PRINCIPLES OF NEURAL SCIENCE

Sixth Edition

Eric R. Kandel
John D. Koester
Sarah H. Mack
Steven A. Siegelbaum

McGraw Hill

PRINCIPLES OF NEURAL SCIENCE

Sixth Edition

Edited by

ERIC R. KANDEL

JOHN D. KOESTER

SARAH H. MACK

STEVEN A. SIEGELBAUM

New York Chicago San Francisco Athens London Madrid Mexico City
Milan New Delhi Singapore Sydney Toronto

ISBN: 978-1-25-964224-1
MHID: 1-25-964224-0

The material in this eBook also appears in the print version of this title: ISBN: 978-1-25-964223-4,
MHID: 1-25-964223-2.

eBook conversion by codeMantra
Version 1.0

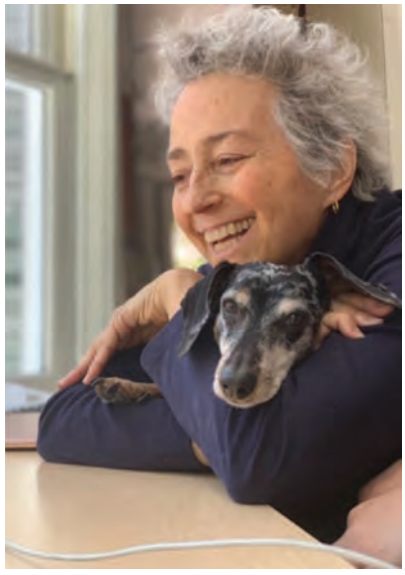

Sarah H. Mack
1962–2020

WE DEDICATE THIS SIXTH EDITION OF *Principles of Neural Science* to our dear friends and colleagues, Thomas M. Jessell and Sarah H. Mack.

Sarah Mack, who contributed to and directed the art program of *Principles of Neural Science* during her more than 30-year tenure, passed away on October 2, 2020. She worked courageously and tirelessly to ensure that all the artwork for this edition met her high standards and could be completed while she still had the strength to continue.

After graduating from Williams College with honors in English literature in 1984, Sarah worked for five years in the field of social work, while taking courses at Columbia in studio art and computer graphics. She first contributed to the art program for the third edition of the book when she joined the Kandel lab as a graphic artist in 1989. Five years later, as the fourth edition went into the planning stage, Sarah, together with Jane Dodd as art editor, completely redesigned the art program, developing and converting hundreds of figures and introducing color. This monumental task required countless aesthetic decisions to develop a stylistic consistency for the various figure elements throughout the book. The result was a set of remarkably clear, didactic, and artistically pleasing diagrams and images. Sarah maintained and extended this high level of excellence as art editor of the fifth and sixth editions of the book. She has thus left an enduring mark on the thousands of students who over the years, as well as in years to come, have been introduced to neuroscience through her work.

Sarah was a most remarkable and gifted artist, who developed a deep understanding and appreciation of neuroscience during the many years she contributed to the book. In addition to her artistic contributions to the figures, she also edited the associated text and legends for maximum clarity. Because her contributions extended far beyond the preparation of the figures, Sarah was made co-editor of the current edition of the book. Sarah also had an amazing ability to juggle huge numbers of negotiations with dozens of authors simultaneously, all the while gently, but firmly, steering them to a final set of elegantly instructive images. She did this with such a spirit of generosity that her interactions with the authors, even those she never met in person, developed into warm friendships.

Over the past three editions, Sarah was the driving force that formed the basis for the aesthetic unifying vision running throughout the chapters of *Principles*. She will be greatly missed by us all.

Thomas M. Jessell
1951–2019

Tom Jessell was an extraordinary neuroscientist who made a series of pioneering contributions to our understanding of spinal cord development, the sensory-motor circuit, and the control of movement. Tom had a deep encyclopedic knowledge and understanding of all that came within his sphere of interest. Equally at home discussing a long-forgotten scientific discovery, quoting Shakespeare by heart, or enthusing about 20th-century British or Italian Renaissance art, Tom was a brilliant polymath.

Tom's interest in neuroscience began with his undergraduate studies of synaptic pharmacology at the University of London, from which he graduated in 1973. He then joined Leslie Iversen's laboratory at the Medical Research Council in Cambridge to pursue his PhD, where he investigated the mechanism by which the newly discovered neuropeptide substance P controls pain sensation. Tom made the pivotal observation that opioids inhibit transmission of pain sensation in the spinal cord by reducing substance P release. After receiving his doctoral degree in 1977, he continued to explore the role of substance P in pain processing as a postdoctoral fellow with Masanori Otsuka in Tokyo, solidifying his lifelong interest in spinal sensory mechanisms while managing to learn rudimentary Japanese. Tom then realized that deeper insights into spinal cord function might best be obtained through an understanding of neural development, prompting him to pursue research on the formation of a classic synapse, the neuromuscular junction, in Gerry Fischbach's laboratory at Harvard.

Tom then joined the faculty of Harvard's Department of Neurobiology as an Assistant Professor in 1981, where he explored the mechanisms of sensory synaptic transmission and the development of the somatosensory input to the spinal cord. In 1985 Tom was recruited to the position of Associate Professor and investigator of the Howard Hughes Medical Institute in the Center for Neurobiology and Behavior (now the Department of Neuroscience) and Department of Biochemistry and Molecular Biophysics at Columbia University's College of Physicians and Surgeons. Over the next 33 years, Tom, together with a remarkable group of students and collaborators, applied a multidisciplinary cellular, biochemical, genetic, and electrophysiological approach to identify and define spinal cord microcircuits that control sensory and motor behavior. His studies revealed the molecular and cellular mechanisms by which spinal neurons acquire their identity and by which spinal circuits are assembled and operate. He defined key concepts and principles of neural development and motor control, and his discoveries generated unprecedented insight into the neural

principles that coordinate movement, paving the way for therapies for motor neuron disease.

Eric Kandel and Jimmy Schwartz, the initial editors of *Principles of Neural Science*, recruited Tom as co-editor as they began to plan the third edition of the book. Tom's role was to expand the treatment of developmental and molecular neural science. This proved to be a prescient choice as Tom's breadth of knowledge, clarity of thought, and precise, elegant style of writing helped shape and define the text for the next three editions. As co-authors of chapters in *Principles* during Tom's tenure, we can attest to the rigor of language and prose that he encouraged his authors to adopt.

In the last years of his life, Tom bravely faced a devasting neurodegenerative disease that prevented him from actively participating in the editing of the current edition. Nonetheless Tom's vision remains in the overall design of *Principles* and its philosophical approach to providing a molecular understanding of the neural bases of behavior and neurological disease. Tom's towering influence on this and future editions of *Principles*, and on the field of neuroscience in general, will no doubt endure for decades to come.

Contents in Brief

Contents

Part IX
Diseases of the Nervous System

This page intentionally left blank

Preface

As in previous editions, the goal of this sixth edition of *Principles of Neural Science* is to provide readers with insight into how genes, molecules, neurons, and the circuits they form give rise to behavior. With the exponential growth in neuroscience research over the 40 years since the first edition of this book, an increasing challenge is to provide a comprehensive overview of the field while remaining true to the original goal of the first edition, which is to elevate imparting basic principles over detailed encyclopedic knowledge.

Some of the greatest successes in brain science over the past 75 years have been the elucidation of the cell biological and electrophysiological functions of nerve cells, from the initial studies of Hodgkin, Huxley, and Katz on the action potential and synaptic transmission to our modern understanding of the genetic and molecular biophysical bases of these fundamental processes. The first three parts of this book delineate these remarkable achievements.

The first six chapters in Part I provide an overview of the broad themes of neural science, including the basic anatomical organization of the nervous system and the genetic bases of nervous system function and behavior. We have added a new chapter (Chapter 5) to introduce the principles by which neurons participate in neural circuits that perform specific computations of behavioral relevance. We conclude by considering how application of modern imaging techniques to the human brain provides a bridge between neuroscience and psychology. The next two parts of the book focus on the basic properties of nerve cells, including the generation and conduction of the action potential (Part II) and the electrophysiological and molecular mechanisms of synaptic transmission (Part III).

We then consider how the activity of neurons in the peripheral and central nervous systems gives rise to sensation and movement. In Part IV, we discuss the various aspects of sensory perception, including how information from the primary organs of sensation is transmitted to the central nervous system and how it is processed there by successive brain regions to generate a sensory percept. In Part V, we consider the neural mechanisms underlying movement, beginning with an overview of the field that is followed by a treatment ranging from the properties of skeletal muscle fibers to an analysis of how motor commands issued by the spinal cord are derived from activity in motor cortex and cerebellum. We include a new treatment that addresses how the basal ganglia regulate the selection of motor actions and instantiate reinforcement learning (Chapter 38).

In the latter parts of the book, we turn to higher-level cognitive processes, beginning in Part VI with a discussion of the neural mechanisms by which subcortical areas mediate homeostatic control mechanisms, emotions, and motivation, and the influence of these processes on cortical cognitive operations, such as feelings, decision-making, and attention. We then consider the development of the nervous system in Part VII, from early embryonic differentiation and the initial establishment of synaptic connections, to their experience-dependent refinement, to the replacement of neurons lost to injury or disease. Because learning and memory can be seen as a continuation of synaptic development, we next consider memory, together with language, and include a new chapter on decision-making and consciousness (Chapter 56) in Part VIII. Finally, in Part IX, we consider the neural mechanisms underlying diseases of the nervous system.

Since the last edition of this book, the field of neuroscience has continued to rapidly evolve, which is reflected in changes in this edition. The continued development of new electrophysiological and light microscopic–based imaging technologies has enabled the simultaneous recording of the activity of large populations of neurons in awake behaving animals. These large data sets have given rise to new computational and theoretical approaches to gain insight into how the activity of populations of neurons produce specific behaviors. Light microscopic imaging techniques

using genetically encoded calcium sensors allow us to record the activity of hundreds or thousands of defined classes of neurons with subcellular resolution as an animal engages in defined behaviors. At the same time, the development of genetically encoded light-activated ion channels and ion pumps (termed optogenetics) or genetically engineered receptors activated by synthetic ligands (termed chemogenetics or pharmacogenetics) can be used to selectively activate or silence genetically defined populations of neurons to examine their causal role in such behaviors. In addition to including such material in chapters throughout the book, we introduce some of these developments in the new Chapter 5, which considers both the new experimental technologies as well as computational principles by which neural circuits give rise to behavior.

Over the past 20 years, there has also been an expansion of new technologies that enable noninvasive and invasive recordings from the human brain. These studies have narrowed the gap between neuroscience and psychology, as exemplified in the expanded discussion of different forms of human memory in Chapter 52. Noninvasive brain imaging methods have allowed scientists to identify brain areas in humans that are activated during cognitive acts. As discussed in a new chapter on the brain–machine interface (Chapter 39), the implantation of electrodes in the brains of patients permits both electrophysiological recordings and local neural stimulation, offering the promise of restoring some function to individuals with damage to the central or peripheral nervous system.

An understanding of basic and higher-order neural mechanisms is critical not only for our understanding of the normal function of the brain, but also for the insights they afford into a range of inherited and acquired neurological and psychiatric disorders. With modern genetic sequencing, it is now clear that inherited or spontaneous mutations in neuronally expressed genes contribute to brain disease. At the same time, it is also clear that environmental factors interact with basic genetic mechanisms to influence disease progression. We now end the book with a new section, Part IX, which presents the neuroscientific principles underlying disorders of the nervous system. In previous editions, many of these chapters were dispersed throughout the book. However, we now group these chapters in their own part based on the increasing appreciation that the underlying causes of what appear to be separate diseases, including neurodegenerative diseases, such as Parkinson and Alzheimer disease, and neurodevelopmental disorders, such as schizophrenia and autism, share certain common principles. Finally, these chapters emphasize the historical tradition of how studies of brain disease provide deep insights into normal brain function, including memory and consciousness.

In writing this latest edition, it is our hope and goal that readers will emerge with an appreciation of the achievements of modern neuroscience and the challenges facing future generations of neuroscientists. By emphasizing how neuroscientists in the past have devised experimental approaches to resolve fundamental questions and controversies in the field, we hope that this textbook will also encourage readers to think critically and not shy away from questioning received wisdom, for every hard-won truth likely will lead to new and perhaps more profound questions in brain science. Thus, it is our hope that this sixth edition of *Principles of Neural Science* will provide the foundation and motivation for the next generation of neuroscientists to formulate and investigate these questions.

Acknowledgments

We were most fortunate to have had the creative editorial assistance of Howard P. Beckman, who passed away earlier this year after having finished his work on this edition. Following graduation from San Francisco State University with a BA in 1968, Howard began his distinguished career as a scientific editor. In 1997, he received a law degree from John F. Kennedy University and began a parallel career in environmental law. Howard has been an integral part of *Principles of Neural Science* since the third edition. Although he was not trained as a scientist, his logical thinking and rigorous intellect helped ensure that the book had a unified style of exposition. Howard's demand for clarity of writing has had an immeasurable impact on each edition of this book, and he will be greatly missed by all who worked with him over the years.

We owe an enormous debt of gratitude to Pauline Henick, who skillfully managed the editorial project with great care, keen intelligence, and the utmost diligence. Pauline somehow managed with good humor and understanding to keep all of the editors and authors of the book on track with their chapters through some very difficult circumstances. The timely publishing of the book would not have been possible without her stellar contributions.

We also wish to thank Jan Troutt of Troutt Visual Services for her superb technical and artistic contributions to the illustrations. We appreciate the artistic expertise and keen eye of Mariah Widman, who helped with the preparation of the figures.

We are indebted to our colleagues at McGraw Hill—Michael Weitz, Kim Davis, Jeffrey Herzich, and Becky Hainz-Baxter—for their invaluable help in the production of this edition. Anupriya Tyagi, Cenveo Publisher Services, did an outstanding job of overseeing the composition of the book, for which we are most grateful.

Many other colleagues have helped the editors by critically reading selected chapters of the book and have helped the authors with assistance in the research and writing of the chapters. We wish to acknowledge the contributions of Katherine W. Eyring to Chapter 15; Jeffrey L. Noebels, MD, PhD, to Chapter 58; and Gabriel Vazquez Velez, PhD, Maxime William C. Rousseaux, PhD, and Vicky Brandt to Chapter 63.

We also wish to acknowledge the important role of authors of chapters in previous editions of *Principles of Neural Science,* whose past contributions continue to be reflected in a number of chapters in the present edition. These legacy authors include Cori Bargmann, Uta Frith, James Gordon, A.J. Hudspeth, Conrad Gilliam, James E. Goldman, Thomas M. Jessell (deceased), Jane M. Macpherson, James H. Schwartz (deceased), Thomas Thach (deceased), and Stephen Warren.

We are especially indebted to the editors of the different sections (parts) of the book—Thomas D. Albright, Randy M. Bruno, Thomas M. Jessell (deceased), C. Daniel Salzman, Joshua R. Sanes, Michael N. Shadlen, Daniel M. Wolpert, and Huda Y. Zoghbi—who played a critical role in planning the overall organization of their sections and working with the authors to shape their chapters. Most importantly, we owe the greatest debt to the contributing authors of this edition.

We finally thank our spouses and families for their support and forbearance during the editorial process.

This page intentionally left blank

Contributors

Laurence F. Abbott, PhD
William Bloor Professor of Theoretical Neuroscience
Co-Director, Center for Theoretical Neuroscience
Zuckerman Mind Brain Behavior Institute
Department of Neuroscience, and Department of Physiology and Cellular Biophysics
Columbia University College of Physicians and Surgeons

Ralph Adolphs, PhD
Bren Professor of Psychology, Neuroscience, and Biology
Division of Humanities and Social Sciences
California Institute of Technology

Thomas D. Albright, PhD
Professor and Conrad T. Prebys Chair
The Salk Institute for Biological Studies

David G. Amaral, PhD
Distinguished Professor
Department of Psychiatry and Behavioral Sciences
The MIND Institute
University of California, Davis

Dora Angelaki, PhD
Center for Neural Science
New York University

Cornelia I. Bargmann, PhD
The Rockefeller University

Ben A. Barres, MD, PhD*
Professor and Chair, Department of Neurobiology
Stanford University School of Medicine

Allan I. Basbaum, PhD, FRS
Professor and Chair
Department of Anatomy
University California San Francisco

Amy J. Bastian, PhD
Professor of Neuroscience, Neurology, and Physical Medicine and Rehabilitation
Department of Neuroscience
Johns Hopkins University
Director of the Motion Analysis Laboratory
Kennedy Krieger Institute

Bruce P. Bean, PhD
Department of Neurobiology
Harvard Medical School

Robert H. Brown, Jr, DPhil, MD
Professor of Neurology
Director, Program in Neurotherapeutics
University of Massachusetts Medical School

Randy M. Bruno, PhD
Associate Professor
Kavli Institute for Brain Science
Mortimer B. Zuckerman Mind Brain Behavior Institute
Department of Neuroscience
Columbia University

Linda B. Buck, PhD
Professor of Basic Sciences
Fred Hutchinson Cancer Research Center
Affiliate Professor of Physiology and Biophysics
University of Washington

*Deceased

Stephen C. Cannon, MD, PhD
Professor and Chair of Physiology
Interim Chair of Molecular and Medical Pharmacology
David Geffen School of Medicine
University of California, Los Angeles

David E. Clapham, MD, PhD
Aldo R. Castañeda Professor of Cardiovascular Research, Emeritus
Professor of Neurobiology, Emeritus
Harvard Medical School
Vice President and Chief Scientific Officer
Howard Hughes Medical Institute

Rui M. Costa, DVM, PhD
Professor of Neuroscience and Neurology
Director/CEO Zuckerman Mind Brain Behavior Institute
Columbia University

Aniruddha Das, PhD
Associate Professor
Department of Neuroscience
Mortimer B. Zuckerman Mind Brain Behavior Institute
Columbia University

J. David Dickman, PhD
Vivian L. Smith Endowed Chair of Neuroscience
Department of Neuroscience
Baylor College of Medicine

Trevor Drew, PhD
Professor
Groupe de Recherche sur le Système Nerveux Central (GRSNC)
Department of Neurosciences
Université de Montréal

Gammon M. Earhart, PT, PhD, FAPTA
Professor of Physical Therapy, Neuroscience, and Neurology
Washington University in St. Louis

Joel K. Elmquist, DVM, PhD
Professor, Departments of Internal Medicine and Pharmacology
Director, Center for Hypothalamic Research
Carl H. Westcott Distinguished Chair in Medical Research
Maclin Family Professor in Medical Science
The University of Texas Southwestern Medical Center

Roger M. Enoka, PhD
Professor
Department of Integrative Physiology
University of Colorado

Gerald D. Fischbach, MD
Distinguished Scientist and Fellow, Simons Foundation
Executive Vice President for Health and Biomedical Sciences, Emeritus
Columbia University

Winrich Freiwald, PhD
Laboratory of Neural Systems
The Rockefeller University

Christopher D. Frith, PhD, FMedSci, FRS, FBA
Emeritus Professor of Neuropsychology, Wellcome Centre for Human Neuroimaging
University College London
Honorary Research Fellow
Institute of Philosophy
School of Advanced Study
University of London

Daniel Gardner, PhD
Professor of Physiology and Biophysics
Departments of Physiology and Biophysics, Neurology, and Neuroscience
Weill Cornell Medical College

Esther P. Gardner, PhD
Professor of Neuroscience and Physiology
Department of Neuroscience and Physiology
Member, NYU Neuroscience Institute
New York University Grossman School of Medicine

Charles D. Gilbert, MD, PhD
Arthur and Janet Ross Professor
Head, Laboratory of Neurobiology
The Rockefeller University

T. Conrad Gilliam, PhD
Marjorie I. and Bernard A. Mitchel Distinguished Service Professor of Human Genetics
Dean for Basic Science
Biological Sciences Division and Pritzker School of Medicine
The University of Chicago

Michael E. Goldberg, MD
David Mahoney Professor of Brain and Behavior
Departments of Neuroscience, Neurology, Psychiatry, and Ophthalmology
Columbia University Vagelos College of Physicians and Surgeons
Zuckerman Mind Brain Behavior Institute

Joshua A. Gordon, MD, PhD
Director, National Institute of Mental Health

David M. Holtzman, MD
Department of Neurology, Hope Center for Neurological Disorders
Knight Alzheimer's Disease Research Center
Washington University School of Medicine

Fay B. Horak, PhD, PT
Professor of Neurology
Oregon Health and Science University

John P. Horn, PhD
Professor of Neurobiology
Associate Dean for Graduate Studies
Department of Neurobiology
University of Pittsburgh School of Medicine

Steven E. Hyman, MD
Stanley Center for Psychiatric Research
Broad Institute of MIT and Harvard University
Department of Stem Cell and Regenerative Biology
Harvard University

Jonathan A. Javitch, MD, PhD
Lieber Professor of Experimental Therapeutics in Psychiatry
Professor of Pharmacology
Columbia University Vagelos College of Physicians and Surgeons
Chief, Division of Molecular Therapeutics
New York State Psychiatric Institute

Thomas M. Jessell, PhD*
Professor (Retired)
Department of Neuroscience and Biochemistry and Biophysics
Columbia University

John Kalaska, PhD
Professeur Titulaire
Département de Neurosciences
Faculté de Médecine
l'Université de Montréal

Eric R. Kandel, MD
University Professor
Kavli Professor and Director, Kavli Institute for Brain Science
Co-Director, Mortimer B. Zuckerman Mind Brain Behavior Institute
Senior Investigator, Howard Hughes Medical Institute
Department of Neuroscience
Columbia University

Ole Kiehn, MD, PhD
Professor, Department of Neuroscience
University of Copenhagen
Professor, Department of Neuroscience
Karolinska Institutet
Stockholm, Sweden

John D. Koester, PhD
Professor Emeritus of Clinical Neuroscience
Vagelos College of Physicians and Surgeons
Columbia University

Patricia K. Kuhl, PhD
The Bezos Family Foundation Endowed Chair in Early Childhood Learning
Co-Director, Institute for Learning and Brain Sciences
Professor, Speech and Hearing Sciences
University of Washington

Joseph E. LeDoux, PhD
Henry And Lucy Moses Professor of Science
Professor of Neural Science and Psychology
Professor of Psychiatry and Child and Adolescent Psychiatry
NYU Langone Medical School
Director of the Emotional Brain Institute
New York University and Nathan Kline Institute

*Deceased

Stephen G. Lisberger, PhD
Department of Neurobiology
Duke University School of Medicine

Attila Losonczy, MD, PhD
Professor, Department of Neuroscience
Mortimer B. Zuckerman Mind Brain Behavior Institute
Kavli-Simons Fellow
Kavli Institute for Brain Science
Columbia University

Bradford B. Lowell, MD, PhD
Professor, Division of Endocrinology, Diabetes, and Metabolism
Department of Medicine
Beth Israel Deaconess Medical Center
Program in Neuroscience
Harvard Medical School

Geoffrey A. Manley, PhD
Professor (Retired), Cochlear and Auditory Brainstem Physiology
Department of Neuroscience
School of Medicine and Health Sciences
Cluster of Excellence "Hearing4all"
Research Centre Neurosensory Science
Carl von Ossietzky University
Oldenburg, Germany

Eve Marder, PhD
Victor and Gwendolyn Beinfield University Professor
Volen Center and Biology Department
Brandeis University

Pascal Martin, PhD
CNRS Research Director
Laboratoire Physico-Chimie Curie
Institut Curie, PSL Research University
Sorbonne Université
Paris, France

Markus Meister, PhD
Professor of Biology
Division of Biology and Biological Engineering
California Institute of Technology

Edvard I. Moser, PhD
Kavli Institute for Systems Neuroscience
Norwegian University of Science and Technology
Trondheim, Norway

May-Britt Moser, PhD
Kavli Institute for Systems Neuroscience
Norwegian University of Science and Technology
Trondheim, Norway

Eric J. Nestler, MD, PhD
Nash Family Professor of Neuroscience
Director, Friedman Brain Institute
Dean for Academic and Scientific Affairs
Icahn School of Medicine at Mount Sinai

Jens Bo Nielsen, MD, PhD
Professor, Department of Neuroscience
University of Copenhagen
The Elsass Foundation
Denmark

Donata Oertel, PhD*
Professor of Neurophysiology
Department of Neuroscience
University of Wisconsin

Franck Polleux, PhD
Professor, Columbia University
Department of Neuroscience
Mortimer B. Zuckerman Mind Brain Behavior Institute
Kavli Institute for Brain Science

Peter Redgrave, PhD
University Professor, Emeritus
Department of Psychology
University of Sheffield
United Kingdom

Lewis P. Rowland, MD*
Professor of Neurology and Chair Emeritus
Department of Neurology
Columbia University

*Deceased

C. Daniel Salzman, MD, PhD
Professor, Departments of Neuroscience and Psychiatry
Investigator, Mortimer B. Zuckerman Mind Brain Behavior Institute
Investigator, Kavli Institute for Brain Science
Columbia University

Joshua R. Sanes, PhD
Jeff C. Tarr Professor of Molecular and Cellular Biology
Paul J. Finnegan Family Director, Center for Brain Science
Harvard University

Clifford B. Saper, MD, PhD
James Jackson Putnam Professor of Neurology and Neuroscience
Harvard Medical School
Chairman, Department of Neurology
Beth Israel Deaconess Medical Center
Editor-in-Chief, *Annals of Neurology*

Nathaniel B. Sawtell, PhD
Associate Professor
Zuckerman Mind Brain Behavior Institute
Department of Neuroscience
Columbia University

Thomas E. Scammell, MD
Professor of Neurology
Beth Israel Deaconess Medical Center
Harvard Medical School

Daniel L. Schacter, PhD
William R. Kenan, Jr. Professor
Department of Psychology, Harvard University

Kristin Scott, PhD
Professor
University of California, Berkeley
Department of Molecular and Cell Biology

Stephen H. Scott, PhD
Professor and GSK Chair in Neuroscience
Centre for Neuroscience Studies
Department of Biomedical and Molecular Sciences
Department of Medicine
Queen's University
Kingston, Canada

Michael N. Shadlen, MD, PhD
Howard Hughes Medical Institute
Kavli Institute of Brain Science
Department of Neuroscience
Zuckerman Mind Brain Behavior Institute
Columbia University Irving Medical Center
Columbia University

Nirao M. Shah, MBBS, PhD
Department of Psychiatry and Behavioral Sciences
Department of Neurobiology
Stanford University

Krishna V. Shenoy, PhD
Investigator, Howard Hughes Medical Institute
Hong Seh and Vivian W. M. Lim Professor
Departments of Electrical Engineering, Bioengineering, and Neurobiology
Wu Tsai Neurosciences Institute and Bio-X Institute
Stanford University

Daphna Shohamy, PhD
Professor, Department of Psychology
Zuckerman Mind Brain Behavior Institute
Kavli Institute for Brain Science
Columbia University

Steven A. Siegelbaum, PhD
Chair, Department of Neuroscience
Gerald D. Fischbach, MD, Professor of Neuroscience
Professor of Pharmacology
Columbia University

Matthew W. State, MD, PhD
Oberndorf Family Distinguished Professor and Chair
Department of Psychiatry and Behavioral Sciences
Weill Institute for Neurosciences
University of California, San Francisco

Beth Stevens, PhD
Boston Children's Hospital
Broad Institute of Harvard and MIT
Howard Hughes Medical Institute

Thomas C. Südhof, MD
Avram Goldstein Professor in the School of Medicine
Departments of Molecular and Cellular Physiology and of Neurosurgery
Howard Hughes Medical Institute
Stanford University

David Sulzer, PhD
Professor, Departments of Psychiatry, Neurology, and Pharmacology
School of the Arts
Columbia University
Division of Molecular Therapeutics
New York State Psychiatric Institute

Larry W. Swanson, PhD
Department of Biological Sciences
University of Southern California

Carol A. Tamminga, MD
Professor and Chairman
Department of Psychiatry
UT Southwestern Medical School

Marc Tessier-Lavigne, PhD
President, Stanford University
Bing Presidential Professor
Department of Biology
Stanford University

Richard W. Tsien, DPhil
Druckenmiller Professor of Neuroscience
Chair, Department of Physiology and Neuroscience
Director, NYU Neuroscience Institute
New York University Medical Center
George D. Smith Professor Emeritus
Stanford University School of Medicine

Nicholas B. Turk-Browne, PhD
Professor, Department of Psychology
Yale University

Anthony D. Wagner, PhD
Professor, Department of Psychology
Wu Tsai Neurosciences Institute
Stanford University

Mark F. Walker, MD
Associate Professor of Neurology
Case Western Reserve University
Staff Neurologist, VA Northeast Ohio Healthcare System

Xiaoqin Wang, PhD
Professor
Laboratory of Auditory Neurophysiology
Department of Biomedical Engineering
Johns Hopkins University

Gary L. Westbrook, MD
Senior Scientist, Vollum Institute
Dixon Professor of Neurology
Oregon Health and Science University

Daniel M. Wolpert, PhD, FMedSci, FRS
Department of Neuroscience
Mortimer B. Zuckerman Mind Brain Behavior Institute
Columbia University

Robert H. Wurtz, PhD
Distinguished Investigator Emeritus
Laboratory of Sensorimotor Research
National Eye Institute
National Institutes of Health

Byron M. Yu, PhD
Department of Electrical and Computer Engineering
Department of Biomedical Engineering Neuroscience Institute
Carnegie Mellon University

Rafael Yuste, MD, PhD
Columbia University
Professor of Biological Sciences
Director, Neurotechnology Center
Co-Director, Kavli Institute of Brain Sciences
Ikerbasque Research Professor
Donostia International Physics Center (DIPC)

Huda Y. Zoghbi, MD
Investigator, Howard Hughes Medical Institute
Professor, Baylor College of Medicine
Director, Jan and Dan Duncan Neurological Research Institute
Texas Children's Hospital

Charles Zuker, PhD
Departments of Neuroscience, and Biochemistry and Molecular Biophysics
Columbia University
Howard Hughes Medical Institute

Part I

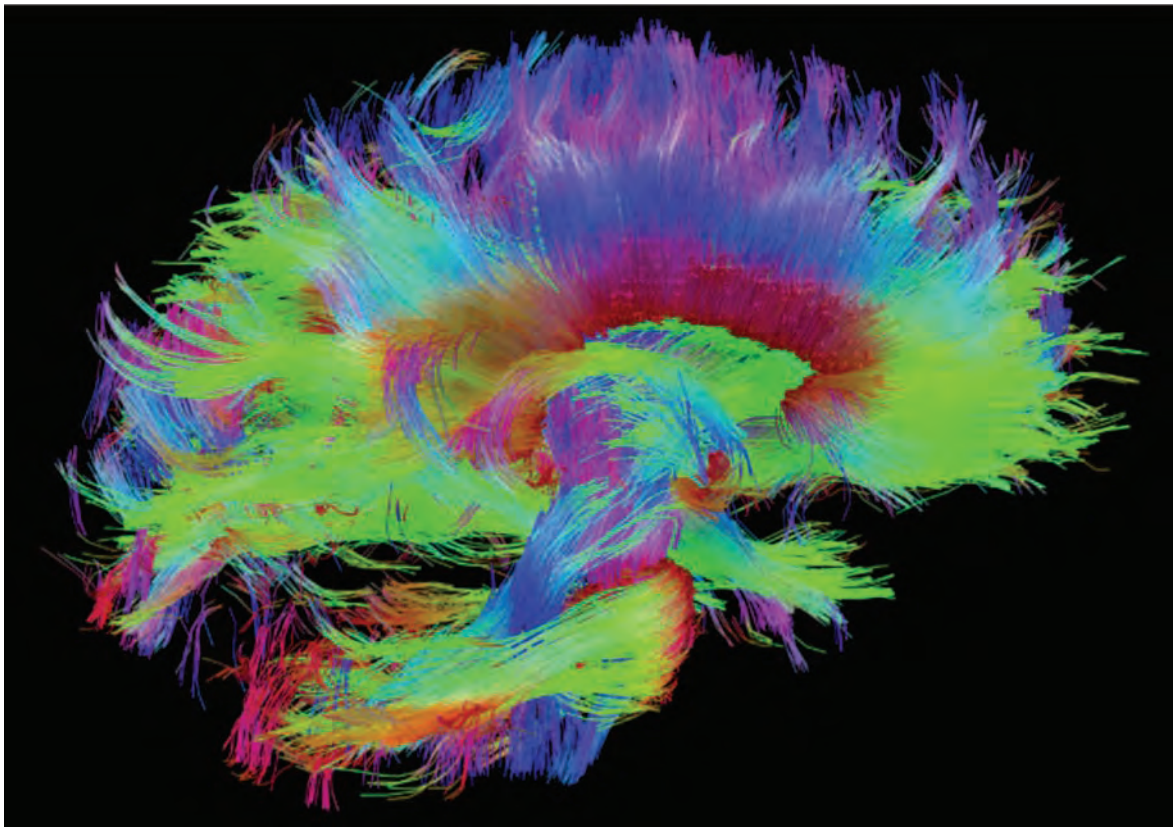

Preceding Page

White matter fiber architecture of the human brain, showing the corpus callosum and brainstem pathways. The image was constructed from magnetic resonance (MR) imaging data with the diffusion spectrum imaging technique, which uses the rate and preferred direction of diffusion of water molecules to generate contrast in MR images to reveal bundles of axons traveling in fiber tracts. The fibers are color-coded by direction: **red**, left-right; **green**, anterior-posterior; **blue**, ascending-descending (RGB = *XYZ* axes). From the Connectome Scanner dataset. (From the Connectome Scanner dataset. Courtesy of the USC Laboratory of Neuro Imaging and Athinoula A. Martinos Center for Biomedical Imaging. Consortium of the Human Connectome Project— www.humanconnectomeproject.org.)

I Overall Perspective

During the second half of the 20th century, the central focus of biology was on the gene. Now in the first half of the 21st century, the focus has shifted to neural science, and specifically to the biology of the mind. We wish to understand the processes by which we perceive, act, learn, and remember. How does the brain—an organ weighing only 1.5 kg—conceive of the infinite, discover new knowledge, and produce the remarkable individuality of human thoughts, feelings, and actions? How are these extraordinary mental capabilities distributed within the organ? What rules relate the anatomical organization and the cellular physiology of a region to its specific role in mentation? What do genes contribute to behavior, and how is gene expression in nerve cells regulated by developmental and learning processes? How does experience alter the way the brain processes subsequent events, and to what degree is that processing unconscious? Finally, what are the neural bases of neurological and psychiatric disorders? In this introductory section of *Principles of Neural Science*, we begin to address these questions. In so doing, we describe how neural science attempts to link the computational logic of neural circuitry to the mind—how the activities of nerve cells within defined neural circuits mediate complex mental processes.

Over the past several decades, technological advances have opened new horizons for the scientific study of the brain. Today, it is possible to link the cellular dynamics of interconnected circuits of neurons to the internal representations of perceptual and motor acts in the brain and to relate these internal mechanisms to observable behavior. New imaging techniques permit us to visualize the human brain in action—to identify specific regions of the brain associated with particular modes of thinking and feeling and their patterns of interconnections.

In the first part of this book, we consider the degree to which mental functions can be localized to specific regions of the brain. We also examine the extent to which such functions can be understood in terms of the properties of individual nerve cells, their molecular constituents, and their synaptic connections. In the later parts of the book, we examine in detail the mechanisms underlying cognitive

and affective functions of the brain: perception, action, motivation, emotion, learning, and memory.

The human brain is a network of more than 80 billion individual nerve cells interconnected in systems—neural circuits—that construct our perceptions of the external world, fix our attention, guide our decisions, and implement our actions. A first step toward understanding the mind, therefore, is to learn how neurons are organized into signaling pathways and how they communicate by means of synaptic transmission. One of the chief ideas we shall develop in this book is that the specificity of the synaptic connections established during development and refined during experience underlie behavior. We must also understand both the innate and environmental determinants of behavior in which genes encode proteins that initially govern the development of the neural circuits that can then be modified by experience-dependent changes in gene expression.

A new science of mind is emerging through the application of modern cell and molecular biological techniques, brain imaging, theory, and clinical observation to the study of cognition, emotion, and behavior. Neural science has reinforced the idea first proposed by Hippocrates more than two millennia ago that the proper study of mind begins with study of the brain. Cognitive psychology and psychoanalytic theory have emphasized the diversity and complexity of human mental experience. These disciplines can now be enriched by insights into brain function from neural science. The task ahead is to produce a study of mental processes, grounded firmly in empirical neural science, concerned with questions of how internal representations and states of mind are generated.

Our goal is to provide not simply the facts but the principles of brain organization, function, and computation. The principles of neural science do not reduce the complexity of human thought to a set of molecules or mathematical axioms. Rather, they allow us to appreciate a certain beauty—a Darwinian elegance—in the complexity of the brain that accounts for mind and behavior. One might ask whether an idea gleaned from the detailed dissection of a more basic neural mechanism contains insight about higher brain function. Does the organization of a simple reflex bear on a volitional movement of the hand? Do the mechanisms that establish circuitry in the developing spinal cord bear on the mechanisms at play in storing a memory? Are the neural processes that awaken us from sleep similar to those that allow an unconscious process to pierce our conscious awareness? We hope readers will delight in the principles as they delve into their factual basis. No doubt, it is a work in progress.

Part Editors: Eric R. Kandel and Michael N. Shadlen

Part I

1

The Brain and Behavior

The last frontier of the biological sciences—the ultimate challenge—is to understand the biological basis of consciousness and the brain processes by which we feel, act, learn, and remember. During the past few decades, a remarkable unification within the biological sciences has set the stage for addressing this great challenge. The ability to sequence genes and infer the amino acid sequences of the proteins they encode has revealed unanticipated similarities between proteins in the nervous system and those encountered elsewhere in the body. As a result, it has become possible to establish a general plan for the function of cells, a plan that provides a common conceptual framework for all of cell biology, including cellular neural science.

The current challenge in the unification within biology is the unification of psychology—the science of the mind—and neural science—the science of the brain. Such a unified approach, in which mind and body are not seen as separate entities, rests on the view that all behavior is the result of brain function. What we commonly call the mind is a set of operations carried out by the brain. Brain processes underlie not only simple motor behaviors such as walking and eating but also all the complex cognitive acts and behavior that we regard as quintessentially human—thinking, speaking, and creating works of art. As a corollary, all the behavioral disorders that characterize psychiatric illness—disorders of affect (feeling) and cognition (thought)—result from disturbances of brain function.

How do the billions of individual nerve cells in the brain produce behavior and cognitive states, and how are those cells influenced by the environment, which includes social experience? Explaining behavior in terms of brain activity is the important task of neural science, and the progress of neural science in this respect is a major theme of this book.

Neural science must continually confront certain fundamental questions. What is the appropriate level of biological description to understand a thought process, the movement of a limb, or the desire to make the movement? Why is a movement smooth or jerky or made unintentionally in certain neurological disease states? Answers to these questions might emerge from looking at the pattern of DNA expression in nerve cells and how this pattern regulates the electrical properties of neurons. However, we will also require knowledge of neural circuits comprising many neurons in specific brain areas and how the activity of specific circuits in many brain areas is coordinated.

Is there a level of biological description that is most apt? The short answer is, it depends. If one's goal is to understand and treat certain genetic epilepsy disorders, then DNA sequencing and measurements of electrical properties of individual neurons might be sufficient to produce an effective therapy.

If one is interested in learning, perception, and exploration, then an analysis of systems of circuits and brain regions is likely to be required.

The goal of modern neural science is to integrate all of these specialized levels into a coherent science. The effort forces us to confront new questions. If mental processes can be localized to discrete brain regions, what is the relationship between the functions of those regions and the anatomy and physiology of those regions? Is one kind of neural circuit required to process visual information, another type to parse speech, and yet another to sequence movements? Or do circuits with different functions share common organizational principles? Are the requisite neural computations best understood as operations on information represented by single neurons or populations of neurons? Is information represented in the electrical activity of individual nerve cells, or is it distributed over ensembles such that any one cell is no more informative than a random bit of computer memory? As we shall see, questions about levels of organization, specialization of cells, and localization of function recur throughout neural science.

To illustrate these points we shall examine how modern neural science describes language, a distinctive cognitive behavior in humans. In so doing, we shall focus broadly on operations in the cerebral cortex, the part of the brain that is most highly developed in humans. We shall see how the cortex is organized into functionally distinct regions, each made up of large groups of neurons, and how the neural apparatus of a highly complex behavior can be analyzed in terms of the activity of specific sets of interconnected neurons within specific regions. In Chapter 3, we describe how the neural circuit for a simple reflex behavior operates at the cellular level, illustrating how the interplay of sensory signals and motor signals leads to a motor act.

Two Opposing Views Have Been Advanced on the Relationship Between Brain and Behavior

Our views about nerve cells, the brain, and behavior emerged during the 20th century from a synthesis of five experimental traditions: anatomy, embryology, physiology, pharmacology, and psychology.

The 2nd century Greek physician Galen proposed that nerves convey fluid secreted by the brain and spinal cord to the body's periphery. His views dominated Western medicine until the microscope revealed the true structure of the cells in nervous tissue. Even so, nervous tissue did not become the subject of a special science until the late 1800s, when the Italian Camillo Golgi and the Spaniard Santiago Ramón y Cajal produced detailed, accurate descriptions of nerve cells but reached two quite different conclusions of how the brain functions.

Golgi developed a method of staining neurons with silver salts that revealed their entire cell structure under the microscope. Based on such studies, Golgi concluded that nerve cells are not independent cells isolated from one another but instead act together in one continuous web of tissue or syncytium. Using Golgi's technique, Ramón y Cajal observed that each neuron typically has a cell body and two types of processes: branching dendrites at one end and a long, cable-like axon at the other. Cajal concluded that nervous tissue is not a syncytium but a network of discrete cells. In the course of this work, Ramón y Cajal developed some of the key concepts and much of the early evidence for the *neuron doctrine*—the principle that individual neurons are the elementary building blocks and signaling elements of the nervous system.

In the 1920s the American embryologist Ross Harrison showed that the dendrites and axons grow from the cell body and do so even when each neuron is isolated from others in tissue culture. Harrison also confirmed Ramón y Cajal's suggestion that the tip of the axon gives rise to an expansion, the *growth cone*, which leads the developing axon to its target, either to other nerve cells or muscles. Both of these discoveries lent strong support to the neuron doctrine. The final definite evidence for the neuron doctrine came in the mid-1950s with the introduction of electron microscopy. A landmark study by Sanford Palay unambiguously demonstrated the existence of synapses, specialized regions of nerve cells that permit chemical or electrical signaling between them.

Physiological investigation of the nervous system began in the late 1700s when the Italian physician and physicist Luigi Galvani discovered that muscle and nerve cells produce electricity. Modern electrophysiology grew out of work in the 19th century by three German physiologists—Johannes Müller, Emil du Bois-Reymond, and Hermann von Helmholtz—who succeeded in measuring the speed of conduction of electrical activity along the axon of the nerve cell and further showed that the electrical activity of one nerve cell affects the activity of an adjacent cell in predictable ways.

Pharmacology made its first impact on our understanding of the nervous system and behavior at the end of the 19th century when Claude Bernard in France, Paul Ehrlich in Germany, and John Langley in England demonstrated that drugs do not act randomly on a cell, but rather bind to discrete receptors typically located in the cell membrane. This insight led to the discovery

that nerve cells can communicate with each other by chemical means.

Psychological thinking about behavior dates back to the beginnings of Western science when the ancient Greek philosophers speculated about the causes of behavior and the relation of the mind to the brain. In subsequent centuries, two major views emerged. In the 17th century, René Descartes distinguished body and mind. In this *dualistic view*, the brain mediates perception, motor acts, memory, appetites, and passions—everything that can be found in the lower animals. But the mind—the higher mental functions, the conscious experience characteristic of human behavior—is not represented in the brain or any other part of the body but in the soul, a spiritual entity. Descartes believed that the soul communicated with the machinery of the brain by means of the pineal gland, a tiny structure in the midline of the brain. Descartes's position has had little sway in modern philosophy or neural science. Indeed, the underlying premise of neural science is that mind is a product of the brain and its neural activity. By this we do not mean that the aim of neural science is to explain *away* the mind by reduction to biological components, but rather to elucidate the biology of mind.

Attempts to join biological and psychological concepts in the study of behavior began as early as 1800, when Franz Joseph Gall, a Viennese physician and neuroanatomist, proposed a radically new idea of body and mind. He advocated that the brain is the organ of the mind and that all mental functions are embodied in the brain. He thus rejected the Cartesian idea that mind and body are separate entities. In addition, he argued that the cerebral cortex was not a unitary organ but contained within it many specialized organs, and that particular regions of the cerebral cortex control specific functions. Gall enumerated at least 27 distinct regions or organs of the cerebral cortex; later many more were added, each corresponding to a specific mental faculty (Figure 1–1). Gall assigned intellectual processes, such as the ability to evaluate causality, to calculate, and to sense order, to the front of the brain. Instinctive characteristics such as romantic love (*amativeness*) and combativeness were assigned to the back of the brain. Even the most abstract of human behaviors—generosity, secretiveness, and religiosity—were assigned a spot in the brain.

Although Gall's theory of the unity of body and mind and his idea that certain functions were localized to specific brain regions proved to be correct, the dominant view today is that many higher functions of mind are most likely highly distributed. Moreover, Gall's experimental approach to localization was extremely

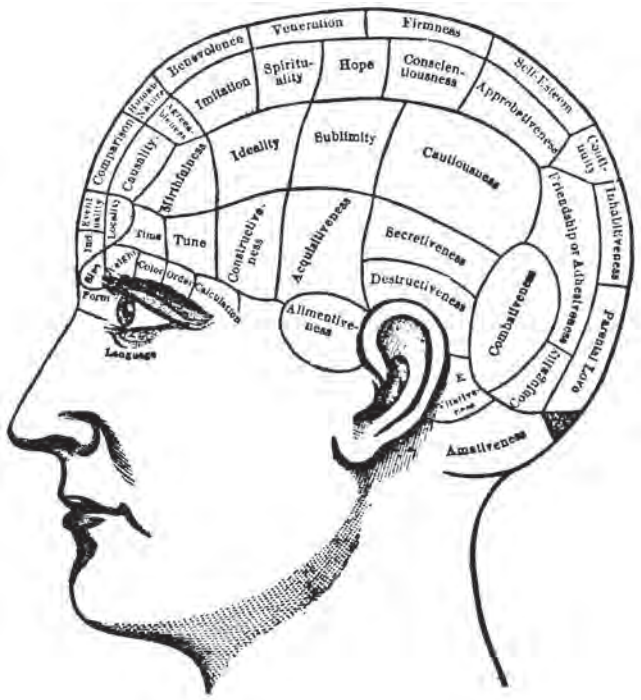

Figure 1–1 An early map of functional localization in the brain. According to the 19th century doctrine of phrenology, complex traits such as combativeness, spirituality, hope, and conscientiousness are controlled by specialized "organs," distinct areas of the cerebral cortex that expand as the traits develop. These enlargements of local areas of the brain were thought to produce characteristic bumps and ridges on the overlying skull, from which an individual's character could be determined. This map, taken from a drawing of the early 1800s, shows 42 intellectual and emotional "organs."

naive. Rather than locate functions empirically, by looking into the brain and correlating defects in mental attributes with lesions in specific regions following tumor or stroke, Gall spurned all evidence derived from studies of brain lesions, whether discovered through clinical examination or produced surgically in experimental animals. Influenced by physiognomy, the popular science based on the idea that facial features reveal character, Gall believed that the bumps and ridges on the skulls of people well endowed with specific cognitive faculties identified the centers for those faculties in the brain. He assumed that the size of an area of brain was related to the relative importance of the mental faculty represented in that area. Accordingly, exercise of a given mental faculty would cause the corresponding brain region to grow, and this growth in turn would cause the overlying skull to protrude.

Gall first had this idea as a young boy when he noticed that those of his classmates who excelled at

memorizing school assignments had prominent eyes. He concluded that this was the result of an overdevelopment of regions in the front of the brain involved in verbal memory. He developed this idea further when, as a young physician, he was placed in charge of an asylum for the insane in Vienna. There he began to study patients suffering from monomania, a disorder characterized by an exaggerated interest in some key idea or a deep urge to engage in some specific behavior—theft, murder, eroticism, extreme religiosity. He reasoned that, because the patient functioned well in all other behaviors, the brain defect must be discrete and in principle could be localized by examining the skulls of these patients. Gall's studies of localized brain functions led to *phrenology*, a discipline concerned with determining personality and character based on the detailed shape of the skull.

In the late 1820s, Gall's ideas were subjected to experimental analysis by the French physiologist Pierre Flourens. Using experimental animals, Flourens destroyed some of Gall's functional centers in the brain, and in turn attempted to isolate the contribution of these "cerebral organs" to behavior. From these experiments, Flourens concluded that specific brain regions are not responsible for specific behaviors, but that all brain regions, especially the cerebral hemispheres of the forebrain, participate in every mental operation. Any part of a cerebral hemisphere, Flourens proposed, contributes to all the hemisphere's functions. Injury to any one area of the cerebral hemisphere should therefore affect all higher functions equally. Thus in 1823 Flourens wrote: "All perceptions, all volitions occupy the same seat in these (cerebral) organs; the faculty of perceiving, of conceiving, of willing merely constitutes therefore a faculty which is essentially one."

The rapid acceptance of this belief, later called the *holistic* view of the brain, was based only partly on Flourens's experimental work. It also represented a cultural reaction against the materialistic view that the human mind is a biological organ. It represented a rejection of the notion that there is no soul, that all mental processes can be reduced to activity within the brain, and that the mind can be improved by exercising it—ideas that were unacceptable to the religious establishment and landed aristocracy of Europe.

The holistic view was seriously challenged, however, in the mid-19th century by the French neurologist Paul Pierre Broca, the German neurologist Carl Wernicke, and the British neurologist Hughlings Jackson. For example, in his studies of focal epilepsy, a disease characterized by convulsions that begin in a particular part of the body, Jackson showed that different motor and sensory functions could be traced to specific parts of the cerebral cortex. The regional studies by Broca, Wernicke, and Jackson were extended to the cellular level by Charles Sherrington and by Ramón y Cajal, who championed the view of brain function called *cellular connectionism.* According to this view, individual neurons are the signaling units of the brain; they are arranged in functional groups and connect to one another in a precise fashion. Wernicke's work and that of the French neurologist Jules Dejerine revealed that different behaviors are produced by different interconnected brain regions.

The first important evidence for localization emerged from studies of how the brain produces language. Before we consider the relevant clinical and anatomical studies, we shall first review the overall structure of the brain, including its major anatomical regions. This requires that we define some essential navigational terms used by neuroanatomists to describe the three-dimensional spatial relationships between parts of the brain and spinal cord. These terms are introduced in Box 1–1 and Figure 1–2.

The Brain Has Distinct Functional Regions

The central nervous system is a bilateral and largely symmetrical structure with two main parts, the spinal cord and the brain. The brain comprises six major structures: the medulla oblongata, pons, cerebellum, midbrain, diencephalon, and cerebrum (Box 1–2 and Figure 1–3). Each of these in turn comprise distinct groups of neurons with distinctive connectivity and developmental origin. In the medulla, pons, midbrain, and diencephalon, neurons are often grouped in distinct clusters termed nuclei. The surface of the cerebrum and cerebellum consists of a large folded sheet of neurons called the cerebral cortex and the cerebellar cortex, respectively, where neurons are organized in layers with stereotyped patterns of connectivity. The cerebrum also contains a number of structures located below the cortex (subcortical), including the basal ganglia and amygdala (Figure 1–4).

Modern brain imaging techniques make it possible to see activity in these structures in living people (see Chapter 6). Brain imaging is commonly used to evaluate the metabolic activity of discrete regions of the brain while people are engaged in specific tasks under controlled conditions. Such studies provide evidence that specific types of behavior recruit the activity of particular regions of the brain more than others. Brain imaging vividly demonstrates that cognitive operations rely primarily on the cerebral cortex, the furrowed gray matter covering the two cerebral hemispheres (Figure 1–5).

Box 1–1 Neuroanatomical Terms of Navigation

The location and orientation of components of the central nervous system within the body are described with reference to three axes: the rostral-caudal, dorsal-ventral, and medial-lateral axes (Figure 1–2). These terms allow the neuroanatomist to describe spatial relations between parts of the brain and spinal cord. They facilitate the comparison of brains of individuals of the same species as they develop or in the case of a disease. They also facilitate the comparison of brains from different species of animals, for example, to understand the brain's evolution.

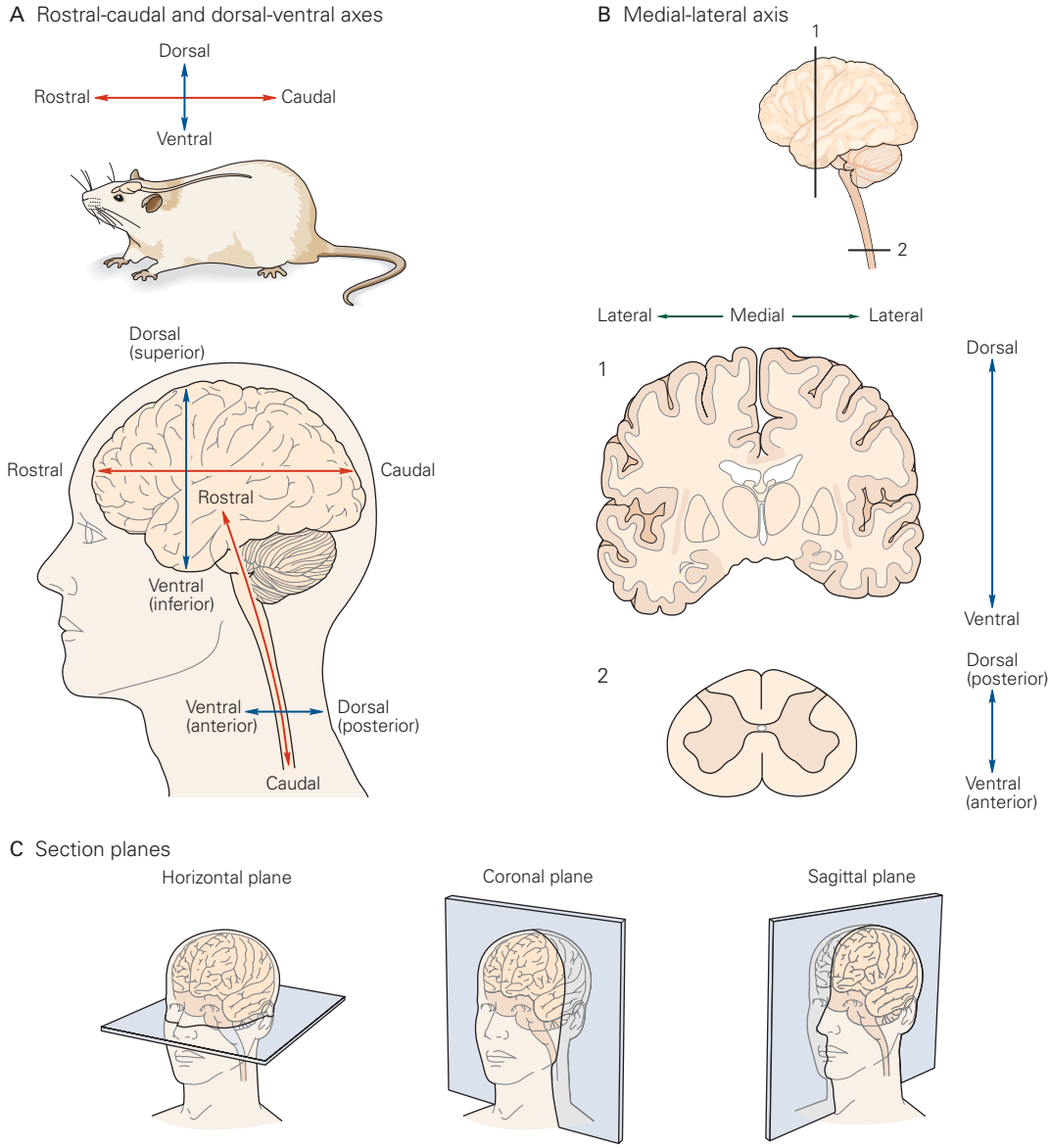

Figure 1–2 The central nervous system is described along three major axes. (Adapted, with permission, from Martin 2003.)

A. *Rostral* means toward the nose and *caudal* toward the tail. *Dorsal* means toward the back of the animal and *ventral* toward the belly. In lower mammals the orientations of these two axes are maintained through development into adult life. In humans and other higher primates, the longitudinal axis is flexed in the brain stem by approximately 110 degrees. Because of this flexure, the same positional terms have different meanings when referring to structures below and above the flexure. Below the flexure, in the spinal cord, rostral means toward the head, caudal means toward the coccyx (the lower end of the spinal column), ventral (anterior) means toward the belly, and dorsal (posterior) means toward the back. Above the flexure, rostral means toward the nose, caudal means toward the back of the head, ventral means toward the jaw, and dorsal means toward the top of the head. The term *superior* is often used synonymously with dorsal, and *inferior* means the same as ventral.

B. *Medial* means toward the middle of the brain and *lateral* toward the side.

C. When brains are sectioned for analysis, slices are typically made in one of three cardinal planes: horizontal, coronal, or sagittal.

Box 1–2 Anatomical Organization of the Central Nervous System

The Central Nervous System Has Seven Main Parts

The **spinal cord,** the most caudal part of the central nervous system, receives and processes sensory information from the skin, joints, and muscles of the limbs and trunk and controls movement of the limbs and the trunk. It is subdivided into cervical, thoracic, lumbar, and sacral regions (Figure 1–3A).

The spinal cord continues rostrally as the **brain stem**, which consists of the medulla oblongata, pons, and midbrain. The brain stem receives sensory information from the skin and muscles of the head and provides the motor control for the head's musculature. It also conveys information from the spinal cord to the brain and from the brain to the spinal cord, and regulates levels of arousal and awareness through the reticular formation.

The brain stem contains several collections of cell bodies, the cranial nerve nuclei. Some of these nuclei receive information from the skin and muscles of the head; others control motor output to muscles of the face, neck, and eyes. Still others are specialized to process information from three of the special senses: hearing, balance, and taste.

The **medulla oblongata,** directly rostral to the spinal cord, includes several centers responsible for vital autonomic functions, such as digestion, breathing, and the control of heart rate.

The **pons,** rostral to the medulla, conveys information about movement from the cerebral hemispheres to the cerebellum.

The **cerebellum,** behind the pons, modulates the force and range of movement and is involved in the learning of motor skills. It is functionally connected to the three main organs of the brain stem: the medulla oblongata, the pons, and the midbrain.

The **midbrain,** rostral to the pons, controls many sensory and motor functions, including eye movement and the coordination of visual and auditory reflexes.

The **diencephalon** lies rostral to the midbrain and contains two structures. The *thalamus* processes most of the information reaching the cerebral cortex from the rest of the central nervous system. The *hypothalamus* regulates autonomic, endocrine, and visceral functions.

The **cerebrum** comprises two cerebral hemispheres, each consisting of a heavily wrinkled outer layer (the *cerebral cortex*) and three deep-lying structures (components of the *basal ganglia,* the *hippocampus,* and *amygdaloid nuclei*). The basal ganglia, which include the caudate, putamen, and globus pallidus, regulate movement execution and motor- and habit-learning, two forms of memory that are referred to as implicit memory; the hippocampus is critical for storage of memory of people, places, things, and events, a form of memory that is referred to as explicit; and the amygdaloid nuclei coordinate the autonomic and endocrine responses of emotional states, including memory of threats, another form of implicit memory.

Each cerebral hemisphere is divided into four distinct lobes: frontal, parietal, occipital, and temporal (Figure 1–3B). These lobes are associated with distinct functions, although the cortical areas are all highly interconnected and can participate in a wide range of brain functions. The occipital lobe receives visual information and is critical for all aspects of vision. Information from the occipital lobe is then processed through two main pathways. The dorsal stream, connecting the occipital lobe to the parietal lobe, is concerned with the location and manipulation of objects in visual space. The ventral stream, connecting the occipital lobe to the temporal lobe, is concerned with object identity, including the recognition of individual faces. The temporal lobe is also important for processing auditory information (and also contains the hippocampus and amygdala buried beneath its surface). The frontal lobes are strongly interconnected with all cortical areas and are important for higher cognitive processing and motor planning.

About two-thirds of the cortex lies in the sulci, and many gyri are buried by overlying cortical lobes. The full extent of the cortex is made visible by separating the hemispheres to reveal the medial surface of the brain and by slicing the brain post mortem, for example in an autopsy (Figure 1–4). Much of this information can be visualized in the living brain through modern brain imaging (Figure 1–5; Chapter 6). These views also afford views of the white matter and subcortical gray matter.

Two important regions of cerebral cortex not visible on the surface include the cingulate cortex and insular cortex. The cingulate cortex lies dorsal to the corpus callosum and is important for regulation of emotion, pain perception, and cognition. The insular cortex, which lies buried within the overlying frontal, parietal, and temporal lobes, plays an important role in emotion, homeostasis, and taste perception. These internal views also afford examination of the *corpus callosum*, the prominent axon *fiber tract* that connects the two hemispheres.

The various brain regions described above are often divided into three broader regions: the *hindbrain* (comprising the medulla oblongata, pons, and cerebellum); *midbrain* (comprising the tectum, substantia nigra, reticular formation, and periaqueductal gray matter); and *forebrain* (comprising the diencephalon and cerebrum). Together the midbrain and hindbrain (minus the cerebellum) include the same structures as the brain stem. The anatomical organization of the nervous system is described in more detail in Chapter 4.

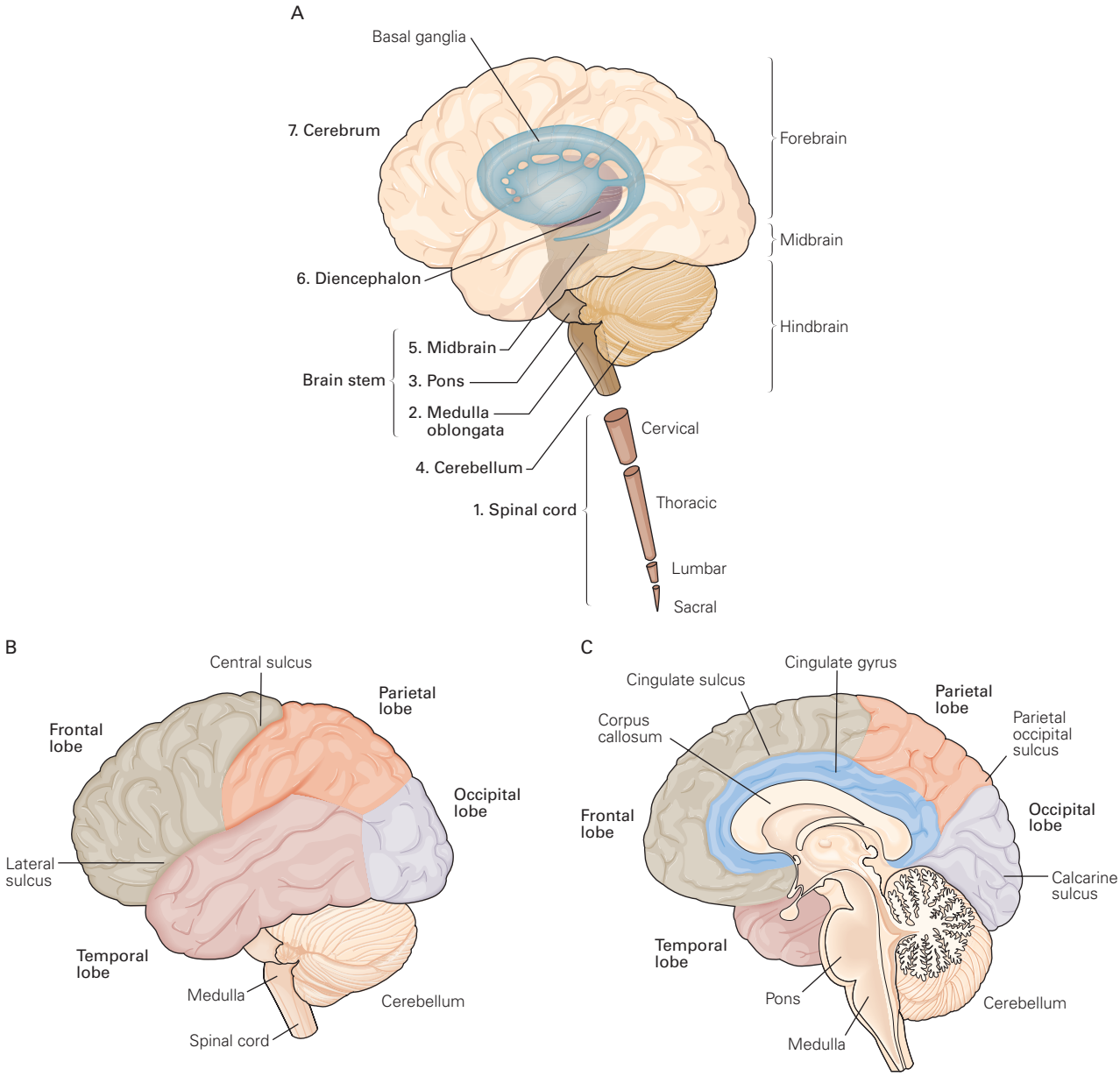

Figure 1–3 The divisions of the central nervous system.

A. The central nervous system can be divided into seven main regions, proceeding from the most caudal region, the spinal cord, to the brain stem (medulla, pons, and midbrain), to the diencephalon (containing the thalamus and hypothalamus), to the telencephalon or cerebrum (cerebral cortex, underlying white matter, subcortical nuclei, and the basal ganglia).

B. The four major lobes of the cerebrum are named for the parts of the cranium that cover them. This lateral view of the brain shows only the left cerebral hemisphere. The central sulcus separates the frontal and parietal lobes. The lateral sulcus separates the frontal from the temporal lobes. The primary motor cortex occupies the gyrus immediately rostral to the central sulcus. The primary somatosensory cortex occupies the gyrus immediately caudal to the central sulcus.

C. Further divisions of the brain are visible when the hemispheres are separated in this medial view of the right hemisphere. The corpus collosum contains a large bundle of axons connecting the two hemispheres. The cingulate cortex is part of the cerebral cortex that surrounds the corpus collosum. The primary visual cortex occupies the calcarine sulcus.

(*continued*)

Box 1–2 Anatomical Organization of the Central Nervous System (continued)

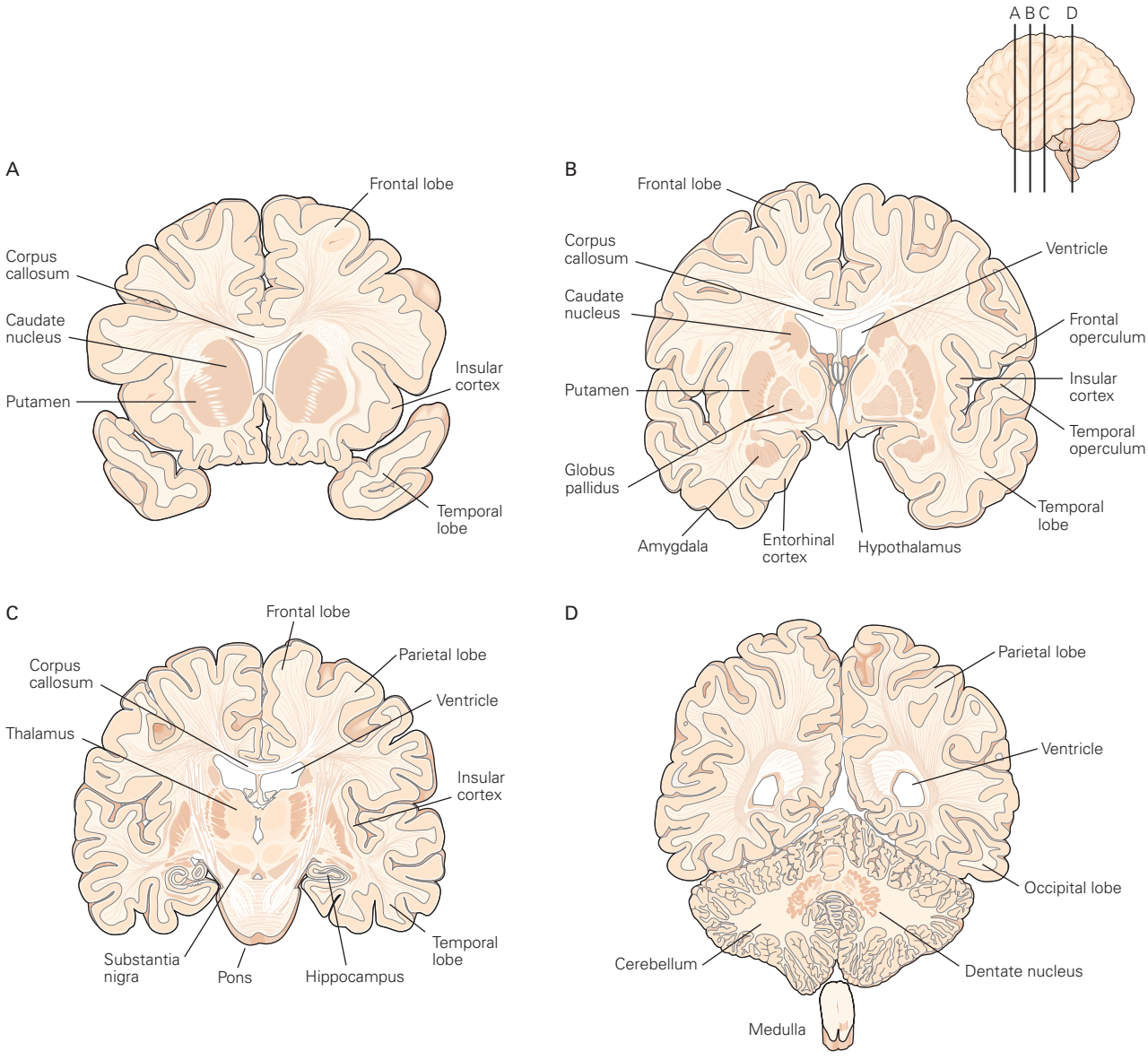

Figure 1–4 Major subcortical and deep cortical regions of the cerebral hemispheres are visible in drawings of brain slices from postmortem tissue.

Four sequential coronal sections (A–D) were made along the rostral-caudal axis indicated on the lateral view of the brain (top right, inset). The basal ganglia comprise the caudate nucleus, putamen, globus pallidus, substantia nigra, and subthalamic nucleus (not shown). The thalamus relays sensory information from the periphery to the cerebral cortex. The amygdala and hippocampus are regions of the cerebral cortex buried within the temporal lobe that are important for emotional responses and memory. The ventricles contain and produce the cerebrospinal fluid, which bathes the sulci, cisterns, and the spinal cord. (Adapted from Nieuwenhuys, Voogd, and van Huijzen 1988.)

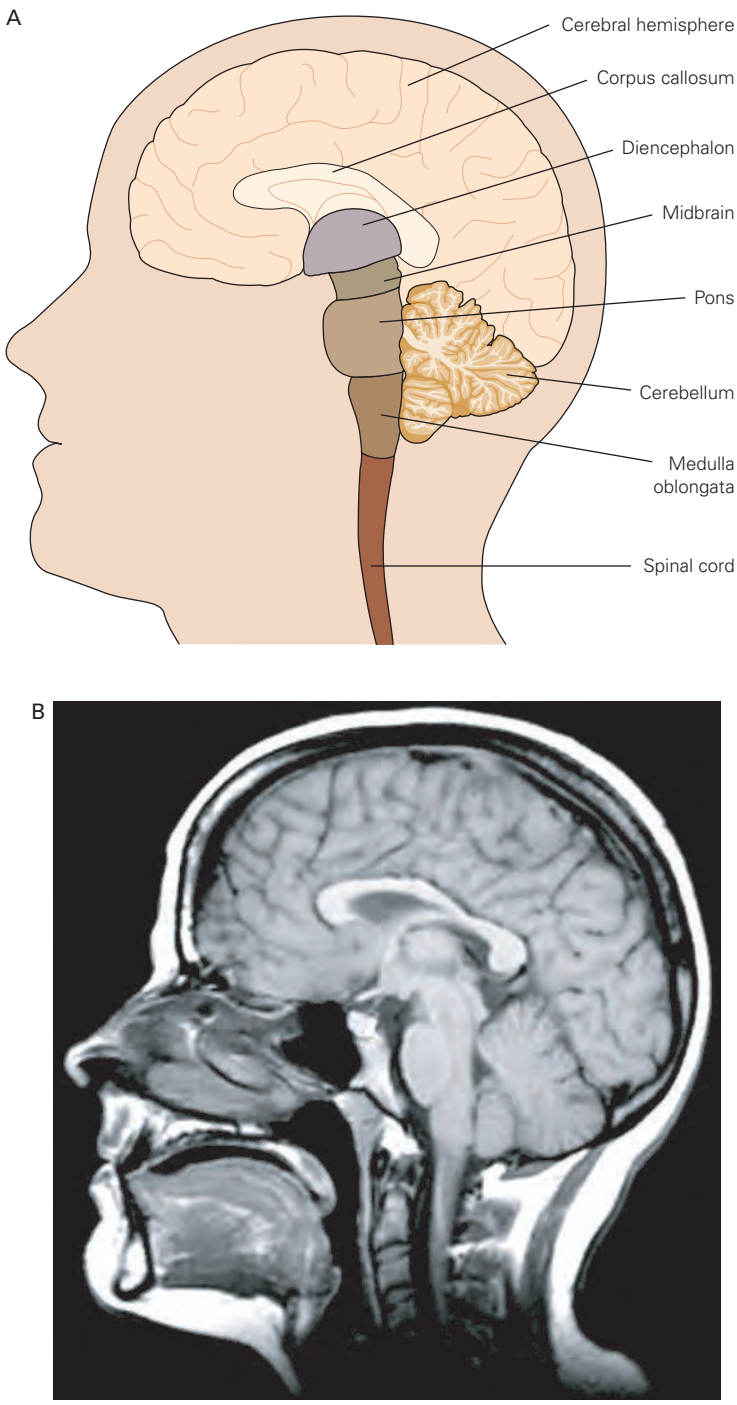

Figure 1–5 The main cortical and subcortical regions can be imaged in the brain of a living individual.

A. This schematic drawing shows, for reference, the major surface and deep regions of the brain, including the rostral end of the spinal cord.

B. The major brain divisions drawn in part A are evident in a magnetic resonance image of a living human brain.

In each of the hemispheres, the overlying cortex is divided into four lobes named for the skull bones that overlie them: *frontal, parietal, occipital*, and *temporal* (Figure 1–3B). Each lobe has several characteristic deep infoldings, an evolutionary strategy for packing a large sheet of cortex into a limited space. The crests of these convolutions are called *gyri,* and the intervening grooves are called *sulci* or *fissures.* The more prominent gyri and sulci, which are quite similar from person to person, bear specific names. For example, the central sulcus separates the precentral gyrus, an area concerned with motor function, from the postcentral gyrus, an area that deals with sensory function (Figure 1–3B). Several prominent gyri are only visible on the medial surface between the two hemispheres (Figure 1–3C), and others are deep within fissures and sulci and therefore only visible when the brain is sliced, either in postmortem tissue (Figure 1–4) or virtually, using magnetic resonance imaging (Figure 1–5), as explained in Chapter 6.

Each lobe has specialized functions. The frontal lobe is largely concerned with short-term memory, planning future actions, and control of movement; the parietal lobe mediates somatic sensation, forming a body image and relating it to extrapersonal space; the occipital lobe is concerned with vision; and the temporal lobe processes hearing, the recognition of objects and faces, and—through its deep structures, the hippocampus and amygdaloid nuclei—learning, memory, and emotion.

Two important features characterize the organization of the cerebral cortex. First, each hemisphere is concerned primarily with sensory and motor processes on the contralateral (opposite) side of the body. Thus sensory information that reaches the spinal cord from the left side of the body crosses to the right side of the nervous system on its way to the cerebral cortex. Similarly, the motor areas in the right hemisphere exert control over the movements of the left half of the body. The second feature is that the hemispheres, although similar in appearance, are not completely symmetrical in structure or function.

The First Strong Evidence for Localization of Cognitive Abilities Came From Studies of Language Disorders

The first areas of the cerebral cortex identified as important for cognition were areas concerned with language. These discoveries came from studies of *aphasia,* a language disorder that most often occurs when certain areas of brain tissue are destroyed by a stroke, the occlusion or rupture of a blood vessel supplying a portion of a cerebral hemisphere. Many of the important discoveries in the study of aphasia occurred in rapid succession during the latter half of the 19th century. Taken together, these advances form one of the most exciting and important chapters in the neuroscientific study of human behavior.

Pierre Paul Broca, a French neurologist, was the first to identify specific areas of the brain concerned with language. Broca was influenced by Gall's efforts to map higher functions in the brain, but instead of correlating behavior with bumps on the skull, he correlated clinical evidence of aphasia with brain lesions discovered post mortem. In 1861 he wrote, "I had thought that if there were ever a phrenological science, it would be the phrenology of convolutions (*in the cortex*), and not the phrenology of bumps (*on the head*)." Based on this insight, Broca founded *neuropsychology,* an empirical science of mental processes that he distinguished from the phrenology of Gall.

In 1861 Broca described a patient, Leborgne, who as a result of a stroke could not speak, although he could understand language perfectly well. This patient had no motor deficits of the tongue, mouth, or vocal cords that would affect his ability to speak. In fact, he could utter isolated words, whistle, and sing a melody without difficulty. But he could not speak grammatically or create complete sentences, nor could he express ideas in writing. Postmortem examination of this patient's brain showed a lesion in a posterior inferior region of the left frontal lobe, now called *Broca's area* (Figure 1–6). Broca studied eight similar patients, all with lesions in this region, and in each case the lesion was located in the left cerebral hemisphere. This discovery led Broca to announce in 1864: "*Nous parlons avec l'hémisphère gauche*!" (We speak with the left hemisphere!).

Broca's work stimulated a search for cortical sites associated with other specific behaviors—a search soon rewarded. In 1870 Gustav Fritsch and Eduard Hitzig galvanized the scientific community when they showed that characteristic limb movements of dogs, such as extending a paw, could be produced by electrically stimulating discrete regions of the precentral gyrus. These regions were invariably located in the contralateral motor cortex. Thus the right hand, the one most used for writing and skilled movements, is controlled by the left hemisphere, the same hemisphere that controls speech. In most people, therefore, the left hemisphere is regarded as *dominant*.

The next step was taken in 1876 by Karl Wernicke, who at age 26 published a now-classic paper,

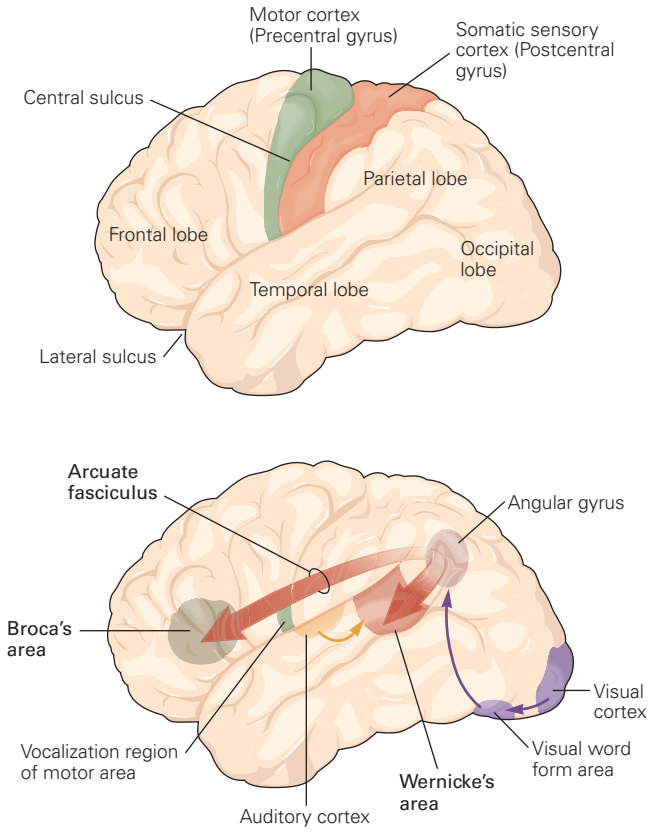

Figure 1–6 Language processing engages several regions of the left cerebral hemisphere.

Broca's area controls the production of speech. It lies near the region of the motor area that controls the mouth and tongue movements that form words. Wernicke's area processes auditory input for language and is important for understanding speech. It lies near the primary auditory cortex and the angular gyrus. The French neurologist Jules Dejerine proposed in the 1890s that a polymodal sensory area in the angular gyrus integrates information from vision and audition to represent words, but more recent studies implicate a more ventral occipitotemporal cortical area for processing of visual words. Wernicke's area communicates with Broca's area by a bidirectional pathway, part of which is made up of the arcuate fasciculus. (Adapted, with permission, from Geschwind 1979.)

"The Symptom-Complex of Aphasia: A Psychological Study on an Anatomical Basis." In it he described another type of aphasia, a failure of comprehension rather than speech: a *receptive* as opposed to an *expressive* malfunction. Whereas Broca's patients could understand language but not speak, Wernicke's patient could form words but could not understand language and produced senseless, yet grammatical, sentences. Moreover, the locus of this new type of aphasia was different from that described by Broca. The lesion occurred in the posterior part of the cerebral cortex where the temporal lobe meets the parietal lobe (Figure 1–6).

On the basis of this discovery, and the work of Broca, Fritsch, and Hitzig, Wernicke formulated a neural model of language that attempted to reconcile and extend the predominant theories of brain function at that time. Phrenologists and cellular connectionists argued that the cerebral cortex was a mosaic of functionally specific areas, whereas the holistic *aggregate-field* school claimed that every mental function involved the entire cerebral cortex. Wernicke proposed that only the most basic mental functions, those concerned with simple perceptual and motor activities, are mediated entirely by neurons in discrete local areas of the cortex. More complex cognitive functions, he argued, result from interconnections between several functional sites. By integrating the principle of localized function within a connectionist framework, Wernicke emphasized the idea that different components of a single behavior are likely to be processed in several regions of the brain. He was thus the first to advance the idea of *distributed processing*, now a central tenet of neural science.

Wernicke postulated that language involves separate motor and sensory programs, each governed by distinct regions of cortex. He proposed that the motor program that governs the mouth movements for speech is located in Broca's area, suitably situated in front of the region of the motor area that controls the mouth, tongue, palate, and vocal cords (Figure 1–6). He next assigned the sensory program that governs word perception to the temporal lobe area that he had discovered, now called *Wernicke's area*. This region is surrounded by the auditory cortex and by areas now known collectively as *association cortex*, integrating auditory, visual, and somatic sensations. According to Wernicke's model, the communication between these two language centers was mediated via a large bundle of axons known as the arcuate fasciculus.

Thus Wernicke formulated the first coherent neural model for language that is still useful today, with important modifications and elaborations described in Chapter 55. According to this model, the neural processing of spoken or written words begins in separate sensory areas of the cortex specialized for auditory or visual information. This information is then conveyed, via intermediate association areas that extract features suitable for recognition of spoken or written words, to Wernicke's area, where it is recognized as language and associated with meaning.

The power of Wernicke's model was not only its completeness but also its predictive utility. This model correctly predicted a third type of aphasia, one that results from disconnection. In this type, the receptive and expressive zones for speech are intact but

the neuronal fibers that connect them (arcuate fasciculus) are destroyed. This *conduction aphasia,* as it is now called, is characterized by frequent, sound-based speech errors (*phonemic paraphasias*), repetition difficulties, and severe limitation in verbal working memory. Patients with conduction aphasia understand words that they hear and read, and have no motor difficulties when they speak. Yet they cannot speak coherently; they omit parts of words or substitute incorrect sounds and experience great difficulties in verbatim repetition of a multisyllabic word, phrase, or sentence that they hear or read or recall from memory. Although painfully aware of their own errors, their successive attempts at self-correction are often unsuccessful.

Inspired in part by Wernicke's advances and led by the anatomist Korbinian Brodmann, a new school of cortical localization arose in Germany at the beginning of the 20th century, one that distinguished functional areas of the cortex based on the shapes of cells and variations in their layered arrangement. Using this *cytoarchitectonic* method, Brodmann distinguished 52 anatomically and functionally distinct areas in the human cerebral cortex (Figure 1–7).

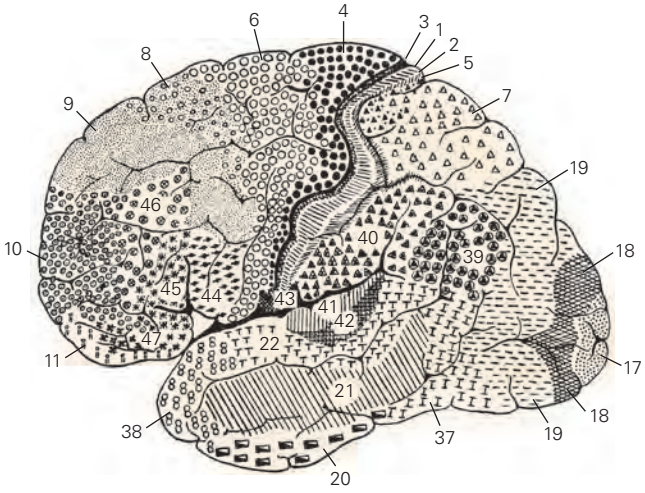

Figure 1–7 Early in the 20th century, the human cerebral cortex was classified into 52 discrete functional areas. The areas shown were identified by the anatomist Korbinian Brodmann on the basis of distinctive nerve cell structures and characteristic arrangements of cell layers. This scheme is still widely used today and is continually updated. Several areas defined by Brodmann have been found to control specific brain functions. For instance, area 4 is the motor cortex, responsible for voluntary movement. Areas 1, 2, and 3 constitute the primary somatosensory cortex, which receives sensory information primarily from the skin and joints. Area 17 is the primary visual cortex, which receives sensory signals from the eyes and relays them to other areas for further processing. Areas 41 and 42 constitute the primary auditory cortex. The drawing shows only areas visible on the outer surface of the cortex.

Even though the biological evidence for functionally discrete areas in the cortex was compelling, by the early 20th century, holistic views of the brain continued to dominate experimental thinking and clinical practice until 1950. This surprising state of affairs owed much to several prominent neural scientists who advocated the holistic view, among them the British neurologist Henry Head, the Russian behavioral physiologist Ivan Pavlov, and the American psychologist Karl Lashley.

Most influential was Lashley, who was deeply skeptical of the cytoarchitectonic approach to functional mapping of the cortex. "The 'ideal' architectonic map is nearly worthless," Lashley wrote. "The area subdivisions are in large part anatomically meaningless, and misleading as to the presumptive functional divisions of the cortex." His skepticism was reinforced by his studies of the effects of various brain lesions on the ability of rats to learn to run a maze. From these studies Lashley concluded that the severity of a learning defect depended on the size of the lesion, not on its precise location. Disillusioned, Lashley—and after him many other psychologists—concluded that learning and other higher mental functions have no special locus in the brain and consequently cannot be attributed to specific collections of neurons.

Based on his observations, Lashley reformulated the aggregate-field view by further minimizing the role of individual neurons, specific neuronal connections, and even specific brain regions in the production of specific behavior. According to Lashley's *theory of mass action,* it is the full mass of the brain, not its regional components, that is crucial for a function such as memory.

Lashley's experiments with rats have now been reinterpreted. A variety of studies have shown that the maze-learning used by Lashley is unsuited to the search for local cortical functions because it involves so many motor and sensory capabilities. Deprived of one sensory capability, say vision, a rat can still learn to run a maze using touch or smell. Besides, as we shall see later in the book, many mental functions are mediated by more than one region or neuronal pathway. Thus a given function may not be eliminated by a single lesion. This is especially germane when considering cognitive functions of the brain. For example, knowledge of space is supported by numerous parietal association areas that link vision to a potential shift of the gaze, turn of the head, reach of the hand, and so on. In principle, any one of these association areas can compensate for damage of another. It takes a large insult to the parietal lobe to produce obvious deficits of spatial knowledge (*spatial agnosia*) (Chapter 59). Such an

observation would have seemed to support theories of mass action, but we now recognize that it is compatible with localization of function that incorporates the idea of redundancy of function.

Soon the evidence for localization of function became overwhelming. Beginning in the late 1930s, Edgar Adrian in England and Wade Marshall and Philip Bard in the United States discovered that touching different parts of a cat's body elicits electrical activity in distinct regions of the cerebral cortex. By systematically probing the body surface, they established a precise map of the body surface in specific areas of the cerebral cortex described by Brodmann. This result showed that functionally distinct areas of cortex could be defined unambiguously according to anatomical criteria such as cell type and cell layering, connections of cells, and—most importantly—behavioral function. As we shall see in later chapters, functional specialization is a key organizing principle in the cerebral cortex, extending even to individual columns of cells within an area of cortex. Indeed, the brain is divided into many more functional regions than Brodmann envisaged.

More refined methods made it possible to learn even more about the function of different brain regions involved in language. In the late 1950s Wilder Penfield, and later George Ojemann, reinvestigated the cortical areas that are essential for producing language. While locally anesthetized during brain surgery for epilepsy, awake patients were asked to name objects (or use language in other ways) while different areas of the exposed cortex were stimulated with small electrodes. If an area of the cortex was critical for language, application of the electrical stimulus blocked the patient's ability to name objects. In this way Penfield and Ojemann were able to confirm the language areas of the cortex described by Broca and Wernicke. As we shall learn in Chapter 55, the neural networks for language are far more extensive and complex than those described by Broca and Wernicke.

Initially almost everything known about the anatomical organization of language came from studies of patients with brain lesions. Today functional magnetic resonance imaging (fMRI) and other noninvasive methods allow analyses to be conducted on healthy people engaged in reading, speaking, and thinking (Chapter 6). fMRI not only has confirmed that reading and speaking activate different brain areas but also has revealed that just *thinking* about a word's meaning in the absence of sensory inputs activates a still different area in the left frontal cortex. Indeed, even within the traditional language areas, individual subregions are recruited to different degrees, depending on the way we think about words, express them, and resolve their meaning from the arrangement of other words (ie, syntax). The new imaging tools promise not only to teach us which areas are involved but also to expose the functional logic of their interconnection.

One of the great surprises emerging from modern methodologies is that so many areas of cortex are activated in language comprehension and production. These include the traditional language areas, identified by Broca, Wernicke, and Dejerine, in the left hemisphere; their homologs in the right hemisphere; and newly identified regions. Functional imaging tends to elucidate areas that are recruited differentially, whereas lesions from stroke, tumor, or injury distinguish brain areas that are essential for one or more functions. Thus it appears that Broca's area, once thought to be dedicated to language production, is in fact also involved in a variety of linguistic tasks including comprehension (Figure 1–6). In some cases, functional imaging invites refinement or revision of the critical areas identified by lesion studies. For example, reading is now thought to recruit specialized regions in the ventral occipitotemporal cortex in addition to the angular gyrus in the parietal cortex (shown in Figure 1–6).

Thus the processing of language in the brain exemplifies not only the principle of localized function but also the more sophisticated elaboration of this principle, that numerous distinct neural structures with specialized functions belong to systems. Perhaps this is the natural reconciliation of the controversy concerning localized and distributed processes—that is, a small number of distinct areas, each identified with a small set of functions and contributing through their interactions to the phenomenology of perception, action, and ideation. The brain may carve up a task differently than our intuition tells us. Who would have guessed that the neural analysis of the movement and color of an object would occur in different pathways rather than a single pathway mediating a unified percept of the object? Similarly, we might expect that the neural organization of language may not conform neatly to the axioms of a theory of universal grammar, yet support the very seamless functionality described by linguistic theory.

Studies of patients with brain damage continue to afford important insight into how the brain is organized for language. One of the most impressive results comes from the study of deaf people who have lost their ability to communicate through the use of a signed language (eg, British Sign Language [BSL] or American Sign Language [ASL]) after suffering cerebral damage. Signed languages use hand movements rather than

vocalizations and are perceived by sight rather than sound, but have the same structural complexity as spoken languages. Sign language processing, as with spoken language processing, localizes to the left hemisphere. Damage to the left hemisphere can have quite specific consequences for signing just as for spoken language, affecting sign comprehension (following damage in Wernicke's area), grammar, or fluency (following damage in Broca's area). These clinical observations are supported by functional neuroimaging. Not surprisingly, production and comprehension of signed and spoken languages do not involve identical brain areas, but the overlap is truly remarkable (Figure 1–8). There is even evidence that processing the constituent parts of signs (eg, handshape used) involves some of the same brain regions involved when making rhyme judgements about speech.

These observations illustrate three points. First, language processing occurs primarily in the left hemisphere, independently of pathways that process the sensory and motor modalities used in language. Second, auditory input is not necessary for the emergence and operation of language capabilities in the left hemisphere. Third, spoken language is only one of a family of language skills mediated by the left hemisphere.

Investigations of other behaviors have provided additional support for the idea that the brain has distinct cognitive systems. These studies demonstrate that complex information processing requires many interconnected cortical and subcortical areas, each concerned with processing particular aspects of sensory stimuli or motor movement and not others. For example, perceptual awareness of an object's location, size, and shape relies on activity in numerous parietal association areas that link vision to potential actions, such as moving the eyes, orienting the head, reaching, and shaping the hand to grasp. The parietal areas do not initiate these actions but evaluate sensory information as evidence bearing on these potentialities. They receive information from the dorsal visual stream—sometimes referred to as the *where pathway*, but more aptly termed a *how pathway*—to construct a state of knowing (gnosia) about the location and other spatial properties of objects. The ventral visual stream, or *what pathway*, is also concerned with possible actions, but these are associated with socializing and foraging. These associations establish *gnosia* about the desirability of objects, faces, foods, and potential mates. In this sense, the *what pathway* might be a *how pathway* too.

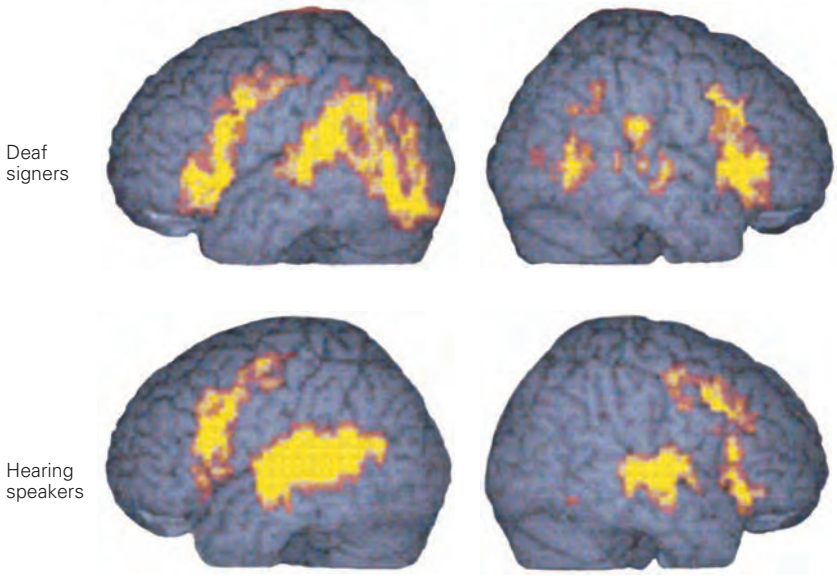

Figure 1–8 Deaf signing and hearing individuals share common language processing areas. Regions of the cortex involved in the recognition of a spoken or signed language, identified by functional magnetic resonance imaging (fMRI). **Yellow** highlight shows the areas of the left and right cerebral hemispheres (*left* and *right columns*, respectively) that were activated more when comprehending language than when performing a perceptual task. For the deaf signers (**top row**), the highlighted regions were more active during comprehension of British Sign Language than during the detection of a visual stimulus superimposed on the same motionless signer. For the hearing speakers (**bottom row**), highlighted regions were more active during comprehension of audio-visual speech than during the detection of a tone while viewing a motionless (silent) speaker. (Adapted, with permission, from MacSweeney et al., 2002. Copyright © 2002 Oxford University Press.)

Mental Processes Are the Product of Interactions Between Elementary Processing Units in the Brain

There are several reasons why the evidence for the localization of brain functions, which seems so obvious and compelling in retrospect, had been rejected so often in the past. Phrenologists introduced the idea of localization in an exaggerated form and without adequate evidence. They imagined each region of the cerebral cortex as an independent mental organ dedicated to a complete and distinct aspect of personality, much as the pancreas and the liver are independent digestive organs. Flourens's rejection of phrenology and the ensuing debate between proponents of the aggregate-field view (against localization) and the cellular connectionists (for localization) were responses to a theory that was simplistic and without adequate experimental evidence.

In the aftermath of Wernicke's discovery of the modular organization of language in the brain—interconnected nodes with distinctive functions—we now think that all cognitive abilities result from the interaction of many processing mechanisms distributed in several regions of the brain. That is, particular brain regions are not fully responsible for specific mental faculties but instead are *elementary processing units* that together have a role. Perception, movement, language, thought, and memory are all made possible by the interlinkage of serial and parallel processing in discrete brain regions—computational modules—within these regions. As a result, damage to a single area need not result in the complete loss of a cognitive function (or faculty) as many earlier neurologists believed. Even if a behavior initially disappears, it may partially return as undamaged parts of the brain reorganize their linkages. Further, when focal damage adversely affects a mental function it may do so indirectly by disrupting the function of other principal loci (*diaschisis*). Indeed, observations of this nature led Wernicke's student Kurt Goldstein to embrace the more holistic view.

Thus it is not accurate to think of a mental function as being mediated strictly by a chain of nerve cells and brain areas—each connected directly to the next—for in such an arrangement the entire process is disrupted when a single connection is damaged. A more realistic metaphor is that of a process consisting of several parallel pathways in a network of modules that interact and ultimately converge upon a common set of targets. The malfunction of a single pathway within a network may affect the information carried by that pathway without disrupting the entire system. The remaining parts of the network may be able to modify their performance to accommodate the breakdown of one pathway.

Modular processing in the brain was slow to be accepted because, until recently, it was difficult to demonstrate which components of a mental operation were mediated by a particular pathway or brain region. Nor is it easy to define mental operations in a manner that leads to testable hypotheses. Nevertheless, with the evolving convergence of modern cognitive psychology and brain science in recent decades, we have begun to appreciate that mental functions can successfully be broken down into subfunctions.

To illustrate this point, consider how we learn, store, and recall information about objects, people, and events. Simple introspection suggests that we store each piece of our knowledge as a single representation that can be recalled by memory-jogging stimuli or even by the imagination alone. Everything you know about an apple, for example, seems to be stored in one complete representation that is equally accessible whether you see a particular apple, a part of an apple, a red or green apple, the written word apple, or an apocryphal story about the discovery of gravity. Our experience, however, is not a faithful guide to how knowledge is stored in memory.

Knowledge about apples is not stored as a single coherent representation but rather is subdivided into distinct categories and stored separately. One region of the brain stores information about the way you would hold the apple, the way you would feel for softness (bearing on freshness), the color (bearing on preference or freshness), the way you might communicate the presence or taste of the apple to another person, as well as its semantic association with computers, physicists, worms, serpents, and biblical gardens. The concept "apple" entails each of these considerations and many more. A natural assumption is that a coherent concept comprising many details must exist in a single place in the brain; however, an equally valid assumption is that a unified concept like "apple" exists in the mind in the form of multiple links between a variety of neural structures, each with a particular kind of information, coordinated through the action of memory retrieval.

The most astonishing example of the modular organization of mental processes is the finding that our very sense of self—a self-aware being, the sum of what we mean when we say "I"—is achieved through the connection of independent circuits in our two cerebral hemispheres, each mediating its own sense of awareness. The remarkable discovery that even consciousness is not a unitary process was made by Roger Sperry, Michael Gazzaniga, and Joseph Bogen

in the course of studying patients in whom the corpus callosum—the major tract connecting the two cerebral hemispheres—was severed as a treatment for epilepsy. They found that each hemisphere had a consciousness that functioned independently of the other.

Thus while one patient was reading a favorite book held in his left hand, the right hemisphere, which controls the left hand but plays only a minor role in language comprehension, found that the raw visual information it received from simply looking at the book was boring. The right hemisphere commanded the left hand to put the book down. Another patient would put on his clothes with the left hand while at the same time taking them off with the other. Each hemisphere has a mind of its own! In addition, the dominant hemisphere sometimes commented on the performance of the nondominant hemisphere, frequently manifesting a false sense of confidence regarding problems to which it could not know the solution, which was provided exclusively to the nondominant hemisphere.

Such findings have brought the study of consciousness, once the domain of philosophy and psychoanalysis, into the fold of neural science. As we shall see in later chapters, many of the issues described in this chapter reemerge in neural theories of consciousness. No one questions the idea that much information processing—perhaps the lion's share—does not reach conscious awareness. When sensory information, a plan of action, or an idea does become conscious, neural science seeks to explain the mechanisms that mediate this transition. While there is as yet no satisfactory explanation, some brain scientists would liken the process to a shift in the focus of attention, mediated by distinct groups of neurons, whereas others believe that awareness requires a qualitative change in the functional interaction between widely separated areas of the brain.

The main reason it has taken so long to understand which mental activities are mediated by which regions of the brain is that we are dealing with biology's deepest riddle: the neural mechanisms that account for consciousness and self-awareness. There is at present no satisfactory theory that explains why only some information that reaches our eyes leads to a state of subjective awareness of an item, person, or scene. We know that we are consciously aware of only a small fraction of our mental deliberations, and those thoughts that do pierce conscious awareness must arise from steps carried out by the brain unconsciously. As we propose in Chapter 56, some answers to the riddles of consciousness may be closer than imagined.

Meanwhile, the current gap in our understanding also poses practical, epistemological challenges for neural science. We cannot help but rely on our conscious experiences of the world, body, and ideation in our characterization of perception, behavior, and cognition. In doing so, however, we risk mischaracterizing many mental processes that do not pierce conscious awareness. For example, we tend to characterize the problem of perception in terms consistent with the subjective experience of sensory information, whereas even sophisticated but nonconscious knowledge of the content of perception may have greater resemblance to a behavioral utility (affordance), in effect an answer to whether this is something I might choose to eat, sit upon, or engage further. Similarly, cognitive processes, such as reasoning, strategizing, and decision making, are likely to be carried out by the brain in ways that only loosely resemble the steps we infer from conscious deliberation.

These cautionary notes have a bright corollary. The insight that many cognitive functions transpire without conscious awareness raises the possibility that principles of neural science revealed in the study of more rudimentary behaviors can furnish insight into more complex cognitive processes. Neural recordings from the brains of animals trained to perform complex tasks have led to an understanding of cognitive processes such as decision making, reasoning, planning, and allocating attention. These experimental models often extrapolate to human functions, and where they fall short, they inspire new hypotheses. For more often than not, there is inspiration if not insight to be gleaned from the gaps in our understanding.

To analyze how the brain gives rise to a specific mental process, we must determine not only which aspects of the process depend on which regions of the brain but also how the relevant information is represented, routed, and transformed. Modern neural science seeks to integrate such understanding across many scales. For example, studies at the level of both the single nerve cell and its molecular constituents elucidate the mechanisms underlying electrical excitability and synaptic connections. Studies of cells and simple circuits lend insights into neural computations, ranging from basic operations, like controlling net excitation, to more masterful feats of computation, such as the derivation of meaningful information from raw sensory data. Studies of the interactions between circuits and brain areas can explain how we coordinate widely separated muscle groups or express a belief in a proposition. Knowledge at all these levels is knit together by mathematical formalizations, computer simulation, and psychological theory. These conceptual tools can now be combined with modern physiological techniques and brain imaging methods, making it possible

to track mental processes as they evolve in real time in living animals and humans. Indeed, the excitement evident in neural science today stems from the conviction that the biological principles that underlie human thought and behavior are within our grasp and may soon be harnessed to elucidate and improve the human condition.

Highlights

1. The neural sciences seek to understand the brain at multiple levels of organization, ranging from the cell and its constituents to the operations of the mind.
2. The fundamental principles of neural science bridge levels of time, complexity, and state—from cell to action and ideation, from development through learning to expertise and forgetting, from normal function to neurological deficits and recovery. As a first step, one must understand the building blocks—the electrical properties of the nerve cell and its connections to other nerve cells—and the organization of the nervous system from supporting cells to pathways.
3. The neuron doctrine states that individual nerve cells (neurons) are the elementary building blocks and signaling elements of the nervous system.
4. Neurons are organized into circuits with specialized functions. The simplest circuits mediate reflexes; more complex cognitive functions require more sophisticated circuits. This organizational principle extends the neuron doctrine to cellular connectionism.
5. Even within complex circuits, critical nodes can be identified as areas associated with a specific function. The first clear evidence for localization of brain function came from the study of a specific impairment of language production.
6. The two cerebral hemispheres receive information from the opposite side of the body and control the actions of the opposite side.
7. While the principle of localization of function in the brain is superior to its main historical alternatives—aggregate-field and the theory of mass action—it is constantly being refined. No area of the cerebral cortex functions independently of other cortical and subcortical structures.
8. A major refinement of localization is the principle of modular functional organization. The brain contains many representations of information organized by both the relevance of certain features for particular computations and by the variety of uses to which such information may be put. This is a form of redundancy with respect to purpose or potential action.
9. The future of brain science will require integration of ideas that cross the boundaries of traditional disciplines. We must open our minds to a wide variety of sources to guide our intuitions and strategies for research, from the sublime—the nature of consciousness—to the seemingly mundane—what general anesthesia does to a calcium sensor in the ring of cells around the thalamus.

Eric R. Kandel
Michael N. Shadlen

Selected Reading

Churchland PS. 1986. *Neurophilosophy: Toward a Unified Science of the Mind-Brain.* Cambridge, MA: MIT Press.

Cooter R. 1984. *The Cultural Meaning of Popular Science: Phrenology and the Organization of Consent in Nineteenth-Century Britain.* Cambridge: Cambridge Univ. Press.

Cowan WM. 1981. Keynote. In: FO Schmitt, FG Worden, G Adelman, SG Dennis (eds). *The Organization of the Cerebral Cortex: Proceedings of a Neurosciences Research Program Colloquium,* pp. xi–xxi. Cambridge, MA: MIT Press.

Crick F, Koch C. 2003. A framework for consciousness. Nat Neurosci 6:119–126.

Dehaene S. 2009. *Reading in the Brain: The Science and Evolution of a Human Invention*. New York: Viking.

Ferrier D. 1890. *The Croonian Lectures on Cerebral Localisation.* London: Smith, Elder.

Geschwind N. 1974. *Selected Papers on Language and the Brain.* Dordrecht, Holland: Reidel.

Glickstein M. 2014. *Neuroscience. A Historical Introduction.* Cambridge, MA: MIT Press.

Gregory RL (ed). 1987. *The Oxford Companion to the Mind*. Oxford: Oxford Univ. Press.

Harrington A. 1987. *Medicine, Mind, and the Double Brain: A Study in Nineteenth-Century Thought.* Princeton, NJ: Princeton Univ. Press.

Harrison RG. 1935. On the origin and development of the nervous system studied by the methods of experimental embryology. Proc R Soc Lond B Biol Sci 118: 155–196.

Hickok G, Small S. 2015. *Neurobiology of Language*. Boston: Elsevier.

Jackson JH. 1884. The Croonian lectures on evolution and dissolution of the nervous system. Br Med J 1:591–593; 660–663; 703–707.

Kandel ER. 1976. The study of behavior: the interface between psychology and biology. In: *Cellular Basis of Behavior: An Introduction to Behavioral Neurobiology,* pp. 3–27. San Francisco: Freeman.

Ojemann GA. 1995. Investigating language during awake neurosurgery. In: RD Broadwell (ed). *Neuroscience, Memory, and Language.* Vol. 1, *Decade of the Brain,* pp. 117–131. Washington, DC: Library of Congress.

Petersen SE. 1995. Functional neuroimaging in brain areas involved in language. In: RD Broadwell (ed). *Neuroscience, Memory, and Language.* Vol. 1, *Decade of the Brain,* pp. 109–116. Washington DC: Library of Congress.

Shepherd GM. 1991. *Foundations of the Neuron Doctrine.* New York: Oxford Univ. Press.

Sperry RW. 1968. Mental unity following surgical disconnection of the cerebral hemispheres. Harvey Lect 62:293–323.

Young RM. 1990. *Mind, Brain and Adaptation in the Nineteenth Century.* New York: Oxford Univ. Press.

References

Adrian ED. 1941. Afferent discharges to the cerebral cortex from peripheral sense organs. J Physiol (Lond) 100:159–191.

Bernard C. 1878–1879. *Leçons sur les Phénomènes de la vie Communs aux Animaux et aux Végétaux.* Vols. 1, 2. Paris: Baillière.

Boakes R. 1984. *From Darwin to Behaviourism: Psychology and the Minds of Animals.* Cambridge: Cambridge Univ. Press.

Broca P. 1865. Sur le siége de la faculté du langage articulé. Bull Soc Anthropol 6:377–393.

Brodmann K. 1909. *Vergleichende Lokalisationslehre der Grosshirnrinde in ihren Prinzipien dargestellt auf Grund des Zeelenbaues.* Leipzig: Barth.

Darwin C. 1872. *The Expression of the Emotions in Man and Animals.* London: Murray.

Dejerine J. 1891. Sur un cas de cécité verbale avec agraphie suivi d'autopsie. Mémoires de la Société de Biologie 3:197–201.

Descartes R. [1649] 1984. *The Philosophical Writings of Descartes.* Cambridge: Cambridge Univ. Press.

Finger S., Koehler PJ, Jagella C. 2004. The Monakow concept of diaschisis: origins and perspectives. Arch Neurol 61:283–288.

Flourens P. [1824] 1953. Experimental research. P Flourens and JMD Olmsted. In: EA Underwood (ed). *Science, Medicine and History,* 2:290–302. London: Oxford Univ. Press.

Flourens P. 1824. *Recherches Expérimentales sur les Propriétés et les Fonctions du Système Nerveux, dans les Animaux Vertébrés.* Paris: Chez Crevot.

Fritsch G, Hitzig E. [1870] 1960. Electric excitability of the cerebrum. In: G. von Bonin (transl). *Some Papers on the Cerebral Cortex,* pp. 73–96. Springfield, IL: Thomas.

Gall FJ, Spurzheim G. 1810. *Anatomie et Physiologie du Système Nerveux en Général, et du Cerveau en Particulier, avec des Observations sur la Possibilité de Reconnoître Plusieurs Dispositions Intellectuelles et Morales de l'Homme et des Animaux, par la Configuration de leurs Têtes.* Paris: Schoell.

Galvani L. [1791] 1953. *Commentary on the Effect of Electricity on Muscular Motion.* RM Green (transl). Cambridge, MA: Licht.

Gazzaniga MS, LeDoux JE. 1978. *The Integrated Mind.* New York: Plenum.

Geschwind N. 1979. Specializations of the human brain. Sci Am 241:180–199.

Goldstein K. 1948. *Language and Language Disturbances: Aphasic Symptom Complexes and Their Significance for Medicine and Theory of Language.* New York: Grune & Stratton.

Golgi C. [1906] 1967. The neuron doctrine: theory and facts. In: *Nobel Lectures: Physiology or Medicine, 1901–1921,* pp. 189–217. Amsterdam: Elsevier.

Langley JN. 1906. On nerve endings and on special excitable substances in cells. Proc R Soc Lond B Biol Sci 78:170–194.

Lashley KS. 1929. *Brain Mechanisms and Intelligence: A Quantitative Study of Injuries to the Brain.* Chicago: Univ. Chicago Press.

Lashley KS, Clark G. 1946. The cytoarchitecture of the cerebral cortex of *Ateles:* a critical examination of architectonic studies. J Comp Neurol 85:223–305.

Loeb J. 1918. *Forced Movements, Tropisms and Animal Conduct.* Philadelphia: Lippincott.

MacSweeney M, Capek CM, Campbell R, Woll B. 2008. The signing brain: the neurobiology of sign language. Trends Cogn Sci 12:432–440.

MacSweeney M, Woll B, Campbell R, et al. 2002. Neural systems underlying British Sign Language and audio-visual English processing in native users. Brain 125:1583–1593.

Marshall WH, Woolsey CN, Bard P. 1941. Observations on cortical somatic sensory mechanisms of cat and monkey. J Neurophysiol 4:1–24.

Martin JH. 2003. *Neuroanatomy: Text and Atlas*, 3rd ed. New York: McGraw Hill.

McCarthy RA, Warrington EK. 1988. Evidence for modality-specific meaning systems in the brain. Nature 334:428–430.

Müller J. 1834–1840. *Handbuch der Physiologie des Menschen für Vorlesungen.* Vols. 1, 2. Coblenz: Hölscher.

Nieuwenhuys R, Voogd J, van Huijzen Chr. 1988. *The Human Central Nervous System: A Synopsis and Atlas,* 3rd rev. ed. Berlin: Springer.

Pavlov IP. 1927. *Conditioned Reflexes: An Investigation of the Physiological Activity of the Cerebral Cortex.* GV Anrep (transl). London: Oxford Univ. Press.

Penfield W. 1954. Mechanisms of voluntary movement. Brain 77:1–17.

Penfield W, Rasmussen T. 1950. *The Cerebral Cortex of Man: A Clinical Study of Localization of Function.* New York: Macmillan.

Penfield W, Roberts L. 1959. *Speech and Brain-Mechanisms.* Princeton, NJ: Princeton Univ. Press.

Ramón y Cajal S. [1892] 1977. A new concept of the histology of the central nervous system. DA Rottenberg (transl). In: DA Rottenberg, FH Hochberg (eds). *Neurological Classics in Modern Translation,* pp. 7–29. New York: Hafner. (See also historical essay by SL Palay, preceding Ramón y Cajal's paper.)

Ramón y Cajal S. [1906] 1967. The structure and connexions of neurons. In: *Nobel Lectures: Physiology or Medicine, 1901–1921,* pp. 220–253. Amsterdam: Elsevier.

Ramón y Cajal S. [1908] 1954. *Neuron Theory or Reticular Theory? Objective Evidence of the Anatomical Unity of Nerve Cells.* MU Purkiss, CA Fox (transl). Madrid: Consejo Superior de Investigaciones Científicas Instituto Ramón y Cajal.

Ramón y Cajal S. 1937. *1852–1934. Recollections of My Life.* EH Craigie (transl). Philadelphia: American Philosophical Society; reprinted 1989. Cambridge, MA: MIT Press.

Rose JE, Woolsey CN. 1948. Structure and relations of limbic cortex and anterior thalamic nuclei in rabbit and cat. J Comp Neurol 89:279–347.

Shadlen MN, Kiani R, Hanks TD, Churchland AK. 2008. Neurobiology of decision making: an intentional framework. In: C Engel, W Singer (eds.). *Better Than Conscious? Decision Making, the Human Mind, and Implications for Institutions,* pp. 71–102. Cambridge, MA: MIT Press.

Sherrington C. 1947. *The Integrative Action of the Nervous System,* 2nd ed. Cambridge: Cambridge Univ. Press.

Spurzheim JG. 1825. *Phrenology, or the Doctrine of the Mind,* 3rd ed. London: Knight.

von Helmholtz H. [1850] 1948. On the rate of transmission of the nerve impulse. In: W Dennis (ed). *Readings in the History of Psychology,* pp. 197–198. New York: Appleton-Century-Crofts.

Wandell BA, Rauschecker AM, Yeatman JD. 2012. Learning to see words. Annu Rev Psychol 63:31–53.

Wernicke C. 1908. The symptom-complex of aphasia. In: A Church (ed). *Diseases of the Nervous System,* pp. 265–324. New York: Appleton.

Yeatman JD, Rauschecker AM, Wandell BA. 2013. Anatomy of the visual word form area: adjacent cortical circuits and long-range white matter connections. Brain Lang 125:146–155.

2

Genes and Behavior

All behaviors are shaped by the interplay of genes and the environment. The most stereotypic behaviors of simple animals are influenced by the environment, while the highly evolved behaviors of humans are constrained by innate properties specified by genes. Genes do not control behavior directly, but the RNAs and proteins encoded by genes act at different times and at many levels to affect the brain. Genes specify the developmental programs that assemble the brain and are essential to the properties of neurons, glia, and synapses that allow neuronal circuits to function. Genes that are stably inherited over generations create the machinery by which new experiences can change the brain during learning.

In this chapter, we ask how genes contribute to behavior. We begin with an overview of the evidence that genes do influence behavior, and then review basic principles of molecular biology and genetic transmission. We then provide examples of the way that genetic influences on behavior have been documented. A deep understanding of the ways that genes regulate behavior has emerged from studies of worms, flies, and mice, animals whose genomes are accessible to experimental manipulation. Many persuasive links between genes and human behavior have emerged from the analysis of human brain development and function. Despite the formidable challenges inherent in studying complex traits in humans, recent progress has

begun to reveal the genetic risk factors in neurodevelopmental and psychiatric syndromes such as autism, schizophrenia, and bipolar disorder, offering another important avenue to clarify the relationship between genes, brain, and behavior.

An Understanding of Molecular Genetics and Heritability Is Essential to the Study of Human Behavior

Many human psychiatric disorders and neurological diseases have a genetic component. The relatives of a patient are more likely than the general population to have the disease. The extent to which genetic factors account for traits in a population is called *heritability*. The strongest case for heritability is based on twin studies, first used by Francis Galton in 1883. Identical twins develop from a single fertilized egg that splits into two soon after fertilization; such monozygotic twins share all genes. In contrast, fraternal twins develop from two different fertilized eggs; these dizygotic twins, like normal siblings, share on average half their genetic information. Systematic comparisons over many years have shown that identical twins tend to be more similar (concordant) for neurological and psychiatric traits than fraternal twins, providing evidence of a heritable component of these traits (Figure 2–1A).

In a variation of the twin study model, the Minnesota Twin Study examined identical twins that were separated early in life and raised in different households. Despite sometimes great differences in their environment, twins shared predispositions for the same psychiatric disorders and even tended to share personality traits, like extraversion. This study provides considerable evidence that genetic variation contributes to normal human differences, not just to disease states.

Heritability for human diseases and behavioral traits is usually substantially less than 100%, demonstrating that the environment is an important factor in acquiring diseases or traits. Estimates of heritability for many neurological, psychiatric, and behavioral traits from twin studies are around 50%, but heritability can be higher or lower for particular traits (Figure 2–1B). Although studies of identical twins and other kinships provide support for the idea that human behavior has a hereditary component, they do not tell us which genes are important, let alone how specific genes influence behavior. These questions are addressed by studies in experimental animals in which genetic and environmental factors are strictly controlled and by modern methods of gene discovery that are now leading to the systematic, reliable identification of specific variations in DNA sequence and structure that contribute to human psychiatric and neurological phenotypes.

The Understanding of the Structure and Function of the Genome Is Evolving

The related fields of molecular biology and transmission genetics are central to our modern understanding of genes. Here we summarize some key ideas in these fields; a glossary at the end of the chapter defines commonly used terms.

Genes are made of DNA, and it is DNA that is passed on from one generation to the next. In most circumstances, exact copies of each gene are provided to all cells in an organism as well as to succeeding generations through DNA replication. The rare exceptions to this general rule—new (de novo) mutations that are introduced into the DNA of either germline or somatic cells and that play an important role in disease risk—are discussed later. DNA is made of two strands, each of which has a deoxyribose-phosphate backbone attached to a series of four subunits: the nucleotides adenine (A), guanine (G), thymine (T), and cytosine (C). The two strands are paired so that an A on one strand is always paired with a T on the complementary strand, and a G with a C (Figure 2–2). This complementarity ensures accurate copying of DNA during DNA replication and drives *transcription* of DNA into lengths of RNA called transcripts. Given that nearly all of the genome is double-stranded, bases or base pairs are used interchangeably as a unit of measurement. A segment of the genome encompassing a thousand base pairs is referred to as 1 kilobase (1 kb) or 1 kilobase pair (1 kbp), whereas a million base pairs are referred to as 1 megabase (1 Mb) or 1 megabase pairs (1 Mbp). RNA differs from DNA in that it is single-stranded, has a ribose rather than a deoxyribose backbone, and uses the nucleoside base uridine (U) in the place of thymine.

In the human genome, approximately 20,000 genes encode protein products, which are generated by *translation* of the linear messenger RNA (mRNA) sequence into a linear polypeptide (protein) sequence composed of amino acids. A typical protein-coding gene consists of a coding region, which is translated into the protein, and noncoding regions (Figure 2–3). The coding region is usually arranged in small coding segments called *exons*, which are separated by noncoding stretches called *introns*. The introns are deleted from the mRNA before its translation into protein.

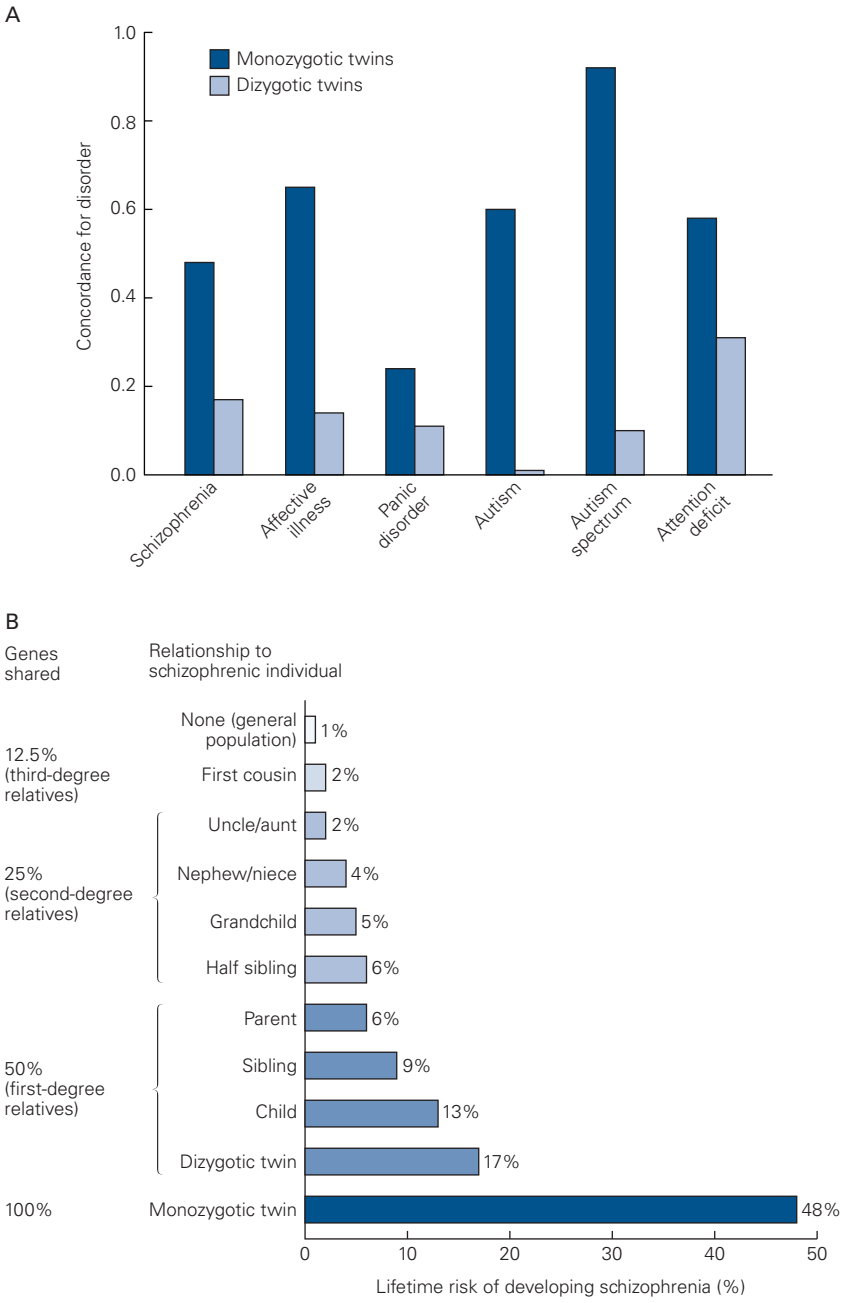

Figure 2–1 Familial risk of psychiatric disorders provides evidence of heritability.

A. Correlations between monozygotic twins for psychiatric disorders are considerably greater than those between dizygotic twins. Monozygotic twins share nearly all genes and have a high (but not 100%) risk of sharing the disease state. Dizygotic twins share 50% of their genetic material. A score of zero represents no correlation (the average result for two random people), whereas a score of 1.0 represents a perfect correlation. (Adapted from McGue and Bouchard 1998.)

B. The risk of developing schizophrenia is greater in close relatives of a schizophrenic patient. Like dizygotic twins, parents and children, as well as brothers and sisters, share 50% of their genetic material. If only a single gene accounted for schizophrenia, the risk should be the same for parents, siblings, children, and dizygotic twins of patients. The variation between family members shows that more complex genetic and environmental factors are in play. (Adapted, with permission, from Gottesman II. 1991.)

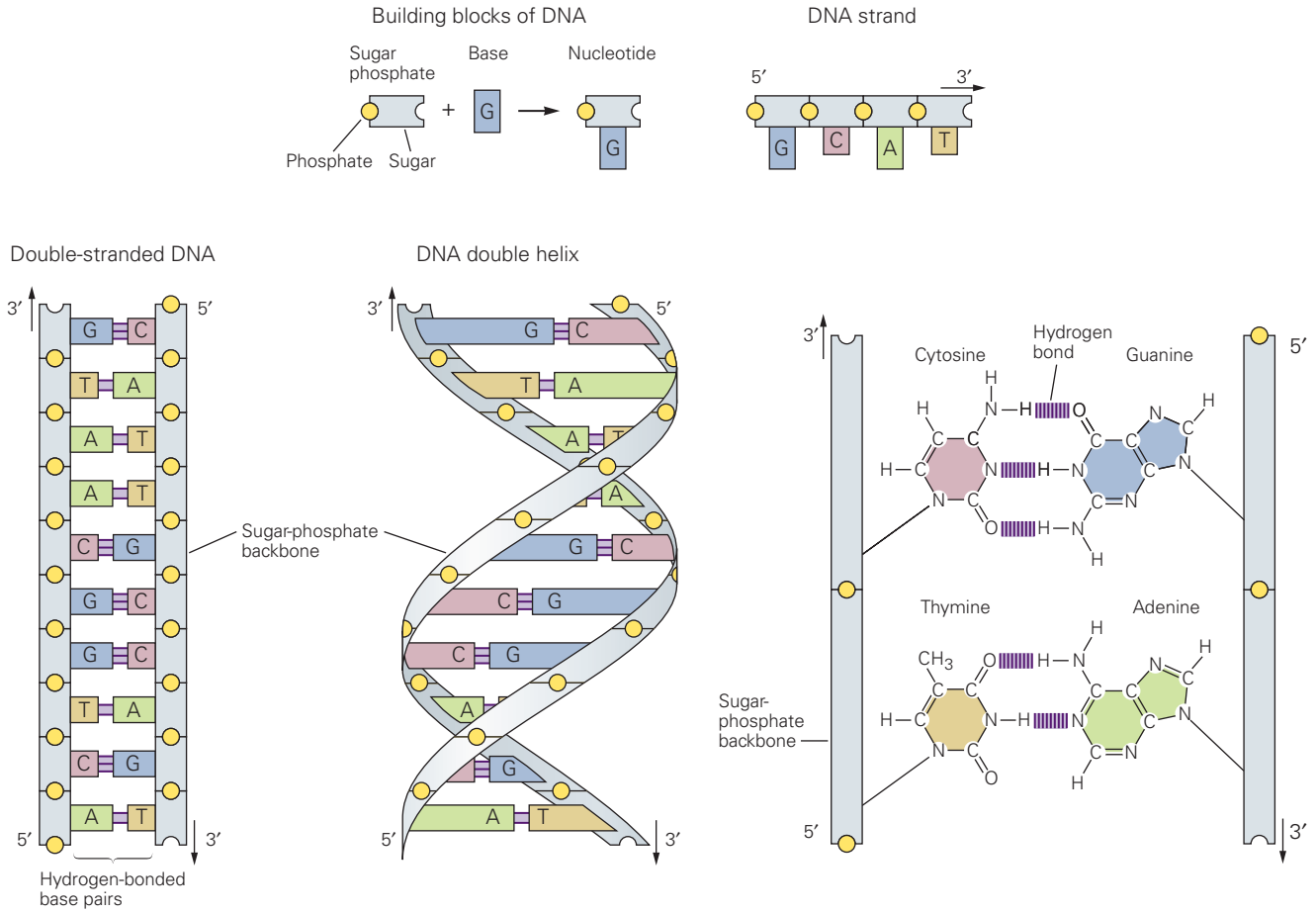

Figure 2–2 Structure of DNA. Four different nucleotide bases, adenine (A), thymine (T), cytosine (C), and guanine (G), are assembled on a sugar phosphate backbone in the double-stranded DNA helix. (Adapted from Alberts et al. 2002.)

Many functional RNA transcripts do not encode proteins. In fact, in the human genome, over 40,000 noncoding transcripts have been characterized as compared with approximately 20,000 protein-coding genes. Such genes include ribosomal RNAs (rRNAs) and transfer RNAs (tRNAs), essential components of the machinery for mRNA translation. Additional noncoding RNAs (ncRNA) include *long noncoding RNAs (lncRNAs)*, arbitrarily defined as longer than 200 bp in length, that do not encode proteins but can have roles in gene regulation; *small noncoding RNAs* of several types, including small nuclear RNAs (snRNAs), that guide mRNA splicing; and microRNAs (miRNAs) that pair with complementary sequences in specific mRNAs to inhibit their translation.

Each cell in the body contains the DNA for every gene but only expresses a specific subset of the genes as RNAs. The part of the gene that is transcribed into RNA is flanked by noncoding DNA regions that may be bound by other proteins, including *transcription factors*, to regulate gene expression. These sequence motifs include *promoters*, *enhancers*, *silencers*, and *insulators*, which together allow accurate expression of the RNA in the right cells at the right time. Promoters are typically found close to the beginning of the region to be transcribed; enhancers, silencers, and insulators may reside at a distance from the gene being regulated. Each type of cell has a unique complement of DNA-binding proteins that interact with promoters and other regulatory sequences to regulate gene expression and the resulting cellular properties.

The brain expresses a greater number of genes than any other organ in the body, and within the brain, diverse populations of neurons express different groups of genes. The selective gene expression controlled by promoters, other regulatory sequences, and the DNA-binding proteins that interact with them

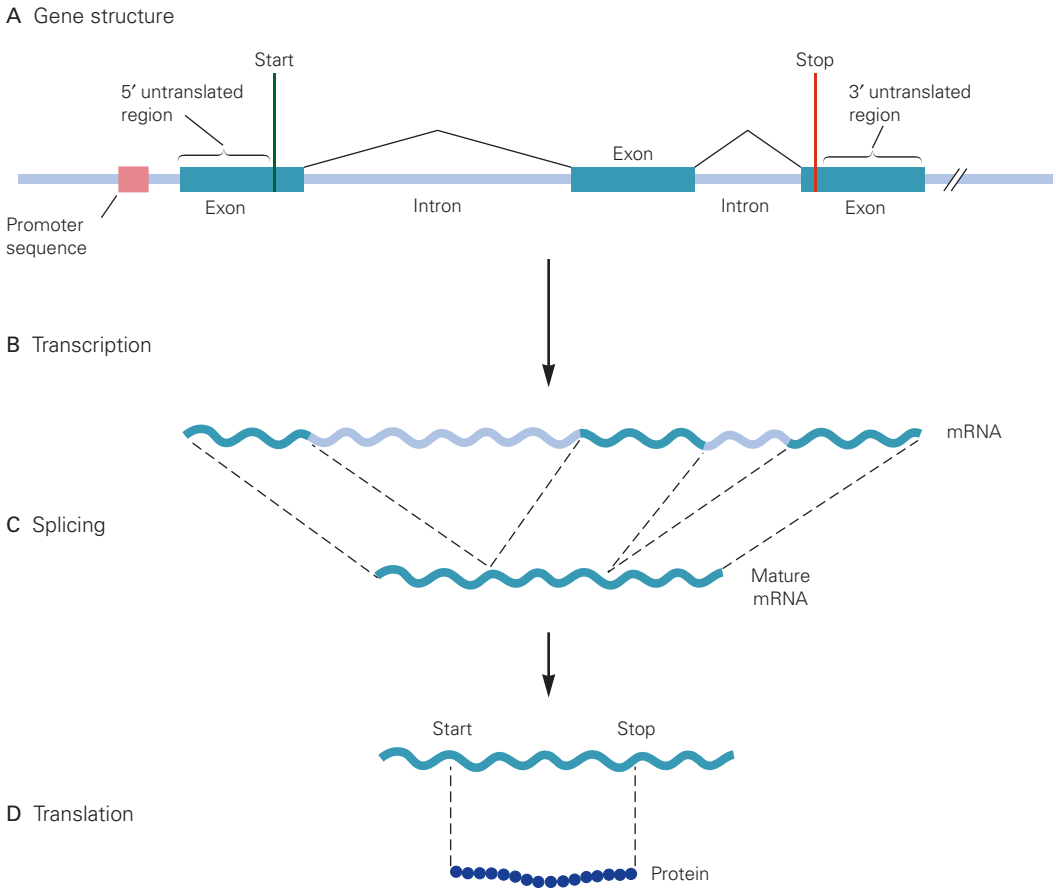

Figure 2–3 Gene structure and expression.

A. A gene consists of coding regions (exons) separated by noncoding regions (introns). Its transcription is regulated by noncoding regions such as promoters and enhancers that are frequently found near the beginning of the gene.

B. Transcription leads to production of a primary single-stranded RNA transcript that includes both exons and introns.

C. Splicing removes introns from the immature transcript and ligates the exons into a mature messenger RNA (**mRNA**), which is exported from the nucleus of the cell.

D. Translation of the mature mRNA produces a protein product.

permits a fixed number of genes to generate a vastly larger number of neuronal cell types and connections in the brain.

Although genes specify the initial development and properties of the nervous system, the experience of an individual and the resulting activity in specific neural circuits can itself alter the expression of genes. In this way, environmental influences are incorporated into the structure and function of neural circuits. Some of the principal goals of genetic studies are to unravel the ways that individual genes affect biological processes, the ways that networks of genes influence each other's activity, and the ways that genes interact with the environment.

Genes Are Arranged on Chromosomes

The genes in a cell are arranged in an orderly fashion on long, linear stretches of DNA called *chromosomes*. Each gene in the human genome is reproducibly located at a characteristic position (locus) on a specific chromosome, and this genetic "address" can be used to associate biological traits with a gene's effects. Most multicellular animals (including worms, fruit flies, and mice, as well as humans) are *diploid*; every somatic cell carries two complete sets of chromosomes, one from the mother and the other from the father.

Humans have about 20,000 genes but only 46 chromosomes: 22 pairs of autosomes (chromosomes

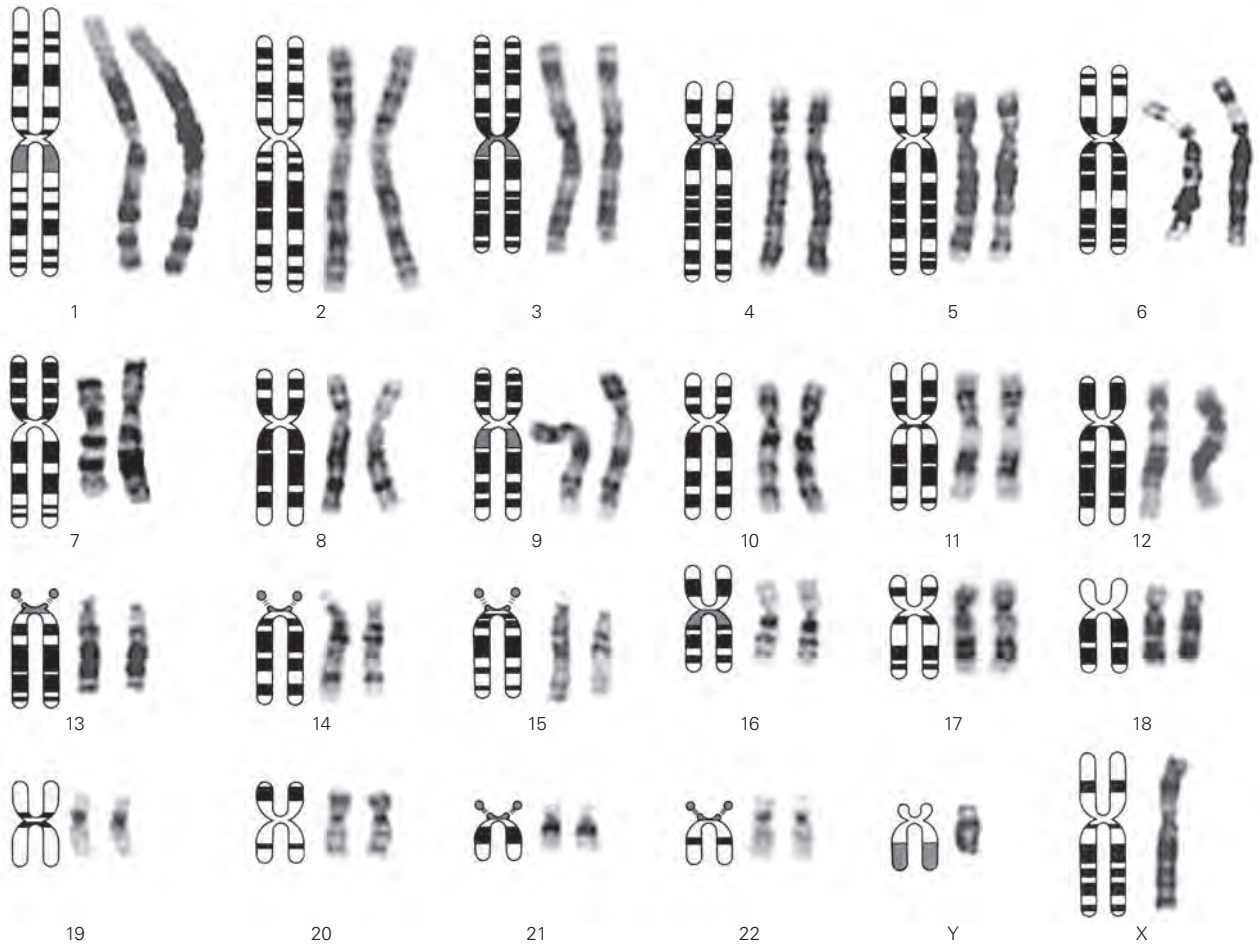

Figure 2–4 A map of normal human chromosomes at metaphase illustrates the distinctive morphology of each chromosome. Characteristic sizes and characteristic light and dark regions allow chromosomes to be distinguished from one another. (Adapted, with permission, from Watson, Tooze, and Kurtz 1983.)

that are present in both males and females) and two sex chromosomes (two X chromosomes in females, one X and one Y chromosome in males) (Figure 2–4). Each parent supplies one copy of each autosome to the diploid offspring. Each parent also supplies one X chromosome to female (XX) offspring, but XY males inherit their single X chromosome from their mothers and their single Y chromosome from their fathers. Sex-linked inheritance was discovered in fruit flies by Thomas Hunt Morgan in 1910. This pattern of sex-linked inheritance associated with the single X chromosome has been highly significant in human genetic studies, where certain X-linked genetic diseases are commonly observed only in males but are genetically transmitted from mothers to their sons.

In addition to the genes on chromosomes, a very small number of an organism's genes are transmitted through *mitochondria*, cytoplasmic organelles that carry out metabolic processes. Mitochondria in all children come from the ovum and therefore are transmitted from the mother to the child. Certain human disorders, including some neuromuscular degenerative diseases, some forms of intellectual disability, and some forms of deafness, are caused by mutations in the mitochondrial DNA.

The Relationship Between Genotype and Phenotype Is Often Complex

The two copies of a particular autosomal gene in an individual are called *alleles*. If the two alleles are identical, the individual is said to be *homozygous* at that locus. If the alleles vary because of mutations, the individual is *heterozygous* at that locus. Males

are *hemizygous* for genes on the X chromosome. A population can have a large number of alleles of a gene; for example, a single gene that affects human eye color, called *OCA2*, can have alleles that encode shades of blue, green, hazel, or brown. Because of this variation, it is important to distinguish the *genotype* of an organism (its genetic makeup) and the *phenotype* (its appearance). In the broad sense, a genotype is the entire set of alleles forming the genome of an individual; in the narrow sense, it is the specific alleles of one gene. By contrast, a phenotype is a description of a whole organism, and is a result of the expression of the organism's genotype in a particular environment.

If a mutant phenotype is expressed only when both alleles of a gene are mutated, the resulting phenotype is called *recessive*. This can occur if individuals are homozygous for the mutant allele or if they are carrying a different damaging allele in a given gene on each of their chromosomes (so-called *compound heterozygote*). Recessive mutations usually result from loss or reduction of a functional protein. Recessive inheritance of mutant traits is commonly observed in humans and experimental animals.

If a mutant phenotype results from a combination of one mutant and one wild-type allele, the phenotypic trait and mutant allele are said to be *dominant.* Some mutations are dominant because 50% of the gene product is not enough for a normal phenotype (*haploinsufficiency*). Other dominant mutations lead to the production of an abnormal protein or to the expression of the wild-type gene product at an inappropriate time or place; if this acts antagonistically to the normal protein product, it is called a *dominant negative* mutation.

The difference between genotype and phenotype is evident when considering the consequences of having one normal (wild-type) allele and one mutant allele of the same gene. Recent progress in gene discovery in a range of neurodevelopmental disorders, including autism and epilepsy, has demonstrated that the human genome is more sensitive to haploinsufficiency than previously appreciated. However, while the complete inactivation of both copies of a gene typically has a reliable effect, the severity and manifestation of haploinsufficiency vary to a greater degree from individual to individual, a phenomenon known as *variable*, *partial*, or *incomplete penetrance*.

Genetic variations that disturb development, cell function, or behavior in humans fall on a continuum between common alleles (also referred to as *polymorphisms*), which generally have small individual effects on biology and behavior, and rare variants, which may have larger biological effects (Box 2–1). While these categorizations are useful generalizations, there are nonetheless important cases in which common polymorphisms carry large disease risks; a common variation in the *APOE* gene, present in 16% of the population, results in a four-fold increase in the risk of late-onset Alzheimer disease.

Genes Are Conserved Through Evolution

The nearly complete nucleotide sequence of the human genome was reported in 2001, and the complete nucleotide sequences of many animal genomes have also been decoded. Comparisons between these genomes lead to a surprising conclusion: the unique human species did not result from the invention of unique new human genes.

Humans and chimpanzees are profoundly different in their biology and behavior, yet they share 99% of their protein-coding genes. Moreover, most of the approximately 20,000 genes in humans are also present in other mammals, such as mice, and over half of all human genes are very similar to genes in invertebrates such as worms and flies (Figure 2–5). The conclusion from this surprising discovery is that ancient genes that humans share with other animals are regulated in new ways to produce novel human properties, like the capacity to generate complex thoughts and language.

Because of this conservation of genes throughout evolution, insights from studies of one animal can often be applied to other animals with related genes, an important fact as animal experiments are often possible when experiments on humans are not. For example, a gene from a mouse that encodes an amino acid sequence similar to a human gene usually has a similar function to the *orthologous* human gene.

Approximately one-half of the human genes have functions that have been demonstrated or inferred from orthologous genes in other organisms (Figure 2–6). A set of genes shared by humans, flies, and even unicellular yeasts encodes the proteins for intermediary metabolism; synthesis of DNA, RNA, and protein; cell division; and cytoskeletal structures, protein transport, and secretion.

The evolution from single-cell organisms to multicellular animals was accompanied by an expansion of genes concerned with intercellular signaling and gene regulation. The genomes of multicellular

Box 2–1 Mutation: The Origin of Genetic Diversity

Although DNA replication generally is carried out with high fidelity, spontaneous errors called *mutations* do occur. Mutations can result from damage to the purine and pyrimidine bases in DNA, mistakes during the DNA replication process, and recombinations that occur during meiosis.

Changes in a single DNA base (also called a point mutation) within a coding region fall into five general categories:

1. A *silent mutation* changes a base but does not result in an obvious change in the encoded protein.
2. A *missense mutation* is a point mutation that results in one amino acid in a protein being substituted for another; increasingly these are being categorized using both informatics and empirical evidence into at least two subclasses: mutations that are damaging to protein function and those that may be functionally neutral.
3. A *nonsense mutation*, where a *codon* (a triplet of nucleotides) within the coding region specifying a specific amino acid is replaced by a stop codon, resulting in a shortened (truncated) protein product.
4. A *canonical splice site mutation* changes a nucleotide that specifies the exon/intron boundary.
5. A *frameshift mutation*, in which small insertions or deletions of nucleotides change the reading frame, leading to the production of a truncated or abnormal protein.

In the current literature, mutations falling into the latter four categories (including damaging missense mutations) are often referred to as *likely gene disrupting (LGD)* mutations.

The frequency of mutations greatly increases when the organism is exposed to chemical mutagens or ionizing radiation during experimental genetic studies. Chemical mutagens tend to induce *point mutations* involving changes in a single DNA base pair or the deletion of a few base pairs. Ionizing radiation can induce large insertions, deletions, or translocations.

In humans, point mutations occur at a low spontaneous rate in oocytes and sperm, leading to mutations present in the child but not in either parent, called de novo mutations. Each generation, between 70 and 90 single base changes are introduced into the entire genome (approximately 3 billion base pairs), of which one, on average, will cause a missense or nonsense mutation in a protein-coding gene. The number of de novo point mutations is increased in the children of older fathers, whereas the frequency of larger chromosome abnormalities is increased in the children of older mothers.

With the sequencing of the human genome in 2001 and increasingly high-resolution methods to detect genetic variation, it is also now clear that point mutations are not the only differences in sequence between humans. Certain sequences may be missing or repeated several times on a chromosome, and thus can have different numbers of copies in different individuals. When such variations encompass more than 1000 base pairs, they are called copy number variations (CNVs). Changes in more than a single base and less than 1000 base pairs are referred to as insertion/deletions (indels).

The contribution of any genetic variation to a disease or syndrome may be referred to as *simple* (or *Mendelian*) or *complex*. In general, a simple or Mendelian mutation is one that is sufficient to confer a phenotype without additional genetic risks. This does not imply that everyone with the mutation will show exactly the same phenotype. However, there is typically a highly reliable relationship between a specific disease allele and a phenotype, one that approaches a one-to-one relationship (as seen in sickle cell anemia or Huntington disease).

In contrast, a complex genetic disorder is one in which genetic risk factors change the probability of a disease but are not fully causal. This genetic contribution may involve rare mutations, common polymorphisms, or both, and is typically quite heterogeneous, with multiple different genes and alleles having the capacity to increase risk or play a protective role. Most complex disorders also involve a contribution from the environment.

animals, such as worms, flies, mice, and humans, typically encode thousands of transmembrane receptors, many more than are present in unicellular organisms. These transmembrane receptors are used in cell-to-cell communication in development, in signaling between neurons, and as sensors of environmental stimuli. The genome of a multicellular animal also encodes 1,000 or more different DNA-binding proteins that regulate the expression of other genes.

Many of the transmembrane receptors and DNA-binding proteins in humans are related to specific orthologous genes in other vertebrates and invertebrates. By enumerating the shared genetic heritage of the animals, we can infer that the basic molecular

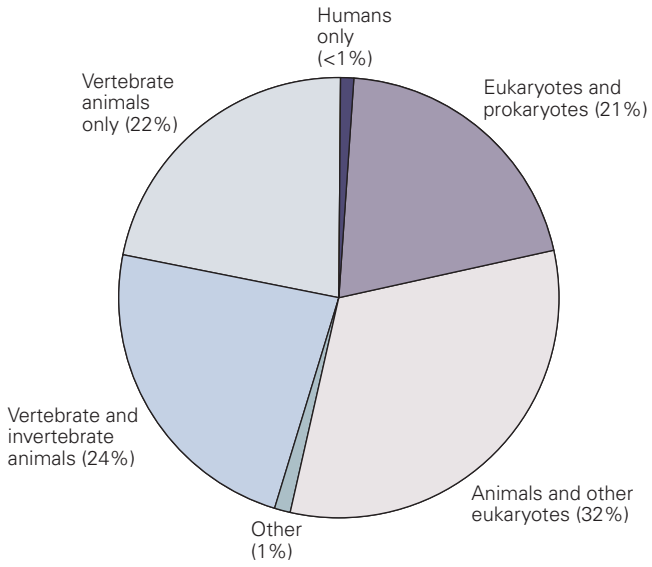

Figure 2–5 **Most human genes are related to genes in other species.** Less than 1% of human genes are specific to humans; other genes may be shared by all living things, by all eukaryotes, by animals only, or by vertebrate animals only. (Adapted, with permission, from Lander et al. 2001. Copyright © 2001 Springer Nature.)

pathways for neuronal development, neurotransmission, electrical excitability, and gene expression were present in the common ancestor of worms, flies, mice, and humans. Moreover, studies of animal and human genes have demonstrated that the most important genes in the human brain are those that are most conserved throughout animal phylogeny. Differences between mammalian genes and their invertebrate counterparts most often result from gene duplication in mammals or subtle changes in gene expression and function, rather than the creation of entirely new genes.

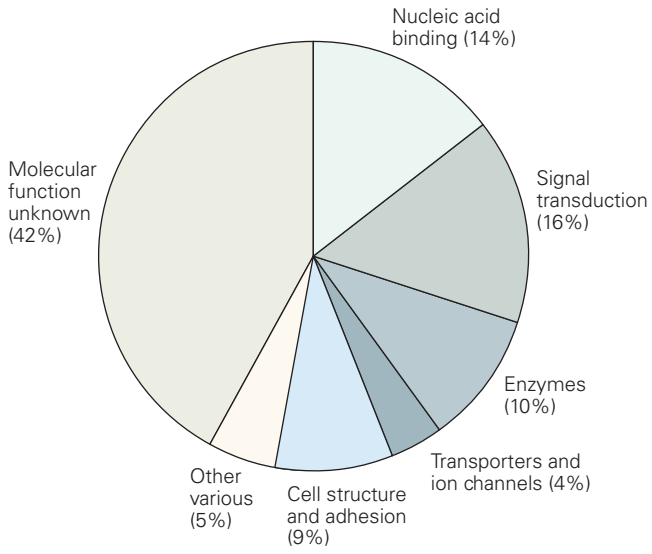

Figure 2–6 **The predicted molecular functions of 26,383 human genes.** (Adapted, with permission, from Venter et al. 2001.)

Genetic Regulation of Behavior Can Be Studied in Animal Models

Because of the evolutionary conservation between human and animal genes, studies in animal models of the relationships between the genes, proteins, and neural circuits that underlie behavior are likely to yield insight into these relationships in humans. Two important strategies have been applied with great success in the study of gene function.

In *classical genetic analysis*, organisms are first subjected to mutagenesis with a chemical or irradiation that induces random mutations and then screened for heritable changes that affect the behavior of interest, say, sleep. This approach does not impose a bias as to the kind of gene involved; it is a random search of all possible mutations that cause detectable changes. Genetic tracing of heritable changes allows the identification of the individual genes that are altered in the mutant organism. Thus the pathway of discovery in classical genetics moves from phenotype to genotype, from organism to gene. In *reverse genetics*, a specific gene of interest is targeted for alteration, a genetically modified animal is produced, and the animals with these altered genes are studied. This strategy is both focused and biased—one begins with a specific gene—and the pathway of discovery moves from genotype to phenotype, from gene to organism.

These two experimental strategies and their more subtle variations form the basis of experimental genetics. Gene manipulation by classical and reverse genetics is conducted in experimental animals, not in humans.

A Transcriptional Oscillator Regulates Circadian Rhythm in Flies, Mice, and Humans

The first large-scale studies of the influence of genes on behavior were initiated by Seymour Benzer and his colleagues around 1970. They used random mutagenesis and classical genetic analysis to identify mutations that affected learned and innate behaviors in the fruit fly *Drosophila melanogaster*: circadian (daily) rhythms, courtship behavior, movement, visual perception, and memory (Box 2–2 and Box 2–3). These induced mutations have had an immense influence on our understanding of the role of genes in behavior.

Box 2–2 Generating Mutations in Experimental Animals

Random Mutagenesis in Flies

Genetic analysis of behavior in the fruit fly (*Drosophila*) is carried out on flies in which individual genes have been mutated. Mutations can be made by chemical mutagenesis or by insertional mutagenesis, strategies that can affect any gene in the genome. Similar random mutagenesis strategies are used to create mutations in the nematode worm *Caenorhabditis elegans*, zebra fish, and mice.

Chemical mutagenesis, for example with ethyl methanesulfonate (EMS), typically creates random point mutations in genes. Insertional mutagenesis occurs when mobile DNA sequences called *transposable elements* randomly insert themselves into other genes.

The most widely used transposable elements in *Drosophila* are the P elements. P elements may be modified to carry genetic markers for eye color, which makes them easy to track in genetic crosses, and they may also be modified to alter expression of the gene into which they are inserted.

To cause P element transposition, *Drosophila* strains that carry P elements are crossed to those that do not. This genetic cross leads to destabilization and transposition of the P elements in the resulting offspring. The mobilization of the P element causes its transposition into a new location in a random gene.

Targeted Mutagenesis in Mice

Advances in molecular manipulation of mammalian genes have permitted precise replacement of a known normal gene with a mutant version. The process of generating a strain of mutant mice involves two separate manipulations. A gene on a chromosome is replaced by homologous recombination in a special cell line known as embryonic stem cells, and the modified cell line is incorporated into the germ cell population of the embryo (Figure 2–7).

The gene of interest must first be cloned. The gene is mutated, and a selectable marker, usually a drug-resistance gene, is then introduced into the mutated fragment. The altered gene is then introduced into embryonic stem cells, and clones of cells that incorporate the altered gene are isolated. DNA samples of each clone are tested to identify a clone in which the mutated gene has been integrated into the homologous (normal) site, rather than some other random site.

When a suitable clone has been identified, the cells are injected into a mouse embryo at the blastocyst stage (3 to 4 days after fertilization), when the embryo consists of approximately 100 cells. These embryos are then reintroduced into a female that has been hormonally prepared for implantation and allowed to come to term. The resulting embryos are chimeric mixtures between the stem cell line and the host embryo.

Embryonic stem cells in the mouse have the capability of participating in all aspects of development, including the germline. The injected cells can become germ cells and pass on the altered gene to future generations of mice. This technique has been used to generate mutations in various genes crucial to development or function in the nervous system.

Restricting Gene Knockout and Regulating Transgenic Expression

To improve the utility of gene knockout technology, methods have been developed that restrict deletions to cells in a specific tissue or at specific points in an animal's development. One method of regional restriction exploits the Cre/loxP system. The Cre/loxP system is a site-specific recombination system, derived from the P1 phage, in which the phage enzyme Cre recombinase catalyzes recombination between 34 bp loxP recognition sequences, which are normally not present in animal genomes.

The loxP sequences can be inserted into the genome of embryonic stem cells by homologous recombination such that they flank one or more exons of a gene of interest (called a floxed gene). When the stem cells are injected into an embryo, one can eventually breed a mouse in which the gene of interest is floxed and still functional in all cells of the animal.

A second line of transgenic mice can then be generated that expresses Cre recombinase under the control of a neural promoter sequence that is normally expressed in a restricted brain region. By crossing the Cre transgenic line of mice with the line of mice with the floxed gene of interest, the gene will only be deleted in those cells that express the Cre transgene.

In the example shown in Figure 2–8A, the gene encoding the NR1 (or GluN1) subunit of the *N*-methyl-D-aspartate (NMDA) glutamate receptor has been flanked with loxP elements and then crossed with a mouse line expressing Cre recombinase under control of the CaMKII promoter, which normally is expressed in forebrain neurons. In this particular line, expression was fortuitously limited to the CA1 region of the hippocampus, resulting in selective deletion of the NR1 subunit in this brain region (Figure 2–8B). Because the CaMKII promoter only activates gene transcription postnatally, early developmental changes are minimized by this strategy.

In addition to regional restriction of gene expression, control over the timing of gene expression gives the investigator an additional degree of flexibility and can exclude the possibility that any abnormality observed in the phenotype of the mature animal is the result of a developmental defect produced by the transgene. This can be done in mice by constructing a gene that can be turned on or off with a drug.

One starts by creating two lines of mice. Line 1 carries a particular transgene that is under control of the promoter tetO, which is ordinarily found only in bacteria. This promoter cannot by itself turn on the gene; it needs to be activated by a specific transcriptional regulator. Thus the second line of mice expresses a second transgene that encodes a hybrid transcription factor,

(*continued*)

Box 2–2 Generating Mutations in Experimental Animals (continued)

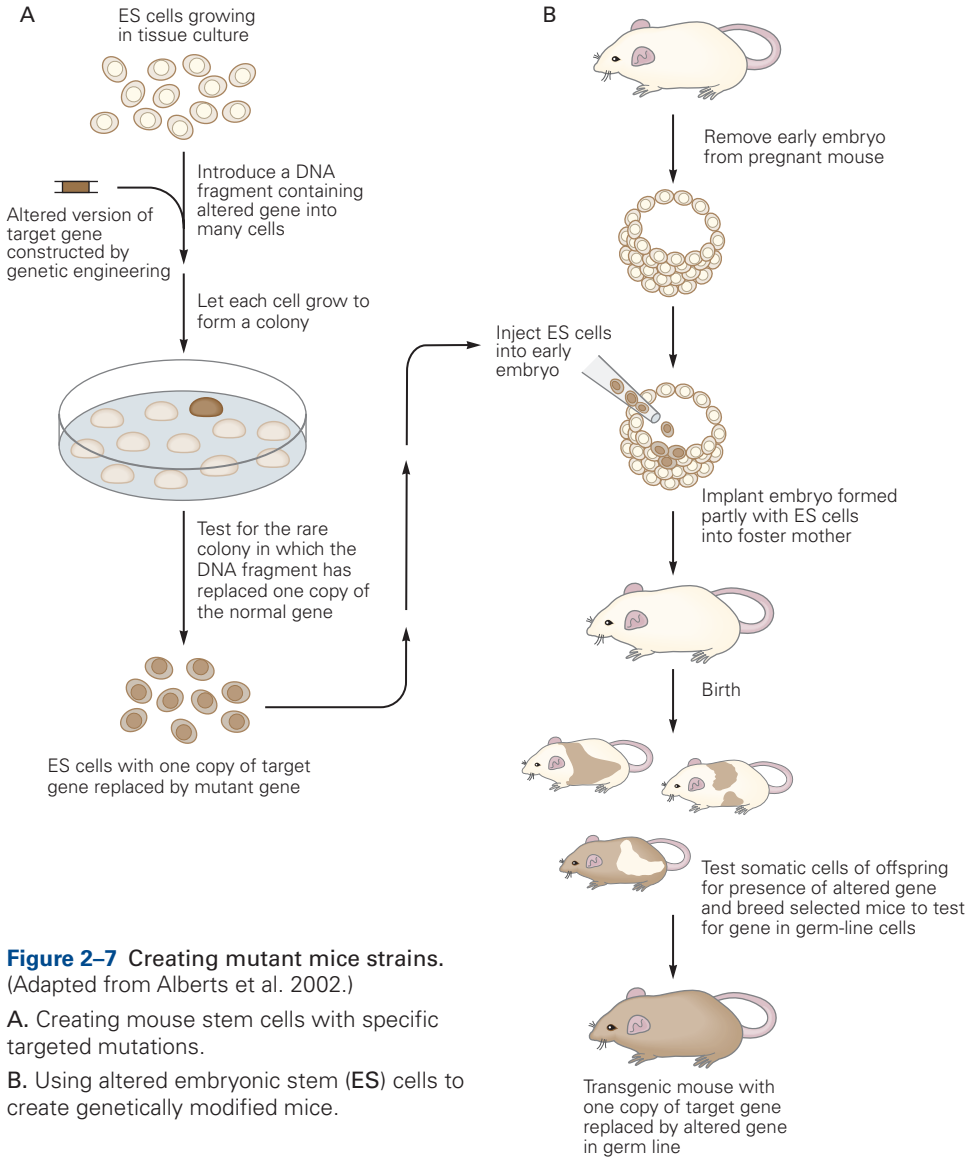

Figure 2–7 Creating mutant mice strains. (Adapted from Alberts et al. 2002.)

A. Creating mouse stem cells with specific targeted mutations.

B. Using altered embryonic stem (ES) cells to create genetically modified mice.

the tetracycline transactivator (tTA), which recognizes and binds to the tetO promoter. Expression of tTA can be placed under the control of a promoter in the mouse genome that normally drives gene transcription in only specific classes of neurons or specific brain regions.

When the two lines of mice are mated, some of the offspring will carry both transgenes. In these mice, the tTA binds to the tetO promoter and activates the downstream transgene. What makes the tTA transcription factor particularly useful is that it becomes inactivated when it binds certain antibiotics, such as tetracycline, allowing transgene expression to be regulated by administering antibiotics to mice. One can also generate mice that express a mutant form of tTA called reverse tTA (rtTA). This transactivator will not bind to tetO unless the animal is fed doxycycline. In this case, the transgene is always turned off unless the drug is given (Figure 2–9).

Altering Gene Function by RNA Interference and CRISPR

Finally, genes can be inactivated by targeting them with modern molecular tools. One such method is RNA interference, which takes advantage of the fact that most double-stranded RNAs in eukaryotic cells are routinely destroyed; the whole RNA is destroyed even if only part of it is double-stranded. By introducing a short RNA sequence that artificially causes a selected mRNA to become double-stranded, researchers can activate this process to reduce the mRNA levels for specific genes.

Another experimental tool is CRISPR, a method in which components of a bacterial immune system are deployed in nonbacterial cells to directly attack a selected DNA sequence. To target a gene with CRISPR,

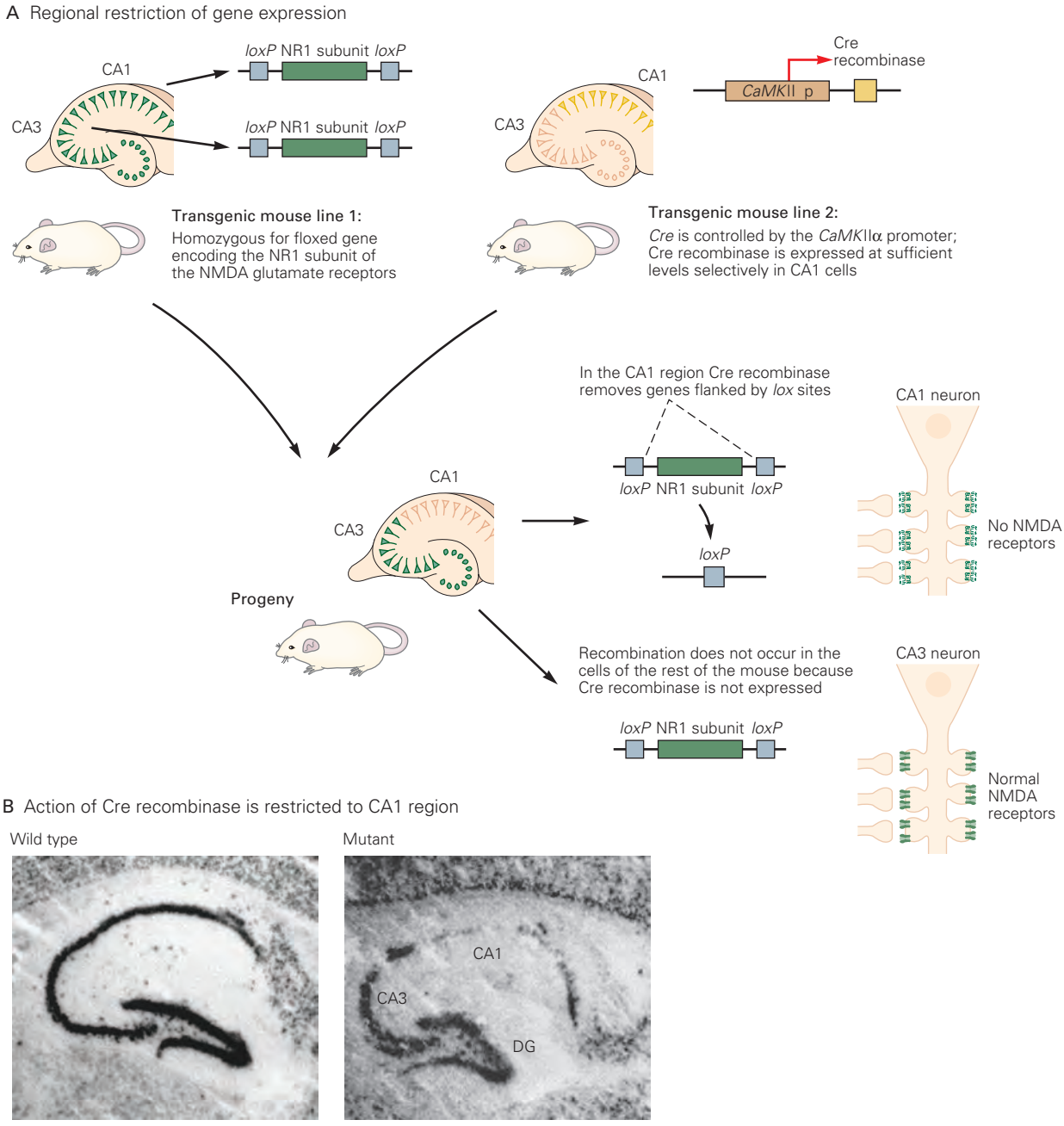

Figure 2–8 The Cre/loxP system for gene knockout in selective regions.

A. A line of mice is bred in which the gene encoding the NR1 subunit of the NMDA receptor has been flanked by loxP genetic elements (transgenic mouse line 1). These so-called "floxed NR1" mice are then crossed with a second line of mice in which a transgene coding for Cre recombinase is placed under the control of a transcriptional promoter specific to a cell type or a tissue type (transgenic mouse line 2). In this example, the promoter from the *CaMKIIα* gene is used to drive expression of the *Cre* gene. In progeny that are homozygous for the floxed gene and that carry the *Cre* recombinase transgene, the floxed gene will be deleted by Cre-mediated loxP recombination only in cell type(s) in which the promoter driving Cre expression is active.

B. In situ hybridization is used to detect mRNA for the NR1 subunit in hippocampal slices from wild-type and mutant mice that contain two floxed NR1 alleles and express Cre recombinase under the control of the CaMKIIα promoter. In the mutant mice, expression of the mRNA for NR1 (dark staining) is greatly reduced in the CA1 region of the hippocampus but remains normal in CA3 and the dentate gyrus (**DG**). (Reproduced, with permission, from Tsien, Huerta, and Tonegawa 1996.)

Box 2–2 Generating Mutations in Experimental Animals (continued)

a bacterial protein (typically but not always a protein called CAS9) is produced together with an engineered guide RNA that has sequence similarity with the target gene. The CAS9-guide RNA complex seeks out and cleaves the target sequence in the genome of the cell of interest. That initial cleavage can induce point mutations, insertions, and deletions at that site, and can also facilitate desired recombination or genetic replacement events. CRISPR tools are increasing in their sophistication and precision to the extent that they are now being considered for repair of hereditary mutations in people with severe inherited genetic diseases.

RNA interference and CRISPR have great potential to increase the power of genetic analysis because they can be used on any species in which DNA or RNA can be delivered to cells, including animals that are not now used in classical genetic analysis, such as long-lived birds, fish, and even primates.

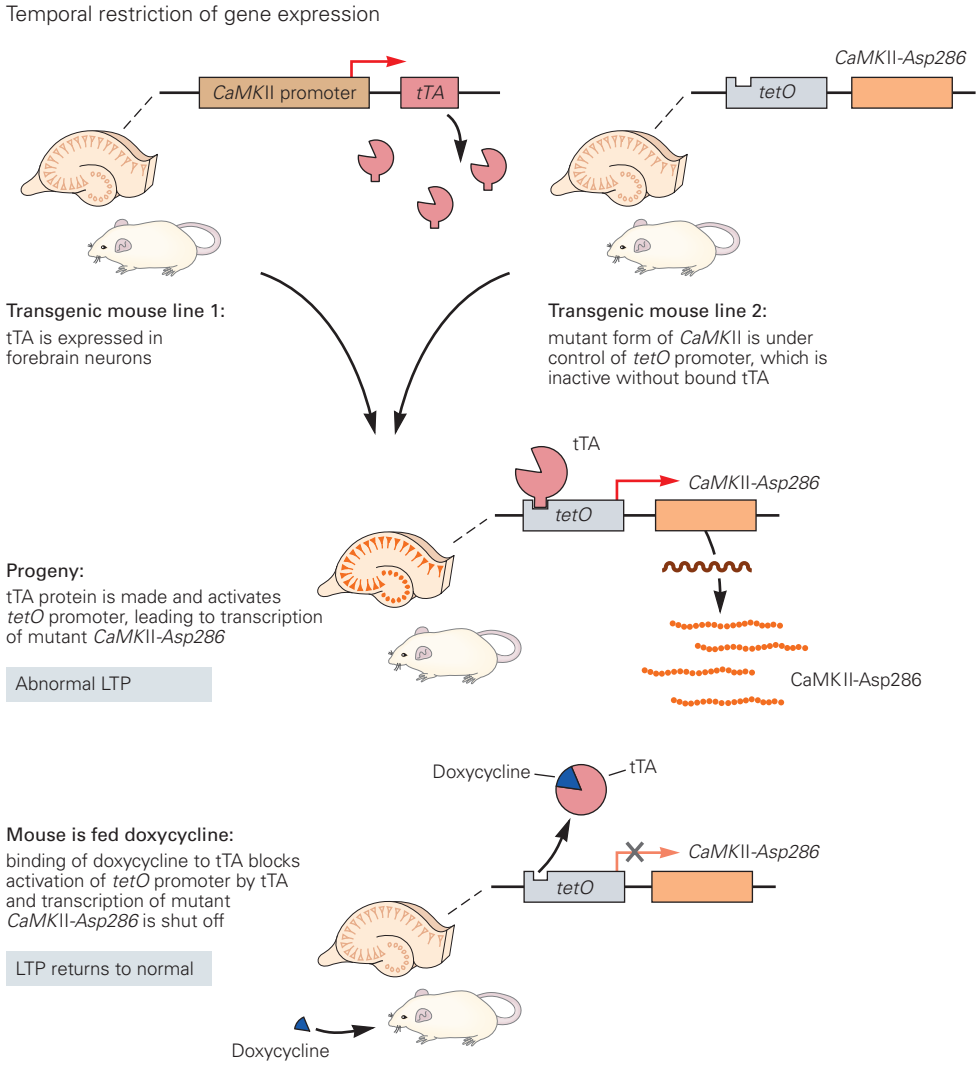

Figure 2–9 The tetracycline system for temporal and spatial regulation of transgene expression. Two independent lines of transgenic mice are bred. One line expresses, under the control of the CaMKIIα promoter, the tetracycline transactivator (**tTA**), an engineered protein incorporating a bacterial transcription factor that recognizes the bacterial tetO operon. The second line contains a transgene of interest—here encoding a constitutively active form of CaMKII (CaMKII–Asp286) that makes the kinase persistently active in the absence of Ca^{2+}—whose expression is under control of tetO. When these two lines are mated, the offspring express the tTA protein in a pattern restricted to the forebrain. When the tTA protein binds to tetO, it will activate transcription of the downstream gene of interest. Tetracycline (or doxycycline) given to the offspring binds to the tTA protein and causes a conformational change that leads to the unbinding of the protein from tetO, blocking transgene expression. In this manner, mice will express CaMKII–Asp286 in the forebrain, and this expression can be turned off by administering doxycycline to the mice. (Reproduced, with permission, from Mayford et al. 1996.)

Box 2–3 Introducing Transgenes in Flies and Mice

Genes can be experimentally introduced in mice by injecting DNA into the nucleus of newly fertilized eggs (Figure 2–10). In some of the injected eggs, the new gene, or transgene, is incorporated into a random site on one of the chromosomes. Because the embryo is at the one-cell stage, the incorporated gene is replicated and ends up in all (or nearly all) of the animal's cells, including the germline.

Gene incorporation is illustrated with a coat color marker gene rescued by injecting a gene for pigment production into an egg obtained from an albino strain. Mice with patches of pigmented fur indicate successful expression of DNA. The transgene's presence is confirmed by testing a sample of DNA from the injected animals.

A similar approach is used in flies. The DNA to be injected is cloned into a transposable element (P element). When injected into the embryo, the DNA becomes inserted into the DNA of germ cell nuclei. P elements can be engineered to express genes at specific times and in specific cells. Transgenes may be wild-type genes that restore function to a mutant or *designer genes* that alter the expression of other genes or code for a specifically altered protein.

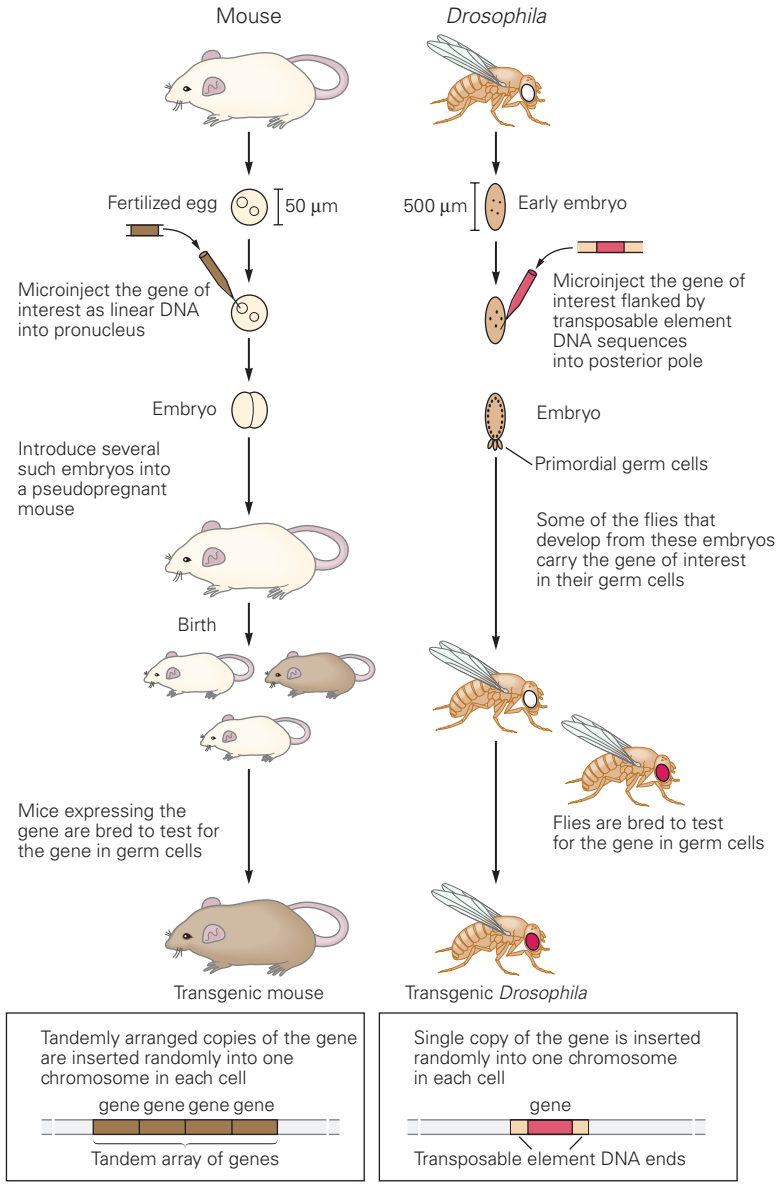

Figure 2–10 Generating transgenic mice and flies. Here the gene injected into the mouse causes a change in coat color, while the gene injected into the fly causes a change in eye color. In some transgenic animals of both species, the DNA is inserted at different chromosomal sites in different cells (see illustration at bottom). (Adapted from Alberts et al. 2002.)

We have a particularly complete picture of the genetic basis of the circadian control of behavior. An animal's circadian rhythm couples certain behaviors to a 24-hour cycle linked to the rising and setting of the sun. The core of circadian regulation is an intrinsic biological clock that oscillates over a 24-hour cycle. Because of the intrinsic periodicity of the clock, circadian behavior persists even in the absence of light or other environmental influences.

The circadian clock can be reset, such that changes in the day-night cycle eventually result in a matching shift in the intrinsic oscillator, a phenomenon familiar to any traveler recovering from jet lag. The clock is reset by light-driven signals transmitted by the eye to the brain. Finally, the clock drives effector pathways for specific behaviors, such as sleep and locomotion.

Benzer's group searched through thousands of mutant flies to look for rare flies that failed to follow circadian rhythms because of mutations in the genes that direct circadian oscillation. From this work emerged the first insight into the molecular machinery of the circadian clock. Mutations in the *period*, or *per*, gene affected all circadian behaviors generated by the fly's internal clock.

Interestingly, *per* mutations could change the circadian clock in several ways (Figure 2–11). Arrhythmic *per* mutant flies, which exhibited no discernible intrinsic rhythms in any behavior, lacked all function of the *per* gene, so *per* is essential for rhythmic behavior. *Per* mutations that maintained some function of the gene resulted in abnormal rhythms. Long-day alleles produced 28-hour behavioral cycles, whereas short-day alleles produced a 19-hour cycle. Thus *per* is not just an essential piece of the clock, it is actually a timekeeper whose activity can change the rate at which the clock runs.

The *per* mutant has no major adverse effects other than the change in circadian behavior. This observation is important because prior to the discovery of *per* many had questioned whether there could be true "behavior genes" that were not required for the physiological needs of an animal. *Per* does seem to be such a "behavior gene."

How does *per* keep time? The protein product PER is a transcriptional regulator that affects the expression of other genes. Levels of PER are regulated throughout the day. Early in the morning, PER and its mRNA are low. Over the course of the day, the PER mRNA and protein accumulate, reaching peak levels after dusk and during the night. The levels then decrease, falling before the next dawn. These observations provide an answer to the circadian rhythm puzzle—a central regulator appears and disappears throughout the day. But they are also unsatisfying because they only push the question back one step—what makes PER cycle? The answer to this question required the discovery of additional clock genes, which were discovered in flies and also in mice.

Emboldened by the success of the fly circadian rhythm screens, Joseph Takahashi began similar but far more labor-intensive genetic screens in mice in the 1990s. He screened hundreds of mutant mice for the rare individuals with alterations in their circadian locomotion period and found a single gene mutation that he called *clock*. When mice homozygous for the *clock* mutation are transferred to darkness, they initially experience extremely long circadian periods and later a complete loss of circadian rhythmicity (Figure 2–12). The *clock* gene therefore appears to regulate two fundamental properties of the circadian rhythm: the length of the circadian period and the persistence of rhythmicity in the absence of sensory input. These properties are conceptually identical to the properties of the *per* gene in flies.

The mouse *clock* gene, like the *per* gene in flies, encodes a transcriptional regulator whose activity oscillates through the day. The mouse CLOCK and fly PER proteins also shared a domain called a *PAS domain*, characteristic of a subset of transcriptional regulators. This observation suggests that the same molecular mechanism—oscillation of PAS-domain transcriptional regulation—controls circadian rhythm in flies and mice.

More significantly, parallel studies of flies and mice showed that similar groups of transcriptional regulators affect the circadian clock in both animals. After the mouse *clock* gene was cloned, a fly circadian rhythm gene was cloned and found to be even more closely related to mouse *clock*, than was *per*. In a different study, a mouse gene similar to fly *per* was identified and inactivated by reverse genetics. The mutant mouse had a circadian rhythm defect, like fly *per* mutants. In other words, both flies and mice use both *clock* and *per* genes to control their circadian rhythms. A group of genes, not one gene, are conserved regulators of the circadian clock.

Characterization of these genes has led to an understanding of the molecular mechanisms of circadian rhythm and a dramatic demonstration of the similarity of these mechanisms in flies and mice. In both flies and mice, the CLOCK protein is a transcriptional activator. Together with a partner protein, it controls the transcription of genes that determine behaviors such as locomotor activity levels. CLOCK and its partner also stimulate the transcription of the *per* gene. However, PER protein represses CLOCK's ability to stimulate *per* gene expression, so as PER protein

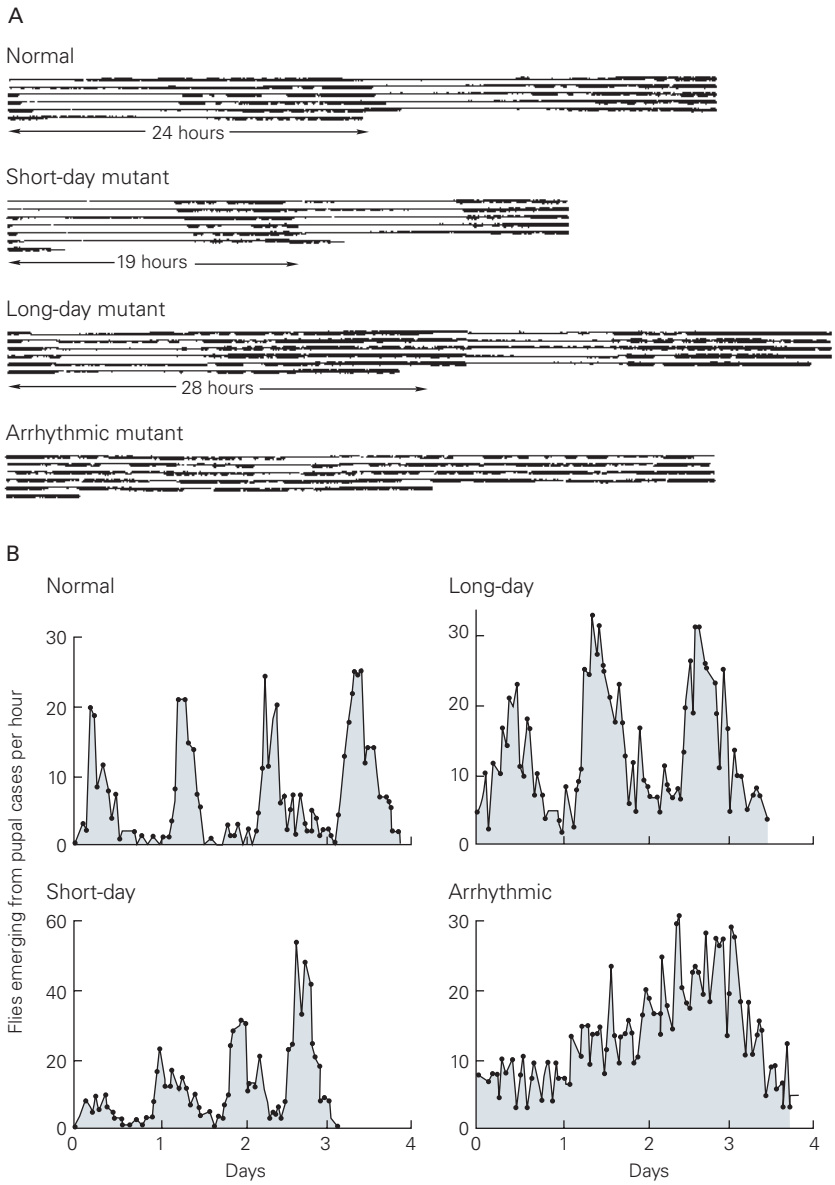

Figure 2–11 A single gene governs the circadian rhythms of behaviors in *Drosophila*. Mutations in the *period*, or *per*, gene affect all circadian behaviors regulated by the fly's internal clock. (Reproduced, with permission, from Konopka and Benzer 1971.)

A. Locomotor rhythms in normal *Drosophila* and three strains of *per* mutants: short-day, long-day, and arrhythmic. Flies were shifted from a cycle of 12 hours of light and 12 hours of dark into continuous darkness, and activity was then monitored under infrared light. Thick segments in the record indicate activity.

B. Normal adult fly populations emerge from their pupal cases in cyclic fashion, even in constant darkness. The plots show the number of flies (in each of four populations) emerging per hour over a 4-day period of constant darkness. The arrhythmic mutant population emerges without any discernible rhythm.

accumulates, *per* transcription falls (Figure 2–13). The 24-hour cycle comes about because the accumulation and activation of PER protein is delayed by many hours after the transcription of *per*, a result of PER phosphorylation, PER instability, and interactions with other cycling proteins.

The molecular properties of *per*, *clock*, and related genes generate all properties essential for circadian rhythm.

1. The transcription of circadian rhythm genes varies with the 24-hour cycle: PER activity is high at night; CLOCK activity is high during the day.

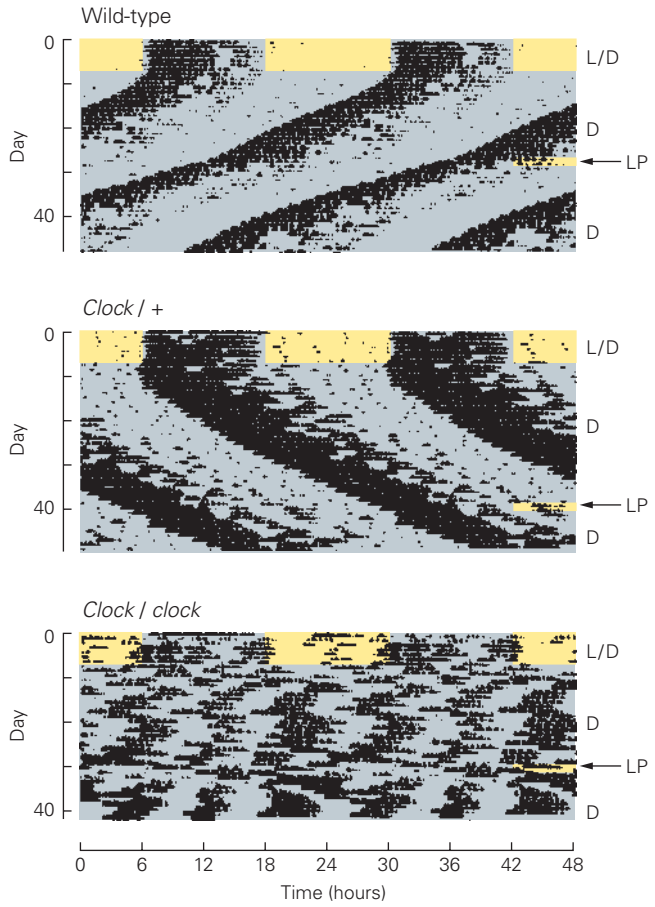

Figure 2–12 Circadian rhythm regulation by the *clock* gene in mice. The records show periods of locomotor activity by three animals: wild-type, heterozygous, and homozygous. All animals were kept on a light-dark (**L/D**) cycle of 12 hours for the first 7 days, then transferred to constant darkness (**D**). They later were exposed to a 6-hour light period (**LP**) to reset the rhythm. The circadian rhythm for the wild-type mouse has a period of 23.1 hours. The period for the heterozygous *clock*/+ mouse is 24.9 hours. The homozygous *clock*/*clock* mice experience a complete loss of circadian rhythmicity on transfer to constant darkness and transiently express a rhythm of 28.4 hours after the light period. (Reproduced, with permission, from Takahashi, Pinto, and Vitaterna. 1994. Copyright © 1994 AAAS.)

2. The circadian rhythm genes are transcription factors that affect each other's mRNA level, generating the oscillations. CLOCK activates *per* transcription and PER represses CLOCK function.
3. The circadian rhythm genes also control the transcription of other genes that in turn affect many downstream responses. For example, in flies, the neuropeptide gene *pdf* controls locomotor activity levels.
4. The oscillation of these genes can be reset by light.

The detailed elucidation of this molecular clock mechanism was recognized by the 2017 Nobel Prize in Physiology or Medicine, awarded to Jeffrey Hall, Michael Rosbash, and Michael Young.

The same genetic network controls circadian rhythm in humans. People with advanced sleep-phase syndrome have short 20-day cycles and an extreme early-to-bed, early-to-rise "morning lark" phenotype. Louis Ptáček and Ying-hui Fu found that these individuals have mutations in a human *per* gene. These results demonstrate that genes for behavior are conserved from insects to humans. Advanced sleep-phase syndrome is discussed in the chapter on sleep (Chapter 44).

Natural Variation in a Protein Kinase Regulates Activity in Flies and Honeybees

In the genetic studies of circadian rhythm described earlier, random mutagenesis was used to identify genes of interest in a biological process. All normal individuals have functional copies of *per*, *clock*, and the related genes; only after mutagenesis were different alleles generated. Another, more subtle question about the role of genes in behavior is to ask which genetic changes may be responsible for behavioral variation among normal individuals. Work by Marla Sokolowski and her colleagues led to the identification of the first gene associated with variation in behavior among normal individuals in a species.

Larvae of *Drosophila* vary in activity level and locomotion. Some larvae, called rovers, move over long distances (Figure 2–14). Others, called sitters, are relatively stationary. *Drosophila* larvae isolated from the wild can be either rovers or sitters, indicating that these are natural variations and not laboratory-induced mutations. These traits are heritable; rover parents have rover offspring and sitter parents have sitter offspring.

Sokolowski used crosses between different wild flies to investigate the genetic differences between rover and sitter larvae. These crosses showed that the difference between rover and sitter larvae lies in a single major gene, the *for* (forager) locus. The *for* gene encodes a signal transduction enzyme, a protein kinase activated by the cellular metabolite cGMP (cyclic guanosine 3′,5′-monophosphate). Thus this natural variation in behavior arises from altered regulation of signal transduction pathways. Many neuronal functions are regulated by protein kinases such as the cGMP-dependent kinase encoded by the *for* gene. Molecules such as protein kinases are particularly significant at transforming short-term neural signals into long-term changes in the property of a neuron or circuit.

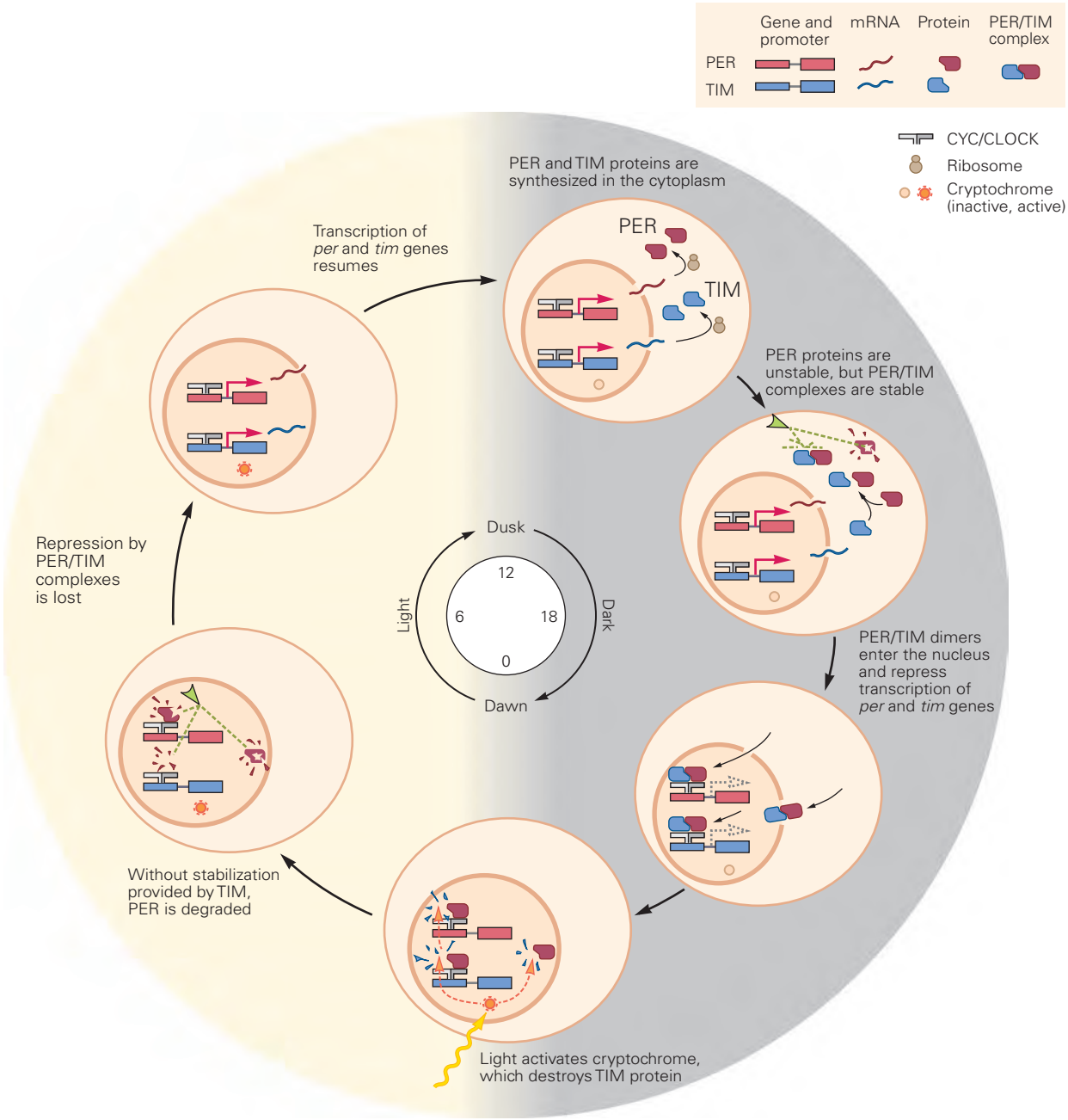

Figure 2–13 **Molecular events that drive circadian rhythm.** The genes that control the circadian clock are regulated by two nuclear proteins, PER and TIM. These proteins slowly accumulate and then bind to one another to form dimers. Once they form dimers, they enter the nucleus and shut off the expression of circadian genes including their own. They do so by inhibiting CLOCK and CYCLE, which stimulate the transcription of *per* and *tim* genes.

PER protein is highly unstable; most of it is degraded so quickly that it never has a chance to repress CLOCK-dependent *per* transcription. The degradation of PER is regulated by at least two different phosphorylation events by different protein kinases. When PER binds to TIM, PER is protected from degradation. As CLOCK drives more and more *per* and *tim* expression, enough PER and TIM eventually accumulate that the two can bind and stabilize each other, at which point they enter the nucleus where their own transcription is repressed. As a result, *per* and *tim* mRNA levels fall; thereafter, PER and TIM protein levels fall and CLOCK can (once again) drive expression of *per* and *tim* mRNA. During daylight, TIM protein is degraded by signaling pathways that are regulated by light (including cryptochrome), so PER/TIM complexes form only at night. The CLOCK protein induces PER and TIM expression but is inhibited by PER and TIM proteins.

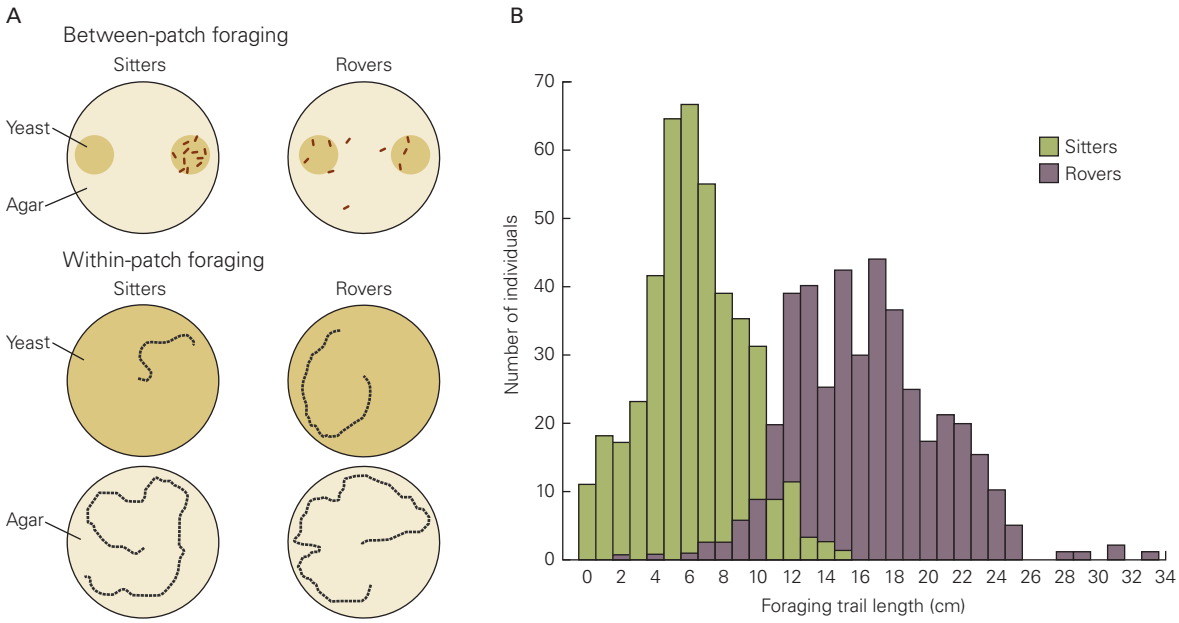

Figure 2–14 Foraging behavior of *Drosophila melanogaster* rover and sitter larvae differs while feasting on patches of yeast. (Reproduced, with permission, from Sokolowski. 2001. Copyright © 2001 Springer Nature.)

A. Rover-type larvae move from patch to patch, whereas sitter-type larvae stay put on a single patch for a long time. When foraging within a single patch, rover larvae move about more than sitter larvae. On agar alone, rover and sitter larvae move about equally.

B. While foraging within a patch of food, rovers have longer trail lengths than sitters (trail lengths were measured over a period of 5 minutes).

This difference in foraging behavior maps to a single protein kinase gene, *for*, which varies in activity in different fly larvae.

Why would variability in signaling enzymes be preserved in wild populations of *Drosophila*, which typically include both rovers and sitters? The answer is that variations in the environment create pressure for balanced selection for alternative behaviors. Crowded environments favor the rover larva, which is more effective at moving to new, unexploited food sources in advance of competitors, whereas sparse environments favor the sitter larva, which exploits the current source more thoroughly.

The *for* gene is also found in honeybees. Honeybees exhibit different behaviors at different stages of their life; in general, young bees are nurses, while older bees become foragers that leave the hive. The *for* gene is expressed at high levels in the brains of active foraging honeybees and at low levels in the younger and more stationary nurse bees. Activation of cGMP signaling in young bees can cause them to enter the forager stage prematurely; this change could be induced by an environmental stimulus or the bee's advancing age.

Thus the same gene controls variation in a behavior in two different insects, but in different ways. In the fruit fly, variations in the behavior are expressed in different individuals, whereas in the honeybee, they are expressed in one individual at different ages. The difference illustrates how an important regulatory gene can be recruited to different behavioral strategies in different species.

Neuropeptide Receptors Regulate the Social Behaviors of Several Species

Many aspects of behavior are associated with an animal's social interactions with other animals. Social behaviors are highly variable between species, yet have a large innate component within a species that is controlled genetically. A simple form of social behavior has been analyzed in the roundworm *Caenorhabditis elegans*. These animals live in soil and eat bacteria.

Different wild-type strains exhibit profound differences in feeding behavior. Animals from the standard laboratory strain are solitary, dispersing across a lawn of bacterial food and failing to interact with each other. Other strains have a social feeding pattern, joining large feeding groups of dozens or hundreds of animals (Figure 2–15). The difference between these strains is genetic, as both feeding patterns are stably inherited.

The difference between social and solitary worms is caused by a single amino acid substitution in a single gene, a member of a large family of genes involved in

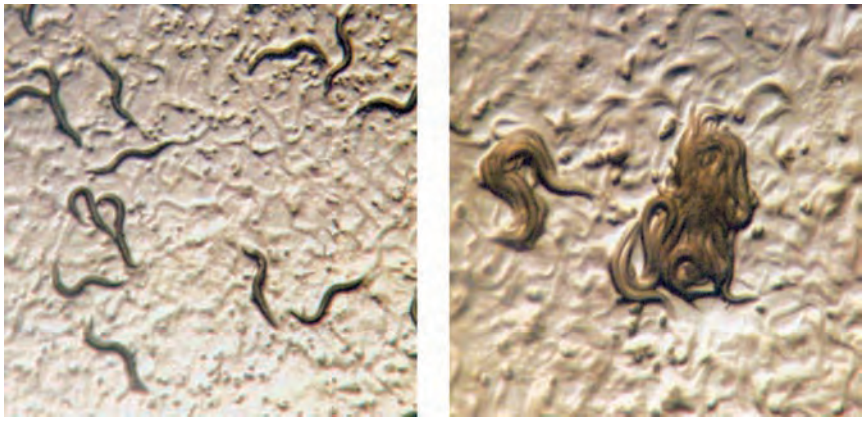

Figure 2–15 Feeding behavior of the roundworm *Caenorhabditis elegans* depends on the level of activity of the gene coding for a neuropeptide receptor. In one strain, individual worms graze in isolation (*left*), whereas in another strain, individuals mass together to feed. The difference is explained by a single amino acid substitution in the neuropeptide receptor gene. (Reproduced, with permission, from De Bono and Bargmann 1998.)

signaling between neurons. This gene, *npr-1*, encodes a neuropeptide receptor. Neuropeptides have long been appreciated for their roles in coordinating behaviors across networks of neurons. For example, a neuropeptide hormone of the marine snail *Aplysia* stimulates a complex set of movements and behavior patterns associated with a single behavior, egg laying. Mammalian neuropeptides have been implicated in feeding behavior, sleep, pain, and many other behaviors and physiological processes. The existence of a mutation in the neuropeptide receptor that alters social behavior suggests that this kind of signaling molecule is important both for generating the behavior and for generating the variation between individuals.

Neuropeptide receptors have also been implicated in the regulation of mammalian social behavior. The neuropeptides oxytocin and vasopressin stimulate mammalian affiliative behaviors such as pair bonding and parental bonding with offspring. In mice, oxytocin is required for social recognition, the ability to identify a familiar individual. Oxytocin and vasopressin have been studied in depth in prairie voles, rodents that form lasting pairs to raise their young. Oxytocin released in the brain of female prairie voles during mating stimulates pair-bond formation. Likewise, vasopressin released in the brain of male prairie voles during mating stimulates pair-bond formation and paternal behavior.

The extent of pair-bonding varies substantially between mammalian species. Male prairie voles form long-lasting pair-bonds with females and help them raise their offspring and are described as monogamous, but the closely related male montane voles breed widely and do not engage in paternal behavior. The difference between the behaviors of males in these species correlates with differences in the expression of the V1a class of vasopressin receptors in the brain. In prairie voles, V1a vasopressin receptors are expressed at high levels in a specific brain region, the ventral pallidum (Figure 2–16). In montane voles, the levels are much lower in this region, although high in other brain regions.

The importance of oxytocin and vasopressin and their receptors has been confirmed and extended by reverse genetic studies in mice, which are easier than voles to manipulate genetically. Introducing the V1a vasopressin receptor gene from prairie voles into male mice, which behave more like montane voles, increases the expression of the V1a vasopressin receptor in the ventral pallidum and increases the affiliative behavior of the male mice toward females. Thus differences between species in the pattern of expression of the vasopressin receptor can contribute to differences in social behaviors.

The analysis of vasopressin receptors in different rodents provides insight into the mechanisms by which genes and behaviors can change during evolution. Thus evolutionary changes in the pattern of expression of the V1a vasopressin receptor in the ventral forebrain have altered the activity of a neural circuit, linking the function of the ventral forebrain to the function of the vasopressin-secreting neurons that are activated by mating. As a result, social behaviors are altered.

The importance of oxytocin and vasopressin in human social behavior is not known, but the central role of pair-bonding and pup rearing in mammalian species suggests that these molecules might play a role in our species as well.

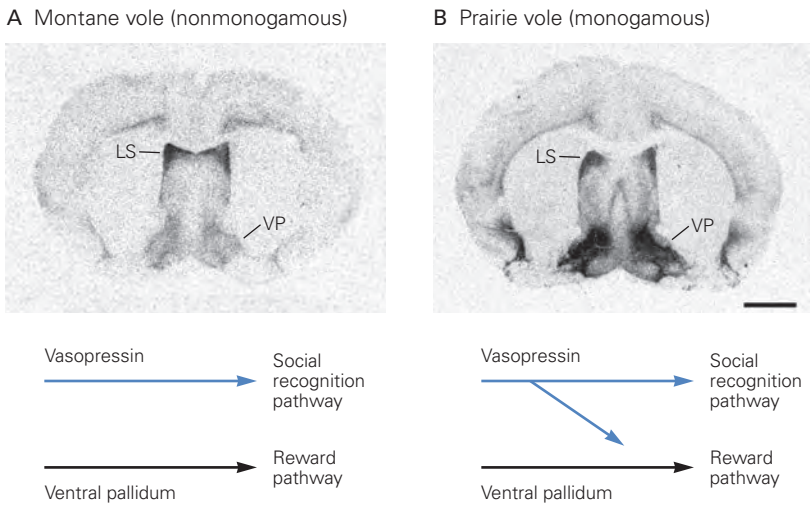

Figure 2–16 Distribution of vasopressin receptors (V1a) in two closely related rodent species. (Adapted, with permission, from Young et al. 2001. Copyright © 2001 Academic Press.)

A. Receptor expression is high in the lateral septum (LS) but low in the ventral pallidum (VP) in the montane vole, which does not form pair bonds.

B. Expression is high in the ventral pallidum of the monogamous prairie vole. Expression of the receptor in the ventral pallidum allows vasopressin to link the social recognition pathway to the reward pathway.

Studies of Human Genetic Syndromes Have Provided Initial Insights Into the Underpinnings of Social Behavior

Brain Disorders in Humans Result From Interactions Between Genes and the Environment

The first gene discovered for a neurological disease in humans clearly illustrates the interaction of genes and environment in determining cognitive and behavioral phenotypes. Phenylketonuria (PKU), described by Asbørn Følling in Norway in 1934, affects one in 15,000 children and results in severe impairment of cognitive function.

Children with this disease have two abnormal copies of the *PKU* gene that codes for phenylalanine hydroxylase, the enzyme that converts the amino acid phenylalanine to tyrosine. The mutation is recessive and heterozygous carrier individuals have no symptoms. Children who lack normal function in both copies of the gene accumulate high blood concentrations of phenylalanine from dietary proteins, which in turn leads to the production of toxic metabolites that interfere with neuronal function. The specific biochemical processes by which phenylalanine adversely affects the brain are still not understood.

The PKU phenotype (intellectual disability) results from the interaction of the genotype (the homozygous *pku* mutation) and the environment (the diet). The treatment for PKU is thus simple and effective: developmental delay can be prevented by a low-protein diet. The molecular and genetic analysis of gene function in PKU has led to dramatic improvements in the life of affected individuals. Since the early 1960s, the United States has instituted mandatory testing for PKU in newborns. Identifying children with the genetic disorder and modifying their diet before the disease appears prevents many aspects of the disorder.

Later chapters of this book describe many examples of single-gene traits that, like PKU, have led to insights into brain function and dysfunction. Certain themes have emerged from these studies. For example, a number of rare neurodegenerative disorders such as Huntington disease and spinocerebellar ataxia result from the pathological, dominant expansion of glutamate residues within proteins. The discovery of these polyglutamine repeat disorders highlighted the danger to the brain of unfolded and aggregated proteins. The discovery that epileptic seizures can be caused by a variety of mutations in ion channels led to the realization that these disorders are primarily disorders of neuronal excitability.

Rare Neurodevelopmental Syndromes Provide Insights Into the Biology of Social Behavior, Perception, and Cognition

Neurological and developmental disorders that manifest themselves in childhood have illuminated the

importance and complexity of genetics in human brain function. Early evidence that genes affect specific cognitive and behavioral circuitry emerged from studies of a rare genetic condition known as Williams syndrome. Individuals with this disorder typically exhibit normal language as well as extreme sociability; early in development, they lack the reticence children typically have in the presence of strangers. At the same time, they are profoundly impaired in spatial processing, show overall intellectual disability, and have very high rates of anxiety (but rarely social anxiety disorder).

The patterns of impairments in Williams syndrome, as compared with for example autism spectrum disorders, suggest that language and social skills can be separated from some other brain functions. Brain areas concerned with language are impaired in children with autism but are active or accentuated in Williams syndrome. By contrast, general and spatial intelligence is more impaired in Williams syndrome than in about half of all children with autism spectrum disorder.

Williams syndrome is caused by a heterozygous deletion of the chromosome region 7q11.23, most often encompassing about 1.5 Mb and 27 genes. The simplest interpretation of this defect is that the level of expression of the genes within the interval is reduced because there is only one copy instead of two of each gene in the region. The precise genes in the interval that influence social communication and spatial processing are not yet known, but they are of great interest because of their potential to provide insight into the genetic regulation of human behavior.

A more recent discovery in studies of autism spectrum disorders has further highlighted the complex relationship between genetic variation and social and intellectual functioning first illuminated by Williams syndrome. Within about the past decade, advances in genomic technology have allowed for high-throughput methods to screen the genome for variations in chromosomal structure, and at much higher resolution than was allowed by the light microscope (see Box 2–1). Seminal studies in 2007 and 2008 demonstrated that individuals with autism spectrum disorder carry new (de novo) copy number variations much more often than unaffected individuals. These findings led to some of the first discoveries of specific genomic intervals contributing to common forms of the syndrome (ie, autism spectrum disorder without evidence of syndromal features, also known as *idiopathic* or *nonsyndromic* autism spectrum disorder).

In 2011, two simultaneous large-scale studies of de novo copy number variations in a very well-characterized cohort found that precisely the same region deleted in Williams syndrome conferred substantial risk for autism spectrum disorder in an individual. However, in these cases, it was rare duplications (one excess copy of the region), and not deletions, that dramatically increased the risk for social disability. These findings, that losses and gains in the identical set of genes may lead to contrasting social phenotypes (while both typically lead to intellectual disability), further support the notion that domains of cognitive and behavioral functioning are separable but may share important molecular mechanisms.

Fragile X syndrome is another neurodevelopmental disorder of childhood that provides insight into the genetics of cognitive function; unlike Williams syndrome, it has been mapped to a single gene on the X chromosome. Fragile X syndrome varies in its presentation. Affected children may have intellectual disability, poor social cognition, high social anxiety, and repetitive behavior; about 30% of boys with fragile X syndrome meet diagnostic criteria for autism spectrum disorder. Fragile X syndrome is also associated with a broader range of traits, including physical characteristics such as an elongated face and protruding ears.

Fragile X syndrome has been shown to result from mutations that reduce expression of a gene called *fragile X mental retardation protein (FMRP)*. Because the gene falls on the X chromosome, males lose all expression of the gene when their one copy is mutated. FMRP protein regulates the translation of mRNAs into proteins in neurons, in a process that is itself regulated by neuronal activity. Regulated translation in neurons is an important component of the synaptic plasticity required for learning. The fragile X defect at the level of translation thus cascades up to affect neuronal function, learning, and higher-order cognitive processes. Interestingly, a large proportion of the other genes associated with increased risk for autism spectrum disorder as well as schizophrenia are regulated by the FMRP protein.

Another Mendelian disorder whose genetic basis is well understood is Rett syndrome (discussed in detail in Chapter 62). Rett syndrome is an X-linked, progressive neurodevelopmental disorder and one of the most common causes of intellectual disability in females. The disorder is almost always confined to females because canonical Rett mutations are very often lethal in the developing male embryo, which has a single X chromosome. Affected girls develop typically until they are 6 to 18 months of age, when they fail to acquire speech, show regression in intellectual functioning, and display compulsive, uncontrolled hand wringing instead of purposeful hand movement. In addition, girls with Rett syndrome often show a

period of markedly impaired social interaction that may be indistinguishable from autism spectrum disorder, although it is thought that social functioning is largely preserved in later life. Huda Zoghbi and her colleagues found that the major cause of this syndrome results from mutations in the *methyl CpG binding protein 2 (MeCP2)* gene. Methylation of specific CpG sequences in DNA alters expression of nearby genes, and one of the established functions of *MeCP2* is that it binds methylated DNA as part of a process that regulates mRNA transcription.

Rare syndromes have also offered some of the first insights into the genetic substrates of schizophrenia (Chapter 60). For example, as first described by Robert Shprintzen and colleagues in 1978, deletions of chromosome 22q11 lead to a wide range of physical and behavioral symptoms, including psychosis, now often referred to as velocardiofacial syndrome (VCFS), DiGeorge syndrome, or 22q11 deletion syndrome. The initial descriptions by Shprintzen were met with some skepticism as a result of the extremely broad range of phenotypes associated with the identical deletion. It is now widely appreciated that the 22q11 deletion is the most common chromosomal abnormality associated with schizophrenia and childhood-onset schizophrenia. Moreover, chromosomal losses of the identical region have been found to be associated with large individual risks for autism. To date, the specific genes within the region responsible for the psychiatric phenotype(s) have not been definitively established. Moreover, recent evidence from the autism literature suggests that it is likely that a combination of multiple genes within this interval, each conferring relatively small individual effects, is responsible for the social disability phenotype.

Psychiatric Disorders Involve Multigenic Traits

As mentioned earlier, single-gene syndromes are rare compared to the total burden of neurodegenerative and psychiatric disease. Consequently, one might question the rationale for studying rare disorders if they represent just a fraction of the total disease burden. The reason is that rare conditions can provide insight into the biological processes involved in more common, complex forms of a disease. For example, among the prominent successes of human genetics has been the discovery of rare genetic variants that lead to early-onset Alzheimer disease or Parkinson disease. Individuals with these severe rare variants represent a tiny subset of all individuals with these conditions, but the identification of rare disease variants uncovered cellular processes that are also disrupted in the larger patient pool, pointing to general therapeutic avenues. Similarly, pursuit of the pathophysiological mechanisms underlying Rett, fragile X, and other neurodevelopmental disorders has already led to some of the first attempts at rational drug development in psychiatric syndromes.

In the remainder of this chapter, we expand the discussion of the genetics of two complex neurodevelopmental and psychiatric phenotypes: autism spectrum disorders and schizophrenia. Compared to the rare Mendelian examples discussed earlier, the genetics of common forms of these conditions are indeed more diverse, varied, and heterogeneous, involving many different genes in different individuals as well as multiple risk genes conferring liability in combinations. Moreover, for both diagnoses, while the support for a genetic contribution is substantial, there is also compelling evidence for a contribution from environmental factors.

Progress in understanding these disorders came from the combination of rapidly advancing genomic technologies and statistical methods, a culture of open data sharing, and the consolidation of very large patient cohorts providing adequate power to detect very rare highly penetrant alleles as well as common genetic variants carrying small increments of risk. Importantly, recent successes in understanding both syndromes have provided a solid foundation for the pursuit of their biological consequences and the molecular, cellular, and circuit-level pathophysiology conveyed by these genetic risk factors.

Advances in Autism Spectrum Disorder Genetics Highlight the Role of Rare and De Novo Mutations in Neurodevelopmental Disorders

Autism spectrum disorders are a collection of developmental syndromes of varying severity affecting approximately 2% to 3% of the population and characterized by impairment in reciprocal social communication as well as stereotyped interests and repetitive behaviors. There is a significant male predominance; on average, three times as many boys as girls are affected. The clinical symptoms of autism spectrum disorders, by definition, emerge in the first 3 years of life, although highly reliable differences between affected and unaffected children are very often identifiable within the first months of life.

There is considerable phenotypic variability between those affected, leading to the development of the quite broad diagnostic classification of autism spectrum disorders. In addition, affected individuals have a higher frequency of seizures and cognitive

problems than the general population and often have serious impairments in adaptive functioning. However, many autistic individuals are not as profoundly affected and lead highly successful lives.

Autism has a very strong heritable component (see Figure 2–1A), which is likely to account for its being among the first genetically complex neuropsychiatric syndromes to yield to modern gene discovery tools and methods. Autism spectrum disorder has broader significance because it provides insight into behaviors that are quintessentially human: language, complex intelligence, and interpersonal interactions. Importantly, the fact that the defects in social communication seen in autism spectrum disorders can coexist with normal intelligence and typical functioning in other domains suggests that the brain is to some degree modular with distinct cognitive functions that can vary independently.

While syndromic forms of autism spectrum disorder account for a small fraction of all cases, the first findings in more common so-called "idiopathic" or "nonsyndromic" forms of the disorder also demonstrated a role for rare mutations carrying large biological effects. For example, in 2003, the sequencing of genes within a region on the X chromosome deleted in a very small number of females with autistic features led to the discovery of rare, loss-of-function mutations in the gene *neuroligin 4X (NLGN4X)*, a gene encoding a synaptic adhesion molecule in excitatory neurons and found in several affected male family members. Soon thereafter, a linkage analysis of a large pedigree with intellectual disability and autism spectrum disorder showed that affected family members all carried a loss-of-function *NLGN4X* mutation.

De novo submicroscopic deletions and duplications in chromosomal structure may dramatically increase an individual's risk for autism spectrum disorder. These copy number variations (CNVs) cluster in specific regions of the genome, identifying specific risk intervals. The earliest reports using this approach showed that the de novo CNVs at chromosome 16p11.2, although present in only about 0.5% to 1% of affected individuals, carried substantial (greater than 10-fold) risk of autism spectrum disorder. Subsequent studies have now identified a dozen or more de novo CNVs that carry risk, including at chromosomes 16p11.2, 1q21, 15q11-13, and 3q29; deletions at 22q11, 22q13 (deleting the gene *SHANK3*), and 2p16 (deleting the gene *NXRN1*); and de novo duplications of 7q11.23 (the Williams syndrome region).

Interestingly, although these CNVs carry large risks for autism spectrum disorder, studies of other psychiatric disorders, including schizophrenia and bipolar disorder, have found that many of the same regions increase the risk for these conditions as well. Moreover, studies of individuals ascertained by genotype (eg, 16p11.2 deletions and duplications) have found a wide variety of associated behavioral phenotypes, ranging from specific language impairment to intellectual disability to schizophrenia. This "one-to-many" phenomenon presents important challenges to illuminating specific pathophysiological mechanisms in psychiatric illness and to conceptualizing the steps from gene discovery to therapies.

The widespread and replicable findings that de novo rare CNVs increase the risk for autism spectrum disorder and other developmental disorders immediately raised the question of whether rare de novo mutations in single genes might carry similar risks. Indeed, the development of technology for low-cost, high-throughput DNA sequencing, initially focused on the coding portion of the genome, led to the identification of an excess of de novo mutations deemed likely to disrupt gene function (LGD mutations) in affected individuals. The repeated occurrence of these mutations in close proximity among unrelated individuals has now been exploited as a means to identify specific risk genes for autism spectrum disorders.

Large-scale studies of de novo mutations in autism spectrum disorders have now identified more than 100 associated genes, with about 45 of these reaching the highest confidence level of statistical significance. These genes have a wide range of known functions, but analyses reveal a statistically significant overrepresentation of genes involved in synaptic formation and function, and in regulation of transcription. Moreover, there are a greater than expected number of risk genes that encode RNAs that are targets of fragile X mental retardation protein and/or proteins that are active in early brain development.

Identification of Genes for Schizophrenia Highlights the Interplay of Rare and Common Risk Variants

Schizophrenia affects about 1% of all young adults, causing a pattern of thought disorders and emotional withdrawal that profoundly impairs life. It is strongly heritable (see Figure 2–1B) and also has a strong environmental component that is associated with stress on a developing fetus. Children born just after the Dutch Hunger Winter famine of World War II had a greatly increased risk of schizophrenia many years later, and children whose mothers were infected with the rubella virus during pregnancy in the 1960s pandemic were also at considerably increased risk.

Genes, as well as the environment, contribute to schizophrenia. As with autism, the sequencing of the human genome, the development of inexpensive methods for genome-wide genotyping of common variants and detection of CNVs, and the consolidation of very large patient cohorts have all resulted in a transformation in the genetics of schizophrenia. First, essentially in parallel with the findings in autism spectrum disorders noted earlier, rare and de novo CNVs began to be implicated in the risk for schizophrenia by the early 2000s. A small percentage of cases are associated with chromosomal abnormalities that carry large risks, including, for example, deletions at chromosome 22q11. These chromosomal abnormalities overlap entirely, or nearly so, with those loci implicated in autism spectrum disorders, but the distribution of risk among deletions and duplications at these loci does not appear to be identical. For instance, although duplications and deletions of the 16p11.2 region are both associated with autism spectrum disorders and schizophrenia, duplications of the region are more likely to lead to schizophrenia, whereas deletions are more likely to be seen with autism spectrum disorders and intellectual disability.

With regard to schizophrenia, the most important development of the last decade and a half has been the emergence of common variant genome-wide association studies (GWASs). In contrast to studies of hypothesis-driven candidate genes described earlier, genome-wide association relies on assaying polymorphisms at every gene in the genome simultaneously. This hypothesis-free approach, when used with well-powered cohorts and appropriate correction for multiple comparisons, has proven to be a highly reliable and reproducible strategy for identifying common risk alleles in common disorders across all of medicine.

GWASs involving nearly 40,000 cases and 113,000 controls have resulted in the identification of 108 risk loci for schizophrenia. The effects attributable to any individual genetic variant in this set have been quite modest, typically accounting for a less than 25% increase in risk. Moreover, many of the genetic polymorphisms assayed in GWASs map to regions outside of the coding segment of the genome. Consequently, although 108 risk loci have been identified, it is not yet entirely clear which genes correspond to all of these risk variants. In some cases, the variations mapped sufficiently close to a single gene that such a relationship could be reasonably inferred; in other cases, this remains to be determined.

The genes implicated in schizophrenia risk provide a starting point for determining the biology underlying the disorder. For example, since the late 1990s, evidence has pointed to the involvement of a region called the major histocompatibility complex (MHC) in schizophrenia risk. Accordingly, the MHC region has the strongest GWAS signal of any part of the human genome in the schizophrenia cohort. Detailed studies made possible by the very large number of patients in the cohort resolved this robust risk association signal in the MHC region into three different loci (and likely three different genes). Among these three loci, one gene, encoding the complement C4 factor, has a strong and definable effect on disease risk. Steven McCarroll and his colleagues showed that the complement C4 locus represents a natural case of CNV, that healthy individuals vary substantially in the number of copies of the gene they have, and that the level of expression of the C4A allele correlates with increasing schizophrenia risk. Subsequent follow-up studies showed that mice with knockouts of the C4 gene had a deficit in synaptic pruning during development, suggesting the hypothesis that excess C4A in humans might cause excessive synaptic pruning, a process that has long been of interest in the schizophrenia literature.

This finding represents an important demonstration of the ability to link genomics to a possible biological mechanism for increased disease risk. Even so, an individual with the highest-risk C4 haplotype who did not have a family history of schizophrenia would on average increase from having a 1% chance of being affected to approximately a 1.3% chance of being affected as a result of this allele. To get a sense of scale, having a first-degree relative with schizophrenia results in an approximately 10-fold increase in risk. This promising start and its limits reflect the challenges that geneticists and neurobiologists now face in moving from successful common variant gene discovery to the elaboration of the specific mechanisms leading to human pathology.

In addition to identifying numerous specific risk loci, GWASs in schizophrenia have repeatedly found that the small individual effects of many common alleles add up to increase risk. These results provide an additional, powerful avenue to study genotype-phenotype relationships in aggregate. Indeed, it is already clear that the number of risk alleles that an individual carries can have a significant (and additive) impact on the risk of developing the disorder. For instance, those in the top decile for a so-called polygenic risk score—a summary statistic relating to the overall amount of additive genetic risk an individual carries—are at 8- to 20-fold increased risk compared to the general population. Although the biology of the cumulative effect is not yet known, the observation nonetheless sets the stage for studying a series

of interesting questions related to disease trajectory and treatment response and will almost certainly reinvigorate studies combining neuroimaing and genomics. These latter types of investigations, similar to early efforts at common variant discovery, have suffered from poor reliability due to the inherent limitations of studying selected, biologically plausible candidate genes.

Finally, high-throughput sequencing methods, similar to those employed in autism spectrum disorders, have begun to yield results in schizophrenia as well. Specifically, exome sequencing in search of rare and de novo risk alleles has been pursued with some success. However, such studies require much larger cohorts to identify statistically significant risks for LGD mutations compared to autism spectrum disorders, suggesting that the overall effect size of these types of variations is likely to be substantially less in schizophrenia. To date, these investigations have identified a handful of risk genes and implicated key neurobiological pathways. In particular, recent exome studies have pointed to the importance of the molecules within the activity-regulated cytoskeleton (ARC) complex, as well as the gene *set domain containing 1A (SETDIA)*, as relevant for schizophrenia pathogenesis.

Perspectives on the Genetic Bases of Neuropsychiatric Disorders

Genes affect many aspects of behavior. There are remarkable similarities in personality traits and psychiatric illnesses in human twins, even those raised separately. Domestic and laboratory animals can be bred for particular, stable behavioral traits; and increasingly, the contributions of a wide range of genetic variations for neurodevelopmental and psychiatric disorders are being discovered.

A series of parallel advances have ushered in an era of remarkable opportunity to understand the relationship between genes, brain, and behavior. The armamentarium available to manipulate and study model systems has been revolutionized. At the same time, progress in defining the genetic risk factors for human neuropsychiatric disorders has advanced considerably. Although the field remains in an early stage in this process, multiple examples of the value of successful gene discovery, and its application to deep biological understanding, have emerged.

Among the many striking findings from recent genetic studies of neurodevelopmental and psychiatric conditions is the overlap in genetic risks across a wide range of diagnostic boundaries. While it may not come as much of a surprise that biology does not hew to categorical diagnostic criteria, it is nonetheless a formidable conceptual challenge to consider how the field will trace these effects and arrive at new therapeutic strategies.

In addition, it is worthwhile noting that for many other psychiatric conditions that have not yet seen the type of progress noted earlier, the calculus is straightforward: greater investment and larger sample sizes will lead to greater insight. For example, recent studies of de novo mutations in Tourette syndrome and obsessive-compulsive disorder clearly demonstrate that the rate-limiting factor for the identification of high confidence risk genes is the availability for sequencing of parent-child trios. In a similar vein, GWAS studies of major depression have only very recently reached sample sizes adequate to confirm statistically significant associated common variants. These studies have included hundreds of thousands of individuals and, not surprisingly, have identified risk alleles carrying very small individual effects.

This last point highlights the idea that one size does not fit all for the genomics of behavioral, developmental, and psychiatric disorders. From the investigations of model systems, to the illumination of rare Mendelian disorders, to the disentangling of both common and rare variants contributing to common disorders, the tools and opportunities available today are unprecedented. The coming years should see deep insights into the biology of psychiatric and neurodevelopmental disorders, and perhaps therapies with the potential to help patients and their families.

Highlights

1. Rare genetic syndromes such as fragile X syndrome, Rett syndrome, and Williams syndrome have provided important insights into the molecular mechanisms of complex human behaviors. Moreover, while considerable work remains to be done, the study of these syndromes has already challenged the notion that associated cognitive and behavioral deficits are immutable and has demonstrated the utility of a wide range of model systems in illuminating conserved biological mechanisms.
2. The sequencing of the human genome, the development of high-throughput genomic assays, and simultaneous computing and methodological advances have led to a profound change in the understanding of the genetics of human behavior and psychiatric illness. Several paradigmatic disorders, including schizophrenia and autism,

have seen dramatic progress, leading to the identification of dozens of definitive risk genes and chromosomal regions.

3. The maturation of the field of psychiatric genetics and genomics over the past decade has revealed the frailty of testing pre-specified candidate genes. These types of studies have now been supplanted by genome-wide scans of both common and rare alleles. Coupled with rigorous statistical frameworks and consensus statistical thresholds, these are yielding highly reliable and reproducible results.
4. At present, the cumulative evidence suggests that the full range of genetic variations underlies complex behavioral syndromes, including common and rare, transmitted and de novo, germline and somatic, and sequence and chromosomal structural variation. However, the relative contributions of these various types of genetic changes vary for a given disorder.
5. A striking finding from recent advances in the genetics of human behavior has been the overlap of genetic risks for syndromes with distinct symptoms and natural histories. Understanding how and why an identical mutation may lead to highly diverse phenotypic outcomes in different individuals will be a major challenge for the future.
6. Findings across common psychiatric disorders point to extremely high rates of genetic heterogeneity. This, coupled with the biological pleiotropy of the risk genes that have been identified to date, as well as the dynamism and complexity of human brain development, all point to important challenges ahead in moving from an understanding of risk genes to an understanding of behavior. Similarly, at present, an important distinction can be made between illuminating the biology of risk genes and unraveling the pathophysiology of behavioral syndromes.

Glossary[1]

Allele. Humans carry two sets of chromosomes, one from each parent. Equivalent genes in the two sets might be different, for example, because of single nucleotide polymorphisms. An allele is one of the two (or more) forms of a particular gene.

Centromere. Chromosomes contain a compact region known as a centromere, where sister chromatids (the two exact copies of each chromosome that are formed after replication) are joined.

Cloning. The process of generating sufficient copies of a particular piece of DNA to allow it to be sequenced or studied in some other way.

Complementary DNA (cDNA). A DNA sequence made from a messenger RNA molecule, using an enzyme called *reverse transcriptase*. cDNAs can be used experimentally to determine the sequence of messenger RNAs after their introns (non–protein-coding sections) have been spliced out.

Conservation of genes. Genes that are present in two distinct species are said to be conserved, and the two genes from the different species are called *orthologous genes*. Conservation can be detected by measuring the similarity of the two sequences at the base (RNA or DNA) or amino acid (protein) level. The more similarities there are, the more highly conserved the two sequences.

Copy number variation (CNV). A deletion or duplication of a limited genetic region that results in an individual having more or fewer than the usual two copies of some genes. Copy number variations are observed in some neurological and psychiatric disorders.

CRISPR (Clustered Regularly Interspaced Short Palindromic Repeats). An enzyme-RNA system in which the enzyme cleaves target sequences that match an RNA guide; the RNA guide can be engineered to recognize a desired gene or sequences within a cell for mutation.

Euchromatin. The gene-rich regions of a genome (see also heterochromatin).

Eukaryote. An organism with cells that have a complex internal structure, including a nucleus. Animals, plants, and fungi are all eukaryotes.

Genome. The complete DNA sequence of an organism.

Genotype. The set of genes that an individual carries; usually refers to the particular pair of alleles (alternative forms of a gene) that a person has at a given region of the genome.

Haplotype. A particular combination of alleles (alternative forms of genes) or sequence variations that are closely linked—that is, are likely to be inherited together—on the same chromosome.

Heterochromatin. Compact, gene-poor regions of a genome, which are enriched in simple sequence repeats.

Introns and exons. Genes are transcribed as continuous sequences, but only some segments of the resulting messenger RNA molecules contain information that encodes a protein product. These segments are called *exons*. The regions between exons are known as *introns* and are spliced from the RNA before the product is made.

[1]Based on Bork P, Copley R. 2001. Genome speak. Nature 409:815.

Long and short arms. The regions on either side of the centromere are known as arms. As the centromere is not in the center of the chromosome, one arm is longer than the other.
Messenger RNA (mRNA). Proteins are not synthesized directly from genomic DNA. Instead, an RNA template (a precursor mRNA) is constructed from the sequence of the gene. This RNA is then processed in various ways, including splicing. Spliced RNAs destined to become templates for protein synthesis are known as mRNAs.
Mutation. An alteration in a genome compared to some reference state. Mutations do not always have harmful effects.
Phenotype. The observable properties and physical characteristics of an organism.
Polymorphism. A region of the genome that varies between individual members of a population. To be called a polymorphism, a variant should be present in a significant number of people in the population.
Prokaryote. A single-celled organism with a simple internal structure and no nucleus. Bacteria and archaebacteria are prokaryotes.
Proteome. The complete set of proteins encoded by the genome.
Recombination. The process by which DNA is exchanged between pairs of equivalent chromosomes during egg and sperm formation. Recombination has the effect of making the chromosomes of the offspring distinct from those of the parents.
Restriction endonuclease. An enzyme that cleaves DNA at a particular short sequence. Different types of restriction endonuclease cleave at different sequences.
RNA interference (RNAi). A method for reducing the function of a specific gene by introducing into a cell small RNAs with complementarity to the targeted mRNA. Pairing of the mRNA with the small RNA leads to destruction of the endogenous mRNA.
Single nucleotide polymorphism (SNP). A polymorphism caused by the change of a single nucleotide. SNPs are often used in genetic mapping studies.
Splicing. The process that removes introns (noncoding portions) from transcribed RNAs. Exons (protein-coding portions) can also be removed. Depending on which exons are removed, different proteins can be made from the same initial RNA or gene. Different proteins created in this way are *splice variants* or *alternatively spliced*.
Transcription. The process of copying a gene into RNA. This is the first step in turning a gene into a protein, although not all transcripts lead to proteins.
Transcriptome. The complete set of RNAs transcribed from a genome.
Translation. The process of using a messenger RNA sequence to synthesize a protein. The messenger RNA serves as a template on which transfer RNA molecules, carrying amino acids, are lined up. The amino acids are then linked together to form a protein chain.

Matthew W. State
Cornelia I. Bargmann
T. Conrad Gilliam

Selected Reading

Alberts B, Johnson A, Lewis J, Raff M, Roberts K, Walter P. 2002. *Molecular Biology of the Cell,* 4th ed. New York: Garland Publishing. Also searchable at http://www.ncbi.nlm.nih.gov/entrez/query.fcgi?db=Books.

Allada R, Emery P, Takahashi JS, Rosbash M. 2001. Stopping time: the genetics of fly and mouse circadian clocks. Annu Rev Neurosci 24:1091–1119.

Bouchard TJ Jr, Lykken DT, McGue M, Segal NL, Tellegen A. 1990. Sources of human psychological differences: the Minnesota Study of Twins Reared Apart. Science 250:222–228.

Cong L, Ran FA, Cox D, et al. 2013. Multiplex genome engineering using CRISPR/Cas systems. Science 339:819–823.

Griffiths AJF, Gelbart WM, Miller JH, Lewontin RC. 1999. *Modern Genetic Analysis*. New York: Freeman. Also searchable at http://www.ncbi.nlm.nih.gov/entrez/query.fcgi?db=Books.

International Human Genome Sequencing Consortium. 2001. Initial sequencing and analysis of the human genome. Nature 409:860–921.

Jinek M, Chylinski K, Fonfara I, Hauer M, Doudna JA, Charpentier E. 2012. A programmable dual-RNA-guided DNA endonuclease in adaptive bacterial immunity. Science 337:816–821.

Online Mendelian Inheritance in Man, OMIM. McKusick-Nathans Institute of Genetic Medicine, Johns Hopkins University (Baltimore, MD) and National Center for Biotechnology Information, National Library of Medicine (Bethesda, MD). http://www.ncbi.nlm.nih.gov/omim/.

Venter JG, Adams MD, Myers EW, et al. 2001. The sequence of the human genome. Science 291:1304–1351.

References

Alberts B, Johnson A, Lewis J, Raff M, Roberts K, Walter P. 1998. *Molecular Biology of the Cell,* 3rd ed. New York: Garland Publishing.

Amir RE, Van den Veyver IB, Wan M, Tran CQ, Francke U, Zoghbi HY. 1999. Rett syndrome is caused by mutations in X-linked MECP2, encoding methyl-CpG-binding protein 2. Nat Genet 23:185–188.

Antoch MP, Song EJ, Chang AM, et al. 1997. Functional identification of the mouse circadian Clock gene by transgenic BAC rescue. Cell 89:655–667.

Arnold SE, Talbot K, Hahn CG. 2004. Neurodevelopment, neuroplasticity, and new genes for schizophrenia. Prog Brain Res 147:319–345.

Bear MF, Huber KM, Warren ST. 2004. The mGluR theory of fragile X syndrome. Trends Neurosci 27:370–377.

Bellugi U, Lichtenberger L, Jones W, Lai Z, St George M. 2000. I. The neurocognitive profile of Williams Syndrome: a complex pattern of strengths and weaknesses. J Cogn Neurosci 12:7–29. Suppl.

Ben-Shahar Y, Robichon A, Sokolowski MB, Robinson GE. 2002. Influence of gene action across different time scales on behavior. Science 296:741–744.

Caron H, van Schaik B, van der Mee M, et al. 2001. The human transcriptome map: clustering of highly expressed genes in chromosomal domains. Science 291:1289–1292.

De Bono M, Bargmann CI. 1998. Natural variation in a neuropeptide Y receptor homolog modifies social behavior and food responses in *C. elegans*. Cell 94:679–689.

De Rubeis S, He X, Goldberg AP, et al. 2014. Synaptic, transcriptional and chromatin genes disrupted in autism. Nature 515:209–215.

Fromer M, Pocklington AJ, Kavanagh DH, et al. 2014. De novo mutations in schizophrenia implicate synaptic networks. Nature 506:179–184.

Genovese G, Fromer M, Stahl EA, et al. 2016. Increased burden of ultra-rare protein-altering variants among 4,877 individuals with schizophrenia. Nat Neurosci 19:1433–1441.

Gottesman II. 1991. *Schizophrenia Genesis. The Origins of Madness*. New York: Freeman.

Iossifov I, O'Roak BJ, Sanders SJ, et al. 2014. The contribution of de novo coding mutations to autism spectrum disorder. Nature 515:216–221.

Jamain S, Quach H, Betancur C, et al. 2003. Mutations of the X-linked genes encoding neuroligins NLGN3 and NLGN4 are associated with autism. Nat Genet 34:27–29.

Kahler SG, Fahey MC. 2003. Metabolic disorders and mental retardation. Am J Med Genet C Semin Med Genet 117:31–41.

Khaitovich P, Muetzel B, She X, et al. 2004. Regional patterns of gene expression in human and chimpanzee brains. Genome Res 14:1462–1473.

Konopka RJ, Benzer S. 1971. Clock mutations of *Drosophila melanogaster*. Proc Natl Acad Sci U S A 68:2112–2116.

Lai CS, Fisher SE, Hurst JA, Vargha-Khadem F, Monaco AP. 2001. A forkhead-domain gene is mutated in a severe speech and language disorder. Nature 413:519–523.

Lander ES, Linton LM, Birren B, et al. 2001. Initial sequencing and analysis of the human genome. Nature 409:860-921.

Laumonnier F, Bonnet-Brilhault F, Gomot M, et al. 2004. X-linked mental retardation and autism are associated with a mutation in the NLGN4 gene, a member of the neuroligin family. Am J Hum Genet 74:552–557.

Lim MM, Wang Z, Olazabal DE, Ren X, Terwilliger EF, Young LJ. 2004. Enhanced partner preference in a promiscuous species by manipulating the expression of a single gene. Nature 429:754–757.

Mayford M, Bach ME, Huang Y-Y, Wang L, Hawkins RD, Kandel ER. 1996. Control of memory formation through regulated expression of a CaMKII transgene. Science 274:1678-1683.

McGue M, Bouchard TH Jr. 1998. Genetic and environmental influences on human behavioral differences. Ann Rev Neurosci 21:1–24.

Mendel G. 1866. Versuche über Pflanzen-hybriden. Verh Naturforsch 4:2–47. Translated in: C Stern, ER Sherwood (eds). *The Origin of Genetics: A Mendel Source Book*, 1966. San Francisco: Freeman.

Neale BM, Kou Y, Liu L, et al. 2012. Patterns and rates of exonic de novo mutations in autism spectrum disorders. Nature 485:242–245.

O'Roak BJ, Vives L, Girirajan S, et al. 2012. Sporadic autism exomes reveal a highly interconnected protein network of de novo mutations. Nature 485:246–250.

Sanders SJ, Ercan-Sencicek AG, Hus V, et al. 2011. Multiple recurrent de novo CNVs, including duplications of the 7q11.23 Williams syndrome region, are strongly associated with autism. Neuron 70:863–885.

Sanders SJ, He X, Willsey AJ, et al. 2015. Insights into autism spectrum disorder genomic architecture and biology from 71 risk loci. Neuron 87:1215–1233.

Sanders SJ, Murtha MT, Gupta AR, et al. 2012. De novo mutations revealed by whole exome sequencing are strongly associated with autism. Nature 485:237–241.

Satterstrom FK, Kosmicki JA, Wang J, et al. 2020. Large-scale exome sequencing study implicated both developmental and functional changes in the neurobiology of autism. Cell 180:568–594.

Schizophrenia Working Group of the Psychiatric Genomics Consortium. 2014. Biological insights from 108 schizophrenia-associated genetic loci. Nature 511:421–427.

Sebat J, Lakshmi B, Malhotra D, et al. 2007. Strong association of de novo copy number variation with autism. Science 316:445–449.

Sekar A, Bialas AR, de Rivera H, et al. 2016. Schizophrenia risk from complex variation of complement component 4. Nature 530:177–183.

Singh T, Kurki MI, Curtis D, et al. 2016. Rare loss-of-function variants in SETD1A are associated with schizophrenia and developmental disorders. Nat Neurosci 19:571–577.

Sokolowski MB. 1980. Foraging strategies of *Drosophila melanogaster*: a chromosomal analysis. Behav Genet 10: 291–302.

Sokolowski MB. 2001. *Drosophila*: genetics meets behavior. Nat Rev Genet 2:879–890.

Sztainberg Y, Zoghbi HY. 2016. Lessons learned from studying syndromic autism spectrum disorders. Nat Neurosci 19:1408–1417.

Takahashi JS, Pinto LH, Vitaterna MH. 1994. Forward and reverse genetic approaches to behavior in the mouse. Science 264:1724–1733.

Toh KL, Jones CR, He Y, et al. 2001. An hPer2 phosphorylation site mutation in familial advanced sleep phase syndrome. Science 291:1040–1043.

Tsien JZ, Huerta PT, Tonegawa S. 1996. The essential role of hippocampal CA1 NMDA receptor-dependent synaptic plasticity in spatial memory. Cell 87:1327–1338.

Walter J, Paulsen M. 2003. Imprinting and disease. Semin Cell Dev Biol 14:101–110.

Watson JD, Tooze J, Kurtz DT (eds). 1983. *Recombinant DNA: A Short Course*. New York: Scientific American.

Whitfield CW, Cziko AM, Robinson GE. 2003. Gene expression profiles in the brain predict behavior in individual honey bees. Science 302:296–299.

Young LJ, Lim MM, Gingrich B, Insel TR. 2001. Cellular mechanisms of social attachment. Horm Behav 40:132–138.

Zondervan KT, Cardon LR. 2004. The complex interplay among factors that influence allelic association. Nat Rev Genet 5:89–100.

3

Nerve Cells, Neural Circuitry, and Behavior

The remarkable range of human behavior depends on a sophisticated array of sensory receptors connected to the brain, a highly flexible neural organ that selects from among the stream of sensory signals those events in the environment and in the internal milieu of the body that are important for the individual. The brain actively organizes sensory information for perception, action, decision-making, aesthetic appreciation, and future reference—that is to say, memory. It also ignores and discards information judiciously, one hopes, and reports to other brains about some of these operations and their psychological manifestations. All this is accomplished by interconnected nerve cells.

Individual nerve cells, or neurons, are the basic signaling units of the brain. The human brain contains a huge number of these cells, on the order of 86 billion neurons, that can be classified into at least a thousand different types. Yet this great variety of neurons is less of a factor in the complexity of human behavior than is their organization into anatomical circuits with precise functions. Indeed, one key organizational principle of the brain is that nerve cells with *similar* properties can produce different actions because of the way they are interconnected.

Because relatively few principles of organization of the nervous system give rise to considerable functional complexity, it is possible to learn a great deal about how the nervous system produces behavior by focusing on five basic features of the nervous system:

1. The structural components of individual nerve cells;
2. The mechanisms by which neurons produce signals within themselves and between each other;
3. The patterns of connection between nerve cells and between nerve cells and their targets (muscle and gland effectors);
4. The relationship of different patterns of interconnection to different types of behavior; and
5. How neurons and their connections are modified by experience.

The parts of this book are organized around these five major topics. In this chapter, we introduce these topics in turn in an overview of the neural control of behavior. We first consider the structure and function of neurons and the glial cells that surround and support them. We then examine how individual cells organize and transmit signals and how signaling between a few interconnected nerve cells produces a simple behavior, the knee-jerk reflex. We then extend these ideas to more complex behaviors, mediated by more complex and malleable circuits.

The Nervous System Has Two Classes of Cells

There are two main classes of cells in the nervous system: nerve cells, or neurons, and glial cells, or glia.

Nerve Cells Are the Signaling Units of the Nervous System

A typical neuron has four morphologically defined regions: (1) the cell body, (2) dendrites, (3) an axon, and (4) presynaptic terminals (Figure 3–1). As we shall see, each region has a distinct role in generating signals and communicating with other nerve cells.

The cell body or *soma* is the metabolic center of the cell. It includes the nucleus, which contains the genes of the cell, and the endoplasmic reticulum, an extension of the nucleus where the cell's proteins are synthesized. The cell body usually gives rise to two kinds of processes: several short *dendrites* and one long, tubular *axon*. Dendrites branch out in tree-like fashion and are the main apparatus for receiving incoming signals

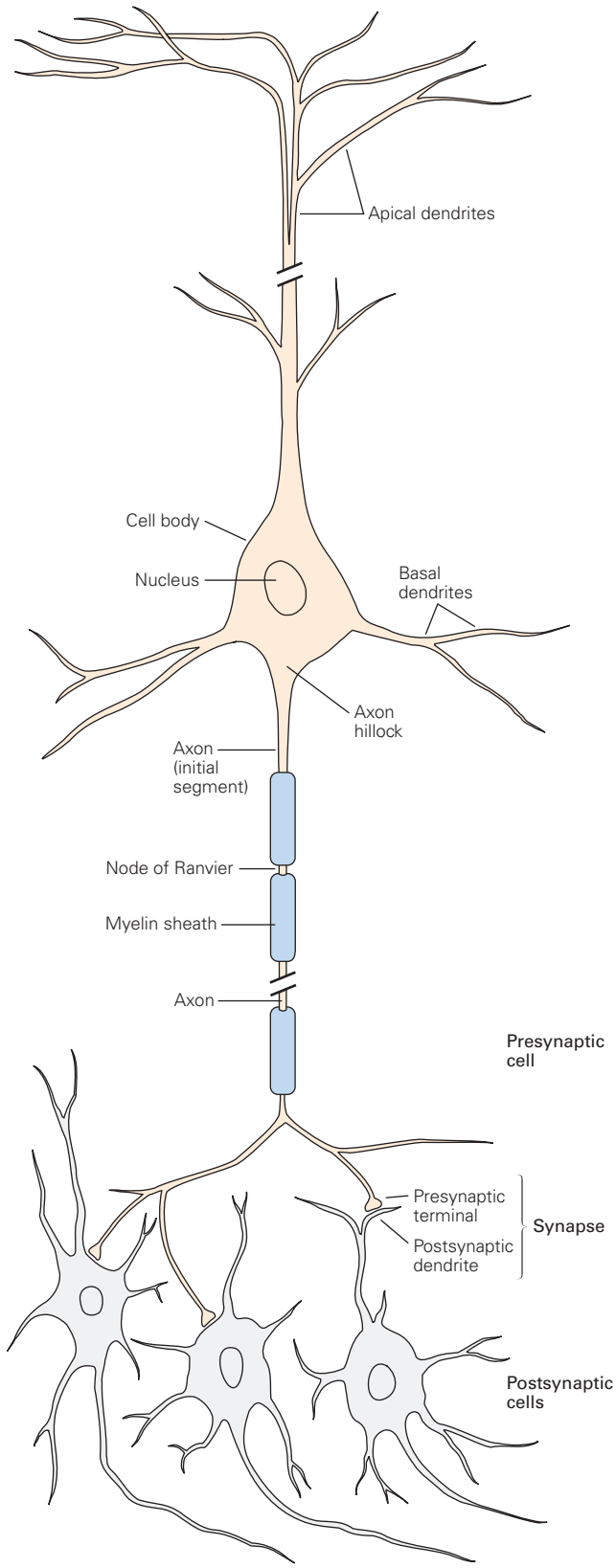

Figure 3–1 (Right) The structure of a neuron. Most neurons in the vertebrate nervous system have several main features in common. The cell body contains the nucleus, the storehouse of genetic information, and gives rise to two types of cell processes: axons and dendrites. Axons are the transmitting element of neurons; they vary greatly in length, some extending more than 1 m within the body. Most axons in the central nervous system are very thin (between 0.2 µm and 20 µm in diameter) compared with the diameter of the cell body (50 µm or more). Many axons are insulated by a sheath of fatty myelin that is regularly interrupted at gaps called the nodes of Ranvier. The action potential, the cell's conducting signal, is initiated at the initial segment of the axon and propagates to the synapse, the site at which signals flow from one neuron to another. Branches of the axon of the presynaptic neuron transmit signals to the postsynaptic cell. The branches of a single axon may form synapses with as many as 1,000 postsynaptic neurons. The apical and basal dendrites together with the cell body are the input elements of the neuron, receiving signals from other neurons.

from other nerve cells. The axon typically extends some distance from the cell body before it branches, allowing it to carry signals to many target neurons. An axon can convey electrical signals over distances ranging from 0.1 mm to 1 m. These electrical signals, or *action potentials*, are initiated at a specialized trigger region near the origin of the axon called the *initial segment* from which the action potentials propagate down the axon without failure or distortion at speeds of 1 to 100 m/s. The amplitude of an action potential traveling down the axon remains constant at 100 mV because the action potential is an all-or-none impulse that is regenerated at regular intervals along the axon (Figure 3–2).

Action potentials are the signals by which the brain receives, analyzes, and conveys information. These signals are highly stereotyped throughout the nervous system, even though they are initiated by a great variety of events in the environment that impinge on our bodies—from light to mechanical contact, from odorants to pressure waves. The physiological signals that convey information about vision are identical to those that carry information about odors. Here we see a key principle of brain function: the type of information conveyed by an action potential is determined not by the form of the signal but by the pathway the signal travels in the brain. The brain thus analyzes and interprets patterns of incoming electrical signals carried over specific pathways, and in turn creates our sensations of sight, touch, taste, smell, and sound.

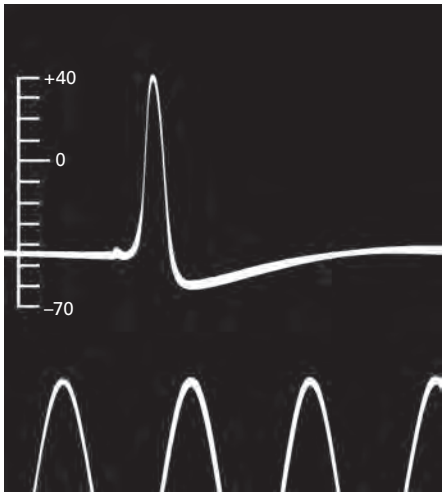

Figure 3–2 This historic tracing is the first published intracellular recording of an action potential. It was recorded in 1939 by Alan Hodgkin and Andrew Huxley from a squid giant axon, using glass capillary electrodes filled with sea water. The timing pulses (bottom) are separated by 2 ms. The vertical scale indicates the potential of the internal electrode in millivolts, the sea water outside being taken as zero potential. (Reproduced, with permission, from Hodgkin and Huxley 1939.)

To increase the speed by which action potentials are conducted, large axons are wrapped in an insulating sheath of a lipid substance, myelin. The sheath is interrupted at regular intervals by the nodes of Ranvier, uninsulated spots on the axon where the action potential is regenerated. (Myelination is discussed in detail in Chapters 7 and 8 and action potentials in Chapter 10.)

Near its end, the axon divides into fine branches that contact other neurons at specialized zones of communication known as *synapses*. The nerve cell transmitting a signal is called the *presynaptic cell*; the cell receiving the signal is the *postsynaptic cell*. The presynaptic cell transmits signals from specialized enlarged regions of its axon's branches, called *presynaptic terminals* or *nerve terminals*. The presynaptic and postsynaptic cells are separated by a very narrow space, the *synaptic cleft*. Most presynaptic terminals end on the postsynaptic neuron's dendrites, but some also terminate on the cell body or, less often, at the beginning or end of the axon of the postsynaptic cell (see Figure 3–1). Some presynaptic neurons excite their postsynaptic target cells; other presynaptic neurons inhibit their target cells.

The neuron doctrine (Chapter 1) holds that each neuron is a discrete cell with distinctive processes arising from its cell body and that neurons are the signaling units of the nervous system. In retrospect, it is hard to appreciate how difficult it was for scientists to accept this elementary idea when first proposed. Unlike other tissues, whose cells have simple shapes and fit into a single field of the light microscope, nerve cells have complex shapes. The elaborate patterns of dendrites and the seemingly endless course of some axons made it extremely difficult to establish a relationship between these elements. Even after the anatomists Jacob Schleiden and Theodor Schwann put forward the cell theory in the early 1830s—and the idea that cells are the structural units of all living matter became a central dogma of biology—most anatomists did not accept that the cell theory applied to the brain, which they thought of as a continuous, web-like reticulum of very thin processes.

The coherent structure of the neuron did not become clear until late in the 19th century, when Ramón y Cajal began to use the silver-staining method introduced by Golgi. Still used today, this method has two advantages. First, in a random manner that is not understood, the silver solution stains only about 1% of the cells in any particular brain region, making it possible to examine a single neuron in isolation from

its neighbors. Second, the neurons that do take up the stain are delineated in their entirety, including the cell body, axon, and full dendritic tree. The stain reveals that there is no cytoplasmic continuity between neurons, and Cajal concluded, prophetically and correctly, that there is no continuity even at synapses between two cells.

Ramón y Cajal applied Golgi's method to the embryonic nervous systems of many animals as well as humans. By examining the structure of neurons in almost every region of the nervous system, he could describe classes of nerve cells and map the precise connections between many of them. In this way, Ramón y Cajal deduced, in addition to the neuron doctrine, two other principles of neural organization that would prove particularly valuable in studying communication in the nervous system.

The first of these, the *principle of dynamic polarization*, states that electrical signals within a nerve cell flow in only one direction: from the postsynaptic sites of the neuron, usually the dendrites and cell body, to the trigger region at the axon. From there, the action potential is propagated along the entire length of the axon to its terminals. In most neurons studied to date, electrical signals in fact travel along the axon in one direction.

The second principle advanced by Ramón y Cajal, *connectional specificity*, states that nerve cells do not connect randomly with one another in the formation of networks but make specific connections—at particular contact points—with certain postsynaptic target cells and not with others. The principles of dynamic polarization and connectional specificity are the basis of the modern cellular-connectionist approach to studying the brain.

Ramón y Cajal was also among the first to realize that the feature that most distinguishes one type of neuron from another is form, specifically the number of the processes arising from the cell body. Neurons are thus classified into three large groups: unipolar, bipolar, and multipolar.

Unipolar neurons are the simplest because they have a single primary process, which usually gives rise to many branches. One branch serves as the axon; other branches function as receiving structures (Figure 3–3A). These cells predominate in the nervous systems of invertebrates; in vertebrates, they occur in the autonomic nervous system.

Bipolar neurons have an oval soma that gives rise to two distinct processes: a dendritic structure that receives signals from other neurons and an axon that carries information toward the central nervous system (Figure 3–3B). Many sensory cells are bipolar, including those in the retina and olfactory epithelium of the nose. The receptor neurons that convey touch, pressure, and pain signals to the spinal cord develop initially as bipolar cells, but the two cell processes fuse into a single continuous structure that emerges from a single point in the cell body, and the dendrite is endowed with the specializations that render it an axon. In these so-called pseudo-unipolar cells, one axon transmits information from the sensory receptors in the skin, joints, and muscle toward the cell body, while the other carries this sensory information to the spinal cord (Figure 3–3C).

Multipolar neurons predominate in the nervous system of vertebrates. They typically have a single axon and many dendritic structures emerging from various points around the cell body (Figure 3–3D). Multipolar cells vary greatly in shape, especially in the length of their axons and in the extent, dimensions, and intricacy of their dendritic branching. Usually the extent of branching correlates with the number of synaptic contacts that other neurons make onto them. A spinal motor neuron with a relatively modest number of dendrites receives about 10,000 contacts—1,000 on the cell body and 9,000 on dendrites. In Purkinje cells in the cerebellum, the dendritic tree is much larger and bushier, receiving as many as a million contacts!

Nerve cells are also classified into three major functional categories: sensory neurons, motor neurons, and interneurons. *Sensory neurons* carry information from the body's peripheral sensors into the nervous system for the purpose of both perception and motor coordination. Some primary sensory neurons are called *afferent neurons*, and the two terms are used interchangeably. The term *afferent* (carried toward the central nervous system) applies to all information reaching the central nervous system from the periphery, whether or not this information leads to sensation. The term *sensory* designates those afferent neurons that convey information to the central nervous system from the sensory epithelia, from joint sensory receptors, or from muscle, but the concept has been expanded to include neurons in primary and secondary cortical areas that respond to changes in a sensory feature, such as displacement of an object in space, a shift in sound frequency, or the angular rotation of the head (via vestibular organs in the ear) or even something as complex as a face.

The term *efferent* applies to all information carried from the central nervous system toward the motor organs, whether or not this information leads to action. *Motor neurons* carry commands from the brain or spinal cord to muscles and glands (efferent information). The traditional definition of a *motor neuron* (or motoneuron) is a neuron that excites a muscle, but the designation of motor neuron now includes other

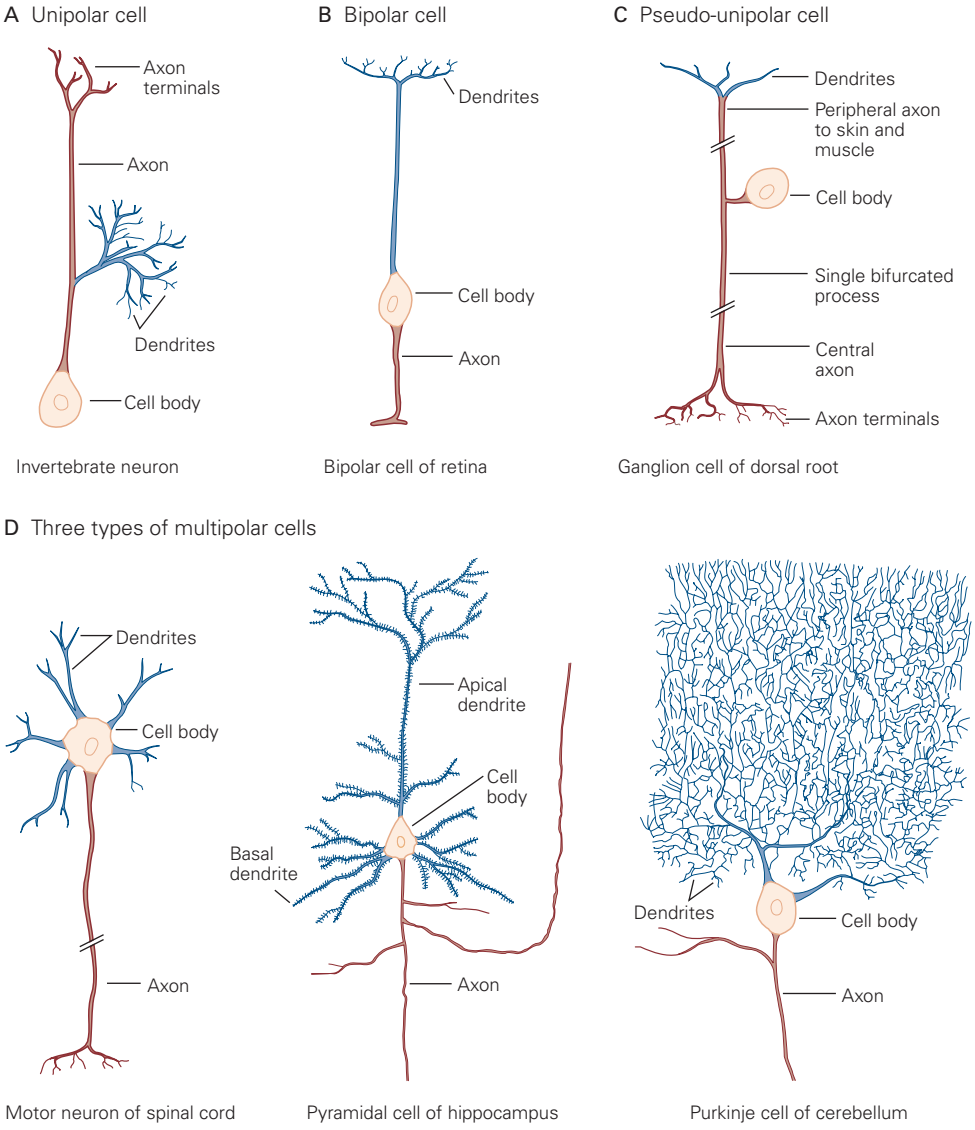

Figure 3–3 Neurons are classified as unipolar, bipolar, or multipolar according to the number of processes that originate from the cell body.

A. Unipolar cells have a single process emanating from the cell. Different segments serve as receptive surfaces or releasing terminals. Unipolar cells are characteristic of the invertebrate nervous system.

B. Bipolar cells have two types of processes that are functionally specialized. The dendrite receives electrical signals and the axon transmits signals to other cells.

C. Pseudo-unipolar cells, which are variants of bipolar cells, carry somatosensory information to the spinal cord. During development, the two processes of the embryonic bipolar cell fuse and emerge from the cell body as a single process that has two functionally distinct segments. Both segments function as axons; one extends to peripheral skin or muscle, the other to the central spinal cord. (Adapted, with permission, from Ramón y Cajal 1933.)

D. Multipolar cells have a single axon and many dendrites. They are the most common type of neuron in the mammalian nervous system. Three examples illustrate the large diversity of these cells. Spinal motor neurons innervate skeletal muscle fibers. Pyramidal cells have a roughly triangular cell body; dendrites emerge from both the apex (the apical dendrite) and the base (the basal dendrites). Pyramidal cells are found in the hippocampus and throughout the cerebral cortex. Purkinje cells of the cerebellum are characterized by a rich and extensive dendritic tree that accommodates an enormous number of synaptic inputs. (Adapted, with permission, from Ramón y Cajal 1933.)

neurons that do not innervate muscle directly but that command action indirectly. A useful characterization of motor and sensory neurons alike is their temporal fidelity to matters outside the nervous system. Their activity keeps up with changes in external stimuli and dynamical forces exerted by the body musculature. Sensory neurons supply the brain with data, whereas motor neurons convert ideation into praxis. Together they compose our interface with the world.

Interneurons comprise the most numerous functional category and are subdivided into two classes: relay and local. Relay or projection interneurons have long axons and convey signals over considerable distances, from one brain region to another. Local interneurons have short axons because they form connections with nearby neurons in local circuits. Since almost every neuron can be regarded as an interneuron, the term is often used to distinguish between neurons that project to another neuron within a local circuit as opposed to neurons that project to a separate neural structure. The term is also sometimes used as shorthand for an inhibitory neuron, especially in studies of cortical circuits, but for clarity, the term *inhibitory interneuron* should be used when appropriate.

Each functional classification can be subdivided further. Sensory system interneurons can be classified according to the type of sensory stimuli to which they respond; these initial classifications can be broken down still further, according to location, density, and size as well as patterns of gene expression. Indeed, our view of neuronal complexity is rapidly evolving due to advances in mRNA sequence analysis that have enabled the molecular profiling of individual neurons. Such analyses have recently revealed a much greater heterogeneity of neuronal types than previously thought (Figure 3–4).

Glial Cells Support Nerve Cells

Glial cells greatly outnumber neurons—there are 2 to 10 times more glia than neurons in the vertebrate central nervous system. Although the name for these cells derives from the Greek for glue, glia do not commonly hold nerve cells together. Rather they surround the cell bodies, axons, and dendrites of neurons. Glia differ from neurons morphologically; they do not form dendrites and axons.

Glia also differ functionally. Although they arise from the same embryonic precursor cells, they do not have the same membrane properties as neurons and thus are not electrically excitable. Hence, they are not directly involved in electrical signaling, which is the function of nerve cells. Yet they play a role in allowing electrical signals to move quickly along the axons

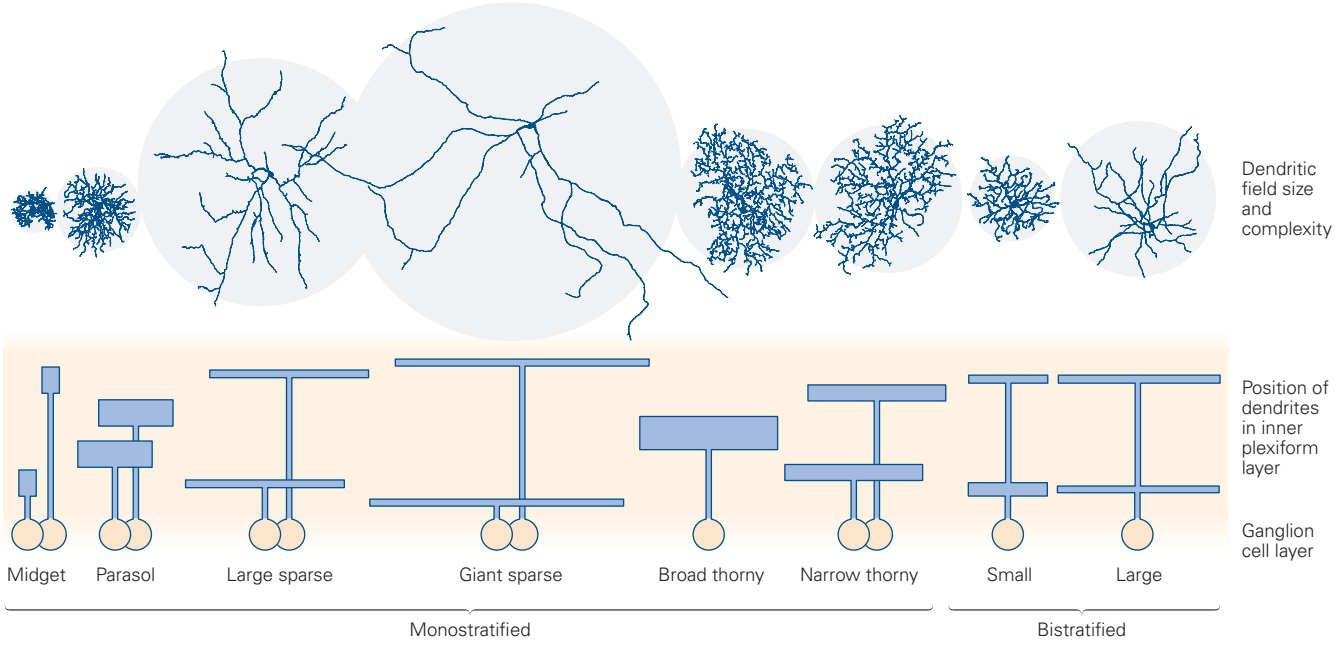

Figure 3–4 Sensory neurons can be subdivided into functionally distinct groups. For example, at least 13 types of retinal ganglion cells are distinguished based on the size and shape of their dendrites combined with the depth within the retina at which they receive their inputs. The inner plexiform layer contains the connections between interneurons of the retina (bipolar and amacrine cells) and the ganglion cells. (Reproduced, with permission, from Dacey et al. 2003. Copyright © 2003 Elsevier.)

of neurons, and they appear to play an important role in guiding connectivity during early development and stabilizing new or altered connections between neurons that occur through learning. Over the past decade, interest in the diverse functions of glia has accelerated, and their characterization has changed from support cells to functional partners of neurons (Chapter 7).

Each Nerve Cell Is Part of a Circuit That Mediates Specific Behaviors

Every behavior is mediated by specific sets of interconnected neurons, and every neuron's behavioral function is determined by its connections with other neurons. A simple behavior, the knee-jerk reflex, will illustrate this. The reflex is initiated when a transient imbalance of the body stretches the quadriceps extensor muscles of the leg. This stretching elicits sensory information that is conveyed to motor neurons, which in turn send commands to the extensor muscles to contract so that balance is restored.

This reflex is used clinically to test the integrity of the nerves as well as the cerebrospinal control of the reflex amplitude (or gain). The underlying mechanism is important because it maintains normal tone in the quadriceps and prevents our knees from buckling when we stand or walk. The tendon of the quadriceps femoris, an extensor muscle that moves the lower leg, is attached to the tibia through the tendon of the patella (kneecap). Tapping this tendon just below the patella stretches the quadriceps femoris. This stretch initiates reflex contraction of the quadriceps muscle to produce the familiar knee jerk. By increasing the tension of a select group of muscles, the stretch reflex changes the position of the leg, suddenly extending it outward (Figure 3–5).

The cell bodies of the sensory neurons involved in the knee-jerk reflex are clustered near the spinal cord in the dorsal root ganglia. They are pseudo-unipolar cells; one branch of each cell's axon runs to the quadriceps muscle at the periphery, while the other runs centrally into the spinal cord. The branch that innervates the quadriceps makes contact with stretch-sensitive receptors (muscle spindles) and is excited when the muscle is stretched. The branch reaching the spinal cord forms excitatory connections with the motor neurons that innervate the quadriceps and control its contraction. This branch also contacts local interneurons that *inhibit* the motor neurons controlling the opposing flexor muscles (Figure 3–5). Although these local interneurons are not involved in producing the stretch reflex itself, they increase the stability of the reflex by coordinating the actions of opposing muscle groups.

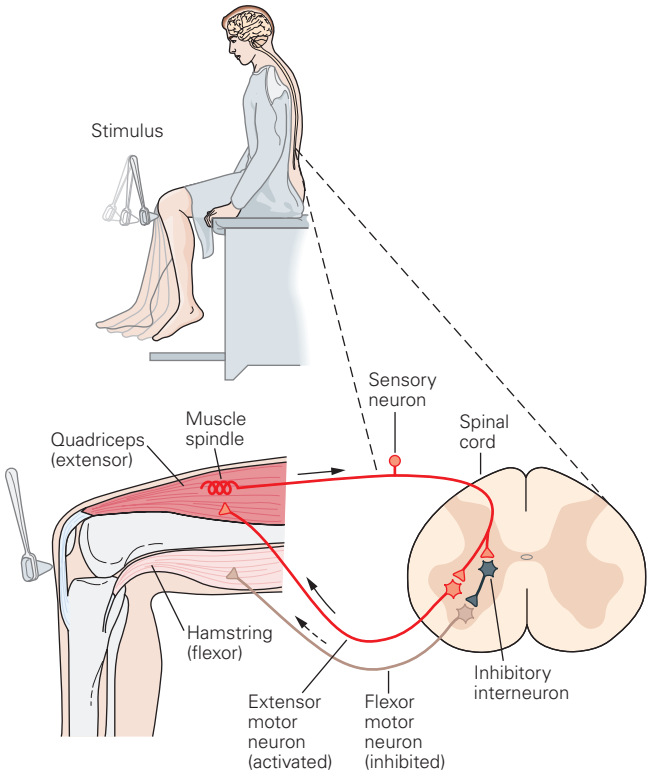

Figure 3–5 The knee-jerk reflex is controlled by a simple circuit of sensory and motor neurons. Tapping the kneecap with a reflex hammer pulls on the tendon of the quadriceps femoris, a muscle that extends the lower leg. When the muscle stretches in response to the pull of the tendon, information regarding this change in the muscle is conveyed to the central nervous system by sensory neurons. In the spinal cord, the sensory neurons form excitatory synapses with extensor motor neurons that contract the quadriceps, the muscle that was stretched. The sensory neurons act indirectly, through interneurons, to inhibit flexor motor neurons that would otherwise contract the opposing hamstring muscles. These actions combine to produce the reflex behavior. In the drawing, each extensor and flexor motor neuron represents a population of many cells.

Thus, the electrical signals that produce the stretch reflex carry four kinds of information:

1. Sensory information is conveyed to the central nervous system (the spinal cord) from muscle.
2. Motor commands from the central nervous system are issued to the muscles that carry out the knee jerk.
3. Inhibitory commands are issued to motor neurons that innervate opposing muscles.
4. Information about local neuronal activity related to the knee jerk is sent to higher centers of the central nervous system, permitting the brain to coordinate different behaviors simultaneously or in series.

In addition, the brain asserts context-dependent control of the reflex to adjust its gain. For example, when we run, the hamstring muscles flex the knee, thereby stretching the quadriceps. The brain and spinal cord suppress the stretch reflex to allow the quadriceps to relax. When these descending pathways are disrupted, as in some strokes, the reflex is exaggerated and the joint has stiffness.

The stretching of just one muscle, the quadriceps, activates several hundred sensory neurons, each of which makes direct contact with 45 to 50 motor neurons. This pattern of connection, in which one neuron activates many target cells, is called *divergence* (Figure 3–6A). It is especially common in the input stages of the nervous system; by distributing its signals to many target cells, a single neuron can exert wide and diverse influence. Conversely, a single motor cell in the knee-jerk circuit receives 200 to 450 input contacts from approximately 130 sensory cells. This pattern of connection is called *convergence* (Figure 3–6B). It is common at the output stages of the nervous system; a target motor cell that receives information from many sensory neurons is able to integrate information from many sources. Each sensory neuron input produces relatively weak excitation, so convergence also ensures that a motor neuron is activated only when a sufficient number of sensory neurons are activated together.

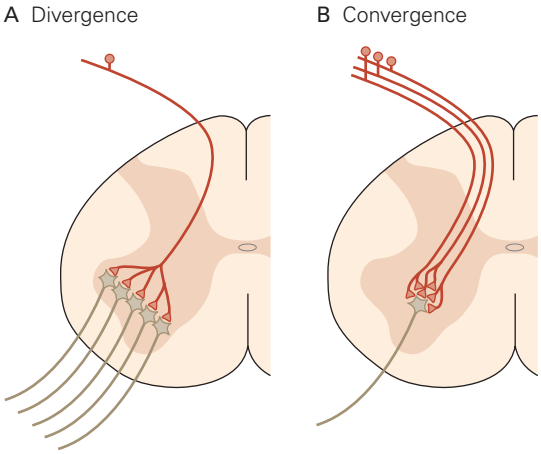

Figure 3–6 Diverging and converging neuronal connections are a key organizational feature of the brain.

A. In the sensory systems, each receptor neuron usually contacts several neurons that represent the second stage of processing. At subsequent processing stages, the incoming connections diverge even more. This allows sensory information from a single site to be distributed more widely in the spinal cord and brain.

B. By contrast, motor neurons are the targets of progressively converging connections. With this arrangement, input from many presynaptic cells is required to activate the motor neuron.

A stretch reflex such as the knee-jerk reflex is a simple behavior produced by two classes of neurons connecting at excitatory synapses. But not all important signals in the brain are excitatory. Many neurons produce inhibitory signals that reduce the likelihood of firing. Even in the simple knee-jerk reflex, the sensory neurons make both excitatory and inhibitory connections. Excitatory connections in the leg's extensor muscles cause these muscles to contract, whereas connections with inhibitory interneurons prevent the antagonist flexor muscles from contracting. This feature of the circuit is an example of *feedforward inhibition* (Figure 3–7A). In the knee-jerk reflex, feedforward

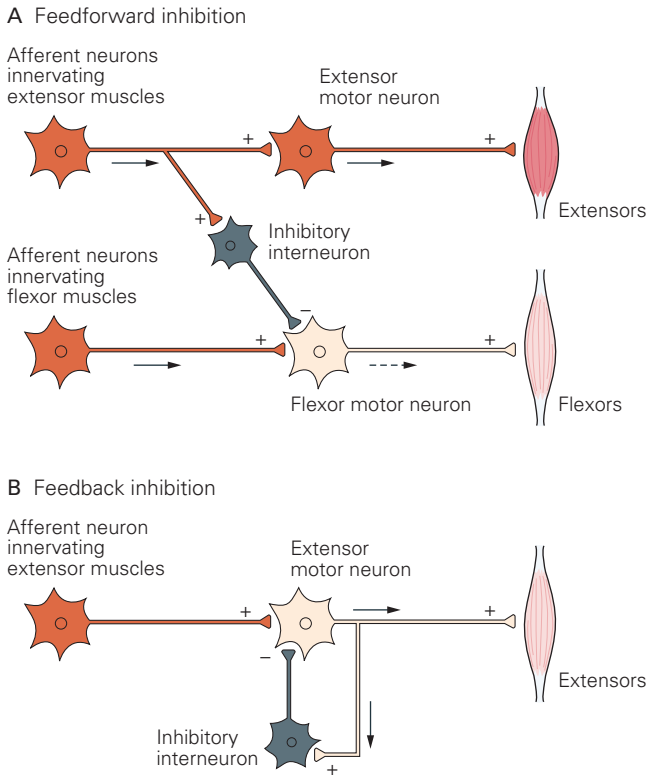

Figure 3–7 Inhibitory interneurons can produce either feedforward or feedback inhibition.

A. Feedforward inhibition enhances the effect of the active pathway by suppressing the activity of pathways mediating opposing actions. Feedforward inhibition is common in monosynaptic reflex systems. For example, in the knee-jerk reflex circuit (**Figure 3–5**) afferent neurons from extensor muscles excite not only the extensor motor neurons but also inhibitory interneurons that prevent the firing of the motor cells innervating the opposing flexor muscles.

B. Feedback inhibition is a self-regulating mechanism. Here extensor motor neurons act on inhibitory interneurons that in turn act on the extensor motor neurons themselves and thus reduce their probability of firing. The effect is to dampen activity within the stimulated pathway and prevent it from exceeding a certain critical level.

inhibition is *reciprocal*, ensuring that the flexor and extensor pathways always inhibit each other so that only muscles appropriate for the movement and not those opposed to it are recruited.

Some circuits provide *feedback inhibition*. For example, a motor neuron may have excitatory connections with both a muscle and an inhibitory interneuron that itself forms a connection with the motor neuron. When the inhibitory interneuron is excited by the motor neuron, the interneuron is able to limit the ability of the motor neuron to excite the muscle (Figure 3–7B). We will encounter many examples of feedforward and feedback inhibition when we examine more complex behaviors in later chapters.

Signaling Is Organized in the Same Way in All Nerve Cells

To produce a behavior, a stretch reflex for example, each participating sensory and motor nerve cell must generate four different signals in sequence, each at a different site within the cell. Despite variations in cell size and shape, transmitter biochemistry, or behavioral function, almost all neurons can be described by a model neuron that has four functional components that generate the four types of signals: a receptive component for producing graded input signals, a summing or integrative component that produces a trigger signal, a conducting long-range signaling component that produces all-or-none conducting signals, and a synaptic component that produces output signals to the next neuron in line or to muscle or gland cells (Figure 3–8).

The different types of signals generated in a neuron are determined in part by the electrical properties of the cell membrane. Every cell, including a neuron, maintains a certain difference in the electrical potential on either side of the plasma membrane when the cell is at rest. This is called the *resting membrane potential*. In a typical resting neuron, the voltage of the inside of the cell is about 65 mV more negative than the voltage outside the cell. Because the voltage outside the membrane is defined as zero, we say the resting membrane potential is –65 mV. The resting potential in different nerve cells ranges from –40 to –80 mV; in muscle cells, it is greater still, about –90 mV. As described in detail in Chapter 9, the resting membrane potential results from two factors: the unequal distribution of electrically charged ions, in particular the positively charged Na^+ and K^+ ions, and the selective permeability of the membrane.

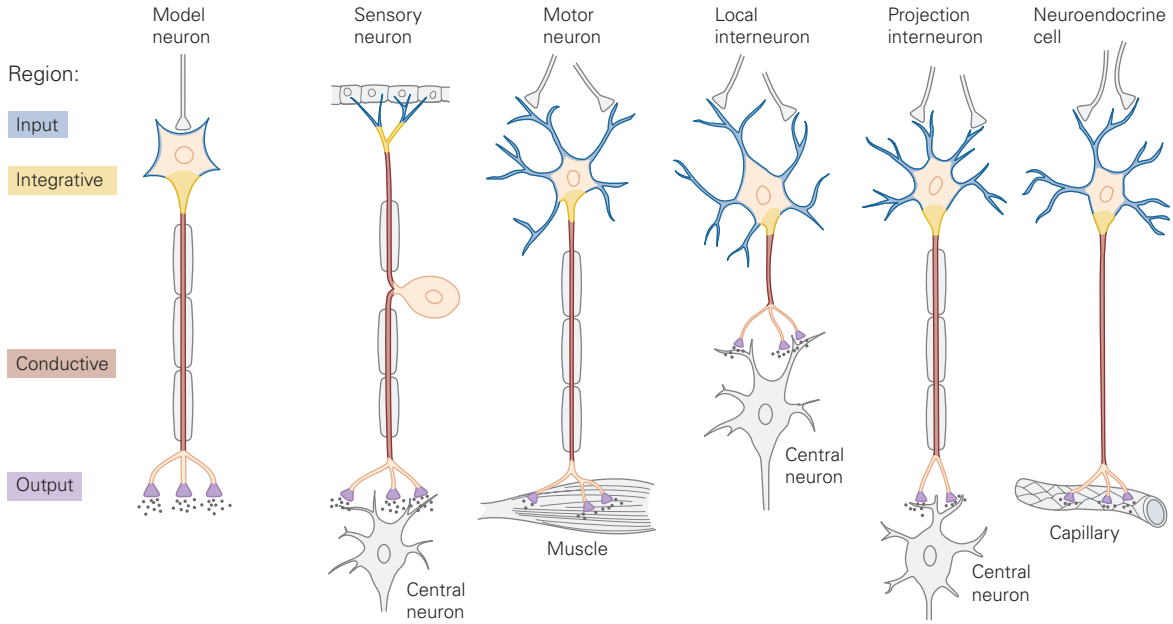

Figure 3–8 **Most neurons have four functional regions in which different types of signals are generated.** Thus, the functional organization of most neurons, regardless of type, can be represented schematically by a model neuron. This model neuron is the physiological expression of Ramón y Cajal's principle of dynamic polarization. The input, integrative, and conductive signals are all electrical and integral to the cell, whereas the output signal is a chemical substance ejected by the cell into the synaptic cleft. Not all neurons share all of these features; for example, some local interneurons lack a conductive component.

The unequal distribution of positively charged ions on either side of the cell membrane is maintained by two main mechanisms. Intracellular Na^+ and K^+ concentrations are largely controlled by a membrane protein that actively pumps Na^+ out of the cell and K^+ back into it. This *Na^+-K^+ pump*, about which we shall learn more in Chapter 9, keeps the Na^+ concentration in the cell low (about one-tenth the concentration outside the cell) and the K^+ concentration high (about 20 times the concentration outside). The extracellular concentrations of Na^+ and K^+ are maintained by the kidneys and the astroglial cells, also known as astrocytes.

The otherwise impermeable cell membrane contains proteins that form pores called *ion channels*. The channels that are active when the cell is at rest are highly permeable to K^+ but considerably less permeable to Na^+. The K^+ ions tend to leak out of these open channels, down the ion's concentration gradient. As K^+ ions exit the cell, they leave behind a cloud of unneutralized negative charge on the inner surface of the membrane, so that the net charge inside the membrane is more negative than that outside. With this state of affairs, the membrane potential is typically maintained at around –65 mV relative to outside of the neuron, and the neuron is said to be at rest.

The resting state is perturbed when the cell begins to take up Na^+ (or Ca^{2+}), which are at a higher concentration outside the cell. The inward movement of these positively charged ions (*inward current*) partially neutralizes the negative voltage inside the cell. We will say more about these events below. What happens next, however, holds the key to understanding what it is about neurons that makes signaling suitable for conveying information.

A cell, such as nerve and muscle, is said to be excitable when its membrane potential can be quickly and significantly altered. In many neurons, a 10-mV change in membrane potential (from –65 to –55 mV) makes the membrane much more permeable to Na^+ than to K^+. The resultant influx of Na^+ further neutralizes the negative charge inside the cell, leading to even more permeability to Na^+. The result is a brief and explosive change in membrane potential to +40 mV, the *action potential*. This potential is actively conducted down the cell's axon to the axon's terminal, where it initiates an elaborate chemical interaction with postsynaptic neurons or muscle cells. Since the action potential is actively propagated, its amplitude does not diminish by the time it reaches the axon terminal. An action potential typically lasts approximately 1 ms, after which the membrane returns to its resting state, with its normal separation of charges and higher permeability to K^+ than to Na^+.

The mechanisms underlying the resting potential and action potential are discussed in detail in Chapters 9 and 10. In addition to the long-distance signals represented by the action potential, nerve cells also produce local signals—receptor potentials and synaptic potentials—that are not actively propagated and that typically decay within just a few millimeters (see next section).

Changes in membrane potential that generate long-range and local signals can be either a decrease or an increase from the resting potential. That is, the resting membrane potential is the baseline from which all signaling occurs. A reduction in membrane potential, called *depolarization*, enhances a cell's ability to generate an action potential and is thus excitatory. In contrast, an increase in membrane potential, called *hyperpolarization*, makes a cell less likely to generate an action potential and is therefore inhibitory.

The Input Component Produces Graded Local Signals

In most neurons at rest, no current flows from one part of the cell to another, so the resting potential is the same throughout. In sensory neurons, current flow is typically initiated by a physical stimulus, which activates specialized receptor proteins at the neuron's receptive surface. In our example of the knee-jerk reflex, stretching of the muscle activates specific ion channels that open in response to stretch of the sensory neuron membrane, as we shall learn in Chapter 18. The opening of these channels when the cell is stretched permits the rapid influx of Na^+ ions into the sensory cell. This ionic current changes the membrane potential, producing a local signal called the *receptor potential*.

The amplitude and duration of a receptor potential depend on the intensity of the muscle stretch: The larger or longer-lasting the stretch, the larger or longer-lasting is the resulting receptor potential (Figure 3–9A). That is, receptor potentials are graded, unlike the all-or-none action potential. Most receptor potentials are depolarizing (excitatory); hyperpolarizing (inhibitory) receptor potentials are found in the retina.

The receptor potential is the first representation of stretch to be coded in the nervous system. However, because this depolarization spreads passively from the stretch receptor, it does not travel far. The distance is longer if the diameter of the axon is bigger, shorter if the diameter is smaller. Also, the distance is shorter if current can pass easily through the membrane, and longer if the membrane is insulated by myelin. The receptor potential from the stretch receptor therefore travels only 1 to 2 mm. In fact, just 1 mm away, the

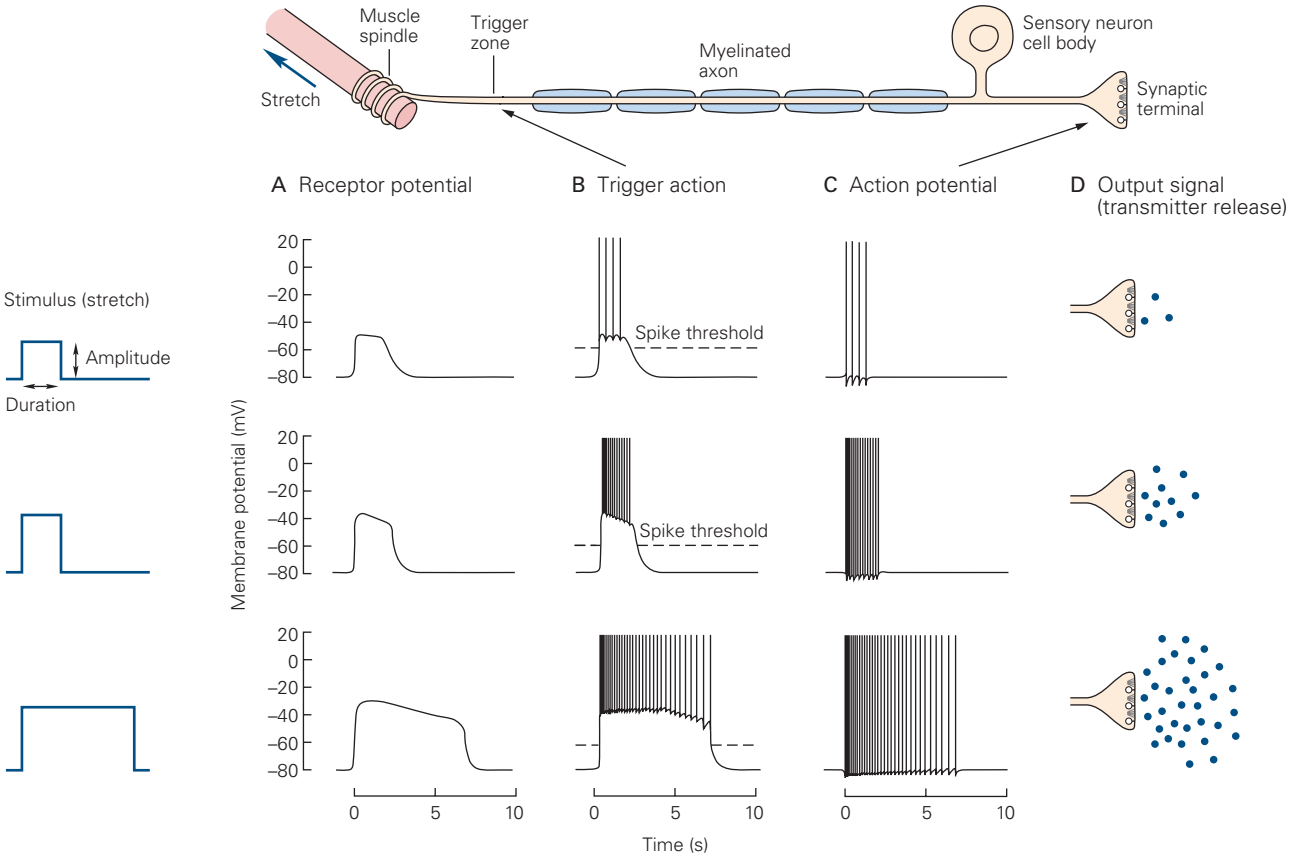

Figure 3–9 Each of the neuron's four signaling components produces a characteristic signal. The figure shows a sensory neuron activated by stretching of a muscle, which the neuron senses through a specialized receptor, the muscle spindle.

A. The input signal, called a receptor potential, is graded in amplitude and duration, proportional to the amplitude and duration of the stimulus.

B. The trigger zone sums the depolarization generated by the receptor potential. An action potential is generated only if the receptor potential exceeds a certain voltage threshold. Once this threshold is surpassed, any further increase in amplitude of the receptor potential can only increase the frequency with which the action potentials are generated, because action potentials have a constant amplitude. The duration of the receptor potential determines the duration of the train of action potentials. Thus, the graded amplitude and duration of the receptor potential are translated into a frequency code in the action potentials generated at the trigger zone. All action potentials produced are propagated faithfully along the axon.

C. Action potentials are all-or-none. Because all action potentials have a similar amplitude and duration, the frequency and duration of firing encodes the information carried by the signal.

D. When the action potential reaches the synaptic terminal, it initiates the release of a neurotransmitter, the chemical substance that serves as the output signal. The frequency of action potentials in the presynaptic cell determines how much neurotransmitter is released by the cell.

amplitude of the signal is only about one-third what it was at the site of generation. To be carried successfully to the spinal cord, the local signal must be amplified—it must generate an action potential. In the knee-jerk reflex, if the receptor potential in the sensory neuron reaches the first node of Ranvier in the axon and is large enough, it will trigger an action potential (Figure 3–9B), which then propagates without failure to the axon terminals in the spinal cord (Figure 3–9C). At the synapse between the sensory neuron and a motor neuron, the action potential produces a chain of events that results in an input signal to the motor neuron.

In the knee-jerk reflex, the action potential in the presynaptic terminal of the sensory neuron initiates the release of a chemical substance, or neurotransmitter, into the synaptic cleft (Figure 3–9D). After diffusing across the cleft, the transmitter binds to receptor proteins in the postsynaptic membrane of the motor neuron, thereby directly or indirectly opening ion channels. The ensuing flow of current briefly alters the membrane potential of the motor cell, a change called the *synaptic potential*.

Like the receptor potential, the synaptic potential is graded; its amplitude depends on how much transmitter is released. In the same cell, the synaptic

Table 3–1 Comparison of Local (Passive) and Propagated Signals

Signal type	Amplitude (mV)	Duration	Summation	Effect of signal	Type of propagation
Local (passive) signals					
Receptor potentials	Small (0.1–10)	Brief (5–100 ms)	Graded	Hyperpolarizing or depolarizing	Passive
Synaptic potentials	Small (0.1–10)	Brief to long (5 ms–20 min)	Graded	Hyperpolarizing or depolarizing	Passive
Propagated (active) signals					
Action potentials	Large (70–110)	Brief (1–10 ms)	All-or-none	Depolarizing	Active

potential can be either depolarizing or hyperpolarizing depending on the type of receptor molecule that is activated. Synaptic potentials, like receptor potentials, spread passively. Thus, the change in potential will remain local unless the signal reaches beyond the axon's initial segment where it can give rise to an action potential. Some dendrites are not entirely passive but contain specializations that boost the synaptic potential, thereby increasing its efficacy to produce an action potential (Chapter 13). The features of receptor and synaptic potentials are summarized in Table 3–1.

The Trigger Zone Makes the Decision to Generate an Action Potential

Sherrington first pointed out that the function of the nervous system is to weigh the consequences of different types of information and then decide on appropriate responses. This *integrative* function of the nervous system is clearly seen in events at the trigger zone of the neuron, the initial segment of the axon.

Action potentials are generated by a sudden influx of Na^+ through channels in the cell membrane that open and close in response to changes in membrane potential. When an input signal (a receptor potential or synaptic potential) depolarizes an area of membrane, the local change in membrane potential opens local Na^+ channels that allow Na^+ to flow down its concentration gradient, from outside the cell where the Na^+ concentration is high to inside where it is low.

Because the initial segment of the axon has the highest density of voltage-sensitive Na^+ channels and therefore the lowest threshold for generating an action potential, an input signal spreading passively along the cell membrane is more likely to give rise to an action potential at the initial segment of the axon than at other sites in the cell. This part of the axon is therefore known as the *trigger zone*. It is here that the activity of all receptor (or synaptic) potentials is summed and where, if the sum of the input signals reaches threshold, the neuron generates an action potential.

The Conductive Component Propagates an All-or-None Action Potential

The action potential is all-or-none: Stimuli below the threshold do not produce a signal, but stimuli above the threshold all produce signals of the same amplitude. Regardless of variation in intensity or duration of stimuli, the amplitude and duration of each action potential are pretty much the same, and this holds for each regenerated action potential at a node of Ranvier along a myelinated axon. In addition, unlike receptor and synaptic potentials, which spread passively and decrease in amplitude, the action potential, as we have seen, does not decay as it travels along the axon to its target—a distance that can be as great as 1 m—because it is periodically regenerated. This conducted signal can travel at rates as fast as 100 m/s. Indeed, the remarkable feature of action potentials is that they are highly stereotyped, varying only subtly (but in some cases importantly) from one nerve cell to another. This feature was demonstrated in the 1920s by Edgar Adrian, one of the first to study the nervous system at the cellular level. Adrian found that all action potentials have a similar shape or waveform (see Figure 3–2). The action potentials carried into the nervous system by a sensory axon often are indistinguishable from those carried out of the nervous system to the muscles by a motor axon.

Only two features of the conducting signal convey information: the number of action potentials and the time intervals between them (Figure 3–9C). As Adrian put it in 1928, summarizing his work on sensory fibers: "all impulses are very much alike, whether the message is destined to arouse the sensation of light, of touch, or of pain; if they are crowded together the sensation is intense, if they are separated by long intervals the sensation is correspondingly feeble." Thus, what determines

the intensity of sensation or speed of movement is the frequency of the action potentials. Likewise, the duration of a sensation or movement is determined by the period over which action potentials are generated.

In addition to the frequency of the action potentials, the pattern of action potentials also conveys important information. For example, some neurons are spontaneously active in the absence of stimulation. Some spontaneously active nerve cells (beating neurons) fire action potentials regularly; others (bursting neurons) fire in brief bursts of action potentials. These diverse cells respond differently to the same excitatory synaptic input. An excitatory synaptic potential may initiate one or more action potentials in a cell that is not spontaneously active, whereas that same input to spontaneously active cells will simply increase the existing rate of firing.

An even more dramatic difference is seen when the input signal is inhibitory. Inhibitory inputs have little information value in a silent cell. By contrast, in spontaneously active cells, inhibition can have a powerful *sculpting* role. By establishing periods of silence in otherwise ongoing activity, inhibition can produce a complex pattern of alternating firing and silence where none existed. Such subtle differences in firing patterns may have important functional consequences for the information transfer between neurons. Mathematical modelers of neuronal networks have attempted to delineate neural codes in which information is also carried by the fine-grained pattern of firing—the exact timing of each action potential.

If signals are stereotyped and reflect only the most elementary properties of the stimulus, how can they carry the rich variety of information needed for complex behavior? How is a message that carries visual information about a bee distinguished from one that carries pain information about the bee's sting, and how are these sensory signals distinguished from motor signals for voluntary movement? The answer is simple and yet is one of the most important organizational principles of the nervous system: Interconnected neurons form anatomically and functionally distinct pathways—labeled lines—and it is these pathways of connected neurons, these labeled lines, not individual neurons, that convey information. The neural pathways activated by receptor cells in the retina that respond to light are completely distinct from the pathways activated by sensory cells in the skin that respond to touch.

The Output Component Releases Neurotransmitter

When an action potential reaches a neuron's terminal, it stimulates the release of chemical substances from the cell. These substances, called *neurotransmitters*, can be small organic molecules, such as L-glutamate and acetylcholine, or peptides like substance P or LHRH (luteinizing hormone–releasing hormone).

Neurotransmitter molecules are held in subcellular organelles called *synaptic vesicles*, which accumulate in the terminals of the axon at specialized release sites called *active zones*. To eject their transmitter substance into the synaptic cleft, the vesicles move up to and fuse with the neuron's plasma membrane, then burst open to release the transmitter into the synaptic cleft (the extracellular space between the pre- and postsynaptic cell) by a process known as *exocytosis*. The molecular machinery of neurotransmitter release is described in Chapters 14 and 15.

The released neurotransmitter molecules are the neuron's output signal. The output signal is thus graded according to the amount of transmitter released, which is determined by the number and frequency of the action potentials that reach the presynaptic terminals (Figure 3–9C,D). After release, the transmitter molecules diffuse across the synaptic cleft and bind to receptors on the postsynaptic neuron. This binding causes the postsynaptic cell to generate a synaptic potential. Whether the synaptic potential has an excitatory or inhibitory effect depends on the type of receptor in the postsynaptic cell, not on the particular chemical neurotransmitter. The same transmitter substance can have different effects at different receptors.

The Transformation of the Neural Signal From Sensory to Motor Is Illustrated by the Stretch-Reflex Pathway

As we have seen, the properties of a signal are transformed as the signal moves from one component of a neuron to another or between neurons. In the stretch reflex, when a muscle is stretched, the amplitude and duration of the stimulus are reflected in the amplitude and duration of the receptor potential generated in the sensory neuron (Figure 3–10A). If the receptor potential exceeds the threshold for an action potential in that cell, the graded signal is transformed at the trigger zone into an action potential. Although individual action potentials are all-or-none signals, the more the receptor potential exceeds threshold, the greater the depolarization and consequently the greater the frequency of action potentials in the axon. The duration of the input signal also determines the duration of the train of action potentials.

The information encoded by the frequency and duration of firing is faithfully conveyed along the axon to its terminals, where the firing of action potentials determines the amount of transmitter released.

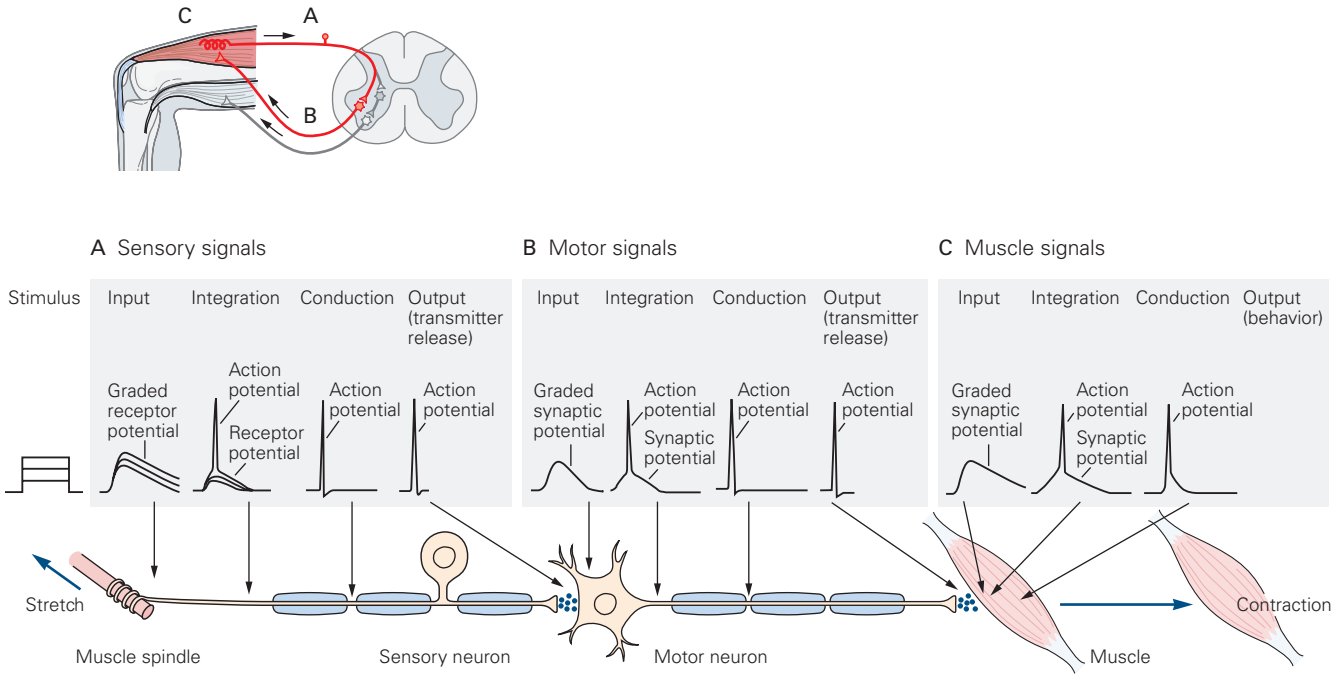

Figure 3–10 The sequence of signals that produces a reflex action.

A. The stretching of a muscle produces a receptor potential in the specialized receptor (the muscle spindle). The amplitude of the receptor potential is proportional to the intensity of the stretch. This potential spreads passively to the integrative or trigger zone at the first node of Ranvier. If the receptor potential is sufficiently large, it triggers an action potential that then propagates actively and without change along the axon to the axon terminal. At specialized sites in the terminal, the action potential leads to the release of a chemical neurotransmitter, the output signal. The transmitter diffuses across the synaptic cleft between the axon terminal and a target motor neuron that innervates the stretched muscle; it then binds to receptor molecules on the external membrane of the motor neuron.

B. This interaction initiates a synaptic potential that spreads passively to the trigger zone of the motor neuron's axon, where it initiates an action potential that propagates actively to the terminal of the motor neuron's axon. At the axon terminal, the action potential leads to release of a neurotransmitter near the muscle fiber.

C. The neurotransmitter binds receptors on the muscle fiber, generating a synaptic potential. The synaptic potential triggers an action potential in the muscle, which causes a contraction.

These stages of signaling have their counterparts in the motor neuron (Figure 3–10B) and in the muscle (Figure 3–10C).

Nerve Cells Differ Most at the Molecular Level

The model of neuronal signaling we have outlined is a simplification that applies to most neurons, but there are some important variations. For example, some neurons do not generate action potentials. These are typically local interneurons without a conductive component; they have no axon or such a short one that regeneration of the signal is not required. In these neurons, the input signals are summed and spread passively to the presynaptic terminal region near where transmitter is released. Neurons that are spontaneously active do not require sensory or synaptic inputs to fire action potentials because they have a special class of ion channels that permit Na^+ current flow even in the absence of excitatory synaptic input.

Even cells that are similar morphologically can differ importantly in molecular details. For example, they can have different combinations of ion channels. As we shall learn in Chapter 10, different ion channels provide neurons with various thresholds, excitability properties, and firing patterns. Such neurons can encode synaptic potentials into different firing patterns and thereby convey different information.

Neurons also differ in the chemical substances they use as transmitters and in the receptors that receive transmitter substances from other neurons. Indeed, many drugs that act on the brain do so by modifying the actions of specific chemical transmitters or receptors. Because of physiological differences among neurons, a disease may affect one class of neurons but

not others. Certain diseases strike only motor neurons (amyotrophic lateral sclerosis and poliomyelitis), whereas others affect primarily sensory neurons (leprosy and tabes dorsalis, a late stage of syphilis). Parkinson disease, a disorder of voluntary movement, damages a small population of neurons that use dopamine as a neurotransmitter. Some diseases are selective even within the neuron, affecting only the receptive elements, the cell body, or the axon. In Chapter 57, we describe how research into myasthenia gravis, a disease caused by a faulty transmitter receptor in the muscle membrane, has provided important insights into synaptic transmission. Indeed, because the nervous system has so many cell types and variations at the molecular level, it is susceptible to more diseases (psychiatric as well as neurological) than any other organ system of the body.

Despite the morphological differences among nerve cells, the molecular mechanisms of electrical signaling are surprisingly similar. This simplicity is fortunate, for understanding the molecular mechanisms of signaling in one kind of nerve cell aids the understanding of these mechanisms in many other nerve cells.

The Reflex Circuit Is a Starting Point for Understanding the Neural Architecture of Behavior

The stretch reflex illustrates how interactions between just a few types of nerve cells can constitute a functional circuit that produces a simple behavior, even though the number of neurons involved is large (the stretch reflex circuit has perhaps a few hundred sensory neurons and a hundred motor neurons). Some invertebrate animals are capable of behavior as sophisticated as reflexes using far fewer neurons. Moreover, in some instances, just one critical command neuron can trigger a complex behavior such as the withdrawal of a body part from a noxious stimulus.

For more complex behaviors, especially in higher vertebrates, many neurons are required, but the basic neural structure of the simple reflex is often preserved. First, there is often an identifiable group of neurons whose firing rate changes in response to a particular type of environmental stimulus, such as a tone of a certain frequency, or the juxtaposition of light and dark at a particular angle. Just as the firing rate of the stretch receptor neurons encodes the degree of muscle tension, the firing rates of cortical neurons in sensory areas of the cortex encode the intensity of a sensory feature (eg, the degree of contrast of the contour). As we shall see in later chapters, it is possible to change the features of a percept just by changing the firing rate of small groups of neurons.

Second, there is often an identifiable group of neurons whose firing rate changes before an animal performs a motor act. Just as the spike rate of motor neurons controls the magnitude of the contraction of the quadriceps muscle—hence the knee jerk—so does the firing rate of neurons in the motor cortex affect the latency and type of movement that will be performed. Exactly what aspect of the movement is encoded by such neurons remains an area of active inquiry, but it is well established that groups of neurons affect the ensuing action in a graded fashion by adjusting their firing rate. In other association areas of the cerebral cortex, the graded firing rates of neurons encode quantities that are essential for thought processes, such as the amount of evidence bearing on a choice (Chapter 56).

Although sophisticated mental operations are far more complicated than a simple stretch reflex, it may nevertheless prove useful to consider the extent to which cognitive functions are supported by neural mechanisms that are organized in any way that resembles a simple reflex. What types of elaborations might be required to mediate a sophisticated behavior and thought? Unlike a simple reflex, with a sophisticated behavior, activation of sensory neurons would not give rise to an immediate reflexive action. There is more contingency to the process. Although simple reflexes are modulated by context, mental functions are more deeply shaped by a complex repertoire of contingencies, allowing for many possible effects of any one stimulus and many possible precipitants of any one action. In light of these contingencies, we are forced to conceive of a flexible routing between the brain's data acquisition systems—not just the sensory systems but also the memory systems—and effector systems. As we shall see in later chapters, this is the role of the higher association areas of the cerebral cortex, acting in concert with several subcortical brain structures.

Perhaps a more salient difference between a complex mental function and a reflex is the timing of action. Once activated, a reflex circuit leads to action almost immediately after the sensory stimulus. Any delay depends mainly on the conduction velocity of the action potentials in the afferent and efferent limbs of the reflex (eg, the ankle jerk is slower than the knee jerk because the spinal cord is further from the stretch receptors of the calf muscles than it is from the thigh extensors). For more complex behaviors, action need not occur more or less instantaneously with the arrival of sensory information. It might be delayed to await additional information or be expressed only when specific circumstances occur.

Interestingly, the neurons in the association areas of the cortex of primates have the capacity to sustain graded firing rates for durations of many seconds. These neurons are abundant in the parts of the brain that mediate the flexible linkage between sensory and motor areas. They afford a freedom from the instantaneous nature of reflexive behavior and therefore may furnish the essential circuit properties that distinguish cognitive functions from more straightforward sensorimotor transformations like a reflex.

Neural Circuits Can Be Modified by Experience

Learning can result in behavioral changes that endure for years, even a lifetime. But even simple reflexes can be modified, albeit for a much briefer period of time. The fact that much behavior can be modified by learning raises an interesting question: How is it that behavior can be modified if the nervous system is wired so precisely? How can changes in the neural control of behavior occur when connections between the signaling units, the neurons, are set during early development?

Several solutions for this dilemma have been proposed. The proposal that has proven most farsighted is the *plasticity hypothesis*, first put forward at the turn of the 20th century by Ramón y Cajal. A modern form of this hypothesis was advanced by the Polish psychologist Jerzy Konorski in 1948.

> The application of a stimulus leads to changes of a twofold kind in the nervous system … [T]he first property, by virtue of which the nerve cells *react* to the incoming impulse … we call *excitability*, and … changes arising … because of this property we shall call *changes due to excitability*. The second property, by virtue of which certain permanent functional transformations arise in particular systems of neurons as a result of appropriate stimuli or their combination, we shall call *plasticity* and the corresponding changes *plastic changes*.

There is now considerable evidence for functional plasticity at chemical synapses. These synapses often have a remarkable capacity for short-term physiological changes (lasting seconds to hours) that increase or decrease synaptic effectiveness. Long-term physiological changes (lasting days or longer) can give rise to anatomical alterations, including pruning of synapses and even growth of new ones. As we shall see in later chapters, chemical synapses are functionally and anatomically modified during critical periods of early development but also throughout life. This functional plasticity of neurons endows each of us with a characteristic manner of interacting with the surrounding world, both natural and social.

Highlights

1. Nerve cells are the signaling units of the nervous system. The signals are mainly electrical within the cell and chemical between cells. Despite variations in size and shape, nerve cells share certain common features. Each has specialized receptors or transducers that receive input from other nerve cells or from the senses respectively; a mechanism to convert input to electrical signals; a threshold mechanism to generate an all-or-none electrical impulse, the action potential, which can be regenerated along the axon that connects the nerve cell to its synaptic target (another nerve cell, a muscle, or gland); and the ability to produce the release of a chemical (neurotransmitter) that affects the target.
2. Glial cells support nerve cells. One type provides the insulation that speeds propagation of the action potential along the axon. Others help establish the chemical milieu for the nerve cells to operate, and still others couple nerve activity to the vascular supply of the nervous system.
3. Nerve cells differ in their morphology, the connections they make, and where they make them. This is clearest in specialized structures like the retina. Perhaps the largest difference between neurons is at the molecular level. Examples of molecular diversity include expression of different receptors, enzymes for synthesis of different neurotransmitters, and different expressions of ion channels. Differences in gene expression furnish the starting point for understanding why certain diseases affect some neurons and not others.
4. Each nerve cell is part of a circuit that has one or more behavioral functions. The stretch reflex circuit is an example of a simple circuit that produces a behavior in response to a stimulus. Its simplicity belies integrative functions, such as relaxation of muscles that oppose the stretched muscle.
5. Modern neural science aspires to explain mental processes far more complex than reflexes. A natural starting point is to understand the ways that circuits must be elaborated to support sensorymotor transformations, which unlike a reflex, are contingent, flexible and not beholden to the immediacy of sensory processing and movement control.
6. Neural connections can be modified by experience. In simple circuits, this process is a simple change in the strength of connections between neurons. A working hypothesis in modern neuroscience is that the "plastic" mechanisms at play

in simple circuits also play a critical role in the learning of more complex behavior and cognitive function.

Michael N. Shadlen
Eric R. Kandel

Selected Reading

Adrian ED. 1928. *The Basis of Sensation: The Action of the Sense Organs.* London: Christophers.

Jack JJB, Noble D, Tsien RW. 1983. *Electric Current Flow in Excitable Cells*. Oxford: Clarendon Press.

Jones EG. 1988. The nervous tissue. In: L Weiss (ed). *Cell and Tissue Biology: A Textbook of Histology,* 6th ed., pp. 277–351. Baltimore: Urban and Schwarzenberg.

Poeppel D, Mangun GR, Gazzaniga MS. 2020. *The Cognitive Neurosciences*. Cambridge, MA: The MIT Press.

Ramón y Cajal S. [1937] 1989. *Recollections of My Life.* EH Craigie (transl). Philadelphia: American Philosophical Society; 1989. Reprint. Cambridge, MA: MIT Press.

References

Adrian ED. 1932. *The Mechanism of Nervous Action: Electrical Studies of the Neurone.* Philadelphia: Univ. Pennsylvania Press.

Alberts B, Johnson A, Lewis J, Raff M, Roberts K, Walter JD. 2002. *Molecular Biology of the Cell,* 4th ed. New York: Garland.

Dacey DM, Peterson BB, Robinson FR, Gamlin PD. 2003. Fireworks in the primate retina: in vitro photodynamics reveals diverse LGN-projecting ganglion cell types. Neuron 37:15–27.

Erlanger J, Gasser HS. 1937. *Electrical Signs of Nervous Activity.* Philadelphia: Univ. Pennsylvania Press.

Hodgkin AL, Huxley AF. 1939. Action potentials recorded from inside a nerve fiber. Nature 144:710–711.

Kandel ER. 1976. The study of behavior: the interface between psychology and biology. In: *Cellular Basis of Behavior: An Introduction to Behavioral Neurobiology,* pp. 3–27. San Francisco: WH Freeman.

Konorski J. 1948. *Conditioned Reflexes and Neuron Organization.* Cambridge: Cambridge Univ. Press.

Martinez PFA. 1982. *Neuroanatomy: Development and Structure of the Central Nervous System.* Philadelphia: Saunders.

McCormick DA. 2004. Membrane potential and action potential. In: JH Byrne, JL Roberts (eds). *From Molecules to Networks: An Introduction to Cellular Neuroscience*, 2nd ed., p. 130. San Diego: Elsevier.

Newman EA. 1986. High potassium conductance in astrocyte endfeet. Science 233:453–454.

Nicholls JG, Wallace BG, Fuchs PA, Martin AR. 2001. *From Neuron to Brain,* 4th ed. Sunderland, MA: Sinauer.

Penfield W (ed). 1932. *Cytology & Cellular Pathology of the Nervous System,* Vol. 2. New York: Hoeber.

Ramón y Cajal S. 1933. *Histology,* 10th ed. Baltimore: Wood.

Sears ES, Franklin GM. 1980. Diseases of the cranial nerves. In: RN Rosenberg (ed). *The Science and Practice of Clinical Medicine.* Vol. 5, *Neurology,* pp. 471–494. New York: Grune & Stratton.

Sherrington C. 1947. *The Integrative Action of the Nervous System,* 2nd ed. Cambridge: Cambridge Univ. Press.

4

The Neuroanatomical Bases by Which Neural Circuits Mediate Behavior

The human brain carries out actions in ways no current computer can begin to approach. Merely to see—to look onto the world and recognize a face or facial expression—entails amazing computational achievements. Indeed, all our perceptual abilities—seeing, hearing, smelling, tasting, and touching—are analytical triumphs. Similarly, all of our voluntary actions are triumphs of engineering. Sensation and movement, while wondrous in their own right, pale in comparison to complex cognitive behaviors such as forming memories or understanding social conventions.

The brain accomplishes these computational feats because its nerve cells are wired together in very precise functional circuits. The brain is hierarchically organized such that information processed at one level is passed to higher-level circuits for more complex and refined processing. In essence, the brain is a network of networks. Different brain areas work in an integrated fashion to accomplish purposeful behavior.

In this chapter, we outline the neuroanatomical organization of some of the circuits that enable the brain to process sensory input and produce motor output. We focus on touch as a sensory modality because the somatosensory system is particularly well understood and because touch clearly illustrates the interaction of sensory processing circuits at several levels, from the spinal cord to the cerebral cortex. Our purpose here is to illustrate the basic principles of how circuits control behavior. In the next chapter, we consider the functional properties of these circuits, including the computations by which they process information. In subsequent chapters, we consider in more detail the

anatomy and function of the various sensory modalities and how sensory input regulates movement.

Finally, we provide a preview of the brain circuits that are instrumental in producing the memories of our daily lives, called explicit memory (see Chapters 52 and 54). We do this to make the point that while many of the neurons in the memory circuits are similar to those in the sensory and motor circuits, not all are. Moreover, the organization of the pathways between circuits is different in the memory system than it is in the motor and sensory systems. This highlights a basic neurobiological tenet that different circuits of the brain have evolved an organization to most efficiently carry out specific functions.

Comprehending the functional organization of the brain might at first seem daunting. But as we saw in the previous chapter, the organization of the brain is simplified by three anatomical considerations. First, there are relatively few types of neurons. Each of the many thousands of spinal motor neurons or millions of neocortical pyramidal cells has a similar anatomical structure and serves a similar function. Second, neurons in the brain and spinal cord are clustered in functional groups called nuclei or discrete areas of the cerebral cortex, which form networks or functional systems. Third, the discrete areas of the cerebral cortex are specialized for sensory, motor, or associative functions such as memory.

Local Circuits Carry Out Specific Neural Computations That Are Coordinated to Mediate Complex Behaviors

Neurons are interconnected to form functional circuits. Within the spinal cord, for example, simple reflex circuits receive sensory information from stretch receptors and send output to various muscle groups. For more complex behavioral functions, different stages of information processing are carried out in networks in different regions of the nervous system. Connections between neurons within the nervous system can be of different lengths.

Within a brain region, local connections, which may be excitatory or inhibitory, integrate many of the neurons into functional networks. Such local networks may then provide outputs to one or more other brain regions through longer projections. Many of these longer pathways have names. For example, projections from the lateral geniculate nucleus of the thalamus to the visual cortex are called the optic radiations. Connections from the neocortex—the region of the cerebral cortex nearest the surface of the brain—of one side of the brain to the other side of the brain form the corpus callosum. Information carried by these long pathways integrates the output of many local circuits (Figure 4–1).

Consider the simple act of hitting a tennis ball (Figure 4–2). Visual information about the motion of the approaching ball is analyzed in the visual system, which is itself a hierarchically organized system extending from the retina to the lateral geniculate nucleus of the thalamus to dozens of cortical areas in the occipital and temporal lobes (Chapter 21). This information is combined in the motor cortex with proprioceptive information about the position of the arms, legs, and trunk to calculate the movement necessary to intercept the ball. Once the swing is initiated, many minor adjustments of the motor program are made by other brain regions dedicated to movement, such as the cerebellum, based on a steady stream of sensory information about the trajectory of the approaching ball and the position of the arm.

Like most motor behaviors, hitting a tennis ball is not hardwired into brain circuits but requires learning and memory. The memory for motor tasks, termed procedural or implicit memory, requires modifications to circuits in motor cortex, the basal ganglia, and the cerebellum. Finally, this entire act is accessible to consciousness and may elicit conscious recall of past similar experiences, termed explicit memory, and emotions. Explicit memory depends on circuits in the hippocampus (Chapters 52 and 54), whereas emotions are regulated by the amygdala (Chapters 42 and 53) and portions of the orbitofrontal, cingulate, and insular cortices. Of course, as the swing is being executed, the brain is also engaged in coordinating the player's heart rate, respiration, and other homeostatic functions through equally complex networks.

Sensory Information Circuits Are Illustrated in the Somatosensory System

Complex behaviors, such as differentiating the motor acts required to grasp a ball versus a book, require the integrated action of several nuclei and cortical regions. Information is processed in the brain in a hierarchical fashion. Thus, information about a stimulus is conveyed through a succession of subcortical and then cortical regions; at each level of processing, the information becomes increasingly more complex.

In addition, different types of information, even within a single sensory modality, are processed in several anatomically discrete pathways. In the somatosensory system, a light touch and a painful pin prick to the same area of skin are mediated by different sensory receptors in the skin that connect to distinct pathways

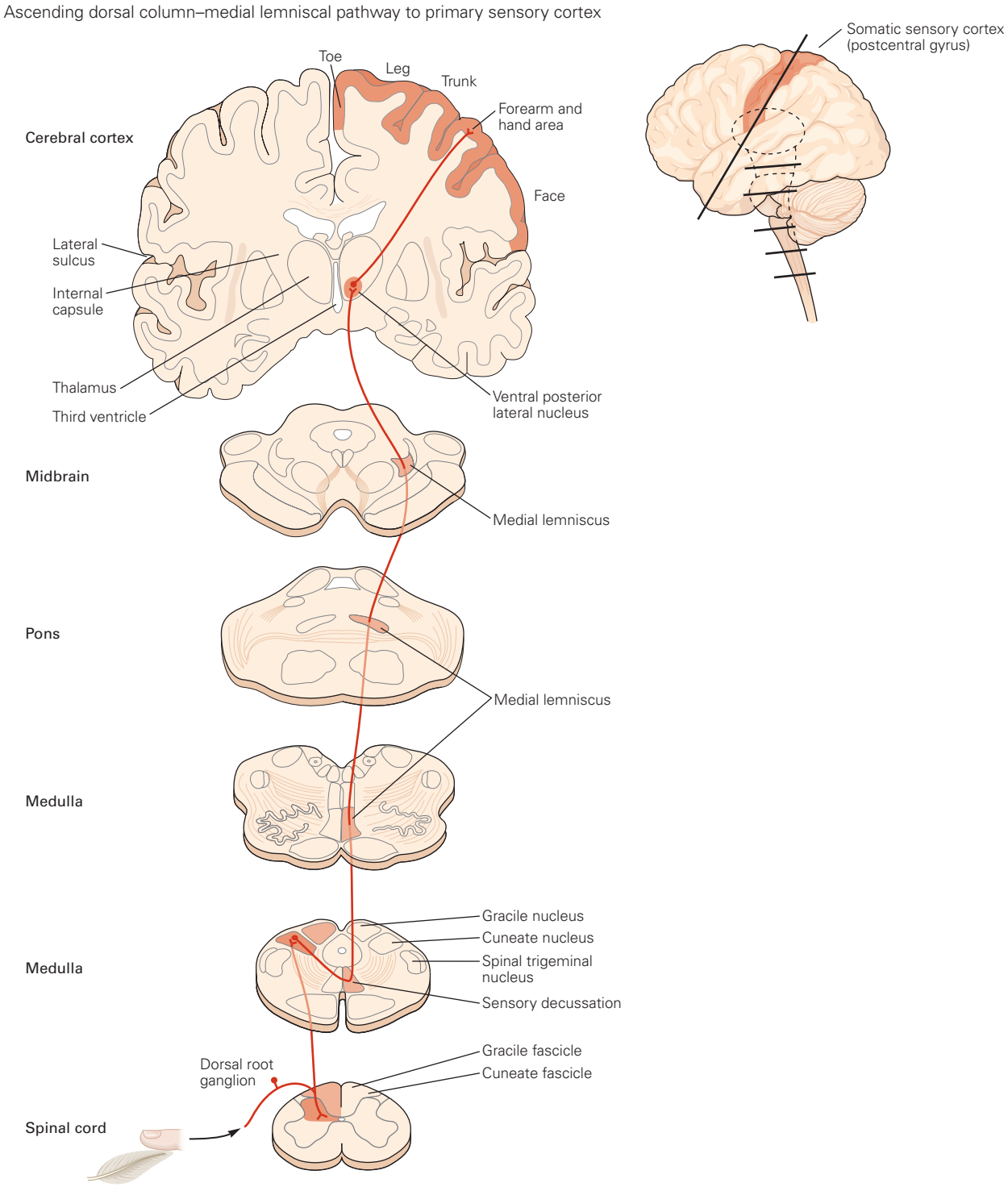

Figure 4–1 **The dorsal column–medial lemniscal pathway is the major afferent pathway for somatosensory information.** Somatosensory information enters the central nervous system through the dorsal root ganglion cells. The flow of information ultimately leads to the somatosensory cortex. Fibers that relay information from different parts of the body maintain an orderly relationship to each other and form a neural map of the body surface in their pattern of termination at each synaptic relay.

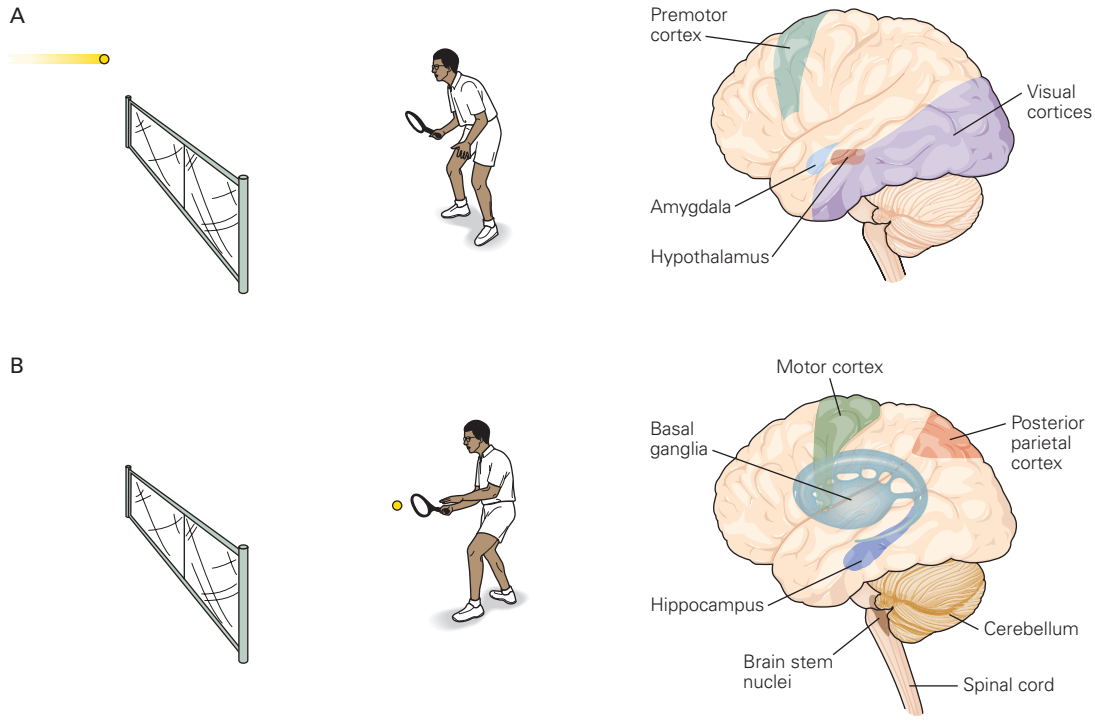

Figure 4–2 A simple behavior is mediated by many parts of the brain.

A. A tennis player watching an approaching ball uses the visual cortex to judge the size, direction, and velocity of the ball. The premotor cortex develops a motor program to return the ball. The amygdala acts in conjunction with other brain regions to adjust the heart rate, respiration, and other homeostatic mechanisms and also activates the hypothalamus to motivate the player to hit well.

B. To execute the shot, the player must use all of the structures illustrated in part **A** as well as others. The motor cortex sends signals to the spinal cord that activate and inhibit many muscles in the arms and legs. The basal ganglia become involved in initiating motor patterns and perhaps recalling learned movements to hit the ball properly. The cerebellum adjusts movements based on proprioceptive information from peripheral sensory receptors. The posterior parietal cortex provides the player with a sense of where his body is located in space and where his racket arm is located with respect to his body. Brain stem neurons regulate heart rate, respiration, and arousal throughout the movement. The hippocampus is not involved in hitting the ball but is involved in storing the memory of the return so that the player can brag about it later.

in the brain. The system for fine touch, pressure, and proprioception is called the epicritic system, whereas the system for pain and temperature is called the protopathic system.

Somatosensory Information From the Trunk and Limbs Is Conveyed to the Spinal Cord

All forms of somatosensory information from the trunk and limbs enter the spinal cord, which has a core H-shaped region of gray matter where neuronal cell bodies are located. The gray matter is surrounded by white matter formed by myelinated axons that make up both short and long connections. The gray matter on each side of the cord is divided into dorsal (or posterior) and ventral (or anterior) horns (Figure 4–3).

The dorsal horn contains groups of secondary sensory neurons (sensory nuclei) whose dendrites receive stimulus information from primary sensory neurons that innervate the body's skin, muscles, and joints. The ventral horn contains groups of motor neurons (motor nuclei) whose axons exit the spinal cord and innervate skeletal muscles. The spinal cord has circuits that mediate behaviors ranging from the stretch reflex to coordination of limb movements.

As we discussed in Chapter 3, when considering the knee-jerk reflex, interneurons of various types in the gray matter regulate the output of the spinal cord motor neurons (see Figure 3–5). Some of these interneurons are excitatory, whereas others are inhibitory. These interneurons modulate both sensory information flowing toward the brain and motor commands descending from the brain to the spinal motor neurons. Motor neurons can also adjust the output of other motor neurons via the interneurons. These

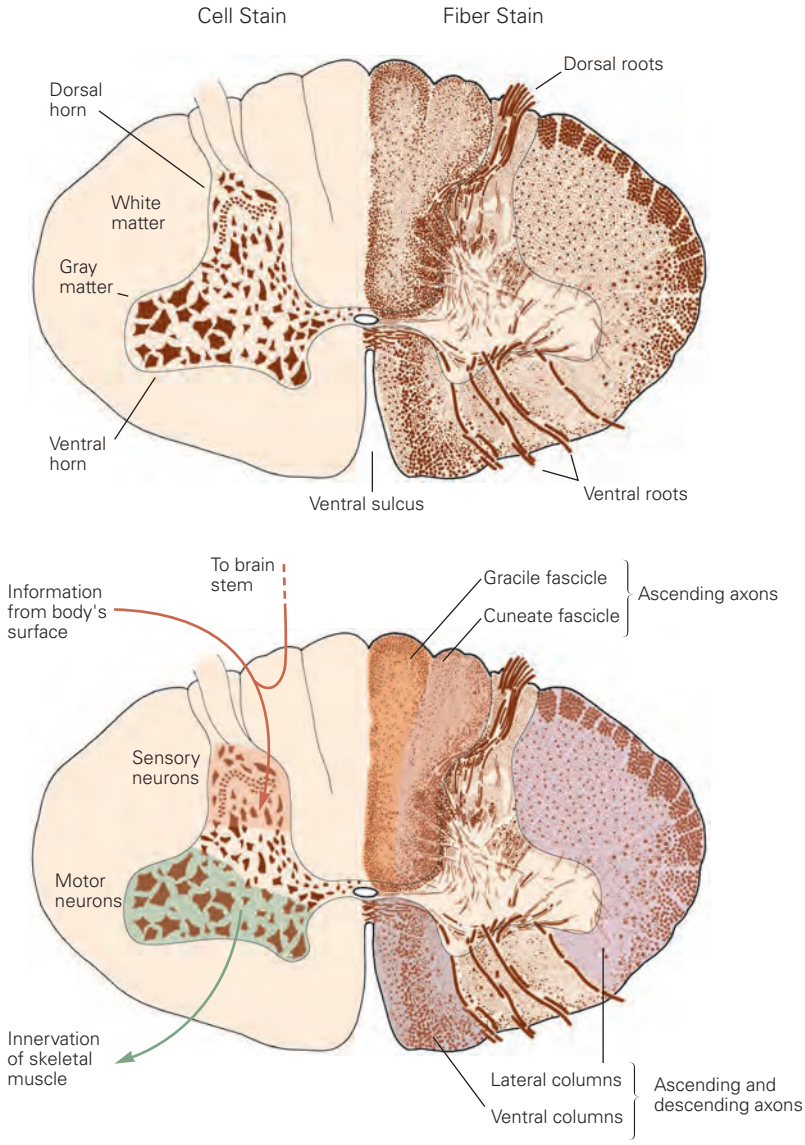

Figure 4–3 The major anatomical features of the spinal cord. The ventral horn (**green**) contains large motor neurons, whereas the dorsal horn (**orange**) contains smaller neurons. Fibers of the gracile fascicle carry somatosensory information from the lower limbs, whereas fibers of the cuneate fascicle carry somatosensory information from the upper body. Fiber bundles of the lateral and ventral columns include both ascending and descending fiber bundles.

circuits will be considered in more detail when we discuss the spinal cord in Chapter 32.

The white matter surrounding the gray matter contains bundles of ascending and descending axons that are divided into dorsal, lateral, and ventral columns. The dorsal columns, which lie between the two dorsal horns of the gray matter, contain only ascending axons that carry somatosensory information to the brain stem (Figure 4–1). The lateral columns include both ascending and descending axons from the brain stem and neocortex that innervate spinal interneurons and motor neurons (Figure 4–3). This demonstrates a general principle about central nervous system connections. Processing tends to be hierarchical: Projections from a lower to a higher processing region are said to be feedforward, while descending projections can modulate spinal reflexes and are considered to be feedback. The motif in which region A projects to region B and, in turn, also receives return projections from B, is recapitulated throughout the nervous

system. The ventral columns also include ascending and descending axons. The ascending somatosensory axons in the lateral and ventral columns constitute parallel pathways that convey information about pain and thermal sensation to higher levels of the central nervous system. The descending axons control axial muscles and posture.

The spinal cord is divided along its length into four major regions: cervical, thoracic, lumbar, and sacral (Figure 4–4). Connections arising from these regions

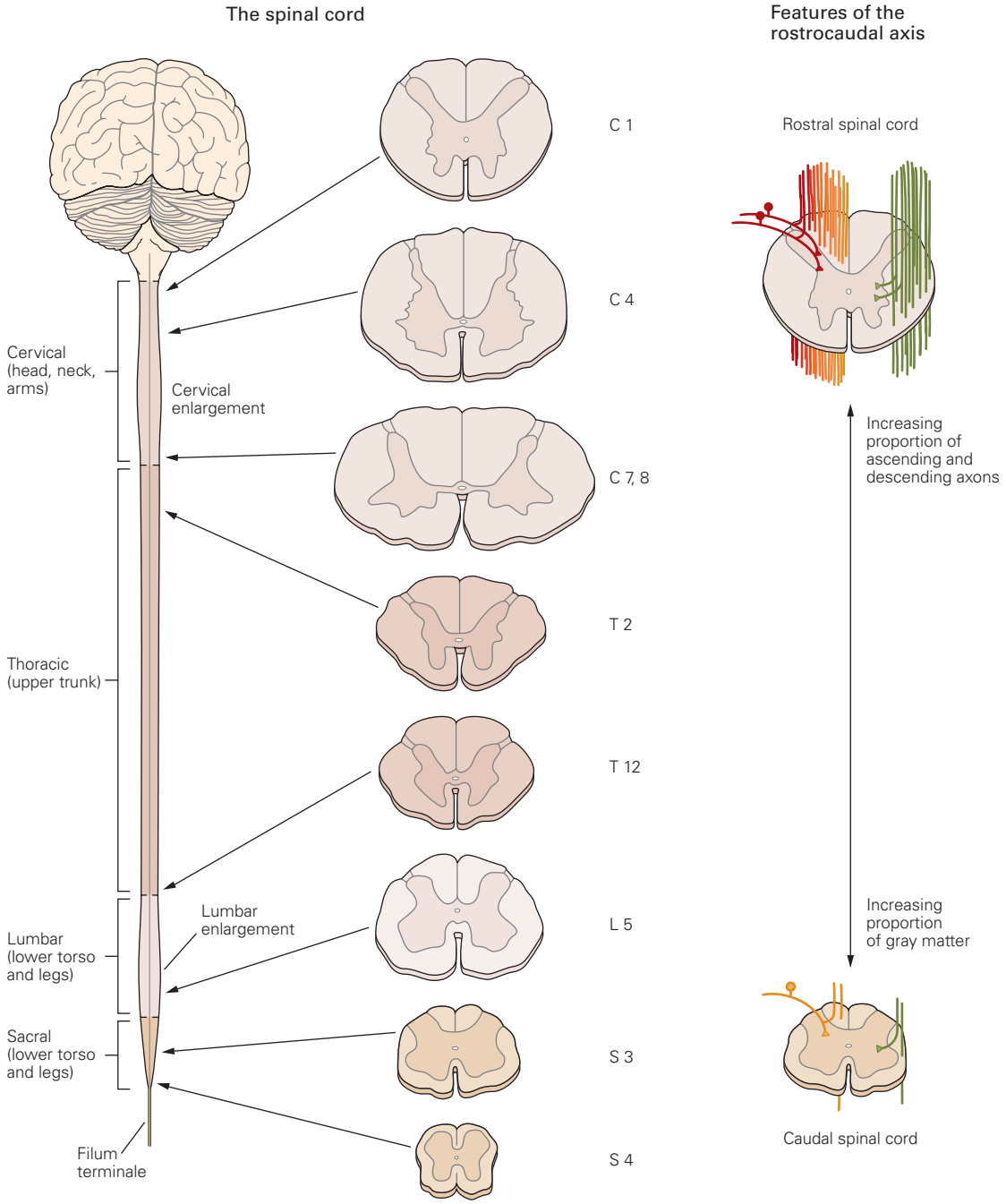

Figure 4–4 The internal and external appearances of the spinal cord vary at different levels. The proportion of gray matter (the H-shaped area within the spinal cord) to white matter is greater at sacral levels than at cervical levels. At sacral levels, very few incoming sensory axons have joined the spinal cord, whereas most of the motor axons have already terminated at higher levels of the spinal cord. The cross-sectional enlargements at the lumbar and cervical levels are regions where the large number of fibers innervating the limbs enter or leave the spinal cord.

are segregated according to the embryological somites from which muscles, bones, and other components of the body develop (Chapter 45). Axons projecting from the spinal cord to body structures that develop at the same segmental level join with axons entering the spinal cord in the intervertebral foramen to form spinal nerves. Spinal nerves at the cervical level are involved with sensory perception and motor function of the back of the head, neck, and arms; nerves at the thoracic level innervate the upper trunk; lumbar and sacral spinal nerves innervate the lower trunk, back, and legs.

Each of the four regions of the spinal cord contains multiple segments corresponding approximately to the different vertebrae in each region; there are 8 cervical segments, 12 thoracic segments, 5 lumbar segments, and 5 sacral segments. The actual substance of the mature spinal cord does not look segmented, but the segments of the four spinal regions are nonetheless defined by the number and location of the dorsal and ventral roots that enter or exit the spinal cord. The spinal cord varies in size and shape along its rostrocaudal axis because of two organizational features.

First, relatively few sensory axons enter the cord at the sacral level. The number of sensory axons entering the cord increases at progressively higher levels (lumbar, thoracic, and cervical). Conversely, most descending axons from the brain terminate at cervical levels, with progressively fewer descending to lower levels of the spinal cord. Thus, the number of fibers in the white matter is highest at cervical levels (where there are the highest numbers of both ascending and descending fibers) and lowest at sacral levels. As a result, sacral levels of the spinal cord have much less white matter than gray matter, whereas the cervical cord has more white matter than gray matter (Figure 4–4).

The second organizational feature is variation in the size of the ventral and dorsal horns. The ventral horn is larger at the levels where the motor nerves innervate the arms and legs. The number of ventral motor neurons dedicated to a body region roughly parallels the dexterity of movements of that region. Thus, a larger number of motor neurons is needed to innervate the greater number of muscles and to regulate the greater complexity of movement in the limbs as compared with the trunk. Likewise, the dorsal horn is larger where sensory nerves from the limbs enter the cord. Limbs have a greater density of sensory receptors to mediate finer tactile discrimination and thus send more sensory fibers to the cord. These regions of the cord are known as the lumbosacral and cervical enlargements (Figure 4–4).

The Primary Sensory Neurons of the Trunk and Limbs Are Clustered in the Dorsal Root Ganglia

The sensory neurons that convey information from the skin, muscles, and joints of the limbs and trunk to the spinal cord are clustered together in dorsal root ganglia within the vertebral column, immediately adjacent to the spinal cord (Figure 4–5). These neurons are pseudo-unipolar in shape; they have a bifurcated axon with central and peripheral branches. The peripheral branch innervates the skin, muscle, or other tissue as a free nerve ending or in association with specialized receptors for sensing touch, proprioception (stretch receptors), pain, and temperature.

The somatosensory system and its pathways from receptors to perception are more fully described in Chapters 17 to 20. Suffice it to say at this point that there are essentially two somatosensory pathways from the periphery that carry either touch and stretch (epicritic system) or pain and temperature (protopathic system). Epicritic fibers travel in the posterior column–medial lemniscal system (Figure 4–6). The centrally directed axons from neurons in the dorsal root ganglion ascend in the dorsal (or posterior) column white matter and terminate in the gracile nucleus or cuneate nucleus of the medulla. The centrally directed axons of the pain and temperature pathway form the spinothalamic

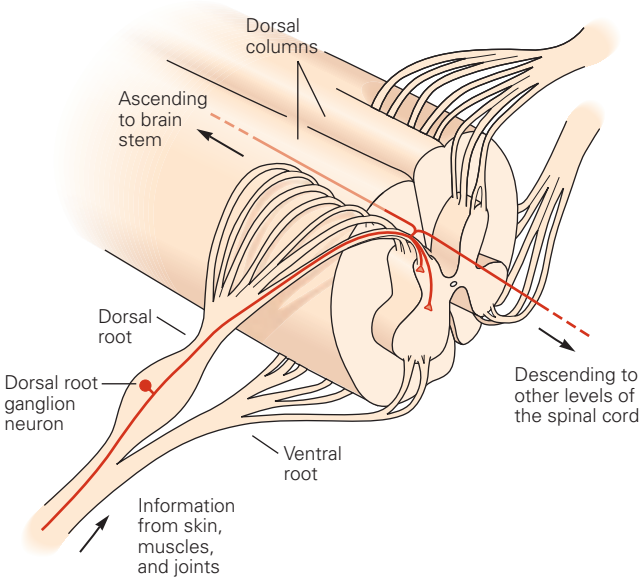

Figure 4–5 Dorsal root ganglia and spinal nerve roots. The cell bodies of neurons that bring sensory information from the skin, muscles, and joints lie in the dorsal root ganglia, clusters of cells that lie adjacent to the spinal cord. The axons of these neurons are bifurcated into peripheral and central branches. The central branch enters the dorsal portion of the spinal cord.

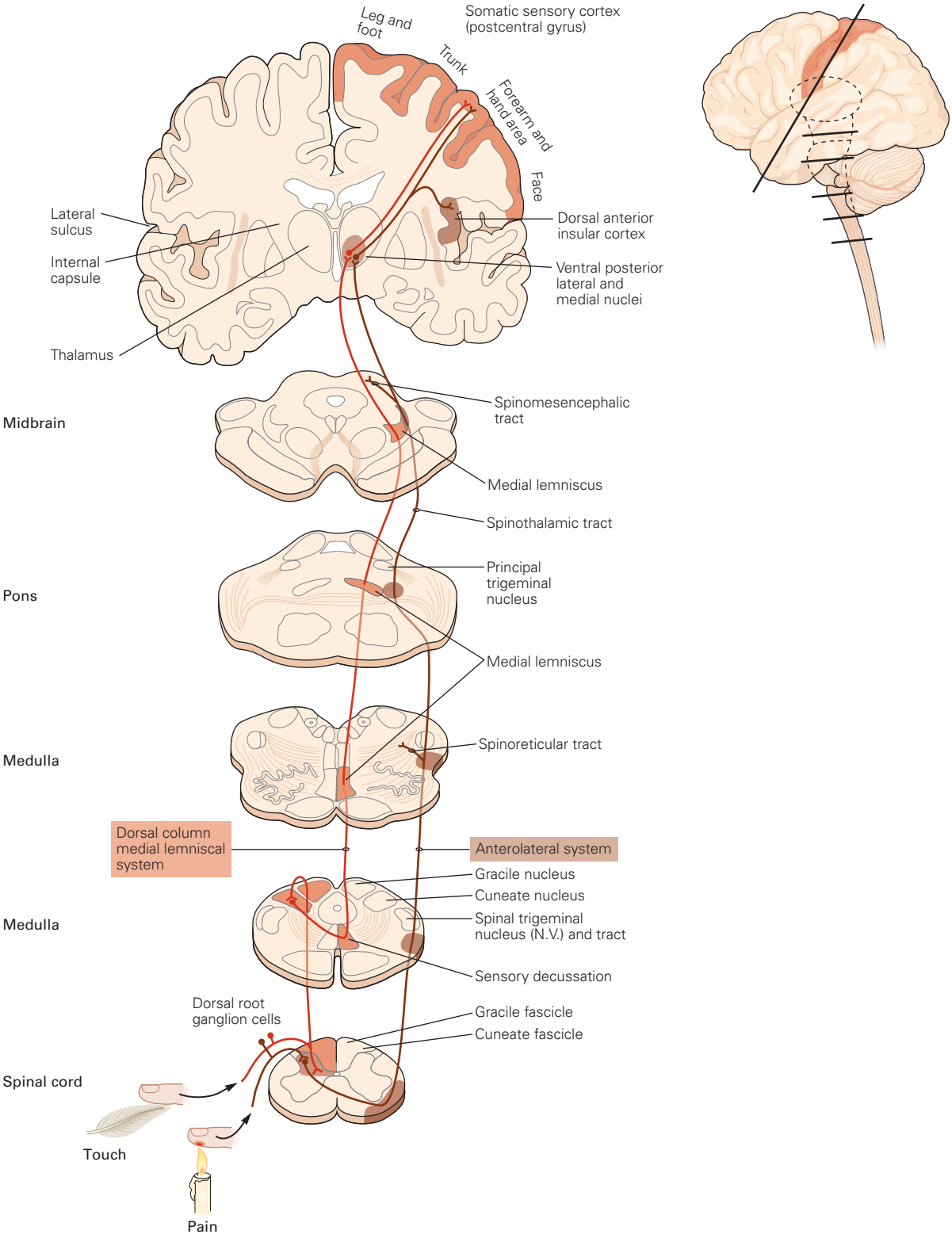
Somatic sensory cortex (postcentral gyrus)
Leg and foot
Trunk
Forearm and hand area
Face
Lateral sulcus
Internal capsule
Thalamus
Dorsal anterior insular cortex
Ventral posterior lateral and medial nuclei
Midbrain
Spinomesencephalic tract
Medial lemniscus
Spinothalamic tract
Pons
Principal trigeminal nucleus
Medial lemniscus
Medulla
Spinoreticular tract
Dorsal column medial lemniscal system
Anterolateral system
Medulla
Gracile nucleus
Cuneate nucleus
Spinal trigeminal nucleus (N.V.) and tract
Sensory decussation
Dorsal root ganglion cells
Gracile fascicle
Cuneate fascicle
Spinal cord
Touch
Pain

pathway. They terminate within the gray matter of the dorsal horn of the spinal cord. Second-order neurons cross to the other side of the spinal cord and ascend in the anterior and lateral spinothalamic tracts (Figure 4–6). Both pathways ultimately terminate in the thalamus, which sends projections to the primary somatosensory area of the cerebral cortex. In the next section, we focus on the epicritic system.

The local and ascending branches from touch and proprioceptive sensory neurons provide two functional pathways for somatosensory information entering the spinal cord from dorsal root ganglion cells. The local branches can activate local reflex circuits that modulate motor output, while the ascending branches carry information into the brain, where this information is further processed in the thalamus and cerebral cortex.

The Terminals of Central Axons of Dorsal Root Ganglion Neurons in the Spinal Cord Produce a Map of the Body Surface

The manner in which the central axons of the dorsal root ganglion cells terminate in the spinal cord forms a neural map of the body surface. This orderly somatotopic distribution of inputs from different portions of the body surface is maintained throughout the entire ascending somatosensory pathway. This arrangement illustrates another important principle of neural organization. Neurons that make up neural circuits at any particular level are often connected in a systematic fashion and appear similar from individual to individual. Similarly, fiber bundles that connect different processing regions at different levels of the nervous system are also arranged in a highly organized and stereotypical fashion.

Axons that enter the cord in the sacral region ascend in the dorsal column near the midline, whereas those that enter at successively higher levels ascend at progressively more lateral positions within the dorsal columns. Thus, in the cervical cord, where axons from all portions of the body have already entered, sensory fibers from the lower body are located medially in the dorsal column, while fibers from the trunk, arm and shoulder, and finally the neck occupy progressively more lateral areas. In the cervical spinal cord, the axons forming the dorsal columns are divided into two bundles: a medially situated gracile fascicle and a more laterally situated cuneate fascicle (Figure 4–1).

Each Somatic Submodality Is Processed in a Distinct Subsystem From the Periphery to the Brain

The submodalities of somatic sensation—touch, pain, temperature, and position sense—are processed in the brain through different pathways that end in different brain regions. We illustrate the specificity of these parallel pathways by the path of information for the submodality of touch.

The primary afferent fibers that carry information about touch enter the ipsilateral dorsal column and ascend to the medulla. Fibers from the lower body run in the gracile fascicle and terminate in the gracile nucleus, whereas fibers from the upper body run in the cuneate fascicle and terminate in the cuneate nucleus. Neurons in the gracile and cuneate nuclei give rise to axons that cross to the other side of the brain and ascend to the thalamus in a long fiber bundle called the medial lemniscus (Figure 4–1).

As in the dorsal columns of the spinal cord, the fibers of the medial lemniscus are arranged somatotopically. Because the fibers carrying sensory information

Figure 4–6 (Opposite) Somatosensory information from the limbs and trunk is conveyed to the thalamus and cerebral cortex by two ascending pathways. Brain slices along the neuraxis from the spinal cord to the cerebrum illustrate the anatomy of the two principal pathways conveying somatosensory information to the cerebral cortex. The two pathways are separated until they reach the pons, where they are juxtaposed.

Dorsal column–medial lemniscal system (**orange**). Touch and limb proprioception signals are conveyed to the spinal cord and brain stem by large-diameter myelinated nerve fibers and transmitted to the thalamus in this system. In the spinal cord, the fibers for touch and proprioception divide, one branch going to the ipsilateral spinal gray matter and the other ascending in the ipsilateral dorsal column to the medulla. The second-order fibers from neurons in the dorsal column nuclei cross the midline in the medulla and ascend in the contralateral medial lemniscus toward the thalamus, where they terminate in the lateral and medial ventral posterior nuclei. Thalamic neurons in these nuclei convey tactile and proprioceptive information to the primary somatosensory cortex.

Anterolateral system (**brown**). Pain, itch, temperature, and visceral information is conveyed to the spinal cord by small-diameter myelinated and unmyelinated fibers that terminate in the ipsilateral dorsal horn. This information is conveyed across the midline by neurons within the spinal cord and transmitted to the brain stem and the thalamus in the contralateral anterolateral system. Anterolateral fibers terminating in the brain stem compose the spinoreticular and spinomesencephalic tracts; the remaining anterolateral fibers form the spinothalamic tract.

cross the midline to the other side of the brain, the right side of the brain receives sensory information from the left side of the body, and vice versa. The fibers of the medial lemniscus end in a specific subdivision of the thalamus called the ventral posterior lateral nucleus (Figure 4–1). There the fibers maintain their somatotopic organization such that those carrying information from the lower body end laterally and those carrying information from the upper body end medially.

The Thalamus Is an Essential Link Between Sensory Receptors and the Cerebral Cortex

The thalamus is an egg-shaped structure that constitutes the dorsal portion of the diencephalon. It contains a class of excitatory neurons called thalamic relay cells that convey sensory input to the primary sensory areas of the cerebral cortex. However, the thalamus is not merely a relay. It acts as a gatekeeper for information to the cerebral cortex, preventing or enhancing the passage of specific information depending on the behavioral state of the organism.

The cerebral cortex has feedback projections that terminate, in part, in a special portion of the thalamus called the thalamic reticular nucleus. This nucleus forms a thin sheet around the thalamus and is made up almost totally of inhibitory neurons that synapse onto the relay cells. It does not project to the neocortex at all. In addition to receiving feedback projections from the neocortex, the reticular nucleus receives input from axons leaving the thalamus en route to the neocortex, enabling the thalamus to modulate the response of its relay cells to incoming sensory information.

The thalamus is a good example of a brain region made up of several well-defined nuclei. As many as 50 thalamic nuclei have been identified (Figure 4–7). Some nuclei receive information specific to a sensory modality and project to a specific area of the neocortex. For example, cells in the ventral posterior lateral nucleus (where the medial lemniscus terminates) process somatosensory information, and their axons project to the primary somatosensory cortex (Figures 4–1 and 4–7). Projections from the retinal ganglion cells terminate in another portion of the thalamus called the lateral geniculate nucleus (Figure 4–7). Neurons in this nucleus project in turn to the visual cortex. Other portions of the thalamus participate in motor functions, transmitting information from the cerebellum and basal ganglia to the motor regions of the frontal lobe. Axons from cells of the thalamus that project to the neocortex travel in the corona radiata, a large

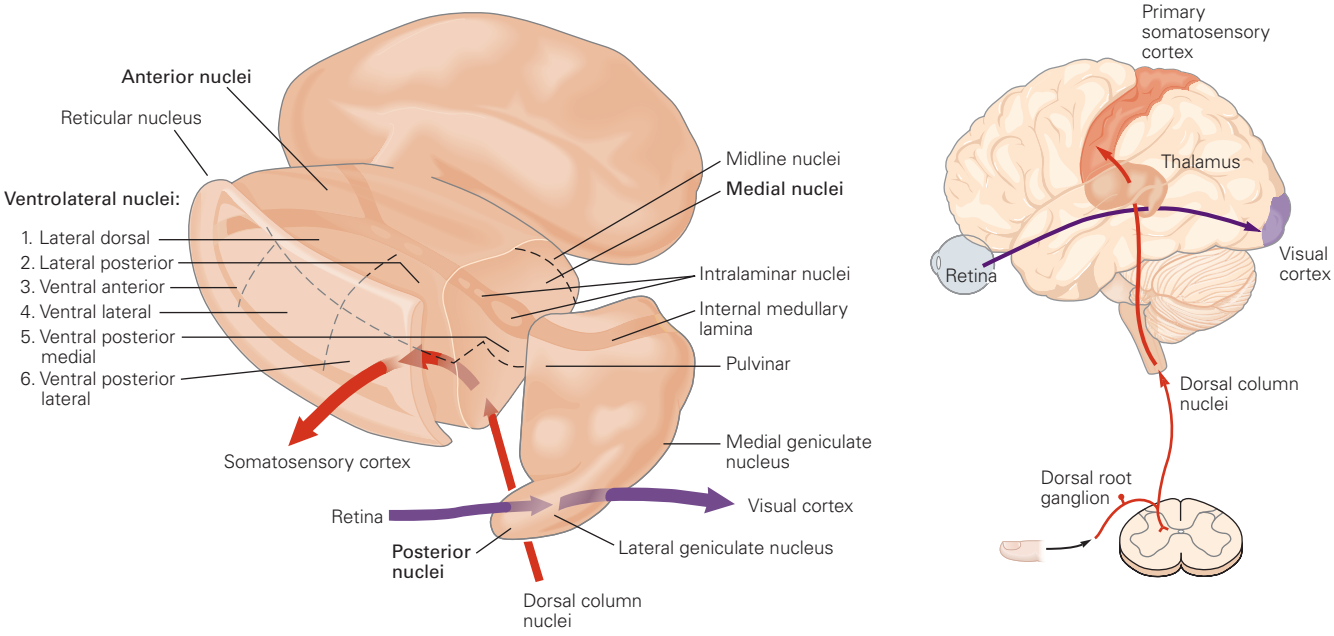

Figure 4–7 **The major subdivisions of the thalamus.** The thalamus is the critical relay for the flow of sensory information from peripheral receptors to the neocortex. Somatosensory information is conveyed from dorsal root ganglia to the ventral posterior lateral nucleus and from there to the primary somatosensory cortex. Likewise, visual information from the retina reaches the lateral geniculate nucleus, from which it is conveyed to the primary visual cortex in the occipital lobe. Each of the sensory systems, except olfaction, has a similar processing step within a distinct region of the thalamus.

fiber bundle that carries most of the axons running to and from the cerebral hemispheres. Through its connections with the frontal lobe and hippocampus, the thalamus may play a role in cognitive functions, such as memory. Some nuclei that may play a role in attention project diffusely to large but distinctly different regions of cortex.

The nuclei of the thalamus are most commonly classified into four groups—anterior, medial, ventrolateral, and posterior—with respect to the internal medullary lamina, a sheet-like bundle of fibers that runs the rostrocaudal length of the thalamus (Figure 4–7). Thus, the medial group of nuclei is located medial to the internal medullary lamina, whereas the ventrolateral and posterior groups are located lateral to it. At the rostral pole of the thalamus, the internal medullary lamina splits and surrounds the anterior group. The caudal pole of the thalamus is occupied by the posterior group, dominated by the pulvinar nucleus. Groups of neurons are also located within the fibers of the internal medullary lamina and are collectively referred to as the intralaminar nuclei.

The *anterior group* receives its major input from the mammillary nuclei of the hypothalamus and from the presubiculum of the hippocampal formation. The role of the anterior group is uncertain, but because of its connections, it is thought to be related to memory and emotion. The anterior group is mainly interconnected with regions of the cingulate and frontal cortices.

The *medial group* consists mainly of the mediodorsal nucleus. This large thalamic nucleus has three subdivisions, each of which is connected to a particular portion of the frontal cortex. The nucleus receives inputs from portions of the basal ganglia, the amygdala, and midbrain and has been implicated in memory and emotional processing.

The nuclei of the *ventrolateral group* are named according to their positions within the thalamus. The ventral anterior and ventral lateral nuclei are important for motor control and carry information from the basal ganglia and cerebellum to the motor cortex. The ventral posterior nuclei convey somatosensory information to the neocortex. The ventroposterior lateral nucleus conveys information from the spinal cord tracts, as described earlier. The ventroposterior medial nucleus conveys information from the face, which enters the brain stem mainly through the trigeminal nerve (cranial nerve V).

The *posterior group* includes the medial and lateral geniculate nuclei, the lateral posterior nucleus, and the pulvinar. The medial geniculate nucleus is a component of the auditory system and is organized tonotopically based on the sound frequency information carried by its inputs; it conveys auditory information to the primary auditory cortex in the superior temporal gyrus of the temporal lobe. The lateral geniculate nucleus receives information from the retina and conveys it to the primary visual cortex in the occipital lobe. Compared to rodents, the pulvinar is enlarged disproportionately in the primate brain, especially in the human brain, and its development seems to parallel the enlargement of the association regions of the parietal, occipital, and temporal cortices. It has been divided into at least three subdivisions and is extensively interconnected with widespread regions of the parietal, temporal, and occipital lobes, as well as with the superior colliculus and other nuclei of the brain stem related to vision.

As noted previously, the thalamus not only projects to the neocortex (feedforward connections) but also receives extensive return inputs back from the neocortex (feedback connections). For example, in the lateral geniculate nucleus, the number of synapses formed by axons from the feedback projection from the visual cortex is actually greater than the number of synapses that the lateral geniculate nucleus receives from the retina! This feedback is thought to play an important modulatory role in the processing of sensory information, although the exact function is not yet understood. Although this feedback is mainly from cortical neurons that are activated by both eyes, the neurons in the lateral geniculate nucleus are responsive to only one or the other eye. The implication is that they are primarily driven by input from the retina (which is from different eyes in different layers), not the feedback from the cortex, despite its numerical advantage. Most nuclei of the thalamus receive a similarly prominent return projection from the cerebral cortex, and the significance of these projections is one of the unsolved mysteries of neuroscience.

The thalamic nuclei described thus far are called the *relay* (or *specific*) *nuclei* because they have a specific and selective relationship with a particular portion of the neocortex. Other thalamic nuclei, called *nonspecific nuclei*, project to several cortical and subcortical regions. These nuclei are located either on the midline of the thalamus (the midline nuclei) or within the internal medullary lamina (the intralaminar nuclei). The largest of the midline nuclei are the paraventricular, paratenial, and reuniens nuclei; the largest of the intralaminar cell groups is the centromedian nucleus. The intralaminar nuclei project to medial temporal lobe structures, such as the amygdala and hippocampus, but also send projections to portions of the basal ganglia. These nuclei receive inputs from a variety of sources in the spinal cord, brain stem, and cerebellum and are thought to mediate cortical arousal.

The thalamus is an important step in the hierarchy of sensory processing, not a passive relay station where information is simply passed on to the neocortex. It is a complex brain region where substantial information processing takes place (Figure 4–1). To give but one example, the output of somatosensory information from the ventral posterior lateral nucleus is subject to four types of processing: (1) local processing within the nucleus; (2) modulation by brain stem inputs, such as from the noradrenergic and serotonergic systems; (3) inhibitory input from the reticular nucleus; and (4) modulatory feedback from the neocortex.

Sensory Information Processing Culminates in the Cerebral Cortex

Somatosensory information from the ventral posterior lateral nucleus is conveyed mainly to the primary somatosensory cortex (Figure 4–1). The neurons here are exquisitely sensitive to tactile stimulation of the skin surface. The somatosensory cortex, like earlier stages in tactile sensory processing, is somatotopically organized (Figure 4–8).

When the neurosurgeon Wilder Penfield stimulated the surface of the somatosensory cortex in patients undergoing brain surgery in the late 1940s and early 1950s, he found that sensation from the lower limbs is mediated by neurons located near the midline of the brain, whereas sensations from the upper body, hands and fingers, face, lips, and tongue are mediated by neurons located laterally. Penfield found that, although all parts of the body are represented in the cortex somatotopically, the amount of surface area of cortex devoted to each body part is not proportional to its mass. Instead, it is proportional to the fineness of discrimination in the body part, which in turn is related to the density of innervation of sensory fibers (Chapter 19). Thus, the area of cortex devoted to the fingers is larger than that for the arms. Likewise, the representation of the lips and tongue occupies more cortical surface than that of the remainder of the face (Figure 4–8). As we shall see in Chapter 53, the amount of cortex devoted to a particular body part is not fixed but can be modified by experience, as seen in concert violinists, where there is an expansion of the region of somatosensory cortex devoted to the fingers of the hand used to finger the strings. This illustrates

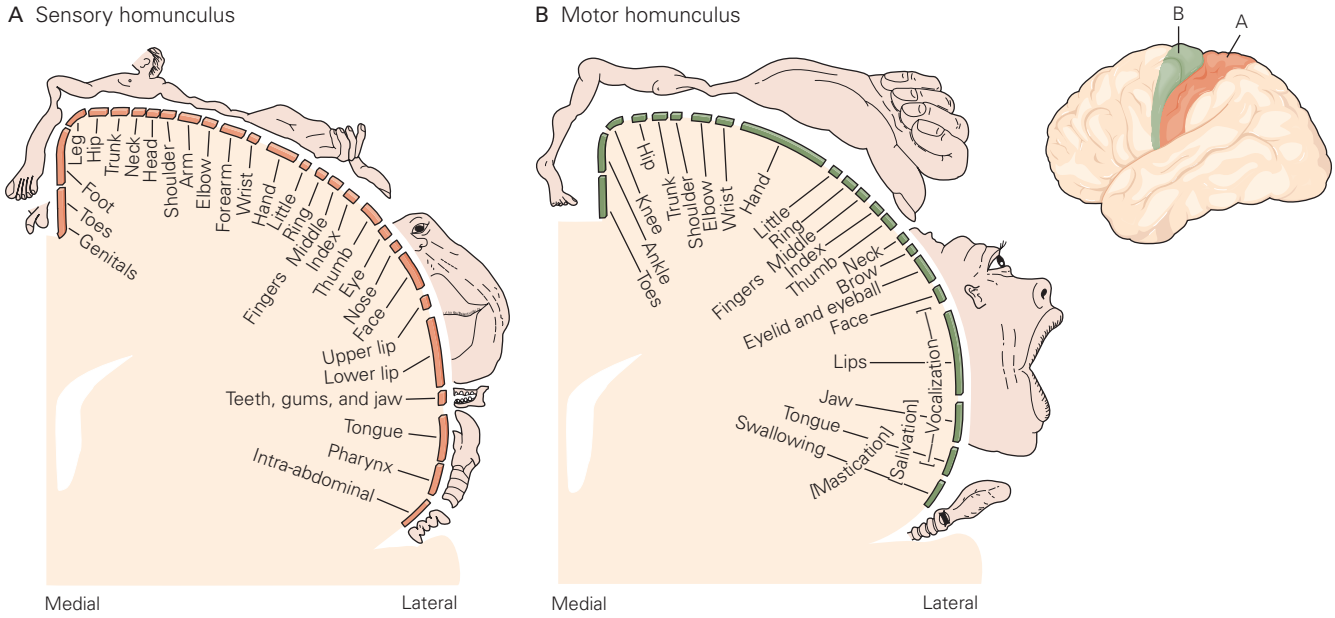

Figure 4–8 Homunculi illustrate the relative amounts of cortical area dedicated to sensory and motor innervation of individual parts of the body. The entire body surface is represented in an orderly array of somatosensory inputs in the cortex. (From Penfield and Rasmussen 1950. Reproduced by permission of the Osler Library of the History of Medicine, McGill University.)

A. The area of cortex dedicated to processing sensory information from a particular part of the body is not proportional to the mass of the body part but instead reflects the density of sensory receptors in that part. Thus, sensory input from the lips and hands occupies more area of cortex than, say, that from the elbow.

B. Output from the motor cortex is organized in similar fashion. The amount of cortical surface dedicated to a part of the body is related to the degree of motor control of that part. Thus, in humans, much of the motor cortex is dedicated to controlling the muscles of the fingers and the muscles related to speech.

an important aspect of brain circuitry: It is capable of plastic changes in response to use or disuse. Such changes are important for various forms of learning, including the ability to recover function after a stroke.

The region of cerebral cortex nearest the surface of the brain is organized in layers and columns, an arrangement that increases its computational efficiency. The cortex has undergone dramatic expansion in evolution. The more recent neocortex comprises most of the cortex of mammals. In larger brains of primates and cetaceans, the neocortical surface is a sheet that is folded with deep wrinkles, thus allowing for three times more cortical surface to be packed into an only modestly enlarged head. Indeed, approximately two-thirds of the neocortex is along the deep wrinkles of the cortex, termed sulci. The remainder of neocortex is at the external folds of the sheet, termed gyri. The neocortex receives inputs from the thalamus, other cortical regions on both sides of the brain, and other subcortical structures. Its output is directed to other regions of the cortex, basal ganglia, thalamus, pontine nuclei, and spinal cord.

These complex input–output relationships are efficiently organized in the orderly layering of cortical neurons; each layer contains different inputs and outputs. Many regions of the neocortex, in particular the primary sensory areas, contain six layers, numbered from the outer surface of the brain to the white matter (Figure 4–9).

Layer I, the molecular layer, is occupied by the dendrites of cells located in deeper layers and axons that travel through this layer to make connections in other areas of the cortex.

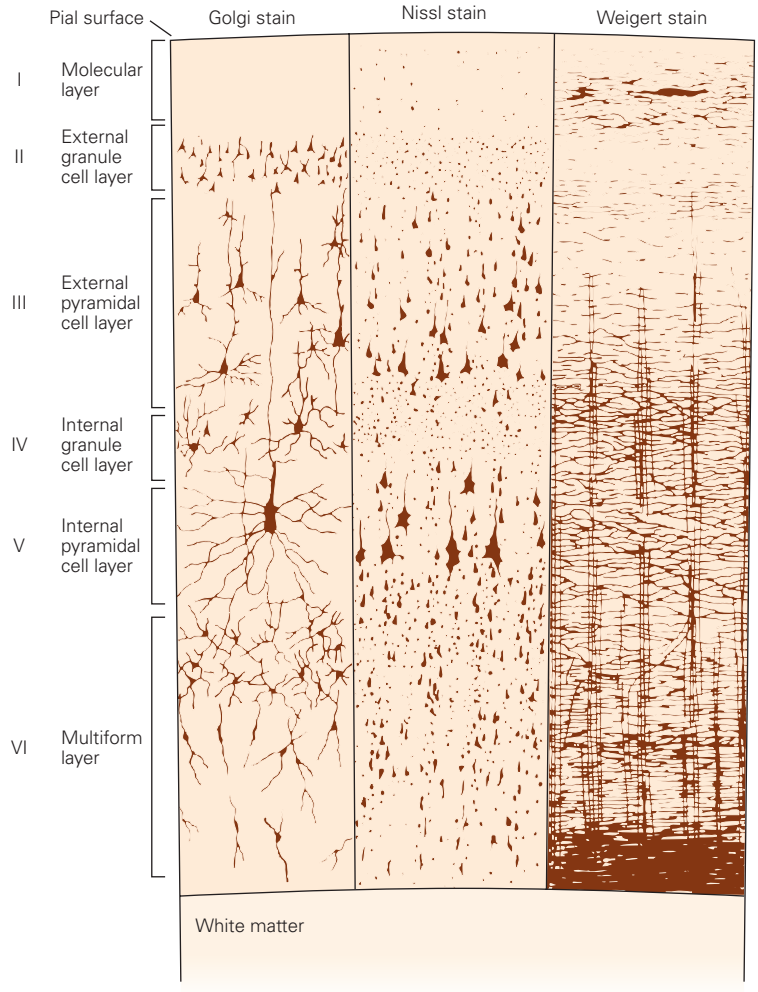

Figure 4–9 **The neurons of the neocortex are arranged in distinctive layers.** The appearance of the neocortex depends on what is used to stain it. The Golgi stain (*left*) reveals a subset of neuronal cell bodies, axons, and dendritic trees. The Nissl method (*middle*) shows cell bodies and proximal dendrites. The Weigert stain (*right*) reveals the pattern of myelinated fibers. (Reproduced, with permission, from Heimer 1994.)

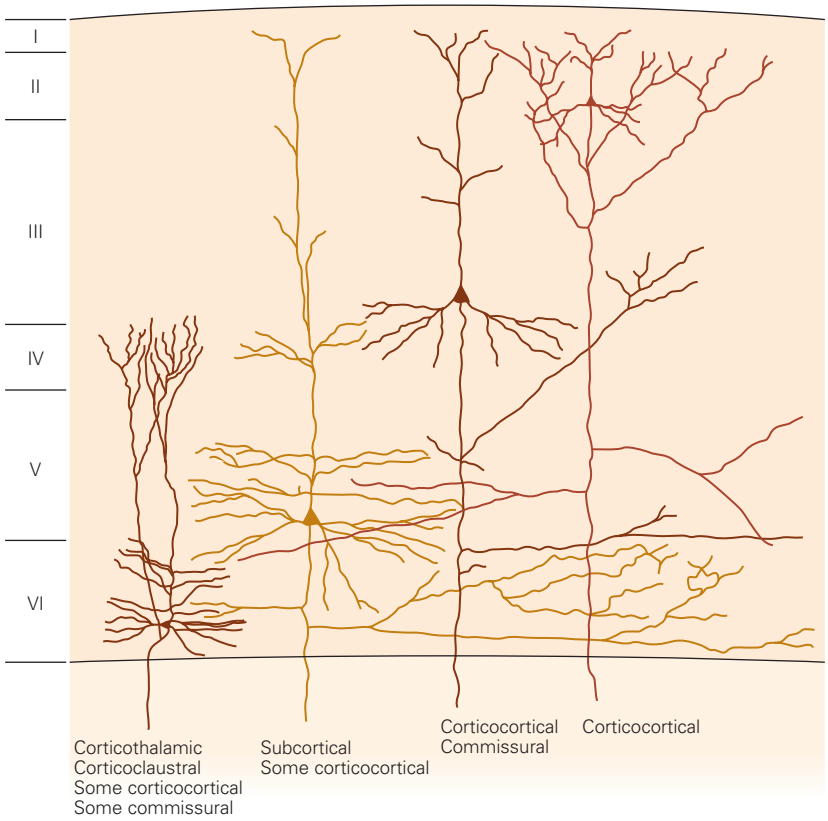

Figure 4–10 Neurons in different layers of neocortex project to different parts of the brain. Projections to all other parts of the neocortex, the so-called corticocortical or associational connections, arise primarily from neurons in layers II and III. Projections to subcortical regions arise mainly from layers V and VI. (Reproduced, with permission, from Jones 1986.)

Layers II and III contain mainly small pyramidal shaped cells. Layer II, the external granular cell layer, is one of two layers that contain small spherical neurons. Layer III is called the external pyramidal cell layer (an internal pyramidal cell layer lies at a deeper level). The neurons located deeper in layer III are typically larger than those located more superficially. The axons of pyramidal neurons in layers II and III project locally to other neurons within the same cortical area as well as to other cortical areas, thereby mediating intracortical communication (Figure 4–10).

Layer IV contains a large number of small spherical neurons and thus is called the internal granular cell layer. It is the main recipient of sensory input from the thalamus and is most prominent in primary sensory areas. For example, the region of the occipital cortex that functions as the primary visual cortex has an extremely prominent layer IV. Layer IV in this region is so heavily populated by neurons and so complex that it is typically divided into three sublayers. Areas with a prominent layer IV are called granular cortex. In contrast, the precentral gyrus, the site of the primary motor cortex, has essentially no layer IV and is thus part of the so-called agranular frontal cortex. These two cortical areas are among the easiest to identify in histological sections (Figure 4–11).

Layer V, the internal pyramidal cell layer, contains mainly pyramidally shaped cells that are typically larger than those in layer III. Pyramidal neurons in this layer give rise to the major output pathways of the cortex, projecting to other cortical areas and to subcortical structures (Figure 4–9).

The neurons in layer VI are fairly heterogeneous in shape, so this layer is called the polymorphic or multiform layer. It blends into the white matter that forms the deep limit of the cortex and carries axons to and from areas of cortex.

The thickness of individual layers and the details of their functional organization vary throughout the cortex. An early student of the cerebral cortex, Korbinian Brodmann, used the relative prominence of the layers above and below layer IV, cell size, and packing

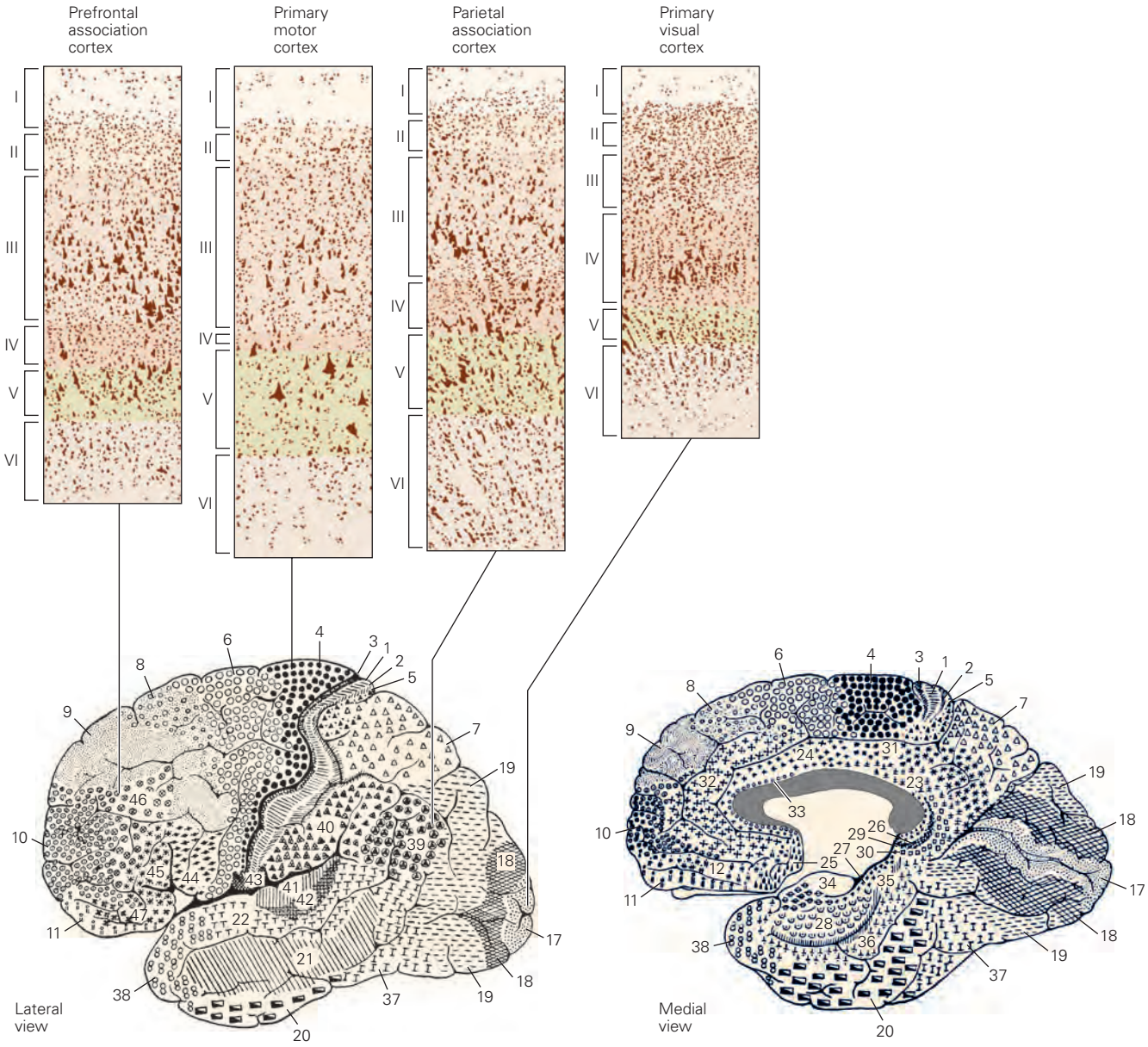

Figure 4–11 **The extent of each cell layer of the neocortex varies throughout the cortex.** Sensory areas of cortex, such as the primary visual cortex, tend to have a very prominent internal granular cell layer (layer IV), the site of sensory input. Motor areas of cortex, such as the primary motor cortex, have a very meager layer IV but prominent output layers, such as layer V. These differences led Korbinian Brodmann and others working at the turn of the 20th century to divide the cortex into various cytoarchitectonic regions. Brodmann's 1909 subdivision shown here is a classic analysis but was based on a single human brain. (Reproduced, with permission, from Martin 2012.)

characteristics to distinguish different areas of the neocortex. Based on such cytoarchitectonic differences, in 1909, Brodmann divided the cerebral cortex into 47 regions (Figure 4–11).

Although Brodmann's demarcation coincides in part with information on localized functions in the neocortex, the cytoarchitectonic method alone does not capture the subtlety or variety of function of all the distinct regions of the cortex. For example, Brodmann identified five regions (areas 17–21) as being concerned with visual function in the monkey. In contrast, modern connectional neuroanatomy and electrophysiology have identified more than 35 functionally distinct cortical regions within the five regions recognized by Brodmann.

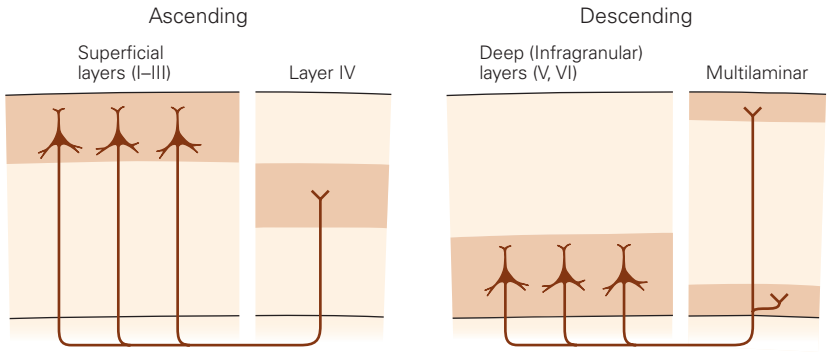

Figure 4–12 Ascending and descending cortical pathways are distinguished by the organization of their origins and terminations within the cortical layers. Ascending or feedforward pathways generally originate in superficial layers of the cortex and invariably terminate in layer IV. Descending or feedback pathways generally originate from deep layers and terminate in layers I and VI. (Adapted, with permission, from Felleman and Van Essen 1991.)

Within the neocortex, information passes from one synaptic relay to another using feedforward and feedback connections. In the visual system, for example, feedforward projections from the primary visual cortex to secondary and tertiary visual areas originate mainly in layer III and terminate mainly in layer IV of the target cortical area. In contrast, feedback projections to earlier stages of processing originate from cells in layers V and VI and terminate in layers I, II, and VI (Figure 4–12).

The cerebral cortex is organized functionally into columns of cells that extend from the white matter to the surface of the cortex. (This columnar organization is not particularly evident in standard histological preparations and was first discovered in electrophysiological studies.) Each column is about one-third of a millimeter in diameter. The cells in each column form a computational module with a highly specialized function. Neurons within a column tend to have very similar response properties, presumably because they form a local processing network. The larger the area of cortex dedicated to a function, the greater the number of computational columns that are dedicated to that function (Chapter 23). The highly discriminative sense of touch in the fingers is a result of many cortical columns in the large area of cortex dedicated to processing somatosensory information from the hand.

Beyond the identification of the cortical column, a second major insight from the early electrophysiological studies was that the somatosensory cortex contains not one but several somatotopic maps of the body surface. The primary somatosensory cortex (anterior parietal cortex) has four complete maps of the skin, one each in Brodmann areas 3a, 3b, 1, and 2. The thalamus sends, in parallel, a lot of deep receptor information (eg, from muscles) to area 3a and most of its cutaneous information to areas 3b and 1. Area 2 receives input from these thalamorecipient cortical areas and may be responsible for our integrated perception of three-dimensional solid objects, termed stereognosis. Neurons in the primary somatosensory cortex project to neurons in adjacent areas, and these neurons in turn project to other adjacent cortical regions (Figure 4–13). At higher levels in the hierarchy of cortical connections, somatosensory information is used in motor control, eye–hand coordination, and memory related to touch.

The cortical areas involved in the early stages of sensory processing are concerned primarily with a single sensory modality. Such regions are called primary sensory or unimodal (sensory) association areas. Information from the unimodal association areas converges on multimodal association areas of the cortex concerned with combining sensory modalities (Figure 4–13). These multimodal association areas, which are heavily interconnected with the hippocampus, appear to be particularly important for two functions: (1) the production of a unified percept and (2) the representation of the percept in memory (we will return to this at the end of this chapter).

Thus, from the mechanical pressure on a receptor in the skin to the perception that a finger has been touched by a friend shaking your hand, somatosensory information is processed in a series of increasingly more complex circuits (networks) from the dorsal root ganglia to the somatosensory cortex, to unimodal association areas, and finally to multimodal association areas. One of the primary purposes of somatosensory information is to guide directed movement. As one might imagine, there is a close linkage between the somatosensory and motor functions of the cortex.

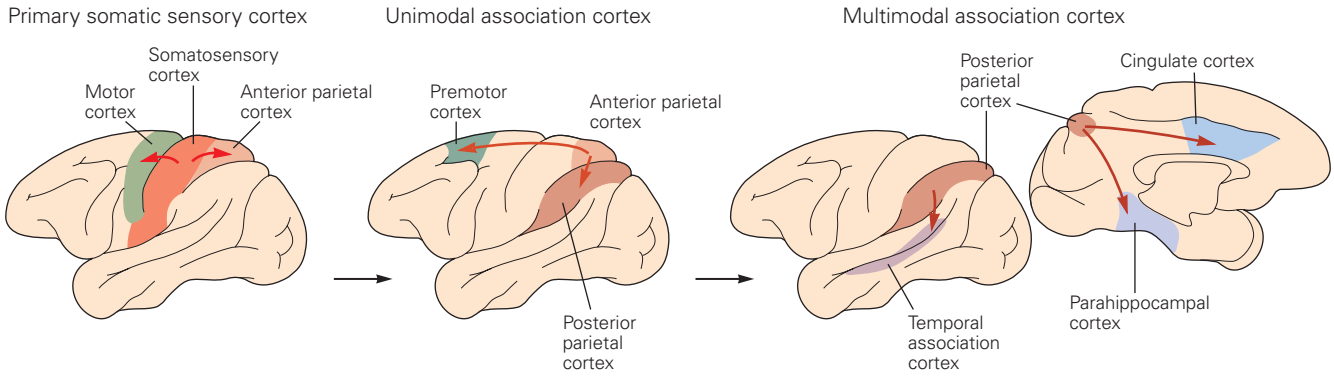

Figure 4–13 The processing of sensory information in the cerebral cortex begins with primary sensory areas, continues in unimodal association areas, and is further elaborated in multimodal association areas. Sensory systems also communicate with portions of the motor cortex. For example, the primary somatosensory cortex projects to the motor area in the frontal lobe and to the somatosensory association area in the parietal cortex. The somatosensory association area, in turn, projects to higher-order somatosensory association areas and to the premotor cortex. Information from different sensory systems converges in the multimodal association areas, which include the parahippocampal, temporal association, and cingulate cortices.

Voluntary Movement Is Mediated by Direct Connections Between the Cortex and Spinal Cord

As we shall see in Chapters 25 and 30, a major function of the perceptual systems is to provide the sensory information necessary for the actions mediated by the motor systems. The primary motor cortex is organized somatotopically like the somatosensory cortex (Figure 4–8B). Specific regions of the motor cortex influence the activity of specific muscle groups (Chapter 34).

The axons of neurons in layer V of the primary motor cortex provide the major output of the neocortex to control movement. Some layer V neurons influence movement directly through projections in the corticospinal tract to motor neurons in the ventral horn of the spinal cord. Others influence motor control by synapsing onto motor output nuclei in the medulla or onto striatal neurons in the basal ganglia. The human corticospinal tract consists of approximately one million axons, of which approximately 40% originate in the motor cortex. These axons descend through the subcortical white matter, the internal capsule, and the cerebral peduncle in the midbrain (Figure 4–14). In the medulla, the fibers form prominent protuberances on the ventral surface called the medullary pyramids, and thus the entire projection is sometimes called the pyramidal tract.

Like the ascending somatosensory system, the descending corticospinal tract crosses to the opposite side of the spinal cord. Most of the corticospinal fibers cross the midline in the medulla at a location known as the pyramidal decussation. However, approximately 10% of the fibers do not cross until they reach the level of the spinal cord at which they will terminate. The corticospinal fibers make monosynaptic connections with motor neurons, connections that are particularly important for individuated finger movements. They also form synapses with both excitatory and inhibitory interneurons in the spinal cord, connections that are important for coordinating larger groups of muscles in behaviors such as reaching and walking.

The motor information carried in the corticospinal tract is significantly modulated by both sensory information and information from other motor regions. A continuous stream of tactile, visual, and proprioceptive information is needed to make voluntary movement both accurate and properly sequenced. In addition, the output of the motor cortex is under the substantial influence of other motor regions of the brain, including the cerebellum and basal ganglia, structures that are essential for smoothly executed movements. These two subcortical regions, which are described in detail in Chapters 37 and 38, provide feedback essential for the smooth execution of skilled movements and thus are also important for the improvement in motor skills through practice (Figure 4–15).

Modulatory Systems in the Brain Influence Motivation, Emotion, and Memory

Some areas of the brain are neither purely sensory nor purely motor, but instead modulate specific sensory or motor functions. Modulatory systems are often involved in behaviors that respond to a primary need such as hunger, thirst, or sleep. For example, sensory

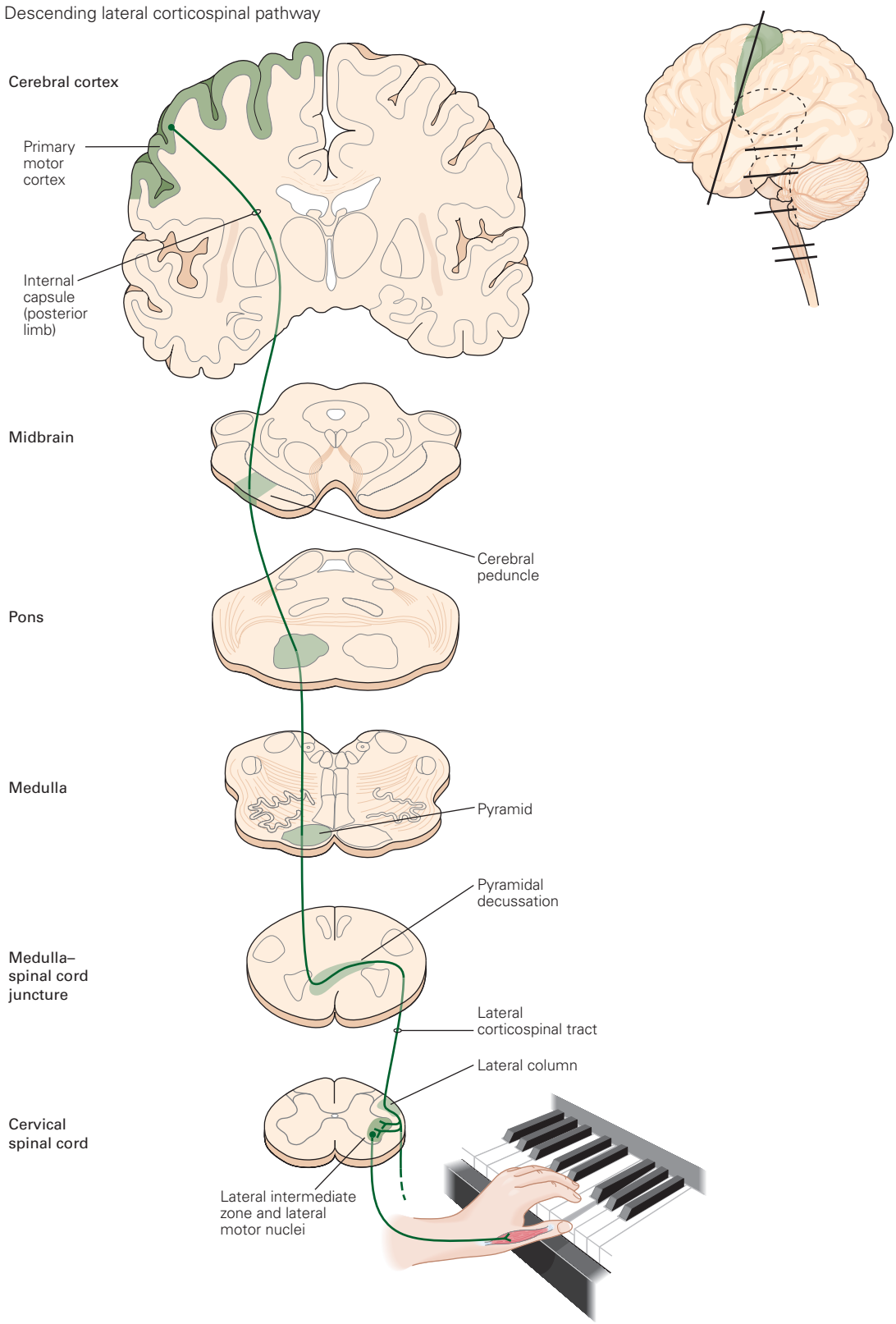

Figure 4–14 A significant number of fibers in the corticospinal tract originate in the primary motor cortex and terminate in the ventral horn of the spinal cord. The same axons are, at various points in their projections, part of the internal capsule, the cerebral peduncle, the medullary pyramid, and the lateral corticospinal tract.

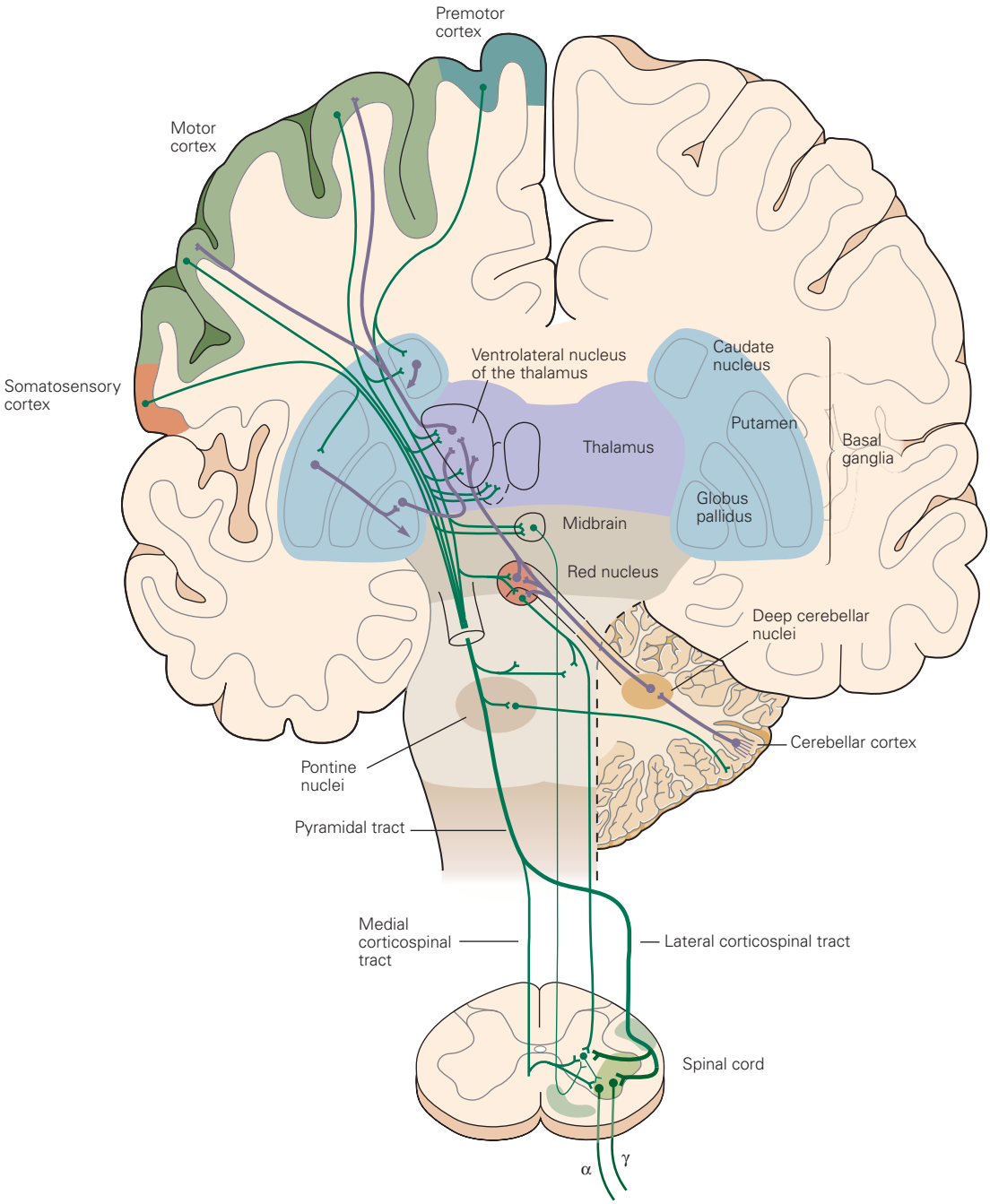

Figure 4–15 **Voluntary movement requires coordination of all components of the motor system.** The principal components are the motor cortex, basal ganglia, thalamus, midbrain, cerebellum, and spinal cord. The principal descending projections are shown in **green**; feedback projections and local connections are shown in **purple**. All of this processing is incorporated in the inputs to the motor neurons of the ventral horn of the spinal cord, the so-called "final common pathway" that innervates muscle and elicits movements. (This figure is a composite view made from sections of the brain taken at different angles.)

and modulatory systems in the hypothalamus determine blood glucose levels (Chapter 41). When blood sugar drops below a certain critical level, we feel hunger. To satisfy hunger, modulatory systems in the brain focus vision, hearing, and smell on stimuli that are relevant to feeding.

Distinct modulatory systems within the brain stem modulate attention and arousal (Chapter 40). Small

nuclei in the brain stem contain neurons that synthesize and release the modulatory neurotransmitter norepinephrine (the locus coeruleus) and serotonin (the dorsal raphe nucleus). Such neurons set the general arousal level of an animal through their widespread connections with forebrain structures. A group of cholinergic modulatory neurons, the basal nucleus of Meynert, is involved in arousal or attention (Chapter 40). This nucleus is located beneath the basal ganglia in the basal forebrain portion of the telencephalon. The axons of its neurons project to essentially all portions of the neocortex.

If a predator finds potential prey, a variety of cortical and subcortical systems determine whether the prey is edible. Once food is recognized, other cortical and subcortical systems initiate a comprehensive voluntary motor program to bring the animal into contact with the prey, capture it and place it in the mouth, and chew and swallow.

Finally, the physiological satisfaction the animal experiences in eating reinforces the behaviors that led to the successful predation. A group of dopaminergic neurons in the midbrain are important for monitoring reinforcements and rewards. The power of the dopaminergic modulatory systems has been demonstrated by experiments in which electrodes were implanted into the reward regions of rats and the animals were freely allowed to press a lever to electrically stimulate their brains. They preferred this self-stimulation to obtaining food or water, engaging in sexual behavior, or any other naturally rewarding activity. The role of the dopaminergic modulatory system in learning through reinforcement of exploratory behavior is described in Chapter 38.

How the brain's modulatory systems, concerned with reward, attention and motivation, interact with the sensory and motor systems is one of the most interesting questions in neuroscience, one that is also fundamental to our understanding of learning and memory storage (Chapter 40).

The Peripheral Nervous System Is Anatomically Distinct From the Central Nervous System

The peripheral nervous system supplies the central nervous system with a continuous stream of information about both the external environment and the internal environment of the body. It has somatic and autonomic divisions (Figure 4–16).

The *somatic division* includes the sensory neurons that receive information from the skin, muscles, and

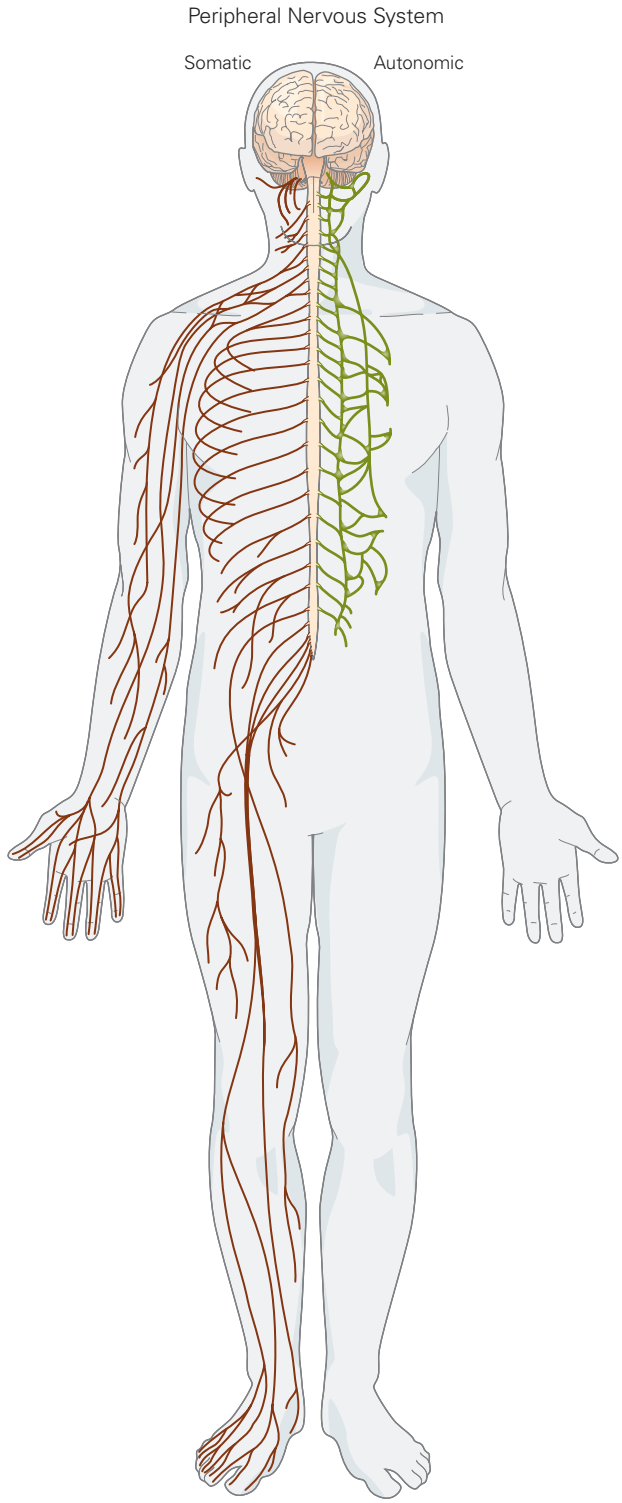

Figure 4–16 The peripheral nervous system has somatic and autonomic divisions. The somatic division carries information from the skin to the brain and from the brain to muscles. The autonomic division regulates involuntary functions, including activity of the heart and smooth muscles in the gut and glands.

joints. The cell bodies of these sensory neurons lie in the dorsal root ganglia and cranial ganglia. Receptors associated with these cells provide information about muscle and limb position and about touch and pressure at the body surface. In Part IV (Perception), we shall see how remarkably specialized these receptors are in transducing one or another type of physical energy (eg, deep pressure or heat) into the electrical signals used by the nervous system. In Part V (Movement), we shall see that sensory receptors in the muscles and joints are crucial to shaping coherent movement of the body.

The *autonomic division* of the peripheral nervous system mediates visceral sensation as well as motor control of the viscera, vascular system, and exocrine glands. It consists of the sympathetic, parasympathetic, and enteric systems. The sympathetic system participates in the body's response to stress, whereas the parasympathetic system acts to conserve body resources and restore homeostasis. The enteric nervous system, with neuronal cell bodies located in or adjacent to the viscera, controls the function of smooth muscle and secretions of the gut. The functional organization of the autonomic nervous system is described in Chapter 41 and its role in emotion and motivation in Chapter 42.

Memory Is a Complex Behavior Mediated by Structures Distinct From Those That Carry Out Sensation or Movement

Research over the past 50 years has provided a sophisticated view of memory systems in the brain. We now know that different forms of memory (eg, fear memory versus skill memory) are mediated by different brain regions. Here we contrast the organization of the system responsible for coding and storing our experiences of other individuals, places, facts, and episodes, a process called explicit memory.

We know that a structure called the hippocampus (or more properly the hippocampal formation, since it is several cortical regions) is a key component of a medial temporal lobe memory system that encodes and stores memories of our lives (Figure 4–17). This understanding is based largely on the analysis of the

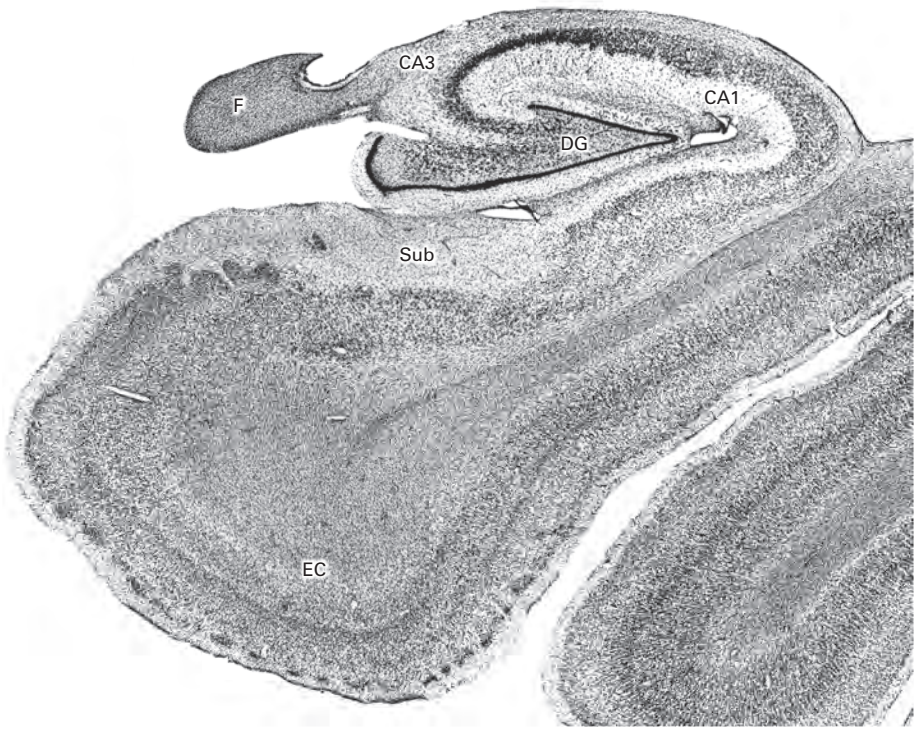

Figure 4–17 Coronal section of the human hippocampal formation stained by the Nissl methods to demonstrate cell bodies. The main cytoarchitectonic fields are shown in this section of the human hippocampal formation. (Abbreviations: **CA3** and **CA1**, subdivisions of the hippocampus; **DG**, dentate gyrus; **EC**, entorhinal cortex; **F**, fimbria; **Sub**, subiculum.)

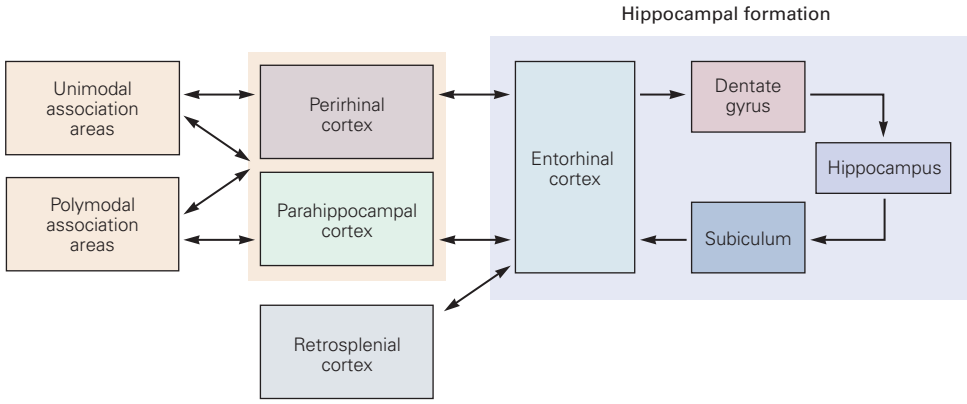

Figure 4–18 Hierarchical organization of connections to the hippocampal formation. The hippocampal formation receives highly processed sensory information, primarily through the entorhinal cortex, from multimodal association regions such as the perirhinal, parahippocampal, and retrosplenial cortices.

famous patient Henry Molaison (referred to as HM by the scientists who studied him during his life), who in the early 1950s had bilateral temporal lobe surgery to reduce his life-threatening epilepsy. In contrast to the six-layered neocortex, the hippocampus, along with olfactory cortex (piriform cortex), is a three-layered cortical structure referred to as archicortex, one of the phylogenetically older areas of cortex.

The reason we briefly describe the hippocampal formation in this chapter is to emphasize that not all brain circuits are alike. In fact, whether one talks about the olfactory bulb, where the sense of smell begins to be processed, or the cerebellum, where fine motor movements are refined, the general principle is that the structure of a circuit is specific to the function that it mediates. And the hippocampal circuit is as different from the circuits that mediate sensory perception or motor movement as one could imagine. Hippocampal circuitry of the brain will be dealt with in much more detail in later chapters. Chapter 5 introduces the idea that the hippocampus encodes information about an animal's spatial location in its environment and that the encoding of explicit memory (including spatial memory) requires plastic changes in synaptic function. Chapters 52 and 54 explore human memory function and the cellular and molecular bases of explicit memory and spatial representation, respectively.

The Hippocampal System Is Interconnected With the Highest-Level Polysensory Cortical Regions

Sensory systems are hierarchical and process progressively more complex stimuli at higher levels, particularly of the neocortex. Moreover, from the highest levels of each modality, circuits connect with polysensory cortical regions located at various places around the cortex, where information from many sensory modalities converges onto single neurons. The hippocampal system receives most of its input, the raw material with which it makes memories, from a few specific polysensory regions. These include the perirhinal and parahippocampal cortices, located in the medial temporal lobe, as well as the retrosplenial cortex, located in the caudal portion of the cingulate gyrus. These polysensory regions converge on the entry structure to the hippocampal system, the entorhinal cortex (Figure 4–18). The polysensory information that enters the entorhinal cortex can be thought of as providing summaries of immediate experience.

The Hippocampal Formation Comprises Several Different but Highly Integrated Circuits

The hippocampal formation is made up of a number of distinct cortical regions that are simpler in organization than the neocortex—at least they have fewer layers. The regions include the dentate gyrus, hippocampus, subiculum, and entorhinal cortex. Each of these regions is made up of subregions containing many neuronal cell types. The simplest subregion of the hippocampal formation is the dentate gyrus, which has a single principal neuron called the granule cell. The subregions of the hippocampus termed CA1, CA2, and CA3, consist of a single layer of pyramidal cells whose dendrites extend above and below the cell body layer and receive inputs from several regions. The subiculum (divided into subiculum, presubiculum and parasubiculum) is another region made up largely of pyramidal cells. Finally, the most complex part of the hippocampal formation is the entorhinal cortex, which has multiple layers but still has an organization distinctly different from the neocortex. For example, it lacks a layer IV and has a much more prominent layer II.

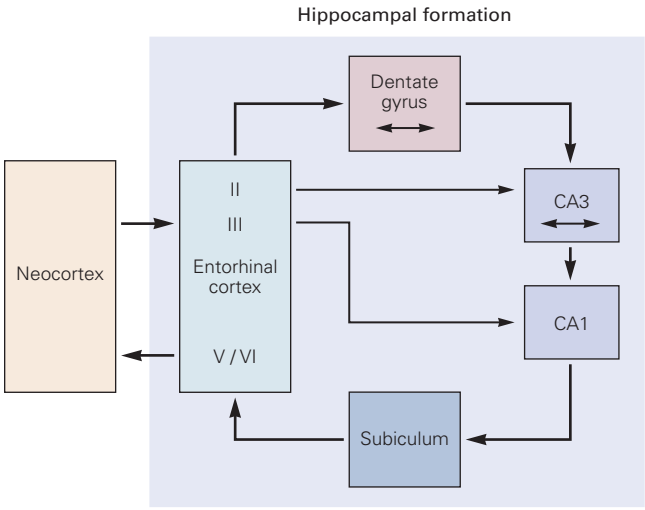

Figure 4–19 Simplified diagram on internal connections within the hippocampal formation. The circuit begins from cells in layer II of the entorhinal cortex to the dentate gyrus, which then projects to the CA3 region of the hippocampus. The CA3 portion of the hippocampus projects to CA1, and CA1 then projects to the subiculum. The hippocampal circuit is closed when the subiculum projects to the deep layers of the entorhinal cortex. Not shown are the feedback pathways from entorhinal cortex to the same multimodal areas from which it receives sensory information.

The Hippocampal Formation Is Made Up Mainly of Unidirectional Connections

Here we describe the fundamental circuitry of the hippocampal formation. The circuitry is described in more detail in Chapter 54. The simplified version of the hippocampal circuit shown in Figure 4–19 emphasizes its stepwise serial processing of multimodal sensory information, with each hippocampal region contributing to the formation of explicit memories. This serial processing implies that damage to any one of the components of this system would lead to memory impairment. And, in fact, another famous patient, known by the initials R.B., did suffer profound memory impairment due to loss of cells in the CA1 region after an ischemic episode.

As it turns out, while the hippocampal formation is essential for the initial formation of memories of our lives, these memories are ultimately stored elsewhere in the brain. In patients such as HM, in whom the entorhinal cortex and much of the rest of the hippocampal system was removed, memories prior to the surgery were largely intact. Thus, to achieve creation and long-term storage of the memories of our lives, the hippocampus and entorhinal cortex must communicate with circuits in the cerebral cortex. Where and precisely how that happens remain a mystery.

Highlights

1. Individual neurons are not able to carry out behavior. They must be incorporated into circuits that comprise different types of neurons that are interconnected by excitatory, inhibitory, and modulatory connections.
2. Sensory and motor information is processed in the brain in a variety of discrete brain regions that are active simultaneously.
3. A functional pathway is formed by the serial connection of identifiable brain regions, and each brain region's circuits process more complex or specific information than the preceding brain region.
4. The sensations of touch and pain are mediated by pathways that run between different circuits in the spinal cord, brain stem, thalamus, and neocortex.
5. All sensory and motor systems follow the pattern of hierarchical and reciprocal processing of information, whereas the hippocampal memory system is organized largely for serial processing of very complex, polysensory information. A general principle is that circuits in the brain have an organizational structure that is suited for the functions that they are carrying out.
6. Contrary to an intuitive analysis of our personal experience, perceptions are not precise copies of the world around us. Sensation is an abstraction, not a replication, of reality. The brain's circuits construct an internal representation of external physical events after first analyzing various features of those events. When we hold an object in the hand, the shape, movement, and texture of the object are simultaneously analyzed in different brain regions according to the brain's own rules, and the results are integrated in a conscious experience.
7. How sensation is integrated in a conscious experience—the *binding problem*—and how conscious experience emerges from the brain's analysis of incoming sensory information are two of the most intriguing questions in cognitive neuroscience (Chapter 56). An even more complex issue is how these conscious impressions are encoded into memories that are stored for decades.

David G. Amaral

Selected Reading

Brodal A. 1981. *Neurological Anatomy in Relation to Clinical Medicine,* 3rd ed. New York: Oxford Univ. Press.

Carpenter MB. 1991. *Core Text of Neuroanatomy,* 4th ed. Baltimore: Williams and Wilkins.

England MA, Wakely J. 1991. *Color Atlas of the Brain and Spinal Cord: An Introduction to Normal Neuroanatomy.* St. Louis: Mosby Year Book.

Martin JH. 2012. *Neuroanatomy: Text and Atlas,* 4th ed. New York: McGraw Hill.

Nieuwenhuys R, Voogd J, van Huijzen Chr. 1988. *The Human Central Nervous System: A Synopsis and Atlas,* 3rd rev. ed. Berlin: Springer-Verlag.

Peters A, Jones EG (eds). 1984. *Cerebral Cortex.* Vol. 1, *Cellular Components of the Cerebral Cortex*. New York: Plenum.

Peters A, Palay S, Webster H de F. 1991. *The Fine Structure of the Nervous System,* 3rd ed. New York: Oxford Univ. Press.

References

Brodmann K. 1909. *Vergleichende Lokalisationslehre der Grosshirnrinde in ihren Prinzipien dargestellt auf Grund des Zellenbaues.* Leipzig: Barth.

Felleman DJ, Van Essen DC. 1991. Distributed hierarchical processing in the primate cerebral cortex. Cereb Cortex 1: 1–47.

Heimer L. 1994. *The Human Brain and Spinal Cord: Functional Neuroanatomy and Dissection Guide*, 2nd ed. New York: Springer.

Jones EG. 1988. The nervous tissue. In: *Cell and Tissue Biology: A Textbook of Histology*, 6th ed., pp. 305–341. Baltimore: Urban & Schwarzenberg.

Jones EG. 1986. Connectivity of the primate sensory-motor cortex. In: EG Jones, A Peters (eds), Cerebral Cortex, Vol. 5, Chapter 4: Sensory-Motor Areas and Aspects of Cortical Connectivity, pp. 113–183. New York/London: Plenum.

Kaas JH. 2006. Evolution of the neocortex. Curr Biol 16: R910–914.

Kaas JH, Qi HX, Burish MJ, Gharbawie OA, Onifer SM, Massey JM. 2008. Cortical and subcortical plasticity in the brains of humans, primates, and rats after damage to sensory afferents in the dorsal columns of the spinal cord. Exp Neurol 209:407–416.

McKenzie AL, Nagarajan SS, Roberts TP, Merzenich MM, Byl NN. 2003. Somatosensory representation of the digits and clinical performance in patients with focal hand dystonia. Am J Phys Med Rehabil 82:737–749.

Penfield W, Boldrey E. 1937. Somatic motor and sensory representation in the cerebral cortex of man as studied by electrical stimulation. Brain 60:389–443.

Penfield W, Rasmussen T. 1950. *The Cerebral Cortex of Man: A Clinical Study of Localization of Function*. New York: Macmillan.

Ramón y Cajal S. 1995. *Histology of the Nervous System of Man and Vertebrates*. 2 vols. N Swanson, LW Swanson (transl). New York: Oxford Univ. Press.

Rockland KS, Ichinohe N. 2004. Some thoughts on cortical minicolumns. Exp Brain Res 158:265–277.

Zola-Morgan S, Squire LR, Amaral DG. 1986. Human amnesia and the medial temporal region: enduring memory impairment following a bilateral lesion limited to field CA1 of the hippocampus. J Neurosci 6:2950–2967.

5

The Computational Bases of Neural Circuits That Mediate Behavior

The previous chapter focused on the neuroanatomy of the brain and the connections between different brain regions. An understanding of how these connections mediate behavior requires insight into how the information represented by the activity of different populations of neurons is communicated and processed. Much of this understanding has come from recordings of the minute electrical signals generated by individual neurons.

Although much has been learned by recording from just one or a few neurons at a time, advances in miniaturization and electronics technology now make it possible to record action potentials simultaneously from many hundreds of individual neurons across multiple brain areas, often in the context of a sensory, motor, or cognitive task (Box 5–1). Such advances, together with computational approaches for managing and making sense of large data sets, promise to revolutionize our understanding of neural function.

At the same time, modern genetic approaches based on mRNA sequencing from individual neurons are revealing the numerous types of cells that contribute to population activity. Genetic-based approaches also allow defined types of neurons to be activated or silenced during an experiment, supporting tests of causality (Box 5–2).

High-throughput anatomical methods, at the scales of both light and electron microscopy, are providing information about circuit wiring at an unprecedented level of detail and completeness. The complexity of neural circuits and the large data sets collected from them has motivated the development and application of statistical, computational, and theoretical methods for extracting, analyzing, modeling, and interpreting results. These methods are used to study a broad range of issues: experimental design, the extraction of signals from raw data, the analysis of large complex data sets, the construction and analysis of models simulating the data, and, finally and most importantly, building some form of understanding from the results.

Signal extraction is often done on the basis of a Bayesian approach, inferring the most likely signal

Box 5–1 Optical Neuroimaging

Optical imaging methods are a rapidly advancing field of technology for large-scale monitoring of neural circuit dynamics. Most of these approaches use fluorescent sensors—synthetic dyes or genetically engineered and encoded proteins—that signal changes in neural activity via changes in the magnitude or the wavelength of their emitted light following excitation. Various florescence imaging approaches have been developed, depending on the source of fluorescence excitation, including single-photon, multiphoton, and super-resolution fluorescent microscopic imaging.

The most commonly used fluorescence indicators signal changes in intracellular calcium levels as a proxy for the electrical activity of neurons. While the temporal resolution of fluorescence calcium imaging is generally lower than that of electrophysiology, fluorescent imaging with genetically encoded calcium indicators enables simultaneous monitoring of many thousands of individually identified neurons in the behaving animal over several days to weeks and months.

In addition to calcium imaging, synthetic and genetically encoded fluorescent indicators of electrical activity (eg, genetically encoded voltage indicators [GEVIs]), neurotransmitter concentration reporters (eg, glutamate-sensing fluorescent reporter [GluSnFR]), activity states of intracellular signaling molecules, and gene expression provide rapidly expanding and versatile techniques for monitoring neural activity on multiple spatial and temporal scales.

present in a noisy recording. Data analysis often consists of reducing the dimensionality of a large data set, not simply to make it more compact but to identify the essential components from which it is built.

Models of neural systems range from detailed simulations of the morphology and electrophysiology of individual neurons to more abstract models of large populations of neurons. Whatever the level of detail, the aim of models is to reveal how the measured features of a neuron or network of neurons contribute to the function of the neuron or neural circuit.

In addition, at the highest levels of functionality, such as identifying images, playing games, or performing tasks at human levels, ideas from machine learning are increasingly impacting neuroscience research.

In this chapter, we introduce ideas, techniques, and approaches that are used to characterize and interpret the activity of neural populations and circuits, with examples drawn from a number of areas of brain research. Many of these topics are covered in greater detail later in the book.

Neural Firing Patterns Provide a Code for Information

Sensory Information Is Encoded by Neural Activity

Animals and humans continually accumulate information about the world through their senses, make decisions on the basis of that information, and, when necessary, take action. In order for sensory information to be processed for decision making and action, it must be transformed into electrical signals that produce patterns of neural activity in the brain. Studying such neural representations and their relationship to external sensory cues, known collectively as neural coding, is a major area of neuroscience research. The process through which features of a stimulus are represented by neural activity is called encoding.

The structure of a neural representation plays an important role in how information is further processed by the nervous system. For example, visual information is initially encoded in the retina by photoreceptor responses to the color and light intensity over a small region of the visual field. This information is then transformed in the brain within the primary visual cortex to encode a visual scene on the basis of the edges and shapes that define the scene as well as on where these features are located. Further transformations occur in higher-order visual areas that extract complex shapes and further structure from the scene, including the identification of objects and even individual faces. In other brain areas, auditory encoding reflects the frequency spectrum of sounds, and touch is encoded in maps that represent the surface of the body. The sequence of action potentials fired by a neuron in response to a sensory stimulus represents how that stimulus changes over time. Research on neural coding aims to understand both the stimulus features that drive a neuron to respond and the temporal structure of the response and its relationship to changes in the external world.

Box 5–2 Optogenetic and Chemogenetic Manipulation of Neuronal Activity

Functional analysis of neural circuits relies on the ability to accurately manipulate identified circuit elements to elucidate their roles in physiology and behavior. Genetically encoded neural perturbation tools have been developed for remotely controlling neuron function using light (optogenetics) or small molecules (chemogenetics) that activate engineered receptors.

Genetically encoded foreign proteins can be expressed in molecularly, genetically, or spatially specified subsets of neurons using viruses or transgenic animals for subsequent selective perturbations of these cell populations. Optogenetic approaches involve the expression of light-sensitive proteins and subsequent light delivery to the resulting photosensitized neurons. Depending on the type of optogenetic actuator, light activation will then enhance neural activity (eg, light-gated ion channels like channelrhodopsin) or suppress it (eg, light-gated ion pumps like halorhodopsin and archaerhodopsin) by depolarizing or hyperpolarizing the cell's membrane, respectively.

Alternatively, selected neuronal populations can be remotely activated or silenced using chemogenetic actuators, which are genetically engineered receptors that are targeted to defined neuronal populations using genetic methods; they can be activated via small-molecule synthetic ligands that selectively interact with these receptors upon delivery (eg, DREADDs [designer receptors exclusively activated by designer drugs]).

These optogenetic and chemogenetic tools offer precise spatiotemporal control over neuronal activity to probe the causal relationship between neuronal cell types, circuit physiology, and behavior.

Information Can Be Decoded From Neural Activity

Sensory neurons encode information by firing action potentials in response to sensory features. Other brain areas, such as those that lead to decisions or generate motor actions, must correctly interpret the meaning of action potential sequences that they receive from sensory areas in order to respond appropriately. The process by which information is extracted from neural activity is called decoding.

The decoding of neural signals can be done experimentally and in clinical contexts by neuroscientists. Such decoding can infer what an animal or a human is seeing or hearing from recordings of visual or auditory neurons, for example. In practice, only certain features of the stimulus are likely to be inferred, but the results can nevertheless be impressive. A large number of decoding procedures have been developed, ranging from simple weighted sums of neuronal firing rates to sophisticated statistical methods.

Decoding methods are central to the development of neuroprosthetics for people with various nervous system impairments that result in extensive paralysis (Chapter 39). To accomplish this, neurons are recorded in the parietal or motor cortices through implanted electrodes, and online decoding procedures are used to interpret the movement intentions that are represented by the recorded neural activity. The inferred intentions are then used to control a computer cursor or drive a robotic limb.

Decoding recorded neural activity also gives us a remarkable view of what is going on in a neural circuit, which in turn provides insight into memory storage and retrieval, planning and decision making, and other cognitive functions. The following section illustrates these insights using a particularly interesting neural representation, the encoding of spatial location in the rodent hippocampus.

Hippocampal Spatial Cognitive Maps Can Be Decoded to Infer Location

One of the most complex cognitive challenges an animal faces is identifying and remembering its location in an environment relative to the location of other salient objects. For example, seed-caching birds can remember the location of hundreds of different places where they have stored food over a period of several months. The neural circuitry involved in formation of explicit memory—the memory of people, places, things, and events—was briefly introduced in the previous chapter. This form of memory requires the hippocampus, entorhinal cortex, and related structures in the temporal lobe. In 1971, John O'Keefe discovered physiological evidence of a neural representation of the spatial environment in the hippocampus. In 2014, he was awarded the Nobel Prize in Physiology or Medicine, together with May-Britt Moser and Edvard Moser, for their discoveries concerning the neuronal representation of space.

O'Keefe discovered that individual cells in the rat hippocampus, termed place cells, fire only when the animal traverses a particular area of the environment, termed the cell's place field (Figure 5–1). Subsequent research uncovered place cell–like activity in

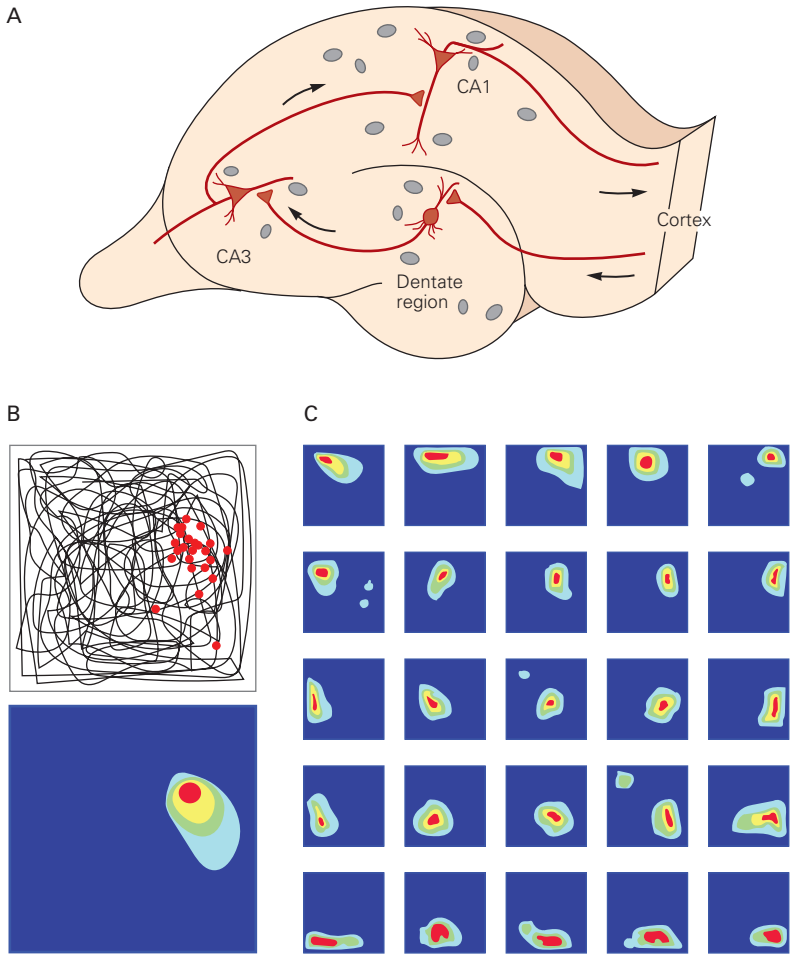

Figure 5–1 Hippocampal place cells and place cell maps.

A. Input–output transformations occur in the trisynaptic circuitry of the mammalian hippocampus, proceeding from the dentate gyrus input region, to the CA3 area, and to the CA1 output region, with principal excitatory neurons (**red**) in each region as primary processing units. Activity of principal cells is modulated by local circuit GABAergic interneurons (**gray**).

B. Place cell firing in the hippocampus. The path taken by a rat is shown in **black** as it traverses a square arena. Electrodes were implanted within the hippocampus to record from individual cells. **Above**: A single place cell increases firing (each action potential represented by a red dot) at discrete locations in the environment. **Below**: A color-coded heat map of firing frequency of the schematic place cell. Lower wavelength colors (**yellow** and **red**) represent higher firing rates on a background of no activity (**dark blue**).

C. Color-coded heat maps showing the firing of 25 different place cells recorded simultaneously in the hippocampal CA1 region as the rat explores a square box.

the hippocampus of several other mammalian species, including bats, monkeys, and humans. Distinct sets of place cells are activated by distinct locations in a given environment. Consequently, although individual place cells represent relatively small spatial areas, the full diverse population of place cells in the hippocampus tiles the entire environment, and any given location is encoded by a unique ensemble of cells. The hippocampal place coding network provides an example of a cognitive map, initially postulated by the psychologist Edward Tolman, that enables an animal to successfully remember and then navigate its environment. The role of the hippocampus in memory formation and the mechanisms by which the hippocampal spatial map is encoded are explored in detail in Chapters 52 and 54.

The electrophysiological methods available to O'Keefe in 1971 were limited to recording one place cell at a time, but subsequent advances allowed investigators to record dozens, and more recently hundreds, of place cells simultaneously. Critically, while single place cells encode only specific parts of the environment and are prone to occasional noisy firing outside of their place fields, entire populations of place cells provide more complete spatial coverage and the

reliability of redundant place coding. These features of population coding have paved the way for new and powerful computational analyses. In particular, it is possible to decode the activity of populations of place cells and estimate an animal's location within an environment. This is accomplished by determining each cell's spatial selectivity and using this selectivity as a template to decode ongoing activity. In practice, this decoding is often performed by weighting each cell's contribution to the final estimate of the animal's position by a factor proportional to that cell's spatial coding reliability. Using this and similar techniques, one can reconstruct an animal's location from second to second within room-sized environments with a precision of a few centimeters (Figure 5–1C).

Hippocampal function has been strongly implicated in spatial and declarative memory based on studies using spatial decoding techniques. During active exploration of an environment, hippocampal activity reflects place coding, but during immobile or resting behavior, the hippocampus enters a different regime in which neural activity is instead dominated by discrete semi-synchronous population bursts termed sharp-wave ripples (Figure 5–2A). These events are thought to be internally generated by circuitry within the hippocampus.

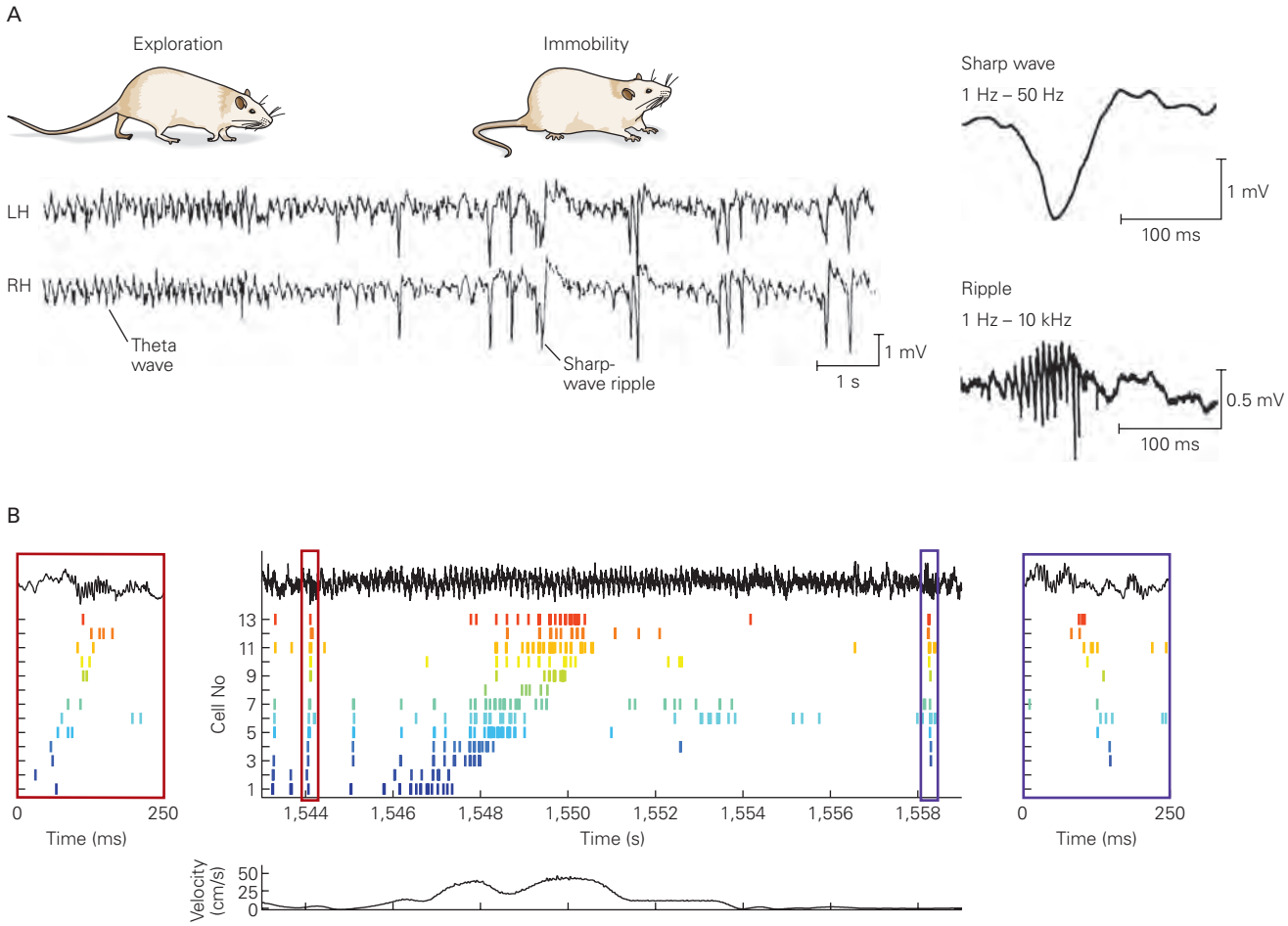

Figure 5–2 Hippocampal sharp-wave ripples and sequence replay.

A. *Left*: Behavior dependence of hippocampal local field potential activity (**LH** and **RH**, left and right hippocampus). Theta waves are present during exploration, and large negative sharp waves during immobility. *Right*: Sharp waves and ripples recorded from the hippocampal CA1 region. (Adapted, with permission, from Buzsaki 2015; and reproduced, with permission, from Buzsaki et al. 1992. Copyright © 1992 AAAS.)

B. Place cell sequences experienced during behavior (*middle*) are replayed in both forward (*left*) and reverse (*right*) direction during sharp-wave ripples. The rat moved from left to right on a familiar track. Spike trains for place fields of 13 CA3 pyramidal cells while the rat is on the track are shown before (forward replay; **red box**), during (*middle*), and after (reverse replay; **blue box**) a single traversal. The CA1 local field potential is shown on top (**black traces**), and the animal's velocity is shown below. (Adapted, with permission, from Diba and Buzsaki 2007. Copyright © 2007 Springer Nature.)

Notably, sharp-wave ripples are prominent during resting periods after recent learning, for example after exploration of an environment. Spatial decoding of the activity of place cells active within these short (50 to 500 ms) sharp-wave ripples reveals that hippocampal neurons recapitulate or replay discrete trajectories through the recently explored environment. Although these trajectories replicate paths taken through space, the replayed activity sequences differ from those observed during active exploration in several ways.

First, replayed sequences within sharp-wave ripples are time compressed, occurring about 10 to 20 times faster than during exploration (Figure 5–2B). Second, they can occur either in the same direction as behavioral spatial trajectories (forward replay) or in the opposite direction (reverse replay). Thus, decoding a single postexploration, 200-ms, sharp-wave ripple-replay event may reveal a virtual mental trajectory spanning 2 to 4 seconds of behavioral time replayed *backward* from how it was experienced. Replay is thought to represent a form of mental rehearsal by which certain memories are gradually consolidated and thus may be a crucial aspect of the role of the hippocampus in memory.

Neural Circuit Motifs Provide a Basic Logic for Information Processing

Neurons tend to be highly interconnected, both with nearby neurons and with neurons in distal brain areas. Knowledge of neuronal connections, called connectomics, is expanding rapidly due to a number of new methods for uncovering fine-scale anatomical structure. Patterns of neuronal interconnection come in several varieties.

Connections from one area to another, for example from the thalamus to primary visual cortex, are termed feedforward (Figure 5–3A). The forward direction is defined as extending from a more peripheral or primary area, such as the retina, thalamus, or primary visual cortex, to a higher area with more complex response properties, such as the visual areas that respond selectively to particular objects. In most cases, two areas that have feedforward connections also have feedback connections; for example, there are numerous connections from primary visual cortex back to the thalamus. Local connections often extend from one neuron to another, ultimately looping back onto the original neuron. Such looping connectivity is called recurrent. Many neurons are involved in all of these types of connectivity—feedforward, feedback, and recurrent—but it is useful to consider the functional implications of these different connectivity motifs separately.

Connections between neurons can be either excitatory or inhibitory. Normally, excitatory connections lead to increased neural firing and inhibitory connections lead to decreased neural firing. Many neural circuits receive strong excitatory drive from hundreds or thousands of synapses. If not checked by inhibition, this synaptic excitation would lead to unstable neural activity. A near balance of excitation and inhibition is a common feature of neural circuits that may enhance their computational capacity. However, this fine tuning may make the circuits prone to generating seizure activity if the balance between excitation and inhibition is not properly maintained, as occurs during epilepsy.

In mammals, visual information is processed in a series of brain areas that are often approximated as having feedforward circuitry. Feedforward circuits can process information in sophisticated ways, for example

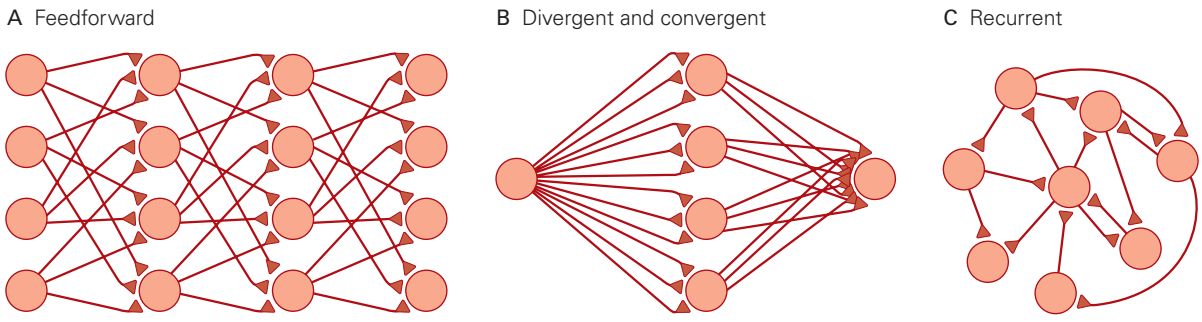

Figure 5–3 Four basic neural circuit motifs.

A. A feedforward circuit in which synaptic connections extend in a single direction from one processing level of neurons to another.

B. Divergent feedforward connections describe a small number of presynaptic neurons connecting to a larger number. Convergent connections describe a large number of presynaptic neurons connecting to a smaller number.

C. In a recurrent network, synaptic connections occur in multiple directions between neurons, forming looping pathways through the circuit.

extracting and identifying objects from a complex visual scene, but they cannot produce ongoing, dynamic patterns of activity. For this purpose, recurrent circuitry is needed (Figure 5–3C).

Within feedforward circuitry, two submotifs can be identified: divergent and convergent connections (Figure 5–3B). In divergent connections, the number of neurons that receive a given type of input exceeds the number of neurons providing that input, so the information encoded in the presynaptic input neurons is expanded in the postsynaptic output neurons. In convergent connections, many presynaptic neurons send input to a smaller number of postsynaptic neurons. The most prominent example of both divergent and convergent connectivity is provided by the cerebellum, as discussed later.

Visual Processing and Object Recognition Depend on a Hierarchy of Feed-Forward Representations

Visual information is processed within a large number of brain regions arranged hierarchically (Figure 5–4). Moving up the hierarchy from the primary sensory input generated by the retina, neurons respond to increasingly complex combinations of visual features, culminating in selectivity for complex objects, such as

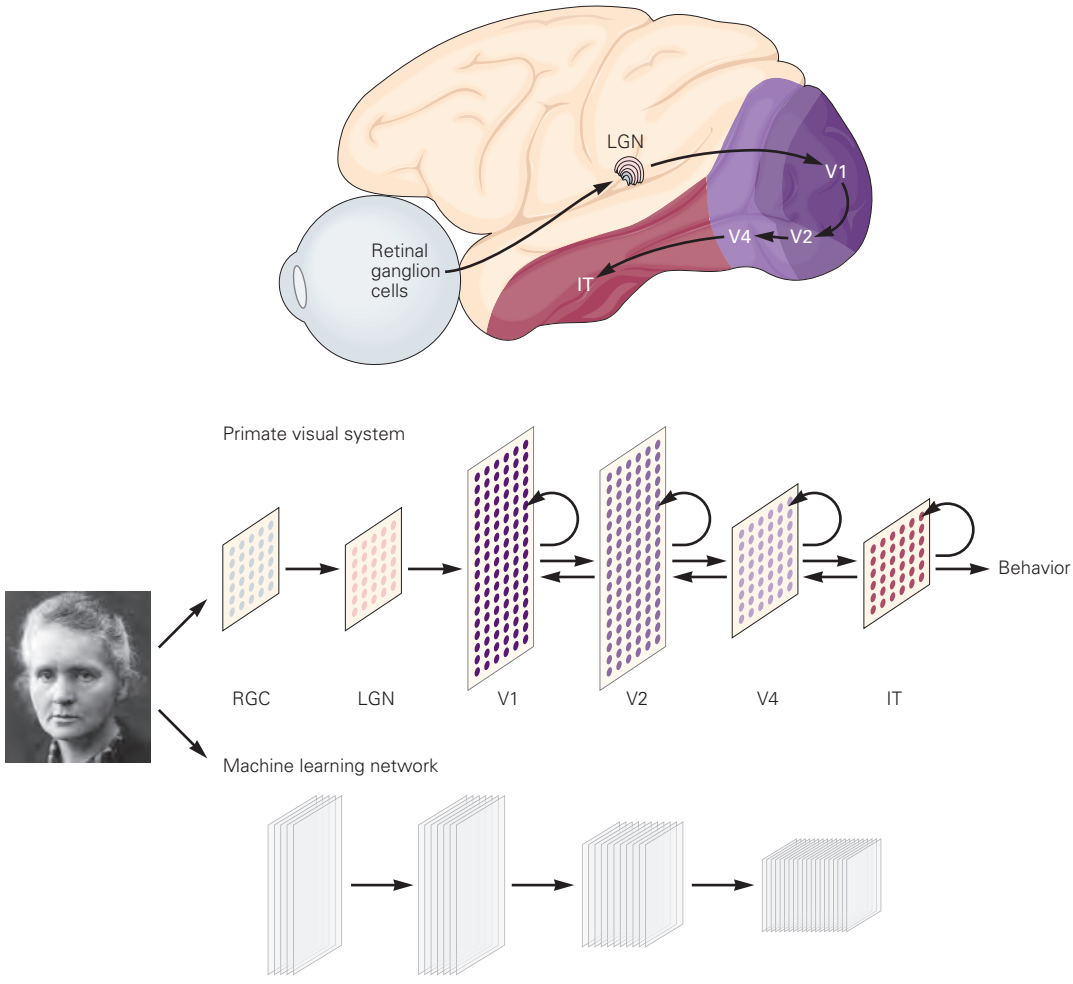

Figure 5–4 Comparison of biological and machine learning networks. In the visual system, multiple brain regions form a hierarchy in which neurons in series become progressively selective to more complex objects. The regions in the primate visual system pathway represent retinal ganglion cells (**RGC**), the lateral geniculate nucleus (**LGN**) of the thalamus, ventral stream visual areas (**V1**, **V2**, and **V4**), and the inferotemporal cortex (**IT**). The number of neurons per region varies (represented by the **colored dots**), but their selectivity steadily increases. The machine learning network pathway represents layers of a feedforward network trained to identify objects in images. Increased selectivity in the different regions of the machine learning network is indicated by the growing numbers of stacked sublayers, reflecting selectivity to a richer array of visual features. The hierarchy of response selectivities recorded in different visual areas resembles the activities seen in corresponding layers of the machine learning network. (Adapted, with permission, from Schrimpf et al. 2018.)

faces. Considerable research is devoted to identifying principles upon which the structure of the visual hierarchy is based. The development of artificial neural network models in machine vision has proven to be an instructive analogy for addressing this issue.

From the retina, to the thalamus, to the primary visual cortex, onto the highest visual areas associated with cognition in inferotemporal cortex, visual neurons respond selectively to particular patterns of light, dark, and color in regions of the visual field called their receptive fields. From the lowest to highest stages of visual processing, neurons have increasingly larger receptive fields and higher degrees of selectivity. At each stage, neurons with a particular type of selectivity tend to have receptive fields that tile the visual scene, providing full coverage for the selected feature. Moreover, the arrangement of the receptive fields in each visual brain area is topographically matched to the layout of the image of the external world on the retina, that is, the cortex forms a map of the visual field.

As receptive fields enlarge and selectivity increases, neural responses depend less on the precise location of the selected object or pattern and more on its overall features. In general, neurons in higher stages of visual processing respond more selectively to a larger portion of the visual field and depend less on features such as location, size, and orientation. This correlates with our ability to recognize objects independent of their location, size, and orientation in a scene. At the highest stages of the hierarchy, neurons can, for example, respond selectively to particular faces located across the visual field, independent of the size of the face or its angular pose (ie, head direction).

The ideas of tiling, increased receptive field size, increased selectivity, and decreased dependence on view-dependent factors are central to the construction of artificial networks for machine vision. Such networks can reach human-level performance on some object recognition tasks. Furthermore, the pattern of errors that the machines make on difficult images matches, to some degree, the errors made by human subjects. Nonhuman primates can also perform these tasks at levels comparable to humans, and interestingly, recordings from different visual areas along the object recognition pathway correspond to activity seen in the artificial networks at similar stages in visual processing (Figure 5–4).

Diverse Neuronal Representations in the Cerebellum Provide a Basis for Learning

The most abundant class of neurons in our brains are the roughly 50 billion granule cells at the input stage of the cerebellum, composing more than half of all the neurons in the brain. The cerebellum is a hindbrain structure vital for motor coordination but also implicated in the adaptive regulation of autonomic, sensory, and cognitive functions (Figure 5–5). Malfunction of cerebellar circuits may contribute to various neurological disorders, including autism. In contrast to the thousands of inputs that most brain neurons receive, each granule cell receives just a handful of inputs (four on average).

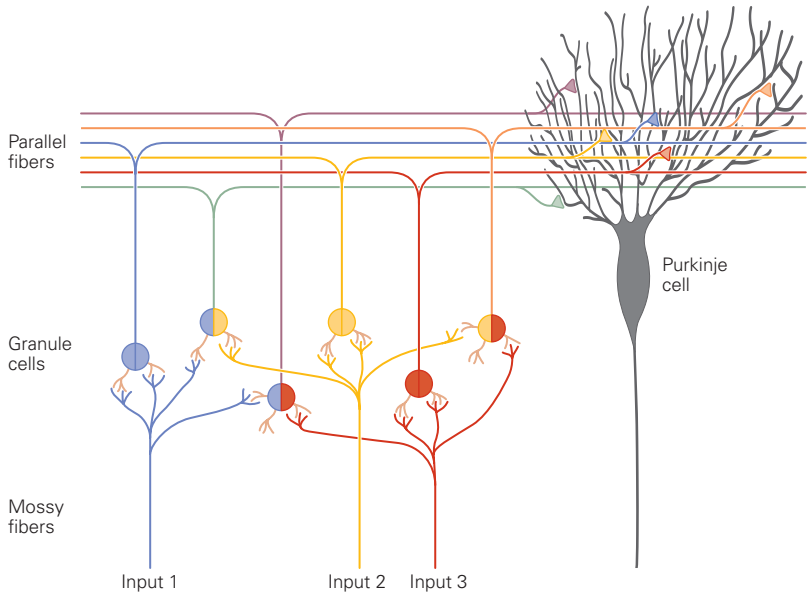

Figure 5–5 The cerebellum receives input from many regions of the brain and spinal cord. These inputs, known collectively as mossy fibers, are recoded in a vast number of granule cells, an example of divergent connectivity, allowing for many possible mixtures of the input signals. Dendrites of Purkinje cells receive convergent input from hundreds of thousands of granule cells relayed by their axons, known as parallel fibers. Parallel fiber to Purkinje cell synapses are modifiable, which is believed to be an important mechanism underlying motor and possibly other forms of learning.

Recent experimental findings using neuroanatomical tracing and electrophysiological recording indicate that inputs converging onto a single granule cell often originate from distinct brain regions. As a result, the firing of individual granule cells may represent any one of an enormous range of combinations of stimuli or events. For example, a cell may fire only during the conjunction of a specific visual stimulus (such as a moving tennis ball) with the movement of a particular body part (such as the flexing of the wrist). Representations that combine different types of information in this way are called mixed.

Cerebellar granule cells provide an extreme example of divergent feedforward connectivity, with the information carried by approximately 200 million input fibers (called mossy fibers) mixed and expanded onto the 50 billion granule cells. Such a large representation is needed to handle the many different ways that multiple channels of information can be combined. For example, representing all possible combinations of 2 out of just 100 different input channels requires $100 \times 99/2$, or 4,950, different response types. Requiring a representation of all triplets pushes this number up over 150,000, and the number increases rapidly for four and more combinations. Because the large number of possible combinations would be difficult to specify genetically, it is generally thought that the assignment of mossy fibers to their granule cell targets is largely random.

This analysis suggests that the role of the cerebellar granule cells is to combine a large number of input channels in many possible ways. Such a representation clearly would be useful for making inferences and generating actions that depend on the co-occurrence of combinations of stimuli and actions. However, to be useful, this information must somehow be read out from the huge number of granule cells.

Read-out from the cerebellar cells is accomplished by Purkinje cells, the output neurons of the cerebellar cortex. In contrast to the highly divergent connectivity at the inputs to granule cells, connections between granule cells and Purkinje cells provide an extreme example of convergence. A single Purkinje cell receives input from over a hundred thousand granule cells. Theories of cerebellar function developed in the 1970s by David Marr and James Albus posited that this convergence allows Purkinje cells to extract useful information from the extremely rich representation provided by granule cells. By doing this, Purkinje cells may, for example, underlie the amazing human capacity to form the many complex associations required for motor skills, such as riding a bicycle or playing a musical instrument. However, to extract information that is useful for a number of purposes under a variety of conditions, the read-out provided by Purkinje cells must be adaptable. This adaptability is provided by the plasticity of the synapse between a granule cell and Purkinje cell synapse, as discussed in a later section.

Recurrent Circuitry Underlies Sustained Activity and Integration

Neurons are inherently forgetful. Transient synaptic input typically evokes a brief response that decays within a few tens of milliseconds. The time course of this decay is determined by an intrinsic property of neurons known as the membrane time constant (Chapter 9). How then do patterns of neural activity persist long enough to support cognitive operations such as memory or decision making that play out over seconds, minutes, or even longer periods of time?

Consider, for example, trying to detect whether you hear a familiar voice in a crowded room full of people talking loudly. As you listen, you may occasionally detect a bit of sound that resembles the voice you are searching for but that by itself is inconclusive. Nevertheless, over time, you may be able to accumulate enough evidence to arrive at a conclusion. This process of evidence accumulation requires integration, meaning that a running sum must be maintained and augmented as additional evidence is detected. Integration requires both a computation (addition) and memory to compute and maintain a running total (Chapter 56).

For a neural circuit to perform integration, a transient input must produce activity that is sustained at a constant level even after the input is gone. This sustained activity provides a memory of the transient input. As outlined in the previous paragraph, circuits that integrate can be useful for accumulating information, but they are also needed for noncognitive tasks such as maintaining the constant muscle tension required to hold a fixed body posture. One of the best studied neural integrators is the circuitry that allows humans and animals to maintain a constant gaze direction with their eyes, even in the dark. The fact that eye movements can be studied across a wide range of species, from fish to primates, has greatly facilitated progress. Moreover, the relative simplicity of the oculomotor system has fostered fruitful dialog between experimental and theoretical studies. (The oculomotor system is described in more detail in Chapter 35.)

The existence of integrator circuits in the oculomotor system was first suggested by a puzzling observation from neuronal recordings (Figure 5–6A). Oculomotor neurons that control the eye muscles increase action potential firing transiently to evoke

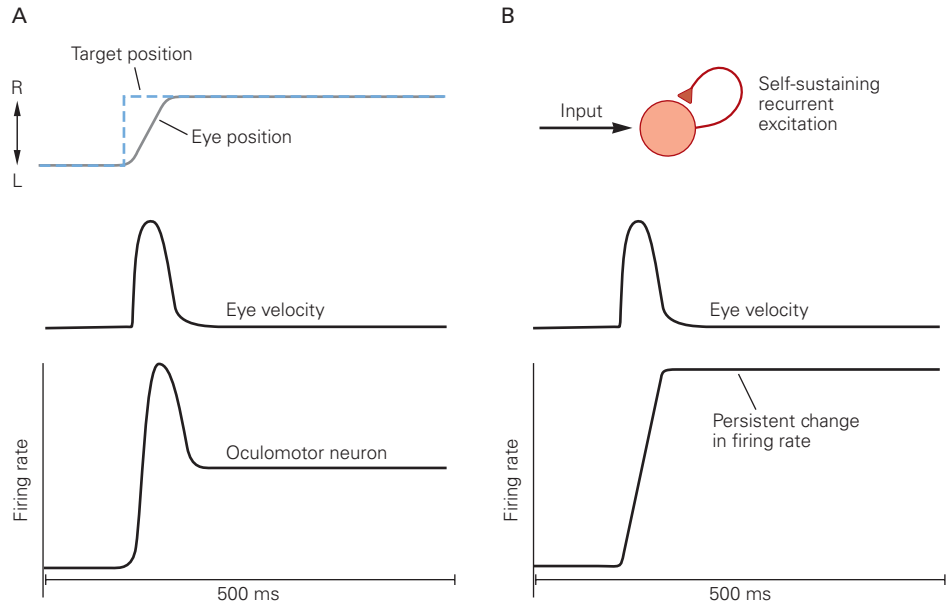

Figure 5–6 Recurrent circuitry and sustained neural activity are required for maintaining eye position.

A. *Above:* A saccadic eye movement consists of a rapid movement change in eye velocity to bring a target back to the center of gaze. This is followed by a sustained change in eye position to maintain the fovea on the target. The **dashed blue line** shows the location of the target, and the **gray line** shows the eye movement and subsequent fixation on the target at its new position. *Below*: An oculomotor neuron exhibits a brief burst of activity related to eye velocity along with sustained activity related to eye position.

B. Recurrent excitation can explain how a brief pulse of input, such as an eye velocity signal, can lead to a persistent change in firing rate through a process akin to mathematical integration.

movements of the eye but also exhibit sustained action potential firing needed to hold the eye in fixed position. For example, a motor neuron that projects to an eye muscle that moves that eye to the left will fire at a high rate when gaze is maintained left of center and at a low rate when gaze is maintained right of center. The puzzle is that the premotor neurons in the superior colliculus and brain stem that project to the oculomotor neurons only fire transiently before eye movements. They do not show any sustained activity related to eye position. How then is this sustained activity generated?

An early conjecture, now strongly supported, is that steady eye position signals are computed by brain stem neurons that integrate the transient eye velocity signals. Such neurons receive velocity information and provide the steady output to the oculomotor neurons that maintain eye position. Lesions or inactivation of certain brain stem nuclei in monkeys, including the medial vestibular nucleus and the nucleus prepositus hypoglossi, result in a failure to maintain steady horizontal eye position following eye movements, suggesting that the neural integrator circuit lies within these structures. Damage to these brain stem structures in humans leads to the same problem, known clinically as gaze-evoked nystagmus (Chapter 35).

How do neural circuits perform integration? One possibility is that integration is supported by specialized intrinsic neuronal properties that effectively lengthen neuronal membrane time constants, allowing brief inputs to generate sustained output. A variety of candidate mechanisms have been described involving different voltage-activated ion channels. However, studies using intracellular recordings, which allow for direct control over the membrane voltage of the recorded neuron, have shown that sustained position-related signals persist even when the neuron's voltage-activated channels are blocked. A second possibility is that integration arises from interactions among a network of synaptically coupled neurons. Intracellular recordings in goldfish support this idea by showing that levels of synaptic input vary with eye position.

The question of what types of neural networks are capable of performing integration has been explored extensively in theoretical studies. One class of models that has been considered relies on recurrent connectivity, specifically a population of neurons that excite each other. A weakly coupled network of this type responds to an input pulse with activity that rapidly decays away. Increasing the strength of the recurrent excitation adds back some of the activity that would

otherwise decay, lengthening the duration of the population response. If recurrent excitation is increased to the point where the recurrent excitation set up by a transient input precisely cancels the decay, the response can last indefinitely. This requires fine-tuning of network parameters.

In a perfectly tuned network, a transient pulse of input produces a change in firing rate that lasts forever in the absence of further input. Equivalently, such a population computes a running integral of the input it receives (Figure 5–6B). If the transient excitation in the network is not perfectly tuned but instead is slightly weaker, the input produces a change in firing rate that decays slowly. Eye position, in the dark, tends to drift back to the center in about 20 seconds, suggesting that the neural integrator is not tuned perfectly, but it is tuned well enough to extend the roughly 20-ms time constant of a typical neuron by a factor of about 1,000.

The fact that recurrent network models reproduce some of the core properties observed in biological integrator circuits has launched development of more detailed and realistic network models and testing the predictions of such models experimentally. These efforts also highlight the challenges involved in forging detailed links between the structure and function of neural circuits. Key questions remain even after decades of intensive study using a variety of systems and approaches.

For example, oculomotor integrator circuits typically contain two opposing classes of neurons, one increasing and the other decreasing their firing rates as eye position changes in a given direction. This arrangement is not restricted to oculomotor integrators but is also found in cortical regions implicated in decision making and working memory. Models have shown that mutual inhibition between these opposing populations can play a role in sustaining activity and integration. Although anatomical studies provide some support for this idea, studies in the goldfish showed that integration remains intact even when connections between the opposing populations are removed.

Another key question regards the mechanisms for tuning integrator networks. Experimental studies suggest that integrator networks are subject to modification via experience; in other words, they are tuneable. Although such tuning presumably occurs via changes in the strength of synaptic connections between neurons, direct evidence for this has yet to be obtained. In short, although much has been learned about how integration *could* be implemented, the details of the network architecture that actually support integration in any particular instance remain to be definitively established.

A detailed understanding of how we maintain the position of our eyes is an important end unto itself, with clinical relevance. However, as pointed out earlier, the solutions found here may apply equally to cognitive functions including short-term memory and decision making. Optical imaging of large populations of neurons along with temporally precise manipulations of their activity and detailed anatomical reconstructions, combined with theoretical models of network function, may soon provide the answers.

Learning and Memory Depend on Synaptic Plasticity

Experience can modify neural circuits to support memory and learning (Chapter 3). It is generally believed that experience-dependent changes responsible for learning and memory occur primarily at synapses. Multiple forms of synaptic plasticity have been identified, and each of these presumably supports a different set of functions.

Just as there are multiple forms of plasticity, there are multiple forms of learning. Different forms of learning can be defined based on the amount and type of information provided. In supervised learning, explicit instruction is given about the behavior needed to perform a task. In reinforcement learning, on the other hand, only a positive reward or a negative punishment is provided to indicate whether that task is being performed properly. Finally, unsupervised learning involves no instructive information at all, but rather organizes input data on the basis of its intrinsic structure without supervision. In the following sections, we discuss an example of unsupervised learning involving Hebbian plasticity and an example of reinforcement learning in the cerebellum. (The various types of learning and memory and their cellular and circuit mechanisms are described in detail in Chapters 52–54.)

Dominant Patterns of Synaptic Input Can be Identified by Hebbian Plasticity

Cortical neurons receive synaptic input from thousands of other neurons and combine this information in patterns of action potentials. The strength of synaptic transmission at each of the synapses determines how the information arriving from many inputs is combined to affect the firing of the neuron. Setting the strength of all the synapses to zero would obviously make for a noninformative neuron of no functional use. Similarly, setting them to nonzero values that extract a signal dominated by random noise would also not produce a signal of value. Instead, neurons can best serve a useful function by extracting the most

interesting aspects of the information carried by their inputs. Theoretical analysis of a form of plasticity known as Hebbian indicates one way that this could happen in an unsupervised manner.

In 1949, Donald Hebb proposed that synapses should strengthen when a given presynaptic input to a neuron cooperates with a sufficient number of coactive inputs to cause that neuron to fire an action potential. Evidence for Hebbian synaptic plasticity has been obtained from many studies (Chapter 54). By itself, Hebbian plasticity would keep making synapses stronger and stronger, so some other form of plasticity must exist to prevent this from happening. Such compensatory forms of plasticity are called homeostatic, and experiments have revealed these forms of plasticity as well. Theoretical analysis indicates that a combination of Hebbian and homeostatic plasticity can adjust synapses, without any additional supervisory signal, so that they extract the combination of a neuron's inputs that is most highly modulated relative to other combinations (Figure 5–7). This is a reasonable candidate for the most interesting signal carried by those inputs, and thus, Hebbian plasticity provides a way for neurons to determine and extract such signals.

Synaptic Plasticity in the Cerebellum Plays a Key Role in Motor Learning

Although a detailed understanding of how the cerebellum contributes to complex human motor skills is lacking, a great deal is known about its role in simple forms of motor learning. Among the most thoroughly studied is a paradigm known as *delay eyeblink conditioning*, in which a neutral sensory stimulus such as a light or a tone is repeatedly paired with an aversive unconditioned stimulus (US) such as an air puff to the eye. After several days of such training, animals learn to close their eye in response to the previously neutral stimulus (the light or tone), known as the conditioned stimulus (CS), in anticipation of the US (the air puff). The timing of the eyelid closure is highly specific to the delay between the onset of the CS and the US.

Eyelid conditioning has been an extremely useful paradigm for understanding cerebellar function because it maps onto the structure of cerebellar circuitry in a particularly clear way (Figure 5–8). Information about the CS is first encoded by cerebellar granule cells and then relayed to Purkinje cells. The US is encoded by a completely separate input pathway, known as the olivocerebellar or climbing fiber system. In contrast to the many thousands of inputs from granule cells, each Purkinje cell receives a single powerful climbing fiber input from a brain stem nucleus known as the inferior olive. Electrophysiological recordings revealed that climbing fiber inputs to one particular region of the cerebellum signal the occurrence of the US, that is, a stimulus that is irritating to the cornea. This discovery was made possible by the fact that the climbing fiber evokes a distinct suprathreshold response in the Purkinje cell known as a complex spike.

A key to understanding how the cerebellum mediates learning was the discovery that the complex spike triggers plasticity at synapses between granule cells and Purkinje cells. Specifically, the co-occurrence of input from a presynaptic granule cell and a complex spike in the postsynaptic Purkinje cell results in a persistent weakening of the granule cell input, a form of plasticity known as cerebellar

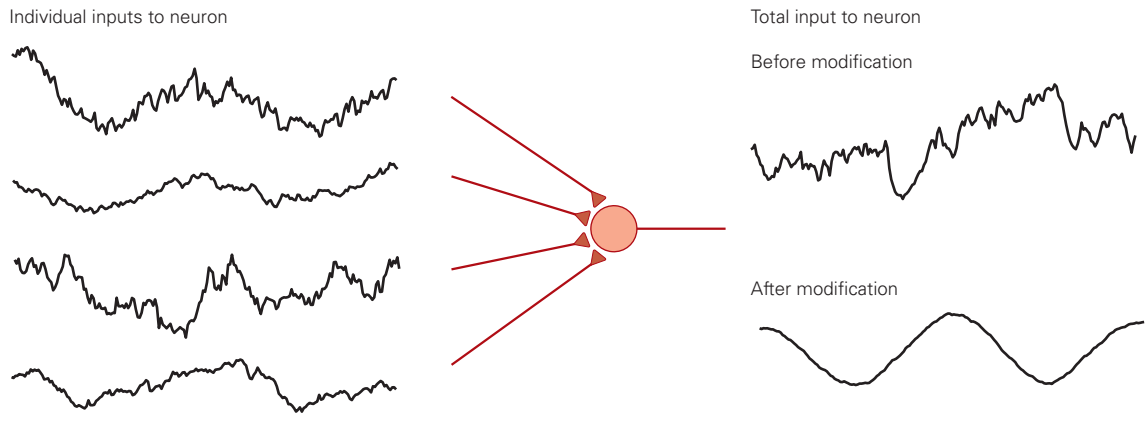

Figure 5–7 Hebbian plasticity can identify relevant input signals to a neuron. In this example, a neuron receives 100 inputs; firing rates for four of them are shown (*left*). Each of the input rates is noisy but contains, within the noise, a sinusoidal signal. The input rates are multiplied by synaptic strengths (brown triangles) and then summed to produce the total input to the neuron (*right*). Before Hebbian plasticity occurs, the synapses have random weights, resulting in the noisy trace; after modification, the total input reveals the underlying sinusoidal signal.

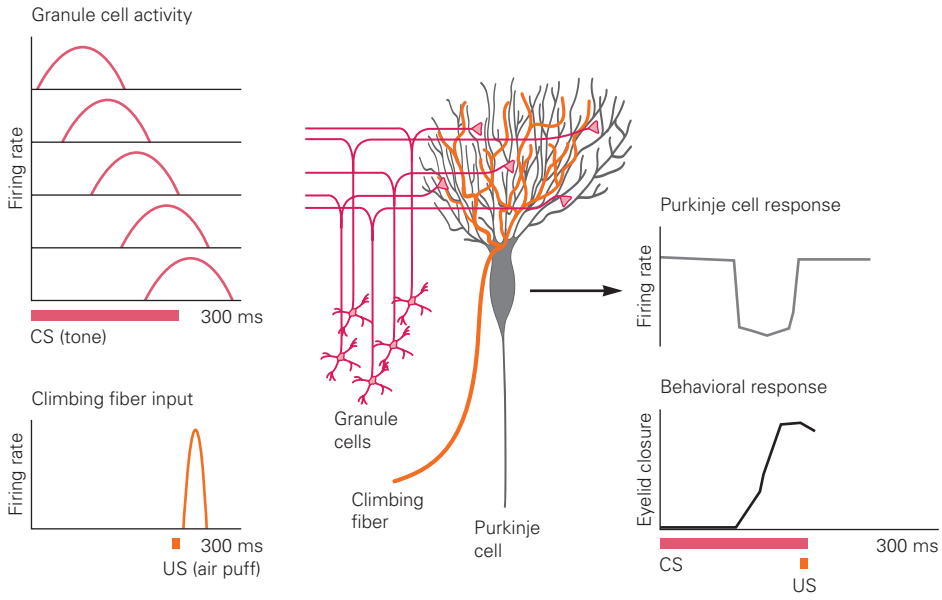

Figure 5–8 Hypothetical role of the cerebellum in eyeblink conditioning. Information about the conditioned stimulus (**CS**) and unconditioned stimulus (**US**) is relayed via mossy and climbing fiber pathways, respectively. Granule cell synapses active before presentation of the US are gradually weakened by long-term depression induced by climbing fiber input. This contributes to a pause in Purkinje cell firing that is precisely timed to occur just before the US. Since Purkinje cells are inhibitory, this pause excites downstream neurons in the cerebellar nucleus and red nucleus that drive eyelid closure.

long-term depression (Figure 5–8). Hence, for each occurrence of the US, the strength of granule–Purkinje cell synapses active immediately prior to the US is reduced. This plasticity leads to the gradual emergence of a learned pause in Purkinje cell firing due to the decrease in granule cell excitation just before the expected time of arrival of the US.

How does a decrease in Purkinje cell firing lead to a learned motor response? Purkinje cells are normally spontaneously active, and they inhibit their downstream targets. Purkinje cells in regions of the cerebellum receiving climbing fiber input related to noxious stimuli to the eye form synapses with neurons that indirectly activate the muscles that produce eyelid closure. Hence the learned pause in Purkinje cell firing causes the eyelid to close at just the right moment to protect the eye. Appropriate timing of the pause is thought to be mediated by a diversity of temporal response patterns in granule cells. Computer simulations have shown that learning of appropriately timed responses can be explained by plasticity in the granule–Purkinje cell synapse if individual granule cells are active at different delays after the CS or exhibit a variety of distinct, but repeatable, temporal patterns locked to the CS.

Due to technical challenges, direct evidence for such temporal representations has not yet been obtained for granule cells in the region of the mammalian cerebellum involved in eyeblink conditioning. However, a diversity of temporal patterns has been observed in granule cells in a structure analogous to the cerebellum in fish. More broadly, studies of the cerebellum, including those of eyeblink conditioning, provide a concrete illustration of how neural circuits can mediate learning though trial and error, even for learning more complex motor skills such as playing a musical instrument. Purkinje cells integrate a rich diversity of signals related both to the external world and internal state of the animal (conveyed by granule cells), with highly specific information about errors or unexpected events (conveyed by the climbing fibers). The climbing fiber acts as a teacher, weakening synapses that were active before, and hence could have contributed to errors. These changes in synaptic strength alter the firing patterns of Purkinje cells and, by virtue of specific wiring patterns, alter behavior such that errors are gradually reduced.

The cerebellum and cerebral cortex, including the hippocampal region, are foci of intense experimental and theoretical research on learning and memory. Technological advances are opening up new approaches for studying the contributions of synaptic actions, individual cells, and circuits to memory-related phenomena.

Highlights

1. Neural coding describes how stimulus features or intended actions are represented by neuronal activity. Decoding refers to the inverse process through which neural activity is interpreted to reveal the encoded signals. Mathematical decoding of neural responses can be used to interpret computations being performed by neural circuits and to drive prosthetic devices.
2. Neural circuits are highly interconnected, but a few basic motifs are used to characterize their functions and modes of operation. Feedforward circuits process information to extract structure and meaning from a sensory stream. Recurrent circuits can perform temporal processing and generate dynamic activity to drive motor responses.
3. Most neurons receive a finely tuned balance of excitatory and inhibitory inputs. Small changes in this balance in response to a sensory stimulus can evoke an action potential output.
4. Levels of neural activity must often be maintained for many seconds. Networks of recurrent excitation provide one mechanism to produce long-lasting changes in neural output.
5. Synaptic plasticity supports longer-lasting changes in neural circuits that underlie learning and memory. Hebbian plasticity can extract interesting signals from a complex set of inputs without the need for supervision (a "teacher"). Synaptic plasticity in the cerebellar cortex is driven by error signals (a form of supervision) and is used to tune motor responses and learn timing relationships.

Larry F. Abbott
Attila Losonczy
Nathaniel B. Sawtell

Selected Reading

Abbott LF. 2008. Theoretical neuroscience rising. Neuron 60:489–495.

Dayan P, Abbott LF. 2001. *Theoretical Neuroscience: Computational and Mathematical Modeling of Neural Systems*. Cambridge, MA: MIT Press.

Hebb DO. 1949. *The Organization of Behavior: A Neuropsychological Theory*. New York: Wiley.

LeCunn Y, Bengio Y, Hinton G. 2015. Deep learning. Nature 521:436–444.

Marr D. 1969. A theory of cerebellar cortex. J Physiol 202:437–470.

References

Buzsaki G. 2015. Hippocampal sharp wave-ripple: a cognitive biomarker for episodic memory and planning. Hippocampus 25:1073–1188.

Buzsaki G, Horváth Z, Urioste R, Hetke J, Wise K. 1992. High-frequency network oscillation in the hippocampus. Science 256:1025–1027.

Diba K, Buzsaki G. 2007. Forward and reverse hippocampal place-cell sequences during ripples. Nat Neurosci 10:1241–1242.

Fusi S, Miller EK, Rigotti M. 2016. Why neurons mix: high dimensionality for higher cognition. Curr Opin Neurobiol 37:66–74.

Litwin-Kumar A, Harris KD, Axel R, Sompolinsky H, Abbott LF. 2017. Optimal degrees of synaptic connectivity. Neuron 93:1153–1164.

Medina JF, Mauk MD. 2000. Computer simulation of cerebellar information processing. Nat Neurosci 3:1205–1211.

Miri A, Daie K, Arrenberg AB, Baier H, Aksay E, Tank DW. 2011. Spatial gradients and multidimensional dynamics in a neural integrator circuit. Nat Neurosci 14:1150–1159.

Oja E. 1982. A simplified neuron model as a principal component analyzer. J Math Biol 15:267–273.

O'Keefe J, Dostrovky J. 1971. The hippocampus as a spatial map. Preliminary evidence from unit activity in the freely-moving rat. Brain Res 34:171–175.

Schrimpf M, Kubilius J, Hong H, et al. 2018. Brain-Score: which artificial neural network for object recognition is most brain-like? bioRxiv doi:10.1101/407007.

Tolman EC. 1948. Cognitive maps in rats and men. Psychol Rev 55:189–208.

Wilson MA, McNaughton BL. 1994. Reactivation of hippocampal ensemble memories during sleep. Science 265:676–679.

Yamins DLK, DiCarlo JJ. 2016. Using goal-driven deep learning models to understand sensory cortex. Nat Neurosci 19:356–365.

6

Imaging and Behavior

To explain an organism's behavior in biological terms, it is necessary to reconcile measures of biological processes (eg, action potentials, blood flow, release of neurotransmitters) with measures of cognitive and motor outputs. Relating biological and behavioral measures is challenging, however. Precise neural measurements and invasive techniques are possible in nonhuman animals, but many of these species have a relatively constrained behavioral repertory. Moreover, it is far more difficult to directly measure or invasively manipulate neural activity in healthy humans, the species with the most advanced and varied behavior. Thus, a central effort of modern neuroscience has been to develop new methods for obtaining precise biological measures from the human brain and for modeling human behaviors in nonhuman animals.

The dominant approach in humans for measuring biological processes and linking them to behavior is functional magnetic resonance imaging (fMRI). Other imaging methods for measuring human brain function such as electroencephalography, positron emission tomography, and near-infrared spectroscopy have their own strengths. However, fMRI is particularly well suited for studying the neural underpinnings of human behavior for several reasons. First, it is noninvasive: It does not require surgery, ionizing radiation, or other disruptive intervention. Second, it can measure brain function over short periods of time (in seconds), which allows it to capture dynamic aspects of mental processes and behavior. Third, it measures activity across the whole brain simultaneously, providing the opportunity to examine how multiple brain regions interact to mediate complex behaviors. Thus, the focus of this chapter is fMRI.

We start by explaining the technicalities of how an fMRI experiment works and how the data are typically collected. We then explain how fMRI data are analyzed

and how they provide insight into human behavior and thought. We then turn to a more conceptual overview of what has been learned from fMRI, using examples from the fields of perception, memory, and decision-making. Finally, we consider the strengths and limitations of fMRI and discuss what kinds of inferences about brain and behavior it can support.

Although the focus of this chapter is on imaging and behavior in the healthy brain, fMRI also has the potential to change the way we diagnose and treat psychiatric and neurological disorders. Virtually all such disorders (eg, autism, schizophrenia, depression, eating disorders) involve changes in large-scale circuit dynamics, in addition to the disruption of particular brain regions and cell types. Basic research into how healthy brain circuits mediate mental processes and behavior, combined with the ability to measure activity in these same circuits in clinical populations, holds tremendous promise for understanding disease and dysfunctional behavior.

Functional MRI Experiments Measure Neurovascular Activity

fMRI experiments enable investigators to track brain function based on changes in local blood oxygen levels that occur in response to neural activity. Like all forms of magnetic resonance imaging (MRI), fMRI requires both highly specialized equipment and sophisticated computer programs. In this section, we first consider the basic principles of how MRI can be used to image brain structure and then explain how fMRI extends this capability to image brain activity.

At the core of every MRI machine is a powerful magnet. The strength of the magnetic field is quantified in Tesla (T) units, and most modern MRI machines are 3T. The use of higher field strengths, such as 7T, offers some advantages, including the possibility of higher-resolution imaging of cortical layers. Such machines are not yet widespread, and layer-specific imaging is in its infancy, so we focus on the capabilities and configuration of 3T machines.

The outside of an MRI machine looks like a tunnel, known as the "bore" of the magnet. Subjects lie on a bed with their head in a helmet-like head coil, which receives signals from the brain. Visual stimuli are typically viewed through a mirror on the head coil angled toward a screen at the back of the bore. Auditory stimuli are presented through headphones. Behavior is typically measured in terms of manual responses with a button box and/or eye movements with an eye tracker. This apparatus constrains which experimental tasks are possible. However, fMRI is flexible in other ways, including that it can be performed and repeated without harm in many different types of subjects, from children to the elderly, whether healthy or suffering from a disorder.

What does fMRI measure? There are two fundamental concepts that we will discuss in turn, first magnetic resonance and then neurovascular coupling (Figure 6–1).

fMRI Depends on the Physics of Magnetic Resonance

In general, MRI exploits the magnetic properties of hydrogen atoms, the dominant source of protons in the body, specifically the way each atom's proton interacts with a strong magnetic field. A key property of protons is that they intrinsically rotate around an axis. This *spin* gives protons angular momentum and a magnetic dipole along the axis, their own north and south poles. Under normal circumstances, the directions of these dipoles are random for different protons. When placed in a strong external magnetic field, however, a subset of the protons (how many is proportional to the field strength) align with the direction of this field, which extends from foot to head when lying in an MRI bore.

An important step toward measuring a signal from protons is to push them out of alignment with this main field. To understand why, it is helpful to think about a familiar object, the gyroscope. If a still gyroscope is tipped out of vertical balance, it will just fall over. However, if you spin the gyroscope before tipping it, inertial forces will prevent it from falling over. The axis around which the gyroscope is spinning will itself begin to rotate around the vertical axis. This *precession* occurs because gravity exerts a vertical torque on the tilted gyroscope, pulling its center of mass down so that it pivots around its bottom point and traces out a circle in the transverse plane (looking from above). Something similar happens to a proton that is tilted with respect to the strong magnetic field: The field applies a torque and the orientation of the rotational axis precesses around the field direction. The speed of precession, or the *resonant frequency*, is determined by the Larmor equation, according to the field strength and a *gyromagnetic ratio* specific to each type of atom. In the case of a 3T magnet and hydrogen atoms, this speed is in the radiofrequency (RF) range.

But how do protons get tipped out of alignment in the first place to enable precession? The answer depends upon the same principle of torque. A second, weaker magnetic field is applied in a perpendicular direction (eg, front to back of the head), introducing

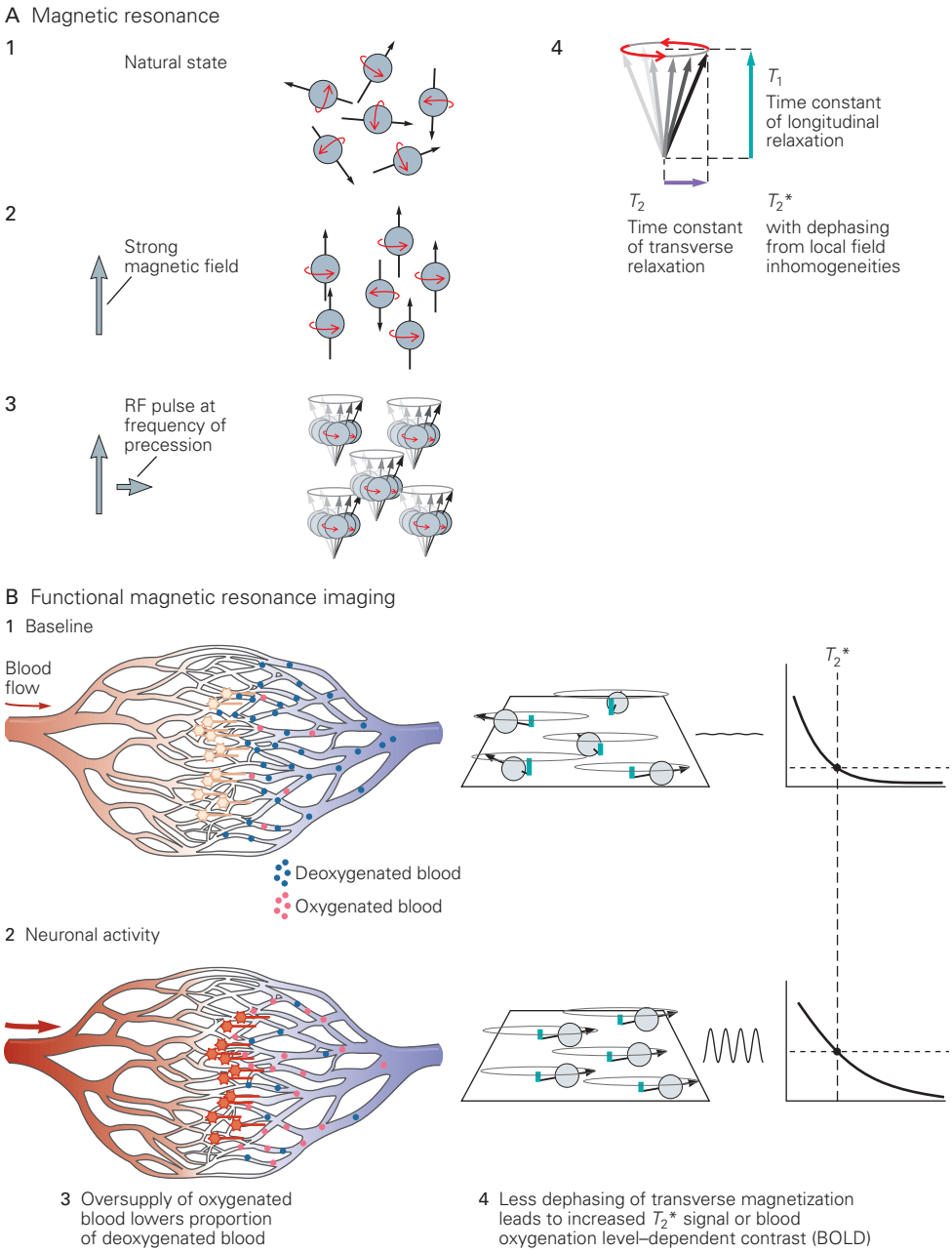

Figure 6–1 How fMRI measures neural activity.

A. Outside of the MRI environment, protons in hydrogen atoms in the brain spin around axes that point in random directions (**1**). When a brain enters the strong magnetic field of the MRI bore, a subset of these axes aligns with this field, which is known as longitudinal magnetization (**2**). These protons can be measured by transmitting a radiofrequency (**RF**) pulse that induces a weaker magnetic field perpendicular to the strong field. This misaligns the protons with the strong field, which now acts as a torque, causing the proton spin axes to precess in an arc on the transverse plane. The frequency of the RF pulse is chosen to resonate with the precession rate of the protons, which in turn depends on the strength of the magnetic field (**3**). When the RF pulse is stopped, the protons initially continue to precess synchronously, inducing alternating current at the same frequency in receiver coils surrounding the head. These signals can be used to generate an image by applying magnetic gradients that adjust the field strength in orthogonal directions across the brain. This results in different resonant frequencies at different points in the brain, allowing the source of the received signals to be identified. The transverse magnetization dissipates over time, and signal is lost. This relaxation occurs as the protons give off thermodynamic energy and their axes return to the longitudinal direction (T_1), and as the protons become desynchronized in the transverse plane from local interactions with other atoms and molecules (T_2), and because of inhomogeneities in the magnetic field (T_2^*) (**4**).

B. Magnetic resonance can be used to estimate neuronal activity in *functional* MRI because of the magnetic properties of blood. When a brain region is in a baseline state, there is a higher proportion of deoxygenated to oxygenated blood than when the region is active. Deoxygenated blood interacts with the magnetic field, causing local inhomogeneities that distort the rate of precession and disrupt the synchrony of protons in the transverse plane, leading to more rapid T_2^* decay and lower BOLD signal (**1**). Neuronal activity leads to metabolic demand (**2**), which in turn results in the delivery of excess oxygenated blood (**3**). Oxygenated blood does not interact with the magnetic field, and so the increased amount in active brain regions reduces field inhomogeneities. In turn, this reduces the dephasing of protons precessing in the transverse plane, leading to slower T_2^* decay and higher BOLD signal (**4**).

another torque that pulls protons away from alignment with the strong field. This misalignment causes precession about the direction of the strong field by allowing the strong field to act as a torque. Complicating matters, this precession makes protons a moving target for the weaker magnetic field that is needed to cause misalignment in the first place. This is solved by generating the second field using a transmit coil in the MRI machine, through which alternating current is passed to deliver an RF pulse at the resonant frequency of the protons. This induces a perpendicular magnetic field that rotates in lockstep with the precession. This RF pulse is sustained as long as needed to generate a specified change in the spin orientation of protons away from the strong field direction (eg, 90°). This change is known as the *flip angle* and is often chosen to maximize signal according to the Ernst equation.

Once the desired flip angle has been achieved, the RF pulse is stopped in order to measure the composition of tissue. At this point, protons are precessing around the strong magnetic field and tilted heavily into the transverse plane. This is akin to a bar magnet spinning on a table, where the north and south poles take turns passing any given location. If a coil is placed nearby, the spinning magnet induces a current in the wire that reverses as the poles alternate. This is what the receiver head coil in an MRI machine measures: alternating current induced by protons precessing synchronously (note: this is the same principle as described earlier for how the transmit coil works, just reversed). The amount of current indicates the concentration of precessing protons.

Critically, the frequency of these measured signals reflects the speed of precession, which in turn depends on the strength of the magnetic field experienced by the tissue. This can be used to generate three-dimensional images by imposing different gradients on the magnetic field (think of a staircase from higher to lower strength) that cause the Larmor frequency to vary systematically over space in the brain. During fMRI, one gradient is applied in a specific direction to select a slice of brain tissue. The RF pulse can be tailored to the resonant frequency for the exact field strength at this gradient step, such that only protons in this slice are excited. The same logic is used with additional gradients in orthogonal directions to impose a two-dimensional matrix on the selected slice, with each unit volume in the matrix or *voxel* having a unique frequency and phase. The head coil receives a composite signal with a mixture of these frequencies, but the signal can be decomposed to identify protons at every voxel in the slice.

There is another important property of precessing protons that contributes to MRI: The alternating current induced in the head coil begins to decay right after the RF pulse. There are different sources of decay. One source is that precessing protons give off thermodynamic energy (heat) to the surrounding tissue, just like a gyroscope will eventually lose energy to friction and topple over. As this occurs, the spin orientation of protons gradually relaxes back to the direction of the strong magnetic field, causing them to precess less in the transverse plane and thus generate less signal. This is called longitudinal relaxation and occurs with time constant T_1. A second type of decay occurs while protons are still precessing in the transverse plane. Individual protons are surrounded by a variable neighborhood of other atoms, which carry their own weak magnetic fields. This subtly changes the field strength the proton experiences, causing its Larmor frequency to vary unpredictably. Whereas right after the RF pulse protons precess in synchrony, these local interactions cause some protons to precess faster or slower. Because they get increasingly out of sync, the induced current alternates less reliably and signal is lost. This is called transverse relaxation and occurs with time constant T_2. This dephasing of protons can also result from inhomogeneities in the strong magnetic field itself, including how it is distorted by tissue placed into the field. The signal decay from both local interactions and field distortions has time constant T_2^* (pronounced "T2-star").

These different sources of decay are important because T_1 and T_2 time constants vary depending on tissue type. MRI can thus exploit signal decay to identify gray matter, white matter, fat, and/or cerebrospinal fluid. Depending on the configuration and timing of RF pulses, gradients, and other parameters set on the MRI machine (collectively known as a *pulse sequence*), the signals received from different voxels can highlight the contrast between tissues with different T_1 values (T_1-weighted image) and/or different T_2 values (T_2-weighted image). For example, white matter is brighter than gray matter in T_1-weighted images and vice versa for T_2-weighted images.

The standard pulse sequence for measuring brain function is the echo planar imaging (EPI) sequence. EPI has two desirable properties for fMRI: It is extremely fast, allowing an entire slice to be acquired from one RF pulse in less than 100 ms, and it is sensitive to T_2^*, which, as we will see later, is how MRI measures neural activity. When designing an fMRI study, several parameters of the EPI sequence need to be chosen, including how many slices to acquire in the brain volume (typically 30–90); how much time per volume (repetition time, typically 1–2 s); what voxel resolution to use (typically 2–3 mm in each dimension); and

whether to use parallel acquisition (eg, acquire multiple parts of a slice and/or multiple slices at once). These choices are interdependent, imposing trade-offs between speed, precision, and signal-to-noise.

fMRI Depends on the Biology of Neurovascular Coupling

We have described general principles of magnetic resonance, but what about the second part of the story, neurovascular coupling? Active neurons consume energy obtained from oxygen in blood. Thus, when a brain area is active, blood oxygenation drops in that moment. To replenish these metabolic resources, the flow of blood to the local area increases over the next few seconds. Supply exceeds demand, and so, counterintuitively, there is a higher proportion of oxygenated (versus deoxygenated) blood in active brain areas.

To link this to magnetic resonance, remember that T_2^* decay reflects dephasing of protons caused by field inhomogeneities. Blood has different magnetic properties depending on oxygenation: Deoxygenated blood interacts with the magnetic field because the iron in hemoglobin is unbound, whereas oxygenated blood in which the iron is bound to oxygen does not. Deoxygenated blood thus causes faster T_2^* decay and reduces signal relative to oxygenated blood. This difference in signal is referred to as the *blood oxygenation level–dependent* (BOLD) contrast. Putting everything together, increased signal in a voxel measured with an EPI sequence indicates recent neuronal activity because of the relative increase in local blood oxygenation that accompanies such activity. The temporal profile of this BOLD response, known as the *hemodynamic response function*, looks like a bell curve with a long tail, peaking around 4 to 5 seconds after local neural activity and returning to baseline after 12 to 15 seconds.

There are many more details about the physics and biology of fMRI. In addition, our understanding of how it all works is still evolving. For example, it is unclear whether BOLD is more closely tied to the firing of individual neurons or to the activity of neural populations. Likewise, it may be difficult to distinguish whether increased blood oxygenation is caused by increases in local excitation or inhibition. More generally, the mechanisms of neurovascular coupling—how the brain knows when and where to deliver oxygenated blood—remain mysterious, with a growing focus on the functional role of astrocytes. There is also the possibility of obtaining better temporal and spatial resolution by measuring the initial consumption of oxygen at the precise site of neuronal activity (the "initial dip"), reflected in an immediate and focal rise in deoxygenated blood rather than the delayed and more diffuse oversupply of oxygenated blood. Nevertheless, even with an incomplete understanding, fMRI has utility as a tool to localize changes in neural activity in the human brain induced by mental operations.

Functional MRI Data Can Be Analyzed in Several Ways

When performing an fMRI experiment, researchers link the neurovascular measurements described earlier to cognitive tasks programmed into a computer script that a human subject performs. The script generally produces a series of *runs* that correspond to a continuous period of data collection (ie, several fMRI volumes in a row), typically lasting 5 to 10 minutes. Within each run, several *trials* are presented to the subject, often by showing a visual stimulus or playing an auditory stimulus. Depending on the task, the subject may, for example, passively view or listen to the stimulus, make a decision about it, or store it in memory. A button press or eye movement response is often collected as a behavioral index of cognitive processing on that trial. These trials are typically drawn from two or more task *conditions*, which determine the stimulus type, task difficulty, or other experimental parameters. In a basic subtraction design, trials are divided between an experimental condition and a control condition, which are identical but for one critical difference whose neural basis is being investigated. Trials usually last 2 to 10 seconds, often separated by a variable or "jittered" interval of several seconds. In all, such sessions typically last up to 2 hours.

Each fMRI session produces a large amount of raw data, with BOLD responses sampled thousands of times at hundreds of thousands of locations in the brain. How are these data translated into insights about cognition and behavior? Numerous approaches to fMRI analysis are possible (Box 6–1), but for the most part, they break down into three categories (Figure 6–2). We first describe preprocessing steps common to all three types and then explain how each is conducted and what it can tell us.

fMRI Data First Need to Be Prepared for Analysis by Following Preprocessing Steps

Before the data can be analyzed, they must be prepared for processing. This is accomplished with a series of

Box 6–1 Brain Imaging as Data Science

Compared to many areas of science, the basic methods of brain imaging have enjoyed remarkable standardization. A major reason for this has been the availability of widely adopted software packages since the earliest days of fMRI in the mid-1990s. These packages were created and released by research groups, and—before it was fashionable—most were open-source.

At first, they included tools for preprocessing, alignment, analysis models, and statistical corrections. They have since incorporated new tools developed by researchers, including nonlinear alignment, field map correction, nonparametric statistics, and parallelization.

As a result, virtually all fMRI researchers use one or more of these packages, at least for part of their analysis pipeline. The following are popular free software packages for fMRI analysis:

AFNI: https://afni.nimh.nih.gov

FSL: https://fsl.fmrib.ox.ac.uk

SPM: https://www.fil.ion.ucl.ac.uk/spm

Beyond these specialized packages, fMRI is increasingly being viewed through the more general lens of data science. There are two reasons for this. First, fMRI produces a huge amount of data, both within each session but also aggregated across the thousands of studies that have been conducted. Making sense of fMRI data can thus be considered a big-data problem. Second, the data are incredibly complex and noisy, and the cognitive signals of interest are weak and hard to find. This creates a data mining challenge that has inspired many computer scientists.

The most concrete manifestation of this trend is the rise of machine learning in fMRI analysis. Other points of contact with data science include the challenges associated with the real-time analysis of streaming data, the application of network analysis and graph theoretic approaches, the use of high-performance computing clusters and cloud systems, and the growing practice of researchers publicly sharing data (eg, https://openneuro.org), code (on services such as GitHub), and educational materials (eg, https://brainiak.org/tutorials). Thus, the field of brain imaging will continue to benefit from advances in computer science, engineering, applied math, and statistics.

steps referred to as *preprocessing*. Preprocessing seeks to remove known sources of noise in the data, caused by either the subject or the MRI machine. Standard practice includes five basic steps known as motion correction, slice-time correction, temporal filtering, spatial smoothing, and anatomical alignment.

Motion correction seeks to address inevitable noise in the data due to a subject's head movement. Even the best subjects move their heads a few millimeters over the course of a scan, such that the voxels across three-dimensional brain volumes become somewhat misaligned. This movement can be corrected for using a spatial interpolation algorithm that lines up all of the volumes within each run. This algorithm quantifies the amount of movement at each point during the scan, including the translation in the x, y, and z dimensions, and the amount of rotation about these axes (*pitch*, *roll*, and *yaw*, respectively). These six time courses can later be included in the data analysis as *regressors*, to further remove motion artifacts.

Slice-time correction is applied to deal with differences in the timing of the acquisition of samples across different slices. EPI sequences collect the slices that make up each brain volume sequentially, often in an interleaved order to avoid contamination of adjacent slices. Thus, there is a large difference in the timing of the first- and last-acquired slices of the same volume, which are closer in time to the preceding and subsequent volumes, respectively, than to each other. Correcting for this difference in the timing of the slices can be accomplished with temporal interpolation to estimate what the signal would have been if all slices were acquired simultaneously.

Temporal filtering and *spatial smoothing* aim to increase the signal-to-noise ratio. Temporal filtering removes components of the time course in each voxel that are highly likely to be noise rather than meaningful variance, such as very low frequencies (>100-second period) that typically result from scanner drift. Spatial smoothing applies a kernel (typically 4–8 mm wide) to blur individual volumes, averaging out noise across adjacent voxels and improving the odds that functions will overlap across subjects after anatomical alignment.

This *anatomical alignment* is accomplished by registering data across runs and subjects, usually with simple transformations (eg, shift, rotate, scale), to a standard template such as Montreal Neurological Institute or Talairach space. Typically, fMRI data are

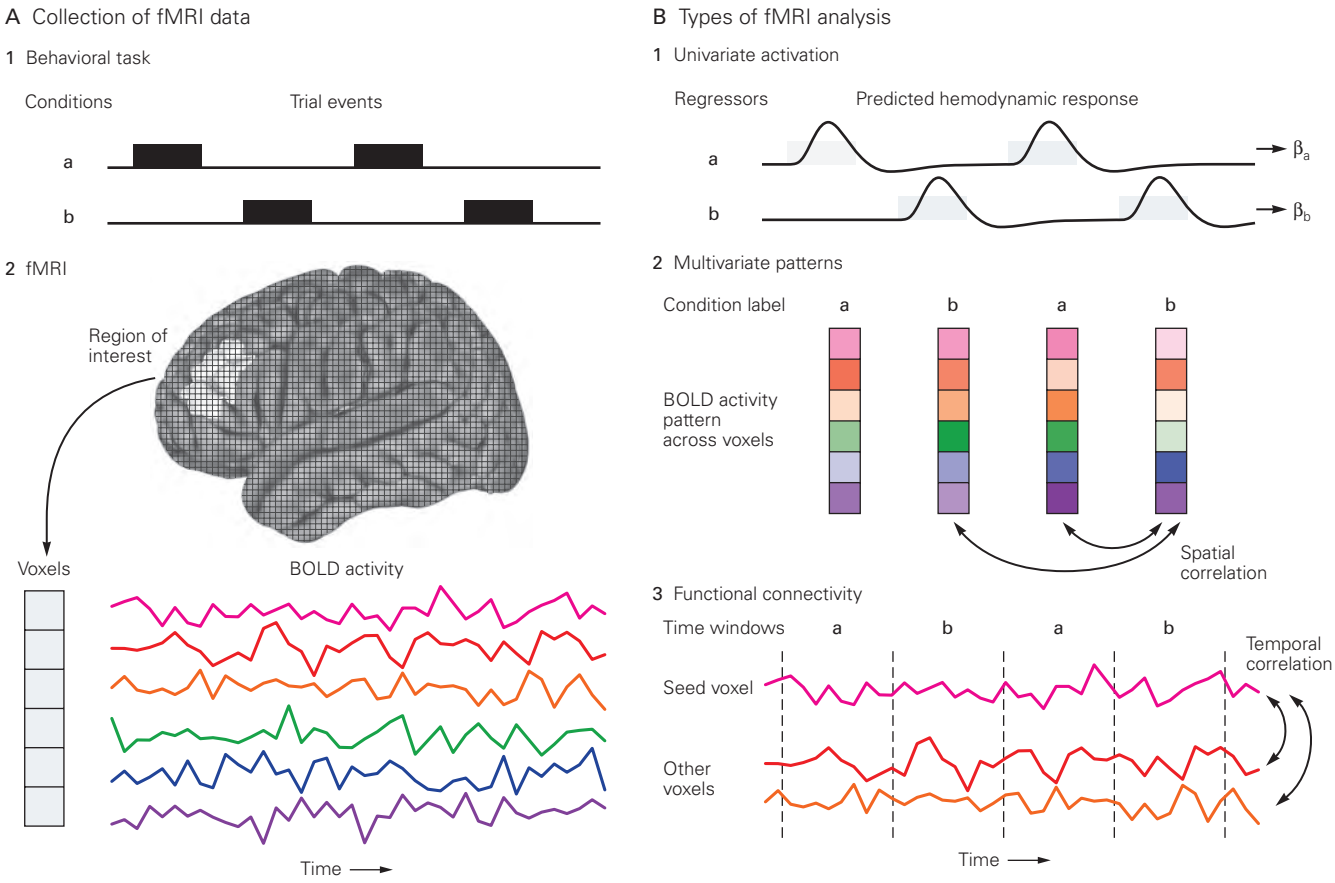

Figure 6–2 Collecting and analyzing fMRI data.

A. An fMRI experiment typically involves subjects performing a behavioral task while BOLD activity is measured from the brain.

1. The example task consists of two conditions (**a**, **b**) that alternate in time, each with two events depicted (**black rectangles**).

2. The time course of BOLD activity in six example voxels (different colors) from a region of interest (**ROI**) during the task. Analysis often focuses on an ROI or other subset of voxels in the brain to reduce the number of statistical tests performed. When all voxels in the brain are analyzed, statistical corrections are applied to reduce the number of false positives. The results of such analyses are often overlaid on a structural MRI as a color-coded heat map. The map is the result of extensive preprocessing and analysis and does not directly reflect neuronal activity or even blood oxygenation. Rather, voxels are colored to indicate that they have passed the threshold of being considered significant in a statistical test.

B. Three analysis approaches are often used in fMRI experiments such as the one depicted in **A**.

1. Univariate activation analysis attempts to explain the BOLD activity of each individual voxel in terms of what happened in the task. This is accomplished using a statistical model that contains a regressor for each task condition specifying the predicted hemodynamic response (**bell curves**) for trial events from that condition (**gray rectangles**). The result of fitting the model to BOLD activity is a beta value for each regressor in every voxel, quantifying the average response of the voxel to trials of that condition. The beta values for a voxel can be subtracted to measure whether there is a greater response in one condition than another. To determine statistical significance, this difference in activation between conditions in each voxel is compared across subjects.

2. Multivariate pattern analysis considers the pattern of BOLD activity across voxels. These spatial patterns are extracted for each trial from a subset of voxels (six depicted) and at a particular moment in time, often the peak of the predicted hemodynamic response (color saturation indicates amplitude of BOLD activity in each voxel on that trial). There are two common ways of analyzing these patterns. The first (shown) involves calculating the spatial correlation of patterns from a pair of trials to explore how similarly voxels responded to the trials. If a brain region represents different information across conditions, this pattern similarity should be higher for pairs of trials from the same versus different conditions. The second type of multivariate pattern analysis (not shown) uses a type of machine learning known as pattern classification. Some of the patterns and their corresponding condition labels are used to train a classifier model, assigning weights to voxels based on how useful they are at distinguishing between conditions. The model is then tested with other patterns on which it was not trained. If a brain region represents different information across conditions, the model should be able to correctly guess from which condition the patterns were extracted. To determine statistical significance, spatial correlations or classification accuracies in a region are compared across subjects.

3. Functional connectivity analysis examines how BOLD activity is correlated between voxels over time. Typically, a seed voxel or ROI is chosen and its time course (**pink curve**) is correlated with the time courses of other voxels (two shown here). This can be performed while the subject is resting, resulting in a correlation value for every voxel that can be used to identify brain networks in a baseline state. Functional connectivity can also be calculated in different time windows of a task (**dashed lines**), resulting in a correlation value for each trial that can be used to understand the dynamics of these networks. To determine statistical significance, temporal correlations for each voxel are compared across subjects between conditions or against zero.

first aligned to a structural scan from the same subject, and then this structural scan is aligned to the standard template.

Once these five steps are completed, the data are ready for analysis.

fMRI Can Be Used to Localize Cognitive Functions to Specific Brain Regions

The first kind of fMRI analysis seeks to localize functions in the brain and to determine what brain regions are associated with a behavior. This is based on having subjects complete a task during fMRI and then examining the relationship between different phases of the experiment and changes in BOLD activity in different parts of the brain. Based on researchers' knowledge of what happened at different times in the experiment, the function of the regions can be inferred.

A series of statistical analyses are performed to quantify this relationship and to determine its significance. Typically, this is accomplished using a statistical regression method known as a *general linear model* (GLM). The GLM attempts to explain observed data (here, the time course of the BOLD activity in each voxel) as a linear combination of regressors that reflect independent variables (eg, task conditions) and covariates (eg, movement parameters).

The regressors that model task conditions serve as a hypothesis about how a voxel should respond if involved in the cognitive function manipulated by that task. The regressor for each condition is generated by marking the onset and duration of each trial of that condition in the experimental time line, corresponding to the expected neuronal activity, and then accounting for the delayed hemodynamic response. All regressors are fit simultaneously to the fMRI activity in each voxel, and the result is a parameter estimate (or "beta") for each condition and voxel, reflecting how much of the temporal variance of the voxel is uniquely explained by that condition's trials on average.

To localize a function, betas from two or more conditions are compared in a contrast. The most basic form of contrast is to subtract one beta (eg, control condition) from another (eg, experimental condition). Contrasts are typically averaged over runs within each subject and then entered into a t-test to assess reliability across subjects. Because statistics are calculated for every voxel, there is a high risk of false positives, and a correction for multiple comparisons is required (eg, by giving voxels more credence if they cluster together with other significant voxels). Alternatively, a more constrained analysis can be performed, focusing on a limited number of regions of interest (ROIs) that are defined a priori. Contrast values can then be averaged over the voxels in an ROI to produce regional estimates, rather than examining all voxels in the brain, thereby reducing the number of comparisons.

This general family of approaches is often described as measuring *univariate activation*—"univariate" because each voxel or region is treated independently and "activation" because the result is a measure of the relative activity evoked by one condition versus another. This kind of analysis is typically used to localize a cognitive function to a set of voxels or regions in the brain.

However, univariate activation can be used for more than localization. For example, a GLM can make quantitative predictions about BOLD activity by assigning a continuous weight, rather than a categorical one, to each trial in a regressor based on an experimental parameter (eg, working memory load), behavioral measurement (eg, response time), or computational model (eg, prediction error in reinforcement learning). The resulting beta reflects how much a voxel correlates with the variable of interest.

Another use of univariate activation is for measuring changes in BOLD activity as a function of repeating a stimulus. Such studies take advantage of *adaptation* (or *repetition suppression*)—the tendency of stimulus-selective neurons to respond less to repeated versus new stimuli. This fact allows the tuning of a brain region to be inferred by conducting an experiment in which related and unrelated stimuli are presented sequentially. In some trials, one stimulus is followed by a near-repetition of the same stimulus, but with a feature changed (eg, its location or size). A univariate analysis tests whether BOLD activity in voxels from the region is lower on these trials compared to other trials in which either (1) the first stimulus is followed by an unrelated second stimulus or (2) the changed stimulus is preceded by an unrelated stimulus. If such a BOLD reduction is observed, the region can be interpreted as not tuned for the changed feature (eg, the region could be considered location or size invariant).

fMRI Can Be Used to Decode What Information Is Represented in the Brain

The second category of fMRI analysis seeks to characterize what kinds of information are represented in different regions of the brain to guide behavior. Rather than analyze voxels independently or average over voxels within an ROI, these analyses examine the information carried by spatial *patterns* of BOLD activity over multiple voxels. This is typically referred to as *multivariate pattern analysis* (MVPA). There are two

types of MVPA, based on the similarity or classification of activity patterns.

Similarity-based MVPA tries to understand what information is contained or "represented" in a brain region. This is accomplished by examining how similarly the region processes different conditions or stimuli in an experiment. This similarity is calculated from the pattern of activation across voxels in an ROI, defined as either the pattern of beta values from a GLM or the pattern of raw BOLD activity from preprocessed data. Once these patterns have been defined for multiple conditions or stimuli, the correlation or distance of each pair of patterns is calculated. This produces a matrix of the pairwise similarities between conditions or stimuli within the ROI. With this matrix, it is possible to infer to what information the ROI is most sensitive. For example, if subjects are shown photos of different objects (eg, a banana, canoe, taxi), a matrix of distances between the activity patterns evoked by these objects can be computed for different brain regions. An ROI in which there is less distance between banana and canoe than between either of them and taxi could be interpreted to mean that the region represents shape (ie, concavity); another region in which the lowest distance is between banana and taxi might represent color (ie, yellow); or one with the lowest distance between canoe and taxi might be interpreted as representing function (ie, transportation).

Neural similarity from fMRI can also be compared with similarity calculated in other ways for the same conditions or stimuli, including from human judgments, computational models, or neural measures in other species. For example, if human subjects rate a large set of stimuli in terms of how similar they look to each other, a brain region with a matching similarity structure could be considered a candidate source of this behavior. This approach of calculating *second-order* correlations between neural and behavioral similarity matrices, or between neural similarity matrices from two sources, is called *representational similarity analysis* (RSA).

Classifier-based MVPA uses techniques from machine learning (discussed in Chapter 5) to decode what information is present in a brain region. The first step is to train a classifier model on a subset of the fMRI data to discriminate between conditions or stimulus classes from patterns of BOLD activity across voxels in an ROI. These patterns are usually obtained from individual trials, and each is labeled according to the condition or stimulus on the corresponding trial. This training set thus contains several brain pattern examples of each class. Classifier training can use many different algorithms, the two most common being support vector machine and regularized logistic regression. The result is typically a weight for each voxel reflecting how activity in that voxel contributes to classification collectively with the other voxels. The second step after training is to test the classifier by examining how well it can decode patterns from a held-out and independent subset of fMRI data (eg, from a different run or subject). The pattern of BOLD activity on each test trial is multiplied by the learned classifier weights and summed to produce a guess about how the pattern should be labeled. Classification accuracy is quantified as the proportion of these guesses that match the correct labels. Importantly, this approach can be used to understand how different brain regions give rise to behavior, such as by attempting to classify which action was performed, which decision was made, or which memory was retrieved.

fMRI Can Be Used to Measure Correlated Activity Across Brain Networks

The third category of fMRI analysis seeks to understand the organization of the brain as a network. Knowing what brain regions do individually does not fully explain how the brain as a whole generates behavior. It is additionally critical to know how brain regions relate to each other—that is, where do the inputs to a region come from and where do the outputs go? This requires an understanding of which regions communicate with each other and when and how they transmit information. This is difficult to determine definitively with fMRI but can be estimated by measuring the correlation of BOLD activity between voxels or regions over time. If two parts of the brain have correlated activity, they may be sharing the same information or participating in the same process. Such correlations are interpreted as measures of *functional connectivity*.

One way to study functional connectivity with fMRI is to measure BOLD correlations in a resting state. Subjects are scanned while they lie still without performing a task, and then the time course of BOLD activity from one "seed" ROI is extracted and correlated with the time courses from other ROIs or from all voxels in the brain. Alternatively, clustering or component analyses can be used without a seed to identify collections of voxels with similar temporal profiles. Resting functional connectivity defined in these ways has helped reveal that the brain contains several large-scale networks of regions. The most widely studied of these networks is referred to as the default mode network, which includes the posterior medial cortex, lateral parietal cortex, and medial prefrontal cortex.

By definition, resting connectivity cannot be linked to concurrent behavior. Nor is it static, as telling subjects not to do anything does not restrict what they think about. Nevertheless, resting connectivity can be linked to behavior indirectly by examining how it goes awry in disease or disorders and how it relates to cognitive differences between people.

Functional connectivity can be linked more directly to behavior if it is measured during tasks rather than at rest. One difficulty in interpreting such correlations between regions is that two regions might be correlated during a task not because they are communicating with each other, but because of a third variable. For example, the regions might be responding independently but coincidentally to the same stimulus. Thus, task-based functional connectivity is typically calculated after removing, or otherwise accounting for, BOLD responses evoked by stimuli. This approach allows functional connectivity to be manipulated experimentally and compared across task conditions. These comparisons provide insight into how the involvement and interaction of brain regions in a network change dynamically to support different behaviors. This has proven useful for understanding cognitive functions such as attention, motivation, and memory, which depend on some brain regions modulating others.

Functional connectivity can also be viewed as a pattern (of correlations rather than activity) and submitted to MVPA. Correlation patterns are larger in scale than activity patterns: If there are n voxels in an activity pattern, there are on the order of n^2 voxel pairs in a correlation pattern. Thus, it can be helpful to summarize the properties of correlation patterns using graph theory, where individual voxels or regions are treated as the nodes in the graph and the functional connectivity between these nodes determines the edge strengths.

Functional MRI Studies Have Led to Fundamental Insights

Functional MRI has changed our understanding of the basic neurobiological building blocks of human behavior. Combining experimental manipulations and computational models from cognitive psychology with precise neurobiological measurements has expanded existing theories of the mind and brain and has stimulated new ideas. Discoveries from fMRI have impacted not just our understanding of behaviors presumed to be uniquely human, but also behaviors that have long been investigated in animals.

In this section, we review three examples of this progress. The study of face perception reveals how human fMRI studies have inspired research in animals. The study of memory illustrates how fMRI has challenged theories from cognitive psychology and systems neuroscience. The study of decision-making shows how animal studies and computational models have advanced fMRI research.

fMRI Studies in Humans Have Inspired Neurophysiological Studies in Animals

Our understanding of how the brain perceives faces has grown tremendously over the past two decades (Chapter 24). The advances described below provide an example of how findings from fMRI in humans inspired follow-up studies with neuronal recordings and causal interventions in nonhuman primates. This synergy across species and techniques led to a more complete understanding of the fundamental process by which faces are recognized.

Some classes of stimuli are more important for survival than others. Does the brain have dedicated machinery for the processing of such stimuli? Faces are an obvious case in humans. The development of fMRI combined with careful and systematic experimental designs led to important insights into how and where faces are processed in the human brain. One region in the fusiform gyrus, often referred to as the fusiform face area (FFA), was found to show robust and selective BOLD activity when humans view faces.

Early fMRI studies that led to this discovery relied on simple designs in which subjects were presented with a series of different types of visual stimuli. To measure the face selectivity of brain areas, the BOLD response to faces was compared with the BOLD responses for the other categories (eg, places, objects). An area of the lateral fusiform gyrus, most reliably in the right hemisphere, was strongly activated by faces. These findings fit with earlier findings of individual neurons in nonhuman primates that respond to faces, but inspired a new wave of animal studies to examine a larger-scale network of brain regions. These newer animal studies, borrowing experimental designs from the human studies, first used fMRI to find orthologs of the FFA. The resulting face patches were then probed invasively with neuronal recording and stimulation. This revealed insights into the distributed neural circuitry for face processing in primates.

In addition to responding selectively to face stimuli, does the FFA contribute to the behavior of face recognition? This question has been addressed using stimulus variations that are known to affect face recognition

(eg, presenting faces that are inverted or presenting parts of faces). Initial fMRI studies using simple comparisons of stimulus categories (inverted versus upright faces) produced weak and mixed results. Follow-up studies used an adaptation design to determine how BOLD activity changes when a face is repeated intact or altered. The findings suggested that the FFA represents intact faces differently than when the same visual features are reconfigured in a way that disrupts behavioral recognition.

Another way to examine the behavioral significance of a region is to study patients who have behavioral deficits—in this case, an impairment of face recognition known as prosopagnosia. Surprisingly, some fMRI studies found an intact FFA in these patients, casting doubt on its necessity for face perception. However, here too follow-up studies using an adaptation design proved informative: The otherwise intact FFA of prosopagnosics did not adapt when the same face was repeated. This suggests that the FFA responds differently in people with prosopagnosia, consistent with its importance to face recognition.

The finding that visual categories, or mental processes more generally, can be mapped to one or a small number of regions like the FFA was important for thinking about the relationship between mind and brain. Whether specific functions are localized or broadly distributed has been a central question regarding brain organization throughout the history of neuroscience (Chapter 1). The discovery of the FFA and the face patch system provided new evidence of localization, and encouraged researchers to pursue the hypothesis that other complex cognitive functions might be localized in specific brain areas or small sets of nodes, but also to question whether localization is the right way to think about brain organization. For example, further studies showed that faces produce widely distributed responses over visual cortex and that the FFA can be co-opted for recognition of other kinds of objects with which we have expertise. These debates reflect the transformative nature of this original work, both for studies of the human brain and for related questions in animal models.

fMRI Studies Have Challenged Theories From Cognitive Psychology and Systems Neuroscience

Many theoretical models from cognitive psychology were originally agnostic about the brain. However, there are now several examples of fMRI findings that changed our understanding of the organization and mechanisms of cognition.

One prominent example is the study of memory. The overall goal of memory research, beginning in the 19th century, has been to understand how a memory is created, retrieved, and used, and whether these processes differ across types of memory. A key discovery came from research on patient H.M. and the realization that damage to the hippocampus causes a loss of the ability to form new autobiographical memories but does not impact the ability to learn certain skills (Chapter 52). These findings led to the idea that memory can be divided into two broad classes, conscious versus unconscious (also known as declarative versus procedural or explicit versus implicit). In the tradition of localization, these and other types of memory were mapped onto distinct brain regions, based on where in the brain a patient had damage and which behavioral symptoms they exhibited.

Later fMRI studies of the healthy human brain helped reveal that this dichotomy was oversimplified. First, several studies using what came to be known as the *subsequent memory task* showed that regions beyond the hippocampus are implicated in the successful formation of declarative memory. In such studies, subjects are presented with a series of stimuli (pictures or words) while being scanned. Later, usually outside of the MRI machine, their memory for these stimuli is tested. The BOLD responses from when a stimulus was initially encoded are then sorted based on whether it was subsequently remembered or forgotten. These conditions are contrasted to reveal which brain regions show more (or less) activity during successful memory formation. In addition to finding such differences in the hippocampus and surrounding medial temporal lobe, BOLD activity in prefrontal and parietal cortices is also predictive of later memory. By measuring the whole brain of healthy individuals, fMRI revealed that declarative memory is served by more than one brain system—processes linked to prefrontal cortex (eg, semantic elaboration) and parietal cortex (eg, selective attention) are also involved in encoding.

The traditional taxonomy of memory organization was challenged in another way by fMRI studies. fMRI revealed that a wide range of tasks that were previously assumed to not involve the hippocampus (or declarative memory) in fact do consistently engage this region. These studies often use learning tasks that would classically be considered unconscious, in which subjects have the opportunity to learn but are never asked to report their memories and, in some instances, are unable to do so if prompted. For example, in the *probabilistic classification task*, subjects learn by trial and error to sort visual cues into categories, even when the relationship between cues and categories is sometimes unreliable. BOLD activity during such learning trials is estimated and compared to

a baseline task that does not involve trial-and-error learning (eg, studying cues with their categories provided). Such comparisons generally reveal activation in the striatum, but also reliably in the hippocampus (see Chapter 52).

In summary, fMRI studies of tasks thought to rely on declarative memory often recruit regions outside of the hippocampus, and tasks thought to rely on procedural memory can recruit the hippocampus. In both cases, these discoveries were serendipitous and made possible only because data were obtained from the whole brain with fMRI. Although these began as unexpected results, they led to systematic follow-up studies that have updated our understanding of the organization of memory. Chiefly, they challenged the original emphasis on conscious awareness as the defining characteristic of hippocampal processing. This in turn helped relate the findings from human studies to those from animal studies, where the notion of conscious memory is less central and where tasks that engage the hippocampus often involve spatial navigation. Thus, fMRI findings in humans have been transformative for our understanding of theoretical models of memory, in terms of both neural structures and cognitive behaviors.

fMRI Studies Have Tested Predictions From Animal Studies and Computational Models

The integration of computational models with fMRI has been an important development in cognitive neuroscience. One example of this comes from studies of how the brain learns to predict and obtain rewards, combined with models of reinforcement learning that formalize this process. These models co-evolved with studies of reward-based decision-making in animals, which also inspired later human studies.

Central to these studies and theories, midbrain dopaminergic neurons increase their firing in response to unexpected rewards, such as juice (Chapter 43). Once a predictive cue has been reliably paired with a reward, the neurons shift their response in time to this predictive cue. If a predicted reward fails to occur, firing decreases. This pattern of responses suggests that midbrain dopaminergic neurons signal the difference between expected and actual rewards. This difference is commonly known as *reward prediction error* and has been modeled using equations based on reinforcement learning theory. When this model is applied to human tasks involving rewards, hypothesized reward prediction errors can be estimated on a trial-by-trial basis. These estimates can then be used to predict BOLD activity and identify voxels and regions that may be involved in reinforcement learning in the human brain.

In a typical study of this type, subjects perform a learning task during fMRI, making a series of choices about visual cues to predict possible rewards. They learn the outcome immediately after each choice. For example, a subject might view two shapes (eg, circle, triangle), choose one by pressing a button, and then learn whether the choice led to a monetary reward. The key feature of such tasks is that the association between shapes and rewards is probabilistic and changes over the course of the experiment. Because of this noisy relationship, subjects must learn to track the likelihood of reward for each shape. Reward prediction error can be calculated on each trial based on the history of the subject's choices and rewards and then included in the analysis of their fMRI data. Many studies using this approach have found that trial-by-trial reward prediction error correlates with BOLD activity in the ventral striatum, an area that receives input from midbrain dopaminergic neurons.

Other computational models, such as *deep neural networks*, which integrate cognitive psychology, computer science, and neuroscience, have also served an important theoretical purpose by generating novel hypotheses about brain activity. Because these models are often inspired by the architecture and functions of the brain, they help bridge levels of analysis, from physiological recordings in animals to fMRI in humans. They also serve a useful purpose in data analysis by simulating variables of psychological and neurobiological interest that can be sought in the brain, an approach often referred to as model-based analysis.

Functional MRI Studies Require Careful Interpretation

The examples provided earlier illustrate how fMRI can improve our understanding of the links between brain and behavior. At the interface with psychology, fMRI can complement purely behavioral measurements. Many complex human behaviors (eg, memory recall, decision-making) depend on multiple processing stages and components. Measuring these processes with fMRI can provide richer and more mechanistic explanations of behavior than those based on simple behavioral measurements such as accuracy or response time alone. At the interface with systems neuroscience, fMRI complements direct neuronal recordings. Most brain areas (eg, hippocampus) support multiple behaviors and do so in concert with other regions. The ability to image the whole brain with fMRI makes it

possible to arrive at a more complete understanding of neural mechanisms at the network level.

What does it mean then to find BOLD activity in a region during a task? The multiplicity of mappings between brain and behavior poses serious challenges to interpretation of fMRI results (Figure 6–3). One fundamental consideration is the type of inference. Most fMRI studies use *forward inference*, in which an experiment compares BOLD activity between task conditions that manipulate the engagement of a particular mental process (eg, comparing the effects of face versus nonface stimuli to study face recognition). Brain regions that differ between these conditions can be inferred to take part in the manipulated process. Forward inference relies on a task manipulation and therefore allows a researcher to infer that differences in brain activity are related to the mental process of interest.

With *reverse inference*, differences in neural activity are the basis for inferring which specific mental process is active, even when the conditions that gave rise to the differences were not designed to manipulate that process. For example, in the previous face versus nonface contrast, a researcher might interpret differential activity in the striatum as evidence that faces are rewarding. This kind of reverse inference is often unjustified, as reward was neither measured nor manipulated—the interpretation is based on other studies that manipulated reward and found striatal activity. The problem arises because each brain region generally supports more than one function, meaning that it is unclear from the observation of activity alone which function(s) were engaged. Indeed, the striatum is also strongly implicated in movement, so perhaps faces are engaging motor rather than reward processes? The logically sound conclusion in this example, reflecting forward inference, is that the striatum is involved in some (as yet unresolved) aspect of face recognition.

One solution therefore is not to use reverse inference in fMRI studies. However, there are some situations in which reverse inference can be desirable or even necessary. For example, reverse inference can allow researchers to perform exploratory analyses and generate new hypotheses, even from data that were collected for other purposes. This may be especially important for getting the most out of fMRI data that are hard to collect, such as from children, the elderly, and patients (Box 6–2). Motivated by this need, statistical tools have been developed to support reverse inference. For example, the web-based tool Neurosynth uses a large database of published studies to assign a probability that a specific mental process (eg, reward) is involved given that BOLD activity has been observed in a particular region (eg, striatum).

It is also important to make a distinction between a correlation of brain activity with behavior versus a cause-and-effect relationship between the brain activity and the behavior. If a brain region is selectively and consistently involved in a specific mental process, this correlation does not license the conclusion that it plays a necessary or sufficient role in the process. With respect to sufficiency, the brain region might (and likely does) work with one or more other brain regions to accomplish the process. With respect to necessity, activity in the region might be a secondary by-product of processing elsewhere.

One approach to bolstering the interpretation of an fMRI study is to evaluate how the findings converge with those from more invasive methods, such as electrical stimulation in epilepsy patients. Because every tool has limitations, including other correlational measures such as neuronal recordings, this principle of converging evidence is central to advancing understanding of how the brain supports behavior. In addition to converging evidence across studies and tools, there are also efforts to manipulate brain function simultaneously with fMRI, using transcranial magnetic stimulation or real-time neurofeedback.

Future Progress Depends on Technological and Conceptual Advances

Functional MRI is the best technology we have so far for probing the healthy human brain. It allows measurement of the whole brain at reasonably high resolution as well as many aspects of the mind in large subject samples without harm. However, in other ways, it is far from what we ultimately need if we are to obtain a deeper and more precise understanding of how the brain works. When compared to tools available in animals, fMRI provides relatively noisy, slow, and indirect measurements of neuronal activity and circuit dynamics.

Efforts are underway to address these limitations, both technically and biologically. On the technical front, multiband imaging sequences can enhance the temporal and spatial resolution of fMRI data by enabling the acquisition of multiple slices through the brain in parallel. However, faster measurements are inherently limited by the slow speed of the hemodynamic response and smaller voxels still average across hundreds of thousands of neurons.

On the biological front, we have a rudimentary understanding of how BOLD activity emerges from physiological mechanisms in the brain, such as single neuron activity, population activity, the function of

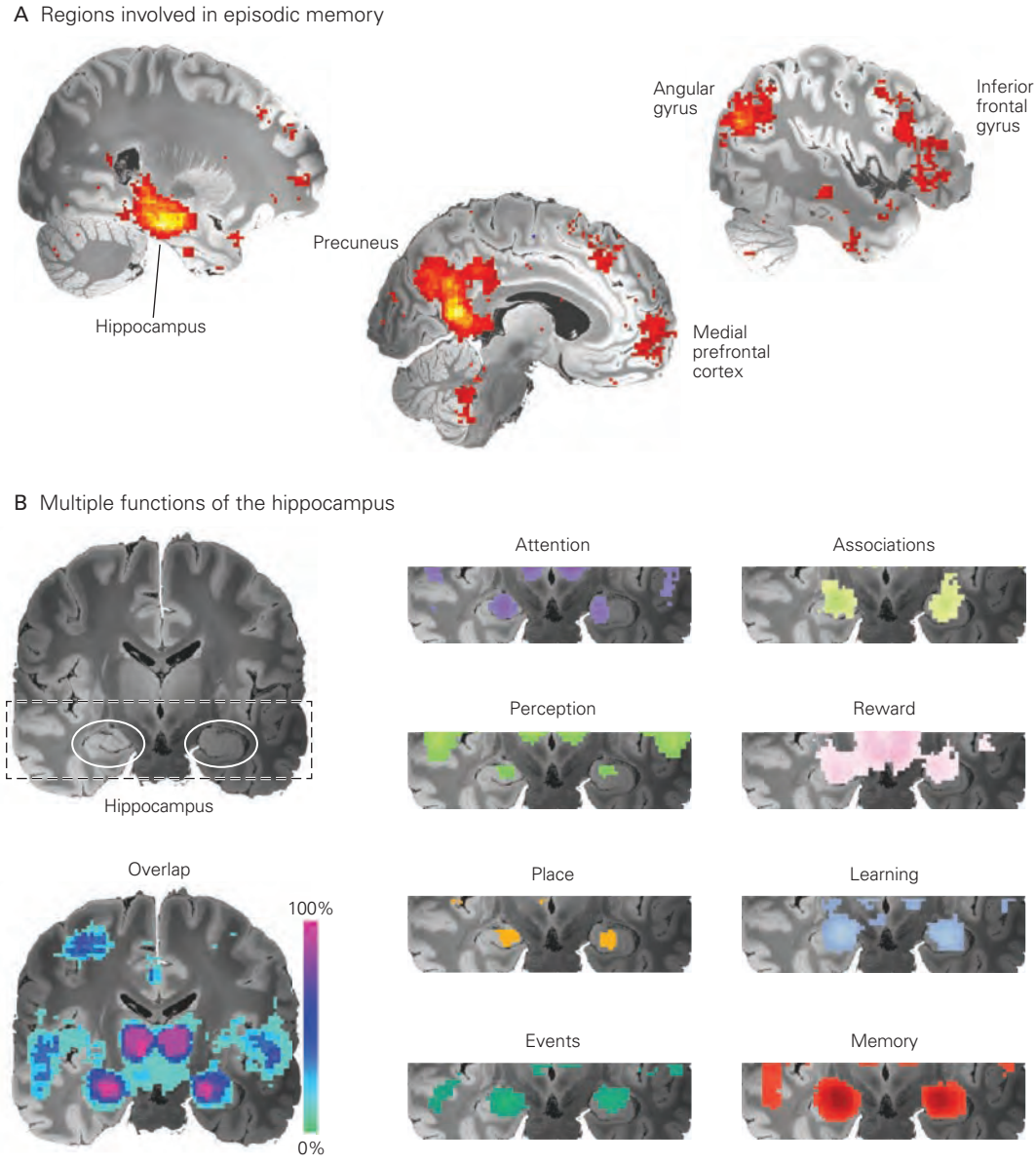

Figure 6–3 **Challenges of mapping mind and brain.** Any interpretation of data from fMRI must consider the complexity of the relationship between cognitive functions and brain regions. This complexity is illustrated here with a meta-analysis from a database containing more than 14,000 published fMRI studies. (Data retrieved in 2019 from http://neurosynth.org, displayed on brain from Edlow et al. 2019; figure updated and adapted from Shohamy and Turk-Browne 2013 by Tristan Yates.)

A. This map shows that multiple brain regions are engaged by episodic memory—that is, encoding and retrieval of specific events from one's past. Colored voxels indicate a high probability of the term "episodic" in studies that reported activation in these voxels (reverse inference). This example illustrates how a single cognitive function can be associated with multiple brain regions (one-to-many mapping).

B. These maps show that multiple cognitive functions engage the hippocampus (circled in white in each hemisphere). Colored voxels in each inset brain indicate a high probability that these voxels were activated in studies that examined the corresponding term (forward inference). The overlap map shows the percentage of these terms that activated each voxel. This example illustrates how a single brain region can be associated with multiple cognitive functions and behaviors (many-to-one mapping).

Box 6–2 Brain Imaging in the Real World

The ability to image the human brain with noninvasive tools and to measure internal mental processes has led to interest in applying fMRI to a variety of real-world problems, such as clinical diagnosis and treatment, law and justice, artificial intelligence, marketing and economics, and politics.

In the clinical realm, one interesting direction is the use of fMRI to examine patients in a vegetative state. Studies suggest that some such patients exhibit brain activity that reflects mental processing. For example, a patient might appear comatose—unconscious, noncommunicative, and unreactive to external stimuli—yet exhibit neural activity in the motor cortex when asked to think of an action or in category-specific visual regions when asked to imagine specific visual cues. Such findings could influence the prognosis and treatment of patients by clinicians.

Another potential real-world application of fMRI is lie detection. The ability to accurately distinguish truth from lies based on brain activity could have significant value in the courtroom. Some laboratory studies have reported differential brain activity when groups of subjects are instructed to lie repeatedly. To be useful, however, fMRI would need to provide highly reliable evidence about whether an *individual* person is lying about a *specific* event, in a way that is immune from strategies or countermeasures. This is not possible at present, and indeed, fMRI evidence is generally inadmissible in court.

These and other applications of fMRI raise ethical and privacy concerns. For example, authorities could use fMRI data to justify consequential decisions (eg, guilt or innocence), exploiting the public's bias to believe biological explanations, even when the underlying science is not settled. More troubling, humans currently have autonomy over whether we share our internal thoughts and feelings, but devices that sense this information could change that. As a result, an important challenge for neuroscientists when considering practical applications is to accurately convey that fMRI is powerful but has limitations and that our understanding of the human brain is a work in progress.

astrocytes and other glia, neuromodulatory systems, and the vascular system. A better understanding of the relationship between BOLD activity and these processes is essential for knowing when and why measurements of different types align and diverge. Although some experimental conditions lead to an increase in both neuronal activity and BOLD activity, others do not. For example, although the presentation of a visual cue increases both blood flow in the visual cortex and neuronal firing, if this visual cue is highly expected but not presented, blood flow can still increase but without an increase in neuronal activity. This suggests that there are important nuances to the coupling of neural and vascular activity that may have functional significance and that the vascular signals themselves may be more complex than previously appreciated.

As the history of fMRI shows, scientific discoveries in one field can lead to unexpected breakthroughs in other fields. The discovery of MRI in the 1970s (which 20 years later led to fMRI) came from physics and chemistry, and was so profound and far-reaching that it was recognized by the Nobel Prize in Physiology or Medicine in 2003 to Paul Lauterbur and Peter Mansfield. This in turn was made possible by the discovery of nuclear magnetic resonance decades earlier, which resulted in the Nobel Prize in Physics in 1944 to Isidor Rabi and in 1952 to Felix Bloch and Edward Purcell. These discoveries had no initial connection to neuroscience but came to spark a revolution in the study of mind, brain, and behavior.

Highlights

1. Functional brain imaging methods in cognitive neuroscience seek to record activity in the human brain associated with mental processes as they unfold in the human mind, linking biological and behavioral measures. Currently, the dominant technique is fMRI.
2. fMRI is based on two main concepts: the physics of magnetic resonance and the biology of neurovascular coupling. Combined, they allow fMRI to measure the BOLD response to neuronal activity. When human subjects perform cognitive tasks during fMRI, measurements of BOLD activity can be linked to particular mental processes and behaviors over time.
3. The link between BOLD activity and behavior is inferred through a series of preprocessing steps and statistical analyses. These analyses can answer

a range of questions, such as which brain regions are active during specific tasks, what information is coded in the spatial pattern of activity within a region, and how regions interact with each other over time as part of a network.

4. Human brain imaging has led to fundamental insights about the neural mechanisms of behavior across many domains. Some prominent examples are understanding how the human brain processes faces, how memories are stored and retrieved, and how we learn from trial and error. Across these domains, data from fMRI have converged with findings from neuronal recordings in animals and with theoretical predictions from computational models, providing a more complete picture of the relationship between brain and mind.
5. fMRI records brain activity but does not directly modify activity. Therefore, it does not support inferences about whether a brain region is necessary for a behavior, but rather whether the region is involved in that behavior. Most studies support forward inferences about this involvement, whereby activity in the brain can be linked to a mental process because the experiment manipulates that process.
6. fMRI provides an opportunity to study the function of the human brain as it engages in a variety of mental processes, in both health and disease. This technology and analyses of the data it generates are undergoing continual development to improve the temporal and spatial resolution of biological measurements and to clarify the links between these measurements, mental processes, and behavior.

Daphna Shohamy
Nick Turk-Browne

Suggested Reading

Bandettini PA. 2012. Twenty years of functional MRI: the science and the stories. NeuroImage 62:575–588.

Bullmore E, Sporns O. 2009. Complex brain networks: graph theoretical analysis of structural and functional systems. Nat Rev Neurosci 10:186–198.

Cohen JD, Daw N, Engelhardt B, et al. 2017. Computational approaches to fMRI analysis. Nat Neurosci 20:304–313.

Daw ND, Doya K. 2006. The computational neurobiology of learning and reward. Curr Opin Neurobiol 16:199–204.

Kanwisher N. 2010. Functional specificity in the human brain: a window into the functional architecture of the mind. Proc Natl Acad Sci U S A 107:11163–11170.

Poldrack RA, Mumford JA, Nichols TE. 2011. *Handbook of Functional MRI Data Analysis*. Cambridge: Cambridge Univ. Press.

Shohamy D, Turk-Browne NB. 2013. Mechanisms for widespread hippocampal involvement in cognition. J Exp Psychol Gen 142:1159–1170.

References

Aly M, Ranganath C, Yonelinas AP. 2013. Detecting changes in scenes: the hippocampus is critical for strength-based perception. Neuron 78:1127–1137.

Aly M, Turk-Browne NB. 2016. Attention stabilizes representations in the human hippocampus. Cereb Cortex 26:783–796.

Brewer JB, Zhao Z, Desmond JE, Glover GH, Gabrieli JD. 1998. Making memories: brain activity that predicts how well visual experience will be remembered. Science 281:1185–1187.

Dricot L, Sorger B, Schiltz C, Goebel R, Rossion B. 2008. The roles of "face" and "non-face" areas during individual face perception: evidence by fMRI adaptation in a brain-damaged prosopagnosic patient. NeuroImage 40:318–332.

Edlow BL, Mareyam A, Horn A, et al. 2019. 7 Tesla MRI of the ex vivo human brain at 100 micron resolution. Sci Data 30:244.

Farah MJ, Hutchinson JB, Phelps EA, Wagner AD. 2014. Functional MRI-based lie detection: scientific and societal challenges. Nat Rev Neurosci 15:123–131.

Foerde K, Shohamy D. 2011. Feedback timing modulates brain systems for learning in humans. J Neurosci 31:13157–13167.

Fox MD, Raichle ME. 2007. Spontaneous fluctuations in brain activity observed with functional magnetic resonance imaging. Nat Rev Neurosci 8:700–711.

Friston KJ, Holmes AP, Worsley KJ, Poline JP, Frith CD, Frackowiak, RS. 1994. Statistical parametric maps in functional imaging: a general linear approach. Hum Brain Mapp 2:189–210.

Grill-Spector K, Henson R, Martin A. 2006. Repetition and the brain: neural models of stimulus-specific effects. Trends Cogn Sci 10:14–23.

Hannula DE, Ranganath C. 2009. The eyes have it: hippocampal activity predicts expression of memory in eye movements. Neuron 63:592–599.

Huettel SA, Song AW, McCarthy G. 2014. *Functional Magnetic Resonance Imaging*. Sunderland, Massachusetts: Sinauer Associates, Inc.

Kanwisher N, McDermott J, Chun MM. 1997. The fusiform face area: a module in human extrastriate cortex specialized for face perception. J Neurosci 17:4302–4311.

Kim H. 2011. Neural activity that predicts subsequent memory and forgetting: a meta-analysis of 74 fMRI studies. NeuroImage 54:2446–2461.

Kriegeskorte N, Mur M, Bandettini P. 2008. Representational similarity analysis—connecting the branches of systems neuroscience. Front Syst Neurosci 2:4.

McCarthy G, Puce A, Gore JC, Allison T. 1997. Face-specific processing in the human fusiform gyrus. J Cog Neurosci 9:605–610.

Moeller S, Freiwald WA, Tsao DY. 2008. Patches with links: a unified system for processing faces in the macaque temporal lobe. Science 320:1355–1359.

Norman KA, Polyn SM, Detre GJ, Haxby JV. 2006. Beyond mind-reading: multi-voxel pattern analysis of fMRI data. Trends Cogn Sci 10:424–430.

O'Doherty JP, Hampton A, Kim H. 2007. Model-based fMRI and its application to reward learning and decision making. Ann NY Acad Sci 1104:35–53.

Owen AM, Coleman MR, Boly M, Davis MH, Laureys S, Pickard JD. 2006. Detecting awareness in the vegetative state. Science 313:1402.

Schapiro AC, Kustner LV, Turk-Browne NB. 2012. Shaping of object representations in the human medial temporal lobe based on temporal regularities. Curr Biol 22:1622–1627.

Sirotin Y, Das A. 2009. Anticipatory haemodynamic signals in sensory cortex not predicted by local neuronal activity. Nature 457:475–479.

Squire LR. 1992. Memory and the hippocampus: a synthesis from findings with rats, monkeys, and humans. Psychol Rev 99:195–231.

Turk-Browne NB. 2013. Functional interactions as big data in the human brain. Science 342:580–584.

Wagner AD, Schacter DL, Rotte M, et al. 1998. Building memories: remembering and forgetting of verbal experiences as predicted by brain activity. Science 281:1188–1191.

Wimmer GE, Shohamy D. 2012. Preference by association: how memory mechanisms in the hippocampus bias decisions. Science 338:270–273.

Yarkoni T, Poldrack RA, Nichols TE, Van Essen DC, Wager TD. 2011. Large-scale automated synthesis of human functional neuroimaging data. Nat Methods 8:665–670.

This page intentionally left blank

Part II

Preceding Page

Crystal structure of the MthK Ca^{2+}-regulated K^+ channel from the archaeon *Methanobacterium thermoautotrophicum*, a thermophilic microbe. The view is from the extracellular side of the channel in the Ca^{2+}-bound open state. MthK consists of two major functional domains. An integral membrane protein forms an aqueous pore (**blue**), which selects and conducts K^+ ions, and has a gate that switches between open and closed conformations; an intracellular Ca^{2+}-binding gating ring (**gray**) controls the gate. When it binds Ca^{2+}, the resulting conformational change is mechanically transmitted to the pore, causing it to switch to the open state. (Used with permission of Kenton Swartz, based on PDB code 1LNQ, from Jian Y, Lee A, Chen J, et al. 2002. Nature 417:523–526.)

II Cell and Molecular Biology of Cells of the Nervous System

In all biological systems, from the most primitive to the most advanced, the basic building block is the cell. Cells are often organized into functional modules that are repeated in complex biological systems. The vertebrate brain is the most complex example of a modular system. Complex biological systems have another basic feature: They are architectonic—that is, their anatomy, fine structure, and dynamic properties all reflect a specific physiological function. Thus, the construction of the brain and the cell biology, biophysics, and biochemistry of its component cells reflect its fundamental function, which is to mediate behavior.

The nervous system is made up of glial cells and nerve cells. Earlier views of glia as purely structural elements have been supplanted by our current understanding that there are several types of glial cells, each of which is specialized to regulate one or more particular aspects of neuronal function. Different varieties of glial cells play essential roles in enabling and guiding neural development, insulating axonal processes, controlling the extracellular milieu, supporting synaptic transmission, facilitating learning and memory, and modulating pathological processes within the nervous system. Some glial cells have receptors for neurotransmitters and voltage-gated ion channels that enable them to communicate with one another and with neurons to support neuronal signaling.

In contrast to glial cells, the great diversity of nerve cells—the fundamental units from which the modules of the nervous systems are assembled—are variations on one basic cell plan. Four features of this plan give nerve cells the unique ability to communicate with one another precisely and rapidly over long distances. First, the neuron is polarized, possessing receptive dendrites on one end and communicating axons with presynaptic terminals at the other. This polarization of functional properties restricts the predominant flow of voltage impulses to one direction. Second, the neuron is electrically excitable. Its cell membrane contains specialized proteins—ion channels and receptors—that permit the influx and efflux of specific inorganic ions, thus creating electrical currents that generate the voltage signals across the membrane. Third, the neuron contains proteins and organelles that endow it with specialized secretory

properties that allow it to release neurotransmitters at synapses. Fourth, this system for rapid signaling over the long distances between the cell body and its terminals is enabled by a cytoskeletal structure that mediates, on a slower time scale, efficient transport of various proteins, mRNAs, and organelles between the two compartments.

In this part of the book, we shall be concerned with the distinctive cell biological properties that allow neurons and glia to fulfill their various specialized functions. A major emphasis will be on properties of ion channels that endow neurons with the ability to generate and propagate electrical signals in the form of action potentials. We begin the discussion of neurons by considering general properties shared by ion channels—the ability to select and conduct ions, and to gate between open and closed conformations. Neurons use four major classes of channels for signaling: (1) resting channels generate the resting potential and underlie the passive electrical properties of neurons that determine the time course of synaptic potentials, their spread along dendrites, and the threshold for firing an action potential; (2) sensory receptor channels respond to certain sensory stimuli to generate local receptor potentials; (3) ligand-gated channels open in response to neurotransmitters, generating local synaptic potentials; and (4) voltage-gated channels produce the currents that generate self-propagating action potentials. In this part, we focus mainly on resting and voltage-gated channels. In Part III, we consider in more detail ligand-gated channels, and the neurotransmitters and second messengers that control their activity. The channels that are activated by sensory stimuli will be examined in Part IV.

Part Editors: John D. Koester and Steven A. Siegelbaum

Part II

7

The Cells of the Nervous System

THE CELLS OF THE NERVOUS SYSTEM— neurons and glia—share many characteristics with cells in general. However, neurons are specially endowed with the ability to communicate precisely and rapidly with other cells at distant sites in the body. Two features give neurons this ability.

First, they have a high degree of morphological and functional asymmetry: Neurons have receptive dendrites at one end and a transmitting axon at the other. This arrangement is the structural basis for unidirectional neuronal signaling.

Second, neurons are both electrically and chemically excitable. The cell membrane of neurons contains specialized proteins—ion channels and receptors—that facilitate the flow of specific inorganic ions, thereby redistributing charge and creating electrical currents that alter the voltage across the membrane. These changes in charge can produce a wave of depolarization in the form of action potentials along the axon, the usual way a signal travels within the neuron. Glia are less excitable, but their membranes contain transporter proteins that facilitate the uptake of ions as well as proteins that remove neurotransmitter molecules from the extracellular space, thus regulating neuronal function.

There are hundreds of distinct types of neurons depending on their dendritic morphology, pattern of axonal projections, and electrophysiological properties. This structural and functional diversity is largely specified by the genes expressed by each neuronal cell type. Although neurons all inherit the same complement of genes, each expresses a restricted set and thus produces only certain molecules—enzymes, structural proteins, membrane constituents, and secretory products—and not others. In large part, this expression depends on the cell's developmental history. In essence, each cell *is* the set of molecules it expresses.

There are also many kinds of glial cells that can be identified based on their unique morphological,

physiological, and biochemical features. The diverse morphologies of glial cells suggest that glia are probably as heterogeneous as neurons. Nonetheless, glia in the vertebrate nervous system can be divided into two major classes: macroglia and microglia. There are three main types of macroglia: oligodendrocytes, Schwann cells, and astrocytes. In the human brain, about 90% of all glial cells are macroglia. Of these, approximately half are myelin-producing cells (oligodendrocytes and Schwann cells) and half are astrocytes. *Oligodendrocytes* provide the insulating myelin sheaths of the axons of some neurons in the central nervous system (CNS) (Figure 7–1A). *Schwann cells* myelinate the axon of neurons in the peripheral nervous system (Figure 7–1B); nonmyelinating Schwann cells have other functions, including promoting development, maintenance, and repair at the neuromuscular synapse. *Astrocytes* owe their name to their irregular, roughly star-shaped cell bodies and large numbers of processes; they support neurons and modulate neuronal signaling in several ways (Figure 7–1C). *Microglia* are the brain's resident immune cells and phagocytes, but also have homeostatic functions in the healthy brain.

Neurons and Glia Share Many Structural and Molecular Characteristics

Neurons and glia develop from common neuroepithelial progenitors of the embryonic nervous system and share many structural characteristics (Figure 7–2). The boundaries of these cells are defined by the cell membrane or *plasmalemma,* which has the asymmetric bilayer structure of all biological membranes and provides a hydrophobic barrier impermeable to most water-soluble substances. Cytoplasm has two main components: cytosol and membranous organelles.

Cytosol is the aqueous phase of cytoplasm. In this phase, only a few proteins are actually free in solution. With the exception of some enzymes that catalyze metabolic reactions, most proteins are organized into functional complexes. A recent subdiscipline called *proteomics* has determined that these complexes can consist of many distinct proteins, none of which are covalently linked to another. For example, the cytoplasmic tail of the *N*-methyl-D-aspartate (NMDA)-type glutamate receptor, a membrane-associated protein that mediates excitatory synaptic transmission in the

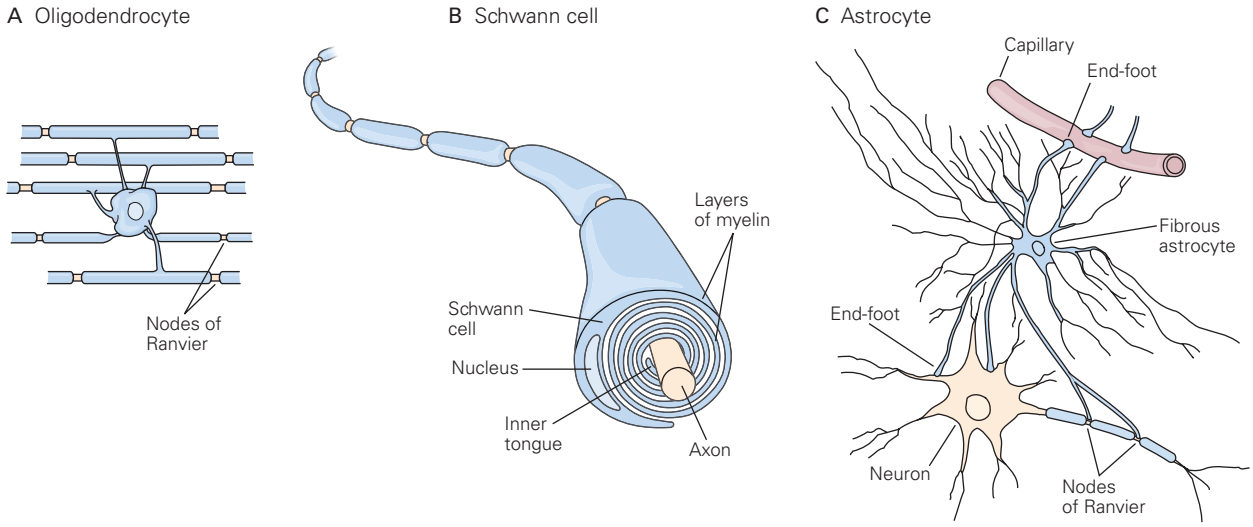

Figure 7–1 The principal types of glial cells are oligodendrocytes and astrocytes in the central nervous system and Schwann cells in the peripheral nervous system.

A. Oligodendrocytes are small cells with relatively few processes. In the white matter of the brain, as shown here, they provide the myelin sheaths that insulate axons. A single oligodendrocyte can wrap its membranous processes around many axons. In the gray matter, perineural oligodendrocytes surround and support the cell bodies of neurons.

B. Schwann cells furnish the myelin sheaths for axons in the peripheral nervous system. During development, several Schwann cells are positioned along the length of a single axon. Each cell forms a myelin sheath approximately 1 mm long between two nodes of Ranvier. The sheath is formed as the inner tongue of the Schwann cell turns around the axon several times, wrapping the axon in layers of membrane. In actuality, the layers of myelin are more compact than what is shown here. (Adapted from Alberts et al. 2002.)

C. Astrocytes, a major class of glial cells in the central nervous system, are characterized by their star-like shape and the broad end-feet on their processes. Because these end-feet put the astrocyte into contact with both capillaries and neurons, astrocytes are thought to have a nutritive function. Astrocytes also play an important role in maintaining the blood–brain barrier (described later in the chapter).

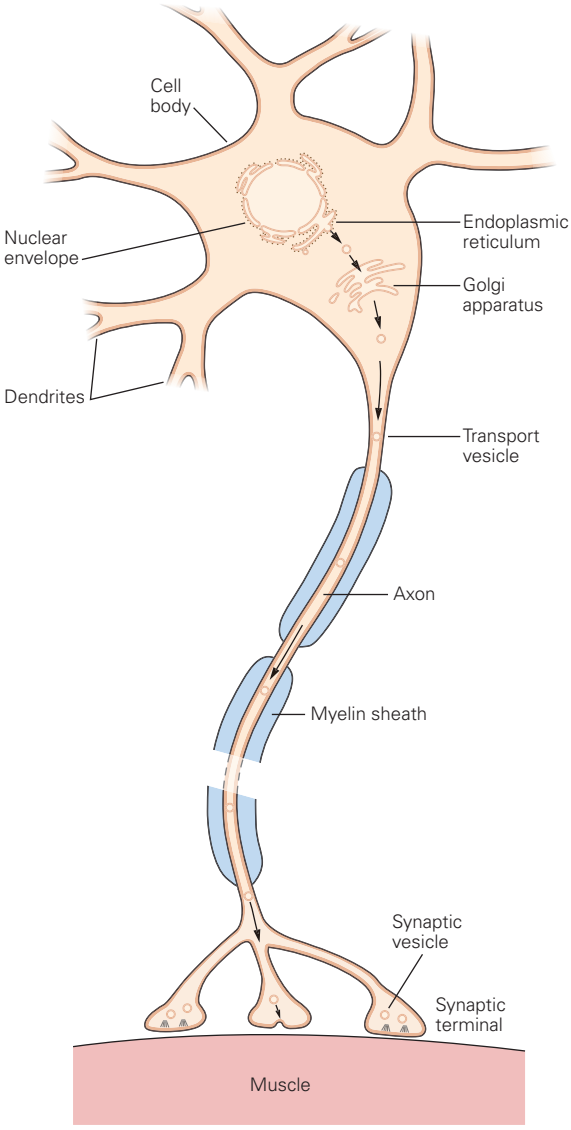

Figure 7–2 **The structure of a neuron.** The cell body and nucleus of a spinal motor neuron are surrounded by a double-layered membrane, the nuclear envelope, which is continuous with the endoplasmic reticulum. The space between the two membrane layers that constitutes the nuclear envelope is continuous with the lumen of the endoplasmic reticulum. Dendrites emerge from the basal aspect of the neuron, the axon from the apical aspect. (Adapted, with permission, from Williams et al. 1989.)

CNS, is anchored in a large complex of more than 100 scaffold proteins and protein-modifying enzymes. (Many cytosolic proteins involved in second-messenger signaling, discussed in later chapters, are embedded in the cytoskeletal matrix immediately below the plasmalemma.) *Ribosomes*, the organelle on which messenger RNA (mRNA) molecules are translated, are made up of several protein subunits. *Proteasomes*, large multi-enzyme organelles that degrade ubiquitinated proteins (a process described later in this chapter), are also present throughout the cytosol of neurons and glia.

Membranous organelles, the second main component of cytoplasm, include mitochondria and peroxisomes as well as a complex system of tubules, vesicles, and cisternae called the *vacuolar apparatus*. Mitochondria and peroxisomes process molecular oxygen. Mitochondria generate adenosine triphosphate (ATP), the major molecule by which cellular energy is transferred or spent, whereas peroxisomes prevent accumulation of the strong oxidizing agent hydrogen peroxide. Mitochondria, which are derived from symbiotic archeobacteria that invaded eukaryotic cells early in evolution, are not functionally continuous with the vacuolar apparatus. Mitochondria also play other essential roles in Ca^{2+} homeostasis and lipid biogenesis.

The vacuolar apparatus includes the smooth endoplasmic reticulum, the rough endoplasmic reticulum, the Golgi complex, secretory vesicles, endosomes, lysosomes, and a multiplicity of transport vesicles that interconnect these various compartments (Figure 7–3). Their lumen corresponds topologically to the outside of the cell; consequently, the inner leaflet of their lipid bilayer corresponds to the outer leaflet of the plasmalemma.

The major subcompartments of this system are anatomically discontinuous but functionally connected because membranous and lumenal material is moved from one compartment to another by means of transport vesicles. For example, proteins and phospholipids synthesized in the rough endoplasmic reticulum (the portion of the reticulum studded with ribosomes) and the smooth endoplasmic reticulum are transported to the Golgi complex and then to secretory vesicles, which empty their contents when the vesicle membrane fuses with the plasmalemma (a process called *exocytosis*). This secretory pathway adds membranous components to the plasmalemma and also releases the contents of these secretory vesicles into the extracellular space.

Conversely, components of cell membrane are taken into the cell through endocytic vesicles (*endocytosis*). These are incorporated into early endosomes, sorting compartments that are concentrated at the cell's periphery. The endocytosed membrane, which typically contains specific proteins such as transmembrane receptors, can be either directed back to the plasma membrane by maturing into recycling endosomes or can mature into late endosomes which are targeted for degradation by fusion with lysosomes. (Exocytosis and endocytosis are discussed in detail later in this

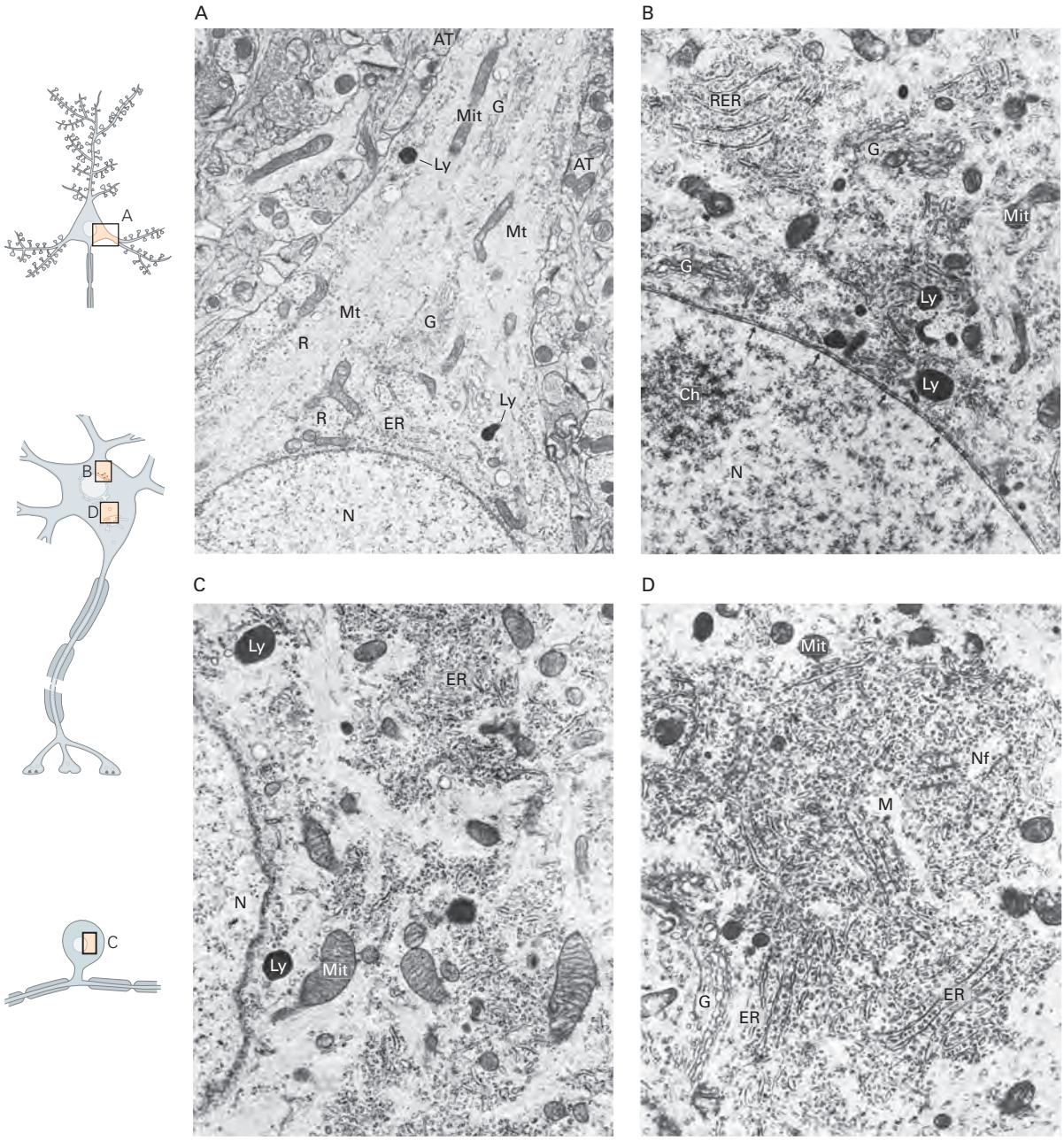

Figure 7–3 Organelles of the neuron. Electron micrographs show cytoplasm in four different regions of the neuron. (Adapted, with permission, from Peters et al. 1991.)

A. A dendrite emerges from a pyramidal neuron's cell body, which includes the endoplasmic reticulum (**ER**) above the nucleus (**N**) and a portion of the Golgi complex (**G**) nearby. Some Golgi cisternae have entered the dendrite, as have mitochondria (**Mit**), lysosomes (**Ly**), and ribosomes (**R**). Microtubules (**Mt**) are prominent cytoskeletal filaments in the cytosol. Axon terminals (**AT**) making contact with the dendrite are seen at the top and right.

B. Some components of a spinal motor neuron that participate in the synthesis of macromolecules. The nucleus (**N**) contains masses of chromatin (**Ch**) and is bounded by the nuclear envelope, which contains many nuclear pores (**arrows**). The mRNA leaves the nucleus through these pores and attaches to ribosomes that either remain free in the cytoplasm or attach to the membranes of the endoplasmic reticulum to form the rough endoplasmic reticulum (**RER**). Regulatory proteins synthesized in the cytoplasm are imported into the nucleus through the pores. Several parts of the Golgi apparatus (**G**) are seen, as are lysosomes (**Ly**) and mitochondria (**Mit**).

C, D. Micrographs of a dorsal root ganglion cell (**C**) and a motor neuron (**D**) show the organelles in the cell body that are chiefly responsible for synthesis and processing of proteins. The mRNA enters the cytoplasm through the nuclear envelope and is translated into proteins. Free polysomes, strings of ribosomes attached to a single mRNA, generate cytosolic proteins and proteins to be imported into mitochondria (**Mit**) and peroxisomes. Proteins destined for the endoplasmic reticulum are formed after the polysomes attach to the membrane of the endoplasmic reticulum (**ER**). The particular region of the motor neuron shown here also includes membranes of the Golgi apparatus (**G**), in which membrane and secretory proteins are further processed. Some of the newly synthesized proteins leave the Golgi apparatus in vesicles that move down the axon to synapses; other membrane proteins are incorporated into lysosomes (**Ly**) and other membranous organelles. The microtubules (**M**) and neurofilaments (**Nf**) are components of the cytoskeleton.

chapter.) The smooth endoplasmic reticulum also acts as a regulated internal Ca^{2+} store throughout the neuronal cytoplasm (see the discussion of Ca^{2+} release in Chapter 14).

A specialized portion of the rough endoplasmic reticulum forms the *nuclear envelope*, a spherical flattened cisterna that surrounds chromosomal DNA and its associated proteins (histones, transcription factors, polymerases, and isomerases) and defines the nucleus (Figure 7–3). Because the nuclear envelope is continuous with other portions of the endoplasmic reticulum and other membranes of the vacuolar apparatus, it is presumed to have evolved as an invagination of the plasmalemma to ensheathe eukaryotic chromosomes. The nuclear envelope is interrupted by nuclear pores, where fusion of the inner and outer membranes of the envelope results in the formation of hydrophilic channels through which proteins and RNA are exchanged between the cytoplasm proper and the nuclear cytoplasm.

Even though nucleoplasm and cytoplasm are continuous domains of cytosol, only molecules with molecular weights less than 5,000 can pass through the nuclear pores freely by diffusion. Larger molecules need help. Some proteins have special nuclear localization signals, domains that are composed of a sequence of basic amino acids (arginine and lysine) that are recognized by soluble proteins called *nuclear import receptors* (importins). At a nuclear pore, this complex is guided into the nucleus by another group of proteins called *nucleoporins.*

The cytoplasm of the nerve cell body extends into the dendritic tree without functional differentiation. Generally, all organelles in the cytoplasm of the cell body are also present in dendrites, although the densities of the rough endoplasmic reticulum, Golgi complex, and lysosomes rapidly diminish with distance from the cell body. In dendrites, the smooth endoplasmic reticulum is prominent at the base of thin processes called *spines* (Figures 7–4 and 7–5), the receptive portion of excitatory synapses. Concentrations of polyribosomes in dendritic spines mediate local protein synthesis (see below).

In contrast to the continuity of the cell body and dendrites, a sharp functional boundary exists between the cell body at the axon hillock, where the axon emerges. The organelles that compose the main biosynthetic machinery for proteins in the

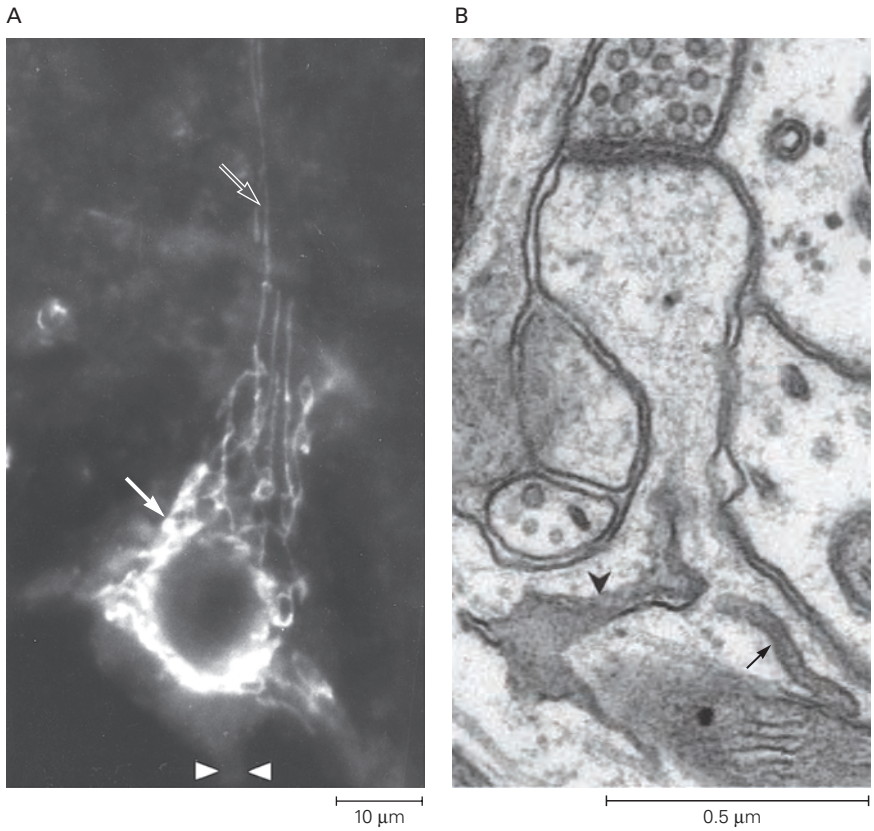

Figure 7–4 Golgi and endoplasmic reticulum membranes extend from the cell body into dendrites.

A. The Golgi complex (**solid arrow**) appears under the light microscope as several filaments that extend into the dendrites (**open arrow**) but not into the axon. The **arrowheads** at the bottom indicate the axon hillock. For this micrograph, a large neuron of the brain stem was immunostained with antibodies specifically directed against the Golgi complex. (Reproduced, with permission, from De Camilli et al. 1986. Copyright © 1986 Rockefeller University Press.)

B. Smooth endoplasmic reticulum (**arrowhead**) extends into the neck of a dendritic spine, while another membrane compartment sits at the origin of the spine (**arrow**). (Reproduced, with permission, from Cooney et al. 2002. Copyright © 2002 Society for Neuroscience.)

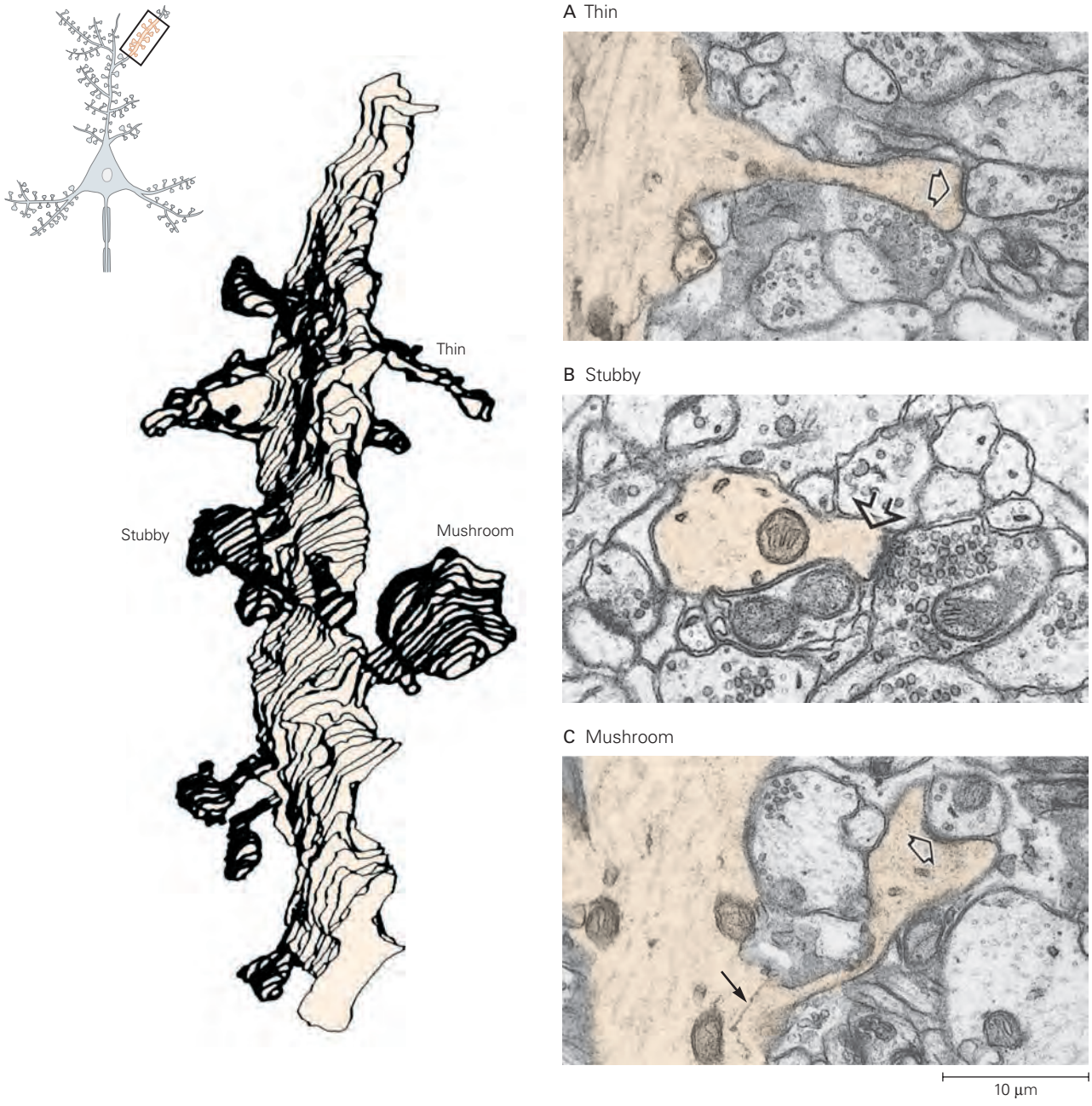

Figure 7–5 Types of dendritic spines. Three types of dendritic spine shapes are shown in a mature dendrite in a pyramidal cell in the CA1 region of the hippocampus. The drawing at left is based on a series of electron micrographs. (Drawing reproduced, with permission, from Harris and Stevens 1989; A, B, and C are reproduced, with permission, from Sorra and Harris 1993. Copyright © 1993 Society for Neuroscience.)

A. In this thin dendritic spine, the thickened receptive surface (**arrow**), located across from the presynaptic axon, contains synaptic receptors. The tissue shown here and in **B** and **C** is from the hippocampus of a postnatal day-15 rat brain.

B. Stubby spines containing postsynaptic densities (**arrow**) are both small and rare in the mature hippocampus. Their larger counterparts (not shown) predominate in the immature brain.

C. Mushroom-shaped spines have a larger head. The immature spine shown here contains flat cisternae of smooth endoplasmic reticulum, some with a beaded appearance (**solid arrow**). The postsynaptic density is indicated by the **open arrow**.

neuron—ribosomes, rough endoplasmic reticulum, and the Golgi complex—are generally excluded from axons (Figure 7–4), as are lysosomes and certain proteins. However, axons are rich in smooth endoplasmic reticulum, individual synaptic vesicles, and their precursor membranes.

The Cytoskeleton Determines Cell Shape

The cytoskeleton determines the shape of a cell and is responsible for the asymmetric distribution of organelles within the cytoplasm. It includes three filamentous structures: microtubules, neurofilaments, and microfilaments. These filaments and associated proteins account for approximately a quarter of the total protein in the cell.

Microtubules form long scaffolds that extend from one end of a neuron to the other and play a key role in developing and maintaining cell shape. A single microtubule can be as long as 0.1 mm. Microtubules consist of protofilaments, each of which consists of multiple pairs of *α- and β-tubulin* subunits arranged longitudinally along the microtubule (Figure 7–6A). Tubulin subunits bind to neighboring subunits along the protofilament and also laterally between adjacent protofilaments. Microtubules are polarized with a plus end (or growing end) and a minus end (where microtubules can be depolymerized). Interestingly, microtubule orientations differ between axons and dendrites. In the axon, microtubules display a single orientation with the plus end directed away from the cell body. In proximal dendrites, microtubules can be oriented both ways, with a plus end oriented toward or away from the cell body.

Microtubules grow by addition of guanosine triphosphate (GTP)-bound tubulin dimers at their plus end. Shortly after polymerization, the GTP is hydrolyzed to guanosine diphosphate (GDP). When a microtubule stops growing, its positive end is capped by a GDP-bound tubulin monomer. The low affinity of the GDP-bound tubulin for the polymer would lead to catastrophic depolymerization, were not for the fact that the microtubules are stabilized by interaction with other proteins.

In fact, while microtubules undergo rapid cycles of polymerization and depolymerization in dividing cells, a phenomenon referred to as *dynamic instability*, in mature dendrites and axons, they are more stable. This stability is thought to be caused by *microtubule-associated proteins* (MAPs) that promote the oriented polymerization and assembly of the tubulin polymers. MAPs in axons differ from those in dendrites. For example, MAP2 is present in dendrites but not in axons, where tau proteins (see Box 7–1) and MAP1b are present. Furthermore, microtubule stability is also tightly regulated by many different types of reversible tubulin posttranslational modifications such as acetylation, detyrosination, and polyglutamylation. In Alzheimer disease and some other degenerative disorders, tau proteins are modified and abnormally polymerized, forming a characteristic lesion called the *neurofibrillary tangle* (Box 7–1).

Tubulins are encoded by a multigene family. At least six genes code the α- and β-subunits. Because of the expression of the different genes or posttranscriptional modifications, more than 20 isoforms of tubulin are present in the brain.

Neurofilaments, 10 nm in diameter, are the bones of the cytoskeleton (Figure 7–6B). Neurofilaments are related to intermediate filaments of other cell types, including the cytokeratins of epithelial cells (hair and nails), glial fibrillary acidic protein in astrocytes, and desmin in muscle. Unlike microtubules, neurofilaments are stable and almost totally polymerized in the cell.

At 3 to 7 nm in diameter, *microfilaments* are the thinnest of the three main types of fibers that make up the cytoskeleton (Figure 7–6C). Like thin filaments of muscle, microfilaments are made up of two strands of polymerized globular actin monomers, each bearing an ATP or adenosine diphosphate (ADP), wound into a double-stranded helix. Actin is a major constituent of all cells, perhaps the most abundant animal protein in nature. There are several closely related molecular forms: the α actin of skeletal muscle and at least two other molecular forms, β and γ. Each is encoded by a different gene. Neural actin in higher vertebrates is a mixture of the β and γ species, which differ from muscle actin by a few amino acid residues. Most actin molecules are highly conserved, not only in different cell types of a species but also in organisms as distantly related as humans and protozoa.

Unlike microtubules and neurofilaments, actin filaments are short. They are concentrated at the cell's periphery in the cortical cytoplasm just beneath the plasmalemma, where they form a dense network with many actin-binding proteins (eg, spectrin-fodrin, ankyrin, talin, and actinin). This matrix plays a key role in the dynamic function of the cell's periphery, such as the motility of growth cones (the growing tips of axons) during development, generation of specialized microdomains at the cell surface, and the formation of pre- and postsynaptic morphological specializations.

Like microtubules, microfilaments undergo cycles of polymerization and depolymerization. At any one

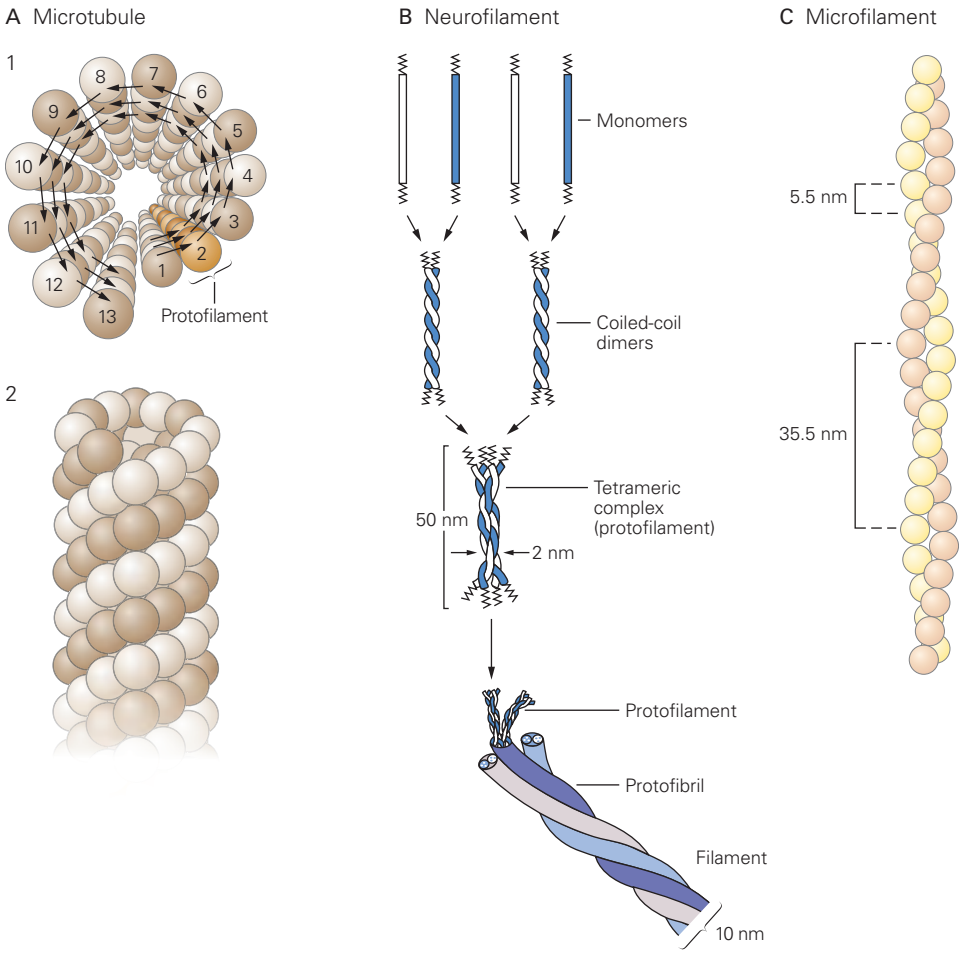

Figure 7–6 Atlas of fibrillary structures.

A. Microtubules, the largest-diameter fibers (25 nm), are helical cylinders composed of 13 protofilaments, each 5 nm in width. Each protofilament is made up of a column of alternating α- and β-tubulin subunits; each subunit has a molecular weight of approximately 50,000 Da. Adjacent subunits bind to each other along the longitudinal protofilaments and laterally between subunits of adjacent protofilaments.

A tubulin molecule is a heterodimer consisting of one α- and one β-tubulin subunit. **1.** View of a microtubule. The **arrows** indicate the direction of the right-handed helix. **2.** A side view of a microtubule shows the alternating α- and β-subunits.

B. Neurofilaments are built with fibers that twist around each other to produce coils of increasing thickness. The thinnest units are monomers that form coiled-coil heterodimers. These dimers form a tetrameric complex that becomes the protofilament. Two protofilaments become a protofibril, and three protofibrils are helically twisted to form the 10-nm diameter neurofilament. (Adapted, with permission, from Bershadsky and Vasiliev 1988.)

C. Microfilaments, the smallest-diameter fibers (approximately 7 nm), are composed of two strands of polymerized globular actin (G-actin) monomers arranged in a helix. At least six different (but closely related) actins are found in mammals; each variant is encoded by a separate gene. Microfilaments are polar structures because the globular monomers are asymmetric.

time, approximately half of the total actin in a cell can exist as unpolymerized monomers. The state of actin is controlled by binding proteins, which facilitate assembly and limit polymer length by capping the rapidly growing end of the filament or by severing it. Other binding proteins crosslink or bundle actin filaments. The dynamic state of microtubules and microfilaments permits a mature neuron to retract old axons and dendrites and extend new ones. This structural plasticity is thought to be a major factor in changes of synaptic connections and efficacy and, therefore, cellular mechanisms of long-term memory and learning.

Box 7–1 Abnormal Accumulations of Proteins Are Hallmarks of Many Neurological Disorders

Tau is a microtubule-binding protein normally present in nerve cells. In Alzheimer disease, abnormal aggregates of tau are visible in the light microscope in neurons and glia as well as in the extracellular space. Highly phosphorylated tau molecules arranged in long, thin polymers wind around one another to form paired helical filaments (Figure 7–7A and Chapter 64). Bundles of the polymers, known as *neurofibrillary tangles*, accumulate in neuronal cell bodies, dendrites, and axons (Figure 7–7A).

In normal neurons, tau is either bound to microtubules or free in the cytosol. In the tangles, it is not bound to microtubules but is highly insoluble. The tangles form at least in part because tau is not proteolytically degraded. The accumulations disturb the polymerization of tubulin and therefore interfere with axonal transport. Consequently, the shape of the neuron is not maintained.

Tau accumulations are also found in neurons of patients with progressive supranuclear palsy, a movement disorder, and in patients with frontotemporal dementias, a group of neurodegenerative disorders that affect the frontal and temporal lobes (Chapter 63). The familial forms of frontotemporal dementias are caused by mutations in the *tau* gene. Abnormal aggregates are also found in glial cells, both astrocytes and oligodendrocytes, in progressive supranuclear palsy, cortico-basoganglionic degeneration, and frontotemporal dementias.

The peptide *β-amyloid* also accumulates in the extracellular space in Alzheimer disease (Figure 7–7B and Chapter 64). It is a small proteolytic product of a much larger integral membrane protein, amyloid precursor protein, which is normally processed by several proteolytic enzymes associated with intracellular membranes. The proteolytic pathway that generates β-amyloid requires the enzyme β-secretase.

For unknown reasons, in Alzheimer disease, abnormal amounts of the amyloid precursor are processed by β-secretase. Some patients with early-onset familial Alzheimer disease either have mutations in the amyloid precursor gene or in the genes coding for the membrane proteins presenilin 1 and 2, which are closely associated with secretase activity.

In Parkinson disease, abnormal aggregates of α-synuclein accumulate in cell bodies of neurons. Like tau, *α-synuclein* is a normal soluble constituent of the cell. But in Parkinson disease, it becomes insoluble, forming spherical inclusions called *Lewy bodies* (Figure 7–7C and Chapter 63).

These abnormal inclusions also contain ubiquitin. Because ubiquitin is required for proteasomal degradation of proteins, its presence suggests that affected neurons have attempted to target α-synuclein or other molecular constituents for proteolysis. Apparently, degradation does not occur, possibly because of misfolding or the abnormal aggregation of the proteins or because of faulty proteolytic processing in the cell.

Do these abnormal protein accumulations affect the physiology of the neurons and glia? On the one hand, the accumulations may form in response to altered posttranslational processing of the proteins and serve to isolate the abnormal proteins, permitting normal cell activities. On the other hand, the accumulations may disrupt cellular activities such as membrane trafficking, axonal and dendritic transport, and the maintenance of synaptic connections between specific classes of neurons. In addition, the altered proteins themselves, aside from the aggregations, may have deleterious effects. With β-amyloid, there is evidence that the peptide itself is toxic.

(*continued*)

In addition to serving as the cytoskeleton, microtubules and actin filaments act as tracks along which organelles and proteins are rapidly driven by molecular motors. The motors used by the actin filaments, the *myosins*, also mediate other types of cell motility, including extension of the cell's processes and translocation of membranous organelles from the bulk cytoplasm to the region adjacent to the plasma membrane. (Actomyosin is responsible for muscle contraction.) Because the microtubules and actin filaments are polar, each motor drives its organelle cargo in only one direction.

As already mentioned, microtubules are arranged in parallel in the axon with plus ends pointing away from the cell body and minus ends facing the cell body. This regular orientation allows some organelles to move toward and others to move away from nerve endings, the direction being determined by the specific type of molecular motor, thus maintaining the distinctive distribution of axonal organelles (Figure 7–8). In dendrites, however, microtubules with opposite polarities are mixed together, explaining why the organelles of the cell body and dendrites are similar.

Box 7–1 Abnormal Accumulations of Proteins Are Hallmarks of Many Neurological Disorders (continued)

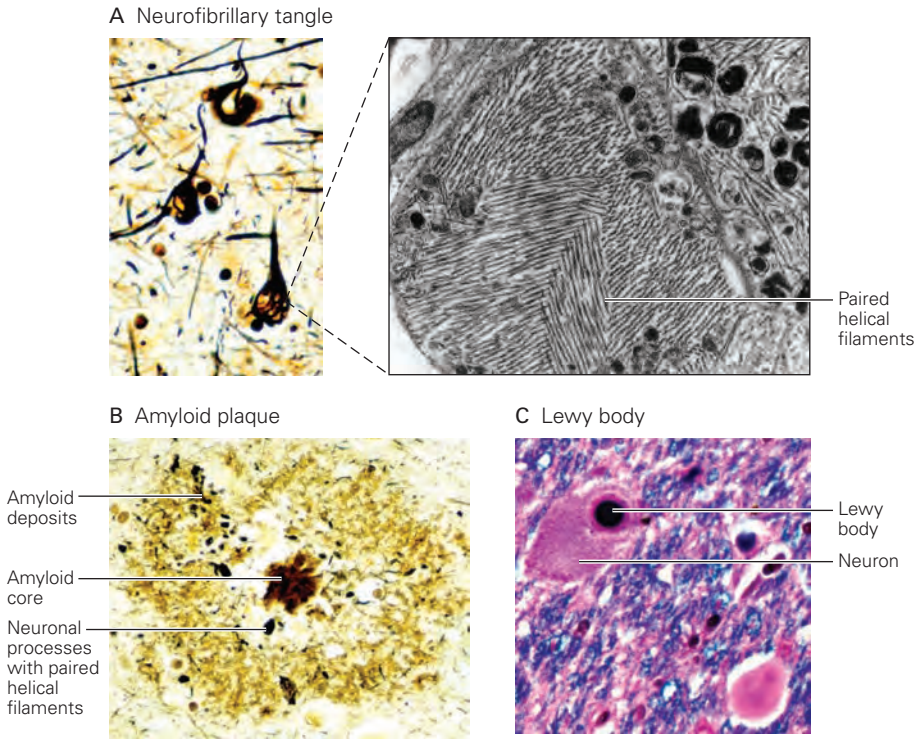

Figure 7–7 Abnormal aggregates of proteins inside neurons in Alzheimer and Parkinson diseases.

A. *Left:* Intracellular neurofibrillary tangles of Alzheimer disease, labeled here with a dark silver stain. (Reproduced, with permission, from J.P. Vonsattel.) *Right:* An electron micrograph of a tangle shows bundles of abnormal filaments, filling a dendrite. The filaments are composed of altered tau protein. (Used, with permission, from Dr. L. Carrasco, formerly of Runwell Hospital, Wickford, UK.)

B. In Alzheimer disease, amyloid plaque is created by extracellular deposits of polymerized β-amyloid peptides. The plaque shown here has a dense core of amyloid as well as a surrounding halo of deposits. Some neuronal processes in the plaque exhibit tangle pathology. (Reproduced, with permission, from J.P. Vonsattel.)

C. A Lewy body in the substantia nigra of a patient with Parkinson disease contains accumulations of abnormal filaments made up of α-synuclein, among other proteins. (Reproduced, with permission, from J.P. Vonsattel.)

Protein Particles and Organelles Are Actively Transported Along the Axon and Dendrites

In neurons, most proteins are made in the cell body from mRNAs. Important examples are neurotransmitter biosynthetic enzymes, synaptic vesicle membrane components, and neurosecretory peptides. Because axons and terminals often lie at great distances from the cell body, sustaining the function of these remote regions presents a challenge. Passive diffusion would be far too slow to deliver vesicles, particles, or even single macromolecules over this great distance.

The axon terminal, the site of secretion of neurotransmitters, is particularly distant from the cell body. In a motor neuron that innervates a muscle of the leg in humans, the distance of the nerve terminal from the cell body can exceed 10,000 times the cell body diameter. Thus, membrane and secretory products formed in the cell body must be actively transported to the end of the axon (Figure 7–9).

In 1948, Paul Weiss first demonstrated axonal transport when he tied off a sciatic nerve and observed that axoplasm in the nerve accumulated with time on the proximal side of the ligature. He concluded that axoplasm

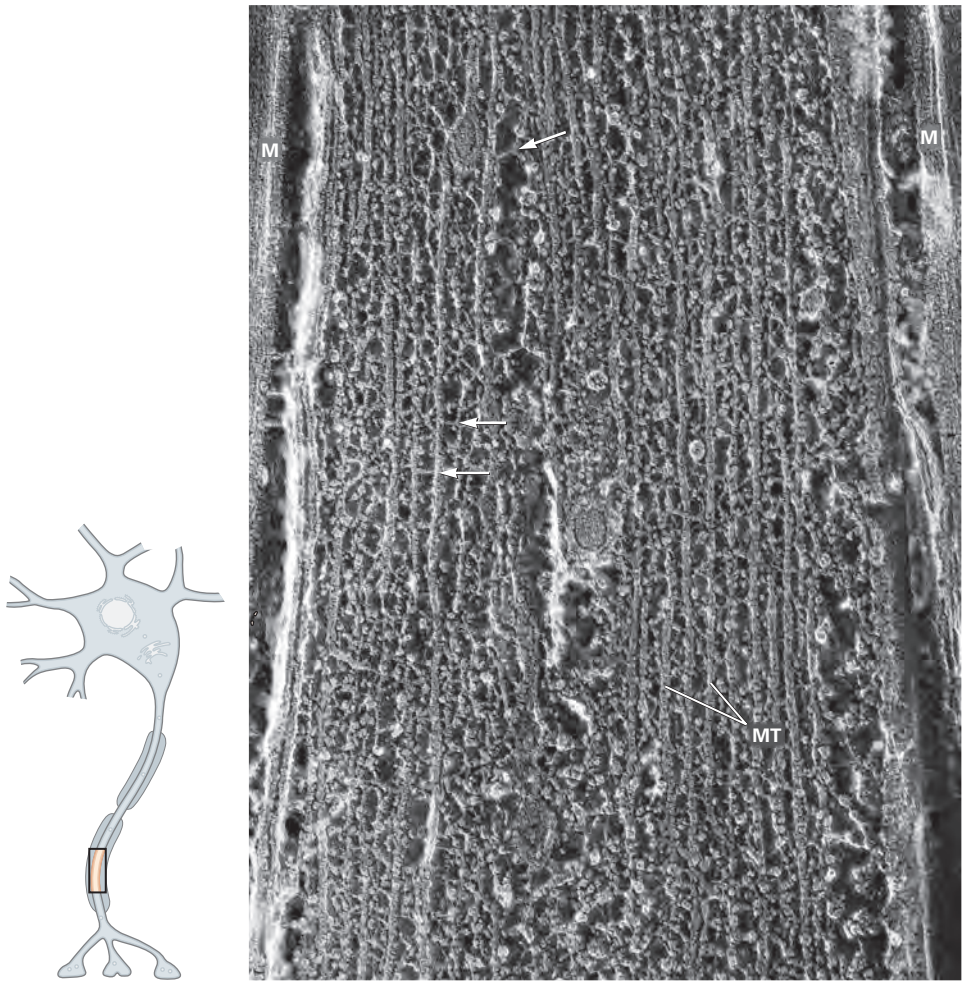

Figure 7–8 The cytoskeletal structure of an axon. The micrograph shows the dense packing of microtubules and neurofilaments linked by cross bridges (**arrows**). Organelles are transported in both the anterograde and retrograde directions in the microtubule-rich domains. Visualization in the micrograph was achieved by quick freezing and deep etching. **M**, myelin sheath; **MT**, microtubules. ×105,000. (Adapted, with permission, from Schnapp and Reese 1982. Copyright © 1982 Rockefeller University Press.)

moves at a slow, constant rate from the cell body toward terminals in a process he called *axoplasmic flow.* Today we know that the flow Weiss observed consists of two discrete mechanisms, one fast and the other slow.

Membranous organelles move toward axon terminals (anterograde direction) and back toward the cell body (retrograde direction) by *fast axonal transport*, a form of transport that is up to 400 mm per day in warm-blooded animals. In contrast, cytosolic and cytoskeletal proteins move only in the anterograde direction by a much slower form of transport, *slow axonal transport.* These transport mechanisms in neurons are adaptations of processes that facilitate intracellular movement of organelles in all secretory cells. Because all these mechanisms operate along axons, they have been used by neuroanatomists to trace the course of individual axons as well as interconnections between neurons (Box 7–2).

Fast Axonal Transport Carries Membranous Organelles

Large membranous organelles are carried to and from the axon terminals by fast transport (Figure 7–11). These organelles include synaptic vesicle precursors, large dense-core vesicles, mitochondria, elements of the smooth endoplasmic reticulum, and protein particles carrying RNAs. Direct microscopic analysis reveals that fast transport occurs in a stop-and-start (saltatory) fashion along linear tracks of microtubules aligned with the main axis of the axon. The saltatory nature of the movement results from the periodic dissociation

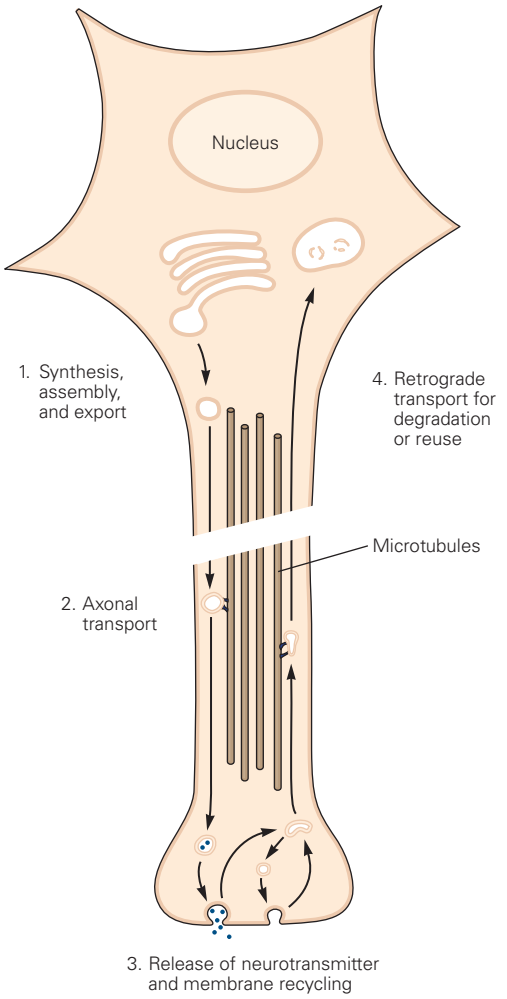

Figure 7–9 Membrane trafficking in the neuron. **1.** Proteins and lipids of secretory organelles are synthesized in the endoplasmic reticulum and transported to the Golgi complex, where large dense-core vesicles (peptide-containing secretory granules) and synaptic vesicle precursors are assembled. **2.** Large dense-core vesicles and transport vesicles carry synaptic vesicle proteins down the axon via axonal transport. **3.** At the nerve terminals, the synaptic vesicles are assembled and loaded with nonpeptide neurotransmitters. Synaptic vesicles and large dense-core vesicles release their contents by exocytosis. **4.** Following exocytosis, large dense-core vesicle membranes are returned to the cell body for reuse or degradation. Synaptic vesicle membranes undergo many cycles of local exocytosis and endocytosis in the presynaptic terminal.

of an organelle from the track or from collisions with other particles.

Early experiments on dorsal root ganglion cells showed that anterograde fast transport depends critically on ATP, is not affected by inhibitors of protein synthesis (once the injected labeled amino acid is incorporated), and does not depend on the cell body, because it occurs in axons severed from their cell bodies. In fact, active transport can occur in reconstituted cell-free axoplasm.

Microtubules provide an essentially stationary track on which specific organelles can be moved by molecular motors. The idea that microtubules are involved in fast transport emerged from the finding that certain alkaloids that disrupt microtubules and block mitosis, which depends on microtubules, also interfere with fast transport.

Molecular motors were first visualized in electron micrographs as cross bridges between microtubules and moving particles (Figure 7–8). More advanced fluorescence time-lapse microscopy techniques are able to visualize the dynamics of axon transport for specific cargos such as mitochondria and synaptic vesicles. The motor molecules for anterograde transport are plus-end-directed motors called *kinesin* and a variety of kinesin-related proteins. The kinesins represent a large family of adenosine triphosphatases (ATPase), each of which transports different cargos. Kinesin is a heterotetramer composed of two heavy chains and two light chains. Each heavy chain has three domains: (1) a globular head (the ATPase domain) that acts as the motor when attached to microtubules, (2) a coiled-coil helical stalk responsible for dimerization with the other heavy chain, and (3) a fan-like carboxyl-terminus that interacts with the light chains. This end of the complex attaches indirectly to the organelle that is moved through specific families of proteins referred to as cargo adapters.

Fast retrograde transport primarily moves endosomes generated by endocytic activity at nerve endings, mitochondria, and elements of the endoplasmic reticulum. Many of these components are degraded through fusion with lysosomes. Fast retrograde transport also delivers signals that regulate gene expression in the neuron's nucleus. For example, activated growth factor receptors at nerve endings are taken up into vesicles and carried back along the axon to the nucleus. Transport of transcription factors informs the gene transcription apparatus in the nucleus of conditions in the periphery. Retrograde transport of these molecules is especially important during nerve regeneration and axon regrowth (Chapter 47). Certain toxins (tetanus toxin) as well as pathogens (herpes simplex, rabies, and polio viruses) are also transported toward the cell body along the axon.

The rate of retrograde fast transport is approximately one-half to two-thirds that of anterograde fast transport. As in anterograde transport, particles move along microtubules during retrograde flow. The motor molecules for retrograde axonal transport are minus-end-directed motors called *dyneins*, similar to those found in cilia and

Box 7–2 Neuroanatomical Tracing Makes Use of Axonal Transport

Neuroanatomists typically locate axons and terminals of specific nerve cell bodies by microinjection of dyes; expression of fluorescent proteins; or autoradiographically tracing specific proteins soon after administering radioactively labeled amino acids, certain labeled sugars (fucose or amino sugars, precursors of glycoprotein), or specific transmitter substances.

Similarly, particles, proteins, or dyes that are readily taken up at nerve terminals by endocytosis and transported back to cell bodies are used to identify the cell bodies. The enzyme horseradish peroxidase has been most widely used for this type of study because it readily undergoes retrograde transport and its reaction product is conveniently visualized histochemically.

Axonal transport is also used by neuroanatomists to label material exchanged between neurons, making it possible to identify neuronal networks (Figure 7–10).

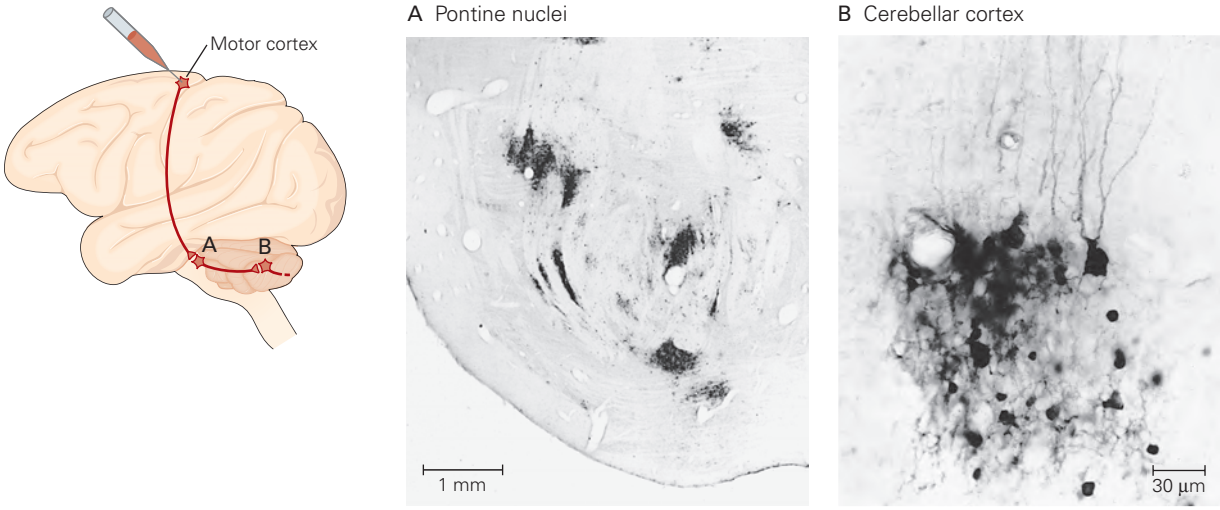

Figure 7–10 Axonal transport of the herpes simplex virus (HSV) is used to trace cortical pathways in monkeys. Depending on the strain, the virus moves in the anterograde or retrograde direction by axonal transport. In either direction, it enters a neuron with which the infected cell makes synaptic contact. Here the projections of cells in the primary motor cortex to the cerebellum in monkeys were traced using an anterograde-moving strain (HSV-1 [H129]). Monkeys were injected in the region of the primary motor cortex that controls the arm. After 4 days, the brain was sectioned and immunostained for viral antigen. Micrographs show the virus was transported from the primary motor cortex to second-order neurons in pontine nuclei (**A**) and then to third-order neurons in the cerebellar cortex (**B**). (Reproduced, with permission, from P.L. Strick.)

flagella of nonneuronal cells. They consist of a multimeric ATPase protein complex with two globular heads on two stalks connected to a basal structure. The globular heads attach to microtubules and act as motors, moving toward the minus end of the polymer. As with kinesin, the other end of the complex attaches to the transported organelle through specialized cargo adapters.

Microtubules also mediate anterograde and retrograde transport of mRNAs and ribosomal RNA carried in particles formed with RNA-binding proteins. These proteins have been characterized in both vertebrate and invertebrate nervous systems and include the cytoplasmic polyadenylation element binding protein (CPEB), the fragile X protein, Hu proteins, NOVA, and Staufen. The activities of these proteins are critical. For example, CPEB keeps select mRNAs dormant during transport from the cell body to nerve endings; once there (upon stimulation), the binding protein can facilitate the local translation of the RNA by mediating polyadenylation and activation of the messenger. Both CPEB and Staufen were discovered in *Drosophila*, where they maintain maternal mRNAs dormant in

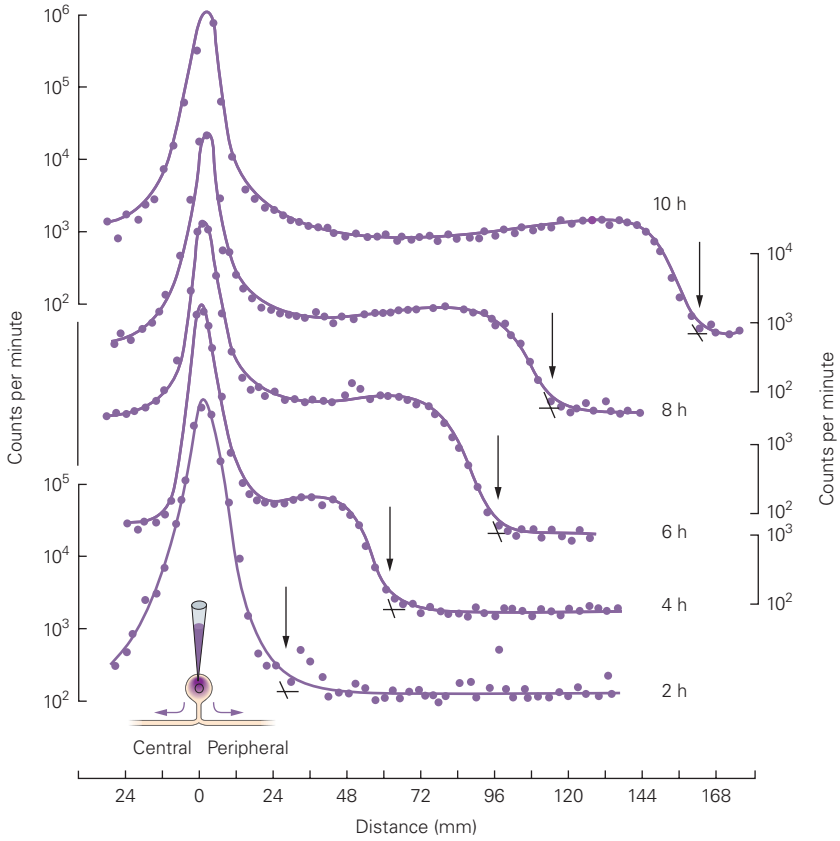

Figure 7–11 Early experiments on anterograde axonal transport used radioactive labeling of proteins. In the experiment illustrated here, the distribution of radioactive proteins along the sciatic nerve of the cat was measured at various times after injection of [^{3}H]-leucine into dorsal root ganglia in the lumbar region of the spinal cord. To show transport curves for various times (2, 4, 6, 8, and 10 hours after the injection) in one figure, several ordinate scales (in logarithmic units) are used. Large amounts of labeled protein stay in the ganglion cell bodies but, with time, move out along axons in the sciatic nerve, so the advancing front of the labeled protein is progressively farther from the cell body (**arrows**). The velocity of transport can be calculated from the distance of the front at the various times. From experiments of this kind, Sidney Ochs found that the rate of fast axonal transport is constant at 410 mm per day at body temperature. (Adapted, with permission, from Ochs 1972. Copyright © 1972 AAAS.)

unfertilized eggs and, upon fertilization, distribute and localize mRNA to various regions of the dividing embryo. Loss-of-function mutations in the fragile X (*FMR1*) gene lead to a severe form of mental retardation.

Proteins, ribosomes, and mRNA are concentrated at the base of some dendritic spines (Figure 7–12). Only a select group of mRNAs are transported into the dendrites from the soma. These include mRNAs that encode actin- and cytoskeletal-associated proteins, MAP2, and the α-subunit of the Ca^{2+}/calmodulin-dependent protein kinase. They are translated in the dendrites in response to activity in a presynaptic neuron. This local protein synthesis is thought to be important in sustaining the molecular changes at the synapse that underlie long-term memory and learning. Likewise, the mRNA for myelin basic protein is transported to the distant ends of the oligodendrocytes, where it is translated as the myelin sheath grows, as discussed later in this chapter.

Slow Axonal Transport Carries Cytosolic Proteins and Elements of the Cytoskeleton

Cytosolic proteins and cytoskeletal proteins are moved from the cell body by slow axonal transport. Slow transport occurs only in the anterograde direction and consists of at least two kinetic components that carry different proteins at different rates.

The slower component travels at 0.2 to 2.5 mm per day and carries the proteins that make up the fibrillar elements of the cytoskeleton: the subunits of

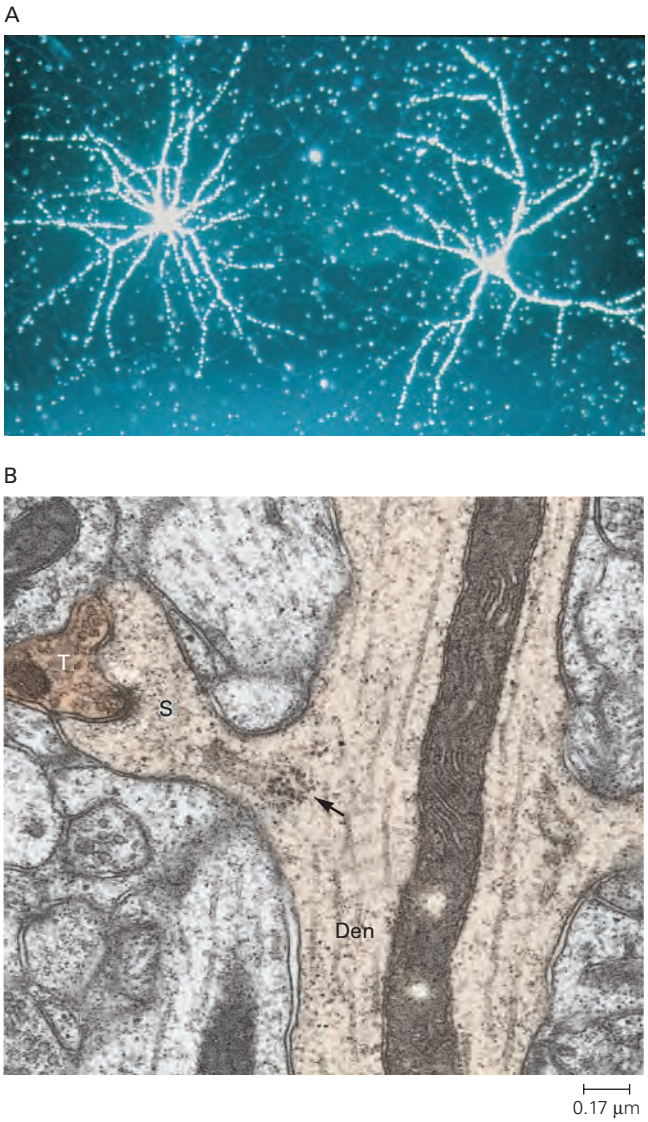

Figure 7–12 Ribosomes in the dendritic arbor. (Images reproduced, with permission, from Oswald Steward.)

A. Some ribosomes are dispatched from the cell body to dendrites where they are used in local protein synthesis. This autoradiograph shows the distribution of ribosomal RNA (rRNA) in hippocampal neurons in low-density cultures using in situ hybridization. The image was made with dark field illumination, in which silver grains reflect light and thus appear as bright spots. Silver grains, denoting the rRNA, are heavily concentrated over cell bodies and dendrites but are not detectable over the axons that crisscross among the dendrites.

B. Ribosomes in dendrites are selectively concentrated at the junction of the spine and main dendritic shaft (**arrow**), where the spine contacts the axon terminal of a presynaptic neuron. This electron micrograph shows a mushroom-shaped spine of a neuron in the hippocampal dentate gyrus. Note the absence of ribosomes in the dendritic shaft. **S**, spine head; **T**, presynaptic terminal; **Den**, main shaft of the dendrite containing a long mitochondrion. ×60,000.

neurofilaments and α- and β-tubulin subunits of microtubules. These fibrous proteins constitute approximately 75% of the total protein moved in the slower component. Microtubules are transported in polymerized form by a mechanism involving microtubule sliding in which relatively short preassembled microtubules move along existing microtubules. Neurofilament monomers or short polymers move passively together with the microtubules because they are crosslinked by protein bridges.

The other component of slow axonal transport is approximately twice as fast as the slower component. It carries clathrin, actin, and actin-binding proteins as well as a variety of enzymes and other proteins.

Proteins Are Made in Neurons as in Other Secretory Cells

Secretory and Membrane Proteins Are Synthesized and Modified in the Endoplasmic Reticulum

The mRNAs for secretory and membrane proteins are translated through the membrane of the rough endoplasmic reticulum, and their polypeptide products are processed extensively within the lumen of the endoplasmic reticulum. Most polypeptides destined to become proteins are translocated across the membrane of the rough endoplasmic reticulum during synthesis, a process called *cotranslational transfer.*

Transfer is possible because ribosomes, the site where proteins are synthesized, attach to the cytosolic surface of the reticulum (Figure 7–13). Complete transfer of the polypeptide chain into the lumen of the reticulum produces a secretory protein (recall that the inside of the reticulum is related to the outside of the cell). Important examples are the neuroactive peptides. If the transfer is incomplete, an integral membrane protein results. Because a polypeptide chain can thread its way through the membrane many times during synthesis, several membrane-spanning configurations are possible depending on the primary amino acid sequence of the protein. Important examples are neurotransmitter receptors and ion channels (Chapter 8).

Some proteins transported into the endoplasmic reticulum remain there. Others are moved to other compartments of the vacuolar apparatus or to the plasmalemma, or are secreted into the extracellular space. Proteins that are processed in the endoplasmic reticulum are extensively modified. One important modification is the formation of intramolecular disulfide linkages (Cys-S-S-Cys) caused by oxidation of pairs of free sulfhydryl side chains, a process that cannot occur

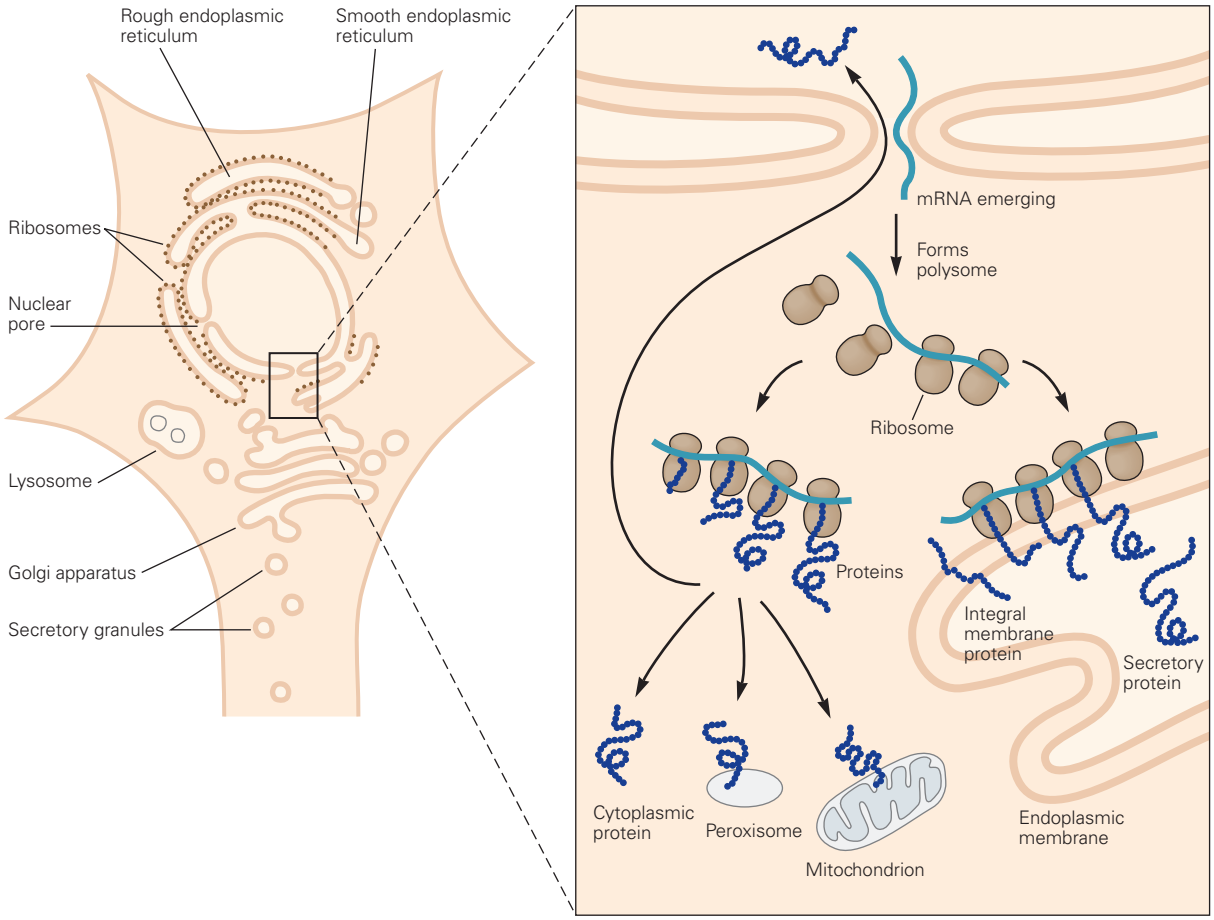

Figure 7–13 Protein synthesis in the endoplasmic reticulum. Free and membrane-bound polysomes translate mRNA that encodes proteins with a variety of destinations. Messenger RNA, transcribed from genomic DNA in the neuron's nucleus, emerges into the cytoplasm through nuclear pores to form polyribosomes (see enlargement). The polypeptides that become secretory and membrane proteins are translocated across the membrane of the rough endoplasmic reticulum.

in the reducing environment of the cytosol. Disulfide linkages are crucial to the tertiary structure of these proteins.

Proteins may be modified by cytosolic enzymes either during synthesis (cotranslational modification) or afterward (posttranslational modification). One example is *N*-acylation, the transfer of an acyl group to the N-terminus of the growing polypeptide chain. Acylation by a 14-carbon fatty acid myristoyl group permits the protein to anchor in membranes through the lipid chain.

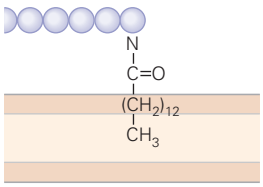

Other fatty acids can be conjugated to the sulfhydryl group of cysteine, producing a thioacylation:

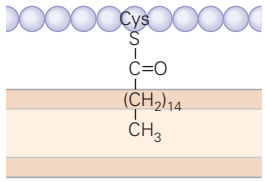

Isoprenylation is another posttranslational modification important for anchoring proteins to the cytosolic side of membranes. It occurs shortly after synthesis of the protein is completed and involves a series of enzymatic steps that result in thioacylation by one of two long-chain hydrophobic polyisoprenyl moieties (farnesyl, with 15 carbons, or geranyl-geranyl, with 20) of the sulfhydryl group of a cysteine at the C-terminus of proteins.

Some posttranslational modifications are readily reversible and thus used to regulate the function of a protein transiently. The most common of these modifications is the phosphorylation at the hydroxyl group in serine, threonine, or tyrosine residues by protein kinases. Dephosphorylation is catalyzed by protein phosphatases. (These reactions are discussed in Chapter 14.) As with all posttranslational modifications, the sites to be phosphorylated are determined by particular sequences of amino acids around the residue to be modified. Phosphorylation can alter physiological processes in a reversible fashion. For example, protein phosphorylation–dephosphorylation reactions regulate the kinetics of ion channels, the activity of transcription factors, and the assembly of the cytoskeleton.

Still another important posttranslational modification is the addition of *ubiquitin*, a highly conserved protein with 76 amino acids, to the ∈-amino group of specific lysine residues in the protein molecule. Ubiquitination, which regulates protein degradation, is mediated by three enzymes. E1 is an activating enzyme that uses the energy of ATP. The activated ubiquitin is next transferred to a conjugase, E2, which then transfers the activated moiety to a ligase, E3. The E3, alone or together with E2, transfers the ubiquitinyl group to the lysine residue in a protein. Specificity arises because a given protein molecule can only be ubiquinated by a specific E3 or combination of E3 and E2. Some E3s also require special cofactors—ubiquitination occurs only in the presence of E3 and a cofactor protein.

Monoubiquitination tags a protein for degradation in the endosomal–lysosomal system. This is especially important in endocytosis and recycling of surface receptors. Ubiquitinyl monomers are successively linked to the ∈-amino group of a lysine residue in the previously added ubiquitin moiety. Addition of more than five ubiquitins to the multiubiquitin chain tags the protein for degradation by the proteasome, a large complex containing multifunctional protease subunits that cleave proteins into short peptides.

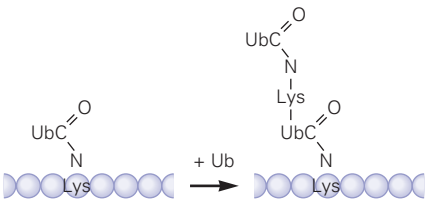

The ATP–ubiquitin–proteasome pathway is a mechanism for the selective and regulated proteolysis of proteins that operates in the cytosol of all regions of the neuron—dendrites, cell body, axon, and terminals. Until recently, this process was thought to be primarily directed to poorly folded, denatured, or aged and damaged proteins. We now know that ubiquitin-mediated proteolysis can be regulated by neuronal activity and plays specific roles in many neuronal processes, including synaptogenesis and long-term memory storage.

Another important protein modification is glycosylation, which occurs on amino groups of asparagine residues (N-linked glycosylation) and results in the addition en bloc of complex polysaccharide chains. These chains are then trimmed within the endoplasmic reticulum by a series of reactions controlled by chaperones, including heat shock proteins, calnexin, and calreticulin. Because of the great chemical specificities of oligosaccharide moieties, these modifications can have important implications for cell function. For example, cell-to-cell interactions that occur during development rely on molecular recognition between glycoproteins on the surfaces of the two interacting cells. Also, because a given protein can have somewhat different oligosaccharide chains, glycosylation can diversify the function of a protein. It can increase the hydrophilicity of the protein (useful for secretory proteins), fine-tune its ability to bind macromolecular partners, and delay its degradation.

An interesting posttranslational modification of mRNA is RNA interference (RNAi), the targeted destruction of double-stranded RNAs. This mechanism, which is believed to have arisen to protect cells against viruses and other rogue fragments of nucleic acids, shuts down the synthesis of any targeted protein. Double-stranded RNAs are taken up by an enzyme complex that cleaves the molecule into oligomers. The RNA sequences are retained by the complex. As a result, any homologous hybridizing RNA strands, either double- or single-stranded, will be destroyed. The process is regenerative: The complex retains a hybridizing fragment and goes on to destroy another RNA molecule until none remain in the cell. Although the physiological role of RNAi in normal cells is unclear, transfection or injection of RNAi into cells is of great research and clinical importance (Chapter 2).

Secretory Proteins Are Modified in the Golgi Complex

Proteins from the endoplasmic reticulum are carried in transport vesicles to the Golgi complex where they are modified and then moved to synaptic terminals and other parts of the plasma membrane. The Golgi complex appears as a grouping of membranous sacks aligned with one another in long ribbons.

The mechanism by which vesicles are transported between stations of the secretory and endocytic

pathways has been remarkably conserved from simple unicellular prokaryotes (yeast) to neurons and glia of multicellular organisms. Transport vesicles develop from membrane, beginning with the assembly of proteins that form *coats*, or coat proteins, at selected patches of the cytosolic surface of the membrane. A coat has two functions. It forms rigid cage-like structures that produce evagination of the membrane into a bud shape, and it selects the protein cargo to be incorporated into the vesicles.

There are several types of coats. *Clathrin coats* assist in evaginating Golgi complex membrane and plasmalemma during endocytosis. Two other coats, COPI and COPII, cover transport vesicles that shuttle between the endoplasmic reticulum and the Golgi complex. Coats usually are rapidly dissolved once free vesicles have formed. The fusion of vesicles with the target membrane is mediated by a cascade of molecular interactions, the most important of which is the reciprocal recognition of small proteins on the cytosolic surfaces of the two interacting membranes: vesicular soluble *N*-ethylmaleimide–sensitive factor attachment protein receptors (v-SNAREs) and t-SNAREs (target-membrane SNAREs). The role of SNARE proteins in neurotransmitter release through synaptic vesicle fusion with the plasma membrane is discussed in Chapter 15.

Vesicles from the endoplasmic reticulum arrive at the *cis* side of the Golgi complex (the aspect facing the nucleus) and fuse with its membranes to deliver their contents into the Golgi complex. These proteins travel from one Golgi compartment (cisterna) to the next, from the *cis* to the *trans* side, undergoing a series of enzymatic reactions. Each Golgi cisterna or set of cisternae is specialized for a particular type of reaction. Several types of protein modifications, some of which begin in the endoplasmic reticulum, occur within the Golgi complex proper or within the transport station adjacent to its *trans* side, the *trans-Golgi network* (the aspect of the complex typically facing away from the nucleus toward the axon hillock). These modifications include the addition of N-linked oligosaccharides, O-linked (on the hydroxyl groups of serine and threonine) glycosylation, phosphorylation, and sulfation.

Both soluble and membrane-bound proteins that travel through the Golgi complex emerge from the trans-Golgi network in a variety of vesicles that have different molecular compositions and destinations. Proteins transported from the trans-Golgi network include secretory products as well as newly synthesized components for the plasmalemma, endosomes, and other membranous organelles (see Figure 7–2). One class of vesicles carries newly synthesized plasmalemmal proteins and proteins that are continuously secreted (*constitutive secretion*). These vesicles fuse with the plasma membrane in an unregulated fashion. An important type of these vesicles delivers lysosomal enzymes to late endosomes.

Still other classes of vesicles carry secretory proteins that are released by an extracellular stimulus (*regulated secretion*). One type stores secretory products, primarily neuroactive peptides, in high concentrations. Called *large dense-core vesicles* because of their electron-dense (osmophilic) appearance in the electron microscope, these vesicles are similar in function and biogenesis to peptide-containing granules of endocrine cells. Large dense-core vesicles are targeted primarily to axons but can be seen in all regions of the neuron. They accumulate in the cytoplasm just beneath the plasma membrane and are highly concentrated at axon terminals, where their contents are released through Ca^{2+}-regulated exocytosis.

Recent work has demonstrated that *small synaptic vesicles*—the electron-lucent vesicles responsible for the rapid release of neurotransmitter at axon terminals—are actively transported toward the synaptic terminals as individual cargoes. It is thought that protein components of small synaptic vesicles originate from large precursor vesicles from the trans-Golgi network. These synaptic vesicles already incorporate most of the proteins that enable their fusion at the presynaptic active zone. The neurotransmitter molecules stored in these synaptic vesicles are released by exocytosis regulated by Ca^{2+} influx through channels close to the release site. The vesicles can then undergo cycles of recycling/exocytosis as described in Chapter 15. Importantly, these vesicles are refilled through specialized transporters called vesicular transporters that are specific for each neurotransmitter (eg, glutamate, γ-aminobutyric acid [GABA], acetylcholine).

Surface Membrane and Extracellular Substances Are Recycled in the Cell

Vesicular traffic toward the cell surface is continuously balanced by *endocytic traffic* from the plasma membrane to internal organelles. This traffic is essential for maintaining the area of the membrane in a steady state. It can alter the activity of many important regulatory molecules on the cell surface (eg, by removing receptors and adhesion molecules). It also removes nutrients and molecules, such as expendable receptor ligands and damaged membrane proteins, to the degradative compartments of the cells. Finally, it serves to recycle synaptic vesicles at nerve terminals (Chapter 15).

A significant fraction of endocytic traffic is carried in clathrin-coated vesicles. The clathrin coat interacts selectively through transmembrane receptors with extracellular molecules that are to be taken up into the cell. For this reason, clathrin-mediated uptake is often referred to as *receptor-mediated endocytosis.* The vesicles eventually shed their clathrin coats and fuse with the early endosomes, in which proteins to be recycled to the cell surface are separated from those destined for other intracellular organelles. Patches of the plasmalemma can also be recycled through larger, uncoated vacuoles that also fuse with early endosomes (*bulk endocytosis*).

Glial Cells Play Diverse Roles in Neural Function

Ramón y Cajal recognized the close association of glia with neurons and synapses in the brain (Figure 7–14). Although their function was at that time a mystery, he predicted that glia must do more than hold neurons together. Indeed, it is now clear that glial cells are critical players in brain development, function, and disease.

Glia Form the Insulating Sheaths for Axons

A major function of oligodendrocytes and Schwann cells is to provide the insulating material that allows rapid conduction of electrical signals along the axon. These cells produce thin sheets of myelin that wrap concentrically, many times, around the axon. CNS myelin, produced by oligodendrocytes, is similar, but not identical, to peripheral nervous system myelin, produced by Schwann cells.

Both types of glia produce myelin only for segments of axons. This is because the axon is not continuously wrapped in myelin, a feature that facilitates propagation of action potentials (Chapter 9). One Schwann cell produces a single myelin sheath for one segment of one axon, whereas one oligodendrocyte produces myelin sheaths for segments of as many as 30 axons (Figures 7–1 and 7–15).

The number of layers of myelin on an axon is proportional to the diameter of the axon—larger axons have thicker sheaths. Axons with very small diameters are not myelinated; nonmyelinated axons conduct action potentials much more slowly than do myelinated axons because of their smaller diameter and lack of myelin insulation (Chapter 9).

The regular lamellar structure and biochemical composition of the sheath are consequences of how

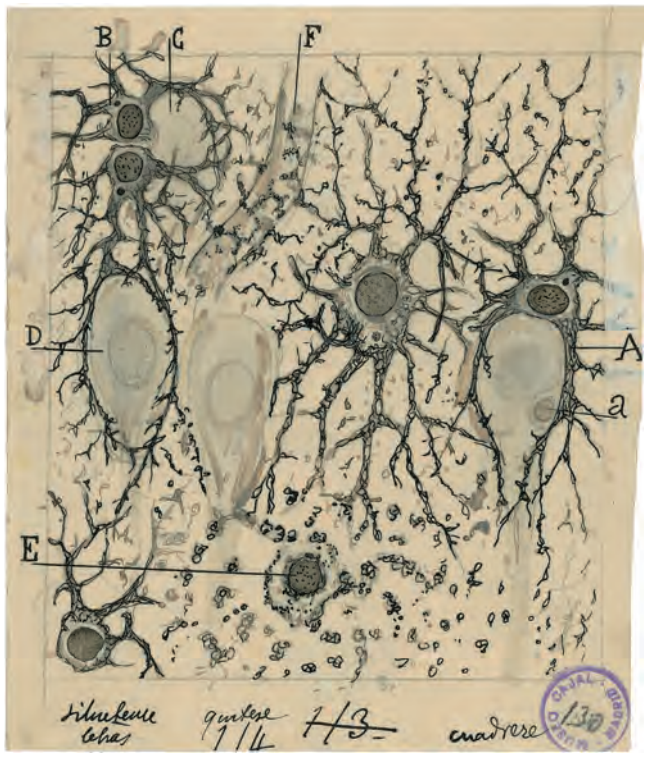

Figure 7–14 Astrocytes interact with neurons and synapses in the brain. This drawing by Ramón y Cajal (based on tissue stained with the sublimated gold chloride method) shows astrocytes of the pyramidal layer and stratum radiatum of Ammon's horn in the human brain. (**A**) A large astrocyte ensheathes a pyramidal neuron. (**B**) Twin astrocytes form a nest around a nerve cell body (**C**). One of the astrocytes sends two branches to form another nest (**D**). (**E**) A cell shows signs of autolysis. (**F**) Capillary vessel. (Reproduced, with permission, from the Instituto Cajal, Madrid, Spain.)

myelin is formed from the glial plasma membrane. In the development of the peripheral nervous system, before myelination takes place, the axon lies within a trough formed by Schwann cells. Schwann cells line up along the axon at regular intervals that become the myelinated segments of axon. The external membrane of each Schwann cell surrounds the axon to form a double membrane structure called the *mesaxon*, which elongates and spirals around the axon in concentric layers (Figure 7–15C). As the axon is ensheathed, the cytoplasm of the Schwann cell is squeezed out to form a compact lamellar structure.

The regularly spaced segments of myelin sheath are separated by unmyelinated gaps, called *nodes of Ranvier*, where the plasma membrane of the axon is exposed to the extracellular space for approximately 1 µm (Figure 7–16). This arrangement greatly increases the speed at which nerve impulses are conducted

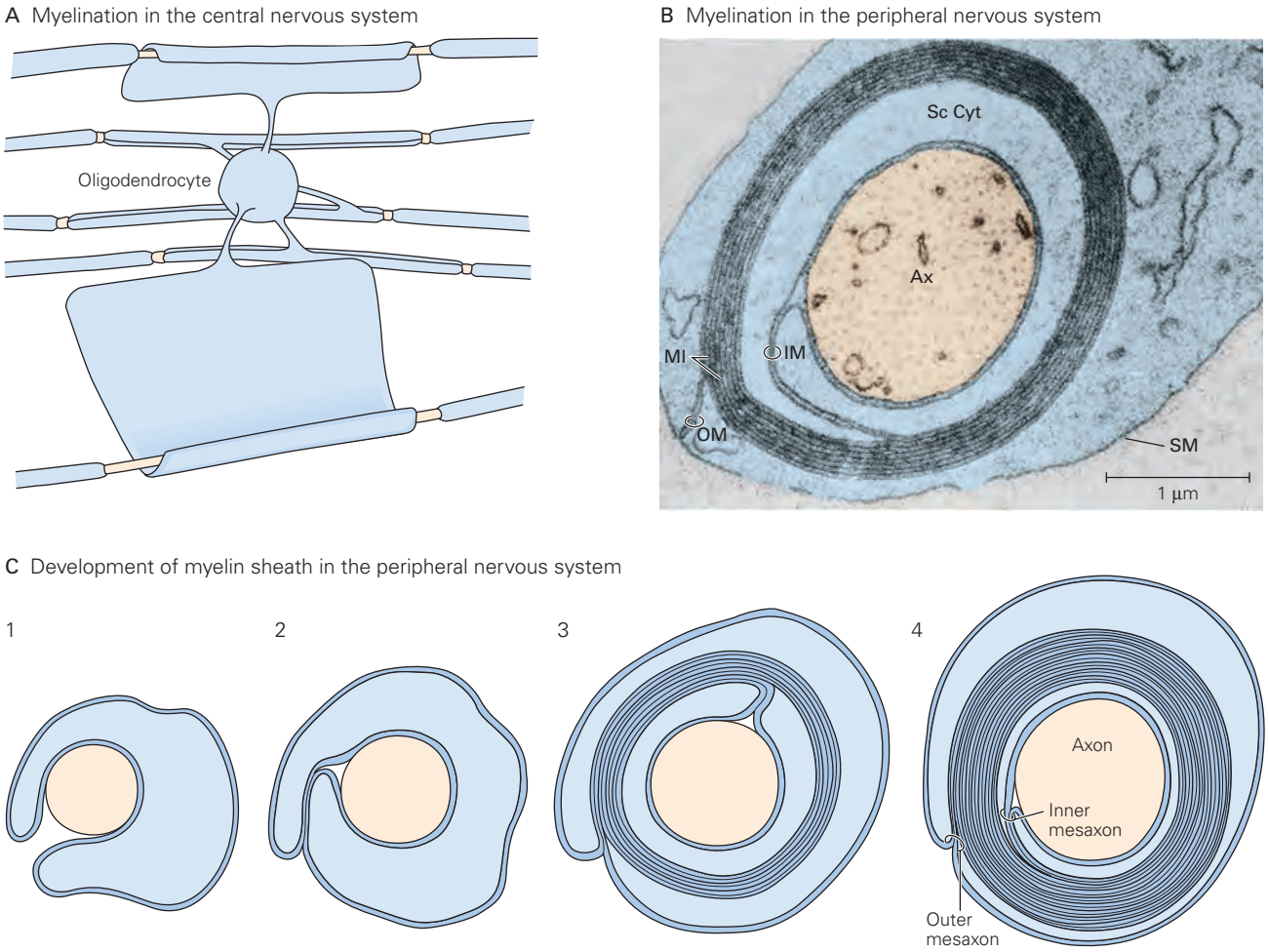

Figure 7–15 Glial cells produce the myelin that insulates the axons of central and peripheral neurons.

A. Axons in the central nervous system are wrapped in several layers of myelin produced by oligodendrocytes. Each oligodendrocyte can myelinate many axons. (Adapted from Raine 1984.)

B. This electron micrograph of a transverse section through an axon (**Ax**) in the sciatic nerve of a mouse shows the origin of a sheet of myelin (**MI**) at a structure called the inner mesaxon (**IM**). The myelin arises from the surface membrane (**SM**) of a Schwann cell, which is continuous with the outer mesaxon (**OM**). In this image, the Schwann cell cytoplasm (**Sc Cyt**) still surrounds the axon; eventually it is squeezed out and the myelin layers become compact, as shown in part **C**. (Reproduced, with permission, from Dyck et al. 1984.)

C. A peripheral nerve fiber is myelinated by a Schwann cell in several stages. In stage 1, the Schwann cell surrounds the axon. In stage 2, the outer aspects of the plasma membrane have become tightly apposed in one area. This membrane fusion reflects early myelin membrane formation. In stage 3, several layers of myelin have formed because of continued rotation of the Schwann cell cytoplasm around the axon. In stage 4, a mature myelin sheath has formed; much of the Schwann cell cytoplasm has been squeezed out of the innermost loop. (Adapted, with permission, from Williams et al. 1989.)

(up to 100 m/s in humans) because the signal jumps from one node to the next, a mechanism called *saltatory conduction* (Chapter 9). Nodes are easily excited because the density of Na^+ channels, which generate the action potential, is approximately 50 times greater in the axon membrane at the nodes than in myelin-sheathed regions of membrane. Cell adhesion molecules around nodes keep the myelin boundaries stable.

In the human femoral nerve, the primary sensory axon is approximately 0.5 m long and the internodal distance is 1 to 1.5 mm; thus, approximately 300 to 500 nodes of Ranvier occur along a primary afferent fiber between the thigh muscle and the cell body in the

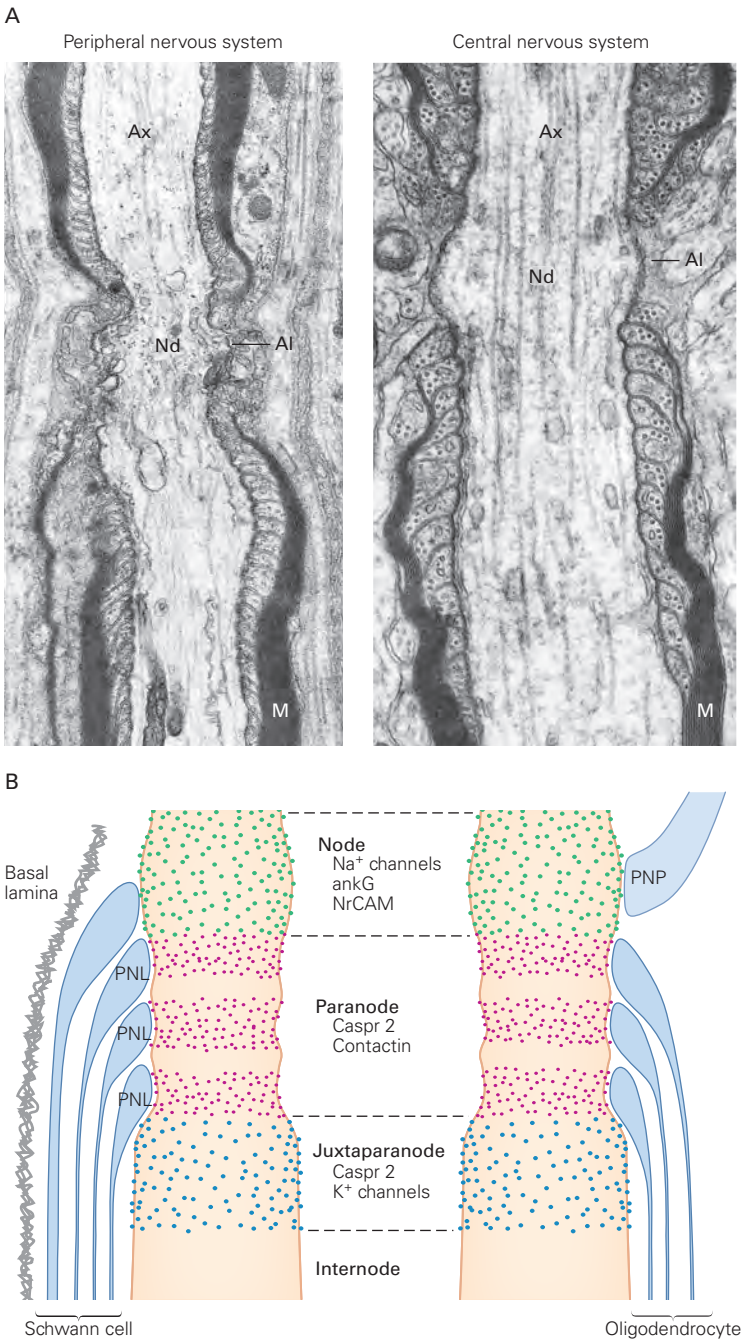

Figure 7–16 The myelin sheath of axons has regular gaps called the *nodes of Ranvier.*

A. Electron micrographs show the region of nodes in axons from the peripheral nervous system and spinal cord. The axon (**Ax**) runs vertically in both micrographs. The layers of myelin (**M**) are absent at the nodes (**Nd**), where the axon's membrane (axolemma, **Al**) is exposed. (Reproduced, with permission, from Peters et al. 1991.)

B. Regions on both sides of a node of Ranvier are rich in stable contacts between myelinating cells and the axon, to ensure that the nodes do not move or change in size and to restrict the localization of K^+ and Na^+ channels in the axon. Potassium-permeable channels and the adhesion protein Caspr2 are concentrated in the juxtaparanode. Paranodal loops (**PNL**) of Schwann cell or oligodendrocyte cytoplasm form a series of stable junctions with the axon. The paranode region is rich with adhesion proteins such as Caspr2, contactin, and neurofascin (NF155). At the nodes in central axons, perinodal astroglial processes (**PNP**) contact the axonal membrane, which is enormously enriched with Na^+ channels. This localization of Na^+ permeability is a major basis for the saltatory conduction in myelinated axons. The membrane-cytoskeletal linker ankyrin G (**ankG**) and the cell adhesion molecules NrCAM and NF186 are also concentrated at the nodes. (Reproduced, with permission, from Peles and Salzer 2000. Copyright © 2000 Elsevier.)

dorsal root ganglion. Because each internodal segment is formed by a single Schwann cell, as many as 500 Schwann cells participate in the myelination of each peripheral sensory axon.

Myelin has bimolecular layers of lipid interspersed between protein layers. Its composition is similar to that of the plasmalemma, consisting of 70% lipid and 30% protein with high concentrations of cholesterol and phospholipid. In the CNS, myelin has two major proteins: myelin basic protein, a small, positively charged protein that is situated on the cytoplasmic surface of compact myelin, and proteolipid protein, a hydrophobic integral membrane protein. Presumably, both provide structural stability for the sheath.

Both have also been implicated as important autoantigens against which the immune system can react to produce the demyelinating disease multiple sclerosis. In the peripheral nervous system, myelin contains a major protein, P_0, as well as the hydrophobic protein PMP22. Autoimmune reactions to these proteins produce a demyelinating peripheral neuropathy, the *Guillain-Barré syndrome*. Mutations in myelin protein genes also cause a variety of demyelinating diseases in both peripheral and central axons (Box 7–3). Demyelination slows down, or even stops, conduction of the action potential in an affected axon, because it allows electrical current to leak out of the axonal membrane. Demyelinating diseases thus have devastating effects on neuronal circuits in the central and peripheral nervous systems (Chapter 57).

Astrocytes Support Synaptic Signaling

Astrocytes are found in all areas of the brain; indeed, they constitute nearly half the number of brain cells. They play important roles in nourishing neurons and in regulating the concentrations of ions and neurotransmitters in the extracellular space. But astrocytes and neurons also communicate with each other to modulate synaptic signaling in ways that are still poorly understood. Astrocytes are generally divided into two main classes, which are distinguished by morphology, location, and function. *Protoplasmic astrocytes* are found in gray matter, and their processes are closely associated with synapses as well as blood vessels. *Fibrillary (or fibrous) astrocytes* in white matter contact axons and nodes of Ranvier. In addition, specialized astrocytes include Bergmann glia in the cerebellum and Müller glia in the retina.

Astrocytes have large numbers of thin processes that enfold all the blood vessels of the brain and ensheathe synapses or groups of synapses. By their intimate physical association with synapses, often closer than 1 μm, astrocytes are positioned to regulate extracellular concentrations of ions, neurotransmitters, and other molecules (Figure 7–19). In fact, astrocytes express many of the same voltage-gated ion channels and neurotransmitter receptors that neurons do and are thus well equipped to receive and transmit signals that could affect neuronal excitability and synaptic function.

How do astrocytes regulate axonal conduction and synaptic activity? The first recognized physiological role was that of K^+ buffering. When neurons fire action potentials, they release K^+ ions into the extracellular space. Because astrocytes have high concentrations of K^+ channels in their membranes, they can act as *spatial buffers*: They take up K^+ at sites of neuronal activity, mainly synapses, and release it at distant contacts with blood vessels. Astrocytes can also accumulate K^+ locally within their cytoplasmic processes along with Cl^- ions and water. Unfortunately, accumulation of ions and water in astrocytes can contribute to severe brain swelling after head injury.

Astrocytes also regulate neurotransmitter concentrations in the brain. For example, high-affinity transporters located in the astrocyte's plasma membrane rapidly clear the neurotransmitter glutamate from the synaptic cleft (Figure 7–19C). Once within the glial cell, glutamate is converted to glutamine by the enzyme glutamine synthetase. Glutamine is then transferred to neurons, where it serves as an immediate precursor of glutamate (Chapter 16). Interference with these uptake mechanisms results in high concentrations of extracellular glutamate that can lead to the death of neurons, a process termed excitotoxicity. Astrocytes also degrade dopamine, norepinephrine, epinephrine, and serotonin.

Astrocytes sense when neurons are active because they are depolarized by the K^+ released by neurons and have neurotransmitter receptors similar to those of neurons. For example, Bergmann glia in the cerebellum express glutamate receptors. Thus, the glutamate released at cerebellar synapses affects not only postsynaptic neurons but also astrocytes near the synapse. The binding of these ligands to glial receptors increases the intracellular free Ca^{2+} concentration, which has several important consequences. The processes of one astrocyte connect to those of neighboring astrocytes through intercellular aqueous channels called gap junctions (Chapter 11), allowing transfer of ions and small molecules between many cells. An increase in free Ca^{2+} within one astrocyte increases Ca^{2+} concentrations in adjacent astrocytes. This spread of Ca^{2+} through the astrocyte network occurs over hundreds of micrometers. It is likely that this Ca^{2+} wave modulates

Box 7–3 Defects in Myelin Proteins Disrupt Conduction of Nerve Signals

Because in myelinated axons normal conduction of the nerve impulse depends on the insulating properties of the myelin sheath, defective myelin can result in severe disturbances of motor and sensory function.

Many diseases that affect myelin, including some animal models of demyelinating disease, have a genetic basis. The *shiverer* (or *shi*) mutant mice have tremors and frequent convulsions and tend to die young. In these mice, the myelination of axons in the central nervous system is greatly deficient and the myelination that does occur is abnormal.

The mutation that causes this disease is a deletion of five of the six exons of the gene for myelin basic protein, which in the mouse is located on chromosome 18. The mutation is recessive; a mouse develops the disease only if it has inherited the defective gene from both parents. *Shiverer* mice that inherit both defective genes have only approximately 10% of the myelin basic protein (MBP) found in normal mice (Figure 7–17A).

When the wild-type gene is injected into fertilized eggs of the *shiverer* mutant with the aim of rescuing the mutant, the resulting transgenic mice express the wild-type gene but produce only 20% of the normal amounts of MBP. Nevertheless, myelination of central neurons in the transgenic mice is much improved. Although they still have occasional tremors, the transgenic mice do not have convulsions and have a normal life span (Figure 7–17B).

In both the central and peripheral nervous systems, myelin contains a protein termed *myelin-associated glycoprotein* (MAG). MAG belongs to the immunoglobulin superfamily that includes several important cell surface proteins thought to be involved in cell-to-cell recognition, eg, the major histocompatibility complex of antigens, T-cell surface antigens, and the neural cell adhesion molecule (NCAM).

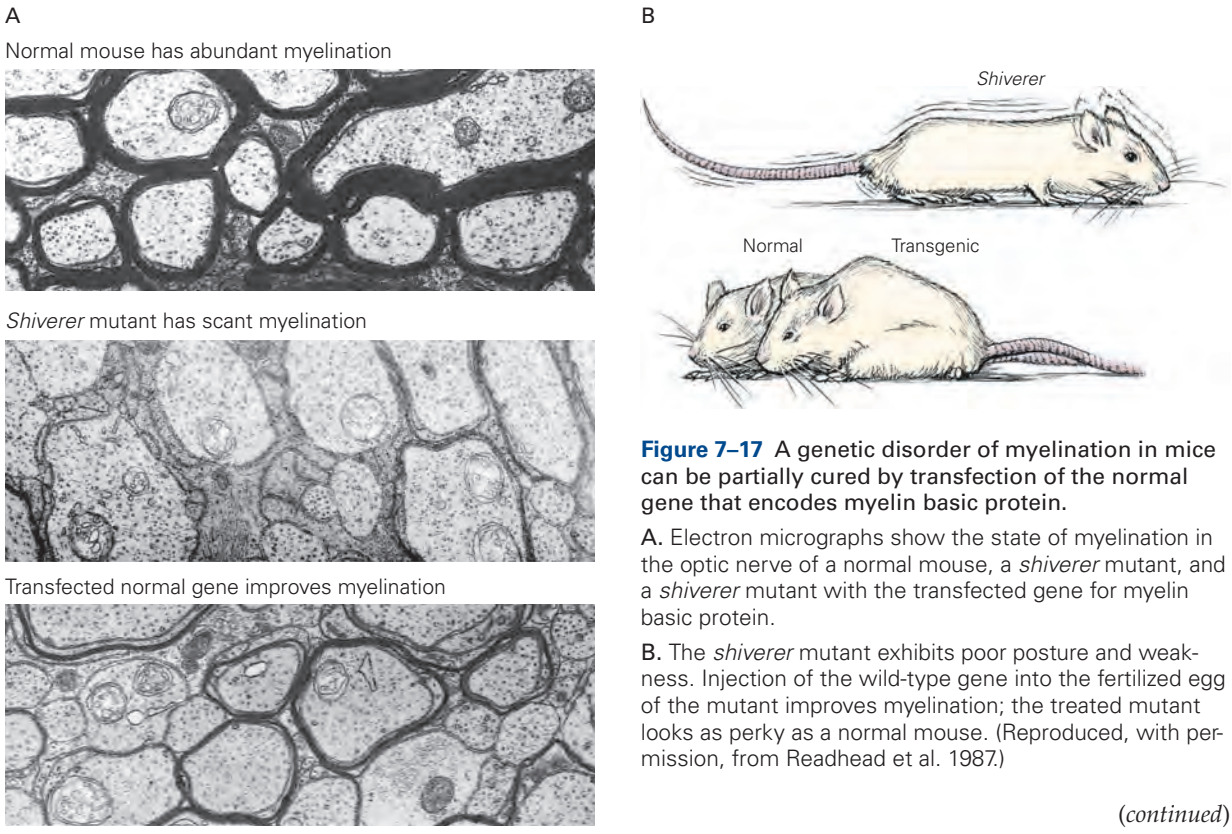

Figure 7–17 A genetic disorder of myelination in mice can be partially cured by transfection of the normal gene that encodes myelin basic protein.

A. Electron micrographs show the state of myelination in the optic nerve of a normal mouse, a *shiverer* mutant, and a *shiverer* mutant with the transfected gene for myelin basic protein.

B. The *shiverer* mutant exhibits poor posture and weakness. Injection of the wild-type gene into the fertilized egg of the mutant improves myelination; the treated mutant looks as perky as a normal mouse. (Reproduced, with permission, from Readhead et al. 1987.)

(*continued*)

Box 7–3 Defects in Myelin Proteins Disrupt Conduction of Nerve Signals (continued)

In the peripheral nervous system, MAG is expressed by Schwann cells early during production of myelin and eventually becomes a component of mature (compact) myelin. Its early expression, subcellular location, and structural similarity to other surface recognition proteins suggest that it is an adhesion molecule important for the initiation of the myelination process. Two isoforms of MAG are produced from a single gene through alternative RNA splicing.

The major protein in mature peripheral myelin, *myelin protein zero* (MPZ or P_0), spans the plasmalemma of the Schwann cell. It has a basic intracellular domain and, like MAG, is a member of the immunoglobulin superfamily. The glycosylated extracellular part of the protein, which contains the immunoglobulin domain, functions as a homophilic adhesion protein during myelin-ensheathing by interacting with identical domains on the surface of the apposed membrane. Genetically engineered mice in which the function of P_0 has been eliminated have poor motor coordination, tremors, and occasional convulsions.

Observation of *trembler* mouse mutants led to the identification of *peripheral myelin protein 22* (PMP22). This Schwann cell protein spans the membrane four times and is normally present in compact myelin. PMP22 is altered by a single amino acid in the mutants. A similar protein is found in humans, encoded by a gene on chromosome 17.

Mutations of the *PMP22* gene on chromosome 17 produce several hereditary peripheral neuropathies, while a duplication of this gene causes one form of *Charcot-Marie-Tooth disease* (Figure 7–18). This disease is the most common inherited peripheral neuropathy and is characterized by progressive muscle weakness, greatly decreased conduction in peripheral nerves, and cycles of demyelination and remyelination. Because both duplicated genes are active, the disease results from *increased* production of PMP22 (a two- to three-fold increase in gene dosage). Mutations in a number of genes expressed by Schwann cells can produce inherited peripheral neuropathies.

In the central nervous system, more than half of the protein in myelin is the proteolipid protein (PLP), which has five membrane-spanning domains. Proteolipids differ from lipoproteins in that they are insoluble in water. Proteolipids are soluble only in organic solvents because they contain long chains of fatty acids that are covalently linked to amino acid residues throughout the proteolipid molecule. In contrast, lipoproteins are noncovalent complexes of proteins with lipids and often serve as soluble carriers of the lipid moiety in the blood.

Many mutations of PLP are known in humans as well as in other mammals, eg, the *jimpy* mouse. One example is Pelizaeus-Merzbacher disease, a heterogeneous X-linked disease in humans. Almost all PLP mutations occur in a membrane-spanning domain of the molecule. Mutant animals have reduced amounts of (mutated) PLP, hypomyelination, and degeneration and death of oligodendrocytes. These observations suggest that PLP is involved in the compaction of myelin.

A

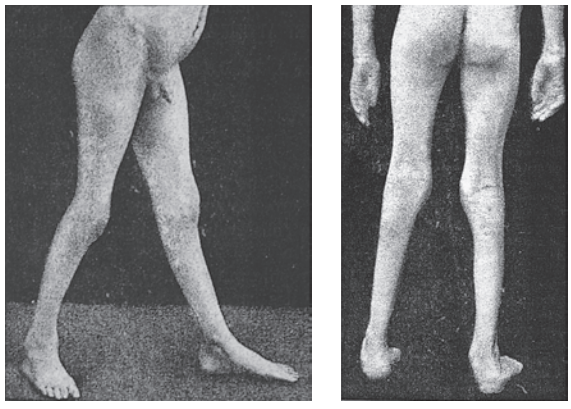

Figure 7–18 Charcot-Marie-Tooth disease (type 1A) results from increased production of peripheral myelin protein 22.

A. A patient with Charcot-Marie-Tooth disease shows impaired gait and deformities. (Reproduced, with permission, from Charcot's original description of the disease, Charcot and Marie 1886.)

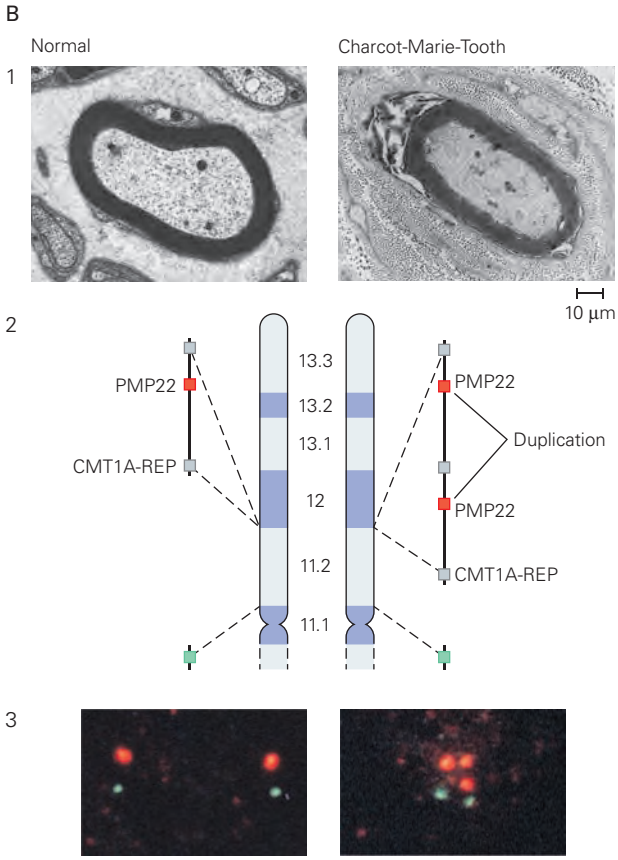

B. The disordered myelination in Charcot-Marie-Tooth disease (type 1A) results from increased production of peripheral myelin protein 22 (PMP22).

1. Sural nerve biopsies from a normal individual (reproduced, with permission, from A.P. Hays) and from a patient with Charcot-Marie-Tooth disease (reproduced, with permission, from Lupski and Garcia 1992). In the patient's biopsy, the myelin sheath is slightly thinner than normal and is surrounded by concentric rings of Schwann cell processes. These changes are typical of the recurrent demyelination and remyelination seen in this disorder.

2. The increase in PMP22 is caused by a duplication of a normal 1.5-Mb region of the DNA on the short arm of chromosome 17 at 17p11.2-p12. The *PMP22* gene is flanked by two similar repeat sequences (CMT1A-REP), as shown in the normal chromosome 17 on the *left*. Normal individuals have two normal chromosomes. In patients with the disease (*right*), the duplication results in two functioning *PMP22* genes, each flanked by a repeat sequence. The normal and duplicated regions are shown in the expanded diagrams indicated by the **dashed lines**. (The repeats are thought to have given rise to the original duplication, which was then inherited. The presence of two similar flanking sequences with homology to a transposable element is believed to increase the frequency of unequal crossing over in this region of chromosome 17 because the repeats enhance the probability of mispairing of the two parental chromosomes in a fertilized egg.)

3. Although a large duplication (3 Mb) cannot be detected in routine examination of chromosomes in the light microscope, evidence for the duplication can be obtained using fluorescence in situ hybridization. The *PMP22* gene is detected with an oligonucleotide probe tagged with the dye Texas Red. An oligonucleotide probe that hybridizes with DNA from region 11.2 (indicated by the green segment close to the centromere) is used for in situ hybridization on the same sample. A nucleus from a normal individual (*left*) shows a pair of chromosomes, each with one red site (*PMP22* gene) for each green site. A nucleus from a patient with the disease (*right*) has one extra red site, indicating that one chromosome has one *PMP22* gene and the other has two *PMP22* genes. (Adapted, with permission, from Lupski et al. 1991.)

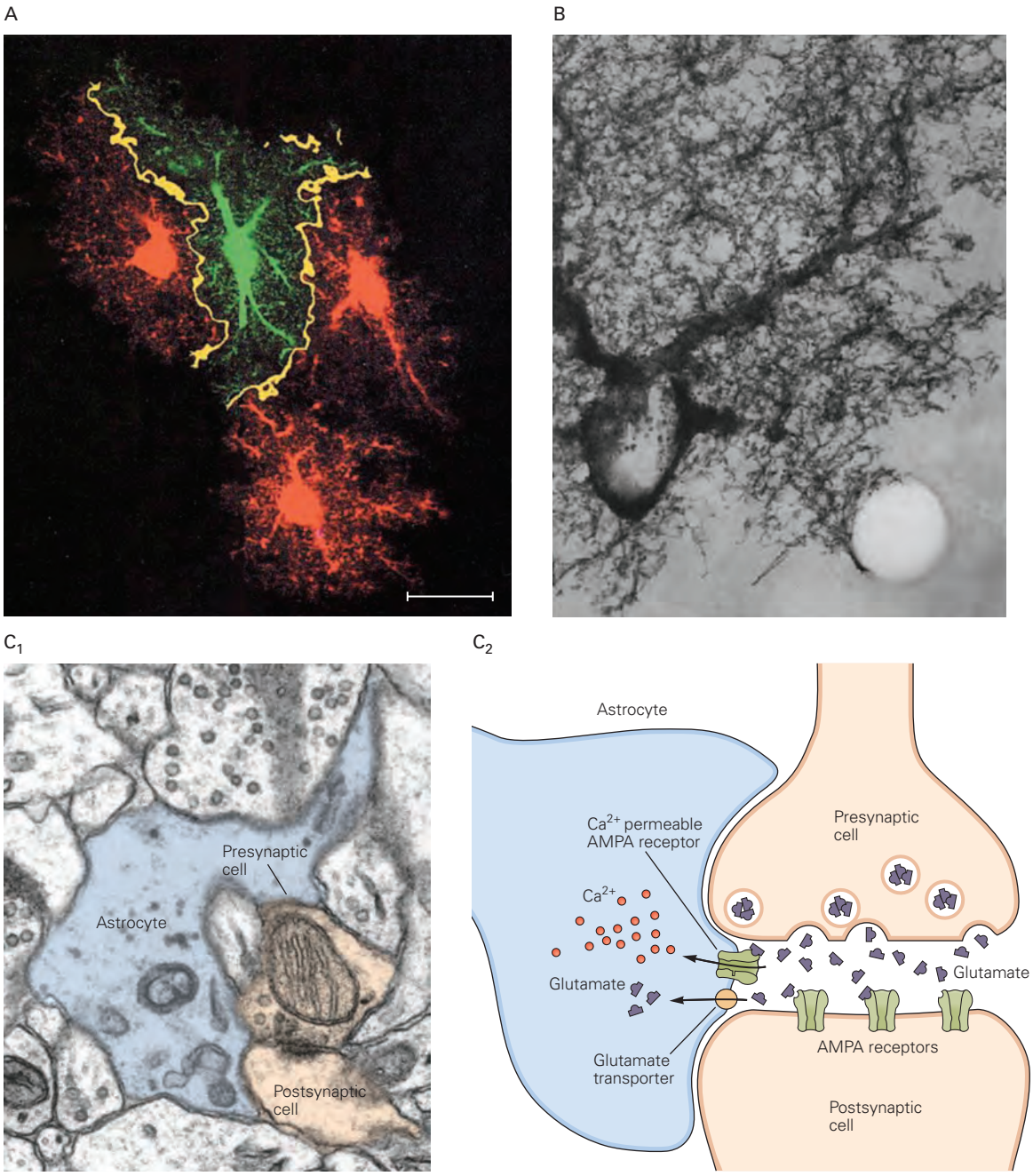

Figure 7–19 Astrocyte processes are intimately associated with synapses.

A. Astrocytes occupy discrete volumes. The central astrocyte (**green**) is shown to occupy a volume distinct from its three neighbors (**red**), with only a small overlap (**yellow**) at the ends of their processes, which are interconnected by gap junctions Bar = 20 µm. (Reproduced, with permission, from Bushong et al. 2002. Copyright © 2002 Society for Neuroscience.)

B. This high-voltage electron micrograph shows several thick processes emanating from the cell body of an astrocyte and branching into extraordinarily fine processes. The typical envelopment of a blood vessel is shown at lower right. (Reproduced, with permission, from Hama et al. 1994. Copyright © 1994 Wiley.)

C. The processes of astrocytes are intimately associated with both presynaptic and postsynaptic elements. **1.** The close association between astrocyte processes and synapses is seen in this electron micrograph of hippocampal cells. (Reproduced, with permission, from Ventura and Harris 1999. Copyright © 1999 Society for Neuroscience.) **2.** Glutamate released from the presynaptic neuron activates not only receptors on the postsynaptic neuron but also AMPA-type (α-amino-3-hydroxy-5-methylisoxazole-4-propionate) receptors on astrocytes. Astrocytes remove glutamate from the synaptic cleft by uptake through high-affinity transporters. (Adapted from Gallo and Chittajallu 2001.)

nearby neuronal activity by triggering the release of nutrients and regulating blood flow. An increase in Ca^{2+} in astrocytes leads to the secretion of signals that enhance synaptic function and even behavior. Thus astrocyte–neuron signaling contributes to normal neural circuit functioning.

Astrocytes also are important for the development of synapses. Their appearance at synapses in the postnatal brain coincides with periods of synaptogenesis and synapse maturation. Astrocytes prepare the surface of the neuron for synapse formation and stabilize newly formed synapses. For example, astrocytes secrete several synaptogenic factors, including thrombospondins, hevin, and glycipans, that promote the formation of new synapses. Astrocytes can also help remodel and eliminate excess synapses during development by phagocytosis (Chapter 48). In the adult CNS, astrocytes continue to phagocytose synapses, and as this phagocytosis is dependent on neuronal activity, it is possible that this remodeling of synapses contributes to learning and memory. In pathological states, such as chromatolysis produced by axonal damage, astrocytes and presynaptic terminals temporarily retract from the damaged postsynaptic cell bodies. Astrocytes release neurotrophic and gliotrophic factors that promote the development and survival of neurons and oligodendrocytes. They also protect other cells from the effects of oxidative stress. For example, the glutathione peroxidase in astrocytes detoxifies toxic oxygen free radicals released during hypoxia, inflammation, and neuronal degeneration.

Finally, astrocytes ensheathe small arterioles and capillaries throughout the brain, forming contacts between the ends of astrocyte processes and the basal lamina around endothelial cells. The CNS is sequestered from the general circulation so that macromolecules in the blood do not passively enter the brain and spinal cord (the *blood–brain barrier*). The barrier is largely the result of tight junctions between endothelial cells and cerebral capillaries, a feature not shared by capillaries in other parts of the body. Nevertheless, endothelial cells have a number of transport properties that allow some molecules to pass through them into the nervous system. Because of the intimate contacts of astrocytes and blood vessels, the transported molecules, such as glucose, can be taken up by astrocyte end-feet.

Following brain injury and disease, astrocytes undergo a dramatic transformation called *reactive astrocytosis*, which involves changes in gene expression, morphology, and signaling. The functions of reactive astrocytes are complex and poorly understood, as they both hinder and support CNS recovery. Recent studies have found evidence for at least two kinds of reactive astrocytes; one type helps to promote repair and recovery, whereas another is harmful, actively contributing to the death of neurons after acute CNS injury; however there are likely other subtypes. These neurotoxic reactive astrocytes are prominent in patients with Alzheimer disease and other neurodegenerative diseases and thus are an attractive target for new therapies. An interesting question is why the brain ever generates a neurotoxic reactive astrocyte. Quite possibly, removal of injured or sick neurons allows synapses to reorganize to help preserve neural circuit function. In addition, removal of virally infected neurons could help limit the spread of viral infections.

Microglia Have Diverse Functions in Health and Disease

Microglia compose about 10% of glia in the CNS and exist in multiple morphological states in the healthy and damaged brain. Despite being described by Rio Hortega over 100 years ago, the functions of microglia are poorly understood compared to other cell types. Unlike neurons, astrocytes, and oligodendrocytes, microglia do not belong to the neuroectodermal lineage. Long thought to derive from the bone marrow, recent fate mapping studies reveal that microglia are in fact derived from myeloid progenitors in the yolk sac.

Microglia colonize brain very early in embryonic development and reside in all regions of the brain throughout life (Figure 7–20). During development, microglia help sculpt developing neural circuits by engulfing pre- and postsynaptic structures (Figure 7–21), and emerging evidence suggests microglia may modulate other aspects of brain development and brain homeostasis. Recent in vivo imaging studies have revealed dynamic interactions between microglia and neurons. In the healthy adult cerebral cortex, microglia processes continuously survey their surrounding extracellular environment and contact neurons and synapses, but the functional significance of this activity remains unknown.

Following injury and disease, microglia undergo a dramatic increase in the motility of their processes and changes in morphology and gene expression and can be rapidly recruited to sites of damage where they can have beneficial roles. For example, they serve to bring lymphocytes, neutrophils, and monocytes into the CNS and expand the lymphocyte population, important immunological activities in infection, stroke, and immunologic demyelinating disease. They also protect the brain by phagocytosing debris as well as unwanted

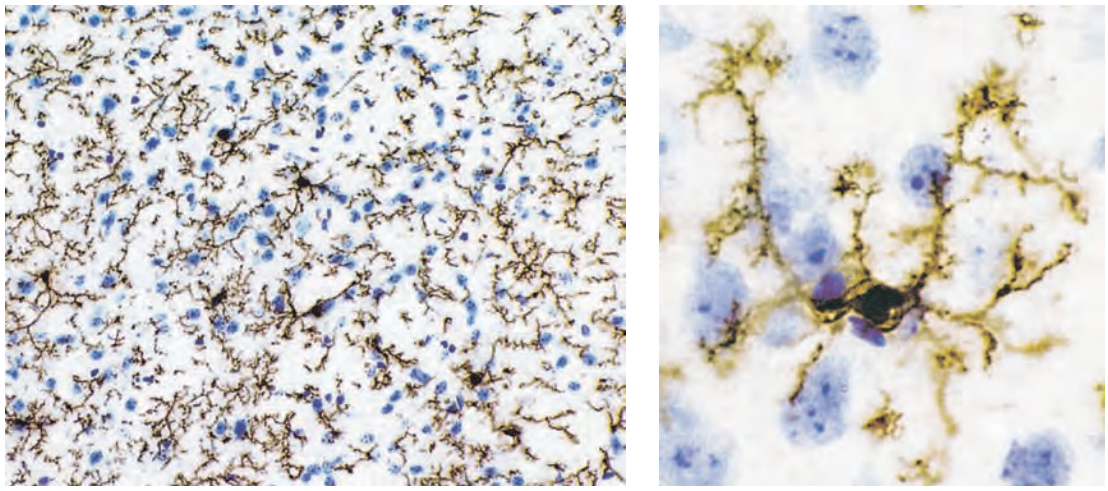

Figure 7–20 Large numbers of microglia reside in the mammalian central nervous system. The micrograph on the *left* shows microglia (in **brown,** immunocytochemistry) in the cerebral cortex of an adult mouse. The **blue** blobs are the nuclei of nonmicroglial cells. The microglial cells have fine, lacy processes, as shown in the higher magnification micrograph on the *right*. (Reproduced, with permission, from Berry et al. 2002.)

and dying cells and toxic proteins, actions that are critical for preventing further damage and maintaining brain homeostasis. Although critical for the immune response to infection or trauma, microglia also contribute to pathological neuroinflammation by releasing cytokines and neurotoxic proteins and by inducing neurotoxic reactive astrocytes. They also contribute to synapse loss and dysfunction in models of Alzheimer disease and neurodegenerative disease.

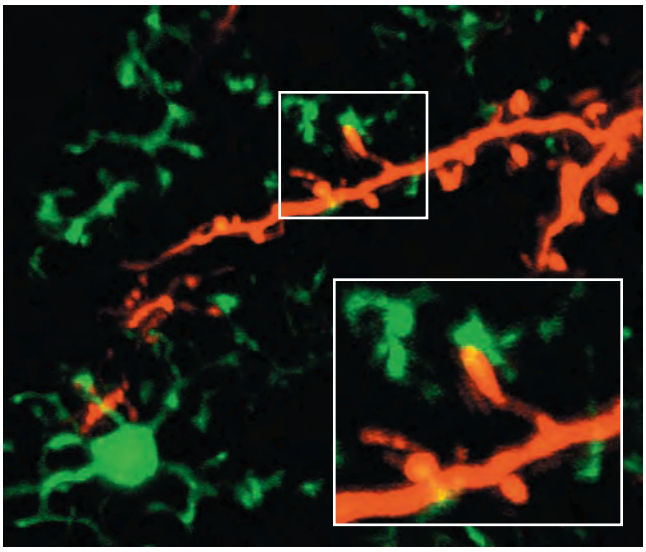

Figure 7–21 Microglia interact with and sculpt synaptic elements in the healthy brain. Two-photon imaging in the olfactory bulb of adult mice shows microglial processes expressing a fractalkine receptor–GFP fusion (CX3CR1-GFP) (**green**) connecting to tdTomato-labeled neurons (**red**). (Reproduced, with permission, from Hong and Stevens 2016.)

Choroid Plexus and Ependymal Cells Produce Cerebrospinal Fluid

The function of neurons and glia is tightly regulated by the extracellular environment of the CNS. *Interstitial fluid* (ISF) fills spaces between neurons and glia in the parenchyma. *Cerebrospinal fluid* (CSF) bathes the brain's ventricles, the subarachnoid space of the brain and spinal cord, and the major cisterns of the CNS. The ISF and CSF deliver nutrients to cells in the CNS, maintain ion homeostasis, and serve as a removal system for metabolic waste products. In conjunction with the meningeal layers that surround the brain and spinal cord, the CSF provides a cushion that protects CNS tissues from mechanical damage. The fluid environment of the CNS is maintained by endothelial cells of the blood–brain barrier and choroid plexus epithelial cells of the blood–CSF barrier. These barriers not only serve to regulate the extracellular environment of the brain and spinal cord but also relay critical information between the CNS and the periphery.

The cells of the *choroid plexus* and the *ependymal layer* contribute to CSF production, composition, and dynamics. The choroid plexuses appear as epithelial invaginations soon after neural tube closure where the lateral, third, and fourth ventricles will eventually

form. Through embryonic development, the choroid plexuses mature, each forming a ciliated cuboidal epithelial layer that encapsulates a stromal and immune cell network and an extensive capillary bed. The ependyma is a single layer of ciliated cuboidal cells, a type of glia cell that lines the ventricles of the brain. At several places in the lateral and fourth ventricles, specialized ependymal cells form the epithelial layer that surrounds the choroid plexus (Figure 7–22B).

The choroid plexus produces most of the CSF that bathes the brain. Loose junctions between ependymal cells provide access for CSF to the brain's interstitial space. Ciliary motion in the ependymal cells helps to move CSF through the ventricular system (Figure 7–22A), facilitating long-range delivery of molecules to other cells in the CNS and transport of waste from the CNS to the periphery.

The choroid plexus transports fluid and solutes from the serum into the CNS to generate CSF. The fenestrated capillaries that traverse the choroid plexus allow free passage of water and small molecules from the blood into the stromal space of the choroid plexus. The choroid plexus epithelial cells, however, form tight junctions, preventing further unregulated movement of these molecules into the brain. Instead, import of water, ions, metabolites, and protein mediators that compose the CSF is tightly regulated by transporters and channels in the choroid plexus epithelium. Active transport mechanisms in the epithelium are bidirectional, additionally mediating the flux of molecules from the CSF back into the peripheral circulation.

The choroid plexus epithelial cells also synthesize and secrete many proteins into the CSF. In the healthy

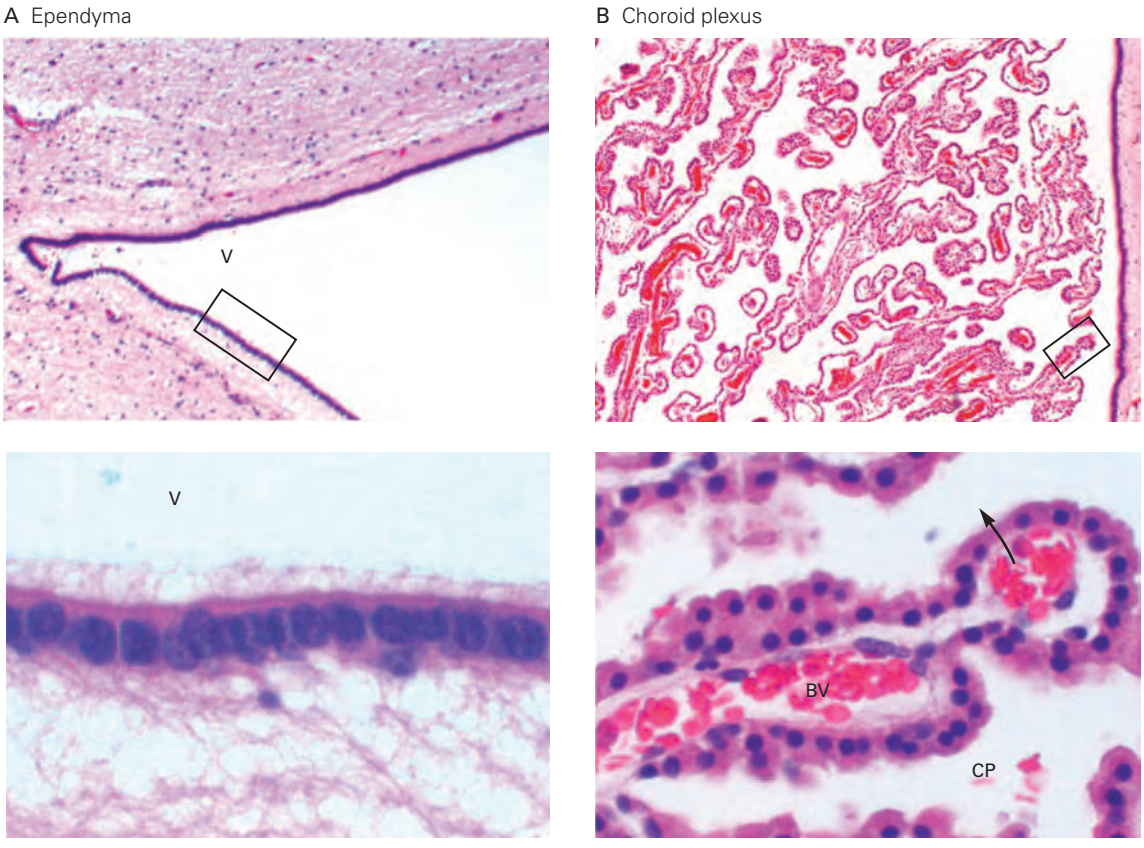

Figure 7–22 Ependyma and choroid plexus.

A. The ependyma is a single layer of ciliated, cuboidal cells lining the cerebral ventricles (**V**). The lower image, a high magnification of the ependymal lining (rectangle in upper image), shows the cilia on the ventricular side of the ependymal cells.

B. The choroid plexus is continuous with the ependyma but projects into the ventricles, where it covers thin blood vessels and forms a highly branched papillary structure. This is the site of cerebrospinal fluid formation. High magnification (lower image) shows the blood vessel core (**BV**) and overlying choroid plexus (**CP**). The arrow denotes the direction of fluid flow from capillary into ventricle during the formation of cerebrospinal fluid.

embryonic and postnatal brain, these proteins modulate development of neural stem cells and may regulate processes such as cortical plasticity. The choroid plexus epithelial cell secretome can also be altered by inflammatory signals from the periphery or from within the brain, with consequences for neuronal function during infection and in aging. Functional roles for other choroid plexus–derived factors in the healthy and diseased brain—including microRNAs, long noncoding RNAs, and extracellular vesicles—are beginning to emerge, further underlining the important contribution of this structure to brain development and homeostasis.

Highlights

1. The morphology of neurons is elegantly suited to receive, conduct, and transmit information in the brain. Dendrites provide a highly branched, elongated surface for receiving signals. Axons conduct electrical impulses rapidly over long distances to their synaptic terminals, which release neurotransmitters onto target cells.
2. Although all neurons conform to the same basic cellular architecture, different subtypes of neurons vary widely in their specific morphological features, functional properties, and molecular identities.
3. Neurons in different locations differ in the complexity of their dendritic trees, extent of axon branching, and the number of synaptic terminals that they form and receive. The functional significance of these morphological differences is plainly evident. For example, motor neurons must have a more complex dendritic tree than sensory neurons, as even simple reflex activity requires integration of many excitatory and inhibitory inputs. Different types of neurons use different neurotransmitters, ion channels, and neurotransmitter receptors. Together, these biochemical, morphological, and electrophysiological differences contribute to the great complexity of information processing in the brain.
4. Neurons are among the most highly polarized cells in our body. The considerable size and complexity of their dendritic and axonal compartments represent significant cell biological challenges for these cells, including transport of various organelles, proteins, and mRNA over long distances (up to a meter for some axons). Most neuronal proteins are synthesized in the cell body, but some synthesis occurs in dendrites and axons. The newly synthesized proteins are folded with the assistance of chaperones, and their final structure is often modified by permanent or reversible posttranslational modifications. The final destination of a protein in the neuron depends on signals encoded in its amino acid sequence.
5. Transport of proteins and mRNA occurs with great specificity and results in the vectorial transport of selected membrane components. The cytoskeleton provides an important framework for the transport of organelles to different intracellular locations in addition to controlling axonal and dendritic morphology.
6. All these fundamental cell biological processes are profoundly modifiable by neuronal activity, which produces the dramatic changes in cell structure and function by which neural circuits adapt to experience (learning).
7. The nervous system also contains several types of glial cells. Oligodendrocytes and Schwann cells produce the myelin insulation that enables axons to conduct electrical signals rapidly. Astrocytes and nonmyelinating Schwann cells ensheathe other parts of the neuron, particularly synapses. Astrocytes control extracellular ion and neurotransmitter concentrations and actively participate in the formation and function of synapses. Microglia resident immune cells and phagocytes dynamically interact with neurons and glial cells and have diverse roles in health and disease.
8. The cells of the choroid plexus and the ependymal layer contribute to CSF production, composition, and dynamics.
9. New advances in genomics and single-cell RNA sequencing are beginning to define the immense diversity of cell types, not only among neurons but also among glial cells.
10. Recent progress in genetics, cell biology, and in vivo microscopy (two-photon microscopy, light-sheet microscopy) is providing new insights into the unique mechanisms by which neurons establish and maintain their polarity throughout an individual's life span.
11. These new insights provide important clues into the cell biological steps, including for example defects in axon transport, that trigger neurodegenerative diseases such as Huntington, Parkinson, and Alzheimer disease.

Beth Stevens
Franck Polleux
Ben A. Barres

Selected Reading

Alberts B, Johnson A, Lewis J, Raff M, Roberts K, Walter P (eds). 2002. *Molecular Biology of the Cell*, 4th ed. New York: Garland.

Chung WS, Allen NJ, Eroglu C. 2015. Astrocytes control synapse formation, function, and elimination. Cold Spring Harb Perspect Biol 7:a020370.

Damkier HH, Brown P, Praetorius J. 2013. Cerebrospinal fluid secretion by the choroid plexus. Physiol Rev 93:1847–1892.

Dyck PJ, Thomas PK, Griffin JW, Low PA, Poduslo JF (eds). 1993. *Peripheral Neuropathy*, 3rd ed. Philadelphia: Saunders.

Dyck PJ, Thomas PK, Lambert EH, Bunge R (eds). 1984. *Peripheral Neuropathy,* 2nd ed., Vols. 1, 2. Philadelphia: Saunders.

Glickman MH, Ciechanover A. 2002. The ubiquitin-proteasome proteolytic pathway: destruction for the sake of construction. Physiol Rev 82:373–428.

Hartl FU. 1996. Molecular chaperones in cellular protein folding. Nature 381:571–579.

Kapitein LC, Hoogenraad CC. 2015. Building the neuronal microtubule cytoskeleton. Neuron 87:492–506.

Kelly RB. 1993. Storage and release of neurotransmitters. Cell 72:43–53.

Kreis T, Vale R (eds). 1999. *Guidebook to the Cytoskeletal and Motor Proteins*, 2nd ed. Oxford: Oxford Univ. Press.

Lun MP, Monuki ES, Lehtinen MK. 2015. Development and functions of the choroid plexus-cerebral fluid system. Nature Rev Neurosci 16:445–457.

Nigg EA. 1997. Nucleocytoplasmic transport: signals, mechanisms and regulation. Nature 386:779–787.

Pemberton LF, Paschal BM. 2005. Mechanisms of receptor-mediated nuclear import and nuclear export. Traffic 6:187–198.

Rothman JE. 2002. Lasker Basic Medical Research Award: the machinery and principles of vesicle transport in the cell. Nat Med 8:1059–1062.

Schafer DP, Stevens B. 2015. Microglia function in central nervous system development and plasticity. Cold Spring Harb Perspect Biol 7:a020545.

Schatz G, Dobberstein B. 1996. Common principles of protein translocation across membranes. Science 271:1519–1526.

Schwartz JH. 2003. Ubiquitination, protein turnover, and long-term synaptic plasticity. Sci STKE 190:26.

Siegel GJ, Albers RW, Brady S, Price DL (eds). 2005. *Basic Neurochemistry: Molecular, Cellular, and Medical Aspects*, 7th ed. Amsterdam: Elsevier.

Signor D, Scholey JM. 2000. Microtubule-based transport along axons, dendrites and axonemes. Essays Biochem 35:89–102.

St Johnston D. 2005. Moving messages: the intracellular localization of mRNAs. Nat Rev Mol Cell Biol 6: 363–375.

Stryer L. 1995. *Biochemistry,* 4th ed. New York: Freeman.

Tahirovic S, Bradke F. 2009. Neuronal polarity. Cold Spring Harb Perspect Biol 1:a001644.

Zhou L, Griffin JW. 2003. Demyelinating neuropathies. Curr Opin Neurol 16:307–313.

References

Barnes AP, Polleux F. 2009. Establishment of axon-dendrite polarity in developing neurons. Ann Rev Neurosci 32:347–381.

Berry M, Butt AM, Wilkin G, Perry VH. 2002. Structure and function of glia in the central nervous system. In: Graham DI and Lantos PL (eds). *Greenfield's Neuropathology.* 7th ed., pp. 104–105. London: Arnold.

Bershadsky AD, Vasiliev JM. 1988. *Cytoskeleton.* New York: Plenum.

Brendecke SM, Prinz M. 2015. Do not judge a cell by its cover—diversity of CNS resident, adjoining and infiltrating myeloid cells in inflammation. Semin Immunopathol 37:591–605.

Bushong EA, Martone ME, Jones YZ, Ellisman MH. 2002. Protoplasmic astrocytes in CA1 stratum radiatum occupy separate anatomical domains. J Neurosci 22:183–192.

Charcot J-M, Marie P. 1886. Sur une forme particulière d'atrophie musculaire progressive, souvent familiale, débutant par les pieds et les jambes et atteignant plus tard les mains. Rev Med 6:97–138.

Christopherson KS, Ullian EM, Stokes CC, et al. 2005. Thrombospondins are astrocyte-secreted proteins that promote CNS synaptogenesis. Cell 120:421–433.

Chung WS, Clarke LE, Wang GX, et al. 2013. Astrocytes mediate synapse elimination through MEGF10 and MERTK pathways. Nature 504:394–400.

Ciechanover A, Brundin P. 2003. The ubiquitin proteasome system in neurodegenerative diseases: sometimes the chicken, sometimes the egg. Neuron 40:427–446.

Cooney JR, Hurlburt JL, Selig DK, Harris KM, Fiala JC. 2002. Endosomal compartments serve multiple hippocampal dendritic spines from a widespread rather than a local store of recycling membrane. J Neurosci 22:2215–2224.

De Camilli P, Moretti M, Donini SD, Walter U, Lohmann SM. 1986. Heterogeneous distribution of the cAMP receptor protein RII in the nervous system: evidence for its intracellular accumulation on microtubules, microtubule-organizing centers, and in the area of the Golgi complex. J Cell Biol 103:189–203.

Divac I, LaVail JH, Rakic P, Winston KR. 1977. Heterogeneous afferents to the inferior parietal lobule of the rhesus monkey revealed by the retrograde transport method. Brain Res 123:197–207.

Duxbury MS, Whang EE. 2004. RNA interference: a practical approach. J Surg Res 117:339–344.

Esiri MM, Hyman BT, Beyreuther K, Masters C. 1997. Ageing and dementia. In: DI Graham, PL Lantos (eds). *Greenfield's Neuropathology*, 6th ed. Vol II. London: Arnold.

Gallo V, Chittajallu R. 2001. Neuroscience. Unwrapping glial cells from the synapse: what lies inside? Science 292:872–873.

Giraudo CG, Hu C, You D, et al. 2005. SNAREs can promote complete fusion and hemifusion as alternative outcomes. J Cell Biol 170:249–260.

Goldberg AL. 2003. Protein degradation and protection against misfolded or damaged proteins. Nature 426:895–899.

Görlich D, Mattaj IW. 1996. Nucleocytoplasmic transport. Science 271:1513–1518.

Hama K, Arii T, Kosaka T. 1994. Three-dimensional organization of neuronal and glial processes: high voltage electron microscopy. Microsc Res Tech 29:357–367.

Harris KM, Jensen FE, Tsao B. 1992. Three-dimensional structure of dendritic spines and synapses in rat hippocampus (CA1) at postnatal day 15 and adult ages: implications for the maturation of synaptic physiology and long-term potentiation. J Neurosci 12:2685–2705.

Harris KM, Stevens JK. 1989. Dendritic spines of CA1 pyramidal cells in the rat hippocampus: serial electron microscopy with reference to their biophysical characteristics. J Neurosci 9:2982–2997.

Hirokawa N. 1997. The mechanisms of fast and slow transport in neurons: identification and characterization of the new Kinesin superfamily motors. Curr Opin Neurobiol 7:605–614.

Hirokawa N, Pfister KK, Yorifuji H, Wagner MC, Brady ST, Bloom GS. 1989. Submolecular domains of bovine brain kinesin identified by electron microscopy and monoclonal antibody decoration. Cell 56:867–878.

Hoffman PN, Lasek RJ. 1975. The slow component of axonal transport: identification of major structural polypeptides of the axon and their generality among mammalian neurons. J Cell Biol 66:351–366.

Hong S, Stevens B. 2016. Microglia: phagocytosing to clear, sculpt and eliminate. Dev Cell 38:126–128.

Ko CO, Robitaille R. 2015. Perisynaptic Schwann cells at the neuromuscular synapse: adaptable, multitasking glial cells. Cold Spring Harb Perspect Biol 7:a020503.

Lemke G. 2001. Glial control of neuronal development. Annu Rev Neurosci 24:87–105.

Liddelow SA,Guttenplan KA, Clarke LE, et al. 2016 Neurotoxic reactive astrocytes are induced by activated microglia. Nature 541:481–487.

Lupski JR, de Oca-Luna RM, Slaugenhaupt S, et al. 1991. DNA duplication associated with Charcot-Marie-Tooth disease type 1A. Cell 66:219–232.

Lupski JR, Garcia CA. 1992. Molecular genetics and neuropathology of Charcot-Marie-Tooth disease type 1A. Brain Pathol 2:337–349.

Ma Z, Stork T, Bergles DE, Freeman MR. 2016. Neuromodulators signal through astrocytes to alter neural circuit activity and behaviour. Nature 539:428–432.

Maday S, Twelvetrees AE, Moughamian AJ, Holzbaur EL. 2014. Axonal transport: cargo-specific mechanisms of motility and regulation. Neuron 84:292–309.

McNew JA, Goodman JM. 1996. The targeting and assembly of peroxisomal proteins: some old rules do not apply. Trends Biochem Sci 21:54–58.

Mirra SS, Hyman BT. 2002. Aging and dementia. In: DI Graham, PL Lantos (eds). *Greenfield's Neuropathology*, 7th ed., Vol. 2, p. 212. London: Arnold.

Ochs S. 1972. Fast transport of materials in mammalian nerve fibers. Science 176:252–260.

Peles E, Salzer JL. 2000. Molecular domains of myelinated axons. Curr Opin Neurobiol 10:558–565.

Peters A, Palay SL, Webster H de F. 1991. *The Fine Structure of the Nervous System*, 3rd ed. New York: Oxford University Press.

Raine CS. 1984. Morphology of myelin and myelination. In: P Morell (ed). *Myelin*. New York: Plenum Press.

Ransohoff RM, Cardona AE. 2010. The myeloid cells of the central nervous system parenchyma. Nature 468:253–262.

Ramón y Cajal S. [1901] 1988. Studies on the human cerebral cortex. IV. Structure of the olfactory cerebral cortex of man and mammals. In: J DeFelipe, EG Jones (eds, transl). *Cajál on the Cerebral Cortex*, pp. 289–362. New York: Oxford Univ. Press.

Ramón y Cajal S. [1909] 1995. *Histology of the Nervous System of Man and Vertebrates*. N Swanson, LW Swanson (transl). Vols. 1, 2. New York: Oxford Univ. Press.

Readhead C, Popko B, Takahashi N, et al. 1987. Expression of a myelin basic protein gene in transgenic Shiverer mice: correction of the dysmyelinating phenotype. Cell 48:703–712.

Roa BB, Lupski JR. 1994. Molecular genetics of Charcot-Marie-Tooth neuropathy. Adv Human Genet 22:117–152.

Schafer DP, Lehrman EK, Kautzman AG, et al. 2012. Microglia sculpt postnatal neural circuits in an activity and complement-dependent manner. Neuron 74:691–705.

Schnapp BJ, Reese TS. 1982. Cytoplasmic structure in rapid-frozen axons. J Cell Biol 94:667–679.

Silva-Vargas V, Maldonado-Soto AR, Mizrak D, Codega P, Doetsch F. 2016. Age-dependent niche signals from the choroid plexus regulate adult neural stem cells. Cell Stem Cell 19:643–652.

Sorra KE, Harris KM. 1993. Occurrence and three-dimensional structure of multiple synapses between individual radiatum axons and their target pyramidal cells in hippocampal area CA1. J Neurosci 13:3736–3748.

Sossin W. 1996. Mechanisms for the generation of synapse specificity in long-term memory: the implications of a requirement for transcription. Trends Neurosci 19:215–218.

Takei K, Mundigl O, Daniell L, De Camilli P. 1996. The synaptic vesicle cycle: a single vesicle budding step involving clathrin and dynamin. J Cell Biol 1335:1237–1250.

Ventura R, Harris KM. 1999. Three-dimensional relationships between hippocampal synapses and astrocytes. J Neurosci 19:6897–6906.

Weiss P, Hiscoe HB. 1948. Experiments on the mechanism of nerve growth. J Exp Zool 107:315–395.

Wells DG, Richter JD, Fallon JR. 2000. Molecular mechanisms for activity-regulated protein synthesis in the synaptodendritic compartment. Curr Opin Neurobiol 10:132–137.

Williams PL, Warwick R, Dyson M, Bannister LH (eds). 1989. *Gray's Anatomy*, 37th ed., pp 859–919. Edinburgh: Churchill Livingstone.

Zemanick MC, Strick PL, Dix RD. 1991. Direction of transneuronal transport of herpes simplex virus 1 in the primate motor system is strain-dependent. Proc Natl Acad Sci U S A 88:8048–8051.

8

Ion Channels

Signaling in the brain depends on the ability of nerve cells to respond to very small stimuli with rapid and large changes in the electrical potential difference across the cell membrane. In sensory cells, the membrane potential changes in response to minute physical stimuli: Receptors in the eye respond to a single photon of light; olfactory neurons detect a single molecule of odorant; and hair cells in the inner ear respond to tiny movements of atomic dimensions. These sensory responses ultimately lead to the firing of an action potential during which the membrane potential changes at up to 500 volts per second.

The rapid changes in membrane potential that underlie signaling throughout the nervous system are mediated by specialized pores or openings in the membrane called ion channels, a class of integral membrane proteins found in all cells of the body. The ion channels of nerve cells are optimally tuned to respond to specific physical and chemical signals. They are also heterogeneous—in different parts of the nervous system different types of channels carry out specific signaling tasks.

Because of their key roles in electrical signaling, malfunctioning of ion channels can cause a wide variety of neurological diseases (Chapters 57 and 58). Diseases caused by ion channel malfunction are not limited to the brain; for example, cystic fibrosis, skeletal muscle disease, and certain types of cardiac arrhythmia are also caused by ion channel malfunction. Moreover, ion channels are often the site of action of drugs, poisons, or toxins. Thus, ion channels have crucial roles in both the normal physiology and pathophysiology of the nervous system.

In addition to ion channels, nerve cells contain a second important class of proteins specialized for moving ions across cell membranes, the ion transporters and pumps. These proteins do not participate in rapid neuronal signaling but rather are important for establishing and maintaining the concentration gradients of physiologically important ions between the inside and outside of the cell. As we will see in this and

the next chapters, ion transporters and pumps differ in important aspects from ion channels, but also share certain common features.

Ion channels have three important properties: (1) They recognize and select specific ions; (2) they open and close in response to specific electrical, chemical, or mechanical, signals; and (3) they conduct ions across the membrane. The channels in nerve and muscle conduct ions across the cell membrane at extremely rapid rates, thereby providing a large flow of electric charge. Up to 100 million ions can pass through a single channel each second. This current causes the rapid changes in membrane potential required for signaling (Chapter 10). The fast flow of ions through channels is comparable to the turnover rate of the fastest enzymes, catalase and carbonic anhydrase, which are limited by diffusion of substrate. (The turnover rates of most other enzymes are considerably slower, ranging from 10 to 1,000 per second.)

Despite such an extraordinary rate of ion flow, channels are surprisingly selective for the ions they allow to permeate. Each type of channel allows only one or a few types of ions to pass. For example, the negative resting potential of nerve cells is largely determined by a class of K^+ channels that are 100-fold more permeable to K^+ than to Na^+. In contrast, generation of the action potential involves a class of Na^+ channels that are 10- to 20-fold more permeable to Na^+ than to K^+. Thus, a key to the great versatility of neuronal signaling is the regulated activation of different classes of ion channels, each of which is selective for specific ions.

Many channels open and close in response to a specific event: Voltage-gated channels are regulated by changes in membrane potential, ligand-gated channels by binding of chemical transmitters, and mechanically gated channels by membrane stretch. Other channels are normally open when the cell is at rest. The ion flux through these "resting" channels largely determines the resting potential.

The flux of ions through ion channels is passive, requiring no expenditure of metabolic energy by the channels. Ion channels are limited to catalyzing the passive movement of ions down their thermodynamic concentration and electrical gradients. The direction of this flux is determined not by the channel itself, but rather by the electrostatic and diffusional driving forces across the membrane. For example, Na^+ ions flow into a cell through voltage-gated Na^+ channels during an action potential because the external Na^+ concentration is much greater than the internal concentration; the open channels allow Na^+ to diffuse into the cell down its concentration gradient. With such passive ion movement, the Na^+ concentration gradient would eventually dissipate were it not for ion pumps. Different types of ion pumps maintain the concentration gradients for Na^+, K^+, $Ca^{2+}$and other ions.

These pumps differ from ion channels in two important details. First, whereas open ion channels have a continuous water-filled pathway through which ions flow unimpeded from one side of the membrane to the other, each time a pump moves an ion or group of ions across the membrane, it must undergo a series of conformational changes. As a result, the rate of ion flow through pumps is 100 to 100,000 times slower than through channels. Second, pumps that maintain ion gradients use chemical energy, often in the form of adenosine triphosphate (ATP), to transport ions against their electrical and chemical gradients. Such ion movements are termed *active transport*. The function and structure of ion pumps and transporters are considered in detail at the end of this chapter and in Chapter 9.

In this chapter, we examine six questions: Why do nerve cells have channels? How can channels conduct ions at such high rates and still be selective? How are channels gated? How are the properties of these channels modified by various intrinsic and extrinsic conditions? How does channel structure explain function? Finally, how do ion movements through channels differ from ion movements through transporters? In succeeding chapters, we consider how resting channels and pumps generate the resting potential (Chapter 9), how voltage-gated channels generate the action potential (Chapter 10), and how ligand-gated channels produce synaptic potentials (Chapters 11, 12, and 13).

Ion Channels Are Proteins That Span the Cell Membrane

To appreciate why nerve cells use channels, we need to understand the nature of the plasma membrane and the physical chemistry of ions in solution. The plasma membrane of all cells, including nerve cells, is approximately 6 to 8 nm thick and consists of a mosaic of lipids and proteins. The core of the membrane is formed by a double layer of phospholipids approximately 3 to 4 nm thick. Embedded within this continuous lipid sheet are integral membrane proteins, including ion channels.

The lipids of the membrane do not mix with water—they are hydrophobic. In contrast, the ions within the cell and those outside strongly attract water

molecules—they are hydrophilic (Figure 8–1). Ions attract water because water molecules are dipolar: Although the net charge on a water molecule is zero, charge is separated within the molecule. The oxygen atom in a water molecule tends to attract electrons and so bears a small net negative charge, whereas the hydrogen atoms tend to lose electrons and therefore carry a small net positive charge. As a result of this unequal distribution of charge, positively charged ions (cations) are strongly attracted electrostatically to the oxygen atoms of water, and negatively charged ions (anions) are attracted to the hydrogen atoms. Similarly, ions attract water; they become surrounded by electrostatically bound *waters of hydration* (Figure 8–1).

An ion cannot move from water into the uncharged hydrocarbon tails of the lipid bilayer in the membrane unless a large amount of energy is expended to overcome the attraction between the ion and the surrounding water molecules. For this reason, it is extremely unlikely that an ion will move from solution into the lipid bilayer, and therefore, the bilayer itself is almost completely impermeable to ions. Rather, ions cross the membrane through ion channels, where the energetics favor ion movement.

Although their molecular nature has been known with certainty for only approximately 35 years, the idea of ion channels dates to the work of Ernst Brücke at the end of the 19th century. Physiologists had long known that, despite the fact that the cell membrane acts as a barrier, cell membranes are nevertheless permeable to water and many small solutes, including some ions. To explain osmosis, the flow of water across biological membranes, Brücke proposed that membranes contain channels or pores that allow water but not larger solutes to flow. Over 100 years later, Peter Agre found that a family of proteins termed *aquaporins* form channels with a highly selective permeability to water. At the beginning of the 20th century, William Bayliss suggested that water-filled channels would permit ions to cross the cell membrane easily, as the ions would not need to be stripped of their waters of hydration.

The idea that ions move through channels leads to a question: How can a water-filled channel conduct ions at high rates and yet be selective? How, for instance, does a channel allow K^+ ions to pass while excluding Na^+ ions? Selectivity cannot be based solely on the diameter of the ion because K^+, with a crystal radius of 0.133 nm, is larger than Na^+ (crystal radius of 0.095 nm). One important factor that determines ion selectivity is the size of an ion's shell of waters of hydration, because the ease with which an ion moves in solution (its mobility) depends on the size of the ion together with the shell of water surrounding it. The smaller an ion, the more highly localized is its charge and the stronger its electric field. As a result, smaller ions attract water more strongly. Thus, as Na^+ moves through solution, its stronger electrostatic attraction for water causes it to have a larger water shell, which tends to slow it down relative to K^+. Because of its larger water shell, Na^+ behaves as if it is larger than K^+. The smaller an ion, the lower its mobility in solution. Therefore, we can construct a model of a channel that selects K^+ rather than Na^+ simply on the basis of the interaction of the two ions with water in a water-filled channel (Figure 8–1).

Although this model explains how a channel can select K^+ and exclude Na^+, it does not explain how a channel could select Na^+ and exclude K^+. This problem led many physiologists in the 1930s and 1940s to abandon the channel theory in favor of the idea that ions cross cell membranes by first binding to a specific carrier protein, which then shuttles the ion through the membrane. In this carrier model, selectivity is based on the chemical binding between the ion and the carrier protein, not on the mobility of the ion in solution.

Even though we now know that ions can cross membranes by means of a variety of transport macromolecules, the Na^+-K^+ pump being a well-characterized example (Chapter 9), many properties of membrane ion permeability do not fit the carrier model. Most important is the rapid rate of ion transfer across membranes. An example is provided by the transmembrane current that is initiated when the neurotransmitter acetylcholine (ACh) binds its receptor in the postsynaptic membrane of the nerve–muscle synapse. As described later, the current conducted by a single ACh receptor is 12.5 million ions per second. In contrast, the Na^+-K^+ pump transports at most 100 ions per second.

If the ACh receptor acted as a carrier, it would have to shuttle an ion across the membrane in 0.1 µs (one ten-millionth of a second), an implausibly fast rate. The 100,000-fold difference in rates between the Na^+-K^+ pump and ACh receptor strongly suggests that the ACh receptor (and other ligand-gated receptors) must conduct ions through a channel. Later measurements in many voltage-gated pathways selective for K^+, Na^+, and Ca^{2+} also demonstrated large currents carried by single macromolecules, indicating that they too are channels.

But we are still left with the problem of what makes a channel selective. To explain selectivity, Bertil Hille extended the pore theory by proposing that channels have narrow regions that act as molecular sieves. At this *selectivity filter*, an ion must shed most of its waters of hydration to traverse the channel; in their place, weak chemical bonds (electrostatic interactions) form

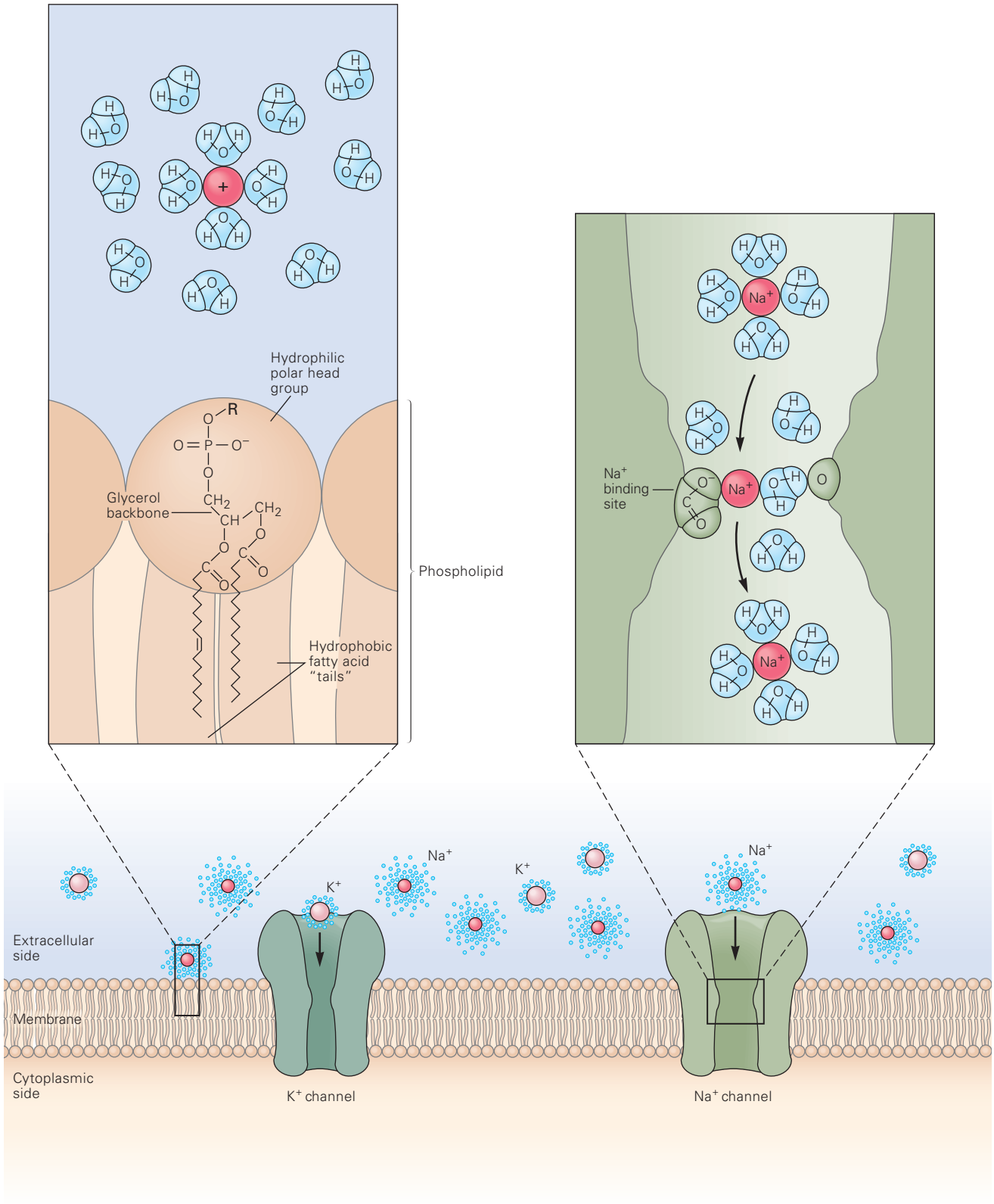
Hydrophilic
polar head
group
Glycerol
backbone
Hydrophobic
fatty acid
"tails"
Phospholipid
Na+
binding
site
Extracellular
side
Membrane
Cytoplasmic
side
K+ channel
Na+ channel

with polar (charged) amino acid residues that line the walls of the channel (Figure 8–1). Because shedding its waters of hydration is energetically unfavorable, the ion will traverse a channel only if its energy of interaction with the selectivity filter compensates for the loss of the energy of interaction with its waters of hydration. Ions traversing the channel are normally bound to the selectivity filter for only a short time (less than 1 μs), after which electrostatic and diffusional forces propel the ion through the channel. In channels where the pore diameter is large enough to accommodate several water molecules, an ion need not be stripped completely of its water shell.

How is this chemical recognition and specificity established? One theory was developed in the early 1960s by George Eisenman to explain the properties of ion-selective glass electrodes. According to this theory, a binding site with high negative field strength—for example, one formed by negatively charged carboxylic acid groups of glutamate or aspartate—will bind Na^+ more tightly than K^+. This selectivity results because the electrostatic interaction between two charged groups, as governed by Coulomb's law, depends inversely on the distance between the two groups.

Because it has a smaller crystal radius than K^+, Na^+ can approach a binding site with a high negative field strength more closely than K^+ can and thus will derive a more favorable free-energy change on binding. This compensates for the requirement that Na^+ lose some of its waters of hydration in order to traverse the narrow selectivity filter. In contrast, a binding site with a low negative field strength—one that is composed, for example, of polar carbonyl or hydroxyl oxygen atoms—would select K^+ over Na^+. At such a site, the binding of Na^+ would not provide a sufficient free-energy change to compensate for the loss of the ion's waters of hydration, which Na^+ holds strongly. However, such a site would be able to compensate for the loss of a K^+ ion's waters of hydration since the larger K^+ ions interact more weakly with water. It is currently thought that ion channels are selective both because of such specific chemical interactions and because of molecular sieving based on pore diameter.

Ion Channels in All Cells Share Several Functional Characteristics

Most cells are capable of local signaling, but only nerve and muscle cells are specialized for rapid signaling over long distances. Although nerve and muscle cells have a particularly rich variety and high density of membrane ion channels, their channels do not differ fundamentally from those of other cells in the body. Here we describe the general properties of ion channels in a wide variety of cells determined by recording current flow through channels under various experimental conditions.

Currents Through Single Ion Channels Can Be Recorded

Studies of ion channels were originally limited to recording the total current through the entire population of a class of ion channels, an approach that obscures some details of channel function. Later developments

Figure 8–1 (Opposite) **The permeability of the cell membrane to ions is determined by the interaction of ions with water, the membrane lipid bilayer, and ion channels.** Ions in solution are surrounded by a cloud of water molecules (waters of hydration) that are attracted by the net charge of the ion. This cloud is carried along by the ion as it diffuses through solution, increasing the effective size of the ion. It is energetically unfavorable, and therefore improbable, for the ion to leave this polar environment to enter the nonpolar environment of the lipid bilayer formed from phospholipids.

Phospholipids have a hydrophilic head and a hydrophobic tail. The hydrophobic tails join to exclude water and ions, whereas the polar hydrophilic heads face the aqueous environments of the extracellular fluid and cytoplasm. The phospholipid is composed of a backbone of glycerol in which two –OH groups are linked by ester bonds to fatty acid molecules. The third –OH group of glycerol is linked to phosphoric acid. The phosphate group is further linked to one of a variety of small, polar alcohol head groups (**R**).

Ion channels are integral membrane proteins that span the lipid bilayer, providing a pathway for ions to cross the membrane. The channels are selective for specific ions.

Potassium channels have a narrow pore that excludes Na^+. Although a Na^+ ion is smaller than a K^+ ion, in solution, the effective diameter of Na^+ is larger because its local field strength is more intense, causing it to attract a larger cloud of water molecules. The K^+ channel pore is too narrow for the hydrated Na^+ ion to permeate.

Sodium channels have a selectivity filter that weakly binds Na^+ ions. According to the hypothesis developed by Bertil Hille and colleagues, a Na^+ ion binds transiently at an active site as it moves through the filter. At the binding site, the positive charge of the ion is stabilized by a negatively charged amino acid residue on the channel wall and also by a water molecule that is attracted to a second polar amino acid residue on the other side of the channel wall. It is thought that a K^+ ion, because of its larger diameter, cannot be stabilized as effectively by the negative charge and therefore will be excluded from the filter. (Adapted from Hille 1984.)

Box 8–1 Recording Current in Single Ion Channels: The Patch Clamp

The *patch-clamp* technique was developed in 1976 by Erwin Neher and Bert Sakmann to record current from single ion channels. It is a refinement of the original voltage clamp technique (see Box 10–1).

A small fire-polished glass micropipette with a tip diameter of approximately 1 µm is pressed against the membrane of a skeletal muscle fiber. A metal electrode in contact with the electrolyte in the micropipette connects the pipette to a special electrical circuit that measures the current through channels in the membrane under the pipette tip (Figure 8–2A).

In 1980, Neher discovered that applying a small amount of suction to the patch pipette greatly increased the tightness of the seal between the pipette and the membrane. The result was a seal with extremely high resistance between the inside and the outside of the pipette. The seal lowered the electronic noise and extended the usefulness of the patch-clamp technique to the whole range of ion channels. Since this discovery, the patch-clamp technique has been used to study all the major classes of ion channels in a variety of neurons and other cells (Figure 8–2B).

Christopher Miller independently developed a method for incorporating ion channels from biological membranes into artificial lipid bilayers. He first homogenized the membranes in a blender; using centrifugation of the homogenate, he then separated out a fraction composed only of membrane vesicles. He studied the functional components of these vesicles using a technique developed by Paul Mueller and Donald Rudin in the 1960s. They discovered how to create an artificial lipid bilayer by painting a thin drop of phospholipid over a hole in a nonconducting barrier separating two salt solutions. Miller found that under appropriate ionic conditions his membrane vesicles fused with the planar phospholipid membrane, incorporating any ion channel in the vesicle into the planar membrane.

This technique has two experimental advantages. First, it allows recording from ion channels in regions of cells that are inaccessible to patch clamp; for example, Miller has successfully studied a K^+ channel isolated from the internal membrane of skeletal muscle (the sarcoplasmic reticulum). Second, it allows researchers to study how the composition of the membrane lipids influences channel function.

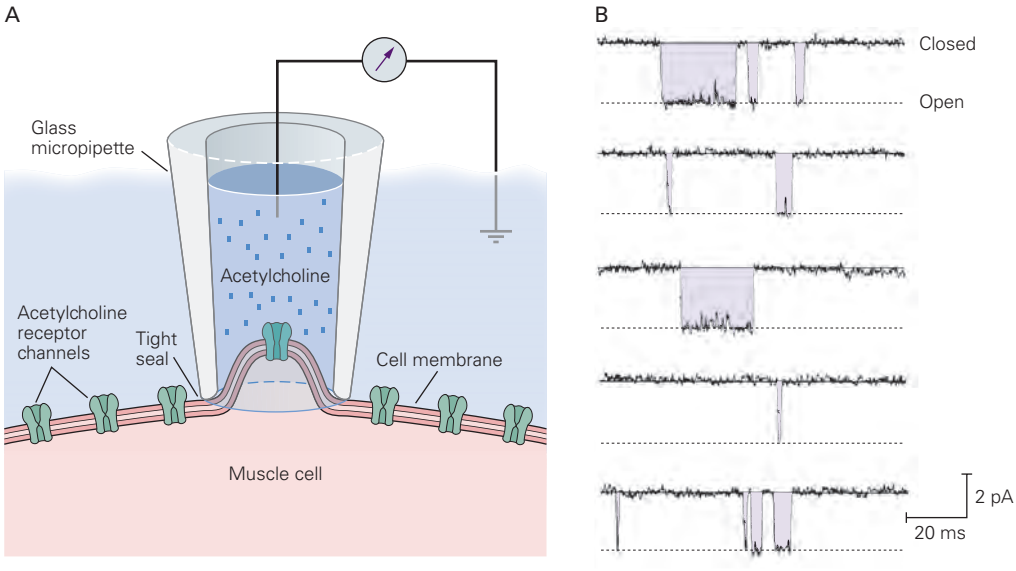

Figure 8–2 Patch-clamp setup and recording.

A. A pipette containing a low concentration of acetylcholine (**ACh**) in saline solution is used to record current through ACh receptor channels in skeletal muscle. (Adapted from Alberts et al. 1994.)

B. Patch-clamp recording of the current through a single ACh receptor channel as the channel switches between closed and open states. (Reproduced, with permission, from B. Sakmann.)

have made it possible to obtain much higher resolution by recording the current through single ion channels. The first direct recordings of individual ion channels in biological membranes were obtained by Erwin Neher and Bert Sakmann in 1976. A glass micropipette containing ACh—the neurotransmitter that activates the ACh receptors in the membrane of skeletal muscle—was pressed tightly against a muscle membrane. Small unitary current pulses representing the opening and closing of a single ACh receptor channel were recorded from the membrane under the pipette tip. The current pulses all had the same amplitude, indicating that the channels open in an all-or-none fashion (Box 8–1).

The pulses measured 2 pA (2×10^{-12} A) at a membrane potential of –80 mV, which according to Ohm's law ($I = V/R$) indicates that the channels had a resistance of 5×10^{11} ohms. In dealing with ion channels, it is more useful to speak of conductance, the reciprocal of resistance ($\gamma = 1/R$), as this provides an electrical measure related to ion permeability. Thus, Ohm's law for a single ion channel can be expressed as $i = \gamma \times V$. The conductance of the ACh receptor channel is approximately 25×10^{-12} siemens (S), or 25 picosiemens (pS), where 1 S equals 1/ohm.

The Flux of Ions Through a Channel Differs From Diffusion in Free Solution

The kinetic properties of ion permeation are best described by the channel's conductance, which is determined by measuring the current (ion flux) through the open channel in response to an electrochemical driving force. The net electrochemical driving force is determined by two factors: the electrical potential difference across the membrane and the concentration gradients of the permeant ions across the membrane. Changing either one can change the net driving force (Chapter 9).

In some open channels, the current varies linearly with driving force—that is, the channels behave as simple resistors. In others, the current is a nonlinear function of driving force. This type of channel behaves as a rectifier—it conducts ions more readily in one direction than in the other because of asymmetry in the channel's structure or ionic environment (Figure 8–3).

The rate of net ion flux (current) through a channel depends on the concentration of the permeant ions in the surrounding solution. At low concentrations, the current increases almost linearly with concentration. At higher concentrations, the current tends to reach a point at which it no longer increases. At this point, the current is said to *saturate*. This saturation effect indicates that ion flux across the cell membrane is not like electrochemical diffusion in free solution but involves the binding of ions to specific polar sites within the pore of the channel. A simple electrodiffusion model would predict that the ionic current should increase in proportion to increases in concentration.

The relation between current and ionic concentration for a wide range of ion channels is well described by a simple chemical binding equation, identical to the Michaelis-Menten equation for enzymes, suggesting that a single ion binds within the channel during permeation. The ionic concentration at which current reaches half its maximum defines the *dissociation constant*, the concentration at which half of the channels will be occupied by a bound ion. The dissociation constant in plots of current versus concentration is typically quite high, approximately 100 mM, indicating weak binding. (In typical interactions between enzymes and substrates, the dissociation constant is below 1 μM.) The rapid rate at which an ion unbinds is necessary for the channel to achieve the very high conduction rates responsible for the rapid changes in membrane potential during signaling.

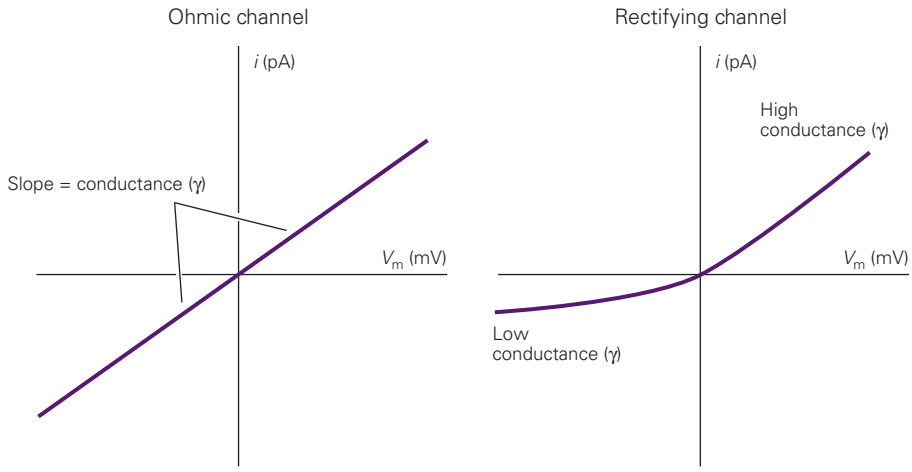

Figure 8–3 Current–voltage relations. In many ion channels, the relation between current (i) through the open channel and membrane voltage (V_m) is linear (left plot). Such channels are said to be "ohmic" because they follow Ohm's law, $i = V_m/R$ or $V_m \times \gamma$, where γ is conductance. In other channels, the relation between current and membrane potential is nonlinear. This kind of channel is said to "rectify," in the sense that it conducts current more readily in one direction than the other. The right plot shows an outwardly rectifying channel for which positive current (right side) is larger than the negative current (left side) for a given absolute value of voltage.

Some ion channels can be blocked by certain free ions or molecules in the cytoplasm or extracellular fluid that bind either to the mouth of the aqueous pore or somewhere within the pore. If the blocker is an ion that binds to a site within the pore, it will be influenced by the membrane electric field as it enters the channel. For example, if a positively charged blocker enters the channel from outside the membrane, then making the cytoplasmic side of the membrane more negative will drive the blocker into the channel by electrostatic attraction, increasing the block. Although some blockers are toxins or drugs that originate outside the body, others are common ions normally present in the cell or its environment. Physiological blockers of certain classes of channels include Mg^{2+}, Ca^{2+}, Na^{+}, and polyamines such as spermine.

The Opening and Closing of a Channel Involve Conformational Changes

In ion channels that mediate electrical signaling, the channel protein has two or more conformational states that are relatively stable. Each conformation represents a different functional state. For example, each ion channel has at least one open state and one or two closed states. The transition of a channel between these different states is called *gating*.

The molecular mechanisms of gating are only partially understood. In some cases, such as the voltage-gated Cl^{-} channel described later in the chapter, a local conformational change along the channel lumen gates the channel (Figure 8–4A). In most cases, channel gating involves widespread changes in the channel's conformation (Figure 8–4B). For example, concerted movements, such as twisting, bending, or tilting, of the subunits that line the channel pore mediate the opening and closing of some ion channels (see Figure 8–14 and Chapters 11 and 12). The molecular rearrangements that occur during the transition from closed to open states appear to enhance ion conduction through the channel not only by creating a wider lumen, but also by positioning relatively more polar amino acid constituents at the surface that lines the aqueous pore. In other cases (eg, inactivation of K^{+} channels described in Chapter 10), part of the channel protein acts as a particle that can close the channel by blocking the pore (Figure 8–4C).

Three major transduction mechanisms have evolved to control channel opening in neurons. Certain channels are opened by the binding of chemical ligands, known as agonists (Figure 8–5A). Some ligands bind directly to the channel either at an extracellular or intracellular site; transmitters bind at extracellular sites, whereas certain cytoplasmic constituents, such as Ca^{2+}, cyclic nucleotides, and GTP-binding proteins, bind at intracellular sites, as do certain dynamically regulated mobile lipid components of the membrane (Chapter 14). Other ligands activate intracellular second messenger signaling cascades that can covalently modify channel gating through protein phosphorylation (Figure 8–5B). Many ion channels are regulated by changes in membrane potential (Figure 8–5C). Some voltage-gated channels act as temperature sensors; changes in temperature shift their voltage gating to higher or lower membrane potentials, giving rise to heat- or cold-sensitive channels. Finally, some channels are regulated by mechanical force (Figure 8–5D).

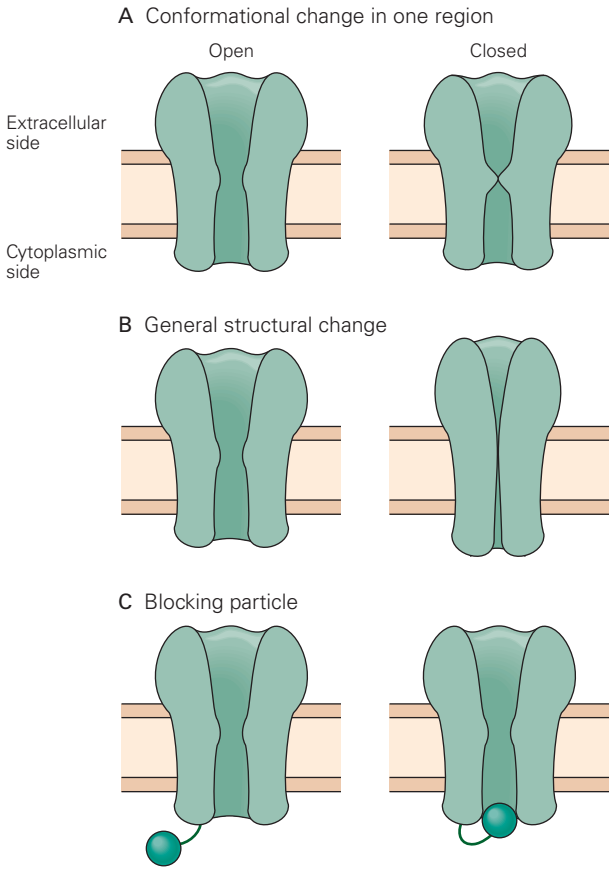

Figure 8–4 Three physical models for the opening and closing of ion channels.

A. A localized conformational change occurs in one region of the channel.

B. A generalized structural change occurs along the length of the channel.

C. A blocking particle swings into and out of the channel mouth.

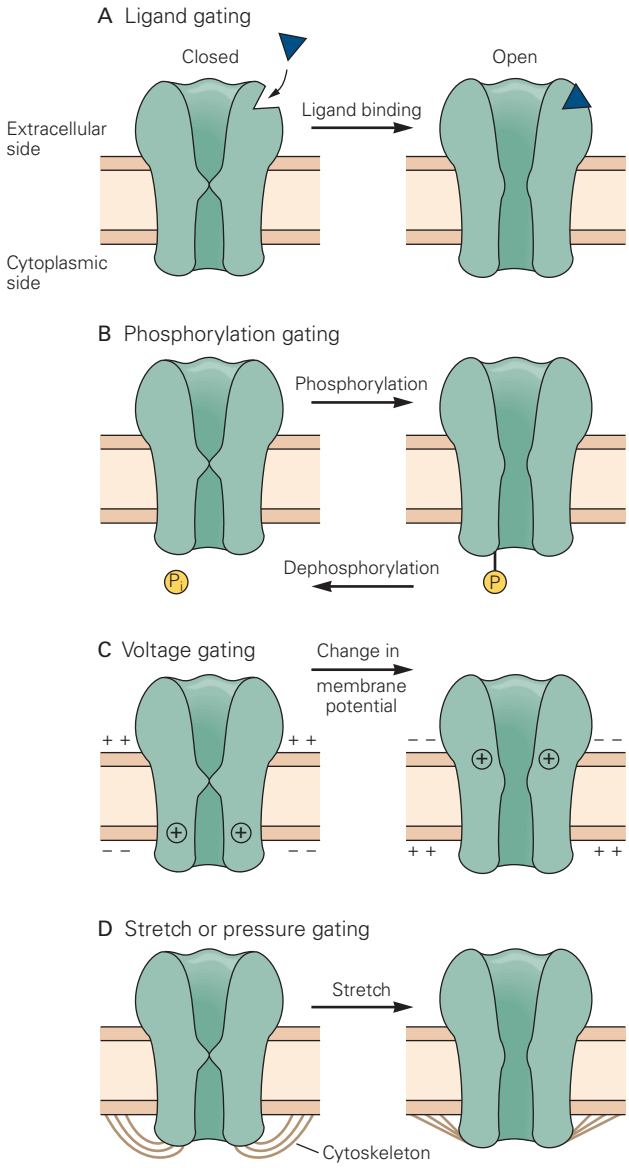

Figure 8–5 Several types of stimuli control the opening and closing of ion channels.

A. A ligand-gated channel opens when a ligand binds a receptor site on the external surface of the channel protein. The energy from ligand binding drives the channel toward an open state.

B. Some channels are regulated by protein phosphorylation and dephosphorylation. The energy for channel opening comes from the transfer of the high-energy phosphate, P_i.

C. Voltage-gated channels open and close with changes in the electrical potential difference across the membrane. The change in membrane potential causes a local conformational change by acting on a region of the channel that has a net charge.

D. Some channels open and close in response to membrane stretch or pressure. The energy for gating may come from mechanical forces that are passed to the channel either directly by distortion of the membrane lipid bilayer or by protein filaments attached to the cytoskeleton or surrounding tissues.

The rapid gating actions necessary for moment-to-moment signaling may also be influenced by certain long-term changes in the metabolic state of the cell. For example, the gating of some K^+ channels is sensitive to intracellular levels of ATP. Some channel proteins contain a subunit with an integral oxidoreductase catalytic domain that is thought to alter channel gating in response to the redox state of the cell.

These regulators control the entry of a channel into one of three functional states: closed and activatable (resting), open (active), or closed and nonactivatable (*inactivated* or *refractory*). A change in the functional state of a channel requires energy. In voltage-gated channels, the energy is provided by the movement of a charged region of the channel protein through the membrane's electric field. This region, the *voltage sensor*, contains a net electric charge, called a *gating charge*, resulting from the presence of basic (positively charged) or acidic (negatively charged) amino acids. The movement of the charged voltage sensor through the electric field in response to a change in membrane potential imparts a change in free energy to the channel that alters the equilibrium between the closed and open states of the channel. For most voltage-gated channels, channel opening is favored by making the inside of the membrane more positive (depolarization).

In transmitter-gated channels, gating is driven by the change in chemical free energy that results when the transmitter binds to a receptor site on the channel protein. Finally, mechanosensitive channels are gated by force transmitted by the distortion of the surrounding lipid bilayer or by protein tethers.

The stimuli that gate the channel also control the rates of transition between the open and closed states of a channel. For voltage-gated channels, the rates are steeply dependent on membrane potential. Although the time scale can vary from several microseconds to a minute, the transition tends to require a few milliseconds on average. Thus, once a channel opens, it stays open for a few milliseconds, and after closing, it stays closed for a few milliseconds before reopening. Once the transition between open and closed states begins, it proceeds virtually instantaneously (in less than 10 µs, the present limit of experimental measurements), thus giving rise to abrupt, all-or-none, step-like changes in current through the channel (Figure 8–2 in Box 8–1).

Ligand-gated and voltage-gated channels enter refractory states through different processes. Ligand-gated channels can enter the refractory state when their exposure to the agonist is prolonged, a process called *desensitization*—an intrinsic property of the interaction between ligand and channel.

Many, but not all, voltage-gated channels enter a refractory state after opening, a process termed *inactivation*. In the inactivated state, the channel is closed and can no longer be opened by positive voltages. Rather, the membrane potential must be returned to its initial negative resting level before the channel can recover from inactivation so that it can again open in response to depolarization. Inactivation of voltage-gated Na^+ and K^+ channels is thought to result from a conformational change, controlled by a subunit or region of the channel separate from that which controls activation. In contrast, the inactivation of certain voltage-gated Ca^{2+} channels is thought to require Ca^{2+} influx. An increase in cytoplasmic Ca^{2+} concentration inactivates the Ca^{2+} channel by binding to the regulatory molecule calmodulin, which is permanently associated with the Ca^{2+} channel protein (Figure 8–6).

Some mechanically gated ion channels that mediate touch sensation inactivate in response to a prolonged stimulus or to a train of brief stimuli. Although the molecular mechanism of this inactivation is not known, it is thought to be an intrinsic property of the channel.

Exogenous factors, such as drugs and toxins, can also affect the gating control sites of an ion channel. Most of these agents tend to inhibit channel opening, but a few facilitate opening. *Competitive antagonists* interfere with normal gating by binding to the same site at which the endogenous agonist normally binds. Antagonist binding, which does not open the channel, blocks access of agonist to the binding site, thereby preventing channel opening. The antagonist binding can be weak and reversible, as in the blockade of the nicotinic ACh-gated channel in skeletal muscle by the plant alkaloid curare, a South American arrow poison (Chapters 11 and 12), or it can be strong and virtually irreversible, as in the blockade of the same channel by the snake venom α-bungarotoxin.

Some exogenous substances modulate gating in a noncompetitive manner, without directly interacting with the transmitter-binding site. For example, binding of the drug diazepam (Valium) to a regulatory site on Cl^- channels that are gated by γ-aminobutyric acid (GABA), an inhibitory neurotransmitter, enhances the frequency with which the channels open in response to GABA binding (Figure 8–7B). This type of indirect, allosteric modulatory effect is found in some voltage- and mechanically gated channels as well.

The Structure of Ion Channels Is Inferred From Biophysical, Biochemical, and Molecular Biological Studies

What do ion channels look like? How does the channel protein span the membrane? What happens to the structure of the channel when it opens and closes? Where along the length of the channel protein do drugs and transmitters bind?

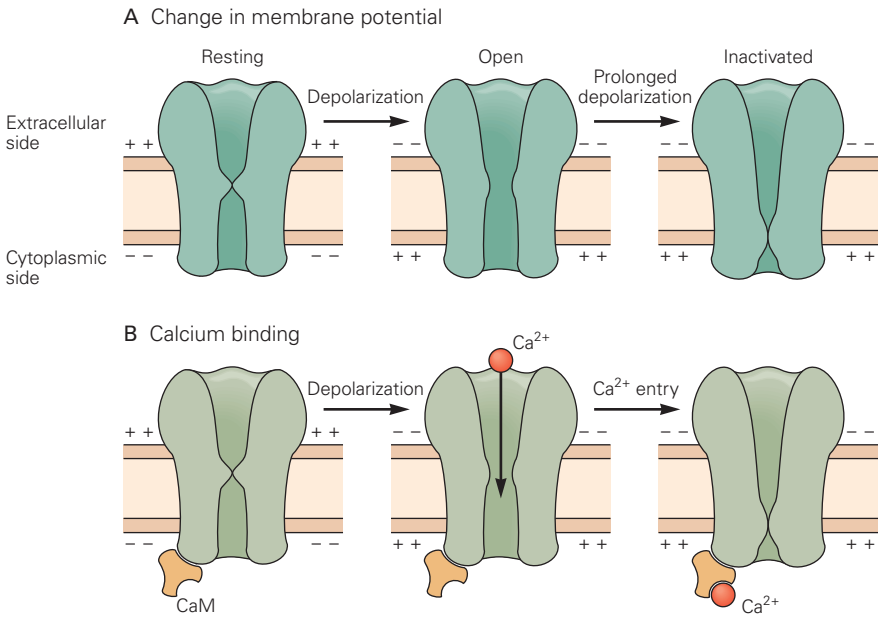

Figure 8–6 Voltage-gated channels are inactivated by two mechanisms.

A. Many voltage-gated channels enter a refractory (inactivated) state after briefly opening in response to depolarization of the membrane. They recover from the refractory state and return to the resting state only after the membrane potential is restored to its resting value.

B. Some voltage-dependent Ca^{2+} channels become inactivated when the internal Ca^{2+} level increases following channel opening. The internal Ca^{2+} binds to calmodulin (**CaM**), a specific regulatory protein associated with the channel.

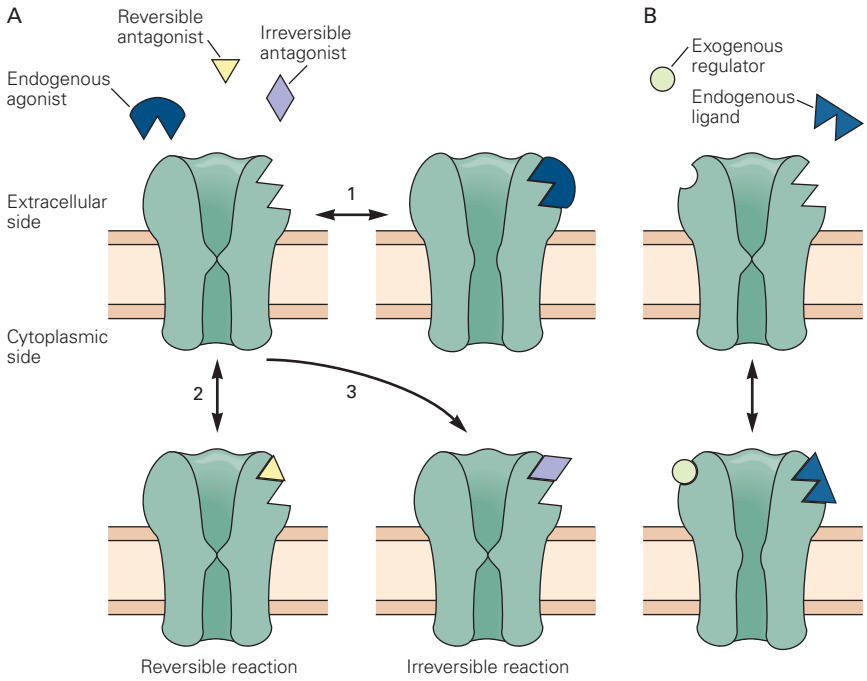

Figure 8–7 Exogenous ligands, such as drugs, can bias an ion channel toward an open or closed state.

A. In channels that are normally opened by the binding of an endogenous ligand (1), a drug or toxin may block the binding of the agonist by means of a reversible (2) or irreversible (3) reaction.

B. Some exogenous agents can bias a channel toward the open state by binding to a regulatory site, distinct from the ligand-binding site that normally opens the channel.

Biophysical, biochemical, and molecular biological studies have provided a basic understanding of channel structure and function. More recent studies using X-ray crystallography and cryo-electron microscopy have provided information about the structure of an increasing number of channels at the atomic level. All ion channels are large integral-membrane proteins with a core transmembrane domain that contains a central aqueous pore spanning the entire width of the membrane. The channel protein often contains carbohydrate groups attached to its external surface. The pore-forming region of many channels is made up of two or more subunits, which may be identical or different. In addition, some channels have auxiliary subunits that may have a variety of effects, including facilitating cell surface expression of the channel, targeting the channel to its appropriate location on the cell surface, and modifying gating properties of the channel. These subunits may be attached to the cytoplasmic end or embedded in the membrane (Figure 8–8).

The genes for all the major classes of ion channels have been cloned and sequenced. The amino acid

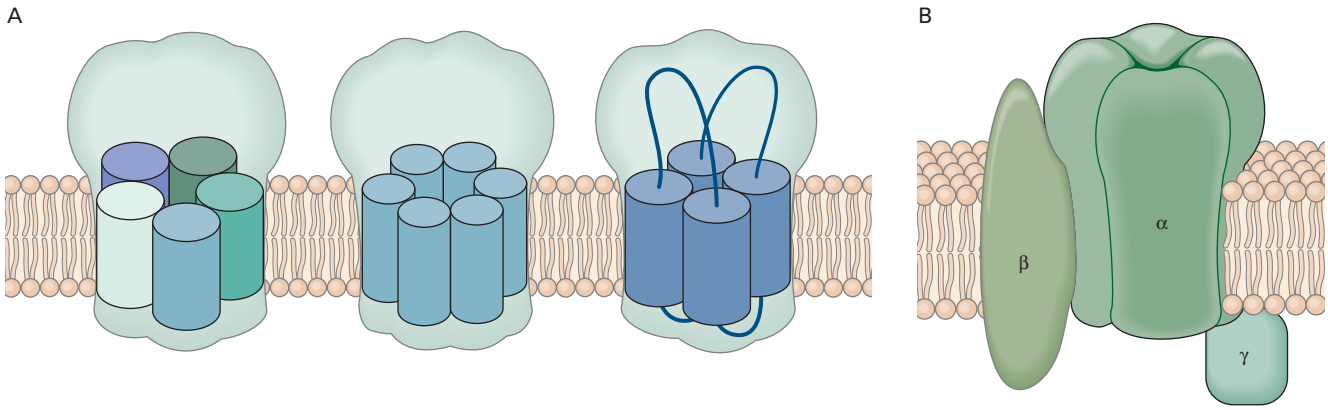

Figure 8–8 Ion channels are integral membrane proteins composed of several subunits.

A. Ion channels can be constructed as hetero-oligomers from distinct subunits (*left*), as homo-oligomers from a single type of subunit (*middle*), or from a single polypeptide chain organized into repeating motifs, where each motif functions as the equivalent of one subunit (*right*).

B. In addition to one or more α-subunits that form a central pore, some channels contain auxiliary subunits (β or γ) that modulate pore gating, channel expression, and membrane localization.

sequence of a channel, inferred from its DNA sequence, can be used to create a structural model of the channel protein. Regions of secondary structure—the arrangement of the amino acid residues into α-helixes and β-sheets—as well as regions that are likely to correspond to membrane-spanning domains of the channel are then predicted based on the structures of related proteins that have been experimentally determined using electron and X-ray diffraction analysis. This type of analysis has identified, for example, the presence of four hydrophobic regions, each around 20 amino acids in length, in the amino acid sequence of a subunit of the ACh receptor channel. Each of these regions is thought to form an α-helix that spans the membrane (Figure 8–9).

Comparing the amino acid sequences of the same type of channel from different species provides additional insights into channel structure and function. Regions that show a high degree of sequence similarity (that is, have been highly conserved throughout evolution) are likely to be important in determining the structure and function of the channel. Likewise, conserved regions in different but related channels are likely to serve a common biophysical function.

The functional consequences of changes in a channel's primary amino acid sequence can be explored through a variety of techniques. One particularly versatile approach is to use genetic engineering to construct channels with parts that are derived from the genes of different species—so-called *chimeric channels*. This technique takes advantage of the fact that the same type of channel can have somewhat different properties in different species. For example, the bovine ACh receptor channel has a slightly greater single-channel conductance than the ACh receptor channel in electric fish. By comparing the properties of a chimeric channel

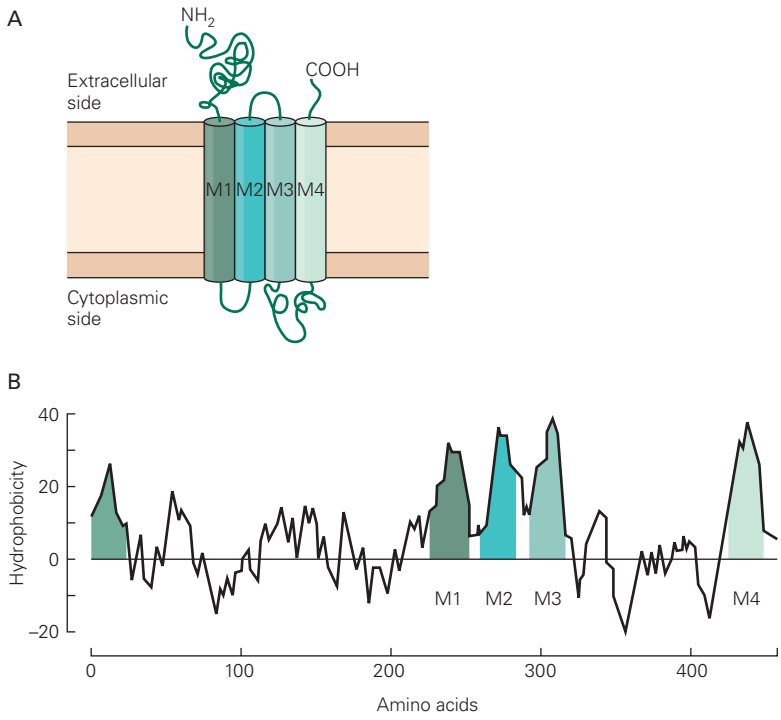

Figure 8–9 The secondary structure of membrane-spanning proteins.

A. A proposed secondary structure for a subunit of the nicotinic acetylcholine (ACh) receptor channel present in skeletal muscle. Each cylinder (**M1–M4**) represents a putative membrane-spanning α-helix comprised of approximately 20 hydrophobic amino acid residues. The membrane segments are connected by cytoplasmic or extracellular segments (loops) of hydrophilic residues. The amino terminus (NH_2) and carboxyl terminus (**COOH**) of the protein lie on the extracellular side of the membrane.

B. The membrane-spanning regions of an ion channel protein can be identified using a hydrophobicity plot. The amino acid sequence of the α-subunit of the nicotinic ACh receptor was inferred from the nucleotide sequence of the cloned receptor subunit gene. Then a running average of hydrophobicity was plotted for the entire amino acid sequence of the subunit. Each point in the plot represents an average hydrophobic index of a sequence of 19 amino acids and corresponds to the midpoint of the sequence. Four of the hydrophobic regions (M1–M4) correspond to the membrane-spanning segments. The hydrophobic region at the far left in the plot is the signal sequence, which positions the hydrophilic amino terminus of the protein on the extracellular surface of the cell during protein synthesis. The signal sequence is cleaved from the mature protein. (Reproduced, with permission, from Schofield et al. 1987.)

to those of the two original channels, one can assess the functions of specific regions of the channel. This technique has been used to identify the membrane-spanning segment that forms the lining of the pore of the ACh receptor channel (Chapter 12).

The roles of different amino acid residues or stretches of residues can be tested using *site-directed mutagenesis*, a type of genetic engineering in which specific amino acid residues are substituted or deleted. Finally, one can exploit the naturally occurring mutations in channel genes. A number of inherited and spontaneous mutations in the genes that encode ion channels in nerve or muscle produce changes in channel function that can underlie certain neurological diseases. Many of these mutations are caused by localized changes in single amino acids within channel proteins, demonstrating the importance of that region for channel function. The detailed functional changes in such channels can then be examined in an artificial expression system.

Ion Channels Can Be Grouped Into Gene Families

The great diversity of ion channels in a multicellular organism is illustrated by the human genome. Our genome contains nine genes encoding variants of voltage-gated Na^+ channels, 10 genes for different Ca^{2+} channels, 80 genes for K^+ channels, 70 genes for ligand-gated channels, and more than a dozen genes for Cl^- channels. Fortunately, the evolutionary relationships between the genes that encode ion channels provide a relatively simple framework with which to categorize them.

Most of the ion channels that have been described in nerve and muscle cells fall into a few gene superfamilies. Members of each gene superfamily have similar amino acid sequences and transmembrane topology and, importantly, related functions. Each superfamily is thought to have evolved from a common ancestral gene by gene duplication and divergence. Several superfamilies can be further subdivided into families of genes encoding channels with more closely related structure and function.

One superfamily encodes ligand-gated ion channels that are receptors for the neurotransmitters ACh, GABA, glycine, or serotonin (Chapter 12). All of these receptors are composed of five subunits, each of which has four transmembrane α-helixes (Figure 8–10A). In addition, the N-terminal extracellular domain that forms the receptor for the ligand contains a conserved loop of 13 amino acids flanked by a pair of cysteine residues that form a disulfide bond. As a result, this receptor superfamily is referred to as the *cys-loop receptors*. Ligand-gated channels can be classified by their ion selectivity in addition to their agonist. The genes that encode glutamate receptor channels belong to a separate gene family.

Gap-junction channels, which bridge the cytoplasm of two cells at electrical synapses (Chapter 11), are encoded by a separate gene superfamily. A gap-junction channel is composed of two hemi-channels, one from each connected cell. A hemi-channel has six identical subunits, each of which has four membrane-spanning segments (Figure 8–10B).

The genes that encode the voltage-gated ion channels responsible for generating the action potential belong to another superfamily (Chapter 10). These channels are selective for Ca^{2+}, Na^+, or K^+. Comparative DNA sequence data suggest that most voltage-sensitive cation channels stem from a common ancestral channel—perhaps a K^+ channel—that can be traced to a single-cell organism living more than 1.4 billion years ago, before the evolution of separate plant and animal kingdoms.

All voltage-gated cation channels have a similar four-fold symmetric architecture, with a core motif composed of six transmembrane α-helical segments termed S1–S6. A seventh hydrophobic region, the *P-region*, connects the S5 and S6 segments by dipping into and out of the extracellular side of the membrane (Figures 8–10C and 8–11A); it forms the channel's selectivity filter. Voltage-gated Na^+ and Ca^{2+} channels are composed of a large subunit that contains four repeats of this basic motif (Figure 8–10C). Voltage-gated K^+ channels are tetramers, with each separate subunit containing one copy of the basic motif (Figure 8–11A). Each subunit contributes one P-region to the pore of the fully assembled channel. This structural configuration is also shared by other, more distantly related channel families described later and in Chapter 10.

The S4 segment is thought to play a particularly important role in voltage gating. It contains an unusual pattern of amino acids in which every third position contains a positively charged arginine or lysine residue. This region was originally proposed to be the voltage sensor because, according to fundamental biophysical principles, voltage-gating must involve the movement of intramembrane gating charges within the membrane electric field. Additional evidence implicating S4 as the voltage sensor comes from the finding that this pattern of positive charges is highly conserved in all voltage-gated cation-selective channels but is absent in channels that are not voltage-gated. Further support comes from site-directed mutagenesis experiments showing that neutralization of these positive charges in S4 decreases the voltage sensitivity of channel activation.

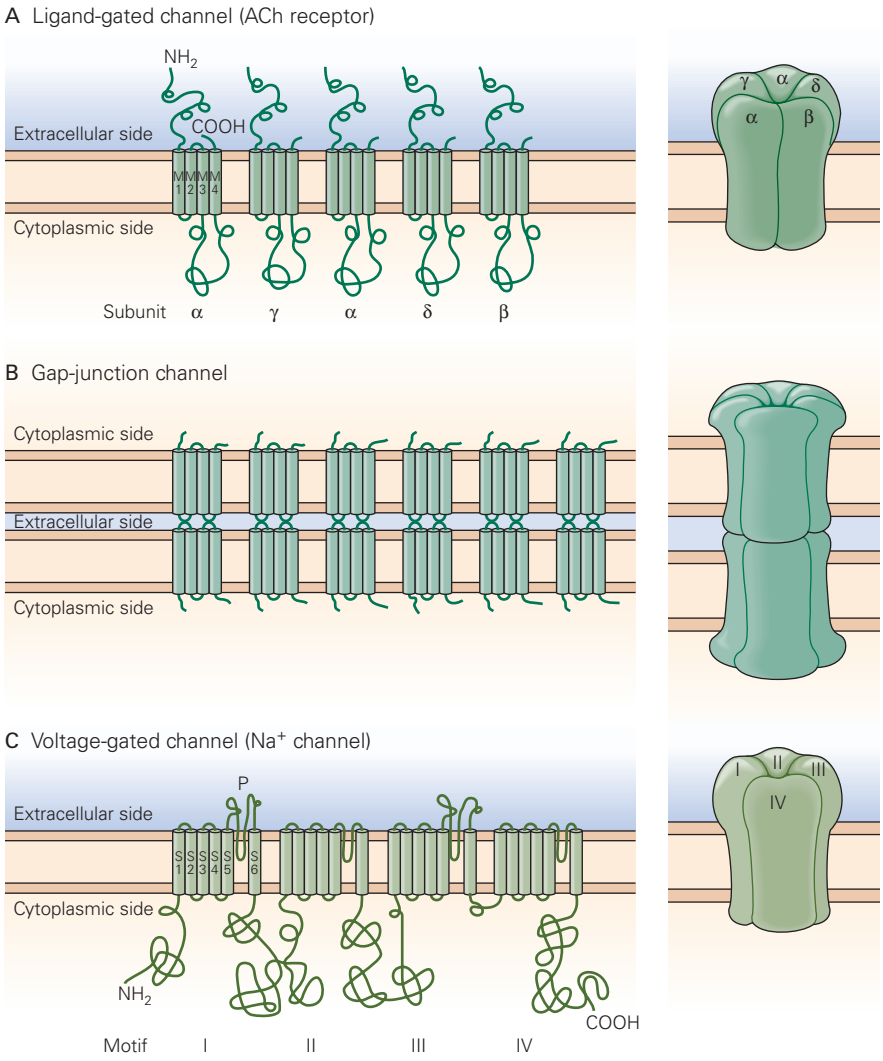

Figure 8–10 Three superfamilies of ion channels.

A. Members of a large family of ligand-gated channels, such as the acetylcholine receptor channel, are composed of five identical or closely related subunits, each of which contains four transmembrane α-helixes (M1–M4). Each cylinder in the figure represents a single transmembrane α-helix.

B. The gap-junction channel is formed from a pair of hemichannels, one each in the pre- and postsynaptic cell membranes, that join in the space between two cells. Each hemichannel is made of six identical subunits, each containing four transmembrane α-helixes. Gap-junction channels serve as conduits between the cytoplasm of the pre- and postsynaptic cells at electrical synapses (Chapter 11).

C. The voltage-gated Na^+ channel is formed from a single polypeptide chain that contains four homologous domains or repeats (motifs I–IV), each with six membrane-spanning α-helixes (**S1–S6**). The S5 and S6 segments are connected by an extended strand of amino acids, the **P**-region, which dips into and out of the external surface of the membrane to form the selectivity filter of the pore. Voltage-gated Ca^{2+} channels share the same general structural pattern, although the amino sequences are different.

The major gene family encoding the voltage-gated K^+ channels is related to three additional families of K^+ channels, each with distinctive properties and structure. One family includes genes encoding three types of channels activated by either intracellular Na^+ or Ca^{2+} or by intracellular Ca^{2+} plus depolarization. A second family consists of the genes encoding inward-rectifying K^+ channels. Because they are open at the resting potential and rapidly occluded by cytosolic cations during depolarization, they conduct ions more readily in the inward than in the outward direction. Each channel subunit has only two transmembrane segments connected by a pore-forming P-region. A third family of genes encodes K2P channels composed of subunits with two repeated pore-forming segments (Figure 8–11). Various members are regulated by temperature, mechanical force, and intracellular ligands. These channels may also contribute to the K^+ permeability of the resting membrane.

The sequencing of the genomes of a variety of species, from bacteria to humans, has led to the identification of additional ion channel gene families. These include channels with related P-regions but that are only very distantly related to the family of voltage-gated channels. An example is the excitatory postsynaptic glutamate-gated channel, in which the P-region is inverted, entering and leaving the internal surface of the membrane (Figure 8–11D).

Finally, the transient receptor potential (TRP) family of nonselective cation channels (named after a mutant *Drosophila* strain in which light evokes a brief receptor potential in photoreceptors) comprises a very large and diverse group of tetrameric channels that contain P-regions. Like the voltage-gated K^+ channels,

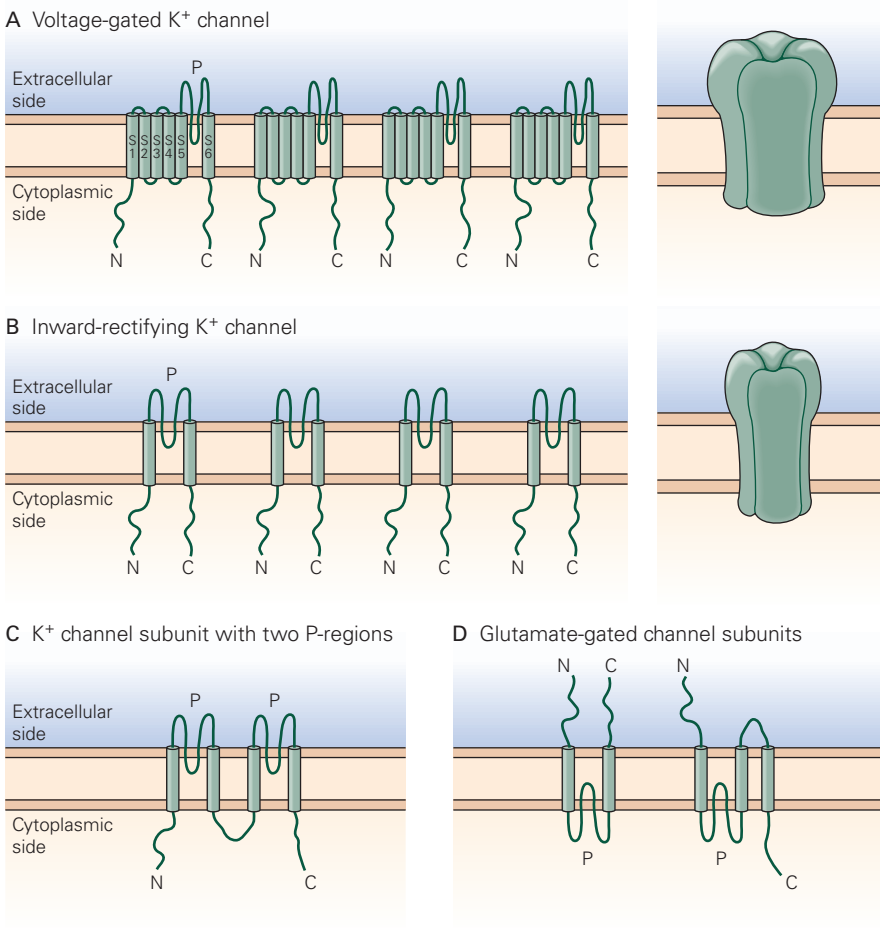

Figure 8–11 Four related families of ion channels with P-regions.

A. Voltage-gated K^+ channels are composed of four subunits, each of which corresponds to one repeated domain of voltage-gated Na^+ or Ca^{2+} channels, with six transmembrane segments and a pore-forming P-region (see Figure 8–10C).

B. Inward-rectifying K^+ channels are composed of four subunits, each of which has only two transmembrane segments connected by a P-region.

C. The K2P K^+ channels are composed of subunits that contain two repeats similar to the inward-rectifying K^+ channel subunit, with each repeat containing a P-region. Two of these subunits combine to form a channel with four P-regions.

D. Glutamate receptors constitute a distinct family of tetrameric channels with P-regions. Their pore regions are nonselectively permeable to cations. In these receptors, the amino terminus is extracellular and the P-region enters and exits the cytoplasmic side of the membrane. The distantly related bacterial GluR0 K^+-permeable glutamate receptor has four subunits, which contain two transmembrane segments (*left*); in higher organisms, the subunits contain three (*right*).

TRP channels also contain six transmembrane segments, but are in most cases gated by intracellular or intramembrane ligands. TRP channels are important for Ca^{2+} metabolism in all cells, visual signaling in insects, and pain, heat, and cold sensation in the nervous system of higher animals (Chapter 18). TRP channels have been implicated in osmoreception and certain taste sensations in mammals.

A number of other families of channels have been identified, structurally unrelated to those considered earlier. These include CLC Cl^- channels that help set the resting potential of skeletal muscle cells and certain neurons, nonspecific cation-permeable Piezo channels that are activated by mechanical stimuli (Chapter 18), Na^+ channels that are activated by H^+ ions released during inflammation, and ligand-gated cation channels that are activated by ATP, which functions as a neurotransmitter at certain excitatory synapses. With the completion of the human genome project, it is likely that nearly all of the major classes of ion channel genes have now been identified.

The diversity of ion channels is even greater than the large number of ion channel genes. Because most channels in a subfamily are composed of multiple subunits, each type of which may be encoded by a family of closely related genes, combinatorial permutations of these subunits can generate a diverse array of heteromultimeric channels with different functional properties. Additional diversity can be produced by posttranscriptional and posttranslational modifications. These subtle variations in structure and function presumably allow channels to perform highly specific functions. As with enzyme isoforms, variants of a channel with slightly different properties may be expressed at distinct stages of development, in different cell types throughout the brain, and even in different regions within a cell. Changes in neuronal activity can also lead to changes in ion channel expression patterns (Chapter 10).

Biochemical, biophysical, and molecular biological approaches have been important in defining structure–function relationships among the large variety of ion

channels. The use of X-ray crystallography and cryo-electron microscopy to define the structure of channels at atomic resolution provides a framework for achieving greater understanding of the mechanisms of ion channel function and malfunction due to disease-causing mutations. Combining a wide array of data from these various approaches makes possible the construction of detailed molecular models, which can be tested by further experiments, as well as by theoretical approaches such as molecular dynamics simulation.

X-Ray Crystallographic Analysis of Potassium Channel Structure Provides Insight Into Mechanisms of Channel Permeability and Selectivity

The first high-resolution X-ray crystallographic analysis of the molecular architecture of the pore region of an ion-selective channel was provided by Rod MacKinnon and his colleagues. To overcome the difficulties inherent in obtaining crystals of large integral membrane proteins, they initially focused on a non–voltage-gated K^+ channel, termed KcsA, from a bacterium. This channel is advantageous for crystallography as it can be expressed at high levels for purification, is relatively small, and has a simple transmembrane topology similar to that of the inward-rectifying K^+ channel in higher organisms, including mammals (Figure 8–11B).

The crystal structure of the KcsA protein provides several important insights into the mechanisms by which the channel facilitates the movement of K^+ ions across the hydrophobic lipid bilayer. The channel is made up of four identical subunits arranged symmetrically around a central pore (Figure 8–12A). Each subunit has two membrane-spanning α-helixes, an inner and outer helix. They are connected by the P-loop, which forms the selectivity filter of the channel. The amino acid sequence of these subunits is homologous to that of the S5-P-S6 region of vertebrate voltage-gated K^+ channels. The two α-helixes of each subunit tilt away from the central axis of the pore such that the structure resembles an inverted tepee (Figure 8–12B,C).

The four inner α-helixes from each of the subunits line the cytoplasmic end of the pore. At the intracellular mouth of the channel, these four helixes cross, forming a very narrow opening—the "smoke hole" of the tepee. Because this hole is too small to allow passage of K^+ ions, the crystal structure is presumed to represent the channel in the closed state. The inner helixes are homologous to the S6 membrane-spanning segment of voltage-gated K^+ channels (Figure 8–11A). At the extracellular end of the channel, the transmembrane helixes in each subunit are connected by a region consisting of three elements: (1) a chain of amino acids that surrounds the mouth of the channel (the turret region), (2) an abbreviated α-helix (the pore helix) approximately 10 amino acids in length that projects toward the central axis of the pore, and (3) a stretch of 5 amino acids near the C-terminal end of the P-region that forms the selectivity filter.

The shape and structure of the pore determine its ion-conducting properties. Both the inner and outer mouths of the pore are lined with acidic amino acids whose negative charges help attract cations from the bulk solution. Going from inside to outside, the pore consists of a medium-wide tunnel, 18 Å in length, which leads into a wider (10 Å diameter) spherical inner chamber. This chamber is lined predominantly by the side chains of hydrophobic amino acids. These relatively wide regions are followed by the very narrow selectivity filter, only 12 Å in length, which is rate-limiting for the passage of K^+ ions. A high K^+ ion throughput rate is ensured by the fact that the inner 28 Å of the pore, from the cytoplasmic entrance to the selectivity filter, lacks polar groups that could delay ion passage by binding and unbinding the ion (Figure 8–12C,D).

An ion passing from the polar solution through the nonpolar lipid bilayer encounters the least energetically favorable region in the middle of the bilayer. The large energy difference between these two regions for a K^+ ion is minimized by two details of channel structure. The inner chamber is filled with water, which provides a highly polar environment, and the pore helixes provide dipoles whose electronegative carboxyl ends point toward this inner chamber (Figure 8–12C).

The high energetic cost incurred as a K^+ ion sheds its waters of hydration is partially compensated by the presence of 20 electronegative oxygen atoms that line the walls of the selectivity filter and form favorable electrostatic interactions with the permeant ions. Each of the four subunits contributes four main-chain carbonyl oxygen atoms from the protein backbone and one side-chain hydroxyl oxygen atom to form a total of four binding sites for K^+ ions. Each bound K^+ ion is thus stabilized by interactions with a total of eight oxygen atoms, which lie in two planes above and below the bound cation. In this way, the channel is able to compensate for the loss of the K^+ ion's waters of hydration. The selectivity filter is stabilized at a critical width, such that it provides optimal electrostatic interactions with K^+ ions as they pass but is too wide for the smaller Na^+ ions to interact effectively with all eight oxygen atoms at any point along the length of the filter (Figure 8–12C).

In light of the extensive interactions between a K^+ ion and the channel, how does the KcsA channel

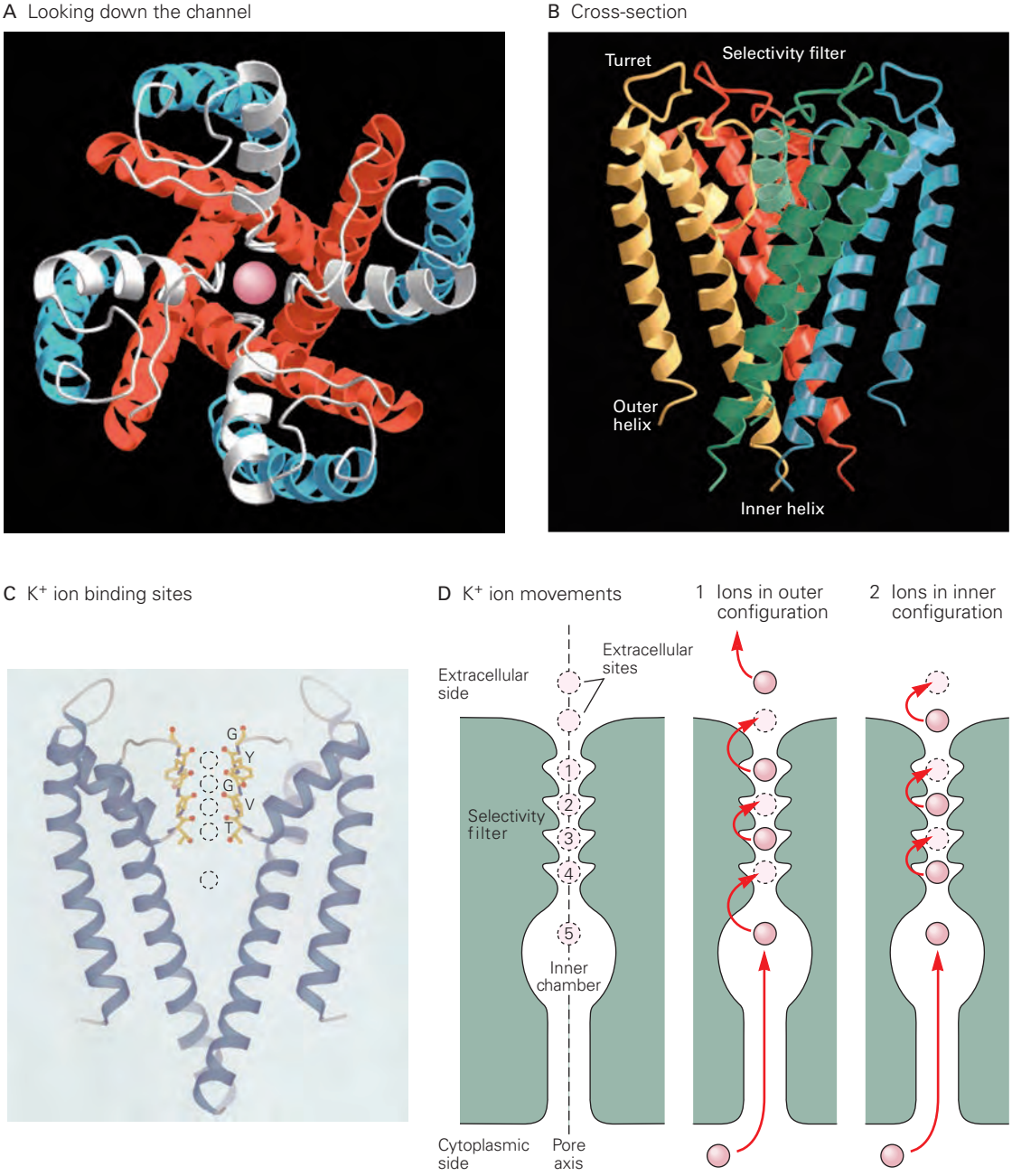

Figure 8–12 The X-ray crystal structure of a bacterial potassium channel. (Reproduced, with permission, from Doyle et al. 1998. Copyright © 1998 AAAS.)

A. The view is looking down the channel pore from outside the cell. Each of the four subunits of the KcsA K^+ channel contributes two membrane-spanning helixes, an outer helix (**blue**) and an inner helix (**red**). The P-region (**white**) lies near the extracellular surface of the channel pore and consists of a short α-helix (pore helix) and a loop that forms the selectivity filter of the channel. In the center of the pore is a K^+ ion (**pink**).

B. The channel is seen in a side view within a cross section of the membrane. The four subunits are shown in different colors.

C. Another view in the same orientation as in **part B** shows only two of the four subunits. The channel contains five K^+ binding sites (**dashed**). Four of the sites lie in the selectivity filter (**yellow**), while the fifth site lies in an inner chamber near the center of the channel. The four K^+ binding sites of the selectivity filter are formed by successive rings of oxygen atoms (**red**) from five amino acid residues per subunit. Four of the rings are formed by carbonyl oxygen atoms from the main chain backbone of four consecutive amino acid residues—glycine (**G**), tyrosine (**Y**), glycine (**G**), and valine (**V**). A fifth ring of oxygen near the internal end of the selectivity filter is formed by the side-chain hydroxyl oxygen of threonine (**T**). Each ring contains four oxygen atoms, one from each subunit. Only the oxygen atoms from two of the four subunits are shown in this view. (Reproduced, with permission, from Morais-Cabral et al. 2001. Copyright © 2001 Springer Nature.)

D. A view of K^+ ion permeation through the channel illustrates the sequence of changes in occupancy of the various K^+ binding sites. A pair of ions hops in concert between a pair of binding sites in the selectivity filter. In the initial state, the "outer configuration," a pair of ions is bound to sites 1 and 3. As an ion enters the inner mouth of the channel, the ion in the inner chamber jumps to occupy the innermost binding site of the selectivity filter (site 4). This causes the pair of ions in the outer configuration to hop outward, expelling an ion from the channel. The two ions now in the inner configuration (sites 2 and 4) can hop to binding sites 1 and 3, returning the channel to its initial state (the outer configuration), from which it can conduct a second K^+ ion. (Adapted, with permission, from Miller 2001. Copyright © 2001 Springer Nature.)

manage its high rate of conduction? Although the channel contains a total of five potential binding sites for K^+ ions, X-ray analysis shows that the channel can be occupied by at most three K^+ ions at any instant. One ion is normally present in the wide inner chamber, and two ions occupy two of the four binding sites within the selectivity filter (Figure 8–12D).

These structural data led to the following hypothesis. Because of electrostatic repulsion, two K^+ ions never simultaneously occupy adjacent binding sites within the selectivity filter; rather, a water molecule is always interposed between K^+ ions. During conduction, a pair of K^+ ions within the selectivity filter hop in tandem between pairs of binding sites. If only one ion were in the selectivity filter, it would be bound rather tightly, and the throughput rate for ion permeation would be compromised. But the mutual electrostatic repulsion between two K^+ ions occupying nearby sites ensures that the ions will linger only briefly, thus resulting in a high overall rate of K^+ conduction.

The form of the KcsA selectivity filter appears to be highly conserved among various types of mammalian voltage-gated K^+ channels. However, more recent studies by MacKinnon and colleagues have revealed how variations in geometric and surface charge features below the selectivity filter of this canonical pore can cause some voltage-gated K^+ channels to differ markedly in single-channel conductance and in affinity for various open channel blockers.

The snug fit between the K^+ channel selectivity filter and K^+ ions that helps explain the unusually high selectivity of these channels is not representative of all channel types. As we shall see in later chapters, in many channels pore diameters are significantly wider than the principal permeating ion, contributing to a lower degree of selectivity.

X-Ray Crystallographic Analysis of Voltage-Gated Potassium Channel Structures Provides Insight into Mechanisms of Channel Gating

As described earlier, the S4 segment of voltage-gated ion channels is thought to be the voltage sensor that detects changes in membrane potential. How do the positive charges in S4 move through the membrane electric field in response to a change in membrane potential? How is S4 movement coupled to gating? What is the relationship of the voltage-sensing region to the pore-forming region of the channel? What is the configuration of the open channel? Some answers to these questions have come from X-ray crystallographic analyses of mammalian voltage-gated K^+ channels, as well as from a number of studies using mutagenesis and other biophysical approaches. MacKinnon and colleagues studied the mammalian voltage-gated Kv1.2 K^+ channel, as well as a closely related chimera Kv1.2-Kv2.1, which yielded higher-resolution images.

Their analysis of X-ray crystal structures of the Kv1.2 channel and the Kv1.2-2.1 chimera showed that a K^+ channel subunit has two domains. The S1–S4 segments form a voltage-sensing domain at the periphery of the channel, whereas the S5-P–S6 segments form the pore domain at the central axis of the channel. The two domains are linked at their intracellular ends by the short S4–S5 coupling helix (Figure 8–13). The idea that the S1–S4 voltage sensor is a separate domain is supported by the fact that certain bacterial proteins contain S1–S4 domains but lack a pore domain. One such protein is a voltage-sensitive phosphatase, while another forms a voltage-gated proton channel. Conversely, the inward-rectifying K^+ channels (Figure 8–11B) have a high K^+ selectivity but are not directly gated by voltage because they lack the voltage sensor domain.

The crystal structures also help clarify what happens when the channel opens. Studies by Clay Armstrong in the 1960s suggested that a gate exists at the intracellular mouth of voltage-gated K^+ channels of higher organisms. He found that small organic cations such as tetraethylammonium (TEA) can enter and block the channel only when this internal gate is opened by depolarization. As described earlier, in the closed bacterial K^+ channels the four inner transmembrane helixes, which correspond to the S6 helixes in voltage-gated K^+ channels, meet at a tight bundle crossing at their cytoplasmic ends to form the closed gate of the channel (Figure 8–12). In contrast, the S6 helix of the Kv1.2–2.1 chimera is bent at a flexible three-amino-acid hinge (proline-valine-proline), causing the inner end of the helix to bend outward. This configuration results in an open channel conformation with an internal orifice that is dilated to 12 Å in diameter, wide enough to pass fully hydrated K^+ ions as well as larger cations such as TEA (Figures 8–13 and 8–14C). Once inside the channel lumen, TEA blocks K^+ permeation because it is too large to pass through the selectivity filter. It is not surprising that the Kv channel is in the open state, as there is no voltage gradient across the channel in the crystals. This is similar to the situation in a membrane that has been depolarized to 0 mV, a voltage at which the channels are normally open. This opening mechanism is likely to be a general one because the inner helixes of many K^+ channels in bacteria and higher organisms also have a flexible hinge at this position.

One long-standing question concerns the placement and movement of the gating charges on the S4

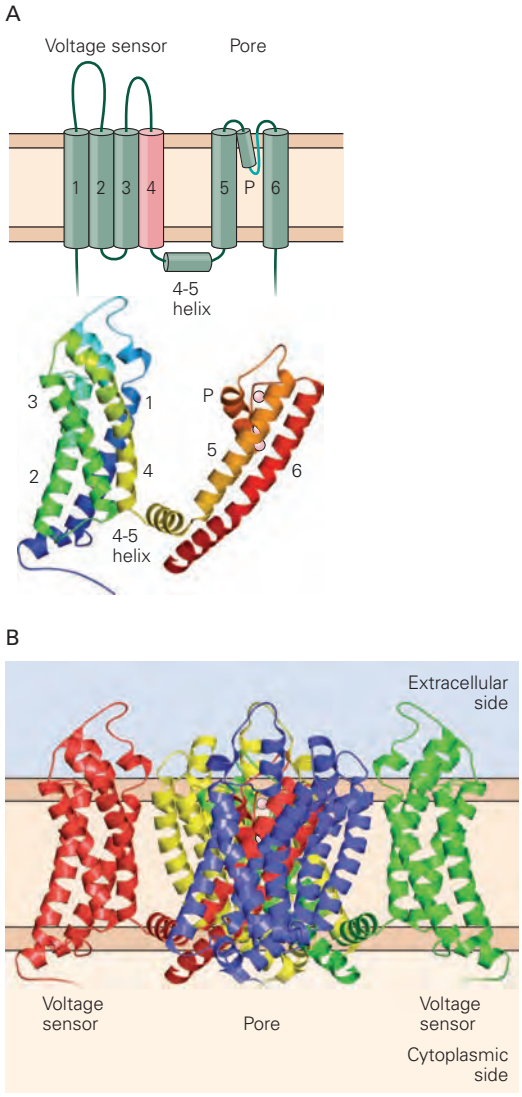

Figure 8–13 X-ray crystal structure of a voltage-gated potassium channel. (Adapted, with permission, from Long et al. 2007. Copyright © 2007 Springer Nature.)

A. *Top*: In addition to its six transmembrane α-helixes (**S1–S6**), a voltage-gated K^+ channel subunit contains a short α-helix (the **P** helix) that is part of the P-region selectivity filter, as well as an α-helix on the cytoplasmic side of the membrane that connects transmembrane helixes S4 and S5 (4–5 coupling helix). *Bottom*: An X-ray structural model of a single subunit shows the positions of the six membrane-spanning helixes, the P helix, and the 4–5 coupling helix. The S1–S4 voltage-sensing region and S5-P–S6 pore-forming regions are localized in separate domains. Two K^+ ions bound in the pore are shown in **pink**.

B. In this side view of the channel, each subunit is a different color. Subunit 6 (**red**) is in the same orientation as in **part A**.

segment voltage sensor. As mentioned earlier, movement of these charges within the plane of the membrane in response to changes in membrane potential is thought to couple membrane depolarization to channel gating. However, placement of charges within the hydrophobic membrane results in an unfavorable energy state, as discussed earlier for free ions in solutions. How do ion channels compensate for this unfavorable free energy?

The crystal structure provides some answers to this question. Mutagenesis studies indicate that four positively charged arginine residues in the external half of the S4 segment are likely to carry most of the gating charge. In the open state, the four positive charges face outward toward the extracellular side of the membrane, where they may undergo energetically favorable interactions with water or with the negatively charged head groups of the phospholipid bilayer. Positive charges on other S4 residues that lie more deeply within the lipid bilayer are stabilized by interactions with negatively charged acidic residues on the S1–S3 transmembrane helixes.

At present, a crystal structure for the closed state of the Kv1.2–Kv2.1 chimera is lacking. However, MacKinnon and colleagues have proposed a plausible model for voltage gating based on the structures of the open voltage-gated K^+ channel and the closed bacterial K^+ channel KcsA (Figure 8–14). According to this model, a negative voltage inside the cell exerts a force on the positively charged S4 helix that causes it to move inward by about 1.0 to 1.5 nm. As a result, the four positively charged S4 residues, which in the depolarized state face the external environment and sense the extracellular potential, now face the intracellular side of the membrane and sense the intracellular potential. In this manner, movement of each S4 segment will translocate 3 to 4 gating charges across the membrane electric field as the channel transitions between the closed and open states, for a total of 12 to 16 charges moved per tetrameric channel. This number is similar to the total gating charge movement determined from biophysical measurements (Chapter 10).

How are S4 movements coupled to the gate of the channel? According to the model, when the membrane voltage becomes negative, the resulting inward movement of the S4 segment exerts a downward force on the S4–S5 coupling helix. This helix, which lies roughly parallel to the membrane at its cytoplasmic surface, rests on the inner end of the S6 helix gate in the open state. As the S4–S5 helix moves downward, it acts as a lever, applying force to S6 and closing the gate. Thus, voltage-gating is thought to rely on the electromechanical coupling between the voltage-sensing domain and the

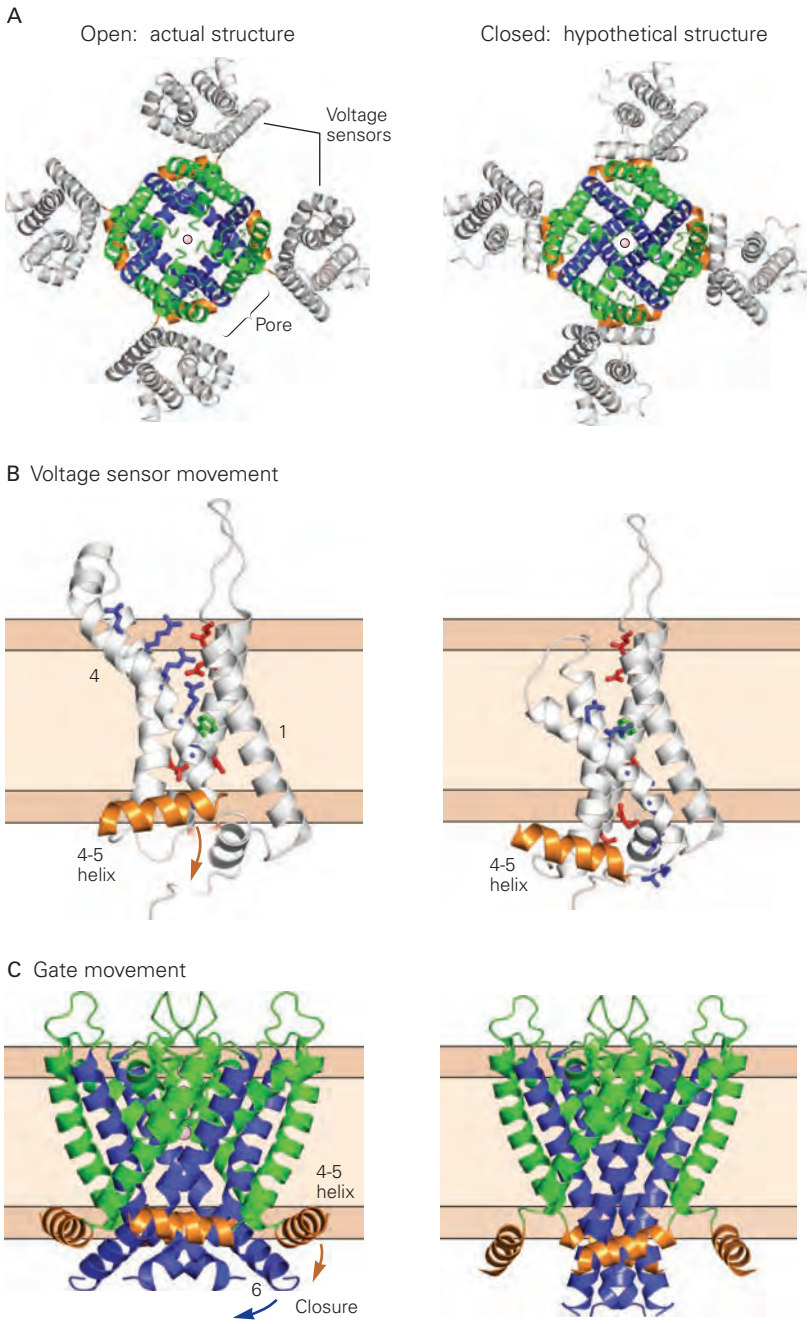

Figure 8–14 Model for voltage gating based on X-ray crystal structures of two potassium channels. In each part of the figure, the drawing on the *left* shows the actual structure of the open voltage-gated Kv1.2-2.1 chimera, while the drawing on the *right* shows the hypothetical structure of a closed voltage-gated K^+ channel, based in part on the structure of the pore region of the bacterial K^+ channel KcsA in the closed state. (Adapted, with permission, by Yuhang Chen from Long et al. 2007. Copyright © 2007 Springer Nature.)

A. A view looking down on the open and closed channel from outside the cell. The central pore is constricted in the closed state, preventing K^+ flow through the channel.

B. A view of the S1–S4 voltage-sensing domain from the side, parallel to the plane of the membrane. Positively charged residues in S4 are shown as **blue sticks**. In the open state, when the membrane is depolarized, four positive charges on the S4 helix are located in the external half of the membrane, facing the external solution. The positive charges in the interior of the membrane are stabilized by interactions with negatively charged residues in S1 and S2 (**red sticks**). In the closed state, when the membrane potential is negative, the S4 region moves inward so that its positive charges now lie in the inner half of the membrane. The inward movement of S4 causes the cytoplasmic S4–S5 coupling helix (**orange**) to move downward.

C. The putative conformational change in the channel pore upon voltage gating. A side view of the tetrameric S5-P–S6 pore region of the channel shows the S4–S5 coupling helix. Membrane repolarization causes the downward movement of the S4–S5 helix, applying force to the S6 inner helix of the pore (**blue**). This causes the S6 helix to bend at its pro-val-pro hinge, thereby closing the gate of the channel.

pore domain of the channel. Although this electromechanical coupling model provides a satisfying picture of how changes in membrane voltage lead to channel gating, a definitive answer to this key problem will require resolution of the structure of the closed state of a related voltage-gated mammalian K^+ channel.

Such a direct coupling between the sensing element of a channel (S4/S4–S5 linker) and the pore gate (S6) is found in most voltage-gated K^+ channels, as well as in voltage-gated Na^+ and Ca^{2+} channels. However, in many cases, the element of a channel that responds directly to the gating signal is not in direct contact with the channel gate, and instead, an allosteric mechanism propagates the response indirectly by more remote conformational changes. For example, in the voltage-gated K^+ channel Kv10, the S4–S5 linker is not in a position to act as a lever on S6. Rather, the inward movement of S4 in response to a negative potential closes the S6

gate indirectly, by laterally compressing the S5 helix, which is packed against the S6 helix. Additional cases of allosteric gating mechanisms are discussed later in the context of inactivation of voltage-gated Na^+ channels (Chapter 10) and activation of ligand-gated (Chapters 12 and 13) and mechanically gated channels (Chapter 18).

The Structural Basis of the Selective Permeability of Chloride Channels Reveals a Close Relation Between Channels and Transporters

Ions move across cell membranes by active transport by ion transporters or pumps, as well as by passive diffusion through ion channels. Ion transporters are distinguished from ion channels because (1) they use a source of energy to actively transport ions against their electrochemical gradients, and (2) they transport ions at rates much lower than ion channels, too low to support fast neuronal signaling. Nevertheless, some types of transporters and certain ion channels have similar structures, according to studies of the CLC family of proteins.

The CLC proteins expressed in vertebrates consist of a family of Cl^- channels and a closely related family of Cl^--H^+ cotransporters. Cotransporters use the electrochemical gradient of one ion to move another ion against its electrochemical gradient. The CLC Cl^--H^+ cotransporters, which are expressed in intracellular organelles, transfer two Cl^- ions across the membrane in exchange for one proton. This type of transporter is termed an ion exchanger.

The human voltage-gated ClC-1 channels are important for maintaining the resting potential in skeletal muscle (Chapter 57).

The crystal structures of the human ClC-1 channel and the homologous *E. coli* CLC exchangers have been determined by MacKinnon and colleagues. They found a close similarity in amino acid sequence to be reflected in a marked overall structural resemblance. Both types of CLC proteins consist of a homodimer composed of two identical subunits. Each subunit forms a separate ion pathway, and the two subunits function independently (Figure 8–15). The structures of the CLC proteins are quite different from those of K^+ channels. Unlike the pore of a K^+ channel, which is widest in the central region, each pore of the CLC protein has an hourglass profile. The neck of the hourglass, a tunnel 12 Å in length which forms the selectivity filter, is just wide enough to contain three fully dehydrated Cl^- ions.

Although the ion permeation pathways of the CLC proteins and the K^+ channel differ in significant respects, they have evolved four similar features that are critical to their function. First, their selectivity filters contain multiple sequential binding sites for the permeating ion. Multi-ion occupancy creates a metastable state that facilitates rapid ion passage. Second, the ion binding sites are formed by polar, partially charged atoms, not by fully ionized atoms. The resultant relatively weak binding energy ensures that the permeating ions do not become too tightly bound. Third, permeant ions are stabilized in the center of the membrane by the positively polarized ends of two α-helixes. Fourth, wide, water-filled vestibules at either end of the selectivity filter allow ions to approach the filter in a partially hydrated state. Thus although the K^+ channels and CLC proteins differ fundamentally in amino acid sequence and overall structure, strikingly

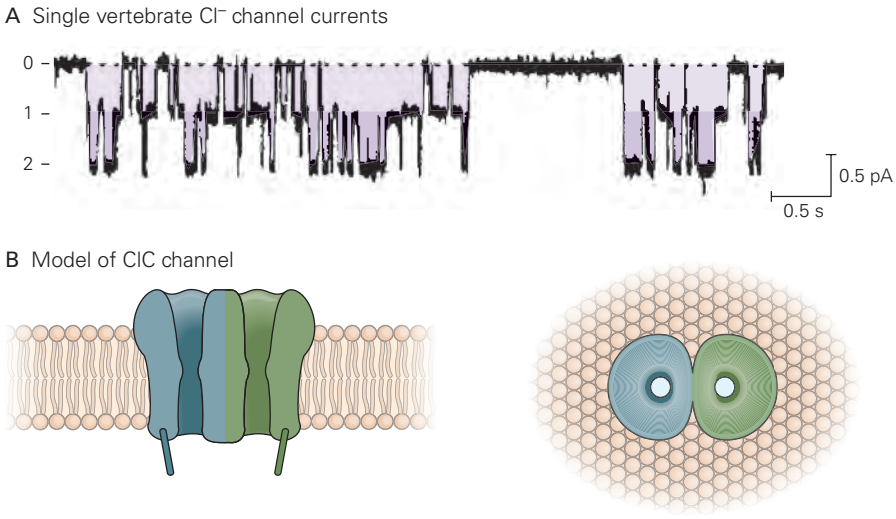

Figure 8–15 The vertebrate CLC family of chloride channels and transporters are double-barrel channels with two identical pores.

A. Recordings of current through a single vertebrate Cl^- channel show three levels of current: both pores closed (**0**), one pore open (**1**), and both pores open (**2**). (Adapted from Miller 1982.)

B. The channel is shown from the side (*left*) and looking down on the membrane from outside the cell (*right*). Each subunit contains its own ion transport pathway and gate. In addition, the dimer has a gate shared by both subunits (not shown).

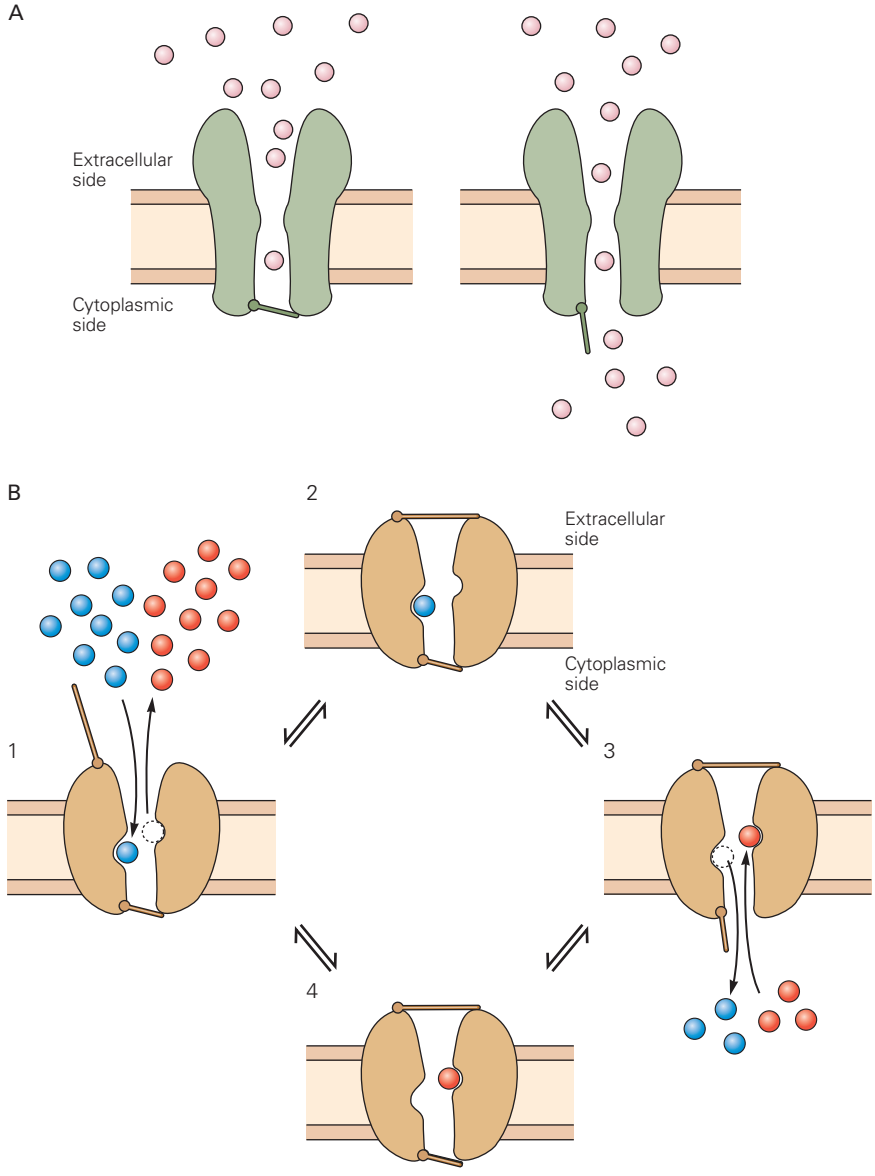

Figure 8–16 The functional difference between ion channels and transporters or pumps. (Adapted, with permission, from Gadsby 2004. Copyright © 2004 Springer Nature.)

A. Ion channels have a continuous aqueous pathway for ion conduction across the membrane. This pathway can be occluded by the closing of a gate.

B. Ion pumps and transporters have two gates in series that control ion flux. The gates are never open simultaneously, but both can close to trap one or more ions in the pore. The type of transporter illustrated here moves two different types of ions in opposite directions and is termed an *exchanger* or *antiporter*. Ion movement is tightly linked to a cycle of opening and closing of the two gates. When the external gate is open, one type of ion leaves while the other type enters the pore (**1**). This triggers a conformational change, causing the external gate to shut, thereby trapping the incoming ion (**2**). A second conformational change then causes the internal gate to open, allowing the trapped ion to leave and a new ion to enter (**3**). A further conformational change closes the internal gate, allowing the cycle to continue (**4**). With each cycle, one type of ion is transported from the outside to the inside of the cell, whereas the other type is transported from the inside to the outside of the cell. By coupling the movements of two or more ions, an exchanger can use the energy stored in the electrochemical gradient of one ion to actively transport another ion against its electrochemical gradient.

similar functional features have evolved in these two classes of membrane proteins that promote both a high degree of ion selectivity and efficient throughput. These features have been conserved with surprising fidelity from prokaryotes through humans.

More detailed structural studies will be needed to understand how some CLC proteins function as Cl^--H^+ exchangers whereas others act as conventional channels. Most exchangers and pumps, such as the Na^+-K^+ pump (Chapter 9), are thought to have two gates, one external and one internal, which are never open simultaneously. Instead, ion movements and gate movements are presumed to be part of a tightly coupled reaction cycle (Figure 8–16). CLC exchangers apparently have two gates that control Cl^- flux, coupled to the protonation-deprotonation cycle of a flexible glutamate residue in the selectivity filter that shuttles protons across the membrane. The resultant conformational changes enable transport of Cl^- against its concentration gradient, driven by the flux of H^+ ions down their electrochemical gradient. CLC channels are apparently built on a very similar structure as the transporters, but with modified gates and small structural changes in the ion transport pathway that allow much more rapid movement of Cl^- down its electrochemical gradient.

Highlights

1. Ions cross cell membranes through two main classes of integral membrane proteins—ion channels and ion pumps or transporters.
2. Ion channels act as catalysts for the passive flux of ions across the membrane. Channels have a central water-filled pore that substitutes for the polar environment on either side of the membrane. It allows the electrically charged ions to rapidly cross the nonpolar environment of the cell membrane, driven by the ion's electrochemical gradient.
3. Most ion channels are selectively permeable to certain ions. The portion of the channel pore called the selectivity filter determines which ions can penetrate based on the ion's charge, size, and physicochemical interactions with the amino acids that line the wall of the pore.
4. Ion channels have gates that open and close in response to different signals. In the open state, channels generate ionic currents that produce rapid voltage signals that carry information in the nervous system and in other excitable cells.
5. Most ion channels have three states: open, closed, and inactivated or desensitized. Transitioning between these states is termed gating. Depending on the type of channel, gating is controlled by various factors, including membrane voltage, ligand binding, mechanical force, phosphorylation state, and temperature.
6. The most common ion channels in nerve and muscle cells belong to three major gene superfamilies, the members of which are related by gene sequence homology and, in most cases, by functional properties.
7. Most ion channels are composed of multiple subunits. Combinatorial permutations of these subunits can generate a diverse array of channels with different functional properties. Post-transcriptional modifications generate additional diversity.
8. The various types of ion channels are differentially expressed in different types of neurons and different regions of neurons, contributing to the functional complexity and computational power of the nervous system. The expression patterns of some ion channels and transporters change during development and in response to changes in neuronal activity patterns.
9. The rich variety of ion channels in different types of neurons has stimulated intensive efforts to develop drugs that can activate or block specific channel types in nerve and muscle cells. Such drugs would, in principle, maximize therapeutic effectiveness with minimal side effects.
10. Structure-function and X-ray crystallographic studies of voltage-gated ion channels have provided key insights into the molecular and atomic-level details of K^+ channel conduction, selectivity, and gating. Recent technical advances in single-particle cryo-electron microscopy have led to rapid progress in studies of a wide range of ion channels.
11. Active transport, which is mediated by integral membrane proteins called transporters or pumps, enables ions to move across the membrane against their electrochemical gradient. The driving force that generates active ion fluxes comes either from chemical energy (the hydrolysis of ATP) or from the favorable electrochemical potential difference for a cotransported ion.
12. Most ion transporters and pumps do not provide a continuous pathway for ions. Rather, they undergo conformational changes for the different phases of the transport cycle, thereby providing alternating access of the molecule's central lumen to the two sides of the membrane. Because these conformational changes are relatively slow,

they are much less efficient than ion channels in mediating ion fluxes.

John D. Koester
Bruce P. Bean

Selected Reading

Hille B. 2001. *Ion Channels of Excitable Membranes,* 3rd ed. Sunderland, MA: Sinauer.

Isacoff EY, Jan LY, Minor DL. 2013. Conduits of life's spark: a perspective on ion channel research since the birth of *Neuron*. Neuron 80:658–674.

Jentsch TJ, Pusch M. 2018. CLC chloride channels and transporters: structure, function, physiology and disease. Physiol Rev 98:1493–1590.

Miller C. 1987. How ion channel proteins work. In: LK Kaczmarek, IB Levitan (eds). *Neuromodulation: The Biological Control of Neuronal Excitability,* pp. 39–63. New York: Oxford Univ. Press.

Yu FH, Yarov-Yarovoy V, Gutman GA, Catterall WA. 2005. Overview of molecular relationships in the voltage-gated ion channel superfamily. Pharmacol Rev 57:387–395.

References

Accardi A, Miller C. 2004. Secondary active transport mediated by a prokaryotic homologue of ClC Cl^- channels. Nature 427:803–807.

Alberts B, Bray D, Lewis J, Raff M, Roberts K, Watson JD. 1994. *Molecular Biology of the Cell,* 3rd ed. New York: Garland.

Armstrong CM. 1971. Interaction of tetraethylammonium ion derivatives with the potassium channels of giant axons. J Gen Physiol 58:413–437.

Basilio D, Noack K, Picollo A, Accardi A. 2014. Conformational changes required for H^+/Cl^- exchange mediated by a CLC transporter. Nat Struct Mol Biol 21:456–464.

Bayliss WM. 1918. *Principles of General Physiology,* 2nd ed., rev. New York: Longmans, Greene.

Boscardin E, Alijevic O, Hummler E, Frateschi S, Kellenberger S. 2016. The function and regulation of acid-sensing ion channels (ASICs) and the epithelial Na+ channel (ENaC): IUPHAR Review 19. Br J Pharmacol. 173:2671–2701.

Brücke E. 1843. Beiträge zur Lehre von der Diffusion tropfbarflüssiger Korper durch poröse Scheidenwände. Ann Phys Chem 58:77–94.

Coste B, Xiao B, Santos JS, et al. 2012. Piezo proteins are pore-forming subunits of mechanically activated channels. Nature 483:176–181.

Doyle DA, Cabral JM, Pfuetzner RA, et al. 1998. The structure of the potassium channel: molecular basis of K^+ conduction and selectivity. Science 280:69–77.

Eisenman G. 1962. Cation selective glass electrodes and their mode of operation. Biophys J 2:259–323. Suppl 2.

Enyedi P, Gabor G. 2010. Molecular background of leak K^+ currents: two-pore domain potassium channels. Physiol Rev 90:550–605.

Feng L, Campbell EB, MacKinnon R. 2012. Molecular mechanism of proton transport in CLC Cl^-/H^+ exchange transporters. Proc Natl Acad Sci U S A 109:11699–11704.

Gadsby DC. 2004. Ion transport: spot the difference. Nature 427:795–797.

Hamill OP, Marty A, Neher E, Sakmann B, Sigworth FJ. 1981. Improved patch-clamp techniques for high-resolution current recording from cells and cell-free membrane patches. Pflugers Arch 391:85–100.

Hansen SB. 2015. Lipid antagonism: the PIP2 paradigm of ligand-gated ion channels. Biochim Biophys Acta 1851:620–628.

Henderson R, Unwin PNT. 1975. Three-dimensional model of purple membrane obtained by electron microscopy. Nature 257:28–32.

Hille B. 1973. Potassium channels selective permeability to small cations. J Gen Physiol 61:669–686.

Hille B. 1984. *Ion Channels of Excitable Membranes,* Sunderland, MA: Sinauer.

Isom LL, DeJongh KS, Catterall WA. 1994. Auxiliary subunits of voltage-gated ion channels. Neuron 12:1183–1194.

Kaczmarek LK. 2013. Slack, slick, and sodium-activated potassium channels. ISRN Neurosci 2013:354262.

Katz B, Thesleff S. 1957. A study of the "desensitization" produced by acetylcholine at the motor end-plate. J Physiol (Lond) 138:63–80.

Kyte J, Doolittle RF. 1982. A simple method for displaying the hydropathic character of a protein. J Mol Biol 157:105–132.

Lau C, Hunter MJ, Stewart A, Perozo E, and Vandenberg JI. 2019. Never at rest: insights into the conformational dynamics of ion channels from cryo-electron microscopy. J Physiol 596:1107–1119.

Lewis AH, Cui AF, McDonald MF, Grandl J. 2017. Transduction of repetitive mechanical stimuli by Piezo1 and Piezo2 ion channels. Cell Rep 19:2572–2585.

Long SB, Tao X, Campbell EB, MacKinnon R. 2007. Atomic structure of a voltage-dependent K^+ channel in a lipid membrane-like environment. Nature 450:376–382.

Miller C. 1982. Open-state substructure of single chloride channels from *Torpedo electroplax*. Philos Trans R Soc Lond B Biol Sci 299:401–411.

Miller C (ed). 1986. *Ion Channel Reconstitution.* New York: Plenum.

Miller C. 2001. See potassium run. Nature 414:23–24.

Morais-Cabral JH, Zhou Y, MacKinnon R. 2001. Energetic optimization of ion conduction rate by the K^+ selectivity filter. Nature 414:37–42.

Moran Y, Barzilai MG, Liebeskind BJ, Zakon HH. 2015. Evolution of voltage-gated ion channels at the emergence of Metazoa. J Exp Biol 218:515–525.

Murata Y, Iwasaki H, Sasaki M, Inaba K, Okamura Y. 2005. Phosphoinositide phosphatase activity coupled to an intrinsic voltage sensor. Nature 435:1239–1243.

Neher E, Sakmann B. 1976. Single-channel currents recorded from membrane of denervated frog muscle fibres. Nature 260:799–802.

Nishida M, MacKinnon R. 2002. Structural basis of inward rectification: cytoplasmic pore of the G protein-gated inward rectifier GIRK1 at 1.8 Å resolution. Cell 111:957–965.

Noda M, Takahashi H, Tanabe T, et al. 1983. Structural homology of *Torpedo californica* acetylcholine receptor subunits. Nature 302:528–532.

Noda M, Shimizu S, Tanabe T, et al. 1984. Primary structure of *Electrophorus electricus* sodium channel deduced from cDNA sequence. Nature 312:121–127.

Park E, MacKinnon R. 2018. Structure of the CLC chloride channel from *Homo sapiens*. eLife 7:36629.

Payandeh J, Scheuer T, Zheng N, Catterall WA. 2011. The crystal structure of a voltage-gated sodium channel. Nature 475:353–359.

Peterson BZ, DeMaria CD, Yue DT. 1999. Calmodulin is the Ca^{2+} sensor for Ca^{2+}-dependent inactivation of L-type calcium channels. Neuron 22:549–558.

Pongs O, Schwarz JR. 2010. Ancillary subunits associated with voltage-dependent K^+ channels. Physiol Rev 90:755–796.

Prager-Khoutorsky M, Arkady Khoutorsky A, Bourque CW. 2014. Unique interweaved microtubule scaffold mediates osmosensory transduction via physical interaction with TRPV1. Neuron 83:866–878.

Preston GM, Agre P. 1992. Appearance of water channels in *Xenopus* oocytes expressing red cell CHIP28 protein. Science 256:385–387.

Ramsey IS, Moran MM, Chong JA, Clapham DE. 2006. A voltage-gated proton-selective channel lacking the pore domain. Nature 440:1213–1216.

Rogers CJ, Twyman RE, MacDonald RL. 1994. Benzodiazepine and β-carboline regulation of single $GABA_A$ receptor channels of mouse spinal neurones in culture. J Physiol (Lond) 475:69–82.

Schofield PR, Darlison MG, Fujita N, et al. 1987. Sequence and functional expression of the $GABA_A$ receptor shows a ligand-gated receptor super-family. Nature 328:221–227.

Tao X, Hite RK, MacKinnon R. 2017. Cryo-EM structure of the open high-conductance Ca^{2+}-activated K^+ channel. Nature 541:46–51.

Voets T, Droogmans T, Wissenbach U, Janssens A, Flockerzi V, Nillus B. 2004. The principle of temperature-dependent gating in cold- and heat-sensitive TRP channels. Nature 430:748–754.

Wang W, MacKinnon R. 2017. Cryo-EM structure of the open human ether-à-go-go-related K^+ channel hERG. Cell 169:422–430.

Wu LJ, Sweet TB, Clapham DE. 2010. Current progress in the mammalian TRP ion channel family. Pharmacol Rev 62:381–404.

Yang N, George AL Jr, Horn R. 1996. Molecular basis of charge movement in voltage-gated sodium channels. Neuron 16:113–122.

Zhou Y, Morais-Cabral JH, Kaufman A, MacKinnon R. 2001. Chemistry of ion coordination and hydration revealed by a K^+ channel-Fab complex at 2.0 Å resolution. Nature 414:43–48.

9

Membrane Potential and the Passive Electrical Properties of the Neuron

Information is carried within neurons and from neurons to their target cells by electrical and chemical signals. Transient electrical signals are particularly important for carrying time-sensitive information rapidly and over long distances. These transient electrical signals—receptor potentials, synaptic potentials, and action potentials—are all produced by temporary changes in the electric current into and out of the cell, changes that drive the electrical potential across the cell membrane away from its resting value. This current represents the flow of negative and positive ions through ion channels in the cell membrane.

Two types of ion channels—resting and gated—have distinctive roles in neuronal signaling. Resting channels are primarily important in maintaining the resting membrane potential, the electrical potential across the membrane in the absence of signaling. Some types of resting channels are constitutively open and are not gated by changes in membrane voltage; other types are gated by changes in voltage but are also open at the negative resting potential of neurons. Most voltage-gated channels, in contrast, are closed when the membrane is at rest and require membrane depolarization to open.

In this and the next several chapters, we consider how transient electrical signals are generated in the neuron. We begin by discussing how particular ion channels establish and maintain the membrane potential when the membrane is at rest and briefly describe the mechanism by which the resting potential can be perturbed, giving rise to transient electrical signals

such as the action potential. We then consider how the passive electrical properties of neurons—their resistive and capacitive characteristics—contribute to the integration and local propagation of synaptic and receptor potentials within the neuron. In Chapter 10 we examine the detailed mechanisms by which voltage-gated Na^+, K^+, and Ca^{2+} channels generate the action potential, the electrical signal conveyed along the axon. Synaptic potentials are considered in Chapters 11 to 14, and receptor potentials are discussed in Part IV in connection with the actions of sensory receptors.

The Resting Membrane Potential Results From the Separation of Charge Across the Cell Membrane

The neuron's cell membrane has thin clouds of positive and negative ions spread over its inner and outer surfaces. At rest, the extracellular surface of the membrane has an excess of positive charge and the cytoplasmic surface an excess of negative charge (Figure 9–1). This separation of charge is maintained because the lipid bilayer of the membrane is a barrier to the diffusion of ions (Chapter 8). The charge separation gives rise to the *membrane potential* (V_m), a difference of electrical potential, or voltage, across the membrane defined as

$$V_m = V_{in} - V_{out},$$

where V_{in} is the potential on the inside of the cell and V_{out} the potential on the outside.

The membrane potential of a cell at rest, the *resting membrane potential* (V_r), is equal to V_{in} since by convention the potential outside the cell is defined as zero. Its usual range is –60 mV to –70 mV. All electrical signaling involves brief changes away from the resting membrane potential caused by electric currents across the cell membrane.

The electric current is carried by ions, both positive (cations) and negative (anions). The direction of current is conventionally defined as the direction of *net movement of positive charge.* Thus, in an ionic solution, cations move in the direction of the electric current and anions move in the opposite direction. In the nerve cell at rest, there is no net charge movement across the membrane. When there is a net flow of cations or anions into or out of the cell, the charge separation across the resting membrane is disturbed, altering the electrical potential of the membrane. A reduction or reversal of charge separation, leading to a less negative membrane potential, is called *depolarization.* An increase in charge separation, leading to a more negative membrane potential, is called *hyperpolarization.*

Changes in membrane potential that do not lead to the opening of gated ion channels are passive responses of the membrane and are called *electrotonic potentials.* Hyperpolarizing responses are almost always passive, as are small depolarizations. However, when depolarization approaches a critical level, or threshold, the cell responds actively with the opening of voltage-gated ion channels, which produces an all-or-none *action potential* (Box 9–1).

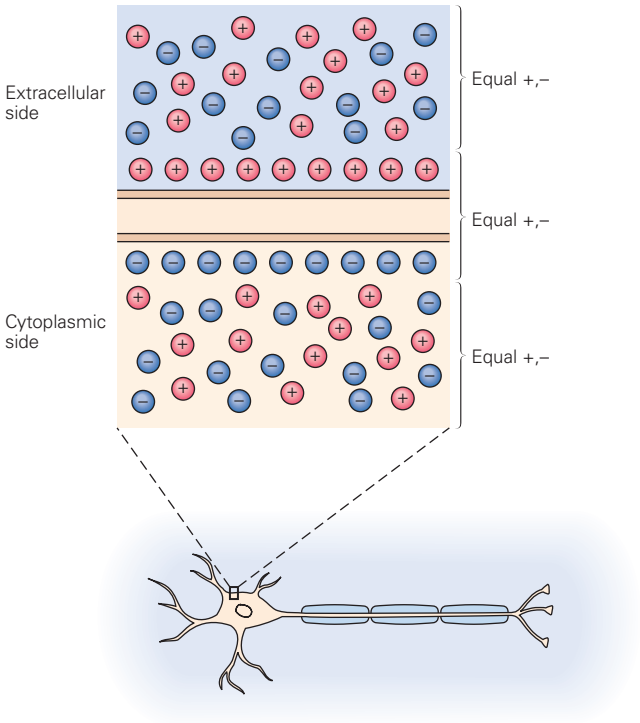

Figure 9–1 **The cell membrane potential results from the separation of net positive and net negative charges on either side of the membrane.** The excess of positive ions outside the membrane and negative ions inside the membrane represents a small fraction of the total number of ions inside and outside the cell at rest.

The Resting Membrane Potential Is Determined by Nongated and Gated Ion Channels

The resting membrane potential is the result of the passive flux of individual ion species through several classes of resting channels. Understanding how this passive ionic flux gives rise to the resting potential enables us to understand how the gating of different

Box 9–1 Recording the Membrane Potential

Reliable techniques for recording the electrical potential across cell membranes were developed in the late 1940s. These techniques allow accurate recordings of both the resting membrane potential and action potentials (Figure 9–2).

Glass micropipettes filled with a concentrated salt solution serve as electrodes and are placed on either side of the cell membrane. Wires inserted into the back ends of the pipettes are connected via an amplifier to an oscilloscope, which displays the amplitude of the membrane potential in volts. Because the diameter of such a *microelectrode* tip is minute (<1 μm), it can be inserted into a cell with relatively little damage to the cell membrane (Figure 9–2A).

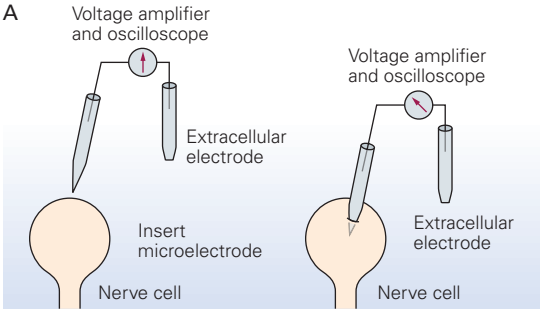

Figure 9–2A Recording setup.

When both electrodes are outside the cell, no electrical potential difference is recorded. But as soon as one microelectrode is inserted into the cell, the oscilloscope shows a steady voltage, the resting membrane potential. In most nerve cells at rest, the membrane potential is approximately −65 mV (Figure 9–2B).

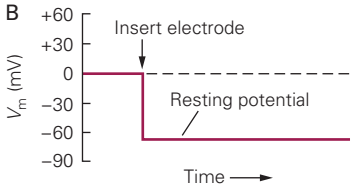

Figure 9–2B Oscilloscope display.

The membrane potential can be experimentally changed using a current generator connected to a second pair of electrodes—one intracellular and one extracellular. When the intracellular electrode is made positive with respect to the extracellular one, a pulse of positive current from the current generator causes positive charge to flow into the neuron from the intracellular electrode. This current returns to the extracellular electrode by flowing outward across the membrane.

As a result, the inside of the membrane becomes more positive while the outside of the membrane becomes more negative. This decrease in the separation of charge is called *depolarization*.

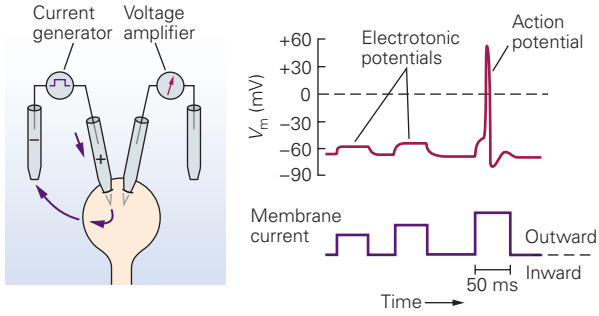

Figure 9–2C Depolarization.

Small depolarizing current pulses evoke purely electrotonic (passive) potentials in the cell—the size of the change in potential is proportional to the size of the current pulses. However, a sufficiently large depolarizing current triggers the opening of voltage-gated ion channels. The opening of these channels leads to the action potential, which differs from electrotonic potentials in the way in which it is generated as well as in magnitude and duration (Figure 9–2C).

Reversing the direction of current—making the intracellular electrode negative with respect to the extracellular electrode—makes the membrane potential more negative. This increase in charge separation is called *hyperpolarization*.

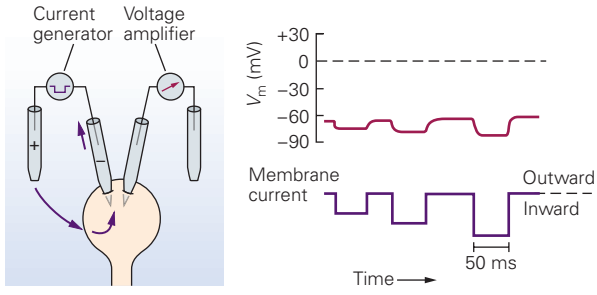

Figure 9–2D Hyperpolarization.

Hyperpolarization does not trigger an active response in the cell. The responses of the cell to hyperpolarization are usually purely electrotonic. As the size of the current pulse increases, the hyperpolarization increases proportionately (Figure 9–2D).

Table 9–1 Distribution of the Major Ions Across a Neuronal Membrane at Rest: The Giant Axon of the Squid

Species of ion	Concentration in cytoplasm (mM)	Concentration in extracellular fluid (mM)	Equilibrium potential[1] (mV)
K^+	400	20	–75
Na^+	50	440	+55
Cl^-	52	560	–60
A^- (organic anions)	385	None	None

[1]The membrane potential at which there is no net flux of the ion species across the cell membrane.

types of ion channels generates the action potential, as well as the receptor and synaptic potentials.

No single ion species is distributed equally on the two sides of a nerve cell membrane. Of the four most abundant ions found on either side of the cell membrane, Na^+ and Cl^- are concentrated outside the cell and K^+ and A^- (organic anions, primarily amino acids and proteins) inside. Table 9–1 shows the distribution of these ions inside and outside of one particularly well-studied nerve cell process, the giant axon of the squid, whose extracellular fluid has a salt concentration similar to that of seawater. Although the absolute values of the ionic concentrations for vertebrate nerve cells are two- to three-fold lower than those for the squid giant axon, the *concentration gradients* (the ratio of the external to internal ion concentration) are similar.

The unequal distribution of ions raises several important questions. How do ionic gradients contribute to the resting membrane potential? What prevents the ionic gradients from dissipating by diffusion of ions across the membrane through the resting channels? These questions are interrelated, and we shall answer them by considering two examples of membrane permeability: the resting membranes of glial cells, which are permeable to only one species of ion, and the resting membranes of nerve cells, which are permeable to three. For the purposes of this discussion, we shall only consider the resting channels that are not gated by voltage and thus are always open.

Open Channels in Glial Cells Are Permeable to Potassium Only

The permeability of a cell membrane to a particular ion species is determined by the relative proportions of the various types of ion channels that are open. The simplest case is that of the glial cell, which has a resting potential of approximately –75 mV. Like most cells, a glial cell has high concentrations of K^+ and A^- on the inside and high concentrations of Na^+ and Cl^- on the outside. However, most resting channels in the membrane are permeable only to K^+.

Because K^+ ions are present at a high concentration inside the cell, they tend to diffuse across the membrane from the inside to the outside of the cell down their chemical concentration gradient. As a result, the outside of the membrane accumulates a net positive charge (caused by the slight excess of K^+) and the inside a net negative charge (because of the deficit of K^+ and the resulting slight excess of anions). Because opposite charges attract each other, the excess positive charges on the outside and the excess negative charges on the inside collect locally on either surface of the membrane (Figure 9–1).

The flux of K^+ out of the cell is self-limiting. The efflux of K^+ gives rise to an electrical potential difference—positive outside, negative inside. The greater the flow of K^+, the more charge is separated and the greater is the potential difference. Because K^+ is positive, the negative potential inside the cell tends to oppose the further efflux of K^+. Thus, K^+ ions are subject to two forces driving them across the membrane: (1) a *chemical driving force,* a function of the concentration gradient across the membrane, and (2) an *electrical driving force,* a function of the electrical potential difference across the membrane.

Once K^+ diffusion has proceeded to a certain point, the electrical driving force on K^+ exactly balances the chemical driving force. That is, the outward movement of K^+ (driven by its concentration gradient) is equal to the inward movement of K^+ (driven by the electrical potential difference across the membrane). This potential is called the K^+ *equilibrium potential*, E_K (Figure 9–3). In a cell permeable only to K^+ ions, E_K determines the resting membrane potential, which in most glial cells is approximately –75 mV.

The equilibrium potential for any ion *X* can be calculated from an equation derived in 1888 from basic

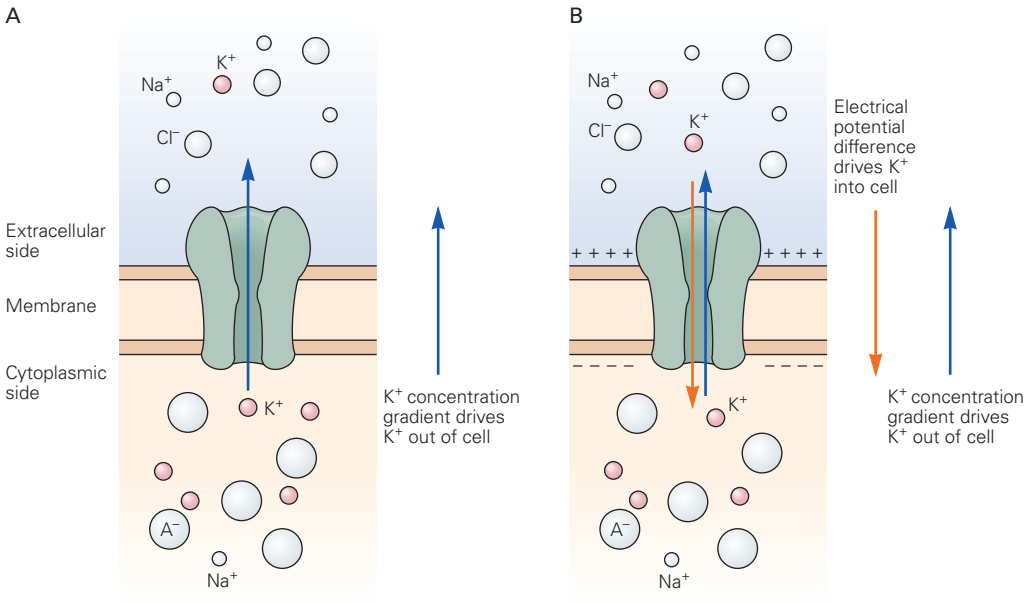

Figure 9–3 The flux of K^+ across a cell membrane is determined by both the K^+ concentration gradient and the membrane potential.

A. In a cell permeable only to K^+, the resting potential is generated by the efflux of K^+ down its concentration gradient.

B. The continued efflux of K^+ builds up an excess of positive charge on the outside of the cell and leaves behind an excess of negative charge inside the cell. This buildup of charge leads to a potential difference across the membrane that impedes the further efflux of K^+, so eventually an equilibrium is reached: The electrical and chemical driving forces are equal and opposite, so as many K^+ ions move in as move out.

thermodynamic principles by the German physical chemist Walter Nernst:

$$E_x = \frac{RT}{zF} \ln \frac{[X]_o}{[X]_i}, \qquad \textbf{Nernst Equation}$$

where R is the gas constant, T the temperature (in degrees Kelvin), z the valence of the ion, F the Faraday constant, and $[X]_o$ and $[X]_i$ the concentrations of the ion outside and inside the cell. (To be precise, chemical activities rather than concentrations should be used.)

Since RT/F is 25 mV at 25°C (77°F, room temperature), and the constant for converting from natural logarithms to base 10 logarithms is 2.3, the Nernst equation can also be written as follows:

$$E_x = \frac{58\,\text{mV}}{z} \log \frac{[X]_o}{[X]_i}.$$

Thus, for K^+, since $z = +1$ and given the concentrations inside and outside the squid axon in Table 9–1:

$$E_K = \frac{58\,\text{mV}}{1} \log \frac{[20]}{[400]} = -75\,\text{mV}.$$

The Nernst equation can be used to find the equilibrium potential of any ion that is present on both sides of a membrane permeable to that ion (the potential is sometimes called the *Nernst potential*). The equilibrium potentials for the distributions of Na^+, K^+, and Cl^- ions across the squid giant axon are given in Table 9–1.

In our discussion so far, we have treated the generation of the resting potential as a passive mechanism—the diffusion of ions down their chemical gradients—one that does not require the expenditure of energy by the cell. However, energy from hydrolysis of adenosine triphosphate (ATP) is required to set up the initial concentration gradients and to maintain them in neurons, as we shall see below.

Open Channels in Resting Nerve Cells Are Permeable to Three Ion Species

Unlike glial cells, nerve cells at rest are permeable to Na^+ and Cl^- ions in addition to K^+ ions. Of the abundant ion species in nerve cells, only the large organic anions (A^-) are unable to permeate the cell membrane. How are the concentration gradients for the three permeant ions (Na^+, K^+, and Cl^-) maintained across the membrane of a single cell, and how do these three

gradients interact to determine the cell's resting membrane potential?

To answer these questions, it is easiest to examine first only the diffusion of K^+ and Na^+. Let us return to the simple example of a cell having only K^+ channels, with concentration gradients for K^+, Na^+, Cl^-, and A^- as shown in Table 9–1. Under these conditions, the resting membrane potential V_r is determined solely by the K^+ concentration gradient and is equal to E_K (–75 mV) (Figure 9–4A).

Now consider what happens if a few resting Na^+ channels are added to the membrane, making it slightly permeable to Na^+. Two forces drive Na^+ into the cell: Na^+ tends to flow into the cell down its chemical concentration gradient, and it is driven into the cell by the negative electrical potential difference across the membrane (Figure 9–4B). The influx of Na^+ depolarizes the cell, but only slightly from the K^+ equilibrium potential (–75 mV). The new membrane potential does not come close to the Na^+ equilibrium potential of +55 mV because there are many more resting K^+ channels than Na^+ channels in the membrane.

As soon as the membrane potential begins to depolarize from the value of the K^+ equilibrium potential, K^+ flux is no longer in equilibrium across the membrane. The reduction in the electrical force driving K^+ into the cell means that there is now a net flow of K^+ out of the cell, tending to counteract the Na^+ influx. The more the membrane potential is depolarized and driven away from the K^+ equilibrium potential, the greater is the net electrochemical force driving K^+ out of the cell and consequently the greater the net K^+ efflux. Eventually the membrane potential reaches a new resting level at which the increased outward movement of K^+ just balances the inward movement of Na^+ (Figure 9–4C). This balance point (usually approximately –65 mV) is far from the Na^+ equilibrium potential (+55 mV) and is only slightly more positive than the K^+ equilibrium potential (–75 mV).

To understand how this balance point is determined, bear in mind that the magnitude of the flux of an ion across a cell membrane is the product of its *electrochemical driving force* (the sum of the electrical and chemical driving forces) and the conductance of the membrane to the ion:

$$\text{ion flux} = (\text{electrical driving force} + \text{chemical driving force}) \times \text{membrane conductance}.$$

In a resting nerve cell, relatively few Na^+ channels are open, so the membrane conductance of Na^+ is quite low. Thus, despite the large chemical and electrical forces driving Na^+ into the cell, the influx of Na^+ is small. In contrast, many K^+ channels are open in the membrane of a resting cell so that the membrane conductance of K^+ is relatively large. Because of the high conductance of K^+ relative to Na^+ in the cell at rest, the small net outward force acting on K^+ is enough to produce a K^+ efflux equal to the Na^+ influx.

The Electrochemical Gradients of Sodium, Potassium, and Calcium Are Established by Active Transport of the Ions

As we have seen, the passive movement of K^+ out of the resting cell through open channels balances the passive movement of Na^+ into the cell. However, this steady leakage of ions cannot be allowed to continue unopposed for any appreciable length of time because the Na^+ and K^+ gradients would eventually run down, reducing the resting membrane potential.

Dissipation of ionic gradients is prevented by the sodium-potassium pump (*Na^+-K^+ pump*), which moves Na^+ and K^+ *against* their electrochemical gradients: It extrudes Na^+ from the cell while taking in K^+. The pump therefore requires energy, and the energy comes from hydrolysis of ATP. Thus, at the resting membrane potential, the cell is not in equilibrium but rather in a *steady state*: There is a continuous passive influx of Na^+ and efflux of K^+ through resting channels that is exactly counterbalanced by the Na^+-K^+ pump.

As we saw in the previous chapter, pumps are similar to ion channels in that they catalyze the movement of ions across cell membranes. However, they differ in two important respects. First, whereas ion channels are passive conduits that allow ions to move down their electrochemical gradient, pumps require a source of chemical energy to transport ions against their electrochemical gradient. Second, ion transport is much faster in channels: Ions typically flow through channels at a rate of 10^7 to 10^8 per second, whereas pumps operate at speeds more than 10,000 times slower.

The Na^+-K^+ pump is a large membrane-spanning protein with catalytic binding sites for Na^+ and ATP on its intracellular surface and for K^+ on its extracellular surface. With each cycle, the pump hydrolyzes one molecule of ATP. (Because the Na^+-K^+ pump hydrolyzes ATP, it is also referred to as the Na^+-K^+ ATPase.) It uses this energy of hydrolysis to extrude three Na^+ ions from the cell and bring in two K^+ ions. The unequal flux of Na^+ and K^+ ions causes the pump to generate a net outward ionic current. Thus, the pump is said to be *electrogenic.* This pump-driven efflux of positive charge tends to set the resting potential a few millivolts more negative than would be achieved by the passive

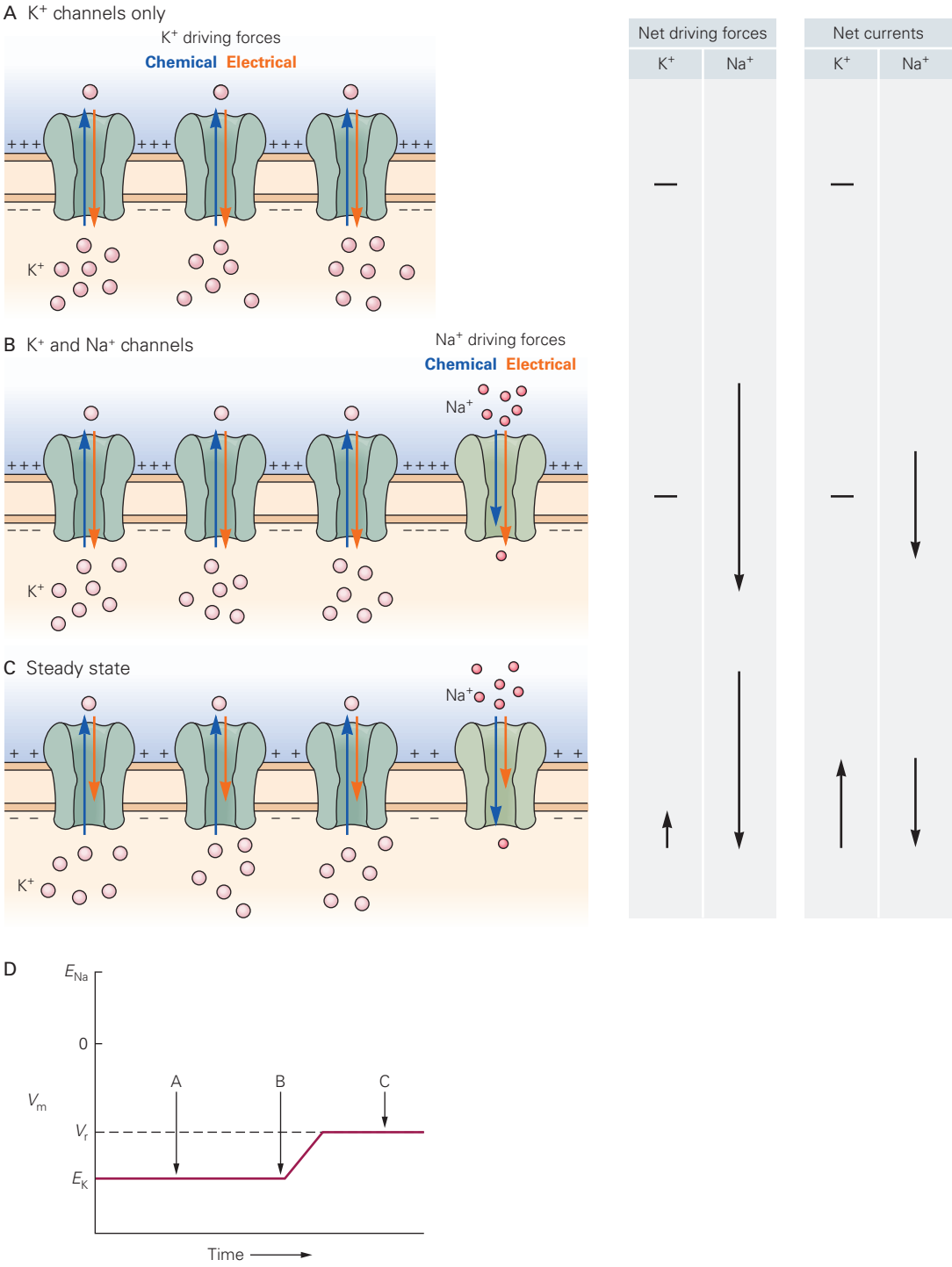

Figure 9–4 **The resting potential of a cell is determined by the proportions of different types of ion channels that are open, together with the value of their equilibrium potentials.** The channels in the figures represent the entire complement of K^+ or Na^+ channels in this hypothetical cell membrane. The lengths of the arrows within the channels represent the relative amplitudes of the electrical (**red**) and chemical (**blue**) driving forces acting on Na^+ or K^+. The lengths of the arrows in the diagram on the right denote the relative sizes of the net driving force (the sum of the electrical and chemical driving forces) for Na^+ and K^+ and the net ion currents. Three hypothetical situations are illustrated.

A. In a resting cell in which only K^+ channels are present, K^+ ions are in equilibrium and $V_m = E_K$.

B. Adding a few Na^+ channels to the resting membrane allows Na^+ ions to diffuse into the cell, and this influx begins to depolarize the membrane.

C. The resting potential settles at a new level (V_r), where the influx of Na^+ is balanced by the efflux of K^+. In this example, the aggregate conductance of the K^+ channels is much greater than that of the Na^+ channels because the K^+ channels are more numerous. As a result, a relatively small net driving force for K^+ drives a current equal and opposite to the Na^+ current driven by the much larger net driving force for Na^+. This is a steady-state condition, in which neither Na^+ nor K^+ is in equilibrium but the net flux of charge is null.

D. Membrane voltage changes during the hypothetical situations illustrated in parts **A**, **B**, and **C**.

diffusion mechanisms discussed earlier. During periods of intense neuronal activity, the increased influx of Na^+ leads to an increase in Na^+-K^+ pump activity that generates a prolonged outward current, leading to a hyperpolarizing after-potential that can last for several minutes, until the normal Na^+ concentration is restored. The Na^+-K^+ pump is inhibited by ouabain or digitalis plant alkaloids, an action that is important in the treatment of heart failure.

The Na^+-K^+ pump is a member of a large family of pumps known as *P-type ATPases* (because the phosphoryl group of ATP is temporarily transferred to the pump). P-type ATPases include a *Ca^{2+} pump* that transports Ca^{2+} across cell membranes (Figure 9–5A). All cells normally maintain a very low cytoplasmic Ca^{2+} concentration, between 50 and 100 nM. This concentration is more than four orders of magnitude lower than the external concentration, which is approximately 2 mM in mammals. Calcium pumps in the plasma membrane transport Ca^{2+} out of the cell; other Ca^{2+} pumps located in internal membranes, such as the smooth endoplasmic reticulum, transport Ca^{2+} from the cytoplasm into these intracellular Ca^{2+} stores. Calcium pumps are thought to transport two Ca^{2+} ions for each ATP molecule that is hydrolyzed, with two protons transported in the opposite direction.

The Na^+-K^+ pump and Ca^{2+} pump have similar structures. They are formed from 110 kD α-subunits, whose large transmembrane domain contains 10 membrane-spanning α-helixes (Figure 9–5A). In the Na^+-K^+ pump, an α-subunit associates with an obligatory β-subunit that is required for proper assembly and membrane expression of the pump. In humans, four genes encode highly related Na^+-K^+ pump α-subunits (*ATP1A1*, *ATP1A2*, *ATP1A3*, *ATP1A4*). Mutations in *ATP1A2* result in familial hemiplegic migraine, a form

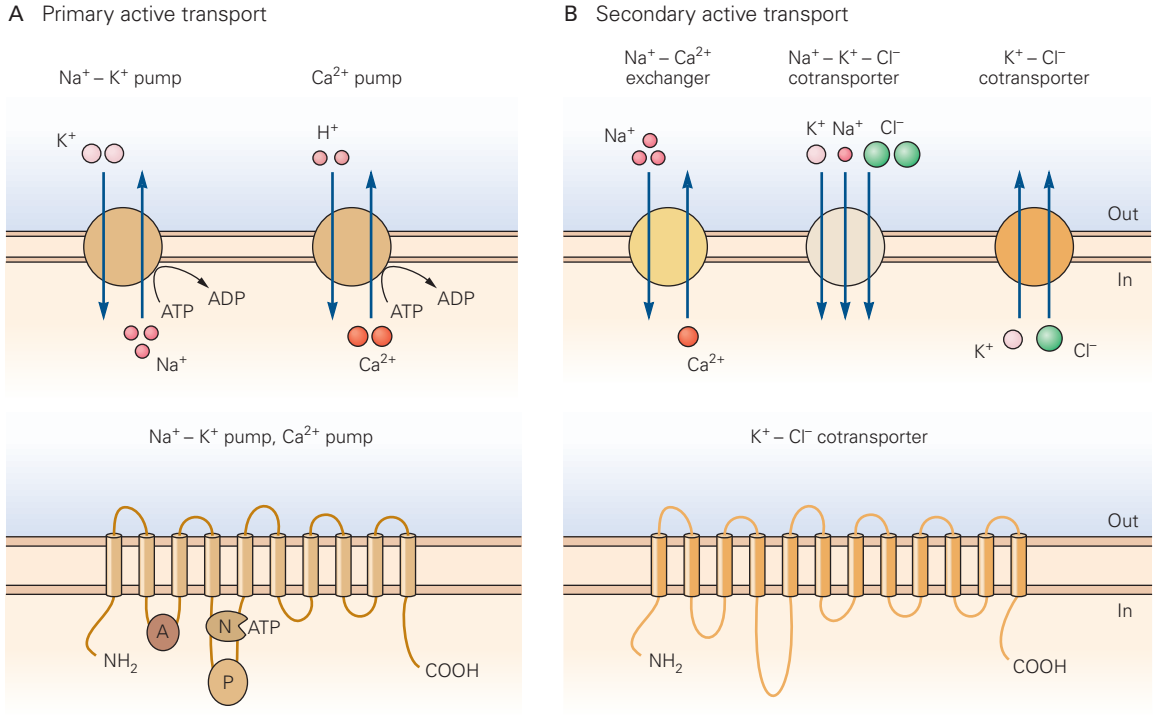

Figure 9–5 Pumps and transporters regulate the chemical concentration gradients of Na^+, K^+, Ca^{2+}, and Cl^- ions.

A. The Na-K^+ pump and Ca^{2+} pump are two examples of active transporters that use the energy of adenosine triphosphate (**ATP**) hydrolysis to transport ions against their concentration gradient. The α-subunit of a Na-K^+ pump or homologous Ca^{2+} pump (**below**) has 10 transmembrane segments, a cytoplasmic amino terminus, and a cytoplasmic carboxyl terminus. There are also cytoplasmic loops important for binding ATP (**N**), ATP hydrolysis and phosphorylation of the pump (**P**), and transducing phosphorylation to transport (**A**). The Na^+-K^+ pump also contains a smaller β-subunit with a single transmembrane domain plus a small accessory integral membrane protein **FXYD**, which modulates pump kinetics (not shown).

B. The Na^+-Ca^{2+} exchanger uses the potential energy of the electrochemical gradient of Na^+ to transport Ca^{2+} out of a cell. The Na^+-Ca^{2+} exchanger contains nine transmembrane segments, two reentrant membrane loops important for ion transport, and a large cytoplasmic regulatory loop. Chloride ions are transported into the cell by the Na^+-K^+-Cl^- cotransporter and out of the cell by the K^+-Cl^- cotransporter. These transporters are members of a family of Cl^- transport proteins with 12 transmembrane segments (**below**).

of migraine associated with an aura and muscle weakness. Certain mutations in the neuron-specific *ATP1A3* isoform lead to rapid-onset dystonia parkinsonism, a movement disorder that first occurs in late adolescence or early adulthood. A different set of mutations lead to a distinct neurological disorder, alternating hemiplegia of childhood, a paralysis that affects one side of the body and develops in children under the age of 2.

Most neurons have relatively few Ca^{2+} pumps in the plasma membrane. Instead, Ca^{2+} is transported out of the cell primarily by the *Na^+-Ca^{2+} exchanger* (Figure 9–5B). This membrane protein is not an ATPase but a different type of molecule called a *cotransporter*. Cotransporters move one type of ion against its electrochemical gradient by using the energy stored in the electrochemical gradient of a second ion. (The CLC Cl^--H^+ cotransporter discussed in Chapter 8 is a type of exchanger.) In the case of the Na^+-Ca^{2+} exchanger, the electrochemical gradient of Na^+ drives the efflux of Ca^{2+}. The exchanger transports three or four Na^+ ions into the cell (down the electrochemical gradient for Na^+) for each Ca^{2+} ion it removes (against the electrochemical gradient of Ca^{2+}). Because Na^+ and Ca^{2+} are transported in opposite directions, the exchanger is termed an *antiporter.* Ultimately, it is the hydrolysis of ATP by the Na^+-K^+ pump that provides the energy (stored in the Na^+ gradient) to maintain the function of the Na^+-Ca^{2+} exchanger. For this reason, ion flux driven by cotransporters is often referred to as *secondary active transport*, to distinguish it from the *primary active transport* driven directly by ATPases.

Chloride Ions Are Also Actively Transported

So far, for simplicity, we have ignored the contribution of chloride (Cl^-) to the resting potential. However, in most nerve cells, the Cl^- gradient across the cell membrane is controlled by one or more active transport mechanisms so that E_{Cl} differs from V_r. As a result, the presence of open Cl^- channels will bias the membrane potential toward its Nernst potential. *Chloride transporters* typically use the energy stored in the gradients of other ions—they are cotransporters.

Cell membranes contain a number of different types of Cl^- cotransporters (Figure 9–5B). Some transporters increase intracellular Cl^- to levels greater than those that would be passively reached if the Cl^- Nernst potential was equal to the resting potential. In such cells, E_{Cl} is positive to V_r so that the opening of Cl^- channels depolarizes the membrane. An example of this type of transporter is the Na^+-K^+-Cl^- cotransporter. This protein transports two Cl^- ions into the cell together with one Na^+ and one K^+ ion. As a result, the transporter is electroneutral. The Na^+-K^+-Cl^- cotransporter differs from the Na^+-Ca^{2+} exchanger in that the former transports all three ions in the same direction—it is a *symporter.*

In most neurons, the Cl^- gradient is determined by cotransporters that move Cl^- out of the cell. This action lowers the intracellular concentration of Cl^- so that E_{Cl} is typically more negative than the resting potential. As a result, the opening of Cl^- channels leads to an influx of Cl^- that hyperpolarizes the membrane. The K^+-Cl^- cotransporter is an example of such a transport mechanism; it moves one K^+ ion out of the cell for each Cl^- ion it exports.

Interestingly, in early neuronal development, cells tend to express primarily the Na^+-K^+-Cl^- cotransporter. As a result, at this stage the neurotransmitter γ-aminobutyric acid (GABA), which activates ligand-gated Cl^- channels, typically has an excitatory (depolarizing) effect. As neurons develop, they begin to express the K^+-Cl^- cotransporter, such that in most mature neurons GABA typically hyperpolarizes the membrane and thus acts as an inhibitory neurotransmitter. In some pathological conditions in adults, such as certain types of epilepsy or chronic pain syndromes, the expression pattern of the Cl^- cotransporters may revert to that of the immature nervous system. This will lead to aberrant depolarizing responses to GABA that can produce abnormally high levels of excitation.

The Balance of Ion Fluxes in the Resting Membrane Is Abolished During the Action Potential

In the nerve cell at rest, the steady Na^+ influx is balanced by a steady K^+ efflux, so that the membrane potential is constant. This balance changes when the membrane is depolarized toward the threshold for an action potential. As the membrane potential approaches this threshold, voltage-gated Na^+ channels open rapidly. The resultant increase in membrane conductance to Na^+ causes the Na^+ influx to exceed the K^+ efflux once threshold is exceeded, creating a net influx of positive charge that causes further depolarization. The increase in depolarization causes still more voltage-gated Na^+ channels to open, resulting in a greater influx of Na^+, which accelerates the depolarization even further.

This regenerative, positive feedback cycle develops explosively, driving the membrane potential rapidly toward the Na^+ equilibrium potential of +55 mV:

$$E_{Na} = \frac{RT}{F} \ln \frac{[Na]_o}{[Na]_i} = 58 \text{ mV} \times \log \frac{[440]}{[50]} = +55 \text{ mV}.$$

However, the membrane potential never quite reaches E_{Na} because K^+ efflux continues throughout the depolarization. A slight influx of Cl^- into the cell also counteracts the depolarizing effect of the Na^+ influx. Nevertheless, so many voltage-gated Na^+ channels open during the rising phase of the action potential that the cell membrane's Na^+ conductance is much greater than the conductance of either Cl^- or K^+. Thus, at the peak of the action potential, the membrane potential approaches the Na^+ equilibrium potential, just as at rest (when permeability to K^+ is predominant), the membrane potential tends to approach the K^+ equilibrium potential.

The Contributions of Different Ions to the Resting Membrane Potential Can Be Quantified by the Goldman Equation

Although K^+, Na^+, and Cl^- fluxes set the value of the resting potential, V_m is not equal to E_K, E_{Na}, or E_{Cl} but lies at some intermediate value. As a general rule, when V_m is determined by two or more species of ions, the contribution of one species is determined not only by the concentrations of the ion inside and outside the cell but also by the ease with which the ion crosses the membrane.

One convenient measure of how readily the ion crosses the membrane is the *permeability* (P) of the membrane to that ion, which has units of velocity (cm/s). This measure is similar to that of a diffusion constant, which determines the rate of solute movement in solution driven by a local concentration gradient. The dependence of membrane potential on ionic permeability and concentration is given by the Goldman equation:

$$V_m = \frac{RT}{F} \ln \frac{P_K[K^+]_o + P_{Na}[Na^+]_o + P_{Cl}[Cl^-]_i}{P_K[K^+]_i + P_{Na}[Na^+]_i + P_{Cl}[Cl^-]_o}.$$

Goldman Equation

This equation applies only when V_m is not changing. It states that the greater the concentration of an ion species and the greater its membrane permeability, the greater is its contribution to determining the membrane potential. In the limit, when permeability to one ion is exceptionally high, the Goldman equation reduces to the Nernst equation for that ion. For example, if $P_K >> P_{Cl}$ or P_{Na}, as in glial cells, the equation becomes as follows:

$$V_m \cong \frac{RT}{F} \ln \frac{[K^+]_o}{[K^+]_i}.$$

Alan Hodgkin and Bernard Katz used the Goldman equation to analyze changes in membrane potential in the squid giant axon. They measured the variations in membrane potential in response to systematic changes in the extracellular concentrations of Na^+, Cl^-, and K^+. They found that if V_m is measured shortly after the extracellular concentration is changed (before the internal ionic concentrations are altered), $[K^+]_o$ has a strong effect on the resting potential, $[Cl^-]_o$ has a moderate effect, and $[Na^+]_o$ has little effect. The data for the membrane at rest could be fit accurately by the Goldman equation using the following permeability ratios:

$$P_K : P_{Na} : P_{Cl} = 1.0 : 0.04 : 0.45.$$

At the peak of the action potential, there is an instant in time when V_m is not changing and the Goldman equation is applicable. At that point, the variation of V_m with external ionic concentrations is fit best if a quite different set of permeability ratios is assumed:

$$P_K : P_{Na} : P_{Cl} = 1.0 : 20 : 0.45.$$

For these values of permeability, the Goldman equation approaches the Nernst equation for Na^+:

$$V_m \cong \frac{RT}{F} \ln \frac{[Na^+]_o}{[Na^+]_i} = +55 \text{ mV}.$$

Thus, at the peak of the action potential, when the membrane is much more permeable to Na^+ than to any other ion, V_m approaches E_{Na}. However, the finite permeability of the membrane to K^+ and Cl^- results in K^+ efflux and Cl^- influx that partially counterbalance Na^+ influx, thereby preventing V_m from quite reaching E_{Na}.

The Functional Properties of the Neuron Can Be Represented as an Electrical Equivalent Circuit

The utility of the Goldman equation is limited because it cannot be used to determine how membrane potential changes with time or distance within a neuron in response to a local change in permeability. It is also inconvenient for determining the magnitude of the individual Na^+, K^+, and Cl^- currents. This information can be obtained using a simple mathematical model derived from electric circuit theory. The model, called an *equivalent circuit*, represents all of the important electrical properties of the neuron by a circuit consisting of conductors or resistors, batteries, and capacitors. Equivalent circuits provide us with an intuitive understanding as well as a quantitative description of

how current caused by the movement of ions generates electrical signals in nerve cells.

The first step in developing an equivalent circuit is to relate the membrane's discrete physical properties to its electrical properties. The lipid bilayer endows the membrane with electrical *capacitance*, the ability of an electrical nonconductor (insulator) to separate electrical charges on either side of it. The nonconducting phospholipid bilayer of the membrane separates the cytoplasm and extracellular fluid, both of which are highly conductive environments. The separation of charges on the inside and outside surfaces of the cell membrane (the capacitor) gives rise to the electrical potential difference across the membrane. The electrical potential difference or voltage across a capacitor is

$$V = Q/C,$$

where Q is the net excess positive or negative charge on each side of the capacitor and C is the capacitance.

Capacitance is measured in units of farads (F), and charge is measured in coulombs (where 96,500 coulombs of a univalent ion is equivalent to 1 mole of that ion). A charge separation of 1 coulomb across a capacitor of 1 F produces a potential difference of 1 volt. A typical value of membrane capacitance for a nerve cell is approximately 1 μF per cm^2 of membrane area. Very few charges are required to produce a significant potential difference across such a capacitance. For example, the excess of positive and negative charges separated by the membrane of a spherical cell body with a diameter of 50 μm and a resting potential of −60 mV is 29×10^6 ions. Although this number may seem large, it represents only a tiny fraction (1/200,000) of the total number of positive or negative charges in solution within the cytoplasm. The bulk of the cytoplasm and the bulk of the extracellular fluid are electroneutral.

The membrane is a *leaky capacitor* because it is studded with ion channels that can conduct charge. Ion channels endow the membrane with conductance and with the ability to generate an electrical potential difference. The lipid bilayer itself has effectively zero conductance or infinite resistance. However, because ion channels are highly conductive, they provide pathways of finite electrical resistance for ions to cross the membrane. Because neurons contain many types of channels selective for different ions, we must consider each class of ion channel separately.

In an equivalent circuit we can represent each K^+ channel as a resistor or conductor of ionic current with a single-channel conductance γ_K (remember, conductance = 1/resistance) (Figure 9–6A). If there were no K^+ concentration gradient, the current through a single K^+ channel would be given by Ohm's law: $i_K = \gamma_K \times V_m$. However, normally there is a K^+ concentration gradient, and thus also a chemical force driving K^+ across the membrane, represented in the equivalent circuit by a battery. (A source of electrical potential is called an *electromotive force* [EMF], and an electromotive force generated by a difference in chemical potentials is called a battery.) The electromotive force of this battery is given by E_K, the Nernst potential for K^+ (Figure 9–6).

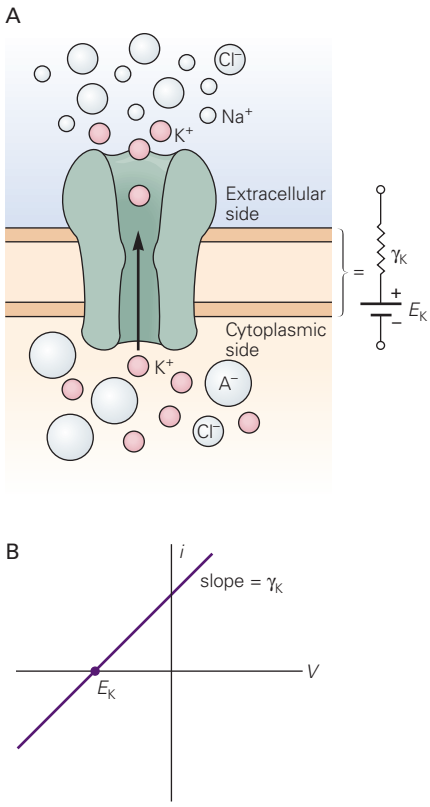

Figure 9–6 Chemical and electrical forces contribute to current through an ion channel.

A. A concentration gradient for K^+ gives rise to an electromotive force, which has a value equal to E_K, the Nernst potential for K^+. This can be represented by a battery. In this circuit, the battery E_K is in series with the conductor γ_K, representing the conductance of the K^+ channel.

B. The current-voltage relation for a K^+ channel in the presence of both electrical and chemical driving forces. The membrane potential at which the current is zero is equal to the K^+ Nernst potential.

In the absence of voltage across the membrane, the normal K^+ concentration gradient causes an outward K^+ current. According to our convention for current, an outward movement of positive charge across the membrane corresponds to a positive current. According to the Nernst equation, when the concentration gradient for a positively charged ion, such as K^+, is directed

outward (ie, the K^+ concentration inside the cell is higher than outside), the equilibrium potential for that ion is negative. Thus, the K^+ current that flows solely because of its concentration gradient is given by $i_K = -\gamma_K \times E_K$ (the negative sign is required because a negative equilibrium potential produces a positive current at 0 mV).

Finally, for a real neuron that has both a membrane potential and a K^+ concentration gradient, the net K^+ current is given by the sum of the currents caused by the electrical and chemical driving forces:

$$i_K = (\gamma_K \times V_m) - (\gamma_K \times E_K) = \gamma_K \times (V_m - E_K). \quad \textbf{(9–1)}$$

The factor $(V_m - E_K)$ is called the *electrochemical driving force.* It determines the direction of ionic current and (along with the conductance) its magnitude. This equation is a modified form of Ohm's law that takes into account the fact that ionic current through a membrane is determined not only by the voltage across the membrane but also by the ionic concentration gradients.

A cell membrane has many resting K^+ channels, all of which can be combined into a single equivalent circuit element consisting of a conductor in series with a battery. In this equivalent circuit, the total conductance of all the K^+ channels (g_K), ie, the K^+ conductance of the cell membrane in its resting state, is equal to the number of resting K^+ channels (N_K) multiplied by the conductance of an individual K^+ channel (γ_K):

$$g_K = N_K \times \gamma_K.$$

Because the battery in this equivalent circuit depends solely on the concentration gradient for K^+ and is independent of the number of K^+ channels, its value is the equilibrium potential for K^+, E_K.

Like the population of resting K^+ channels, all the resting Na^+ channels can be represented by a single conductor in series with a single battery, as can the resting Cl^- channels. Because the K^+, Na^+, and Cl^- channels account for the bulk of the passive ionic current through the membrane in the cell at rest, we can calculate the resting potential by incorporating these three pathways into a simple equivalent circuit of a neuron (Figure 9–7).

To complete this circuit, we first connect the elements representing each type of channel at their two ends with elements representing the extracellular fluid and cytoplasm. The extracellular fluid and cytoplasm are both good conductors (compared with the membrane) because they have relatively large cross-sectional areas and many ions available to carry charge. In a small region of a neuron, the extracellular and cytoplasmic resistances can be approximated by a *short circuit*—a conductor with zero resistance. The membrane capacitance (C_m) is determined by the insulating properties of the lipid bilayer and its area.

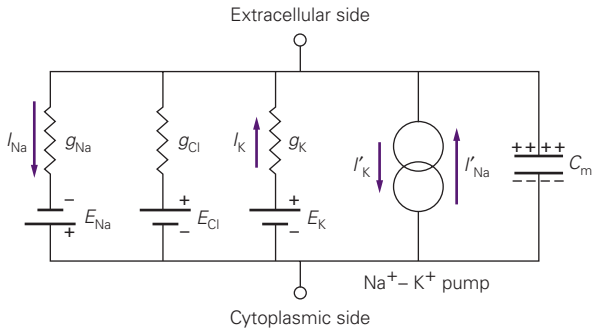

Figure 9–7 An equivalent circuit of passive and active current in a resting neuron. The total K^+ conductance represented by the symbol g_K is the product of $\gamma_K \times N$, the total number of open K^+ channels in the resting membrane. The total conductances for Na^+ and Cl^- channels are determined in a similar fashion. Under steady-state conditions, the passive Na^+ and K^+ currents are balanced by active Na^+ and K^+ fluxes (I'_{Na} and I'_K) driven by the Na-K^+ pump. The active Na^+ flux (I'_{Na}) is 50% greater than the active K^+ flux (I'_K) because the Na^+-K^+ pump transports three Na^+ ions out for every two K^+ ions it transports into the cell. As a result, for the cell to remain in a steady state, I_{Na} must be 50% greater than I_K (arrow size is proportional to current magnitude). There is no current through the Cl^- channels because in this example V_m is at E_{Cl}, the Cl^- equilibrium potential.

Finally, the equivalent circuit can be made complete by incorporating the active ion fluxes driven by the Na^+-K^+ pump, which extrudes three Na^+ ions from the cell for every two K^+ ions it pumps in. This electrogenic ATP-dependent pump, which keeps the ionic batteries charged, is represented in the equivalent circuit by the symbol for a current generator (Figure 9–7). The use of the equivalent circuit to analyze neuronal properties quantitatively is illustrated in Box 9–2, where the equivalent circuit is used to calculate the resting potential.

The Passive Electrical Properties of the Neuron Affect Electrical Signaling

Once an electrical signal is generated in part of a neuron, for example in response to a synaptic input on a branch of a dendrite, it is integrated with the other inputs to the neuron and then propagated to the axon initial segment, the site of action potential generation. When synaptic potentials, receptor potentials, or action potentials are generated in a neuron, the membrane potential changes rapidly.

Box 9–2 Using the Equivalent Circuit Model to Calculate Resting Membrane Potential

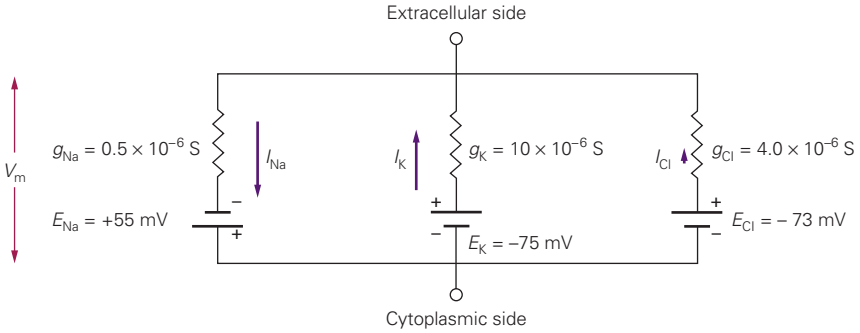

Figure 9–8 The electrical equivalent circuit used to calculate the resting membrane potential. In this example, it is assumed that the Cl^- cotransporter maintains intracellular Cl^- at a relatively low value. As a result, the Cl^- equilibrium potential is more negative than the resting potential.

An equivalent circuit model of the resting membrane can be used to calculate the resting potential (Figure 9–8). To simplify the calculation, we ignore the electrogenic influence of the Na^+-K^+ pump because it is small. We also ignore membrane capacitance because V_m is unchanging, so the charge on the capacitance is also not changing.

Because there are more resting channels for K^+ than for Na^+, the membrane conductance for K^+ is much greater than that for Na^+. In the equivalent circuit in Figure 9–8, g_K (10×10^{-6} S) is 20 times higher than g_{Na} (0.5×10^{-6} S). For most nerve cells, the value of g_{Cl} ranges from one-fourth to one-half of g_K. In this example, g_{Cl} equals 4.0×10^{-6} S. Given these values and the values of E_K, $E_{Cl,}$ and E_{Na}, we can calculate V_m as follows.

Since the membrane potential is constant, there is no net current through the three sets of ion channels:

$$I_K + I_{Cl} + I_{Na} = 0. \qquad \textbf{(9–2)}$$

We can easily calculate each current in two steps. First, we add up the separate potential differences across each branch of the circuit. For example, in the K^+ branch, the total potential difference is the sum of the the battery E_K and the voltage drop across g_K given by Ohm's law ($V_m = I_K/g_K$):*

$$V_m = E_K + I_K/g_K$$

Similarly, for the Na^+ and Cl^- conductance branches:

$$V_m = E_{Cl} + I_{Cl}/g_{Cl}$$

$$V_m = E_{Na} + I_{Na}/g_{Na}$$

Next, we rearrange and solve for the ionic current I in each branch:

$$I_{Na} = g_{Na} \times (V_m - E_{Na}) \qquad \textbf{(9–3a)}$$

$$I_K = g_K \times (V_m - E_K) \qquad \textbf{(9–3b)}$$

$$I_{Cl} = g_{Cl} \times (V_m - E_{Cl}). \qquad \textbf{(9–3c)}$$

These equations are similar to Equation 9–1, in which the net current through a single ion channel is derived from the currents caused by the individual

*Because we have defined V_m as $V_{in} - V_{out}$, the following convention must be used for these equations. Outward current (in this case I_K) is positive and inward current is negative. Batteries whose positive pole is directed toward the inside of the membrane (eg, E_{Na}) are given positive values in the equations. The reverse is true for batteries whose negative pole is directed toward the inside, such as the K^+ battery.

What determines the rate of change in potential with time or distance? What determines whether a stimulus will or will not produce an action potential? Here we consider the neuron's passive electrical properties and geometry and how these relatively constant properties affect the cell's electrical signaling. The actions of the gated channels and the ionic currents that change the membrane potential are described in the next five chapters.

Neurons have three passive electrical properties that are important for electrical signaling. We have already described the resting membrane conductance or resistance ($g_r = 1/R_r$) and the membrane capacitance, C_m. A third important property that determines signal propagation along dendrites or axons is their intracellular axial resistance (r_a). Although the resistivity of cytoplasm is much lower than that of the membrane, the axial resistance along the entire length of an

driving forces. As these equations illustrate, the ionic current through each conductance branch is equal to the conductance of that branch multiplied by the net electrochemical driving force. Thus, for the K^+ current, the conductance is proportional to the number of open K^+ channels, and the driving force is equal to the difference between V_m and E_K. If V_m is more positive than E_K (−75 mV), the driving force is positive and the current is outward; if V_m is more negative than E_K, the driving force is negative and the current is inward.

Similar equations are used in a variety of contexts throughout this book to relate the magnitude of a particular ionic current to its membrane conductance and driving force.

As we saw in Equation 9–2, $I_{Na} + I_K + I_{Cl} = 0$. If we now substitute Equations 9–3a,b,c for I_{Na}, I_K, and I_{Cl} in Equation 9–2, multiply through, and rearrange, we obtain the following expression:

$$V_m \times (g_{Na} + g_K + g_{Cl}) = (E_{Na} \times g_{Na}) + (E_K \times g_K) + (E_{Cl} \times g_{Cl}).$$

Solving for V_m, we obtain an equation for the resting membrane potential that is expressed in terms of membrane conductances g and batteries E:

$$V_m = \frac{(E_{Na} \times g_{Na}) + (E_K \times g_K) + (E_{Cl} \times g_{Cl})}{g_{Na} + g_K + g_{Cl}}. \qquad \textbf{(9–4)}$$

From this equation, using the values in our equivalent circuit (Figure 9–8), we calculate that $V_m = -70$ mV.

Equation 9–4 states that V_m approaches the value of the ionic batteries that have the greater conductance. This principle can be illustrated by considering what happens during the action potential. At the peak of the action potential, g_K and g_{Cl} are essentially unchanged from their resting values, but g_{Na} increases as much as 500-fold. This increase in g_{Na} is caused by the opening of voltage-gated Na^+ channels. In the equivalent circuit in Figure 9–8, a 500-fold increase would change g_{Na} from 0.5×10^{-6} S to 250×10^{-6} S.

If we substitute this new value of g_{Na} into Equation 9–4 and solve for V_m, we obtain +48 mV. V_m is closer to E_{Na} than to E_K at the peak of the action potential because g_{Na} is now 25-fold greater than g_K and 62.5-fold greater than g_{Cl}, so that the Na^+ battery becomes much more important than the K^+ and Cl^- batteries in determining V_m.

Equation 9–4 is similar to the Goldman equation in that the contribution to V_m of each ionic battery is weighted in proportion to the conductance of the membrane for that particular ion. In the limit, if the conductance for one ion is much greater than that for the other ions, V_m approaches the value of that ion's Nernst potential.

The equivalent circuit can be further simplified by lumping the conductance of all the resting channels that contribute to the resting potential into a single conductance, g_r, and replacing the battery for each conductance channel with a single battery E_r, whose value is given by Equation 9–4 (Figure 9–9). Here the subscript r stands for the resting channel pathway. Because the resting channels provide a pathway for the steady leakage of ions across the membrane, they are sometimes referred to as *leakage channels* (Chapter 10). This consolidation of resting pathways will prove useful when we consider the effects on membrane voltage of current through voltage-gated and ligand-gated channels in later chapters.

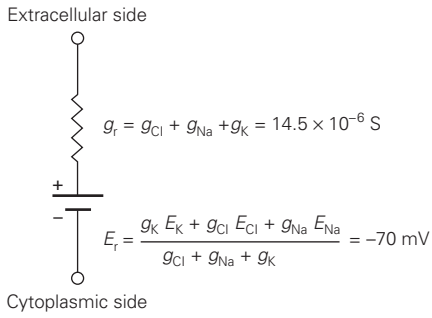

Figure 9–9 The Na^+, K^+, and Cl^- resting channels can be simplified to a single conductance and battery. For an equivalent circuit model of the resting membrane (eg, Figure 9–8), the total membrane conductance (g_r) is calculated from the sum of the Na^+, K^+, and Cl^- conductances, and the value of the resting potential battery (E_r) is calculated from Equation 9–4.

extended thin neuronal process can be considerable. Because these three elements provide the return pathway to complete the electrical circuit when active ionic currents flow into or out of the cell, they determine the time course of the change in synaptic potential generated by the synaptic current. They also determine whether a synaptic potential generated in a dendrite will depolarize the trigger zone at the axon initial segment enough to fire an action potential. Finally, the passive properties influence the speed at which an action potential is conducted.

Membrane Capacitance Slows the Time Course of Electrical Signals

The steady-state change in a neuron's voltage in response to subthreshold current resembles the behavior of a simple resistor, but the *time course* of the change

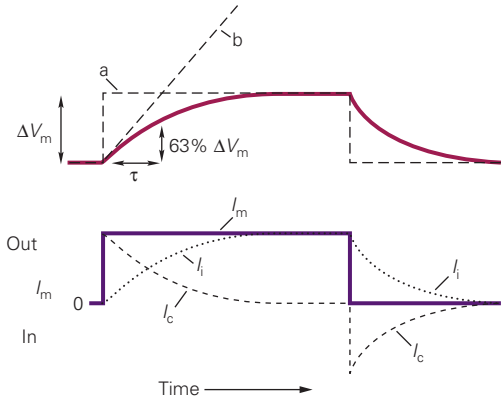

Figure 9–10 **The rate of change in the membrane potential is slowed by the membrane capacitance.** The **upper** plot shows the response of the membrane potential (ΔV_m) to a step current pulse (I_m). The shape of the actual voltage response (**red line**) combines the properties of a purely resistive element (**dashed line a**) and a purely capacitive element (**dashed line b**). The time taken to reach 63% of the final voltage defines the membrane time constant, τ. The **lower** plot shows the two elements of the total membrane current (I_m) during the current pulse: the ionic current (I_i) across the resistive elements of the membrane (ion channels) and the capacitive current (I_c).

does not. A true resistor responds to a step change in current with a similar step change in voltage, but the neuron's membrane potential rises and decays more slowly than the step change in current because of its *capacitance* (Figure 9–10).

To understand how the capacitance slows down the voltage response, recall that the voltage across a capacitor is proportional to the charge stored on the capacitor. To alter the voltage, charge Q must be added to or removed from the capacitor C:

$$\Delta V = \Delta Q/C.$$

To change the charge across the capacitor (the membrane lipid bilayer), there must be current across the capacitor (I_c). Since current is the flow of charge per unit time ($I_c = \Delta Q/\Delta t$), the change in voltage across a capacitor is a function of the magnitude and duration of the current:

$$\Delta V = I_c \cdot \Delta t/C.$$

Thus, the magnitude of the change in voltage across a capacitor in response to a current pulse depends on the duration of the current, because time is required to deposit and remove charge from the capacitor.

If the membrane had only resistive properties, a step pulse of outward current would change the membrane potential instantaneously. Conversely, if the membrane had only capacitive properties, the membrane potential would change linearly with time in response to the same step of current. Because the membrane has both capacitive and resistive properties in parallel, the actual change in membrane potential combines features of the two pure responses. The initial slope of the change reflects a purely capacitive element, whereas the final slope and amplitude reflect a purely resistive element (Figure 9–10, upper plot).

In the simple case of the spherical cell body of a neuron, the time course of the potential change is described by the following equation:

$$\Delta V_m\,(t) = I_m R_m (1 - e^{-t/\tau}),$$

where e is the base of the system of natural logarithms with a value of approximately 2.72, and τ is the *membrane time constant*, given by the product of the membrane resistance and capacitance ($R_m C_m$). The time constant can be measured experimentally as the time it takes the membrane potential to rise to $1 - 1/e$, or approximately 63% of its steady-state value (Figure 9–10, upper plot). Typical values of τ for neurons range from 20 to 50 ms. We shall return to the time constant in Chapter 13 where we consider the temporal summation of synaptic inputs in a cell.

Membrane and Cytoplasmic Resistance Affect the Efficiency of Signal Conduction

So far, we have considered the effects of the passive properties of neurons on signaling only within the cell body. Distance is not a factor in the propagation of a signal in the neuron's soma because the cell body can be approximated as a sphere whose membrane voltage is uniform. However, a subthreshold voltage signal traveling along extended structures (dendrites, axons, and muscle fibers) decreases in amplitude with distance from the site of initiation because some charge leaks out of the resting membrane conductance as it flows along the dendrite or axon. To show how this attenuation occurs, we will consider how the geometry of a neuron influences the distribution of current.

If current is injected into a dendrite at one point, how will the membrane potential change along its length? For simplicity, consider how membrane potential varies with distance after a constant-amplitude current pulse has been on for some time ($t >> \tau$). Under these conditions, the membrane capacitance is fully charged, so membrane potential reaches a steady value. The variation of the potential with distance depends on the fraction of charge that leaks out of the dendrite compared to the fraction that flows inside the dendrite towards the soma. Since charge flows along the path of least resistance, this depends on the relative values of the *membrane resistance* in a unit length of dendrite r_m

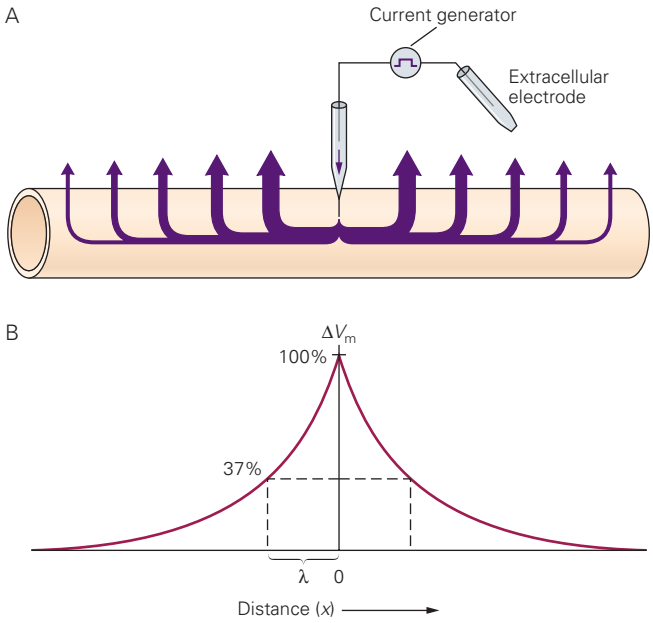

Figure 9–11 The change in membrane potential along a neuronal process during electrotonic conduction decreases with distance.

A. Current injected into a neuronal process by a microelectrode follows the path of least resistance to the return electrode in the extracellular fluid. (The thickness of the arrows represents the magnitude of membrane current.)

B. The change in V_m decays exponentially with distance from the site of current injection. The distance at which ΔV_m has decayed to 37% of its value at the point of current injection defines the length constant, λ.

(units of Ω · cm) and the *axial resistance* per unit length of dendrite r_a (units of Ω/cm). The change in membrane potential along the dendrite becomes smaller with distance from the current electrode (Figure 9–11A). This decay with distance is exponential and expressed by

$$\Delta V(x) = \Delta V_0 \, e^{-x/\lambda},$$

where λ is the membrane *length constant*, x is the distance from the site of current injection, and ΔV_0 is the change in membrane potential produced by the current at the site of injection ($x = 0$). The length constant is the distance along the dendrite to the site where ΔV_m has decayed to $1/e$, or 37% of its initial value (Figure 9–11B). It is a measure of the efficiency of electrotonic conduction—the passive spread of voltage changes along the neuron—and is determined by the values of membrane and axial resistance as follows:

$$\lambda = \sqrt{(r_m / r_a)}.$$

The better the insulation of the membrane (that is, the greater r_m) and the better the conducting properties of the inner core (the lower r_a), the greater the length constant of the dendrite. That is because current is able to spread farther along the inner conductive core of the dendrite before leaking across the membrane at some point x to alter the local membrane potential:

$$\Delta V(x) = i(x) \cdot r_m.$$

The length constant is also a function of the diameter of the neuronal process. Neuronal processes vary greatly in diameter, from as much as 1 mm for the squid giant axon to 1 μm for fine dendritic branches in the mammalian brain. For neuronal processes with similar ion channel surface densities (number of channels per unit membrane area) and cytoplasmic composition, thicker axons and dendrites have longer length constants than do narrower processes and hence can transmit passive electrical signals for greater distances. Typical values for neuronal length constants for unmyelinated axons range from about 0.5 to 1.0 mm. Myelinated axons have longer length constants—up to about 1.5 mm—because the insulating properties of myelin lead to an increase in the effective r_m of the axon.

To understand how the diameter of a process affects the length constant, we must consider how the diameter (or radius) affects r_m and r_a. Both r_m and r_a are measures of resistance for a unit length of a neuronal process of a given radius. The axial resistance r_a of the process depends inversely on the number of charge carriers (ions) in a cross section of the process. Therefore, given a fixed cytoplasmic ion concentration, r_a depends inversely on the cross-sectional area of the process $1/(\pi \cdot \text{radius}^2)$. The resistance of a unit length of membrane r_m depends inversely on the total number of channels in a unit length of the neuronal process.

Channel density, the number of channels per μm^2 of membrane, is often similar among different-sized processes. As a result, the number of channels per unit length of a neuronal process increases in direct proportion to increases in membrane area, which depends on the circumference of the process times its length; therefore, r_m varies as $1/(2 \cdot \pi \cdot \text{radius})$. Because r_m/r_a varies in direct proportion to the radius of the process, the length constant is proportional to the square root of the radius. In this analysis, we have assumed that dendrites have only passive electrical properties. As discussed in Chapter 13, however, voltage-gated ion channels endow most dendrites with active properties that modify their purely passive length constants.

The efficiency of electrotonic conduction has two important effects on neuronal function. First, it influences spatial summation, the process by which synaptic potentials generated in different regions of the

neuron are added together at the trigger zone of the axon (Chapter 13). Second, electrotonic conduction is a factor in the propagation of the action potential. Once the membrane at any point along an axon has been depolarized beyond threshold, an action potential is generated in that region. This local depolarization spreads passively down the axon, causing successive adjacent regions of the membrane to reach the threshold for generating an action potential (Figure 9–12). Thus, the depolarization spreads along the length of the axon by local current driven by the difference in potential between the active and resting regions of the axon membrane. In axons with longer length constants, local current spreads a greater distance down the axon, and therefore, the action potential propagates more rapidly.

Large Axons Are More Easily Excited Than Small Axons

The influence of axonal geometry on action potential conduction plays an important role in a common neurological exam. In the examination of a patient for diseases of peripheral nerves, the nerve often is stimulated by passing current between a pair of external cutaneous electrodes placed over the nerve, and the population of resulting action potentials (the *compound action potential*) is recorded farther along the nerve by a second pair of cutaneous voltage-recording electrodes. In this situation, the total number of axons that generate action potentials varies with the amplitude of the current pulse (Chapter 57).

To drive a cell to threshold, a stimulating current from the positive electrode must pass through the cell membrane into the axon. There it travels along the axoplasmic core, eventually exiting the axon into the extracellular fluid through the membrane to reach the second (negative) electrode. However, most of the stimulating current does not even enter the axon, moving instead through neighboring axons or through the low-resistance pathway of the extracellular fluid. Thus, the axons into which current enters most easily are the ones most excitable.

In general, axons with the largest diameter have the lowest threshold for such excitation. The greater the

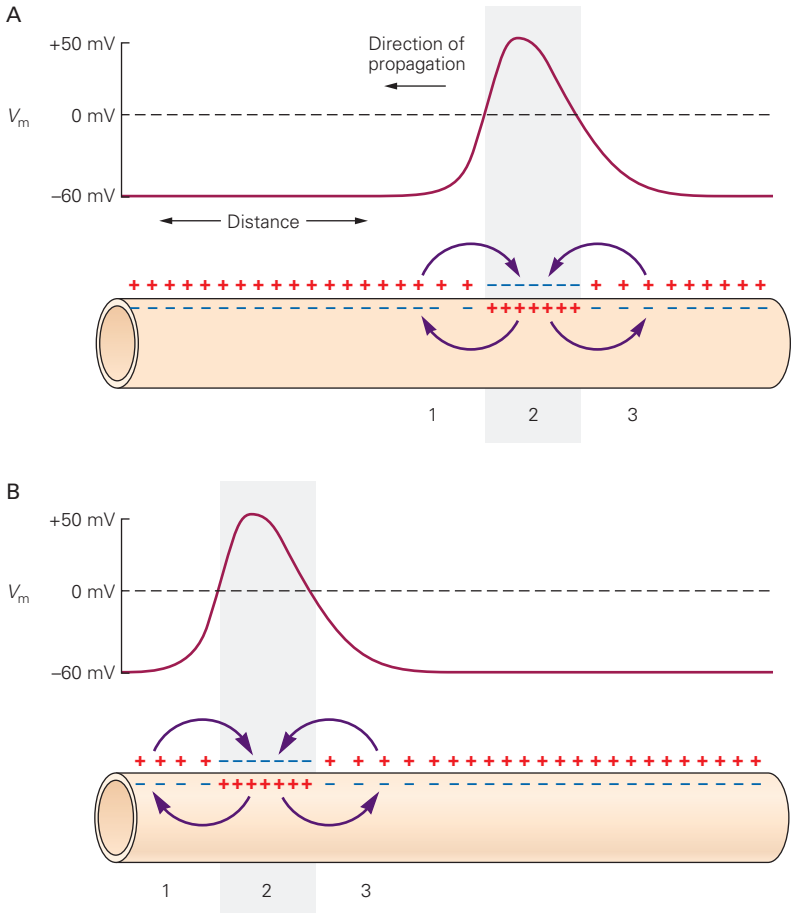

Figure 9–12 Electrotonic conduction contributes to propagation of the action potential.

A. An action potential propagating from right to left causes a difference in membrane potential between two adjacent regions of the axon. The difference creates a local-circuit current that causes the depolarization to spread passively. Current spreads from the more positive active region (**2**) to the less positive resting region *ahead* of the action potential (**1**), as well as to the less positive area *behind* the action potential (**3**). However, because there is also an increase in membrane K^+ conductance in the wake of the action potential (Chapter 10), the buildup of positive charge along the inner side of the membrane in area 3 is more than balanced by the local efflux of K^+, allowing this region of membrane to repolarize.

B. A short time later, the action potential has traveled down the axon and the process is repeated.

diameter of the axon, the lower is the axial resistance to the flow of current down the axon because the number of charge carriers (ions) per unit length of the axon is greater. Because more current enters the larger axon, the axon is depolarized more efficiently than a smaller axon. For these reasons, larger axons are recruited at low values of current; axons with smaller diameter are recruited only at relatively greater current strengths.

The fact that larger axons conduct more rapidly and have a lower current threshold for excitation aids in the interpretation of clinical nerve-stimulation tests. Neurons that convey different types of information (eg, motor versus sensory) often differ in axon diameter and thus conduction velocity (Chapter 18). In addition, a specific disease may preferentially affect certain functional classes of axons. Thus, using conduction velocity as a criterion to determine which classes of axons have defective conduction properties can help one infer the neuronal basis for the neurological deficit.

Passive Membrane Properties and Axon Diameter Affect the Velocity of Action Potential Propagation

The passive spread of depolarization during conduction of the action potential is not instantaneous. In fact, electrotonic conduction is a rate-limiting factor in the propagation of the action potential. We can understand this limitation by considering a simplified equivalent circuit of two adjacent segments of axon membrane connected by a segment of axoplasm.

An action potential generated in one segment of membrane supplies depolarizing current to the adjacent membrane, causing it to depolarize gradually toward threshold (Figure 9–12). According to Ohm's law, the larger the axoplasmic resistance, the smaller is the current between adjacent membrane segments ($I = V/R$) and thus the longer it takes to change the charge on the membrane capacitance of the adjacent segment.

Recall that, since $\Delta V = \Delta Q/C$, the membrane potential changes slowly if the current is small because ΔQ, equal to the magnitude of the current multiplied by time, changes slowly. Similarly, the larger the membrane capacitance, the more charge must be deposited on the membrane to change the potential across the membrane, so the current requires a longer time to produce a given depolarization. Therefore, the time it takes for depolarization to spread along the axon is determined by both the axial resistance r_a and the capacitance per unit length of the axon c_m (units F/cm). The rate of passive spread of charge varies inversely with the product $r_a c_m$. If this product is reduced, the rate of passive spread increases and the action potential propagates faster.

Rapid propagation of the action potential is functionally important, and two adaptations have evolved to increase it. One is an increase in the diameter of the axon core. Because r_a decreases in proportion to the square of axon diameter, whereas c_m increases in direct proportion to diameter, the net effect of an increase in diameter is a decrease in $r_a c_m$. This adaptation has been carried to an extreme in the giant axon of the squid, which can reach a diameter of 1 mm. No larger axons have evolved, presumably because of the competing need to keep neuronal size small so that many cells can be packed into a limited space.

The second adaptation that increases conduction velocity is the wrapping of a myelin sheath around an axon (Chapter 7). This process is functionally equivalent to increasing the thickness of the axonal membrane by as much as 100-fold. Because the capacitance of a parallel-plate capacitor such as the membrane is inversely proportional to the thickness of the insulation, myelination decreases c_m and thus $r_a c_m$. Each layer of myelin is extremely thin—only 80 Å. Therefore, myelination results in a proportionately much greater decrease in $r_a c_m$ than does the same increase in the diameter of a bare axon core, because the many layers of membrane in the myelin sheath produce a large decrease in c_m with a relatively small increase in overall axon diameter. For this reason, conduction in myelinated axons is faster than in nonmyelinated axons of the same diameter.

In a neuron with a myelinated axon, the action potential is triggered at the nonmyelinated initial segment of the axon. The inward current through this region of membrane is available to discharge the capacitance of the myelinated axon ahead. Even though the capacitance of the axon is quite small (because of the myelin insulation), the amount of current down the core of the axon from the trigger zone is not enough to discharge the capacitance along the entire length of the myelinated axon.

To prevent the action potential from dying out, the myelin sheath is interrupted every 1 to 2 mm by the nodes of Ranvier, bare patches of axon membrane approximately 1 µm in length (Chapter 7). Although the area of membrane at each node is quite small, the nodal membrane is rich in voltage-gated Na^+ channels and thus can generate an intense depolarizing inward Na^+ current in response to the passive spread of depolarization down the axon. These regularly distributed nodes thus periodically boost the amplitude of the action potential, preventing it from decaying with distance.

The action potential, which spreads quite rapidly along the internodal region because of the low capacitance of the myelin sheath, slows down as it crosses the high-capacitance region of each bare node. Consequently, as the action potential moves down the axon, it jumps quickly from node to node (Figure 9–13A). For this

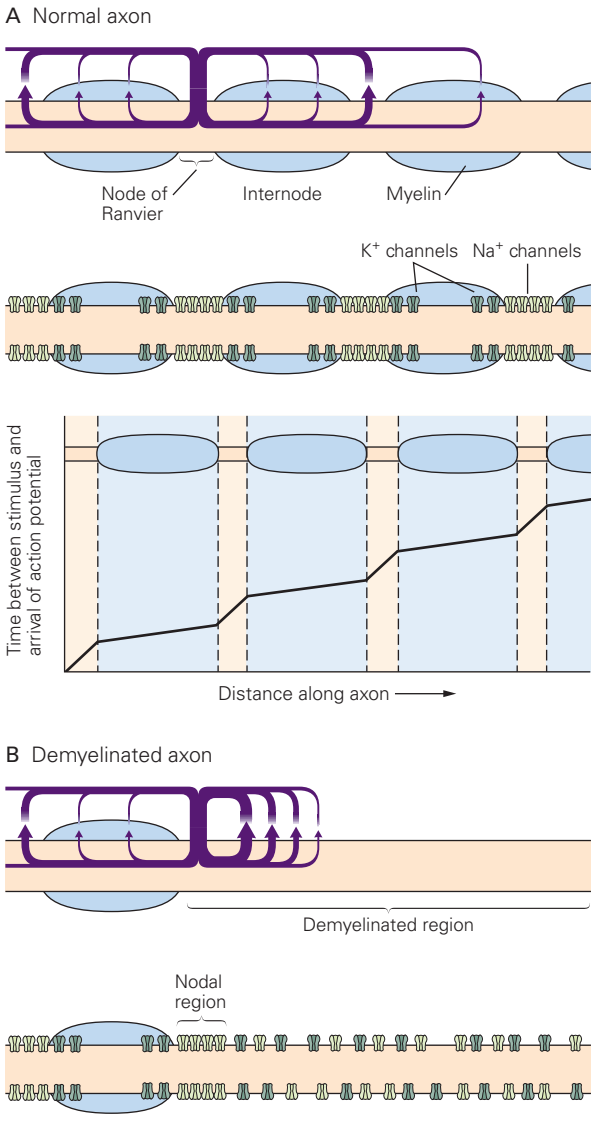

Figure 9–13 Action potentials in myelinated nerves are regenerated at the nodes of Ranvier.

A. The densities of capacitive and ionic membrane currents (membrane current per unit area of membrane) are much higher at the nodes of Ranvier than in the myelin-insulated internodal regions. (The density of membrane current at any point along the axon is represented by the thickness of the arrows.) Because of the higher capacitance of the axon membrane at the nodes, the action potential slows down as it approaches each node and thus appears to skip rapidly from node to node as it propagates from left to right.

B. In regions of the axon that have lost their myelin, the spread of the action potential is slowed down or blocked. The local-circuit currents must discharge a larger membrane capacitance, and because of the shorter length constant (caused by the low membrane resistance in demyelinated stretches of axon), they do not spread as well down the axon. In response to demyelination, additional voltage-gated Na^+ and K^+ ion channels are inserted into the membrane that is normally myelinated.

reason, the action potential in a myelinated axon is said to move by *saltatory conduction* (from the Latin *saltare*, to jump). Because ions flow across the membrane only at the nodes in myelinated fibers, saltatory conduction is also favorable from a metabolic standpoint. Less energy must be expended by the Na^+-K^+ pump to restore the Na^+ and K^+ concentration gradients, which tend to run down as the action potential is propagated.

The distribution of conduction velocities varies widely among neurons and even between different branches of an axon, depending on axon diameter and degree of myelination. Additional geometric features of myelinated axons, such as internodal length and nodal diameter, can also affect velocity. Evolution has adapted conduction velocities to optimize the behavioral functions of each neuron. In general, axons that are involved in rapid sensory and motor computations generally have high rates of conduction. More specifically, in certain neural circuits in the auditory system, an optimal behavioral response depends on the precise temporal relationship of presynaptic action potentials in two pathways that converge on the same postsynaptic neuron (Chapter 28). In such cases, values of the geometrical parameters of myelinated axons in the two input pathways can result in different conduction velocities that compensate for the differences in the input path lengths.

Various diseases of the nervous system are caused by demyelination, such as multiple sclerosis and Guillain-Barré syndrome. As an action potential goes from a myelinated region to a bare stretch of demyelinated axon, it encounters a region of relatively high c_m and low r_m. The inward current generated at the node just before the demyelinated segment may be too small to provide the capacitive current required to depolarize the segment of demyelinated membrane to threshold. In addition, this local-circuit current does not spread as far as it normally would because it encounters a segment of axon that has a relatively short length constant resulting from its low r_m (Figure 9–13B). These two factors can combine to slow, and in some cases actually block, the conduction of action potentials, causing devastating effects on behavior (Chapter 57).

Highlights

1. When the cell is at rest, passive fluxes of ions into and out of the cell through ion channels are balanced, such that the charge separation across the membrane remains constant and the membrane potential is maintained at its resting value.

2. The permeability of the cell membrane for an ion species is proportional to the number of open channels that allow passage of that ion. According to the Goldman equation, the value of the resting membrane potential in nerve cells is determined by resting channels that conduct K^+, Cl^-, and Na^+; the membrane potential is closest to the equilibrium (Nernst) potential of the ion or ions with the greatest membrane permeability.
3. Changes in membrane potential that generate neuronal electrical signals (action potentials, synaptic potentials, and receptor potentials) are caused by changes in the membrane's relative permeabilities to these three ions and to Ca^{2+} ions.
4. Although the changes in permeability caused by the opening of gated ion channels change the net charge separation across the membrane, they typically produce only negligible changes in the bulk concentrations of ions.
5. The functional properties of a neuron can be described by an electrical equivalent circuit, which includes the membrane capacitance, the ionic conductances, the EMF–generating properties of ion channels, and cytoplasmic resistance. In this model, membrane potential is determined by the ion or ions with the greatest membrane conductances.
6. Ion pumps prevent the ionic batteries from running down due to passive fluxes through the ion channels. The Na^+-K^+ pump uses the chemical energy of one molecule of ATP to exchange three intracellular Na^+ ions for two extracellular K^+ ions, an example of primary active transport. Secondary active transport by cotransporters is powered by coupling the downhill ionic gradients of one or two types of ions to drive the uphill transport of another ion. The coupling may take the form of symtransport (in the same direction) or antitransport (opposite directions).
7. The Na^+-Ca^{2+} antitransporter exchanges internal Ca^{2+} ion for external Na^+ ions. There are two types of Cl^- cotransporters in the cell membrane. The Cl^--K^+ symtransporter, which transports Cl^- and K^+ out of the cell, maintains E_{Cl} at a relatively negative potential, and is the most common variant of Cl^- transporter found in mature neurons. The Cl^--Na^+-K^+ symtransporter, which transports Cl^-, Na^+, and K^+ into the cell, generates an E_{Cl} that is relatively positive. It is expressed in immature neurons and in certain adult neurons.
8. The details of the molecular transitions during primary and secondary active transport are an area of active investigation.
9. The nerve cell membrane has a relatively high capacitance per unit of membrane area. As a result, when a channel opens and ions begin to flow, the membrane potential changes more slowly than the membrane current.
10. The currents that change the charge on the membrane capacitance along the length of an axon or dendrite pass through a relatively poor conductor—a thin column of cytoplasm. These two factors combine to slow down the conduction of voltage signals. Moreover, the various ion channels that are open at rest and that give rise to the resting potential also degrade the signaling function of the neuron, as they make the cell leaky and limit how far a signal can travel passively.
11. To overcome the physical constraints on long-distance signaling, neurons use sequential transient opening of voltage-gated Na^+ and K^+ channels to generate action potentials. The action potential is continually regenerated along the axon and thus conducted without attenuation.
12. For pathways in which rapid signaling is particularly important, conduction of the action potential is enhanced by myelination of the axon, an increase in axon diameter, or both. Conduction velocities can vary between or within axons in ways that optimize the timing of neuronal signals within a neuronal circuit.

John D. Koester
Steven A. Siegelbaum

Selected Reading

Clausen MV, Hilbers F, Poulsen H. 2017. The structure and function of the Na,K-ATPase isoforms in health and disease. Front Physiol 8:371.

Hille B. 2001. *Ionic Channels of Excitable Membranes,* 3rd ed. Sunderland, MA: Sinauer.

Hodgkin AL. 1964. Saltatory conduction in myelinated nerve. In: *The Conduction of the Nervous Impulse. The Sherrington Lecture, VII,* pp. 47–55. Liverpool: Liverpool University Press.

Jack JB, Noble D, Tsien RW. 1975. *Electric Current Flow in Excitable Cells*, pp. 1–4, 83–97, 131–224, 276–277. Oxford: Clarendon.

Johnston D, Wu M-S. 1995. Functional properties of dendrites. In: *Foundations of Cellular Neurophysiology,* pp. 55–120. Cambridge, MA: MIT Press.

Koch C. 1999. *Biophysics of Computation,* pp. 25–48. New York: Oxford Univ. Press.

References

Debanne D, Campanac E, Bialowas A, Carlier E, Alcaraz G. 2011. Axon physiology. Physiol Rev 91:555–602.

Ford MC, Alexandrova O, Cossell L, et al. 2015. Tuning of Ranvier node and internode properties in myelinated axons to adjust action potential timing. Nat Commun 6:8073.

Friedrich T, Tavraz NN, Junghans C. 2016. ATP1A2 mutations in migraine: seeing through the facets of an ion pump onto the neurobiology of disease. Front Physiol 7:239.

Gadsby DC. 2009. Ion channels versus ion pumps: the principal difference, in principle. Nat Rev Mol Cell Biol 10:344–352.

Goldman DE. 1943. Potential, impedance, and rectification in membranes. J Gen Physiol 27:37–60.

Hodgkin AL, Katz B. 1949. The effect of sodium ions on the electrical activity of the giant axon of the squid. J Physiol 108:37–77.

Hodgkin AL, Rushton WAH. 1946. The electrical constants of a crustacean nerve fibre. Proc R Soc Lond Ser B 133:444–479.

Huxley AF, Stämpfli R. 1949. Evidence for saltatory conduction in peripheral myelinated nerve fibres. J Physiol 108:315–339.

Jorgensen PL, Hakansson KO, Karlish SJ. 2003. Structure and mechanism of Na,K-ATPase: functional sites and their interactions. Annu Rev Physiol 65:817–849.

Kaila K, Price T, Payne J, Puskarjov M, Voipio J. 2014. Cation-chloride cotransporters in neuronal development, plasticity and disease. Nat Rev Neurosci 15:637–654.

Lytton J. 2007. Na^+/Ca^{2+} exchangers: three mammalian gene families control Ca^{2+} transport. Biochem J 406:365–382.

Moore JW, Joyner RW, Brill MH, Waxman SD, Najar-Joa M. 1978. Simulations of conduction in uniform myelinated fibers: relative sensitivity to changes in nodal and internodal parameters. Biophys J 21:147–160.

Nernst W. [1888] 1979. Zur Kinetik der in Lösung befindlichen Körper. [On the kinetics of substances in solution.] Z Physik Chem 2:613–622, 634–637. English translation in: GR Kepner (ed). 1979. *Cell Membrane Permeability and Transport*, pp. 174–183. Stroudsburg, PA: Dowden, Hutchinson & Ross.

Ren D. 2011. Sodium leak channels in neuronal excitability and rhythmic behaviors. Neuron 72:899–911.

Seidl AH, Rubel EW, Barría A. 2014. Differential conduction velocity regulation in ipsilateral and contralateral collaterals innervating brainstem coincidence detector neurons. J Neurosci 34:4914–4919.

Stokes DL, Green NM. 2003. Structure and function of the calcium pump. Annu Rev Biophys Biomol Struct 32:445–468.

Toyoshima C, Flemming F. 2013. New crystal structures of PII-type ATPases: excitement continues. Curr Op Struct Biol 23:507–514.

10

Propagated Signaling: The Action Potential

Nerve cells are able to carry electrical signals over long distances because the long-distance signal, the action potential, is continually regenerated and thus does not attenuate as it moves down the axon. In Chapter 9, we saw how an action potential arises from sequential changes in the membrane's permeability to Na^+ and K^+ ions and how the membrane's passive properties influence the speed at which the action potential is conducted. In this chapter, we describe in detail the voltage-gated ion channels that are critical for generating and propagating action potentials and consider how these channels are responsible for important features of a neuron's electrical excitability.

Action potentials have four properties important for neuronal signaling. First, they can be initiated only when the cell membrane voltage reaches a *threshold*. As we saw in Chapter 9, in many nerve cells, the membrane behaves as a simple resistor in response to small hyperpolarizing or depolarizing current steps. The membrane voltage changes in a graded manner as a function of the size of the current step according to Ohm's law, $\Delta V = \Delta I \cdot R$ (in terms of conductance, $\Delta V = \Delta I / G$). However, as the size of the depolarizing current increases, the membrane voltage will eventually reach a threshold, typically at around –50 mV, at which an action potential can be generated (see Figure 9–2C). Second, the action potential is an all-or-none event. The size and shape of an action potential initiated by a large depolarizing current is the same as that of an action potential evoked by a current that just surpasses the

threshold.[1] Third, the action potential is conducted without decrement. It has a self-regenerative feature that keeps the amplitude constant, even when it is conducted over great distances. Fourth, the action potential is followed by a *refractory period*. For a brief time after an action potential is generated, the neuron's ability to fire a second action potential is suppressed. The refractory period limits the frequency at which a nerve can fire action potentials, and thus limits the information-carrying capacity of the axon.

These four properties of the action potential—initiation threshold, all-or-none amplitude, conduction without decrement, and refractory period—are unusual for biological processes, which typically respond in a graded fashion to changes in the environment. Biologists were puzzled by these properties for almost 100 years after the action potential was first recorded in the mid-1800s. Finally, in the late 1940s and early 1950s, studies of the membrane properties of the giant axon of the squid by Alan Hodgkin, Andrew Huxley, and Bernard Katz provided the first quantitative insight into the mechanisms underlying the action potential.

The Action Potential Is Generated by the Flow of Ions Through Voltage-Gated Channels

An important early insight into how action potentials are generated came from an experiment performed by Kenneth Cole and Howard Curtis that predated the studies by Hodgkin, Huxley, and Katz. While recording from the giant axon of the squid, they found that the conductance of the membrane increases dramatically during the action potential (Figure 10–1). This discovery provided evidence that the action potential results from a dramatic increase in the ion permeability of the cell membrane. It also raised two central questions: Which ions are responsible for the action potential, and how is the permeability of the membrane regulated?

Hodgkin and Katz provided a key insight into this problem by demonstrating that the amplitude of the action potential is reduced when the external Na^+ concentration is lowered, indicating that Na^+ influx is responsible for the rising phase of the action potential. They proposed that depolarization of the cell above the threshold for an action potential causes a brief increase in the cell membrane's Na^+ conductance, during which the Na^+ conductance overwhelms the K^+ conductance that predominates in the cell at rest, thereby driving the membrane potential towards E_{Na}. Their data also suggested that the falling phase of the action potential was caused by a later increase in K^+ permeability.

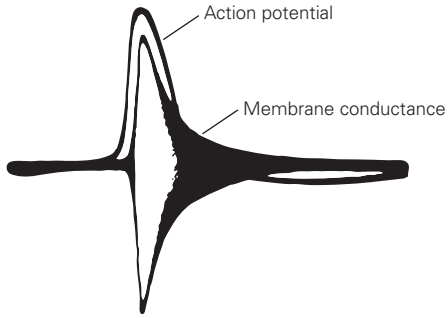

Figure 10–1 The action potential results from an increase in ion conductance of the axon membrane. This historic recording from an experiment conducted in 1939 by Kenneth Cole and Howard Curtis shows the oscilloscope record of an action potential superimposed on a simultaneous record of axonal membrane conductance.

Sodium and Potassium Currents Through Voltage-Gated Channels Are Recorded With the Voltage Clamp

This insight of Hodgkin and Katz raised a further question. What mechanism is responsible for regulating the changes in the Na^+ and K^+ permeabilities of the membrane? Hodgkin and Andrew Huxley reasoned that the Na^+ and K^+ permeabilities were regulated directly by the membrane voltage. To test this hypothesis, they systematically varied the membrane potential in the squid giant axon and measured the resulting changes in the conductance of voltage-gated Na^+ and K^+ channels. To do this, they made use of a new apparatus, the voltage clamp, developed by Kenneth Cole.

Prior to the availability of the voltage-clamp technique, attempts to measure Na^+ and K^+ conductance as a function of membrane potential had been limited by the strong interdependence of the membrane potential and the gating of Na^+ and K^+ channels. For example, if the membrane is depolarized sufficiently to open some voltage-gated Na^+ channels, the influx of Na^+ through these channels causes further depolarization. The additional depolarization causes still more

[1]The all-or-none property describes an action potential that is generated under a specific set of conditions. The size and shape of the action potential *can* be affected by changes in membrane properties, ion concentrations, temperature, and other variables, as discussed later in the chapter. The shape can also be affected slightly by the current that is used to evoke it, if measured near the point of stimulation.

Na^+ channels to open and consequently induces more inward Na^+ current:

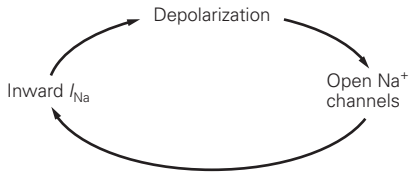

This positive feedback cycle drives the membrane potential to the peak of the action potential, making it impossible to achieve a stable membrane potential.

The voltage clamp interrupts the interaction between the membrane potential and the opening and closing of voltage-gated ion channels. It does so by adding or withdrawing a current from the axon that is equal to the current through the voltage-gated membrane channels. In this way, the voltage clamp prevents the membrane potential from changing. Thus, the amount of current that must be generated by the voltage clamp to keep the membrane potential constant provides a direct measure of the current through the voltage-gated channels (Box 10–1). Using the voltage-clamp technique, Hodgkin and Huxley were able to completely describe the ionic mechanisms underlying the action potential.

One advantage of the voltage clamp is that it readily allows the ionic and capacitive components of membrane current to be analyzed separately. As described in Chapter 9, the membrane potential V_m is proportional to the charge Q_m on the membrane capacitance C_m. When V_m is not changing, Q_m is constant, and no capacitive current ($\Delta Q_m/\Delta t$) flows. Capacitive current flows *only* when V_m is changing. Therefore, when the membrane potential changes in response to a commanded depolarizing step, capacitive current flows only at the beginning and end of the step. Because the capacitive current is essentially instantaneous, the ionic currents that subsequently flow through the voltage-gated channels can be analyzed separately.

Measurements of these ionic currents can be used to calculate the voltage and time dependence of changes in membrane conductance caused by the opening and closing of Na^+ and K^+ channels. This information provides insights into the properties of these two types of channels.

A typical voltage-clamp experiment starts with the membrane potential clamped at its resting value. When a small (10 mV) depolarizing step is applied, a very brief outward current instantaneously discharges the membrane capacitance by the amount required for a 10 mV depolarization. This capacitive current (I_c) is followed by a smaller outward current that persists for the duration of the voltage step. This steady ionic current flows through the nongated resting ion channels of the membrane, which we refer to here as *leakage channels* (see Box 9–2). The current through these channels is called the *leakage current*, I_l, and the total conductance of this population of channels is called the *leakage conductance* (g_l). At the end of the step, a brief inward capacitive current repolarizes the membrane to its initial voltage and the total membrane current returns to zero (Figure 10–3A).

If a large depolarizing step is commanded, the current record is more complicated. The capacitive and leakage currents both increase in amplitude. In addition, shortly after the end of the capacitive current and the start of the leakage current, an inward (negative) current develops; it reaches a peak within a few milliseconds, declines, and gives way to an outward current. This outward current reaches a plateau that is maintained for the duration of the voltage step (Figure 10–3B).

A simple interpretation of these results is that the depolarizing voltage step sequentially turns on two types of voltage-gated channels, each selective for a distinct ion species. One type of channel conducts ions that generate a rapidly rising inward current, while the other conducts ions that generate a more slowly rising outward current. Because these two oppositely directed currents partially overlap in time, the most difficult task in analyzing voltage-clamp experiments is to determine their separate time courses.

Hodgkin and Huxley achieved this separation by changing ions in the bathing solution. By replacing Na^+ with a larger, impermeant cation (choline $\cdot$ H^+), they eliminated the inward Na^+ current. Later the task of separating inward and outward currents was made easier by the discovery of drugs or toxins that selectively block the different classes of voltage-gated channels. Tetrodotoxin, a poison from a certain Pacific puffer fish, blocks the voltage-gated Na^+ channel with a very high potency in the nanomolar range of concentration. (Ingestion of only a few milligrams of tetrodotoxin from improperly prepared puffer fish, consumed as the Japanese sashimi delicacy *fugu*, can be fatal.) The cation tetraethylammonium (TEA) specifically blocks some voltage-gated K^+ channels.

When TEA is applied to the axon to block the K^+ channels, the total membrane current (I_m) consists of I_c, I_l, and I_{Na}. The leakage conductance g_l is constant; it does not vary with V_m or with time. Therefore, the leakage current I_l can be readily calculated and subtracted from I_m, leaving I_{Na} and I_c. Because I_c occurs only briefly at the beginning and end of the pulse, it is easily isolated by visual inspection, revealing the pure I_{Na}.

Box 10–1 Voltage-Clamp Technique

The voltage clamp permits the experimenter to "clamp" the membrane potential at predetermined levels, preventing changes in membrane current from influencing the membrane potential. By controlling the membrane potential, one can measure the effect of changes in membrane potential on the membrane conductance of individual ion species.

The voltage clamp is connected to a pair of electrodes (one intracellular and one extracellular) used to measure the membrane potential and another pair of electrodes used to pass current across the membrane (Figure 10–2A). Through the use of a negative feedback amplifier, the voltage clamp is able to pass the correct amount of current across the cell membrane to rapidly step the membrane to a constant predetermined potential.

Depolarization opens voltage-gated Na^+ and K^+ channels, initiating movement of Na^+ and K^+ across the membrane. This change in membrane current ordinarily would change the membrane potential, but the voltage clamp maintains the membrane potential at the predetermined (commanded) level.

When Na^+ channels open in response to a moderate depolarizing voltage step, an inward ionic current

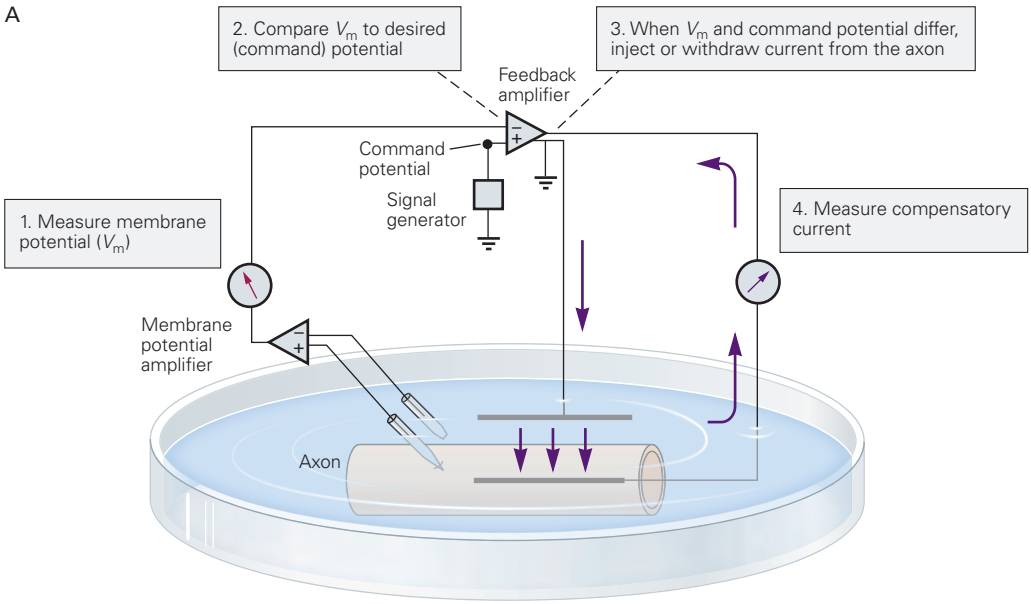

Figure 10–2 The negative feedback mechanism of the voltage clamp.

A. Membrane potential (V_m) is measured by two electrodes, one intracellular and one in the bath, connected to an amplifier. The membrane potential signal is displayed on an oscilloscope and also fed into the negative terminal of the feedback amplifier. The command potential, which is selected by the experimenter and can be of any desired amplitude and waveform, is fed into the positive terminal of the feedback amplifier. The feedback amplifier subtracts the membrane potential from the command potential and amplifies any difference between these two signals. The voltage output of the amplifier is connected to an internal current electrode, a thin wire that runs the length of the axon core. The negative feedback ensures that the voltage output of the amplifier will drive a current across the resistance of the current electrode that eliminates any difference between V_m and the command potential. To accurately measure the current–voltage relationship of the cell membrane, the membrane potential must be uniform along the entire surface of the axon. This is made possible by the highly conductive internal current electrode, which short-circuits the axoplasmic resistance, reducing axial resistance to near zero (see Chapter 9). This low-resistance pathway eliminates all variations in electrical potential along the axon core.

develops because Na^+ ions are driven through these channels by their electrochemical driving force. This Na^+ influx would normally depolarize the membrane by increasing the positive charge on the inside of the membrane and reducing the positive charge on the outside.

The voltage clamp intervenes in this process by simultaneously withdrawing positive charges from the cell and depositing them in the external solution. By generating a current that is equal and opposite to the ionic current through the membrane, the voltage-clamp circuit automatically prevents the ionic current from changing the membrane potential from the commanded value. As a result, the *net* amount of charge separated by the membrane does not change, and therefore, no significant change in V_m occurs.

The voltage clamp is a negative feedback system, a type of system in which the value of the output of the system (V_m in this case) is fed back as the input to the system and compared to a reference value (the command signal). Any difference between the command signal and the output signal activates a "controller" (the feedback amplifier in this case) that automatically reduces the difference. Thus, the actual membrane potential automatically and precisely follows the command potential.

For example, assume that an inward Na^+ current through the voltage-gated Na^+ channels ordinarily causes the membrane potential to become more positive than the command potential. The input to the feedback amplifier is equal to ($V_{command} - V_m$). The amplifier generates an output voltage equal to this error signal multiplied by the gain of the amplifier. Thus, both the input and the resulting output voltage at the feedback amplifier will be negative.

This negative output voltage will make the internal current electrode negative, withdrawing net positive charge from the cell through the voltage-clamp circuit. As the current flows around the circuit, an equal amount of net positive charge will be deposited into the external solution through the other current electrode.

Today, most voltage-clamp experiments use a patch-clamp amplifier. The patch-clamp technique uses a feedback amplifier to control the voltage in a saline-filled micropipette and measures the current flowing through a patch of membrane to which the pipette is sealed. This allows the functional properties of single ion channels to be analyzed (see Box 8–1 and Figure 10–9).

If the pipette is sealed onto a cell and the patch under the membrane is ruptured by a pulse of suction, the result is a "whole-cell patch clamp" recording in which the intracellular voltage of the cell is controlled by the patch-clamp amplifier and the current flowing through the entire cell membrane is measured (Figure 10–2B). Whole-cell patch clamp recording allows voltage-clamp measurements in small cell bodies of neurons and is widely used to study the electrophysiological properties of neurons in cell culture, in brain slice preparations, and, recently, in vivo.

B

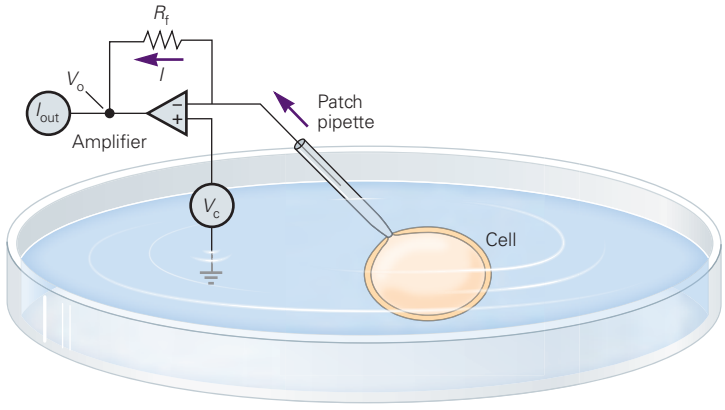

B. Voltage clamp of a neuronal cell body using the whole-cell mode of a patch-clamp amplifier. The patch pipette is sealed onto the cell and the membrane under the pipette is ruptured, providing electrical continuity between the inside of the cell and the pipette. An electrode in the pipette controls V_m, with an amplifier providing current (I) through a feedback resistor (R_f) to clamp the electrode (and therefore the pipette solution and the inside of the cell) to the command voltage (V_c), which is applied to the other amplifier input. The voltage on the output of the amplifier (V_o) is proportional to current flowing through the electrode and through the membrane.

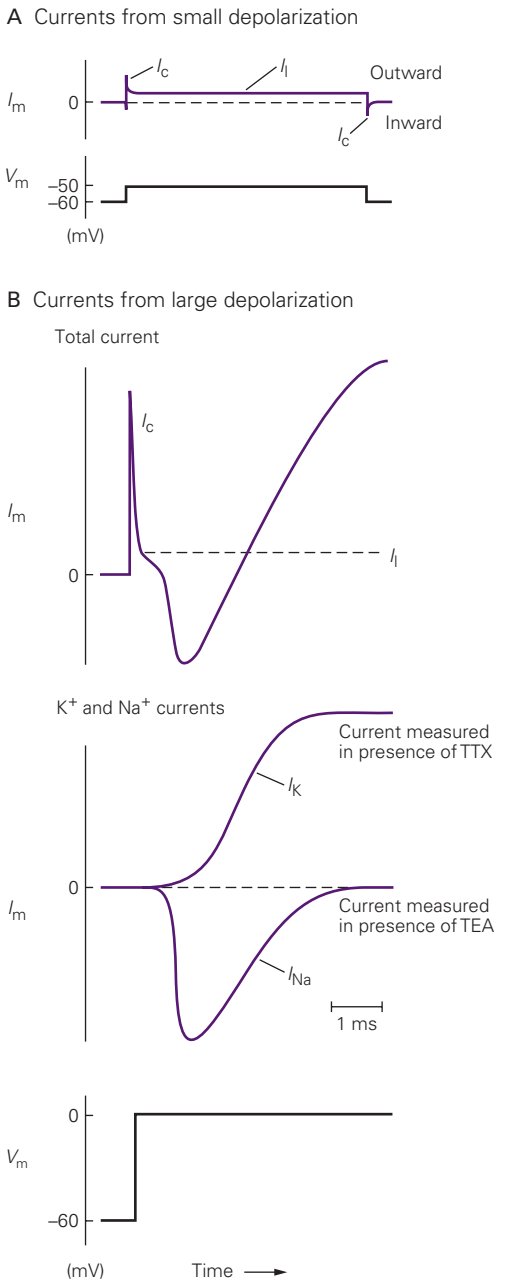

Figure 10–3 A voltage-clamp experiment demonstrates the sequential activation of voltage-gated sodium and potassium channels.

A. A small depolarization (10 mV) elicits capacitive and leakage currents (I_c and I_l, respectively), the components of the total membrane current (I_m).

B. A larger depolarization (60 mV) results in larger capacitive and leakage currents, plus a time-dependent inward ionic current followed by a time-dependent outward ionic current.

Top: Total (net) current in response to the depolarization. *Middle*: Individual Na^+ and K^+ currents. Depolarizing the cell in the presence of tetrodotoxin (**TTX**), which blocks the Na^+ current, or in the presence of tetraethylammonium (**TEA**), which blocks the K^+ current, reveals the pure K^+ and Na^+ currents (I_K and I_{Na}, respectively) after subtracting I_c and I_l. *Bottom*: Voltage step.

Similarly, I_K can be measured when the Na^+ channels are blocked by tetrodotoxin (Figure 10–3B).

By stepping the membrane through a wide range of potentials, Hodgkin and Huxley were able to measure the Na^+ and K^+ currents over the entire voltage extent of the action potential (Figure 10–4). They found that the Na^+ and K^+ currents vary as a graded function of the membrane potential. As the membrane voltage is made more positive, the outward K^+ current becomes larger. The inward Na^+ current also becomes larger with increases in depolarization, up to a certain extent. However, as the voltage becomes more and more positive, the Na^+ current eventually declines in amplitude. When the membrane potential is +55 mV, the Na^+ current is zero. Positive to +55 mV, the Na^+ current reverses direction and becomes outward.

Hodgkin and Huxley explained this behavior by a simple model in which the size of the Na^+ and K^+ currents is determined by two factors. The first is the magnitude of the Na^+ or K^+ conductance, g_{Na} or g_K, which reflects the number of Na^+ or K^+ channels open at any instant (Chapter 9). The second factor is the electrochemical driving force on Na^+ ions ($V_m - E_{Na}$) or K^+ ions ($V_m - E_K$). The model is thus expressed as:

$$I_{Na} = g_{Na} \times (V_m - E_{Na})$$

$$I_K = g_K \times (V_m - E_K).$$

According to this model, the amplitudes of I_{Na} and I_K change as the voltage is made more positive because there is an increase in g_{Na} and g_K. The conductances increase because the opening of the Na^+ and K^+ channels is voltage-dependent. The currents also change in response to changes in the electrochemical driving forces.

Both I_{Na} and I_K initially increase in amplitude as the membrane is made more positive because g_{Na} and g_K increase steeply with voltage. However, as the membrane potential approaches E_{Na} (+55 mV), I_{Na} declines because of the decrease in inward driving force, even though g_{Na} is large. That is, the positive membrane voltage now opposes the influx of Na^+ down its chemical concentration gradient. At +55 mV the chemical and electrical driving forces are in balance so there is no net I_{Na}, even though g_{Na} is quite large. As the membrane is made positive to E_{Na}, the driving force on Na^+ becomes positive. That is, the electrical driving force pushing Na^+ out is now greater than the chemical driving force pulling Na^+ in, so I_{Na} becomes outward. The behavior of I_K is simpler; E_K is quite negative (–75 mV), so in addition to an increase in g_K, the outward driving force on K^+ also becomes larger as the membrane

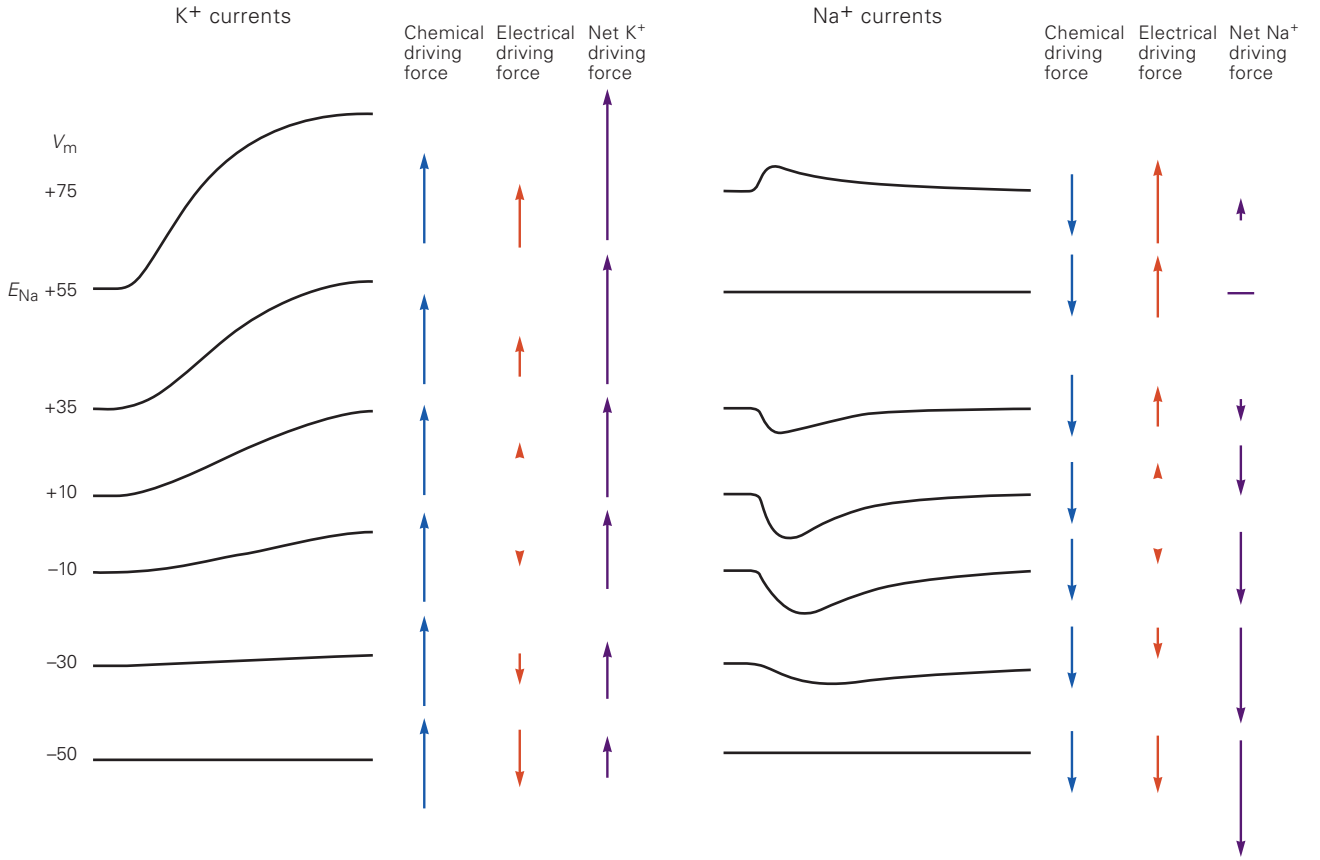

Figure 10–4 The magnitude and polarity of the sodium and potassium membrane currents vary with the amplitude of membrane depolarization. *Left*: With progressive depolarization, the voltage-clamped membrane K^+ current increases monotonically, because both g_K and $(V_m - E_K)$, the driving force for K^+, increase with increasing depolarization. The voltage during the depolarization is indicated at left. The direction and magnitude of the chemical (E_K) and electrical driving force on K^+, as well as the net driving force, are given by arrows at the right of each trace. (**Up arrows** = outward force; **down arrows** = inward force.) *Right*: At first, the Na^+ current becomes increasingly inward with greater depolarization due to the increase in g_{Na}. However, as the membrane potential approaches E_{Na} (+55 mV), the magnitude of the inward Na^+ current begins to decrease due to the decrease in inward driving force $(V_m - E_{Na})$. Eventually, I_{Na} goes to zero when the membrane potential reaches E_{Na}. At depolarizations positive to E_{Na}, the sign of $(V_m - E_{Na})$ reverses and I_{Na} becomes outward.

is made more positive, thereby increasing the outward K^+ current.

Voltage-Gated Sodium and Potassium Conductances Are Calculated From Their Currents

From the two preceding equations, Hodgkin and Huxley were able to calculate g_{Na} and g_K by dividing measured Na^+ and K^+ currents by the known Na^+ and K^+ electrochemical driving forces. Their results provided direct insight into how membrane voltage controls channel opening because the values of g_{Na} and g_K reflect the number of open Na^+ and K^+ channels (Box 10–2).

Measurements of g_{Na} and g_K at various levels of membrane potential reveal two functional similarities and two differences between the Na^+ and K^+ channels. Both types of channels open in response to depolarization. Also, as the size of the depolarization increases, the extent and rate of opening increase for both types of channels. The Na^+ and K^+ channels differ, however, in the rate at which they open and in their responses to prolonged depolarization. At all levels of depolarization, the Na^+ channels open more rapidly than K^+ channels (Figure 10–6). When the depolarization is maintained for some time, the Na^+ channels begin to close, leading to a decrease of inward current. The process by which Na^+ channels close during a prolonged depolarization is termed *inactivation*.

Thus, depolarization causes Na^+ channels to switch between three different states—resting, activated, or inactivated—which represent three different conformations of the Na^+ channel protein (see Figure 8–6).

Box 10–2 Calculation of Membrane Conductances From Voltage-Clamp Data

Membrane conductances can be calculated from voltage-clamp currents using equations derived from an equivalent circuit (Figure 10–5) that includes the membrane capacitance (C_m); the leakage conductance (g_l), representing the conductance of all of the resting (nongated) K^+, Na^+, and Cl^- channels (Chapter 9); and g_{Na} and g_K, the conductances of the voltage-gated Na^+ and K^+ channels.

In the equivalent circuit, the ionic battery of the leakage channels, E_l, is equal to the resting membrane potential, and g_{Na} and g_K are in series with their appropriate ionic batteries.

The current through each class of voltage-gated channel can be calculated from a modified version of Ohm's law that takes into account the electrical driving force (V_m) and chemical driving forces (E_{Na} or E_K) on Na^+ and K^+ (Chapter 9):

$$I_K = g_K \times (V_m - E_K)$$
$$I_{Na} = g_{Na} \times (V_m - E_{Na}).$$

Rearranging and solving for g gives two equations that can be used to compute the conductances of the active Na^+ and K^+ channel populations:

$$g_K = \frac{I_K}{(V_m - E_K)}$$

$$g_{Na} = \frac{I_{Na}}{(V_m - E_{Na})}.$$

In these equations, the independent variable V_m is set by the experimenter. The dependent variables I_K and I_{Na} can be calculated from the records of voltage-clamp experiments (see Figure 10–4). The parameters E_K and E_{Na} can be determined empirically by finding the values of V_m at which I_K and I_{Na} reverse their polarities, that is, their *reversal potentials*.

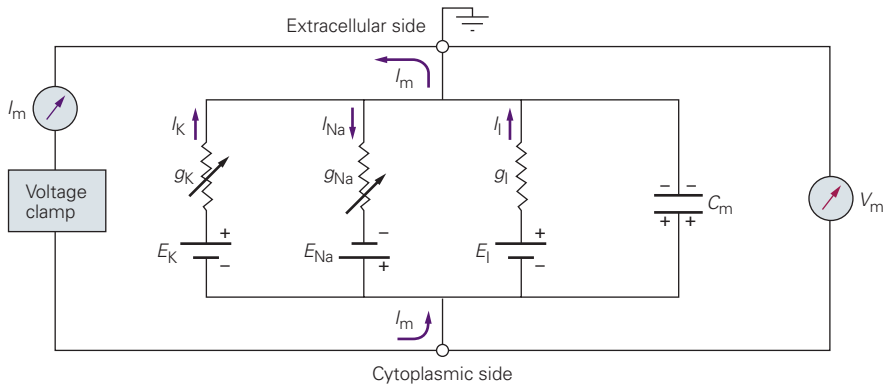

Figure 10–5 Equivalent circuit of a voltage-clamped neuron. The voltage-gated conductance pathways (g_K and g_{Na}) are represented by the symbol for a variable conductance—a conductor (resistor) with an arrow through it. The conductance is variable because of its dependence on time and voltage. These conductances are in series with batteries representing the chemical gradients for Na^+ and K^+. In addition, there are parallel pathways for leakage current (g_l and E_l) and capacitive current (C_m). Arrows indicate current flow during a depolarizing step that has activated g_K and g_{Na}.

In contrast, squid axon K^+ channels do not inactivate; they remain open as long as the membrane is depolarized, at least for voltage-clamp depolarizations lasting up to tens of milliseconds (Figure 10–6).

In the inactivated state, the Na^+ channel cannot be opened by further membrane depolarization. The inactivation can be reversed only by repolarizing the membrane to its negative resting potential, whereupon the channel switches to the resting state. This switch takes some time.

These variable, time-dependent effects of depolarization on g_{Na} are determined by the kinetics of two gating mechanisms in Na^+ channels. Each Na^+ channel has an *activation gate* that is closed while the membrane is at the resting potential and opened by depolarization. An *inactivation gate* is open at the resting potential

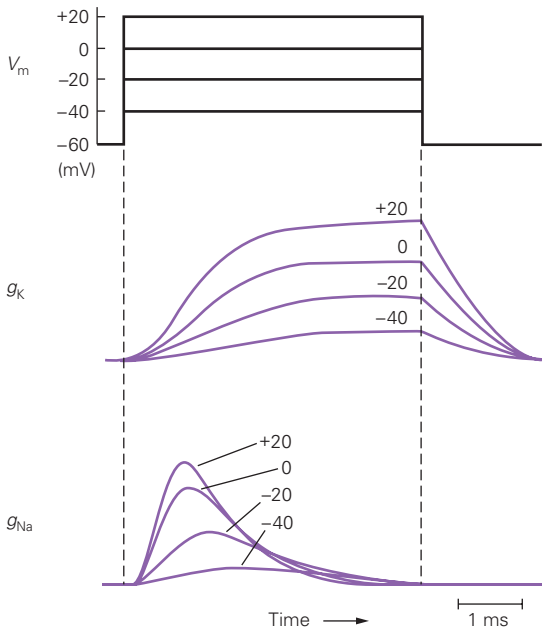

Figure 10–6 The responses of potassium and sodium ion channels to prolonged depolarization. Increasing depolarizations elicit graded increases in K^+ and Na^+ conductance (g_{Na} and g_K), which reflect the proportional opening of thousands of voltage-gated K^+ and Na^+ channels. The Na^+ channels open more rapidly than the K^+ channels. During a maintained depolarization, the Na^+ channels close after opening because of the closure of an inactivation gate. The K^+ channels remain open because they lack a fast inactivation process. At very positive V_m, the K^+ and Na^+ conductances approach a maximal value because the depolarization is sufficient to open nearly all available channels.

and closes after the channel opens in response to depolarization. The channel conducts Na^+ only for the brief period during depolarization when *both* gates are open.

The Action Potential Can Be Reconstructed From the Properties of Sodium and Potassium Channels

Hodgkin and Huxley were able to fit their measurements of membrane conductance to a set of empirical equations that completely describe the Na^+ and K^+ conductances as a function of membrane potential and time. Using these equations and measured values for the passive properties of the axon, they computed the shape and conduction velocity of the action potential. Remarkably, these equations also provided insights into the biophysical bases for voltage-gating that were confirmed over 50 years later when the structure of certain voltage-gated channels was elucidated through X-ray crystallography.

The calculated waveform of the action potential matched the waveform recorded in the unclamped axon almost perfectly. This close agreement indicates that the mathematical model developed by Hodgkin and Huxley accurately describes the properties of the channels that are responsible for generating and propagating the action potential. More than a half-century later, the Hodgkin-Huxley model stands as the most successful quantitative model in neural science if not in all of biology.

According to the model, an action potential involves the following sequence of events. Depolarization of the membrane causes Na^+ channels to open rapidly (an increase in g_{Na}), resulting in an inward Na^+ current. This current, by discharging the membrane capacitance, causes further depolarization, thereby opening more Na^+ channels, resulting in a further increase in inward current. This regenerative process drives the membrane potential toward E_{Na}, causing the rising phase of the action potential. The depolarization limits the duration of the action potential in two ways: (1) It gradually inactivates the voltage-gated Na^+ channels, thus reducing g_{Na}, and (2) it opens, with some delay, the voltage-gated K^+ channels, thereby increasing g_K. Consequently, the inward Na^+ current is followed by an outward K^+ current that tends to repolarize the membrane (Figure 10–7).

Two features of the action potential predicted by the Hodgkin-Huxley model are its threshold and all-or-none behavior. A fraction of a millivolt can be the difference between a subthreshold stimulus and a stimulus that generates a full-sized action potential.

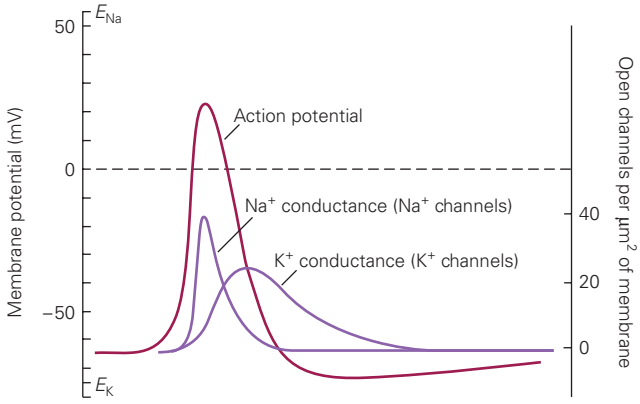

Figure 10–7 The sequential opening of voltage-gated Na^+ and K^+ channels generates the action potential. One of Hodgkin and Huxley's great achievements was to dissect the change in conductance during an action potential into separate components attributable to the opening of Na^+ and K^+ channels. The shape of the action potential and the underlying conductance changes can be calculated from the properties of the voltage-gated Na^+ and K^+ channels. (Adapted, with permission, from Hille 2001.)

This all-or-none phenomenon may seem surprising when one considers that Na^+ conductance increases in a strictly *graded* manner as depolarization increases (Figure 10–6). Each increment of depolarization increases the number of voltage-gated Na^+ channels that open, thereby gradually increasing Na^+ current. How then can there be a discrete threshold for generating an action potential?

Although a small subthreshold depolarization increases the inward I_{Na}, it also increases two *outward* currents, I_K and I_l, by increasing the electrochemical driving forces acting on K^+ and Cl^-. In addition, the depolarization augments K^+ conductance by gradually opening more voltage-gated K^+ channels (Figure 10–6). As the outward K^+ and leakage currents increase with depolarization, they tend to repolarize the membrane and thereby resist the depolarizing action of the Na^+ influx. However, because of the high voltage sensitivity and more rapid kinetics of activation of the Na^+ channels, the depolarization eventually reaches the point at which the increase in inward I_{Na} exceeds the increase in outward I_K and I_l. At this point, there is a net inward ionic current. This produces a further depolarization, opening even more Na^+ channels, so that the depolarization becomes regenerative, rapidly driving the membrane potential V_m all the way to the peak of the action potential. The specific value of V_m at which the net ionic current ($I_{Na} + I_K + I_l$) changes from outward to inward, depositing a positive charge on the inside of the membrane capacitance, is the threshold.

Early experiments with extracellular stimulation of nerve fibers showed that, for a short time after an action potential (typically a few milliseconds), it is impossible to generate another action potential. This *absolute refractory period* is followed by a period when it is possible to stimulate another action potential, but only with a stimulus larger than what was needed for the first. This *relative refractory period* typically lasts 5 to 10 ms.

The Hodgkin-Huxley analysis provided a mechanistic explanation of two factors underlying the refractory period. In the immediate aftermath of an action potential, it is impossible to evoke another one, even with a very strong stimulus, because the Na^+ channels remain inactivated. After repolarization, Na^+ channels recover from inactivation and reenter the resting state, a transition that takes several milliseconds (Figure 10–8). The relative refractory period corresponds to partial recovery from inactivation.

The relative refractory period is also influenced by a residual increase in K^+ conductance that follows the action potential. It takes several milliseconds for all of the K^+ channels that open during the action potential to return to their closed state. During this period, when the K^+ conductance remains somewhat elevated, V_m is slightly more negative than its normal resting value, as V_m approaches E_K (Figure 10–7, Equation 9–4). This *afterhyperpolarization* and residual increase in g_K contribute to the increase in depolarizing current required to drive V_m to threshold during the relative refractory period.

The Mechanisms of Voltage Gating Have Been Inferred From Electrophysiological Measurements

The empirical equations derived by Hodgkin and Huxley are quite successful in describing how the flow of ions through the Na^+ and K^+ channels generates the action potential. However, these equations describe the process of excitation in terms of changes in membrane conductance and current. They tell little about the mechanisms that activate or inactivate channels in response to changes in membrane potential or about channel selectivity for specific ions.

We now know that the voltage-dependent conductances described by Hodgkin and Huxley are generated by ion channels that open in a voltage- and time-dependent manner. Patch-clamp recordings from a variety of nerve and muscle cells have provided detailed information about the properties of the voltage-dependent Na^+ channels that generate the action potential. Recordings of single voltage-gated Na^+ channels show that, in response to a depolarizing step, each channel opens in an all-or-none fashion, conducting brief current pulses of constant amplitude but variable duration.

Each channel opening is associated with a current of about 1 pA (at voltages near −30 mV), and the open state is rapidly terminated by inactivation. Each channel behaves stochastically, opening after a variable time and staying open for a variable time before inactivating. If the openings of all the channels in a cell membrane in response to a step depolarization are summed or the openings of a single channel to multiple trials of the same depolarization are summed (Figure 10–9), the result is an averaged current with the same time course as the macroscopic Na^+ current recorded in voltage-clamp experiments (see Figure 10–4B).

To explain how changes in membrane potential lead to an increase in Na^+ conductance, Hodgkin and Huxley deduced from basic thermodynamic considerations that a conformational change in some membrane component that regulates the conductance must move charged particles through the membrane electric field. As a result, membrane depolarization would exert a force causing the charged particles to move, thereby opening the channel. For a channel with positively charged mobile particles, the depolarization

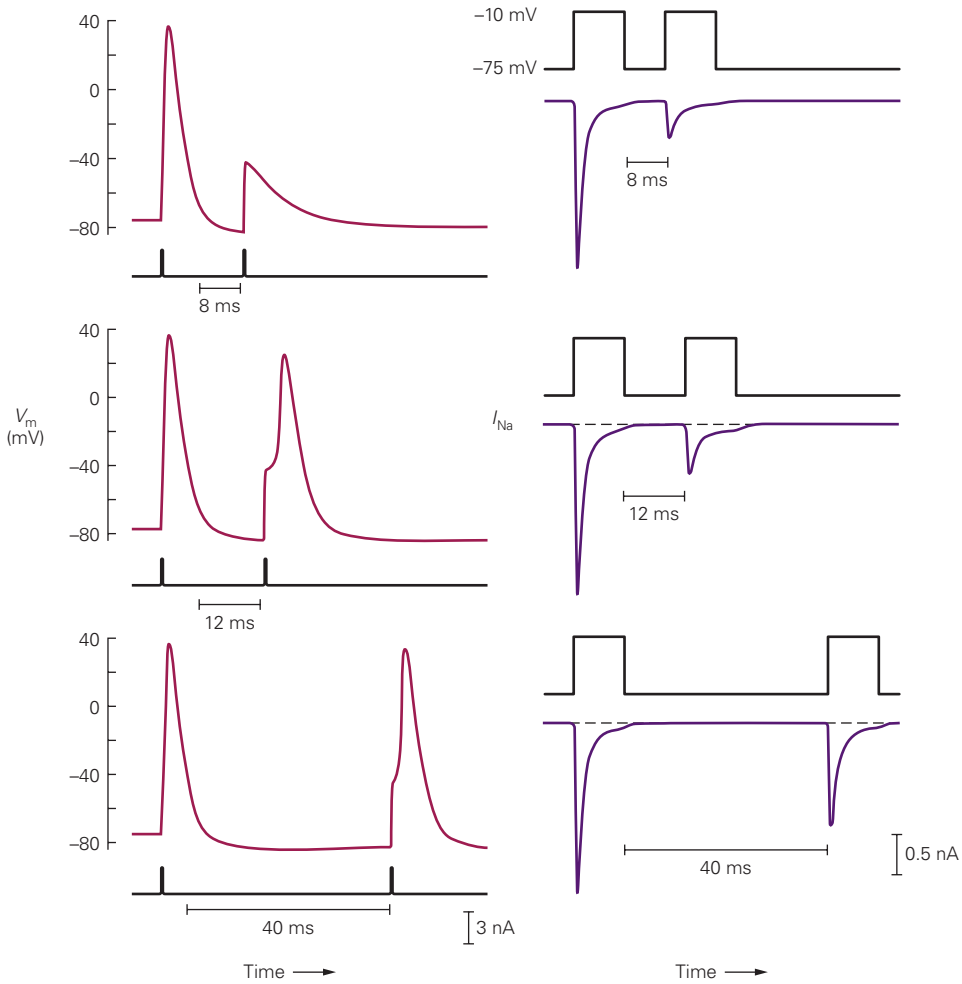

Figure 10–8 The refractory period is associated with recovery of the sodium channels from inactivation. *Left:* The voltage response of a mouse dorsal root ganglion neuron to two current pulses (**bottom traces**). The first triggers an action potential; the second triggers a variable voltage response depending on the delay between the current pulses. *Right*: Sodium currents recorded under voltage clamp in the same cell evoked by two depolarizing voltage pulses separated by the intervals indicated in the records on the left. In this neuron, the refractory period corresponds to the time needed for recovery of about 20% of the sodium channels. (Data from Pin Liu and Bruce Bean.)

would produce an outward movement of charge that should precede the opening of the channel. Upon membrane repolarization the charge would move in the opposite direction, closing the channel. Because the mobile charge movement is confined to the membrane, it is a type of capacitive current. This *gating charge* movement was predicted to generate a small outward current (or *gating current*), which was later confirmed when the membrane current was examined using very sensitive techniques. Blocking the inward ionic current with tetrodotoxin revealed a small outward capacitive current during the time the channels were activating (Figure 10–10A). In later experiments, this gating current (I_g) was progressively reduced by mutating the positively charged lysine and arginine residues in the four S4 transmembrane regions of the Na^+ channel to neutral residues. Thus, the gating current is produced by outward movement of the positively charged residues in the S4 regions through the membrane electric field (Chapter 8). Voltage-gated K^+ and Ca^{2+} channels also generate gating currents during channel opening.

Recent experiments have shown that the four S4 transmembrane regions of the Na^+ channel move with different time courses. Movement of the S4 regions of the first three domains (DI, DII, DIII) occurs first and is associated with channel activation. Movement of the S4 region of domain IV occurs more slowly and is associated with inactivation. Inactivation of Na^+ channels likely involves a series of conformational changes whereby outward movement of the S4 region of domain IV enables binding of the cytoplasmic linker connecting domains III and IV to a binding site near the intracellular ends of the pore-forming S6 helices, stabilizing a nonconducting inactivated state of the pore (Figure 10–10B,C).

Control of channel activation by gating charges results in a characteristic feature of voltage-dependent channels: The conductance change occurs over a relatively narrow range of V_m with a saturating value for larger depolarizations. When peak I_{Na} is measured over a wide range of V_m and then converted to a conductance, as illustrated in Figure 10–6, the voltage dependence of peak conductance has a sigmoid shape (Figure 10–11). Activation of voltage-dependent

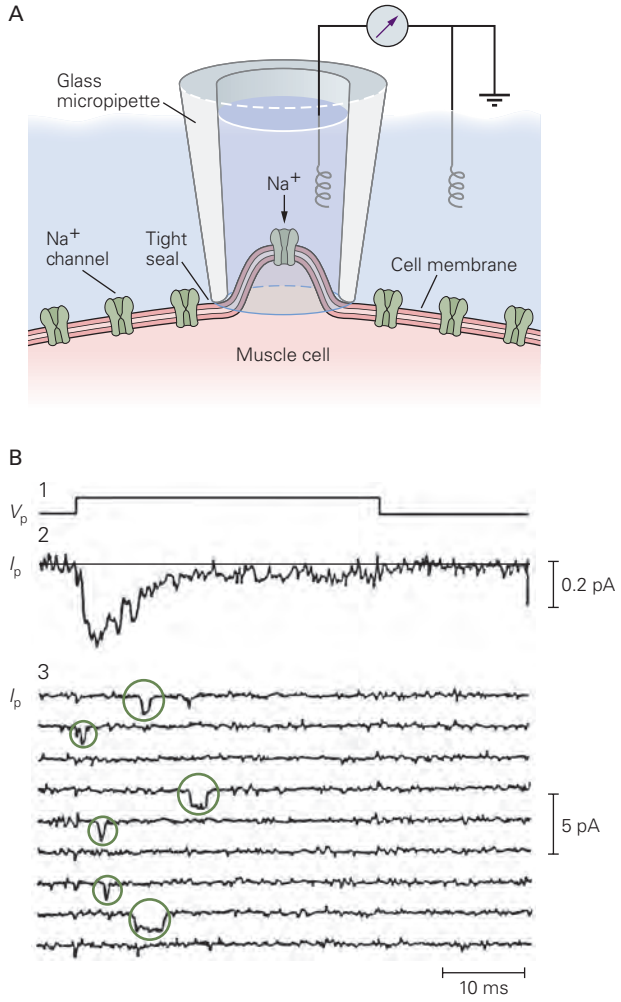

Figure 10–9 Individual voltage-gated ion channels open in an all-or-none fashion.

A. A small patch of membrane containing a single voltage-gated Na^+ channel is electrically isolated from the rest of the cell by the patch electrode. The Na^+ current that enters the cell through the channel is recorded by a monitor connected to the patch electrode (see Box 8–1).

B. Recordings of single Na^+ channels in cultured muscle cells of rats. (**1**) Time course of a 10 mV depolarizing voltage step applied across the isolated patch of membrane (V_p = potential difference across the patch). (**2**) The sum of the inward current through the Na^+ channel in the patch during 300 trials (I_p = current through the patch). The trace was obtained by blocking the K^+ channels with tetraethylammonium and subtracting the leakage and capacitive currents electronically. (**3**) Nine individual trials from the set of 300, showing six openings of the channel (**circled**). These data demonstrate that the total Na^+ current recorded in a conventional voltage-clamp record (see Figure 10–3B) can be accounted for by the statistical nature of the all-or-none opening and closing of a large number of Na^+ channels. (Reproduced, with permission, from Sigworth and Neher 1980.)

sodium conductance begins at about –50 mV (near the threshold for action potential firing), reaches a midpoint near –25 mV, and saturates at about 0 mV. The saturation of conductance occurs when the S4 regions of the entire population of Na^+ channels have moved to the activated conformation.

The relationship of conductance to voltage can be approximately fit by the Boltzmann function, an equation from statistical mechanics that describes the distribution of a population of molecules that can exist in distinct states with different potential energies. In the case of Na^+ channels, the channels move between closed and open states that differ in potential energy because of the work done when the S4 region gating charges move through the electric field of the membrane (Figure 10–10C). The two parameters of the fitted Boltzmann curve, the midpoint and the slope factor, provide a convenient characterization of the voltage dependence with which channels open. The curve is steeper if more gating charge moves as channels convert between closed and open states. The voltage dependence of activation and inactivation of many other types of voltage-dependent channels can also be approximated by Boltzmann curves with characteristic midpoints and slopes.

Voltage-Gated Sodium Channels Select for Sodium on the Basis of Size, Charge, and Energy of Hydration of the Ion

In Chapter 8, we saw how the structure of the K^+ channel pore could explain how such channels are able to select for K^+ over Na^+ ions. The narrow diameter of the K^+ channel selectivity filter (around 0.3 nm) requires that a K^+ or Na^+ ion must shed nearly all of its waters of hydration to enter the channel, an energetically unfavorable event.

The energetic cost of dehydration of a K^+ ion is well compensated by its close interaction with a cage of electronegative carbonyl oxygen atoms contributed by the peptide backbones of the four subunits of the K^+ channel selectivity filter. Because of its smaller radius, a Na^+ ion has a higher local electric field than does a K^+ ion and therefore interacts more strongly with its waters of hydration than does K^+. On the other hand, the small diameter of the Na^+ ion precludes close interaction with the cage of carbonyl oxygen atoms in the selectivity filter; the resultant high energetic cost of dehydrating the Na^+ ion excludes it from entering the channel.

How then does the selectivity filter of the Na^+ channel select for Na^+ over K^+ ions? Bertil Hille deduced a model for the Na^+ channel's selectivity mechanism from measurements of the channel's relative

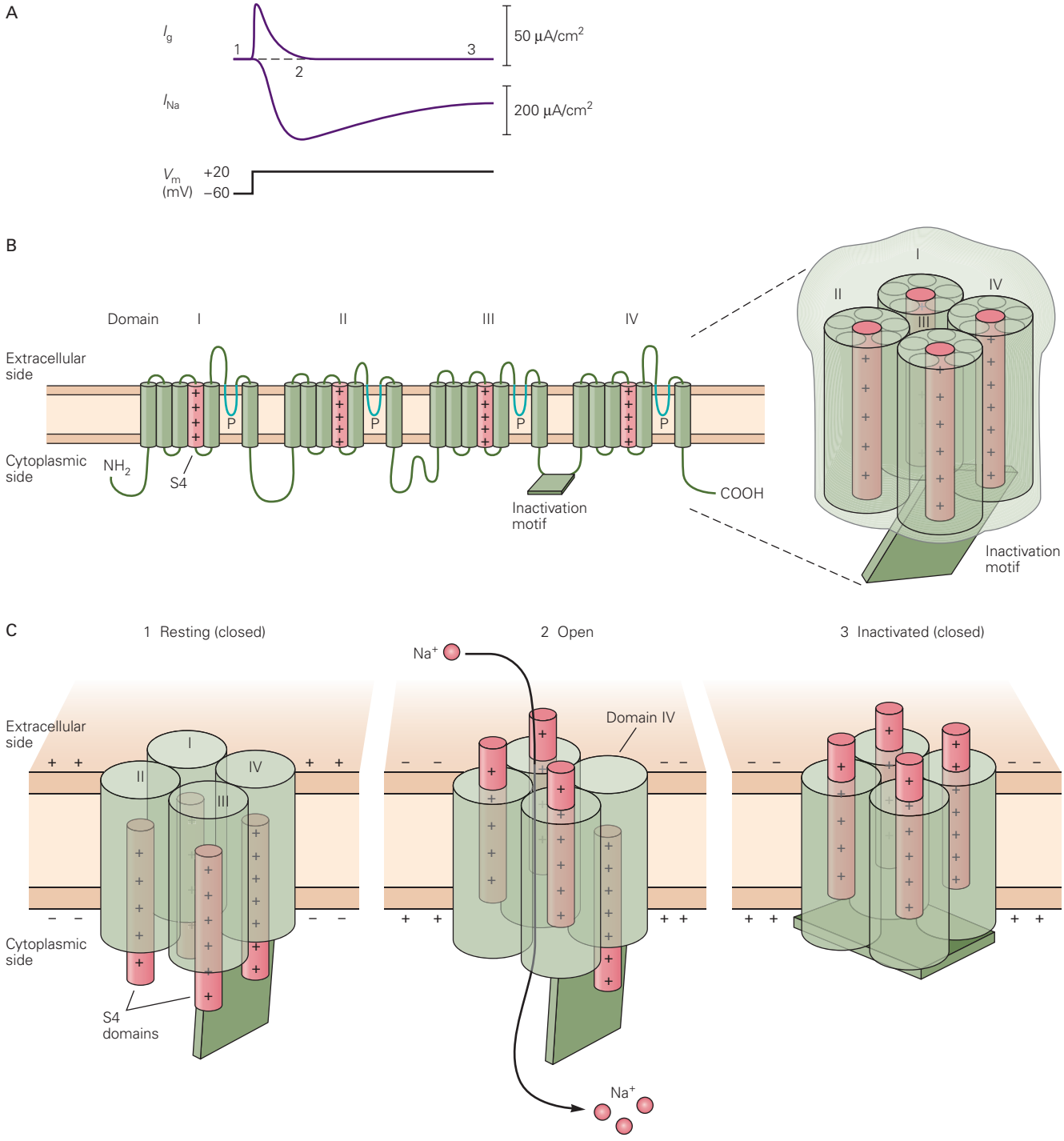

Figure 10–10 The opening and closing of the sodium channel are associated with a redistribution of charges.

A. When the membrane is depolarized, the Na^+ current (I_{Na}) is activated and then inactivated. The activation of the Na^+ current is preceded by a brief capacitive *gating current* (I_g), reflecting the outward movement of positive charges within the walls of the Na^+ channels. To detect this small gating current, it is necessary to block the flow of ionic current through the Na^+ and K^+ channels and subtract the capacitive current that depolarizes the lipid bilayer. (Adapted, with permission, from Armstrong and Gilly 1979.)

B. Secondary structure of the α-subunit of mammalian sodium channels showing location of gating charges. The sodium channel α-subunit is a single polypeptide consisting of four repeated domains, each containing six transmembrane regions. The fourth transmembrane region (S4 region) of each domain contains positively charged arginine and lysine residues that form the gating charge of the channels. (Adapted, with permission, from Ahern et al. 2016. Permission conveyed through Copyright Clearance Center, Inc.)

C. Diagrams depict the redistribution of gating charge and positions of the activation and inactivation gates when the channel is at rest, open, and inactivated. The **red** cylinders represent the S4 regions containing the positive gating charges. Depolarization of the cell membrane from the resting state causes the gating charge to move outward. Outward movement of the S4 regions of domains I, II, and III is associated with activation (**1–2**), whereas slower movement of the S4 region of domain IV is associated with inactivation (**2–3**). The movement of the S4 region of domain IV allows an intracellular loop between domains III and IV (depicted as a **green** rectangle) to bind to a docking site near the S6 helices at the inside of the pore, allosterically stabilizing an inactivated closed state. (Adapted from Ahern et al. 2016.)

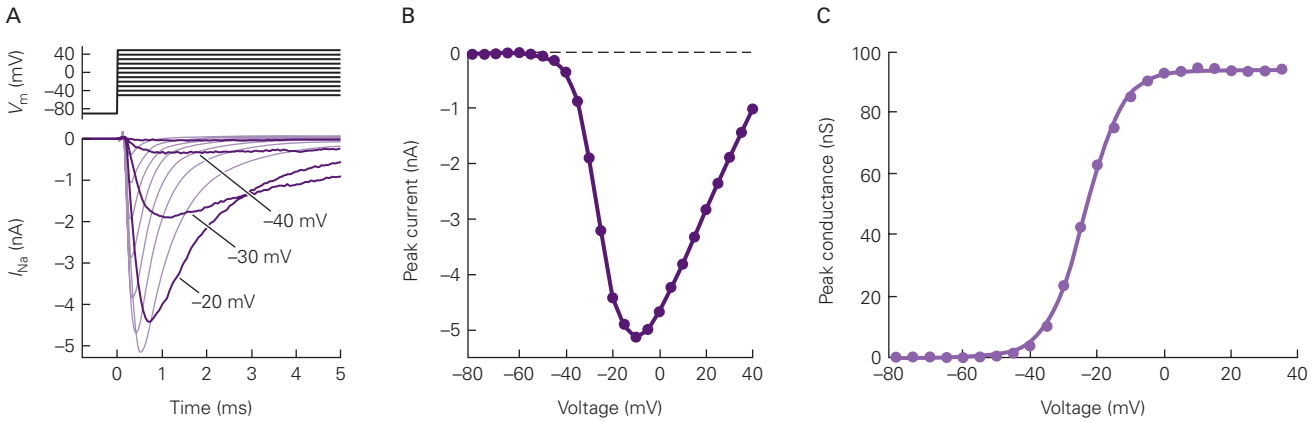

Figure 10–11 The voltage dependence of sodium channel activation is determined by the number of gating charges.

A. Whole-cell patch-clamp recordings of voltage-gated Na^+ currents were made in a dissociated hippocampal pyramidal neuron. Sodium channel currents were isolated by blocking currents through K^+ and Ca^{2+} channels and then subtracting the capacitive and leakage currents that remained after blocking Na^+ currents.

B. Current–voltage curve for peak Na^+ current.

C. Peak Na^+ conductance versus membrane potential. Increases in peak g_{Na} in response to a series of depolarizing voltage steps were calculated from peak current, as in Box 10–2. The experimental data points are fit by the Boltzmann relation with the form $g_{Na}/g_{Na(max)} = 1/[1 + \exp - (V_m - V_h)/k]$, where $V_h = -24$ mV is the midpoint of the activation curve and $k = 5.5$ is the "slope factor," with units of mV, and $g_{Na(max)}$ is the maximal sodium conductance at positive voltages. The greater the number of gating charges that must move to open the channel, the smaller is the slope factor. The voltage dependence of most voltage-gated channels can be fit by similar Boltzmann curves. (Data from Indira M. Raman.)

permeability to a range of organic and inorganic cations. As we learned in Chapter 8, the channel behaves as if it contains a selectivity filter, or recognition site, which selects partly on the basis of size, thus acting as a molecular sieve (see Figure 8–1). Based on the size and hydrogen-bonding characteristics of the largest organic cation that could readily permeate the channel, Hille deduced that the selectivity filter has rectangular dimensions of 0.3 × 0.5 nm. This cross section is just large enough to accommodate one Na^+ ion contacting one water molecule (see Figure 8–1). Because a K^+ ion in contact with one water molecule is larger than the size of the selectivity filter, it cannot readily permeate.

According to Hille's model, negatively charged carboxylic acid groups of glutamate or aspartate residues at the outer mouth of the pore perform the first step in the selection process by attracting cations and repelling anions. The negative carboxylic acid groups, as well as other oxygen atoms that line the pore, can substitute for waters of hydration, but the degree of effectiveness of this substitution varies among ion species. The negative charge of a carboxylic acid is able to form a stronger coulombic interaction with the smaller Na^+ ion than with the larger K^+ ion. Because the Na^+ channel is large enough to accommodate a cation in contact with several water molecules, the energetic cost of dehydration is not as great as it is in a K^+ channel. As a result of these two features, the Na^+ channel is able to select for Na^+ over K^+, but not perfectly, with $P_{Na}/P_K \sim 12/1$. Structures of bacterial and vertebrate voltage-gated Na^+ channels obtained by X-ray crystallography and cryo-electron microscopy have confirmed many of the key features of Hille's model.

Individual Neurons Have a Rich Variety of Voltage-Gated Channels That Expand Their Signaling Capabilities

The basic mechanism of electrical excitability identified by Hodgkin and Huxley in the squid giant axon is common to most excitable cells: Voltage-gated channels conduct an inward Na^+ current followed by an outward K^+ current. However, we now know that the squid axon is unusually simple in expressing only two types of voltage-gated ion channels. In contrast, the genomes of both vertebrates and invertebrates include large families of voltage-gated Na^+, K^+, and Ca^{2+} channels encoded by sub-families of related genes that are widely expressed in different kinds of nerve and muscle cells.

A neuron in the mammalian brain typically expresses a dozen or more different types of voltage-gated ion channels. The voltage dependence and kinetic properties of various Na^+, Ca^{2+}, and K^+ channels can differ widely. Moreover, the distribution of these

channels varies between different types of neurons and even between different regions of a single neuron. The great variety of voltage-gated channels in the membranes of most neurons enables a neuron to fire action potentials with a much greater range of frequencies and patterns than is possible in the squid axon, and thus allows much more complex information-processing abilities and modulatory control than is possible with just two types of channels.

The Diversity of Voltage-Gated Channel Types Is Generated by Several Genetic Mechanisms

The conservative mechanism by which evolution proceeds—creating new structural or functional entities by duplicating, modifying, shuffling, and recombining existing gene-coding sequences—is illustrated by the diversity and modular design of the members of the extended gene superfamily that encodes the voltage-gated Na^+, K^+, and Ca^{2+} channels. This family also includes genes that encode calcium-activated K^+ channels, the hyperpolarization-activated HCN nonselective cation channels, and a voltage-independent cyclic nucleotide-gated cation channel important for phototransduction and olfaction.

The functional differences between these channels are produced by differences in amino acid sequences in their core transmembrane domains as well as by the addition of regulatory elements in cytoplasmic domains. For example, some K^+ channels have a mechanism of inactivation mediated by a tethered plug formed by the cytoplasmic N-terminus of the channel protein, which binds to the inner mouth of the channel when the activation gate opens. The C-terminal cytoplasmic end of the channel proteins is a particularly rich locus for regulatory elements, including domains that bind either Ca^{2+} or cyclic nucleotides, enabling these agents to regulate channel gating. Inward-rectifying K^+ channels, which are tetramers of subunits with only a P-region and flanking transmembrane regions, have an internal cation-binding site that produces rectification. When the cell is depolarized, cytoplasmic Mg^{2+} or positively charged polyamines (small organic molecules that are normal constituents of the cytoplasm) are electrostatically driven to this binding site from the cytoplasm, plugging the channel (Figure 10–12).

Figure 10–12 represents large families of channels within which there is considerable structural and functional diversity. Five different mechanisms contribute to diversity in voltage-gated channels.

1. Multiple genes encode related principal subunits within each class of channel. For example, in mammalian neurons and muscle, at nine different genes encode voltage-gated Na^+ channel α-subunits.
2. The four α-subunits that form a voltage-gated K^+ channel (Figure 8–11) can be encoded by different genes. After translation, the α-subunits are in some cases mixed and matched in various combinations, thus forming different subclasses of heteromeric channels.
3. A single gene product may be alternatively spliced, resulting in variations in the messenger RNA (mRNA) molecules that encode the α-subunit.
4. The mRNA that encodes an α-subunit may be edited by chemical modification of a single nucleotide, thereby changing the composition of a single amino acid in the channel subunit.
5. Principal pore-forming α-subunits of all channel types are commonly combined with different accessory subunits to form functionally different channel types.

These accessory subunits (often termed β-, γ-, or δ-subunits) may be either cytoplasmic or membrane-spanning and can produce a wide range of effects on channel function. For example, some β-subunits enhance the efficiency with which the channel protein is transported from the rough endoplasmic reticulum to the membrane, as well determining its final destination on the cell surface. Other subunits can regulate the voltage sensitivity or kinetics of channel gating. In contrast to the α-subunits, there is no known homology among the β-, γ-, and δ-subunits from the three major subfamilies of voltage-gated channels.

These various sources of channel diversity also vary widely between different areas of the nervous system, between different types of neurons, and within different subcellular compartments of a given neuron. A corollary of this regional differentiation is that mutations or epigenetic mechanisms that alter voltage-gated channel function can have very selective effects on neuronal or muscular function. The result is a large array of neurological diseases called channelopathies (Chapters 57 and 58).

Voltage-Gated Sodium Channels

The α-subunits of mammalian voltage-dependent Na^+ channels are encoded by nine genes. Three of the α-subunits encoded by these genes (Nav1.1, Nav1.2, and Nav1.6) are widely expressed in neurons in the mature mammalian brain, while four others have more restricted expression in neurons. Nav1.3 is strongly expressed early in development, with little expression in the mature brain, but can be reexpressed in injured

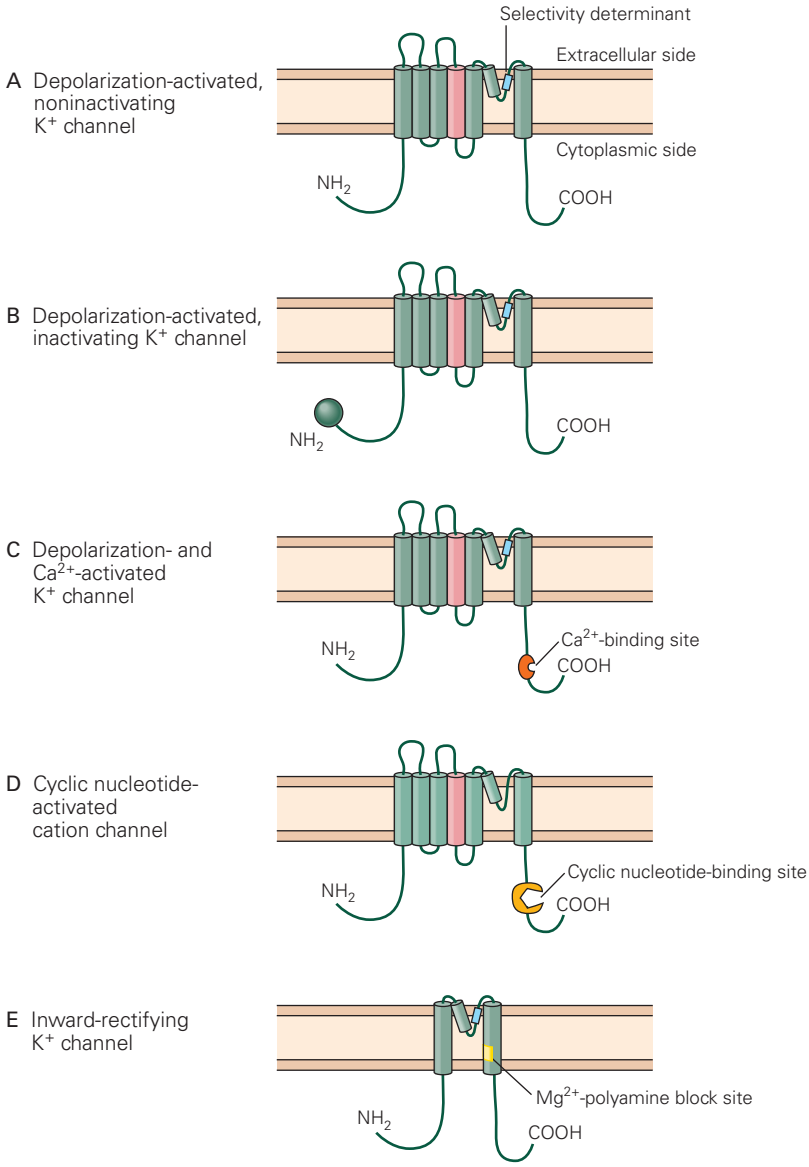

Figure 10–12 **The extended gene family of voltage-gated channels produces variants of a common molecular design.**

A. The basic transmembrane topology of an α-subunit of a voltage-gated K^+ channel. The S4 membrane-spanning α-helix is labeled in **red**.

B. Many K^+ channels that are first activated and then inactivated by prolonged depolarization have a ball-and-chain segment at their N-terminal end that inactivates the channel by plugging its inner mouth.

C. Some K^+ channels that require both depolarization and an increase in intracellular Ca^{2+} to activate have a Ca^{2+}-binding sequence attached to the C-terminal end of the channel.

D. Cation channels gated by cyclic nucleotides have a cyclic nucleotide-binding domain attached to the C-terminal end. One subclass of such channels includes the voltage-independent, cyclic nucleotide-gated channels important in the transduction of olfactory and visual sensory signals. Another subclass consists of the hyperpolarization-activated cyclic nucleotide-gated (HCN) channels important for pacemaker activity (see Figure 10–15D). The P loops in these channels lack key amino acid residues required for K^+ selectivity. As a result, these channels do not show a high degree of discrimination between Na^+ and K^+.

E. Inward-rectifying K^+ channels, which are gated by blocking particles available in the cytoplasm, are formed from a truncated version of the basic building block, with only two membrane-spanning regions and a P-region.

tissue, for example following spinal cord injury. Nav1.7 channels are confined to autonomic and sensory neurons in the peripheral nervous system. Nav1.8 and Nav1.9 channels are largely restricted to a subset of peripheral sensory neurons, with particularly prominent expression in pain-sensing primary sensory neurons (nociceptors). Nav1.1, Nav1.2, Nav1.3, Nav1.6, and Nav1.7 channels have generally similar voltage dependence and relatively fast activation and inactivation kinetics compared to Nav1.8 and Nav1.9 channels. Nav1.4 channels in skeletal muscle fibers and Nav1.5 channels in cardiac muscle conduct the voltage-gated Na^+ current that generates action potentials in these tissues.

Although Nav1.1, Nav1.2, and Nav1.6 are all widely expressed in mammalian central neurons, they are expressed in different proportions in different types of neurons. Nav1.1 channels are particularly strongly expressed in some inhibitory GABAergic interneurons, and some loss-of-function mutations in Nav1.1 channels can lead to epilepsy, as in Dravet syndrome, perhaps reflecting greater loss of excitability of inhibitory neurons relative to excitatory neurons.

Voltage-Gated Calcium Channels

Virtually all neurons contain voltage-gated Ca^{2+} channels that open in response to membrane depolarization. A strong electrochemical gradient drives Ca^{2+} into the cell, so these channels give rise to an inward current that helps depolarize the cell.

A single neuron typically expresses at least four or five different types of voltage-gated Ca^{2+} channels with different voltage dependence, kinetic properties, and subcellular localization. Calcium channels that are widely expressed in central and peripheral neurons include Cav1.2 and Cav1.3 channels (collectively known as L-type channels), Cav2.1 (P/Q-type channels), Cav2.2 (N-type channels), and Cav2.3 (R-type channels). The various Cav1 and Cav2 family channels are collectively known as *high-threshold* or *high-voltage activated* (HVA) Ca^{2+} channels because activation generally requires relatively large depolarizations.

Members of the Cav3 family, collectively known as *T-type* or *low-voltage activated* (LVA) channels, are more selectively expressed in certain neurons. They are opened by small depolarizations (as negative as −65 mV) and undergo inactivation over tens of milliseconds. At normal resting potentials, Cav3 channels are typically inactivated. Hyperpolarization of the membrane voltage (as by inhibitory synaptic input) removes resting inactivation, which enables transient activation of the LVA channels following the hyperpolarization as the membrane voltage moves back toward its resting level. This activation can produce a regenerative depolarization that triggers a burst of Na^+ action potentials, which terminates when the Cav3 channels inactivate. Such postinhibitory burst firing is common in some regions of the thalamus and can help drive synchronized burst firing in neural circuits (see Figure 44–2). Similar rebound activation of Cav3 channels following the hyperpolarizing phase of a slow pacemaker potential contributes to spontaneous rhythmic bursting in some thalamocortical neurons (see Figure 10–15).

Voltage-Gated Potassium Channels

Voltage-dependent K^+ channels comprise an especially varied group of channels that differ in their kinetics of activation, voltage-activation range, and sensitivity to various ligands. Mammalian neurons typically express members of at least five families of voltage-dependent K^+ channels: Kv1, Kv2, Kv3, Kv4, and Kv7 (Figure 10–13). Each family consists of multiple gene products, with each channel composed of four α-subunits. For example, there are eight closely-related genes encoding the members of the Kv1 gene family (Kv1.1–Kv1.8).

The subunits can be of the same type (a homomeric channel) or of different gene products from within the same Kv family (a heteromeric channel). For example, Kv1 channels can be formed by heteromeric combinations of at least five different gene products that have wide expression in central neurons, with each combination possessing different properties of kinetics and voltage dependence. The possible functional variation provided by different combinations of α-subunits in heteromeric channels is immense, although not all possible combinations actually occur.

One way of distinguishing different components of voltage-dependent K^+ currents in a neuron is by the presence or absence of inactivation. Non-inactivating K^+ current, like that described in the squid axon by Hodgkin and Huxley, is called *delayed rectifier* K^+ current. In the squid axon, delayed rectifier current flows through a single Kv1 family channel type. In most mammalian neurons, delayed rectifier current includes multiple components from Kv1, Kv2, and Kv3 family channels, each with different kinetics and voltage dependence. Kv3 channels are unusual in requiring large depolarizations to become activated and also in having very rapid kinetics of activation. As a result, Kv3 channels are not activated until the action potential is near its peak, but they activate quickly enough to help terminate the action potential.

In addition to delayed rectifier current, many neurons also have a component of inactivating K^+ current known as A-type current. In cell bodies and dendrites,

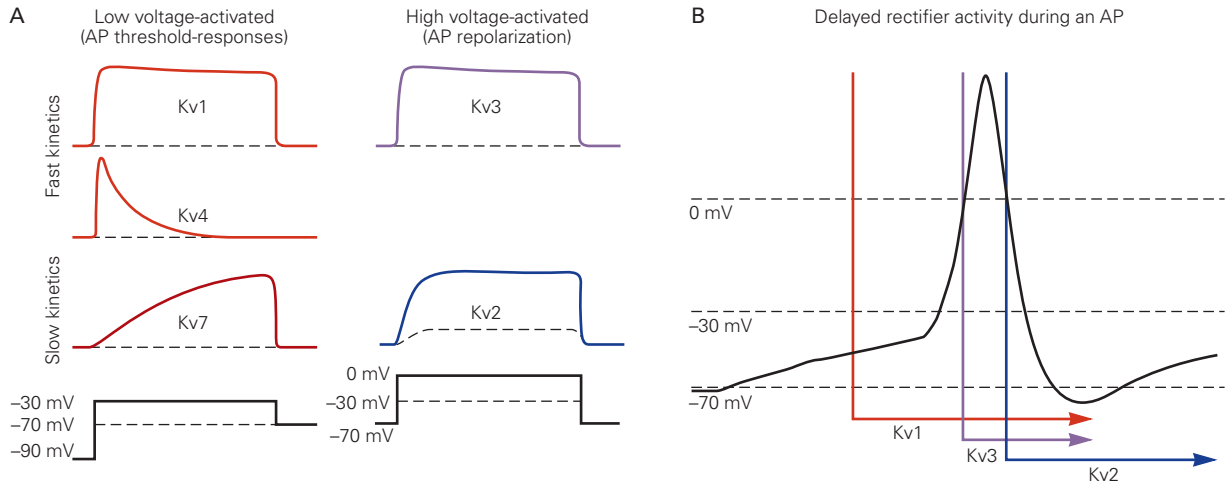

Figure 10–13 Different voltage dependence and kinetics of major classes of mammalian voltage-activated potassium channels.

A. Simplified generalization of the voltage dependence and kinetics of the major voltage-gated K^+ families. Because Kv1, Kv4, and Kv7 channels can be activated by relatively small depolarizations, they often help control action potential (AP) threshold. Kv2 and Kv3 channels require larger depolarizations to be activated. Kv1, Kv3, and Kv4 channels are activated relatively rapidly, whereas Kv7 and Kv2 channels are activated more slowly.

B. Simplified generalization of the differing activation times of the major components of delayed rectifier K^+ channels during an action potential. Kv1 channels require small depolarizations and are activated rapidly, sometimes significantly in advance of the action potential. Kv3 channels require large depolarizations and are activated late in the rising phase of the action potential and deactivated very rapidly thereafter. Kv2 channels are activated relatively slowly during the falling phase of the action potential and remain open during the afterhyperpolarization. (Adapted, with permission, from Johnston et al. 2010.)

A-type current is formed primarily by Kv4 family α-subunits, which form channels that inactivate over a range of time scales from a few milliseconds to tens of milliseconds. Kv1 channels that include Kv1.4 subunits or the auxiliary subunit Kvβ1 also mediate an inactivating component of current, which is highly expressed in some nerve terminals as well as some cell bodies.

As is the case for Na^+ channels and Cav3 family channels, A-type K^+ current not only inactivates during large depolarizations but is also subject to steady-state inactivation by small depolarizations from rest, providing a mechanism by which its amplitude can be modulated by small voltage changes around resting potential (see Figure 10–15B).

Kv7 subunits form non-inactivating channels that require only small depolarizations from rest to be activated and can even be activated significantly at the resting potential. In some neurons, Kv7 channels are downregulated by the transmitter acetylcholine acting through muscarinic G protein–coupled receptors (thus the origin of an alternative name of "M-current"). Kv7 channels typically activate relatively slowly, over tens of milliseconds, and provide little current during a single action potential but tend to suppress firing of subsequent action potentials (Chapter 14).

The KCNH gene family consists of three subfamilies of voltage-gated K^+ channels (Kv10, Kv11, and Kv12), which are also expressed in the brain. They influence resting potential, action potential threshold, and frequency and pattern of firing.

Voltage-Gated Hyperpolarization-Activated Cyclic Nucleotide-Gated Channels

Many neurons have cation channels that are slowly activated by hyperpolarization. This sensitivity to hyperpolarization is enhanced when intracellular cyclic nucleotides bind to the channel. Because these hyperpolarization-activated cyclic nucleotide-gated (HCN) channels have only two of the four negative binding sites found in the selectivity filter of K^+ channels, they are permeable to both K^+ and Na^+ and have a reversal potential around –40 to –30 mV. As a result, hyperpolarization from rest, as during strong synaptic inhibition or following an action potential, opens the channels to generate an inward depolarizing current referred to as I_h (see Figure 10–15D).

Gating of Ion Channels Can Be Controlled by Cytoplasmic Calcium

In a typical neuron, the opening and closing of certain ion channels can be modulated by various cytoplasmic factors, thus affording the neuron's excitability

properties greater flexibility. Changes in the levels of such cytoplasmic factors can result from the activity of the neuron itself or from the influences of other neurons (Chapters 14 and 15).

Intracellular Ca^{2+} concentration is one important factor that modulates ion channel activity. Although ionic currents through membrane channels during an action potential generally do not result in appreciable changes in the intracellular concentrations of most ion species, calcium is a notable exception to this rule. The concentration of free Ca^{2+} in the cytoplasm of a resting cell is extremely low, about 10^{-7} M, several orders of magnitude below the external Ca^{2+} concentration, which is approximately 2 mM. Thus, intracellular Ca^{2+} concentration may increase many-fold above its resting value as a result of voltage-gated Ca^{2+} influx.

Intracellular Ca^{2+} concentration controls the gating of a number of channels. Several kinds of channels are activated by increases in intracellular Ca^{2+}. For example, the Ca^{2+}-activated *BK channels* (named for their big single-channel conductance), which are widely expressed in neurons, are voltage-dependent K^+ channels that require a very large, nonphysiological depolarization to open in the absence of Ca^{2+}. The binding of Ca^{2+} to a site on the cytoplasmic surface of the channel shifts its voltage gating to allow the channel to open at more negative potentials. With the influx of Ca^{2+} during an action potential, BK channels can open and help repolarize the action potential. Another family of calcium-activated K^+ channels, the *SK channels* (named for their small single-channel conductance), are not voltage dependent but open only in response to increases in intracellular Ca^{2+}. SK channels can open in response to relatively small changes in intracellular Ca^{2+} but gate slowly, so their activation gradually builds up as more Ca^{2+} enters the cell during repeated action potential firing. Some Ca^{2+} channels are themselves sensitive to levels of intracellular Ca^{2+}, becoming inactivated when intracellular Ca^{2+} increases as a result of entry through the channel itself.

As is described in later chapters, changes in the intracellular concentration of Ca^{2+} can also influence a variety of cellular metabolic processes, as well as neurotransmitter release and gene expression.

Excitability Properties Vary Between Types of Neurons

Through the expression of a distinct complement of ion channels, the electrical properties of different neuronal types have evolved to match the dynamic demands of information processing. Thus, the function of a neuron is defined not only by its synaptic inputs and outputs but also by its intrinsic excitability properties.

Different types of neurons in the mammalian nervous system generate action potentials that have different shapes and fire in different characteristic patterns, reflecting different expression of voltage-gated channels. For example, cerebellar Purkinje neurons and GABAergic cortical interneurons are associated with high levels of expression of Kv3 channels. The rapid activation of these channels produces narrow action potentials. In dopaminergic and other monoaminergic neurons, there is a high level of expression of voltage-activated Ca^{2+} channels that open during the falling phase of the action potential. The inward Ca^{2+} current from these channels slows repolarization, resulting in broader action potentials.

In the squid axon, the action potential is followed by an *afterhyperpolarization* (see Figure 10–7). In some mammalian neurons, the afterhyperpolarization has slow components lasting tens or even hundreds of milliseconds, generated by calcium-activated K^+ channels or voltage-activated K^+ channels with slow deactivation kinetics. Slow afterhyperpolarizations mediated by SK channels can be enhanced by repeated action potentials, reflecting buildup in intracellular Ca^{2+} concentrations.

In many pyramidal neurons in the cortex and hippocampus, the action potential is followed by an *afterdepolarization*, a transient depolarization that sometimes follows an earlier faster afterhyperpolarization. If the afterdepolarization is large enough, it can trigger a second action potential, resulting in all-or-none burst firing. The afterdepolarization can be caused by a variety of ionic currents, including Na^+ and Ca^{2+} currents from a number of voltage-dependent channels.

The shape of the action potential in a neuron is not always invariant. In some cases it can be dynamically regulated either intrinsically (eg, by repetitive firing) or extrinsically (eg, by synaptic modulation) (Chapter 15).

The pattern of action potential firing evoked by depolarization varies widely between neurons. The input-output function of a neuron can be characterized by the frequency and pattern of action potential firing in response to a series of current injections of different magnitudes. In the mammalian cerebral cortex, glutamatergic pyramidal neurons typically fire rapidly at the beginning of the current pulse followed by progressive slowing of firing, a pattern known as *adaptation* (Figure 10–14A). In contrast, many GABAergic interneurons fire with very little change in frequency (Figure 10–14B). Other neurons have more complex firing patterns. Some pyramidal neurons in the cerebral cortex tend to fire with an initial burst of action potentials (Figure 10–14C); "chattering" cells respond with repetitive brief bursts of high-frequency firing (Figure 10–14D).

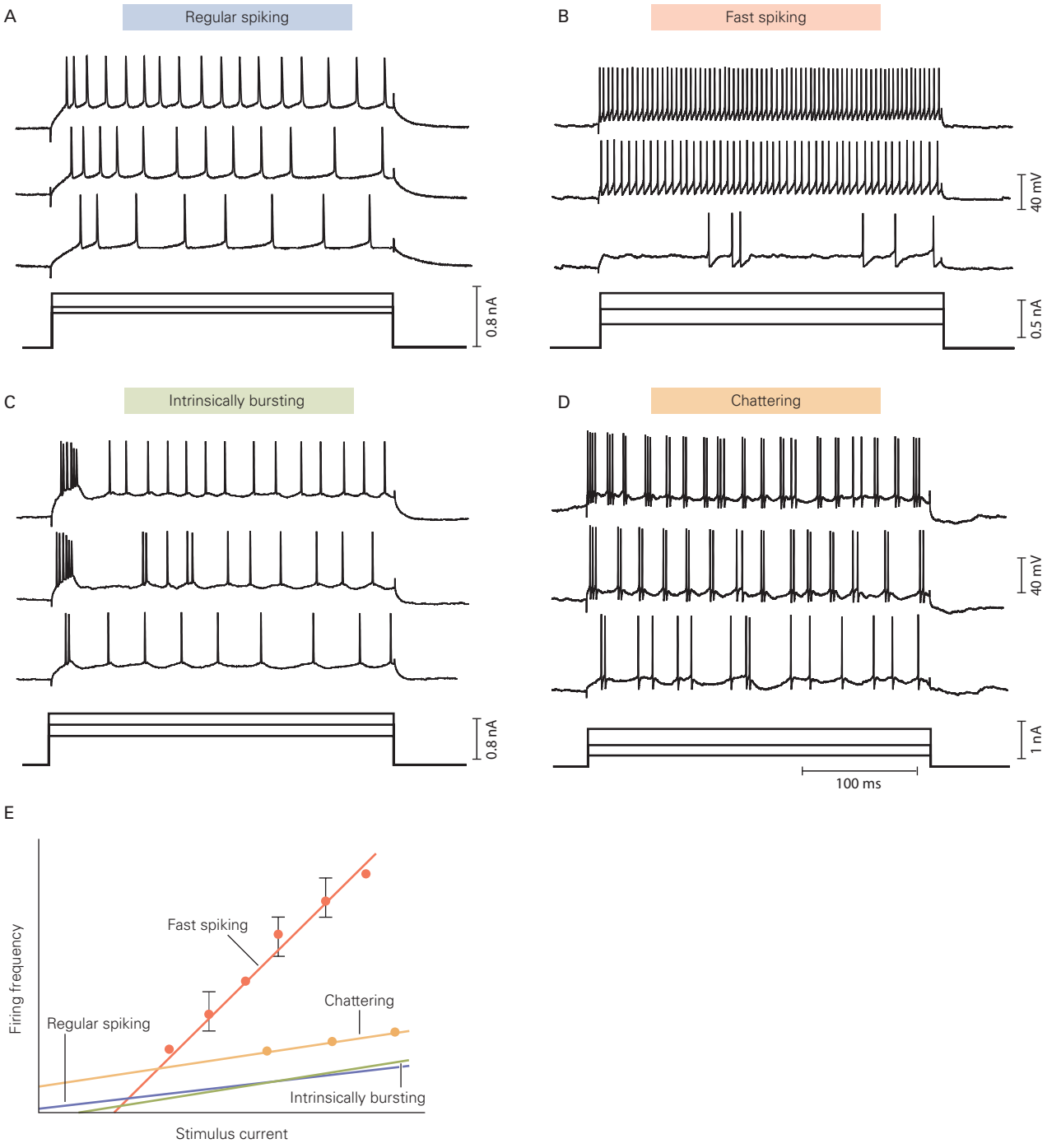

Figure 10–14 Different firing patterns in four types of cortical neurons. Three steps of depolarizing current, each of different amplitude, were injected into each cell to evoke firing. (Adapted, with permission, from Nowak et al. 2003.)

A. A cortical neuron with a firing pattern typical of many glutamatergic cortical pyramidal neurons, illustrating characteristic adaptation.

B. A firing pattern typical of many GABAergic interneurons, illustrating maintained high-frequency repetitive firing.

C. Firing in an intrinsically bursting neuron, a subtype of pyramidal neuron in cortical layer II/III.

D. Firing in a chattering cell, a subtype of pyramidal neuron in cortical layer V.

E. Firing frequency versus stimulus current for these four cell types, showing their different sensitivities to increasing stimulus strength.

The sensitivity of these four classes of neurons to excitatory input can also be characterized by their frequency–current relationships. The fast spiking neurons are the most sensitive to increases in depolarizing excitatory current.

Some neurons can sustain repetitive firing at high frequencies up to 500 Hz. Such *fast-spiking* neurons occur throughout the mammalian central nervous system, including many principal neurons in the auditory system, where neurons must respond to sound waves of very high frequencies. The ability to fire repetitively at high frequencies is correlated with high expression levels of Kv3 family channels, which produce rapid repolarization and close extremely rapidly following repolarization, resulting in a minimal afterhyperpolarization and a brief refractory period.

The different firing patterns of neurons can be understood in terms of the expression and gating properties of particular channels. For example, adaptation of firing frequency during a maintained current pulse can be produced by activation of particular Kv1 family channels, which are strongly activated following an action potential and thus impede firing of a subsequent spike (Figure 10–15A). Because many channels are controlled by a process of inactivation that regulates their availability for activation, synaptic inputs that produce small voltage changes around the resting potential can greatly modify the cell's excitability. For example, in some neurons, a steady hyperpolarizing synaptic input makes the cell less excitable by reducing the extent of inactivation of the A-type K^+ channels at the normal resting potential of the cell (Figure 10–15B). In other neurons, such a steady hyperpolarization makes the cell *more* excitable because it reduces the inactivation of Cav3 voltage-gated Ca^{2+} channels (Figure 10–15C).

A surprisingly large number of neurons in the mammalian brain fire spontaneously in the absence of any synaptic input. When such activity is regular and rhythmic, it is often referred to as "pacemaking," by analogy to the rhythmic spontaneous firing of the cardiac pacemaker in the sinoatrial node of the heart. Many neurons that release modulatory neurotransmitters, such as dopamine, serotonin, norepinephrine, and acetylcholine, fire spontaneously, typically at frequencies of 0.5 to 5 Hz, resulting in constant tonic release of transmitter in the target areas of the neuron.

One mechanism causing spontaneous firing is exemplified by neurons in the suprachiasmatic nucleus of the hypothalamus, which helps control the circadian rhythm of overall metabolism and the sleep–wake cycle. These neurons fire spontaneously, with faster firing during the daytime than the nighttime (Chapter 44). Pacemaking in these cells is driven in part by subthreshold *persistent Na^+ current*, a small voltage-dependent current which flows through Na^+ channels at voltages as negative as –70 mV. This current can slowly depolarize the neuron to the point where a fast action potential fires (Figure 10–15E). In the same neurons, there are non–voltage-dependent channels that conduct Na^+ "leak" current, which depolarizes the cells into the voltage range where voltage-dependent persistent Na^+ current is activated. The higher expression level in the cell membrane of such Na^+ leakage channels during the daytime leads to the day–night difference in firing rate.

In dopaminergic neurons of the substantia nigra, pacemaking is unusual in being driven partly by voltage-dependent Ca^{2+} currents. The continual entry of Ca^{2+} during the lifetime of the neurons may contribute to metabolic stress associated with death of these neurons in Parkinson disease (Chapter 63).

Excitability Properties Vary Between Regions of the Neuron

Different regions of a neuron have different types of ion channels that support the specialized functions of each region. The axon, for example, functions as a relatively simple relay line. In contrast, the input, integrative, and output regions of a neuron typically perform more complex processing of the information they receive before passing it along (Chapter 3).

The trigger zone at the axon initial segment has the lowest threshold for action potential generation, in part because it has an exceptionally high density of voltage-gated Na^+ channels. In addition, it typically has voltage-gated ion channels that are sensitive to relatively small deviations from the resting potential. These channels thus play a critical role in transforming graded synaptic or receptor potentials into a train of all-or-none action potentials. Channels highly expressed at the axon initial segment of many neurons include Nav1.6, Kv1, Kv7, and low voltage-activated T-type Ca^{2+} channels.

Dendrites in many types of neurons have voltage-gated ion channels, including Ca^{2+}, K^+, HCN, and Na^+ channels (Chapter 13). When activated, these channels help shape the amplitude, time course, and propagation of the synaptic potentials to the cell body. In some neurons, the density of voltage-gated channels in the dendrites is sufficient to support local action potentials, typically with relatively high threshold voltages.

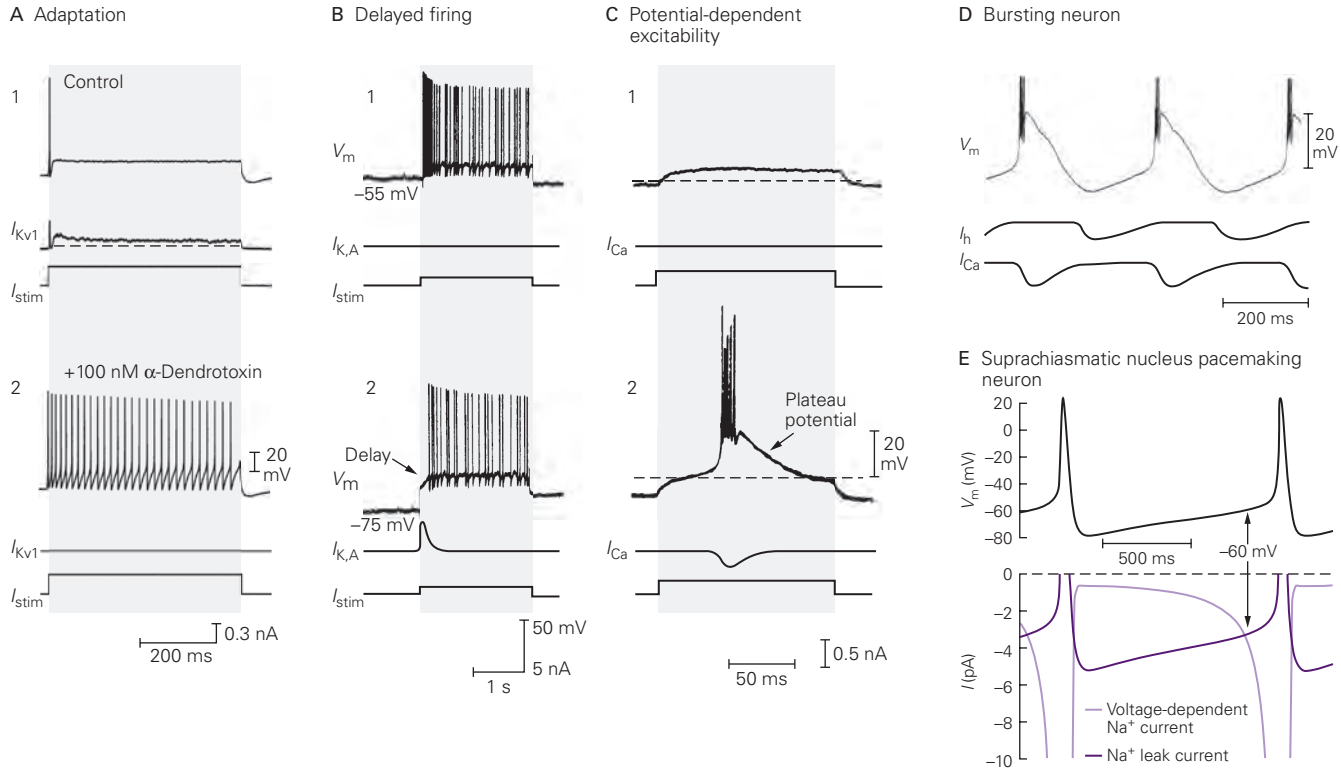

Figure 10–15 Regulation of firing pattern by a variety of voltage-gated channels.

A. Activation of Kv1 channels normally prevents firing of a second action potential by increasing spike threshold in a mouse dorsal root ganglion neuron (**1**). Blocking Kv1 channels with the snake toxin α-dendrotoxin changes the firing pattern from strong adaptation to maintained repetitive firing in response to a steady stimulating current (I_{stim}) (**2**). (Data from Pin Liu.)

B. Injection of a depolarizing current pulse (I_{stim}) into a neuron in the nucleus tractus solitarius normally triggers an immediate train of action potentials (**1**). If the cell is first held at a hyperpolarized membrane potential, the spike train is delayed (**2**). The delay is caused when A-type K^+ channels are activated by the depolarizing current pulse. The channels generate a transient outward K^+ current, $I_{K,A}$, that briefly slows the approach of V_m to threshold. These channels typically are inactivated at the resting potential (–55 mV), but steady hyperpolarization removes the inactivation. (Adapted with permission, from Dekin and Getting 1987.)

C. A small depolarizing current pulse injected into a thalamic neuron at rest generates a subthreshold depolarization (**1**). If the membrane potential is held at a hyperpolarized level, the same current pulse triggers a burst of action potentials (**2**). The effectiveness of the current pulse is enhanced because the hyperpolarization causes a type of voltage-gated Ca^{2+} channel to recover from inactivation. Depolarizing inward current through these Ca^{2+} channels (I_{Ca}) generates a plateau potential of about 20 mV that triggers a burst of action potentials. The **dashed line** indicates the level of the normal resting potential. (Adapted with permission, from Llinás and Jahnsen 1982.)

The data in parts **B** and **C** demonstrate that steady hyperpolarization, such as might be produced by inhibitory synaptic input to a neuron, can profoundly affect the spike train pattern of a neuron. This effect varies greatly among cell types and depends on the presence or absence of particular types of voltage-gated Ca^{2+} and K^+ channels.

D. In the absence of synaptic input, thalamocortical relay neurons can fire spontaneously in brief bursts of action potentials. These bursts are produced by current through two types of voltage-gated ion channels. The gradual depolarization that leads to a burst is driven by inward current (I_h) through HCN channels, which open in response to hyperpolarization. The burst is triggered by an inward Ca^{2+} current through voltage-gated Cav3 channels, which are activated at relatively low levels of depolarization. This Ca^{2+} influx generates sufficient depolarization to reach threshold and drive a brief burst of Na^+-dependent action potentials. The strong depolarization during the burst causes the HCN channels to close and inactivates the Ca^{2+} channels, allowing hyperpolarization to develop between bursts of firing. This hyperpolarization then opens the HCN channels, initiating the next cycle in the rhythm. (Adapted, with permission, from McCormick and Huguenard 1992.)

E. Neurons from the suprachiasmatic nucleus of the hypothalamus generate spontaneous pacemaker potentials. Following an action potential, the neuron spontaneously depolarizes, first slowly and then more rapidly, resulting in another action potential. The depolarization is driven by two inward Na^+ currents during the interspike interval. One is "persistent Na^+ current," which flows through voltage-dependent sodium channels sensitive to block by tetrodotoxin, probably the same population of channels that underlie the much larger sodium current during the upstroke of the action potential. The second current flows through non–voltage-activated sodium leak nonselective (*NALCN*) channels, which provide a steady conductance pathway for Na^+ and K^+ ions. At negative voltages, Na^+ driving force is large and K^+ driving force is small, so the leak current is carried predominantly by Na^+ ions. This inward current depolarizes the neuron to the point at which voltage-dependent persistent Na^+ current becomes dominant (around –60 mV). (Adapted, with permission, from Jackson et al. 2004. Copyright © 2004 Society for Neuroscience.)

With moderate synaptic stimulation, full-blown action potentials are first generated at the trigger zone at the initial segment of the axon and then propagate back into the dendrites, serving as a signal to the synaptic regions that the cell has fired.

Conduction of the action potential down the axon is mediated primarily by voltage-gated Na^+ and K^+ channels that function much like those in the squid axon. In myelinated axons, the nodes of Ranvier have a high density of Na^+ channels but a low density of voltage-activated K^+ channels. There is a higher density of voltage-activated K^+ channels under the myelin sheath near the two ends of each internodal segment. The normal function of these K^+ channels is to suppress generation of action potentials in portions of the axon membrane under the myelin sheath. In demyelinating diseases, these channels become exposed and thus may inhibit the ability of the bare axon to conduct action potentials (Chapters 9 and 57).

Presynaptic nerve terminals at chemical synapses have a high density of voltage-gated Ca^{2+} channels, most commonly Cav2.1 (P/Q-type) channels, Cav2.2 (N-type) channels, or a mixture of the two. Arrival of an action potential in the terminal opens these channels, causing an influx of Ca^{2+} that triggers transmitter release (Chapter 15).

Neuronal Excitability Is Plastic

The expression, localization, and functional state of voltage-gated ion channels controlling the rate and pattern of action potential firing in a particular neuron are not always fixed, but can change in response to changes in the neuron's synaptic input, its activity, or its environment, as well as in response to injury or disease. For example, synaptic input that causes channel phosphorylation via second messenger pathways can lead to transient changes in a channel's functional properties, which in turn modulate cell excitability (Chapter 14). Plasticity can also occur on a longer time scale, such as when increased activity of a neuronal network as a whole leads to decreased excitability of individual neurons—a homeostatic feedback system. In some cases, activity-induced structural changes, such as change in length of the axon initial segment or its migration relative to the soma, can also affect excitability. The molecular mechanisms of homeostatic changes in neuronal excitability are not well understood but likely involve intracellular calcium signaling pathways that control transcription or cellular trafficking of specific ion channels. Dysfunction of such regulatory pathways may underlie some types of epilepsy and hyperexcitability associated with conditions such as neuropathic pain.

Highlights

1. An action potential is a transient depolarization of membrane voltage lasting about 1 ms that is produced when ions move across the cell membrane through voltage-gated channels and thereby change the charge separation across the membrane.
2. The depolarizing phase of the action potential results from rapid, regenerative opening of voltage-activated Na^+ channels. Repolarization is due to inactivation of Na^+ channels and activation of K^+ channels.
3. The sharp threshold for action potential generation occurs at a voltage at which inward Na^+ channel current just exceeds outward currents through leak channels and voltage-gated K^+ channels.
4. The refractory period reflects Na^+ channel inactivation and K^+ channel activation continuing after the action potential. The refractory period limits the action potential firing rate.
5. The conformational changes of channel proteins underlying voltage-dependent activation and inactivation are not yet completely understood, but key regions involved in channel gating have been identified.
6. Voltage-gated sodium channels select for sodium on the basis of size, charge, and energy of hydration of the ion.
7. Most neurons express multiple kinds of voltage-gated Na^+, Ca^{2+}, K^+, HCN, and Cl^- channels, with especially large diversity in the properties of K^+ channels.
8. The diversity of voltage-dependent channels reflects the expression of multiple genes, formation of heteromeric channels from multiple gene products, alternative splicing of gene transcripts, mRNA editing, and combination of pore-forming subunits with a variety of accessory proteins.
9. Activity of some voltage-gated ion channels can be modulated by cytoplasmic Ca^{2+}.
10. The diversity in expression of voltage-gated ion channels results in differences in excitability properties of different types of neurons and in different regions of the same neuron.
11. The regional expression and functional state of ion channels can be regulated in response to cell

activity, changes in cell environment, or pathological processes, resulting in plasticity of the intrinsic excitability of neurons.

Bruce P. Bean
John D. Koester

Selected Reading

Ahern CA, Payandeh J, Bosmans F, Chanda B. 2016. The hitchhiker's guide to the voltage-gated sodium channel galaxy. J Gen Physiol 147:1–24.

Armstrong CM, Hille B. 1998. Voltage-gated ion channels and electrical excitability. Neuron 20:371–380.

Bezanilla F. 2008. How membrane proteins sense voltage. Nat Rev Mol Cell Biol 9:323–332.

Duménieu M, Oulé M, Kreutz MR, Lopez-Rojas J. 2017. The segregated expression of voltage-gated potassium and sodium channels in neuronal membranes: functional implications and regulatory mechanisms. Front Cell Neurosci 11:115.

Hille B. 2001. *Ion Channels of Excitable Membranes*, 3rd ed. Sunderland, MA: Sinauer.

Hodgkin AL. 1992. *Chance & Design: Reminiscences of Science in Peace and War*. Cambridge: Cambridge Univ. Press.

Johnston J, Forsythe ID, Kopp-Scheinpflug C. 2010. Going native: voltage-gated potassium channels controlling neuronal excitability. J Physiol 588:3187–3200.

Llinás RR. 1988. The intrinsic electrophysiological properties of mammalian neurons: insights into central nervous system function. Science 242:1654–1664.

Rudy B, McBain C. 2001. Kv3 channels: voltage-gated K^+ channels designed for high-frequency repetitive firing. Trends Neurosci 24:517–526.

Turrigiano GG, Nelson SB. 2004. Homeostatic plasticity in the developing nervous system. Nat Rev Neurosci 5:97–107.

Vacher H, Mohapatra DP, Trimmer JS. 2008. Localization and targeting of voltage-dependent ion channels in mammalian central neurons. Physiol Rev 88:1407–1447.

References

Aplizar SA, Cho H, Hoppa M. 2019. Subcellular control of membrane excitability in the axon. Curr Opin Neurobiol 57:117–125.

Armstrong CM, Gilly WF. 1979. Fast and slow steps in the activation of sodium channels. J Gen Physiol 59:691–711.

Battefeld A, Tran BT, Gavrilis J, Cooper EC, Kole MH. 2014. Heteromeric Kv7.2/7.3 channels differentially regulate action potential initiation and conduction in neocortical myelinated axons. J Neurosci 34:3719–3732.

Bauer CK, Schwarz JR. 2018. Ether-à-go-go K^+ channels: effective modulators of neuronal excitability. J Physiol (Lond) 596:769–783.

Bender KJ, Trussell LO. 2012. The physiology of the axon initial segment. Annu Rev Neurosci 35:249–265.

Capes DL, Goldschen-Ohm MP, Arcisio-Miranda M, Bezanilla F, Chanda B. 2013. Domain IV voltage-sensor movement is both sufficient and rate limiting for fast inactivation in sodium channels. J Gen Physiol 142:101–112.

Carrasquillo Y, Nerbonne JM. 2014. I_A channels: diverse regulatory mechanisms. Neuroscientist 20:104–111.

Catterall WA. 1988. Structure and function of voltage-sensitive ion channels. Science 242:50–61.

Catterall WA. 2010. Ion channel voltage sensors: structure, function, and pathophysiology. Neuron 67:915–928.

Catterall WA. 2011. Voltage-gated calcium channels. Cold Spring Harb Perspect Biol 3:a003947.

Catterall WA, Few AP. 2008. Calcium channel regulation and presynaptic plasticity. Neuron 59:882–8901.

Cole KS, Curtis HJ. 1939. Electric impedance of the squid giant axon during activity. J Gen Physiol 22:649–670.

Dekin MS, Getting PA. 1987. In vitro characterization of neurons in the vertical part of the nucleus tractus solitarius. II. Ionic basis for repetitive firing patterns. J Neurophysiol 58:215–229.

Erisir A, Lau D, Rudy B, Leonard CS. 1999. Function of specific K^+ channels in sustained high-frequency firing of fast-spiking neocortical interneurons. J Neurophysiol 82:2476–2489.

Flourakis M, Kula-Eversole E, Hutchison AL, et al. 2015. A conserved bicycle model for circadian clock control of membrane excitability. Cell 162:836–848.

Hodgkin AL, Huxley AF. 1952. A quantitative description of membrane current and its application to conduction and excitation in nerve. J Physiol 117:500–544.

Hodgkin AL, Katz B. 1949. The effect of sodium ions on the electrical activity of the giant axon of the squid. J Physiol 108:37–77.

Isom LL, DeJongh KS, Catterall WA. 1994. Auxiliary subunits of voltage-gated ion channels. Neuron 12:1183–1194.

Jackson AC, Yao GL, Bean BP. 2004. Mechanism of spontaneous firing in dorsomedial suprachiasmatic nucleus neurons. J Neurosci 24:7985–7998.

Joseph A, Turrigiano GG. 2017. All for one but not one for all: excitatory synaptic scaling and intrinsic excitability are coregulated by CaMKIV, whereas inhibitory synaptic scaling is under independent control. J Neurosci 37:6778–6785.

Kaczmarek LK. 2012. Gradients and modulation of K^+ channels optimize temporal accuracy in networks of auditory neurons. PLoS Comput Biol 8:e1002424.

Kole MH, Ilschner SU, Kampa BM, Williams SR, Ruben PC, Stuart GJ. 2008. Action potential generation requires a high sodium channel density in the axon initial segment. Nat Neurosci 11:178–186.

Lee C-H, MacKinnon R. 2017. Structures of the human HCN1 hyperpolarization-activated channel. Cell 168:111–120.

Llinás R, Jahnsen H. 1982. Electrophysiology of mammalian thalamic neurones in vitro. Nature 297:406–408.

McCormick DA, Connors BW, Lighthall JW, Prince DA. 1985. Comparative electrophysiology of pyramidal and sparsely spiny stellate neurons of the neocortex. J Neurophysiol 54:782–806.

McCormick DA, Huguenard JR. 1992. A model of electrophysiological properties of thalamocortical relay neurons. J Neurophysiol 68:1384–1400.

Nowak LG, Azouz R, Sanchez-Vives MV, Gray CM, McCormick DA. 2003. Electrophysiological classes of cat primary visual cortical neurons in vivo as revealed by quantitative analyses. J Neurophysiol 89:1541–1566.

Pan X, Li Z, Zhou Q, et al. 2018. Structure of the human voltage-gated sodium channel Na(v)1.4 in complex with β1. Science 362:eaau2486.

Payandeh J, Scheuer T, Zheng N, Catterall WA. 2011. The crystal structure of a voltage-gated sodium channel. Nature 475:353–359.

Proft J, Weiss N. 2015. G protein regulation of neuronal calcium channels: back to the future. Mol Pharmacol 87:890–906.

Puopolo M, Raviola E, Bean BP. 2007. Roles of subthreshold calcium current and sodium current in spontaneous firing of mouse midbrain dopamine neurons. J Neurosci 27:645–656.

Sigworth FJ, Neher E. 1980. Single Na^+ channel currents observed in cultured rat muscle cells. Nature 287:447–449.

Tai C, Abe Y, Westenbroek RE, Scheuer T, Catterall WA. 2014. Impaired excitability of somatostatin- and parvalbumin-expressing cortical interneurons in a mouse model of Dravet syndrome. Proc Natl Acad Sci U S A 111:E3139–E3148.

Tateno T, Harsch A, Robinson HP. 2004. Threshold firing frequency-current relationships of neurons in rat somatosensory cortex: type 1 and type 2 dynamics. J Neurophysiol 92:2283–2294.

Vassilev PM, Scheuer T, Catterall WA. 1988. Identification of an intracellular peptide segment involved in sodium channel inactivation. Science 241:1658–1661.

Yamada R, Kuba H. 2016, Structural and functional plasticity at the axon initial segment. Front Cell Neurosci 10:250.

Yang N, George AL Jr, Horn R. 1996. Molecular basis of charge movement in voltage-gated sodium channels. Neuron 16:113–122.

Yu FH, Catterall WA. 2003. Overview of the voltage-gated sodium channel family. Genome Biol 4:207.

This page intentionally left blank

Part III

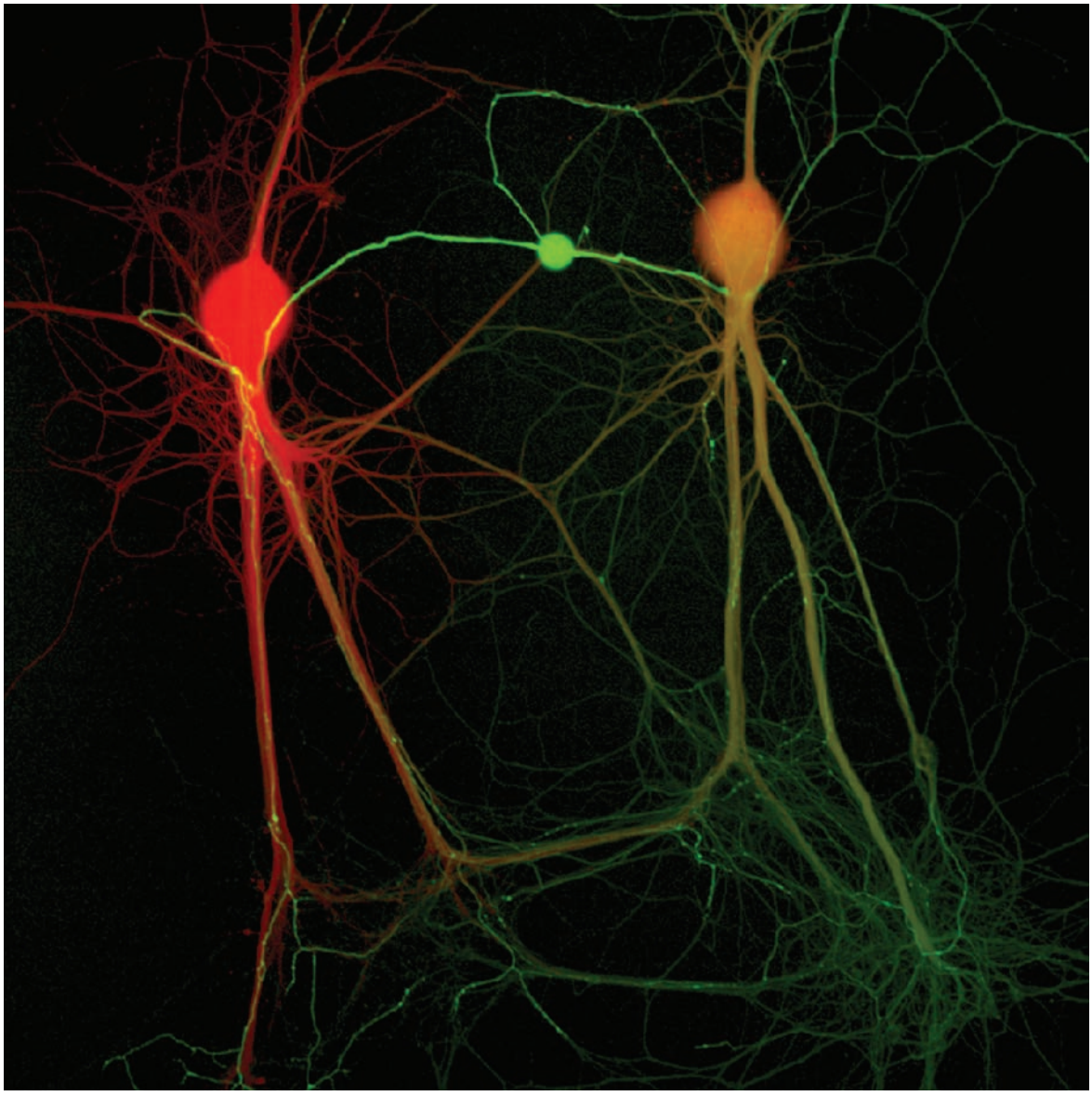

Preceding Page

A mechanosensory neuron (center, **green**) sends its axon to form excitatory synaptic connections with two motor neurons (**red**, **orange**) in cell culture, recapitulating the connections in the living animal. The neurons were isolated from the marine snail *Aplysia californica*. (Reproduced, with permission, from Harshad Vishwasrao and Eric R. Kandel.)

III Synaptic Transmission

In Part II, we examined how electrical signals are initiated and propagated within an individual neuron. We now turn to synaptic transmission, the process by which one nerve cell communicates with another.

With some exceptions, the synapse consists of three components: (1) the terminals of the presynaptic axon, (2) a target on the postsynaptic cell, and (3) a zone of apposition. Based on the structure of the apposition, synapses are categorized into two major groups: electrical and chemical. At electrical synapses, the presynaptic terminal and the postsynaptic cell are in very close apposition at regions termed *gap junctions*. The current generated by an action potential in the presynaptic neuron directly enters the postsynaptic cell through specialized bridging channels called *gap junction channels*, which physically connect the cytoplasm of the presynaptic and postsynaptic cells. At chemical synapses, a cleft separates the two cells, and the cells do not communicate through bridging channels. Rather, an action potential in the presynaptic cell leads to the release of a chemical transmitter from the nerve terminal. The transmitter diffuses across the synaptic cleft and binds to receptor molecules on the postsynaptic membrane, which regulates the opening and closing of ion channels in the postsynaptic cell. This leads to changes in the membrane potential of the postsynaptic neuron that can either excite or inhibit the firing of an action potential.

Receptors for transmitters can be classified into two major groups depending on how they control ion channels in the postsynaptic cell. One type, the ionotropic receptor, is an ion channel that opens when the transmitter binds. The second type, the metabotropic receptor, acts indirectly on ion channels by activating a biochemical second-messenger cascade within the postsynaptic cell. Both types of receptors can result in excitation or inhibition. The sign of the signal depends not on the identity of the transmitter but on the properties of the receptor with which the transmitter interacts. Most transmitters are low-molecular-weight molecules, but certain peptides also can act as messengers at synapses. The methods of electrophysiology, biochemistry, and molecular biology have been used to characterize the receptors in postsynaptic cells that respond to these various chemical messengers. These methods have also clarified how second-messenger pathways transduce signals within cells.

In this part of the book, we consider synaptic transmission in its most elementary forms. We first compare and contrast the two major classes of synapses, chemical and electrical (see Chapter 11). We then focus on a model chemical synapse in the peripheral nervous system, the neuromuscular junction between a presynaptic motor neuron and a postsynaptic skeletal muscle fiber (see Chapter 12). Next we examine chemical synapses between neurons in the central nervous system, focusing on the postsynaptic cell and its integration of synaptic signals from multiple presynaptic inputs acting on both ionotropic receptors (see Chapter 13) and metabotropic receptors (see Chapter 14). We then turn to the presynaptic terminal and consider the mechanisms by which neurons release transmitter from their presynaptic terminals, how transmitter release can be regulated by neural activity (see Chapter 15), and the chemical nature of the neurotransmitters (see Chapter 16). Because the molecular architecture of chemical synapses is complex, many inherited and acquired diseases can affect chemical synaptic transmission, which we consider in detail later in Chapter 57.

One key theme running throughout the chapters of this section, and indeed throughout the book, is the concept of plasticity. At all synapses, the strength of a synaptic connection is not fixed but can be modified in various ways by behavioral context or experience, through a variety of mechanisms referred to as synaptic plasticity. Some modifications result from the activity of the synapse itself (homosynaptic plasticity). Other modifications depend on extrinsic factors, often due to the release of a modulatory transmitter (heterosynaptic plasticity). In Chapters 53 and 54, we will see how such modifications provide a cellular substrate for different forms of memory storage that range in duration from seconds to a lifetime. In the chapters of Part IX, we will see how dysfunction in synaptic plasticity can contribute to a variety of neurological and psychiatric disorders.

Part Editor: Steven A. Siegelbaum

Part III

11

Overview of Synaptic Transmission

WHAT GIVES NERVE CELLS THEIR SPECIAL ABILITY to communicate with one another rapidly and with such great precision? We have already seen how signals are propagated *within* a neuron, from its dendrites and cell body to its axonal terminals. With this chapter, we begin to consider the signaling *between* neurons through the process of synaptic transmission. Synaptic transmission is fundamental to the neural functions we consider in this book, such as perception, voluntary movement, and learning.

Neurons communicate with one another at a specialized site called a *synapse*. The average neuron forms several thousand synaptic connections and receives a similar number of inputs. However, this number can vary widely depending on the particular type of neuron. Whereas the Purkinje cell of the cerebellum receives up to 100,000 synaptic inputs, the neighboring granule neurons, the most numerous class of neurons in the brain, receive only around four excitatory inputs. Although many of the synaptic connections in the central and peripheral nervous systems are highly specialized, all neurons make use of one of the two basic forms of synaptic transmission: electrical or chemical. Moreover, the strength of both forms of synaptic transmission is not fixed, but can be enhanced or diminished by neuronal activity. This synaptic *plasticity* is crucial for memory and for other higher brain functions.

Electrical synapses are employed primarily to send rapid and stereotyped depolarizing signals. In contrast, chemical synapses are capable of more variable signaling and thus can produce more complex interactions. They can produce either excitatory or inhibitory actions in postsynaptic cells and initiate changes in the postsynaptic cell that last from milliseconds to hours. Chemical synapses also serve to amplify neuronal signals, so even a small presynaptic nerve terminal can alter the response of large postsynaptic cells. Because chemical synaptic transmission is so central to understanding brain and behavior, it is examined in detail in the next four chapters.

Synapses Are Predominantly Electrical or Chemical

The term *synapse* was introduced at the beginning of the 20th century by Charles Sherrington to describe the specialized zone of contact at which one neuron communicates with another. This site had first been

Table 11–1 Distinguishing Properties of Electrical and Chemical Synapses

Type of synapse	Distance between pre- and postsynaptic cell membranes	Cytoplasmic continuity between pre- and postsynaptic cells	Ultrastructural components	Agent of transmission	Synaptic delay	Direction of transmission
Electrical	4 nm	Yes	Gap-junction channels	Ion current	Virtually absent	Usually bidirectional
Chemical	20–40 nm	No	Presynaptic vesicles and active zones; postsynaptic receptors	Chemical transmitter	Significant: at least 0.3 ms, usually 1–5 ms or longer	Unidirectional

described histologically at the level of light microscopy by Ramón y Cajal in the late 19th century.

All synapses were initially thought to operate by means of electrical transmission. In the 1920s, however, Otto Loewi discovered that a chemical compound, most likely acetylcholine (ACh), conveys signals from the vagus nerve to slow the beating heart. Loewi's discovery provoked considerable debate in the 1930s over whether chemical signaling existed at the fast synapses between motor nerve and skeletal muscle as well as synapses in the brain.

Two schools of thought emerged, one physiological and the other pharmacological. Each championed a single mechanism for all synaptic transmission. Led by John Eccles (Sherrington's student), the physiologists argued that synaptic transmission is electrical, that the action potential in the presynaptic neuron generates a current that flows passively into the postsynaptic cell. The pharmacologists, led by Henry Dale, argued that transmission is chemical, that the action potential in the presynaptic neuron leads to the release of a chemical substance that in turn initiates current in the postsynaptic cell. When physiological and ultrastructural techniques improved in the 1950s and 1960s, it became clear that both forms of transmission exist. While most neurons initiate electrical signaling with a chemical transmitter, many others produce an electrical signal directly in the postsynaptic cell.

Once the fine structure of synapses was made visible with the electron microscope, chemical and electrical synapses were found to have different structures. At chemical synapses, the presynaptic and postsynaptic neurons are completely separated by a small space, the synaptic cleft; there is no continuity between the cytoplasm of one cell and the next. In contrast, at electrical synapses, the pre- and postsynaptic cells communicate through special channels that directly connect the cytoplasm of the two cells.

The main functional properties of the two types of synapses are summarized in Table 11–1. The most important difference can be observed by injecting a positive current into the presynaptic cell to elicit a depolarization. At both types of synapses, outward current across the presynaptic cell membrane deposits positive charge on the inside of its membrane, thereby depolarizing the cell (Chapter 9). At electrical synapses, some of the current will enter the postsynaptic cell through the gap-junction channels, depositing a positive charge on the inside of the membrane and depolarizing it. The current leaves the postsynaptic cell across the membrane through resting channels (Figure 11–1A). If the depolarization exceeds threshold, voltage-gated ion channels in the postsynaptic cell open and generate an action potential. By contrast, at chemical synapses, there is no direct low-resistance pathway between the pre- and postsynaptic cells. Instead, the action potential in the presynaptic neuron initiates the release of a chemical transmitter, which diffuses across the synaptic cleft and binds with receptors on the membrane of the postsynaptic cell (Figure 11–1B).

Electrical Synapses Provide Rapid Signal Transmission

During excitatory synaptic transmission at an electrical synapse, voltage-gated ion channels in the presynaptic cell generate the current that depolarizes the postsynaptic cell. Thus, these channels not only depolarize the presynaptic cell above the threshold for an action potential but also generate sufficient ionic current to produce a change in potential in the postsynaptic cell. To generate such a large current, the presynaptic terminal must be big enough for its membrane to contain many ion channels. At the same time, the postsynaptic cell must be relatively small. This is because a small cell has a higher input resistance (R_{in}) than a large cell

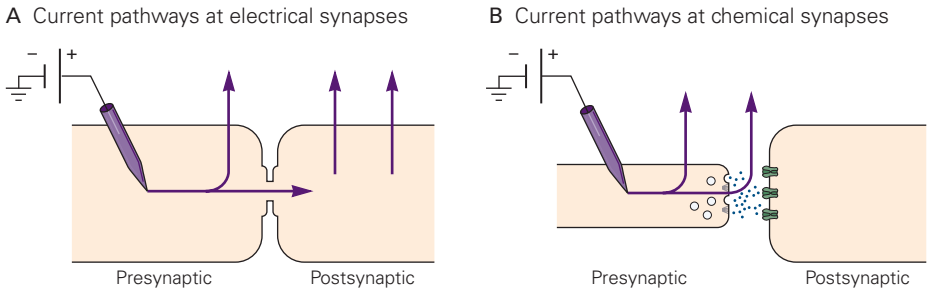

Figure 11–1 Functional properties of electrical and chemical synapses.

A. At an electrical synapse, some current injected into the presynaptic cell escapes through resting (nongated) ion channels in the cell membrane. However, some current also enters the postsynaptic cell through gap-junction channels that connect the cytoplasm of the pre- and postsynaptic cells and that provide a low-resistance (high-conductance) pathway for electrical current.

B. At chemical synapses, all current injected into the presynaptic cell escapes into the extracellular fluid. However, the resulting depolarization of the presynaptic cell membrane can produce an action potential that causes the release of neurotransmitter molecules that bind receptors on the postsynaptic cell. This binding opens ion channels that initiate a change in membrane potential in the postsynaptic cell.

and, according to Ohm's law ($\Delta V = I \times R_{in}$), undergoes a greater voltage change (ΔV) in response to a given presynaptic current (I).

Electrical synaptic transmission was first described by Edwin Furshpan and David Potter in the giant motor synapse of the crayfish, where the presynaptic fiber is much larger than the postsynaptic fiber (Figure 11–2A). An action potential generated in the presynaptic fiber produces a depolarizing postsynaptic potential that often exceeds the threshold to fire an action

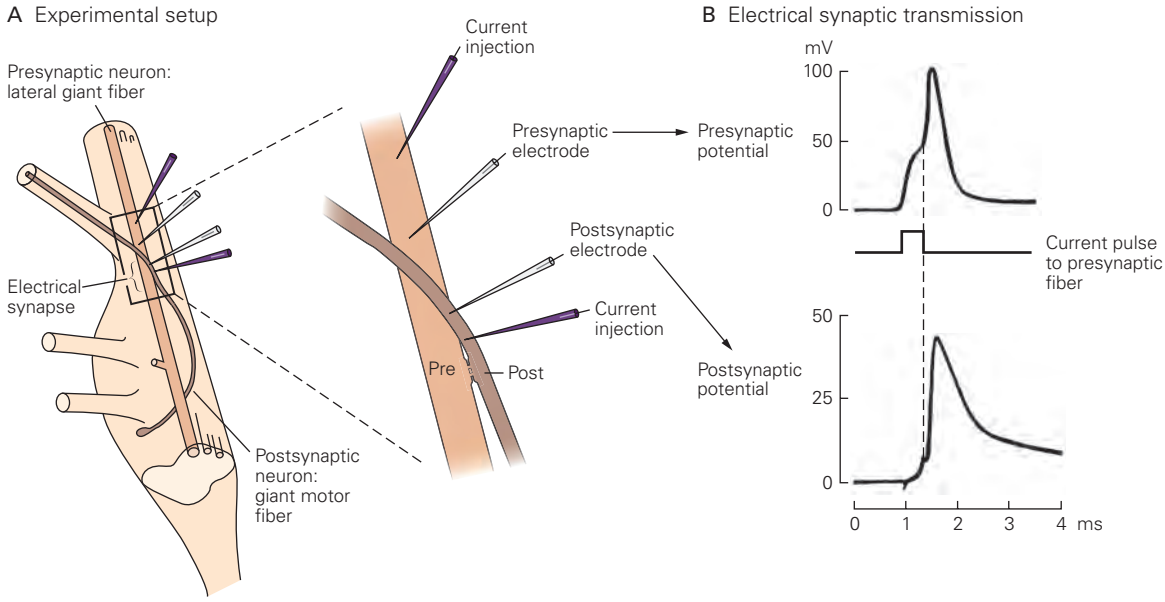

Figure 11–2 Electrical synaptic transmission was first demonstrated at the giant motor synapse in the crayfish. (Adapted, with permission, from Furshpan and Potter 1957 and 1959.)

A. The lateral giant fiber running down the nerve cord is the presynaptic neuron. The giant motor fiber, which projects from the cell body in the ganglion to the periphery, is the postsynaptic neuron. Electrodes for passing current and for recording voltage are placed within the pre- and postsynaptic cells.

B. Transmission at an electrical synapse is virtually instantaneous—the postsynaptic response follows presynaptic stimulation in a fraction of a millisecond. The **dashed line** shows how the responses of the two cells correspond in time. At chemical synapses, there is a delay (the synaptic delay) between the pre- and postsynaptic potentials (see Figure 11–8).

potential. At electrical synapses, the synaptic delay—the time between the presynaptic spike and the postsynaptic potential—is remarkably short (Figure 11–2B).

Such a short latency is not possible with chemical transmission, which requires several biochemical steps: release of a transmitter from the presynaptic neuron, diffusion of transmitter molecules across the synaptic cleft to the postsynaptic cell, binding of transmitter to a specific receptor, and subsequent gating of ion channels (all described in this and the next chapter). Only current passing directly from one cell to another can produce the near-instantaneous transmission observed at the giant motor electrical synapse.

Another feature of electrical transmission is that the change in potential of the postsynaptic cell is directly related to the size and shape of the change in potential of the presynaptic cell. Even when a weak subthreshold depolarizing current is injected into the presynaptic neuron, some current enters the postsynaptic cell and depolarizes it (Figure 11–3). In contrast, at a chemical synapse, the current in the presynaptic cell must reach the threshold for an action potential before it can release transmitter and elicit a response in the postsynaptic cell.

Most electrical synapses can transmit both depolarizing and hyperpolarizing currents. A presynaptic action potential with a large hyperpolarizing afterpotential produces a biphasic (depolarizing-hyperpolarizing) change in potential in the postsynaptic cell. Signal transmission at electrical synapses is similar to the passive propagation of subthreshold electrical signals along axons (Chapter 9) and therefore is also referred to as *electrotonic transmission*. At some specialized gap junctions, the channels have voltage-dependent gates that permit them to conduct depolarizing current in only one direction, from the presynaptic cell to the postsynaptic cell. These junctions are called *rectifying synapses*. (The crayfish giant motor synapse is an example.)

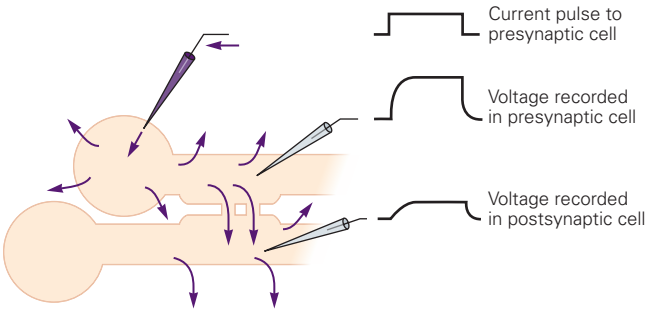

Figure 11–3 Electrical transmission is graded. It occurs even when the current in the presynaptic cell is below the threshold for an action potential. As demonstrated by single-cell recordings, a subthreshold depolarizing stimulus causes a passive depolarization in the presynaptic and postsynaptic cells. (Depolarizing or outward current is indicated by an upward deflection.)

Cells at an Electrical Synapse Are Connected by Gap-Junction Channels

At an electrical synapse, the pre- and postsynaptic components are apposed at the *gap junction*, where the separation between the two neurons (4 nm) is much less than the normal nonsynaptic space between neurons (20 nm). This narrow gap is bridged by *gap-junction channels*, specialized protein structures that conduct ionic current directly from the presynaptic to the postsynaptic cell.

A gap-junction channel consists of a pair of *hemichannels*, or *connexons*, one in the presynaptic and the other in the postsynaptic cell membrane. These hemichannels thus form a continuous bridge between the two cells (Figure 11–4). The pore of the channel has a large diameter of approximately 1.5 nm, much larger than the 0.3- to 0.5-nm diameter of ion-selective ligand-gated or voltage-gated channels. The large pore of gap-junction channels does not discriminate among inorganic ions and is even wide enough to permit small organic molecules and experimental markers such as fluorescent dyes to pass between the two cells.

Each connexon is composed of six identical subunits, called *connexins*. Connexins in different tissues are encoded by a large family of 21 separate but related genes. In mammals, the most common connexon in neurons is formed from the product of *connexin 36.* Connexin genes are named for their predicted molecular weight, in kilodaltons, based on their primary amino acid sequence. All connexin subunits have an intracellular N- and C-terminus with four interposed α-helixes that span the cell membrane (Figure 11–4C).

Many gap-junction channels in different cell types are formed by the products of different connexin genes and thus respond differently to modulatory factors that control their opening and closing. For example, although most gap-junction channels close in response to lowered cytoplasmic pH or elevated cytoplasmic Ca^{2+}, the sensitivity of different channel isoforms to these factors varies widely. The closing of gap-junction channels in response to pH and Ca^{2+} plays an important role in the decoupling of damaged cells from healthy cells, as damaged cells contain elevated Ca^{2+} levels and a high concentration of protons. Finally, neurotransmitters released from nearby chemical synapses can modulate the opening of gap-junction channels through intracellular metabolic reactions (Chapter 14).

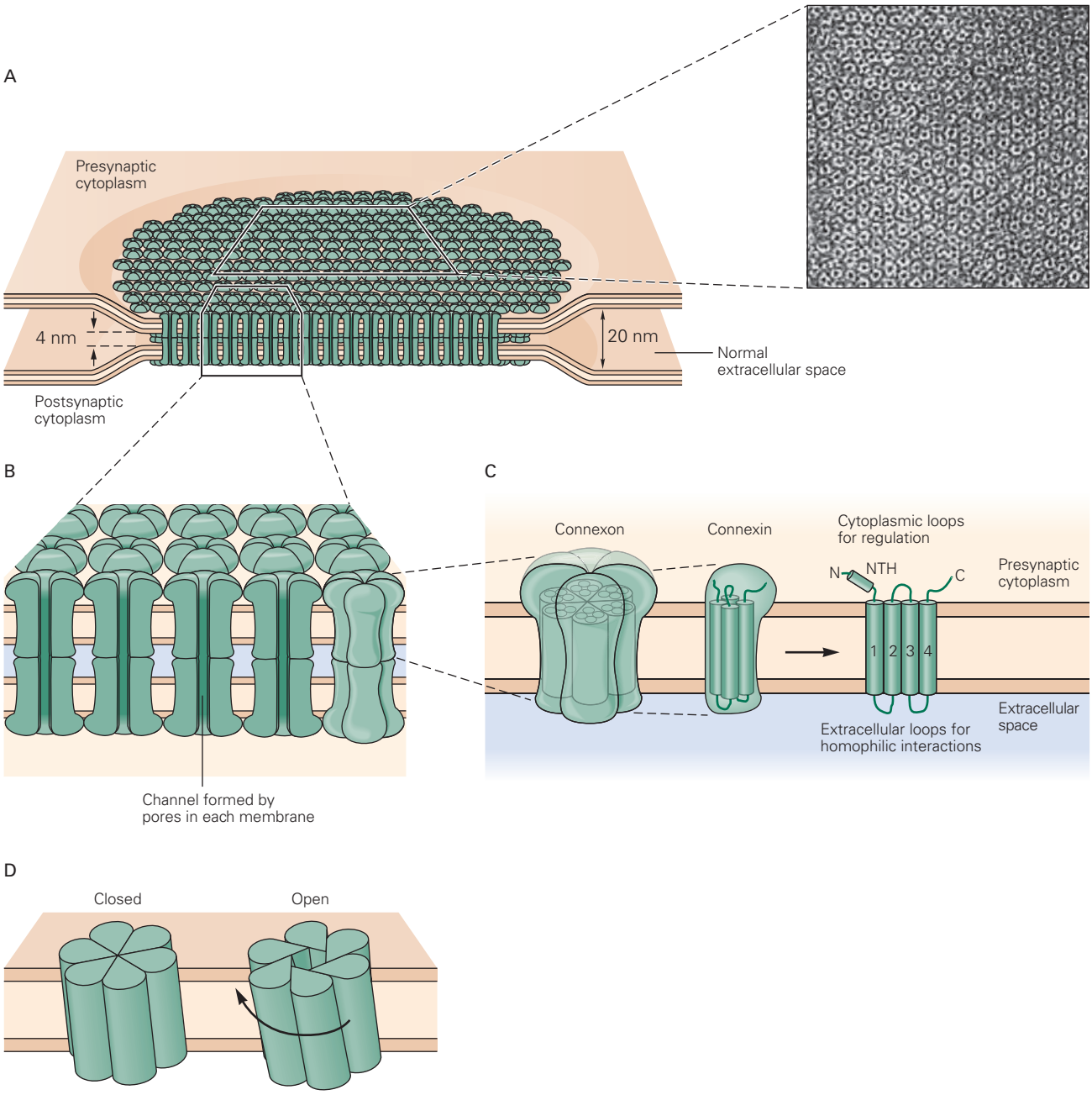

Figure 11–4 A three-dimensional model of the gap-junction channel, based on X-ray and electron diffraction studies.

A. The electrical synapse, or gap junction, is composed of numerous specialized channels that span the membranes of the pre- and postsynaptic neurons. These gap-junction channels allow current to pass directly from one cell to the other. The array of channels in the electron micrograph was isolated from the membrane of a rat liver cell that had been negatively stained, a technique that darkens the area around the channels and in the pores. Each channel appears hexagonal in outline. Magnification ×307,800. (Reproduced, with permission, from N. Gilula.)

B. A gap-junction channel is actually a pair of hemichannels, one in each apposite cell that connects the cytoplasm of the two cells. (Adapted from Makowski et al. 1977.)

C. Each hemichannel, or connexon, is made up of six identical subunits called connexins. Each connexin is approximately 7.5 nm long and spans the cell membrane. A single connexin has intracellular N- and C-terminals, including a short intracellular N-terminal α-helix (**NTH**), and four membrane-spanning α-helixes (**1–4**). The amino acid sequences of gap-junction proteins from many different kinds of tissue have regions of similarity that include the transmembrane helixes and the extracellular regions, which are involved in the homophilic matching of apposite hemichannels.

D. The connexins are arranged in such a way that a pore is formed in the center of the structure. The resulting connexon, with a pore diameter of approximately 1.5 to 2 nm, has a characteristic hexagonal outline, as shown in the photograph in part A. In some gap-junction channels, the pore is opened when the subunits rotate approximately 0.9 nm at the cytoplasmic base in a clockwise direction. (Reproduced, with permission, from Unwin and Zampighi 1980. Copyright © 1980 Springer Nature.)

The three-dimensional structure of a gap-junction channel formed by the human connexin 26 subunit has been determined by X-ray crystallography. This structure shows how the membrane-spanning α-helixes assemble to form the central pore of the channel and how the extracellular loops connecting the transmembrane helixes interdigitate to connect the two hemichannels (Figure 11–5). The pore is lined with polar residues that facilitate the movement of ions. An N-terminal α-helix may serve as the voltage gate of the connexin 26 channel, plugging the cytoplasmic mouth of the pore in the closed state. A separate gate

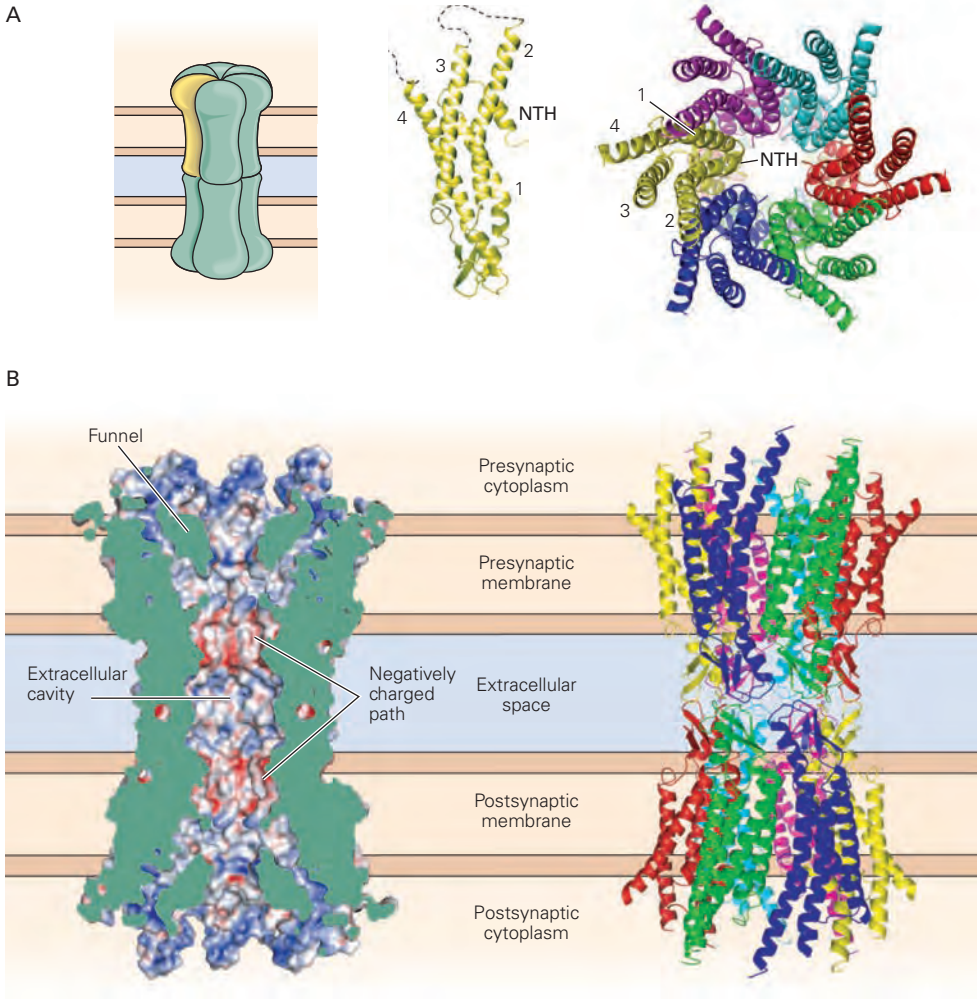

Figure 11–5 High-resolution three-dimensional structure of a gap-junction channel. All structures were determined by X-ray crystallography of gap-junction channels formed by the human connexin 26 subunit. (Reproduced, with permission, from Maeda et al. 2009. Copyright © 2009 Springer Nature.)

A. *Left:* Diagram of an intact gap-junction channel showing the pair of apposed hemichannels. *Middle:* This high-resolution structure of a single connexin subunit shows four transmembrane α-helixes (**1–4**) and a short N-terminal helix (**NTH**). The orientation of the subunit corresponds to that of the yellow subunit in the diagram to the right. *Right:* Bottom-up view looking into a hemichannel from the cytoplasm. Each of the six subunits has a different color. The helixes of the yellow subunit are numbered. The orientation corresponds to that of the yellow hemichannel in the diagram at left, following a 90-degree rotation toward the viewer.

B. Two side views of the gap-junction channel in the plane of the membrane show the two apposed hemichannels. The orientation is the same as in part A. *Left:* Cross section through the channel shows the internal surface of the channel pore. **Blue** indicates positively charged surfaces; **red** indicates negatively charged surfaces. The **green mass** inside the pore at the cytoplasmic entrance (funnel) is thought to represent the channel gate formed by the N-terminal helix. *Right:* A side view of the channel shows each of the six connexin subunits in the same color scheme as in part A. The entire gap-junction channel is approximately 9 nm wide by 15 nm tall.

at the extracellular side of the channel, formed by the extracellular loop connecting the first two membrane helixes, has been inferred from functional studies. This loop gate is thought to close isolated hemichannels that are not docked to a hemichannel partner in the apposing cell.

Electrical Transmission Allows Rapid and Synchronous Firing of Interconnected Cells

How are electrical synapses useful? As we have seen, electrical synaptic transmission is rapid because it results from the direct passage of current between cells. Speed is important for escape responses. For example, the tail-flip response of goldfish is mediated by a giant neuron in the brain stem (known as the Mauthner cell), which receives sensory input at electrical synapses. These electrical synapses rapidly depolarize the Mauthner cell, which in turn activates the motor neurons of the tail, allowing rapid escape from danger.

Electrical transmission is also useful for orchestrating the actions of groups of neurons. Because current crosses the membranes of all electrically coupled cells at the same time, several small cells can act together as one large cell. Moreover, because of the electrical coupling between the cells, the effective resistance of the network is smaller than the resistance of an individual cell. Thus, from Ohm's law, the synaptic current required to fire electrically coupled cells is larger than that necessary to fire an individual cell. That is, electrically coupled cells have a higher firing threshold. Once this high threshold is surpassed, however, electrically coupled cells fire synchronously because voltage-activated Na^+ currents generated in one cell are very rapidly conducted to other cells.

Thus, a behavior controlled by a group of electrically coupled cells has an important adaptive advantage: It is triggered explosively. For example, when seriously perturbed, the marine snail *Aplysia* releases massive clouds of purple ink that provide a protective screen. This stereotypic behavior is mediated by three electrically coupled motor cells that innervate the ink gland. Once the action potential threshold is exceeded in these cells, they fire synchronously (Figure 11–6). In certain fish, rapid eye movements (called saccades) are also mediated by electrically coupled motor neurons

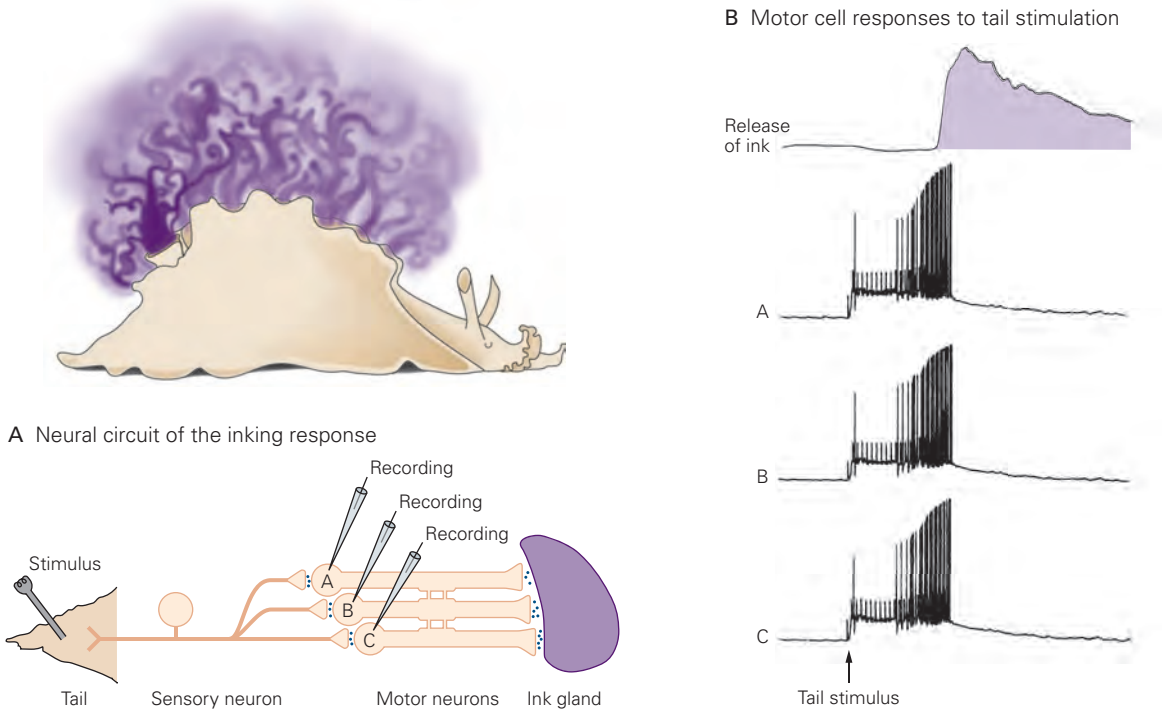

Figure 11–6 Electrically coupled motor neurons firing together can produce synchronous behaviors. (Adapted, with permission, from Carew and Kandel 1976.)

A. In the marine snail *Aplysia*, sensory neurons from the tail ganglion form synapses with three motor neurons that innervate the ink gland. The motor neurons are interconnected by electrical synapses.

B. A train of stimuli applied to the tail produces a synchronized discharge in all three motor neurons that results in the release of ink.

firing together. Gap junctions are also important in the mammalian brain, where the synchronous firing of electrically coupled inhibitory interneurons generates synchronous 40- to 100-Hz (gamma) oscillations in large populations of cells.

In addition to providing speed or synchrony in neuronal signaling, electrical synapses also can transmit metabolic signals between cells. Because of their large-diameter pore, gap-junction channels conduct a variety of inorganic cations and anions, including the second messenger Ca^{2+}, and even conduct moderate-sized organic compounds (<1 kDa molecular weight) such as the second messengers inositol 1,4,5-trisphosphate (IP_3), cyclic adenosine monophosphate (cAMP), and even small peptides.

Gap Junctions Have a Role in Glial Function and Disease

Gap junctions are formed between glial cells as well as between neurons. In glia, the gap junctions mediate both intercellular and intracellular signaling. In the brain, individual astrocytes are connected to each other through gap junctions forming a glial cell network. Electrical stimulation of neuronal pathways in brain slices can release neurotransmitters that trigger a rise in intracellular Ca^{2+} in certain astrocytes. This produces a wave of Ca^{2+} that propagates from astrocyte to astrocyte at a rate of approximately 1–20 μm/s, about a million-fold slower than the propagation of an action potential (10–100 m/s). Although the precise function of the waves is unknown, their existence suggests that glia may play an active role in intercellular signaling in the brain.

Gap-junction channels also enhance communication *within* certain glial cells, such as the Schwann cells that produce the myelin sheath of axons in the peripheral nervous system. Successive layers of myelin formed by a single Schwann cell are connected by gap junctions. These gap junctions may help to hold the layers of myelin together and promote the passage of small metabolites and ions across the many layers of myelin. The importance of the Schwann cell gap-junction channels is underscored by certain genetic diseases. For example, the X chromosome–linked form of Charcot-Marie-Tooth disease, a demyelinating disorder, is caused by single mutations that disrupt the function of *connexin 32*, the gene expressed in Schwann cells. Inherited mutations that prevent the function of a connexin in the cochlea (connexin 26), which normally forms gap-junction channels that are important for fluid secretion in the inner ear, underlie up to half of all instances of congenital deafness.

Chemical Synapses Can Amplify Signals

In contrast to electrical synapses, at chemical synapses, there is no structural continuity between presynaptic and postsynaptic neurons. In fact, the separation between the two cells at a chemical synapse, the synaptic cleft, is usually slightly wider (20–40 nm) than the nonsynaptic intercellular space (20 nm). Chemical synaptic transmission depends on a neurotransmitter, a chemical substance that diffuses across the synaptic cleft and binds to and activates receptors in the membrane of the target cell. At most chemical synapses, transmitter is released from specialized swellings of the presynaptic axon—synaptic boutons—that typically contain 100 to 200 synaptic vesicles, each of which is filled with several thousand molecules of neurotransmitter (Figure 11–7).

The synaptic vesicles are clustered at specialized regions of the synaptic bouton called *active zones.* During a presynaptic action potential, voltage-gated Ca^{2+} channels at the active zone open, allowing Ca^{2+} to enter the presynaptic terminal. The rise in intracellular Ca^{2+}concentration triggers a biochemical reaction that causes the vesicles to fuse with the presynaptic membrane and release neurotransmitter into the synaptic cleft, a process termed *exocytosis*. The transmitter molecules then diffuse across the synaptic cleft and bind

Figure 11–7 The fine structure of a presynaptic terminal. This electron micrograph shows an axon terminal in the cerebellum. The large dark structures are mitochondria. The many small round bodies are vesicles that contain neurotransmitter. The fuzzy dark thickenings along the presynaptic membrane (**arrows**) are the active zones, specialized areas that are thought to be docking and release sites for synaptic vesicles. The synaptic cleft is the space separating the pre- and postsynaptic cell membranes. (Reproduced, with permission, from Heuser and Reese 1977.)

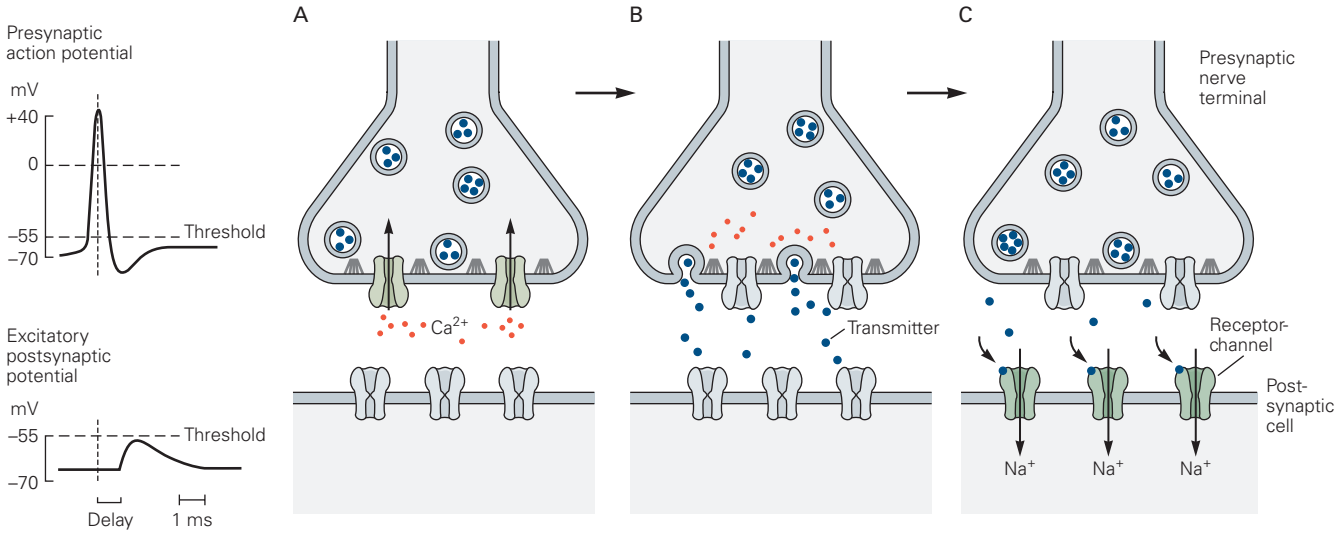

Figure 11–8 Synaptic transmission at chemical synapses involves several steps. The complex process of chemical synaptic transmission accounts for the delay between an action potential in the presynaptic cell and the synaptic potential in the postsynaptic cell, as compared with the virtually instantaneous transmission of signals at electrical synapses (see Figure 11–2B).

A. An action potential arriving at the terminal of a presynaptic axon causes voltage-gated Ca^{2+} channels at the active zone to open. The **gray filaments** represent the docking and release sites of the active zone.

B. The Ca^{2+} channel opening produces a high concentration of intracellular Ca^{2+} near the active zone, causing vesicles containing neurotransmitter to fuse with the presynaptic cell membrane and release their contents into the synaptic cleft (a process termed *exocytosis*).

C. The released neurotransmitter molecules then diffuse across the synaptic cleft and bind specific receptors on the postsynaptic membrane. These receptors cause ion channels to open (or close), thereby changing the membrane conductance and membrane potential of the postsynaptic cell.

to their receptors on the postsynaptic cell membrane. This in turn activates the receptors, leading to the opening or closing of ion channels. The resulting flux of ions alters the membrane conductance and potential of the postsynaptic cell (Figure 11–8).

These several steps account for the synaptic delay at chemical synapses. Despite its biochemical complexity, the release process is remarkably efficient—the synaptic delay is usually only 1 ms or less. Although chemical transmission lacks the immediacy of electrical synapses, it has the important property of *amplification*. Just one synaptic vesicle releases several thousand molecules of transmitter that together can open thousands of ion channels in the target cell. In this way, a small presynaptic nerve terminal, which generates only a weak electrical current, can depolarize a large postsynaptic cell.

The Action of a Neurotransmitter Depends on the Properties of the Postsynaptic Receptor

Chemical synaptic transmission can be divided into two steps: a transmitting step, in which the presynaptic cell releases a chemical messenger, and a receptive step, in which the transmitter binds to and activates the receptor molecules in the postsynaptic cell. The transmitting process in neurons resembles endocrine hormone release. Indeed, chemical synaptic transmission can be seen as a modified form of hormone secretion. Both endocrine glands and presynaptic terminals release a chemical agent with a signaling function, and both are examples of regulated secretion (Chapter 7). Similarly, both endocrine glands and neurons are usually some distance from their target cells.

There is one important difference, however, between endocrine and synaptic signaling. Whereas the hormone released by a gland travels through the blood stream until it interacts with all cells that contain an appropriate receptor, a neuron usually communicates only with the cells with which it forms synapses. Because the presynaptic action potential triggers the release of a chemical transmitter onto a target cell across a distance of only 20 nm, the chemical signal travels only a small distance to its target. Therefore, neuronal signaling has two special features: It is fast and it is precisely directed.

In most neurons, this directed or focused release is accomplished at the active zones of synaptic boutons.

In presynaptic neurons neurons without active zones, the distinction between neuronal and hormonal transmission becomes blurred. For example, the neurons in the autonomic nervous system that innervate smooth muscle reside at some distance from their postsynaptic cells and do not have specialized release sites in their terminals. Synaptic transmission between these cells is slower and relies on a more widespread diffusion of transmitter. Furthermore, the same transmitter substance can be released differently from different cells. A substance can be released from one cell as a conventional transmitter acting directly on neighboring cells. From other cells, it can be released in a less focused way as a modulator, producing a more diffuse action; and from still other cells, it can be released into the blood stream as a neurohormone.

Although a variety of chemicals serve as neurotransmitters, including both small molecules and peptides (Chapter 16), the action of a transmitter depends on the properties of the postsynaptic receptors that recognize and bind the transmitter, not the chemical properties of the transmitter. For example, ACh can excite some postsynaptic cells and inhibit others, and at still other cells, it can produce both excitation and inhibition. It is the receptor that determines the action of ACh, including whether a cholinergic synapse is excitatory or inhibitory.

Within a group of closely related animals, a transmitter substance binds conserved families of receptors and is often associated with specific physiological functions. In vertebrates, ACh acts on excitatory ACh receptors at all neuromuscular junctions to trigger contraction while also acting on inhibitory ACh receptors to slow the heart.

The distinction between the transmitting and receptive processes is not absolute; many presynaptic terminals contain transmitter receptors that can modify the release process. In some instances, these presynaptic receptors are activated by the transmitter released from the same presynaptic terminal. In other instances, the presynaptic terminal can be contacted by presynaptic terminals from other classes of neurons that release distinct neurotransmitters.

The notion of a receptor was introduced in the late 19th century by the German bacteriologist Paul Ehrlich to explain the selective action of toxins and other pharmacological agents and the great specificity of immunological reactions. In 1900, Ehrlich wrote: "Chemical substances are only able to exercise an action on the tissue elements with which they are able to establish an intimate chemical relationship … [This relationship] must be specific. The [chemical] groups must be adapted to one another … as lock and key."

In 1906, the English pharmacologist John Langley postulated that the sensitivity of skeletal muscle to curare and nicotine was caused by a "receptive molecule." A theory of receptor function was later developed by Langley's students (in particular, A.V. Hill and Henry Dale), a development that was based on concurrent studies of enzyme kinetics and cooperative interactions between small molecules and proteins. As we shall see in the next chapter, Langley's "receptive molecule" has been isolated and characterized as the ACh receptor of the neuromuscular junction.

All receptors for chemical transmitters have two biochemical features in common:

1. They are membrane-spanning proteins. The region exposed to the external environment of the cell recognizes and binds the transmitter from the presynaptic cell.
2. They carry out an effector function within the target cell. The receptors typically influence the opening or closing of ion channels.

Activation of Postsynaptic Receptors Gates Ion Channels Either Directly or Indirectly

Neurotransmitters control the opening of ion channels in the postsynaptic cell either directly or indirectly. These two classes of transmitter actions are mediated by receptor proteins derived from different gene families.

Receptors that gate ion channels directly, such as the ACh receptor at the neuromuscular junction, are composed of four or five subunits that form a single macromolecule. Such receptors contain both an extracellular domain that forms the binding site for the transmitter and a membrane-spanning domain that forms an ion-conducting pore (Figure 11–9A). This kind of receptor is often referred to as *ionotropic* because the receptor directly controls ion flux. Upon binding neurotransmitter, the receptor undergoes a conformational change that opens the ion channel. The actions of ionotropic receptors, also called *receptor-channels* or *ligand-gated channels*, are discussed in detail in Chapters 12 and 13.

Receptors that gate ion channels indirectly, like the several types of receptors for norepinephrine or dopamine in neurons of the cerebral cortex, are normally composed of one or at most two subunits that are distinct from the ion channels they regulate. These receptors, which commonly have seven membrane-spanning α-helixes, act by altering intracellular metabolic reactions and are often referred to as *metabotropic receptors*. Activation of these receptors often stimulates

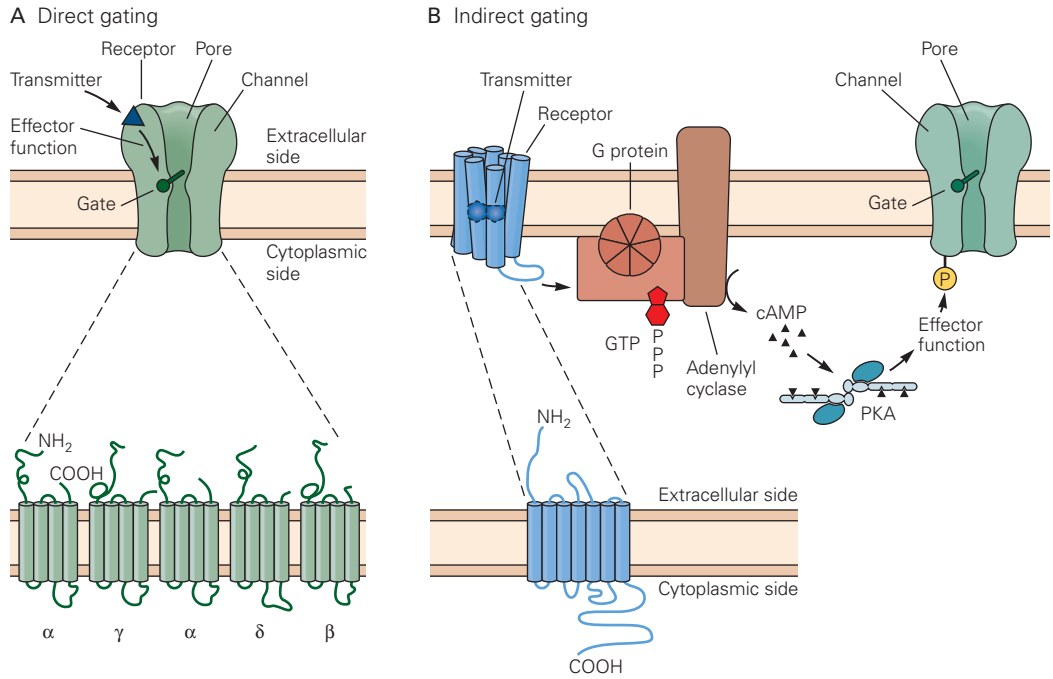

Figure 11–9 Neurotransmitters open postsynaptic ion channels either directly or indirectly.

A. A receptor that directly opens ion channels is an integral part of the macromolecule that also forms the channel. Many such ligand-gated channels are composed of five subunits, each of which is thought to contain four membrane-spanning α-helical regions.

B. A receptor that indirectly opens an ion channel is a distinct macromolecule separate from the channel it regulates. In one large family of such receptors, the receptors are composed of a single subunit with seven membrane-spanning α-helical regions that bind the ligand within the plane of the membrane. These receptors activate a guanosine triphosphate (**GTP**)–binding protein (**G protein**), which in turn activates a second-messenger cascade that modulates channel activity. In the cascade illustrated here, the G protein stimulates adenylyl cyclase, which converts adenosine triphosphate (**ATP**) to cyclic adenosine monophosphate (**cAMP**). The cAMP activates the cAMP-dependent protein kinase (**PKA**), which phosphorylates the channel (**P**), leading to a change in opening.

the production of second messengers, small freely diffusible intracellular metabolites such as cAMP or diacylglycerol. Many of these second messengers activate protein kinases, enzymes that phosphorylate different substrate proteins. In many instances, the protein kinases directly phosphorylate ion channels, including gap-junction channels and ionotropic receptors, modulating their opening or closing (Figure 11–9B). The actions of metabotropic receptors are examined in detail in Chapter 14.

Ionotropic and metabotropic receptors have different functions. The ionotropic receptors produce relatively fast synaptic actions lasting only milliseconds. These are commonly found at synapses in neural circuits that mediate rapid behaviors, such as the stretch receptor reflex. The metabotropic receptors produce slower synaptic actions, lasting hundreds of milliseconds to minutes. These slower actions can modulate a behavior by altering the excitability of neurons and the strength of the synaptic connections in the neural circuit that mediates the behavior. Such modulatory synaptic actions often act as crucial reinforcing pathways in the process of learning.

Electrical and Chemical Synapses Can Coexist and Interact

As we now realize, both Henry Dale and John Eccles were correct about the existence of chemical and electrical synapses, respectively. Furthermore, we now know that both forms of synaptic transmission can coexist in the same neuron and that electrical and chemical synapses can modify each other's efficacy. For example, during development, many neurons are initially connected by electrical synapses, whose presence helps in the formation of chemical synapses. As chemical

synapses begin to form, they often initiate the down-regulation of electrical transmission.

Both types of synapses also can coexist in neurons in the mature nervous system. The role of these two types of synapses is perhaps best understood in the circuitry of the retina. There, rod and cone photoreceptors release the neurotransmitter glutamate and form chemical synapses on a class of interneurons called bipolar cells. Each bipolar cell extends its dendrites horizontally, receiving chemical synaptic input from a number of overlying rods and cones that respond to light from a very small region of the visual field. The receptive field of a bipolar neuron, however, extends about twice as far as the receptive field of the photoreceptors from which it receives chemical synaptic input. This is a result of electrical synapses formed between neighboring bipolar cells and between bipolar cells and a second type of interneuron, the amacrine cell (Chapter 22).

Finally, the efficacy of gap junctions can be regulated by phosphorylation through different protein kinases, which generally enhances gap-junction coupling. For example, dopamine and other transmitters can increase or decrease gap-junction coupling by acting on metabotropic G protein–coupled receptors to regulate levels of cAMP and thereby enhance or decrease channel phosphorylation. Such complex signaling loops are a hallmark of many neural circuits and greatly expand their computational powers.

Highlights

1. Neurons communicate by two major mechanisms: electrical and chemical synaptic transmission.
2. Electrical synapses are formed at regions of tight apposition called gap junctions, which provide a direct pathway for charge to flow between the cytoplasm of communicating neurons. This results in very rapid synaptic transmission that is suited for synchronizing the activity of populations of neurons.
3. Neurons at electrical synapses are connected through gap-junction channels, which are formed from a pair of hemichannels, called connexons, one each contributed by the presynaptic and postsynaptic cells. Each connexon is a hexamer, composed of six subunits termed connexins.
4. At chemical synapses, a presynaptic action potential triggers the release of a chemical transmitter from the presynaptic cell through the process of exocytosis. Transmitter molecules then rapidly diffuse across the synaptic cleft to bind to and activate transmitter receptors in the postsynaptic cell.
5. Although slower than electrical synaptic transmission, chemical transmission allows for amplification of the presynaptic action potential through the release of tens of thousands of molecules of transmitter and the activation of hundreds to thousands of receptors in the postsynaptic cell.
6. There are two major classes of transmitter receptors. Ionotropic receptors are ligand-gated ion channels. Binding of transmitter to an extracellular binding site triggers a conformational change that opens the channel pore, generating an ionic current that excites (depolarizes) or inhibits (hyperpolarizes) the postsynaptic cell, depending on the receptor. Ionotropic receptors underlie fast chemical synaptic transmission that mediates rapid signaling in the nervous system.
7. Metabotropic receptors are responsible for the second major class of chemical synaptic actions. These receptors activate intracellular metabolic signaling pathways, often leading to the synthesis of second messengers, such as cAMP, that regulate levels of protein phosphorylation. Metabotropic receptors underlie slow, modulatory synaptic actions that contribute to changes in behavioral state and arousal.

Steven A. Siegelbaum
Gerald D. Fischbach

Selected Reading

Bennett MV, Zukin RS. 2004. Electrical coupling and neuronal synchronization in the mammalian brain. Neuron 19:495–511.

Colquhoun D, Sakmann B. 1998. From muscle endplate to brain synapses: a short history of synapses and agonist-activated ion channels. Neuron 20:381–387.

Cowan WM, Kandel ER. 2000. A brief history of synapses and synaptic transmission. In: MW Cowan, TC Südhof, CF Stevens (eds). *Synapses,* pp. 1–87. Baltimore and London: The Johns Hopkins Univ. Press.

Curti S, O'Brien J. 2016. Characteristics and plasticity of electrical synaptic transmission. BMC Cell Biol 17:13. Suppl 1.

Eccles JC. 1976. From electrical to chemical transmission in the central nervous system. The closing address of the

Sir Henry Dale Centennial Symposium. Notes Rec R Soc Lond 30:219–230.
Furshpan EJ, Potter DD. 1959. Transmission at the giant motor synapses of the crayfish. J Physiol 145:289–325.
Goodenough DA, Paul DL. 2009. Gap junctions. Cold Spring Harb Perspect Biol 1:a002576.
Jessell TM, Kandel ER. 1993. Synaptic transmission: a bidirectional and a self-modifiable form of cell-cell communication. Cell 72:1–30.
Nakagawa S, Maeda S, Tsukihara T. 2010. Structural and functional studies of gap junction channels. Curr Opin Struct Biol 20:423–430.
Pereda AE. 2014. Electrical synapses and their functional interactions with chemical synapses. Nat Rev Neurosci 15:250–263.

References

Beyer EC, Paul DL, Goodenough DA. 1987. Connexin 43: a protein from rat heart homologous to a gap junction protein from liver. J Cell Biol 105:2621–2629.
Bruzzone R, White TW, Scherer SS, Fischbeck KH, Paul DL. 1994. Null mutations of connexin 32 in patients with X-linked Charcot-Marie-Tooth disease. Neuron 13:1253–1260.
Carew TJ, Kandel ER. 1976. Two functional effects of decreased conductance EPSP's: synaptic augmentation and increased electrotonic coupling. Science 192:150–153.
Cornell-Bell AH, Finkbeiner SM, Cooper MS, Smith SJ. 1990. Glutamate induces calcium waves in cultured astrocytes: long-range glial signaling. Science 247:470–473.
Dale H. 1935. Pharmacology and nerve-endings. Proc R Soc Lond 28:319–332.
Eckert R. 1988. Propagation and transmission of signals. In: *Animal Physiology: Mechanisms and Adaptations,* 3rd ed., pp. 134–176. New York: Freeman.
Ehrlich P. 1900. On immunity with special reference to cell life. Croonian Lect Proc R Soc Lond 66:424–448.
Furshpan EJ, Potter DD. 1957. Mechanism of nerve-impulse transmission at a crayfish synapse. Nature 180:342–343.
Harris AL. 2009. Gating on the outside. J Gen Physiol 133:549–553.
Heuser JE, Reese TS. 1977. Structure of the synapse. In: ER Kandel (ed). *Handbook of Physiology: A Critical, Comprehensive Presentation of Physiological Knowledge and Concepts,* Sect. 1. *The Nervous System,* Vol. 1 *Cellular Biology of Neurons,* Part 1, pp. 261–294. Bethesda, MD: American Physiological Society.
Jaslove SW, Brink PR. 1986. The mechanism of rectification at the electrotonic motor giant synapse of the crayfish. Nature 323:63–65.
Langley JN. 1906. On nerve endings and on special excitable substances in cells. Proc R Soc Lond B Biol Sci 78:170–194.
Loewi O, Navratil E. [1926] 1972. On the humoral propagation of cardiac nerve action. Communication X. The fate of the vagus substance. English translation in: I Cooke, M Lipkin Jr (eds). *Cellular Neurophysiology: A Source Book,* pp. 4711–485. New York: Holt, Rinehart and Winston.
Maeda S, Nakagawa S, Suga M, et al. 2009. Structure of the connexin 26 gap junction channel at 3.5 Å resolution. Nature 458:597–602.
Makowski L, Caspar DL, Phillips WC, Goodenough DA. 1977. Gap junction structures. II. Analysis of the X-ray diffraction data. J Cell Biol 74:629–645.
Pappas GD, Waxman SG. 1972. Synaptic fine structure: morphological correlates of chemical and electronic transmission. In: GD Pappas, DP Purpura (eds). *Structure and Function of Synapses,* pp. 1–43. New York: Raven.
Ramón y Cajal S. 1894. La fine structure des centres nerveux. Proc R Soc Lond 55:444–468.
Ramón y Cajal S. 1911. *Histologie du Système Nerveux de l'Homme & des Vertébrés,* Vol. 2. L Azoulay (transl). Paris: Maloine, 1955. Reprint. Madrid: Instituto Ramón y Cajal.
Sherrington C. 1947. *The Integrative Action of the Nervous System,* 2nd ed. New Haven: Yale Univ. Press.
Unwin PNT, Zampighi G. 1980. Structure of the junction between communicating cells. Nature 283:545–549.
Whittington MA, Traub RD. 2003. Interneuron diversity series: inhibitory interneurons and network oscillations in vitro. Trends Neurosci 26:676–682.

12

Directly Gated Transmission: The Nerve-Muscle Synapse

MUCH OF OUR UNDERSTANDING of the principles that govern chemical synapses in the brain is based on studies of synapses formed by motor neurons on skeletal muscle cells. The landmark work of Bernard Katz and his colleagues over three decades beginning in 1950 defined the basic parameters of synaptic transmission and opened the door to modern molecular analyses of synaptic function. Therefore, before we examine the complexities of synapses in the central nervous system, we will examine the basic features of chemical synaptic transmission at the simpler nerve-muscle synapse.

The early studies capitalized on several experimental advantages offered by nerve-muscle preparations of various species. Muscles and attached motor axons are easy to dissect and maintain for several hours in vitro. Muscle cells are large enough to be penetrated with two or more fine-tipped microelectrodes, enabling precise analyses of synaptic potentials and underlying ionic currents. In most species, innervation is restricted to one site, the motor end-plate, and in adult animals that site is innervated by only one motor axon. In contrast, central neurons receive many convergent inputs that are distributed throughout the dendritic arbor and the soma, and thus the impact of single inputs is more difficult to discern.

Most important, the chemical transmitter that mediates synaptic transmission between nerve and muscle, acetylcholine (ACh), was identified early in the 20th century. We now know that signaling at the nerve-muscle synapse involves a relatively simple mechanism: Neurotransmitter released from the presynaptic nerve binds to a single type of receptor in the postsynaptic membrane,

the nicotinic ACh receptor.[1] Binding of transmitter to the receptor directly opens an ion channel; both the receptor and channel are components of the same macromolecule. Synthetic and natural agents that activate or inhibit nicotinic ACh receptors have proven useful in analyzing not only the ACh receptors in muscle, but also cholinergic synapses in peripheral ganglia and in the brain. Moreover, such ligands can be useful therapeutic agents, including the treatment of inherited and acquired neurological diseases resulting from alterations in ACh receptor function or genetic mutations.

The Neuromuscular Junction Has Specialized Presynaptic and Postsynaptic Structures

As the motor axon approaches the *end-plate*, the site of contact between nerve and muscle (also known as the *neuromuscular junction*), it loses its myelin sheath and divides into several fine branches. At their ends, these fine branches form multiple expansions or varicosities called *synaptic boutons* (Figure 12–1) from which the motor axon releases its transmitter. Although myelin ends some distance from the sites of transmitter release, Schwann cells cover and partially enwrap the nerve terminal. A terminal "arbor" defines the area of the motor end-plate. In different species, end-plates range from compact elliptical structures about 20 µm across to linear arrays more than 100 µm in length.

The nerve terminals lie in grooves, the primary folds, along the muscle surface. The membrane under each synaptic bouton is further invaginated to form a series of secondary or junctional folds (Figure 12–1). The muscle cytoplasm beneath the nerve terminals contains many round muscle nuclei that likely are involved in synthesis of synapse-specific molecules. They are different from the flat nuclei located away from the synapse along the length of the muscle fiber.

Action potentials in the axon are conducted to the tips of the fine branches where they trigger the release of ACh. The synaptic boutons contain all the machinery required to synthesize and release ACh. This includes the synaptic vesicles containing the transmitter ACh and the active zones where the synaptic vesicles are clustered. In addition, each active zone contains voltage-gated Ca^{2+} channels that conduct Ca^{2+} into the terminal with each action potential. This influx of Ca^{2+} triggers the fusion of the synaptic vesicles with the plasma membrane at the active zones, releasing the contents of the synaptic vesicles into the synaptic cleft by the process of exocytosis (Chapter 15).

The distribution of ACh receptors can be studied using α-bungarotoxin (αBTX), a peptide isolated from the venom of the snake *Bungarus multicinctus* that binds tightly and specifically to the ACh receptors at the neuromuscular junction (Figure 12–2B). Quantitative autoradiography of iodinated BTX (^{125}I-αBTX) showed that the ACh receptors are packed at the crests of the secondary folds at a surface density in excess of 10,000/µm^2 (Figure 12–3). The factors responsible for localizing the receptor are discussed in Chapter 48, where we consider the development of synaptic connections.

Presynaptic and postsynaptic membranes at the neuromuscular junction are separated by a cleft approximately 100 nm wide. Although such a gap was postulated by Ramón y Cajal in the last years of the 19th century, it was not visualized until synapses were examined by electron microscopy more than 50 years later! A basement membrane (basal lamina) composed of collagen and other extracellular matrix proteins is present throughout the synaptic cleft. Acetylcholinesterase (AChE), an enzyme that rapidly hydrolyzes ACh, is anchored to collagen fibrils within the basement membrane. The ACh released into the synaptic cleft must run a "gauntlet" of AChE before it reaches the ACh receptors in the muscle membrane. As AChE is inhibited by high concentrations of ACh, most molecules get through. Nevertheless, the enzyme limits the action of ACh to "one hit" because AChE hydrolyzes transmitter as soon as it dissociates from its receptor in the postsynaptic membrane.

The Postsynaptic Potential Results From a Local Change in Membrane Permeability

Once ACh is released from a synaptic terminal, it rapidly binds to and opens the ACh receptor-channels in the end-plate membrane. This produces a dramatic increase in the permeability of the muscle membrane to cations, which leads to the entry of positive charge into the muscle fiber and a rapid depolarization of the end-plate membrane. The resulting excitatory postsynaptic potential (EPSP) is very large; stimulation of a single motor axon produces an EPSP of approximately 75 mV. At the nerve-muscle synapse, the EPSP is also referred to as the *end-plate potential*.

This change in membrane potential usually is large enough to rapidly activate the voltage-gated Na^+

[1]There are two basic types of receptors for ACh: nicotinic and muscarinic, so called because the alkaloids nicotine and muscarine bind exclusively to and activate one or the other type of ACh receptor. The nicotinic ACh receptor is ionotropic, whereas the muscarinic receptor is metabotropic. We shall learn more about muscarinic ACh receptors in Chapter 14.

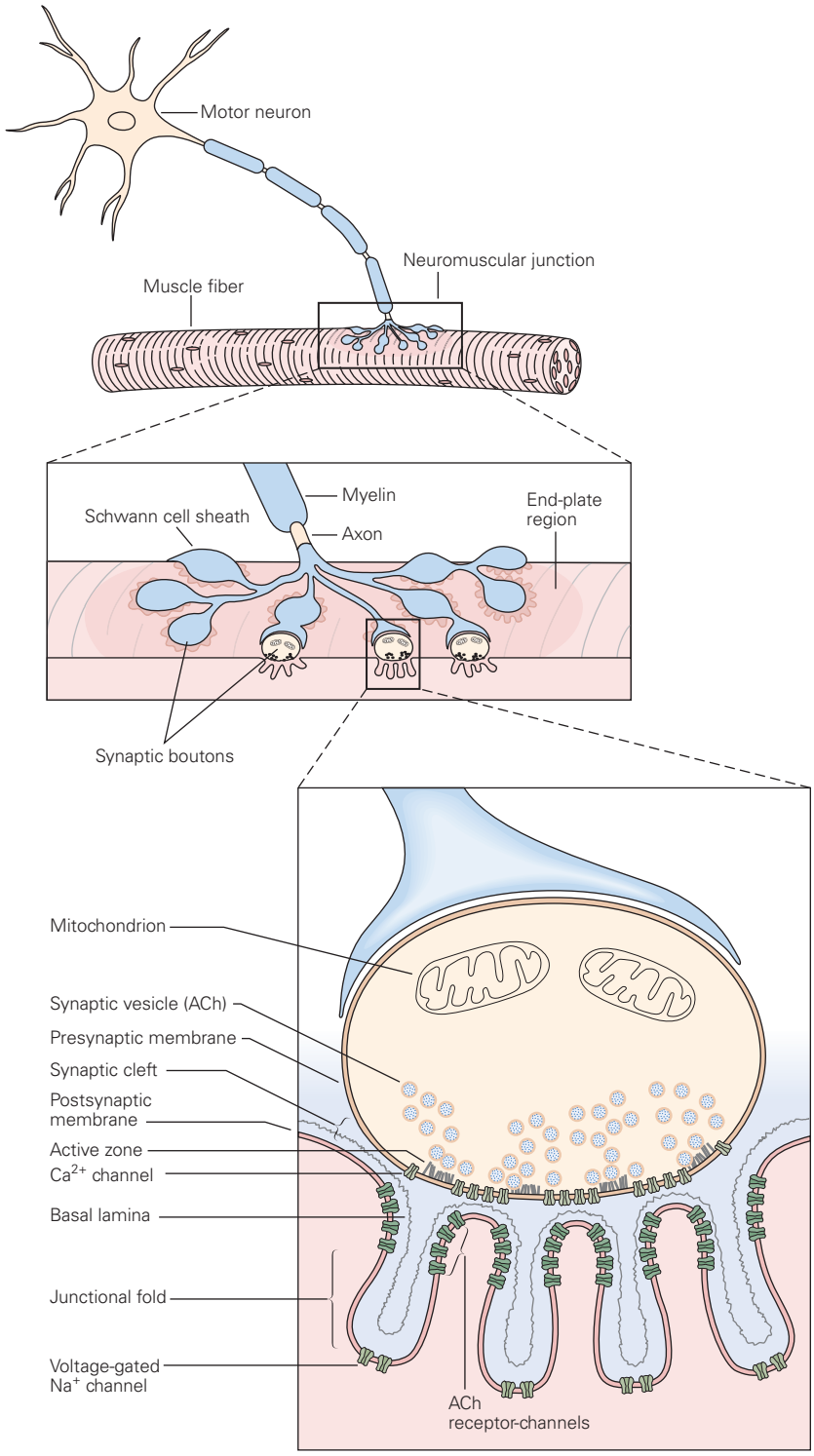

Figure 12–1 The neuromuscular junction is an ideal site for studying chemical synaptic signaling. At the muscle, the motor axon ramifies into several fine branches approximately 2 μm thick. Each branch forms multiple swellings called *synaptic boutons*, which are covered by a thin layer of Schwann cells. The boutons contact a specialized region of the muscle fiber membrane, the *end-plate*, and are separated from the muscle membrane by a 100-nm synaptic cleft. Each bouton contains mitochondria and synaptic vesicles clustered around *active zones*, where the neurotransmitter acetylcholine (**ACh**) is released. Immediately under each bouton in the end-plate are several junctional folds, the crests of which contain a high density of ACh receptors.

The muscle fiber and nerve terminal are covered by a layer of connective tissue, the basal lamina, consisting of collagen and glycoproteins. Unlike the cell membrane, the basal lamina is freely permeable to ions and small organic compounds, including the ACh transmitter. Both the presynaptic terminal and the muscle fiber secrete proteins into the basal lamina, including the enzyme acetylcholinesterase, which inactivates the ACh released from the presynaptic terminal by breaking it down into acetate and choline. The basal lamina also organizes the synapse by aligning the presynaptic boutons with the postsynaptic junctional folds. (Adapted from McMahan and Kuffler 1971.)

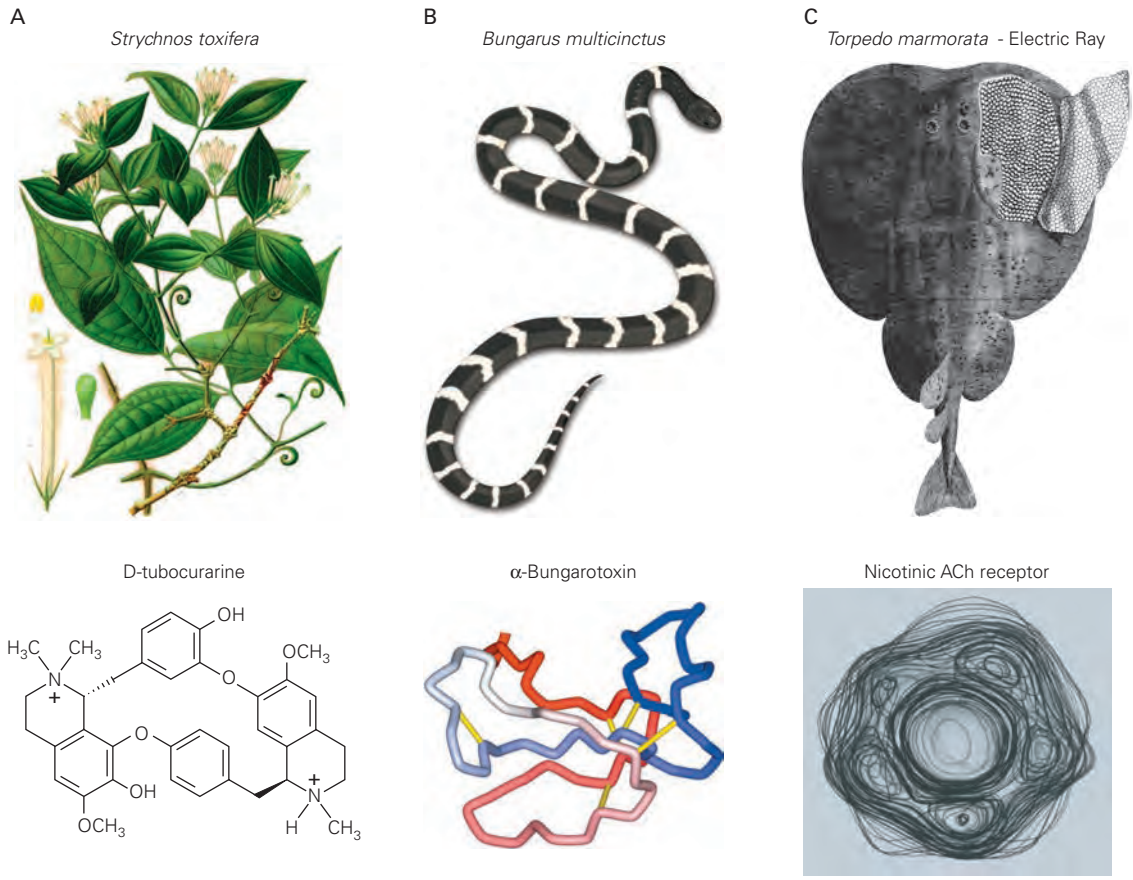

Figure 12–2 Poisons, venoms, and high-voltage electric fish help elucidate the structure and function of the nicotinic ACh receptor.

A. Curare is a mixture of toxins extracted from the leaves of *Strychnos toxifera* and is used by South American indigenous people on arrowheads to paralyze their quarry. The active compound, D-tubocurarine, is a complex multiring structure with positively charged amine groups that bear some similarity to ACh. It binds tightly to the ACh binding site on the nicotinic receptor, where it acts as a competitive antagonist for ACh. (Reproduced from Pabst, G (ed). 1898. *Köhler's Medizinal-Pflanzen*, Vol. 3, Plate 45. Gera-Untermhaus, Germany: Franz Eugen Köhler.)

B. The toxin α-bungarotoxin is obtained from the venom of the banded krait, *Bungarus*. It is a 74-amino acid polypeptide that contains five disulfide bonds (**yellow lines**), producing a rigid structure (From https://en.wikipedia.org/wiki/Alpha-bungarotoxin. Adapted from Zeng et al. 2001.). The toxin binds extremely tightly to the ACh binding site and acts as an irreversible, noncompetitive antagonist of ACh.

C. The electric ray *Torpedo marmorata* has a specialized structure, the electric organ, which consists of a large number of small, flat, muscle-like cells, or electroplaques, arranged in series like a stack of batteries. When a motor nerve releases ACh, a large current is generated by the opening of a very large number of nicotinic ACh receptor-channels, which produces a very large voltage drop of up to 200 V outside the fish, thereby stunning nearby prey. The electroplaques provide a rich source of ACh receptors for biochemical purification and characterization. (From Walsh 1773.)

channels in the muscle membrane, converting the end-plate potential into an action potential, which then propagates along the muscle fiber. The threshold for generating an action potential in the muscle is particularly low at the end-plate, owing to a high density of voltage-gated Na^+ channels in the bottom of the junctional folds. The combination of a very large EPSP and low threshold results in a high safety factor for triggering an action potential in the muscle fiber. In contrast, in the central nervous system, most presynaptic neurons produce postsynaptic potentials less than 1 mV in amplitude, such that inputs from many presynaptic neurons are needed to generate an action potential in most central neurons.

The end-plate potential was first studied in detail in the 1950s by Paul Fatt and Bernard Katz using intracellular voltage recordings. Fatt and Katz were able to isolate the end-plate potential by applying the drug curare (Figure 12–2A) to reduce the amplitude of the postsynaptic potential below the threshold for the action potential (Figure 12–4). At the end-plate, the synaptic potential rises within 1 to 2 ms but decays more slowly.

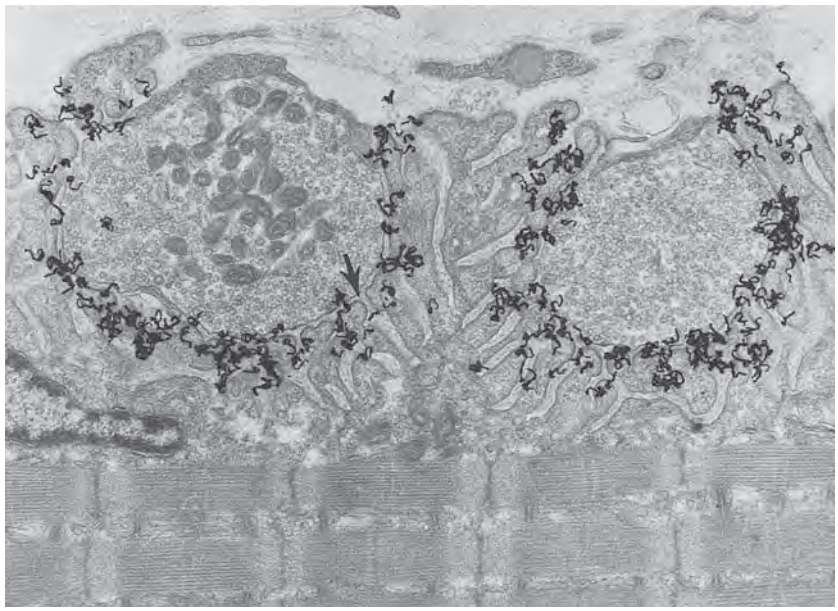

Figure 12–3 Acetylcholine receptors in the vertebrate neuromuscular junction are concentrated at the top one-third of the junctional folds. This receptor-rich region is characterized by an increased density of the postjunctional membrane (**arrow**). The autoradiograph shown here was made by first incubating the membrane with radiolabeled α-bungarotoxin, which binds to the ACh receptor. Radioactive decay results in the emittance of a particle that causes overlaid silver grains to become fixed along its trajectory (**black grains**). Magnification ×18,000. (Reproduced, with permission, from Salpeter 1987.)

By recording at different points along the muscle fiber, Fatt and Katz found that the EPSP is maximal at the end-plate and decreases progressively with distance (Figure 12–5). In addition, the time course of the EPSP slows progressively with distance.

From this, Fatt and Katz concluded that the end-plate potential is generated by an inward ionic current that is confined to the end-plate and then spreads passively away. (An inward current corresponds to an influx of positive charge, which depolarizes the inside of the membrane.) Inward current is confined to the end-plate because the ACh receptors are concentrated there, opposite the presynaptic terminal from which transmitter is released. The decrease in amplitude and slowing of the EPSP as a function of distance is a result of the passive cable properties of the muscle fiber.

Electrophysiological evidence that the ACh receptors are localized to the end-plate was provided by Stephen Kuffler and his colleagues, who applied ACh to precise points on the muscle membrane

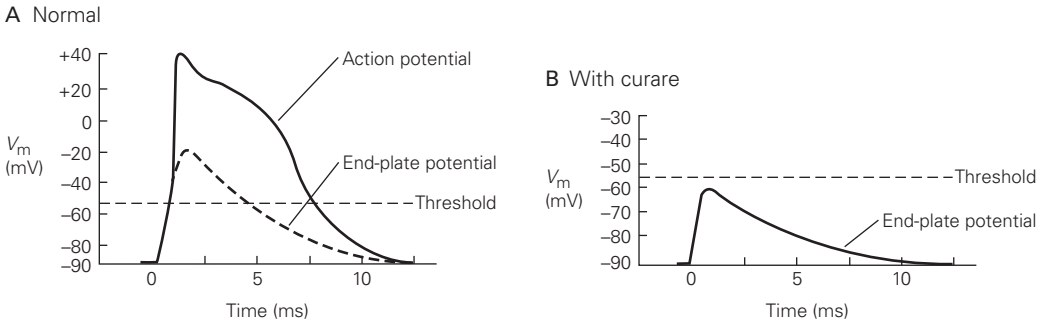

Figure 12–4 The end-plate potential can be isolated pharmacologically for study.

A. Under normal circumstances, stimulation of the motor axon produces an action potential in a skeletal muscle cell. The **dashed curve** in the plot shows the inferred time course of the end-plate potential that triggers the action potential. The lighter **dashed line** shows the action potential threshold.

B. Curare blocks the binding of ACh to its receptor and so prevents the end-plate potential from reaching the threshold for an action potential. In this way, the currents and channels that contribute to the end-plate potential, which are different from those producing an action potential, can be studied. The end-plate potential shown here was recorded in the presence of a low concentration of curare, which blocks only a fraction of the ACh receptors. The values for the resting potential (–90 mV), end-plate potential, and action potential in these intracellular recordings are typical of a vertebrate skeletal muscle.

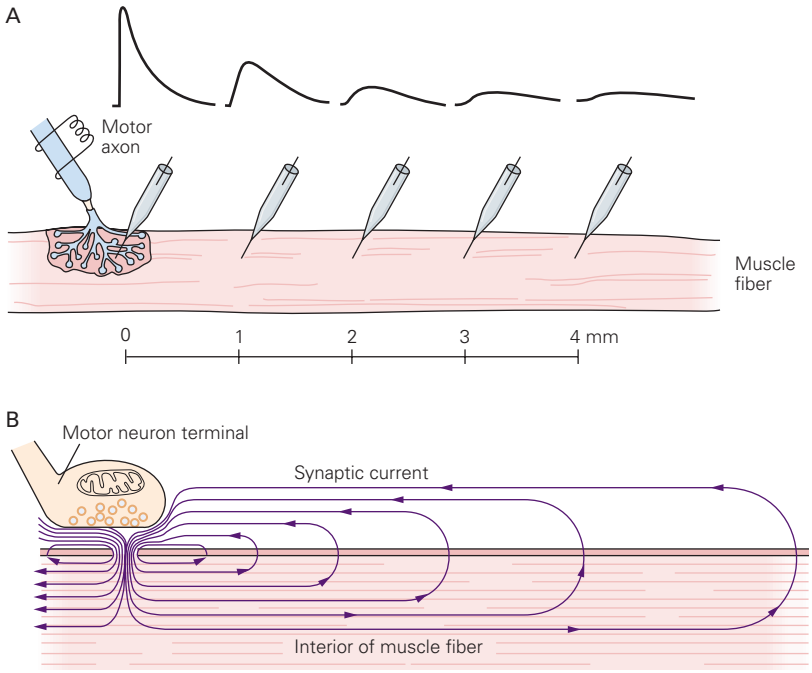

Figure 12–5 The end-plate potential decreases with distance as it passively propagates away from the end-plate. (Adapted, with permission, from Miles 1969.)

A. The amplitude of the postsynaptic potential decreases and the time course of the potential slows with distance from the site of initiation in the end-plate.

B. The decay results from leakiness of the muscle fiber membrane. Because charge must flow in a complete circuit, the inward synaptic current at the end-plate gives rise to a return outward current through resting channels and across the lipid bilayer (the capacitor). This return outward flow of positive charge depolarizes the membrane. Because current leaks out all along the membrane, the outward current and resulting depolarization decreases with distance from the end-plate.

using a technique called micro-iontophoresis. In this approach, the positively charged ACh is ejected from an ACh-filled extracellular microelectrode by applying a positive voltage to the inside of the electrode. Exposing the end-plate region to proteolytic enzymes allows the nerve terminal to be pulled away from the muscle surface and the ACh to be applied directly to the postsynaptic membrane directly under the tip of the small microelectrode. Using this technique, Kuffler found that the postsynaptic depolarizing response to ACh declined steeply within a few micrometers of the synaptic terminal.

Voltage-clamp experiments have revealed that the end-plate current rises and decays more rapidly than the resultant end-plate potential (Figure 12–6). The time course of the end-plate current is directly determined by the rapid opening and closing of the ACh receptor-channels. Because it takes time for an ionic

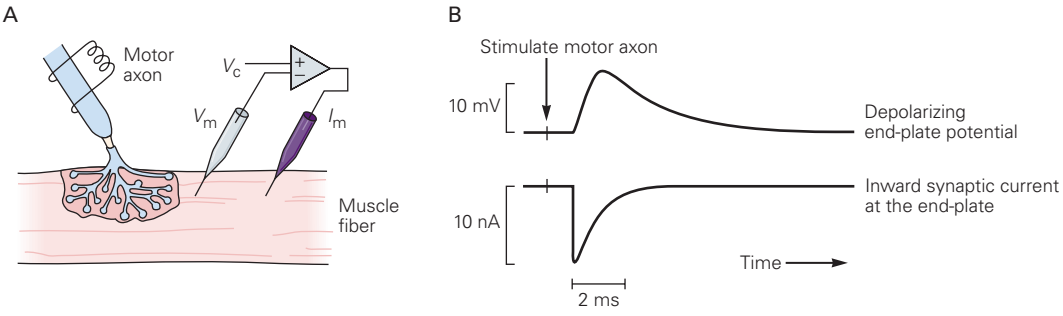

Figure 12–6 The end-plate current increases and decays more rapidly than the end-plate potential.

A. The membrane at the end-plate is voltage-clamped by inserting two microelectrodes into the muscle near the end-plate. One electrode measures membrane potential (V_m), and the second passes current (I_m). Both electrodes are connected to a negative feedback amplifier, which ensures that sufficient current (I_m) is delivered so that V_m will remain clamped at the command potential V_c. The synaptic current evoked by stimulating the motor nerve can then be measured at constant V_m, for example, –90 mV (see Box 10–1).

B. The end-plate potential (measured when V_m is not clamped) changes relatively slowly and lags behind the more rapid inward synaptic current (measured under voltage-clamp conditions). This is because synaptic current must first alter the charge on the muscle membrane capacitance before the muscle membrane can be depolarized.

current to charge or discharge the muscle membrane capacitance, and thus alter the membrane voltage, the EPSP lags behind the synaptic current (see Figure 9–10 and the Postscript at the end of this chapter).

The Neurotransmitter Acetylcholine Is Released in Discrete Packets

During their first microelectrode recordings at frog motor end-plates in the 1950s, Fatt and Katz observed small spontaneous depolarizing potentials (0.5–1.0 mV) that occurred at an average rate of about 1/s. Such spontaneous potentials were restricted to the end-plate, exhibited the same time course as stimulus-evoked EPSPs, and were blocked by curare. Hence, they were named "miniature" end-plate potentials (mEPPs, or mEPSPs in our current terminology).

What could account for the small, fixed size of the miniature end-plate potential? Del Castillo and Katz tested the possibility that an mEPSP represents the action of a *single* ACh molecule. This hypothesis was quickly dismissed, because applying very small amounts of ACh to the end-plate could elicit depolarizing responses that were much smaller than the 1.0-mV mEPSP. The low doses of ACh did produce an increase in baseline fluctuations or "noise." Later analysis of the statistical components of this noise led to estimates that the underlying unitary postsynaptic response was a depolarization of 0.3 μV in amplitude and 1.0 ms in duration. This was the first hint of the electrical signaling properties of a single ACh receptor-channel (described later).

Del Castillo and Katz concluded that each mEPSP must represent the action of a multimolecular packet or "quantum" of transmitter. Further, they suggested that the large, stimulus-evoked EPSP was made up of an integral number of quanta. Evidence for this quantal hypothesis is presented in Chapter 15.

Individual Acetylcholine Receptor-Channels Conduct All-or-None Currents

What are the properties of the ACh receptor-channels that produce the inward current that generates the depolarizing end-plate potential? Which ions move through the channels to produce this inward current? And what does the current carried by a single ACh receptor-channel look like?

In 1976, Erwin Neher and Bert Sakmann obtained key insights into the biophysical nature of ACh receptor-channel function from recordings of the current conducted by single ACh receptor-channels in skeletal muscle cells, the unitary or elementary current. They found that the opening of an individual channel generates a very small rectangular step of ionic current (Figure 12–7A). At a given resting potential, each channel opening generates the same-size current pulse. At –90 mV, the current steps are approximately –2.7 pA in amplitude. Although this is a very small current, it corresponds to a flow of approximately 17 million ions per second!

Whereas the amplitude of the current through a single ACh receptor-channel is constant for every opening, the duration of each opening and the time between openings vary considerably. These variations occur because channel openings and closings are stochastic; they obey the same statistical law that describes the exponential time course of radioactive decay. Because channels and ACh undergo random thermal motions and fluctuations, it is impossible to predict exactly how long it will take any one channel to bind ACh or how long that channel will stay open before the ACh dissociates and the channel closes. However, the average length of time a particular type of channel stays open is a well-defined property of that channel, just as the half-life of radioactive decay is an invariant property of a particular isotope. The mean open time for ACh receptor-channels is approximately 1 ms. Thus, each channel opening permits the movement of approximately 17,000 ions. Once a channel closes, the ACh molecules dissociate and the channel remains closed until it binds ACh again.

The Ion Channel at the End-Plate Is Permeable to Both Sodium and Potassium Ions

Once a receptor-channel opens, which ions flow through the channel, and how does this lead to depolarization of the muscle membrane? One important means of identifying the ion (or ions) responsible for the synaptic current is to measure the value of the chemical driving force (the chemical battery) propelling ions through the channel. Remember, the current through a single open channel is given by the product of the single-channel conductance and the electrochemical driving force on the ions conducted through the channel (Chapter 9). Thus, the current generated by a single ACh receptor-channel is given by:

$$I_{EPSP} = \gamma_{EPSP} \times (V_m - E_{EPSP}), \qquad \textbf{(12–1)}$$

where I_{EPSP} is the amplitude of current through one channel, γ_{EPSP} is the conductance of a single open channel, E_{EPSP} is membrane potential at which the net flux of ions through the channel is zero, and $V_m - E_{EPSP}$ is the electrochemical driving force for ion flux. The current steps change in

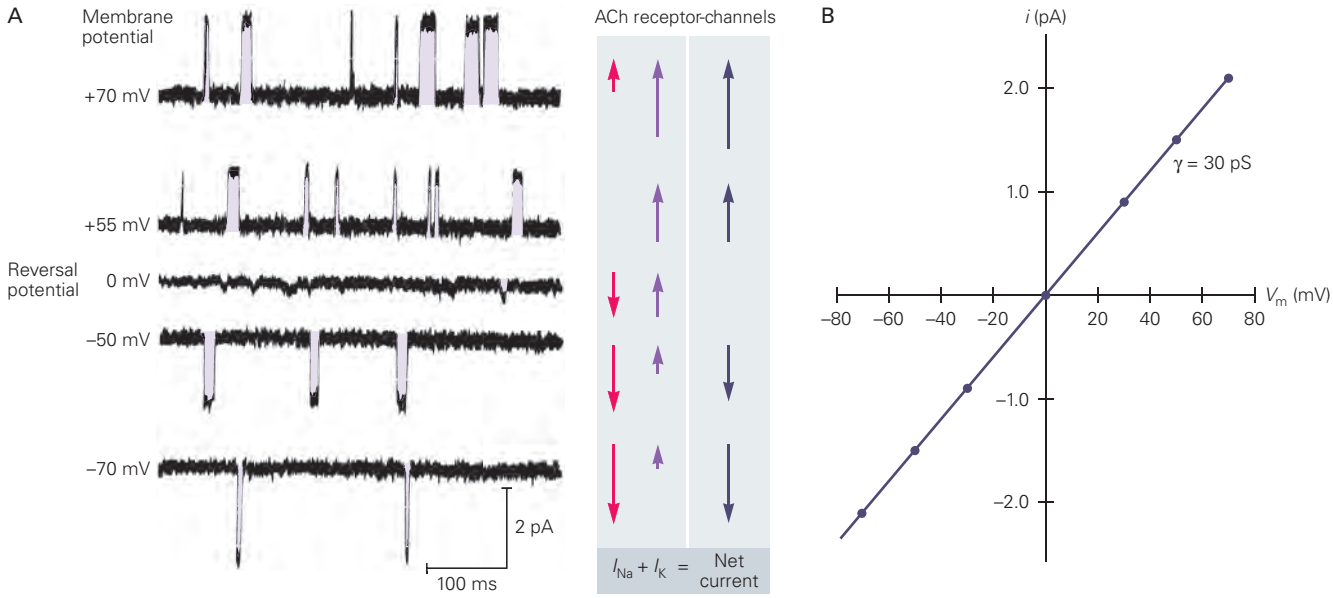

Figure 12–7 Individual acetylcholine (ACh) receptor-channels conduct an all-or-none elementary current.

A. The patch-clamp technique is used to record currents from single ACh receptor-channels. The patch electrode is filled with salt solution that contains a low concentration of ACh and is then brought into close contact with the surface of the muscle membrane (see Box 8–1). At a fixed membrane potential, each time a channel opens, it generates a relatively constant elementary current. At the resting potential of –90 mV, the current is approximately –2.7 pA (1 pA = 10^{-12} A). As the voltage across a patch of membrane is systematically varied, the resultant current varies in amplitude as a result of changes in driving force. The current is inward at voltages negative to 0 mV and outward at voltages positive to 0 mV, thus defining 0 mV as the reversal potential. The arrows on the right side of the traces illustrate the individual sodium and potassium fluxes and resultant net current as a function of voltage.

B. The linear relation between current through a single ACh receptor-channel and membrane voltage shows that the channel behaves as a simple resistor having a single-channel conductance (γ) of about 30 pS.

size as the membrane potential changes because of the change in driving force. For the ACh receptor-channels, the relationship between I_{EPSP} and membrane voltage is linear, indicating that the single-channel conductance is constant and does not depend on membrane voltage; that is, the channel behaves as a simple ohmic resistor. From the slope of this relation, the channel is found to have a conductance of 30 pS (Figure 12–7B). As we saw in Chapter 9, the total conductance, g, due to the opening of a number of receptor-channels (n) is given by:

$$g = n \times \gamma.$$

The current–voltage relation for a single channel shows that the reversal potential for ionic current through ACh receptor-channels, obtained from the intercept of the membrane voltage axis, is 0 mV, which is not equal to the equilibrium potential for Na^+ or any of the other major cations or anions. This is due to the fact that this chemical potential is produced not by a single ion species but by a combination of two species: The ligand-gated channels at the end-plate are almost equally permeable to both major cations, Na^+ and K^+. Thus, during the end-plate potential, Na^+ flows into the cell and K^+ flows out. The reversal potential is at 0 mV because this is a weighted average of the equilibrium potentials for Na^+ and K^+ (Box 12–1). At the reversal potential, the influx of Na^+ is balanced by an equal efflux of K^+ (Figure 12–7A).

The ACh receptor-channels at the end-plate are not selective for a single ion species, as are the voltage-gated Na^+ or K^+ channels, because the diameter of the pore of the ACh receptor-channel is substantially larger than that of the voltage-gated channels. Electrophysiological measurements suggest that it may be 0.6 nm in diameter, an estimate based on the size of the largest organic cation that can permeate the channel. For example, tetramethylammonium (TMA) is approximately 0.6 nm in diameter and yet still permeates the channel. In contrast, the voltage-gated Na^+ channel is only permeant to organic cations that are smaller than 0.5 × 0.3 nm in cross section, and voltage-gated K^+ channels will only conduct ions less than 0.3 nm in diameter.

The relatively large diameter of the ACh receptor-channel pore is thought to provide a water-filled

Box 12–1 Reversal Potential of the End-Plate Potential

The reversal potential of a membrane current carried by more than one ion species, such as the end-plate current through the ACh receptor-channels, is determined by two factors: (1) the relative conductance for the permeant ions (g_{Na} and g_K in the case of the end-plate current) and (2) the equilibrium potentials of the ions (E_{Na} and E_K).

At the reversal potential for the ACh receptor-channel current, inward current carried by Na^+ is balanced by outward current carried by K^+:

$$I_{Na} + I_K = 0. \quad \textbf{(12–2)}$$

The individual Na^+ and K^+ currents can be obtained from

$$I_{Na} = g_{Na} \times (V_m - E_{Na}) \quad \textbf{(12–3a)}$$

and

$$I_K = g_K \times (V_m - E_K). \quad \textbf{(12–3b)}$$

We can substitute Equations 12–3a and 12–3b for I_{Na} and I_K in Equation 12–2, replacing V_m with E_{EPSP} (because at the reversal potential $V_m = E_{EPSP}$):

$$g_{Na} \times (E_{EPSP} - E_{Na}) + g_K \times (E_{EPSP} - E_K) = 0. \quad \textbf{(12–4)}$$

Solving this equation for E_{EPSP} yields

$$E_{EPSP} = \frac{(g_{Na} \times E_{Na}) + (g_K \times E_K)}{g_{Na} + g_K}. \quad \textbf{(12–5)}$$

This equation can also be used to solve for the ratio g_{Na}/g_K if one knows E_{EPSP}, E_K, and E_{Na}. Thus, rearranging Equation 12–5 yields

$$\frac{g_{Na}}{g_K} = \frac{E_{EPSP} - E_K}{E_{Na} - E_{EPSP}}. \quad \textbf{(12–6)}$$

At the neuromuscular junction, E_{EPSP} = 0 mV, E_K = –100 mV, and E_{Na} = +55 mV. Thus, from Equation 12–6, g_{Na}/g_K has a value of approximately 1.8, indicating that the conductance of the ACh receptor-channel for Na^+ is slightly higher than for K^+. A comparable approach can be used to analyze the reversal potential and the movement of ions during excitatory and inhibitory synaptic potentials in central neurons (Chapter 13).

environment that allows cations to diffuse through the channel relatively unimpeded, much as they would in free solution. This explains why the pore does not discriminate between Na^+ and K^+ and why even divalent cations, such as Ca^{2+}, are able to pass through. Anions are excluded by the presence of fixed negative charges in the channel, as described later in this chapter. Recent X-ray crystallographic data have provided a direct view of the large pore of the ACh receptor-channel (see Figure 12–12).

Four Factors Determine the End-Plate Current

How do the rectangular current steps carried by single ACh receptor-channels produce the large synaptic current at the end-plate in response to motor nerve stimulation? Stimulation of a motor nerve releases a large quantity of ACh into the synaptic cleft. The ACh rapidly diffuses across the cleft and binds to the ACh receptors, causing more than 200,000 receptor-channels to open almost simultaneously. (This number is obtained by comparing the total end-plate current, approximately –500 nA, with the current through a single channel, approximately –2.7 pA).

The rapid opening of so many channels causes a large increase in the total conductance of the end-plate membrane, g_{EPSP}, and produces the fast rising phase of the end-plate current. As the ACh in the cleft decreases rapidly to zero (in <1 ms), because of enzymatic hydrolysis and diffusion, the channels begin to close randomly. Although each closure produces only a small step-like decrease in end-plate current, the random closing of large numbers of small unitary currents causes the total end-plate current to appear to decay smoothly (Figure 12–8).

The Acetylcholine Receptor-Channels Have Distinct Properties That Distinguish Them From the Voltage-Gated Channels That Generate the Muscle Action Potential

The ACh receptors that produce the end-plate potential differ in two important ways from the voltage-gated channels that generate the action potential in

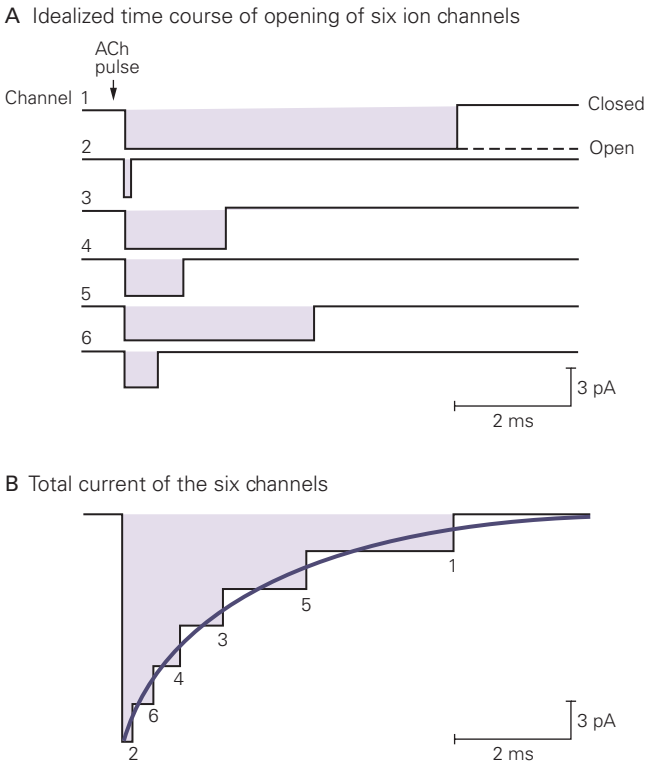

Figure 12–8 **The time course of the total current at the end-plate reflects the summation of contributions of many individual acetylcholine receptor-channels.** (Reproduced, with permission, from Colquhoun 1981. Copyright © 1981 Elsevier.)

A. Individual ACh receptor-channels open in response to a brief pulse of ACh. In this idealized example, the membrane contains six ACh receptor-channels, all of which open rapidly and nearly simultaneously. The channels remain open for varying times and close independently.

B. The stepped trace shows the sum of the six single-channel current records in part A. It represents the current during the sequential closing of each channel (the number indicates which channel has closed). In the final period of current, only channel one is open. In a current record from a whole muscle fiber, with thousands of channels, individual channel closings are not detectable because the scale needed to display the total end-plate current (hundreds of nanoamperes) is so large that the contributions of individual channels cannot be resolved. As a result, the total end-plate current appears to decay smoothly.

muscle. First, the action potential is generated by sequential activation of two distinct classes of voltage-gated channels, one selective for Na^+ and the other for K^+. In contrast, a single type of ion channel, the ACh receptor-channel, generates the end-plate potential by allowing both Na^+ and K^+ to pass with nearly equal permeability.

Second, the Na^+ flux through voltage-gated channels is regenerative: By increasing the depolarization of the cell, the Na^+ influx opens more voltage-gated Na^+ channels. This regenerative feature is responsible for the all-or-none property of the action potential. In contrast, the number of ACh receptor-channels opened during the synaptic potential is fixed by the amount of ACh available. The depolarization produced by Na^+ influx through the ACh-gated channels does not lead to the opening of more ACh receptor-channels and cannot produce an action potential. To trigger an action potential, a synaptic potential must recruit neighboring voltage-gated Na^+ channels (Figure 12–9).

As might be expected from these two differences in physiological properties, the ACh receptor-channels and voltage-gated channels are formed by different macromolecules that exhibit different sensitivities to drugs and toxins. Tetrodotoxin, which blocks the voltage-gated Na^+ channel, does not block the influx of Na^+ through the nicotinic ACh receptor-channels. Similarly, α-bungarotoxin binds tightly to the nicotinic receptors and blocks the action of ACh but does not interfere with voltage-gated Na^+ or K^+ channels.

Transmitter Binding Produces a Series of State Changes in the Acetylcholine Receptor-Channel

Each ACh receptor has two binding sites for ACh; both must be occupied by transmitter for the channel to open efficiently. However, during prolonged applications of ACh, the channel enters a desensitized state where it no longer conducts. The time course of desensitization of the muscle nicotinic receptor is too slow to contribute to the time course of the EPSP under normal conditions, where ACh is present in the synaptic cleft for only a very brief period of time. However, desensitization can play a more important role in determining the time course of the postsynaptic response at certain neuronal synapses, where the transmitter may persist in the synaptic cleft for more prolonged times or where the postsynaptic receptors undergo more rapid desensitization.

For example, the persistence of ACh in the synaptic cleft at cholinergic synapses in the brain may lead to significant desensitization of certain subtypes of neuronal nicotinic receptors. Heavy smokers can build up sufficient levels of nicotine to desensitize receptors in the brain. Desensitization also plays a role in the action of the drug succinylcholine, a dimer of ACh that is resistant to acetylcholinesterase and is used during general anesthesia to produce muscle relaxation. Succinylcholine does so through its ability to produce both receptor desensitization and prolonged depolarization, which blocks muscle action potentials by inactivating voltage-gated Na^+ channels.

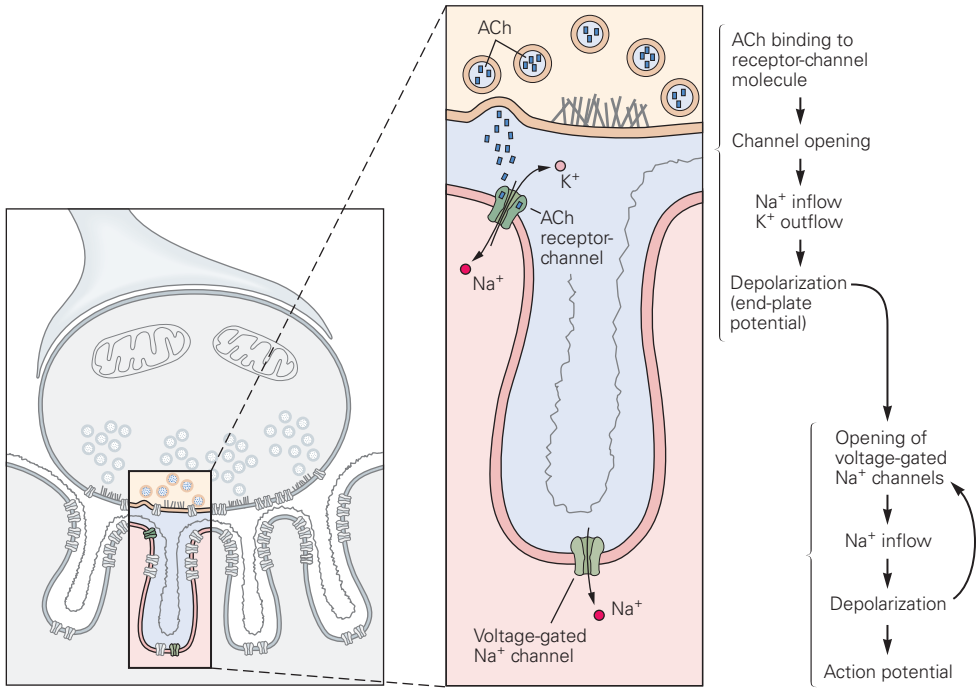

Figure 12–9 The end-plate potential resulting from the opening of acetylcholine receptor-channels opens voltage-gated sodium channels. The end-plate potential is normally large enough to open a sufficient number of voltage-gated Na^+ channels to exceed the threshold for an action potential. (Adapted from Alberts et al. 1989.)

A minimal reaction model, first proposed by Katz and his colleagues, captures many (but not all) of the key steps of ACh receptor-channel function, in which a closed receptor-channel (R) successively binds two molecules of ACh (A) prior to undergoing a rapid conformational change to an open state (R*). This is followed by a slower conformational change to the nonconducting desensitized state (D). The model also incorporates the finding that there is a small probability that an individual receptor may enter the desensitized state even in the absence of ACh. These binding and gating reactions can be summarized by the following scheme:

$$\begin{array}{ccccccc} A + R & \longleftrightarrow & AR + A & \longleftrightarrow & A_2R & \longleftrightarrow & A_2R^* \\ \updownarrow & & \updownarrow & & \updownarrow & & \updownarrow \\ A + D & \longleftrightarrow & AD + A & \longleftrightarrow & A_2D & \longleftrightarrow & A_2D^* \end{array}$$

X-ray crystal structure models have now been obtained for all three states of the ACh receptor (described later).

The Low-Resolution Structure of the Acetylcholine Receptor Is Revealed by Molecular and Biophysical Studies

The nicotinic ACh receptor at the nerve-muscle synapse is part of a single macromolecule that includes the pore in the membrane through which ions flow. Where in the molecule is the binding site located? How is the pore of the channel formed? How is ACh binding coupled to channel gating?

Insights into these questions have been obtained from molecular and biophysical studies of the ACh receptor proteins and their genes, beginning with the purification of the macromolecule from the electric ray *Torpedo marmorata* (Figure 12–2). Using different biochemical approaches, Arthur Karlin and Jean Pierre Changeux purified the receptor from electroplaques, specialized muscle-like cells whose stack-like packing enables their individual EPSPs to summate in series to generate the large voltages (>100 V) used by the electric ray to stun its prey. Their studies indicate that the mature nicotinic ACh receptor is a membrane glycoprotein formed from five subunits of similar molecular weight: two α-subunits and one β-, one γ-, and one δ-subunit (Figure 12–10).

Karlin and his colleagues identified two extracellular binding sites for ACh on each receptor protein in the clefts between each α-subunit and its neighboring γ- or δ-subunit. One molecule of ACh must bind at each of the two sites for the channel to open efficiently (Figure 12–10). Because α-bungarotoxin binds remarkably tightly to the same binding site on the α-subunit as does ACh, the toxin acts as an irreversible transmitter antagonist.

Further insights into the structure of the ACh receptor-channel come from the analysis of the primary amino acid sequence of the receptor's four different

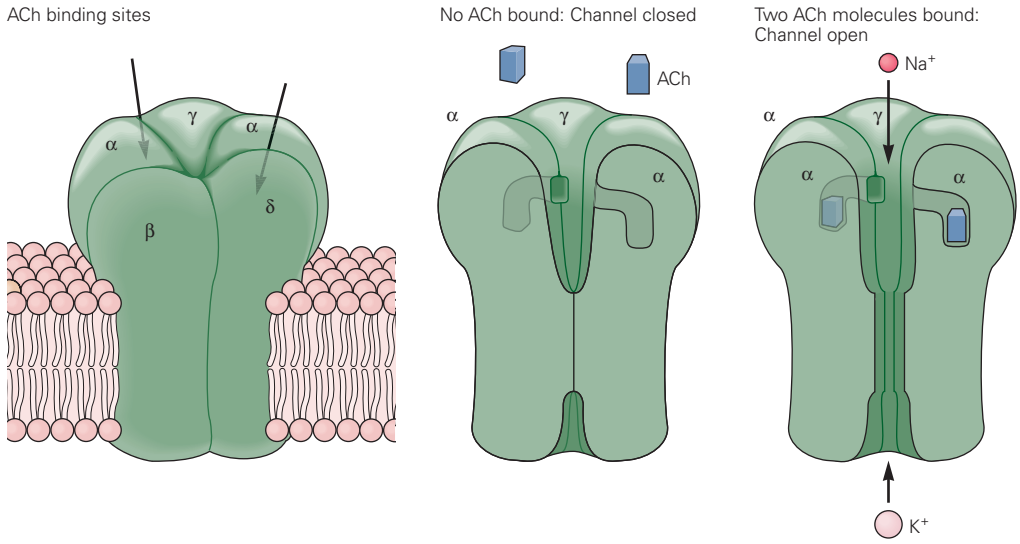

Figure 12–10 The nicotinic ACh receptor-channel is a pentameric macromolecule. The receptor and channel are components of a single macromolecule consisting of five subunits: two identical α-subunits and one each of β-, γ-, and δ-subunits. The subunits form a pore through the cell membrane. When two molecules of ACh bind to the extracellular binding sites—formed at the interfaces of the two α-subunits and their neighboring γ- and δ-subunits—the conformation of the receptor-channel molecule changes (see Figure 12–12). This change opens the pore through which K^+ and Na^+ flow down their electrochemical gradients.

subunits and from biophysical studies. Molecular cloning by Shosaku Numa and colleagues demonstrated that the four subunits are encoded by distinct but related genes. Sequence comparison of the subunits shows a high degree of similarity—one-half of the amino acid residues are identical or conservatively substituted—which suggests that all subunits have a similar structure. Furthermore, all four of the genes for the subunits are homologous; that is, they are derived from a common ancestral gene. Nicotinic ACh receptors in neurons are encoded by a set of distinct but related genes. All of these receptors are pentamers; however, their subunit composition and stoichiometry vary. Whereas most neuronal receptors are composed of two α-subunits and three β-subunits, some neuronal receptors are composed of five identical α-subunits (the α7 isoform) and so can bind five molecules of ACh.

All nicotinic ACh receptor subunits contain a highly conserved sequence near the extracellular binding site for ACh consisting of two disulfide-bonded cysteine (cys) residues with 13 intervening amino acids. The resultant 15-amino acid loop forms a signature sequence both for nicotinic ACh receptor subunits and for related receptors for other transmitters in neurons. The *cys-loop receptor family*, also known as *pentameric ligand-gated ion channels* (pLGIC), includes receptors for the neurotransmitters γ-aminobutyric acid (GABA), glycine, and serotonin.

The distribution of the polar and nonpolar amino acids of the subunits provided the first clues as to how the subunits are threaded through the membrane bilayer. Each subunit contains four hydrophobic regions of approximately 20 amino acids called M1 to M4, each of which forms an α-helix that spans the membrane (Figure 12–11A). The amino acid sequences of the subunits suggest that the subunits are arranged such that they create a central pore through the membrane (Figure 12–11B).

The walls of the channel pore are formed by the M2 membrane-spanning segment and by the loop connecting M2 to M3. Three rings of negative charges that flank the external and internal boundaries of the M2 segment play an important role in the channel's selectivity for cations. Certain local anesthetic drugs block the channel by interacting with one ring of polar serine residues and two rings of hydrophobic residues in the central region of the M2 helix, midway through the membrane.

Three-dimensional models of the entire receptor-channel complex were initially proposed by Karlin based on low-resolution neutron scattering and by Nigel Unwin based on electron diffraction images. The complex is divided into three regions: a large

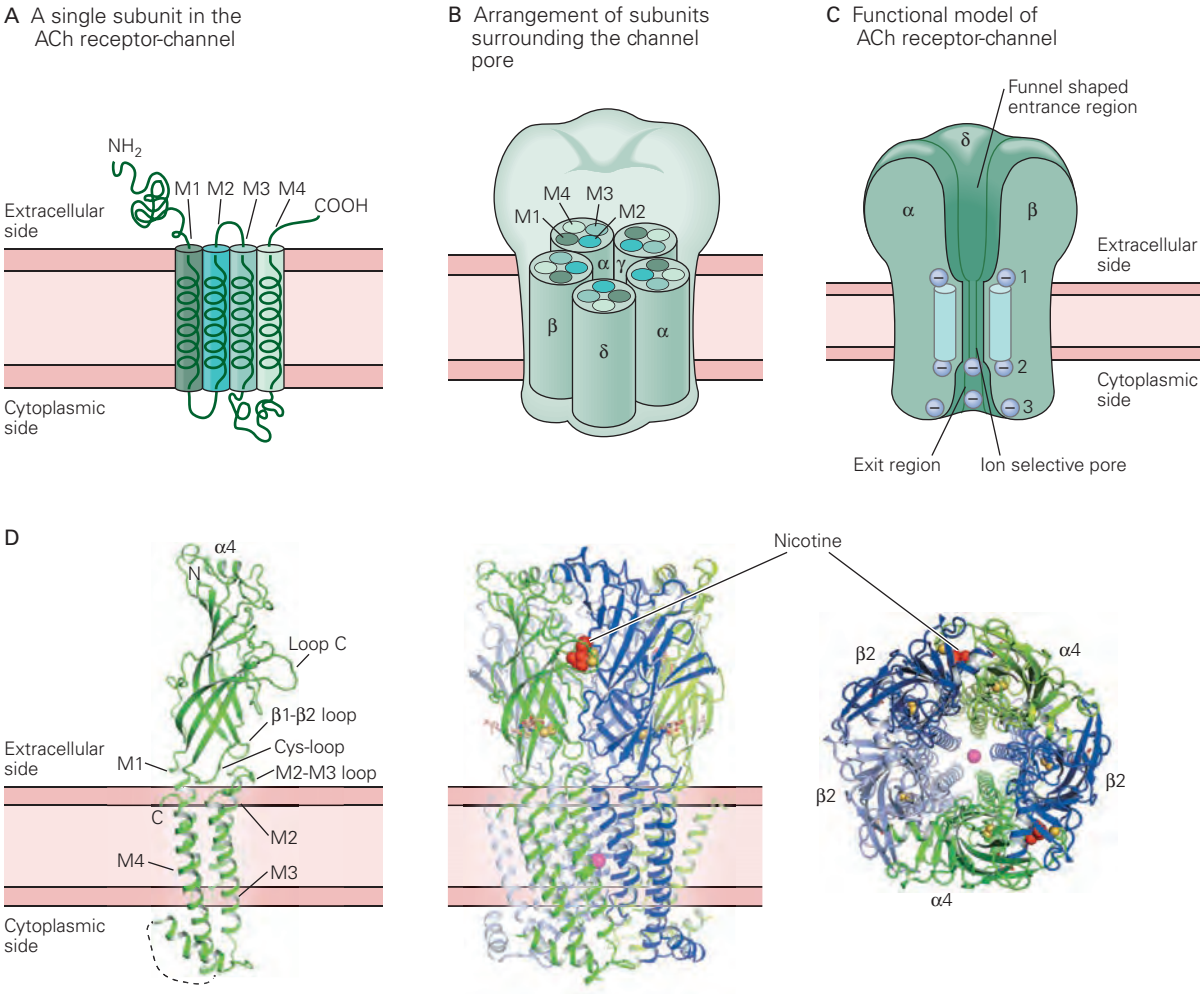

Figure 12–11 The ACh receptor subunits are homologous membrane-spanning proteins.

A. Each subunit contains a large extracellular N-terminus, four membrane-spanning α-helixes (M1–M4), and a short extracellular C-terminus. The N-terminus contains the ACh-binding site, and the membrane helixes form the pore.

B. The five subunits are arranged such that they form a central aqueous channel, with the M2 segment of each subunit forming the lining of the pore. The γ-subunit lies between the two α-subunits. (Dimensions are not to scale.)

C. Negatively charged amino acids on each subunit form three rings of negative charge around the pore. As an ion traverses the channel, it encounters these rings of charge. The rings at the external and internal surfaces of the cell membrane (**1**, **3**) may serve as prefilters that help repel anions and form divalent cation blocking sites. The central ring near the cytoplasmic side of the membrane bilayer (**2**) may contribute more importantly to establishing the specific cation selectivity of the selectivity filter, which is the narrowest region of the pore.

D. A high-resolution X-ray crystal structure model of a human neuronal nicotinic ACh receptor-channel. *Right:* A top-down view of the open channel, which is composed of two α_4-subunits and three β_2-subunits arranged around the central pore. These subunits are closely related variants of the α- and β-subunits of the muscle receptor. Two molecules of nicotine (atoms shown as **red** spheres) are bound to the receptor. A permeating cation is shown as a **pink** sphere. *Center:* A side view of the receptor showing the location of the phospholipid bilayer of the membrane and bound nicotine. *Left:* A side view of a single α_4-subunit in the plane of the membrane. The amino-terminus of the subunit consists of a large extracellular domain. Loop C helps form the ligand-binding site. The β_1-β_2 and cys-loops at the interface between the extracellular domain and the M1–M4 membrane-spanning α-helixes transmit a conformational change from the ligand-binding site to the pore to open the channel. (Reproduced, with permission, from Morales-Perez et al. 2016. Copyright © 2016 Springer Nature.)

extracellular portion that contains the ACh binding site, a narrow transmembrane pore selective for cations, and a large exit region at the internal membrane surface (Figure 12–11C). The extracellular region is surprisingly large, approximately 6 nm in length. In addition, the extracellular end of the pore has a wide mouth approximately 2.5 nm in diameter. Within the bilayer of the membrane, the pore gradually narrows.

The autoimmune disorder myasthenia gravis results from the production of antibodies that bind to the extracellular domain of the ACh receptor, leading to a decrease in the number or function of the nicotinic ACh receptors at the neuromuscular junction. If the change is severe enough, this can decrease the EPSP below the threshold for triggering an action potential, resulting in debilitating weakness. Several congenital forms of myasthenia result from mutations in nicotinic ACh receptor subunits that can also alter receptor number or channel function. For example, a mutation in an amino acid residue in the M2 segment leads to a prolonged channel open time, termed the slow channel syndrome, which results in excessive postsynaptic excitation that leads to degeneration of the end-plate (Chapter 57).

The High-Resolution Structure of the Acetylcholine Receptor-Channel Is Revealed by X-Ray Crystal Studies

A deeper understanding of the fine details of the ACh binding site initially came from high-resolution X-ray crystallographic studies of a molluscan ACh-binding protein, which is homologous to the extracellular amino terminus of nicotinic ACh receptor subunits. Remarkably, unlike typical ACh receptors, the molluscan ACh-binding protein is a soluble protein secreted by glial cells into the extracellular space. At cholinergic synapses in snails, it acts to reduce the size of the EPSP, perhaps by buffering the free concentration of ACh in the synaptic cleft.

Further insights into the structure of the complete receptor-channel have come from X-ray crystal structures of related pentameric ligand-gated channels from bacteria and multicellular animals, culminating with a recent X-ray crystal structure of a human neuronal nicotinic ACh receptor in complex with nicotine. Combined with knowledge of structures of related proteins, we now have a remarkably detailed knowledge of the structure and mechanisms underlying ligand binding, channel gating, and ion permeation of the ACh receptor-channel and related ligand-gated channels.

In the neuronal ACh receptor, two α-subunits combine with three β-subunits to form the pentamer (Figure 12–11D). The large extracellular domain of the receptor contains two ACh binding sites and forms a pentameric ring that surrounds a large central vestibule, which presumably funnels ions toward the narrow transmembrane domain of the receptor. Each α-subunit binds one molecule of nicotine at a site located at the interface with a neighboring β-subunit. Electron diffraction data from Nigel Unwin's higher-resolution structures of related cys-loop receptors and from the high-resolution structure of the desensitized state of the neuronal nicotinic receptor show that the four transmembrane segments of each subunit are indeed α-helixes that traverse the 3-nm length of the lipid bilayer (Figure 12–12). In the desensitized state, the M2 segments from the five subunits form a narrow constriction near the intracellular side of the membrane, preventing ion permeation.

Our picture of the transmembrane region of the nicotinic ACh receptor-channel in the open and closed state is still incomplete. However, by comparison with structures of related pLGICs, a coherent picture of the receptor is beginning to emerge. In the closed state, the pore-lining M2 segments lie roughly parallel to each other, forming a narrow central pore. The pore is further constricted to a diameter of 0.3 to 0.4 nm by a ring of highly conserved hydrophobic leucine residues near the middle of the M2 segment (Figure 12–12). This hydrophobic constriction is thought to provide a high-energy barrier that restricts the passage of hydrated cations whose diameter is greater than the constriction in the pore. At present the discrepancy in pore diameter inferred from electrophysiological measuements (0.6 nm) and the narrower value from the crystal structure remains unresolved.

In the open state, the M2 segments are thought to tilt outward and rotate, widening the constriction of the leucine residues in the middle of M2, thus enabling ion permeation. The narrowest constriction in the open pore lies near the intracellular mouth of the channel, where the electronegative hydroxyl side chains from one ring of threonine residues (serine and threonine residues in the muscle ACh receptor) and a second ring of negatively charged glutamate residues are thought to form the selectivity filter. In the desensitized state the M2 segments tilt further, causing the selectivity filter to constrict even more, preventing ion permeation.

A detailed picture of how ligand binding leads to channel opening is now emerging based on various structural and functional studies. Binding of ligand is thought to promote the closure of the cleft between neighboring subunits, leading to the tightening of the extracellular domain of the pentamer, similar to the closing of the petals of a flower. This results in a twisting motion that causes the bottom of the extracellular domain of the receptor to push on the M1 segment and extracellular loop connecting the M2 and

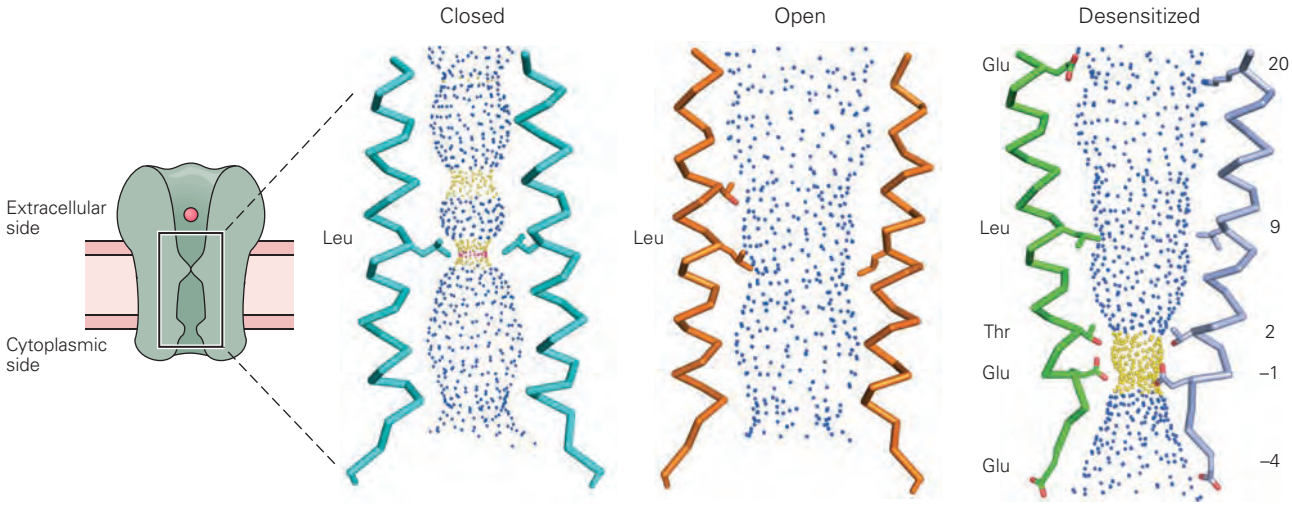

Figure 12–12 A high-resolution three-dimensional structural model of a neuronal nicotinic ACh receptor-channel. High-resolution models of the pentameric family of ligand-gated channels are shown for the closed, open, and desensitized states of the receptor-channel. Two out of five of the M2 α-helixes are shown. The desensitized structure is from the human neuronal ACh receptor. The closed and open states are based on structures of neuronal glycine receptors, which are closely related in amino acid sequence to ACh receptor subunits. Key amino acid side chains are illustrated for the desensitized ACh receptor with position numbering on the right and amino acid abbreviations on the left. According to convention, position 0 is near the intracellular surface of the phospholipid bilayer; other positions are labeled according to relative position in the primary amino acid sequence. A conserved leucine in the middle of the M2 segment (position 9) forms a gate that constricts the pore in the closed state. Ligand binding causes the subunits to tilt outward and twist, opening up the leucine gate. A further conformational change during desensitization causes the subunits to tilt inward near the bottom, constricting the pore near the intracellular side of the channel and thereby producing a nonconducting state. The negatively charged glutamates at positions 20, –1, and –4 correspond to the external (**1**), middle (**2**), and internal (**3**) rings of charge in Figure 12–11C. The negatively charged glutamate at position –1 and the electronegative threonine at position 2 form the selectivity filter of the channel. (Reproduced, with permission, from Morales-Perez et al. 2016. Copyright © 2016 Springer Nature.)

M3 transmembrane segments. This motion exerts a force on the M2 segment that leads to its rotation and tilting, thereby opening up the hydrophobic leucine gate in the middle of the pore and allowing ion permeation. Although future studies will no doubt refine our understanding of the structural bases for nicotinic receptor-channel and function, these recent advances give us an unprecedented molecular understanding of one of the most fundamental processes in the nervous system: synaptic transmission and, specifically, the signaling of information from nerve to muscle.

Highlights

1. The terminals of motor neurons form synapses with muscle fibers at specialized regions in the muscle membrane called end-plates. When an action potential reaches the terminals of a presynaptic motor neuron, it causes the release of ACh.
2. ACh diffuses across the narrow (100-nm) synaptic cleft in a matter of microseconds and binds to nicotinic ACh receptors in the end-plate membrane. The energy of binding is translated into a conformational change that opens a cation-selective channel in the protein, allowing Na^+, K^+, and Ca^{2+} to flow across the postsynaptic membrane. The net effect, due largely to the influx of Na^+ ions, produces a depolarizing synaptic potential called the end-plate potential.
3. Because the ACh receptor-channels are concentrated at the end-plate, the opening of these channels produces a local depolarization. This local depolarization is large enough (75 mV) to exceed the threshold for action potential generation by a factor of three to four.
4. It is important that the safety factor of nerve-muscle transmission be at a high level, as it determines our ability to move, breath, and escape from danger. Decreases in ACh receptor number or function as a result of autoimmune disease or genetic mutations can contribute to neurological disorders.
5. Patch-clamp recordings have revealed the step-like increase and decrease in current in response to the opening and closing of single ACh receptor-channels. A typical excitatory postsynaptic current

at the neuromuscular junction is generated by the opening of approximately 200,000 individual channels.

6. The biochemical structure of the muscle nicotinic ACh receptor has been determined. The receptor is a pentamer composed of two α-subunits and one β-γ-, and δ-subunit. The four genes encoding the subunits are closely related, and more distantly related to the genes encoding other pentameric ligand-gated channels for other transmitters.
7. Higher-resolution structures have provided a detailed view of the ACh ligand-binding pocket and the pore of the channel and further insight into how ligand binding leads to conformational changes associated with receptor-channel opening and desensitization gating reactions.

Postscript: The End-Plate Current Can Be Calculated From an Equivalent Circuit

The current through a population of ACh receptor-channels can be described by Ohm's law. However, to describe how the current generates the end-plate potential, the conductance of the resting channels in the surrounding membrane must also be considered. We must also take into consideration the capacitive properties of the membrane and the ionic batteries determined by the distribution of Na^+ and K^+ inside and outside the cell.

The dynamic relationships between these various components can be explained using the same rules we used in Chapter 9 to analyze the current in passive electrical devices that consist only of resistors, capacitors, and batteries. We can represent the end-plate region with an equivalent circuit that has three parallel current paths: (1) one for the synaptic current through the transmitter-gated channels, (2) one for the return current through resting channels (the nonsynaptic membrane), and (3) one for the capacitive current across the lipid bilayer (Figure 12–13). For simplicity, we ignore the voltage-gated channels in the surrounding nonsynaptic membrane.

Because the end-plate current is carried by both Na^+ and K^+ flowing through the same ion channel, we combine the Na^+ and K^+ current pathways into a single conductance (g_{EPSP}) representing the ACh receptor-channels. The conductance of this pathway is proportional to the number of channels opened, which in turn depends on the concentration of transmitter in the synaptic cleft. In the absence of transmitter, no channels are open and the conductance is zero. When a presynaptic action potential causes the release

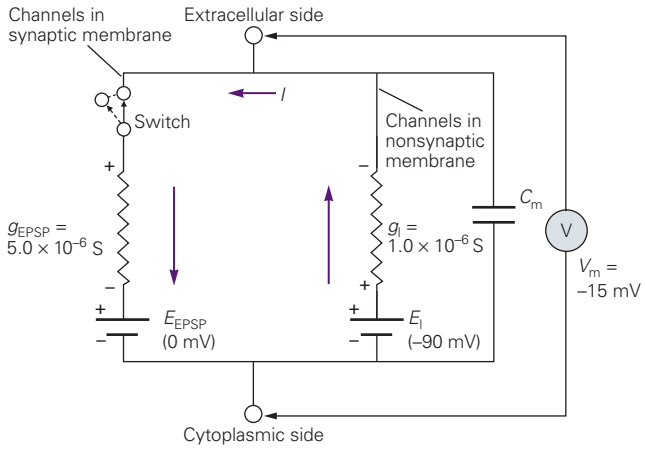

Figure 12–13 The equivalent circuit of the end-plate. The circuit has three parallel current pathways. One conductance pathway carries the end-plate current and consists of a battery (E_{EPSP}) in series with the conductance of the ACh receptor-channels (g_{EPSP}). Another conductance pathway carries current through the nonsynaptic membrane and consists of a battery representing the resting potential (E_l) in series with the conductance of the resting channels (g_l). In parallel with both of these conductance pathways is the membrane capacitance (C_m). The voltmeter (V) measures the potential difference between the inside and the outside of the cell.

When no ACh is present, the ACh receptor-channels are closed and carry no current. This state is depicted as an open electrical circuit in which the synaptic conductance is not connected to the rest of the circuit. The binding of ACh opens the synaptic channels. This event is electrically equivalent to throwing the switch that connects the gated conductance pathway (g_{EPSP}) with the resting pathway (g_l). In the steady state, an inward current through the ACh receptor-channels is balanced by an outward current through the resting channels. With the indicated values of conductances and batteries, the membrane will depolarize from –90 mV (its resting potential) to –15 mV (the peak of the end-plate potential).

of ACh, the conductance of this pathway increases to approximately 5×10^{-6} S, which is about five times the conductance of the parallel branch representing the resting (leakage) channels (g_l).

The end-plate conductance is in series with a battery (E_{EPSP}) with a value given by the reversal potential for synaptic current (0 mV) (Figure 12–13). This value is the weighted algebraic sum of the Na^+ and K^+ equilibrium potentials (see Box 12–1). The current during the excitatory postsynaptic potential (I_{EPSP}) is given by

$$I_{EPSP} = g_{EPSP} \times (V_m - E_{EPSP}).$$

Using this equation and the equivalent circuit of Figure 12–13, we can now analyze the EPSP in terms of its components (Figure 12–14).

At the onset of the EPSP (the dynamic phase), an inward current (I_{EPSP}) flows through the ACh

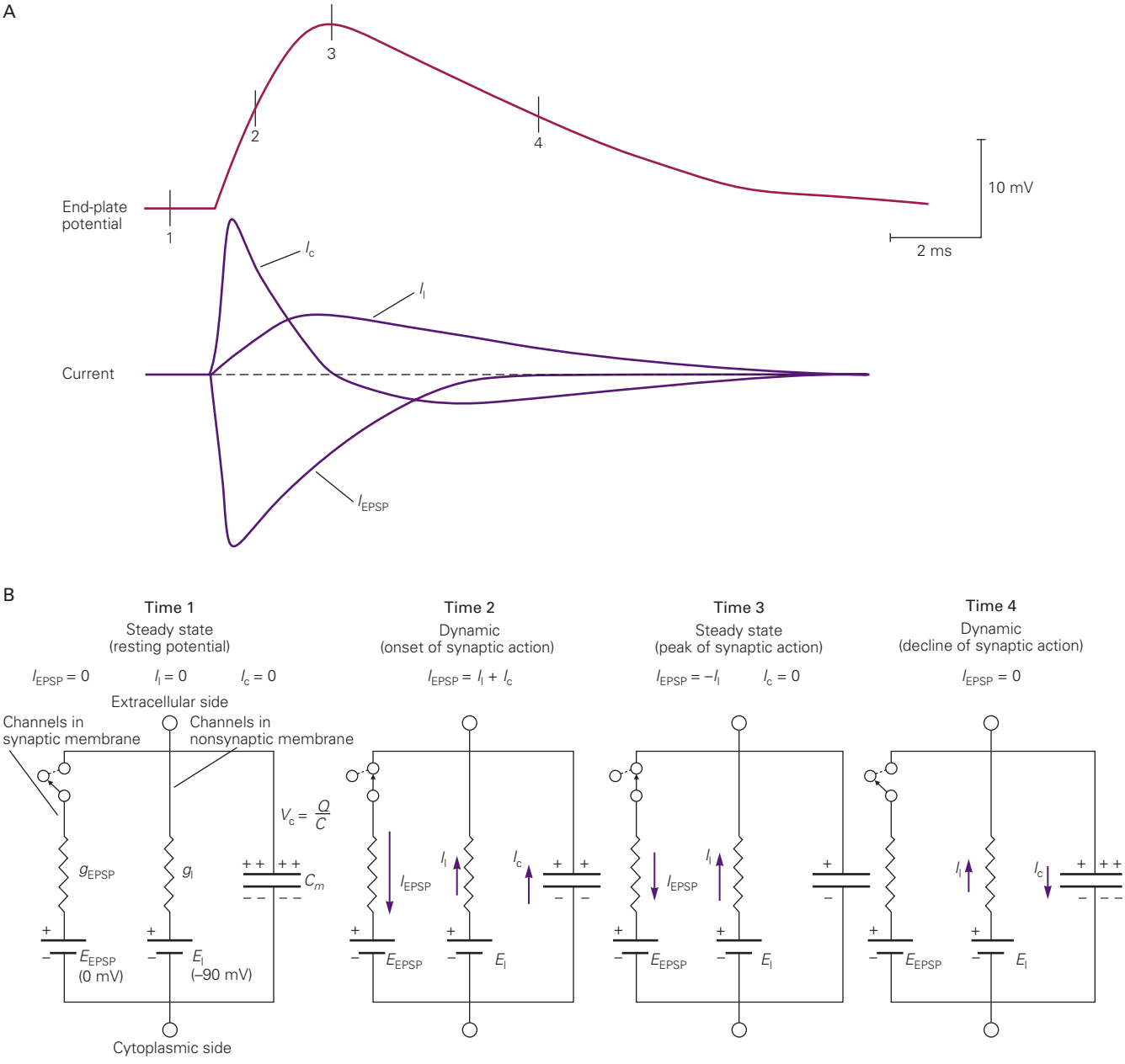

Figure 12–14 The time course of the end-plate potential is determined by both the ACh-gated synaptic conductance and the passive membrane properties of the muscle cell.

A. The time course of the end-plate potential and the component currents through the ACh receptor-channels (I_{EPSP}), the resting (or leakage) channels (I_l), and the capacitor (I_c). There is a capacitive current only when the membrane potential is changing. In the steady state, such as at the peak of the end-plate potential, the inward flow of positive charge through the ACh receptor-channels is exactly balanced by the outward ionic current across the resting channels, and there is no capacitive current.

B. Equivalent circuits for the current at times 1, 2, 3, and 4 shown in part A. (The relative magnitude of a current is represented by the arrow length.)

receptor-channels because of the increased conductance to Na^+ and K^+ and the large inward driving force on Na^+ at the resting potential of –90 mV (Figure 12–14B, time 2). Because charge flows in a closed loop, the inward synaptic current leaves the cell as outward current through two parallel pathways: a pathway for ionic current (I_l) through the resting (or leakage) channels and a pathway for capacitive current (I_c) across the lipid bilayer. Thus,

$$I_{EPSP} = -(I_l + I_c).$$

During the earliest phase of the EPSP, the membrane potential, V_m, is still close to its resting value, E_l. As a result, the outward driving force on current through the resting channels ($V_m - E_l$) is small. Therefore, most of the outward current leaves the cell as capacitive current and the membrane depolarizes rapidly (Figure 12–14B, time 2). As the cell depolarizes, the outward driving force on current through the resting channels increases, while the inward driving force on synaptic current through the ACh receptor-channels decreases. Concomitantly, as the concentration of ACh in the synapse decreases, the ACh receptor-channels begin to close, and eventually the inward current through the gated channels is exactly balanced by outward current through the resting channels ($I_{EPSP} = -I_l$). At this point, no charge flows into or out of the capacitor ($I_c = 0$). Because the rate of change of membrane potential is directly proportional to I_c,

$$I_c / C_m = \Delta V_m / \Delta t,$$

the membrane potential will have reached a peak or new steady-state value, $\Delta V_m / \Delta t = 0$ (Figure 12–14B, time 3).

As the ACh receptor-channels close, I_{EPSP} decreases further. Now I_{EPSP} and I_l are no longer in balance and the membrane potential starts to repolarize, because the outward current through leak channels (I_l) becomes larger than the inward synaptic current. During most of the declining phase of the synaptic action, the ACh receptor-channels carry no current because they are all closed. Instead, current is conducted through the membrane only as outward current carried by resting channels, balanced by inward capacitive current (Figure 12–14B, time 4).

When the EPSP is at its peak or steady-state value, $I_c = 0$, and therefore the value of V_m can be easily calculated. The inward current through the ACh receptor-channels (I_{EPSP}) must be exactly balanced by outward current through the resting channels (I_l):

$$I_{EPSP} + I_l = 0. \qquad \textbf{(12–7)}$$

The current through the ACh receptor-channels (I_{EPSP}) and resting channels (I_l) is given by Ohm's law:

$$I_{EPSP} = g_{EPSP} \times (V_m - E_{EPSP}),$$

and

$$I_l = g_l \times (V_m - E_l).$$

By substituting these two expressions into Equation 12–7, we obtain

$$g_{EPSP} \times (V_m - E_{EPSP}) + g_l \times (V_m - E_l) = 0.$$

Solving for V_m, we obtain

$$V_m = \frac{(g_{EPSP} \times E_{EPSP}) + (g_l \times E_l)}{g_{EPSP} + g_l}. \qquad \textbf{(12–8)}$$

This equation is similar to that used to calculate the resting and action potentials (Chapter 9). According to Equation 12–8, the peak voltage of the EPSP is a weighted average of the electromotive forces of the two batteries for the ACh receptor-channels and the resting (leakage) channels. The weighting factors are given by the relative magnitude of the two conductances. Since g_l is a constant, the greater the value of g_{EPSP} (ie, the more ACh channels are open), the more closely V_m will approach the value of E_{EPSP}.

We can now calculate the peak EPSP for the specific case shown in Figure 12–13, where $g_{EPSP} = 5 \times 10^{-6}$ S, $g_l = 1 \times 10^{-6}$ S, $E_{EPSP} = 0$ mV, and $E_l = -90$ mV. Substituting these values into Equation 12–8 yields

$$V_m = \frac{[(5 \times 10^{-6}\ \text{S}) \times (0\ \text{mV})] + [(1 \times 10^{-6}\ \text{S}) \times (-90\ \text{mV})]}{(5 \times 10^{-6}\ \text{S}) + (1 \times 10^{-6}\ \text{S})}.$$

or

$$V_m = \frac{(1 \times 10^{-6}\ \text{S}) \times (-90\ \text{mV})}{(6 \times 10^{-6}\ \text{S})} = -15\ \text{mV}.$$

The peak amplitude of the EPSP is then

$$\Delta V_{EPSP} = V_m - E_l = -15\ \text{mV} - (-90\ \text{mV}) = 75\ \text{mV}.$$

Gerald D. Fischbach
Steven A. Siegelbaum

Selected Reading

Fatt P, Katz B. 1951. An analysis of the end-plate potential recorded with an intracellular electrode. J Physiol 115:320–370.

Heuser JE, Reese TS. 1977. Structure of the synapse. In: ER Kandel (ed). *Handbook of Physiology: A Critical, Comprehensive Presentation of Physiological Knowledge and Concepts*, Sect. 1 *The Nervous System*, Vol. 1 *Cellular Biology of Neurons*, Part 1, pp. 261–294. Bethesda, MD: American Physiological Society.

Hille B. 2001. *Ion Channels of Excitable Membranes*, 3rd ed., pp. 169–199. Sunderland, MA: Sinauer.

Imoto K, Busch C, Sakmann B, et al. 1988. Rings of negatively charged amino acids determine the acetylcholine receptor-channel conductance. Nature 335:645–648.

Karlin A. 2002. Emerging structure of the nicotinic acetylcholine receptors. Nat Rev Neurosci 3:102–114.

Neher E, Sakmann B. 1976. Single-channel currents recorded from membrane of denervated frog muscle fibres. Nature 260:799–802.

Nemecz Á, Prevost MS, Menny A, Corringer PJ. 2016. Emerging molecular mechanisms of signal transduction in pentameric ligand-gated ion channels. Neuron 90:452–470.

References

Akabas MH, Kaufmann C, Archdeacon P, Karlin A. 1994. Identification of acetylcholine receptor-channel lining residues in the entire M2 segment of the α-subunit. Neuron 13:919–927.

Alberts B, Bray D, Lewis J, Raff M, Roberts K, Watson JD. 1989. *Molecular Biology of the Cell*, 2nd ed. New York: Garland.

Brejc K, van Dijk WJ, Klaassen RV, et al. 2001. Crystal structure of an ACh-binding protein reveals the ligand-binding domain of nicotinic receptors. Nature 411:269–276.

Charnet P, Labarca C, Leonard RJ, et al. 1990. An open channel blocker interacts with adjacent turns of α-helices in the nicotinic acetylcholine receptor. Neuron 4:87–95.

Claudio T, Ballivet M, Patrick J, Heinemann S. 1983. Nucleotide and deduced amino acid sequences of *Torpedo californica* acetylcholine receptor γ-subunit. Proc Natl Acad Sci U S A 80:1111–1115.

Colquhoun D. 1981. How fast do drugs work? Trends Pharmacol Sci 2:212–217.

Dwyer TM, Adams DJ, Hille B. 1980. The permeability of the endplate channel to organic cations in frog muscle. J Gen Physiol 75:469–492.

Fertuck HC, Salpeter MM. 1974. Localization of acetylcholine receptor by ^{125}I-labeled α-bungarotoxin binding at mouse motor endplates. Proc Natl Acad Sci U S A 71:1376–1378.

Heuser JE, Salpeter SR. 1979. Organization of acetylcholine receptors in quick-frozen, deep-etched, and rotary-replicated Torpedo postsynaptic membrane. J Cell Biol 82:150–173.

Ko C-P. 1984. Regeneration of the active zone at the frog neuromuscular junction. J Cell Biol 98:1685–1695.

Kuffler SW, Nicholls JG, Martin AR. 1984. *From Neuron to Brain: A Cellular Approach to the Function of the Nervous System*, 2nd ed. Sunderland, MA: Sinauer.

McMahan UJ, Kuffler SW. 1971. Visual identification of synaptic boutons on living ganglion cells and of varicosities in postganglionic axons in the heart of the frog. Proc R Soc Lond B Biol Sci 177:485–508.

Miles FA. 1969. *Excitable Cells*. London: Heinemann.

Miyazawa A, Fujiyoshi Y, Unwin N. 2003. Structure and gating mechanism of the acetylcholine receptor pore. Nature 424:949–955.

Morales-Perez CL, Noviello CM, Hibbs RE. 2016. X-ray structure of the human α4β2 nicotinic receptor. Nature 538:411–415.

Noda M, Furutani Y, Takahashi H, et al. 1983. Cloning and sequence analysis of calf cDNA and human genomic DNA encoding α-subunit precursor of muscle acetylcholine receptor. Nature 305:818–823.

Noda M, Takahashi H, Tanabe T, et al. 1983. Structural homology of *Torpedo californica* acetylcholine receptor subunits. Nature 302:528–532.

Palay SL. 1958. The morphology of synapses in the central nervous system. Exp Cell Res 5:275–293. Suppl.

Revah F, Galzi J-L, Giraudat J, Haumont PY, Lederer F, Changeux J-P. 1990. The noncompetitive blocker [3H] chlorpromazine labels three amino acids of the acetylcholine receptor gamma subunit: implications for the alpha-helical organization of regions MII and for the structure of the ion channel. Proc Natl Acad Sci U S A 87:4675–4679.

Salpeter MM (ed). 1987. *The Vertebrate Neuromuscular Junction*, pp. 1–54. New York: Liss.

Takeuchi A. 1977. Junctional transmission. I. Postsynaptic mechanisms. In: ER Kandel (ed). *Handbook of Physiology: A Critical, Comprehensive Presentation of Physiological Knowledge and Concepts*, Sect. 1 *The Nervous System*, Vol. 1 *Cellular Biology of Neurons*, Part 1, pp. 295–327. Bethesda, MD: American Physiological Society.

Verrall S, Hall ZW. 1992. The N-terminal domains of acetylcholine receptor subunits contain recognition signals for the initial steps of receptor assembly. Cell 68:23–31.

Villarroel A, Herlitze S, Koenen M, Sakmann B. 1991. Location of a threonine residue in the alpha-subunit M2 transmembrane segment that determines the ion flow through the acetylcholine receptor-channel. Proc R Soc Lond B Biol Sci 243:69–74.

Walsh J. 1773. Of the electric property of the torpedo. Phil Trans 63(1773):480.

Zeng H, Moise L, Grant MA, Hawrot E. 2001. The solution structure of the complex formed between alpha-bungarotoxin and an 18-mer cognate peptide derived from the alpha 1 subunit of the nicotinic acetylcholine receptor from Torpedo californica. J Biol Chem 276: 22930–22940.

13

Synaptic Integration in the Central Nervous System

Like synaptic transmission at the neuromuscular junction, most rapid signaling between neurons in the central nervous system involves ionotropic receptors in the postsynaptic membrane. Thus, many principles that apply to the synaptic connection between the motor neuron and skeletal muscle fiber at the neuromuscular junction also apply in the central nervous system. Nevertheless, synaptic transmission between central neurons is more complex for several reasons.

First, although most muscle fibers are typically innervated by only one motor neuron, a central nerve cell (such as pyramidal neurons in the neocortex) receives connections from thousands of neurons. Second, muscle fibers receive only excitatory inputs, whereas central neurons receive both excitatory and inhibitory inputs. Third, all synaptic actions on muscle fibers are mediated by one neurotransmitter, acetylcholine (ACh), which activates only one type of receptor (the ionotropic nicotinic ACh receptor). A single central neuron, however, can respond to many different types of inputs, each mediated by a distinct transmitter that activates a specific type of receptor.

These receptors include ionotropic receptors, where binding of transmitter directly opens an ion channel, and metabotropic receptors, where transmitter binding indirectly regulates a channel by activating second messengers. As a result, unlike muscle fibers, central neurons must integrate diverse inputs into a single coordinated action.

Finally, the nerve–muscle synapse is a model of efficiency—every action potential in the motor neuron produces an action potential in the muscle fiber. In comparison, connections made by a presynaptic neuron onto a central neuron are only modestly effective—in many cases at least 50 to 100 excitatory neurons must fire together to produce a synaptic potential large enough to trigger an action potential in postsynaptic neurons.

The first insights into synaptic transmission in the central nervous system came from experiments by John Eccles and his colleagues in the 1950s on the synaptic inputs onto spinal motor neurons that control the stretch reflex, the simple behavior we considered in Chapter 3. The spinal motor neurons have been particularly useful for examining central synaptic mechanisms because they have large, accessible cell bodies and, most important, they receive both excitatory and inhibitory connections and therefore allow us to study the integrative action of the nervous system at the cellular level.

Central Neurons Receive Excitatory and Inhibitory Inputs

To analyze the synapses that mediate the stretch reflex, Eccles activated a large population of axons of the sensory cells that innervate the stretch receptor organs in the quadriceps (extensor) muscle (Figure 13–1A,B). Nowadays the same experiments can be done by stimulating a single sensory neuron.

Passing sufficient current through a microelectrode into the cell body of a stretch-receptor sensory neuron that innervates the extensor muscle generates an action potential. This in turn produces a small excitatory postsynaptic potential (EPSP) in the motor neuron that innervates precisely the same muscle (in this case the quadriceps) monitored by the sensory neuron (Figure 13–1B, upper panel). The EPSP produced by one sensory cell, the unitary EPSP, depolarizes the extensor motor neuron by less than 1 mV, often only 0.2 to 0.4 mV, far below the threshold for generating an action potential. Typically, a depolarization of 10 mV or more is required to reach threshold.

The generation of an action potential in a motor neuron thus requires the near-synchronous firing of a number of sensory neurons. This can be observed in an experiment in which a population of sensory neurons is stimulated by passing current through an extracellular electrode. As the strength of the extracellular stimulus is increased, more sensory afferent fibers are excited, and the depolarization produced by the EPSP becomes larger. The depolarization eventually becomes large enough to bring the membrane potential of the motor neuron axon initial segment (the region with the lowest threshold) to the threshold for an action potential.

In addition to the EPSP produced in the extensor motor neuron, stimulation of extensor stretch-receptor neurons also produces a small inhibitory postsynaptic potential (IPSP) in the motor neuron that innervates the flexor muscle, which is antagonistic to the extensor muscle (Figure 13–1B, lower panel). This hyperpolarizing action is generated by an inhibitory interneuron, which receives excitatory input from the sensory neurons of the extensor muscle and in turn makes synapses with the motor neurons that innervate the flexor muscle. In the laboratory, a single interneuron can be stimulated intracellularly to directly elicit a small unitary IPSP in the motor neuron. Extracellular activation of an entire population of interneurons elicits a larger IPSP. If strong enough, IPSPs can counteract the EPSP and prevent the membrane potential from reaching threshold.

Excitatory and Inhibitory Synapses Have Distinctive Ultrastructures and Target Different Neuronal Regions

As we learned in Chapter 11, the effect of a synaptic potential—whether it is excitatory or inhibitory—is determined not by the type of transmitter released from the presynaptic neuron but by the type of ion channels in the postsynaptic cell activated by the transmitter. Although some transmitters can produce both EPSPs and IPSPs, by acting on distinct classes of ionotropic receptors at different synapses, most transmitters produce a single predominant type of synaptic response; that is, a transmitter is usually inhibitory or excitatory. For example, in the vertebrate central nervous system, neurons that release glutamate typically act on receptors that produce excitation; neurons that release γ-aminobutyric acid (GABA) or glycine act on receptors that produce inhibition.

The synaptic terminals of excitatory and inhibitory neurons can be distinguished by their ultrastructure.

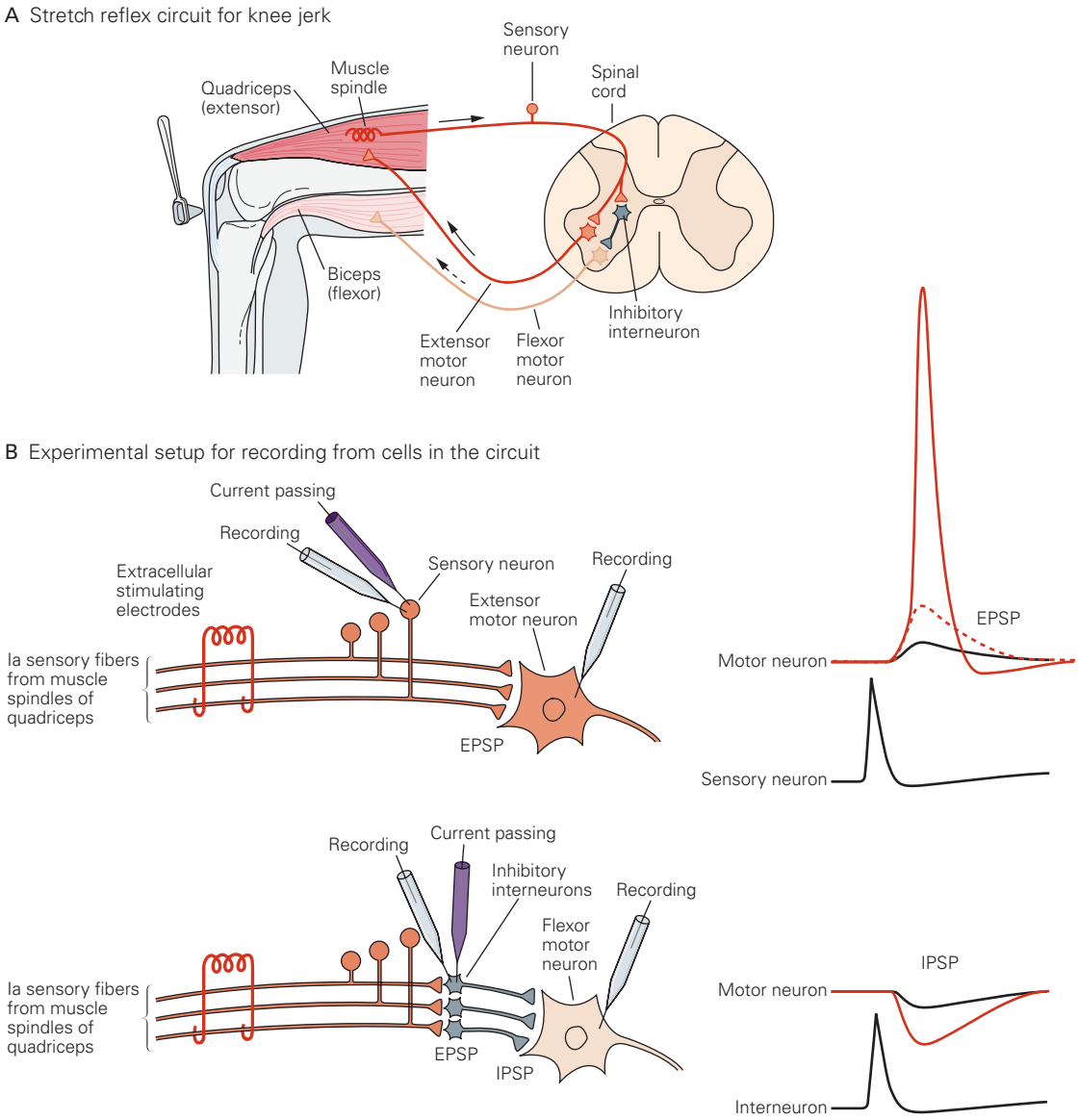

Figure 13–1 **The combination of excitatory and inhibitory synaptic connections mediating the stretch reflex of the quadriceps muscle is typical of circuits in the central nervous system.**

A. A sensory neuron activated by a stretch receptor (muscle spindle) at the extensor (quadriceps) muscle makes an excitatory connection with an extensor motor neuron in the spinal cord that innervates this same muscle group. It also makes an excitatory connection with an interneuron, which in turn makes an inhibitory connection with a flexor motor neuron that innervates the antagonist (biceps femoris) muscle group. Conversely, an afferent fiber from the biceps (not shown) excites an interneuron that makes an inhibitory synapse on the extensor motor neuron.

B. This idealized experimental setup shows the approaches to studying the inhibition and excitation of motor neurons in the pathway illustrated in part A. **Upper panel:** Two alternatives for eliciting excitatory postsynaptic potentials (**EPSPs**) in the extensor motor neuron. A single presynaptic axon can be stimulated by inserting a current-passing electrode into the sensory neuron cell body. An action potential in the sensory neuron stimulated in this way triggers a small EPSP in the extensor motor neuron (**black trace**). Alternatively, the whole afferent nerve from the quadriceps can be stimulated electrically with an extracellular electrode. The excitation of many afferent neurons through the extracellular electrode generates a synaptic potential (**dashed trace**) large enough to initiate an action potential (**red trace**). **Lower panel:** The setup for eliciting and measuring inhibitory potentials in the flexor motor neuron. Intracellular stimulation of a single inhibitory interneuron receiving input from the quadriceps pathway produces a small inhibitory (hyperpolarizing) postsynaptic potential (**IPSP**) in the flexor motor neuron (**black trace**). Extracellular stimulation recruits numerous inhibitory neurons and generates a larger IPSP (**red trace**). (Action potentials in the sensory neuron and interneuron appear smaller because they were recorded at lower amplification than those in the motor neuron.)

Two morphological types of synapses are common in the brain: Gray types I and II (named after E. G. Gray, who described them using electron microscopy). Most type I synapses are glutamatergic and excitatory, whereas most type II synapses are GABAergic and inhibitory. Type I synapses have round synaptic vesicles, an electron-dense region (the *active zone*) on the presynaptic membrane, and an even larger electron-dense region in the postsynaptic membrane opposed to the active zone (known as the *postsynaptic density*), which gives type I synapses an asymmetric appearance. Type II synapses have oval or flattened synaptic vesicles and less obvious presynaptic membrane specializations and postsynaptic densities, resulting in a more symmetric appearance (Figure 13–2). (Although type I synapses are mostly excitatory and type II inhibitory, the two morphological types have proved to be only a first approximation to transmitter biochemistry. Immunocytochemistry affords much more reliable distinctions between transmitter types, as discussed in Chapter 16).

Although dendrites are normally postsynaptic and axon terminals presynaptic, all four regions of the nerve cell—axon, presynaptic terminals, cell body, and dendrites—can be presynaptic or postsynaptic sites of chemical synapses. The most common types of contact, illustrated in Figure 13–2, are axodendritic, axosomatic, and axo-axonic (by convention, the presynaptic element is identified first). Excitatory synapses are typically axodendritic and occur mostly on dendritic spines. Inhibitory synapses are normally formed on dendritic shafts, the cell body, and the axon initial segment. Dendrodendritic and somasomatic synapses are also found, but they are rare.

As a general rule, the proximity of a synapse to the axon initial segment is thought to determine its effectiveness. A given postsynaptic current generated at a site near the cell body will produce a greater change in membrane potential at the trigger zone of the axon initial segment, and therefore have a greater influence on action potential output than an equal current generated at more remote sites in the dendrites. This is because some of the charge entering the postsynaptic membrane at a remote site will leak out of the dendritic membrane as the synaptic potential propagates to the cell body (Chapter 9). Some neurons compensate for this effect by placing

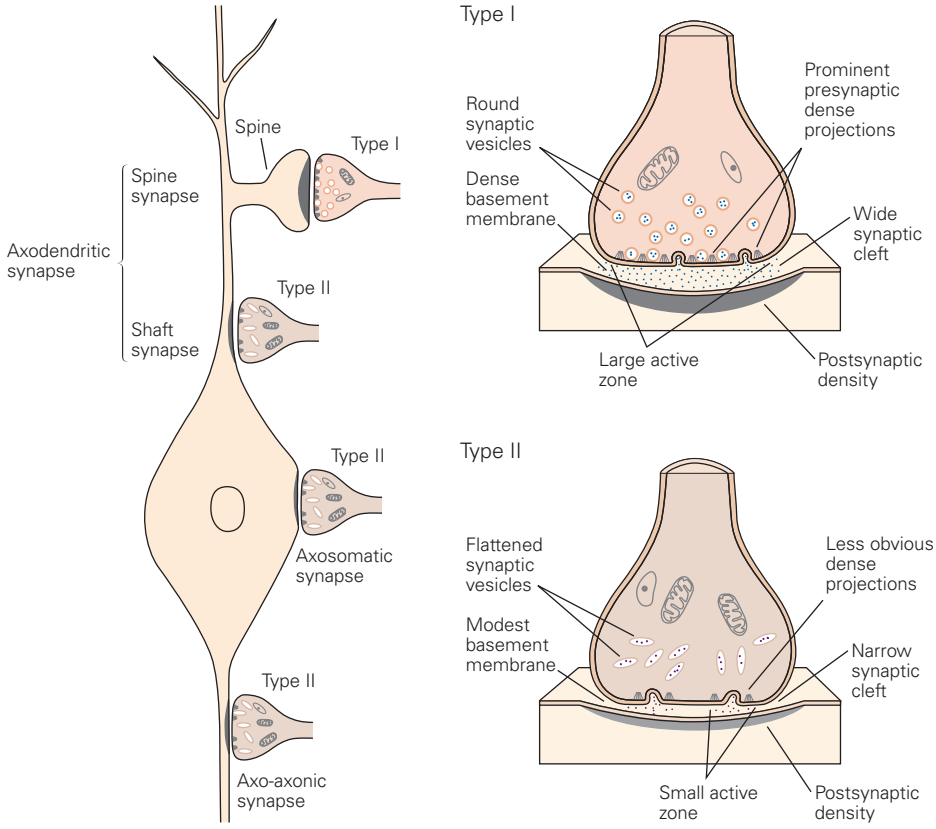

Figure 13–2 The two most common morphological types of synapses in the central nervous system are Gray type I and type II. Type I is usually excitatory, whereas type II is usually inhibitory. Differences include the shape of vesicles, the prominence of presynaptic densities, total area of the active zone, width of the synaptic cleft, and presence of a dense basement membrane. Type I synapses typically contact specialized dendritic projections, called spines, and less commonly contact the shafts of dendrites. Type II synapses contact the cell body (axosomatic), dendritic shaft (axodendritic), axon initial segment (axo-axonic), and presynaptic terminals of another neuron (not shown).

more glutamate receptors at distal synapses than at proximal synapses, ensuring that inputs at different locations along the dendritic tree will have a more equivalent influence at the initial segment. In contrast to axodendritic and axosomatic input, most axoaxonic synapses have no direct effect on the trigger zone of the postsynaptic cell. Instead, they affect neural activity by controlling the amount of transmitter released from the presynaptic terminals (Chapter 15).

Excitatory Synaptic Transmission Is Mediated by Ionotropic Glutamate Receptor-Channels Permeable to Cations

The excitatory transmitter released from the presynaptic terminals of the stretch-receptor sensory neurons is the amino acid L-glutamate, the major excitatory transmitter in the brain and spinal cord. Eccles and his colleagues discovered that the EPSP in spinal motor cells results from the opening of ionotropic glutamate receptor-channels, which are permeable to both Na^+ and K^+. This ionic mechanism is similar to that produced by ACh at the neuromuscular junction described in Chapter 12. Like the ACh receptor-channels, glutamate receptor-channels conduct both Na^+ and K^+ with nearly equal permeability. As a result, the reversal potential for current flow through these channels is 0 mV (see Figure 12–7).

Glutamate receptors can be divided into two broad categories: ionotropic receptors and metabotropic receptors (Figure 13–3). There are three major types of ionotropic glutamate receptors: *AMPA*, *kainate*, and *NMDA*, named according to the types of pharmacological agonists that activate them (α-amino-3-hydroxy-5-methylisoxazole-4-propionic acid, kainate, and *N*-methyl-D-aspartate, respectively). These receptors are also differentially sensitive to antagonists. The NMDA receptor is selectively blocked by the drug *APV* (2-amino-5-phosphonovaleric acid). The AMPA and kainate receptors are not affected by APV, but both are blocked by the drug *CNQX* (6-cyano-7-nitroquinoxaline-2,3-dione). Because of this shared pharmacological sensitivity, these two types are sometimes called the *non-NMDA receptors*. Another important distinction between NMDA and non-NMDA receptors is that the NMDA receptor channel is highly permeable to Ca^{2+}, whereas most non-NMDA receptors are not. There are several types of metabotropic glutamate receptors, most of which can be activated by *trans*-(1S,3R)-1-amino-1,3-cyclopentanedicarboxylic acid (*ACPD*).

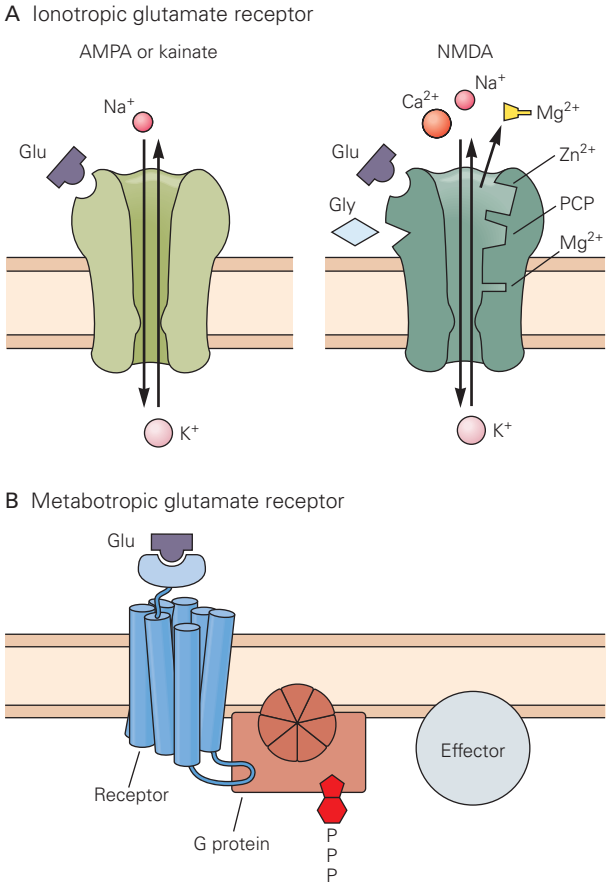

Figure 13–3 Different classes of glutamate receptors regulate excitatory synaptic actions in neurons in the spinal cord and brain.

A. Ionotropic glutamate receptors directly gate ion channels permeable to cations. The AMPA and kainate types bind the glutamate agonists AMPA or kainate, respectively; these receptors contain a channel that is permeable to Na^+ and K^+. The NMDA receptor binds the glutamate agonist NMDA; it contains a channel permeable to Ca^{2+}, K^+, and Na^+. It has binding sites for glutamate, glycine, Zn^{2+}, phencyclidine (**PCP**, or angel dust), MK801 (an experimental drug), and Mg^{2+}, each of which regulates the functioning of the channel differently.

B. Binding of glutamate (**Glu**) to metabotropic glutamate receptors indirectly gates ion channels by activating a GTP-binding protein (**G protein**), which in turn interacts with effector molecules that alter metabolic and ion channel activity (Chapter 11).

The action of all ionotropic glutamate receptors is excitatory or depolarizing because the reversal potential of their ionic current is near zero, causing channel opening to produce a depolarizing inward current at negative membrane potentials. In contrast, metabotropic receptors can produce either excitation or inhibition, depending on the reversal potential of the ionic currents that they regulate and whether they promote channel opening or channel closing.

The Ionotropic Glutamate Receptors Are Encoded by a Large Gene Family

Over the past 30 years, a large variety of genes coding for the subunits of all the major neurotransmitter receptors have been identified. In addition, many of these subunit genes are alternatively spliced, generating further diversity. This molecular analysis demonstrates evolutionary linkages among the structure of receptors that enable us to classify them into three distinct families (Figure 13–4).

The ionotropic glutamate receptor family includes the AMPA, kainate, and NMDA receptors. The genes encoding the AMPA and kainate receptors are more closely related to one another than are the genes encoding the NMDA receptors. Surprisingly, the glutamate receptor family bears little resemblance to the two other gene families that encode ionotropic receptors (one of which encodes the nicotinic ACh, GABA, and glycine receptors, and the other the ATP receptors, as described later).

The AMPA, kainate, and NMDA receptors are tetramers composed of two or more types of related subunits, with all four subunits arranged around a central pore. The AMPA receptor subunits are encoded by four separate genes (*GluA1–GluA4*), whereas the kainate receptor subunits are encoded by five different genes (*GluK1–GluK5*). Autoantibodies to the GluA3 subunit of the AMPA receptor are thought to play an important role in some forms of epilepsy. These antibodies actually mimic glutamate by activating GluA3-containing receptors, resulting in excessive excitation and seizures. NMDA receptors, on the other hand, are encoded by a family consisting of five genes that fall

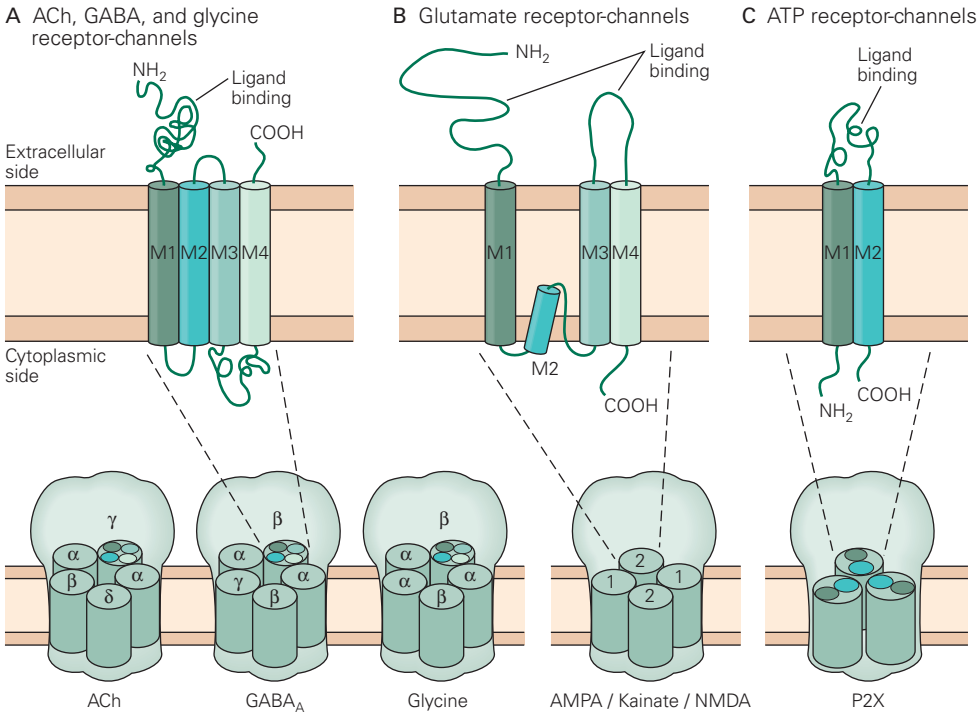

Figure 13–4 The three families of ionotropic receptors.

A. The nicotinic ACh, $GABA_A$, and glycine receptor-channels are all pentamers composed of several types of related subunits. As shown here, the ligand-binding domain is formed by the extracellular amino-terminal region of the protein. Each subunit has a membrane domain with four membrane-spanning α-helixes (M1–M4) and a short extracellular carboxyl terminus. The M2 helix lines the channel pore.

B. The glutamate receptor-channels are tetramers, often composed of two different types of closely related subunits (here denoted **1** and **2**). The subunits have a large extracellular amino terminus, a membrane domain with three membrane-spanning α-helixes (M1, M3, and M4), a large extracellular loop connecting the M3 and M4 helixes, and an intracellular carboxyl terminus. The M2 segment forms a loop that dips into and out of the cytoplasmic side of the membrane, contributing to the selectivity filter of the channel. The glutamate binding site is formed by residues in the extracellular amino terminus and in the M3–M4 extracellular loop.

C. The adenosine triphosphate (**ATP**) receptor-channels (or purinergic P2X receptors) are trimers. Each subunit possesses two membrane-spanning α-helixes (M1 and M2) and a large extracellular loop that binds ATP. The M2 helix lines the pore.

into two groups: The *GluN1* gene encodes one type of subunit, whereas four distinct *GluN2* genes (*A–D*) encode a second type. Each NMDA receptor contains two GluN1 subunits and two GluN2 subunits.

Glutamate Receptors Are Constructed From a Set of Structural Modules

All ionotropic glutamate receptor subunits share a common architecture with similar motifs. Eric Gouaux and colleagues have provided important insights into the structure of the ionotropic glutamate receptors, initially through an X-ray crystallographic model of an AMPA receptor composed of four GluA2 subunits. The subunits have a large extracellular amino-terminal domain, which is followed in the primary amino acid sequence by an extracellular ligand-binding domain and a transmembrane domain (Figures 13–4B and 13–5). The transmembrane domain contains three transmembrane α-helixes (M1, M3, and M4) and a loop (M2) between the M1 and M3 helixes that dips into and out of the cytoplasmic side of the membrane. This M2 loop resembles the pore-lining P loop of K^+ channels and helps form the selectivity filter of the channel (see Figure 8–12).

Both extracellular domains are homologous to bacterial amino acid binding protein domains. The ligand-binding domain is a bi-lobed clamshell-like structure (Figure 13–5A), whereas the amino-terminal domain is homologous to the glutamate-binding domain of metabotropic glutamate receptors but does not bind glutamate. Instead, in the ionotropic glutamate receptors, this domain is involved in subunit assembly, the modulation of receptor function by ligands other than glutamate, and/or the interaction with other synaptic proteins to regulate synapse development.

The ligand-binding domain is formed by two distinct regions in the linear sequence of the protein. One region comprises the end of the amino-terminal domain up to the M1 transmembrane helix; the second region is formed by the large extracellular loop connecting the M3 and M4 helixes (Figure 13–5A). In the ionotropic receptors, the binding of a molecule of glutamate within the clamshell triggers the closure of the lobes of the clamshell; competitive antagonists also bind to the clamshell but fail to trigger clamshell closure. This suggests that the conformational change associated with clamshell closure is important for opening the ion channel.

In addition to the core subunits that form the receptor-channel, AMPA receptors contain additional (or auxiliary) subunits that regulate receptor trafficking to the membrane and function. One important class of auxiliary subunits comprises the *transmembrane AMPA receptor regulatory proteins* (TARPs). A TARP subunit has four transmembrane domains, and its association with the pore-forming AMPA receptor subunits enhances the surface membrane trafficking, synaptic localization, and gating of the AMPA receptors. The first TARP family member to be identified was stargazin, which was isolated through a genetic screen in the *stargazer* mutant mouse, so named because these animals have a tendency to tip their heads backward and stare upward. Loss of stargazin leads to a complete loss of AMPA receptors from cerebellar granule cells, which results in cerebellar ataxia and frequent seizures. Other members of the TARP family are similarly required for AMPA receptor trafficking to the surface membrane in other types of neurons.

High-resolution cryo-electron microscopy has revealed the structure of TARP subunits in association with the AMPA receptor subunits (Figure 13–5D,E). These studies suggest that interactions between a TARP subunit and the ligand-binding domain clamshell of an AMPA receptor can stabilize the receptor in the glutamate-bound open state, thereby enhancing the channel open time, single-channel conductance, and affinity for glutamate.

Given the homology among the various subtypes of glutamate receptors, it is not surprising that the overall structure of the kainate and NMDA receptors is similar to that of the homomeric GluA2 receptor. However, there are some important differences that give rise to the distinct physiological functions of the different receptors. The high permeability of the NMDA receptor-channels to Ca^{2+} has been localized to a single amino acid residue in the pore-forming M2 loop. All NMDA receptor subunits contain the neutral residue asparagine at this position in the pore. In most types of AMPA receptor subunits, the residue at this position is the uncharged amino acid glutamine; in the GluA2 subunit, however, the corresponding M2 residue is arginine, a positively charged basic amino acid. Inclusion of even a single GluA2 subunit prevents the AMPA receptor-channel from conducting Ca^{2+} (Figure 13–6B), most likely as a result of strong electrostatic repulsion by the arginine. The opening of AMPA receptor-channels in cells that lack the GluA2 subunit can produce a significant Ca^{2+} influx because the pores of these receptors lack the positively charged arginine residue.

Interestingly, the DNA of the *GluA2* gene does not encode an arginine residue at this position in the M2 loop but rather codes for a glutamine residue. After transcription, the codon for glutamine in the *GluA2* mRNA is replaced with one for arginine through an enzymatic process termed RNA editing (Figure 13–6A). The importance of this RNA editing was investigated using a genetically modified mouse whose *GluA2* gene was engineered so that the relevant nucleotide in the

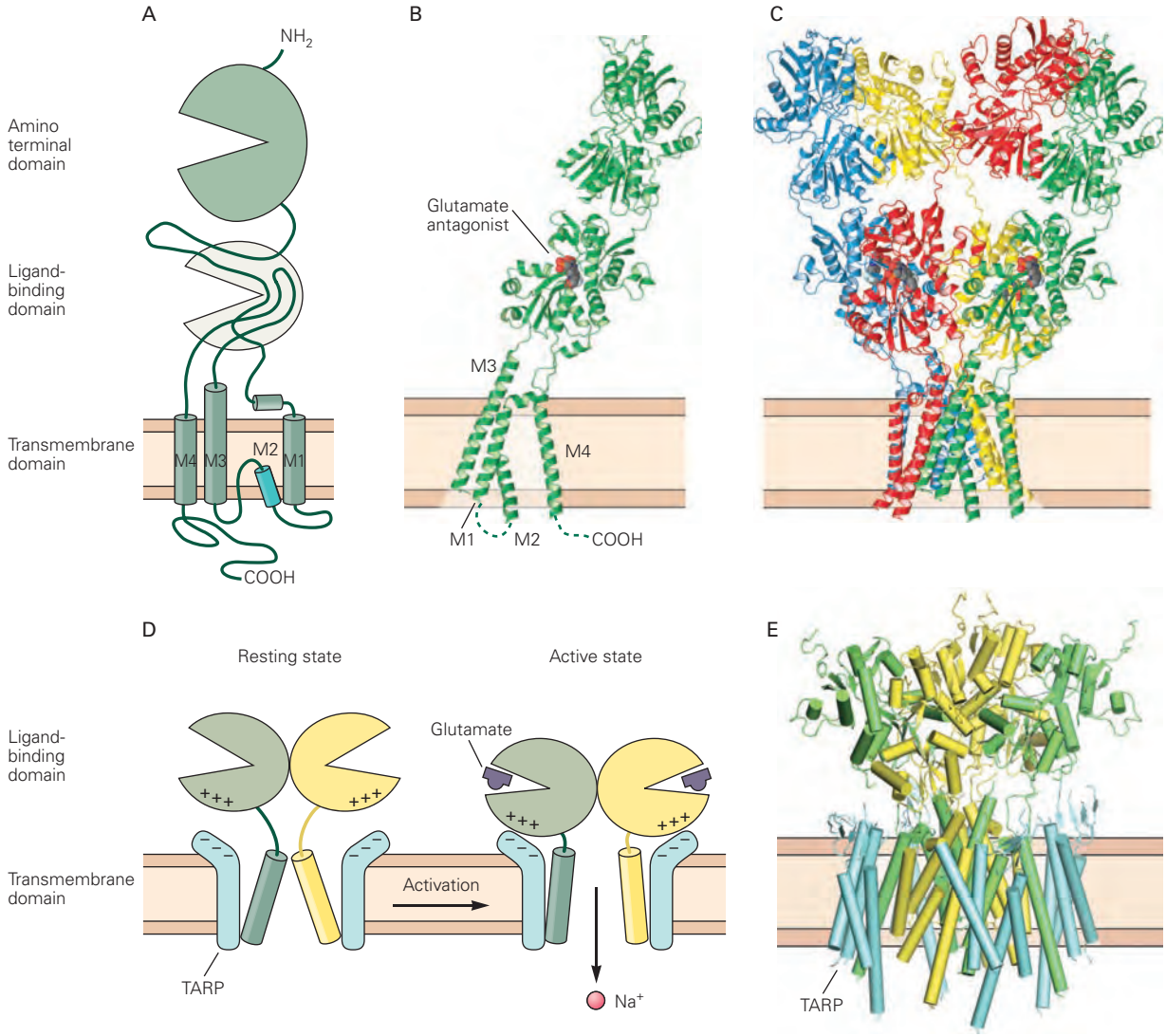

Figure 13–5 Atomic structure of an ionotropic glutamate receptor.

A. Schematic organization of the ionotropic glutamate receptors. The receptors contain a large extracellular amino terminus, a transmembrane domain containing three membrane-spanning α-helixes (M1, M3, and M4), and a loop that dips into the cytoplasmic side of the membrane (M2). The ligand-binding domain is formed by the extracellular region of the receptor on the amino-terminal side of the M1 segment and by the extracellular loop connecting M3 and M4. These two regions intertwine to form a clamshell-like structure that binds glutamate and various pharmacological agonists and competitive antagonists. A similar structure is formed at the extreme amino terminus of the receptor. In ionotropic glutamate receptors, this amino-terminal domain does not bind glutamate but is thought to modulate receptor function and synapse development. (Reproduced, with permission, from Armstrong et al. 1998.)

B. Three-dimensional X-ray crystal structure of a single AMPA receptor GluA2 subunit. This side view shows the amino-terminal, ligand-binding, and transmembrane domains (compare to panel A). The M1, M3, and M4 transmembrane α-helixes are indicated, as is a short α-helix in the M2 loop. A molecule of a competitive antagonist of glutamate bound to the ligand-binding domain is shown (**red space-filling representation**). The cytoplasmic loops connecting the membrane α-helixes were not resolved in the structure and have been drawn as **dashed lines**. (Reproduced, with permission, from Sobolevsky, Rosconi, and Gouaux 2009.)

C. This side view shows the structure of a receptor assembled from four identical GluA2 subunits (the subunits are colored differently for illustrative purposes). The subunits associate through their extracellular domains as a pair of dimers (two-fold symmetry). In the amino-terminal domain, one dimer is formed by the **blue** and **yellow** subunits, the other dimer by the **red** and **green** subunits. In the ligand-binding domain, the subunits change partners. In one dimer, the blue subunit associates with the red subunit, whereas in the other dimer, the yellow subunit associates with the green subunit. In the transmembrane region, the subunits associate as a four-fold symmetric tetramer. The significance of this highly unusual subunit arrangement is not fully understood. (Reproduced, with permission, from Sobolevsky, Rosconi, and Gouaux 2009.)

D. Cartoon side view of auxiliary TARP subunits (**blue**) associated with pore-forming GluA2 subunits. For simplicity, only the transmembrane and ligand-binding domain of two of the four GluA2 subunits is shown. Two of four TARP subunits are also shown. Binding of glutamate causes the clamshell-like ligand-binding domain to close, leading to a conformational change in the transmembrane domain that opens the pore. An electrostatic interaction between TARP and GluA2 stabilizes the receptor in the open state. (Adapted, with permission, from Mayer 2016. Copyright © 2016 Elsevier Ltd.)

E. Three-dimensional structure of the TARP-GluA2 complex. The α-helixes are shown as cylinders. The four TARP subunits are shown in blue. Transmembrane and ligand-binding domains of GluA2 subunits are shown in **yellow** and **green**. (Adapted, with permission, from Mayer 2016. Copyright © 2016 Elsevier Ltd.)

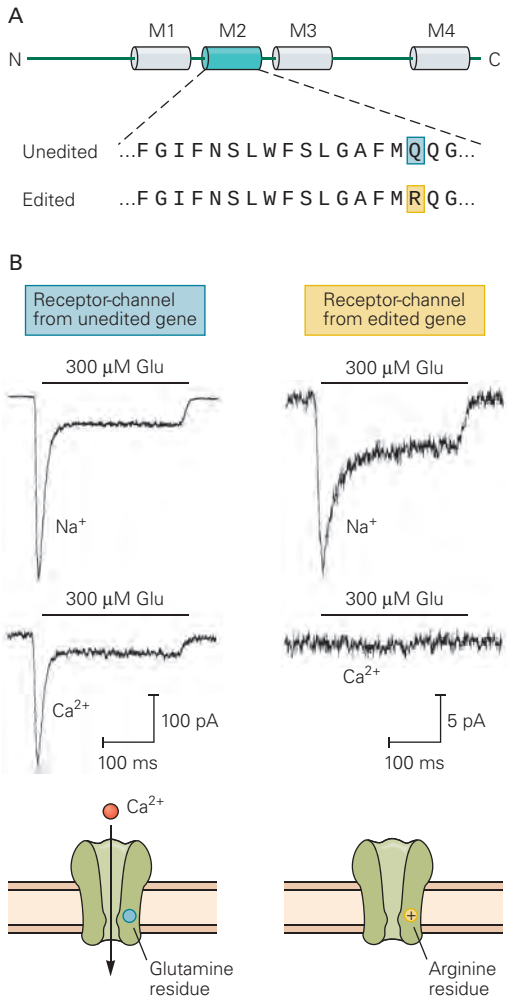

Figure 13–6 Determinants of calcium ion permeability of the AMPA receptor-channel.

A. Comparison of amino acid sequences in the M2 region of the AMPA receptor-channel coded by the *GluA2* gene before and after RNA editing. The unedited transcript codes for the polar residue glutamine (**Q**, the single-letter amino acid notation), whereas the edited transcript codes for the positively charged residue arginine (**R**). In adults, the GluA2 protein exists almost exclusively in the edited form.

B. AMPA receptor-channels expressed from unedited transcripts conduct Ca^{2+} (*left traces*), whereas those expressed from edited transcripts do not (*right traces*). The traces show currents elicited by glutamate with either extracellular Na^+ (*top*) or Ca^{2+} (*bottom*) as the predominant permeant cation. (Reproduced, with permission, from Sakmann 1992. Copyright © 1992 Elsevier.)

glutamine codon could no longer be changed to arginine. Such mice develop seizures and die within a few weeks after birth, presumably because the high Ca^{2+} permeability of all the AMPA receptors results in an excess of intracellular Ca^{2+}.

NMDA and AMPA Receptors Are Organized by a Network of Proteins at the Postsynaptic Density

How are the different glutamate receptors localized and arranged at excitatory synapses? Like most ionotropic receptors, glutamate receptors are normally clustered at postsynaptic sites in the membrane, precisely opposed to glutamatergic presynaptic terminals. The vast majority of excitatory synapses in the mature nervous system contain both NMDA and AMPA receptors, whereas in early development, synapses containing only NMDA receptors are common. The pattern of receptor localization and expression at individual synapses depends on a large number of regulatory proteins that constitute the postsynaptic density and help organize the three-dimensional structure of the postsynaptic cell membrane.

The postsynaptic density (PSD) is a remarkably stable structure, permitting its biochemical isolation, purification, and characterization. Electron microscopic studies of intact and isolated PSDs provide a strikingly detailed view of their structure (Figure 13–7A). By using gold-labeled antibodies, it is possible to identify specific protein components of the postsynaptic membrane, including the location and number of glutamate receptors. A typical PSD is around 350 nm in diameter and contains about 20 NMDA receptors, which tend to be localized near the center of the PSD, and 10 to 50 AMPA receptors, which are less centrally localized. The metabotropic glutamate receptors are located on the periphery, outside the main area of the PSD. All three receptor types interact with a wide array of cytoplasmic and membrane proteins to ensure their proper localization (Figure 13–7C).

One of the most prominent proteins in the PSD important for the clustering of glutamate receptors is PSD-95 (PSD protein of 95 kD molecular weight). PSD-95 is a membrane-associated protein that contains three repeated regions—the so-called PDZ domains—important for protein–protein interactions. (The PDZ domains are named after the three proteins in which they were first identified: PSD-95, the DLG tumor suppressor protein in *Drosophila*, and a protein termed ZO-1.) The PDZ domains bind to specific sequences at the carboxy terminus of a number of proteins. In PSD-95, the PDZ domains bind the NMDA receptor and Shaker-type voltage-gated K^+ channels, thereby localizing and concentrating these channels at postsynaptic sites. PSD-95 also interacts with the postsynaptic membrane protein neuroligin, which contacts the presynaptic membrane protein neurexin in the synaptic cleft, an interaction important for synapse development. Mutations in neuroligin are thought to contribute to some cases of autism.

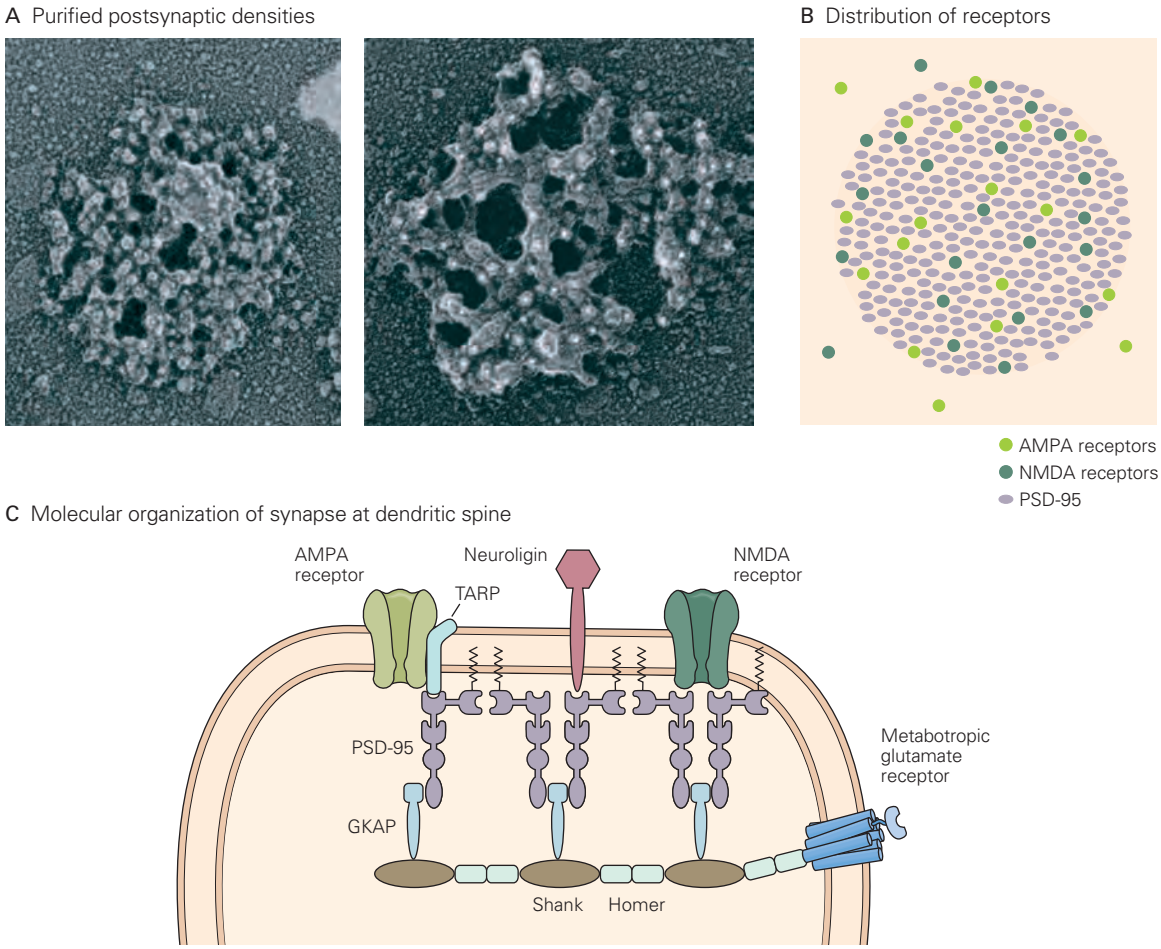

Figure 13–7 The postsynaptic cell membrane is organized into a macromolecular complex at excitatory synapses. Proteins containing PDZ domains help organize the distribution of AMPA and NMDA glutamate receptors at the postsynaptic density. (Reproduced, with permission, from Sheng and Hoogenrad 2007. Micrographs provided by Thomas S. Reese and Xiaobing Chen; National Institutes of Health, USA.)

A. Electron microscope images of biochemically purified post-synaptic densities, showing organization of the protein network. The membrane lipid bilayer is no longer present. *Left:* View of postsynaptic density from what would normally be the outside of the cell. This image consists of the extracellular domains of various receptors and membrane proteins. *Right:* View of a postsynaptic density from what would normally be the cytoplasmic side of the membrane. **White dots** show immunolabeled guanylate kinase anchoring protein, an important component of the postsynaptic density.

B. The distribution of NMDA receptors, AMPA receptors, and PSD-95, a prominent postsynaptic density protein, at a synapse.

C. The network of receptors and their interacting proteins in the postsynaptic density. PSD-95 contains three PDZ domains at its amino terminus and two other protein-interacting motifs at its carboxyl terminus, an SH3 domain and guanylate kinase (GK) domain. Certain PDZ domains of PSD-95 bind to the carboxyl terminus of the GluN2 subunit of the NMDA receptor. PSD-95 does not directly interact with AMPA receptors but binds to the carboxyl terminus of the TARP family of membrane proteins, which interact with the AMPA receptors as auxiliary subunits. PSD-95 also acts as a scaffold for various cytoplasmic proteins by binding to GK-associated protein (**GKAP**), which interacts with Shank, a large protein that associates into a meshwork linking the various components of the postsynaptic density. PSD-95 also interacts with the cytoplasmic region of neuroligin. The metabotropic glutamate receptor is localized on the periphery of the synapse where it interacts with the protein Homer, which in turn binds to Shank.

Although PSD-95 does not directly bind to AMPA receptors, it does interact with the TARP subunits. The proper localization of AMPA receptors in the postsynaptic membrane depends on the interaction between the carboxy terminus of the TARP subunit and PSD-95. AMPA receptors also bind to a distinct PDZ domain protein called GRIP, and metabotropic glutamate receptors interact with yet another PDZ domain protein called Homer. In addition to interacting with receptors, proteins with PDZ domains interact with

many other cellular proteins, including proteins that bind to the actin cytoskeleton, providing a scaffold around which a complex of postsynaptic proteins is constructed. Indeed, a biochemical analysis of the PSD has identified dozens of proteins that participate in NMDA or AMPA receptor complexes.

NMDA Receptors Have Unique Biophysical and Pharmacological Properties

The NMDA receptor has several interesting properties that distinguish it from AMPA receptors. As mentioned earlier, NMDA receptors have a distinctively high permeability to Ca^{2+}. In addition, the NMDA receptor is unique among ligand-gated channels thus far characterized because its opening depends on membrane voltage as well as transmitter binding.

The voltage dependence is caused by a mechanism that is quite different from that employed by the voltage-gated channels that generate the action potential. In the latter, changes in membrane potential are translated into conformational changes in the channel by an intrinsic voltage sensor. In the NMDA receptors, however, depolarization removes an extrinsic plug from the channel. At the resting membrane potential (–65 mV), extracellular Mg^{2+} binds tightly to a site in the pore of the channel, blocking ionic current. But when the membrane is depolarized (for example, by the opening of AMPA receptor-channels), Mg^{2+} is expelled from the channel by electrostatic repulsion, allowing Na^+, K^+, and Ca^{2+} to flow (Figure 13–8). The NMDA receptor has the further interesting property of being inhibited by the hallucinogenic drug *phencyclidine* (PCP, also known as angel dust) and the experimental compound MK801. Both drugs bind to a site in the pore of the channel that is distinct from the Mg^{2+} binding site (Figure 13–3A).

At most glutamatergic central synapses, the postsynaptic membrane contains both NMDA and AMPA receptors. The relative contributions of current through

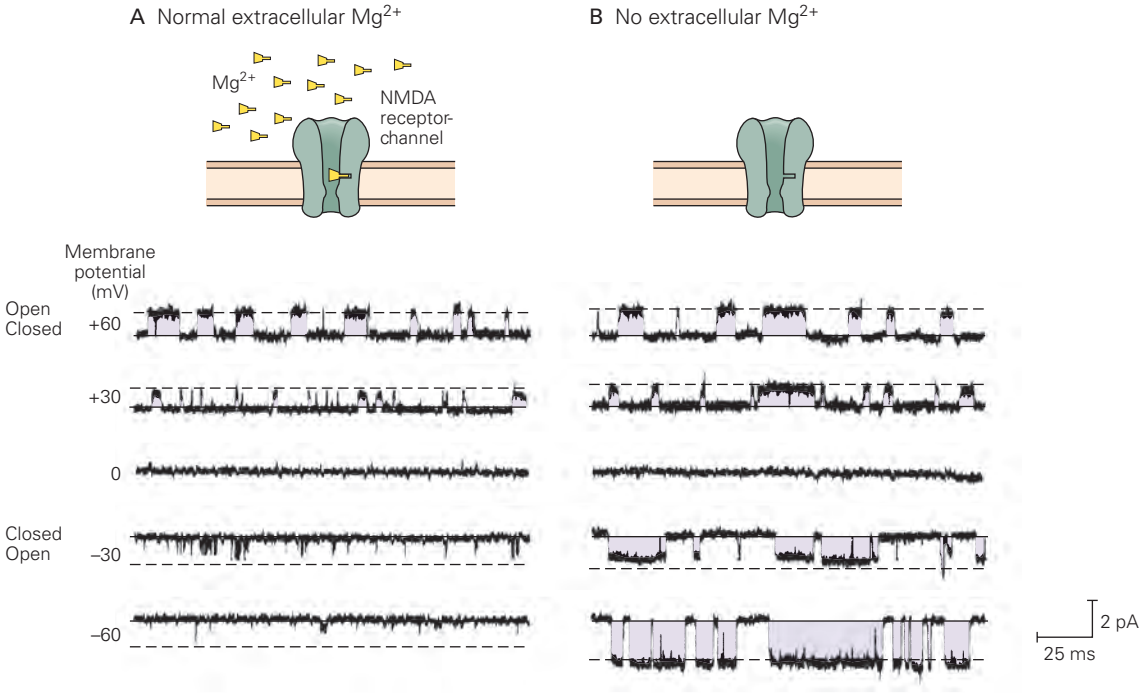

Figure 13–8 Opening of individual NMDA receptor-channels depends on membrane potential in addition to glutamate. These patch-clamp recordings are from individual NMDA receptor-channels (from rat hippocampal cells in culture). **Downward** deflections indicate pulses of inward (negative) current; **upward** deflections indicate outward (positive) current. (Reproduced, with permission, from J. Jen and C.F. Stevens.)

A. When Mg^{2+} is present in normal concentration in the extracellular solution (1.2 mM), the channel is largely blocked at the resting potential (–60 mV). At negative membrane potentials, only brief, flickering, inward currents are seen upon channel opening because of the Mg^{2+} block. Substantial depolarization to voltages positive to the reversal potential of 0 mV (to +30 mV or +60 mV) relieves the Mg^{2+} block, permitting longer-lasting pulses of outward current through the channel.

B. When Mg^{2+} is removed from the extracellular solution, the opening and closing of the channel do not depend on voltage. The channel is open at the resting potential of –60 mV, and the synaptic current reverses near 0 mV, like the total synaptic current (see Figure 13–9B).

NMDA and AMPA receptors to the total excitatory postsynaptic current (EPSC) can be quantified using pharmacological antagonists in a voltage-clamp experiment (Figure 13–9). Since NMDA receptors are largely inhibited by Mg^{2+} at the normal resting potential of most neurons, the EPSC is predominantly determined by charge flow through the AMPA receptors. This current has very rapid rising and decay phases. However, as a neuron becomes depolarized and Mg^{2+} is driven out of the mouth of the NMDA receptors, more charge flows through them. Thus, the NMDA receptor-channel conducts current maximally when two conditions are met: Glutamate is present, and the cell is depolarized. That is, the NMDA receptor acts as a molecular "coincidence detector," opening during the concurrent activation of the presynaptic and postsynaptic cells. In addition, because of its intrinsic kinetics of ligand gating, the current through the NMDA receptor-channel rises and decays with a much slower time course than the current through AMPA receptor-channels. As a result, the NMDA receptors contribute to a late, slow phase of the EPSC and EPSP.

As most glutamatergic synapses contain AMPA receptors that are capable of triggering an action potential by themselves, what is the function of the NMDA receptor? At first glance, the function of these receptors is even more puzzling because their intrinsic channel is normally blocked by Mg^{2+} at the resting potential. However, the high permeability of the NMDA receptor-channels to Ca^{2+} endows them with the special ability to produce a marked rise in intracellular [Ca^{2+}] that can activate various calcium-dependent signaling cascades, including several different protein kinases (Chapters 15 and 53). Thus, NMDA receptor activation can translate electrical signals into biochemical ones. Some of these biochemical reactions lead to long-lasting changes in synaptic strength through a set of processes called long-term synaptic plasticity, which are important for refining synaptic connections during early development and regulating neural circuits in the adult brain, including circuits critical for long-term memory.

The Properties of the NMDA Receptor Underlie Long-Term Synaptic Plasticity

In 1973, Tim Bliss and Terje Lomo found that a brief period of high-intensity and high-frequency synaptic stimulation (known as a tetanus) leads to *long-term potentiation* (LTP) of excitatory synaptic transmission in the hippocampus, a region of the mammalian brain required for many forms of long-term memory (Figure 13–10; see Chapters 53 and 54). Subsequent studies demonstrated that LTP requires Ca^{2+} influx through the NMDA receptor-channels, which open in response to the combined effect of glutamate release and strong postsynaptic depolarization during the tetanic stimulation. LTP is blocked if the tetanus is delivered in the presence of APV, which blocks the NMDA receptors, or if the postsynaptic neuron is injected with a compound that chelates intracellular Ca^{2+}.

The rise of Ca^{2+} in the postsynaptic cell is thought to potentiate synaptic transmission by activating postsynaptic biochemical cascades that trigger the insertion of additional AMPA receptors into the postsynaptic membrane. Under some circumstances, postsynaptic Ca^{2+} can trigger production of a retrograde messenger, a chemical signal that enhances transmitter release from the presynaptic terminal (Chapter 14). As we will discuss later, the Ca^{2+} accumulation and biochemical activation are largely restricted to the individual spines that are activated by the tetanic stimulation. As a result, LTP is input-specific; only those synapses that are activated during the tetanic stimulation are potentiated.

The prolonged high-frequency presynaptic firing required to induce LTP is unlikely to be achieved under physiological conditions. However, a more physiologically relevant form of plasticity, termed spike-timing-dependent plasticity (STDP), can be induced if a single presynaptic stimulus is paired at low frequency with the triggered firing of one or more postsynaptic action potentials, providing sufficient depolarization to relieve Mg^{2+} block of the NMDA receptor pore. The presynaptic activity must precede postsynaptic firing, following a rule proposed in 1949 by the psychologist Donald Hebb for how individual neurons could become grouped together into functional assemblies during associative memory storage. A number of lines of evidence now suggest that LTP, STDP, or related processes provide an important cellular mechanism for memory storage (Chapters 53 and 54) and fine-tuning synaptic connections during development (Chapter 49).

NMDA Receptors Contribute to Neuropsychiatric Disease

Unfortunately, there is also a downside to recruiting Ca^{2+} through the NMDA receptors. Excessively high concentrations of glutamate are thought to result in an overload of Ca^{2+} in the postsynaptic neurons, a condition that can be toxic to neurons. In tissue culture, even a brief exposure to high concentrations of glutamate can kill many neurons, an action called *glutamate excitotoxicity.* High concentrations of intracellular Ca^{2+} are thought to activate calcium-dependent proteases and phospholipases and lead to the production of free radicals that are toxic to the cell.

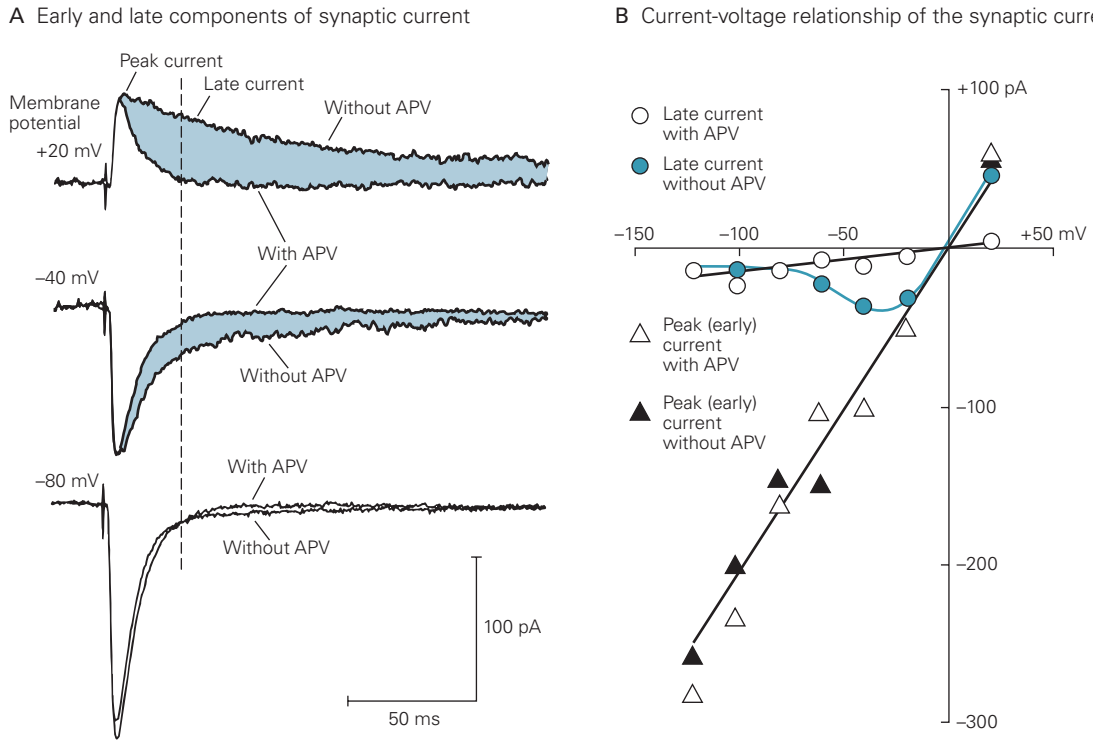

Figure 13–9 The contributions of the AMPA and NMDA receptor-channels to the excitatory postsynaptic current. These voltage-clamp current records are from a cell in the rat hippocampus. Similar receptor-channels are present in motor neurons and throughout the brain. (Adapted, with permission, from Hestrin et al. 1990.)

A. The drug APV selectively binds to and blocks the NMDA receptor. Shown here is the excitatory postsynaptic current (EPSC) before and during application of 50 μM APV at three different membrane potentials. The difference between the traces (**blue region**) represents the contribution of the NMDA receptor-channel to the EPSC. The current that remains in the presence of APV is the contribution of the AMPA receptor-channels. At –80 mV, there is no current through the NMDA receptor-channels because of pronounced Mg^{2+} block (see Figure 13–8). At –40 mV, a small late inward current through NMDA receptor-channels is evident. At +20 mV, the late component is more prominent and has reversed to become an outward current. The time 25 ms after the peak of the synaptic current (**dashed line**) is used for the calculations of late current in part B.

B. The postsynaptic currents through the NMDA and AMPA receptor-channels differ in their dependence on the membrane potential. The current through the AMPA receptor-channels contributes to the early phase of the synaptic current (**filled triangles**). The early phase is measured at the peak of the synaptic current and plotted here as a function of membrane potential. The current through the NMDA receptor-channels contributes to the late phase of the synaptic current (**filled circles**). The late phase is measured 25 ms after the peak of the synaptic current, a time at which the AMPA receptor component has decayed almost to zero (see part A). Note that the AMPA receptor-channels behave as simple resistors; current and voltage have a linear relationship. In contrast, current through the NMDA receptor-channels is nonlinear and increases as the membrane is depolarized from –80 to –40 mV, owing to progressive relief of the Mg^{2+} block. The reversal potential of both receptor-channel types is at 0 mV. The components of the synaptic current in the presence of 50 μm APV are indicated by the **unfilled circles** and **triangles**. Note how APV blocks the late (NMDA receptor) component of the EPSC but not the early (AMPA receptor) component.

Glutamate toxicity may contribute to cell damage after stroke, to the cell death that occurs with episodes of rapidly repeated seizures experienced by patients who have status epilepticus, and to degenerative diseases such as Huntington disease. Agents that selectively block the NMDA receptor may protect against the toxic effects of glutamate and have been tested clinically. The hallucinations that accompany NMDA receptor blockade have so far limited the usefulness of such compounds. A further complication of attempts to control excitotoxicity by blocking NMDA receptor function is that physiological levels of NMDA receptor activation may actually protect neurons from damage and cell death.

Not all of the physiological and pathophysiological effects mediated by the NMDA receptor may result from Ca^{2+} influx. There is increasing evidence that binding of glutamate to the NMDA receptor may cause a conformational change in the receptor that activates downstream intracellular signaling pathways independently of ion

flux. Such metabotropic functions of the NMDA receptor may contribute to long-term depression, a form of synaptic plasticity in which low-frequency synaptic activity produces a long-lasting decrease in glutamatergic synaptic transmission, the opposite of LTP. Metabotropic actions of the NMDA receptor may also contribute to the effect of β-amyloid, the peptide fragment implicated in Alzheimer disease, in depressing synaptic function.

A number of lines of evidence implicate NMDA receptor malfunction in schizophrenia. Pharmacological blockade of NMDA receptors with drugs such as phencyclidine or the general anesthetic ketamine, a derivative of PCP, produces symptoms that resemble the hallucinations associated with schizophrenia; in contrast, certain antipsychotic drugs enhance current through the NMDA receptor-channels. A particularly

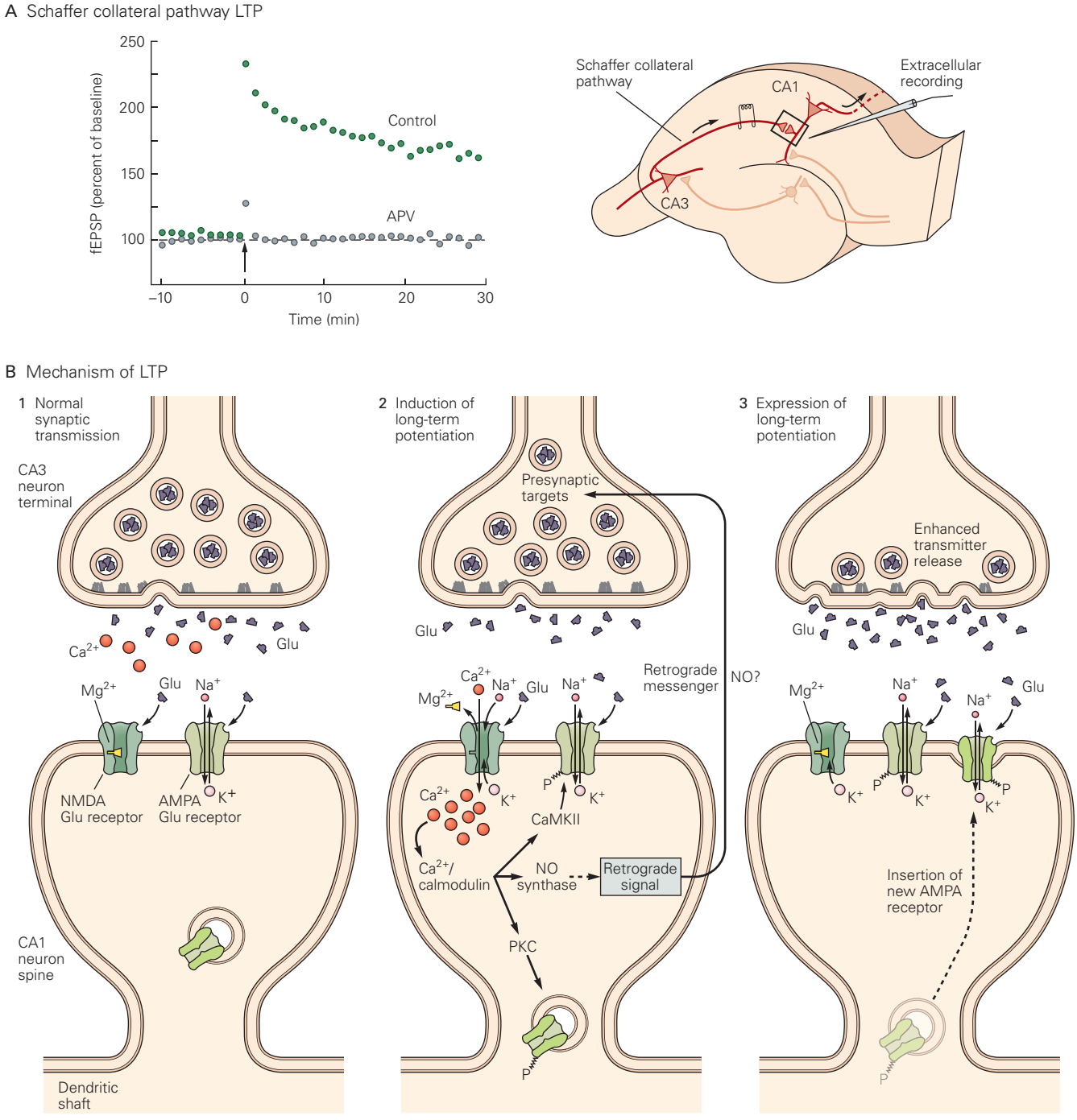

striking link with schizophrenia is seen in anti-NMDA receptor encephalitis, an autoimmune disorder in which the production of antibodies to the NMDA receptor reduces levels of the receptor in the membrane. Individuals with this disorder often experience severe seizures, most likely a result of the loss of inhibitory tone because of a reduction in NMDA receptor excitation in GABAergic interneurons, as well as psychoses, including hallucinations and other symptoms resembling schizophrenia. Treatments that reduce antibody levels often lead to complete remission of these symptoms. The idea that a decrease in NMDA receptor function may contribute to the symptoms of schizophrenia is further supported by recent genome-wide linkage analysis suggesting an association between the *NR2A* gene and schizophrenia. One additional link between the NMDA receptor and neuropsychiatric disorders is provided by the finding that low doses of ketamine exert a rapid and powerful antidepressant action.

Fast Inhibitory Synaptic Actions Are Mediated by Ionotropic GABA and Glycine Receptor-Channels Permeable to Chloride

Although glutamatergic excitatory synapses account for the vast majority of synapses in the brain, inhibitory synapses play an essential role in the nervous system both by preventing too much excitation and by regulating the firing patterns of networks of neurons. IPSPs in spinal motor neurons and most central neurons are generated by the amino acid neurotransmitters GABA and glycine.

GABA acts on both ionotropic and metabotropic receptors. The $GABA_A$ receptor is an ionotropic receptor that directly opens a Cl^- channel. The $GABA_B$ receptor is a metabotropic receptor that activates a second-messenger cascade, which often indirectly activates a K^+ channel (Chapter 15). Glycine, a less common inhibitory transmitter in the brain, also activates ionotropic receptors that directly open Cl^- channels. Glycine is the major transmitter released in the spinal cord by the interneurons that inhibit antagonist motorneurons.

Ionotropic Glutamate, GABA, and Glycine Receptors Are Transmembrane Proteins Encoded by Two Distinct Gene Families

The individual subunits that form the $GABA_A$ and glycine receptors are encoded by two distinct but closely related sets of genes. More surprisingly, these receptor subunits are structurally related to the nicotinic ACh receptor subunits, even though the latter select for cations and are therefore excitatory. Thus, as we saw above (Figure 13–4), the three types of receptor subunits are members of one large gene family.

Figure 13–10 (Opposite) NMDA receptor-dependent long-term potentiation of synaptic transmission at Schaffer collateral synapses.

A. Tetanic stimulation of the Schaffer collateral pathway for 1 second (**arrow**) induces LTP at the synapses between the presynaptic terminals of CA3 pyramidal neurons and the postsynaptic dendritic spines of CA1 pyramidal neurons. The graph shows the size of the synaptic response (extracellular field EPSP or **fEPSP**) as a percentage of the initial response prior to induction of LTP. At these synapses, LTP requires activation of the NMDA receptor-channels in the CA1 neurons; LTP is completely blocked when the tetanus is delivered in the presence of the NMDA receptor antagonist APV. (Adapted from Morgan and Teyler 2001.)

B. A model for the mechanism of long-term potentiation at Schaffer collateral synapses.

1. During normal, low-frequency synaptic transmission, glutamate (**Glu**) released from the terminals of CA3 Schaffer collateral axons binds to both NMDA and AMPA receptors in the postsynaptic CA1 neurons (specifically at the postsynaptic membrane of dendritic spines, the site of excitatory input). Sodium and potassium ions flow through the AMPA receptors but not through the NMDA receptor-channels, because their pores are blocked by Mg^{2+} at negative membrane potentials.

2. During a high-frequency tetanus, the large depolarization of the postsynaptic membrane (caused by the large amount of glutamate release resulting in strong activation of the AMPA receptors) relieves the Mg^{2+} blockade of the NMDA receptor-channels, allowing Ca^{2+}, Na^+, and K^+ to flow through these channels. The resulting increase of Ca^{2+} in the dendritic spine activates calcium-dependent protein kinases—calcium/calmodulin–dependent kinase (**CaMKII**) and protein kinase C (**PKC**)—leading to induction of LTP.

3. Second-messenger cascades activated during induction of LTP have two main effects on synaptic transmission. Phosphorylation through activation of protein kinases, including PKC, enhances current through the AMPA receptor-channels, in part by causing insertion of new receptors into the postsynaptic CA1 neuron. In addition, the postsynaptic cell releases (in ways that are still not understood) retrograde messengers that diffuse to the presynaptic terminal to enhance subsequent transmitter release. One such retrograde messenger may be nitric oxide (**NO**), produced by the enzyme NO synthase (shown in panel B-2).

Like the nicotinic ACh receptor-channels, the $GABA_A$ and glycine receptor-channels are pentamers. The $GABA_A$ receptors are usually composed of two α-, two β-, and one γ- or δ-subunit and are activated by the binding of two molecules of GABA in clefts formed between the two α- and β-subunits. The glycine receptors are composed of three α- and two β-subunits and require the binding of up to three molecules of ligand to open. The transmembrane topology of each $GABA_A$ and glycine receptor subunit is similar to that of a nicotinic ACh receptor subunit, consisting of a large extracellular ligand-binding domain followed by four hydrophobic transmembrane α-helices (labeled M1, M2, M3, and M4), with the M2 helix forming the lining of the channel pore (Figure 13–4A). However, the amino acids flanking the M2 domain are strikingly different from those of the nicotinic ACh receptor. As discussed in Chapter 12, the pore of the ACh receptor contains rings of negatively charged acidic residues that help the channel select for cations over anions. In contrast, the GABA and glycine receptor-channels contain either neutral or positively charged basic residues at the homologous positions, which contribute to the selectivity of these channels for anions.

Most of the major classes of receptor subunits are encoded by multiple related genes. Thus, there are six types of $GABA_A$ α-subunits (α1–α6), three β-subunits (β1–β3), three γ-subunits (γ1–γ3), and one δ-subunit. The genes for these different subtypes are often differentially expressed in different types of neurons, endowing their inhibitory synapses with distinct properties. The possible combinatorial arrangements of these subunits in a fully assembled pentameric receptor provides an enormous potential diversity of receptors.

The $GABA_A$ and glycine receptors play important roles in disease and in the actions of drugs. $GABA_A$ receptors are the target for several types of drugs that are clinically important and socially abused, including general anesthetics, benzodiazepines, barbiturates, and alcohol. General anesthetics, either gases or injectable compounds, induce loss of consciousness and are therefore widely used during surgery. Benzodiazepines are antianxiety agents and muscle relaxants that include diazepam (Valium), lorazepam (Ativan), and clonazepam (Klonopin). Zolpidem (Ambien) is a benzodiazepine compound that promotes sleep. The barbiturates comprise a distinct group of hypnotics that includes phenobarbital and secobarbital.

The different classes of compounds—GABA, general anesthetics, benzodiazepines, barbiturates, and alcohol—bind to different sites on the receptor but act similarly to increase the opening of the GABA receptor-channel. For example, whereas GABA binds to a cleft between the α- and β-subunits, benzodiazepines bind to a cleft between the α- and γ-subunits. In addition, the binding of any one of these classes of drug influences the binding of the others. For example, a benzodiazepine (or a barbiturate) binds more strongly to the receptor-channel when GABA also is bound, and this tight binding helps stabilize the channel in the open state. In this manner, the various compounds all enhance inhibitory synaptic transmission.

How do these different compounds, all acting on $GABA_A$ receptors to promote channel opening, produce such diverse behavioral and psychological effects, for example, reducing anxiety versus promoting sleep? It turns out that many of these compounds bind selectively to specific subunit types, which can be expressed in different types of neurons in different regions of the brain. For example, zolpidem binds selectively to $GABA_A$ receptors containing the α_1- subunit. In contrast, the anxiolytic effect of benzodiazepines requires binding to the α_2- and γ-subunits.

In addition to being important pharmacological targets, the $GABA_A$ and glycine receptors are targets of disease and poisons. Missense mutations in the α-subunit of the glycine receptor underlie an inherited neurological disorder called *familial startle disease* (or *hyperekplexia*), characterized by abnormally high muscle tone and exaggerated responses to noise. These mutations decrease the opening of the glycine receptor and so reduce the normal levels of inhibitory transmission in the spinal cord. The poison strychnine, a plant alkaloid compound, causes convulsions by blocking the glycine receptor and decreasing inhibition. Nonsense mutations that result in truncations of $GABA_A$ receptor α- and γ-subunits have been implicated in congenital forms of epilepsy.

Chloride Currents Through $GABA_A$ and Glycine Receptor-Channels Normally Inhibit the Postsynaptic Cell

The function of GABA receptors is intimately linked to their biophysical properties. Eccles and his colleagues determined the ionic mechanism of the IPSP in spinal motor neurons by systematically changing the level of the resting membrane potential in a motor neuron while stimulating a presynaptic inhibitory interneuron (Figure 13–11).

When the motor neuron membrane is held at the normal resting potential (−65 mV), a small hyperpolarizing potential is generated when the presynaptic interneuron is stimulated. When the motor neuron membrane is held at −70 mV, no change in potential

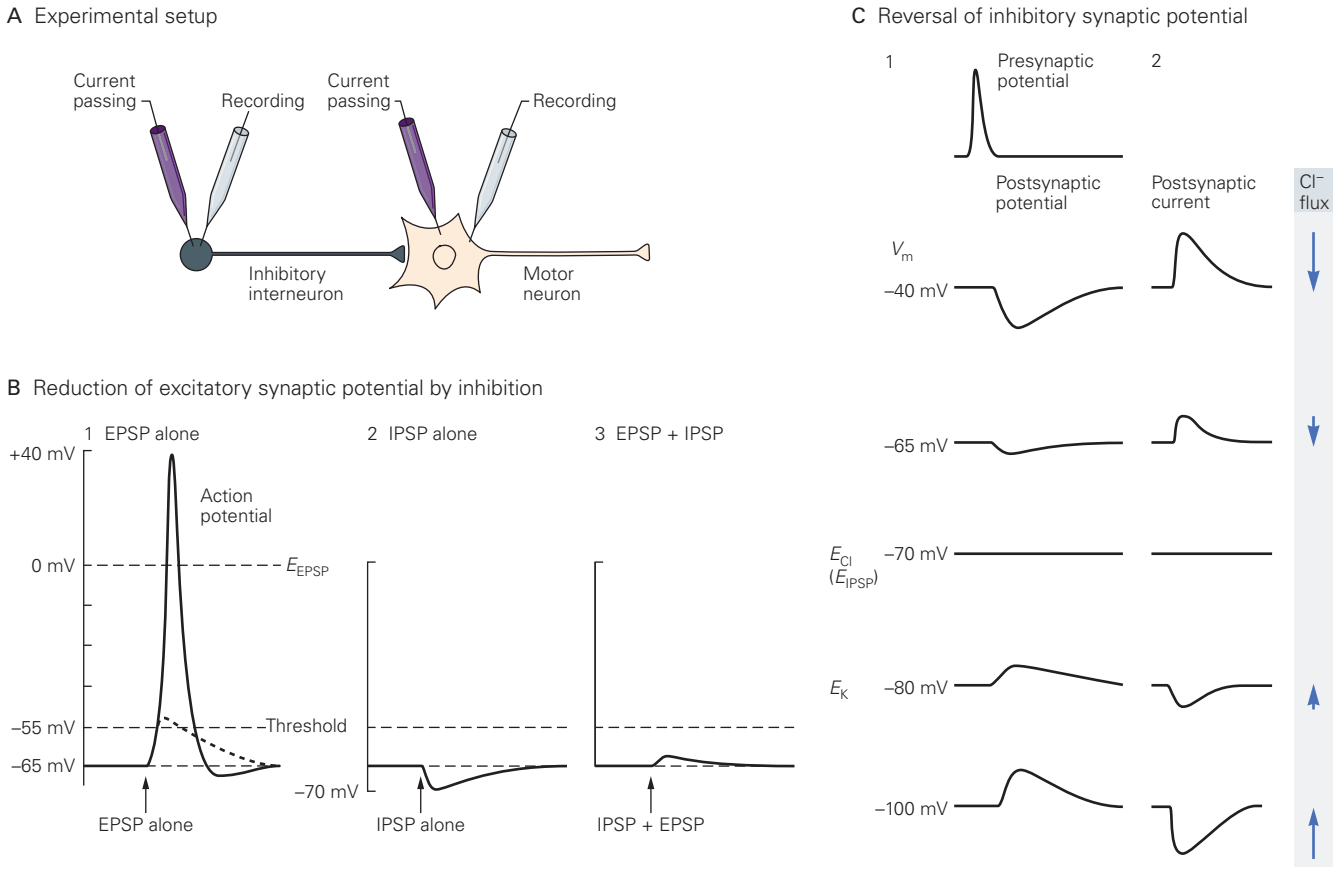

Figure 13–11 Inhibitory actions at chemical synapses result from the opening of ion channels selective for chloride.

A. In this hypothetical experiment, two electrodes are placed in the presynaptic interneuron and two in the postsynaptic motor neuron. The current-passing electrode in the presynaptic cell is used to produce an action potential; in the postsynaptic cell, it is used to alter the membrane potential systematically prior to the presynaptic input.

B. Inhibitory actions counteract excitatory actions. **1.** A large EPSP occurring alone depolarizes the membrane toward E_{EPSP} and exceeds the threshold for generating an action potential. **2.** An IPSP alone moves the membrane potential away from the threshold toward E_{Cl}, the equilibrium potential for Cl^- (–70 mV). **3.** When inhibitory and excitatory synaptic potentials occur together, the effectiveness of the EPSP is reduced and prevented from reaching the threshold for an action potential.

C. The IPSP and inhibitory synaptic current reverse at E_{Cl}. **1.** A presynaptic spike produces a hyperpolarizing IPSP at the resting membrane potential (–65 mV). The IPSP is larger when the membrane potential is set at –40 mV due to the increased inward driving force on Cl^-. When the membrane potential is set at –70 mV the IPSP is nullified. This reversal potential for the IPSP occurs at E_{Cl}. With further hyperpolarization of the membrane, the IPSP is inverted to a depolarizing postsynaptic potential (at –80 and –100 mV) because the membrane potential is negative to E_{Cl}. **2.** The reversal potential of the inhibitory postsynaptic current measured under voltage clamp. An inward (negative) current flows at membrane potentials negative to the reversal potential (corresponding to an efflux of Cl^-), and an outward (positive) current flows at membrane potentials positive to the reversal potential (corresponding to an influx of Cl^-). (**Up arrows** = efflux; **down arrows** = influx.)

is recorded when the interneuron is stimulated. But at potentials more negative than –70 mV, the motor neuron generates a *depolarizing* response following stimulation of the inhibitory interneuron. This reversal potential of –70 mV corresponds to the Cl^- equilibrium potential in spinal motor neurons (the extracellular concentration of Cl^- is much greater than the intracellular concentration). Thus, at –70 mV, the tendency of Cl^- to diffuse into the cell down its chemical concentration gradient is balanced by the electrical force (the negative membrane potential) that opposes Cl^- influx. Replacement of extracellular Cl^- with an impermeant anion reduces the size of the IPSP and shifts the reversal potential to more positive values in accord with the predictions of the Nernst equation. Thus, the IPSP results from an increase in Cl^- conductance.

The currents through single GABA and glycine receptor-channels, the unitary currents, have been measured using the patch-clamp technique. Both transmitters activate Cl^- channels that open in an all-or-none manner, similar to the opening of ACh and glutamate-gated channels. The inhibitory effect of GABA and glycine on neuronal firing depends on two related mechanisms. First, in a typical neuron, the resting potential of −65 mV is slightly more positive than E_{Cl} (−70 mV). At this resting potential, the chemical force driving Cl^- into the cell is slightly greater than the electrical force opposing Cl^- influx—that is, the electrochemical driving force on Cl^- ($V_m - E_{Cl}$) is positive. As a result, the opening of Cl^- channels leads to a positive current, based on the relation $I_{Cl} = g_{Cl}\ (V_m - E_{Cl})$. Because the charge carrier is the negatively charged Cl^- ion, the positive current corresponds to an influx of Cl^- into the neuron, down its electrochemical gradient. This causes a net increase in the negative charge on the inside of the membrane—the membrane becomes hyperpolarized.

However, some central neurons have a resting potential that is approximately equal to E_{Cl}. In such cells, an increase in Cl^- conductance does not change the membrane potential—the cell does not become hyperpolarized—because the electrochemical driving force on Cl^- is nearly zero. However, the opening of Cl^- channels in such a cell still inhibits the cell from firing an action potential in response to a near-simultaneous EPSP. This is because the depolarization produced by an excitatory input depends on a weighted average of the batteries for all types of open channels—that is, the batteries for the excitatory and inhibitory synaptic conductances and the resting conductances—with the weighting factor equal to the total conductance for a particular type of channel (see Chapter 12, Postscript). Because the battery for Cl^- channels lies near the resting potential, opening these channels helps hold the membrane near its resting potential during the EPSP by increasing the weighting factor for the Cl^- battery.

The effect that the opening of Cl^- channels has on the magnitude of an EPSP can also be described in terms of Ohm's law. Accordingly, the amplitude of the depolarization during an EPSP, ΔV_{EPSP} is given by:

$$\Delta V_{EPSP} = I_{EPSP}/g_l$$

where I_{EPSP} is the excitatory synaptic current and g_l is the conductance from all other channels open in the membrane, including resting channels and transmitter-gated Cl^- channels. Because the opening of the Cl^- channels increases the resting conductance, ie, makes the neuron more leaky, the depolarization during the EPSP decreases. This consequence of synaptic inhibition is called the *short-circuiting* or *shunting* effect.

By counteracting synaptic excitation, synaptic inhibition can exert powerful control over action potential firing in neurons that are spontaneously active because of the presence of intrinsic pacemaker channels. This function, called the *sculpting* role of inhibition, shapes the pattern of firing in such cells (Figure 13–12). In fact, this sculpting role of inhibition likely happens in all neurons, leading to the temporal patterning of neuronal spiking and to the control of the synchronization of neural circuits.

The different biophysical properties of synaptic conductances can be understood as distinct mathematical operations carried out by the postsynaptic neuron. Thus, inhibitory inputs that hyperpolarize the cell perform a *subtraction* on the excitatory inputs, whereas the shunting effect of the conductance increase performs a *division.* Adding excitatory inputs (or removing nonshunting inhibitory inputs) results in *summation.* Finally, the combination of an excitatory input with the removal of an inhibitory shunt produces a *multiplication.* These arithmetic effects, however, are often mixed and can vary with time as the membrane potential of neurons constantly varies, leading to changes in the driving force on Cl^- through $GABA_A$ receptor-channels.

In some cells, such as those with metabotropic $GABA_B$ receptors, inhibition is caused by the opening of K^+ channels. Because the K^+ equilibrium potential of neurons (E_K = −80 mV) is always negative to the resting potential, opening K^+ channels inhibits the cell even

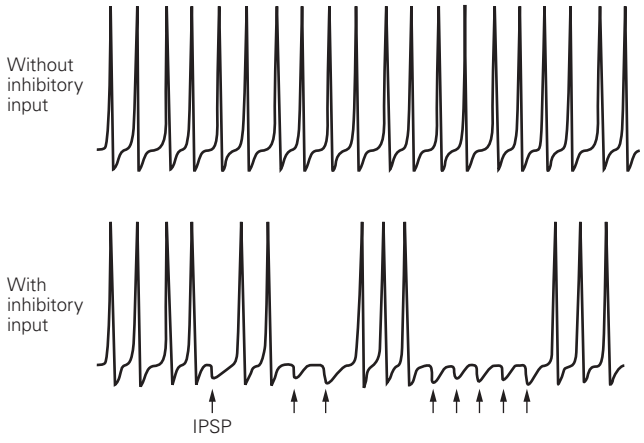

Figure 13–12 Inhibition can shape the firing pattern of a spontaneously active neuron. Without inhibitory input, the neuron fires continuously at a fixed interval. With inhibitory input (**arrows**), some action potentials are inhibited, resulting in a distinctive pattern of impulses.

more profoundly than opening Cl^- channels (assuming a similar-size synaptic conductance), generating a more "subtractive" inhibition. $GABA_B$ responses turn on more slowly and persist for a longer time compared with $GABA_A$ responses.

Paradoxically, under some conditions, the activation of $GABA_A$ receptors in brain cells can cause excitation. This is because the influx of Cl^- after intense periods of stimulation can be so great that the intracellular Cl^- concentration increases substantially. It may even double. As a result, the Cl^- equilibrium potential may become more positive than the resting potential. Under these conditions, the opening of Cl^- channels leads to Cl^- efflux and depolarization of the neuron. Such depolarizing Cl^- responses occur normally in many neurons in newborn animals, where the intracellular Cl^- concentration tends to be high even at rest. This is because the K^+-Cl^- cotransporter responsible for maintaining low intracellular Cl^- is expressed at low levels during early development (Chapter 9). Depolarizing Cl^- responses may also occur in the distal dendrites of more mature neurons and perhaps also at their axon initial segment. Such excitatory $GABA_A$ receptor actions in adults may contribute to epileptic discharges in which large, synchronized, and depolarizing GABA responses are observed.

Some Synaptic Actions in the Central Nervous System Depend on Other Types of Ionotropic Receptors

A minority of fast excitatory synaptic actions in the brain are mediated by the neurotransmitter serotonin (5-HT) acting at the $5\text{-}HT_3$ class of ionotropic receptor-channels. These pentameric receptors, which are made up of subunits with four transmembrane segments, are structurally similar to nicotinic ACh receptors. Like the ACh receptor-channels, $5\text{-}HT_3$ receptor-channels are permeable to monovalent cations and have a reversal potential near 0 mV.

Ionotropic receptors for adenosine triphosphate (ATP) serve an excitatory function at other selected synapses and constitute a third family of transmitter-gated ion channels. These so-called purinergic receptors (named for the purine ring in adenosine) occur on smooth muscle cells innervated by sympathetic neurons of the autonomic ganglia as well as on certain central and peripheral neurons. At these synapses, ATP activates an ion channel that is permeable to both monovalent cations and Ca^{2+}, with a reversal potential near 0 mV. Several genes coding for this family of ionotropic ATP receptors (termed the *P2X receptors*) have been identified. The amino acid sequence and subunit structure of these ATP receptors are different from the other two ligand-gated channel families. An X-ray crystal structure of the P2X receptor reveals that it has an exceedingly simple organization in which three subunits, each containing only two transmembrane segments, surround a central pore (Figure 13–4C).

Excitatory and Inhibitory Synaptic Actions Are Integrated by Neurons Into a Single Output

Each neuron in the central nervous system is constantly bombarded by an array of synaptic inputs from many other neurons. A single motor neuron, for example, may be the target of as many as 10,000 different presynaptic terminals. Some are excitatory, others inhibitory; some are strong, others weak. Some inputs contact the motor cell on the tips of its apical dendrites, others on proximal dendrites, some on the dendritic shaft, others on the soma. The different inputs can reinforce or cancel one another. How does a given neuron integrate these signals into a coherent output?

As we saw earlier, the synaptic potentials produced by a single presynaptic neuron typically are not large enough to depolarize a postsynaptic cell to the threshold for an action potential. The EPSPs produced in a motor neuron by most stretch-sensitive afferent neurons are only 0.2 to 0.4 mV in amplitude. If the EPSPs generated in a single motor neuron were to sum linearly, at least 25 afferent neurons would have to fire together and release transmitter to depolarize the trigger zone by the 10 mV required to reach threshold. But at the same time the postsynaptic cell is receiving excitatory inputs, it may also be receiving inhibitory inputs that prevent the firing of action potentials by either a subtractive or shunting effect.

The net effect of the inputs at any individual excitatory or inhibitory synapse will therefore depend on several factors: the location, size, and shape of the synapse; the proximity and relative strength of other synergistic or antagonistic synapses; and the resting potential of the cell. And, in addition, all of this is exquisitely dependent on the timing of the excitatory and inhibitory input. Inputs are coordinated in the postsynaptic neuron by a process called *neuronal integration.* This cellular process reflects the task that confronts the nervous system as a whole. A cell at any given moment has two options: to fire or not to fire an action potential. Charles Sherrington described the brain's ability to choose between competing alternatives as the *integrative action of the nervous system.*

He regarded this decision making as the brain's most fundamental operation (see Chapter 56).

Synaptic Inputs Are Integrated at the Axon Initial Segment

In most neurons, the decision to initiate an action potential output is made at one site: the axon initial segment. Here, the cell membrane has a lower threshold for action potential generation than at the cell body or dendrites because it has a higher density of voltage-dependent Na^+ channels (Figure 13–13). With each increment of membrane depolarization, more Na^+ channels open, providing a higher density of inward current (per unit area of membrane) at the axon initial segment than elsewhere in the cell.

At the initial segment, the depolarization increment required to reach the threshold for an action potential (–55 mV) is only 10 mV from the resting level of –65 mV. In contrast, the membrane of the cell body must be depolarized by 30 mV before reaching its threshold (–35 mV). Therefore, synaptic excitation first discharges the region of membrane at the initial segment, also called the *trigger zone.* The action potential generated at this site then depolarizes the membrane of the cell body to threshold and at the same time is propagated along the axon .

Because neuronal integration involves the summation of synaptic potentials that spread to the trigger zone, it is critically affected by two passive membrane properties of the neuron (Chapter 9). First, the membrane time constant helps determine the time course of the synaptic potential in response to the EPSC, thereby controlling *temporal summation*, the process by which consecutive synaptic potentials are added together in the postsynaptic cell. Neurons with a large membrane time constant have a greater capacity for temporal summation than do neurons with a shorter time constant (Figure 13–14A). As a result, the longer the time constant, the greater is the likelihood that two consecutive inputs will summate to bring the cell membrane to its threshold for an action potential.

Second, the *length* constant of the cell determines the degree to which the EPSP decreases as it spreads

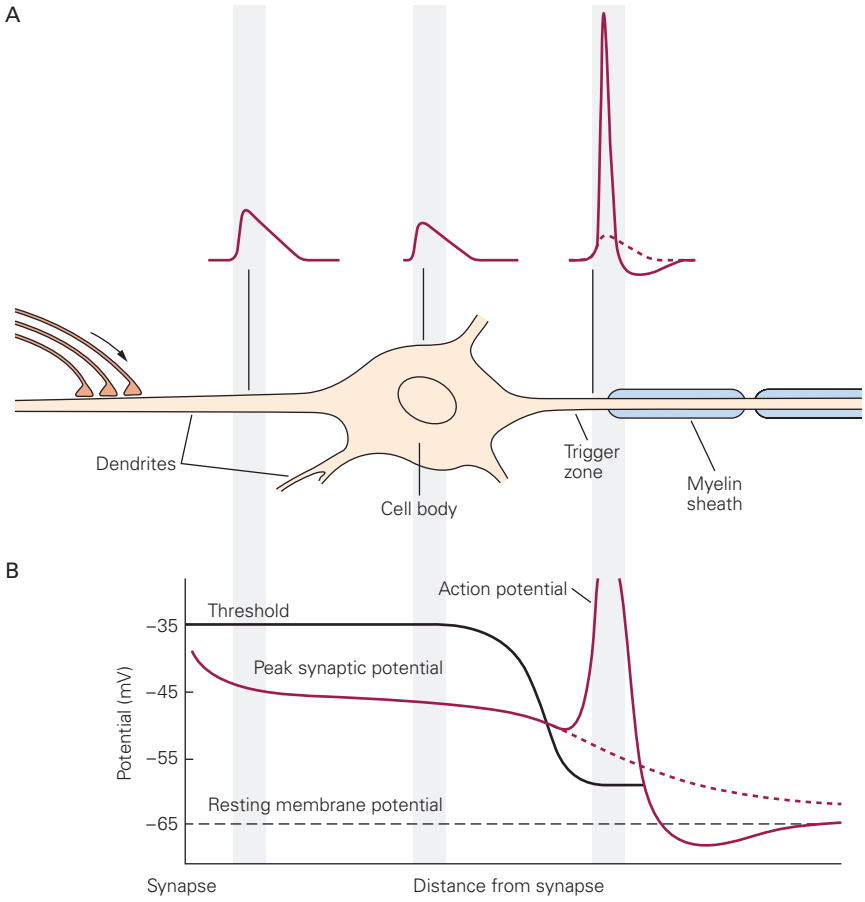

Figure 13–13 A synaptic potential arising in a dendrite can generate an action potential at the axon initial segment. (Adapted, with permission, from Eckert et al. 1988.)

A. An excitatory synaptic potential originating in the dendrites decreases with distance as it propagates passively to the soma. Nevertheless, an action potential can be initiated at the trigger zone (the axon initial segment) because the density of the Na^+ channels in this region is high and thus the threshold for an action potential is low.

B. Comparison of the threshold for initiation of the action potential at different sites in the neuron (corresponding to drawing A). An action potential is generated when the amplitude of the synaptic potential exceeds the threshold. The **dashed line** shows the decay of the synaptic potential if no action potential is generated at the axon initial segment.

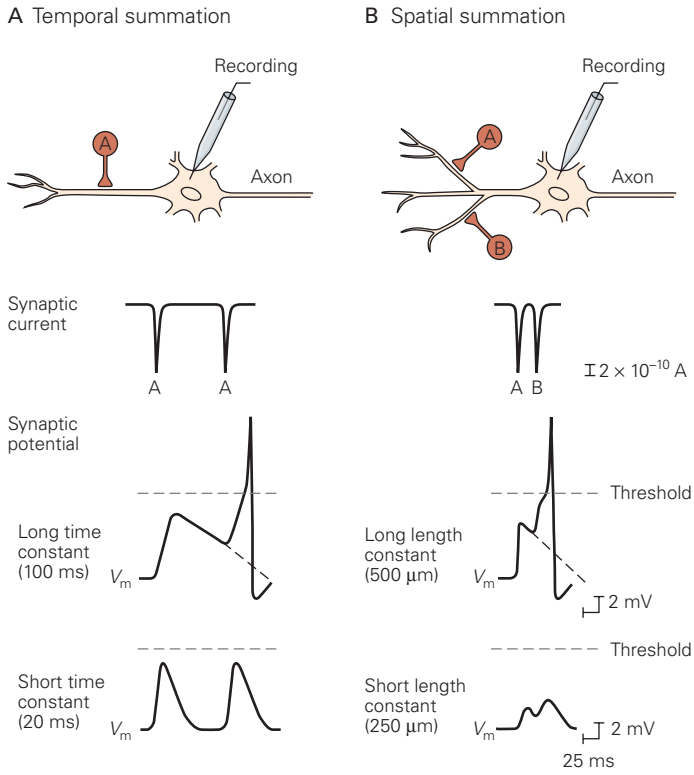

Figure 13–14 Central neurons are able to integrate a variety of synaptic inputs through temporal and spatial summation of synaptic potentials.

A. Temporal summation. The time constant of a postsynaptic cell (see Figure 9–10) affects the amplitude of the depolarization caused by consecutive EPSPs produced by a single presynaptic neuron (cell A). Here the synaptic current generated by the presynaptic neuron is nearly the same for both EPSPs. In a cell with a *long* time constant, the first EPSP does not fully decay by the time the second EPSP is triggered. In that instance, the depolarizing effects of both potentials are additive, bringing the membrane potential above the threshold and triggering an action potential. In a cell with a *short* time constant, the first EPSP decays to the resting potential before the second EPSP is triggered, and in that instance, the second EPSP alone does not cause enough depolarization to trigger an action potential.

B. Spatial summation. The length constant of a postsynaptic cell (see Figure 9–11B) affects the amplitudes of two excitatory postsynaptic potentials produced by two presynaptic neurons (cells A and B). For illustrative purposes, both synapses are the same distance (500 µm) from the postsynaptic cell's trigger zone, and the current produced by each synaptic contact is the same. If the distance between the site of synaptic input and the trigger zone in the postsynaptic cell is only one length constant (that is, the postsynaptic cell has a long length constant of 500 µm), the synaptic potentials produced by each of the two presynaptic neurons will decrease to 37% of their original amplitude by the time they reach the trigger zone. Summation of the two potentials results in enough depolarization to exceed threshold, triggering an action potential. If the distance between the synapse and the trigger zone is equal to two length constants (ie, the postsynaptic cell has a short length constant of
250 µm), each synaptic potential will be less than 15% of its initial amplitude, and summation will not be sufficient to trigger an action potential.

passively from a synapse along the length of the dendrite to the cell body and axon initial segment (the trigger zone). In cells with a longer length constant, signals spread to the trigger zone with minimal decrement; in cells with a short length constant, the signals decay rapidly with distance. Because the depolarization produced by one synapse is almost never sufficient to trigger an action potential at the trigger zone, the inputs from many presynaptic neurons acting at different sites on the postsynaptic neuron must be added together. This process is called *spatial summation.* Neurons with a large length constant are more likely to be brought to threshold by inputs arising from different sites than are neurons with a short length constant (Figure 13–14B).

Subclasses of GABAergic Neurons Target Distinct Regions of Their Postsynaptic Target Neurons to Produce Inhibitory Actions With Different Functions

In contrast to the relatively few types of glutamatergic pyramidal neurons, the mammalian central nervous

system has a large variety of GABAergic inhibitory interneurons that differ in developmental origin, molecular composition, morphology, and connectivity (Figure 13–15). Up to 20 different subtypes of GABAergic neurons have been identified in one subregion of the hippocampus alone. The different types of GABAergic interneurons form extensive synaptic connections with their neighboring excitatory and inhibitory neurons. Thus, even though only 20% of all neurons are inhibitory, the overall levels of inhibition and excitation tend to be nearly balanced in most brain regions. This results in the tuning of neural circuits to respond to only the most salient excitatory information. While the diversity of interneurons is challenging to understand, it is clear that different types of interneurons selectively target different regions of their postsynaptic neurons.

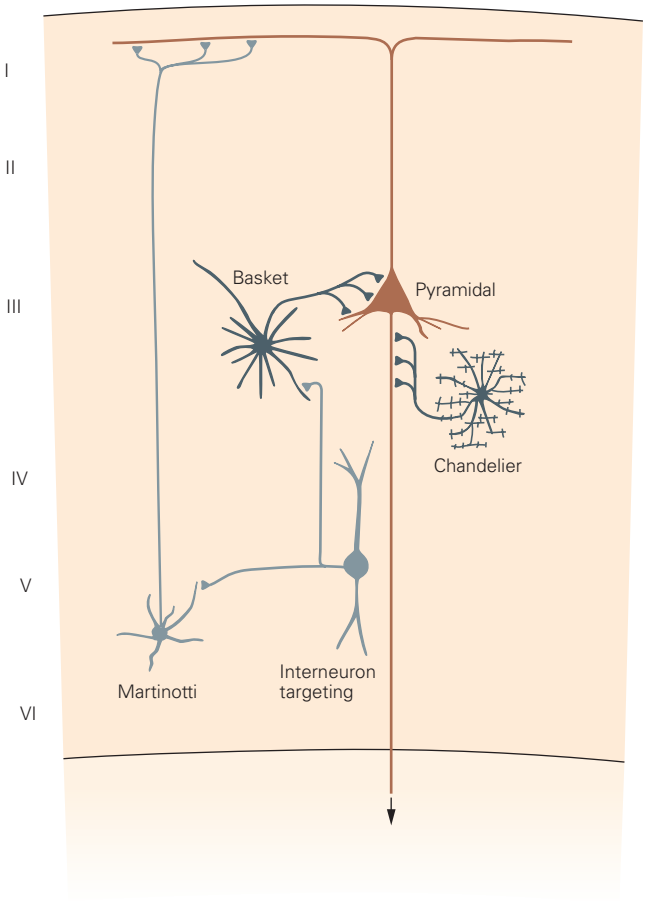

Figure 13–15 Different GABAergic inhibitory neurons target different regions of a postsynaptic cell. A diverse array of interneurons can be distinguished by their morphology, expression of different molecular markers, and their preferred site of targeting of postsynaptic neurons. *Basket cells* send their axons to form synapses on the cell body and proximal dendrites of postsynaptic neurons. The dendrites of the basket cells are shown as short lines radiating from the soma. *Axo-axonic cells*, also called *chandelier cells*, send their axons to form clusters of synapses along the axon initial segment of their targets. Both basket cells and chandelier cells express the calcium-binding protein parvalbumin. *Dendrite-targeting cells*, also called *Martinotti cells*, send their axons to form synapses on the distal dendrites of pyramidal cells. These cells also release the neuropeptide somatostatin. Other classes of GABAergic neurons selectively form synapses onto other inhibitory interneurons. These interneuron-targeting inhibitory neurons often release neuropeptide Y in addition to GABA.

This selective targeting is important because the location of inhibitory inputs in relation to excitatory synapses is critical in determining the effectiveness of inhibition (Figure 13–16). Inhibition of action potential output in response to excitatory input is more effective when inhibition is initiated at the cell body or near the axon trigger zone. The depolarization produced by an excitatory current from a dendrite must pass along the cell body membrane as it moves toward the axon. Inhibitory actions at the cell body or axon initial segment open Cl^- channels, thus increasing Cl^- conductance and reducing (by shunting) much of the depolarization produced by the spreading excitatory current. In addition, the size of the hyperpolarization at the cell body in response to an IPSP is largest when the inhibitory input targets the cell body, not a dendrite, owing to the attenuation of the dendritic IPSP by the cable properties of the dendrite.

Two classes of inhibitory neurons, basket cells and chandelier cells, exert strong control over neuronal output by specifically targeting the soma and axon initial segment, respectively (Figure 13–15). Basket cells often express the calcium-binding protein parvalbumin and are the most common type of inhibitory neuron in the brain. Chandelier cells, which also express parvalbumin, have axonal arbors with a branching pattern and clustering of synaptic terminals that resemble the numerous candles of a chandelier. Under some circumstances, the chandelier cells may paradoxically enhance neuronal firing because the Cl^- reversal potential in some axons can be positive to the threshold for action potential firing.

A third class of interneurons, the Martinotti cells, specifically targets distal dendrites and spines. These common interneurons release the neuropeptide somatostatin in addition to GABA. Inhibitory actions at a remote part of a dendrite act to decrease the local depolarization produced by a nearby excitatory input, with less of an effect on EPSPs generated on other dendritic branches. Somatostatin-positive interneurons activate slowly in response to an excitatory input and generate IPSPs that increase in size with repetitive activation (synaptic facilitation). In contrast, parvalbumin-expressing interneurons fire rapidly and generate

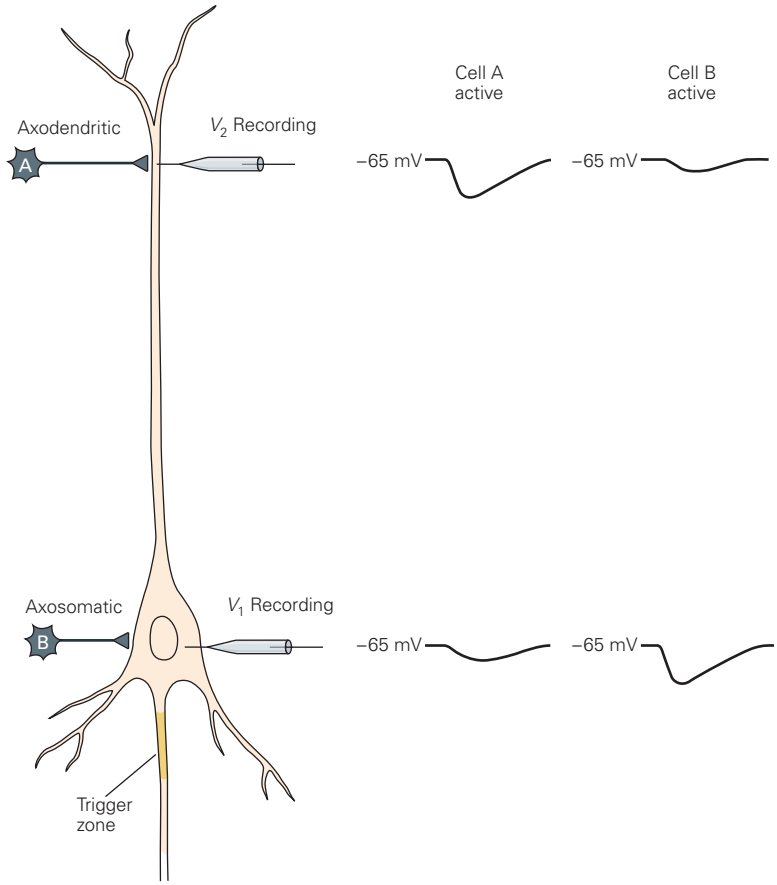

Figure 13–16 **The effect of an inhibitory current in the postsynaptic neuron depends on the distance the current travels from the synapse to the cell's trigger zone.** In this hypothetical experiment, the inputs from inhibitory axosomatic and axodendritic synapses are compared by recording from both the cell body (V_1) and a dendrite (V_2) of the postsynaptic cell. Stimulating cell B (the axosomatic synapse) produces a large IPSP in the cell body. The IPSP decays as it propagates up the dendrite, producing only a small hyperpolarization at the site of dendritic recording. Stimulating cell A activates an axodendritic synapse, producing a large local IPSP in the dendrite but only a small IPSP in the cell body, because the synaptic potential decays as it propagates down the dendrite. Thus, the axosomatic IPSP is more effective than the axodendritic IPSP in inhibiting action potential firing in the postsynaptic cell, whereas the axodendritic IPSP is more effective in preventing local dendritic depolarization.

IPSPs that decrease in size with repetitive activation (synaptic depression). These properties allow the somatostatin and parvalbumin interneurons to control the spread through neural circuits of later and earlier phases of neural signals, respectively.

A fourth major type of inhibitory interneuron expresses the neuropeptide vasoactive intestinal peptide (VIP). These interneurons selectively target other interneurons and thus serve to decrease the level of inhibition in a neural circuit, thereby enhancing overall excitation, a process termed disinhibition.

Dendrites Are Electrically Excitable Structures That Can Amplify Synaptic Input

Propagation of signals in dendrites was originally thought to be purely passive. However, intracellular recordings from the cell body of neurons in the 1950s and from dendrites beginning in the 1970s demonstrated that dendrites could produce action potentials. Indeed, we now know that the dendrites of most neurons contain voltage-gated Na^+, K^+, and Ca^{2+} channels in addition to ligand-gated channels and resting channels. In fact, the rich diversity of dendritic conductances suggests that central neurons rely on a sophisticated repertory of electrophysiological properties to integrate synaptic inputs.

One function of the voltage-gated Na^+ and Ca^{2+} channels in dendrites is to amplify the EPSP. In some neurons, there is a sufficient density of voltage-gated channels in the dendritic membrane to serve as a local trigger zone. This can produce nonlinear electrical responses that enhance the depolarization generated by excitatory inputs that arrive at remote parts of the dendrite. When a cell has several dendritic trigger zones, each one sums the local excitation and inhibition produced by nearby synaptic inputs; if the net input is above threshold, a dendritic action potential may be generated, usually by voltage-gated Na^+ or Ca^{2+} channels (Figure 13–17A). Nevertheless, the number of voltage-gated Na^+ or Ca^{2+} channels in the dendrites is usually not sufficient to support all-or-none regenerative propagation of an action potential to the cell body. Rather, action potentials generated in the dendrites are usually local events that spread electrotonically to the cell body and axon initial segment, producing a

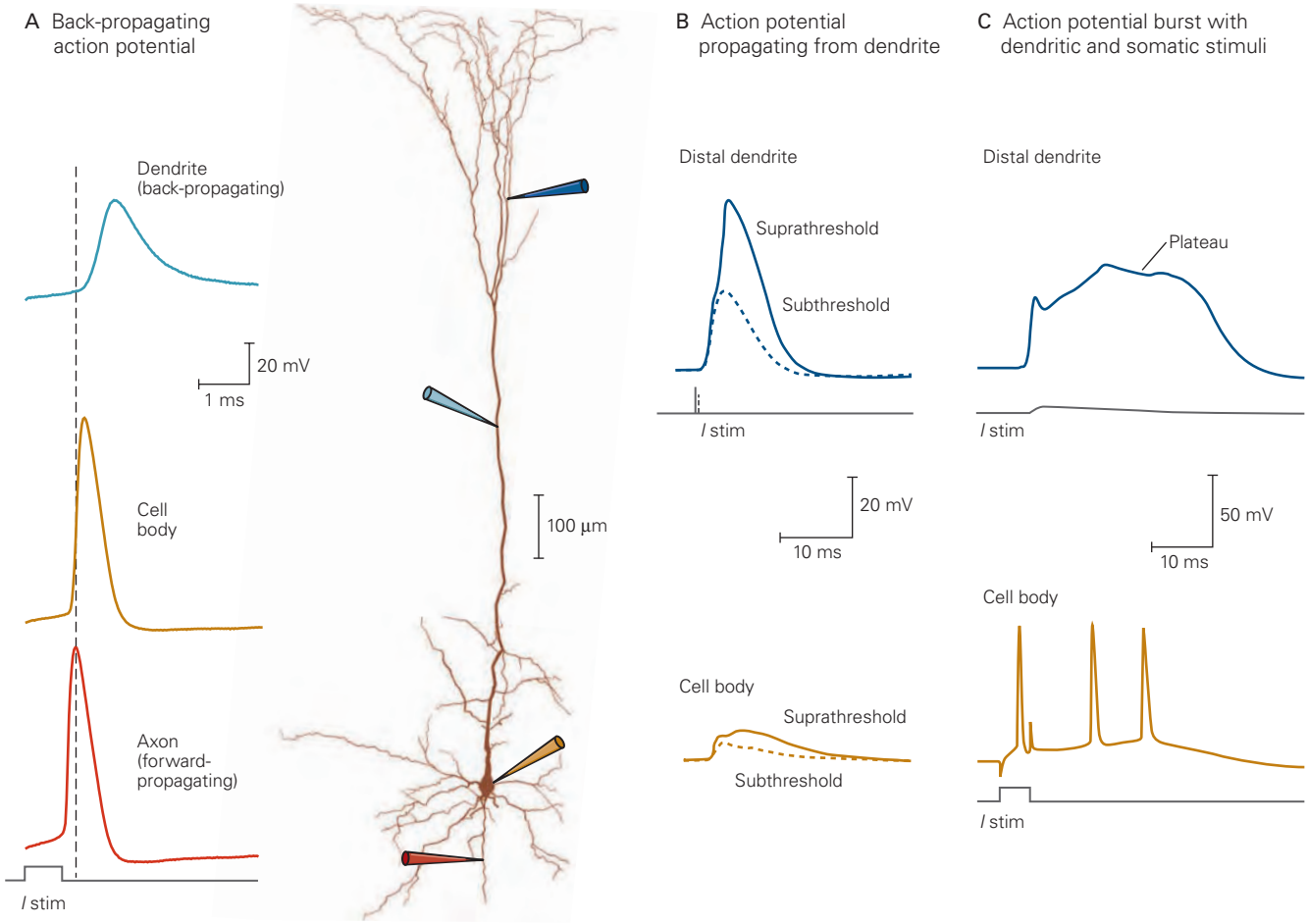

Figure 13–17 Active properties of dendrites can amplify synaptic inputs and support propagation of electrical signals to and from the axon initial segment. The figure illustrates an experiment in which several electrodes are used to record membrane voltage and pass stimulating current in the axon, cell body, and at several locations along the dendritic tree. The recording electrodes and corresponding voltage traces are matched by color. Stimulating current pulses are also indicated (***I* stim**). (Panels A and B adapted from Stuart et al. 2016.)

A. An action potential initiated in the axon initial segment can propagate to the dendrites. Such backpropagation depends on activation of voltage-gated Na^+ channels in the dendrites. Unlike the nondecrementing action potential that is continually regenerated along an axon, the amplitude of a back-propagating action potential decreases as it travels along a dendrite due to its relatively low density of voltage-gated Na^+ channels.

B. A strong depolarizing EPSP at a dendrite can generate a dendritic action potential that travels to the cell body. Such action potentials are often generated by dendritic voltage-gated Ca^{2+} channels and have a high threshold. They propagate relatively slowly and attenuate with distance, often failing to reach the cell body. The **solid blue line** shows a suprathreshold response generated in the dendrite in response to a large depolarizing current pulse, and the **dotted blue line** shows a subthreshold response to a weaker current stimulus. The **solid and dotted orange lines** show the corresponding voltage responses recorded in the cell body.

C. Near simultaneous injection of a subthreshold stimulating current resembling a weak EPSC into the dendrite and a strong brief suprathreshold stimulating current into the cell body (which by itself evokes a single somatic action potential) triggers a long-lasting plateau potential in the dendrite and the firing of a burst of action potentials in the cell body. (Adapted, with permission from Larkum et al. 1999. Copyright © 1999 Springer Nature.)

subthreshold somatic depolarization that is integrated with other input signals in the cell.

Dendritic voltage-gated channels also permit action potentials generated at the axon initial segment to propagate backward into the dendritic tree (Figure 13–17B). These *backpropagating* action potentials are largely generated by dendritic voltage-gated Na^+ channels. Although the precise role of these action

potentials is unclear, they may provide a temporally precise mechanism for enhancing current through NMDA receptor-channels by providing the depolarization necessary to remove the Mg^{2+} block, thereby contributing to the induction of synaptic plasticity (Figure 13–10).

NMDA receptors are able to mediate another type of nonlinear integration in dendrites as a result of their voltage dependence. Moderate synaptic stimuli are able to activate a sufficient number of AMPA receptors to produce an intermediate level of depolarization that is able to lead to expulsion of Mg^{2+} from a fraction of NMDA receptors. As these receptors begin to conduct cations into the postsynaptic dendrite, they produce a further depolarization that leads to even greater unblocking of Mg^{2+}, increasing further the size of the NMDA receptor EPSC, resulting in even greater depolarization. In some instances, this leads to a local regenerative depolarization, referred to as an NMDA spike. Such NMDA spikes are purely local events—they cannot propagate actively in the absence of synaptic stimulation because they require glutamate release. NMDA spikes have been implicated in different forms of synaptic plasticity and in the enhancement of dendritic integration of synaptic inputs.

Under what conditions do active conductances influence dendritic integration? There is now evidence that dendrites may switch between passive and active integration depending on the precise timing and strength of synaptic inputs. One interesting example of such a switch is the way some cortical neurons respond to inputs arriving at their distal and proximal dendrites. In many neurons, inputs from relatively nearby neurons arrive at more proximal regions of the dendrites, closer to the cell body. Inputs from more distant brain areas arrive at the distal tips of dendrites. Although excitatory synaptic inputs to the distal dendrites usually produce only a very small depolarizing response at the soma, due to electronic decay along the dendritic cable, these inputs can significantly enhance spike firing when paired with excitatory inputs to more proximal regions of the dendrites. Thus, a single strong EPSP at a proximal site (or a single brief somatic current pulse) normally produces a single action potential at the axon initial segment, which can then backpropagate into the dendrites. However, when a distal stimulus is paired with a proximal stimulus, the backpropagating spike summates with the distal EPSP to trigger a long-lasting type of dendritic spike called a plateau potential, which depends on activation of voltage-gated Ca^{2+} channels and NMDA receptors. When the plateau potential arrives at the cell body, it can trigger a brief burst of three or more spikes at rates as high as 100 Hz (Figure 13–17C). These spike bursts are thought to provide a very potent means of inducing long-term synaptic plasticity and releasing transmitter as the burst propagates to the presynaptic terminal.

A more localized form of synaptic integration occurs in dendritic spines. Even though some excitatory inputs occur on dendritic shafts, close to 95% of all excitatory inputs in the brain terminate on spines, surprisingly avoiding dendritic shafts (see Figure 13–2). Although the function of spines is not completely understood, their thin necks provide a barrier to diffusion of various signaling molecules from the spine head to the dendritic shaft. As a result, a relatively small Ca^{2+} current through the NMDA receptors can lead to a relatively large increase in $[Ca^{2+}]$ that is localized to the head of the individual spine that is synaptically activated (Figure 13–18A). Moreover, because action potentials can backpropagate from the cell body to the dendrites, spines also serve as sites at which information about presynaptic and postsynaptic activity is integrated.

Indeed, when a backpropagating action potential is paired with presynaptic stimulation, the spine Ca^{2+} signal is greater than the linear sum of the individual Ca^{2+} signals from synaptic stimulation alone or action potential stimulation alone. This "supralinearity" is specific to the activated spine and occurs because depolarization during the action potential causes Mg^{2+} to be expelled from the NMDA receptor-channel, allowing it to conduct Ca^{2+} into the spine. The resultant Ca^{2+} accumulation thus provides, at an individual synapse, a biochemical detector of the near simultaneity of the input (EPSP) and output (backpropagating action potential), which is thought to be a key requirement of memory storage (Chapter 54).

Because the thin spine neck restricts, at least partly, the rise in Ca^{2+} and, thus, long-term plasticity to the spine that receives the synaptic input, spines also ensure that activity-dependent changes in synaptic function, and thus memory storage, are restricted to the synapses that are activated. The ability of spines to implement such synapse-specific local learning rules may be of fundamental importance for the ability of neural networks to store meaningful information (Chapter 54). Finally, in some spines, local synaptic potentials are filtered as they propagate through the spine neck and enter the dendrite, such that the size of the EPSP at the cell body is reduced. The regulation of this electrical filtering could provide another means of controlling the efficacy with which a given synaptic conductance is able to excite the cell body.

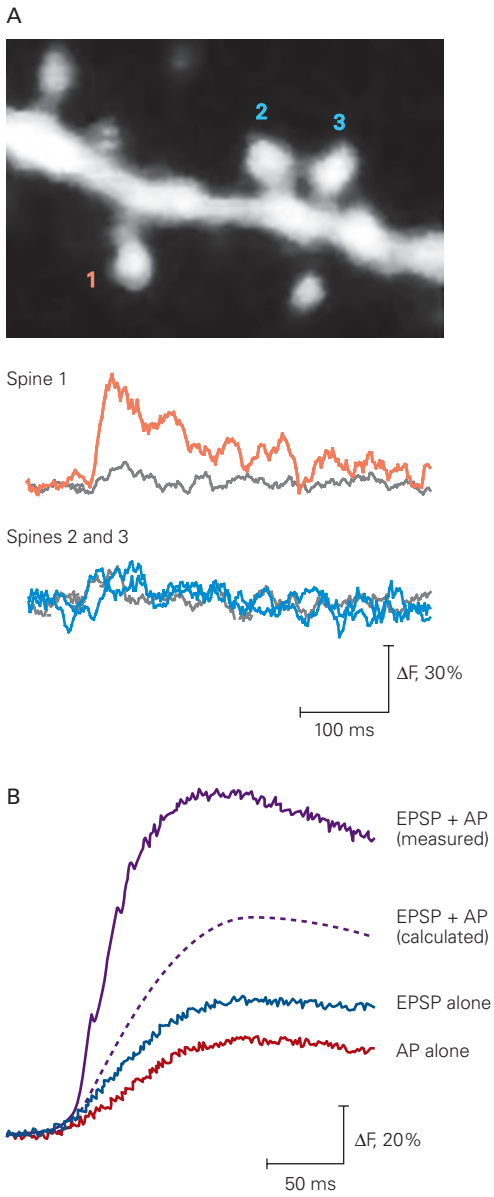

Figure 13–18 Dendritic spines compartmentalize calcium influx through NMDA receptors.

A. This fluorescence image of a hippocampal CA1 pyramidal neuron filled with a calcium-sensitive dye shows the outline of a dendritic shaft with several spines. When the dye binds Ca^{2+}, its fluorescence intensity increases. The traces plot fluorescence intensity over the time following the extracellular stimulation of the presynaptic axon. Spine 1 shows a large, rapid increase in fluorescence (**ΔF**) in response to synaptic stimulation (**red trace**), reflecting Ca^{2+} influx through the NMDA receptors. In contrast, there is little change in the fluorescence intensity in the neighboring dendrite shaft (**gray trace**), showing that Ca^{2+} accumulation is restricted to the head of the spine. Spines 2 and 3 show little increase in fluorescence in response to synaptic stimulation because their presynaptic axons were not activated. (Reproduced, with permission, from Lang et al. 2004. Copyright © 2004 National Academy of Sciences.)

B. Calcium accumulation is greatest in spines when synaptic stimulation is paired with postsynaptic action potentials. The Ca^{2+} signal generated when an EPSP and a backpropagating action potential are evoked at the same time is greater than the expected sum of the individual Ca^{2+} signals when either an EPSP or a backpropagating action potential (**AP**) alone is evoked. (Adapted, with permission, from Yuste and Denk 1995.)

Highlights

1. A typical central neuron integrates a large number of excitatory and inhibitory synaptic inputs. The amino acid transmitter glutamate is responsible for most excitatory synaptic actions in the central nervous system, with the inhibitory amino acids GABA and glycine mediating inhibitory synaptic actions.
2. Glutamate activates families of ionotropic and metabotropic receptors. The three major classes of ionotropic glutamate receptors—AMPA, NMDA, and kainate—are named for the chemical agonists that activate them.
3. The ionotropic glutamate receptors are tetramers composed of subunits encoded by homologous genes. Each subunit has a large extracellular amino terminus, with three membrane-spanning segments and a large cytoplasmic tail. A pore-forming loop dips into and out of the membrane between the first and second transmembrane segments.
4. Binding of glutamate to all three ionotropic receptors opens a nonselective cation channel equally permeable to Na^+ and K^+. The NMDA receptor-channel also has a high permeability to Ca^{2+}.
5. The NMDA receptor acts as a coincidence detector. It is normally blocked by extracellular Mg^{2+}

lodged in its pore; it only conducts when glutamate is released *and* the postsynaptic membrane is sufficiently depolarized to expel the Mg^{2+} ion by electrostatic repulsion.

6. Calcium influx through the NMDA receptor during strong synaptic activation can trigger intracellular signaling cascades, leading to long-term synaptic plasticity, which can potentiate synaptic transmission for a period of hours to days, providing a potential mechanism for memory storage.
7. Inhibitory synaptic actions in the brain are mediated by the binding of GABA to both ionotropic ($GABA_A$) and metabotropic ($GABA_B$) receptors. The $GABA_A$ receptors are pentamers, whose subunits are homologous to those of the nicotinic ACh receptors. Glycine ionotropic receptors are structurally similar to $GABA_A$ receptors and are largely confined to inhibitory synapses in the spinal cord.
8. Binding of GABA or glycine to its receptor activates a Cl^- selective channel. In most cells, the Cl^- equilibrium potential is slightly negative to the resting potential. As a result, inhibitory synaptic actions hyperpolarize the cell membrane away from threshold for firing an action potential.
9. The decision as to whether a neuron fires an action potential depends on spatial and temporal summation of the various excitatory and inhibitory inputs and is determined by the size of the resulting depolarization at the axon initial segment, the region of the neuron with the lowest threshold.
10. Dendrites also have voltage-gated channels, enabling them to fire local action potentials in some circumstances. This can amplify the size of the local EPSP to produce a larger depolarization at the cell body.

Rafael Yuste
Steven A. Siegelbaum

Selected Reading

Arundine M, Tymianski M. 2004. Molecular mechanisms of glutamate-dependent neurodegeneration in ischemia and traumatic brain injury. Cell Mol Life Sci 61:657–668.

Basu J, Siegelbaum SA. 2015. The corticohippocampal circuit, synaptic plasticity, and memory. Cold Spring Harb Perspect Biol 7:11.

Colquhoun D, Sakmann B. 1998. From muscle endplate to brain synapses: a short history of synapses and agonist-activated ion channels. Neuron 20:381–387.

Granger AJ, Gray JA, Lu W, Nicoll RA. 2011. Genetic analysis of neuronal ionotropic glutamate receptor subunits. J Physiol 589:4095–4101.

Herring BE, Nicoll RA. 2016. Long-term potentiation: from CaMKII to AMPA receptor trafficking. Annu Rev Physiol 78:351–365.

Karnani M, Agetsuma M, Yuste R. 2014. A blanket of inhibition: functional inferences from dense inhibitory connectivity. Curr Opin Neurobiol 26:96–102.

Martenson JS, Tomita S. 2015. Synaptic localization of neurotransmitter receptors: comparing mechanisms for AMPA and $GABA_A$ receptors. Curr Opin Pharmacol 20:102–108.

Mayer ML. 2016. Structural biology of glutamate receptor ion channel complexes. Curr Opin Struct Biol 41:119–127.

Olsen RW, Sieghart W. 2009. $GABA_A$ receptors: subtypes provide diversity of function and pharmacology. Neuropharmacology 56:141–148.

Peters A, Palay SL, Webster HD. 1991. *The Fine Structure of the Nervous System.* New York: Oxford Univ. Press.

Sheng M, Hoogenraad CC. 2007. The postsynaptic architecture of excitatory synapses: a more quantitative view. Ann Rev Biochem 76:823–847.

Stuart GJ, Spruston N. 2015. Dendritic integration: 60 years of progress. Nat Neurosci 18:1713–1721.

Valbuena S, Lerma J. 2016. Non-canonical signaling, the hidden life of ligand-gated ion channels. Neuron 92:316–329.

References

Araya R, Vogels T, Yuste R. 2014. Activity-dependent dendritic spine neck changes are correlated with synaptic strength. Proc Natl Acad Sci U S A 111:E2895–E2904.

Armstrong N, Sun Y, Chen GQ, Gouaux E. 1998. Structure of a glutamate-receptor ligand-binding core in complex with kainate. Nature 395:913–917.

Bormann J, Hamill O, Sakmann B. 1987. Mechanism of anion permeation through channels gated by glycine and γ-aminobutyric acid in mouse cultured spinal neurones. J Physiol 385:243–286.

Cash S, Yuste R. 1999. Linear summation of excitatory inputs by CA1 pyramidal neurons. Neuron 22:383–394.

Coombs JS, Eccles JC, Fatt P. 1955. The specific ionic conductances and the ionic movements across the motoneuronal membrane that produce the inhibitory post-synaptic potential. J Physiol 130:326–373.

Eccles JC. 1964. *The Physiology of Synapses.* New York: Academic.

Eckert R, Randall D, Augustine G. 1988. Propagation and transmission of signals. In: *Animal Physiology: Mechanisms and Adaptations,* 3rd ed., pp. 134–176. New York: Freeman.

Finkel AS, Redman SJ. 1983. The synaptic current evoked in cat spinal motoneurones by impulses in single group Ia axons. J Physiol 342:615–632.

Gray EG. 1963. Electron microscopy of presynaptic organelles of the spinal cord. J Anat 97:101–106.

Grenningloh G, Rienitz A, Schmitt B, et al. 1987. The strychnine-binding subunit of the glycine receptor shows homology with nicotinic acetylcholine receptors. Nature 328:215–220.

Hamill OP, Bormann J, Sakmann B. 1983. Activation of multiple-conductance state chloride channels in spinal neurones by glycine and GABA. Nature 305:805–808.

Hestrin S, Nicoll RA, Perkel DJ, Sah P. 1990. Analysis of excitatory synaptic action in pyramidal cells using whole-cell recording from rat hippocampal slices. J Physiol 422:203–225.

Heuser JE, Reese TS. 1977. Structure of the synapse. In: ER Kandel (ed), *Handbook of Physiology: A Critical, Comprehensive Presentation of Physiological Knowledge and Concepts,* Sect. 1 *The Nervous System.* Vol. 1, *Cellular Biology of Neurons,* Part 1, pp. 261–294. Bethesda, MD: American Physiological Society.

Hollmann M, O'Shea-Greenfield A, Rogers SW, Heinemann S. 1989. Cloning by functional expression of a member of the glutamate receptor family. Nature 342:643–648.

Jia H, Rochefort NL, Chen X, Konnerth A. 2010. Dendritic organization of sensory input to cortical neurons in vivo. Nature 464:1307–1312.

Kayser MS, Dalmau J. 2016. Anti-NMDA receptor encephalitis, autoimmunity, and psychosis. Schizophr Res 176:36–40.

Lang C, Barco A, Zablow L, Kandel ER, Siegelbaum SA, Zakharenko SS. 2004. Transient expansion of synaptically connected dendritic spines upon induction of hippocampal long-term potentiation. Proc Natl Acad Sci U S A 101:16665–16670.

Larkum ME, Zhu JJ, Sakmann B. 1999. A new cellular mechanism for coupling inputs arriving at different cortical layers. Nature 398:338–341.

Llinas R. 1988. The intrinsic electrophysiological properties of mammalian neurons: insights into central nervous system function. Science 242:1654–1664.

Llinas R, Sugimori M. 1980. Electrophysiological properties of in vitro Purkinje cell dendrites in mammalian cerebellar slices. J Physiol 305:197–213.

Markram H, Lubke J, Frotscher M, Sakmann B. 1997. Regulation of synaptic efficacy by coincidence of postsynaptic APs and EPSPs. Science 275:213–215.

Morgan SL, Teyler TJ. 2001. Electrical stimuli patterned after the theta-rhythm induce multiple forms of LTP. J Neurophysiol 86:1289–1296.

Palay SL. 1958. The morphology of synapses in the central nervous system. Exp Cell Res Suppl 5:275–293.

Pfeffer CK, Xue M, He M, Huang ZJ, Scanziani M. 2013. Inhibition of inhibition in visual cortex: the logic of connections between molecularly distinct interneurons. Nat Neurosci 16:1068–1076.

Pritchett DB, Sontheimer H, Shivers BD, et al. 1989. Importance of a novel $GABA_A$ receptor subunit for benzodiazepine pharmacology. Nature 338:582–585.

Redman S. 1979. Junctional mechanisms at group Ia synapses. Prog Neurobiol 12:33–83.

Sakmann B. 1992. Elementary steps in synaptic transmission revealed by currents through single ion channels. Neuron 8:613–629.

Schiller J, Schiller Y. 2001. NMDA receptor-mediated dendritic spikes and coincident signal amplification. Curr Opin Neurobiol 11:343–348.

Sheng M, Hoogenraad C. 2007. The postsynaptic architecture of excitatory synapses: a more quantitative view. Ann Rev Biochem 76:823–847.

Sherrington CS. 1897. The central nervous system. In: M Foster (ed). *A Text Book of Physiology,* 7th ed. London: Macmillan.

Sobolevsky AI, Rosconi MP, Gouaux E. 2009. X-ray structure, symmetry and mechanism of an AMPA-subtype glutamate receptor. Nature 462:745–756.

Sommer B, Köhler M, Sprengel R, Seeburg PH. 1991. RNA editing in brain controls a determinant of ion flow in glutamate-gated channels. Cell 67:11–19.

Stuart G, Spruston N, Häuser M (eds). 2016. *Dendrites*, 3rd ed. Oxford, England, and New York: Oxford Univ. Press.

Yuste R. 2010. *Dendritic Spines*. Cambridge, MA and London, England: MIT Press.

Yuste R, Denk W. 1995. Dendritic spines as basic functional units of neuronal integration. Nature 375:682–684.

14

Modulation of Synaptic Transmission and Neuronal Excitability: Second Messengers

The binding of neurotransmitter to postsynaptic receptors produces a postsynaptic potential either directly, by opening ion channels, or indirectly, by altering ion channel activity through changes in the postsynaptic cell's biochemical state. As we saw in Chapters 11 to 13, the type of postsynaptic action depends on the type of receptor. Activation of an *ionotropic receptor* directly opens an ion channel that is part of the receptor macromolecule itself. In contrast, activation of *metabotropic receptors* regulates the opening of ion channels indirectly through biochemical signaling pathways; the metabotropic receptor and the ion channels regulated by the receptor are distinct macromolecules (Figure 14–1).

Whereas the action of ionotropic receptors is fast and brief, metabotropic receptors produce effects that begin slowly and persist for long periods, ranging from hundreds of milliseconds to many minutes. The two types of receptors also differ in their functions. Ionotropic receptors underlie fast synaptic signaling that is the basis of all behaviors, from simple reflexes to complex cognitive processes. Metabotropic receptors

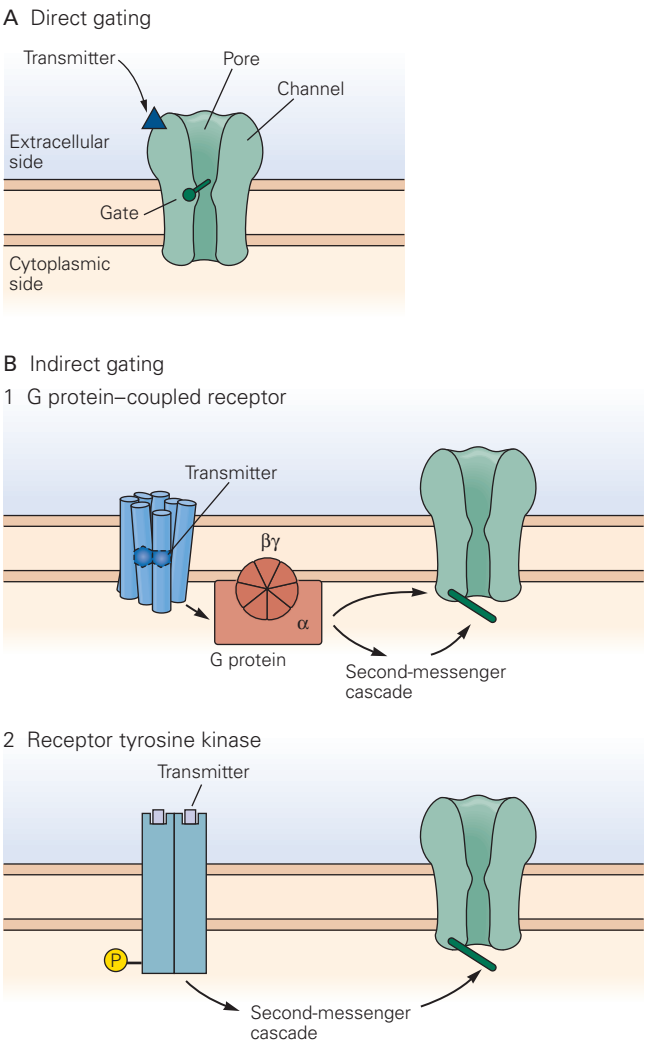

Figure 14–1 Neurotransmitter actions can be divided into two groups according to the way receptor and effector functions are coupled.

A. Direct transmitter actions are produced by the binding of transmitter to *ionotropic receptors*, ligand-gated channels in which the receptor and ion channel are domains within a single macromolecule. The binding of transmitter to the receptor on the extracellular aspect of the receptor-channel protein directly opens the ion channel embedded in the cell membrane.

B. Indirect transmitter actions are caused by binding of transmitter to *metabotropic receptors*, macromolecules that are separate from the ion channels they regulate. There are two families of these receptors. 1. G protein–coupled receptors activate guanosine triphosphate (GTP)-binding proteins that engage a second-messenger cascade or act directly on ion channels. 2. Receptor tyrosine kinases initiate a cascade of protein phosphorylation reactions, beginning with autophosphorylation (P) of the kinase itself on tyrosine residues.

modulate behaviors; they modify reflex strength, activate motor patterns, focus attention, set emotional states, and contribute to long-lasting changes in neural circuits that underlie learning and memory. Metabotropic receptors are responsible for many of the actions of transmitters, hormones, and growth factors. The actions of these neuromodulators can produce remarkable and dramatic changes in neuronal excitability and synaptic strength and, in so doing, can profoundly alter the state of activity in an entire circuit important for behavior.

Ionotropic receptors change the membrane potential quickly. As we have seen, this change is local at first but is propagated as an action potential along the axon if the change in membrane potential is suprathreshold. Activation of metabotropic receptors also begins as a local action that can spread to a wider region of the cell. The binding of a neurotransmitter with a metabotropic receptor activates proteins that in turn activate effector enzymes. The effector enzymes then often produce second-messenger molecules that can diffuse within a cell to activate still other enzymes that catalyze modifications of a variety of target proteins, greatly changing their activities.

There are two major families of metabotropic receptors: G protein–coupled receptors and receptor tyrosine kinases. We first describe the G protein–coupled receptor family and later discuss the receptor tyrosine kinase family.

The G protein–coupled receptors are coupled to an effector by a trimeric guanine nucleotide-binding protein, or G protein (Figure 14–1B). This receptor family comprises α- and β-adrenergic receptors for norepinephrine, muscarinic acetylcholine (ACh) receptors, γ-aminobutyric acid B ($GABA_B$) receptors, certain glutamate and serotonin receptors, all receptors for dopamine, receptors for neuropeptides, odorant receptors, rhodopsin (the protein that reacts to light, initiating visual signals; see Chapter 22), and many others. Many of these receptors are thought to be involved in neurological and psychiatric diseases and are key targets for the actions of important classes of therapeutic drugs.

G protein–coupled receptors activate a variety of effectors. The typical effector is an enzyme that produces a diffusible second messenger. These second messengers in turn trigger a biochemical cascade, either by activating specific protein kinases that phosphorylate the hydroxyl group of specific serine or threonine residues in various proteins or by mobilizing Ca^{2+} ions from intracellular stores, thereby initiating reactions that change the cell's biochemical state. In some instances, the G protein or the second messenger acts directly on an ion channel.

The Cyclic AMP Pathway Is the Best Understood Second-Messenger Signaling Cascade Initiated by G Protein–Coupled Receptors

The adenosine 3′,5′-cyclic monophosphate (cyclic AMP or cAMP) pathway is a prototypic example of a G protein–coupled second-messenger cascade. It was the first second-messenger pathway to be discovered, and our conception of other second-messenger pathways is based on it.

The binding of transmitter to receptors linked to the cAMP cascade first activates a specific G protein, G_s (named for its action to *stimulate* cAMP synthesis). In its resting state, G_s, like all G proteins, is a trimeric protein consisting of an α-, β-, and γ-subunit. The α-subunit is only loosely associated with the membrane and is usually the agent that couples the receptor to its primary effector enzyme. The β- and γ-subunits form a strongly bound complex that is more tightly associated with the membrane. As described later in this chapter, the βγ complex of G proteins can regulate the activity of certain ion channels directly.

In the resting state, the α-subunit binds a molecule of guanosine diphosphate (GDP). Upon the binding of ligand, a G protein–coupled receptor undergoes a conformational change that enables it to bind to the α-subunit, thereby promoting the exchange of GDP with a molecule of guanosine triphosphate (GTP). This leads to a conformational change that causes the α-subunit to dissociate from the βγ complex, thereby activating the α-subunit.

The particular class of α-subunit that is coupled to the cAMP cascade is termed α_s, which stimulates the integral membrane protein adenylyl cyclase to catalyze the conversion of adenosine triphosphate (ATP) to cAMP. When associated with the cyclase, α_s also acts as a GTPase, hydrolyzing its bound GTP to GDP. When GTP is hydrolyzed, α_s becomes inactive. It dissociates from adenylyl cyclase and reassociates with the βγ complex, thereby stopping the synthesis of cAMP (Figure 14–2A). A G_s protein typically remains active for a few seconds before its bound GTP is hydrolyzed.

Once a G protein–coupled receptor binds a ligand, it can interact sequentially with more than one G protein macromolecule. As a result, the binding of relatively few molecules of transmitter to a small number of receptors can activate a large number of cyclase complexes. The signal is further amplified in the next step in the cAMP cascade, the activation of the protein kinase.

The major target of cAMP in most cells is the cAMP-dependent protein kinase (also called protein kinase A or PKA). This kinase, identified and characterized by Edward Krebs and colleagues, is a heterotetrameric enzyme consisting of a dimer of two regulatory (R) subunits and two catalytic (C) subunits. In the absence of cAMP, the R subunits bind to and inhibit the C subunits. In the presence of cAMP, each R subunit binds two molecules of cAMP, leading to a conformational change that causes the R and C subunits to dissociate (Figure 14–2B). Dissociation frees the C subunits to transfer the γ-phosphoryl group of ATP to the hydroxyl groups of specific serine and threonine residues in substrate proteins. The action of PKA is terminated by phosphoprotein phosphatases, enzymes that cleave the phosphoryl group from proteins, producing inorganic phosphate.

Protein kinase A is distantly related through evolution to other serine and threonine protein kinases that we shall consider: the calcium/calmodulin-dependent protein kinases and protein kinase C. These kinases also have regulatory and catalytic domains, but both domains are within the same polypeptide molecule (see Figure 14–4).

In addition to blocking enzymatic activity, the regulatory subunits of PKA also target the catalytic subunits to distinct sites within cells. Human PKA has two types of R subunits, R_I and R_{II}, each with two subtypes: $R_{I\alpha}$, $R_{I\beta}$, $R_{II\alpha}$, and $R_{II\beta}$. The genes for each derive from a common ancestor but have different properties. For example, type II PKA (containing R_{II}-type subunits) is targeted to the membrane by *A kinase attachment proteins* (AKAPs). One type of AKAP targets PKA to the *N*-methyl-D-aspartate (NMDA)-type glutamate receptor by binding both PKA and the postsynaptic density protein PSD-95, which binds to the cytoplasmic tail of the NMDA receptor (Chapter 13). In addition, this AKAP also binds a protein phosphatase, which removes the phosphate group from substrate proteins. By localizing PKA and other signaling components near their substrate, AKAPs form local signaling complexes that increase the specificity, speed, and efficiency of second-messenger cascades. Because AKAPs have only a weak affinity for R_I subunits, most type I PKA is free in the cytoplasm.

Kinases can only phosphorylate proteins on serine and threonine residues that are embedded within a context of specific *phosphorylation consensus sequences* of amino acids. For example, phosphorylation by PKA usually requires a sequence of two contiguous basic amino acids—either lysine or arginine—followed by any amino acid, and then by the serine or threonine residue that is phosphorylated (for example, Arg-Arg-Ala-Thr).

Several important protein substrates for PKA have been identified in neurons. These include voltage-gated

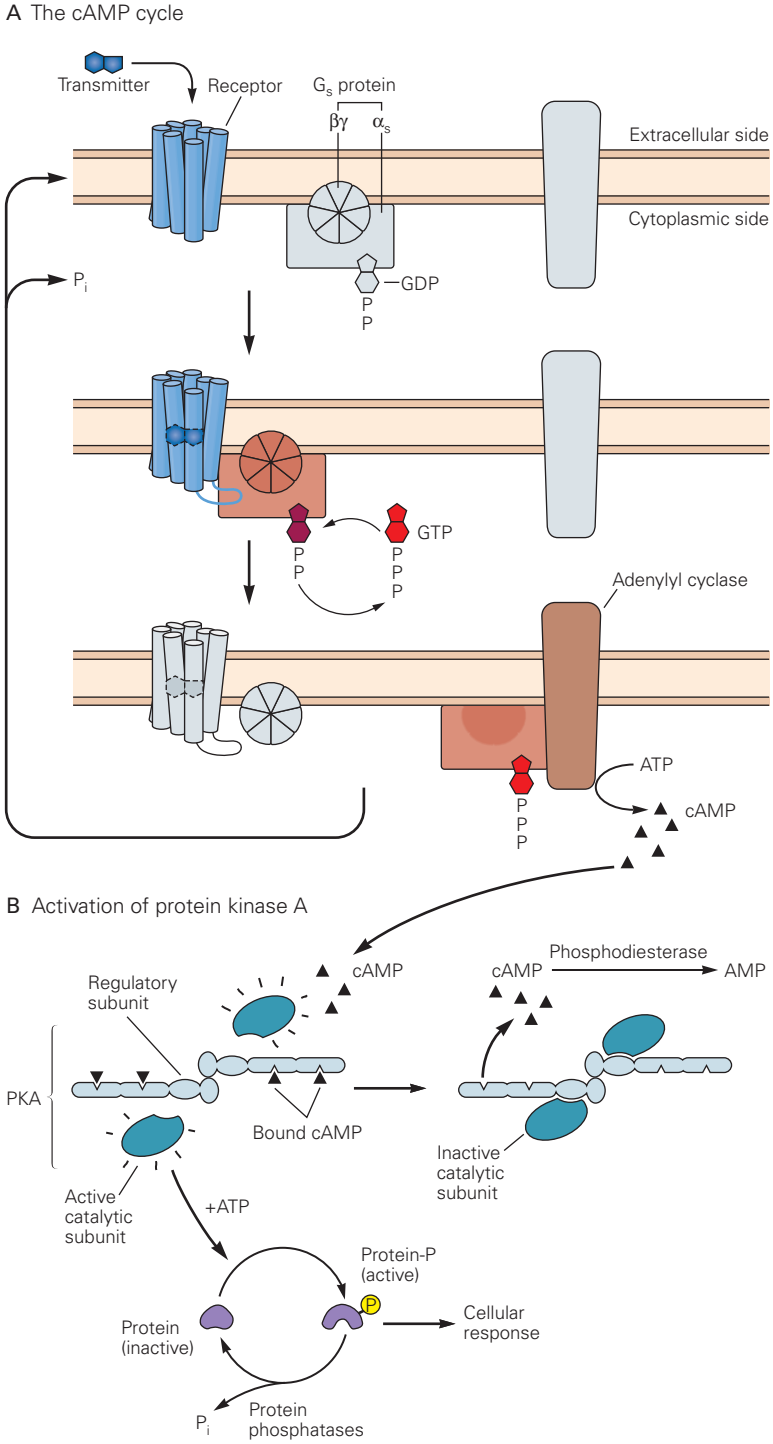

Figure 14–2 Activation of G protein–coupled receptors stimulates cyclic adenosine monophosphate (cAMP) production and protein kinase A. (Adapted from Alberts et al. 1994.)

A. The binding of a transmitter to certain receptors activates the stimulatory G protein (G_s), consisting of α_s-, β-, and γ-subunits. When activated, the α_s-subunit exchanges its bound guanosine diphosphate (**GDP**) for guanosine triphosphate (**GTP**), causing α_s to dissociate from the βγ complex. Next, α_s associates with an intracellular domain of adenylyl cyclase, thereby stimulating the enzyme to produce cAMP from adenosine triphosphate (**ATP**). The hydrolysis of GTP to GDP and inorganic phosphate (P_i) leads to dissociation of α_s from the cyclase and its reassociation with the βγ complex. The cyclase then stops producing the second messenger. As transmitter dissociates from the receptor, the three subunits of the G protein reassociate, and the guanine nucleotide-binding site on the α-subunit is occupied by GDP.

B. Four cAMP molecules bind to the two regulatory subunits of protein kinase A (**PKA**), liberating the two catalytic subunits, which are then free to phosphorylate specific substrate proteins on certain serine or threonine residues, thereby regulating protein function to produce a given cellular response. Two kinds of enzymes regulate this pathway. Phosphodiesterases convert cAMP to adenosine monophosphate (which is inactive), and protein phosphatases remove phosphate groups (**P**) from the substrate proteins, releasing inorganic phosphate, P_i. Phosphatase activity is, in turn, decreased by the protein inhibitor-1 (not shown), when it is phosphorylated by PKA.

and ligand-gated ion channels, synaptic vesicle proteins, enzymes involved in transmitter biosynthesis, and proteins that regulate gene transcription. As a result, the cAMP pathway has widespread effects on the electrophysiological and biochemical properties of neurons. We shall consider some of these actions later in this chapter.

The Second-Messenger Pathways Initiated by G Protein–Coupled Receptors Share a Common Molecular Logic

Approximately 3.5% of genes in the human genome code for G protein–coupled receptors. Although many of these are odorant receptors in olfactory neurons (Chapter 29), many others are receptors for well-characterized neurotransmitters used throughout the nervous system. Despite their enormous diversity, all G protein–coupled receptors consist of a single polypeptide with seven characteristic membrane-spanning regions (serpentine receptors) (Figure 14–3A). Recent results from X-ray crystallography have provided detailed insights into the three-dimensional structure of these receptors in contact with their respective G proteins (Figure 14–3B).

The number of substances that act as second messengers in synaptic transmission is much fewer than the number of transmitters. More than 100 substances serve as transmitters; each can activate several types of receptors present in different cells. The few second messengers that have been well characterized fall into two categories, intracellular and transcellular. Intracellular messengers are molecules whose actions are confined to the cell in which they are produced. Transcellular messengers are molecules that can readily cross the cell membrane and thus can leave the cell in which they are produced to act as intercellular signals, or first messengers, on neighboring cells.

A Family of G Proteins Activates Distinct Second-Messenger Pathways

Approximately 20 types of α-subunits have been identified, 5 types of β-subunits, and 12 types of γ-subunits. G proteins with different α-subunits couple different classes of receptors and effectors and therefore have different physiological actions. For example, the inhibitory *G_i proteins*, which contain the α_i-subunit, inhibit adenylyl cyclase and decrease cAMP levels. Other G proteins ($G_{q/11}$ proteins, which contain α_q- or α_{11}-subunits) activate phospholipase C and probably other signal transduction mechanisms not yet identified. The G_o protein, which contains the α_o-subunit, is expressed at particularly high levels in the brain, but its exact targets are not known. Compared with other organs of the body, the brain contains an exceptionally large variety of G proteins. Even so, because of the limited number of classes of G proteins compared to the much larger number of receptors, one type of G protein can often be activated by different classes of receptors.

The number of known effector targets for G proteins is even more limited than the types of G proteins. Important effectors include certain ion channels that are activated by the βγ complex, adenylyl cyclase in the cAMP pathway, phospholipase C in the diacylglycerol-inositol polyphosphate pathway, and phospholipase A_2 in the arachidonic acid pathway. Each of these effectors (except for the ion channels) initiates changes in specific target proteins within the cell, either by generating second messengers that bind to the target protein or by activating a protein kinase that phosphorylates it.

Hydrolysis of Phospholipids by Phospholipase C Produces Two Important Second Messengers, IP_3 and Diacylglycerol

Many important second messengers are generated through the hydrolysis of phospholipids in the inner leaflet of the plasma membrane. This hydrolysis is catalyzed by three enzymes—phospholipase C, D, and A_2—named for the ester bonds they hydrolyze in the phospholipid. The phospholipases each can be activated by different G proteins coupled to different receptors.

The most commonly hydrolyzed phospholipid is *phosphatidylinositol 4,5-bisphosphate* (PIP_2), which typically contains the fatty acid stearate esterified to the glycerol backbone in the first position and the unsaturated fatty acid arachidonate in the second. Activation of receptors coupled to G_q or G_{11} stimulates *phospholipase C*, which leads to the hydrolysis of PIP_2 (specifically the phosphodiester bond that links the glycerol backbone to the polar head group) and production of two second messengers, *diacylglycerol* (DAG) and *inositol 1,4,5-trisphosphate* (IP_3).

Diacylglycerol, which is hydrophobic, remains in the membrane when formed, where it recruits the cytoplasmic protein kinase C (PKC). Together with DAG and certain membrane phospholipids, PKC forms an active complex that can phosphorylate many protein substrates in the cell, both membrane-associated and cytoplasmic (Figure 14–4A). Activation of some isoforms of PKC requires elevated levels of cytoplasmic Ca^{2+} in addition to DAG.

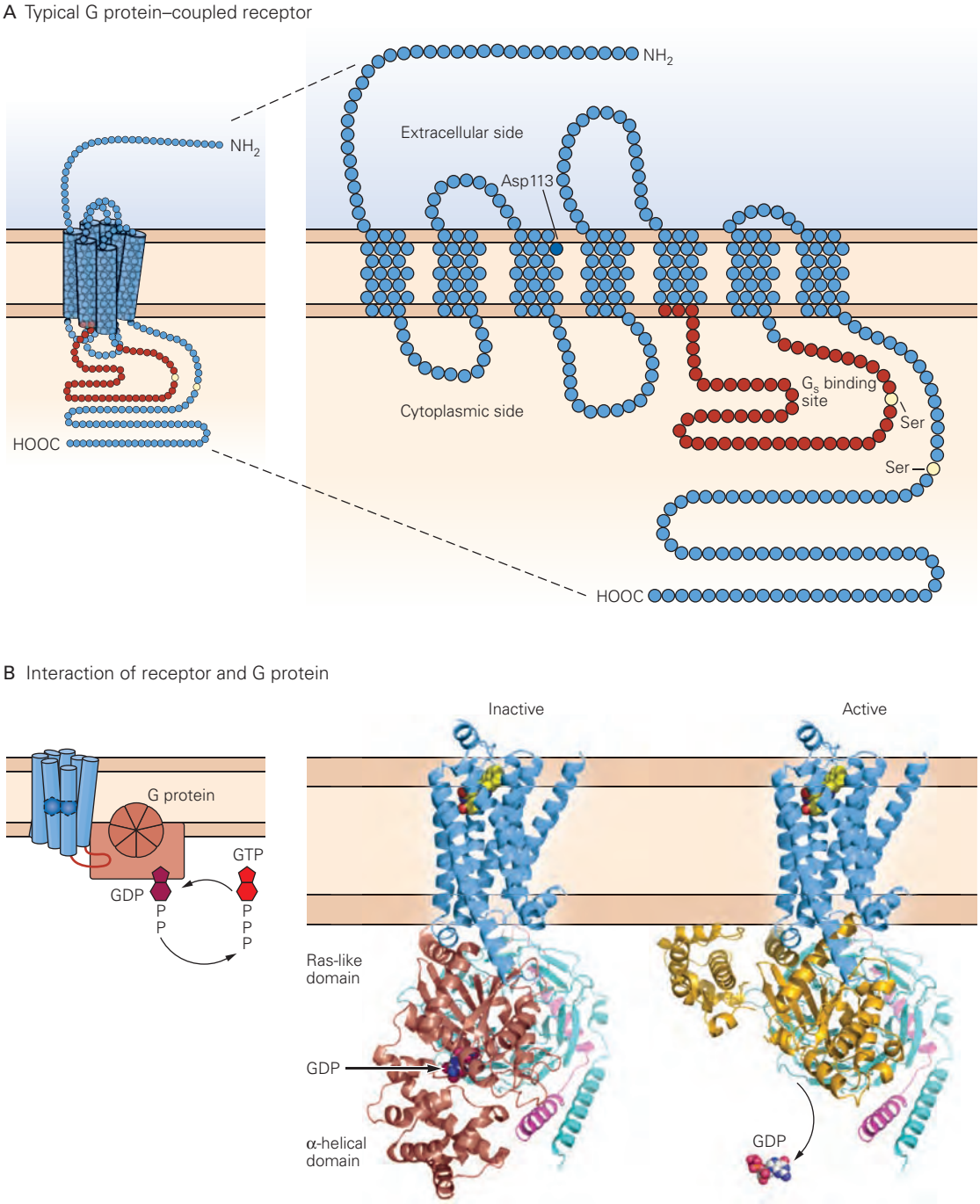

Figure 14–3 G protein–coupled receptors contain seven membrane-spanning domains.

A. The β_2-adrenergic receptor shown here is representative of G protein–coupled receptors, including the β_1-adrenergic and muscarinic acetylcholine (ACh) receptors and rhodopsin. It consists of a single subunit with an extracellular amino terminus, intracellular carboxy terminus, and seven membrane-spanning α-helixes. The binding site for the neurotransmitter lies in a cleft in the receptor formed by the transmembrane helixes. The amino acid residue aspartic acid (**Asp**)-113 participates in binding. The part of the receptor indicated in **brown** associates with G_s protein α-subunits. Two serine (**Ser**) residues in the intracellular carboxy-terminal tail are sites for phosphorylation by specific receptor kinases, which helps inactivate the receptor. (Adapted, with permission, from Frielle et al. 1989.)

B. Models based on X-ray crystal structures of the β_2-adrenergic receptor (**blue**) interacting with the G_s protein in the inactive guanosine diphosphate (**GDP**)-bound state and the active guanosine triphosphate (**GTP**)-bound state. A high-affinity synthetic agonist is bound in the transmembrane region near the extracellular surface of the membrane (space-filling model). The α_s-, β-, and γ-subunits of the inactive G_s protein are shown in **brown**, **cyan**, and **purple**, respectively. In the active state, α_s (**gold**) undergoes a conformational change that enables it to interact with adenylyl cyclase. (Adapted, with permission, from Kobilka 2013. Copyright © 2013 Wiley-VCH Verlag GmbH & Co. KGaA, Weinheim.)

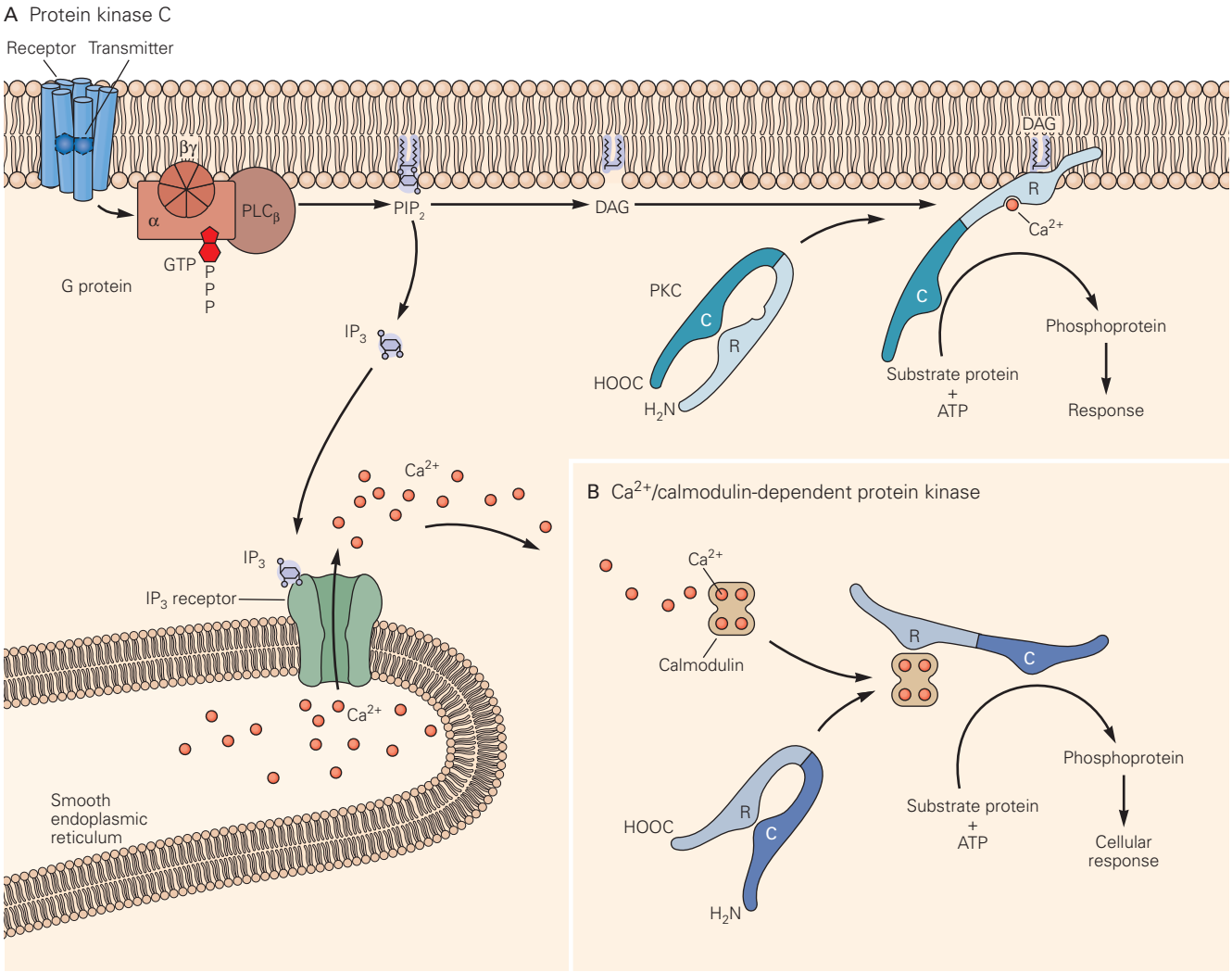

Figure 14–4 Hydrolysis of phospholipids in the cell membrane activates three major second-messenger cascades.

A. The binding of transmitter to a receptor activates a G protein that activates phospholipase C_β (**PLC_β**). This enzyme cleaves phosphatidylinositol 4,5-bisphosphate (**PIP_2**) into the second messengers inositol 1,4,5-trisphosphate (**IP_3**) and diacylglycerol (**DAG**). IP_3 is water soluble and diffuses into the cytoplasm, where it binds to the IP_3 receptor-channel on the smooth endoplasmic reticulum, thereby releasing Ca^{2+} from internal stores. DAG remains in the membrane, where it recruits and activates protein kinase C (**PKC**). Membrane phospholipid is also a necessary cofactor for PKC activation. Some isoforms of PKC also require Ca^{2+} for activation. PKC is composed of a single protein molecule that has both a regulatory domain that binds DAG and a catalytic domain that phosphorylates proteins on serine or threonine residues. In the absence of DAG the regulatory domain inhibits the catalytic domain.

B. The calcium/calmodulin-dependent protein kinase is activated when Ca^{2+} binds to calmodulin and the calcium/calmodulin complex then binds to a regulatory domain of the kinase. The kinase is composed of many similar subunits (only one of which is shown here), each having both regulatory and catalytic functions. The catalytic domain phosphorylates proteins on serine or threonine residues. (**ATP**, adenosine triphosphate; **C**, catalytic subunit; **COOH**, carboxy terminus; **H_2N**, amino terminus; **R**, regulatory subunit.)

The second product of the phospholipase C pathway, IP_3, stimulates the release of Ca^{2+} from intracellular membrane stores in the lumen of the smooth endoplasmic reticulum. The membrane of the reticulum contains a large integral membrane macromolecule, the IP_3 receptor, which forms both a receptor for IP_3 on its cytoplasmic surface and a Ca^{2+} channel that spans the membrane of the reticulum. When this macromolecule binds IP_3, the channel opens, releasing Ca^{2+} into the cytoplasm (Figure 14–4A).

The increase in intracellular Ca^{2+} triggers many biochemical reactions and opens calcium-gated channels

in the plasma membrane. Calcium can also act as a second messenger to trigger the release of additional Ca^{2+} from internal stores by binding to another integral protein in the membrane of the smooth endoplasmic reticulum, the *ryanodine receptor* (so called because it binds the plant alkaloid ryanodine, which inhibits the receptor; in contrast, caffeine opens the ryanodine receptor). Like the IP_3 receptor to which it is distantly related, the ryanodine receptor forms a Ca^{2+} channel that spans the reticulum membrane; however, cytoplasmic Ca^{2+}, not IP_3, opens the ryanodine receptor-channel.

Calcium often acts by binding to the small cytoplasmic protein calmodulin. An important function of the calcium/calmodulin complex is to activate *calcium/calmodulin-dependent protein kinase* (CaM kinase). This enzyme is a complex of many similar subunits, each containing both regulatory and catalytic domains within the same polypeptide chain. When the calcium/calmodulin complex is absent, the C-terminal regulatory domain of the kinase binds and inactivates the catalytic portion. Binding to the calcium/calmodulin complex causes conformational changes of the kinase molecule that unfetter the catalytic domain for action (Figure 14–4B). Once activated, CaM kinase can phosphorylate itself through intramolecular reactions at many sites in the molecule. Autophosphorylation has an important functional effect: It converts the enzyme into a form that is independent of calcium/calmodulin and therefore persistently active, even in the absence of Ca^{2+}.

Persistent activation of protein kinases is a general and important mechanism for maintaining biochemical processes that underlie long-term changes in synaptic function associated with certain forms of memory. In addition to the persistent activation of calcium/calmodulin-dependent protein kinase, PKA can also become persistently active following a prolonged increase in cAMP because of a slow enzymatic degradation of free regulatory subunits through the ubiquitin pathway. The decline in regulatory subunit concentration results in the long-lasting presence of free catalytic subunits, even after cAMP levels have declined, leading to the continued phosphorylation of substrate proteins. PKC can also become persistently active through proteolytic cleavage of its regulatory and catalytic domains or through the expression of a PKC isoform that lacks a regulatory domain. Finally, the duration of phosphorylation can be enhanced by certain proteins that act to inhibit the activity of phosphoprotein phosphatases. One such protein, inhibitor-1, inhibits phosphatase activity only when the inhibitor is itself phosphorylated by PKA.

Receptor Tyrosine Kinases Compose the Second Major Family of Metabotropic Receptors

The *receptor tyrosine kinases* represent a distinct family of receptors from the G protein–coupled receptors. The receptor tyrosine kinases are integral membrane proteins composed of a single subunit with an extracellular ligand-binding domain connected to a cytoplasmic region by a single transmembrane segment. The cytoplasmic region contains a protein kinase domain that phosphorylates both itself (autophosphorylation) and other proteins on tyrosine residues (Figure 14–5A). This phosphorylation results in the activation of a large number of proteins, including other kinases that are capable of acting on ion channels.

Receptor tyrosine kinases are activated when bound by peptide hormones, including epidermal growth factor (EGF), fibroblast growth factor (FGF), nerve growth factor (NGF), brain-derived neurotrophic factor (BDNF), and insulin. Cells also contain important nonreceptor cytoplasmic tyrosine kinases, such as the protooncogene *src*. These nonreceptor tyrosine kinases are often activated by interactions with receptor tyrosine kinases and are important in regulating growth and development.

Many (but not all) of the receptor tyrosine kinases exist as monomers in the plasma membrane in the absence of ligand. Ligand binding causes two monomeric receptor subunits to form a dimer, thereby activating the intracellular kinase. Each monomer phosphorylates its counterpart at a tyrosine residue, an action that enables the kinase to phosphorylate other proteins. Like the serine and threonine protein kinases, tyrosine kinases regulate the activity of neuronal proteins they phosphorylate, including the activity of certain ion channels. Tyrosine kinases also activate an isoform of phospholipase C, phospholipase Cγ, which like PLCβ cleaves PIP_2 into IP_3 and DAG.

Receptor tyrosine kinases initiate cascades of reactions involving several adaptor proteins and other protein kinases that often lead to changes in gene transcription. The mitogen-activated protein kinases (MAP kinases) are an important group of serine-threonine kinases that can be activated by a signaling cascade initiated by receptor tyrosine kinase. MAP kinases are activated by cascades of protein-kinase reactions (kinase kinases), each cascade specific to one of three types of MAP kinase: extracellular signal-regulated kinase (ERK), p38 MAP kinase, and *c-Jun* N-terminal kinase (JNK). Activated MAP kinases have several important actions. They translocate to the nucleus where they

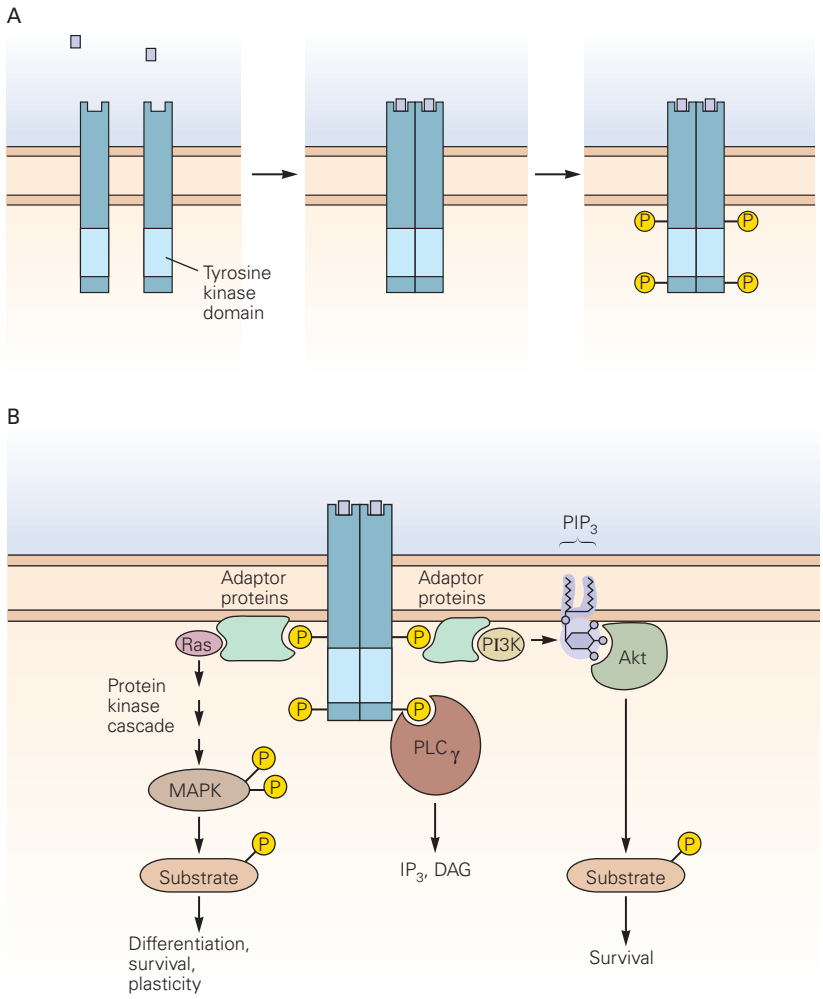

Figure 14–5 Receptor tyrosine kinases.

A. Receptor tyrosine kinases are monomers in the absence of a ligand. The receptor contains a large extracellular binding domain that is connected by a single transmembrane segment to a large intracellular region that contains a catalytic tyrosine kinase domain. Ligand binding to the receptor often causes two receptor subunits to form dimers, enabling the enzyme to phosphorylate itself on various tyrosine residues on the cytoplasmic side of the membrane.

B. After the receptor is autophosphorylated, several downstream signaling cascades become activated through the binding of specific adaptor proteins to the receptor phosphotyrosine residues (**P**). *Left:* Activation of mitogen-activated protein kinase (**MAPK**). A series of adaptor proteins recruits the small guanosine triphosphate (GTP)-binding protein Ras, which activates a protein kinase cascade, leading to the dual phosphorylation of MAP kinase on nearby threonine and tyrosine residues. The activated MAP kinase then phosphorylates substrate proteins on serine and threonine residues, including ion channels and transcription factors. *Center:* Phospholipase C_γ (**PLC_γ**) becomes activated on binding to a different phosphotyrosine residue, providing a mechanism for producing inositol 1,4,5-trisphosphate (**IP_3**) and diacylglycerol (**DAG**) that does not rely on G proteins. *Right:* Activation of the **Akt** protein kinase (also called PKB). Adaptor proteins first activate phosphoinositide 3-kinase (**PI3K**), which adds a phosphate group to PIP_2, yielding PIP_3, which then enables Akt activation.

turn on gene transcription by phosphorylating certain transcription factors. This action is thought to be important in stabilizing long-term memory formation (Chapters 53 and 54). MAP kinases also phosphorylate cytoplasmic and membrane proteins to produce short-term modulatory actions (Figure 14–5B).

Several Classes of Metabolites Can Serve as Transcellular Messengers

The metabolic products we have considered so far in response to metabotropic receptor actions do not readily cross the cell membrane. As a result, they act as true intracellular second messengers: They only affect the cell that produces them. However, cells can also synthesize metabolites that are lipid soluble and so can both act on the cell that produces them and diffuse across the plasma membrane to affect neighboring cells. We refer to such molecules as transcellular messengers.

Although these molecules have some functional resemblance to neurotransmitters, they differ in a number of important ways. They are not contained within vesicles and are not released at specialized synaptic contacts. They often do not act on membrane receptors but cross the plasma membrane of neighboring cells to reach intracellular targets. And their release and actions are much slower than those at fast synapses. We will consider three broad classes of transcellular messengers: the cyclooxygenase and lipoxygenase metabolites of the lipid molecule arachidonic acid, the endocannabinoids, and the gas nitric oxide.

Hydrolysis of Phospholipids by Phospholipase A_2 Liberates Arachidonic Acid to Produce Other Second Messengers

Phospholipase A_2 hydrolyzes phospholipids that are distinct from PIP_2, cleaving the fatty acyl bond between the 2′ position of the glycerol backbone and arachidonic acid. This releases *arachidonic acid*, which is then converted through enzymatic action to one of a family of active metabolites called *eicosanoids*, so called because of their 20 (Greek *eicosa*) carbon atoms.

Three types of enzymes metabolize arachidonic acid: (1) cyclooxygenases, which produce prostaglandins and thromboxanes; (2) several lipoxygenases, which produce a variety of other metabolites; and (3) the cytochrome P450 complex, which oxidizes arachidonic acid itself as well as cyclooxygenase and lipoxygenase metabolites (Figure 14–6). Synthesis of prostaglandins and thromboxanes in the brain is dramatically increased by nonspecific stimulation such as electroconvulsive shock, trauma, or acute cerebral ischemia (localized absence of blood flow). These metabolites can all be released by the cell that synthesizes them and thus act as transcellular signals. Many of the actions of prostaglandins are mediated by acting in the plasma membrane on a family of G protein–coupled receptors. The members of this receptor family can, in turn, activate or inhibit adenylyl cyclase or activate phospholipase C.

Endocannabinoids Are Transcellular Messengers That Inhibit Presynaptic Transmitter Release

In the early 1990s, researchers identified two types of G protein–coupled receptors, CB1 and CB2, which bind with high affinity the active compound in marijuana, Δ^9-tetrahydrocannabinol (THC). Both classes of receptors are coupled to G_i and G_o types of G proteins. The CB1 receptors are the most abundant type of G protein–coupled receptor in the brain and are found predominantly on axons and presynaptic terminals in both the central and peripheral nervous systems. Activation of these receptors inhibits release of several types of neurotransmitters, including both GABA and glutamate. The CB2 receptors are found mainly on lymphocytes, where they modulate the immune response.

The identification of the cannabinoid receptors led to the purification of their endogenous ligands, the *endocannabinoids*. Two major endocannabinoids have been identified; both contain an arachidonic acid moiety and bind to both CB1 and CB2 receptors. *Anandamide* (Sanskrit *ananda*, bliss) consists of arachidonic acid coupled to ethanolamine (arachidonyl-ethanolamide); *2-arachidonylglycerol* (2-AG) consists of arachidonic acid esterified at the 2 position of glycerol. Both are produced by the enzymatic hydrolysis of phospholipids containing arachidonic acid, a process that is initiated either when certain G protein–coupled receptors are stimulated or the internal Ca^{2+} concentration is elevated (Figure 14–6). However, whereas 2-AG is synthesized in nearly all neurons, the sources of anandamide are less well characterized.

Because the endocannabinoids are lipid metabolites that can diffuse through the membrane, they function as transcellular signals that act on neighboring cells, including presynaptic terminals. Production of these metabolites is often stimulated in postsynaptic neurons by the increase in intracellular Ca^{2+} that results from postsynaptic excitation. Once produced, the endocannabinoids diffuse through the cell membrane to nearby presynaptic terminals, where they bind to CB1 receptors and inhibit transmitter release. In this manner, the postsynaptic cell can control activity of the presynaptic neuron. There is now intense interest in understanding how the activation of these receptors in the brain leads to the various behavioral effects of marijuana.

The Gaseous Second Messenger Nitric Oxide Is a Transcellular Signal That Stimulates Cyclic GMP Synthesis

Nitric oxide (NO) acts as a transcellular messenger in neurons as well as in other cells of the body. The modulatory function of NO was discovered through its action as a local hormone released from the endothelial cells of blood vessels, causing relaxation of the smooth muscle of vessel walls. Like the metabolites of arachidonic acid, NO readily passes through cell membranes and can affect nearby cells without acting on a surface receptor. Nitric oxide is a free radical and so is highly reactive and short-lived.

Nitric oxide produces many of its actions by stimulating the synthesis of guanosine 3′,5′-cyclic monophosphate (cyclic GMP or cGMP), which like cAMP is a cytoplasmic second messenger that activates a protein kinase. Specifically, NO activates guanylyl cyclase, the enzyme that converts GTP to cGMP. There are two types of guanylyl cyclase. One is an integral membrane protein with an extracellular receptor domain and an intracellular catalytic domain that synthesizes cGMP. The other is cytoplasmic (soluble guanylyl cyclase) and is the isoform activated by NO. In some instances, NO is thought

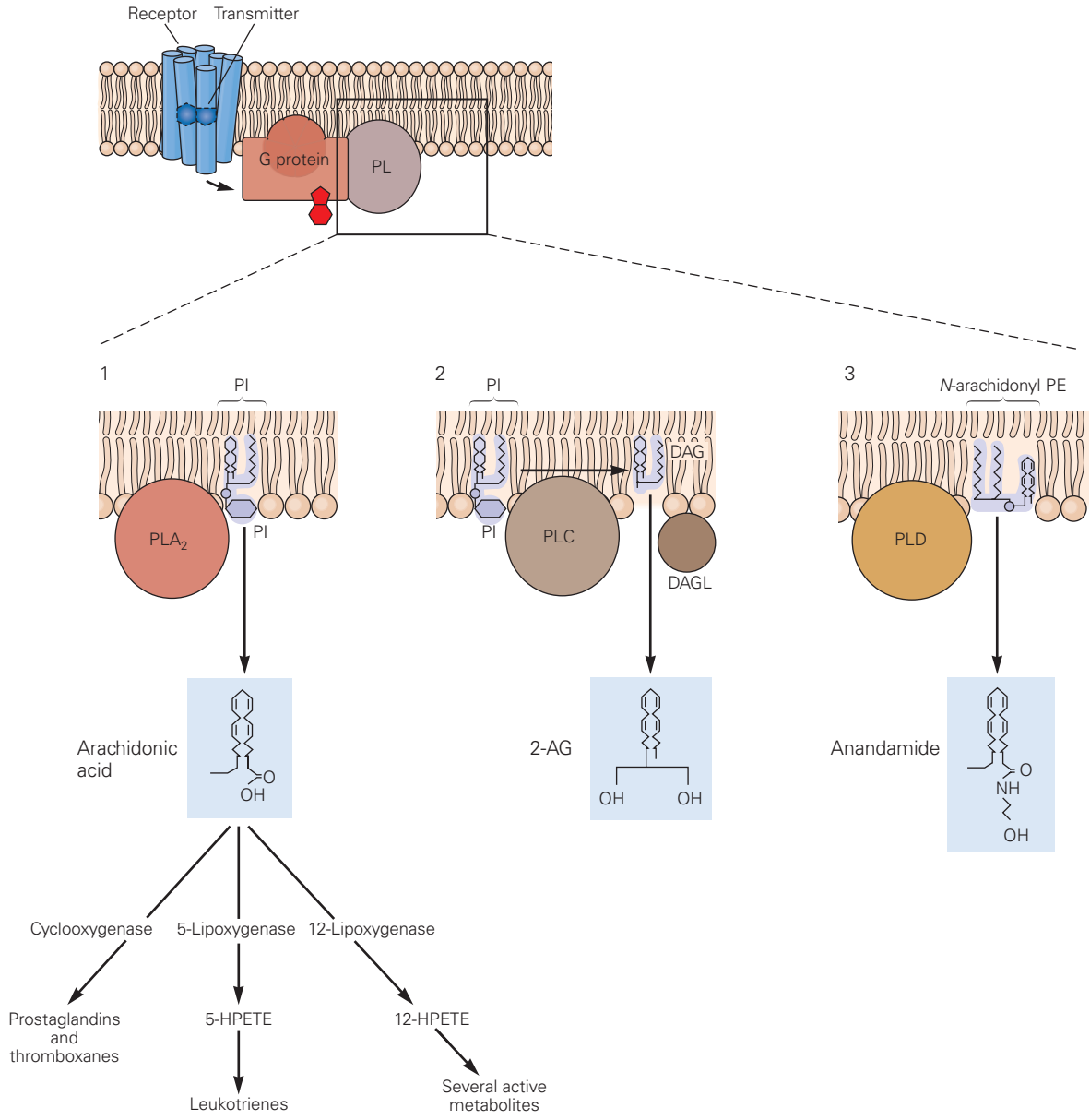

Figure 14–6 Three phospholipases generate distinct second messengers by hydrolysis of phospholipids containing arachidonic acid.

Pathway 1. Stimulation of G protein–coupled receptors leads to activation of phospholipase A_2 (**PLA_2**) by the free βγ-subunit complex. Phospholipase A_2 hydrolyzes phosphatidylinositol (**PI**) in the plasma membrane, leading to the release of arachidonic acid, a 20-carbon fatty acid with four double bonds that is a component of many phospholipids. Once released, arachidonic acid is metabolized through several pathways, three of which are shown. The 12- and 5-lipoxygenase pathways both produce several active metabolites; the cyclooxygenase pathway produces prostaglandins and thromboxanes. Cyclooxygenase is inhibited by indomethacin, aspirin, and other nonsteroidal anti-inflammatory drugs. Arachidonic acid and many of its metabolites modulate the activity of certain ion channels. (**HPETE**, hydroperoxyeicosatetraenoic acid.)

Pathway 2. Other G proteins activate phospholipase C (**PLC**), which hydrolyzes PI in the membrane to generate DAG (see Figure 14–4). Hydrolysis of DAG by a second enzyme, diacylglycerol lipase (**DAGL**), leads to production of 2-arachidonylglycerol (**2-AG**), an endocannabinoid that is released from neuronal membranes and then activates G protein–coupled endocannabinoid receptors in the plasma membrane of other neighboring neurons.

Pathway 3. Elevation of intracellular Ca^{2+} activates phospholipase D (**PLD**), which hydrolyzes phospholipids that have an unusual polar head group containing arachidonic acid (*N*-arachidonylphosphatidylethanolamine [***N*-arachidonyl PE**]). This action generates a second endocannabinoid termed anandamide (arachidonylethanolamide).

to act directly by modifying sulfhydryl groups on cysteine residues of various proteins, a process termed nitrosylation.

Cyclic GMP has two major actions. It acts directly to open cyclic nucleotide-gated channels (important for phototransduction and olfactory signaling, as described in Chapters 22 and 29, respectively), and it activates the *cGMP-dependent protein kinase* (PKG), which like PKA phosphorylates substrate proteins on certain serine or threonine residues. PKG differs from the PKA in that it is a single polypeptide with both regulatory (cGMP-binding) and catalytic domains, which are homologous to regulatory and catalytic domains in other protein kinases. It also phosphorylates a distinct set of substrates from PKA.

Cyclic GMP–dependent phosphorylation of proteins is prominent in Purkinje cells of the cerebellum, large neurons with copiously branching dendrites. There, the cGMP cascade is activated by NO produced and released from the presynaptic terminals of granule cell axons (the parallel fibers) that make excitatory synapses onto the Purkinje cells. This increase in cGMP in the Purkinje neuron reduces the response of the AMPA receptors to glutamate, thereby depressing fast excitatory transmission at the parallel fiber synapse.

The Physiological Actions of Metabotropic Receptors Differ From Those of Ionotropic Receptors

Second-Messenger Cascades Can Increase or Decrease the Opening of Many Types of Ion Channels

The functional differences between metabotropic and ionotropic receptors reflect the differences in their properties. For example, metabotropic receptor actions are much slower than ionotropic ones (Table 14–1). The physiological actions of the two classes of receptors also differ.

Ionotropic receptors are channels that function as simple on-off switches; their main job is either to excite a neuron to bring it closer to the threshold for firing or inhibit the neuron to decrease its likelihood to fire. Because these channels are normally confined to the postsynaptic region of the membrane, the action of ionotropic receptors is local. Metabotropic receptors, on the other hand, because they activate diffusible second messengers, can act on channels some distance from the receptor. Moreover, metabotropic receptors regulate a variety of channel types, including resting channels, ligand-gated channels, and voltage-gated channels that generate action potentials, underlie pacemaker potentials, and provide Ca^{2+} influx for neurotransmitter release.

Finally, whereas transmitter binding leads to an increase in the opening of ionotropic receptor-channels, the activation of metabotropic receptors can lead to an increase or decrease in channel opening. For example, MAP kinase phosphorylation of an inactivating (A-type) K^+ channel in the dendrites of hippocampal pyramidal neurons decreases channel opening and, thus, K^+ current magnitude, thereby enhancing dendritic action potential firing.

The binding of transmitter to metabotropic receptors can greatly influence the electrophysiological properties of a neuron (Figure 14–7). Metabotropic receptors in a presynaptic terminal can alter transmitter release by regulating either Ca^{2+} influx or the efficacy of the synaptic release process itself (Figure 14–7A). Metabotropic receptors in the postsynaptic cell can influence the strength of a synapse by modulating the ionotropic receptors that mediate the postsynaptic potential (Figure 14–7B). By acting on resting and voltage-gated channels in the postsynaptic neuron's cell body, dendrites, and axon, metabotropic receptor actions can also alter the resting potential, membrane resistance, length and time constants, threshold potential, action potential

Table 14–1 Comparison of Synaptic Excitation Produced by the Opening and Closing of Ion Channels

	Ion channels involved	Effect on total membrane conductance	Contribution to action potential	Time course	Second messenger	Nature of synaptic action
EPSP caused by opening of channels	Nonselective cation channel	Increase	Triggers action potential	Usually fast (milliseconds)	None	Mediating
EPSP caused by closing of channels	K^+ channel	Decrease	Modulates action potential	Slow (seconds or minutes)	Cyclic AMP (or other second messengers)	Modulating

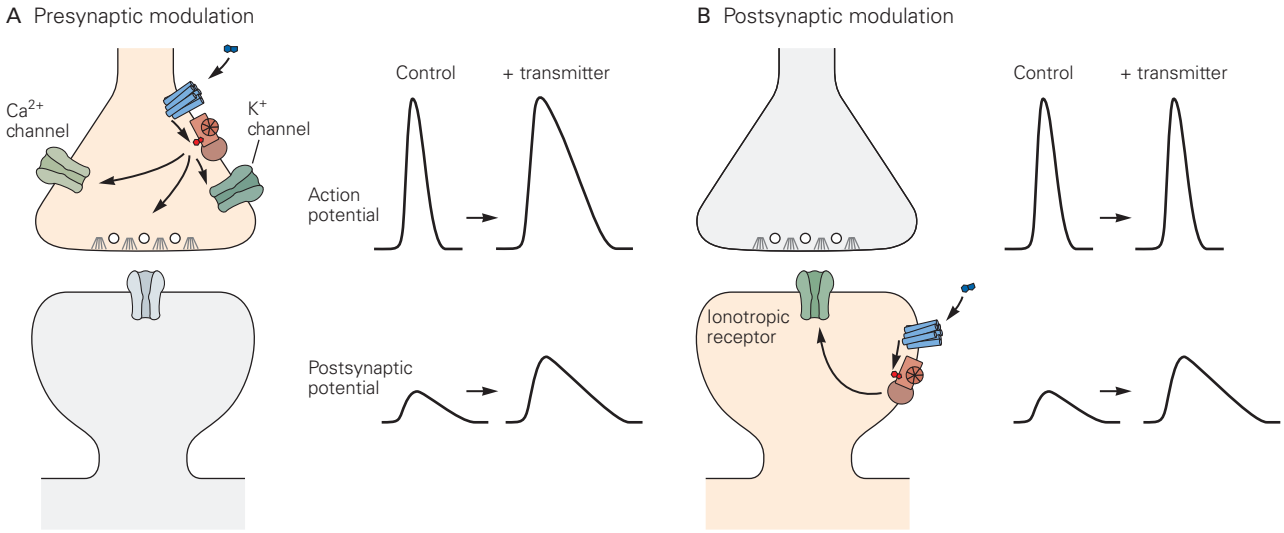

Figure 14–7 The modulatory actions of second messengers can regulate fast synaptic transmission by acting at two synaptic sites.

A. In the presynaptic terminal, second messengers can regulate the efficacy of transmitter release and thus the size of the fast postsynaptic potential mediated by ionotropic receptors. This can occur by altering presynaptic Ca^{2+} influx, either directly by modulating presynaptic voltage-gated Ca^{2+} channels or indirectly by modulating presynaptic K^+ channels, which alters Ca^{2+} influx by controlling action potential duration as illustrated (and thereby the length of time Ca^{2+} channels remain open). Some modulatory transmitters act to directly modulate the efficacy of the release machinery.

B. In the postsynaptic terminal, second messengers can alter directly the amplitude of postsynaptic potentials by modulating ionotropic receptors.

duration, and repetitive firing characteristics. Such modulation of the intrinsic excitability of neurons can play an important role in regulating information flow through neuronal circuits to alter behavior.

The distinction between direct and indirect regulation of ion channels is nicely illustrated by cholinergic synaptic transmission in autonomic ganglia of the peripheral nervous system. Stimulation of the presynaptic nerve releases ACh from the nerve terminals, directly opening nicotinic ACh receptor-channels in the postsynaptic neuron, thereby producing a fast excitatory postsynaptic potential (EPSP). The fast EPSP is followed by a slow EPSP that takes approximately 100 ms to develop but then lasts for several seconds. The slow EPSP is produced by an action of ACh on metabotropic muscarinic receptors that leads to the closing of a delayed-rectifier K^+ channel called the muscarine-sensitive (or M-type) K^+ channel (Figure 14–8A). These voltage-gated channels, which are formed by members of the KCNQ gene family, are partially activated when the cell is at rest; as a result, the current they carry helps determine the cell resting potential and membrane resistance.

The M-type K^+ channel differs from other delayed-rectifier K^+ channels by its much slower activation. It requires several hundred milliseconds to fully activate on depolarization. Because M-type channels are partially open at the resting potential, their closure in response to muscarinic stimulation causes a decrease in resting K^+ conductance, thus depolarizing the cell (Figure 14–8B). How far will the membrane depolarize? This can be calculated using the equivalent circuit form of the Goldman equation (Chapter 9) by decreasing the g_K term from its initial value. As the change in g_K due to closure of M-type K^+ channels is relatively modest, the depolarization at the peak of the slow EPSP is small, only a few millivolts. Nonetheless, M-type K^+ channel closure by ACh can lead to a striking increase in action potential firing in response to a depolarizing input.

What are the special properties of M-type K^+ channel closure that dramatically enhance excitability? First, the depolarization resulting from the reduction in resting g_K drives the membrane closer to threshold. Second, the increase in membrane resistance decreases the amount of excitatory current necessary to depolarize the cell to a given voltage. Third, the reduction in the delayed K^+ current enables the cell to produce a more sustained firing of action potentials in response to a prolonged depolarizing stimulus.

In the absence of ACh, a ganglionic neuron normally fires only one or two action potentials and then stops firing in response to prolonged excitatory stimulation that is just above threshold. This process, termed *spike-frequency adaptation*, results in part from

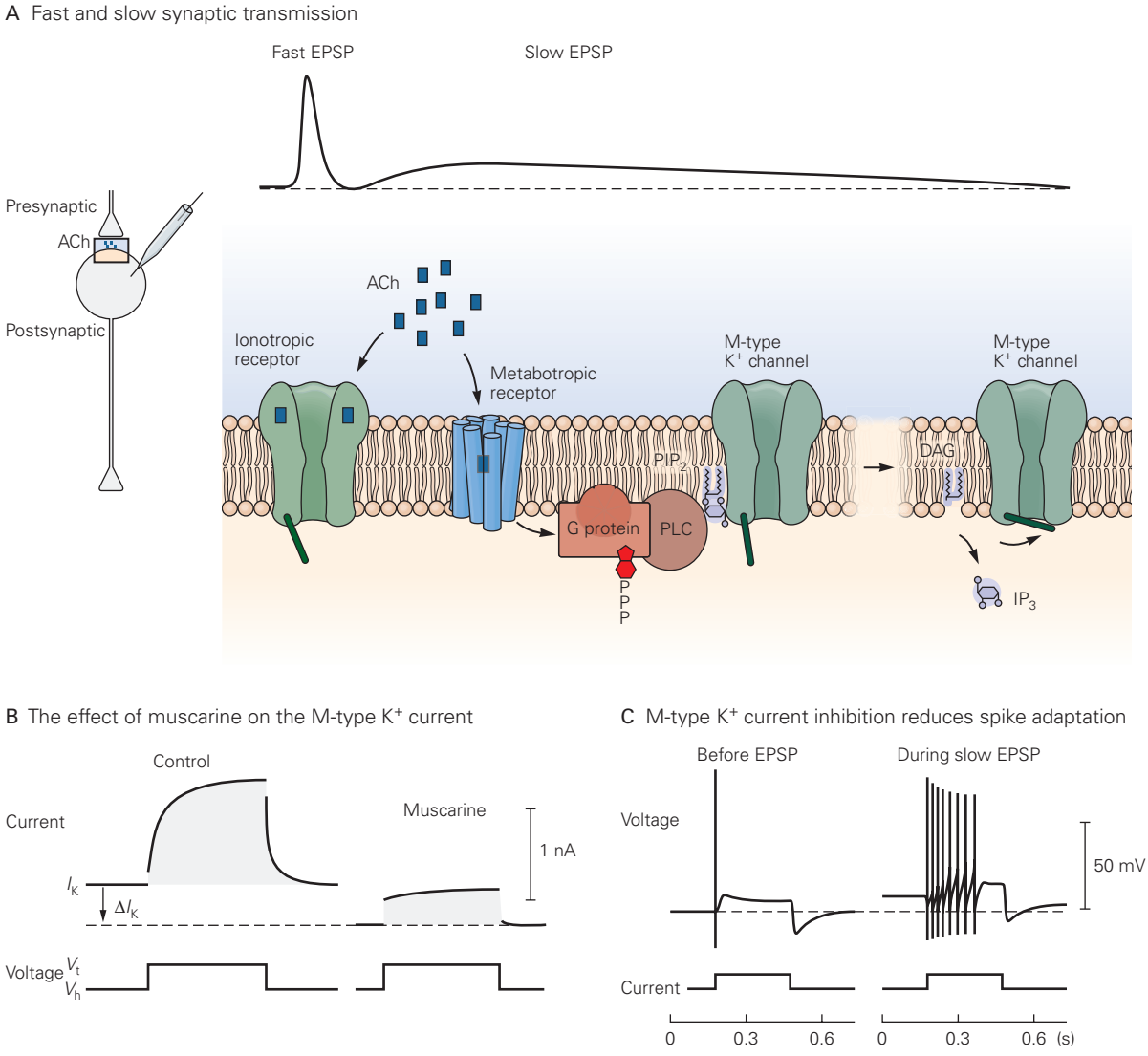

Figure 14–8 Fast ionotropic and slow metabotropic synaptic actions at autonomic ganglia.

A. The release of ACh onto a postsynaptic neuron in autonomic ganglia produces a fast EPSP followed by a slow EPSP. The fast EPSP is produced by activation of ionotropic nicotinic ACh receptors, the slow EPSP by activation of metabotropic muscarinic ACh receptors. The metabotropic receptor stimulates PLC to hydrolyze PIP_2, yielding IP_3 and DAG. The decrease in PIP_2 causes the closure of M-type delayed-rectifier K^+ channels.

B. Voltage-clamp recordings from an autonomic ganglion neuron indicate that ACh decreases the magnitude of the current carried by the voltage-gated M-type K^+ channels. In this experiment, the cell is initially clamped at a holding potential (V_h) near the resting potential in the absence of ACh (typically –60 mV). At this potential, the M-type K^+ channels are partially open, leading to a steady outward K^+ current. The voltage is then stepped for 1 second to a more positive test potential (V_t, typically –40 mV), which normally causes a slow increase in outward K^+ current (I_K) as the M-type K^+ channels respond to the more positive voltage by increasing their opening (control). Application of muscarine, a plant alkaloid that selectively stimulates the muscarinic ACh receptor, causes a fraction of the M-type K^+ channels to close. This decreases the outward K^+ current at the holding potential (note the shift in baseline current, ΔI_K), by closing the M-type K^+ channels that are open at rest, and decreases the magnitude of the slowly activating K^+ current in response to the step depolarization. (Adapted from Adams et al. 1986.)

C. In the absence of muscarinic ACh receptor stimulation, the neuron fires only a single action potential in response to a prolonged depolarizing current stimulus, a process termed spike-frequency adaptation (*left*). This is because the slow activation of the M-type K^+ channel during the depolarization generates an outward current that repolarizes the membrane below threshold. When the same current stimulus is applied during a slow EPSP, when a large fraction of M-type channels are now unable to open, the neuron fires a more sustained train of action potentials (*right*). (Adapted from Adams et al. 1986.)

the increase in M-type K^+ current in response to the prolonged depolarization, which helps repolarize the membrane below threshold. As a result, if the same prolonged stimulus is applied during a slow EPSP (when the M-type K^+ channels are closed), the neuron remains depolarized above threshold during the entire stimulus and thus fires a prolonged burst of impulses (Figure 14–8C). As this modulation by ACh illustrates, the M-type K^+ channels do more than help set the resting potential—they also control excitability.

Although it has been known for some time that muscarinic receptor actions in autonomic ganglia result in the activation of PLC and the production of DAG and IP_3, the precise mechanism by which this signaling cascade produces M-type channel closure remained mysterious. However, it is now clear that M-channel closure upon muscarinic receptor activation is not due to the production of a second messenger. Rather, the M-channels, as well as a number of other types of channels (eg, see Figure 14–10), bind membranous PIP_2 as a cofactor for their proper functioning. Thus, muscarinic receptor activation closes M-type channels by activating PLC, and thereby decreasing the levels of PIP_2 in the membrane due to hydrolysis by PLC. We shall next discuss the mechanisms by which other signaling cascades are capable of modulating other types of ion channels. We start by describing the simplest mechanism, the direct gating of ion channels by G proteins, and then consider a more complex mechanism dependent on protein phosphorylation by PKA.

G Proteins Can Modulate Ion Channels Directly

The simplest mechanism for the indirect gating of a channel occurs when transmitter binding to a metabotropic receptor releases a G protein subunit that directly interacts with the channel to modify its opening. This mechanism is used to gate two kinds of ion channels: the *G protein–gated inward-rectifier K^+* channels (GIRK1–4; encoded by the *KCNJ1–4* genes) and a voltage-dependent Ca^{2+} channel. With both kinds of channels, it is the G protein's βγ complex that binds to and regulates channel opening (Figure 14–9A).

The GIRK channel, like other inward-rectifier channels, passes current more readily in the inward than the outward direction, although in physiological situations, K^+ current is always outward. Inward-rectifier channels resemble a truncated voltage-gated K^+ channel in having two transmembrane regions connected by a P-region loop that forms the selectivity filter in the channel (see Figure 8–11).

In the 1920s, Otto Loewi described how the release of ACh in response to stimulation of the vagus nerve slows the heart rate (Figure 14–9B). We now know that ACh activates muscarinic receptors to stimulate G protein activity, which directly opens the GIRK channel. For many years, this transmitter action was puzzling because it has properties of both ionotropic and metabotropic receptor actions. The time course of activation of the K^+ current following release of ACh is slower (50- to 100-ms rise time) than that of ionotropic receptors (rise time <1 ms). However, the rate of GIRK channel activation is much faster than that of second-messenger-mediated actions that depend on protein phosphorylation (which can take many seconds to turn on). Although biochemical and electrophysiological studies clearly demonstrated that a G protein was required for this action, patch-clamp experiments showed that the G protein did not trigger production of a diffusible second messenger (Figure 14–9C). These findings were reconciled when it was found that the GIRK channel was activated directly by the G protein's βγ-subunit complex, which becomes available to interact with the GIRK channel when it dissociates from the G protein α-subunit upon activation of the muscarinic receptors.

The mechanism by which the βγ-subunits activate the GIRK channel was recently elucidated at the atomic resolution through the solving of the X-ray crystal structure of the GIRK channel in a complex with the βγ-subunits. Each of the four GIRK channel subunits binds a single βγ-subunit complex, which interacts with the cytoplasmic surface of the channel, leading to a conformational change that promotes channel opening (Figure 14–10).

Activation of GIRK channels hyperpolarizes the membrane in the direction of E_K (–80 mV). In certain classes of spontaneously active neurons, the outward K^+ current through these channels acts predominantly to decrease the neuron's intrinsic firing rate, opposing the slow depolarization caused by excitatory pacemaker currents carried by the hyperpolarization-activated, cyclic nucleotide-regulated channels, which are encoded by the *HCN* gene family (Chapter 10). Because GIRK channels are activated by neurotransmitters, they provide a means for synaptic modulation of the firing rate of excitable cells. These channels are regulated in a wide variety of neurons by a large number of transmitters and neuropeptides that act on different G protein–coupled receptors to activate either G_i or G_o, thereby releasing the βγ-subunits.

Several G protein–coupled receptors also act to inhibit the opening of certain voltage-gated Ca^{2+} channels, again as a result of the direct binding of the βγ complex of G_i or G_o to the channel. Because Ca^{2+} influx through voltage-gated Ca^{2+} channels normally has a depolarizing effect, the dual action of G protein βγ-subunits—Ca^{2+} channel inhibition and K^+ channel activation—strongly inhibits neuronal firing. As we will see in Chapter 15, inhibition

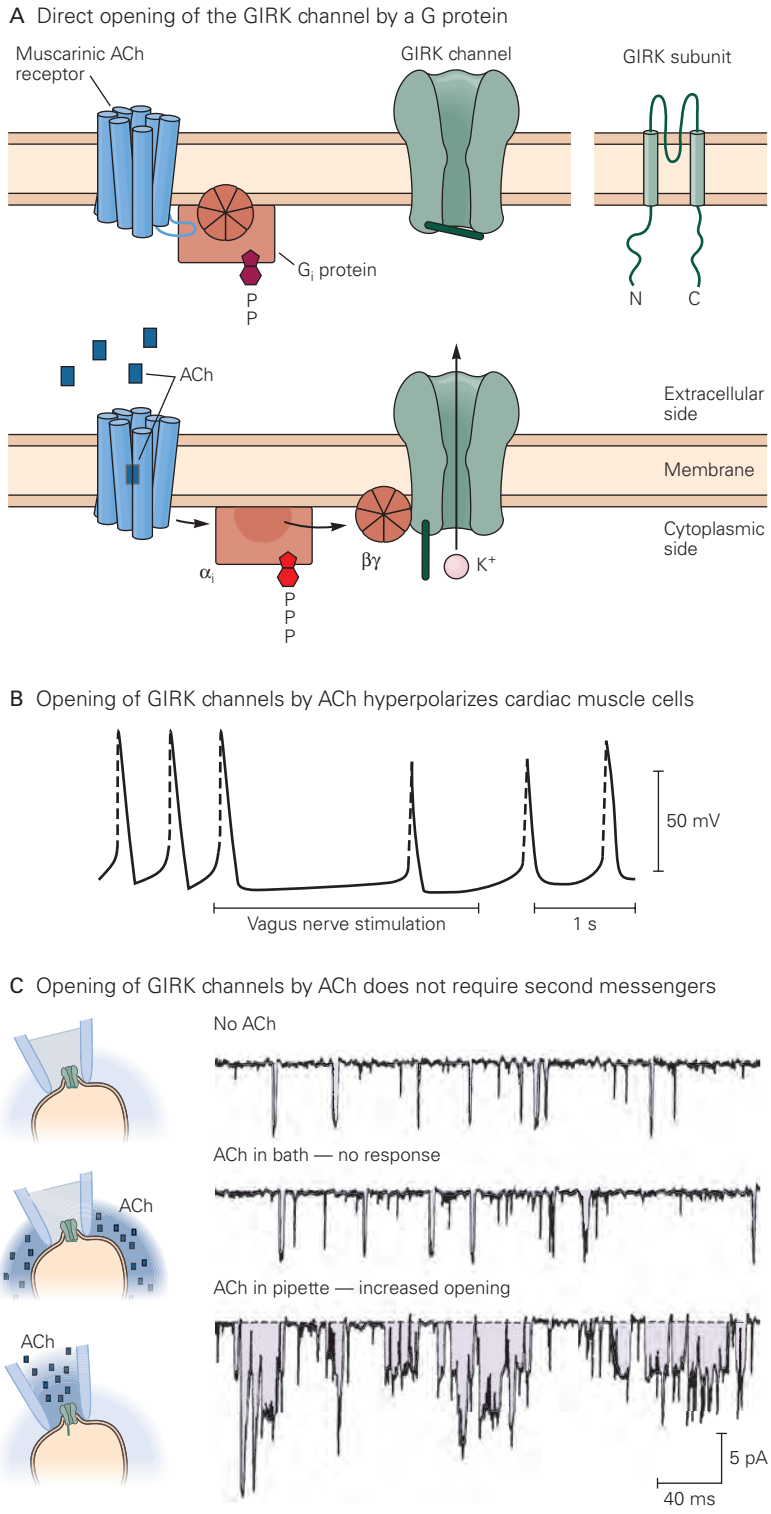

Figure 14–9 Some G proteins can open ion channels directly without employing second messengers.

A. An inward-rectifying K^+ channel (**GIRK**) is opened directly by a G protein. Binding of ACh to a muscarinic receptor causes the G_i protein and $\alpha_i\beta\gamma$ complex to dissociate; the free $\beta\gamma$-subunits bind to a cytoplasmic domain of the channel, causing the channel to open.

B. Stimulation of the parasympathetic vagus nerve releases ACh, which acts at muscarinic receptors to open GIRK channels in cardiac muscle cell membranes. The current through the GIRK channel hyperpolarizes the cells, thus slowing the heart rate. (Adapted from Toda and West 1967.)

C. Three single-channel records show that opening of GIRK channels does not involve a freely diffusible second messenger. In this experiment, the pipette contained a high concentration of K^+, which makes E_K less negative. As a result, when GIRK channels open, they generate brief pulses of inward (downward) current. In the absence of ACh, channels open briefly and infrequently (**top record**). Application of ACh in the bath (outside the pipette) does not increase channel opening in the patch of membrane under the pipette (**middle record**). This is because the free $\beta\gamma$-subunits, released by the binding of ACh to its receptor, remain tethered to the membrane near the receptor and can only activate nearby channels. The subunits are not free to diffuse to the channels under the patch pipette. The ACh must be in the pipette to activate the channel (**bottom record**). (Reproduced, with permission, from Soejima and Noma 1984. Copyright © 1984 Springer Nature.)

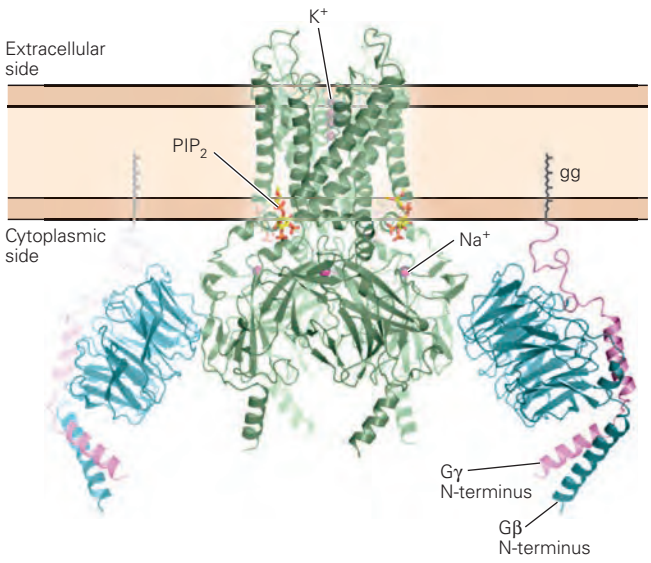

Figure 14–10 G protein βγ-subunits can directly bind and activate GIRK channels. A high-resolution structure of a GIRK channel (**green**) interacting with the G protein β-subunit (**Gβ**, **cyan**) and γ-subunit (**Gγ**, **purple**). A geranylgeranyl lipid molecule (**gg**) is attached to the C-terminus of Gγ. The structure illustrates that Na^+ ions and the phospholipid PIP_2 also bind to the channel, thereby enhancing channel opening. The **pink spheres** inside the channel represent K^+ ions. (Adapted with permission from Whorton and MacKinnon 2013. Copyright © 2013 Springer Nature.)

of voltage-gated Ca^{2+} channels in presynaptic terminals can suppress the release of neurotransmitter.

Cyclic AMP–Dependent Protein Phosphorylation Can Close Potassium Channels

In the marine mollusk *Aplysia*, a group of mechanoreceptor sensory neurons initiates defensive withdrawal reflexes in response to tactile stimuli through fast excitatory synapses with motor neurons. Certain interneurons form serotonergic synapses with these sensory neurons, and the serotonin released by the interneurons sensitizes the withdrawal reflex, enhancing the animal's response to a stimulus and thus producing a simple form of learning (Chapter 53).

The modulatory action of serotonin depends on its binding to a G protein–coupled receptor that activates a G_s protein, which elevates cAMP and thus activates PKA. This leads to the direct phosphorylation and subsequent closure of the serotonin-sensitive (or S-type) K^+ channel that acts as a resting channel (Figure 14–11). Like the closing of the M-type K^+ channel by ACh, closure of the S-type K^+ channel decreases K^+ efflux from the cell, thereby depolarizing the cell and decreasing its resting membrane conductance. Conversely, the opening of the same S-type K^+ channels can be enhanced by the neuropeptide FMRFamide, acting through 12-lipoxygenase metabolites of arachidonic acid. This enhanced channel opening leads to a slow hyperpolarizing inhibitory postsynaptic potential (IPSP) associated with an increase in resting membrane conductance.

Thus, a single channel can be regulated by distinct second-messenger pathways that produce opposite effects on neuronal excitability. Likewise, a resting K^+ channel with two pore-forming domains in each subunit (the TREK-1 channel) in mammalian neurons is dually regulated by PKA and arachidonic acid in a manner very similar to the dual regulation of the S-type channel in *Aplysia*.

Second Messengers Can Endow Synaptic Transmission with Long-Lasting Consequences

So far, we have described how synaptic second messengers alter the biochemistry of neurons for periods lasting seconds to minutes. Second messengers can also produce long-term changes lasting days to weeks as a result of alterations in a cell's expression of specific genes (Figure 14–12). Such changes in gene expression result from the ability of second-messenger cascades to control the activity of transcription factors, regulatory proteins that control mRNA synthesis.

Some transcription factors can be directly regulated by phosphorylation. For example, the cAMP response element-binding protein (CREB) is activated when phosphorylated by PKA, calcium/calmodulin-dependent protein kinases, PKC, or MAP kinases. Once activated, CREB enhances transcription by binding to specific DNA sequences, the cAMP response elements or CRE, and recruiting a component of the transcription machinery, the CREB-binding protein (CBP). CBP activates transcription by recruiting RNA polymerase II and by functioning as a histone acetylase, adding acetyl groups to certain histone lysine residues. The acetylation weakens the binding between histones and DNA, thus opening up the chromatin structure and enabling specific genes to be transcribed. The changes in transcription and chromatin structure are important for regulating neuronal development, as well as for long-term learning and memory (Chapters 53 and 54).

Modulators Can Influence Circuit Function by Altering Intrinsic Excitability or Synaptic Strength

Most of this chapter has been devoted to understanding the cellular mechanisms and signal transduction pathways that allow neuromodulator-activated

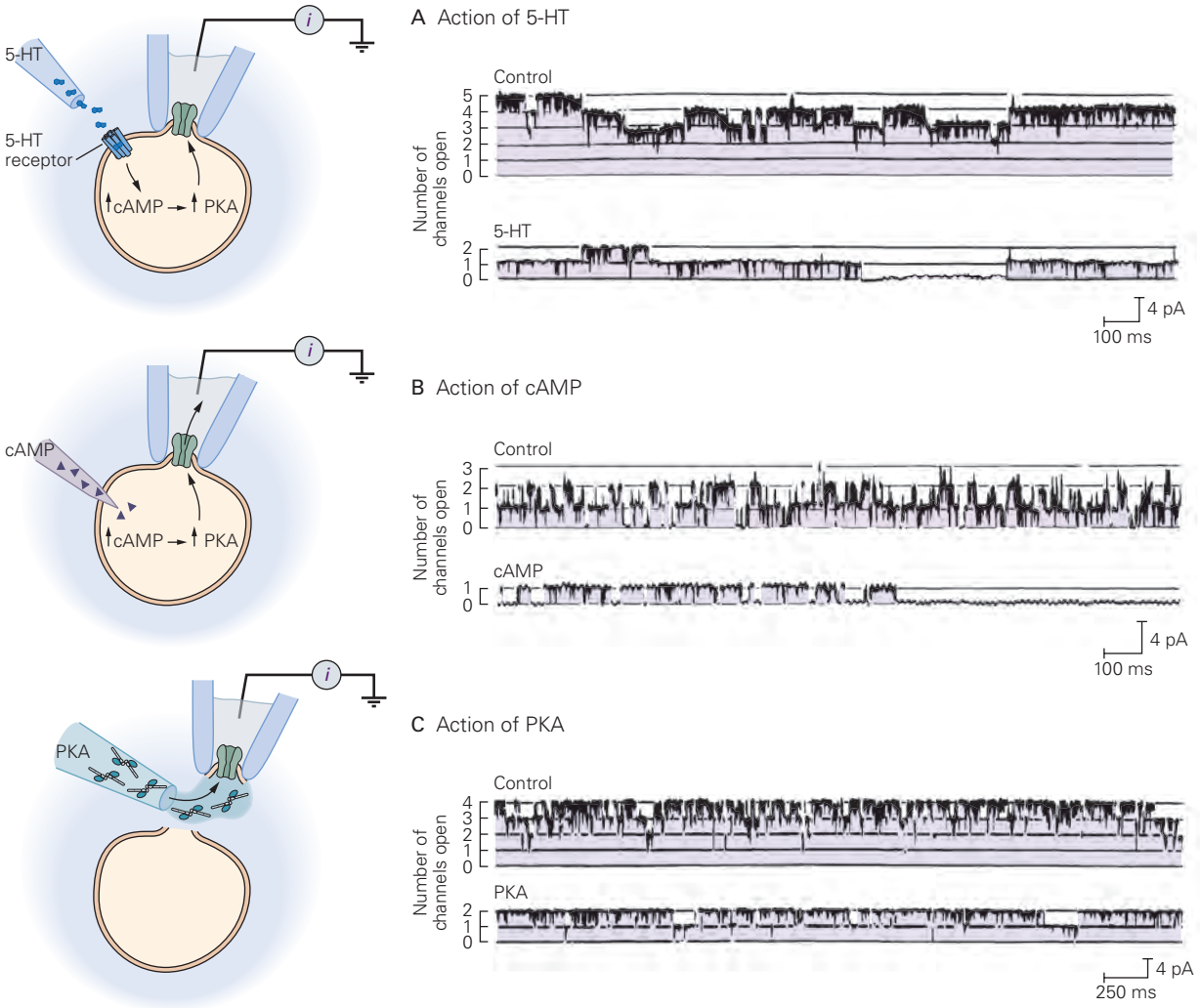

Figure 14–11 Serotonergic interneurons close a K^+ channel through the diffusible second-messenger cAMP. Serotonin (**5-HT**) produces a slow EPSP in *Aplysia* sensory neurons by closing the serotonin-sensitive or S-type K^+ channels. The 5-HT receptor is coupled to G_s, which stimulates adenylyl cyclase. The increase in cAMP activates cAMP-dependent protein kinase A (**PKA**), which phosphorylates the S-type channel, leading to its closure. Single-channel recordings illustrate the actions of 5-HT, cAMP, and PKA on the S-type channels.

A. Addition of 5-HT to the bath closes three of five S-type K^+ channels active in this cell-attached patch of membrane. The experiment implicates a diffusible messenger, as the 5-HT applied in the bath has no direct access to the S-type channels in the membrane under the pipette. Each channel opening contributes an outward (positive) current pulse. (Adapted, with permission, from Siegelbaum, Camardo, and Kandel 1982.)

B. Injection of cAMP into a sensory neuron through a microelectrode closes all three active S-type channels in this patch. The bottom trace shows the closure of the final active channel in the presence of cAMP. (Adapted, with permission, from Siegelbaum, Camardo, and Kandel 1982.)

C. Application of the purified catalytic subunit of PKA to the cytoplasmic surface of the membrane closes two out of four active S-type K^+ channels in this cell-free patch. ATP was added to the solution bathing the inside surface of the membrane to provide the source of phosphate for protein phosphorylation. (Adapted, with permission, from Shuster et al. 1985.)

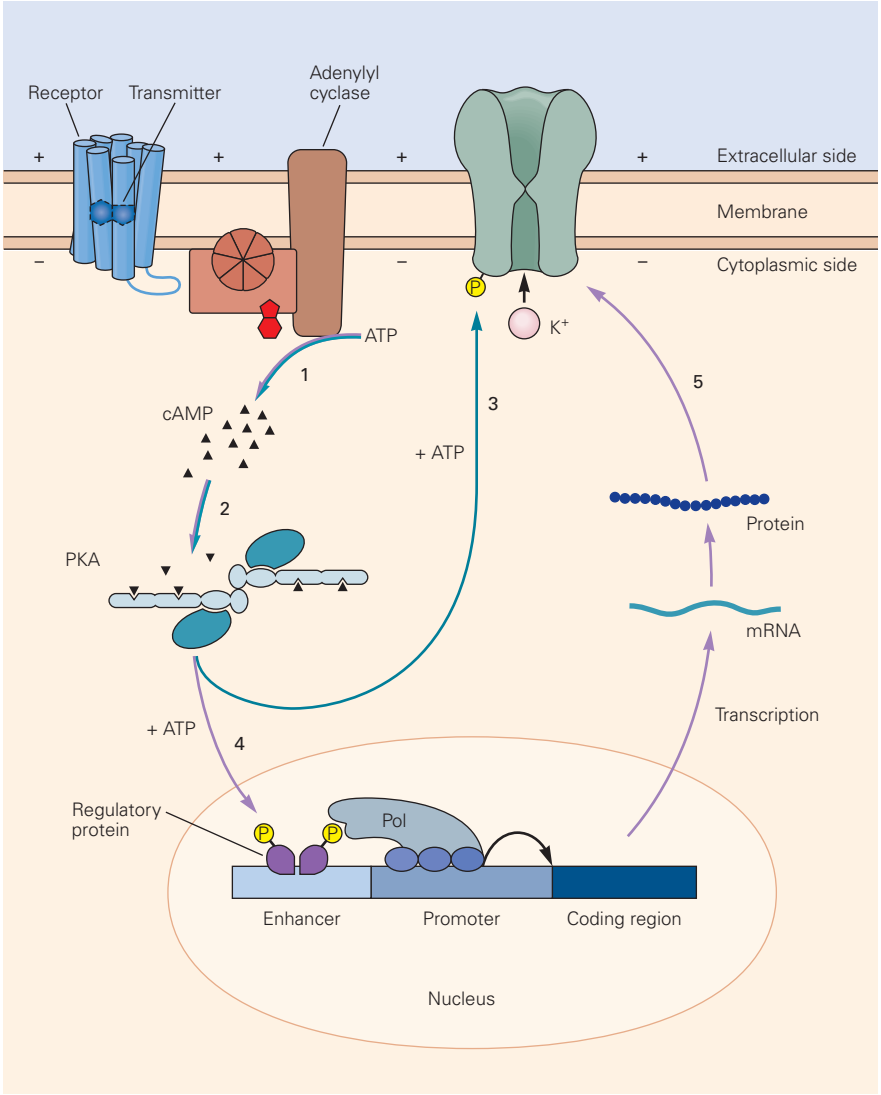

Figure 14–12 A single neurotransmitter can have either short-term or long-term effects on an ion channel. In this example, a short exposure to transmitter activates the cAMP second-messenger system (**1**), which in turn activates PKA (**2**). The kinase phosphorylates a K^+ channel; this leads to a synaptic potential that lasts for several minutes and modifies the excitability of the neuron (**3**). With sustained activation of the receptor, the kinase translocates to the nucleus, where it phosphorylates one or more transcription factors that turn on gene expression (**4**). As a result of the new protein synthesis, the synaptic actions are prolonged—closure of the channel and changes in neuronal excitability last days or longer (**5**). (**Pol**, polymerase.)

pathways to alter the activity of ion channels, receptors, and synapses in individual neurons. However, in the intact brain, modulatory transmitters released either from diffuse projections over large areas of the brain (Chapter 16) or from more locally targeted connections can alter the dynamics of brain circuits in a number of important ways. In this section, we examine one well-studied example of modulatory control of circuit function—the control of crustacean feeding behavior by the neurons of the stomatogastric ganglion to illustrate the following general properties.

1. Modulatory projection neurons or neurohormones can coordinately influence the properties of large numbers of neurons to change the state of a neural circuit or of the entire animal. For example, modulators released from a relatively small number of neurons are important in the control of the transitions between sleep and wakefulness (Chapter 44).
2. Neuromodulators act over intermediate time scales, ranging from many milliseconds to hours. Fast synaptic transmission and rapid action potential propagation are well suited for rapid computation of all kinds of processes important for behavior. Nevertheless, modulators that act over longer time scales can bias a circuit's dynamics to expand its dynamic range or to adapt it to the behavioral needs of the animal. For example, many sensory processes will evoke very different responses depending on the behavioral state of the animal, and modulators that alter synaptic strength and intrinsic excitability are often involved in such actions.

Multiple Neuromodulators Can Converge Onto the Same Neuron and Ion Channels

We have seen in our discussion of the *Aplysia* S-channel how the same ion channel can be regulated by different modulatory agents. This is a common theme, as the M-type K^+ channel is modulated by acetylcholine, substance P, and a variety of other peptides.

One particularly striking example of convergence is seen in the modulatory control of the neurons of the crustacean stomatogastric ganglion. There, a large number of structurally diverse neuropeptides converge to modulate a voltage-dependent inward current (I_{MI}). Although I_{MI} is a small current, it plays an important role in regulating excitability and the generation of plateau and burst potentials. Many neurons express a large number of different receptor types, giving these cells the ability to respond flexibly to different modulatory inputs during different brain states.

The crustacean stomatogastric ganglion (STG) contains 26 to 30 neurons and generates two rhythmic motor patterns important for feeding—the gastric rhythm and the pyloric rhythm. One set of STG neurons generates the pyloric rhythm, which is important for filtering food and is continuously active throughout the animal's life. Another set of neurons generates the gastric mill rhythm, which moves three teeth inside of the stomach that are used to chew and grind food. The gastric mill rhythm is activated in response to food and is therefore only intermittently active in vivo. Whether a particular rhythm is active at any time is under the control of a variety of neuromodulators, some of which activate the pyloric and gastric mill rhythms, while others inhibit them. These modulators can be released at specific synaptic contacts or can act diffusely as neurohormones. Interestingly, modulators can also cause individual neurons to switch between these two circuits, thereby increasing the computational power that this small number of neurons can achieve.

The fundamental circuit (the kernel) that serves as the pacemaker of the STG pyloric rhythm consists of a single anterior burster (AB) neuron and two pyloric dilator (PD) neurons. Both types of neurons make inhibitory synaptic connections with a third type of neuron, the pyloric (PY) neuron. During bursting, a slowly depolarizing pacemaker potential (slow wave) triggers a burst of action potentials in both AB and PD neurons. As these neurons are strongly coupled by electrical (gap-junction) synapses, they depolarize and synchronously fire bursts of action potentials, resulting in transient inhibition of the downstream PY neuron (Figure 14–13A).

Dopamine, which functions both as a fast neurotransmitter and as a neurohormone in crustaceans, influences feeding behavior by acting on many neurons and synapses to influence synaptic strength and neuronal and muscle excitability. For example, application of dopamine decreases the slow-wave amplitude in the PD neurons but increases the amplitude of the slow wave in the AB neurons. Ron Harris-Warrick found that dopamine modulates different sets of membrane currents in the two neurons, providing a clear example of how a single modulatory transmitter can exert distinct actions in different postsynaptic cells (Figure 14–13B).

Dopamine also alters the relative timing of the activity of these neurons. Although the PY neuron receives inhibitory input from both the AB and PD neurons, the inhibitory synaptic action from the AB neuron is faster than that from the PD neuron. Thus, dopamine, by inhibiting the PD neuron and suppressing the slow component of the IPSP, acts to speed the time course of the combined IPSP in the PY neurons (Figure 14–13A), contributing to a change in the timing of the activity of the PY neurons relative to that of the pacemaker group. Dopamine also enhances firing in the PY neuron by modulating its intrinsic *excitability*, by decreasing the transient A-type K^+ current ($I_{K,A}$) while increasing the *excitatory* slow inward current carried by the HCN channels (I_h) (Figure 14–13B). Thus, the effects of a modulator on the circuit result from its selective actions on a number of voltage-gated channels and synapses in distributed circuit elements.

Why So Many Modulators?

We now know that the STG is the direct target of 50 or more different neuromodulatory substances, including biogenic amines, amino acids, NO, and a host of neuropeptides that are released from descending modulatory projection neurons and sensory neurons and that circulate as hormones in the hemolymph. Many of these modulators are released as cotransmitters from the terminals of certain descending fibers that are activated by sensory neurons. Many neuromodulators are both released synaptically in the STG neuropil and also function as neurohormones.

Why should a small ganglion composed of only 26 to 30 neurons be modulated by so many substances? At first, it was thought that the richness of the modulatory innervation was important for producing different behaviorally relevant motor outputs. This remains true, but it is now also evident that some modulators may be used exclusively in special circumstances, such as molting, and that different modulators with similar effects ensure that important functions are preserved even if one modulatory system is lost. Thus, diverse modulators may be used in the service of both plasticity and stability.

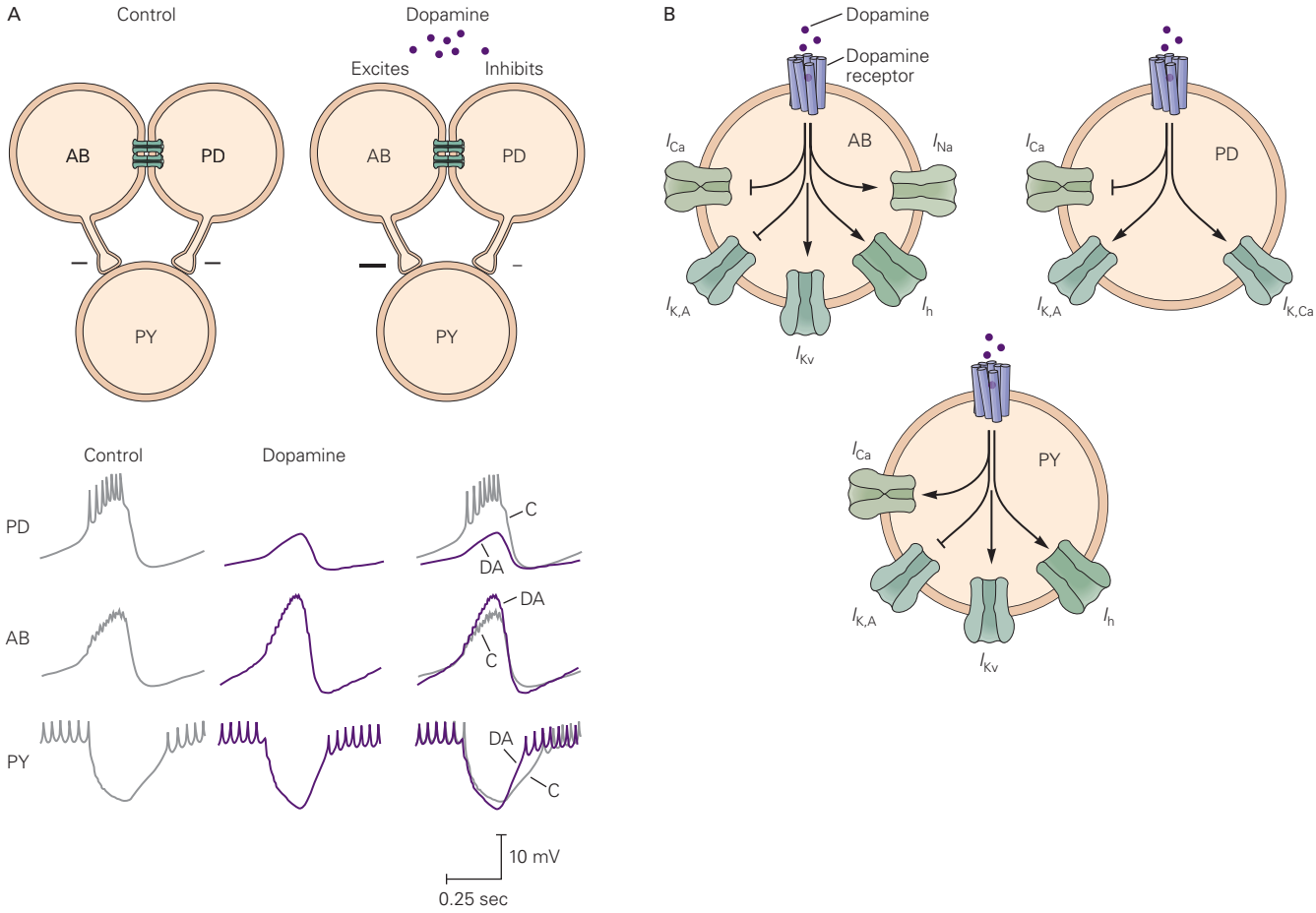

Figure 14–13 The modulatory action of dopamine on the pyloric rhythm of the lobster stomatogastric ganglion results from numerous actions.

A. A circuit diagram shows the interactions between three of the pyloric circuit neurons. The anterior burster (**AB**) and pyloric dilator (**PD**) neurons are strongly electrically coupled by gap-junction channels. Both the AB and PD neurons form inhibitory synapses with the pyloric (**PY**) neuron that generate inhibitory postsynaptic potentials (IPSPs) in this cell. Intracellular voltage recordings illustrate phases of pyloric rhythm from PD, AB, and PY neurons without dopaminergic input (control) and with dopamine. On the *right*, the voltage traces from control cells (**C**) and cells with dopaminergic input (**DA**) are overlaid. Dopamine enhances the amplitude of the slow-wave burst in the AB neuron (in this neuron, axonal action potentials are highly attenuated by the cable properties of the neuron and appear in the soma as faint ripples) but hyperpolarizes and decreases the amplitude of the slow wave in the PD neurons. These combined actions result in a shorter IPSP in the PY neuron, enabling it to fire earlier relative to the PD neurons. (Adapted, with permission, from Eisen and Marder 1984.)

B. Dopamine modulates a number of different voltage-dependent channels in the AB, PD, and PY neurons. These include Ca^{2+} currents (I_{Ca}), a calcium-activated K^+ current ($I_{K,Ca}$), an inactivating K^+ current ($I_{K,A}$), a delayed rectifier K^+ current (I_{Kv}), the hyperpolarization-activated cation current (I_h), and a persistent Na^+ current (I_{Na}). **Lines with arrowheads** indicate current increase, **lines ending in short line segment** indicate current decrease. (Adapted, with permission, from Marder and Bucher 2007. For effects of dopamine on the complete pyloric circuit, see Harris-Warrick, 2011.)

Highlights

1. Neuromodulators are substances that bind to receptors, most of which are metabotropic, to alter the excitability of neurons, the likelihood of transmitter release, or the functional state of receptors on postsynaptic neurons.
2. When neuromodulators activate second-messenger pathways, the modulator can influence the properties of ion channels and other targets at some distance from the site of release.
3. Some neuromodulatory systems have widespread and pronounced actions over many neurons and many brain areas.
4. There are two major families of metabotropic receptors: G protein–coupled receptors and receptor tyrosine kinases. Many important brain signaling molecules, such as norepinephrine,

ACh, GABA, glutamate, serotonin, dopamine, and many diverse neuropeptides, activate metabotropic receptors; many of these same substances also activate ionotropic receptors.

5. The cyclic AMP pathway is among the best-understood second-messenger signaling cascades. Metabotropic receptor activation triggers a sequence of biochemical reactions that result in activation of adenylyl cyclase, which synthesizes cAMP, which in turn activates protein kinase A. The kinase then phosphorylates target proteins, altering their functional state. Important targets for PKA include voltage- and ligand-gated ion channels as well as proteins important in vesicle release.
6. Hydrolysis of phospholipids by phospholipase C produces DAG and IP_3, which plays an important role in intracellular Ca^{2+} handling. Endocannabinoids are synthesized from lipid precursors and can act across synapses as retrograde messengers. Another generalized signaling molecule is the gas nitric oxide, which diffuses across membranes and stimulates cyclic GMP synthesis.
7. The receptor tyrosine kinases also gate ion channels indirectly in response to binding a variety of peptide hormones.
8. Neuromodulators can close ion channels, thus producing decreases in membrane conductance. The M-type current is a slowly activating voltage-gated K^+ current that underlies action potential adaptation. ACh and several neuropeptides decrease M-type current amplitude, thereby producing a slow depolarization and decreasing adaptation. The S-type K^+ channel contributes to the resting K^+ conductance of certain neurons, including a class of sensory neurons mediating the *Aplysia* gill withdrawal reflex. Closure of the channel by serotonin, acting through a cAMP signaling cascade, depolarizes the resting membrane, increases excitability, and enhances transmitter release from sensory neuron terminals. Prolonged exposure to serotonin can alter gene transcription to produce long-term changes in synaptic strength.
9. Modulators can alter the output of neuronal circuits by acting on numerous circuit targets.
10. Given that all brain neurons and synapses are likely to be modulated by one or more substances, it is remarkable that brain circuits are only rarely "overmodulated" so that they lose their function. Much additional research is needed to understand the rules that allow robust and stable network performance in the face of the modulators that allow network plasticity.
11. Except in a few notable cases such as small ganglia or the retina, it is likely that we still have only a partial catalog of the total number of neuromodulatory substances that are present and active.
12. Much of what we know about neuromodulatory actions comes from in vitro studies. Much less is known about how neuromodulatory concentrations are controlled in behaving animals.

Steven A. Siegelbaum
David E. Clapham
Eve Marder

Selected Reading

Berridge MJ. 2016. The inositol trisphosphate/calcium signaling pathway in health and disease. Physiol Rev 96:1261–1296.

Greengard P. 2001. The neurobiology of slow synaptic transmission. Science 294:1024–1030.

Hille B, Dickson EJ, Kruse M, Vivas O, Suh BC. 2015. Phosphoinositides regulate ion channels. Biochim Biophys Acta 1851:844–856.

Kobilka B. 2013. The structural basis of G-protein-coupled receptor signaling (Nobel Lecture). Angew Chem Int Ed Engl 52:6380–6388.

Levitan IB. 1999. Modulation of ion channels by protein phosphorylation. How the brain works. Adv Second Messenger Phosphoprotein Res 33:3–22.

Lu HC, Mackie K. 2016. An introduction to the endogenous cannabinoid system. Biol Psychiatry 79:516–525.

Marder E. 2012. Neuromodulation of neuronal circuits: back to the future. Neuron 76:1–11.

Schwartz JH. 2001. The many dimensions of cAMP signaling. Proc Natl Acad Sci U S A 98:13482–13484.

Syrovatkina V, Alegre KO, Dey R, Huang XY. 2016. Regulation, signaling, and physiological functions of G-proteins. J Mol Biol 428:3850–3868.

Takemoto-Kimura S, Suzuki K, Horigane SI, et al. 2017. Calmodulin kinases: essential regulators in health and disease. J Neurochem 141:808–818.

References

Adams PR, Jones SW, Pennefather P, Brown DA, Koch C, Lancaster B. 1986. Slow synaptic transmission in frog sympathetic ganglia. J Exp Biol 124:259–285.

Alberts B, Bray D, Lewis J, Raff M, Roberts K, Watson JD. 1994. *Molecular Biology of the Cell,* 3rd ed. New York: Garland.

Eisen JS, Marder E. 1984. A mechanism for the production of phase shifts in a pattern generator. J Neurophysiol 51:1375–1393.

Fantl WJ, Johnson DE, Williams LT. 1993. Signalling by receptor tyrosine kinases. Annu Rev Biochem 62:453–481.

Frielle T, Kobilka B, Dohlman H, Caron MG, Lefkowitz RJ. 1989. The β-adrenergic receptor and other receptors coupled to guanine nucleotide regulatory proteins. In: S Chien (ed). *Molecular Biology in Physiology,* pp. 79–91. New York: Raven.

Halpain S, Girault JA, Greengard P. 1990. Activation of NMDA receptors induces dephosphorylation of DARPP-32 in rat striatal slices. Nature 343:369–372.

Harris-Warrick, RM. 2011. Neuromodulation and flexibility in central pattern generating networks. Curr Opin Neurobiol 21:685-692.

Logothetis DE, Kurachi Y, Galper J, Neer EJ, Clapham DE. 1987. The βγ subunits of GTP-binding proteins activate the muscarinic K^+ channel in heart. Nature 325:321–326.

Marder E, Bucher D. 2007. Understanding circuit dynamics using the stomatogastric nervous system of lobsters and crabs. Annu Rev Physiol 69:291–316.

Nusbaum MP, Blitz DM, Marder E. 2017. Functional consequences of neuropeptide/small molecule cotransmission. Nature Rev Neurosci 18:389–403.

Osten P, Valsamis L, Harris A, Sacktor TC. 1996. Protein synthesis-dependent formation of protein kinase Mzeta in long-term potentiation. J Neurosci 16:2444–2451.

Pfaffinger PJ, Martin JM, Hunter DD, Nathanson NM, Hille B. 1985. GTP-binding proteins couple cardiac muscarinic receptors to a K channel. Nature 317:536–538.

Phillis JW, Horrocks LA, Farooqui AA. 2006. Cyclooxygenases, lipoxygenases, and epoxygenases in CNS: their role and involvement in neurological disorders. Brain Res Rev 52:201–243.

Shuster MJ, Camardo JS, Siegelbaum SA, Kandel ER. 1985. Cyclic AMP-dependent protein kinase closes the serotonin-sensitive K^+ channels of *Aplysia* sensory neurones in cell-free membrane patches. Nature 313:392–395.

Siegelbaum SA, Camardo JS, Kandel ER. 1982. Serotonin and cyclic AMP close single K^+ channels in *Aplysia* sensory neurones. Nature 299:413–417.

Soejima M, Noma A. 1984. Mode of regulation of the ACh-sensitive K-channel by the muscarinic receptor in rabbit atrial cells. Pflugers Arch 400:424–431.

Tedford HW, Zamponi GW. 2006. Direct G protein modulation of Cav2 calcium channels. Pharmacol Rev 58: 837–862.

Toda N, West TC. 1967. Interactions of K, Na, and vagal stimulation in the S-A node of the rabbit. Am J Physiol 212:416–423.

Whorton MR, MacKinnon R. 2013. X-ray structure of the mammalian GIRK2-betagamma G-protein complex. Nature 498:190–197.

Zeng L, Webster SV, Newton PM. 2012. The biology of protein kinase C. Adv Exp Med Biol 740:639–661.

15

Transmitter Release

Some of the brain's most remarkable abilities, such as learning and memory, are thought to emerge from the elementary properties of chemical synapses, where the presynaptic cell releases chemical transmitters that activate receptors in the membrane of the postsynaptic cell. At most central synapses, transmitter is released from the presynaptic cell at presynaptic boutons, varicosities along the axon (like beads on a string) filled with synaptic vesicles and other organelles that contact postsynaptic targets. At other synapses, including the neuromuscular junction, transmitter is released from presynaptic terminals at the end of the axon. For convenience, we will refer to both types of release sites as presynaptic terminals. In the last three chapters, we saw how postsynaptic receptors control ion channels that generate the postsynaptic potential. Here we consider how electrical and biochemical events in the presynaptic terminal lead to the rapid release of small-molecule neurotransmitters, such as acetylcholine (ACh), glutamate, and γ-aminobutyric acid (GABA), that underlie fast synaptic transmission. In the next chapter, we examine the chemistry of the neurotransmitters themselves as well as the biogenic amines (serotonin, norepinephrine, and dopamine) and neuropeptides, which underlie slower forms of intercellular signaling.

Transmitter Release Is Regulated by Depolarization of the Presynaptic Terminal

What event at the presynaptic terminal leads to the release of transmitter? Bernard Katz and Ricardo Miledi first demonstrated the importance of depolarization of the presynaptic membrane. For this purpose, they used

the giant synapse of the squid, a synapse large enough to permit insertion of electrodes into both pre- and postsynaptic structures. Two electrodes are inserted into the presynaptic terminal—one for stimulating and one for recording—and one electrode is inserted into the postsynaptic cell for recording the excitatory postsynaptic potential (EPSP), which provides an index of transmitter release (Figure 15–1A).

After the presynaptic neuron is stimulated and fires an action potential, an EPSP large enough to trigger an action potential is recorded in the postsynaptic cell. Katz and Miledi then asked how the presynaptic action potential triggers transmitter release. They found that as voltage-gated Na^+ channels are blocked by application of tetrodotoxin, successive action potentials become progressively smaller. As the action potential is reduced in size, the EPSP decreases accordingly (Figure 15–1B). When the Na^+ channel blockade becomes so profound as to reduce the amplitude of the presynaptic spike below 40 mV (positive to the resting potential), the EPSP disappears altogether. Thus, the amount of transmitter release (as measured by the size of the postsynaptic depolarization) is a steep function of the amount of presynaptic depolarization (Figure 15–1C).

Katz and Miledi next investigated how presynaptic depolarization triggers transmitter release. The action potential is produced by an influx of Na^+ and an efflux of K^+ through voltage-gated channels. To determine

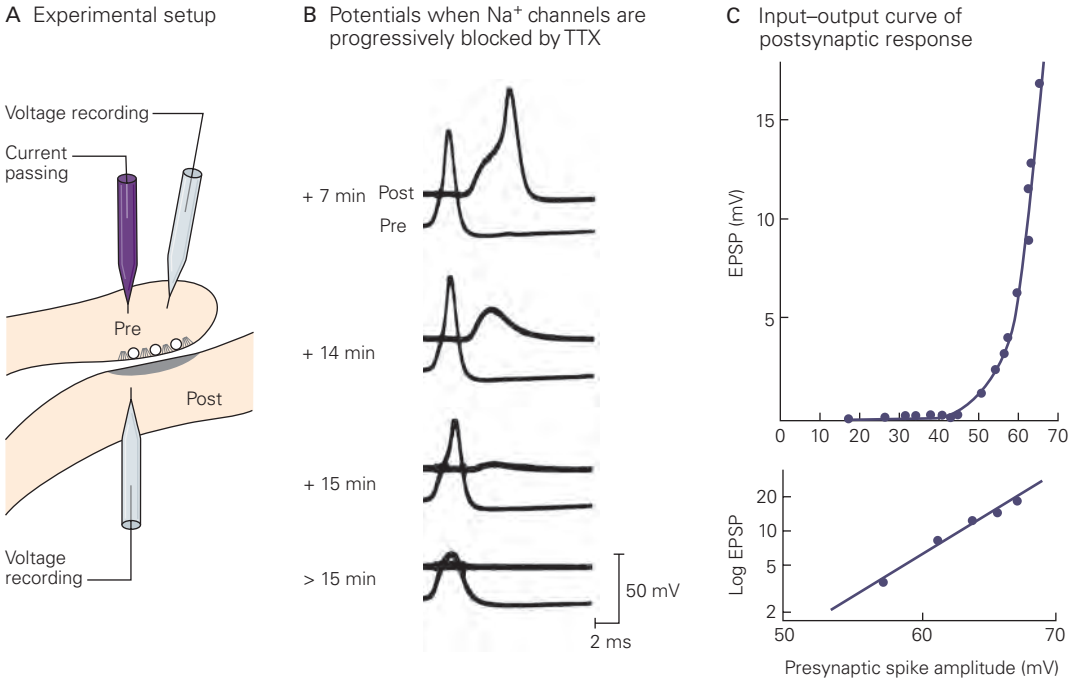

Figure 15–1 Transmitter release is triggered by changes in presynaptic membrane potential. (Adapted, with permission, from Katz and Miledi 1967a.)

A. Voltage recording electrodes are inserted in both the pre- and postsynaptic fibers of the giant synapse in the stellate ganglion of a squid. A current-passing electrode is also inserted presynaptically to elicit a presynaptic action potential.

B. Tetrodotoxin (TTX) is added to the solution bathing the cell to block the voltage-gated Na^+ channels that underlie the action potential. The amplitudes of both the presynaptic action potential and the excitatory postsynaptic potential (EPSP) gradually decrease as more and more Na^+ channels are blocked. After 7 minutes, the presynaptic action potential can still produce a suprathreshold EPSP that triggers an action potential in the postsynaptic cell. After about 14 to 15 minutes, the presynaptic spike gradually becomes smaller and produces smaller postsynaptic depolarizations. When the presynaptic spike is reduced to 40 mV or less, it fails to produce an EPSP. Thus, the size of the presynaptic depolarization (here provided by the action potential) controls the magnitude of transmitter release.

C. The dependence of the amplitude of the EPSP on the amplitude of the presynaptic action potential is the basis for the input–output curve for transmitter release. This relation is obtained by stimulating the presynaptic nerve during the onset of the blockade by TTX of the presynaptic Na^+ channels, when there is a progressive reduction in the amplitude of the presynaptic action potential and postsynaptic depolarization. The upper plot demonstrates that a 40-mV presynaptic action potential is required to produce a postsynaptic potential. Beyond this threshold, there is a steep increase in amplitude of the EPSP in response to small increases in the amplitude of the presynaptic potential. The relationship between the presynaptic spike and the EPSP is logarithmic, as shown in the lower plot. A 13.5-mV increase in the presynaptic spike produces a 10-fold increase in the EPSP.

whether Na^+ influx or K^+ efflux is required to trigger transmitter release, Katz and Miledi first blocked the Na^+ channels with tetrodotoxin. They then asked whether direct depolarization of the presynaptic membrane, by current injection, would still trigger transmitter release. Indeed, depolarization of the presynaptic membrane beyond a threshold of about 40 mV positive to the resting potential elicits an EPSP in the postsynaptic cell even with the Na^+ channels blocked. Beyond that threshold, progressively greater depolarization leads to progressively greater amounts of transmitter release. This result shows that presynaptic Na^+ influx is not necessary for release; it is important only insofar as it depolarizes the membrane enough for transmitter release to occur (Figure 15–2B).

To examine the contribution of K^+ efflux to transmitter release, Katz and Miledi blocked the voltage-gated K^+ channels with tetraethylammonium at the same time that they blocked the voltage-sensitive Na^+ channels with tetrodotoxin. They then injected a depolarizing current into the presynaptic terminals and found that the EPSPs were of normal size, indicating that normal transmitter release occurred (Figure 15–2C). Thus, neither Na^+ nor K^+ flux is required for transmitter release.

In the presence of tetraethylammonium, the current pulse elicits presynaptic depolarization throughout the duration of the pulse because the K^+ current that normally repolarizes the presynaptic membrane is blocked. As a result, transmitter release is sustained throughout the current pulse as reflected in the prolonged depolarization of the postsynaptic cell (Figure 15–2C). Quantification of the sustained depolarization was used by Katz and Miledi to determine a complete input–output curve relating presynaptic depolarization to transmitter release (Figure 15–2D). They confirmed the steep dependence of transmitter release on presynaptic depolarization. In the range of depolarization over which transmitter release increases (40–70 mV

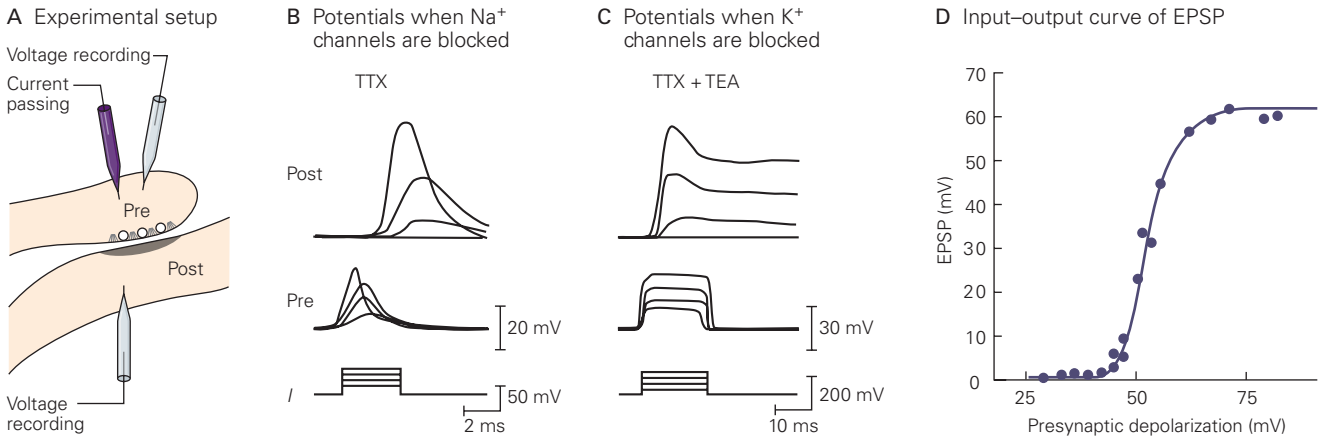

Figure 15–2 Transmitter release is not directly triggered by the opening of presynaptic voltage-gated Na^+ or K^+ channels. (Adapted, with permission, from Katz and Miledi 1967a.)

A. Voltage recording electrodes are inserted in both the pre- and postsynaptic fibers of the giant synapse in the stellate ganglion of a squid. A current-passing electrode has also been inserted into the presynaptic cell.

B. Depolarizing the presynaptic terminal with direct current injection through a microelectrode can trigger transmitter release even after the voltage-gated Na^+ channels are completely blocked by adding tetrodotoxin (**TTX**) to the cell-bathing solution. Three sets of traces represent (from bottom to top) the depolarizing current pulse (*I*) injected into the presynaptic terminal, the resulting potential in the presynaptic terminal (**Pre**), and the EPSP generated by the release of transmitter onto the postsynaptic cell (**Post**). Progressively stronger current pulses in the presynaptic cell produce correspondingly greater depolarizations of the presynaptic terminal. The greater the presynaptic depolarization, the larger is the EPSP. The presynaptic depolarizations are not maintained throughout the duration of the depolarizing current pulse because delayed activation of the voltage-gated K^+ channels causes repolarization.

C. Transmitter release occurs even after the voltage-gated Na^+ channels have been blocked with TTX *and* the voltage-gated K^+ channels have been blocked with tetraethylammonium (**TEA**). In this experiment, TEA was injected into the presynaptic terminal. The three sets of traces represent the same measurements as in part B. Because the presynaptic K^+ channels are blocked, the presynaptic depolarization is maintained throughout the current pulse. The large sustained presynaptic depolarization produces large sustained EPSPs.

D. Blocking both the Na^+ and K^+ channels permits accurate control of presynaptic voltage and the determination of a complete input–output curve. Beyond a certain threshold (40 mV positive to the resting potential), there is a steep relationship between presynaptic depolarization and transmitter release, as measured from the size of the EPSP. Depolarizations greater than a certain level do not cause any additional release of transmitter. The initial presynaptic resting membrane potential was approximately −70 mV.

positive to the resting level), a 10-mV increase in presynaptic depolarization produces as much as a 10-fold increase in transmitter release. Depolarization of the presynaptic membrane above an upper limit produces no further increase in the postsynaptic potential.

Release Is Triggered by Calcium Influx

Katz and Miledi next turned their attention to Ca^{2+} ions. Earlier, Katz and José del Castillo had found that increasing the extracellular Ca^{2+} concentration enhanced transmitter release, whereas lowering the concentration reduced and ultimately blocked synaptic transmission. Because transmitter release is an intracellular process, these findings implied that Ca^{2+} must enter the cell to influence transmitter release.

Previous work on the squid giant axon membrane had identified a class of voltage-gated Ca^{2+} channels, the opening of which results in a large Ca^{2+} influx because of the large inward electrochemical driving force on Ca^{2+}. The extracellular Ca^{2+} concentration, approximately 2 mM in vertebrates, is normally four orders of magnitude greater than the intracellular concentration, approximately 10^{-7} M at rest. However, because these Ca^{2+} channels are sparsely distributed along the axon, they cannot, by themselves, provide enough current to produce a regenerative action potential.

Katz and Miledi found that the Ca^{2+} channels were much more abundant at the presynaptic terminal. There, in the presence of tetraethylammonium and tetrodotoxin, a depolarizing current pulse was sometimes able to trigger a regenerative depolarization that required extracellular Ca^{2+}, a *calcium spike*. Katz and Miledi therefore proposed that Ca^{2+} serves dual functions. It is a carrier of depolarizing charge during the action potential (like Na^+), and it is a special chemical signal—a second messenger—conveying information about changes in membrane potential to the intracellular machinery responsible for transmitter release. Calcium ions are able to serve as an efficient chemical signal because of their low intracellular resting concentration, approximately 10^5-fold lower than the resting concentration of Na^+. As a result, the small amount of Ca^{2+} ions that enter or leave a cell during an action potential can lead to large percentage changes in intracellular Ca^{2+} that can trigger various biochemical reactions. Proof of the importance of Ca^{2+} channels in release has come from more recent experiments showing that specific toxins that block Ca^{2+} channels also block release.

The properties of the voltage-gated Ca^{2+} channels at the squid presynaptic terminal were measured by Rodolfo Llinás and his colleagues. Using a voltage clamp, Llinás depolarized the terminal while blocking the voltage-gated Na^+ channels with tetrodotoxin and the K^+ channels with tetraethylammonium. He found that graded depolarizations activated a graded inward Ca^{2+} current, which in turn resulted in graded release of transmitter (Figure 15–3). The Ca^{2+} current is graded because the Ca^{2+} channels are voltage-dependent like the voltage-gated Na^+ and K^+ channels. Calcium ion channels in squid terminals differ from Na^+ channels, however, in that they do not inactivate quickly but stay open as long as the presynaptic depolarization lasts.

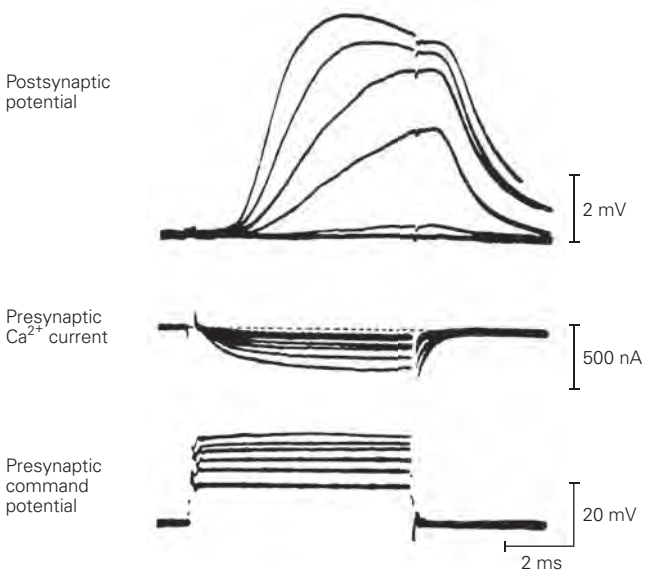

Figure 15–3 Transmitter release is regulated by Ca^{2+} influx into the presynaptic terminals through voltage-gated Ca^{2+} channels. The voltage-sensitive Na^+ and K^+ channels in a squid giant synapse were blocked by tetrodotoxin and tetraethylammonium. The membrane of the presynaptic terminal was voltage-clamped and membrane potential stepped to six different command levels of depolarization (**bottom**). The amplitude of the postsynaptic depolarization (**top**) varies with the size of the presynaptic inward Ca^{2+} current (**middle**) because the amount of transmitter release is a function of the concentration of Ca^{2+} in the presynaptic terminal. The notch in the postsynaptic potential trace is an artifact that results from turning off the presynaptic command potential. (Adapted, with permission, from Llinás and Heuser 1977.)

Calcium channels are largely localized in presynaptic terminals at *active zones*, the sites where neurotransmitter is released, exactly opposite the postsynaptic receptors (Figure 15–4). This localization is important as Ca^{2+} ions do not diffuse long distances from their site of entry because free Ca^{2+} ions are rapidly buffered by Ca^{2+}-binding proteins. As a result, Ca^{2+} influx creates a sharp local rise in Ca^{2+} concentration at the active zones. This rise in Ca^{2+} in the presynaptic terminals can be visualized using Ca^{2+}-sensitive

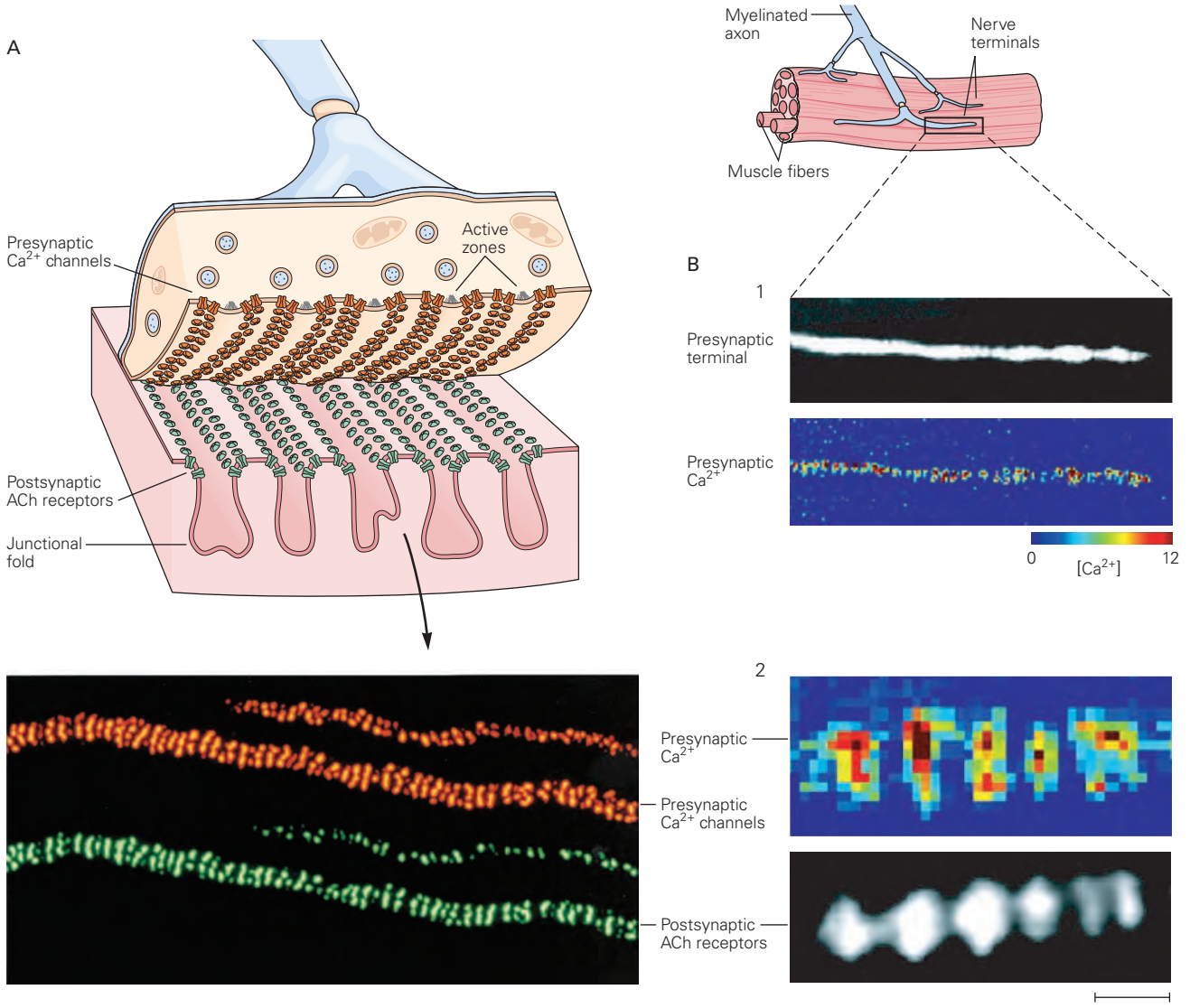

Figure 15–4 **Calcium flowing into the presynaptic nerve terminal during synaptic transmission at the neuromuscular junction is concentrated at the active zone.** Calcium channels in presynaptic terminals at the end-plate are concentrated opposite clusters of nicotinic acetylcholine (**ACh**) receptors on the postsynaptic muscle membrane. Two drawings show the frog neuromuscular junction.

A. The enlarged view shows the microanatomy of the neuromuscular junction with the presynaptic terminal peeled back. A fluorescent image shows the presynaptic Ca^{2+} channels (labeled with a Texas red-coupled marine snail toxin that binds to Ca^{2+} channels) and postsynaptic ACh receptors (labeled with fluorescently tagged α-bungarotoxin, which binds selectively to ACh receptors). The two images are normally superimposed but have been separated for clarity. The patterns of labeling with both probes are in almost precise register, indicating that the active zone of the presynaptic neuron is in almost perfect alignment with the postsynaptic membrane containing the high concentration of ACh receptors. (Reproduced, with permission, from Robitaille, Adler, and Charlton 1990.)

B. Calcium influx in presynaptic terminals is localized at active zones. Calcium can be visualized using Ca^{2+}-sensitive fluorescent dyes. **1.** A presynaptic terminal at a neuromuscular junction filled with the dye fura-2 under resting conditions is shown in the black and white image. The fluorescence intensity of the dye changes as it binds Ca^{2+}. In the color image, color-coded fluorescence intensity changes show local hotspots of intracellular Ca^{2+} in response to a single presynaptic action potential. **Red** indicates regions with a large increase in Ca^{2+}; **blue** indicates regions with little increase in Ca^{2+}. Regular peaks in Ca^{2+} concentration are seen along the terminal, corresponding to the localization of Ca^{2+} channels at the active zones. **2.** The color image shows a high-magnification view of the peak increase in terminal Ca^{2+} levels. The corresponding black and white image shows fluorescence labeling of nicotinic ACh receptors in the postsynaptic membrane, illustrating the close spatial correspondence between areas of presynaptic Ca^{2+} influx and areas of postsynaptic receptors. Scale bar = 2 μm. (Reproduced, with permission, from Wachman et al. 2004. Copyright © 2004 Society for Neuroscience.)

fluorescent dyes (Figure 15–4B). One striking feature of transmitter release at all synapses is its steep and nonlinear dependence on Ca^{2+} influx; a 2-fold increase in Ca^{2+} influx can increase the amount of transmitter released by more than 16-fold. This relationship indicates that at some regulatory site, the *calcium sensor*, the cooperative binding of several Ca^{2+} ions is required to trigger release.

The Relation Between Presynaptic Calcium Concentration and Release

How much Ca^{2+} is necessary to induce release of neurotransmitters? To address this question, Bert Sakmann and Erwin Neher and their colleagues measured synaptic transmission in the calyx of Held, a large synapse in the mammalian auditory brain stem, composed of axons from the cochlear nucleus to the medial nucleus of the trapezoid body. This synapse is specialized for very rapid and reliable transmission to allow for precise localization of sound in the environment.

The calyx forms a cup-like presynaptic terminal that engulfs a postsynaptic cell body (Figure 15–5A). The calyx synapse includes almost a thousand active zones that function as independent release sites. This enables a presynaptic action potential to release a large amount of transmitter that results in a reliably large postsynaptic depolarization. In contrast, individual synaptic boutons of a typical neuron in the brain contain only a single active zone. Because the calyx terminal is large, it is possible to insert electrodes into both the pre- and postsynaptic structures, much as with the squid giant synapse, and directly measure the synaptic coupling between the two compartments. This paired recording allows a precise determination of the time course of activity in the presynaptic and postsynaptic cells (Figure 15–5B).

These recordings revealed a brief lag of 1 to 2 ms between the onset of the presynaptic action potential and the EPSP, which accounts for what Sherrington termed the *synaptic delay.* Because Ca^{2+} channels open more slowly than Na^{+} channels, and the inward Ca^{2+} driving force increases as the neuron repolarizes, Ca^{2+} does not begin to enter the presynaptic terminal in full force until the membrane has begun to repolarize. Surprisingly, once Ca^{2+} enters the terminal, transmitter is rapidly released with a delay of only a few hundred microseconds. Thus, the synaptic delay is largely attributable to the time required to open Ca^{2+} channels. The astonishing speed of Ca^{2+} action indicates that, prior to Ca^{2+} influx, the biochemical machinery underlying the release process must already exist in a primed and ready state. Such rapid kinetics are vital for neuronal information processing and require elegant molecular mechanisms that we shall consider later.

A presynaptic action potential normally produces only a brief rise in presynaptic Ca^{2+} concentration because the Ca^{2+} channels open only for a short time. In addition, Ca^{2+} influx is localized at the active zone. These two properties contribute to a concentrated local pulse of Ca^{2+} that induces a burst of transmitter release (Figure 15–5B). As we shall see later in this chapter, the duration of the action potential regulates the amount of Ca^{2+} that flows into the terminal and thus the amount of transmitter release.

To determine how much Ca^{2+} is needed to trigger release, the Neher and Sakmann groups introduced into the presynaptic terminal an inactive form of Ca^{2+} complexed within a light-sensitive *chemical cage.* They also loaded the terminals with a Ca^{2+}-sensitive fluorescent dye to assay the intracellular free Ca^{2+} concentration. By uncaging the Ca^{2+} ions with a flash of light, they could trigger transmitter release by a uniform and quantifiable increase in Ca^{2+} concentration. These experiments revealed that a rise in Ca^{2+} concentration of less than 1 μM is sufficient to induce release of some transmitter, but approximately 10 to 30 μM Ca^{2+} is required to release the amount normally observed during an action potential. Here again, the relationship between Ca^{2+} concentration and transmitter release is highly nonlinear, consistent with a model in which at least four or five Ca^{2+} ions must bind to the Ca^{2+} sensor to trigger release (Figure 15–5C,D).

Several Classes of Calcium Channels Mediate Transmitter Release

Calcium channels are found in all nerve cells and in many nonneuronal cells. In skeletal and cardiac muscle cells, they are important for excitation-contraction coupling; in endocrine cells, they mediate release of hormones. Neurons contain five broad classes of voltage-gated Ca^{2+} channels: the L-type, P/Q-type, N-type, R-type, and T-type, which are encoded by distinct but closely related genes that can be divided into three gene families based on amino acid sequence similarity. L-type channels are encoded by the Ca_V1 family. Members of the Ca_V2 family comprise P/Q- ($Ca_V2.1$), N- ($Ca_V2.2$), and R-type ($Ca_V2.3$) channels. Finally, T-type channels are encoded by the Ca_V3 gene family. Each channel type has specific biophysical and pharmacological properties and physiological functions (Table 15–1).

Calcium channels are multimeric proteins whose distinct properties are determined by their pore-forming subunit, the α_1-subunit. The α_1-subunit is homologous to the α-subunit of the voltage-gated Na^{+}

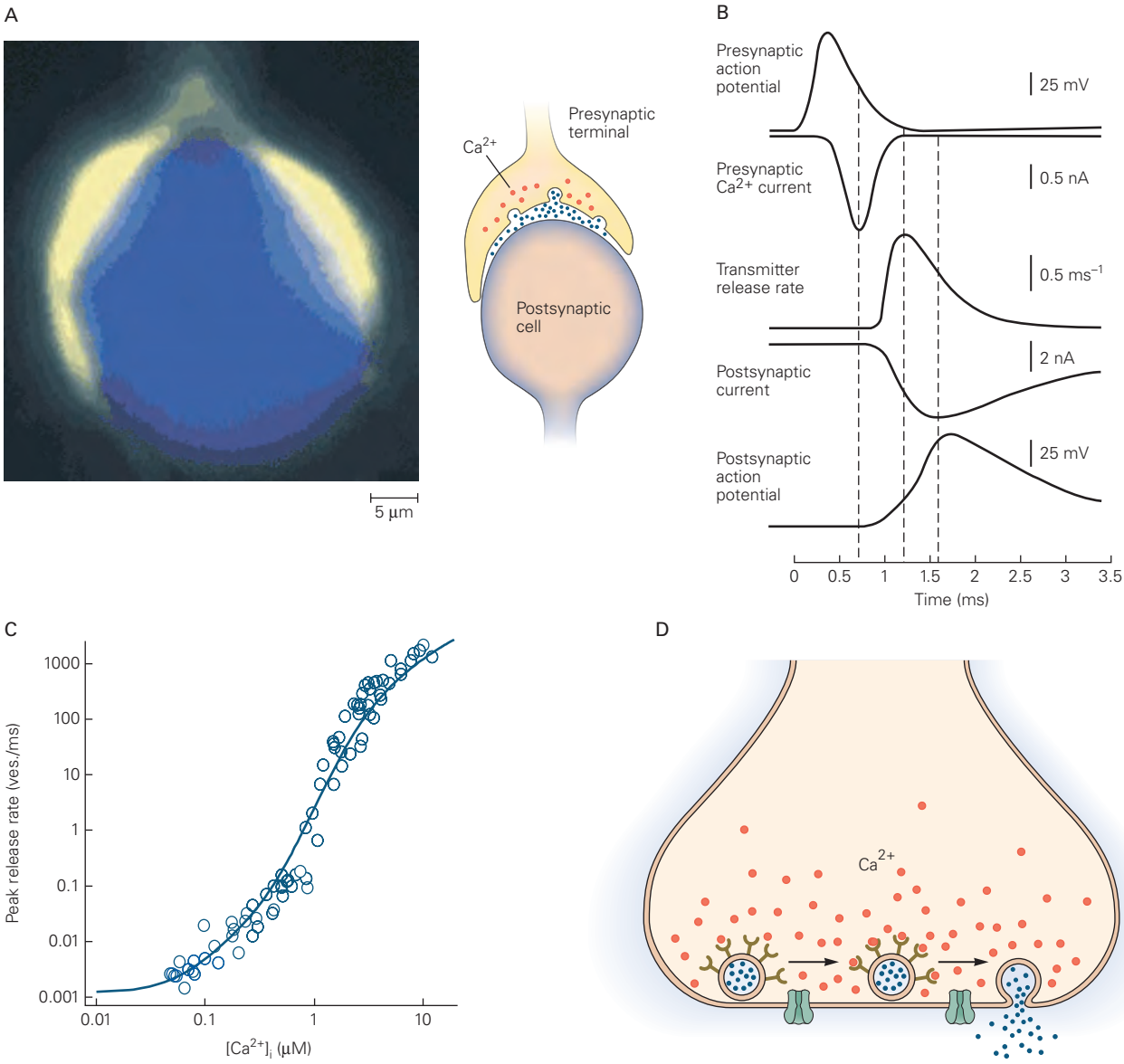

Figure 15–5 The precise relation between presynaptic Ca^{2+} and transmitter release at a central synapse has been measured. (Reproduced, with permission, from Meinrenken, Borst, and Sakmann 2003, and Sun et al. 2007. Parts A and B: Copyright © 2003 John Wiley and Sons.)

A. The large presynaptic terminal of the calyx of Held in the mammalian brain stem engulfs a postsynaptic cell body. The fluorescence image at left shows a calyx filled with a Ca^{2+}-sensitive dye.

B. Time courses for several synaptic events. The **dashed lines** indicate the timing of the peak responses for the Ca^{2+} current, transmitter release, and postsynaptic current.

C. Transmitter release is steeply dependent on the Ca^{2+} concentration in the presynaptic terminal. The calyx was loaded with a caged Ca^{2+} compound that releases its bound Ca^{2+} in response to a flash of ultraviolet light and with a Ca^{2+}-sensitive dye that allows the intracellular Ca^{2+} concentration to be measured. By controlling the intensity of light, one can regulate the increase in Ca^{2+} in the presynaptic terminal. The plot, on a logarithmic scale, shows the relation between the rate of vesicle release and intracellular Ca^{2+} concentration. The **blue line** depicts a fit of the data by a model that assumes that release is triggered by a major Ca^{2+} sensor that binds five Ca^{2+} ions, resulting in a Ca^{2+} cooperativity of five. Due to the nonlinear relationship between $Ca^{2+}$and release, small increments in Ca^{2+} at concentrations of more than 1 µm cause massive increases in release.

D. The release of transmitter from a vesicle requires the binding of five Ca^{2+} ions to a Ca^{2+}-sensing synaptic vesicle protein. In the figure, Ca^{2+} ions bind to five sensors present on a single vesicle; in reality, each sensor molecule binds multiple Ca^{2+} ions.

Table 15–1 Voltage-Gated Ca^{2+} Channels of Neurons

Channel	Former name	Ca^{2+} channel type	Tissue	Blocker	Voltage dependence[1]	Function
$Ca_V1.1–1.4$	$\alpha_{1C,D,F,S}$	L	Muscle, neurons	Dihydropyridines	HVA	Contraction, slow and some limited fast release
$Ca_V2.1$	α_{1A}	P/Q	Neurons	ω-Agatoxin (spider venom)	HVA	Fast release +++
$Ca_V2.2$	α_{1B}	N	Neurons	ω-Conotoxin (cone snail venom)	HVA	Fast release ++
$Ca_V2.3$	α_{1E}	R	Neurons	SNX-482 (tarantula venom)	HVA	Fast release +
$Ca_V3.1–3.3$	$\alpha_{1G,H,I}$	T	Muscle, neurons	Mibefradil (limited selectivity)	LVA	Pacemaker firing

[1]HVA, high voltage activated; LVA, low voltage activated.

channel, comprised of four repeats of a domain with six membrane-spanning segments that includes the S4 voltage-sensor and pore-lining P-region (see Figure 8–10). Calcium channels also have auxiliary subunits (termed α_2, β, γ, and δ) that modify the properties of the channel formed by the α_1-subunit. The subcellular localization in neurons of different types of calcium channels also varies. The N- and P/Q-type Ca^{2+} channels are found predominantly in the presynaptic terminal, whereas L-, R-, and T-type channels are found largely in the soma and dendrites.

Four of the types of voltage-gated Ca^{2+} channels—the L-type, P/Q-type, N-type, and R-type—generally require fairly strong depolarization to be activated (voltages positive to −40 to −20 mV are required) and thus are sometimes loosely referred to as *high-voltage-activated* Ca^{2+} channels (Table 15–1). In contrast, T-type channels open in response to small depolarizations around the threshold for generating an action potential (−60 to −40 mV) and are therefore called *low-voltage-activated* Ca^{2+} channels. Because they are activated by small changes in membrane potential, the T-type channels help control excitability at the resting potential and are an important source of the excitatory current that drives the rhythmic pacemaker activity of certain cells in both the brain and heart.

In neurons, the rapid release of conventional transmitters during fast synaptic transmission is mediated mainly by P/Q-type and N-type Ca^{2+} channels, the channel types most concentrated at the active zone. The localization of N-type Ca^{2+} channels at the frog neuromuscular junction has been visualized using a fluorescence-labeled snail toxin that binds selectively to these channels (see Figure 15–4A). The L-type channels are not found in the active zone and thus do not normally contribute to the fast release of conventional transmitters such as ACh and glutamate. However, Ca^{2+} influx through L-type channels is important for slower forms of release that do not occur at specialized active zones, such as the release of neuropeptides from neurons and of hormones from endocrine cells. As we shall see later, regulation of Ca^{2+} influx into presynaptic terminals controls the amount of transmitter release and hence the strength of synaptic transmission.

Mutations in voltage-gated Ca^{2+} channels are responsible for certain acquired and genetic diseases. Timothy syndrome, a developmental disorder characterized by a severe form of autism with impaired cognitive function and a range of other pathophysiological changes, results from a mutation in the α_1-subunit of L-type channels that alters their voltage-dependent gating, thereby affecting dendritic integration. Different point mutations in the P/Q-type channel α_1-subunit give rise to hemiplegic migraine or epilepsy. Patients with Lambert-Eaton syndrome, an autoimmune disease associated with muscle weakness, make antibodies to the P/Q-type channel α_1-subunit that decrease total Ca^{2+} current (Chapter 57).

Transmitter Is Released in Quantal Units

How does the influx of Ca^{2+} trigger transmitter release? Katz and his colleagues provided a key insight into this question by showing that transmitter is released in discrete amounts they called *quanta.* Each quantum of transmitter produces a postsynaptic potential of fixed size, called the *quantal synaptic potential.* The total postsynaptic potential is made up of a large number of quantal potentials. EPSPs seem smoothly graded in amplitude only because each quantal (or unit) potential is small relative to the total potential.

Katz and Fatt obtained the first clue as to the quantal nature of synaptic transmission in 1951 when they observed spontaneous postsynaptic potentials of approximately 0.5 mV at the nerve-muscle synapse of the frog. Like end-plate potentials evoked by nerve stimulation, these small depolarizing responses are largest at the site of nerve-muscle contact and decay electrotonically with distance (see Figure 12–5). Small spontaneous potentials have since been observed in mammalian muscle and in central neurons. Because postsynaptic potentials at vertebrate nerve-muscle synapses are called end-plate potentials, Fatt and Katz called these spontaneous potentials *miniature end-plate potentials*.

Several results convinced Fatt and Katz that the miniature end-plate potentials represented responses to the release of small amounts of ACh, the neurotransmitter used at the nerve-muscle synapse. The time course of the miniature end-plate potentials and the effects of various drugs on them are indistinguishable from the properties of the end-plate potential. Like the end-plate potentials, the miniature end-plate potentials are enhanced and prolonged by prostigmine, a drug that blocks hydrolysis of ACh by acetylcholinesterase. Conversely, they are abolished by agents that block the ACh receptor, such as curare. The miniature end-plate potentials represent responses to small packets of transmitter that are spontaneously released from the presynaptic nerve terminal in the absence of an action potential. Their frequency can be increased by a small depolarization of the presynaptic terminal. They disappear if the presynaptic motor nerve degenerates and reappear when a new motor synapse is formed.

What could account for the small, fixed size of the miniature end-plate potential? Del Castillo and Katz first tested the possibility that each event represents a response to the opening of a *single* ACh receptor-channel. However, application of very small amounts of ACh to the frog muscle end-plate elicited depolarizing postsynaptic responses that were much smaller than the 0.5 mV response of a miniature end-plate potential. This finding made it clear that the miniature end-plate potential represents the opening of more than one ACh receptor-channel. In fact, Katz and Miledi were later able to estimate the voltage response to the elementary current through a single ACh receptor-channel as being only approximately 0.3 μV (Chapter 12). Based on this estimate, a miniature end-plate potential of 0.5 mV would represent the summation of the elementary currents of approximately 2,000 channels. Later work showed that a miniature end-plate potential is the response to the synchronous release of approximately 5,000 molecules of ACh.

What is the relationship of the large end-plate potential evoked by nerve stimulation and the small, spontaneous miniature end-plate responses? This question was first addressed by del Castillo and Katz in a study of synaptic signaling at the nerve-muscle synapse bathed in a solution low in Ca^{2+}. Under this condition, the end-plate potential is reduced markedly, from the normal 70 mV to about 0.5 to 2.5 mV. Moreover, the amplitude of each successive end-plate potential now varies randomly from one stimulus to the next; often, no response can be detected at all (termed *failures*). However, the minimum response above zero—the unit end-plate potential in response to a presynaptic action potential—is identical in amplitude (approximately 0.5 mV) and shape to the spontaneous miniature end-plate potentials. Importantly, the amplitude of each end-plate potential is an integral multiple of the unit potential (Figure 15–6).

Now del Castillo and Katz could ask: How does the rise of intracellular Ca^{2+} that accompanies each action potential affect the release of transmitter? They found that increasing the external Ca^{2+} concentration does not change the amplitude of the unit synaptic potential. However, the proportion of failures decreases and the incidence of higher-amplitude responses (composed of multiple quantal units) increases. These observations show that an increase in external Ca^{2+} concentration does not enhance the *size* of a quantum of transmitter (that is, the number of ACh molecules in each quantum) but rather acts to increase the average number of quanta that are released in response to a presynaptic action potential. The greater the Ca^{2+} influx into the terminal, the larger the number of transmitter quanta released.

Thus, three findings led del Castillo and Katz to conclude that transmitter is released in packets with a fixed amount of transmitter, a quantum: The amplitude of the end-plate potential varies in a stepwise manner at low levels of ACh release, the amplitude of each step increase is an integral multiple of the unit potential, and the unit potential has the same mean amplitude and shape as that of the spontaneous miniature end-plate potentials. Moreover, by analyzing the statistical distribution of end-plate potential amplitudes, del Castillo and Katz and other subsequent researchers were able to show that a single action potential produced a transient increase in the probability that a given quantum of transmitter is released according to a random process, similar to that governing the outcome of a coin toss (Box 15–1).

In the absence of an action potential, the rate of quantal release is low—only one quantum per second is released spontaneously at the end-plate. In contrast, the firing of an action potential releases approximately 150 quanta, each approximately 0.5 mV in amplitude, resulting in a large end-plate potential. Thus, the influx of Ca^{2+} into the presynaptic terminal during an action potential dramatically increases the rate of quantal release by a factor of 150,000, triggering the synchronous release of about 150 quanta in about 1 ms.

Transmitter Is Stored and Released by Synaptic Vesicles

What morphological features of the cell might account for the quantal release of transmitter? The physiological observations indicating that transmitter is released in fixed quanta coincided with the discovery, through electron microscopy, of accumulations of small clear vesicles in the presynaptic terminal. Del Castillo and Katz speculated that the vesicles were organelles for the storage of transmitter, each vesicle stored one quantum of transmitter (amounting to several thousand molecules), and each vesicle released its entire contents into the synaptic cleft in an all-or-none manner at sites specialized for release.

The sites of release, the active zones, contain a cloud of synaptic vesicles that cluster above a fuzzy electron-dense material attached to the internal face of the presynaptic membrane (see Figure 15–4A). At all synapses, the vesicles are typically clear, small, and ovoid, with a diameter of approximately 40 nm (in distinction with the large dense-core vesicles described in Chapter 16). Although most synaptic vesicles do not contact the active zone, some are physically bound. These are called the *docked* vesicles and are thought to

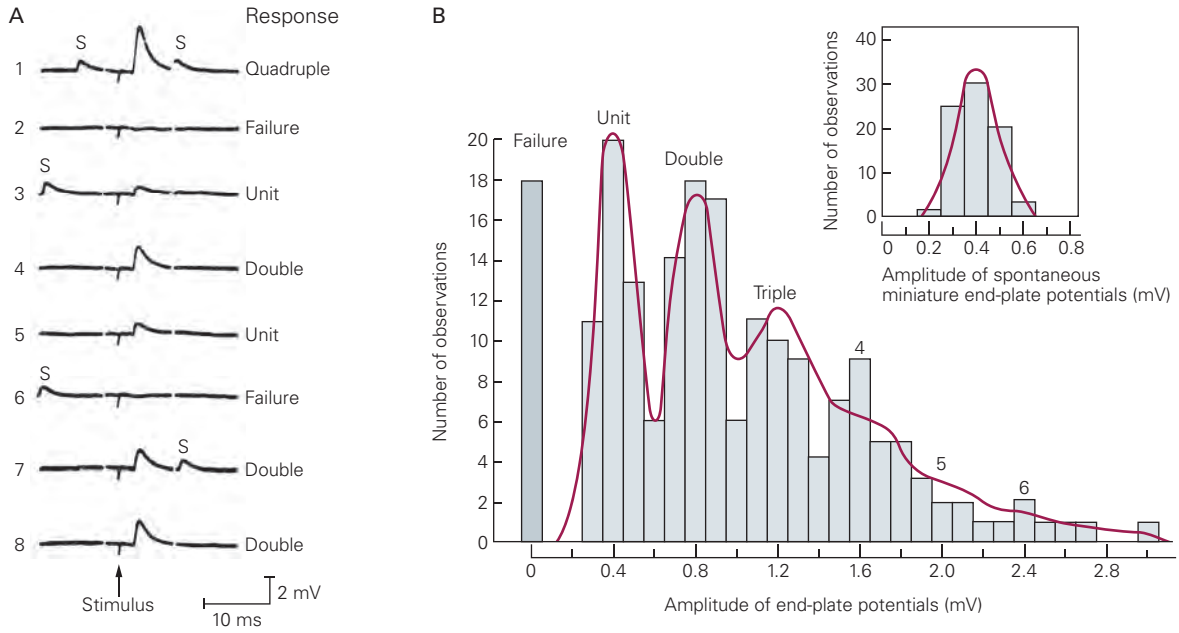

Figure 15–6 **Neurotransmitter is released in fixed increments. Each increment or quantum of transmitter produces a unit end-plate potential of fixed amplitude.** The amplitude of the response evoked by nerve stimulation is thus equal to the amplitude of the unit end-plate potential multiplied by the number of quanta of transmitter released.

A. Intracellular recordings from a muscle fiber at the end-plate show the change in postsynaptic potential when eight consecutive stimuli of the same size are applied to the motor nerve. To reduce transmitter release and to keep the end-plate potentials small, the tissue is bathed in a Ca^{2+}-deficient (and magnesium-rich) solution. The postsynaptic responses to the nerve stimulus vary. Two of the eight presynaptic stimuli elicit no EPSP (failures), two produce unit potentials, and the others produce EPSPs that are approximately two to four times the amplitude of the unit potential. Note that the spontaneous miniature end-plate potentials (**S**), which occur at random intervals in the traces, are the same size as the unit potential. (Adapted, with permission, from Liley 1956.)

B. After many end-plate potentials are recorded, the number of responses with a given amplitude is plotted as a function of this amplitude in the histogram shown here. The distribution of responses falls into a number of peaks. The first peak, at 0 mV, represents failures. The first peak of responses, at 0.4 mV, represents the unit potential, the smallest elicited response. The unit response has the same amplitude as the spontaneous miniature end-plate potentials (inset), indicating that the unit response is caused by the release of a single quantum of transmitter. The other peaks in the histogram are integral multiples of the amplitude of the unit potential; that is, responses are composed of two, three, four, or more quantal events.

The number of responses under each peak divided by the total number of events in the entire histogram is the probability that a single presynaptic action potential triggers the release of the number of quanta that comprise the peak. For example, if there are 30 events in the peak corresponding to the release of two quanta out of a total of 100 events recorded, the probability that a presynaptic action potential releases exactly two quanta is 30/100 or 0.3. This probability follows a Poisson distribution (**red curve**). This theoretical distribution is composed of the sum of several Gaussian functions. The spread of the unit peak (standard deviation of the Gaussian function) reflects the fact that the amount of transmitter in a quantum, and hence the amplitude of the quantal postsynaptic response, varies randomly about a mean value. The successive Gaussian peaks widen progressively because the variability (or variance) associated with each quantal event increases linearly with the number of quanta per event. The distribution of amplitudes of the spontaneous miniature potentials (inset) is fit by a Gaussian curve whose width is identical to that of the Gaussian curve for the unit synaptic responses. (Adapted, with permission, from Boyd and Martin 1956.)

be the ones immediately available for release (sometimes referred to as the *readily releasable pool*). At the neuromuscular junction, the active zones are linear structures (see Figure 15–4), whereas in central synapses, they are disc-shaped structures approximately 0.1 μm^2 in area with dense projections pointing into the cytoplasm. Active zones are generally found in precise apposition to the postsynaptic membrane patches that contain the neurotransmitter receptors (see Figure 13–2). Thus, presynaptic and postsynaptic specializations are functionally and morphologically attuned to each other, sometimes precisely aligned in structural "nanocolumns." As we shall learn later, several key active zone proteins involved in transmitter release have now been identified and characterized.

Box 15–1 Synaptic Strength Depends on the Probability of Transmitter Release and Other Quantal Parameters

The mean size of a synaptic response E evoked by an action potential has often been described as the product of the total number of releasable quanta (n), the probability that an individual quantum of transmitter is released (p), and the size of the response to a quantum (a):

$$E = n \cdot p \cdot a.$$

These parameters are statistical terms, useful for describing the size and variability of the postsynaptic response. At some but not all central synapses, they can also be assigned to biological processes. We begin by focusing on synapses of the kind envisioned by Katz and colleagues, where the interpretation of the parameters is most straightforward. At these synapses, the presynaptic terminal typically contains multiple active zones, and each active zone releases at most a single vesicle in response to an action potential (*univesicular release*).

We then consider another kind of synapse that requires a different interpretation. At these synapses, each active zone can release multiple vesicles in response to a single action potential (*multivesicular release*), leading to very high concentrations of transmitter in the synaptic cleft that can cause the postsynaptic receptors to become saturated with transmitter.

Univesicular Release at Multiple Active Zones

In the simplest case, the parameter a is the response of the postsynaptic membrane to the release of a single vesicle's contents of transmitter. It is assumed that transmitter is packaged in synaptic vesicles, that release of the contents of a vesicle is a stereotyped, all-or-none event, and that single release events occur in physical isolation from each other. Quantal size depends on the amount of transmitter in a vesicle and on the properties of the postsynaptic cell, such as the membrane resistance and capacitance (which can be independently estimated) and the responsiveness of the postsynaptic membrane to the transmitter substance. This can also be measured experimentally by the postsynaptic membrane's response to the application of a known amount of transmitter.

The parameter n describes the maximum number of quantal units that can be released in response to a single action potential if the probability p reaches 1.0. At some central synapses, this maximum may be imposed by the number of release sites (active zones) in the terminals of a presynaptic neuron that contact a given postsynaptic neuron. Multiple studies have found that for this kind of connection n corresponds with the number of release sites determined by electron microscopy, as if those sites obeyed a rough rule wherein a presynaptic action potential triggers the exocytosis of at most one vesicle per active zone.

The parameter p represents the likelihood of vesicle release. This likelihood encompasses a series of events necessary for a particular release site to contribute a quantal event: (1) The active zone must be loaded with at least one releasable vesicle (a process referred to as vesicle mobilization); (2) the presynaptic action potential must evoke Ca^{2+} influx in sufficient quantity and proximity to the vesicle; and (3) the Ca^{2+}-sensitive synaptotagmin and SNARE machinery must cause the vesicle to fuse and discharge its contents.

Here, we focus mainly on the determinants of p. We can treat quantal release at a single active zone as a random event with only two possible outcomes in response to an action potential—the quantum of transmitter is or is not released. Because the quantal responses from different active zones are thought to occur independently of each other in some situations, this is similar to tossing a set of n coins in the air and counting the number of heads or tails. The equivalent of individual coin flips (Bernoulli trials) are then totaled up in a binomial distribution, where p stands for the average probability of success (that is, the probability that any given quantum will be released) and q (equal to $1 - p$) stands for the mean probability of failure.

Both the average probability (p) that an individual quantum will be released and the maximal number (n)

(*continued*)

Quantal transmission has been demonstrated at all chemical synapses so far examined. Nevertheless, the efficacy of transmitter release from a single presynaptic cell onto a single postsynaptic cell varies widely in the nervous system and depends on several factors: (1) the number of individual synapses between a pair of presynaptic and postsynaptic cells (that is, the number of presynaptic boutons that contact the postsynaptic cell); (2) the number of active zones in an individual synaptic terminal; and (3) the probability that a presynaptic action potential will trigger release of one or more quanta of transmitter

Box 15–1 Synaptic Strength Depends on the Probability of Transmitter Release and Other Quantal Parameters (continued)

of releasable quanta are assumed to be constant. (Any reduction in the store of vesicles is assumed to be quickly replenished after each stimulus.) The product of n and p yields an estimate m of the mean number of quanta that will be released. This mean is called the *quantal content* or *quantal output.*

Calculation of the probability of transmitter release can be illustrated with the following example. Consider a terminal that has a releasable store of five quanta ($n = 5$). Assuming $p = 0.1$, then the probability that an individual quantum will not be released from the terminals (q) is $1 - p$, or 0.9. We can now determine the probability that a stimulus will release no quanta (failure), a single quantum, or any other number of quanta (up to n).

The probability that none of the five available quanta will be released by a given stimulus is the product of the individual probabilities that each quantum will not be released: $q^5 = (0.9)^5$, or 0.59. We would thus expect to see 59 failures in a hundred stimuli. The probabilities of observing zero, one, two, three, four, or five quanta are represented by the successive terms of the binomial expansion:

$$(q + p)^5 = q^5 \text{ (failures)} + 5\,q^4p \text{ (1 quantum)} + 10\,q^3p^2 \text{ (2 quanta)} + 10\,q^2p^3 \text{ (3 quanta)} + 5\,qp^4 \text{ (4 quanta)} + p^5 \text{ (5 quanta).}$$

Thus, in 100 stimuli, the binomial expansion would predict 33 single unit responses, 7 double responses, 1 triple response, and 0 quadruple or quintuple responses.

Values for the quantal output m vary from approximately 100 to 300 at the vertebrate nerve-muscle synapse, the squid giant synapse, and *Aplysia* central synapses, to as few as 1 to 4 in the synapses of the sympathetic ganglion and spinal cord of vertebrates. The probability of release p also varies, ranging from as high as 0.7 at the neuromuscular junction in the frog and 0.9 in the crab down to around 0.1 at some mammalian central synapses. Estimates for n range from as much as 1,000 (at the vertebrate nerve-muscle synapse) to 1 (at single terminals of mammalian central neurons).

This numerical example illustrates a characteristic feature of synapses with simple binomial features—their substantial variability. This holds just as strongly whether p is high or low. For example, for $p = 0.9$ and 100 stimuli, the binomial expansion predicts 0 failures, 0 single unit responses, 1 double response, 7 triple responses, 33 quadruple responses, and 59 quintuple responses, the mirror-image of the distribution for $p = 0.1$. Even if each sequential event that supports vesicle release is highly likely, the aggregate strength of the synapse will vary widely.

Multivesicular Release with Receptor Saturation

One well-studied mechanism for achieving high synaptic reliability is through the release of multiple vesicles onto a single postsynaptic site. In the extreme, this can release sufficient amounts of transmitter in the synaptic cleft to cause the postsynaptic receptor binding sites to become fully occupied by transmitter (receptor saturation).

Under these conditions, the postsynaptic response will reach a maximal amplitude. Further release of transmitter, for example in response to a modulatory neurotransmitter, would fail to increase the postsynaptic response. Variability in response size would shrink greatly if, say, three to five vesicles worth of transmitter activated the same number of receptors as a single vesicle. The postsynaptic response would be highly stereotyped (it would appear to result from release of a single quantum of transmitter) even though the presynaptic terminal was releasing multiple vesicles. However, the binomial treatment could still retain some usefulness as a way of adding up the contributions of multiple synapses of this kind, so long as each synapse released transmitter simultaneously and independently. But in such a case, n, p, and a would take on biological meanings different from those in which only a single vesicle could be released per synapse.

at an active zone. As we will see later, release probability can be powerfully regulated as a function of neuronal activity.

In the central nervous system, most presynaptic boutons have only a single active zone where an action potential usually releases at most a single quantum of transmitter in an all-or-none manner. However, at some central synapses, such as the calyx of Held, transmitter is released from a large presynaptic terminal that may contain many active zones and thus can release a large number of quanta in response to a single presynaptic action potential. Central neurons also vary in

the number of synapses that a typical presynaptic cell forms with a typical postsynaptic cell. Whereas most central neurons form only a few synapses with any one postsynaptic cell, a single climbing fiber from neurons in the inferior olive forms up to 10,000 terminals on a single Purkinje neuron in the cerebellum! Finally, the mean probability of transmitter release from a single active zone also varies widely among presynaptic terminals, from less than 0.1 (that is, a 10% chance that a presynaptic action potential will trigger release of a vesicle) to greater than 0.9. This wide range of probabilities can even be seen among the boutons at individual synapses between a specific type of presynaptic cell and a specific type of postsynaptic cell.

Thus, central neurons vary widely in the efficacy and reliability of synaptic transmission. Synaptic *reliability* is defined as the probability that an action potential in a presynaptic cell leads to some measurable response in the postsynaptic cell—that is, the probability that a presynaptic action potential will release one or more quanta of transmitter. *Efficacy* refers to the mean amplitude of the synaptic response, which depends on both the reliability of synaptic transmission and on the mean size of the response when synaptic transmission does occur.

Most central neurons communicate at synapses that have a low probability of transmitter release. The high failure rate of release at most central synapses (that is, their low release probability) is not a *design defect* but serves a purpose. As we discuss later, this feature allows transmitter release to be regulated over a wide dynamic range, which is important for adapting neural signaling to different behavioral demands. In synaptic connections where a low probability of release is deleterious for function, this limitation can be overcome by simply having many active zones in one synapse, as is the case at the calyx of Held and the nerve-muscle synapse. Both contain hundreds of independent active zones, so an action potential reliably releases 150 to 250 quanta, ensuring that a presynaptic signal is always followed by a postsynaptic action potential. Reliable transmission at the neuromuscular junction is essential for survival. An animal would not survive if its ability to move away from a predator was hampered by a low-probability response. Another strategy for increasing reliability is to use multivesicular release, the simultaneous fusion of multiple vesicles at a single active zone, to ensure that postsynaptic receptors are consistently exposed to a saturating concentration of neurotransmitter (see Box 15–1).

Not all chemical signaling between neurons depends on the synaptic machinery described earlier. Some substances, such as certain lipid metabolites and the gas nitric oxide (Chapter 14), can diffuse across the lipid bilayer of the membrane. Others can be moved out of nerve endings by carrier proteins if their intracellular concentration is sufficiently high. Plasma membrane transporters for glutamate or GABA normally take up transmitter into a cell from the synaptic cleft following a presynaptic action potential (Chapter 13). However, in some glial cells of the retina, the direction of glutamate transport can be reversed under certain conditions, causing glutamate to leave the cell through the transporter into the synaptic cleft. Still other substances simply leak out of nerve terminals at a low rate. Surprisingly, approximately 90% of the ACh that leaves the presynaptic terminals at the neuromuscular junction does so through continuous leakage. This leakage is ineffective, however, because it is diffuse and not targeted to receptors at the end-plate region and because it is continuous and low level rather than synchronous and concentrated.

Synaptic Vesicles Discharge Transmitter by Exocytosis and Are Recycled by Endocytosis

The quantal hypothesis of del Castillo and Katz has been amply confirmed by direct experimental evidence that synaptic vesicles do indeed package neurotransmitter and that they release their contents by directly fusing with the presynaptic membrane, a process termed *exocytosis*.

Forty years ago, Victor Whittaker discovered that the synaptic vesicles in the motor nerve terminals of the electric organ of the electric fish *Torpedo* contain a high concentration of ACh. Later, Thomas Reese and John Heuser and their colleagues obtained electron micrographs that caught vesicles in the act of exocytosis. To observe the brief exocytotic event, they rapidly froze the nerve-muscle synapse by immersing it in liquid helium at precisely defined intervals after the presynaptic nerve was stimulated. In addition, they increased the number of quanta of transmitter discharged with each nerve impulse by applying the drug 4-aminopyridine, a compound that blocks certain voltage-gated K^+ channels, thus increasing the duration of the action potential and enhancing Ca^{2+} influx. (The spike broadening produced by this pharmacological intervention resembles spike broadening resulting from cumulative inactivation of K^+ channels during repetitive firing; see Figure 15–15C.) In both cases, prolonged action potentials evoke greater opening of presynaptic Ca^{2+} channels.

These techniques provided clear images of synaptic vesicles at the active zone during exocytosis. Using a technique called *freeze-fracture electron microscopy*,

Reese and Heuser noted deformations of the presynaptic membrane along the active zone immediately after synaptic activity, which they interpreted as invaginations of the cell membrane caused by fusion of synaptic vesicles. These deformations lay along one or two rows of unusually large intramembranous particles, visible along both margins of the presynaptic density. Many of these particles are now thought to be voltage-gated Ca^{2+} channels (Figure 15–7). The particle density (approximately 1,500 per μm^2) is similar to the Ca^{2+} channel density that is thought to be present in the presynaptic plasma membrane at the active zone. Moreover, the proximity of the particles to the release site is consistent with the short time interval between the onset of the Ca^{2+} current and the release of transmitter.

Finally, Heuser and Reese found that these deformations are transient; they occur only when vesicles are discharged and do not persist after transmitter has been released. Thin-section electron micrographs revealed a number of omega-shaped (Ω) structures with the appearance of synaptic vesicles that have just fused with the membrane, prior to the complete collapse of the vesicle membrane into the plasma membrane (Figure 15–7B). Heuser and Reese confirmed this idea by showing that the number of Ω-shaped structures is directly correlated with the size of the EPSP when they varied the concentration of 4-aminopyridine to alter the amount of transmitter release. These morphological studies provide striking evidence that transmitter is released from synaptic vesicles by means of exocytosis.

Following exocytosis, the excess membrane added to the presynaptic terminal is retrieved. In images of presynaptic terminals made 10 to 20 seconds after stimulation, Heuser and Reese observed new structures at the plasma membrane, the coated pits, which are formed by the protein *clathrin* that helps mediate membrane retrieval through the process of endocytosis (Figure 15–7C). Several seconds later, the coated pits are seen to pinch off from the membrane and appear as coated vesicles in the cytoplasm. As we will see later, endocytosis through coated pit formation represents one of several means of vesicle membrane retrieval.

Capacitance Measurements Provide Insight Into the Kinetics of Exocytosis and Endocytosis

In certain neurons with large presynaptic terminals, the increase in surface area of the plasma membrane during exocytosis can be detected in electrical measurements as increases in membrane capacitance. As we saw in Chapter 9, the capacitance of the membrane is proportional to its surface area. Erwin Neher discovered that one could use measurements of capacitance to monitor exocytosis in secretory cells.

In adrenal chromaffin cells (which release epinephrine and norepinephrine) and in mast cells of the rat peritoneum (which release histamine and serotonin), individual dense-core vesicles are large enough to permit measurement of the increase in capacitance associated with fusion of a single vesicle. Release of transmitter in these cells is accompanied by stepwise increases in capacitance, followed somewhat later by stepwise decreases, which reflect the retrieval and recycling of the excess membrane (Figure 15–8).

In neurons, the changes in capacitance caused by fusion of single, small synaptic vesicles are usually too small to resolve. In certain favorable synaptic preparations that release large numbers of vesicles (such as the giant presynaptic terminals of bipolar neurons in the retina), membrane depolarization triggers a transient smooth rise and fall in the total capacitance of the terminal as a result of the exocytosis and retrieval of the membrane from hundreds of individual synaptic vesicles (Figure 15–8C). These results provide direct measurements of the rates of membrane fusion and retrieval.

Exocytosis Involves the Formation of a Temporary Fusion Pore

Morphological studies of mast cells using rapid freezing suggest that exocytosis depends on the formation of a temporary fusion pore that spans the membranes of the vesicle and plasma membranes. In electrophysiological studies of capacitance increases in mast cells, a channel-like fusion pore was detected in the electrophysiological recordings prior to complete fusion of vesicles and cell membranes. This fusion pore starts out with a single-channel conductance of approximately 200 pS, similar to that of gap-junction channels, which also bridge two membranes. During exocytosis, the pore rapidly dilates, probably from around 5 to 50 nm in diameter, and the conductance increases dramatically (Figure 15–9A).

The fusion pore is not just an intermediate structure leading to exocytosis of transmitter, as transmitter can be released through the pore prior to pore expansion and vesicle collapse. This was first shown by amperometry, a method that uses an extracellular carbon-fiber electrode to detect certain amine neurotransmitters, such as serotonin, based on an electrochemical reaction between the transmitter and the electrode that generates an electrical current proportional to the local transmitter concentration. Firing of an action potential in serotonergic cells leads to a large transient increase in electrode

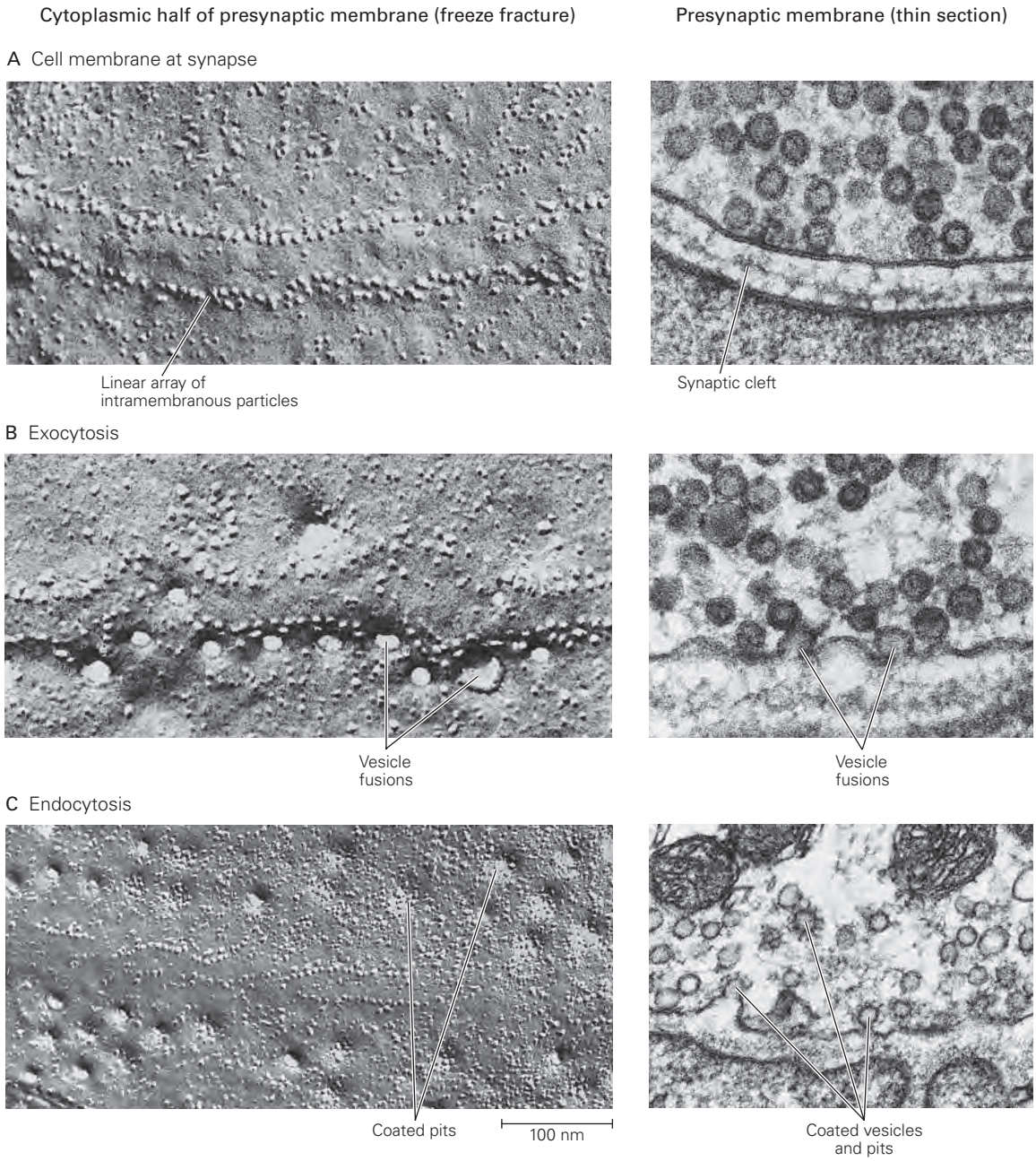

Figure 15–7 **Synaptic vesicles release transmitter by exocytosis and are retrieved by endocytosis.** The images on the left are freeze-fracture electron micrographs at a neuromuscular junction. The freeze-fracture technique exposes the intramembranous area to view by splitting the membrane along the hydrophobic interior of the lipid bilayer. The views shown are of the cytoplasmic leaflet of the bilayer presynaptic membrane looking up from the synaptic cleft (see Figure 15–4A). Conventional thin-section electron micrographs on the right show cross-section views of the presynaptic terminal, synaptic cleft, and postsynaptic muscle membrane. (Reproduced, with permission, from Heuser and Reese 1981. Permission conveyed through Copyright Clearance Center, Inc.)

A. Parallel rows of intramembranous particles arrayed on either side of an active zone are thought to be the voltage-gated Ca^{2+} channels essential for transmitter release (see Figure 15–4A). The thin-section image at right shows the synaptic vesicles adjacent to the active zone.

B. Synaptic vesicles release transmitter by fusing with the plasma membrane (exocytosis). Here, synaptic vesicles are caught in the act of fusing with the plasma membrane by rapid freezing of the tissue within 5 ms after a depolarizing stimulus. Each depression in the plasma membrane represents the fusion of one synaptic vesicle. In the micrograph at right, fused vesicles are seen as Ω-shaped structures.

C. After exocytosis, synaptic vesicle membrane is retrieved by endocytosis. Within approximately 10 seconds after fusion of the vesicles with the presynaptic membrane, coated pits form. After another 10 seconds, the coated pits begin to pinch off by endocytosis to form coated vesicles. These vesicles store the membrane proteins of the original synaptic vesicle and also molecules captured from the extracellular medium. The vesicles are recycled at the terminals or are transported to the cell body, where the membrane constituents are degraded or recycled (see Chapter 7).

A Mast cell before and after exocytosis of secretory vesicles

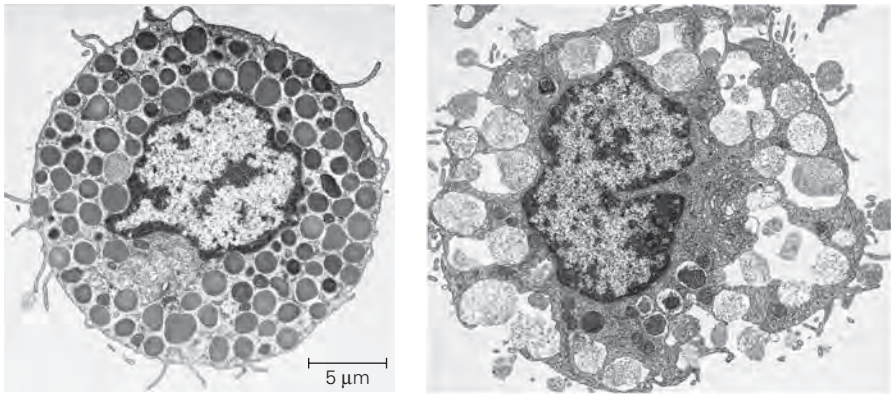

B Membrane capacitance during and after exocytosis of mast cell vesicles

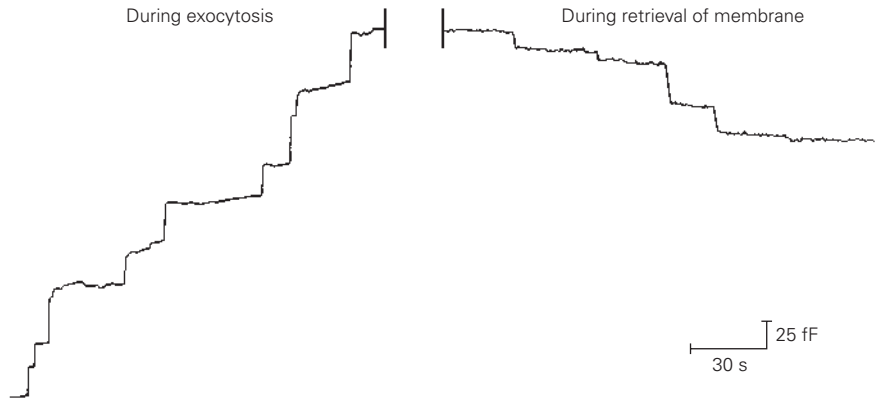

C Retinal bipolar neuron terminal

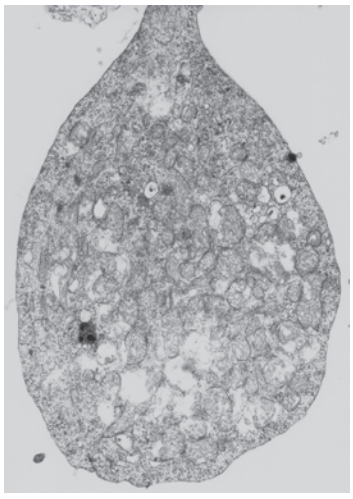

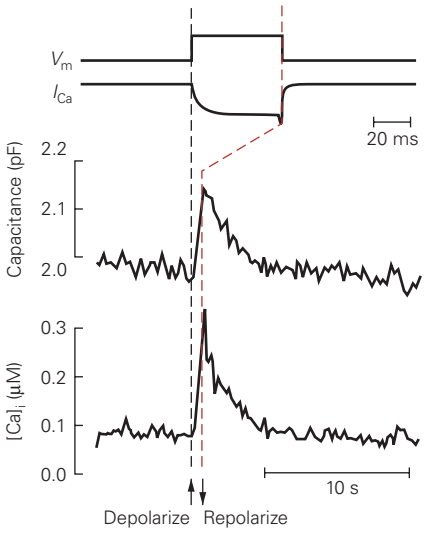

current, corresponding to the exocytosis of the contents of a single dense-core vesicle. In some instances, these large transient increases are preceded by smaller, longer-lasting current signals that reflect leakage of transmitter through a fusion pore that flickers open and closed several times prior to complete fusion (Figure 15–9B).

It is possible that transmitter can also be released solely through transient fusion pores that fleetingly connect vesicle lumen and extracellular space without full collapse of the vesicle membrane into the plasma membrane. Capacitance measurements for exocytosis of large dense-core vesicles in neuroendocrine cells show that the fusion pore can open and close rapidly and reversibly. The reversible opening and closing of a fusion pore represents a very rapid method of membrane retrieval. The circumstances under which the small clear vesicles at fast synapses discharge transmitter through a fusion pore, as opposed to full membrane collapse, are uncertain.

The Synaptic Vesicle Cycle Involves Several Steps

When firing at high frequency, a typical presynaptic neuron is able to maintain a high rate of transmitter release. This can result in the exocytosis of a large number of vesicles over time, more than the number morphologically evident within the presynaptic terminal. To prevent the supply of vesicles from being rapidly depleted during fast synaptic transmission, used vesicles are rapidly retrieved and recycled. Because nerve terminals are usually some distance from the cell body, replenishing vesicles by synthesis in the cell body and transport to the terminals would be too slow to be practical at fast synapses.

Synaptic vesicles are released and reused in a simple cycle. Vesicles fill with neurotransmitter and cluster in the nerve terminal. They then dock at the active zone where they undergo a complex *priming* process that makes vesicles competent to respond to the Ca^{2+} signal that triggers the fusion process (Figure 15–10A). Numerous mechanisms exist for retrieving the synaptic vesicle membrane following exocytosis, each with a distinct time course (Figure 15–10B).

The first, most rapid mechanism involves the reversible opening and closing of the fusion pore, without the full fusion of the vesicle membrane with the plasma membrane. In the *kiss-and-stay* pathway, the vesicle remains at the active zone after the fusion pore closes, ready for a second release event. In the *kiss-and-run* pathway, the vesicle leaves the active zone after the fusion pore closes, but is competent for rapid rerelease. These pathways are thought to be used preferentially during stimulation at low frequencies.

Jorgensen and colleagues have described a second pathway of *ultrafast* clathrin-independent endocytosis that is 200 times faster than the classical clathrin-mediated pathway. Beginning just 50 ms after exocytosis, ultrafast endocytosis occurs just outside of the active zone.

Stimulation at higher frequencies recruits a third, slower recycling pathway that uses clathrin to retrieve the vesicle membrane after fusion with the plasma membrane. Clathrin forms a lattice-like structure that surrounds the membrane during endocytosis, giving rise to the appearance of a coat around the coated pits observed by Heuser and Reese. In this pathway, the retrieved vesicular membrane must be recycled through an endosomal compartment before the vesicles can be reused. Clathrin-mediated recycling requires up

Figure 15–8 (Opposite) Changes in capacitance reveal the time course of exocytosis and endocytosis.

A. Electron micrographs show a mast cell before (*left*) and after (*right*) exocytosis. Mast cells are secretory cells of the immune system that contain large dense-core vesicles filled with the transmitters histamine and serotonin. Exocytosis of the secretory vesicles is normally triggered by the binding of antigen complexed to an immunoglobulin (IgE). Under experimental conditions, massive exocytosis can be triggered by the inclusion of a nonhydrolyzable analog of guanosine triphosphate (GTP) in an intracellular recording electrode. (Reproduced, with permission, from Lawson et al. 1977. Permission conveyed through Copyright Clearance Center, Inc.)

B. Stepwise increases in capacitance reflect the successive fusion of individual secretory vesicles with the mast cell membrane. The step increases are unequal because of variability in the membrane area of the vesicles. After exocytosis, the membrane added through fusion is retrieved through endocytosis. Endocytosis of individual vesicles gives rise to the stepwise decreases in membrane capacitance. In this way, the cell maintains a constant size. (Units are femtofarads, where 1 fF = 0.1 μm^2 of membrane area.) (Adapted, with permission, from Fernandez, Neher, and Gomperts 1984.)

C. The giant presynaptic terminals of bipolar neurons in the retina are more than 5 µm in diameter, permitting direct patch-clamp recordings of membrane capacitance and Ca^{2+} current. A brief depolarizing voltage-clamp step in membrane potential (V_m) elicits a large sustained Ca^{2+} current (I_{Ca}) and a rise in the cytoplasmic Ca^{2+} concentration, $[Ca]_i$. This results in the fusion of several thousand small synaptic vesicles with the cell membrane, leading to an increase in total membrane capacitance. The increments in capacitance caused by fusion of individual vesicles are too small to resolve. As the internal Ca^{2+} concentration falls back to its resting level upon repolarization, the extra membrane area is retrieved and capacitance returns to its baseline value. The increases in capacitance and Ca^{2+} concentration outlast the brief depolarization and Ca^{2+} current (note different time scales) because of the relative slowness of endocytosis and Ca^{2+} metabolism. (Micrograph reproduced, with permission, from Zenisek et al. 2004. Copyright © 2004 Society for Neuroscience.)

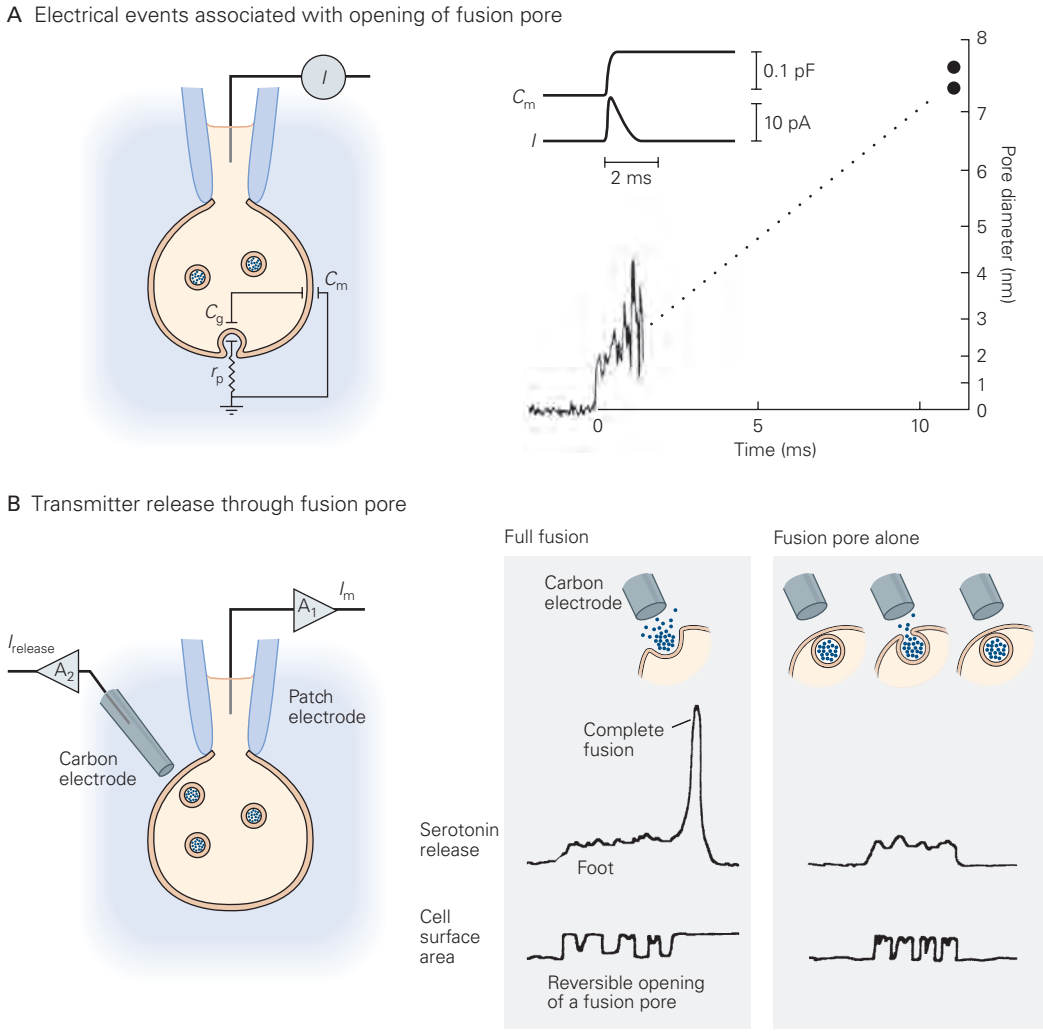

Figure 15–9 Reversible opening and closing of fusion pores.

A. A whole cell patch clamp is used to record membrane current associated with the opening of a fusion pore. As a vesicle fuses with the plasma membrane, the capacitance of the vesicle (C_g) is initially connected to the capacitance of the rest of the cell membrane (C_m) through the high resistance of the fusion pore (r_p). Because the membrane potential of the vesicle (lumenal side negative) is normally much more negative than the membrane potential of the cell, charge flows from the vesicle to the cell membrane during fusion. This transient current (I) is associated with the increase in membrane capacitance (C_m).

The magnitude of the conductance of the fusion pore (g_p) can be calculated from the time constant of the transient current according to $\tau = C_g r_p = C_g / g_p$. The pore diameter can be calculated from the pore conductance, assuming that the pore spans two lipid bilayers and is filled with a solution whose resistivity is equal to that of the cytoplasm. The plot on the right shows the pore has an initial conductance of approximately 200 pS, similar to the conductance of a gap-junction channel, corresponding to a pore diameter of approximately 2 nm. The pore diameter and conductance rapidly increase as the pore dilates to approximately 7 to 8 nm in 10 ms (**filled circles**). (Reproduced, with permission, from Monck and Fernandez 1992. Permission conveyed through Copyright Clearance Center, Inc; and adapted, with permission, from Spruce et al. 1990.)

B. Transmitter release is measured by amperometry. A cell is voltage-clamped with a whole cell patch electrode while an extracellular carbon fiber is pressed against the cell surface. A large voltage applied to the tip of the carbon electrode oxidizes certain amine transmitters (such as serotonin or norepinephrine). This oxidation of one molecule generates one or more free electrons, which results in an electrical current that is proportional to the amount of transmitter release. The current can be recorded through an amplifier (A_2) connected to the carbon electrode. Membrane current and capacitance are recorded through the patch electrode amplifier (A_1). Recordings of serotonin release (**top traces**) and capacitance measurements (**bottom traces**) from mast cell secretory vesicles are shown at the *right*. The records indicate that serotonin may be released through the reversible opening and closing of the fusion pore prior to full fusion (*traces on left*). During these brief openings, small amounts of transmitter escape through the pore, resulting in a low-level signal (a *foot*) that precedes a large spike of transmitter release upon full fusion. During the foot, the cell surface area (proportional to membrane capacitance) undergoes reversible step-like changes as the fusion pore opens and closes. Sometimes the reversible opening and closing of the fusion pore are not followed by full fusion (*traces on right*). (Adapted, with permission, from Neher 1993.)

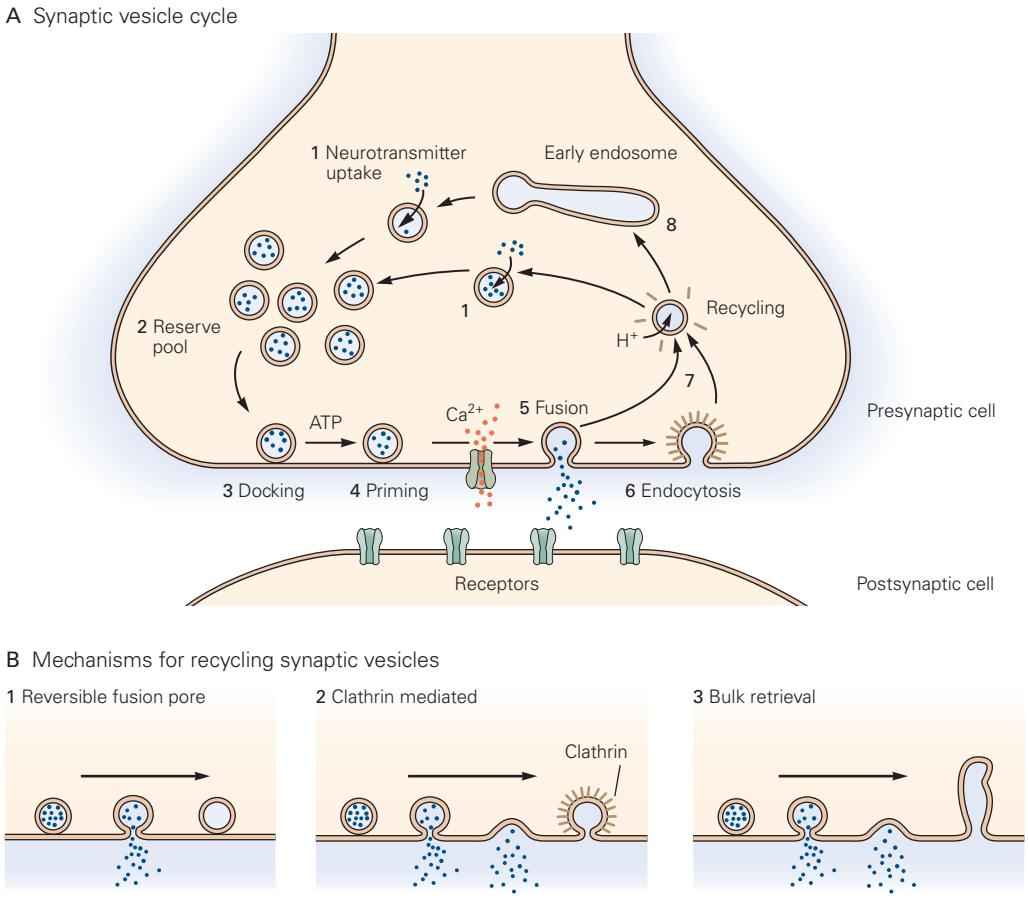

Figure 15–10 The synaptic vesicle cycle.

A. Synaptic vesicles are filled with neurotransmitters by active transport (**step 1**) and join the vesicle cluster that may represent a reserve pool (**step 2**). Filled vesicles dock at the active zone (**step 3**) where they undergo an ATP-dependent priming reaction (**step 4**) that makes them competent for Ca^{2+}-triggered fusion (**step 5**). After discharging their contents, synaptic vesicles are recycled through one of several routes (see part B). In one common route, vesicle membrane is retrieved via clathrin-mediated endocytosis (**step 6**) and recycled directly (**step 7**) or via endosomes (**step 8**).

B. Retrieval of vesicles after transmitter discharge is thought to occur via three mechanisms, each with distinct kinetics. **1.** A reversible fusion pore is the most rapid mechanism for reusing vesicles. The vesicle membrane does not completely fuse with the plasma membrane, and transmitter is released through the fusion pore. Vesicle retrieval requires only the closure of the fusion pore and thus can occur rapidly, in tens to hundreds of milliseconds. This pathway may predominate at lower to normal release rates. The spent vesicle may either remain at the membrane (kiss-and-stay) or relocate from the membrane to the reserve pool of vesicles (kiss-and-run). **2.** In the classical pathway, excess membrane is retrieved through endocytosis by means of clathrin-coated pits. These pits are found throughout the axon terminal except at the active zones. This pathway may be important at normal to high rates of release. **3.** In the bulk retrieval pathway, excess membrane reenters the terminal by budding from uncoated pits. These uncoated cisternae are formed primarily at the active zones. This pathway may be used only after high rates of release and not during the usual functioning of the synapse. (Adapted, with permission, from Schweizer, Betz, and Augustine 1995; Südhof 2004.)

to a minute for completion and also appears to shift from the active zone to the membrane surrounding the active zone (see Figure 15–7). A fourth mechanism operates after prolonged high-frequency stimulation. Under these conditions, large membranous invaginations into the presynaptic terminal are visible, which are thought to reflect membrane recycling through a process called *bulk retrieval*.

Exocytosis of Synaptic Vesicles Relies on a Highly Conserved Protein Machinery

Many key proteins of synaptic vesicles as well as their interacting partners in the plasma membrane have been isolated and purified. Proteomic analysis of isolated synaptic vesicles has provided a census of the many types of proteins they contain (Figure 15–11).

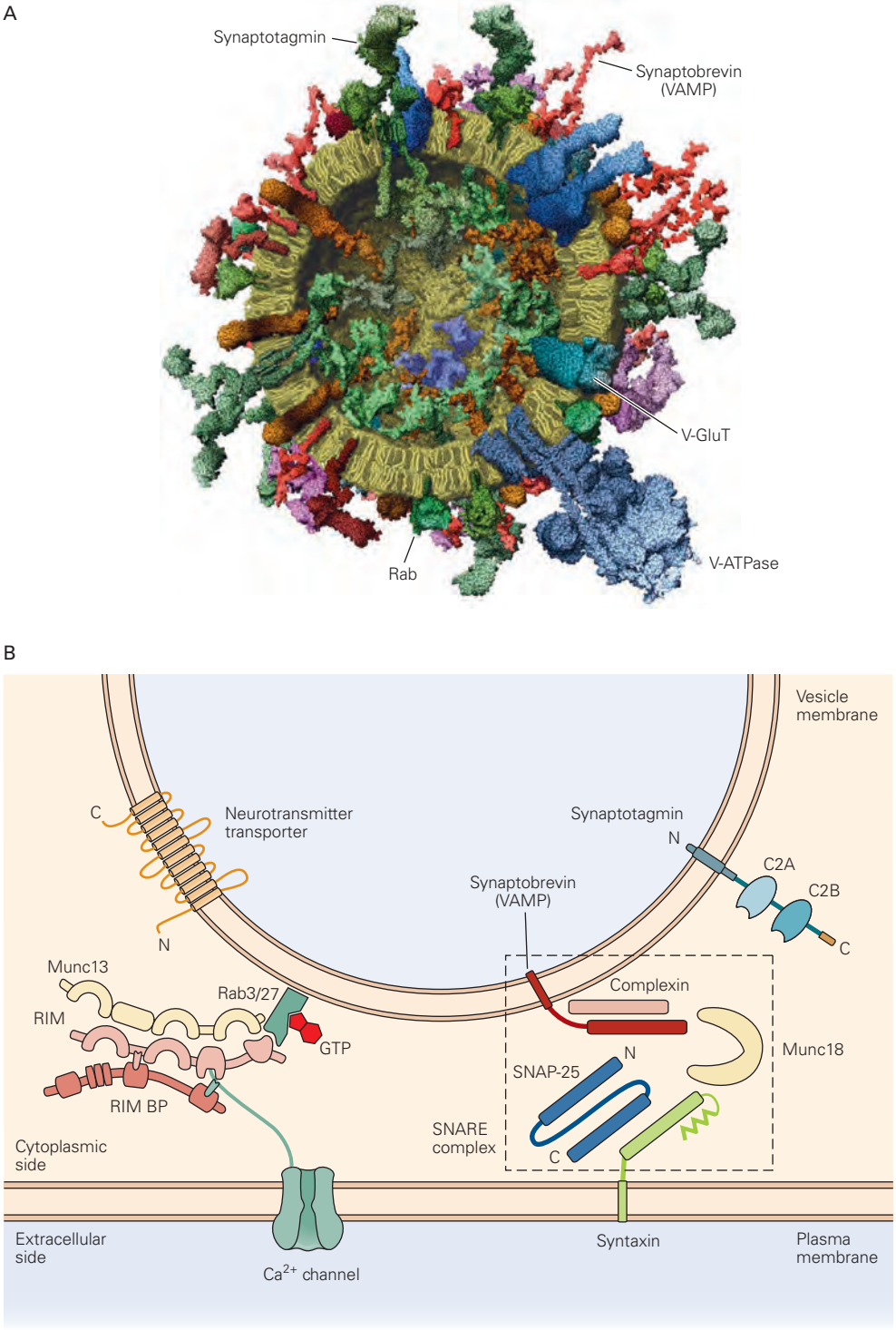

Figure 15–11 Molecular components of exocytosis.

A. Depiction of protein constituents of a glutamatergic synaptic vesicle (and their approximate copy numbers). Proteins are shown embedded in a synaptic vesicle, drawn to scale. Components include the vesicular ATPase (**V-ATPase**; 1–2 per vesicle), vesicular glutamate transporter (**V-GluT**; ~10 per vesicle), synaptobrevin/VAMP (~70 per vesicle), synaptotagmin (~15 per vesicle) and the small GTPases Rab3 and/or Rab27. Estimates are obtained as an average over many vesicles. (Reproduced from Takamori et al. 2006. Copyright © 2006 Elsevier.)

B. The molecular machinery mediating Ca^{2+}-triggered vesicle fusion with the presynaptic cell membrane. This depiction of a portion of a docked synaptic vesicle and the presynaptic active zone illustrates the interactions of several key functional proteins of the neurotransmitter release machinery. *Right:* The dotted box shows the core fusion machine, which is comprised of the SNARE proteins synaptobrevin/VAMP, syntaxin-1, and SNAP-25, along with Munc18-1. The Ca^{2+} sensor synaptotagmin-1 functions in coordination with complexin (shown bound to the SNARE complex). *Left:* The active zone protein complex also contains RIM, Munc13, and RIM-BP and a Ca^{2+} channel in the presynaptic plasma membrane. RIM plays a central role in this complex, coordinating multiple functions of the active zone by binding to specific target proteins: (1) vesicular Rab proteins (Rab3 and Rab27) to mediate vesicle docking; (2) Munc13 to activate vesicle priming; and (3) the Ca^{2+} channel, both directly and indirectly via RIM-BP, to tether Ca^{2+} channels within 100 nm of docked vesicles. The active zone protein complex puts into close proximity key elements that enable vesicles to dock, prime, and fuse rapidly in response to action potential–triggered Ca^{2+} entry near the docked vesicle. (Reproduced from Südhof 2013.)

Two of the most abundant proteins, *synaptobrevin* and *synaptotagmin-1*, are involved in vesicle fusion and are discussed later. Another key class of vesicle proteins are the neurotransmitter transporters (Chapter 16). These transmembrane proteins (exemplified by the *glutamate transporter* v-GluT) harness energy stored in the electrochemical gradient for protons to pump transmitter molecules against their concentration gradient from the cytoplasm into the vesicle. The protonmotive force is generated by a vesicular H^+ pump, the V-ATPase, that pumps protons into the lumen of the vesicle from the cytoplasm, leading to an acidic vesicular pH of around 5.0.

Other synaptic vesicle proteins direct vesicles to their release sites, participate in the discharge of transmitter by exocytosis, and mediate recycling of the vesicle membrane. The protein machinery involved in these three steps has been conserved throughout evolution, in species ranging from worms to humans, and forms the basis for the regulated release of neurotransmitter. We consider each of these steps in turn.

The Synapsins Are Important for Vesicle Restraint and Mobilization

The vesicles outside the active zone represent a reserve pool of transmitter. Paul Greengard discovered a family of proteins, *synapsins*, that are thought to be important regulators of the reserve pool of vesicles. Synapsins are peripheral membrane proteins that are bound to the cytoplasmic surface of synaptic vesicles. Synapsins contain a conserved central ATPase domain that accounts for most of their structure, but whose function remains unknown. In addition, synapsin-1 binds actin.

The synapsins are substrates for both protein kinase A and Ca^{2+}/calmodulin-dependent protein kinase II. When the nerve terminal is depolarized and Ca^{2+} enters, the synapsins become phosphorylated by the kinase and are thus released from the vesicles. Strikingly, stimulation of synapsin phosphorylation, genetic deletion of synapsins or intracellular injection of a synapsin antibody leads to a decrease in the number of synaptic vesicles in the nerve terminal and a resulting decrease in the ability of a terminal to maintain a high rate of transmitter release during repetitive stimulation.

SNARE Proteins Catalyze Fusion of Vesicles With the Plasma Membrane

Because a membrane bilayer is a stable structure, fusion of the synaptic vesicle and plasma membrane must overcome a large unfavorable activation energy. This is accomplished by a family of fusion proteins now referred to as *SNAREs* (soluble *N*-ethylmaleimide–sensitive factor attachment receptors) (Figure 15–12).

SNAREs are universally involved in membrane fusion, from yeast to humans. They mediate both constitutive membrane trafficking during the movement of proteins from the endoplasmic reticulum to the Golgi apparatus to the plasma membrane, as well as synaptic vesicle trafficking important for regulated exocytosis. SNAREs have a conserved protein sequence, the SNARE motif, that is 60 residues long. They come in two forms. Vesicle SNAREs, or v-SNAREs (also referred to as R-SNAREs because they contain an important central arginine residue), reside in the vesicle membranes. Target-membrane SNAREs, or t-SNAREs (also referred to as Q-SNAREs because they contain an important glutamine residue), are present in target membranes, such as the plasma membrane.

Each synaptic vesicle contains a v-SNARE called *synaptobrevin* (also called vesicle-associated membrane protein or VAMP). By contrast, the presynaptic active zone contains two types of t-SNARE proteins, *syntaxin* and *SNAP-25*. (Synaptobrevin and syntaxin have one SNARE motif; SNAP-25 has two.) The first clue that synaptobrevin, syntaxin, and SNAP-25 are all involved in fusion of the synaptic vesicle with the plasma membrane came from the finding that all three proteins are substrates for botulinum and tetanus toxins, bacterial proteases that are potent inhibitors of transmitter release. James Rothman then provided the crucial insight that these three proteins interact in a tight biochemical complex. In experiments using purified v-SNAREs and t-SNAREs in solution, four SNARE motifs bind tightly to each other to form an α-helical coiled-coil complex (Figure 15–12B).

How does formation of the SNARE complex drive synaptic vesicle fusion? During exocytosis, the SNARE motif of synaptobrevin on the synaptic vesicle forms a tight complex with the SNARE motifs of SNAP-25 and syntaxin on the plasma membrane (Figure 15–12B). The crystal structure of the SNARE complex suggests that this complex draws the membranes together. The ternary complex of synaptobrevin, syntaxin, and SNAP-25 is extraordinarily stable. The energy released in its assembly is thought to draw the negatively charged phospholipids of the vesicle and plasma membranes in close apposition, forcing them into a prefusion intermediate state (Figure 15–12). Such an unstable state may start the formation of the fusion pore and generate the rapid opening and closing (flickering) of the fusion pore observed in electrophysiological measurements.

However, the SNAREs do not fully account for fusion of the synaptic vesicle and plasma membranes. Reconstitution experiments with purified proteins in

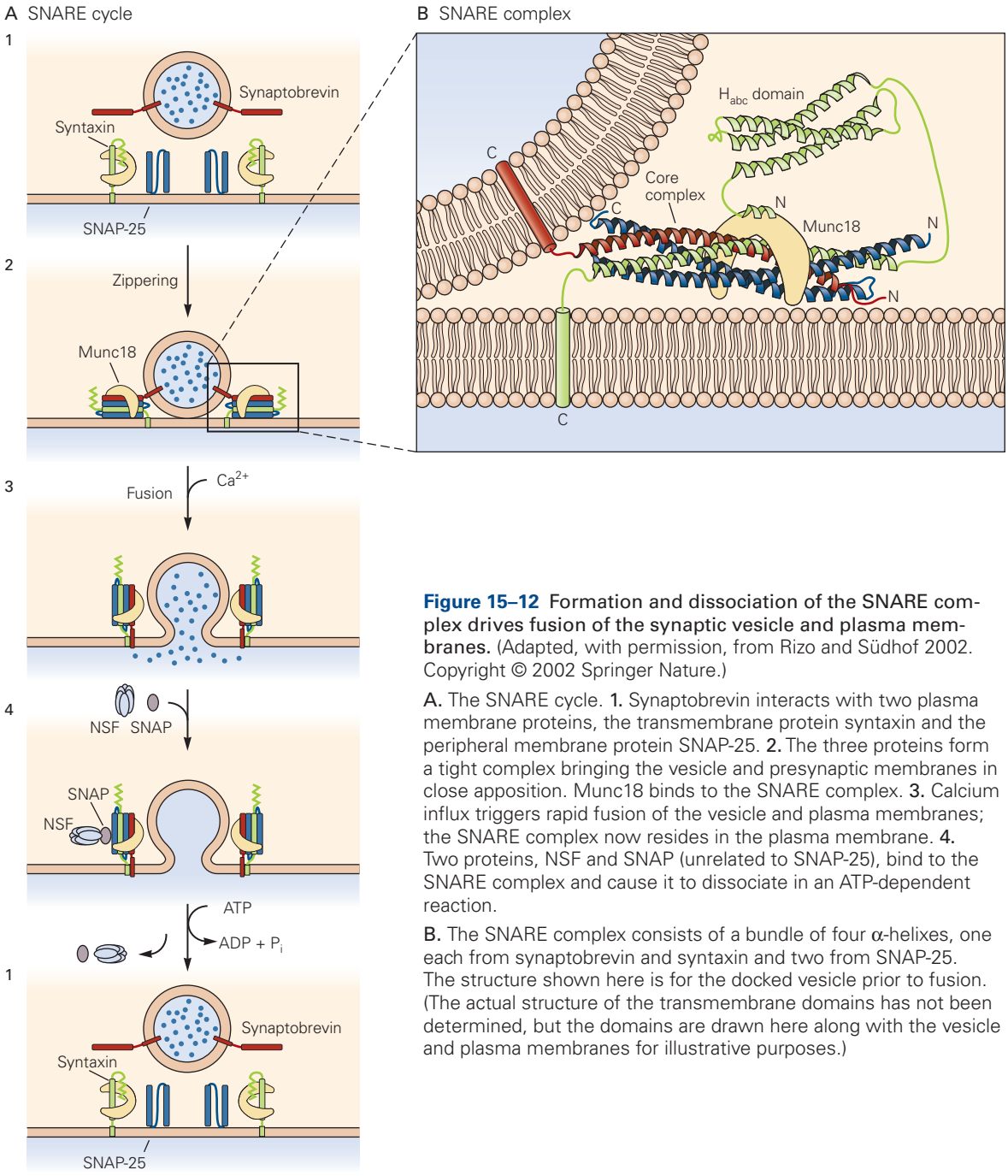

Figure 15–12 **Formation and dissociation of the SNARE complex drives fusion of the synaptic vesicle and plasma membranes.** (Adapted, with permission, from Rizo and Südhof 2002. Copyright © 2002 Springer Nature.)

A. The SNARE cycle. **1.** Synaptobrevin interacts with two plasma membrane proteins, the transmembrane protein syntaxin and the peripheral membrane protein SNAP-25. **2.** The three proteins form a tight complex bringing the vesicle and presynaptic membranes in close apposition. Munc18 binds to the SNARE complex. **3.** Calcium influx triggers rapid fusion of the vesicle and plasma membranes; the SNARE complex now resides in the plasma membrane. **4.** Two proteins, NSF and SNAP (unrelated to SNAP-25), bind to the SNARE complex and cause it to dissociate in an ATP-dependent reaction.

B. The SNARE complex consists of a bundle of four α-helixes, one each from synaptobrevin and syntaxin and two from SNAP-25. The structure shown here is for the docked vesicle prior to fusion. (The actual structure of the transmembrane domains has not been determined, but the domains are drawn here along with the vesicle and plasma membranes for illustrative purposes.)

lipid vesicles indicate that synaptobrevin, syntaxin, and SNAP-25 can catalyze fusion, but the in vitro reaction shows little regulation by Ca^{2+}, and the reaction is much slower and less efficient than vesicle fusion in a real synapse. One important additional protein required for exocytosis of synaptic vesicles is Munc18 (mammalian unc18 homolog). Homologs of Munc18, referred to as SM proteins (sec1/Munc18-like proteins), are essential for all SNARE-mediated intracellular fusion reactions. Munc18 binds to syntaxin before the SNARE complex assembles. Deletion of Munc18 prevents all synaptic fusion in neurons. The core fusion machinery is thus composed of SNARE and SM proteins that are modulated by various accessory factors specific for particular fusion reactions. Finally, the synaptic SNARE complex also interacts with a small soluble protein called *complexin*, which suppresses the spontaneous release of transmitter but enhances Ca^{2+}-dependent evoked release.

After fusion, the SNARE complex must be disassembled for efficient vesicle recycling to occur. Rothman discovered that a cytoplasmic ATPase called *NSF* (*N*-ethylmaleimide-sensitive fusion protein) binds to SNARE complexes via an adaptor protein called *SNAP* (soluble NSF-attachment protein, not related to the SNARE protein SNAP-25). NSF and SNAP use the energy of ATP hydrolysis to dissociate SNARE complexes, thereby regenerating free SNARE (Figure 15–12A). SNAREs and NSF also participate in the cycling of postsynaptic AMPA-type glutamate receptors in dendritic spines.

Calcium Binding to Synaptotagmin Triggers Transmitter Release

Because fusion of synaptic vesicles with the plasma membrane must occur within a fraction of a millisecond, it is thought that most proteins responsible for fusion are assembled prior to Ca^{2+} influx. According to this view, once Ca^{2+} enters the presynaptic terminal, it binds a Ca^{2+} sensor on the vesicle, triggering immediate fusion of the membranes.

Members of a family of closely related proteins, the synaptotagmins, have been identified as the major Ca^{2+} sensors that trigger fusion of synaptic vesicles. Synaptotagmins are membrane proteins with a single N-terminal transmembrane region that anchors them to the synaptic vesicle (Figure 15–13A,B). The cytoplasmic region of each synaptotagmin protein is largely composed of two domains, the C2 domains, which are a common protein motif homologous to the Ca^{2+} and phospholipid-binding C2 domain of protein kinase C. The finding that the C2 domains bind not only Ca^{2+} but also phospholipids is consistent with their importance in Ca^{2+}-dependent exocytosis. Synaptotagmin-1, -2, and -9 have been identified as Ca^{2+} sensors for fast and synchronous vesicle fusion. Each exhibits distinct Ca^{2+} binding affinities and kinetics, endowing different synapses with distinct release properties on the basis of the particular synaptotagmin isoform that is expressed. In contrast, synaptotagmin-7 mediates a slower form of Ca^{2+}-triggered exocytosis that is important for synaptic transmission during prolonged periods of activity periods of repeated firing of action potential. All of these synaptotagmins also function as Ca^{2+} sensors in other forms of exocytosis, such as exocytosis in endocrine cells and the insertion of AMPA-type glutamate receptors into the postsynaptic cell membrane from a pool of intracellular vesicles during NMDA-receptor-dependent long-term potentiation.

Studies with mutant mice in which synaptotagmin-1 is deleted or in which its Ca^{2+} affinity is altered through genetic engineering provide important evidence that synaptotagmin is the physiological Ca^{2+} sensor. When the affinity of synaptotagmin for Ca^{2+} is decreased two-fold, the Ca^{2+} required for transmitter release is changed by the same amount. When synaptotagmin-1 is deleted in mice, flies, or worms, an action potential is no longer able to trigger fast synchronous release. However, Ca^{2+} is still capable of stimulating a slower form of transmitter release referred to as asynchronous release (Figure 15–13A), mediated by synaptotagmin-7. Thus, nearly all Ca^{2+}-triggered neurotransmitter release depends on the synaptotagmins.

How does Ca^{2+} binding to synaptotagmin trigger vesicle fusion? The two C2 domains bind a total of five Ca^{2+} ions, the same minimal number of Ca^{2+} ions required to trigger release of a quantum of transmitter (Figure 15–13B). However, as multiple synaptotagmins may be engaged to trigger release, more than five bound Ca^{2+} ions may be distributed among the multiple synaptotagmin molecules on a single vesicle.

The binding of the Ca^{2+} ions to synaptotagmin is thought to act as a switch, promoting the interaction of the C2 domains with phospholipids. The C2 domains of synaptotagmin also interact with SNARE proteins and complexin. Crystal structures of synaptotagmin reveal a conserved primary interface with the associated SNARE complex. In addition, a second molecule of synaptotagmin forms a tripartite interaction with the same SNARE complex and complexin. Brunger and colleagues found that both the primary SNARE complex/synaptotagmin interface and the tripartite SNARE complex/synaptotagmin/complexin interface are essential for fast Ca^{2+}-triggered fusion. These findings have led to the hypothesis that: (1) at rest, synaptotagmin of primed vesicles exists in a complex with partially pre-zippered SNARE proteins and complexin; (2) upon action potential–triggered Ca^{2+} influx, Ca^{2+} binds to synaptotagmin. This triggers an interaction between synaptotagmin and the plasma membrane that causes the complex to rotate en bloc, which induces complexin to partly dissociate from the SNARE complex; (3) this rotation causes a dimpling of the plasma membrane, rearrangement of its cytoplasm-facing lipids, and ultimately the fusion of plasma and vesicle membranes (Figure 15–13C). In this way, the energy of the favorable interaction of synaptotagmin, Ca^{2+}, and the membrane can be harnessed to both relieve the complexin-mediated lock on fusion and promote the energetically unfavorable merging of a vesicle membrane with the plasma membrane.

The Fusion Machinery Is Embedded in a Conserved Protein Scaffold at the Active Zone

As we have seen, a defining feature of fast synaptic transmission is that neurotransmitters are released by

A

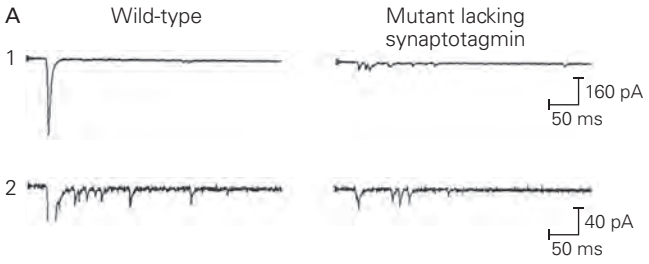

B1 Calcium-bound synaptotagmin

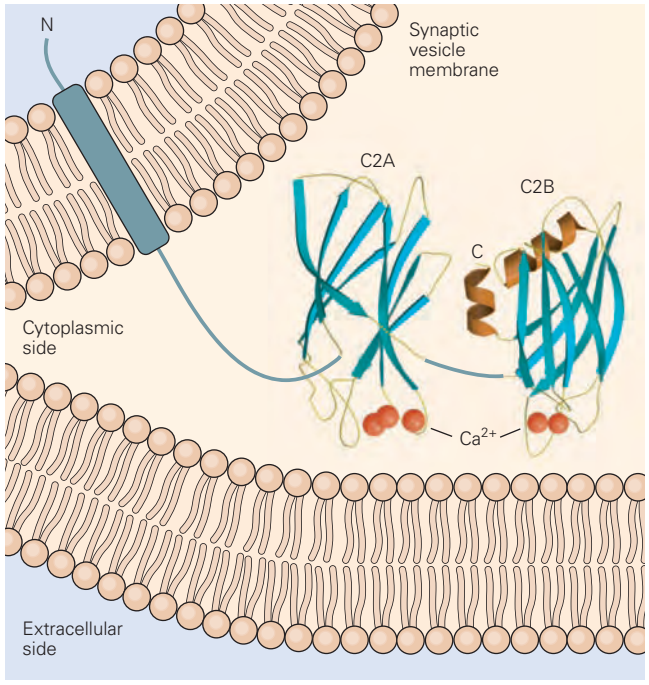

B2 Synaptotagmin/SNARE complex

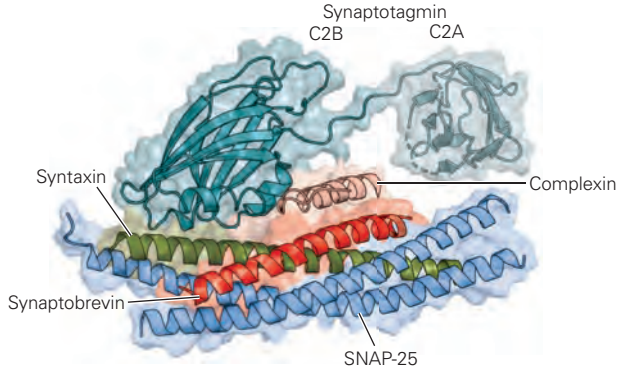

C

Locked

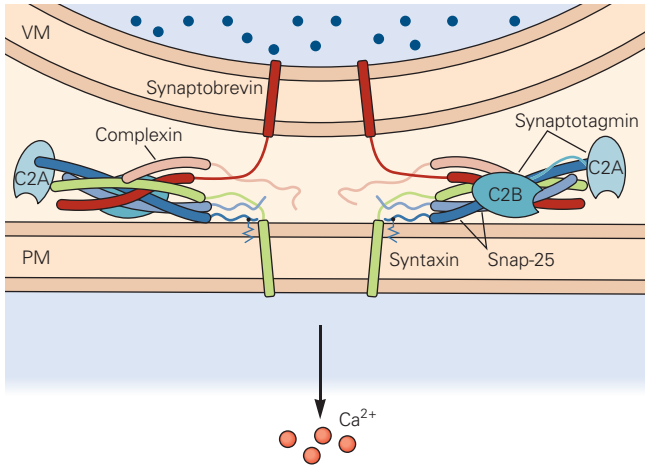

Unlocking and triggering

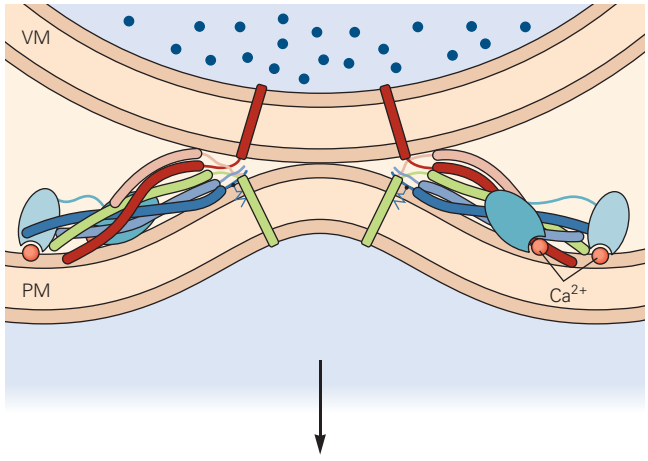

Fusion pore formation

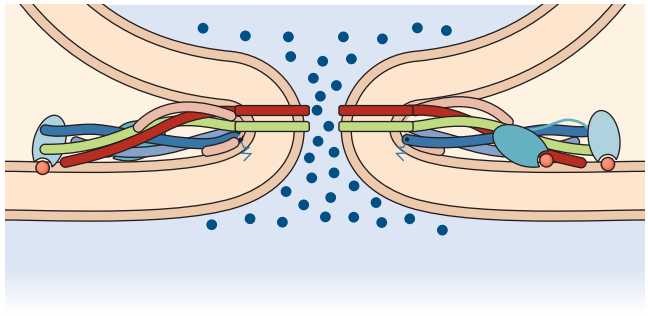

exocytosis at the active zone. Other types of exocytosis, such as that which occurs in the adrenal medulla, do not require a specialized domain of the plasma membrane. The active zone is thought to coordinate and regulate the docking and priming of synaptic vesicles to enable the speed and tight regulation of release. This is accomplished through a conserved set of proteins that form one large macromolecular structure at active zones.

An exquisitely detailed view of the active zone at the frog neuromuscular junction was obtained by Jack MacMahan using a powerful ultrastructural technique called electron microscopic tomography. This technique has shown how synaptic vesicles are tethered to the membrane by a series of distinctive structural entities, termed *ribs* and *beams*, that attach to defined sites on the vesicles and to particles (*pegs*) in the presynaptic membrane that may correspond to voltage-gated Ca^{2+} channels (Figure 15–14).

A key goal in understanding how the various synaptic vesicle and active zone proteins are coordinated during exocytosis is to match up the various proteins that have been identified with elements of this electron microscopic structure. Several cytoplasmic proteins have been identified that are thought to be components of a structural matrix at the active zone. These include three large cytoplasmic multidomain proteins, *Munc13* (not related to the Munc18 protein discussed earlier), *RIM*, and *RIM-binding proteins* (RIM-BPs), which form a tight complex with each other and may comprise part of the ribs and beams. The binding of synaptic vesicles to RIM and Munc13 is essential for priming the vesicles for exocytosis. Phosphorylation of RIM by cAMP-dependent protein kinase is implicated in the enhancement of transmitter release associated with certain forms of long-term synaptic plasticity that may contribute to learning and memory. As we will see later, regulation of Munc13 by second messengers is involved in shorter-term forms of synaptic plasticity.

RIM binds the synaptic vesicle proteins *Rab3* and *Rab27*, members of the family of low-molecular-weight guanosine triphosphatases (GTPases). Rab3 and Rab27 proteins transiently associate with synaptic vesicles as a GTP-bound Rab3 complex (Figure 15–11B). The binding of RIM to Rab3 or Rab27 is thought to tether synaptic vesicles to the active zone during the vesicle cycle prior to SNARE-complex assembly. Moreover, RIM and RIM-BP together mediate the recruitment of Ca^{2+} channels to the active zone, allowing tight coupling of Ca^{2+} influx to vesicle release. This general machinery is conserved through evolution and is present in invertebrates, although with modifications.

At the *Drosophila* neuromuscular junction, Sigrist and colleagues identified another protein, Bruchpilot, as a major component of the electron-dense active zone "T-bar" structure; Bruchpilot is associated with the fly homolog of RIM-binding protein, which also serves to recruit Ca^{2+} channels to active zones in *Drosophila*. As coordinators of both presynaptic Ca^{2+} channels and synaptic vesicles, these proteins act as essential regulators of presynaptic release in the fly. In *Caenorhabditis elegans*, RIM plays a central role for the same processes.

Figure 15–13 (Opposite) Synaptotagmin mediates Ca^{2+}-dependent transmitter release by forming a protein complex that favors vesicle fusion.

A. Fast Ca^{2+}-triggered transmitter release is absent in mutant mice lacking synaptotagmin-1. Recordings show excitatory postsynaptic currents evoked in vitro by stimulation of cultured hippocampal neurons from wild-type mice and from mutant mice in which synaptotagmin-1 has been deleted by homologous recombination (**1**). Neurons from wild-type mice show large, fast excitatory postsynaptic currents evoked by presynaptic action potentials, reflecting the fact that synaptic transmission is dominated by the rapid synchronous release of transmitter from a large number of synaptic vesicles. In the **bottom trace** (**2**), where the synaptic current is shown at a highly expanded scale, one can see that a small, prolonged phase of asynchronous release of transmitter follows the fast phase of synchronous release. During this slow phase, there is a prolonged increase in frequency of individual quantal responses. In neurons from a mutant mouse, a presynaptic action potential triggers only the slow asynchronous phase of release; the rapid synchronous phase has been abolished. (Reproduced, with permission, from Geppert et al., 1994).

B. The X-ray crystal structure synaptotagmin. **B1.** A ribbon diagram shows that the C2A domain binds three Ca^{2+} ions and the C2B domain two Ca^{2+} ions. The **blue arrows** show β-strands. There are two short α-helixes (**orange**) at the C-terminus of the C2B domain. The structures of the other regions of synaptotagmin have not yet been determined and are drawn here for illustrative purposes. The membrane and structures are drawn to scale. (Adapted, with permission, from Fernandez et al., 2001). **B2.** The X-ray crystal structure of synaptotagmin (**light blue**) bound to the SNARE complex (synaptobrevin, syntaxin and SNAP-25) and complexin. The transmembrane domain of synaptotagmin is not shown. (Adapted, with permission, from Zhou et al, 2017.)

C. Zippering of the synaptotagmin-complexin-SNARE complex mediates vesicle fusion. **Top**, in the absence of Ca^{2+}, the α-helixes of the SNARE complex and complexin, with the bound synaptotagmin, are only partially zippered. **Middle**, binding of Ca^{2+} to the C2A and C2B domains of synaptotagmin allows them to interact with the plasma membrane, applying force to bring the vesicle and plasma membranes closer together. **Bottom**, synaptotagmin-mediated proximity and the final zippering of the complexin-SNARE-synaptotagmin complex triggers membrane fusion. (Adapted, with permission, from Zhou et al., 2017.)

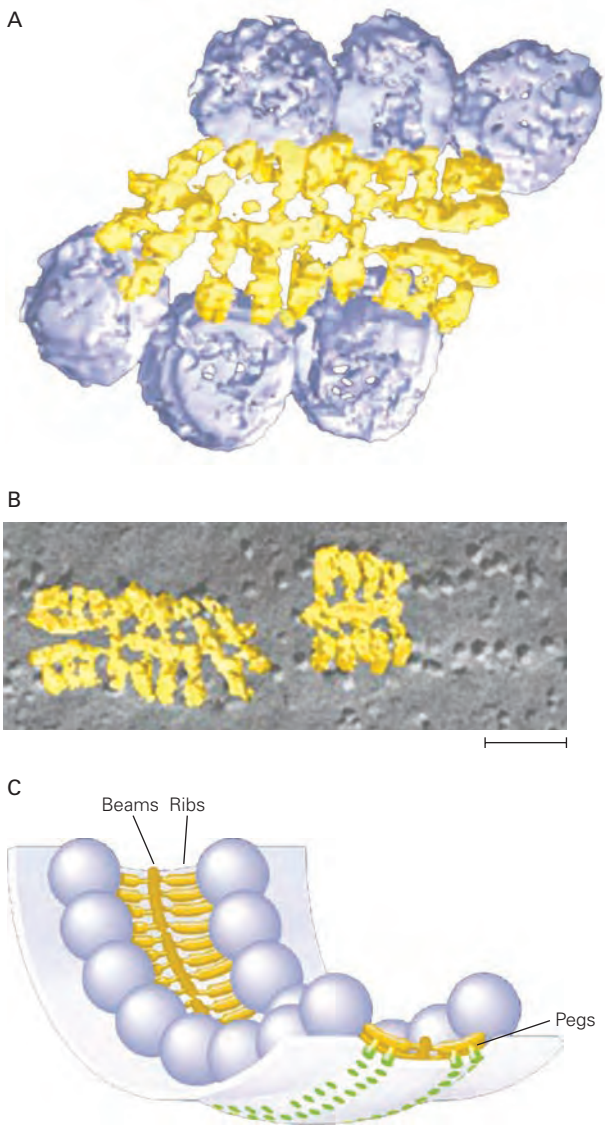

Figure 15–14 Synaptic vesicles at the active zone. The images are obtained from electron microscopic tomography. (Reproduced, with permission, from Harlow et al. 2001. Copyright © 2001 Springer Nature.)

A. Vesicles are tethered to filamentous proteins of the active zone. Three distinct filamentous structures are resolved: pegs, ribs, and beams. Ribs protruding from the vesicles are attached to long horizontal beams, which are anchored to the membrane by vertical pegs.

B. Ribs and beams superimposed on a freeze fracture view of intramembranous particles at the active zone show how the ribs are aligned with the particles, some of which are presumed to be voltage-gated Ca^{2+} channels. Scale bar = 100 nm.

C. A model for the structure of the active zone shows the relation between synaptic vesicles, pegs, ribs, and beams.

Modulation of Transmitter Release Underlies Synaptic Plasticity

The effectiveness of chemical synapses can be modulated dramatically and rapidly—by several-fold in a matter of seconds—and this change can be maintained for seconds, to hours, or even days or longer, a property called *synaptic plasticity.*

Synaptic strength can be modified presynaptically, by altering the release of neurotransmitter, postsynaptically, by modulating the response to transmitter (as discussed in Chapter 13), or both. Long-term changes in presynaptic and postsynaptic mechanisms are crucial for the refinement of synaptic connections during development (Chapter 49) and for storing information during learning and memory (Chapters 53 and 54). Here, we focus on how synaptic strength can be changed through modulation of the amount of transmitter released. In principle, changes in transmitter release can be mediated by two different mechanisms: changes in Ca^{2+} influx or changes in the amount of transmitter released in response to a given Ca^{2+} concentration. As we will see later, both types of mechanisms contribute to different forms of plasticity.

Synaptic strength is often altered by the pattern of activity of the presynaptic neuron. Trains of action potentials produce successively larger postsynaptic currents at some synapses and successively smaller currents in others (Figure 15–15A). A decrease in the size of the postsynaptic response to repeated stimulation is referred to as *synaptic depression* (Figure 15–15A, upper); the opposite, enhancement of transmission with repeated stimulation, is called *synaptic facilitation* or *potentiation* (Figure 15–15A, lower, 15–15E). Various synapses exhibit these disparate forms of *short-term synaptic plasticity*—sometimes overlapping and sometimes with one predominating—resulting in characteristic patterns of short-term dynamics in individual synapse types (Figure 15–15A).

Whether a synapse facilitates or depresses often is determined by the probability of release in response to the first action potential of a train. Synapses with an initial high probability of release normally undergo depression because the high rate of release transiently depletes docked vesicles at the active zone. Synapses with an initial low probability of release undergo synaptic facilitation, in part because the buildup in intracellular Ca^{2+} during the train increases the probability of release (see later). The importance of release probability in controlling the sign of plasticity can be seen by the effect of genetic mutations. Synapses formed by hippocampal neurons in cell culture have an initially high release probability and so normally depress in

response to 20-Hz stimulation. However, a mutation that reduces by approximately two-fold the Ca^{2+}-binding affinity of synaptotagmin-1, thus reducing the initial probability of release, converts the depressing synapse into a facilitating one (Figure 15–15B).

Mechanisms that affect the concentration of free Ca^{2+} in the presynaptic terminal also affect the amount of transmitter released. For example, the buildup of inactivation of certain voltage-gated K^+ channels during high-frequency firing leads to a gradual increase in the duration of the action potential. Prolongation of the action potential increases the time that voltage-gated Ca^{2+} channels stay open, which leads to enhanced entry of Ca^{2+} and a subsequent increase in transmitter release, resulting in a larger postsynaptic potential (Figure 15–15C).

Most studies of the functional implications of short-term synaptic dynamics have been performed in vitro or are based on computational results. However, recent in vivo experiments are beginning to shed light on the behavioral importance of short-term plasticity. For example, in vivo recordings in rodents from thalamocortical synapses have suggested that synaptic depression may contribute to sensory adaptation during repeated whisker stimulation. The time course of this sensory adaptation parallels the attenuation of cortical spiking to whisker stimulation and the synaptic depression of EPSPs at thalamocortical synapses (Figure 15–15D).

High-frequency stimulation of the presynaptic neuron, which in some cells can generate up to 500 to 1,000 action potentials per second, is called *tetanic stimulation.* Such intense stimulation can cause dramatic changes in synaptic strength. The increase in size of the EPSP during tetanic stimulation is called *potentiation*; the increase that persists after tetanic stimulation is called *posttetanic potentiation* (Figure 15–15E). In contrast to synaptic facilitation, which lasts milliseconds to seconds, posttetanic potentiation usually lasts several minutes, but it can persist for an hour or more at some synapses.

Synapses utilize a complex containing Munc13 and RIM, two of the active zone proteins discussed earlier, to counteract vesicle depletion during high-frequency stimulation. The rise in presynaptic Ca^{2+} during tetanic stimulation activates phospholipase C, which produces inositol 1,4,5-trisphosphate (IP_3) and diacylglycerol. Diacylglycerol directly interacts with a protein domain on Munc13 called the C1 domain (homologous to the diacylglycerol-binding domain in protein kinase C but distinct from the C2 domain of synaptotagmin), thereby accelerating the rate of synaptic vesicle recycling. At the same time, IP_3 causes additional release of Ca^{2+} from intracellular stores, and the increase in Ca^{2+} further activates Munc13 by binding to its C2 domain, which resembles the C2 domain of synaptotagmin but acts as an agent of short-term synaptic plasticity.

Activity-Dependent Changes in Intracellular Free Calcium Can Produce Long-Lasting Changes in Release

Several Ca^{2+}-dependent mechanisms contribute to longer-lasting changes in transmitter release that persist after a high-frequency tetanus is terminated. Normally the rise in Ca^{2+} in the presynaptic terminal in response to an action potential is rapidly buffered by cytoplasmic Ca^{2+}-binding proteins and mitochondria. Calcium ions are also actively transported out of the neuron by pumps and transporters. However, during tetanic stimulation, so much Ca^{2+} flows into the axon terminals that the Ca^{2+} buffering and clearance systems can become saturated.

This leads to a temporary excess of Ca^{2+} called *residual* Ca^{2+}. The residual free Ca^{2+} enhances synaptic transmission for many minutes or longer by activating certain enzymes that are sensitive to enhanced levels of resting Ca^{2+}, including the Ca^{2+}/calmodulin-dependent protein kinases. Activation of such Ca^{2+}-dependent enzymatic pathways is thought to increase the priming of synaptic vesicles in the terminals. Here, then, is the simplest kind of cellular memory! The presynaptic cell can store information about the history of its activity in the form of residual free Ca^{2+} in its terminals (or residual Ca^{2+} bound to sensor proteins).

This Ca^{2+} acts by multiple pathways that have different half-times of decay. In Chapter 13, we saw how posttetanic potentiation at certain synapses is followed by an even longer-lasting process (also initiated by Ca^{2+} influx), called *long-term potentiation,* which can last for many hours or even days. The importance of long-term potentiation for learning and memory will be considered in Chapters 53 and 54.

Axo-axonic Synapses on Presynaptic Terminals Regulate Transmitter Release

Synapses are formed on axon terminals as well as the cell body and dendrites of neurons (see Chapter 13). Although axosomatic synaptic actions affect all branches of the postsynaptic neuron's axon (because they affect the probability that the neuron will fire an action potential), axo-axonic actions selectively control individual terminals of the axon. One important action of axo-axonic synapses is to increase or decrease Ca^{2+} influx into the presynaptic terminals of the postsynaptic cell, thereby enhancing or depressing transmitter release, respectively.

As we saw in Chapter 13, when one neuron releases transmitter that hyperpolarizes the cell body (or

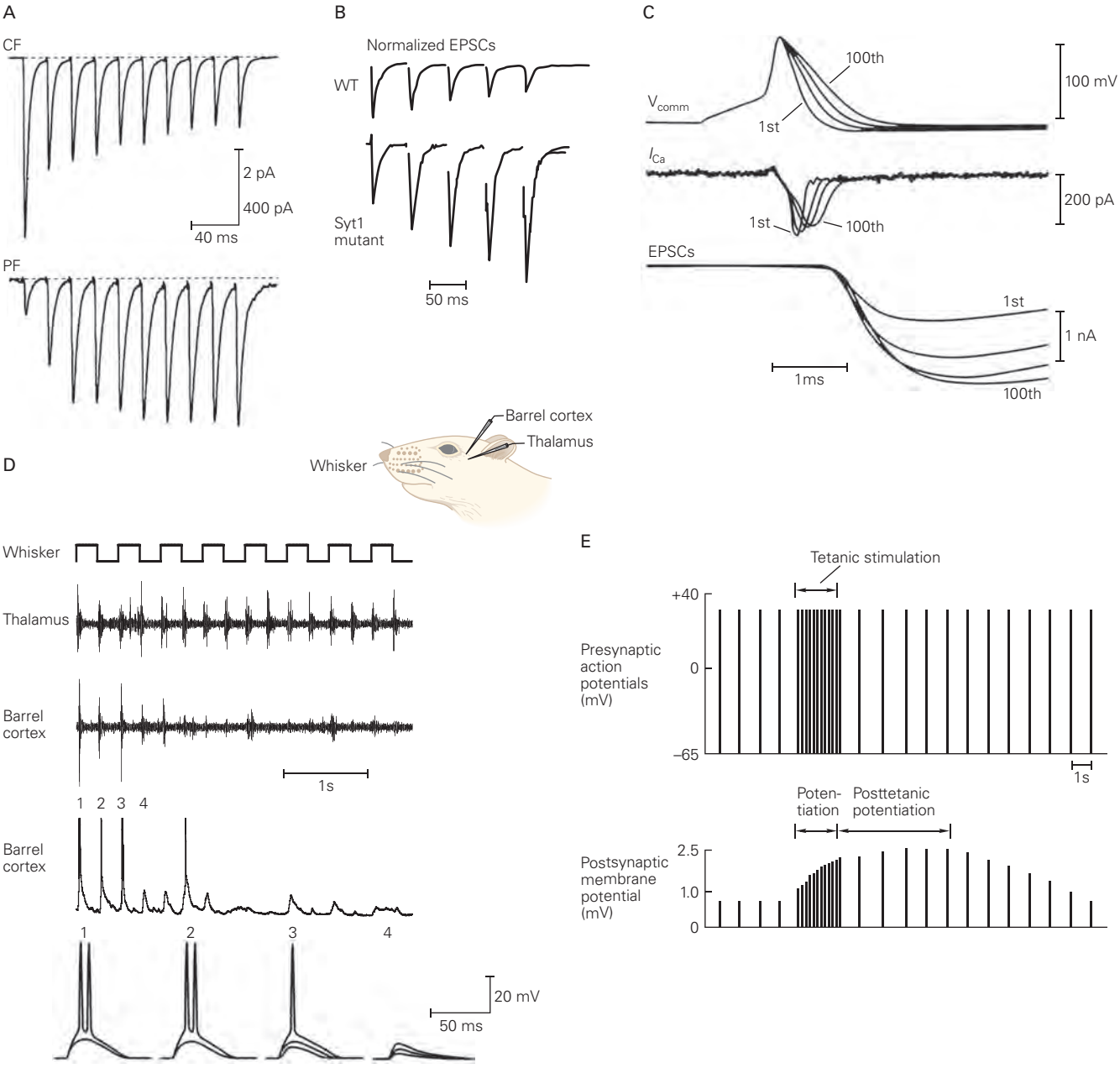
A
CF
2 pA
400 pA
40 ms
PF
B
Normalized EPSCs
WT
Syt1
mutant
50 ms
C
100th
100 mV
V_{comm}
1st
I_{Ca}
200 pA
1st
100th
EPSCs
1st
1 nA
1ms
100th
Barrel cortex
Thalamus
Whisker
D
Whisker
Thalamus
Barrel
cortex
1s
1 2 3 4
Barrel
cortex
1
2
3
4
20 mV
50 ms
E
Tetanic stimulation
+40
0
–65
Presynaptic
action
potentials
(mV)
1s
Poten-
tiation
Posttetanic
potentiation
2.5
1.0
0
Postsynaptic
membrane
potential
(mV)

dendrites) of another, it decreases the likelihood that the postsynaptic cell will fire; this action is called *postsynaptic inhibition.* In contrast, when a neuron forms synapses on the axon terminal of another cell, it can reduce the amount of transmitter that will be released by the postsynaptic cell onto a third cell; this action is called *presynaptic inhibition* (Figure 15–16A). Other axo-axonic synaptic actions can increase the amount of transmitter released by the postsynaptic cell; this action is called *presynaptic facilitation* (Figure 15–16B). Both presynaptic inhibition and facilitation can occur in response to activation of ionotropic or metabotropic receptors in the membrane of the presynaptic terminals.

The best-analyzed mechanisms of presynaptic inhibition and facilitation are found in invertebrate neurons and vertebrate mechanoreceptor neurons (whose axons project to neurons in the spinal cord). Three mechanisms for presynaptic inhibition have been identified in these cells. One depends on the activation of inhibitory interneurons that form axo-axonic synapses on the sensory neuron presynaptic terminals, where they activate ionotropic $GABA_A$ receptor-channels. Because the Cl^- reversal potential in the presynaptic terminals is relatively positive, the increased Cl^- conductance resulting from activation of $GABA_A$ channels depolarizes the presynaptic terminal. This voltage change, termed the primary afferent depolarization, is thought to inactivate voltage-gated Na^+ channels, reducing the amplitude of the presynaptic action potential, which decreases the activation of voltage-gated Ca^{2+} channels and thereby decreases the amount of transmitter release.

The other two mechanisms for presynaptic inhibition both result from the activation of presynaptic G protein–coupled metabotropic receptors. One type of action results from the modulation of ion channels. As we saw in Chapter 14, the βγ-subunit complex of G proteins can simultaneously close voltage-gated Ca^{2+} channels and open K^+ channels. This decreases the influx of Ca^{2+} and enhances repolarization of the presynaptic terminal following an action potential, thus diminishing transmitter release. A second type of G protein–dependent action depends on a direct action by the βγ-subunit complex on the release machinery itself, independent of any changes in ion channel activity or Ca^{2+} influx. This second action is thought to involve a decrease in the Ca^{2+} sensitivity of the release machinery.

In contrast, presynaptic facilitation can be caused by enhanced influx of Ca^{2+}. In certain molluscan neurons, serotonin acts through cAMP-dependent protein phosphorylation to close K^+ channels in the presynaptic

Figure 15–15 (Opposite) Diversity of short-term plasticity in the central nervous system.

A. Excitatory postsynaptic currents (**EPSCs**) were recorded from a cerebellar Purkinje neuron under voltage clamp in response to repetitive stimulation of either the climbing fiber (**CF**) or parallel fiber (**PF**) inputs to the Purkinje cells. In both cases EPSCs were recorded while afferents were stimulated 10 times at 50 Hz. Note that the CF EPSC depresses whereas the PF EPSC facilitates during repetitive stimulation. (Reproduced, with permission, from Dittman et al. 2000. Copyright © 2000 Society for Neuroscience.)

B. EPSCs were recorded from hippocampal neurons in culture during stimulation at 20 Hz. EPSC size was normalized by dividing each response by peak amplitude of first EPSC in each individual train. The EPSC depresses in neurons cultured from wild-type mice (**WT**) whereas the EPSC facilitates in neurons from mice harboring a mutated form of synaptotagmin-1 that reduces its Ca^{2+} binding affinity (**Syt1 mutant**, R233Q). (Reproduced, with permission, from Fernandez-Chacon et al. 2001. Copyright © 2001 Springer Nature.)

C. The action potential recorded at the presynaptic terminals of dentate gyrus granule neurons broadens progressively during a 2-s long train of 50 Hz stimulation. This results in enhanced synaptic transmission from the granule neurons onto their CA3 postsynaptic target. The 1st, 25th, 50th, and 100th action potentials are shown. These action potential waveforms were then used as the command waveforms (**Vcomm, top**) to voltage clamp the presynaptic nerve terminal ("action potential clamp"), eliciting the voltage-gated Ca^{2+} current (I_{Ca}) recorded in the terminal (**middle**) and the EPSCs in a postsynaptic CA3 neuron (**bottom**). As the action potential, waveform increases in duration, the duration of I_{Ca} increases, increasing the amplitude of the EPSCs. (Adapted, with permission, from Geiger and Jonas, 2000. Copyright © 2000 Cell Press.)

D. Simultaneous extracellular multiunit recordings of action potentials from thalamus and barrel cortex (*second* and *third traces* from top) during a train of 4-Hz mechanical stimulation of the primary whisker (**top trace**). Cortical and thalamic responses both depress during stimulation, although cortical responses depress faster. Intracellular voltage responses of a cortical neuron in a whisker barrel to 4-Hz stimulation of the primary whisker (**bottom two traces**). The first of the two traces shows responses to successive whisker stimuli in one train. Time scale same as top traces. The bottom trace shows an expanded view of the first four responses to whisker stimulation in three separate trains. Note there is variability from trial to trial in the spiking responses to the second and third stimuli in the train, likely due to the probabilistic nature of transmitter release. (Reproduced from Chung et al. 2002. Copyright © 2002 Cell Press.)

E. A brief burst of high-frequency stimulation leads to sustained enhancement in transmitter release. The time scale of the experimental records here has been compressed (each presynaptic and postsynaptic potential appears as a single line indicating its amplitude). A stable excitatory postsynaptic potential (EPSP) of around 1 mV is produced when the presynaptic neuron is stimulated at a relatively low rate of one action potential per second. The presynaptic neuron is then stimulated for a few seconds at a higher rate of 50 action potentials per second. During this *tetanic stimulation*, the EPSP increases in size because of enhanced transmitter release, a phenomenon known as *potentiation.* After several seconds of stimulation, the presynaptic neuron is returned to the initial rate of stimulation (one per second). However, the EPSPs remain enhanced for minutes and, in some cells, for several hours. This persistent increase is called *posttetanic potentiation.*

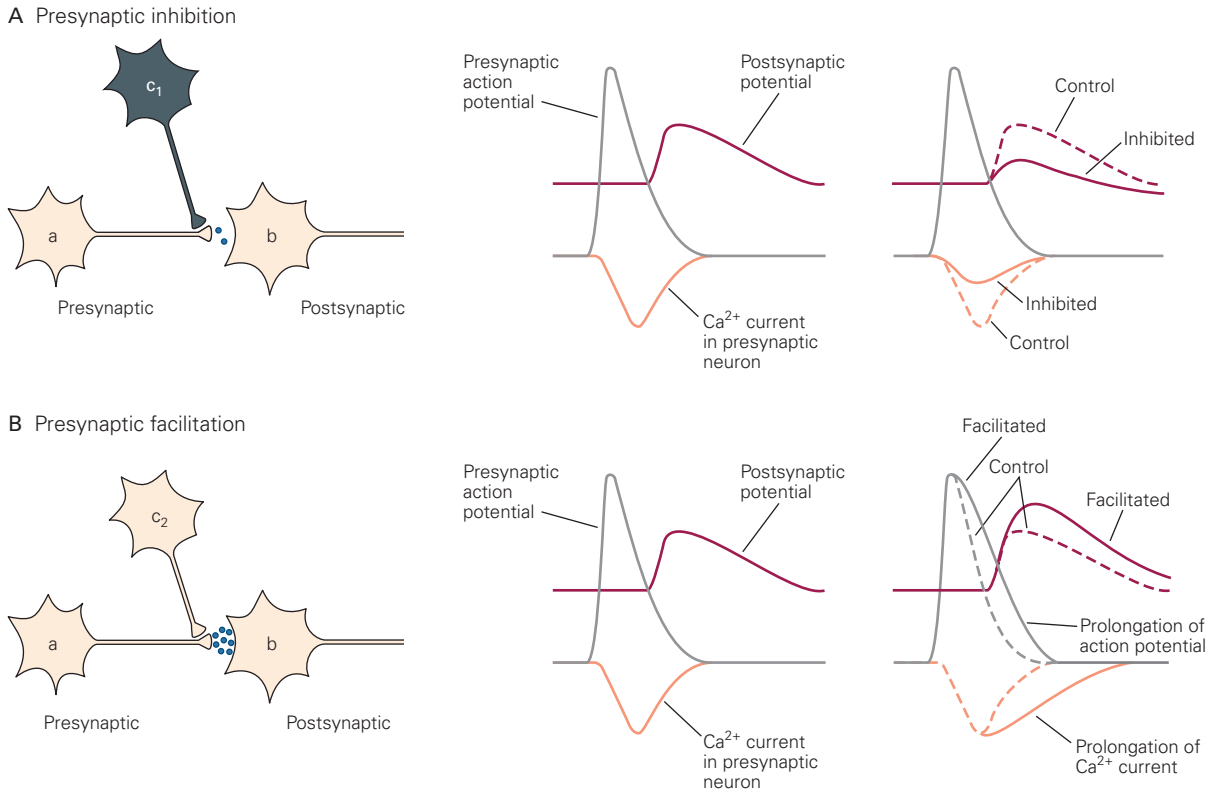

Figure 15–16 Axo-axonic synapses can inhibit or facilitate transmitter release by the presynaptic cell.

A. An inhibitory neuron (c_1) forms a synapse on an axon terminal of neuron **a**. Release of transmitter by cell c_1 activates metabotropic receptors on the terminal, thus inhibiting the Ca^{2+} current in the terminal and reducing the amount of transmitter released by cell a onto cell **b**. The reduction of transmitter release from cell a in turn reduces the amplitude of the excitatory postsynaptic potential in cell b, a process termed presynaptic inhibition.

B. A facilitating neuron (c_2) forms a synapse on an axon terminal of neuron **a**. Release of transmitter by cell c_2 activates metabotropic receptors on the terminal, thus decreasing a K^+ current in the terminals and thereby prolonging the action potential and increasing Ca^{2+} influx into cell a. This increases transmitter release from cell a onto cell **b**, thereby increasing the size of the EPSP in cell b, a process termed presynaptic facilitation.

terminal (including the *Aplysia* S-type K^+ channel discussed in Chapter 14). This action increases the duration of the presynaptic action potential, thereby increasing Ca^{2+} influx by enabling the voltage-dependent Ca^{2+} channels to remain open for a longer period. In other cells, activation of presynaptic ionotropic receptors increases transmitter release. Activation of presynaptic Ca^{2+}-permeable ionotropic receptor-channels, including presynaptic NMDA-type glutamate receptors, can increase release by directly enhancing Ca^{2+} influx. Activation of presynaptic ionotropic receptor-channels that are not permeable to Ca^{2+} can indirectly increase presynaptic Ca^{2+} levels by depolarizing the terminal and activating voltage-gated Ca^{2+} channels.

Thus, presynaptic terminals are endowed with a variety of mechanisms that allow for the fine-tuning of the strength of synaptic transmission. Although we know a fair amount about the mechanisms of short-term changes in synaptic strength—changes that last seconds, minutes, and hours—we are only beginning to learn about their functional roles. The mechanisms that support changes that persist for days, weeks, and longer also remain mysterious. These long-term changes often require alterations in gene expression and growth of presynaptic and postsynaptic structures in addition to alterations in Ca^{2+} influx and enhancement of transmitter release from existing terminals. We will discuss how such changes may contribute to different forms of long-term learning and memory in Chapters 53 and 54.

Highlights

1. Chemical neurotransmission is the primary mechanism by which neurons communicate, and process information; it occurs throughout the nervous system. Release of neurotransmitter is

stimulated by a series of electrical and biochemical processes in the presynaptic nerve terminal.

2. Neurotransmitter release is steeply dependent on depolarization of the presynaptic terminal. While the action potential is controlled by sodium and potassium conductances, it is the depolarization itself, rather than opening of either voltage-gated sodium or potassium channels, that triggers release.
3. Depolarization of the presynaptic terminal opens voltage-gated Ca^{2+} channels (VGCCs), resulting in Ca^{2+} influx. These channels are concentrated at presynaptic "active zones," very close to the sites at which release occurs. The relationship between Ca^{2+} influx and neurotransmitter release is tightly coupled and steeply nonlinear. The peak Ca^{2+} entry lags slightly behind the peak of the action potential and quickly produces a marked rise in the rate of transmitter release.
4. VGCCs are heterogeneous—five classes have been described with distinct biophysical, biochemical, and pharmacological properties. Multiple classes of VGCCs can contribute to neurotransmitter release at individual nerve terminals and are targets of disease-causing mutations. P/Q- and N-type Ca^{2+} channels are particularly prominent at active zones in the central nervous system.
5. Chemical transmission generally involves the release of quantal packets of neurotransmitter, with a quantum corresponding to the contents of a single synaptic vesicle. Under conditions that decrease transmitter release, such as lowered extracellular Ca^{2+}, a presynaptic action potential triggers the probabilistic release of a few quanta, which produce postsynaptic responses of variable amplitude that are integral multiples of the unitary response to a single quantum, interspersed by complete failures of transmission.
6. The unitary events are driven by the fusion of individual synaptic vesicles of relatively homogeneous size and transmitter content. Visualized as small, clear, spherical membrane organelles, single vesicles contain thousands of small-molecule neurotransmitters. Other neurotransmitters, including the biogenic amines and neuropeptides, are packaged into a distinct class of larger, dense-core vesicles that mediate slower forms of synaptic transmission. A typical presynaptic terminal in the mammalian central nervous system involved in fast synaptic transmission contains 100 to 200 vesicles. A small number of vesicles dock along the presynaptic membrane of the active zone and are the most ready to fuse.
7. At many synaptic connections, the amplitude of a postsynaptic potential can be described as a product of multiple factors: (1) the number of presynaptic sites occupied by a readily releasable vesicle (n), (2) the release probability of individual sites (p), and (3) the size of the postsynaptic response to the release of a single vesicle (a). On individual trials, the number of vesicles released can be described by a binomial distribution reflecting the likelihood of release of zero, one, two, or more vesicles, as if we were to count the number of heads when n coins were being flipped.
8. Exocytosis, the process by which vesicles fuse with the presynaptic membrane, and endocytosis, the process that retrieves vesicles, occur in rapid succession in nerve terminals and other secretory structures. These events are evident in morphological studies and are studied in real time by electrical measurements of membrane surface area.
9. Exocytosis is mediated by evolutionarily conserved SNARE proteins. Together, the presynaptic plasma membrane proteins syntaxin and SNAP-25 and the synaptic vesicle membrane protein synaptobrevin contribute to the SNARE complex, a set of four helical domains. Formation of this complex is critical for vesicle fusion as shown by the ability of various neurotoxins to block transmitter release through the cleavage of SNARE proteins. SNARE complex assembly is modulated by a family of SM proteins, exemplified by Munc18.
10. Synaptotagmins, such as synaptotagmin-1 (syt1), are abundant vesicular proteins that act as Ca^{2+} sensors for regulation of vesicle release. Syt1 binds multiple Ca^{2+} ions and thus forms a close association with the plasma membrane following Ca^{2+} influx. By binding to the SNARE complex even before the rise in presynaptic Ca^{2+}, it may enable that complex to cause fusion quickly.
11. Synaptic vesicle exocytosis is exquisitely precise and rapid because its molecular machinery is embedded in an active zone protein scaffold consisting of RIM, RIM-BP, and Munc-13. The complex: 1. Tethers vesicles to the plasma membrane through binding of RIM to Rab3 and Rab27 vesicle proteins; 2. Recruits calcium channels to the vicinity of tethered vesicles via binding to RIM and RIM-BP; and 3. Facilitates SNARE complex assembly via interaction with Munc13. The active zone complex also mediates many forms of short- and long-term synaptic plasticity.
12. Rapid endocytosis of vesicle membranes after release enables fast recycling of vesicles for a continuous supply during prolonged stimulation.
13. Synaptic terminals are diverse and vary in their release properties. Active zone scaffolding proteins differ across synapses and species, as does

expression of presynaptic Ca^{2+} channels and synaptotagmins. At some synapses, vesicles and Ca^{2+} channels appear aligned by an intricate structural network.

14. Transmitter release can be modulated intrinsically or extrinsically as an aspect of synaptic plasticity. Synaptic strength can be strongly influenced intrinsically by the pattern of firing in phenomena known as "depression" and "facilitation." In addition, extrinsic neuromodulators can alter the dynamics of release by regulation of Ca^{2+} channels or events downstream of Ca^{2+} entry.

Steven A. Siegelbaum
Thomas C. Südhof
Richard W. Tsien

Selected Reading

Katz B. 1969. *The Release of Neural Transmitter Substances.* Springfield, IL: Thomas.

Lonart G. 2002. RIM1: an edge for presynaptic plasticity. Trends Neurosci 25:329–332.

Meinrenken CJ, Borst JG, Sakmann B. 2003. Local routes revisited: the space and time dependence of the Ca^{2+} signal for phasic transmitter release at the rat calyx of Held. J Physiol 547:665–689.

Reid CA, Bekkers JM, Clements JD. 2003. Presynaptic Ca^{2+} channels: a functional patchwork. Trends Neurosci 26:683–687.

Stevens CF. 2003. Neurotransmitter release at central synapses. Neuron 40:381–388.

Südhof TC. 2014. The molecular machinery of neurotransmitter release (Nobel lecture). Angew Chem Int Ed Engl 53:12696–12717.

References

Acuna C, Liu X, Südhof TC. 2016. How to make an active zone: unexpected universal functional redundance between RIMs and RIM-BPs. Neuron 91:792–807.

Akert K, Moor H, Pfenninger K. 1971. Synaptic fine structure. Adv Cytopharmacol 1:273–290.

Bacaj T, Wu D, Yang X, et al. 2013. Synaptotagmin-1 and -7 trigger synchronous and asynchronous phases of neurotransmitter release. Neuron 80:947–959.

Baker PF, Hodgkin AL, Ridgway EB. 1971. Depolarization and calcium entry in squid giant axons. J Physiol 218:709–755.

Bollmann JH, Sakmann B, Gerard J, Borst G. 2000. Calcium sensitivity of glutamate release in a calyx-type terminal. Science 289:953–957.

Borst JG, Sakmann B. 1996. Calcium influx and transmitter release in a fast CNS synapse. Nature 383:431–434.

Boyd IA, Martin AR. 1956. The end-plate potential in mammalian muscle. J Physiol 132:74–91.

Chung S, Li X, Nelson SB. 2002. Short-term depression at thalamocortical synapses contributes to rapid adaptation of cortical sensory responses in vivo. Neuron 34:437–446.

Couteaux R, Pecot-Dechavassine M. 1970. Vésicules synaptiques et poches au niveau des "zones actives" de la jonction neuromusculaire. C R Acad Sci Hebd Seances Acad Sci D 271:2346–2349.

Del Castillo J, Katz B. 1954. The effect of magnesium on the activity of motor nerve endings. J Physiol 124:553–559.

Dittman JS, Kreitzer AC, Regehr WG. 2000. Interplay between facilitation, depression and residual calcium at three presynaptic terminals. J Neurosci 20:1374–1385.

Enoki R, Hu YL, Hamilton D, Fine A. 2009. Expression of long-term plasticity at individual synapses in hippocampus is graded, bidirectional, and mainly presynaptic: optical quantal analysis. Neuron 62:242–253.

Fatt P, Katz B. 1952. Spontaneous subthreshold activity at motor nerve endings. J Physiol 117:109–128.

Fawcett DW. 1981. *The Cell,* 2nd ed. Philadelphia: Saunders.

Fernandez I, Araç D, Ubach J, et al. 2001. Three-dimensional structure of the synaptotagmin 1 C2B-domain: synaptotagmin 1 as a phospholipid binding machine. Neuron 32:1057–1069.

Fernandez JM, Neher E, Gomperts BD. 1984. Capacitance measurements reveal stepwise fusion events in degranulating mast cells. Nature 312:453–455.

Fernandez-Chacon R, Konigstorfer A, Gerber SH, et al. 2001. Synaptotagmin I functions as a calcium regulator of release probability. Nature 410:41–49.

Geiger JR, Jonas P. 2000. Dynamic control of presynaptic Ca(2+) inflow by fast-inactivating K(+) channels in hippocampal mossy fiber boutons. Neuron 28:927–939.

Geppert M, Goda Y, Hammer RE, et al. 1994. Synaptotagmin I: a major Ca^{2+} sensor for transmitter release at a central synapse. Cell 79:717–727.

Harlow LH, Ress D, Stoschek A, Marshall RM, McMahan UJ. 2001. The architecture of active zone material at the frog's neuromuscular junction. Nature 409:479–484.

Heuser JE, Reese TS. 1981. Structural changes in transmitter release at the frog neuromuscular junction. J Cell Biol 88:564–580.

Hille B. 2001. *Ionic Channels of Excitable Membranes,* 3rd ed. Sunderland, MA: Sinauer.

Kaeser PS, Deng L, Wang Y, et al. 2011. RIM proteins tether Ca^{2+} channels to presynaptic active zones via a direct PDZ-domain interaction. Cell 144:282–295.

Kandel ER. 1981. Calcium and the control of synaptic strength by learning. Nature 293:697–700.

Katz B, Miledi R. 1967a. The study of synaptic transmission in the absence of nerve impulses. J Physiol 192:407–436.

Katz B, Miledi R. 1967b. The timing of calcium action during neuromuscular transmission. J Physiol 189:535–544.

Klein M, Shapiro E, Kandel ER. 1980. Synaptic plasticity and the modulation of the Ca^{2+} current. J Exp Biol 89:117–157.

Kretz R, Shapiro E, Connor J, Kandel ER. 1984. Post-tetanic potentiation, presynaptic inhibition, and the modulation of the free Ca^{2+} level in the presynaptic terminals. Exp Brain Res Suppl 9:240–283.

Kuffler SW, Nicholls JG, Martin AR. 1984. *From Neuron to Brain: A Cellular Approach to the Function of the Nervous System,* 2nd ed. Sunderland, MA: Sinauer.

Lawson D, Raff MC, Gomperts B, Fewtrell C, Gilula NB. 1977. Molecular events during membrane fusion. A study of exocytosis in rat peritoneal mast cells. J Cell Biol 72:242–259.

Liley AW. 1956. The quantal components of the mammalian end-plate potential. J Physiol 133:571–587.

Llinás RR. 1982. Calcium in synaptic transmission. Sci Am 247:56–65.

Llinás RR, Heuser JE. 1977. Depolarization-release coupling systems in neurons. Neurosci Res Program Bull 15:555–687.

Llinás R, Steinberg IZ, Walton K. 1981. Relationship between presynaptic calcium current and postsynaptic potential in squid giant synapse. Biophys J 33:323–351.

Lynch G, Halpain S, Baudry M. 1982. Effects of high-frequency synaptic stimulation on glumate receptor binding studied with a modified in vitro hippocampal slice preparation. Brain Res 244:101–111.

Magee JC, Johnston D. 1997. A synaptically controlled, associative signal for Hebbian plasticity in hippocampal neurons. Science 275:209–213.

Magnus CJ, Lee PH, Atasoy D, Su HH, Looger LL, Sternson SM. 2011. Chemical and genetic engineering of selective ion channel-ligand interactions. Science 333:1292–1296.

Martin AR. 1977. Junctional transmission. II. Presynaptic mechanisms. In: ER Kandel (ed). *Handbook of Physiology: A Critical, Comprehensive Presentation of Physiological Knowledge and Concepts,* Sect. 1 *The Nervous System,* Vol. 1 *Cellular Biology of Neurons,* Part 1, pp. 329–355. Bethesda, MD: American Physiological Society.

Monck JR, Fernandez JM. 1992. The exocytotic fusion pore. J Cell Biol 119:1395–1404.

Neher E. 1993. Cell physiology. Secretion without full fusion. Nature 363:497–498.

Nicoll RA. 1982. Neurotransmitters can say more than just "yes" or "no." Trends Neurosci 5:369–374.

Park M, Penick EC, Edwards JG, Kauer JA, Ehlers MD. 2004. Recycling endosomes supply AMPA receptors for LTP. Science 305:1972–1975.

Peters A, Palay SL, Webster H deF. 1991. *The Fine Structure of the Nervous System: Neurons and Supporting Cells,* 3rd ed. Philadelphia: Saunders.

Redman S. 1990. Quantal analysis of synaptic potentials in neurons of the central nervous system. Physiol Rev 70:165–198.

Rhee JS, Betz A, Pyott S, et al. 2002. Beta phorbol ester- and diacylglycerol-induced augmentation of transmitter release is mediated by Munc13s and not by PKCs. Cell 108:121–133.

Rizo J, Südhof TC. 2002. Snares and Munc18 in synaptic vesicle fusion. Nat Rev Neurosci 3:641–653.

Robitaille R, Adler EM, Charlton MP. 1990. Strategic location of calcium channels at transmitter release sites of frog neuromuscular synapses. Neuron 5:773–779.

Schneggenburger R, Neher E. 2000. Intracellular calcium dependence of transmitter release rates at a fast central synapse. Nature 406:889–893.

Schoch S, Castillo PE, Jo T, et al. 2002. RIM1alpha forms a protein scaffold for regulating neurotransmitter release at the active zone. Nature 415:321–326.

Schoch S, Deak F, Konigstorfer A, et al. 2001. SNARE function analyzed in synaptobrevin/VAMP knockout mice. Science 294:1117–1122.

Schweizer FE, Betz H, Augustine GJ. 1995. From vesicle docking to endocytosis: intermediate reactions of exocytosis. Neuron 14:689–696.

Smith SJ, Augustine GJ, Charlton MP. 1985. Transmission at voltage-clamped giant synapse of the squid: evidence for cooperativity of presynaptic calcium action. Proc Natl Acad Sci U S A 82:622–625.

Söllner T, Whiteheart SW, Brunner M, et al. 1993. SNAP receptors implicated in vesicle targeting and fusion. Nature 362:318–324.

Spruce AE, Breckenridge LJ, Lee AK, Almers W. 1990. Properties of the fusion pore that forms during exocytosis of a mast cell secretory vesicle. Neuron 4:643–654.

Sudhof TC. 2004. The synaptic vesicle cycle. Annu Rev Neurosci. 27:509–547.

Südhof TC. 2013. Neurotransmitter release: the last millisecond in the life of a synaptic vesicle. Neuron 80:675–690.

Sun J, Pang ZP, Qin D, Fahim AT, Adachi R, Südhof TC. 2007. A dual-Ca2+-sensor model for neurotransmitter release in a central synapse. Nature 450:676–682.

Sun JY, Wu LG. 2001. Fast kinetics of exocytosis revealed by simultaneous measurements of presynaptic capacitance and postsynaptic currents at a central synapse. Neuron 30: 171–182.

Sutton RB, Fasshauer D, Jahn R, Brunger AT. 1998. Crystal structure of a SNARE complex involved in synaptic exocytosis at 2.4 A resolution. Nature 395:347–353.

Takamori S, Holt M, Stenius K, et al. 2006. Molecular anatomy of a trafficking organelle. Cell 127:831–846.

von Gersdorff H, Matthews G. 1994. Dynamics of synaptic vesicle fusion and membrane retrieval in synaptic terminals. Nature 367:735–739.

Wachman ES, Poage RE, Stiles JR, Farkas DL, Meriney SD. 2004. Spatial distribution of calcium entry evoked by single action potentials within the presynaptic active zone. J Neurosci 24:2877–2885.

Wernig A. 1972. Changes in statistical parameters during facilitation at the crayfish neuromuscular junction. J Physiol 226:751–759.

Whittaker VP. 1993. Thirty years of synaptosome research. J Neurocytol. 22:735–742.

Zenisek D, Horst NK, Merrifield C, Sterling P, Matthews G. 2004. Visualizing synaptic ribbons in the living cell. J Neurosci 24:9752–9759.

Zhou Q, Zhou P, Wang AL, et al. 2017. The primed SNARE-complexin-synaptotagmin complex for neuronal exocytosis. Nature. 548:420–425.

Zucker RS. 1973. Changes in the statistics of transmitter release during facilitation. J Physiol 229:787–810.

16

Neurotransmitters

Chemical synaptic transmission can be divided into four steps: (1) synthesis and storage of a transmitter substance, (2) release of the transmitter, (3) interaction of the transmitter with receptors at the postsynaptic membrane, and (4) removal of the transmitter from the synapse. In the previous chapters, we considered steps 2 and 3. We now turn to the initial and final steps of chemical synaptic transmission: the synthesis and storage of transmitter molecules and their removal from the synaptic cleft after synaptic action.

A Chemical Messenger Must Meet Four Criteria to Be Considered a Neurotransmitter

Before considering the biochemical processes involved in synaptic transmission, it is important to make clear what is meant by a chemical transmitter. The concept is empirical and has changed over the years with increased understanding of synaptic transmission and a corresponding expansion of signaling agents. The concept that a released chemical could act as a transmitter was introduced by the British physician George Oliver and his colleague Edward Albert Schaefer, who in 1894 reported that injection of an adrenal gland extract increases blood pressure (Sir Henry Dale claimed that Oliver discovered this by injecting the extract into his own son). The constituent responsible was independently identified by three laboratories in 1897, and competing claims for priority provide one reason that this transmitter has 38 different names in the Merck Index, including adrenaline (as it was obtained from the adrenal gland) and epinephrine.

Experiments reported in 1904 by Thomas Elliott, a student in the lab of the physiologist John Langley, are generally credited as the first report of chemical neurotransmission. Elliott concluded that "adrenaline might then be the chemical stimulant liberated on each occasion when the impulse arrives at the periphery." Not incidentally, Elliott also proposed as early as 1914 that nerves could accumulate transmitter by an uptake system, suggesting that adrenal gland signaling might "depend on what could be picked up from the circulating blood and stored in its nerve endings," although uptake mechanisms were not demonstrated until more than 40 years later.

In 1913, Arthur Ewins, working with Henry Dale, discovered acetylcholine (ACh) as a component of the ergot fungus. In 1921, Otto Loewi demonstrated that stimulation of the vagus nerve terminals in frog hearts released "vagustoff," which was later shown to be ACh. Dale and Loewi later shared the Nobel Prize in 1946. The terms *cholinergic* and *adrenergic* were introduced to indicate that a neuron makes and releases ACh or norepinephrine (or epinephrine), respectively, the two substances first recognized as neurotransmitters. The term *catecholaminergic*, encompassing dopamine and the adrenergic transmitters, was derived from one of many natural sources, the catechu tree of India. Since that time, many other substances have been identified as transmitters.

The first secretory vesicles shown to accumulate and release neurotransmitters were the chromaffin vesicles of the adrenal gland, named in 1902 by Alfred Kohn due to their colorimetric reaction with chromate. William Cramer later showed that these organelles accumulate epinephrine. More recently, Mark Wightman provided direct evidence that these vesicles released epinephrine using carbon fiber electrodes as an electrochemical detector to measure catecholamine molecules released following fusion of chromaffin vesicles with the plasma membrane.

As a first approximation, a neurotransmitter can be defined as a substance that is released by a neuron that affects a specific target in a specific manner. A target can be either another neuron or an effector organ, such as muscle or gland. As with many other operational concepts in biology, the concept of a transmitter is not precise. Although the actions of hormones and neurotransmitters are quite similar, neurotransmitters usually act on targets that are close to the site of transmitter release, whereas hormones are released into the bloodstream to act on distant targets.

Neurotransmitters typically act on a target other than the releasing neuron itself, whereas substances termed autacoids act on the cell from which they are released. Nevertheless, at many synapses, transmitters activate not only postsynaptic receptors but also autoreceptors at the presynaptic release site. Autoreceptors usually modulate synaptic transmission that is in progress, for example, by limiting further release of transmitter or inhibiting subsequent transmitter synthesis. Receptors can also exist on presynaptic release sites that receive synaptic input from another neuron. These receptors function as heteroreceptors that regulate presynaptic excitability and transmitter release (Chapters 13 and 15).

Following release, the interaction of neurotransmitters with receptors is typically transient, lasting for periods ranging from less than a millisecond to several seconds. Nevertheless, neurotransmitter actions can result in long-term changes within target cells lasting hours or days, often by activating gene transcription. Moreover, nonneural cells, including astrocytes and microglia, can also synthesize, store, and release neurotransmitters, as well as express receptors that modulate their own function.

A limited number of substances of low molecular weight are generally accepted as classical neurotransmitters, and these exclude many neuropeptides, as well as other substances that are not released by exocytosis. Even so, it is often difficult to demonstrate that a specific neurotransmitter operates at a particular synapse, particularly given the diffusion and rapid reuptake or degradation of transmitters at the synaptic cleft.

A classical neurotransmitter is considered to meet four criteria:

1. It is synthesized in the presynaptic neuron.
2. It is accumulated within vesicles present in presynaptic release sites and is released via exocytosis in amounts sufficient to exert a defined action on the postsynaptic neuron or effector organ.
3. When administered exogenously in reasonable concentrations, it mimics the action of the endogenous transmitter (for example, it activates the same ion channels or second-messenger pathway in the postsynaptic cell).
4. A specific mechanism usually exists for removing the substance from the extracellular environment. This may be the synaptic cleft in the case of "wired" or "private" neurotransmission (in which the action of the substance is limited to a single synapse) or the extrasynaptic space in the case of "volume" or "social" neurotransmission (in which the substance diffuses to multiple synapses).

The nervous system makes use of two main classes of chemical substances that fit these criteria for signaling: small-molecule transmitters and neuropeptides. Neuropeptides are short polymers of amino acids processed in the Golgi apparatus, where they are packaged in large dense-core vesicles (approximately 70–250 nm in diameter). Small-molecule transmitters are packaged in small vesicles (~40 nm in diameter) that are usually electron-lucent. Vesicles are closely associated with specific Ca^{2+} channels at active zones and release their contents through exocytosis in response to a rise in intracellular Ca^{2+} evoked by an action potential (Chapter 15). Vesicle membrane is retrieved through endocytosis and recycled locally in the axon to produce new synaptic vesicles. Large dense-core vesicles

can contain both small-molecule transmitters and neuropeptides and do not undergo local recycling following full fusion with the plasma membrane.

Both types of vesicles are found in most neurons but in different proportions. Small synaptic vesicles are characteristic of neurons that use ACh, glutamate, γ-aminobutyric acid (GABA), and glycine as transmitters, whereas neurons that use catecholamines and serotonin as transmitters often have both small and large dense-core vesicles. The adrenal medulla—the tissue in which most discoveries on secretion were made and still widely used as a model for studying exocytosis—contains only large dense-core vesicles that contain both catecholamines and neuroactive peptides.

Only a Few Small-Molecule Substances Act as Transmitters

A relatively small number of low-molecular-weight substances are generally accepted as neurotransmitters. These include ACh, the excitatory amino acid glutamate, the inhibitory amino acids GABA and glycine, amine containing amino acid derivatives, and adenosine triphosphate (ATP) and its metabolites (Table 16–1). A small set of small molecules, such as the gas nitric oxide lipid metabolites are not released from vesicles and tend to break all of the classical rules (Chapter 14).

Table 16–1 Small-Molecule Neurotransmitter Substances and Their Precursors

Transmitter	Precursor
Acetylcholine	Choline
Biogenic amines	
Dopamine	Tyrosine
Norepinephrine	Tyrosine via dopamine
Epinephrine	Tyrosine via norepinephrine
Octopamine	Tyrosine via tyramine
Serotonin	Tryptophan
Histamine	Histidine
Melatonin	Tryptophan via serotonin
Amino acids	
Aspartate	Oxaloacetate
γ-Aminobutyric acid	Glutamine
Glutamate	Glutamine
Glycine	Serine
Adenosine triphosphate (ATP)	Adenosine diphosphate (ADP)
Adenosine	ATP
Endocannabinoids	Phospholipids
Nitric oxide	Arginine

The amine messengers share many biochemical similarities. All are charged small molecules that are formed in relatively short biosynthetic pathways and synthesized either from essential amino acids or from precursors derived from the major carbohydrate substrates of intermediary metabolism. Like other pathways of intermediary metabolism, synthesis of these neurotransmitters is catalyzed by enzymes that, with the notable exception of dopamine β-hydroxylase, are cytosolic. ATP, which originates in mitochondria, is abundantly present throughout the cell.

As in any biosynthetic pathway, the overall synthesis of amine transmitters typically is regulated at one rate-limiting enzymatic reaction. The rate-limiting step often is characteristic of one type of neuron and usually is absent in other types of mature neurons. The classical small-molecule neurotransmitters released from a particular neuron are thus determined by their presence in the cytosol due to synthesis and reuptake and to the selectivity of the vesicular transporter.

Acetylcholine

Acetylcholine is the only low-molecular-weight aminergic transmitter substance that is not an amino acid or derived directly from one. The biosynthetic pathway for ACh has only one enzymatic reaction, catalyzed by choline acetyltransferase (step 1 below):

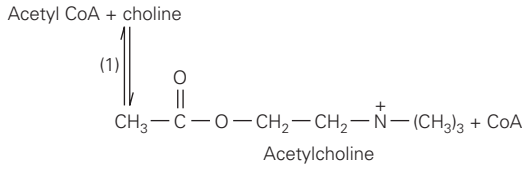

This transferase is the characteristic and limiting enzyme in ACh biosynthesis. Nervous tissue cannot synthesize choline, which is derived from the diet and delivered to neurons through the bloodstream. The co-substrate, acetyl coenzyme A (acetyl CoA), participates in many general metabolic pathways and is not restricted to cholinergic neurons.

Acetylcholine is released at all vertebrate neuromuscular junctions by spinal motor neurons (Chapter 12). In the autonomic nervous system, it is the transmitter released by all preganglionic neurons and by parasympathetic postganglionic neurons (Chapter 41). Cholinergic neurons form synapses throughout the brain; those in the nucleus basalis have particularly

widespread projections to the cerebral cortex. Acetylcholine (together with a noradrenergic component) is a principal neurotransmitter of the reticular activating system, which modulates arousal, sleep, wakefulness, and other critical aspects of human consciousness.

Biogenic Amine Transmitters

The terms *biogenic amine* or *monoamine,* although chemically imprecise, have been used for decades to designate certain neurotransmitters. This group includes the catecholamines and serotonin. Histamine, an imidazole, is also often included with biogenic amine transmitters, although its biochemistry is remote from the catecholamines and the indolamines.

Catecholamine Transmitters

The catecholamine transmitters—dopamine, norepinephrine, and epinephrine—are all synthesized from the essential amino acid tyrosine in a biosynthetic pathway containing five enzymes: tyrosine hydroxylase, pteridine reductase, aromatic amino acid decarboxylase, dopamine β-hydroxylase, and phenylethanolamine-*N*-methyl transferase. Catecholamines contain a catechol nucleus, a 3,4-dihydroxylated benzene ring.

The first enzyme, tyrosine hydroxylase (step 1 below), is an oxidase that converts tyrosine to L-dihydroxyphenylalanine (L-DOPA):

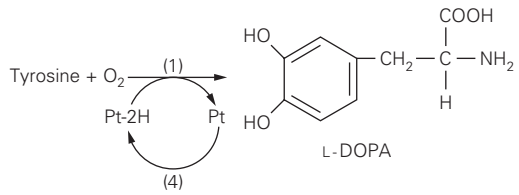

This enzyme is rate-limiting for the synthesis of both dopamine and norepinephrine. A distinct pathway is used to synthesize L-DOPA for production of the melanin pigments found throughout the plant and animal kingdoms, while the neuromelanin pigment found in some dopamine and norepinephrine neurons are metabolites of the oxidized neurotransmitters.

L-DOPA is present in all cells producing catecholamines, and its synthesis requires a reduced pteridine cofactor, Pt-2H, which is regenerated from pteridine (Pt) by another enzyme, pteridine reductase, which uses nicotinamide adenine dinucleotide (NADH) (step 4 above). This reductase is not specific to neurons.

Based on the finding that individuals with Parkinson disease have lost dopamine neurons of the substantia nigra, L-DOPA has been used to restore dopamine and motor function in patients. L-DOPA, whether exogenous or produced by tyrosine hydroxylase, is decarboxylated by a widespread enzyme known as aromatic amino acid decarboxylase, also called L-DOPA decarboxylase (step 2 below), to yield dopamine and carbon dioxide:

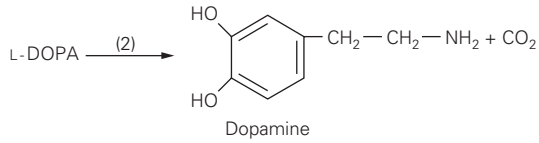

Interestingly, dopamine was initially thought to be present in neurons only as a precursor to norepinephrine. That dopamine also functions as a neurotransmitter itself was demonstrated in 1957 by Aarvid Carlsson, who found that rabbits treated with the synaptic vesicle dopamine uptake blocker, reserpine, exhibited floppy ears, but that L-DOPA, under conditions that produced dopamine but not norepinephrine, restored the normal erect ear posture.

In adrenergic neurons, the third enzyme in the sequence, dopamine β-hydroxylase (step 3 below), further converts dopamine to norepinephrine:

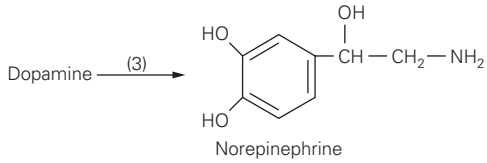

Unlike all other enzymes in the biosynthetic pathways of small-molecule neurotransmitters, dopamine β-hydroxylase is membrane-associated. It is bound tightly to the inner surface of aminergic vesicles as a peripheral protein. Consequently, norepinephrine is the only transmitter synthesized within vesicles.

In the central nervous system, norepinephrine is used as a transmitter by neurons with cell bodies in the locus coeruleus, a nucleus of the brain stem with many complex modulatory functions (Chapter 40). Although these adrenergic neurons are relatively few in number, they project widely throughout the cortex, cerebellum, hippocampus, and spinal cord. In many cases, neurons that release norepinephrine can also release the precursor dopamine, and thus can act at neurons expressing receptors for dopamine or norepinephrine. In the peripheral nervous system, norepinephrine is the transmitter of the postganglionic neurons in the sympathetic nervous system (Chapter 41).

In addition to these four catecholaminergic biosynthetic enzymes, a fifth enzyme, phenylethanolamine-*N*-methyltransferase (step 5 below), methylates

norepinephrine to form epinephrine (adrenaline) in the adrenal medulla:

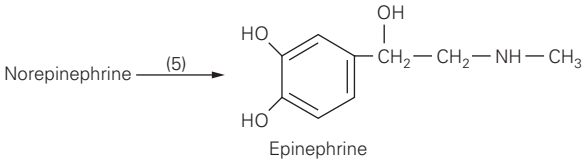

This reaction requires *S*-adenosyl-methionine as a methyl donor. The transferase is a cytoplasmic enzyme. Thus, for epinephrine to be formed, its immediate precursor norepinephrine must exit from vesicles into the cytoplasm. For epinephrine to be released, it must then be taken back up into vesicles. Only a small number of neurons in the brain use epinephrine as a transmitter.

The production of these catecholamine neurotransmitters is controlled by feedback regulation of the first enzyme in the pathway, tyrosine hydroxylase (Box 16–1). Not all cells that release catecholamines express all five biosynthetic enzymes, although cells that release epinephrine do. During development, the expression of the genes encoding these synthetic enzymes is independently regulated and the particular catecholamine that is produced by a cell is determined by which enzyme(s) in the step-wise pathway is not

Box 16–1 Catecholamine Production Varies With Neuronal Activity

Norepinephrine neurotransmission is far more active during awake states than sleep or anesthesia, with locus coeruleus noradrenergic neurons nearly silenced during rapid eye movement (REM) sleep. The production of catecholamine is able to keep up with wide variations in neuronal activity because catecholamine synthesis is highly regulated. Circadian changes in extracellular dopamine in the striatum have been suggested to result from altered activity of the dopamine uptake transporter.

In autonomic ganglia, the amount of norepinephrine in postganglionic neurons is regulated transsynaptically. Activity in the presynaptic neurons, which are both cholinergic and peptidergic, first induces short-term changes in second messengers in the postsynaptic adrenergic cells. These changes increase the supply of norepinephrine through the cAMP-dependent phosphorylation of tyrosine hydroxylase, the first enzyme in the catecholamine biosynthetic pathway.

Phosphorylation enhances the affinity of the hydroxylase for the pteridine cofactor and diminishes feedback inhibition by end products such as norepinephrine. Phosphorylation of tyrosine hydroxylase lasts only as long as cAMP remains elevated, as the phosphorylated hydroxylase is quickly dephosphorylated by protein phosphatases.

If presynaptic activity is sufficiently prolonged, however, other changes in the production of norepinephrine will occur. Severe stress to an animal results in intense presynaptic activity and persistent firing of the postsynaptic adrenergic neuron, placing a greater demand on transmitter synthesis. To meet this challenge, the tyrosine hydroxylase gene is induced to increase transcription and thus production of the protein. Elevated amounts of tyrosine hydroxylase are observed in the cell body within hours after stimulation and at nerve endings days later.

This induction of increased levels of tyrosine hydroxylase begins with the persistent release of chemical transmitters from the presynaptic neurons and prolonged activation of the cAMP pathway in postsynaptic adrenergic cells, which activates the cAMP-dependent protein kinase (PKA). This kinase phosphorylates not only existing tyrosine hydroxylase molecules but also the transcription factor, cAMP response element binding protein (CREB).

Once phosphorylated, CREB binds a specific DNA enhancer sequence called the cAMP-recognition element (CRE), which lies upstream (5′) of the gene for the hydroxylase. Binding of CREB to CRE facilitates the binding of RNA polymerase to the gene's promoter, increasing tyrosine hydroxylase transcription. Induction of tyrosine hydroxylase was the first known example of a neurotransmitter altering gene expression.

Based on similarity in portions of the amino acid and nucleic acid sequences encoding three of the biosynthetic enzymes—tyrosine hydroxylase, dopamine β-hydroxylase, and phenylethanolamine-*N*-methyltransferase—it has been suggested that the three enzymes may have arisen from a common ancestral protein. Moreover, long-term changes in the synthesis of these enzymes are coordinately regulated in adrenergic neurons.

At first, this discovery suggested that the genes encoding these enzymes might be located sequentially along the same chromosome and be controlled by the same promoter, like genes in a bacterial operon. But in humans, the genes for the biosynthetic enzymes for norepinephrine are not located on the same chromosome. Therefore, coordinate regulation is likely achieved by parallel activation through similar but independent transcription activator systems.

expressed. Thus, neurons that release norepinephrine do not express the methyltransferase, and neurons that release dopamine do not express the transferase or dopamine β-hydroxylase. Some neurons that express tyrosine hydroxylase, and thus produce dopamine, do not express the vesicular monoamine transporter (VMAT), the transporter that accumulates dopamine in synaptic vesicles, and thus do not appear to release dopamine as a transmitter.

Of the four major dopaminergic nerve tracts, three arise in the midbrain (Chapters 40 and 43). Dopaminergic neurons in the substantia nigra that project to the striatum are important for the control of movement and are affected in Parkinson disease and other disorders of movement, but projections to the associative striatum have also been implicated more recently in dopamine dysfunction in schizophrenia. The mesolimbic and mesocortical tracts are critical for affect, emotion, attention, and motivation and are implicated in drug addiction and schizophrenia. A fourth dopaminergic tract, the tuberoinfundibular pathway, originates in the arcuate nucleus of the hypothalamus and projects to the pituitary gland, where it regulates secretion of hormones (Chapter 41).

The synthesis of biogenic amines is highly regulated and can be rapidly increased. As a result, the amounts of transmitter available for release can keep up with wide variations in neuronal activity. Mechanisms for regulating both the synthesis of catecholamine transmitters and the production of enzymes in the step-wise catecholamine pathway are discussed in Box 16–1.

Trace amines, naturally occurring catecholamine derivatives, may also serve as transmitters. In invertebrates, the tyrosine derivatives tyramine and octopamine (so called because it was originally identified in the octopus salivary gland) play key roles in numerous physiological processes including behavioral regulation. Trace amine receptors also have been identified in mammals, where their functional role is still being characterized. In particular, trace amine-associated receptor 1 (TAAR1) has been shown to modulate aspects of biogenic amine neurotransmission as well as to play a role in the immune system.

Serotonin

Serotonin (5-hydroxytryptamine or 5-HT) and the essential amino acid tryptophan from which it is derived belong to a group of aromatic compounds called indoles, with a five-member ring containing nitrogen joined to a benzene ring. Two enzymes are needed to synthesize serotonin: tryptophan (Trp) hydroxylase (step 1 below), an oxidase similar to tyrosine hydroxylase, and aromatic amino acid decarboxylase, also called 5-hydroxytryptophan (5-HTP) decarboxylase (step 2 below):

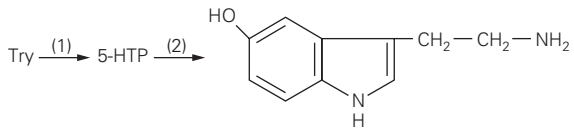

Serotonin

As with the catecholamines, the limiting reaction in serotonin synthesis is catalyzed by the first enzyme in the pathway, tryptophan hydroxylase. Tryptophan hydroxylase is similar to tyrosine hydroxylase not only in catalytic mechanism but also in amino acid sequence. The two enzymes are thought to stem from a common ancestral protein by gene duplication because the two hydroxylases are encoded by genes close together on the same chromosome (tryptophan hydroxylase, 11p15.3-p14; tyrosine hydroxylase, 11p15.5). The second enzyme in the pathway, 5-hydroxytryptophan decarboxylase, is identical to L-DOPA decarboxylase. Enzymes with similar activity, L-aromatic amino acid decarboxylases, are present in nonnervous tissues as well.

The cell bodies of serotonergic neurons are found in and around the midline raphe nuclei of the brain stem and are involved in regulating affect, attention, and other cognitive functions (Chapter 40). These cells, like the noradrenergic cells in the locus coeruleus, project widely throughout the brain and spinal cord. Serotonin and the catecholamines norepinephrine and dopamine are implicated in depression, a major mood disorder. Antidepressant medications inhibit the uptake of serotonin, norepinephrine, and dopamine, thereby increasing the magnitude and duration of the action of these transmitters, which in turn leads to altered cell signaling and adaptations (Chapter 61).

Histamine

Histamine, derived from the essential amino acid histidine by decarboxylation, contains a characteristic five-member ring with two nitrogen atoms. It has long been recognized as an autacoid, active when released from mast cells in the inflammatory reaction and in the control of vasculature, smooth muscle, and exocrine glands (eg, secretion of highly acidic gastric juice). Histamine is a transmitter in both invertebrates and vertebrates. It is concentrated in the hypothalamus, one of the brain centers for regulating the secretion of hormones (Chapter 41). The decarboxylase catalyzing its synthesis (step 1 below), although not extensively analyzed, appears to be characteristic of histaminergic neurons.

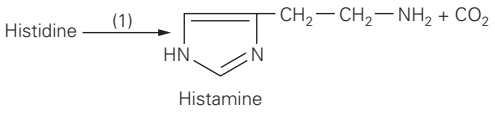

As described in the next section, the biogenic amines are loaded into synaptic and secretory vesicles by two transporters, VMAT1, mostly in peripheral cells, and VMAT2, mostly in the central nervous system. As the transporters are not selective for a given biogenic amine, a mixture of transmitters can be present. Some neurons co-release dopamine with norepinephrine, whereas secretory vesicles from the adrenal medulla can co-release epinephrine and norepinephrine.

Amino Acid Transmitters

In contrast to acetylcholine and the biogenic amines, which are not intermediates in general metabolic pathways and are produced only in certain neurons, the amino acids glutamate and glycine are not only neurotransmitters but also universal cellular constituents. Because they can be synthesized in neurons and other cells, neither is an essential amino acid.

Glutamate, the neurotransmitter most frequently used at excitatory synapses throughout the central nervous system, is produced from α-ketoglutarate, an intermediate in the tricarboxylic acid cycle of intermediary metabolism. After it is released, glutamate is taken up from the synaptic cleft by specific transporters in the membrane of both neurons and glia (see later). The glutamate taken up by astrocytes is converted to glutamine by the enzyme glutamine synthase. This glutamine is transported back into neurons that use glutamate as a transmitter, where it is hydrolyzed to glutamate by the enzyme glutaminase. Cytoplasmic glutamate is then loaded into synaptic vesicles by the vesicular glutamate transporter, VGLUT.

Glycine is the major transmitter used by inhibitory interneurons of the spinal cord. It is also a necessary cofactor for activation of the *N*-methyl-D-aspartate (NMDA) glutamate receptors (Chapter 13). Glycine is synthesized from serine by the mitochondrial form of the serine hydroxymethyltransferase. The amino acid GABA is synthesized from glutamate in a reaction catalyzed by glutamic acid decarboxylase (step 1 below):

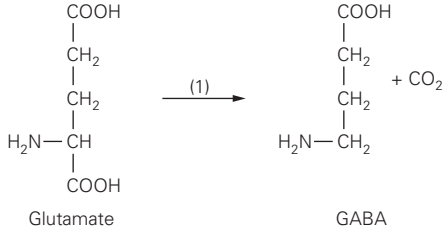

GABA is present at high concentrations throughout the central nervous system and is detectable in other tissues. It is used as a transmitter by an important class of inhibitory interneurons in the spinal cord. In the brain, GABA is the major transmitter of a wide array of inhibitory neurons and interneurons. Both GABA and glycine are loaded into synaptic vesicles by the same transporter, VGAT, and thus can be co-released from the same vesicles.

ATP and Adenosine

ATP and its degradation products (eg, adenosine) act as transmitters at some synapses by binding to several classes of G protein–coupled receptors (the P1 and P2Y receptors). ATP can also produce excitatory actions by binding to ionotropic P2X receptors. Caffeine's stimulatory effects depend on its inhibition of adenosine binding to the P1 receptors. Adenine and guanine and their sugar-containing derivatives are called purines; the evidence for transmission at purinergic receptors is especially strong for autonomic neurons that innervate the vas deferens, bladder, and muscle fibers of the heart; for nerve plexuses on smooth muscle in the gut; and for some neurons in the brain. Purinergic transmission is particularly important for nerves mediating pain (Chapter 20).

ATP released by tissue damage acts to transmit pain sensation through one type of ionotropic purine receptor present on the terminals of peripheral axons of dorsal root ganglion cells that act as nociceptors. ATP released from terminals of the central axons of these dorsal root ganglion cells excites another type of ionotropic purine receptor on neurons in the dorsal horn of the spinal cord. ATP and other nucleotides also act at the family of P2Y G protein–coupled receptors to modulate various downstream signaling pathways.

Small-Molecule Transmitters Are Actively Taken Up Into Vesicles

Common amino acids act as transmitters in some neurons but not in others, indicating that the presence of a substance in a neuron, even in substantial amounts, is not in itself sufficient evidence that the substance is used as a transmitter. For example, at the neuromuscular junction of the lobster (and other arthropods), GABA is inhibitory and glutamate is excitatory. The concentration of GABA is approximately 20 times greater in inhibitory cells than in excitatory cells,

supporting the idea that GABA is the inhibitory transmitter at the lobster neuromuscular junction. In contrast, the concentration of the excitatory transmitter glutamate is similar in both excitatory and inhibitory cells. Glutamate therefore must be compartmentalized within these neurons; that is, *transmitter* glutamate must be kept separate from *metabolic* glutamate. In fact, transmitter glutamate is compartmentalized in synaptic vesicles.

Although the presence of a specific set of biosynthetic enzymes can determine whether a small molecule can be used as a transmitter, the presence of the enzymes does not mean that the molecule will be used. Before a substance can be released as a transmitter, it usually must first be concentrated in synaptic vesicles. Transmitter concentrations within vesicles are high, on the order of several hundred millimolar. Neurotransmitter substances are concentrated in vesicles by transporters that are specific to each type of neuron and energized by a vacuolar-type H^+-ATPase (V-ATPase) that is found not only in synaptic and secretory vesicles but also in all organelles in the secretory pathway, including endosomes and lysosomes.

Using the energy generated by the hydrolysis of cytoplasmic ATP, the V-ATPase creates an H^+ electrochemical gradient by promoting the influx of protons into the vesicle. Transporters use this proton gradient to drive transmitter molecules into the vesicles against their concentration gradient through a proton-antiport mechanism. A number of different vesicular transporters in mammals are responsible for concentrating different transmitter molecules in vesicles (Figure 16–1). These proteins span the vesicle membrane 12 times and are distantly related to a class of bacterial transporters that mediate drug resistance. (Vesicular transporters differ structurally and mechanistically from the transporters in the plasma membrane, as discussed later.)

Transmitter molecules are classically modeled to be taken up into a vesicle by vesicular transporters in exchange for the transport of two protons out of the vesicle. Because the maintenance of the pH gradient requires the hydrolysis of ATP, the uptake of transmitter into vesicles is energy-dependent. Vesicular transporters can concentrate some neurotransmitters such as dopamine up to 100,000-fold relative to their concentration in the cytoplasm. Uptake of transmitters by the transporters is rapid, enabling vesicles to be quickly refilled after they release their transmitter and are retrieved by endocytosis; this is important for maintaining the supply of releasable vesicles during periods of rapid nerve firing (Chapter 15).

The specificity of transporters for substrate is quite variable. The vesicular ACh transporter (VAChT) does not transport choline or other transmitters. Likewise, the vesicular glutamate transporters, for which there are three types (VGLUT1, 2, and 3) that are differentially expressed in the CNS, carry negligible amounts of the other acidic amino acid, aspartate. However, VMAT2 can transport all of the biogenic amines as well as drugs including amphetamine and even some neurotoxic compounds such as *N*-methyl-4-phenylpyridinium (MPP^+). 1-Methyl-4-phenyl-1,2,3,6-tetrahydropyridine (MPTP), a contaminant of a synthetic opiate drug of abuse, is metabolized to MPP^+ by the enzyme monoamine oxidase (MAO) type B. In fact, VMAT1 was cloned by Robert Edwards and colleagues based on the ability of the transporter to protect cells from the neurotoxic effects of MPP^+; cells expressing VMAT were able to sequester the toxin in vesicle-like compartments, thereby lowering its cytoplasmic concentration and promoting cell survival. By expressing genes obtained from a cDNA library from adrenal pheochromocytoma cells in a mammalian cell line sensitive to MPP^+, Edwards was able to identify cells that expressed VMAT1 based on their selective survival. VMAT2 was subsequently identified by homology cloning, as well as directly by a number of other groups.

Transporters and V-ATPases are present in the membranes of both small synaptic vesicles and large dense-core vesicles. Vesicular transporters are the targets of several important pharmacological agents. Reserpine and tetrabenazine inhibit uptake of amine transmitters by binding to the vesicular monoamine transporter. The psychostimulants amphetamine, methamphetamine, and 3,4-methylenedioxy-*N*-methylamphetamine (MDMA or ecstasy) act to deplete vesicles of amine transmitter molecules, but also cause their efflux from the cytoplasm into the extracellular space via the plasma membrane biogenic amine transporters (see below). These compounds accumulate inside vesicles through proton-antiport–driven transport mediated by VMAT, which diminishes the proton gradient necessary for loading amine transmitters into vesicles.

Drugs that are sufficiently similar to the normal transmitter substance can act as *false transmitters.* These are packaged in vesicles and released by exocytosis as if they were true transmitters, but they often bind only weakly or not at all to the postsynaptic receptor for the natural transmitter, and thus their release decreases the efficacy of transmission. Several drugs historically used to treat hypertension, such as α-methyldopa and guanethidine, are taken up into adrenergic synapses

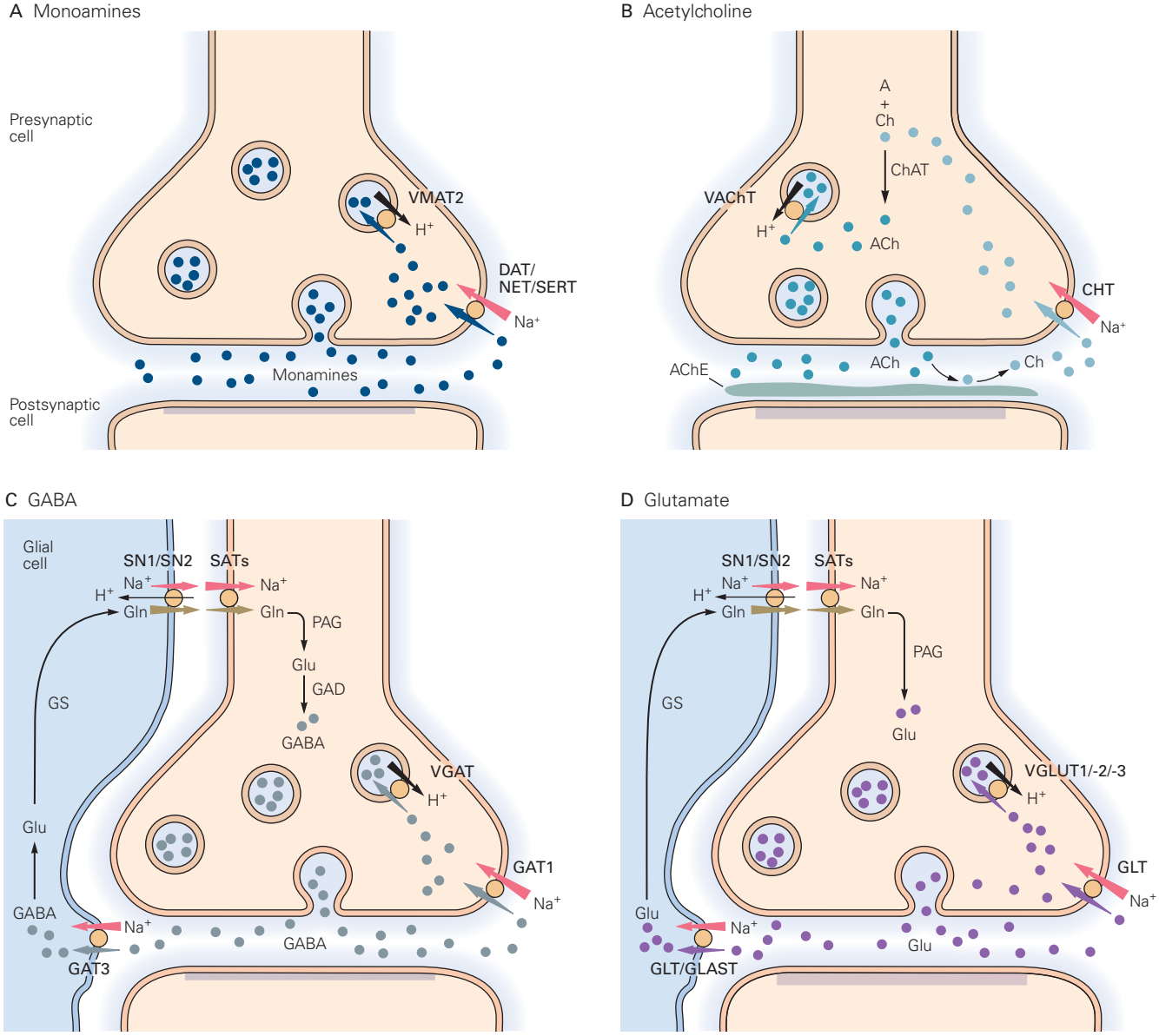

Figure 16–1 **Small-molecule transmitters are transported from the cytosol into vesicles or from the synaptic cleft to the cytosol by transporters.** Most small-molecule neurotransmitters are released by exocytosis from the nerve terminal and act on specific postsynaptic receptors. The signal is terminated and transmitter recycled by specific transporter proteins located at the nerve terminal or in surrounding glial cells. Transport by these proteins (**orange circles**) is driven by the electrochemical gradients of H^+ (**black arrows**) or Na^+ (**red arrows**). (Adapted, with permission, from Chaudhry et al. 2008. Copyright © 2008 Springer-Verlag.)

A. Three distinct transporters mediate reuptake of monoamines across the plasma membrane. The dopamine transporter (**DAT**), norepinephrine transporter (**NET**), and serotonin transporter (**SERT**) are responsible for the reuptake (**dark blue arrows**) of their cognate transmitters. The vesicular monoamine transporter (**VMAT2**) transports all three monoamines into synaptic vesicles for subsequent exocytotic release.

B. Cholinergic signaling is terminated by metabolism of acetylcholine (**ACh**) to the inactive choline and acetate by acetylcholinesterase (**AChE**), which is located in the synaptic cleft (**green bar**). Choline (**Ch**) is transported by the choline transporter (**CHT**) back into the nerve terminal (**light blue arrow**) where choline acetyltransferase (**ChAT**) subsequently catalyzes acetylation of choline to reconstitute ACh. The ACh is transported into the vesicle by the vesicular ACh transporter (**VAChT**).

C. At GABAergic and glycinergic nerve terminals, the GABA transporter (**GAT1**) and glycine transporter (GLYT2, not shown) mediate reuptake of GABA and glycine (**gray arrow**), respectively. GABA may also be taken up by surrounding glial cells (eg, by GAT3). In the glial cells, GABA is first converted to glutamate (**Glu**) by GAD. Glu is then is converted by glial glutamine synthetase (**GS**) to glutamine (**Gln**). Glutamine is transported back to the nerve terminal by the concerted action of the system N transporter (**SN1/SN2**) and system A transporter (**SAT**) (**brown arrows**). In the nerve terminal, phosphate-activated glutaminase (**PAG**) converts glutamine to glutamate, which is converted to GABA by glutamate decarboxylase (**GAD**). VGAT then transports GABA into vesicles. The glial transporter GLYT1 (not shown) also contributes to the clearance of glycine.

D. After release from excitatory neuronal terminals, the majority of glutamate is taken up by surrounding glial cells (eg, by **GLT** and **GLAST**) for conversion to glutamine, which is subsequently transported back to the nerve terminals by SN1/SN2 and a type of SAT (**SATx**) (**brown arrows**). Reuptake of glutamate at glutamatergic terminals also has been demonstrated for a GLT isoform (**purple arrows**). Glutamate is transported into vesicles by **VGLUT**.

(and converted into α-methyldopamine in the case of α-methyldopa) and replace norepinephrine in synaptic vesicles. When released, these drugs fail to stimulate postsynaptic adrenergic receptors, thereby relaxing vascular smooth muscle by inhibiting adrenergic tone. Tyramine, which is found in high quantities in dietary red wine and cheese, also acts as a false transmitter; however, it also can act as a stimulant by releasing biogenic amines through a mechanism akin to amphetamine. Another false transmitter, 5-hydroxydopamine, can produce an electron-dense reaction product and has been used to identify synaptic vesicles that acquire biogenic amines.

More recently, several fluorescent false neurotransmitters have been designed, enabling researchers to use imaging methods to monitor the uptake and release of neurotransmitter derivatives during synaptic activity in rodent and fly brain (see Figure 16–5 in Box 16–2).

An unexpected finding is that dopamine can be released from dendrites as well as from axons, despite the lack of synaptic vesicles in dendrites. Organelles that express VMAT2 seem likely to be the source of the release, albeit with different requirements for intracellular Ca^{2+} than classical neurotransmission at presynaptic terminals. For technical reasons, this phenomenon has been studied mostly in dendrites of dopaminergic neurons of the substantia nigra: dopamine can be measured directly by electrochemical techniques, and the dendrites are well separated from the cell bodies. However, it is possible that dendritic neurotransmitter release occurs more widely throughout the nervous system.

Many Neuroactive Peptides Serve as Transmitters

The enzymes that catalyze the synthesis of the low-molecular-weight neurotransmitters, with the exception of dopamine β-hydroxylase, are found in the cytoplasm. These enzymes are synthesized on free polysomes in the cell body and probably in dendrites and are distributed throughout the neuron by axoplasmic flow. Thus, small-molecule transmitter substances can be formed in all parts of the neuron; most importantly, they can be synthesized at axonal presynaptic sites from which they are released.

In contrast, neuroactive peptides are derived from secretory proteins that are formed in the cell body. More than 50 short peptides are produced by neurons or neuroendocrine cells and exert physiological actions (Table 16–2). Some act as hormones

Table 16–2 Neuroactive Mammalian Peptides

Category	Peptide
Hypothalamic neuropeptides	Thyrotropin-releasing hormone Gonadotropin-releasing hormone Corticotropin-releasing factor (CRF) Growth hormone–releasing hormone Melanocyte-stimulating hormone Melanocyte-inhibiting factor Somatostatin β-Endorphin Dynorphin Galanin Neuropeptide Y Orexin Oxytocin Vasopressin
Neurohypophyseal neuropeptides	Oxytocin Vasopressin
Pituitary peptides	Adrenocorticotropic hormone β-Endorphin α-MSH Prolactin Luteinizing hormone Growth hormone Thyrotropin
Pineal hormones	Melatonin
Basal ganglia	Substance P Enkephalin Dynorphin Neuropeptide Y Neurotensin Cholecystokinin Glucagon-like peptide-1 Cocaine- and amphetamine-regulated transcript (CART)
Gastrointestinal peptides	Vasoactive intestinal polypeptide Cholecystokinin Gastrin Substance P Neurotensin Methionine-enkephalin Leucine-enkephalin Insulin Glucagon Bombesin Secretin Somatostatin Thyrotropin-releasing hormone Motilin
Heart	Atrial natriuretic peptide
Other	Angiotensin II Bradykinin Calcitonin Calcitonin gene-related peptide (CGRP) Galanin Leptin Sleep peptide(s) Substance K (neurokinin A)

on targets outside the brain (eg, angiotensin and gastrin) or are products of neuroendocrine secretion (eg, oxytocin, vasopressin, somatostatin, luteinizing hormone, and thyrotropin-releasing hormone). In addition, many neuropeptides act as neurotransmitters when released close to a target neuron, where they can cause inhibition, excitation, or both.

Neuroactive peptides have been implicated in modulating sensory perception and affect. Some peptides, including substance P and the enkephalins, are preferentially located in regions of the central nervous system involved in the perception of pain. Other neuropeptides regulate complex responses to stress; these peptides include γ-melanocyte-stimulating hormone, corticotropin-releasing hormone (CRH), adrenocorticotropin (ACTH), dynorphin, and β-endorphin.

Although the diversity of neuroactive peptides is enormous, as a class these chemical messengers share a common cell biology. A striking generality is that neuroactive peptides are grouped in families with members that have similar sequences of amino acid residues. At least 10 have been identified; the seven main families are listed in Table 16–3.

Several different neuroactive peptides can be encoded by a single continuous messenger RNA (mRNA), which is translated into one large polyprotein precursor (Figure 16–2). Polyproteins can serve as a mechanism for amplification by providing more than one copy of the same peptide from the one precursor. For example, the precursor of glucagon contains two copies of the hormone. Polyproteins also generate diversity by producing several distinct peptides cleaved from one precursor, as in the case of the opioid peptides. The opioid peptides are derived from polyproteins encoded by three distinct genes. These peptides are endogenous ligands for a family of G protein–coupled receptors. In addition to endogenous agonists, the mu opioid receptor also binds drugs with analgesic and addictive properties, such as morphine and synthetic derivatives, including heroin and oxycodone.

The processing of more than one functional peptide from a single polyprotein is not unique to neuroactive peptides. The mechanism was first described for proteins encoded by small RNA viruses. Several viral polypeptides are produced from the same viral polyprotein, and all contribute to the generation of new virus particles. As with the virus, where the different proteins obviously serve a common biological purpose (formation of new viruses), a neuronal polypeptide will in many instances yield peptides that work together to serve a common physiological goal. Sometimes the biological functions appear to be more complex, as peptides with related or antagonistic activities can be generated from the same precursor.

A particularly striking example of this form of synergy is the group of peptides formed from the precursor of egg-laying hormone (ELH), a set of neuropeptides that govern diverse reproductive behaviors in the marine mollusk *Aplysia*. Egg-laying hormone can act as a hormone causing the contraction of oviduct muscles; it can also act as a neurotransmitter to alter the firing of several neurons involved in producing behaviors, as do the other peptides cut from the polyprotein.

The processing of neuroactive peptides takes place within the neuron's intracellular membrane system and in vesicles. Several peptides are produced from a single polyprotein by limited and specific proteolytic cleavage, catalyzed by proteases within these internal membrane systems. Some of these enzymes are serine proteases, a class that also includes the pancreatic enzymes trypsin and chymotrypsin. As with trypsin, the cleavage site of the peptide bond is determined by basic amino acid residues (lysine and arginine) in the substrate protein. Although cleavage is most common at dibasic residues, it can also occur at single basic residues, and polyproteins sometimes are cleaved at other peptide bonds.

Table 16–3 The Main Families of Neuroactive Peptides

Family	Peptide members
Opioids	Opiocortin, enkephalins, dynorphin, FMRFamide (Phe-Met-Arg-Phe-amide)
Neurohypophyseal neuropeptides	Vasopressin, oxytocin, neurophysins
Tachykinins	Substance P, physalaemin, kassinin, uperolein, eledoisin, bombesin, substance K
Secretins	Secretin, glucagon, vasoactive intestinal peptide, gastric inhibitory peptide, growth hormone–releasing factor, peptide histidine isoleucine amide
Insulins	Insulin, insulin-like growth factors I and II
Somatostatins	Somatostatins, pancreatic polypeptide
Gastrins	Gastrin, cholecystokinin

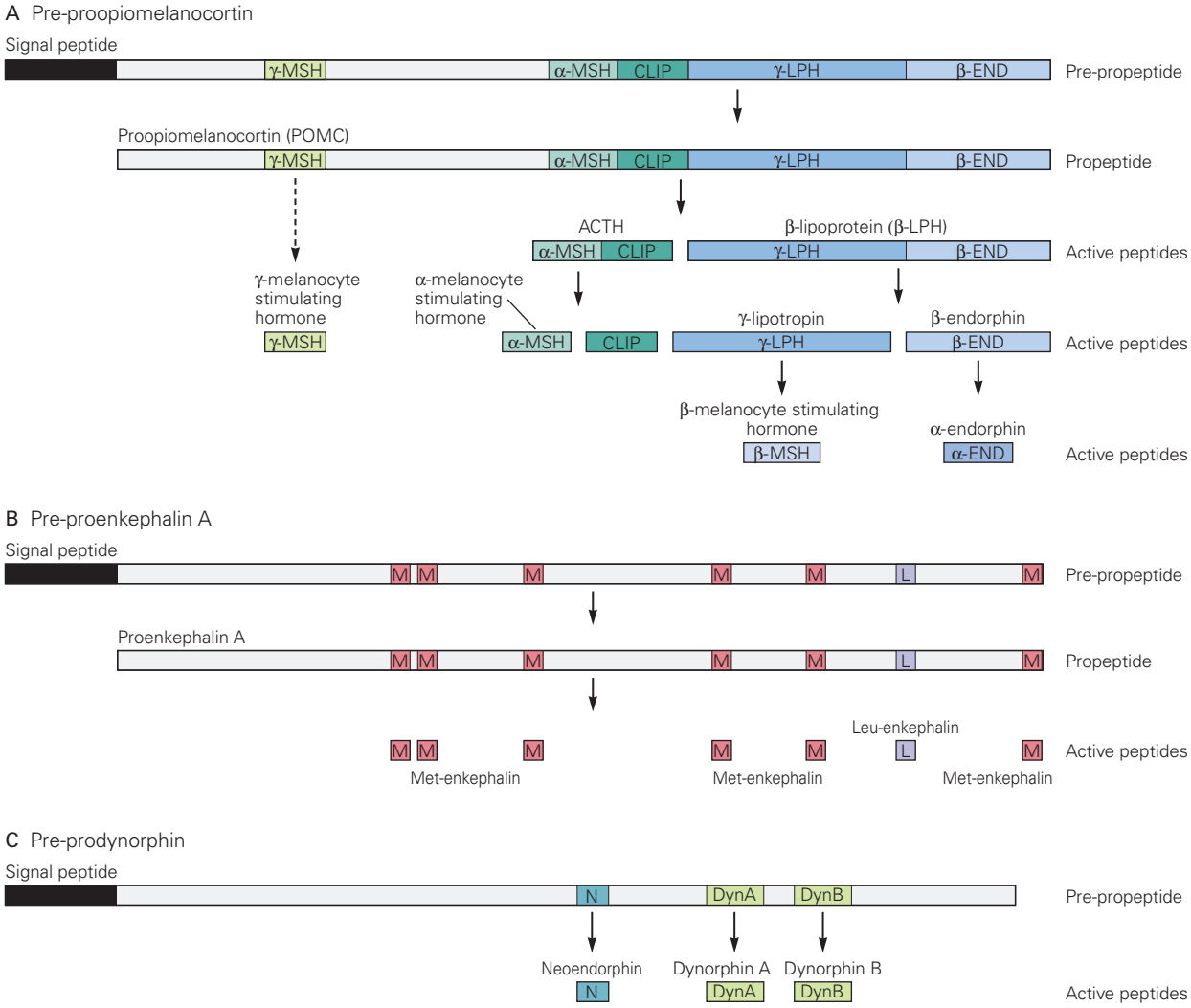

Figure 16–2 Hormone and neuropeptide precursors are processed differentially: The opioid family of neuropeptides. The opioid neuropeptides are derived from larger precursor molecules that require multiple rounds of protease-mediated cleavage. These precursors are processed differentially to yield their specific peptide products. Transport of these precursors through the membrane of the endoplasmic reticulum is initiated by a hydrophobic signal sequence. Internal cleavages often occur at basic residues within the polypeptide. Moreover, these precursors have key cysteine residues and sugar moieties that play roles in their processing and function. Generally, the first iteration of processing begins with the newly synthesized polyprotein precursor (known as the pre-propeptide form). Cleavage of an amino-terminal signal sequence generates a smaller molecule, the propeptide. Three major opioid peptide precursor proteins are encoded by three genes: *proopiomelanocortin* (***POMC***), *proenkephalin* (***PENK***), and *prodynorphin* (***PDYN***) (not shown). Differential processing of the three resultant pre-propeptides gives rise to the major opioid peptides—endorphins, enkephalins, and dynorphins.

A. The POMC precursor is processed differently in different lobes of the pituitary gland, resulting in α-melanocyte-stimulating hormone (**α-MSH**) and **γ-MSH**, corticotropin-like intermediate lobe peptide (**CLIP**), and β-lipotropin (**β-LPH**). β-LPH is cleaved to yield **γ-LPH** and β-endorphin (**β-END**), which themselves yield β-melanocyte-stimulating hormone (**β-MSH**) and α-endorphin (**α-END**), respectively. The endoproteolytic cleavages within adrenocorticotropic hormone (**ACTH**) and β-LPH take place in the intermediate lobe but not the anterior lobe.

B. Similar principles are evident in the processing of the enkephalin precursor, which gives rise to six Met-enkephalin peptides and one Leu-enkephalin peptide.

C. The dynorphin precursor is cleaved into at least three peptides that are related to Leu-enkephalin since the amino-terminal sequences of all three peptides contain the sequence of Leu-enkephalin.

Other types of peptidases also catalyze the limited proteolysis required for processing neuroactive peptides. Among these are thiol endopeptidases (with catalytic mechanisms like that of pepsin), amino peptidases (which remove the N-terminal amino acid of the peptide), and carboxy-peptidase B (an enzyme that removes an amino acid from the C-terminal end of the peptide if it is basic).

Different neurons that produce the same polyprotein may release different neuropeptides because of differences in the way the polyprotein is processed. An example is proopiomelanocortin (POMC), one of the three branches of the opioid family. POMC is found in neurons of the anterior and intermediate lobes of the pituitary, in the hypothalamus, and in several other regions of the brain, as well as in the placenta and gut. The same mRNA for POMC is found in all of these tissues, but different peptides are produced from POMC in different tissues in a regulated manner. One possibility is that two neurons that process the same polyprotein might differently express proteases with different specificities within the lumina of the endoplasmic reticulum, Golgi apparatus, or vesicles. Alternatively, the two neurons might contain the same processing proteases, but each cell might glycosylate the common polyprotein at different sites, thereby protecting different regions of the polypeptide from cleavage.

Peptides and Small-Molecule Transmitters Differ in Several Ways

Large dense-core vesicles are homologous to the secretory granules of nonneuronal cells. These vesicles are formed in the trans-Golgi network, where they are loaded with neuropeptides and other proteins that enable formation of the dense core. The dense-core vesicles are then transported from the soma to presynaptic sites in axons. In addition to containing neuropeptides, these vesicles often contain small molecule transmitters due to their expression of vesicular transporters. After large dense-core vesicles release their contents through exocytosis, the membrane is not recycled to form new large dense core vesicles. Rather the vesicles must be replaced by transport from the soma. In contrast, mature small synaptic vesicles are not synthesized in the soma. Rather, their protein components are delivered to release sites by transport of large dense-core precursor vesicles. To form a mature small synaptic vesicle, the precursor vesicles must first fuse with the plasma membrane. Following endocytosis, mature synaptic vesicles are then produced by local processing. Once their contents are released by exocytosis, synaptic vesicles can be rapidly recycled to maintain their local concentration during periods of sustained neural firing.

Although both types of vesicles contain many similar proteins, dense-core vesicles lack several proteins needed for release at the active zones. The membranes from dense-core vesicles are used only once; new dense-core vesicles must be synthesized in the cell body and transported to the axonal terminals by anterograde transport. Moreover, no uptake mechanisms exist for neuropeptides. Thus, once a peptide is released, a new supply must arrive from the cell body. Although there is evidence for local protein synthesis in some axons, it has not been shown that this provides new peptides for release.

The large dense-core vesicles release their contents by an exocytotic mechanism that is not specialized to nerve cells and does not require active zones; release can thus take place anywhere along the membrane of the axon that has the appropriate fusion machinery. As in other examples of regulated secretion, exocytosis of the dense-core vesicles depends on a general elevation of intracellular Ca^{2+} through voltage-gated Ca^{2+} channels that are not localized to the site of release. As a result, this form of exocytosis is slow and requires high stimulation frequencies to raise Ca^{2+} to levels sufficient to trigger release. This is in contrast to the rapid exocytosis of synaptic vesicles following a single action potential, which initiates the large, rapid increase in Ca^{2+} through voltage-gated Ca^{2+} channels tightly clustered at the active zone (Chapter 15).

Peptides and Small-Molecule Transmitters Can Be Co-released

Neuroactive peptides, small-molecule transmitters, and other neuroactive molecules coexist in the same dense-core vesicles of some neurons (Chapters 7 and 15). In mature neurons, the combination usually consists of one of the small-molecule transmitters and one or more peptides derived from a polyprotein. For example, ACh and vasoactive intestinal peptide (VIP) can be released together and work synergistically on the same target cells.

Another example is calcitonin gene–related peptide (CGRP), which in most spinal motor neurons is packaged together with ACh, the transmitter used at

the neuromuscular junction. CGRP activates adenylyl cyclase, raising cyclic adenosine monophosphate (cAMP) levels and cAMP-dependent protein phosphorylation in the target muscles (Chapter 14). Increased protein phosphorylation results in an increase in the force of contraction. Another example is the co-release of glutamate and dynorphin in neurons of the hippocampus, where glutamate is excitatory and dynorphin inhibitory. Because postsynaptic target cells have receptors for both chemical messengers, all of these examples of co-release are also examples of cotransmission.

As already described, the dense-core vesicles that release peptides differ from the small clear vesicles that release only small-molecule transmitters. The peptide-containing vesicles may or may not contain small-molecule transmitter, but both types of vesicles contain ATP. As a result, ATP is released by exocytosis of both large dense-core vesicles and synaptic vesicles. Moreover, it appears that ATP may be stored and released in a number of distinct ways: (1) ATP is co-stored and co-released with transmitters, (2) ATP release is simultaneous but independent of transmitter release, and (3) ATP is released alone. Co-release of ATP (which after release can be degraded to adenosine) may be an important illustration that coexistence and co-release do not necessarily signify cotransmission. ATP, like many other substances, can be released from neurons but still not be involved in signaling if there are no receptors nearby.

As mentioned earlier, one criterion for judging whether a particular substance is used as a transmitter is that the substance is present in high concentrations in a neuron. Identification of transmitters in specific neurons has been important in understanding synaptic transmission, and a variety of histochemical methods are used to detect chemical messengers in neurons (Box 16–2).

The glutamate synaptic vesicle transporters VGLUT2 and VGLUT3 are expressed in neurons that release other classes of neurotransmitter, particularly cholinergic, serotonergic, and catecholaminergic neurons. An interesting example of co-release of two small-molecule transmitters is that of glutamate and dopamine by neurons projecting to the ventral striatum, cortex, and elsewhere. This co-release may have important implications for modulation of motivated behaviors and for establishing the patterns of axonal projections. In some cases, glutamate is released together with dopamine in response to different patterns of dopaminergic neuron firing. While there is a controversy regarding whether the same synaptic vesicles can accumulate both neurotransmitters, in isolated synaptic vesicles, glutamate uptake enhances vesicular monoamine storage by increasing the pH gradient that drives vesicular monoamine transport, providing a presynaptic mechanism to regulate quantal size.

Removal of Transmitter From the Synaptic Cleft Terminates Synaptic Transmission

Timely removal of transmitters from the synaptic cleft is critical to synaptic transmission. If transmitter molecules released in one synaptic action were allowed to remain in the cleft after release, this would impede the normal spatial and temporal dynamics of signaling, initially boosting the signal but preventing new signals from getting through. The synapse would ultimately become refractory, mainly because of receptor desensitization resulting from continued exposure to transmitter.

Transmitter substances are removed from the cleft by three mechanisms: diffusion, enzymatic degradation, and reuptake. Diffusion removes some fraction of all chemical messengers, but in brain regions with very high innervation and thus a high requirement for neurotransmitter release, diffusion can play a relatively small role in tapering signaling. In contrast, in regions of low innervation, diffusion is a major means by which signaling is decreased.

At cholinergic synapses, the dominant means of clearing ACh is enzymatic degradation of the transmitter by acetylcholinesterase. At the neuromuscular junction, the active zone of the presynaptic nerve terminal is situated just above the junctional folds of the muscle membrane. The ACh receptors are located at the surface of the muscle facing the release sites and do not extend deep into the folds (see Figure 12–1), whereas acetylcholinesterase is anchored to the basement membrane within the folds. This anatomical arrangement of transmitter, receptor, and degradative enzyme serves two functions.

First, on release, ACh reacts with its receptor; after dissociation from the receptor, the ACh diffuses into the cleft and is hydrolyzed to choline and acetate by acetylcholinesterase. As a result, the transmitter molecules are used only once. Thus, one function of the esterase is to punctuate the synaptic message. Second, the choline that otherwise might be lost by diffusion away from the synaptic cleft is recaptured. Once hydrolyzed by the esterase, the choline lingers in the reservoir provided by the junctional folds and is taken back up into cholinergic nerve endings by a high-affinity choline transporter. (Unlike the biogenic amines, there is no uptake mechanism for ACh itself at the plasma membrane.) In addition to acetylcholinesterase, ACh is also degraded by another esterase,

Box 16–2 Detection of Chemical Messengers and Their Processing Enzymes Within Neurons

Powerful histochemical techniques are available for detecting both small-molecule transmitter substances and neuroactive peptides in histological sections of nervous tissue.

Catecholamines and serotonin, when reacted with formaldehyde vapor, form fluorescent derivatives. In an early example of transmitter histochemistry, the Swedish neuroanatomists Bengt Falck and Nils Hillarp found that the reaction can be used to locate transmitters with fluorescence microscopy under properly controlled conditions.

Because individual vesicles are too small to be resolved by the light microscope, the exact position of the vesicles containing the transmitter was inferred by comparing the fluorescence under the light microscope with the position of vesicles under the electron microscope. A number of fluorescent false transmitters, particularly those that mimic catecholamines, are substrates for plasma membrane and/or vesicular transporters, enabling their use to label vesicles and assess their turnover in living tissue. In addition, a variety of genetically expressed neurotransmitter reporters based on green fluorescent protein can be used to detect extracellular levels of neurotransmitters.

Histochemical analysis can be extended to the ultrastructure of neurons under special conditions. Fixation of nervous tissue in the presence of potassium permanganate, chromate, or silver salts, or the dopamine analog

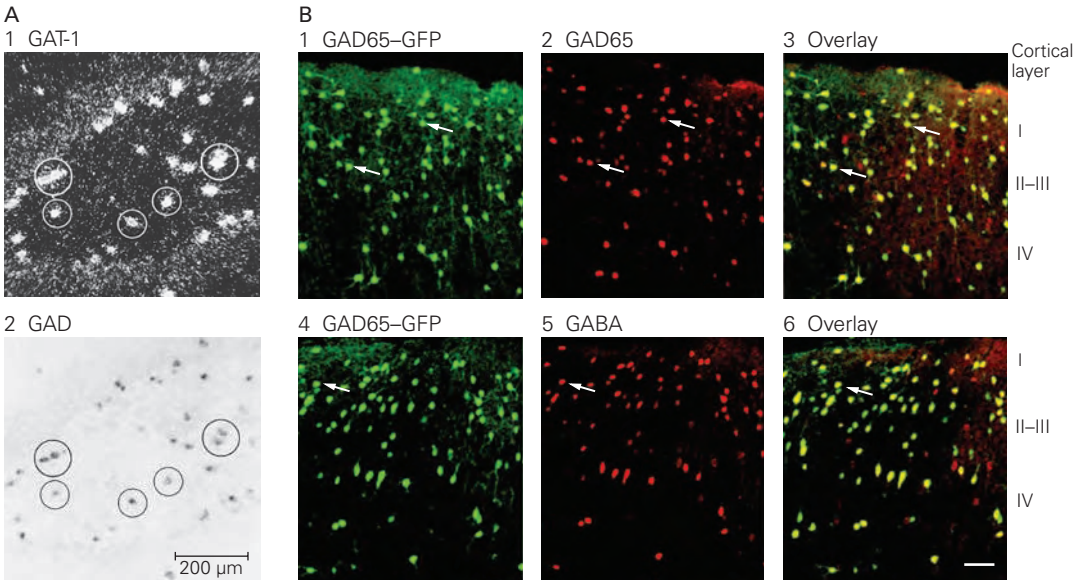

Figure 16–3 Techniques for visualizing chemical messengers.

A. A light-microscope section of the hippocampus of a rat. **1.** In situ hybridization using a probe for the mRNA encoding GAT-1, a GABA transporter. The probe was end-labeled with α-^{35}S-dATP and visualized by clusters of silver grains in the overlying autoradiographic photographic emulsion. **2.** In situ hybridization of the mRNA for glutamic acid decarboxylase (**GAD**), the specific biosynthetic enzyme for GABA, was carried out with an oligonucleotide probe linked to the enzyme alkaline phosphatase. The GAD probe was visualized by accumulation of colored alkaline phosphatase reaction product in the cytoplasm. Neurons expressing both GAT-1 and GAD transcripts were labeled by silver grains and the phosphatase reaction, respectively, and are indicated by circles enclosing cells bodies that contain both labels. (Used with permission of Sarah Augood.)

B. Images of neocortex from a GAD65-GFP transgenic mouse in which green fluorescent protein (**GFP**) is expressed under the control of the GAD65 promotor. GFP is co-localized with GAD65 (1–3) and GABA (4–6) (both detected by indirect immunofluorescence) in neurons in the different layers. Most of the GFP-positive neurons are immunopositive for GAD65 and GABA (**arrows** show selected examples). Scale bar = 100 µm. (Adapted, with permission, from López-Bendito et al. 2004. Copyright © 2004 Oxford University Press.)

5-hydroxdopamine, which forms an electron-dense product, intensifies the electron density of vesicles containing biogenic amines and thus reveals the large number of dense-core vesicles that are characteristic of aminergic neurons.

It is also possible to identify neurons that express the gene for a particular transmitter enzyme or peptide precursor. Many methods for detecting specific mRNAs depend on nucleic acid hybridization. One such method is in situ hybridization.

Two single strands of a nucleic acid polymer will pair if their sequence of bases is complementary. With in situ hybridization, the strand of noncoding DNA (the negative or antisense strand or its corresponding RNA) is applied to tissue sections under conditions suitable for hybridizing with endogenous (sense) mRNA. If the probes are radiolabeled, autoradiography reveals the locations of neurons that contain the complex formed by the labeled complementary nucleic acid strand and the mRNA.

Hybrid oligonucleotides synthesized with nucleotides containing base analogs tagged chemically, fluorescently, or with antibodies can be detected histochemically. Multiple labels can be used at the same time (Figure 16–3A). RNAscope, a more recent mRNA hybridization method, allows for simultaneous detection of different mRNAs with lower background and single-molecule sensitivity. Another approach to detecting the synthetic proteins involves viral or transgenic expression of proteins fused to variants of green fluorescent protein (Figure 16–3B).

Transmitter substances can also be detected using immunohistochemical techniques. Amino acid transmitters, biogenic amines, and neuropeptides have a primary amino group that becomes covalently fixed within the neurons; this group becomes cross-linked to proteins by aldehydes, the usual fixatives used in microscopy for immunohistochemical techniques.

Specific antibodies against the transmitter substances are necessary. Antibodies specific to serotonin, histamine, and many neuroactive peptides can be detected by a second antibody (in a technique called *indirect immunofluorescence*). As an example, if the first antibody is rabbit-derived, the second antibody can be goat antibody raised against rabbit immunoglobulin.

These commercially available secondary antibodies are tagged with fluorescent dyes and used under the fluorescence microscope to locate antigens in regions of individual neurons—cell bodies, axons, and presynaptic release sites (Figure 16–3).

Immunohistochemical techniques are also used with electron microscopy to locate chemical transmitters in the ultrastructure of neurons. Such techniques

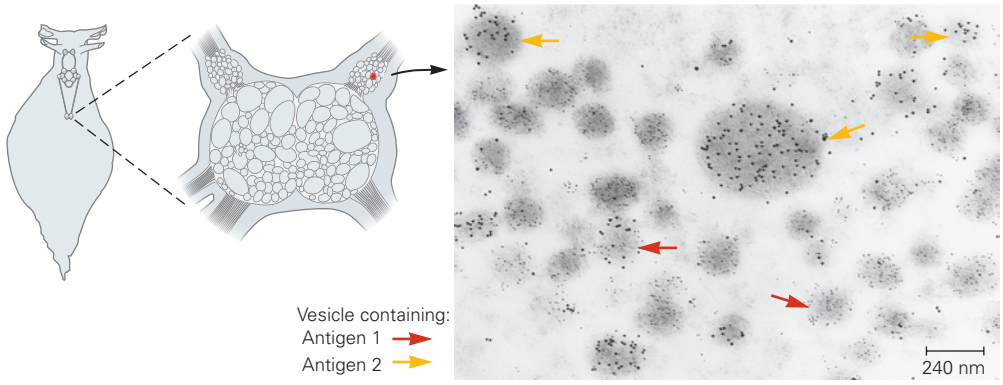

Figure 16–4 Electron-opaque gold particles linked to antibody are used to locate antigens in tissue at the ultrastructural level. The electron micrograph shows a section through the cell body of an *Aplysia* bag cell. Bag cells control reproductive behavior by releasing a group of neuropeptides cleaved from the egg-laying hormone (ELH) precursor. The cells contain several kinds of dense-core vesicles. The cell shown here was treated with two antibodies against different amino acid sequences contained in different regions of the ELH precursor. One antibody was raised in rabbits and the other in rats. These antibodies were detected with anti-rabbit or anti-rat immunoglobulins (secondary antibodies) raised in goats. Each secondary antibody was coupled to colloidal gold particles of a distinct size. Vesicles identified by antigen 1 (labeled with the smaller gold particles) are smaller than vesicles identified by antigen 2 (labeled with the larger gold particles), indicating that the specific fragments cleaved from the precursor are localized in different vesicles. (Reproduced, with permission, from Fisher et al. 1988.)

(*continued*)

Box 16–2 Detection of Chemical Messengers and Their Processing Enzymes Within Neurons (continued)

usually involve a peroxidase-antiperoxidase system that produces an electron-dense reaction product. Another method is to use antibodies linked to electron-dense gold particles. Spheres of colloidal gold can be generated with precise diameters in the nanometer range. When coated with an appropriate antibody, these gold particles can be used to detect proteins and peptides with high resolution. This technique has the additional useful feature that more than one specific antibody can be examined in the same tissue section if each antibody is linked to gold particles of different sizes (Figure 16–4).

A number of fluorescent vesicular transporter substrates have been used as fluorescent false neurotransmitters (FFNs) to monitor transmitter release in mouse brain slice or whole fly brain (Figure 16–5). This approach allows visualization of nerve terminals in which synaptic vesicles have been loaded with FFNs; release can then be monitored optically in real time in response to either depolarization, which leads to exocytosis and synaptic vesicle emptying, or amphetamine, which leads to nonexocytic release of vesicular contents into the cytoplasm in response to vesicle deacidification.

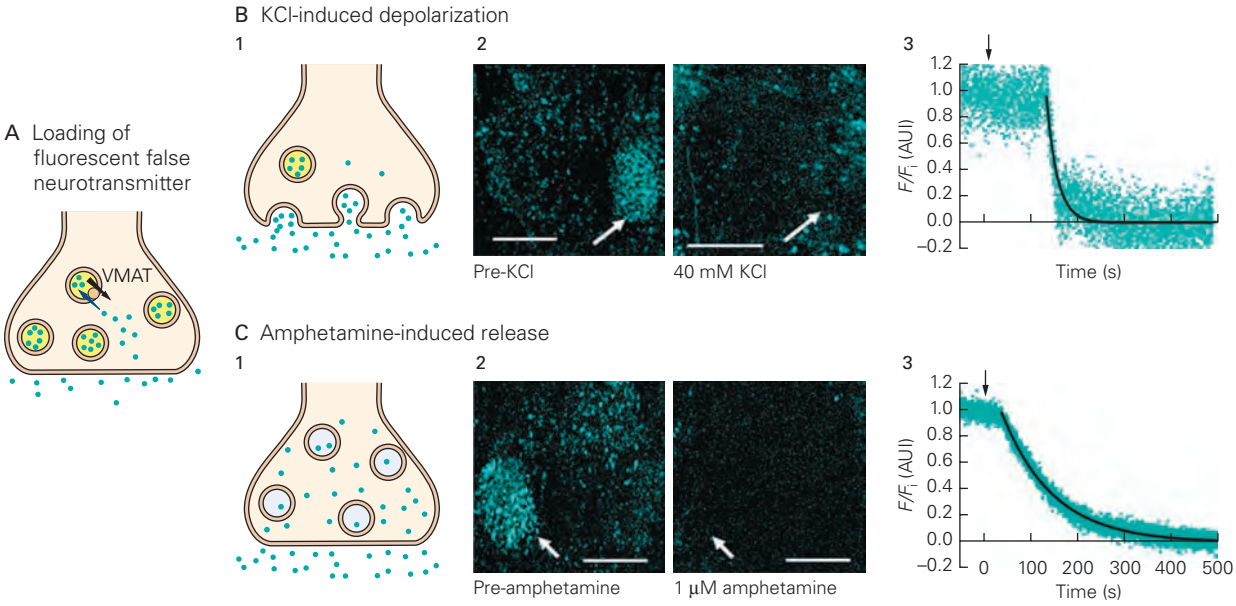

Figure 16–5 Fluorescent false neurotransmitter (FFN) labeling permits optical monitoring of neurotransmitter release.

A. FFN (**blue dots**) is transported by VMAT into synaptic vesicles in dopamine nerve terminals. Vesicles at steady state are acidic, as indicated by **yellow shading**.

B. 1. Raising the extracellular KCl concentration leads to depolarization and release of vesicles through exocytosis, resulting in the loss of fluorescent label (destaining). **2.** KCl (40 mM) depolarization caused rapid FFN206 destaining in presynaptic dopamine nerve terminals. Whole fly brains were loaded to steady state with FFN206 (300 nM) and treated with KCl. Projected image stacks of the neuropil before (*left*) and after (*right*) KCl-induced depolarization. **3.** Kinetics of fluorescence decay from representative experiments. **Black arrow** indicates initiation of KCl addition. Scale bar = 25 µm.

C. 1. Amphetamine leads to deacidification of vesicles (**loss of yellow shading**) and their destaining through a nonexocytic mechanism discussed in the text. **2.** Amphetamine (1 µM) caused FFN206 destaining. Whole fly brains were loaded to steady state with FFN206 (300 nM) and treated with amphetamine. Projected image stacks of neuropil before (*left*) and after (*right*) treatment. **3.** Kinetics of fluorescence decay from representative experiments. **Black arrow** indicates initiation of drug addition. Scale bar = 25 µm. (Reproduced, with permission, from Freyberg et al. 2016.)

butyrylcholinesterase, which can also degrade other molecules including cocaine and the paralytic drug succinylcholine. However, the precise functions of butyrylcholinesterase are not fully understood.

Many other enzymatic pathways that degrade released transmitters are not directly involved in terminating synaptic transmission but are important for controlling the concentration of the transmitter within the neuron or for inactivating transmitter molecules that have diffused away from the synaptic cleft. Many of these degradative enzymes are important clinically—they provide sites for drug action and serve as diagnostic indicators. For example, inhibitors of MAO, an intracellular enzyme that degrades amine transmitters, are used to treat depression and Parkinson disease. Catechol-*O*-methyltransferase (COMT) is another cytoplasmic enzyme that is important for degrading biogenic amines. Measurement of its metabolites provides a useful clinical index of the efficacy of drugs that affect the synthesis or degradation of the biogenic amines in nervous tissue. COMT is thought to play a particularly critical role in regulating cortical dopamine levels because of the low levels of the dopamine uptake transporter. The relevance of this enzyme is underscored by the finding that a functional polymorphism in the COMT gene has been related to cognitive performance.

Neuropeptides are removed relatively slowly from the synaptic cleft by slow diffusion and proteolysis by extracellular peptidases. In contrast, small-molecule transmitters are removed more quickly from the synaptic cleft and extrasynaptic space. The critical mechanism for inactivation of most small molecule neurotransmitters is reuptake at the plasma membrane. This mechanism serves the dual purposes of terminating the synaptic action of the transmitter as well as recapturing transmitter molecules for subsequent reuse. Although Elliott had hypothesized in 1914 that uptake transporters might exist, their discovery waited until 1958 when F. Barbara Hughes and Benjamin Brodie found that blood platelets accumulated norepinephrine and serotonin, which could compete with each other for uptake. Julius Axelrod,* also a member of Brodie's group, soon afterward characterized norepinephrine uptake into neurons using a radiolabeled substrate.

High-affinity uptake is mediated by transporter molecules in the membranes of nerve terminals and glial cells. Unlike vesicular transporters, which are powered by the H^+ electrochemical gradient in an antiport mechanism, plasma membrane transporters are driven by the Na^+ electrochemical gradient through a symport mechanism in which Na^+ ions and transmitter move in the same direction.

Each type of neuron has its own characteristic uptake mechanism. For example, noncholinergic neurons do not take up choline with high affinity. Certain powerful psychotropic drugs can block uptake processes. For example, cocaine blocks the uptake of dopamine, norepinephrine, and serotonin; the tricyclic antidepressants block uptake of serotonin and norepinephrine. The selective serotonin reuptake inhibitors, such as fluoxetine (Prozac), were an important therapeutic innovation and are generally better tolerated than tricyclic antidepressants, although treatment-resistant depression remains a critical problem. The application of appropriate drugs that block transporters can prolong and enhance synaptic signaling by the biogenic amines and GABA. In some instances, drugs act both on transporters on the neuron's surface and on vesicular transporters within the cell. For example, amphetamines are actively taken up by the dopamine or other biogenic amine transporters on the external membrane of the neuron as well as by VMAT2.

Transporter molecules for neurotransmitters belong to two distinct groups that are different in both structure and mechanism. High-resolution structures of bacterial homologs from each of these families have been solved, which has greatly advanced our understanding of transporter mechanisms.

One group of transporters is the neurotransmitter sodium symporters (NSS), a superfamily of transmembrane proteins that thread through the plasma membrane 12 times (11 times for many prokaryotic homologs). These proteins are comprised of a pseudo-symmetric inverted repeat in which membrane-spanning segments 1 to 5 are homologous to membrane-spanning segments 6 to 10. The NSS family includes the transporters of GABA, glycine, norepinephrine, dopamine, serotonin, osmolytes, and amino acids. Crystal structures for the human serotonin transporter and the fly dopamine transporter, which share the same structure and general mechanism as the bacterial homologs crystallized previously, have recently been solved.

The second family consists of transporters of glutamate. These proteins traverse the plasma membrane eight times and contain two helical hairpins that are

*Axelrod received a bachelor's degree in chemistry and wrote many of his celebrated papers as a technician in Brodie's lab before entering graduate school and receiving a PhD 21 years later. He was awarded a share of the Nobel Prize in 1970 for his co-discovery of neuronal norepinephrine uptake and his discovery of COMT. His co-recipients of the prize that year were Bernard Katz, who described quantal neurotransmission, and Ulf von Euler, who also studied vesicular uptake and epinephrine release.

thought to serve a role in gating access of substrate from each side of the membrane (see Figure 8–16). Each group includes several transporters for each transmitter substance; for example, there are multiple GABA, glycine, and glutamate transporters, each with somewhat different localization, function, and pharmacology.

The two groups can be distinguished functionally. Although both are driven by the electrochemical potential provided by the Na^+ gradient, transport of glutamate requires the countertransport of K^+, whereas transport by NSS proteins often requires the cotransport of Cl^- (or H^+ antiport in the case of prokaryotic homologs). During transport of glutamate, one negatively charged molecule of the transmitter is imported with three Na^+ ions and one proton (symport) in exchange for the export of one K^+. This leads to a net influx of two positive charges for each transport cycle, generating an inward current. As a result of this charge transfer, the negative resting potential of the cell generates a large inward driving force that results in an enormous gradient of glutamate across the cell membrane. In contrast, the NSS proteins transport one to three Na^+ ions and one Cl^- ion together with their substrates. While under most conditions the electrochemical driving force is sufficient for NSS transporters to carry transmitter into the cell, thereby increasing the cytoplasmic transmitter concentration, the concentration of transmitter in the cytoplasm is quite low and ultimately determined by the action of vesicular transporters to load transmitter into synaptic vesicles.

A fascinating aspect of the function of the NSS proteins is the ability of these transporters to run backward, allowing them to generate transmitter efflux. This is best characterized for the neurotransmitter dopamine, as amphetamine and related analogs lead to massive release of dopamine through a nonexocytotic mechanism. As discussed earlier, at pharmacological doses, amphetamine is actively transported by both the plasma membrane dopamine transporter (DAT) and the vesicular VMAT2; the latter effect dissipates the vesicular H^+ gradient, leading to the escape of dopamine to the cytoplasm. This dopamine then moves "backward", out of the cell, through DAT, a process that requires phosphorylation of its N-terminus. While essential for amphetamine function, the normal physiological role of this phosphorylation remains a mystery, as it does not seem essential for dopamine uptake. Computational studies suggest that phosphorylation-regulated interactions of the N-terminus with acidic lipids in the inner leaflet play a role in modulating transporter function. Nevertheless, the ultimate answer may require atomic resolution structures that include the N-terminal domain coupled with biophysical data on N-terminal dynamics.

Highlights

1. Information carried by a neuron is encoded in electrical signals that travel along its axon to a synapse, where these signals are transformed and carried across the synaptic cleft by one or more chemical messengers.
2. Two major classes of chemical messengers, small-molecule transmitters and neuroactive peptides, are packaged in vesicles within the presynaptic neuron. After their synthesis in the cytoplasm, small-molecule transmitters are taken up and highly concentrated in vesicles, where they are protected from degradative enzymes in the cytoplasm.
3. Synaptic vesicles in the periphery are highly concentrated in nerve endings and, in the brain, tend to be at varicosities along the axon at presynaptic sites. Classical excitatory synapses with ionotropic glutamate receptors are examples of "private" synapses that communicate with a closely apposed postsynaptic structure such as a dendritic spine. In contrast, the dopamine system exemplifies "social" synapses that can interact with extrasynaptic receptors on many neurons.
4. To prevent depletion of small molecule transmitters during rapid synaptic transmission, most are synthesized locally at terminals.
5. The protein precursors of neuroactive peptides are synthesized only in the cell body, the site of transcription and translation. The neuropeptides are packaged in secretory granules and vesicles that are carried from the cell body to the terminals by axoplasmic transport. Unlike the vesicles that contain small-molecule transmitters, these vesicles are not refilled at the terminal.
6. The enzymes that regulate transmitter biosynthesis are under tight regulatory control, and changes in neuronal activity can produce homeostatic changes in the levels and activity of these enzymes. This regulation can occur both posttranslationally in the cytoplasm, as a result of phosphorylation and dephosphorylation reactions, as well as by transcriptional control in the nucleus.
7. Precise mechanisms for terminating transmitter actions represent a key step in synaptic

transmission that is nearly as important as transmitter synthesis and release. Some released transmitter is lost as a result of simple diffusion out of the synaptic cleft. However, for the most part, transmitter actions are terminated by specific molecular reactions.

8. Acetylcholine is rapidly hydrolyzed by acetylcholinesterase to choline and acetate. Glutamate, GABA, glycine, and the biogenic amines are taken up into presynaptic terminals and/or glia by specific transporters at the plasma membrane that are driven by the Na^+ gradient.
9. Some of the most potent psychoactive compounds act at neurotransmitter transporters. The psychostimulatory effects of cocaine result from its action to prevent reuptake of dopamine, thereby increasing its extracellular levels. In contrast, amphetamine and its derivatives promote nonexocytotic release of dopamine through a mechanism involving both the plasma membrane DAT and the vesicular transporter VMAT2.
10. The first step in understanding the molecular strategy of chemical transmission usually involves identifying the contents of synaptic vesicles. Except for those instances in which transmitter is released by transporter molecules or by diffusion through the membrane (in the case of gases and lipid metabolites, see Chapter 14), only molecules suitably packaged in vesicles can be released from a neuron's terminals. However, not all molecules released by a neuron are chemical messengers—only those that bind to appropriate receptors and initiate functional changes in that target neuron can usefully be considered neurotransmitters.
11. Information is transmitted when transmitter molecules bind to receptor proteins in the membrane of another cell, causing them to change conformation, leading either to increased ion conductance in the case of ligand-gated ion channels or to alterations in downstream signaling pathways in the case of G protein–coupled receptors.
12. The co-release of several neuroactive substances onto appropriate postsynaptic receptors permits great diversity of information to be transferred in a single synaptic action.

Jonathan A. Javitch
David Sulzer

Selected Reading

Alberts B, Johnson A, Lewis J, Raff M, Roberts K, Walter P. 2002. Membrane transport of small molecules and the electrical properties of membranes. In: *Molecular Biology of the Cell*, 4th ed. New York and Oxford: Garland Science.

Axelrod J. 2003. Journey of a late blooming biochemical neuroscientist. J Biol Chem 278:1–13.

Burnstock G. 1986. Purines and cotransmitters in adrenergic and cholinergic neurones. Prog Brain Res 68:193–203.

Chaudhry FA, Boulland JL, Jenstad M, Bredahl MK, Edwards RH. 2008. Pharmacology of neurotransmitter transport into secretory vesicles. Handb Exp Pharmacol 184:77–106.

Cooper JR, Bloom FE, Roth RH. 2003. *The Biochemical Basis of Neuropharmacology*, 8th ed. New York: Oxford Univ. Press.

Dale H. 1935. Pharmacology and nerve endings. Proc R Soc Med (Lond) 28:319–332.

Edwards RH. 2007. The neurotransmitter cycle and quantal size. Neuron 55:835–858.

Falck B, Hillarp NÅ, Thieme G, Torp A. 1982. Fluorescence of catecholamines and related compounds condensed with formaldehyde. Brain Res Bull 9:11–15.

Fatt P, Katz B. 1950. Some observations on biological noise. Nature 166:597–598.

Jiang J, Amara SG. 2011. New views of glutamate transporter structure and function: advances and challenges. Neuropharmacology 60:172–181.

Johnson RG. 1988 Accumulation of biological amines into chromaffin granules: a model for hormone and neurotransmitter transport. Physiol Rev 68:232–307.

Katz B. 1966. *Nerve, Muscle, and Synapse*. New York: McGraw-Hill.

Koob GF, Sandman CA, Strand FL (eds). 1990. A decade of neuropeptides: past, present and future. Ann N Y Acad Sci 579:1–281.

Loewi O. 1960. An autobiographic sketch. Perspect Biol Med 4:3–25.

Lohr KM, Masoud ST, Salahpour A, Miller GW. 2017. Membrane transporters as mediators of synaptic dopamine dynamics: implications for disease. Eur J Neurosci 45:20–33.

Pereira D, Sulzer D. 2012. Mechanisms of dopamine quantal size regulation. Front Biosci 17:2740–2767.

Sames D, Dunn M, Karpowicz RJ Jr, Sulzer D. 2013. Visualizing neurotransmitter secretion at individual synapses. ACS Chem Neurosci 4:648–651.

Siegel GJ, Agranoff BW, Albers RW, Molinoff PB (eds). 1998. *Basic Neurochemistry: Molecular, Cellular, and Medical Aspects*, 6th ed. Philadelphia: Lippincott.

Snyder SH, Ferris CD. 2000. Novel neurotransmitters and their neuropsychiatric relevance. Am J Psychiatry 157:1738–1751.

Sossin WS, Fisher JM, Scheller RH. 1989. Cellular and molecular biology of neuropeptide processing and packaging. Neuron 2:1407–1417.

Sulzer D, Cragg SJ, Rice ME. 2016. Striatal dopamine neurotransmission: regulation of release and uptake. Basal Ganglia 6:123–148.

Sulzer D, Pothos EN. 2000. Regulation of quantal size by presynaptic mechanisms. Rev Neurosci 11:159–212.
Toei M, Saum R, Forgac M. 2010. Regulation and isoform function of the V-ATPases. Biochemistry 49:4715–4723.
Torres GE, Amara SG. 2007. Glutamate and monoamine transporters: new visions of form and function. Curr Opin Neurobiol 17:304–312.
Van der Kloot W. 1991 The regulation of quantal size. Prog Neurobiol 36:93–130.
Weihe E, Eiden LE. 2000. Chemical neuroanatomy of the vesicular amine transporters. FASEB J 15:2435–2449.

References

Augood SJ, Herbison AE, Emson PC. 1995. Localization of GAT-1 GABA transporter mRNA in rat striatum: cellular coexpression with GAD_{67} mRNA, GAD_{67} immunoreactivity, and parvalbumin mRNA. J Neurosci 15:865–874.
Coleman JA, Green EM, Gouaux E. 2016. X-ray structures and mechanism of the human serotonin transporter. Nature 532:334–339.
Danbolt NC, Chaudhry FA, Dehnes Y, et al. 1998. Properties and localization of glutamate transporters. Prog Brain Res 116:23–43.
Fisher JM, Sossin W, Newcomb R, Scheller RH. 1988. Multiple neuropeptides derived from a common precursor are differentially packaged and transported. Cell 54:813–822.
Freyberg Z, Sonders MS, Aguilar JI, et al. 2016. Mechanisms of amphetamine action illuminated through in vivo optical monitoring of dopamine synaptic vesicles. Nat Commun 7:10652.
Hnasko TS, Chuhma N, Zhang H, et al. 2010. Vesicular glutamate transport promotes dopamine storage and glutamate corelease in vivo. Neuron 65:643–656.
Khoshbouei, H, Sen N, Guptaroy B, et al. 2004. N-terminal phosphorylation of the dopamine transporter is required for amphetamine-induced efflux. PLoS Biol 2(3): E78.
Krieger DT. 1983. Brain peptides: what, where, and why? Science 222:975–985.
Liu Y, Kranz DE, Waites C, Edwards RH. 1999. Membrane trafficking of neurotransmitter transporters in the regulation of synaptic transmission. Trends Cell Biol 9:356–363.
Lloyd PE, Frankfurt M, Stevens P, Kupfermann I, Weiss KR. 1987. Biochemical and immunocytological localization of the neuropeptides FMRFamide SCPA, SCPB, to neurons involved in the regulation of feeding in *Aplysia*. J Neurosci 7:1123–1132.
López-Bendito G, Sturgess K, Erdélyi F, Szabó G, Molnár Z, Paulsen O. 2004. Preferential origin and layer destination of GAD65-GFP cortical interneurons. Cereb Cortex 14:1122–1133.
Okuda T, Haga T. 2003. High-affinity choline transporter. Neurochem Res 28:483–488.
Otsuka M, Kravitz EA, Potter DD. 1967. Physiological and chemical architecture of a lobster ganglion with particular reference to γ-aminobutyrate and glutamate. J Neurophysiol 30:725–752.
Palay SL. 1956. Synapses in the central nervous system. J Biophys Biochem Cytol 2:193–202.
Pereira DB, Schmitz Y, Mészáros J, et al. 2016. Fluorescent false neurotransmitter reveals functionally silent dopamine vesicle clusters in the striatum. Nat Neurosci 19:578–586.
Rubin RP. 2007. A brief history of great discoveries in pharmacology: in celebration of the centennial anniversary of the founding of the American Society of Pharmacology and Experimental Therapeutics. Pharmacol Rev 59:289–359.
Yamashita A, Singh SK, Kawate T, Jin Y, Gouaux E. 2005. Crystal structure of a bacterial homologue of Na^+/Cl^--dependent neurotransmitter transporters. Nature 437:205–223.
Yernool D, Boudker O, Jin Y, Gouaux E. 2004. Structure of a glutamate transporter homologue from *Pyrococcus horikoshii*. Nature 431:811–818.

Part IV


LVX VENIT IN MVNDVN ET DILEXERVNT HOMINES MAGIS TENEBRAS QVAM LVCEM. Io.3.19.
ANTRVM PLATONICVM

Preceding Page

In Plato's "Allegory of the Cave," which addresses the origin of knowledge, his early insight into the constructive nature of perception offers illuminating metaphors for the process. The parable begins with the premise that a group of prisoners has never seen the outside world. Their experience is limited to shadows cast upon the wall of the cave by objects passing before a fire. The causes of those shadows—even the fact that they are shadows—is unknown to the prisoners. Nonetheless, over time, the shadows become imbued with meaning in the prisoners' minds. Metaphorically, the shadows represent sensations, which are fleeting and incoherent. The assignment of meaning represents the construction of intelligible percepts. The prisoner turning the corner of the wall has been freed to witness the larger world of causes, which he reports back to those still imprisoned. In a novel metaphorical take on this ancient story, this returning prisoner represents the field of modern neuroscience, which sheds light on the relationship between our shadowy sensations and our rich perceptual experience of the world. (Plato's Cave, 1604. Jan Pietersz Saenredam, after Cornelis Cornelisz van Haarlem. National Gallery, Washington D.C.)

IV Perception

> I understood that the world was nothing: a mechanical chaos of casual, brute enmity on which we stupidly impose our hopes and fears. I understand that, finally and absolutely, I alone exist. All the rest, I saw, is merely what pushes me, or what I push against, blindly—as blindly as all that is not myself pushes back. I create the whole universe, blink by blink…. Nevertheless, something will come of all this.[1]

JOHN GARDNER'S HEARTRENDING TALE OF THE TORMENTED MONSTER Grendel's perspective on life captures the fundamental nature of perceptual experience: It is a construct that we alone impose. Or, as Grendel keenly observes, "The mountains are what I define them as." Isolated and tortured by loneliness, Grendel sees the world as do the shackled prisoners in Plato's Cave, where mere shadows are what is sensed, but those shadows are imbued with meaning, utility, agency, beauty, joy, and sadness, all through the constructive process of perception: "What I see, I inspire with usefulness . . . and all that I do not see is useless, void."

Like the prisoner who escapes from Plato's Cave to view a larger world of causes, or the all-knowing dragon who fills Grendel with ideas from another dimension—"But dragons, my boy, have a whole different kind of mind. . . . We see from the mountaintop: all time, all space"—modern neuroscience promises a mountaintop understanding of perceptual experience, an understanding not simply of the things we construct from our shadowy sensations, but how we do so, and for what purpose.

This section on perception offers that expansive mountaintop view. For each of the sensory modalities in turn, these chapters begin by examining environmental stimuli—light, sound, gravity, touch, and chemicals—that are the origins of human experience and knowledge of the world. In hierarchical fashion, the chapters survey the mechanisms that enable stimulus detection and discrimination, the perceptual processes that fill evanescent sensations with meaning, and the operations that support attention, decision, and action, based on what is perceived.

Vision—a sense both particularly well understood and heavily utilized by humans—acquires information through properties of light. Light reflected from objects in the environment varies in wavelength and intensity and fluctuates over space and time, and through

[1]Gardner J. 1971. *Grendel*. Alfred A. Knopf, New York.

those physical properties conveys evidence of the world around us. Cast as patterned images upon the retina, luminous energy is transduced into neuronal signals by dedicated receptor cells. The evidential properties of these images are detected by a collection of specialized neuronal systems that sense forms of contrast and convey this information to the rest of the brain.

Similarly, the auditory system acquires information about the world through the simple compression and rarefaction of air, as caused by spoken language, music, or environmental sounds. This sensory evidence is detected—even in minute quantities and with incredibly precise timing—by an extraordinarily intricate amplification system consisting of small drums, levers, tubes, and hair cells, whose bendable stereocilia transduce mechanical energy into neuronal signals. Similar motion-detecting hair cells serve the vestibular senses of balance, acceleration, and rotation of the head.

The somatosensory system acquires information about physical stimuli impinging on the body in the form of pressure, vibration, and temperature—and, in the extreme, pain—as would be caused by touch, movement of the skin across a textured surface, or contact with a source of heat. The peripheral nerve endings of a variety of specialized detector neurons embedded in skin, viscera, and muscle transduce this mechanical energy into neuronal signals, which are carried via the spinal cord and cranial nerves to the brain.

Finally, the senses of taste and smell acquire information about the chemical composition of the world, in the form of form of food, drink, and airborne molecules. From one of the most exciting and rapidly developing areas of sensory biology today, we now know that there are hundreds of olfactory receptors that have unique patterns of affinity for airborne molecules, which accounts for the human ability to detect and discriminate a staggering number and diversity of odors.

All of these receptive systems serve as filters, characterized by neural "receptive fields" that highlight certain forms of information and restrict others. These selective filters are tunable over different timescales, enhancing attention to salient stimuli and adapting to the statistics of the sensory world. This flexibility accommodates variations in both behavioral goals and environmental conditions.

Like the shackled prisoners in Plato's cave, our sensory systems initially convey simple filtered representations of sensory input, which are fundamentally ambiguous, noisy, and incomplete. Alone they have no meaning. Quite remarkably, our brain enables us to ultimately experience this sensory information as the environmental objects and events that *cause* those patterns. The constructive transition from a world of sensory evidence to one of meaning lies at the heart of perception and has long been one of the most engaging mysteries of human cognition. The 19th-century English philosopher John Stuart Mill wrote "perception reflects the permanent possibilities of sensation," and in doing so reclaims from transient

sensory events the enduring structural and relational properties of the world.

This section reveals how perception overcomes the vagaries of sensory evidence to develop hypotheses or inferences about the causes of sensation, by reference to past knowledge. Much of this happens through the machinery of the cerebral cortex, where sensory signals are linked both within and between modalities and to feedback from the memory store. Like a detective viewing a crime scene, informed by memory and context, the activity of cortical neurons begins to yield what William James aptly called the "perception of probable things."

With this perceptual transformation also comes the ability to recognize objects familiar to us. We readily generalize across different sensory manifestations of the same or similar objects, in the form of perceptual constancies and categorical percepts, and we link these with other meaningful events. The sound of the coffee grinder in the morning, the smell of a lover's perfume or the sight of her face expands our experience beyond the immediate to a realm of recall and imagination. The chapters in this collection review the brain structures and computations that underlie these associative functions, which include highly specialized neuronal systems for recognizing and interpreting complex and behaviorally significant objects, such as faces.

Perceptual experience of the world around us is a prerequisite for meaningful interaction with that world. Decisions are made based on the accumulation of sensory evidence in support of one percept versus another. Is that my suitcase on the carousel? Is this where we turn? Was that aria from Wagner or Strauss? Is that the fragrance of jasmine or gardenia? Cortical neurons form salience maps, which represent the outcome of these perceptual decisions with respect to behavioral goals and rewards and prioritize actions accordingly.

Perception is generally treated—as it is herein—as a distinct subdiscipline of neuroscience. Increasingly we see this compartmentalization breaking down. The relationship of perception to other brain functions—learning, memory, emotion, motor control, language, development—is ever clearer with the explosive growth of new concepts and experimental methods for monitoring and manipulating brain structure and function, and for revealing the extensive anatomical and functional neural connections between seemingly distinct brain regions. Thus have we begun to fully appreciate how the brain's system for acquiring and interpreting information, for becoming aware of and understanding the world—for *perceiving*—is the functional centerpiece of human cognition and behavior.

Part Editors: Thomas D. Albright and Randy M. Bruno

Part IV

17

Sensory Coding

Our senses enlighten and empower us. Through sensation, we form an immediate and relevant picture of the world and our place in it, informed by our past experience and preparing us for probable futures. Sensation provides immediate answers to three ongoing and essential questions: *Is something there? What is it?* and *What's changed?* To answer these questions, all sensory systems perform two fundamental functions: *detection* and *discrimination*. Because our world and our needed responses to it change with time, sensory systems can both *preferentially respond* and *adapt* to changing stimuli in the short term, and also *learn* to modify our responses to stimuli as our needs and circumstances change.

Since ancient times, humans have been fascinated by the nature of sensory experience. Aristotle defined five senses—vision, hearing, touch, taste, and smell—each linked to specific sense organs in the body: eyes, ears, skin, tongue, and nose. Pain was not considered to be a specific sensory modality but rather an affliction of the soul. Intuition, often referred to colloquially as a "sixth sense," was not yet understood to depend upon the experience of the classic sensory systems. Today, neurobiologists recognize intuition as inferences derived from previous experience and thus the result of cognitive as well as sensory processes.

In this chapter, we consider the organizational principles and coding mechanisms that are universal to all sensory systems. *Sensory information* is defined as neural activity originating from stimulation of receptor cells in specific parts of the body. Our senses include the classic five senses plus a variety of modalities not recognized by the ancients but essential to bodily function: the *somatic* sensations of pain, itch, temperature, and proprioception (posture and movement of our own body); *visceral* sensations (both conscious and

unconscious) necessary for homeostasis; and the *vestibular* senses of balance (the position of the body in the gravitational field) and head movement.

Sensation informs and enriches all life, and the fundamentals of sensory processing have been conserved throughout vertebrate evolution. Specialized receptors in each of the sensory systems provide the first neural representation of the external and internal world, transforming a specific type of stimulus energy into electrical signals (Figure 17–1). All sensory information is then transmitted to the central nervous system by trains of action potentials that represent particular aspects of the stimulus. This information flows centrally to regions of the brain involved in the processing of individual senses, multisensory integration, and cognition.

The sensory pathways have both serial and parallel components, consisting of fiber tracts with

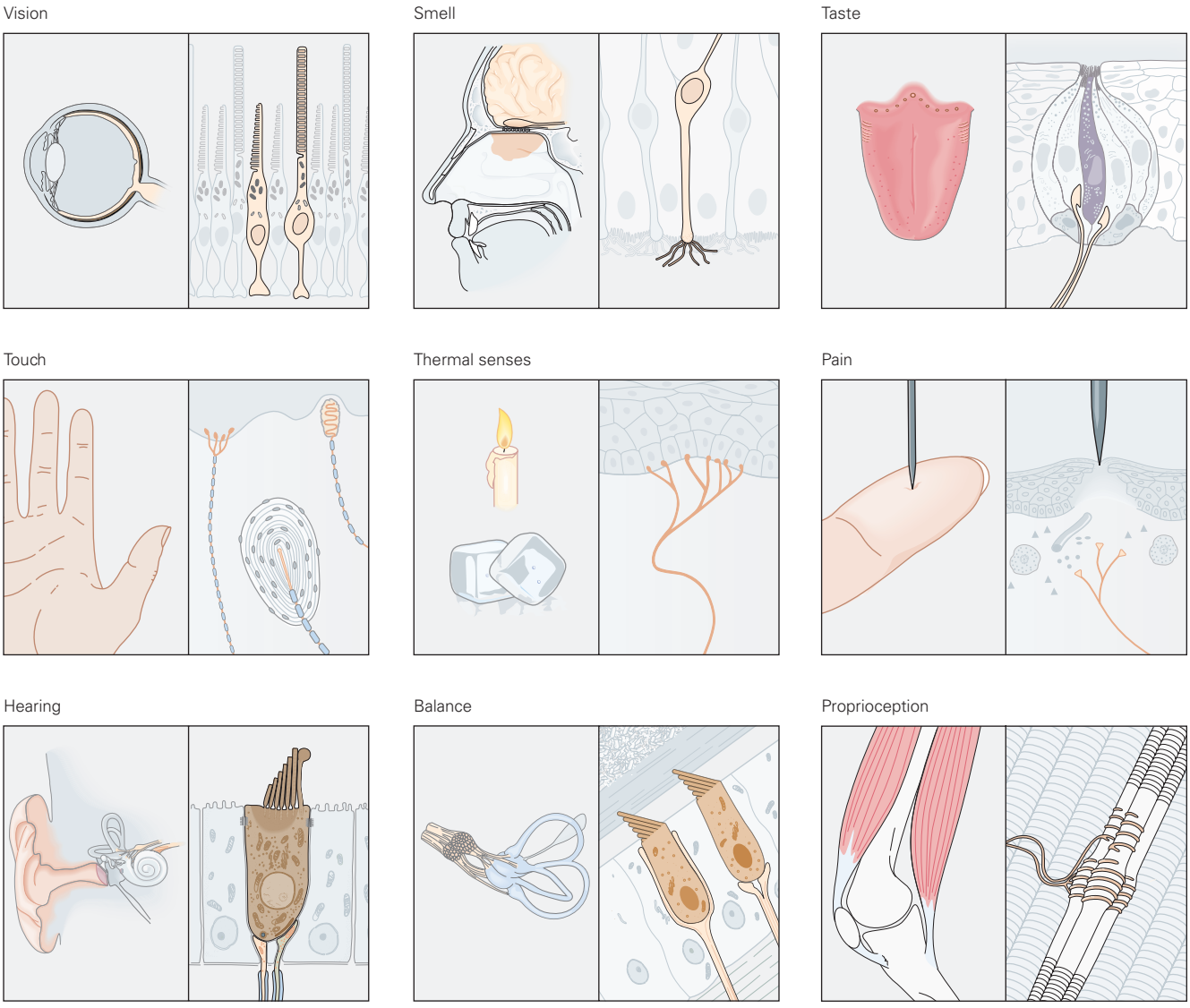

Figure 17–1 The major sensory modalities in humans are mediated by distinct classes of receptor neurons located in specific sense organs. Each class of receptor cell transforms one type of stimulus energy into electrical signals that are encoded as trains of action potentials (see Figure 17–4). The principal receptor cells include photoreceptors (vision), chemoreceptors (smell, taste, and pain), thermal receptors, and mechanoreceptors (touch, hearing, balance, and proprioception). The classic five senses—vision, smell, taste, touch, and hearing—and the sense of balance are mediated by receptors in the eye, nose, mouth, skin, and inner ear, respectively. The other somatosensory modalities—thermal senses, pain, visceral sensations, and proprioception—are mediated by receptors distributed throughout the body.

thousands or millions of axons linked by synapses that both transmit and transform information. Relatively simple forms of neural coding of stimuli by receptors are modulated by complex mechanisms in the brain to form the basis of cognition. Sensory pathways are also controlled by higher centers in the brain that modify and regulate incoming sensory signals by feeding information back to earlier stages of processing. Thus, perception is the product not simply of "raw" physical sensory information but also cognition and experience.

Both scientists and philosophers have examined the extent to which the sensations we experience accurately reflect the stimuli that produce them, and how they are altered by our inherently subjective and imprecise knowledge of the world. In prior centuries, the interest of European philosophers in sensation and perception was related to the question of human nature itself. Two schools of thought eventually dominated: empiricism, represented by John Locke, George Berkeley, and David Hume, and idealism, represented by René Descartes, Immanuel Kant, and Georg Wilhelm Friedrich Hegel.

Locke, the preeminent empiricist, advanced the idea that the mind at birth is a blank slate, or *tabula rasa*, void of any ideas. Knowledge, he asserted, is obtained only through sensory experience—what we see, hear, feel, taste, and smell. Berkeley extended this topic by questioning whether there was any sensory reality beyond the experiences and knowledge acquired through the senses. He famously asked: Does a falling tree make a sound if no one is near enough to hear it?

Idealists argued that the human mind possesses certain innate abilities, including logical reasoning itself. Kant classified the five senses as categories of human understanding. He argued that perceptions were not direct records of the world around us but rather were products of the brain and thus depended on the architecture of the nervous system. Kant referred to these brain properties as *a priori knowledge*.

Thus, in Kant's view, the mind was not the passive receiver of sense impressions envisaged by the empiricists. Rather, it had evolved to conform to certain universal conditions such as space, time, and causality. These conditions were independent of any physical stimuli detected by the body. For Kant and other idealists, this meant that knowledge is based not only on sensory stimulation alone but also on our ability to organize and interpret sensory experience. If sensory experience is inherently subjective and personal, they said, it may not be subject to empirical analysis. As the empirical investigation of perception matured, both schools proved partially correct.

Psychophysics Relates Sensations to the Physical Properties of Stimuli

The modern study of sensation and perception began in the 19th century with the emergence of experimental psychology as a scientific discipline. The first scientific psychologists—Ernst Weber, Gustav Fechner, Hermann Helmholtz, and Wilhelm Wundt—focused their experimental study of mental processes on sensation, which they believed was the key to understanding the mind. Their findings gave rise to the fields of psychophysics and sensory physiology.

Psychophysics describes the relationship between the physical characteristics of a stimulus and attributes of the sensory experience. *Sensory physiology* examines the neural consequences of a stimulus—how the stimulus is transduced by sensory receptors and processed in the brain. Some of the most exciting advances in our understanding of perception have come from merging these two approaches in both human and animal studies. For example, functional magnetic resonance imaging (fMRI) and positron emission tomography (PET) have been used in controlled experiments to identify regions of the human brain involved in the perception of pain or the identification of specific types of objects or particular persons and places.

Psychophysics Quantifies the Perception of Stimulus Properties

Early scientific studies of the mind focused not on the perception of complex qualities such as color or taste but on phenomena that could be isolated and measured precisely: the size, shape, amplitude, velocity, and timing of stimuli. Weber and Fechner developed simple experimental paradigms to study how and under what conditions humans are able to distinguish between two stimuli of different amplitudes. They quantified the intensity of sensations in the form of mathematical laws that allowed them to predict the relationship between the magnitude of a stimulus and its detectability, including the ability to discriminate between different stimuli.

In 1953, Stanley S. Stevens demonstrated that the subjective experience of the intensity (I) of a stimulus (S) is best described by a power function. Stevens's law states that,

$$I = K(S - S_0)^n,$$

where the *sensory threshold* (S_0) is the lowest stimulus strength a subject can detect, and K is a constant. For some sensations, such as the sense of pressure on

the hand, the relationship between the stimulus magnitude and its perceived intensity is linear, that is, a power function with a unity exponent ($n = 1$).

All sensory systems have a threshold, and thresholds have two essential functions. First, by asking if a sensation is large enough to have a high enough probability of being of interest or relevance, they reduce unwanted responses to noise. Second, the specific nonlinearity introduced by thresholds aids encoding and processing, even if the rest of the primary sensory response scales linearly with the stimulus. Sensory thresholds are a feature, not a bug. Thresholds are normally determined statistically by presenting a subject with a series of stimuli of random amplitude. The percentage of times the subject reports detecting the stimulus is plotted as a function of stimulus amplitude, forming a relation called the *psychometric function* (Figure 17–2). By convention, threshold is defined as the stimulus amplitude detected in half of the trials.

The measurement of sensory thresholds is a useful technique for diagnosing sensory function in individual modalities. An elevated threshold may signal an abnormality in sensory receptors (such as loss of hair cells in the inner ear caused by aging or exposure to very loud noise), deficits in nerve conduction properties (as in multiple sclerosis), or a lesion in sensory-processing areas of the brain. Sensory thresholds may also be altered by emotional or psychological factors related to the conditions in which stimulus detection is measured. Thresholds can also be determined by the method of limits, in which the subject reports the intensity at which a progressively decreasing stimulus is no longer detectable or an increasing stimulus becomes detectable. This technique is widely used in audiology to measure hearing thresholds.

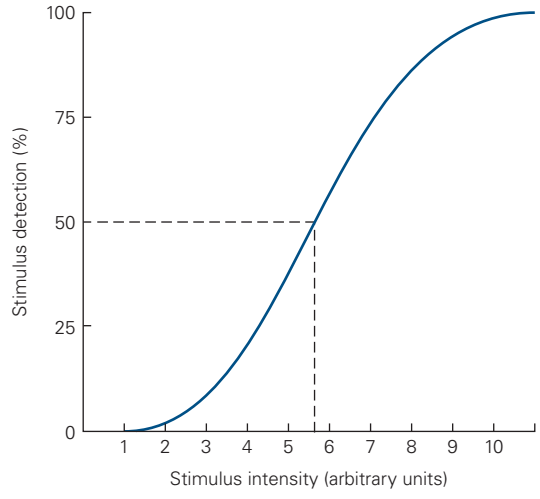

Figure 17–2 The psychometric function. The psychometric function plots the percentage of stimuli detected by a human observer as a function of the stimulus magnitude. Threshold is defined as the stimulus intensity detected on 50% of the trials, which in this example would be about 5.5 (arbitrary units). Psychometric functions are also used to measure the *just noticeable difference* (JND) between stimuli that differ in intensity, frequency, or other parametric properties.

Subjects can also provide nonverbal responses in sensory detection or discrimination tasks using levers, buttons, or other devices that allow accurate measurement of decision times. Experimental animals can be trained to respond to controlled sensory stimuli using such devices, allowing neuroscientists to investigate the underlying neural mechanisms by combining electrophysiological and behavioral studies in the same experiment. Methods for quantifying responses to stimuli are summarized in Box 17–1.

Stimuli Are Represented in the Nervous System by the Firing Patterns of Neurons

Psychophysical methods provide objective techniques for analyzing sensations evoked by stimuli. These quantitative measures have been combined with neurophysiological techniques to study the neural mechanisms that transform sensory neural signals into percepts. The goal of sensory neuroscience is to follow the flow of sensory information from receptors toward the cognitive centers of the brain, to understand the processing mechanisms that occur at successive synapses, and to decipher how this shapes our internal representation of the external world. The neural coding of sensory information is better understood at the early stages of processing than at later stages in the brain.

This approach to the *neural coding problem* was pioneered in the 1960s by Vernon Mountcastle, who showed that single-cell recordings of spike trains from peripheral and central sensory neurons provide a statistical description of the neural activity evoked by a physical stimulus. He then investigated which quantitative aspects of neural responses might correspond to the psychophysical measurements of sensory tasks and, just as important, which do not.

The study of neural coding of information is fundamental to understanding how the brain works. A neural code describes the relationship between the activity in a specified neural population and its functional consequences for perception or action. Sensory systems are ideal for the study of neural coding because both the physical properties of the stimulus input and the neural or behavioral output of these systems can be precisely defined and quantified in a controlled setting.

Box 17–1 Signal Detection Theory: Quantifying Detection and Discrimination

Two major functions of our sensory systems are to tell us if something is there and what it is. To test our ability and the ability of our sensory systems to answer these questions, experimental protocols, tools, and methods have been developed to quantify the response of sensory systems to stimuli. These include *decision theory* and *signal detection theory*. Each uses statistical methods to quantify the variability of subjects' responses.

In an "Is something there?" task, for example, subjects or experimental animals can correctly detect a specific stimulus (a "hit" or "true positive"), respond incorrectly in the absence of that stimulus ("false positive" or "false alarm"), fail to respond to a true stimulus ("miss"), or correctly decline to respond in the absence of the stimulus ("true negative" or "correct rejection"). With repeated presentations, these choices can be tabulated in a four-cell stimulus–response matrix (Figure 17–3A).

This quantifies *sensitivity*, defined as the number of true positives divided by the number of stimuli presented, and *specificity*, defined as the number of true negatives divided by the number of presentations without a stimulus.

In 1927, L. L. Thurstone proposed that the variability of sensations evoked by stimuli could be represented as normal or Gaussian probability functions, equating the physical distance between the amplitudes of two stimuli to a psychological scale value of inferred intensity called the *discrimination index* or *d'*.

Decision theory methods were first applied to psychophysical studies in 1954 by the psychologists Wilson Tanner and John Swets. They developed a series of experimental protocols for stimulus detection that allowed accurate calculation of *d'* as well as techniques for quantitative analyses of sensations in both human and animal subjects. Such studies can be designed to measure not just "Is something there?" as in the earlier example, but also comparative judgments of a physical property of a stimulus such as its intensity, size, or temporal frequency, thereby measuring a *two-alternative forced-choice* analog of "What is it?"

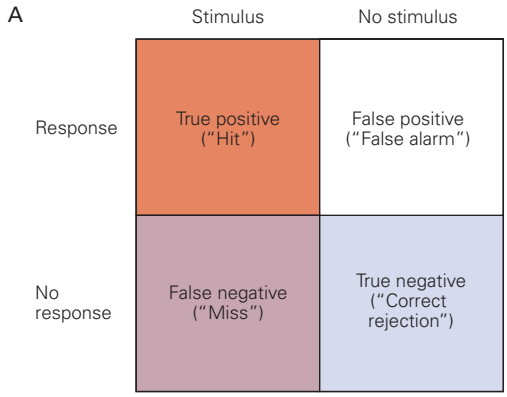

Figure 17–3A The stimulus–response matrix for data collected during a yes–no stimulus detection task ("Is a particular stimulus there?"). Each trial updates one of the four totals. For example, correct detection of the stimulus would update the count of true positives (hits), but an incorrect positive response in the absence of the stimulus would count as a false positive. From such a table, important measures such as the sensitivity and false-positive rate can be calculated.

When subjects are asked to report whether the second stimulus is stronger or weaker, higher or lower, larger or smaller, or same or different than the first stimulus, responses in each trial can again be tabulated in a four-cell stimulus–response matrix similar to the one in Figure 17–3A, but with the terms "stimulus" or "no stimulus" replaced by the two distinct stimuli.

(*continued*)

By recording neuronal activity at various stages of sensory processing, neuroscientists attempt to decipher the mechanisms used by various sensory modalities to represent information and the transformations needed to convey these signals to the brain encoded by sequences of action potentials. Additional analyses are performed of the transformation of signals by neural networks along pathways to and within the cerebral cortex. Neuroscientists can also modify activity within sensory circuits by direct stimulation with electrical pulses, chemical neurotransmitters, and modulators, or can use genetically encoded light-activated ion channels (optogenetics) to depolarize or hyperpolarize sensory neurons. How sensory stimuli are encoded by neurons may lead to insight into the coding principles that underlie cognition.

It is often said that the power of the brain lies in the millions of neurons processing information in parallel. That formulation, however, does not capture the essential difference between the brain and all the other organs of the body. In the kidney or a muscle, most cells do similar things; if we understand typical

Box 17–1 Signal Detection Theory: Quantifying Detection and Discrimination (continued)

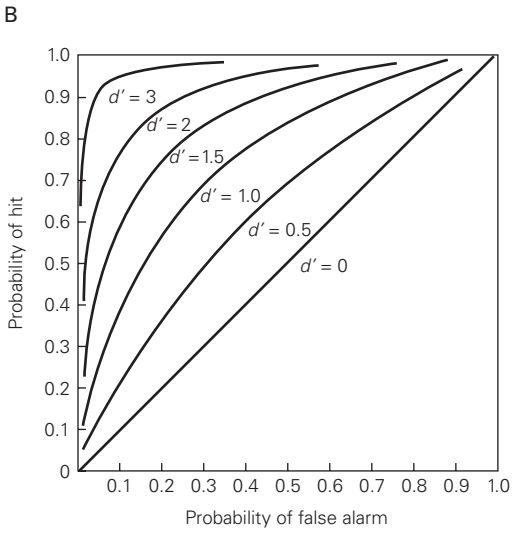

Figure 17–3B A receiver operating characteristic (ROC) plot displays the results of sets of trials, each collected in matrices such as those in Figure 17–3A. The vertical axis plots the fraction or probability of hits as a function of fraction or probability of false alarms on the horizontal axis. It is also common to label the vertical axis TPR (true-positive rate), or sensitivity, and the horizontal axis FPR (false-positive rate), or (1 – specificity). A set of trials in which yes or no responses are delivered randomly (discriminability [d'] = 0) plots as a straight line from the origin to the upper right corner. The area under such an ROC curve (AUC) would be 0.5. A perfect set of trials, in which observers accurately detect the presence of every stimulus and fail to be fooled by any trials without stimuli ($d' > 3$), would rise sharply along the left axis, and the AUC would be 1.0. AUC values are increasingly quoted as single-number measures of confidence. The (theoretical) curves shown demonstrate how higher values of d' result in larger AUC. (Adapted, with permission, from Swets 1973. Copyright © 1973 AAAS.)

Discriminability (d') in these studies is measured with *receiver operating characteristic* (ROC) analyses that compare the neural firing rates or choice probability evoked by pairs of stimuli that differ in some property. The assumption is that one of the two stimuli evokes higher responses than the other. ROC graphs of neural or psychophysical data plot the proportion of trials judged correctly (hits) and incorrectly (false positives) when the decision criteria are set at various firing levels or choice rates (Figure 17–3B). The area under the ROC curve provides an accurate estimate of d' for each stimulus pair.

Signal detection methods have been applied by William Newsome, Michael Shadlen, and J. Anthony Movshon in studies of neural responses to visual stimuli that differ in orientation, spatial frequency, or coherence of motion in order to correlate changes in neural firing rates with sensory processing. The neurometric function, plotting neural discriminability as a function of stimulus differences, corresponds closely to the psychometric function obtained in forced-choice paradigms testing the same stimuli, thereby providing a physiological basis for the observed behavioral responses.

Many of these tools, developed in part to study sensory systems, have been generalized to apply broadly beyond neuroscience. ROC curves, sensitivity, and specificity are essential in quantification of diagnosis and treatment of disease. The area under an ROC curve, or *AUC*, is today used much more than d'. Values of AUC close to 1 characterize high sensitivity and high specificity. The *false positive rate* (1 – specificity, or the number of false positives divided by the number of presentations without a stimulus) is, for many experiments or clinical investigations in which true positive findings are rare, a more meaningful measure than the classical p value.

muscle cells, we essentially understand how whole muscles work. In the brain, millions of cells each do something *different*. To understand the brain, we need to understand how its tasks are organized in networks of neurons.

Sensory Receptors Respond to Specific Classes of Stimulus Energy

Functional differences between sensory systems arise from two features: the different stimulus energies that drive them and the discrete pathways that compose each system. Each neuron performs a specific task, and the train of action potentials it produces has a specific functional significance for all postsynaptic neurons in that circuit. This basic idea was expressed in the theory of specificity set forward by Charles Bell and Johannes Müller in the 19th century, and remains one of the cornerstones of sensory neuroscience.

When analyzing sensory experience, it is important to realize that our conscious sensations differ qualitatively from the physical properties of stimuli because,

as Kant and the idealists predicted, the nervous system extracts only certain features of each stimulus while ignoring others. It then interprets this information within the constraints of the brain's intrinsic structure and previous experience. Thus, we *receive* electromagnetic waves of different frequencies, but we *see* them as colors. We receive pressure waves from objects vibrating at different frequencies but we hear sounds, words, and music. We encounter chemical compounds floating in the air or water but we experience them as odors and tastes. Colors, tones, odors, and tastes are mental creations constructed by the brain out of sensory experience. They do not exist as such outside the brain but are linked to specific physical properties of stimuli.

The richness of sensory experience begins with millions of highly specific sensory receptors. Sensory receptors are found in specialized epithelial structures called sense organs, principally the eye, ear, nose, tongue, and skin. Each receptor responds to a specific kind of energy at specific locations in the sense organ and sometimes only to energy with a particular temporal or spatial pattern. The receptor transforms the stimulus energy into electrical energy; thus, all sensory systems use a common signaling mechanism. The amplitude and duration of the electrical signal produced by the receptor, termed the *receptor potential*, are related to the intensity and time course of stimulation of the receptor. The process by which a specific stimulus energy is converted into an electrical signal is called *stimulus transduction*.

Sensory receptors are morphologically specialized to transduce specific forms of energy, and each receptor has a specialized anatomical region within the sense organ where stimulus transduction occurs (Figure 17–4). Most receptors are optimally selective for a single type of stimulus energy, a property termed

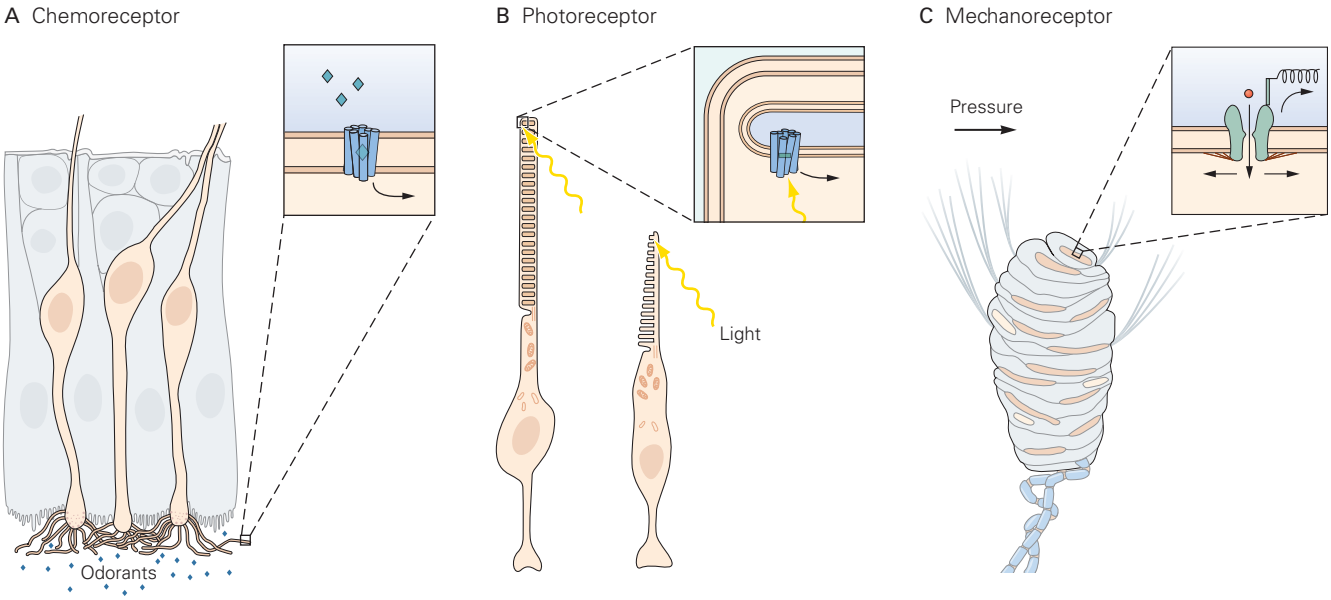

Figure 17–4 Sensory receptors are specialized to transduce a particular type of stimulus energy into electrical signals. Sensory receptors are classified as chemoreceptors, photoreceptors, or mechanoreceptors depending on the class of stimulus energy that excites them. They transform that energy into an electrical signal that is transmitted along pathways that serve one sensory modality. The inset in each panel illustrates the location of the ion channels that are activated by stimuli.

A. The olfactory hair cell responds to chemical molecules in the air. The olfactory cilia on the mucosal surface bind specific odorant molecules and depolarize the sensory nerve through a second-messenger system. The firing rate signals the concentration of odorant in the inspired air.

B. Rod and cone cells in the retina respond to light. The outer segment of both receptors contains the photopigment rhodopsin, which changes configuration when it absorbs light of particular wavelengths. Stimulation of the chromophore by light reduces the concentration of cyclic guanosine 3′,5′-monophosphate (cGMP) in the cytoplasm, closing cation channels and thereby hyperpolarizing the photoreceptor. (Adapted from Shepherd 1994.)

C. Meissner's corpuscles respond to mechanical pressure. The fluid-filled capsule (**pale blue**) surrounding the sensory nerve endings (**pink**) is linked by collagen fibers to the fingerprint ridges. Pressure or motion on the skin opens stretch-sensitive ion channels in the nerve fiber endings, thus depolarizing them. (Adapted, with permission, from Andres and von Düring 1973.)

receptor specificity. We see particular colors, for example, because we have receptors that are selectively sensitive to photons with specific ranges of wavelengths, and we smell particular odors because we have receptors that bind specific odorant molecules.

In all sensory systems, each receptor encodes the type of energy applied to its receptive field, the local stimulus magnitude, and how it changes with time. For example, photoreceptors in the retina encode the hue, brightness, and duration of light striking the retina from a specific location in the visual field. Hair cell receptors in the cochlea encode the tonal frequency, loudness, and duration of sound-pressure waves hitting the ear. The neural representation of an object, sound, or scene is therefore composed of a mosaic of individual receptors that collectively signal its size, contours, texture, temporal frequency, color, and temperature.

The arrangement of receptors in the sense organ allows further specialization of function within each sensory system. Mammalian sensory receptors are classified as mechanoreceptors, chemoreceptors, photoreceptors, or thermoreceptors (Table 17–1). Mechanoreceptors and chemoreceptors are the most widespread and the most varied in form and function.

Four different kinds of *mechanoreceptors* that sense skin deformation, motion, stretch, and vibration are responsible for the sense of touch in the human hand and elsewhere (Chapters 18 and 19). Muscles contain three kinds of mechanoreceptors that signal muscle length, velocity, and force, whereas other mechanoreceptors in the joint capsule signal joint angle (Chapter 31). Hearing is based on two kinds of mechanoreceptors, inner and outer hair cells, that transduce motion of the basilar membrane in the inner ear (Chapter 26). Other hair cells in the vestibular labyrinth sense motion and acceleration of the fluids of the inner ear to signal head motion and orientation (Chapter 27). Visceral mechanoreceptors detect the distension of internal organs such as the bowel and bladder. Osmoreceptors in the brain, which sense the state of hydration, are activated when a cell swells. Certain mechanoreceptors report extreme distortion that threatens to damage tissue; their signals reach pain centers in the brain (Chapter 20).

Table 17–1 Classification of Sensory Receptors

Sensory system	Modality	Stimulus	Receptor class	Receptor cells
Visual	Vision	Light (photons)	Photoreceptor	Rods and cones
Auditory	Hearing	Sound (pressure waves)	Mechanoreceptor	Hair cells in cochlea
Vestibular	Head motion	Gravity, acceleration, and head motion	Mechanoreceptor	Hair cells in vestibular labyrinths
Somatosensory				Cranial and dorsal root ganglion cells with receptors in:
	Touch	Skin deformation and motion	Mechanoreceptor	Skin
	Proprioception	Muscle length, muscle force, and joint angle	Mechanoreceptor	Muscle spindles, Golgi tendon organs, and joint capsules
	Pain	Noxious stimuli (thermal, mechanical, and chemical stimuli)	Thermoreceptor, mechanoreceptor, and chemoreceptor	All tissues except central nervous system
	Itch	Histamine, pruritogens	Chemoreceptor	Skin
	Visceral (not pain)	Wide range (thermal, mechanical, and chemical stimuli)	Thermoreceptor, mechanoreceptor, and chemoreceptor	Cardiovascular, gastrointestinal tract, urinary bladder, and lungs
Gustatory	Taste	Chemicals	Chemoreceptor	Taste buds, intraoral thermal, and chemoreceptors
Olfactory	Smell	Odorants	Chemoreceptor	Olfactory sensory neurons

Chemoreceptors are responsible for olfaction, gustation, itch, pain, and many visceral sensations. A significant part of pain is due to chemoreceptors that detect molecules spilled into the extracellular fluid by tissue injury and molecules that are part of the inflammatory response. Several kinds of *thermoreceptors* in the skin sense skin warming and cooling. Another thermoreceptor, which monitors blood temperature in the hypothalamus, is mainly responsible for whether we feel warm or cold.

Vision is mediated by five kinds of *photoreceptors* in the retina. The light sensitivities of these receptors define the visible spectrum. The photopigments in rods and cones detect electromagnetic energy of wavelengths that span the range of 390 to 670 nm (Figure 17–5A), the principal wavelengths of sunlight and moonlight reaching the earth and informing our visual world. Unlike some other species, such as birds or reptiles, humans do not detect ultraviolet light or infrared radiation because we lack receptors that detect the appropriate short or long wavelengths. Likewise, we do not perceive radio waves and microwave energy bands because we have not evolved receptors for these wavelengths.

Multiple Subclasses of Sensory Receptors Are Found in Each Sense Organ

Each major sensory system has several *submodalities*. For example, taste can be sweet, sour, salty, savory, or bitter; visual objects have qualities of color, shape, and pattern; and touch includes qualities of temperature, texture, and rigidity. Some submodalities are mediated by discrete subclasses of receptors that respond to limited ranges of stimulus energies of that modality; others are derived by combining information from different receptor types.

The receptor behaves as a filter for a narrow range or bandwidth of energy. For example, an individual photoreceptor is not sensitive to all wavelengths of light but only to a small part of the spectrum. We say that a receptor is *tuned* to an optimal or best stimulus, the *preferred* stimulus that activates the receptor at low energy and evokes the strongest neural response. As a result, we can plot a *tuning curve* for each receptor based on physiological experiments (see the light absorbance curves for photoreceptors in Figure 17–5A). The tuning curve shows the range of sensitivity of the receptor, including its preferred stimulus. For example, blue cone cells in the retina are most sensitive to light of 430 to 440 nm, green cone cells respond best to 530 to 540 nm, and red cone cells respond most vigorously to light of 560 to 570 nm. Responses of the three cone cells to other wavelengths of light are weaker as the incident wavelengths differ from these optimal ranges (Chapter 22).

Each rod and cone cell thus responds to a wide spectrum of colors. The graded sensitivity of photoreceptors encodes specific wavelengths by the amplitude of the evoked receptor potential. However, this amplitude also depends upon the intensity or brightness of the light, so a green cone responds similarly to bright orange or dimmer green light. How are these distinguished? Stronger stimuli activate more photoreceptors than do weaker ones, and the resulting population code of multiple receptors, combined with receptors of different wavelength preferences, distinguishes intensity from hue. Such neural ensembles enable individual visual neurons to multiplex signals of color and brightness in the same pathway.

Additionally, because the tuning curve of a photoreceptor is roughly symmetric around the best frequency, wavelengths of greater or lesser values may evoke similar responses. For example, red cones respond similarly to light of 520 and 600 nm. How does the brain interpret these signals? The answer again lies with multiple receptors, in this case the green and blue cones. Green cones respond very strongly to light of 520 nm, as it is close to their preferred wavelength, but respond weakly to 600 nm light. Blue cones do not respond to 600 nm light and are barely activated at 520 nm. As a result, 520 nm light is perceived as green, whereas 600 nm is seen as orange. Thus, through varying combinations of photoreceptors, we are able to perceive a spectrum of colors.

Similarly, the complex flavors we perceive when eating are a result of combinations of chemoreceptors with different affinities for natural ligands. The broad tuning curves of a large number of distinct olfactory and gustatory receptors afford many combinatorial possibilities.

The existence of submodalities points to an important principle of sensory coding, namely that the range of stimulus energies—such as the wavelength of light—is deconstructed into smaller, simpler components whose intensity is monitored over time by specialized receptors that transmit information in parallel to the brain. The brain eventually integrates these diverse components of the stimulus to convey an ensemble representation of the sensory event. The ensemble hypothesis is even more important when we examine the representation of sensory events in the central nervous system. Although most studies of sensory processing have examined how individual neurons respond to temporally varying stimuli, the current challenge is to decipher how sensory information is

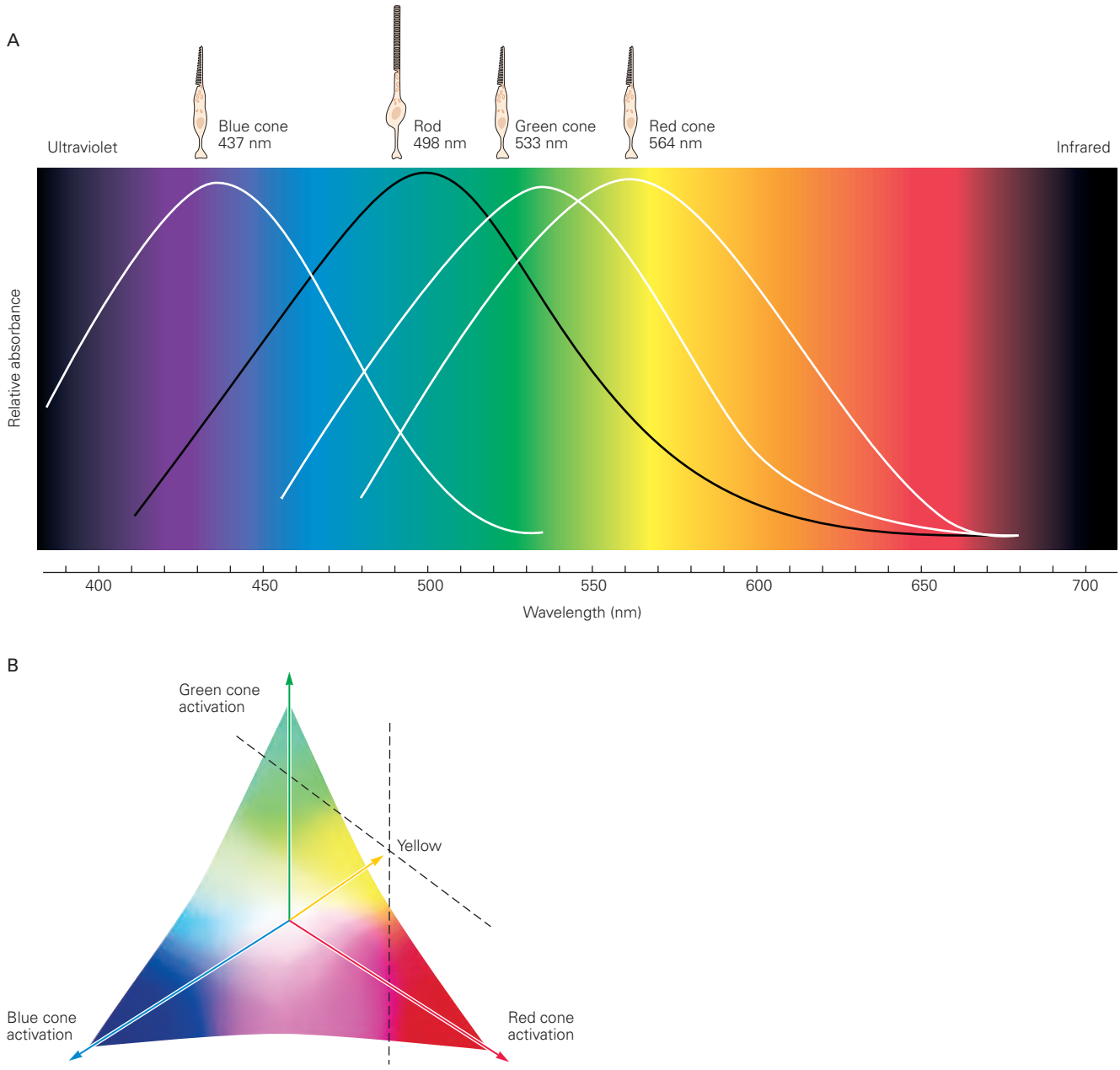

Figure 17–5 Human perception of colors results from the simultaneous activation of three different classes of photoreceptors in the retina.

A. The visible spectrum of light spans wavelengths of 390 to 670 nm. Individual photoreceptors are sensitive to a broad range of wavelengths, but each is most responsive to light in a particular spectral band. Thus, cone cells are classified as red, green, or blue type photoreceptors. Changes in the relative activation of each of the three cone types account for the perception of specific colors. (Adapted from Dowling 1987.)

B. The neural coding of color and brightness in the retina can be portrayed as a three-dimensional vector in which the strength of activation of each cone type is plotted along one of the three axes. Each point in the vector space represents a unique pattern of activation of the three cone types. Direction in the vector indicates the relative activity of each cone type and the color seen. In the example shown here, strong activation of **red cones** along with moderate stimulation of **green cones** and weak activation of **blue cones** produces the perception of **yellow**. The length of the vector from the origin to the point represents the intensity or brightness of light in that region of the retina.

distributed across populations of neurons responding to the same event at the same time.

Receptor Population Codes Transmit Sensory Information to the Brain

The receptor potential generated by an adequate stimulus produces a local depolarization or hyperpolarization of the sensory receptor neuron whose amplitude is proportional to the stimulus intensity. However, the sense organs are located at distances far enough from the central nervous system that passive propagation of receptor potentials is insufficient to transmit signals there. To communicate sensory information to the brain, a second step in neural coding must occur. The receptor potential produced by the stimulus must be transformed into sequences of action potentials that can be propagated along axons. The analog signal of stimulus magnitude in the receptor potential is transformed into a digital pulse code in which the frequency of action potentials is proportional to the intensity of the stimulus (Figure 17–6A). This is spike train *encoding*.

The recognition of an analog-to-digital transformation dates back to 1925 when Edgar Adrian and Yngve Zotterman discovered the all-or-none properties of the action potential in sensory neurons. Despite the simple recording instruments available at that time, Adrian and Zotterman discovered that the frequency of firing—the number of action potentials per second—varies with the strength of the stimulus and its duration; stronger stimuli evoke larger receptor potentials that generate a greater number and a higher frequency of action potentials. This signaling mechanism is termed *rate coding*.

In later years, as recording technology improved and digital computers allowed precise quantification of the timing of action potentials, Vernon Mountcastle and his colleagues demonstrated a precise correlation between sensory thresholds and neural responses, as well as the parametric relationship between neural firing rates and the perceived intensity of sensations (Figure 17–6B). They also found that the intensity of a stimulus is represented in the brain by all active neurons in the receptor population. This type of *population code* depends on the fact that individual receptors in a

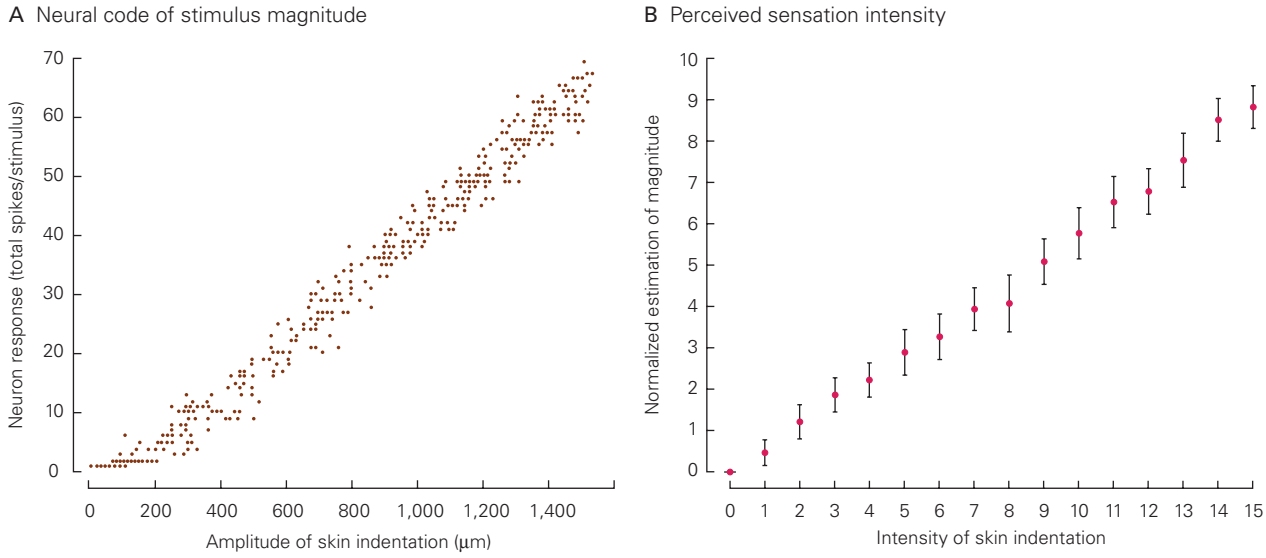

Figure 17–6 The firing rates of sensory neurons encode the stimulus magnitude. The two plots indicate that the neural coding of stimulus intensity is faithfully transmitted from peripheral receptors to cortical centers that mediate conscious sensation. (Adapted, with permission, from Mountcastle, Talbot, and Kornhuber 1966.)

A. The number of action potentials per second recorded from a touch receptor in the hand is proportional to the amplitude of skin indentation. Each dot represents the response of the receptor to pressure applied by a small probe. The relationship between the neural firing rate and the pressure stimulus is linear. This receptor does not respond to stimuli weaker than 200 μm, its touch threshold.

B. Estimates made by human subjects of the magnitude of sensation produced by pressure on the hand increase linearly as a function of skin indentation. The relation between a subject's estimate of the intensity of the stimulus and its physical strength resembles the relation between the discharge frequency of the sensory neuron and the stimulus amplitude.

sensory system differ in their sensory thresholds or in their affinity for particular molecules.

Most sensory systems have low- and high-threshold receptors. When stimulus intensity changes from weak to strong, low-threshold receptors are first recruited, followed by high-threshold receptors. For example, rod cells in the retina are activated by very low light levels and reach their maximal receptor potentials and firing rates in dim daylight. Cone cells do not respond in very dim light but do report differences in daylight brightness. The combination of the two types of photoreceptors allows us to perceive light intensity over several orders of magnitude. Parallel processing by low- and high-threshold receptors thus extends the dynamic range of a sensory system.

Distributed patterning of firing in neural ensembles allows the use of vector algebra to quantify how stimulus properties are distributed across populations of active neurons. For example, although humans possess only three types of cone cells in the retina, we can clearly identify colors across the entire spectrum of visible light. In Figure 17–5B, we see that the color yellow can be synthesized in the mind by specific combinations of activity in red, green, and blue cone cells (Figure 17–5B). Likewise, the color magenta results from other combinations of the same photoreceptor classes. Mathematically, the perceived hue can be represented in a three-dimensional vector space in which the strengths of activation of each receptor class are combined to yield a unique sensation.

High-dimensional multineuronal representation of stimuli across large populations of neurons is beginning to be analyzed as new techniques are developed for simultaneous recording and imaging of activity in neural ensembles. Ideally, the firing rates of each neuron in a population can be plotted in a coordinate system with multiple axes such as modality, location, intensity, and time. The neural components along these axes combine to form a vector that represents the population's activity. The vector interpretation is useful because it makes available powerful analytic techniques.

The possibilities for information coding through *temporal patterning* within and between neurons in a population are enormous. For example, the timing of action potentials in a presynaptic neuron can determine whether the postsynaptic cell fires. Two action potentials that arrive near synchronously will alter the postsynaptic neuron's probability of firing more than would action potentials arriving at different times. The relative timing of action potentials between neurons also has a profound effect on mechanisms of learning and synaptic plasticity, including long-term potentiation and depression at synapses (Chapter 54).

Sequences of Action Potentials Signal the Temporal Dynamics of Stimuli

The instantaneous firing patterns of sensory neurons are as important to sensory perception as the total number of spikes fired over long periods. Steady rhythmic firing in nerves innervating the hand is perceived as steady pressure or vibration depending upon which touch receptors are activated (Chapter 19). Bursting patterns may be perceived as motion. The patterning of spike trains plays an important role in encoding temporal fluctuations of the stimulus, such as the frequency of vibration or auditory tones, or changes in rate of movement. Humans can report changes in sensory experience that correspond to alterations within a few milliseconds in the firing patterns of sensory neurons.

Sensory systems detect *contrasts*, changes in the temporal and spatial patterns of stimulation. If a stimulus persists unchanged for several minutes without a change in position or amplitude, the neural response and corresponding sensation diminishes, a condition called *receptor adaptation*. Receptor adaptation is thought to be an important neural basis of perceptual adaptation, whereby a constant stimulus fades from consciousness. Receptors that respond to prolonged and constant stimulation—known as *slowly adapting* receptors—encode stimulus duration by generating action potentials throughout the period of stimulation (Figure 17–7A). In contrast, *rapidly adapting* receptors respond only at the beginning and end of a stimulus; they *cease* firing in response to constant amplitude stimulation and are active only when the stimulus intensity increases or decreases (Figure 17–7B). Rapidly and slowly adapting sensors illustrate another important principle of sensory coding: Neurons signal important properties of stimuli not only when they fire but also when they slow or stop firing.

The temporal properties of a changing stimulus are encoded as changes in the firing pattern, including the *interspike intervals*, of sensory neurons. For example, the touch receptors illustrated in Figure 17–7 fire at higher rates when a probe initially contacts the skin than when the pressure is maintained. The time interval between spikes is shorter when the skin is indented rapidly than when pressure is applied gradually. The firing rate of these neurons is proportional to both the speed at which the skin is indented and the total amount of pressure applied. During steady pressure, the firing rate slows to a level proportional to skin indentation (Figure 17–7A) or ceases entirely (Figure 17–7B). Firing of both neurons stops after the probe is retracted.

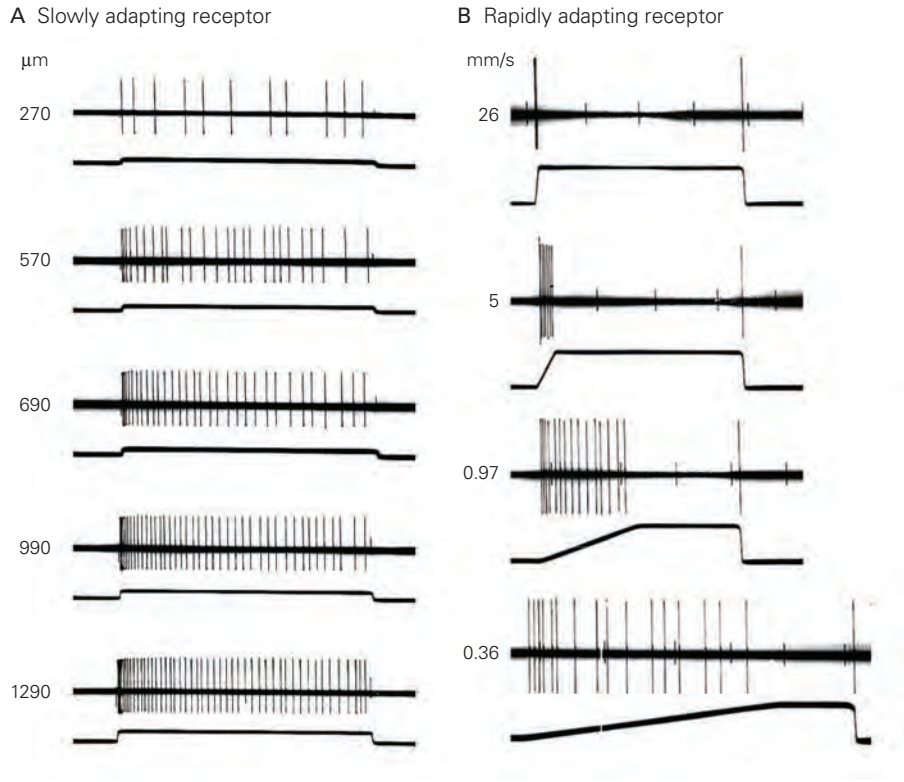

Figure 17–7 Firing patterns of sensory neurons convey information about the stimulus intensity and time course. These records illustrate responses of two different classes of touch receptors to a probe pressed into the skin. The stimulus amplitude and time course are shown in the lower trace of each pair; the upper trace shows the action potentials recorded from the sensory nerve fiber in response to the stimulus.

A. A slowly adapting mechanoreceptor responds as long as pressure is applied to the skin. The total number of action potentials discharged during the stimulus is proportional to the amount of pressure applied to the skin. The firing rate is higher at the beginning of skin contact than during steady pressure, as this receptor also detects how rapidly pressure is applied to the skin. When the probe is removed from the skin, the spike activity ceases. (Adapted, with permission, from Mountcastle, Talbot, and Kornhuber 1966.)

B. A rapidly adapting mechanoreceptor responds at the beginning and end of the stimulus, signaling the rate at which the probe is applied and removed; it is silent when pressure is maintained at a fixed amplitude. Rapid motion evokes a brief burst of high-frequency spikes, whereas slow motion evokes a longer-lasting, low-frequency spike train. (Adapted, with permission, from Talbot et al. 1968.)

The Receptive Fields of Sensory Neurons Provide Spatial Information About Stimulus Location

The position of a sensory neuron's input terminals in the sense organ is a major component of the specific information conveyed by that neuron. The skin area, location in the body, retinal area, or tonal domain in which stimuli can activate a sensory neuron is called its *receptive field* (Figure 17–8). The region from which a sensation is perceived to arise is called the neuron's *perceptive field*. The two usually coincide.

The dimensions of receptive fields play an important role in the ability of a sensory system to encode detailed spatial information. The objects that we see with our eyes or hold in our hands are much larger than the receptive field of an individual sensory neuron, and therefore stimulate groups of adjacent receptors. The size of the stimulus therefore determines the total number of receptors that are activated. In this manner, the spatial distribution of active and silent receptors provides a neural image of the size and contours of the stimulus.

The spatial resolution of a sensory system depends on the total number of receptor neurons and the distribution of receptive fields across the area covered. The projection neurons for regions of the body with a high density of receptors, such as the retinal ganglion cells representing the central retina (the fovea), have small receptive fields because they receive inputs from a small number of bipolar cells, each of which receives input from a few closely packed photoreceptors. Because of the high density of receptors in the

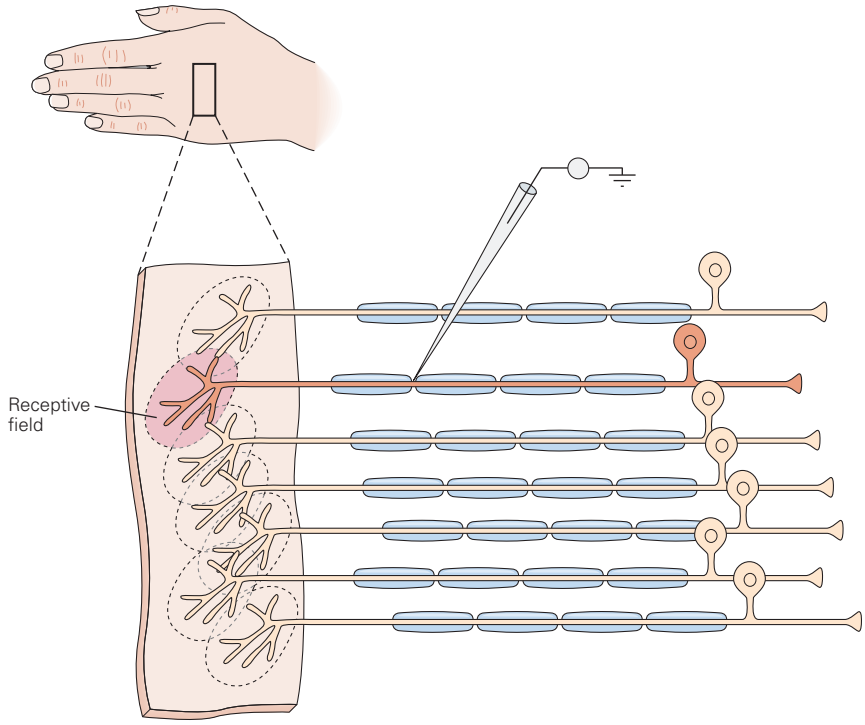

Figure 17–8 The receptive field of a sensory neuron. The receptive field of a touch-sensitive neuron denotes the region of skin where gentle tactile stimuli evoke action potentials in that neuron. It encompasses all of the receptive endings and terminal branches of the sensory nerve fiber. If the fiber is stimulated electrically with a microelectrode, the subject experiences touch localized on the skin. The area from which the sensation is perceived to arise is called the *perceptive field*. A patch of skin contains many overlapping receptive fields, allowing sensations to shift smoothly from one sensory neuron to the next in a continuous sweep. The axon terminals of sensory neurons in the central nervous system are arranged somatotopically, providing an orderly map of the innervated region of the body.

fovea, the population of neurons transmits a very detailed representation of the visual scene. Ganglion cells in the periphery of the retina have larger receptive fields because the receptor density is much lower. The dendrites of these ganglion cells receive information from a wider area of the retina, and thus integrate light intensity over a greater portion of the visual field. This arrangement yields a less detailed image of the visual scene (Figure 17–9). Similarly, the region of the body most often used to touch objects is the hand. Not surprisingly, mechanoreceptors for touch are concentrated in the fingertips, and the receptive fields on the hand are smaller than those on the arm or trunk.

Central Nervous System Circuits Refine Sensory Information

The central connections of a sensory neuron determine how that neuron's signals influence our sensory experience. Action potentials in nerve fibers of the cochlea, for example, evoke the sensation of a tone whether they are initiated by sound waves acting on hair cells or by electrical stimulation with a neural prosthesis.

The parcellation of a stimulus into its components, each encoded by an individual type of sensory receptor or projection neuron, is an initial step in sensory processing. These components are integrated into a representation of an object or scene by neural networks in the brain. This process allows the brain to select certain abstract features of an object, person, scene, or external event from the detailed input of many receptors. As a result, the representation formed in the brain may enhance the saliency of features that are important at the moment while ignoring others. In this sense, our percepts are not merely reflections of environmental events, but also constructs of the mind.

How we experience the sensations reported by primary receptors is also subject to modification or learning. Initially aversive odors and tastes, for example, can become attractive over time because of familiarity or changes in context or association. The pleasure elicited by photos of a respected baseball player can be converted to disdain should he subsequently appear in the uniform of a rival team.

In the early stages of sensory information processing in the central nervous system, each class of peripheral receptors provides input to clusters of neurons in relay nuclei that are dedicated to one sensory modality. That is, each sensory modality is represented by an ensemble of central neurons connected to a specific class of receptors. Such ensembles are referred to as *sensory systems*, and include the somatosensory, visual, auditory, vestibular, olfactory, and gustatory systems (see Table 17–1).

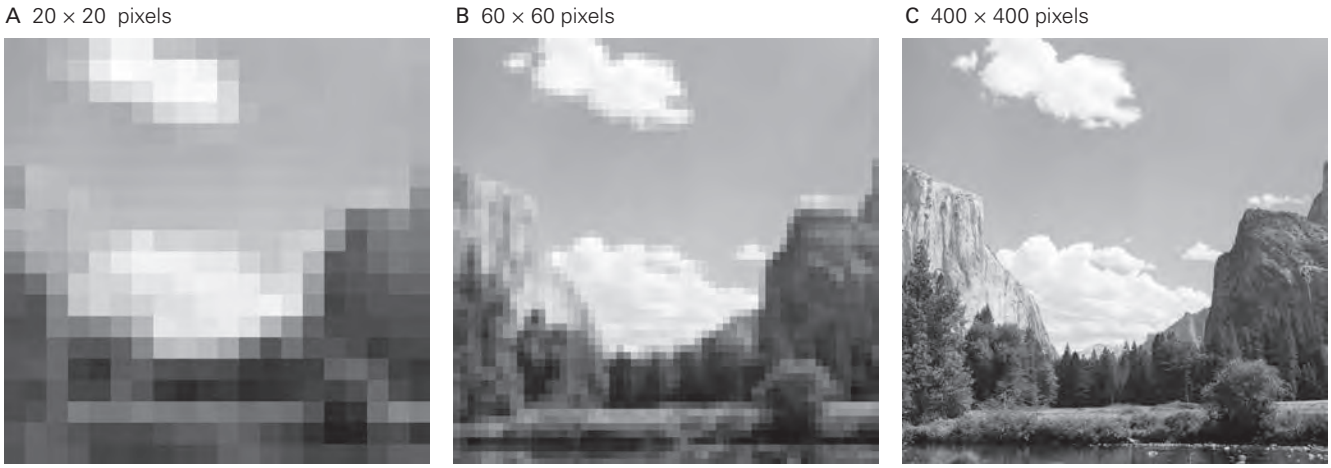

Figure 17–9 The visual resolution of scenes and objects depends on the density of photoreceptors that mediate the image. The resolution of detail is inversely correlated with the area of the receptive field of individual neurons. Each square or pixel in these images represents a receptive field. The gray scale in each pixel is proportional to the average light intensity in the corresponding receptive field. If there are a small number of neurons, and each spans a large area of the image, the result is a very schematic representation of the scene (**A**). As the density of neurons increases, and the size of each receptive field decreases, the spatial detail becomes clearer (**B, C**). The increased spatial resolution comes at the cost of the larger number of neurons required to transmit the information. (Photographs reproduced, with permission, from Daniel Gardner.)

The brain has evolved to process and respond to this rich ensemble of sensory information. The activation of sensory, cognitive, and motor systems in the human brain can be visualized in real time with fMRI techniques. Maurizio Corbetta, Marcus Raichle, and colleagues discovered coherent fluctuations in low-frequency (0.01–0.1 Hz) components of the blood oxygen level–dependent (BOLD) signal during the "resting" state in brain areas that are anatomically connected and activated together during specific behaviors. Figure 17–10 highlights three functionally specialized networks of brain areas that respond to auditory (in red), somatomotor (in green), and visual (in blue) inputs. Other areas are multisensory, integrating information from several different modalities. Spontaneous correlation of firing of these networks in the absence of direct sensory stimuli or performance of motor tasks suggests that excitability within resting state sensory or motor networks may signal readiness to process information for future sensation or action. Deficits in sensory, cognitive, or motor function following local brain injury may result not just from impairment of one specific area, or node, but rather disruption of the circuit or circuits that include that node.

Synapses in sensory pathways provide an opportunity to modify the signals from receptors. Most neurons in relay nuclei receive convergent excitatory inputs from many presynaptic neurons (Figure 17–11A), integrate those inputs, combine them with inhibitory and top-down signals, and transmit the processed information to higher brain areas. Horace Barlow proposed that sensory systems demonstrate *efficient coding*, which includes sensory relays recoding sensory messages so that their redundancy is reduced, but comparatively little information is lost. Likewise, each receptor neuron excites multiple postsynaptic relay neurons.

Convergent excitatory networks provide a mechanism for spatial summation of inputs, strengthening signals of functional importance. One example of how such circuits are used is detection of synchronous inputs from multiple nearby locations but not others, thereby providing the first step toward *orientation tuning* of central neurons. Relay neurons are also interconnected with their neighbors, forming recurrent excitatory connections that amplify sensory signals. Such *recurrent networks* are also a feature of some deep learning algorithms used by artificial neural networks to classify sensory patterns.

A relay neuron's receptive field is also shaped by inhibitory input. The inhibitory region of a receptive field provides an important mechanism for enhancing the contrast between stimuli, giving the sensory system additional power to resolve spatial detail. Inhibitory interneurons modulate the excitability of neurons in relay nuclei, thereby regulating the amount of sensory information transmitted to higher levels of

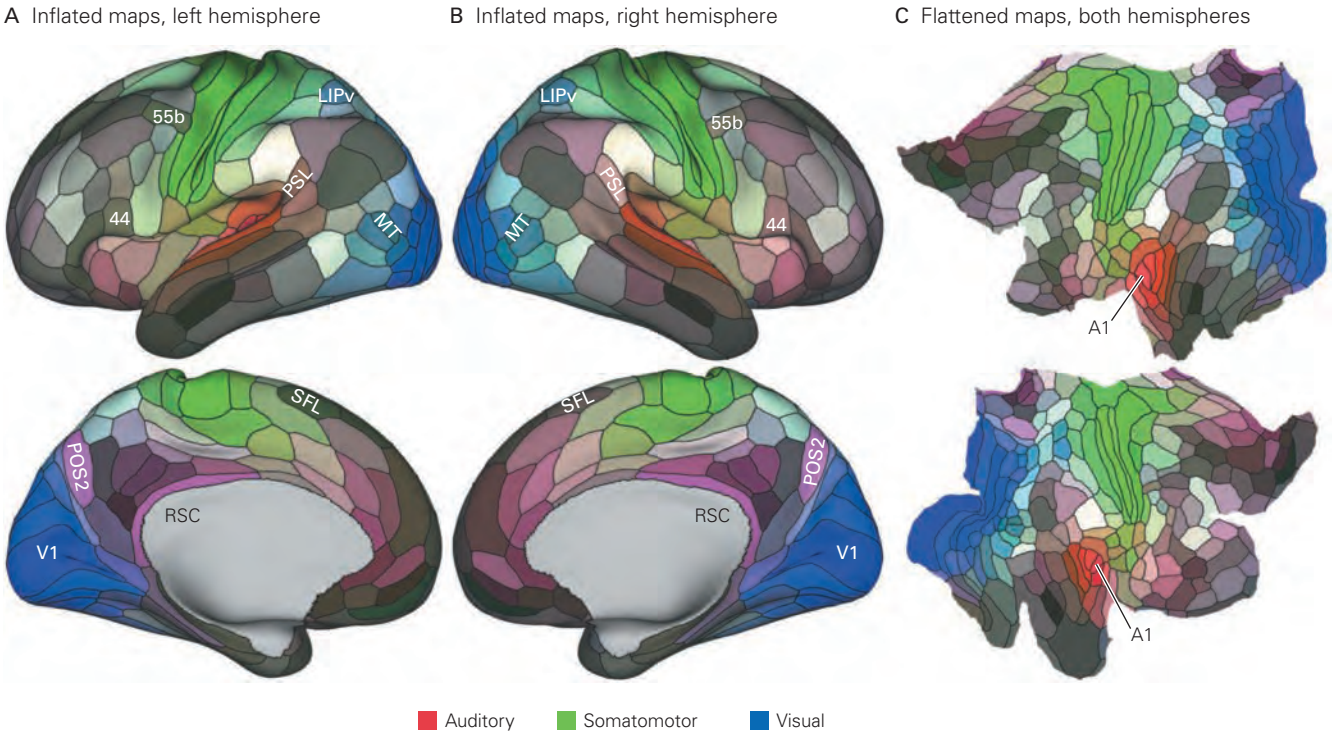

Figure 17–10 **Distinct regions of the human brain process information for individual sensory modalities, multisensory systems, motor activity, or cognitive function.** The human cerebral cortex has been divided into 180 functional areas by the Human Connectome Project based largely on a variety of fMRI techniques and neuroanatomy. Early auditory areas (**red**), somatosensory and motor areas (**green**), and visual areas (**blue**) are shaded in primary colors. Mixed colors indicate multisensory areas: visual and somatosensory/motor (**blue-green, LIPv, MT**); or visual and auditory (**pink to purple, POS2, RSC**). Language networks include areas 55b, 44, SFL, and PSL in both hemispheres. Gray-scaled regions serve cognitive functions; they comprise the anticorrelated "task-positive" (**light shading**) and "default mode" (**dark shading**) networks. The maps show brain regions located on the surface gyri and within adjacent cortical sulci. Note the similarity of brain organization between the two hemispheres. Data available at https://balsa.wustl.edu/study/RVVG. (Reproduced, with permission, from Glasser et al. 2016. Copyright © 2016 Springer Nature.)

A. Inflated maps of the left hemisphere. The top map is a lateral view and the bottom map is a medial view.

B. Similar maps of the right hemisphere.

C. Flattened maps show the functional organization of both hemispheres (left at top, right at bottom).

(Abbreviations: **A1**, primary auditory cortex; **LIPv,** lateral intraparietal area, ventral portion; **MT,** middle temporal area; **POS2**, parieto-occipital sulcus area 2; **PSL**, perisylvian language area; **RSC**, retrosplenial complex; **SFL**, superior frontal language area; **V1**, primary visual cortex; **Area 55b**, newly identified language area; **Area 44**, part of Broca's area.)

a network (Figure 17–11B). Inhibitory circuits are also useful for suppressing irrelevant information during goal-directed behaviors, thereby focusing attention on specific task-related inputs. Additionally, inhibitory networks allow the context of a stimulus to modify the strength of excitation evoked by that stimulus, an important process called *normalization*.

The responses of central neurons to sensory stimuli are more variable from trial to trial than those of peripheral receptors. Central sensory neurons also fire irregularly before and after stimulation and during periods when no stimuli are present. The variability of the evoked central responses is a result of several factors: the subject's state of alertness, whether attention is engaged (Figure 17–12), previous experience of that stimulus, and recent activation of the pathway by similar stimuli. Similarly, the context of stimulus presentation, subjective intentions, motor plans that may require feedback, or intrinsic oscillations of the neuron's membrane potential can all modify incoming sensory information.

The Receptor Surface Is Represented Topographically in the Early Stages of Each Sensory System

The axons of sensory projection neurons terminate in the brain in an orderly manner that retains their spatial arrangement in the receptor sheet. Sensory neurons for

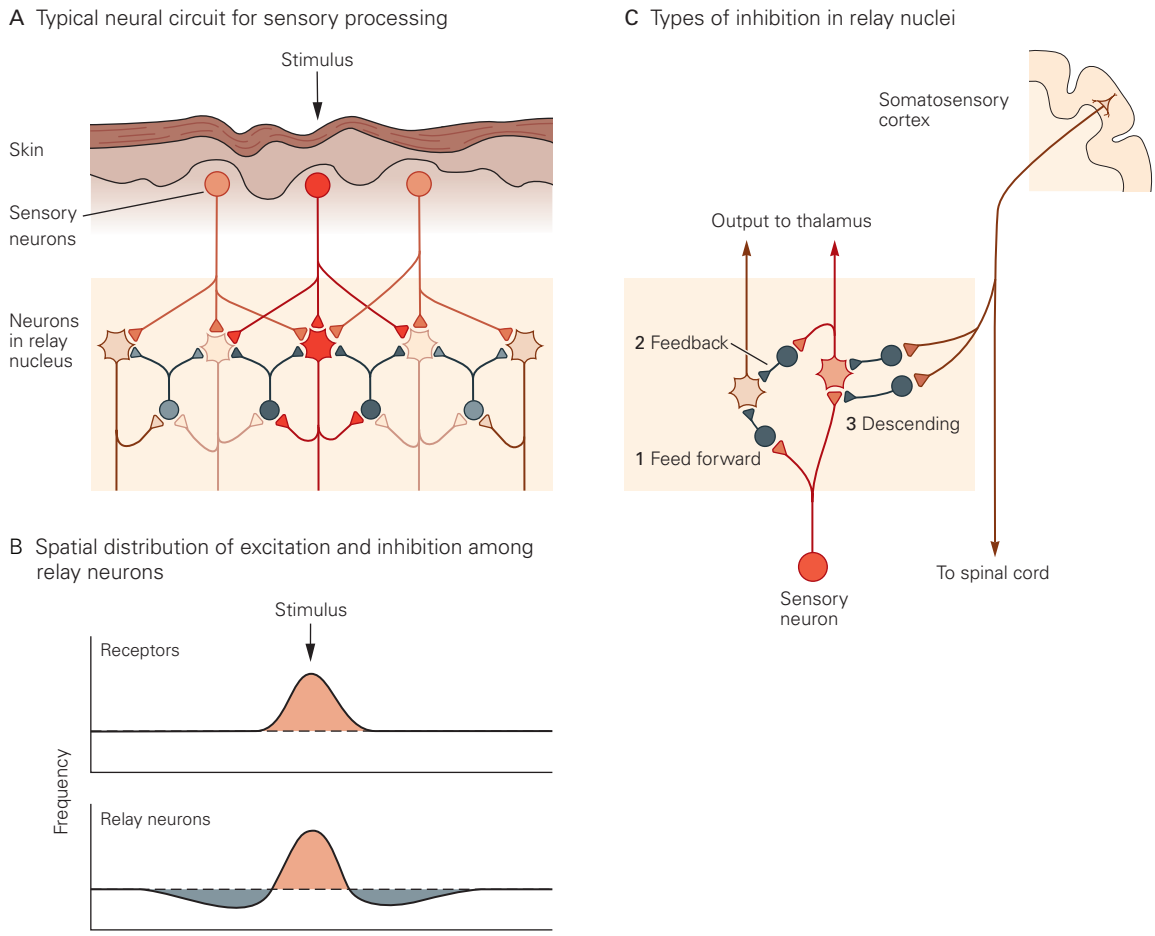

Figure 17–11 Relay neurons in sensory systems integrate a variety of inputs that shape stimulus information.

A. Sensory information is transmitted in the central nervous system through hierarchical processing networks. Neural signaling initiated by a stimulus to the skin reaches a large group of postsynaptic neurons in relay nuclei in the brain stem and thalamus and is most strong in neurons in the center of the array of postsynaptic cells (**red neuron**). (Adapted, with permission, from Dudel 1983.)

B. Inhibition (**gray areas**) mediated by local interneurons (**gray**) confines excitation (**orange area**) to the central zone in the array of relay neurons where stimulation is strongest. This pattern of inhibition within the relay nucleus enhances the contrast between strongly and weakly stimulated relay neurons.

C. Inhibitory interneurons in a relay nucleus are activated by three distinct excitatory pathways. **1. Feed-forward** inhibition is initiated by the afferent fibers of sensory neurons that terminate on the inhibitory interneurons. **2. Feedback** inhibition is initiated by recurrent collateral axons of neurons in the output pathway from the nucleus that project back to interneurons in the source nucleus. The interneurons in turn inhibit nearby output neurons, creating sharply defined zones of excitatory and inhibitory activity in the relay nucleus. In this way, the most active relay neurons reduce the output of adjacent, less active neurons, thus ensuring that only one of two or more active neurons will send out signals. **3. Descending** inhibition is initiated by neurons in other brain regions such as the cerebral cortex. The descending commands allow cortical neurons to control the afferent relay of sensory information, providing a mechanism by which attention can select sensory inputs.

touch in adjacent regions of the skin project to neighboring neurons in the central nervous system, and this topographic arrangement of receptive fields is preserved throughout the early somatosensory pathways. Each primary sensory area in the brain thus contains a topographic, spatially organized map of the sense organ. This topography extends to all levels of a sensory system. Within these maps, specificity—the qualities to which neurons are most narrowly tuned—provides clues to the functional organization of that region of the brain.

In the first and subsequent relay nuclei of the somatosensory, visual, and auditory systems, adjacent neurons represent adjacent areas of the body,

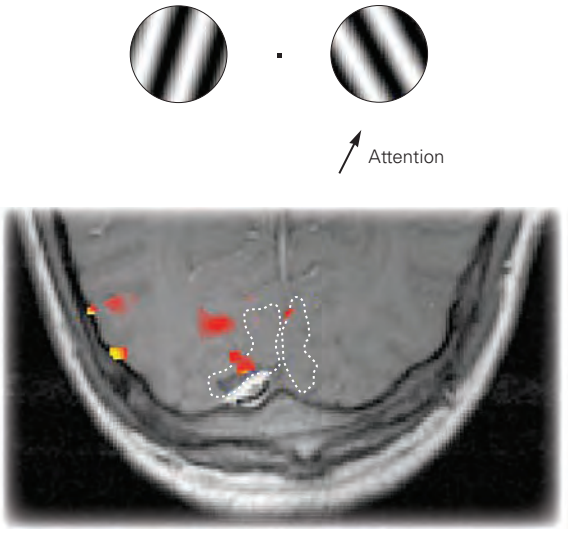

Figure 17–12 Attention to a visual stimulus alters responses of neurons in visual cortical areas. When we pay attention to a stimulus, we select certain sensory inputs for cognitive processing and ignore or suppress other information. Functional MRI is used in this study to measure the effects of attention to visual stimuli on neural responses in human primary visual (V1) cortex (**white dashed lines** on the brain anatomical section, **lower panel**). Moving grating stimuli (**upper panel**) were presented simultaneously to the right and left visual fields while subjects stared at a central fixation point (**black dot**). The subjects performed a motion discrimination task, attending (without moving their eyes) to one of the two oriented gratings. When stimuli were attended in the right visual field, neural activity (**red**) increased significantly in the left hemisphere, but not in the right hemisphere, even though the stimuli were presented to both eyes. When the subject attended to the grating in the left visual field, a similar focus of activity occurred in the right V1 cortex, and activity dropped in the left hemisphere (not shown). (Adapted from Gandhi, Heeger, and Boynton, 1999.)

retina, and cochlea, respectively. The organization of these nuclei is thus said to be somatotopic, retinotopic, or tonotopic. Nuclei in the auditory system are tonotopic because the cochlear hair cells of the inner ear are arranged to create an orderly shift in frequency sensitivity from cell to cell (Figure 26–2). Neurons in the primary sensory areas of the cerebral cortex maintain these location-specific features of a stimulus, and the functional maps of these early cortical areas are likewise somatotopic, retinotopic, or tonotopic.

Sensory information flows serially through hierarchical pathways, including multiple levels of the cerebral cortex, before ending in brain regions that are concerned with cognition and action. Forming the percepts that inform these regions requires integration of lower-level inputs that report only information from small areas of the sense organ. Neurons in the cerebral cortex are specialized to integrate and so detect specific features of stimuli beyond merely their location in the sense organ. Such neurons are said to be *tuned* to combined stimulus features represented by ensembles of sensory receptors. These neurons respond preferentially to stimulus properties such as the orientation of edges (eg, simultaneous activation of specific groups of receptors), direction of motion, or tonal sequences of frequencies (temporal pattern of receptor activation). Central auditory neurons are less selective for frequency and more selective for certain kinds of sound. For example, some neurons are specific for vocalizations by members of the same species. In each successive stage of cortical processing, the spatial organization of stimuli is progressively lost as neurons become less concerned with the descriptive features of stimuli and more concerned with properties of behavioral importance. Details of these central sensory transformations are presented in succeeding chapters that describe specific sensory systems.

Sensory Information Is Processed in Parallel Pathways in the Cerebral Cortex

Distributed spatial coding is ubiquitous in sensory systems for two reasons. First, it takes advantage of the parallel architecture of the nervous system. There are approximately 100 million neurons in each primary sensory area of the cerebral cortex, and the possible number of combinatorial patterns of neural activity far exceeds the number of atoms in the universe. Second, each neuron codes the intensity and timing of a stimulus as well as its location in the receptor sheet. It fires only when many of its excitatory synapses receive action potentials and most of the inhibitory synapses do not, firing in response to specific patterns of stimulation but not to others. Since many cortical neurons receive input from 1,000 to 10,000 synapses, the information coding potential is enormous.

One of the most important insights into feature detection in the cortex arose from combined physiological and anatomical studies of the cortical visual pathways by Mortimer Mishkin and Leslie Ungerleider in the early 1980s. They discovered that sensory information arriving in the primary visual areas is divided in two parallel pathways.

One pathway carries information needed for classification of images, while the other conveys information needed for immediate action. Visual features that identify *what* an object is are transmitted in a *ventral pathway* to the temporal lobe and eventually to the hippocampus and entorhinal cortex. Visual information

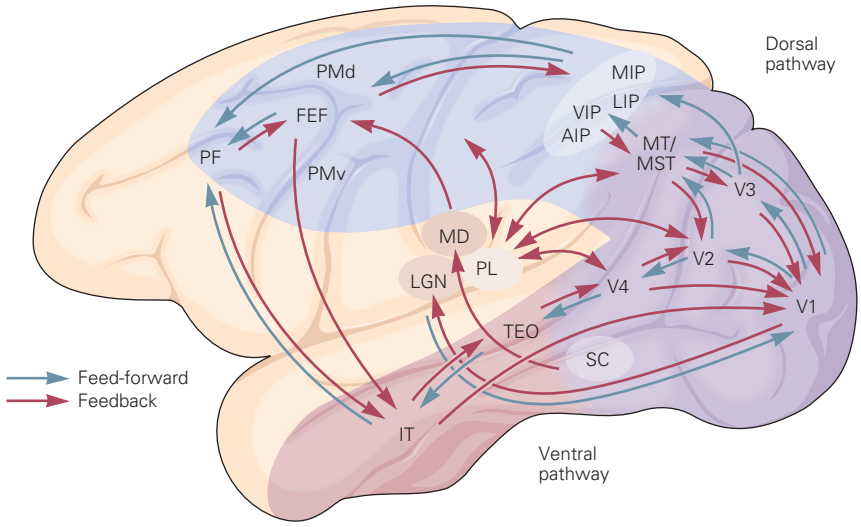

Figure 17–13 Visual stimuli are processed by serial and parallel networks in the cerebral cortex. When you read this text, the spatial pattern of the letters is sent to the cerebral cortex through successive synaptic links comprising photoreceptors, bipolar cells of the retina, retinal ganglion cells, cells in the lateral geniculate nucleus (**LGN**) of the thalamus, and neurons of the primary visual cortex (**V1**). Within the cortex, there is a gradual divergence to successive processing areas called ventral and dorsal streams that are neither wholly serial nor parallel. The ventral stream in the temporal lobe (**red shading**) analyzes and encodes information about the form and structure of the visual scene and objects within it, delivering this information to the parahippocampal cortex (not shown) and prefrontal cortex (**PF**). The dorsal stream in the parietal lobe (**blue shading**) analyzes and represents information about stimulus location and motion and delivers this information to motor areas of the frontal cortex that control movements of the eyes, hand, and arm. The anatomical connections between these areas are reciprocal, involving both feedforward and feedback circuits. The zone of overlap (**purple**) shows that both pathways originate from the same source in **V1**. Connections to subcortical structures in the thalamus and midbrain are defined in Figure 21–7B. (Abbreviations: **V1**, **V2**, **V3**, and **V4**, occipital visual areas; **MT**, middle temporal; **MST**, medial superior temporal; **AIP**, **VIP**, **LIP**, and **MIP**, anterior, ventral, lateral, and medial intraparietal; **TEO**, temporal-occipital; **IT**, inferior temporal; **PMd** and **PMv**, dorsal and ventral premotor; **FEF**, frontal eye fields.) (Adapted from Albright and Stoner 2002.)

about *where* an object is located, its size and shape, and *how* it might be acquired and used is transmitted in a more *dorsal pathway* to the parietal lobe and eventually to the motor areas of frontal cortex (Figure 17–13).

Ventral and dorsal streams are evident in other sensory systems as well. In the auditory system, acoustic information from speech is transmitted to Wernicke's area in the temporal lobe, which has a strong role in language comprehension, and to Broca's area in the frontal cortex, which is involved in speech production. In the somatosensory system, information about an object's size and shape is transmitted to ventral areas of parietal cortex for object recognition. Tactile information about object size, weight, and texture is also communicated to posterior parietal and frontal motor areas, where it is needed to plan the handling of the object.

Ventral and dorsal streams of sensory information also contribute to two major forms of memory: semantic (also called explicit) memory, which we use to talk about objects or persons, and procedural (also called implicit) memory, which we use to interact with objects, persons, or the immediate environment.

Ventral stream information generates *nouns* that we use to identify and classify persons, places, and objects, such as spheres, bricks, and cars. Dorsal stream information motivates *verbs* enabling the actions performed based on sensory inputs and subjective intentions, such as grasping, lifting, or driving.

Feedback Pathways From the Brain Regulate Sensory Coding Mechanisms

Sensory systems are not simply automated assembly lines that reassemble fragmented neural representations of environmental events (eg, light, sound, odor) into more coherent percepts. We have enormous control over our own experience of sensation and perception, and even our conscious attention.

We can to some extent control which sensations reach our consciousness. We may, for example, watch television to take our minds off the pain of a sprained ankle.

Direct, volitional control of the sensory information that reaches consciousness can be readily demonstrated by suddenly directing your attention to a body part, such as the fingers of your left hand, to which you were initially oblivious as you were attending to this text. Sensations from the fingers flood consciousness until attention is redirected to the text. Neural recordings in somatosensory and visual cortex confirm that neurons change their sensitivity, as reflected in their firing rates, much more so than their selectivity for particular stimuli. At a more abstract level, for example, we can switch our attention from the subject matter of a painting to the artist's technique.

Each primary sensory area of cortex has extensive projections back to its principal afferent relay nucleus in the thalamus. In fact, the number of feedback axons exceeds the number of afferent axons from the thalamus to the cortex. These projections have an important function that is not yet clear. One possibility is that they modulate the activity of certain neurons when attention and vigilance change or during motor tasks.

Centers in the brain are also able to modulate the responsiveness of sensory receptors. For example, neurons in the motor cortex can alter the sensitivity of sensory receptors in skeletal muscle that signal muscle length. Activation of gamma motor neurons by corticospinal pathways enhances the sensory responses of muscle spindle afferents to stretch. Neurons in the brain stem can directly modulate the frequency sensitivity of hair cells in the cochlea. Thus, information about a stimulus sent from peripheral sensory neurons to the brain is conditioned by the entire organism.

Top-Down Learning Mechanisms Influence Sensory Processing

What we perceive is always some combination of the sensory stimulus itself and the memories it both evokes and builds upon. The relationship between perception and memory was originally developed by empiricists, particularly the associationist philosophers James and John Stuart Mill. Their idea was that sensory and perceptual experiences that occur together or in close succession, particularly those that do so repeatedly, become associated so that thereafter the one triggers the other. Association is a powerful mechanism, and much of learning consists of forging associations through repetition.

Contemporary neuroscientists using multineuronal recordings discovered that sensory events evoke sequences of neuronal activation. These patterns of neural activity are believed to trigger memories of previous experiences of such stimulation patterns. For example, as we hear a work of music over and over again, the circuits of our auditory system are modified by the experience, and we learn to anticipate what comes next, completing the phrase before it occurs. Familiarity with the phrasing and harmonies used by a composer allows us to distinguish the operas of Verdi from those of Mozart, and the symphonies of Bruckner from those of Brahms. Likewise, when we drive to an unknown destination, our visual system is initially overwhelmed by new landmarks, as we assess which are important and which are not. With repeated trips, the journey becomes second nature and seems to take less time.

Percepts are uniquely subjective. When we look at a work of art, we superimpose our personal experience on the view; what we see is not just the image projected on the retina, but its contextual meaning to us as individuals. For example, when we view a historic photograph of important events in our lives, or persons we admired or detested, we recall not only the event in the image but also the words spoken and our emotional reactions in the past. The emotional response is muted or absent if we did not experience a direct connection to the event or person illustrated.

How can a network of neurons "recognize" a specific pattern of inputs from a population of presynaptic neurons? One potential mechanism is called *template matching*. Each neuron in the target population has a pattern of excitatory and inhibitory presynaptic connections. If the pattern of arriving action potentials fits the postsynaptic neuron's pattern of synaptic connections even approximately—activating many of its excitatory synapses but mostly avoiding activating its inhibitory synapses—the target neuron fires. The codes may also be combinatorial: the overall activity of a region remains the same with different stimuli, but the specific subset of neurons that are active when a particular input is presented constitute a "tag" specifying that input.

Charles F. Stevens has identified these in very different sensory systems and noted that such *maximum entropy* codes are highly efficient, able to represent many different stimuli for a set number of neurons. Refining our understanding of efficient coding, the Carandini and Harris labs have recently shown that the neural code in mouse visual cortex is indeed efficient and preserves fine detail, but in a manner that retains the ability to generalize by responding similarly to closely related visual stimuli. Such computational or algorithmic views have great promise for our understanding of sensory systems. *Artificial neural networks*, simulated using computers, can be trained on images and taught to "see." Daniel L. Yamins and James J.

DiCarlo have pointed out that as these artificial networks evolve the ability to recognize objects and faces, the properties of neuron-like "units" in particular layers begin to resemble the distribution of activity seen in corresponding cortical areas. Such artificial neural networks are trained by machine learning algorithms that modify the connection strength between units, similar to neuronal learning with repetition and synapse modification.

Precisely how the brain solves the recognition problem is uncertain. There is currently much evidence that the neural representation of a stimulus in the initial pathways of sensory systems is an isomorphic representation of the stimulus. Successive synaptic regions transform these initial representations into abstractions of our environment that we are beginning to decipher. In contrast, we barely understand the top-down mechanisms by which incoming sensory information invokes memories of past occurrences and activates our prejudices and opinions.

One view of these processes is Bayesian: Our experience and understanding of the world inform a top-down *sensory prior* that describes our likely environment. The primary insight of Bayes's rule is that decisions are made by the likelihood ratio of current evidence from a test stimulus and the subject's previous experience of similar stimuli (priors), all modified by the task contingencies (rewards and hazards). Ongoing sensory information contributes immediate data, and the two combine to form an up-to-the-moment *posterior* estimate of our surroundings and our place in them. When we do understand these neural codes and the algorithms and mechanisms that generate and interpret them, it is likely that we will be on the verge of understanding cognition, the way in which information is coded in our memory and our understanding. That is what makes the study of neural coding so challenging and exciting.

Highlights

1. Our sensory systems provide the means by which we perceive the external world, remain alert, form a body image, and regulate our movements. Sensations arise when external stimuli interact with some of the billion sensory receptors that innervate every organ of the body. The information detected by these receptors is conveyed to the brain as trains of action potentials traveling along individual sensory axons.
2. All sensory systems respond to four elementary features of stimuli—modality, location, intensity, and duration. The diverse sensations we experience—the sensory modalities—reflect different forms of energy that are transformed by receptors into depolarizing or hyperpolarizing electrical signals called receptor potentials. Receptors specialized for particular forms of energy, and sensitive to particular ranges of the energy bandwidth, allow humans to sense many kinds of mechanical, thermal, chemical, and electromagnetic events.
3. The intensity and duration of stimulation are represented by the amplitude and time course of the receptor potential and by the total number of receptors activated. In order to transmit sensory information over long distances, the receptor potential is transformed into a digital pulse code, sequences of action potentials whose frequency of firing is proportional to the strength of the stimulus. The pattern of action potentials in peripheral nerves and in the brain gives rise to sensations whose qualities can be measured directly using a variety of psychophysical paradigms such as magnitude estimation, signal detection methods, and discrimination tasks. The temporal features of a stimulus, such as its duration and changes in magnitude, are signaled by the dynamics of the spike train.
4. The location and spatial dimensions of a stimulus are conveyed through each receptor's receptive field, the precise area in the sensory domain in which stimulation activates the receptor. The identity of the active sensory neurons therefore signals not only the modality of a stimulus but also the place where it occurs.
5. These messages are analyzed centrally by several million sensory neurons performing different, specific functions in parallel. Each sensory neuron extracts highly specific and localized information about the external or internal environment, and in turn has a specific effect on sensation and cognition because it projects to specific places in the brain that have specific sensory, motor, or cognitive functions. To maintain the specificity of each modality within the nervous system, receptor axons are segregated into discrete anatomical pathways that terminate in unimodal nuclei.
6. Sensory information in the central nervous system is processed in stages, in the sequential relay nuclei of the spinal cord, brain stem, thalamus, and cerebral cortex. Each nucleus integrates sensory inputs from adjacent receptors and, using networks of inhibitory neurons, emphasizes the strongest signals. After about a dozen synaptic steps in each sensory system, neural activity

converges on neuronal groups whose function is multisensory and more directly cognitive.

7. Processing of sensory information in the cerebral cortex occurs in multiple cortical areas in parallel and is not strictly hierarchical. Feedback connections from areas of the brain involved in cognition, memory, and motor planning control the incoming stream of sensory information, allowing us to interpret sensory stimulation in the context of past experience and current goals.
8. The richness of sensory experience—the complexity of sounds in a Mahler symphony, the subtle layering of color and texture in views of the Grand Canyon, or the multiple flavors of a salsa—requires the activation of large ensembles of receptors acting in parallel, each one signaling a particular aspect of a stimulus. The neural activity in a set of thousands or millions of neurons should be thought of as coordinated activity that conveys a "neural image" of specific properties of the external world.
9. Our sensory systems are increasingly appreciated as computational and algorithmic encoders, processors, and decoders of information. Insights from machine learning, information theory, artificial neural networks, and Bayesian inference continue to inform our understanding of what we perceive in our bodies and from the world around us.

Esther P. Gardner
Daniel Gardner

Selected Reading

Basbaum AI, Kaneko JH, Shepherd GM, Westheimer G (eds). 2008. *The Senses: A Comprehensive Reference* (6 vols). Oxford: Elsevier.

Dowling JE. 1987. *The Retina: An Approachable Part of the Brain.* Cambridge, MA: Belknap.

Gerstein GL, Perkel DH, Dayhoff JE. 1985. Cooperative firing activity in simultaneously recorded populations of neurons: detection and measurement. J Neurosci 5:881–889.

Green DM, Swets JA. 1966. *Signal Detection Theory and Psychophysics.* New York: Wiley. (Reprinted 1974, Huntington, NY: Robert E. Krieger.)

Kandel ER. 2016. *Reductionism in Art and Brain Science: Bridging the Two Cultures.* New York: Columbia Univ. Press.

Moore GP, Perkel DH, Segundo JP. 1966. Statistical analysis and functional interpretation of neuronal spike data. Annu Rev Physiol 28:493–522.

Mountcastle VB. 1998. *Perceptual Neuroscience: The Cerebral Cortex*. Cambridge, MA: Harvard Univ. Press.

Singer W. 1999. Neuronal synchrony: a versatile code for the definition of relations? Neuron 24:49–65.

Stevens SS. 1961. The psychophysics of sensory function. In: WA Rosenblith (ed). *Sensory Communication*, pp. 1–33. Cambridge, MA: MIT Press.

Stevens SS. 1975. *Psychophysics: Introduction to Its Perceptual, Neural, and Social Prospects*. New York: Wiley.

References

Adrian ED, Zotterman Y. 1926. The impulses produced by sensory nerve-endings. Part 2. The response of a single end-organ. J Physiol (Lond) 61:151–171.

Albright TD, Stoner GR. 2002. Contextual influences on visual processing. Annu Rev Neurosci 25:339–379.

Andres KH, von Düring M. 1973. Morphology of cutaneous receptors. In: Iggo A (ed). *Handbook of Sensory Physiology*, Vol. 2, *Somatosensory System*, pp. 3–28. Berlin: Springer-Verlag.

Barch DM, Burgess GC, Harms MP, et al. 2013. Function in the human connectome: task-fMRI and individual differences in behavior. Neuroimage 80:169–189.

Berkeley G. [1710] 1957. *A Treatise Concerning the Principles of Human Knowledge*. K Winkler (ed). Indianapolis: Bobbs-Merrill.

Britten KH, Shadlen MN, Newsome WT, Movshon JA. 1992. The analysis of visual motion: a comparison of neuronal and psychophysical performance. J Neurosci 12:4745–4768.

Carandini M, Heeger DJ. 2011. Normalization as a canonical neural computation. Nat Rev Neurosci 13:51–62.

Chang L, Tsao DY. 2017. The code for facial identity in the primate brain. Cell 169:1013–1028.

Colquhoun D. 2014. An investigation of the false discovery rate and the misinterpretation of *p*-values. Royal Soc Open Sci 1:140216.

DiCarlo JJ, Zoccolan D, Rust NC. 2012. How does the brain solve visual object recognition? Neuron 73:415–434.

Dudel J. 1983. General sensory physiology. In: RF Schmitt, G Thews (eds). *Human Physiology*, pp. 177–192. Berlin: Springer-Verlag.

Gandhi SP, Heeger DJ, Boynton GM. 1999. Spatial attention affects brain activity in human primary visual cortex. Proc Natl Acad Sci U S A 96:3314–3319.

Gazzaniga MS (ed). 2009. *The Cognitive Neurosciences*, 4th ed. Cambridge, MA: MIT Press.

Glasser MF, Coalson TS, Robinson EC, et al. 2016. A multimodal parcellation of human cerebral cortex. Nature 536:171–178.

Hubel DH, Wiesel TN. 1968. Receptive fields and functional architecture of monkey striate cortex. J Physiol 195:215–243.

Hume D. [1739] 1984. *A Treatise of Human Nature*. EC Mossner (ed). New York: Penguin.

Johansson RS, Vallbo AB. 1979. Detection of tactile stimuli. thresholds of afferent units related to psychophysical thresholds in the human hand. J Physiol 297:405–422.

Johnson KO, Hsiao SS, Yoshioka T. 2002. Neural coding and the basic law of psychophysics. Neuroscientist 8:111–121.

Kant I. [1781/1787] 1961. *Critique of Pure Reason*. NK Smith (transl.). London: Macmillan.

Kirkland KL, Gerstein GL. 1999. A feedback model of attention and context dependence in visual cortical networks. J Comput Neurosci 7:255–267.

LaMotte RH, Mountcastle VB. 1975. Capacities of humans and monkeys to discriminate between vibratory stimuli of different frequency and amplitude: a correlation between neural events and psychophysical measurements. J Neurophysiol 38:539–559.

Li HH, Rankin J, Rinzel J, Carrasco M, Heeger DJ. 2017. Attention model of binocular rivalry. Proc Natl Acad Sci U S A 114:E6192-E6201.

Livingstone MS, Hubel DH. 1987. Psychophysical evidence for separate channels for the perception of form, color, movement, and depth. J Neurosci 7:3416–3468.

Locke J. 1690. *An Essay Concerning Human Understanding: In Four Books*, Book 2, Chapter 1. London.

Mountcastle VB, Talbot WH, Kornhuber HH. 1966. The neural transformation of mechanical stimuli delivered to the monkey's hand. In: AVS de Reuck, J Knight (eds). *Ciba Foundation Symposium: Touch, Heat and Pain*, pp. 325–351. London: Churchill.

Ochoa J, Torebjörk E. 1983. Sensations evoked by intraneural microstimulation of single mechanoreceptor units innervating the human hand. J Physiol 342:633–654.

Raichle ME. 2011. The restless brain. Brain Connect 1:3–12.

Roy A, Steinmetz PN, Hsiao SS, Johnson KO, Niebur E. 2007. Synchrony: a neural correlate of somatosensory attention. J Neurophysiol 98:1645–1661.

Shepherd GM. 1994. *Neurobiology*, 3rd ed. New York: Oxford Univ. Press.

Smith SM, Beckmann CF, Andersson J, et al. 2013. Resting-state fMRI in the Human Connectome Project. Neuroimage 80:144–168.

Stevens CF. 2015. What the fly's nose tells the fly's brain. Proc Natl Acad Sci U S A 112:9460–9465.

Stevens CF. 2018. Conserved features of the primate face code. Proc Natl Acad Sci U S A 115:584–588.

Stringer C, Pachitariu M, Steinmetz N, Carandini M, Harris KD. 2019. High-dimensional geometry of population responses in visual cortex. Nature 571:361–365.

Swets JA. 1973. The relative operating characteristic in psychology: a technique for isolating effects of response bias finds wide use in the study of perception and cognition. Science 182:990–1000.

Swets JA. 1986. Indices of discrimination or diagnostic accuracy: their ROCs and implied models. Psychol Bull 99:100–117.

Talbot WH, Darian-Smith I, Kornhuber HH, Mountcastle VB. 1968. The sense of flutter-vibration: comparison of the human capacity with response patterns of mechanoreceptive afferents from the monkey hand. J Neurophysiol 31:301–334.

Tanner WP, Swets JA. 1954. A decision-making theory of visual detection. Psychol Rev 61:401–409.

Thurstone LL. 1927. A law of comparative judgment. Psychol Rev 34:273–286.

Ungerleider LG, Mishkin M. 1982. Two cortical visual systems. In: DG Ingle, MA Goodale, RJW Mansfield (eds). *Analysis of Visual Behavior*, pp. 549–586. Cambridge, MA: MIT Press.

Yamins DLK, DiCarlo JJ. 2016. Using goal-driven deep learning models to understand sensory cortex. Nat Neurosci 19:356–365.

18

Receptors of the Somatosensory System

Neurophysiological studies of the individual sensory modalities were first conducted in the somatosensory system (Greek *soma*, the body), the system that transmits information coded by receptors distributed throughout the body. Charles Sherrington, one of the earliest investigators of these bodily senses, noted that the somatosensory system serves three major functions: proprioception, exteroception, and interoception.

Proprioception is the sense of oneself (Latin *proprius*, one's own). Receptors in skeletal muscle, joint capsules, and the skin enable us to have conscious awareness of the posture and movements of our own body, particularly the four limbs and the head. Although one can move parts of the body without sensory feedback from proprioceptors, the movements are often clumsy, poorly coordinated, and inadequately adapted to complex tasks, particularly if visual guidance is absent.

Exteroception is the sense of direct interaction with the external world as it impacts the body. The principal mode of exteroception is the sense of *touch*, which includes sensations of contact, pressure, stroking, motion, and vibration, and is used to identify objects. Some touch involves an active motor component—stroking, tapping, grasping, or pressing—whereby a part of the body is moved against another surface or organism. The sensory and motor components of touch are intimately connected anatomically in the brain and are important in guiding behavior.

Exteroception also includes the *thermal senses* of heat and cold. Thermal sensations are important controllers of behavior and homeostatic mechanisms needed to maintain the body temperature near 37°C (98.6°F). Finally, exteroception includes the sense of *pain*, or nociception, a response to external events that damage or harm the body. Nociception is a prime motivator of actions necessary for survival, such as fight or flight.

The third component of somatic sensation, *interoception*, is the sense of the function of the major organ systems of the body and its internal state.

The information conveyed by receptors in the viscera is crucial for regulating autonomic functions, particularly in the cardiovascular, respiratory, digestive, and renal systems, although most of the stimuli registered by these receptors do not lead to conscious sensations. Interoceptors are primarily chemoreceptors that monitor organ function through such indicators as blood gases and pH, and mechanoreceptors that sense tissue distention, which may be perceived as painful.

This diverse group of sensory functions may seem an unlikely combination to form a sensory system. We treat all of the somatic senses in one introductory chapter because they are mediated by one class of sensory neurons, the dorsal root ganglion (DRG) neurons. Somatosensory information from the skin, muscles, joint capsules, and viscera is conveyed by DRG neurons innervating the limbs and trunk or by trigeminal sensory neurons that innervate cranial structures (the face, lips, oral cavity, conjunctiva, and dura mater). These sensory neurons perform two major functions: the transduction and encoding of stimuli into electrical signals and the transmission of those signals to the central nervous system.

The study of somatic sensation has been revolutionized in the past 10 years by three important advances. First, the development of transgenic mice with fluorescent reporters of gene expression in DRG neurons has allowed neuroscientists to assess the physiological responses of specific receptor classes and their anatomical projections to sensory receptors in the body and in the central nervous system. Functional imaging of individual DRG neurons expressing genetically encoded calcium sensors such as GCaMP6 enables simultaneous optical recordings of activity from populations of receptor neurons innervating a specific region of the body, thereby providing a useful tool for analyzing ensemble responses to somatosensory stimuli. Second, studies of isolated DRG neurons in vitro, or in reduced skin-nerve preparations, enable biophysical assessment of receptor responses and characterization of ion channels expressed in individual somatosensory neurons. Third, the identification of Piezo protein ion channels as the molecular transducers of touch and proprioception in mammalian mechanoreceptors has provided a novel system for assessing the role of these channels in the senses of touch, proprioception, and visceral function.

In this chapter, we consider the principles common to all DRG neurons and those that distinguish their individual sensory function. We begin with a description of the peripheral nerves and their organization, followed by a survey of the receptor classes responsible for each of the major bodily senses. We also examine the sensory transduction mechanisms that convert various stimulus energies into electrical signals. We then describe the integration of information by the parent axon from multiple receptors in its receptive field and conclude with a discussion of the central processing centers for each submodality in the spinal cord and brain stem. Higher-order processing of touch, pain, proprioception, and autonomic regulation of viscera is described in later chapters.

Dorsal Root Ganglion Neurons Are the Primary Sensory Receptor Cells of the Somatosensory System

The cell body of a DRG neuron lies in a ganglion on the dorsal root of a spinal or cranial nerve. Dorsal root ganglion neurons originate from the neural crest and are intimately associated with the nearby segment of the spinal cord. Individual neurons in a DRG respond selectively to specific types of stimuli because of morphological and molecular specializations of their peripheral terminals.

Dorsal root ganglion neurons are a type of bipolar cell, called pseudo-unipolar cells. The axon of a DRG neuron has two branches, one projecting to the periphery and one projecting to the central nervous system (Figure 18–1). The peripheral terminals of individual DRG neurons innervate the skin, muscle, joint capsules, or viscera and contain receptors specialized for particular kinds of stimuli. The region of the body innervated by these sensory endings is called a *dermatome* (see Figure 18-13). Sensory peripheral nerve endings differ in receptor morphology and stimulus selectivity, allowing them to detect mechanical, thermal, or chemical events. The central branches terminate in the spinal cord or brain stem, forming the first synapses in somatosensory pathways. Thus, the axon of each DRG cell serves as a single transmission line with one polarity between the receptor terminal and the central nervous system. This axon is called the *primary afferent fiber*.

Individual primary afferent fibers innervating a particular region of the body, such as the thumb or fingers, are grouped together into bundles or fascicles of axons forming the *peripheral nerves*. They are guided during development to a specific location in the body by various trophic factors such as brain-derived neurotrophic factor (BDNF), neurotrophin-3 (NT3), neurotrophin-4 (NT4), or nerve growth factor (NGF). The peripheral nerves also include motor axons innervating nearby muscles, blood vessels, glands, or viscera.

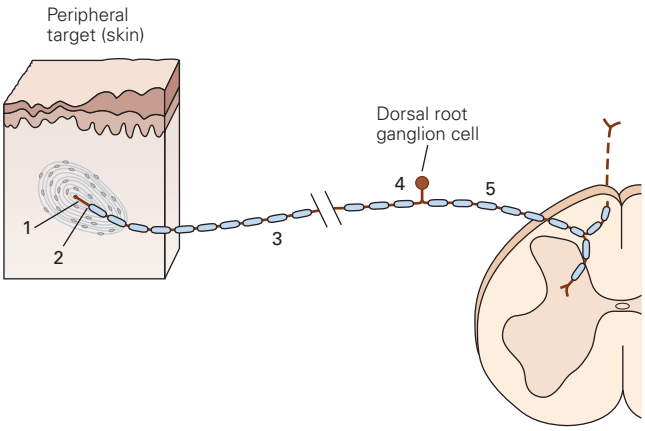

Figure 18–1 The dorsal root ganglion neuron is the primary sensory cell of the somatosensory system. The cell body is located in a dorsal root ganglion (**DRG**) adjacent to the spinal cord. The axon has two branches, one projecting to the body, where its specialized terminal contains receptors for a particular form of stimulus energy, and one projecting to the spinal cord or brain stem, where the afferent signals are processed. All DRG neurons contain five functional zones: **1.** The *distal terminals* in skin, muscle, or viscera contain specialized receptor-channels that convert specific types of stimulus energy (mechanical, thermal, or chemical) into a depolarizing receptor potential. DRG neurons typically have multiple sensory endings. **2.** The *spike generation site* contains voltage-gated Na^+ and K^+ channels (Na_V and K_V) that are located near the initial segment of the axon within the receptor capsule; they convert the receptor potential into a stream of action potentials. **3.** The *peripheral nerve fiber* transmits action potentials from the spike initiation site to the DRG cell body. **4.** The *cell body* of the DRG neuron is contained within a ganglion adjacent to the spinal cord or brain stem. **5.** A *spinal or cranial nerve* connects the DRG or trigeminal neuron to the ipsilateral spinal cord or brain stem.

Damage to peripheral nerves or their targets in the brain may produce sensory deficits in more than one somatosensory submodality or motor deficits in specific muscle groups. Knowledge of where somatosensory modalities overlap morphologically, and where they diverge, facilitates diagnosis of neurological disorders and malfunction.

Each DRG neuron can be subdivided into five functional zones: the receptive zone, the spike generation site, the peripheral nerve fiber, the DRG cell body, and the spinal or cranial nerve (Figure 18–1). The receptive zone, at the distal end of the DRG axon, contains specialized receptor proteins that sense mechanical force, thermal events, or chemicals in the local environment and translate these signals into a local depolarization of the axonal terminals, called the *receptor potential* (see Figure 3–9A). This local depolarization spreads passively toward the central axon where action potentials are generated, usually at the initial segment (distal to the first node of Ranvier in myelinated fibers) (see Figure 3–10A). Stimuli of sufficient strength produce action potentials that are transmitted along the peripheral nerve fiber, through the cell soma, and into the central branch that terminates in the spinal cord or brain stem.

The soma of a DRG neuron contains the cell nucleus. Sensory receptor proteins are expressed in the soma, providing a convenient expression system for characterizing their conductance properties in vitro. Isolated DRG neurons have been widely used in patch-clamp studies of sensory receptor currents and voltage-gated action potential channels.

DRG neurons differ in the size of their cell soma, gene expression profile, conduction velocity of their axons, sensory transduction molecule(s), innervation pattern in the body, and physiological function. For example, DRGs that innervate mechanoreceptors that sense touch and proprioception have the largest cell bodies and large myelinated axons; they express proteins such as Npy2r or parvalbumin (PV) (Figure 18–2). In contrast, DRG neurons that sense temperature or irritant chemicals have small cell bodies and unmyelinated axons; they express calcitonin gene-related peptide (CGRP) or the lectin IB4 (Figure 18–2C,D). As these fluorescent molecular labels extend through the axons to their peripheral endings in the body and in the central nervous system, David Ginty and colleagues were able to characterize the pattern of somatosensory nerve endings in the body (Figure 18–2H) and trace their central projections to the spinal cord (Figure 18–2G) and brain stem.

Peripheral Somatosensory Nerve Fibers Conduct Action Potentials at Different Rates

The peripheral nerves that transmit spike trains from the site of spike generation to the central nervous system have classically served as the primary recording sites for neurophysiological studies of somatosensory receptor mechanisms. Individual peripheral nerve fibers in animals are typically dissected from the main axon bundle and placed on fine wires that serve as recording electrodes. Microelectrodes—manufactured from sharpened tungsten or platinum wires—have also been inserted through the skin into the peripheral nerves of humans (a technique known as *microneurography*) to measure sensory responses to various somatic stimuli (Chapter 19).

Peripheral nerve fibers are classified into functional groups based on properties related to axon diameter

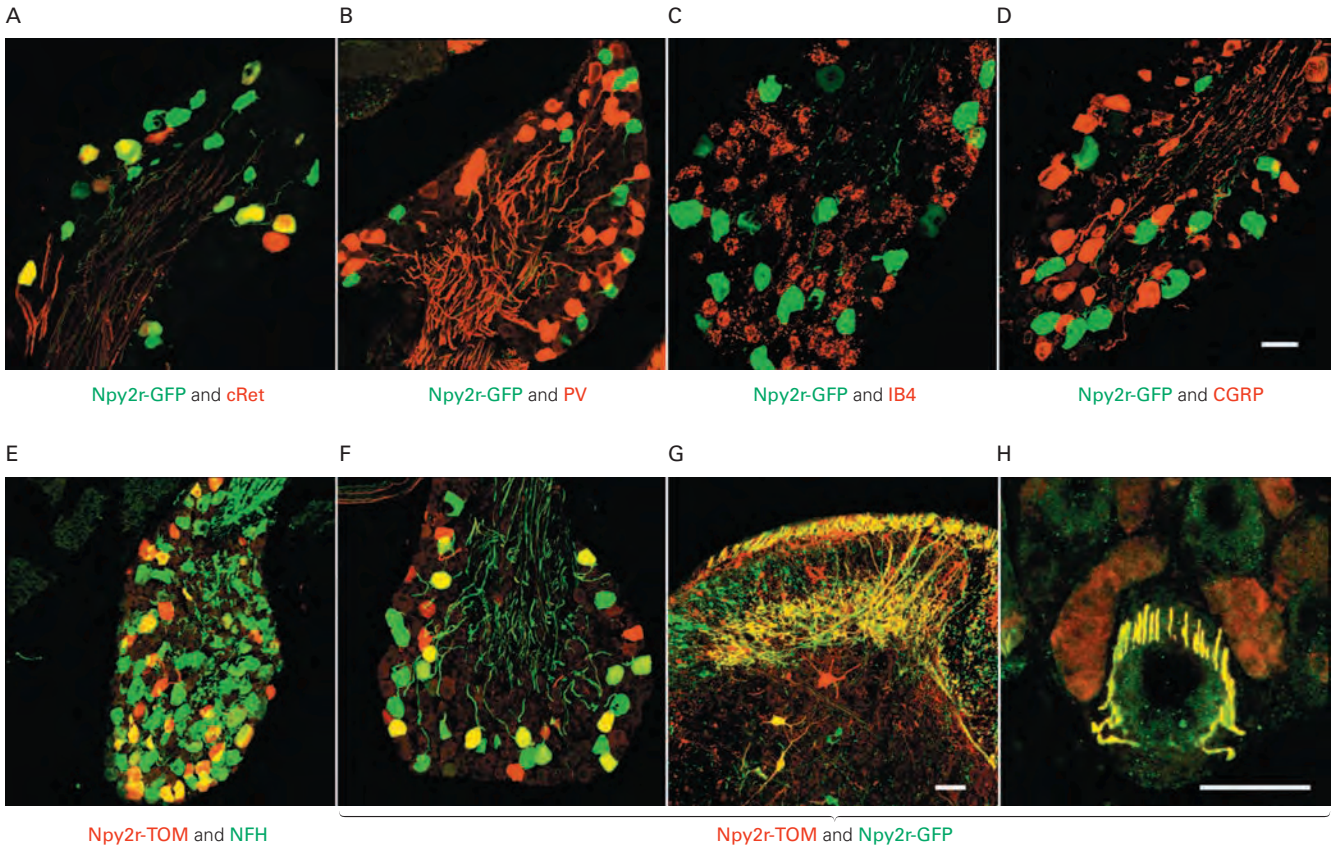

Figure 18–2 Dorsal root ganglion neurons differ in size, gene expression, and skin innervation patterns. (Reproduced, with permission, from Li et al. 2011. Copyright © 2011 Elsevier Inc.)

Panels **A–F** show double immunostaining of histological sections through a thoracic dorsal root ganglion. Individual dorsal root ganglion (DRG) neurons in these sections express genetic markers for specific classes of somatosensory nerve fibers. The G protein–coupled receptor Npy2r-GFP (**green**) or Npy2r-TOM (**red**) labels physiologically identified Aβ rapidly adapting low-threshold mechanoreceptors (Aβ RA-LTMRs). These fibers also express neurofilament heavy polypeptide (**NFH**), a marker of heavily myelinated axons (**E**), form longitudinal lanceolate (comb-like) endings surrounding individual guard hairs or awl/auchene hairs in hairy skin (**H**), and terminate in laminae III to V of the dorsal horn (**G**). Double-labeled neurons or fibers are stained **yellow.**

A. Aβ RA-LTMRs express the receptor tyrosine kinase *Ret* early in development (named early *Ret* and stained **red**). A majority of these neurons also express Npy2r-GFP (**green**); neurons that express both markers are stained **yellow**. Aβ RA-LTMRs have medium-sized cell bodies.

B. Aβ RA-LTMRs (**green**) have smaller cell bodies than proprioceptors such as muscle spindle afferents and Golgi tendon organs that express parvalbumin (**PV**, **red**).

C, D. Aβ RA-LTMRs (Npy2r-GFP, **green**) have larger cell bodies than unmyelinated purinergic C fibers that release ATP as cotransmitters (**IB4, red**) and peptidergic Aδ LTMRs that express calcitonin gene-related peptide (**CGRP, red**).

E. Heavily myelinated peripheral nerve fibers with large cell bodies express neurofilament heavy polypeptide (**NFH**, **green**). These include group Ia and Ib muscle afferents, Aβ SA-LTMRs, and Aβ RA-LTMRs (also labeled with Npy2r-tdTom [**red**]). Only Aβ RA-LTMRs express both markers and are stained **yellow**.

F–H. Double immunostaining with Npy2r-GFP (**green**) and Npy2r-tdTomato (**red**) of thoracic DRG neurons (**F**), their central processes in lamina III through V in the spinal cord dorsal horn (**G**), and their peripheral lanceolate endings at hair follicles in hairy skin sections (**H**) shows that the labeled peripheral and central Aβ RA-LTMR neurons largely overlap with each other (**yellow**) and that such genetic markers are useful for tracing sensory nerve endings.

and myelination, conduction velocity, and whether they are sensory or motor. The first nerve classification scheme was devised in 1894 by Charles Sherrington, who measured the diameter of myelin-stained axons in sensory nerves, and subsequently codified by David Lloyd (Table 18–1). They found two or three overlapping groups of axonal diameters (Figure 18–3). It was later discovered that these anatomical groupings are functionally important. Group I axons in *muscle* nerves innervate muscle spindle receptors and Golgi tendon

Table 18–1 Classification of Sensory Fibers in Peripheral Nerves[1]

	Muscle nerve	Cutaneous nerve[2]	Fiber diameter (μm)	Conduction velocity (m/s)
Myelinated				
Large diameter	I	Aα	12–20	72–120
Medium diameter	II	Aβ	6–12	36–72
Small diameter	III	Aδ	1–6	4–36
Unmyelinated	IV	C	0.2–1.5	0.4–2.0

[1]Sensory fibers from muscle are classified according to their diameter, whereas those from the skin are classified by conduction velocity.
[2]The types of receptors innervated by each type of fiber are listed in Table 18–2.

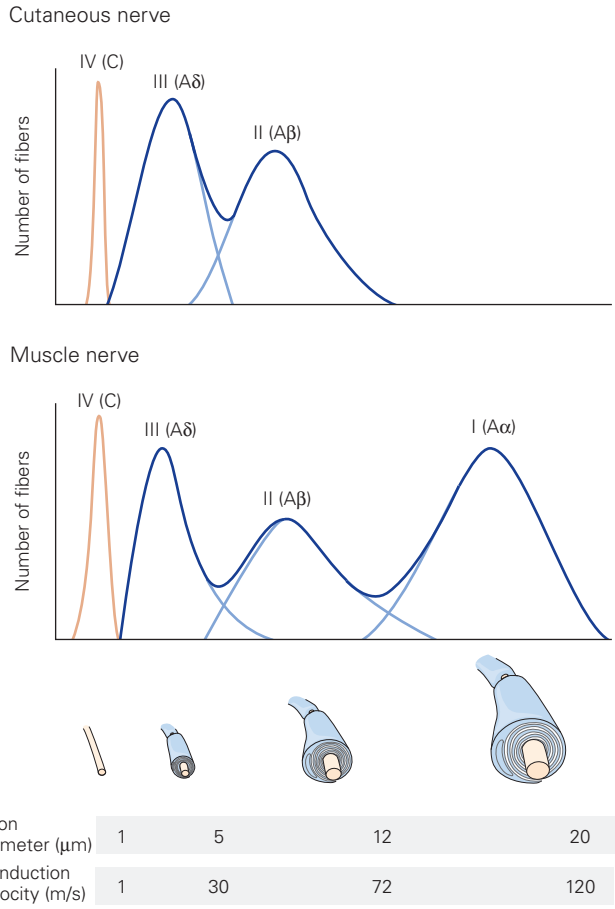

Figure 18–3 Classification of mammalian peripheral nerve fibers. The histograms illustrate the distribution of axon diameter for four groups of sensory nerve fibers innervating skeletal muscle and the skin. Each group has a characteristic axon diameter and conduction velocity (see Table 18–1). **Light blue lines** mark the boundaries of fiber profiles in each group in the zones of overlap. The conduction velocity (m/s) of myelinated peripheral nerve fibers is approximately six times the fiber diameter (μm). (Adapted, with permission, from Boyd and Davey 1968.)

organs, which signal muscle length and contractile force. Group II fibers innervate secondary spindle endings and receptors in joint capsules; these receptors also mediate proprioception. Group III fibers, the smallest myelinated muscle afferents, and the unmyelinated group IV afferents signal trauma or injuries in muscles and joints that are sensed as painful.

Nerves that innervate the skin contain two sets of myelinated fibers: Group II fibers innervate cutaneous mechanoreceptors that respond to touch, and group III fibers mediate thermal and noxious stimuli, as well as light touch in hairy skin. Unmyelinated group IV cutaneous afferents, like those in muscle, also mediate thermal and noxious stimuli.

Another method for classifying peripheral nerve fibers is based on electrical stimulation of whole nerves. In this widely used diagnostic technique, nerve conduction velocities are measured between pairs of stimulating and recording electrodes placed on the skin above a peripheral nerve. When studying conduction in the median or ulnar nerve, for example, the stimulation electrode might be placed at the wrist and the recording electrode on the upper arm. Brief electrical pulses applied through the stimulating electrode evoke action potentials in the nerve. The neural signal recorded a short time later in the arm represents the summed action potentials of all of the nerve fibers excited by the stimulus pulse and is called the *compound action potential* (Chapter 9). It increases in amplitude as more nerve fibers are stimulated; the summed activity is roughly proportional to the total number of active nerve fibers.

Electrical stimuli of increasing strength evoke action potentials first in the largest axons, because they have the lowest electrical resistance, and then progressively in smaller axons (Figure 18–4). Large-diameter fibers conduct action potentials more rapidly because

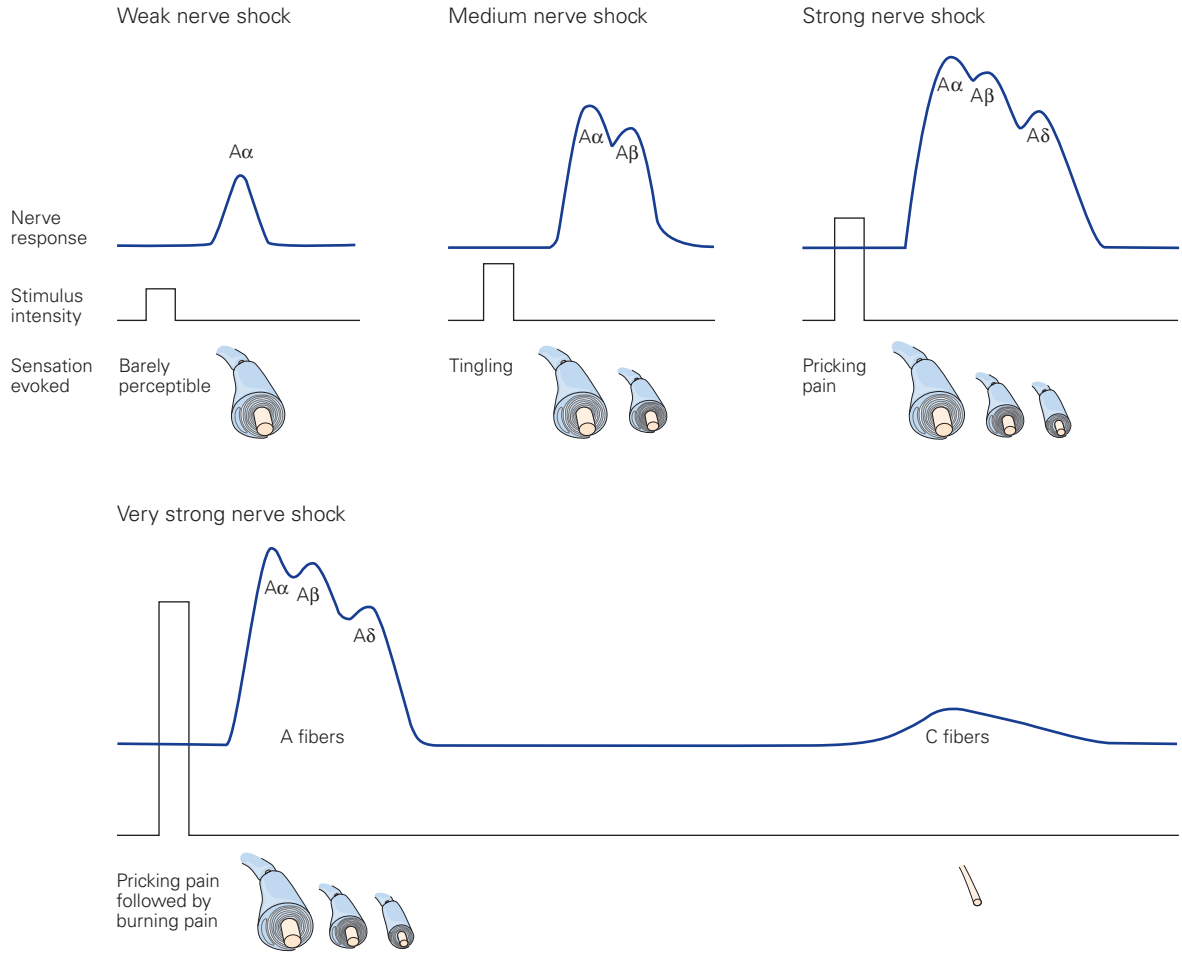

Figure 18–4 Conduction velocities of peripheral nerves are measured clinically from compound action potentials. Electrical stimulation of a peripheral nerve at varying intensities activates different types of nerve fibers. The action potentials of all the nerves stimulated by a particular amount of current are summed to create the compound action potential. The distinct conduction velocities of different classes of sensory and motor axons produce multiple peaks. (Adapted from Erlanger and Gasser 1938.)

the internal resistance to current flow along the axon is low, and the nodes of Ranvier are widely spaced along its length (Chapter 9). The conduction velocity of large myelinated fibers (in meters per second) is approximately six times the axon diameter (in micrometers), whereas thinly myelinated fibers conduct at five times the axon diameter. For unmyelinated fibers, the factor for converting axon diameter to conduction velocity is 1.5 to 2.5.

Following the stimulus artifact, the earliest neural signal recorded in the compound action potential occurs in fibers with conduction velocities greater than 90 m/s. Called the Aα wave (Figure 18–4), this signal reflects the action potentials generated in group I fibers and in motor neurons innervating skeletal muscle. The sensation is barely perceived by the subject in the region innervated.

As more large fibers are recruited, a second signal, the Aβ wave, appears. This component corresponds to group II fibers in skin or muscle nerves that innervate mechanoreceptors mediating touch and proprioception and becomes larger as the shock intensity is increased. At higher voltages, when axons in the smaller Aδ range are recruited, the stimulus becomes painful, resembling an electric shock produced by static electricity. Voltages sufficient to activate unmyelinated C fibers evoke sensations of burning pain. As we shall learn later in this chapter, some Aδ and C fibers also respond to light touch on hairy skin, but such gentle tactile stimuli are masked by concurrent activation of

pain fibers when whole nerves are stimulated electrically. Stimulation of motor neurons innervating the intrafusal fibers of muscle spindles (see Figure 18–9) evokes an intermediate wavelet called the Aγ wave, but this is usually difficult to discern because the conduction velocities of these motor neurons overlap those of Aβ and Aδ sensory axons. These differences in fiber diameter and conduction velocity of peripheral nerves allow signals of touch and proprioception to reach the spinal cord and higher brain centers earlier than noxious or thermal signals.

The clinician takes advantage of the known distribution of the conduction velocities of the various afferent fibers to diagnose diseases that result in sensory-fiber degeneration or motor neuron loss. In certain conditions, the loss of peripheral nerve axons is selective; in the neuropathy characteristic of diabetes, for example, the large-diameter sensory fibers degenerate. Such a selective loss is reflected in a reduction in the appropriate peak of the compound action potential, a slowing of nerve conduction, and a corresponding diminution of sensory capacity. Similarly, in multiple sclerosis, degeneration of the myelin sheath of large-diameter afferent fibers in the central nervous system results in slowing and, if severe enough, failure of nerve conduction.

A Variety of Specialized Receptors Are Employed by the Somatosensory System

The functional specialization of individual DRG neurons is determined by the molecular mechanisms of sensory transduction that occur at the distal nerve terminals in the body. When a somatic receptor is activated by an appropriate stimulus, its sensory terminal is typically depolarized. The amplitude and time course of the depolarization reflect the strength of the stimulus and its duration (see Figure 3–9A). Stimuli of sufficient strength produce action potentials that are transmitted along the peripheral branch of the DRG neuron's axon and into the central branch that terminates in the spinal cord or brain stem.

The sensory neurons that mediate touch and proprioception terminate in a nonneural capsule (Figure 18–1) or form morphologically distinctive endings surrounding hair follicles (Figure 18–2H) or intrafusal muscle fibers (see Figure 18–9A). They sense mechanical stimuli that indent or stretch their receptive surface. In contrast, the peripheral axons of neurons that detect noxious, thermal, or chemical events have unsheathed endings with multiple branches that terminate in the epidermis or in the viscera.

Several different morphologically specialized receptors underlie the various somatosensory submodalities. For example, the median nerve that innervates the skin of the hand and some of the muscles controlling the hand contains tens of thousands of nerve fibers that can be classified into 30 functional types. Of these, 22 types are afferent fibers (sensory axons conducting impulses toward the spinal cord), and eight types are efferent fibers (motor axons conducting impulses away from the spinal cord to skeletal muscle, blood vessels, and sweat glands). The afferent fibers convey signals from eight kinds of cutaneous mechanoreceptors that are sensitive to different kinds of skin deformation; five kinds of proprioceptors that signal information about muscle force, muscle length, and joint angle; four kinds of thermoreceptors that report the temperatures of objects touching the skin; and four kinds of nociceptors that signal potentially injurious stimuli. The major receptor groups within each submodality are listed in Table 18–2.

Mechanoreceptors Mediate Touch and Proprioception

A mechanoreceptor senses physical deformation of the tissue surrounding it. Mechanical distension—such as pressure on the skin, stretch of muscles, suction applied directly to cell membranes, or osmotic swelling of tissue—is transduced into electrical energy by the physical action of the stimulus on mechanoreceptor ion channels in the membrane. Mechanical stimulation deforms the receptor protein, thus opening stretch-sensitive ion channels and increasing nonspecific cation conductances that depolarize the receptor neuron (see Figure 3–9A). Removal of the stimulus relieves mechanical stress on the receptor and allows stretch-sensitive channels to close.

Various mechanisms for activation of mechanoreceptor ion channels have been proposed. Some mechanoreceptors appear to respond to forces conveyed through tension or deformation of the lipids of the plasma membrane, a mechanism called *force from lipids* (Figure 18–5A). Here, deformation of membrane lipids changes the cell surface curvature, exposing hydrophobic residues in the receptor protein to the membrane phospholipids, thereby opening the channel pore to cation flow. This may be the mechanism for detection of cellular swelling, which plays an important role in osmoregulation, or changes in shear stress on the walls of blood vessels due to altered fluid flow.

Another postulated mechanism for activation of mechanoreceptors involves linking the channel protein to the surrounding tissue through structural proteins,

Table 18–2 Receptor Types Active in Somatic Sensory Processing

Receptor type	Fiber group[1]	Fiber name	Receptor	Marker(s)	Modality
Cutaneous mechanoreceptors					Touch
Meissner corpuscle	Aα,β	RA1	Piezo2	*cRet*/*Npy2r*/NFH	Stroking, flutter
Merkel disk receptor	Aα,β	SA1	Piezo2	Troma1/Keratin8/*Npy2r*	Pressure, texture
Pacinian corpuscle[2]	Aα,β	RA2	Piezo2	*cRet*/*Npy2r*/NFH	Vibration
Ruffini ending	Aα,β	SA2	Piezo2		Skin stretch
Hair (guard)	Aα,β	Aβ RA-LTMR	Piezo2	*cRet*/*Npy2r*/NFH	Stroking, hair movement
Hair (awl/auchene)	Aδ	Aδ-LTMR	Piezo2	TrkB	Light stroking, air puff
Field receptor (circumferential endings)	Aβ	Aβ Field-LTMR	Piezo2	NFH	Skin stretch
Hair (zigzag)	C	C-LTMR		TH	Slow stroking, gentle touch
Thermal receptors					Temperature
Cool receptors	Aδ	III	TRPM8		Skin cooling (<25°C)
Warm receptors	C	IV	TRPV3		Skin warming (>35°C)
Heat nociceptors	Aδ	III	TRPV1/TRPV2		Hot temperature (>45°C)
Cold nociceptors	C	IV	TRPA1/TRPM8		Cold temperature (<5°C)
Nociceptors					Pain
Mechanical	Aδ	III		CGRP	Sharp, pricking pain
Thermal-mechanical (heat)	Aδ	III	TRPV2		Burning pain
Thermal-mechanical (cold)	C	IV	TRPV1/TRPA1	IB4	Freezing pain
Polymodal	C	IV	TRPV1/TRPA1		Slow, burning pain
Muscle and skeletal mechanoreceptors					Limb proprioception
Muscle spindle primary	Aα	Ia	Piezo2	PV/NFH	Muscle length and speed
Muscle spindle secondary	Aβ	II	Piezo2	PV/NFH	Muscle stretch
Golgi tendon organ	Aα	Ib	Piezo2	PV/NFH	Muscle contraction
Joint capsule receptors	Aβ	II			Joint angle
Stretch-sensitive free endings	Aδ	III			Excess stretch or force

[1]See Table 18–1.
[2]Pacinian corpuscles are also located in the mesentery, between layers of muscle, and on interosseous membranes.

a mechanism termed *force from filaments* (Figure 18–5B). In this arrangement, mechanical force applied to the skin or muscle by direct pressure or lateral stretch of the tissue distorts the extracellular matrix or intracellular cytoskeletal proteins (actin, integrins, microtubules). These tethering molecules interact with the receptor-channel proteins, change their conformation, and open cation channels. The extracellular linkage to the channel proteins is elastic and often represented as a spring-loaded gate. Direct channel gating in this model may be produced by forces that stretch the extracellular linkage protein. The channel closes when the force is removed. This type of direct channel gating is used by hair cells of the inner ear and by some touch receptors in the skin.

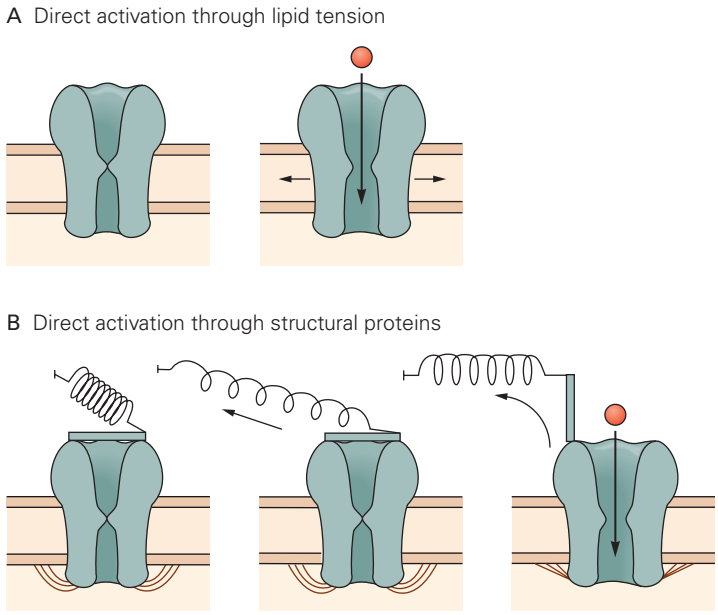

Figure 18–5 Ion channels in mechanoreceptor nerve terminals are activated by mechanical stimuli that stretch or deform the cell membrane. Mechanical displacement leads to channel opening, permitting the influx of cations. (Adapted, with permission, from Lin and Corey 2005. Copyright © 2005 Elsevier Ltd.)

A. Force from lipids. Channels can be directly activated by forces conveyed through lipid tension in the cell membrane, such as changes in blood pressure.

B. Force from filaments. Forces conveyed through structural proteins linked to the ion channel can also directly activate mechanosensory channels. The linking structural proteins may be extracellular (attached to the surrounding tissue) or intracellular (bound to the cytoskeleton) or both.

It is remarkable that although the receptor end organs for touch in the skin were first studied by Edgar Adrian and Yngve Zotterman in the 1920s and receptor potentials were recorded from isolated touch receptors from the mesentery (Pacinian corpuscles) in the 1960s, there was little consensus about the molecular biology of mechanosensation in mammalian touch. The leading candidates were derived from invertebrate model organisms such as the nematode worm *Caenorhabditis elegans* whose touch receptors were identified as members of the degenerin superfamily of ion channels and are similar to vertebrate epithelial Na^+ channels (DEG/ENac channels). Other candidate molecules included TRPV4 receptors (members of the transient receptor potential [TRP] receptors that are also involved in thermal senses), and NOMPC, a *Drosophila* member of the TRPN family. However, these molecules are not expressed in mammalian DRG neurons.

The Piezo protein family of transmembrane ion channels was recently identified by Ardem Patapoutian and colleagues as molecular mediators of mechanoreception in mammals. Piezo1 proteins are composed of approximately 2,500 amino acids, with at least 26 transmembrane α-helices (Figure 18–6A). The ion channel is a trimer formed from three identical Piezo protein subunits, with two pore-forming α-helices at the C-terminal end of each Piezo protein. The N-terminals of the subunits form a propeller-like structure (Figure 18–6B), which is thought to be involved in coupling mechanical stimuli to channel gating. Piezo proteins form nonspecific cation-permeable channels that conduct excitatory depolarizing current.

Two different isoforms of the Piezo proteins serve as mechanosensors: Piezo1 is found primarily in nonneural tissue, such as epithelia in blood vessels, the kidney, and bladder, and in red blood cells. Piezo2 is expressed in mechanosensory DRG and trigeminal neurons that mediate the senses of touch and proprioception and in vagal afferents innervating smooth muscle of the lung, where they mediate the Hering-Breuer reflex by sensing lung stretch (Chapter 32).

Specialized End Organs Contribute to Mechanosensation

In addition to the molecular composition of the ion channels expressed in the distal nerve endings, components of surrounding tissue such as epithelial cells or muscle fibers play a significant role in mechanotransduction. The specialized nonneural end organs that surround the nerve terminals of a DRG neuron must be deformed in specific ways to excite the fiber. For example, individual mechanoreceptors respond selectively to pressure or motion, and thereby detect the direction of force applied to the skin, joints, or muscle fibers. The end organ can also amplify or modulate the sensitivity of the receptor axon to mechanical displacement.

Specialized epithelial cells in the skin—such as Merkel cells, the epithelium lining hair follicles, and the papillary ridges that form the fingerprints of glabrous

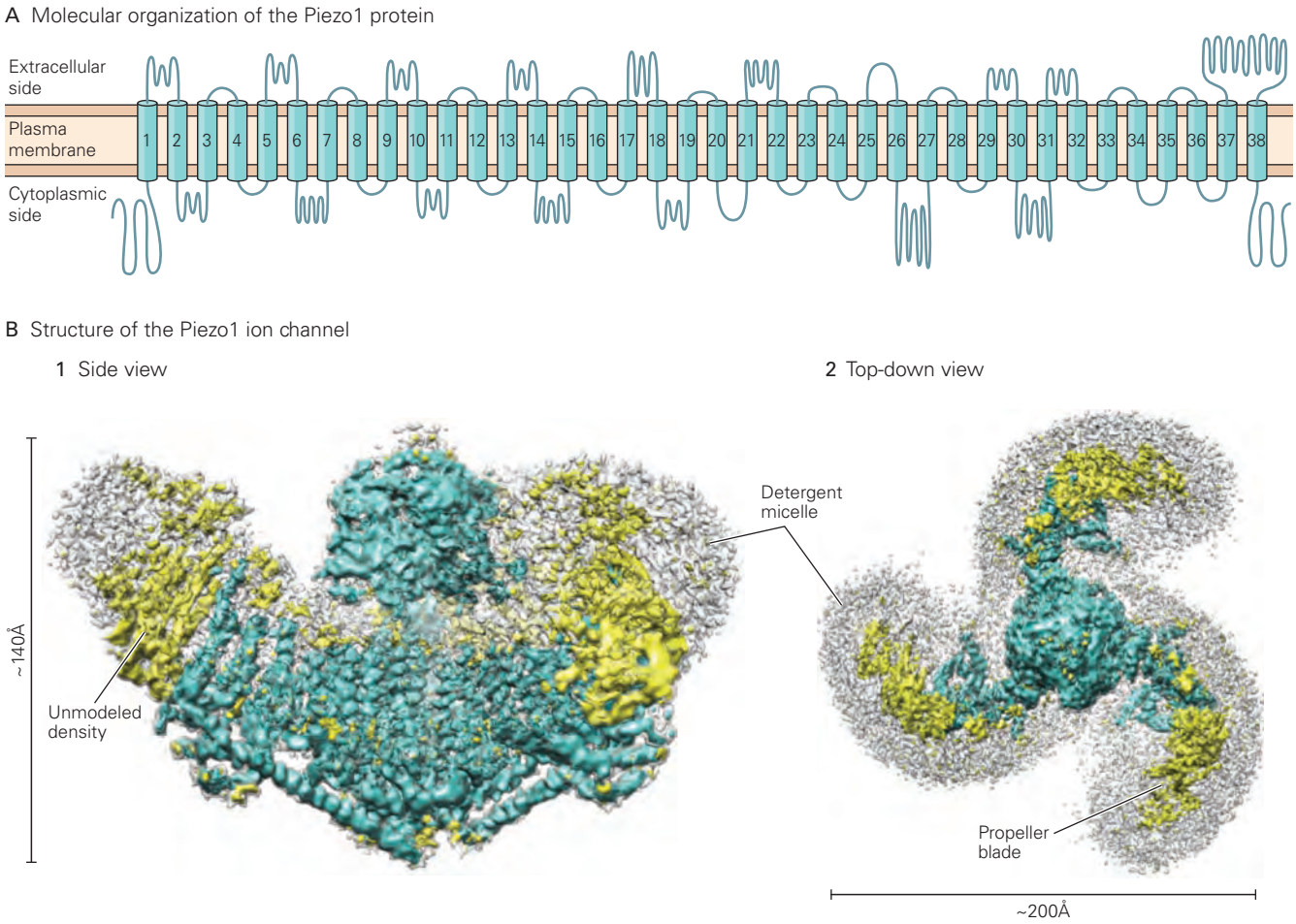

Figure 18–6 Structure and molecular organization of Piezo1 ion channels.

A. Piezo1 and Piezo2 have homologous protein structures, containing approximately 2,500 amino acids, with at least 26 putative transmembrane segments. Combined as trimers, they form the largest membrane ion channels in mammals. (Adapted, with permission, from Murthy, Dubin, and Patapoutian 2017. Copyright © 2017 Springer Nature.)

B. Putative structure of the Piezo1 ion channel deduced from cryo-electron microscopy. **1.** Side view, cytoplasmic surface down. **2.** Top-down view from extracellular side. The receptor is a triskelion made up of three identical Piezo1 subunits. The C-terminals of the three Piezo proteins form a central extracellular cap tethered to the extracellular surface of the transmembrane pore, which extends beyond the membrane into a cytoplasmic tail domain. The aqueous pore through the channel extends through the central axis of the cap, the transmembrane pore, and the cytoplasmic tail domain. The N-terminals of the three protein subunits are arrayed peripherally, forming a propeller-like helical structure. **Blue** indicates area of high-resolution modeling. (Adapted, with permission, from Saotome et al. 2018. Copyright © 2018 Springer Nature.)

skin—play important auxiliary roles in the sense of touch. The best studied of these end organs are Merkel cells—sensory epithelial cells that form close contacts with the terminals of large-diameter (Aβ) sensory nerve axons at the epidermal–dermal junction, forming Merkel cell–neurite complexes. Merkel cells cluster in swellings of the epidermis in hairy skin called touch domes (Figure 18–7A) and near the center of the fingerprint ridges in glabrous skin (see Figure 19–3). When a probe contacts the touch dome, the sensory nerve responds with a train of action potentials whose frequency is proportional to the velocity and amplitude of pressure applied to the skin (Figure 18–7A2). These spike trains typically last throughout the period of stimulation and are termed *slowly adapting* because the firing persists for periods of up to 30 minutes. Likewise, the sensory nerve is called an *SA1 fiber* (slowly adapting type 1 fiber).

Merkel cells serve a similar receptive function in the sense of touch as auditory hair cells in the cochlea

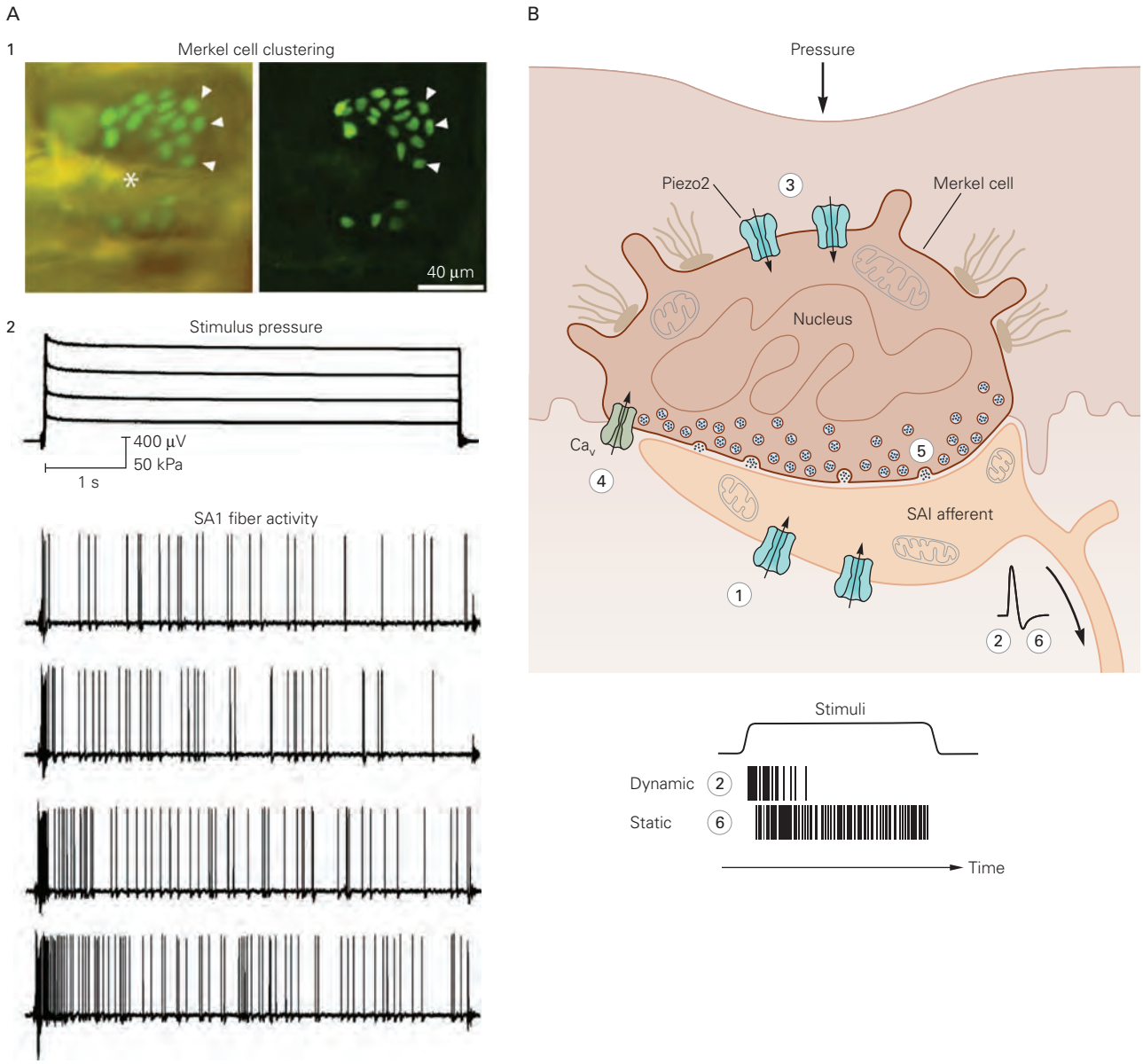

Figure 18–7 Afferent fibers innervating Merkel cells respond continuously to pressure on the skin.

A. 1. An individual slowly adapting type 1 (**SA1**) mechanoreceptive fiber innervates a cluster of 22 Merkel cells (each labeled with enhanced green fluorescent protein [eGFP]) in a touch dome of the hairy skin. *Left*: In vivo epifluorescent images of the isolated skin-nerve recording preparation. Asterisk (*) indicates the location of the associated guard hair within the touch dome. *Right*: Confocal z-series projections of the entire touch dome innervated by the SA1 fiber. **Arrowheads** are used to align Merkel cells in the two images. **2.** The SA1 fiber responds to 5-second duration steps of pressure (measured in kilopascals [**kPa**]) applied over the touch dome (upper records) with irregular, slowly adapting spike trains (recorded extracellularly), whose mean frequency of firing is proportional to the applied force (lower records). The neuron fires at its highest rate at the start of stimulation and fires fewer spikes during maintained pressure. (Reproduced, with permission, from Wellnitz et al. 2010.)

B. A model of sensory transduction in SA1 mechanoreceptors. Pressure on the skin opens Piezo2 channels (**blue**) in the Merkel cell and in the peripheral neurite of the SA1 fiber that receives synaptic input from the Merkel cell. Piezo2 channels in the neurite open at the onset of stimulation (**1**) generating the initial dynamic response to touch (**2**). Skin deformation simultaneously activates Piezo2 channels in the Merkel cell (**3**), depolarizing it and allowing voltage-gated Ca_V channels in the Merkel cell (**4**) to open and release neurotransmitter continuously (**5**). Binding of the neurotransmitter further depolarizes the SA1 neurite, producing sustained firing in the principal axon (**6**). (Reproduced, with permission, from Maksimovic et al. 2014. Copyright © 2014 Springer Nature.)

(Chapter 26) and taste cells in the tongue (Chapter 32). Merkel cells studied in vitro respond to mechanical force such as pressure or suction with depolarizing currents that are similar in time course and conductance to those evoked in isolated DRG neurons. They express synaptic release proteins and contain vesicles that release excitatory neurotransmitters during sustained pressure. Merkel cells express Piezo2 proteins and show increased cytoplasmic Ca^{2+} levels when stimulated by pressure.

The importance of Merkel cells for physiological responses to touch is seen in mice that fail to develop Merkel cells in the epidermis (*Atoh1* conditional knockout mice). The firing rates of SA1 fibers in these animals are reduced in amplitude and duration compared to wild-type. These experiments indicate that Merkel cells are responsible for the sustained response to static touch. Recently, Ellen Lumpkin and colleagues used optogenetic stimulation of Merkel cells rather than direct pressure on the skin to demonstrate that SA1 fibers innervating touch domes use a dual-mechanism to sense pressure on the skin (Figure 18–7B). The initial dynamic response to touch is generated primarily by current flow through Piezo2 channels in the SA1 nerve terminal. The subsequent static response results from excitatory synaptic transmission from Merkel cells that express Piezo2 channels and continuously release neurotransmitter during sustained pressure on the skin.

Hairs that protrude from the surface of the skin provide another important set of touch end organs. Sensory hair fibers are extremely sensitive to motion. Deflection of hairs by light breezes or air puffs evokes one or more action potentials from hair follicle afferent fibers. Humans can perceive motion of individual hairs and localize the sensation to the base of the hair, where it emerges from the skin. Sensory hairs serve an important protective function as they detect objects, other organisms, or obstacles in the environment at a distance before they impact the body. Hairs or sensory antennae detect important object features such as texture, curvature, and rigidity that aid recognition as friend or foe. These neurons are named *rapidly adapting low-threshold mechanoreceptors* (RA-LTMRs) because they respond to gentle touch or hair movement with brief bursts of spikes when the hair is moved by external forces.

Hairs are embedded in skin invaginations called hair follicles. Three types of hairs are found in mammalian skin (Figure 18–8A). The largest, longest, and stiffest hairs (named guard hairs) are the first to emerge from the skin during development. *Guard hairs* are innervated by the largest-diameter and fastest-conducting sensory nerve fibers (type Aβ); these fibers form lanceolate (comb-like) endings in the epidermis of the follicle surrounding the hair (Figure 18–2H). Aβ RA-LTMR nerve fibers also innervate intermediate-sized hairs (called *awl/auchene hairs*) with lanceolate endings. Awl/auchene hairs are triply innervated: They provide inputs to fast-conducting (Aβ) myelinated fibers; smaller-diameter, slower-conducting myelinated (Aδ) fibers; and unmyelinated C fibers. The smallest and most numerous hairs (called *zigzag* or *down hairs*) are also innervated by Aδ and C fibers.

Until recently, Aδ and C fibers were thought to mediate only thermal or painful sensations. However, microneurography studies in humans by Johan Wessberg, Håkan Olausson, and Åke Vallbo demonstrated that hairy skin is also innervated by unmyelinated C-LTMR fibers that respond to slowly moving tactile stimuli and are thought to mediate social or pleasurable touch. They may also play a role in pain inhibition in the spinal cord dorsal horn.

The innervation pattern of hair follicles in the skin illustrates two important principles of sensory innervation of the body: convergence and divergence. Each individual hair follicle in the skin provides input to multiple sensory afferent fibers. This pattern of overlap provides redundancy of sensory input from a small patch of skin. Shared lines of communication innervate each hair follicle, rather than a single labeled line. Tactile information from the skin is therefore transmitted in parallel by an ensemble of sensory neurons.

The skin area innervated by the sensory nerve terminals of a DRG neuron defines the cell's *receptive field*, the region of the body that can excite the cell. Each sensory nerve fiber collects information from a wide area of skin because its distal terminals have multiple branches that can be activated independently. This morphology enables each afferent fiber to provide unique patterns of sensory input to the brain.

The diversity of receptive field sizes and territories encompassed by individual classes of DRG neurons is illustrated in Figure 18–8B. Because of the large size of tactile receptive fields, gentle touch excites many different sensory fibers at the site of contact, each conveying a specific sensory message. The smallest tactile receptive fields are the touch domes innervated by SA1 fibers (see Figure 19–8B Aβ SA1). An individual SA1 fiber innervates all of the Merkel cells in a touch dome and typically collects information from one to three touch domes in adjacent skin regions. Hair follicles innervated by individual RA fibers are spread further apart and the sensory endings differ somewhat in size, with the largest-diameter Aβ fibers encompassing the

A Hairy skin innervation

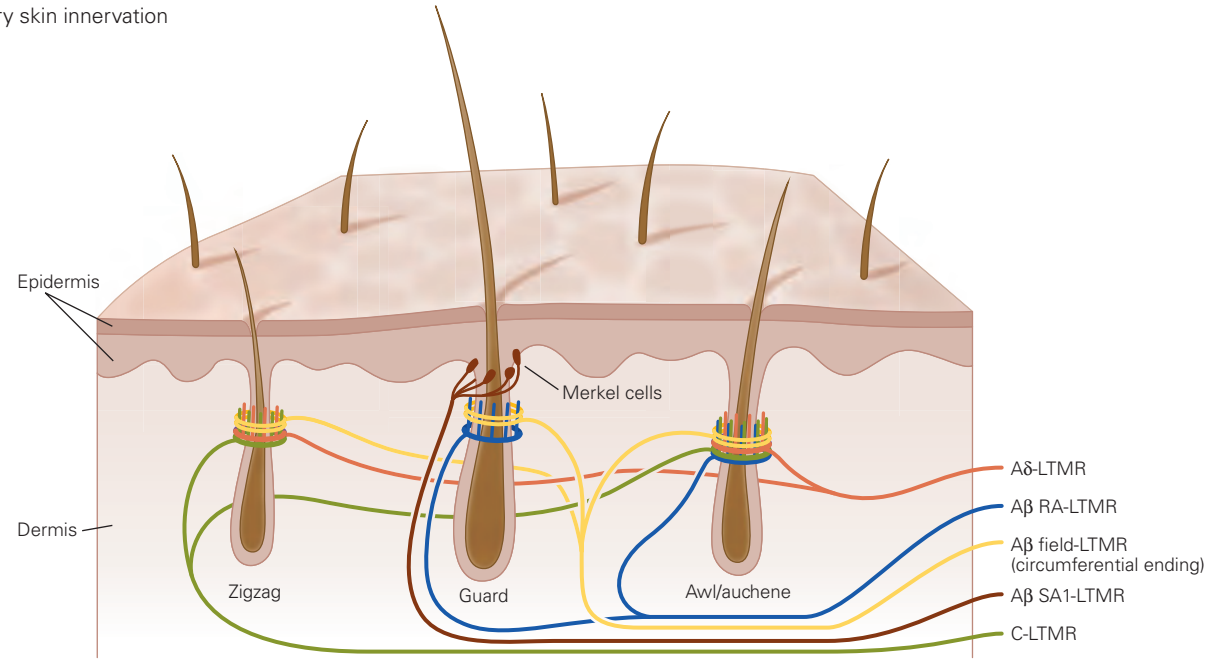

B Receptive fields of low-threshold mechanoreceptors

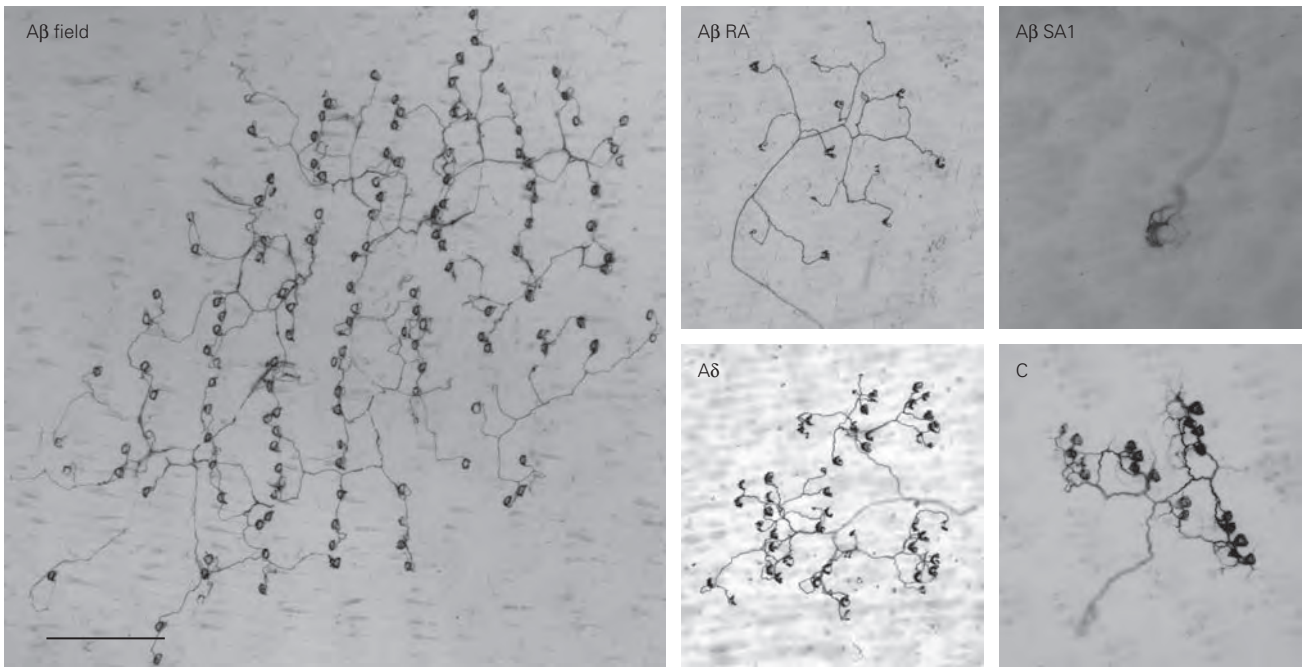

smallest hair follicle receptive fields (see Figure 19–8B Aβ RA). The largest receptive fields in the skin are those of Aβ field receptors (see Figure 19–8B Aβ Field). These fibers form circumferential endings around hair follicles but do not respond to hair movement or air puffs. Instead, field receptors respond to stroking or stretching of the skin in their receptive fields. Field receptors are also excited by painful stimuli such as pulling hairs or strong pressure, suggesting that they may also mediate sensations of mechanical pain.

Proprioceptors Measure Muscle Activity and Joint Positions

Mechanoreceptors in muscles and joints convey information about the posture and movements of the body and thereby play an important role in proprioception and motor control. Mechanical coupling of sensory nerve terminals to skeletal muscle, tendons, joint capsules, and the skin is thought to underlie proprioception. These receptors include two types of muscle-length sensors, the type Ia and II muscle spindle endings; one muscle force sensor, the Golgi tendon organ; joint-capsule receptors, which transduce tension in the joint capsule; and Ruffini endings that sense skin stretch over joints.

The muscle spindle consists of a bundle of thin muscle fibers, or intrafusal fibers, that are aligned parallel to the larger fibers of the muscle and enclosed within a capsule (Figure 18–9A). The intrafusal fibers are entwined by a pair of sensory axons that detect muscle stretch because of mechanoreceptive ion channels in the nerve terminals. Intrafusal muscles also receive inputs from motor axons that regulate contractile force and receptor sensitivity. (See Box 32–1 for details on muscle spindles.)

Although the receptor potential and firing rates of muscle spindle afferent fibers are proportional to muscle length (Figure 18–9B), these responses can be modulated by higher centers in the brain that regulate contraction of intrafusal muscles. Spindle afferent fibers are thus able to encode the amplitude and speed of internally generated voluntary movements as well as passive limb displacement by external forces (Chapter 32).

Golgi tendon organs, located at the junction between skeletal muscle and tendons, measure the forces generated by muscle contraction. (See Box 32–4 for details on Golgi tendon organs.) Although these receptors play an important role in reflex circuits modulating muscle force, they appear to contribute little to conscious sensations of muscle activity. Psychophysical experiments in which muscles are fatigued or partially paralyzed have shown that perceived muscle force is mainly related to centrally generated effort rather than to actual muscle force.

Recent studies by Ardem Patapoutian and colleagues suggest that Piezo2 mediates the signals transmitted by afferent fibers from muscle spindles and Golgi tendon organs, as these fibers express the Piezo2 protein in their distal terminals and cell body.

Joint receptors play little if any role in postural sensations of joint angle. Instead, perception of the angle of proximal joints such as the elbow or knee

Figure 18–8 (Opposite) Innervation of the hairy skin by low-threshold mechanoreceptors.

A. Hairy skin of mammals is innervated by specific combinations of low-threshold mechanoreceptors (**LTMRs**); these multiple classes of nerve fibers allow touch information to be transmitted along multiple parallel nerve fibers to the central nervous system. Touch domes of Merkel cells are located at the epidermal–dermal boundary surrounding large-diameter guard hairs. The axons of Merkel cells are classified as Aβ SA1-LTMRs, and they compose approximately 3% of sensory fibers innervating hairy skin. Guard hair follicles are innervated by rapidly adapting touch fibers, classified as Aβ RA-LTMRs, which form longitudinal lanceolate (comb-like) endings surrounding the hair follicle. They compose another 3% of sensory fibers innervating hairy skin. Aβ RA-LTMR fibers also form lanceolate endings on medium size awl/auchene hairs; each fiber innervates multiple hair follicles in neighboring regions of skin. Awl/auchene hairs are innervated by lanceolate endings from three different classes of sensory fibers; Aβ RA-LTMRs (**blue**), Aδ-LTMRs (**red**, 7% of fibers), and C-LTMRs (**green**, 15%–27% of fibers). Zigzag, or down hairs, are the most numerous type; they are innervated by the smallest-diameter, slowest-conducting peripheral nerve fibers (Aδ- and C-LTMRs). All three types of hair follicles are also innervated by circumferential endings (**yellow**). (Reproduced with permission from Zimmerman, Bai, and Ginty 2014. Copyright © 2014 AAAS.)

B. Whole mount sections of skin illustrate the spread of LTMR sensory nerve terminals in hairy skin and the skin region that can activate an individual sensory fiber. All five classes innervate multiple hair follicles and have branched sensory nerve endings. Scale bar (which applies to all images) = 500 μm. Firing rates in each of these axons reflect inputs from multiple receptor end organs in the skin. Aβ field-LTMRs form circumferential endings around all classes of hair follicles; they have the largest receptive fields in hairy skin, innervating up to 180 hair follicles/fibers and spanning areas up to 6 mm^2. Aβ SA1-LTMRs have the smallest receptive fields but innervate all of the Merkel cells within a touch dome; each touch dome is innervated by only a single Aβ SA1-LTMR. Aβ RA- Aδ-, and C-LTMRs form lanceolate endings enclosing up to 40 individual hair follicles and span skin areas of 0.5 to 4 mm^2. (Reproduced, with permission, from Bai et al. 2015. Copyright © 2015 Elsevier Inc.)

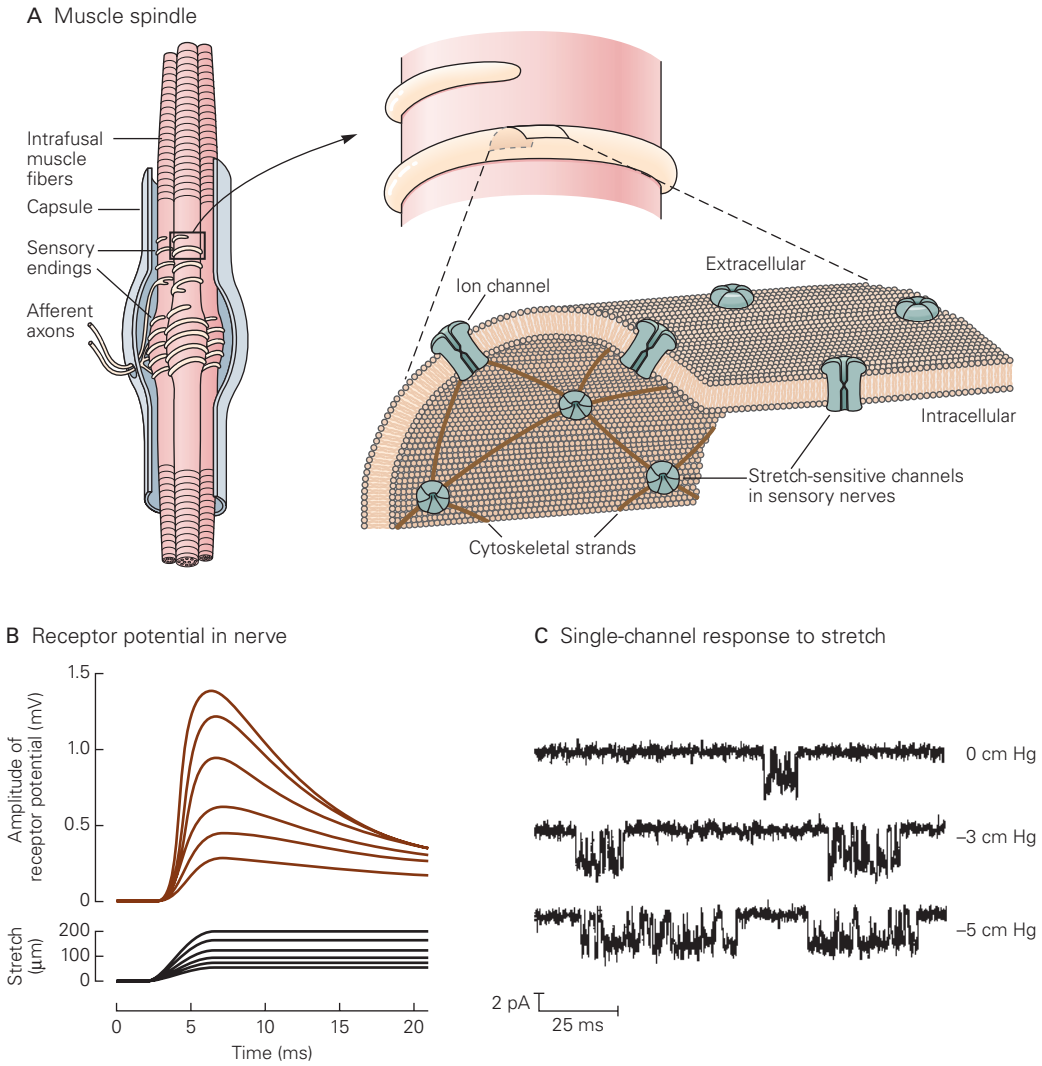

Figure 18–9 The muscle spindle is the principal receptor for proprioception.

A. The muscle spindle is located within skeletal muscle and is excited by stretch of the muscle. It consists of a bundle of thin (intrafusal) muscle fibers entwined by a pair of sensory axons. It is also innervated by several motor axons (not shown) that produce contraction of the intrafusal muscle fibers. Stretch-sensitive ion channels in the sensory nerve terminals are linked to the cytoskeleton by the protein spectrin. (Adapted, with permission, from Sachs 1990.)

B. The depolarizing receptor potential recorded in a group Ia fiber innervating the muscle spindle is proportional to both the velocity and amplitude of muscle stretch parallel to the myofilaments. When stretch is maintained at a fixed length, the receptor potential decays to a lower value. (Adapted, with permission, from Ottoson and Shepherd 1971.)

C. Patch-clamp recordings of a single stretch-sensitive channel in myocytes. Pressure is applied to the receptor cell membrane by suction. At rest (0 cm Hg) the channel opens sporadically for short time intervals. As the pressure applied to the membrane increases, the channel opens more often and remains in the open state longer. This allows more current to flow into the receptor cell, resulting in higher levels of depolarization. (Adapted, with permission, from Guharay and Sachs 1984. Copyright © 1984 The Physiological Society.)

depends on afferent signals from muscle spindle receptors and efferent motor commands. Additionally, conscious sensations of finger position and hand shape depend on cutaneous stretch receptors as well as muscle spindles.

Thermal Receptors Detect Changes in Skin Temperature

Although the size, shape, and texture of objects held in the hand can be apprehended visually as well as

by touch, the thermal qualities of objects are uniquely somatosensory. Humans recognize four distinct types of thermal sensation: cold, cool, warm, and hot. These sensations result from differences between the normal skin temperature of approximately 32°C (90°F) and the external temperature of the air or of objects contacting the body. Temperature sense, like the other *protopathic* modalities of pain and itch, is mediated by a *combinatorial code* of multiple receptor types, transmitted by small-diameter afferent fibers.

Although humans are exquisitely sensitive to sudden changes in skin temperature, we are normally unaware of the wide swings in skin temperature that occur as our cutaneous blood vessels expand or contract to discharge or conserve body heat. If skin temperature changes slowly, we are unaware of changes in the range 31° to 36°C (88–97°F). Below 31°C (88°F), the sensation progresses from cool to cold and, finally, beginning at 10° to 15°C (50–59°F), to pain. Above 36°C (97°F), the sensation progresses from warm to hot and then, beginning at 45°C (113°F), to pain.

Thermal sensations are mediated by free nerve endings in the epidermis. The temperature ranges signaled by these nerve fibers are determined by the molecular composition of receptor molecules expressed in the distal nerve terminals and cell bodies of small-diameter DRG neurons. Studies by David Julius and his colleagues revealed that thermal stimuli activate specific classes of *transient receptor potential (TRP) channels* in these neurons (Figure 18–10). TRP channels are encoded by genes belonging to the same gene superfamily as the voltage-gated channels that give rise to the action potential (Chapter 8). They form nonselective cation channels that mediate inward depolarizing current. TRP channels comprise four identical protein subunits, each of which contains six transmembrane α-helices,

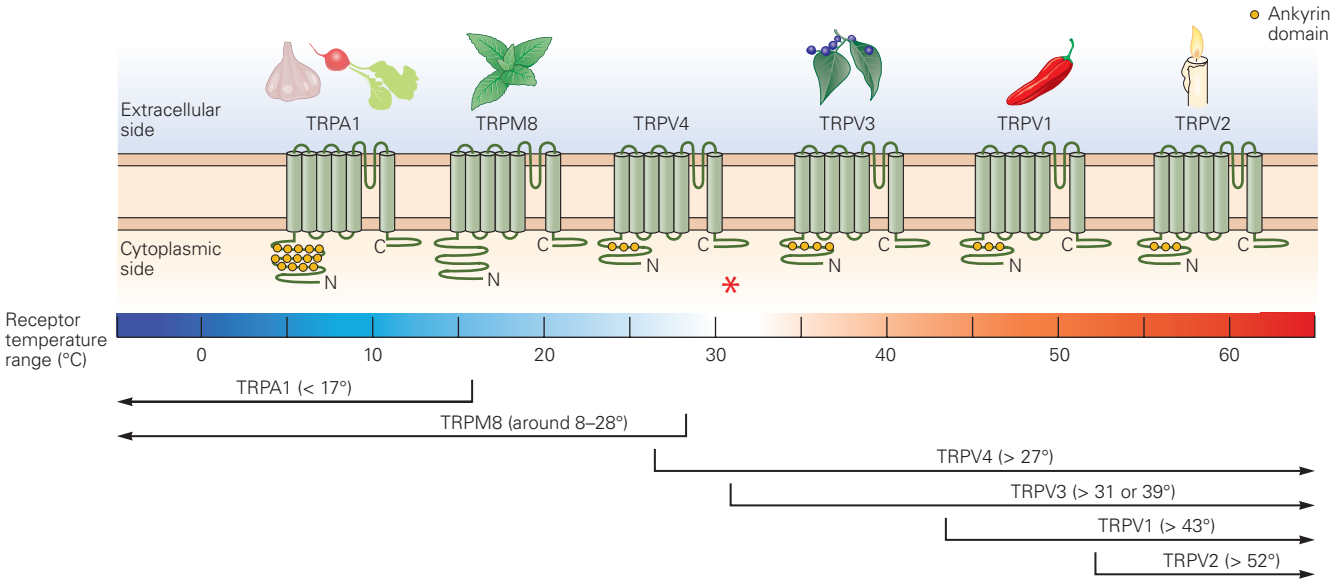

Figure 18–10 **Transient receptor potential ion channels.** TRP channels consist of membrane proteins with six transmembrane α-helices. A pore is formed between the fifth (S5) and sixth (S6) helices from the four subunits. Most of these receptors contain ankyrin repeats in the N-terminal domains and a common 25-amino acid motif adjacent to S6 in the C-terminal domain. Individual TRP channels are composed of four identical TRP proteins. All TRP channels are gated by temperature and various chemical ligands, but different types respond to different temperature ranges and have different activation thresholds. At least six types of TRP receptors have been identified in sensory neurons; the thermal sensitivity of a neuron is determined by the particular TRP receptors expressed in its nerve terminals. At 32°C (90°F), the resting skin temperature (**asterisk**), only TRPV4 and some TRPV3 receptors are stimulated. TRPA1 and TRPM8 receptors are activated by cooling and cold stimuli. TRPM8 receptors also respond to menthol and various mints; TRPA1 receptors respond to allium-expressing plants such as garlic and radishes. TRPV3 receptors are activated by warm stimuli and also bind camphor. TRPV1 and TRPV2 receptors respond to heat and produce burning pain sensations. TRPV1 channels also respond to a variety of substances, temperatures, or forces that can elicit pain. Their sites of action on the receptor include binding sites for chili peppers' active ingredient (capsaicin), acids (lemon juice), spider venoms, and phosphorylation sites for second messenger-activated kinases. TRPV4 receptors are active at normal skin temperatures and respond to touch. (Adapted, with permission, from Jordt, McKemy, and Julius 2003; adapted from Dhaka, Viswanath, and Patapoutian 2006.)

with a pore-forming element between the fifth and sixth helices. Individual TRP receptors are distinguished by their sensitivity to heat or cold, showing sharp increases in conductance to cations when their thermal threshold is exceeded. Their names specify the genetic subfamily of TRP receptors and the member number. Examples include TRPV1 (for TRP vanilloid-1), TRPM8 (for TRP melastatin-8), and TRPA1 (for TRP ankyrin-1).

Two classes of TRP receptors are activated by cold temperatures and inactivated by warming. TRPM8 receptors respond to temperatures below 25°C (77°F); such temperatures are perceived as cool or cold. TRPA1 receptors have thermal thresholds below 17°C (63°F); this range is described as cold or frigid. Both TRPM8 and TRPA1 receptors are expressed in high-threshold cold receptor terminals, but only TRPM8 receptors are expressed in low-threshold cold receptor terminals.

Thermal signals from low-threshold cold receptors are transmitted by small-diameter, myelinated Aδ fibers with unmyelinated endings within the epidermis. These fibers express the transient receptor potential channel TRPM8 and respond to menthol applied to the skin. Cold receptors are approximately 100 times more sensitive to sudden drops in skin temperature than to gradual changes. This extreme sensitivity to change allows humans to detect a draft from a distant open window.

Four types of TRP receptors are activated by warm or hot temperatures and inactivated by cooling. TRPV3 receptors are expressed in warm type fibers; they respond to warming of the skin above 35°C (95°F) and generate sensations ranging from warm to hot. TRPV1 and TRPV2 receptors respond to temperatures exceeding 45°C (113°F) and mediate sensations of burning pain; they are expressed in heat nociceptors. TRPV4 receptors are active at temperatures above 27°C and signal normal skin temperatures.

Warm receptors are located in the terminals of C fibers that end in the dermis. Unlike the cold receptors, warm receptors act more like simple thermometers; their firing rates rise monotonically with increasing skin temperature up to the threshold of pain and then saturate at higher temperatures. Warm receptors are less sensitive to rapid changes in skin temperature than cold receptors. Consequently, humans are less responsive to warming than cooling; the threshold change for detecting sudden skin warming, even in the most sensitive subject, is about 0.1°C.

Heat nociceptors are activated by temperatures exceeding 45°C (113°F) and inactivated by skin cooling. The burning pain caused by high temperatures is transmitted by both myelinated Aδ fibers and unmyelinated C fibers.

The role of TRP receptors in thermal sensation was originally discovered by analyses of natural substances such as capsaicin and menthol that produce burning or cooling sensations when applied to the skin or injected subcutaneously. Capsaicin, the active ingredient in chili peppers, has been used extensively to activate nociceptive C fiber afferents that mediate sensations of burning pain. These studies indicate that the various TRP receptors also bind other molecules that induce painful sensations, such as toxins, venoms, and substances released by diseased or injured tissue. TRPA1 receptors bind pungent substances such as horseradish (wasabi), garlic, onions, and similar allium-expressing plants. These substances behave as irritants that may produce pain or itch through covalent modification of cysteines in the TRPA1 protein.

TRP channels are polymodal sensory integrators, because different sections of the protein respond directly to changes in temperature, pH, or osmolarity; to the presence of noxious substances such as capsaicin or toxins; or to phosphorylation by intracellular second messengers (see Figure 20–2). Their molecular structure and role in pain are detailed in Chapter 20.

Nociceptors Mediate Pain

The receptors that respond selectively to stimuli that can damage tissue are called *nociceptors* (Latin *nocere*, to injure). They respond directly to mechanical and thermal stimuli and indirectly to other stimuli by means of chemicals released from cells in the traumatized tissue. Nociceptors signal impending tissue injury, and more important, they provide a constant reminder of tissues that are already injured and must be protected.

Abnormal function in major organ systems resulting from disease or trauma evokes conscious sensations of pain. Much of our knowledge of the neural mechanisms of pain is derived from studies of cutaneous nociceptors because the mechanisms are easier to study in cutaneous nerves than in visceral nerves. Nevertheless, the neural mechanisms underlying visceral pain are similar to those for pain arising from the surface of the body.

Nociceptors in the skin, muscle, joints, and visceral receptors fall into two broad classes based on the myelination of their afferent fibers. Nociceptors innervated by thinly myelinated Aδ fibers produce short-latency pain that is described as sharp and pricking. The majority are called mechanical nociceptors or *high-threshold mechanoreceptors* (HTMRs) because they are excited by sharp objects that penetrate, squeeze, or pinch the skin

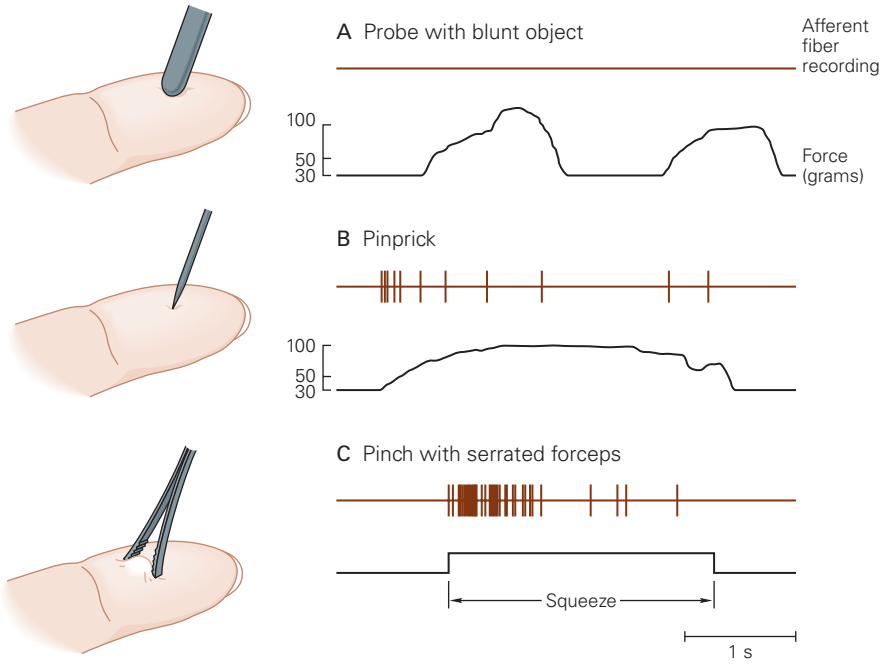

Figure 18–11 Mechanical nociceptors respond to stimuli that puncture, squeeze, or pinch the skin. Sensations of sharp, pricking pain result from stimulation of Aδ fibers with free nerve endings in the skin. These receptors respond to sharp objects that puncture the skin (**B**), but not to strong pressure from a blunt probe (**A**). The strongest responses are produced by pinching the skin with serrated forceps that damage the tissue in the region of contact (**C**). (Adapted, with permission, from Perl 1968.)

(Figure 18–11) or by pulling hairs in hairy skin. Many of these fibers also respond to temperatures above 45°C (113°F) that burn the skin; these Aδ fibers also express the heat-sensitive TRPV2 channel.

Nociceptors innervated by C fibers produce dull, burning pain that is diffusely localized and poorly tolerated. The most common type encompasses polymodal nociceptors that respond to a variety of noxious mechanical, thermal, and chemical stimuli, such as pinch or puncture, noxious heat and cold, and irritant chemicals applied to the skin. As detailed in Chapter 20, most C-polymodal nociceptors express TRPV1 and/or TRPA1 receptors. Electrical stimulation of these fibers in humans evokes prolonged sensations of burning pain. In the viscera, nociceptors are activated by distension or swelling, producing sensations of intense pain.

Itch Is a Distinctive Cutaneous Sensation

Itch is a common sensory experience that is confined to the skin, the ocular conjunctiva, and the mucosa. It has some properties in common with pain and, until recently, was thought to result from low firing rates in nociceptive fibers. Like pain, itch is inherently unpleasant whatever its intensity; even at the expense of inducing pain, we attempt to eliminate it by scratching.

Recent studies by Diana Bautista and Sarah Wilson indicate that C fibers that express both TRPV1 and TRPA1 receptors mediate itch sensations evoked by pruritic (itch-producing) agents. Itch induced by intradermal injection of histamine or by procedures that release endogenous histamine activates a subset of TRPV1-expressing neurons that also contain the H1 histamine receptor; these itch sensations are blocked by antihistamines. Histamine-independent itch appears to be mediated by C fiber DRGs that express TRPA1 channels. Itch sensations in this pathway are triggered by dry skin or by pruritogens that bind to members of the Mas-related G protein–coupled receptor (Mrgpr) family, such as the antimalarial drug chloroquine.

How can TRPA1 receptors mediate itch when they are also involved in sensing noxious cold temperatures (<15°C)? Why do some TRPV1-expressing fibers mediate itch sensations rather than sensations of noxious heat? The answer lies in the use of *combinatorial* codes by small-diameter sensory nerve fibers. For example, noxious cold is sensed when both TRPA1 and TRPM8

receptors are excited, but itch is perceived when TRPM8 receptors are silent. Likewise, heat pain is sensed when TRPV1-, TRPV2-, and TRPV3-expressing fibers are co-activated, but itch may be perceived when only TRPV1-expressing fibers respond and TRPV2 and TRPV3 receptors are silent. Similar combinatorial codes using multiple receptors are commonly used by other chemical senses such as olfaction and taste.

Visceral Sensations Represent the Status of Internal Organs

Visceral sensations are important because they drive behaviors critical for survival, such as respiration, eating, drinking, and reproduction. The same molecular genetic strategies described earlier to study touch, pain, thermal senses, and proprioception in the dorsal root and trigeminal ganglia have been used to classify visceral afferents in the vagal sensory ganglia. Stephen Liberles and colleagues recently analyzed sensory responses in the vagal sensory ganglia (nodose/jugular complex) that receive mechanosensory or chemosensory information from the lungs, cardiovascular, immune, or digestive systems.

Vagal afferent fibers express a variety of G protein–coupled receptors (GPCRs) that have been labeled with fluorescent antibodies to identify their peripheral sensory receptor sites in specific viscera, as well as mark their distinctive central projections to specific zones in the nucleus of the solitary tract in the medulla. By expressing genetic markers of calcium transients (GCaMPs) in identified vagal ganglia neurons, Liberles and colleagues measured their physiological responses to mechanical stimuli such as stretch or their activation by nutrients or gastric hormones (serotonin, glucagon-like peptide 1, or cholecystokinin). The ability to label specific vagal afferents provides important tools for analyzing neural regulation of visceral function and tracing the pathways used to modulate these important bodily functions.

Although their cell bodies seem to be scattered randomly in the vagal nucleus, individual vagal neurons perform different sensory functions in specific organ systems. For example optogenetic stimulation of identified vagal sensory neurons reveals that there are at least two populations of vagal neurons controlling respiration. Neurons that express the GPCR *P2ry1* induce apnea, trapping the lung in expiration, while those expressing the GPCR *Npy2r* produce rapid shallow breathing. Stimulation of these neurons has no effect on heart rate or digestive function. Another set of GPCRs are used to label neurons that regulate gastrointestinal function. One set of gastric afferents are mechanoreceptors that sense distension of the stomach and upper intestine and modulate gastric motility, while other gastric afferents are chemoreceptors that sense specific nutrients in the gut and aid their absorption.

Action Potential Codes Transmit Somatosensory Information to the Brain

In the previous sections, we learned that a variety of stimuli, such as mechanical forces, temperature, and various chemicals, interact with receptor molecules at the distal axon terminals of DRG neurons to produce local depolarization of the sensory endings. As noted in Chapter 17, these receptor potentials are transformed into a digital pulse code of action potentials for transmission to the central nervous system.

The sensory terminal regions of peripheral nerve fibers are usually unmyelinated and do not express the voltage-gated Na^+ and K^+ channels that underlie action potential generation. For example, the lanceolate endings of hair follicle afferents are unmyelinated (Figure 18–2H). This design optimizes information gathering in the receptive field by dedicating the highly branched terminal membrane area to sensory transduction channels such as Piezo2 or TRP receptors.

The most distal action potential ion channels in myelinated fibers are usually located near the initial myelin segment (see Figure 3–10) or at the intersection of branches in unmyelinated fibers. This has important consequences for information transmission. Depolarizing sensory signals from multiple branches can summate more easily if channels involved in action potential generation are absent from receptive terminals, because of the regenerative properties of action potentials and the subsequent inactivation of the voltage-gated Na^+ channels. Sensory messages arriving from later-activated receptors may be extinguished by collision with backward-propagating action potentials traveling along another branch of the fiber. Thus, the signals transmitted along a primary afferent axon may be a nonlinear reflection of the sensory stimulus, reflecting either spatial summation of excitation from multiple branches or winner-take-all suppression of late-generated activity. Sequential activation of different neurite branches can also aid detection of moving stimuli by generating long trains of action potentials if individual endings are stimulated at optimal rates so that their responses are not shunted by spikes generated earlier in other branches.

Action potential transmission along peripheral nerves depends on whether the axon is myelinated or

unmyelinated and on the expression of specific subclasses of voltage-dependent Na_V and K_V channels in each nerve fiber. Steven Waxman and colleagues reported that large-diameter Aα and Aβ fibers that innervate proprioceptors and low-threshold mechanoreceptors (LTMRs) express primarily $Na_V1.1$ and $Na_V1.6$ isoforms; these fibers generally fire action potentials at high rates, in part because they also express $K_V1.1$ and $K_V1.2$ channels that enable rapid repolarization of axons. Small-diameter peripheral nerves that mediate pain and itch sensations express $Na_V1.7$, $Na_V1.8$, and $Na_V1.9$ channels. The latter two Na_V subtypes have kinetic and voltage sensitivities that promote repetitive firing, thereby enhancing painful sensations: Na_V 1.8 channels inactivate incompletely during action potentials and recover rapidly following them; Na_V 1.9 channels activate at relatively negative potentials and undergo negligible inactivation, resulting in persistent inward currents that can amplify subthreshold stimuli.

Sensory Ganglia Provide a Snapshot of Population Responses to Somatic Stimuli

We conclude this survey of DRG neurons by examining the distribution of sensory responses within an individual mammalian somatosensory ganglion. Typically, peripheral nerve fibers have been studied one at a time, usually with optimal stimuli for particular receptor classes. However, even weak voices contribute to the neural chorale, and those have been largely ignored with classic single-cell recording techniques.

New in vivo functional imaging techniques provide useful tools for labeling, visualizing, and measuring ensemble responses to various types of somatosensory stimuli. For example, the Ca^{2+} currents evoked by sensory stimuli provide an alternative to electrophysiological recordings of spike trains in individual neurons. In the experiment illustrated in Figure 18–12, the genetically encoded Ca^{2+} sensor GCaMP6f was expressed in cells of the mouse trigeminal ganglia that also expressed the polymodal TRPV1 receptor, allowing researchers to visualize and quantify the activity of populations of neurons activated by a variety of somatosensory stimuli. Using a battery of tactile, noxious, and thermal stimuli first developed by William Willis to analyze somatosensory responses of neurons in the spinal cord, Nima Ghitani, Alexander Chesler, and colleagues recorded responses of 213 trigeminal neurons simultaneously. Their findings were quite remarkable. As shown in the heat map of Figure 18–12B1, neuronal responses are diverse, varying considerably in the intensity and duration of firing patterns to identical stimuli. Such ensemble recording techniques indicate that even at the receptor level there are no canonical responses to somatic stimuli, but rather common patterns of responses.

Furthermore, individual somatosensory neurons appear to be polysensory, responding to more than one modality, such as touch and pain. This study shows that individual trigeminal neurons distinguish noxious heat from mechanical pain (hair pull) and may respond, albeit weakly, to gentle touch or moderate thermal stimuli (Figure 18–12A). The most prevalent type of trigeminal ganglion neurons (49%) distinguish light touch (stroking the cheek) from thermal stimuli (Figure 18–12B). The next most common types are mechanical nociceptors (18%) or thermoreceptors (16%). Less common are polymodal types that respond to thermal and nociceptive stimuli (total 9%).

These new imaging techniques will enable neuroscientists to quantify sensory interactions in populations of somatosensory afferents, define combinatorial codes used by members of the active population, and thereby identify specific neural populations engaged in somatic sensation. Recording neurons simultaneously rather than one at a time is essential for decoding population activity and defining the circuits underlying diverse sensory modalities.

Lastly, we note that neurons in the dorsal root, trigeminal, and vagal ganglia do not appear to be spatially clustered or segregated functionally by modality such as mechanosensation or thermal or chemical events (Figure 18–12A). The principal organizational feature of these sensory ganglia is one of body topography: which particular area of skin or which muscle or visceral structure is innervated by particular sensory neurons. Such geographical specificity extends centrally to higher structures in the brain that analyze the sensory information and that organize specific behaviors.

Somatosensory Information Enters the Central Nervous System Via Spinal or Cranial Nerves

As the peripheral nerve fibers exit the dorsal root ganglia and approach the spinal cord, the large- and small-diameter fibers separate into medial and lateral divisions, to form the *spinal nerves* that project to distinct locations in the spinal cord and brain stem. The medial division includes large myelinated Aα and Aβ fibers, which transmit proprioceptive and tactile information from the innervated body region. The lateral division of a spinal nerve includes small, thinly myelinated Aδ fibers and unmyelinated C fibers, which transmit noxious, thermal, pruritic, and visceral

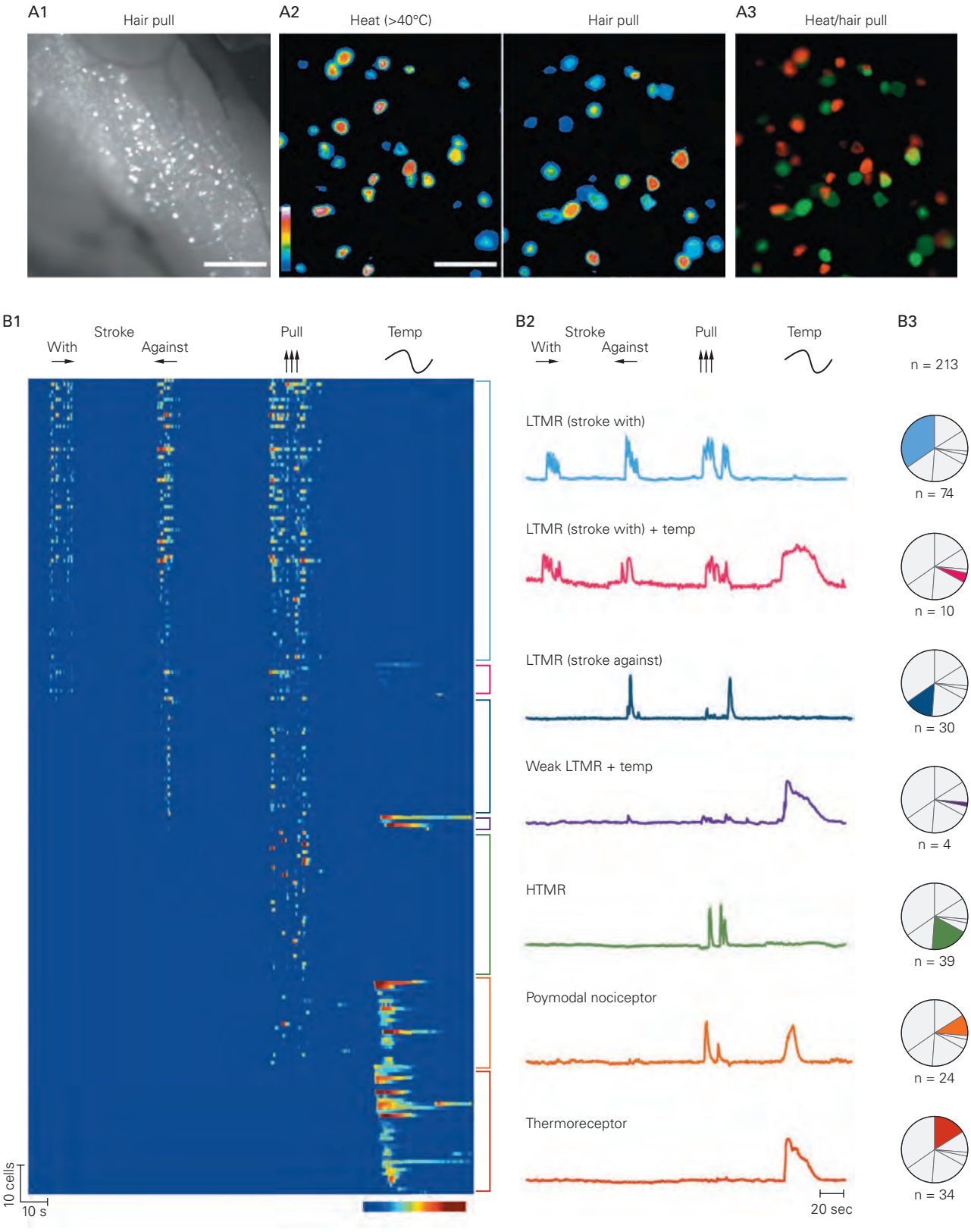
A1
Hair pull
A2
Heat (>40°C)
Hair pull
A3
Heat/hair pull
B1
Stroke
With
Against
Pull
Temp
10 cells
10 s
B2
Stroke
With
Against
Pull
Temp
LTMR (stroke with)
LTMR (stroke with) + temp
LTMR (stroke against)
Weak LTMR + temp
HTMR
Poymodal nociceptor
Thermoreceptor
20 sec
B3
n = 213
n = 74
n = 10
n = 30
n = 4
n = 39
n = 24
n = 34

information from the same region of the body, as well as some tactile information.

Somatosensory information from the limbs and trunk reaches the central nervous system through the 31 spinal nerves, which enter the spinal cord through openings between the vertebrae of the spine. Individual spinal nerves are named for the vertebrae below the foramen through which they pass in cervical nerves or for the foramen above their entry point in thoracic, lumbar, and sacral nerves.

Somatosensory information from the head and neck is transmitted through the trigeminal, facial, glossopharyngeal, and vagus nerves, which enter through openings in the cranium. The trigeminal nerve conveys somatosensory information from the lips, mouth, cornea, and skin on the anterior half of the head, as well as the muscles of mastication. The facial and glossopharyngeal nerves innervate the taste buds of the tongue, the skin of the ear, and some of the skin of the tongue and pharynx. The glossopharyngeal and vagus nerves provide some cutaneous information, but their main sensory role is visceral. Vagal afferents regulating respiration and those regulating gastric motility project to distinct regions of the nucleus of the solitary tract.

Each spinal or cranial nerve receives sensory inputs from a particular region of the body called a *dermatome* (Figure 18–13); the muscles innervated by motor fibers in the corresponding peripheral nerve constitute a *myotome*. These are the skin and muscle regions affected by damage to peripheral nerves. Because the dermatomes overlap, three adjacent spinal nerves often have to be blocked to anesthetize a particular area of skin. The distribution of spinal nerves in the body forms the anatomical basis of the topographic maps of sensory receptors in the brain that underlie our ability to localize specific sensations.

Individual spinal or cranial nerve fibers terminate on neurons in specific zones of the spinal cord gray matter or the medullary dorsal horn (Figure 18–14). The spinal neurons that receive sensory input are either interneurons, which terminate upon other spinal neurons within the same or neighboring segments, or projection neurons, which serve as the cells of origin of major ascending pathways to higher centers in the brain.

The spinal gray matter is subdivided anatomically into 10 laminae (or layers), numbered I to X from dorsal to ventral, based on differences in cell and fiber composition. As a general rule, the largest fibers (Aα) terminate in or near the ventral horn, the medium-size fibers (Aβ) from the skin and muscle terminate in intermediate layers of the dorsal horn, and the smallest fibers (Aδ and C) terminate in the most dorsal portion of the spinal gray matter.

Lamina I consists of a thin layer of neurons capping the dorsal horn of the spinal cord and pars caudalis of the spinal trigeminal nucleus. Individual neurons of lamina I receive monosynaptic inputs from small myelinated fibers (Aδ) or unmyelinated C fibers of a

Figure 18–12 (Opposite) **The distribution of somatosensory modalities among trigeminal ganglion neurons that innervate the hairy skin of the face.** (Adapted, with permission, from Ghitani et al. 2017.)

A. In vivo epifluorescent imaging of a trigeminal ganglion in a TRPV1-GCaMP6f–expressing mouse. Calcium-sensitive dyes (GCaMP6f) fluoresce in response to Ca^{2+} entry through voltage-gated channels in individual trigeminal ganglion neurons. **A1.** Anatomical positions of 213 GCaMP6f-expressing neurons in the trigeminal ganglion of a mouse. Scale bar = 500 µm. These neurons are widely distributed within the trigeminal ganglion. **A2.** Higher magnification images of calcium signals in a subset of neurons that respond to heat pulses >40°C or to hair pull; the color bar in the left image indicates the strength of the calcium signal in each neuron. The strongest activity is shown in **white** or **red**; the weakest response in **blue**. Scale bar = 100 µm. **A3.** An overlay of the two population maps labeled in pseudocolor (**red** for heat, **green** for hair pulling) shows which neurons responded to each stimulus. These neurons were usually selective for heat or hair pull, but two responded to both modalities (**yellow**).

B. Quantification of the responses of all TRPV1-expressing neurons visualized in this trigeminal ganglion to various modes of tactile, noxious, and thermal stimuli. **B1.** Heatmap of the simultaneously recorded responses of all 213 labeled neurons to stroking the cheek, noxious mechanical (hair pull), and thermal stimuli. Each row illustrates the response of an individual neuron to these stimuli; the pixel color indicates the strength of each neuron's response (Δf/F). (Color range = 10%–60% Δf/F.) Neuronal responses are ordered vertically by the temporal onset of increased firing rates. The symbols above the heat map indicate the type and sequence of stimulation: stroking the cheek **with** or **against** the direction of hair growth, hair pull, and thermal stimuli ranging from 25°C to 47°C to 12°C. Although more than half of these neurons responded to gentle touch (stroking), they generally responded more vigorously to noxious mechanical stimuli (hair pull) than to stroking the skin. The strongest responses were observed to noxious heat, but such neurons composed only 30% of the population studied. At the end of the experiment, records from each neuron were sorted into one of the seven response categories identified in B2. **B2.** Averaged response amplitude and time course of Ca^{2+} signals for the seven categories of trigeminal sensory responses. Note the polymodal nature of responses using this objective mode of neuronal classification. (Abbreviations: **LTMR**, low-threshold mechanoreceptor; **HTMR**, high-threshold nociceptor-mechanoreceptor.) **B3.** Pie charts illustrate the number and fraction of neurons in each category.

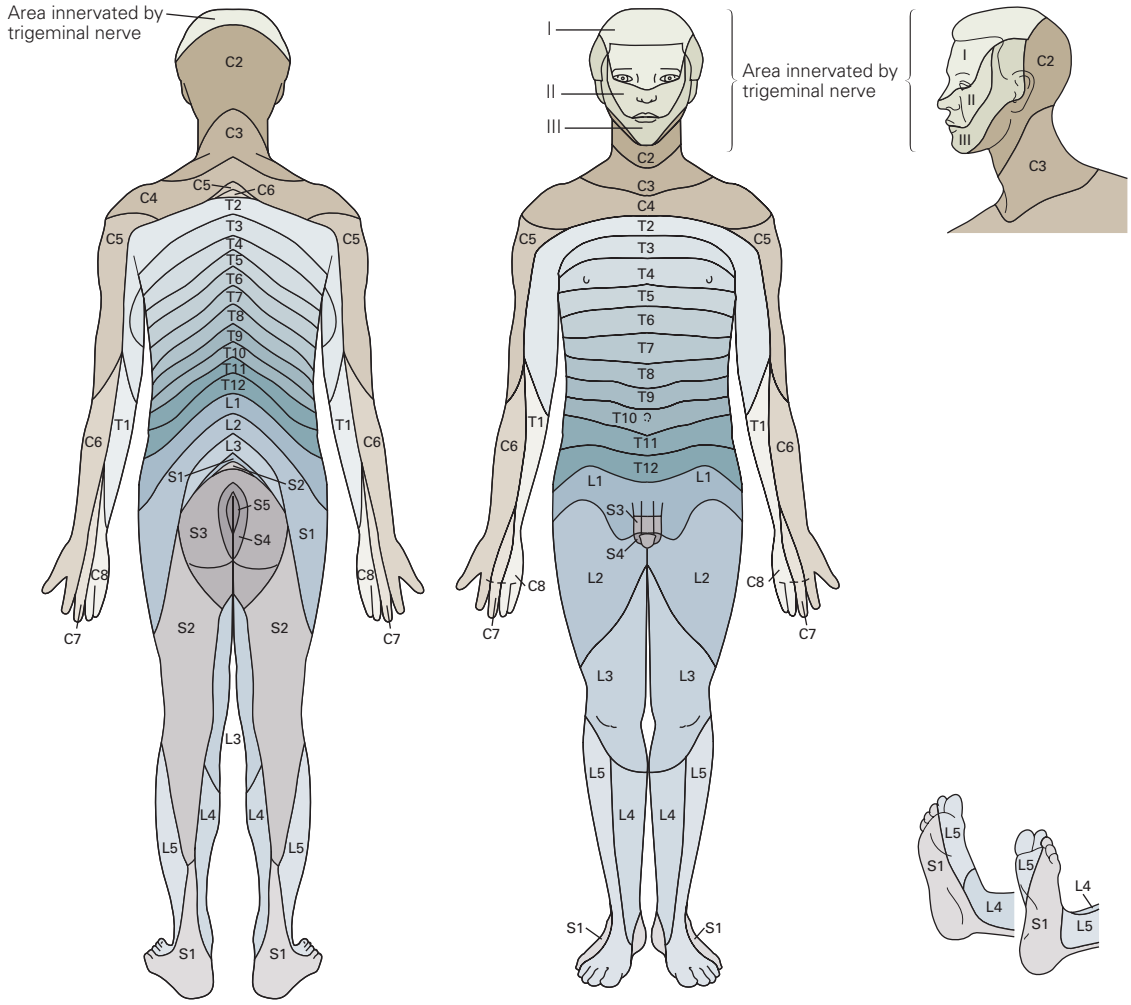

Figure 18–13 The distribution of dermatomes in the spinal cord and brain stem. A dermatome is the area of skin and deeper tissues innervated by a single dorsal root or branch of the trigeminal nerve. The dermatomes of the 31 pairs of dorsal root nerves are projected onto the surface of the body and labeled by the foramen through which each nerve enters the spinal cord. The 8 cervical (C), 12 thoracic (T), 5 lumbar (L), 5 sacral (S), and single coccygeal roots are numbered rostrocaudally for each division of the vertebral column. The facial skin, cornea, scalp, dura, and intraoral regions are innervated by the ophthalmic (I), maxillary (II), and mandibular (III) divisions of the trigeminal nerve (cranial nerve V). Level C1 has no dorsal root, only a ventral (or motor) root. Dermatome maps provide an important diagnostic tool for localizing the site of injury to the spinal cord and dorsal roots. However, the boundaries of the dermatomes are less distinct than shown here because the axons comprising a dorsal root originate from several different peripheral nerves, and each peripheral nerve contributes fibers to several adjacent dorsal roots.

single type (Figure 18–14) and therefore transmit information about noxious, thermal, or visceral stimuli. Inputs from warm, cold, itch, and pain receptors have been identified in lamina I, and some neurons have unique cellular morphologies that correlate with sensory modalities. Lamina I neurons generally have small receptive fields localized to one dermatome.

Neurons in lamina II are interneurons that receive inputs from Aδ and C fibers and make excitatory or inhibitory connections to neurons in laminae I, IV, and V that project to higher brain centers. The more superficial portion of lamina II receives input from peptidergic nociceptors that release substance P or CGRP together with glutamate at their central synapses. Fibers terminating in the deeper part of lamina II are purinergic; they release ATP at their central synapses and express the lectin IB4. Co-transmitters such as ATP provide useful immunostaining markers for identifying specific classes of sensory nerve fibers (Figure 18–2C,D).

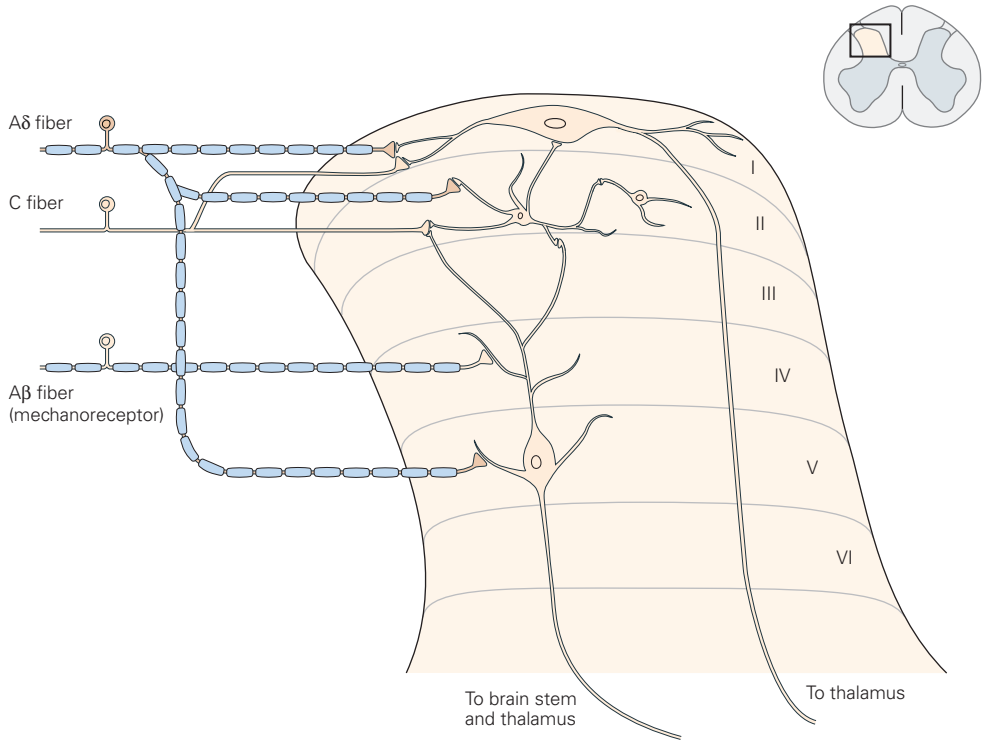

Figure 18–14 Touch and pain fiber projections to the spinal cord dorsal horn. The spinal gray matter in the dorsal horn and intermediate zone of the spinal cord is divided into six layers of cells (laminae I–VI), each with functionally distinct populations of neurons. Neurons in the marginal zone (lamina I) and in lamina II receive nociceptive or thermal inputs from receptors innervated by Aδ or C fibers. The zone for inputs from low-threshold mechanoreceptors (LTMR) is located below lamina II and spans laminae III to V, with the smallest fibers (C-LTMRs) located dorsally, and the largest fibers (Aβ LTMRs) terminating ventrally. LTMRs innervating a particular patch of skin are aligned to form a narrow cell column in the spinal dorsal horn, terminating on spinal interneurons or on projection neurons that send their axons to the brain stem. The medial-lateral arrangement of spinal nerves in the dorsal horn provides a somatotopic representation of adjacent skin areas in the body. The spinal nerve projections of Aβ LTMRs extend to multiple spinal segments along the rostrocaudal axis, whereas those of Aδ or C fibers are more localized to the immediate entry segment (not shown). Aβ LTMRs also send branches to the dorsal column nuclei in the brain stem (Chapters 19 and 20).

Neurons in laminae III to V are the main targets of LTMRs, particularly the large myelinated sensory (Aβ) fibers from cutaneous mechanoreceptors (Figure 18–14). Spinal cord circuits of the dorsal horn have been characterized anatomically and functionally by Victoria Abraira and David Ginty. These local spinal networks enable sensory integration of multiple modalities within a local zone of the body, enabling motoneuron pools to react rapidly to local sensory feedback. Large-diameter fibers mediating touch (Aβ) or proprioception (Aα) also send ascending branches to the medulla through the dorsal columns or dorsolateral funiculi.

Additionally, neurons of the cerebral cortex project to the dorsal horn, permitting direct cortical regulation of local sensorimotor circuits and thus coordinating purposeful behaviors. These higher-order, top-down pathways are supplemented by intraspinal circuits between dermatomes that enable coordinated movements of different fingers or distal and proximal joints.

Neurons in lamina V typically respond to more than one modality—low-threshold mechanical stimuli, visceral stimuli, or noxious stimuli—and are therefore named *wide-dynamic-range neurons*.

Many of the dorsal horn circuits also transmit somatosensory information directly to higher structures in the brain stem, such as the dorsal column, parabrachial, and raphe nuclei, and to the cerebellum or various thalamic nuclei.

Afferent C fibers from the viscera have widespread projections in the spinal cord that terminate ipsilaterally in laminae I, II, V, and X; some also cross the midline and terminate in lamina V and X of the contralateral gray matter. The extensive spinal distribution of visceral C fibers appears to be responsible for the poor localization of visceral pain sensations.

Afferent fibers from the pelvic viscera make important connections to cells in the central gray matter (lamina X) of spinal segments L5 and S1. Lamina X neurons in turn project their axons along the midline of the dorsal columns to the nucleus gracilis in a postsynaptic dorsal column pathway for visceral pain.

Primary afferent fibers that terminate in the deepest laminae in the ventral horn provide sensory information from proprioceptors (muscle spindles and Golgi tendon organs) that is required for somatic motor control, such as spinal reflexes (Chapter 32).

Somatosensory information is conveyed by several ascending pathways to higher centers in the brain, particularly the thalamus and cerebral cortex. The dorsal column–medial lemniscal system transmits tactile and proprioceptive information to the thalamus (Chapter 19), and the spinothalamic (anterolateral) tract conveys pain and thermal information to the midbrain parabrachial nucleus or to the thalamus (Chapter 20). A third pathway, the dorsolateral tract, conveys somatosensory information from the lower half of the body to the cerebellum. The anatomical and functional roles of these networks are described in detail in later chapters.

Highlights

1. The bodily senses mediate a wide range of experiences that are important for normal bodily function and for survival. Although diverse, they share common pathways and common principles of organization. The most important of those principles is *specificity*: Each of the bodily senses arises from specific types of receptors distributed throughout the body.
2. Dorsal root ganglion (DRG) neurons are the sensory receptor cells of the somatosensory system. The functional role of an individual DRG neuron is determined by the sensory receptor molecules expressed in its distal terminals in the body. Mechanoreceptors are sensitive to specific aspects of local tissue distortion, thermoreceptors to particular temperature ranges and shifts in temperature, and chemoreceptors to particular molecular structures. Recordings of physiological responses from these neurons reveal the cellular and molecular mechanisms underlying the senses of touch, pain, temperature, and proprioception, as well as visceral senses.
3. Mechanosensation is mediated by Piezo2 proteins that form ion channels in the axon terminals of DRG fibers sensitive to compression or stretch. These include touch fibers that innervate hair follicles or specialized epithelia such as Merkel cells, Meissner and Pacinian corpuscles, or Ruffini endings. Muscle stretch is signaled by intramuscular spindle receptors and contractile force by Golgi tendon organs. These receptors transmit sensory information via rapidly conducting Aα and Aβ peripheral nerve fibers.
4. Thermoreceptors are excited by transient receptor potential (TRP) ion channels in the axon terminals that are gated in response to local temperature gradients and respond selectively to particular ranges of temperature: cold, cool, warm, or hot. Chemoreceptors change their conductance when binding specific chemicals, both natural and exogenous, giving rise to sensations of pain, itch, or visceral function. Thermosensory and chemosensory information is conveyed centrally via Aδ and C fiber pathways.
5. Activation of somatosensory receptors produces local depolarization of the distal nerve terminals, called the *receptor potential*, whose amplitude is proportional to the strength of the stimulus. Receptor potentials are converted near the distal nerve terminals to trains of action potentials whose frequency is linked to the strength of the stimulus, much as synaptic potentials at synapses produce complex firing patterns in postsynaptic neurons.
6. Individual DRG neurons have multiple sensory endings in the skin, muscle, or viscera, forming complex receptive fields with overlapping territories. The combination of divergent distal terminals and innervation of sense organs by multiple axons enables redundant, parallel pathways for information transmission to the brain.
7. The information transmitted from each type of somatosensory receptor in a particular part of the body is conveyed in discrete pathways to the spinal cord or brain stem by the axons of DRG neurons with cell bodies that generally lie in ganglia close to the point of entry. The axons are gathered together in peripheral nerves. Axon diameter and myelination, both of which determine the speed of action potential conduction, vary in different sensory pathways according to the need for rapid signaling.
8. When DRG axons enter the central nervous system, they separate to terminate in distinct layers of the spinal cord gray matter and/or project directly to higher centers in the brain stem. These circuits form the foundation of five separate sensory pathways with different properties. In three of those systems (the medial lemniscal, lamina I

spinothalamic, and solitary tract systems), the pathways for submodalities appear to be segregated until they reach the cerebral cortex.

9. Future studies of the peripheral nervous system will likely engage high-resolution optical methods for identification of specific receptor classes in the DRG that are labeled with genetic markers. Functional studies of these neurons will also employ optical imaging of entire sensory ganglia labeled with voltage-sensitive or calcium-sensitive fluorescent dyes that enable quantitative temporal monitoring of ensemble responses to specific somatosensory modalities. These receptor neurons will thereby be studied as identified physiological populations rather than one at a time in isolation.

Esther P. Gardner

Selected Reading

Abraira VE, Ginty DD. 2013. The sensory neurons of touch. Neuron 79:618–639.

Abraira VE, Kuehn ED, Chirila AM, et al. 2017. The cellular and synaptic architecture of the mechanosensory dorsal horn. Cell 168:295–310.

Bautista DM, Siemens J, Glazer JM, et al. 2007. The menthol receptor TRPM8 is the principal detector of environmental cold. Nature 448:204–208.

Delmas P, Hao J, Rodat-Despoix L. 2011. Molecular mechanisms of mechanotransduction in mammalian sensory neurons. Nat Rev Neurosci 12:139–153.

Dhaka A, Viswanath V, Patapoutian A. 2006. TRP ion channels and temperature sensation. Annu Rev Neurosci 29:135–161.

Iggo A, Andres KH. 1982. Morphology of cutaneous receptors. Annu Rev Neurosci 5:1–31.

Julius D. 2013. TRP channels and pain. Annu Rev Cell Dev Biol 29:355–384.

Kaas JH, Gardner EP (eds). 2008. *The Senses: A Comprehensive Reference*, Vol. 6, *Somatosensation*. Oxford: Elsevier.

LaMotte RH, Dong X, Ringkamp M. 2014. Sensory neurons and circuits mediating itch. Nat Rev Neurosci 15:19–31.

Lechner SG, Lewin GR. 2013. Hairy sensation. Physiology 28:142–150.

Li L, Rutlin M, Abraira VE, et al. 2011. The functional organization of cutaneous low-threshold mechanosensory neurons. Cell 147:1615–1627.

Patapoutian A, Tate S, Woolf CJ. 2009. Transient receptor potential channels: targeting pain at the source. Nat Rev Drug Discov 8:55–68.

Ranade SS, Syeda R, Patapoutian A. 2015. Mechanically activated ion channels. Neuron 87:1162–1179.

Vallbo ÅB, Hagbarth KE, Torebjörk HE, Wallin BG. 1979. Somatosensory, proprioceptive, and sympathetic activity in human peripheral nerves. Physiol Rev 59:919–957.

Vallbo ÅB, Hagbarth KE, Wallin BG. 2004. Microneurography: how the technique developed and its role in the investigation of the sympathetic nervous system. J Appl Physiol 96:1262–1269.

References

Bai L, Lehnert BP, Liu J, et al. 2015. Genetic identification of an expansive mechanoreceptor sensitive to skin stroking. Cell 163:1783–1795.

Bandell M, Macpherson LJ, Patapoutian A. 2007. From chills to chilis: mechanisms for thermosensation and chemesthesis via thermoTRPs. Curr Opin Neurobiol 17:490–497.

Bennett DL, Clark AJ, Huang J, Waxman SG, Dib-Hajj SD. 2019. The role of voltage-gated sodium channels in pain signaling. Physiol Rev 99:1079–1151.

Boyd IA, Davey MR. 1968. *Composition of Peripheral Nerves*. Edinburgh: Livingston.

Cao E, Liao M, Cheng Y, Julius D. 2013. TRPV1 structures in distinct conformations reveal activation mechanisms. Nature 504:113–118.

Chang RB, Strochlic DE, Williams EK, Umans BD, Liberles SD. 2015. Vagal sensory neuron subtypes that differentially control breathing. Cell 161:622–633.

Collins DF, Refshauge KM, Todd G, Gandevia SC. 2005. Cutaneous receptors contribute to kinesthesia at the index finger, elbow, and knee. J Neurophysiol 94:1699–1706.

Coste B, Xiao B, Santos JS, et al. 2012. Piezo proteins are pore-forming subunits of mechanically activated channels. Nature 483:176–181.

Cox CD, Bae C, Ziegler L, et al. 2016. Removal of the mechanoprotective influence of the cytoskeleton reveals PIEZO1 is gated by bilayer tension. Nat Commun 7:10366.

Darian-Smith I, Johnson KO, Dykes R. 1973. "Cold" fiber population innervating palmar and digital skin of the monkey: responses to cooling pulses. J Neurophysiol 36:325–346.

Darian-Smith I, Johnson KO, LaMotte C, Shigenaga Y, Kenins P, Champness P. 1979. Warm fibers innervating palmar and digital skin of the monkey: responses to thermal stimuli. J Neurophysiol 42:1297–1315.

Dib-Hajj SD, Cummins TR, Black JA, Waxman SG. 2010. Sodium channels in normal and pathological pain. Annu Rev Neurosci 33:325–347.

Edin BB, Vallbo AB. 1990. Dynamic response of human muscle spindle afferents to stretch. J Neurophysiol 63:1297–1306.

Erlanger J, Gasser HS. 1938. *Electrical Signs and Nervous Activity*. Philadelphia: Univ. of Pennsylvania Press.

Gandevia SC, McCloskey DI, Burke D. 1992. Kinaesthetic signals and muscle contraction. Trends Neurosci 15:62–65.
Gandevia SC, Smith JL, Crawford M, Proske U, Taylor JL. 2006. Motor commands contribute to human position sense. J Physiol 571:703–710.
Ghitani N, Barik A, Szczot M, et al. 2017. Specialized mechanosensory nociceptors mediating rapid responses to hair pull. Neuron 95:944–954.
Guharay F, Sachs F. 1984. Stretch-activated single ion channel currents in tissue-cultured embryonic chick skeletal muscle. J Physiol 352:685–701.
Guo YR, MacKinnon R. 2017. Structure-based membrane dome mechanism for Piezo mechanosensitivity. Elife 6:e33660.
Johansson RS, Vallbo ÅB. 1983. Tactile sensory coding in the glabrous skin of the human hand. Trends Neurosci 6:27–32.
Jordt S-E, McKemy DD, Julius D. 2003. Lessons from peppers and peppermint: the molecular logic of thermosensation. Curr Opin Neurobiol 13:487–492.
Liao M, Cao E, Julius D, Cheng Y. 2013. Structure of the TRPV1 ion channel determined by electron cryo-microscopy. Nature 504:107–112.
Lin S-Y, Corey DP. 2005. TRP channels in mechanosensation. Curr Opin Neurobiol 15:350–357.
Macefield VG. 2005. Physiological characteristics of low-threshold mechanoreceptors in joints, muscle and skin in human subjects. Clin Exp Pharmacol Physiol 32:135–144.
Macefield G, Gandevia SC, Burke D. 1990. Perceptual responses to microstimulation of single afferents innervating joints, muscles and skin of the human hand. J Physiol 429:113–129.
Maksimovic S, Nakatani M, Baba Y, et al. 2014. Epidermal Merkel cells are mechanosensory cells that tune mammalian touch receptors. Nature 509:617–621.
McGlone F, Wessberg J, Olausson H. 2014. Discriminative and affective touch: sensing and feeling. Neuron 82:737–755.
Murthy SE, Dubin AE, Patapoutian A. 2017. Piezos thrive under pressure: mechanically activated ion channels in health and disease. Nat Rev Mol Cell Biol 18:771–783.
Ochoa J, Torebjörk E. 1989. Sensations evoked by intraneural microstimulation of C nociceptor fibres in human skin nerves. J Physiol 415:583–599.
Ottoson D, Shepherd GM. 1971. Transducer properties and integrative mechanisms in the frog's muscle spindle. In: WR Lowenstein (ed). *Handbook of Sensory Physiology*, Vol. 1 *Principles of Receptor Physiology*, pp. 442–499. Berlin: Springer-Verlag.
Perl ER. 1968. Myelinated afferent fibers innervating the primate skin and their response to noxious stimuli. J Physiol (Lond) 197:593–615.
Perl ER. 1996. Cutaneous polymodal receptors: characteristics and plasticity. Prog Brain Res 113:21–37.
Ranade SS, Woo SH, Dubin AE, et al. 2014. Piezo2 is the major transducer of mechanical forces for touch sensation in mice. Nature 516:121–125.
Sachs F. 1990. Stretch-sensitive ion channels. Sem Neurosci 2:49–57.
Saotome K, Murthy SE, Kefauver JM, Whitwam T, Patapoutian A, Ward AB. 2018. Structure of the mechanically activated ion channel Piezo1. Nature 554:481–486.
Torebjörk HE, Vallbo ÅB, Ochoa JL. 1987. Intraneural microstimulation in man. Its relation to specificity of tactile sensations. Brain 110:1509–1529.
Wellnitz SA, Lesniak DR, Gerling GJ, Lumpkin EA. 2010. The regularity of sustained firing reveals two populations of slowly adapting touch receptors in mouse hairy skin. J Neurophysiol 103:3378–3388.
Wessberg J, Olausson H, Fernström KW, Vallbo ÅB. 2003. Receptive field properties of unmyelinated tactile afferents in the human skin. J Neurophysiol 89:1567–1575.
Williams EK, Chang RB, Strochlic DE, Umans BD, Lowell BB, Liberles SD. 2016. Sensory neurons that detect stretch and nutrients in the digestive system. Cell 166:209–221.
Wilson SR, Gerhold KA, Bifolck-Fisher A, et al. 2011. TRPA1 is required for histamine-independent, Mas-related G protein-coupled receptor-mediated itch. Nat Neurosci 14:595–602.
Wilson SR, Nelson AM, Batia L, et al. 2013. The ion channel TRPA1 is required for chronic itch. J Neurosci 33:9283–9294.
Woo SH, Lukacs V, de Nooij JC, et al. 2015. Piezo2 is the principal mechanotransduction channel for proprioception. Nat Neurosci 18:1756–1762.
Woo SH, Ranade S, Weyer AD, et al. 2014. Piezo2 is required for Merkel-cell mechanotransduction. Nature 509:622–626.
Zhao Q, Zhou H, Chi S, et al. 2018. Structure and mechanogating mechanism of the Piezo1 channel. Nature 554:487–492.
Zimmerman A, Bai L, Ginty DD. 2014. The gentle touch receptors of mammalian skin. Science 346:950–954.

19

Touch

In this chapter on the sense of touch, we focus on the hand because of its importance for this modality, in particular its role in the appreciation of object properties and in performance of skilled motor tasks. The human hand is one of evolution's great creations. The fine manipulative capacity provided by our fingers is possible because of their fine sensory capacity; if we lose tactile sensation in our fingers, we lose manual dexterity.

The softness and compliance of the glabrous skin play a major role in the sense of touch. When an object contacts the hand, the skin conforms to its contours, forming a mirror image of the object's surface. The resultant displacement and indentation of the skin stretches the tissue, thereby stimulating the sensory endings of mechanoreceptors at or near the region of contact.

These receptors are highly sensitive and are continually active as we manipulate objects and explore the world with our hands. They provide information to the brain about the object's position in the hand, its shape and surface texture, the amount of force applied at the contact points, and how these features change over time when the hand or the object moves. The fingertips are among the most densely innervated parts of the body, providing extensive and redundant somatosensory information about objects manipulated by the hand.

Moreover, the anatomical structure of the hand, with its multiple joints and apposable digits, enables humans to shape the hand in ways that mirror an object's overall shape, providing a hand-centered proprioceptive representation of the external world. This ability to internalize the shape of objects allows us to create tools that extend the abilities of our hands alone.

When we become skilled in the use of a tool, such as a scalpel or a pair of scissors, we feel conditions at

the working surface of the tool as though our fingers were there because two groups of touch receptors monitor the vibrations and forces produced by those distant conditions. When we scan our fingers across a surface, we feel its form and texture because another group of mechanoreceptors has high spatial and temporal acuity. A blind person uses this capacity to read Braille at a hundred words per minute. When we grip and manipulate an object, we do so delicately, with only as much force as needed, because specific mechanoreceptors continually monitor slip and adjust our grip appropriately.

We are also able to recognize objects placed in the hand from touch alone. When we are handed a baseball, we recognize it instantly without having to look at it because of its shape, size, weight, density, and texture. We do not have to think about the information provided by each finger to deduce that the object must be a baseball; the information flows to memory and instantly matches previously stored representations of baseballs. Even if we have never previously handled a baseball, we perceive it as a single object, not as a collection of discrete features. The somatosensory pathways of the brain have the daunting task of integrating information from thousands of sensors in each hand and transforming it to a form suitable for cognition and action.

Sensory information is extracted for the purpose of motor control as well as cognition, and different kinds of information are extracted for those purposes. We can, for example, shift our attention from the baseball's shape to its location in the hand to readjust our grip for an effective throw or pitch. This selective attention to different aspects of the sensory information is brought about by cortical mechanisms.

Active and Passive Touch Have Distinct Goals

Touch is defined as direct contact between two physical bodies. In neuroscience, touch refers to the special sense by which contact with the body is perceived consciously. Touch can be active, as when you move your hand or some other part of the body against another surface, or passive, as when someone or something else touches you. Active touch is fundamentally a top-down process in which the subject has agency, seeks particular information, and controls what occurs. Subjects select relevant salient features of objects to determine subsequent behaviors. They choose which object to grasp and the most efficient hand shape needed to acquire it, and decide how to manipulate it to achieve particular goals. During active touch, somatosensory information depicts the physical properties of objects as well as the motor actions of the subject's hand and arm, and their relation to the task goals. Importantly, active manipulation of objects is based upon the concept of touch as a three-dimensional modality designed to capture the volumetric, topographic, and elastic properties of objects, as first proposed by Roberta Klatzky and Susan Lederman. These three-dimensional qualities are best appreciated by active manipulation including grasping, rotation, and contour tracing by the hand.

Passive touch engages a bottom-up process in which subjects react to external stimuli specified by the experimenter or clinician. The experimenter selects and controls the location, amplitude, force, timing, duration, and spatial spread of stimuli delivered to the skin. Subsequent behaviors are guided by instructions provided in the paradigm. Tactile stimuli are classified into experimenter-selected categories and/or rated along an intensive or hedonic scale. Subjects therefore need to analyze all of the transmitted somatosensory information and select specific features guided in part by the task instructions.

Active and passive modes of tactile stimulation excite the same population of receptors in the skin and evoke similar responses in afferent fibers. They differ somewhat in cognitive features that reflect attention and behavioral goals during the period of stimulation. Passive touch is tested by naming objects or describing sensations; active touch is used when the hand manipulates objects. The sensory and motor components of touch are intimately connected anatomically in the brain and are important functionally in guiding motor behavior.

During active touch, descending fibers from motor centers of the cerebral cortex terminate on interneurons in the medial dorsal horn that receive tactile information from the skin. Similar fibers from cortical motor areas terminate in the dorsal column nuclei, providing an *efference copy* (or corollary discharge) of the motor commands that generate behavior (Chapter 30). In this manner, tactile signals from the hand resulting from active hand movements may be distinguished centrally from passively applied stimuli in the neurological exam or in psychophysical tests.

The distinction between active and passive touch is important clinically when patients have deficits in hand use. Motor deficits such as weakness, stiffness, or clumsiness may result from sensory loss, which is why passive sensory testing is important in the neurological examination. Common neurological tests for touch include measurements of detection thresholds, vibration sense, two-point or texture discrimination, and

the ability to recognize form through touch (*stereognosis*). These tests measure the sensitivity and function of various receptors for touch. Deviations from expected values may help diagnose sensory deficits or lesions that underlie somatosensory dysfunction. The neural mechanisms underlying these tests are discussed in this chapter. Other common tests of somatosensory function—tendon reflexes, pinprick, and thermal tests—are discussed in other chapters.

The Hand Has Four Types of Mechanoreceptors

Tactile sensations in the human hand arise from four kinds of mechanoreceptors: Meissner corpuscles, Merkel cells, Pacinian corpuscles, and Ruffini endings (Figure 19–1). Each receptor responds in a distinctive manner depending on its morphology, innervation pattern, and depth in the skin. The sense of touch can be understood as the combined result of the information provided by these four systems acting in concert.

Touch receptors are innervated by slowly adapting or rapidly adapting axons. Slowly adapting (SA) fibers respond to steady skin indentation with a sustained discharge, whereas rapidly adapting (RA) fibers stop firing when indentation becomes stationary (Figure 19–1 and Table 19–1). Sustained mechanical sensations from the hand must accordingly arise from the SA fibers; the sensation of motion on or across the skin is signaled primarily by RA fibers.

Touch receptors in the hand are further subdivided into two types based on size and location in the skin.

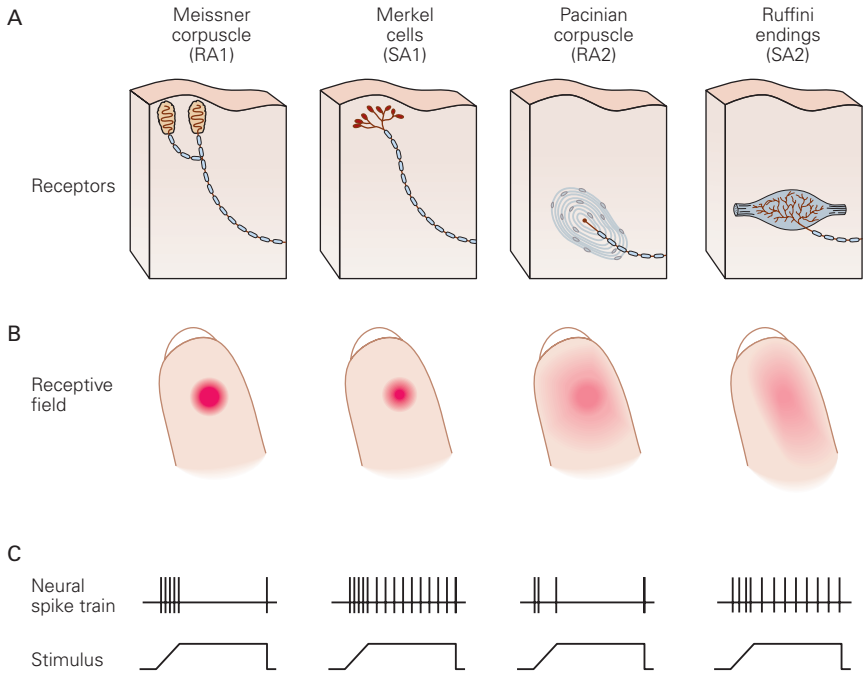

Figure 19–1 Four types of mechanoreceptors are responsible for the sense of touch in the human hand. The terminals of myelinated sensory nerves innervating the hand are surrounded by specialized structures that detect contact on the skin. The receptors differ in morphology, innervation patterns, location in the skin, receptive field size, and physiological responses to touch. (Adapted, with permission, from Johansson and Vallbo 1983.)

A. The superficial and deep layers of the glabrous (hairless) skin of the hand each contain distinct types of mechanoreceptors. The superficial layers contain small receptor cells: Meissner corpuscles (**RA1**, rapidly adapting type 1) and Merkel cells (**SA1**, slowly adapting type 1). The sensory nerve fibers that innervate these receptors have branching terminals that innervate multiple receptors of one type. The deep layers of the skin and subcutaneous tissue contain large receptors: Pacinian corpuscles (**RA2**, rapidly adapting type 2) and Ruffini endings (**SA2**, slowly adapting type 2). Each of these receptors is innervated by a single nerve fiber, and each fiber innervates only one receptor.

B. The receptive field of a mechanoreceptor reflects the location and distribution of its terminals in the skin. Touch receptors in the superficial layers of the skin have smaller receptive fields than those in the deep layers.

C. The nerve fibers innervating each type of mechanoreceptor respond differently when activated. The schematic spike trains show responses of each type of nerve when its receptor is activated by slowly increasing and constant pressure against the skin. The rapidly adapting fibers respond to motion at the onset and end of a pressure stimulus and adapt rapidly to constant stimulation, whereas the slowly adapting fibers respond to both steady pressure and motion and adapt slowly.

Table 19–1 Cutaneous Mechanoreceptors in Glabrous Skin

	Type 1		Type 2	
	SA1	**RA1**[1]	**SA2**	**RA2**[2]
Receptor	Merkel cell/neurite complex (multiple endings)	Meissner corpuscle (multiple endings)	Ruffini ending (single ending)	Pacinian corpuscle (single ending)
Location	Base of intermediate ridge surrounding sweat duct	Dermal papillae (adjacent to limiting ridge)	Skin folds, skin over joints, nail bed	Dermis (deep tissue)
Axon diameter (μm)	7–11	6–12	6–12	6–12
Conduction velocity (ms)	40–65	35–70	35–70	35–70
Best stimulus	Edges, points	Lateral motion	Skin stretch	Vibration
Response to sustained indentation	Sustained with slow adaptation (irregular firing pattern)	Phasic at stimulus onset	Sustained with slow adaptation (regular firing rate)	Phasic at stimulus onset
Frequency range (Hz)	0–100	1–300		5–1,000
Best frequency (Hz)	5	50		200
Threshold for rapid indentation or vibration (best) (μm)	8	2	40	0.01

[1]Also called RA, QA, or FA1.
[2]Also called PC or FA2.
RA1, rapidly adapting type 1; **RA2**, rapidly adapting type 2; **SA1**, slowly adapting type 1; **SA2**, slowly adapting type 2.

Type 1 touch fibers terminate in clusters of small receptor organs (Meissner corpuscles or Merkel cells) in the superficial layers of the skin at the margin between the dermis and epidermis (Figure 19–2, Box 19–1.). RA1 fibers are the most numerous tactile afferents in the hand, reaching a density of approximately 150 per cm^2 at the fingertip in man and monkey; SA1 fibers are also widely distributed in the hand, at densities of 70 per cm^2 in the fingertips.

Type 2 fibers innervate the skin sparsely and terminate in single large receptors (Pacinian corpuscles and Ruffini endings) located in the dermis or in subcutaneous tissue. These receptors are larger and less numerous than the receptor organs of the type 1 fibers. The large size of type 2 receptors allows them to sense mechanical displacement of the skin at some distance from the sensory nerve endings. The density of RA2 fibers in human fingers is only 21 per cm^2; SA2 fibers are the least abundant, providing only 9 fibers per cm^2.

A Cell's Receptive Field Defines Its Zone of Tactile Sensitivity

Individual mechanoreceptor fibers convey information from a limited area of skin called the *receptive field* (Chapter 18). Tactile receptive fields in the human hand were first studied by Åke Vallbo and Roland Johansson using microneurography. They inserted microelectrodes through the skin into the median or ulnar nerves in the human forelimb and recorded the responses of individual afferent fibers. They found that in humans, as in other primates, there are important differences between touch receptors, both in their physiological responses and in the structure of their receptive fields.

Type 1 fibers have small, highly localized receptive fields with multiple spots of high sensitivity that reflect the branching patterns of their axon terminals in the skin (Figure 19–5). An RA1 axon typically innervates 10 to 20 Meissner corpuscles, integrating information from several adjacent fingerprint ridges. An SA1 fiber innervates approximately 20 Merkel cells in young adults (Figure 19–4B); the number of Merkel cells drops significantly as we age.

In contrast, type 2 fibers innervating the deep layers of skin are connected to only a single Pacinian corpuscle or Ruffini ending. As these receptors are large, they collect information from a broader area of skin. Their receptive fields typically contain a single

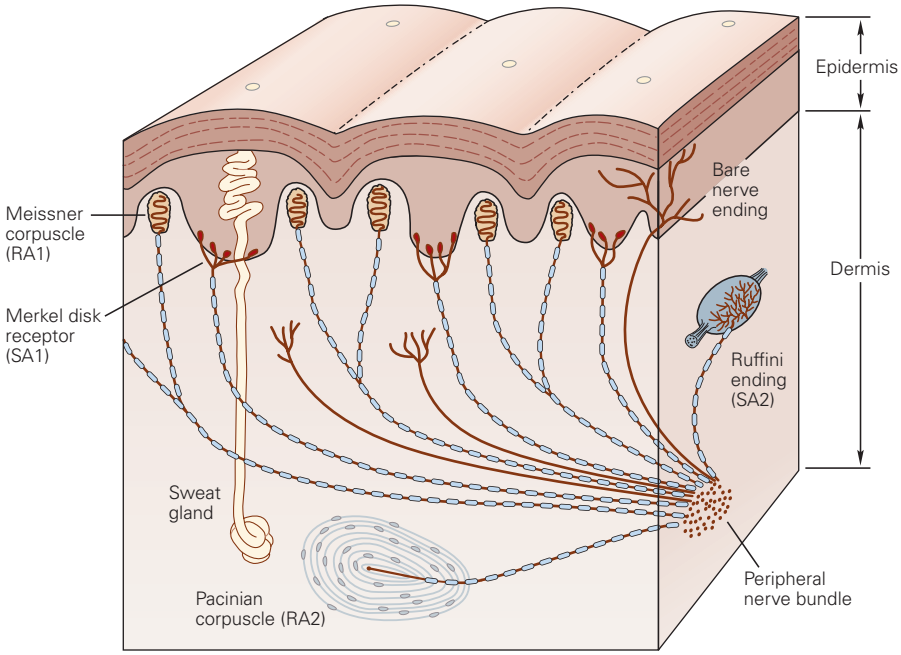

Figure 19–2 Tactile innervation of the glabrous skin in humans. A cross section of the glabrous skin shows the principal receptors for touch in the human hand. All of these receptors are innervated by large-diameter Aβ myelinated fibers. The Meissner corpuscles and Merkel cells lie in the superficial layers of the skin at the base of the epidermis, 0.5 to 1.0 mm below the skin surface. The Meissner corpuscles are located in the dermal papillae that border the edges of each papillary ridge. The Merkel cells form dense bands below the intermediate ridge surrounding the sweat gland ducts along the center of the papillary ridges. The RA1 and SA1 fibers that innervate these receptors branch at their terminals so that each fiber innervates several nearby receptor organs. The Pacinian and Ruffini corpuscles lie within the dermis (2–3 mm thick) and in deeper tissues. The RA2 and SA2 fibers that innervate these receptors each innervate only one receptor organ. (Abbreviations: **RA1**, rapidly adapting type 1; **RA2**, rapidly adapting type 2; **SA1**, slowly adapting type 1; **SA2**, slowly adapting type 2.)

"hot spot" where sensitivity to touch is greatest; this point is located directly above the receptor (Figure 19–5).

Receptive fields on the fingertips are the smallest on the body, averaging 11 mm^2 for SA1 fibers and 25 mm^2 for RA1 fibers. The small fields complement the high density of receptors in the fingertips. Receptive fields become progressively larger on the proximal phalanges and the palm, consistent with the lower density of mechanoreceptors in these regions. Importantly, the receptive fields of type 1 fibers are significantly smaller than most objects that contact the hand, and therefore signal the spatial properties of only a limited portion of an object. As in the visual system, the spatial features of objects are distributed across a population of stimulated receptors whose responses are integrated in the brain to form a unified percept.

Each RA2 axon terminates without branching in a single Pacinian corpuscle, and each Pacinian corpuscle receives but a single RA2 axon. Pacinian corpuscles are large onion-like structures in which successive layers of connective tissue are separated by fluid-filled spaces (see Figure 19–8A1). These layers surround the unmyelinated RA2 ending and its myelinated axon up to one or more nodes of Ranvier. The capsule amplifies high-frequency vibration, a role that is important for tool use. Estimates of the number of Pacinian corpuscles in the human hand range from 2,400 in the young to 300 in the elderly.

The SA2 fibers innervate Ruffini endings concentrated at the finger and wrist joints, the skin surrounding the fingernails, and along the skin folds in the palm. The Ruffini endings are elongated fusiform structures that enclose collagen fibrils extending from the subcutaneous tissue to folds in the skin at the joints, in the palm, or at the fingernail borders. The SA2 nerve endings are intertwined between the collagen fibers in the capsule, as in Golgi tendon organs (Box 32–4), and are excited by stimuli that stretch the skin along its long axis.

Two-Point Discrimination Tests Measure Tactile Acuity

The ability of humans to resolve spatial details of textured surfaces depends on which region of the body is

Box 19–1 Fingerprint Structure Enhances Touch Sensitivity in the Hand

The histological structure of glabrous skin—the smooth, hairless skin of the palm and fingertips—plays a crucial role in the hand's sensitivity to touch. The fingerprints are formed by a regular array of parallel ridges in the epidermis, the papillary ridges (Figure 19–3). Regularly spaced Merkel cells below sweat ducts that emerge from the center of each ridge provide a spatial grid that allows us to localize stimuli precisely on our fingertips.

Each ridge is bordered by epidermal folds—the limiting ridges—that are visible as thin lines on the fingers, palms, and feet. The limiting ridges increase the stiffness and rigidity of the skin, protecting it from damage when contacting objects or when walking barefooted. Meissner corpuscles are typically located in dermal papillae adjacent to the limiting ridges; each dermal papilla contains several Meissner corpuscles and is innervated by two to five RA1 axons (Figure 19–4A).

Merkel cells, innervated by an SA1 fiber, are densely clustered in the center of each papillary ridge, at the base of the intermediate ridge surrounding the epidermal sweat ducts (Figure 19–4A), placing them in an excellent position to detect deformation of the epidermis from pressure or lateral stretch. They perform similar tactile receptive functions as Merkel cells in the touch domes of hairy skin (Chapter 18).

The fingerprints give the glabrous skin a corrugated, rough structure that increases friction, allowing us to grasp objects without slippage. Frictional forces are augmented further when these ridges contact the textured surfaces of objects. Smooth surfaces slide easily underneath the fingers

Figure 19–3 The skin of the human fingertip.

A. Scanning electron micrograph of the fingerprints in the human index finger. The glabrous skin of the hand is structured as arrays of papillary ridges and intervening sulci (limiting ridges) that recur at regular intervals. Globules of sweat exude from ducts at the center of the papillary ridges, forming a regularly spaced grid-like pattern along the center of each ridge. The Merkel cells are located in dense clusters below the sweat ducts at the base of the epidermis along the center of the papillary ridges (see Figure 19–2). (Adapted, with permission, from Quilliam 1978.)

B. Histological section of the glabrous skin cut parallel to the skin surface. The Meissner corpuscles, here immunostained for cholinesterase, form regularly spaced chains along both sides of each papillary ridge adjacent to the limiting ridge. Thus, Meissner corpuscles and Merkel cells form alternating bands of rapidly adapting type 1 (RA1) and slowly adapting type 1 (SA1) touch receptors that span each fingerprint ridge. (Adapted, with permission, from Bolanowski and Pawson 2003.)

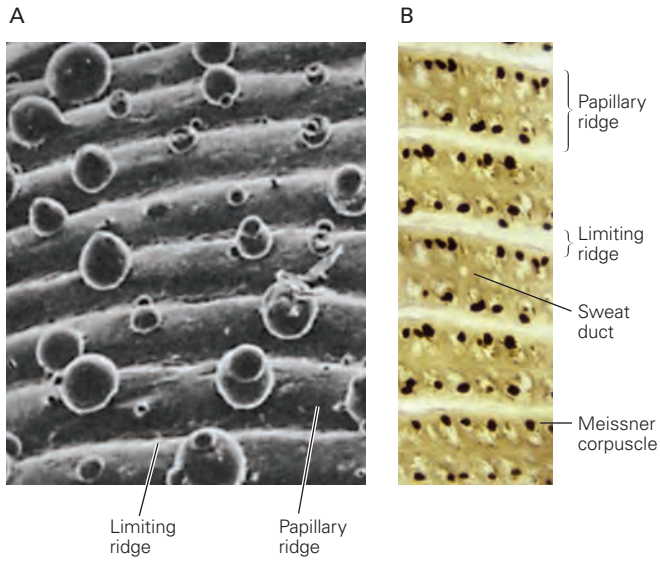

contacted. When a pair of probes is spaced several millimeters apart on the hand, each probe is perceived as a distinct point because it produces a separate dimple in the skin and stimulates nonoverlapping populations of receptors. As the probes are moved closer together, the two sensations become blurred because both probes are contained within the same receptive fields. The spatial interactions between tactile stimuli form the basis of neurological tests of *two-point discrimination* and texture recognition.

The threshold for *tactile acuity*—the separation that defines performance midway between chance and perfect discrimination—is approximately 1 mm on the fingertips of young adults, but declines in the elderly to about 2 mm. Tactile acuity is highest on the fingertips and the lips, where receptive fields are smallest.

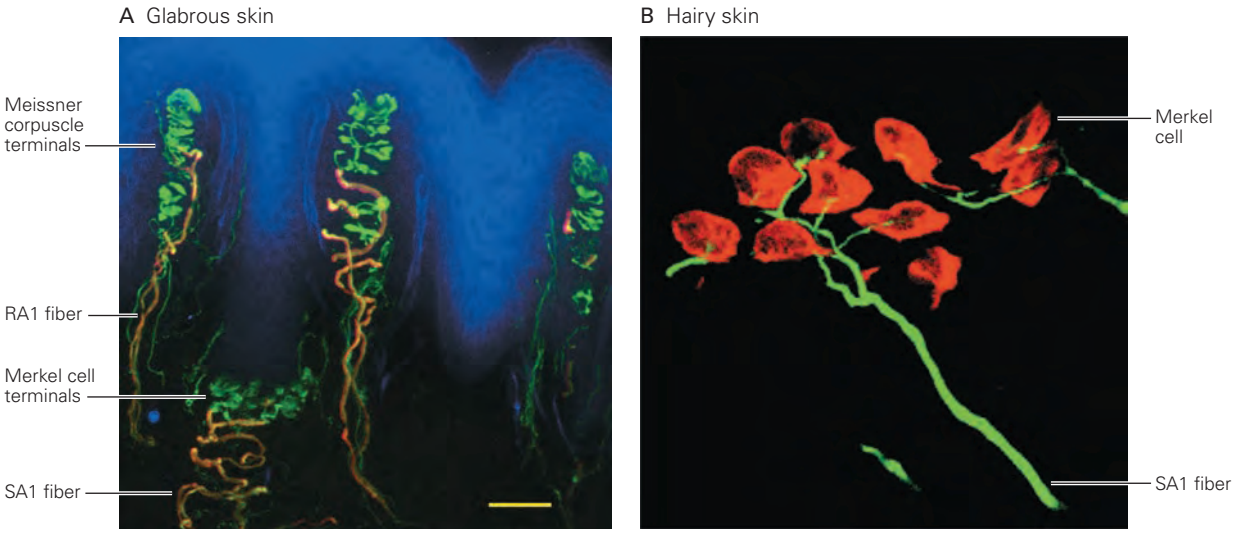

Figure 19–4 Innervation pattern of Meissner corpuscles and Merkel cells in glabrous and hairy skin.

A. A confocal transverse section of a papillary ridge in the human fingertip skin shows the innervation pattern of mechanoreceptors. Meissner corpuscles are located in dermal papillae just below the epidermis (**blue**) bordering the limiting ridge and are innervated by two or more rapidly adapting type 1 (**RA1**) fibers. The fibers lose their myelin sheaths (**orange**) when entering the receptor capsule, exposing broad terminal bulbs (**green**) at which sensory transduction occurs. Individual slowly adapting type 1 (**SA1**) fibers innervate groups of Merkel cells clustered at the base of the intermediate ridge, providing localized signals of pressure applied to that ridge. Scale bar = 50 µm. (Adapted, with permission, from Nolano et al. 2003. Copyright © 2003 American Neurological Association.)

B. A higher-magnification micrograph portrays keratin-8 antibody-labeled Merkel cells (**red**) innervated by an SA1 fiber (**green**) labeled with neurofilament heavy polypeptide (NFH^+). Each nerve fiber extends multiple branches parallel to the surface of the skin that allow it to integrate tactile information from multiple receptor cells in a small zone of skin. The diameter of each Merkel cell is approximately 10 µm. (Adapted, with permission, from Snider 1998. Copyright © 1998 Springer Nature.)

and thus require greater grip force to maintain stability in the hand; the screw caps on bottles are often ridged to make them easy to turn. Frictional forces between the limiting ridges and objects also amplify our sensations of surface features when we palpate objects, generating vibrations that allow us to detect small irregularities such as the grain of wood and threads of fabrics.

The regular spacing of the papillary ridges—and the precise localization of specific receptors within this grid—allows us to repeatedly scan surfaces with back-and-forth hand movements while preserving a constant spatial alignment of adjacent surface features. They also provide an anatomical grid for referencing the precise location of tactile stimuli.

Tactile acuity on proximal parts of the body decreases in parallel with the size of receptive fields of SA1 and RA1 fibers (Figure 19–6A).

When we grasp or touch an object, we can discriminate features of its surface separated by as little as 0.5 mm. Humans are able to distinguish horizontal and vertical orientations of gratings with remarkably narrow spacing of the ridges (Figure 19–6B). Long edges, such as the ridges of a grating, evoke stronger responses from RA1 and SA1 afferents when they stimulate multiple sensory endings in the receptive field simultaneously, stressing the importance of multisensor receptive fields for tactile information processing. Roland Johansson and Andrew Pruszynski recently found that RA1 and SA1 fibers respond more intensely to edges that contact multiple sensory

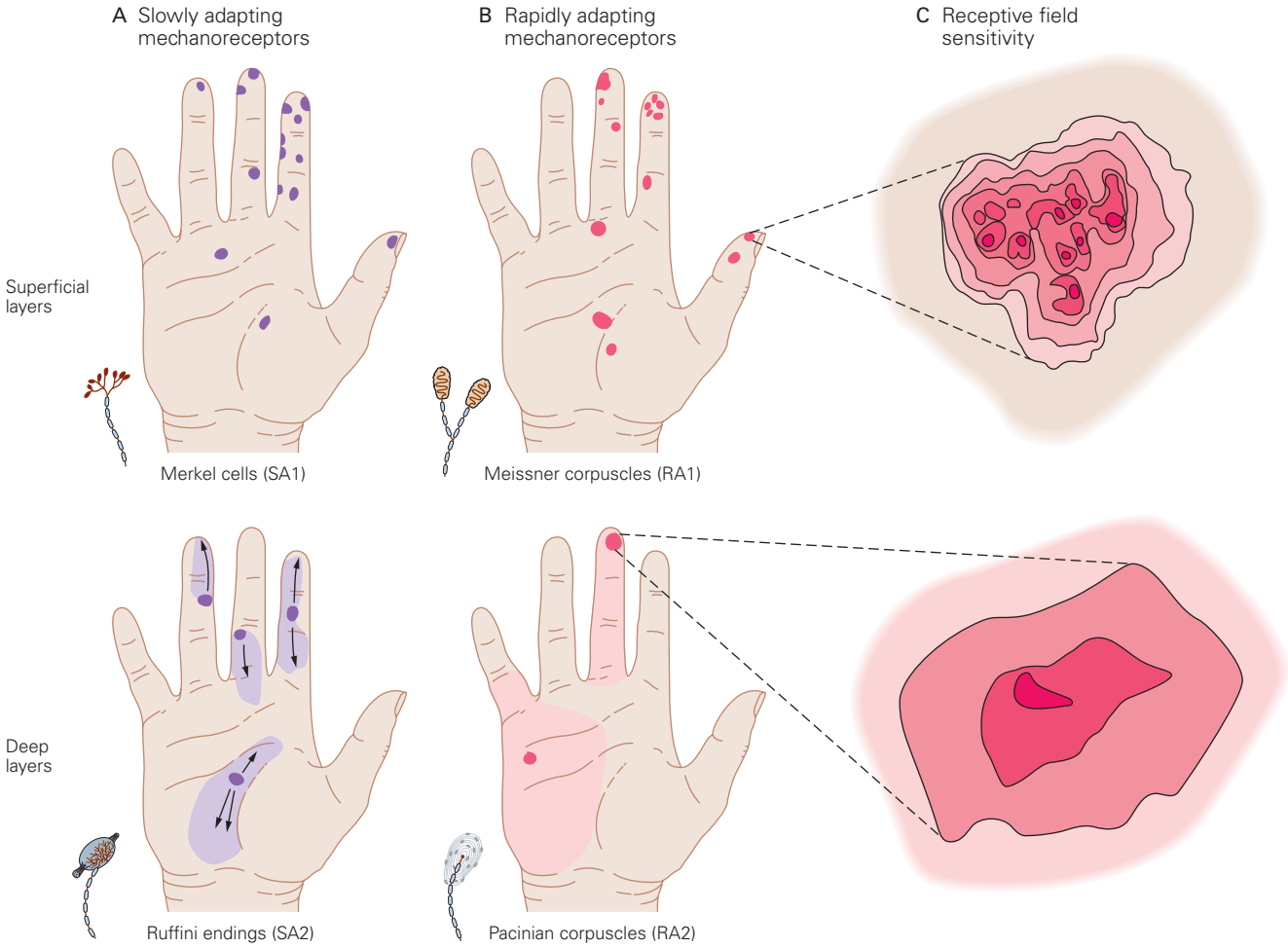

Figure 19–5 Receptive fields in the human hand are smallest at the fingertips. Each colored area on the hands indicates the receptive field of an individual sensory nerve fiber. (Adapted, with permission, from Johansson and Vallbo 1983.)

A–B. In the superficial layers of skin, the receptive fields of type 1 receptors encompass spot-like patches of skin. In the deep layers, type 2 receptive fields extend across wide regions of skin (**light shading**), but responses are strongest in the skin directly over the receptor (**dark spots**). The **arrows** indicate the directions of skin stretch that activate slowly adapting type 2 (**SA2**) fibers.

C. Pressure sensitivity throughout the receptive field is shown as a contour map. The most sensitive regions are indicated in **deep red** and the least sensitive areas in **pale pink**. The receptive field of a rapidly adapting type 1 (**RA1**) fiber (**above**) has many points of high sensitivity, marking the positions of the group of Meissner corpuscles innervated by the fiber. The receptive field of a rapidly adapting type 2 (**RA2**) fiber (**below**) has a single point of maximum sensitivity overlying the Pacinian corpuscle. The receptive field contour map of slowly adapting type 1 (**SA1**) fibers is similar to that of RA1 fibers. Likewise, the receptive field map of SA2 fibers resembles that of RA2 fibers.

endings, allowing these afferents to distinguish vertical, horizontal, or oblique orientations.

Tactile acuity is slightly greater in women than in men and varies between fingers but not between hands; the gender difference is related primarily to the smaller papillary ridge diameter in women, and the resultant higher density of SA1 fibers per cm^2 of skin. The distal pad of the index finger has the keenest sensitivity; spatial acuity declines progressively from the index to the little finger and falls rapidly at locations proximal to the distal finger pads. Tactile spatial resolution is 50% poorer at the distal pad of the little finger and six to eight times coarser on the palm.

Blind individuals use the fine spatial sensitivity of SA1 and RA1 fibers to read Braille. The Braille alphabet represents letters as simple dot patterns that are easy to distinguish by touch. A blind person reads Braille by moving the fingers over the dot patterns. This hand

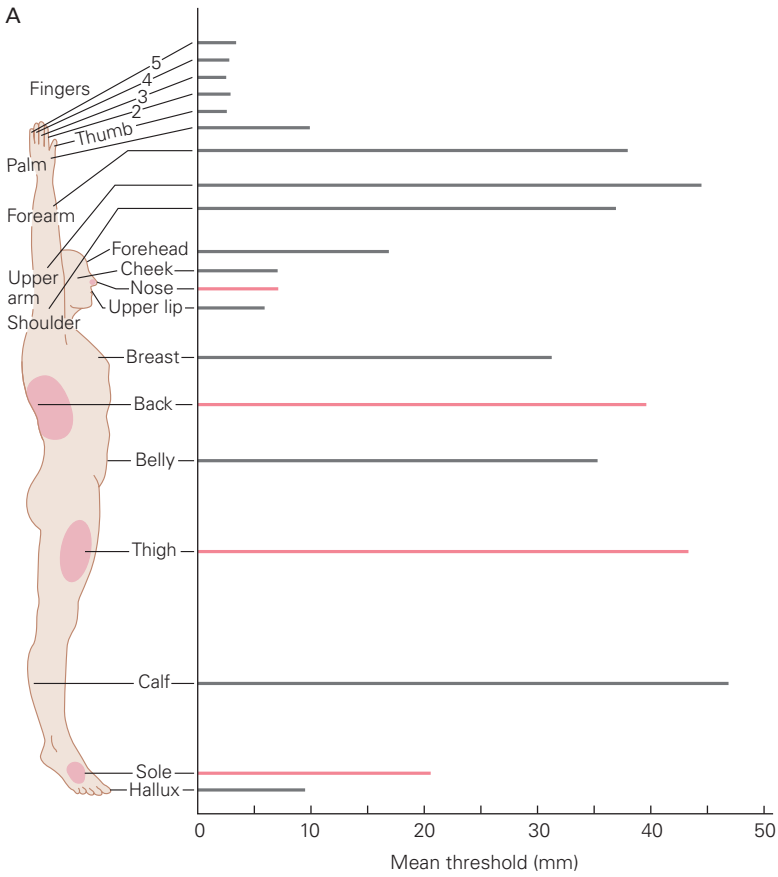

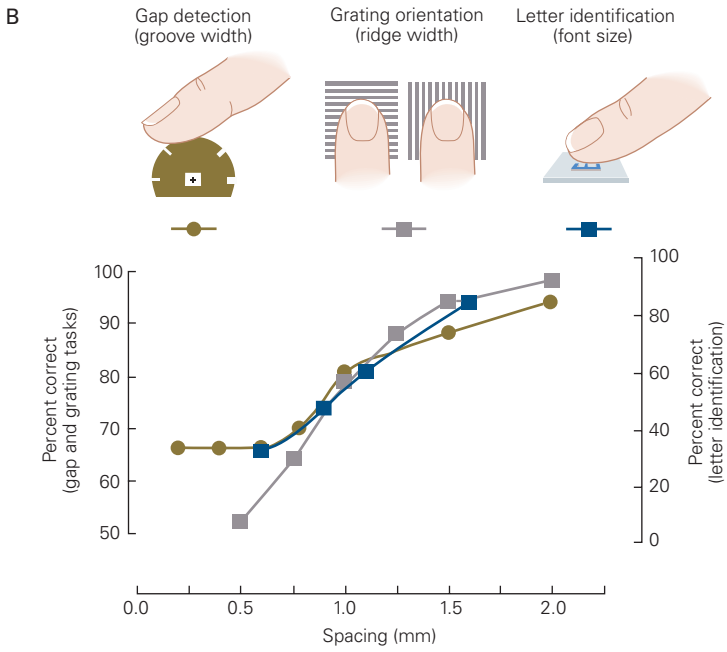

Figure 19–6 Tactile acuity in the human hand is highest on the fingertip.

A. The two-point threshold measures the minimum distance at which two stimuli are resolved as distinct. This distance varies for different body regions; it is approximately 2 mm on the fingers, but as much as 10 mm on the palm and 40 mm on the arm, thigh, and back. The mean two-point perceptual thresholds of different body parts, indicated by **pink** lines in the bar graph, match the mean receptive field diameters of the corresponding pink zones on the body. The greatest discriminative capacity is afforded in the fingertips, lips, and tongue, which have the smallest receptive fields. (Adapted, with permission, from Weinstein 1968. © Charles C. Thomas Publisher, Ltd.)

B. Spatial acuity is measured in psychophysical experiments by having a blindfolded subject touch a variety of textured surfaces. As shown here, the subject is asked to determine whether the surface of a wheel is smooth or contains a gap, whether the ridges of a grating are oriented across the finger or parallel to its long axis, or which letters appear on raised type used in letterpress printing. The tactile acuity threshold is defined as the groove width, ridge width, or font size that yields 75% correct performance (detectable midway between chance and perfect accuracy). The threshold spacing on the human fingertip is 1.0 mm in each of these tests. (Adapted, with permission, from Johnson and Phillips 1981.)

movement enhances the sensations produced by the dots. Because the Braille dots are spaced approximately 3 mm apart, a distance greater than the receptive field diameter of an SA1 fiber, each dot stimulates a different set of SA1 fibers. An SA1 fiber fires a burst of action potentials as a dot enters its receptive field and is silent once the dot leaves the field (Figure 19–7). Specific combinations of SA1 fibers that fire synchronously signal the spatial arrangement of the Braille dots. RA1 fibers also discriminate the dot patterns, enhancing the signals provided by SA1 fibers.

Although Pacinian corpuscles (RA2 fibers) respond to scanning Braille dots over the skin, their spike trains do not reflect the periodicity of dots in the Braille patterns. Instead, they signal the skin vibrations evoked by motion of the Braille dots over the skin. Sliman Bensmaia and colleagues recently found that when fine textures such as fabrics are tested with this method, RA2 afferents signal the periodicity of threads in the weave by generating their spike trains in phase with these surface features. SA1 fibers are less responsive to motion of textiles because the thread size is usually too small to indent the skin at sufficient amplitude. Nevertheless, all three types of tactile afferents contribute to human percepts of roughness and smoothness.

Slowly Adapting Fibers Detect Object Pressure and Form

The most important function of SA1 and SA2 fibers is their ability to signal skin deformation and pressure. The sensitivity of SA1 receptors to edges, corners, points, and curvature provides information about an object's compliance, shape, size, and surface texture. We perceive an object as hard or rigid if it indents the skin when we touch it, and soft if we deform the object.

Paradoxically, as an object's size and diameter increase, its surface curvature decreases. The responses of individual SA1 fibers are weaker and the resulting sensations feel less distinct. For example, the tip of a pencil pressed 1 mm into the skin feels sharp, unpleasant, and highly localized at the contact point, whereas a 1-mm indentation by the eraser feels blunt and broad. The weakest sensation is evoked by a flat surface pressed against the finger pad.

To understand why these objects evoke different sensations, we need to consider the physical events that occur when the skin is touched. When a pencil tip is pressed against the skin, it dimples the surface at the contact point and forms a shallow, sloped basin in the surrounding region (approximately 4 mm in radius). Although the indentation force is concentrated in the center, the surrounding region is also perturbed by local stretch, called tensile strain. SA1 receptors at both the center and the surrounding "hillsides" of skin are stimulated, firing spike trains proportional to the degree of local stretch.

If a second probe is pressed close to the first one, more SA1 fibers are stimulated but the neural response of each fiber is reduced because the force needed to displace the skin is shared between the two probes. Ken Johnson and his colleagues have shown that as more probes are added within the receptive field, the response intensity at each sensory ending becomes progressively weaker because the displacement forces on the skin are distributed across the entire contact zone. Thus, the skin mechanics result in a case of "less is more." Individual SA1 fibers respond more vigorously to a small object than to a large one because the force needed to indent the skin is concentrated at a small contact point. In this manner, each SA1 fiber integrates the local skin indentation profile within its receptive field.

The sensitivity of SA1 receptors to local strain on the skin enables them to detect edges, the places where an object's curvature changes abruptly. SA1 firing rates are many times greater when a finger touches an edge than when it touches a flat surface because the force applied by an object boundary displaces the skin asymmetrically, beyond the edge as well as at the edge. This asymmetric distribution of force enhances responses from receptive fields located along the edges of an object. As edges are often perceived as sharp, we tend to grasp objects on flat or gently curved surfaces rather than by their edges.

The SA2 fibers that innervate Ruffini endings respond more vigorously to stretch of the skin than to indentation, because of their anatomical location along the palmar folds or at the finger joints. They provide information about the shape of large objects grasped with the entire hand, the "power grasp" in which an object is pressed against the palm.

The SA2 system may play a central role in stereognosis—the recognition of three-dimensional objects using touch alone—as well as other perceptual tasks in which skin stretch is a major cue. Benoni Edin has shown that SA2 innervation of the hairy skin on the dorsum of the hand plays a substantial role in the perception of hand shape and finger position. The SA2 fibers aid the perception of finger joint angle by detecting skin stretch over the knuckles, or in the webbing between the fingers. The Ruffini endings near these joints are aligned such that different groups of receptors are stimulated as the fingers move in specific directions (Figure 19–5A, bottom panel). In this manner, the SA2 system provides a neural representation

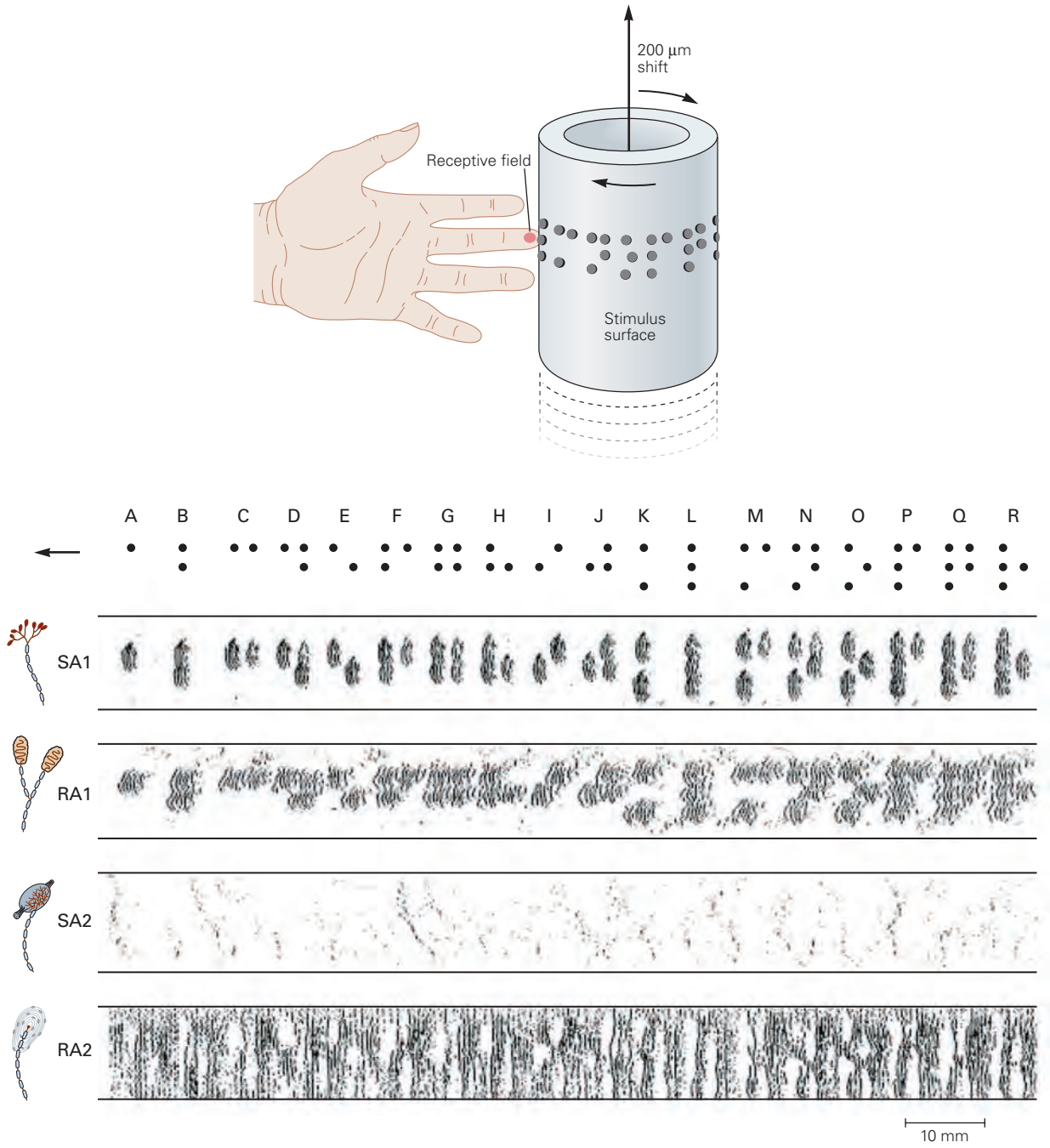

Figure 19–7 Responses of touch receptors to Braille dots scanned by the fingers. The Braille symbols for the letters A through R were mounted on a drum that was repeatedly rotated against the fingertip of a human subject. Following each revolution, the drum was shifted upward so that another portion of the symbols was scanned across the finger. Microelectrodes placed in the median nerve of this subject recorded the responses of the mechanoreceptive fibers innervating the fingertip. The action potentials discharged by the nerve fibers as the Braille symbols moved over the receptive field are represented in these records by small dots; each horizontal row of dots represents the responses of the fiber to a single revolution of the drum. The SA1 receptors register the sharpest image of the Braille symbols, representing each Braille dot with a series of action potentials and falling silent when the spaces between Braille symbols provide no stimulation. RA1 receptors provide a blurred image of the Braille symbols because their receptive fields are larger, but the individual dot patterns are still recognizable. Neither RA2 nor SA2 receptors are able to encode the spatial characteristics of the Braille patterns because their receptive fields are larger than the dot spacing. The high firing rate of the RA2 fibers reflects the keen sensitivity of Pacinian corpuscles to vibration. (Abbreviations: **RA1**, rapidly adapting type 1; **RA2**, rapidly adapting type 2; **SA1**, slowly adapting type 1; **SA2**, slowly adapting type 2.) (Reproduced, with permission, from Phillips, Johansson, and Johnson 1990. Copyright © 1990 Society for Neuroscience.)

of skin stretch over the entire hand, a proprioceptive rather than exteroceptive function.

The SA2 fibers also provide proprioceptive information about hand shape and finger movements when the hand is empty. If the fingers are fully extended and abducted, we feel the stretch in the palm and proximal phalanges as the glabrous skin is flattened. Similarly, if the fingers are fully flexed, forming a fist, we feel the stretch of the skin on the back of the hand, particularly over the metacarpal-phalangeal and proximal interphalangeal joints. Humans use this proprioceptive information to preshape their hand to grasp objects efficiently, opening the fingers just wide enough to clear the object and grasp it skillfully without too much force.

Rapidly Adapting Fibers Detect Motion and Vibration

Tests of vibration sense form an important component of the neurological exam. Touching the skin with a tuning fork that oscillates at a particular frequency evokes a periodic buzzing sensation because most touch receptors fire synchronized, periodic trains of action potentials in phase with the stimulus frequency (Figure 19–8A2). Vibration sense is a useful measurement of dynamic sensitivity to touch, particularly in cases of localized nerve damage.

The RA2 receptor, the Pacinian corpuscle, is the most sensitive mechanoreceptor in the somatosensory system. It is exquisitely responsive to high-frequency (30–500 Hz) vibratory stimuli and can detect vibration of 250 Hz in the nanometer range (Figure 19–8B2). The ability of Pacinian corpuscles to filter and amplify high-frequency vibration allows us to feel conditions at the working surface of a tool in our hand as if our fingers themselves were touching the object under the tool. The clinician uses this exquisite sensitivity to guide a needle into a blood vessel and to probe tissue stiffness. The auto mechanic uses vibratory sense to position wrenches on unseen bolts. We can write in the dark because we feel the vibration of the pen as it contacts the paper and transmits the frictional forces from the surface roughness to our fingers.

Although Pacinian corpuscles have the lowest vibration thresholds for frequencies greater than 40 Hz (Figure 19–8B2), vibratory stimuli of higher amplitude also excite SA1 and RA1 fibers, even if their evoked spike trains are weaker than those of Pacinian afferents. Figure 19–9A illustrates the evoked firing patterns of 15 different peripheral nerve fibers stimulated at 20 Hz at weak, moderate, and high amplitudes. Although these fibers differ in sensitivity to vibration, their spike trains have certain important characteristics in common. First, each neuron fires at a particular phase of the vibratory cycle, usually when the probe indents the skin, and its phasic pattern of spikes replicates the vibratory frequency: when stimulated at 20 Hz, the spike bursts recur at intervals of approximately 50 ms. The patterning of the spike trains is further reinforced because the population of fibers fires synchronously, enabling the frequency information to be preserved centrally due to synaptic integration.

The total number of spikes per burst also increases as the stimulus amplitude rises, allowing each fiber to multiplex signals of vibratory frequency and intensity: the frequency information is conveyed by the temporal pattern of the spike train, and the vibratory amplitude is encoded by the total number of spikes fired per second by each fiber, as well as the total spike output of the ensemble of activated fibers. Finally, note that the spike trains of each neuron are very similar in time course and spike count from trial to trial for each condition, indicating the high reliability of sensory signaling provided by tactile afferent fibers. This reliability and predictability of sensory coding make vibration a particularly useful technique for assessing the sense of touch.

Both Slowly and Rapidly Adapting Fibers Are Important for Grip Control

In addition to their role sensing the physical properties of objects, touch receptors provide important information concerning hand actions during skilled movements. Roland Johansson and Gören Westling used microneurography to determine the role of touch receptors when objects are grasped in the hand. By placing microelectrodes in the median nerve, they were able to record the firing patterns of touch fibers as an object was initially contacted by the fingers, and when it was grasped between the thumb and index finger, lifted, held above a table, lowered, and returned to rest.

They found that all four classes of touch fibers respond to grasp and that each fiber type monitors a particular function. The RA1, RA2, and SA1 fibers are normally silent in the absence of tactile stimuli. They detect contact when an object is first touched (Figure 19–10). The SA1 fibers signal the amount of grip force applied by each finger, and the RA1 fibers sense how quickly the grasp is applied. The RA2 fibers detect the small shock waves transmitted through the object when it is lifted from the table and when it is returned. We know when an object makes contact with the table top because of these vibrations and therefore can

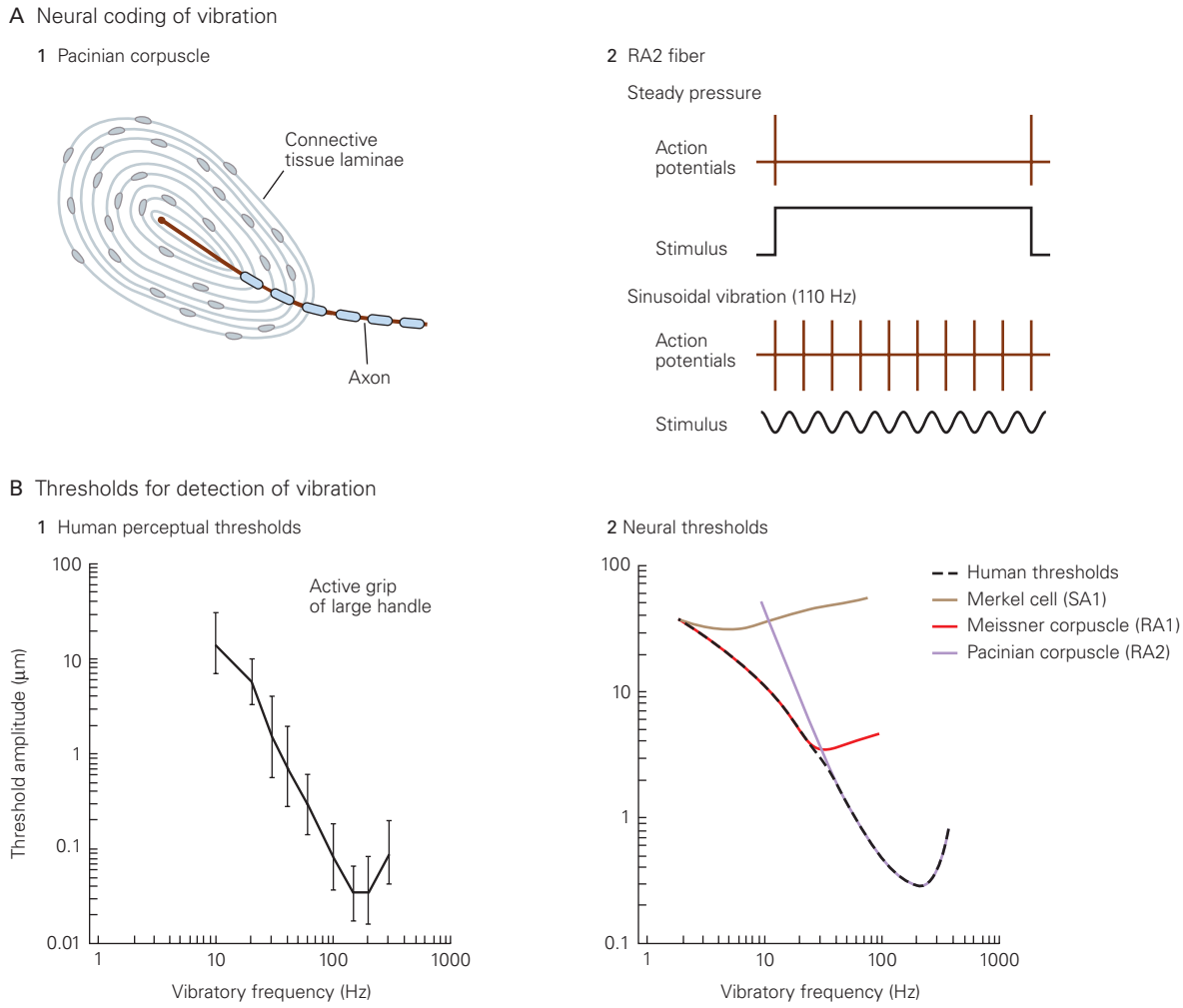

Figure 19–8 **Rapidly adapting type 2 (RA2) fibers have the lowest threshold for vibration.** Vibration is the sensation produced by sinusoidal stimulation of the skin, as by the hum of an electric motor, the strings of a musical instrument, or a tuning fork used in the neurological examination.

A. **1.** The Pacinian corpuscle consists of concentric, fluid-filled lamellae of connective tissue that encapsulate the terminal of an RA2 fiber. This structure is uniquely suited to the detection of motion. Sensory transduction in the RA2 fiber occurs in stretch-sensitive cation channels linked to the inner lamellae of the capsule. **2.** When steady pressure is applied to the skin, the RA2 fiber fires a burst at the start and end of stimulation. In response to sinusoidal stimulation (vibration), the fiber fires at regular intervals such that each action potential signals one cycle of the stimulus. Our perception of vibration as a rhythmically repeating event results from the simultaneous activation of many RA2 units, which fire in synchrony. (Adapted from Talbot et al. 1968.)

B. **1.** Psychophysical thresholds for detection of vibration depend on the stimulation frequency. As shown here, humans can detect vibrations as small as 30 nm at 200 Hz when grasping a large object; the threshold is higher at other frequencies and when tested with small probes. (Adapted, with permission, from Brisben, Hsiao, and Johnson 1999.) **2.** Human thresholds for vibration, measured by a small probe tip indenting the skin, match those of the most sensitive touch fibers in each frequency range. Each type of mechanosensory fiber is most sensitive to a specific range of frequencies. Slowly adapting type 1 (**SA1**) fibers are the most sensitive population below 5 Hz, rapidly adapting type 1 (**RA1**) fibers between 10 Hz and 50 Hz, and RA2 fibers above 50 Hz and 400 Hz. (Adapted, with permission, from Mountcastle, LaMotte, and Carli 1972, and Johansson, Landström, and Lundström 1982.)

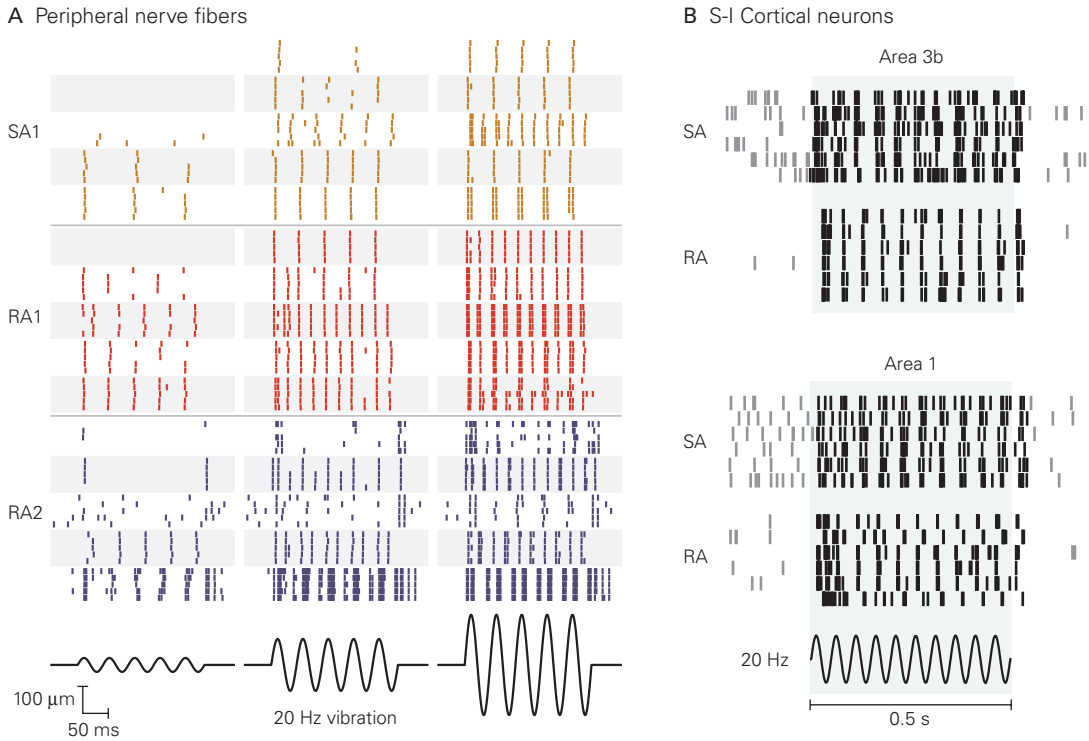

Figure 19–9 Suprathreshold vibration activates multiple classes of touch receptors.

A. Rasters of spike trains recorded from 15 different somatosensory fibers in macaque monkeys stimulated by 20-Hz vibratory stimuli with amplitudes of 35 (*left*), 130 (*center*), and 250 µm (*right*). The alternating **shaded and white bands** indicate the responses of individual slowly adapting type 1 (**SA1**), rapidly adapting type 1 (**RA1**), and rapidly adapting type 2 (**RA2**) touch fibers to five presentations of the same stimulus. Neural responses are grouped in bursts of one or more spikes that occur in phase with the indentation phase of each vibratory cycle. The total number of spikes per cycle in each fiber is correlated with the amplitude of the vibration; the total number of spikes fired across this population also reflects the vibratory amplitude. Although the individual neurons differ in the intensity of their responses, the spike trains of each touch fiber are very similar from trial to trial and occur synchronously between neurons. (Adapted, with permission, from Muniak et al. 2007. Copyright © 2007 Society for Neuroscience.)

B. S-I cortical responses to 20-Hz vibration. Rasters of spike trains evoked in two neurons in area 3b (**top**) and two neurons in area 1 (**bottom**) of S-I cortex of a macaque monkey. The **shaded area** indicates the period of vibratory stimulation. As in the peripheral nerves, S-I cortical neurons respond to low-frequency vibration with bursts of impulses in phase with the stimulation rate. Note that the spike trains vary somewhat from trial to trial and are less periodic in area 1 than in area 3b. The periodicity of firing is even less pronounced in S-II cortex (see Figure 19–21) than in S-I. (Abbreviations: **RA**, rapidly adapting; **SA**, slowly adapting.) (Adapted, with permission, from Salinas et al. 2000. Copyright © 2000 Society for Neuroscience.)

manipulate the object without looking at it. The RA1 and RA2 fibers cease responding after grasp is established. The SA2 fibers signal flexion or extension of the fingers during grasp or release of the object and thereby monitor the hand posture as these movements proceed.

Signals from the hand that report on the shape, size, and texture of an object are important factors governing the application of force during grasping. Johansson and his colleagues found that we lift and manipulate an object with delicacy—with grip forces that just exceed the forces that result in overt slip—and that the grip force is adjusted automatically to compensate for differences in the frictional coefficient between the fingers and object surface. Subjects predict how much force is required to grasp and lift an object and modify these forces based on tactile information provided by SA1 and RA1 afferents. Objects with smooth surfaces are grasped more firmly than those with rough textures, properties coded by RA1 afferents during initial contact of the hand with an object. The significance of the tactile information in grasping is seen in cases of nerve injury or during local anesthesia of the hand; patients apply unusually high grip forces, and coordination between the grip and load forces applied by the fingers is poor.

The information supplied by the RA1 receptors to monitor grasping actions is critical for grip control,

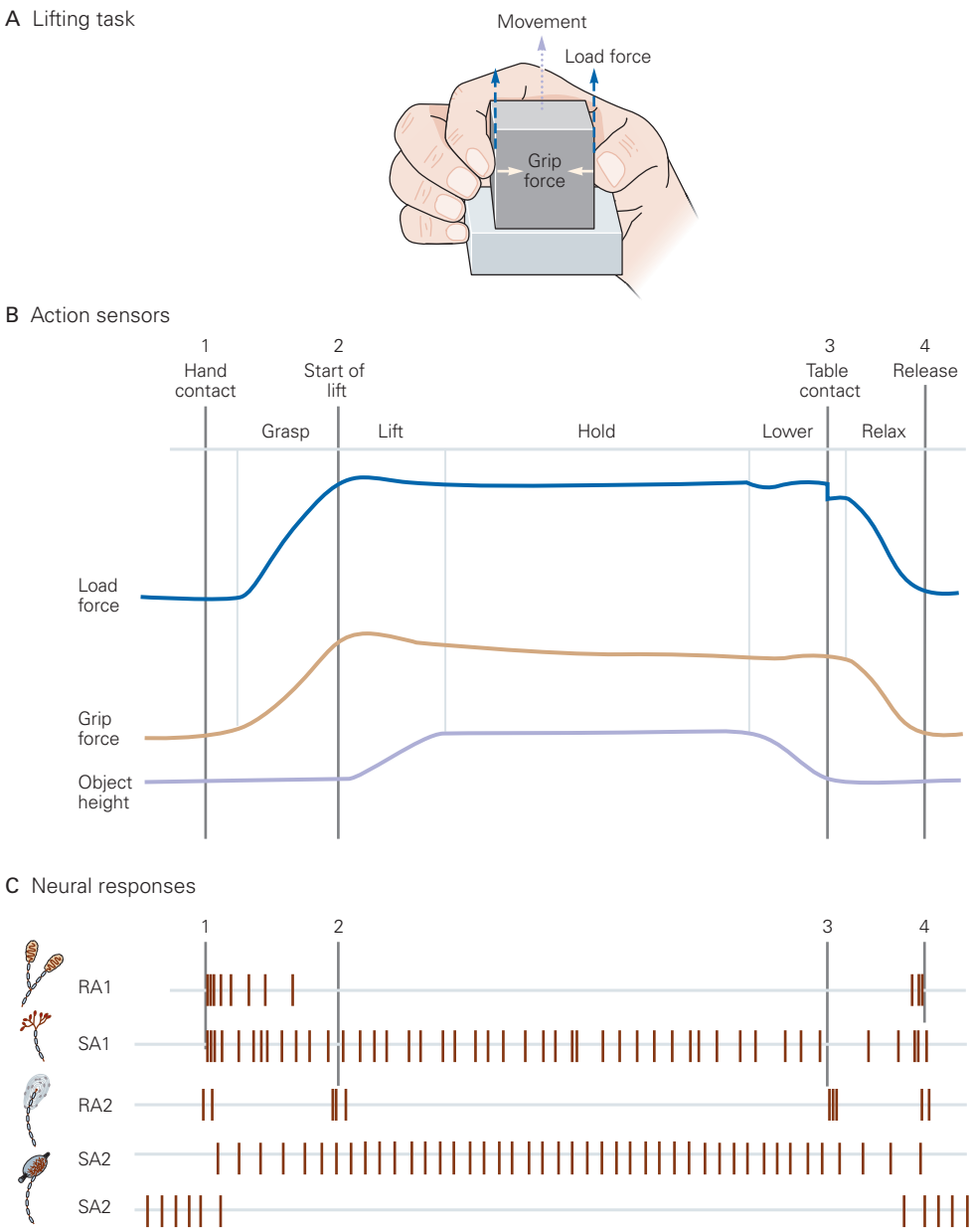

Figure 19–10 Sensory information from the hand during grasping and lifting. (Adapted, with permission, from Johansson 1996.)

A. The subject grasps and lifts a block between the thumb and fingertips, holds it above a table, and then returns it to the resting position. The normal (grip) force secures the object in the hand, and the tangential (load) force overcomes gravity. The grip force is adapted to the surface texture and weight of the object.

B. The grip and load forces are monitored with sensors in the object. These forces are coordinated following contact with the object, stabilize as lift begins, and relax in concert after the object is returned to the table.

C. All four mechanoreceptors detect hand contact with the object, but each monitors a different aspect of the action as the task progresses. SA1 fibers encode the grip force and SA2 fibers the hand posture. RA1 fibers encode the rate of force application and movement of the hand on the object. RA2 fibers sense vibrations in the object during each task phase: at hand contact, lift-off, table contact, and release of grasp. (Abbreviations: **RA1**, rapidly adapting type 1; **RA2**, rapidly adapting type 2; **SA1**, slowly adapting type 1; **SA2**, slowly adapting type 2.)

allowing us to hold on to objects when perturbations cause them to slip unexpectedly. RA1 fibers are silent during steady grasp and usually remain quiet until the object is returned to rest and the grasp released. However, if the object is unexpectedly heavy or jolted by external forces and begins to slip from the hand, the RA1 fibers fire in response to the small tangential slip movements of the object. The net result of this RA1 activity is that grip force is increased by signals from the motor cortex.

Tactile Information Is Processed in the Central Touch System

Sensory afferent fibers innervating the hand transmit tactile and other somatosensory information to the central nervous system through the median, ulnar, and superficial radial nerves. These nerves terminate ipsilaterally in spinal segments C6 to T1; other branches of these fibers project through the ipsilateral dorsal columns directly to the medulla, where they make synaptic connections to neurons in the cuneate nucleus, the lateral division of the dorsal column nuclei (Figure 19–11).

Spinal, Brain Stem, and Thalamic Circuits Segregate Touch and Proprioception

Fibers in the dorsal columns, and neurons in the dorsal column nuclei, are organized topographically, with the upper body (including the hand) represented laterally in the cuneate fascicle and nucleus and the lower body represented medially in the gracile fascicle and nucleus. The somatosensory submodalities of touch and proprioception are also segregated functionally in these regions, as individual spinal and brain stem neurons receive synaptic inputs from afferents of a single type, and neurons of distinct types are spatially separated. The rostral third of the dorsal column nuclei is dominated by neurons that process proprioceptive information from muscle afferents; tactile inputs predominate more caudally. Modality segregation is a consistent feature of the projection pathways to the primary somatosensory cortex.

Neurons in the dorsal column nuclei project their axons across the midline in the medulla to form the *medial lemniscus*, a prominent fiber tract that transmits tactile and proprioceptive information from the contralateral side of the body through the pons and midbrain to the thalamus. As a result of this crossing (or decussation) of sensory fibers, the left side of the brain receives somatosensory input from mechanoreceptors on the right side of the body, and vice versa. In transit, the somatotopic representation of the body in the medial lemniscus and within the thalamus becomes inverted; the topographic map of the body displays the face medially, the lower body laterally, and the upper body and hands in between.

Tactile and proprioceptive information from the hand and other regions of the body is processed in distinct subnuclei of the thalamus. Touch signals from the limbs and trunk are sent via the medial lemniscus to the ventral posterior lateral (VPL) nucleus, while those from the face and mouth are conveyed to the ventral posterior medial (VPM) nucleus. Proprioceptive information from muscles and joints, including those of the hand, is transmitted to the ventral posterior superior (VPS) nucleus. These nuclei send their outputs to different subregions of the parietal lobe of the cerebral cortex. The VPL and VPM nuclei transmit cutaneous information primarily to area 3b of the primary somatosensory

Figure 19–11 (Opposite) Somatosensory information from the limbs and trunk is conveyed to the thalamus and cerebral cortex by two ascending pathways. Brain slices along the neuraxis from the spinal cord to the cerebrum illustrate the anatomy of the two principal pathways conveying somatosensory information to the cerebral cortex. The two pathways are separated until they reach the pons, where they are juxtaposed.

Dorsal column—medial lemniscal system (orange). Touch and limb proprioception signals are conveyed to the spinal cord and brain stem by large-diameter myelinated nerve fibers and transmitted to the thalamus in this system. In the spinal cord, the fibers for touch and proprioception divide, one branch going to the ipsilateral spinal gray matter and the other ascending in the ipsilateral dorsal column to the medulla. The second-order fibers from neurons in the dorsal column nuclei cross the midline in the medulla and ascend in the contralateral medial lemniscus toward the thalamus, where they terminate in the lateral and medial ventral posterior nuclei. Thalamic neurons in these nuclei convey tactile and proprioceptive information to the primary somatosensory cortex.

Anterolateral system (brown). Pain, itch, temperature, and visceral information is conveyed to the spinal cord by small-diameter myelinated and unmyelinated fibers that terminate in the ipsilateral dorsal horn. This information is conveyed across the midline by neurons within the spinal cord and transmitted to the brain stem and the thalamus in the contralateral anterolateral system. Anterolateral fibers terminating in the brain stem compose the spinoreticular and spinomesencephalic tracts; the remaining anterolateral fibers form the spinothalamic tract.

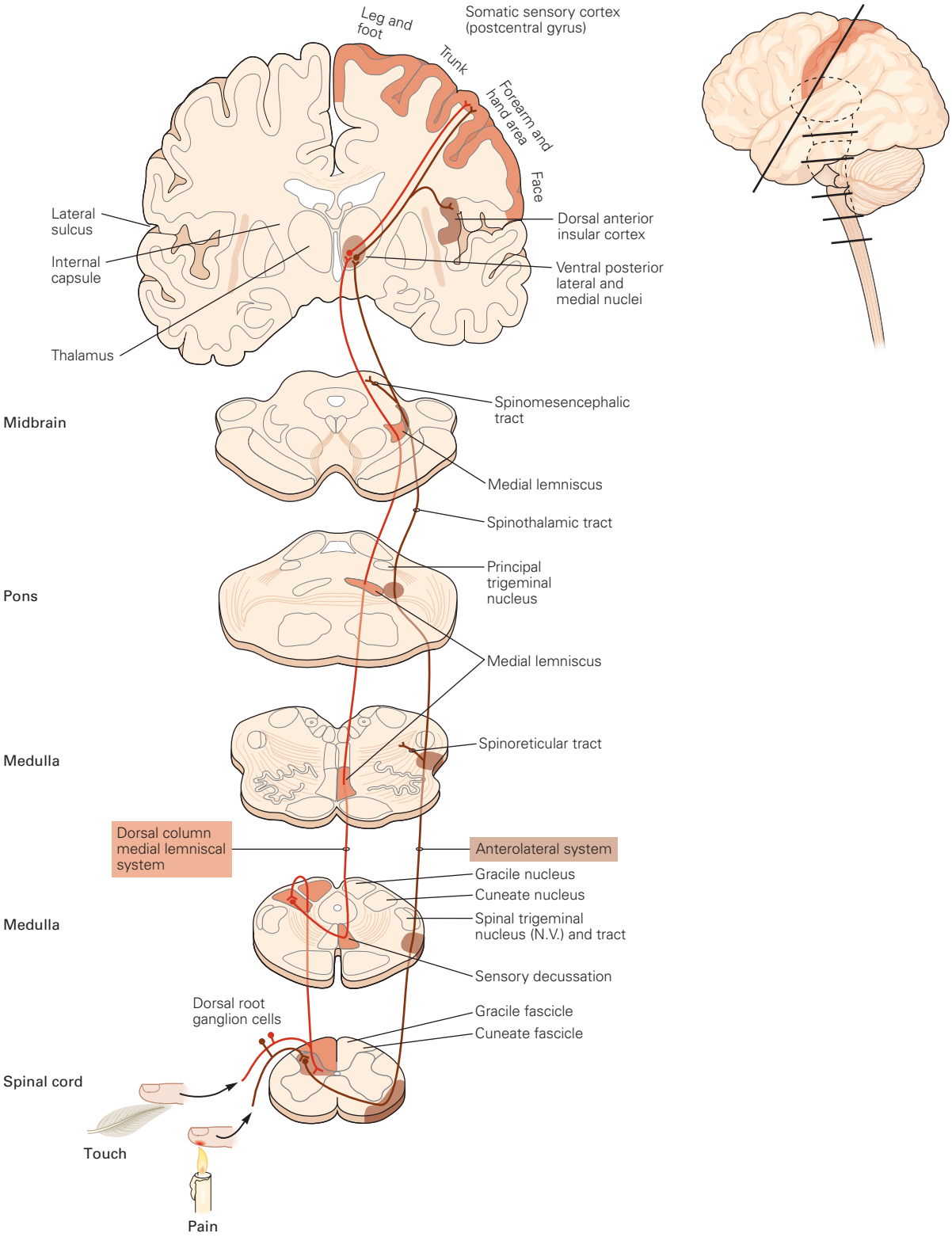
Leg and foot
Somatic sensory cortex (postcentral gyrus)
Trunk
Forearm and hand area
Face
Lateral sulcus
Internal capsule
Thalamus
Dorsal anterior insular cortex
Ventral posterior lateral and medial nuclei
Midbrain
Spinomesencephalic tract
Medial lemniscus
Spinothalamic tract
Pons
Principal trigeminal nucleus
Medial lemniscus
Medulla
Spinoreticular tract
Dorsal column medial lemniscal system
Anterolateral system
Medulla
Gracile nucleus
Cuneate nucleus
Spinal trigeminal nucleus (N.V.) and tract
Sensory decussation
Dorsal root ganglion cells
Gracile fascicle
Cuneate fascicle
Spinal cord
Touch
Pain

cortex (S-I), whereas the VPS nucleus conveys proprioceptive information principally to area 3a.

The Somatosensory Cortex Is Organized Into Functionally Specialized Columns

Conscious awareness of touch is believed to originate in the cerebral cortex. Tactile information enters the cerebral cortex through the primary somatosensory cortex (S-I) in the postcentral gyrus of the parietal lobe. The primary somatic sensory cortex comprises four cytoarchitectural areas: Brodmann's areas 3a, 3b, 1, and 2 (Figure 19–12). These areas are interconnected such that processing of sensory information in S-I involves both serial and parallel processing.

In a series of pioneering studies of the cerebral cortex, Vernon Mountcastle discovered that S-I cortex is organized into vertical columns or slabs. Each column is 300 to 600 μm wide and spans all six cortical layers from the pial surface to the white matter (Figure 19–13). Neurons within a column receive inputs from the same local area of skin and respond to the same class or classes of touch receptors. A column therefore comprises an elementary functional module of the neocortex; it provides an anatomical structure that organizes sensory inputs to convey related information about location and modality.

The columnar organization of the cortex is a direct consequence of intrinsic cortical circuitry, the projection patterns of thalamocortical axons, and migration pathways of neuroblasts during cortical development. The pattern of connections within a column is oriented vertically, perpendicular to the cortical surface. Thalamocortical axons terminate primarily on clusters of stellate cells in layer IV, whose axons project vertically toward the surface of the cortex, as well as on star pyramid cells. Thus, thalamocortical inputs are relayed to a narrow column of pyramidal cells that are contacted by the layer IV cell axons. The apical dendrites and axons of cortical pyramidal cells in other cortical layers are also largely oriented vertically, parallel to the thalamocortical axons and stellate cell axons (Figure 19–14). This allows the same information to be processed by a column of neurons throughout the thickness of the cortex.

Pyramidal neurons form the principal excitatory class of somatosensory cortex; they compose approximately 80% of S-I neurons. Pyramidal neurons in

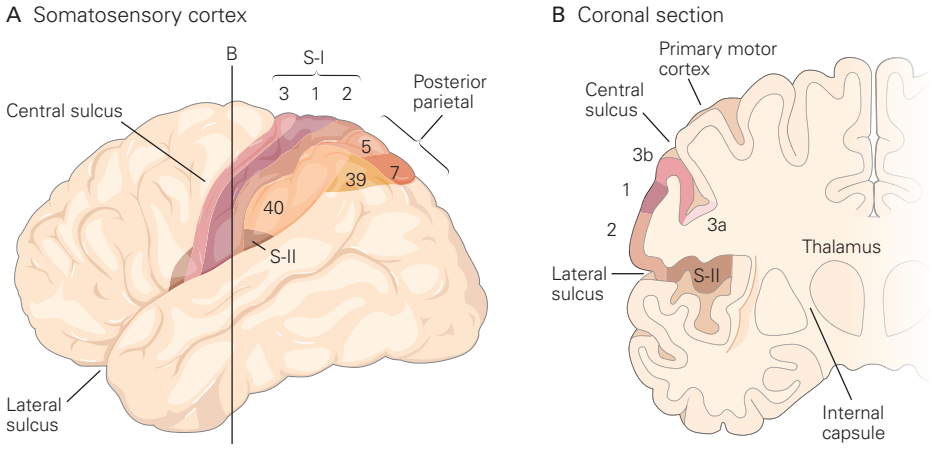

Figure 19–12 The somatosensory areas of the cerebral cortex in the human brain.

A. The somatosensory areas of cortex lie in the parietal lobe and consist of three major divisions. The *primary somatosensory cortex* (**S-I**) forms the anterior part of the parietal lobe. It extends throughout the postcentral gyrus beginning at the bottom of the central sulcus, extending posteriorly to the postcentral sulcus, and into the medial wall of the hemisphere to the cingulate gyrus (not shown). The S-I cortex comprises four distinct cytoarchitectonic regions: Brodmann's areas 3a, 3b, 1, and 2. The *secondary somatosensory cortex* (**S-II**) is located on the upper bank of the lateral sulcus (Sylvian fissure) and on the parietal operculum; it covers Brodmann's area 43. The *posterior parietal cortex* surrounds the intraparietal sulcus on the lateral surface of the hemisphere, extending from the postcentral sulcus to the parietal-occipital sulcus and medially to the precuneus. The superior parietal lobule (Brodmann's areas 5 and 7) is a somatosensory area; the inferior parietal lobule (areas 39 and 40) receives both somatosensory and visual inputs.

B. A coronal section through the postcentral gyrus illustrates the anatomical relationship of S-I, S-II, and the primary motor cortex (area 4). S-II lies adjacent to area 2 in S-I and extends medially along the upper bank of the lateral sulcus to the insular cortex. The primary motor cortex lies rostral to area 3a within the anterior wall of the central sulcus.

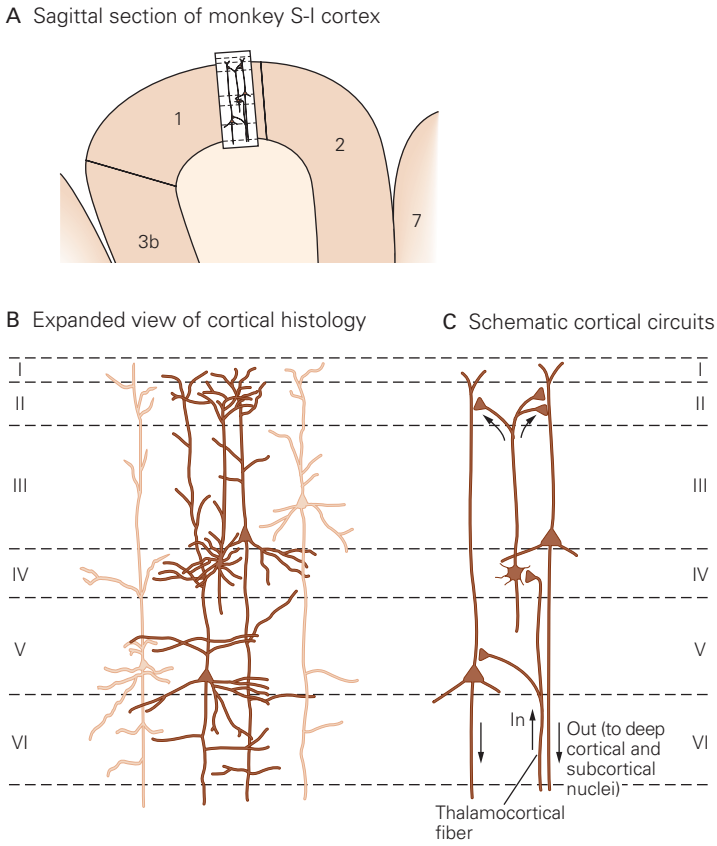

Figure 19–13 Organization of neuronal circuits within a column of somatosensory cortex. Sensory inputs from the skin or deep tissue are organized in columns of neurons that run from the surface of the brain to the white matter. Each column receives thalamic input primarily in layer IV from one part of the body. Excitatory neurons in layer IV send their axons vertically toward the surface of the cortex, contacting the dendrites of pyramidal neurons in layers II and III (supragranular layers) as well as the apical dendrites of pyramidal cells in the infragranular layers (layers V and VI). In this manner, tactile information from a body part such as a finger is distributed vertically within a column of neurons.

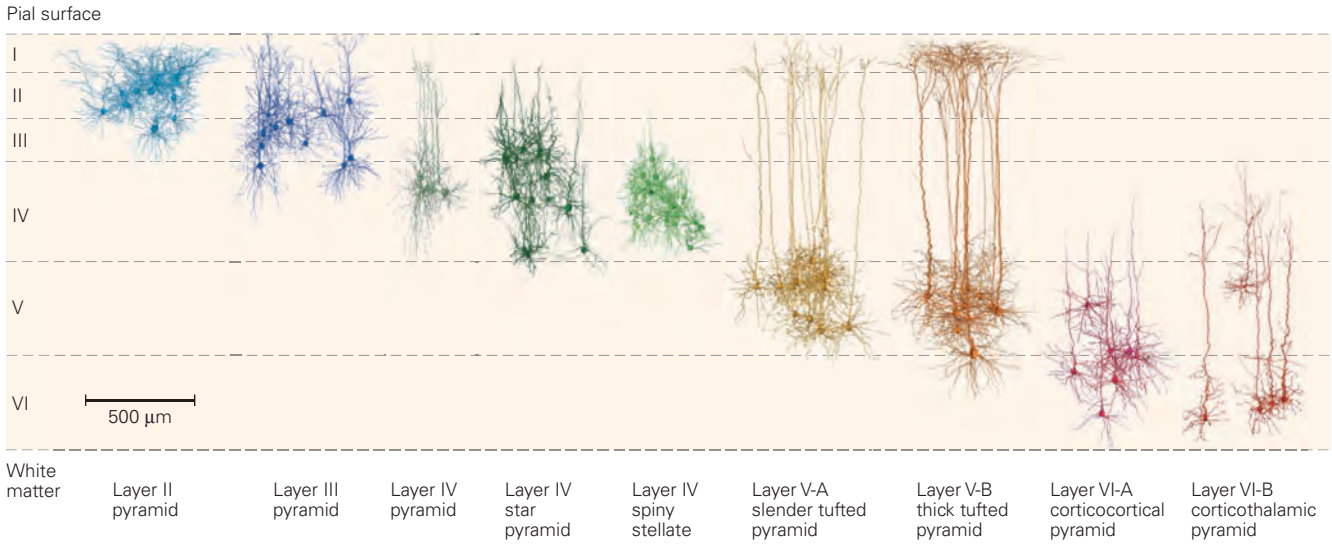

Figure 19–14 Columnar organization of the somatosensory cortex. Cortical excitatory neurons in the six layers have distinctive pyramidal-type shapes with large cell bodies, a single apical dendrite that projects vertically toward the cortical surface and arborizes in more superficial layers, and multiple basal dendrites that arborize close to the cell body. Pyramidal neurons differ in size, gene expression patterns, the length and thickness of their apical dendrite, and the projection targets of their axons. All of these neurons synapse on targets within the cerebral cortex. Additionally, the pyramidal neurons in layer V project subcortically to the spinal cord, brain stem, midbrain, and basal ganglia. Corticothalamic neurons in layer VI project back to the afferent thalamic nucleus providing sensory input to that column. Spiny stellate neurons in layer IV are the only excitatory cells shown that are not pyramidal neurons. (Adapted, with permission, from Oberlaender et al. 2012.)

each of the six cortical layers project to specific targets (Figure 19–14). Recurrent horizontal connections link pyramidal neurons in the same or neighboring columns, allowing them to share information when activated simultaneously by the same stimulus. Neurons in layers II and III also project to layer V in the same column, to higher cortical areas in the same hemisphere, and to mirror-image locations in the opposite hemisphere. These feedforward connections to higher cortical areas allow complex signal integration, as described later in this chapter.

Pyramidal neurons in layer V provide the principal output from each column. They receive excitatory inputs from neurons in layers II and III in the same and adjacent columns as well as sparse thalamocortical inputs. Neurons in the superficial portion of layer V (layer V-A) send feedforward outputs bilaterally to layer IV of higher-order cortical areas (see Figure 19–17C) as well as to the striatum. Neurons deeper in layer V (layer V-B) project to subcortical structures, including the basal ganglia, superior colliculus, pontine and other brain stem nuclei, the spinal cord, and dorsal column nuclei. Layer VI neurons project to local cortical neurons, and back to the thalamus, particularly to regions of the ventral posterior nuclei providing inputs to that column.

In addition to feedforward signals of information from touch receptors, feedback signals from layers II and III of higher somatosensory cortical areas are provided to layer I in lower cortical areas, regulating their excitability. Such feedback signals originate not only in somatosensory cortical areas but also in sensorimotor areas of the posterior parietal cortex, frontal motor areas, limbic areas, and regions of the medial temporal lobe involved in memory formation and storage. These feedback signals are thought to play a role in the selection of sensory information for cognitive processing (by the mechanisms of attention) and in short-term memory tasks. Feedback pathways may also gate sensory signals during motor activity. Various local inhibitory interneurons within each column serve to focus columnar output.

Cortical Columns Are Organized Somatotopically

The columns within the primary somatic sensory cortex are arranged topographically such that there is a complete somatotopic representation of the body in each of the four areas of S-I (Figure 19–15). The cortical map of the body corresponds roughly to the spinal dermatomes (see Figure 18–13). Sacral segments are represented medially, lumbar and thoracic segments centrally, cervical segments more laterally, and the trigeminal representation of the face at the most lateral portion of S-I cortex. Knowledge of the neural map of the body in the brain is important for localizing damage to the cortex from stroke or head trauma.

The body surface is represented in at least 10 distinct neural maps in the parietal lobe: four in S-I, four in S-II, and at least two in the posterior parietal cortex. As a result, these regions mediate different aspects of tactile sensation. Neurons in areas 3b and 1 of S-I process details of surface texture, whereas those in area 2 represent the size and shape of objects. These attributes of somatic sensation are further elaborated in S-II and the posterior parietal cortex, where neurons are engaged in object discrimination and manipulation, respectively.

Another important feature of somatotopic maps is the amount of cerebral cortex devoted to each body part. The neural map of the body in the human brain, termed the *homunculus*, does not duplicate exactly the spatial topography of the skin. Rather, each part of the body is represented in proportion to its importance to the sense of touch. Disproportionately large areas are

Figure 19–15 (Opposite) Each region of the primary somatosensory cortex contains a topographic neural map of the entire body surface. (Adapted, with permission, from Nelson et al. 1980. Copyright © 1980 Alan R. Liss, Inc.)

A. The primary somatosensory cortex in the macaque monkey lies caudal to the central sulcus as in the human brain. The colored areas on the macaque cortex correspond to the homologous Brodmann's areas of the human brain in Figure 19–12. Area 5 in the macaque monkey is homologous to areas 5 and 7 in humans. Area 7 in macaques is homologous to areas 39 and 40 in humans.

B. The flat map diagram on the right shows the somatosensory cortex of the macaque monkey unfolded along the central sulcus (**dotted line** that parallels the border between areas 3b and 1). The upper part of the diagram includes cortex unfolded from the medial wall of the hemisphere. Body maps were obtained from microelectrode recordings in the postcentral gyrus. The body surface is mapped to columns within rostrocaudal bands arranged in the order of the spinal dermatomes. The body maps in areas 3b and 1 form mirror images of the distal-proximal or dorsal-ventral axes of each dermatome. Each finger (D5–D1) has its own representation along the medial-lateral axis of the cortex in areas 3b and 1, but inputs from several adjacent fingers converge in the receptive fields of neurons in areas 2 and 5.

C. Cortical magnification of highly innervated skin areas. Although the trunk (**violet**) is covered by a greater area of skin than the fingers (**red**), the number of cortical columns responding to touch on the fingers is nearly three times the number activated by touching the trunk because of the higher innervation density of the fingers.

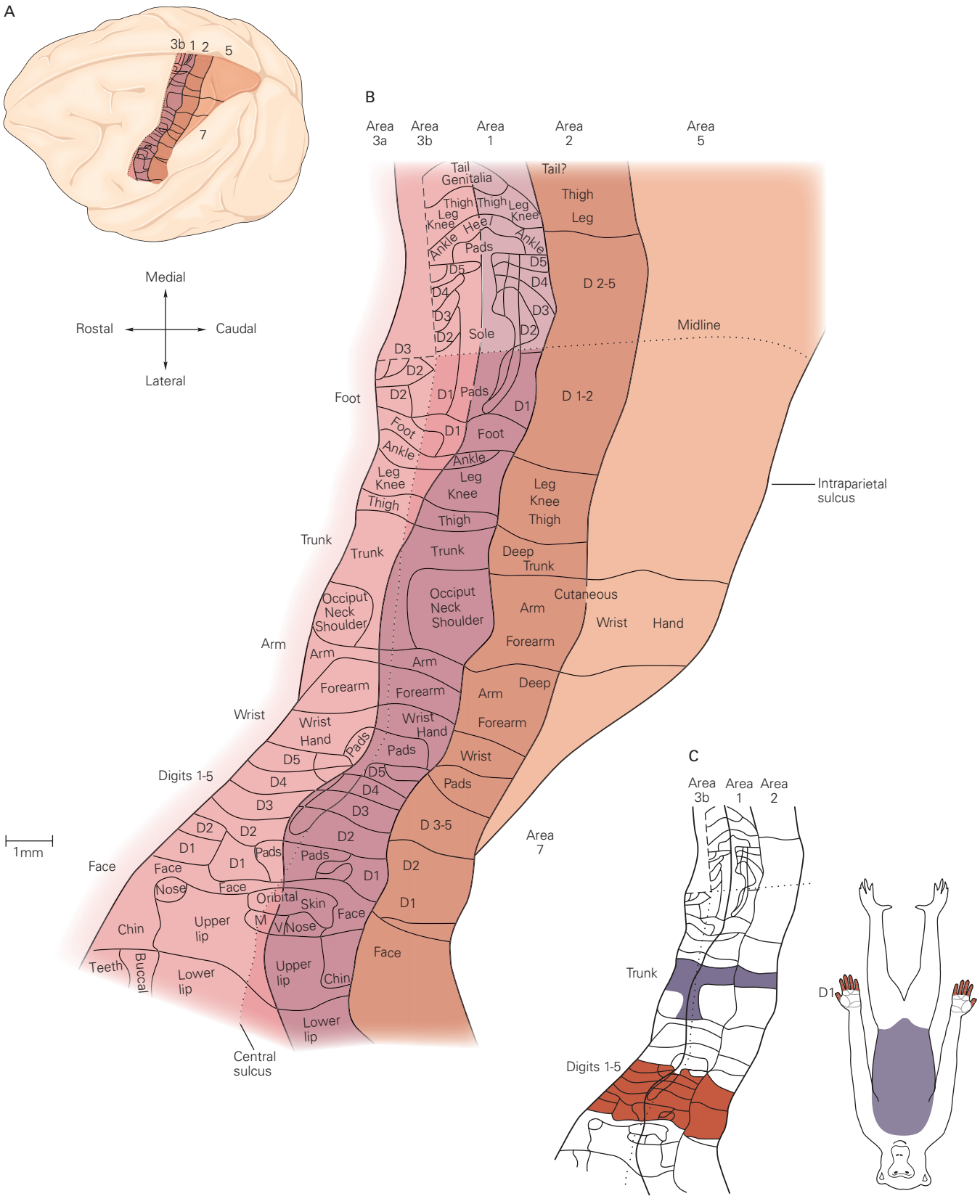
A
3b 1 2 5
7
Medial
Rostral
Caudal
Lateral
B
Area 3a
Area 3b
Area 1
Area 2
Area 5
Tail
Genitalia
Tail?
Thigh
Leg
Knee
Ankle
Hee
Pads
D5
D4
D3
D2
D1
Sole
D 2-5
D 1-2
Midline
Foot
Trunk
Occiput
Neck
Shoulder
Arm
Forearm
Wrist
Hand
Deep
Cutaneous
Intraparietal sulcus
Digits 1-5
Face
Nose
Oribital
Skin
M
V
Chin
Upper lip
Lower lip
Teeth
Buccal
Central sulcus
D 3-5
Area 7
1mm
C
Area 3b
Area 1
Area 2
Trunk
Digits 1-5
D1

devoted to certain body regions, particularly the hand, foot, and mouth, and relatively smaller areas to more proximal body parts. In humans and monkeys, more cortical columns are devoted to the fingers than to the entire trunk (Figure 19–15C).

The amount of cortical area devoted to a unit area of skin—called the *cortical magnification*—varies by more than a hundredfold across different body surfaces. It is closely correlated with the innervation density and thus the spatial acuity of the touch receptors in an area of skin. The areas with greatest magnification in the human brain—the lips, tongue, fingers, and toes—have tactile acuity thresholds of 0.5, 0.6, 1.0, and 4.5 mm, respectively.

Rodents and other mammals that probe the environment with their whiskers have a large number of columns in S-I, named *barrels*, that receive inputs from individual vibrissae on the face (Box 19–2). Barrel cortex provides a widely used experimental preparation for studying cortical circuitry.

Box 19–2 The Rodent Whisker-Barrel System

The rodent whisker-barrel system is a widely used animal model in modern neuroscience. Most mammals and all primates except man possess specialized tactile hairs on their face called *vibrissae*. Distinct from other hairs on the skin, vibrissae grow from a follicle that is densely innervated by the trigeminal cranial nerve and surrounded by a blood-filled sinus.

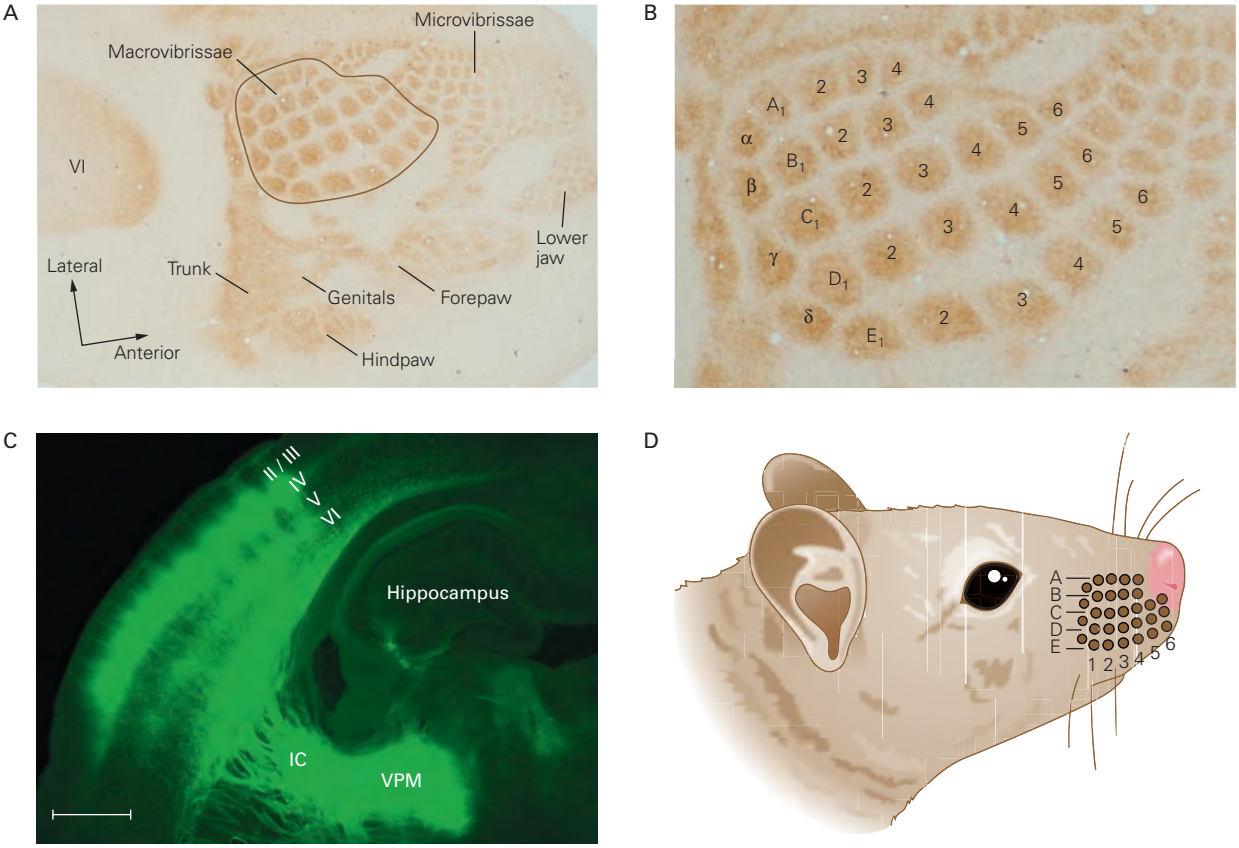

The Receptive Fields of Cortical Neurons Integrate Information From Neighboring Receptors

The neurons in S-I are at least three synapses beyond touch receptors in the skin. Their inputs represent information processed in the dorsal column nuclei, the thalamus, and the cortex itself. Each cortical neuron receives inputs arising from receptors in a specific area of the skin, and these inputs together are its receptive field. We perceive that a particular location on the skin is touched because specific populations of neurons in the cortex are activated. This experience can be induced experimentally by electrical or optogenetic stimulation of the same cortical neurons.

The receptive fields of cortical neurons are much larger than those of somatosensory fibers in peripheral nerves. For example, the receptive fields of SA1 and RA1 fibers innervating the fingertip are tiny spots on the skin (Figure 19–5), whereas those of the cortical neurons receiving these inputs cover an entire fingertip or several adjacent fingers (Figure 19–17B). The receptive field of a neuron in area 3b represents a

Many mammalian species actively move these large facial whiskers using specialized muscles that wrap like slings around each individual follicle. Mice and rats, two of the most commonly used vertebrate model organisms, rely more heavily on their sense of whisker-mediated touch than on their other senses during exploration.

Rodents rhythmically sweep their whiskers across objects in much the same way that humans palpate objects with their fingertips. Despite their structural differences, vibrissae and fingertips afford similar psychophysical thresholds and discriminative sensitivities. Whiskers mediate diverse abilities, including localizing objects in space, discriminating textures and shapes, navigating the environment, interacting socially, and capturing prey.

The rodent somatosensory cortex has evolved proportional to this system's high ethological relevance. For instance, the rat somatosensory cortex is thicker than the primary visual cortex of the cat, a highly visual animal.

The representation of the largest whiskers (macrovibrissae) in rodent S-I is enlarged relative to that of other parts of the body (Figure 19–16). In contrast to the continuous representations of the skin or retina, the cortical networks dedicated to processing information from individual whiskers are discrete and anatomically identifiable. Each whisker maps one-to-one onto a distinct cluster of excitatory neurons visible in cortical layer IV called a *barrel*.

Barrels are densely interconnected networks that are established during development by the interaction of thalamocortical axons with cortical neurons. This unique correspondence facilitates diverse studies of cortical microcircuits, development, experience-dependent plasticity, sensorimotor integration, tactile behavior, and disease.

Randy M. Bruno

Figure 19–16 (Opposite) The "barrel cortex" of rodents represents the vibrissae in topographic patterns. The barrel cortex, a subregion of the rodent primary somatosensory (S-I) cortex that represents the facial vibrissae, is a widely studied structure used to decipher cortical circuits. (Adapted from Bennett-Clarke et al. 1997 and Wimmer et al. 2010.)

A. Tangential histological section through layer IV of the somatosensory cortex of a juvenile rat stained for serotonin. The darker immunoreactive patches correspond to cortical representations of specific body parts. The largest part of the rodent somatosensory cortical map is devoted to the vibrissae.

B. Enlarged view of the macrovibrissae representation in S-I. The spatial pattern of the whiskers on the face is stereotyped from animal to animal, allowing each cortical "barrel" to be identified by row with the letter, and by arc (column) with the number of the corresponding whisker. Neurons in each barrel are most responsive to motion of this principal whisker.

C. A rat brain section cut obliquely along the path axons travel from the ventroposterior medial (**VPM**) thalamic nucleus to S-I. Green fluorescent protein–labeled VPM axons project through the internal capsule (**IC**) to the subcortical white matter and travel parallel to the pial surface before entering the cortex. The axons densely innervate layer IV where they form discrete barrels and more sparsely and diffusely innervate the border of layers V and VI. Scale bar = 1 mm.

D. The topographic arrangement of the barrels in the cortex matches the spatial arrangement of vibrissae on the face in rows (letters) and arcs (numbers).

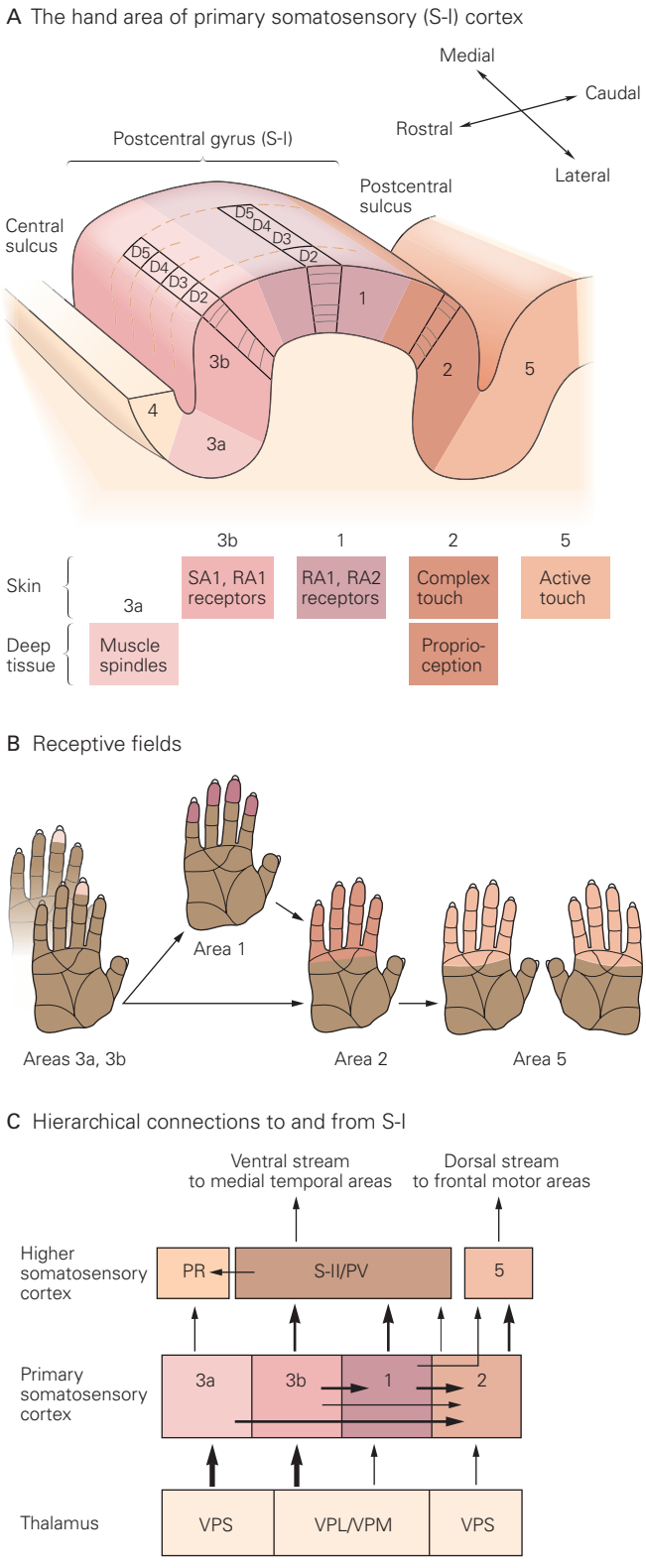

Figure 19–17 The hand area of S-I cortex.

A. This sagittal section through the hand representation illustrates the rostrocaudal anatomy of the four subregions of S-I (areas 3a, 3b, 1, and 2) in the human brain and the adjacent primary motor cortex (area 4) and posterior parietal cortex (area 5). Labels on the cortical surface indicate columns representing individual fingers (D2–D5); arrows to the right denote the section orientation in the brain. The four S-I regions process different types of somatosensory information indicated by color-matched rectangles below the cortical section. Neurons in area 5 respond mainly to goal-directed active hand movements. (Abbreviations: **RA1**, rapidly adapting type 1; **RA2**, rapidly adapting type 2; **SA1**, slowly adapting type 1.)

B. Typical receptive fields of neurons in each area of S-I of macaque monkeys are shown as colored patches on the hand icons. The fields are outlined by applying light touch to the skin or moving individual joints. Receptive fields are smallest in areas 3a and 3b, where tactile information first enters the cortex, and are progressively larger in areas 1, 2, and 5, reflecting convergent inputs from neurons in area 3b that are stimulated together when the hand is used. Neurons in area 5 and in S-II cortex often have bilateral receptive fields because they respond to touch at mirror-image locations on both hands. (Adapted from Gardner 1988; Iwamura et al. 1993; Iwamura, Iriki, and Tanaka 1994.)

C. Feedforward hierarchical connections between somatosensory cortical areas. The strength of thalamocortical and corticocortical connections is indicated by the thickness of arrows interconnecting these areas. Neurons in the thalamus send their axons mainly to areas 3a and 3b, but some also project to areas 1 and 2. In turn, neurons in cortical areas 3a and 3b project to areas 1 and 2. Information from the four areas of S-I is conveyed to neurons in the posterior parietal cortex (area 5) and in S-II. Many of these connections are bidirectional; neurons in higher order cortical areas project back to lower order regions, particularly to layer I. (**PR**, parietal rostroventral cortex; **PV**, parietal ventral cortex; **VPL**, ventral posterior lateral nuclei; **VPM**, ventral posterior medial nuclei; **VPS**, ventral posterior superior nuclei). (Adapted, with permission, from Felleman and Van Essen 1991. Copyright © 1991, Oxford University Press.)

composite of inputs from 300 to 400 nerve fibers, and typically covers a single phalanx or palm pad. Inputs from SA1 and RA1 touch receptors in the same skin region converge on common neurons in area 3b.

Receptive fields in higher cortical areas are even larger, spanning functional regions of skin that are activated simultaneously during motor activity. These include the tips of several adjacent fingers, or an entire finger, or both the fingers and the palm. Neurons in areas 1 and 2 of S-I are concerned with information more abstract than just their innervation sites on the body. Neurons whose receptive fields include more than one finger fire at higher rates when several fingers are touched simultaneously and, in this way, signal the size and shape of objects held in the hand. These large receptive fields allow cortical neurons to integrate the fragmented information from individual touch receptors, enabling us to recognize the overall shape of an object. For example, such neurons may distinguish the handle of a screwdriver from its blade.

Convergent inputs from different sensory receptors in S-I may also allow individual neurons to detect the size and shape of objects. Whereas neurons in areas 3b and 1 respond only to touch and neurons in area 3a respond to muscle stretch, many of the neurons in area 2 receive both inputs. Thus, neurons in area 2 can integrate information about the hand shape used to grasp an object, the grip force applied by the hand, and the tactile stimulation produced by the object; this integrated information may be sufficient to recognize the object.

The receptive fields of cortical neurons usually have an excitatory zone surrounded by or superimposed upon inhibitory zones (Figure 19–18A). Stimulation of regions of skin outside the excitatory zone may reduce the neuron's responses to tactile stimulation within the receptive field. Similarly, repeated stimulation within the receptive field may also decrease neuronal responsiveness because the excitability of the pathway is diminished by longer lasting inhibition mediated by local interneurons.

Inhibitory receptive fields result from feedforward and feedback connections through interneurons in the dorsal column nuclei, the thalamus, and the cortex itself that limit the spread of excitation. Inhibition generated by strong activity in one circuit reduces the output of nearby neurons that are only weakly excited. The inhibitory networks ensure that the strongest of

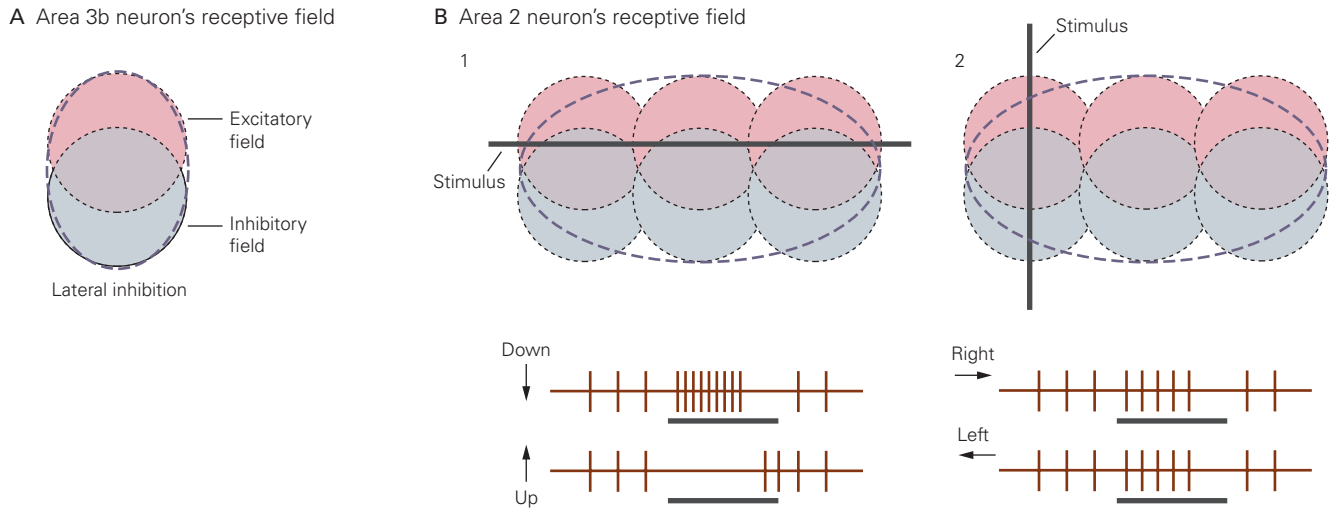

Figure 19–18 The spatial arrangement of excitatory and inhibitory inputs to a cortical neuron determines which stimulus features are encoded by the neuron.

A. A neuron in area 3b of the primary somatosensory cortex has overlapping excitatory and inhibitory zones within its receptive field. (Adapted, with permission, from DiCarlo et al. 1998; Sripati et al. 2006. Copyright © Society for Neuroscience.)

B. Convergence of three presynaptic neurons with the same arrangement of excitatory and inhibitory zones allows direction and orientation selectivity in a neuron in area 2. **1.** Downward motion of a horizontal bar across the receptive field of the postsynaptic cell produces a strong excitatory response because the excitatory fields of all three presynaptic neurons are contacted simultaneously. Upward motion of the bar strongly inhibits firing because it enters all three inhibitory fields first. The neuron responds poorly to upward motion through the excitatory field because the initial inhibition outlasts the stimulus. **2.** Motion of a vertical bar across the receptive field evokes a weak response because it simultaneously crosses the excitatory and inhibitory receptive fields of the input neurons. Motion to the left or right cannot be distinguished in this example.

several competing responses is transmitted, permitting a winner-take-all strategy. These circuits prevent blurring of tactile details such as texture when large populations of touch neurons are stimulated. In addition, higher centers in the brain use inhibitory circuits to focus attention on relevant information from the hand when it is used in skilled tasks, by suppressing unwanted, distracting inputs.

The size and position of receptive fields on the skin are not fixed permanently but can be modified by experience or injury to sensory nerves (Chapter 53). Cortical receptive fields appear to be formed during development and maintained by simultaneous activation of the input pathways. If a peripheral nerve is injured or transected, its cortical projection targets acquire new receptive fields from less effective sensory inputs that are normally suppressed by inhibitory networks, or from newly developed connections from neighboring skin areas that retain innervation. Likewise, extensive stimulation of afferent pathways through repeated practice may strengthen synaptic inputs, improving perception and thereby performance.

Touch Information Becomes Increasingly Abstract in Successive Central Synapses

Somatosensory information is conveyed in parallel from the four areas of S-I to higher centers in the cortex, such as the secondary somatosensory cortex (S-II), the posterior parietal cortex, and the primary motor cortex (Figure 19–17C). As information flows toward higher-order cortical areas, specific combinations of stimulus patterns are needed to excite individual neurons.

Signals from neighboring neurons are combined in higher cortical areas to discern global properties of objects such as their orientation on the hand, or the direction of motion (Figure 19–19). In general, cortical neurons in higher cortical areas are concerned with sensory features that are independent of the stimulus position in their receptive field, abstracting object properties common to a particular class of stimuli.

A cortical neuron is able to detect the orientation of an edge or the direction of motion because of the spatial arrangement of the presynaptic receptive fields. The receptive fields of the excitatory presynaptic neurons are typically aligned along a common axis that generates the preferred orientation of the postsynaptic neuron. In addition, the receptive fields of inhibitory presynaptic neurons at one side of the excitatory fields reinforce the orientation and direction selectivity of postsynaptic neurons (Figure 19–18B).

Cognitive Touch Is Mediated by Neurons in the Secondary Somatosensory Cortex

An S-I neuron's response to touch depends primarily on input from within the neuron's receptive field. This feedforward pathway is often described as a *bottom-up* process because the receptors in the periphery are the principal source of excitation of S-I cortical neurons.

Higher-order somatosensory areas not only receive information from peripheral receptors but are also strongly influenced by top-down cognitive processes, such as goal-setting and attentional modulation. Data obtained from a variety of studies—single-neuron studies in monkeys, neuroimaging studies in humans, and clinical observations of patients with lesions in higher-order somatosensory areas—suggest that the ventral and dorsal regions of the parietal lobe serve complementary functions in the touch system similar to the "what" and "where" pathways of the visual system (see Figure 17–13).

S-II is located on the upper bank and adjacent parietal operculum of the lateral sulcus in both humans and monkeys (Figures 19–12B and 19–20B). Like S-I, the S-II cortex contains four distinct anatomical subregions with separate maps of the body. The central zone—consisting of S-II proper and the adjacent parietal ventral area—receives its major input from areas 3b and 1, largely tactile information from the hand and face. A more rostral region, the parietal rostroventral area, receives information from area 3a about active hand movements as well as tactile information from areas 3b and 1 (Figure 19–20). The most caudal somatosensory region of the lateral sulcus extends onto the parietal operculum (Figure 19–12A). This region abuts the posterior parietal cortex and plays a role in integrating somatosensory and visual properties of objects.

Physiological studies indicate that S-II plays key roles in tactile recognition of objects placed in the hand (stereognosis), distinguishing spatial features, such as shape and texture, and temporal properties, such as vibratory frequency. The receptive fields of neurons in S-II are larger than those in S-I, covering the entire surface of the hand, and are often bilateral, representing symmetric, mirror-image locations on the contralateral and ipsilateral hands. Such large receptive fields enable us to sense the shape of an entire large object grasped in one hand, allowing us to integrate the overall contours of a tool as it contacts the palm and different fingers. Bilateral receptive fields enable us to perceive still larger objects with two hands, such as a watermelon or basketball, sharing the load between them.

The large receptive fields of S-II neurons also influence their physiological responses to motion and vibration. S-II neurons do not represent vibration as

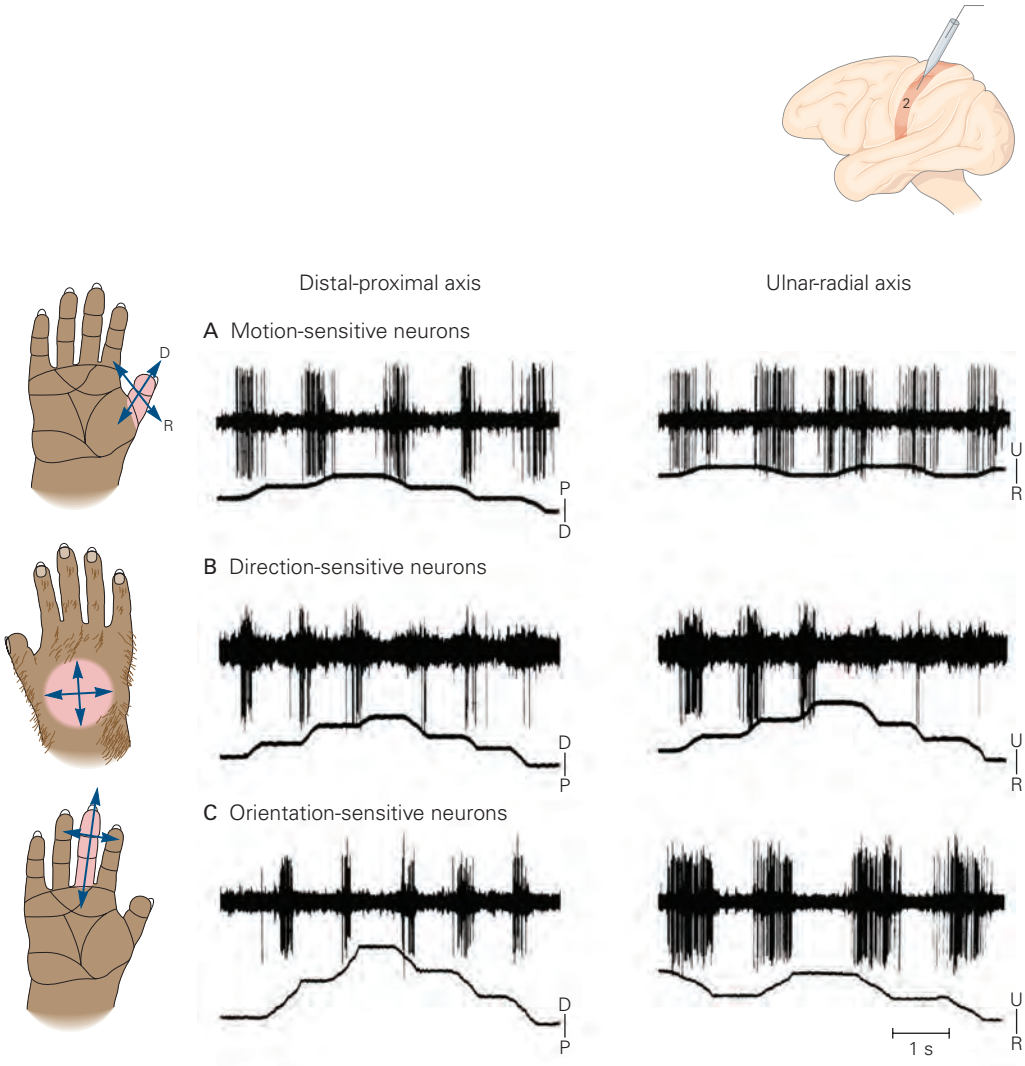

Figure 19–19 Neurons in area 2 encode complex tactile information. These neurons respond to motion of a probe across the receptive field but not to touch at a single point. The lower trace indicates the direction of motion by upward and downward deflections. (Adapted, with permission, from Warren, Hämäläinen, and Gardner 1986.)

A. A motion-sensitive neuron responds to stroking the skin in all directions.

B. A direction-sensitive neuron responds strongly to motion toward the ulnar side of the palm but fails to respond to motion in the opposite direction. Responses to distal or proximal movements are weaker.

C. An orientation-sensitive neuron responds better to motion across a finger (ulnar-radial) than to motion along the finger (distal-proximal), but does not distinguish ulnar from radial or proximal from distal directions.

periodic spike trains linked to the oscillatory frequency, as do the sensory fibers from the skin or S-I neurons (Figure 19–9). Instead, S-II neurons abstract temporal or intensive properties of the vibratory stimulus, firing at different mean rates for different frequencies. A similar frequency-dependent transition from temporal- to rate-coding neurons underlies sound processing in primary auditory cortex (Chapter 28), a brain region juxtaposed to S-II cortex in the parietal operculum.

Importantly, the firing rates of S-II neurons depend on the behavioral context or motivational state of the subject. In elegant recent studies, Ranulfo Romo and his colleagues compared responses to vibratory stimuli of neurons in S-I, S-II, and various regions of the frontal lobe of monkeys while the animals performed a two-alternative forced-choice task. The animals were rewarded if they correctly recognized which of two vibratory stimuli was higher in frequency.

Neurons in S-I faithfully represent the vibratory cycles of each stimulus using a temporal code: they fire brief spike bursts in phase with each cycle (Figure 19–9B).

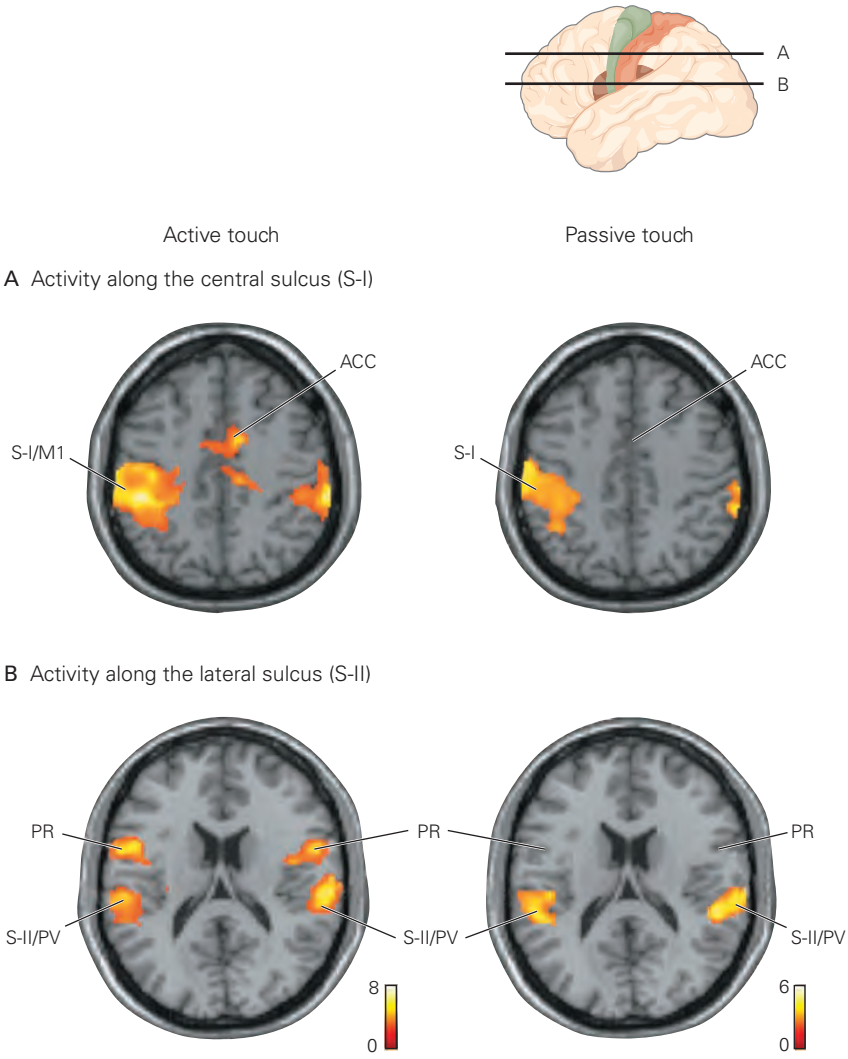

Figure 19–20 Responses in S-I and S-II to active touch are more complex than those evoked by passive touch. Cortical regions in the human brain stimulated by passive and active touch are localized using functional magnetic resonance imaging (fMRI). (Adapted, with permission, from Hinkley et al. 2007.)

A. Axial views of activity along the central sulcus during passive stroking of the right hand with a sponge (*right panel*) and during active touching of the sponge (*left panel*). Areas 3b and 1 are activated in the left hemisphere in both conditions. Active touch also engages the primary motor cortex (**M1**) in the left hemisphere, the anterior cingulate cortex (**ACC**), and evokes weak activity in the ipsilateral S-I (right hemisphere). These sites were confirmed independently using magnetoencephalography in the same subjects.

B. Axial views of activity along the Sylvian fissure in the same experiment. Bilateral activity occurs in S-II and the parietal ventral (**PV**) area during passive stroking and is stronger when the subject actively moves the hand. The parietal rostroventral area (**PR**) is active only during active touch. Magnetoencephalographic responses in S-II/PV and PR occur later than in S-I, reflecting serial processing of touch from S-I to S-II/PV and from S-II/PV to PR.

In contrast, S-II neurons respond to the first stimulus with nonperiodic spike trains in which their mean firing rates are directly or inversely correlated with the vibratory frequency (Figure 19–21A). Their responses to the second stimulus are even more abstract. S-II spike trains combine the frequencies of both stimuli (Figure 19–21B). In other words, S-II responses to vibration depend on the stimulus context: the same vibratory stimulus can evoke different firing rates depending on whether the preceding stimulus is higher or lower in frequency.

Even more interesting, Romo's group found that neurons in S-II send copies of the spike trains evoked by the first stimulus to the prefrontal and premotor cortex in order to preserve a memory of that response. Neurons in these frontal cortical areas continue to fire during the delay period after the first stimulus ends. Romo and colleagues proposed that these regions in the frontal lobe send the memory signal back to S-II when the second stimulus occurs, thereby modifying the response of S-II neurons to the direct tactile signals from the hand. In this manner, sensorimotor memories of previous stimuli influence sensory processing in the brain, allowing subjects to make cognitive judgments about newly arriving tactile stimuli.

S-II is the gateway to the temporal lobe via the insular cortex. Regions of the medial temporal lobe, particularly the hippocampus, are vital to the storage of explicit memory (Chapter 53). We do not store in memory every scintilla of tactile information that enters the nervous system, only that which has some behavioral significance. In light of the demonstration that the firing patterns of S-II neurons are modified by selective attention, S-II could make the decision whether a particular bit of tactile information is remembered.

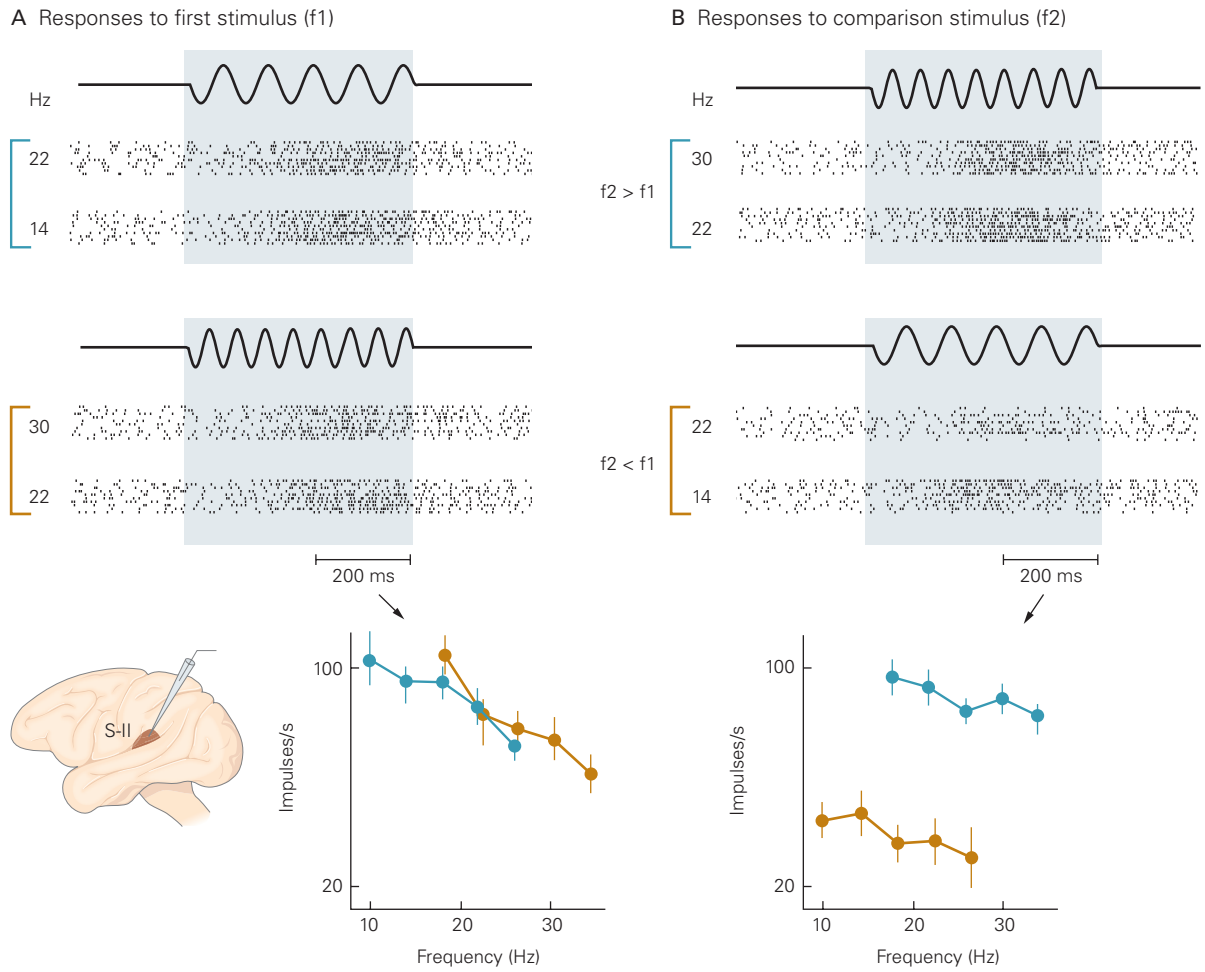

Figure 19–21 **The sensitivity of an S-II neuron to vibratory stimuli is modulated by attention and behavioral conditions.** A monkey was trained to compare two vibratory stimuli applied at a 3-second interval to the fingertips (**f1** and **f2**) and to indicate which had the higher frequency. The plots show the mean firing rates of the neuron during each of the two stimuli. The animal's decision about which frequency is higher can be predicted from the neural data during each type of trial. The mean firing rates of this neuron are significantly higher at each stimulation frequency when f2 is greater than f1 than when f2 is less than f1. (Adapted, with permission, from Romo et al. 2002. Copyright © 2002 Springer Nature.)

A. Raster plots show the responses of an S-II neuron to various sample stimuli (f1). The vertical tick marks in each row denote action potentials, and individual rows are separate trials of the stimulus pairs. Trials are grouped according to the frequencies tested. The firing rate of the neuron encodes the vibratory frequency of the sample stimulus; it is higher for low-frequency vibration regardless of the subsequent events. Note that the firing patterns recorded in S-II are not phase-locked to the vibratory cycle as in S-I (see Figure 19–9B).

B. Each row in the raster plots illustrates responses to the comparison stimulus (f2) during the same trials shown in A. The neuron's response to f2 reflects the frequency of both f2 and f1. When f2 > f1, the neuron fires at high rates during f2 and the animal reports that f2 is the higher frequency. When f2 < f1, the neuron fires at low rates during f2 and the animal reports that f1 is the higher frequency. In this manner, the responses of S-II neurons reflect the animal's memory of an earlier event.

Active Touch Engages Sensorimotor Circuits in the Posterior Parietal Cortex

Studies in the mid-1970s by Vernon Mountcastle, Juhani Hyvärinen, and others demonstrated that regions of the posterior parietal cortex surrounding the intraparietal sulcus play an important role in the sensory guidance of movement rather than in discriminative touch. These regions include areas 5 and 7 in monkeys and the superior parietal lobule (Brodmann's areas 5 and 7) and inferior parietal cortex (areas 39 and 40) in humans. These and subsequent studies demonstrated that neural activity in the posterior parietal cortex during reaching and grasping coincides with activation of neurons in motor and premotor areas of the frontal cortex and precedes activity in S-I. Areas 5 and 7

are postulated to be engaged in the planning of hand actions, because the posterior parietal cortex receives convergent central and peripheral signals that allow it to compare central motor commands with somatosensory feedback during reaching and grasping behaviors. Sensory feedback from S-I to the posterior parietal cortex is used to confirm the goal of the planned action, thereby reinforcing previously learned skills or correcting those plans when errors occur.

Predicting the sensory consequences of hand actions is an important component of active touch. For example, when we view an object and reach for it, we predict how heavy it should be and how it should feel in the hand; we use such predictions to initiate grasping. Daniel Wolpert and Randy Flanagan have proposed that during active touch the motor system controls the afferent flow of somatosensory information to the brain so that subjects can predict when tactile information should arrive in S-I and reach consciousness. Convergence of central and peripheral signals allows neurons to compare planned and actual movements. Corollary discharge from motor areas to somatosensory regions of the cortex may play a key role in active touch. It provides posterior parietal cortex neurons with information on intended actions, allowing them to learn new skills and perform them smoothly.

Lesions in Somatosensory Areas of the Brain Produce Specific Tactile Deficits

Patients with lesions in S-I cortex have difficulty responding to simple tactile tests: touch thresholds, vibration and joint position sense, and two-point discrimination (Figure 19–22A). These patients also perform poorly on more complex tasks, such as texture discrimination, stereognosis, and visual–tactile matching tests.

Loss of tactile sensation in the hand produces significant motor as well as sensory deficits. Motor deficits are less pronounced than sensory losses, particularly during tests of force and position control. Exploratory movements and skilled tasks such as catching a ball or pinching small objects between the fingertips are also abnormal.

Local anesthesia of sensory nerve fibers in the hand provides a direct way to appreciate the sensorimotor role of touch. Under local anesthesia of the median and ulnar nerves, hand movements are clumsy and poorly coordinated, and force generation during grasping is abnormally slow. With the loss of tactile sensibility, one is completely reliant on vision for directing the hand. Loss of touch does not cause paralysis or weakness because much of skilled movement is predictive, relying on sensory feedback for adjustment if necessary. The motor system in these subjects compensates for the absence of tactile information by generating more force than necessary.

These motor problems are exacerbated by long-term, chronic loss of tactile function because of injury to peripheral nerves or dorsal column lesions. Deafferentation produces major changes in the afferent connections in the brain, as do certain diseases. Myelinated afferent fibers in the dorsal columns degenerate in patients with demyelinating diseases, such as multiple sclerosis. In late-stage syphilis, the large-diameter neurons in the dorsal root ganglia are destroyed (tabes dorsalis). These patients have severe chronic deficits in touch and proprioception but often little loss of temperature perception and nociception. The somatosensory losses are accompanied by motor deficits: clumsy and poorly coordinated movements and dystonia. Similar impairments occur in patients with damage to S-I caused by stroke or head trauma, or following surgical excision of the postcentral gyrus.

Patients with lesions in the posterior parietal cortex usually have only mild difficulty with simple tactile tests. However, they have profound difficulty with complex tactile recognition tasks and use few exploratory and skilled movements (Figure 19–22B). They display kinematic deficits when interacting with objects, failing to shape and orient the hand properly to grasp them and misdirecting the arm during reaching. They typically use too much grip force when an object is placed in their hand and are unable to direct the fingers properly when asked to evaluate its size and shape. These deficits are described clinically as the "useless hand" syndrome (tactile apraxia).

Studies of sensory deficits in human patients are complicated by the fact that disease states or trauma rarely produce damage confined to one localized brain area. For this reason, analyses of experimentally controlled lesions in animals have been useful for understanding the etiology of the sensory deficits observed in human patients. For example, macaque monkeys with a lesion of the cuneate fascicle show chronic losses in tactile discrimination, such as higher touch thresholds, impaired vibration sense, and poor two-point discrimination. They also display major deficits in the control of fine finger movements during grooming, scratching, and object manipulation. A similar deficit in skilled movements can be produced experimentally in monkeys by inhibiting the neurons in the hand-representation region of area 2.

Experimental ablation of somatosensory areas of the cortex in monkeys has provided valuable information about the function of these areas. Small lesions

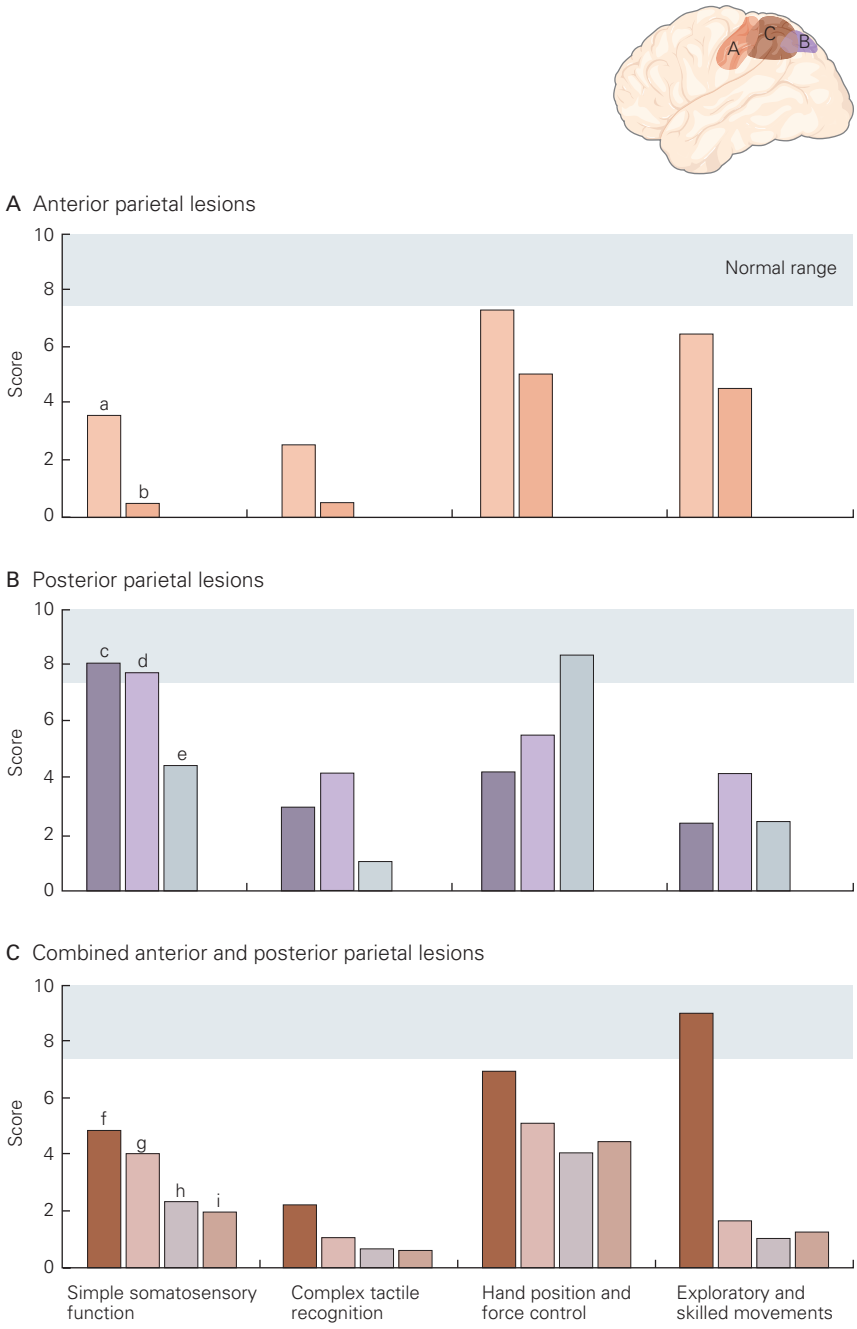

Figure 19–22 **Lesions of anterior and posterior regions of the parietal lobe produce characteristic sensory and motor deficits of the hand.** Bar graphs rank the performance of nine patients (a–i) with unilateral parietal cortex brain lesions on four sets of standardized tests of sensory and motor function of the contralateral hand. The behavioral scores are ranked from normal (10) to maximal deficit (0). The normal range shown is the performance score of these patients for the ipsilateral hand. Tests of *simple somatosensory function* include light touch from a 1-g force-calibrated probe, two-point discrimination on the finger and palm, vibration sense, and position sense of the index finger metacarpophalangeal joint. Tests of *complex tactile recognition* assess texture discrimination, form recognition, and size discrimination. Tests of *hand position and force control* measure grip force, tapping, and reaching to a target. Tests of *exploratory and skilled movements* evaluate insertion of pegs in slots, pincer grip of small objects, and exploratory movements when palpating objects. (Adapted, with permission, from Pause et al. 1989. Copyright © 1989, Oxford University Press.)

A. Two patients with lesions to the anterior parietal lobe show severe impairment in both sets of tactile tests but only moderate impairment in the motor tasks.

B. Three patients with posterior parietal lesions show only minor deficits in simple somatosensory tests but severe impairment in complex tests of stereognosis and form. Motor deficits are greater in skilled tasks.

C. Four patients with combined lesions to anterior and posterior parietal cortex show severe impairment in all tests. Interestingly, the patient who showed the least impairment in this group (patient f) suffered brain damage at birth; the developing brain was able to compensate for the loss of major somatosensory areas. Lesions in the other patients resulted from strokes later in life.

limited to area 3b produce major deficits in touch sensation from a particular part of the body. Lesions in area 1 produce a defect in the assessment of the texture of objects, whereas lesions in area 2 alter the ability to differentiate the size and shape of objects. The damage to tactile function is less severe when such lesions are made in infant animals, apparently because in the developing brain S-II cortex may take over functions normally assumed by S-I.

Removal of S-II cortex in monkeys causes severe impairment in the discrimination of both shape and texture and prevents the animals from learning new tactile discriminations. Ablation or inhibition of areas 2 or 5 produces deficits in roughness discrimination but few other alterations in passive touch. However, motor performance is impaired as these animals misdirect reaching toward objects, fail to preshape the hand to grasp objects skillfully, and have difficulty coordinating finger movements because tactile feedback is absent (Figure 19–23).

The similarity between impairments observed in humans and monkeys is an important basis for understanding clinical losses of somatosensory function. We shall learn in later chapters that lesioning studies of other cortical areas in monkeys have also provided insight into higher-order sensory and motor functions of the brain.

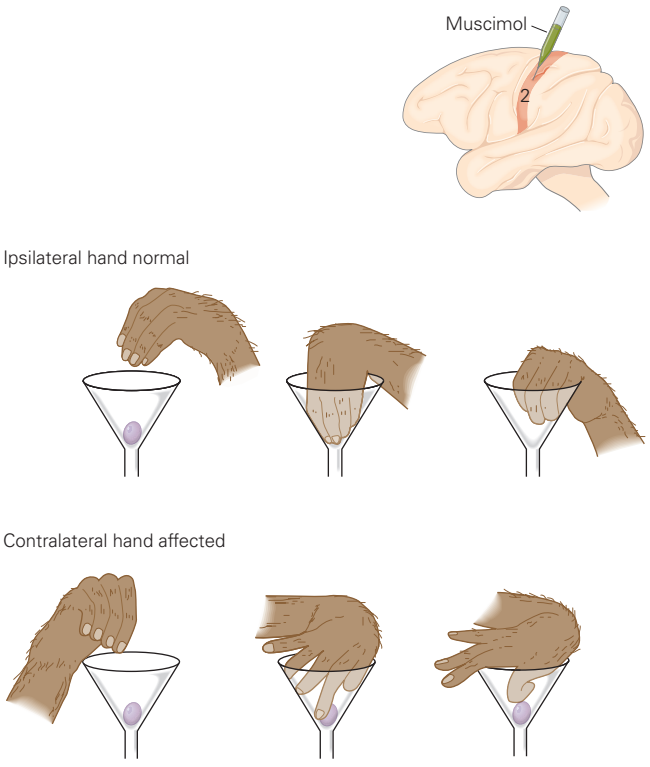

Figure 19–23 Finger coordination is disrupted when synaptic transmission in the somatic sensory cortex is inhibited in a monkey. Muscimol, a γ-aminobutyric acid (GABA) agonist that inhibits cortical cells, was injected into Brodmann's area 2 on the left side of a monkey's brain. Within minutes after injection, the finger coordination of the right hand (contralateral) was severely disrupted; the monkey was unable to pick up a grape from a funnel. The injection effects are shown to be specific to the injected hemisphere because the left hand (ipsilateral) continues to perform normally. (Adapted, with permission, from Hikosaka et al. 1985. Copyright © 1985 Elsevier B.V.)

Highlights

1. When we explore an object with our hands, a large part of the brain may become engaged by the sensory experience, by the thoughts and emotions it evokes, and by motor responses to it. These sensations result from the parallel actions of multiple cortical areas engaged in feedforward and feedback networks.
2. At the first touch, the peripheral sensory apparatus deconstructs the object into tiny segments, distributed over a large population of approximately 20,000 sensory nerve fibers. The SA1 system provides high-fidelity information about the object's spatial structure that is the basis of form and texture perception. The SA2 system provides information about the hand conformation and posture during grasping and other hand movements. The RA1 system conveys information about motion of the object in the hand, which enables us to manipulate it skillfully. Together with RA2 receptors, they sense vibration of objects that allows us to use them as tools.
3. The information from touch receptors is conveyed to consciousness by the dorsal column fiber tracts of the spinal cord, relay nuclei in the brain stem and thalamus, and a hierarchy of intracortical pathways. By analyzing patterns of activity across the entire population, the brain constructs a neural representation of objects and actions of the hand.
4. Computations in central pathways are complex and accomplished serially, beginning in the dorsal column nuclei, progressing through the thalamus and several cortical stages, and terminating in regions of the medial temporal cortex concerned with memory and perception and in motor areas of the frontal lobe that mediate voluntary movements.
5. The brain's processing of touch is aided by the topographic, somatotopic organization of the neurons involved at each relay. Adjacent skin areas that

are stimulated together are linked anatomically and functionally in central relays. Body parts that are especially sensitive to touch—the hands, feet, and mouth—are represented in large areas of the brain, reflecting the importance of tactile information conveyed from these regions.

6. Another function of the central pathways is the transformation of the disaggregated representation of object properties among thousands of neurons to an integrated representation of complex object properties in a few neurons. Convergent excitatory connections between neurons representing neighboring skin areas and intracortical inhibitory circuits enable higher-order cortical cells to integrate global features of objects. In this manner, the somatosensory areas of the brain represent properties common to particular classes of objects.
7. A third function is regulating the afferent flow of somatosensory information. The peripheral fibers deliver much more information than can be handled at any one moment; the central neural pathways compensate by selecting information for delivery to the mechanisms of perception and memory. Recurrent pathways from higher brain areas modify the ascending information provided by touch receptors, thus fitting the stream of sensory information to previous experience and task goals.
8. Finally, the touch system provides information necessary for the control and guidance of movement. Interactions between sensory and motor areas of parietal and frontal cortex provide a neural mechanism for planning desired actions, for predicting the sensory consequences of motor behaviors, and for skill learning from repeated experience.

Esther P. Gardner

Selected Reading

Freund HJ. 2003. Somatosensory and motor disturbances in patients with parietal lobe lesions. Adv Neurol 93:179–193.

Harris KD, Shepherd GMG. 2015. The neocortical circuit: themes and variations. Nat Neurosci 18:170–181.

Johnson KO. 2001. The roles and functions of cutaneous mechanoreceptors. Curr Opin Neurobiol 11:455–461.

Jones EG. 2000. Cortical and subcortical contributions to activity-dependent plasticity in primate somatosensory cortex. Annu Rev Neurosci 23:1–37.

Jones EG, Peters A (eds). 1986. *Cerebral Cortex.* Vol 5, *Sensory-Motor Areas and Aspects of Cortical Connectivity.* New York: Plenum Press.

Kaas JH, Gardner EP (eds). 2008. *The Senses: A Comprehensive Reference.* Vol 6, *Somatosensation.* Oxford: Elsevier.

Milner AD, Goodale MA. 1995. *The Visual Brain in Action*. Oxford: Oxford Univ. Press.

Mountcastle VB. 1995. The parietal system and some higher brain functions. Cerebral Cortex 5:377–390.

Mountcastle VB. 2005. *The Sensory Hand: Neural Mechanisms of Somatic Sensation*. Cambridge, MA: Harvard Univ. Press.

Romo R, Salinas E. 2003. Flutter discrimination: neural codes, perception, memory and decision making. Nat Rev Neurosci 4:203–218.

Wing AM, Haggard P, Flanagan JR (eds). 1996. *Hand and Brain.* San Diego, CA: Academic Press.

References

Bennett-Clarke CA, Chiaia NL, Rhodes RW. 1997. Contributions of raphe-cortical and thalamocortical axons to the transient somatotopic pattern of serotonin immunoreactivity in rat cortex. Somatosens Mot Res 14:27–33.

Birznieks I, Macefield VG, Westling G, Johansson RS. 2009. Slowly adapting mechanoreceptors in the borders of the human fingernail encode fingertip forces. J Neurosci 29:9370–9379.

Bolanowski SJ, Pawson L. 2003. Organization of Meissner corpuscles in the glabrous skin of monkey and cat. Somatosens Mot Res 20:223–231.

Brisben AJ, Hsiao SS, Johnson KO. 1999. Detection of vibration transmitted through an object grasped in the hand. J Neurophysiol 81:1548–1558.

Brochier T, Boudreau M-J, Paré M, Smith AM. 1999. The effects of muscimol inactivation of small regions of motor and somatosensory cortex on independent finger movements and force control in the precision grip. Exp Brain Res 128:31–40.

Carlson M. 1981. Characteristics of sensory deficits following lesions of Brodmann's areas 1 and 2 in the postcentral gyrus of *Macaca mulatta*. Brain Res 204:424–430.

Chapman CE, Meftah el-M. 2005. Independent controls of attentional influences in primary and secondary somatosensory cortex. J Neurophysiol 94:4094–4107.

Connor C, Hsiao SS, Phillips J, Johnson KO. 1990. Tactile roughness: neural codes that account for psychophysical magnitude estimates. J Neurosci 10:3823–3836.

Costanzo RM, Gardner EP. 1980. A quantitative analysis of responses of direction-sensitive neurons in somatosensory cortex of alert monkeys. J Neurophysiol 43:1319–1341.

DiCarlo JJ, Johnson KO, Hsaio SS. 1998. Structure of receptive fields in area 3b of primary somatosensory cortex in the alert monkey. J Neurosci 18:2626–2645.

Edin BB, Abbs JH. 1991. Finger movement responses of cutaneous mechanoreceptors in the dorsal skin of the human hand. J Neurophysiol 65:657–670.

Felleman DJ, Van Essen DC. 1991. Distributed hierarchical processing in the primate cerebral cortex. Cereb Cortex 1:1–47.

Fitzgerald PJ, Lane JW, Thakur PH, Hsiao SS. 2006. Receptive field properties of the macaque second somatosensory cortex: representation of orientation on different finger pads. J Neurosci 26:6473–6484.

Flanagan JR, Vetter P, Johansson RS, Wolpert DM. 2003. Prediction precedes control in motor learning. Curr Biol 13:146–150.

Fogassi L, Luppino G. 2005. Motor functions of the parietal lobe. Curr Opin Neurobiol 15:626–631.

Gardner EP. 1988. Somatosensory cortical mechanisms of feature detection in tactile and kinesthetic discrimination. Can J Physiol Pharmacol 66:439–454.

Gardner EP. 2008. Dorsal and ventral streams in the sense of touch. In: JH Kaas, EP Gardner (eds). *The Senses: A Comprehensive Reference.* Vol. 6, *Somatosensation*, pp. 233–258. Oxford: Elsevier.

Gardner EP, Babu KS, Ghosh S, Sherwood A, Chen J. 2007. Neurophysiology of prehension: III. Representation of object features in posterior parietal cortex of the macaque monkey. J Neurophysiol 98:3708–3730.

Hikosaka O, Tanaka M, Sakamoto M, Iwamura Y. 1985. Deficits in manipulative behaviors induced by local injections of muscimol in the first somatosensory cortex of the conscious monkey. Brain Res 325:375–380.

Hinkley LB, Krubitzer LA, Nagarajan SS, Disbrow EA. 2007. Sensorimotor integration in S2, PV, and parietal rostroventral areas of the human Sylvian fissure. J Neurophysiol 97:1288–1297.

Hyvärinen J, Poranen A. 1978. Movement-sensitive and direction and orientation-selective cutaneous receptive fields in the hand area of the post-central gyrus in monkeys. J Physiol (Lond) 283:523–537.

Iwamura Y, Iriki A, Tanaka M. 1994. Bilateral hand representation in the postcentral somatosensory cortex. Nature 369:554–556.

Iwamura Y, Tanaka M, Sakamoto M, Hikosaka O. 1993. Rostrocaudal gradients in neuronal receptive field complexity in the finger region of the alert monkey's postcentral gyrus. Exp Brain Res 92:360–368.

Jenmalm P, Birznieks I, Goodwin AW, Johansson RS. 2003. Influence of object shape on responses of human tactile afferents under conditions characteristic of manipulation. Eur J Neurosci 18:164–176.

Johansson RS. 1996. Sensory control of dexterous manipulation in humans. In: AM Wing, P Haggard, JR Flanagan (eds). *Hand and Brain,* pp. 381–414. San Diego, CA: Academic Press.

Johansson RS, Flanagan JR. 2009. Coding and use of tactile signals from the fingertips in object manipulation tasks. Nat Rev Neurosci 10:345–359.

Johansson RS, Landström U, Lundström R. 1982. Responses of mechanoreceptive afferent units in the glabrous skin of the human hand to sinusoidal skin displacements. Brain Res 244:17–25.

Johansson RS, Vallbo ÅB. 1983. Tactile sensory coding in the glabrous skin of the human hand. Trends Neurosci 6:27–32.

Johnson KO, Phillips JR. 1981. Tactile spatial resolution: I. Two-point discrimination, gap detection, grating resolution and letter recognition. J Neurophysiol 46:1177–1191.

Jones EG, Powell TPS. 1969. Connexions of the somatic sensory cortex of the rhesus monkey. I. Ipsilateral cortical connexions. Brain 92:477–502.

Klatzky RA, Lederman SJ, Metzger VA. 1985. Identifying objects by touch: an "expert system." Percept Psychophys 37:299–302.

Koch KW, Fuster JM. 1989. Unit activity in monkey parietal cortex related to haptic perception and temporary memory. Exp Brain Res 76:292–306.

LaMotte RH, Mountcastle VB. 1979. Disorders in somethesis following lesions of parietal lobe. J Neurophysiol 42:400–419.

Lederman SJ, Klatzky RL. 1987. Hand movements: a window into haptic object recognition. Cogn Psychol 19: 342–368.

Lieber JD, Xia X, Weber AI, Bensmaia SJ. 2017. The neural code for tactile roughness in the somatosensory nerves. J Neurophysiol 118:3107–3117.

Manfredi LR, Saal, HP, Brown KJ, et al. 2014. Natural scenes in tactile texture. J Neurophysiol 111:1792–1802.

Mountcastle VB. 1997. The columnar organization of the neocortex. Brain 120:701–722.

Mountcastle VB, LaMotte RH, Carli G. 1972. Detection thresholds for stimuli in humans and monkeys: comparison with threshold events in mechanoreceptive afferent fibers innervating the monkey hand. J Neurophysiol 35:122–136.

Mountcastle VB, Lynch JC, Georgopoulos AP, Sakata H, Acuna C. 1975. Posterior parietal association cortex of the monkey: command functions for operations within extrapersonal space. J Neurophysiol 38:871–908.

Muniak MA, Ray S, Hsiao SS, Dammann JF, Bensmaia SJ. 2007. The neural coding of stimulus intensity: linking the population response of mechanoreceptive afferents with psychophysical behavior. J Neurosci 27:11687–11699.

Murray EA, Mishkin M. 1984. Relative contributions of SII and area 5 to tactile discrimination in monkeys. Behav Brain Res 11:67–83.

Nelson RJ, Sur M, Felleman DJ, Kaas JH. 1980. Representations of the body surface in postcentral parietal cortex of *Macaca fascicularis.* J Comp Neurol 192:611–643.

Nolano M, Provitera V, Crisci C, et al. 2003. Quantification of myelinated endings and mechanoreceptors in human digital skin. Ann Neurol 54:197–205.

Oberlaender M, de Kock CP, Bruno RM, et al. 2012. Cell type-specific three-dimensional structure of thalamocortical circuits in a column of rat vibrissal cortex. Cereb Cortex 22:2375–2391.

Pandya DN, Seltzer B. 1982. Intrinsic connections and architectonics of posterior parietal cortex in the rhesus monkey. J Comp Neurol 204:196–210.

Pause M, Kunesch E, Binkofski F, Freund H-J. 1989. Sensorimotor disturbances in patients with lesions of the parietal cortex. Brain 112:1599–1625.

Pei Y-C, Denchev P V, Hsiao SS, Craig JC, Bensmaia SJ. 2009. Convergence of submodality-specific input onto neurons in primary somatosensory cortex. J Neurophysiol 102:1843–1853.

Peters RM, Hackeman E, Goldreich D. 2009. Diminutive digits discern delicate details: fingertip size and the sex difference in tactile spatial acuity. J Neurosci 29:15756–15761.

Phillips JR, Johansson RS, Johnson KO. 1990. Representation of braille characters in human nerve fibres. Exp Brain Res 81:589–592.

Pons TP, Garraghty PE, Mishkin M. 1992. Serial and parallel processing of tactual information in somatosensory cortex of rhesus monkeys. J Neurophysiol 68:518–527.

Pons TP, Garraghty PE, Ommaya AK, Kaas JH, Taub E, Mishkin M. 1991. Massive cortical reorganization after sensory deafferentation in adult macaques. Science 252:1857–1860.

Pruszynski JA, Johansson RS. 2014. Edge-orientation processing in first-order tactile neurons. Nat Neurosci 17:1404–1409.

Quilliam TA. 1978. The structure of finger print skin. In: G Gordon (ed). *Active Touch*, pp. 1–18. Oxford: Pergamon Press.

Robinson CJ, Burton H. 1980. Somatic submodality distribution within the second somatosensory (SII), 7b, retroinsular, postauditory and granular insular cortical areas of *M. fascicularis*. J Comp Neurol 192:93–108.

Romo R, Hernandez A, Zainos A, Lemus L, Brody CD. 2002. Neuronal correlates of decision-making in secondary somatosensory cortex. Nat Neurosci 5:1217–1235.

Saal HP, Bensmaia SJ. 2014. Touch is a team effort: interplay of submodalities in cutaneous sensibility. Trends Neurosci 37:689–697.

Salinas E, Hernandez A, Zainos A, Romo R. 2000. Periodicity and firing rate as candidate neural codes for the frequency of vibrotactile stimuli. J Neurosci 20:5503–5515.

Snider WD. 1998. How do you feel? Neurotrophins and mechanotransduction. Nat Neurosci 1:5–6.

Srinivasan MA, Whitehouse JM, LaMotte RH. 1990. Tactile detection of slip: surface microgeometry and peripheral neural codes. J Neurophysiol 63:1323–1332.

Sripati AP, Yoshioka T, Denchev P, Hsiao SS, Johnson KO. 2006. Spatiotemporal receptive fields of peripheral afferents and cortical area 3b and 1 neurons in the primate somatosensory system. J Neurosci 26:2101–2114.

Talbot WH, Darian-Smith I, Kornhuber HH, Mountcastle VB. 1968. The sense of flutter-vibration: comparison of the human capacity with response patterns of mechanoreceptive afferents from the monkey hand. J Neurophysiol 31:301–334.

Vega-Bermudez F, Johnson KO. 1999. Surround suppression in the responses of primate SA1 and RA mechanoreceptive afferents mapped with a probe array. J Neurophysiol 81:2711–2719.

Warren S, Hämäläinen HA, Gardner EP. 1986. Objective classification of motion- and direction-sensitive neurons in primary somatosensory cortex of awake monkeys. J Neurophysiol 56:598–622.

Weber AI, Saal HP, Lieber JD, et al. 2013. Spatial and temporal codes mediate the tactile perception of natural textures. Proc Nat Acad Sci USA 110:17107–17112.

Weinstein S. 1968. Intensive and extensive aspects of tactile sensitivity as a function of body part, sex, and laterality. In: DR Kenshalo (ed). *The Skin Senses*, pp. 195–222. Springfield, IL: Thomas.

Westling G, Johansson RS. 1987. Responses in glabrous skin mechanoreceptors during precision grip in humans. Exp Brain Res 66:128–140.

Wimmer VC, Bruno RM, de Kock CP, Kuner T, Sakmann B. 2010. Dimensions of a projection column and architecture of VPM and POm axons in rat vibrissal cortex. Cereb Cortex 20:2265–2276.

20

Pain

According to the International Association for the Study of Pain, pain is an unpleasant sensation and emotional experience associated with actual or potential tissue damage, or described in terms of such damage. Pricking, burning, aching, stinging, and soreness are among the most distinctive of all the sensory modalities. As with the other somatosensory modalities—touch, pressure, and position sense—pain serves an important protective function, alerting us to injuries that require evasion or treatment. In children born with insensitivity to pain, severe injuries often go unnoticed and can lead to permanent tissue damage. Yet pain is unlike other somatosensory modalities, or vision, hearing, and smell, in that it has an urgent and primitive quality, possessing a powerful emotional component.

The perception of pain is subjective and is influenced by many factors. An identical sensory stimulus can elicit quite distinct responses in the same individual under different conditions. Many wounded soldiers, for example, do not feel pain until they have been removed from the battlefield; injured athletes are often not aware of pain until a game is over. Simply put, there are no purely "painful" stimuli, sensory stimuli that invariably elicit the perception of pain in all individuals. The variability of the perception of pain is yet another example of a principle that we have encountered in earlier chapters: Pain is not the direct expression of a sensory event but rather the product of elaborate processing in the brain of a variety of neural signals.

When pain is experienced, it can be acute, persistent, or, in extreme cases, chronic. Persistent pain characterizes many clinical conditions and is usually the reason that patients seek medical attention. In contrast, chronic pain appears to have no useful purpose; it only makes patients miserable. Pain's highly individual and subjective nature is one of the factors that make it so difficult to define objectively and to treat clinically.

In this chapter, we discuss the neural processes that underlie the perception of pain in normal individuals and explain the origins of some of the abnormal pain states that are encountered clinically.

Noxious Insults Activate Thermal, Mechanical, and Polymodal Nociceptors

Many organs in the periphery, including skin and subcutaneous structures such as joints and muscles, possess specialized sensory receptors that are activated by noxious insults. Unlike the specialized somatosensory receptors for light touch and pressure, most of these *nociceptors* are simply the free nerve endings of primary sensory neurons. There are three main classes of nociceptors—thermal, mechanical, and polymodal—as well as a more enigmatic fourth class, termed silent nociceptors.

Thermal nociceptors are activated by extremes in temperature, typically greater than 45°C (115°F) or less than 5°C (41°F). They include the peripheral endings of small-diameter, thinly myelinated Aδ axons that conduct action potentials at speeds of 5 to 30 m/s and unmyelinated C-fiber axons that conduct at speeds less than 1.0 m/s (Figure 20–1A). *Mechanical nociceptors* are activated optimally by intense pressure applied to the skin; they too are the endings of thinly myelinated Aδ axons. *Polymodal nociceptors* can be activated by high-intensity mechanical, chemical, or thermal (both hot and cold) stimuli. This class of nociceptors consists predominantly of unmyelinated C fibers (Figure 20–1A).

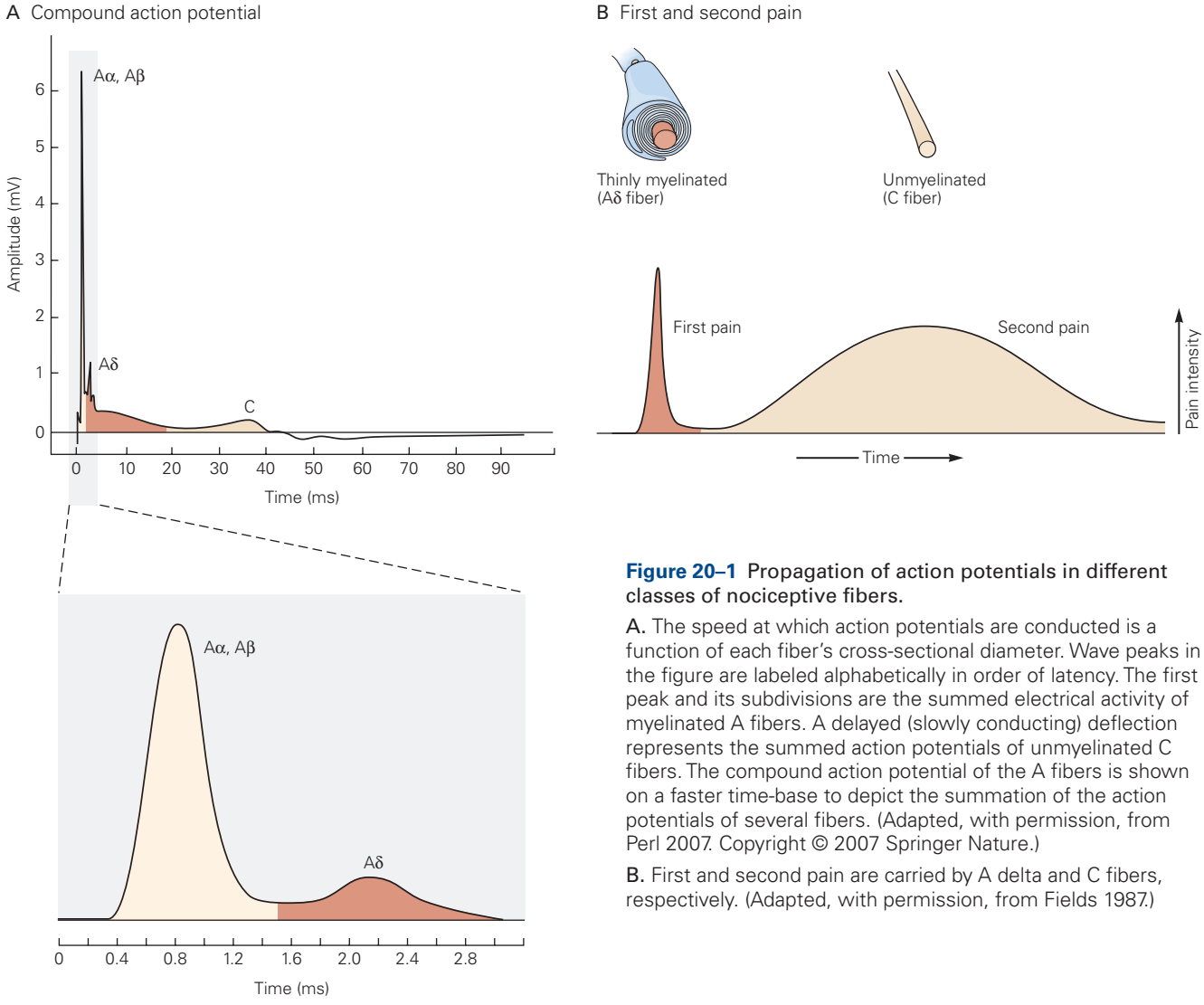

Figure 20–1 Propagation of action potentials in different classes of nociceptive fibers.

A. The speed at which action potentials are conducted is a function of each fiber's cross-sectional diameter. Wave peaks in the figure are labeled alphabetically in order of latency. The first peak and its subdivisions are the summed electrical activity of myelinated A fibers. A delayed (slowly conducting) deflection represents the summed action potentials of unmyelinated C fibers. The compound action potential of the A fibers is shown on a faster time-base to depict the summation of the action potentials of several fibers. (Adapted, with permission, from Perl 2007. Copyright © 2007 Springer Nature.)

B. First and second pain are carried by A delta and C fibers, respectively. (Adapted, with permission, from Fields 1987.)

These three classes of nociceptors are widely distributed in skin and deep tissues and are often co-activated. When a hammer hits your thumb, you initially feel a sharp pain ("first pain") followed by a more prolonged aching and sometimes burning pain ("second pain") (Figure 20–1B). The fast sharp pain is transmitted by Aδ fibers that carry information from damaged thermal and mechanical nociceptors. The slow dull pain is transmitted by C fibers that convey signals from polymodal nociceptors.

Silent nociceptors are found in the viscera. This class of receptors is not normally activated by noxious stimulation; instead, inflammation and various chemical agents dramatically reduce their firing threshold. Their activation is thought to contribute to the emergence of secondary hyperalgesia and central sensitization, two prominent features of chronic pain.

Noxious stimuli depolarize the bare nerve endings of afferent axons and generate action potentials that are propagated centrally. How is this achieved? The membrane of the nociceptor contains receptors that convert the thermal, mechanical, or chemical energy of noxious stimuli into a depolarizing electrical potential. One such protein is a member of a large family of so-called transient receptor potential (TRP) ion channels. This receptor-channel, TRPV1, is expressed selectively by nociceptive neurons and mediates the pain-producing actions of capsaicin, the active ingredient of hot peppers and many other pungent chemicals. The TRPV1 channel is also activated by noxious thermal stimuli, with a threshold for activation around 45°C, the temperature that provokes heat pain. Importantly, TRPV1-mediated membrane currents are enhanced by a reduction in pH, a characteristic of the chemical milieu of inflammation.

Other receptor-channels of the TRP channel family are expressed by nociceptors and underlie the perception of a wide range of temperatures, from cold to intense heat. Of particular interest is TRPM8, a menthol-responsive and cold-sensing channel that likely mediates the extreme cold hypersensitivity produced by many chemotherapeutic drugs (such as oxaliplatin). TRPA1 responds to a variety of irritants, from mustard oil to garlic and even air pollutants (Figure 20–2). Very recently, a family of mechanical transducers (Piezo1 and Piezo2) was described (Chapter 18). These channels may be important contributors to the mechanical hypersensitivity that is a prominent feature of many chronic pain conditions.

In addition to this constellation of TRP channels, sensory neurons express many other receptors and ion channels involved in the transduction of peripheral stimuli. Nociceptors selectively express many different voltage-gated Na^{2+} channels, which are the target of local anesthetics that so effectively block pain. (Think of the dentist who can completely eliminate tooth pain.) Nociceptors express Na^{2+} channels that are sensitive or resistant to tetrodotoxin (TTX). One type of TTX-sensitive channel, Nav1.7, is a key molecular mechanism in the perception of pain in humans, as revealed in the rare individuals who have a loss-of-function mutation in the corresponding *SCN9A* gene. These individuals are insensitive to pain but are otherwise healthy and exhibit normal sensory responses to touch, temperature, proprioception, tickle, and pressure. A second class of mutations in the *SCN9A* gene result in hyperexcitability of nociceptors; individuals with these mutations exhibit an inherited condition called erythromelalgia, in which there is intense, ongoing burning pain of the extremities, accompanied by profound redness (vasodilation). Since Nav1.7, unlike many other voltage-gated Na^{+} channels, is not found in the central nervous system, pharmaceutical companies are developing antagonists that will hopefully provide a novel approach to regulating pain processing without the adverse side effects that can occur with systemic administration of lidocaine, which blocks all subtypes of voltage-gated Na^{+} channels.

Nociceptors also express an ionotropic purinergic receptor, PTX3, which is activated by adenosine triphosphate (ATP) released from peripheral cells after tissue damage. In addition, they express members of the Mas-related G protein–coupled receptor (Mrg) family, which are activated by peptide ligands and serve to sensitize nociceptors to other chemicals released in their local environment (see Figure 20–7). Subsets of these unmyelinated afferents also include receptor-channels that respond to a variety of itch-provoking substances, including the pruritogens histamine and chloroquine. It follows that these receptors and channels are attractive targets for the development of drugs selective for sensory neurons responsive to pain and itch-provoking stimuli.

Uncontrolled activation of nociceptors is associated with several pathological conditions. Two common pain states that result from alterations in nociceptor activity are allodynia and hyperalgesia. Patients with *allodynia* feel pain in response to stimuli that are normally innocuous: a light stroking of sunburned skin, the movement of joints in patients with rheumatoid arthritis, and even the act of getting out of bed in the morning after a vigorous workout. Nevertheless, patients with allodynia do not feel pain constantly; in the absence of a peripheral stimulus, there is no pain. In contrast, patients with *hyperalgesia*—an exaggerated

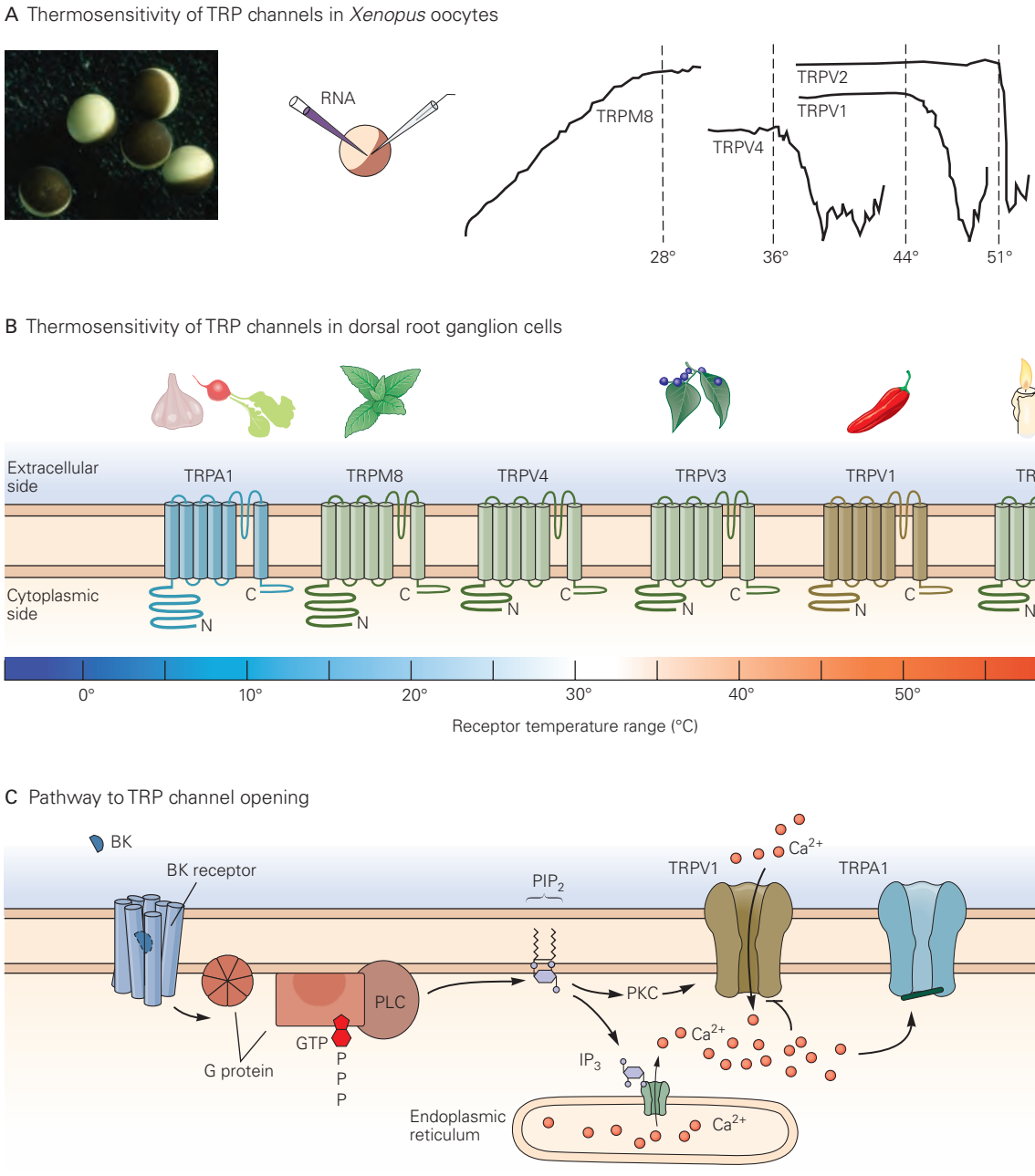

Figure 20–2 Transient receptor potential ion channels in nociceptive neurons.

A. Recordings from *Xenopus* oocytes injected with mRNA encoding transient receptor potential (**TRP**) channels reveal the thermosensitivity of the channels. The temperature (centigrade) at which a specific TRP channel is activated is shown by the downward deflection of the recording. (Photograph on left reproduced, with permission, from Erwin Siegel 1987; traces on the right reproduced, with permission, from Tominaga and Caterina 2004.)

B. Temperature response profiles of different TRP channels expressed by dorsal root ganglion neurons. (Adapted, with permission, from Jordt, McKemy, and Julius 2003; Dhaka, Viswanath, and Patapoutian 2006.)

C. Bradykinin (**BK**) binds to G protein–coupled receptors on the surface of primary afferent neurons to activate phospholipase C (**PLC**), leading to the hydrolysis of membrane phosphatidylinositol bisphosphate (PIP_2), the production of inositol 1,4,5-trisphosphate (IP_3), and the release of Ca^{2+} from intracellular stores. Activation of protein kinase C (**PKC**) regulates TRP channel activity. The TRPV1 channel is sensitized, leading to channel opening and Ca^{2+} influx. (Source: Bautista et al. 2006.)

response to noxious stimuli—typically report persistent pain in the absence of sensory stimulation.

Persistent pain can be subdivided into two broad classes, nociceptive and neuropathic. *Nociceptive pain* results from the activation of nociceptors in the skin or soft tissue in response to tissue injury, and it usually occurs with inflammation. Sprains and strains produce mild forms of nociceptive pain, whereas arthritis or a tumor that invades soft tissue produce a much more severe nociceptive pain. Typically, nociceptive pain is treated with nonsteroidal anti-inflammatory drugs (NSAIDS; see later discussion) or, when severe, with opiates such as morphine.

Neuropathic pain results from direct injury to nerves in the peripheral or central nervous system, and is often accompanied by a burning or electric sensation. Neuropathic pains include complex regional pain syndrome, which can follow even very minor damage to a limb peripheral nerve; post-herpetic neuralgia, the severe pain experienced by many patients after a bout of shingles; or trigeminal neuralgia, an intense, shooting pain in the face that results from an as yet unknown pathology of the trigeminal nerve. Other neuropathic pains include phantom limb pain, which can occur after limb amputation (see Figure 20–14). In some instances, spontaneous, ongoing, often burning pain can even occur without a peripheral stimulus, a phenomenon termed *anesthesia dolorosa*. This syndrome can be triggered following attempts to treat trigeminal neuralgia by ablating trigeminal sensory neurons. Neuropathic pains do not respond to NSAIDS and are generally poorly responsive to opiates. Finally, lesions of the central nervous system, for example, in multiple sclerosis, after stroke, or after spinal cord injury, can also result in central neuropathic pain states. Since loss of inhibitory controls (as occurs in epilepsy) is an important contributor to neuropathic pain, the first-line therapy for neuropathic pain, not surprisingly, involves anticonvulsants, notably the gabapentinoids. (The reference to γ-aminobutyric acid [GABA] was based on a structural similarity of gabapentin to GABA. However, gabapentin in fact exerts its action by binding to the $\alpha_2\delta$-subunit of voltage-gated Ca^{2+} channels, ultimately decreasing neurotransmitter release.)

Signals From Nociceptors Are Conveyed to Neurons in the Dorsal Horn of the Spinal Cord

The sensation of noxious stimuli arises from signals in the peripheral axonal branches of nociceptive sensory neurons whose cell bodies are located in dorsal root ganglia. The central branches of these neurons terminate in the spinal cord in a highly orderly manner. Most terminate in the dorsal horn. Primary afferent neurons that convey distinct sensory modalities terminate in different laminae (Figure 20–3B) such that there is a tight link between the anatomical organization of dorsal horn neurons, their receptive properties, and their function in sensory processing.

Many neurons in the most superficial lamina of the dorsal horn, termed *lamina I* or the *marginal layer*, respond to noxious stimuli conveyed by Aδ and C fibers. Because they respond selectively to noxious stimulation, they have been called *nociceptive-specific neurons*. This set of neurons projects to the midbrain and thalamus. A second class of lamina I neurons receives input from C fibers that are activated selectively by cool stimuli. Other classes of lamina I neurons respond in a graded fashion to both innocuous and noxious mechanical stimulation and thus are termed *wide dynamic range neurons*.

Lamina II, the substantia gelatinosa, is a densely packed layer that contains many different classes of local interneurons, some excitatory and others inhibitory. Some of these interneurons respond selectively to pain-provoking inputs, whereas others are selectively activated by itch-provoking stimuli. Laminae III and IV contain a mixture of local interneurons and supraspinal projection neurons. Many of these neurons receive input from Aβ afferent fibers that respond to innocuous cutaneous stimuli, such as deflection of hairs and light pressure. Lamina V contains neurons that respond to a wide variety of noxious stimuli and project to the brain stem and thalamus. These neurons receive direct inputs from Aβ and Aδ fibers and, because their dendrites extend into lamina II, are also innervated by C-fiber nociceptors (Figure 20–3B).

Neurons in lamina V also receive input from nociceptors in visceral tissues. The convergence of somatic and visceral nociceptive inputs onto individual lamina V neurons provides one explanation for a phenomenon called "referred pain," a condition in which pain from injury to a visceral tissue is perceived as originating from a region of the body surface. Patients with myocardial infarction, for example, frequently report pain from the left arm as well as the chest (Figure 20–4). This phenomenon occurs because a single lamina V neuron receives sensory input from both regions, and thus a signal from this neuron does not inform higher brain centers about the source of the input. As a consequence, the brain often incorrectly attributes the pain to the skin, possibly because cutaneous inputs predominate. Another anatomical explanation for instances of referred pain is that the axons of nociceptive sensory

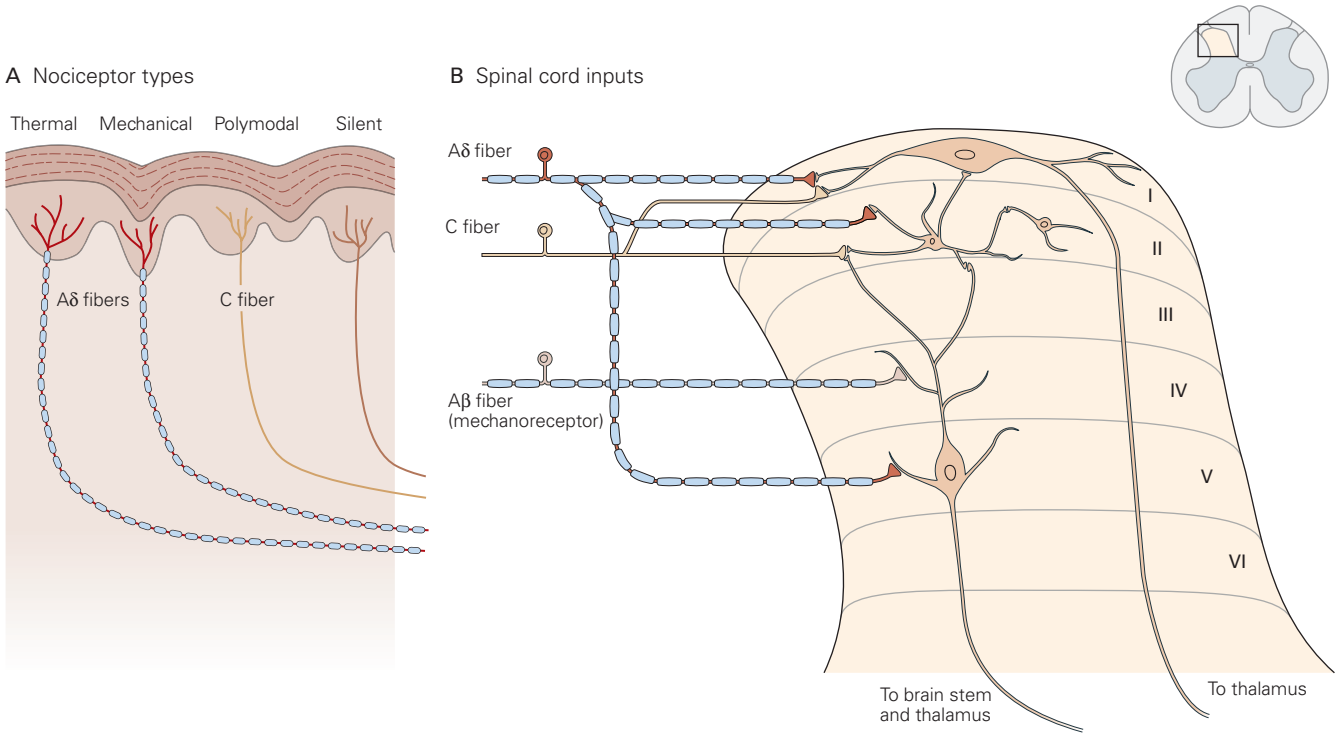

Figure 20–3 Nociceptive fibers terminate in different laminae of the dorsal horn of the spinal cord.

A. There are three main classes of peripheral nociceptor as well as the silent nociceptors, which are activated by inflammation and various chemical substances.

B. Neurons in lamina I of the dorsal horn receive direct input from myelinated (Aδ) nociceptive fibers and both direct and indirect input from unmyelinated (C) nociceptive fibers via interneurons in lamina II. Lamina V neurons receive low-threshold input from large-diameter myelinated Aβ mechanoreceptive fibers as well as inputs from nociceptive Aδ and C fibers. Lamina V neurons send dendrites to lamina IV, where they are contacted by the terminals of Aβ primary afferents. Axon terminals of lamina II interneurons can make contact with dendrites in lamina III that arise from cells in lamina V. Aα primary afferents contact motor neurons and interneurons in the ventral spinal cord (not shown). (Adapted, with permission, from Fields 1987.)

neurons branch in the periphery, innervating both skin and visceral targets.

Neurons in lamina VI receive inputs from large-diameter primary afferent fibers that innervate muscles and joints. These neurons are activated by innocuous joint movement and do not contribute to the transmission of nociceptive information. Many neurons in laminae VII and VIII, the intermediate and ventral regions of the spinal cord, do respond to noxious stimuli. These neurons typically have complex response properties because the inputs from nociceptors to these neurons are conveyed through many intervening synapses. Neurons in lamina VII often respond to stimulation of either side of the body, whereas most dorsal horn neurons receive unilateral input. The activation of lamina VII neurons is therefore thought to contribute to the diffuse quality of many pain conditions.

Nociceptive sensory neurons that activate neurons in the dorsal horn of the spinal cord release two major classes of neurotransmitters. Glutamate is the primary neurotransmitter of all primary sensory neurons, regardless of sensory modality. Neuropeptides are released as cotransmitters by many nociceptors with unmyelinated axons. These peptides include substance P, calcitonin gene–related peptide (CGRP), somatostatin, and galanin (Figure 20–5). Glutamate is stored in small, electron-lucent vesicles, whereas peptides are sequestered in large, dense-core vesicles at the central terminals of nociceptive sensory neurons (Figure 20–6). Separate storage sites permit these two classes of neurotransmitters to be selectively released under different physiological conditions.

Of the neuropeptide transmitters released by nociceptive sensory neurons, the actions of substance P, a member of the neurokinin peptide family, have been studied in most detail. Substance P is released from the central terminals of nociceptive afferents in response to tissue injury or after intense stimulation of peripheral

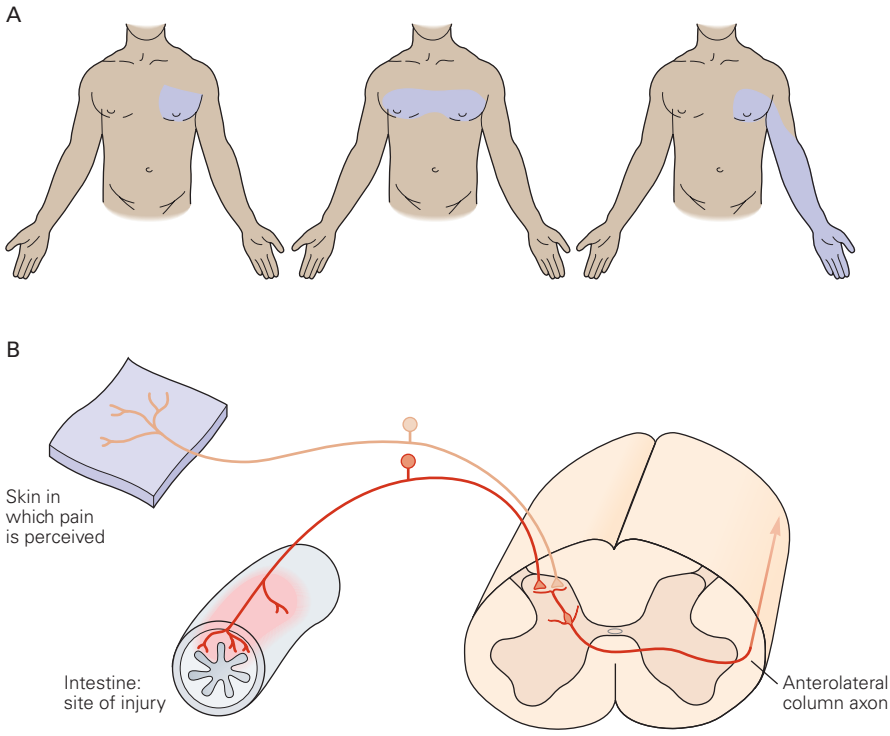

Figure 20–4 Signals from nociceptors in the viscera can be felt as "referred pain" elsewhere in the body.

A. Myocardial infarction and angina can be experienced as deep referred pain in the chest and left arm. The source of the pain cannot be readily predicted from the site of referred pain.

B. Convergence of visceral and somatic afferent fibers may account for referred pain. Nociceptive afferent fibers from the viscera and fibers from specific areas of the skin converge on the same projection neurons in the dorsal horn. The brain has no way of knowing the actual site of the noxious stimulus and mistakenly associates a signal from a visceral organ with an area of skin. (Adapted, with permission, from Fields 1987.)

nerves. Its interaction with neurokinin receptors on dorsal horn neurons elicits slow excitatory postsynaptic potentials that prolong the depolarization elicited by glutamate. Although the physiological actions of glutamate and neuropeptides on dorsal horn neurons are different, these transmitters act coordinately to regulate the firing properties of dorsal horn neurons.

Details of the interaction of neuropeptides with their receptors on dorsal horn neurons have suggested strategies for chronic pain regulation. Infusion of substance P coupled to a neurotoxin into the dorsal horn of experimental animals results in selective destruction of neurons that express neurokinin receptors. Animals treated in this way fail to develop the central sensitization that is normally associated with peripheral injury. This method of neuronal ablation is more selective than traditional surgical interventions such as partial spinal cord transection (anterolateral cordotomy) and is being considered as a treatment for patients suffering from otherwise intractable chronic pain.

Hyperalgesia Has Both Peripheral and Central Origins

Up to this point, we have considered the conveyance of noxious signals in the normal physiological state. But the normal process of sensory signaling can be dramatically altered when peripheral tissue is damaged, resulting in an increase in pain sensitivity or hyperalgesia. This condition can be elicited by sensitizing peripheral nociceptors through repetitive exposure to noxious stimuli (Figure 20–7).

The sensitization is triggered by a complex mix of chemicals released from damaged cells that accumulate at the site of tissue injury. This cocktail contains peptides and proteins such as bradykinin, substance P, and nerve growth factor, as well as molecules such as ATP, histamine, serotonin, prostaglandins, leukotrienes, and acetylcholine. Many of these chemical mediators are released from distinct cell types, but together they act to decrease the threshold of nociceptor activation.

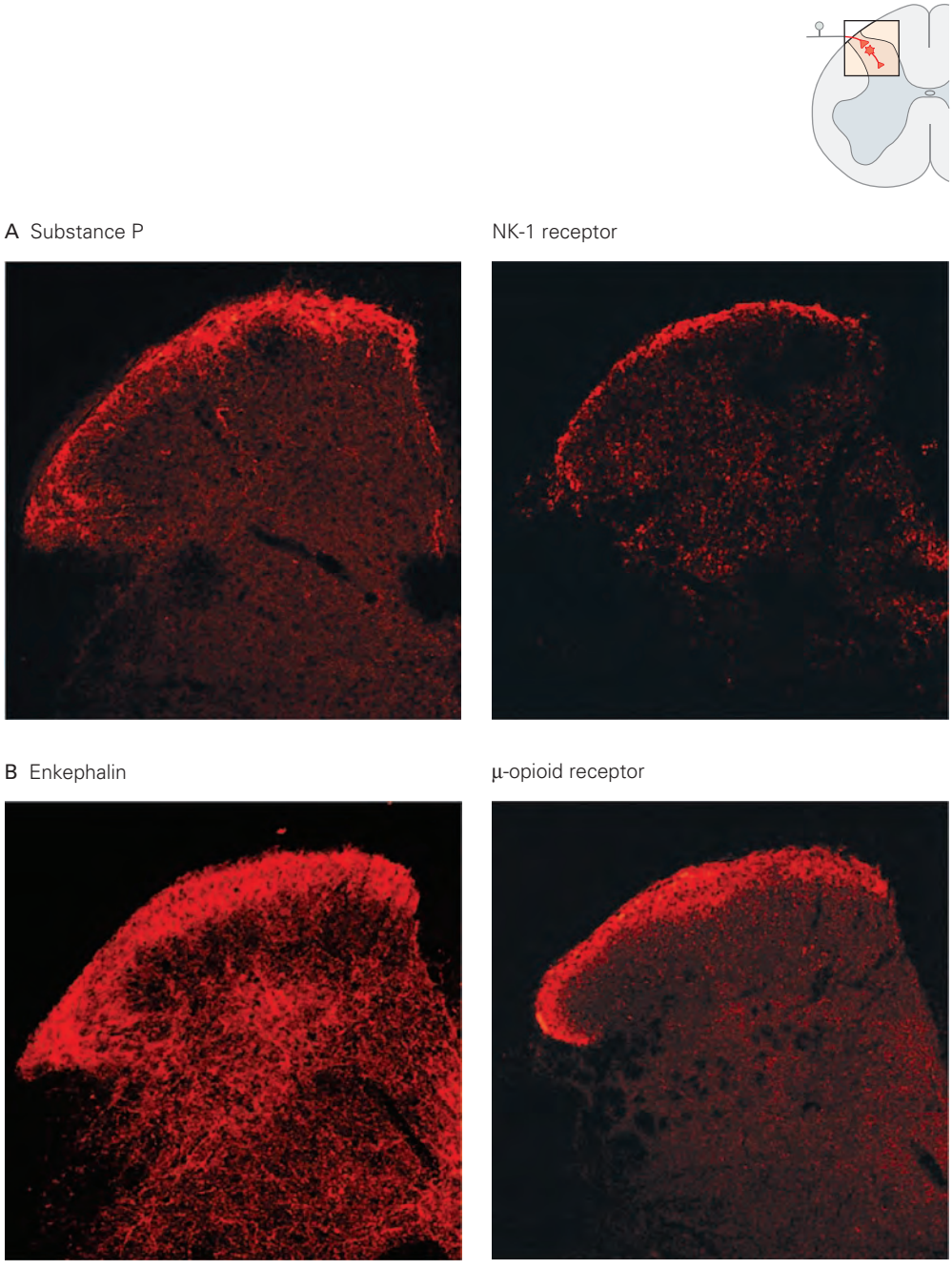

Figure 20–5 Neuropeptides and their receptors in the superficial dorsal horn of the rat spinal cord. (Images reproduced, with permission, from A. Basbaum.)

A. The terminals of unmyelinated primary sensory neurons are a major source of substance P in the superficial dorsal horn. Substance P activates the neurokinin-1 (**NK1**) receptor, which is expressed by neurons in the superficial dorsal horn, the majority of which are projection neurons.

B. Enkephalin is localized in interneurons and found in the same region of the dorsal horn as terminals containing substance P. The μ-opioid receptor, which is targeted by enkephalins, is expressed by neurons in the superficial dorsal horn and also, presynaptically, on the terminals of sensory neurons.

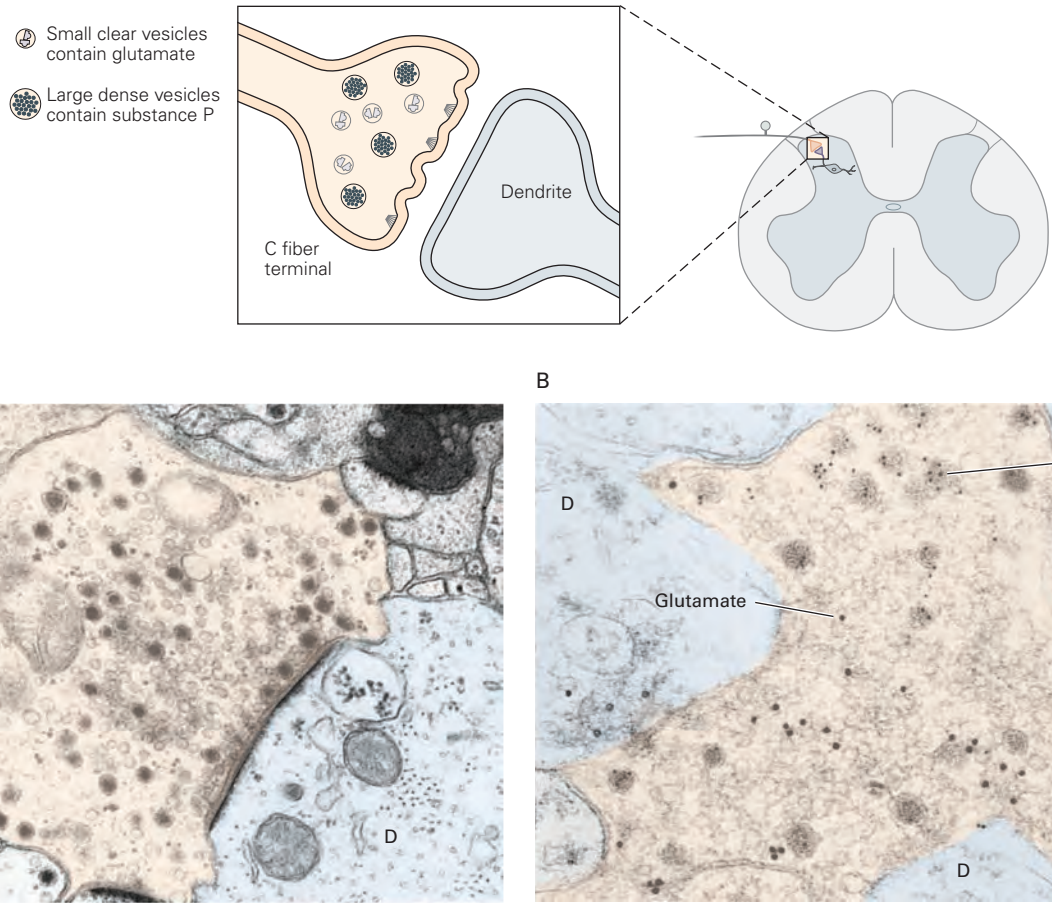

Figure 20–6 Transmitter storage in the synaptic terminals of primary nociceptive neurons in the dorsal spinal cord.

A. The terminal of a C fiber on the dendrite (D) of a dorsal horn neuron has two classes of synaptic vesicles that contain different transmitters. Small electron-lucent vesicles contain glutamate, whereas large dense-cored vesicles store neuropeptides. (Image reproduced, with permission, from H. J. Ralston III.)

B. Glutamate and the peptide substance P (marked by large and small gold particles, respectively) are scattered in the axoplasm of a sensory neuron terminal in lamina II of the dorsal horn. Dense core vesicles also store calcitonin gene–related peptide (CGRP). (Reproduced, with permission, from De Biasi and Rustioni 1990.)

Where do these chemicals come from, and what exactly do they do? Histamine is released from mast cells after tissue injury and activates polymodal nociceptors. The lipid anandamide, an endogenous cannabinoid agonist, is released under conditions of inflammation, activates the TRPV1 channel, and may trigger pain associated with inflammation. ATP, acetylcholine, and serotonin are released from damaged endothelial cells and platelets; they act indirectly to sensitize nociceptors by triggering the release of chemical agents such as prostaglandins and bradykinin from peripheral cells.

Bradykinin is one of the most active pain-producing agents. Its potency stems in part from the fact that it directly activates Aδ and C nociceptors and increases the synthesis and release of prostaglandins from nearby cells. Prostaglandins are metabolites of arachidonic acid that are generated through the activity of cyclooxygenase (COX) enzymes that cleave arachidonic acid (Chapter 14). The COX-2 enzyme is preferentially induced under conditions of peripheral inflammation, contributing to enhanced pain sensitivity. The enzymatic pathways of prostaglandin synthesis are targets of commonly used analgesic drugs. Aspirin and other nonsteroidal anti-inflammatory analgesics, such as ibuprofen and naproxen, are effective in controlling pain because they block the activity of the COX enzymes, reducing prostaglandin synthesis.

Activity of peripheral nociceptors can also produce all of the cardinal signs of inflammation, including heat

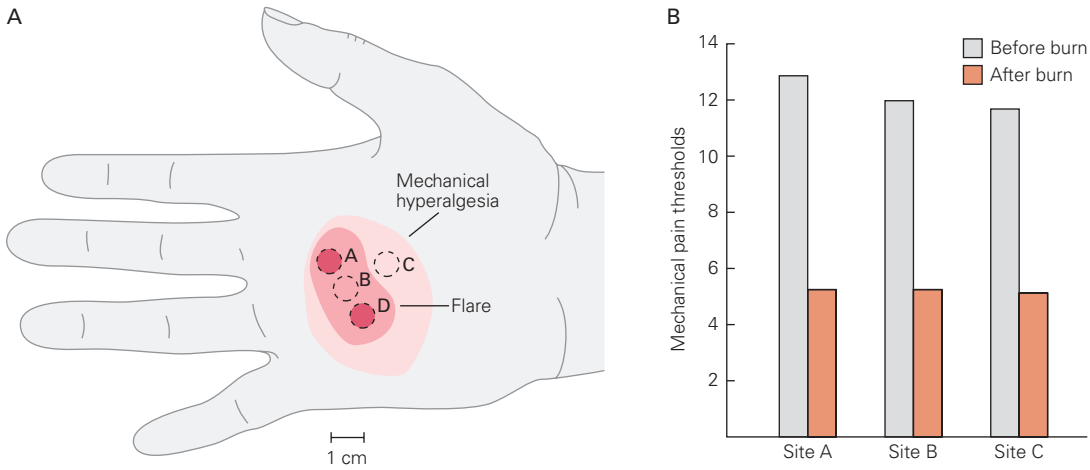

Figure 20–7 Hyperalgesia results from sensitization of nociceptors. (Reproduced, with permission, from Raja, Campbell, and Meyer 1984. Copyright © 1984, Oxford University Press.)

A. Mechanical thresholds for pain were recorded at sites A, B, and C before and after burns at sites A and D. The areas of reddening (flare) and mechanical hyperalgesia resulting from the burns are shown on the hand of one subject. In all subjects, the area of mechanical hyperalgesia was larger than the area of flare. Mechanical hyperalgesia was present even after the flare disappeared.

B. Mean mechanical pain thresholds before and after burns. The mechanical threshold for pain is significantly decreased after the burn.

(calor), redness (rubor), and swelling (tumor). Heat and redness result from the dilation of peripheral blood vessels, whereas swelling results from plasma extravasation, a process in which proteins, cells, and fluids are able to penetrate postcapillary venules. Release of the neuropeptides substance P and CGRP from the peripheral terminals of C fibers provokes plasma extravasation and vasodilation, respectively. Because this form of inflammation depends on neural activity, it has been termed *neurogenic inflammation* (Figure 20–8). Importantly, as profound peripheral vasodilation is a critical trigger of many migraine headaches, the development of antibodies to CGRP, which counteract the vasodilation by scavenging CGRP, offers significant hope for a new migraine therapy.

The release of substance P and CGRP from the peripheral terminals of sensory neurons is also responsible for the *axon reflex*, a physiological process characterized by vasodilation in the vicinity of a cutaneous injury. Pharmacological antagonists of substance P are able to block neurogenic inflammation and vasodilation in humans; this discovery illustrates how knowledge of nociceptive mechanisms can be applied in improving clinical therapies for pain.

In addition to these small molecules and peptides, neurotrophins are causative agents in pain. Nerve growth factor (NGF) and brain-derived neurotrophic factor (BDNF) are particularly active in inflammatory pain states. The synthesis of BDNF is upregulated in many inflamed peripheral tissues (Figure 20–9). NGF-neutralizing molecules are effective analgesic agents in animal models of persistent pain. Indeed, inhibition of NGF function and signaling blocks pain sensation as effectively as COX inhibitors and opiates. Several promising clinical trials using antibodies to NGF for the management of knee osteoarthritis have been reported, once again demonstrating the translation of basic science to the clinic.

What accounts for the enhanced sensitivity of dorsal horn neurons to nociceptor signals? Under conditions of persistent injury, C fibers fire repetitively and the response of dorsal horn neurons increases progressively (Figure 20–10A). The gradual enhancement in the excitability of dorsal horn neurons has been termed "windup" and is thought to involve *N*-methyl-D-aspartate (NMDA)-type glutamate receptors (Figure 20–10B).

Repeated exposure to noxious stimuli therefore results in long-term changes in the response of dorsal horn neurons through mechanisms that are similar to those underlying the long-term potentiation of synaptic responses in many circuits in the brain. In essence, these prolonged changes in the excitability of dorsal horn neurons constitute a "memory" of the state of C-fiber input. This phenomenon has been termed *central sensitization* to distinguish it from sensitization at the peripheral terminals of the dorsal horn neurons, a process that involves activation of the enzymatic pathways of prostaglandin synthesis.

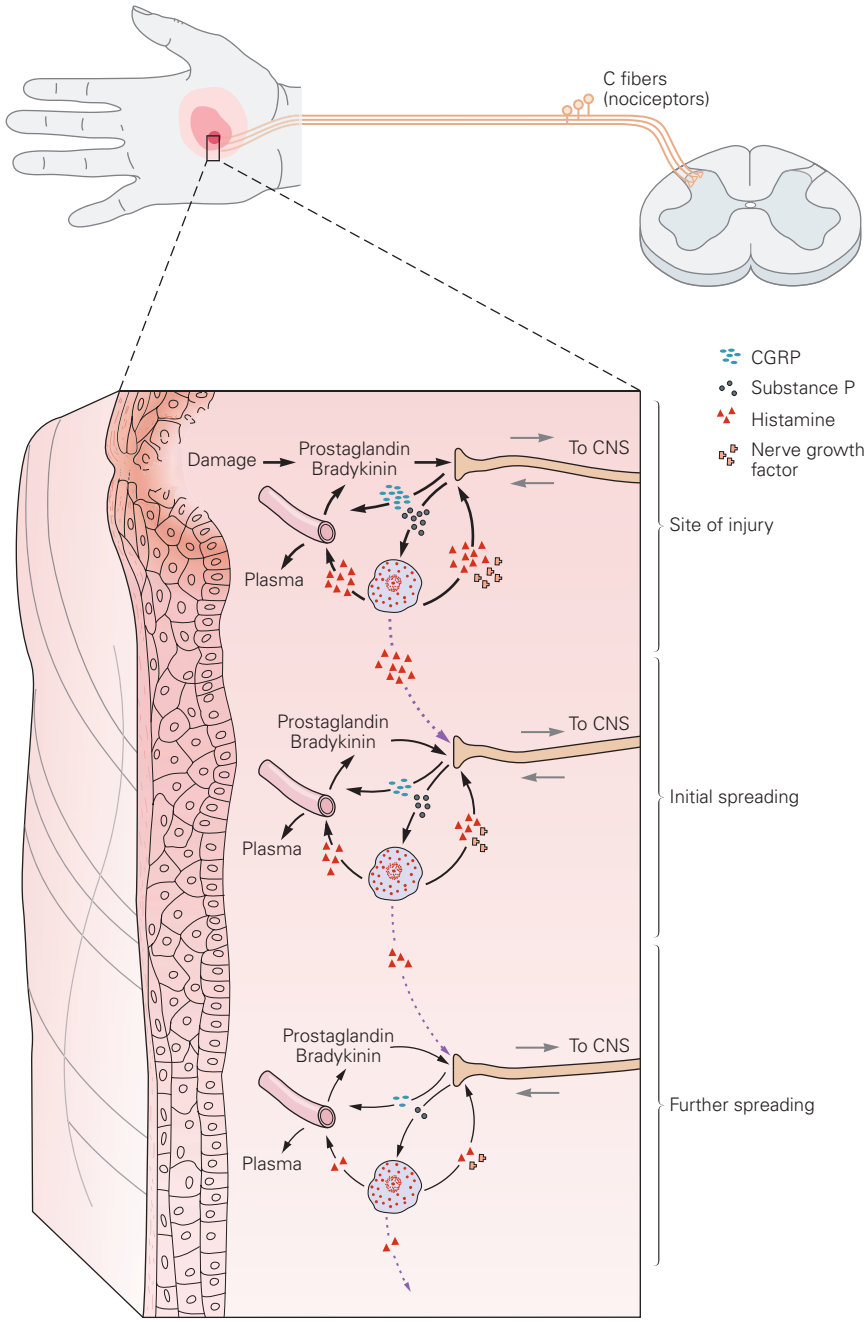

Figure 20–8 **Neurogenic inflammation.** Injury or tissue damage releases bradykinin and prostaglandins, which activate or sensitize nociceptors. Activation of nociceptors leads to the release of substance P and calcitonin gene–related peptide (**CGRP**). Substance P acts on mast cells (**light blue**) in the vicinity of sensory endings to evoke degranulation and the release of histamine, which directly excites nociceptors. Substance P also produces plasma extravasation and edema, and CGRP produces dilation of peripheral blood vessels (leading to reddening of the skin); the resultant inflammation causes additional liberation of bradykinin. These mechanisms also occur in healthy tissue, where they contribute to secondary or spreading hyperalgesia. (Abbreviation: **CNS**, central nervous system.)

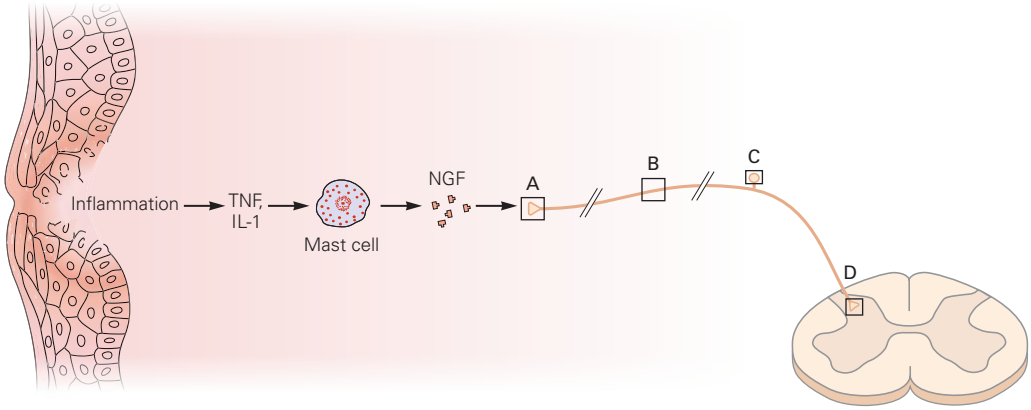

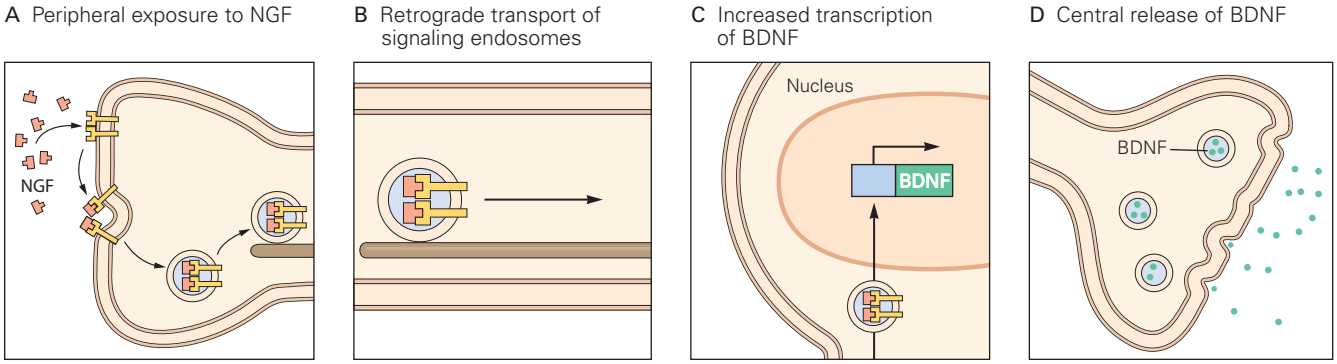

Figure 20–9 **Neurotrophins are pain mediators.** Local production of inflammatory cytokines such as interleukin-1 (**IL-1**) and tumor necrosis factor (**TNF**) promotes the synthesis and release of nerve growth factor (**NGF**) from several cell types in the periphery. Nerve growth factor binds to TrkA receptors on primary nociceptive terminals (**A**), triggering upregulation in expression of ion channels that increase nociceptor excitability. Retrograde transport of signaling endosomes to the cell body (**B**) results in enhanced expression of brain-derived neurotrophic factor (**BDNF**) (**C**), and its release from sensory terminals in the spinal cord (**D**) further increases excitability of dorsal horn neurons.

The sensitization of dorsal horn neurons also involves recruitment of second-messenger pathways and activation of protein kinases that have been implicated in memory storage in other regions of the central nervous system. One consequence of this enzymatic cascade is the expression of immediate-early genes that encode transcription factors such as *c-fos*, which are thought to activate effector proteins that sensitize dorsal horn neurons to sensory inputs. Most importantly, central sensitization of "pain" transmission circuitry in the dorsal horn is the process that can decrease pain thresholds (allodynia) and lead to *spontaneous pain* (ie, ongoing pain in the absence of peripheral stimulation).

Central sensitization is also a major contributor to neuropathic pain due to nerve injury. Here again, there is increased excitability of dorsal horn circuits mediated by NMDA receptors. There is also loss of inhibitory controls in the dorsal horn. Under normal conditions, GABAergic inhibitory interneurons in the dorsal horn are not only tonically active but are also turned on by activity of large-diameter, nonnociceptive Aβ fibers (Figure 20–11A). Peripheral nerve damage decreases the GABAergic controls, thus exacerbating the hyperactivity of these nociceptive pathways (Figure 20–11B). Recent studies also implicate nerve injury–induced activation of microglia and consequent reduced GABAergic inhibition in the central sensitization process (Figures 20–11C and 20–12). Together, these changes contribute to *mechanical allodynia* (ie, pain provoked by normally innocuous mechanical stimulation). Mechanical allodynia can also develop because of an inappropriate engagement of dorsal horn nociceptive pathway circuits by the Aβ myelinated afferents. In fact, spread of pain (secondary hyperalgesia) can occur because uninjured Aβ afferents outside of

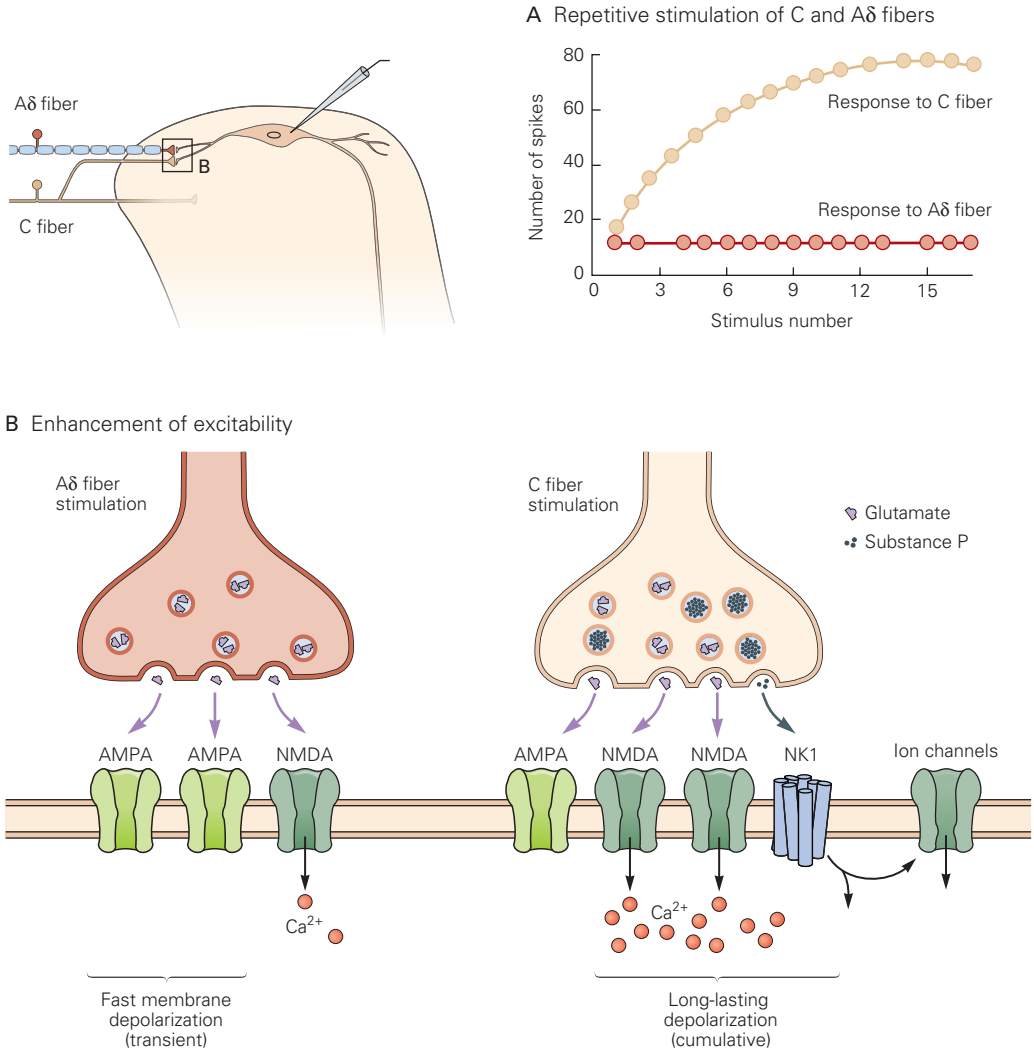

Figure 20–10 Mechanisms for enhanced excitability of dorsal horn neurons.

A. Typical responses of a dorsal horn neuron in the rat to electrical stimuli delivered transcutaneously at a frequency of 1 Hz. With repetitive stimulation, the long-latency component evoked by a C fiber increases gradually, whereas the short-latency component evoked by an A fiber remains constant.

B. Dorsal horn neurons receive mono- and polysynaptic input from Aδ and C fiber nociceptors. Elevation of residual Ca^{2+} in the presynaptic terminal leads to increased release of glutamate and substance P (and CGRP, not shown). *Left:* Activation of postsynaptic AMPA receptors by Aδ fibers causes a fast transient membrane depolarization, which relieves the Mg^{2+} block of the NMDA receptors. *Right*: Activation of the postsynaptic NMDA receptors and neurokinin-1 (**NK1**) receptors by C fibers generates a long-lasting cumulative depolarization. The cytosolic Ca^{2+} concentration in the dorsal horn neuron increases because of Ca^{2+} entry through the NMDA receptor channels and voltage-sensitive Ca^{2+} channels. The elevated Ca^{2+} and activation by NK1 receptors of second-messenger systems enhance the performance of the NMDA receptors. Activation of NK1 receptors, cumulative depolarization, elevated cytosolic Ca^{2+}, and other factors regulate the behavior of voltage-gated ion channels responsible for action potentials, resulting in enhanced excitability, all of which contribute to the process of central sensitization. (Abbreviations: **AMPA**, α-amino-3-hydroxy-5-methylisoxazole-4-propionate; **NMDA**, *N*-methyl-D-aspartate)

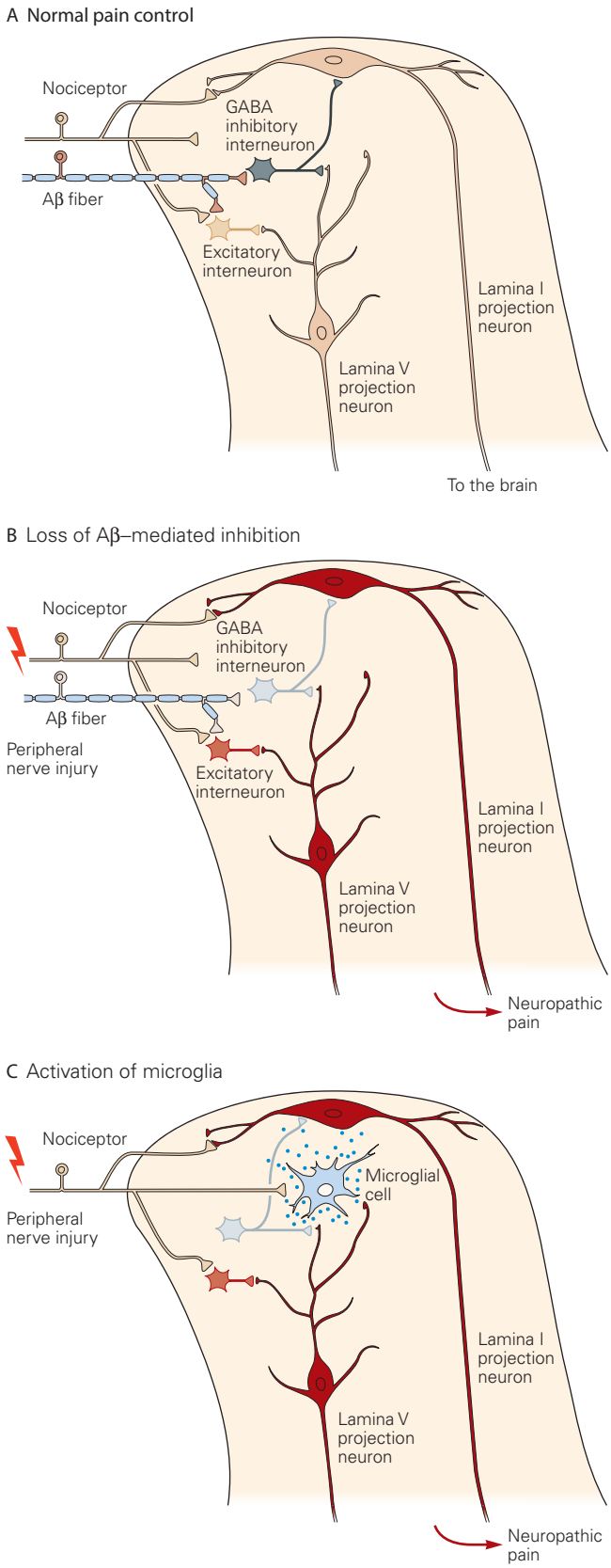

Figure 20–11 Nerve injury triggers multiple dorsal horn central sensitization mechanisms that contribute to neuropathic pain.

A. Under normal conditions, nociceptors engage dorsal horn pain transmission circuits, via both monosynaptic and polysynaptic (excitatory) inputs to projection neurons of laminae I and V that transmit nociceptive information to the brainstem and thalamus. (See Figure 20–13.) The output of the projection neurons is regulated by GABAergic inhibitory interneurons, which can be activated by nonnociceptive, large-diameter, myelinated Aβ afferent fibers.

B. Peripheral nerve injury can result in a loss of the inhibitory control exerted by the Aβ afferents, via loss of GABAergic interneurons, reduced production of GABA, or reduced expression of GABAergic receptors by the projection neurons. Pathophysiological sprouting of Aβ afferents may also permit nonnociceptive inputs to directly engage the projection neurons (not shown), resulting in the condition of Aβ-mediated mechanical hypersensitivity/allodynia, a hallmark of neuropathic pain.

C. Peripheral nerve injury not only activates dorsal horn neurons directly but also activates microglia, which in turn release a host of mediators that enhance neuronal excitability and reduce the inhibitory controls exerted by GABAergic interneurons. Thus, targeting the mediators released from microglia introduces yet another potential approach to the pharmacotherapy of chronic pain.

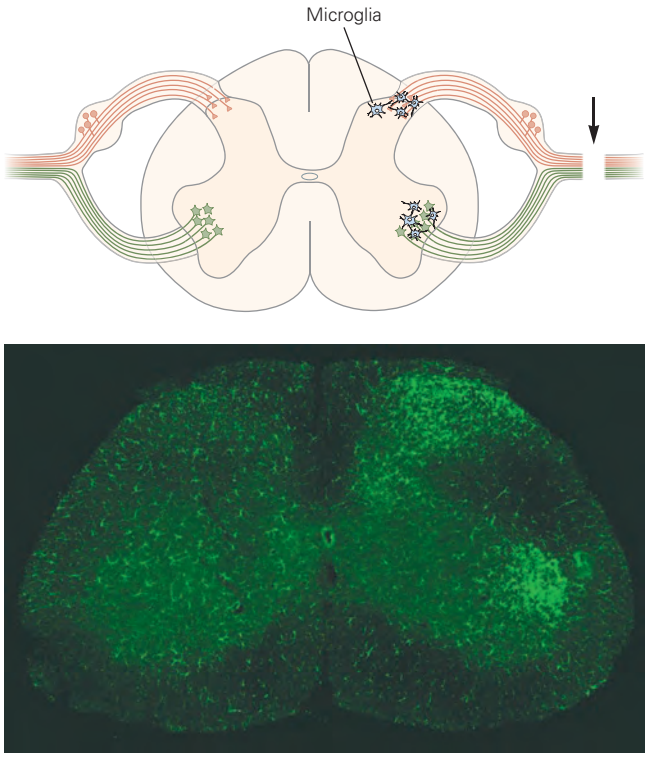

Figure 20–12 Peripheral nerve injury activates microglia in the dorsal and ventral horns. Schematic drawing and photomicrograph illustrate the location where microglia are activated after peripheral nerve injury. Activation of microglia in the dorsal horn results from damage (**arrow**) to the peripheral branch of primary sensory neurons (**orange cells**). Microglial activation around motor neuron cell bodies in the ventral horn occurs because the same injury damages efferent axons of the motor neurons (**green cells**). (Micrograph reproduced, with permission, from Julia Kuhn.)

the area of injury can inappropriately activate dorsal horn circuits that have undergone central sensitization.

Four Major Ascending Pathways Convey Nociceptive Information From the Spinal Cord to the Brain

Four major ascending pathways—the spinothalamic, spinoreticular, spinoparabrachial, and spinohypothalamic tracts—contribute sensory information to the central processes that generate pain.

The *spinothalamic tract* is the most prominent ascending nociceptive pathway in the spinal cord. It includes the axons of nociceptive-specific, thermosensitive, and wide-dynamic-range neurons in laminae I and V through VII of the dorsal horn. These axons cross the midline of the spinal cord near their segment of origin and ascend in the anterolateral white matter before terminating in thalamic nuclei (Figure 20–13). The spinothalamic tract has a crucial role in the transmission of nociceptive information. Cells at the origin of this tract typically have discrete, unilateral receptive fields that underlie our ability to localize painful stimuli. Not surprisingly, electrical stimulation of the tract is sufficient to elicit the sensation of pain; conversely, lesioning this tract (anterolateral cordotomy), a procedure that is generally only used for intractable pain in terminal cancer patients, can result in a marked reduction in pain sensation on the side of the body contralateral to that of the lesion.

The *spinoreticular tract* contains the axons of projection neurons in laminae VII and VIII. This tract ascends in the anterolateral quadrant of the spinal cord with spinothalamic tract axons, and terminates in both the reticular formation and the thalamus. As neurons at the origin of the spinoreticular tract generally have large, often bilateral receptive fields, this pathway has been implicated more in the processing of diffuse, poorly localized pains.

The *spinoparabrachial tract* contains the axons of projection neurons in laminae I and V. Information transmitted along this tract is thought to contribute to the affective component of pain. This tract projects in the anterolateral quadrant of the spinal cord to the parabrachial nucleus at the level of the pons (Figure 20–13). This pathway has extensive collaterals to the mesencephalic reticular formation and periaqueductal gray matter. Parabrachial neurons project to the amygdala, a critical nucleus of the limbic system, which regulates emotional states (Chapter 42).

The *spinohypothalamic tract* contains the axons of neurons found in spinal cord laminae I, V, VII, and VIII. These axons project to hypothalamic nuclei that serve as autonomic control centers involved in the regulation of the neuroendocrine and cardiovascular responses that accompany pain syndromes (Chapter 41).

Several Thalamic Nuclei Relay Nociceptive Information to the Cerebral Cortex

The thalamus contains several relay nuclei that participate in the central processing of nociceptive information. Two of the most important regions of the thalamus are the lateral and medial nuclear groups. The *lateral nuclear group* comprises the ventroposterolateral (VPL), ventroposteromedial (VPM) and posterior/pulvinar nuclei. The VPL and VPM, respectively, receive inputs via the spinothalamic tract from nociception-specific and wide-dynamic-range neurons in laminae I and V of the dorsal horn and via the trigeminothalamic tract

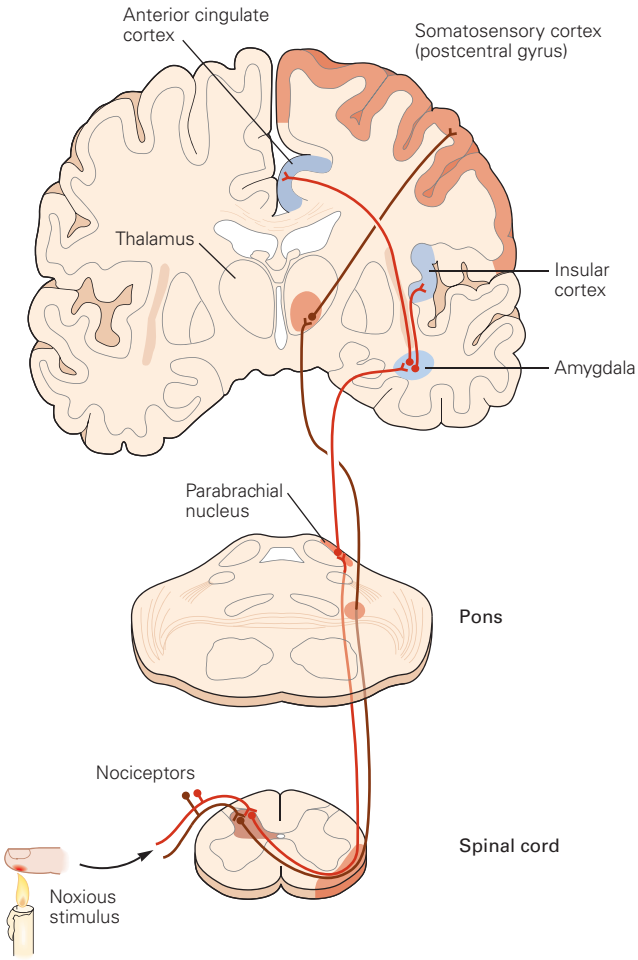

Figure 20–13 Major ascending pathways that transmit nociceptive information. Sensory discriminative features of the pain experience are transmitted from the spinal cord to the ventroposterolateral thalamus via the spinothalamic tract (**brown**). From there, information is transmitted predominantly to the somatosensory cortex. A second pathway, (the spinoparabrachial tract (**red**), carries information from the spinal cord to the parabrachial nucleus of the dorsolateral pons. These neurons in turn target limbic forebrain regions, including the insular and anterior cingulate cortex, which process emotional features of the pain experience.

from the trigeminal nucleus caudalis, the trigeminal homolog of the dorsal horn that processes nociceptive information from orofacial regions. The lateral thalamus processes information about the precise location of an injury, information usually conveyed to consciousness as acute pain. Consistent with this view, neurons in the lateral thalamic nuclei have small receptive fields, matching those of the presynaptic spinal neurons.

A cerebrovascular infarct that destroys the lateral thalamus can produce a central neuropathic pain condition called the Dejerine-Roussy (thalamic pain) syndrome. Patients with this syndrome experience spontaneous burning pain as well as abnormal sensations (called dysesthesias) contralateral to the infarct. Electrical stimulation of the thalamus can also result in intense pain. In one dramatic clinical case, electrical stimulation of the thalamus rekindled sensations of angina pectoris that were so realistic that the anesthesiologist thought the patient was experiencing a heart attack. This and other clinical observations suggest that in chronic neuropathic pain conditions there is a fundamental change in thalamic and cortical circuitry. This hypothesis is consistent with studies demonstrating that the topographic map of the body in the thalamus and somatosensory cortex is not fixed, but can change with use and disuse. Loss of a limb can lead to shrinking and even disappearance of the cortical representation of the limb. Abnormal reorganization likely contributes to the phantom limb pain (Figure 20–14).

The *medial nuclear group* of the thalamus comprises the medial dorsal and central lateral nucleus of the thalamus and the intralaminar complex. Its major input is from neurons in laminae VII and VIII of the dorsal horn. The pathway to the medial thalamus was the first spinothalamic projection evident in the evolution of mammals and is therefore known as the *paleospinothalamic tract.* It is also sometimes referred to as the spinoreticulothalamic tract because it includes indirect connections through the reticular formation of the brain stem. The projection from the lateral thalamus to the ventroposterior lateral and medial nuclei is most developed in primates, and thus is termed the *neospinothalamic tract.* Many neurons in the medial thalamus respond optimally to noxious stimuli and project to many regions of the limbic system, including the anterior cingulate cortex.

The Perception of Pain Arises From and Can Be Controlled by Cortical Mechanisms

Anterior Cingulate and Insular Cortex Are Associated With the Perception of Pain

Imaging studies now show that no single area of the cortex is responsible for pain perception. Rather, many regions are activated when an individual experiences pain. In the somatosensory cortex, neurons typically have small receptive fields and may not contribute greatly to the diffuse perception of aches and pains that characterize most clinical syndromes. The anterior cingulate gyrus and insular cortex also contain neurons that are activated strongly and selectively by noxious somatosensory stimuli (Box 20–1).

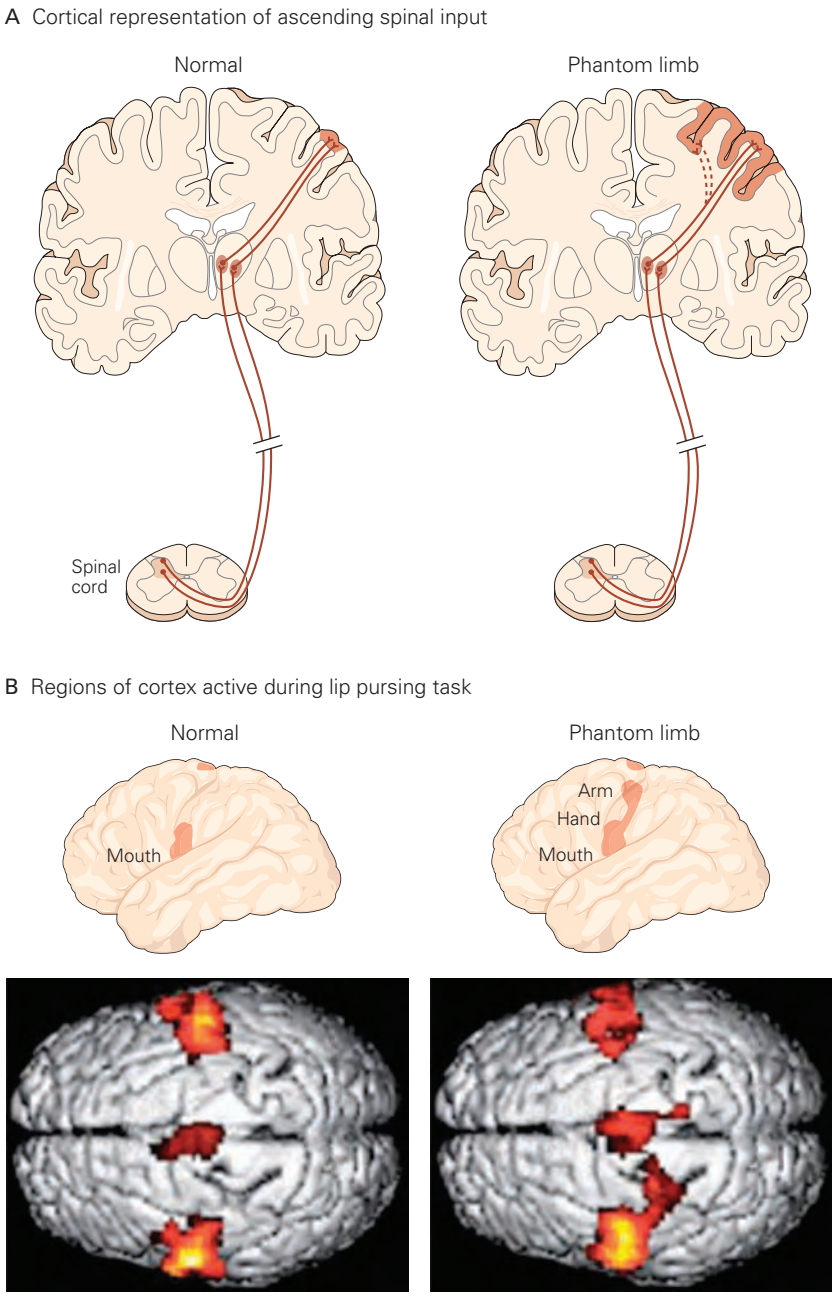

Figure 20–14 Changes in neural activation in phantom limb pain.

A. The domain of cerebral cortex activated by ascending spinal sensory inputs is expanded in patients with phantom limb pain.

B. Functional magnetic resonance imaging (fMRI) of patients with phantom limb pain and healthy controls during a lip-pursing task. In amputees with phantom limb pain, cortical representation of the mouth has extended into the regions of the hand and arm. In amputees without pain, the areas of primary somatosensory and motor cortices that are activated are similar to those in healthy controls (image not shown). (Adapted, with permission, from Flor, Nokolajsen, and Jensen 2006. Copyright © 2006 Springer Nature.)

The anterior cingulate gyrus is part of the limbic system and is involved in processing emotional states associated with pain. The insular cortex receives direct projections from the thalamus as well as from the amygdala. Neurons in the insular cortex process information about the internal state of the body and contribute to the autonomic component of pain responses. Importantly, neurosurgical procedures that ablate the cingulate cortex or the pathway from the frontal cortex to the cingulate cortex reduce the affective features of pain without eliminating the ability to recognize the intensity and location of the injury. Patients with lesions of the insular cortex present the striking syndrome of asymbolia for pain. They perceive noxious stimuli as painful and can distinguish sharp from dull pain but fail to display appropriate emotional responses. These observations implicate the insular cortex as an area in which

Box 20–1 Localizing Illusory Pain in the Cerebral Cortex

Thunberg's illusion, first demonstrated in 1896, is a strong, often painful heat felt after placing the hand on a grill of alternating warm and cool bars (Figure 20–15A).

One hypothesis proposes that this illusory sensation occurs as a result of differential grill responses of two classes of spinothalamic tract neurons, one sensitive to innocuous and another to noxious cold. This finding has led to a model of pain perception based on a central disinhibition or unmasking process in the cerebral cortex. The model predicts perceptual similarities between grill-evoked and cold-evoked pain, a prediction that has been verified psychophysically. The thalamocortical integration of pain and temperature stimuli may explain the burning sensation felt when nociceptors are activated by cold.

To identify the anatomical site of the unmasking phenomenon described above, positron emission tomography (PET) was used to compare the cortical areas activated by Thunberg's grill with those activated by cool, warm, noxious cold, and noxious heat stimuli separately. All thermal stimuli activate the insula and somatosensory cortices. The anterior cingulate cortex is activated by Thunberg's grill and by noxious heat and cold, but not by discrete warm and cool stimuli (Figure 20–15B).

A

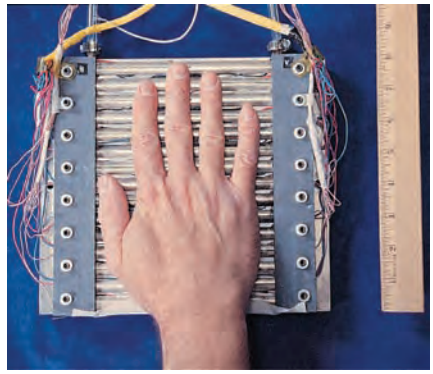

Figure 20–15A Thunberg's thermal grill. The stimulus surface (20 × 14 cm) is made of 15 sterling silver bars, each 1 cm wide, set approximately 3 mm apart. Underneath each bar are three longitudinally spaced thermoelectric (Peltier) elements (1 cm^2), and on top of each bar is a thermocouple. Alternate (even- and odd-numbered) bars can be controlled independently. (Adapted, with permission, from Craig and Bushnell 1994. Copyright © 1994 AAAS.)

B

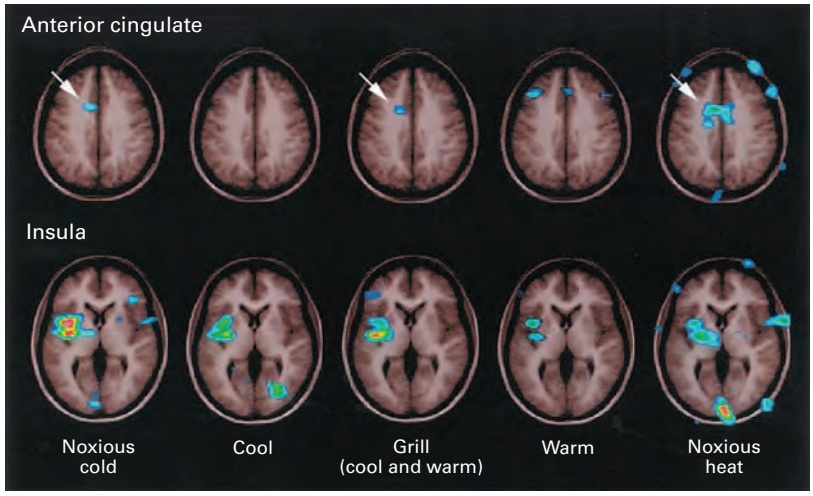

Figure 20–15B Cortical areas activated by Thunberg's grill. The anterior cingulate and insula regions of the cerebral cortex are activated when the hand is placed on the grill but not when warm and cool stimuli are applied separately. (Reproduced, with permission, from Craig AD, Reiman EM, Evans A, et al. 1996. Functional imaging of an illusion of pain. Nature 384:258–260. Copyright © 1996 Springer Nature.)

the sensory, affective, and cognitive components of pain are integrated.

Pain Perception Is Regulated by a Balance of Activity in Nociceptive and Nonnociceptive Afferent Fibers

Many projection neurons in the dorsal horn of the spinal cord respond selectively to noxious inputs, but others receive convergent inputs from both nociceptive and nonnociceptive afferents. The concept that the convergence of sensory inputs onto spinal projection neurons regulates pain processing first emerged in the 1960s.

Ronald Melzack and Patrick Wall proposed that the relative balance of activity in nociceptive and nonnociceptive afferents might influence the transmission and perception of pain. In particular, they proposed that activation of nonnociceptive sensory neurons, by engaging inhibitory interneurons in the dorsal horn, closes a "gate" for afferent transmission of nociceptive signals that can be opened by the activation of nociceptive sensory neurons. In the original and simplest form of this gate-control theory, the interaction between large and small fibers occurred at the first possible site of convergence on projection neurons in the dorsal horn of the spinal cord (Figure 20–16). We now know that such interactions can also occur at many supraspinal relay centers.

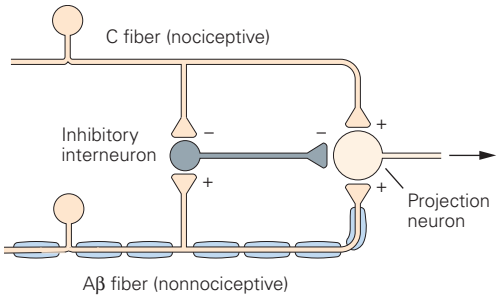

Figure 20–16 The gate control theory of pain. The gate-control hypothesis was proposed in the 1960s to account for the fact that activation of low-threshold primary afferent fibers can attenuate pain. The hypothesis focused on the interaction of neurons in the dorsal horn of the spinal cord: the nociceptive (**C**) and nonnociceptive (**Aβ**) sensory neurons, projection neurons, and inhibitory interneurons. In the original version of the model, as shown here, the projection neuron is excited by both classes of sensory neurons and inhibited by interneurons in the superficial dorsal horn. The two classes of sensory fibers also terminate on the inhibitory interneurons; the C fibers indirectly inhibit the interneurons, thus increasing the activity of the projection neurons (thereby "opening the gate"), whereas the Aβ fibers excite the interneurons, thus suppressing the output of the projection neurons (and "closing the gate").

The concept of convergence of different sensory modalities has provided an important basis for the design of new pain therapies. Viewed in its broadest sense, the convergence of high- and low-threshold inputs at spinal or supraspinal sites provided a plausible explanation for several empirical observations about the perception of pain. The shaking of the hand that follows a hammer blow or burn is a reflexive behavior and may alleviate pain by activating large-diameter afferent fibers that suppress the transmission of information about noxious stimuli.

The idea of convergence also helped to promote the use of transcutaneous electrical nerve stimulation (TENS) and spinal cord stimulation for the relief of pain. With TENS, stimulating electrodes placed at peripheral locations activate large-diameter afferent fibers that innervate areas that overlap but also surround the region of injury and pain. The region of the body in which pain is reduced maps to those segments of the spinal cord in which nociceptive and nonnociceptive afferents from that body region terminate. This makes intuitive sense: You do not shake your left leg to relieve pain in your right arm.

Electrical Stimulation of the Brain Produces Analgesia

Several sites of endogenous pain regulation are located in the brain. One effective means of suppressing nociception involves stimulation of the periaqueductal gray region, the area of the midbrain that surrounds the third ventricle and the cerebral aqueduct. In experimental animals, stimulation of this region elicits a profound and selective analgesia. This *stimulation-produced analgesia* is remarkably modality-specific; animals still respond to touch, pressure, and temperature within the body area that is not sensitive to pain. Stimulation-evoked analgesia has proved to be an effective way of relieving pain in a limited number of human pain conditions.

Stimulation of the periaqueductal gray matter blocks spinally mediated withdrawal reflexes that are normally evoked by noxious stimulation. Few of the neurons in the periaqueductal gray matter project directly to the dorsal horn of the spinal cord. Most make excitatory connections with neurons of the rostroventral medulla, including serotonergic neurons in a midline region called the nucleus raphe magnus. The axons of these serotonergic neurons project through the dorsal region of the lateral funiculus to the spinal cord, where they form inhibitory connections with neurons in laminae I, II, and V of the dorsal horn (Figure 20–17). Stimulation of the rostroventral

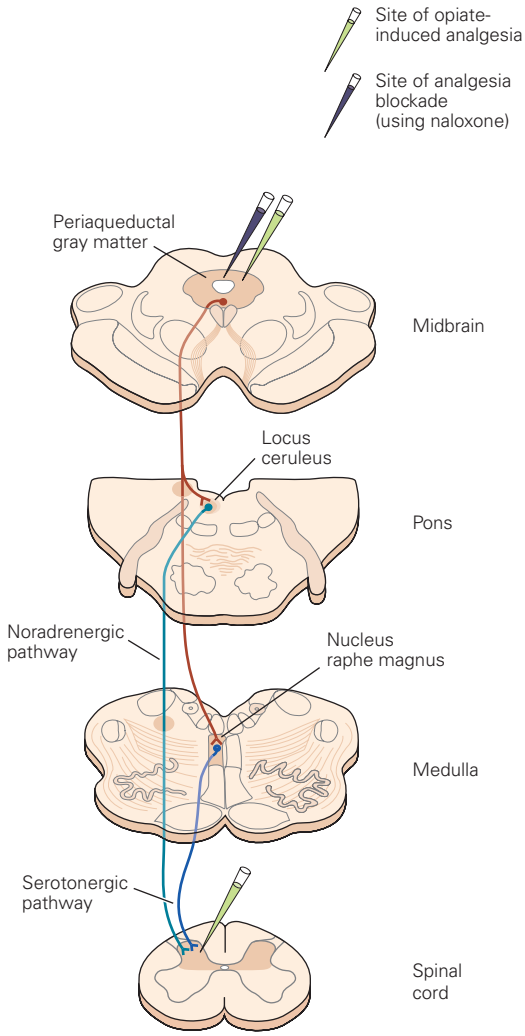

Figure 20–17 Descending monoaminergic pathways regulate nociceptive relay neurons in the spinal cord. A serotonergic pathway arises in the nucleus raphe magnus and projects through the dorsolateral funiculus to the dorsal horn of the spinal cord. A noradrenergic system arises in the locus ceruleus and other nuclei in the pons and medulla. (See Figure 40–11A for the locations and projections of monoaminergic neurons.) In the spinal cord, these descending pathways inhibit nociceptive projection neurons through direct connections as well as through interneurons in the superficial layers of the dorsal horn. Both the serotonergic nucleus raphe magnus and noradrenergic nuclei receive input from neurons in the periaqueductal gray region. Sites of opioid peptide expression and actions of exogenously administered opioids are shown.

medulla thus inhibits the firing of many classes of dorsal horn neurons, including projection neurons of the major ascending pathways that convey afferent nociceptive signals to the brain.

A second major monoaminergic descending system can also suppress the activity of nociceptive neurons in the dorsal horn. This noradrenergic system originates in the locus ceruleus and other nuclei of the medulla and pons (Figure 20–17). Through direct and indirect synaptic actions, these projections inhibit neurons in laminae I and V of the dorsal horn.

Opioid Peptides Contribute to Endogenous Pain Control

Since discovery of the opium poppy by the Sumerians in 3300 BC, the plant's active ingredients, opiates such as morphine and codeine, have been recognized as powerful analgesic agents. Over the past two decades, we have begun to understand many of the molecular mechanisms and neural circuits through which opiates exert their analgesic actions. In addition, we have come to realize that the neural networks involved in stimulation-produced and opiate-induced analgesia are intimately related.

Two key discoveries led to these advances. The first was the recognition that morphine and other opiates interact with specific receptors on neurons in the spinal cord and brain. The second was the isolation of endogenous neuropeptides with opiate-like activities at these receptors. The observation that the opiate antagonist, naloxone, blocks stimulation-produced analgesia provided the first clue that the brain contains endogenous opioids.

Endogenous Opioid Peptides and Their Receptors Are Distributed in Pain-Modulatory Systems

Opioid receptors fall into four major classes: mu (μ), delta (δ), kappa (κ), and orphanin FQ. The genes encoding each of these receptor types constitute a subfamily of G protein–coupled receptors. The μ receptors are particularly diverse; numerous μ receptor isoforms have been identified, many with different patterns of expression. This finding has prompted a search for analgesic drugs that target specific isoforms.

The opioid receptors were originally defined on the basis of the binding affinity of different agonist compounds. Morphine and other opioid alkaloids are potent agonists at μ receptors, and there is a tight correlation between the potency of an analgesic and its affinity of binding to μ receptors. Mice in which the gene for the μ receptor has been inactivated are insensitive to morphine and other opiate agonists. Many opiate antagonist drugs, such as naloxone, also bind to the μ receptor and compete with morphine for receptor occupancy without activating receptor signaling.

The μ receptors are highly concentrated in the superficial dorsal horn of the spinal cord, the ventral

Table 20–1 Four Major Classes of Endogenous Opioid Peptides

Propeptide	Peptide(s)	Preferential receptor
POMC	β-Endorphin	μ/δ
	Endomorphin-1	μ
	Endomorphin-2	μ
Proenkephalin	Met-enkephalin	δ
	Leu-enkephalin	δ
Prodynorphin	Dynorphin A	κ
	Dynorphin B	κ
Pro-orphanin FQ	Orphanin FQ	Orphan receptor

POMC, pro-opiomelanocortin.

medulla, and the periaqueductal gray matter—important anatomical sites for the regulation of pain. Nevertheless, like other classes of opioid receptors, they are also found at many other sites in the central and peripheral nervous systems. Their widespread distribution explains why systemically administered morphine influences many physiological processes in addition to the perception of pain.

The discovery of opioid receptors and their expression by neurons in the central and peripheral nervous systems led to the definition of four major classes of endogenous opioid peptides, each interacting with a specific class of opioid receptors (Table 20–1).

Three classes—the enkephalins, β-endorphins, and dynorphins—are the best characterized. These opioid peptides are formed from large polypeptide precursors by enzymatic cleavage (Figure 20–18) and encoded by distinct genes. Despite differences in amino acid sequence, each contains the sequence Tyr-Gly-Gly-Phe. β-Endorphin is a cleavage product of a precursor that also generates the active peptide adrenocorticotropic hormone (ACTH). Both β-endorphin and ACTH are synthesized by cells in the pituitary and are released into the bloodstream in response to stress. Dynorphins are derived from the polyprotein product of the *dynorphin* gene.

Members of the four classes of opioid peptides are distributed widely in the central nervous system, and individual peptides are located at sites associated with the processing or modulation of nociceptive information. Neuronal cell bodies and axon terminals containing enkephalin and dynorphin are found in the dorsal horn of the spinal cord, particularly in laminae I and II, as well as in the rostral ventral medulla and the periaqueductal gray matter. Neurons that synthesize β-endorphin are confined primarily to the hypothalamus; their axons terminate in the periaqueductal gray region and on noradrenergic neurons in the brain stem. Orphanin FQ appears to participate in a broad range of other physiological functions.

Morphine Controls Pain by Activating Opioid Receptors

Microinjection of low doses of morphine, other opiates, or opioid peptides directly into specific regions of the rat brain produces a powerful analgesia. The periaqueductal gray region is among the most sensitive sites, but local administration of morphine into other regions, including the spinal cord, also elicits a powerful analgesia.

Systemic morphine-induced analgesia can be blocked by injection of the opiate antagonist naloxone into the periaqueductal gray region or the nucleus raphe magnus (Figure 20–17). In addition, bilateral transection of the dorsal lateral funiculus in the spinal cord blocks analgesia induced by central administration of morphine. Thus, the central analgesic actions of morphine involve the activation of descending pathways to the spinal cord, the same descending pathways that mediate the analgesia produced by electrical brain stimulation and morphine.

In the spinal cord, as elsewhere, morphine acts by mimicking the actions of endogenous opioid peptides. The superficial dorsal horn of the spinal cord contains interneurons that express enkephalin and dynorphin, and the terminals of these neurons lie close to synapses formed by nociceptive sensory neurons and spinal projection neurons (Figure 20–19A). Moreover, the μ, δ, and κ receptors are located on the terminals of the nociceptive sensory neurons as well as on the dendrites of dorsal horn neurons that receive afferent nociceptive input, thus placing endogenous opioid peptides in a strategic position to regulate sensory input. The C-fiber nociceptors, which mediate slow persistent pain or "second pain," have more μ receptors than the Aδ nociceptors, which mediate fast and acute pain or "first pain" (Figure 20–1). This may help to explain why morphine is more effective in the treatment of persistent rather than acute pains.

Opioids (both opiates and opioid peptides) regulate nociceptive transmission at synapses in the dorsal horn through two main mechanisms. First, they increase membrane K^+ conductances in dorsal horn neurons, hyperpolarizing the neurons and increasing their threshold for activation. Second, by binding to receptors on presynaptic sensory terminals, opioids block voltage-gated Ca^{2+} channels, which reduces Ca^+

Figure 20–18 Four families of endogenous opioid peptides arise from large precursor polyproteins.

A. Proteolytic enzymes cleave each of the precursor proteins to generate shorter, biologically active peptides, some of which are shown in this diagram. The proenkephalin precursor protein contains multiple copies of methionine-enkephalin (**M**), leucine-enkephalin (**L**), and several extended enkephalins. Proopiomelanocortin (POMC) contains β-endorphin (**β-END**, melanocyte-stimulating hormone (**MSH**), adrenocorticotropic hormone (ACTH), and corticotropin-like intermediate-lobe peptide (**CLIP**). The prodynorphin precursor can produce dynorphin (**D**) and α-neoendorphin (**N**). The pro-orphanin precursor contains the orphanin FQ peptide (**O**), also called nociceptin. The **black domains** indicate a signal peptide.

B. Amino acid sequences of proteolytically processed bioactive peptides. The amino acid residues shown in **bold type** mediate interaction with opioid receptors. (Adapted, with permission, from Fields 1987.)

entry into the sensory nerve terminal (Figure 20–19B). This effect in turn inhibits the release of neurotransmitter and thereby decreases activation of postsynaptic dorsal horn neurons.

The wide distribution of opioid receptors within the brain and periphery accounts for the many side effects produced by opiates. Activation of opioid receptors expressed by muscles of the bowel and anal sphincter results in constipation. Similarly, opioid receptor–mediated inhibition of neuronal activity in the nucleus of the solitary tract underlies the respiratory depression and cardiovascular side effects. For this reason, direct spinal administration of opiates has significant advantages. Morphine injected into the cerebrospinal fluid of the spinal cord subarachnoid space interacts with opioid receptors in the dorsal horn to elicit a profound and prolonged analgesia. Spinal administration of morphine is now commonly used in the treatment of postoperative pain, notably the pain associated with cesarean section during childbirth. In addition to producing prolonged analgesia, intrathecal morphine has fewer side effects because the drug does not diffuse far from its site of injection. Continuous local infusion of morphine to the spinal cord has also been used for the treatment of certain cancer pains.

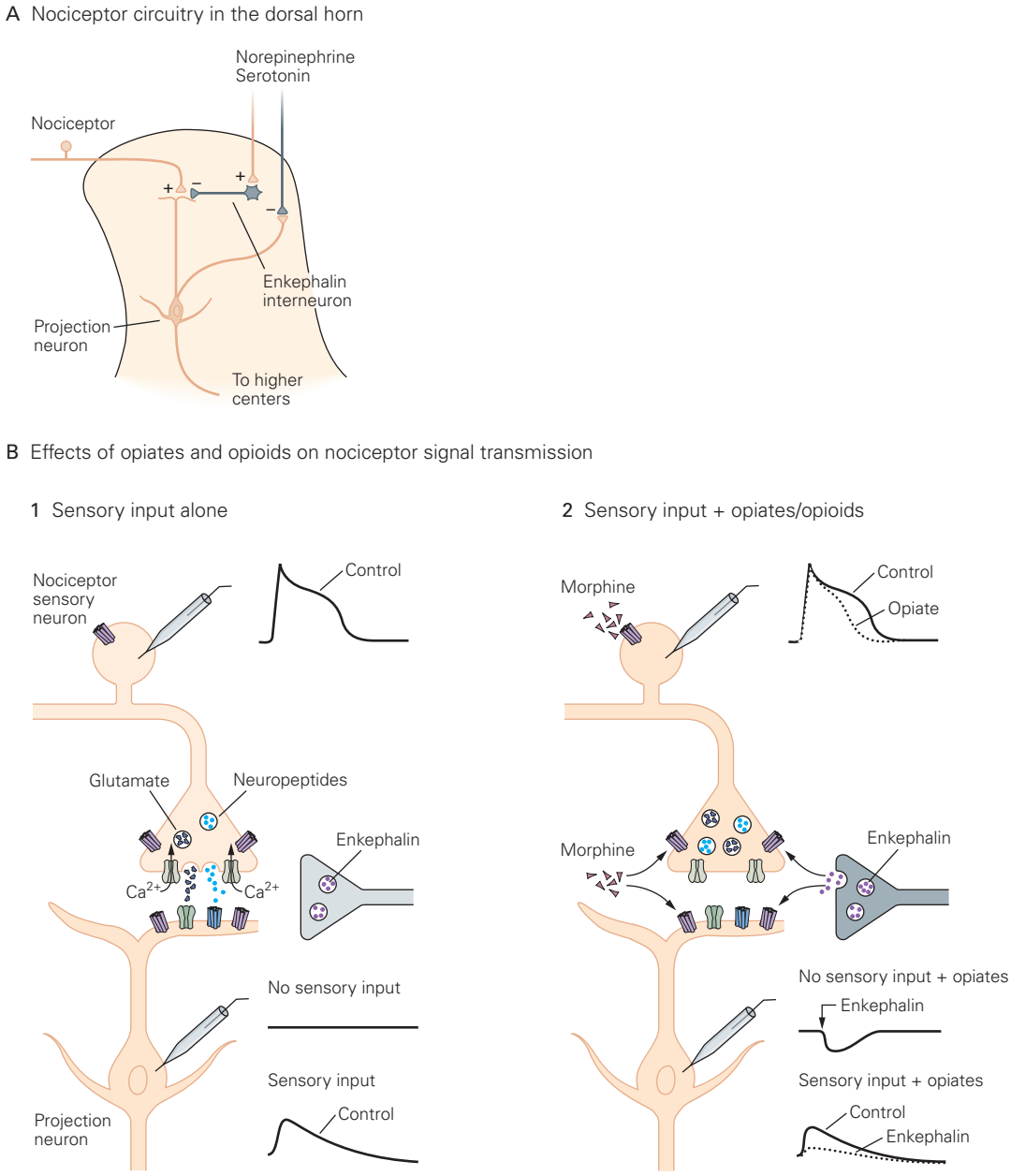

Figure 20–19 Local interneurons in the spinal cord integrate descending and afferent nociceptive pathways.

A. Nociceptive afferent fibers, local interneurons, and descending fibers interconnect in the dorsal horn of the spinal cord (see also Figure 20–3B). Nociceptive fibers terminate on second-order projection neurons. Local GABAergic and enkephalin-containing inhibitory interneurons exert both pre- and postsynaptic inhibitory actions at these synapses. Serotonergic and noradrenergic neurons in the brain stem activate the local interneurons and also suppress the activity of the projection neurons. Loss of these inhibitory controls contributes to ongoing pain and pain hypersensitivity.

B. Regulation of nociceptive signals at dorsal horn synapses. **1.** Activation of a nociceptor leads to the release of glutamate and neuropeptides from the primary sensory neuron, producing an excitatory postsynaptic potential in the projection neuron. **2.** Opiates decrease the duration of the postsynaptic potential, probably by reducing Ca^{2+} influx, and thus decrease the release of transmitter from the primary sensory terminals. In addition, opiates hyperpolarize the dorsal horn neurons by activating a K^+ conductance and thus decrease the amplitude of the postsynaptic potential in the dorsal horn neuron.

Opiates also act on receptors in the cerebral cortex. There is evidence, for example, that opiates can influence the affective component of the pain experience by an action in the anterior cingulate gyrus. Most interestingly, there is considerable evidence that placebo analgesia involves endorphin release and can be reversed by naloxone. This finding emphasizes that responses to a placebo do not indicate that the pain was somehow imaginary. Moreover, placebo analgesia is a component of the overall analgesic action of any pain-relieving drug, including morphine, provided that the patient believes that the treatment will be effective. On the other hand, some other psychological interventions to relieve pain, namely hypnosis, do not appear to involve release of endorphins.

Tolerance to and Dependence on Opioids Are Distinct Phenomena

The chronic use of morphine invites major problems, most notably tolerance and psychological dependence (addiction) (Chapter 43). The repeated use of morphine for pain relief can cause patients to develop resistance to the analgesic effects of the drug, such that progressively higher drug doses are required to achieve the same therapeutic effect. One theory holds that tolerance results from uncoupling of the opioid receptor from its G protein transducer. However, as the binding of naloxone to μ-opioid receptors can precipitate withdrawal symptoms in tolerant subjects, it appears that the opioid receptor is still active in the tolerance state. Tolerance may therefore also reflect a cellular response to the activation of opioid receptors, a response that counteracts the effects of the opiate and resets the system. It follows that when the opiate is abruptly removed or naloxone is administered, this compensatory response is unmasked and withdrawal results.

Such physiological tolerance differs from dependence/addiction, which is a psychological craving for the drug, one that is associated with its misuse and that contributes to opiate use disorders. Given the alarming increases in opiate-related deaths, either because of misuse and overdose of prescription opioids or a host of socioeconomic factors, further studies of the mechanisms that contribute to the development of and distinguish between tolerance and addiction are essential. Unquestionably, morphine and other opiate drugs are very useful in the management of postoperative pain. Whether they are equally effective for the management of chronic pain in noncancer patients remains controversial and needs further study.

Highlights

1. Peripheral nociceptive axons, with cell bodies in dorsal root ganglia, include small-diameter unmyelinated (C) and myelinated (Aδ) afferents. Larger diameter Aβ afferents respond only to innocuous stimulation but, following injury, can activate central nervous system pain circuitry.
2. All nociceptors use glutamate as their excitatory neurotransmitter; many also express an excitatory neuropeptide cotransmitter, such as substance P or CGRP.
3. Nociceptors are also molecularly distinguished by their expression of different receptors sensitive to temperature, plant products, mechanical stimuli, or ATP. As many of these molecules, including the Nav1.7 subtype of voltage-gated Na^+ channels, are exclusively expressed in sensory neurons, their selective pharmacological targeting suggests a novel approach to analgesic drug development.
4. Nociceptors terminate in the dorsal horn of the spinal cord where they excite interneurons and projection neurons. Neuropeptides are also released from the peripheral terminals of nociceptors and contribute to neurogenic inflammation, including vasodilatation of and extravasation from peripheral vessels. The development of antibodies to CGRP, to block vasodilation, is a new approach to managing migraine.
5. A major brain target of dorsal horn projection neurons is the ventroposterolateral thalamus, which processes location and intensity features of the painful stimulus. Other neurons target the parabrachial nucleus (PB) of the dorsolateral pons. PB neurons, in turn, project to limbic regions of the brain, which process affective/emotional features of the pain experience.
6. Allodynia, pain produced by an innocuous stimulus, results in part from peripheral sensitization of nociceptors. Peripheral sensitization occurs when there is tissue injury and inflammation and involves NSAID-sensitive production of prostaglandins, which lower the threshold for activating nociceptors. A great advantage of NSAIDs is that they act in the periphery, illustrating the importance of efforts to develop pharmacotherapies, such as antibodies to NGF, which cannot cross the blood–brain barrier, thus reducing their likelihood of having adverse side effects in the central nervous system.
7. Hyperalgesia (exacerbated pain in response to a painful stimuli) and allodynia also arise from

altered activity in the dorsal horn—a central sensitization process that contributes to spontaneous activity of pain-transmission neurons and amplification of nociceptive signals. Glutamate activation of spinal cord NMDA receptors and activation of microglia and astrocytes contribute, in particular, to the neuropathic pains that can occur after peripheral nerve injury. Understanding the consequences of central sensitization is critical to preventing the transition from acute to chronic pain.

8. Under normal conditions, input carried by large-diameter, nonnociceptive afferents can reduce the transmission of nociceptive information to the brain by engaging GABAergic inhibitory circuits in the dorsal horn. This inhibitory control is the basis of the pain relief produced by vibration and transcutaneous electrical stimulation. However, when injury induces central sensitization, Aβ input mediates mechanical allodynia.
9. Opiates are the most effective pharmacological tool for the management of severe pain. The inhibitory action of opiates and the related endogenous opioid peptides result from reduced neurotransmitter release or by hyperpolarization of postsynaptic neurons. All opioid actions can be blocked by the opiate receptor antagonist naloxone.
10. Endogenous opioids, including enkephalin and dynorphin, and their opioid receptor targets are not expressed only in pain-relevant areas of the brain. As a result, systemic administration of opiates is associated with many adverse side effects, including constipation, respiratory depression, and activation of the reward system. The latter can lead to psychological dependence and eventual misuse. Many of these adverse side effects limit opiate use for long-term pain control.
11. The brain not only receives nociceptive information leading to a perception of pain, but also regulates the output of the spinal cord to reduce pain by an endorphin-mediated pain control system. Electrical stimulation of the midbrain periaqueductal gray can engage a descending inhibitory control system, likely involving endorphins, which reduces the transmission of pain messages from the spinal cord to the brain.
12. The pain relief produced by some psychological manipulations (e.g., placebo analgesia) involves endorphin release; other manipulations, such as hypnosis, do not.
13. Tolerance and psychological dependence can arise after prolonged opiate use. Tolerance is manifested as a requirement for higher doses of the opiate to achieve the same physiological endpoint. Psychological dependence, in contrast, involves activation of the brain's reward system and the development of craving that can lead to misuse of opiates. Development of nonrewarding opioid analgesics, which can regulate the sensory-discriminative but not the emotional features of the pain experience, may significantly impact the ongoing opioid epidemic.

Allan I. Basbaum

Selected Reading

Basbaum AI, Bautista DM, Scherrer G, Julius D. 2009 Cellular and molecular mechanisms of pain. Cell 139:267–284.

Basbaum AI, Fields HL. 1984. Endogenous pain control systems: brainstem spinal pathways and endorphin circuitry. Annu Rev Neurosci 7:309–338.

Dib-Hajj SD, Geha P, Waxman SG. 2017. Sodium channels in pain disorders: pathophysiology and prospects for treatment. Pain 158(Suppl 1):S97–S107.

Grace PM, Hutchinson MR, Maier SF, Watkins LR. 2014. Pathological pain and the neuroimmune interface. Nat Rev Immunol 14:217–231.

Ji RR, Chamessian A, Zhang YQ. 2016. Pain regulation by non-neuronal cells and inflammation. Science 354:572–577.

Peirs C, Seal RP. 2016. Neural circuits for pain: recent advances and current views. Science 354:578–584.

Tracey I. 2017. Neuroimaging mechanisms in pain: from discovery to translation. Pain 158:S115–S122.

References

Akil H, Mayer DJ, Liebeskind JC. 1976. Antagonism of stimulation-produced analgesia by naloxone, a narcotic antagonist. Science 191:961–962.

Bautista DM, Jordt SE, Nikai T, et al. 2006. TRPA1 mediates the inflammatory actions of environmental irritants and proalgesic agents. Cell 124:1269–1282.

Bautista DM, Siemens J, Glazer JM, et al. 2007. The menthol receptor TRPM8 is the principal detector of environmental cold. Nature 44:204–208.

Benedetti F. 2014. Placebo effects: from the neurobiological paradigm to translational implications. Neuron 84:623–637.

Bliss TV, Collingridge GL, Kaang BK, Zhuo M. 2016. Synaptic plasticity in the anterior cingulate cortex in acute and chronic pain. Nat Rev Neurosci 17:485–496.

Caterina MJ, Schumacher MA, Tominaga M, Rosen TA, Levine JD, Julius D. 1997. The capsaicin receptor: a

heat-activated ion channel in the pain pathway. Nature 389:816–824.
Colloca L, Ludman T, Bouhassira D, et al. 2017. Neuropathic pain. Nat Rev Dis Primers 3:17002.
Cox JJ, Reimann F, Nicholas AK, et al. 2006. An SCN9A channelopathy causes congenital inability to experience pain. Nature 444:894–898.
Craig AD, Bushnell MC. 1994. The thermal grill illusion: unmasking the burn of cold pain. Science 265:252–255.
Darland T, Heinricher MM, Grandy DK. 1988. Orphanin FQ/nociceptin: a role in pain and analgesia, but so much more. Trends Neurosci 21:215–221.
De Biasi S, Rustioni A 1990. Ultrastructural immunocytochemical localization of excitatory amino acids in the somatosensory system. J Histochem Cytochem 38: 1745–1754.
De Felice M, Eyde N, Dodick D, et al. 2013. Capturing the aversive state of cephalic pain preclinically. Ann Neurol 74:257–265.
Dejerine J, Roussy G. 1906. Le syndrome thalamique. Rev Neurol 14:521–532.
Dhaka A, Viswanath V, Patapoutian A. 2006. Trp ion channels and temperature sensation. Annu Rev Neurosci 29:135–161.
Fields H. 1987 *Pain*. New York: McGraw-Hill.
Flor H, Nikolajsen L, Jensen TS. 2006. Phantom limb pain: a case of maladaptive CNS plasticity? Nature Rev Neurosci 7:873–881.
Günther T, Dasgupta P, Mann A, et al. 2017. Targeting multiple opioid receptors—improved analgesics with reduced side effects? Br J Pharmacol 2018:2857–2868.
Han L, Ma C, Liu Q, et al. 2013. A subpopulation of nociceptors specifically linked to itch. Nat Neurosci 16:174–182.
Hosobuchi Y. 1986. Subcortical electrical stimulation for control of intractable pain in humans: report of 122 cases 1970–1984. J Neurosurg 64:543–553.
Jordt SE, Bautista DM, Chuang HH, et al. 2004. Mustard oils and cannabinoids excite sensory nerve fibres through the TRP channel ANKTM1. Nature 427:260–265.
Jordt SE, McKemy DD, Julius D. 2003. Lessons from peppers and peppermint: the molecular basis of thermosensation. Curr Opin Neurobiol 13:487–492.
Kelleher JH, Tewari D, McMahon SB. 2017. Neurotrophic factors and their inhibitors in chronic pain treatment. Neurobiol Dis 97:127–138.
Kuner R, Flor H. 2016. Structural plasticity and reorganisation in chronic pain. Nat Rev Neurosci 18:20–30.
Lane NE, Schnitzer TJ, Birbara CA, et al. 2010. Tanezumab for the treatment of pain from osteoarthritis of the knee. N Engl J Med 363:1521–1531.
Lenz FA, Gracely RH, Romanoski AJ, Hope EJ, Rowland LH, Dougherty PM. 1995. Stimulation in the human somatosensory thalamus can reproduce both the affective and sensory dimensions of previously experienced pain. Nat Med 1:910–913.
Mantyh PW, Rogers SD, Honore P, et al. 1997. Inhibition of hyperalgesia by ablation of lamina I spinal neurons expressing the substance P receptor. Science 278:275–279.
Matthes HW, Maldonado R, Simonin F, et al. 1996. Loss of morphine-induced analgesia, reward effect and withdrawal symptoms in mice lacking the μ-opioid-receptor gene. Nature 383:819–823.
McDonnell A, Schulman B, Ali Z, et al. 2016. Inherited erythromelalgia due to mutations in SCN9A: natural history, clinical phenotype and somatosensory profile. Brain 39:1052–1065.
Melzack R, Wall PD. 1965. Pain mechanisms: a new theory. Science 150:971–979.
Merzenich MM, Jenkins WM. 1993. Reorganization of cortical representations of the hand following alterations of skin inputs induced by nerve injury, skin island transfers, and experience. J Hand Ther 6:89–104.
Perl ER. 2007. Ideas about pain, a historical review. Nat Rev Neurosci 8:71–80.
Raja SN, Campbell JN, Meyer RA. 1984. Evidence for different mechanisms of primary and secondary hyperalgesia following heat injury to the glabrous skin. Brain 107:1179–1188.
Ross SE, Mardinly AR, McCord AE, et al. 2010. Loss of inhibitory interneurons in the dorsal spinal cord and elevated itch in Bhlhb5 mutant mice. Neuron 65:886–898.
Sorge RE, Mapplebeck JC, Rosen S, et al. 2015. Different immune cells mediate mechanical pain hypersensitivity in male and female mice. Nat Neurosci 18:1081–1083.
Talbot JD, Marrett S, Evans AC, Meyer E, Bushnell MC, Duncan GH. 1991. Multiple representations of pain in human cerebral cortex. Science 251:1355–1358.
Todd AJ. 2010. Neuronal circuitry for pain processing in the dorsal horn. Nat Rev Neurosci. 11:823–836.
Tominaga M, Caterina MJ. 2004. Thermosensation and pain. J Neurobiol 61:3–12.
Tracey I, Mantyh PW. 2007. The cerebral signature for pain perception and its modulation. Neuron 55:377–391.
Tso AR, Goadsby PJ. 2017. Anti-CGRP monoclonal antibodies: the next era of migraine prevention? Curr Treat Options Neurol 19:27.
Wercberger R. Basbaum AI. 2019. Spinal cord projection neurons: A superficial, and also deep analysis. Curr Opin Physiol 11:109–115.
Woo SH, Ranade S, Weyer AD, et al. 2014. Piezo2 is required for Merkel-cell mechanotransduction. Nature 509: 622–626.
Woolf CJ. 1983. Evidence for a central component of post-injury pain hypersensitivity. Nature 306:686–688.
Yaksh TL, Fisher C, Hockman T, Wiese A. 2017. Current and future issues in the development of spinal agents for the management of pain. Curr Neuropharmacol 15:232–259.
Zeilhofer HU, Wildner H, Yévenes GE. 2012. Fast synaptic inhibition in spinal sensory processing and pain control. Physiol Rev 92:193–235.

21

The Constructive Nature of Visual Processing

We are so familiar with seeing, that it takes a leap of imagination to realize that there are problems to be solved. But consider it. We are given tiny distorted upside-down images in the eyes and we see separate solid objects in surrounding space. From the patterns of stimulation on the retina we perceive the world of objects and this is nothing short of a miracle.

—Richard L. Gregory, *Eye and Brain*, 1966

Most of our impressions of the world and our memories of it are based on sight. Yet the mechanisms that underlie vision are not at all obvious. How do we perceive form and movement? How do we distinguish colors? Identifying objects in complex visual environments is an extraordinary computational achievement that artificial vision systems have yet to duplicate. Vision is used not only for object recognition but also for guiding our movements, and these separate functions are mediated by at least two parallel and interacting pathways.

The existence of parallel pathways in the visual system raises one of the central questions of cognition, the binding problem: How are different types of information carried by discrete pathways brought together into a coherent visual image?

Visual Perception Is a Constructive Process

Vision is often incorrectly compared to the operation of a camera. A camera simply reproduces point-by-point the light intensities in one plane of the visual field. The visual system, in contrast, does something fundamentally different. It interprets the scene and parses it into distinct components, separating foreground from background. The visual system is less accurate than a camera at certain tasks, such as quantifying the absolute level of brightness or identifying spectral color. However, it excels at tasks such as recognizing a charging animal (or a speeding car) whether in bright sunlight or at dusk, in an open field or partly occluded by trees (or other cars). And it does so rapidly to let the viewer respond and, if necessary, escape.

A potentially unifying insight reconciling the visual system's remarkable ability to grasp the bigger picture with its inaccuracy regarding details of the input is that vision is a biological process that has evolved in step with our ecological needs. This insight helps

explain why the visual system is so efficient at extracting useful information such as the identities of objects independent of lighting conditions, while giving less importance to aspects like the exact nature of the ambient light. Moreover, vision does so using previously learned rules about the structure of the world. Some of these rules appeared to have become wired into our neural circuits over the course of evolution. Others are more plastic and help the brain guess at the scene presented to the eyes based on the individual's past experience. This complex, purposeful processing happens at all levels of the visual system. It starts even at the retina, which is specialized to pick out object boundaries rather than creating a point-by-point representation of uniform surfaces.

This *constructive* nature of visual perception has only recently been fully appreciated. Earlier thinking about sensory perception was greatly influenced by the British empiricist philosophers, notably John Locke, David Hume, and George Berkeley, who thought of perception as an atomistic process in which simple sensory elements, such as color, shape, and brightness, were assembled in an additive way, component by component. The modern view that perception is an active and creative process that involves more than just the information provided to the retina has its roots in the philosophy of Immanuel Kant and was developed in detail in the early 20th century by the German psychologists Max Wertheimer, Kurt Koffka, and Wolfgang Köhler, who founded the school of Gestalt psychology.

The German term *Gestalt* means configuration or form. The central idea of the Gestalt psychologists is that what we see about a stimulus—the perceptual interpretation we make of any visual object—depends not just on the properties of the stimulus but also on its context, on other features in the visual field. The Gestalt psychologists argued that the visual system processes sensory information about the shape, color, distance, and movement of objects according to computational rules inherent in the system. The brain has a way of looking at the world, a set of expectations that derives in part from experience and in part from built-in neural wiring.

Max Wertheimer wrote: "There are entities where the behavior of the whole cannot be derived from its individual elements nor from the way these elements fit together; rather the opposite is true: the properties of any of the parts are determined by the intrinsic structural laws of the whole." In the early part of the 20th century, the Gestalt psychologists worked out the laws of perception that determine how we group elements in the visual scene, including similarity, proximity, and good continuation.

We see a uniform six-by-six array of dots as either rows or columns because of the visual system's tendency to impose a pattern. If the dots in each row are similar, we are more likely to see a pattern of alternating rows (Figure 21–1A). If the dots in each column are closer together than those in the rows, we are more disposed to see a pattern of columns (Figure 21–1B). The principle of good continuation is an important basis for linking line elements into unified shapes (Figure 21–1C). It is also seen in the phenomenon of contour saliency, whereby smooth contours tend to pop out from complex backgrounds (Figure 21–1D). The Gestalt features that we are disposed to pick out are also ones that characterize objects in natural scenes. Statistical studies of natural scenes show that object boundaries are likely to contain visual elements that lie in close proximity, are continuous across intersections, or form smooth contours. It is tempting to speculate that the formal features of objects in natural scenes created evolutionary pressure on our visual systems to develop neural circuits that have made us sensitive to those features.

Separating the figure and background in a visual scene is an important step in object recognition. At different moments, the same elements in the visual field can be organized into a recognizable figure or serve as part of the background for other figures (Figure 21–2). This process of segmentation relies not only on certain geometric principles, but also on cognitive influences such as attention and expectation. Thus, a priming stimulus or an internal representation of object shape can facilitate the association of visual elements into a unified percept (Figure 21–3). This internal representation can take many different forms reflecting the wide range of time scales and mechanisms of neural encoding. It could consist of transient reverberating spiking activity selective to a shape or a decision, lasting a fraction of a second, or the selective modulation of synaptic weights during a particular context of a task or an expected shape, or circuit changes that could comprise a long-term memory.

The brain analyzes a visual scene at three levels: low, intermediate, and high (Figure 21–4). At the lowest level, which we consider in the next chapter (Chapter 22), visual attributes such as local contrast, orientation, color, and movement are discriminated. The intermediate level involves analysis of the layout of scenes and of surface properties, parsing the visual image into surfaces and global contours, and distinguishing foreground from background (Chapter 23). The highest level involves object recognition (Chapter 24). Once a scene has been parsed by the brain and objects recognized, the objects can be matched with memories of

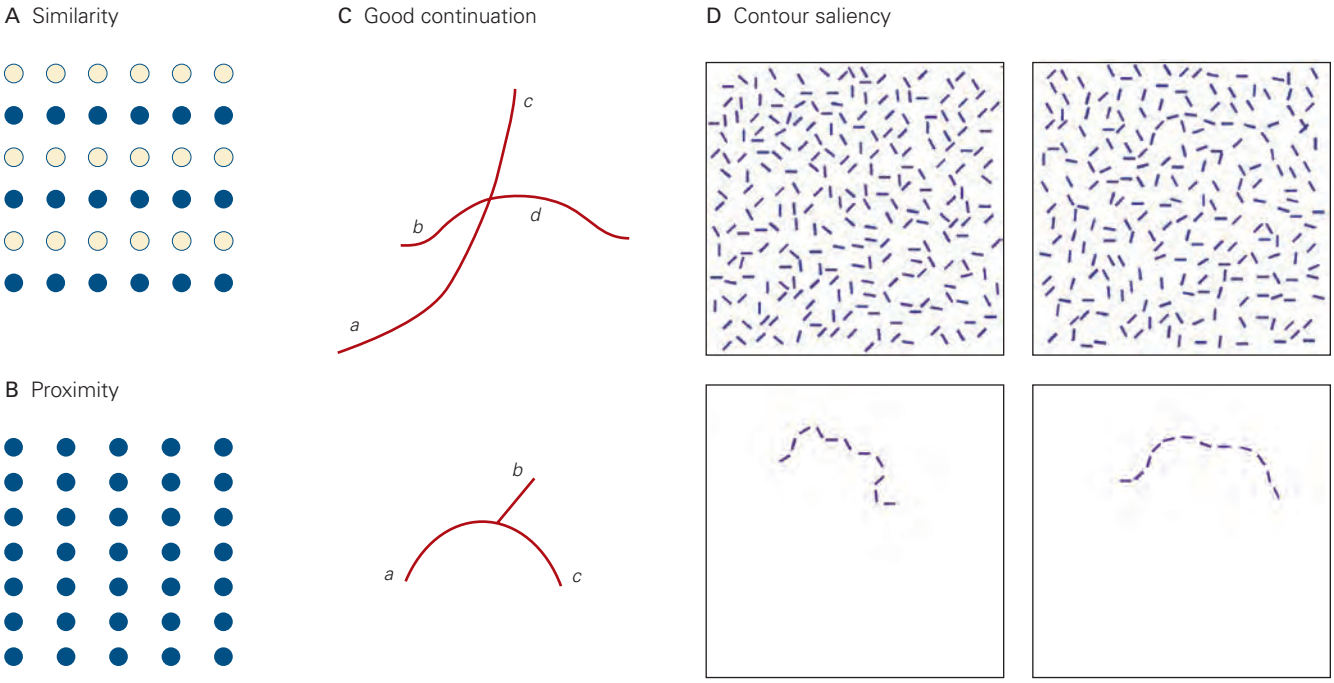

Figure 21–1 **Organizational rules of visual perception.** To link the elements of a visual scene into unified percepts, the visual system relies on organizational rules such as similarity, proximity, and good continuation.

A. Because the dots in alternating rows have the same color, an overall pattern of blue and white rows is perceived.

B. The dots in the columns are closer together than those in the rows, leading to the perception of columns.

C. Line segments are perceptually linked when they are collinear. In the top set of lines, one is more likely to see line segment **a** as belonging with **c** rather than **d**. In the bottom set, **a** and **c** are perceptually linked because they maintain the same curvature, whereas **a** and **b** appear to be discontinuous.

D. The principle of good continuation is also seen in contour saliency. On the right, a smooth contour of line elements pops out from the background, whereas the jagged contour on the left is lost in the background. (Adapted, with permission, from Field, Hayes, and Hess 1993. Copyright © 1993 Elsevier Ltd.)

Figure 21–2 **Object recognition depends on segmentation of a scene into foreground and background.** Recognition of the white salamanders in this image depends on the brain "locating" the white salamanders in the foreground and the brown and black salamanders in the background. The image also illustrates the role of higher influences in segmentation: One can consciously select any of the three colors as the foreground. (Reproduced, with permission, from M.C. Escher's "Symmetry Drawing E56" © 2010 The M.C. Escher Company-Holland. All rights reserved. www.mcescher.com.)

Figure 21–3 Expectation and perceptual task play a critical role in what is seen. It is difficult to separate the dark and white patches in this figure into foreground and background without additional information. This figure immediately becomes recognizable after viewing the priming image on page 501. In this example, higher-order representations of shape guide lower-order processes of surface segmentation. (Reproduced, with permission, from Porter 1954. Copyright 1954 by the Board of Trustees of the University of Illinois. Used with permission of the University of Illinois Press.)

shapes and their associated meanings. Vision also has an important role in guiding body movement, particularly hand movement (Chapter 25).

In vision, as in other cognitive operations, various features—motion, depth, form, and color—occur together in a unified percept. This unity is achieved not by one hierarchical neural system but by multiple areas in the brain that are fed by parallel but interacting neural pathways. Because distributed processing is one of the main organizational principles in the neurobiology of vision, one must have a grasp of the anatomical pathways of the visual system to understand fully the physiological description of visual processing in later chapters.

In this chapter, we lay the foundation for understanding the neural circuitry and organizational principles of the visual pathways. These principles apply quite broadly and are relevant not only for the multiple areas of the brain concerned with vision but also for other types of sensory information processing by the brain.

Visual Processing Is Mediated by the Geniculostriate Pathway

The brain's analysis of visual scenes begins in the two retinas, which transform visual input using a strategy of parallel processing (Chapter 22). This important neural computation strategy is utilized at all stages of the visual pathway as well as in other sensory areas. The pixel-like bits of visual input falling on individual photoreceptors—rods and cones—are analyzed by retinal circuits to extract some 20 local features, such as the local contrasts of dark versus light, red versus green, and blue versus yellow. These features are computed by different populations of specialized neural circuits forming independent processing modules that separately cover the visual field. Thus, each point in the visual field is processed in multiple channels that extract distinct aspects of the visual input simultaneously and in parallel. These parallel streams are then sent out along the axons of the retinal ganglion cells, the projection neurons of the retina, which form the optic nerves.

From the eye, the optic nerve extends to a midline crossing point, the optic chiasm. Beyond the chiasm, the fibers from each temporal hemiretina proceed to the ipsilateral hemisphere along the ipsilateral optic tract; fibers from the nasal hemiretinas cross to the contralateral hemisphere along the contralateral optic tract (Figure 21–5). Because the temporal hemiretina of one eye sees the same half of the visual field (hemifield) as the nasal hemiretina of the other, the partial decussation of fibers at the chiasm ensures that all the information about each hemifield is processed in the visual cortex of the contralateral hemisphere. The layout of the pathway also forms the basis for useful diagnostic information. As a consequence of the particular anatomy of this visual pathway, lesions at different points along the pathway lead to visual deficits with different geometric shapes (Figure 21–5) that can be distinguished reliably through clinical examination. The deficit could be entirely monocular; if present in both eyes, it could affect noncorresponding or corresponding parts of the visual field in the two eyes; it could be restricted to either the upper or the lower visual field or may extend into both, etc. Thus, the shape of the deficit could give valuable clues about type and location of the

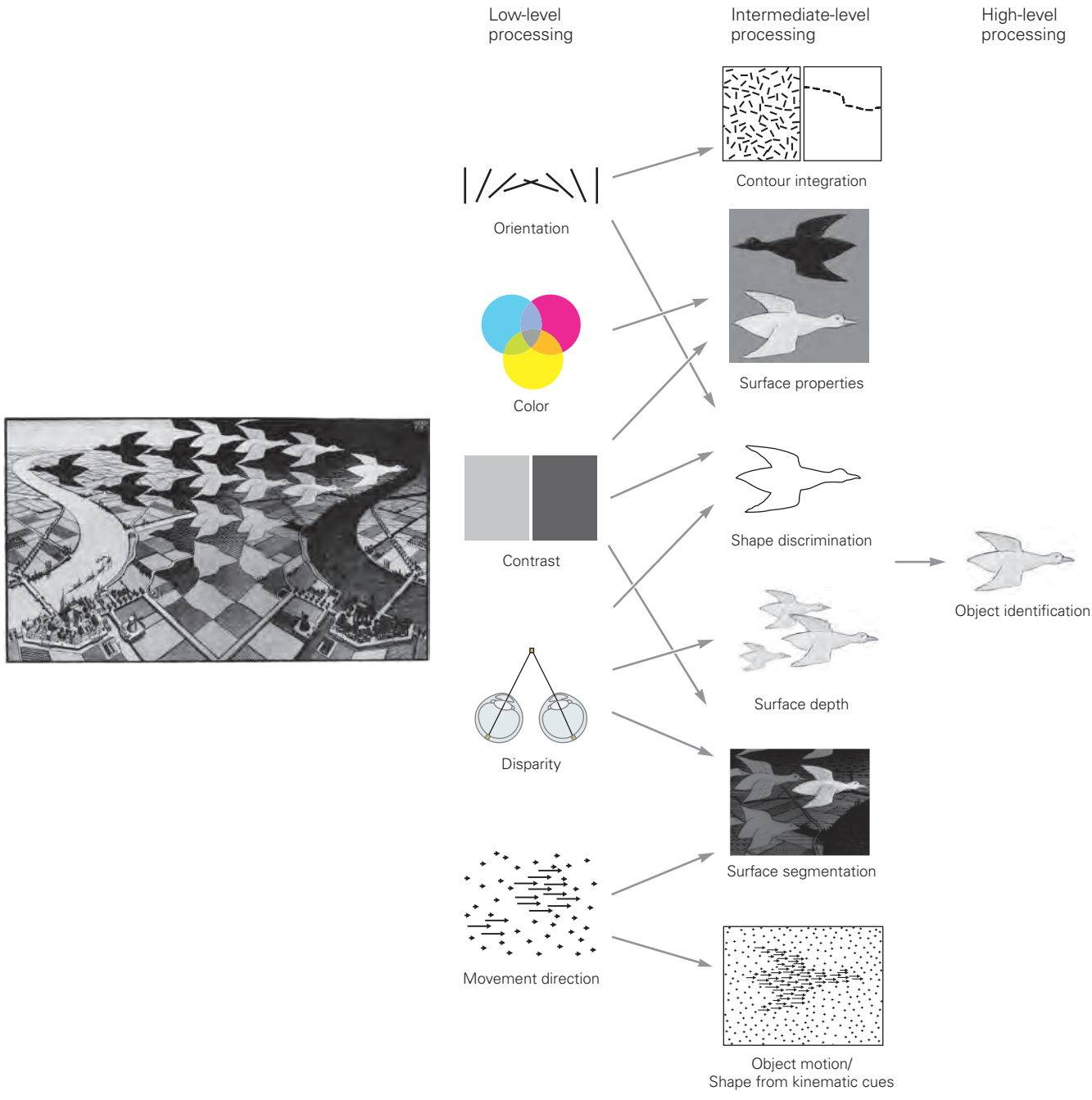

Figure 21–4 **A visual scene is analyzed at three levels.** Simple attributes of the visual environment are analyzed (low-level processing), and these low-level features are then used to parse the visual scene (intermediate-level processing): Local visual features are assembled into surfaces, objects are segregated from background (surface segmentation), local orientation is integrated into global contours (contour integration), and surface shape is identified from shading and kinematic cues. Finally, surfaces and contours are used to identify the object (high-level processing). (M.C. Escher's "Day and Night". © 2020 The M.C. Escher Company—The Netherlands. All rights reserved. www.mcescher.com)

Priming image for Figure 21–3

underlying nerve damage or occlusion (ranging from optic nerve degeneration, such as due to multiple sclerosis, to tumors, strokes, or physical trauma).

Beyond the optic chiasm, the axons from nasal and temporal hemiretinas carrying input from one hemifield join in the optic tract, which extends to the lateral geniculate nucleus (LGN) of the thalamus. The LGN in primates consists of six primary layers: four parvocellular (Latin *Parvus*, small) and two magnocellular, each paired with a thin but dense intercalated or koniocellular (Greek *konio*, dust) layer (see Figure 21–14). The term "koniocellular" refers to the substantially smaller cell bodies in these layers relative to those of magnocellular or parvocellular layers. The parallel channels established in the retinas remain anatomically segregated through the LGN. Parvocellular layers get input from the midget retinal ganglion cells, which are the most numerous in the primate retina (~70%) and carry red-green opponent information (Chapter 22). Magnocellular layers get achromatic contrast information from the parasol ganglion cells (~10%). Koniocellular layers get input from the small and large bistratified ganglion cells, carrying blue-yellow information, that together make up the third most populous set of retinal projections to the LGN (~8%). Koniocellular layers also get inputs from a number of other numerically much smaller classes of retinal ganglion cells.

Each geniculate layer receives input from either the ipsilateral or the contralateral eye (see Figure 21–12) but is aligned so as to come from a matching region of the contralateral hemifield. Thus, they form a set of concordant maps stacked atop one another. The thalamic neurons then relay retinal information to the primary visual cortex. But the LGN is not simply a relay; the retinal information it receives can be strongly modulated by attention and arousal through inhibitory connections to this brain region and by feedback from the visual cortex.

The primary visual pathway is also called the geniculostriate pathway (Figure 21–6A) because it passes through the LGN on its way to the primary visual cortex (V1), also known as the striate cortex because of the myelin-rich stripe that runs through its middle layers. A second pathway extends from the retina to the pretectal area of the midbrain, where neurons mediate the pupillary reflexes that control the amount of light entering the eyes (Figure 21–6B). A third pathway from the retina runs to the superior colliculus and is important in controlling eye movements. This pathway continues to the pontine formation in the brain stem and then to the extraocular motor nuclei (Figure 21–6C).

Each LGN projects to the primary visual cortex through a pathway known as the optic radiation. These afferent fibers form a complete neural map of the contralateral visual field in the primary visual cortex. Beyond the striate cortex lie the extrastriate areas, a set of higher-order visual areas that are also organized as neural maps of the visual field. The preservation of the spatial arrangement of inputs from the retina is called retinotopy, and a neural map of the visual field is described as retinotopic or having a retinotopic frame of reference.

The primary visual cortex constitutes the first level of cortical processing of visual information. From there, information is transmitted over two major pathways. A ventral pathway into the temporal lobe carries information about what the stimulus is, and a dorsal

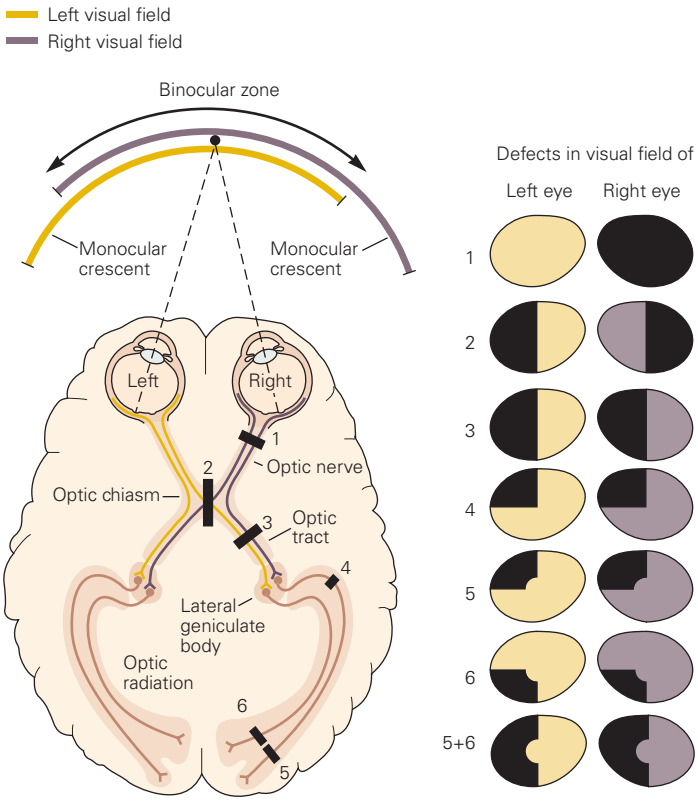

Figure 21–5 Representation of the visual field along the visual pathway. Each eye sees most of the visual field, with the exception of a portion of the peripheral visual field known as the monocular crescent. The axons of retinal neurons (ganglion cells) carry information from each visual hemifield along the optic nerve up to the optic chiasm, where fibers from the nasal hemiretina cross to the opposite hemisphere. Fibers from the temporal hemiretina stay on the same side, joining the fibers from the nasal hemiretina of the contralateral eye to form the optic tract. The optic tract carries information from the opposite visual hemifield originating in both eyes and projects into the lateral geniculate nucleus. Cells in this nucleus send their axons along the optic radiation to the primary visual cortex.

Lesions along the visual pathway produce specific visual field deficits, as shown on the *right*:

1. A lesion of an optic nerve causes a total loss of vision in one eye.

2. A lesion of the optic chiasm causes a loss of vision in the temporal half of each visual hemifield (bitemporal hemianopsia).

3. A lesion of the optic tract causes a loss of vision in the opposite half of the visual hemifield (contralateral hemianopsia).

4. A lesion of the optic radiation fibers that curve into the temporal lobe (Meyer's loop) causes loss of vision in the upper quadrant of the contralateral visual hemifield in both eyes (upper contralateral quadrantic anopsia).

5, 6. Partial lesions of the visual cortex lead to deficits in portions of the contralateral visual hemifield. For example, a lesion in the upper bank of the calcarine sulcus (**5**) causes a partial deficit in the inferior quadrant, while a lesion in the lower bank (**6**) causes a partial deficit in the superior quadrant. The central area of the visual field tends to be unaffected by cortical lesions because of the extent of the representation of the fovea and the duplicate representation of the vertical meridian in the hemispheres.

pathway into the parietal lobe carries information about where the stimulus is, information that is critical for guiding movement.

A major fiber bundle called the corpus callosum connects the two hemispheres, transmitting information across the midline. The primary visual cortex in each hemisphere represents slightly more than half the visual field, with the two hemifield representations overlapping at the vertical meridian. One of the functions of the corpus callosum is to unify the perception of objects spanning the vertical meridian by linking the cortical areas that represent opposite hemifields.

Form, Color, Motion, and Depth Are Processed in Discrete Areas of the Cerebral Cortex

In the late 19th and early 20th centuries, the cerebral cortex was differentiated into discrete regions by the anatomist Korbinian Brodmann and others using

anatomical criteria. The criteria included the size, shape, and packing density of neurons in the cortical layers and the thickness and density of myelin. The functionally distinct cortical areas we have considered heretofore correspond only loosely to Brodmann's classification. The primary visual cortex (V1) is identical to Brodmann's area 17. In the extrastriate cortex, the secondary visual area (V2) corresponds to area 18. Beyond that, however, area 19 contains several functionally distinct areas that generally cannot be defined by anatomical criteria.

The number of functionally discrete areas of visual cortex varies between species. Macaque monkeys have more than 30 areas. Although not all visual areas in humans have yet been identified, the number is likely to be at least as great as in the macaque. If one includes oculomotor areas and prefrontal areas contributing to visual memory, almost half of the cerebral cortex is involved with vision. Functional magnetic resonance imaging (fMRI) has made it possible to establish homologies between the visual areas of the macaque and human brains (Figure 21–7). Based on pathway tracing studies in monkeys, we now appreciate that these areas are organized in functional streams (Figure 21–7B).

The visual areas of cortex can be differentiated by the functional properties of their neurons. Studies of

A Visual processing

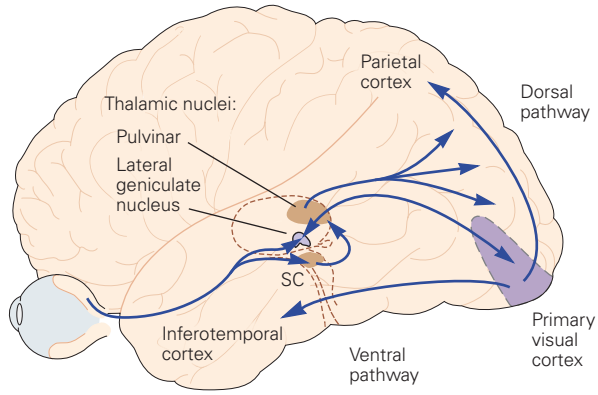

B Pupillary reflex and accommodation

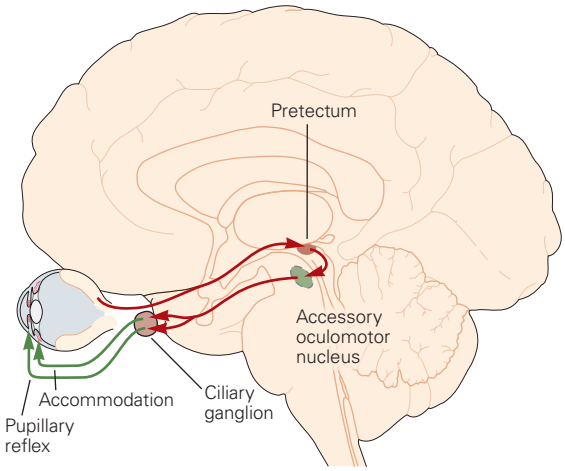

C Eye movement (horizontal)

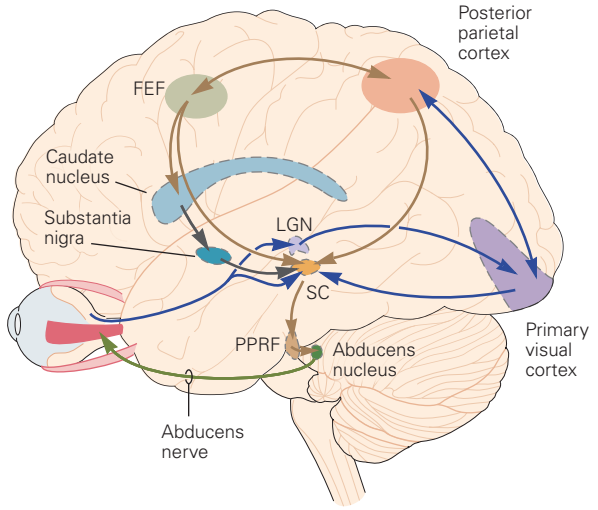

Figure 21–6 Pathways for visual processing, pupillary reflex and accommodation, and control of eye position.

A. *Visual processing.* The eye sends information first to thalamic nuclei, including the lateral geniculate nucleus and pulvinar, and from there to cortical areas. Cortical projections go forward from the primary visual cortex to areas in the parietal lobe (the dorsal pathway, which is concerned with visually guided movement) and areas in the temporal lobe (the ventral pathway, which is concerned with object recognition). The pulvinar also serves as a relay between cortical areas to supplement their direct connections. (Abbreviation: **SC**, superior colliculus).

B. *Pupillary reflex and accommodation.* Light signals are relayed through the midbrain pretectum, to preganglionic parasympathetic neurons in the accessory oculomotor (Edinger-Westphal) nucleus, and out through the parasympathetic outflow of the oculomotor nerve to the ciliary ganglion. Postganglionic neurons innervate the smooth muscle of the pupillary sphincter, as well as the muscles controlling the lens.

C. *Eye movement.* Information from the retina is sent to the superior colliculus (**SC**) directly along the optic nerve and indirectly through the geniculostriate pathway to cortical areas (primary visual cortex, posterior parietal cortex, and frontal eye fields) that project back to the superior colliculus. The colliculus projects to the pons (**PPRF**), which then sends control signals to oculomotor nuclei, including the abducens nucleus, which controls lateral movement of the eyes. (Abbreviations: **FEF**, frontal eye field; **LGN**, lateral geniculate nucleus; **PPRF**, paramedian pontine reticular formation.)

A Cortical visual areas in humans

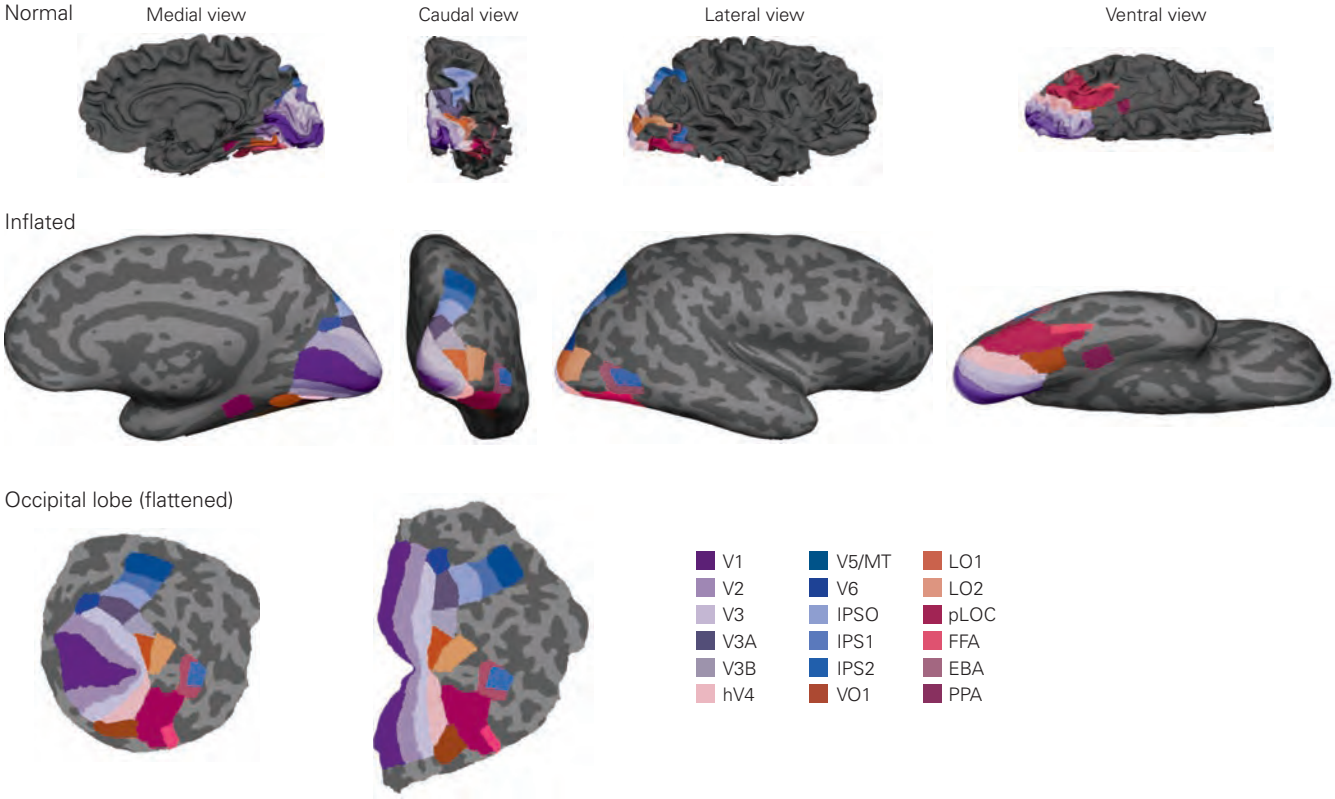

B Visual pathways in the macaque monkey

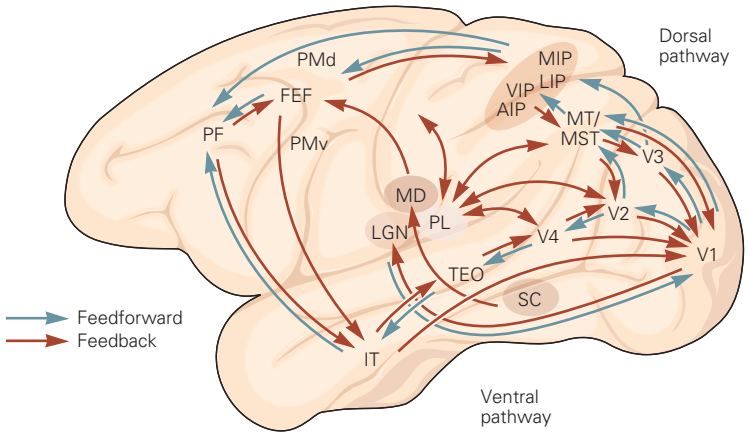

such functional properties have revealed that the visual areas are organized in two hierarchical pathways, a ventral pathway involved in object recognition and a dorsal pathway dedicated to the use of visual information for guiding movements. The ventral or object-recognition pathway extends from the primary visual cortex to the temporal lobe; it is described in detail in Chapter 24. The dorsal or movement-guidance pathway connects the primary visual cortex with the parietal lobe and then with the frontal lobes.

The pathways are interconnected so that information is shared. For example, movement information in the dorsal pathway can contribute to object recognition through kinematic cues. Information about movements in space derived from areas in the dorsal pathway is therefore important for the perception of object shape and is fed into the ventral pathway.

All connections between cortical areas are reciprocal—each area sends information back to the areas from which it receives input. These feedback connections provide information about cognitive functions, including spatial attention, stimulus expectation, and emotional content, to earlier levels of visual processing. The pulvinar in the thalamus serves as a relay between cortical areas (see Figure 21–7B).

The dorsal pathway courses through the parietal cortex, a region that uses visual information to direct the movement of the eyes and limbs, that is, for visuomotor integration. The lateral intraparietal area, named for its location in the intraparietal sulcus, is involved in representing points in space that are the targets of eye movements or reaching. Patients with lesions of parietal areas fail to attend to objects on one side of the body, a syndrome called *unilateral neglect* (see Figure 59–1 in Chapter 59).

The ventral pathway extends into the temporal lobe. The inferior temporal cortex stores information about the shapes and identities of objects; one portion represents faces, for damage to that region results in the inability to recognize faces (*prosopagnosia*).

The dorsal and ventral pathways each comprise a hierarchical series of areas that can be delineated by several criteria. First, at many relays, the array of inputs forms a map of the visual hemifield. The boundaries of these maps can be used to demarcate the boundaries of visual areas. This is particularly useful at early levels of the pathway where the receptive fields of neurons

Figure 21–7 Visual pathways in the cerebral cortex.

A. Functional magnetic resonance imaging shows areas of the human cerebral cortex involved in visual processing. The **top row** shows areas on the gyri and sulci of a normal view of a brain; the **middle row** shows "inflated" views of the brain following a computational process that simulates inflating the brain like a balloon so as to stretch out the "wrinkles" of gyri and sulci into a smooth surface while minimizing local distortions. Light and dark gray regions identify gyri and sulci, respectively; the **bottom row** shows a two-dimensional representation of the occipital lobe (*left*) and a representation with less distortion by making a cut along the calcarine fissure. Different approaches are required for demarcating different functional areas. Retinotopic areas, by definition, contain continuous maps of visual space and are identified using stimuli such as rotating spirals or expanding circles that sweep through visual space. Maps in adjacent cortical areas run in opposite directions on the cortical surface and meet along boundaries of local mirror reversals. These mirror reversals can be used to identify area boundaries and thus demarcate each area. These retinotopic areas, including early visual areas V1, V2, and V3, and areas V3A, V3B, V6, hV4, VO1, LO1, LO2, and V5/MT, share boundaries in pairs; these boundaries converge (at the representation of the fovea) at the occipital pole. A different approach, identifying loci of attention, is used to map areas IPS1 and IPS2. Yet further sets of approaches or responsiveness to specific attributes or classes of objects (such as faces) are used for less strictly retinotopic areas. Functional specificity has been demonstrated for a number of visual areas: VO1 is implicated in color processing, the lateral occipital complex (**LO2**, **pLOC**) codes object shape, fusiform face area (**FFA**) codes faces, the parahippocampal place area (**PPA**) responds more strongly to places than to objects, the extrastriate body area (**EBA**) responds more strongly to body parts than objects, and V5/MT is involved in motion processing. Areas in the intraparietal sulcus (**IPS1** and **IPS2**) are involved in control of spatial attention and saccadic eye movements. (Images courtesy of V. Piech, reproduced with permission.)

B. In the macaque monkey, V1 is located on the surface of the occipital lobe and sends axons in two pathways. A dorsal pathway courses through a number of areas in the parietal lobe and into the frontal lobe and mediates attentional control and visually guided movements. A ventral pathway projects through V4 into areas of the inferior temporal cortex and mediates object recognition. In addition to feedforward pathways extending from primary visual cortex into the temporal, parietal, and frontal lobes (**blue arrows**), reciprocal or feedback pathways run in the opposite direction (**red arrows**). Feedforward and feedback can operate directly, between cortical areas, or indirectly, via the thalamus, in particular the pulvinar, which acts as a relay between cortical areas. The subcortical pathways involved include thalamic nuclei—the lateral geniculate nucleus (**LGN**), pulvinar nucleus (**PL**), and mediodorsal nucleus (**MD**)—and the superior colliculus (**SC**). (Abbreviations: **AIP**, anterior intraparietal area; **FEF**, frontal eye field; **IT**, inferior temporal cortex; **LIP**, lateral intraparietal area; **MIP**, medial intraparietal area; **MT**, middle temporal area; **PF**, prefrontal cortex; **PMd**, dorsal premotor cortex; **PMv**, ventral premotor cortex; **TEO**, posterior division of area IT; **V1**, primary visual cortex, Brodmann's area 17; **V2**, secondary visual area, Brodmann's area 18; **V3**, **V4**, third and fourth visual areas; **VIP**, ventral intraparietal area.)

are small and visuotopic maps are precisely organized (see the next section for the definition of receptive field). At higher levels, however, the receptive fields become larger, the maps less precise, and visuotopic organization is therefore a less reliable basis to delineate the boundaries of an area.

Another means to differentiate one area from another, as shown by experiments in monkeys, depends upon the distinctive functional properties exhibited by the neurons in each area. The clearest example of this is an area in the dorsal pathway, the middle temporal area (MT or V5), which contains neurons with a strong selectivity for the direction of movement across their receptive fields. Consistent with the idea that the middle temporal area is involved in the analysis of motion, lesions of this area produce deficits in the ability to track moving objects.

A classical view of the organization of visual cortical areas is a hierarchical one, where the areas at the bottom of the hierarchy, such as V1 and V2, represent the visual primitives of orientation, direction of movement, depth, and color. In this view, the top of the ventral pathway's hierarchy would represent whole objects, with the areas in between representing intermediate level vision. This idea of "complexification" along the hierarchy suggests a mapping between the levels of visual perception and stages in the sequence of cortical areas. But more recent findings indicate a more complex story, where even the primary visual cortex plays a role in intermediate-level vision, and neurons in the higher areas may process information on components of objects. Moreover, as shown in Figure 21–7, one also has to take into account the fact that there is a powerful reverse flow of information, or feedback, from the "higher" to the "lower" cortical areas. As will be described in Chapter 23, this reverse direction of information contains higher order "top-down" cognitive influences including attention, object expectation, perceptual task, perceptual learning, and efference copy. Top-down influences may play a role in scene segmentation, object relationships, and perception of object details, as well as object recognition itself.

The Receptive Fields of Neurons at Successive Relays in the Visual Pathway Provide Clues to How the Brain Analyzes Visual Form

In 1906, Charles Sherrington coined the term *receptive field* in his analysis of the scratch withdrawal reflex: "The whole collection of points of skin surface from which the scratch-reflex can be elicited is termed the receptive field of that reflex." When it became possible to record from single neurons in the eye, H. Keffer Hartline applied the concept of the receptive field in his study of the retina of the horseshoe crab, *Limulus:* "The region of the retina which must be illuminated in order to obtain a response in any given fiber . . . is termed the receptive field of that fiber." In the visual system, a neuron's receptive field represents a small window on the visual field (Figure 21–8).

But responses to only one spot of light yielded a limited understanding of a cell's receptive field. Using two small spots of light, both Hartline and Stephen Kuffler, who studied the mammalian retina, found an inhibitory surround or lateral inhibitory region in the receptive field. In 1953, Kuffler observed that "not only the areas from which responses can actually be set up by retinal illumination may be included in a definition of the receptive field but also all areas which show a functional connection, by an inhibitory or excitatory effect on a ganglion cell." Kuffler thus demonstrated that the receptive fields of retinal ganglion cells have functionally distinct subareas. These receptive fields have a center-surround organization and fall into one of two categories: *on-center* and *off-center*. Later work demonstrated that neurons in the LGN have similar receptive fields.

The on-center cells fire when a spot of light is turned on within a circular central region. Off-center cells fire when a spot of light in the center of their receptive field is turned off. The surrounding annular region has the opposite sign. For on-center cells, a light stimulus anywhere in the annulus surrounding the center produces a response when the light is turned off, a response termed *on-center, off-surround*. The center and surround areas are mutually inhibitory (Figure 21–9). When both center and surround are illuminated with diffuse light, there is little or no response. Conversely, a light–dark boundary across the receptive field produces a brisk response. Because these neurons are most sensitive to borders and contours—to differences in illumination as opposed to uniform surfaces—they encode information about contrast in the visual field.

The size on the retina of a receptive field varies both according to the field's *eccentricity*—its position relative to the fovea, the central part of the retina where visual acuity is highest—and the position of neurons along the visual pathway. Receptive fields with the same eccentricity are relatively small at early levels in visual processing and become progressively larger at later levels. The size of the receptive field is expressed in terms of degrees of visual angle; the entire visual field covers nearly 180° (Figure 21–10A). In early relays of visual processing, the receptive fields near the fovea are the smallest. The receptive

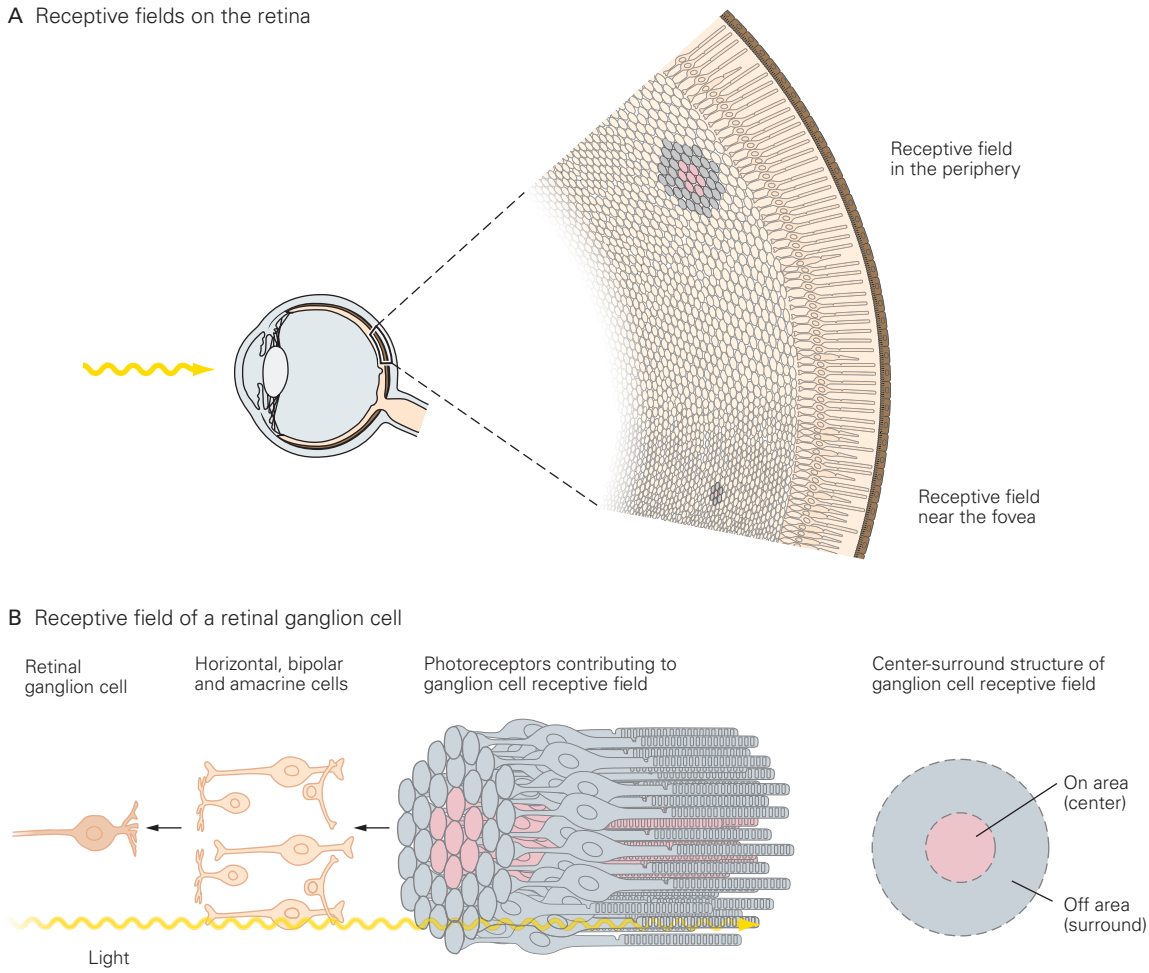

Figure 21–8 Receptive fields of retinal ganglion cells in relation to photoreceptors.

A. The number of photoreceptors contributing to the receptive field of a retinal ganglion cell varies depending on the location of the receptive field on the retina. A cell near the fovea receives input from fewer receptors covering a smaller area, whereas a cell farther from the fovea receives input from many more receptors covering a larger area (see Figure 21–10).

B. Light passes through nerve cell layers to reach the photoreceptors at the back of the retina. Signals from the photoreceptors are then transmitted by neurons in the outer and inner nuclear layers to a retinal ganglion cell.

fields for retinal ganglion cells that monitor portions of the fovea subtend approximately 0.1°, whereas those in the visual periphery can be a couple of orders of magnitude larger.

The amount of cortex dedicated to a degree of visual space changes with eccentricity. More area of cortex is dedicated to the central part of the visual field, where the receptive fields are smallest and the visual system has the greatest spatial resolution (Figure 21–10C).

Receptive-field properties change from relay to relay along a visual pathway. By determining these properties, one can assay the function of each relay nucleus and how visual information is progressively analyzed by the brain. For example, the change in receptive-field structure that occurs between the LGN and cerebral cortex reveals an important mechanism in the brain's analysis of visual form. The key property of the form pathway is selectivity for the orientation of contours in the visual field. This is an emergent property of signal processing in primary visual cortex; it is not a property of the cortical input but is generated within the cortex itself.

Whereas retinal ganglion cells and neurons in the LGN have concentric center-surround receptive fields, those in the cortex, although equally sensitive to contrast, also analyze contours. David Hubel and Torsten Wiesel discovered this characteristic in 1958

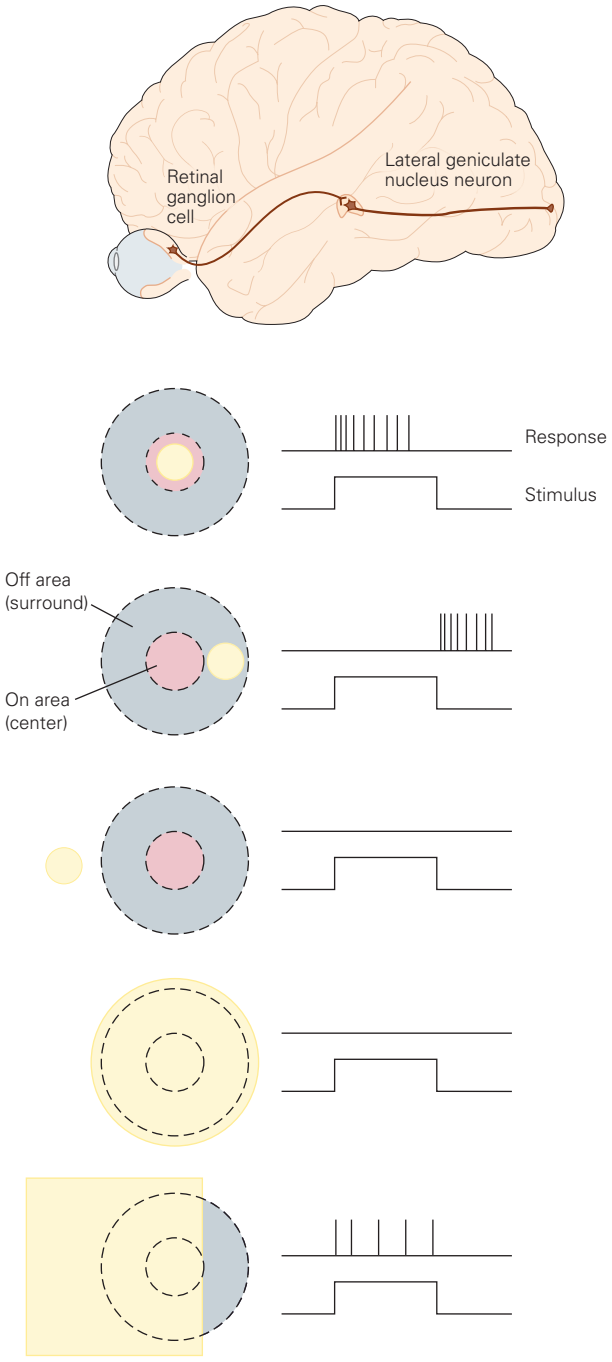

Figure 21–9 Receptive fields of neurons at early relays of visual pathways. A circular symmetric receptive field with mutually antagonistic center and surround is characteristic of retinal ganglion cells and neurons in the lateral geniculate nucleus of the thalamus. The center can respond to the turning on or turning off of a spot of light (**yellow**) depending on whether the receptived field belongs to an "on-center" or "off-center" class, respectively. The surround has the opposite response. Outside the surround, there is no response to light, thus defining the receptive field boundary. The response is weak when light covers both the center and surround, so these neurons respond optimally to contrast (a light–dark boundary) in the visual field.

while studying what visual stimuli provoked activity in neurons in the primary visual cortex. While showing an anesthetized animal slides containing a variety of images, they recorded extracellularly from individual neurons in the visual cortex. As they switched from one slide to another, they found a neuron that produced a brisk train of action potentials. The cell was responding not to the image on the slide but to the edge of the slide as it was moved into position.

The Visual Cortex Is Organized Into Columns of Specialized Neurons

The dominant feature of the functional organization of the primary visual cortex is the visuotopic organization of its cells: the visual field is systematically represented across the surface of the cortex (Figure 21–11A).

In addition, cells in the primary visual cortex with similar functional properties are located close together in columns that extend from the surface of the cortex to the white matter. The columns are concerned with the functional properties that are analyzed in any given cortical area and thus reflect the functional role of that area in vision. The properties that are developed in the primary visual cortex include orientation specificity and the integration of inputs from the two eyes, which is measured as the relative strength of input from each eye, or ocular dominance.

Ocular-dominance columns reflect the segregation of thalamocortical inputs arriving from different layers of the LGN. Alternating layers of this nucleus receive input from retinal ganglion cells located in either the ipsilateral or contralateral retina (Figure 21–12). This segregation is maintained in the inputs from the LGN to the primary visual cortex, producing the alternating left-eye and right-eye ocular dominance bands (Figure 21–11B).

Cells with similar orientation preferences are also grouped into columns. Across the cortical surface, there is a regular clockwise and counterclockwise cycling of orientation preference, with the full 180° cycle repeating every 750 µm (Figure 21–11C). Likewise, the left- and right-eye dominance columns alternate with a periodicity of 750 to 1,000 µm. One full cycle of orientation columns, or a full pair of left- and right-eye dominance columns, is called a *hypercolumn*. The orientation and ocular dominance columns at each point on the cortical surface are locally roughly orthogonal to each other. Thus, a cortical patch one hypercolumn in extent contains all possible combinations of orientation preference and left- and right-eye dominance.

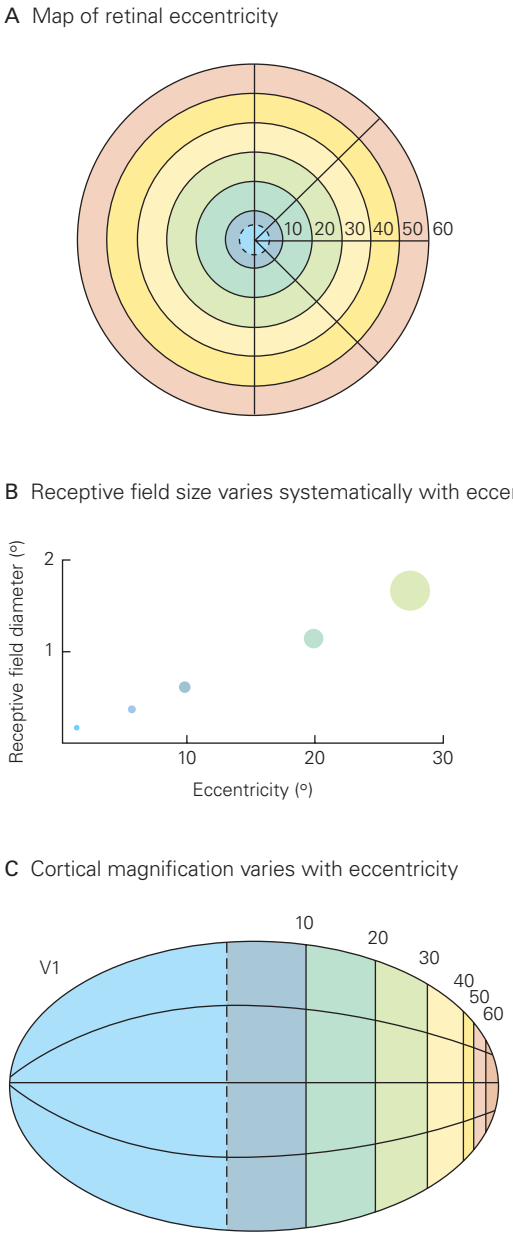

Figure 21–10 **Receptive field size, eccentricity, retinotopic organization, and magnification factor.** The color code refers to position in visual space or on the retina.

A. The distance of a receptive field from the fovea is referred to as the eccentricity of the receptive field.

B. Receptive field size varies with distance from the fovea. The smallest fields lie in the center of gaze, the fovea, where the visual resolution is highest; fields become progressively larger with distance from the fovea.

C. The amount of cortical area dedicated to inputs from within each degree of visual space, known as the magnification factor, also varies with eccentricity. The central part of the visual field commands the largest area of cortex. For example, in area V1, more area is dedicated to the central 10° of visual space than to all the rest. The map of V1 shows the cortical sheet unfolded.

Both types of columns were first mapped by recording the responses of neurons at closely spaced electrode penetrations in the cortex. The ocular-dominance columns were also identified by making lesions or tracer injections in individual layers of the LGN. More recently, a technique known as optical imaging has enabled researchers to visualize a surface representation of the orientation and ocular dominance columns in living animals. Developed for studies of cortical organization by Amiram Grinvald, this technique visualizes changes in surface reflectance associated with the metabolic requirements of active groups of neurons, known as intrinsic-signal optical imaging, or changes in fluorescence of voltage-sensitive dyes. Intrinsic-signal imaging depends on activity-associated changes in local blood flow and alterations in the oxidative state of hemoglobin and other intrinsic chromophores. These techniques are also now being complemented with imaging at cellular resolution using genetically encoded markers of neural activity.

An experimenter can visualize the distribution of cells with left or right ocular dominance, for example, by subtracting the image obtained while stimulating one eye from that acquired while stimulating the other. When viewed in a plane tangential to the cortical surface, the ocular dominance columns appear as alternating left- and right-eye stripes, each approximately 750 µm in width (Figure 21–11B).

The cycles of orientation columns form various structures, from parallel stripes to pinwheels. Sharp jumps in orientation preference occur at the pinwheel centers and "fractures" in the orientation map (Figure 21–11C).

Embedded within the orientation and ocular-dominance columns are clusters of neurons that have poor orientation selectivity but strong color preferences. These units of specialization, located within the superficial layers, were revealed by a histochemical label for the enzyme cytochrome oxidase, which is distributed in a regular patchy pattern of blobs and interblobs. In the primary visual cortex, these blobs are a few hundred micrometers in diameter and 750 µm apart (Figure 21–11D). The blobs correspond to clusters of color-selective neurons. Because they are rich in cells with color selectivity and poor in cells with orientation selectivity, the blobs are specialized to provide information about surfaces rather than edges.

In area V2, thick and thin dark stripes separated by pale stripes are evident with cytochrome oxidase labeling (Figure 21–11D). The thick stripes contain neurons selective for direction of movement and for binocular disparity as well as cells that are responsive to illusory contours and global disparity cues. The thin stripes hold cells specialized for color. The pale stripes contain orientation-selective neurons.

A Visuotopic map

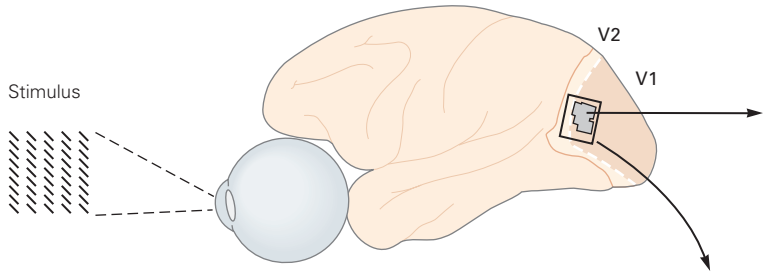

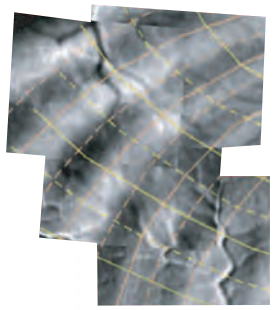

Pattern of excitation in response to striped stimulus

B Ocular dominance columns

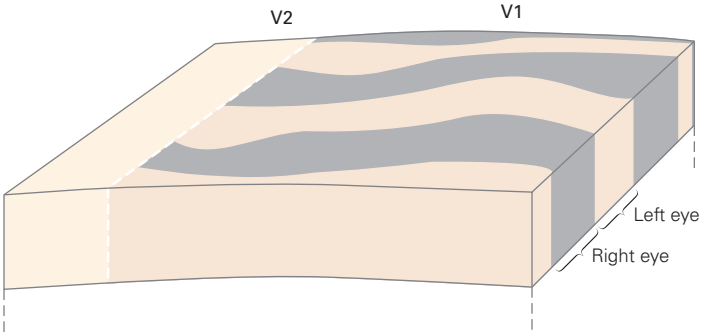

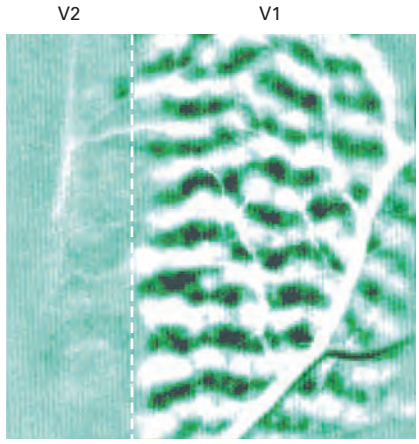

C Orientation columns

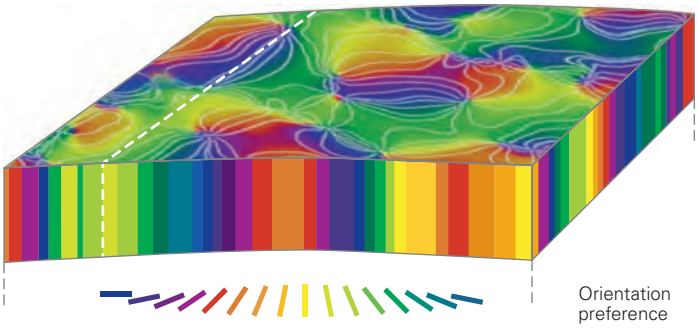

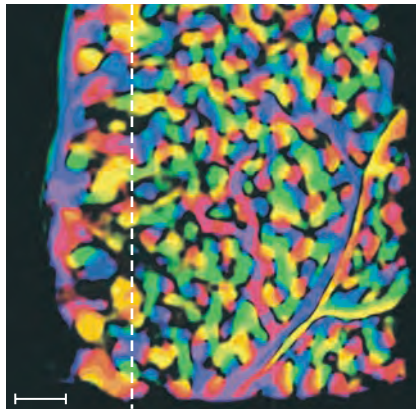

D Blobs, interblobs (V1), and stripes (V2)

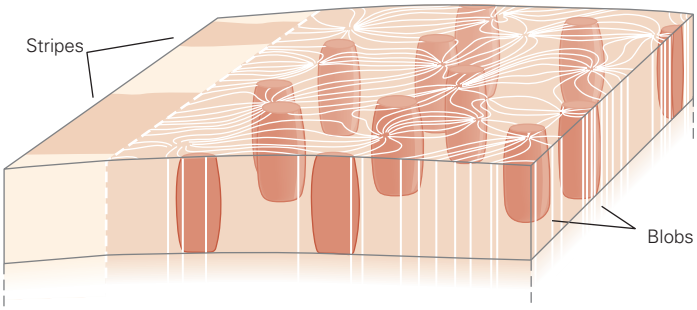

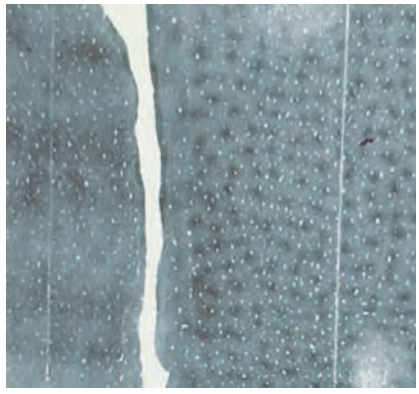

Figure 21–11 (Opposite) **Functional architecture of the primary visual cortex.** (Courtesy of M. Kinoshita and A. Das, reproduced with permission.)

A. The surface of the primary visual cortex is functionally organized as a map of the visual field. The elevations and azimuths of visual space are organized in a regular grid that is distorted because of variation in the magnification factor (see Figure 21–10). The grid is visible here in the dark stripes (visualized with intrinsic-signal optical imaging), which reflect the pattern of neurons that responded to a series of vertical candy stripes. Within this surface map, one finds repeated superimposed cycles of functionally specific columns of cells, as illustrated in **B**, **C**, and **D**.

B. The dark and light stripes represent the surface view of the left and right ocular dominance columns. These stripes intersect the border between areas V1 and V2, the representation of the vertical meridian, at right angles.

C. Some columns contain cells with similar selectivity for the orientation of stimuli. The different colors indicate the orientation preference of the columns. The orientation columns in surface view are best described as pinwheels surrounding singularities of sudden changes in orientation (the center of the pinwheel). The scale bar represents 1 mm. (Surface image of orientation columns on the left courtesy of G. Blasdel, reproduced with permission.)

D. Patterns of blobs in V1 and stripes in V2 represent other modules of functional organization. These patterns are visualized with cytochrome oxidase.

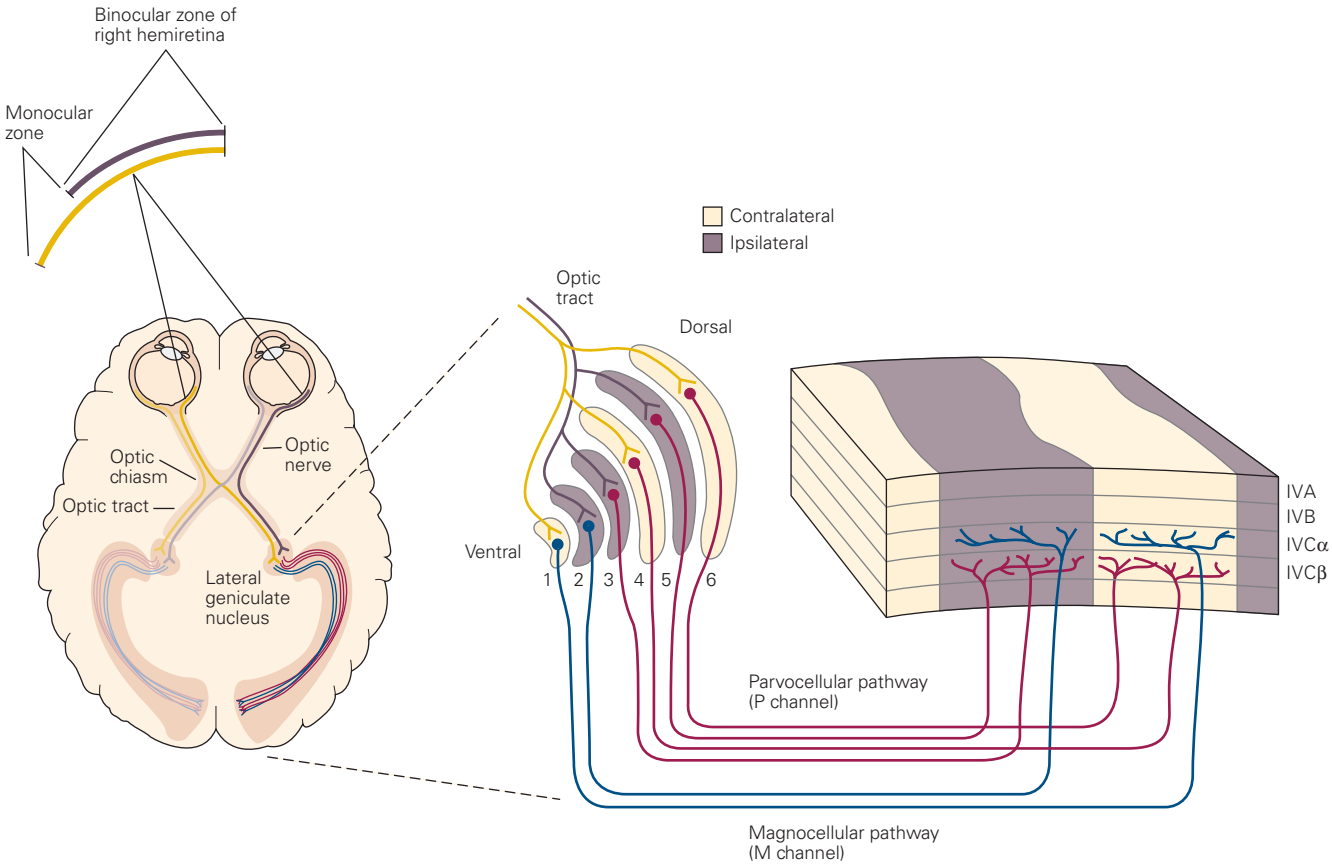

Figure 21–12 **Projections from the lateral geniculate nucleus to the visual cortex.** The lateral geniculate nucleus in each hemisphere receives input from the temporal retina of the ipsilateral eye and the nasal retina of the contralateral eye. The nucleus is a layered structure comprising four parvocellular layers (layers 3 to 6) and two magnocellular layers (layers 1 and 2). Each is paired with an intercalated koniocellular layer. (These layers are represented here by the gaps separating the primary layers. They are unlabeled to avoid clutter. See Figure 21–14.) The inputs from the two eyes terminate in different geniculate layers: The contralateral eye projects to layers 1, 4, and 6, whereas the ipsilateral eye sends input to layers 2, 3, and 5. Neurons from these geniculate layers then project to different layers of cortex. The parvocellular geniculate neurons project to layer IVCβ, the magnocellular ones project to layer IVCα, and the koniocellular ones project to "blobs" in the upper cortical layers (see Figures 21–14 and 21–15). In addition, the afferents from the ipsilateral and contralateral layers of the lateral geniculate nucleus are segregated into alternating ocular-dominance columns.

For every visual attribute to be analyzed at each position in the visual field, there must be adequate tiling, or coverage, of neurons with different functional properties. As one moves in any direction across the cortical surface, the progression of the visuotopic location of receptive fields is gradual, whereas the cycling of columns occurs more rapidly. Any given position in the visual field can therefore be analyzed adequately in terms of the orientation of contours, the color and direction of movement of objects, and stereoscopic depth by a single computational module. The small segment of visual cortex that comprises such a module represents all possible values of all the columnar systems (Figure 21–13).

The columnar systems serve as the substrate for two fundamental types of connectivity along the visual pathway. *Serial processing* occurs in the successive connections between cortical areas, connections that run from the back of the brain forward. At the same time, *parallel processing* occurs simultaneously in subsets of fibers that process different submodalities such as form, color, and movement, continuing the neural processing strategy started in the retina.

Many areas of visual cortex reflect this arrangement; for example, functionally specific cells in V1 communicate with cells of the same specificity in V2. These pathways are not absolutely segregated, however, for there is some mixing of information between different visual attributes (Figure 21–14).

Columnar organization confers several advantages. It minimizes the distance required for neurons with similar functional properties to communicate with one another and allows them to share inputs from discrete pathways that convey information about particular sensory attributes. This efficient connectivity economizes on the use of brain volume and maximizes processing speed. The clustering of neurons into functional groups, as in the columns of the cortex, allows the brain to minimize the number of neurons required for analyzing different attributes. If all neurons were tuned for every attribute, the resultant combinatorial explosion would require a prohibitive number of neurons.

Intrinsic Cortical Circuits Transform Neural Information

Each area of the visual cortex transforms information gathered by the eyes and processed at earlier synaptic relays into a signal that represents the visual scene. This transformation is accomplished by local circuits comprising both excitatory and inhibitory neurons.

The principal input to the primary visual cortex comes from three parallel pathways that originate in the parvocellular, magnocellular, and the blue/yellow channels of koniocellular layers of the LGN (see Figure 21–12). Neurons in the parvocellular layers project to cortical layers IVCβ and 6, those in the

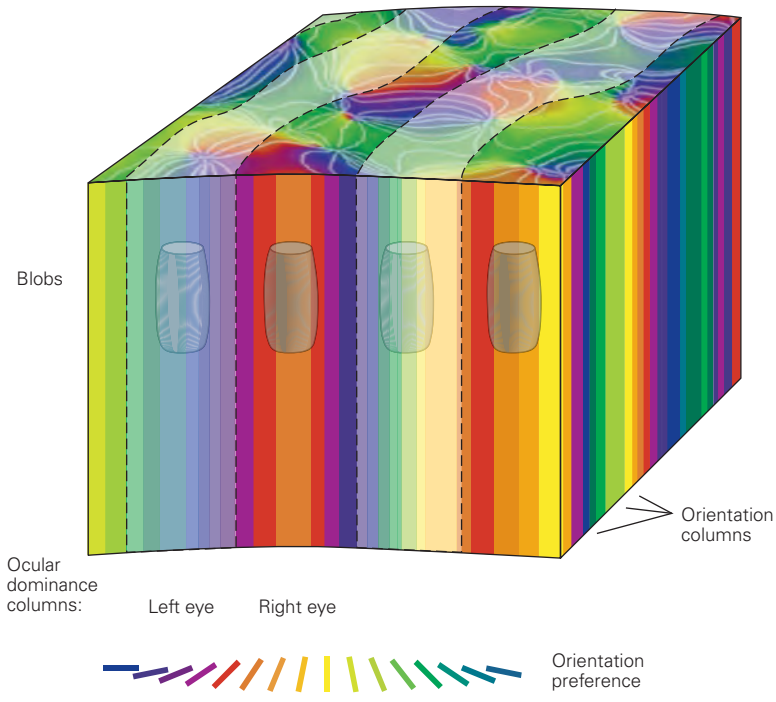

Figure 21–13 A cortical computational module. A chunk of cortical tissue roughly 1 mm square contains an orientation hypercolumn (a full cycle of orientation columns), one cycle of left- and right-eye ocular-dominance columns, and blobs and interblobs. This module would presumably contain all of the functional and anatomical cell types of primary visual cortex, which would be repeated hundreds of times to cover the visual field. (Adapted from Hubel 1988.)

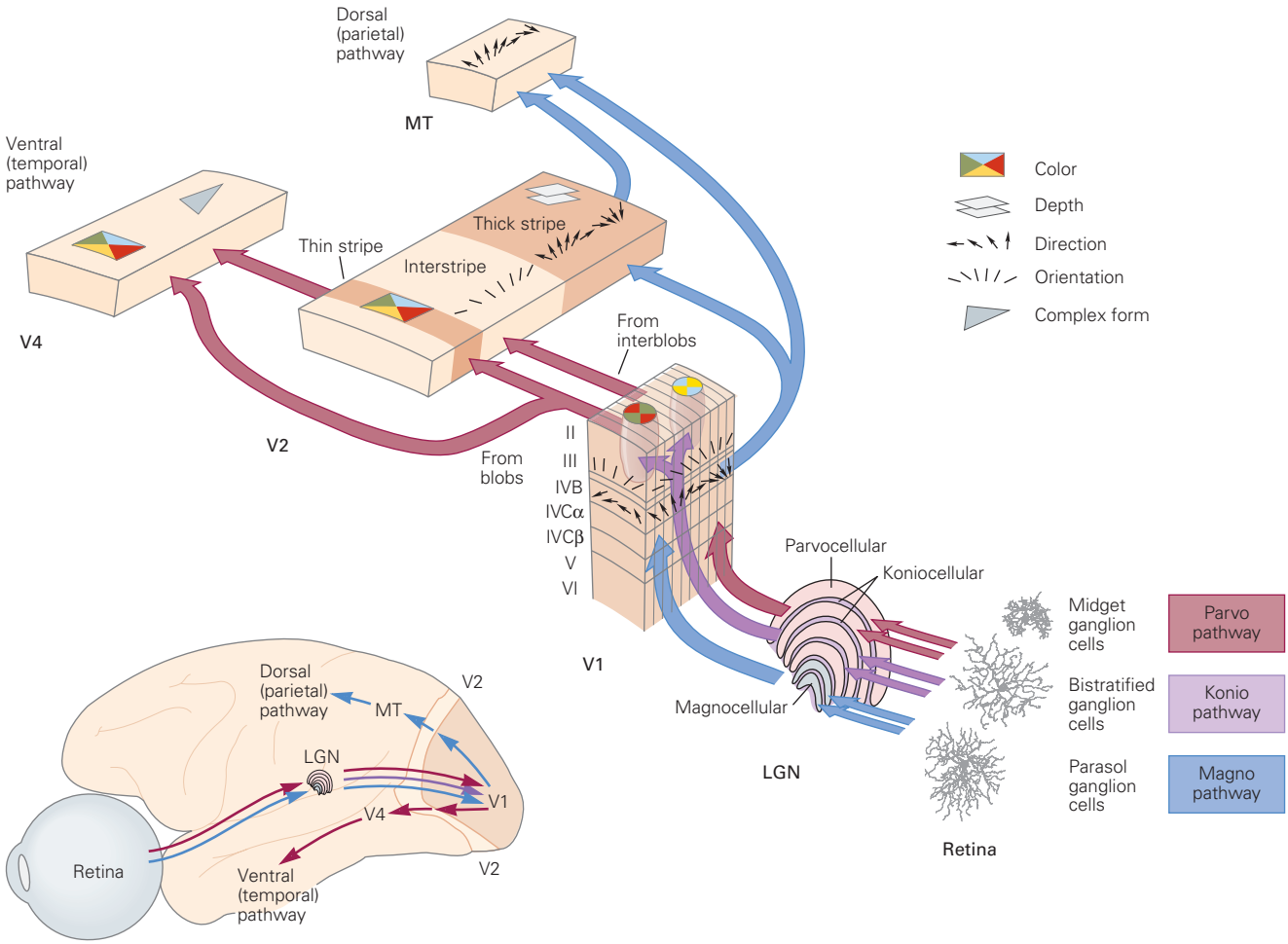

Figure 21–14 Parallel processing in visual pathways. The ventral stream is primarily concerned with object identification, carrying information about form and color. The dorsal pathway is dedicated to visually guided movement, with cells selective for direction of movement. These pathways are not strictly segregated, however, and there is substantial interconnection between them even in the primary visual cortex. (Abbreviations: **LGN**, lateral geniculate nucleus; **MT**, middle temporal area.) (Retinal ganglion cell images courtesy of Dennis Dacey, reproduced with permission.)

magnocellular layers project to layer IVCα and 6, while the koniocellular neurons project to layer 1 and to the cytochrome oxidase blobs in layers 2 and 3. From there, a sequence of interlaminar connections, mediated by the excitatory spiny stellate neurons, processes visual information over a stereotyped set of connections (Figure 21–15).

This characterization of parallel pathways is only an approximation, as there is considerable interaction between the pathways. This interaction is the means by which various visual features—color, form, depth, and movement—are linked, leading to a unified visual percept. One way this linkage, or binding, may be accomplished is through cells that are tuned to more than one attribute.

At each stage of cortical processing, pyramidal neurons extend output to other brain areas. Superficial-layer cells are responsible for connections to higher-order areas of cortex. Layer V pyramidal neurons project to the superior colliculus and pons in the brain stem. Layer VI cells are responsible for feedback projections, both to the thalamus and to lower-order cortical areas.

Neurons in different layers have distinctive receptive-field properties. Neurons in the superficial layer of V1 have small receptive fields, whereas neurons in deeper layers have large ones. The superficial-layer neurons are specialized for high-resolution pattern recognition. Neurons in the deeper layers, such as those in layer V that are selective for the direction of movement, are specialized for the tracking of objects in space.

A Distribution of cell types in the primary visual cortex

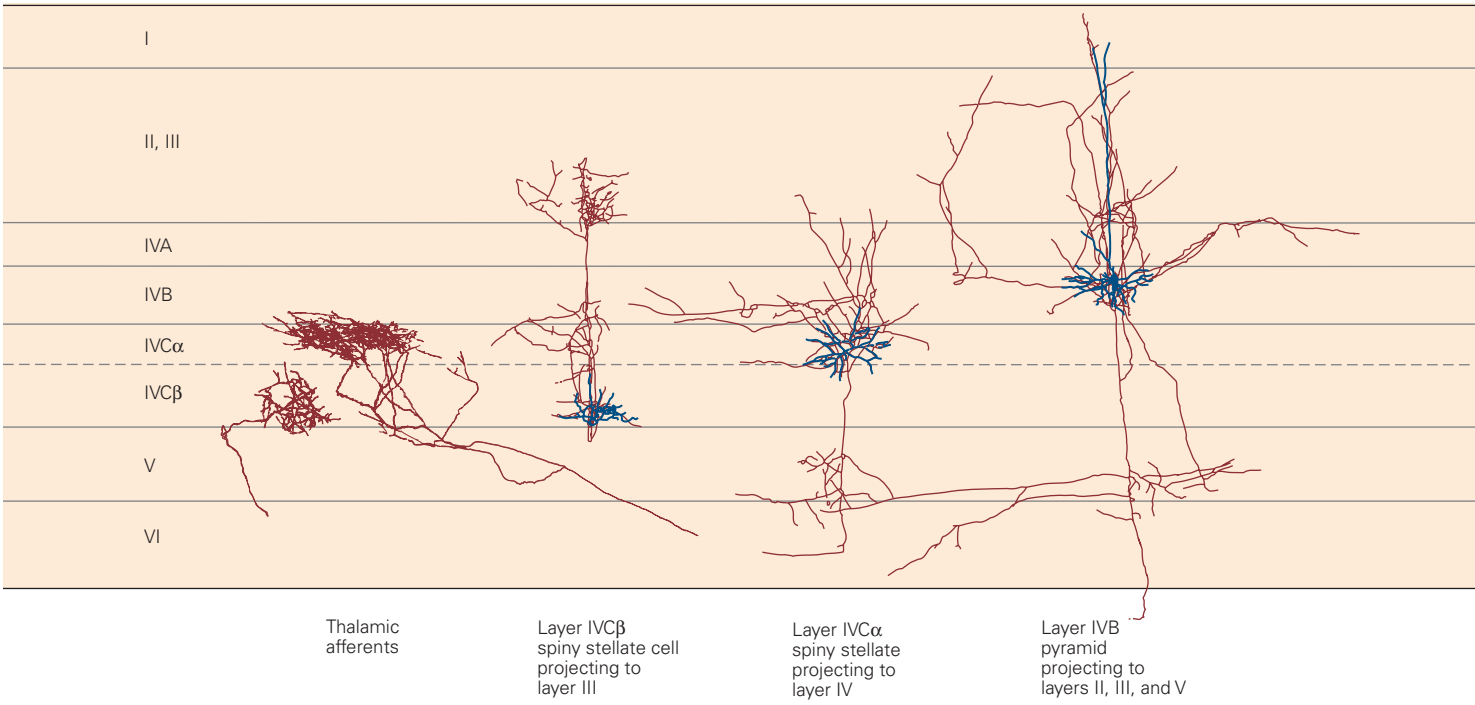

B Simplified diagram of intrinsic circuitry

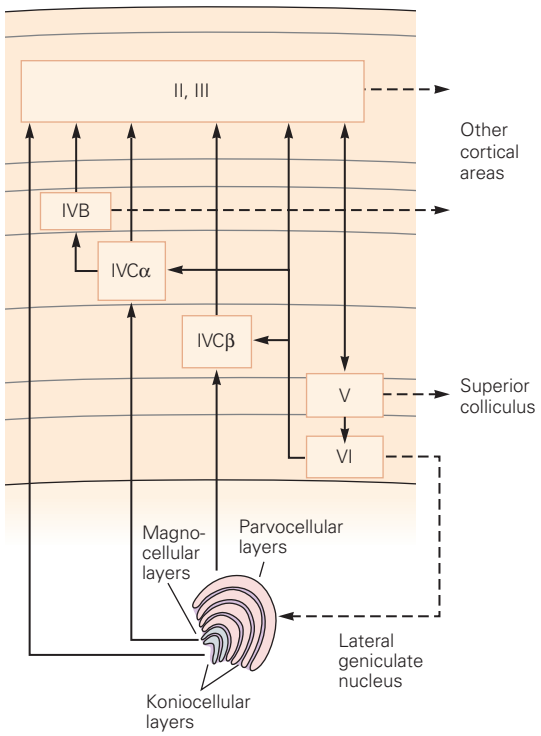

Figure 21–15 The intrinsic circuitry of the primary visual cortex.

A. Examples of neurons in different cortical layers responsible for excitatory connections in cortical circuits. Layer IV is the principal layer of input from the lateral geniculate nucleus of the thalamus. Fibers from the parvocellular layer terminate in layer IVCβ, whereas the magnocellular fibers terminate in layer IVCα. The intrinsic cortical excitatory connections are mediated by spiny stellate and pyramidal cells. A variety of γ-aminobutyric acid (GABA)-ergic smooth stellate cells (not shown) are responsible for inhibitory connections. Dendritic arbors are colored **blue**, and axonal arbors are shown in **brown**. (Cortical neurons courtesy of E. Callaway, reproduced with permission. Thalamic afferents adapted, with permission, from Blasdel and Lund 1983. Copyright © 1983 Society for Neuroscience.)

B. Diagram of excitatory connections within the primary visual cortex. Output to other regions of cortex is sent from every layer of visual cortex.

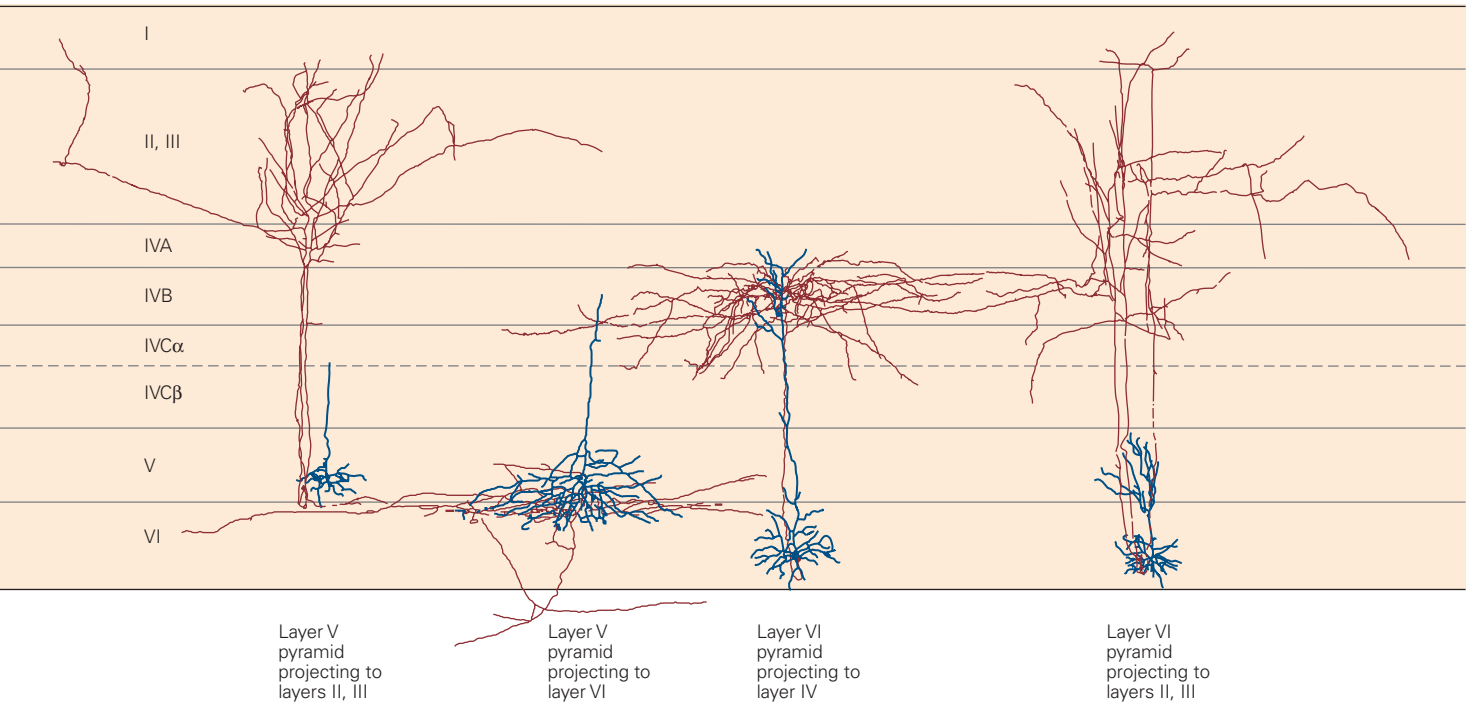

Feedback projections are thought to provide a means whereby higher centers in a pathway can influence lower ones. The number of neurons projecting from the cortex to the LGN is 10-fold the number projecting from the LGN to the cortex. Although this feedback projection is obviously important, its function is largely unknown.

The activity of the excitatory pyramidal and spiny stellate neurons that mediate information flow into or out of cortical regions is also tightly controlled by local networks of inhibitory interneurons. The spike rates of excitatory neurons are constantly nonlinearly balanced by matched inhibition that maintains the stability of the neural response to an input. Inhibitory interneurons come in multiple classes distinguished by their morphology and their coexpression of distinct peptides such as parvalbumin, somatostatin, or vasoactive intestinal polypeptide (VIP). Some of these interneurons form cascading circuits where interneurons of one class target interneurons of another class, which then target excitatory neurons. This leads to multistep control mechanisms in the neural circuit whereby increasing activity in the first class of inhibitory interneurons reduces activity in the second class, disinhibiting and increasing responses in the excitatory targets at the end of the cascade. Such motifs of inhibitory control are likely to be common to multiple cortical sensory areas.

In addition to serial feedforward, feedback, and local recurrent connections, fibers that travel parallel to the cortical surface within each layer provide long-range horizontal connections (Figure 21–16). These connections and their role in the functional architecture of cortex were analyzed by Charles Gilbert and Torsten Wiesel, who used intracellular recordings and dye injection to correlate anatomical features with cortical function. Because the visual cortex is organized visuotopically, the horizontal connections allow target neurons to integrate information over a relatively large area of the visual field and are therefore important in assembling the components of a visual image into a unified percept.

Integration can also be achieved by other means. The considerable convergence and divergence of connections at the synaptic relays of the afferent visual pathway imply that the receptive fields of neurons are larger and more complex at each successive relay and thus have an integrative function. Feedback connections may also support integration, both because of their divergence and because they originate from cells with larger receptive fields.

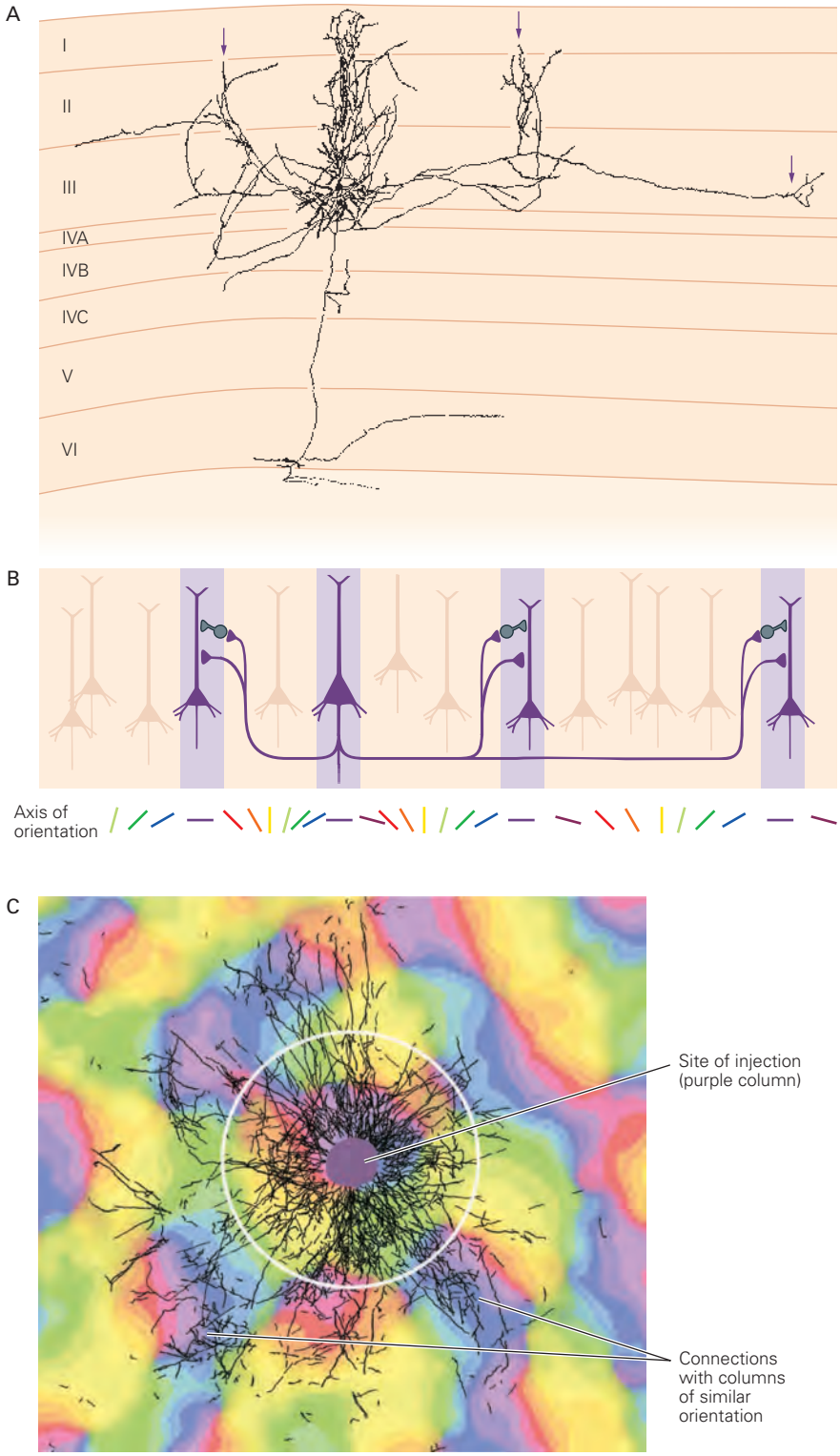

Figure 21–16 Long-range horizontal connections in each layer of the visual cortex integrate information from different parts of the visual field.

A. The axons of pyramidal cells extend for many millimeters parallel to the cortical surface. Axon collaterals form connections with other pyramidal cells as well as with inhibitory interneurons. This arrangement enables neurons to integrate information over large parts of the visual field. An important characteristic of these connections is their relationship to the functional columns. The axon collaterals are found in clusters (**arrows**) at distances greater than 0.5 mm from the cell body. (Reproduced, with permission, from Gilbert and Wiesel 1983. Copyright © 1983 Society for Neuroscience.)

B. Horizontal connections link columns of cells with similar orientation specificity.

C. The pattern of horizontal connections is visualized by injecting an adenoviral vector containing the gene encoding green fluorescent protein into one orientation column and superimposing the labeled image (**black**) on an optically imaged map of the orientation columns in the vicinity of the injection. (Diameter of white circle is 1 mm.) (Reproduced, with permission, from Stettler et al. 2002.)

Visual Information Is Represented by a Variety of Neural Codes

Individual neurons in a sensory pathway respond to a range of stimulus values. For example, a neuron in a color-detection pathway is not limited to responding to one wavelength but is instead tuned to a range of wavelengths. A neuron's response peaks at a particular value and tails off on either side of that value, forming a bell-shaped tuning curve with a particular bandwidth. Thus, a neuron with a peak response at 650 nm and a bandwidth of 100 nm might give identical responses at 600 nm and 700 nm.

To be able to determine the wavelength from neuronal signals, one needs at least two neurons representing filters centered at different wavelengths. Each neuron can be thought of as a *labeled line* in which activity signals a stimulus with a given value. When more than one such neuron fires, the convergent signals at the postsynaptic relay represent a stimulus with a wavelength that is the weighted average of the values represented by all the inputs.

A single visual percept is the product of the activity of a number of neurons operating in a specific combinatorial and interactive fashion called a *population code.* Population coding has been modeled in various ways. The most prevalent model is called *vector averaging*.

We can illustrate population coding with a population of orientation-selective cells, each of which responds optimally to a line with a specific orientation. Each neuron responds not just to the preferred stimulus but rather to any line that falls within a range of orientations described by a Gaussian tuning curve with a particular bandwidth. A stimulus of a particular orientation most strongly activates cells with tuning curves centered at that orientation; cells with tuning curves centered away from but overlapping that orientation are excited less strongly.

Each cell's preferred orientation, the line label, is represented as a vector pointing in the direction of that orientation. Each cell's firing is a "vote" for the cell's line label, and the cell's firing rate represents the weighting of the vote. The cell's signal can thus be represented by a vector pointing in the direction of the cell's preferred orientation with a length proportional to the strength of the cell's response. For all the activated cells, one can calculate a vector sum with a direction that represents the value of the stimulus (Figure 21–17).

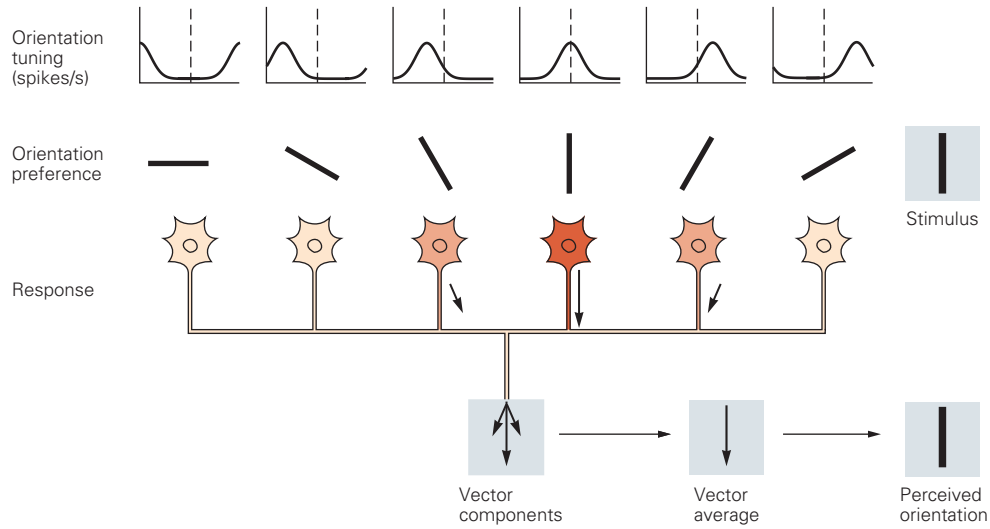

Figure 21–17 Vector averaging is one model for population coding in neural circuits. Vector averages describe the possible relationship between the responses in an ensemble of neurons, the tuning characteristics of individual neurons in the ensemble, and the resultant percept. Individual neurons respond optimally to a particular orientation of a stimulus in the visual field, but also respond at varying rates to a range of orientations. The stimulus orientation to which a neuron fires best can be thought of as a line label—when the cell fires briskly, its activity signifies the presence of a stimulus with that orientation. A number of neurons with different orientation preferences will respond to the same stimulus. Each neuron's response can be represented as a vector whose length indicates the strength of its response and whose direction represents its preferred orientation, or line label. (Adapted, with permission, from Kapadia, Westheimer, and Gilbert 2000.)

Another aspect of the population code is the variability of a neuron's response to the same stimulus. Repeated presentation of a stimulus to a neuron sensitive to that stimulus will elicit a range of responses. The most sensitive part of a neuron's tuning curve lies not at the peak but along the flanks, where the tuning curve is steepest. Here, small changes in the value of a stimulus produce the strongest change in response. Changes in stimulus value must, however, be sufficient to elicit a change in response that significantly exceeds the normal variability in the response of the neuron. One can compare that amount of change to the perceptual discrimination threshold. When many neurons contribute to the discrimination, the signal-to-noise ratio increases, a process known as probability summation, and the critical difference in stimulus value required for a significant change in neuronal response is less.

When the brain represents a piece of information, an important consideration is the number of neurons that participate in that representation. Although all information about a visual stimulus is present in the retina, the retinal representation is not sufficient for object recognition. At the other end of the visual pathway, some neurons in the temporal lobe are selective for complex objects, such as faces. Can an individual cell represent something as complex as a particular face? Such a hypothetical neuron has been dubbed a "grandmother cell" because it would represent exclusively a person's grandmother, or a "pontifical cell" because it would represent the apex of a hierarchical cognitive pathway.

The nervous system does not, however, represent entire objects by the activity of single neurons. Instead, some cells represent parts of an object, and an ensemble of neurons represents an entire object. Each member of the ensemble may participate in different ensembles that are activated by different objects. This arrangement is known as a *distributed code*. Distributed codes can involve a few neurons or many. In any case, a distributed code requires complex connectivity between the cells representing a face and those representing the name and experiences associated with that person.

The foregoing discussion assumes that neurons signal information by their firing rate and their line labels. An alternative hypothesis is that the timing of action potentials itself carries information, analogous to Morse code. The code might be read from the synchronous firing of different sets of neurons over time. At one instant, one group of cells might fire together followed by the synchronous firing of another group. Over a single train of action potentials, a single cell could participate in many such ensembles. Whether sensory information is represented this way and whether the nervous system carries more information than that represented by firing rate alone are not known.

Highlights

1. Vision is a constructive process fundamentally different from the mere recording of visual input as in a camera. Rather, the brain uses visual input to infer information about the world around it, including information about objects, such as their sizes, shapes, distances, and identities and how rapidly they are moving.
2. The tuning of neural circuits for visual features such as contrast, orientation, and motion often matches the distribution of the feature in the natural environment. This suggests an evolutionary, ethologically driven origin for the neural circuitry.
3. Visual circuitry, and thus vision, are modulated by individual visual experience.
4. Vision makes extensive use of parallel processing. The higher visual centers form two distinct pathways. The dorsal pathway, located in parietal cortex, is involved in motion perception, attention, and visually guided action. The ventral pathway, located in temporal cortex, processes form and objects. Further subdivisions of the ventral pathway are specialized, for example, for recognizing faces. These pathways, although distinct, communicate with each other; this is likely important for the perception of objects as coherent wholes.
5. Parallel processing starts at the retina. Distinct retinal circuits analyze each point of the visual input for different local features including local contrasts of achromatic bright versus dark, red versus green, and blue versus yellow. The information is sent out through distinct classes of retinal ganglion cells (magnocelluar, parvocelluar, and koniocellular, respectively, for the three features noted) whose axons form the optic nerves.
6. The optic nerves from the two eyes regroup at the optic chiasm such that all fibers from the left visual hemifield project to the right hemisphere of the brain, and vice versa. However, the parallel retinal channels remain anatomically segregated by eye and by visual feature, past a thalamic relay station, the lateral geniculate nucleus (LGN), up to primary visual cortex (V1).

7. The different channels enter V1 at different layers, although primarily they enter at the major input layers 4 and 6. The visual input is recombined to extract new sets of features. These include tuning for orientation, motion, and object depth (obtained by combining left- and right-eye inputs).
8. V1 neurons sharing basic properties such as spatial location or orientation preference form columns extending vertically from the pia to the white matter.
9. V1 neurons also form systematic horizontal maps of their response properties over cortex. The tuning for location forms a smooth "visuotopic" map of visual space, which changes gradually with distance, and is most finely resolved at the fovea, growing progressively coarser toward the periphery. Superimposed on the spatial map are locally smooth maps of orientation preference and left- versus right-eye preference, with interspersed columns that preferentially process color. These visual response features cycle over relatively short cortical distances, in effect completing one full cycle over each partial shift of the spatial map. Thus, V1 circuits effectively analyze each visual location, in parallel, for the full set of V1 visual features.
10. Neural processing in V1 reflects its architecture, with local vertical processing along columns and lateral processing across columns. In addition, there is long-range processing that spans multiple columns.
11. The output of V1 feeds into progressively higher visual areas comprising more than 30 centers distributed along the dorsal and ventral pathways. The connectivity is reciprocal, with higher loci sending dense feedback targeting lower areas including the LGN.
12. A useful measure of visual processing is provided by changes in neuronal "receptive fields" along the visual pathway. The receptive field is the region of visual space from which the neuron receives input; it is further characterized by the neuron's optimal visual stimulus. Receptive fields grow larger and more complex at successive stages along the visual pathway. Their optimal stimuli also increase in complexity from simple pixel-like dots for photoreceptors, to oriented lines for V1, to faces in higher face-selective centers of the ventral pathway.
13. Looking forward, one of the most important unsolved questions is the interaction between feedforward visual processing through progressively "higher" neural computations and feedback mediated via the dense plexus of connections from higher to lower levels. Understanding this interaction may be the key to understanding how the brain effortlessly forms complex visual percepts.

Charles D. Gilbert
Aniruddha Das

Selected Reading

Hubel DH, Wiesel TN. 1962. Receptive fields, binocular interaction and functional architecture in the cat's visual cortex. J Physiol 160:106–154.

Hubel DH, Wiesel TN. 1977. Functional architecture of macaque monkey visual cortex. Proc R Soc Lond B Biol Sci 198:1–59.

Hubener M, Shohan D, Grinvald A, Bonhoeffer T. 1997. Spatial relationships among three columnar systems in cat area 17. J Neurosci 17:9270–9284.

Isaacson JS, Scanziani M. 2011. How inhibition shapes cortical activity. Neuron 72:231–243.

Nassi JJ, Callaway EM. 2009. Parallel processing strategies of the primate visual system. Nat Rev Neurosci 10:360–372.

Orban GA, Van Essen D, Vanduffel W. 2004. Comparative mapping of higher visual areas in monkeys and humans. Trends Cogn Sci 8:315–324.

Stryker MP. 2014. A neural circuit that controls cortical state, plasticity, and the gain of sensory responses in mouse. Cold Spring Harb Symp Quant Biol 79:1–9.

Tsao DY, Moeller S, Freiwald WA. 2008. Comparing face patch systems in macaques and humans. Proc Natl Acad Sci U S A 105:19514–19519.

VanEssen DC, Anderson CH, Felleman DJ. 1992. Information processing in the primate visual system: an integrated systems perspective. Science 255:419–423.

Wertheimer M. 1938. *Laws of Organization in Perceptual Forms*. London: Harcourt, Brace & Jovanovitch.

Wiesel TN, Hubel DH. 1966. Spatial and chromatic interactions in the lateral geniculate body of the rhesus monkey. J Neurophysiol 29:1115–1156.

References

Blasdel GG, Lund JS. 1983. Termination of afferent axons in macaque striate cortex. J Neurosci 3:1389–1413.

Callaway EM. 1998. Local circuits in primary visual cortex of the macaque monkey. Annu Rev Neurosci 21:47–74.

Field DJ, Hayes A, Hess RF. 1993. Contour integration by the human visual system: evidence for a local "association field." Vision Res 33:173–193.

Gilbert CD, Li W. 2012. Adult visual cortical plasticity. Neuron 75:250–264.
Gilbert CD, Li W. 2013. Top-down influences on visual processing. Nat Rev Neurosci 14:350–363.
Gilbert CD, Wiesel TN. 1983. Clustered intrinsic connections in cat visual cortex. J Neurosci 3:1116–1133.
Hartline HK. 1941. The neural mechanisms of vision. Harvey Lect 37:39–68.
Hubel DH. 1988. *Eye, Brain and Vision*. New York: Scientific American Library.
Hubel DH, Wiesel TN. 1974. Uniformity of monkey striate cortex. A parallel relationship between field size, scatter and magnification factor. J Comp Neurol 158:295–306.
Kapadia MK, Westheimer G, Gilbert CD. 2000. Spatial distribution of contextual interactions in primary visual cortex and in visual perception. J Neurophysiol 84:2048–2062.
Kuffler SF. 1953. Discharge patterns and functional organization of mammalian retina. J Neurophysiol 16:37–68.
Porter PB. 1954. Another puzzle-picture. Am J Psychol 67:550–551.
Stettler DD, Das A, Bennett J, Gilbert CD. 2002. Lateral connectivity and contextual interactions in macaque primary visual cortex. Neuron 36:739–750.

22

Low-Level Visual Processing: The Retina

The retina is the brain's window on the world. All visual experience is based on information processed by this neural circuit in the eye. The retina's output is conveyed to the brain by just one million optic nerve fibers, and yet almost half of the cerebral cortex is used to process these signals. Visual information lost in the retina—by design or deficiency—can never be recovered. Because retinal processing sets fundamental limits on what can be seen, there is great interest in understanding how the retina functions.

On the surface, the vertebrate eye appears to act much like a camera. The pupil forms a variable aperture, and the cornea and lens provide the refractive optics that project a small image of the outside world onto the light-sensitive retina lining the back of the eyeball (Figure 22–1). But this is where the analogy ends. The retina is a thin sheet of neurons, a few hundred micrometers thick, composed of five major cell types that are arranged in three cellular layers separated by two synaptic layers (Figure 22–2).

The photoreceptor cells, in the outermost layer, absorb light and convert it into a neural signal, a process known as phototransduction. These signals are

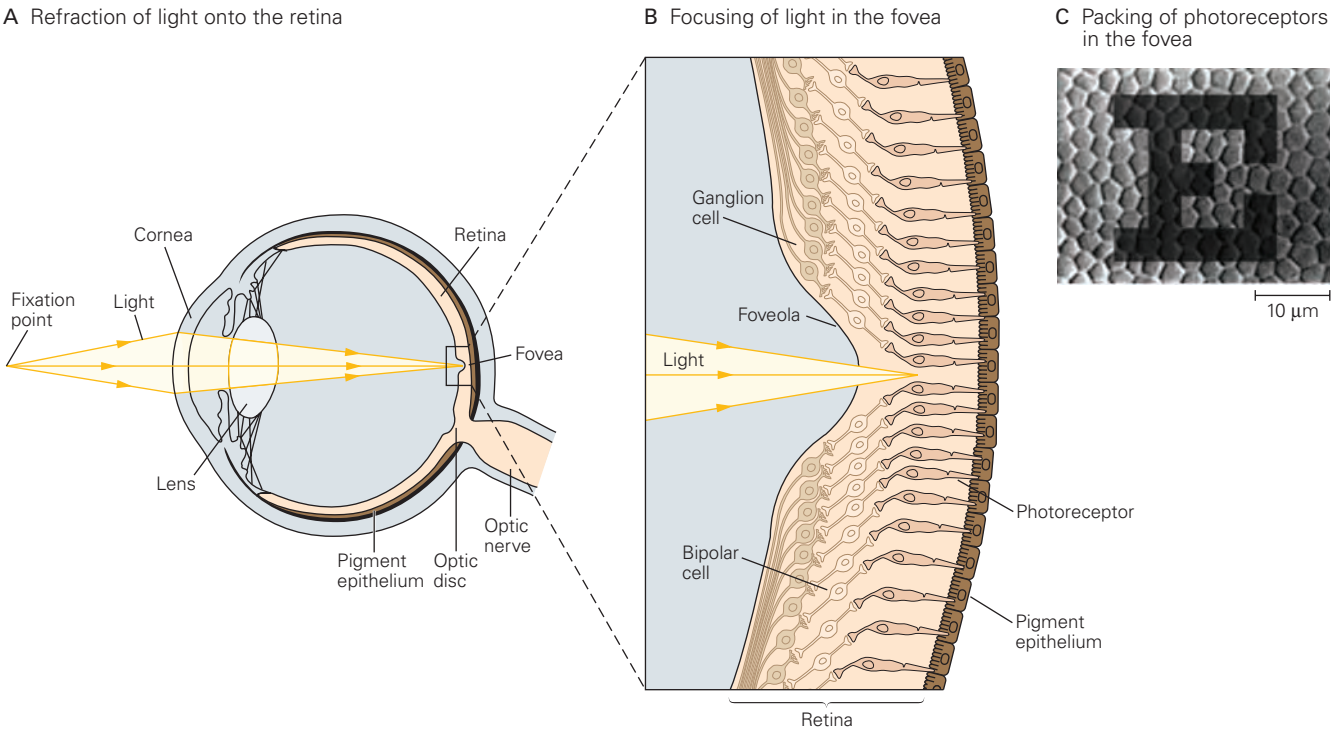

Figure 22–1 The eye projects the visual scene onto the retina's photoreceptors.

A. Light from an object in the visual field is refracted by the cornea and lens and focused onto the retina.

B. In the foveola, corresponding to the very center of gaze, the proximal neurons of the retina are shifted aside so light has direct access to the photoreceptors.

C. A letter from the eye chart used to assess normal visual acuity is projected onto the densely packed photoreceptors in the fovea. Although less sharply focused than shown here as a result of diffraction by the eye's optics, the smallest discernible strokes of the letter are approximately one cone diameter in width. (Adapted, with permission, from Curcio and Hendrickson 1991. Copyright © 1991 Elsevier Ltd.)

passed synaptically to bipolar cells, which in turn connect to retinal ganglion cells in the innermost layer. Retinal ganglion cells are the output neurons of the retina, and their axons form the optic nerve. In addition to this direct pathway from sensory to output neurons, the retinal circuit includes many lateral connections provided by horizontal cells in the outer synaptic layer and amacrine cells in the inner synaptic layer (Figure 22–3).

The retinal circuit performs low-level visual processing, the initial stage in the analysis of visual images. It extracts from the raw images in the eyes certain spatial and temporal features and conveys them to higher visual centers. The rules of this processing are adapted to changes in environmental conditions. In particular, the retina must adjust its sensitivity to ever-changing conditions of illumination. This adaptation allows our vision to remain more or less stable despite the vast range of light intensities encountered during the course of each day.

In this chapter, we discuss in turn the three important aspects of retinal function: phototransduction, preprocessing, and adaptation. We will illustrate both the neural mechanisms by which they are achieved and their consequences for visual perception.

The Photoreceptor Layer Samples the Visual Image

Ocular Optics Limit the Quality of the Retinal Image

The sharpness of the retinal image is determined by several factors: diffraction at the pupil's aperture, refractive errors in the cornea and lens, and scattering due to material in the light path. A point in the outside world is generally focused into a small blurred circle on the retina. As in other optical devices, this blur is smallest near the optical axis, where the image quality

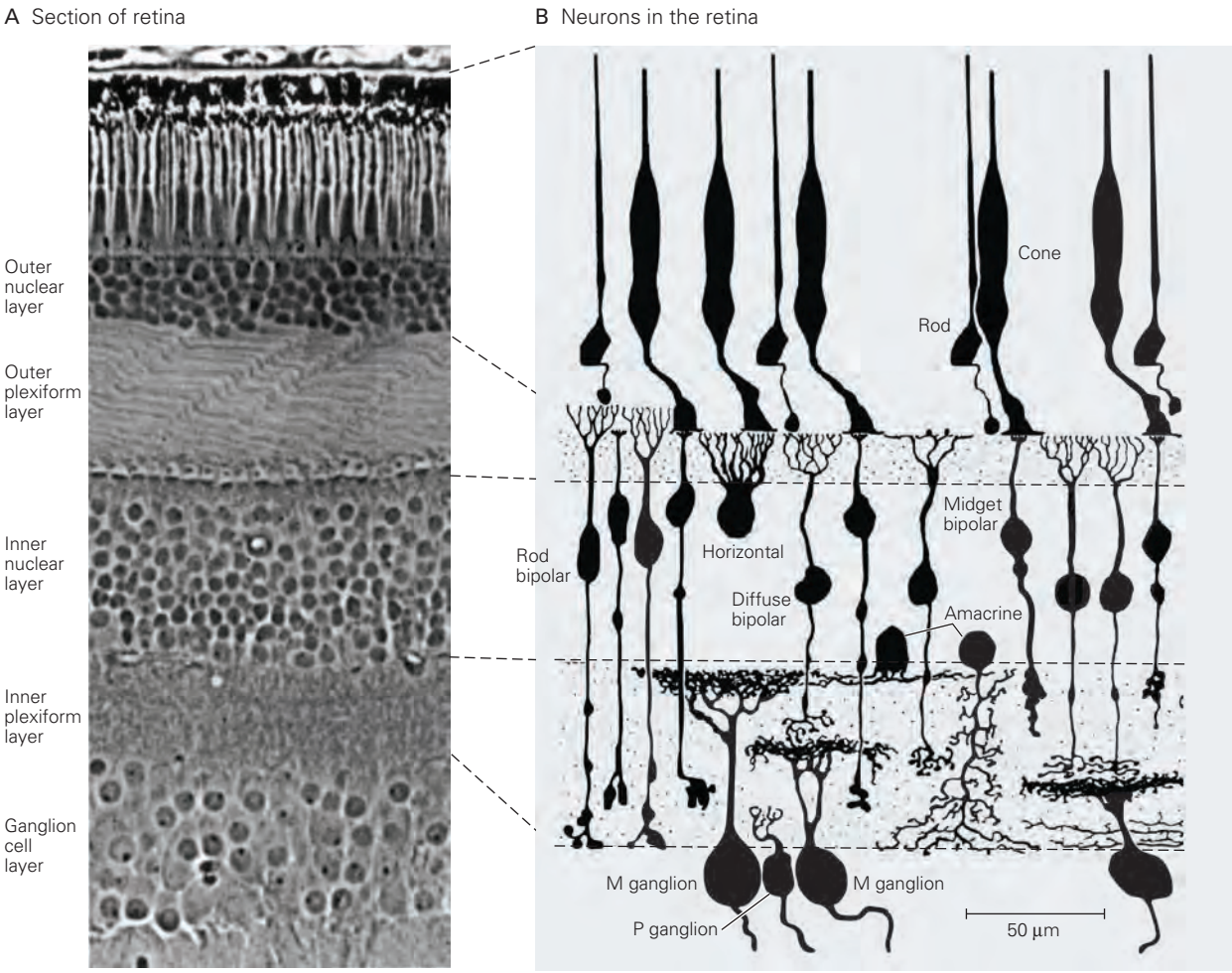

Figure 22–2 The retina comprises five distinct layers of neurons and synapses.

A. A perpendicular section of the human retina seen through the light microscope. Three layers of cell bodies are evident. The outer nuclear layer contains cell bodies of photoreceptors; the inner nuclear layer includes horizontal, bipolar, and amacrine cells; and the ganglion cell layer contains ganglion cells and some displaced amacrine cells. Two layers of fibers and synapses separate these: the outer plexiform layer and the inner plexiform layer. (Reproduced, with permission, from Boycott and Dowling 1969. Permission conveyed through Copyright Clearance Center.)

B. Neurons in the retina of the macaque monkey based on Golgi staining. The cellular and synaptic layers are aligned with the image in part **A**. (Abbreviations: **M ganglion**, magnocellular ganglion cell; **P ganglion**, parvocellular ganglion cell.) (Reproduced, with permission, from Polyak 1941.)

approaches the limit imposed by diffraction at the pupil. Away from the axis, the image is degraded significantly owing to aberrations in the cornea and lens and may be degraded further by abnormal conditions such as light-scattering cataracts or refractive errors such as myopia.

The area of retina near the optical axis, the *fovea*, is where vision is sharpest and corresponds to the center of gaze that we direct toward the objects of our attention. The density of photoreceptors, bipolar cells, and ganglion cells is highest at the fovea (Figure 22–1B). The spacing between photoreceptors there is well matched to the size of the optical blur circle, and thus the image is sampled in an ideal fashion. Light must generally traverse several layers of cells before reaching the photoreceptors, but in the center of the fovea, called the *foveola*, the other cellular layers are pushed aside to reduce additional blur from light scattering (Figure 22–1B). Finally, the back of the eye is lined by a black pigment epithelium that absorbs light and keeps it from scattering back into the eye.

The retina contains another special site, the *optic disc*, where the axons of retinal ganglion cells converge and extend through the retina to emerge from the back of the eye as the optic nerve (Figure 22–1A). By necessity, this area is devoid of photoreceptors and thus

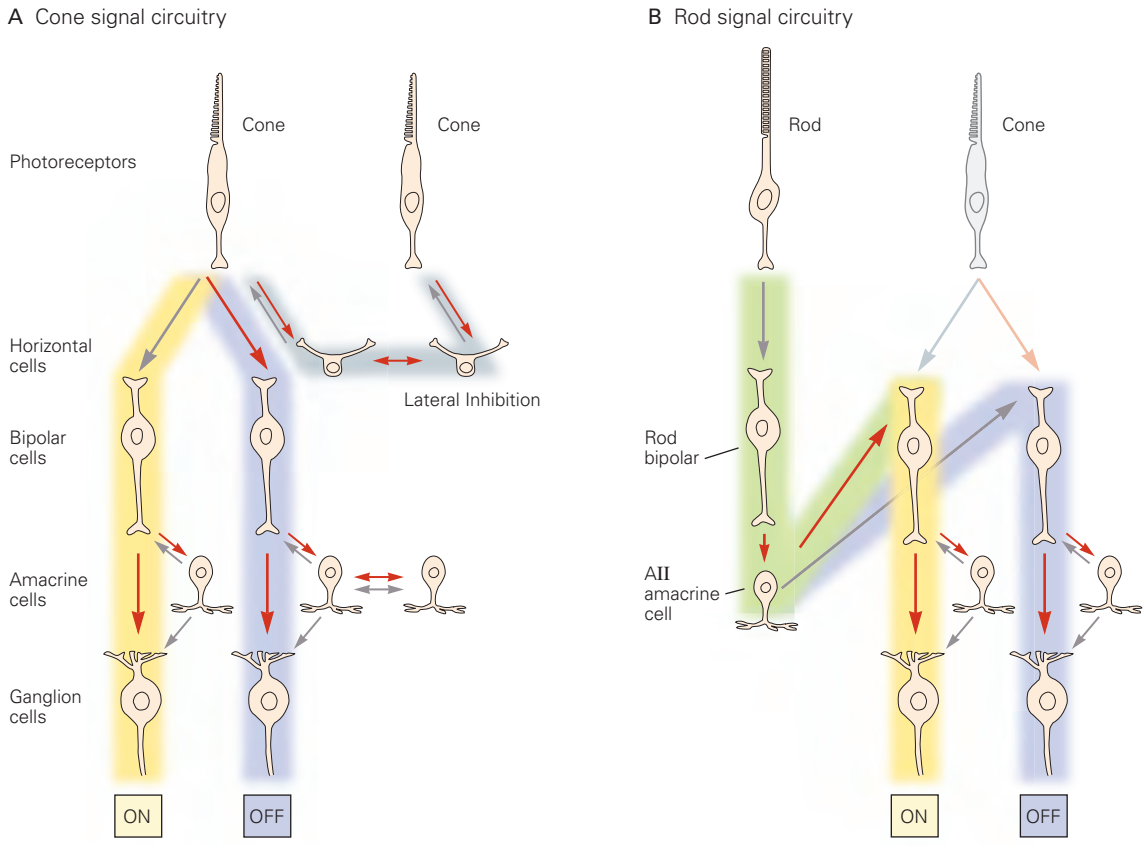

Figure 22–3 The retinal circuitry.

A. The circuitry for cone signals, showing the split into ON cell and OFF cell pathways (see Figure 22–10) as well as the pathway for lateral inhibition in the outer layer. **Red arrows** indicate sign-preserving connections through electrical or glutamatergic synapses. **Gray arrows** represent sign-inverting connections through GABAergic, glycinergic, or glutamatergic synapses.

B. Rod signals feed into the cone circuitry through AII amacrine cells, where the ON and OFF cell pathways diverge.

corresponds to a blind spot in the visual field of each eye. Because the disc lies nasal to the fovea of each eye, light coming from a single point never falls on both blind spots simultaneously, so that normally we are unaware of them. We can experience the blind spot by using only one eye (Figure 22–4). The blind spot demonstrates what blind people experience—not blackness, but simply nothing. This explains why damage to the peripheral retina often goes unnoticed. It is usually through accidents, such as bumping into an unnoticed object, or through clinical testing that a deficit of sight is revealed.

The blind spot is a necessary consequence of the inside-out design of the retina, which has puzzled and amused biologists for generations. The purpose of this organization may be to enable the tight apposition of photoreceptors with the retinal pigment epithelium, which plays an essential role in the turnover of retinal pigment and recycles photoreceptor membranes by phagocytosis.

There Are Two Types of Photoreceptors: Rods and Cones

All photoreceptor cells have a common structure with four functional regions: the outer segment, located at the distal surface of the neural retina; the inner segment, located more proximally; the cell body; and the synaptic terminal (Figure 22–5A).

Most vertebrates have two types of photoreceptors, rods and cones, distinguished by their morphology. A rod has a long, cylindrical outer segment within which the stacks of discs are separated from the plasma membrane, whereas a cone often has a shorter, tapered outer segment, and the discs are continuous with the outer membrane (Figure 22–5B).

Figure 22–4 The blind spot of the human retina. Locate the blind spot in your left eye by shutting the right eye and fixating the cross with the left eye. Hold the book about 12 inches from your eye and move it slightly nearer or farther until the circle on the left disappears. Now place a pencil vertically on the page and sweep it sideways over the circle. Note the pencil appears unbroken, even though no light can reach your retina from the region of the circle. Next, move the pencil lengthwise and observe what happens when its tip enters the circle. (Adapted, with permission, from Hurvich 1981.)

Rods and cones also differ in function, most importantly in their sensitivity to light. Rods can signal the absorption of a single photon and are responsible for vision under dim illumination such as moonlight. But as the light level increases toward dawn, the electrical response of rods becomes saturated and the cells cease to respond to variations in intensity. Cones are much less sensitive to light; they make no contribution to night vision but are solely responsible for vision in daylight. Their response is considerably faster than that of rods. Primates have only one type of rod but three kinds of cone photoreceptors, distinguished by the range of wavelengths to which they respond: the L (long-wave), M (medium-wave), and S (short-wave) cones (Figure 22–6).

The human retina contains approximately 100 million rods and 5 million cones, but the two cell types are differently distributed. The central fovea contains no rods but is densely packed with small cones. A few millimeters outside the fovea, rods greatly outnumber cones. All photoreceptors become larger and more widely spaced toward the periphery of the retina.

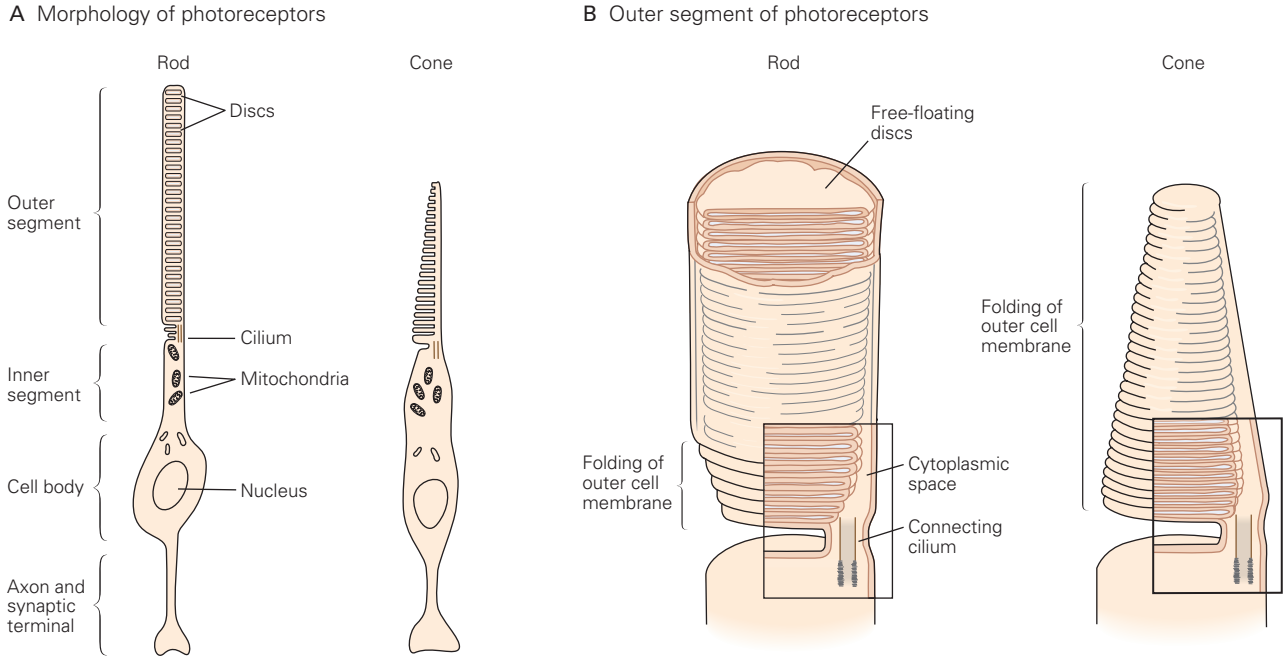

Figure 22–5 Rod and cone photoreceptors have similar structures.

A. Both rod and cone cells have specialized regions called the outer and inner segments. The outer segment is attached to the inner segment by a cilium and contains the light-transducing apparatus. The inner segment holds mitochondria and much of the machinery for protein synthesis.

B. The outer segment consists of a stack of membranous discs that contain the light-absorbing photopigments. In both types of cells, these discs are formed by infolding of the plasma membrane. In rods, however, the folds pinch off from the membrane so that the discs are free-floating within the outer segment, whereas in cones, the discs remain part of the plasma membrane. (Adapted, with permission, from O'Brien 1982. Copyright © 1982 AAAS; Young 1970.)

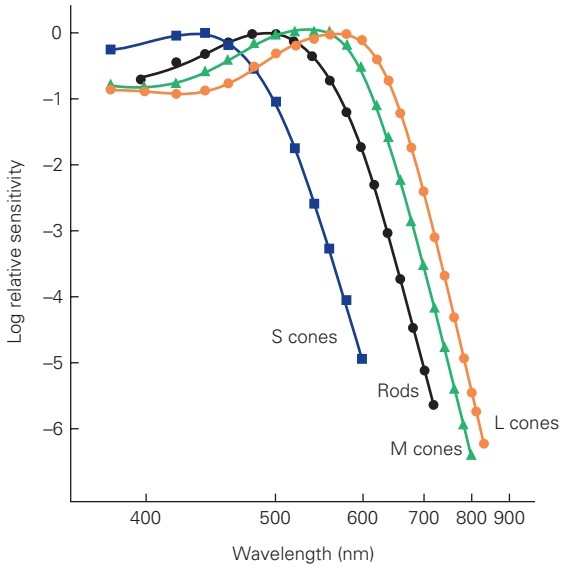

Figure 22–6 Sensitivity spectra for the three types of cones and the rod. At each wavelength, the sensitivity is inversely proportional to the intensity of light required to elicit a criterion response in the sensory neuron. Sensitivity varies over a large range and thus is shown on a logarithmic scale. The different classes of photoreceptors are sensitive to broad and overlapping ranges of wavelengths. (Reproduced, with permission, from Schnapf et al. 1988.)

The S cones make up only 10% of all cones and are absent from the central fovea.

The retinal center of gaze is clearly specialized for daytime vision. The dense packing of cone photoreceptors in the fovea sets the limits of our visual acuity. In fact, the smallest letters we can read on a doctor's eye chart have strokes whose images are just one to two cone diameters wide on the retina, a visual angle of about 1 minute of arc (Figure 22–1C). At night, the central fovea is blind owing to the absence of rods. Astronomers know that one must look just to the side of a dim star to see it at all. During nighttime walks in the forest, we nonastronomers tend to follow our daytime reflex of looking straight at the source of a suspicious sound. Mysteriously, the object disappears, only to jump back into our peripheral field of view as we avert our gaze.

Phototransduction Links the Absorption of a Photon to a Change in Membrane Conductance

As in many other neurons, the membrane potential of a photoreceptor is regulated by the balance of membrane conductances to Na^+ and K^+ ions, whose transmembrane gradients are maintained by metabolically active pumps (Chapter 9). In the dark, Na^+ ions flow into the photoreceptor through nonselective cation channels that are activated by the second messenger cyclic guanosine 3′-5′ monophosphate (cGMP).

Absorption of a photon by the pigment protein sets in motion a biochemical cascade that ultimately lowers the concentration of cGMP, thus closing the cGMP-gated channels and moving the cell closer to the K^+ equilibrium potential. In this way, light hyperpolarizes the photoreceptor (Figure 22–7). Here, we describe this sequence of events in detail. Most of this knowledge derives from studies of rods, but the mechanism in cones is very similar.

Figure 22–7 (Opposite) Phototransduction.

A. The rod cell responds to light. Rhodopsin molecules in the outer-segment discs absorb photons, which leads to the closure of cyclic guanosine 3′-5′ monophosphate (**cGMP**)-gated channels in the plasma membrane. This channel closure hyperpolarizes the membrane and reduces the rate of release of the neurotransmitter glutamate. (Adapted from Alberts 2008.)

B. 1. Molecular processes in phototransduction. cGMP is produced by a guanylate cyclase (**GC**) from guanosine triphosphate (**GTP**) and hydrolyzed by a phosphodiesterase (**PDE**). In the dark, the phosphodiesterase activity is low, the cGMP concentration is high, and the cGMP-gated channels are open, allowing the influx of Na^+ and Ca^{2+}. In the light, rhodopsin (**R**) is excited by absorption of a photon, then activates transducin (**T**), which in turn activates the PDE; the cGMP level drops, the membrane channels close, and less Na^+ and Ca^{2+} enter the cell. The transduction enzymes are all located in the internal membrane discs, and the soluble ligand cGMP serves as a messenger to the plasma membrane.

2. Calcium ions have a negative feedback role in the reaction cascade in phototransduction. Stimulation of the network by light leads to the closure of the cGMP-gated channels. This causes a drop in the intracellular concentration of Ca^{2+}. Because Ca^{2+} modulates the function of at least three components of the cascade—rhodopsin, GC, and the cGMP-gated channel—the drop in Ca^{2+} counteracts the excitation caused by light.

C. Voltage response of a primate rod and cone to brief flashes of light of increasing intensity. Higher numbers on the traces indicate greater intensities of illumination (not all traces are labeled). For dim flashes, the response amplitude increases linearly with intensity. At high intensities, the receptor saturates and remains hyperpolarized steadily for some time after the flash; this leads to the afterimages that we perceive after a bright flash. Note that the response peaks earlier for brighter flashes and that cones respond faster than rods. (Reproduced, with permission, from Schneeweis and Schnapf 1995. Copyright © 1995 AAAS.)

A Phototransduction and neural signaling

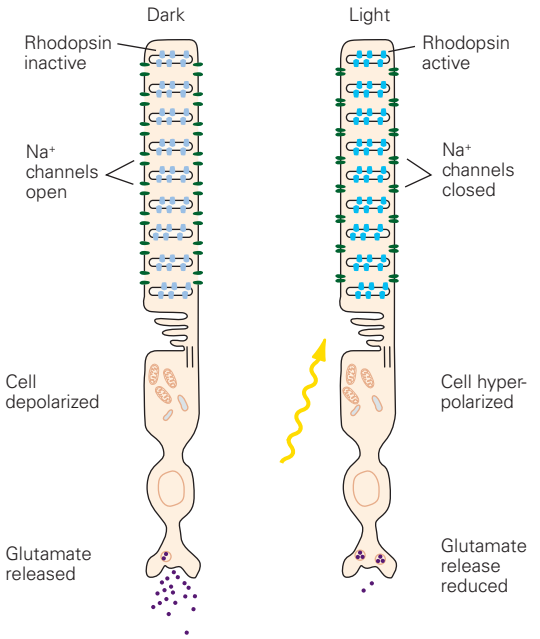

C Voltage response to light

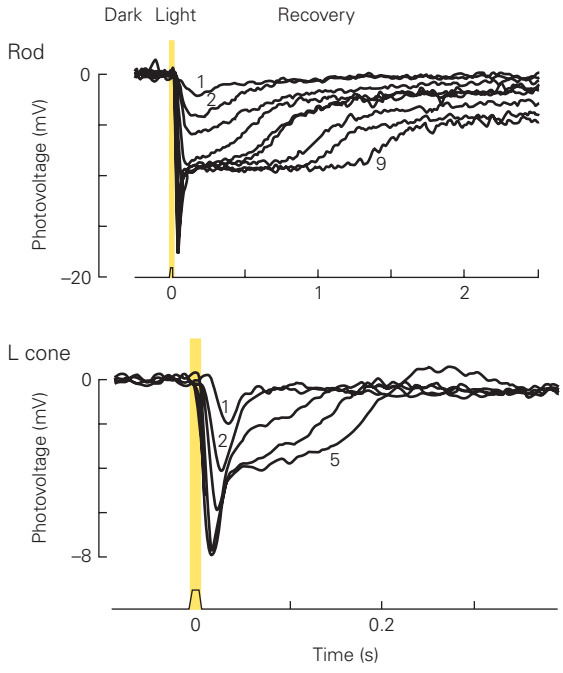

B1 Molecular processes in phototransduction

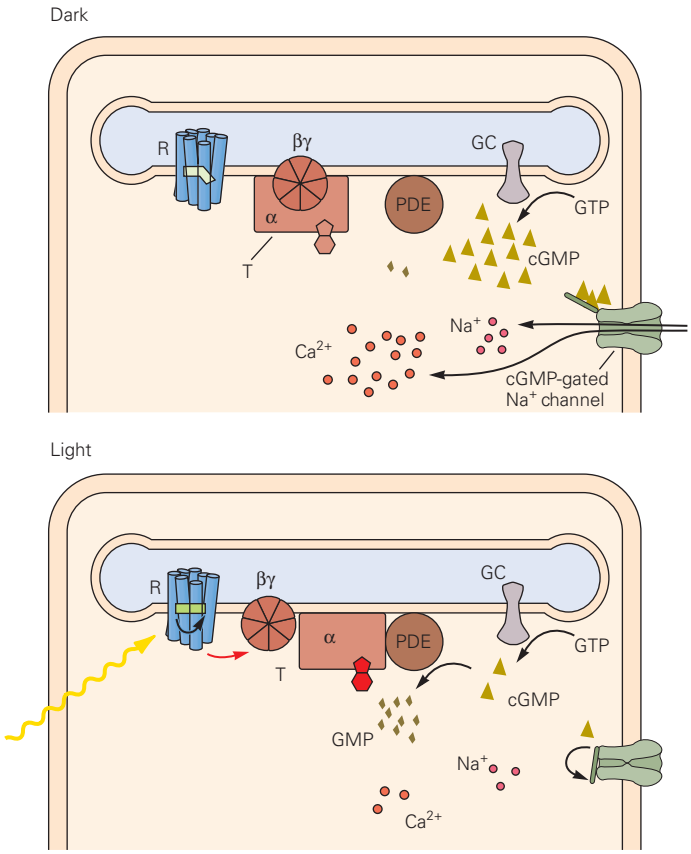

B2 Reaction network in phototransduction

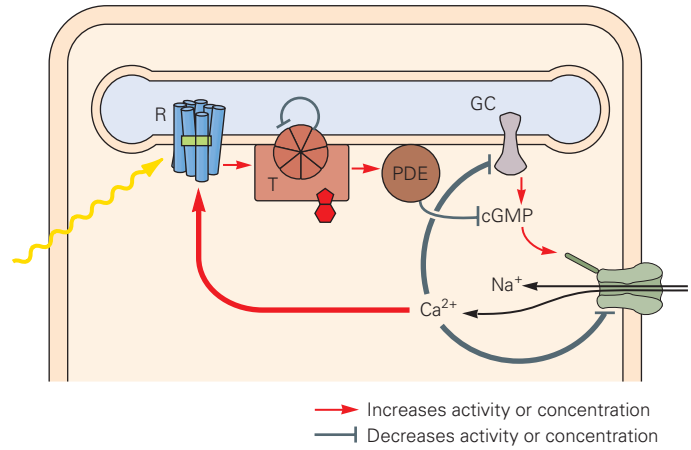

Light Activates Pigment Molecules in the Photoreceptors

Rhodopsin, the visual pigment in rod cells, has two components. The protein portion, *opsin*, is embedded in the disc membrane and does not by itself absorb visible light. The light-absorbing moiety, *retinal*, is a small molecule whose 11-*cis* isomer is covalently linked to a lysine residue of opsin (Figure 22–8A). Absorption of a photon by retinal causes it to flip from the 11-*cis* to the all-*trans* configuration. This reaction is the only light-dependent step in vision.

The change in shape of the retinal molecule causes a conformational change in the opsin to an activated state called *metarhodopsin II*, thus triggering the second

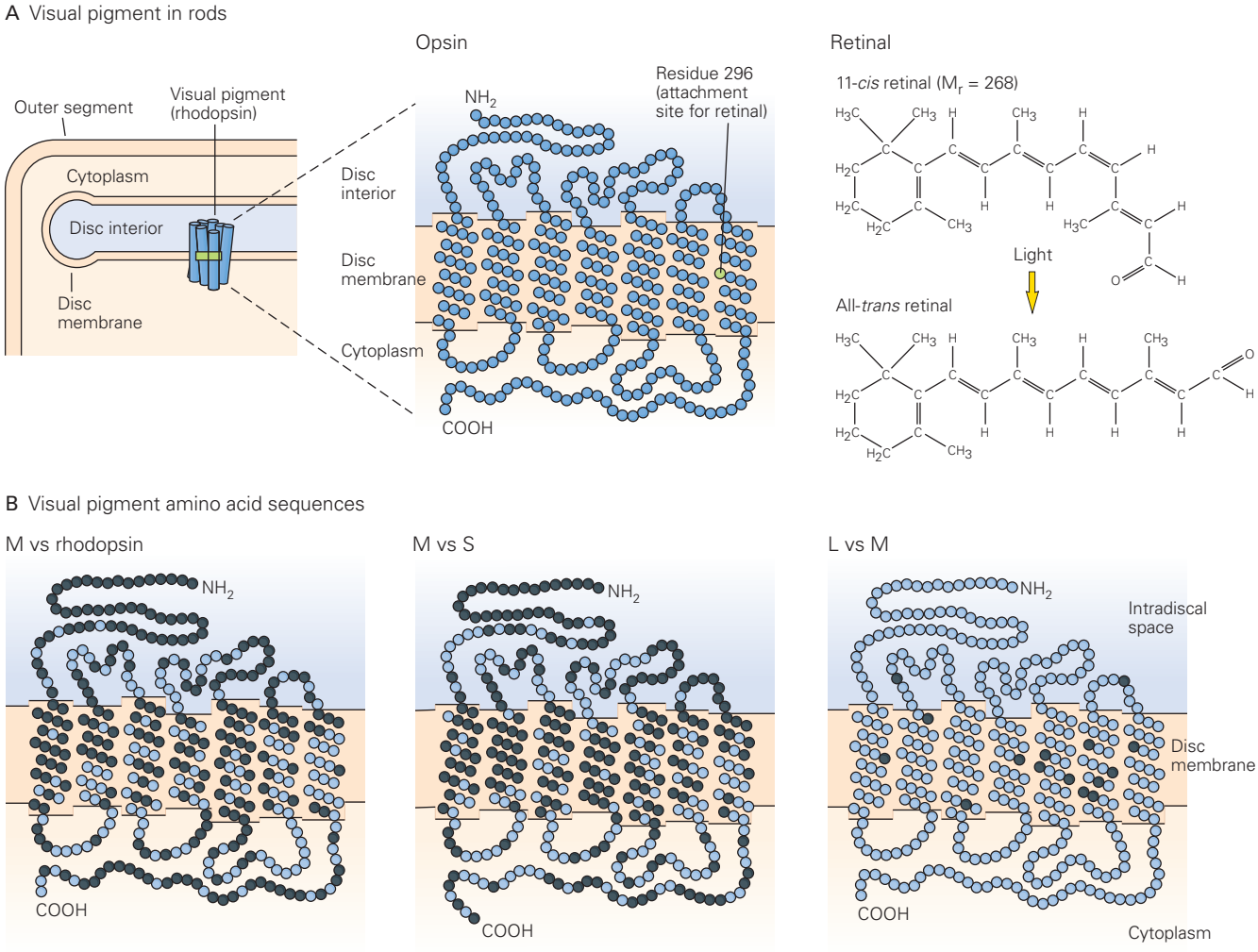

Figure 22–8 Structure of the visual pigments.

A. The visual pigment in rod cells, rhodopsin, is the covalent complex of two components. Opsin is a large protein with 348 amino acids and a molecular mass of approximately 40,000 daltons. It loops back and forth seven times across the membrane of the rod disc. Retinal is a small light-absorbing compound covalently attached to a side chain of lysine 296 in opsin's seventh membrane-spanning region. Absorption of light by 11-*cis* retinal causes a rotation around the double bond. As retinal adopts the more stable all-*trans* configuration, it causes a conformational change in opsin that triggers the subsequent events of visual transduction. (Adapted, with permission, from Nathans and Hogness 1984.)

B. The **blue circles** denote identical amino acids; **black circles** denote differences. The forms of opsin in the three types of cone cells (L, M, and S) resemble each other as well as the rhodopsin in rod cells, suggesting that all four evolved from a common precursor by duplication and divergence. The L and M opsins are most closely related, with 96% identity in their amino acid sequences. They are thought to have evolved from a gene-duplication event approximately 30 million years ago, after Old World monkeys, which have three visual pigments, separated from New World monkeys, which generally have only two.

step of phototransduction. Metarhodopsin II is unstable and splits within minutes, yielding opsin and free all-*trans* retinal. The all-*trans* retinal is then transported from rods to pigment epithelial cells, where it is reduced to all-*trans* retinol (vitamin A), the precursor of 11-*cis* retinal, which is subsequently transported back to rods.

All-*trans* retinal is thus a crucial compound in the visual system. Its precursors, such as vitamin A, cannot be synthesized by humans and so must be a regular part of the diet. Deficiencies of vitamin A can lead to night blindness and, if untreated, to deterioration of receptor outer segments and eventually to blindness.

Each type of cone in the human retina produces a variant of the opsin protein. These three cone pigments are distinguished by their *absorption spectrum*, the dependence on wavelength of the efficiency of light absorption (see Figure 22–6). The spectrum is determined by the protein sequence through the interaction between retinal and certain amino acid side chains near the binding pocket. Red light excites L cones more than the M cones, whereas green light excites the M cones more. Therefore, the relative degree of excitation in these cone types contains information about the spectrum of the light, independent of its intensity. The brain's comparison of signals from different cone types is the basis for color vision.

In night vision, only the rods are active, so all functional photoreceptors have the same absorption spectrum. A green light consequently has exactly the same effect on the visual system as a red light of a greater intensity. Because a single-photoreceptor system cannot distinguish the spectrum of a light from its intensity, "at night all cats are gray." By comparing the sensitivity of a rod to different wavelengths of light, one obtains the absorption spectrum of rhodopsin. It is a remarkable fact that one can measure this molecular property accurately just by asking human subjects about the appearance of various colored lights (Figure 22–9). The quantitative study of perception, or psychophysics, provides similar insights into other mechanisms of brain processing (Chapter 17).

Excited Rhodopsin Activates a Phosphodiesterase Through the G Protein Transducin

Activated rhodopsin in the form of metarhodopsin II diffuses within the disc membrane where it encounters transducin, a member of the G protein family (Chapter 14). As is the case for other G proteins, the inactive form of transducin binds a molecule of guanosine diphosphate (GDP). Interaction with metarhodopsin II promotes the exchange of GDP for guanosine triphosphate (GTP). This leads to dissociation of transducin's subunits into an active α-subunit carrying the GTP (Tα-GTP) and the β- and γ-subunits (Tβγ). Metarhodopsin II can activate hundreds of additional transducin molecules, thus significantly amplifying the cell's response.

The active transducin subunit Tα-GTP forms a complex with a cyclic nucleotide phosphodiesterase, another protein associated with the disc membrane. This interaction greatly increases the rate at which the enzyme hydrolyzes cGMP to 5′-GMP. Each phosphodiesterase molecule can hydrolyze more than 1,000 molecules of cGMP per second, thus increasing the degree of amplification.

The concentration of cGMP controls the activity of the cGMP-gated channels in the plasma membrane of the outer segment. In darkness, when the cGMP concentration is high, a sizeable Na^+ influx through the open channels maintains the cell at a depolarized level

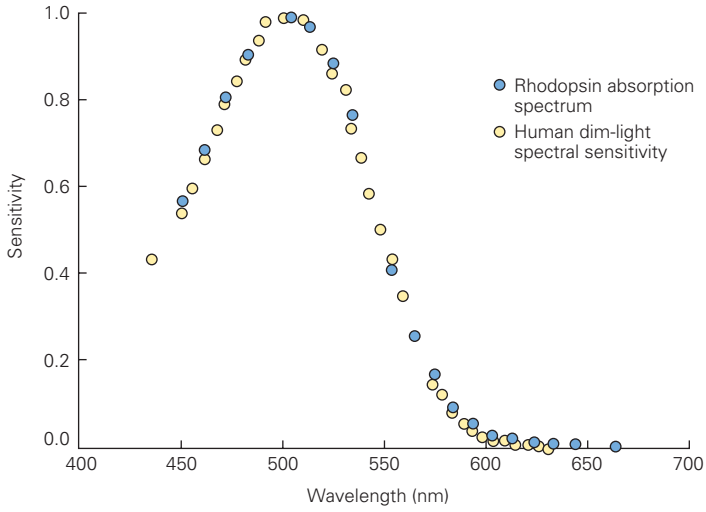

Figure 22–9 Absorption spectrum of rhodopsin. The absorption spectrum of human rhodopsin measured in a cuvette is compared with the spectral sensitivity of human observers to very dim light flashes. The psychophysical data have been corrected for absorption by the ocular media. (Reproduced, with permission, from Wald and Brown 1956. Copyright © 1956 Springer Nature.)

of approximately –40 mV. As a consequence, the cell's synaptic terminal continuously releases the transmitter glutamate. The light-evoked decrease in cGMP results in the closure of the cGMP-gated channels, thus reducing the inward flux of Na^+ ions and hyperpolarizing the cell (Figure 22–7B1). Hyperpolarization slows the release of neurotransmitter from the photoreceptor terminal, thereby initiating a neural signal.

Multiple Mechanisms Shut Off the Cascade

The photoreceptor's response to a single photon must be terminated so that the cell can respond to another photon. Metarhodopsin II is inactivated through phosphorylation by a specific rhodopsin kinase followed by binding of the soluble protein arrestin, which blocks the interaction with transducin.

Active transducin (Tα-GTP) has an intrinsic GTPase activity, which eventually converts bound GTP to GDP. Tα-GDP then releases phosphodiesterase and recombines with Tβγ, ready again for excitation by rhodopsin. Once the phosphodiesterase has been inactivated, the cGMP concentration is restored by a guanylate cyclase that produces cGMP from GTP. At this point, the membrane channels open, the Na^+ current resumes, and the photoreceptor depolarizes back to its dark potential.

In addition to these independent mechanisms that shut off individual elements of the cascade, an important feedback mechanism ensures that large responses are terminated more quickly. This is mediated by a change in the Ca^{2+} concentration in the cell. Calcium ions enter the cell through the cGMP-gated channels and are extruded by rapid cation exchangers. In the dark, the intracellular Ca^{2+} concentration is high, but during the cell's light response, when the cGMP-gated channels close, the Ca^{2+} level drops quickly to a few percent of the dark level.

This reduction in Ca^{2+} concentration modulates the biochemical reactions in three ways (Figure 22–7B2). Rhodopsin phosphorylation is accelerated through the action of the calcium-binding protein recoverin on rhodopsin kinase, thus reducing activation of transducin. The activity of guanylyl cyclase is accelerated by calcium-dependent guanylyl cyclase–activating proteins. Finally, the affinity of the cGMP-gated channel for cGMP is increased through the action of Ca^{2+}-calmodulin. All these effects promote the return of the photoreceptor to the dark state.

Defects in Phototransduction Cause Disease

Not surprisingly, defects in the phototransduction machinery have serious consequences. One prominent defect is color blindness, which results from loss or abnormality in the genes for cone pigments, as discussed later.

Stationary night blindness results when rod function has been lost but cone function remains intact. This disease is heritable, and mutations have been identified in many components of the phototransduction cascade: rhodopsin, rod transducin, rod phosphodiesterase, rhodopsin kinase, and arrestin. In some cases, it appears that the rods are permanently activated, as if exposed to a constant blinding light.

Unfortunately, many defects in phototransduction lead to *retinitis pigmentosa*, a progressive degeneration of the retina that ultimately results in blindness. The disease has multiple forms, many of which have been associated with mutations that affect signal transduction in rods. Why these changes in function lead to death of the rods and subsequent degeneration of the cones is not understood.

Ganglion Cells Transmit Neural Images to the Brain

The photoreceptor layer produces a relatively simple neural representation of the visual scene: Neurons in bright regions are hyperpolarized, whereas those in dark regions are depolarized. Because the optic nerve has only about 1% as many axons as there are receptor cells, the retinal circuit must edit the information in the photoreceptors before it is conveyed to the brain.

This step constitutes *low-level visual processing*, the first stage in deriving visual percepts from the pattern of light falling on the retina. To understand this process, we must first understand the organization of the retina's output and how retinal ganglion cells respond to various patterns of light.

The Two Major Types of Ganglion Cells Are ON Cells and OFF Cells

Many retinal ganglion cells fire action potentials spontaneously even in darkness or constant illumination. If the light intensity is suddenly increased, so-called ON cells fire more rapidly. Other ganglion cells, the OFF cells, fire more slowly or cease firing altogether. When the intensity diminishes again, the ON cells fire less and OFF cells fire more. The retinal output thus includes two complementary representations that differ in the polarity of their response to light.

This arrangement serves to communicate rapidly both brightening and dimming in the visual scene. If the retina had only ON cells, a dark object would be

encoded by a decrease in firing rate. If the ganglion cell fired at a maintained rate of 10 spikes per second and then decreased its rate, it would take about 100 ms for the postsynaptic neuron to notice the change in frequency of action potentials. In contrast, an increase in firing rate to 200 spikes per second is noticeable within only 5 ms.

Many Ganglion Cells Respond Strongly to Edges in the Image

To probe the responses of a ganglion cell in more detail, one can test how the cell's firing varies with the location and time course of a small spot of light focused on different portions of the retina.

A typical ganglion cell is sensitive to light in a compact region of the retina near the cell body called the cell's *receptive field.* Within that area, one can often distinguish a *center* region and *surround* region where light produces opposite responses in the cell. An ON cell, for example, fires faster when a bright spot is focused in the cell's receptive field center but decreases its firing when the spot is focused on the surround. If light covers both the center and the surround, the response is much weaker than for center-only illumination. A bright spot on the center combined with a dark annulus covering the surround elicits very strong firing. For an OFF cell, these relationships are reversed; the cell is strongly excited by a dark spot and a bright annulus (Figure 22–10).

The output produced by a population of retinal ganglion cells thus enhances regions of spatial contrast in the input, such as an edge between two areas of different intensity, and gives less emphasis to regions of homogeneous illumination.

The Output of Ganglion Cells Emphasizes Temporal Changes in Stimuli

When an effective light stimulus appears, a ganglion cell's firing typically increases sharply from the resting level to a peak and then relaxes to an intermediate rate. When the stimulus turns off, the firing rate drops sharply then gradually recovers to the resting level.

The rapidity of decline from the peak to the resting level varies among ganglion cell types. *Transient neurons* produce a burst of spikes only at the onset of the stimulus, whereas *sustained neurons* maintain an almost steady firing rate for several seconds during stimulation (Figure 22–10).

In general, however, the output of ganglion cells favors temporal changes in visual input over periods of constant light intensity. In fact, when an image is stabilized on the retina with an eye-tracking device, it fades from view within seconds. Fortunately, this never happens in normal vision; even when we attempt to fix our gaze, small automatic eye movements (saccades) continually scan the image across the retina and prevent the world from disappearing (Chapter 25).

Retinal Output Emphasizes Moving Objects

Based on these observations, we can understand more generally the response of ganglion cells to visual inputs. For example, the edges of a moving object elicit strong firing in the ganglion cell population because these are the only regions of spatial contrast and the only regions where the light intensity changes over time (Figure 22–11).

We can easily appreciate why the retina selectively responds to these features. The outline of an object is particularly useful for inferring its shape and identity. Similarly, objects that move or change suddenly are more worthy of immediate attention than those that do not. Retinal processing thus extracts low-level features of the scene that are useful for guiding behavior and selectively transmits those to the brain. In fact, the rejection of features that are constant either in space or in time accounts for the spatiotemporal sensitivity of human perception (Box 22–1).

Several Ganglion Cell Types Project to the Brain Through Parallel Pathways

Several different types of ganglion cells have been identified on the basis of their morphology and responses to light. The ON and OFF cells occur in every vertebrate retina, and in the primate retina, two major classes of cells, the P-cells and M-cells, each include ON and OFF types (see Figure 22–2B). At any given distance from the fovea, the receptive fields of M-cells (Latin *magno,* large) are much larger than those of P-cells (Latin *parvo,* small). The M-cells also have faster and more transient responses than P-cells. Some ganglion cells are intrinsically light-sensitive owing to expression of the visual pigment melanopsin.

In total, more than 20 types of ganglion cells have been described. The population of each type covers the retina in a tiled fashion, such that any point on the retina lies within the receptive field center of at least one ganglion cell. One can envision that the signals from each population together send a distinct neural representation of the visual field to the brain. In this view, the optic nerve conveys 20 or more neural representations that differ in polarity (ON or OFF), spatial resolution (fine or coarse), temporal responsiveness

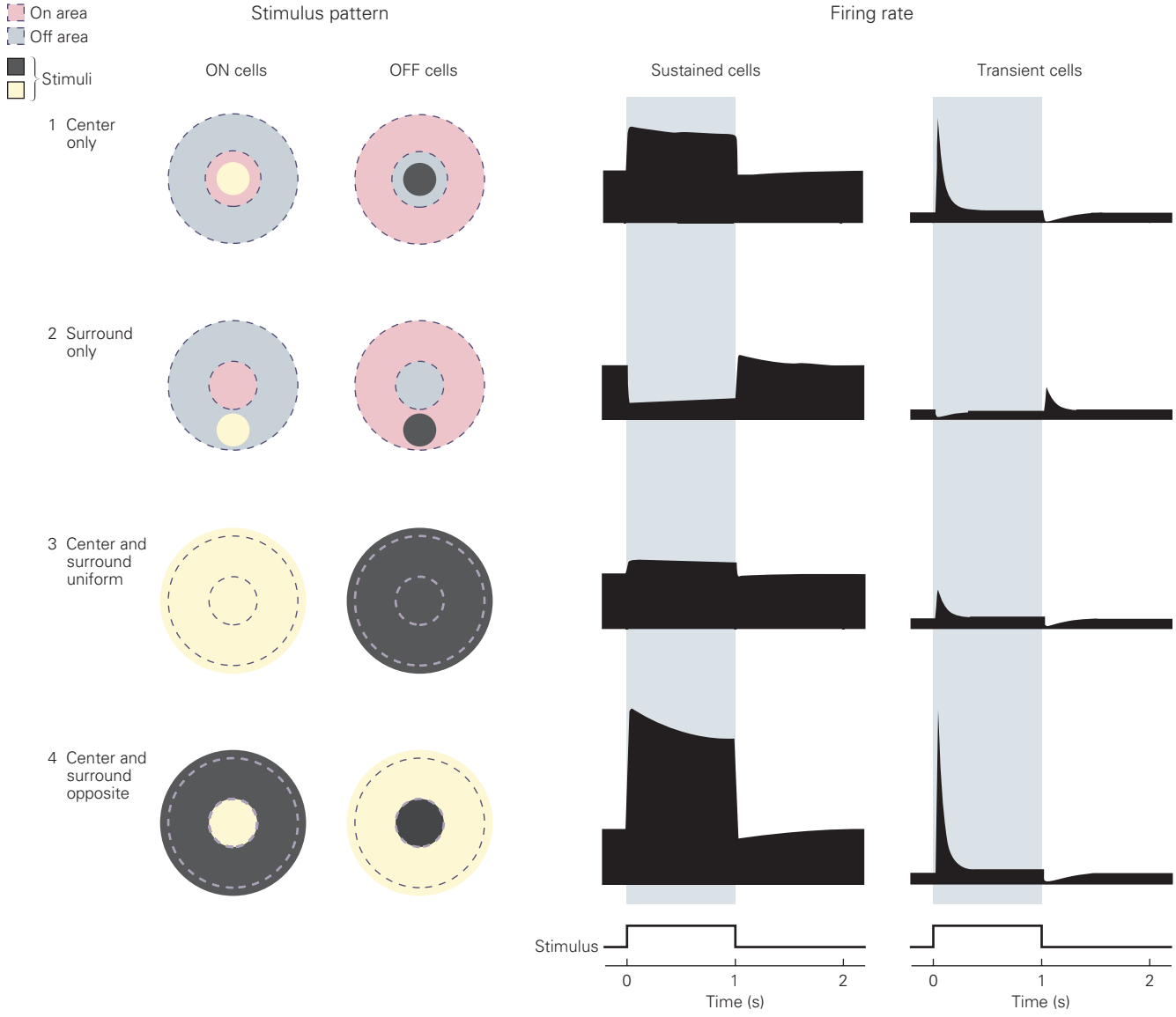

Figure 22–10 **Responses of retinal ganglion cells with center-surround receptive fields.** In these idealized experiments, the stimulus changes from a uniform gray field to the pattern of bright (**yellow**) and dark (**black**) regions indicated on the *left*. This leads to the firing rate responses shown on the *right*. **1.** ON cells are excited by a bright spot in the receptive field center, OFF cells by a dark spot. In *sustained cells*, the excitation persists throughout stimulation, whereas in *transient cells*, a brief burst of spikes occurs just after the onset of stimulation. **2.** If the same stimulus that excites the center is applied to the surround, firing is suppressed. **3.** Uniform stimulation of both center and surround elicits a response like that of the center, but much smaller in amplitude. **4.** Stimulation of the center combined with the opposite stimulus in the surround produces the strongest response.

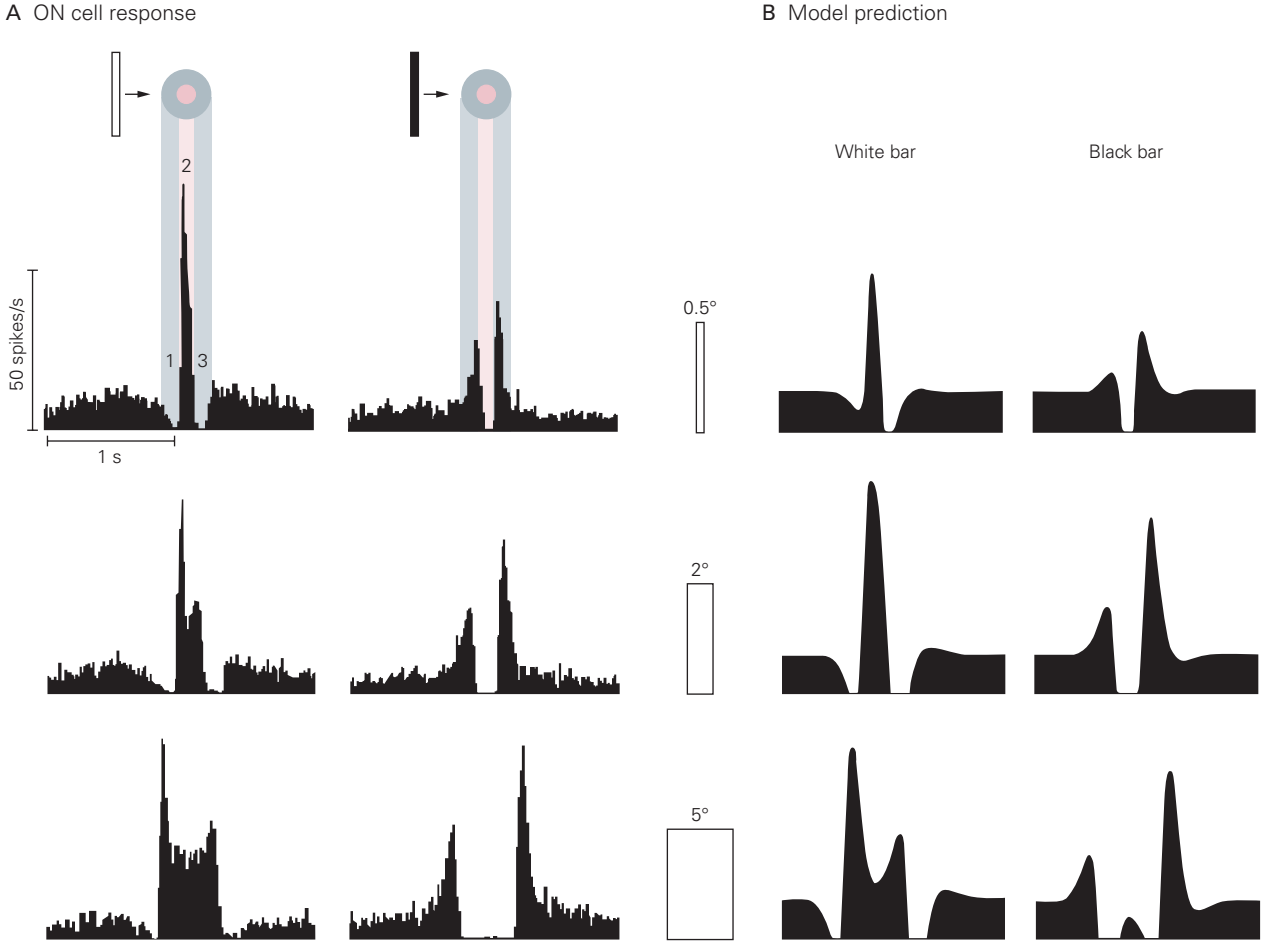

Figure 22–11 Responses of ganglion cells in the cat retina to moving objects.

A. The firing rate of an ON ganglion cell in response to a variety of bars (white or black, various widths) moving across the retina. Each bar moves at 10° per second; 1° corresponds to 180 μm on the retina. In response to the white bar, the firing rate first decreases as the bar passes over the receptive-field surround (**1**), increases as the bar enters the center (**2**), and decreases again as the bar passes through the surround on the opposite side (**3**). The dark bar elicits responses of the opposite sign. Because ganglion cells similar to this one are distributed throughout the retina, one can also interpret this curve as an instantaneous snapshot of activity in a population of ganglion cells, where the horizontal axis represents location on the retina. In effect, this activity profile is the neural representation of the moving bar transmitted to the brain. A complementary population of OFF ganglion cells (not shown here) conveys another neural activity profile in parallel. In this way, both bright and dark edges can be signaled by a sharp increase in firing.

B. A simple model of retinal processing that incorporates center-surround antagonism and a transient temporal filter is used to predict ganglion-cell firing rates. The predictions match the essential features of the responses in part **A**. (Reproduced, with permission, from Rodieck 1965. Copyright © 1965 Elsevier Ltd.)

Box 22–1 Spatiotemporal Sensitivity of Human Perception

Although small spots of light are useful for probing the receptive fields of single neurons in visual pathways, different stimuli are needed to learn about human visual perception. Grating stimuli are commonly used to probe how our visual system deals with spatial and temporal patterns.

The subject views a display in which the intensity varies about the mean as a sinusoidal function of space (Figure 22–12). Then the contrast of the display—defined as the peak-to-peak amplitude of the sinusoid divided by the mean—is reduced to a threshold at which the grating is barely visible. This measurement is repeated for gratings of different spatial frequencies.

When the inverse of this threshold is plotted against the spatial frequency, the resulting *contrast sensitivity curve* provides a measure of sensitivity of visual perception to patterns of different scales (Figure 22–13A). When measured at high light intensity, sensitivity declines sharply at high spatial frequencies, with an absolute threshold at approximately 50 cycles per degree. This sensitivity is limited fundamentally by the quality of the optical image and the spacing of cone cells in the fovea (see Figure 22–1C).

Interestingly, sensitivity also declines at low spatial frequencies. Patterns with a frequency of approximately 5 cycles per degree are most visible. The visual system is said to have *band-pass* behavior because it rejects all but a band of spatial frequencies.

One can use the same techniques to measure the sensitivity of individual retinal ganglion cells in primates. The results resemble those for human subjects (Figure 22–13), suggesting that these basic features of visual perception are determined by the retina.

The band-pass behavior can be understood on the basis of spatial antagonism in center-surround receptive fields. A very fine grating presents many dark and bright stripes within the receptive-field center; their effects cancel one another and thus provide no net excitation. A very coarse grating presents a single stripe to both the center and surround of the receptive field, and their antagonism again provides the ganglion cell little net excitation. The strongest response is produced by a grating of intermediate spatial frequency that just covers the center with one stripe and most of the surround with stripes of the opposite polarity (Figure 22–13B).

In dim light, the visual system's contrast sensitivity declines, but more so at high than at low spatial frequencies (Figure 22–13A). Thus, the peak sensitivity shifts to lower spatial frequencies, and eventually the curve loses its peak altogether. In this state, the visual system has so-called *low-pass* behavior, for it preferentially encodes stimuli of low spatial frequency. The fact that in dim light the receptive fields of ganglion cells lose their antagonistic surrounds explains the transition from band-pass to low-pass spatial filtering (Figure 22–13B).

Similar experiments can be done to test visual sensitivity to temporal patterns. Here, the intensity of a test stimulus flickers sinusoidally in time, while the contrast is gradually brought to the threshold level of detection. For humans, contrast sensitivity declines sharply at very high flicker frequencies, but declines also at very low frequencies (Figure 22–14A). Flicker at approximately 10 Hz is the most effective stimulus. One finds similar band-pass behavior in the flicker sensitivity of macaque retinal ganglion cells (Figure 22–14B).

Sensitivity to temporal contrast also depends on the mean light level. For human subjects, the optimum flicker frequency shifts downward at lower stimulus intensities and the peak in the curve becomes less and less prominent (Figure 22–14). The fact that primate retinal ganglion cells duplicate this behavior suggests that retinal processing limits the performance of the entire visual system in these simple tasks.

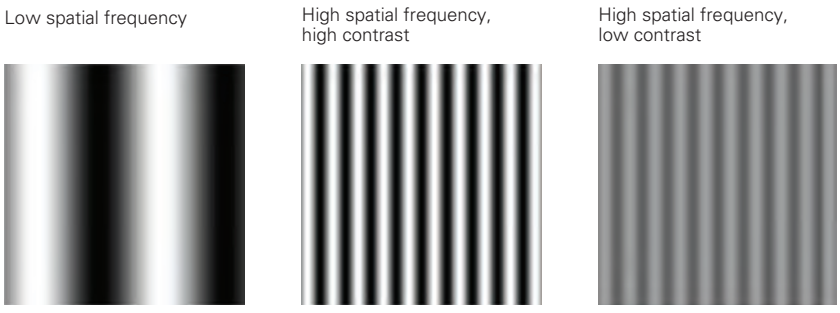

Figure 22–12 Sinusoid grating displays used in psychophysical experiments with human subjects. Such stimuli were used in the experiments discussed in Figure 22–13.

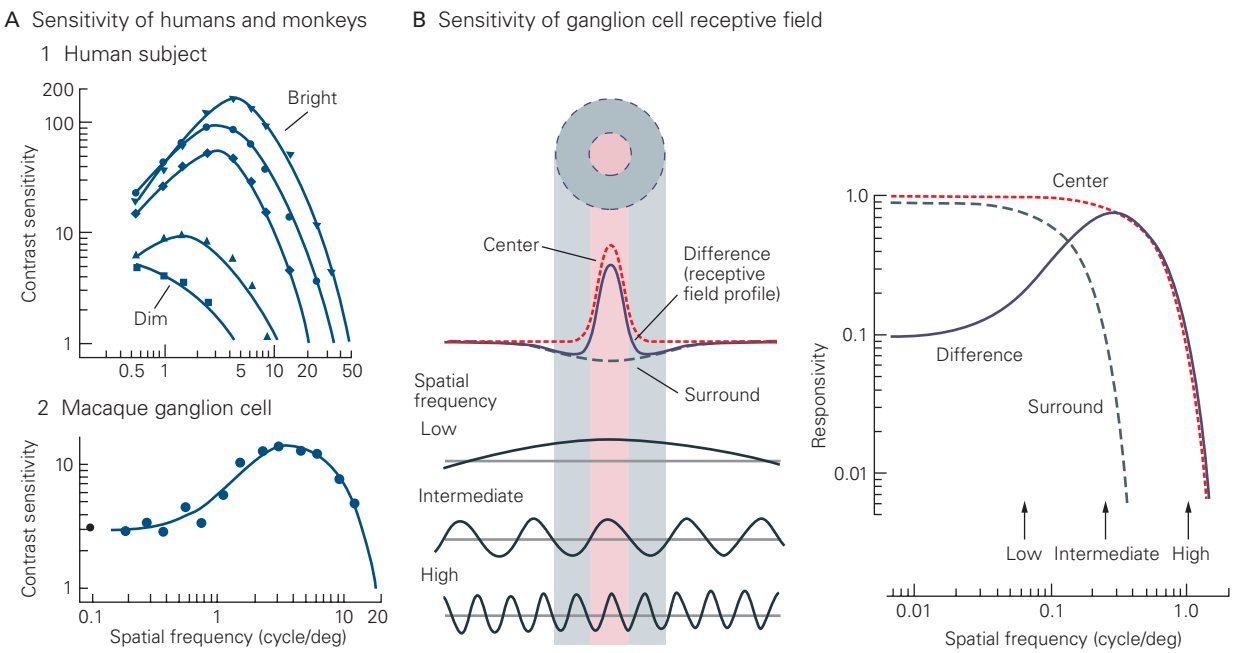

Figure 22–13 Spatial contrast sensitivity.

A. 1. The contrast sensitivity of human subjects was measured using gratings with different spatial frequencies (see Figure 22–12). At each frequency, the contrast was increased to the threshold for detection, and the inverse of that contrast value was plotted against spatial frequency, as shown here. The curves were obtained at different mean intensities, decreasing by factors of 10 from the top to the bottom curve. (Reproduced, with permission, from De Valois, Morgan, and Snodderly 1974.) 2. Contrast sensitivity of a P-type ganglion cell in the macaque retina measured at high intensity. At each spatial frequency, the contrast was gradually increased until it produced a detectable change in the neuron's firing rate. The inverse of that threshold contrast was plotted as in part A-1. The isolated dot at left marks the sensitivity at zero spatial frequency, a spatially uniform field. (Reproduced, with permission, from Derrington and Lennie 1984.)

B. Stimulation of a center-surround receptive field with sinusoid gratings. The neuron's sensitivity to light at different points on the retina is modeled as a "difference-of-Gaussians" receptive field, with a narrow positive Gaussian for the excitatory center and a broad negative Gaussian for the inhibitory surround. Multiplying the profile of the grating stimulus (intensity vs position) with the profile of the receptive field (sensitivity vs position) and integrating over all space calculates the stimulus strength delivered by a particular grating. The resulting sensitivity of the receptive field to gratings of different frequency is shown in the plot on the right. At low spatial frequencies, the negative contribution from the surround cancels the contribution from the center, leading to a drop in the difference curve. (Reproduced, with permission, from Enroth-Cugell and Robson 1984.)

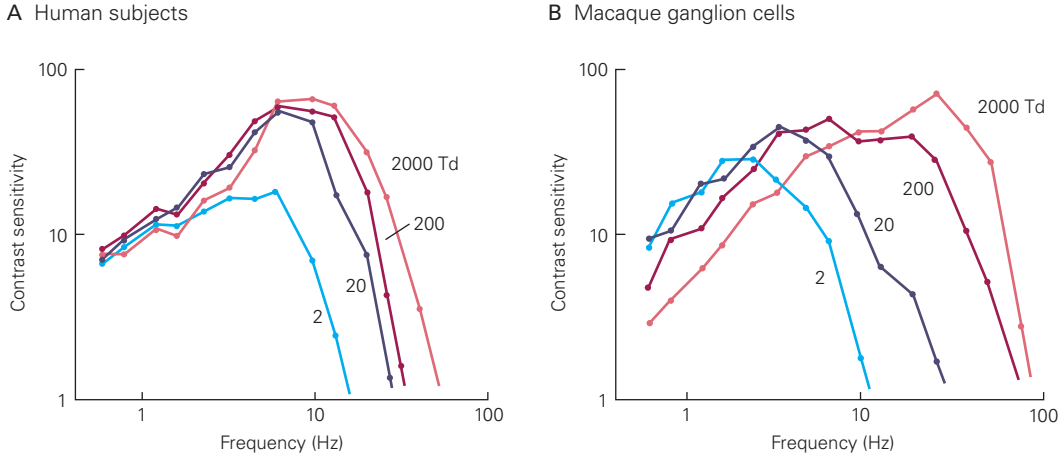

Figure 22–14 Temporal contrast sensitivity. (Reproduced, with permission, from Lee et al. 1990.)

A. The sensitivity of human subjects to temporal flicker was measured by methods similar to those in Figure 22–13A, but the stimulus was a large spot whose intensity varied sinusoidally in time rather than in space. The inverse of the threshold contrast required for detection is plotted against the frequency of the sinusoidal flicker. Sensitivity declines at both high and low frequencies. The mean light level varied, decreasing by factors of 10 from the top to the bottom trace.

B. The flicker sensitivity of M-type ganglion cells in the macaque retina was measured by the same method applied to human subjects in part A. The detection threshold for the neural response was defined as a variation of 20 spikes per second in the cell's firing rate in phase with the flicker.

(sustained or transient), spectral filtering (broadband or dominated by red, green, or blue), and selectivity for other image features such as motion.

These neural representations are directed to various visual centers in the brain, including the lateral geniculate nucleus of the thalamus, a relay to the visual cortex; the superior colliculus, a midbrain region involved in spatial attention and orienting movements; the pretectum, involved in control of the pupil; the accessory optic system, which analyzes self-motion to stabilize gaze; and the suprachiasmatic nucleus, a central clock that directs circadian rhythm and whose phase can be set by light cues (Chapter 44). In many cases, the axons of one type of ganglion cell extend collaterals to multiple areas of the central nervous system. M-cells, for example, project to the thalamus and the superior colliculus.

A Network of Interneurons Shapes the Retinal Output

We now consider in more detail the retinal circuit and how it accounts for the intricate response properties of retinal ganglion cells.

Parallel Pathways Originate in Bipolar Cells

The photoreceptor forms synapses with bipolar cells and horizontal cells (see Figure 22–3A). In the dark, the photoreceptor's synaptic terminal releases glutamate continuously. When stimulated by light, the photoreceptor hyperpolarizes, less calcium enters the terminal, and the terminal releases less glutamate. Photoreceptors do not fire action potentials; like bipolar cells, they release neurotransmitter in a graded fashion using a specialized structure, the *ribbon synapse.* In fact, most retinal processing is accomplished with graded membrane potentials: Action potentials occur primarily in certain amacrine cells and in the retinal ganglion cells.

The two principal varieties of bipolar cells, ON and OFF cells, respond to glutamate at the synapse through distinct mechanisms. The OFF cells use ionotropic receptors, namely glutamate-gated cation channels of the AMPA-kainate variety (AMPA = α-amino-3-hydroxy-5-methylisoxazole-4-propionate). The glutamate released in darkness depolarizes these cells. The ON cells use metabotropic receptors that are linked to a G protein whose action ultimately closes cation channels. Glutamate activation of these receptors thus hyperpolarizes the cells in the dark.

Bipolar ON and OFF cells differ in shape and especially in the levels within the inner plexiform layer where their axons terminate. The axons of ON cells end in the proximal (lower) half, while those of OFF cells end in the distal (upper) half (Figure 22–15). There, they form specific synaptic connections on the dendrites of amacrine and ganglion cells. The ON bipolar cells excite ON ganglion cells, while OFF bipolar cells excite OFF ganglion cells (see Figure 22–3A). Thus, the two principal subdivisions of retinal output, the ON and OFF pathways, are already established at the level of bipolar cells.

Bipolar cells can also be distinguished by the morphology of their dendrites (Figure 22–15). In the central region of the primate retina, the *midget bipolar cell* receives input from a single cone and excites a P-type ganglion cell. This explains why the centers of P-cell receptive fields are so small. The *diffuse bipolar cell* receives input from many cones and excites an M-type ganglion cell. Accordingly, the receptive-field centers of M-cells are much larger. Thus, stimulus representations in the ganglion cell population originate in dedicated bipolar cell pathways that are differentiated by their selective connections to photoreceptors and postsynaptic targets.

Spatial Filtering Is Accomplished by Lateral Inhibition

Signals in the parallel on and off pathways are modified by interactions with horizontal and amacrine cells (see Figure 22–3A). Horizontal cells have broadly arborizing dendrites that spread laterally in the outer plexiform layer. Photoreceptors contact the tips of these arbors at glutamatergic terminals shared with bipolar cells. In addition, horizontal cells are electrically coupled to each other through gap junctions.

A horizontal cell effectively measures the average level of excitation of the photoreceptor population over a broad region. This signal is fed back to the photoreceptor terminal through an inhibitory synapse. Thus, the photoreceptor terminal is under two opposing influences: light falling on the receptor hyperpolarizes it, but light falling on the surrounding region depolarizes it through the sign-inverting synapses from horizontal cells. As a result, the bipolar cell has an antagonistic receptive-field structure.

This spatial antagonism in the receptive field is enhanced by lateral inhibition from amacrine cells in the inner retina. Amacrine cells are neurons whose processes ramify only in the inner plexiform layer. Approximately 30 types of amacrine cells are known, some with small arbors only tens of micrometers across, and others with processes that extend across the entire retina. Amacrine cells generally receive

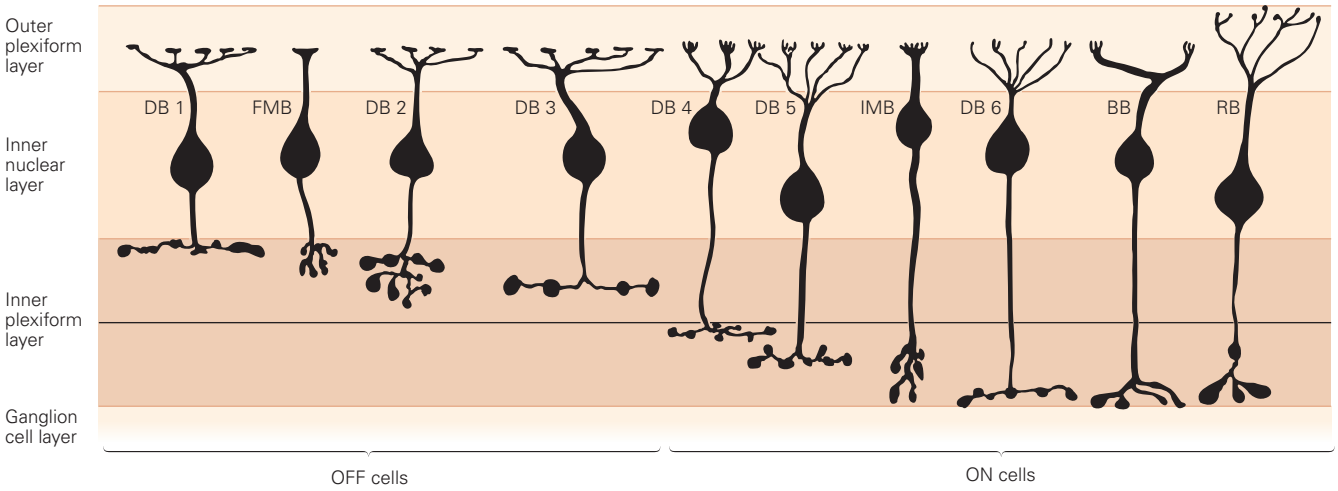

Figure 22–15 Bipolar cells in the macaque retina. The cells are arranged according to the depth of their terminal arbors in the inner plexiform layer. The horizontal line dividing the distal (**upper**) and proximal (**lower**) levels of this layer represents the border between the axonal terminals of OFF and ON type cells. Terminals in the upper half are presumed to be those of OFF cells, and those in the lower half ON cells. Cell types are diffuse bipolar cells (**DB**), ON and OFF midget bipolars (**IMB, FMB**), S-cone ON bipolar (**BB**), and rod bipolar (**RB**). (Reproduced, with permission, from Boycott and Wässle 1999.)

excitatory signals from bipolar cells at glutamatergic synapses. Some amacrine cells feed back directly to the presynaptic bipolar cell at a *reciprocal inhibitory synapse.* Some amacrine cells are electrically coupled to others of the same type, forming an electrical network much like that of the horizontal cells.

Through this inhibitory network, a bipolar cell terminal can receive inhibition from distant bipolar cells, in a manner closely analogous to the lateral inhibition of photoreceptor terminals (see Figure 22–3A). Amacrine cells also inhibit retinal ganglion cells directly. These lateral inhibitory connections contribute substantially to the antagonistic receptive field component of retinal ganglion cells.

Temporal Filtering Occurs in Synapses and Feedback Circuits

For many ganglion cells, a step change in light intensity produces a transient response, an initial peak in firing that declines to a smaller steady rate (see Figure 22–10). Part of this sensitivity originates in the negative-feedback circuits involving horizontal and amacrine cells. For example, a sudden decrease in light intensity depolarizes the cone terminal, which excites the horizontal cell, which in turn repolarizes the cone terminal (see Figure 22–3A). Because this feedback loop involves a brief delay, the voltage response of the cone peaks abruptly and then settles to a smaller steady level. Similar processing occurs at the reciprocal synapses between bipolar and amacrine cells in the inner retina.

In both cases, the delayed-inhibition circuit favors rapidly changing inputs over slowly changing inputs. The effects of this filtering, which can be observed in visual perception, are most pronounced for large stimuli that drive the horizontal and amacrine cell networks most effectively. For example, a large spot can be seen easily when it flickers at a rate of 10 Hz but not at a low rate (see Figure 22–14).

In addition to these circuit properties, certain cellular processes contribute to shaping the temporal response. For example, the AMPA-kainate type of glutamate receptor undergoes strong desensitization. A step increase in the concentration of glutamate at the dendrite of a bipolar or ganglion cell leads to an immediate opening of additional glutamate receptors. As these receptors desensitize, the postsynaptic conductance decreases again. The effect is to render a step response more transient.

Retinal circuits seem to go to great lengths to speed up their responses and emphasize temporal changes. One likely reason is that the very first cell in the retinal circuit, the photoreceptor, is exceptionally slow (see Figure 22–7C). Following a flash of light, a cone takes about 40 ms to reach the peak response, an intolerable delay for proper visual function. Through the various filtering mechanisms in retinal circuitry, subsequent neurons respond most vigorously during the rising phase of the cone's response. Indeed, some ganglion cells have a response peak only 20 ms after the flash. Temporal processing in the retina clearly helps to reduce visual reaction times, a life-extending trait as

important in highway traffic as on the savannas of our ancestors.

Color Vision Begins in Cone-Selective Circuits

Throughout recorded history, philosophers and scientists have been fascinated by color perception. This interest was originally driven by the relevance of color to art, later by its relation to the physical properties of light, and finally by commercial interests in television and photography. The 19th century witnessed a profusion of theories to explain color perception, of which two have survived modern scrutiny. They are based on careful psychophysics that placed strong constraints on the underlying neural mechanisms.

Early experiments demonstrated that any given natural light could be color-matched by mixing together appropriate amounts of three primary lights. This led to the trichromatic theory of color perception based on absorption of light by three mechanisms, each with a different sensitivity spectrum. These correspond to the three cone types (see Figure 22–6), whose measured absorption spectra fully explain the color-matching results both in normal individuals and those with genetic anomalies in the pigment genes.

The so-called opponent-process theory was proposed to explain our perception of different hues. According to this theory, color vision involves three processes that respond in opposite ways to light of different colors: (y–b) would be stimulated by yellow and inhibited by blue light; (r–g) stimulated by red and inhibited by green; and (w–bk) stimulated by white and inhibited by black. We recognize some of these 19th century postulates in the postreceptor circuitry of the retina.

In the central 10° of the human retina, a single midget bipolar cell that receives input from a single cone excites each P-type ganglion cell. An L-ON ganglion cell, for example, has a receptive field center consisting of a single L cone and an antagonistic surround involving a mixture of L and M cones. When this neuron's receptive field is stimulated with a large uniform spot of light that extends over both the center and the surround, this neuron is depolarized by red light and hyperpolarized by green light. Similar antagonism holds for the three other P-cells: L-OFF, M-ON, and M-OFF. These P-cells send their signals to the parvocellular layers of the lateral geniculate nucleus.

A dedicated type of S-ON bipolar cell collects the signals of S-cones selectively and transmits them to ganglion cells of the small bistratified type. Because this ganglion cell also receives excitation from L-OFF and M-OFF bipolar cells, it is depolarized by blue light and hyperpolarized by yellow light. Another type of ganglion cell shows the opposite signature: S-OFF and (L + M)-ON. These signals are transmitted to the koniocellular layers of the lateral geniculate nucleus.

The M-cells are excited by diffuse bipolar cells, which in turn collect inputs from many cones regardless of pigment type. These ganglion cells therefore have large receptive fields with broad spectral sensitivity. Their axons project to the magnocellular layers of the lateral geniculate nucleus.

In this way, chromatic signals are combined and encoded by the retina for transmission to the thalamus and cortex. In circuits of the primary visual cortex, these signals are recombined in different ways, leading to a great variety of receptive field layouts. Only about 10% of cortical neurons are preferentially driven by color contrast rather than luminance contrast. This likely reflects the fact that color vision—despite its great aesthetic appeal—makes only a small contribution to our overall fitness. As an illustration of this, recall that colorblind individuals, who in a sense have lost half of their color space, can grow up without ever noticing that defect.

Congenital Color Blindness Takes Several Forms

Few people are truly colorblind in the sense of being wholly unable to distinguish a change in color from a

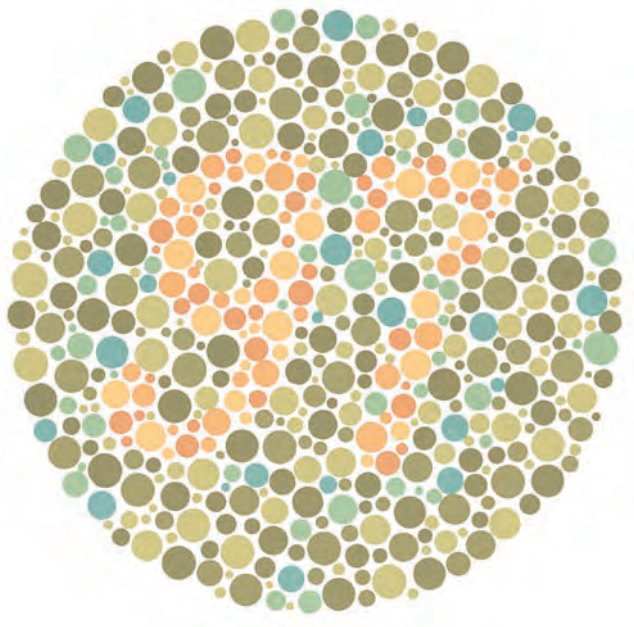

Figure 22–16 A test for some forms of color blindness. The numerals embedded in this color pattern can be distinguished by people with trichromatic vision but not by dichromats who are weak in red–green discrimination. If you don't see any numbers please have your vision tested. (Reproduced, with permission, from Ishihara 1993.)

change in the intensity of light, but many individuals have impaired color vision and experience difficulties in making distinctions that for most of us are trivial, for example between red and green. Most such abnormalities of color vision are congenital and have been characterized in detail; some other abnormalities result from injury or disease of the visual pathway.

Some people have only two classes of cones instead of three. These dichromats find it difficult or impossible to distinguish some surfaces whose colors appear distinct to trichromats. The dichromat's problem is that every surface reflectance function is represented by a two-value description rather than a three-value one, and this reduced description causes dichromats to confuse many more surfaces than do trichromats. Simple tests for color blindness exploit this fact (Figure 22–16).

Although there are three forms of dichromacy, corresponding to the loss of each of the three types of cones, two kinds are much more common than the third. The common forms correspond to the loss of the L cones or M cones and are called *protanopia* and *deuteranopia*, respectively. Protanopia and deuteranopia almost always occur in males, each with a frequency of about 1%. The conditions are transmitted by women who are not themselves affected, and so implicate genes on the X chromosome. A third form of dichromacy, *tritanopia*, involves loss or dysfunction of the S cone. It affects only about 1 in 10,000 people, afflicts women and men with equal frequency, and involves a gene on chromosome 7.

Because the L and M cones exist in large numbers, one might think that the loss of one or the other type would impair vision more broadly than just weakening color vision. In fact, this does not happen because the total number of L and M cones in the dichromat retina is not altered. All cells destined to become L or M cones are probably converted to L cones in deuteranopes and to M cones in protanopes.

In addition to the relatively severe forms of colorblindness represented by dichromacy, there are milder forms, again affecting mostly males. These so-called anomalous trichromats have cones whose spectral sensitivities differ from those in normal trichromats. Anomalous trichromacy results from the replacement of one of the normal cone pigments by an altered protein with a different spectral sensitivity. Two common forms, protanomaly and deuteranomaly, together affect about 7% of males and represent, respectively, the replacement of the L or M cones by a pigment with some intermediate spectral sensitivity.

The genetics of color vision defects are well understood. The genes for the L and M pigments reside on the X chromosome in a head-to-tail arrangement (Figure 22–17A). The pigment proteins have very similar structures, differing in only 4% of their amino acids. People with normal color vision possess a single copy of the gene for the L pigment and from one to three—occasionally as many as five—nearly identical copies of the gene for the M pigment.

The proximity and similarity of these genes predisposes them to varied forms of recombination, leading either to the loss of a gene or to the formation of hybrid genes that account for the common forms of red–green defect (Figure 22–17B). Examination of these genes in dichromats reveals a loss of the L-pigment gene in protanopes and a loss of one or more M-pigment genes in deuteranopes. Anomalous trichromats have L-M or M-L hybrid genes that code for visual pigments with shifted spectral sensitivity; the extent of the shift

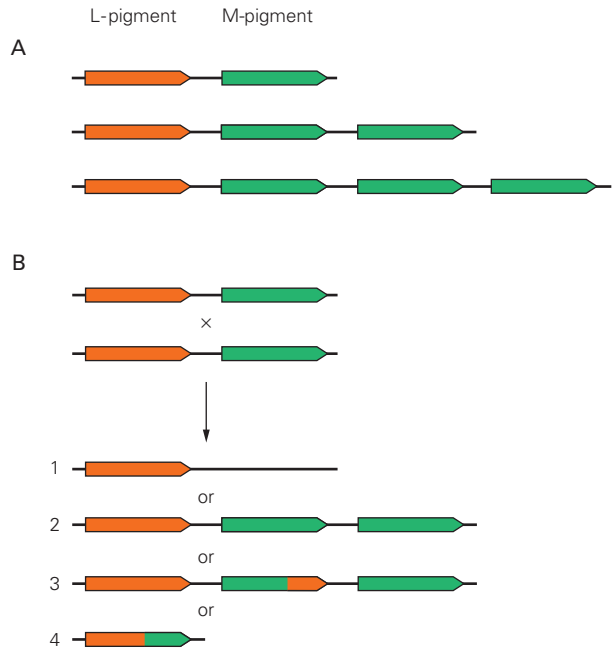

Figure 22–17 L- and M-pigment genes on the X chromosome.

A. The L- and M-pigment genes normally lie next to each other on the chromosome. The base of each arrow corresponds to the 5′ end of the gene, and the tip corresponds to the 3′ end. Males with normal color vision can have one, two, or three copies of the gene for the M pigment on each X chromosome. (Adapted, with permission, from Nathans, Thomas, and Hogness 1986. Copyright © 1986 AAAS.)

B. Recombinations of the L- and M-pigment genes can lead to the generation of a hybrid gene (3 and 4) or the loss of a gene (1), the patterns observed in colorblind men. Spurious recombination can also cause gene duplication (2), a pattern observed in some people with normal color vision. (Adapted from Streyer 1988. Used with permission from J. Nathans.)

depends on the point of recombination. In tritanopes, the loss of S-cone function arises from mutations in the S-pigment gene.

Rod and Cone Circuits Merge in the Inner Retina

For vision under low-light conditions, the mammalian retina has an ON bipolar cell that is exclusively connected to rods (see Figure 22–3B). By collecting inputs from up to 50 rods, this rod bipolar cell can pool the effects of dispersed single-photon absorptions in a small patch of retina. There is no corresponding OFF bipolar cell dedicated to rods.

Unlike all other bipolar cells, the rod bipolar cell does not contact ganglion cells directly but instead excites a dedicated neuron, the AII amacrine cell. This amacrine cell receives inputs from several rod bipolar cells and conveys its output to cone bipolar cells. It provides excitatory signals to ON bipolar cells through gap junctions as well as glycinergic inhibitory signals to OFF bipolar cells. These cone bipolar cells in turn excite ON and OFF ganglion cells, as described earlier. Thus, the rod signal is fed into the cone system after a detour that produces the appropriate signal polarities for the ON and OFF pathways. The purpose of the added interneurons may be to allow greater pooling of rod signals than of cone signals.

Rod signals also enter the cone system through two other pathways. Rods can drive neighboring cones directly through electrical junctions, and they make connections with an OFF bipolar cell that services primarily cones. Once the rod signal has reached the cone bipolars through these pathways, it can take advantage of the same intricate circuitry of the inner retina. Thus, the rod system of the mammalian retina may have been an evolutionary afterthought added to the cone circuits.

The Retina's Sensitivity Adapts to Changes in Illumination

Vision operates under many different lighting conditions. The intensity of the light coming from an object depends on the intensity of the ambient illumination and the fraction of this light reflected by the object's surface, called the *reflectance*. The range of intensities encountered in a day is enormous, with variation spanning 10 orders of magnitude, but most of this variation is useless for the purpose of guiding behavior.

The illumination intensity varies by about nine orders of magnitude, mostly because our planet turns about its axis once a day, while the object reflectance varies much less, by about one order of magnitude in a typical scene. But this reflectance is the interesting quantity for vision, for it characterizes objects and distinguishes them from the background. In fact, our visual system is remarkably good at calculating surface reflectances independently of ambient illumination (Figure 22–18).

With an overall increase in ambient illumination, all points in the visual scene become brighter by the same factor. If the eye could simply reduce its sensitivity by that same factor, the neural representation of the image would remain unchanged at the level of the ganglion cells and could be processed by the rest of the brain in the same way as before the change in illumination. Moreover, the retinal ganglion cells would only need to encode the 10-fold range of image intensities owing to the different object reflectances, instead of the 10-billion-fold range that includes variations in ambient illumination. Some of this adjustment in sensitivity is performed by the pupil, which contracts in bright light, reducing retinal illumination by up to a factor of 10. In addition, the retina itself performs an automatic gain control, called *light adaptation*, that approaches the ideal normalization we have imagined here.

Light Adaptation Is Apparent in Retinal Processing and Visual Perception

When flashes of light of different intensity are presented with a constant background illumination, the responses of a retinal ganglion cell fit a sigmoidal curve (Figure 22–19A). The weakest flashes elicit no response, a graded increase in flash intensity elicits graded responses, and the brightest flashes elicit saturation. When the background illumination is increased, the response curve maintains the same shape but is shifted to higher flash intensities. Compensating for the increase in background illumination, the ganglion cell is now less sensitive to light variations: In the presence of a higher background, a larger change is needed to cause the same response. This lateral shifting of the stimulus–response relationship is a hallmark of light adaptation in the retina.

The consequences of this gain change for human visual perception are readily apparent in psychophysical experiments. When human subjects are asked to detect a flash in a background field of constant illumination, detection on a brighter background necessitates a brighter flash (Figure 22–19B). Under the ideal gain-control mechanism discussed earlier, two stimuli would produce the same response if they caused the same fractional change from the background intensity. In that case, the threshold flash intensity should

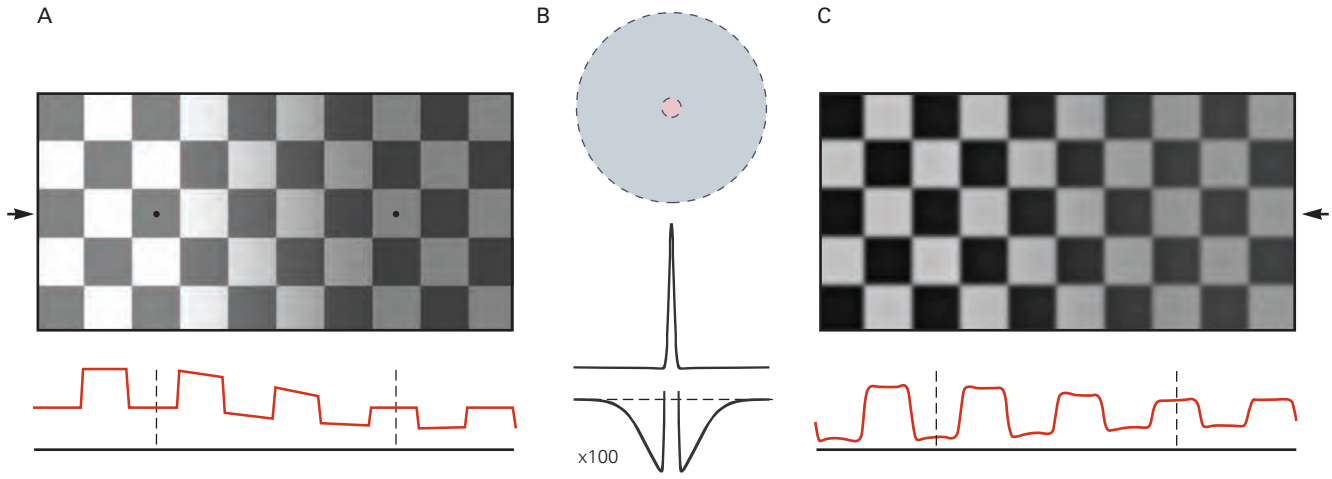

Figure 22–18 A brightness illusion.

A. The two tiles marked with small dots appear to have different color but actually reflect the same light intensity. (To see this, fold the page so they touch.) The trace underneath plots a profile of light intensity at the level of the **arrowheads**. Your visual system interprets this retinal image as a regular tile pattern under spatially varying illumination with a diffuse shadow in the right half. Under that interpretation, the right tile must have a lighter color than the left, which is what you perceive. This process is automatic and requires no conscious analysis.

B. Retinal processing contributes to the perception of "lightness" by discounting the shadow's smooth gradients of illumination and accentuating the sharp edges between checkerboard fields. The receptive field for a visual neuron with an excitatory center and inhibitory surround is shown at the top. As shown in a hundredfold magnification at the bottom, the surround is weak but extends over a much larger area than the center.

C. The result when a population of visual neurons with receptive fields as in B processes the image in A. This operation—the convolution of the image in A with the profile in B—subtracts from each point in the visual field the average intensity in a large surrounding region. The neural representation of the object has largely lost the effects of shading, and the two tiles in question do indeed have different brightness values in this representation.

be proportional to the background intensity, a relationship known as *Weber's law of adaptation*, which we encountered in considering somatic receptor sensitivity (Chapter 17). The visual system follows Weber's law approximately: Over the entire range of vision, sensitivity decreases somewhat less steeply with increasing background intensity (Figure 22–19B).

Multiple Gain Controls Occur Within the Retina

The enormous change in gain required for light adaptation arises at multiple sites within the retina. In starlight, a single rod cell is stimulated by a photon only every few seconds, a rate insufficient to alter the cell's adaptation status. However, a retinal ganglion cell combines signals from many rods, thus receiving a steady stream of photon signals that can elicit a light-dependent gain change in the cell.

At somewhat higher light intensities, a rod bipolar cell begins to adapt, changing its responsiveness depending on the average light level. Next, we reach a light intensity at which the gain of individual rod cells gradually decreases. Beyond that, the rods saturate: All their cGMP-dependent channels are closed, and the membrane potential no longer responds to the light stimulus. By this time, around dawn, the much less sensitive cone cells are being stimulated effectively and gradually take over from the rods. As the ambient light increases further, toward noon, light adaptation results principally from gain changes within the cones.

The cellular mechanisms of light adaptation are best understood in the photoreceptors. The calcium-dependent feedback pathways discussed earlier have a prominent role. Recall that when a light flash closes the cGMP-gated channels, the resulting decrease in intracellular Ca^{2+} accelerates several biochemical reactions that terminate the response to the flash (see Figure 22–7B). When illumination is continuous, however, the Ca^{2+} concentration remains low, and all these reactions are therefore in a steady state that both lowers the gain and accelerates the time course of the receptor's response to light (Figure 22–19C). As a result, the light-adapted photoreceptor can respond to rapid changes in intensity much more quickly. This has important consequences for human visual perception; the contrast sensitivity to high-frequency flicker increases with intensity, an effect observed in primate retinal ganglion cells as well (see Figure 22–14).

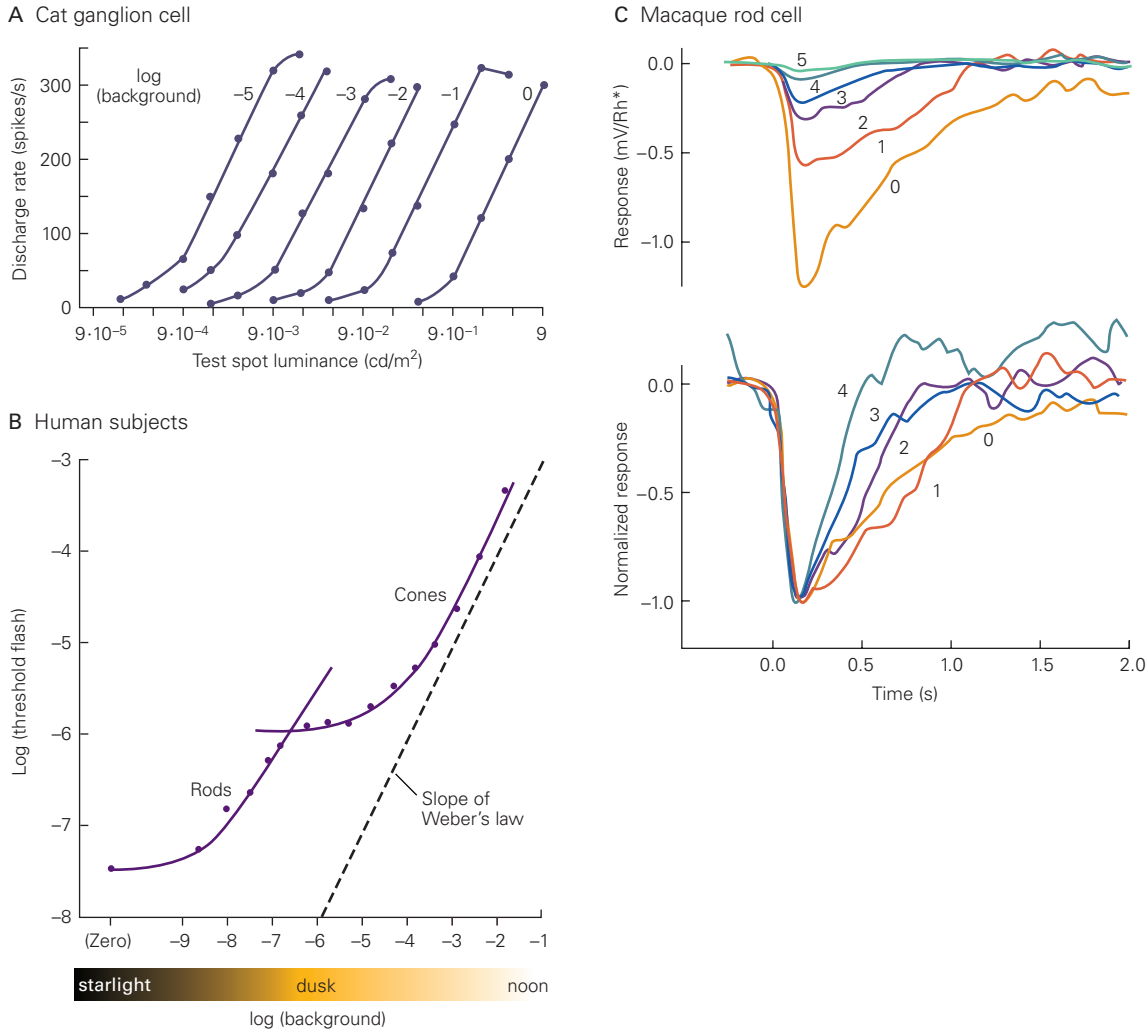

Figure 22–19 Light adaptation.

A. The receptive field of a cat retinal ganglion cell was illuminated uniformly at a steady background intensity, and a test spot was flashed briefly on the receptive field center. The peak firing rate following the flash was measured and plotted against the logarithm of the flash intensity. Each curve corresponds to a different background intensity, increasing by factors of 10 from left to right. (Reproduced, with permission, from Sakmann and Creutzfeldt 1969. Copyright © 1969 Springer.)

B. A small test spot was flashed briefly on a steadily illuminated background, and the flash intensity gradually increased to where a human subject could just detect it. The procedure was repeated at different background intensities. Here, the threshold flash intensity is plotted against the background intensity. The curve has two branches connected by a distinct kink: These correspond to the regimes of rod and cone vision. The slope of Weber's law represents the idealization when the threshold intensity is proportional to the background intensity. (Adapted from Wyszecki and Stiles 1982.)

C. The top plot shows the responses of a macaque monkey's rod cell to flashes presented at varying background intensities. The cell's single-photon response was calculated from the recorded membrane potential divided by the number of rhodopsins (**Rh**) activated by the flash. The gain of the single-photon response decreases substantially with increasing background intensity. The background intensity, in photon/μm^2/s, is 0 for trace 0, 3.1 for trace 1, 12 for trace 2, 41 for trace 3, 84 for trace 4, and 162 for trace 5. In the bottom plot, the same data (except for the smallest response) are normalized to the same amplitude, showing that the time course of the single-photon response accelerates at high intensity. (Reproduced, with permission, from Schneeweis and Schnapf 2000.)

Light Adaptation Alters Spatial Processing

In addition to the sensitivity and speed of the retinal response, light adaptation also changes the rules of spatial processing. In bright light, many ganglion cells have a sharp center-surround structure in their receptive fields (see Figure 22–10). As the light dims, the antagonistic surround becomes broad and weak and eventually disappears. Under these conditions, the circuits of the retina function to simply accumulate the rare photons rather than computing local intensity gradients. These changes in receptive-field properties occur because of changes in the lateral inhibition produced by the networks of horizontal and amacrine cells (see Figure 22–3). An important regulator of these processes is dopamine, released in a light-dependent manner by specialized amacrine cells.

These retinal effects leave their signature on human perception. In bright light, our visual system prefers fine gratings to coarse gratings. But in dim light, we are most sensitive to coarse gratings: With the loss of center-surround antagonism, the low spatial frequencies are no longer attenuated (see Box 22–1 and Figure 22–13).

In conclusion, light adaptation has two important roles. One is to discard information about the intensity of ambient light while retaining information about object reflectances. The other is to match the small dynamic range of firing in retinal ganglion cells to the large range of light intensities in the environment. These large gain changes must be accomplished with graded neuronal signals before action potentials are produced in optic nerve fibers, because the firing rates of these fibers can vary effectively over only two orders of magnitude. In fact, the crucial need for light adaptation may be why this neural circuitry resides in the eye and not in the brain at the other end of the optic nerve.

Highlights

1. The retina transforms light patterns projected onto photoreceptors into neural signals that are conveyed through the optic nerve to specialized visual centers in the brain. Different populations of ganglion cells transmit multiple neural representations of the retinal image along parallel pathways.
2. The retina discards much of the stimulus information available at the receptor level and extracts certain low-level features of the visual field useful to the central visual system. Fine spatial resolution is maintained only in a narrow region at the center of gaze. Intensity gradients in the image, such as object edges, are emphasized over spatially uniform portions; temporal changes are enhanced over unchanging parts of the scene.
3. The retina adapts flexibly to the changing conditions for vision, especially the large diurnal changes in illumination. Information about the absolute light level is largely discarded, favoring the subsequent analysis of object reflectances within the scene.
4. The transduction of light stimuli begins in the outer segment of the photoreceptor cell when a pigment molecule absorbs a photon. This sets in motion an amplifying G protein cascade that ultimately reduces the membrane conductance, hyperpolarizes the photoreceptor, and decreases glutamate release at the synapse. Multiple feedback mechanisms, in which intracellular Ca^{2+} has an important role, serve to turn off the enzymes in the cascade and terminate the light response.
5. Rod photoreceptors are efficient collectors of light and serve nocturnal vision. Cones are much less sensitive and function throughout the day. Cones synapse onto bipolar cells that in turn excite ganglion cells. Rods connect to specialized rod bipolar cells whose signals are conveyed through amacrine cells to the cone bipolar cells.
6. The vertical excitatory pathways are modulated by horizontal connections that are primarily inhibitory. Through these lateral networks, light in the receptive-field surround of a ganglion cell counteracts the effect of light in the center. The same negative-feedback circuits also sharpen the transient response of ganglion cells.
7. The segregation of information into parallel pathways and the shaping of response properties by inhibitory lateral connections are pervasive organizational principles in the visual system.

Markus Meister
Marc Tessier-Lavigne

Selected Reading

Dowling JE. 2012. *The Retina: An Approachable Part of the Brain.* Cambridge, MA: Harvard Univ. Press.

Fain GL, Matthews HR, Cornwall MC, Koutalos Y. 2001. Adaptation in vertebrate photoreceptors. Physiol Rev 81:117–151.

Field GD, Chichilnisky EJ. 2007. Information processing in the primate retina: circuitry and coding. Ann Rev Neurosci 30:1–30.
Gollisch T, Meister M. 2010. Eye smarter than scientists believed: neural computations in circuits of the retina. Neuron 65:150–164.
Lamb TD. 2016. Why rods and cones? Eye (Lond) 30:179–185.
Masland RH. 2012. The tasks of amacrine cells. Vis Neurosci 29:3–9.
Meister M, Berry MJ. 1999. The neural code of the retina. Neuron 22:435–450.
Oyster CW. 1999. *The Human Eye: Structure and Function.* Sunderland, MA: Sinauer.
Roof DJ, Makino CL. 2000. The structure and function of retinal photoreceptors. In: DM Albert, FA Jakobiec (eds). *Principles and Practice of Ophthalmology*, pp. 1624–1673. Philadelphia: Saunders.
Shapley R, Enroth-Cugell C. 1984. Visual adaptation and retinal gain controls. Prog Retin Eye Res 3:223–346.
Wandell BA. 1995. *Foundations of Vision.* Sunderland, MA: Sinauer.
Wässle H. 2004. Parallel processing in the mammalian retina. Nat Rev Neurosci 5:747–757.
Williams DR. 2011. Imaging single cells in the living retina. Vision Res 51:1379–1396.

References

Alberts B, Johnson A, Lewis J, Raff M, Roberts K, Walter P. 2008. *Molecular Biology of the Cell,* 5th ed. New York: Garland Science.
Boycott BB, Dowling JE. 1969. Organization of the primate retina: light microscopy. Philos Trans R Soc Lond B Biol Sci 255:109–184.
Boycott B, Wässle H. 1999. Parallel processing in the mammalian retina: the Proctor Lecture. Invest Ophthalmol Vis Sci 40:1313–1327.
Curcio CA, Hendrickson A. 1991. Organization and development of the primate photoreceptor mosaic. Prog Retinal Res 10:89–120.
Derrington AM, Lennie P. 1984. Spatial and temporal contrast sensitivities of neurones in lateral geniculate nucleus of macaque. J Physiol 357:219–240.
De Valois RL, Morgan H, Snodderly DM. 1974. Psychophysical studies of monkey vision. 3. Spatial luminance contrast sensitivity tests of macaque and human observers. Vision Res 14:75–81.
Enroth-Cugell C, Robson JG. 1984. Functional characteristics and diversity of cat retinal ganglion cells. Basic characteristics and quantitative description. Invest Ophthalmol Vis Sci 25:250–227.
Hurvich LM. 1981. *Color Vision.* Sunderland, MA: Sinauer.
Ishihara S. 1993. *Ishihara's Tests for Colour-Blindness*. Tokyo: Kanehara.
Lee BB, Pokorny J, Smith VC, Martin PR, Valberg A. 1990. Luminance and chromatic modulation sensitivity of macaque ganglion cells and human observers. J Opt Soc Am A 7:2223–2236.
Nathans J, Hogness DS. 1984. Isolation and nucleotide sequence of the gene encoding human rhodopsin. Proc Natl Acad Sci U S A 81:4851–4855.
Nathans J, Thomas D, Hogness DS. 1986. Molecular genetics of human color vision: the genes encoding blue, green, and red pigments. Science 232:193–202.
O'Brien DF. 1982. The chemistry of vision. Science 218:961–966.
Polyak SL. 1941. *The Retina.* Chicago: Univ. Chicago Press.
Rodieck RW. 1965. Quantitative analysis of cat retinal ganglion cell response to visual stimuli. Vision Res 5:583–601.
Sakmann B, Creutzfeldt OD. 1969. Scotopic and mesopic light adaptation in the cat's retina. Pflügers Arch 313: 168–185.
Schnapf JL, Kraft TW, Nunn BJ, Baylor DA. 1988. Spectral sensitivity of primate photoreceptors. Vis Neurosci 1:255–221.
Schneeweis DM, Schnapf JL. 1995. Photovoltage of rods and cones in the macaque retina. Science 228:1053–1056.
Schneeweis DM, Schnapf JL. 2000. Noise and light adaptation in rods of the macaque monkey. Vis Neurosci 17:659–666.
Solomon GS, Lennie P. 2007. The machinery of color vision. Nat Rev Neurosci 8:276–286.
Stryer L. 1988. *Biochemistry,* 3rd ed. New York: Freeman.
Wade NJ. 1998. *A Natural History of Vision.* Cambridge: MIT Press.
Wald G, Brown PK. 1956. Synthesis and bleaching of rhodopsin. Nature 177:174–176.
Wyszecki G, Stiles WS. 1982. *Color Science: Concepts and Methods, Quantitative Data and Formulas,* Chapter 7 "Visual Thresholds." 2nd ed. New York: Wiley.
Young RW. 1970. Visual cells. Sci Am 223:80–91.

23

Intermediate-Level Visual Processing and Visual Primitives

We have seen in Chapters 21 and 22 that the eye is not a mere camera, but instead contains sophisticated retinal circuitry that decomposes the retinal image into signals representing contrast and movement. These data are conveyed through the optic nerve to the primary visual cortex, which uses this information to analyze the shape of objects. It first identifies the boundaries of objects, represented by numerous short line segments, each with a specific orientation. The cortex then integrates this information into a representation of specific objects, a process referred to as *contour integration.*

These two steps, local analysis of orientation and contour integration, exemplify two distinct stages of visual processing. Computation of local orientation is an example of low-level visual processing, which is concerned with identifying local elements of the light structure of the visual field. Contour integration is an example of intermediate-level visual processing, the first step in generating a representation of the unified visual field. At the earliest stages of analysis in the cerebral cortex, these two levels of processing are accomplished together.

A visual scene comprises many thousands of line segments and surfaces. Intermediate-level visual processing is concerned with determining which boundaries and surfaces belong to specific objects and which are part of the background (see Figure 21–4). It is also involved in distinguishing the brightness and color of a surface from the intensity and wavelength of light reflected from that surface. The physical characteristics of reflected light result as much from the intensity and color balance of the light that illuminates a surface as from the color of that surface. Determining the actual surface color of a single object requires comparison of the wavelengths of light reflected from multiple surfaces in a scene.

Intermediate-level visual processing thus involves assembling local elements of an image into a unified percept of objects and background. Although determining which elements belong together in a single object is a highly complex problem with an astronomical number of potential solutions, each relay in the visual circuity of the brain has built-in logic that

allows assumptions to be made about the likely spatial relationships between elements. In certain cases, these inherent rules can lead to the illusion of contours and surfaces that do not actually exist in the visual field (Figure 23–1).

Three features of visual processing help overcome ambiguity in the signals from the retina. First, the way in which a visual feature is perceived depends on everything that surrounds it. The perception of a point, line, or surface, for example, depends on the relationship between that feature and what else is present in the scene. That is, the response of a neuron in the visual cortex is context-dependent: It depends as much on the presence of contours and surfaces outside the cell's receptive field as on the attributes within it. Second, the functional properties of neurons in the visual cortex can be altered by visual experience or perceptual learning. Finally, visual processing in the cortex is subject to the influence of cognitive functions, specifically attention, expectation, and "perceptual task" (the active engagement in visual discrimination or detection). The interaction between these three factors—the context or entire set of signals representing a scene, experience-dependent changes in cortical circuitry,

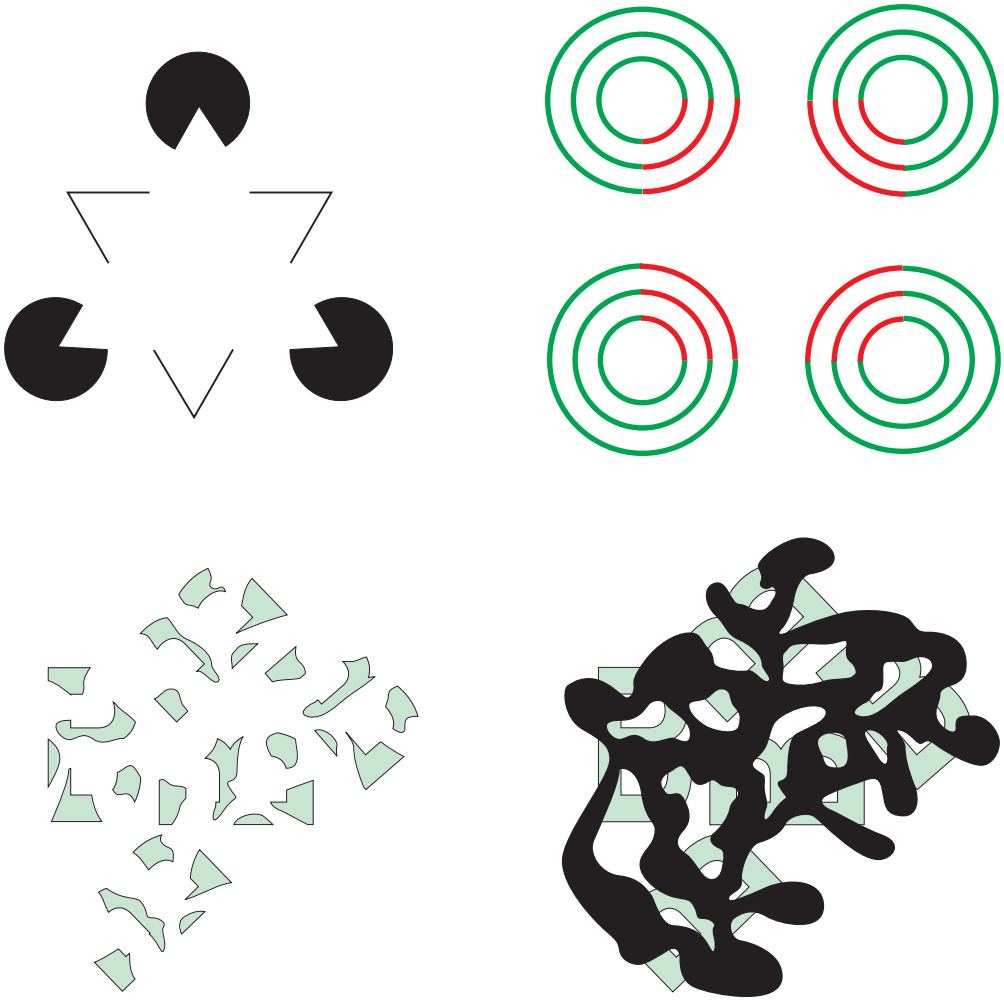

Figure 23–1 Illusory contours and perceptual fill-in. The visual system uses information about local orientation and contrast to construct the contours and surfaces of objects. This constructive process can lead to the perception of contours and surfaces that do not appear in the visual field, including those seen in illusory figures. **Top left:** In the Kanizsa triangle illusion, one perceives continuous boundaries extending between the apices of a white triangle, even though the only real contour elements are those formed by the Pac-Man–like figures and the acute angles. **Top right:** The inside and outside of the illusory pink square are the same white color as the page, but a continuous transparent pink surface within the square is perceived. **Bottom:** Occluding surfaces can also facilitate contour integration and surface segmentation. The irregular shapes on the left appear to be unrelated, but when they are partially occluded by black shapes (right), they are easily seen as fragments of the letter B.

and expectation—is vital to the visual system's analysis of complex scenes.

In this chapter, we examine how the brain's analysis of the local features in a visual scene, or *visual primitives,* proceeds in parallel with the analysis of more global features. Visual primitives include contrast, line orientation, brightness, color, movement, and depth. Each type of visual primitive is subject to the integrative action of intermediate-level processing. Lines with particular orientations are integrated into object contours, local contrast information into surface brightness and surface segmentation, wavelength selectivity into color constancy, and directional selectivity into object motion.

The analysis of visual primitives begins in the retina with the detection of brightness and color and continues in the primary visual cortex with the analysis of orientation, direction of movement, and stereoscopic depth. Properties related to intermediate-level visual processing are analyzed together with visual primitives in the visual cortex starting in the primary visual cortex (V1), which plays a role in contour integration and surface segmentation. Other areas of the visual cortex specialize in different aspects of this task: V2 analyzes properties related to object surfaces, V4 integrates information about color and object shape, and V5—the middle temporal area or MT—integrates motion signals across space (Figure 23–2).

Internal Models of Object Geometry Help the Brain Analyze Shapes

A first step in determining an object's contour is identification of the orientation of local parts of the contour. This step commences in V1, which plays a critical role in both local and global analysis of form.

Neurons in the visual cortex respond selectively to specific local features of the visual field, including orientation, binocular disparity or depth, and direction of movement, as well as to properties already analyzed in the retina and lateral geniculate nucleus, such as contrast and color. Orientation selectivity, the first emergent property identified in the receptive fields of cortical neurons, was discovered by David Hubel and Torsten Wiesel in 1959.

Neurons in both the retina (Chapter 22) and the lateral geniculate nucleus (Chapter 21) have circular receptive fields with a center-surround organization. They respond to the light–dark contrasts of edges or lines in the visual field but are not selective for the orientations of those edges (see Figure 21–9). In the visual cortex, however, neurons respond selectively to lines of particular orientations. Each neuron responds to a narrow range of orientations, approximately 40°, and different neurons respond optimally to distinct orientations. Hubel and Wiesel proposed that this orientation selectivity reflects the arrangement of the inputs

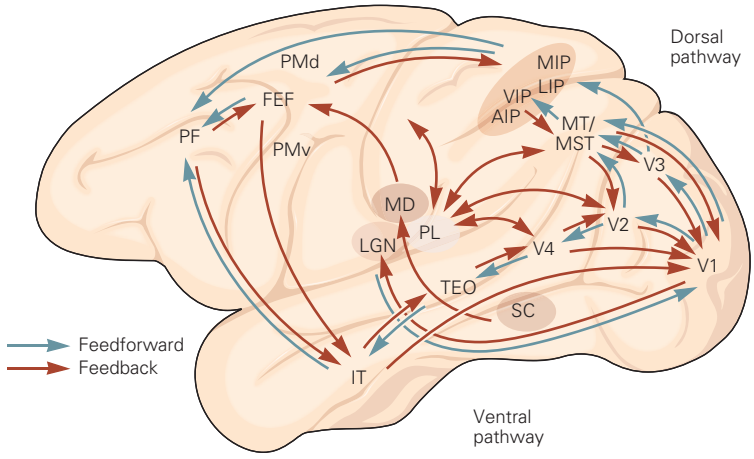

Figure 23–2 Cortical areas involved with intermediate-level visual processing. Many cortical areas in the macaque monkey, including V1, V2, V3, V4, and middle temporal area (**MT**), are involved with integrating local cues to construct contours and surfaces and segregating foreground from background. The shaded areas extend into the frontal and temporal lobes because cognitive output from these areas, including attention, expectation, and behavioral task, contributes to the process of scene segmentation. (Abbreviations: **AIP**, anterior intraparietal cortex; **FEF**, frontal eye fields; **IT**, inferior temporal cortex; **LGN**, lateral geniculate nucleus; **LIP**, lateral intraparietal cortex; **MD**, medial dorsal nucleus of thalamus; **MIP**, medial intraparietal cortex; **MST**, medial superior temporal cortex; **MT**, middle temporal cortex; **PF**, prefrontal cortex; **PL**, pulvinar; **PMd**, dorsal premotor cortex; **PMv**, ventral premotor cortex; **SC**, superior colliculus; **TEO**, occipitotemporal cortex; **VIP**, ventral intraparietal cortex; **V1**, **V2**, **V3**, **V4**, primary, secondary, third, and fourth visual areas.)

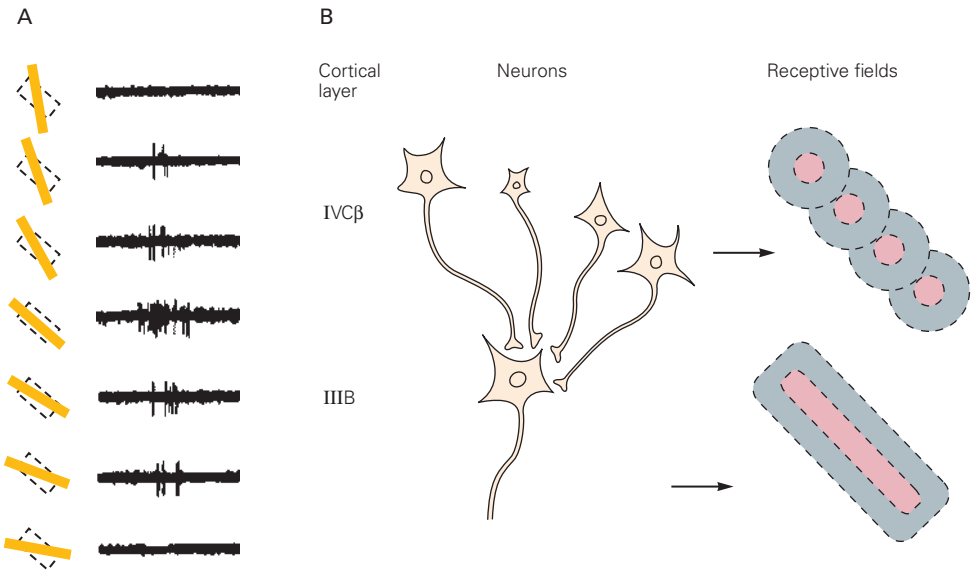

Figure 23–3 Orientation selectivity and mechanisms.

A. A neuron in the primary visual cortex responds selectively to line segments that fit the orientation of its receptive field. This selectivity is the first step in the brain's analysis of an object's form. (Reproduced, with permission, from Hubel and Wiesel 1968. Copyright © 1968 The Physiological Society.)

B. The orientation of the receptive field is thought to result from the alignment of the circular center-surround receptive fields of several presynaptic cells in the lateral geniculate nucleus. In the monkey, individual neurons in layer IVCβ of V1 have unoriented receptive fields. However, when several neighboring IVCβ cells project to a neuron in layer IIIB they create a receptive field with a specific orientation for that postsynaptic cell.

from the lateral geniculate nucleus, and there is now a body of supportive evidence for the idea. Each V1 neuron receives input from several neighboring geniculate neurons whose center-surround receptive fields are aligned so as to represent a particular axis of orientation (Figure 23–3). Two principal types of orientation-selective neurons, simple and complex, have been identified.

Simple cells have receptive fields divided into ON and OFF subregions (Figure 23–4). When a visual stimulus such as a bar of light enters the receptive field's ON subregion, the neuron fires; the cell also responds when the bar leaves the OFF subregion. Simple cells have a characteristic response to a moving bar; they discharge briskly when a bar of light leaves an OFF region and enters an ON region. The responses of these cells are therefore highly selective for the position of a line or edge in space.

Complex cells are less selective for the position of object boundaries. They lack discrete ON and OFF subregions (Figure 23–4) and respond similarly to light and dark at all locations across their receptive fields. They fire continuously as a line or edge stimulus traverses their receptive fields. Hubel and Wiesel proposed that the complex cells are a second stage of the elaboration of receptive fields after simple receptive fields and are built by overlapping simple receptive fields.

As one considers the range of receptive field properties that have been described in the early visual cortical areas, it is important to point out phylogenetic differences, with different species differing in the location in which these properties are first expressed and in the kinds of properties that are represented. In the cat, the target layer of the visual cortex for lateral geniculate neurons has oriented simple cells; it had been presumed that these cortical cells represent an obligatory first stage in the cortical processing of visual information, between the center-surround circularly symmetric receptive fields in the lateral geniculate nucleus and the receptive fields of complex cells in the superficial cortical layers. In primates, however, the geniculate target layers, 4Cα and β, have circularly symmetric, unoriented receptive fields. The postsynaptic target of the layer 4C cells, predominantly the superficial layers of the cortex, is populated with complex cells, therefore skipping a simple cell stage. In the mouse, orientation selectivity is seen in the lateral geniculate nucleus. The preceding comparison points out a few characteristics of the evolution of visual processing. One is the encephalization of function, where properties such as orientation are shifted to later stages of processing over stages of evolution. Another is the development of new pathways. It has been suggested that the

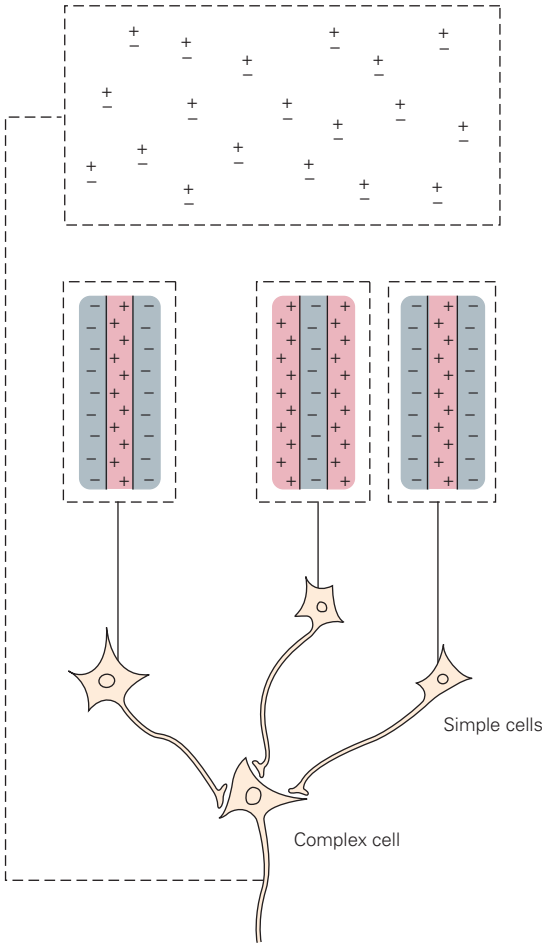

Figure 23–4 Simple and complex cells in the visual cortex. The receptive fields of simple cells are divided into subfields with opposite response properties. In an ON subfield (indicated by +), the onset of a light triggers a response in the neuron; in an OFF subfield (indicated by –), the extinction of a bar of light triggers a response. Complex cells have overlapping ON and OFF regions and respond continuously as a line or edge traverses the receptive field along an axis perpendicular to the receptive-field orientation.

magnocellular pathway in the monkey is equivalent to the entire geniculostriate pathway in the cat, whereas the parvocellular pathway, which mediates higher-resolution vision and color vision, is new to the primate.

Moving stimuli are often used to study the receptive fields of visual cortex neurons, not only to simulate the conditions under which an object moving in space is detected but also to simulate the conditions produced by eye movements. As we scan the visual environment, the boundaries of stationary objects move across the retina. In fact, visual perception requires eye movement. Visual cortex neurons do not respond to an image that is stabilized on the retina. These neurons require transient stimulation (moving or flashing stimuli) in order to be activated.

Some visual cortex neurons have receptive fields in which an excitatory center is flanked by inhibitory regions. Inhibitory regions along the axis of orientation, a property known as *end-inhibition*, restrict a neuron's responses to lines of a certain length (Figure 23–5). End-inhibited neurons respond well to a line that does not extend into the inhibitory flanks but lies entirely within the excitatory part of the receptive field. Because the inhibitory regions share the orientation preference of the central excitatory region, end-inhibited cells are selective for line curvature and also respond well to corners.

To define the shape of the object as a whole, the visual system must integrate the information on local orientation and curvature into object contours. The way in which the visual system integrates contours reflects the geometrical relationships present in the natural world (Figure 23–6). As originally pointed out by Gestalt psychologists early in the 20th century, contours that are immediately recognizable tend to follow the rule of good continuation (curved lines maintain a constant radius of curvature and straight lines stay straight). In a complex visual scene, such smooth contours tend to "pop out," whereas more jagged contours are difficult to detect.

The responses of a visual cortex neuron can be modulated by stimuli that themselves do not activate the cell and therefore lie outside the receptive field's core. This *contextual modulation* endows a neuron with selectivity for more complex stimuli than would be predicted by placing the components of a stimulus at different positions in and around the receptive field. The same visual features that facilitate the detection of an object in a complex scene (Figure 23–6A) also apply to contextual modulation. The properties of the features that confer perception of contours, even illusory ones, are reflected in the responses of neurons in the primary visual cortex, which are sensitive to the global characteristics of contours, even those that extend well outside their receptive fields.

Contextual influences over large regions of visual space are likely to be mediated by connections between multiple columns of neurons in the visual cortex that have similar orientation selectivity (Figure 23–6B). These connections are formed by pyramidal-cell axons that run parallel to the cortical surface (see Figure 21–16). The extent and orientation dependency of these horizontal connections provide the interactions that could mediate contour saliency (see Figure 21–14).

Central to the process of contour integration is the idea of the association field. The association field refers

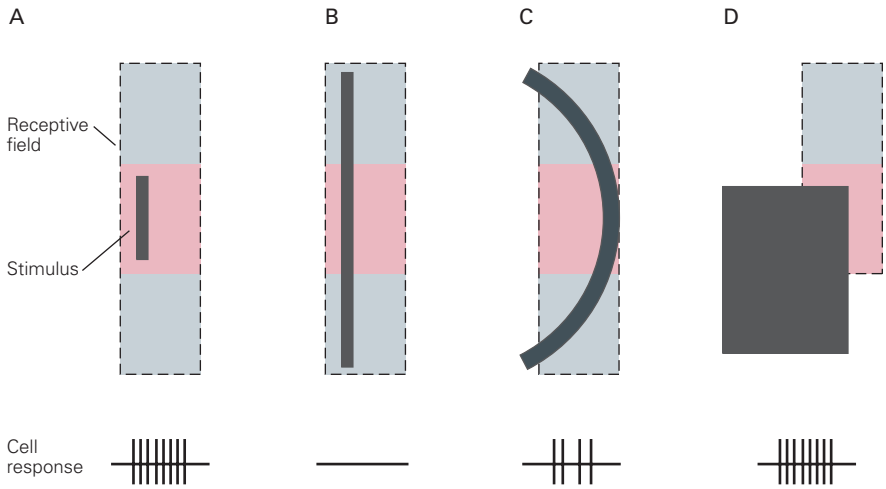

Figure 23–5 End-inhibited receptive fields. Some receptive fields have a central excitatory region flanked by inhibitory regions that have the same orientation selectivity. Thus, a short line segment or a long curved line will activate the neuron (**A** and **C**), but a long straight line will not (**B**). A neuron with a receptive field that displays only one inhibitory region in addition to the excitatory region can signal the presence of corners (**D**).

to the interactions across visual space required to perceptually link contour elements into global contours. It underlies the Gestalt principle of good continuation and the perceptual saliency of smooth contours embedded in complex scenes. Physiologically, it underlies the facilitation of neuronal responses by contour elements extending outside their "classical" receptive fields. Anatomically, it is mediated in part by the relationship between long-range horizontal connections and cortical functional architecture. Though it has been investigated most extensively in primary visual cortex, because of the ubiquity of horizontal connections across all areas of cortex, it is likely to be a strategy for associating bits of information that are mapped within every cortical area. The functional role of the association field in cortical areas outside of V1 depends on how information is mapped across the cortical surface and the relationship between these maps and the plexus of horizontal connections.

Depth Perception Helps Segregate Objects From Background

Depth is another key feature in determining the perceived shape of an object. An important cue for the perception of depth is the difference between the two eyes' views of the world, which must be computed and reconciled by the brain. The integration of binocular input begins in the primary visual cortex, the first level at which individual neurons receive signals from both eyes. The balance of input from the two eyes, a property known as ocular dominance, varies among cells in V1.

Binocular neurons in many visual cortical areas are also selective for depth, which is computed from the relative retinal positions of objects placed at different distances from the observer. An object that lies in the *plane of fixation* produces images at corresponding positions on the two retinas (Figure 23–7). The images of objects that lie in front of or behind the plane of fixation fall on slightly different locations in the two eyes, a property known as binocular disparity. Individual neurons can be selective for a narrow range of disparities and therefore positions in depth. Some are selective for objects lying on the plane of fixation (tuned excitatory or inhibitory cells), whereas others respond only when objects lie in front of the plane of fixation (near cells) or behind that plane (far cells).

Depth plays an important role in the perception of object shape, in surface segmentation, and in establishing the three-dimensional properties of a scene. Objects that are placed near an observer can partially occlude those situated farther away. A surface passing behind an object is perceived as continuous even though its two-dimensional image on each retina represents two surfaces separated by the occluder. When the brain encounters a surface interrupted by gaps that have appropriate alignment and contrast, and lying in the near-depth plane, it fills in the gaps to create a continuous surface (Figure 23–8).

Although the depth of a single object can be established easily, determining the depths of multiple objects within a scene is a much more complex problem that requires linking the retinal images of all objects in the two eyes. The disparity calculation is therefore a global one: The calculation in one part of the visual image influences the calculation for other parts. When the assignment of depth is unambiguous in one part of an image, that information is applied to other parts of the image where there is insufficient information to

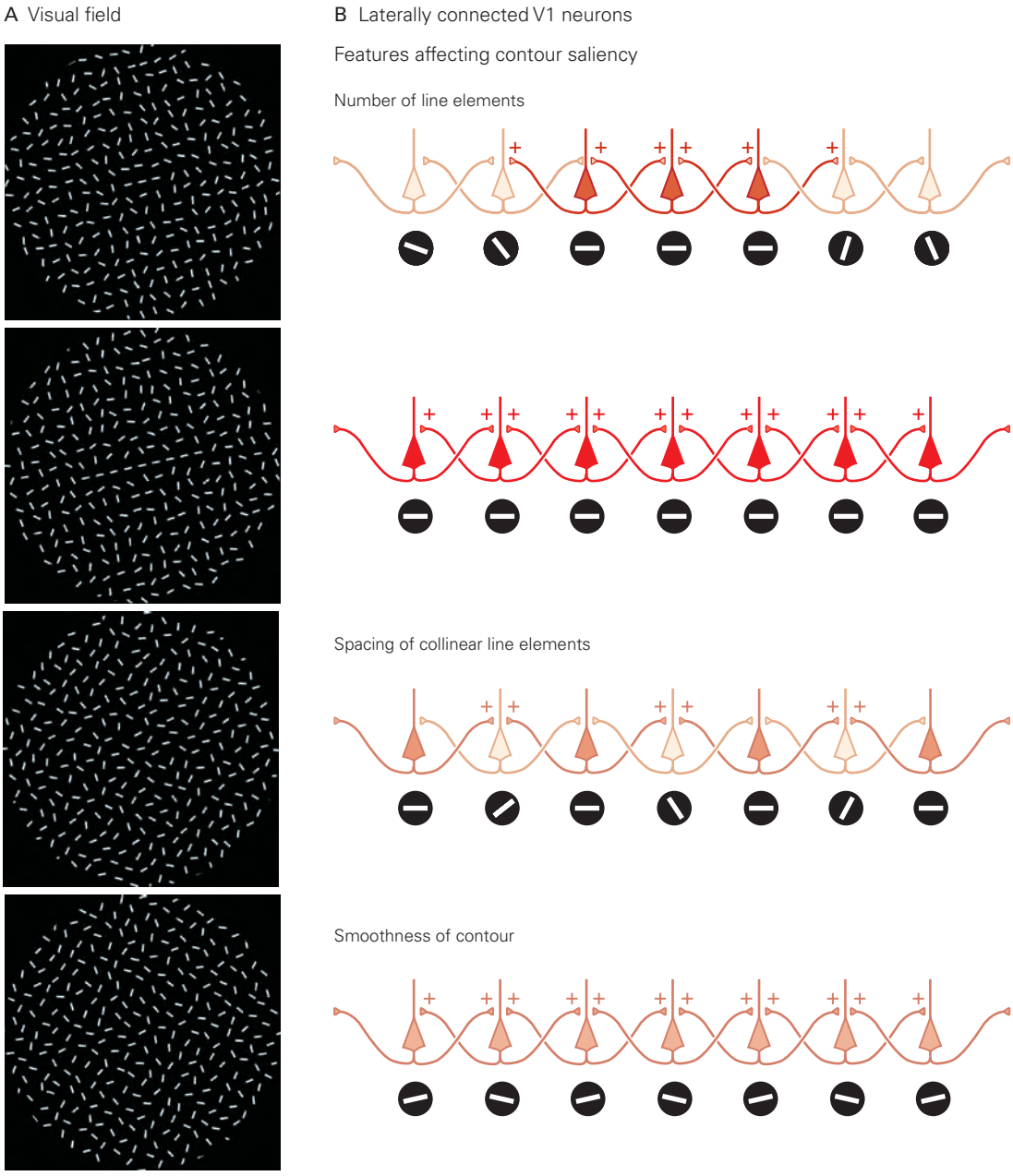

Figure 23–6 Contour integration reflects the perceptual rules of proximity and good continuation. (Adapted, with permission, from Li and Gilbert 2002.)

A. A straight line composed of one or more contour elements with the same oblique orientation appears in the center of each of the four images here. In some images, the line pops out more or less immediately, without searching. Factors that contribute to contour saliency include the number of contour elements (compare the first and second frames), the spacing of the elements (third frame), and the smoothness of the contour (bottom frame). When the spacing between elements is too large or the orientation difference between them too great, one must search the image to find the contour.

B. These perceptual properties are reflected in the horizontal connections between columns of V1 neurons with similar orientation selectivity. As long as the visual elements are spaced sufficiently close together, excitation can propagate from cell to cell, thus facilitating the responses of V1 neurons. Each neuron in the network then augments the responses of neurons on either side, and the facilitated responses propagate across the network.

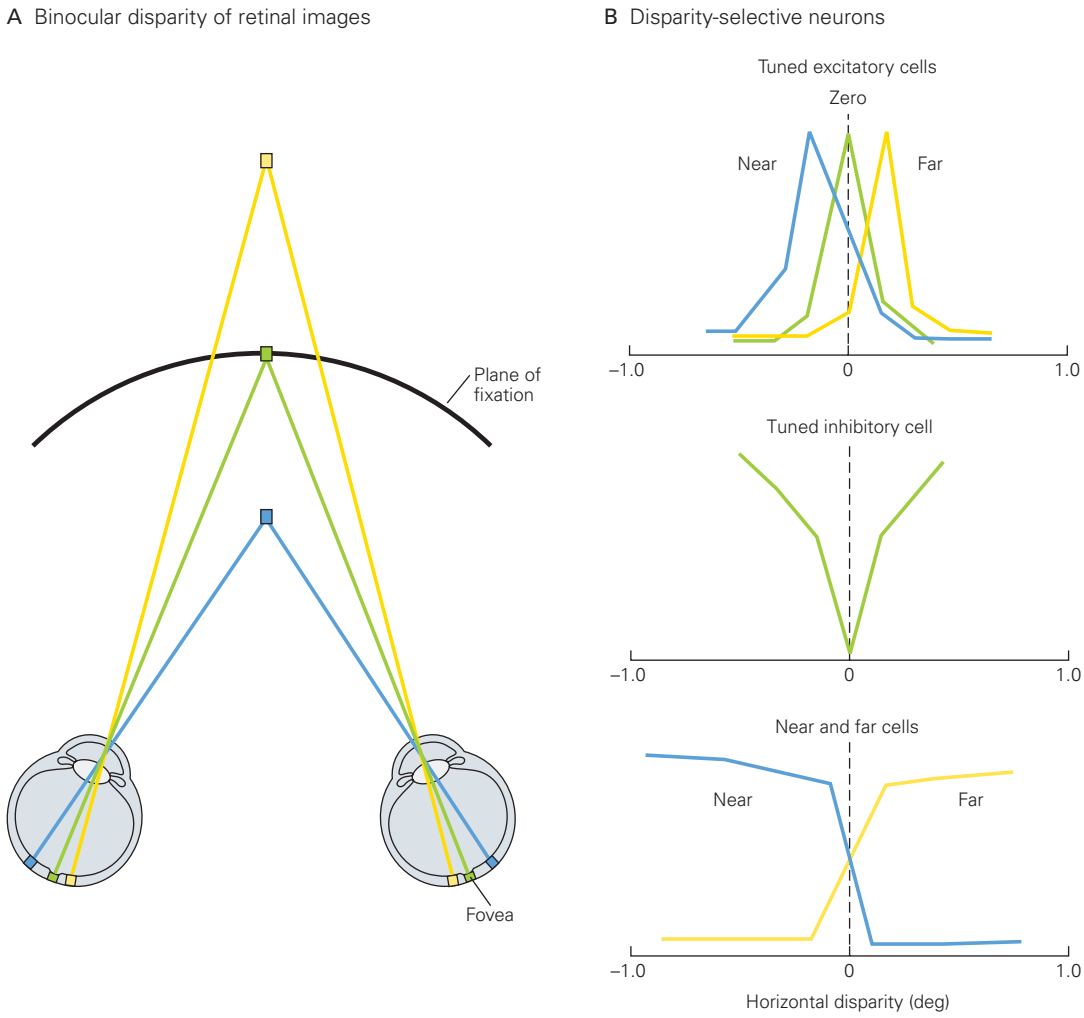

Figure 23–7 Stereopsis and binocular disparity.

A. Depth is computed from the positions at which images occur in the two eyes. The image of an object lying in the plane of fixation (**green**) falls on corresponding points on the two retinas. Images of objects lying in front of the plane of fixation (**blue**) or behind it (**yellow**) fall on noncorresponding locations on the two retinas, a phenomenon termed *binocular disparity*.

B. Neurons in many visual cortical areas are selective for particular ranges of disparity. Each plot shows the responses of a neuron to binocular stimuli with different disparities (abscissa). Some neurons are tuned to a narrow range of disparities and thus have particular disparity preferences (tuned excitatory or tuned inhibitory neurons), whereas others are tuned broadly for objects in front of the fixation plane (near cells) or beyond the plane (far cells). (Adapted, with permission, from Poggio 1995. Copyright © 1995 Oxford University Press.)

determine depth, a phenomenon known as disparity capture.

Random-dot stereograms provide a dramatic demonstration of the global scope of disparity analysis. The visual information presented to each eye appears to be incoherent, but when the stereogram is viewed binocularly, the disparity between the random array of dots in the two images allows an embedded shape to become visible (Figure 23–8C). The calculation underlying this percept is not simple, but requires determining which features shown to the left eye correspond to features seen by the right eye and propagating local disparity information across the image.

Neurons in area V2 display sensitivity to global disparity cues. Distant depth cues can be used to link contour elements that belong to an object, and to separate them from the object background (Figure 23-B).

In addition to binocular disparity, the visual system also uses many monocular cues to discriminate depth. Depth determination through monocular

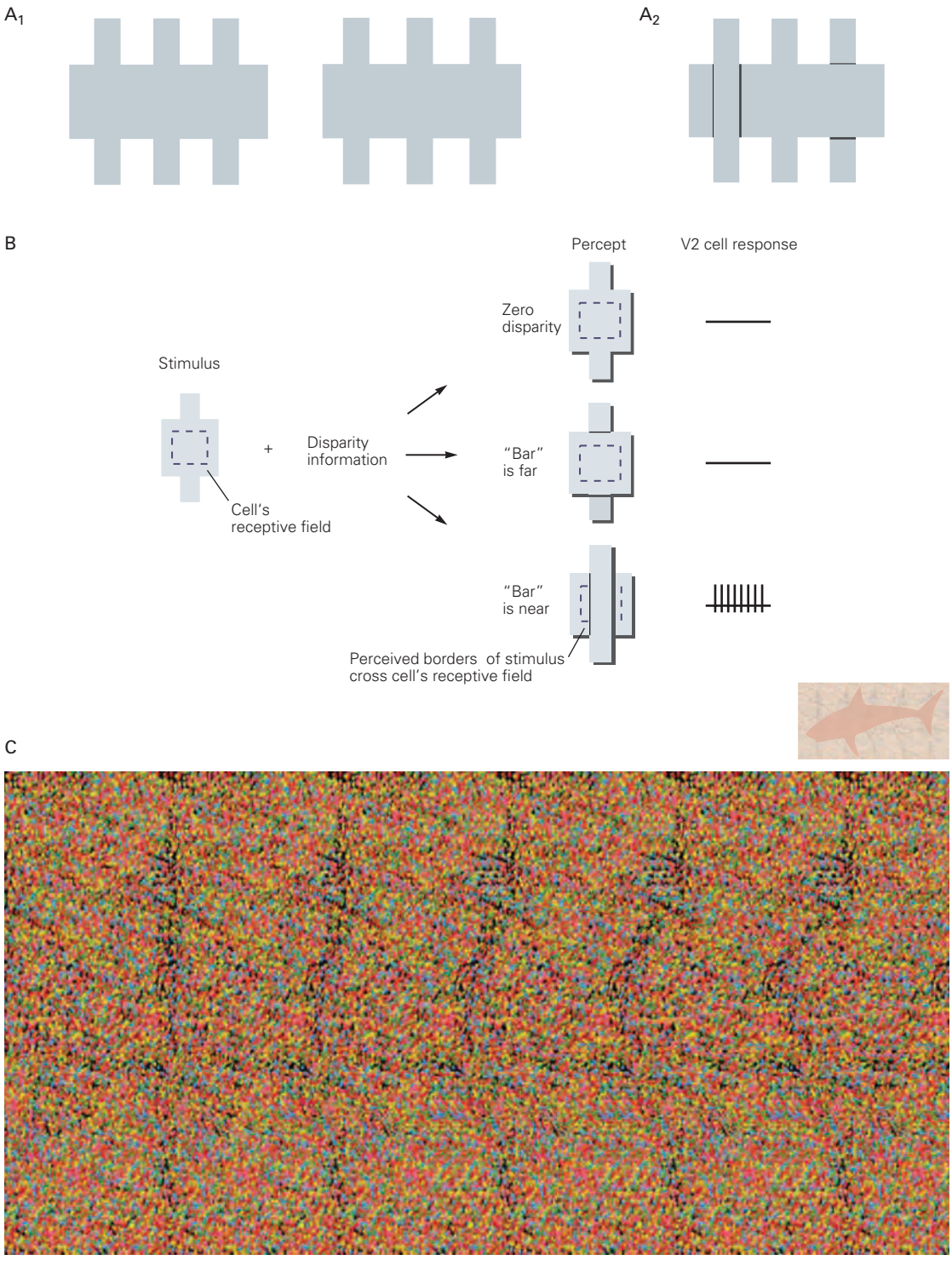

Figure 23–8 Global analysis of binocular disparity.

A. 1. Depth cues contribute to surface segmentation. If you view one of the images of three gray vertical bars crossing a gray horizontal rectangle, you see a uniform gray area within the rectangle. 2. However, if you fuse the two rectangles with diverged eyes, the three vertical bars fall on the two retinas with near, zero, and far disparity. Seen this way, the bar at the left appears to hover in front of the rectangle with an illusory vertical edge crossing the rectangle, whereas the bar at the right appears to lie behind the edges of the horizontal rectangle.

B. A neuron in area V2 responds to illusory edges formed by binocular disparity cues. When the cell's receptive field is centered in the gray square, the cell does not respond to a vertical bar that has far disparity or the same disparity as the square. When the vertical bar has near disparity, the cell responds as the illusory vertical edge crosses its receptive field. (Reproduced, with permission, from Bakin, Nakayama, and Gilbert 2000. Copyright © 2000 Society for Neuroscience.)

C. A random-dot stereogram is seen as a random array of colored dots until you diverge or converge your eyes to bring the adjacent dark vertical stripes into register, producing a three-dimensional image of a shark that emerges from the background. This effect stems from systematic disparity for selected sets of dots. (© Fred Hsu/ Wikimedia Commons/CC-BY-SA-3.0.)

cues, such as size, perspective, occlusion, brightness, and movement, is not difficult. Another cue that originates outside the visual system is vergence, the angle between the optical axes of the two eyes for objects at varying distances. Yet another binocular cue, known as DaVinci stereopsis, is the presence of features visible to one eye but occluded in the other eye's view.

Neurons in areas V1 and V2 also signal foreground–background relationships. A cell with its receptive field in the center of a pattern within a larger surface may respond even when the boundary of that surface is distant from the receptive field. This response helps differentiate the object from its background. In making sense of an image, the brain must identify which edge belongs to which object and differentiate the edge of each object from the background. Some cells in area V2 have the property of "border ownership," firing only when a figure but not the background is to one side of the edge, even when the local edge information is identical in both instances (Figure 23–9).

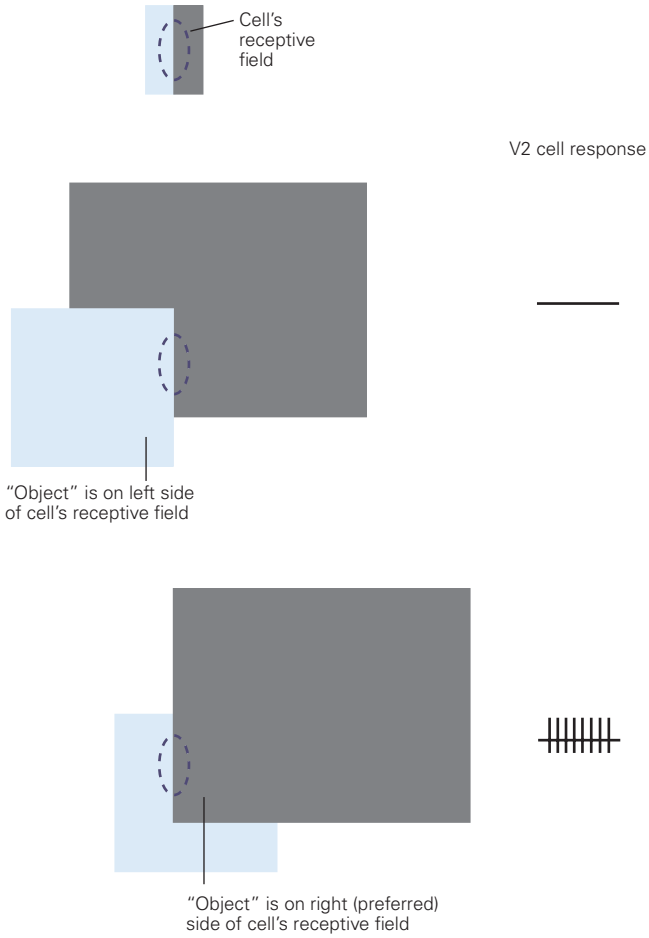

Figure 23–9 Border ownership. Cells in area V2 are sensitive to the boundaries of whole objects. Even though the local contrast is the same for the two rectangles within a cell's receptive field, the cell responds only when the boundary is part of the full rectangle that lies on the preferred side of the receptive field. (Adapted, with permission, from Zhou, Friedman, and von der Heydt 2000. Copyright © 2000 Society for Neuroscience.)

Local Movement Cues Define Object Trajectory and Shape

The primary visual cortex determines the direction of movement of objects. Directional selectivity in neurons likely involves sequential activation of regions on different sides of the receptive field.

If an object moving at an appropriate velocity first encounters a region of a neuron's receptive field with long response latencies and then passes into regions with progressively shorter latencies, signals from throughout the receptive field will arrive at the cell simultaneously and the neuron will fire vigorously. If the object moves in the opposite direction, signals from the different regions will not summate and the cell may never reach the threshold for firing (Figure 23–10).

Early in the visual pathways, analysis of the movement of an object is limited by the size of the receptive fields of the sensory neurons. Even in the initial cortical areas V1 and V2, the receptive fields of neurons are small and might encompass only a fraction of an object. Eventually, however, information about the direction and speed of movement of discrete aspects of an object must be integrated into a computation of the movement of a whole object. This problem is more difficult than one might expect.

If one observes a complex shape moving through a small aperture, the part of the object's boundary within the aperture appears to move in a direction perpendicular to the boundary's orientation (Figure 23–11A). One cannot detect a line's true direction of movement if the line's ends are not visible. The image of a line appears the same if it is moving slowly along an axis perpendicular to its orientation or more quickly along an oblique axis. This is the quandary presented by the receptive field of a V1 neuron. The visual system's solution is to assume that the movement of a contour is perpendicular to its orientation. Thus, an object is first presented to the visual system in countless small pieces with boundaries of different orientations, all of which appear to be moving in

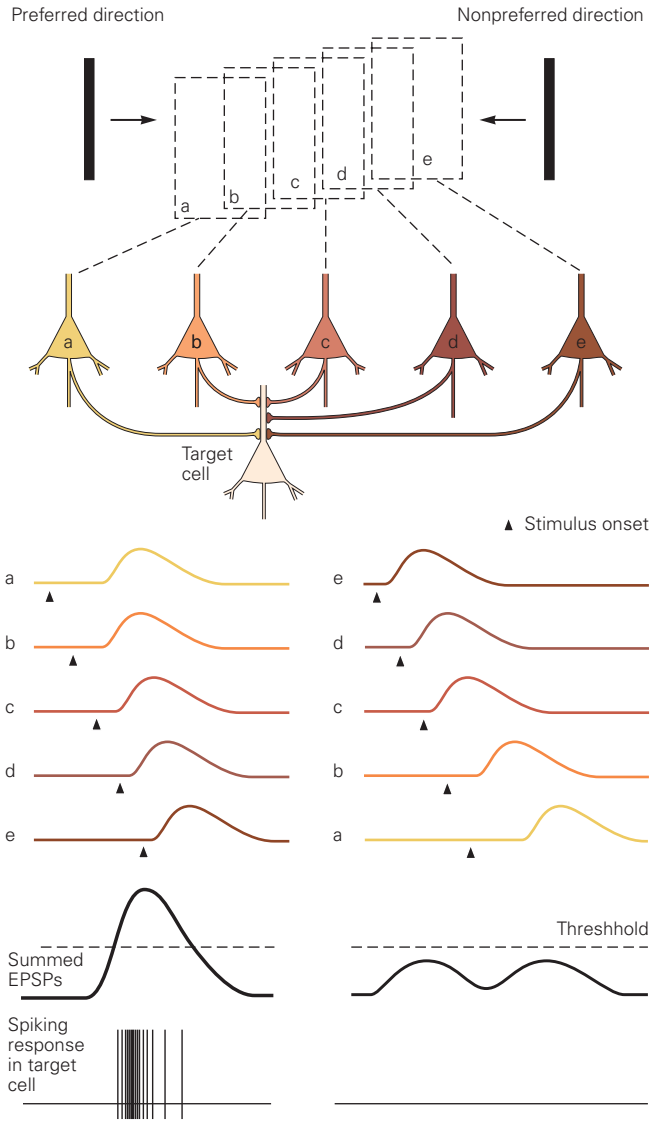

Figure 23–10 Directional selectivity of movement. A neuron's selectivity for direction of movement depends on the response latencies of presynaptic neurons relative to the onset of a stimulus. The response latencies of presynaptic neurons *a* and *b* are somewhat longer than those of neurons *d* and *e*. When a stimulus moves from left to right, neurons *a* and then *b* are activated first, but because their response latencies are longer, their inputs arrive at the target neuron superimposed with the inputs from neurons *d* and *e*, and the summated inputs cause the neuron to fire. In contrast, stimuli moving leftward produce signals that arrive in the target neuron at different times and therefore do not reach the cell's threshold for firing. (Abbreviation: **EPSP**, excitatory postsynaptic potential.) (Adapted, with permission, from Priebe and Ferster 2008. Copyright © 2008 Elsevier.)

different directions and at different velocities (Figure 23–11A).

Determining the direction of motion of an object requires resolving multiple cues. This can be demonstrated readily by placing one grating on top of another and moving the two in different directions. The resulting checkerboard pattern appears to move in an intermediate direction between the trajectories of the individual gratings (Figure 23–11B). This percept depends on the relative contrast of the gratings and the area of grating overlap. With large relative contrasts, the gratings appear to slide across each other, moving in their individual directions rather than together in a common direction.

An important determinant of perceived direction is scene segmentation, the separation of moving elements into foreground and background. In a scene with moving objects, segmentation is not based on local cues of direction; instead, perception of direction depends on scene segmentation. The barber-pole illusion provides another example of the predominance of global relationships over the perception of simple attributes. The rotating stripes are perceived as moving vertically along the long axis of the pole (Figure 23–11C). The perception of motion in the visual field uses a complex algorithm that integrates the bottom-up analysis of local motion signals with top-down scene segmentation.

Integration of local motion signals in monkeys has been observed in the middle temporal area (area MT or V5), an area specializing in motion. The neurons in this area are selective for a particular direction of movement of an overall pattern, rather than individual components of the pattern. This dependency on the overall pattern is also seen in the correspondence of their responses with the perceived direction in the barber-pole effect.

Context Determines the Perception of Visual Stimuli

Brightness and Color Perception Depend on Context

The visual system measures the surface characteristics of objects by comparing the light arriving from different parts of the visual field. As a result, the perception of brightness and color is highly dependent on context. In fact, perceived brightness and color can be quite different from what is expected from the physical properties of an object. At the same time, perceptual constancies make objects appear similar even when the brightness and wavelength distribution of the light

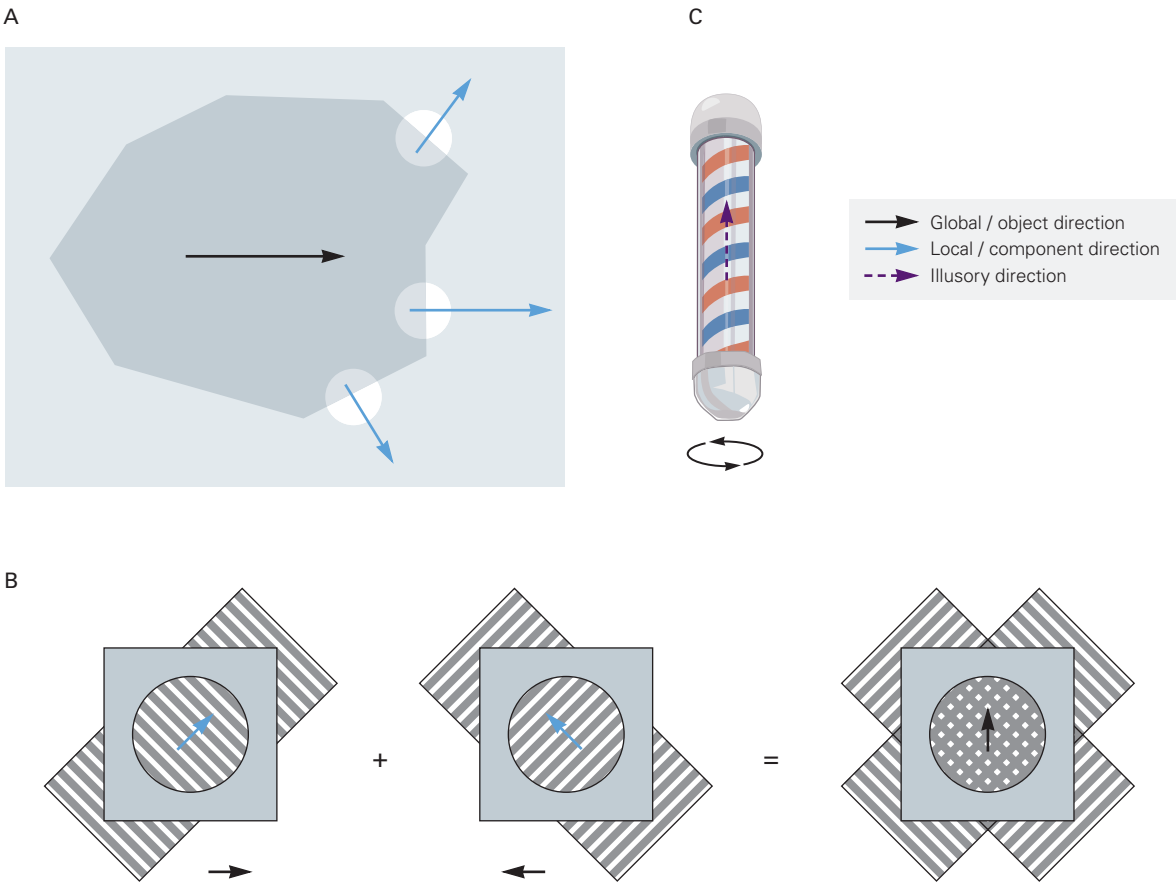

Figure 23–11 The aperture problem and barber-pole illusion.

A. Although an object moves in one direction, each component edge when viewed through a small aperture appears to move in a direction perpendicular to its orientation. The visual system must integrate such local motion signals into a unified percept of a moving object.

B. Gratings are used to test whether a neuron is sensitive to local or global motion signals. When the gratings are superimposed and moved independently in different directions, one does not see the two gratings sliding past each other but rather a plaid pattern moving in a single, intermediate direction. Neurons in the middle temporal area of monkeys are responsive to such global motion rather than to local motion.

C. Motion perception is influenced by scene segmentation cues, as seen in the barber-pole illusion. Even though the pole rotates around its axis, one perceives the stripes as moving vertically, due to the global vertical rectangle surround of the barber pole enclosure.

that illuminates them changes from natural to artificial light, from sunlight to shadow, or from dawn to midday (Figure 23–12A).

As we move about or as the ambient illumination changes, the retinal image of an object—its size, shape, and brightness—also changes. Yet under most conditions, we do not perceive the object itself to be changing. As we move from a brightly lit garden into a dimly lit room, the intensity of light reaching the retina may vary a thousandfold. Both in the room's dim illumination and in the sun's glare, we nevertheless see a white shirt as white and a red tie as red. Likewise, as a friend walks toward you, she is seen as coming closer; you do not perceive her to be growing larger even though the image on your retina does expand. Our ability to perceive an object's size and color as constant illustrates again a fundamental principle of the visual system: It does not record images passively, like a camera, but instead uses transient and variable stimulation of the retina to construct representations of a stable, three-dimensional world.

Another example of contextual influence is color induction, whereby the appearance of a color in one region shifts toward that in an adjoining region. Shape also plays an important role in the perception of surface brightness. Because the visual system assumes that illumination comes from above, gray patches on a folded surface appear very different when they lie on

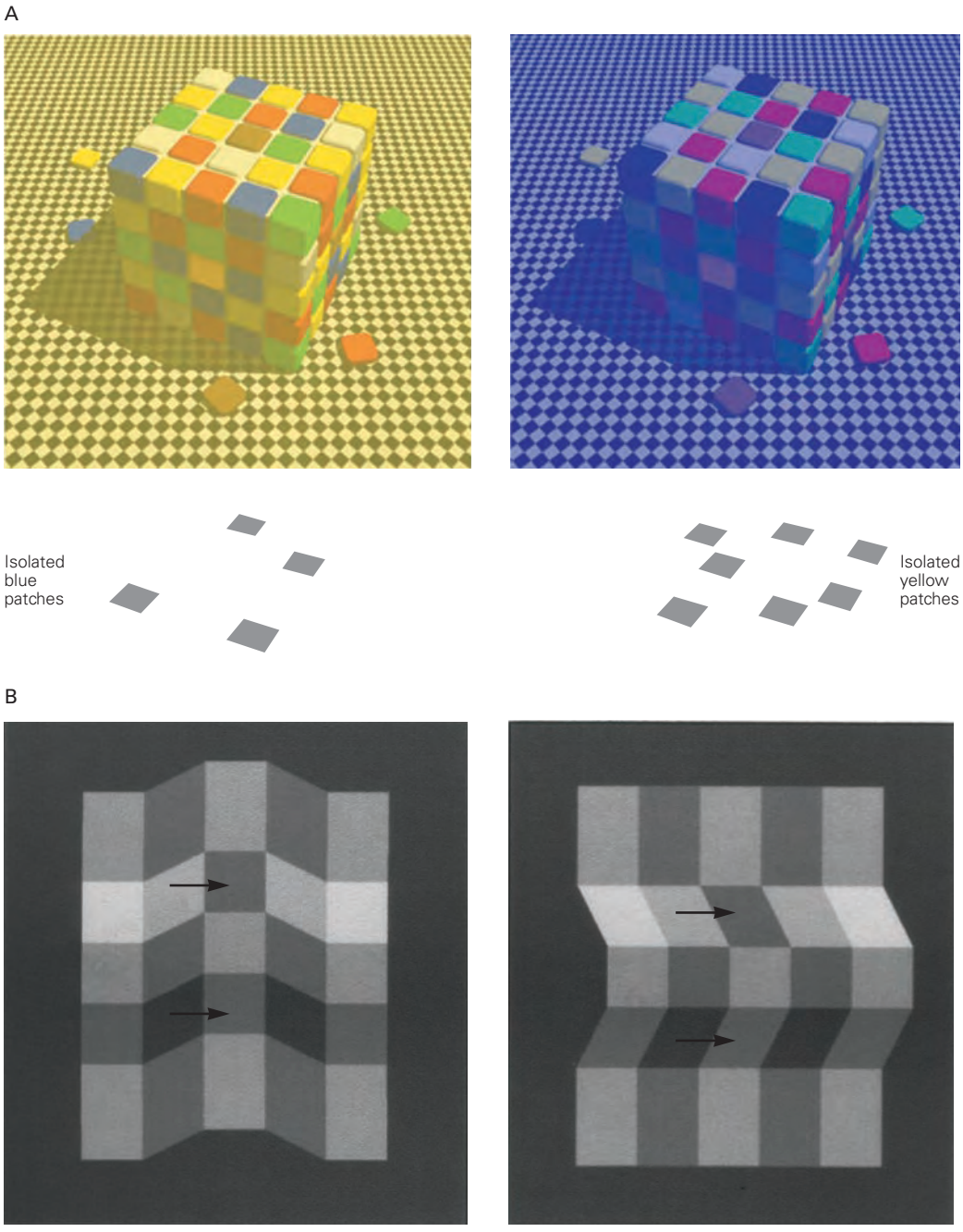

Figure 23–12 Color and brightness perception depend on contextual cues.

A. Perceived surface colors remain relatively stable under different illumination conditions and the consequent changes in wavelength of the light reflected from the surface. The **yellow squares** on the left and right cubes appear similar despite the fact that the wavelengths of light coming from the two sets of surfaces are very different. In fact, if the **blue squares** on the top of the left cube and the **yellow squares** on the top of the right cube are isolated from their contextual squares, their colors appear identical. (Reproduced, with permission, from www.lottolab.org.)

B. Brightness perception is also influenced by three-dimensional shape. The four gray squares indicated by **arrows** all have the same luminance. The apparent brightnesses are similar in the left illustration but different in the right illustration. This is because the visual system has an inherent expectation that illumination comes from above (the position of the sun relative to us), and thus the perception that the surface below the fold in the illustration on the right is brighter than the surface of the same luminance that lies above. (Reproduced, with permission, from Adelson 1993. Copyright © 1993 AAAS.)

the top or bottom of the surface, even when they are in fact the same shade of gray (Figure 23–12B).

The responses of some neurons in the visual cortex correlate with perceived brightness. Most visual neurons respond to surface boundaries; the center-surround structure of the receptive fields of retinal ganglion cells and geniculate neurons is suited to capturing boundaries. Most such cells do not respond to the interior parts of surfaces, for uniform interiors produce no contrast gradients across receptive fields. However, a small percentage of neurons do respond to the interiors of surfaces, signaling local brightness, texture, or color, and the responses of these neurons are influenced by context. The cell's response changes as the brightness of surfaces *outside* a cell's receptive field change, even when the brightness of the surface within the receptive field remains fixed.

Because most neurons respond to surface boundaries and not to areas of uniform brightness, the visual system calculates the brightness of surfaces from information about contrast at the edges of surfaces. The brain's analysis of surface qualities from boundary information is known as perceptual fill-in. If one fixates the boundary between a dark disk and a surrounding bright area for a few seconds, the disk will "fill in" with the same brightness as the surrounding area. This occurs because the cells that respond to edges fire only when the eye or stimulus moves. They gradually cease to respond to a stabilized image and no longer signal the presence of the boundary. Neurons with receptive fields within the disk gradually begin to respond in a fashion similar to those with receptive fields in the surrounding area, demonstrating short-term plasticity in their receptive-field properties.

An object's color always appears more or less the same despite the fact that under different conditions of illumination the wavelength distribution of light reflected from the object varies widely. To identify an object, we must know the properties of its surface rather than those of the reflected light, which are constantly changing. Computation of an object's color is therefore more complex than analyzing the spectrum of reflected light. To determine a surface's color, the wavelength distribution of the incident light must be determined. In the absence of that information, surface color can be estimated by determining the balance of wavelengths coming from different surfaces in a scene. Some neurons in V4 respond similarly to different illumination wavelengths if the perceived color remains constant. By being responsive to the light across an extensive surface, these neurons are selective for surface color rather than wavelength.

Receptive-Field Properties Depend on Context

The distinction between local and global effects—between stimuli that occur within a receptive field and those beyond—poses the problem of how the receptive field itself is defined. Because the original characterization of the receptive fields of visual cortex neurons did not take into account contextual influences, some investigators now distinguish between "classical" and "nonclassical" receptive fields.

However, even the earliest description of the sensory receptive field allowed for the possibility of influences from portions of the sensory surface outside the narrowly defined receptive field. In 1953, Steven Kuffler, in his pioneering observations on the receptive-field properties of retinal ganglion cells, noted that "not only the areas from which responses can actually be set up by retinal illumination may be included in a definition of the receptive field but also all areas which show a functional connection, by an inhibitory or excitatory effect on a ganglion cell. This may well involve areas which are somewhat remote from a ganglion cell and by themselves do not set up discharges."

A more useful distinction contrasts the response of a neuron to a simple stimulus, such as a short line segment, with its response to a stimulus with multiple components. Even in the primary visual cortex, neurons are highly nonlinear; their response to a complex stimulus cannot be predicted from their responses to a simple stimulus placed in different positions around the visual field. Their responses to local features are instead dependent on the global context within which the features are embedded. Contextual influences are pervasive in intermediate-level visual processing, including contour integration, scene segmentation, and the determination of object shape, object motion and surface properties.

Cortical Connections, Functional Architecture, and Perception Are Intimately Related

Intermediate-level visual processing requires sharing of information from throughout the visual field. The relationship of interconnections within the primary visual cortex to the functional architecture of this area suggests that this circuitry mediates contour integration.

Cortical circuits include a plexus of long-range horizontal connections formed by the axons of pyramidal neurons running parallel to the cortical surface. Horizontal connections exist in every area of the cerebral cortex, but their function varies from one area to

the next depending on the functional architecture of each area. In the visual cortex, these connections mediate interactions between orientation columns of similar specificity, thus integrating information over a large area of visual cortex that represents a great expanse of the visual field (see Figure 21–16).

The fact that these horizontal connections link neurons similar in function but representing distant locations in the visual field suggests that these connections have a role in contour integration. Contour integration and the related property of contour saliency reflect the Gestalt principle of good continuation. Both are mediated by the horizontal connections in V1 (see Figure 23–6).

A final feature of cortical connectivity important for visuospatial integration is feedback projections from higher-order cortical areas. Feedback connections are as extensive as the feedforward connections that originate in the thalamus or at earlier stages of cortical processing. Little is known about the function of these feedback projections. They likely play a role in mediating the top-down influences of attention, expectation, and perceptual task, all of which are known to affect early stages in cortical processing.

Perceptual Learning Requires Plasticity in Cortical Connections

The synaptic connections in ocular-dominance columns are adaptable to experience only during a critical period in development (Chapter 49). This suggests that the functional properties of visual cortex neurons are fixed in adulthood. Nevertheless, many properties of cortical neurons remain mutable throughout life. For example, changes in the visual cortex can occur following retinal lesions.

When focal lesions occur in corresponding positions on the two retinas, the corresponding part of the cortical map, referred to as the lesion projection zone, is initially deprived of visual input. Over a period of several months, however, the receptive fields of cells within this region shift from the lesioned part of the retina to the functioning area surrounding the lesion. As a result, the cortical representation of the lesioned part of the retina shrinks while that of the surrounding region expands (Figure 23–13).

The plasticity of cortical maps and connections did not evolve as a response to lesions but as a neural mechanism for improving our perceptual skills. Many of the attributes analyzed by the visual cortex, including stereoscopic acuity, direction of movement, and orientation, become sharper with practice. Hermann von Helmholtz stated in 1866 that "the judgment of the senses may be modified by experience and by training derived under various circumstances, and may be adapted to the new conditions. Thus, persons may learn in some measure to utilize details of the sensation which otherwise would escape notice and not contribute to obtaining any idea of the object." This perceptual learning is a variety of implicit learning that does not involve conscious processes (Chapter 52).

Perceptual learning involves repeating a discrimination task many times and does not require error feedback to improve performance. Improvement manifests itself, for example, as a decrease in the threshold for discriminating small differences in the attributes of a target stimulus or in the ability to detect a target in a complex environment. Several areas of visual cortex, including the primary visual cortex, participate in perceptual learning.

An important aspect of perceptual learning is its specificity: Training on one task does not transfer to other tasks. For example, in a three-line bisection task, the subject must determine whether the centermost of three parallel lines is closer to the line on the left or the one on the right. The amount of offset from the central position required for accurate responses decreases substantially after repeated practice.

Learning of this task is specific to the location in the visual field and to the orientation of the lines. This specificity suggests that early stages of visual processing are responsible, for in the early stages, receptive fields are smallest, visuotopic maps are most precise, and orientation tuning is sharpest. The learning is also specific for the stimulus configuration. Training on three-line bisection does not transfer to a vernier discrimination task in which the context is a line that is collinear with the target line (Figure 23–14A).

The response properties of neurons in the primary visual cortex change during the course of perceptual learning in a way that tracks the perceptual improvement. An example of this is seen in contour saliency. With practice, subjects can more easily detect contours embedded in complex backgrounds. Detection improves with contour length, as do the responses of neurons in V1. With practice, subjects improve their ability to detect shorter contours and V1 neurons become correspondingly more sensitive to shorter contours (Figure 23–14B).

Visual Search Relies on the Cortical Representation of Visual Attributes and Shapes

The detectability of features such as color, orientation, and shape is related to the process of visual search. In a complex image, certain objects stand out or "pop out"

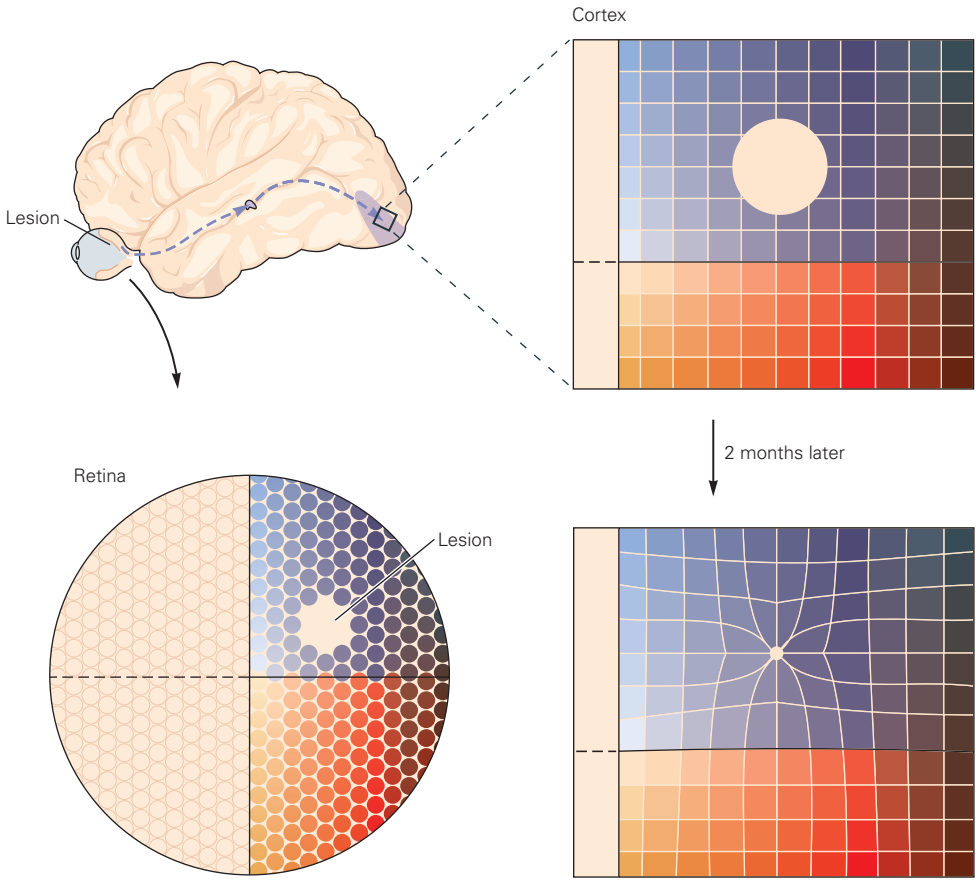

Figure 23–13 Adult cortical plasticity. When corresponding positions in both eyes are lesioned, the cortical area receiving input from the lesioned areas—the lesion projection zone—is initially silenced. The receptive fields of neurons in the lesion projection zone eventually shift from the area of the lesion to the surrounding, intact retina. This occurs because neurons surrounding the lesion projection zone sprout collaterals that form synaptic connections with neurons inside the zone. As a result, the cortical representation of the lesioned part of the retina shrinks while that of the surrounding retina expands.

because the visual system processes simultaneously, in parallel pathways, the features of the target and the surrounding distractors (Figure 23–15). When the features of a target are complex, the target can be identified only through careful inspection of an entire image or scene.

The pop-out phenomenon can be influenced by training. A stimulus that initially cannot be found without effortful searching will pop out after training. The neuronal correlate of such a dramatic change is not certain. Parallel processing of the features of an object and its background is possible because feature information is encoded in retinotopically mapped areas at multiple locations in the visual cortex. Pop-out probably occurs early in the visual cortex. The pop-out of complex shapes such as numerals supports the idea that early in visual processing neurons can represent, and be selective for, shapes more complex than line segments with a particular orientation.

Cognitive Processes Influence Visual Perception

Scene segmentation—the parsing of a scene into different objects—involves a combination of bottom-up processes that follow the Gestalt rule of good continuation and top-down processes that create object expectation.

One strong top-down influence is spatial attention, which can change focus without any movement of an observer's eyes. Spatial attention can be object-oriented in that the focus of attention is distributed over the area occupied by the attended object, allowing the visual cortex to analyze the shape and attributes of objects one at a time.

Attentional mechanisms can solve the superposition problem. Before we can recognize an object in a scene that includes many objects, we must determine which features correspond to which objects. Our sense that we identify all objects in the visual field simultaneously is illusory. Instead, we serially process objects in rapid succession by

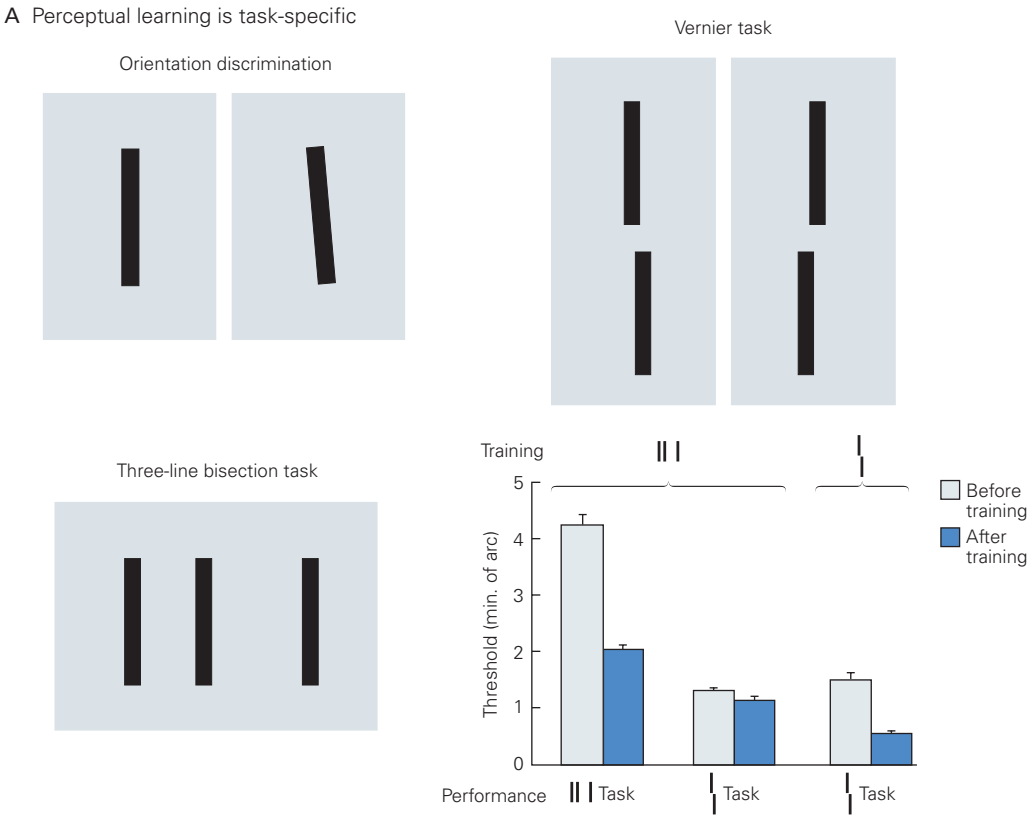

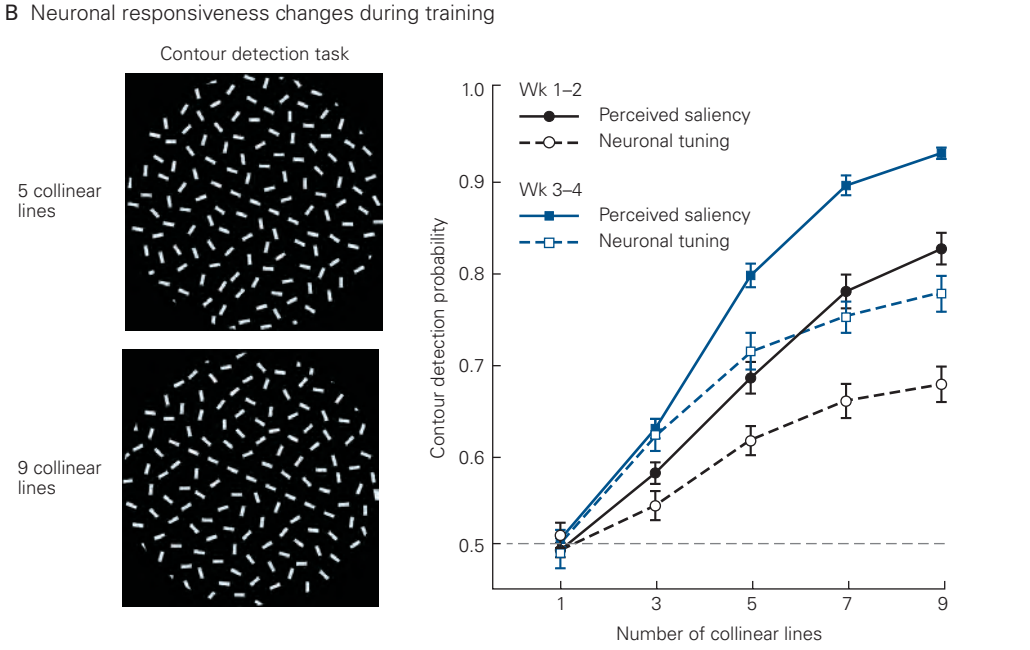

Figure 23–14 **Perceptual learning.** Perceptual learning is a form of implicit learning. With practice, one can learn to discriminate smaller differences in orientation, position, depth, and direction of movement of objects.

A. The improvement is seen as a reduction in the amount of change required to reliably detect a tilted line or one positioned to the left or right of a nearly collinear line (vernier task). Perceptual learning is highly specific, so that training on a three-line bisection task leads to substantial improvement in that task (*left pair of bars* in the bar graph) without affecting performance on the vernier discrimination task (*central pair of bars*). However, training specifically on vernier discrimination does enhance performance on that task (*right pair of bars*).

B. Subjects can detect collinear line segments embedded in a random background more easily as the number of collinear segments is increased. The responses of neurons in V1 grow correspondingly stronger with the increase in the number of line segments. After practice, a line with fewer segments stands out more easily, and with this improvement, the responses in V1 also increase. (Reproduced, with permission, from Crist, Li, and Gilbert 2001; Li, Piech, and Gilbert 2008.)

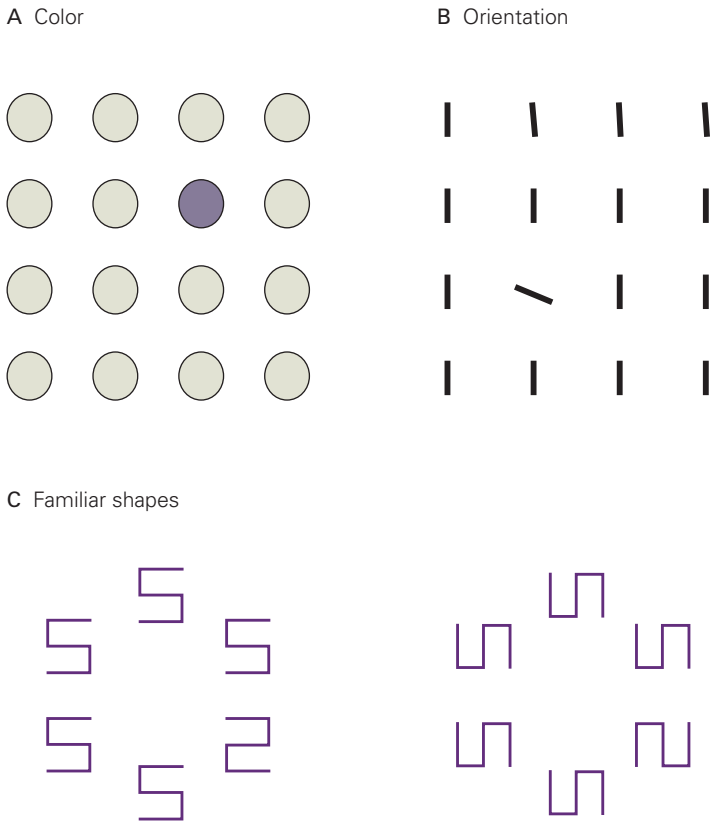

Figure 23–15 One object in a complex image stands out under certain conditions.

A. A differently colored object pops out.

B. A differently oriented line also pops out.

C. More complex shapes can pop out when they are very familiar, such as the numeral 2 embedded in a field of 5s. Rotating the image by 90° renders the elements of the figure less recognizable, making it more difficult to find the one figure that differs from the rest. (Reproduced, with permission, from Wang, Cavanagh, and Green 1994. Copyright © 1994 Springer Nature.)

shifting attention from one to the next. The results of each analysis build up the perception of a complex environment populated with many distinct objects. A dramatic demonstration of the importance of attention in object recognition is *change blindness.* If a subject rapidly shifts between two slightly different views of the same scene, he will not be able to detect the absence of an important component of the scene in one view without considerable scrutiny (see Figure 25–8).

Another top-down influence is perceptual task. At early stages in visual processing, the properties of the same neuron vary with the type of visual discrimination being performed. Object identification involves a process of hypothesis testing in which information arriving from the retina is compared with internal representations of objects. This process is reflected in studies that have shown that early stages in processing, such as the primary visual cortex, are activated when scenes are imagined without visual input.

Highlights

1. Vision requires segregating objects from their backgrounds, a process involving contour integration and surface segmentation.
2. This process is simplified by relying on the statistical properties of natural forms. As recognized by the Gestalt psychologists early in the 20th century, we naturally link scene components based on grouping rules of similarity, proximity, and contour smoothness (referred to as "good continuation").
3. Neurons in visual cortical areas have properties consonant with Gestalt grouping rules. They perform a local and global analysis of scene properties in parallel. The local properties are the visual primitives, which include orientation selectivity, direction selectivity, contrast sensitivity, disparity selectivity, and color selectivity. The corresponding global properties include contour integration, object movement, border ownership, disparity capture, and color constancy.
4. Perception of visual features is dependent on context; similarly, neuronal responses are context dependent. The principle underlying these interactions is the association field, a pattern of interactions between bits of information that are mapped across each cortical area. The association field mediates contour integration in visual cortex but is likely to be a general feature of processing throughout the cerebral cortex. The anatomical

substrate for the association field includes a network of long-range horizontal connections formed by the axons of cortical pyramidal cells, which extend for long distances parallel to the cortical surface.

5. Different visual cortical areas contribute to the various global properties, and interactions between areas, including top-down influences, are required for their development. Though there has been considerable emphasis on selectivity for increasing stimulus complexity as one ascends a hierarchy of cortical areas through feedforward connections extending from the primary visual cortex to areas in the temporal (ventral pathway) and parietal (dorsal pathway) cortex, feedback connections are of equal importance.
6. Future studies will elucidate the relative contributions of intrinsic, feedforward, and feedback cortical connections, and the interactions between them, in cortical processing. Evidence is emerging that rather than having fixed functions, neurons are adaptive processors, taking on different functional roles under different behavioral contexts. Neurons may mediate this functional diversity by input selection, expressing task-relevant inputs and suppressing task-irrelevant inputs. When operating abnormally, these functional and connectivity dynamics may account for perceptual and behavioral phenomena associated with disorders such as autism and schizophrenia.

Charles D. Gilbert

Selected Reading

Albright TD, Stoner GR. 2002. Contextual influences on visual processing. Annu Rev Neurosci 25:339–379.

Gilbert CD, Sigman M. 2007. Brain states: top-down influences in sensory processing. Neuron 54:677–696.

Gilbert CD, Sigman M, Crist R. 2001. The neural basis of perceptual learning. Neuron 31:681–697.

Li W, Piech V, Gilbert CD. 2004. Perceptual learning and top-down influences in primary visual cortex. Nat Neurosci 7:651–657.

Li W, Piech V, Gilbert CD. 2006. Contour saliency in primary visual cortex. Neuron 50:951–962.

Priebe NJ, Ferster D. 2008. Inhibition, spike threshold, and stimulus selectivity in primary visual cortex. Neuron 57:482–497.

References

Adelson EH. 1993. Perceptual organization and the judgment of brightness. Science 262:2042–2044.

Bakin JS, Nakayama K, Gilbert CD. 2000. Visual responses in monkey areas V1 and V2 to three-dimensional surface configurations. J Neurosci 20:8188–8198.

Crist RE, Li W, Gilbert CD. 2001. Learning to see: experience and attention in primary visual cortex. Nat Neurosci 4:519–525.

Cumming BG, DeAngelis GC. 2001. The physiology of stereopsis. Annu Rev Neurosci 24:203–238.

Ferster D, Miller KD. 2000. Neural mechanisms of orientation selectivity in the visual cortex. Annu Rev Neurosci 23:441–471.

He ZJ, Nakayama K. 1994. Apparent motion determined by surface layout not by disparity or three-dimensional distance. Nature 367:173–175.

Hubel DH, Wiesel TN. 1968. Receptive fields and functional architecture of monkey striate cortex. J Physiol 195:215–243.

Li W, Gilbert CD. 2002. Global contour saliency and local colinear interations. J Neurophysiol 88:2846–2856.

Li W, Piech V, Gilbert CD. 2008. Learning to link visual contours. Neuron 57:442–451.

Movshon JA, Adelson EH, Gizzi MS, Newsome WT. 1985. The analysis of moving visual patterns. In: C Chagas, R Gattass, CG Gross (eds). *Study Group on Pattern Recognition Mechanisms*, pp. 67–86. Vatican City: Pontifica Academia Scientiarum.

Nakayama K. 1996. Binocular visual surface perception. Proc Natl Acad Sci U S A 93:634–639.

Nakayama K, Joseph JS. 2000. Attention, pattern recognition and popout in visual search. In: R Parasuraman (ed). *The Attentive Brain*. Cambridge, MA: MIT Press.

Poggio GE. 1995. Mechanisms of stereopsis in monkey visual cortex. Cereb Cortex 5:193–204.

Purves D, Lotto RB, Nundy S. 2002. Why we see what we do. Am Sci 90:236–243.

Wang Q, Cavanagh P, Green M. 1994. Familiarity and pop-out in visual search. Percept Psychophys 56:495–500.

Zhou H, Friedman HS, von der Heydt R. 2000. Coding of border ownership in monkey visual cortex. J Neurosci 20:6594–6611.

24

High-Level Visual Processing: From Vision to Cognition

As we have seen, low-level visual processing is responsible for detecting various types of contrasts in the patterns of light projected onto the retina. Intermediate-level processing is concerned with the identification of so-called visual primitives, such as contours and fields of motion, and the segregation of surfaces. High-level visual processing integrates information from a variety of sources and is the final stage in the visual pathway leading to visual perception.

High-level visual processing is concerned with identifying behaviorally meaningful features of the environment and thus depends on descending signals that convey information from short-term working memory, long-term memory, and executive areas of cerebral cortex.

High-Level Visual Processing Is Concerned With Object Recognition

Our visual experience of the world is fundamentally object-centered. We can recognize the same object even when the patterns of light it casts onto the retina vary greatly with viewing conditions, such as lighting, angle, position, and distance. And this is the case even for visually complex objects, those that include a large number of conjoined visual features.

Moreover, objects are not mere visual entities, but are commonly associated with specific experiences, other remembered objects, and sensations—such as the hum of the coffee grinder or the aroma of a lover's perfume—and a variety of emotions. It is the behavioral significance of objects that guides our action based on visual information. In short, object recognition establishes a nexus between vision and cognition (Figure 24–1).

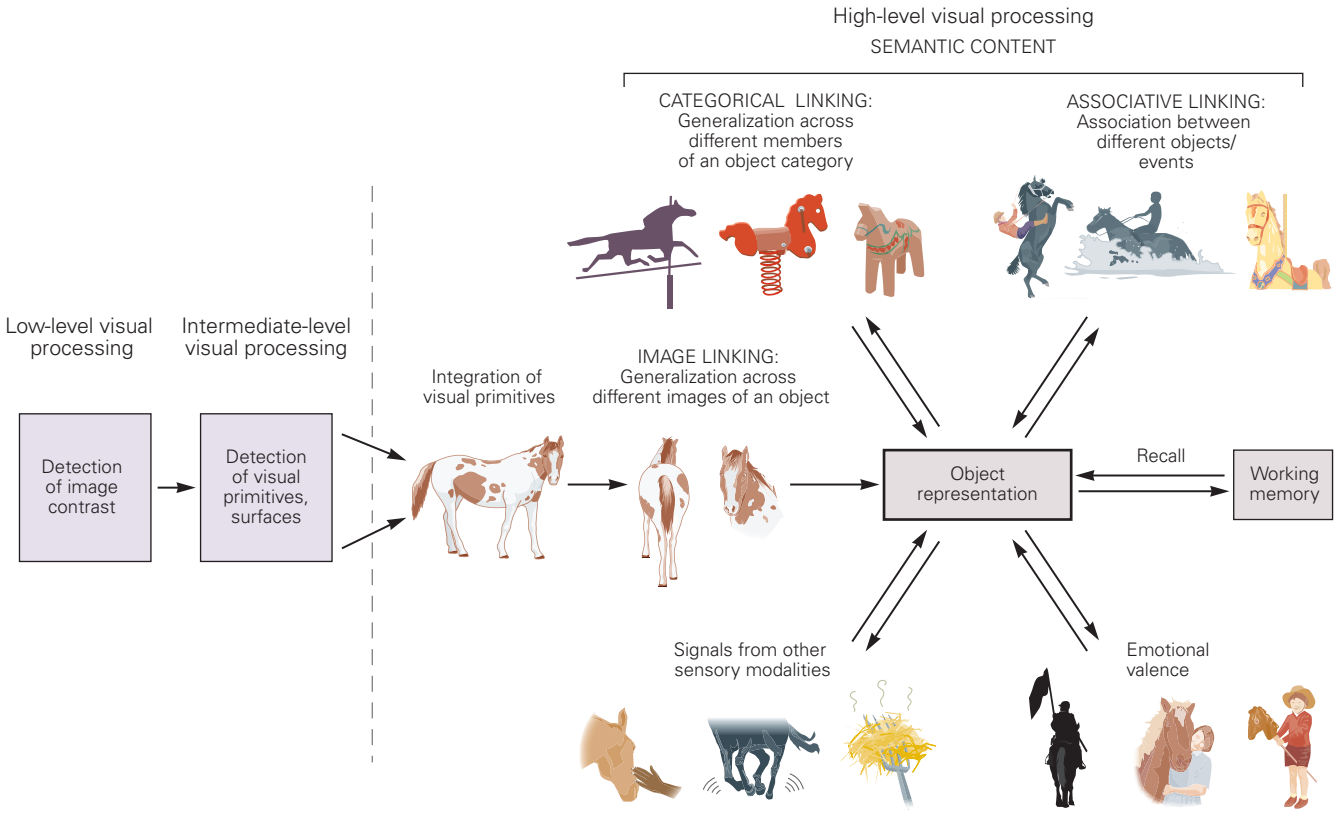

Figure 24–1 Representation of entire objects is central to high-level visual processing. Representation of entire objects involves integration of visual features extracted at earlier stages in the visual pathways. This integration is a generalization of the numerous retinal images generated by the same object and of different members of an object category. The representation also incorporates information from other sensory modalities, attaches emotional valence, and associates the object with the memory of other objects or events. Object representations can be stored in working memory and recalled in association with other memories.

The Inferior Temporal Cortex Is the Primary Center for Object Recognition

Primate studies implicate neocortical regions of the temporal lobe, principally the inferior temporal cortex, in object perception. Because the hierarchy of synaptic relays in the cortical visual system extends from the primary visual cortex to the temporal lobe, the temporal lobe is a site of convergence of many types of visual information.

Neuropsychological studies have found that damage to the inferior temporal cortex can produce specific failures of object recognition. Neurophysiological and functional imaging studies have, in turn, yielded remarkable insights into the ways in which the activity of inferior temporal neurons represents objects, how these representations relate to perceptual and cognitive events, and how they are modified by experience.

Visual signals originating in the retina are processed in the lateral geniculate nucleus of the thalamus before reaching the primary visual cortex (V1). Ascending visual pathways from V1 follow two main parallel and hierarchically organized streams: the ventral and dorsal streams (Chapter 21). The ventral stream extends ventrally and anteriorly from V1 through V2, via V4, into inferior temporal cortex, which, in macaque monkeys, comprises the lower bank of the superior temporal sulcus and the ventrolateral convexity of the temporal lobe (Figure 24–2). Neurons at each synaptic relay in this ventral stream receive convergent input from the preceding stage. At the top of the hierarchy, inferior temporal neurons are in a position to integrate a large and diverse quantity of visual information over a vast region of visual space.

The inferior temporal cortex is a large brain region. The patterns of anatomical connections to and from this region indicate that it comprises at least two main functional subdivisions—the posterior area temporo-occipital cortex and the anterior area temporal cortex—and functional evidence suggests further subdivisions

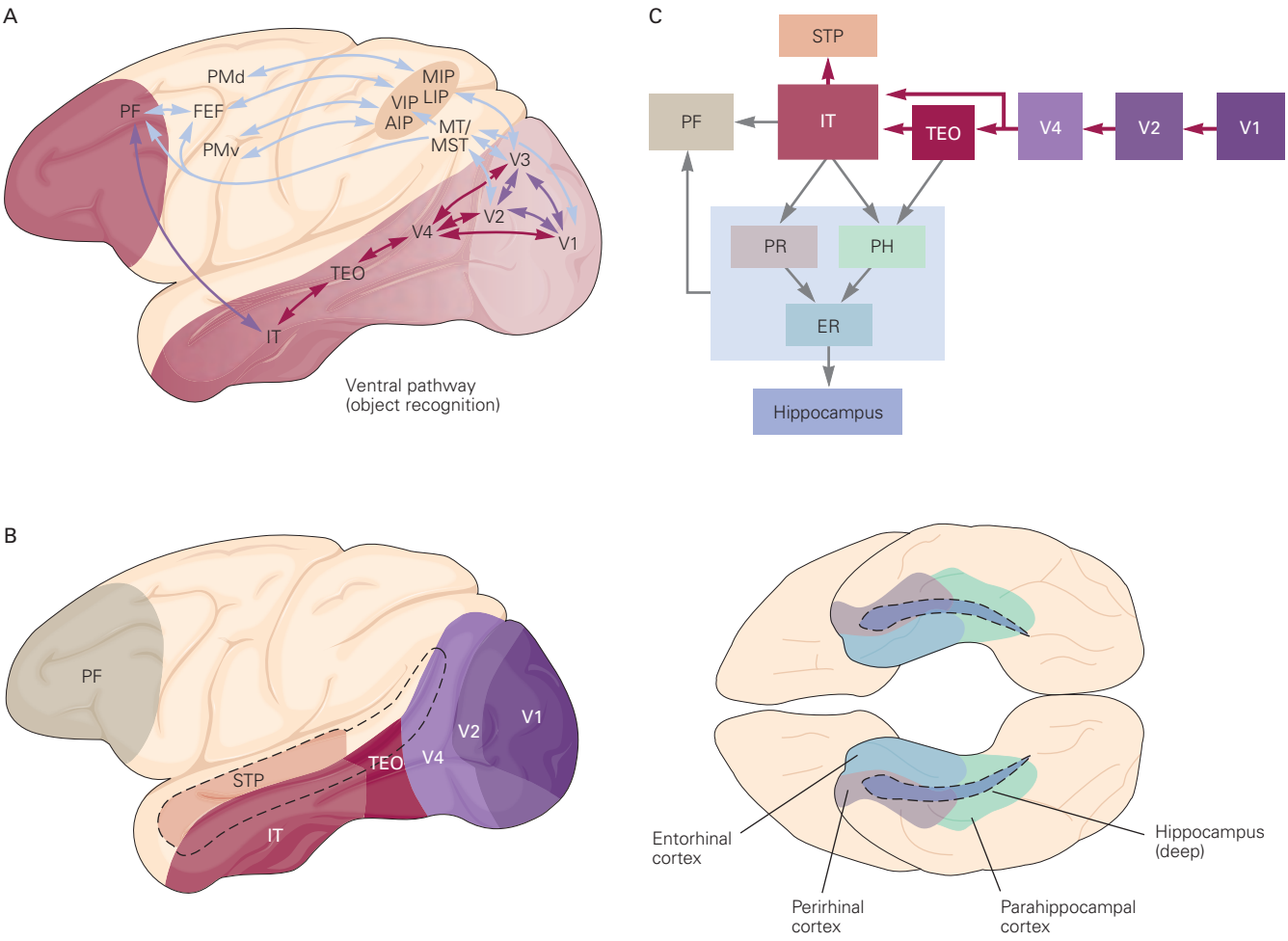

Figure 24–2 Cortical pathway for object recognition.

A. A lateral view of the macaque brain shows the major pathways involved in visual processing, including the pathway for object recognition (**red**). (Abbreviations: **AIP**, anterior intraparietal cortex; **FEF**, frontal eye fields; **IT**, inferior temporal cortex; **LIP**, lateral intraparietal cortex; **MIP**, medial intraparietal cortex; **MST**, medial superior temporal cortex; **MT**, middle temporal cortex; **PF**, prefrontal cortex; **PMd**, dorsal premotor cortex; **PMv**, ventral premotor cortex; **TEO**, temporo-occipital cortex; **VIP**, ventral intraparietal cortex.)

B. Lateral and ventral views of the macaque monkey brain show the cortical areas involved in object recognition. (Abbreviations: **IT**, inferior temporal cortex; **PF**, prefrontal cortex; **STP**, superior temporal polysensory area; **TEO**, temporo-occipital cortex.)

C. The inferior temporal cortex (**IT**) is the end stage of the ventral stream (**red arrows**) and is reciprocally connected with neighboring areas of the medial temporal lobe and prefrontal cortex (**gray arrows**). This chart illustrates the main connections and predominant direction of information flow. (Abbreviations: **ER**, entorhinal cortex; **PF**, prefrontal cortex; **PH**, parahippocampal cortex; **PR**, perirhinal cortex; **STP**, superior temporal polysensory area; **TEO**, temporo-occipital cortex.)

into multiple functionally specialized areas. As we shall see, the distinction between anterior and posterior parts of the inferior temporal cortex is supported by both neuropsychological and neurophysiological evidence.

Clinical Evidence Identifies the Inferior Temporal Cortex as Essential for Object Recognition

The first clear insight into the neural pathways mediating object recognition was obtained in the late 19th century when the American neurologist Sanger Brown and the British physiologist Edward Albert Schäfer found that experimental lesions of the temporal lobe in primates abolished the ability to recognize objects. Unlike the deficits that accompany lesions of occipital cortical areas, temporal lobe lesions do not impair sensitivity to basic visual attributes, such as color, motion, and distance. Because of the unusual type of visual loss, the impairment was originally called psychic blindness, but this term was later replaced by *visual agnosia* ("without visual knowledge"), a term coined by Sigmund Freud.

In humans, there are two basic categories of visual agnosia, apperceptive and associative, the description of which led to a two-stage model of object recognition in the visual system. With apperceptive agnosia, the ability to match or copy complex visual shapes or objects is impaired (Figure 24–3). This impairment results from disruption of the first stage of object recognition: integration of visual features into sensory representations of entire objects. With associative agnosia, the ability to match or copy complex objects remains intact, but the ability to identify objects is impaired. This impairment results from disruption of the second stage of object recognition: association of the sensory representation of an object with knowledge of the object's meaning or function.

Consistent with this functional hierarchy, apperceptive agnosia is most common following damage to the posterior inferior temporal cortex, whereas associative agnosia, a higher-order perceptual deficit, is more common following damage to the anterior inferior temporal cortex. Neurons in the anterior subdivision exhibit a variety of memory-related properties not seen in the posterior area.

More focal lesions within temporal cortex can lead to specific deficits. Damage to a small region of the human temporal lobe results in an inability to

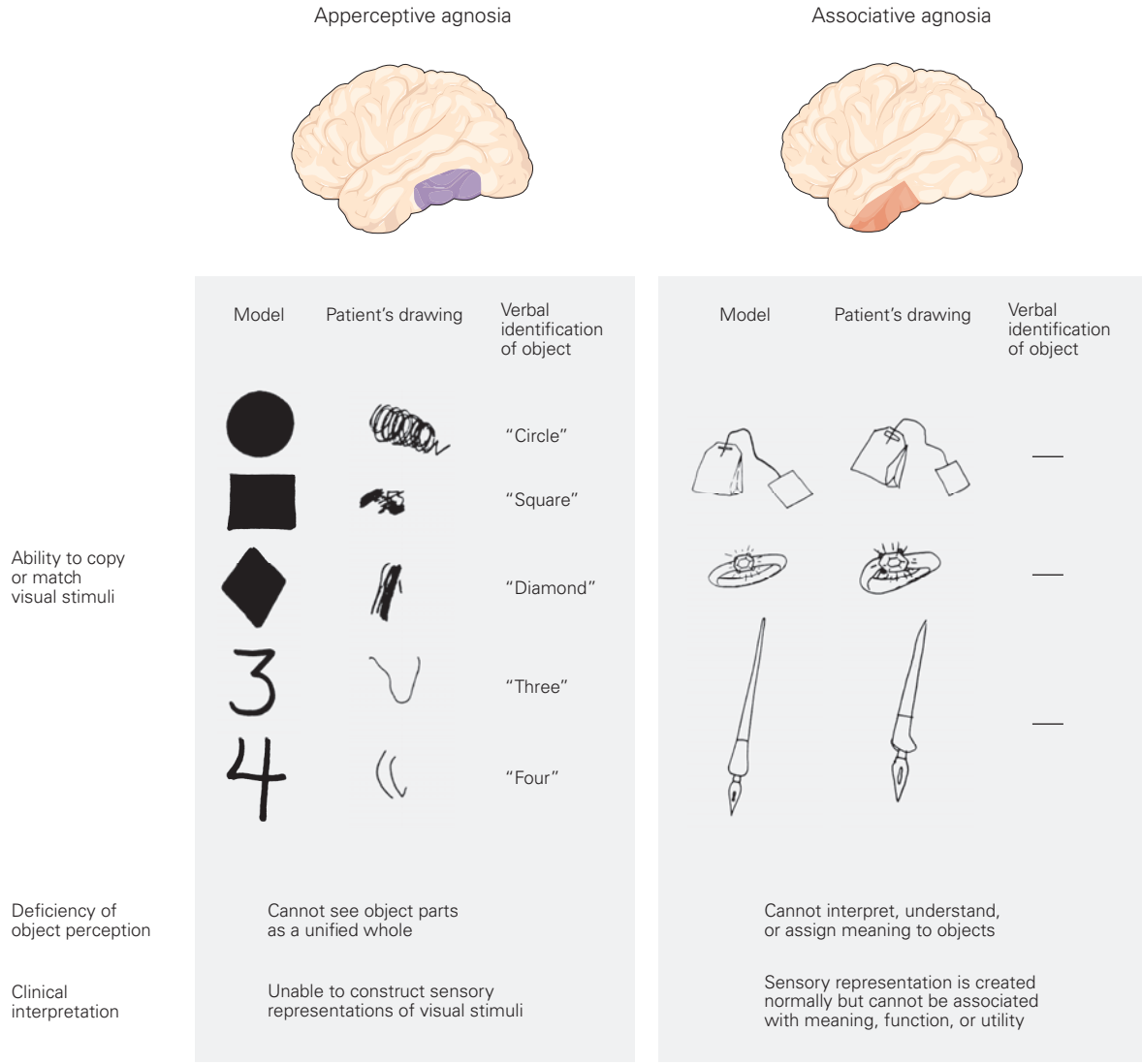

Figure 24–3 Neurons in the temporal lobe of humans are involved in object recognition. Damage to the inferior temporal cortex impairs the ability to recognize visual objects, a condition known as visual agnosia. There are two major categories of visual agnosia: Apperceptive agnosia results from damage to the posterior region, and associative agnosia results from damage of the anterior region. (Reproduced, with permission, from Farah 1990. © 1990 Massachusetts Institute of Technology.)

recognize faces, a form of associative agnosia known as *prosopagnosia.* Patients with prosopagnosia can identify a face as a face, recognize its parts, and even detect specific emotions expressed by the face, but they are unable to identify a particular face as belonging to a specific person.

Prosopagnosia is an example of a *category-specific agnosia*, in which patients with temporal lobe damage fail to recognize particular items belonging to a specific semantic category. Category-specific agnosias for living things, fruits, vegetables, tools, or animals have also been reported. Owing to the pronounced behavioral significance of faces and the normal ability of people to recognize an extraordinarily large number of faces, prosopagnosia may simply be the most commonly diagnosed variety of category-specific agnosia.

Neurons in the Inferior Temporal Cortex Encode Complex Visual Stimuli and Are Organized in Functionally Specialized Columns

The coding of visual information in the temporal lobe has been studied extensively using electrophysiological techniques, beginning with the work of Charles Gross and colleagues in the 1970s. Neurons in this region have distinctive response properties. They are relatively insensitive to simple stimulus features such as orientation and color. Instead, the vast majority possess large, centrally located receptive fields and encode complex stimulus features. These selectivities often appear somewhat arbitrary. An individual neuron might, for example, respond strongly to a crescent-shaped pattern of a particular color and texture. Cells with such unique selectivities likely provide inputs to higher-order neurons that respond to specific meaningful objects.

In fact, within the inferior temporal cortex, several small subpopulations of neurons are activated by highly meaningful objects, such as faces and hands (Figure 24–4), as Charles Gross discovered. For cells that respond to the sight of a hand, individual fingers are particularly critical. Among cells that respond to faces, the most effective stimulus for some cells is a frontal view of the face, whereas for others it is a side view. Although some neurons respond preferentially to faces in general, others respond only to specific

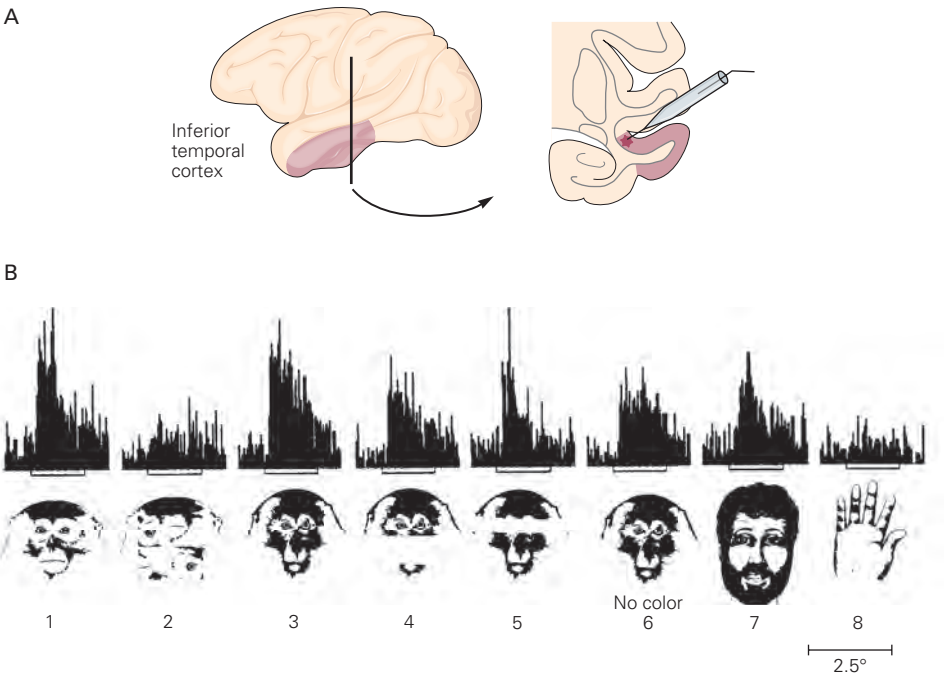

Figure 24–4 Neurons in the inferior temporal cortex of the monkey are involved in face recognition. (Reproduced, with permission, from Desimone et al. 1984. Copyright © 1984 Society for Neuroscience.)

A. The location of the inferior temporal cortex of the monkey is shown in a lateral view and coronal section. The colored area is the location of the recorded neurons.

B. Peristimulus time histograms illustrate the frequency of action potentials in a single neuron in response to different images (shown below the histograms). This neuron responded selectively to faces. Masking of critical features, such as the mouth or eyes (**4**, **5**), led to a substantial but not complete reduction in response. Scrambling the parts of the face (**2**) nearly eliminated the response.

facial expressions. It seems likely that such cells contribute directly to face recognition.

In initial relays in the cortical visual system, neurons that respond to the same stimulus features, such as orientation or direction of motion, but from different parts of the visual field are organized in columns. Cells within the inferior temporal cortex are similarly organized. Columns of neurons representing the same or similar stimulus properties commonly extend throughout the cortical thickness and over a range of approximately 400 μm. The columns are arranged such that different stimuli that possess some similar features are represented in partially overlapping columns (Figure 24–5). Thus, one stimulus can activate multiple columns. Horizontal connections can span many millimeters and may facilitate the formation of distributed networks for encoding objects.

The Primate Brain Contains Dedicated Systems for Face Processing

Prosopagnosia often occurs in the absence of any other form of agnosia. Such a highly specific perceptual deficit could be explained by focal lesions of face-selective neurons located in exclusive clusters. This idea was strengthened by the discovery of face-selective regions in the human brain by Nancy Kanwisher and colleagues using functional magnetic resonance imaging (fMRI) and by Gregory McCarthy and colleagues using direct electrophysiological recordings from the surface of the human brain. Kanwisher and colleagues found that during the presentation of pictures of faces and other objects one area in the human temporal lobe, the fusiform face area, responded significantly more during the presentation of faces compared to other objects.

Subsequently, several more face-selective areas were found, primarily in temporal but also in prefrontal cortex. Early studies of these areas provided circumstantial evidence for clustering of face-selective neurons. In later studies, Doris Tsao, Winrich Freiwald, and colleagues directly demonstrated such clustering and showed that face processing might be performed by a dedicated face-processing network spanning from the posterior part of inferior temporal cortex to prefrontal cortex. Using fMRI, they found six areas in temporal cortex and three in prefrontal cortex of the macaque monkey that responded more selectively to faces than to other objects. These areas, called face patches, are found at highly consistent locations across individuals and thus are named based on their location. Each face patch is a few millimeters in diameter and thus differs organizationally from the inferior temporal columns. Intracellular recordings from the face patches

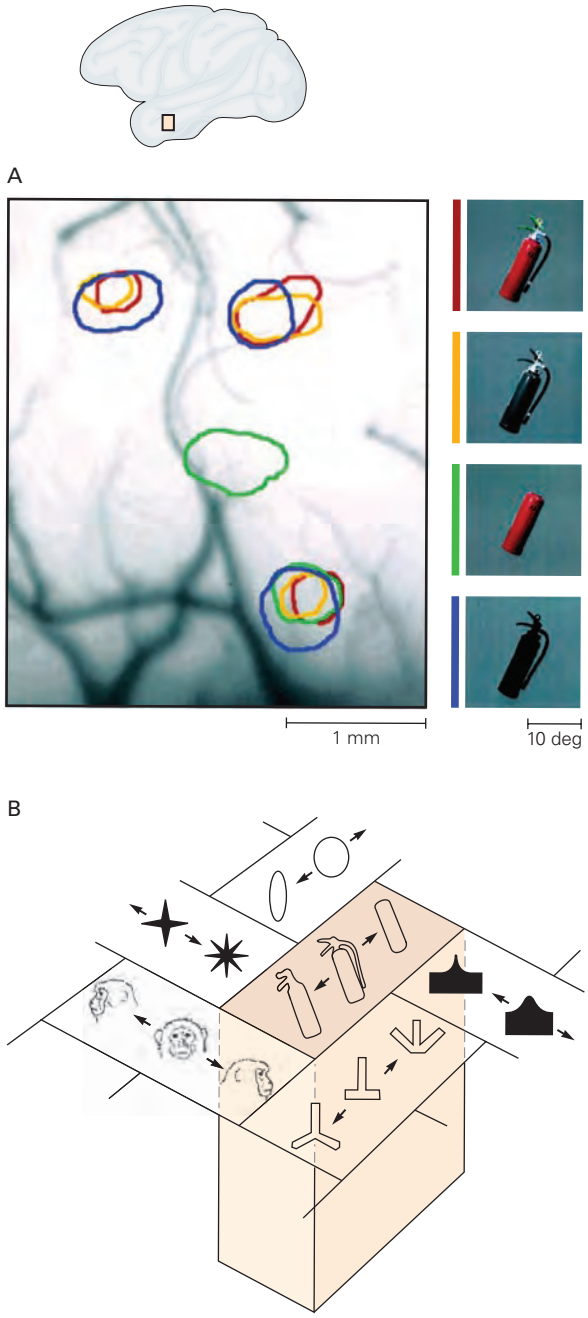

Figure 24–5 Neurons in the anterior portion of the inferior temporal cortex that respond to complex visual stimuli are organized into columns. (Reproduced, with permission, from Tanaka 2003. Copyright © 2003 Oxford University Press.)

A. Optical images of the surface of the anterior inferior temporal cortex illustrate regions selectively activated by the objects shown at the right.

B. Neurons of the inferior temporal cortex are organized in functionally specialized columns that extend from the surface of the cortex. According to this model, each column includes neurons that respond to a specific visually complex object. Columns of neurons that represent variations of an object, such as different faces or different fire extinguishers, constitute a hypercolumn.

revealed that the vast majority of cells respond selectively more to faces than to other objects. Thus, millions of face cells are clustered into a fixed number of small areas. These areas are directly connected to each other, thus forming a face-processing network. Within this network, each node appears to be functionally specialized. From posterior to anterior locations within the temporal lobe, the initial face patches respond to particular views of the face, and then face patches become gradually more selective to identity and less selective for angle of view. Furthermore, dorsal face areas within the temporal lobe exhibit a selectivity for natural facial motion, which ventral areas lack. Thus, a highly specialized network, located primarily in temporal cortex, processes the multiple dimensions of information conveyed by a face (Figure 24–6).

The Inferior Temporal Cortex Is Part of a Network of Cortical Areas Involved in Object Recognition

Object recognition is intimately intertwined with visual categorization, visual memory, and emotion, and the outputs of the inferior temporal cortex contribute to these functions (see Figure 24–2). Among the principal projections are those to the perirhinal and parahippocampal cortices, which lie medially adjacent to the ventral surface of the inferior temporal cortex (Figure 24–2C). These regions project, in turn, to the entorhinal cortex and the hippocampal formation, both of which are involved in long-term memory storage and retrieval. A second major projection from the inferior temporal cortex is to the prefrontal cortex, an important site for high-level visual processing. As we shall see, prefrontal neurons play important roles in object categorization, visual working memory, and memory recall.

The inferior temporal cortex also provides input—directly and indirectly via the perirhinal cortex—to the amygdala, which is believed to apply emotional valence to sensory stimuli and to engage the cognitive and visceral components of emotion (Chapter 42). Finally, the inferior temporal cortex is a major source of input to multimodal sensory areas of cortex such as the superior temporal polysensory area (Figure 24–2B), which lies dorsally adjacent to the inferior temporal cortex.

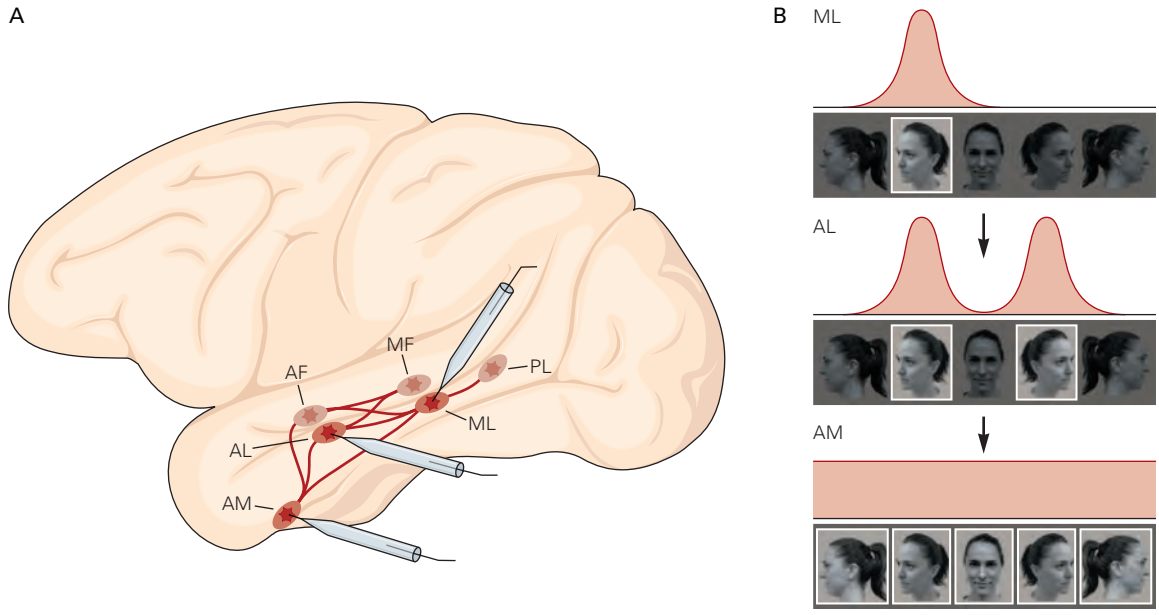

Figure 24–6 The temporal lobe contains a network of face-selective areas.

A. Functional magnetic resonance imaging of macaque monkeys watching pictures of faces and other objects identified six face-selective areas in the temporal lobe, inside and around the superior temporal sulcus. These areas occur at the same locations across subjects and have been given names based on their anatomical location (**PL**, posterior lateral; **ML**, medial lateral; **MF**, medial fundus of the superior temporal sulcus; **AL**, anterior lateral; **AF**, anterior fundus; **AM**, anterior medial). These areas are interconnected to form a face-processing network.

B. Single-neuron recordings from areas ML, AL, and AM show tuning to head orientation. ML cells are tuned to specific head orientations, many AL cells are tuned to multiple orientations that are mirror-symmetric versions of each other, and AM cells are broadly and more weakly tuned to head orientation. These three representations in interconnected areas can be thought of as transformations of each other (**arrows**).

Object Recognition Relies on Perceptual Constancy

The ability to recognize objects as the same under different viewing conditions, despite the sometimes markedly different retinal images, is one of the most functionally important requirements of visual experience. The invariant attributes of an object—for example, spatial and chromatic relationships between image features or characteristic features such as the stripes of a zebra—are cues to the identity and meaning of the objects.

For object recognition to take place, these invariant attributes must be represented independently of other image properties. The visual system does this with proficiency, and its behavioral manifestation is termed *perceptual constancy*. Perceptual constancy has many forms ranging from invariance across simple transformations of an object, such as changes of size or position, to more difficult ones, such as rotation in depth or changes in lighting, and even to the sameness of objects within a category: All zebras look alike.

One of the best examples is *size constancy.* An object placed at different distances from an observer is perceived as having the same size, even though the object produces images of different absolute size on the retina. Size constancy has been recognized for centuries, but only in the past several decades has it been possible to identify the neural mechanisms responsible. An early study found that lesions of the inferior temporal cortex lead to failures of size constancy in monkeys, suggesting that neurons in this area play a critical role in size constancy. Indeed, one of the most striking properties of individual inferior temporal neurons is the invariance of their shape selectivity even to very big changes in stimulus size (Figure 24–7A).

Another type of perceptual constancy is *position constancy*, in which objects are recognized as the same regardless of their location in the visual field. The pattern of selective response of many inferior temporal neurons does not vary when an object changes position within their large receptive fields (Figure 24–7B). *Form-cue invariance* refers to the constancy of a form when the cues that define the form change. The silhouette of Abraham Lincoln's head, for example, is readily recognizable whether it is black on white, white on black, or red on green. The responses of many inferior temporal neurons do not change with changes in contrast polarity (Figure 24–7C), color, or texture.

Viewpoint invariance refers to the perceptual constancy of three-dimensional objects observed from different angles. Because most objects we see are three-dimensional and opaque, when looked at from different viewpoints, some parts become invisible, while others are revealed, and all others change in appearance. Yet despite the limitless range of retinal images that might be cast by a familiar object, an observer can readily recognize an object independently of the angle at which it is viewed. There are notable exceptions to this rule, which generally occur when an object is viewed from an angle that yields an uncharacteristic retinal image, such as a bucket viewed from directly above.

Thus, object recognition mechanisms must infer the identity of objects from apparent complex shapes. Many neurons in inferior temporal cortex do not exhibit viewpoint invariance. In fact, many are systematically tuned to viewing angle. Yet at more anterior locations, neurons are not only more size and position invariant, but they also exhibit greater invariance to viewpoint. The face-processing system is a case in point. Neurons in posterior face patches are tuned to viewing angle, while neurons in anterior face patches exhibit great robustness to changes in viewpoint. Thus, population responses in posterior face areas contain more information about head orientation than those in anterior areas, while the anterior face patches provide more information about face identity across head orientations compared to posterior face areas. The degree of viewpoint invariance achieved in anterior inferior temporal cortex, by individual neurons and populations of neurons, might be sufficient to account for perceptual viewpoint invariance. But this has not been directly shown yet. Alternatively, viewpoint invariance may be achieved at a higher stage of cortical processing, such as the prefrontal cortex.

Studies of the conditions under which viewpoint invariance fails may lead to insights into the neural mechanisms of the behavior. One such condition is presentation of mirror images. Although mirror images are not identical, they are frequently perceived as such, a confusion reflecting a false-positive identification by the system for viewpoint invariance. Carl Olson and colleagues examined the responses of neurons in a particular region of the inferior temporal cortex to stimuli that were mirror images. Consistent with the perceptual confusion, many inferior temporal neurons responded similarly to both images. Similarly, in one face area between the posterior and anterior ones described earlier, profile-selective cells respond similarly to the left and right profile of a face. These results reinforce the conclusion that activity in the inferior temporal cortex reflects perceptual invariance, albeit incorrectly in this case, rather than the actual features of a stimulus.

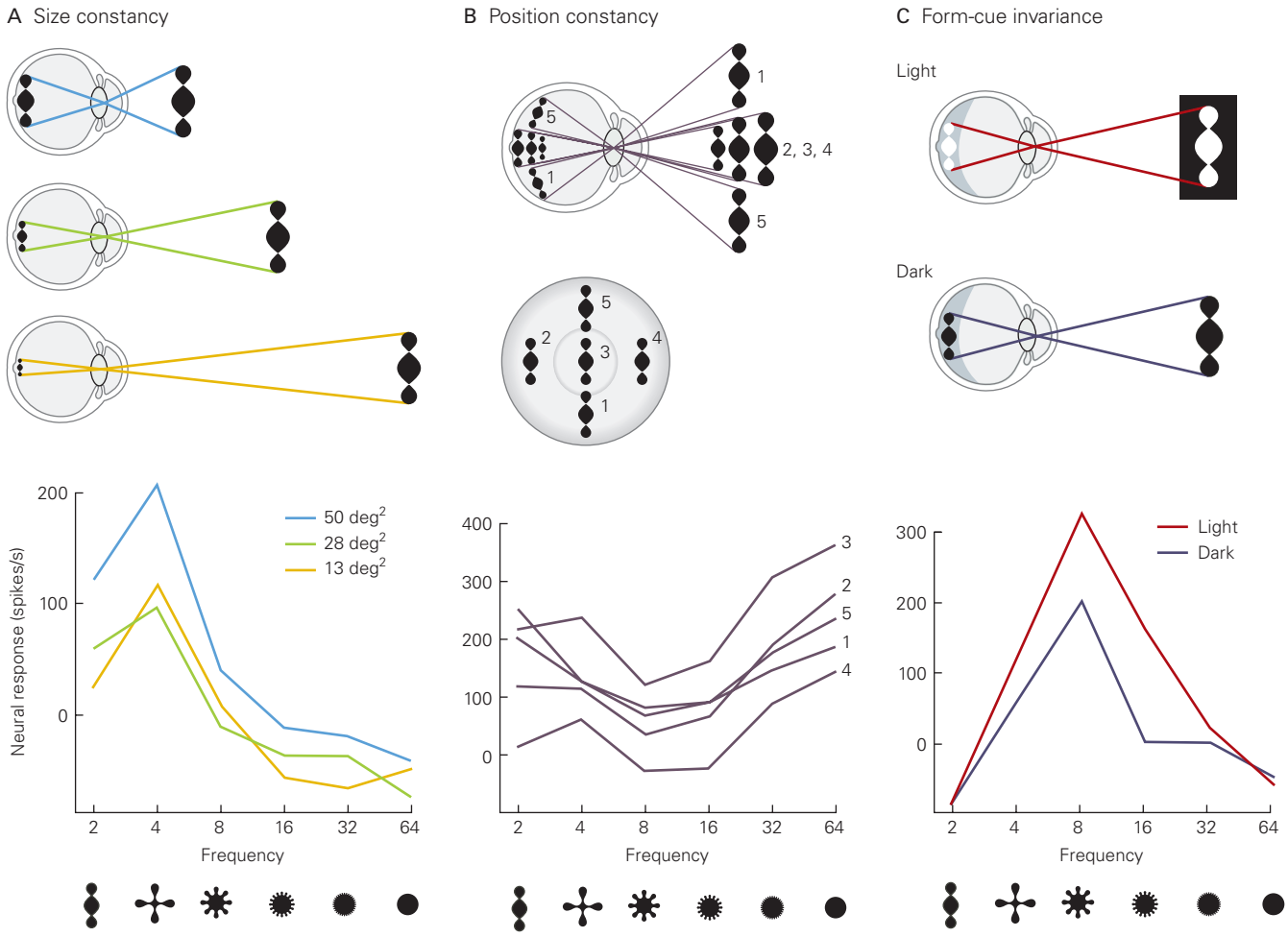

Figure 24–7 Perceptual constancy is reflected in the behavior of neurons in the inferior temporal cortex. The responses of many inferior temporal neurons are selective for stimuli with a particular frequency (number) of lobes but invariant to object size, position, and reflectance. (Reproduced, with permission, from Schwartz et al. 1983.)

A. *Size constancy.* An object is perceived to be the same even when the retinal image size decreases with the distance of the object in the visual field. The response of the vast majority of inferior temporal neurons to substantial changes in retinal image size is invariant, as illustrated here by the record of a single cell.

B. *Position constancy.* An object is perceived to be the same despite changes in position in the retinal image. Almost all inferior temporal neurons respond similarly to the same stimulus in different positions in the visual field, as illustrated here by the record of a single neuron.

C. *Form-cue invariance.* An object is perceived to be the same despite changes in reflectance. Most inferior temporal neurons respond similarly to the two images illustrated, as shown in the record of an individual neuron.

Categorical Perception of Objects Simplifies Behavior

All forms of perceptual constancy are the product of the visual system's attempts to generalize across different retinal images generated by a single object. A still more general type of constancy is the perception of individual objects as belonging to the same semantic category. The apples in a basket or the many appearances of the letter *A* in different fonts, for example, are physically distinct but are effortlessly perceived as *categorically* identical.

Categorical perception is classically defined as the ability to distinguish objects of different categories better than objects of the same category. For example, it is more difficult to discriminate between two red lights that differ in wavelength by 10 nm than to discriminate between red and orange lights with the same wavelength difference.

Categorical perception simplifies behavior. For example, it usually does not matter whether an apple

is completely spherical or slightly mottled on the left side or whether the seat we are offered is a Windsor or a Chippendale side chair. Similarly, reading ability requires that one be able to recognize the alphabet in a broad variety of type styles. Like the simpler forms of perceptual constancy, categorical perception relies on the brain's ability to extract invariant features of objects seen.

Is there a population of neurons that respond uniformly to objects within a category and differentially to objects of different categories? To test this, David Freedman and Earl Miller and colleagues created a set of images in which features of dogs and cats were merged; the proportions of dog and cat in the composite images varied continuously from one extreme to the other. Monkeys were trained to identify these stimuli reliably as either dog or cat. Miller and colleagues then recorded from visually responsive neurons in the dorsolateral prefrontal cortex, a region that receives direct input from the inferior temporal cortex. Not only did these neurons exhibit the predicted category-selective responses—responding well to cat but not dog, or vice versa—but the neuronal category boundary also corresponded to the behaviorally learned boundary (Figure 24–8). By contrast, neurons in inferior temporal cortex represented similarity of features, not categories.

The fact that category-specific agnosias sometimes follow damage to the temporal lobe suggests there are neurons in the inferior temporal cortex that are category-selective similar to those of neurons in the prefrontal cortex. Face-selective cells in the temporal cortex appear to meet this criterion, because their responses to a range of faces are often similar. Yet, these may constitute a special case, whereas for most stimulus conditions, category-selective responses may be characteristic of neurons in the prefrontal cortex, where visual responses are more commonly linked to the behavioral significance of the stimuli.

Visual Memory Is a Component of High-Level Visual Processing

Visual experience can be stored as memory, and visual memory influences the processing of incoming visual information. Object recognition in particular relies on the observer's previous experiences with objects. Thus, the contributions of the inferior temporal cortex to object recognition must be modifiable by experience.

Studies of the role of experience in visual perception have focused on two distinct types of experience-dependent plasticity. One stems from repeated exposure or practice, which leads to improvements in visual discrimination and object recognition ability. These experience-dependent changes constitute a form of implicit learning known as perceptual learning (Chapter 23). The other occurs in connection with the storage of explicit learning, the learning of facts or events that can be recalled consciously (Chapter 54).

Implicit Visual Learning Leads to Changes in the Selectivity of Neuronal Responses

The ability to discriminate complex visual stimuli is highly modifiable by experience. For example, individuals who attend to fine differences between automobile models improve their ability to recognize such differences.

In the inferior temporal cortex, neuronal selectivity for complex objects can undergo change that parallels change in the ability to distinguish objects. For example, in a study by Logothetis and colleagues, monkeys were trained to identify novel three-dimensional objects, such as randomly bent wire forms, from two-dimensional views of the objects. Extensive training led to pronounced improvements in the ability to recognize the objects from two-dimensional views. After training, a population of neurons was found that exhibited marked selectivity for the views seen earlier but not for other two-dimensional views of the same objects (Figure 24–9).

Other studies with monkeys have shown that familiarization with novel faces alters the tuning of face-selective neurons in the inferior temporal cortex. Similarly, when an animal has experience with novel objects formed from simple features, inferior temporal neurons become selective for those objects. Such neuronal changes have been found as a consequence of the animal engaging in active discrimination or simply passive viewing of visual stimuli, and they are often manifested as a sharpening of neural selectivity rather than changes in absolute firing rate. Sharpening is precisely the sort of neuronal change that could underlie improvements in perceptual discrimination of visual stimuli.

The Visual System Interacts With Working Memory and Long-Term Memory Systems

Object recognition and learning are intricately linked. In fact, learning can generate entire areas of functional specialization within inferior temporal cortex. For example, monkeys who learn at a young age to associate specific shapes (eg, a number symbol) with particular reward magnitudes develop specialized brain areas that process these specific shapes. These brain regions

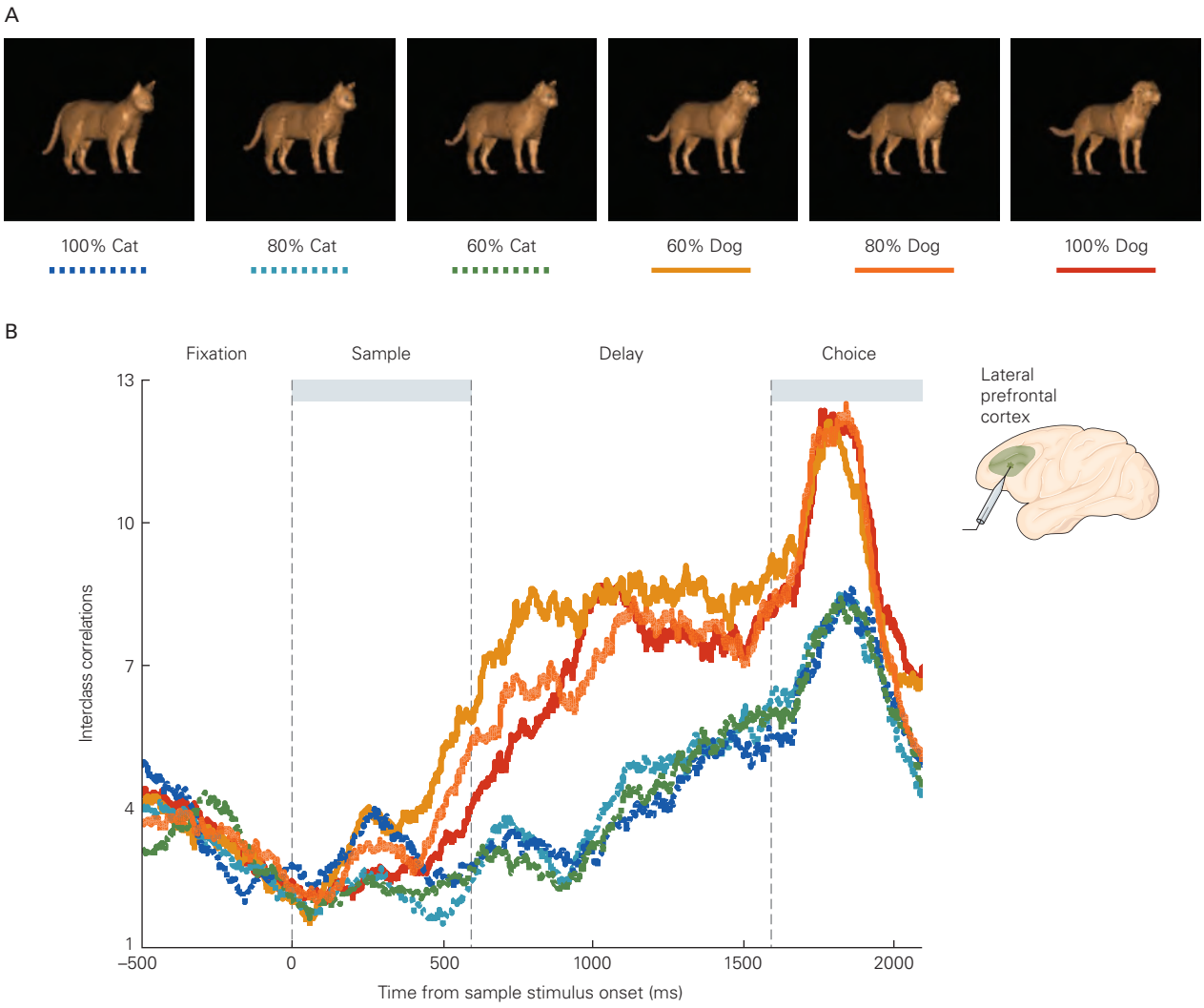

Figure 24–8 Neural coding for categorical perception. (Reproduced, with permission, from Freedman et al. 2002.)

A. The images combine cat and dog features in varying proportions. Monkeys were trained to categorize an image as cat or dog if it had 50% or more features of that animal.

B. Peristimulus time histograms illustrate the responses of a prefrontal cortex neuron to the images shown in part A. The neuron responded much more weakly to images of cats (100%, 80%, and 60%) than to images of dogs (60%, 80%, and 100%). Responses to images from the same category were very similar despite variations in retinal images that were as large as or even larger than the differences in retinal images between categories. Thus, the cell was category-specific. Such category-specific responses were common among visual neurons of the lateral prefrontal cortex.

develop close to the temporal lobe face patches discussed earlier.

Two issues concerning interaction between vision and memory have been investigated. First, how is visual information maintained in short-term working memory? Working memory has a limited capacity, acting like a buffer in a computer operating system, and consolidation into long-term memory is susceptible to interference (Chapter 54). Second, how are long-term visual memories and the associations between them stored and recalled?

In a visual delayed-response task requiring access to stimulus information beyond the duration of the stimulus (Box 24–1), many vision-related neurons in both the inferior temporal and prefrontal cortices continue firing during the delay. This delay-period activity is thought to maintain information in short-term working memory (Figure 24–11). Delay-period activity in the inferior temporal and prefrontal cortices differs in a number of ways. For one, activity in the inferior temporal cortex is associated with the short-term storage of visual patterns and color information, whereas

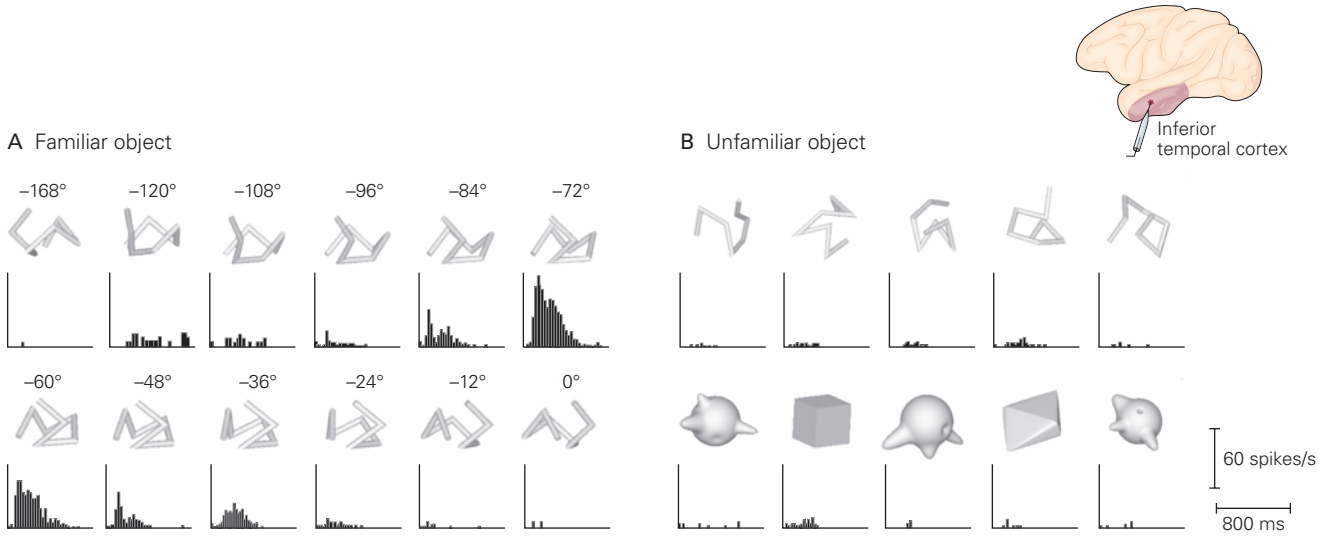

Figure 24–9 Familiarity with particular complex objects leads inferior temporal neurons to respond selectively for those objects. (Reproduced, with permission, from Logothetis and Pauls 1995. Copyright © 1995 Oxford University Press.)

A. Monkeys were trained to recognize a randomly bent wire from a set of two-dimensional views of the wire. The wire form was rotated 12° in successive views. Once recognition performance was stable at a high level, recordings were made from neurons in the inferior temporal cortex while each view was presented. Peristimulus time histograms show the responses of a typical neuron to each view. This neuron responded selectively to views that represented a small range of rotation of the object.

B. When the same neuron was tested with two sets of stimuli that were unfamiliar to the monkey, it failed to respond to any of these stimuli.

activity in the prefrontal cortex encodes visuospatial information as well as information received from other sensory modalities. Delay-period activity in the inferior temporal cortex also appears to be closely attuned to visual perception, for it encodes the sample image, but can be eliminated by the appearance of another image.

In the prefrontal cortex, by contrast, delay-period activity depends more on task requirements and is not terminated by intermittent sensory inputs, suggesting that it may play a role in the recall of long-term memories. Experiments by Earl Miller and colleagues support this view. In these experiments, monkeys were trained to associate multiple pairs of objects. They were then tested on whether they had learned these pairwise associations, using the following procedure. First, a single (sample) object was presented; then, after a brief delay, a second (test) object appeared. The monkey was instructed to indicate whether the test object was the object paired with the sample during previous training.

There are two possible ways to solve this task. During the delay, the animal could use a sensory code and keep a representation of the sample object online until the appearance of the test object, or it could remember the sample object's associate and keep information about the associate object online in a "prospective code" of what might appear as the test object. Remarkably, neuronal activity appears to transition from one to the other during the delay. Neurons in the prefrontal cortex initially encode the sensory properties of the sample object—the one just seen—but later begin to encode the expected (associated) object. As we shall see, such prospective coding in the prefrontal cortex may be the source of top-down signals to the inferior temporal cortex, activating neurons that represent the expected object and thus giving rise to conscious recall of that object.

The relation between long-term declarative memory storage and visual processing has been explored extensively in the context of remembered associations between visual stimuli. Over a century ago, William James, a founder of the American school of experimental psychology, suggested that learning visual associations might be mediated by enhanced connectivity between the neurons encoding individual stimuli. To test this hypothesis, Thomas Albright and colleagues trained monkeys to associate pairs of objects that had no prior physical or semantic relatedness. The monkeys were later tested while extracellular recordings of neurons in the inferior temporal cortex were made. Objects that had been paired often elicited similar neuronal

Box 24–1 Investigating Interactions Between Vision and Working Memory

The relationship between vision and memory can be studied by combining a neuropsychological approach with single-cell electrophysiological methods.

One behavioral paradigm used to study memory is the *delayed-response task*. A subject is required to make a specific response based on information remembered during a brief delay. In one form of this task, known as *delayed match-to-sample*, the subject must indicate whether a visual stimulus is the same or different from a previously viewed cue stimulus (sample) (Figure 24–10A).

When used in conjunction with single-cell recording, this task allows the experimenter to isolate three key components of a neuronal response: (1) the sensory component, the response elicited by the cue stimulus; (2) the short-term or working-memory component, the response that occurs during the delay between the cue and the match; and (3) the recognition-memory or familiarity component, the difference between the response elicited by the match stimulus and the earlier response to the cue stimulus.

A second behavioral paradigm, the *visual paired-association task*, has been used in conjunction with electrophysiology to explore the cellular mechanisms underlying the long-term storage and recall of associations. This task differs from the delayed match-to-sample task in that the match and cue are two different stimuli (Figure 24–10B).

The sample stimulus might consist of the letter *A* and the match stimulus the letter *B*. Through repeated temporal pairing and conditional reinforcement, subjects learn that *A* and *B* are predictive of one another: They are associated.

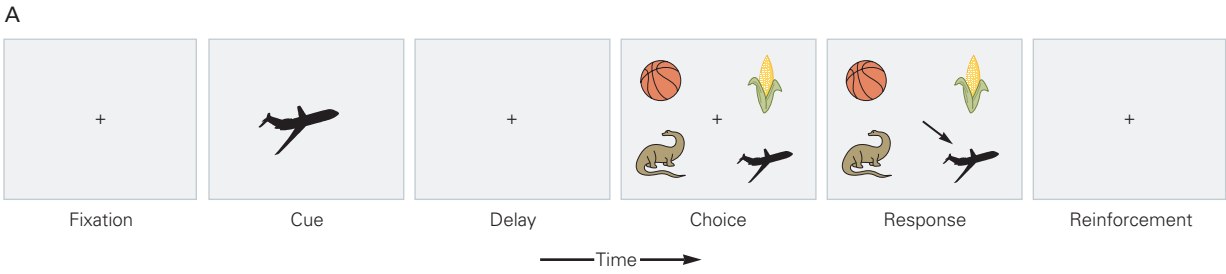

Figure 24–10A Delayed match-to-sample task. In this paradigm, a trial begins with the appearance of a fixation spot that directs the subject's attention and gaze to the center of the computer screen. A cue stimulus (the "sample") then appears briefly, typically for 500 ms, followed by a delay in which the display is blank. The delay can be varied to fit the experimental goals. Following the delay, the choice display appears, which contains several images, one of which is the cue (the "match"). The subject must respond by choosing the cue stimulus, typically either by pressing a button or by a saccade to the stimulus. In the task illustrated here, all of the test images appear at once (a simultaneous match-to-sample task). They can also be presented sequentially (a sequential match-to-sample task). Although the trial's duration may be longer for the sequential task, this paradigm can be advantageous for electrophysiological studies by limiting the visual stimuli present at any time.

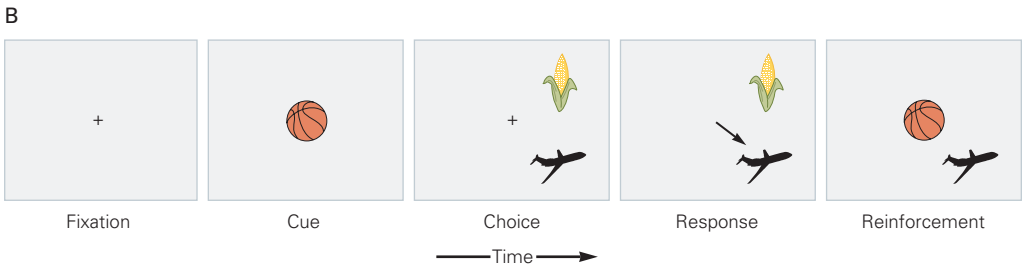

Figure 24–10B The paired-association task. This paradigm resembles the match-to-sample paradigm except that the cue and match are different stimuli. In the illustrated example, the basketball is the cue stimulus and the airplane is the experimenter-designated match stimulus. Because these stimuli have no inherent association, the subject must discover the designated association through trial-and-error learning. The task is thus to establish an association between nonidentical stimuli. The paired-association task can also incorporate a delay between presentation of the sample and test stimuli, and it can be used in both simultaneous (shown) and sequential forms.

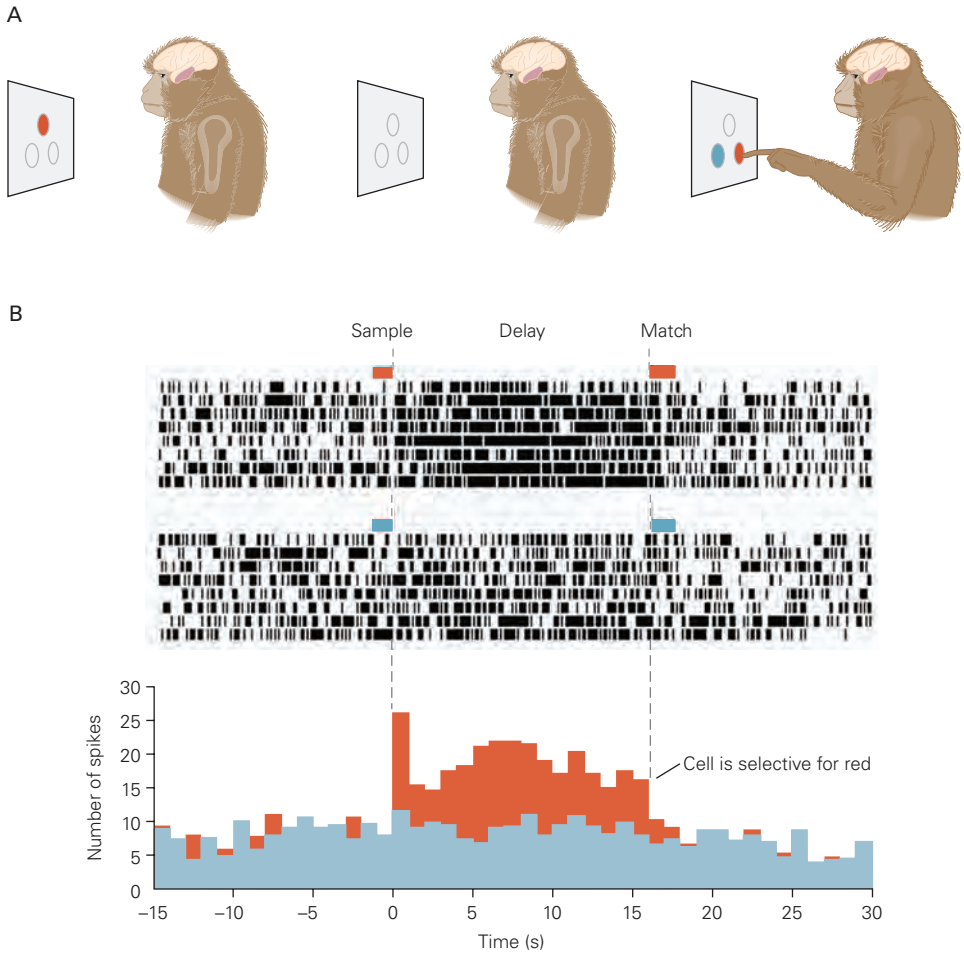

Figure 24–11 Neural activity representing an object is sustained while the object is held in working memory. (Reproduced, with permission, from Fuster and Jervey 1982. Copyright © 1982 Society for Neuroscience.)

A. Monkeys were trained to perform a color match-to-sample task. For example, a red stimulus was first presented and the animal later had to choose a red stimulus from among many colored stimuli. The task incorporated a brief delay (1–2 seconds) between display of the sample and the match, during which information about the correct target color had to be maintained in working memory. The **purple** area in the monkey's brain indicates the inferior temporal cortex.

B. Peristimulus time histograms and raster plots of action potentials illustrate responses of a single neuron in the inferior temporal cortex during the delayed match-to-sample task. The upper record is from trials in which the sample was red, and the lower record is from trials in which it was green (shown here as **blue**). The recordings show that the cell responds preferentially to red stimuli. In trials with a green sample, the activity of the neuron does not change, whereas in trials with a red sample, the cell exhibited a brief burst of activity following presentation of the sample and continued firing throughout the delay. Many visual neurons in the inferior temporal and prefrontal cortices exhibit this kind of behavior.

responses, as one would expect if functional connections had been enhanced, whereas responses elicited by unpaired objects were unrelated. Recordings from individual inferior temporal neurons while monkeys were learning new visual associations showed that a cell's responses to paired objects became more similar over the course of training (Figure 24–12). Most importantly, the changes in neuronal activity occurred on the same timescale as the changes in behavior, and the changes in neural activity depended on successful learning.

These learning-dependent changes in the stimulus selectivity of inferior temporal cortex neurons are long-lasting, suggesting that this cortical region is part of the neural circuitry for associative visual memories. The experimental results also support the view that learned associations are implemented rapidly by changes in the strength of synaptic connections between neurons representing the associated stimuli.

We know that the hippocampus and neocortical areas of the medial temporal lobe—the perirhinal, entorhinal, and parahippocampal cortices—are

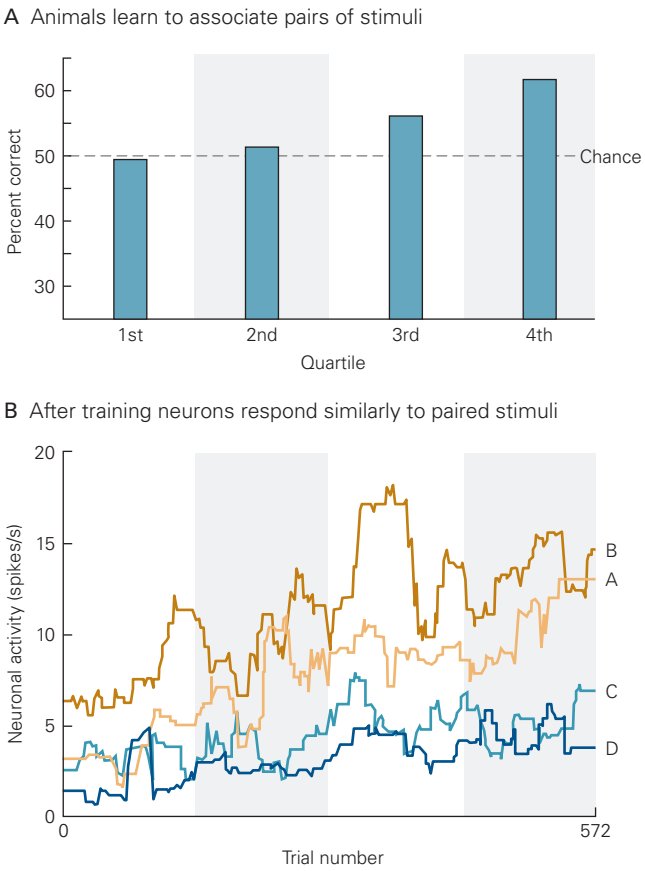

Figure 24–12 Object recognition is linked to associative memory. Monkeys learned associations between pairs of visual stimuli while activity was recorded from a neuron in the inferior temporal cortex. (Reproduced, with permission, from Messinger et al. 2001. © 2001 National Academy of Sciences.)

A. Behavioral performance on a paired-association task is plotted for each quartile of a single training session (572 trials). The animal was presented with four novel stimuli (A, B, C, D) and was required to learn two paired associations (A–B, C–D). As expected, performance began at chance (50% correct) and gradually climbed as the animal learned the associations.

B. Mean firing rates of an inferior temporal neuron recorded during the behavioral task described in part A. Each trace represents the firing rate during presentation of one of the four stimuli (A, B, C, or D). The responses to all stimuli were of similar magnitude at the outset. As the paired associations were learned, the neuronal responses to the paired stimuli A and B began to cluster at a different level from responses to the paired stimuli C and D. The neuron's activity thus corresponded to the learned associations between the two pairs.

essential both for the acquisition of associative visual memories and for the functional plasticity of the inferior temporal cortex. In fact, work by Yasushi Miyashita and colleagues showed that the aforementioned pair-association neurons are much more prevalent in perirhinal cortex than in anterior inferior temporal cortex. Thus, although learning changes the stimulus selectivity of neurons in both areas, the association between visually associated pairs grows stronger from inferior temporal to perirhinal cortex (Figure 24–2C). The hippocampus and medial temporal lobe may facilitate the reorganization of local neuronal circuitry in the inferior temporal cortex necessary to store associative visual memories. The reorganization itself may be a form of Hebbian plasticity (Chapter 49) initiated by the temporal coincidence of the associated visual stimuli.

Associative Recall of Visual Memories Depends on Top-Down Activation of the Cortical Neurons That Process Visual Stimuli

One of the most intriguing features of high-level visual processing is the fact that the detection of an image in one's visual field and the recall of the same image are subjectively similar. The former depends on the bottom-up flow of visual information and is what we traditionally regard as vision. The latter, by contrast, is a product of top-down information flow. This distinction is anatomically accurate but obscures the fact that under normal conditions afferent and descending signals collaborate to yield visual experience.

The study of associative visual memory has provided valuable insights into the cellular mechanisms underlying visual recall. As we have seen, visual associative memories are stored in the visual cortex through changes in the functional connectivity between neurons that independently represent the associated stimuli. The practical consequence of this change is that a neuron that responded only to stimulus *A* prior to learning will respond to both *A* and *B* after these stimuli have been associated (Figure 24–13). Activation of an *A*-responsive neuron by stimulus *B* can be viewed as the neuronal correlate of top-down recall of stimulus *A*.

Neurons in the inferior temporal cortex exhibit precisely this behavior. The activity correlated with cued recall is nearly identical to the bottom-up activation by the stimulus. These neurophysiological findings are supported by a number of brain imaging studies that have identified selective activity in the visual cortex during cued and spontaneous recall of objects.

Although learned associations between images are likely to be stored through circuit changes in the inferior temporal cortex, activation of these circuits for conscious recall depends on input from the prefrontal cortex. The afferent signal for one of a pair of images might be received by the inferior temporal cortex and relayed to prefrontal cortex, where the information

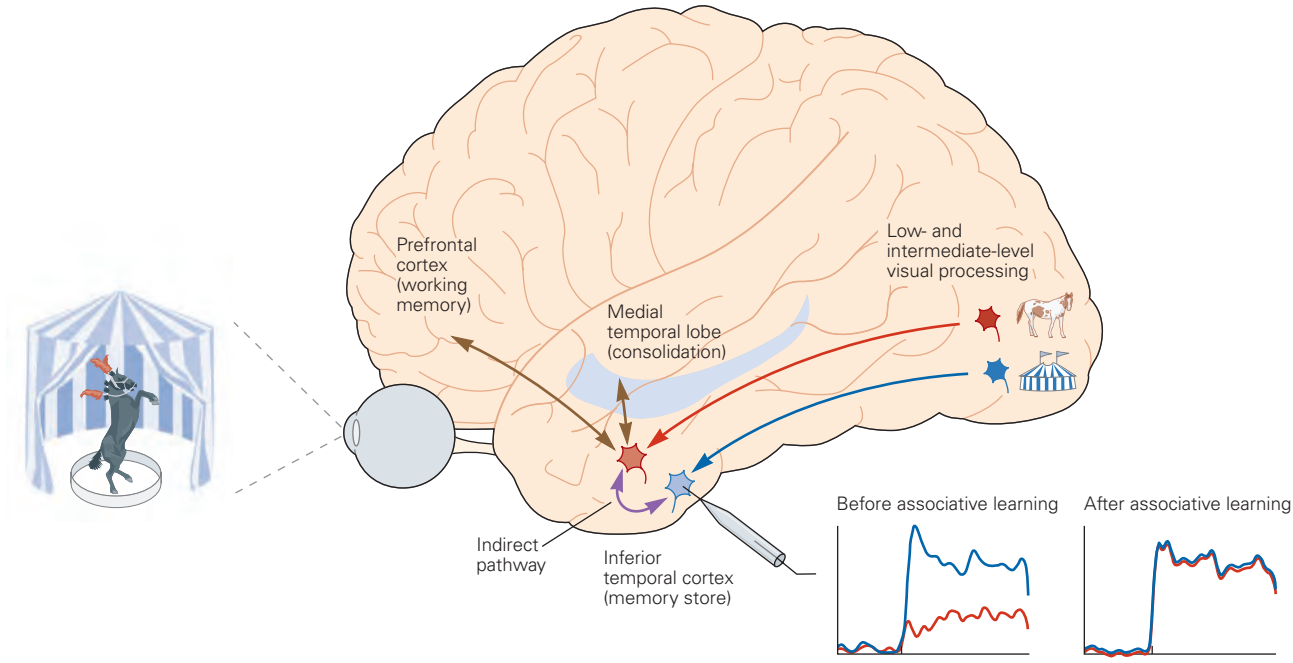

Figure 24–13 Circuits for visual association and recall. Bottom-up signals—afferent signals conveying information about objects in the observer's visual field—are combined into object representations in the inferior temporal cortex. Before associative learning, a neuron (**blue**) responds well to the circus tent but not to the horse. Learned associations between objects are mediated in the inferior temporal cortex by strengthening connections between neurons representing each of the paired objects (the indirect pathway in the figure). Thus, recall of the circus tent following presentation of the horse is achieved by activating the indirect pathway. Indirect activation can also be triggered by the contents of working memory (feedback from the prefrontal cortex). Under normal conditions, visual perception is the product of a combination of direct and indirect inputs to inferior temporal neurons.

would be maintained in working memory. As we have seen, the continued firing of many prefrontal neurons during the delay period of a delayed match-to-sample task initially represents information about the sample image but changes to the associated image that is expected to follow. Signals from prefrontal cortex to the inferior temporal cortex would selectively activate neurons representing the associated image, and that activation would constitute the neural correlate of visual recall.

Highlights

1. A key function of high-level vision is object recognition. Object recognition imbues visual perception with meaning. As the eminent neuropsychologist Hans-Lukas Teuber once wrote, failure of object recognition "would appear in its purest form as a normal percept that has somehow been stripped of its meaning."
2. Object recognition is difficult, primarily because of changes in appearance with changes in position, distance, orientation, or lighting conditions, possibly rendering different objects similar in appearance. Building computer models mimicking primate object recognition capabilities is a major challenge for current and future research.
3. Object recognition relies on a region of the temporal lobe called inferior temporal cortex. Visual information reaching inferior temporal cortex has already been processed through mechanisms of low- and mid-level vision.
4. Lesions to inferior temporal cortex cause visual agnosia, a loss in the ability to recognize objects. Apperceptive agnosia, the inability to match or copy complex objects, is distinguished from associative agnosia, the impairment of the ability to recognize an object's meaning or function. Predicting the exact nature of an agnosia from the pattern of lesioned or inactivated areas, and thus to go from understanding the *correlates* to the *causes* of neural object representations, is a major goal for the field of object recognition and neurology.

5. Individual cells in inferior temporal cortex can be highly shape-selective and respond selectively, eg, to a hand or a face. They can maintain selectivity across position, size, and even rotation—properties that might explain perceptual constancy.
6. Inferotemporal cortex comprises a yet-unknown number of areas with very different functional specializations. While the functional logic of the overall organization remains unknown, we do know that cells with similar selectivity group into cortical columns and that face cells are organized into larger units called face areas.
7. Face recognition is supported by multiple face areas, each with a unique functional specialization. Face areas are selectively coupled to form a face-processing network, which has emerged as a model system for high-level vision.
8. Inferotemporal cortex is interconnected with perirhinal and parahippocampal cortices for memory formation, with the amygdala for the assignment of emotional valence to objects, and with prefrontal cortex for object categorization and visual working memory. If associative memories are stored as patterns of connections between neurons, what then are the specific contributions of hippocampus and neocortical structures of the medial temporal lobe, and by what cellular mechanisms do they exert their influences? The confluence of molecular-genetic, cellular, neurophysiological, and behavioral approaches promises to solve these and other problems.
9. Objects are perceived as members of a category. This simplifies the selection of appropriate behaviors, which often do not depend on stimulus details. Neurons with categorical selectivity are found in dorsolateral prefrontal cortex, a main projection site of inferior temporal cortex.
10. Object recognition relies on past experience. Perceptual learning can improve the ability to discriminate between complex objects and refine neural selectivity in inferior temporal cortex.
11. Visual information can be held in short-term working memory to be available beyond the duration of a sensory stimulus. Neurons in temporal and prefrontal cortex can exhibit delay-period activity after the disappearance of a stimulus. How these networks establish the ability to keep information online is an open question.
12. High-level visual information processing changes with top-down modulation. The sensory experience of an image in view and the recall of the same stimulus from memory are subjectively similar. Neurons in inferior temporal cortex exhibit similar activity during bottom-up activation and cued recall.

Thomas D. Albright
Winrich A. Freiwald

Selected Reading

Freedman DJ, Miller EK. 2008. Neural mechanisms of visual categorization: insights from neurophysiology. Neurosci Biobehav Rev 32:311–329.

Gross CG. 1999. *Brain, Vision, Memory: Tales in the History of Neuroscience.* Cambridge, MA: MIT Press.

Kanwisher N, McDermott J, Chun MM. 1997. The fusiform face area: a module in human extrastriate cortex specialized for face perception. J Neurosci 17:4302–4311.

Logothetis NK, Sheinberg DL. 1996. Visual object recognition. Annu Rev Neurosci 19:577–621.

McCarthy G, Puce A, Gore J, Allison T. 1997. Face-specific processing in the human fusiform gyrus. J Cog Neurosci 9:605–610.

Messinger A, Squire LR, Zola SM, Albright TD. 2005. Neural correlates of knowledge: stable representation of stimulus associations across variations in behavioral performance. Neuron 48:359–371.

Miller EK, Li L, Desimone R. 1991. A neural mechanism for working and recognition memory in inferior temporal cortex. Science 254:1377–1379.

Miyashita Y. 1993. Inferior temporal cortex: where visual perception meets memory. Annu Rev Neurosci 16:245–263.

Schlack A, Albright TD. 2007. Remembering visual motion: neural correlates of associative plasticity and motion recall in cortical area MT. Neuron 53:881–890.

Squire LR, Zola-Morgan S. 1991. The medial temporal lobe memory system. Science 253:1380–1386.

Ungerleider LG, Courtney SM, Haxby JV. 1998. A neural system for human visual working memory. Proc Natl Acad Sci U S A 95:883–890.

References

Baker CI, Behrmann M, Olson CR. 2002. Impact of learning on representation of parts and wholes in monkey inferotemporal cortex. Nat Neurosci 5:1210–1216.

Brown S, Schafer ES. 1888. An investigation into the functions of the occipital and temporal lobes of the monkey's brain. Philos Trans R Soc Lond B Biol Sci 179:303–327.

Damasio AR, Damasio H, Van Hoesen GW. 1982. Prosopagnosia: anatomic basis and behavioral mechanisms. Neurology 32:331–341.

Desimone R, Albright TD, Gross CG, Bruce CJ. 1984. Stimulus selective properties of inferior temporal neurons in the macaque. J Neurosci 8:2051–2062.

Desimone R, Fleming J, Gross CG. 1980. Prestriate afferents to inferior temporal cortex: an HRP study. Brain Res 184:41–55.

Farah MJ. 1990. *Visual Agnosia: Disorders of Object Recognition and What They Tell Us About Normal Vision*. Cambridge, MA: MIT Press.

Felleman DJ, Van Essen DC. 1991. Distributed hierarchical processing in the primate cerebral cortex. Cereb Cortex 1:1–47.

Freedman DJ, Riesenhuber M, Poggio T, Miller EK. 2002. Visual categorization and the primate prefrontal cortex: neurophysiology and behavior. J Neurophysiol 88:929–941.

Freiwald WA, Tsao DY. 2010. Functional compartmentalization and viewpoint generalization within the macaque face-processing system. Science 330:845–851.

Fujita I, Tanaka K, Ito M, Cheng K. 1992. Columns for visual features of objects in monkey inferotemporal cortex. Nature 360:343–346.

Fuster JM, Jervey JP. 1982. Neuronal firing in the inferotemporal cortex of the monkey in a visual memory task. J Neurosci 2:361–375.

Gross CG, Bender DB, Rocha-Miranda CE. 1969. Visual receptive fields of neurons in inferotemporal cortex of the monkey. Science 166:1303–1306.

Kosslyn SM. 1994. *Image and Brain.* Cambridge, MA: MIT Press.

Leibo JZ, Liao Q, Anselmi F, Freiwald WA, Poggio T. 2017. View-tolerant face recognition and Hebbian learning imply mirror-symmetric neural tuning to head orientation. Curr Biol 27:62–67.

Logothetis NK, Pauls J. 1995. Psychophysical and physiological evidence for viewer-centered object representations in the primate. Cereb Cortex 5:270–288.

Messinger A, Squire LR, Zola SM, Albright TD. 2001. Neuronal representations of stimulus associations develop in the temporal lobe during learning. Proc Natl Acad Sci U S A 98:12239–12244.

Miyashita Y, Chang HS. 1988. Neuronal correlate of pictorial short-term memory in the primate temporal cortex. Nature 331:68–70.

Rainer G, Rao SC, Miller EK. 1999. Prospective coding for objects in primate prefrontal cortex. J Neurosci 19:5493–5505.

Rollenhagen JE, Olson CR. 2000. Mirror-image confusion in single neurons of the macaque inferotemporal cortex. Science 287:1506–1508.

Sakai K, Miyashita Y. 1991. Neural organization for the long-term memory of paired associates. Nature 354:152–155.

Schwartz EL, Desimone R, Albright TD, Gross CG. 1983. Shape recognition and inferior temporal neurons. Proc Natl Acad Sci U S A 80:5776–5778.

Suzuki WA, Amaral DG. 2004. Functional neuroanatomy of the medial temporal lobe memory system. Cortex 40:220–222.

Tanaka K. 2003. Columns for complex visual object features in the inferotemporal cortex: clustering of cells with similar but slightly different stimulus selectivities. Cereb Cortex 13:90–99.

Teuber HL. 1968. Disorders of memory following penetrating missile wounds of the brain. Neurology 18:287–288.

Tomita H, Ohbayashi M, Nakahara K, Hasegawa I, Miyashita Y. 1999. Top-down signal from prefrontal cortex in executive control of memory retrieval. Nature 401:699–703.

Tsao DY, Freiwald WA, Tootell RB, Livingstone MS. 2006. A cortical region consisting entirely of face-selective cells. Science 311:670–674.

Wheeler ME, Petersen SE, Buckner RL. 2000. Memory's echo: vivid remembering reactivates sensory-specific cortex. Proc Natl Acad Sci U S A 97:11125–11129.

25

Visual Processing for Attention and Action

The human brain has an amazing ability to direct action to objects in the visual world—a baby reaching for an object, a tennis player hitting a ball, an artist looking at a model. This ability requires that the visual system solve three problems: making a spatially accurate analysis of the visual world, choosing the object of interest from the welter of stimuli in the visual world, and transferring information on the location and details of the object to the motor system.

The Brain Compensates for Eye Movements to Create a Stable Representation of the Visual World

Although the visual system produces vivid representations of our visual world, as described in preceding chapters, a visual image is not like an instantaneous photographic record but is dynamically constructed from information conveyed in several discrete neural pathways from the eyes. When we look at a painting, for example, we explore it with a series of quick eye movements (saccades) that redirect the fovea to different objects of interest in the visual field. The brain must take into account these eye movements in the course of producing an interpretable visual image from the light stimuli in the retina.

As each saccade brings a new object onto the fovea, the image of the entire visual world shifts on the fovea. These shifts occur several times per second, such that after several minutes the record of movement is a jumble (Figure 25–1). With such constant movement, visual images should resemble an amateur video in which the image jerks around because the camera operator is not skilled at holding the camera steady. In fact, however, our vision is so stable that we are ordinarily unaware of the visual effects of saccades. This is so because the brain makes continual adjustments to the images falling on the retina after each saccade.

A simple laboratory experiment, shown in Figure 25–2, illustrates the biological challenge to the brain.

Motor Commands for Saccades Are Copied to the Visual System

The first insight into the brain mechanisms underlying visual stability came from an observation by Hermann von Helmholtz in the 19th century. He saw a patient who could not move his eye horizontally toward his ear because of a paralysis of the lateral rectus muscle. Whenever the patient attempted to look toward his ear, the entire visual world jumped in the opposite direction and then returned to the center of gaze.

Figure 25–1 Eye movements during vision. A subject viewed this painting (*An Unexpected Visitor* by Ilya Repin) for several minutes, making saccades to selected fixation points, primarily to faces. Lines indicate saccades, and spots indicate points of fixation. (Reproduced, with permission, from Yarbus 1967).

Helmholtz postulated that a copy of the motor command for each saccade was fed to the visual system so that the representation of the visual world could be adjusted to compensate for eye movement. This adjustment would lead to a stable image of the visual world. In the 19th century, Helmholtz called such a copy a "sense of effort," and in the 20th century, it was named an efference copy or corollary discharge.

The corollary discharge solves the problem of the double-step saccade. In order for a corollary discharge to affect visual perception across eye movements, motor information has to affect the activity of visual neurons. This is precisely what happens to neurons in the parietal cortex, frontal eye field, prestriate visual cortex, and superior colliculus when a monkey makes a saccade. Each saccade can be considered a vector with two dimensions—direction and amplitude. Although the retinal image is different after each saccade, the brain can use the vector of each saccade to reconstruct the whole visual scene from the sequence of retinal images.

The corollary discharge can be seen at the level of a single cell. Physiological studies in the Rhesus monkey, an animal whose oculomotor and visual systems resemble those of humans, have illuminated the

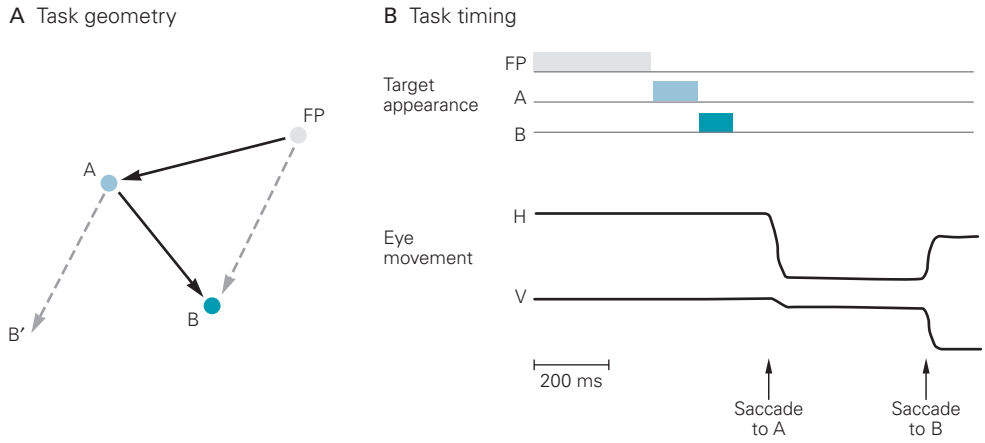

Figure 25–2 The double-step task illustrates how the brain stabilizes images during saccades.

A. A subject starts by looking at a fixation point (**FP**) that disappears, after which two saccade targets **A** and **B** appear and disappear sequentially before the subject can make the saccade. The first saccade (to target A) is simple. The retinal vector (FP→A) and the saccade vectors are the same. After the first saccade, the subject is looking at A. The retinal vector is A→B′, but the monkey must make a saccade whose vector is A→B. The brain must adjust the retinal vector to compensate for the first saccade.

B. Timing. The upper records show when the targets appear (**colored bars**). (Abbreviations: **H**, horizontal; **V**, vertical.)

problem. Every time a monkey makes a saccade, a stimulus currently not in the receptive field of a neuron in the lateral intraparietal area, and therefore incapable of exciting the neuron, will excite the neuron if the impending saccade will bring the stimulus into the receptive field, even before the saccade occurs (Figure 25–3). Thus, a corollary discharge of the impending saccade affects the visual responsiveness of the parietal neuron.

This transient remapping of the receptive field explains how subjects can perform the double-step task. Consider the diagram in Figure 25–2A. The task begins with the monkey directing gaze to the fixation point (FP). After the monkey makes the first saccade, the retinal vector A→B′ is no longer useful for making the A→B saccade. However, the FP→A saccade remaps the activity of the cell describing the vector A→B, so it responds to the target at the retinal location of B, which was not in its receptive field when the monkey was looking at FP. Remapping is found in a number of cortical and subcortical areas, including lateral intraparietal area, frontal eye field, medial intraparietal area, intermediate layers of the superior colliculus, and prestriate areas V4, V3a, and V2. As we shall see, remapping facilitates both visual perception around the time of a saccade and the accuracy of visually guided movement.

The first question this raises is: How does the brain obtain the vector of the saccade that it feeds back to the visual system? We know from decades of research that the motor command for the vector is represented in the superior colliculus on the roof of the midbrain (Chapter 35). Each neuron in the superior colliculus is tuned to saccades of a given vector, such that the neurons collectively provide a map of the vectors of all possible saccades. Inactivation of the superior colliculus affects the monkey's ability to make saccades. Electrical stimulation of the superior colliculus evokes saccades of the vector described by the neurons at the stimulation site. But this provides the vectors that actually drive the eye, not the vectors that inform perception about the vector of the saccade. How does the vector information used to move the eye become available to brain processes that do not move the eye but do require information about how it moved?

Since the vectors for moving the eye have been identified in the superior colliculus, it is reasonable to expect that this also might be the source of a corollary discharge. Indeed, it is. The superior colliculus has both descending pathways for generating the saccades and ascending pathways to the cerebral cortex that could carry the corollary discharge of the impending movement (Figure 25–4). The pathways to the cortex pass through the thalamus, as does all internal and almost all external information reaching the cerebral cortex.

The motor signal in the thalamus is not necessarily a corollary discharge; it could also be a movement command that simply passes through the cerebral cortex. That is not the case, however, because inactivation of this pathway in the thalamus does not alter the amplitude and direction of saccades. It is not driving saccades. It is more likely to be a corollary discharge. After inactivation of the thalamic pathway, monkeys cannot accurately perform the second saccade of the double-step task. In addition, inactivation disrupts the

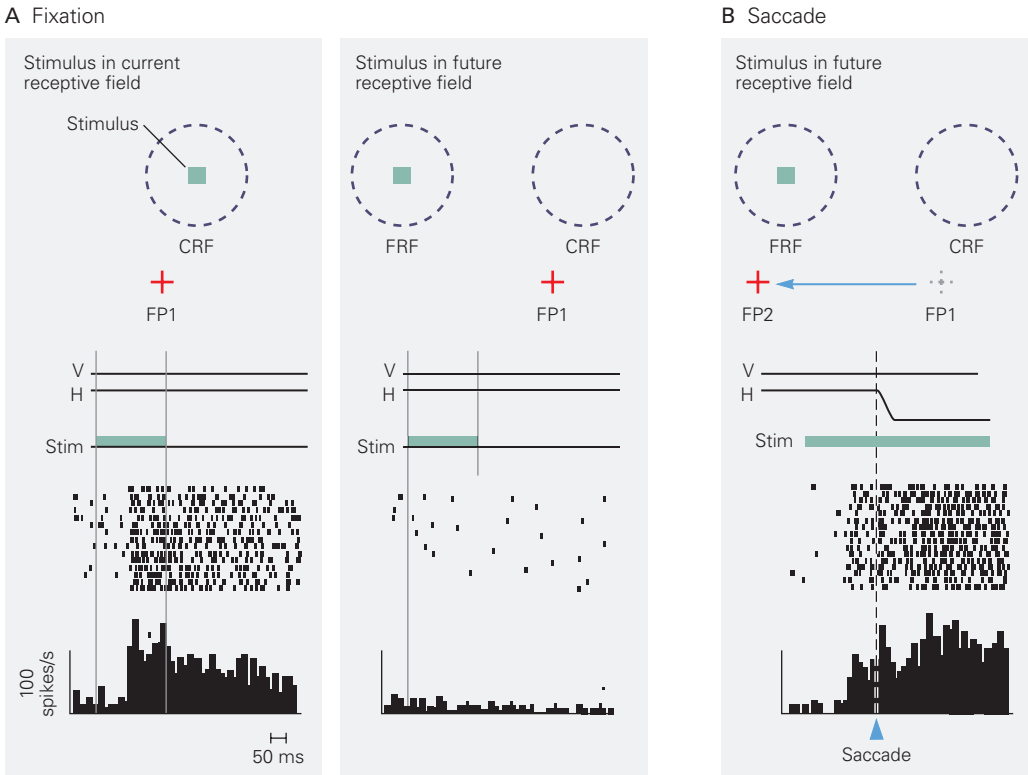

Figure 25–3 Remapping of the receptive field of a visual neuron in the parietal cortex of a monkey in conjunction with saccadic eye movements. (**A** [*left*] and **B** adapted, with permission, from Duhamel, Colby, and Goldberg 1992. **A** [*right*] reproduced with permission, from M.E. Goldberg.)

A. *Left:* The monkey looks at fixation point 1 (**FP1**), and the cell responds to the abrupt onset of a task-irrelevant stimulus in the current receptive field (**CRF**). Successive trials are synchronized on the appearance of the stimulus. (Abbreviations: **H**, horizontal eye position; **V**, vertical eye position.) *Right:* The monkey looks at FP1, and the cell does not respond to a stimulus flashed in the future receptive field (**FRF**).

B. The monkey makes a saccade from FP1 to FP2, which will bring the cell's receptive field onto the stimulus in the FRF. Now the cell fires even before the saccade begins, which means that a corollary discharge of the saccade plan remapped the area of the retina to which the cell responds.

receptive field remapping described earlier (Figure 25–3B). Because disrupting the corollary discharge disrupts both receptive field remapping and the behavioral compensation for eye movements, it is likely that the corollary discharge is essential for solving the problem of spatial accuracy for action.

To determine whether the corollary discharge also provides the information that allows the visual system to perceive the location of objects that appeared before a saccade, the monkey is trained to indicate where it thinks its eyes are directed at the end of the saccade. We can measure where the motor system moved the eye, but what we want to know is the monkey's perception of the change in its eye direction with each saccade. This can be determined using a task developed for humans by Heiner Deubel and his colleagues and adapted for monkeys. In this task, the monkey looks at a fixation point and then makes a saccade to a target (Figure 25–5A). During the saccade, the target temporarily disappears; when it reappears, it has been displaced to a location left or right of the original target. After the trial, the monkey moves a bar to the right or left to indicate the direction of the displacement (Figure 25–5A).

Over a series of trials, the monkey's responses are plotted to generate a psychometric curve (Figure 25–5B). This curve show the actual intrasaccadic target displacement (horizontal axis) in the same (forward) or opposite (backward) direction as the initial saccade, and how frequently the monkey reports that it was moved forward (vertical axis). The monkey responded that the target had moved forward 100% of the time when the target was 3° to the right. When the target moved 3° to the left, the monkey responded that it had never moved forward. The point on the psychometric curve where the monkey reported forward and backward displacements with equal frequency (the 50% horizontal line) was taken as the perceptual null point.

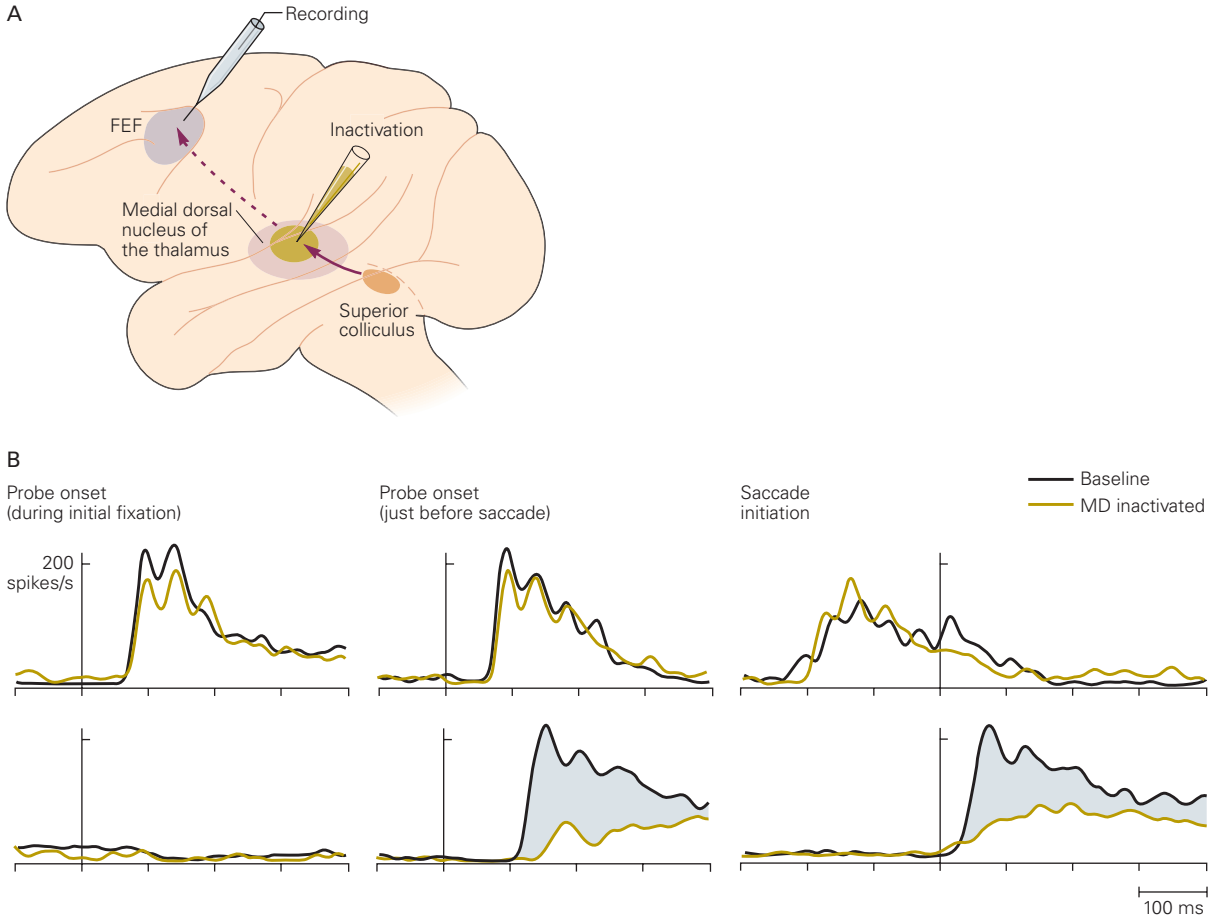

Figure 25–4 A corollary discharge from the motor program for saccades directs a shift in location of the receptive field of frontal eye field neurons prior to the saccade. (Adapted, with permission, from Sommer and Wurtz 2008. Copyright © 2008 by Annual Reviews.)

A. One possible pathway for the corollary discharge originates in saccade-generating neurons in the superior colliculus, passes through the medial dorsal nucleus of the thalamus, and terminates in the frontal eye field (**FEF**) in the frontal cortex.

B. When the medial dorsal nucleus (**MD**) is inactivated, the response of a frontal eye field neuron to a stimulus probe in the cell's current receptive field is unaffected (**upper records**), whereas the response to a stimulus in a future (post-saccade) receptive field is severely impaired (**lower records**). This result demonstrates that a corollary discharge from the saccade motor program directs the shift in the neuron's receptive field properties.

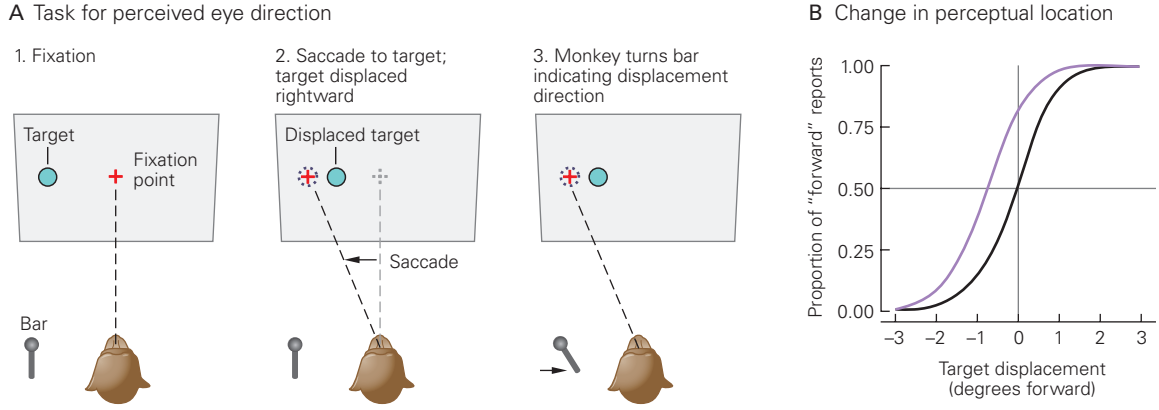

Figure 25–5 Perceived saccade direction changes with disruption of corollary discharge.

A. At the start of each trial, the monkey fixates a target on a screen (**1**). When the fixation point is turned off, the monkey makes a saccade to the target; during the saccade, the target is displaced randomly (up to 3°) either to the left or to the right (**2**). After the saccade to the original target, the monkey receives a reward for manually moving a bar in the direction of the target displacement (**3**).

B. Psychometric curves before (**black**) and after (**purple**) inactivation of the medial dorsal nucleus of the thalamus, which contains the relay neurons for the corollary discharge in its pathway between the superior colliculus and the frontal cortex. The curve shows the proportion of forward (in the direction of the saccade) judgments (y-axis) for each target displacement (x-axis). The post-saccadic target location at which the monkey perceived no displacement is defined as the perceptual null location. (Adapted, with permission, from Cavanaugh et al. 2016.)

We take this point to be the monkey's perception of the original target location. If the target were not perceived to move, it must be in the same location as before the saccade; in a normal monkey, that point is close to zero (Figure 25–5B).

We now have a corollary discharge that can provide the vector for each saccade and a task for a monkey that allows us to determine where it perceives the target to be at the end of the saccade. If the corollary discharge contributes to the monkey's perception, then inactivating the corollary discharge should change the animal's perception of target location. It does. The purple curve in Figure 25–5B represents the perceived location after corollary discharge inactivation; the curve shifts to the left after inactivation of the medial dorsal nucleus of the thalamus. The conclusion is that the corollary discharge does provide the vector of the saccade, which is necessary for the monkey to perceive that the target had moved. With each saccade, corollary discharge information provides perceptual information for determining the amplitude and direction of the current saccade, and it does so with machine-like precision several times per second.

The corollary discharge provides the vector information available before the saccade is made, but it is not the only source of information. Two other types of information must be evaluated after the saccade has taken place: visual cues and eye muscle proprioception. Visual cues are unlikely to be a factor in the perceptual experiment described (Figure 25–5) because the experiment was done in total darkness except for light scattered from the very dim fixation point and saccade target. In the light, however, could visual cues be a factor? In fact, repeating the experiment in the light did not improve the monkey's judgment and frequently made it worse.

Oculomotor proprioception is unlikely to provide the vector information at the end of the saccade because, on average, the metrics of the saccades before and during inactivation do not change, so there is little reason to expect that the muscle proprioception will have changed. In addition, while the corollary discharge begins at least 100 ms before the saccade, neuronal activity from oculomotor proprioception reaches the lateral intraparietal area about 150 ms after the saccade. As we will see in the next section, the role of proprioception in perception might be to provide information long after the saccade ends.

Finally, there is a second potential disruption of vision produced by saccades: a blur as the saccade sweeps the visual scene across the retina. The blur is not seen, however, because neuronal activity in a number of visual areas is suppressed around the time of every saccade. This so-called saccadic suppression was first seen in the superior colliculus and has subsequently been seen in the thalamus and areas of visual cortex beyond primary visual cortex.

A corollary discharge contributes to this neuronal activity suppression because the suppression occurs even in total darkness (no vision) and even if eye movement is blocked (no proprioception). Suppression can also be produced by visual masking, which occurs when one stimulus reduces the perception of a following or preceding stimulus. If a saccade starts in total darkness, and an object is then flashed and extinguished before the saccade ends, a blur can be seen during the saccade. If a mask is flashed after the saccade, the blur is suppressed. A correlate of such a masking effect is clearly seen in neurons in primary visual cortex. The suppression resulting from a corollary discharge is relatively weak but is present with all saccades; that from visual masking is much stronger but is present only in the light.

Oculomotor Proprioception Can Contribute to Spatially Accurate Perception and Behavior

Charles Sherrington suggested that the way the brain compensates for a moving eye is to measure directly where the eyes are in the orbit and adjust the visual signal for changes in position. Richard Andersen and Vernon Mountcastle discovered that the responses of parietal visual neurons with retinotopic receptive fields are modulated by the position of the eye in the orbit in a linear fashion called the *gain field* (Figure 25–6). From this relationship, the position of an object in head-centered (craniotopic) coordinates can easily be calculated.

Where does the eye position signal that creates the gain fields come from? It could come from a corollary discharge of eye position, or it could come from a proprioceptive mechanism. Human eye muscles have two structures that could contribute to oculomotor proprioception: muscle spindles and myotendinous cylinders, or palisade endings, an eye-specific structure. Area 3a, the region of somatosensory cortex to which skeletal muscle spindles project, has a representation of the position of the eye, which arises from proprioceptors in the contralateral orbit (Figure 25–7).

However, the proprioceptive measurement of eye position lags changes in eye position by 60 ms, and for 150 ms after a saccade, the gain fields modulate the visual response as if the monkey were still looking at the presaccadic target, long after the corollary discharge has remapped the visual response. Therefore, the eye position signal creating the gain fields probably arises from a proprioceptive mechanism. The possibility

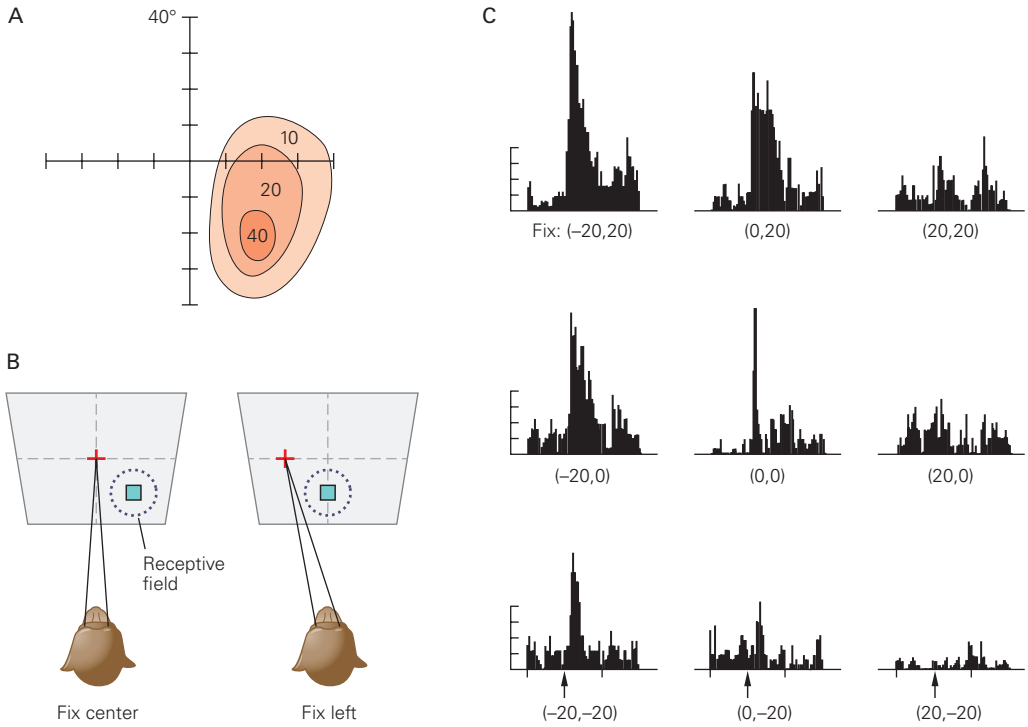

Figure 25–6 The position of the eye in the orbit affects the responses of parietal visual neurons with retinotopic receptive fields.

A. Receptive field relative to the fovea. Contour plot indicates spike rates for different spatial locations. Numbers are spikes per second for each contour at the maximum position.

B. The receptive field moves in space with the eye. On the left the monkey is fixating the center of the screen. On the right the same monkey is fixating 20° to the left of center. For the recordings in C, the stimulus (**blue square**) is always presented in the center of the receptive field.

C. Responses to a stimulus at the optimum location in the receptive field change as a function of the position of the eye in the orbit, from a maximum when the monkey fixates a point at –20°,20° to a minimum when the monkey fixates a point at 20°,–20°. **Arrows** indicate onset of stimulus flash. Trial duration, 1.5 sec; ordinate, 25 spikes/division. (Adapted, with permission, from Andersen, Essick, and Siegel 1985. Copyright © 1985 AAAS.)

exists that the brain calculates the spatial location of an object that appeared before an eye movement using two mechanisms: a corollary discharge that is rapid and a proprioceptive signal that is slow but can be more accurate than the corollary discharge. The proprioceptive signal can also be used to calibrate the corollary discharge.

Visual Scrutiny Is Driven by Attention and Arousal Circuits

In the 19th century, William James described attention as "the taking possession by the mind in clear and vivid form, of one out of what seem several simultaneously possible objects or trains of thought. It implies withdrawal from some things in order to deal effectively with others." James went on to describe two different kinds of attention: "It is either passive, reflex, non-voluntary, effortless or active and voluntary. In passive immediate sensorial attention the stimulus is a sense-impression, either very intense, voluminous, or sudden … big things, bright things, moving things … blood."

Your attention to this page as you read it is an example of voluntary attention. If a bright light suddenly flashed, your attention would probably be pulled away involuntarily from the page. Large changes in the visual scene that occur outside the focus of attention are often missed until the subject directs attention to them, a phenomenon referred to as change blindness (Figure 25–8).

Voluntary attention is closely linked to saccadic eye movements because the fovea has a much denser array of cones than the peripheral retina (Chapter 17) and moving the fovea to an attended object permits a finer-grain analysis than is possible with peripheral vision. Attention that selects a point in space, whether or not it is accompanied by a saccade, is called spatial attention. Searching for a specific kind of object, for

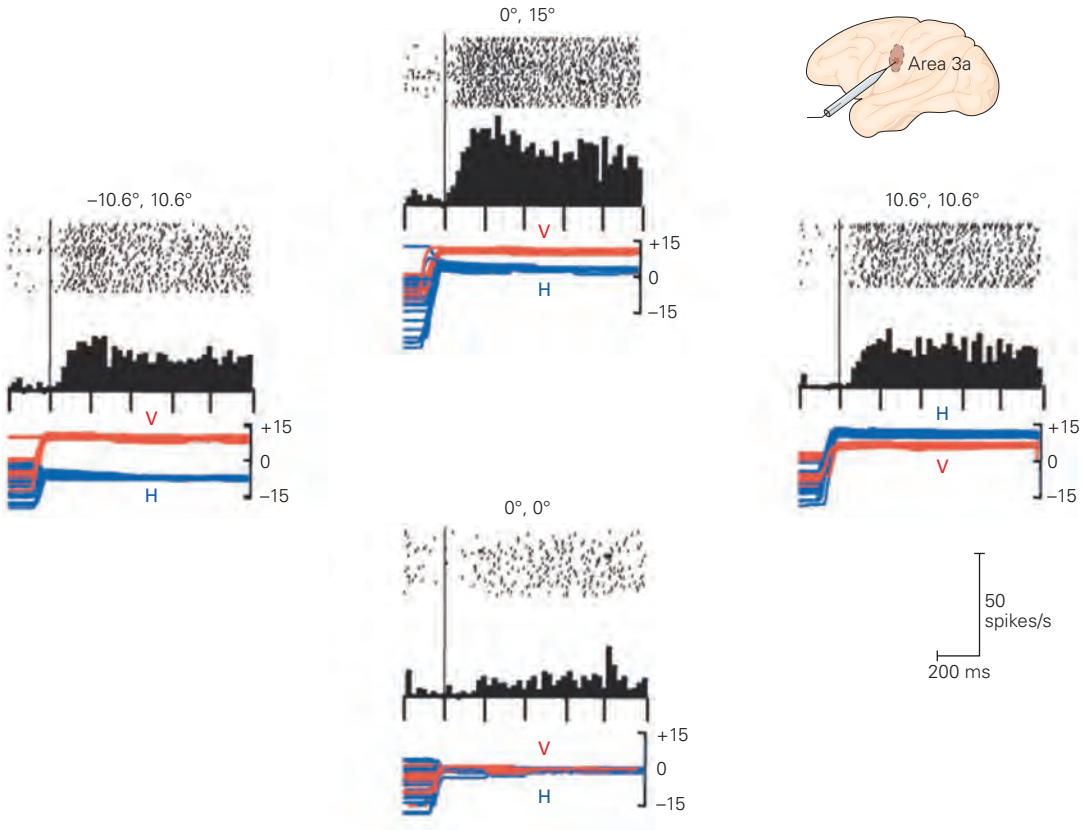

Figure 25–7 Eye position neuron in somatosensory cortex area 3a. Each panel shows horizontal (**H**) and vertical (**V**) eye position and the activity of the neuron after the monkey made a saccade to the eye position indicated above each raster. The neuron responds much more briskly when the eye is at 0°,15° than when it is at 0°,0°. (Reproduced, with permission, from Wang et al. 2007.)

example a red O among red and green Qs, involves a second kind of attention, feature attention: In your search, you ignore the green letters and attend only to the red ones.

Attention, both voluntary and involuntary, shortens reaction time and makes visual perception more sensitive. This increased sensitivity includes the abilities to detect objects at a lower contrast and ignore distracters close to an attended object. The abrupt appearance of a behaviorally irrelevant cue, such as a light flash, reduces the reaction time to a test stimulus presented 300 ms later in the same place. Conversely, when the cue appears away from the test stimulus, the reaction time is increased. The light flash draws involuntary attention to its location, thus accelerating the visual response to the test stimulus. Similarly, when a subject plans a saccade to a particular part of the visual field, the contrast threshold at which any object there can be detected is improved 50% by a cue.

Clinical studies have long implicated the parietal lobe in visual attention. Patients with lesions of the right parietal lobe have normal visual fields. When their visual perception is studied with a single stimulus in an uncomplicated visual environment, their responses are normal. However, when presented with a more complicated visual environment, with objects in the left and right visual hemifields, these patients tend to report less of what lies in the left hemifield (contralateral to their lesion) than in the right hemifield (ipsilateral to their lesion). This deficit, known as *neglect* (Chapter 59), arises because attention is focused on the visual hemifield ipsilateral to the lesion. Even when patients are presented with only two stimuli, one in each hemifield, they report seeing only the stimulus in the ipsilateral hemifield. When attention is focused on one stimulus in the affected hemifield and a second stimulus is presented in the unaffected hemifield, patients do not have the ability to shift attention to the new stimulus, even though the sensory pathway from the eye to the striate and prestriate cortex is intact.

This neglect of the contralateral visual hemifield extends to the neglect of the contralateral half of

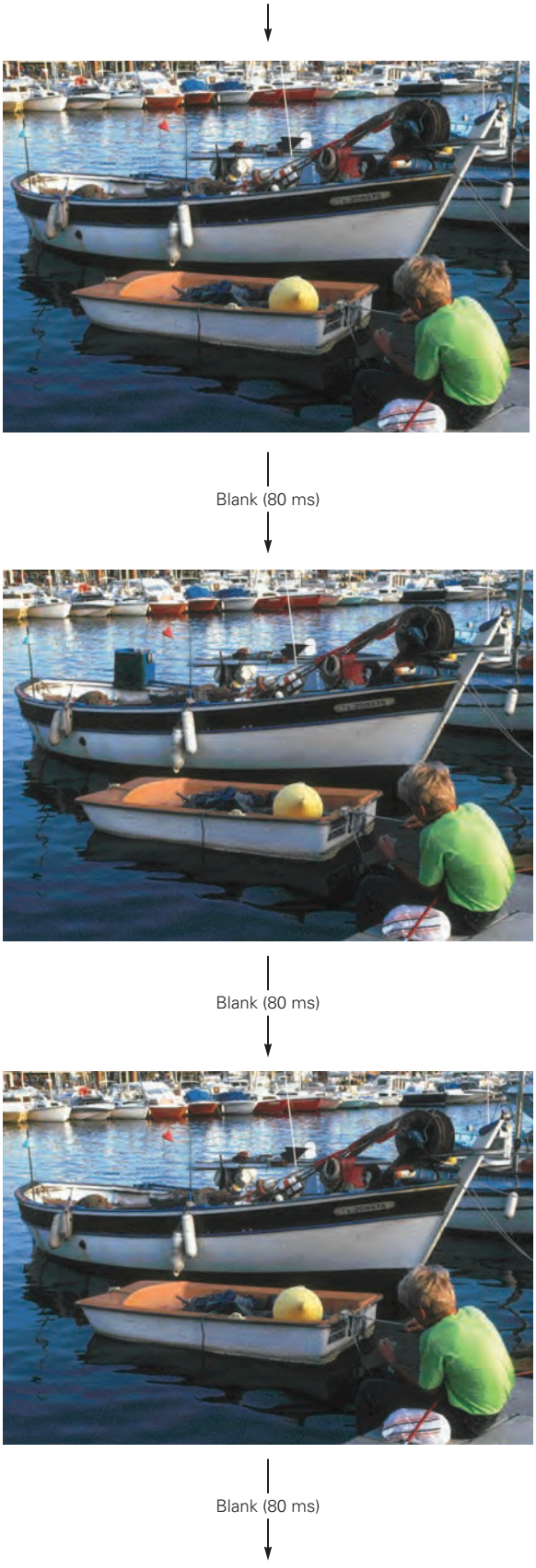

Figure 25–8 Change blindness. In a test for change blindness, one picture is presented followed by a blank screen for 80 ms, followed by the second picture, another blank screen, and a repeat of the cycle (*left*). The subject is asked to report what changed in the scene. Although there is a substantial difference between the two pictures, it takes multiple repetitions for most observers to detect the difference. (Reproduced, with permission, from Ronald Rensink.)

individual objects (Figure 25–9). Patients with right parietal lobe deficits often have difficulty reproducing drawings. When asked to draw a clock, for example, they may force all of the numbers into the right side of the clock's face, or when asked to bisect a line, they may place the midline well to the right of the line's actual center.

The process of attentional selection is evident at the level of single parietal neurons in the monkey. The responses of neurons in the lateral intraparietal area to a visual stimulus depend not only on the physical properties of the stimulus but also on its importance

Figure 25–9 Drawing of a candlestick by a patient with a lesion of the right parietal lobe. The patient neglects the left side of the candlestick, drawing only its right half. (Reproduced, with permission, from Halligan and Marshall 2001. Copyright © 2001 Academic Press.)

to the monkey. Thus, the responses to a behaviorally irrelevant stimulus are much smaller than for any event that evokes attention, such as the abrupt onset of a visual stimulus in the receptive field or the planning of a saccade to the receptive field of the neuron.

Although neurons in the lateral intraparietal area collectively represent the entire visual hemifield, the neurons active at any one moment represent only the important objects in the hemifield, a priority map of the visual field. The lateral intraparietal area acts as a summing junction for a number of different signals: saccade planning, abrupt stimulus onset, and the cognitive aspects of a searched-for feature.

The absolute value of the neuronal response evoked by an object does not by itself determine whether that animal is attending to that object. When a monkey plans a saccade to a stimulus in the visual field, attention is on the goal of the saccade, and the activity evoked by the saccade plan lies at the peak of the priority map. However, if a bright light appears elsewhere in the visual field, attention is involuntarily drawn to the bright light, which evokes more neuronal activity than does the saccade plan. Thus, the locus of attention can be identified only by examining the entire priority map and choosing its peak; it cannot be identified by monitoring activity at any one point alone (Box 25–1).

Box 25–1 The Priority Map in Parietal Cortex

Neurons in the lateral intraparietal area of the monkey represent only those objects of potential importance to the monkey, a priority map of the visual field. This selectivity for objects of behavioral importance can be demonstrated by recording from neurons in a monkey while the animal makes eye movements across a stable array of objects.

Stable objects in the visual world are rarely the objects of attention. In the lateral intraparietal area, as in most other visual centers of the brain, neuronal receptive fields are retinotopic; that is, they are defined relative to the center of gaze. As a monkey scans the visual field, fixed objects enter and leave the receptive fields of neurons with every eye movement without disrupting the monkey's attention (Figure 25–10).

The abrupt appearance of a visual stimulus involuntarily evokes attention. When a task-irrelevant light flashes in the receptive field of a lateral intraparietal

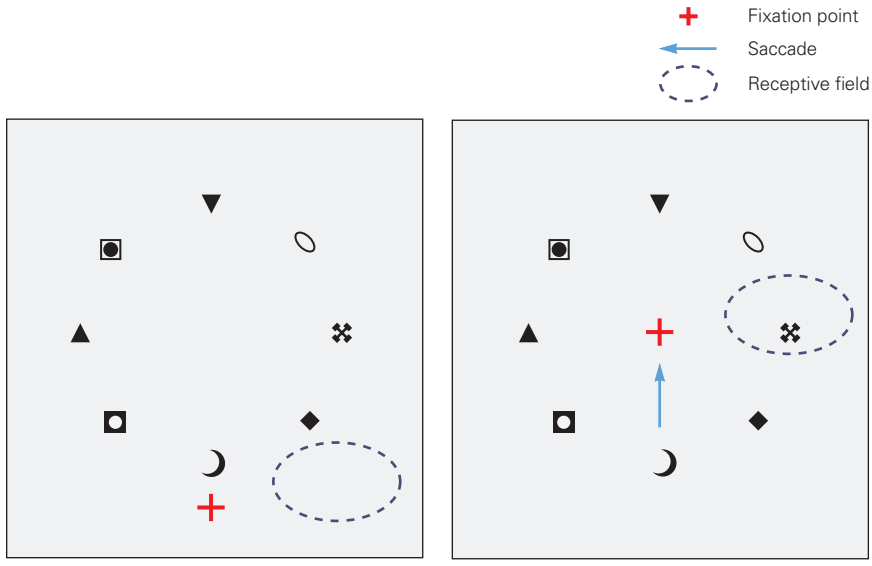

Figure 25–10 Exploring a stable array of objects. The monkey views a screen with a number of objects that remain in place throughout the experiment. The monkey's gaze can be positioned so that none of the objects are included in the receptive field of a neuron (*left*), or the monkey can make a saccade that brings one of the objects into the receptive field (*right*). (Reproduced, with permission, from Kusunoki, Gottlieb, and Goldberg 2000.)

(*continued*)

The Parietal Cortex Provides Visual Information to the Motor System

Vision interacts with the supplementary and premotor cortices to prepare the motor system for action. For example, when you pick up a pencil, your fingers are separated from your thumb by the width of the pencil; when you pick up a drink, your fingers are separated from your thumb by the width of the glass. The visual system helps to adjust the grip width before your hand arrives at the object. Similarly, when you insert a letter into a mail slot, your hand is aligned to place the letter in the slot. If the slot is tilted, your hand tilts to match.

Patients with lesions of the parietal cortex cannot adjust their grip width or wrist angle using visual information alone, even though they can verbally describe the size of the object or the orientation of the slot. Conversely, patients with intact parietal lobes and deficits in the ventral stream cannot describe the size of an object or its orientation but can adjust their grip width and orient their hands as well as normal subjects can. Neurons in parietal cortex are a critical source of information needed to manipulate or move objects.

Box 25–1 The Priority Map in Parietal Cortex (continued)

neuron, that cell responds briskly (Figure 25–11A). In contrast, a stable, task-irrelevant stimulus evokes little response when eye movement brings it into the neuron's receptive field (Figure 25–11B).

It is possible that the saccade that brings the stable object into the receptive field suppresses the visual response. This is not the case. A second experiment uses a similar array, except there is no stimulus at the location to which the saccade had brought the receptive field in the stable array experiment. The monkey fixates so that no member of the array is in the receptive field, and then the task-irrelevant stimulus suddenly appears at the post-saccade location of the receptive field. Now the monkey makes a saccade to the center of the array, bringing the recently appeared stimulus into the receptive field, and the cell fires intensely (Figure 25–11C). When the monkey makes the saccade, the two arrays are identical. However, the stable stimulus is presumably unattended,

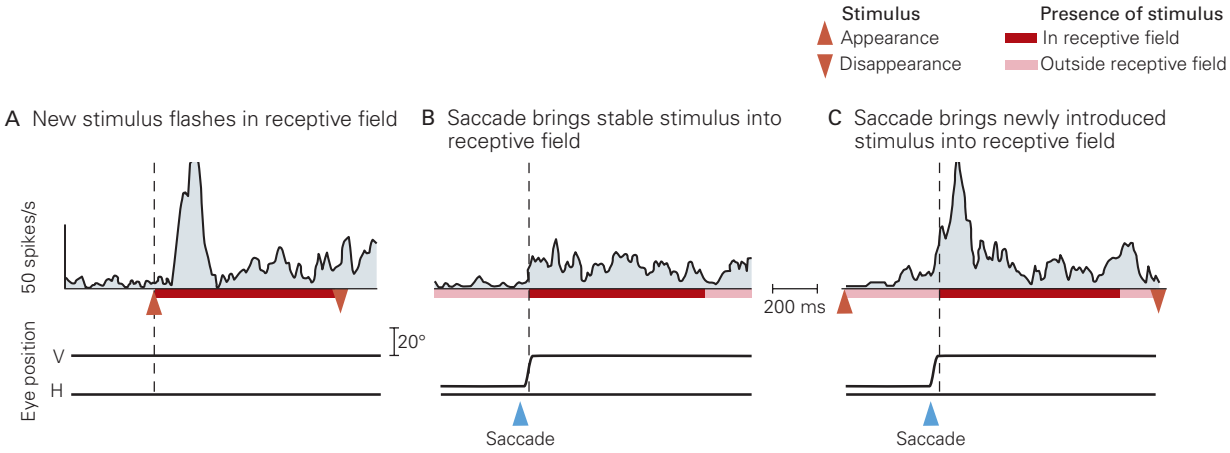

Figure 25–11 A neuron in the lateral intraparietal area fires only in response to salient stimuli. In each panel, neuronal activity and eye positions are plotted across time.

A. A stimulus flashes in the receptive field while the monkey fixates.

B. The monkey makes a saccade that brings a stable, task-irrelevant stimulus into the receptive field.

C. The monkey makes a saccade that brings the location of the recent light flash into the receptive field.

The neural operations behind visually guided movements involve identifying targets, specifying their qualities, and ultimately generating a motor program to accomplish the movement. Neurons in the parietal cortex provide the visual information necessary for independent movement of the fingers.

The representation of space in the parietal cortex is not organized into a single map like the retinotopic map in primary visual cortex. Instead, it is divided into at least four areas (LIP, MIP, VIP, AIP) that analyze the visual world in ways appropriate for individual motor systems. These four areas project visual information to the areas of premotor and frontal cortex that control individual voluntary movements (Figure 25–13).

Neurons in the medial intraparietal area describe the targets for reaching movements and project to the premotor area that controls reaching movements. The anterior intraparietal cortex has neurons that signal the size, depth, and orientation of objects that can be grasped. Neurons in this area respond to stimuli that could be the targets for a grasping movement, and these neurons are also active when the animal makes the movement (Figure 25–14). Neurons in the lateral

whereas the recently flashed stimulus evokes attention and a much larger response. Stable objects can evoke enhanced responses when they become relevant to the animal's current behavior.

A stable object can also be made behaviorally important. In that case, the neurons increase their firing rate when the monkey has to attend to the stable object brought into the receptive field by the saccade (Figure 25–12).

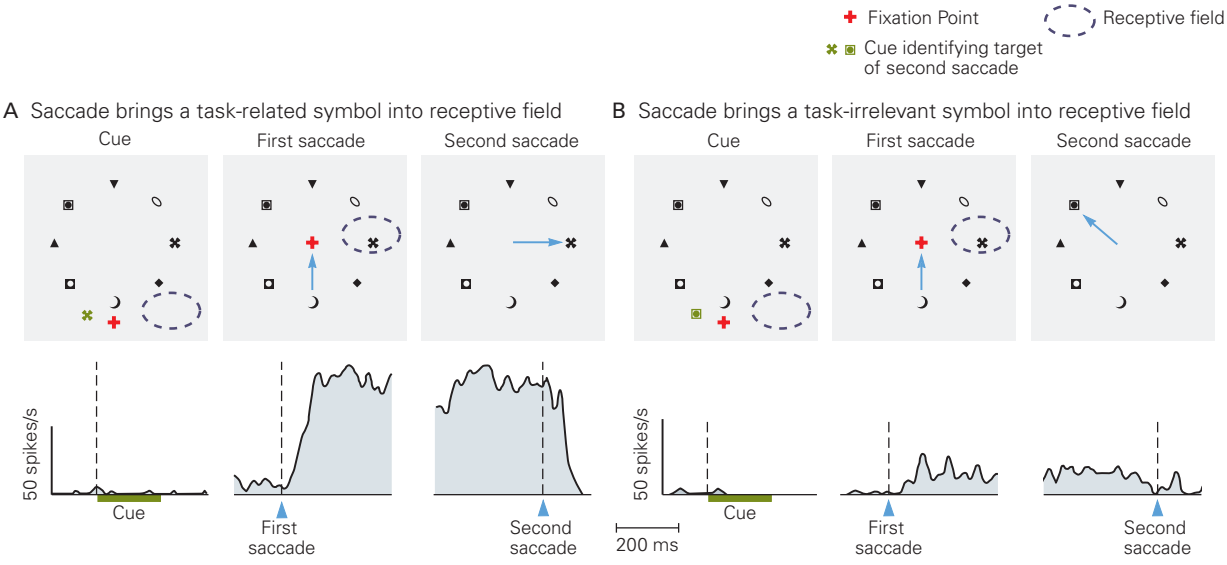

Figure 25–12 A neuron in the lateral intraparietal area fires before a saccade to a significant stable object. On each trial, one object in a stable array becomes significant to the monkey because the monkey must make a saccade to it. The monkey fixates a point outside the array, and a cue that matches an object in the array appears outside the neuron's receptive field. The monkey must then make a saccade to the center of the array and a second saccade to the object that matches the cue. Two experiments are shown (in parts A and B). The *left* panel shows the neuron's response to the appearance of the cue outside the receptive field, the *center* panel shows the response after the first saccade brings the cued object into the receptive field, and the *right* panel shows the response just before the second saccade to the cued object. The cues are shown here in **green** for clarity but were black in the experiment. The visual scene at the time of the saccade is identical in both experiments.

A. The monkey is trained to make the second saccade to the cued object; the cell fires intensely when the first saccade brings the object into the receptive field.

B. The monkey is trained to make the second saccade to an object outside the receptive field; the cell fires much less when the saccade brings the task-irrelevant stimulus into the receptive field.

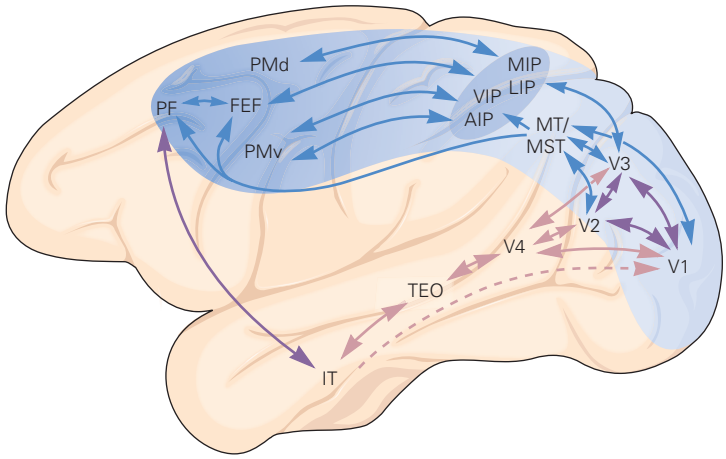

Figure 25–13 **Pathways involved in visual processing for action.** The dorsal visual pathway (**blue**) extends to the posterior parietal cortex and then to the frontal cortex. The ventral visual pathway (**pink**) is considered in Chapter 24. There are bidirectional projections from the inferior temporal cortex to the prefrontal cortex. (Abbreviations: **AIP**, anterior intraparietal cortex; **FEF**, frontal eye field; **IT**, inferior temporal cortex; **LIP**, lateral intraparietal cortex; **MIP**, medial intraparietal cortex; **MST**, medial superior temporal cortex; **MT**, middle temporal cortex; **PF**, prefrontal cortex; **PMd**, **PMv**, dorsal and ventral premotor cortices; **TEO**, occipitotemporal cortex; **VIP**, ventral intraparietal cortex; **V1–V4**, areas of visual cortex.)

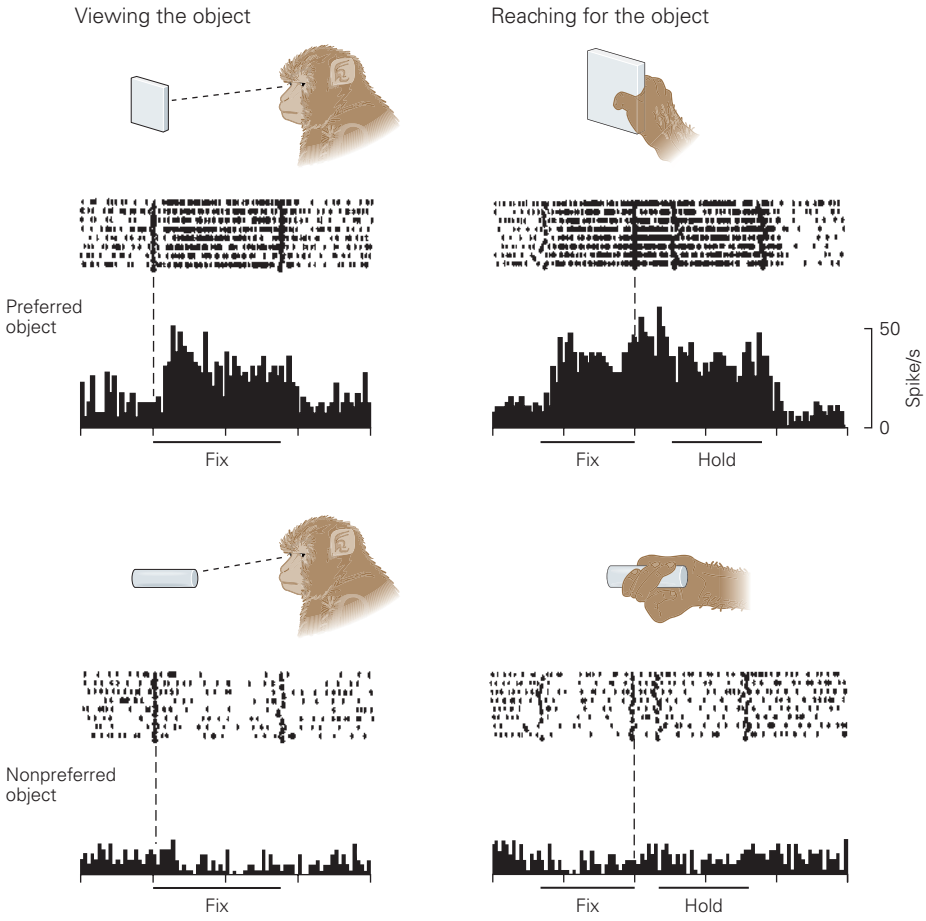

Figure 25–14 **Neurons in the anterior intraparietal cortex respond selectively to specific shapes.** The neuron shown here is selective for a rectangle, whether viewing the object or reaching for it. The neuron is not responsive to the cylinder in either case. (Reproduced, with permission, from Murata et al. 2000.)

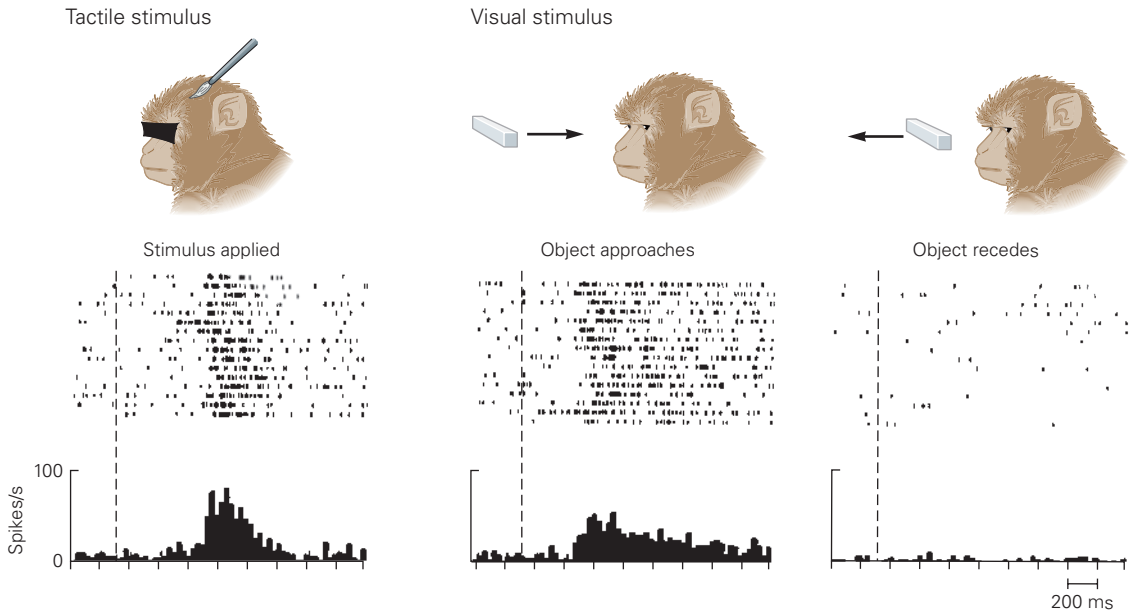

Figure 25–15 Bimodal neurons in the ventral intraparietal cortex of a monkey respond to both visual and tactile stimuli. The neuron shown here responds to tactile stimulation of the monkey's head or to a visual stimulus coming toward the head, but not to the same stimulus moving away from the head. (Reproduced, with permission, from Duhamel, Colby, and Goldberg 1998.)

intraparietal area specify the targets for saccades, and project to the frontal eye field.

Because a monkey cannot see its mouth, the ventral intraparietal area has bimodal neurons that respond to tactile stimuli on the face (Figure 25–15) and to objects in the visual world that are approaching the tactile receptive field, allowing the brain to estimate that an object is near the mouth. The ventral intraparietal area projects to the face area of premotor cortex.

Highlights

1. The image of the world enters the brain via the eye, which is constantly moving in the head. The visual system must compensate for changes in eye position to calculate spatial locations from retinal locations. Helmholtz postulated that the brain solves this problem by feeding back the motor signal that drives the eye to the visual system, to compensate for the effect of the eye movement. This motor feedback to the visual system is called corollary discharge.
2. Neurons in the lateral intraparietal area, which provides visual information to the oculomotor system, show evidence of this corollary discharge. Neurons that ordinarily do not respond to a particular stimulus in space will respond to it if an impending saccade will bring that stimulus into its receptive field.
3. This receptive field remapping depends on a pathway that goes from the intermediate layers of the superior colliculus to the medial dorsal nucleus of the thalamus to the frontal eye field. Medial dorsal nucleus inactivation impairs monkeys' ability to identify where their eyes land after a saccade, suggesting the corollary discharge has a perceptual as well as a motor role.
4. Sherrington postulated that the brain uses eye position to calculate the spatial location of objects from the position of their images on the retina. There is a representation of eye position in somatosensory cortex. Eye position modulates the visual responses of parietal neurons, and target position in space is simple to calculate from this modulation.
5. An unanswered question is how the brain chooses between the eye position and corollary discharge mechanisms to determine spatial position. Because corollary discharge precedes the change in eye position and proprioception follows it, could the brain use both positions at different times?
6. Attention is the ability of the brain to select objects in the world for further analysis. Without attention, spatial perception is severely limited. For

example, humans have great difficulty noticing a change in the visual world unless their attention is drawn to the spatial location of a change.

7. The activity of neurons in the parietal cortex predicts a monkey's locus of spatial attention as measured by their perceptual thresholds. The parietal cortex sums a number of different signals—motor, visual, cognitive—to create a priority map of the visual field. The motor system uses this map to choose targets for movement. The visual system uses the same map to find the locus of visual attention.
8. Lesions in the parietal cortex cause a neglect of the contralateral visual world.
9. Visual information provided by the parietal cortex enables the motor system to adjust hand grip to match the size of the object to which it reaches before the hand actually lands on the target. By contrast, patients with perceptual deficits caused by lesions in inferior temporal cortex adjust their grip perfectly well even though they cannot describe the nature or size of the object to which they reach perfectly.
10. There are at least four different visual maps in the intraparietal sulcus, each of which corresponds to a particular motor workspace.
11. Neurons in the anterior intraparietal area respond to targets for grasping, respond even when monkeys make grasping movements in total darkness, and project to the grasp region of premotor cortex.
12. Neurons in the ventral intraparietal area respond to objects coming toward the mouth, have tactile receptive fields on the face, and project to the mouth area of premotor cortex.
13. Neurons in the medial intraparietal area have a representation of arm position and respond to targets for reaching.
14. Neurons in the lateral intraparietal area respond to targets for eye movements and objects of visual attention, discharge before eye movements, and have a representation of eye position. Activity of these neurons is modulated by the position of the eyes in the orbit.
15. Neurons in the face region of area 3a in the somatosensory cortex have a representation of the position of the eye in the orbit that arises from the contralateral eye.

Michael E. Goldberg
Robert H. Wurtz

Selected Reading

Bisley JW, Goldberg ME. 2010. Attention, intention, and priority in the parietal lobe. Annu Rev Neurosci 33:1–21.

Cohen YE, Andersen RA. 2002. A common reference frame for movement plans in the posterior parietal cortex. Nat Rev Neurosci 3:553–562.

Colby CL, Goldberg ME. 1999. Space and attention in parietal cortex. Annu Rev Neurosci 23:319–349.

Henderson JM, Hollingworth A. 1999. High-level scene perception. Annu Rev Psychol 50:243–271.

Milner AD, Goodale MA. 1996. *The Visual Brain in Action.* Oxford: Oxford Univ. Press.

Rensink RA. 2002. Change detection. Annu Rev Psychol 53:245–277.

Ross J, Ma-Wyatt A. 2004. Saccades actively maintain perceptual continuity. Nat Neurosci 7:65–69.

Sommer MA, Wurtz RH. 2008. Brain circuits for the internal monitoring of movements. Annu Rev Neurosci 31:317–338.

Sun LD, Goldberg ME. 2016. Corollary discharge and oculomotor proprioception: cortical mechanisms for spatially accurate vision. Annu Rev Vis Sci 2:61–84.

Wurtz RH. 2008. Neuronal mechanisms of visual stability. Vision Res 48:2070–2089.

Yarbus AL. 1967. *Eye Movements and Vision.* New York: Plenum.

References

Andersen RA, Essick GK, Siegel RM. 1985. Encoding of spatial location by posterior parietal neurons. Science 230:456–458.

Bisley JW, Goldberg ME. 2003. Neuronal activity in the lateral intraparietal area and spatial attention. Science 299:81–86.

Cavanaugh J, Berman RA, Joiner WM, Wurtz RH. 2016. Saccadic corollary discharge underlies stable visual perception. J Neurosci 36:31–42.

Cohen YE, Andersen RA. 2002. A common reference frame for movement plans in the posterior parietal cortex. Nat Rev Neurosci 3:553–562.

Deubel H, Schneider WX, Bridgeman B. 1996. Postsaccadic target blanking prevents saccadic suppression of image displacement. Vision Res 36:985–996.

Duhamel J-R, Colby CL, Goldberg ME. 1992. The updating of the representation of visual space in parietal cortex by intended eye movements. Science 255:90–92.

Duhamel J-R, Colby CL, Goldberg ME. 1998. Ventral intraparietal area of the macaque: congruent visual and somatic response properties. J Neurophysiol 79:126–136.

Duhamel J-R, Goldberg ME, FitzGibbon EJ, Sirigu A, Grafman J. 1992. Saccadic dysmetria in a patient with a right frontoparietal lesion: the importance of corollary discharge for accurate spatial behavior. Brain 115:1387–1402.

Goodale MA, Meenan JP, Bulthoff HH, Nicolle DA, Murphy KJ, Racicot CI. 1994. Separate neural pathways for the visual analysis of object shape in perception and prehension. Curr Biol 4:604–610.

Hallett PE, Lightstone AD. 1976. Saccadic eye movements to flashed targets. Vision Res 16:107–114.

Halligan PW, Marshall JC. 2001. Graphic neglect—more than the sum of the parts. Neuro Image 14:S91–S97.

Henderson JM, Hollingworth A. 2003. Global transsaccadic change blindness during scene perception. Psychol Sci 14:493–497.

Kusunoki M, Gottlieb J, Goldberg ME. 2000. The lateral intraparietal motion, and task relevance. Vision Res 40:1459–1468.

Morrone MC, Ross J, Burr DC. 1997. Apparent position of visual targets during real and simulated saccadic eye movements. J Neurosci 17:7941–7953.

Murata A, Gallese V, Luppino G, Kaseda M, Sakata H. 2000. Selectivity for the shape, size, and orientation of objects for grasping in neurons of monkey parietal area AIP. J Neurophysiol 83:2580–2601.

Nakamura K, Colby CL. 2002. Updating of the visual representation in monkey striate and extrastriate cortex during saccades. Proc Natl Acad Sci U S A 99:4026–4031.

Perenin MT, Vighetto A. 1988. Optic ataxia: a specific disruption in visuomotor mechanisms. I. Different aspects of the deficit in reaching for objects. Brain 111:643–674.

Rensink RA. 2002. Change detection. Annu Rev Psychol 53:245–277.

Rizzolatti G, Luppino G, Matelli M. 1998. The organization of the cortical motor system: new concepts. Electroencephalogr Clin Neurophysiol 106:283–296.

Snyder LH, Batista AP, Andersen RA. 1997. Coding of intention in the posterior parietal cortex. Nature 386:167–170.

Thiele A, Henning P, Kubischik M, Hoffmann KP. 2002. Neural mechanisms of saccadic suppression. Science 295:2460–2462.

Umeno MM, Goldberg ME. 1997. Spatial processing in the monkey frontal eye field. I. Predictive visual responses. J Neurophysiol 78:1373–1383.

Walker MF, Fitzgibbon EJ, Goldberg ME. 1995. Neurons in the monkey superior colliculus predict the visual result of impending saccadic eye movements. J Neurophysiol 73:1988–2003.

Wang X, Zhang M, Cohen IS, Goldberg ME. 2007. The proprioceptive representation of eye position in monkey primary somatosensory cortex. Nat Neurosci 10:640–646.

Xu B, Karachi C, Goldberg M. 2012. The postsaccadic unreliability of gain fields renders it unlikely that the motor system can use them to calculate target position in space. Neuron 76:1201–1209.

26

Auditory Processing by the Cochlea

Human experience is enriched by the ability to distinguish a remarkable range of sounds—from the intimacy of a whisper to the warmth of a conversation, from the complexity of a symphony to the roar of a stadium. Hearing begins when the sensory cells of the cochlea, the receptor organ of the inner ear, transduce sound energy into electrical signals and forward them to the brain. Our ability to recognize small differences in sounds stems from the cochlea's capacity to distinguish among frequency components, their amplitudes, and their relative timing.

Hearing depends on the remarkable properties of hair cells, the cellular microphones of the inner ear. Hair cells transduce mechanical vibrations elicited by sounds into electrical signals, which are then relayed to the brain for interpretation. The hair cells can measure motions of atomic dimensions and transduce stimuli ranging from static inputs to those at frequencies of tens of kilohertz. Remarkably, hair cells can also serve as mechanical amplifiers that augment auditory sensitivity. Each of the paired cochleae contains approximately 16,000 of these cells. Deterioration of hair cells and their innervation accounts for most of the hearing loss that afflicts about 10% of the population in industrialized countries.

The Ear Has Three Functional Parts

Sound consists of alternating compressions and rarefactions propagated by an elastic medium, the air, at a speed of approximately 340 m/s. This wave of pressure changes carries mechanical energy that stems from the work produced on air by our vocal apparatus or some other sound source. The mechanical energy is captured and transmitted to the receptor organ, where it is transduced into electrical signals suitable for neural analysis. These three tasks are associated with the external ear, the middle ear, and the cochlea of the inner ear, respectively (Figure 26–1).

The most obvious component of the human external ear is the auricle, a prominent fold of cartilage-supported skin. The auricle acts as a reflector to capture sound efficiently and focus it into the external auditory meatus, or ear canal. The ear canal ends at the tympanum, or eardrum, a diaphragm approximately 9 mm in diameter and 50 µm in thickness.

The external ear is not uniformly effective at capturing sound from all directions; the auricle's corrugated surface collects sounds best when they originate at different, but specific, positions with respect to the head. Our capacity to localize sounds in space, especially along the vertical axis, depends critically on these sound-gathering properties. Each auricle has a unique topography; its effect on sound reflections at different frequencies is learned by the brain early in life.

The middle ear is an air-filled pouch connected to the pharynx by the Eustachian tube. Airborne sound traverses the middle ear as vibrations of the auditory ossicles, three tiny bones that are linked together: the malleus (hammer), incus (anvil), and stapes (stirrup; Figure 26–1). A long extension of the malleus is attached to the tympanic membrane; its other extreme makes a ligamentous connection to the incus, which is similarly connected to the stapes. The flattened base of the stapes, the footplate, is seated in an opening—the oval window—in the bony covering of the cochlea. The auditory ossicles are relics of evolution. The stapes was originally a component of the gill support of ancient fish; the malleus and incus were components of the primary jaw joint in reptilian ancestors.

The inner ear includes the auditory sensory organ, the cochlea (Greek *cochlos,* snail), a coiled structure of progressively diminishing diameter wound around a conical bony core (Figure 26–1). In humans, the cochlea is approximately 9 mm across, the size of a chickpea, and is embedded within the temporal bone. The interior of the cochlea consists of three parallel liquid-filled compartments termed *scalae*. In a cross section of the cochlea at any position along its spiral course, the top compartment is the *scala vestibuli* (Figure 26–2). At the broad, basal end of this chamber is the oval window, the opening that is sealed by the footplate of the stapes. The bottom compartment is the *scala tympani;* it too has a basal aperture, the round window, which is closed by

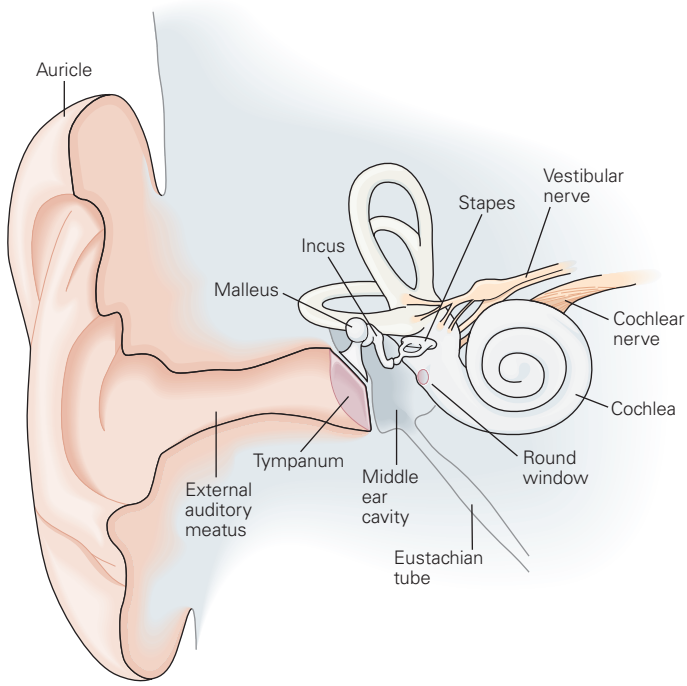

Figure 26–1 The structure of the human ear. The external ear, especially the prominent auricle, focuses sound into the external auditory meatus. Alternating increases and decreases in air pressure vibrate the tympanum. These vibrations are conveyed across the air-filled middle ear by three tiny, linked bones: the malleus, the incus, and the stapes. Vibration of the stapes stimulates the cochlea, the hearing organ of the inner ear.

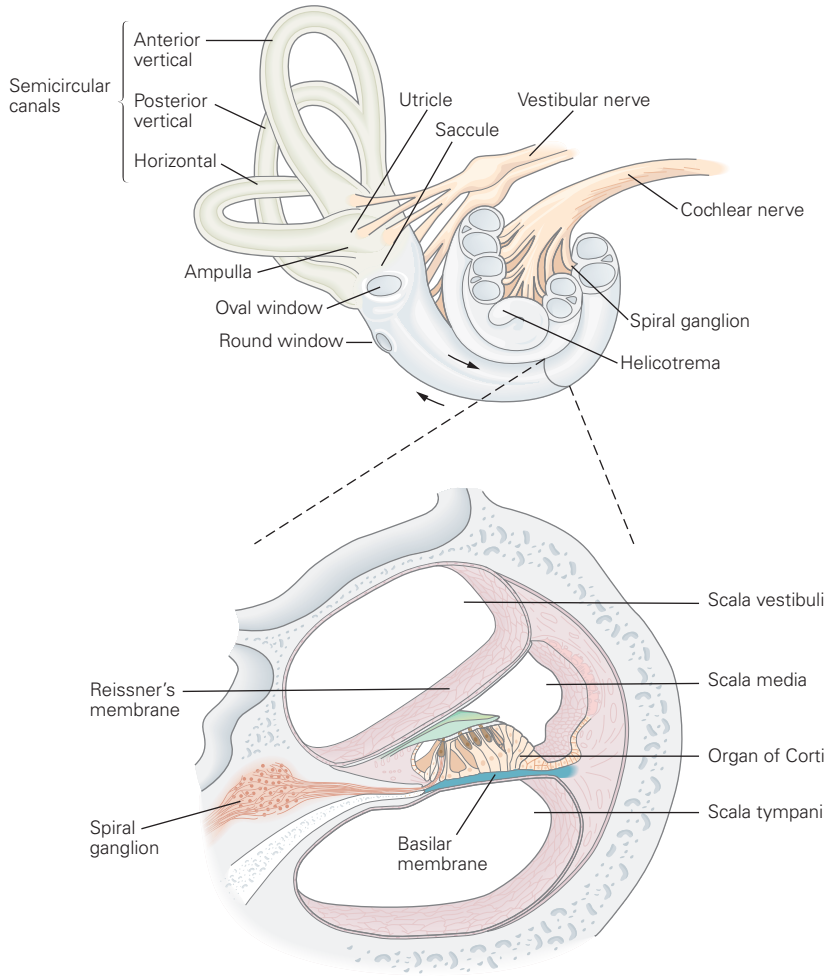

Figure 26–2 The structure of the cochlea. A cross section of the cochlea shows the arrangement of the three liquid-filled ducts or scalae, each of which is approximately 33 mm long. The scala vestibuli and scala tympani communicate through the helicotrema at the apex of the cochlea. At the base, each duct is closed by a sealed aperture. The scala vestibuli is closed by the oval window, against which the stapes pushes in response to sound; the scala tympani is closed by the round window, a thin, flexible membrane. Between these two compartments lies the scala media, an endolymph-filled tube whose epithelial lining includes the 16,000 hair cells in the organ of Corti surmounting the basilar membrane (**blue**). The hair cells are covered by the tectorial membrane (**green**). The cross section in the lower diagram has been rotated so that the cochlear apex is oriented toward the top.

a thin, elastic diaphragm beyond which lies the air of the middle-ear cavity. The two chambers are separated along most of their length by the cochlear partition but communicate with one another at the very tip of the cochlea, through the helicotrema.

The cochlear partition contains the third liquid-filled cavity, the *scala media,* and is delimited by two membranes. The thin Reissner's, or vestibular, membrane divides the scala media from the scala vestibuli. The basilar membrane separates the cochlear partition from the scala tympani and supports the complex sensory structure involved in auditory transduction, the organ of Corti (Figure 26–2).

Hearing Commences With the Capture of Sound Energy by the Ear

Psychophysical experiments have established that we perceive an approximately equal increment in loudness for each 10-fold increase in the magnitude of a sound stimulus. This type of relation is characteristic

of many of our senses and is the basis of the Weber-Fechner law (Chapter 17). A logarithmic scale is therefore useful in relating the magnitude of sound pressure to perceived loudness. Sound pressure corresponds to the sound-evoked modulation of the air pressure with respect to the mean atmospheric pressure; the louder the sound, the larger is the modulation. The sound-pressure level, L, of any sound may be expressed in decibels (dB) as

$$L = 20 \cdot \log_{10}(P / P_{REF}),$$

in which P, the magnitude of the stimulus, is the root-mean-square sound pressure (in units of pascals, abbreviated Pa, or newtons per square meter). For a sinusoidal stimulus, the amplitude exceeds the root-mean-square value by a factor of $\sqrt{2}$. The arbitrary reference level on this scale, 0 dB sound-pressure level (SPL), corresponds to a root-mean-square sound pressure, P_{REF}, of 20 μPa. This level represents the approximate threshold of human hearing at 1 to 4 kHz, the frequency range in which our ears are most sensitive.

Sound consists of very small alternating changes in the local air pressure. The loudest sound tolerable to humans, approximately 120 dB SPL, transiently alters the local atmospheric pressure by only ±0.01%. In contrast, a sound at the threshold level causes a change in the local pressure of much less than one part in a billion. From the faintest sounds that can be detected to sounds so intense that they hurt, the sound pressure increases by one millionfold, which correspond to a trillionfold range in stimulus power. The dynamic range of hearing is enormous.

Despite their small magnitude, sound-induced increases and decreases in air pressure move the tympanum inward and outward (Figure 26–3A,B). Near threshold, the amplitude of vibration is in the picometer range, which is comparable to the tympanum's own thermal fluctuations. Even loud sounds elicit vibrations of the tympanum that do not exceed 1 μm in amplitude. The resulting motions of the ossicles are essentially like those of two interconnected levers (the malleus and incus) and a piston (the stapes). The vibration of the incus alternately drives the stapes deeper into the oval window and retracts it, like a piston that pushes and pulls cyclically upon the liquid in the scala vestibuli. In humans, the area of the eardrum is about 20-fold larger than that of the stapes footplate. As a result, pressure changes applied on the liquid of scala vestibuli by the stapes footplate are larger than those pushing and pulling the tympanum. Pressures are further magnified by the lever operating between the malleus and the incus, the incus in humans being only about 70% of the length of the malleus.

The action of the stapes produces pressure changes that propagate through the liquid of the scala vestibuli at the speed of sound in water. Because liquids are virtually incompressible, however, the primary effect of the stapes's motion is to displace the liquid in the scala vestibuli in the one direction that is not restricted by a rigid boundary: toward the elastic cochlear partition (Figure 26–3B). The deflection of the cochlear partition downward increases the pressure in the scala tympani, displacing a liquid mass that causes outward bowing of the round window. Each cycle of a sound stimulus thus evokes a cycle of up-and-down movement of a minuscule volume of liquid in each of the cochlea's three chambers, thus displacing the sensory organ.

By increasing the magnitude of pressure changes by up to 30-fold, the overall effect of the middle ear is to match the low impedance of the air outside the ear to the higher impedance of the cochlear partition, thus ensuring the efficient transfer of sound energy from the first medium to the second. The pressure gain afforded by the middle ear depends on sound frequency, which determines the U-shape tuning curve of auditory threshold.

Changes of the middle ear's normal structure that reduce its displacement amplitudes can lead to *conductive hearing loss*, of which two forms are especially common. First, scar tissue caused by middle-ear infection (*otitis media*) can immobilize the tympanum or ossicles. Second, a proliferation of bone in the ligamentous attachments of the ossicles can reduce their normal freedom of motion. This chronic condition of unknown origin, termed *otosclerosis*, can lead to severe deafness.

A clinician may test for conductive hearing loss by the simple Rinné test. A patient is asked to assess the loudness of a vibrating tuning fork under two conditions: when the tuning fork is held in the air or when it is pressed against the head just behind the ear. For the second stimulus, sound is conducted through bone to the cochlea. If the second stimulus is perceived to be louder, the patient's conductive pathway through the middle ear may be damaged, but the inner ear is likely to be intact. In contrast, if bone conduction is not more efficient than airborne stimulation, the patient may have inner-ear damage, that is, sensorineural hearing loss. The diagnosis of conductive hearing loss is important, because surgical intervention can be highly effective: Removal of scar tissue or reconstitution of the conductive pathway with a prosthesis may restore excellent hearing.

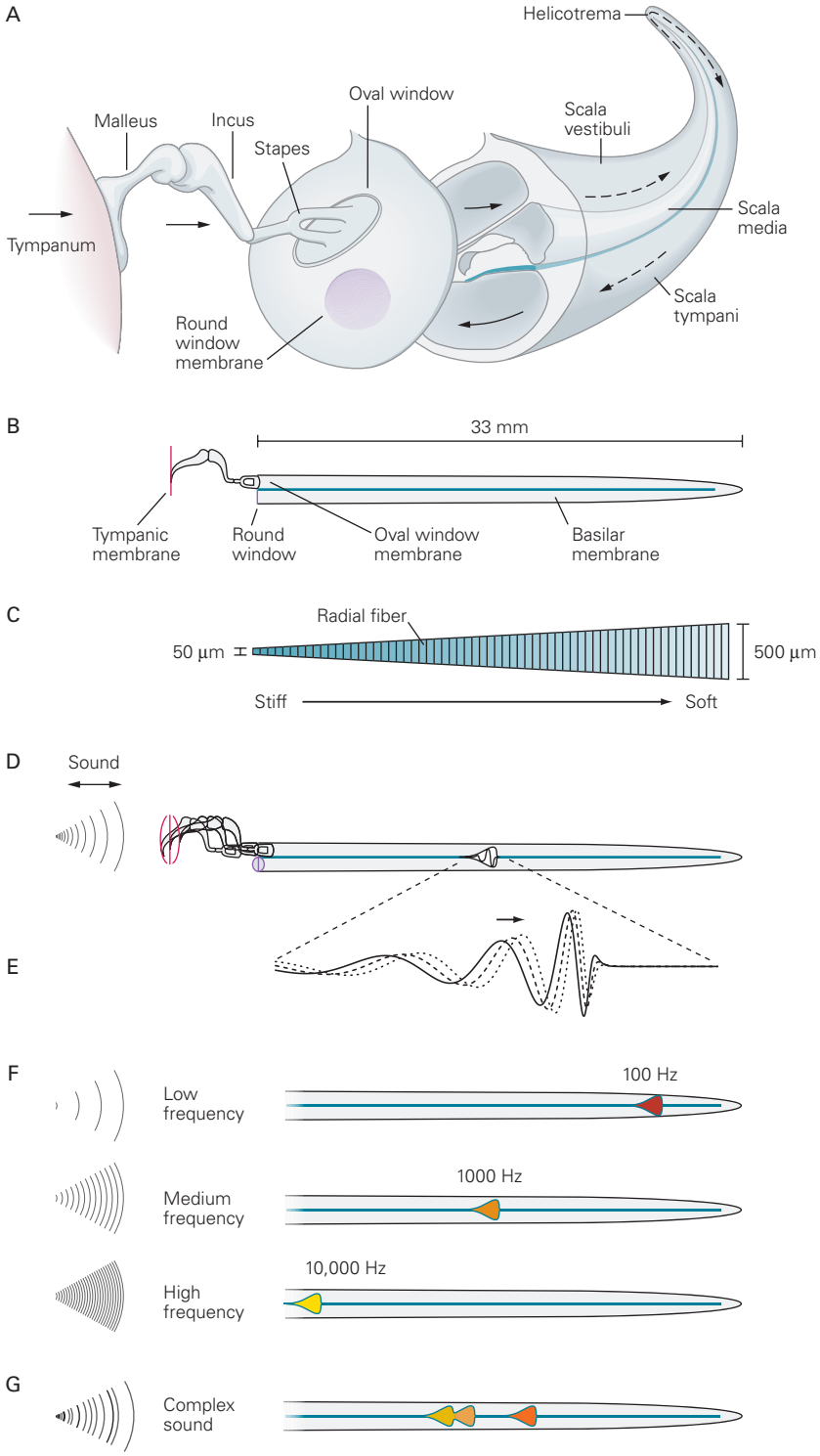
A
Helicotrema
Oval window
Malleus
Incus
Stapes
Scala vestibuli
Scala media
Tympanum
Scala tympani
Round window membrane
B
33 mm
Tympanic membrane
Round window
Oval window membrane
Basilar membrane
C
Radial fiber
50 µm
500 µm
Stiff
Soft
D
Sound
E
F
Low frequency
100 Hz
Medium frequency
1000 Hz
High frequency
10,000 Hz
G
Complex sound

The Hydrodynamic and Mechanical Apparatus of the Cochlea Delivers Mechanical Stimuli to the Receptor Cells

The Basilar Membrane Is a Mechanical Analyzer of Sound Frequency

The continuous variation of the mechanical properties of the basilar membrane along the cochlea's length, approximately 33 mm, is key to the cochlea's operation. The basilar membrane at the base of the human cochlea is less than one-fifth as broad as at the apex. Thus, although the cochlear chambers become progressively smaller from the organ's base toward its apex, the basilar membrane *increases* in width (Figure 26–3C). Moreover, the basilar membrane is relatively thick toward the base of the cochlea but thinner at the apex. Both morphological gradients contribute to a base-to-apex decrease in basilar-membrane stiffness. Radial collagen fibers within the membrane determine most of its elasticity. The basilar membrane may schematically be regarded as a set of weakly coupled radial segments of increasing length along the longitudinal axis of the cochlea, with the shortest segment at the base and the longest segment at the apex, analogous to the multiple strings of a piano.

Stimulation with a pure tone evokes a complex and elegant movement of the basilar membrane. Over one complete cycle of a tone, each affected segment along the basilar membrane undergoes a single cycle of vibration (Figure 26–3D,E). The various segments of the membrane do not, however, oscillate in phase with one another. As first demonstrated by Georg von Békésy using stroboscopic illumination, each segment reaches its maximal amplitude of motion slightly later than its basal neighbor. The normalized sinusoidal movement of the basilar membrane reproduces that of the stapes, but with a time delay that increases with the distance from the cochlear base.

The overall pattern of motion of the membrane is that of a traveling wave that traverses the cochlea from the stiff base toward the floppier apex. As each wave advances toward the apex, the amplitude of vibration grows to a maximum and then declines rapidly. The position at which the traveling wave reaches its maximal amplitude depends on sound frequency. The basilar membrane at the base of the cochlea responds best to the highest audible frequencies—in humans approximately 20 kHz. At the cochlear apex, the membrane responds to frequencies as low as 20 Hz. The intervening frequencies are represented along the basilar

Figure 26–3 (Opposite) Motion of the basilar membrane.

A. An uncoiled cochlea, with its base displaced to show its relation to the scalae, indicates the flow of stimulus energy. Sound vibrates the tympanum, which sets the three ossicles of the middle ear in motion. The piston-like action of the stapes, a bone inserted partially into the elastic oval window, produces oscillatory pressure differences that rapidly propagate along the scala vestibuli and scala tympani. Low-frequency pressure differences are shunted through the helicotrema, where the two ducts communicate.

B. The functional properties of the cochlea are conceptually simplified if the cochlea is viewed as a linear structure with only two liquid-filled compartments separated by the elastic basilar membrane.

C. The basilar membrane, here represented in a surface view, increases in width from approximately 50 μm near the base to 500 μm near the apex of the cochlea. Radial collagen fibers run from the neural to the abneural edge of the membrane. As the result of its morphological gradients, the basilar membrane's mechanical properties vary continuously along its length.

D. The oscillatory stimulation of a sound causes a traveling wave on the basilar membrane, shown here within the envelope of maximal displacement over an entire cycle. The magnitude of movement is grossly exaggerated in the vertical direction; the loudest tolerable sounds move the basilar membrane by only ±150 nm, a scaled distance less than one-hundredth the width of the lines representing the basilar membrane in these figures.

E. An enlargement of the active region in D demonstrates the motion of the basilar membrane in response to stimulation with sound of a single frequency. The continuous curve depicts a traveling wave at one instant; the vertical scale of basilar-membrane deflection is exaggerated about one-millionfold. The **dashed** and **dotted curves** portray the traveling wave at successively later times as it progresses from the cochlear base (*left*) toward the apex (*right*). As the wave approaches the characteristic place for the stimulus frequency, it slows and grows in amplitude. The stimulus energy is then transferred to hair cells at positions within the wave's peak.

F. Each frequency of stimulation excites maximal motion at a particular position along the basilar membrane. Low-frequency sounds produce basilar-membrane motion near the apex, where the membrane is relatively broad and soft. Mid-frequency sounds excite the membrane in its middle. The highest frequencies that we can hear excite the basilar membrane at its narrow, stiff base. The mapping of sound frequency onto the basilar membrane is approximately logarithmic.

G. The basilar membrane performs spectral analysis of complex sounds. In this example, a sound with three prominent frequencies, such as the three formants of a vowel sound, excites basilar-membrane motion in three regions, each of which represents a particular frequency. Hair cells in the corresponding positions transduce the basilar-membrane oscillations into receptor potentials, which in turn excite the nerve fibers that innervate these particular regions.

membrane in a continuous array (Figure 26–3F). In the 19th century, the German physiologist Hermann von Helmholtz was the first to appreciate that the basilar membrane's operation is essentially the inverse of a piano's. The piano synthesizes a complex sound by combining the pure tones produced by numerous vibrating strings; the cochlea, by contrast, deconstructs a complex sound by isolating the component tones at the appropriate segments of the basilar membrane.

For any frequency within the auditory range, there is a characteristic place along the basilar membrane at which the magnitude of vibration is maximal. Although the morphological gradients of the basilar membrane are key to the process, the actual dispersion of a sound's frequency components along the cochlea's longitudinal axis depends on the mechanical properties of the cochlear partition as a whole. In particular, as we shall detail later, the hair cells within the organ of Corti provide active mechanical feedback that sharpens mechanical tuning of the basilar membrane and enhances its sensitivity to sound. The arrangement of vibration frequencies along the basilar membrane is an example of a *tonotopic map.* The relationship between frequency and position along the basilar membrane varies monotonically, but is not linear; the logarithm of the frequency decreases roughly in proportion to the distance from the cochlea's base. The frequencies from 20 kHz to 2 kHz, those between 2 kHz and 200 Hz, and those spanning 200 Hz to 20 Hz are each represented by approximately one-third of the basilar membrane's extent.

Analysis of the response to a complex sound illustrates how the basilar membrane operates in daily life. A vowel sound in human speech, for example, ordinarily comprises three dominant frequency components termed formants. Each frequency component of the stimulus establishes a traveling wave that, to a first approximation, is independent of the waves evoked by the others (Figure 26–3G) and reaches its peak excursion at a point on the basilar membrane appropriate for that frequency component. The basilar membrane thus acts as a mechanical frequency analyzer by distributing the energies associated with the different frequency components of the stimulus to hair cells arrayed along its length. In doing so, the basilar membrane begins the encoding of the frequencies in a sound.

The Organ of Corti Is the Site of Mechanoelectrical Transduction in the Cochlea

The organ of Corti, a ridge of epithelium extending along the basilar membrane, is the receptor organ of the inner ear. Each organ of Corti contains approximately 16,000 hair cells that are innervated by approximately 30,000 *afferent* nerve fibers; these are fibers that carry information into the brain along the eighth cranial nerve. Like the basilar membrane itself, each hair cell is most sensitive to a particular frequency, and these frequencies are logarithmically mapped in descending order from the cochlea's base to its apex. Thus, the information transmitted by these sensory cells to their innervating nerve fibers is also tonotopically organized.

The organ of Corti includes a variety of cells, some of unknown function, but four types have obvious importance. First, there are two types of hair cells. The *inner hair cells* form a single row of approximately 3,500 cells, whereas approximately 12,000 *outer hair cells* lie in three rows farther from the central axis of the cochlear spiral (Figure 26–4). The space between the inner and outer hair cells is delimited and mechanically supported by pillar cells. The outer hair cells are supported at their bases by Deiters's (phalangeal) cells.

A second epithelial ridge adjacent to the organ of Corti, but nearer the cochlea's central axis, gives rise to the tectorial membrane, a gelatinous shelf that covers the organ of Corti (Figure 26–4). The tectorial membrane is anchored at its base, and its tapered distal edge forms a fragile connection with the organ of Corti.

Hair cells are not neurons; they lack both dendrites and axons (Figure 26–5A). A special saline solution, the endolymph that fills scala media, bathes the cell's apical aspect. Tight junctions between hair cells and supporting cells separate this liquid from the standard extracellular fluid, or perilymph, that contacts the basolateral surface of the cell. Immediately below the tight junctions, a desmosomal junction provides a strong mechanical attachment for the hair cell to its neighbors.

The hair bundle, which serves as a receptive antenna for mechanical stimuli, projects from the flattened apical surface of the hair cell. Each bundle comprises a few tens to a few hundred cylindrical processes, the *stereocilia*, arranged in 2 to 10 parallel rows and extending several micrometers from the cell surface. Successive stereocilia across a cell's surface vary monotonically in height; a hair bundle is beveled like the tip of a hypodermic needle (Figure 26–5B). The inner hair-cell bundles of the mammalian cochlea, when viewed from above, have a roughly linear form. Outer hair-cell bundles, in contrast, have a V or W shape (Figure 26–6).

Each stereocilium is a rigid cylinder whose core consists of a fascicle of actin filaments that are heavily cross-linked by the proteins plastin (fimbrin), fascin, and epsin. Cross-linking renders a stereocilium

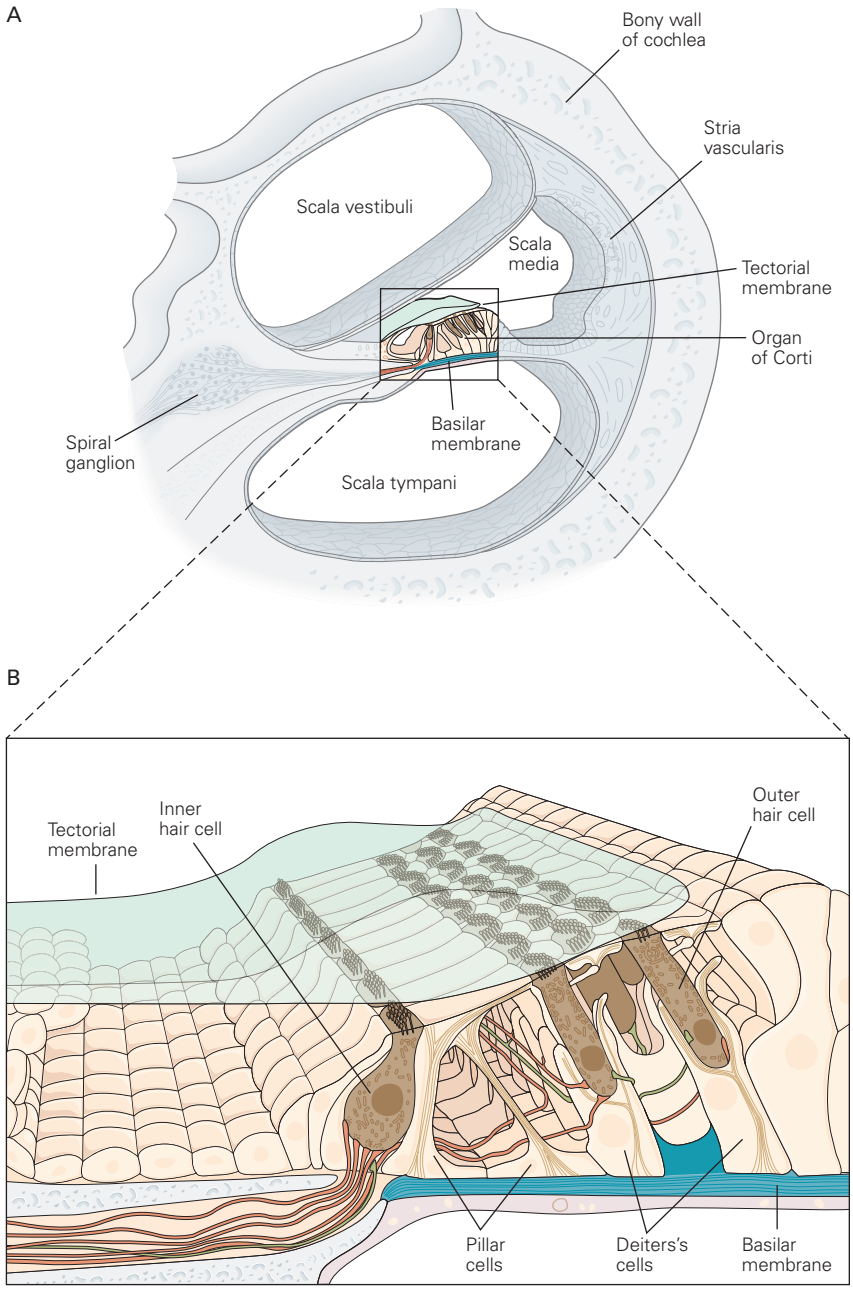

Figure 26–4 Cellular architecture of the human organ of Corti. Although there are differences among species, the basic plan is similar for all mammals.

A. The organ of Corti, the inner ear's receptor organ, is an epithelial strip that surmounts the elastic basilar membrane. The organ contains some 16,000 hair cells arrayed in four rows: a single row of inner hair cells and three rows of outer hair cells. The mechanically sensitive hair bundles of these receptor cells protrude into endolymph, the liquid within the scala media. Reissner's membrane, which provides the upper boundary of the scala media, separates the endolymph from the perilymph in the scala vestibuli. The hair bundles of outer hair cells are attached at their tops to the lower surface of the tectorial membrane, a gelatinous shelf that extends the full length of the basilar membrane.

B. The hair cells are separated and supported by pillar cells and Deiters's cells. One hair cell has been removed from the middle row of outer hair cells to reveal the three-dimensional relationship between supporting cells and hair cells. Afferent and efferent nerve endings are colored in **red** and **green**, respectively.

much more rigid than would be expected for a bundle of unconnected actin filaments. The actin core of the stereocilium is covered by a tubular sheath of plasma membrane. Although a stereocilium is of constant diameter along most of its length, it tapers just above its basal insertion (see Figure 25–5B). Correspondingly, the number of actin filaments diminishes from several hundred to only a few dozen. This thin cluster of microfilaments anchors the stereocilium in the cuticular plate, a thick mesh of interlinked actin filaments beneath the apical cell membrane. Because of this tapered structure, a mechanical force applied at the tip causes the stereocilium to pivot around its basal insertion. Horizontal top connectors interconnect adjacent stereocilia near their tips. These extracellular filaments restrict the bundle to move as a unit during stimulation at low frequencies. At high frequencies, the viscosity of the liquid between the stereocilia also opposes their separation and thus ensures the unitary motion of the hair bundle.

During its early development, every hair bundle includes at its tall edge a single true cilium, the *kinocilium* (Figure 26–5). Like other cilia, this structure possesses at its core an axoneme, or array of nine paired microtubules, and often an additional central pair of microtubules. The kinocilium is not essential for mechanoelectrical transduction, for in mammalian cochlear hair cells, it degenerates around the time of birth.

Hair Cells Transform Mechanical Energy Into Neural Signals

Deflection of the Hair Bundle Initiates Mechanoelectrical Transduction

Just as in vestibular organs (Chapter 27), mechanical deflection of the hair bundle is the stimulus that excites hair cells of the cochlea. Stimuli elicit an electrical response, the receptor potential, by opening or closing—a process termed "gating"—mechanically sensitive ion channels. The hair cell's response depends on the direction and magnitude of the stimulus.

In an unstimulated cell, 10% to 50% of the channels involved in stimulus transduction are open. As a result, the cell's resting potential, which lies within a range of approximately –70 to –30 mV, is determined in part by the influx of cations through these channels. A stimulus that displaces the bundle toward its tall edge opens additional channels, thereby depolarizing the cell (Figure 26–7). In contrast, a stimulus that displaces the bundle toward its short edge shuts transduction channels that are open at rest, thus hyperpolarizing

A

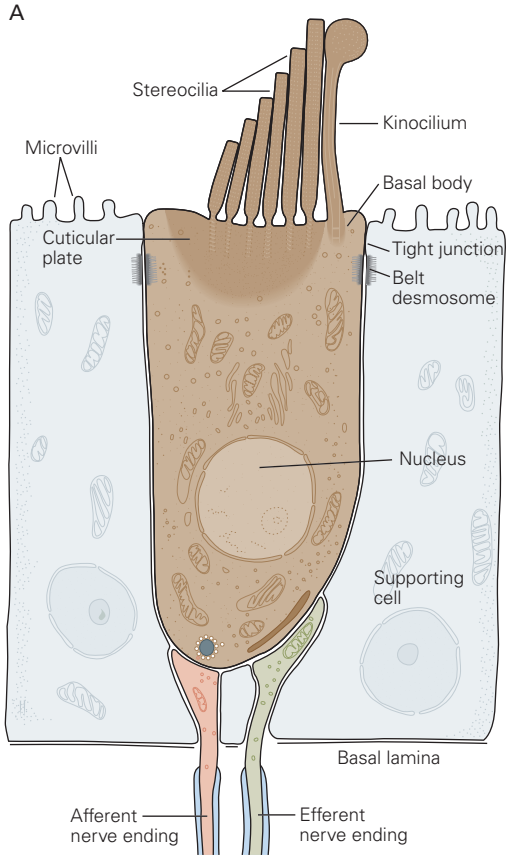

B

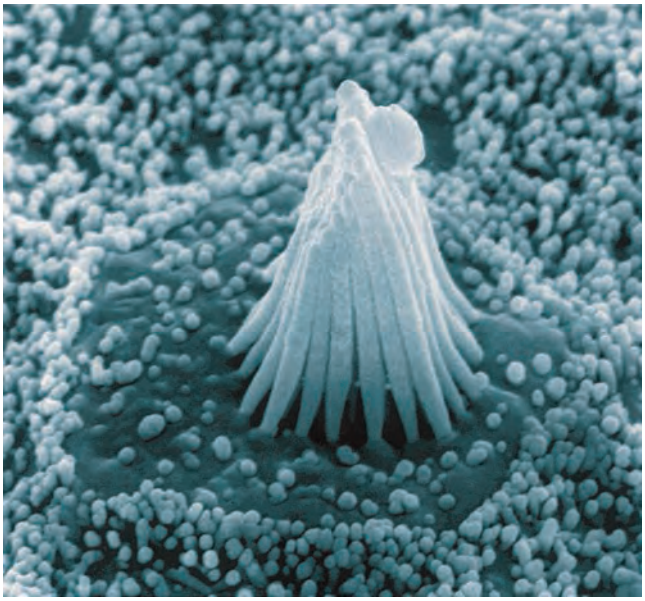

Figure 26–5 (Left) Structure of a vertebrate hair cell.

A. The epithelial character of the hair cell is evident in this drawing of the sensory epithelium from a frog's internal ear. The cylindrical hair cell is joined to adjacent supporting cells by a junctional complex around its apex. The hair bundle, a mechanically sensitive organelle, extends from the cell's apical surface. The bundle comprises some 60 stereocilia arranged in stepped rows of varying length. At the bundle's tall edge stands the single kinocilium, an axonemal structure with a bulbous swelling at its tip; in the mammalian cochlea, this organelle degenerates around the time of birth. Deflection of the hair bundle's top to the right depolarizes the hair cell; movement in the opposite direction elicits hyperpolarization. The hair cell is surrounded by supporting cells, whose apical surfaces bear a stubble of microvilli. Afferent and efferent synapses contact the basolateral surface of the plasma membrane.

B. This scanning electron micrograph of a hair cell's apical surface reveals the hair bundle protruding approximately 8 μm into the endolymph. (Image reproduced, with permission, from A.J. Hudspeth.)

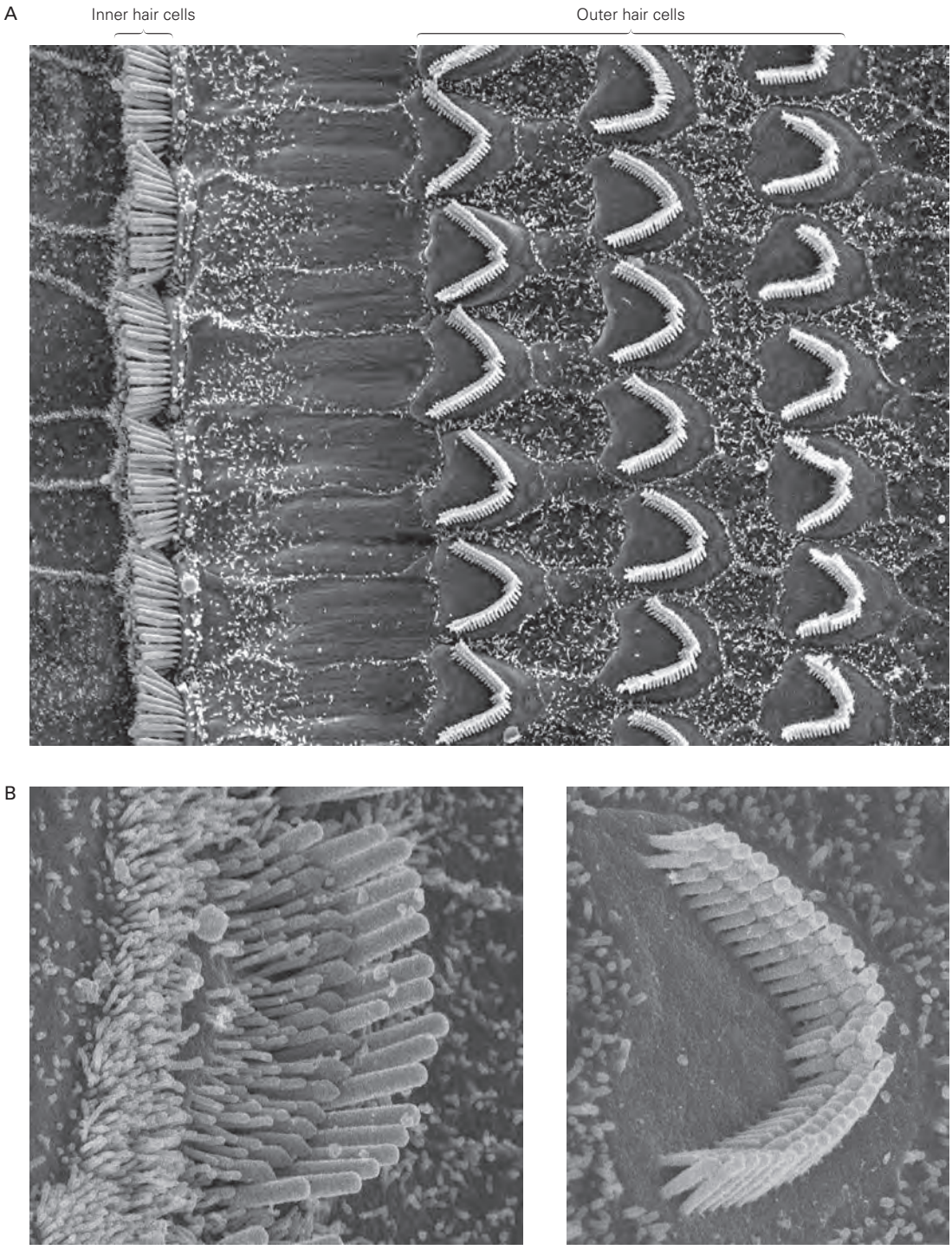

Figure 26–6 Arrangement of the hair cells in the organ of Corti. (Images reproduced, with permission, from D. Furness, Keele University, United Kingdom.)

A. Inner hair cells form a single row, and the stereocilia of each cell are arranged linearly. In contrast, outer hair cells are distributed in three rows, and the stereocilia of each cell are arranged in a V configuration. The apical surfaces of several other cells are visible: from left to right, inner spiral sulcus cells, pillar cells, Deiters's cells, and Hensen's cells (see Figure 26–4).

B. Higher magnification shows the linear configuration of the hair bundle atop an inner hair cell (*left*) and the V configuration of an outer hair-cell bundle (*right*), as well as the arrangement of the stereocilia in rows of increasing heights.

the cell. Hair cells respond most to stimuli parallel to the hair bundle's axis of morphological mirror symmetry: Stimuli at right angles to the axis produce little change from the resting potential. An oblique stimulus elicits a response proportional to its vectorial projection along the axis of sensitivity.

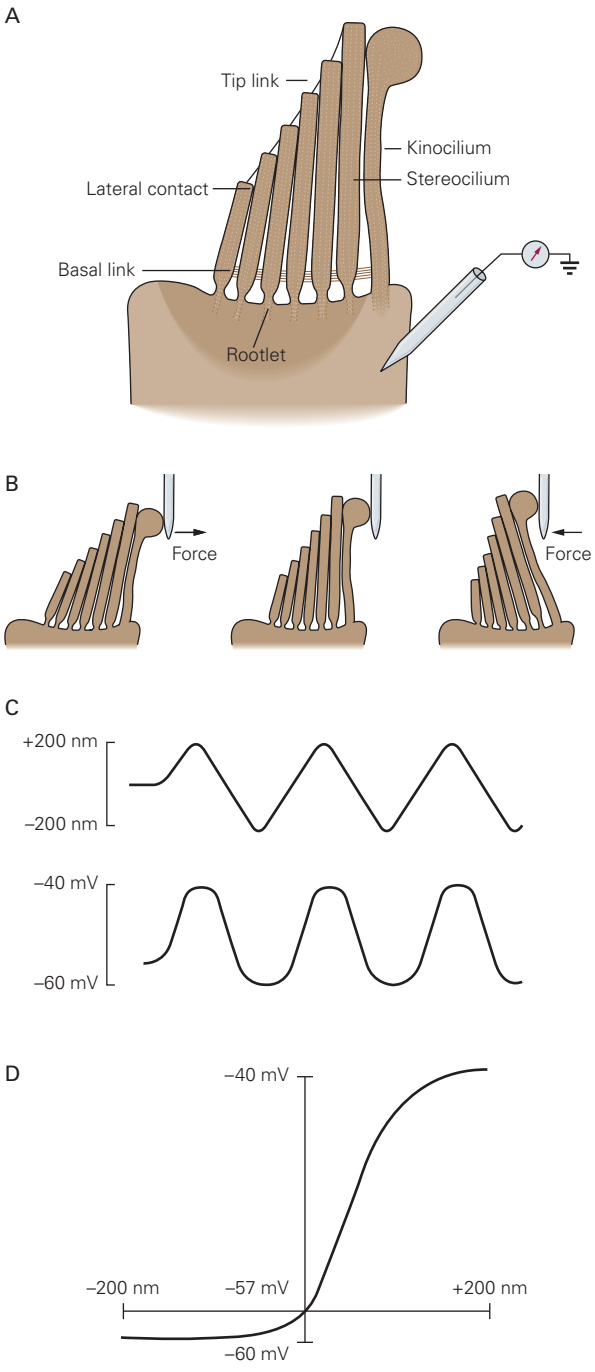

A hair cell's receptor potential is graded. As the stimulus amplitude increases, the receptor potential grows progressively larger up to the point of saturation. The receptor potential of an inner hair cell can be as great as 25 mV in peak-to-peak magnitude. The relation between a bundle's deflection and the resulting electrical response is sigmoidal (Figure 26–7D). A displacement of only ±100 nm represents approximately 90% of the response range. During normal stimulation, a hair bundle moves through an angle of ±1° or so, that is, by much less than the diameter of one stereocilium.

When observed in vitro, a hair bundle exhibits Brownian motion of approximately ±3 nm, whereas the threshold of hearing corresponds to basilar-membrane movements of as little as ±0.3 nm. There are at least three mechanisms that explain how the hair bundle may respond to motion smaller than its own noise. First, because the cochlear partition does not move as a rigid body, the movement of the hair bundle is larger than that of the basilar membrane. Second, frequency-selective amplification of low stimuli actively pulls the signal out of the noise. Finally, mechanical coupling to a group of neighbors results in synchronization that effectively reduces noise. At hearing threshold, a stimulus evokes a receptor potential near 100 μV in amplitude.

The ion channels in hair cells that mediate mechanoelectrical transduction are relatively nonselective, cation-passing pores with a conductance near 100 pS. From the known size of small organic cations and fluorescent molecules that can traverse the channel, the transduction channel's pore must be about 1.3 nm in diameter. Most of the transduction current is carried by K^+, the cation with the highest concentration in the endolymph bathing the hair bundle. Although

Figure 26–7 (Left) Mechanical sensitivity of a hair cell.

A. A recording electrode is inserted into a frog hair cell.

B. A probe attached to the bulbous tip of the stereocilium is moved by a piezoelectric stimulator, deflecting the elastic hair bundle from its resting position. The actual deflections are generally only one-tenth as large as those portrayed.

C. When the top of a hair bundle is displaced back and forth (**upper trace**), the opening and closing of mechanically sensitive ion channels produce an oscillatory receptor potential (**lower trace**) that—as here—may saturate in both the depolarizing and the hyperpolarizing directions.

D. The relation between hair-bundle deflection (abscissa) and receptor potential (ordinate) is sigmoidal. The entire operating range is only approximately 100 nm, less than the diameter of an individual stereocilium. At rest, the hair bundle operates within the steep region of the sigmoid, which ensures significant receptor potentials in response to weak stimuli.

endolymph is relatively poor in Ca^{2+}, a small fraction of the transduction current is carried by this ion. Fluorescent indicators indicate that Ca^{2+} entry, and thus mechanoelectrical transduction, occurs precisely at the stereociliary tips of a deflected hair bundle. Single-channel recordings, together with the observation that the magnitude of the transduction current is roughly proportional to the number of functional stereocilia remaining in a microdissected bundle, indicate that there are probably only two active transduction channels per stereocilium.

The large diameter and poor selectivity of the pore permit transduction channels to be blocked by aminoglycoside antibiotics such as streptomycin, gentamicin, and tobramycin. When used in large doses to counter bacterial infections, these drugs have a toxic effect on hair cells; the antibiotics damage hair bundles and eventually kill hair cells. These drugs pass through transduction channels at a low rate and thus cause long-term toxic effects by interfering with protein synthesis on the mitochondrial ribosomes, which resemble bacterial ribosomes. Consistent with this hypothesis, human sensitivity to aminoglycosides is maternally inherited, as are the mitochondria, and in many instances reflects a single base change in the 12S ribosomal RNA gene of the mitochondrion.

Mechanical Force Directly Opens Transduction Channels

The mechanism for gating of transduction channels in hair cells differs fundamentally from the mechanisms used for electrical signals in neurons such as the action potential or postsynaptic potential. Many ion channels respond to changes in membrane potential or to specific ligands (Chapters 8, 10, and 12–14). In contrast, two lines of evidence suggest that the mechanoelectrical transduction channels in the hair cell are activated by mechanical strain.

First, a bundle is stiffer along its axis of mechanical sensitivity than at a right angle. This observation suggests that a portion of the work done in deflecting a bundle goes into elastic elements, termed *gating springs,* which pull on the molecular gates of the transduction channels. Because the gating springs contribute over half of a hair bundle's stiffness, the transduction channels efficiently capture the energy supplied when a bundle is deflected. In addition, the mechanical properties of a hair bundle vary during channel gating: When channels open or close, stiffness decreases and friction increases. Both phenomena are expected if the channels are gated directly through a mechanical linkage to the hair bundle.

A second indication that transduction channels are directly controlled by gating springs is the rapidity with which hair cells respond. The response latency is so brief, only a few microseconds, that gating is more likely to be direct than to involve a second messenger (Chapter 14). Moreover, the electrical responses of hair cells to a series of step stimuli of increasing magnitude become both larger and faster. This behavior favors a kinetic scheme in which mechanical force controls the rate constant for channel gating.

The *tip link* is a probable component of the gating spring. A tip link is a fine molecular braid joining the distal end of one stereocilium to the side of the longest adjacent process (Figure 26–8A). Deflection of a hair bundle toward its tall edge tenses the tip link and promotes channel opening; movement in the opposite direction slackens the link and allows the associated channels to close (Figure 26–8B).

Three experimental results suggest that the tip links are components of the gating springs. First, tip links are universal features of hair bundles and are situated at the site of transduction. The transduction channels are indeed located at the stereociliary tips, thus near the lower insertion point of the tip link. Second, the orientation of the links is consistent with the vectorial sensitivity of transduction. The links invariably interconnect stereocilia in a direction parallel with the hair bundle's axis of mechanosensitivity. Finally, when tip links are disrupted by exposing hair cells to Ca^{2+} chelators, transduction vanishes. As the tip links regenerate over the course of approximately 12 hours, a hair cell regains mechanosensitivity. It remains unclear whether the elasticity of gating springs resides primarily in the tip links or in the structures at their two insertions.

In the mammalian cochlea, hair bundles are deflected through their linkage to the tectorial membrane. When the basilar membrane oscillates up and down in response to a sound, the organ of Corti and the overlying tectorial membrane move with it. Because the basilar and tectorial membranes pivot about different lines of insertion, however, their up-and-down motion is accompanied by a back-and-forth shearing motion between the upper surface of the organ of Corti and the lower surface of the tectorial membrane. This is the motion that is detected by hair cells (Figure 26–9).

The hair bundles of outer hair cells, whose tips are firmly attached to the tectorial membrane, are directly deflected by this movement. The hair bundles of inner hair cells, which do not contact the tectorial membrane, are deflected by movement of the liquid beneath the membrane. This mode of stimulation affords some mechanical magnification of the signals reaching hair

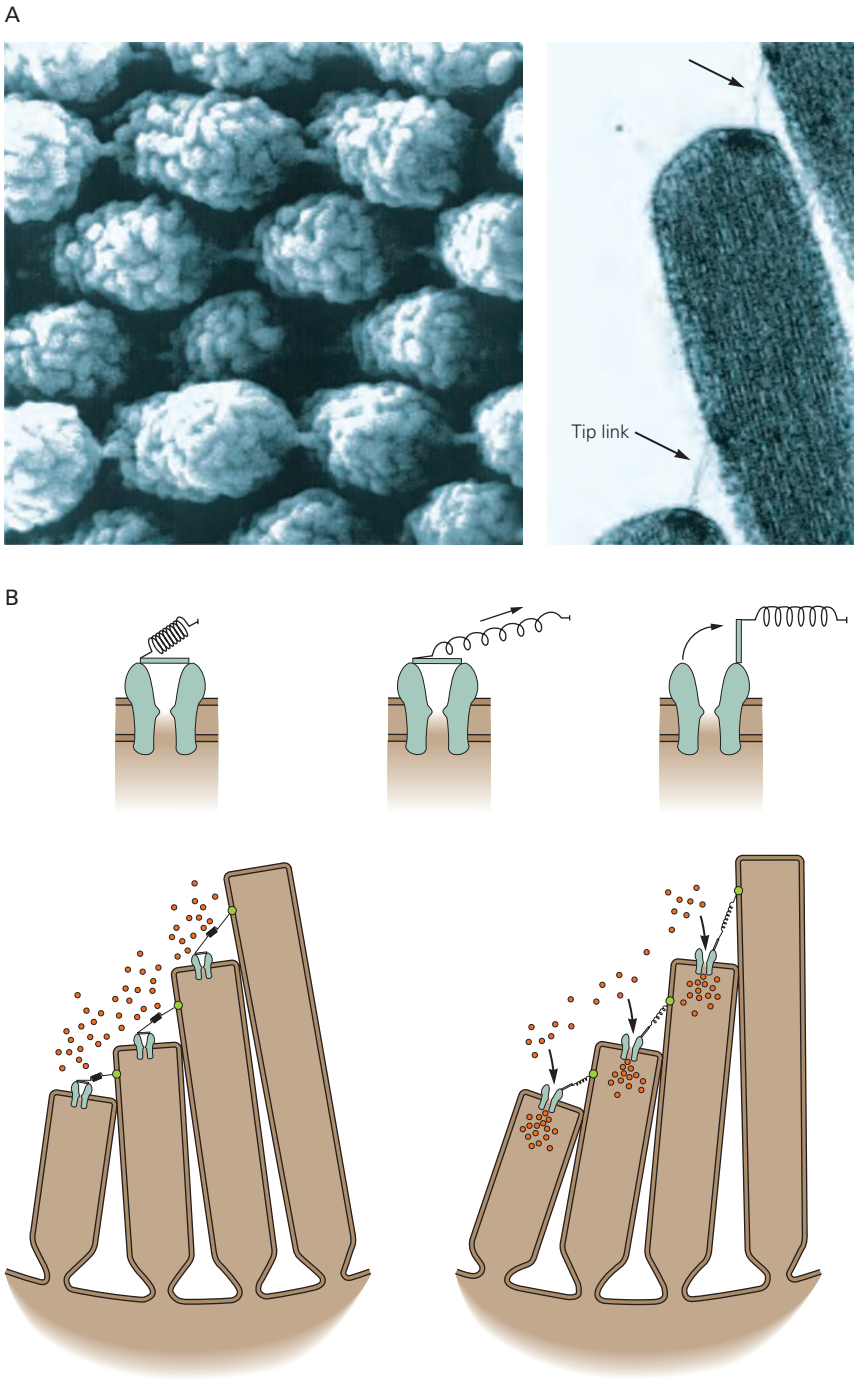

Figure 26–8 Mechanoelectrical transduction by hair cells.

A. A tip link connects each stereocilium to the side of the longest adjacent stereocilium, as seen in a scanning electron micrograph (*left*) and a transmission electron micrograph (*right*) of a hair bundle's top surface. Each tip link is only 3 nm in diameter and 150 to 200 nm in length. The links appear stouter in the illustration on the left because of metallic coating during specimen preparation. (Reproduced, with permission, from Assad, Shepherd, and Corey 1991; reproduced, with permission, from Hudspeth and Gillespie 1994.)

B. Top: Ion flux through the channel that underlies mechanoelectrical transduction in hair cells is regulated by a molecular gate. The opening and closing of the gate are controlled by the tension in an elastic element, the gating spring, which senses hair-bundle displacement. (Adapted, with permission, from Howard and Hudspeth 1988.)

Bottom: When the hair bundle is at rest, each transduction channel fluctuates between closed and open states, spending most of its time shut. Displacement of the bundle in the positive direction increases the tension in the gating spring, here assumed to be in part a tip link, attached to each channel's molecular gate. The enhanced tension promotes channel opening and the influx of cations, thereby producing a depolarizing receptor potential. (Adapted, with permission, from Hudspeth 1989.)

bundles. At least for high-frequency stimuli, the movements of hair bundles are thought to be severalfold greater than that of the basilar membrane.

Direct Mechanoelectrical Transduction Is Rapid

Hair cells operate much more quickly than do other sensory receptor cells of the vertebrate nervous system and, indeed, more quickly than neurons themselves. To deal with the frequencies of biologically relevant sounds, transduction by hair cells must be rapid. Given the behavior of sound in air and the dimensions of sound-emitting and sound-absorbing organs such as vocal cords and eardrums, optimal auditory communication occurs in the frequency range of 10 Hz to 100 kHz. Much higher frequencies propagate

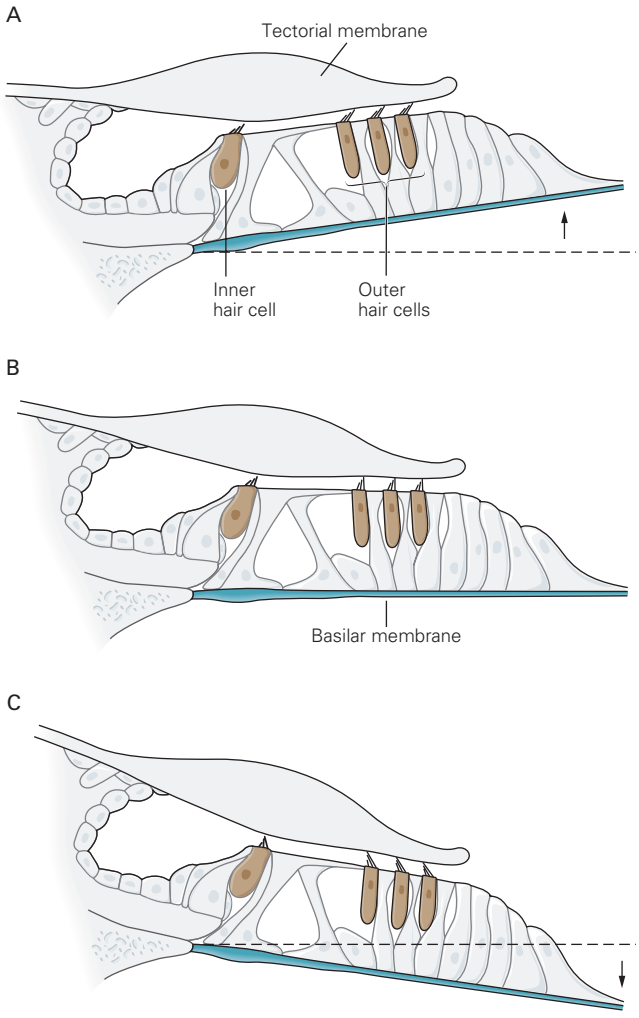

Figure 26–9 Forces acting on cochlear hair cells. Hair cells in the cochlea are stimulated when the basilar membrane is driven up and down by differences in the pressure between the scala vestibuli and scala tympani. This motion is accompanied by shearing movements between the tectorial membrane and organ of Corti. These motions deflect the hair bundles of outer hair cells, which are attached to the lower surface of the tectorial membrane. The hair bundles of inner hair cells, which are not attached to the tectorial membrane, are deflected by the movement of liquid in the space beneath that structure. In both instances, the deflection initiates mechanoelectrical transduction of the stimulus.

A. When the basilar membrane is driven upward, shear between the hair cells and the tectorial membrane deflects hair bundles in the excitatory direction, toward their tall edge.

B. At the midpoint of an oscillation, the hair bundles resume their resting position.

C. When the basilar membrane moves downward, the hair bundles are driven in the inhibitory direction.

poorly through air; much lower frequencies are inefficiently produced and poorly captured by animals of moderate size. Even in animals sensitive to relatively low frequencies, such as frogs, the in vitro transduction current in response to a step stimulus of moderate intensity rises with a time constant of only 80 µs at room temperature. For mammals to be able to respond to frequencies greater than 100 kHz, the hair cells evidently display gating times that are an order of magnitude smaller. Locating sound sources, one of the most important functions of hearing, sets even more stringent limits on the speed of transduction (Chapter 28). A sound from a source directly to one side of a person reaches the nearer ear somewhat sooner than the farther, by at most 700 µs in humans. An observer can locate sound sources on the basis of much smaller delays, about 10 µs. For this to occur, hair cells must be capable of transducing acoustic waveforms with microsecond-level resolution.

Deafness Genes Provide Components of the Mechanotransduction Machinery

Genetic studies of deafness in both humans and mouse models have provided entry points into the molecular composition of the mechanotransduction machinery of the hair cell. In particular, the upper two-thirds of the tip link consist of two parallel molecules of cadherin-23, whereas the lower third comprises two parallel molecules of protocadherin-15 (Figure 26–10). The two components are joined at their tips in a Ca^{2+}-sensitive manner; lowering the extracellular Ca^{2+} concentration below approximately 1 µM disrupts their association. In humans, mutations in the genes coding for cadherin 23 (*USH1D*) and protocadherin 15 (*USH1F*) lead to the most severe form of the Usher syndrome, an autosomal recessive disorder that associates severe-to-profound congenital deafness, constant vestibular dysfunction, and retinitis pigmentosa with a prepubertal onset. The study of other genes involved in this type of Usher syndrome has revealed that the upper end of the tip link is anchored to the actin core of a stereocilium by a protein complex that includes the scaffolding proteins sans (*USH1G*) and harmonin (*USH1C*), as well as the molecular motor myosin 7a (*USH1B*).

The small number of channels in a hair cell, along with the lack of high-affinity ligands with which to label them, explains why the biochemical identity of the transduction channels has long remained uncertain. However, recent genetic, biochemical, and biophysical experiments indicate that four integral transmembrane proteins are intimately related to the transduction channel: transmembrane channel-like proteins 1 and

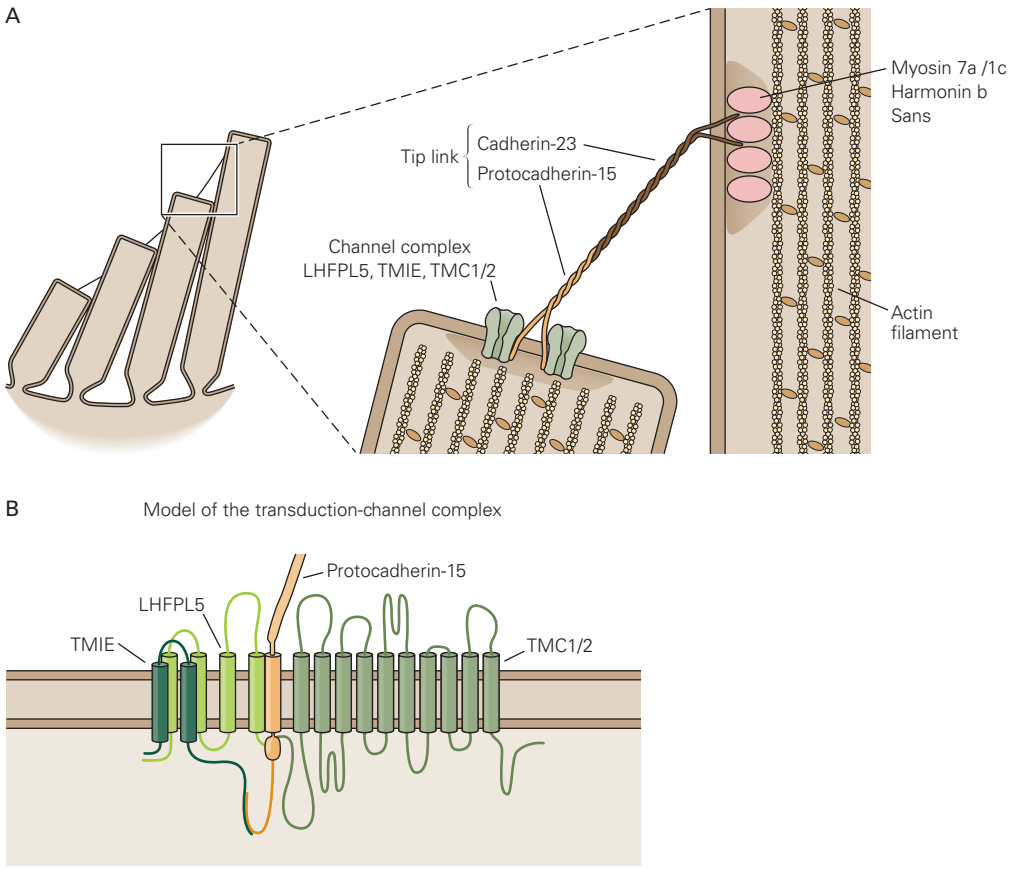

Figure 26–10 Molecular composition of the transduction machinery.

A. The tip link is composed of the heterophilic association of protocadherin 15 and cadherin 23. Two transduction channels are localized near the lower insertion point of the tip link at the tip of the shorter stereocilium. Each channel is part of a molecular complex that includes the proteins TMC1/2, LHFPL5, and TMIE. At the upper insertion point on the flank of the longer stereocilium, cadherin 23 interacts with harmonin b and the molecular motor myosin 7a, which both bind to actin and thus anchor the tip link. The protein sans serves as a scaffolding protein. In vestibular hair cells, myosin 1c may set the tip link under tension, but the presence of this motor protein is uncertain in cochlear hair cells.

B. Model of the transduction-channel complex. TMC1/2, LHFPL5, and TMIE interact with protocadherin 15 and, thus, with the lower end of the tip link. TMIE also interacts with LHFPL5. The detailed arrangement of these proteins within the transduction apparatus is still unknown. Unlike what the figure suggests, TMC1 has been proposed to assemble as a dimer, with each TMC1 molecule contributing a permeation pathway for cations. (Adapted, with permission, from Wu and Müller 2016 and Pan et al. 2018.)

2 (TMC1 and TMC2), tetraspan membrane protein in hair-cell stereocilia (TMHS; official nomenclature LHFPL5), and transmembrane inner-ear-expressed gene (TMIE; Figure 26–10). Mechanotransduction is abolished in mouse hair cells lacking TMIE, even though all other known components of the transduction machinery appear to be properly in place. However, because TMIE contains only two predicted transmembrane domains, it seems highly unlikely that this protein alone constitutes an ion channel. In the absence of LHFPL5, the conductance of the transduction channel is reduced, but significant transduction currents can still be measured, suggesting that this protein is not an essential part of the channel pore.

Multiple lines of evidence advocate for TMC1 and TMC2 as components of the transduction channel. Both proteins are localized near the lower insertion point of the tip link, where the transduction current enters the hair cell, interact with the tip-link constituent protocadherin 15, and their onset of expression coincides with that of mechanoelectrical transduction. In addition, transduction channels in a mouse carrying a single point mutation in the *Tmc1* gene show lower conductance and Ca^{2+} permeability, indicating that TMC1 is very close to the channel's pore. Individual

cysteine substitutions made at sites that are predicted to be in or near the channel pore confirm that TMC1 belongs to the main conductive pathway. Indeed, covalent modification of the cysteine residues with a positively charged reagent leads to a reduction of the single-channel conductance in several TMC1 mutants. The cysteine-modifying reagent has no effect when the reagent is applied after the hair bundle has been deflected towards its short edge (to close the transduction channels) or when access to the channel pore is prevented by a channel blocker. TMC1 is thus unlikely to constitute an accessory channel subunit that forms a vestibule to the pore-forming protein(s). Instead, the evidence is strong that TMC1 forms at least part of the pore of the transduction channel. In cochlear hair cells, TMC1 and TMC2 are coexpressed during neonatal development, but only TMC1 expression is maintained through adulthood.

Dynamic Feedback Mechanisms Determine the Sensitivity of the Hair Cells

Hair cells must cope with acoustic stimuli that have a very low energy content. If the stimulus consists of a periodic signal, such as the sinusoidal pressure of a pure tone, a detection system can increase the signal-to-noise ratio by enhancing selectively the response to a relevant frequency. Hair cells respond best at a characteristic frequency of acoustic stimulation. The frequency selectivity of a given hair cell results in part from passive extrinsic filtering of its mechanical input, in particular as a result of the tonotopic arrangement of the mammalian basilar membrane. In addition, when it is appropriate that low-frequency inputs be disregarded, hair cells possess a unique mechanism of adaptation that acts as a high-pass filter. Hair cells also employ mechanical amplification that enhances and further tunes their mechanosensitivity.

Hair Cells Are Tuned to Specific Stimulus Frequencies

Every cochlear hair cell is most sensitive to stimulation at a specific frequency, termed its characteristic, natural, or best frequency. On average, the characteristic frequencies of adjacent inner hair cells differ by approximately 0.2%; adjacent piano strings, in comparison, are tuned to frequencies some 6% apart. Because the traveling wave evoked even by a pure sinusoidal stimulus spreads somewhat along the basilar membrane, the sensitivity of a cochlear hair cell extends within a limited range above and below its characteristic frequency, the more so with a greater level of stimulation. At low levels, a pure tone recruits approximately 100 hair cells. The frequency sensitivity of a hair cell may be displayed as a tuning curve. To construct a tuning curve, an experimenter stimulates the ear with pure tones at numerous frequencies below, at, and above the cell's characteristic frequency. The level of stimulation is adjusted for each frequency until the cell's response reaches a predefined criterion magnitude. The tuning curve is then a graph of sound level, presented logarithmically in decibels SPL, as a function of stimulus frequency.

The tuning curve for an inner hair cell is typically V-shaped (Figure 26–11). The curve's tip represents the cell's characteristic frequency, the frequency that produces the criterion response for the lowest level of the stimulus. Sounds of greater or lesser frequencies require higher levels to excite the cell to the criterion response. As a consequence of the traveling wave's shape, the slope of a tuning curve is far steeper on its high-frequency flank than on its low-frequency flank.

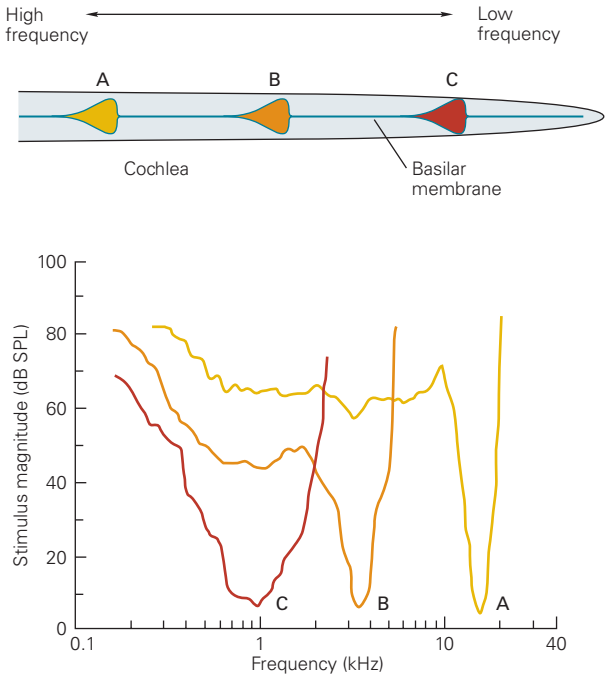

Figure 26–11 Tuning curves for cochlear hair cells. To construct a curve, the experimenter presents sound at several frequencies. At each frequency, the stimulus intensity is adjusted until the cell produces a criterion response, here 1 mV. The curve thus reflects the threshold of the cell for stimulation over a range of frequencies. Each cell is most sensitive to a specific frequency, its characteristic frequency. The threshold rises briskly—the sensitivity falls rapidly—as the stimulus frequency is raised or lowered. The characteristic frequency depends on the position of the hair cell along the longitudinal axis of the cochlea. (Reproduced, with permission, from Kiang 1980. Copyright © 1980 Acoustical Society of America.)

In the same way as a tuning fork's resonant frequency depends on the size of its tines, the heights of the hair bundles vary systematically along the tonotopic axis. Hair cells that respond to low-frequency stimuli have the tallest bundles, whereas those that respond to the highest-frequency signals possess the shortest bundles. In the human cochlea, for example, an inner hair cell with a characteristic frequency of 20 kHz bears a 4-μm hair bundle. At the opposite extreme, a cell sensitive to a 20-Hz stimulus has a bundle more than 7 μm high. A similar morphological gradient is observed with outer hair cells, supplementing the extrinsic tuning accomplished by the basilar membrane.

Hair Cells Adapt to Sustained Stimulation

Despite the precision with which a hair bundle grows, it cannot develop in such a way that the sensitive transduction apparatus is always perfectly poised at its position of greatest mechanosensitivity. Some mechanism must compensate for developmental irregularities, as well as for environmental changes, by adjusting the gating springs so that transduction channels are responsive to weak stimuli at the bundle's resting position. To ensure this, an adaptation process continuously resets the hair bundle's range of mechanical sensitivity. As a result of adaptation, a hair cell can maintain a high sensitivity to transient stimuli while rejecting static inputs a million times as large.

Adaptation manifests itself as a progressive decrease in the receptor potential during protracted deflection of the hair bundle (Figure 26–12). The process is not one of desensitization, for the responsiveness of the receptor persists. Instead, during a prolonged step stimulus, the sigmoidal relationship between the initial receptor potential and the bundle's position shifts in the direction of the applied stimulus. As a result, the membrane potential of the hair cell progressively returns to near its resting value. Adaptation is incomplete, however; the relation between the membrane potential and the bundle position shifts by approximately 80% of the deflected position.

How does adaptation occur? Because the mechanical force exerted by a hair bundle changes as adaptation proceeds, the process evidently involves an adjustment in the tension borne by the gating springs. It appears likely that the structure anchoring the upper end of each tip link, the *insertional plaque,* is repositioned during adaptation by an active molecular motor (Figure 26–12). The transduction channels are inherently more stable in a closed state, for they close when the tip links are disrupted. A motor is thus also required to maintain a significant fraction (10%–50%) of the transduction channels open at rest by continuously pulling on the gating springs. Several dozen myosin molecules associated with the upper end of each tip link are thought to maintain tension by ascending the actin core of the stereocilium and pulling the link's insertion with them.

When a stimulus step increases the tension in a gating spring, the associated transduction channel opens, permitting an influx of cations. As Ca^{2+} ions accumulate in the stereociliary cytoplasm, they reduce the upward force of the myosin molecules, thereby shortening the gating spring. When the spring reaches its resting tension, closure of the channel reduces the Ca^{2+} influx to its original level, restoring a balance between the upward force of myosin and the downward tension in the spring.

Hair bundles contain at least five isoforms of myosin, the motor molecule associated with motility along actin filaments (Chapter 31). In vestibular hair cells, immunohistochemical studies and site-directed mutagenesis implicate myosin 1c in adaptation. In cochlear hair cells, the role of myosin 1c in adaptation has remained elusive. Another motor protein, myosin 7a, is present near the upper insertion point of the tip link and mutations in the corresponding gene (*USH1B*) are associated with deafness. Hair-cell bundles defective for myosin 7a are disorganized, suggesting that this motor is involved at least in hair-bundle development.

If it were only to set the operating point of the transduction apparatus, adaptation could afford to operate on much slower timescales than the period of acoustic stimuli. This is the case in response to large deflections of the hair bundle, for which the time constant of adaptation is approximately 20 ms or more when endolymph bathes the hair bundle. This slow adaptation is compatible with the activity of a myosin-based motor driven by the cyclical hydrolysis of adenosine triphosphate (ATP). Yet, after being pulled open by an excitatory step stimulus of small magnitude, transduction channels reclose with typical timescales of less than 1 ms and thus short enough to be compatible with auditory frequencies. Current models posit that Ca^{2+} ions entering a hair cell through a transduction channel bind to or near the channel's pore, thereby energetically favoring channel closure. The kinetics of this fast adaptation varies systematically along the tonotopic axis of auditory organs, indicating that adaptation may help in setting the hair cell's characteristic frequency of maximal responsiveness. In addition, the reciprocal relationship between channel gating and tip-link tension means that adaptive channel rearrangements evoke internal forces that drive active hair-bundle movements. The mechanical correlate of adaptation

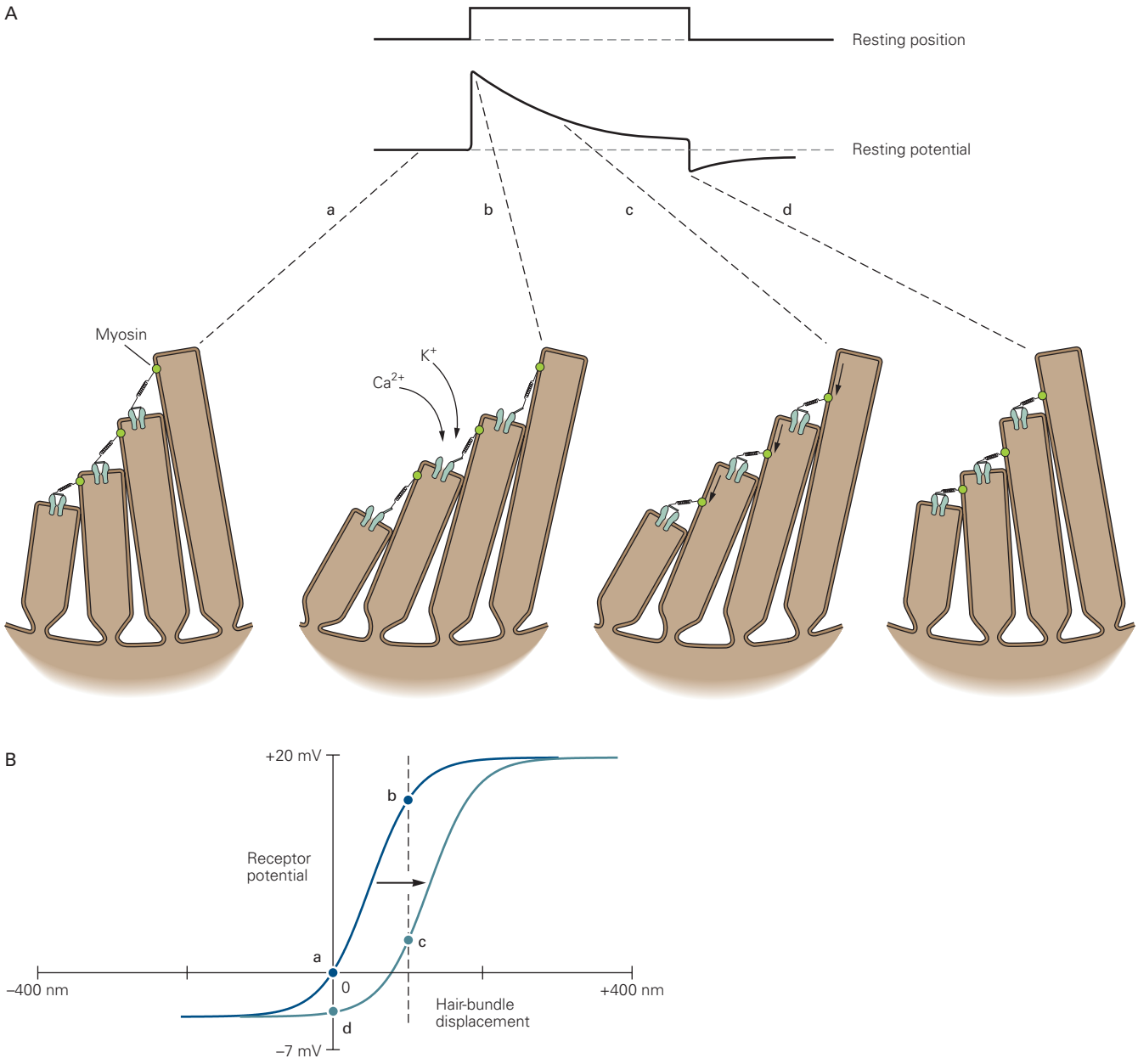

Figure 26–12 Adaptation of mechanoelectrical transduction in hair cells. **A.** Prolonged deflection of the hair bundle in the positive direction (**upper trace**) elicits an initial depolarization followed by a decline to a plateau and an undershoot at the cessation of the stimulus (**lower trace**). The four schematic hair-cell bundles illustrate the states of the transduction channels before (**a**) and during the illustrated phases of the adaptation (**b–d**). Initially, the stimulation increases tension in the tip link (second bundle), thus opening transduction channels. As stimulation continues, however, a tip link's upper attachment is thought to slide down the stereocilium, allowing each channel to close during adaptation (third bundle). Prolonged deflection of the hair bundle in the negative direction elicits a complementary response. The cell is slightly hyperpolarized at first but shows a rebound depolarization at the end of stimulation; tension is restored to the initially slack tip link as myosin molecules actively pull up the link's upper insertion. **B.** As adaptation proceeds, the sigmoidal relation between hair bundle displacement and the receptor potential of the hair cell shifts to the right along the abscissa, in the direction of the new hair-bundle position (**dashed line**), without substantial changes in the curve's shape or amplitude. The shift explains why the receptor potential decreases over time as shown in **A** between states **b** and **c**, restoring the membrane potential of the hair cell to near its value when there is no stimulus. This result implies that adaptation restores mechanical sensitivity to small rapid deflections of the hair bundle in the presence of a protracted stimulus that would otherwise saturate mechanoelectrical transduction. The four states of the transduction channels shown in **A** are marked (**a–d**). (Adapted, with permission, from Hudspeth and Gillespie 1994.)

thus provides feedback that can enhance the stimulus to the hair cell.

Sound Energy Is Mechanically Amplified in the Cochlea

The inner ear faces an important obstacle to efficient operation: A large portion of the energy in an acoustic stimulus goes into overcoming the damping effects of cochlear liquids on hair-cell and basilar-membrane motion rather than into excitation of hair cells. The sensitivity of the cochlea is too great, and auditory frequency selectivity too sharp, to result solely from the inner ear's passive mechanical properties. The cochlea must therefore possess some means of actively amplifying sound energy.

One indication that amplification occurs in the cochlea comes from measurements of the basilar membrane's movements with sensitive laser interferometers. In a preparation stimulated with low-level sound, the basilar-membrane motion is highly dependent on frequency. The movement is maximal at the appropriate frequency for the position at which the measurement is made—the characteristic frequency—but drops abruptly at higher or lower frequencies. As the sound level is increased, however, the frequency selectivity of the vibration becomes less sharp; the peak in the relationship between amplitude and frequency broadens. In addition, the membrane's sensitivity to sound, defined as the vibration amplitude per unit of sound pressure, declines precipitously. When stimulated at the characteristic frequency, the sensitivity of basilar-membrane motion to stimulation at 80 dB SPL is less than 1% of that for 10 dB SPL excitation. The basilar membrane displays a compressive nonlinearity that accommodates the millionfold variation of sound pressure that characterizes audible sounds (0–120 dB SPL) into only two to three orders of magnitude of vibration amplitude (±0.3–300 nm). The sensitivity and frequency selectivity predicted in modeling studies of a passive cochlea correspond to those observed with high-level stimuli. This result implies that the motion of the basilar membrane is augmented more than 100-fold during low-level stimulation at the characteristic frequency, but that amplification diminishes progressively as the stimulus grows in strength. Consequently, amplification lowers the threshold of hearing by more than 40 to 50 dB SPL.

In addition to this circumstantial evidence, experimental observations support the idea that the cochlea contains a mechanical amplifier. When a normal human ear is stimulated with a click, that ear emits one to several measurable pulses of sound within

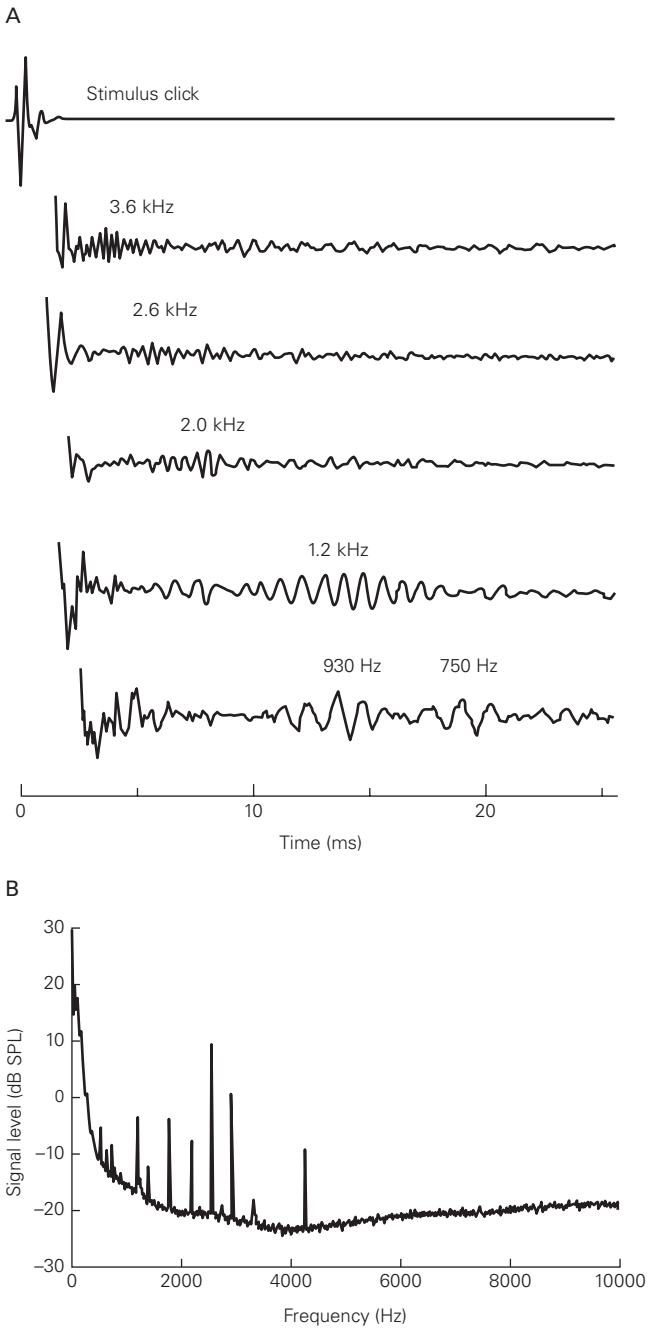

Figure 26–13 The cochlea actively emits sounds.

A. The records display evoked otoacoustic emissions from the ears of five human subjects. A brief click (**top trace**) was played into each ear through a miniature speaker. A few milliseconds later, a tiny microphone in the external auditory meatus detected one or more bursts of sound emission from the ear. (Adapted, with permission, from Wilson 1980. Copyright © 1980 Elsevier B.V.)

B. Under suitably quiet recording conditions, spontaneous otoacoustic emissions occur in most normal human ears. This spectrum displays the acoustic power of six prominent emissions and several smaller ones from one ear. (Reproduced, with permission, from Murphy et al. 1995. Copyright © 1995, Acoustical Society of America.)

milliseconds (Figure 26–13A). Because they can carry more energy than the stimulus, these so-called *evoked otoacoustic emissions* cannot simply be echoes; they represent the emission of mechanical energy by the cochlea, triggered by acoustic stimulation. In accordance with the compressive nonlinearity associated with cochlear amplification, the relative level of the emissions decreases with the stimulus level.

A still more compelling manifestation of the cochlea's active amplification is *spontaneous otoacoustic emission.* When a suitably sensitive microphone is used to measure sound pressure in the ear canals of subjects in a quiet environment, at least 70% of normal human ears continuously emit one or more pure tones (Figure 26–13B). Although these sounds are generally too faint to be directly audible by others, physicians have reported actually hearing sounds emanating from the ears of newborns!

What is the source of evoked and spontaneous otoacoustic emissions, and thus presumably of cochlear amplification as well? Several lines of evidence implicate outer hair cells as the elements that enhance cochlear sensitivity and frequency selectivity and hence act as the motors for amplification. The afferent nerve fibers that extensively innervate the inner hair cells make only minimal contacts with the outer hair cells (Figure 26–4). Instead, the outer hair cells receive an extensive efferent innervation that, when activated, decreases cochlear sensitivity and frequency discrimination. In addition, when stimulated electrically, an isolated outer hair cell displays the unique phenomenon of electromotility: The cell body shortens by up to several micrometers when depolarized and elongates when hyperpolarized (Figure 26–14). This response can occur at frequencies exceeding 80 kHz, an attractive feature for a process postulated to assist high-frequency hearing.

The energy for these movements is drawn from the experimentally imposed electrical field rather than from hydrolysis of an energy-rich substrate such as ATP. Movement occurs when changes in the electric field across the membrane reorient molecules of the protein prestin. The concerted movement of several million of these molecules, which are packed in the lateral cell membranes of outer hair cells, changes the membrane's area and thus the cell's length. When an outer hair cell transduces mechanical stimulation of its hair bundle into receptor potentials, cochlear amplification might then occur when voltage-induced movement of the cell body augments basilar-membrane motion. Consistent with this hypothesis, mutation of certain amino acid residues required for the voltage sensitivity of prestin abolishes the active process in mice.

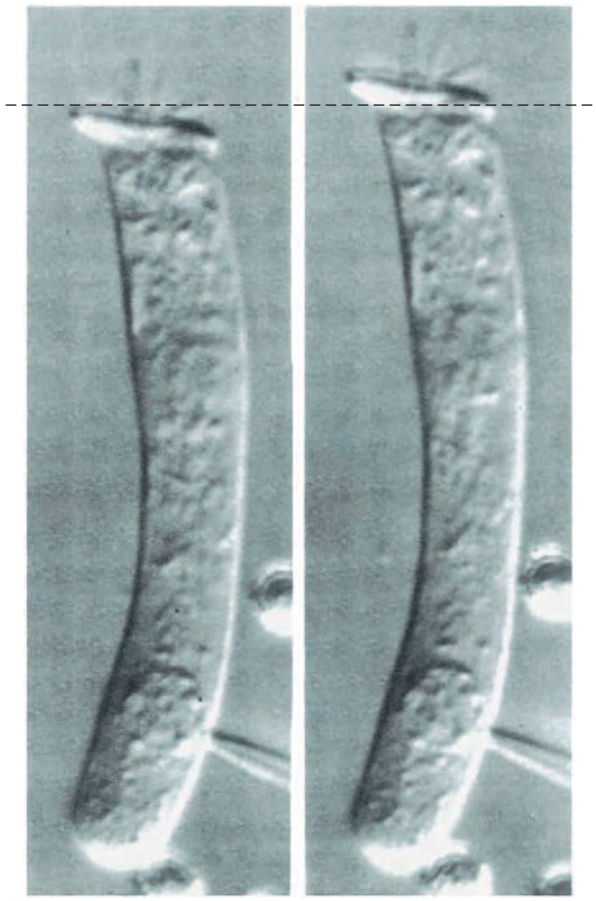

Figure 26–14 Voltage-induced motion of an outer hair cell. Depolarization of an isolated outer hair cell through the electrode at its base causes the cell body to shorten (*left*); hyperpolarization causes it to lengthen (*right*). The oscillatory motions of outer hair cells may provide the mechanical energy that amplifies basilar-membrane motion and thus enhances the sensitivity of human hearing. (Reproduced, with permission, from Holley and Ashmore 1988.)

Because sharp frequency selectivity, high sensitivity, and otoacoustic emissions are also observed in animal species that lack outer hair cells and lack high concentrations of prestin, electromotility cannot be the only form of mechanical amplification by hair cells. In addition to detecting stimuli, hair bundles are also mechanically active and contribute to amplification. Hair bundles can make spontaneous back-and-forth movements that have been shown in some nonmammals to underlie spontaneous otoacoustic emissions. Under experimental conditions, bundles can exert force against stimulus probes, performing mechanical work and thereby amplifying the input. In vitro experiments indicate that active hair-bundle motility

contributes to the cochlear active process even in the mammalian ear.

Active hair-bundle movements can be fast enough to mediate otoacoustic emissions at sound frequencies at least as high as a few kilohertz. However, it remains uncertain whether bundles can generate forces at the very high frequencies at which sharp frequency selectivity and otoacoustic emissions are observed in the mammalian cochlea. Active hair-bundle motility and somatic electromotility may function synergistically, with the former serving metaphorically as a tuner and preamplifier and the latter as a power amplifier. Alternatively, hair-bundle motility may dominate at relatively low frequencies but be superseded by electromotility at higher frequencies.

Cochlear Amplification Distorts Acoustic Inputs

When stimulated by two tones at nearby frequencies f_1 and f_2 ($f_1 < f_2$), the basilar membrane vibrates not only at these frequencies but also at additional frequencies—the distortion products—that are not present in the acoustic stimulus. As reported by the Italian violinist Giuseppe Tartini in the 18th century, distortion products can be heard as phantom tones in the auditory percept. Remarkably, the cubic difference tone $2f_1 - f_2$ is heard even at very low sound levels, and its magnitude grows in proportion to the stimulus. Correspondingly, the relative level of distortion remains practically constant over a broad range of sound levels. This phenomenon is explained by the particular form of the compressive nonlinearity associated with cochlear amplification. Clearly, the cochlea does not work as a high-fidelity sound receiver. Distorted cochlear vibrations are strong enough to be reemitted from the ear canal as *distortion-product otoacoustic emissions*. Because they are a property of healthy ears, these emissions are extensively used to screen hearing in newborns.

The Hopf Bifurcation Provides a General Principle for Sound Detection

Detailed in vivo and in vitro studies have revealed four cardinal features of auditory responsiveness. First, an active amplification process lowers the detection threshold. Second, because amplification operates only near a characteristic frequency, the input to the sensory system is actively filtered, which sharpens frequency selectivity. Third, for stimulation near the characteristic frequency, the response displays a compressive nonlinearity that represents a wide range of stimulus levels by a much narrower range of vibration amplitudes. Finally, even in the absence of a stimulus, mechanical activity can produce self-sustained oscillations that result in otoacoustic emissions.

These features have been recognized as signatures of an active dynamical system—a critical oscillator—that operates on the verge of an oscillatory instability termed the Hopf bifurcation (Box 26–1). They are generic: They do not depend on the subcellular and molecular details of the candidate mechanism that brings the system to the brink of spontaneous oscillation. The fact that active hair-bundle motility demonstrates a Hopf bifurcation in vitro provides further evidence that this mechanism contributes to cochlear amplification.

Within this framework, the characteristic frequency is set by that of the critical oscillator. The cochlear partition may be viewed as a set of active oscillatory modules that are hydrodynamically coupled by the cochlear fluids and with characteristic frequencies tonotopically distributed along the longitudinal axis of the cochlea. The hypothesis of critical oscillation facilitates modeling of the traveling wave and cochlear amplification. This is because the generic behaviors of a critical oscillator can be described by a single equation termed the "normal form" (Box 26–1). A critical oscillator is ideally suited for auditory detection, even if its inherent nonlinearity yields pronounced distortions in response to complex sound stimuli. Nonlinear interference between the frequency components of complex stimuli in fact appears as a necessary price to pay for the exquisite sensitivity, sharp frequency selectivity, and wide dynamic range of auditory detection afforded by a critical oscillator. The Hopf bifurcation provides generic properties that account for numerous disparate experimental observations at the level of a single hair bundle, of the basilar membrane, and even in psychoacoustics. This physical principle of auditory detection thus greatly simplifies our understanding of hearing. Although this chapter focusses primarily on mammalian hearing, the common necessity to hear with high sensitivity and sharp frequency selectivity poses similar physical constraints to the ears of all land vertebrates. These constraints have led to the independent evolution of ears that share similar structural features and whose operation is based on similar physical principles, including the use of critical oscillators to amplify sound (Box 26–2).

Hair Cells Use Specialized Ribbon Synapses

Being sensory receptors, hair cells form synapses with sensory neurons. The basolateral membrane of each cell contains several presynaptic active zones at which

Box 26–1 Generic Properties Near a Hopf Bifurcation

A dynamical system displays a Hopf bifurcation when it abruptly transits from quiescence to a state of spontaneous oscillation while subject to continuous variation of a control parameter C. If the system is poised in the vicinity of the critical point, at which $C = C_C$, its steady-state response to sinusoidal forces can be described by a single equation—the "normal form"—of a complex variable Z:

$$\Lambda \frac{dZ}{dt} \cong -\Lambda(C_c - C - 2i\pi f_c)Z - B|Z|^2 Z + F \qquad \textbf{(26–1)}$$

Here, the real part of Z may represent the position of the basilar membrane or of the hair bundle, Λ is a friction coefficient, and F is the external force provided by a sound stimulus. In the absence of an external force ($F = 0$), spontaneous oscillations emerge when the control parameter becomes larger than the critical value C_C (Figure 26-15A); the parameter f_C corresponds to the frequency of spontaneous oscillation at the critical point. A Hopf bifurcation must be driven by an active process, whereby the system mobilizes internal resources of energy to power spontaneous movements. A system operating precisely at the critical point is called a critical oscillator. The response of a critical oscillator to sinusoidal stimuli is endowed with generic properties (Figure 26–15B,C) that are characteristic of sound detection in the ear.

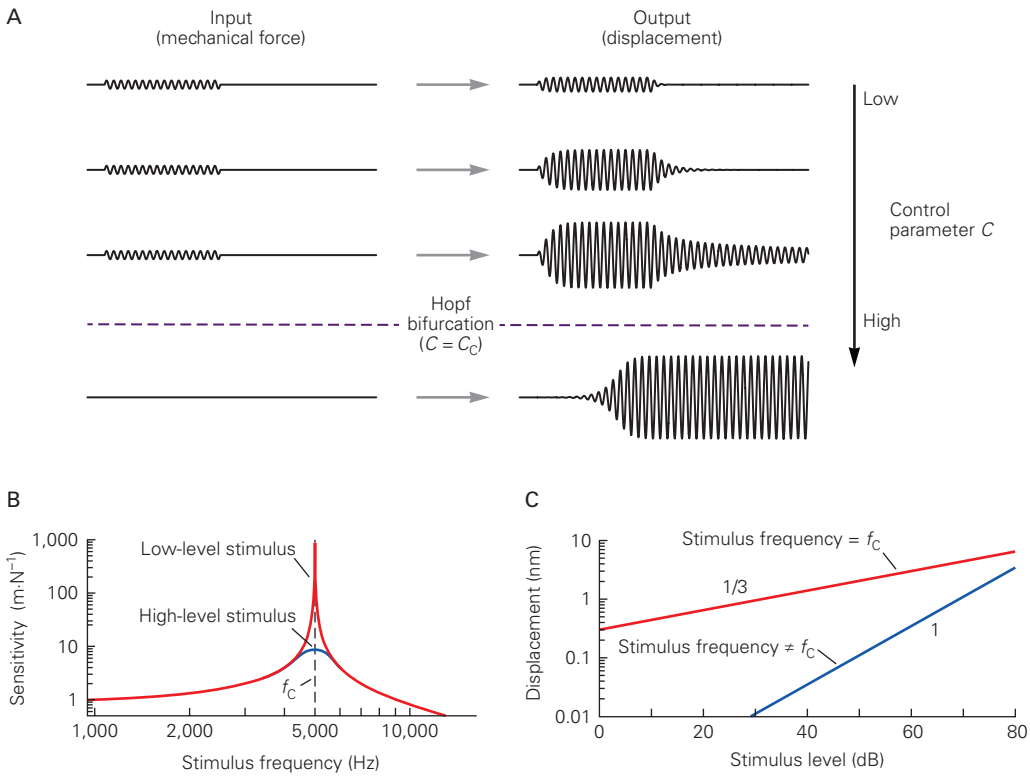

Figure 26–15 Frequency-selective amplification near a Hopf bifurcation.

A. As the control parameter C increases to approach the critical value C_C, the response to a sinusoidal stimulus of constant amplitude increases: The system gets more sensitive. For $C > C_C$, the system oscillates spontaneously at a constant amplitude and frequency, even if no stimulus is applied. The Hopf bifurcation corresponds to $C = C_C$. (Reproduced, with permission, from Hudspeth 2014.)

B. When the system is poised at the bifurcation ($C = C_C$), the sensitivity to a low-level stimulus is greatly enhanced near the characteristic frequency f_C (here 5000 Hz; **dashed line**), but drops rapidly if the stimulus is detuned from this frequency (**red line**). For a stimulus 60 dB more intense, the maximal sensitivity is 100-fold lower, and the peak in sensitivity is 100-fold broader (**blue line**): A critical oscillator enhances the weakest stimuli much more than the strongest and with much sharper frequency selectivity. (Adapted, with permission, from Hudspeth, Jülicher, and Martin 2010.)

C. At the characteristic frequency f_C, the response—here displacement—displays a compressive growth that corresponds to a line of slope 1/3 in this doubly logarithmic plot (**red line**): A large range of stimulus levels is represented by a much narrower range of response amplitudes. In contrast, when the frequency of the stimulus departs significantly from the characteristic frequency (**blue line**), the response is proportional to the input, corresponding to a line of slope unity. By amplifying weak inputs near its characteristic frequency, the critical oscillator lowers the stimulus level required to elicit a threshold vibration, here by 60 dB for a threshold of 0.3 nm. (Adapted, with permission, from Hudspeth, Jülicher, and Martin 2010.)

Box 26–2 The Evolutionary History of Hearing Resulted in Similarities Between Groups

Mammals are not alone in possessing sensitive and frequency-selective hearing. Amphibians and reptiles, including birds, also do. It is a remarkable fact that these various groups of land vertebrates actually acquired their good hearing systems largely independently. The small, dedicated auditory receptor organ was present in the inner ear of their common ancestor. Much later, the ancestors of modern lizards, birds, and mammals each independently evolved middle-ear systems with eardrums collecting sound from the outside world. Some species, such as birds and their relatives, even evolved two groups of sensory hair cells that have a division of labor similar to that of mammalian inner and outer hair cells. Comparison of middle-ear and inner-ear structures and functions across all living vertebrate groups has revealed that they share many common features and that hearing performance is largely comparable between them. Sound amplification associated with active hair-bundle motility was already present in the very first hair cells that evolved, even before the first fishes. This amplifying system was inherited by all groups and, as described earlier, plays a critical role in improving hearing sensitivity and sharpening frequency selectivity. The greatest difference between mammals and the other groups is that the upper frequency limit of hearing is generally higher in mammals. Nonmammalian ears are limited in response to frequencies lower than about 12 to 14 kHz, whereas some mammals can hear beyond 100 kHz.

In addition to active hair-bundle motility, the second mechanism that tunes individual hair cells to specific frequencies in many nonmammalian ears is electrical in nature. In many fishes, amphibians, and birds, the membrane potential of each hair cell resonates at a particular frequency. Several factors, including alternative splicing of the mRNA encoding cochlear K^+ channels and expression of these channels' auxiliary β subunit, tune the characteristic frequency of the resonance along the tonotopic axis of the auditory organ. Whether electrical resonance contributes to frequency tuning in the ears of mammals, including humans, remains uncertain. It is plausible that mammalian hair cells use instead an interplay between somatic electromotility, which seems absent in nonmammalian species, and the micromechanical environment, including hair-bundle motility, to actively amplify and filter their inputs.

The key signatures of a Hopf bifurcation have been recognized in spontaneous mechanical oscillations of the hair bundle, in electrical oscillations of the membrane potential, and in sound-evoked vibration of the basilar membrane. It is likely that the parallel evolution of hearing organs in different groups of vertebrates resulted in several ways of benefitting from the generic properties of critical oscillation.

chemical neurotransmitter is released. An active zone is characterized by four prominent morphological features (Figure 26–16).

A presynaptic dense body or synaptic ribbon lies in the cytoplasm adjacent to the release site. This fibrillar structure may be spherical, ovoidal, or flattened, and usually measures a few hundred nanometers across. The dense body resembles the synaptic ribbon of a photoreceptor cell and represents a specialized elaboration of the smaller presynaptic densities found at many other synapses. In addition to molecular components shared with conventional synapses, ribbon synapses contain large amounts of the protein ribeye.

The presynaptic ribbon is surrounded by clear synaptic vesicles, each 35 to 40 nm in diameter, which are attached to the dense body by tenuous filaments. Between the dense body and the presynaptic cell membrane lies a striking presynaptic density that comprises several short rows of fuzzy-looking material. Within the cell membrane, rows of large particles are aligned with the strips of presynaptic density. These particles include the Ca^{2+} channels involved in the release of transmitter as well as the K^+ channels that participate in electrical resonance in nonmammalian vertebrates.

Studies of nonmammalian experimental models show that, as with most other synapses (Chapter 15), the release of transmitter by hair cells is evoked by presynaptic depolarization and requires influx of Ca^{2+} from the extracellular medium. Hair cells lack synaptotagmins 1 and 2, however, and the role of those proteins as rapid Ca^{2+} sensors has probably been assumed by the protein otoferlin, which also promotes the replenishment of synaptic vesicles. Although glutamate is the principal afferent neurotransmitter, other substances are released as well.

The presynaptic apparatus of hair cells has several unusual features that underlie the signaling abilities of

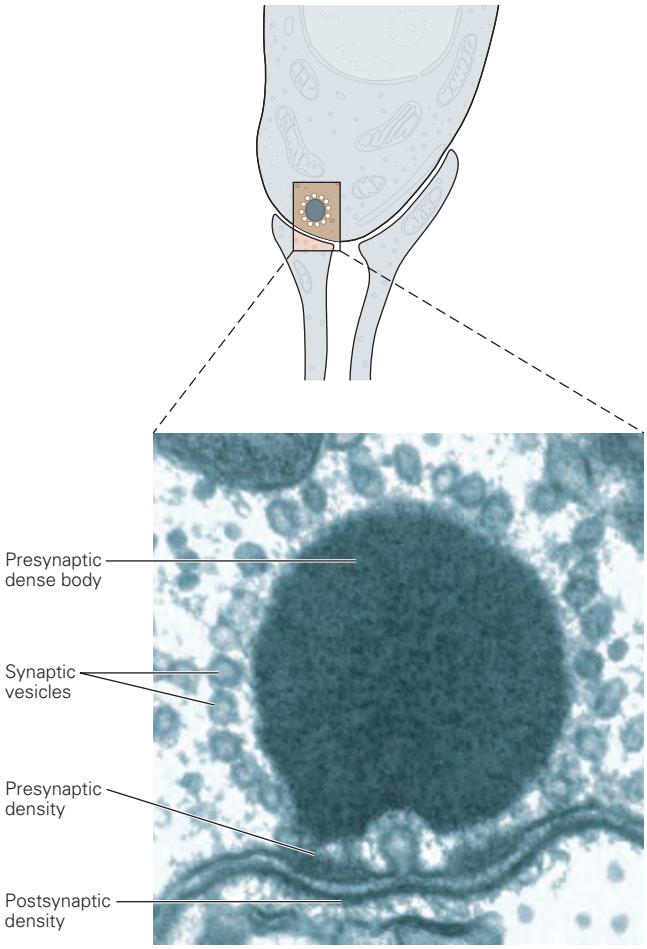

Figure 26–16 The presynaptic active zone of a hair cell. This transmission electron micrograph shows the spherical presynaptic dense body or synaptic ribbon that is characteristic of the hair cell's presynaptic active zone. It is surrounded by clear synaptic vesicles. Beneath the ribbon lies a presynaptic density, in the middle of which one vesicle is undergoing exocytosis. A modest postsynaptic density lies along the inner aspect of the plasmalemma of the afferent terminal. (Reproduced, with permission, from Jacobs and Hudspeth 1990.)

these cells. At rest, inner hair cells continuously release synaptic transmitter. The rate of transmitter release can be modulated upward or downward, depending on whether the hair cell is respectively depolarized or hyperpolarized. Consistent with this observation, some Ca^{2+} channels of hair cells are activated at the resting potential, providing a steady leak of Ca^{2+} that evokes transmitter release from unstimulated cells. Another unusual feature of the hair cell's synapses is that, like those of photoreceptors, they must be able to release neurotransmitter reliably in response to a threshold receptor potential of only 100 μV or so. This feature, too, depends on the fact that the presynaptic Ca^{2+} channels are activated at the resting potential.

Outer hair cells receive inputs from neurons in the brainstem in the form of large boutons on their basolateral surfaces (Figure 26–4). This efferent system desensitizes the cochlea by hyperpolarizing outer hair cells, which turns down the active process. The efferent terminals contain numerous clear synaptic vesicles about 50 nm in diameter, as well as a smaller number of larger, dense-core vesicles. The principal transmitter at these synapses is acetylcholine (ACh); calcitonin gene–related peptide (CGRP) also occurs in efferent terminals and may be co-released with ACh. ACh binds to nicotinic ionotropic receptors consisting of α9 and α10 subunits that have a substantial permeability to Ca^{2+} as well as to Na^+ and K^+. The Ca^{2+} that enters through these channels activates small-conductance Ca^{2+}-sensitive K^+ channels (SK channels), whose opening leads to a protracted hyperpolarization. The cytoplasm of a hair cell immediately beneath each efferent terminal holds a single cisterna of smooth endoplasmic reticulum. This structure may be involved in the reuptake of the Ca^{2+} that enters the cytoplasm in response to efferent stimulation, thus accelerating the return to the cell's resting potential.

Auditory Information Flows Initially Through the Cochlear Nerve

Bipolar Neurons in the Spiral Ganglion Innervate Cochlear Hair Cells

Information flows from cochlear hair cells to neurons whose cell bodies lie in the cochlear ganglion. The central processes of these bipolar neurons form the cochlear division of the vestibulocochlear nerve (eighth cranial nerve). Because this ganglion follows a spiral course around the bony core of the cochlea, it is also called the *spiral ganglion.* Approximately 30,000 ganglion cells innervate the hair cells of each inner ear.

The afferent pathways from the human cochlea reflect the functional distinction between inner and outer hair cells. At least 90% of the spiral ganglion cells terminate on inner hair cells (Figure 26–17). Each axon contacts only a single inner hair cell, but each cell directs its output to many nerve fibers, on average nearly 10. This arrangement has three important consequences.

First, the neural information from which hearing arises originates almost entirely at inner hair cells. Second, because the output of each inner hair cell is

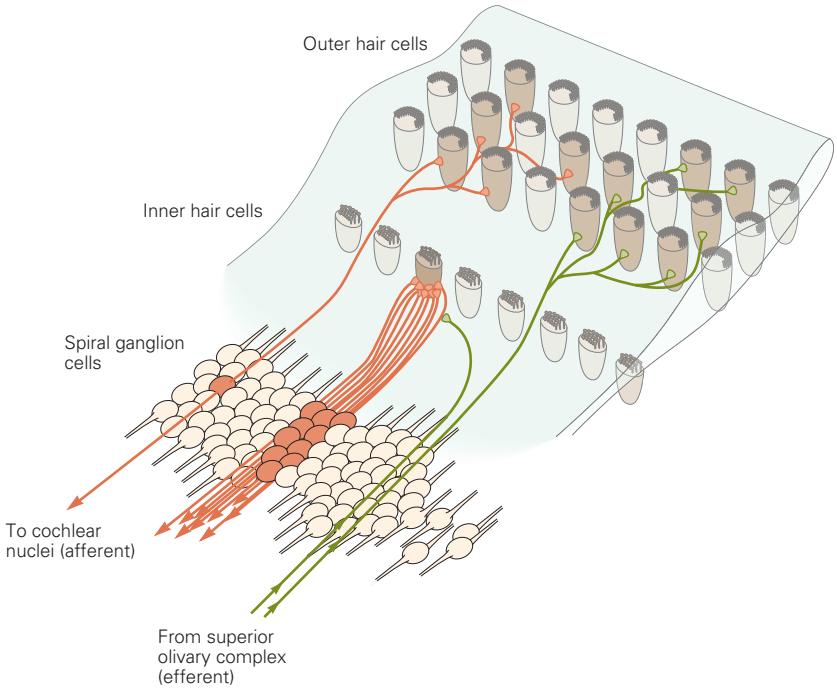

Figure 26–17 Innervation of cochlear hair cells. The great majority of sensory axons (**orange**) in the cochlea carry signals from inner hair cells, each of which constitutes the sole input to an average of 10 axons. A few sensory axons of small caliber transmit information from the outer hair cells. Efferent axons (**green**) largely innervate the outer hair cells and do so directly. In contrast, efferent innervation of inner hair cells is sparse and occurs on the sensory axon terminals. (Adapted, with permission, from Spoendlin 1974.)

sampled by many afferent nerve fibers, the information from one receptor is encoded independently in parallel channels. Third, at any point along the cochlear spiral, or at any position within the spiral ganglion, each ganglion cell responds best to stimulation at the characteristic frequency of the presynaptic hair cell. The tonotopic organization of the auditory neural pathways thus begins at the earliest possible site, immediately postsynaptic to inner hair cells.

Relatively few cochlear ganglion cells contact outer hair cells, and each such neuron extends branching terminals to numerous outer hair cells. Although the ganglion cells that receive input from outer hair cells are known to project into the central nervous system, these neurons are so few that it is not certain whether their projections contribute significantly to the analysis of sound.

The patterns of efferent and afferent connections of cochlear hair cells are complementary. Mature inner hair cells do not receive efferent input; just beneath these cells, however, are extensive axo-axonic synaptic contacts between efferent axon terminals and the endings of afferent nerve fibers. In contrast, other efferent nerves have extensive connections with outer hair cells on their basolateral surfaces. Each outer hair cell receives input from several large efferent terminals, which fill most of the space between the cell's base and the associated supporting cell, leaving little space for afferent terminals.

Cochlear Nerve Fibers Encode Stimulus Frequency and Level

The acoustic sensitivity of axons in the cochlear nerve mirrors the connection pattern of the spiral ganglion cells to the hair cells. Each axon is most responsive to a characteristic frequency. Stimuli of lower or higher frequency also evoke responses, but only when presented at greater levels. An axon's responsiveness may be characterized by a frequency selectivity, or tuning, curve, which is V-shaped like the curves for basilar-membrane motion and hair-cell sensitivity (Figure 26–11). The tuning curves for nerve fibers with different characteristic frequencies resemble one another but are shifted along the frequency axis.

The relationship between sound level in decibels SPL and firing rate in each fiber of the cochlear nerve is approximately linear. Because of the dependence of decibel level on sound pressure, this relation implies that sound pressure is logarithmically encoded by neuronal activity. At the upper end of a fiber's dynamic range, very loud sounds saturate the response. Because an action potential and the subsequent refractory period each last almost 1 ms, the greatest sustainable firing rate is about 500 spikes per second.

Even among nerve fibers with the same characteristic frequency, the threshold of responsiveness varies from axon to axon. The most sensitive fibers, whose response thresholds extend down to approximately

0 dB SPL, characteristically have high rates of spontaneous activity and produce saturating responses for stimulation at moderate intensities, approximately 30 dB SPL. At the opposite extreme, the least sensitive afferent fibers have very little spontaneous activity and much higher thresholds, but respond in a graded fashion to levels even in excess of 100 dB SPL. The activity patterns of most fibers range between these extremes.

The afferent neurons of lowest sensitivity contact the surface of an inner hair cell nearest the axis of the cochlear spiral. The most sensitive afferent neurons, on the other hand, contact the hair cell's opposite side. The multiple innervation of each inner hair cell is therefore not redundant. Instead, the output from a given hair cell is directed into parallel channels of differing sensitivity and dynamic range.

The firing pattern of fibers in the eighth cranial nerve exhibits both phasic and tonic components. Brisk firing occurs at the onset of a tone but, as adaptation occurs, the firing rate declines to a plateau level over a few tens of milliseconds. When stimulation ceases, there is usually a transitory cessation of activity with a similar time course to that of adaptation, before gradual resumption of the spontaneous firing rate (Figure 26–18).

When a periodic stimulus such as a pure tone is presented, the firing pattern of a cochlear nerve fiber encodes information about the periodicity of the stimulus. For example, a relatively low-frequency tone at a moderate intensity might produce one spike in a nerve fiber during each cycle of stimulation. The phase of firing is also stereotyped. Each action potential might occur, for example, during the compressive phase of the stimulus. As the stimulation frequency rises, the stimuli eventually become so rapid that the nerve fiber can no longer produce action potentials on a cycle-by-cycle basis. Up to a frequency in excess of 3 kHz, however, phase-locking persists; a fiber may produce an action potential only every few cycles of the stimulus, but its firing continues to occur at a particular phase in the stimulus cycle.

Periodicity in neuronal firing enhances the information about the stimulus frequency. Any pure tone of sufficient level evokes firing in numerous cochlear nerve fibers. Those fibers whose characteristic frequency coincides with the frequency of the stimulus respond at the lowest stimulus level, but respond still more briskly for stimuli of moderate intensity. Other nerve fibers with characteristic frequencies further from the stimulus also respond, although less vigorously. Regardless of their characteristic frequencies, however, all the responsive fibers may display phase

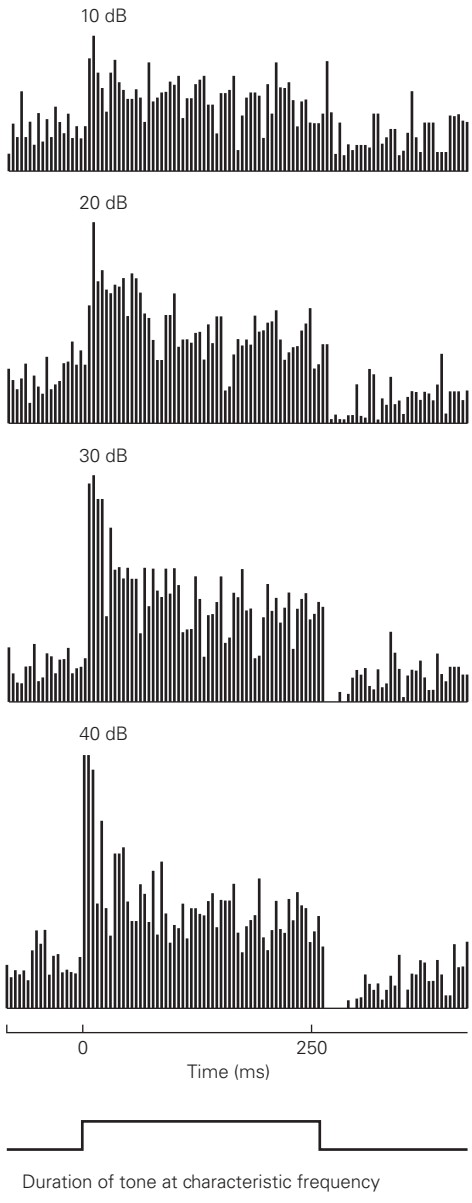

Figure 26–18 The firing pattern of a cochlear nerve fiber. A cochlear nerve fiber is stimulated for somewhat more than 250 ms with a tone burst at about 5 kHz, the cell's characteristic frequency. After a quiet period, the stimulus is repeated. Histograms show the average response patterns of the fiber as a function of stimulus level. The sample period is divided into discrete temporal bins, and the number of spikes occurring in each bin is displayed. An initial, phasic increase in firing is correlated with the onset of the stimulus. The discharge continues during the remainder of the stimulus during adaptation, but decreases following termination. This pattern is evident when the stimulus is 20 dB or more above threshold. Activity gradually returns to baseline during the interval between stimuli. (Adapted, with permission, from Kiang 1965.)

locking: Each tends to fire during a particular part of the stimulus cycle.

The central nervous system can therefore gain information about stimulus frequency in two ways. First, there is a *place code*: The fibers are arrayed in a tonotopic map in which the position is related to characteristic frequency. Second, there is a *frequency code*: The phase-locked firing of the fiber provides information about the frequency of the stimulus, at least for frequencies below 3 kHz.

Sensorineural Hearing Loss Is Common but Is Amenable to Treatment

Whether mild or profound, most deafness falls into the category of *sensorineural hearing loss,* often misnamed "nerve deafness." Although hearing loss can result from direct damage to the eighth cranial nerve, for example from an acoustic neuroma, deafness stems primarily from the loss of cochlear hair cells and their afferent fibers.

The 16,000 hair cells in each human cochlea are not replaced by cell division but must last a lifetime. However, in amphibians and birds, supporting cells can be induced to divide and their progeny to produce new hair cells. In the zebrafish and in birds, some hair cell populations are regenerated continually by the activity of stem or supporting cells. Researchers have recently succeeded in replenishing mammalian hair cells in vitro. Until we understand how hair cells can be restored to the organ of Corti, however, we must cope with hearing loss.

The past few decades have brought remarkable advances in our ability to treat deafness. For the majority of patients who have significant residual hearing, hearing aids can amplify sounds to a level sufficient to activate the surviving hair cells. A modern aid is custom-tailored to compensate for each individual's hearing loss, so that the device amplifies sounds at frequencies to which the wearer is least sensitive, while providing little or no enhancement to those that can still be heard well.

When most or all of a person's cochlear hair cells have degenerated, no amount of amplification can assist hearing. However, a degree of hearing can be restored by bypassing the damaged organ of Corti with a cochlear prosthesis or implant. A user wears a compact unit that picks up sounds, separates their frequency components, and forwards electronic signals representing these constituents along separate wires to small antennae situated just behind the auricle. The signals are then transmitted transdermally to receiving antennae implanted in the temporal bone. From there, fine wires bear the signals to appropriate electrodes implanted as an array in the cochlea at various positions along the scala tympani. Activation of the electrodes excites action potentials in any nearby axons that have survived the degeneration of the hair cells (Figure 26–19).

The cochlear prosthesis takes advantage of the tonotopic representation of stimulus frequency along the cochlea—the *place code* (Figure 26–11 and Chapter 28). The axons innervating each segment of the cochlea are concerned with a specific, narrow range of frequencies. Each electrode in a prosthesis can excite a cluster of nerve fibers that represent similar frequencies. The stimulated neurons then forward their outputs along the eighth nerve to the central nervous system, where these signals are interpreted as a sound of the frequency represented at that position on the basilar membrane. An array of approximately 20 electrodes can mimic a complex sound by appropriately stimulating several clusters of neurons.

The number of implanted cochlear prostheses worldwide is now approaching 350,000. Their effectiveness, however, varies widely from person to person. In the best outcome, an individual can, under quiet conditions, understand speech nearly as well as a normally hearing person and can even conduct telephone conversations. At the other extreme are patients who derive little benefit from prostheses, presumably because of extensive degeneration of the nerve fibers near the electrode array. Most patients find their prostheses of great value. Even if hearing is not completely restored, the devices help in lip reading and alert patients to noises in the environment.

Hearing loss is often accompanied by another distressing symptom, *tinnitus*, or "ringing in the ears." By interfering with concentration and disrupting sleep, tinnitus can exasperate, depress, and even madden its victims. Because on rare occasions tinnitus stems from lesions to the auditory pathways, such as acoustic neuromas, it is important in neurological diagnosis to exclude such causes. Most tinnitus, however, is idiopathic: Its cause is uncertain. More and more studies implicate stress as an important factor. Some drugs also trigger the condition; antimalarial drugs related to quinine and aspirin at the high dosages used in the treatment of rheumatoid arthritis are notorious for this. Often, however, tinnitus occurs at high frequencies to which a damaged ear is no longer sensitive. In these instances, tinnitus may reflect hypersensitivity in the deafferented central nervous system, a phenomenon analogous to phantom limb pain (Chapter 20).

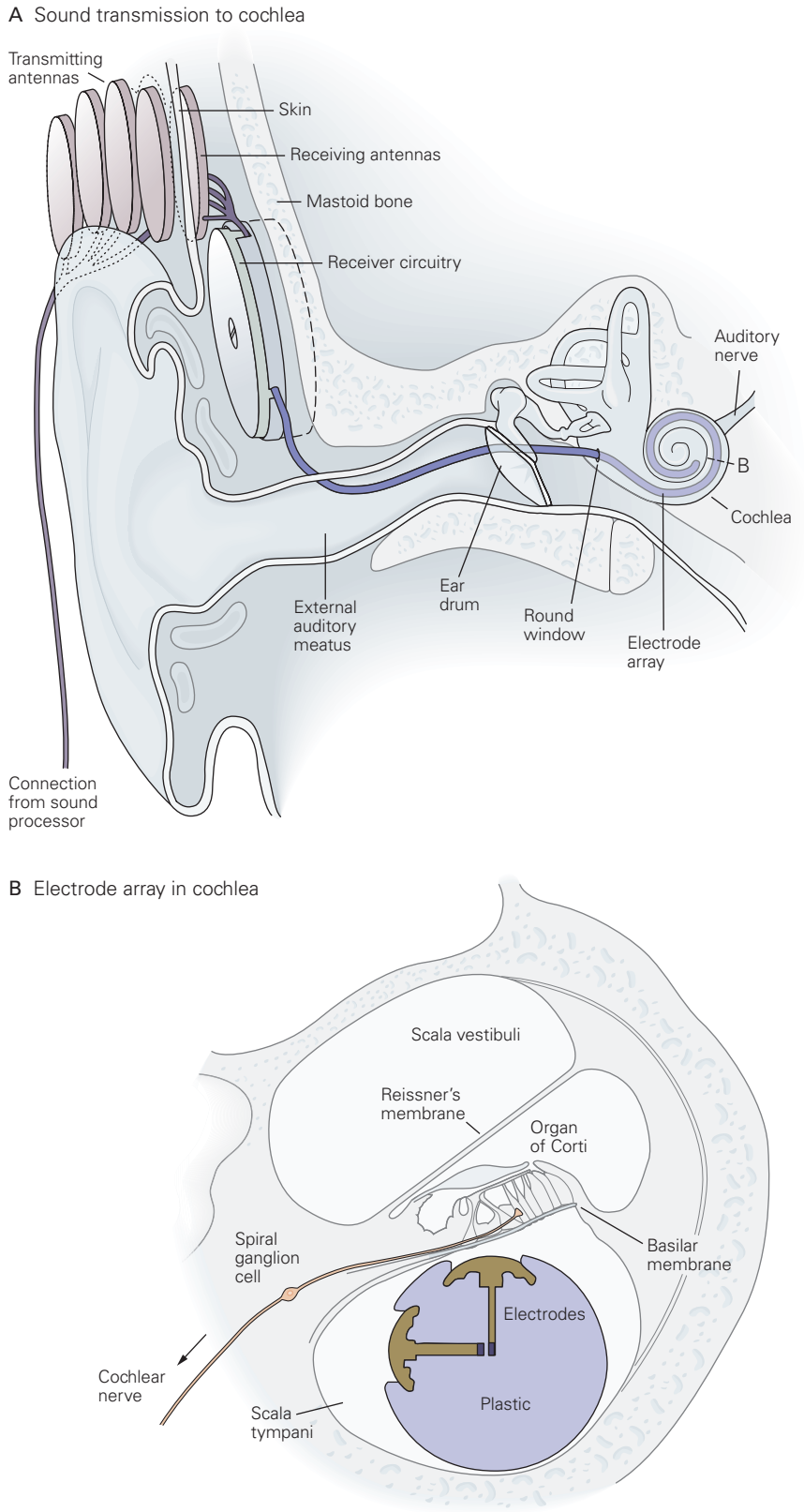

Figure 26–19 A cochlear prosthesis. (Reproduced, with permission, from Loeb et al. 1983.)

A. Transmitting antennas receive electrical signals from a sound processor, located behind the subject's auricle or on the frame of his eyeglasses, and transmit them across the skin to receiving antennas implanted subdermally behind the auricle. The signals are then conveyed in a fine cable (**dark purple**) to an electrode array in the cochlea.

B. This cross section of the cochlea shows the placement of pairs of electrodes in the scala tympani. A portion of the extracellular current passed between an electrode pair is intercepted by nearby cochlear nerve fibers, which are thus excited and send action potentials to the brain.

Highlights

1. Hearing begins with capture of sound by the ear. Mechanical energy captured by the outer ear flows through the middle ear to the cochlea, where it causes the elastic basilar membrane to oscillate.
2. The basilar membrane supports the receptor organ of the inner ear—the organ of Corti, an epithelial strip that contains approximately 16,000 mechanosensory hair cells. Hair cells transduce basilar-membrane vibrations into receptor potentials that cause sensory neurons to fire.
3. The frequency components of a sound stimulus are detected at different locations along the basilar membrane by different hair cells, following a tonotopic map. Mechanical gradients of the basilar membrane contribute to frequency analysis by the cochlea. In addition, each hair cell is tuned at a characteristic frequency according to its morphological, mechanical, and electrical properties, which vary continuously along the tonotopic axis of the cochlea.
4. Hair cells operate much more quickly than do other sensory receptors, which allows them to respond to sound frequencies beyond 100 kHz in some mammalian species. Accordingly, the mechanoelectrical transduction channels in the hair cell are activated directly by mechanical strain.
5. Each hair cell projects from its apical surface a tuft of cylindrical stereocilia—the hair bundle, which works as a mechanical antenna that vibrates in response to sound stimuli. The transduction channels occur at the stereociliary tips. Their open probability is modulated by tension changes in tip links that interconnect neighboring stereocilia.
6. Uniquely among sensory receptors, hair cells amplify their inputs to enhance their sensitivity, sharpen their frequency selectivity, and widen the range of stimulus levels that they can detect. Two forms of cellular motility contribute to this active process. First, receptor potentials evoke length changes of the somata of outer hair cells, a biological analog of piezoelectricity called electromotility. Second, the hair bundle—the mechanosensory antenna of the hair cell—can vibrate autonomously.
7. The ear not only receives sound but also emits sound called otoacoustic emissions. Spontaneous and evoked otoacoustic emissions result from the cochlea's active amplification processes.
8. The cochlea does not work as a high-fidelity sound receiver; instead, it introduces conspicuous distortions that contribute to sound perception. The auditory nonlinearity originates in the cochlea, which amplifies preferentially weak sound stimuli, and constitutes a hallmark of sensitive hearing that is used to screen hearing deficits in newborns.
9. A large variety of experimental observations at the level of a single hair bundle, of the basilar membrane, and in psychoacoustics are readily explained if the cochlea contains active mechanical modules that each operate on the verge of an oscillatory instability—the Hopf bifurcation. The Hopf bifurcation provides a general principle of auditory detection that simplifies our understanding of hearing.
10. The evolutionary history of hearing reveals that the various groups of land vertebrates acquired their hearing systems largely independently, but that their sensitivity and frequency selectivity are similar. In particular, both mammalian and nonmammalian ears benefit from mechanical amplification of sound inputs and show otoacoustic emissions. Mammals most notably differ from other groups in that their hearing range extends to frequencies beyond 12 to 14 kHz.
11. Analysis of the genetic forms of deafness has provided information on dozens of proteins key to the function of the hair cell, in particular those responsible for mechanoelectrical transduction and for synaptic transmission between hair cells and fibers of the auditory nerve. Although these genes may serve as potential targets for future therapies, sensorineural hearing loss is currently treated mostly with hearing aids or cochlear prostheses. New strategies, such as hair-cell replenishment via stem-cell differentiation or optogenetic stimulation of the spiral ganglion, provide promising avenues for research on hearing restoration.

Pascal Martin
Geoffrey A. Manley

Selected Reading

Hudspeth AJ. 1989. How the ear's works work. Nature 341:397–404.
Hudspeth AJ. 2014. Integrating the active process of hair cells with cochlear function. Nat Rev Neurosci 15:600–614.

Hudspeth AJ, Jülicher F, Martin P. 2010. A critique of the critical cochlea: Hopf—a bifurcation—is better than none. J Neurophysiol 104:1219–1229.
Kazmierczak P, Sakaguchi H, Tokita J, et al. 2007. Cadherin 23 and protocadherin 15 interact to form tip-link filaments in sensory hair cells. Nature 449:87–91.
Loeb GE. 1985. The functional replacement of the ear. Sci Am 252:104–111.
Pickles JO. 2008. *An Introduction to the Physiology of Hearing*, 3rd ed. New York: Academic.
Robbles L. Ruggero MA. 2001. Mechanics of the mammalian cochlea. Physiol Rev 81:1305–1352.
Zheng J, Shen W, He DZZ, Long KB, Madison LD, Dallos P. 2000. Prestin is the motor protein of cochlear outer hair cells. Nature 405:149–155.

References

Art JJ, Crawford AC, Fettiplace R, Fuchs PA. 1985. Efferent modulation of hair cell tuning in the cochlea of the turtle. J Physiol 360:397–421.
Ashmore JF. 2008. Cochlear outer-hair-cell motility. Physiol Rev 88:173–210.
Assad JA, Shepherd GM, Corey DP. 1991. Tip-link integrity and mechanical transduction in vertebrate hair cells. Neuron 7:985–994.
Avan P, Buki B, Petit C. 2013. Auditory distortions: origins and functions. Physiol Rev 93:1563–1619.
Barral J, Dierkes K, Lindner B, Jülicher F, Martin P. 2010. Coupling a sensory hair-cell bundle to cyber clones enhances nonlinear amplification. Proc Natl Acad Sci USA 107:8079–8084.
Barral J, Martin P. 2012. Phantom tones and suppressive masking by active nonlinear oscillation of the hair-cell bundle. Proc Natl Acad Sci USA 109:E1344–E1351.
Beurg M, Fettiplace R, Nam J-H, Ricci AJ. 2009. Localization of inner hair cell mechanotransducer channels using high-speed calcium imaging. Nat Neurosci 12:553–558.
Chan DK, Hudspeth AJ. 2005. Ca^{2+} current-driven nonlinear amplification by the mammalian cochlea in vitro. Nat Neurosci 8:149–155.
Corey D, Hudspeth AJ. 1983. Kinetics of the receptor current in bullfrog saccular hair cells. J Neurosci 3:962–976.
Crawford AC, Fettiplace R. 1981. An electrical tuning mechanism in turtle cochlear hair cells. J Physiol 312:377–412.
Fettiplace R, Kim KX. 2014. The physiology of mechanoelectrical transduction channels in hearing. Physiol Rev 94:951–986.
Frolenkov GI, Atzori M, Kalinec F, Mammano F, Kachar, B. 1998. The membrane-based mechanism of cell motility in cochlear outer hair cells. Mol Biol Cell 9:1961–1968.
Glowatzki E, Fuchs PA. 2002. Transmitter release at the hair cell ribbon synapse. Nat Neurosci 5:147–154.
Helmholtz HLF. [1877] 1954. *On the Sensations of Tone as a Physiological Basis for the Theory of Music.* New York: Dover.
Holley MC, Ashmore JF. 1988. On the mechanism of a high-frequency force generator in outer hair cells isolated from the guinea pig cochlea. Proc R Soc Lond B Biol Sci 232:413–429.
Howard J, Hudspeth AJ. 1988. Compliance of the hair bundle associated with gating of mechanoelectrical transduction channels in the bullfrog's saccular hair cell. Neuron 1:189–199.
Hudspeth AJ, Gillespie PG. 1994. Pulling springs to tune transduction: adaptation by hair cells. Neuron 12:1–9.
Jacobs RA, Hudspeth AJ. 1990. Ultrastructural correlates of mechanoelectrical transduction in hair cells of the bullfrog's internal ear. Cold Spring Harbor Symp Quant Biol 55:547–561.
Johnson SL, Beurg M, Marcotti W, Fettiplace R. 2011. Prestin-driven cochlear amplification is not limited by the outer hair cell membrane time constant. Neuron 70:1143–1154.
Kemp DT. 1978. Stimulated acoustic emissions from within the human auditory system. J Acoust Soc Am 64:1386–1391.
Kiang NY-S. 1965. *Discharge Patterns of Single Fibers in the Cat's Auditory Nerve.* Cambridge, MA: MIT Press.
Kiang NY-S. 1980. Processing of speech by the auditory nervous system. J Acoust Soc Am 68:830–835.
Liberman MC. 1982. Single-neuron labeling in the cat auditory nerve. Science 216:1239–1241.
Loeb GE, Byers CL, Rebscher SJ, et al. 1983. Design and fabrication of an experimental cochlear prosthesis. Med Biol Eng Comput 21:241–254.
Manley GA. 2012. Evolutionary paths to mammalian cochleae. J Assoc Res Otolaryngol 13:733–743.
Manley GA, Köppl C. 1998. Phylogenic development of the cochlea and its innervation. Curr Opin Neurobiol 8:468–474.
Martin P, Hudspeth AJ. 1999. Active hair-bundle movements can amplify a hair cell's response to oscillatory mechanical stimuli. Proc Natl Acad Sci USA 96:14306–14311.
Michalski N, Petit C. 2015. Genetics of auditory mechano-electrical transduction. Pflugers Arch 467:49–72.
Murphy WJ, Tubis A, Talmadge CL, Long GR. 1995. Relaxation dynamics of spontaneous otoacoustic emissions perturbed by external forces. II. Suppression of interacting emissions. J Acoust Soc Am 97:3711–3720.
Oshima K, Shin K, Diensthuber M, Peng AW, Ricci AJ, Heller S. 2010. Mechanosensitive hair cell-like cells from embryonic and induced pluripotent stem cells. Cell 141: 704–716.
Pan B, Akyuz N, Liu XP, et al. 2018. TMC1 forms the pore of mechanosensory transduction channels in vertebrate inner ear hair cells. Neuron 99:736–753.
Probst R, Lonsbury-Martin BL, Martin GK. 1991. A review of otoacoustic emissions. J Acoust Soc Am 89:2027–2067.
Reichenbach T, Hudspeth AJ. 2014. The physics of hearing: fluid mechanics and the active process of the inner ear. Rep Prog Phys 77:0706601.
Ricci AJ, Crawford AC, Fettiplace R. 2003. Tonotopic variation in the conductance of the hair cell mechanotransducer channel. Neuron 40:983–990.
Sotomayor M, Weihofen WA, Gaudet R, Corey DP. 2012. Structure of a force-conveying cadherin bond essential for the inner-ear mechanotransduction. Nature 492:128–132.

Spoendlin H. 1974. Neuroanatomy of the cochlea. In: E Zwicker, E Terhardt (eds). *Facts and Models in Hearing*, pp. 18–32. New York: Springer-Verlag.

Stauffer EA, Scarborough JD, Hirono M, et al. 2005. Fast adaptation in vestibular hair cells requires myosin-1c activity. Neuron 47:541–553.

Tinevez JY, Jülicher F, Martin P. 2007. Unifying the various incarnations of active hair-bundle motility by the vertebrate hair cell. Biophys J 93:4053–4067.

von Békésy G. 1960. *Experiments in Hearing*. EG Wever (ed, transl). New York: McGraw-Hill.

Wilson JP. 1980. Evidence for a cochlear origin for acoustic re-emissions, threshold fine-structure and tonal tinnitus. Hear Res 2:233–252.

Wu Z, Müller U. 2016. Molecular identity of the mechanotransduction channel in hair cells: not quiet there yet. J Neurosci 36:10927–10934.

27

The Vestibular System

Modern vehicular travel on earth and through extraterrestrial space relies upon sophisticated guidance systems that integrate acceleration, velocity, and positional information through transducers, computational algorithms, and satellite triangulation. Yet the principles of inertial guidance are ancient: Vertebrates have used analogous systems for 500 million years and invertebrates for even longer. In these animals, the inertial guidance system, termed the vestibular system, serves to detect and interpret motion through space as well as orientation relative to gravity.

Through extensive research over many decades, it is apparent that most, if not all, organisms on Earth have evolved to sense one of the most prevalent "forces" in our universe, gravity. The mechanisms for the sensory transduction are as diverse as nature could devise. Gravity is most precisely referenced as gravitoinertial acceleration (GIA), a distinct form of linear acceleration directed toward the core of our planet. In truth, gravity varies systematically by as much as 0.5% between the equator and the poles; it increases over mineral-dense regions and decreases over mineral-light regions of the Earth's surface. Yet every single behavior that animals perform is referenced to the GIA, and all of our actions and cognitive directives depend

upon knowledge of our motion and orientation relative to it. The first developments of what we refer to as a vestibular system were actually gravity sensors; as behavior became increasingly mobile, sensory organs evolved to process rotational accelerations as well.

In this chapter we will concentrate on the vestibular system of vertebrates, which has remained highly conserved across many species. Vestibular signals originate in the labyrinths of the internal ear (Figure 27–1B). The *bony labyrinth* is a hollow structure within the petrous portion of the temporal bone. Within it lies the *membranous labyrinth,* which contains sensors for both the vestibular and auditory systems.

The vestibular receptors consist of two parts: two otolith organs, the utricle and saccule, which measure linear accelerations, and three semicircular canals, which measure angular accelerations. Rotational motion (angular acceleration) is experienced during head turns, whereas linear acceleration occurs during walking, falling, vehicular travel (ie, translations), or head tilts relative to gravity. These receptors send vestibular information to the brain, where it is integrated into an appropriate signal regarding direction and speed of motion, as well as the position of the head relative to the GIA. Many of the central vestibular neurons at the first junction with receptor afferent fibers also

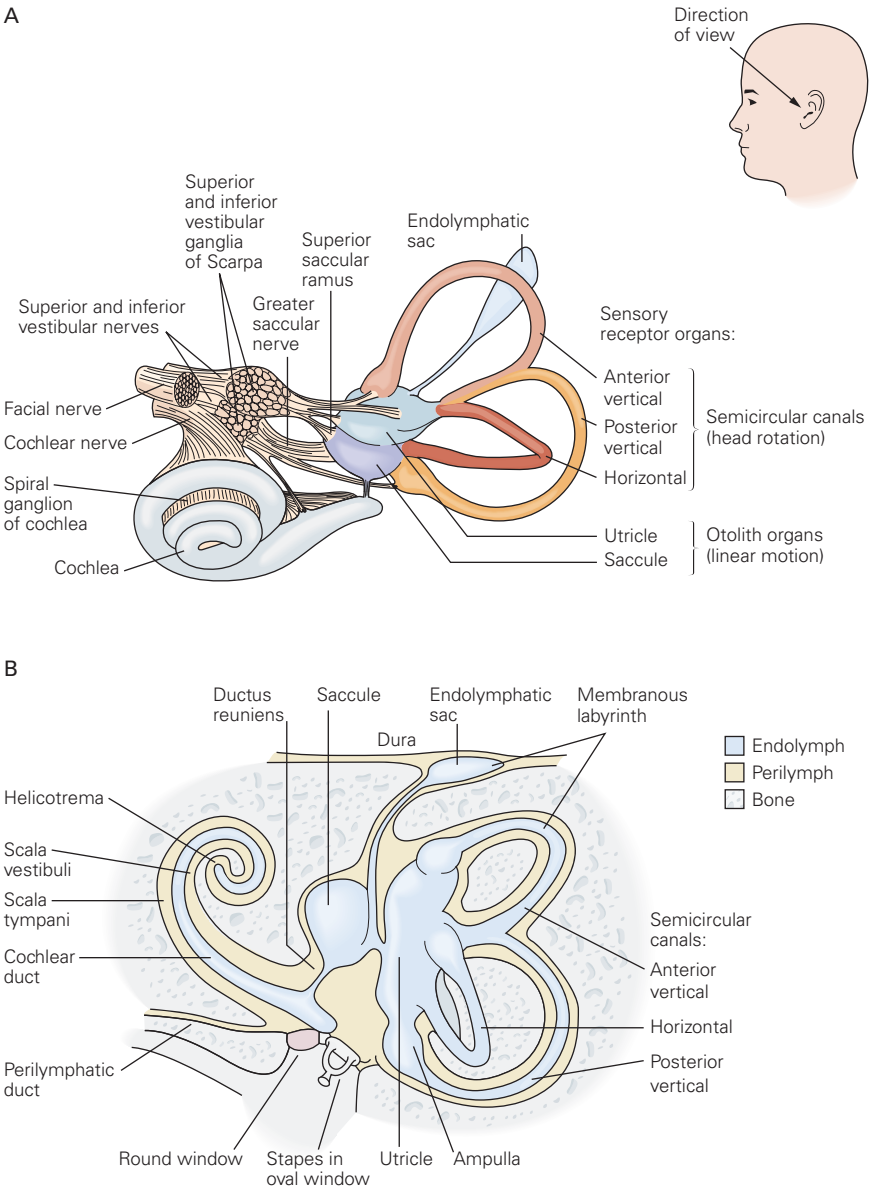

Figure 27–1 The vestibular apparatus of the inner ear.

A. The orientations of the vestibular and cochlear divisions of the inner ear are shown with respect to the head.

B. The inner ear is divided into bony and membranous labyrinths. The bony labyrinth is bounded by the petrosal portion of the temporal bone. Lying within this structure is the membranous labyrinth, which contains the receptor organs for hearing (the cochlea) and equilibrium (the utricle, saccule, and semicircular canals). The space between bone and membrane is filled with perilymph, whereas the membranous labyrinth is filled with endolymph. Sensory cells in the utricle, saccule, and ampullae of the semicircular canals respond to motion of the head. (Adapted from Iurato 1967.)

receive convergent signals from other systems such as proprioceptors, visual signals, and motor commands. Central processing of these multimodal signals occurs very rapidly to ensure adequate coordination of visual gaze and postural responses, autonomic responses, and awareness of spatial orientation.

The Vestibular Labyrinth in the Inner Ear Contains Five Receptor Organs

The membranous labyrinth is supported within the bony labyrinth by a filamentous network of connective tissue. The vestibular portion of the membranous labyrinth lies lateral and posterior to the cochlea. Vestibular receptors are contained in specialized enlarged regions of the membranous labyrinth, termed the ampullae for the semicircular canals and maculae for the otolith organs (Figure 27–1B). Both of the otolith organs lie in a central compartment of the membranous labyrinth, the vestibule, which is surrounded by the bony labyrinth of the same name.

The membranous labyrinth is filled with endolymph, a K^+-rich (150 mM) and Na^+-poor (16 mM) fluid whose composition is maintained by the action of ion pumps in specialized cells. Endolymph bathes the surface of the vestibular receptor cells. Surrounding the membranous labyrinth, in the space between the membranous labyrinth and the wall of the bony labyrinth, is *perilymph.* Perilymph is a high-Na^+ (150 mM), low-K^+ (7 mM) fluid similar in composition to cerebrospinal fluid, with which it is in communication through the cochlear duct. Perilymph bathes the basal surface of the receptor epithelia and the vestibular nerve fibers. Two fluid-tight partitions in the bony labyrinth, the oval and round windows (Figure 27–1B), connect the perilymphatic space to the middle ear cavity. The oval window is connected to the tympanic membrane by the middle ear ossicles. These windows are important for sound transduction (Chapter 26). The endolymph and perilymph are kept separate by a junctional complex of support cells that surrounds the apex of each receptor cell. Disruption of the balance between these two fluids (by trauma or disease) can result in vestibular dysfunction, leading to dizziness, vertigo, and spatial disorientation.

During development, the labyrinth progresses from a simple sac to a complex set of interconnected sensory organs, but retains the same fundamental topological organization. Each organ originates as an epithelium-lined pouch that buds from the otic cyst, and the endolymphatic spaces within the several organs remain continuous in the adult. The endolymphatic spaces of the vestibular labyrinth are also connected to the cochlear duct through the ductus reuniens (Figure 27–1B). In addition, the membranous labyrinth contains a small tube, the endolymphatic duct, which extends through a space in the sigmoid bone, the vestibular aqueduct, to end in a blind sac adjacent to the dura in the epidural space of the posterior cranial fossa. It is thought that the endolymphatic sac has both absorptive and excretive functions to maintain the ionic composition of the endolymphatic fluid.

Hair Cells Transduce Acceleration Stimuli Into Receptor Potentials

Each of the five receptor organs has a cluster of hair cells responsible for transducing head motion into vestibular signals. Hair cells are so named due to an array of nearly 100 staggered height stereocilia. The shortest stereocilia are at one end of the cell and the tallest at the other, ending with the only true cilium of the hair cell, termed the kinocilium. The kinocilium is typically the tallest of all stereocilia. Angular or linear acceleration of the head leads to a deflection of the stereocilia, which together compose the hair bundle (Figure 27–2).

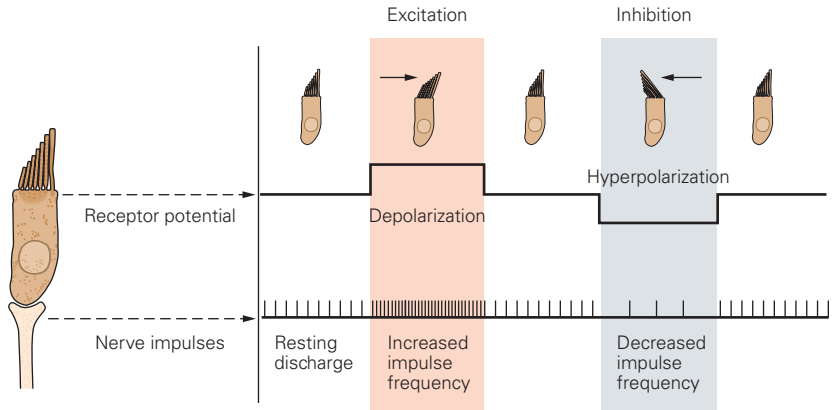

Figure 27–2 Hair cells in the vestibular labyrinth transduce mechanical stimuli into neural signals. At the apex of each cell are the stereocilia, which increase in length toward the single kinocilium. The membrane potential of the receptor cell depends on the direction in which the stereocilia are bent. Deflection toward the kinocilium causes the cell to depolarize and thus increases the rate of firing in the afferent fiber. Bending away from the kinocilium causes the cell to hyperpolarize, thus decreasing the afferent firing rate. (Adapted, with permission, from Flock 1965.)

Specialized ion channels in the tips of the hair bundle stereocilia allow K^+ to enter or be blocked from the surrounding endolymph (Chapter 26). This action allows hair cells to act as mechanoreceptors, where deflection of the stereocilia produces a depolarizing or hyperpolarizing receptor potential depending on which direction the hair bundle moves (Figure 27–2). These depolarizations and hyperpolarizations of the receptor membrane lead to excitation and inhibition, respectively, in the firing rate of the innervating afferent (Figure 27–2). In each vestibular receptor organ, hair cells are arranged so that movement directional specificity is defined by excitation in some cells and inhibition in other cells.

Vestibular signals are carried from the hair cells to the brain stem by branches of the vestibulocochlear nerve (cranial nerve VIII), which enter the brain stem and terminate in the ipsilateral vestibular nuclei, cerebellum, and reticular formation. Cell bodies of the vestibular nerve are located in Scarpa's ganglia within the internal auditory canal (Figure 27–1A). The *superior vestibular nerve* innervates the horizontal and anterior canals and the utricle, whereas the *inferior vestibular nerve* innervates the posterior canal and the saccule. The labyrinth's vascular supply, which arises from the anterior inferior cerebellar artery, travels with nerve VIII. The anterior vestibular artery supplies the structures innervated by the superior vestibular nerve, and the posterior vestibular artery supplies the structures innervated by the inferior vestibular nerve.

All vertebrate receptor hair cells receive efferent inputs from the brain stem. The function of the efferent innervation of vestibular receptors is still a subject of debate. Stimulation of the efferent fibers from the brain stem changes the sensitivity of the afferent axons from the hair cells. It increases the excitability of some afferents and hair cells while inhibiting others, and varies across species.

The Semicircular Canals Sense Head Rotation

An object undergoes angular acceleration when its rate of rotation about an axis changes. Therefore, the head undergoes angular acceleration when it turns or tilts, when the body rotates, and during active or passive locomotion. The three semicircular canals of each vestibular labyrinth detect these angular accelerations and report their magnitudes and motion directions to the brain.

Each semicircular canal is a semicircular tube of membranous labyrinth extending from the vestibule. One end of each canal is open to the vestibule, whereas at the other end, the ampulla, the entire lumen of the canal is traversed by a fluid-tight gelatinous diaphragm, the cupula. The stereocilia and the kinocilium protrude into the gelatinous cupula, while the hair cells are located below in a receptor epithelium, the crista, along with the innervating afferent terminals (Figure 27–3).

The vestibular organs detect accelerations of the head because the inertia of endolymph and cupula results in forces acting on the stereocilia. Consider the simplest situation, a rotation in the plane of a semicircular canal. When the head begins to rotate, the membranous and bony labyrinths move along with it. Because of its inertia, however, the endolymph lags behind the surrounding membranous labyrinth, thus pushing the cupula in a direction opposite that of the head (Figure 27–3B).

The motion of endolymph in a semicircular canal can be demonstrated with a cup of coffee. While gently twisting the cup about its vertical axis, observe a particular bubble near the fluid's outer boundary. As the cup begins to turn, the coffee tends to maintain its initial orientation in space and thus counter-rotates in the cup. If you continue rotating the cup at the same speed, the coffee (and the bubble) eventually catches up to the cup and rotates with it. When the cup decelerates and stops, the coffee keeps rotating, moving in the opposite direction relative to the cup.

In the ampulla, this relative motion of the endolymph creates pressure on the cupula, bending it toward or away from the adjacent vestibule, depending on the direction of endolymph flow. The resulting deflection of the stereocilia alters the membrane potential of the hair cells, thereby changing the firing rates of the associated sensory fibers. Each semicircular canal is maximally sensitive to rotations in its plane. The horizontal canal is oriented approximately 30° elevated above the naso-occipital axis (roughly in the horizontal plane as a person walks and looks at the ground ahead) and thus is most sensitive to rotations in the horizontal plane. The stereocilia are arranged so that leftward rotational motion is excitatory for the left horizontal canal and inhibitory for the right horizontal canal. The anterior and posterior canals are oriented more vertically in the head, at an angle of approximately 45 degrees from the sagittal plane (Figure 27–4). Similar rotational motion downward in the plane of the anterior canals is excitatory for anterior canal hair cells, while upward head motion is excitatory for posterior canals.

Because there is approximate mirror symmetry of the left and right labyrinths, the six canals effectively operate as three coplanar pairs. The two horizontal canals form one pair; each of the other pairs consists of one anterior canal on one side of the head and the contralateral posterior canal. Further, the three

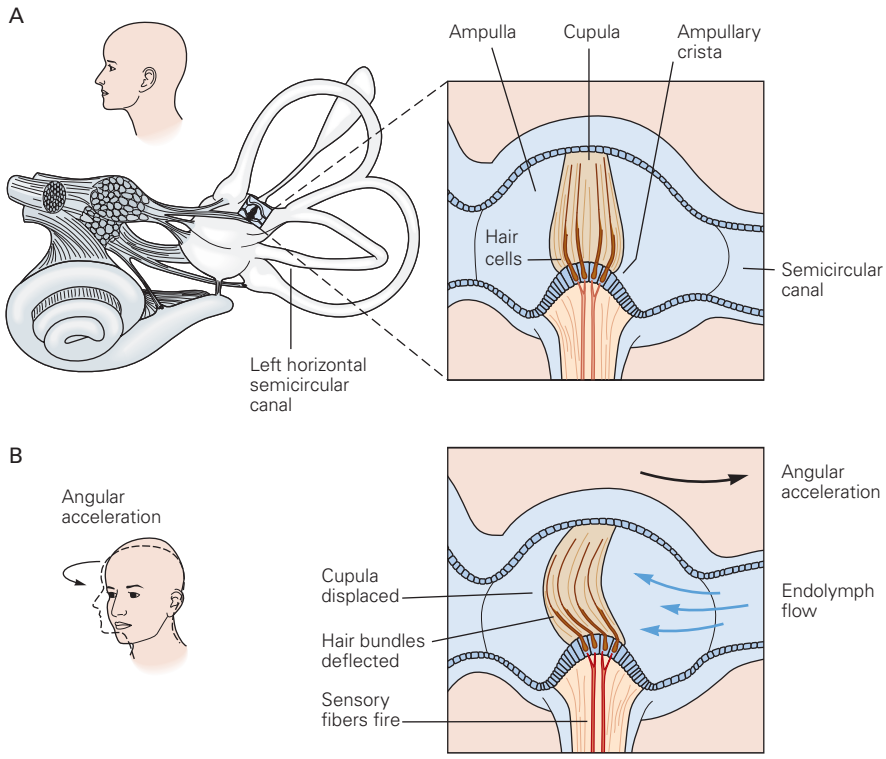

Figure 27–3 The ampulla of a semicircular canal.

A. A thickened zone of epithelium, the ampullary crista, contains the hair cells. The stereocilia and the kinocilia of the hair cells extend into a gelatinous diaphragm, the cupula, which stretches from the crista to the roof of the ampulla.

B. The cupula is displaced by the relative movement of endolymph when the head turns. As a result, the hair bundles are also displaced. Their movement is greatly exaggerated in the diagram.

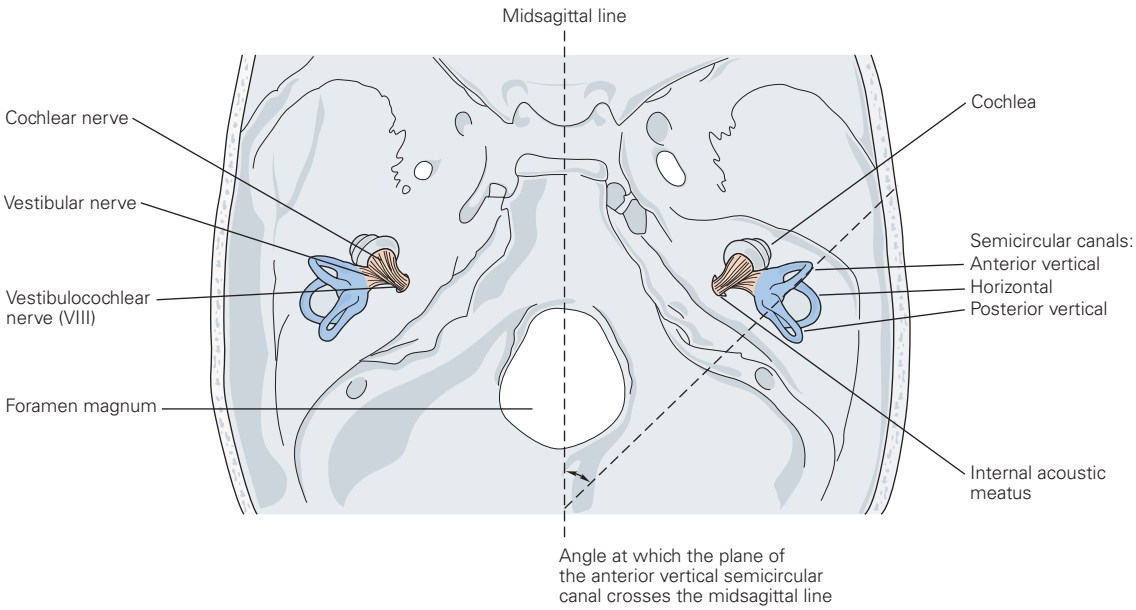

Figure 27–4 The bilateral symmetry of the semicircular canals. The horizontal canals on both sides lie in approximately the same plane and therefore are functional pairs. The bilateral vertical canals have a more complex relationship. The anterior canal on one side and the posterior canal on the opposite side lie in parallel planes and therefore constitute a functional pair. The vertical semicircular canals lie nearly 45° from the midsagittal plane. Each of the semicircular canals on one side of the head lie in approximately orthogonal planes to each other.

semicircular canals on each side of the head lie roughly orthogonal to each other (Figure 27–4). When the head moves toward the receptor hair cells (eg, leftward head turns for the left horizontal semicircular canal), the stereocilia are bent toward the tall kinocilium, thus exciting (depolarizing) the cell. Head motion in the opposite direction causes bending away from the kinocilum and toward the smallest stereocilia, thus closing the channels and inhibiting (hyperpolarizing) the cell.

The left and right ear semicircular canals have opposite polarity; thus, when you turn your head to the left, the receptors in the left horizontal semicircular canal will be excited (increased firing rate), whereas right horizontal canal receptors will be inhibited (decreased firing rate; Figure 27–5). The same relationship is true for the vertical semicircular canals. The canal planes are also roughly aligned to the pulling planes of specific eye muscles. The pair of horizontal canals lies in the pulling plane of the lateral and medial rectus muscles. The left anterior and right posterior canal pair lie in the pulling plane of the left superior and inferior rectus and right superior and inferior oblique muscles. The right anterior and left posterior pair occupies the pulling plane of the left superior and inferior oblique and right superior and inferior rectus muscles.

The Otolith Organs Sense Linear Accelerations

The vestibular system must compensate not only for head rotations but also for linear motion. The two otolith organs, the utricle and saccule, detect linear motion as well as the static orientation of the head relative to gravity, which is itself a linear acceleration. Each organ consists of a sac of membranous labyrinth approximately 3 mm in the longest dimension. The hair cells of each organ are arranged in a roughly elliptical patch called the *macula*. The human utricle contains approximately 30,000 hair cells, whereas the saccule contains some 16,000.

The hair bundles of the otolithic hair cells extend into a gelatinous sheet, the *otolithic membrane*, which

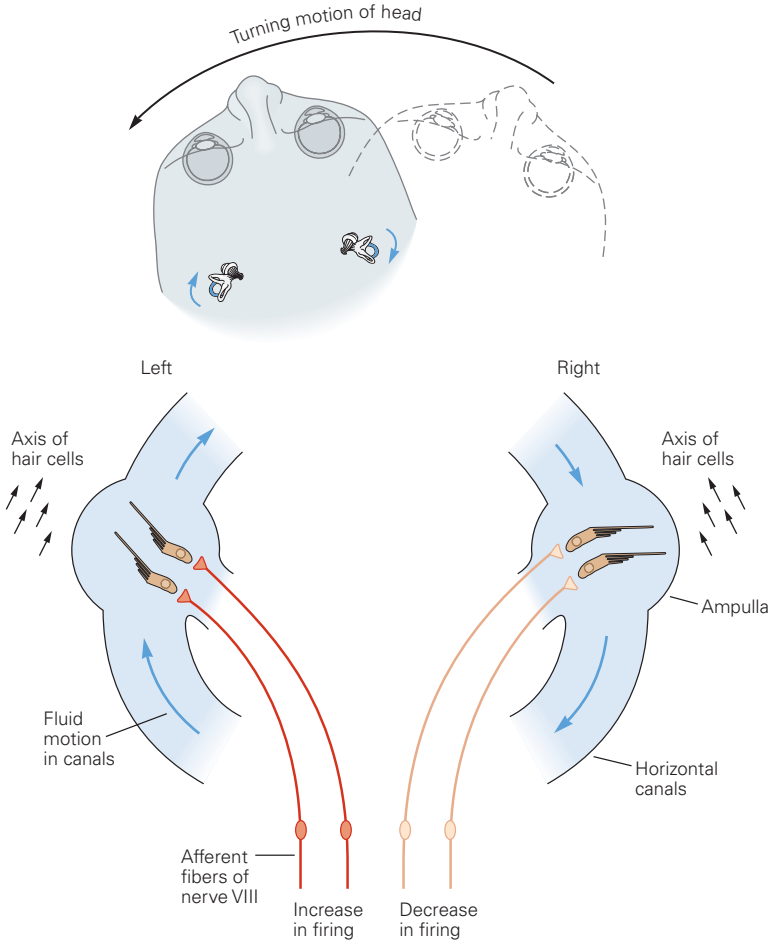

Figure 27–5 The left and right horizontal semicircular canals work together to signal head movement. Because of inertia, rotation of the head in a counterclockwise direction causes endolymph to move clockwise with respect to the canals. This deflects the stereocilia in the left canal in the excitatory direction, thereby exciting the afferent fibers on this side. In the right canal, the afferent fibers are hyperpolarized so that firing decreases.

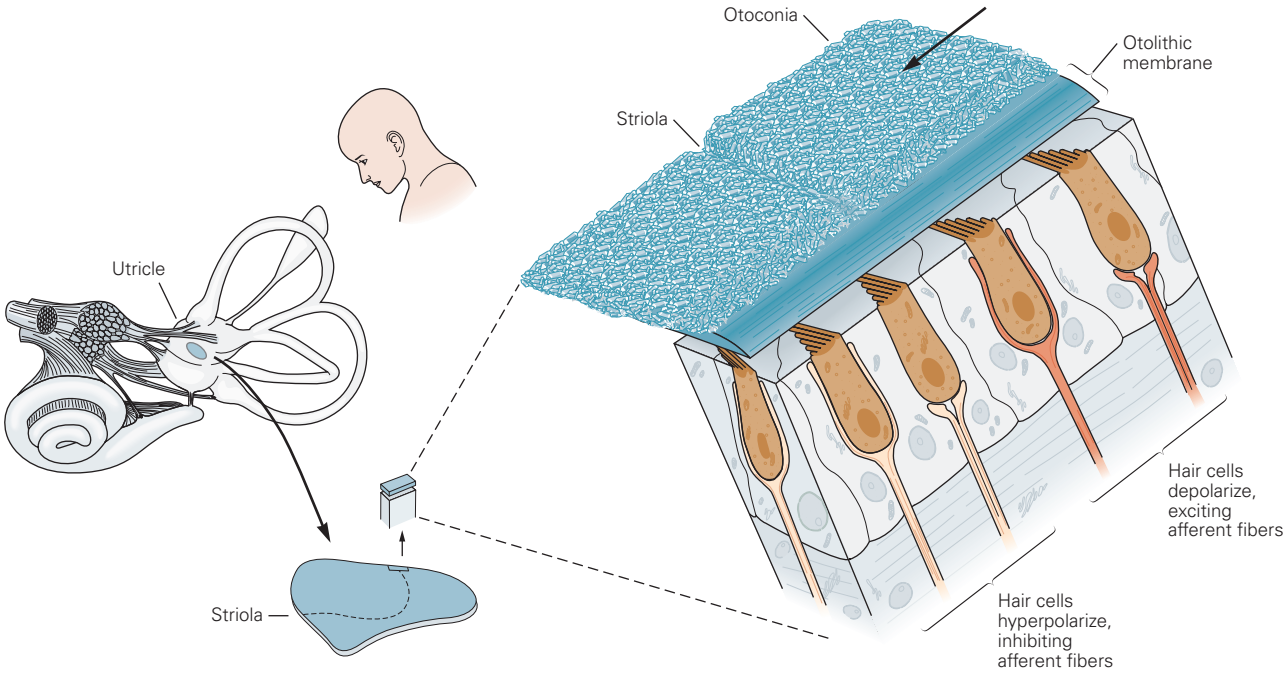

Figure 27–6 The utricle detects tilt of the head. Hair cells in the epithelium of the utricle have apical hair bundles that project into the otolithic membrane, a gelatinous material that is covered by millions of calcium carbonate particles (otoconia). The hair bundles are polarized but are oriented in different directions. The directional polarity of each hair cell is organized relative to a reversal region running through the center of the utricle, termed the striola (see Figure 27–7). Thus, when the head is tilted, the gravitational force on the otoconia bends each hair bundle in a particular direction. When the head is tilted in the direction of a hair cell's axis of polarity, that cell depolarizes and excites the afferent fiber. When the head is tilted in the opposite direction, the same cell hyperpolarizes and inhibits the afferent fiber. (Adapted from Iurato 1967.)

covers the entire macula (Figure 27–6). Embedded on the surface of this membrane are fine, dense particles of calcium carbonate called *otoconia* (Greek root translates to "ear dust"), which give the otolith ("ear stone") organs their name. Otoconia are typically 0.5 to 30 µm long; thousands of these particles are attached to the otolithic membranes of the utricle and saccule.

Gravity and other linear accelerations exert shear forces on the otoconial matrix and the gelatinous otolithic membrane, which can move relative to the membranous labyrinth. This results in a deflection of the hair bundles, altering activity in the vestibular nerve to signal linear acceleration owing to translational motion or gravity. The orientations of the otolith organs and the directional sensitivity of individual hair cells are such that a linear acceleration along any axis can be sensed. For example, with the head in its normal position, the macula of each utricle is raised above the naso-occipital axis by approximately 30°, similar to the horizontal semicircular canal. In normal resting head position, the utricle is deviated to bring the utricle approximately equal to an Earth horizontal plane. Any acceleration in the horizontal plane excites some hair cells in each utricle and inhibits others, according to their orientations (Figures 27–6 and 27–7).

The operation of the paired saccules resembles that of the utricles. The hair cells represent all possible

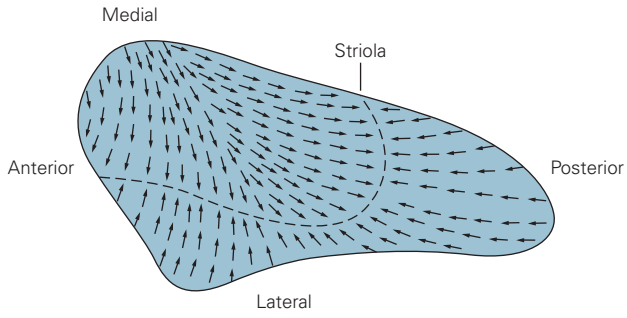

Figure 27–7 The axis of mechanical sensitivity of each hair cell in the utricle is oriented toward the striola. The striola curves across the surface of the macula containing the hair cells, resulting in a characteristic variation in the axes of mechanosensitivity (**arrows**) in the population of hair cells. Because of this arrangement, tilt in any direction depolarizes some cells and hyperpolarizes others, while having no effect on the remainder. (Adapted, with permission, from Spoendlin 1966.)

orientations within the plane of each saccular macula, but the maculae are oriented vertically in nearly parasagittal planes. The saccules are therefore especially sensitive to vertical accelerations. Certain saccular hair cells also respond to accelerations in the horizontal plane, in particular those along the anterior–posterior axis.

Central Vestibular Nuclei Integrate Vestibular, Visual, Proprioceptive, and Motor Signals

The vestibular nerve projects ipsilaterally from the vestibular ganglion mainly to four vestibular nuclei (medial, lateral, superior, and descending) in the dorsal part of the pons and medulla, in the floor of the fourth ventricle. Many vestibular nerve fibers also bifurcate, sending a direct projection to the fastigial nucleus, the nodulus and uvula, and the reticular formation (Figure 27–8A). These nuclei integrate signals from the vestibular organs with signals from the spinal cord, cerebellum, and visual system.

The vestibular nuclei project, in turn, to many central targets, including the oculomotor nuclei, reticular and spinal centers concerned with gaze and postural movement, and the thalamus (Figure 27–9). Many vestibular nuclei neurons have reciprocal connections with the cerebellum, primarily in the floculo-nodular lobe, that form important regulatory mechanisms for eye movements, head movements, and posture (Figures 27–8 and 27–9). The vestibular nuclei receive inputs from the premotor cortex, the accessory optic system (nucleus of the optic tract), the neural integrator nuclei (nucleus prepositus hypoglossi and interstitial nucleus of Cajal), and the reticular formation (Figure 27–8). Further projections from the vestibular nuclei reach the rostral and caudal lateral medulla nuclei that are involved in regulation of blood pressure, heart rate, respiration, and bone remodeling, as well as the parabrachial nucleus for homeostasis modulation. Finally, there are projections from the vestibular nuclei to the medial geniculate (auditory) nuclei, as well as the supragenual nucleus and dorsal tegmental nucleus, which contribute to spatial orientation (Figure 27–9).

The superior and medial vestibular nuclei receive fibers predominantly from the semicircular canals in the medial regions and some otolith input in the lateral regions (Figure 27–8). They send fibers predominantly to the cerebellum, reticular formation, thalamus, oculomotor centers, and spinal cord (Figure 27–9). Oculomotor center outputs include the three oculomotor nuclei (abducens, oculomotor, trochlear), as well as the neural integrators for converting head velocity into head position signals in the nucleus hypoglossi (horizontal eye movements) and interstitial nucleus of Cajal (vertical eye movements). These nuclei are described in some detail later.

Another major output pathway concerned with gaze control arises from the medial vestibular nucleus (as well as lesser projections from the descending and lateral vestibular nuclei) and projects bilaterally to the cervical spinal cord through the medial vestibulospinal tract (Figure 27–9; see Chapter 35). There are two categories of medial vestibulospinal fibers. Vestibulospinal neurons project only to the spinal cord to control neck musculature. Vestibulo-ocular neurons project to both the spinal cord and the oculomotor nuclei and are involved in coordinated eye and head movements to maintain gaze stability.

The lateral vestibular nucleus (Deiters' nucleus) receives fibers from the semicircular canals medially and the otolith organs laterally. There is a major output to all levels of the ipsilateral spinal cord through the lateral vestibulospinal tract that is concerned principally with postural reflexes through modulation of limb and axial musculature (Figure 27–9). Lateral vestibular nuclei neurons also project heavily to the reticular formation. The descending vestibular nucleus receives predominantly otolithic input, but also receives semicircular canal fibers medially, and projects to the cerebellum, reticular formation, and spinal cord (medial vestibulospinal tract). The primary neurotransmitters for excitatory vestibular nuclear projections include glutamate, whereas the inhibitory projections are either glycine or γ-aminobutyric acid (GABA). Vestibular projections to the spinal systems are discussed in more detail in Chapter 36.

The Vestibular Commissural System Communicates Bilateral Information

Many of these vestibular nuclei neurons receive convergent motion information from the opposite ear through an inhibitory commissural pathway that uses GABA as a neurotransmitter (Figure 27–8B). The commissural pathway is highly organized according to the type of receptor from which information is received. For example, cells receiving signals from the ipsilateral horizontal excitatory canal will also receive signals from the contralateral horizontal canal through an inhibitory interneuron. Due to the directional selectivity of the receptors in each ear, the contralateral horizontal canal input will always be decreased during an ipsilateral head turn, in effect "disinhibiting" the inhibitory input from the contralateral side.

The effect of the commissural system is to increase the response of the vestibular nuclei neuron and

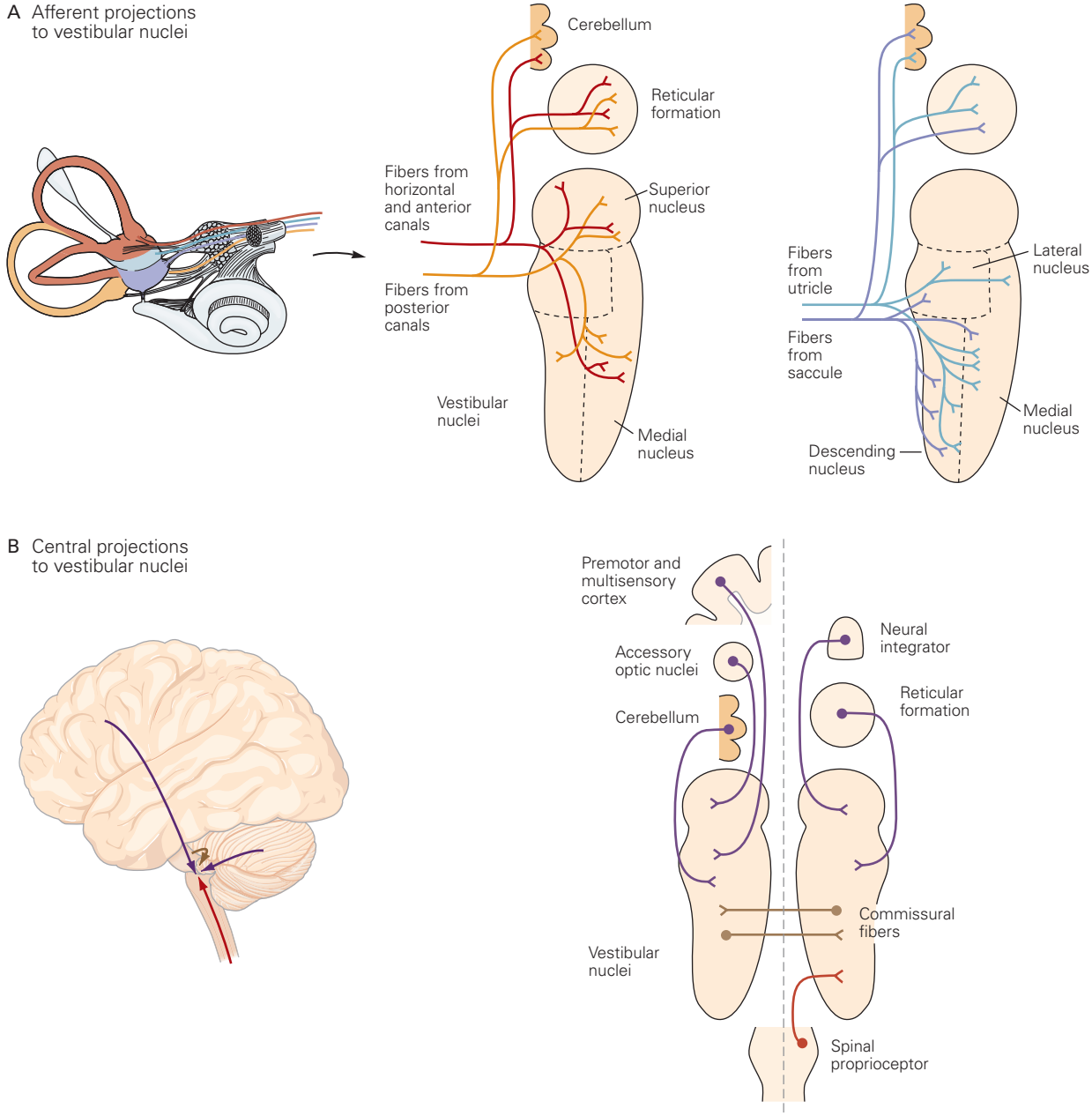

Figure 27–8 Afferent fiber and central projections to the vestibular nuclei.

A. Afferent fibers from vestibular receptors terminate in the brain stem and cerebellum. Fibers from semicircular canals project primarily to the medial portions of the superior and medial vestibular nuclei, the descending vestibular nucleus, the cerebellum (nodulus and uvula), and the reticular formation. Fibers from the otoliths primarily project to the lateral portions of all vestibular nuclei, the nodulus and uvula, and the reticular formation. (Adapted, with permission, from Gacek and Lyon 1974.)

B. Central projections to the vestibular nuclei arise from a number of cortical, brain stem, and spinal cord regions. These include the premotor and multisensory cortices, accessory optic nuclei, cerebellum, neural integrator nuclei, reticular formation, spinal cord, and commissural fibers from the contralateral vestibular nuclei.

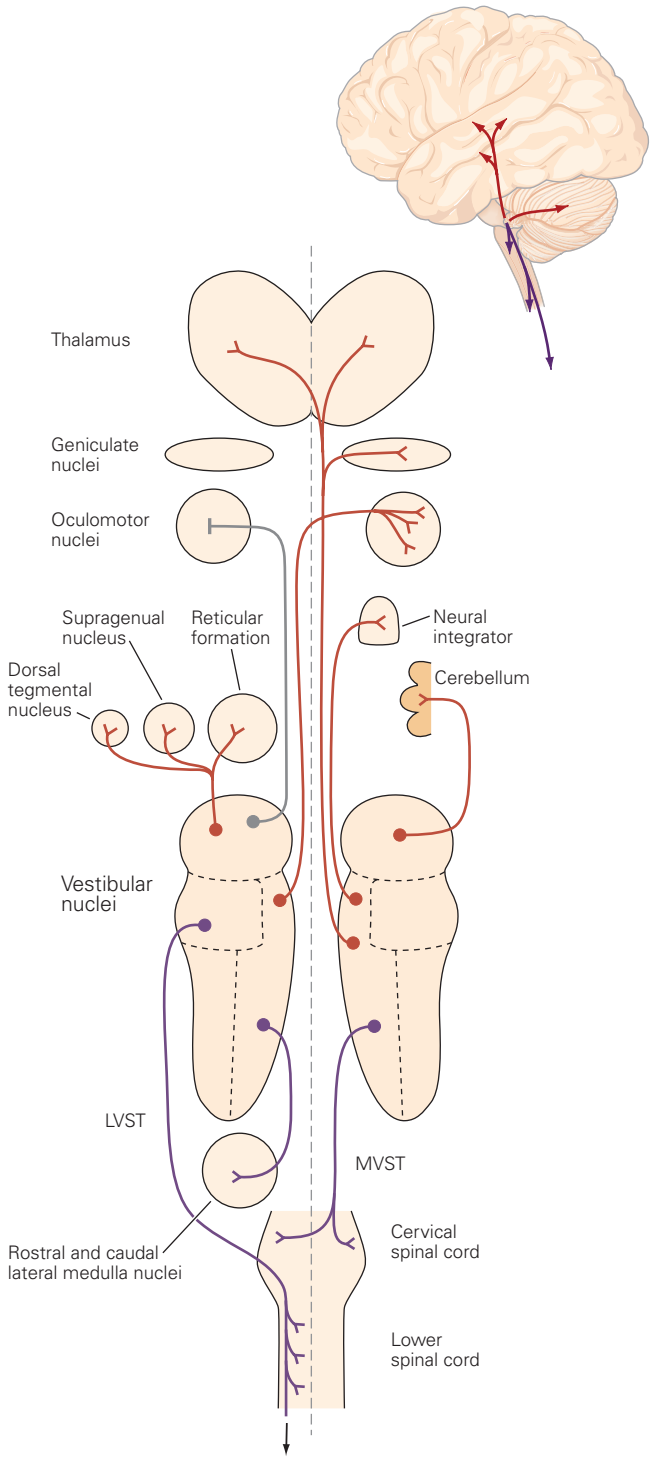

decrease noise from the incoming afferent signal, giving rise to a "push-pull" vestibular function. From an engineering point of view, the "push-pull" set point in the nuclei neurons constantly updates canal signals from the opposing ear to act as a comparator junction and can explain the relatively high spontaneous firing rate of canal afferents at nearly 100 spikes/s. For example, during a leftward head turn, left brain stem nuclei neurons receive high firing rate signals from the left horizontal canal and low firing rate signals from the right horizontal canal. The comparison of activity is interpreted as a left head turn (Figure 27–5). Similar comparisons between signals also occur for inputs from the anterior semicircular canal on one side and the posterior semicircular canal on the opposite ear side. Thus, for rotational motion in any head plane, the comparator is able to determine the direction of movement with great specificity.

Any disruption of the normal balance between left and right ear canal inputs (eg, from trauma or disease in the receptor organs or nerve) will be interpreted by the brain as a head rotation, even though the head is stationary. These effects often lead to illusions of spinning or rotating that can be quite upsetting and may produce nausea or vomiting. However, over time, the commissural fibers provide for vestibular compensation, a process by which the loss of unilateral vestibular receptor function is partially restored centrally and behavioral responses such as the vestibulo-ocular reflex mostly recover.

Combined Semicircular Canal and Otolith Signals Improve Inertial Sensing and Decrease Ambiguity of Translation Versus Tilt

In some instances, the vestibular input from a single receptor may be ambiguous. For example, Einstein (1908) showed that linear accelerations are equivalent whether they arise from translational motion or tilts of the head relative to gravity. The otolith receptors cannot

Figure 27–9 (Left) Output projections from the vestibular nuclei. The vestibular nuclei project to a number of brain regions below the cortical level. Two separate descending pathways project through the lateral and medial vestibulospinal tracts (**LVST, MVST**) to terminate in the spinal cord. The vestibular nuclei also project to the reticular formation and the lateral medullary nuclei in the brain stem. Ascending projections to the supragenual nucleus, the dorsal tegmental nucleus, the oculomotor nuclei (abducens, oculomotor, and trochlear), and the neural integrator nuclei are very prominent (**red line**, excitatory; **gray line**, inhibitory), as are projections to the cerebellum (nuclei, nodulus, and uvula). Other prominent vestibular projections terminate in the geniculate nuclei and the thalamus (ventral lateral, posterior, and intralaminar thalamic regions).

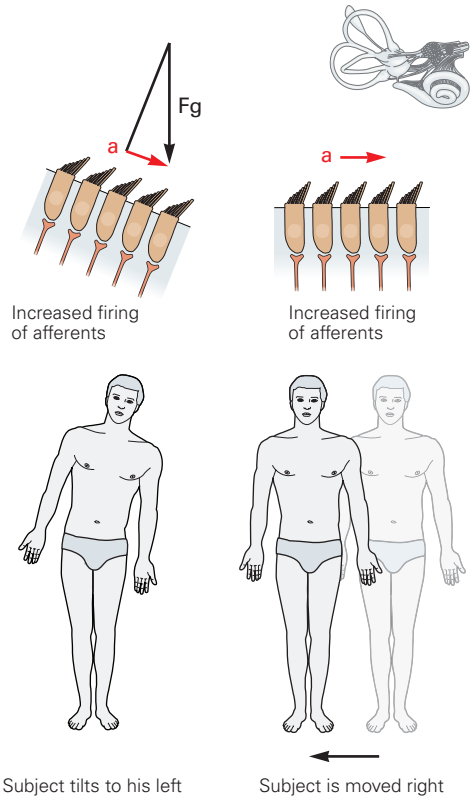

Figure 27–10 Vestibular inputs signaling body posture and motion can be ambiguous. The postural system cannot distinguish between tilt and linear acceleration of the body based on otolithic inputs alone. The same shearing force acting on vestibular hair cells can result from tilting of the head (*left*), which exposes the hair cells to a portion of the acceleration (**a**) owing to gravity (**Fg**), or from horizontal linear acceleration of the body (*right*).

discriminate between the two: So how is it that we can tell the difference between translating rightward and tilting leftward, where the linear acceleration signaled by the otolith afferents is the same (Figure 27–10)?

It is now well established that convergent vestibular nuclei and cerebellar neurons use combined signals from both the semicircular canals and the otolith receptors and some simple computations to discriminate between tilt and translation. As a result, some central vestibular and cerebellar cells encode head tilt, whereas other cells encode translational motion, which, as we will see, is extremely important for the control of head and eye movements.

Vestibular Signals Are a Critical Component of Head Movement Control

An important discovery is the differing responses in some vestibular nuclei neurons to actively versus passively generated head movements. Specifically, in contrast to vestibular afferents, some neurons in the vestibular nuclei and cerebellum well known for responding to vestibular stimuli during passive movement lose or reduce their sensitivity during self-generated movement. The preferential response to passive motion, or to the passive components of combined active and passive motion, has been interpreted as sensory prediction error signals: The brain predicts how self-generated motion activates the vestibular organs and subtracts these predictions from afferent signals. Such error signals are important for the on-line control of head movement, as well as head movement estimation.

Computationally, these properties have been interpreted quantitatively using concepts common to all sensorimotor systems; that is, active and passive motion signals are processed by internal models of the motion sensor (ie, the canals, otolith organs, and neck proprioceptors). The brain uses an internal representation of the laws of physics and sensory dynamics (which can be elegantly modeled as forward internal models of the sensors) to process vestibular signals. Without such error signals, accurate self-motion estimation would be severely compromised. These computational insights suggest that, unlike early interpretations, vestibular signals remain critically important when coupled to self-motion estimation and head movement control during actively generated head movements.

Vestibulo-Ocular Reflexes Stabilize the Eyes When the Head Moves

In order to see clearly and maintain focus on visual objects during head motion, the eyes maintain foveal fixation through a series of vestibulo-ocular reflexes (VORs). If you shake your head back and forth while reading, you can still discern words because of the VORs. If instead you move the book at a similar speed while holding your head steady, you can no longer read the words.

In the latter instance, vision provides the brain with the only corrective feedback for stabilizing of the image on the retina, and visual processing in vertebrates is much slower (around 100 ms latency) and less effective than vestibular processing (around 10 ms) for image stabilization. The vestibular apparatus signals how fast the head is rotating, and the oculomotor system uses this information to stabilize the eyes to fix visual images on the retina.

There are two components of VORs. The *rotational VOR* compensates for head rotation and receives its input predominantly from the semicircular canals. The *translational VOR* compensates for linear head movement. These two VOR responses arise from connections from vestibular nuclei neurons to the abducens, oculomotor, and trochlear nuclei (Figure 27–9).

The Rotational Vestibulo-Ocular Reflex Compensates for Head Rotation

When the semicircular canals sense head rotation in one direction, the eyes rotate in the opposite direction at equal velocity in the orbits (Figure 27–11). This compensatory eye rotation is called the vestibular slow phase, although it is not necessarily slow: The eyes may reach speeds of more than 200 degrees per second if the head's rotation is fast. During fast head movements, the VOR must act quickly to maintain stable gaze. A trisynaptic pathway, the three-neuron arc, connects each semicircular canal to the appropriate eye muscle (Figure 27–11).

The rotational VOR represents a phylogenetically old reflex. Many invertebrates and all vertebrate species, from amphibians, reptiles, fish, and birds to nonhuman primates, have the ability to reflexively rotate their eyes opposite to the direction of head rotation, thus keeping the visual world stable on the retina. Primary afferents from the horizontal semicircular canals send excitatory signals through the vestibular nuclei and the medial longitudinal fasciculus to the contralateral abducens nucleus (Figure 27–11). Abducens motor neurons send impulses via cranial nerve VI to excite the ipsilateral lateral rectus muscle. At the same time, abducens interneurons send excitatory signals to motor neurons in the contralateral oculomotor nucleus, which innervates the medial rectus muscle (see Chapter 35 for details on other projections).

The three-synapse pathway illustrated in Figure 27–11 is not sufficient to elicit appropriate compensatory eye movements. This is because the afferent signal from the semicircular canals is proportional to head velocity, while the compensatory eye movement requires eye position changes. To convert velocity to position requires temporal integration (simple calculus) that occurs through neural networks in the brain stem nuclei for most head motion speeds. However, at high rotation frequencies, the viscoelastic properties of the eyeball, eye muscles, and surrounding tissues provide an additional integration step. Thus, the rotational VOR is thought to consist of two parallel processes.

The first process consists of the direct neural pathway known as the three-neuron arc (Figure 27–11). The second neural integrator process consists of additional parallel pathways that ensure that the correct proportion of velocity and position commands are delivered to the oculomotor nuclei to move the eye appropriately (Figure 27–9 and see Chapter 35). Without this second indirect integrator pathway, the response to a head rotation would initially bring the eye to the correct position, but the eye would drift away from that position since the oculomotor neurons would lack the tonic input to compensate for the elastic restoring forces of the eyeball (Chapter 35). This is exactly what happens after lesions of brainstem and cerebellar structures that are thought to participate in this neural integration (eg, the prepositus hypoglossi and the interstitial nucleus of Cajal; Figure 27–9). It is generally thought that the integrator pathway is shared by all conjugate eye movement systems (saccades, smooth pursuit, and the VOR), although the direct pathway is at least partly segregated for different types of eye movements (ie, VOR, smooth pursuit, saccades).

With continued head rotation, the eyes eventually reach the limit of their orbital range and stop moving. To prevent this, a rapid saccade-like movement called a quick phase displaces the eyes to a new point of fixation in the direction of head rotation.

If rotation is prolonged, the eyes execute alternating slow and quick phases called *nystagmus* (Figure 27–12). Although the slow phase is the primary response of the rotational VOR, the direction of nystagmus is defined in clinical practice by the direction of its quick phase. Since prolonged rightward rotation excites the right horizontal canal and inhibits the left horizontal canal, leftward slow phases and a *right-beating nystagmus* result.

If the angular velocity of the head remains constant, the inertia of the endolymph is eventually overcome, as in the earlier coffee cup example. The cupula relaxes and vestibular nerve discharge returns to its baseline rate. As a consequence, slow-phase velocity decays and the nystagmus stops, although the head is still rotating.

In fact, the nystagmus lasts longer than would be expected based on cupular deflection. By a process called *velocity storage*, a brain stem network provides a velocity signal to the oculomotor system, although the vestibular nerve no longer signals head movement. Eventually, however, the nystagmus does decay and the sense of motion vanishes in darkness. Further, the same rotation in the presence of a visual surround activates the optokinetic reflex (Chapter 35) and elicits a steady-state nystagmus pattern that is sustained indefinitely. The interactions between canal and optokinetic

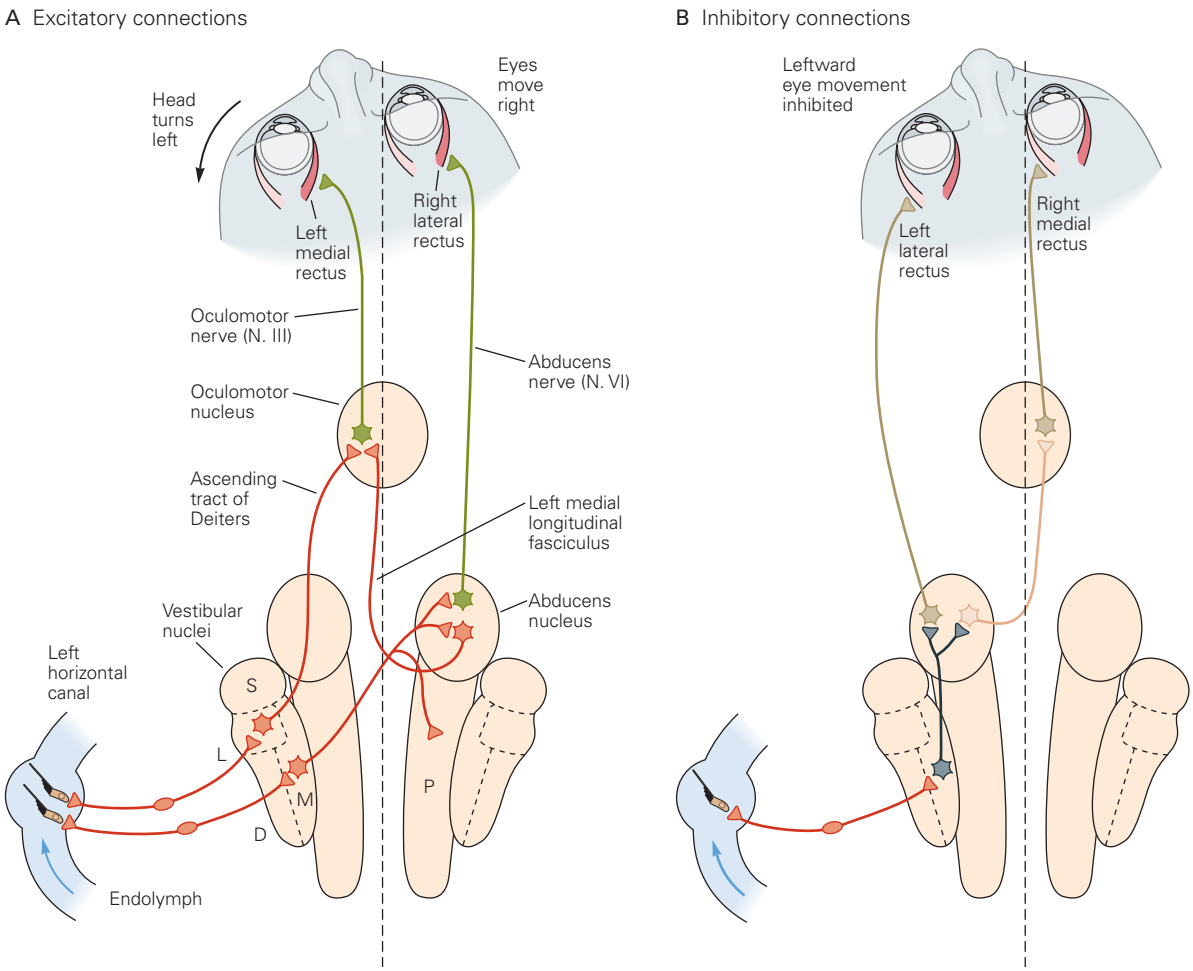

Figure 27–11 The horizontal vestibulo-ocular reflex. Similar pathways connect the anterior and posterior canals to the vertical recti and oblique muscles.

A. Leftward head rotation excites hair cells in the left horizontal canal, thus exciting neurons that evoke rightward eye movement. The vestibular nuclei include two populations of first-order neurons. One lies in the medial vestibular nucleus (**M**); its axons cross the midline and excite neurons in the right abducens nucleus and nucleus prepositus hypoglossi (**P**). The other population is in the lateral vestibular nucleus (**L**); its axons ascend ipsilaterally in the tract of Deiters and excite neurons in the left oculomotor nucleus, which project in the oculomotor nerve to the left medial rectus muscle.

The right abducens nucleus has two populations of neurons. A set of motor neurons projects in the abducens nerve and excites the right lateral rectus muscle. The axons of a set of interneurons cross the midline and ascend in the left medial longitudinal fasciculus to the oculomotor nucleus, where they excite the neurons that project to the left medial rectus muscle. These connections facilitate the rightward horizontal eye movement that compensates for leftward head movement. Other nuclei shown are the superior (**S**) and descending (**D**) vestibular nuclei.

B. During counterclockwise head movement, leftward eye movement is inhibited by sensory fibers from the left horizontal canal. These afferent fibers excite neurons in the medial vestibular nucleus that inhibit motor neurons and interneurons in the left abducens nucleus. This action reduces the excitation of the motor neurons for the left lateral and right medial rectus muscles. The same head movement results in a decreased signal in the right horizontal canal (not shown), which has similar connections. The weakened signal results in decreased inhibition of the right lateral and left medial rectus muscles and decreased excitation of the left lateral and right medial rectus muscles. (Adapted from Sugiuchi et al. 2005.)

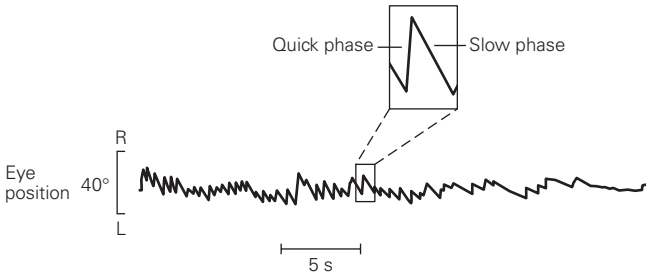

Figure 27–12 Vestibular nystagmus. The trace shows the eye position of a subject in a chair rotated counterclockwise at a constant rate in the dark. At the beginning of the trace, the eye moves slowly at the same speed as the chair (slow phase) and occasionally makes rapid resetting movements (quick phase). The speed of the slow phase gradually decreases until the eye no longer moves regularly. (Reproduced, with permission, from Leigh and Zee 2015.)

signals during rotation occurs through the velocity storage network.

If head rotation stops abruptly, the endolymph continues to be displaced in the same direction that the head had formerly rotated. With rightward rotation, this inhibits the right horizontal canal and excites the left horizontal canal, resulting in a sensation of leftward rotation and a corresponding left-beating nystagmus. However, this occurs only in darkness. In the light, optokinetic reflexes suppress postrotatory nystagmus since there is no visual motion stimulus.

The Translational Vestibulo-Ocular Reflex Compensates for Linear Motion and Head Tilts

When the head rotates, all images move with the same velocity on the retina. When the head moves sideways, however, the image of a close object moves more rapidly across the retina than does the image of a distant object. This can be understood easily by considering what happens when a person looks out the side window of a moving car. Objects near the side of the road move out of view almost with the speed of the car, whereas distant objects disappear more slowly. To compensate for linear head movement, the vestibular system must take into account the distance to the object being viewed—the more distant the object, the smaller the needed eye movement. During linear movements that do not involve head rotation, an appropriate translational VOR is elicited, driven by input from the otolith organs. Neurons in the vestibular nuclei, including some different from those providing the main drive to the rotational VOR, carry this signal to the extraocular motor neuron pools.

Side-to-side head movements result in a horizontal eye movement in a direction opposite to the head movement. Vertical displacements of the body, such as during walking or running, elicit oppositely directed vertical eye movements to stabilize gaze. However, in contrast to the rotational VOR where a head rotation is compensated by an equal but opposite eye rotation, horizontal displacement must be compensated by an eye rotation that depends on the viewed object distance, a nontrivial computation. For example, during a lateral head displacement, nearby objects move on the retina more rapidly than distant ones. So, in order to stabilize a nearby object on the retina, the eyes need to rotate by a larger amount than is needed for a distant object. Thus, the horizontal compensatory eye movements that are elicited during lateral motion scale with target distance; the closer the target, the larger is the compensatory eye movement. Similarly, as in the rotational VOR, compensatory responses to translation occur at relatively short latency (10–12 ms).

Fore-aft translations produce converging and diverging eye movements that bring the eyes together or move them apart. The amount of convergence or divergence is also dependent upon visual target distance, such that close visual objects produce large eye movements and distant visual objects produce little eye movements. Further, the amount of relative left and right eye movement is dependent upon visual object eccentricity relative to straight ahead. Unlike the rotational VOR that is a full-field image stabilization reflex, the goal of the translational VOR is to selectively stabilize visual objects on the fovea. In general, the two eyes move disjunctively, consisting of either a pure vergence movement or a combination of vergence and conjugate eye movements. In practice, although the direction of the evoked eye movement is typically consistent with geometrical predictions, the primate/human translational VOR typically undercompensates for near-target viewing, with gains of only about 0.5.

The translational VOR differs from the rotational VOR in the ability to generate compensatory eye movements during translation that optimize visual acuity on the central retina. These abilities appear to be specific to frontal-eyed animals, such as primates. Many lateral-eyed species, like the rabbit, do not generate eye movements that compensate for the visual consequences of translation during self-motion.

Because gravity exerts a constant linear acceleration force on the head, the otolith organs also sense the orientation of the head relative to gravity. When the head tilts away from the vertical in the roll plane—around the axis running from the occiput to the nose—the eyes rotate in the opposite direction to reduce the

tilt of the retinal image. This ocular counter-rolling reflex—the ability to use a gravity-sensing mechanism to maintain gaze relative to the horizon—is of paramount importance for lateral-eyed, afoveate species that typically lack a well-developed saccadic system. But such functional utility for these tilt responses has lost its advantage in the primate oculomotor system, where static ocular counter-rolling and counter-pitching in humans have a gain of less than 0.1.

Vestibulo-Ocular Reflexes Are Supplemented by Optokinetic Responses

The VORs compensate for head movement imperfectly. They are best at sensing the onset or abrupt change of motion; they compensate poorly for sustained motion at constant speed during translation or constant angular velocity during rotation. In addition, they are insensitive to very slow rotations or low-amplitude linear accelerations.

Thus, vestibular responses during prolonged motion in the light are supplemented by visual stabilization reflexes that maintain nystagmus when vestibular input ceases: optokinetic nystagmus, a full-field stabilization system, and ocular following, a foveal stabilization system. Although the two classes of reflexes are distinct, their pathways overlap.

The Cerebellum Adjusts the Vestibulo-Ocular Reflex

As we have seen, the VOR keeps the gaze constant when the head moves. There are times, however, when the reflex is inappropriate. For example, when you turn your head while walking, you want your gaze to follow. The rotational VOR, however, would prevent your eyes from turning with your head. To prevent this sort of biologically inappropriate response, the VOR is under the control of the cerebellum and cortex, which suppress the reflex during volitional head movements.

In addition, the VOR must be continuously calibrated to maintain its accuracy in the face of changes within the motor system (fatigue, injury to vestibular organs or pathways, eye-muscle weakness, or aging) and differing visual requirements (wearing corrective lenses). Indeed, the VOR is a highly modifiable reflex. The brain continuously monitors its performance by evaluating the clarity of vision during head movements. When head turns are consistently associated with image motion across the retina, the VOR undergoes gain changes in the direction appropriate to improve the compensatory ability of the reflex. For example, when viewing the world through spectacles that magnify or miniaturize the visual scene, the rotational VOR gain (in darkness) increases or decreases accordingly. The reflex behavior can adapt over several minutes, hours, and days. This is accomplished by sensory feedback that modifies the motor output. If the reflex is not working properly, the image moves across the retina. The motor command to the eye muscles must be adjusted until the gaze is again stable, rotational retinal image motion is zero, and there is no error.

Anyone who wears eyeglasses depends on this plasticity of the VOR. Because lenses for nearsightedness shrink the visual image, a smaller eye rotation is needed to compensate for a given head rotation, and the gain of the VOR must be reduced. Conversely, glasses for farsightedness magnify the image, so the VOR gain must increase during their use. More complicated is the instance of bifocal or progressive spectacles, in which the reflex must use different gains for the different magnifications. In the laboratory, the reflex can be conditioned by altering the visual consequences of head motion. For example, if a subject is rotated for a period of time while wearing magnifying glasses, the reflex gain gradually increases (Figure 27–13A).

This process requires changes in synaptic transmission in both the cerebellum and the brain stem. If the flocculus and paraflocculus of the cerebellum are lesioned, the gain of the VOR can no longer be modulated. Mossy fibers carry vestibular, visual, and motor signals from the pontine and vestibular nuclei to the cerebellar cortex; the granule cells, with their parallel fiber axons, relay these signals to the Purkinje cells (Figure 27–13B). The synaptic efficacy of parallel fiber input to a Purkinje cell could be modified by the concurrent action of climbing fiber input. Indeed, the climbing fiber input to the cerebellum carries a retinal error signal, thought to serve as a "teaching" signal enabling the cerebellum to correct the error in the VOR. This adaptation requires long-term plasticity of multiple mechanisms through multiple sites (Chapter 37).

In addition to the Purkinje cell, plasticity is also found in the vestibular nuclei, in a particular class of neurons known as flocculus target neurons, which receive GABAergic inhibitory input from Purkinje cells in the flocculus as well as direct inputs from vestibular sensory fibers. During adaptation of the VOR, these neurons change their sensitivity to the vestibular inputs in the appropriate way, and after adaptation, they can maintain those changes without further input from the cerebellum. The importance of the cerebellum in calibrating eye movements is also evident in patients with cerebellar disease, who are often characterized by a VOR response of abnormal amplitude or direction.

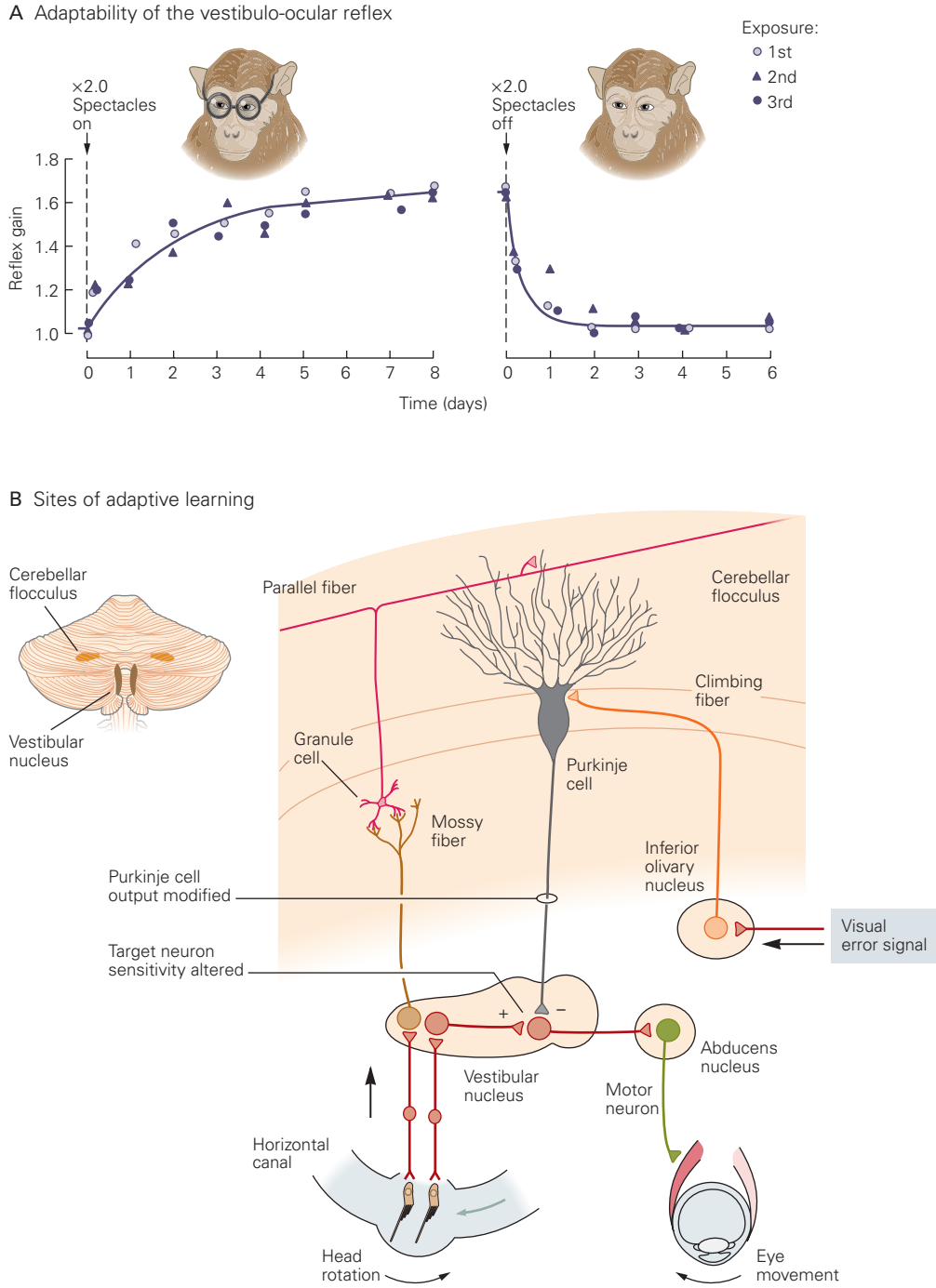

Figure 27–13 The vestibulo-ocular reflex is adaptable.

A. For several days, the monkey continuously wears magnifying spectacles that double the speed of the retinal-image motion evoked by head movement. Each day, the gain of the vestibulo-ocular reflex—the amount the eyes move for a given head movement—is tested in the dark so that the monkey cannot use retinal motion as a clue to modify the reflex. Over a period of 4 days, the gain increases gradually (*left*). It quickly returns to normal when the spectacles are removed (*right*). (Adapted, with permission, from Miles and Eighmy 1980.)

B. Adaptation of the vestibulo-ocular reflex occurs in cerebellar and brain stem circuits. A visual error signal, triggered by motion of the retinal image during head movement, reaches the inferior olivary nucleus. The climbing fiber transmits this error signal to the Purkinje cell, affecting the parallel fiber–Purkinje cell synapse. The Purkinje cell transmits changed information to the floccular target cell in the vestibular nucleus, changing its sensitivity to the vestibular input. After the reflex has been adapted, the Purkinje cell input is no longer necessary.

The Thalamus and Cortex Use Vestibular Signals for Spatial Memory and Cognitive and Perceptual Functions

For decades, vestibular function has been studied primarily in relation to reflexes, both vestibulo-ocular and vestibulospinal. Yet, in the past decade, it has become increasingly clear that the function of the vestibular system is as important for cognitive processes as for reflexes. The difficulty in understanding the vestibular system's role in spatial cognition stems from the fact that these functions are inherently multisensory, arising through convergence of vestibular, visual, somatosensory, and motor cues, following principles that remain poorly understood. Some of these perceptual functions of the vestibular system include tilt perception, visual-vertical perception, and visuospatial constancy.

Tilt perception. Vestibular information is critical for spatial orientation—the perception of how our head and body are positioned relative to the outside world. Nearly all species orient themselves using gravity, which provides a global, external reference. Thus, spatial awareness is governed by our orientation relative to gravity, collectively typically referred to as tilt.

Visual-vertical perception. We commonly experience the visual scene as perceptually oriented relative to earth-vertical orientation, regardless of our spatial orientation in the world. This ability has been studied psychophysically in humans and monkeys using tasks in which a subject is turned ear-down in the dark and asked to orient a dimly lit bar vertically in space (to align it with gravity). The results suggest that the neural representation of the visual scene is modified by static vestibular and proprioceptive signals that indicate the orientation of the head and body.

Visuospatial constancy. Vestibular signals are also important for the perception of a stable visual world despite constantly changing retinal images caused by movement of the eyes, head, and body. The projection of the scene onto the retina continuously changes because of these movements. Despite the changing retinal image, the percept of the scene as a whole remains stable; this stability is critical not only for vison but also for sensorimotor transformations (eg, to update the motor goal of an eye or arm movement).

Vestibular Information Is Present in the Thalamus

Vestibular projections to the thalamus are complicated and overall less clear, partly because of the strong multisensory nature of the responses in these cells and the difficulty in comparing thalamic regions and nomenclature across studies and species. Some neurons in all vestibular nuclei and likely the fastigial cerebellar nuclei project bilaterally to the thalamus, but most fibers terminate in the contralateral thalamic nuclei (Figure 27–9).

Several major thalamic regions receive vestibular projections, including the ventral posterolateral and ventral lateral thalamic nuclei and, to a lesser extent, the ventral posteroinferior nuclei, the posterior group, and the anterior pulvinar. These nuclei are traditionally thought to also receive somatosensory input and project to the primary and secondary somatosensory cortices, as well as the posterior parietal cortex (areas 5 and 7) and the insula of the temporal cortex.

Vestibular Information Is Widespread in the Cortex

A number of cortical areas receiving short-latency vestibular signals either alone or more commonly in concert with proprioceptive, tactile, oculomotor, visual, and auditory signals have been identified (Figure 27–14). Although vestibular signals are widely distributed to a number of cortical regions, all such regions are multimodal and none seems to represent a purely vestibular cortex, similar to other modalities such as vision, proprioception, and audition.

Vestibular modulation has been established in the lateral sulcus (parietoinsular vestibular cortex), somatosensory cortex (areas 3a and 2v), oculomotor cortex (frontal and supplementary eye fields), extrastriate visual motion cortex (dorsal medial superior temporal area), and parietal cortex (ventral intraparietal area and area 7a). In the primary somatosensory cortex, area 2v lies at the base of the intraparietal sulcus just posterior to the areas of the postcentral gyrus representing the hand and mouth. Electrical stimulation of area 2v in humans produces sensations of whole-body motion. Area 3a lies at the base of the central sulcus, adjacent to the motor cortex. Many cells in the parietoinsular vestibular cortex are multisensory, responding to body motion, somatosensory, proprioceptive, and visual motion stimuli. Patients with lesions in this region report episodes of vertigo, unsteadiness, and a loss of perception for visual vertical. Neurons in the medial intraparietal and medial superior temporal areas respond to both visual (optic flow) and vestibular signals. These cells utilize multisensory cue integration (Bayesian) frameworks to assist in the cognitive perception of motion through space.

Imaging studies reveal an even larger portion of cerebral cortex involved in processing vestibular information, including the temporoparietal cortex and the insula, the superior parietal lobe, the

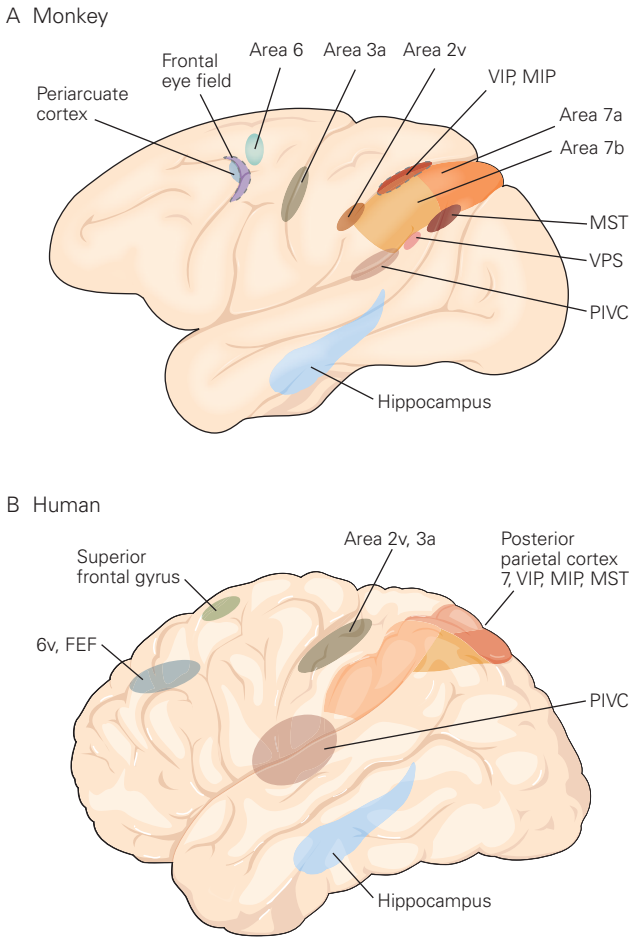

Figure 27–14 The vestibular cortex.

A. This lateral view of a monkey's brain shows the areas of cerebral cortex in which vestibular responses have been recorded. Areas in monkey cortex include periarcuate cortex, area 6, frontal eye fields, areas 3a and 2v, ventral intraparietal area (**VIP**), medial intraparietal area (**MIP**), area 7, visual posterior sylvian area (**VPS**), medial superior temporal area (**MST**), parieto-insular vestibular cortex (**PIVC**), and the hippocampal formation.

B. In the human cortex, areas recording vestibular activity include 6v, frontal eye fields (**FEF**), superior frontal gyrus, 2v, 3a, posterior parietal cortex, PIVC, and the hippocampal formation.

pre- and postcentral gyri, anterior cingulate and posterior middle temporal gyri, premotor and frontal cortices, inferior parietal lobule, putamen, and hippocampal regions. Using electrical stimulation of the vestibular nerve in patients activates the prefrontal lobe and anterior portion of the supplementary motor area at relatively short latencies. However, imaging and, to a lesser extent, single-cell recording studies may overstate the range of vestibular representations. In particular, vestibular stimuli often co-activate the somatosensory and proprioceptive systems, as well as evoke postural and oculomotor responses, which might in turn result in increased cortical activations.

Vestibular Signals Are Essential for Spatial Orientation and Spatial Navigation

Our ability to move about depends on a stable directional orientation. Certain cells in the thalamus, hippocampal region, entorhinal cortex, and subiculum are involved in navigation tasks. Damage to these areas impairs a variety of spatial and directional abilities. At least six cell types contributing to spatial orientation have been identified, including place cells, grid cells, head direction cells, border cells, speed cells, and conjunctive cells. In the hippocampus, place cells discharge relative to the animal's location in the environment (Chapter 54). Head direction cells in the dorsal thalamus, parahippocampal regions, and several regions of the cortex indicate the animal's heading direction like a compass. Grid cells in the entorhinal cortex respond to multiple spatial locations in a unique triangular grid pattern. Border cells in the entorhinal cortex signal environmental boundaries, speed cells discharge in proportion to the animal's running speed, and conjunctive cells exhibit a combination of several of these properties.

These regions are intimately connected and appear to work together in a "navigation network" to provide for spatial orientation, spatial memory, and our ability to move through our surroundings. Think of walking through your house, driving to the store, or knowing which direction to go in a new city. Lesions of central vestibular networks disrupt head direction, place, and grid responses. Patients with disease or trauma to the vestibular system, hippocampus, and anterior thalamus regions often exhibit severe deficits in their ability to orient in familiar environments or even find their way home.

All of these cells depend on a functioning vestibular system to maintain their spatial orientation properties. The pathway by which vestibular signals reach the navigation network and the computational principles determining how vestibular cues influence these spatially tuned cells is not well understood. We know that there are at least three different influences: Semicircular canal signals contribute to the estimate of head direction; gravity signals influence the three-dimensional properties of head direction cells; and translation signals influence the estimate of linear speed, which controls both grid cell properties and the magnitude and frequency of theta oscillations in the hippocampal network. What is clear is that there is no evidence

linking vestibular nuclei response properties directly to head direction or other spatially tuned cell types, and no direct projections from the vestibular nuclei to the brain areas thought to house these spatially tuned neurons have been identified. Furthermore, vestibular nuclei responses are inappropriate for driving these spatially tuned cells, as these signals need to encompass the total head movement, rather than individual components during active or passive head movement.

It has long been recognized that proprioceptive and motor efference cues should participate, together with vestibular signals, to track head direction over time. It has been proposed that internally generated information from vestibular, proprioceptive, and motor efference cues can be utilized to keep track of changes in directional heading. More recent insights have started to shed light on how each of these cues contributes to the final self-motion estimate that can be precisely predicted and quantitatively estimated based on a Bayesian framework. Although as yet difficult to define, quantitative internal models govern the relationship of vestibular and other multisensory self-motion cues for computing the spatial properties of navigation circuit cells.

Clinical Syndromes Elucidate Normal Vestibular Function

As we have seen, rotation excites hair cells in the semicircular canal whose hair bundles are oriented in the direction of motion and inhibits those in the canals oriented away from the motion direction. This imbalance in vestibular signals is responsible for the compensatory eye movements and the sensation of rotation that accompanies head movement. It can also originate from disease of one labyrinth or vestibular nerve, which results in a pattern of afferent vestibular signaling analogous to that stemming from rotation away from the side of the lesion, that is, more discharge from the intact side. There is accordingly a strong feeling of spinning, called vertigo.

Caloric Irrigation as a Vestibular Diagnostic Tool

Nystagmus can be used as a diagnostic indicator of vestibular system integrity. In patients complaining of dizziness or vertigo, the function of the vestibular labyrinth is typically assessed by a caloric test (Figure 27–15). Either warm (44°C) or cold (30°C) water is introduced into the external auditory canal. In normal persons, warm water induces nystagmus that beats toward the ear into which the water has been introduced, whereas cold water induces nystagmus that beats away from the ear into which the water has been introduced. This relationship is encapsulated in the mnemonic COWS: **C**old water produces nystagmus beating to the **O**pposite side; **W**arm water produces nystagmus beating to the **S**ame side. In normal persons, the two ears give equal responses. If there is a unilateral lesion in the vestibular pathway, however, nystagmus will be induced and directed toward the side opposite the lesion.

The vertigo and nystagmus resulting from an acute vestibular lesion typically subside over several days, even if peripheral function does not recover. This is because central compensatory mechanisms restore the balance in vestibular signals in the brain stem, even when peripheral input is permanently lost or unbalanced.

The loss of input from one labyrinth also means that all vestibular reflexes must be driven by a single labyrinth. For the VOR, this condition is quite effective at low speeds because the intact labyrinth can be both excited and inhibited. However, during rapid, high-frequency rotations, inhibition is not sufficient, such that the gain of the reflex is reduced when the head rotates toward the lesioned side. This is the basis of an important clinical test of canal function, the head-impulse test. In this test, the head is moved rapidly one time along the axis of rotation of a single canal. If there is a significant decrease in gain owing to canal dysfunction, the movement of the eyes will lag behind that of the head, and there will be a visible catch-up saccade.

Bilateral Vestibular Hypofunction Interferes With Normal Vision

Vestibular function is sometimes lost simultaneously on both sides, for example, from ototoxicity owing to aminoglycoside antibiotics such as gentamicin or cancer treatment medications such as cisplatin. The symptoms of bilateral vestibular hypofunction are different from those of unilateral loss. First, vertigo is absent because there is no imbalance in vestibular signals; input is reduced equally from both sides. For the same reason, there is no spontaneous nystagmus. In fact, these patients may have no symptoms when they are at rest and the head is still.

In humans, receptor and nerve fiber loss due to disease, trauma, or ototoxicity is permanent. However, in other animal classes such as amphibians, reptiles, and birds, spontaneous regeneration does occur over time. Although the differences in regeneration between animal groups is not yet understood, recent

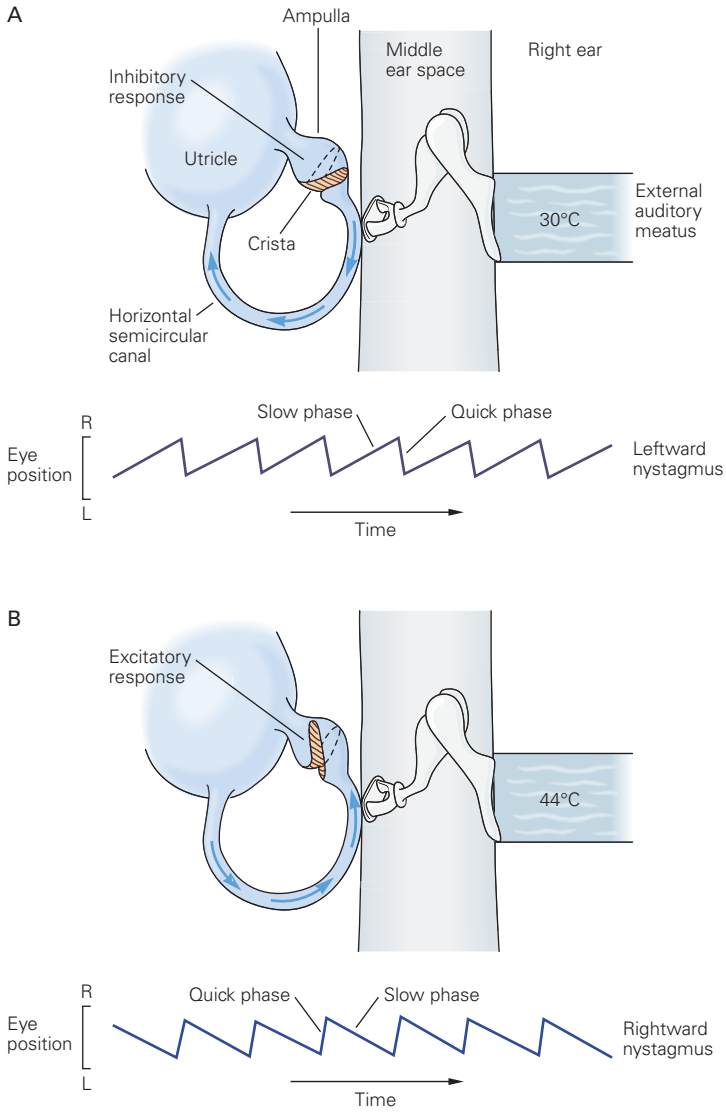

Figure 27–15 **Bithermal caloric test of the vestibulo-ocular reflex.** The vestibular caloric test remains the primary test used today in clinics around the world to determine if there is system dysfunction. The head is elevated 30° to align the horizontal semicircular canals with gravity.

A. Cold water or air introduced into the right ear causes a downward convection current in the endolymph, producing an inhibitory response in the right ear hair cells and afferent fibers. The result is a leftward (opposite side) beating nystagmus (as determined by fast phase direction).

B. Warm water or air introduced into the right ear produces an upward endolymph movement, producing an excitatory response in the hair cells and afferents. The result is a rightward (same side) beating nystagmus.

research shows promise for the future development of regenerative treatments in humans.

For the present, the loss of vestibular reflexes is devastating. A physician who lost his vestibular hair cells because of a toxic reaction to streptomycin wrote a dramatic account of this loss. Immediately after the onset of streptomycin toxicity, he could not read without steadying his head to keep it motionless. Even after partial recovery, he could not read signs or recognize friends while walking in the street; he had to stop to see clearly. Some patients may even "see" their heartbeat if the VOR fails to compensate for the miniscule head movements that accompany each arterial pulse.

Highlights

1. The vestibular system provides the brain with a rapid estimate of head movement. Vestibular signals are used for balance, visual stability, spatial orientation, movement planning, and motion perception.
2. Vestibular receptor hair cells are mechanotransducers that sense rotational and linear accelerations. Through kinematic and neural processing mechanisms, movements are transformed into acceleration, velocity, and position signals. These signals are used throughout the brain efficiently and quickly to guide behavior and cognition.

3. Receptor cells are polarized to detect the direction of motion. Three semicircular canals in each inner ear detect rotational motion and work in bilateral synergistic pairs through convergent commissural pathways in the vestibular nuclei. Two otolith organs in each ear detect linear translations and tilts relative to gravity.
4. Vestibular nuclei neurons receive converging multisensory and motor signals from visual, proprioceptive, cerebellar, and cortical sources. The multisensory integration allows for discrimination between active and passive body motion, as well as appropriate motor responses for reactive or volitional behavior.
5. Projections from the vestibular nuclei to the oculomotor system allow eye muscles to compensate for head movement through the vestibulo-ocular reflex to hold the image of the external world motionless on the retina. Cortical projections to the vestibular and oculomotor nuclei allow volitional eye movements to be separated from reflex eye movements but work through a final common pathway. Motor learning through vestibulocerebellar networks provides compensatory changes in eye movement responses to changing visual conditions through the use of spectacles, disease, or aging.
6. Projections from the vestibular nuclei to motor areas and the spinal cord facilitate postural stability. Gaze stability coordinates eye and neck movements through the medial vestibulospinal pathway. Postural control is exerted through the lateral vestibulospinal pathway.
7. Projections from the vestibular nuclei to the rostral and caudal medulla nuclei are involved in regulation of blood pressure, heart rate, respiration, bone remodeling, and homeostasis.
8. Projections from the vestibular nuclei to thalamus and cortex ensure spatial orientation and influence spatial perception more generally.
9. Vestibular signals processed in the hippocampal regions are crucial for spatial location and navigation functions.
10. Vestibular signals are combined with visual signals in several cortical regions through Bayesian cue integration to provide motion perception.
11. Disease or trauma to the vestibular system can produce nausea, vertigo, dizziness, balance disorders, visual instability, and spatial confusion.
12. We are only beginning to appreciate the role of the vestibular system in cognition. However, it is clear that vestibular signals contribute to our perception of self, conception of body presence, and memory.
13. New approaches in computation and theory promise to provide the lapidary keys needed to unlock our understanding of how vestibular signals contribute to the essence of brain function.

J. David Dickman
Dora Angelaki

Selected Reading

Baloh RW, Honrubia V. 1990. *Clinical Neurology of the Vestibular System*, 2nd ed. Philadelphia: FA Davis.

Beitz AJ, Anderson JH. 2000. *Neurochemistry of the Vestibular System*. Boca Raton, FL: CRC Press.

Goldberg JM, Wilson VJ, Cullen KE, et al. 2012. *The Vestibular System: A Sixth Sense*. New York: Oxford Univ. Press.

Leigh RJ, Zee DS. 2015. *The Neurology of Eye Movements*, 5th ed. New York: Oxford Univ. Press.

References

Angelaki DE, Cullen KE. 2008. Vestibular system: the many facets of a multimodal sense. Ann Rev Neurosci 31:125–150.

Angelaki DE, Shaikh AG, Green AM, Dickman JD. 2004. Neurons compute internal models of the physical laws of motion. Nature 430:560–564.

Brandt T, Dieterich M. 1999. The vestibular cortex. Its locations, functions, and disorders. Ann N Y Acad Sci 871:293–312.

Clark BJ, Taube JS. 2012. Vestibular and attractor network basis of the head direction cell signal in subcortical circuits. Front Neural Circuits 6:1–12.

Crèmer PD, Halmagyi GM, Aw ST, et al. 1998. Semicircular canal plane head impulses detect absent function of individual semicircular canals. Brain 121:699–716.

Cullen KE, Roy JE. 2004. Signal processing in the vestibular system during active versus passive head movements. J Neurophys 91:1919–1933.

Curthoys IS, Halmagyi GM. 1992. Behavioral and neural correlates of vestibular compensation. Behav Clin Neurol 1:345–372.

Dickman JD, Angelaki DE. 2002. Vestibular convergence patterns in vestibular nuclei neurons of alert primates. J Neurophys 88:3518–3533.

Dieterich M, Brandt T. 1995. Vestibulo-ocular reflex. Curr Opin Neurol 8:83–88.

Distler C, Mustari MJ, Hoffmann KP. 2002. Cortical projections to the nucleus of the optic tract and dorsal terminal nucleus and to the dorsolateral pontine nucleus in

macaques: a dual retrograde tracing study. J Comp Neurol 444:144–158.
Einstein A. 1908. Über das Relativitätsprinzip und die aus demselben gezogenen Folgerungen. Jahrbuch Radioaktiv Electronik 4:411–462.
Fernandez C, Goldberg JM. 1971. Physiology of peripheral neurons innervating semicircular canals of the squirrel monkey. II. Response to sinusoidal stimulation and dynamics of peripheral vestibular system. J Neurophysiol 34:661–675.
Fernandez C, Goldberg JM. 1976a. Physiology of peripheral neurons innervating otolith organs of the squirrel monkey. I. Response to static tilts and to long-duration centrifugal force. J Neurophysiol 39:970–984.
Fernandez C, Goldberg JM. 1976b. Physiology of peripheral neurons innervating otolith organs of the squirrel monkey. II. Directional selectivity and force-response relations. J Neurophysiol 39:985–995.
Flock Å. 1965. Transducing mechanisms in the lateral line canal organ receptors. Cold Spring Harbor Symp Quant Biol 30:133–145.
Fukushima K. 1997. Corticovestibular interactions: anatomy, electrophysiology, and functional considerations. Exp Brain Res 117:1–16.
Gacek RR, Lyon M. 1974. The localization of vestibular efferent neurons in the kitten with horseradish peroxidase. Acta Otolaryngol (Stockh) 77:92–101.
Goldberg JM, Fernández C. 1971. Physiology of peripheral neurons innervating semicircular canals of the squirrel monkey. I. Resting discharge and response to constant angular accelerations. J Neurophysiol 34:635–660.
Goldberg ME, Colby CL. 1992. Oculomotor control and spatial processing. Curr Opin Neurobiol 2:198–202.
Grüsser OJ, Pause M, Schreiter U. 1990. Localization and responses of neurons in the parieto-insular vestibular cortex of awake monkeys (*Macaca fascicularis*). J Physiol (Lond) 430:537–557.
Gu Y, Watkins PV, Angelaki DE, DeAngelis GC. 2006. Visual and nonvisual contributions to three-dimensional heading selectivity in the medial superior temporal area. J Neurosci 26:73–85.
Hillman DE, McLaren JW. 1979. Displacement configuration of semicircular canal cupulae. Neuroscience 4:1989–2000.
Hudspeth AJ, Corey DP. 1977. Sensitivity, polarity, and conductance change in the response of vertebrate hair cells to controlled mechanical stimuli. Proc Nat Acad Sci 74:2407–2411.
Iurato S. 1967. *Submicroscopic Structure of the Inner Ear.* Oxford: Pergamon Press.
Laurens J, Kim H, Dickman JD, Angelaki DE. 2016. Gravity orientation tuning in macaque anterior thalamus. Nat Neurosci 19:1566–1568.
Miles FA, Eighmy BB. 1980. Long-term adaptive changes in primate vestibuloocular reflex. I. Behavioral observations. J Neurophysiol 43:1406–1425.
Moser EI, Moser MB. 2008. A metric for space. Hippocampus 18:1142–1156.
Mustari MJ, Fuchs AF. 1990. Discharge patterns of neurons in the pretectal nucleus of the optic tract (NOT) in the behaving primate. J Neurophysiol 64:77–90.
Newlands SD, Vrabec JT, Purcell IM, Stewart CM, Zimmerman BE, Perachio AA. 2003. Central projections of the saccular and utricular nerves in macaques. J Comp Neurol 466:31–47.
O'Keefe J. 1976. Place units in the hippocampus of the freely moving rat. Exp Neurol 51:78–109.
Raymond JL, Lisberger SG. 1998. Neural learning rules for the vestibulo-ocular reflex. J Neurosci 18:9112–9129.
Spoendlin H. 1966. Ultrastructure of the vestibular sense organ. In: RJ Wolfson (ed). *The Vestibular System and Its Diseases,* pp. 39–68. Philadelphia: Univ. of Pennsylvania Press.
Sugiuchi Y, Izawa Y, Ebata S, Shinoda Y. 2005. Vestibular cortical areas in the periarcuate cortex: its afferent and efferent projections. Ann N Y Acad Sci 1039:111–123.
Taube JS. 1995. Head direction cells recorded in the anterior thalamic nuclei of freely moving rats. J Neurosci 15:70–86.
Waespe W, Henn V. 1977. Neuronal activity in the vestibular nuclei of the alert monkey during vestibular and optokinetic stimulation. Exp Brain Res 27:523–538.
Watanuki K, Schuknecht HF. 1976. A morphological study of human vestibular sensory epithelia. Arch Otolaryngol Head Neck Surg 102:583–588.

28

Auditory Processing by the Central Nervous System

Hearing is crucial for localizing and identifying sound; for humans, it is particularly important because of its role in the understanding and production of speech. The auditory system has several noteworthy features. Its subcortical pathway is longer than that of other sensory systems. Unlike the visual system, sounds can enter the auditory system from all directions, day and night, when we are asleep as well as when we are awake. The auditory system processes not only sounds emanating from outside the body (environmental sounds, sounds generated by others) but also self-generated sounds (vocalizations and chewing sounds). The location of sound stimuli in space is not conveyed by the spatial arrangement of

sensory afferent neurons but is instead computed by the auditory system from representations of the physical cues.

Sounds Convey Multiple Types of Information to Hearing Animals

Hearing helps to alert animals to the presence of unseen dangers or opportunities and, in many species, also serves as a means for communication. Information about where sounds arise and what they mean must be extracted from the representations of the physical characteristics of sound at each of the ears. To understand how animals process sound, it is useful first to consider which cues are available.

Most vertebrates take advantage of having two ears for localizing sounds in the horizontal plane. Sound sources at different positions in that plane affect the two ears differentially: Sound arrives earlier and is more intense at the ear nearer the source (Figure 28–1A). Interaural time and intensity differences carry information about where sounds arise.

The size of the head determines how interaural time delays are related to the location of sound sources; the neuronal circuitry determines the precision with which time delays are resolved. Because air pressure waves travel at roughly 340 m/s in air, the maximal interaural delay in humans is approximately 600 μs; in small birds, the greatest delay is only 35 μs. Humans can resolve the location of a sound source directly ahead to within approximately 1 degree, corresponding to an interaural time difference of 10 μs. Interaural time differences are particularly well conveyed by neurons that encode relatively low frequencies. These neurons can fire at the same position in every cycle of the sound and in this way encode the interaural time difference as an interaural phase difference. Sounds of high frequencies produce *sound shadows* or intensity differences between the two ears. For many mammals with small heads, high-frequency sounds provide the primary cue for localizing sound in the horizontal plane.

Mammals can localize sounds in the vertical plane and with a single ear using spectral filtering. High-frequency sounds, with wavelengths that are close to or smaller than the dimensions of the head, shoulders, and external ears, interact with those parts of the body to produce constructive and destructive interference, introducing broad spectral peaks and deep, narrow spectral notches whose frequency changes with the location of the sound (Figure 28–1B). High-frequency sounds from different origins are filtered differently because in mammals the shape of the external ear differs back-to-front as well as top-to-bottom. Animals learn to use these spectral cues to locate sound sources. If the shape of the ear is experimentally altered, even adult humans can learn to make use of a new pattern of spectral cues. If animals lose hearing in one ear, they lose interaural timing and intensity cues and must depend completely on spectral cues for localizing sounds.

How do we make sense of the complex and changing sounds that we hear? Most natural sounds contain energy over a wide range of frequencies and change rapidly with time. The information used to recognize sounds varies among animal species, and depends on listening conditions and experience. Human speech, for example, can be understood in the midst of noise, over electronic devices that distort sounds, and even through cochlear implants. One reason for its robustness is that speech contains redundant cues: The vocal apparatus produces sounds in which multiple parameters covary. At the same time, this makes the task of understanding how animals recognize patterns a complicated one. It is not clear which cues are used by animals under various conditions.

Music is a source of pleasure to human beings. Musical instruments and human voices produce sounds that have energy at the fundamental frequency that corresponds to its perceived pitch, as well as at multiples of that frequency, giving sounds a quality that allows us, for example, to distinguish a flute from a violin when their pitch is the same. Musical pitches are largely in the low-frequency range in which auditory nerve fibers fire in phase with sounds. In music, sounds are combined simultaneously to produce chords and successively to produce melodies. Euphonious, pleasant chords elicit regular, periodic firing in cochlear nerve fibers. In dissonant sounds, there is less regularity both in the sound itself and in the firing of auditory nerve fibers; the component frequencies are so close that they interfere with one another instead of periodically reinforcing one another.

The Neural Representation of Sound in Central Pathways Begins in the Cochlear Nuclei

The neural pathways that process acoustic information extend from the ear to the brain stem, through the midbrain and thalamus, to the cerebral cortex (Figure 28–2). Acoustic information is conveyed from cells in the cochlear ganglion (see Figure 26–17) to the cochlear nuclei in the brain stem. There information is received by several different types of neurons, most of which are arranged tonotopically.

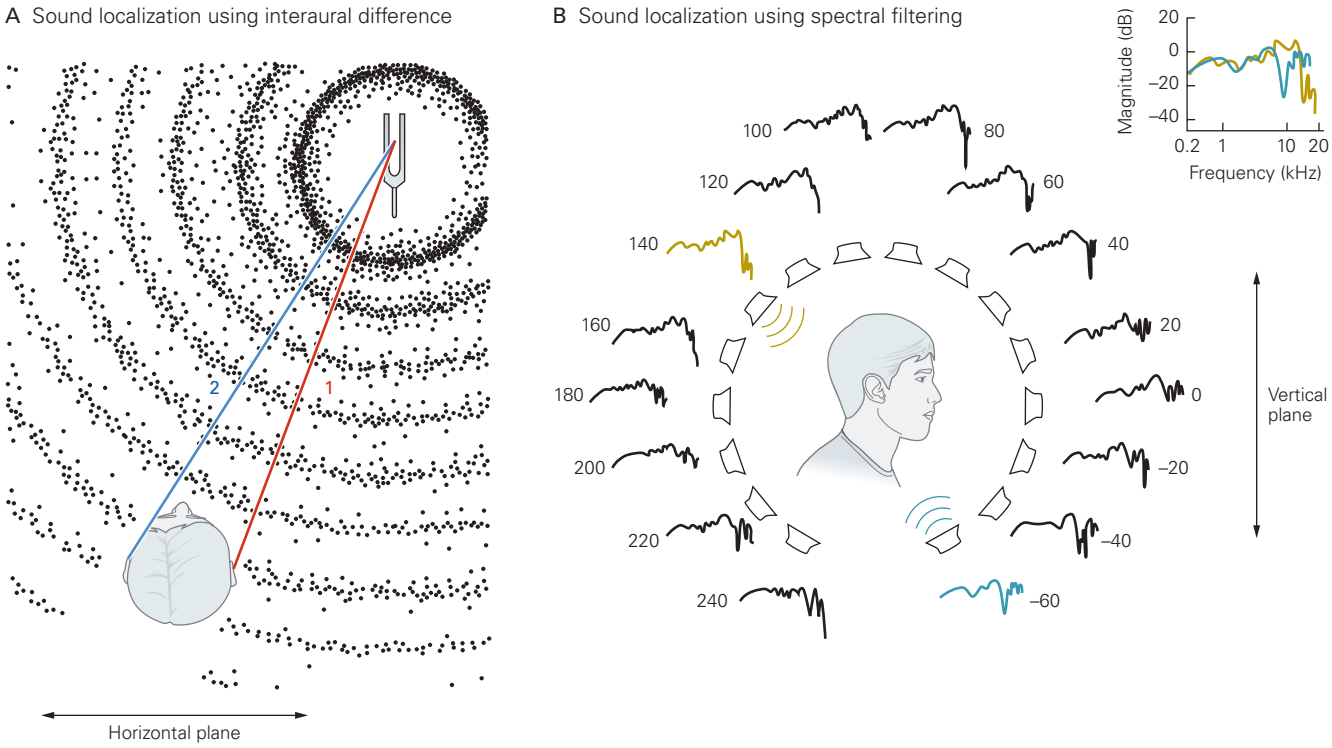

Figure 28–1 Cues for localizing sound sources in the horizontal plane.

A. Interaural time and intensity differences are cues for localizing sound sources in the horizontal plane, or azimuth. A sound arising in the horizontal plane arrives differently at the two ears: Sounds arrive earlier and are louder at the ear nearer the source. A sound that arises directly in the front or back travels the same distance to the right and left ears and thus arrives at both ears simultaneously. Interaural time and intensity do not vary with the movement of sound sources in the vertical plane, so it is impossible to localize a pure sinusoidal tone in the vertical plane. In humans, the maximal interaural time difference is approximately 600 μs. High-frequency sounds, with short wavelengths, are deflected by the head, producing a sound shadow on the far side. (Adapted, with permission, from Geisler 1998.)

B. Mammals can localize broadband sounds in both the vertical and horizontal planes on the basis of spectral filtering. When a noise that has equal energy at all frequencies over the human hearing range (*white noise*) is presented through a speaker, the ear, head, and shoulders cancel energy at some frequencies and enhance others. The white noise that is emitted from the speaker has a flat power spectrum, but by the time the noise has reached the bottom of the ear canal, its spectrum is no longer flat.

In the figure, the sound energy at each frequency at the eardrum relative to that of the white noise is shown by the traces beside each speaker; these traces plot the relative sound magnitude in decibels against spectral frequency (*head-related transfer function*). The small plot in the upper right compares two head-related transfer functions: one for a noise that arises low and in front of a listener (**blue**) and one for a noise from behind the listener's head (**brown**). Head-related transfer functions have deep notches at frequencies greater than 8 kHz, whose frequencies vary depending on where the sounds arose. Sounds that lack energy at high frequencies and narrowband sounds are difficult to localize in the vertical plane. Since spectral filtering also varies in the horizontal plane, it provides the only location cue to animals that have lost hearing in one ear.

You can test the salience of these spectral cues with a simple experiment. Close your eyes as a friend jingles keys directly in front of you at various elevations. Compare your ability to localize sounds under normal conditions and when you distort the shape of both ears by pushing them with your fingers from the back. (Data from D. Kistler and F. Wightman.)

The axons of the different types of neurons take different routes to the brain stem and midbrain, where they terminate on separate targets. Some of the pathways from the cochlear nuclei to the contralateral inferior colliculus are direct; others involve one or two synaptic stages in brain stem auditory nuclei. From the bilateral inferior colliculi, acoustic information flows two ways: to the ipsilateral superior colliculus, where it participates in orienting the head and eyes in response to sounds, and to the ipsilateral thalamus, the relay to auditory areas of the cerebral cortex. The afferent auditory pathways from the periphery to higher brain regions include efferent feedback at many levels.

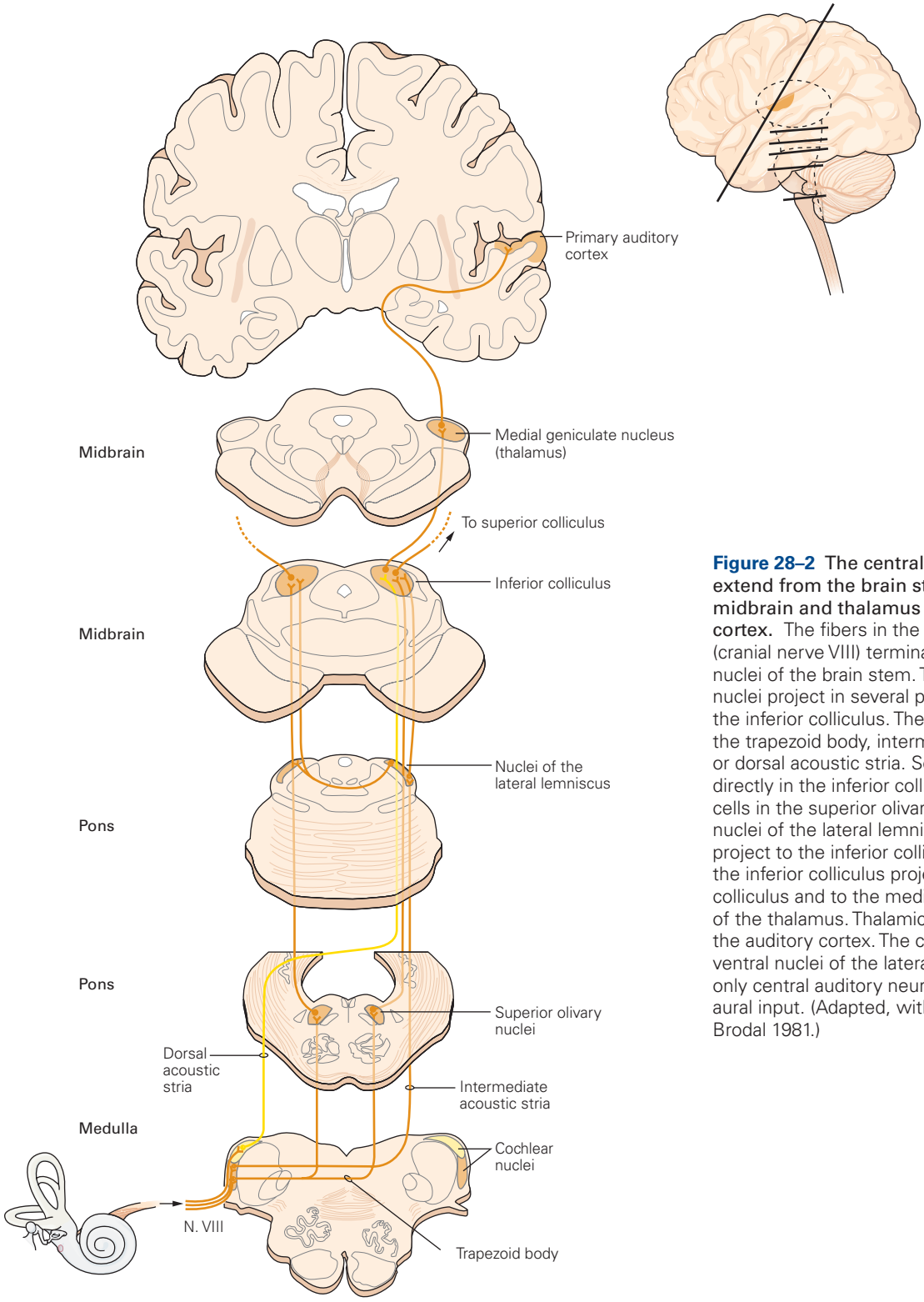

Figure 28–2 **The central auditory pathways extend from the brain stem through the midbrain and thalamus to the auditory cortex.** The fibers in the cochlear nerve (cranial nerve VIII) terminate in the cochlear nuclei of the brain stem. The neurons of these nuclei project in several parallel pathways to the inferior colliculus. Their axons exit through the trapezoid body, intermediate acoustic stria, or dorsal acoustic stria. Some cells terminate directly in the inferior colliculus. Others contact cells in the superior olivary complex and in the nuclei of the lateral lemniscus, which in turn project to the inferior colliculus. Neurons of the inferior colliculus project to the superior colliculus and to the medial geniculate nucleus of the thalamus. Thalamic neurons project to the auditory cortex. The cochlear nuclei and the ventral nuclei of the lateral lemniscus are the only central auditory neurons that receive monaural input. (Adapted, with permission, from Brodal 1981.)

The Cochlear Nerve Delivers Acoustic Information in Parallel Pathways to the Tonotopically Organized Cochlear Nuclei

The afferent nerve fibers from cochlear ganglion cells are bundled in the cochlear or auditory component of the vestibulocochlear nerve (cranial nerve VIII) and terminate exclusively in the cochlear nuclei. The cochlear nerve in mammals contains two groups of fibers: a large number (95%) of myelinated fibers that receives input from inner hair cells and a small number (5%) of unmyelinated fibers that receive input from outer hair cells.

The larger, more numerous, myelinated fibers are much better understood than the unmyelinated fibers. Each type detects energy over a narrow range of frequencies; the tonotopic array of cochlear nerve fibers thus carries detailed information about how the frequency content of sounds varies from moment to moment. The unmyelinated fibers terminate both on the large neurons in the ventral cochlear nuclei and also on the small granule cells that surround the ventral cochlear nuclei. Because it is difficult to record from these tiny fibers, the information they convey to the brain is not well understood. The unmyelinated fibers integrate information from a relatively wide region of the cochlea but are not responsive to sound. It has been suggested that these fibers respond to cochlear damage and contribute to hyperacusis—pain after exposure to loud sounds that damages the cochlea.

Two features of the cochlear nuclei are important. First, these nuclei are organized tonotopically. Fibers that carry information from the apical end of the cochlea, which detects low frequencies, terminate ventrally in the ventral and dorsal cochlear nuclei; those that carry information from the basal end of the cochlea, which detects high frequencies, terminate dorsally (Figure 28–3). Second, each cochlear nerve fiber innervates several different areas within the cochlear nuclei, contacting various types of neurons that have distinct projection patterns to higher auditory centers. As a result, the auditory pathway comprises at least four parallel ascending pathways that simultaneously extract different acoustic information from the signals carried by cochlear nerve fibers. Parallel circuits are a general feature of vertebrate sensory systems.

The Ventral Cochlear Nucleus Extracts Temporal and Spectral Information About Sounds

The principal cells of the unlayered ventral cochlear nucleus sharpen temporal and spectral information and convey it to higher centers of the auditory pathway. Three types of neurons are intermingled and form separate pathways through the brain stem (Figure 28–4).

Bushy cells project bilaterally to the superior olivary complex. This pathway has two parts. One courses through the medial superior olive and compares the time of arrival of sounds at the two ears; the other travels through the medial nucleus of the trapezoid body and the lateral superior olive and compares interaural intensity. Large spherical bushy cells sense low frequencies and project bilaterally to the medial superior olive, forming a circuit that detects interaural time delay and contributes to the localization of low-frequency sounds in the horizontal plane. The small spherical bushy cells and globular bushy cells sense higher frequencies. Small spherical bushy cells excite the lateral superior olive ipsilaterally. The globular bushy cells, through calyceal endings, excite neurons in the contralateral medial nucleus of the trapezoid body that in turn inhibit principal cells of the lateral superior olive. Neurons in the lateral superior olive integrate the ipsilateral excitation and contralateral inhibition to measure interaural intensity and to localize sources of high-frequency sounds in the horizontal plane (see Figure 28–6).

Stellate cells terminate widely. They excite neurons in the ipsilateral dorsal cochlear nucleus, the medial olivocochlear efferent neurons in the ventral nucleus of the trapezoid body, the periolivary nuclei in the vicinity of the ipsilateral lateral superior olive, and the contralateral ventral nucleus of the lateral lemniscus, inferior colliculus, and thalamus. The tonotopic array of stellate cells encodes the spectrum of sounds.

Octopus cells excite targets in the contralateral paraolivary nucleus and terminate in large excitatory calyceal endings on neurons of the ventral nucleus of the lateral lemniscus, which in turn provide sharply timed glycinergic inhibition to the inferior colliculus. Octopus cells detect onsets of sounds that allow animals to detect brief gaps. They mark the spectral components that come from one source that necessarily start together.

The differences in the integrative tasks performed by these pathways through the ventral cochlear nucleus are reflected in cell morphology. The shapes of their dendrites reflect the way they collect information from cochlear nerve fibers. The dendrites of the sharply tuned bushy and stellate cells receive input from relatively few cochlear nerve fibers, whereas those of the broadly tuned octopus cells, in contrast, lie perpendicular to the path of cochlear nerve fibers, poised to receive input from many cochlear nerve fibers. Many of the inputs to bushy cells are from unusually large

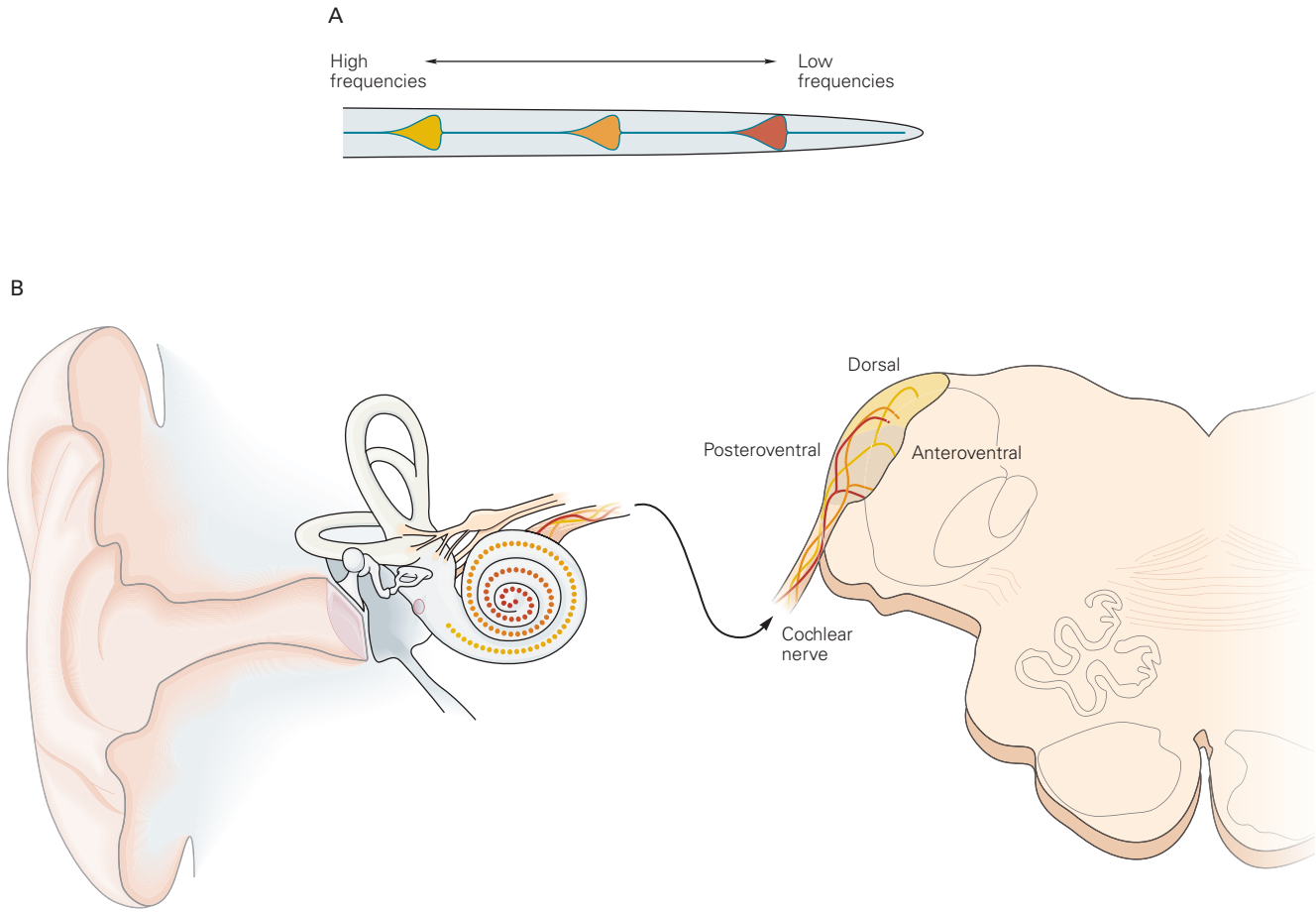

Figure 28–3 The dorsal and ventral cochlear nuclei.

A. Stimulation with three frequencies of sound vibrates the schematically uncoiled basilar membrane at three positions, exciting distinct populations of hair cells and their afferent nerve fibers.

B. Cochlear nerve fibers project in a tonotopic pattern to the cochlear nuclei. Those encoding the lowest frequencies (**red**) terminate most ventrally, whereas those encoding higher frequencies (**yellow**) terminate more dorsally. The cochlear nuclei include the ventral and dorsal nuclei. Each afferent fiber enters at the nerve root and splits into branches that run anteriorly (the ascending branch) and posteriorly (the descending branch). The ventral cochlear nucleus is thus divided functionally into anteroventral and posteroventral divisions.

terminals that envelop the bushy cell bodies, meeting their need for large synaptic currents. The need for large synaptic currents in octopus cells is met by summing inputs from large numbers of small terminals.

The biophysical properties of neurons determine how synaptic currents are converted to voltage changes and over how long a time synaptic inputs are integrated. Octopus and bushy cells in the ventral cochlear nucleus are able to respond with exceptionally rapid and precisely timed synaptic potentials. These neurons have a prominent, low-voltage-activated K^+ conductance that confers a low input resistance and rapid responsiveness and prevents repetitive firing (Figure 28–4C). The large synaptic currents that are required to trigger action potentials in these leaky cells are delivered through rapidly gated, high-conductance, AMPA-type (α-amino-3-hydroxy-5-methylisoxazole-4-propionate) glutamate receptors at many synaptic release sites. In contrast, stellate cells, in which even relatively small depolarizing currents produce large protracted voltage changes, generate slower excitatory postsynaptic potentials (EPSPs) in response to synaptic currents, and *N*-methyl-D-aspartate (NMDA)-type glutamate receptors enhance those responses.

The Dorsal Cochlear Nucleus Integrates Acoustic With Somatosensory Information in Making Use of Spectral Cues for Localizing Sounds

Among vertebrates, only mammals have dorsal cochlear nuclei. The dorsal cochlear nucleus receives input from two systems of neurons that project to different

layers (Figure 28–4A,B). Its principal cells, fusiform cells, integrate those two systems of inputs and convey the result directly to the contralateral inferior colliculus.

The outermost molecular layer is the terminus of a system of parallel fibers, the unmyelinated axons of granule cells that are scattered in and around the cochlear nuclei. This system transmits somatosensory, vestibular, and auditory information from widespread regions of the brain to the molecular layer.

The deep layer receives acoustic information. Not only cochlear nerve fibers but also stellate cells of the ventral cochlear nucleus terminate in the deep layer. Acoustic inputs are tonotopically organized in isofrequency laminae that run at right angles to parallel fibers.

Fusiform cells, the principal cells of the dorsal cochlear nucleus, integrate the two systems of inputs. Parallel fibers in the molecular layer excite fusiform cells through spines on apical dendrites in the molecular layer. Parallel fibers also terminate on spines of dendrites of cartwheel cells, interneurons that bear a strong resemblance to cerebellar Purkinje cells, which in turn inhibit fusiform cells. Cochlear nerve fibers and stellate cells in the ventral cochlear nucleus excite fusiform cells and inhibitory interneurons via synapses on the smooth basal dendrites in the deep layer.

Recent experiments suggest that the circuits of the dorsal cochlear nucleus distinguish between unpredictable and predictable sounds. An animal's own chewing or licking sounds, for example, are predictable and canceled through these circuits. The changes in spectral cues that arise when animals move their heads or ears or shoulders, changing the angle of incidence of sounds to the ears, are unpredictable, especially when an external sound source is moving. Somatosensory and vestibular information about the position of the head and ears, as well as descending information from higher levels of the nervous system about the animal's own movements, pass through the molecular layer to modulate acoustic information that arrives in the deep layer.

The Superior Olivary Complex in Mammals Contains Separate Circuits for Detecting Interaural Time and Intensity Differences

In many vertebrates, including mammals and birds, neurons in the superior olivary complex compare the activity of cells in the bilateral cochlear nuclei to locate sound sources. Separate circuits detect interaural time and intensity differences and project to the inferior colliculi.

The Medial Superior Olive Generates a Map of Interaural Time Differences

Differences in arrival times at the ears are not represented at the cochlea. Instead, they are first represented in the medial superior olive where a map of interaural phase is created by a comparison of the timing of action potentials in the responses to sounds from the two ears. Sounds arrive at the near ear before they arrive at the far ear, with interaural time differences being directly related to the location of sound sources in the horizontal plane (Figure 28–5A).

Cochlear nerve fibers tuned to frequencies below 4 kHz and their bushy cell targets encode sounds by firing in phase with the pressure waves. This property is known as *phase-locking.* Although individual neurons may fail to fire at some cycles, some set of neurons fires with every cycle. In so doing, these neurons carry information about the timing of inputs with every cycle of the sound. Sounds arriving from one side evoke phase-locked firing that is consistently earlier at the near ear than at the far ear, resulting in consistent interaural phase differences (Figure 28–5A).

In 1948, Lloyd Jeffress suggested that an array of detectors of coincident inputs from the two ears, transmitted through *delay lines* comprised of axons with systematically differing lengths, could form a map of interaural time differences and thus a map of the location of sound sources (Figure 28–5B). In such a circuit, conduction delays compensate for the earlier arrival at the near ear. Interaural time delays increase systematically as sounds move from the midline to the side, resulting in coincident firing further toward the edge of the neuronal array.

Such neuronal maps have been found in the barn owl in the homolog of the medial superior olivary nucleus. Mammals and chickens use a variant of this input arrangement. The principal neurons of the medial superior olive form a sheet of one or a few cells' thickness on each side of the midline. Each neuron has two tufts of dendrites, one extending to the lateral face of the sheet, and the other projecting to the medial face of the sheet (Figure 28–5C). The dendrites at the lateral face are contacted by the axons of large spherical bushy cells from the ipsilateral cochlear nucleus, whereas the dendrites at the medial face are contacted by large spherical bushy cells of matching best frequency from the contralateral cochlear nucleus. The axons of bushy cells terminate in the contralateral

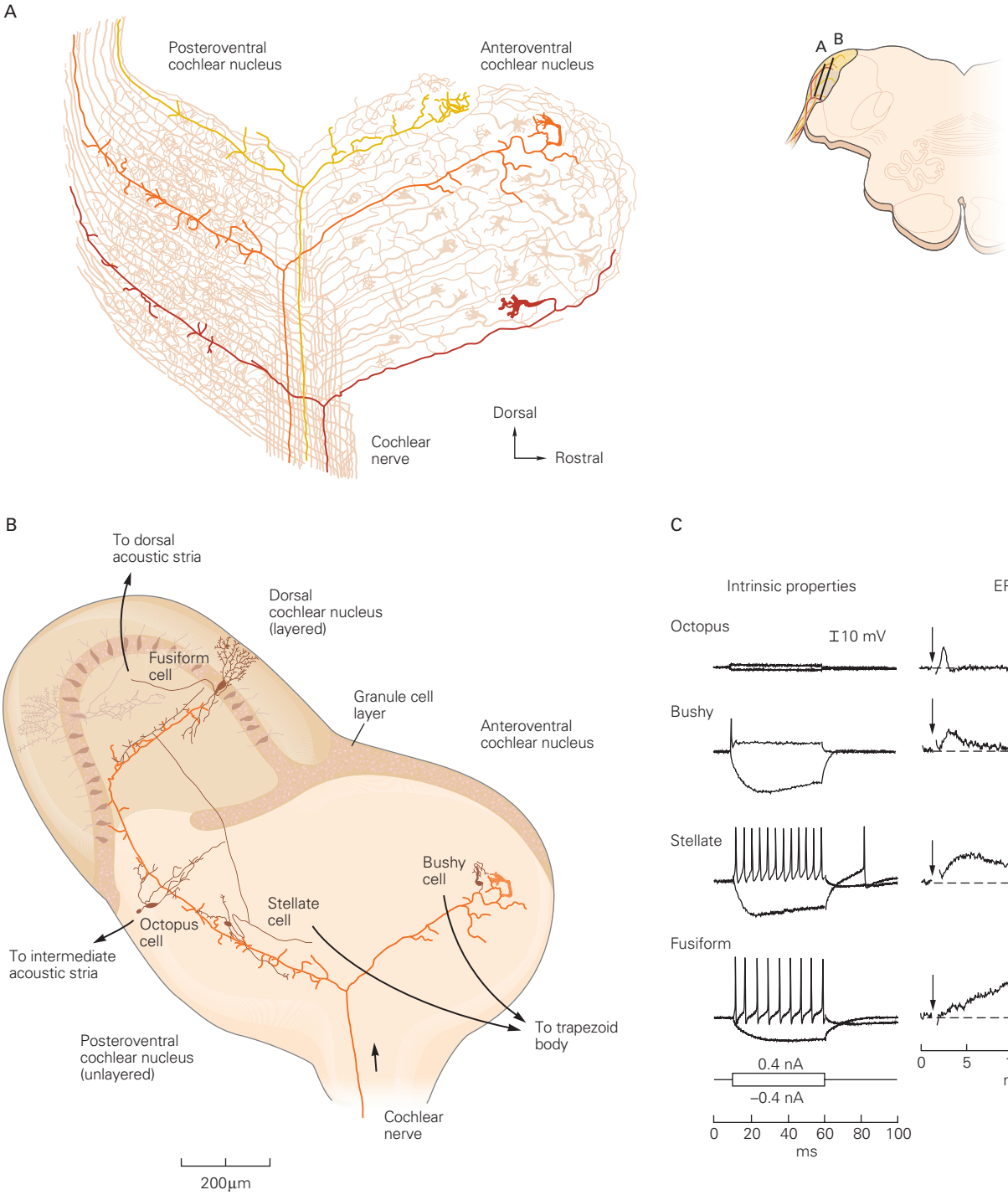
A
Posteroventral cochlear nucleus
Anteroventral cochlear nucleus
Cochlear nerve
Dorsal
Rostral
A B
B
To dorsal acoustic stria
Dorsal cochlear nucleus (layered)
Fusiform cell
Granule cell layer
Anteroventral cochlear nucleus
Bushy cell
Stellate cell
Octopus cell
To intermediate acoustic stria
To trapezoid body
Posteroventral cochlear nucleus (unlayered)
Cochlear nerve
200µm
C
Intrinsic properties
EPSPs
Octopus
10 mV
5 mV
Bushy
Stellate
Fusiform
0.4 nA
–0.4 nA
0 20 40 60 80 100
ms
0 5 10 15 20
ms

medial superior olive with delay lines just as Jeffress had suggested, but the branches that terminate in the ipsilateral medial superior olive are of equal length (see Figure 28–5C).

The conduction delays are such that each medial superior olive receives coincident excitatory inputs from the two ears only when sounds come from the contralateral half of space. As sound sources move from the midline to the most lateral point on the contralateral side of the head, the earlier arrival of sounds at the contralateral ear needs to be compensated by successively longer delay lines. This results in inputs from the two ears coinciding at successively more posterior and lateral regions of the medial superior olive. Inhibition superimposed on these excitatory inputs plays a significant role in sharpening the map of interaural phase.

In encoding interaural phase, individual neurons in the medial superior olive provide ambiguous information about interaural time differences. Phase ambiguities are resolved when sounds have energy at multiple frequencies, as natural sounds almost always do. The sheet of neurons of the medial superior olive forms a representation of interaural phase along the rostrocaudal and lateromedial dimensions. The array of bushy cell inputs also imposes a tonotopic organization in the dorsoventral dimension. Sounds that contain energy at multiple frequencies evoke maximal coincident firing in a single dorsoventral column of neurons that localizes sound sources unambiguously. The beauty of using interaural phase to encode interaural time disparities is that the brain receives information about interaural time differences not just at the beginning and end of the sound but with every cycle of an ongoing sound.

Principal cells of the medial superior olive also receive sharply timed inhibition driven by sounds from both the ipsilateral and contralateral sides through the lateral and medial nuclei of the trapezoid body, respectively. Remarkably, the inhibition through pathways from both sides precedes the arrival of excitation and sharpens the summation of excitation even though inhibition is mediated through a pathway that has an additional synapse. The great conduction speed through the disynaptic pathway through the medial nucleus of the trapezoid body is made possible by the large axons of globular bushy cells and the large calyceal terminals of Held that activate neurons in the medial nucleus of the trapezoid body with short and consistently timed delays. The pathway that brings ipsilateral inhibition through the lateral nucleus of the trapezoid body is less well understood.

Each medial superior olive thus forms a map of the location of sound sources in the contralateral hemifield. The striking difference between this spatial representation of stimuli and those in other sensory systems is that it is not the result of the spatial arrangement of inputs, like retinotopic or somatosensory maps, but is inferred by the brain from computations made in the afferent pathways.

The Lateral Superior Olive Detects Interaural Intensity Differences

Sounds with wavelengths that are similar to or smaller than the head are deflected by the head, causing the

Figure 28–4 (Opposite) Different types of cells in the cochlear nuclei extract distinct types of acoustic information from cochlear nerve fibers.

A. The differing sizes and shapes of terminals along the length of each cochlear nerve fiber in the ventral cochlear nucleus of a newborn dog reflect differences in their postsynaptic targets. The large end bulbs form synapses on bushy cells; smaller boutons contact stellate and octopus cells. The nerve fibers shown here are color-coded as in Figure 28–3: the **yellow** fiber encodes the highest frequencies and the **red** fiber the lowest. (Adapted, with permission, from Cajal 1909.)

B. A layer of mouse granule cells (**light brown**) separates the unlayered ventral cochlear nucleus (**pink**) from the layered dorsal nucleus (**tan and light brown**). In the dorsal cochlear nucleus, the cell bodies of fusiform and granule cells are intermingled in a region between the outermost molecular layer and the deep layer. Cochlear nerve fibers, color-coded for frequency as in Figure 28–3, terminate in both nuclei but with different patterns of convergence on the principal cells. Each bushy, stellate, and fusiform cell receives input from a few auditory nerve fibers and is sharply tuned, whereas individual octopus cells are contacted by many auditory nerve fibers and are broadly tuned.

C. Differences in the intrinsic electrical properties of the principal cells of mouse cochlear nuclei are reflected in the patterns of voltage change in the cells. When steadily depolarized, stellate and fusiform cells fire repetitive action potentials, whereas repetitive firing in bushy and octopus cells is prevented by low-voltage-activated conductances. The low input resistance of bushy and octopus cells in the depolarized voltage range makes depolarizing voltage changes rapid but also small; the rise and fall of voltage changes in stellate and fusiform cells is slower. Synaptic potentials, too, are different. The brief synaptic potentials in bushy and octopus cells require larger synaptic currents but encode the timing of auditory nerve inputs more faithfully than do the longer-lasting synaptic potentials in stellate or fusiform cells. (Reproduced, with permission, from N. Golding.)

A Phase-locked firing in bushy cells

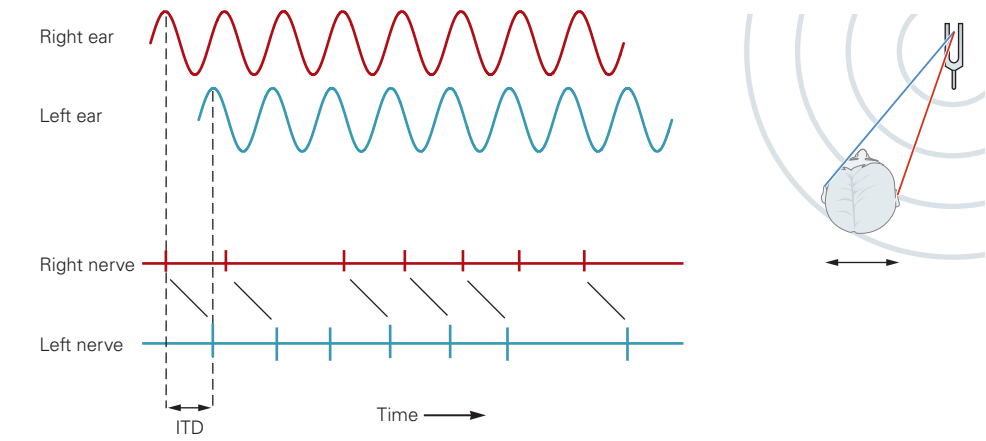

B Mapping of ITD onto array of neuronal coincidence neurons

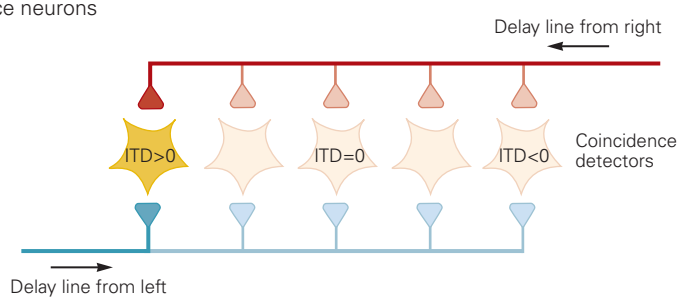

C Bilateral medial superior olivary nuclei

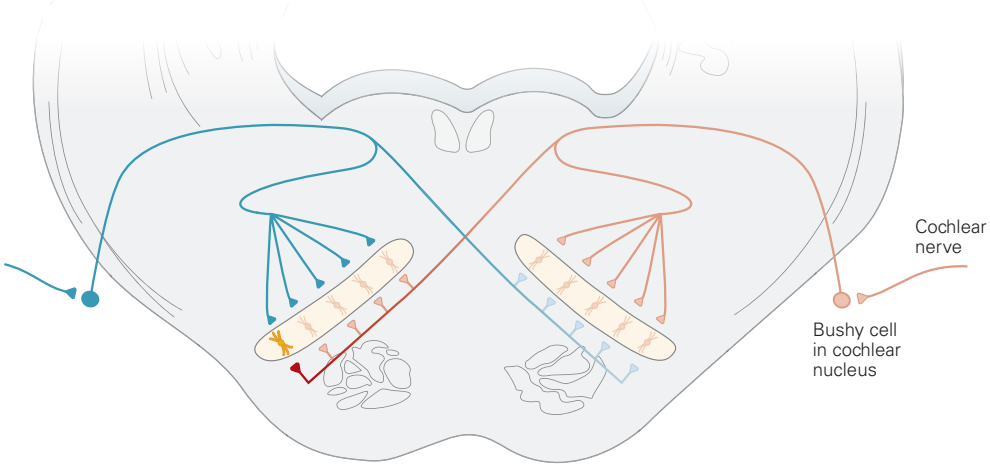

intensity at the near ear to be greater than that at the far ear. In humans, interaural intensities can differ in sounds that have frequencies greater than about 2 kHz. Interaural intensity differences produced by such *head shadowing* are detected by a neuronal circuit that includes the medial nucleus of the trapezoid body and the lateral superior olive.

Although the lateral superior olive does not form a map of the location of sounds in the horizontal plane, it performs the first of several integrative steps that use interaural intensity differences to localize sounds. Neurons in this nucleus balance ipsilateral excitation with contralateral inhibition. Excitation comes from small spherical bushy cells and stellate cells in the ipsilateral ventral cochlear nucleus. Inhibition comes from a disynaptic pathway that includes globular bushy cells in the contralateral ventral cochlear nucleus and principal neurons of the ipsilateral medial nucleus of the trapezoid body (Figure 28–6A). Sounds that arise ipsilaterally generate relatively strong excitation and relatively weak inhibition, whereas those that arise contralaterally generate stronger inhibition than excitation. Neurons in the lateral superior olive are activated more strongly by sounds from the ipsilateral than from the contralateral hemifield. The firing of lateral superior olivary neurons is a function of the location of the sound source and thus carries information about where sounds arise in the horizontal plane (Figure 28–6B).

In order to balance excitation and inhibition stimulated by one sound, the ipsilateral excitation and contralateral inhibition must arrive at neurons in the lateral superior olive at the same time. Thus, excitation that arises monosynaptically from the ipsilateral ventral cochlear nucleus must arrive at the same time as inhibition that arises disynaptically from the contralateral ventral cochlear nucleus. The inhibition comes from the medial nucleus of the trapezoid body whose inputs through large axons of globular bushy cells and large calyces of Held produce synaptic responses

Figure 28–5 (Opposite) Interaural differences in the arrival of a sound help localize sound in the horizontal plane.

A. When a sound such as a pure tone arises from the right, the right ear detects the sound earlier than the left ear. The difference in the time of arrival at the two ears is the interaural time delay (**ITD**). Cochlear nerve fibers and their bushy cell targets fire in phase with pressure changes. Although individual bushy cells may fail to fire at some cycles, a set of cells will encode the timing of a low-frequency sound and its frequency with every cycle. Comparison of the onset of action potentials in the bushy cells at the two sides reveals the ITDs (**slanted black lines**).

B. Interaural time differences can be measured by an array of neurons whose inputs from the two ears are delay lines as proposed by Lloyd Jeffress (1948). Action potentials propagate to reach the nearest terminals before they reach the farthest ones; thus, in the delay line from the right, terminals will generate synaptic potentials sequentially from right to left, and in the delay line from the left, terminals will generate synaptic potentials sequentially from left to right. Suppose that such postsynaptic neurons are coincidence detectors, firing only when they receive excitatory postsynaptic potentials (EPSPs) simultaneously from the right and left. Sounds that arise at the midline reach the right and left ears simultaneously with no interaural time disparity (ITD = 0). The neuron in the middle of the array that receives input from equally long axons from the two sides will thus receive simultaneous EPSPs from the two sides. When sounds come from the right, signals from the right ear arrive at the central nervous system earlier than those from the left ear (ITD >0). Sound from the right generates synchronous EPSPs in the (**yellow**) neuron because the earlier arrival of sound from the right (**red**) is compensated by a longer conduction delay relative to that from the left (**blue**). Likewise, when sound arises from the left, the ITD <0 and conduction delays from the left (**blue**) compensate for the early arrival at the left. Such a neuronal circuit produces a map of interaural time disparities in the coincidence detectors; as sounds move from the right to left, they activate coincidence detectors sequentially from left to right. Such an arrangement of delay lines has been found in the nucleus laminaris of the barn owl, the homolog of the mammalian medial superior olivary nucleus.

C. Mammals use delay lines only in the nucleus contralateral to a sound source to form a map of interaural time differences. The bitufted neurons of the medial superior olivary nucleus form a sheet that is contacted on its lateral face by bushy cells from the ipsilateral cochlear nucleus and on the medial face by bushy cells from the contralateral cochlear nucleus. (Although it is depicted here schematically in a coronal section of the brain stem, the encoding of interaural disparities is in a sheet of neurons that also has a rostrocaudal dimension.) On the ipsilateral side, the branches of the bushy cell axon are of equal length and thus initiate synaptic currents in their targets in the medial superior olive simultaneously. On the contralateral side, the branches deliver synaptic currents sequentially first to the regions closest to the midline, and then to progressively more lateral regions. Neurons of the medial superior olive detect synchronous excitation from the two ears only when sounds arise from the contralateral half of space. When sounds arise from the right side, their early arrival at the right ear is compensated by progressively longer conduction delays to activate neurons more and more toward the lateral end of the left medial superior olive (the **yellow cell** is activated by a sound from the far right, as in part **B**). When sounds arise from the front and there is no interaural time difference, neurons in the anterior end of the medial superior olive are activated synchronously from both sides. Each medial superior olive forms a map of where sounds arise in the contralateral hemifield. (Adapted, with permission, from Yin 2002.)

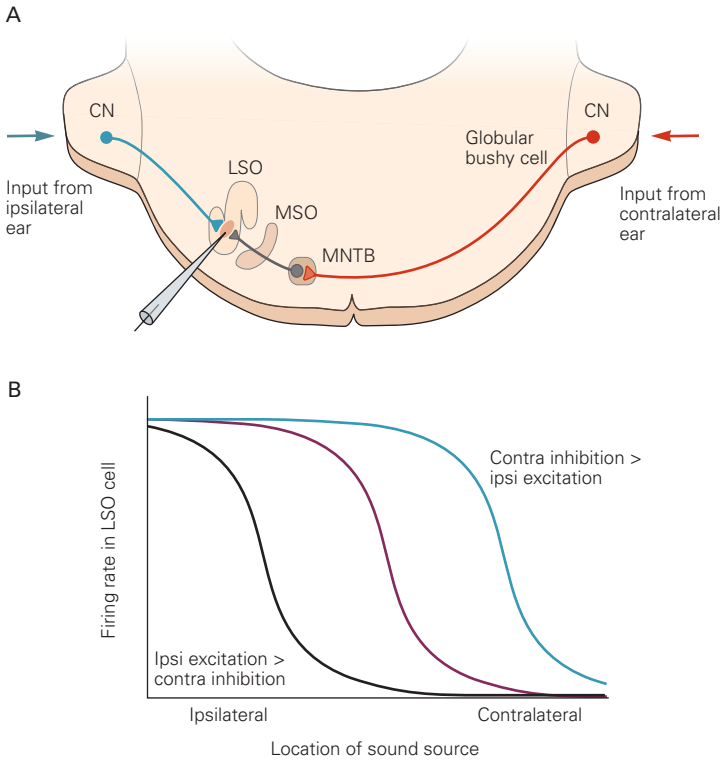

Figure 28–6 Interaural differences in the intensity of a sound also help localize sound in the horizontal plane.

A. Principal cells of the lateral superior olivary nucleus (**LSO**) receive excitatory input from the ipsilateral cochlear nucleus (**CN**) and inhibitory input from the contralateral cochlear nucleus. A coronal section through the brain stem of a cat illustrates the anatomical connections. Small spherical bushy cells and stellate cells in the ipsilateral ventral cochlear nucleus provide direct excitation. Globular bushy cells in the contralateral ventral cochlear nucleus project across the midline and excite neurons in the medial nucleus of the trapezoid body (**MNTB**) via large terminals, the calyces of Held. Cells of the medial nucleus of the trapezoid body inhibit neurons in the lateral superior olive as well as in the medial superior olive (**MSO**). For neurons of the lateral superior olive to compare intensities of the same sound, the timing of the ipsilateral excitatory input must be matched with the timing of the contralateral inhibitory input. To this end, globular bushy cells have particularly large axons that terminate in a calyx of Held in the medial nucleus of the trapezoid body where synaptic transmission is strong and thus the synaptic delay is short and invariant in its timing.

B. The firing of neurons in the lateral superior olive reflects a balance of ipsilateral excitation and contralateral inhibition. When sounds arise from the ipsilateral side, excitation is relatively stronger and inhibition is relatively weaker than when sounds arise from the contralateral side. The transition between the dominance of excitation and inhibition reflects the location of the sound source.

with short and consistently timed delays. The axons of small spherical bushy cells and stellate cells that carry ipsilateral excitation conduct more slowly than those of globular bushy cells.

The terminals of the globular bushy cells, the calyces of Held, engulf the cell bodies of trapezoid-body neurons so dramatically that they caught the attention of early anatomists and modern biophysicists. A single somatic terminal releases neurotransmitter at numerous release sites and generates large synaptic currents. The reliability of pre- and postsynaptic recordings at this synapse makes the site ideal for detailed studies of the mechanisms of synaptic transmission (Chapter 15).

The Superior Olivary Complex Provides Feedback to the Cochlea

Although sensory systems are largely afferent, bringing sensory information to the brain, recent studies have led to an appreciation of the importance of efferent signaling at many levels of the auditory system. Olivocochlear neurons form a feedback loop from the superior olivary complex to hair cells in the cochlea. Their cell bodies lie around the major dense clusters of cell bodies in the olivary nuclei. In mammals, two groups of olivocochlear neurons have been functionally distinguished. The medial olivocochlear neurons' axons terminate on the outer hair cells bilaterally; the lateral olivocochlear neuron axons terminate ipsilaterally on the afferent fibers associated with inner hair cells.

Most medial olivocochlear neurons, with cell bodies that lie ventral and medial within the olivary complex, send their axons to the contralateral cochlea (Figure 28–7), but many also project to the ipsilateral cochlea. These cholinergic neurons act on hair cells through a special class of nicotinic acetylcholine receptor-channels formed from α9 and α10 subunits. The influx of Ca^{2+} through these channels leads to the opening of K^+ channels that hyperpolarize outer hair cells. These neurons thus mediate tuned negative feedback and are binaural, being driven predominantly but not exclusively by stellate cells of the contralateral

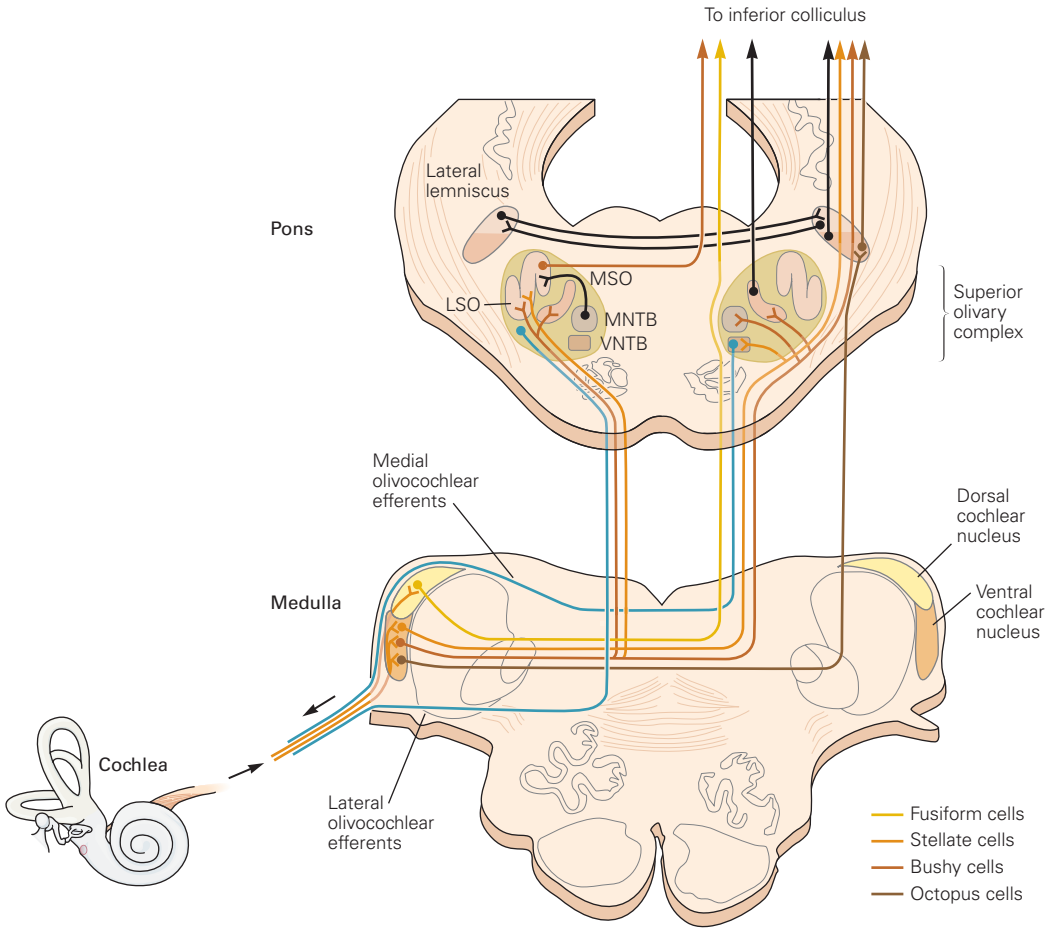

Figure 28–7 **Major components of the ascending and descending auditory pathways.** The auditory pathway is bilaterally symmetrical; the major connections among the nuclei that form the early auditory pathway are shown. The ascending pathway begins in the cochlea and progresses through several parallel pathways through the cochlear nuclei: the cochlear nuclei, the superior olivary nuclei, and the ventral and dorsal nuclei of the lateral lemniscus. These signals converge in the inferior colliculus, which projects to the medial geniculate body of the thalamus and thence to the cerebral cortex (see Figure 28–2). Some of the connections are through excitatory pathways (**colored lines**) and others through inhibitory pathways (**black lines**). These same nuclei are also interconnected through descending pathways (**blue lines**) and bilaterally through commissural projections. (**LSO**, lateral superior olivary nucleus; **MNTB**, medial nucleus of the trapezoid body; **MSO**, medial superior olive; **VNTB**, ventral nucleus of the trapezoid body).

ventral cochlear nucleus. Activity in these efferent fibers reduces the sensitivity of the cochlea and protects it from damage by loud sounds. Collateral branches of medial olivocochlear neurons terminate on stellate cells in the cochlear nucleus, acting on conventional nicotinic and muscarinic acetylcholine receptors, forming an excitatory feedback loop.

Lateral olivocochlear neurons, with cell bodies that lie in and around the lateral superior olive, send their axons exclusively to the ipsilateral cochlea, where they terminate on the afferent fibers from inner hair cells. Charles Liberman and his colleagues demonstrated that these efferents balance the excitability of cochlear nerve fibers at the two ears.

Ventral and Dorsal Nuclei of the Lateral Lemniscus Shape Responses in the Inferior Colliculus With Inhibition

Fibers from the cochlear and superior olivary nuclei run in a band, or lemniscus, along the lateral edge of the brain as they ascend from the brainstem to the inferior colliculus. Along this band of fibers are groups of neurons that form the dorsal and ventral nuclei of the

lateral lemniscus. Neurons in the ventral nuclei of the lateral lemniscus receive input from all major groups of principal cells of the ventral cochlear nuclei and respond predominantly to monaural input, driven by the contralateral ear, while neurons in the dorsal nucleus receive input from the lateral and medial superior olivary nuclei and respond to inputs from both ears. Neurons in both subdivisions are inhibitory and project to the inferior colliculus. Their roles are intriguing but not fully understood.

Since understanding the meaning of sounds is not greatly compromised by the loss of one ear, it would make sense that the largely monaural functions of the ventral nuclei of the lateral lemniscus involve the processing of the meaning of sounds. Furthermore, mammals vary in the information they extract from their acoustic environments, which may account for differences between species in the structure and function of the ventral nuclei of the lateral lemniscus.

A border that is more distinct in some mammalian species than in others separates the ventral and intermediate nuclei and the subdivisions of the ventral nucleus of the lateral lemniscus. Neurons differ in their shapes, biophysical properties, and pattern of convergence of cochlear nuclear inputs. One group of glycinergic neurons is innervated by large calyceal terminals from octopus cells. These could generate inhibitory temporal reference signals in the inferior colliculus. Some broadly tuned neurons fire almost exclusively at the onset of tones with sharply timed action potentials but convey periodicity in complex sounds, raising the question of whether these neurons might have a role in encoding pitch in music and speech. Others respond by firing as long as a tone is present; these neurons track the fluctuations in intensity or the envelopes of sounds, a feature that is useful for understanding the meaning of sounds including speech. Tuning curves of the neurons are variable, with many being broad or W-shaped.

Neurons in the dorsal nucleus are predominantly binaural, receiving input from the ipsilateral medial superior olive and from the lateral superior olive, primarily from the contralateral side. These neurons are GABAergic, targeting the inferior colliculi on both sides and also targeting the contralateral dorsal nucleus of the lateral lemniscus. Excitation in neurons of the dorsal nucleus is amplified by NMDA-type glutamate receptors so that the inhibition they generate in their targets outlasts sound stimuli for tens of milliseconds and thus has been termed persistent inhibition. To localize sounds accurately, animals must ignore the reflections of sounds from surrounding surfaces that arrive after the initial direct wave front. Psychophysical experiments have shown that mammals suppress all but the first-arriving sound, a phenomenon termed the *precedence effect.* It has been proposed that persistent inhibition in the inferior colliculus from the dorsal nucleus of the lateral lemniscus serves to suppress spurious localization cues such as echoes and thus that it contributes to the precedence effect.

Afferent Auditory Pathways Converge in the Inferior Colliculus

The inferior colliculus occupies a central position in the auditory pathway of all vertebrate animals because all auditory pathways ascending through the brain stem converge there (Figure 28–7). The most important sources of excitation are stellate cells from the contralateral ventral cochlear nucleus, fusiform cells from the contralateral dorsal cochlear nucleus, principal cells of the ipsilateral medial superior olive and of the contralateral lateral superior olive, principal cells of ipsilateral and contralateral dorsal nuclei of the lateral lemniscus, commissural connections from the contralateral inferior colliculus, and pyramidal cells in layer V of the auditory cortex. Important sources of inhibition include the nuclei of the lateral lemniscus, the ipsilateral lateral superior olive, the superior paraolivary nucleus, and the contralateral inferior colliculus.

The inferior colliculus of mammals is subdivided into the central nucleus, dorsal cortex, and external cortex. The central nucleus is tonotopically organized. Low frequencies are represented dorsolaterally and high frequencies ventromedially in laminae that have similar best frequencies. Fine mapping has shown that the tonotopic organization is discontinuous; the separation between best frequencies corresponds to psychophysically measured critical bands of approximately one-third octave. Although the central nucleus is organized tonotopically, the spectral range of inputs to these neurons is broader than at earlier stages in the auditory pathway. Inhibition can be broad and narrows the responses of excitatory neurons. Furthermore, tuning can be modulated by descending inputs from the cortex.

Many neurons in the central nucleus carry information about the location of sound sources. The majority of these cells are sensitive to interaural time and intensity differences, essential cues for localizing sounds in the horizontal plane. Neurons are also sensitive to spectral cues that localize sounds in the vertical plane. Physiological correlates of the precedence effect have been measured in the inferior colliculus, where inhibition suppresses simulated reflections of sounds.

The inferior colliculus is not only a convergence point but also a branch point for ascending or outflow pathways. Neurons of the central nucleus project to the external cortex of the inferior colliculus and also to the thalamus and the nucleus of the brachium of the inferior colliculus, both of which then project to the superior colliculus (or the optic tectum in birds).

Sound Location Information From the Inferior Colliculus Creates a Spatial Map of Sound in the Superior Colliculus

The inferior colliculus is not only a convergence point but also a branch point for ascending or outflow pathways. Central nucleus neurons project to the thalamus and also to the external cortex of the inferior colliculus and the nucleus of the brachium of the inferior colliculus, both of which then project to the superior colliculus (or the optic tectum in birds).

The superior colliculus is critical for reflexive orienting movements of the head and eyes to acoustic and visual cues in space. By the time the binaural sound cues and the monaural spectral cues that underlie mammalian sound localization reach the superior colliculus, they have been merged to create a spatial map of sound in which neurons are unambiguously tuned to specific sound directions. This convergence is critical since binaural differences in level and timing alone cannot unambiguously code for a single position in space. The spectral cues that provide information about vertical location must be taken into account, as different locations in the vertical plane can give rise to identical interaural differences in time or intensity. Such unambiguous spatial mapping occurs both in birds and in some mammals (Figure 28–8). In ferrets and guinea pigs, it occurs in the external cortex and the nucleus of the brachium of the inferior colliculus.

Within the superior colliculus, the auditory map is aligned with maps of visual space and the body surface. Unlike the visual and somatosensory spatial maps, the auditory spatial map does not reflect the peripheral receptor surface; instead, it is computed from a combination of cues that identify the specific position of a sound source in space.

Auditory, visual, and somatosensory neurons in the superior colliculus all converge on output pathways in the same structure that controls orienting movements of the eyes, head, and external ears. The motor circuits of the superior colliculus are mapped with respect to motor targets in space and are aligned with the sensory maps. Such sensory-motor correspondence facilitates the sensory guiding of movements.

The Inferior Colliculus Transmits Auditory Information to the Cerebral Cortex

Auditory information ascends from the inferior colliculus to the medial geniculate body of the thalamus and from there to the auditory cortex. The pathways from the inferior colliculus include a lemniscal or core pathway and extralemniscal or belt pathways. Descending projections from the auditory cortex to the medial geniculate body are prominent both anatomically and functionally.

Stimulus Selectivity Progressively Increases Along the Ascending Pathway

A marked feature of auditory neurons at structures along the ascending pathway is their progressively increased stimulus selectivity. An auditory nerve fiber is primarily selective to one stimulus dimension, the frequency of a pure tone. The stimulus selectivity of neurons in the central auditory system may be multidimensional, such as frequency, spectral bandwidth, sound intensity, modulation frequency, and spatial location. In this multidimensional acoustic space, neurons become more selective at successive auditory areas along the ascending pathway.

Many neurons in the auditory cortex (especially those in upper cortical layers) are highly selective to acoustic stimuli, such that the preferred (nearly optimal) stimulus of a neuron occupies only a small region of its receptive field in the multidimensional acoustic space. The region of the preferred stimulus becomes increasingly smaller at structures along the path to the auditory cortex (Figure 28–9A). Pure tones and broadband noises are two extreme cases of a wide range of acoustic stimuli that could preferentially drive auditory cortex neurons. The majority of neurons in the auditory cortex are preferentially driven by stimuli with greater spectral and temporal complexity than pure tones and broadband noises.

The increased stimulus selectivity is also accompanied by changes in a neuron's firing pattern. When neurons are driven by their preferred stimuli, they respond not only with higher firing rates but also with sustained firing throughout the stimulus duration (Figure 28–9B). The receptive field of a cortical neuron contains a "sustained firing region" (corresponding to preferred stimuli) within a larger "onset firing region" (corresponding to nonpreferred stimuli). This explains why it is common for experimenters to observe onset (phasic) responses in auditory cortex when a continuous sound is played.

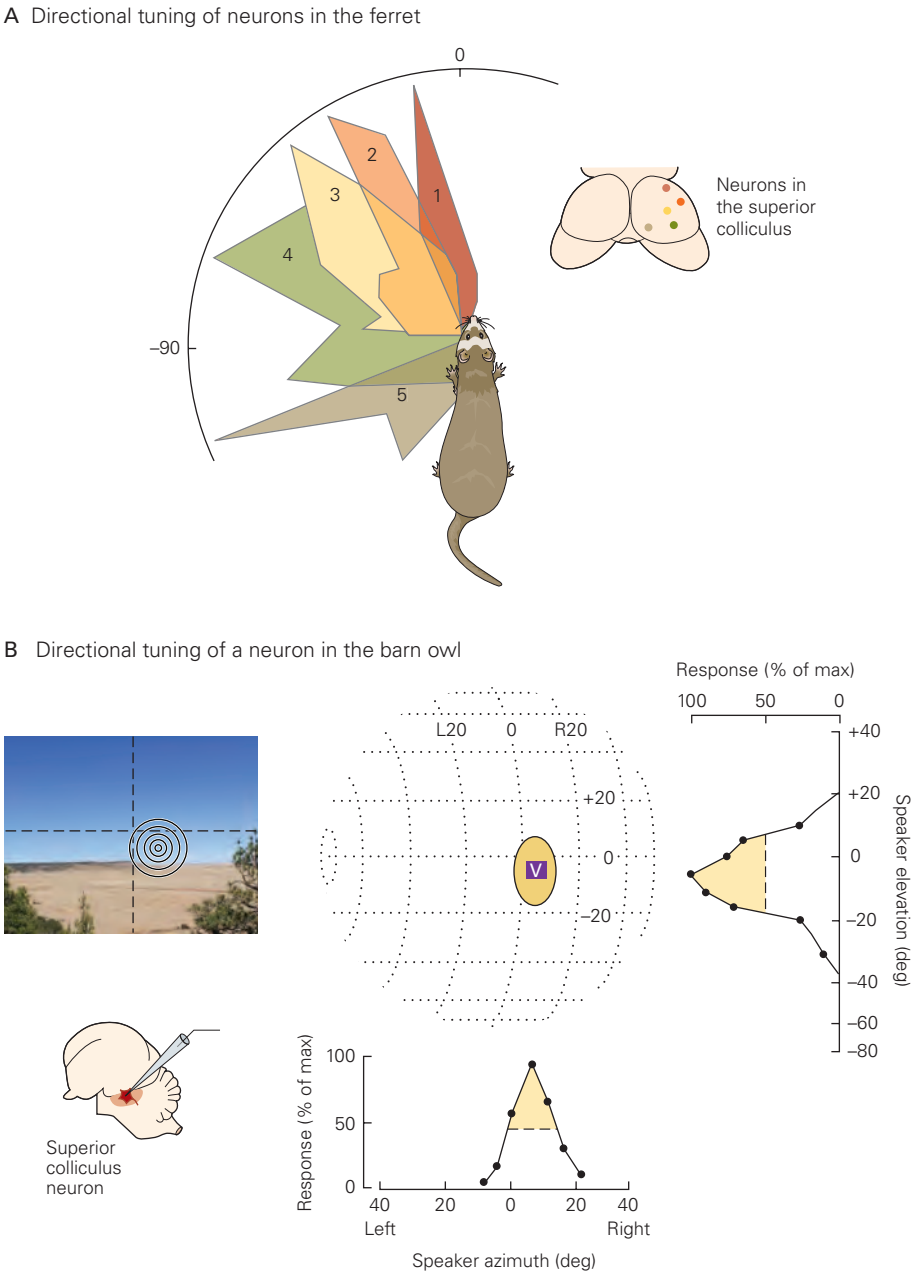

Figure 28–8 A spatial map of sound is formed in the superior colliculus.

A. Neurons in the ferret's superior colliculus are directionally tuned to sound in the horizontal plane. The illustration shows the firing rate profiles of collicular neurons 1 through 5 as a function of where the sounds are located, plotted in polar coordinates centered on the head. The drawing on the right shows the location of the recorded neurons in the colliculus. Note that neuron 1 responds best to sounds in front of the animal, whereas neurons that are located progressively more caudally in the colliculus gradually shift their responses to sounds that originate farther contralaterally. (Adapted, with permission, from King 1999.)

B. The normalized responses of a neuron in the superior colliculus of a barn owl to noise bursts presented at various locations along the horizon are plotted below (*bottom right*). The **yellow areas** in these tuning curves indicate where responses exceed 50% of the maximum. The sensitivity of the neuron to a particular location along the horizon or a particular elevation (*top right*) creates a discrete best auditory area in space for this neuron (*top middle*), shown as the colored ellipse on a plot of spatial locations with respect to a point straight in front of the owl. The neuron also responds to visual cues from the same area (the box labeled **V**). The photo illustrates the neuron's best area in space with respect to the position of the head (the intersection of the vertical and horizontal dotted lines indicates where the owl's head is pointing). The recording site for this neuron is also shown. (Adapted, with permission, from Cohen and Knudsen 1999. Copyright © 1999 Elsevier Science.)

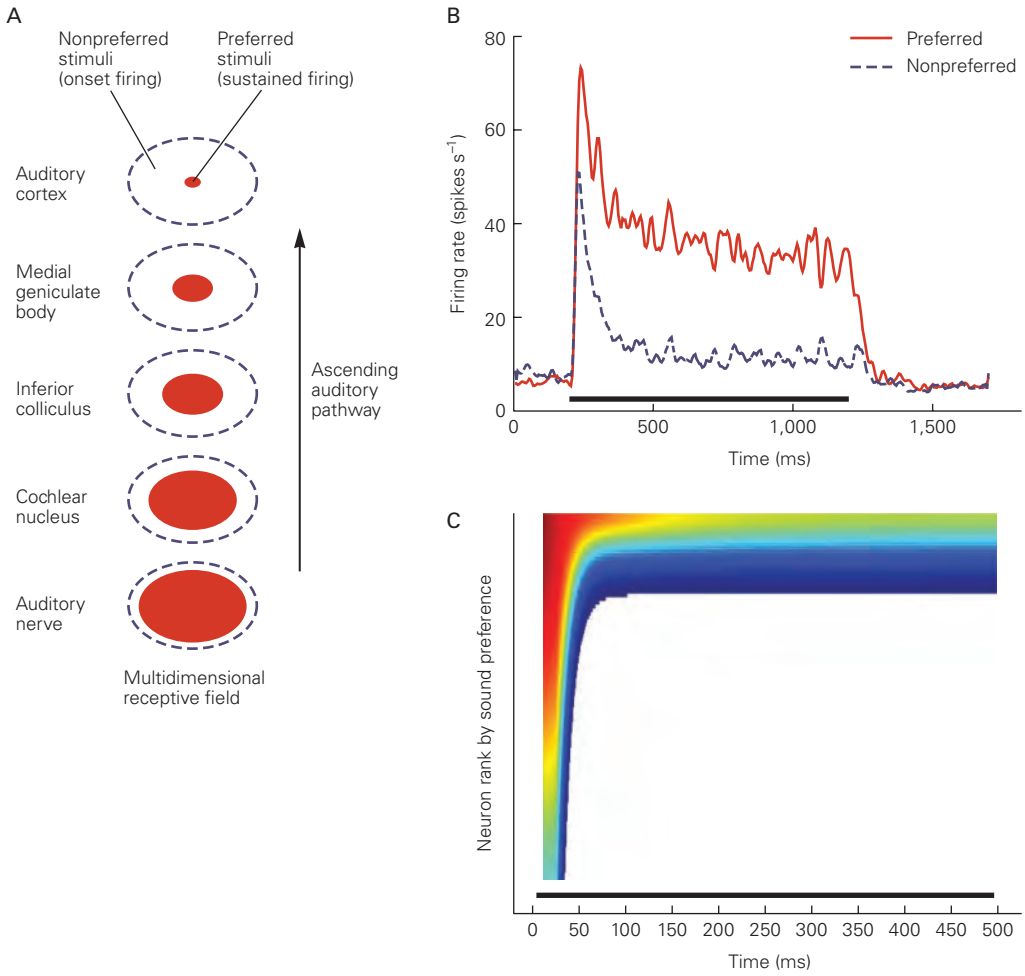

Figure 28–9 Stimulus selectivity increases along the ascending auditory pathway.

A. Stimulus selectivity and the relationship between sustained and onset firings along the ascending auditory pathway. Each open ellipse represents the multidimensional receptive field (RF) of a neuron illustrated on a two-dimensional plane. The filled ellipse represents the "sustained firing region" (corresponding to preferred stimuli) of a neuron's RF. The rest of the area within the RF is the "onset firing region" (corresponding to nonpreferred stimuli). A neuron exhibits sustained or onset firing depending on which region of the RF is stimulated. The neuron does not fire if stimuli fall outside the RF. (Adapted, with permission, from Wang 2018.)

B. Population-averaged firing rate in response to each neuron's preferred and nonpreferred stimuli from primary auditory cortex (A1). Extracellular recordings were made in awake marmoset monkeys. **Thick bar** = stimulus duration. (Adapted, with permission, from Wang et al. 2005. Copyright © 2005 Springer Nature.)

C. Distribution of activity among A1 neurons in response to a sound burst. On the *y*-axis, all A1 neurons are ranked according to their preference for a particular stimulus. The **blue-to-red color gradient** represents increasing firing rate. The neuron with the highest firing rate is located at the top end of the *y*-axis. **Black bar** = stimulus duration. Most neurons show a brief phasic response to the onset of the sound, but only those particularly tuned to the sound maintain their response until the end of the sound. (Adapted, with permission, from Middlebrooks 2005. Copyright © 2005 Springer Nature.)

The discovery of how sustained firing is evoked in the auditory cortex is important because it provides a direct link between neural firing and the perception of a continuous acoustic event. Such sustained firing by auditory cortex neurons has been observed only in awake animals. In contrast, an auditory nerve fiber typically shows sustains firing in response to a wide range of acoustic signals as long as the spectral energy of the stimulus falls within the neuron's receptive field, under either anesthetized or awake conditions. When David Hubel and his colleagues ventured into the auditory cortex more than half a century ago, they

were puzzled by how difficult it was to drive neurons in the auditory cortex of awake cats. Now we know it was because they were probably recording from highly selective neurons and using nonpreferred stimuli. The availability of digital technology since then has made it possible to create and test a large battery of acoustic stimuli in search of the preferred stimulus of a highly selective neuron in auditory cortex. The overall picture elucidated by experimenters is that when a sound is heard, the auditory cortex first responds with transient discharges (encoding the onset of a sound) across a relatively large population of neurons. As the time passes, the activation becomes restricted to a smaller population of neurons that are preferentially driven by the sound (Figure 28–9C), which results in a selective representation of the sound within the neuronal population and over time. Because each neuron has its own preferred stimulus that differs from preferred stimuli of other neurons, neurons in the auditory cortex collectively cover the entire acoustic space with their sustained firing regions. Therefore, any particular sound can evoke sustained firing throughout its duration in a particular population of neurons in the auditory cortex. In other words, the region of auditory cortex activated by acoustic stimulation in whole-brain imaging (eg, functional magnetic resonance imaging [fMRI], positron emission tomography [PET]) comprises neurons that are preferentially driven by the acoustic stimulus.

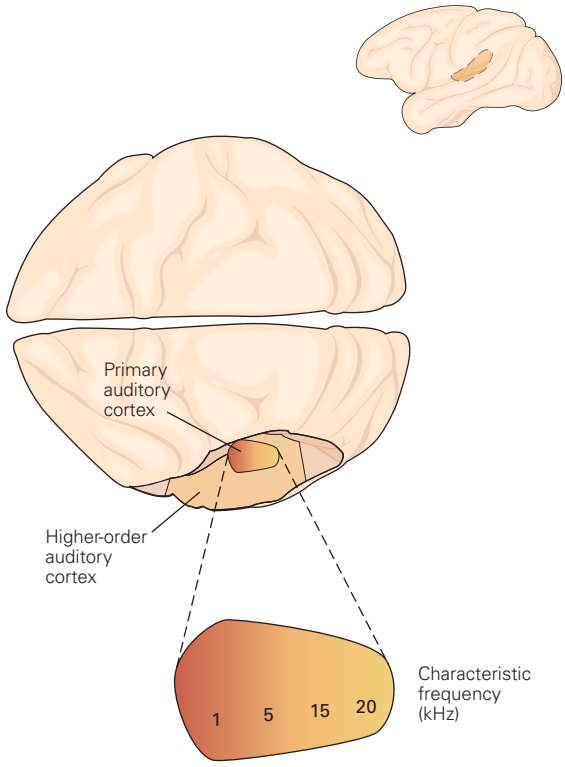

Figure 28–10 The auditory cortex of primates has multiple primary and secondary areas. The expanded figure of the primary auditory cortex shows its tonotopic organization. The primary areas are surrounded by higher-order areas (see Figure 28–11).

The Auditory Cortex Maps Numerous Aspects of Sound

The auditory cortex includes multiple distinct functional areas on the dorsal surface of the temporal lobe. The most prominent projection is from the ventral division of the medial geniculate nucleus to the primary auditory cortex (A1, or Brodmann's area 41). As in the subcortical structures, the neurons in this cytoarchitectonically distinct region are arranged tonotopically. In monkeys, neurons tuned to low frequencies are found at the rostral end of A1, while those responsive to high frequencies are in the caudal region (Figure 28–10). Thus, like the visual and somatosensory cortices, A1 contains a map reflecting the sensory periphery.

Because the cochlea encodes discrete frequencies at different points along the basilar membrane, however, a one-dimensional frequency map from the periphery is spread across the two-dimensional surface of the cortex, with a smooth frequency gradient in one direction and isofrequency contours along the other direction. In many species, subregions of the auditory cortex that represent biologically significant frequencies are larger than others because of extensive inputs, similar to the large area in the primary visual cortex devoted to inputs from the fovea.

In addition to frequency, other features of auditory stimuli are mapped in the primary auditory cortex, although the overall organization is less clear and precise than for vision. Auditory neurons in A1 are excited either by input from both ears (EE neurons), with the contralateral input usually stronger than the ipsilateral contribution, or by a unilateral input (EI). The EI neurons are inhibited by stimulation of the opposite ear.

Certain neurons in A1 also seem to be organized according to bandwidth, that is, according to their responsiveness to a narrow or broad range of frequencies. Neurons near the center of the isofrequency contours are tuned more narrowly to bandwidth or frequency than those located away from the center. Distinct subregions of A1 form clusters of cells with narrow or broadband tuning within individual isofrequency contours. Within intracortical circuits, neurons receive input primarily from neurons with similar bandwidths and characteristic frequencies.

This modular organization of bandwidth selectivity may allow redundant processing of incoming signals through neuronal filters of varying bandwidths as well as center frequencies, which could be useful for the analysis of spectrally complex sounds such as species-specific vocalizations, including speech.

Several other parameters are represented in A1. These include neuronal response latency, loudness, modulation of loudness, and the rate and direction of frequency modulation. Although it remains to be seen how these various maps intersect, this array of parameters clearly endows each neuron and each location in A1 with the ability to represent many independent variables of sound and thus allows for a great diversity of neuronal selectivity.

As is true for visual and somatosensory areas of the cortex, sensory representation in A1 can change in response to alterations in input pathways. After peripheral hearing loss, tonotopic mapping in A1 can be altered so that neurons that were previously responsive to sounds within the lost range of hearing will begin to respond to adjacent frequencies. The work of Michael Merzenich and others has shown that behavioral training of adult animals can also result in large-scale reorganization of the auditory cortex, so that the most behaviorally relevant frequencies—those specifically associated with attention or reinforcement—come to be overrepresented.

The auditory areas of young animals are particularly plastic. In rodents, the frequency organization of A1 emerges gradually during development from an early, crude frequency map. Raising animals in acoustic environments in which they are exposed to repeated tone pulses of a particular frequency results in a persistent expansion of cortical areas devoted to that frequency, accompanied by a general deterioration and broadening of the tonotopic map. This result not only suggests that the development of A1 is experience-dependent but also raises the possibility that early exposure to abnormal sound environments can create long-term disruptions of high-level sensory processing. A greater understanding of how this happens and whether it is also true for human fetuses and infants may provide insights into the origin and remediation of disorders in which central auditory processing is impaired, such as many forms of dyslexia. Moreover, the ability to induce plasticity in the auditory cortex of adults by engaging attention or reward raises new hopes for brain repair even in adulthood.

The primary auditory area of mammals is surrounded by multiple distinct regions, some of which are tonotopic. Adjacent tonotopic fields have mirror-image tonotopy: The direction of tonotopy reverses at the boundary between fields. In monkeys, as many as 7 to 10 secondary (belt) areas surround the three or four primary or primary-like (core) areas (see Figure 28–11). The secondary areas receive input from the core areas of the auditory cortex and, in some cases, from thalamic nuclei. Electrophysiological and imaging studies have confirmed that A1 in humans lies on Heschl's gyrus, in the temporal lobe, medial to the Sylvian fissure. In addition, recent fMRI studies have revealed that in humans, just as in monkeys, pure tones activate primarily core areas, whereas the neurons of belt areas prefer complex sounds such as narrowband noise bursts.

A Second Sound-Localization Pathway From the Inferior Colliculus Involves the Cerebral Cortex in Gaze Control

Many neurons in the auditory cortex have broad spatial tuning, but neurons with narrow spatial tuning are also found when studied in awake animals. In monkeys, auditory cortex neurons are tuned to both frontal space and rear space (outside the coverage of vision), as well as the space above and below the horizontal plane. In contrast to the auditory midbrain, however, there is yet no evidence for a spatially organized map of sound in any of the cortical areas sensitive to sound location.

The sound-localization pathways in the cortex originate in the central nucleus of the inferior colliculus and ascend through the auditory thalamus and the primary and secondary cortical areas, eventually reaching the frontal eye fields involved in gaze control. Eye or head movements can be elicited by stimulating the frontal eye fields, which connect directly to brain stem tegmentum premotor nuclei that mediate gaze changes as well as to the superior colliculus. But why should there be this second sound-localization pathway connected to gaze control circuitry when the midbrain pathway from location-sensitive neurons in the inferior colliculus to the superior colliculus to gaze control circuitry directly controls orientation movements of the head, eyes, and ears?

Behavioral experiments shed light on this question. Although lesions of A1 can result in profound sound-localization deficits, no deficiency is seen when the task is simply to indicate the side of the sound source by pushing a lever. The deficit becomes apparent only when the animal must approach the location of a brief sound source; that is, when the task is the more complex one of forming an image of the source, remembering it, and moving toward it.

Experiments in barn owls have produced particularly compelling evidence. The ability of owls to orient to sounds in space is unaffected by inactivation of the avian equivalent of the frontal eye fields. Similarly, when the midbrain sound localization pathway is disrupted by pharmacological inactivation of the superior colliculus, the probability of an accurate head turn is decreased, but animals still respond correctly more than half of the time. In contrast, when both structures are inactivated, animals are completely unable to orient accurately to acoustic stimuli on the contralateral side. Thus, cortical and subcortical sound-localization pathways have parallel access to gaze control centers, perhaps providing some redundancy. Moreover, when only the frontal eye fields are inactivated, birds lose their ability to orient their gaze toward a target that has been extinguished and must be remembered, just as is seen with mammalian A1 lesions. Thus, in both mammals and birds, cortical pathways are required for more complex sound-localization tasks.

This appears to be a general difference between cortical and subcortical pathways. Subcortical circuits are important for rapid and reliable performance of behaviors that are critical to survival. Cortical circuitry allows for working memory, complex recognition tasks, and selection of stimuli and evaluation of their significance, resulting in slower but more differentiated performance. Examples of this also exist in auditory pathways not involved in localization. Conditioned fear responses to simple auditory stimuli are mediated by direct rapid pathways from the auditory thalamus to the amygdala; they can still be elicited after cortical inactivation. However, fear responses that require more complex discrimination of auditory stimuli require pathways through the cortex and are accordingly slower but more specific.

Auditory Circuits in the Cerebral Cortex Are Segregated Into Separate Processing Streams

In the visual system, the output from the primary visual cortex is segregated into separate dorsal and ventral streams concerned respectively with object location in space and object identification. A similar division of labor is thought to exist in the somatosensory cortex, and recent evidence suggests that the auditory cortex also follows this plan.

Anatomical tracing studies of the three most accessible belt areas in monkeys show that the more rostral and ventral areas connect primarily to the more rostral and ventral areas of the temporal lobe, whereas the more caudal area projects to the dorsal and caudal temporal lobe. In addition, these belt areas and their temporal lobe targets both project to largely different areas of the frontal lobes (Figure 28–11).

The frontal areas receiving anterior auditory projections are generally implicated in nonspatial functions, whereas those that are targets of posterior auditory areas are implicated in spatial processing. Electrophysiological and imaging studies provide support for this. Caudal and parietal areas are more active when a stimulus must be localized or moves, and ventral areas are more active during identification of the same stimulus or analysis of its pitch. Thus anterior-ventral pathways may identify auditory objects by analyzing spectral and temporal characteristics of sounds, whereas the more dorsal-posterior pathways may specialize in sound-source location, detection of sound-source motion, and spatial segregation of sources.

Although the idea that all sensory areas of the cerebral cortex initially segregate object identification and location is attractive, it is likely an oversimplification. It is clear that the medial-belt areas of the auditory cortex project to both dorsal and ventral frontal cortices, and neurons with broad spatial responsiveness are distributed throughout caudal and anterior areas. Nonetheless, although the details may differ between systems, the basic concept holds that sensory systems deconstruct stimuli into features and analyze each type in discrete pathways.

The Cerebral Cortex Modulates Sensory Processing in Subcortical Auditory Areas

An intriguing feature of all mammalian cortical areas, and one shared by the auditory system, is the massive projection from the cortex back to lower areas. There are almost 10 times as many corticofugal fibers entering the sensory thalamus as there are axons projecting from the thalamus to the cortex. Projections from the auditory cortex also innervate the inferior colliculus, olivocochlear neurons, some basal ganglionic structures, and even the dorsal cochlear nucleus.

Insights into possible functions of this feedback have come from the bat's auditory system. Silencing of frequency-specific cortical areas leads to decreased responses in thalamus and inferior colliculus in the corresponding frequency-specific areas, whereas activation of cortical projections increases and sharpens the responses of some neurons. The auditory cortex can therefore actively adjust and improve auditory signal processing in subcortical structures. A variety of evidence suggests that cortical feedback also occurs in other mammals. This challenges the view of ascending

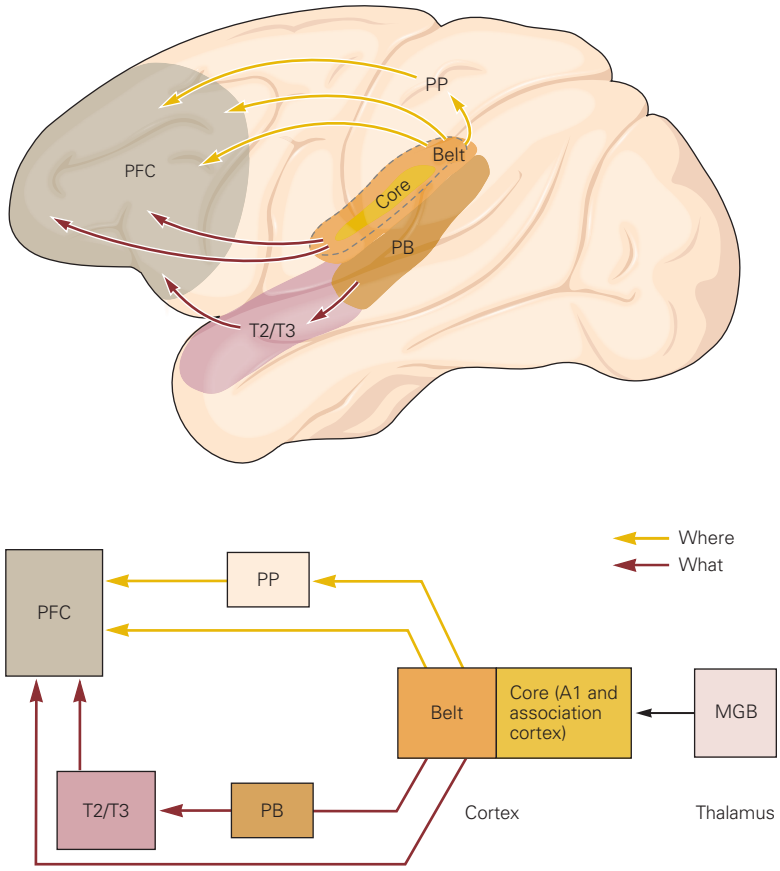

Figure 28–11 The "what" and "where" streams in the auditory cortical system of primates. The ventral "what" stream and dorsal "where" stream originate in different parts of primary and belt cortex and ultimately project to distinct regions of prefrontal cortex through independent paths. (**MGB**, medial geniculate body of the thalamus; **PB**, parabelt cortex; **PFC**, prefrontal cortex; **PP**, posterior parietal cortex; **T2/T3**, areas of temporal cortex.) (Adapted, with permission, from Rauschecker and Tian 2000. Copyright 2000 National Academy of Sciences; adapted from Romanski and Averbeck 2009.)

sensory pathways as purely feedforward circuits and suggests that we should regard the thalamus and cortex as reciprocally and highly interconnected circuits in which the cortex exercises some top-down control of perception.

The Cerebral Cortex Forms Complex Sound Representations

The Auditory Cortex Uses Temporal and Rate Codes to Represent Time-Varying Sounds

An important function of the auditory system is to represent time-varying sounds across multiple time scales, from a few milliseconds to tens and hundreds of milliseconds or even longer. In the auditory nerve, firing patterns largely mirror the temporal structure of sounds, firing in phase with sounds to the limit of the phase-locking. The precision of this temporally based neural representation gradually decreases as information ascends toward the auditory cortex due to synaptic integration at the soma and dendrites.

The upper limit of the phase-locking to periodic sounds progressively decreases along the ascending auditory pathway from approximately 3,000 Hz in the auditory nerve to less than approximately 300 Hz in the medial geniculate body in the thalamus and less than 100 Hz in A1. The upper limit of the phase-locking in A1 is similar to that found in the primary visual and somatosensory areas of cortex. In the auditory cortex, the temporal firing pattern alone is inadequate to represent the entire range of time-varying sounds that are perceived by humans and animals.

Cortical neurons use an alternative method to represent time-varying sounds that change more rapidly than the upper limit of the phase-locking in A1. When an animal listens to a sequence of periodic clicks, two types of neural responses are observed in A1. One population of neurons displays phase-locked periodic firing in response to click trains with long intervals between clicks or slowly varying sounds, but not to click trains with short intervals between clicks or rapidly varying sounds (Figure 28–12A). The second population of neurons does not respond to click trains

at long interclick intervals, but instead fires increasingly rapidly as the interclick interval becomes shorter (Figure 28–12B). These two populations of A1 neurons, referred to as *synchronized* and *nonsynchronized*, respectively, have complementary response properties. Neurons of the synchronized population *explicitly* represent slowly occurring sound events by synchronized neural firing (a temporal code), whereas neurons of the nonsynchronized population *implicitly* represent rapidly changing sound events by changes in average firing rates (a rate code).

The nonsynchronized neurons have been observed in the auditory cortex of awake primates and rodents. In A1, neural representation changes from a temporal code to a rate code at the interclick interval of about 25 ms, corresponding to a repetition rate of approximately 40 Hz (Figure 28–12A,B). This is near the boundary where our perception of a periodic click train changes from being "discrete" to "continuous."

The combination of temporal and rate codes to represent the whole range of time-varying sounds is the consequence of a progressive transformation beginning in the auditory nerve, where only a temporal code (phase-locking) is available. The progressive reduction in the upper limit of the phase-locking along the ascending auditory pathway is accompanied by the emergence of firing-rate-based representations. In the medial geniculate body of the thalamus, the intersection between temporal and rate codes is at a shorter interclick interval than in A1 (Figure 28–12C). This indicates that neurons in the medial geniculate body can phase-lock to more rapidly time-varying sounds than A1 neurons, but still utilize a rate code to represent rapidly changing sounds beyond their phase-locking limit.

The prevalence of rate-coding neurons in A1 has important functional implications. It shows that a considerable transition from temporal to rate coding has taken place by the time auditory signals reach the auditory cortex. The importance of the nonsynchronized neural responses is that they represent transformed instead of preserved temporal information. It suggests that cortical processing of sound streams operates on a segment-by-segment basis rather than on a moment-by-moment basis, as found in the auditory nerve. This is necessary for complex integration because higher-level processing tasks require temporal integration over a time window. The reduction in A1 of the upper limit of phase-locking is a prerequisite for multisensory integration in the cerebral cortex. Auditory information is encoded at the periphery at a much faster temporal modulation rate than visual or tactile information, but phase-locking is similar across

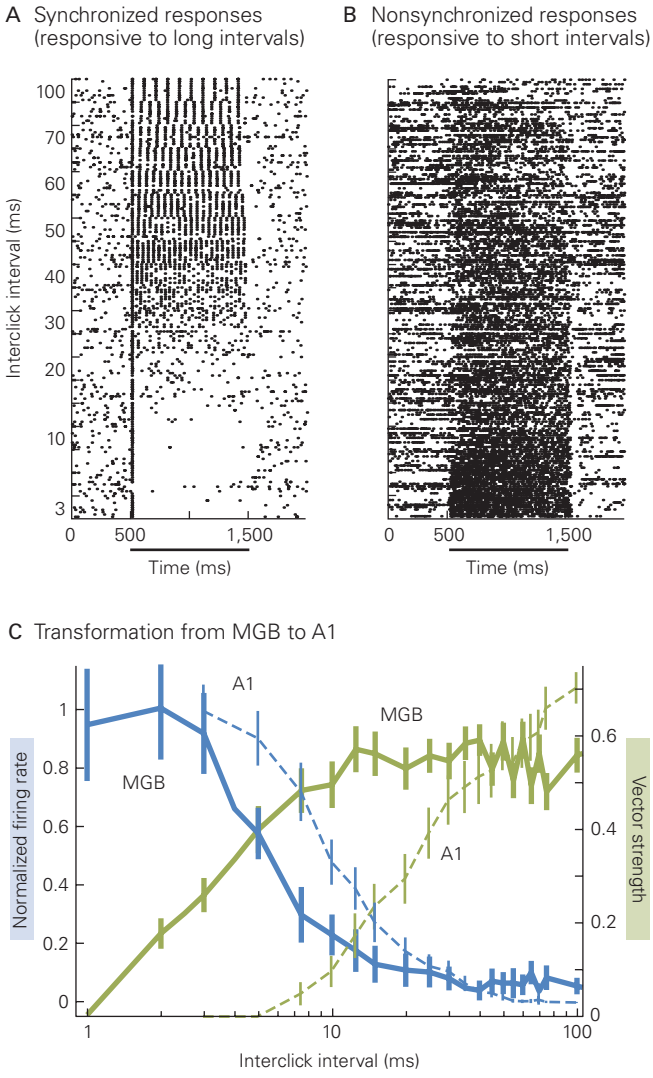

Figure 28–12 Temporal and rate coding of time-varying sounds.

A. Stimulus-synchronized responses of a neuron to periodic click trains recorded from A1 of an awake marmoset. The horizontal bar below the *x*-axis indicates the duration of the stimulus. (Adapted, with permission, from Lu, Liang, and Wang 2001. Copyright © 2001 Springer Nature.)

B. Nonsynchronized responses of a neuron to periodic click trains recorded from A1 in an awake marmoset. (Adapted, with permission, from Lu, Liang, and Wang 2001. Copyright © 2001 Springer Nature.)

C. Comparison of temporal response properties between primary auditory cortex (**A1**) and medial geniculate body of the thalamus (**MGB**). Stimulus-synchronized responses are quantified by vector strength, a measure of the strength of phase-locking. Nonsynchronized responses are quantified by the normalized firing rate (data curves identified as A1 rate and MGB rate). Error bars represent standard error of the mean. (Adapted, with permission, from Bartlett and Wang 2007.)

primary sensory areas of the cortex. The slowing of the phase-locking limit along the ascending auditory pathway and accompanying transition from a temporal code to a rate code are necessary for auditory information to be integrated in the cerebral cortex with information from other sensory modalities that are intrinsically slower.

Primates Have Specialized Cortical Neurons That Encode Pitch and Harmonics

Pitch perception is crucial for perceiving speech and music and for recognizing auditory objects in a complex acoustic environment. Pitch is the percept that allows harmonically structured periodic sounds to be perceived and ordered on a musical scale. Pitch carries crucial linguistic information in tonal languages such as Chinese and prosodic information in European languages. We use pitch to identify a particular voice from a noisy background in a cocktail party. When listening to an orchestra, we hear the melody of the soloist over the background of accompanying instruments.

An important phenomenon for understanding pitch is the perception of "missing fundamental," also referred to as the residue pitch. When the harmonics of a fundamental frequency are played together, the pitch is perceived as the fundamental frequency even if the fundamental frequency is missing. For example, the harmonics of the fundamental frequency of 200 Hz are at 400, 600, 800 Hz, and so on. Playing the frequencies 400, 600, and 800 Hz together will generate a pitch perception of 200 Hz, even though a distinct frequency component of 200 Hz is not physically present in the sound. We encounter this phenomenon routinely when we listen to music over speakers that are too small to generate sounds at low frequencies.

Many combinations of frequencies can give rise to a common fundamental frequency or pitch, making it a particularly valuable auditory cue. This is especially useful when pitch conveys behaviorally important information, as in the case of human speech or animal vocalizations. Sounds propagated through the environment can become spectrally degraded, losing high or low frequencies. While such spectral filtering distorts spectral information, the perception of the missing fundamental is robust despite the loss of some harmonic components.

The ability to perceive pitch is not unique to humans; birds, cats, and monkeys can also pick out pitch. Monkeys are capable of spectral pitch discrimination, melody recognition, and octave generalization, each of which requires the perception of pitch. Marmoset monkeys (*Callithrix jacchus*), a highly vocal New World primate species whose hearing range is similar to that of humans, exhibit human-like pitch perception. Marmosets are able to discriminate a missing fundamental in harmonic sounds with a precision as small as one semitone for the periodicity above 440 Hz.

Given that both humans and some animals experience a pitch that generalizes across a variety of sounds with the same periodicity (including harmonic sounds with a missing fundamental), it is reasonable to expect that some neurons extract pitch from complex sounds. Xiaoqin Wang and his colleagues discovered a decade ago that a small region in the auditory cortex of marmoset monkeys contains "pitch-selective neurons." These neurons are tuned to pure tones with a best frequency and respond to harmonic complexes with a fundamental frequency near its best frequency even when the harmonics lay outside the neuron's excitatory-frequency response area (Figure 28–13A).

A pitch-selective neuron responds to pitch-evoking sounds (eg, harmonic sounds, click trains) when the pitch is near the neuron's preferred best frequency. Pitch-selective neurons increase their firing rates as the behavioral salience of pitch increases and prefer sounds with periodicity over aperiodic sounds. It is important to note that the pitch-selective neurons in marmoset monkeys, which extract and code for pitch embedded in harmonic sounds (a highly nonlinear computation), are distinctly different from neurons in subcortical areas or A1 that merely "reflect" information on pitch in their firing patterns.

The region containing the pitch-selective neurons in marmoset monkeys is confined to the low-frequency border of A1, the rostral auditory cortex (area R), and lateral belt areas (Figure 28–13B). Human imaging studies have identified a restricted region at the lateral end of Heschl's gyrus anterolateral to A1 that extracts pitch of harmonic complex sounds and is sensitive to changes in pitch salience. The location of this region mirrors the location of the pitch center in marmoset monkeys (Figure 28–13B).

The core regions of auditory cortex in marmosets also contain a class of harmonic template neurons that respond weakly or not at all to pure tones or two-tone combinations but respond strongly to particular combinations of multiple harmonics. The harmonic template neurons show stronger responses to harmonic sounds than inharmonic sounds and selectivity for particular harmonic structures. In contrast to the pitch-selective neurons that are localized within a small cortical region lateral to the low-frequency border between A1 and R and have best frequencies

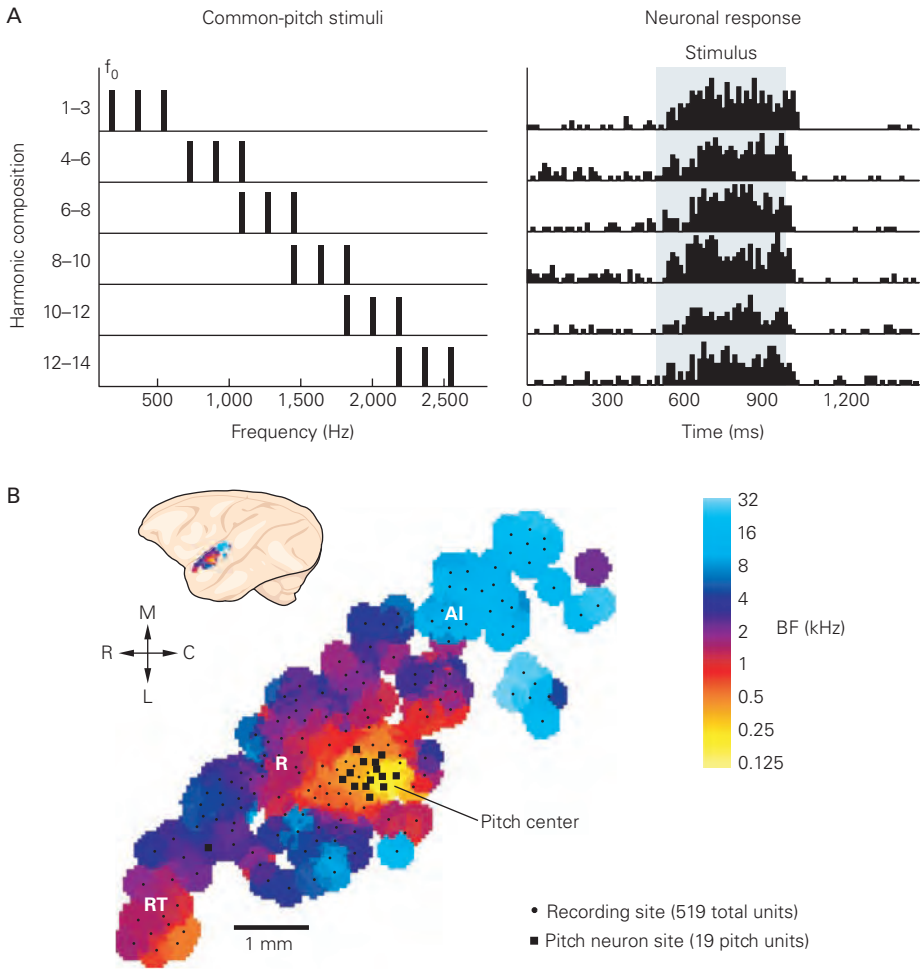

Figure 28–13 Pitch is encoded by specialized neurons in primate auditory cortex.

A. An example of a pitch-selective neuron recorded from marmoset auditory cortex. *Left*: Frequency spectra of a series of harmonic stimuli that share the same fundamental frequency (f_0). *Right*: Peristimulus time histogram of the neuron's response to the stimuli (stimulus duration indicated by the shaded region). (Adapted, with permission, from Bendor and Wang 2005. Copyright © 2005 Springer Nature.)

B. Anatomical organization of the marmoset auditory cortex and the location of a pitch center. **Top:** Side view of the marmoset brain. **Bottom:** Tonotopic map of the left auditory cortex characterized in one marmoset. Pitch-selective neurons (**black squares**) are clustered near the low-frequency border between A1 and area **R** (rostral auditory cortex). Frequency reversals indicate the borders between A1/R and **R/RT** (rostrotemporal auditory cortex). (**BF**: best frequency.) (Adapted from Bendor and Wang 2005. Copyright © 2005 Springer Nature.)

less than 1,000 Hz, the harmonic template neurons are distributed across A1 and R and have best frequencies ranging from approximately 1 kHz to approximately 32 kHz, a range that covers the entire hearing range of marmosets.

Whereas in the periphery single auditory nerve fibers encode individual components of harmonic sounds, the properties of the harmonic template neurons reveal harmonically structured receptive fields for extracting harmonic patterns. The change in neural representation of harmonic sounds from auditory nerve fibers to the auditory cortex reflects a principle of neural coding in sensory systems. Neurons in sensory pathways transform the representation of physical features, such as the frequency of sounds in hearing or luminance of images in vision, into a representation of perceptual features, such as pitch in hearing or curvature in vision. Such features lead to the formation of auditory or visual percepts. The harmonic template neurons in the auditory cortex are key to processing sounds with harmonic structures such as animal vocalizations, human speech, and music.

Insectivorous Bats Have Cortical Areas Specialized for Behaviorally Relevant Features of Sound

Although it is generally assumed that upstream auditory areas perform increasingly specialized functions related to hearing, much less is known about the functions of serial relays in the auditory system compared to the visual system. In humans, one of the most important aspects of audition is its role in processing language, but we know relatively little about how speech sounds are analyzed by neural circuits. New techniques for imaging the human brain are gradually providing insights into the functional specialization of cortical areas associated with language (Chapter 55).

Evidence for specialized analysis of complex auditory signals in the cerebral cortex comes from studies of insectivorous bats. These animals find their prey almost entirely through *echolocation*, emitting ultrasonic pulses of sound that are reflected by flying insects. Bats analyze the timing and structure of the echoes to help locate and identify the targets, and discrete auditory areas are devoted to processing different aspects of the echoes.

Many bats, such as the mustached bat studied by Nobuo Suga and his collaborators, emit echolocating pulses with two components. An initial *constant-frequency* (CF) component consists of several harmonically related sounds. These harmonics are emitted stably for tens to hundreds of milliseconds, akin to human vowel sounds. The constant-frequency component is followed by a sound that decreases steeply in frequency, the *frequency-modulated* (FM) component, which resembles the rapidly changing frequency of human consonants (Figure 28–14A).

The FM sounds are used to determine the distance to the target. The bat measures the interval between the emitted sound and the returning echo, which corresponds to a particular distance, based on the relatively constant speed of sound. Neurons in the FM-FM area of auditory cortex (Figure 28–14B) respond preferentially to pulse-echo pairs separated by a specific delay. Moreover, these neurons respond better to particular combinations of sounds than to the individual sounds in isolation; such neurons are called *feature detectors* (Figure 28–14C). The FM-FM area contains an array of such detectors, with preferred delays systematically ranging from 0.4 to 18 ms, corresponding to target ranges of 7 to 280 cm (Figure 28–14B). These neurons are organized in columns, each of which is responsive to a particular combination of stimulus frequency and delay. In this way, the bat, like the barn owl in its inferior colliculus, is able to represent an acoustic feature that is not directly represented by sensory receptors.

The CF components of bat calls are used to determine both the speed of the target relative to the bat and the acoustic image of the target. When an echolocating bat is flying toward an insect, the sounds reflected from the insect are Doppler-shifted to a higher frequency at the bat's ear, for the bat is moving toward the returning sound waves from the target, causing a relative speeding up of these waves at its ear. Similarly, a receding insect yields reflections of lowered frequency at the bat's ear. Neurons in the CF-CF area (Figure 28–14B) are sharply tuned to a combination of frequencies close to the emitted frequency or its harmonics. Each neuron responds best to a combination of a pulse of a particular fundamental frequency with an echo corresponding to the first or second harmonic of the pulse, Doppler-shifted to a specific extent. As in the FM-FM area, neurons do not respond to the pulse or echo alone, but rather to the combination of the two CF signals.

CF-CF neurons are arranged in columns, each encoding a particular combination of frequencies. These columns are arranged regularly along the cortical surface, with the fundamental frequency along one axis and the echo harmonics along a perpendicular axis. This dual-frequency coordinate system creates a map wherein a specific location corresponds to a particular Doppler shift and thus a particular target velocity, ranging systematically from –2 m/s to 9 m/s.

The CF components of returning echoes are also used for detailed frequency analysis of the acoustic image, presumably important in its identification. The Doppler-shifted constant-frequency area (DSCF) of the mustached bat is a dramatic expansion of the primary auditory cortex's representation of frequencies between 60 kHz and 62 kHz, corresponding well to the set of returning echoes from the major CF component of the bat's call (Figure 28–14B). Within the DSCF area, individual neurons are extremely sharply tuned to frequency, so that the tiny changes in frequency created by fluttering moth wings are easily detected.

Transient inactivation of some of these specialized cortical areas while the bat performs a discrimination task strikingly supports the importance of their functional specialization in behavior. Silencing of the DSCF selectively impairs fine frequency discrimination while leaving time perception intact. Conversely, inactivation of the FM-FM area impairs the bat's ability to detect small differences in the time of arrival of two echoes, while leaving frequency perception unchanged.

Investigation of this auditory system was greatly facilitated by knowledge of the stimuli relevant to bats. It remains to be seen whether these cortical areas are functionally or anatomically analogous to particular

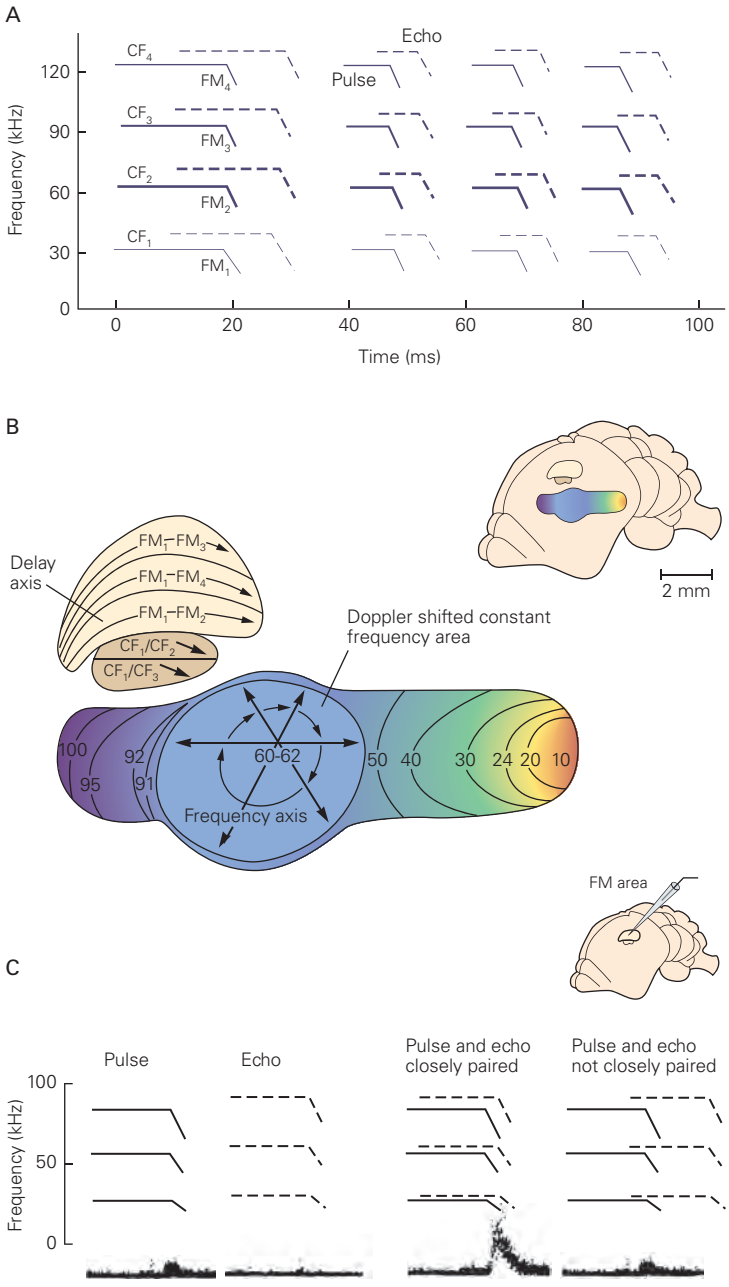

Figure 28–14 The auditory system of the bat has specialized areas for locating sounds.

A. A sonogram of an animal's calls (**solid lines**) and the resultant echoes (**dashed lines**) illustrates the two components of the call: the protracted, harmonically related constant-frequency (**CF**) signal and the briefer frequency-modulated (**FM**) signal. The duration of the calls declines as the animal approaches its target. (Adapted, with permission, from Suga 1984.)

B. A view of the cerebral hemisphere of the mustached bat shows three of the functional areas within the auditory cortex. The FM area is where the distance from the target is computed; the CF area is where the velocity of the target is computed; and the Doppler-shifted CF area is specialized for the identification of small fluttering objects. The expanded cortical representation of Doppler-shifted CF signals near the second harmonic of the call frequency (60–62 kHz) forms the acoustic "fovea." (Adapted, with permission, from Suga 1984.)

C. The FM-FM combination-sensitive neuron shown does not respond significantly to either pulses or echoes alone, but responds very strongly to a closely paired pulse-echo. However, the neuron is also sensitive to the time difference between the pulse and echo, as seen in the record on the right, where the neuron fails to respond to a pulse-echo combination that is not closely paired. (Adapted, with permission, from Suga et al. 1983.)

fields in cats, monkeys, and humans. Regardless, the choice of appropriate stimuli is likely to be as important in studying these other species as it has been in studies of bats.

The Auditory Cortex Is Involved in Processing Vocal Feedback During Speaking

Vocal communication involves both speaking and hearing, often taking place concurrently. When we speak, the sound of our voice is delivered not only to the intended listener but also back to our own ears. Such feedback to our auditory system during vocal production is conducted not only through the air but also through bone and can be loud as a result of the proximity of the mouth and the ears.

The auditory system must distinguish an auditory percept as being self-generated or externally generated. To monitor external sounds from the acoustic environment during speaking, self-generated sounds have to be masked. At the same time, the auditory system must also monitor our own voice in order to detect errors in vocal production. An accurate representation of one's own voice through vocal feedback is crucial to maintaining desired vocal production and to the learning of a new language. In humans and animals, perturbations of the vocal feedback can lead to alterations in vocal production, and interruptions or blockages of the vocal feedback can result in degradation in vocal learning.

The evidence for the involvement of the auditory cortex in processing vocal feedback comes from both human and animal studies. Responses in the auditory cortex of human subjects to their own voice while speaking are smaller than the responses to the playback of the same sounds. This reduction can be observed in electrocorticographical (ECoG) recordings (Figure 28–15A) or with a variety of imaging methods (eg, fMRI, PET, magnetoencephalography [MEG]).

Single-neuron recordings from the auditory cortex of vocalizing monkeys have shown that self-initiated vocalizations result in suppression of cortical responses to monkeys' own vocalizations, of external sounds heard during vocalization, and also spontaneous activity (Figure 28–15B). Because in many instances firing rates are suppressed to below spontaneous activity, the suppression is likely caused by inhibition. Neurons suppressed by self-initiated vocalizations show frequency and intensity tuning, as is typical of auditory cortical neurons, and respond to the playback of vocalizations.

The vocalization-induced suppression begins several hundred milliseconds prior to the onset of vocalization (Figure 28–15B), suggesting that these neurons receive modulatory signals originating in vocal production circuits. In humans, vocal production is carried out by cortical areas in the frontal lobe, from Broca's area to premotor and motor cortex. In humans and monkeys, axons from the premotor cortex to auditory regions of the superior temporal gyrus have been described, and presumably, they mediate the vocalization-induced suppression. This modulatory connection is not active when humans or monkeys simply listen to vocal sounds played to them.

Why do we suppress our auditory cortex when we speak? A simple answer is that this suppression helps reduce the masking effect of our own voice, which can be very loud. A more interesting answer is that this suppression results from a vocal feedback-monitoring network in auditory cortex. In humans, there is less or no suppression of auditory cortex if vocal feedback is experimentally altered through earphones, for example, when the pitch of the voice is shifted (Figure 28–15A). In marmoset monkeys, neurons suppressed by self-initiated vocalizations may become less suppressed or even excited when the animal hears its own frequency-shifted vocalizations (Figure 28–15C). This sensitivity to feedback perturbations suggests that neurons exhibiting vocalization-induced suppression are part of a network responsible for monitoring vocal feedback signals. The presence of vocal feedback-related neural activity in the auditory cortex of both humans and monkeys suggests that the auditory cortex combines both internal modulation and vocal feedback responses, rather than merely responding to sensory signals coming through the ears.

Not all neurons in the auditory cortex are suppressed by speaking or vocalizing. A smaller proportion (~30%) of neurons in marmoset A1 increase their responses during self-initiated vocalizations, consistent with their auditory response characteristics. In contrast to vocalization-induced suppression, vocalization-related excitation begins after the onset of vocalization and is likely the result of feedback through the ascending auditory pathway. The vocalization-related excitation may help maintain the sensitivity of the auditory cortex to the external acoustic environment during speaking or vocalizing.

Vocalization-induced suppression of auditory responses has been observed in several mammalian subcortical structures, including the brain stem and inferior colliculus. Such suppression begins a few milliseconds before or is synchronized with vocal production. In contrast, cortical suppression begins several hundred milliseconds before the vocal onset. It is possible that subcortical suppression of auditory responses during speaking or vocalizing is initiated by cortical commands.

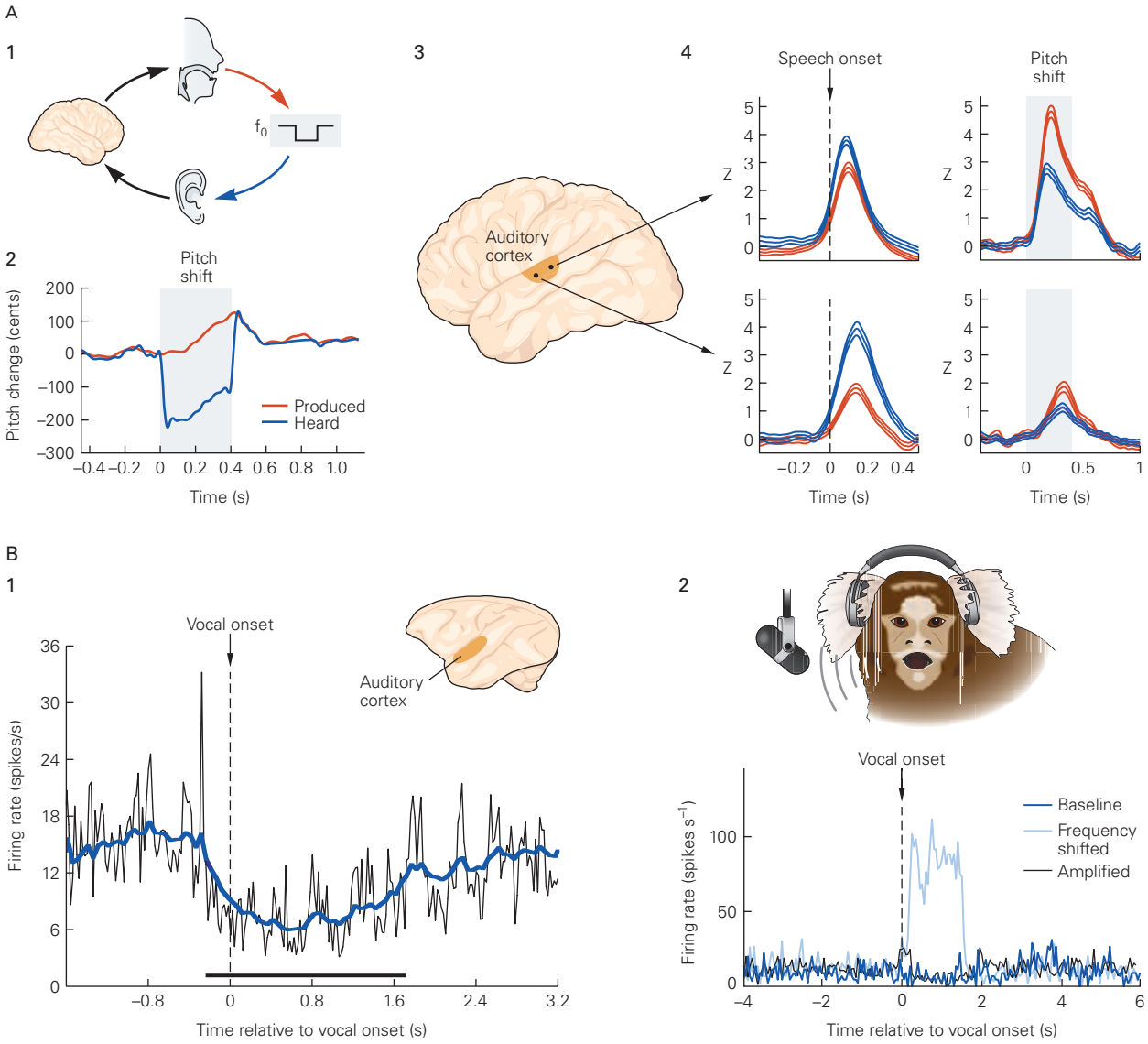

Figure 28–15 Vocal feedback processing in auditory cortex.

A. Examples of vocalization-induced suppression and sensitivity to pitch perturbation in human cerebral cortex. **1.** A subject's vocalizations (**red arrow**) went through a digital signal processor that shifted pitch and delivered the distorted auditory feedback (**blue arrow**) to the subject's earphones. **2.** Pitch track of an example trial shows the pitch recorded by the microphone (produced) and the pitch delivered to the earphones (heard). Shaded region indicates the time interval when the signal processor shifted the pitch by –200 cents (1 cent = 1/1200 octave). **3.** The locations of electrodes that recorded from two sites in the auditory cortex on the surface of the superior temporal gyrus. **4.** The Z variable represents the power in the 50 to 150 Hz (high-γ) range of cortical activity, which has been shown to correlate well with neuronal spiking activity. It was extracted from the signals recorded at each electrode in the speaking (**red**) and listening (**blue**) conditions. Vertical lines in the left column of plots indicate vocalization onset, and shaded regions in the right column of plots indicate the onset and offset of perturbation. The response of a subject's auditory cortex to his or her own self-produced vocalization is generally smaller than the response seen when the subject passively listens to playback of the same vocalization (*left column).* The response of auditory cortex to the perturbation during active phonation (speaking) is enhanced (*right column*). (Adapted, with permission, from Houde and Chang, 2015.)

B. 1. Vocalization-induced suppression of neural activity in marmoset monkey auditory cortex. Population-averaged firing rate of all vocalization-suppressed responses are aligned by vocal onset (a "Phee" call). The **blue line** is a moving average (100 ms window) and shows that suppression begins prior to vocalization (indicated by **arrow**). The **thick bar** indicates the period over which suppression is continuously significant (P <0.05). (Adapted, with permission, from Eliades and Wang 2003.)

2. Neurons subject to vocalization-induced suppression are sensitive to vocal feedback perturbations. **Top:** Self-produced vocalizations with or without feedback alterations were delivered to the marmoset through a customized headphone. **Bottom:** This auditory cortical neuron was suppressed during normal vocalization (**dark blue**) but showed a large increase in firing rate when the auditory feedback of the vocalization was shifted in the frequency domain (**light blue**). Amplifying auditory feedback alone did not generate firing rate changes (**black**). (Adapted, with permission, from Eliades and Wang 2008; Crapse and Sommer 2008.)

Highlights

1. Sound impinging on two ears carries information that the brain uses to compute where sounds arise and what they mean. Sounds are characterized by the amount of energy at one or more frequencies. To determine where sounds arise in the horizontal plane, many mammals compute differences in the time of arrival at the two ears for sounds less than approximately 3,000 Hz. To determine where sounds arise in the vertical dimension and whether they arise from the front or the back, mammals use spectral filtering of sounds greater than approximately 6,000 Hz by the head, shoulders, and external ears.
2. Acoustic information is brought to the brain from the cochlea by auditory nerve fibers, each sharply tuned to a narrow range of frequencies and together representing the entire hearing range of the animal. Auditory nerve fibers terminate in the ventral and dorsal cochlear nuclei, distributing acoustic information to four major groups of principal cells that form parallel ascending pathways through the brain stem. The topographic organization of the auditory nerve inputs imparts a tonotopic organization to the ipsilateral cochlear nuclei that is preserved all along the auditory pathway, including auditory cortex.
3. A marked feature of auditory neurons at processing stations along the ascending pathway is their progressively increasing stimulus selectivity.
4. The ventral cochlear nucleus extracts three features of sounds: (a) The monaural pathways through octopus cells of the ventral cochlear nucleus, the superior paraolivary nucleus, and ventral nucleus of the lateral lemniscus detect coincident firing of auditory nerve fibers that is useful for detecting onsets and gaps in sounds. (b) Stellate cells detect and sharpen the encoding of spectral peaks and valleys and convey that spectral information to the dorsal cochlear nucleus, olivocochlear neurons in the ventral nucleus of the lateral lemniscus, ventral nucleus of the lateral lemniscus, inferior colliculus, and thalamus. Spectral information is used for understanding the meaning of sounds and for localizing their sources. (c) Bushy cells sharpen and convey information about the fine structure of sounds, which is used in the binaural pathways through the medial and lateral superior olivary nuclei to make the interaural comparisons of timing and intensity of sounds at the two ears, which are used to localize sound sources along the azimuth.
5. The dorsal cochlear nucleus integrates acoustic signals with somatosensory information in its principal cells. Somatosensory information helps distinguish the spectral cues generated by an animal's own movements, which are biologically uninteresting, from those that arise from the environment.
6. Auditory brainstem pathways converge in the inferior colliculus. The inferior colliculus feeds acoustic information through the medial geniculate body of the thalamus to auditory cortex.
7. A projection from the inferior colliculus carries information about the location of sounds to the superior colliculus, a part of the brain that controls reflexive orienting movements of the head and eyes.
8. Within auditory cortex, auditory neurons continue to become more selective to the stimuli to which they respond. Subregions of the auditory cortex represent different biologically significant features such as pitch of tones that form harmonic complexes. Auditory cortex also transforms rapidly varying features of sounds into firing-rate-based representations, while representing slowly varying sounds using spike timing.
9. Auditory circuits in the cerebral cortex are segregated into separate processing streams, with dorsal and ventral streams concerned respectively with sound location in space and sound identification.
10. The cerebral cortex modulates processing in subcortical auditory areas. Projections from the auditory cortex innervate the thalamus, inferior colliculus, olivocochlear neurons, some basal ganglionic structures, and even the dorsal cochlear nucleus.
11. Auditory cortex is involved in processing vocal feedback signals during speaking. Speaking induces suppression of neural activity in auditory cortex that begins several hundred milliseconds prior to the vocal onset. This suppression results from a vocal feedback-monitoring network that functions to guide vocal production and learning.

Donata Oertel
Xiaoqin Wang

Selected Reading

Bendor DA, Wang X. 2005. The neuronal representation of pitch in primate auditory cortex. Nature 436:1161–1165.

Chase SM, Young ED. 2006. Spike-timing codes enhance the representation of multiple simultaneous sound-localization cues in the inferior colliculus. J Neurosci 26:3889–3898.

Eliades SJ, Wang X. 2008. Neural substrates of vocalization feedback monitoring in primate auditory cortex. Nature 453:1102–1106.

Gao E, Suga N. 2000. Experience-dependent plasticity in the auditory cortex and the inferior colliculus of bats: role of the corticofugal system. Proc Natl Acad Sci U S A 97:8081–8086.

Hofman PM, Van Riswick JG, Van Opstal AJ. 1998. Relearning sound localization with new ears. Nat Neurosci 1:417–421.

Joris PX, Smith PH, Yin TC. 1998. Coincidence detection in the auditory system: 50 years after Jeffress. Neuron 21:1235–1238.

Joris PX, Yin TCT. 2007. A matter of time: internal delays in binaural processing. Trends Neurosci 30:70–78.

Oertel D, Young ED. 2004. What's a cerebellar circuit doing in the auditory system? Trends Neurosci 27:104–110.

Schneider DM, Mooney R. 2018. How movement modulates hearing. Annu Rev Neurosci 41:553–572.

Schreiner CE, Read HL, Sutter ML. 2000. Modular organization of frequency integration in primary auditory cortex. Annu Rev Neurosci 23:501–529.

Suga N. 1990. Cortical computational maps for auditory imaging. Neural Netw 3:3–21.

Wang X. 2018. Cortical coding of auditory features. Annu Rev Neurosci 41:527–552.

Zhang LI, Bao S, Merzenich MM. 2001. Persistent and specific influences of early acoustic environments on primary auditory cortex. Nat Neurosci 4:1123–1130.

References

Bartlett EL, Wang X. 2007. Neural representations of temporally-modulated signals in the auditory thalamus of awake primates. J Neurophysiol 97:1005–1017.

Bendor DA, Wang X. 2006. Cortical representations of pitch in monkeys and humans. Curr Opin Neurobiol 16:391–399.

Brodal A. 1981. *Neurological Anatomy in Relation to Clinical Medicine*. New York: Oxford Univ. Press.

Cajal SR. 1909. *Histologie du Systeme Nerveux de l'Homme et des Vertebres.* Paris: A. Maloine.

Cariani PA, Delgutte B. 1996. Neural correlates of the pitch of complex tones. I. Pitch and pitch salience. J Neurophysiol 76:1698–1716.

Cohen YE, Knudsen EI. 1999. Maps versus clusters: different representations of auditory space in the midbrain and forebrain. Trends Neurosci 22:128–135.

Crapse TB, Sommer MA. 2008. Corollary discharge circuits in the primate brain. Curr Opin Neurobiol 18:552–557.

Darrow KN, Maison SF, Liberman MC. 2006. Cochlear efferent feedback balances interaural sensitivity. Nat Neurosci 9:1474–1476.

Eliades SJ, Wang X. 2003. Sensory-motor interaction in the primate auditory cortex during self-initiated vocalizations. J Neurophysiol 89:2194–2207.

Feng L, Wang X. 2017. Harmonic template neurons in primate auditory cortex underlying complex sound processing. Proc Natl Acad Sci U S A 114:E840–E848.

Gao L, Kostlan K, Wang Y, Wang X. 2016. Distinct subthreshold mechanisms underlying rate-coding principles in primate auditory cortex. Neuron 91:905–919.

Geisler CD. 1998. *From Sound to Synapse, Physiology of the Mammalian Ear.* New York: Oxford Univ. Press.

Houde JF, Chang EF 2015. The cortical computations underlying feedback control in vocal production. Curr Opin Neurobiol 33:174–181.

Hubel DH, Henson CO, Rupert A, Galambos R. 1959. Attention units in the auditory cortex. Science 129:1279–1280.

Jeffress LA. 1948. A place theory of sound localization. J Comp Physiol Psychol 41:35–39.

Kanold PO, Young ED. 2001. Proprioceptive information from the pinna provides somatosensory input to cat dorsal cochlear nucleus. J Neurosci 21:7848–7858.

King AJ. 1999. Sensory experience and the formation of a computational map of auditory space in the brain. BioEssays 21:900–911.

King AJ, Bajo VM, Bizley JK, et al. 2007. Physiological and behavioral studies of spatial coding in the auditory cortex. Hear Res 229:106–115.

Liberman MC. 1978. Auditory-nerve response from cats raised in a low-noise chamber. J Acoust Soc Am 63:442–455.

Lu T, Liang L, Wang X. 2001. Temporal and rate representations of time-varying signals in the auditory cortex of awake primates. Nature Neurosci 4:1131–1138.

Merzenich MM, Knight PL, Roth GL. 1975. Representation of cochlea within primary auditory cortex in the cat. J Neurophysiol 38:231–249.

Mesgarani N, Cheung C, Johnson K, Chang EF. 2014. Phonetic feature encoding in human superior temporal gyrus. Science 343:1006–1010.

Middlebrooks JC. 2005. Auditory cortex cheers the overture and listens through the finale. Nature Neurosci 8:851–852.

Musicant AD, Chan JCK, Hind JE. 1990. Direction-dependent spectral properties of cat external ear: new data and cross-species comparisons. J Acoust Soc Am 87:757–781.

Oertel D, Bal R, Gardner SM, Smith PH, Joris PX. 2000. Detection of synchrony in the activity of auditory nerve fibers by octopus cells of the mammalian cochlear nucleus. Proc Nat Acad Sci U S A 97:11773–11779.

Palmer AR, King AJ. 1982. The representation of auditory space in the mammalian superior colliculus. Nature 299:248–249.

Penagos H, Melcher JR, Oxenham AJ. 2004. A neural representation of pitch salience in nonprimary human auditory cortex revealed with functional magnetic resonance imaging. J Neurosci 24:6810–6815.

Raman IM, Zhang S, Trussell LO. 1994. Pathway-specific variants of AMPA receptors and their contribution to neuronal signaling. J Neurosci 14:4998–5010.

Rauschecker JP, Tian B. 2000. Mechanisms and streams for processing of "what" and "where" in auditory cortex. Proc Nat Acad Sci U S A 97:11800–11806.

Rauschecker JP, Tian B, Hauser M. 1995. Processing of complex sounds in the macaque nonprimary auditory cortex. Science 268:111–114.

Recanzone GH, Schreiner CE, Merzenich MM. 1993. Plasticity in the frequency representation of primary auditory cortex following discrimination training in adult owl monkeys. J Neurosci 13:87–103.

Remington ED, Wang X. 2019. Neural representations of the full spatial field in auditory cortex of awake marmoset (*Callithrix jacchus*). Cereb Cortex 29:1199–1216.

Riquimaroux H, Gaioni SJ, Suga N. 1991. Cortical computational maps control auditory perception. Science 251: 565–568.

Romanski LM, Averbeck BB. 2009. The primate cortical auditory system and neural representation of conspecific vocalizations. Annu Rev Neurosci 32:315–346.

Sadagopan S, Wang X. 2009. Nonlinear spectrotemporal interactions underlying selectivity for complex sounds in auditory cortex. J Neurosci 29:11192–11202.

Schreiner CE, Winer JA. 2007. Auditory cortex mapmaking: principles, projections, and plasticity. Neuron 56: 356–365.

Scott LL, Mathews PJ, Golding NL. 2005. Posthearing developmental refinement of temporal processing in principal neurons of the medial superior olive. J Neurosci 25: 7887–7895.

Song X, Osmanski MS, Guo Y, Wang X. 2016. Complex pitch perception mechanisms are shared by humans and a New World monkey. Proc Natl Acad Sci U S A 113:781–786.

Spirou GA, Young ED. 1991. Organization of dorsal cochlear nucleus type IV unit response maps and their relationship to activation by bandlimited noise. J Neurophysiol 66:1750–1768.

Suga N, O'Neill WE, Kujirai K, Manabe T. 1983. Specificity of combination-sensitive neurons for processing of complex biosonar signals in auditory cortex of the mustached bat. J Neurophysiol 49:1573–626.

Suga N. 1984. Neural mechanisms of complex-sound processing for echolocation. Trends Neurosci 7:20–27.

Tollin DJ, Yin TC. 2002. The coding of spatial location by single units in the lateral superior olive of the cat. II. The determinants of spatial receptive fields in azimuth. J Neurosci 22:1468–1479.

Wang X, Lu T, Snider RK, Liang L. 2005. Sustained firing in auditory cortex evoked by preferred stimuli. Nature 435:341–346.

Warr WB. 1992. Organization of olivocochlear efferent systems in mammals. In: DB Webster, AN Popper, RR Fay (eds). *The Mammalian Auditory Pathway: Neuroanatomy,* pp. 410–448. New York: Springer.

Winer JA, Saint Marie RL, Larue DT, Oliver DL. 1996. GABAergic feedforward projections from the inferior colliculus to the medial geniculate body. Proc Natl Acad Sci U S A 93:8005–8010.

Yin TCT. 2002. Neural mechanisms of encoding binaural localization cues in the auditory brainstem. In: D Oertel, RR Fay, AN Popper (eds). *Integrative Functions in the Mammalian Auditory Pathway,* pp. 238–288. New York: Springer.

29

Smell and Taste: The Chemical Senses

Through the senses of smell and taste, we are able to perceive a staggering number and variety of chemicals in the external world. These chemical senses inform us about the availability of foods and their potential pleasure or danger. Smell and taste also initiate physiological changes required for the digestion and utilization of food. In many animals, the olfactory system also serves an important social function by detecting pheromones that elicit innate behavioral or physiological responses.

Although the discriminatory ability of humans is somewhat limited compared with that of many other animals, odor chemists estimate that the human olfactory system may be capable of detecting more than 10,000 different volatile chemicals. Perfumers who are highly trained to discriminate odorants can distinguish as many as 5,000 different types of odorants, and wine tasters can discern more than 100 different components of taste based on combinations of flavor and aroma.

In this chapter, we consider how odor and taste stimuli are detected and how they are encoded in patterns of neural signals transmitted to the brain. In recent years, much has been learned about the mechanisms underlying chemosensation in a variety of animal species. Certain features of chemosensation have

been conserved through evolution, whereas others are specialized adaptations of individual species.

A Large Family of Olfactory Receptors Initiate the Sense of Smell

Odorants—volatile chemicals that are perceived as odors—are detected by olfactory sensory neurons in the nose. The sensory neurons are embedded in a specialized olfactory epithelium that lines part of the nasal cavity, approximately 5 cm^2 in area in humans (Figure 29–1), and are interspersed with glia-like supporting cells (Figure 29–2). They are relatively short lived, with a life span of only 30 to 60 days, and are continuously replaced from a layer of basal stem cells in the epithelium.

The olfactory sensory neuron is a bipolar nerve cell. A single dendrite extends from the apical end to the epithelial surface, where it gives rise to numerous

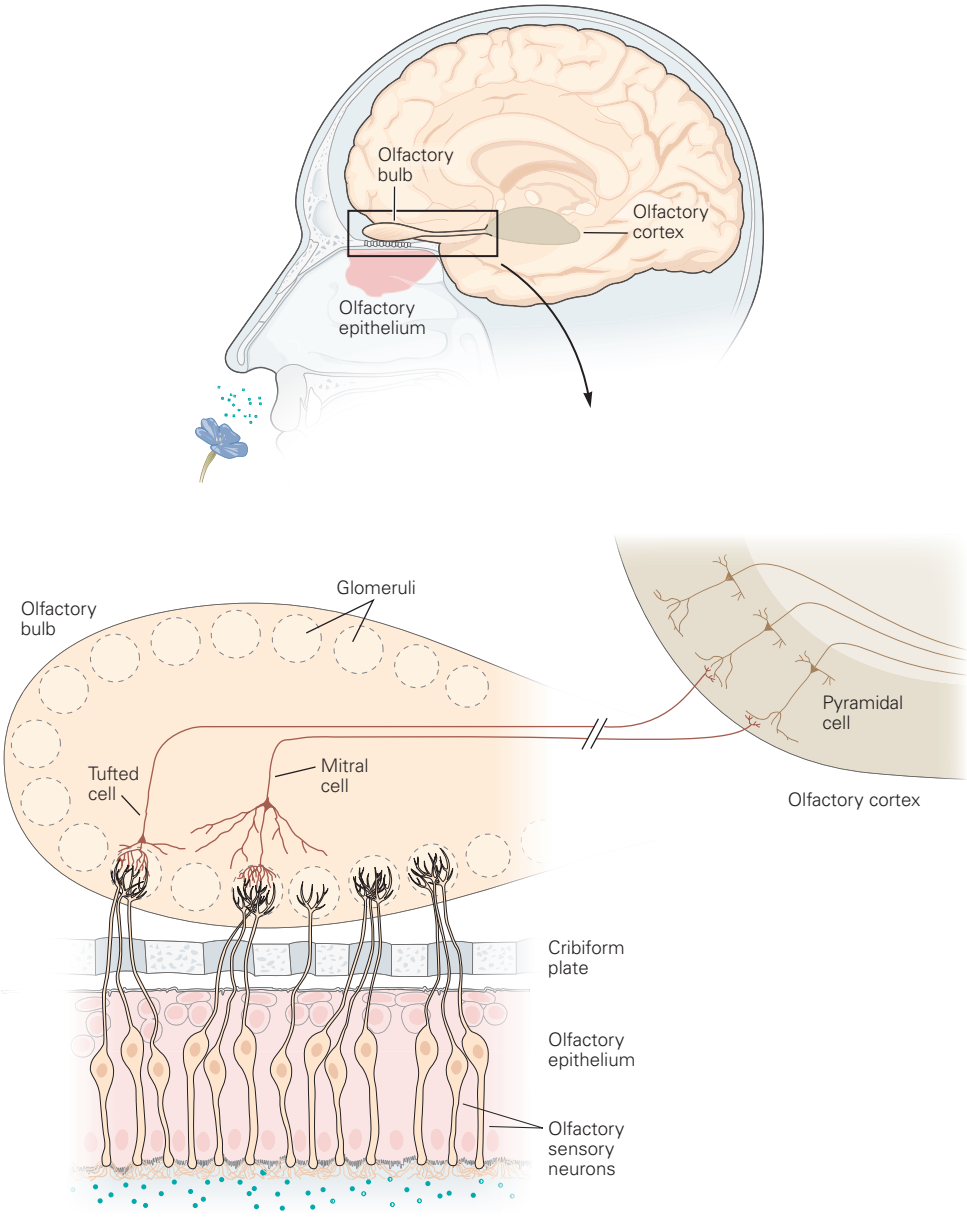

Figure 29–1 The olfactory system. Odorants are detected by olfactory sensory neurons in the olfactory epithelium, which lines part of the nasal cavity. The axons of these neurons project to the olfactory bulb, where they terminate on the dendrites of mitral and tufted cell relay neurons within glomeruli. In turn, the axons of the relay neurons project to the olfactory cortex, where they terminate on the dendrites of pyramidal neurons whose axons project to other brain areas.

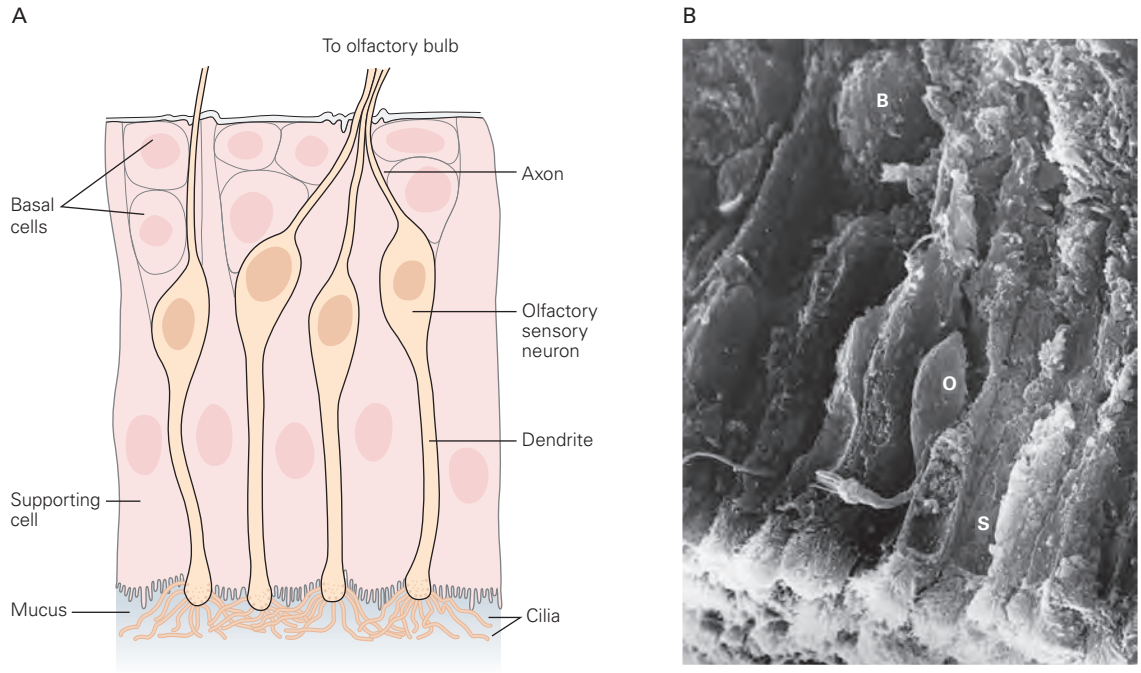

Figure 29–2 The olfactory epithelium.

A. The olfactory epithelium contains sensory neurons interspersed with supporting cells as well as a basal layer of stem cells. A single dendrite extends from the apical end of each neuron; sensory cilia sprout from the end of the dendrite into the mucus lining the nasal cavity. An axon extends from the basal end of each neuron to the olfactory bulb.

B. A scanning electron micrograph of the olfactory epithelium shows the dense mat of sensory cilia at the epithelial surface. Supporting cells (**S**) are columnar cells that extend the full depth of the epithelium and have apical microvilli. Interspersed among the supporting cells is an olfactory sensory neuron (**O**) with its dendrite and cilia, and a basal stem cell (**B**). (Reproduced, with permission, from Morrison and Costanzo 1990. Copyright © 1990 Wiley-Liss, Inc.)

thin cilia that protrude into the mucus that coats the nasal cavity (Figure 29–2). The cilia contain the odorant receptors as well as the transduction machinery needed to amplify sensory signals from the receptors and transform them into electrical signals in the neuron's axon, which projects from the basal pole of the neuron to the brain. The axons of olfactory sensory neurons pass through the cribriform plate, a perforated region in the skull above the nasal cavity, and then terminate in the olfactory bulb (see Figure 29–1).

Mammals Share a Large Family of Odorant Receptors

Odorant receptors are proteins encoded by a multigene family that is evolutionarily conserved and found in all vertebrate species. Humans have approximately 350 different odorant receptors, whereas mice have approximately 1,000. Although odorant receptors belong to the G protein–coupled receptor superfamily, they share sequence motifs not seen in other superfamily members. Significantly, the odorant receptors vary considerably in amino acid sequence (Figure 29–3A).

Like other G protein–coupled receptors, odorant receptors have seven hydrophobic regions that are likely to serve as transmembrane domains (Figure 29–3A). Detailed studies of other G protein–coupled receptors, such as the β-adrenergic receptor, suggest that odorant binding occurs in a pocket in the transmembrane region formed by a combination of the transmembrane domains. The amino acid sequences of odorant receptors are especially variable in several transmembrane domains, providing a possible basis for variability in the odorant binding pocket that could account for the ability of different receptors to recognize structurally diverse ligands.

A second, smaller family of chemosensory receptors is also expressed in the olfactory epithelium. These receptors, called trace amine-associated receptors (TAARs), are G protein–coupled, but their protein sequence is unrelated to that of odorant receptors. They are encoded by a small family of genes present in humans and mice as well as fish. Studies in mice, which have 14 different olfactory TAARs, indicate that TAARs recognize volatile amines, one of which is present in high concentrations in the urine of male

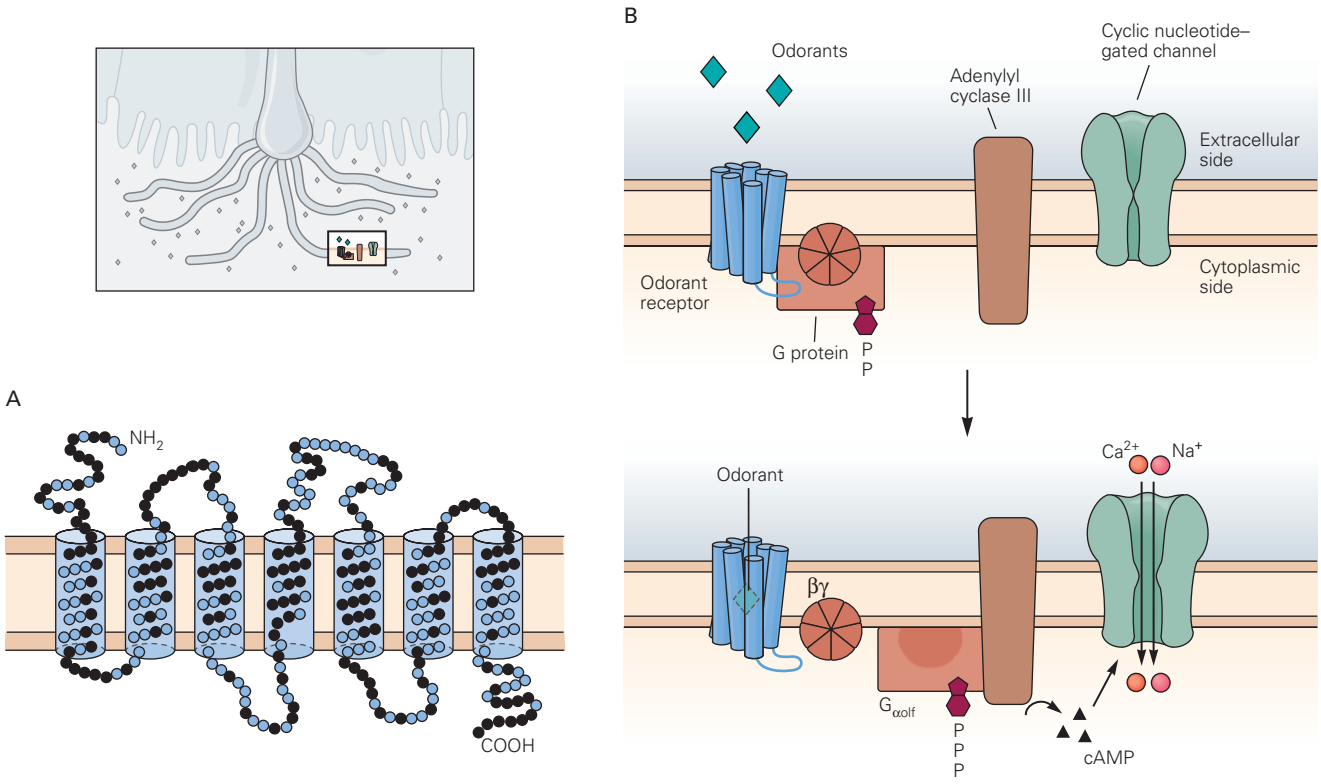

Figure 29–3 Odorant receptors.

A. Odorant receptors have the seven transmembrane domains characteristic of G protein–coupled receptors. They are related to one another but vary in amino acid sequence (positions of highest variability are shown here as **black balls**). (Reproduced, with permission, from Buck and Axel 1991.)

B. Binding of an odorant causes the odorant receptor to interact with $G\alpha_{olf}$, the α-subunit of a heterotrimeric G protein. This causes the release of a guanosine triphosphate (GTP)-coupled $G\alpha_{olf}$, which stimulates adenylyl cyclase III, leading to an increase in cyclic adenosine monophosphate (**cAMP**). The elevated cAMP in turn induces the opening of cyclic nucleotide–gated cation channels, causing cation influx and a change in membrane potential in the ciliary membrane.

mice and another in the urine of some predators. It is possible that this small receptor family has a function distinct from that of the odorant receptor family, perhaps one associated with the detection of animal cues. Another family of 12 receptors, called MS4Rs, is also found in mice, where it may be involved in the detection of pheromones and certain food odors.

The binding of an odorant to its receptor induces a cascade of intracellular signaling events that depolarize the olfactory sensory neuron (Figure 29–3B). The depolarization spreads passively to the cell body and then the axon, where action potentials are generated that are actively conducted to the olfactory bulb.

Humans and other animals rapidly accommodate to odors, as seen for example in the weakening of detection of an unpleasant odor that is continuously present. The ability to sense an odorant rapidly recovers when the odorant is temporarily removed. The adaptation to odorants is caused in part by modulation of a cyclic nucleotide–gated ion channel in olfactory cilia, but the mechanism by which sensitivity is speedily restored is not yet understood.

Different Combinations of Receptors Encode Different Odorants

To be distinguished perceptually, different odorants must cause different signals to be transmitted from the nose to the brain. This is accomplished in two ways. First, each olfactory sensory neuron expresses only one odorant receptor gene and therefore one type of receptor. Second, each receptor recognizes multiple odorants, and conversely, each odorant is detected by multiple different receptors (Figure 29–4). Importantly, however, each odorant is detected, and thereby encoded, by a unique combination of receptors and thus causes a distinctive pattern of signals to be transmitted to the brain.

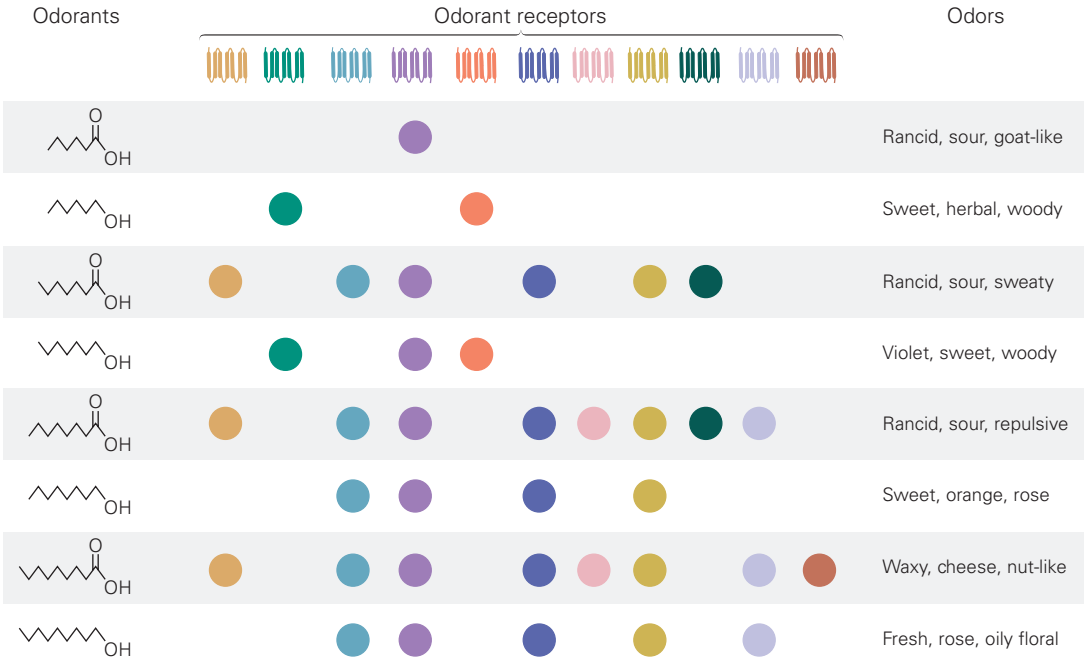

Figure 29–4 Each odorant is recognized by a unique combination of receptors. A single odorant receptor can recognize multiple odorants, but different odorants are detected, and thus encoded, by different combinations of receptors. This combinatorial coding explains how mammals can distinguish odorants with similar chemical structures as having different scents. The data in the figure were obtained by testing mouse olfactory sensory neurons with different odorants and then determining the odorant receptor gene expressed by each responsive neuron. The perceived qualities of these odorants in humans shown on the right illustrate how highly related odorants can have different scents. (Adapted, with permission, from Malnic et al. 1999.)

The combinatorial coding of odorants greatly expands the discriminatory power of the olfactory system. If each odorant were detected by only three different receptors, this strategy could in theory generate millions of different combinatorial receptor codes—and an equivalently vast number of different signaling patterns sent from the nose to the brain. Interestingly, even odorants with nearly identical structures are recognized by different combinations of receptors (Figure 29–4). The fact that highly related odorants have different combinatorial receptor codes explains why a slight change in the chemical structure of an odorant can alter its perceived odor. In some cases, the result is dramatic, for example, changing the perception of a chemical from rose to sour.

A change in concentration of an odorant can also change the perceived odor. For example, a low concentration of thioterpineol smells like tropical fruit, whereas a higher concentration smells like grapefruit and an even higher concentration smells putrid. As the concentration of an odorant is increased, additional receptors with lower affinity for the odorant are recruited into the response and thus change the combinatorial receptor code, providing an explanation for the effects of odorant concentration on perception.

Olfactory Information Is Transformed Along the Pathway to the Brain

Odorants Are Encoded in the Nose by Dispersed Neurons

How are signals from a large array of different odorant receptors organized in the nervous system to generate diverse odor perceptions? This question has been investigated in rodents. Studies in mice have revealed that olfactory information undergoes a series of transformations as it travels from the olfactory epithelium to the olfactory bulb and then to the olfactory cortex.

The olfactory epithelium has a series of spatial zones that express different olfactory receptors. Each receptor type is expressed in approximately 5,000 neurons that are confined to one zone (Figure 29–5). (Recall that each neuron expresses only one odorant receptor gene.) Neurons with the same receptor are randomly scattered within a zone so neurons with different receptors are interspersed. All zones contain a variety of receptors, and a specific odorant may be recognized by receptors in different zones. Thus, despite a rough organization of odorant receptors into spatial

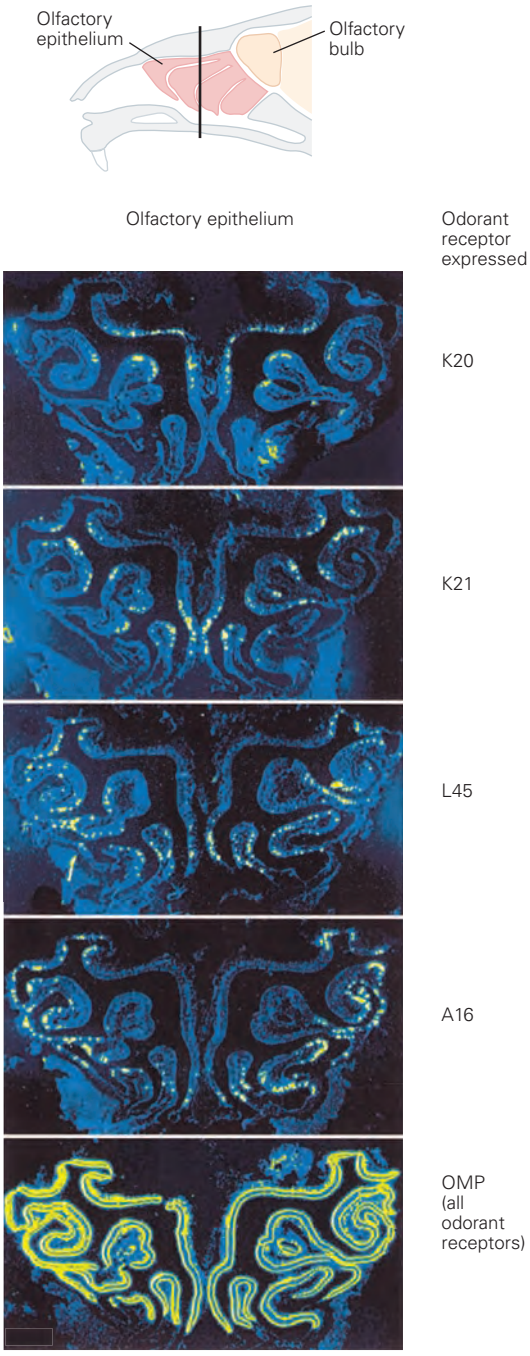

Figure 29–5 Organization of sensory inputs in the olfactory epithelium. The olfactory epithelium has different spatial zones that express different sets of odorant receptor genes. Each sensory neuron expresses only one receptor gene and thus one type of receptor. Neurons with the same receptor are confined to one zone but randomly scattered within that zone, such that neurons with different receptors are interspersed. The micrographs show the distribution of neurons labeled by four different receptor probes in sections through the mouse nose. An olfactory marker protein (**OMP**) probe labels all neurons expressing odorant receptors. (Adapted, with permission, from Ressler, Sullivan, and Buck 1993; Sullivan et al. 1996.)

zones, information provided by the odorant receptor family is highly distributed in the epithelium.

Because each odorant is detected by an ensemble of neurons widely dispersed across the epithelial sheet, receptors in one part of the epithelium will be able to detect a particular odorant even when those in another part are impaired by respiratory infection.

Sensory Inputs in the Olfactory Bulb Are Arranged by Receptor Type

The axons of olfactory sensory neurons project to the ipsilateral olfactory bulb, whose rostral end lies just above the olfactory epithelium. The axons of olfactory sensory neurons terminate on the dendrites of olfactory bulb neurons within bundles of neuropil called glomeruli that are arrayed over the bulb's surface (Figure 29–1). In each glomerulus, the sensory axons make synaptic connections with three types of neurons: mitral and tufted projection (relay) neurons, which project axons to the olfactory cortex, and periglomerular interneurons, which encircle the glomerulus (Figure 29–6).

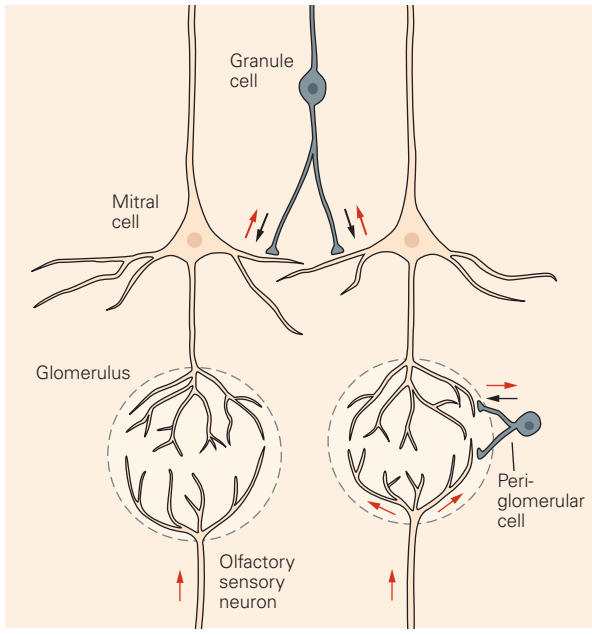

Figure 29–6 Olfactory bulb interneurons. In addition to excitatory mitral and tufted relay neurons, the olfactory bulb contains inhibitory interneurons. Within each glomerulus, the dendrites of GABAergic periglomerular cells receive excitatory input from olfactory sensory neurons and have reciprocal synapses with the primary dendrites of mitral and tufted relay neurons, suggesting a possible role in signal modification. The dendrites of GABAergic granule cells deeper in the bulb have reciprocal excitatory-inhibitory synapses with the secondary dendrites of the relay neurons and are thought to provide negative feedback to relay neurons that shapes the odor response. (Adapted from Shepherd and Greer 1998.)

The axon of an olfactory sensory neuron as well as the primary dendrite of each mitral and tufted relay neuron terminate in a single glomerulus. In each glomerulus, the axons of several thousand sensory neurons converge on the dendrites of approximately 40 to 50 relay neurons. This convergence results in approximately a 100-fold decrease in the number of neurons transmitting olfactory signals.

The organization of sensory information in the olfactory bulb is dramatically different from that of the epithelium. Whereas olfactory sensory neurons with the same odorant receptor are randomly scattered in one epithelial zone, their axons typically converge in two glomeruli at specific locations, one on either side of the olfactory bulb (Figure 29–7C). Each glomerulus, and each mitral and tufted relay neuron connected to it, receives input from just one type of odorant receptor. The result is a precise arrangement of sensory inputs from different odorant receptors, one that is similar between individuals.

Because each odorant is recognized by a unique combination of receptor types, each also activates a particular combination of glomeruli in the olfactory bulb (Figure 29–7B). At the same time, just as one odorant receptor recognizes multiple odorants, a single glomerulus—or a given mitral or tufted cell—is activated by more than one odorant. Owing to the nearly stereotyped pattern of receptor inputs in the olfactory bulb, the patterns of glomerular activation elicited by individual odorants are similar in all individuals and are bilaterally symmetrical in the two adjacent bulbs.

This organization of sensory information in the olfactory bulb is likely to be advantageous in two respects. First, signals from thousands of sensory neurons with the same odorant receptor type always converge on the same few glomeruli, and relay neurons in the olfactory bulb may optimize the detection of odorants present at low concentrations. Second, although olfactory sensory neurons with the same receptor type are dispersed and are continually replaced, the arrangement of inputs in the olfactory bulb remains unaltered. As a result, the neural code for an odorant in the brain is maintained over time, assuring that an odorant encountered previously can be recognized years later.

One mystery that remains unsolved is how all the axons of olfactory sensory neurons with the same type of receptor are directed to the same glomeruli. Studies using transgenic mice indicate that the odorant receptor itself somehow determines the target of the axon, but how it does so is not yet understood.

Sensory information is processed and possibly refined in the olfactory bulb before it is forwarded to the olfactory cortex. Each glomerulus is encircled by periglomerular interneurons that receive excitatory input from sensory axons and form inhibitory dendrodendritic synapses with mitral and tufted cell dendrites in that glomerulus and perhaps adjacent glomeruli. The periglomerular interneurons may therefore have a role in signal modulation. In addition, granule cell interneurons deep in the bulb provide negative feedback onto mitral and tufted cells. The granule cell interneurons are excited by the basal dendrites of mitral and tufted cells and in turn inhibit those relay neurons and others with which they are connected. The lateral inhibition afforded by these connections is thought to dampen signals from glomeruli and relay neurons that respond to an odorant only weakly, thereby sharpening the contrast between important and irrelevant sensory information before its transmission to the cortex.

Other potential sources of signal refinement are the retrograde projections to the olfactory bulb from the olfactory cortex, basal forebrain (horizontal limb of the diagonal band), and midbrain (locus ceruleus and raphe nuclei). These connections may modulate olfactory bulb output according to the physiological or behavioral state of an animal. When the animal is hungry, for example, some centrifugal projections might heighten the perception of the aroma of foods.

The Olfactory Bulb Transmits Information to the Olfactory Cortex

The axons of the mitral and tufted relay neurons of the olfactory bulb project through the lateral olfactory tract to the olfactory cortex (Figure 29–8 and see Figure 29–1). The olfactory cortex, defined roughly as that portion of the cortex that receives a direct projection from the olfactory bulb, comprises multiple anatomically distinct areas. The six major areas are the anterior olfactory nucleus, which connects the two olfactory bulbs through a portion of the anterior commissure; the anterior and posterior-lateral cortical nuclei of the amygdala; the olfactory tubercle; part of the entorhinal cortex; and the piriform cortex, the largest and considered the major olfactory cortical area.

The functions of the different olfactory cortical areas are largely unknown. However, the piriform cortex is thought to be important for odor learning. Recent studies indicate that the posterior-lateral cortical amygdala may have a role in innate attraction and fear behaviors, and the amygdalo-piriform transition area, a minor olfactory cortical area, a role in stress hormone responses to predator odors detected in the nose.

In the piriform cortex, the axons of olfactory bulb mitral and tufted cells leave the lateral olfactory tract

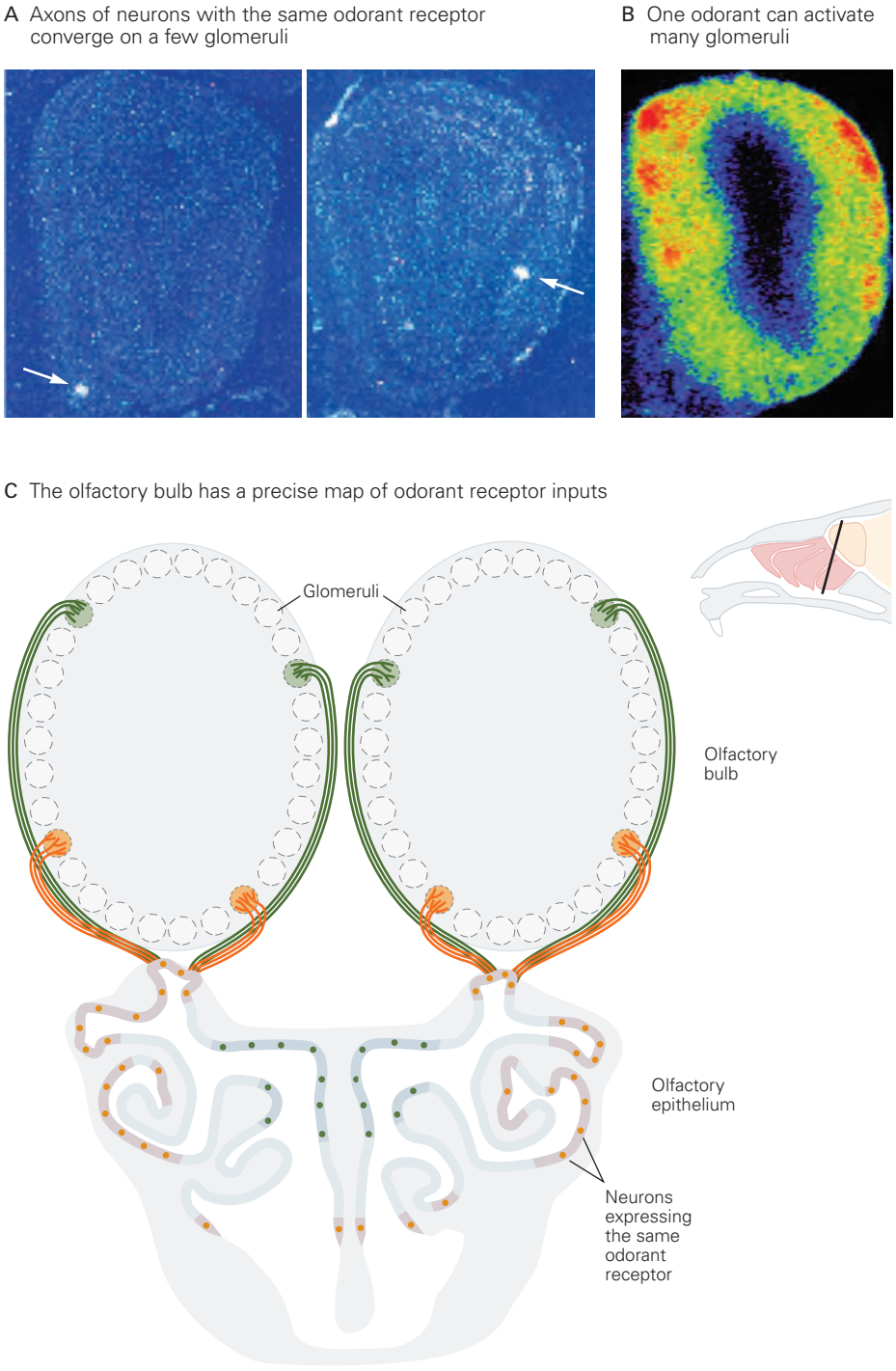

Figure 29–7 Odor responses in the olfactory bulb.

A. The axons of sensory neurons with the same odorant receptor type usually converge in only two glomeruli, one on each side of the olfactory bulb. Here, a probe specific for one odorant receptor gene labeled a glomerulus on the medial side (*left*) and lateral side (*right*) of a mouse olfactory bulb. The probe hybridized to receptor messenger RNAs present in sensory axons in these coronal sections. (Adapted, with permission, from Ressler, Sullivan, and Buck 1994.)

B. A single odorant often activates multiple glomeruli with input from different receptors. This section of a rat olfactory bulb shows the uptake of radiolabeled 2-deoxglucose at multiple foci (**red**) following exposure of the animal to the odorant methyl benzoate. The labeled foci correspond to numerous glomeruli at different locations in the olfactory bulb. (Reproduced, with permission, from Johnson, Farahbod, and Leon 2005. Copyright © 2005 Wiley-Liss, Inc.)

C. The olfactory bulb has a precise map of odorant receptor inputs because each glomerulus is dedicated to only one type of receptor. The maps in the two olfactory bulbs are bilaterally symmetrical and are nearly identical across individuals. The maps on the medial and lateral sides of each bulb are similar, but slightly displaced along the dorsal-ventral and anterior-posterior axes.

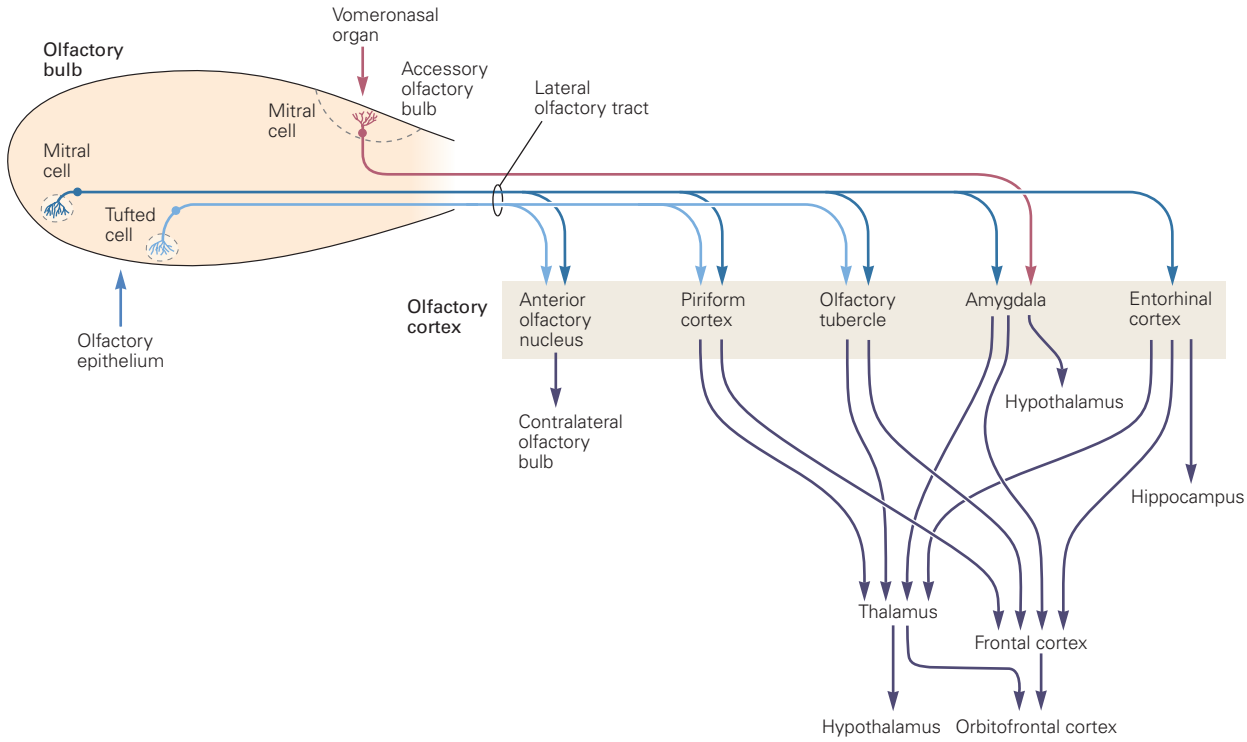

Figure 29–8 Afferent pathways to olfactory cortex. The axons of mitral and tufted relay neurons of the olfactory bulb project through the lateral olfactory tract to the olfactory cortex. The olfactory cortex consists of a number of distinct areas, the largest of which is the piriform cortex. From these areas, olfactory information is transmitted to other brain areas directly as well as indirectly via the thalamus. Targets include frontal and orbitofrontal areas of the neocortex, which are thought to be important for odor discrimination, and the amygdala and hypothalamus, which may be involved in emotional and physiological responses to odors. Mitral cells in the accessory olfactory bulb project to specific areas of the amygdala that transmit signals to the hypothalamus.

to form excitatory glutamatergic synapses with pyramidal neurons, the projection neurons of the cortex. Pyramidal neuron activity appears to be modulated by inhibitory inputs from local GABAergic interneurons as well as by excitatory inputs from other pyramidal neurons in the same and other olfactory cortical areas and the contralateral piriform cortex. The piriform cortex also receives centrifugal inputs from modulatory brain areas, suggesting that its activity may be adjusted according to physiological or behavioral state. Finally, the olfactory cortex projects to the olfactory bulb, providing yet another possible means of signal modulation.

As with the olfactory bulb relay neurons, individual pyramidal neurons can be activated by more than one odorant. However, the pyramidal neurons activated by a particular odorant are scattered across the piriform cortex, an arrangement different from that of the olfactory bulb. Mitral cells in different parts of the olfactory bulb can project axons to the same subregion of the piriform cortex, further indicating that the highly organized map of odorant receptor inputs in the olfactory bulb is not recapitulated in the cortex.

Output From the Olfactory Cortex Reaches Higher Cortical and Limbic Areas

Pyramidal neurons in the olfactory cortex transmit information indirectly to the orbitofrontal cortex through the thalamus and directly to the frontal cortex. These pathways to higher cortical areas are thought to be important in odor discrimination. In fact, people with lesions of the orbitofrontal cortex are unable to discriminate odors. Interestingly, recordings in the orbitofrontal cortex suggest that some individual neurons in that area receive multimodal input, responding, for example, to the smell, sight, or taste of a banana.

Many areas of the olfactory cortex also relay information to nonolfactory areas of the amygdala, which is linked to emotions, and to the hypothalamus, which controls basic drives, such as appetite, as well as a number of innate behaviors. These limbic areas are thought to play a role in the emotional and motivational aspects of smell as well as many of the behavioral and physiological effects of odorants. In animals, they may be important in the generation of

stereotyped behavioral and physiological responses to odors of predators or to pheromones that are detected in the olfactory epithelium.

Olfactory Acuity Varies in Humans

Olfactory acuity can vary as much as 1,000-fold among humans, even among people with no obvious abnormality. The most common olfactory aberration is *specific anosmia*. An individual with a specific anosmia has lowered sensitivity to a specific odorant even though sensitivity to other odorants appears normal. Specific anosmias to some odorants are common, with a few occurring in 1% to 20% of people. For example, 12% of individuals tested in one study exhibited a specific anosmia for musk. Recent studies indicate that specific anosmias can be caused by mutations in particular odorant receptor genes.

Far rarer abnormalities of olfaction, such as *general anosmia* (complete lack of olfactory sensation) or *hyposmia* (diminished sense of smell), are often transient and can derive from respiratory infections. Chronic anosmia or hyposmia can result from damage to the olfactory epithelium caused by infections; from particular diseases, such as Parkinson disease; or from head trauma that severs the olfactory nerves passing through holes in the cribriform plate, which then become blocked by scar tissue. Olfactory hallucinations of repugnant smells (*cacosmia*) can occur as a consequence of epileptic seizures.

Odors Elicit Characteristic Innate Behaviors

Pheromones Are Detected in Two Olfactory Structures

In many animals, the olfactory system detects not only odors but also pheromones, chemicals that are released from animals and influence the behavior or physiology of members of the same species. Pheromones play important roles in a variety of mammals, although they have not been demonstrated in humans. Often contained in urine or glandular secretions, some pheromones modulate the levels of reproductive hormones or stimulate sexual behavior or aggression. Pheromones are detected by two separate structures: the nasal olfactory epithelium, where odorants are detected, and the vomeronasal organ, an accessory olfactory organ thought to be specialized for the detection of pheromones and other animal cues.

The vomeronasal organ is present in many mammals, although not in humans. It is a tubular structure in the nasal septum that has a duct opening into the nasal cavity and one inner wall lined by a sensory epithelium. Signals generated by sensory neurons in the epithelium of the vomeronasal organ follow a distinct pathway. They travel through the accessory olfactory bulb primarily to the medial amygdala and posterior-medial cortical amygdala and from there to the hypothalamus.

Sensory detection in the vomeronasal organ differs from that in the olfactory epithelium. The vomeronasal organ has two different families of chemosensory receptors, the V1R and V2R families. In the mouse, each family has more than 100 members. Variation in amino acid sequence between members of each receptor family suggests that each family may recognize a variety of different ligands. Like odorant receptors, V1R and V2R receptors have the seven transmembrane domains typical of G protein–coupled receptors. The V2R receptor differs from both V1R and odorant receptors in having a large extracellular domain at the N-terminal end (Figure 29–9A). By analogy with receptors with similar structures, ligands may bind V1R receptors in a membrane pocket formed by a combination of transmembrane domains, whereas binding to V2R receptors may occur in the large extracellular domain. Although the V1R receptors are thought to recognize volatile chemicals, at least some V2Rs are thought to recognize proteins. These include a protein pheromone present in tears, mouse urinary proteins that stimulate aggression, and predator proteins from cats and rats that stimulate fear in mice.

The V1R and V2R families are expressed in different spatial zones in the vomeronasal organ that express different G proteins (Figure 29–9B,C). Each *V1R* or *V2R* gene is expressed in a small percentage of neurons scattered throughout one zone, an arrangement similar to that of odorant receptors in the olfactory epithelium. Similar to the main olfactory bulb, vomeronasal neurons with the same receptor type project to the same glomeruli in the accessory olfactory bulb, although the glomeruli for each receptor type are more numerous and their distribution less stereotyped than in the main olfactory bulb. In addition to V1R and V2R receptors, the vomeronasal organ has a family of five formyl peptide-related receptors (FPRs). These receptors are related to immune system FPRs that detect bacterial proteins, raising speculation that they might play a role in detecting diseased animals of the same species.

Invertebrate Olfactory Systems Can Be Used to Study Odor Coding and Behavior

Because invertebrates have simple nervous systems and often respond to olfactory stimuli with stereotyped

behaviors, they are useful for understanding the relationship between the neural representation of odor and behavior.

Certain features of chemosensory systems are highly conserved in evolution. First, all metazoan animals can detect a variety of organic molecules using specialized chemosensory neurons with cilia or microvilli that contact the external environment. Second, the initial events of odor detection are mediated by families of transmembrane receptors with specific expression patterns in peripheral sensory neurons. Other features of the olfactory system differ between species, reflecting selection pressures and evolutionary histories of the animals.

The primary sensory organs of insects are the antennae and appendages known as maxillary palps near the mouth (Figure 29–10A). Whereas mammals have millions of olfactory neurons, insects have a much smaller number. There are approximately 2,600 olfactory neurons in the fruit fly *Drosophila* and approximately 60,000 in the honeybee.

The insect odorant receptors were discovered by finding multigene receptor families in the *Drosophila* genome, and these genes have now been examined in other insect genomes as well. Remarkably, they have little similarity to mammalian odorant receptors save for the presence of many transmembrane domains. Indeed, insect receptors appear to have an independent evolutionary origin from mammalian receptors and may not even be G protein–coupled receptors—an extreme example of the fast evolutionary change observed across all olfactory receptor systems. In *Drosophila*, the main odorant receptor family has only 60 genes, rather than the hundreds characteristic of vertebrates. The malaria mosquito *Anopheles gambiae* and the honeybee have similar numbers (85–95 genes), whereas leaf-cutter ants have more than 350 odorant

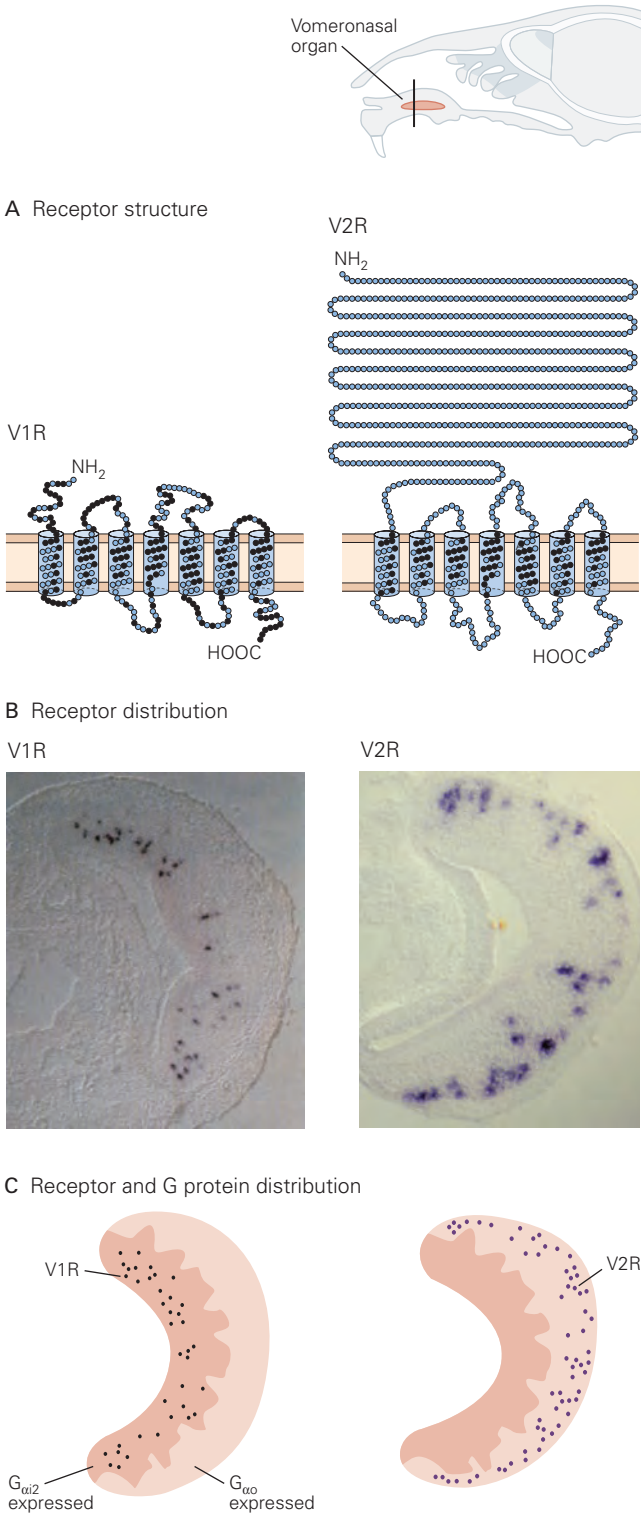

Figure 29–9 (Right) Candidate pheromone receptors in the vomeronasal organ.

A. The V1R and V2R families of receptors are expressed in the vomeronasal organ. In the mouse, each family has more than 100 members, which vary in protein sequence. Members of both families have the seven transmembrane domains of G protein–coupled receptors, but V2R receptors also have a large extracellular domain at the N-terminal end that may be the site of ligand binding.

B. Sections through the vomeronasal organ show individual V1R and V2R probes hybridized to subsets of neurons in two distinct zones. (Reproduced, with permission, from Dulac and Axel 1995; Matsunami and Buck 1997.)

C. The two zones express high levels of different G proteins, $G\alpha_{\alpha i2}$ and $G\alpha_{\alpha o}$.

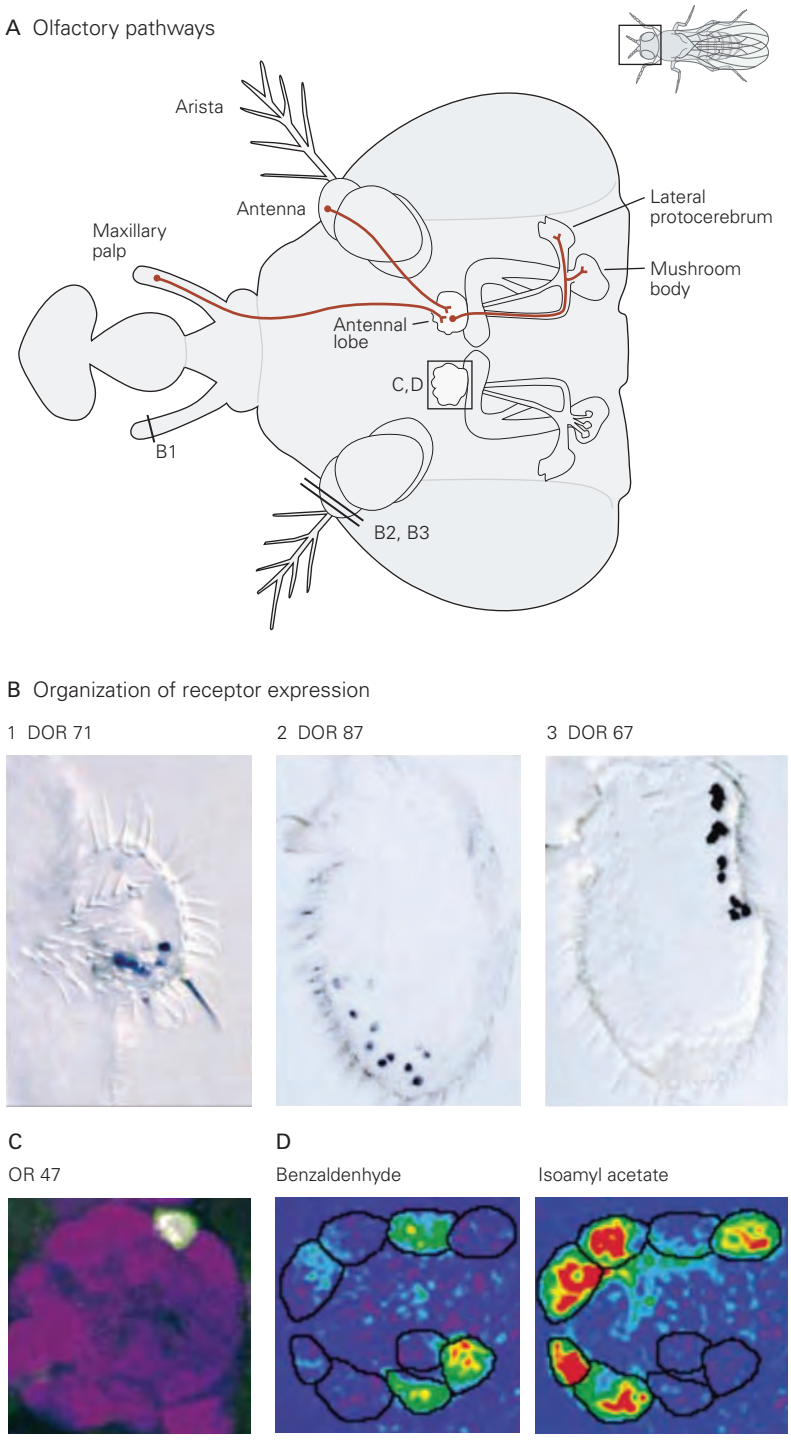

Figure 29–10 Olfactory pathways from the antenna to the brain in *Drosophila*.

A. The axons of olfactory neurons with cell bodies and dendrites in the antenna and maxillary palp project axons to the antennal lobe. Projection neurons in the antennal lobe then project to two regions of the fly brain, the mushroom body and lateral protocerebrum. (Reproduced, with permission, from Takaki Komiyama and Liqun Luo.)

B. The neurons that express one type of olfactory receptor gene, detected by RNA in situ hybridization, are scattered in the maxillary palp (**1**) or antenna (**2**, **3**).

C. All neurons that express the olfactory receptor gene *OR47* converge on a glomerulus in the antennal lobe. (Reproduced, with permission, from Vosshall et al. 1999; Vosshall, Wong, and Axel 2000.)

D. Each odorant elicits a physiological response from a subset of glomeruli in the antennal lobe. Two-photon calcium imaging was used to detect odor-evoked signals. (Reproduced, with permission, from Wang et al. 2003. Copyright © 2003 Elsevier.)

receptor genes, suggesting a wide variation in receptor number in insects.

Despite molecular differences in receptors, the anatomical organization of the fly's olfactory system is quite similar to that of vertebrates. Each olfactory neuron expresses one or sometimes two functional odorant receptor genes. The neurons expressing a particular gene are loosely localized to a region of the antenna but interspersed with neurons expressing other genes (Figure 29–10B). This scattered distribution is

not the case at the next level of organization, the antennal lobe. Axons from sensory neurons that express one type of receptor converge on two invariant glomeruli in the antennal lobe, one each on the left and right sides of the animal (Figure 29–10C). This organization is strikingly similar to that of the first sensory relay in the vertebrate olfactory bulb and is also found in the moth, honeybee, and other insects.

Because there are only a few dozen receptor genes in *Drosophila*, it is possible to characterize the entire repertory of odorant-receptor interactions, a goal that is not yet attainable in mammals. Sophisticated genetic methods can be used to label and record from a *Drosophila* neuron expressing a single known odorant receptor gene. By repeating this experiment with many receptors and odors, the receptive fields of the odorant receptors have been defined and shown to be quite diverse.

In insects, individual odorant receptors can detect large numbers of odorants, including odorants with very different chemical structures. This broad recognition of odorants by "generalist" receptors is necessary if only a small number of receptors is available to detect all biologically significant odorants. A single insect receptor protein that detects many odors can be stimulated by some odors and inhibited by others, often with distinct temporal patterns. A subset of insect odorant receptors that convey information about pheromones or other unusual odors like carbon dioxide are more selective. Thus, the coding potential of each olfactory neuron can be broad or narrow and arises from a combination of stimulatory and inhibitory signals delivered to its receptors.

Information from the olfactory neurons is relayed to the antennal lobe where sensory neurons expressing the same odorant receptor converge onto a small number of projection neurons in one glomerulus (Figure 29–10A). Because *Drosophila* glomeruli are stereotyped in position and have one type of odorant receptor input, the transformation of information across the synapse can be described. Convergence of many olfactory sensory axons onto a few projection neurons leads to a great increase in the signal-to-noise ratio of olfactory signals, so projection neurons are much more sensitive to odor than individual olfactory neurons. Within the antennal lobe, excitatory interneurons distribute signals to projection neurons at distal locations, and inhibitory interneurons feed back onto the olfactory sensory neurons to dampen their input. Thus, while activity of an individual olfactory neuron is conveyed to one glomerulus. its activity is also distributed across the entire antennal lobe, as it is processed by excitatory and inhibitory local interneurons that connect many glomeruli.

The projection neurons from the antennal lobe extend to higher brain centers called mushroom bodies and lateral protocerebrum (Figure 29–10A). These structures may represent insect equivalents of the olfactory cortex. The mushroom bodies are sites of olfactory associative learning and multimodal associative learning; the lateral protocerebrum is important for innate olfactory responses. At this stage, projection neurons form complex connections with a large number of downstream neurons. Neurons in higher brain centers in *Drosophila* have the potential to integrate information from many receptors.

Olfactory Cues Elicit Stereotyped Behaviors and Physiological Responses in the Nematode

The nematode roundworm *Caenorhabditis elegans* has one of the simplest nervous systems in the animal kingdom, with only 302 neurons in the entire animal. Of these, 32 are ciliated chemosensory neurons. Because *C. elegans* has strong behavioral responses to a wide variety of chemicals, it has been a useful experimental animal for relating olfactory signals to behavior. Each chemosensory neuron detects a specific set of chemicals, and activation of the neuron is required for the behavioral responses to those substances. The neuron for a particular response, such as attraction to a specific odor, occurs in the same position in all individuals.

The molecular mechanisms of olfaction in *C. elegans* were elucidated through genetic screens for mutant worms lacking the ability to detect odors (anosmia). The G protein–coupled receptor for the volatile odorant diacetyl emerged from these screens (Figure 29–11). This receptor is one of approximately 1,700 predicted G protein–coupled chemoreceptor genes in *C. elegans*, the largest number of chemoreceptors among known genomes. Other kinds of chemosensory receptors are also present; for example, *C. elegans* senses external oxygen levels indirectly by detecting soluble guanylate cyclases that bind directly to oxygen. With so many chemoreceptors, nematodes are able to recognize a large variety of odors with great sensitivity. Some chemosensory neurons use G proteins to regulate cyclic guanosine 3′,5′-monophosphate (cGMP) and a cGMP-gated channel, a signal transduction pathway like that of vertebrate photoreceptors. Other chemosensory neurons signal through a transient receptor potential vanilloid (TRPV) channel, like vertebrate nociceptive neurons.

The "one neuron, one receptor" principle observed in vertebrates and insects does not operate in nematodes because the number of neurons is much smaller

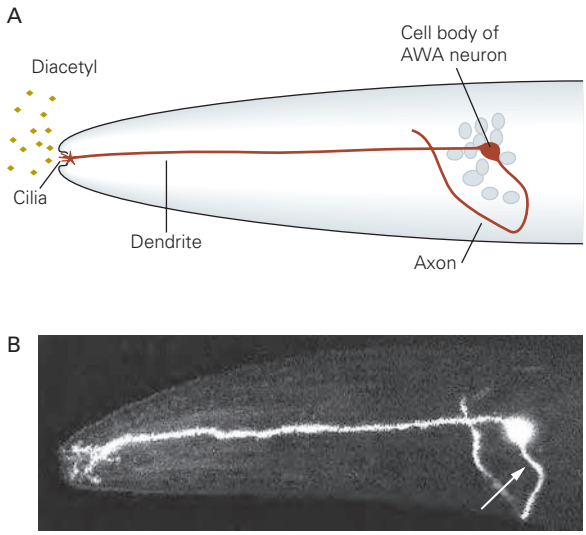

Figure 29–11 The receptor for diacetyl in the *Caenorhabditis elegans* worm.

A. A lateral view of the worm's anterior end shows the cell body and processes of the AWA chemosensory neuron. A dendrite terminates in cilia that are exposed to environmental chemicals. The neuron detects the volatile chemical diacetyl; animals with a mutation in the *odr-10* gene are unable to sense diacetyl.

B. The *odr-10* gene is active only in the AWA neurons. The micrograph here shows the gene product marked with fusion to a fluorescent reporter protein; the **arrow** indicates the neuron's axon. (Reproduced, with permission, from Sarafi-Reinach and Sengupta 2000.)

than the number of receptors. Each chemoreceptor gene is typically expressed in only one pair of chemosensory neurons, but each neuron expresses many receptor genes. The small size of the *C. elegans* nervous system limits olfactory computations. For example, a single neuron responds to many odors, but odors can be distinguished efficiently only if they are sensed by different primary sensory neurons.

The relationship between odor detection and behavior has been explored in *C. elegans* through genetic manipulations. For example, diacetyl is normally attractive to worms, but when the diacetyl receptor is experimentally expressed in an olfactory neuron that normally senses repellents, the animals are instead repelled by diacetyl. This observation indicates that specific sensory neurons encode the hardwired behavioral responses of attraction or repulsion and that a "labeled line" connects specific odors to specific behaviors. Similar ideas have emerged from genetic manipulations of taste systems in mice and flies, where sweet and bitter preference pathways are encoded by different sets of sensory cells.

Olfactory cues are linked to physiological responses as well as behavioral responses in nematodes. Food and pheromone cues that regulate development are detected by specific sensory neurons through G protein–coupled receptors. With low pheromone levels and plentiful food, animals rapidly develop to adulthood, whereas with high pheromone levels and scarce food, animals arrest in a long-lived larval stage called *dauer larvae* (Figure 29–12). Activation of these sensory neurons ultimately regulates the activity of an insulin signaling pathway that controls physiology and growth as well as the life span of the nematode. It is an open question whether the chemosensory systems and physiological systems of other animals are as entangled as they are in nematodes.

Strategies for Olfaction Have Evolved Rapidly

Why have independent families of odorant receptors evolved in mammals, nematodes, and insects? And why have the families changed so rapidly compared to genes involved in other important biological processes? The answer lies in a fundamental difference between olfaction and other senses such as vision, touch, and hearing.

Most senses are designed to detect physical entities with reliable physical properties: photons, pressure, or sound waves. By contrast, olfactory systems are designed to detect organic molecules that are infinitely variable and do not fit into a simple continuum of properties. Moreover, the organic molecules that are detected are produced by other living organisms, which evolve far more rapidly than the world of light, pressure, and sound.

An ancient olfactory system was present in the common ancestor of all animals that exist today. That ancestor lived in the ocean, where it gave rise to different lineages for mammals, insects, and nematodes. Those three phyla of animals came onto land hundreds of millions of years after the phyla diverged. Each phylum independently modified its olfactory system to detect airborne odors, leading to diversification of the receptors.

A consideration of the natural history of dipteran and hymenopteran insects, which have evolved in the last 200 million years, helps explain the rapid diversification of the odorant receptors. These insects include honeybees that pollinate flowers, fruit flies that feed on rotting fruit, flesh flies that arrive within minutes of death, and mosquitoes that prey on living animals. The odorants important for the survival of these insects are radically different, and receptor genes tuned to those odorants have evolved accordingly.

Figure 29–12 Chemosensory cues regulate the development of *C. elegans*. When exposed to different chemosensory cues, two larvae of the same age follow different development paths. A dauer larva, which forms under stressful conditions of low food and high population density, develops into a small slender adult (*left*). It is a nonfeeding, nonreproducing, stress-resistant form of the worm. In contrast, a larva in a rich environment favoring reproductive growth develops into a normal adult (*right*). (Reproduced, with permission, from Manuel Zimmer.)

The Gustatory System Controls the Sense of Taste

Taste Has Five Submodalities That Reflect Essential Dietary Requirements

The gustatory system is a specialized chemosensory system dedicated to evaluating potential food sources. It is the only sensory system that detects sugars and harmful compounds present in foods, and it serves as a main driver of feeding decisions. Unlike the olfactory system, which distinguishes millions of odors, the gustatory system recognizes just a few taste categories.

Humans and other mammals can distinguish five basic taste qualities: sweet, bitter, salty, sour, and umami, a Japanese word meaning delicious and associated with the "savory" taste of amino acids. This limited palate detects all essential dietary requirements of animals: A sweet taste invites consumption of energy-rich foods; bitter taste warns against the ingestion of toxic, noxious chemicals; salty taste promotes a diet that maintains proper electrolyte balance; sour taste signals acidic, unripened, or fermented foods; and umami indicates protein-rich foods.

Consistent with the nutritional importance of carbohydrates and proteins, both sweet and umami tastants elicit innately pleasurable sensations in humans and are attractants for animals in general. In contrast, bitter and sour tastants elicit innately aversive responses in humans and animals.

Taste is often thought to be synonymous with flavor. However, taste refers strictly to the five qualities encoded in the gustatory system, whereas flavor, with its rich and varied qualities, stems from the multisensory integration of inputs from the gustatory, olfactory, and somatosensory systems (eg, texture and temperature).

Tastant Detection Occurs in Taste Buds

Tastants are detected by taste receptor cells clustered in taste buds. Although the majority of taste buds in

humans are located on the tongue surface, some can also be found on the palate, pharynx, epiglottis, and upper third of the esophagus.

Taste buds on the tongue occur in structures called papillae, of which there are three types based on morphology and location. *Fungiform papillae*, located on the anterior two-thirds of the tongue, are peg-like structures that are topped with taste buds. Both the *foliate papillae*, situated on the posterior edge of the tongue, and the *circumvallate papillae*, of which there are only a few in the posterior area of the tongue, are structures surrounded by grooves lined with taste buds (Figure 29–13A). In humans, each fungiform papilla contains one to five taste buds, whereas each foliate and circumvallate papilla may contain hundreds to thousands of taste buds, respectively.

The taste bud is a garlic-shaped structure embedded in the epithelium. A small opening at the epithelial surface, the taste pore, is the point of contact with tastants (Figure 29–13B). Each taste bud contains approximately 100 taste receptor cells (taste cells), elongated cells that stretch from the taste pore to the basal area of the bud. The taste bud also contains other elongated cells that are thought to serve a supporting function, as well as a small number of round cells at the base, which are thought to serve as stem cells. Each taste cell extends microvilli into the taste pore, allowing the cell to contact chemicals dissolved in saliva at the epithelial surface.

At its basal end, the taste cell contacts the afferent fibers of gustatory sensory neurons, whose cell bodies reside in specific sensory ganglia (see Figure 29–17). Although taste cells are nonneural, their contacts with the gustatory sensory neurons have the morphological characteristics of chemical synapses, including clustered presynaptic vesicles. Taste cells also resemble neurons in that they are electrically excitable; they have voltage-gated Na^+, K^+, and Ca^{2+} channels and are capable of generating action potentials. Taste cells are very short-lived (days to weeks) and are continually replaced from the stem cell population. This turnover requires that newborn taste cells differentiate to detect one of the five taste qualities and connect to the terminals of appropriate gustatory sensory neurons, such that a sweet taste cell connects to sweet sensory neurons and a bitter taste cell to bitter sensory neurons.

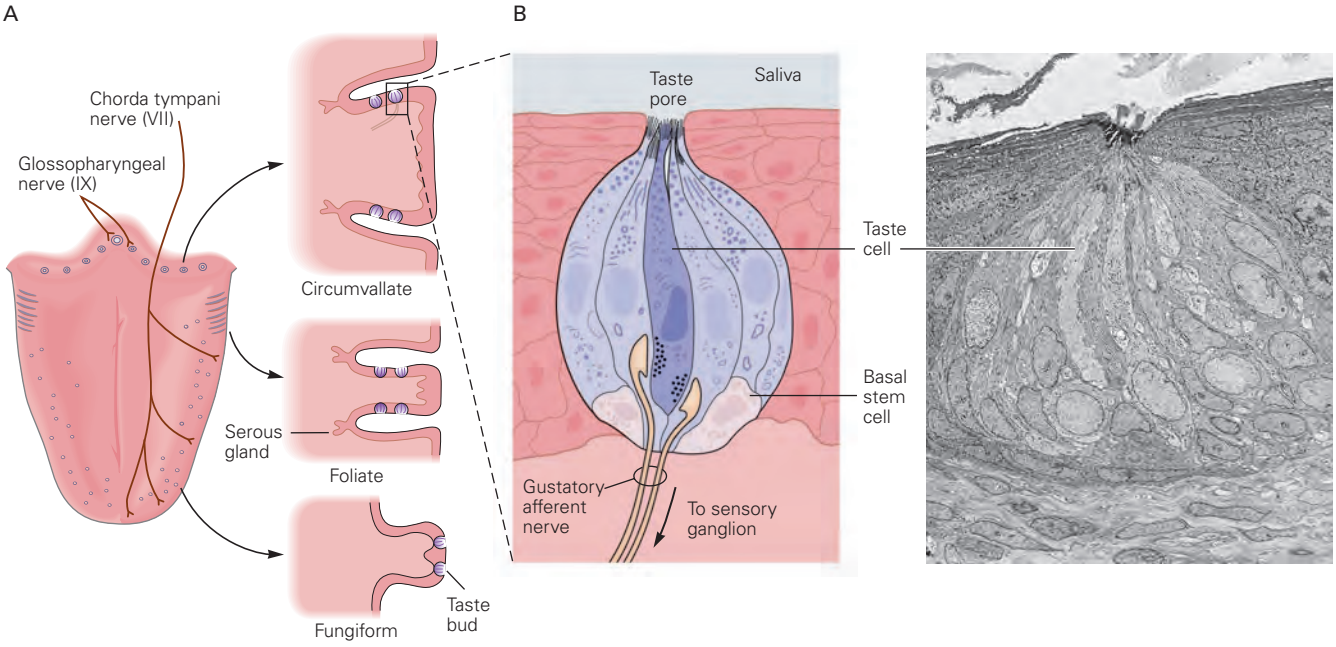

Figure 29–13 Taste buds are clustered in papillae on the tongue.

A. The three types of papillae—circumvallate, foliate, and fungiform—differ in morphology and location on the tongue and are differentially innervated by the chorda tympani and glossopharyngeal nerves.

B. Each taste bud contains 50 to 150 elongated taste receptor cells, as well as supporting cells and a small population of basal stem cells. The taste cell extends microvilli into the taste pore, allowing it to detect tastants dissolved in saliva. At its basal end, the taste cell contacts gustatory sensory neurons that transmit stimulus signals to the brain. The scanning electron micrograph shows a taste bud in a foliate papilla in a rabbit. (Reproduced, with permission, from Royer and Kinnamon 1991. Copyright © 1991 Wiley-Liss, Inc.)

Each Taste Modality Is Detected by Distinct Sensory Receptors and Cells

The five taste qualities are detected by sensory receptors in the microvilli of different taste cells. There are two general types of receptors: Bitter, sweet, and umami tastants interact with G protein–coupled receptors, whereas salty and sour tastants interact directly with specific ion channels (Figure 29–14). These interactions depolarize the taste cell, leading to the generation of action potentials in the afferent gustatory fibers.

Sweet Taste Receptor

Compounds that humans perceive as sweet include sugars, artificial sweeteners such as saccharin and aspartame, a few proteins such as monellin and thaumatin, and several D-amino acids. All of these sweet-tasting compounds are detected by a heteromeric receptor composed of two members of the T1R taste receptor family, T1R2 and T1R3 (Figure 29–15). The T1R receptors are a small family of three related G protein–coupled receptors that participate in sweet and umami detection.

Receptors of the TIR family have a large N-terminal extracellular domain (Figure 29–14) that serves as the main ligand-binding domain, similar to the V2R receptor of vomeronasal neurons. This domain recognizes many different sugars with low-affinity binding in the millimolar range. This ensures that only high sugar concentrations of nutritive value are detected. Changing a single amino acid in this domain in mice can alter an animal's sensitivity to sweet compounds. Indeed, T1R3 was initially discovered by examining genes at the mouse saccharin preference (Sac) locus, a chromosomal region that governs sensitivity to saccharin, sucrose, and other sweet compounds.

In mice, taste cells with T1R2 receptors are found mostly in palate, foliate, and circumvallate papillae; almost invariably, those cells also possess T1R3 receptors (Figure 29–16A). Gene knockout experiments in mice indicate that the T1R2/T1R3 complex mediates

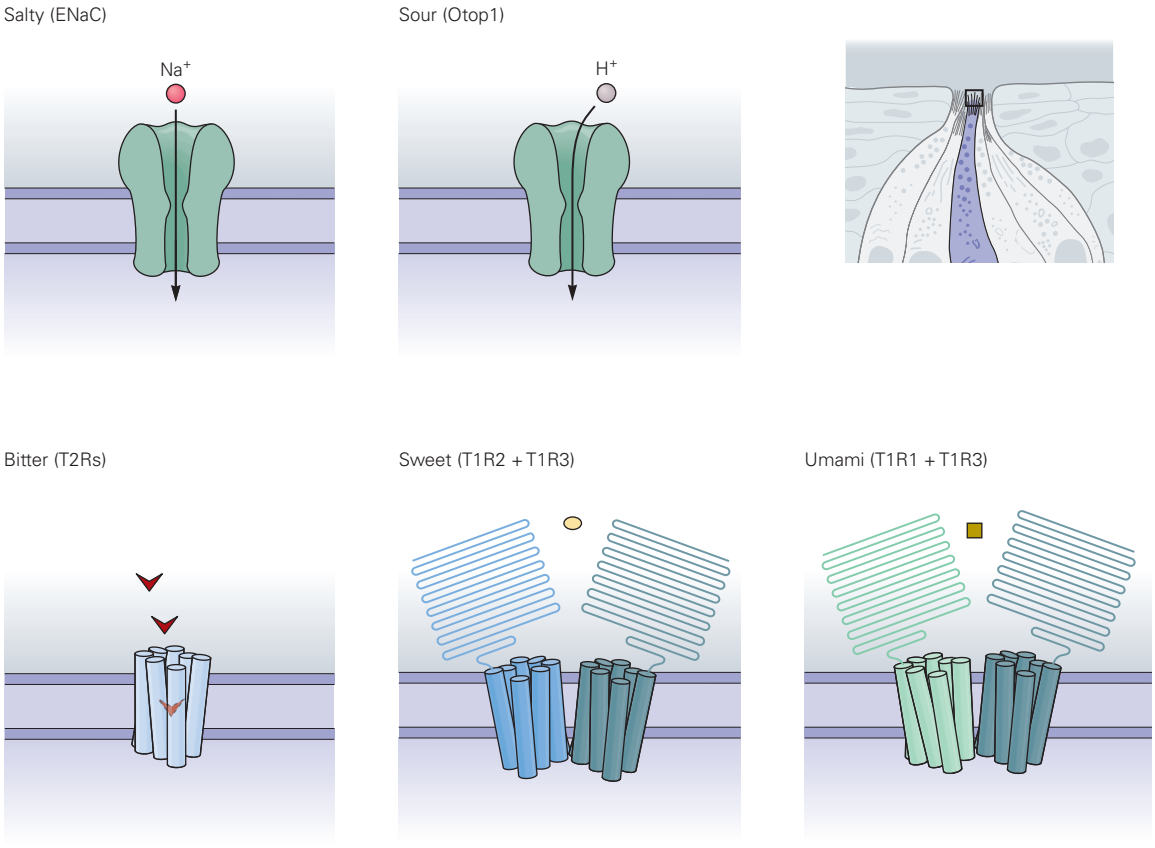

Figure 29–14 Sensory transduction in taste cells. Different taste qualities involve different detection mechanisms in the apical microvilli of taste cells (see Figure 29–13B). Salty and sour tastants directly activate ion channels, whereas tastants perceived as bitter, sweet, or umami activate G protein–coupled receptors. Bitter tastants are detected by T2R receptors, whereas sweet tastants are detected by a combination of T1R2 and T1R3, and umami tastants by a combination of T1R1 and T1R3.

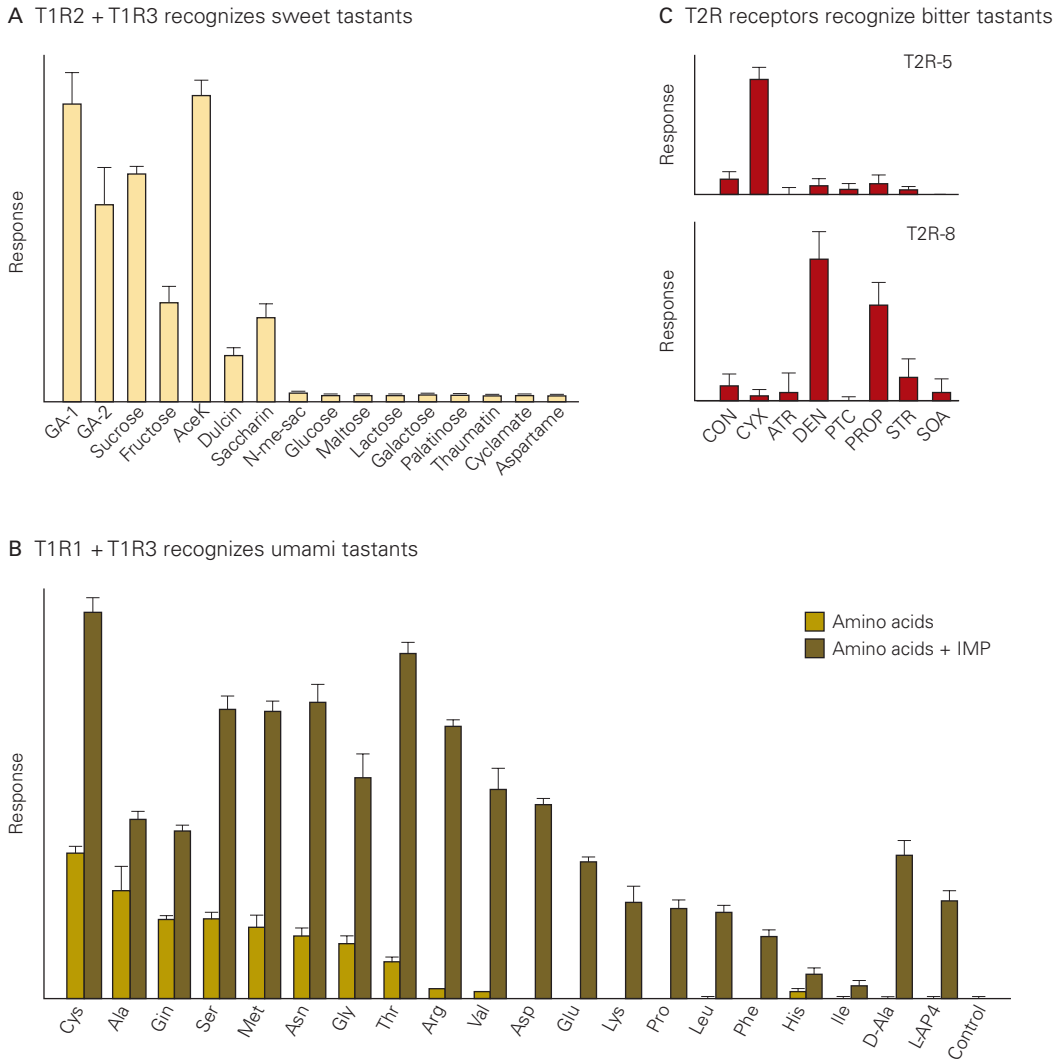

Figure 29–15 Tastants recognized by T1R and T2R receptors. A calcium-sensitive dye was used to test whether T1R and T2R receptors expressed in a tissue culture cell line could detect tastants.

A. Cells expressing both rat T1R2 and rat T1R3 responded to a number of sweet compounds. (Reproduced, with permission, from Nelson et al. 2001.)

B. Cells expressing mouse T1R1 and mouse T1R3 responded to numerous L-amino acids (umami taste). Responses were potentiated by inosine monophosphate (**IMP**). (Reproduced, with permission, from Nelson et al. 2002. Copyright © 2002 Springer Nature.)

C. Cells expressing different T2R receptors responded selectively to different bitter compounds. Cells expressing mouse T2R5 responded most vigorously to cycloheximide (**CYX**), whereas cells expressing mouse T2R8 responded preferentially to denatonium (**DEN**) and 6-n-propyl-2-thiouracil (**PROP**). (**ATR**, atropine; **CON**, control; **PTC**, phenyl thiocarbamide; **SOA**, sucrose octaacetate; **STR**, strychnine.) (Reproduced, with permission, from Chandrashekar et al. 2000.)

the detection of all sweet compounds except for high concentrations of sugars, which may also be detected by T1R3 alone.

Umami Taste Receptor

Umami is the name given to the savory taste of monosodium glutamate, an amino acid widely used as a flavor enhancer. It is believed that the pleasurable sensation associated with umami taste encourages the ingestion of proteins and is thus evolutionarily important for nutrition.

The receptor for umami taste is a complex of two T1R receptor subunits: T1R1, specific to the umami receptor, and T1R3, present in both sugar and umami receptors (Figure 29–14). In mice, the T1R1/T1R3

complex can interact with all L-amino acids (Figure 29–15B), but in humans it is preferentially activated by glutamate. Purine nucleotides, such as inosine 5′-monophosphate (IMP), are often added to monosodium glutamate to enhance its pleasurable umami taste. Interestingly, in vitro studies demonstrated that IMP potentiates the responsiveness of T1R1/T1R3 to L-amino acids, acting as a strong positive allosteric modulator of the receptor (Figure 29–15B).

Taste cells with both T1R1 and T1R3 are concentrated in fungiform papillae (Figure 29–16A). Studies in genetically engineered mice in which individual T1R genes have been deleted indicate that the T1R1/T1R3 complex is solely responsible for umami taste, whereas T1R2/T1R3 is solely responsible for sweet taste. As expected, a genetic knockout of T1R1 selectively abolishes umami taste, a knockout of T1R2 specifically abolishes sweet taste, while a knockout of T1R3 eliminates both sweet and umami taste (exactly as predicted, given that it is a common subunit of both the umami and sweet taste receptors).

Sweet and umami receptors differ significantly among different species. Most interestingly, different T1R subunits have been lost in some species, likely reflecting their evolutionary niche and diet. For example, the giant panda, which feeds almost exclusively on a bamboo diet, lacks a functional umami receptor. On the other hand, domestic cats, tigers, and cheetahs do not have a functional sweet receptor, whereas vampire bats that feed on a blood diet have mutations that have eliminated both sweet and umami functional receptors.

Bitter Taste Receptor

Bitter taste is thought to have evolved as an aversive signal of toxic molecules. Bitter taste sensation is elicited by a variety of compounds, including caffeine, nicotine, alkaloids, and denatonium, the most bitter-tasting chemical known (this compound is sometimes added to toxic products that are odorless and tasteless to prevent their ingestion).

Bitter tastants are detected by a family of approximately 30 G protein–coupled receptors called

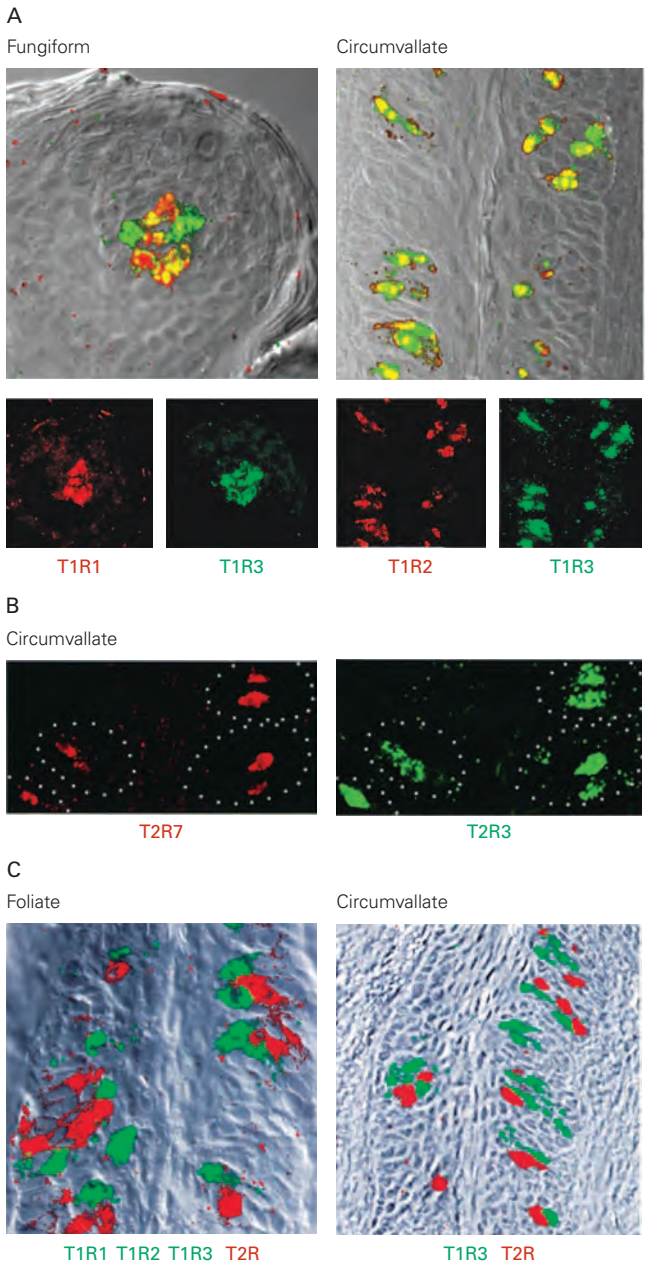

Figure 29–16 (Right) Expression of T1R and T2R receptors on the tongue. Sections of mouse or rat tongue were hybridized to probes that label T1R or T2R mRNAs to detect their sites of expression in taste cells.

A. The T1R3 receptor is expressed in taste cells of all three types of papillae. However, T1R1 is found mostly in fungiform papillae, whereas T1R2 is located predominantly in circumvallate (and foliate) papillae. Overlap between sites of expression appears as yellow cells in the micrographs at the top. The T1R1-T1R3 umami receptor is more frequently found in fungiform papillae, whereas the T1R2-T1R3 sweet receptor is more frequently found in circumvallate and foliate papillae. (Reproduced, with permission, from Nelson et al. 2001.)

B. A taste cell that detects bitter tastants can express several variants of T2R receptors. Here, probes for T2R3 and T2R7 labeled the same taste cells in circumvallate papillae. (Reproduced, with permission, from Adler et al. 2000.)

C. The T1R and T2R receptors are expressed in different taste cells. Taste cells labeled by a T1R3 probe or mixed T1R probes (**green**) did not overlap with cells labeled by a mixture of T2R probes (**red**). (Reproduced, with permission, from Nelson et al. 2001.)

T2Rs (Figure 29–14). However, different animal species contain different numbers of bitter receptors (varying from just a handful in the chicken genome to over 50 in the western clawed frog; humans have 28 T2R genes). These receptors recognize bitter compounds that have diverse chemical structures, with each T2R tuned to detect a small number of bitter compounds (Figure 29–15C). The T2R receptors recognize chemicals with high-affinity binding in the micromolar range, allowing detection of minute quantities of harmful compounds. A single taste cell expresses many, probably most, types of T2R receptors (Figure 29–16B). This arrangement implies that information about different bitter tastants is integrated in individual taste cells. Because different bitter compounds are detected by the same cells, all these compounds elicit the same perceptual bitter taste quality. The degree of bitterness might be caused by a compound's effectiveness in activating bitter taste cells.

Interestingly, genetic differences in the ability to perceive specific bitter compounds have been identified in both humans and mice. For example, humans are either super-tasters, tasters, or taste-blind to the bitter chemical 6-n-propylthiouracil. It was by mapping variation in this trait to specific chromosomal loci, and then by searching for novel G protein–coupled receptor genes within that chromosomal interval, that the T2R receptors were first identified. In the case of 6-n-propylthiouracil detection, the gene responsible for the genetic difference has proven to be a particular T2R gene. Thus, some bitter compounds may be recognized predominantly by only one of the approximately 30 T2R receptor types.

Taste cells expressing T2R receptors are found in both foliate and circumvallate papillae in mice (Figure 29–16C). A given taste cell expresses either T2R or T1R receptors (ie, one taste cell–one receptor class), but a single taste bud can contain taste cells of all types (eg, sweet, umami, bitter). Such mixing of cells accords with the observation that a single taste bud can be activated by more than one class of tastant; for example, sweet as well as bitter.

Salty Taste Receptor

Salt intake is critical to maintaining electrolyte balance. Perhaps because electrolytes must be maintained within a stringent range, the behavioral response to salt is concentration dependent: Low salt concentrations are appetitive, whereas high salt concentrations are aversive. How does the response to salt change based on concentration? It turns out that multiple taste cells detect salt. The essential salt taste receptor cell uses the epithelial sodium channel ENaC (see Figure 29–14). These specialized salt taste receptors are distinct from sweet, bitter, or umami receptors. At much higher salt concentrations, some bitter and sour taste cells also respond to salt, although the molecular details of detection have not been determined. Therefore, appetitive concentrations of salt drive responses via the ENaC salt taste receptor in the salt-sensing cells, whereas high salt concentrations activate the bitter and sour cells and thus trigger behavioral aversion.

Sour Taste Receptor

Sour taste is associated with acidic or fermented foods or drink. As with bitter compounds, animals are innately averse to sour substances, suggesting that the adaptive advantage of sour taste is avoidance of spoiled foods. Sour, like the other 4 taste qualities, is also detected by its own type of taste receptor cells (Figure 29–14). The ion channel Otopetrin-1 (Otop1), a proton-selective channel normally involved in the sensation of gravity in the vestibular system, is the sour-sensing ion channel in the taste system. As expected, a knockout of Otop1 in mice eliminated acid responses from sour taste receptor cells. Furthermore, mice engineered to express Otop1 in sweet taste receptor cells now have sweet cells that also respond to sour stimuli, demonstrating that this channel is sufficient to confer acid sensing.

Molecular-genetic studies have demonstrated that the different taste modalities are detected by distinct subsets of taste cells. As we have seen, a combination of T1R1 and T1R3 is responsible for all umami taste, and a combination of T1R2 and T1R3 is needed for all sweet taste detection except for the detection of high concentrations of sugars, which can be mediated by T1R3 alone. The T1R1 and T1R2 receptors are expressed by separate subsets of taste cells, indicating that the detection of sweet and umami tastants is segregated. Similarly, receptors and molecular markers uniquely define bitter, low salt, and sour taste cells.

A dramatic demonstration that each taste quality is detected by a different category of taste cells comes from studies of mice lacking a specific taste receptor gene or cell type. These studies showed that the loss of one taste modality did not affect the others. For example, mice in which sweet cells have been genetically ablated do not detect sugars but still detect amino acids, bitter compounds, salts, and sour compounds. Similarly, mice engineered to lack specific taste receptors cannot detect the corresponding tastants. For instance, mice lacking selective bitter receptors are not responsive to the corresponding bitter tastants,

and mice lacking ENaC cannot detect the taste of salt. These types of studies have shown that different tastes are detected by different receptors expressed in different classes of taste cells that drive specific behaviors.

Studies in mice further indicate that it is the taste cells rather than the receptors that determine the animal's response to a tastant. The human bitter receptor T2R16 recognizes a bitter tastant that mice cannot detect. When this receptor was expressed in mouse taste cells that normally express T2R bitter receptors, the ligand caused strong taste aversion. However, when that receptor was expressed in cells that express the T1R2/T1R3 sweet complex (ie, sweet cells), the bitter ligand elicited strong taste acceptance. These findings showed that innate responses of mice to different tastants (sweet and bitter in this example) operate via labeled lines that link the activation of different subsets of taste cells to different behavioral outcomes.

Gustatory Information Is Relayed From the Periphery to the Gustatory Cortex

Each taste cell is innervated at its base by the peripheral branches of the axons of primary sensory neurons (Figure 29–13). Each sensory fiber branches many times, innervating several taste cells within taste buds. The release of neurotransmitter from taste cells onto the sensory fibers induces action potentials in the fibers and the transmission of signals to the sensory cell body.

The cell bodies of gustatory sensory neurons lie in the geniculate, petrosal, and nodose ganglia. The peripheral branches of these neurons travel in cranial nerves VII, IX, and X, while the central branches enter the brain stem, where they terminate on neurons in the gustatory area of the nucleus of the solitary tract (Figure 29–17). In most mammals, neurons in this nucleus transmit signals to the parabrachial nucleus of the pons, which in turn sends gustatory information to the ventroposterior medial nucleus of the thalamus. In primates, however, these neurons transmit gustatory information directly to the taste area of the thalamus.

From the thalamus, taste information is transmitted to the gustatory cortex, a region of the cerebral cortex located along the border between the anterior insula and the frontal operculum (Figure 29–17). The gustatory cortex is believed to mediate the conscious perception and discrimination of taste stimuli. The taste areas of the thalamus and cortex also transmit information both directly and indirectly to the hypothalamus, which controls feeding behavior and autonomic responses.

Large-scale calcium imaging revealed that some neurons in the gustatory cortex respond preferentially to one taste modality, such as bitter or sweet. These neurons are localized in segregated cortical fields or hot spots. Interestingly, using a light-activated ion channel to activate neurons in the sweet hot spot elicits innately attractive responses. In contrast, activation of the bitter hot spot evokes suppression of licking and strong aversive orofacial responses, mimicking what is often seen in response to bitter tastants. These experiments showed that direct control of primary taste cortex can evoke specific, reliable, and robust behaviors that mimic responses to natural tastants. They also illustrated that the gustatory pathway can activate innate, immediate responses to sweet and bitter chemicals. To demonstrate that these cortically triggered behaviors are innate (ie, independent of learning or experience), similar stimulation experiments were performed in mutant mice that had never tasted sweet or bitter chemicals (the mutation abolished all sweet and bitter signal transduction). Even in these animals, activation of the corresponding cortical fields triggered the expected behavioral response, thus substantiating the predetermined nature of the sense of taste.

Perception of Flavor Depends on Gustatory, Olfactory, and Somatosensory Inputs

Much of what we think of as the flavor of foods derives from information provided by the integration of the taste and olfactory systems. Volatile molecules released from foods or beverages in the mouth are pumped into the back of the nasal cavity ("retronasal passage") by the tongue, cheek, and throat movements that accompany chewing and swallowing. Although the olfactory epithelium of the nose clearly makes a major contribution to sensations of flavor, such sensations are localized in the mouth rather than in the nose.

The somatosensory system is also thought to be involved in this localization of flavors. The coincidence between taste, somatosensory stimulation of the tongue, and the retronasal passage of odorants into the nose is assumed to cause odorants to be perceived as flavors in the mouth. Sensations of flavor also frequently have a somatosensory component that includes the texture of food as well as sensations evoked by spicy or minty foods and by carbonation.

Insects Have Modality-Specific Taste Cells That Drive Innate Behaviors

Insects have a specialized gustatory system that evaluates potential nutrients and toxins in food. Taste neurons are found on the proboscis, internal mouthparts, legs, wings, and ovipositor, allowing insects to sample

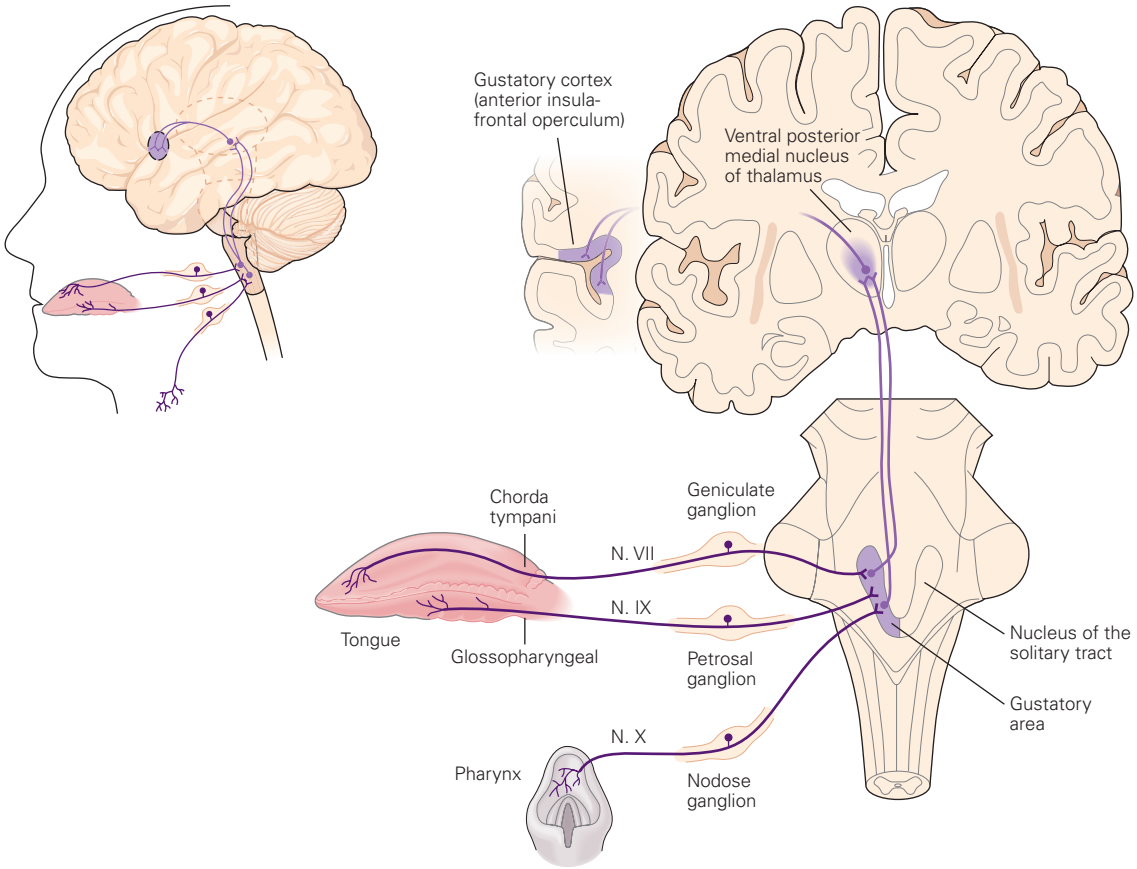

Figure 29–17 The gustatory system. Tastants are detected in taste buds in the oral cavity. Taste buds on the tongue and pharynx are innervated by the peripheral fibers of gustatory sensory neurons, which travel in the glossopharyngeal, chorda tympani and vagus nerves and terminate in the nucleus of the solitary tract in the brain stem. From there, taste information is relayed through the thalamus to the gustatory cortex as well as to the hypothalamus.

the local chemical environment prior to ingestion. As in mammals, only a few different types of taste cells detect different tastes. In the *Drosophila* fly, the different taste cell classes include those that sense sugars, bitter compounds, water, and pheromones. As in mammals, activation of these different taste cells drives different innate behaviors; for example, activation of sugar cells drives food acceptance behavior, whereas activation of bitter cells drives food rejection. Thus, the basic organization of taste detection is remarkably similar in insects and mammals, despite divergent evolutionary histories.

The taste receptors in insects are not related to vertebrate receptors. Members of the gustatory receptor (GR) gene family participate in the detection of sugars and bitter compounds. The GRs are membrane-spanning receptors that are distantly related to the odorant receptors of the fly. The fly has approximately 70 GR genes, a surprisingly large number considering it has approximately 60 olfactory receptor genes. Different GRs are found in sugar cells versus bitter cells, with many GRs present in a single neuron. In addition to GRs, other gene families participate in insect taste, including variants of ionotropic glutamate receptors and other ion channel classes. Similar to olfactory detection, the gene families involved in taste recognition differ across phyla, demonstrating that the gene families for chemical recognition have evolved independently.

Highlights

1. Odor detection in the nose is mediated by a large family of odorant receptors that number approximately 350 in humans and 1,000 in mice. These receptors vary in protein sequence, consistent with an ability to detect structurally diverse odorants.

2. Individual odorant receptors can detect multiple odorants, and different odorants activate different combinations of receptors. This combinatorial strategy explains how we can discriminate a multitude of odorants and how nearly identical odorants can have different scents.
3. Each olfactory sensory neuron in the nose expresses a single type of receptor. Thousands of neurons with the same receptor are dispersed in the olfactory epithelium and intermingled with neurons expressing other receptors.
4. In the olfactory bulb, the axons of the sensory neurons expressing the same receptor converge in a few receptor-specific glomeruli, generating a map of odorant receptor inputs that is similar among individuals.
5. The axons of olfactory bulb projection neurons project broadly to multiple areas of the olfactory cortex, generating a highly distributed organization of cortical neurons responsive to individual odorants. The olfactory cortex transmits information to many other brain areas.
6. In mice, pheromones can be detected in the nose or in the vomeronasal organ, a structure absent in humans. Signals from the nose and vomeronasal organ travel through different neural pathways in the brain.
7. The olfactory system of the fruit fly *Drosophila melanogaster* resembles that of mammals in many aspects. It uses a large number of diverse olfactory receptors, with one or a few olfactory receptors expressed by each olfactory sensory neuron. Moreover, neurons with the same receptor synapse in a few specific glomeruli in the antennal lobe of the brain. From there, olfactory signals are transmitted to two major brain areas involved in innate versus learned odor responses. The ease of using genetic approaches in fruit flies has enabled rapid study of mechanisms underlying odor coding and behavior.
8. The gustatory system detects five basic tastes: sweet, sour, bitter, salty, and umami (amino acids). Tastants that activate these taste qualities are detected by taste receptor cells located primarily in taste buds on the tongue and palate epithelium. The detection of the five different taste modalities is mediated by different taste receptor cells, each dedicated to one modality.
9. Sweet tastants are detected by a single type of receptor, which is composed of two subunits, T1R2 and T1R3. Umami receptors are related but comprise a combination of T1R1 and T1R3 subunits.
10. Bitter taste receptors constitute a family of approximately 30 related but diverse receptors that vary in ligand specificity. Individual taste receptor cells express many or all bitter receptors.
11. In contrast to sweet, umami, and bitter receptors, which are all G protein–coupled receptors, salty and sour tastes are detected by ion channels: ENaC for salt taste and Otopetrin-1 for sour taste.
12. Taste signals travel from taste buds through cranial nerves from gustatory sensory neurons in the geniculate, petrosal, and nodose ganglia via labeled lines (sweet taste receptor cells to sweet neurons, bitter taste cells to bitter neurons, etc.). They then travel to the gustatory area of the nucleus of the solitary tract and parabrachial nucleus, and from there to the taste area of the thalamus and then the gustatory cortex. The gustatory cortex, in turn, projects to many brain areas, including those involved in motor control, feeding, hedonic value, learning, and memory.
13. The gustatory cortex contains hot spots for sweet and bitter taste, which, when directly stimulated, can elicit behavioral responses similar to those obtained with tastants applied to the tongue.
14. The fruit fly *Drosophila* also has a specialized gustatory system that evaluates potential nutrients and toxins in food. Different classes of taste cells sense sugars, bitter compounds, pheromones, or water. Activation of these different peripheral sensors drives different innate behaviors, such as food acceptance or rejection.

Linda Buck
Kristin Scott
Charles Zuker

Selected Reading

Bargmann CI. 2006. Comparative chemosensation from receptors to ecology. Nature 444:295–301.

Giessel AJ, Datta SR. 2014. Olfactory maps, circuits and computations. Curr Opin Neurobiol 24:120–132.

Stowers L, Kuo TH. 2015. Mammalian pheromones: emerging properties and mechanisms of detection. Curr Opin Neurobiol 34:103–109.

Touhara K, Vosshall LB. 2009. Sensing odorants and pheromones with chemosensory receptors. Annu Rev Physiol 71:307–332.

Wilson DA, Sullivan RM. 2011. Cortical processing of odor objects. Neuron 72:506–519.
Yarmolinsky DA, Zuker CS, Ryba NJ. 2009. Common sense about taste: from mammals to insects. Cell 139: 234–244.

References

Adler E, Hoon MA, Mueller KL, Chandrashekar J, Ryba NJ, Zuker CS. 2000. A novel family of mammalian taste receptors. Cell 100:693–702.
Bachmanov AA, Bosak NP, Lin C, et al. 2014. Genetics of taste receptors. Curr Pharm Des 20:2669–2683.
Buck L, Axel R. 1991. A novel multigene family may encode odorant receptors: a molecular basis for odor recognition. Cell 65:175–187.
Chandrashekar J, Kuhn C, Oka Y, et al. 2010. The cells and peripheral representation of sodium taste in mice. Nature 464:297–301.
Chandrashekar J, Mueller KL, Hoon MA, et al. 2000. T2Rs function as bitter taste receptors. Cell 100:703–711.
Chen X, Gabitto M, Peng Y, Ryba NJ, Zuker CS. 2011. A gustotopic map of taste qualities in the mammalian brain. Science 333:1262–1266.
Dulac C, Axel R. 1995. A novel family of genes encoding putative pheromone receptors in mammals. Cell 83:195–206.
Dulac C, Torello AT. 2003. Molecular detection of pheromone signals in mammals: from genes to behaviour. Nat Rev Neurosci 7:551–562.
Glusman G, Yanai I, Rubin I, Lancet D. 2001. The complete human olfactory subgenome. Genome Res 1:685–702.
Godfrey PA, Malnic B, Buck LB. 2004. The mouse olfactory receptor gene family. Proc Natl Acad Sci U S A 101:2156–2161.
Greer PL, Bear DM, Lassance JM, et al. 2016. A family of non-GPCR chemosensors defines an alternative logic for mammalian olfaction. Cell 165:1734–1748.
Hallem EA, Carlson JR. 2006. Coding of odors by a receptor repertoire. Cell 125:143–160.
Herrada G, Dulac C. 1997. A novel family of putative pheromone receptors in mammals with a topographically organized and sexually dimorphic distribution. Cell 90:763–773.
Hoon MA, Adler E, Lindemeier J, Battey JF, Ryba NJ, Zuker CS. 1999. Putative mammalian taste receptors: a class of taste-specific GPCRs with distinct topographic selectivity. Cell 96:541–551.
Johnson BA, Farahbod H, Leon M. 2005. Interactions between odorant functional group and hydrocarbon structure influence activity in glomerular response modules in the rat olfactory bulb. J Comp Neurol 483:205–216.
Keller A, Zhuang H, Chi Q, Vosshall LB, Matsunami H. 2007. Genetic variation in a human odorant receptor alters odour perception. Nature 449:468–472.
Kondoh K, Lu Z, Ye X, Olson DP, Lowell BB, Buck LB. 2016. A specific area of olfactory cortex involved in stress hormone responses to predator odours. Nature 532:103–106.
Liberles SD, Buck LB. 2006. A second class of chemosensory receptors in the olfactory epithelium. Nature 442:645–650.
Liberles SD, Horowitz LF, Kuang D, et al. 2009. Formyl peptide receptors are candidate chemosensory receptors in the vomeronasal organ. Proc Natl Acad Sci U S A 106:9842–9847.
Malnic B, Godfrey PA, Buck LB. 2004. The human olfactory receptor gene family. Proc Natl Acad Sci U S A 101:2584–2589.
Malnic B, Hirono J, Sato T, Buck LB. 1999. Combinatorial receptor codes for odors. Cell 96:713–723.
Matsunami H, Buck LB. 1997. A multigene family encoding a diverse array of putative pheromone receptors in mammals. Cell 90:775–784.
Matsunami H, Montmayeur JP, Buck LB. 2000. A family of candidate taste receptors in human and mouse. Nature 404:601–604.
Mombaerts P, Wang F, Dulac C, et al. 1996. Visualizing an olfactory sensory map. Cell 87:675–686.
Montmayeur JP, Liberles SD, Matsunami H, Buck LB. 2001. A candidate taste receptor gene near a sweet taste locus. Nat Neurosci 4:492–498.
Morrison E, Constanzo R. 1990. Morphology of the human olfactory epithelium. J Comp Neurol 297:1–13.
Mueller KL, Hoon MA, Erlenbach I, Chandrashekar J, Zuker CS, Ryba NJ. 2005. The receptors and coding logic for bitter taste. Nature 434:225–229.
Nelson G, Chandrashekar J, Hoon MA, et al. 2002. An amino-acid taste receptor. Nature 416:199–202.
Nelson G, Hoon MA, Chandrashekar J, et al. 2001. Mammalian sweet taste receptors. Cell 106:381–390.
Neville KR, Haberly LB. 2004. The olfactory cortex. In: GM Shepherd (ed). *The Synaptic Organization of the Brain*, pp. 415–454. New York: Oxford University Press.
Niimura Y, Nei M. 2005. Evolutionary changes of the number of olfactory receptor genes in the human and mouse lineages. Gene 14:23–28.
Northcutt RG. 2004. Taste buds: development and evolution. Brain Behav Evol 64:198–206.
Oka Y, Butnaru M, von Buchholtz L, Ryba NJ, Zuker CS. 2013. High salt recruits aversive taste pathways. Nature 494:472–475.
Peng Y, Gillis-Smith S, Jin H, Tränkner D, Ryba NJ, Zuker CS. 2015. Sweet and bitter taste in the brain of awake behaving animals. Nature 527:512–515.
Ressler KJ, Sullivan SL, Buck LB. 1993. A zonal organization of odorant receptor gene expression in the olfactory epithelium. Cell 73:597–609.
Ressler KJ, Sullivan SL, Buck LB. 1994. Information coding in the olfactory system: evidence for a stereotyped and highly organized epitope map in the olfactory bulb. Cell 79:1245–1255.
Riviere S, Challet L, Fluegge D, Spehr M, Rodriguez I. 2009. Formyl peptide receptor-like proteins are a novel family of vomeronasal chemosensors. Nature 459:574–577.
Root CM, Denny CA, Hen R, Axel R. 2014. The participation of cortical amygdala in innate, odour-driven behaviour. Nature 515:269–273.

Royer SM, Kinnamon JC. 1991. HVEM Serial-section analysis of rabbit foliate taste buds. I. Type III cells and their synapses. J Comp Neurol 306:49–72.

Sarafi-Reinach TR, Sengupta P. 2000. The forkhead domain gene *unc*-130 generates chemosensory neuron diversity in *C. elegans*. Genes Dev 14:2472–2485.

Shepherd GM, Chen WR, Greer CA. 2004. The olfactory bulb. In: GM Shepherd (ed). *The Synaptic Organization of the Brain*, 5th ed., pp. 164–216. New York: Oxford Univ. Press.

Shepherd GM, Greer CA. 1998. The olfactory bulb. In: GM Shepherd (ed). *The Synaptic Organization of the Brain*, 4th ed., pp. 159–203. New York: Oxford Univ. Press.

Stettler DD, Axel R. 2009. Representations of odor in the piriform cortex. Neuron 63:854–864.

Sullivan SL, Adamson MC, Ressler KJ, Kozak CA, Buck LB. 1996. The chromosomal distribution of mouse odorant receptor genes. Proc Natl Acad Sci U S A 93: 884–888.

Teng B, Wilson CE, Tu YH, Joshi NR, Kinnamon SC, Liman ER. 2019. Cellular and neural responses to sour stimuli require the proton channel Otop1. Curr Biol 4:3647–3656.

Troemel ER, Kimmel BE, Bargmann CI. 1997. Reprogramming chemotaxis responses: sensory neurons define olfactory preferences in *C. elegans*. Cell 91:161–169.

Vassar R, Ngai J, Axel R. 1993. Spatial segregation of odorant receptor expression in the mammalian olfactory epithelium. Cell 74:309–318.

Vosshall L, Amrein H, Morozov PS, Rzhetsky A, Axel R. 1999. A spatial map of olfactory receptor expression in the *Drosophila* antenna. Cell 96:725–736.

Vosshall LB, Stocker RF. 2007. Molecular architecture of smell and taste in *Drosophila*. Annu Rev Neurosci 30:505–533.

Vosshall LB, Wong AM, Axel R. 2000. An olfactory sensory map in the fly brain. Cell 102:147–159.

Wang JW, Wong AM, Flores J, Vosshall LB, Axel R. 2003. Two-photon calcium imaging reveals an odor-evoked map of activity in the fly brain. Cell 112:271–282.

Wilson RI. 2013. Early olfactory processing in *Drosophila*: mechanisms and principles. Annu Rev Neurosci 36:217–241.

Zhang X, Firestein S. 2002. The olfactory receptor gene superfamily of the mouse. Nat Neurosci 5:124–133.

Zhang Y, Hoon MA, Chandrashekar J, et al. 2003. Coding of sweet, bitter, and umami tastes: different receptor cells sharing similar signaling pathways. Cell 112:293–301.

Zhang J, Jin H, Zhang W, et al. 2019. Sour Sensing from the Togue to the Brain. Cell 179:392–402.

Zhao GQ, Zhang Y, Hoon MA, et al. 2003. The receptors for mammalian sweet and umami taste. Cell 115:255–266.

Part V

Preceding Page

Fresco of dancing Peucetian women from the Tomb of the Dancers in the Corso Cotugno necropolis of Ruvo di Puglia, 4th–5th century BC. The tomb has a semichamber design. Its six painted panels depict 30 dancing women, moving from left to right with arms interlocked as though they were dancing in a circle around the interior of the tomb. The skeletal remains of the deceased in the tomb clearly belonged to a distinguished male warrior. The tomb is named after the dancing women that appear on the frescoes in the tomb. The panels with the frescoes are now exhibited in the Naples National Archaeological Museum, inv. 9353. (Source: https://en.wikipedia.org/wiki/Tomb_of_the_Dancers.)

V Movement

The capacity for movement, as many dictionaries remind us, is a defining feature of animal life. As Sherrington, who pioneered the study of the motor system pointed out, "to move things is all that mankind can do, for such the sole executant is muscle, whether in whispering a syllable or in felling a forest."*

The immense repertoire of motions that humans are capable of stems from the activity of some 640 skeletal muscles—all under the control of the central nervous system. After processing sensory information about the body and its surroundings, the motor centers of the brain and spinal cord issue neural commands that effect coordinated, purposeful movements.

The task of the motor systems is the reverse of the task of the sensory systems. Sensory processing generates an internal representation in the brain of the outside world or of the state of the body. Motor processing begins with an internal representation: the desired purpose of movement. Critically, however, this internal representation needs to be continuously updated by internally generated information (efference copy) and external sensory information to maintain accuracy as the movement unfolds.

Just as psychophysical analysis of sensory processing tells us about the capabilities and limitations of the sensory systems, psychophysical analyses of motor performance reveal the control rules used by the motor system.

Because many of the motor acts of daily life are unconscious, we are often unaware of their complexity. Simply standing upright, for example, requires continual adjustments of numerous postural muscles in response to the vestibular signals evoked by miniscule swaying. Walking, running, and other forms of locomotion involve the combined action of central pattern generators, gated sensory information, and descending commands, which together generate the complex patterns of alternating excitation and inhibition to the appropriate sets of muscles. Many actions, such as serving a tennis

*Sherrington CS. 1979. 1924 Linacre lecture. In: JC Eccles, WC Gibson (eds). *Sherrington: His Life and Thought*, p. 59. New York: Springer-Verlag.

ball or executing an arpeggio on a piano, occur far too quickly to be shaped by sensory feedback. Instead, centers, such as the cerebellum, make use of predictive models that simulate the consequences of the outgoing commands and allow very short latency corrections. Motor learning provides one of the most fruitful subjects for studies of neural plasticity.

Motor systems are organized in a functional hierarchy, with each level concerned with a different decision. The highest and most abstract level, likely requiring the prefrontal cortex, deals with the purpose of a movement or series of motor actions. The next level, which is concerned with the formation of a motor plan, involves interactions between the posterior parietal and premotor areas of the cerebral cortex. The premotor cortex specifies the spatiotemporal characteristics of a movement based on sensory information from the posterior parietal cortex about the environment and about the position of the body in space. The lowest level of the hierarchy coordinates the spatiotemporal details of the muscle contractions needed to execute the planned movement. This coordination is executed by the primary motor cortex, brain stem, and spinal cord. This serial view has heuristic value, but evidence suggests that many of these processes can occur in parallel.

Some functions of the motor systems and their disturbance by disease have now been described at the level of the biochemistry of specific transmitter systems. In fact, the discovery that neurons in the basal ganglia of parkinsonian patients are deficient in dopamine was the first important clue that neurological disorders in the central nervous system can result from altered chemical transmission. Neurophysiological studies have provided information as to how such transmitters play a critical role in action selection and the reinforcement of successful movements.

Understanding the functional properties of the motor system is not only fundamental in its own right, but it is of further importance in helping us to understand disorders of this system and explore the possibilities for treatment and recovery. As would be expected for such a complex apparatus, the motor system is subject to various malfunctions. Disruptions at different levels in the motor hierarchy produce distinctive symptoms, including the movement-slowing characteristic of disorders of the basal ganglia, such as Parkinson disease, the incoordination seen with cerebellar disease, and the spasticity and weakness typical of spinal cord damage. For this reason, the neurological examination of a patient inevitably includes tests of reflexes, gait, and dexterity, all of which provide information about the status of the nervous system. In addition to pharmacological therapies, the treatment of motor system disorders has been augmented by two new approaches. First, focal stimulation of the basal ganglia has been shown to restore motility to certain patients with Parkinson disease; such deep-brain stimulation is also being tested in the context of other neurological and psychiatric conditions. And

second, the motor systems have become a target for the application of neural prosthetics; neural signals are decoded and used to drive devices that aid patients with paralysis caused by spinal cord injury and stroke.

Part Editors: Daniel M. Wolpert and Thomas M. Jessell

Part V

This page intentionally left blank

30

Principles of Sensorimotor Control

The preceding chapters in this book consider how the brain constructs internal representations of the world around us. These representations are behaviorally meaningful when used to guide movement. Thus, an important function of the sensory representations is to shape the actions of the motor systems. This chapter describes the principles that govern the neural control of movement using concepts derived from behavioral studies and computational models of the brain and musculoskeletal system.

We start by considering the challenges motor systems face in generating skillful actions. We then examine some of the neural mechanisms that have evolved to meet these challenges and produce smooth, accurate, and efficient movements. Finally, we see how motor learning improves our performance and allows us to adapt to new mechanical conditions, such as when using a tool, or to learn novel correspondences between sensory and motor events, such as when using a computer mouse to control a cursor. This chapter focuses on voluntary movement; reflexes and rhythmic movements are discussed in further detail in Chapters 32 and 33.

Voluntary movements are generated by neural circuits that span different levels of the sensory and motor hierarchies, including regions of the cerebral cortex, subcortical areas such as the basal ganglia and cerebellum, and the brain stem and spinal networks. These different structures have unique patterns of neural activity. Moreover, focal damage to different structures can cause distinct motor deficits. Although it is tempting to suggest that these individual structures have distinct functions, these brain and spinal areas normally work together as a network, such that damage to one component likely affects the function of all

others. Many of the principles discussed in this chapter cannot be easily attributed to a single brain or spinal area. Instead, distributed neural processing is likely to underlie the computational mechanisms that subserve sensorimotor control.

The Control of Movement Poses Challenges for the Nervous System

Motor systems produce neural commands that act on the muscles, causing them to contract and generate movement. The ease with which we move, from tying our shoelaces to returning a tennis serve, masks the complexity of the control processes involved. Many factors inherent in sensorimotor control are responsible for this complexity, which becomes clearly evident when we try to build machines to perform human-like movement (Chapter 39). Although computers can now beat the world's best players at chess and Go, no robot can manipulate a chess piece with the dexterity of a 6-year-old child.

The act of returning a tennis serve illustrates why the control of movement is challenging for the brain (Figure 30–1). First, motor systems have to contend with different forms of uncertainty, such as our incomplete knowledge with regard to the state of the world and the rewards we might gain. On the sensory side, although the player may see the serve, she cannot be certain where her opponent will aim or where the ball might strike the racket. On the motor side, there is uncertainty as to the likely success of different possible returns. Skilled performance requires reducing uncertainty by anticipating events we may encounter (the trajectory of an opponent's tennis serve) and by motor planning (adopting an appropriate stance to return the expected serve).

Second, even if the player can reliably estimate the ball's trajectory, she must determine from sensory signals which of the 600 muscles she will use in order to move her body and racket to intercept the ball. Controlling such a system can be challenging as it is hard to explore all possible actions effectively in a system with many degrees of freedom (eg, a large number of individual muscles), making learning difficult. We will see how the motor system reduces the degrees of freedom of the musculoskeletal system by controlling groups of muscles, termed synergies, to simplify control.

Third, unwanted disturbances, termed noise, corrupt many signals and are present at all stages of sensorimotor control, from sensory processing, through planning, to the outputs of the motor system. For example, in a tennis serve, such noise will cause the ball to land in different places even when the server is trying to hit the same location on the court. Both sensory feedback, reflecting the ball's location, and motor outputs are contaminated with noise. The variability inherent in such noise limits our ability to perceive accurately and act precisely. The amount of noise in our motor commands tends to increase with stronger commands (ie, more force). This limits our ability to move rapidly and accurately at the same time and thus

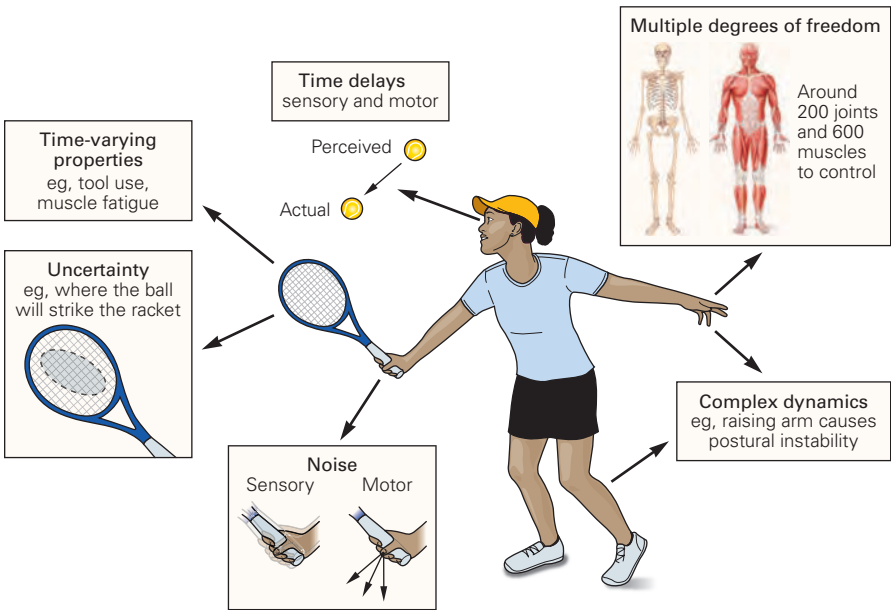

Figure 30–1 The challenges of sensorimotor control.

leads to a trade-off between speed and accuracy. We will see how efficient planning of movement can minimize the deleterious effects of noise on task success.

Fourth, time delays are present at all stages of the sensorimotor system, including the delays arising from receptor dynamics, conduction delays along nerve fibers and synapses, and delays in the contraction of muscles in response to motor commands. Together, these delays, which can be on the order of 100 ms, depend on the particular sensory modality (eg, longer for vision than proprioception) and complexity of processing (eg, longer for face recognition than motion perception). Therefore, we effectively live in the past, with the control system only having access to out-of-date information about the world and our own body. Such delays can result in instability when trying to make fast movements, as we try to correct for errors we perceive but that no longer exist. We will see how the brain makes predictions of the future states of the body and environment to reduce the negative consequences of such delays.

Fifth, the body and environment change both on a short and a long timescale. For example, within the relatively short period of a game, a player must correct for weakening muscles as she fatigues and changes in the court surface when it rains. On a longer timescale, the properties of our motor system change dramatically during growth as our limbs lengthen and increase in weight. As we will see, the ever-changing properties of the motor system place a premium on our ability to use motor learning to adapt control appropriately.

Finally, the relation between motor command and the ensuing action is highly complex. The motion of each body segment produces torques, and potentially motions, at all other body segments through mechanical interactions. For example, when a player raises the racket to hit the ball, she must anticipate destabilizing forces and counteract them to maintain balance. Indeed, when we raise our arms forward while standing, the first muscle to activate is an ankle flexor ensuring you remain upright. We will see how the sensorimotor system controls movement of different segments to maintain fine coordination of actions.

Actions Can Be Controlled Voluntarily, Rhythmically, or Reflexively

Although movements are often classified according to function—as eye movement, prehension (reach and grasp), posture, locomotion, breathing, and speech—many of these functions are subserved by overlapping groups of muscles. Moreover, the same groups of muscles can be controlled voluntarily, rhythmically, or reflexively. For example, the muscles that control respiration can be used to take a deep breath voluntarily before diving under water, to breathe automatically and rhythmically in a regular cycle of inspiration and expiration, or to act reflexively in response to a noxious stimulus in the throat, producing a cough.

Voluntary movements are those that are under conscious control. Rhythmic movements can also be controlled voluntarily but differ from voluntary movements in that their timing and spatial organization are to a larger extent controlled autonomously by spinal or brain stem circuitry. Reflexes are stereotyped responses to specific stimuli that are generated by neural circuits in the spinal cord or brain stem (although some reflexes involve pathways through cortex). These responses occur on a shorter timescale than voluntary responses.

Although we may consciously intend to perform a task or plan a certain sequence of actions, and at times are aware of deciding to move at a particular moment, movements generally seem to occur automatically. Conscious processes are not necessary for moment-to-moment control of movement. We carry out the most complicated movements without a thought to the actual joint motions or muscle contractions required. The tennis player does not consciously decide which muscles to use to return a serve with a backhand or which body parts must be moved to intercept the ball. In fact, thinking about each body movement before it takes place can disrupt the player's performance.

Motor Commands Arise Through a Hierarchy of Sensorimotor Processes

Although the final output to the musculoskeletal system is via motor neurons in the spinal cord, the motor control of muscles for a specific action occurs through a hierarchy of control centers. This arrangement can simplify control: Higher levels can plan more global goals, whereas lower levels are concerned with how these goals are implemented.

At the lowest level, muscles themselves have properties that can contribute to control even without any change in the motor command. Unlike the electric motors of a robot, muscles have substantial passive properties that depend on both the motor command acting on the muscle as well as the muscle's length and rate of change of length (Chapter 31). As a simple approximation, a muscle can be seen as acting like a spring (increasing tension as it is stretched and reducing tension as it is shortened) and damper

(increasing tension as the rate of stretch increases). For small perturbations, these properties tend to act to stabilize the length of a muscle and hence stabilize the joint on which the muscle acts. For example, if an external perturbation extends a joint, the flexor muscles will be stretched, increasing their tension, while the extensor muscles will be shortened, reducing their tension, and the imbalance in tension will tend to bring the joint back toward its original position. A particular advantage of such control is that, unlike higher levels in the motor hierarchy, such changes in force act with minimal delay as they are simply an effect of passive physical properties of the muscles.

In addition to the passive properties of muscles, sensory inputs can cause motor output directly without the intervention of higher brain centers. Sensorimotor responses, such as spinal reflexes, control for local disturbance or noxious stimuli. Reflexes are stereotyped responses to specific stimuli that are generated by simple neural circuits in the spinal cord or brain stem. For example, a spinal flexor withdrawal reflex can remove your hand from a hot stove without any descending input from the brain. The advantage of such reflexes is that they are fast; the disadvantage is they are less flexible than voluntary control systems (Chapter 32). Again, there is a hierarchy of reflex circuits. The fastest is the monosynaptic stretch reflex, which drives contraction of a stretched muscle. In this reflex circuit, sensory neurons that are activated by stretch receptors in the muscle (the muscle spindle) directly synapse onto motor neurons that cause the same muscle to contract. The time from the stimulus to the response is around 25 ms. This reflex can be tested clinically by striking the quadriceps muscle tendon just below the patella.

While this monosynaptic stretch reflex is not adaptable on short timescales, multisynaptic reflexes, which involve higher level structures such as motor cortex, can produce responses at around 70 ms. Unlike the monosynaptic reflex, multisynaptic reflexes are adaptable to changes in behavioral goals because the circuit connecting sensory and motor neurons can be modified by task-dependent properties. The strength of a reflex tends to increase with the tension in a muscle (called gain-scaling), and therefore, reflexes can be amplified by co-contracting the set of muscles around a joint so as to respond to perturbations with a greater force. In fact, we use such co-contraction when holding the hand of a rebellious child when crossing a road. Such a strategy can amplify the reflexes, thereby reducing deviations of the arm caused by random external forces.

Finally, voluntary movements are those that are under conscious control by the brain. Voluntary movements can be generated in the absence of a stimulus or used to compensate for a perturbation. The time to generate a voluntary movement in response to a physical perturbation depends both on the nature of the perturbation (modality and size) as well as whether the response can be specified before the perturbation occurs. For example, a voluntary correction to a small physical perturbation can occur with a latency of about 110 ms.

Although we have described clear distinctions between the different levels of the motor hierarchy, from reflexes through to voluntary control, in reality, such distinctions are blurred in a continuum of responses spanning different latencies. Increasing the response time permits additional neural circuitry to be involved in the sensorimotor loop and tends to increase the sophistication and adaptability of the response, leading to a trade-off between the speed of the response and the sophistication of processing as one ascends the motor hierarchy.

Motor Signals Are Subject to Feedforward and Feedback Control

In this section, we will first illustrate some principles of control that are important for dealing with the problem of sensory delays, sensory noise, and motor noise. For simplicity, we confine our discussion to relatively simple movements, such as moving the eyes in response to head movements or moving the hand from one location to another. We consider two broad classes of control, feedforward and feedback, which differ in their reliance on sensory feedback during the movement.

Feedforward Control Is Required for Rapid Movements

Some movements are executed without monitoring the sensory feedback that arises from the action. In such feedforward control situations, the motor command is generated without regard to the sensory consequences. Such commands are therefore also termed *open-loop*, reflecting the fact that the sensorimotor loop is not completed by sensory feedback (Figure 30–2A).

Open-loop control requires some information about the body so that the appropriate command can be generated. For example, it should include information about the dynamics of the motor system. Here, "dynamics" refers to the relation between the motor command (or the torques or forces) applied and the ensuing motion of the body, for example, joint rotations. For perfect open-loop control, one needs to

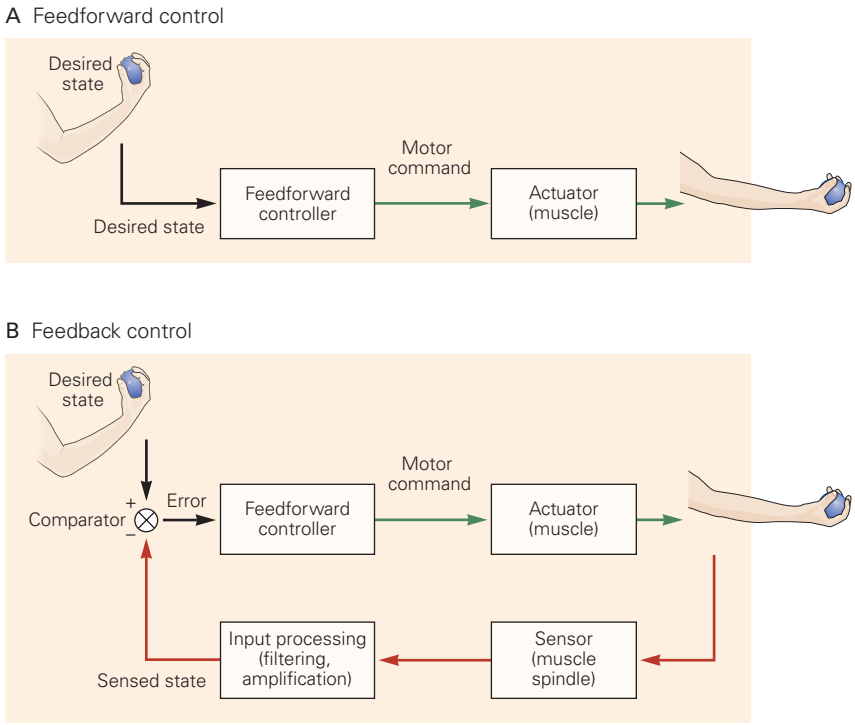

Figure 30–2 Feedforward and feedback control.

A. A feedforward control motor command is based on a desired state. Any errors that arise during the movement are not monitored. Although we illustrate the elements of feedforward control for the arm, only the initial portion of any arm movement is driven by feedforward signals and the movement typically involves feedback control.

B. With feedback control, the desired and sensed states are compared (at the comparator) to generate an error signal, which helps shape the motor command. There can be considerable delay in the feedback of sensory information to the comparator.

invert the dynamics so as to calculate the motor command that will generate the desired motion. The neural mechanism that performs this inversion is called an inverse model, a type of internal model (Box 30–1). An inverse model coupled to open-loop control can determine what motor commands are needed to produce the particular movements necessary to achieve a goal.

Although not monitoring the consequences of an action may seem counterproductive, there are good reasons for not doing so. The main reason, as discussed earlier, is that there are delays in both sensing and acting. That is, the conversion of a stimulus into neural signals by sensory receptors and conveyance of these signals to central neurons take time. For example, visual inputs can take around 60 ms to be processed in the retina and transmitted to the visual cortex. In addition to delays in afferent sensory systems, there are also delays in central processing, in the transmission of efferent signals to motor neurons, and in the response of muscles. In all, the combined sensorimotor loop delay is appreciable, approximately 120 to 150 ms for a motor response to a visual stimulus. This delay means that movements like saccades, which redirect gaze within 30 ms, cannot use sensory feedback to guide movement. Even for slower movements like reaching, which takes on the order of 500 ms, sensory information cannot be used to guide the initial part of a movement, so open-loop control must be used.

Open-loop control also has disadvantages. Any movement errors caused by inaccuracies in planning or execution will not be corrected, and therefore will compound themselves over time or successive movements. The more complex the system under control, the more difficult it is to arrive at an accurate inverse model through learning.

An example of a purely open-loop control system is the control of the eye in response to head rotation. The vestibulo-ocular reflex (Chapter 27) uses open-loop control to fix gaze on an object during head rotation. The vestibular labyrinth senses the head rotation and drives appropriate movements of the eyes through a three-synapse circuit. The reflex does not require (or use) vision during the movement (the eyes maintain a stable gaze when the head is rotated in the dark). Sensory information from the vestibular system does drive the eye movement, but the control is feedforward (any errors that arise are not corrected during the movement). Such precise open-loop control is possible because the dynamic properties of the eye are relatively simple, the rotation of the head can be directly sensed by the vestibular labyrinth, and the eye tends not to be substantially perturbed by external events. In contrast, it is very difficult to optimize an inverse model for a complex musculoskeletal system such as the arm, and thus, the control of arm movement requires some form of error correction.

Box 30–1 Internal Models

The utility of numerical models in the physical sciences has a long history. Numerical models are abstract quantitative representations of complex physical systems. Some start with equations and parameters that represent initial conditions and run *forward*, either in time or space, to generate physical variables at some future state. For example, we can construct a model of the weather that predicts wind speed and temperature 2 weeks from now.

Other models start with a state, a set of physical variables with specific values, and run in the *inverse* direction to determine what parameters in the system account for that state. When we fit a straight line to a set of data points, we are constructing an inverse model that estimates slope and intercept based on the equations of the system being linear. An inverse model thus may allow us to know how to set the parameters of the system to obtain desired outcomes.

Over the past 50 years, the idea that the nervous system has similar predictive models of the physical world to guide behavior has become a major issue in neuroscience. Such a model is termed "internal" because it is instantiated in neural circuits and is therefore internal to the central nervous system. The idea originated in Kenneth Craik's notion of *internal models* for cognitive function. In his 1943 book *The Nature of Explanation*, Craik was perhaps the first to suggest that organisms make use of internal representations of the external world:

> If the organism carries a "small-scale model" of external reality and of its own possible actions within its head, it is able to try out various alternatives, conclude which is the best of them, react to future situations before they arise, use the knowledge of past events in dealing with the present and future, and in every way to react in a much fuller, safer, and more competent manner to the emergencies that face it.

In this view, an internal model allows an organism to contemplate the consequences of potential actions without actually committing itself to those actions. In the context of sensorimotor control, internal models can answer two fundamental questions. First, how can we generate motor commands that act on our muscles so as to control the behavior of our body? Second, how can we predict the consequences of our own motor commands?

The central nervous system must exercise both control and prediction to achieve skilled motor performance. Prediction and control are two sides of the same coin, and the two processes map exactly onto forward and inverse models (Figure 30–3). Prediction turns motor commands into expected sensory consequences, whereas control turns desired sensory consequences into motor commands.

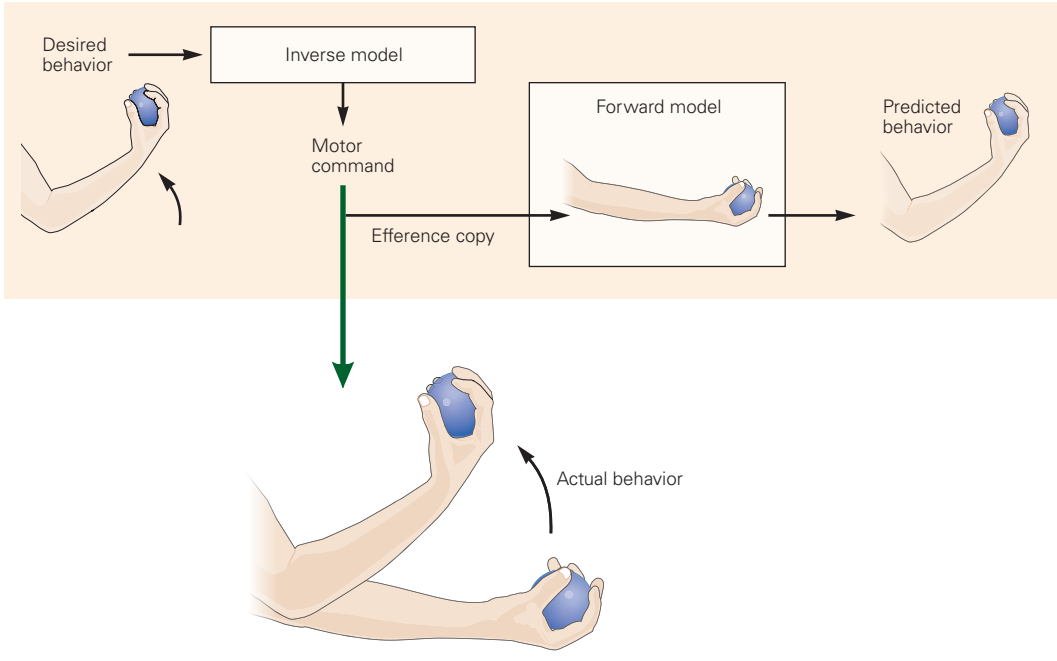

Figure 30–3 Internal sensorimotor models represent relationships of the body and external world. The inverse model determines the motor commands that will produce a behavioral goal, such as raising the arm while holding a ball. A descending motor command acts on the musculoskeletal system to produce the movement. A copy of the motor command is passed to a forward model that simulates the interaction of the motor system and the world and thus can predict behaviors. If both forward and inverse models are accurate, the output of the forward model (the predicted behavior) will be the same as the input to the inverse model (the desired behavior).

Feedback Control Uses Sensory Signals to Correct Movements

To correct movement errors as they arise, movement must be monitored. Systems that perform error correction are known as feedback or closed-loop control because the sensorimotor loop is complete (Figure 30–2B).

The simplest form of feedback control is one in which the control system generates a fixed response when the error exceeds some threshold. Such a system is seen in most central heating systems in which a thermostat is set to a desired temperature. When the house temperature falls below the specified level, the heating is turned on until the temperature reaches that level. Although such a system is simple and can be effective, it has the drawback that the amount of heat being put into the house does not relate to the discrepancy between the actual and desired temperature (the error). A better system is one in which the control signal is proportional to the error.

Such proportional control of movement involves sensing the error between the actual and desired position of, for example, the hand. The size of the corrective motor command is in proportion to the size of the error and in a direction to reduce the error. The amount by which the corrective motor command is increased or decreased per unit of positional error is called the gain. By continuously correcting a movement, feedback control can be robust both to noise in the sensorimotor system and to environmental perturbations.

While feedback control can update commands in response to deviations that arise during the movement, it is sensitive to feedback delays. Without any delay, as the gain of the feedback controller increases, the system will track a desired position with increasing fidelity (Figure 30–4). However, as feedback delay increases, the control system may start to oscillate and eventually become unstable. This is because with a delay the system may respond to errors that no longer exist and may therefore even correct in the wrong direction.

Smooth pursuit eye movement, used to track a moving object, is an example of a movement driven primarily by feedback. Smooth pursuit uses feedback to minimize the velocity error on the retina (the difference between the gaze and target velocity). We can compare the efficiency of feedforward and feedback control in minimizing error. Compare how easy it is to fixate on your outstretched stationary finger when quickly rotating your head back and forth versus trying to track your finger when it is moving it rapidly sinusoidally left and right while your head remains stationary. Although the relative motion of finger to head is the same in both conditions, the former is precise because it uses the vestibulo-ocular reflex, whereas the latter uses feedback (requiring an error in velocity to drive the eye movement) and thus is less precise, particularly as the frequency of motion increases.

In most motor systems, movement control is achieved through a combination of feedforward and feedback processes. We will see later that these two components arise naturally in a unified model of movement production.

Estimation of the Body's Current State Relies on Sensory and Motor Signals

Accurate control of movement requires information about our body's current state, for example, the positions and velocities of the different segments of the body. To grasp an object, we need to know not only the location, shape, and surface properties of the object but also the current configuration of our arm and fingers so as to appropriately shape and position the hand.

Estimating the state of the body is not a trivial problem. First, as we have seen, sensory signals are delayed due to sensory transduction and conduction time. Therefore, signals from our muscles, joints, and vision are all out of date by the time they reach the central nervous system. Second, the sensory signals we receive are often imprecise and corrupted by neural noise. For example, if you touch the underside of a table with the finger of one hand and try to estimate its location on the top of the table with your other hand, you can be off by a considerable distance. Third, we often do not have sensors that directly communicate relevant information. For example, although we have sensors that report muscle length and joint angle, we have no sensors within the limb that directly determine the location of the hand in space. Therefore, sophisticated computation is required to estimate current body states as accurately as possible. Several principles have emerged as to how the brain estimates state.

First, state estimation relies on internal models of sensorimotor transformations. Given the fixed lengths of our limb segments, there is a mathematical relation between the muscle lengths or joint angles of the arm and the location of the hand in space. A neural representation of this relation allows the central nervous system to estimate hand position if it knows the joint angles and segment lengths. Neural circuits that compute such sensorimotor transformations are examples of internal models (Box 30–1).

Second, state estimation can be improved by combining multiple sensory modalities. For example, information about the state of our limbs arrives from

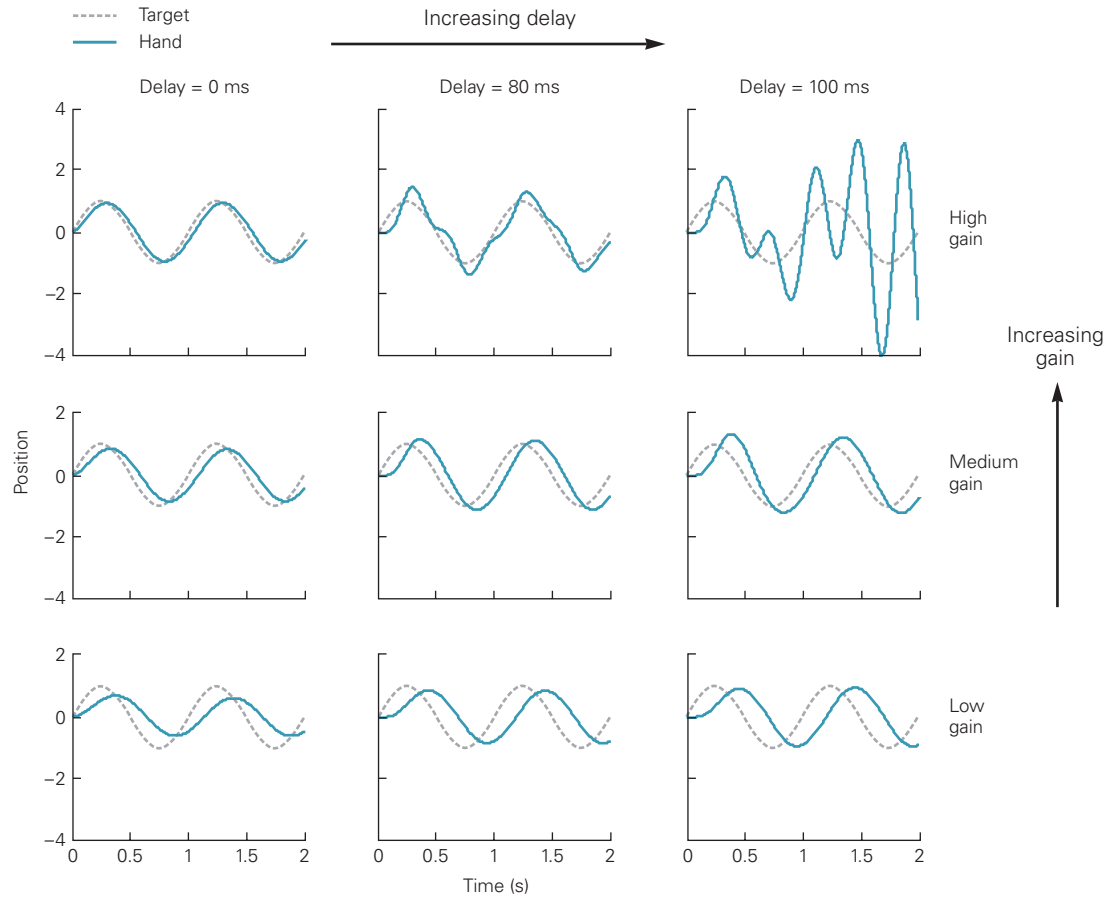

Figure 30–4 The interplay of gain and delay in feedback control. Performance of a feedback controller trying to track a target moving sinusoidally in one dimension. The sensory feedback signal that conveys error in the position arrives after some period of time (the delay), and the motor system tries to correct for the error by increasing or decreasing the size of its command relative to the error (the gain).

The plots show the performance in which there is either instantaneous feedback (no delay) of error (**left column**) or feedback with delay of 80 or 100 ms (**middle and right columns**). When the gain is high and the delay is low, tracking is very good. However, when the delay increases, because the controller is compensating for errors that existed 80 or 100 ms earlier, the correction may be inappropriate for the current error. The gain can be lowered to maintain stability, but as the feedback controller corrects errors only slowly, tracking becomes inaccurate.

At low gain (**bottom row**), the feedback controller corrects errors only slowly and tracking is inaccurate. As the gain increases (**middle row**), the feedback controller corrects errors more rapidly and tracking performance improves. At high gain (**top row**), the system corrects rapidly but is prone to overcorrect, leading to instability when the time delay in feedback is on the order of physiological time delays (**top right**). Because the controller is compensating for errors that existed 100 ms earlier, the correction may therefore be inappropriate for the current error. This overcorrection leads to oscillations and is one mechanism proposed to account for some forms of oscillatory tremor seen in neurological disease.

proprioceptive information from muscle spindles, the stretch of the skin, and the sight of the arm. These modalities have different amounts of variability (or noise) associated with them, and just as we average a set of experimental data to reduce measurement error, these sensory modalities can be combined to reduce the overall uncertainty in the state estimate.

The optimal way to combine these sources is for higher brain centers to take the uncertainty of each modality into account and rely on the more certain modalities. For example, the location of the hand can be sensed both by proprioception and vision. The sight of your hand in front of you tends to be more reliable than proprioception for estimating location along the azimuth (right–left) but less reliable for depth (forward–back). Therefore, visual input should be given greater weight than proprioceptive input when estimating the azimuth location of your hand, and vice versa for depth. By measuring the precision of each modality when used alone, it is possible to predict the increased

Box 30–2 Bayesian Inference

Bayesian inference is a mathematical framework for making estimates about the world based on uncertain information. The fundamental idea is that probabilities (between 0 and 1) can be used to represent the degree of belief in different alternatives, such as the belief that the chance of your rolling a six with fair dice is 1 in 6.

The beauty of Bayesian inference is that by using the rules of probability we can specify how beliefs should be formed and updated based on our experience and new information from sensory input. For example, when playing tennis, we want to estimate where the ball will land. Because vision does not provide perfect information about the ball's position and velocity in flight, there is uncertainty as to the landing location. However, if we know the level of noise in our sensory system, then the current sensory input can be used to compute the *likelihood* (ie, probability) of the particular sensory input for different potential landing locations.

We can learn additional information from repeated experience of the game: The position where the ball lands is not equally probable over the court. For example, bounce locations are likely to be concentrated near the boundary lines where it is most difficult to return the ball. This distribution is termed the *prior*.

The Bayes rule defines how to combine the prior and likelihood to make an optimal estimate of the bounce location. While the Bayesian approach was originally developed in statistics, it now provides a unifying framework to understand how the brain deals with uncertainty in the perceptual, motor, and cognitive domains.

precision when both are used at the same time. Experiments have shown that this process is often close to optimal. Precision can also be improved by combining prior knowledge with sensory inputs using the mathematics of Bayesian inference (Box 30–2).

Third, the motor command can also provide valuable information. If both the current state of the body and the descending motor command are known, the next state of the body can be estimated. This estimate can be derived from an internal model that represents the causal relation between actions and their consequences. This is called a forward model because it estimates future sensory inputs based on motor outputs (Box 30–1). Thus, a forward model can be used to anticipate how the motor system's state will change as the result of a motor command. A copy of a descending motor command is passed into a forward model that acts as a neural simulator of the musculoskeletal system moving in the environment. This copy of the motor command is known as an efference copy (or corollary discharge). Forward and inverse models can be better understood if we place the two in series. If the structure and parameter values of each model are correct, the output of the forward model (the predicted behavior) will be the same as the input to the inverse model (the desired behavior) (Figure 30–3).

Using the motor command to estimate the state of the body is advantageous as, unlike sensory information that is delayed, the motor command is available before it acts on the musculoskeletal system and therefore can be used to anticipate changes in the state. However, this estimate will tend to drift over time if the forward model is not perfectly accurate, and therefore, sensory feedback is used to correct the state estimate, albeit with a delay.

It may seem surprising that the motor command is used in state estimation. In fact, the first demonstration of a forward model used a motor system that relies on only the motor command to estimate state, that is, the position of the eye within the orbit. The concept of motor prediction was first considered by Helmholtz when trying to understand how we localize visual objects. To calculate the location of an object relative to the head, the central nervous system must know both the retinal location of the object and the gaze direction of the eye. Helmholtz's ingenious suggestion was that the brain, rather than sensing the gaze direction, predicted it based on a copy of the motor command to the eye muscles.

Helmholtz used a simple experiment on himself to demonstrate this. If you move your own eye without using the eye muscles (cover one eye and gently press with your finger on your open eye through the eyelid), the retinal locations of visual objects change. Because the motor command to the eye muscles is required to update the estimate of the eye's state, the predicted eye position is not updated. However, because the retinal image has changed, this leads to the false percept that the world must have moved. A more dramatic example is that if the eye muscles are temporarily paralyzed with curare, then trying to move the eyes leads to a percept that the world is moving. This is because

the command leads to a state estimate that the eye has moved, but with a fixed retinal input (due to the paralysis), the only consistent interpretation is that the world has moved.

Finally, the best estimate of state is achieved by combining sensory modalities with motor commands. The drawbacks of using only sensory feedback or only motor prediction can be ameliorated by monitoring both and using a forward model to estimate the current state. A neural apparatus that does this is known as an *observer model.* The major objectives of the observer model are to compensate for sensorimotor delays and to reduce uncertainty in the estimate of current state arising from noise in both the sensory and motor signals (Figure 30–5). Such a model has been supported by empirical studies of how the nervous system estimates hand position, posture, and head orientation. We will see how such models are used to decode neural signals in brain–machine interfaces (Chapter 39).

State estimation is not a passive process. Skilled performance requires the effective and efficient gathering and processing of sensory information relevant to an action. The quality of sensory information depends on our actions because what we see, hear, and touch is

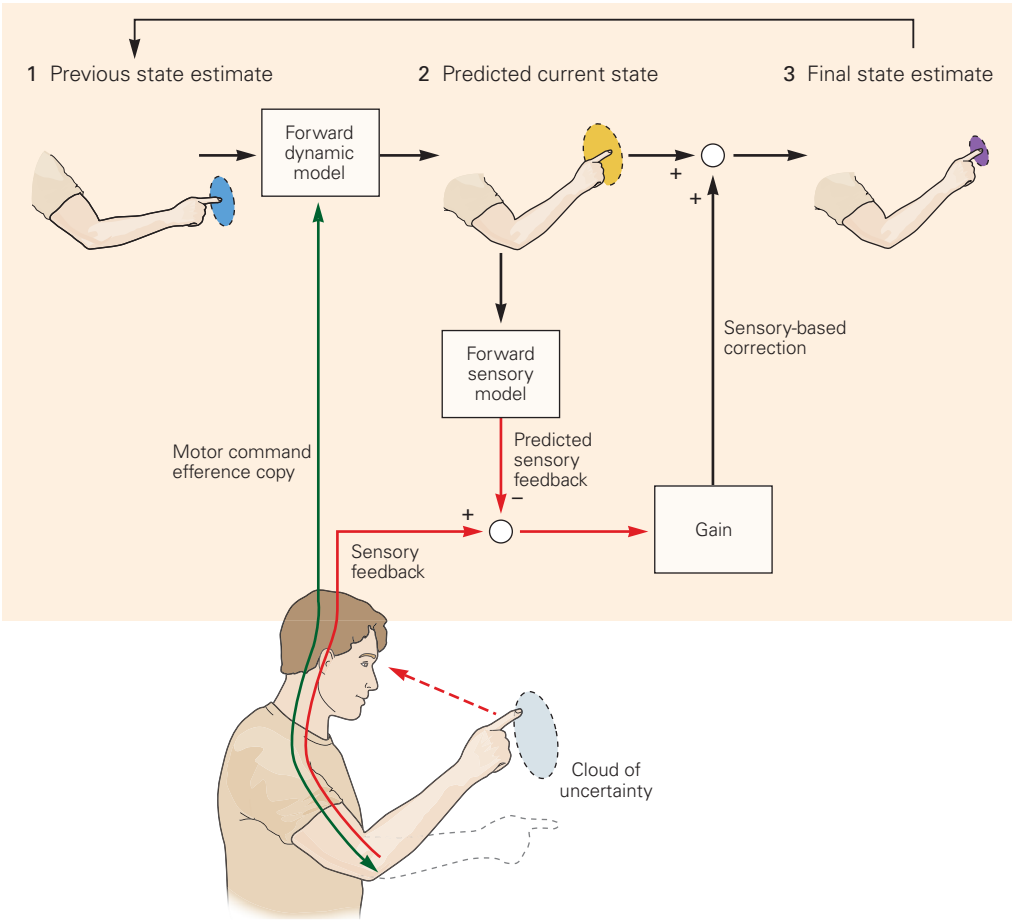

Figure 30–5 **An observer model.** The model is being used to estimate the finger's location during movement of the arm. A previous estimate of the distribution of possible finger positions (**1, blue cloud**) is updated (**2, yellow cloud**) using an efference copy of the motor command and a forward model of the dynamics. The updated distribution of finger positions is larger than that of the previous estimate. The model then uses a forward sensory model to predict the sensory feedback that would occur for these new finger positions, and the error between the predicted and actual sensory feedback is used to correct the estimate of current finger position. This correction changes the sensory error into state errors and also determines the relative reliance on the efference copy and sensory feedback.

The final estimate of current finger position (**3, purple cloud**) has less uncertainty. This estimate will become the new previous estimate for subsequent movement as this sequence is repeated many times. Delays in sensory feedback that must be compensated have been omitted from the diagram for clarity.

influenced by our movements. For example, the ocular motor system controls the eyes' sensory input by orienting the fovea to points of interest within the visual scene. Thus, movement can be used to efficiently gather information, a process termed *active sensing*. Active sensing involves two main processes: perception, by which we process sensory information and make inferences about the world, and action, by which we choose how to sample the world to obtain useful sensory information. Eye movements can betray the difference between skilled and amateur performers. For example, a batsman in the game of cricket will make a predictive saccade to the place where he expects a bowled ball to hit the ground, wait for it to bounce, and use a pursuit eye movement to follow the ball's trajectory after the bounce. A shorter latency for this first saccade distinguishes expert from amateur batsmen. Therefore, the motor system can also be used to improve our sensing of the world so as to gather information that, in turn, helps us achieve our motor goals.

Prediction Can Compensate for Sensorimotor Delays

As we have seen, delays in feedback can lead to problems during a movement, as the delayed information does not reflect the present state of the body and world. Two strategies, intermittency and prediction, can compensate for such delays and thus increase accuracy of information during movement. With intermittency, movement is momentarily interrupted by rest, as in eye saccades and manual tracking. Provided the interval of rest is greater than the time delay of the sensorimotor loop, intermittency fosters more accurate sensory feedback. Prediction is a better strategy and, as we have seen, can form a major component of a state estimator.

The nervous system uses different modes of control that depend on prediction and sensory feedback to different extents. These modes are nicely illustrated by differences in object manipulation under different conditions. When an object's behavior is unpredictable, sensory feedback provides the most useful signal for estimating load. For example, when flying a kite, we need to adjust our grip almost continuously in response to unpredictable wind currents. When dealing with such unpredictability, grip force needs to be high to prevent slippage because adjustments to grip tend to lag behind changes in load force (Figure 30–6A).

However, when handling objects with stable properties, predictive control mechanisms can be effective. For example, when the load is increased by a self-generated action, such as moving the arm, the grip force increases instantaneously with load force (Figure 30–6B). Sensory detection of the load would be too slow to account for this rapid increase in grip force.

Such predictive control is essential for the rapid movements commonly observed in dexterous behavior. Indeed, this predictive ability can be demonstrated easily with the "waiter task." Hold a weighty book on the palm of your hand with an outstretched arm. If you then use your other hand to remove the book (like a waiter removing objects from a tray), the supporting hand remains stationary. This shows our ability to anticipate a change in load caused by our own action and thus generate an appropriate and exquisitely timed change in muscle activity. In contrast, if someone else removes the book from your hand, even though you are watching the removal, it is close to impossible to maintain the hand stationary. We will see how cerebellar lesions affect this ability to predict, leading to a lack of such a coordinated response (Chapter 37).

Detecting any discrepancies between predicted and actual sensory feedback is also essential in motor control. This discrepancy, termed sensory prediction error, can drive learning of internal models and also be used for control. For example, when we pick up an object, we anticipate when the object will lift off the surface. The brain is particularly sensitive to the occurrence of unexpected events or the nonoccurrence of expected events (ie, to sensory prediction errors). Thus, if an object is lighter or heavier than expected and therefore lifts off too early or cannot be lifted, reactive responses are initiated.

In addition to its use in compensating for delays, prediction is a key element in sensory processing. Sensory feedback can arise as a consequence of both external events and our own movements. In the sensory receptors, these two sources are not distinguishable, as sensory signals do not carry a label of "external stimulus" or "internal stimulus." Sensitivity to external events can be amplified by reducing the feedback from our own movement. Thus, subtracting predictions of sensory signals that arise from our own movements from the total sensory feedback enhances the signals that carry information about external events. Such a mechanism is responsible for the fact that self-tickling is a less intense experience than tickling by another. When subjects were asked to tickle themselves using a robotic interface, but a time delay was introduced between the motor command and the resulting tactile input, the ticklishness increased. With such delayed tactile input, the predictions become inaccurate and thus fails to cancel the sensory feedback, resulting in the increased tickle sensation. Such predictive modulation of sensory

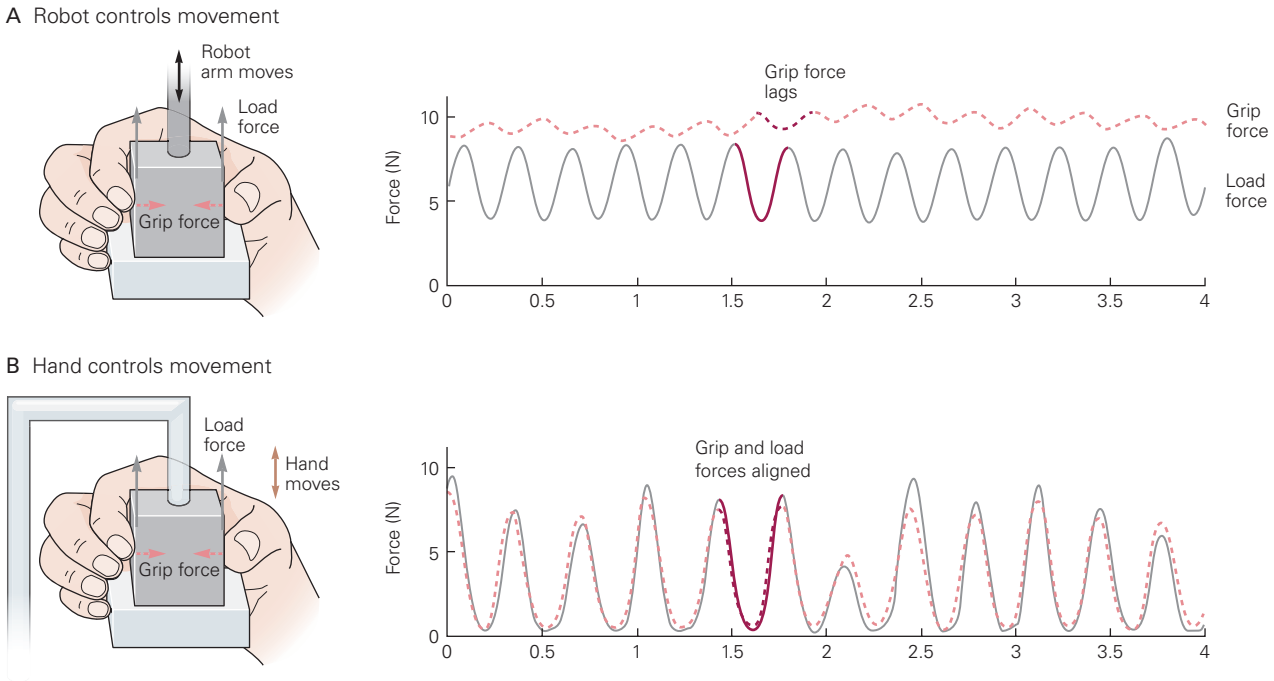

Figure 30–6 Anticipatory control of self-generated actions. (Adapted, with permission, from Blakemore, Goodbody, and Wolpert 1998. Copyright © 1998 Society for Neuroscience.

A. When a subject is instructed to hold an object to which a sinusoidal load force is mechanically applied, the grip force of the fingers is high to prevent slippage, and the grip force modulation lags behind the changes in load force. This is highlighted for a portion of the load force modulation (**dark red solid line**) that leads to a corresponding grip force (**dark red dashed line**), which is delayed. (Trial duration 4 s).

B. When a subject generates a similar load profile by pulling down on the fixed object, the load force can be anticipated, and thus, the grip force is lower and also tracks the load force without delay.

signals by motor actions is a fundamental property of many sensory systems.

Sensory Processing Can Differ for Action and Perception

A growing body of research supports the idea that the sensory information used to control actions is processed in neural pathways that are distinct from the afferent pathways that contribute to perception. It has been proposed that visual information flows in two streams in the brain (Chapter 25). A dorsal stream that projects to the posterior parietal cortex is particularly involved in the use of vision for action (Chapter 34), while a ventral stream that projects to the inferotemporal cortex is involved in conscious visual perception.

This distinction between the uses of vision for action and perception is based on a double dissociation seen in patient studies. For example, the patient D.F. developed visual agnosia after damage to her ventral stream. She is unable, for example, to indicate the orientation of a slot either verbally or with her hand. However, when asked to perform a simple action, such as putting a card through the slot, she has no difficulty orienting her hand appropriately to put the card through the slot (Chapter 59). Conversely, patients with damage to the dorsal stream can develop optic ataxia in which perception is intact but control is affected.

Although the distinction between perception and action arose from clinical observations, it can also be seen in normal people, as in the size–weight illusion. When lifting two objects of different size but equal weight, people report that the smaller object feels heavier. This illusion, first documented more than 100 years ago, is both powerful and robust. It does not lessen when a person is informed that the objects are of equal weight and does not weaken with repeated lifting.

When subjects begin to lift large and small objects that weigh the same, they generate larger grip and load forces for the larger object because they assume that larger objects are heavier. After alternating between the two objects, they rapidly learn to scale their fingertip forces precisely for the true object weight (Figure 30–7). This shows that the sensorimotor system recognizes that the two weights are equal. Nevertheless, the size–weight illusion persists, suggesting not only that

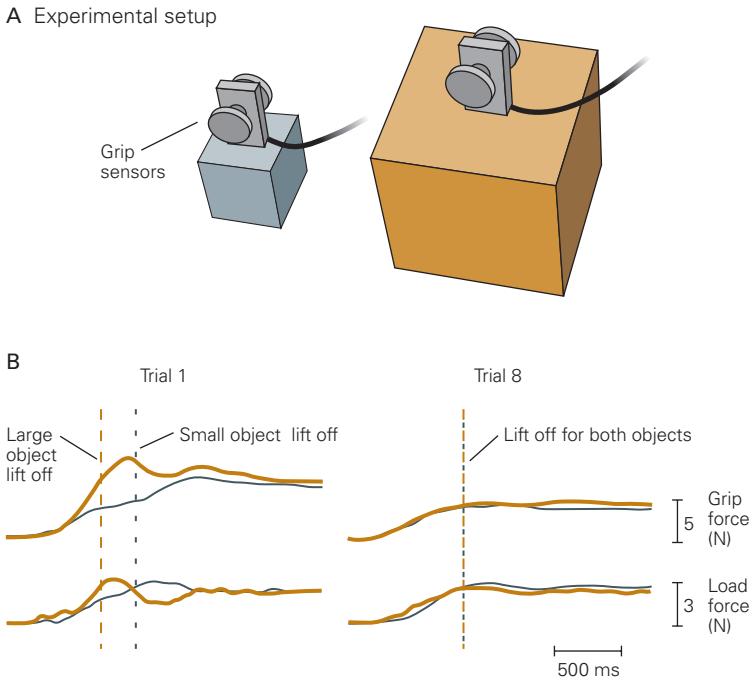

Figure 30–7 The size–weight illusion.

A. In each trial, subjects alternately lifted a large object and a small object that weighed the same. Subjects thought the smaller object felt heavier than it actually was.

B. In the first trial, subjects generated greater grip and load forces for the bigger object (**orange traces**) as it was expected to be heavier than the small object. In the eighth trial, the grip and load forces are the same for the two objects, showing that the sensorimotor system for this action generates grip and load forces appropriate to the weights of the two objects despite the persistent conscious perception of a difference in weight. (Adapted with permission, from Flanagan and Beltzner 2000. Copyright © 2000 Springer Nature.)

the illusion is a result of high-level cognitive centers in the brain but also that the sensorimotor system can operate independently of these centers.

Motor Plans Translate Tasks Into Purposeful Movement

Real-world tasks are expressed as goals: I want to pick up a glass, dance, or have lunch. However, action requires a detailed specification of the temporal sequence of movements powered by the 600 or so muscles in the human body. There is clearly a gap between the statement of a goal and a motor plan that recruits specific muscles in pursuit of that goal.

Stereotypical Patterns Are Employed in Many Movements

The ability of the motor systems to achieve the same task in many different ways is called redundancy. If one way of achieving a task is not practical, there is usually an alternative. For example, the simplest of all tasks, reaching for an object, can be achieved in infinitely many ways.

The duration of the movement can be freely selected from a wide range and, given a particular choice of duration, the path and speed profile of the hand along the path (ie, trajectory) can take on many different patterns. Even selecting one trajectory still allows for infinitely many joint configurations to hold the hand on any given point of the path. Finally, holding the arm in a fixed posture can be achieved with a wide range of muscular co-contraction levels. Therefore, for any movement, a choice must be made from a large number of alternatives.

Do we all choose to move in our own way? The answer is clearly no. Repetitions of the same behavior by one individual as well as comparisons between individuals have shown that the patterns of movement are very stereotypical.

Invariance in stereotypical patterns of movement tells us something about the principles the brain uses when planning and controlling our actions. For example, when reaching, our hand tends to follow roughly a straight path and the hand speed over time is typically smooth, unimodal, and roughly symmetric (bell-shaped, Figure 30–8). The tendency to make straight-line movements characterizes a large class of movements and is surprising given that the muscles act to rotate joints.

To achieve such a straight-line movement of the hand requires complex joint rotations. The motions of the joints in series (the shoulder, elbow, and wrist) are complicated and vary greatly with different initial and final positions. Because rotation at a single joint would

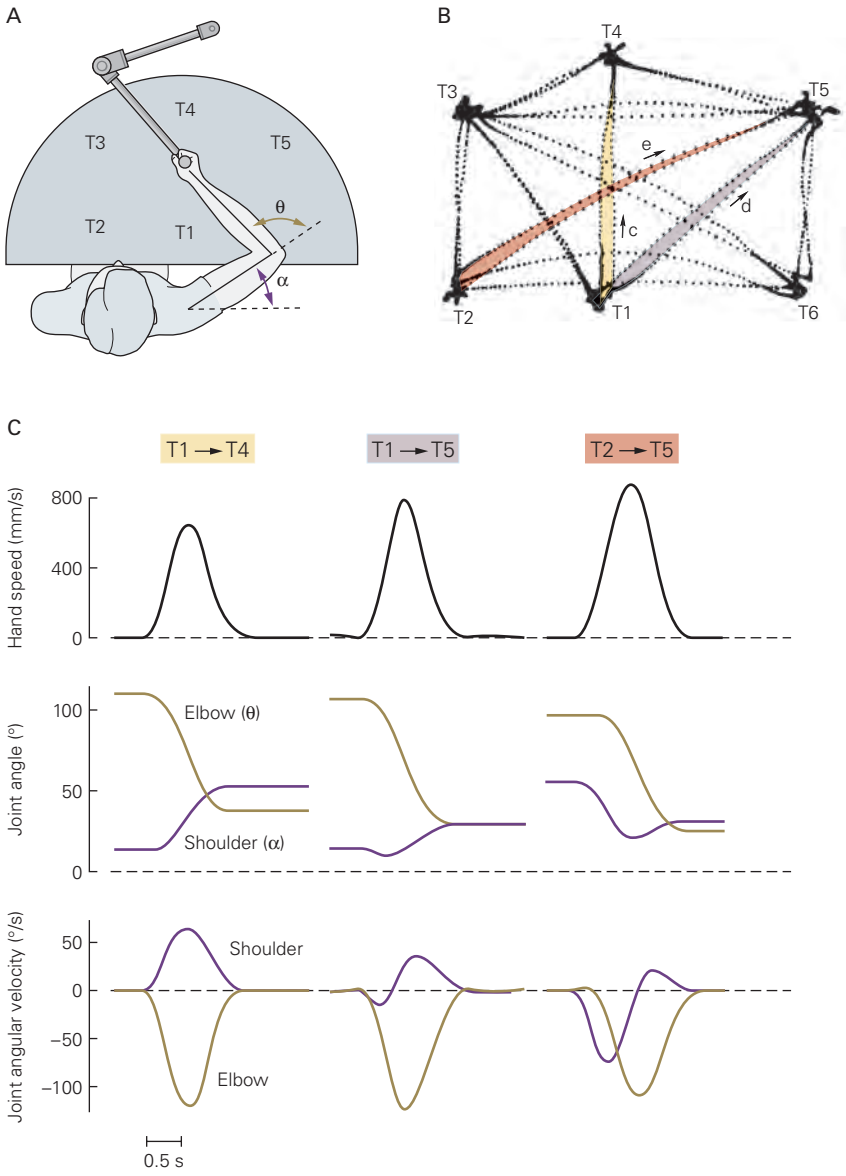

Figure 30–8 Hand path and velocity have stereotypical features. (Adapted, with permission, from Morasso 1981. Copyright © 1981 Springer Nature.)

A. The subject sits in front of a semicircular plate and grasps the handle of a two-jointed apparatus that moves in the horizontal plane and records hand position. The subject is instructed to move the hand between various targets (**T1–T6**).

B. The paths traced by one subject while moving his hand between targets.

C. Kinematic data for three hand paths (**c**, **d**, and **e**) shown in panel **B**. All paths are roughly straight, and all hand speed profiles have the same shape and scale in proportion to the distance covered. In contrast, the profiles for the angular velocity of the elbow and shoulder for the three hand paths differ. The straight hand paths and common profiles for speed suggest that planning is done with reference to the hand because these parameters can be linearly scaled. Planning with reference to joints would require computing nonlinear combinations of joint angles.

produce an arc at the hand, both elbow and shoulder joints must be rotated concurrently to produce a straight path. In some directions, the elbow moves more than the shoulder; in others, the reverse occurs. When the hand is moved from one side of the body to the other (Figure 30–8, movement from T2 to T5), one or both joints may have to reverse direction in midcourse. The fact that hand trajectories are more invariant than joint trajectories suggests that the motor system is more concerned with controlling the hand, even at the cost of generating complex patterns of joint rotations.

Such task-centered motor plans can account for our ability to perform a specific action, such as writing, in different ways with more or less the same result. Handwriting is structurally similar regardless of the size of the letters or the limb or body segment used to produce it (Figure 30–9). This phenomenon, termed motor equivalence, suggests that purposeful movements are represented in the brain abstractly rather than as sets of specific joint motions or muscle contractions. Such abstract representations of movement, which are able to drive different effectors, provide a degree of flexibility of action not practical with preset motor programs.

Motor Planning Can Be Optimal at Reducing Costs

Why do humans choose one particular manner of performing a task out of the infinite number of possibilities?

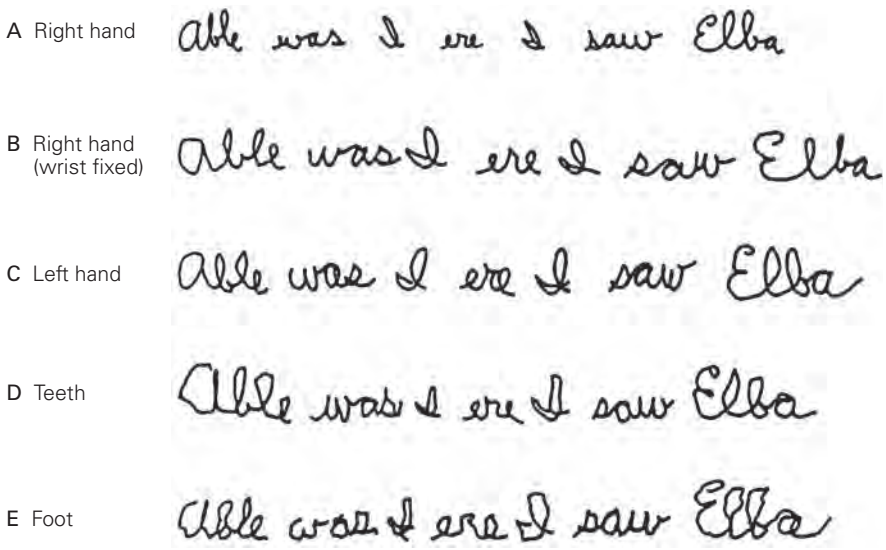

Figure 30–9 Motor equivalence. The ability of different motor systems to achieve the same behavior is called motor equivalence. For example, writing can be performed using different parts of the body. The examples here were written by the same person using the right (dominant) hand (**A**), the right hand with the wrist immobilized (**B**), the left hand (**C**), the pen gripped between the teeth (**D**), and the pen attached to the foot (**E**). (Reproduced, with permission, from Raibert 1977.)

Extensive research has attempted to answer this question, and the fundamental idea that has emerged is that planning can be equated with choosing the best way to achieve a task. Mathematically, this is equivalent to the process of optimizing (ie, minimizing) a cost associated with the movement. The cost is a way of quantifying what is good or bad about a movement (eg, energy, accuracy, stability) with a single number.

Different ways of achieving a task will lead to different costs. This allows all possible solutions to be ranked, thus identifying the one with the lowest cost. Invariances in our movements will reflect the particular cost we care about for that type of movement. Many costs have been proposed, but currently, most successful theories propose that there are two main components to movement cost: task success and effort. The effort component means that we want to achieve success but with minimal energetic cost.

To understand how task success is a component of the cost, it is useful to understand what leads to lack of success. Having inaccurate internal models or processing clearly limits our ability to complete tasks, and motor learning is designed to keep these processes accurate. However, low-level components in the motor system, such as motor noise, limit success. Movements tend to be variable, and the variability tends to increase with the speed or force of the movement. Part of this increase is caused by random variation in both the excitability of motor neurons and the recruitment of additional motor units needed to increase force. Incremental increases in force are produced by progressively smaller sets of motor neurons, each of which produces disproportionately greater increments of force (Chapter 31). Therefore, as force increases, fluctuations in the number of motor neurons lead to greater fluctuations in force.

The consequences of this can be observed experimentally by asking subjects to generate a constant force. The variability of such force production increases with the level of the force. Over a large range, this increase in variability is captured by a constant coefficient of variation (the standard deviation divided by the mean force). This dependence of variability on force also increases the variability of pointing movements as the speed of movement increases (as greater speed requires greater muscle force). The decrease in movement accuracy with increasing speed is known as the speed–accuracy trade-off (Figure 30–10). This relationship is not fixed, and part of skill learning, such as learning to play the piano, involves being able to increase speed without sacrificing accuracy.

In general, effort and accuracy are in conflict. Accuracy requires energy because corrections require muscular activity and thus comes at some cost. The trade-off between accuracy and energy varies for different movements. When walking, we could choose to step gingerly to ensure we never trip, but this would require substantial energy use. Therefore, we are willing to save energy by allowing ourselves the risk of occasionally tripping. In contrast, while eating with a knife and fork, we prioritize accuracy over energy to ensure the fork does not end up in our cheek.

The optimal movement is thus the one that minimizes the bad consequences of noise while saving energy. One way to do this is to specify a desired

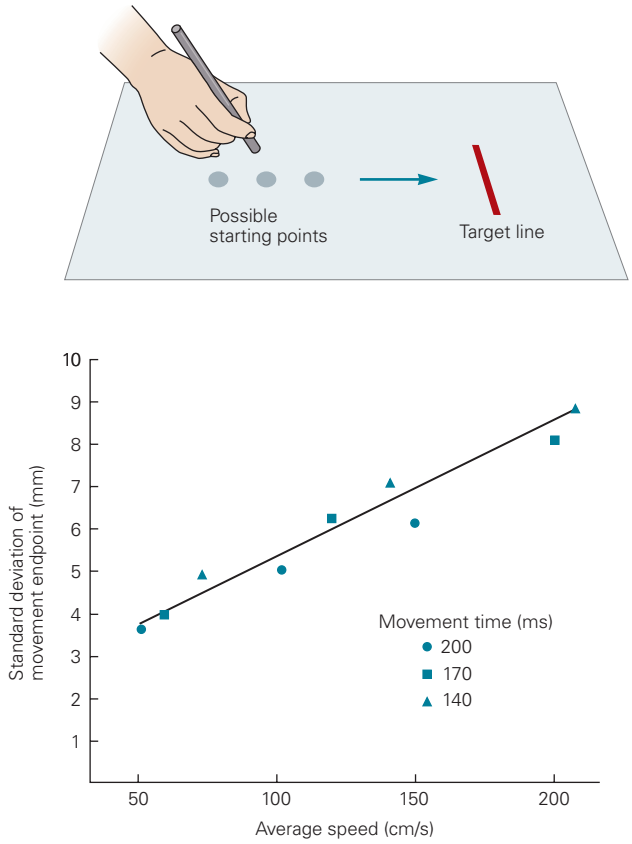

Figure 30–10 Accuracy of movement varies in direct proportion to its speed. Subjects held a stylus and had to hit a straight line lying perpendicular to the direction in which they moved the stylus. Subjects started from one of three different initial positions and were required to complete the movement within three different times (140, 170, or 200 ms). A trial was successful if the subject completed the movement within 10% of the required time. Only successful trials were used for analysis. Subjects were informed when a trial was not successful. The variability in the motion of the subjects' arm movements is shown in the plot as the standard deviation of the movement endpoint plotted against average speed (for each of three movement starting points and three movement times, giving nine data points). The variability in movement increases in proportion to the speed and therefore to the force producing the movement. (Adapted, with permission, from Schmidt et al. 1979.)

movement trajectory or sequence of states that can be considered optimal. Although noise and environmental disturbances can cause the motor system to deviate from the desired behavior, the role of feedback is simply to return the movement back to the desired trajectory. However, this approach is not necessarily computationally efficient. Rather than specifying the desired state of the body, we can specify an optimal feedback controller to generate the movement.

Optimal Feedback Control Corrects for Errors in a Task-Dependent Manner

Optimal feedback control aims to minimize a cost such as a combination of energy and task inaccuracy (Chapter 34). This type of feedback control is based on the idea that people do not plan a trajectory given a particular cost. Instead, the cost is used to create a feedback controller that specifies, for example, how the feedback gain for positional errors (and other errors such as velocity and force) changes over time. Therefore, given the goal of the task, the controller specifies the motor command suitable for different possible states of the body. The trajectory is then simply a consequence of applying the feedback control law to the current estimate of the state of the body (Figure 30–11). The feedback controller is optimal in that it can minimize the cost even in the presence of potential disturbances.

Optimal feedback control, therefore, does not make a hard distinction between feedforward and feedback control. Rather, during a task, the balance between feedforward and feedback control varies along a continuum that depends on the extent to which the estimate of current body state is influenced by predictions (feedforward) or by sensory input (feedback).

An important feature of optimal feedback control is that it will correct only for deviations that are task relevant and allow variation in task-irrelevant deviations. For example, when reaching to open an exit door that has a long horizontal handle, it is of little importance where along the handle one makes contact, so deviations in the horizontal direction can be ignored. Such considerations lead naturally to the minimal intervention principle that one should only intervene in an ongoing task if deviations will affect task success.

Intervening will generally add noise into the system (and require an increased effort), so intervening unnecessarily will lead to a decrement in performance. The aim of optimal feedback control is not to eliminate all variability, but to allow it to accumulate in dimensions that do not interfere with the task while minimizing it in the dimensions relevant for the task completion. The minimal intervention principle is supported by studies that show that feedback does not always return the system to the unperturbed trajectory but often acts in a manner to reduce the effect of the disturbance on the achievement of the task goal and to ensure that corrections are task-dependent.

Optimal feedback control emphasizes the setting of feedback gains, which can be partially instantiated by reflexes that generate rapid motor responses. Optimal feedback control proposes that these rapid responses should be highly tuned to the task at hand.

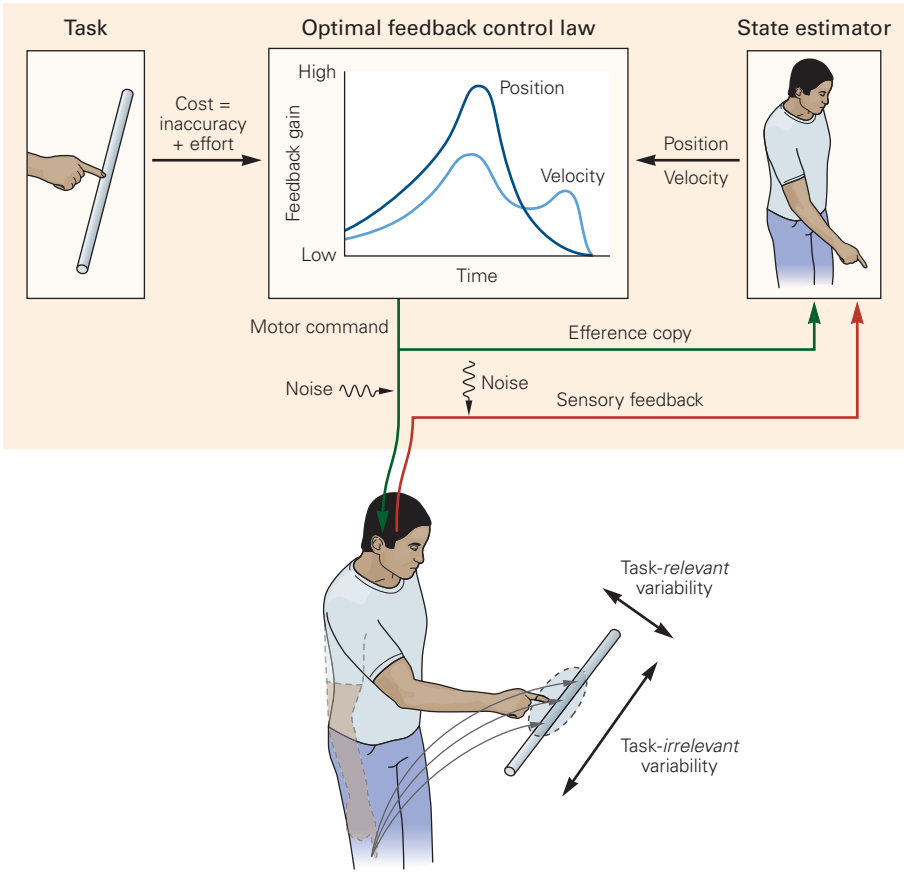

Figure 30–11 Optimal feedback control. In order to generate a movement for a given task, such as touching a horizontal bar, the sensorimotor system specifies a cost that is a combination of accuracy (eg, distance of the finger to the bar) and effort. To generate a movement that minimizes this cost, the sensorimotor system sets up an optimal feedback control rule that specifies the time-varying gains. These gains specify how the motor command should depend on states such as positional error and hand velocity. The form of this feedback control law assures that the movement is the best it can be in the presence of internal noise and external perturbations. The optimal behavior tends to let variability (**blue ellipsoid**, showing the possible final locations of the hand) accumulate in dimensions that do not affect task success (task-irrelevant variability), such as along the axis of the bar, while controlling variability that would lead to the hand missing the bar (task-relevant variability). Three paths for reaching from the same starting point are shown; corrections are made only in the task-relevant dimension.

Although the short-latency (monosynaptic) stretch reflex responds only to muscle stretch, the long-latency response has long been known to respond to task-dependent factors (Chapter 32). Optimal feedback control is important because it combines trajectory generation, noise, and motor cost and provides a clear comparison for the results of experimental work.

Multiple Processes Contribute to Motor Learning

Animals have a remarkable capacity for learning new motor skills simply through everyday interaction with their environment. Although evolution can hard wire some innate behaviors, such as the ability of a foal to stand or a spider to spin a web, motor learning is required to adapt to new and varying environments.

New motor skills cannot be acquired by fixed neural systems. Sensorimotor systems must constantly adapt over a lifetime as body size and proportions change, thereby maintaining an appropriate relationship between motor commands and body mechanics. In addition, learning is the only way to acquire motor skills that are defined by social convention, such as writing or dancing.

Most forms of motor learning involve *procedural* or *implicit* learning, so-called because subjects are generally unable to express what it is they have learned. Implicit learning often takes place without consciously thinking about it and can be retained for extended periods of time without practice (Chapter 52). Typical examples of procedural learning are learning to ride a

bicycle or play the piano. In contrast, *declarative* or *explicit* learning refers to knowledge that can be expressed in statements about the world and is available to introspection (Chapter 52). Memorizing the names of the cranial nerves or the directions to the local hospital are examples of explicit learning. Declarative memory tends to be easily forgotten, although repeated exposure can lead to long-lasting retention. We use explicit learning strategies when initially learning some motor tasks, such as driving a car, but the skill becomes automatic with time and practice.

Motor learning can occur more or less immediately or over time. We learn to pick up an object of unknown weight almost immediately, and we learn to ride a bicycle after a few weeks of practice, but mastering the piano requires years. These different timescales may reflect the intrinsic difficulty of the task as well as evolutionary constraints that have to be unlearned to perform the task. For example, piano playing requires learning precise control of individual fingers, whereas in normal movements, such as reaching and grasping, individuated finger movements are rare. Sensorimotor learning can be divided into two broad, but overlapping, classes: adaptations to alterations in the properties of sensorimotor systems and learning new skills. We focus on each in turn.

Error-Based Learning Involves Adapting Internal Sensorimotor Models

Error-based learning is the driving force behind many well-studied sensorimotor adaptation paradigms. For example, the relation between the visual and proprioceptive location of a limb can be altered by wearing prismatic glasses (or even spectacles). This shifts the visual input so that a person's reach for an object is misdirected. Over repeated attempts, the reach trajectories are adjusted to account for the discrepancy between vision and proprioception, a process termed visuomotor learning. Similarly, to control a computer mouse, we must learn the kinematic relation between the movement of the mouse and the cursor on the screen. In addition, the properties of the limbs change with both growth and tool use. The brain must adapt to such changes by reorganizing or adjusting motor commands.

In error-based learning, the sensorimotor system senses the outcome of each movement and compares this to both the desired outcome and the predicted outcome. For example, when shooting a basketball the desired outcome is for the ball to go through the hoop. However, once you let go of the ball you may predict that the ball will miss to the right of the hoop. The difference between the prediction and actual outcome, termed the sensory prediction error, can be used to update the internal model of how the ball responds to your actions. The difference between the actual and desired outcome, termed the target error, can be used to adjust your plan (i.e. aim direction) to reduce the error. Both sensory prediction errors and target errors are important for driving learning.

Additional transformations may have to be applied to the error signal before it can be used to train an internal model. For example, when we throw a dart, errors are received in visual coordinates. This sensory error must be converted into motor command errors suitable for updating a control process such as an inverse model. Error-based learning tends to lead to trial-by-trial reduction in error as the motor system learns the novel sensorimotor properties.

An example of such error-based learning in reaching occurs when the dynamics of the arm are unexpectedly changed. As we saw earlier, we normally move the hand with a straight-line path to reach an object. Unexpected dynamic interactions can produce curved paths, but subjects learn to anticipate and compensate for these effects. This learning is conveniently studied by having subjects make reaching movements while holding the end of a robotic apparatus that can introduce novel forces on the arm (Figure 30–12A–C). Applying a force that is proportional to the speed of the hand but that acts at right angles to the direction of movement will produce a curved movement before finally reaching the target. Over time, the subject adapts to this perturbation and is able to maintain a straight-line movement (Figure 30–12D).

Subjects might adapt to such a situation in either of two ways. Subjects could co-contract the muscles in their arm, thereby stiffening the arm and reducing the impact of the perturbation, or they could learn an internal model that compensates for the anticipated force. By examining the aftereffects (movements after the robot is turned off), we can distinguish between these two forms of learning. If the arm simply stiffens, it should continue to move in a straight path. If a new internal model is learned, the new model should compensate for a force that no longer exists, thereby producing a path in the direction opposite from the earlier perturbation. Early in learning, co-contraction is used to reduce the errors before an internal model can be learned, but the co-contraction then decreases as the internal model is able to compensate for the perturbation. Therefore, when the force is turned off after learning, subjects normally show a large aftereffect in the opposite direction, demonstrating that they have compensated for the perturbation (Figure 30–12D).

Such error-based processes appear to underlie adaptation across a number of different movement

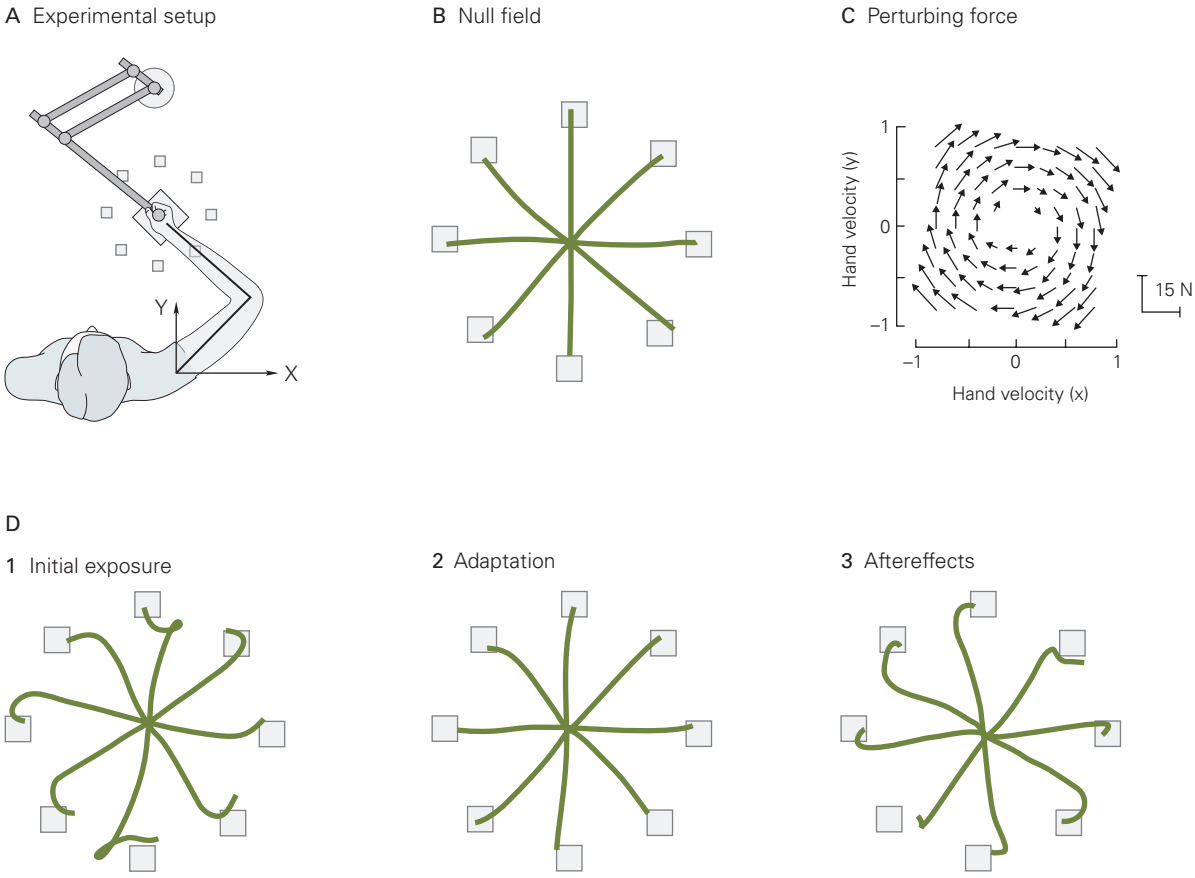

Figure 30–12 Learning improves the accuracy of reaching in a novel dynamic environment. (Adapted, with permission, from Brashers-Krug, Shadmehr, and Bizzi 1996. Copyright © 1996 Springer Nature.)

A. A subject holds a robotic apparatus that measures the position and velocity of the hand and applies forces to the hand.

B. When the motors are off (null field), the subject makes approximately straight movements from the center of the workspace to targets arrayed in a circle.

C. A clockwise force is then applied to the hand, shown as a function of hand velocity. This field produces a force proportional to the speed of the hand that always acts at right angles to the current direction of motion.

D. Initially, the hand paths are severely perturbed in response to the perturbing force (1). After some time, the subject adapts and can again follow a straight path during the entire movement (2). When the motors are then turned off, movement is again perturbed, but in a direction opposite to the earlier perturbation (3).

types and effectors, from the eye to whole-body movements. For example, our normal symmetric pattern of gait seems to rely on error-based learning. When the gait pattern of subjects is perturbed by walking on a split-belt treadmill in which one belt moves faster than the other, they initially limp. However, step by step the gait pattern naturally regains its symmetry (Figure 30–13), thus showing that error-based learning can drive complex whole-body coordinated movements. There is extensive evidence that fast trial-by-trial error-based learning relies on the cerebellum (Chapter 37).

Motor adaptation may not be a single unitary process. Recent evidence suggests that adaptation is driven by interacting processes whose outputs are combined. These interacting processes could have different temporal properties: one process quickly adapting to perturbations but also rapidly forgetting what was learned and the other learning more slowly but retaining learning for a longer period (Figure 30–13B). The advantage of such a mechanism is that the learning processes can be matched to the temporal properties of the perturbations, which can range from short-lived (fatigue) to long-lasting (growth).

Although motor learning often takes much practice, once a task is no longer performed, deadaptation is typically faster. However, the sensory inputs associated with the particular action can be enough to switch behavior. When subjects wear prismatic glasses

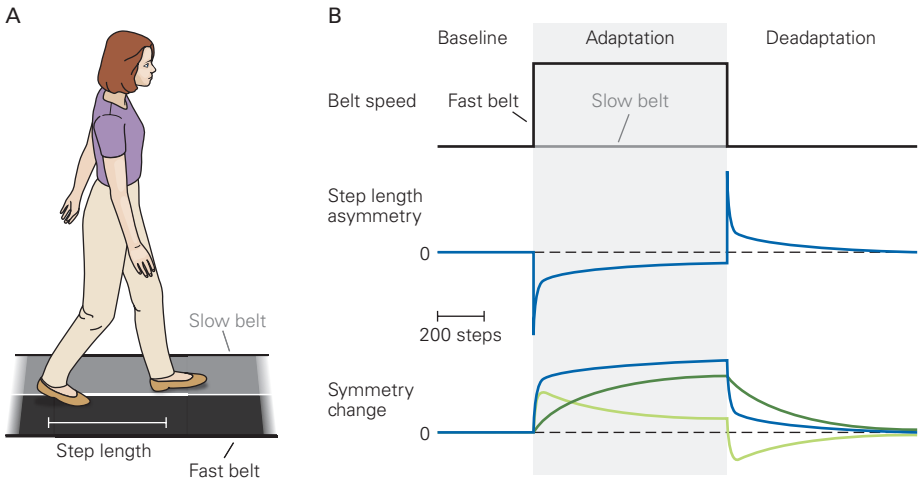

Figure 30–13 Learning new coordination patterns in walking.

A. A subject walks on a split-belt treadmill. When the two belts move at the same speed, subjects have a symmetric gait pattern with equal step lengths.

B. In an adaptation study, the speeds of the belts are initially the same, then become split so that the right belt moves faster than the left, and then finally return to the same speed (**top**). Step length symmetry is initially lost when the belts move at different speeds, causing the subject to limp. Over time, the symmetry is restored and the limping is abolished. When the belts are once again moving at the same speed, an aftereffect is seen (**middle**). Maurice Smith and colleagues have shown that this type of adaptation is composed of multiple underlying processes that adapt on different timescales (**bottom**). The change in the step length symmetry is composed of two processes: a fast process (**light green line**) that adapts quickly but also rapidly forgets what has been learned, and a slow process (**dark green line**) that learns more slowly but has better retention. These processes both adapt to learn from the error, and the sum of these processes is the final adaptation (**blue line**). This dual-rate learning system gives rise to the typical double exponential learning curves seen in many forms of adaptation in which adaptation is initially fast but tends to slow down as learning proceeds. (Adapted, with permission, from Roemmich, Long, and Bastian 2016.)

that shift visual space, for example, they initially miss when reaching to targets but soon learn to reach correctly. After repeated trials, the mere feel of the glasses, without the prisms in place, is sufficient to evoke the adaptive behavior appropriate for the prisms.

In general, we can quantify performance with two measurements, accuracy and precision. Accuracy is a measure of systematic errors or biases, for example, on average how far a series of thrown darts are away from the target. In contrast, precision is a measure of random errors, or statistical variability, in our actions. Both accuracy and precision contribute to performance. In general, accuracy can be improved by adapting or calibrating motor commands so as to reduce systematic errors. Although there is always some variability in movement arising from irreducible sensory and motor noise, the variability, as we have seen, can be reduced through planning so as to have minimal impact on task success. Most motor learning tends to become automatic (ie, implicit) with time, but early learning of some tasks can be aided by explicit learning (ie, strategy), such as a verbal instruction on how best to approach the task.

Not all sensory modalities are equally important in learning all motor tasks. In learning dynamic tasks, proprioception and tactile input are more important than vision. We normally learn dynamic tasks equally well with or without vision. However, individuals who have lost proprioception and tactile input have particular difficulty controlling the dynamic properties of their limbs or learning new dynamic tasks without vision (Box 30–3).

Skill Learning Relies on Multiple Processes for Success

In contrast to error-based learning in which the sensorimotor system adapts to a perturbation to return to preperturbation performance, learning skills such as tying one's shoelaces, juggling, typing, or playing the piano instead involves improving performance in the absence of a perturbation. Such learning tends to improve the speed–accuracy trade-off. Initially, we may be able to hit the correct keys on a keyboard when paced 1 second apart, but with practice, the same accuracy can be achieved at an increasingly quickening pace.

Box 30–3 Proprioception and Tactile Sense Are Critical for Sensorimotor Control

While visual impairment certainly has limiting effects on sensorimotor control, blind people are able to walk normally and reach and grasp known objects with ease. This is in stark contrast to the rare loss of proprioceptive and tactile sense.

Some sensory neuropathies selectively damage the large-diameter sensory fibers in peripheral nerves and dorsal roots that carry most proprioceptive information. Impairments in motor control resulting from loss of proprioception have fascinated neurologists and physiologists for well over a century. Studies of patients with sensory neuropathies provide invaluable insight into the interactions between sensation and movement planning.

As expected, such patients lose joint position sense, vibration sense, and fine tactile discrimination (as well as tendon reflexes), but both pain and temperature senses are fully preserved. Patients with peripheral neuropathies are unable to maintain a steady posture, for example, while holding a cup or standing, with the eyes closed. Movements also become clumsy, uncoordinated, and inaccurate.

Some recovery of function may occur over many months as the patient learns to use vision as a substitute for proprioception, but this compensation still leaves patients completely incapacitated in the dark. Some of this difficulty reflects an inability to detect errors that develop during unseen movements, as occurs if the weight of an object differs from expectation.

Peripheral neuropathies are particularly incapacitating when patients try to make movements with rapid direction reversals. Analyses of the joint torques during these movements show that subjects with intact proprioception anticipate intersegmental torques, whereas those without proprioception fail to do so (Figure 30–14).

However, the same patients easily adapt to drastic kinematic changes, such as tracing a drawing while viewing their hand in a mirror. In fact, they perform better than normal subjects, perhaps because they have learned to guide their movements visually and, because they lack proprioception, do not experience any conflict between vision and proprioception.

Even in normal subjects, the relative importance of tactile input in manipulation tasks can be easily demonstrated. It is relatively easy to light a match with one's eyes closed. However, if the tips of the digits are made numb with local anesthetic, then even under full vision the task is remarkably hard because the match tends to slip from the fingers.

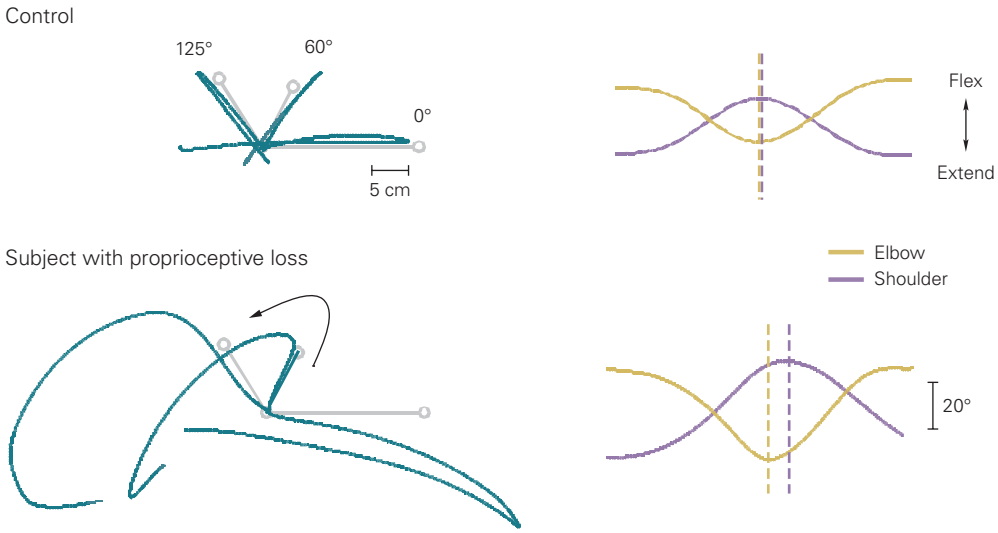

Figure 30–14 Patients lacking proprioception cannot make an accurate movement that requires a rapid reversal in path. (*Left*) The subject tries to trace a template (gray line) while her hand is hidden from view. The joint angles for the elbow and shoulder of a normal subject show good alignment (*Right top*), leading to an accurate reversal (*Left top*). In contrast, the timing of the joint reversal is poor in subjects who lack proprioceptive input (*Right bottom*), leading to large errors in the path (*Left bottom*). These patients cannot anticipate and correct for the intersegmental dynamics that occur around the path reversal. (Adapted, with permission, from Sainburg et al. 1995.)

For some skills, there can be a complex relation between the actions performed and success or failure at the task. For example, when children first sit on a swing, they have to learn the complex sequence of leg and body movements required to make the swing go higher. In contrast to error-based learning, there is no readily available error signal that can be used to adjust the current action because the swing's height is not directly determined by the current action but by a long history of body and leg motion. Learning in such complex scenarios can be achieved using reinforcement learning in which the sensorimotor system adjusts its commands in an effort to maximize reward, that is, task success. In the most general form, the performance measure that the reinforcement learning tries to maximize is the sum of all future rewards. However, as we tend to favor an immediate versus time-delayed reward, the sum is typically weighted to reflect this by progressively discounting future rewards.

Reinforcement learning is more general than error-based learning in that the training signal is success or failure, rather than an error at each point in time. Another distinguishing property of reinforcement learning is that the success or failure that the learning system receives can depend in nontrivial ways on the history of the actions taken. For tasks that require a complex sequence of actions to take place to achieve a goal, such as tying one's shoelaces, and the outcome or reward is removed in time from the action, error-based learning cannot easily be applied. A key problem that reinforcement solves is that of credit assignment: Which action within a sequence should we credit or blame when we eventually succeed or fail? This is just the sort of problem reinforcement learning algorithms are good at solving.

There are two main classes of reinforcement learning, those that depend on an internal model and those that do not. Model-based reinforcement builds a model of the task (eg, the structure of a maze). With such a model, the learner can efficiently plan in a goal-directed manner. In contrast, with model-free reinforcement learning, the learner simply associates movements with success or failure; those that lead to success are more likely to be performed again. Such learning can lead to motor habits. While model-free learning avoids the computational burden of building a model, it is also less able to generalize to novel situations. These two types of reinforcement learning can even act together, and different tasks can rely on them to different extents. Dopaminergic systems in the basal ganglia have been tied to signals that one would expect in reinforcement learning, such as expected reward. Moreover, dysfunction in these systems is related to movement disorders, addiction, and other problems that could be related to reinforcement signals (Chapter 38).

Finally, the development of efficient strategies plays a key part in motor skill acquisition. Skill learning for real-world tasks typically involves a sequence of decision-making processes at different spatiotemporal scales. The skill of a tennis player, for example, is not only determined by the precision with which she can strike the ball but also by the speed with which she can make the correct decision on where to aim it and how well she uses her senses to extract task-relevant information.

Sensorimotor Representations Constrain Learning

The information obtained during a single movement is often too sparse or noisy to unambiguously determine the source of error. For example, if a tennis player hits a shot into the net on the serve, the problem could be that the ball was not thrown high enough, the ball was hit too early, the racquet strings are loose, there was a gust of wind, or the player is fatigued. If the racquet dynamics have changed, the player would do well to adapt to these for the next shot. If a temporary gust of wind was the problem, then no adjustment is needed. To resolve this issue, the sensorimotor learning system constrains the way in which the system is updated in response to errors. These constraints reflect the internal assumptions about the task structure and the source of errors and determine how the system represents the task. Indeed, on a slower timescale, learning itself can alter the representation.

While the final output of the motor system is the contraction of its 600 or so muscles, it is not the case that the brain controls each independently. In current models of sensorimotor control, motor commands are generated by multiple modules that can be selectively engaged depending on the requirements of the task. Examples of modular architectures include multiple internal models, motor primitives, and motor synergies (Chapter 36).

Motor primitives can be thought of as neural control modules that can be flexibly combined to generate a large repertory of behaviors. A primitive might represent the temporal profile of a particular muscle activity or a set of muscles that are activated together, termed a synergy. The overall motor output will be the sum of all primitives, weighted by the level of the activation of each module. The makeup of the population of such primitives then determines which structural constraints are imposed on learning. For example, a behavior for which the motor system has many primitives will be easy to learn, whereas a behavior that cannot be approximated by any existing primitives would be impossible to learn.

Highlights

1. The primary purpose of the elaborate information processing and storage that occurs in the brain is to enable us to interact with our environment through our motor system.
2. Our infinitely varied and purposeful motor behaviors are governed by the integrated actions of the motor systems, including the motor cortex, spinal cord, cerebellum, and basal ganglia.
3. To control action, the central nervous system uses a hierarchy of sensorimotor transformations that convert incoming sensory information into motor outputs.
4. There is a trade-off in the speed versus sophistication of the different levels of sensorimotor response from rapid reflexes to slower voluntary control.
5. The motor systems generate commands using feedforward circuits or error-correcting feedback circuits; most movement involves both types of control.
6. The brain uses internal models of the sensorimotor system to facilitate control.
7. The state of the body is estimated using both sensory and motor signals together with a forward predictive mode to reduce the adverse effects of delays in feedback.
8. Variability in the sensory inputs and motor outputs together with inaccuracies in sensorimotor transformations underlie the errors and variability in movement, leading to the trade-off between speed and accuracy.
9. Motor planning can use the redundancy of the motor system to move in such a way as to reduce the negative consequences of motor noise while reducing effort.
10. Motor control circuits are not static but undergo continual modification and recalibration throughout life.
11. Motor learning improves motor control in novel situations, and different forms of sensory information are vital for learning. Error-based learning is particularly important for adapting to simple sensorimotor perturbations. Reinforcement learning is particularly important for more complex skill learning and can rely on a model (model-based) or on simply reinforcing motor actions directly (model-free).
12. The motor representations used by the brain constrain the way the sensorimotor system updates during learning.
13. Studies of sensorimotor control have focused on developing a detailed understanding of relatively simple tasks, such as reaching and walking. Although these tasks are amenable to analysis and modeling, they do not capture the full complexity of real-world motor control. The challenge will be to determine if these principles can be generalized to tasks such as tying shoelaces and learning to skateboard.

Daniel M. Wolpert
Amy J. Bastian

Selected Reading

Diedrichsen J, Shadmehr R, Ivry RB. 2010. The coordination of movement: optimal feedback control and beyond. Trends Cogn Sci 14:31–39.

Roemmich RT, Bastian AJ. 2018. Closing the loop: From motor neuroscience to neurorehabilitation. Annu Rev Neurosci 41:415–429.

Scott SH. 2016. A functional taxonomy of bottom-up sensory feedback processing for motor actions. Trends Neurosci 39:512–526.

Shadmehr R, Smith MA, Krakauer JW. 2010. Error correction, sensory prediction, and adaptation in motor control. Annu Rev Neurosci 33:89–108.

Wolpert DM, Diedrichsen J, Flanagan JR. 2011. Principles of sensorimotor learning. Nat Rev Neurosci 12:739–751.

Wolpert DM, Flanagan JR. 2016. Computations underlying sensorimotor learning. Curr Opin Neurobiol 37:7–11.

References

Blakemore SJ, Frith CD, Wolpert DM. 1999. Spatio-temporal prediction modulates the perception of self-produced stimuli. J Cogn Neurosci 11:551–559.

Blakemore SJ, Goodbody S, Wolpert DM. 1998. Predicting the consequences of our own actions: the role of sensorimotor context estimation. J Neurosci 18:7511–7518.

Brashers-Krug T, Shadmehr R, Bizzi E. 1996. Consolidation in human motor memory. Nature 382:252–255.

Burdet E, Osu R, Franklin DW, Milner TE, Kawato M. 2001. The central nervous system stabilizes unstable dynamics by learning optimal impedance. Nature 414:446–449.

Craik KJW. 1943. *The Nature of Explanation*. Cambridge: Cambridge Univ. Press.

Crapse TB, Sommer MA. 2008. Corollary discharge across the animal kingdom. Nature Rev Neurosci 9:587.

Crevecoeur F, Scott SH. 2013. Priors engaged in long-latency responses to mechanical perturbations suggest a rapid update in state estimation. PLoS Comput Biol 9:e1003177.

Crevecoeur F, Scott SH. 2014. Beyond muscles stiffness: importance of state-estimation to account for very fast motor corrections. PLoS Comput Biol 10:e1003869.

Diedrichsen J, Kornysheva K. 2015. Motor skill learning between selection and execution. Trends Cogn Sci 19:227–233.

Ernst MO, Bulthoff HH. 2004. Merging the senses into a robust percept. Trends Cogn Sci 8:162–169.

Faisal AA, Selen LP, Wolpert DM. 2008. Noise in the nervous system. Nat Rev Neurosci 9:292–303.

Flanagan JR, Beltzner MA. 2000. Independence of perceptual and sensorimotor predictions in the size-weight illusion. Nat Neurosci 3:737–741.

Goodale MA, Milner AD. 1992. Separate visual pathways for perception and action. Trends Neurosci 15:20–25.

Harris CM, Wolpert DM. 1998. Signal-dependent noise determines motor planning. Nature 394:780–784.

Huberdeau DM, Krakauer JW, Haith AM. 2015. Dual-process decomposition in human sensorimotor adaptation. Curr Opin Neurobiol 33:71–77.

Krakauer JW, Mazzoni P. 2011. Human sensorimotor learning: adaptation, skill, and beyond. Curr Opin Neurobiol 21:636–644.

Land MF, McLeod P. 2000. From eye movements to actions: how batsmen hit the ball. Nat Neurosci 3:1340–1345.

McDougle SD, Ivry RB, Taylor JA. 2016. Taking aim at the cognitive side of learning in sensorimotor adaptation tasks. Trends Cogn Sci 20:535-544.

Morasso P. 1981. Spatial control of arm movements. Exp Brain Res 42:223–227.

Muller H, Sternad D. 2004. Decomposition of variability in the execution of goal-oriented tasks: three components of skill improvement. J Exp Psychol Hum Percept Perform 30:212–233.

O'Doherty JP, Lee SW, McNamee D. 2015. The structure of reinforcement-learning mechanisms in the human brain. Curr Opin Behav Sci 1:94–100.

Pruszynski JA, Scott SH. 2012. Optimal feedback control and the long-latency stretch response. Exp Brain Res 218:341–359.

Raibert MH. 1977. Motor control and learning by the state space model. Ph.D. Dissertation. Cambridge, MA: Artificial Intelligence Laboratory, MIT.

Reisman DS, Block HJ, Bastian AJ. 2005. Interlimb coordination during locomotion: what can be adapted and stored? J Neurophysiol 94:2403–2415.

Roemmich RT, Long AW, Bastian AJ. 2016. Seeing the errors you feel enhances locomotor performance but not learning. Curr Biol 26:1–10.

Rothwell JC, Traub MM, Day BL, Obeso JA, Thomas PK, Marsden CD. 1982. Manual motor performance in a deafferented man. Brain 105:515–542.

Sainburg RL, Ghilardi MF, Poizner H, Ghez C. 1995. Control of limb dynamics in normal subjects and patients without proprioception. J Neurophysiol 73:820–835.

Schmidt RA, Zelaznik H, Hawkins B, Frank JS, Quinn JT. 1979. Motor-output variability: a theory for the accuracy of rapid motor acts. Psychol Rev 47:415–451.

Scott SH, Cluff T, Lowrey CR, Takei T. 2015. Feedback control during voluntary motor actions. Curr Opin Neurobiol 33:85–94.

Sing GC, Joiner WM, Nanayakkara T, Brayanov JB, Smith MA. 2009. Primitives for motor adaptation reflect correlated neural tuning to position and velocity. Neuron 64:575–589.

Smith MA, Ghazizadeh A, Shadmehr R. 2006. Interacting adaptive processes with different timescales underlie short-term motor learning. PLoS Biol 4:e179.

Todorov E, Jordan MI. 2002. Optimal feedback control as a theory of motor coordination. Nat Neurosci 5:1226–1235.

Torres-Oviedo G, Macpherson JM, Ting LH. 2006. Muscle synergy organization is robust across a variety of postural perturbations. J Neurophysiol 96:1530–1546.

Valero-Cuevas FJ, Venkadesan M, Todorov E. 2009. Structured variability of muscle activations supports the minimal intervention principle of motor control. J Neurophysiol 102:59–68.

van Beers RJ, Sittig AC, Gon JJ. 1999. Integration of proprioceptive and visual position-information: an experimentally supported model. J Neurophysiol 81:1355–1364.

Wolpert DM, Flanagan JR. 2001. Motor prediction. Curr Biol 11:R729–732.

Yang SC-H, Wolpert DM, Lengyel M. 2016. Theoretical perspectives on active sensing. Curr Opin Behav Sci 11:100–108.

31

The Motor Unit and Muscle Action

Any action—ascending a flight of stairs, typing on a keyboard, even holding a pose—requires coordinating the movement of body parts. This is accomplished by the interaction of the nervous system with muscle. The role of the nervous system is to activate the muscles that provide the forces needed to move in a particular way. This is not a simple task. Not only must the nervous system decide which muscles to activate, how much to activate them, and the sequence in which they must be activated in order to move one part of the body, but it must also control the influence of the resultant muscle forces on other body parts and maintain the required posture.

This chapter examines how the nervous system controls muscle force and how the force exerted by a limb depends on muscle structure. We also describe how muscle activation changes to perform different types of movement.

The Motor Unit Is the Elementary Unit of Motor Control

A Motor Unit Consists of a Motor Neuron and Multiple Muscle Fibers

The nervous system controls muscle force with signals sent from motor neurons in the spinal cord or brain stem to the muscle fibers. A motor neuron and the muscle fibers it innervates are known as a motor unit, the basic functional unit by which the nervous system controls movement, a concept proposed by Charles Sherrington in 1925.

A typical muscle is controlled by a few hundred motor neurons whose cell bodies are clustered in a motor nucleus in the spinal cord or brain stem. The axon of each motor neuron exits the spinal cord through the ventral root or through a cranial nerve in the brain stem and runs in a peripheral nerve to the

muscle. When the axon reaches the muscle, it branches and innervates from a few to several thousand muscle fibers (Figure 31–1).

Once synaptic input depolarizes the membrane potential of a motor neuron above threshold, the neuron generates an action potential that is propagated along the axon to its terminals in the muscle. The action potential releases acetylcholine at the neuromuscular synapse, triggering an action potential at the sarcolemma of the muscle fiber (Chapter 12). A muscle fiber has electrical properties similar to those of a large-diameter, unmyelinated axon, and thus, action potentials propagate along the sarcolemma, although more slowly due to the higher capacitance of the fiber resulting from the transverse tubules (see Figure 31–9). Because the action potentials in all the muscle fibers of a motor unit occur at approximately the same time, they contribute to extracellular currents that sum to generate a field potential near the active muscle fibers.

Most muscle contractions involve the activation of many motor units, whose currents sum to produce signals (*compound action potentials*) that can be detected by electromyography. The electromyogram (EMG) is typically large and can be easily recorded with electrodes

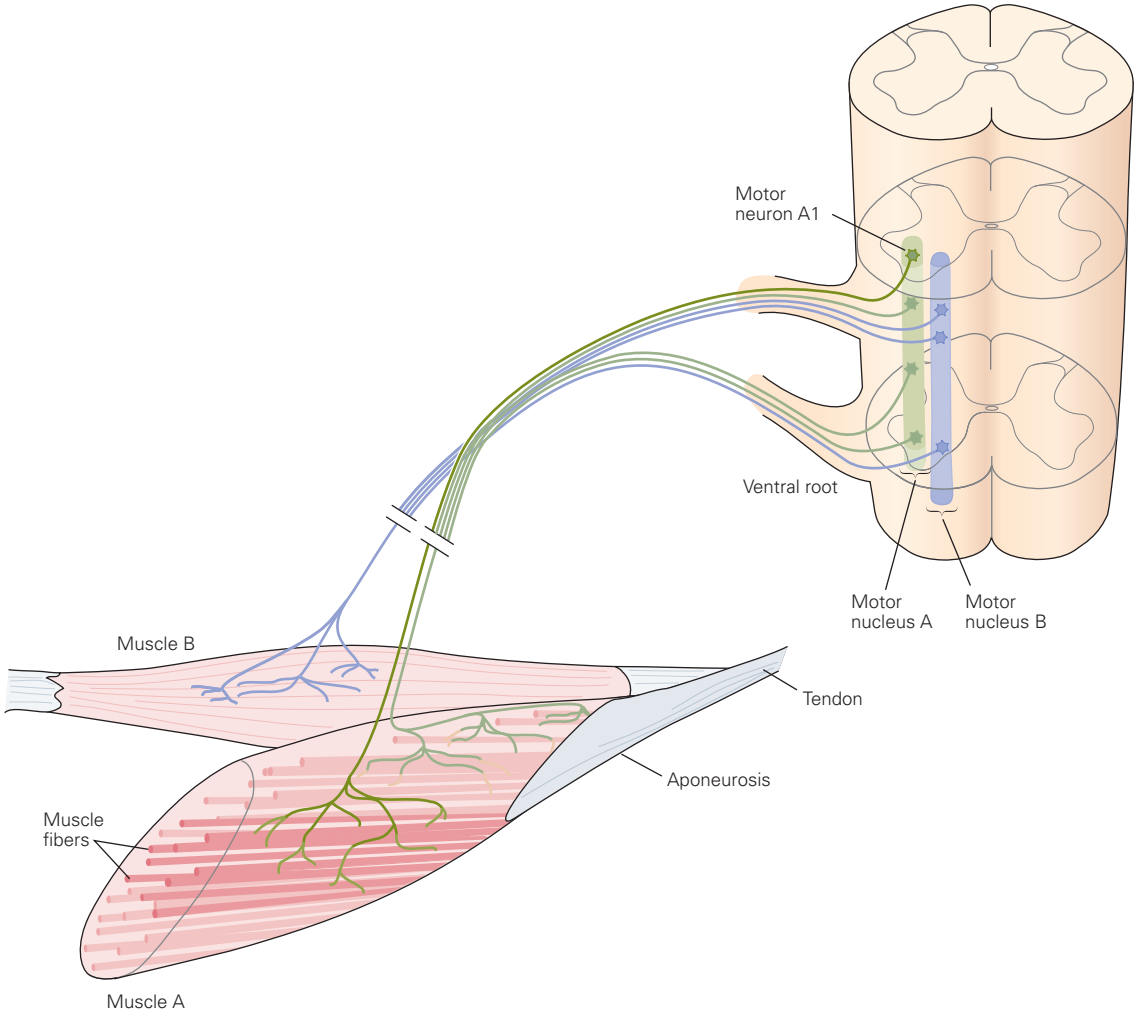

Figure 31–1 A typical muscle consists of many thousands of muscle fibers working in parallel and organized into a smaller number of motor units. A motor unit comprises a motor neuron and the muscle fibers it innervates, illustrated here by motor neuron A1. The motor neurons innervating one muscle are usually clustered into an elongated motor nucleus that may extend over one to four segments within the ventral spinal cord. The axons from a motor nucleus exit the spinal cord in several ventral roots and peripheral nerves but are collected into one nerve bundle near the target muscle. In the figure, motor nucleus A includes all those motor neurons innervating muscle A; likewise, motor nucleus B includes all the motor neurons that innervate muscle B. The extensively branched dendrites of each motor neuron (not shown in the figure) tend to intermingle with those of motor neurons from other nuclei.

placed on the skin over the muscle. The timing and amplitude of EMG activity, therefore, reflect the activation of muscle fibers by the motor neurons. EMG signals are useful for studying the neural control of movement and for diagnosing pathology (Chapter 57).

Each fiber in most mature vertebrate muscles is innervated by a single motor neuron. The number of muscle fibers innervated by one motor neuron, the *innervation number*, varies across muscles. In human skeletal muscles, the innervation number ranges from average values of 5 for an eye muscle to 1,800 for a leg muscle (Table 31–1). Because innervation number denotes the number of muscle fibers within a motor unit, differences in innervation number determine the differences in increments in force produced by activation of different motor units in the same muscle. Thus, the innervation number also indicates the fineness of control of the muscle at low forces; the smaller the innervation number, the finer the control achieved by varying the number of activated motor units.

The differences in innervation numbers between motor units in the same muscle can be substantial. For example, motor units of the first dorsal interosseous muscle of the hand have innervation numbers ranging from approximately 21 to 1,770. The strongest motor unit in the hand's first dorsal interosseous muscle can exert approximately the same force as the average motor unit in the leg's medial gastrocnemius muscle due to different ranges of innervation numbers in the two muscles.

Table 31–1 Innervation Numbers in Human Skeletal Muscles

Muscle	Alpha motor axons	Muscle fibers	Average innervation number
Biceps brachii	774	580,000	750
Brachioradialis	333	129,200	410
Cricothyroid	112	18,550	155
Gastrocnemius (medial)	579	1,042,000	1,800
Interossei dorsales (1)	119	40,500	340
Lumbricales (1)	96	10,269	107
Masseter	1,452	929,000	640
Opponens pollicis	133	79,000	595
Platysma	1,096	27,100	25
Posterior cricoarytenoid	140	16,200	116
Rectus lateralis	4,150	22,000	5
Temporalis	1,331	1,247,000	936
Tensor tympani	146	1,100	8
Tibialis anterior	445	272,850	613
Transverse arytenoid	139	34,470	247

Source: Adapted, with permission, from Enoka 2015. © Human Kinetics, Inc.

The muscle fibers of a single motor unit are distributed throughout the muscle and intermingle with fibers innervated by other motor neurons. The muscle fibers innervated by a single motor unit can be distributed across 8% to 75% of the volume in a limb muscle, with 2 to 5 muscle fibers belonging to the same motor unit among 100 muscle fibers. Therefore, the muscle fibers in a cross-section through the middle of an entire muscle are associated with 20 to 50 different motor units. This distribution and even the number of motor units change with age and with some neuromuscular disorders (Chapter 57). For example, muscle fibers that lose their innervation after the death of a motor neuron can be reinnervated by collateral sprouts from neighboring axons.

Some muscles comprise discrete compartments that are each innervated by a different primary branch of the muscle nerve. Branches of the median and ulnar nerves in the forearm, for example, innervate distinct compartments in three multitendon extrinsic hand muscles that enable the fingers to be moved relatively independently. The muscle fibers belonging to each motor unit in such muscles tend to be confined to one compartment. A muscle can therefore consist of several functionally distinct regions.

The Properties of Motor Units Vary

The force exerted by a muscle depends not only on the number of motor units that are activated during a contraction but also on three properties of motor units: contraction speed, maximal force, and fatigability. These properties are assessed by examining the force exerted by individual motor units in response to variations in the number and rate of evoked action potentials.

The mechanical response to a single action potential is known as a *twitch contraction.* The time it takes the twitch to reach its peak force, the *contraction time,* is one measure of the contraction speed of the muscle fibers that compose a motor unit. The motor units in a muscle typically exhibit a range of contraction times from slow to fast contracting. The mechanical response to a series of action potentials that produce overlapping twitches is known as a *tetanic contraction* or *tetanus.*

The force exerted during a tetanic contraction depends on the extent to which the twitches overlap

and summate (ie, the force varies with the contraction time of the motor unit and the rate at which the action potentials are evoked). At lower rates of stimulation, the ripples in the tetanus denote the peaks of individual twitches (Figure 31–2A). The peak force achieved during a tetanic contraction varies as a sigmoidal function of action potential rate, with the shape of the curve depending on the contraction time of the motor unit (Figure 31–2B). Maximal force is reached at lower action potential rates for slow-contracting motor units than the rates needed to achieve maximal force in fast-contracting units.

The functional properties of motor units vary across the population and between muscles. At one end of the distribution, motor units have long twitch contraction times and produce small forces, but are less fatigable. At the other end of the distribution, motor units have short contraction times, produce large forces, and are

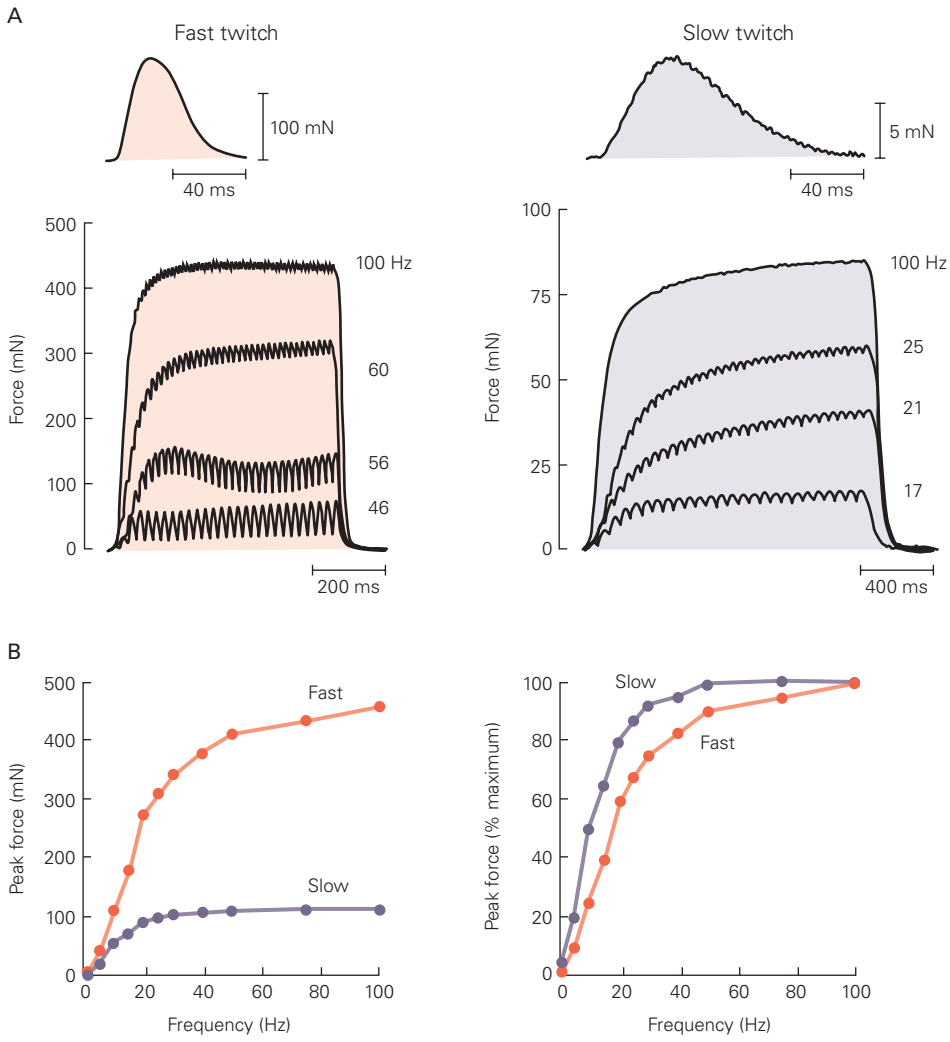

Figure 31–2 The force exerted by a motor unit varies with the rate at which its neuron generates action potentials.

A. Traces show the forces exerted by fast- and slow-contracting motor units in response to a single action potential (**top trace**) and a series of action potentials (set of **four traces below**). The time to the peak twitch force, or contraction time, is briefer in the faster unit. The rates of the action potentials used to evoke the tetanic contractions range from 17 to 100 Hz in the slow-contracting unit to 46 to 100 Hz in the fast-contracting unit. The peak tetanic force evoked by 100-Hz stimulation is greater for the fast-contracting unit. Note the different force scales for the two sets of traces. (Adapted, with permission, from Botterman, Iwamoto, and Gonyea 1986; adapted from Fuglevand, Macefield, and Bigland-Ritchie 1999; and Macefield, Fuglevand, and Bigland-Ritchie 1996.)

B. Relation between peak force and the rate of action potentials for fast- and slow-contracting motor units. The absolute force (*left plot*) is greater for the fast-contracting motor unit at all frequencies. At lower stimulus rates (*right plot*), the force evoked in the slow-contracting motor unit (longer contraction time) sums to a greater relative force (percent of peak force) than in the fast-contracting motor unit (shorter contraction time).

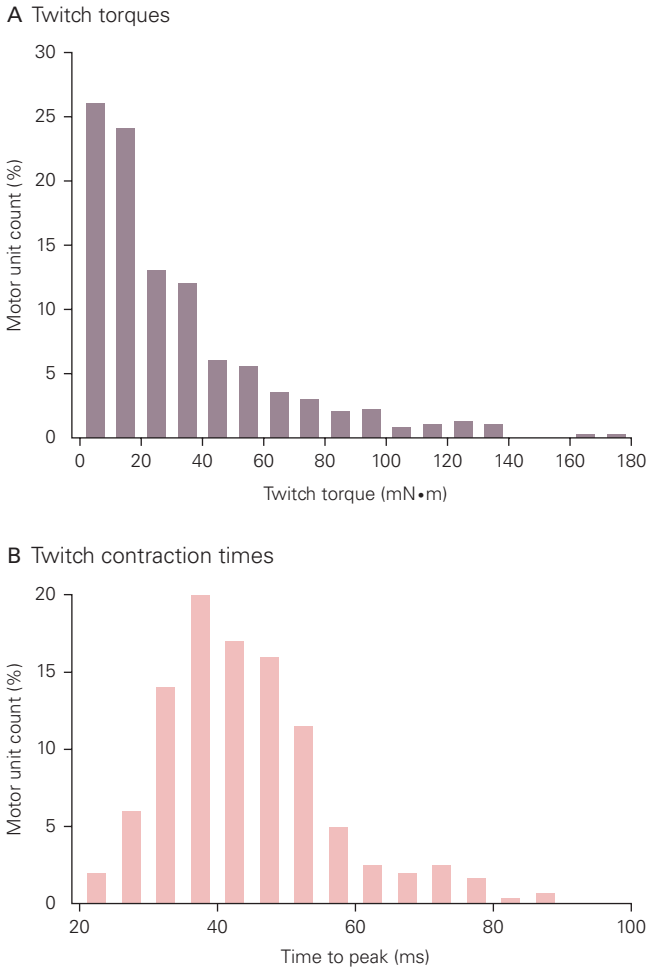

Figure 31–3 Most human motor units produce low forces and have intermediate contraction times. (Reproduced, with permission, from Van Cutsem et al. 1997. © Canadian Science Publishing.)

A. Distribution of twitch torques for 528 motor units in the tibialis anterior muscle obtained from 10 subjects.

B. Distribution of twitch contraction times for 528 motor units in the tibialis anterior muscle.

more fatigable. The order in which motor units are recruited during a voluntary contraction begins with the slow-contracting, low-force units and proceeds up to the fast-contracting, high-force units. As observed by Jacques Duchateau and colleagues, most motor units in humans produce low forces and have intermediate contraction times (Figure 31–3).

The range of contractile properties exhibited by motor units is partly attributable to differences in the structural specializations and metabolic properties of muscle fibers. One commonly used scheme to characterize muscle fibers is based on their reactivity to histochemical assays for the enzyme myosin adenosine triphosphatase (ATPase), which is used as an index of contractile speed. Histochemical stains for myosin ATPase can identify two types of muscle fibers: type I (low levels of myosin ATPase) and type II (high levels of myosin ATPase). Slow-contracting motor units contain type I muscle fibers, and fast-contracting units include type II fibers. The type II fibers can be further classified as being less fatigable (type IIa) or more fatigable (type IIb, IIx, or IId), due to the association between myosin ATPase content and the relative abundance of oxidative enzymes. Another commonly used scheme distinguishes muscle fibers on the basis of genetically defined isoforms of the myosin heavy chain (MHC). Muscle fibers in slow-contracting motor units express MHC-I, those in the less fatigable fast-contracting units express MHC-IIA, and those in the more fatigable fast-contracting units express MHC-IIX.

In actuality, the contractile properties of single muscle fibers are less distinct than the two classification schemes suggest (Figure 31–4). In addition to the variability in the contractile properties of each type of muscle fiber (MHC-I, -IIA, or -IIX), some muscle fibers co-express more than one MHC isoform. Such hybrid muscle fibers exhibit contractile properties that are intermediate between the muscle fibers that compose a

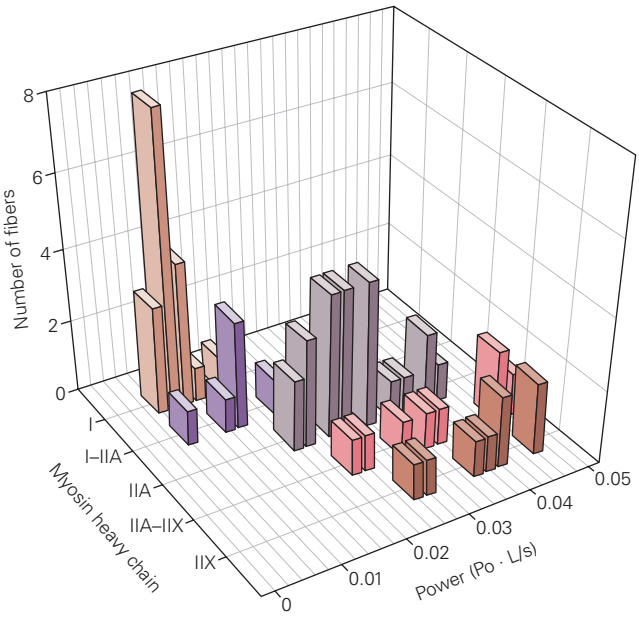

Figure 31–4 The contractile properties of muscle fiber types are distributed continuously. Peak power produced by segments of single muscle fibers from the vastus lateralis muscle with different types of myosin heavy chain (MHC) isoforms. Two types of hybrid fibers (I-IIA and IIA-IIX) contain isoforms of both types of MHCs. Power is calculated as the product of peak tetanic force (P_o) and maximal shortening velocity (segment length per second [L/s]). (Adapted, with permission, from Bottinelli et al. 1996. Copyright © 1996 The Physiological Society.)

single isoform. The relative proportion of hybrid fibers in a muscle increases with age. As with the distribution of contractile properties across motor units (Figure 31–3), the distribution across individual muscle fibers is also continuous, from slow to fast contracting and from least to most powerful (Figure 31–4).

Physical Activity Can Alter Motor Unit Properties

Alterations in habitual levels of physical activity can influence the three contractile properties of motor units (contraction speed, maximal force, and fatigability). A decrease in muscle activity, such as occurs with aging, bed rest, limb immobilization, or space flight, reduces the maximal capabilities of all three properties. The effects of increased physical activity vary with the intensity and duration of the activity. Brief sets of strong contractions performed a few times each week can increase motor unit force (strength training); brief sets of rapid contractions performed a few times each week can increase motor unit discharge rate (power training); and prolonged periods of weaker contractions can reduce motor unit fatigability (endurance training).

Changes in the contractile properties of motor units involve adaptations in the structural specializations and biochemical properties of muscle fibers. The improvement in contraction speed caused by power training, for example, is associated with an increase in the maximal shortening velocity of a muscle fiber caused by an increase in the quantity of myosin ATPase in the fiber. Similarly, the increase in maximal force is associated with the enlarged size and increased intrinsic force capacity of the muscle fibers produced by an increase in the number and density of the contractile proteins.

In contrast, decreases in the fatigability of a muscle fiber can be caused by many different adaptations, such as increases in capillary density, number of mitochondria, efficiency of the processes involved in activating the contractile proteins (excitation-contraction coupling), and oxidative capacity of the muscle fibers. Although the adaptive capabilities of muscle fibers decline with age, the muscles remain responsive to exercise even at 90 years of age.

Despite the efficacy of strength, power, and endurance training in altering the contractile properties of muscle fibers, these training regimens have little effect on the composition of a muscle's fibers. Although several weeks of exercise can change the relative proportion of type IIA and IIX fibers, it produces no change in the proportion of type I fibers. All fiber types adapt in response to exercise, although to varying extents depending on the type of exercise. For example, strength training of leg muscles for 2 to 3 months can increase the cross-sectional area of type I fibers by 0% to 20% and of type II fibers by 20% to 60%, increase the proportion of type IIa fibers by approximately 10%, and decrease the proportion of type IIx fibers by a similar amount. Furthermore, endurance training may increase the enzyme activities of oxidative metabolic pathways without noticeable changes in the proportions of type I and type II fibers, but the relative proportions of type IIa and IIx fibers do change as a function of the duration of each exercise session. Conversely, although several weeks of bed rest or limb immobilization do not change the proportions of fiber types in a muscle, they do decrease the size and intrinsic force capacity of muscle fibers. Adaptations in fiber type properties and proportions in turn alter the distribution of contractile properties in muscle fibers (Figure 31–4) and motor units (Figure 31–3).

Although physical activity has little influence on the proportion of type I fibers in a muscle, more substantial interventions can have an effect. Space flight, for example, exposes muscles to a sustained decrease in gravity that reduces the proportion of type I fibers in some leg muscles and decreases contractile properties. Similarly, surgically changing the nerve that innervates a muscle alters the pattern of activation and eventually causes the muscle to exhibit properties similar to those of the muscle that was originally innervated by the transplanted nerve. Connecting a nerve that originally innervated a rapidly contracting leg muscle to a slowly contracting leg muscle, for example, will cause the slower muscle to become more like a faster muscle. In contrast, a history of performing powerful contractions with leg muscles is associated with a modest reduction in the proportion of type I fibers, a marked increase in the proportion of type IIx fibers, and a huge increase in the power that can be produced by the type IIa and IIx fibers.

Muscle Force Is Controlled by the Recruitment and Discharge Rate of Motor Units

The force exerted by a muscle during a contraction depends on the number of motor units that are activated and the rate at which each of the active motor neurons discharges action potentials. Force is increased during a muscle contraction by the activation of additional motor units, which are recruited progressively from the weakest to the strongest (Figure 31–5). A motor unit's recruitment threshold is the force during the contraction at which the motor unit is activated. Muscle force decreases gradually by terminating the activity of motor units in the reverse order from strongest to weakest.

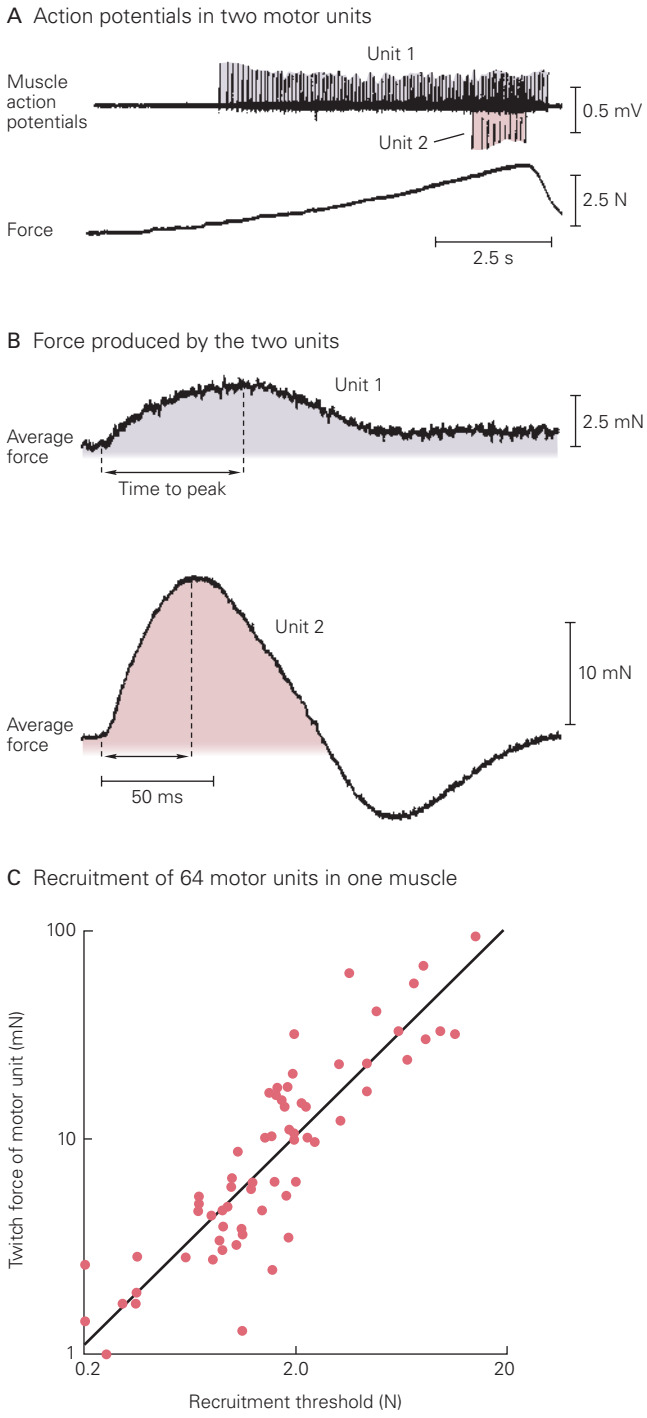

The order in which motor units are recruited is highly correlated with several indices of motor unit size, including the size of the motor neuron cell bodies, the diameter and conduction velocity of the axons, and the amount of force that the muscle fibers can exert. Because individual sources of synaptic input are broadly distributed across most neurons in a motor nucleus, the orderly recruitment of motor neurons is not accomplished by the sequential activation of different sets of synaptic inputs that target specific motor neurons. Rather, recruitment order is determined by intrinsic differences in the responsiveness of individual motor neurons to relatively uniform synaptic input.

One of these factors is the anatomical size of a neuron's soma and dendrites. Smaller neurons have a higher input resistance (R_{in}) to current and, due to Ohm's law ($\Delta V_m = I_{syn} \times R_{in}$), experience a greater change in membrane potential (ΔV_m) in response to a given synaptic current (I_{syn}). Consequently, increases in the net excitatory input to a motor nucleus cause the levels of depolarization to reach threshold in an ascending order of motor neuron size: Contraction force is increased by recruiting the smallest motor neuron first and the largest motor neuron last (Figure 31–6). This effect is known as the size principle of motor neuron recruitment, a concept enunciated by Elwood Henneman in 1957.

The size principle has two important consequences for the control of movement by the nervous system. First, the sequence of motor neuron recruitment is determined by the properties of the spinal neurons and not by supraspinal regions of the nervous system. This means that the brain cannot selectively activate specific motor units. Second, the axons arising from small motor neurons are thinner than those associated with

Figure 31–5 (Left) Motor units that exert low forces are recruited before those that exert greater forces. (Adapted, with permission, from Desmedt and Godaux 1977; Milner-Brown, Stein, and Yemm 1973. Copyright © 1973 The Physiological Society.)

A. Action potentials in two motor units were recorded concurrently with a single intramuscular electrode while the subject gradually increased muscle force. Motor unit 1 began discharging action potentials near the beginning of the voluntary contraction, and its discharge rate increased during the contraction. Motor unit 2 began discharging action potentials near the end of the contraction.

B. Average twitch forces for motor units 1 and 2 as extracted with an averaging procedure during the voluntary contraction.

C. The plot shows the net muscle forces at which 64 motor units in a hand muscle of one person were recruited (recruitment threshold) during a voluntary contraction relative to the twitch forces of the individual motor units.

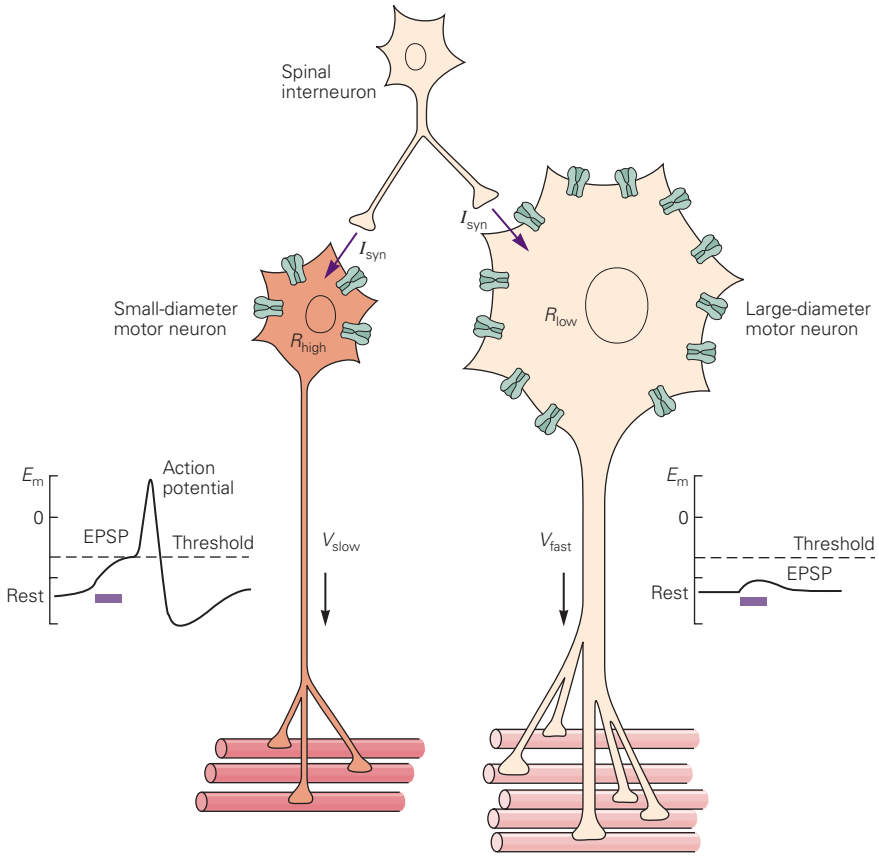

Figure 31–6 The size principle of motor neuron recruitment. Two motor neurons of different sizes have the same resting membrane potential (V_r) and receive the same excitatory synaptic current (I_{syn}) from a spinal interneuron. Because the small motor neuron has a smaller surface area, it has fewer parallel ion channels and therefore a higher input resistance (R_{high}). According to Ohm's law ($V = IR$), I_{syn} in the small neuron produces a large excitatory postsynaptic potential (**EPSP**) that reaches threshold, resulting in the discharge of an action potential. However, the axon of the small motor neuron has a small diameter and thus conducts the action potential at a relatively low velocity (V_{slow}) and to fewer muscle fibers. In contrast, the large motor neuron has a larger surface area, which results in a lower transmembrane resistance (R_{low}) and a smaller EPSP that does not reach threshold in response to I_{syn}; however, when synaptic input does reach threshold, the action potential is conducted relatively rapidly (V_{fast}) (Chapter 9).

large motor neurons and innervate fewer muscle fibers. Because the number of muscle fibers innervated by a motor neuron is a key determinant of motor unit force, motor units are activated in order of increasing strength, so the earliest recruited motor units are the weakest ones.

As suggested by Edgar Adrian in the 1920s, the muscle force at which the last motor unit in a motor nucleus is recruited varies between muscles. In some hand muscles, all the motor units have been recruited when the force reaches approximately 60% of maximum during a slow muscle contraction. In the biceps brachii, deltoid, and tibialis anterior muscles, recruitment continues up to approximately 85% of the maximal force. Beyond the upper limit of motor unit recruitment, changes in muscle force depend solely on variations in the rate at which motor neurons generate action potentials. Over most of the operating range of a muscle, the force it exerts depends on concurrent changes in discharge rate and the number of active motor units (Figure 31–7). Except at low forces, however, variation in

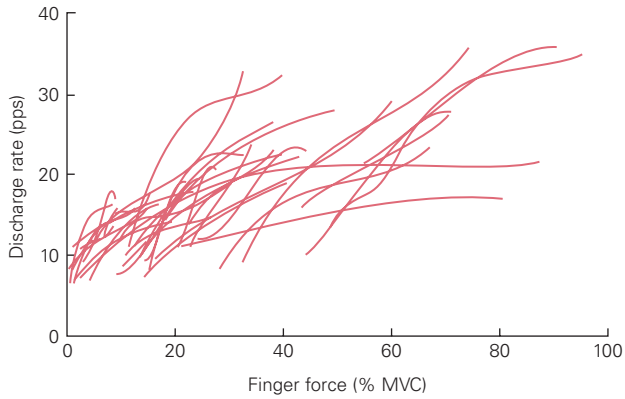

Figure 31–7 Muscle force can be adjusted by varying the number of active motor units and their discharge rate. Each line shows the discharge rate (pulses per second [**pps**]) for a single motor unit in a hand muscle over a range of finger forces (maximal voluntary contraction [**MVC**]). The finger force was produced by the action of a single hand muscle. The leftmost point of each line indicates the threshold force at which the motor unit is recruited, whereas the rightmost point corresponds to the peak force at which the motor unit could be identified. The range of discharge rates was often less for motor units with lower recruitment thresholds. Increases in finger force were produced by concurrent increases in discharge rate and the number of activated motor units. (Adapted, with permission, from Moritz et al. 2005.)

discharge rate has a greater influence on muscle force than does changes in the number of active motor units.

The order in which motor units are recruited does not change with contraction speed. Due to the time involved in excitation-contraction coupling, faster contractions require the action potential for each motor unit to be generated earlier than during a slow contraction. As a result of this adjustment, the upper limit of motor unit recruitment during the fastest muscle contractions is approximately 40% of maximum. Consequently, it is possible to manipulate the rate at which motor units are recruited by varying contraction speed.

The Input–Output Properties of Motor Neurons Are Modified by Input From the Brain Stem

The discharge rate of motor neurons depends on the magnitude of the depolarization generated by excitatory inputs and the intrinsic membrane properties of the motor neurons in the spinal cord. These properties can be profoundly modified by input from monoaminergic neurons in the brain stem (Chapter 40). In the absence of this input, the dendrites of motor neurons passively transmit synaptic current to the cell body, resulting in a modest depolarization that immediately ceases when the input stops. Under these conditions, the relation between input current and discharge rate is linear over a wide range.

The input–output relation becomes nonlinear, however, when the monoamines serotonin and norepinephrine induce a huge increase in conductance by activating L-type Ca^{2+} channels that are located on the dendrites of the motor neurons. The resulting inward Ca^{2+} currents can enhance synaptic currents by three- to five-fold (Figure 31–8). In an active motor neuron, this augmented current can sustain an elevated discharge rate after a brief depolarizing input has ended, a behavior known as *self-sustained firing*. A subsequent brief inhibitory input, such as from a spinal reflex pathway, can terminate such self-sustained firing.

Because the properties of motor neurons are strongly influenced by monoamines, the excitability of the pool of motor neurons innervating a single muscle is partly under control of the brain stem. In the awake state, moderate levels of monoaminergic input to the motor neurons of slowly contracting motor units promote self-sustained firing. This is probably the source of the sustained force exerted by slower motor units to maintain posture (Chapter 36). Conversely, the withdrawal of monoaminergic drive during sleep decreases excitability and helps ensure a relaxed motor state. Thus, monoaminergic input from the brain stem can adjust the gain of the motor unit pool to meet the demands of different tasks. This flexibility does not compromise the size principle of orderly recruitment because the threshold for activation of the persistent inward currents is lowest in the motor neurons of slower contracting motor units, which are the first recruited even in the absence of monoamines.

Muscle Force Depends on the Structure of Muscle

Muscle force depends not only on the amount of motor neuron activity but also on the arrangement of the fibers in the muscle. Because movement involves the controlled variation of muscle force, the nervous system must take into account the structure of muscle to achieve specific movements.

The Sarcomere Is the Basic Organizational Unit of Contractile Proteins

Individual muscles contain thousands of fibers that vary from 1 to 50 mm in length and from 10 to 60 µm in diameter. The variation in fiber dimensions reflects differences in the quantity of contractile protein. Despite this quantitative variation, the organization of contractile proteins is similar in all muscle fibers. The proteins are arranged in repeating sets of thick and thin filaments, each set known as a *sarcomere* (Figure 31–9). The in vivo length of a sarcomere, which is bounded by Z disks, ranges from 1.5 to 3.5 µm within and across muscles. Sarcomeres are arranged in series to form a *myofibril*, and the myofibrils are aligned in parallel to form a muscle fiber (myocyte).

The force that each sarcomere can generate arises from the interaction of the contractile thick and thin filaments. The thick filament consists of several hundred myosin molecules arranged in a structured sequence. Each myosin molecule comprises paired coiled-coil domains that terminate in a pair of globular heads. The myosin molecules in the two halves of a thick filament point in opposite directions and are progressively displaced so that the heads, which extend away from the filament, protrude around the thick filament (Figure 31–9C). The thick filament is anchored in the middle of the sarcomere by the protein titin, which connects each end of the thick filament with neighboring strands of actin in the thin filament and with the Z-disc. To maximize the interaction between the globular heads of myosin and the thin filaments, six thin filaments surround each thick filament.

The primary components of the thin filament are two helical strands of fibrous F-actin, each of which

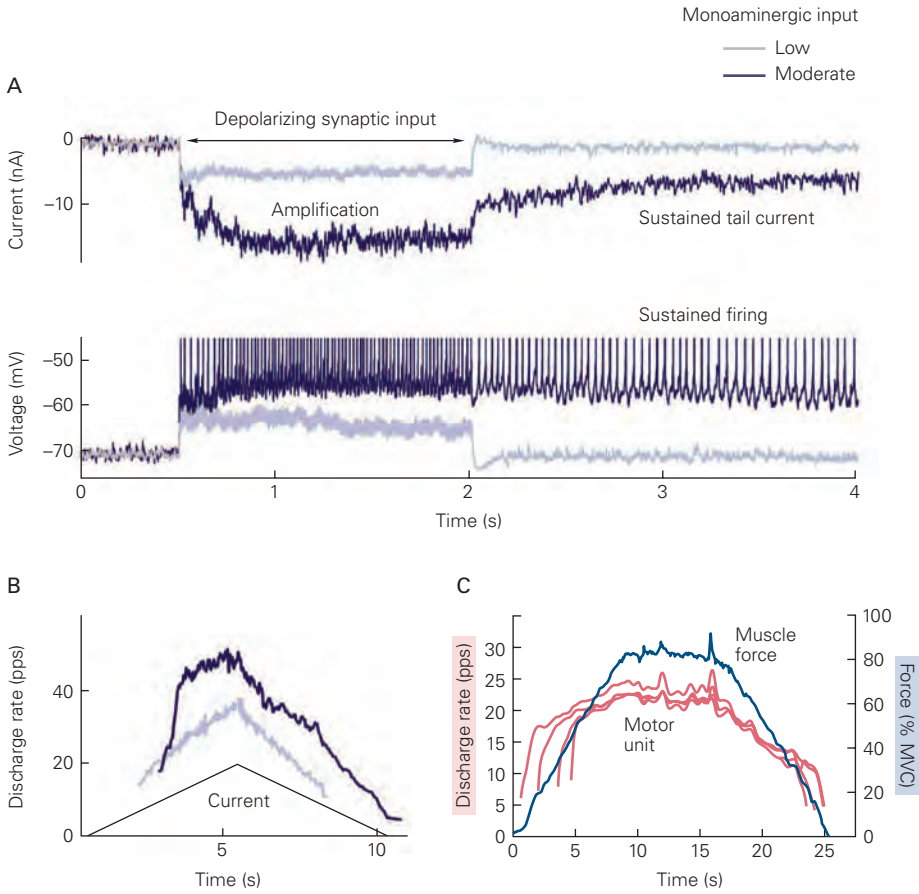

Figure 31–8 **Monoaminergic input enhances the excitability of motor neurons.** (Part **A**, adapted, with permission, of Heckman et al. 2009. Copyright © 2009 International Federation of Clinical Neurophysiology; Part **B**, data from CJ Heckman; Part **C**, adapted, with permission, from Erim et al. 1996. Copyright © 1996 John Wiley & Sons, Inc.)

A. Membrane currents and potentials in spinal motor neurons of adult cats that were either deeply anesthetized (low monoaminergic drive) or decerebrate (moderate monoaminergic drive). When monoaminergic input is absent or low, a brief excitatory input produces an equally brief synaptic current during voltage clamp (**upper record**). This current is not sufficient to bring the membrane potential of the neuron to threshold for generating action potentials in the unclamped condition (**lower record**). The same brief excitatory input during moderate levels of monoaminergic input activates a persistent inward current in the dendrites, which amplifies the excitatory synaptic current and decays slowly following cessation of synaptic input (**upper record**). This persistent inward current causes a high discharge rate during the input and sustains a lesser discharge rate after the input ceases (**lower record**). A brief inhibitory input will return the neuron to its resting state.

B. High levels of monoaminergic input to a motor neuron give rise to a persistent inward current in response to injected current, resulting in a much greater discharge rate for a given amount of current.

C. The **blue** trace represents the force exerted by the dorsiflexor muscle during a contraction that gradually increased to 80% of maximal voluntary isometric contraction (**MVC**) force in a human subject. Each of the four **pink** traces indicates the change in the rate at which a single motor unit discharged action potentials during the contraction. The leftmost point (start) of each of these four traces shows the time when the motor unit was recruited, and the rightmost point (end) denotes the time at which the motor neuron stopped discharging action potentials. The rapid increase in discharge rate during the increase in muscle force is similar to the change in rate observed in the presence of moderate levels of monoaminergic input (see part **B**).

contains approximately 200 actin monomers. Superimposed on F-actin are tropomyosin and troponin, proteins that control the interaction between actin and myosin. Tropomyosin consists of two coiled strands that lie in the groove of the F-actin helix; troponin is a small molecular complex that is attached to tropomyosin at regular intervals (Figure 31–9C).

The thin filaments are anchored to the Z disk at each end of the sarcomere, whereas the thick filaments occupy the middle of the sarcomere (Figure 31–9B). This organization accounts for the alternating light and dark bands of striated muscle. The light band contains only thin filaments, whereas the dark band contains both thick and thin filaments. When a muscle is

activated, the width of the light band decreases but the width of the dark band does not change, suggesting that the thick and thin filaments slide relative to one another during a contraction. This led to the *sliding filament hypothesis* of muscle contraction proposed by A. F. Huxley and H. E. Huxley in the 1950s.

The sliding of the thick and thin filaments is triggered by the release of Ca^{2+} from within the sarcoplasm of a muscle fiber in response to an action potential that travels along the fiber's membrane, the sarcolemma. Varying the amount of Ca^{2+} in the sarcoplasm controls the interaction between the thick and thin filaments. The Ca^{2+} concentration in the sarcoplasm is kept low under resting conditions by active pumping of Ca^{2+} into the sarcoplasmic reticulum, a network of longitudinal tubules and chambers of smooth endoplasmic reticulum. Calcium is stored in the terminal cisternae, which are located next to intracellular extensions of the sarcolemma known as transverse tubules (T-tubules). The transverse tubules, terminal cisternae, and sarcoplasmic reticulum constitute an activation system that transforms an action potential into the sliding of the thick and thin filaments (Figure 31–9A).

As an action potential propagates along the sarcolemma, it invades the transverse tubules and causes the rapid release of Ca^{2+} from the terminal cisternae into the sarcoplasm. Once in the sarcoplasm, Ca^{2+} diffuses among the filaments and binds reversibly to troponin, which results in the displacement of the troponin–tropomyosin complex and enables the sliding of the thick and thin filaments. Because a single action potential does not release enough Ca^{2+} to bind all available troponin sites in skeletal muscle, the strength of a contraction increases with the action potential rate.

The sliding of the filaments depends on mechanical work performed by the globular heads of myosin, work that uses chemical energy contained in adenosine triphosphate (ATP). The actions of the myosin heads are regulated by the *cross-bridge cycle*, a sequence of detachment, activation, and attachment (Figure 31–10). In each cycle, a globular head undergoes a displacement of 5 to 10 nm. Contractile activity continues as long as Ca^{2+} and ATP are present in the cytoplasm in sufficient amounts.

Once the contractile proteins have been activated by the release of Ca^{2+}, sarcomere length may increase, remain the same, or decrease depending on the magnitude of the load against which the muscle is acting. The force generated by an activated sarcomere when its length does not change or decreases can be explained by the cross-bridge cycle involving the thick and thin filaments. When the length of the activated sarcomere increases, however, the force developed by the extension of titin adds significantly to the sarcomere force. The force produced by titin during the stretch of an activated sarcomere is augmented by its ability to increase stiffness, which is accomplished when titin binds Ca^{2+} and then attaches at specific locations on actin to reduce the length that it can be stretched. The force produced by activated sarcomeres therefore depends on the interactions of three filaments (actin, myosin, and titin).

Noncontractile Elements Provide Essential Structural Support

Structural elements of the muscle fiber maintain the alignment of the contractile proteins within the fiber and facilitate the transmission of force from the sarcomeres to the skeleton. A network of proteins (nebulin, titin) maintains the orientation of the thick and thin filaments within the sarcomere, whereas other proteins (desmin, skelemins) constrain the lateral alignment of the myofibrils (Figure 31–9B). These proteins contribute to the elasticity of muscle and maintain the appropriate alignment of cellular structures when the muscle acts against an external load.

Although some of the force generated by the cross bridges is transmitted along the sarcomeres in series, most of it travels laterally from the thin filaments to an extracellular matrix that surrounds each muscle fiber, through a group of transmembrane and membrane-associated proteins called a *costamere* (see inset for Figure 31–9B). The lateral transmission of force follows two pathways through the costamere, one through a dystrophin–glycoprotein complex and the other through vinculin and members of the integrin family. Mutations of genes that encode components of the dystrophin–glycoprotein complex cause muscular dystrophies in humans, which are associated with substantial decreases in muscle force.

Contractile Force Depends on Muscle Fiber Activation, Length, and Velocity

The force that a muscle fiber can exert depends on the number of cross bridges formed and the force produced by each cross bridge. These two factors are influenced by the Ca^{2+} concentration in the sarcoplasm, the amount of overlap between the thick and thin filaments, and the velocity with which the thick and thin filaments slide past one another.

The influx of Ca^{2+} that activates formation of the cross bridges is transitory because continuous pump activity quickly returns Ca^{2+} to the sarcoplasmic reticulum. The release and reuptake of Ca^{2+} in response to a single action potential occurs so quickly that only some

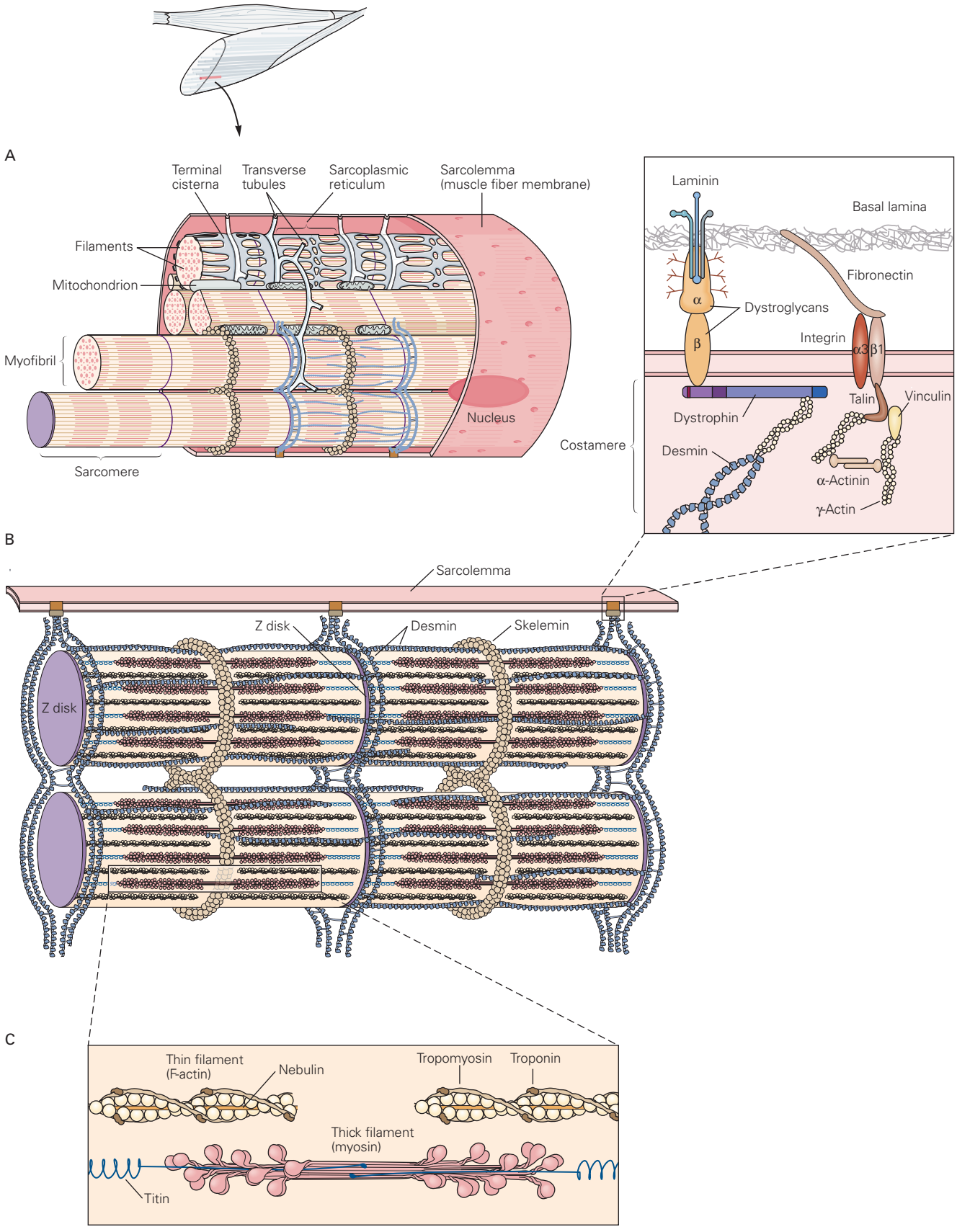
A
Terminal cisterna
Transverse tubules
Sarcoplasmic reticulum
Sarcolemma (muscle fiber membrane)
Filaments
Mitochondrion
Myofibril
Nucleus
Sarcomere
Laminin
Basal lamina
Fibronectin
α
Dystroglycans
β
Integrin
α3β1
Talin
Vinculin
Dystrophin
Costamere
Desmin
α-Actinin
γ-Actin
B
Sarcolemma
Z disk
Desmin
Skelemin
Z disk
C
Thin filament (F-actin)
Nebulin
Tropomyosin
Troponin
Thick filament (myosin)
Titin

of the potential cross bridges are formed. This explains why the peak force of a twitch is less than the maximal force of the muscle fiber (see Figure 31–2A). Maximal force can be achieved only with a series of action potentials that sustains the Ca^{2+} concentration in the sarcoplasm, thus maximizing cross bridge formation.

Although Ca^{2+} activates formation of the cross bridges, cross bridges can be formed only when the thick and thin filaments overlap. This overlap varies as the filaments slide relative to one another (Figure 31–11A). The amount of overlap between actin and myosin is optimal at an intermediate sarcomere length (L_o), and the relative force is maximal. Increases in sarcomere length reduce the overlap between actin and myosin and the force that can be developed. Decreases in sarcomere length cause the thin filaments to overlap, reducing the number of binding sites available to the myosin heads. Although many muscles operate over a narrow range of sarcomere lengths (approximately 94 ± 13% L_o, mean ± standard deviation), among muscles, there is considerable diversity in sarcomere lengths during movement.

Because structures that connect the contractile proteins to the skeleton also influence the force that a muscle can exert, muscle force increases with length over its operating range. This property enables muscle to function like a spring and to resist changes in length. Muscle stiffness, which corresponds to the slope of the relation between muscle force and muscle length (N/m), depends on the structure of the muscle. A stiffer muscle, similar to a stronger spring, is more resistant to changes in length.

Once activated, cross bridges perform work and cause the thick and thin filaments to slide relative to one another. Due to the elasticity of intracellular cytoskeletal proteins and the extracellular matrix, sarcomeres will shorten when the cross bridges are activated and the length of the muscle fiber is held fixed (*isometric contraction*). When the length of the muscle fiber is not kept constant, the direction and rate of change in sarcomere length depend on the amount of muscle fiber force relative to the magnitude of the load against which the fiber acts. Sarcomere length decreases when the muscle fiber force exceeds the load (*shortening contraction*) but increases when the force is less than the load (*lengthening contraction*). The maximal force that a muscle fiber can exert decreases as shortening velocity increases but increases as lengthening velocity increases (Figure 31–11B).

The maximal rate at which a muscle fiber can shorten is limited by the peak rate at which cross bridges can form. The variation in fiber force as contraction velocity changes is largely caused by differences in the average force exerted by each cross bridge. For example, the decrease in force during a shortening contraction is attributable to a reduction in cross-bridge displacement during each power stroke and the failure of some myosin heads to find attachment sites. Conversely, the increase in force during a lengthening contraction reflects the stretching of incompletely activated sarcomeres, the more rapid reattachment of cross bridges after they have been pulled apart, and the attachment of Ca^{2+} to titin.

The rate of cross-bridge cycling depends not only on contraction velocity but also on the preceding activity of the muscle. For example, the rate of cross-bridge cycling increases after a brief isometric contraction. When a muscle is stretched while in this state, such as would occur during a postural disturbance, muscle stiffness is enhanced, and the muscle is more effective at resisting the change in length. This property is known as *short-range stiffness*. Conversely, the cross-bridge cycling rate decreases after shortening contractions, and the muscle does not exhibit short-range stiffness.

Figure 31–9 (Opposite) **The sarcomere is the basic functional unit of muscle.** (Adapted from Bloom and Fawcett 1975.)

A. This section of a muscle fiber shows its anatomical organization. Several myofibrils lie side by side in a fiber, and each myofibril is made up of sarcomeres arranged end to end and separated by Z disks (see part **B**). The myofibrils are surrounded by an activation system (the transverse tubules, terminal cisternae, and sarcoplasmic reticulum) that initiates muscle contraction.

B. Sarcomeres are connected to one another and to the muscle fiber membrane by the cytoskeletal lattice. The cytoskeleton influences the length of the contractile elements, the thick and thin filaments (see part **C**). It maintains the alignment of these filaments within a sarcomere, connects adjacent myofibrils, and transmits force to the extracellular matrix of connective tissue through costameres. One consequence of this organization is that the force generated by the contractile elements in a sarcomere can be transmitted along and across sarcomeres (through desmin and skelemin), within and between sarcomeres (through nebulin and titin), and to the sarcolemma through the costameres. The Z disk is a focal point for many of these connections.

C. The thick and thin filaments comprise different contractile proteins. The thin filament includes polymerized actin along with the regulatory proteins tropomyosin and troponin. The thick filament is an array of myosin molecules; each molecule includes a stem that terminates in a pair of globular heads. The protein titin maintains the position of each thick filament in the middle of the sarcomere.

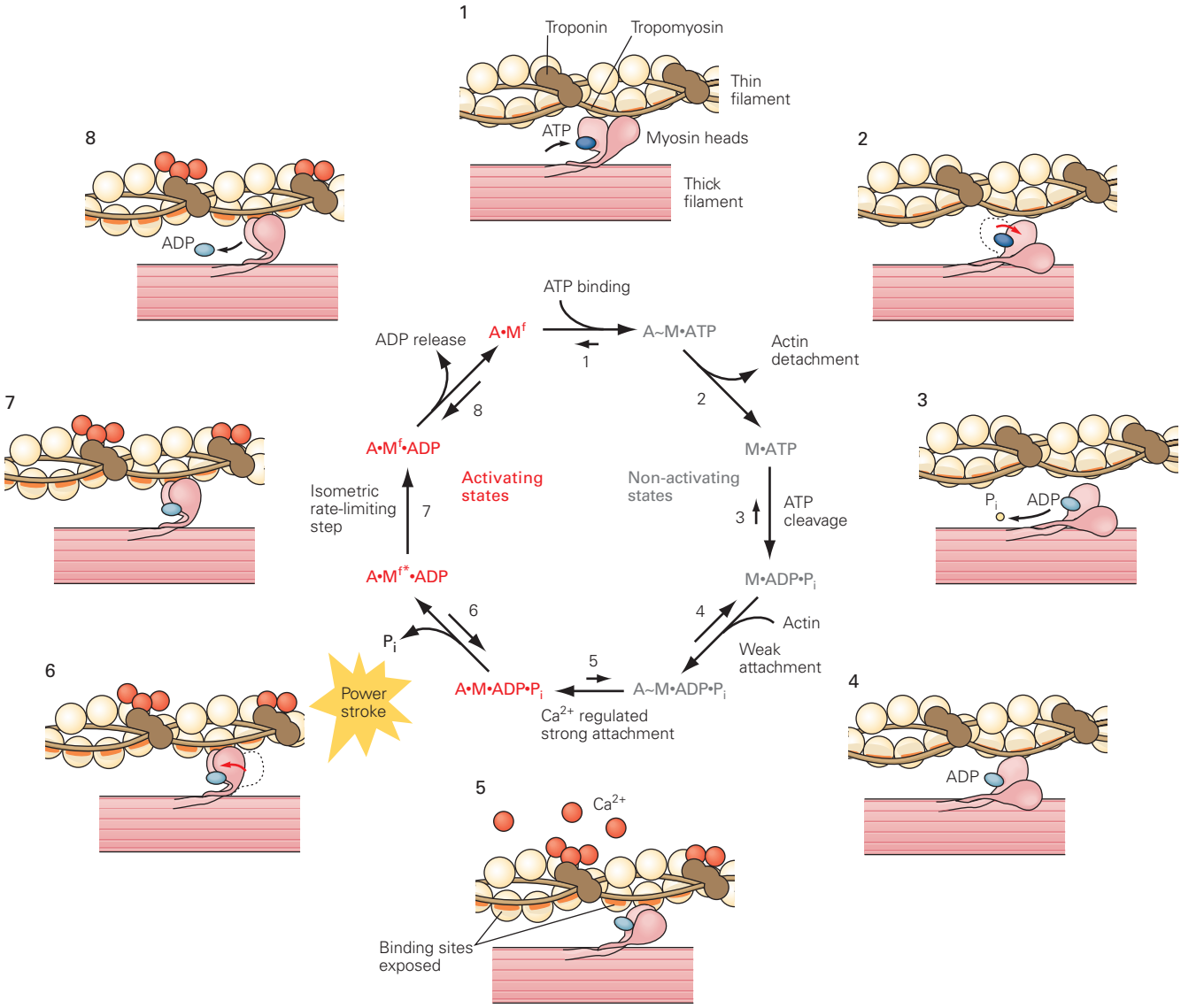

Figure 31–10 **The cross-bridge cycle.** Several nonactivating states are followed by several activating states triggered by Ca^{2+}. The cycle begins at the top (**step 1**) with the binding of adenosine triphosphate (**ATP**) to the myosin head. The myosin head detaches from actin (**step 2**), ATP is cleaved to phosphate (P_i) and adenosine diphosphate (**ADP**) (**step 3**), and the myosin becomes weakly bound to actin (**step 4**). The binding of Ca^{2+} to troponin causes tropomyosin to slide over actin and enables the two myosin heads to close (**step 5**). This results in the release of P_i and the extension of the myosin neck, the power stroke of the cross-bridge cycle (**step 6**). Each cross-bridge exerts a force of approximately 2 pN during a structural change (**step 7**) and the release of ADP (**step 8**). (•, strong binding; ~, weak binding; M^f, cross-bridge force of myosin; and M^{f*}, force-bearing state of myosin.) (Adapted, with permission, from Gordon, Regnier, and Homsher 2001.)

Muscle Torque Depends on Musculoskeletal Geometry

The anatomy of a muscle has a pronounced effect on its force capacity, range of motion, and shortening velocity. The anatomical features that influence function include the arrangement of the sarcomeres in each muscle fiber, the organization of the muscle fibers within the muscle, and the location of the muscle's attachments on the skeleton. These features vary widely among muscles.

At the level of a single muscle fiber, the number of sarcomeres in series and in parallel can vary. The number of sarcomeres in series determines the length

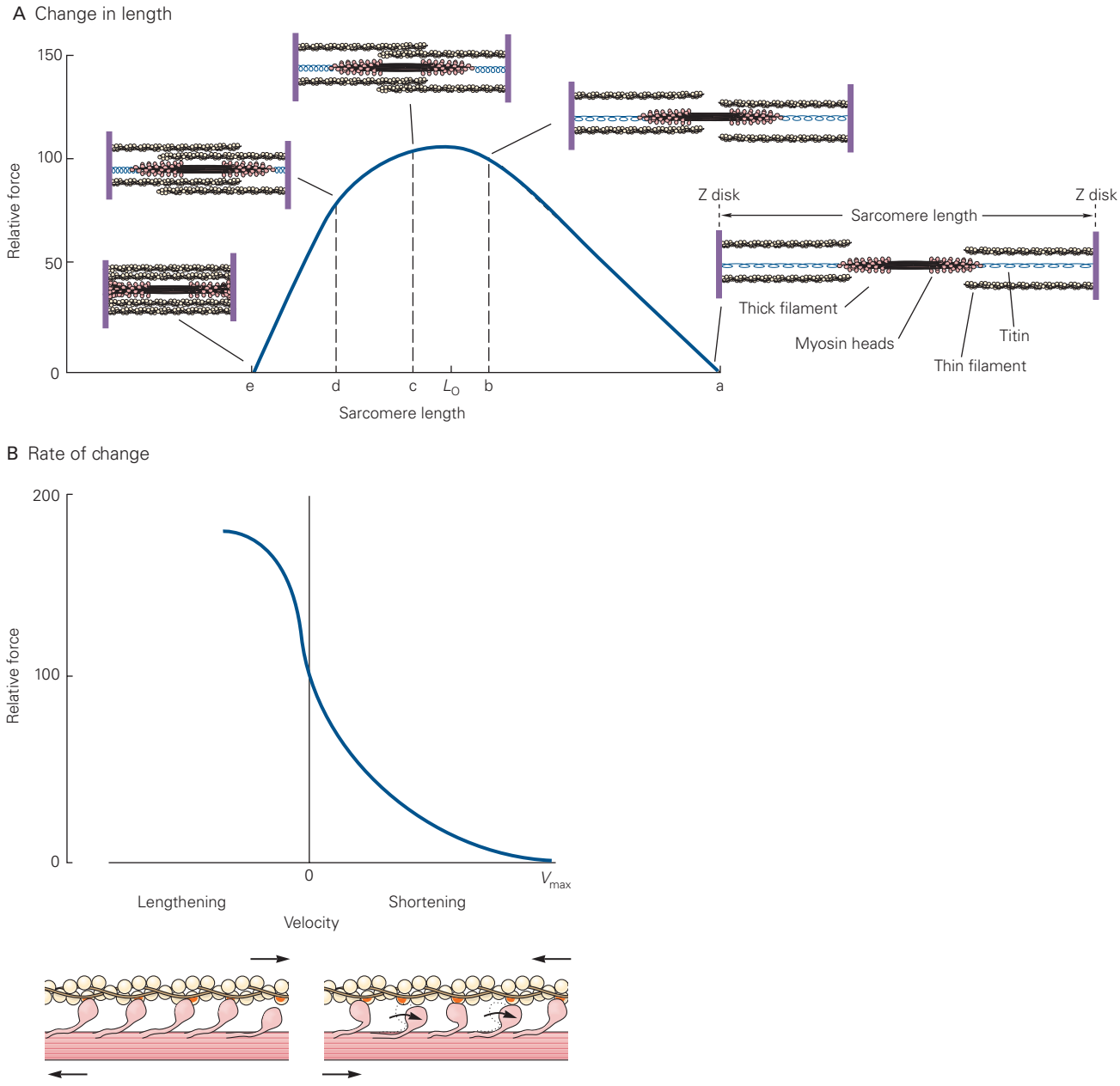

Figure 31–11 Contractile force varies with the change in sarcomere length and velocity.

A. At an intermediate sarcomere length, L_o, the amount of overlap between actin and myosin is optimal and the relative force is maximal. When the sarcomere is stretched beyond the length at which the thick and thin filaments overlap (length **a**), cross bridges cannot form and no force is exerted. As sarcomere length decreases and the overlap of the thick and thin filaments increases (between lengths **a** and **b**), the force increases because the number of cross bridges increases. With further reductions in length (between lengths **c** and **e**), the extreme overlap of the thin filaments with each other occludes potential attachment sites and the force decreases.

B. Contractile force varies with the rate of change in sarcomere length. Relative to the force that a sarcomere can exert during an isometric contraction (zero velocity), the peak force declines as the rate of shortening increases. Muscle force reaches a minimum at the maximal shortening velocity (V_{max}). In contrast, when the sarcomere is lengthened while being activated, the peak force increases to values greater than those during an isometric contraction. Shortening causes the myosin heads to spend more time near the end of their power stroke, where they produce less contractile force, and more time detaching, recocking, and reattaching, during which they produce no force. When the muscle is actively lengthened, the myosin heads spend more time stretched beyond their angle of attachment and little time unattached because they do not need to be recocked after being pulled away from the actin in this manner. Titin also contributes significantly to sarcomere force during lengthening contractions.

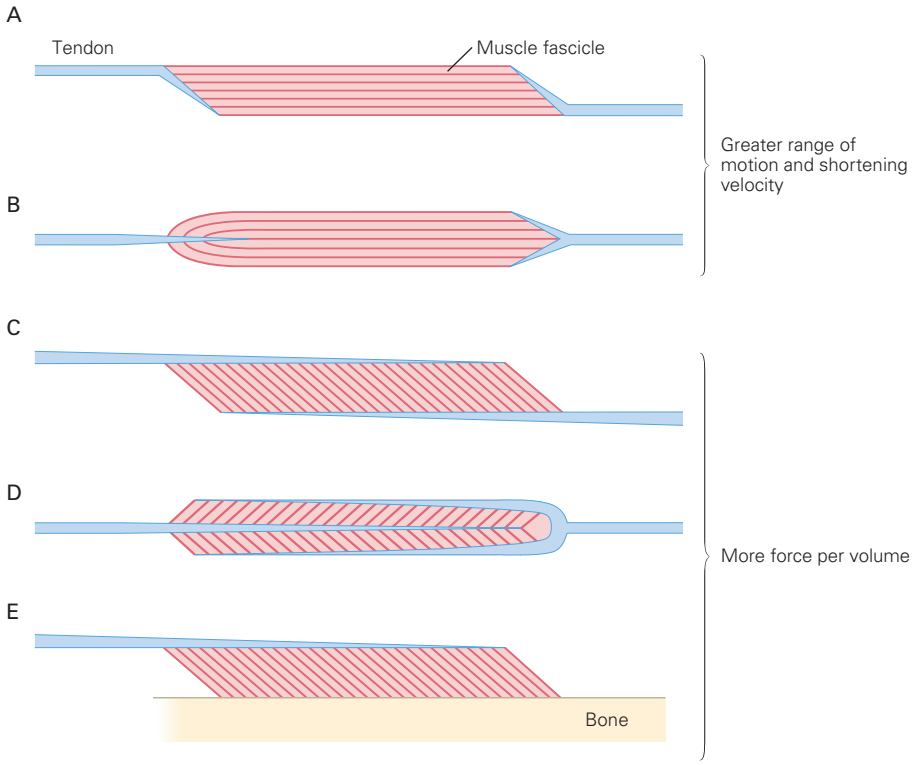

Figure 31–12 Five common arrangements of tendon and muscle. The fundamental distinction between these arrangements is whether or not the muscle fascicles are aligned with the line of pull of the muscles. The fascicles in muscles A and B are parallel to the line of pull (longitudinal axis of the muscle), whereas the fascicles in muscles C, D, and E are rotated away from the line of pull. The magnitude of this rotation is expressed as the pennation angle. (Reproduced, with permission, from Alexander and Ker 1990.)

of the myofibril and thus the length of the muscle fiber. Because one sarcomere can shorten by a certain length with a given maximal velocity, both the range of motion and the maximal shortening velocity of a muscle fiber are proportional to the number of sarcomeres in series. The force that a myofibril can exert is equal to the average sarcomere force and is not influenced by the number of sarcomeres in series. Rather, the force capacity of a fiber depends on the number of sarcomeres in parallel and hence on the diameter or cross-sectional area of the fiber. At the level of the muscle, the functional attributes of the fibers are modified by the orientation of the fascicles (bundles of muscle fibers) to the line of pull of the muscle and the length of the fiber relative to the muscle length. In most muscles, the fascicles are not parallel to the line of pull but fan out in feather-like (pennate) arrangements (Figure 31–12).

The relative orientation, or pennation angle of the fascicles, ranges from close to 0° (biceps brachii, sartorius) to approximately 30° (soleus). Because more fibers can fit into a given volume as the pennation angle increases, muscles with large pennation angles typically have more fascicles in parallel and hence large cross-sectional areas when measured perpendicular to the long axis of individual muscle fibers. Given the linear relation between cross-sectional area (quantity of contractile proteins in parallel) and maximal force (~22.5 N • cm^{-2}), these muscles are capable of a greater maximal force. However, the fibers in pennate muscles are generally short and have a lesser maximal shortening velocity than those in nonpennate muscles.

The functional consequences of this anatomical arrangement can be seen by comparing the contractile properties of two muscles with different numbers of fibers and fiber lengths. If the two muscles have identical fiber lengths but one has twice as many fibers, the range of motion of the two muscles will be similar because it is a function of fiber length, but the maximal force capacity will vary in proportion to the number of muscle fibers. If the two muscles have identical numbers of fibers but the fibers in one muscle are twice as long, the muscle with the longer fibers will have a greater range of motion and a greater maximal shortening velocity, even though the two muscles have a similar force capacity. Because of this effect, the muscle with longer fibers is able to exert more force and produce more power (the product of force and velocity) at a given absolute shortening velocity (Figure 31–13).

Muscle fiber lengths and cross-sectional areas vary substantially throughout the human body, which suggests that the contractile properties of individual muscles also differ markedly (Table 31–2). In the leg,

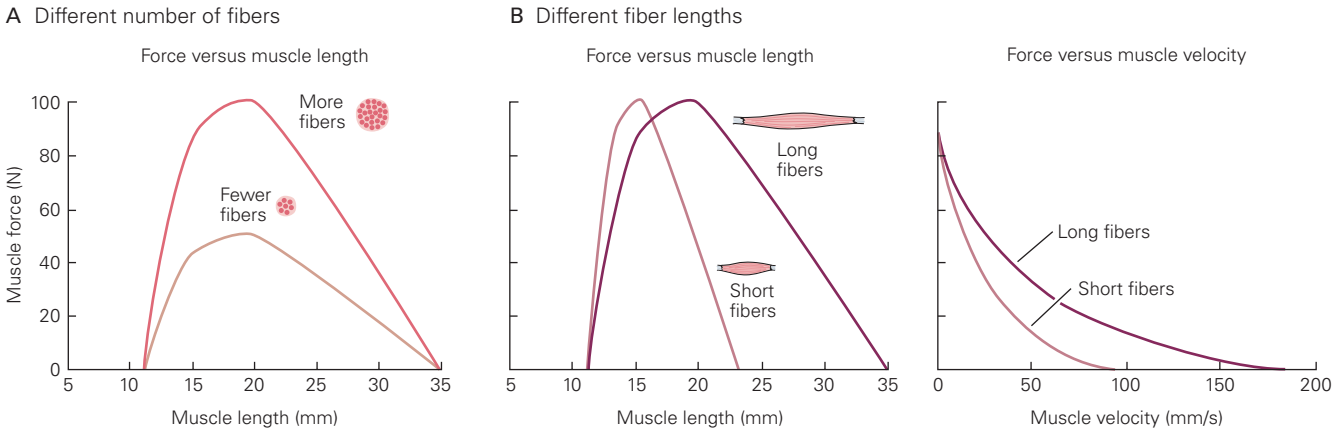

Figure 31–13 **Muscle dimensions influence the peak force and maximal shortening velocity.** (Reproduced, with permission, from Lieber and Fridén 2000. Copyright © 2000 John Wiley & Sons, Inc.)

A. Muscle force at various muscle lengths for two muscles with similar fiber lengths but different numbers of muscle fibers (different cross-sectional area). The muscle with twice as many fibers exerts greater force.

B. Muscle force at various muscle lengths for two muscles with the same cross-sectional area but different fiber lengths. The muscle with longer fibers (approximately twice as long as those of the other muscle) has an increased range of motion (left plot). It also has a greater maximal shortening velocity and exerts greater force at a given absolute velocity (right plot).

Table 31–2 Average Architectural Properties for Some Human Skeletal Leg Muscles

Muscle	Mass (g)	Muscle length (cm)	Fiber length (cm)	Pennation angle (°)	Cross-sectional area (cm^2)
Thigh					
Sartorius	78	45	40	1	2
Rectus femoris	111	36	8	14	14
Vastus lateralis	376	27	10	18	35
Vastus intermedius	172	41	10	5	17
Vastus medialis	239	44	10	30	21
Gracilis	53	29	23	8	2
Adductor longus	75	22	11	7	7
Adductor brevis	55	15	10	6	5
Adductor magnus	325	38	14	16	21
Biceps femoris (long)	113	35	10	12	11
Biceps femoris (short)	60	22	11	12	5
Semitendinosus	100	30	19	13	5
Semimembranosus	134	29	7	15	18
Lower leg					
Tibialis anterior	80	26	7	10	11
Extensor hallucis longus	21	24	7	9	3
Extensor digitorum longus	41	29	7	11	6
Peroneus longus	58	27	5	14	10
Peroneus brevis	24	24	5	11	5
Gastrocnemius (medial)	113	27	5	10	21
Gastrocnemius (lateral)	62	22	6	12	10
Soleus	276	41	4	28	52
Flexor hallucis longus	39	27	5	17	7
Flexor digitorum longus	20	27	4	14	4
Tibialis posterior	58	31	4	14	14

Source: Adapted, with permission, from Ward et al. 2009.

for example, pennation angle ranges from 1° (sartorius) to 30° (vastus medialis), fiber length ranges from 4 mm (soleus) to 40 mm (sartorius), and cross-sectional area ranges from 2 cm^2 (sartorius) to 52 cm^2 (soleus). In addition, the fact that muscle fiber length is usually less than muscle length indicates that muscle fibers are connected serially within a muscle. Functionally coupled muscles tend to have complementary combinations of these properties. For example, the three vasti muscles have similar muscle fiber lengths (10 cm), but they differ in pennation angle (intermedius is the smallest) and cross-sectional area (lateralis is the largest). A similar relation exists for soleus and the two heads (medial and lateral) of gastrocnemius.

Movement involves the muscle-controlled rotation of adjacent body segments, which means that the capacity of a muscle to contribute to a movement also depends on its location relative to the joint that it spans. The rotary force exerted by a muscle about a joint is referred to as *muscle torque* and is calculated as the product of the muscle force and the *moment arm*, the shortest perpendicular distance from the line of pull of the muscle to the joint's center (Figure 31–14).

The moment arm usually changes as a joint rotates through its range of motion; the amount of change depends on where the muscle is attached to the skeleton relative to the joint. If the force exerted by a muscle remains relatively constant throughout the joint's range of motion, muscle torque varies in direct proportion to the change in the moment arm. For many muscles, the moment arm is maximal in the middle of the range of motion, which usually corresponds to the position of maximal muscle force and hence greatest muscle torque.

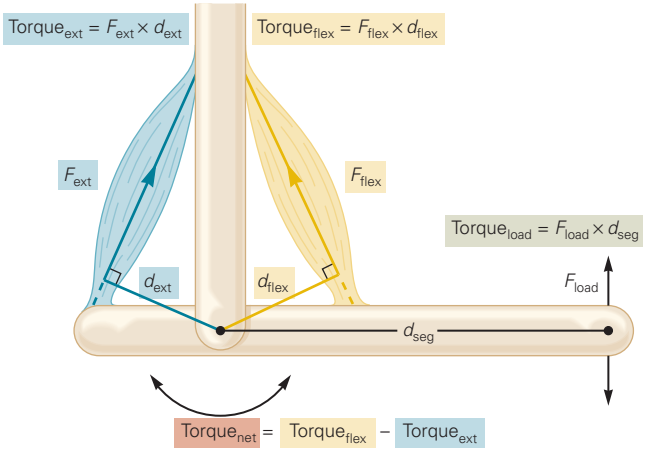

Figure 31–14 Muscle torque varies over the range of motion about a joint. A muscle's torque about a joint is the product of its contractile force (F) and its moment arm relative to the joint (d). The moment arm is the shortest perpendicular distance from the line of pull of the muscle to the center of rotation of the joint. Because the moment arm changes when the joint rotates, muscle torque varies with angular displacement about the joint. The net torque about a joint, which determines the mechanical action, is the difference in the torques exerted by opposing muscles, such as extensors (ext) and flexors (flex). Similarly, a force applied to the limb (F_{load}) will exert a torque about the joint that depends on F_{load} and its distance from the joint (d_{seg}).

Different Movements Require Different Activation Strategies

The human body has approximately 600 muscles, each with a distinct torque profile about one or more joints. To perform a desired movement, the nervous system must activate an appropriate combination of muscles with adequate intensity and timing of activity. The activation must be appropriate for the contractile properties and musculoskeletal geometry of many muscles, as well as the mechanical interactions between body segments. As a result of these demands, activation strategies differ with the details of the movement.

Contraction Velocity Can Vary in Magnitude and Direction

Movement speed depends on the contraction velocity of a muscle. The only ways to vary contraction velocity are to alter either the number of motor units recruited or the rates at which they discharge action potentials. The velocity of a contraction can vary in both magnitude and direction (see Figure 31–11B). To control the velocity of a contraction, the nervous system must scale the magnitude of the net muscle torque relative to the load torque (Figure 31–14), which includes both the weight of the body part and any external load acting on the body.

When muscle torque exceeds load torque, the muscle shortens as it performs a shortening contraction. When muscle torque is less than load torque, the muscle lengthens as it performs a lengthening contraction. For the example shown in Figure 31–14, the load is lifted with a shortening contraction of the flexor and lowered with a lengthening contraction of the flexor. Both types of contractions are common in daily activities.

Shortening and lengthening contractions are not simply the result of adjusting motor unit activity so that the net muscle torque is greater or less than the load torque. When the task involves lifting a load with a prescribed trajectory, activation of the motor units must be aligned so that the sum of the rise times produce the appropriate torque so as to match the desired trajectory while lifting (shortening contractions), whereas while lowering the load (lengthening contractions), the sum of the decay times must be similarly

controlled. The nervous system accomplishes this with different descending input and sensory feedback during the two types of contractions. Because of these differences in required motor unit activity, the control of the two types of contraction respond differently to stresses imposed on the system. Declines in the capacity to control motor unit activity, such as observed in older adults and persons performing rehabilitation exercises after an orthopedic procedure, are associated with greater difficulty in performing lengthening contractions.

The amount of motor unit activity relative to the load also influences the contraction velocity. This effect depends on both the number of motor units recruited and the maximal rates at which the motor units can discharge action potentials. As described previously, physical training with rapid contractions, such as power training, increases the rate at which motor units can discharge trains of action potentials, which can be mimicked by step injections of current into a motor neuron. Changes in the maximal shortening velocity of a muscle after a change in the habitual level of physical activity are the result, at least partly, of factors that influence the ability of motor neurons to discharge action potentials at high rates.

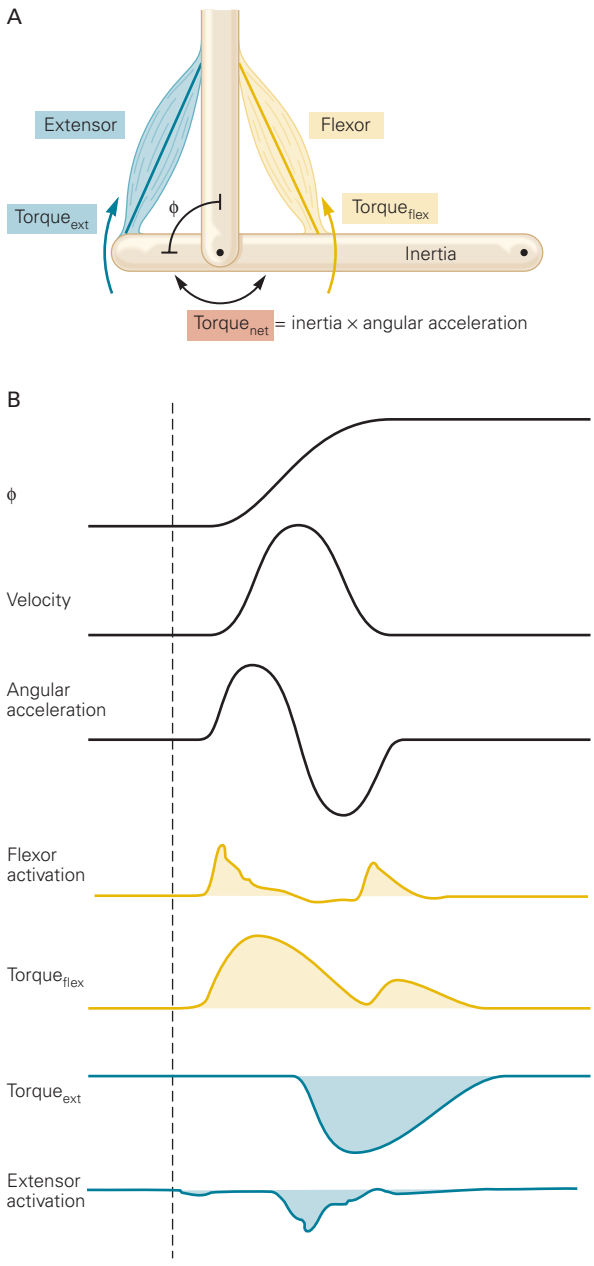

Movements Involve the Coordination of Many Muscles

In the simplest case, muscles span a single joint and cause the attached body segments to accelerate about a single axis of rotation. Because muscles can exert only a pulling force, motion about a single axis of rotation requires at least two muscles or groups of muscles when the action involves shortening contractions (Figure 31–15A).

Because most muscles attach to the skeleton slightly off center from the axis of rotation, they can cause movement about more than one axis of rotation. If one of the actions is not required, the nervous system must activate other muscles to control the unwanted movement. For example, activation of the radial flexor muscle of the wrist can cause the wrist to flex and abduct. If the intended action is only wrist flexion, then the abduction action must be opposed by another muscle, such as the ulnar flexor muscle, which causes wrist flexion and adduction. Depending on the geometry of the articulating surfaces and the attachment sites of the muscles, the multiple muscles that span a joint are capable of producing movements about one to three axes of rotation. Furthermore, some structures

Figure 31–15 (Left) Antagonist muscles spanning a single joint control movement of a limb about a single axis of rotation.

A. According to Newton's law of acceleration (force = mass × acceleration), force is required to change the velocity of a mass. Muscles exert a torque to accelerate the inertial mass of the skeletal segment around a joint. For angular motion, Newton's law is written as torque = rotational inertia × angular acceleration.

B. The angular velocity for movement of a limb from one position to another has a bell-shaped profile. Acceleration in one direction is followed by acceleration in the opposite direction—the flexor and extensor muscles are activated in succession. The records here show the activation profiles and associated muscle torques for a fast elbow flexion movement. Because contractile force decays relatively slowly, the flexor muscle is usually activated a second time to counter the prolonged acceleration generated by the extensor muscle and to stop the limb at the intended joint angle.

can be displaced linearly (eg, the scapula on the trunk), adding to the degrees of freedom about a joint.

The off-axis attachment of muscles enhances the flexibility of the skeletal motor system; the same movement can be achieved by activating different combinations of muscles. However, this additional flexibility requires the nervous system to control the unwanted actions. A solution used by the nervous system is to organize relations among selected muscles to produce specific actions. A particular sequence of muscle activations is known as a *muscle synergy,* and movement is produced through the coordinated activation of these synergies. For example, EMG recordings of human subjects suggest that variations of movements with the same general purpose, such as grasping various objects with the hand, reaching and pointing in different directions, or walking and running at several speeds, are controlled by approximately five muscle synergies.

The number of muscles that participate in a movement also varies with the speed of the movement. For example, slow lifting of a load requires only that the muscle torque slightly exceed the load torque (see Figure 31–14), and thus, only the flexor muscle is activated. This strategy is used when lifting a handheld weight with the elbow flexor muscles. In contrast, to perform this movement rapidly with an abrupt termination at an intended joint angle, both the flexor and extensor muscles must be activated. First, the flexor muscle is activated to accelerate the limb in the direction of flexion, followed by activation of the extensor muscle to accelerate the limb in the direction of extension, and finally a burst of activity by the flexor muscle to increase the angular momentum of the limb and the handheld weight in the direction of flexion so that it arrives at the desired joint angle (Figure 31–15B). The amount of extensor muscle activity increases with the speed of the movement.

Increases in movement speed introduce another factor that the nervous system must control: unwanted accelerations in other body segments. Because body parts are connected to one another, motion in one part can induce motion in another. The induced motion is often controlled with lengthening contractions, such as

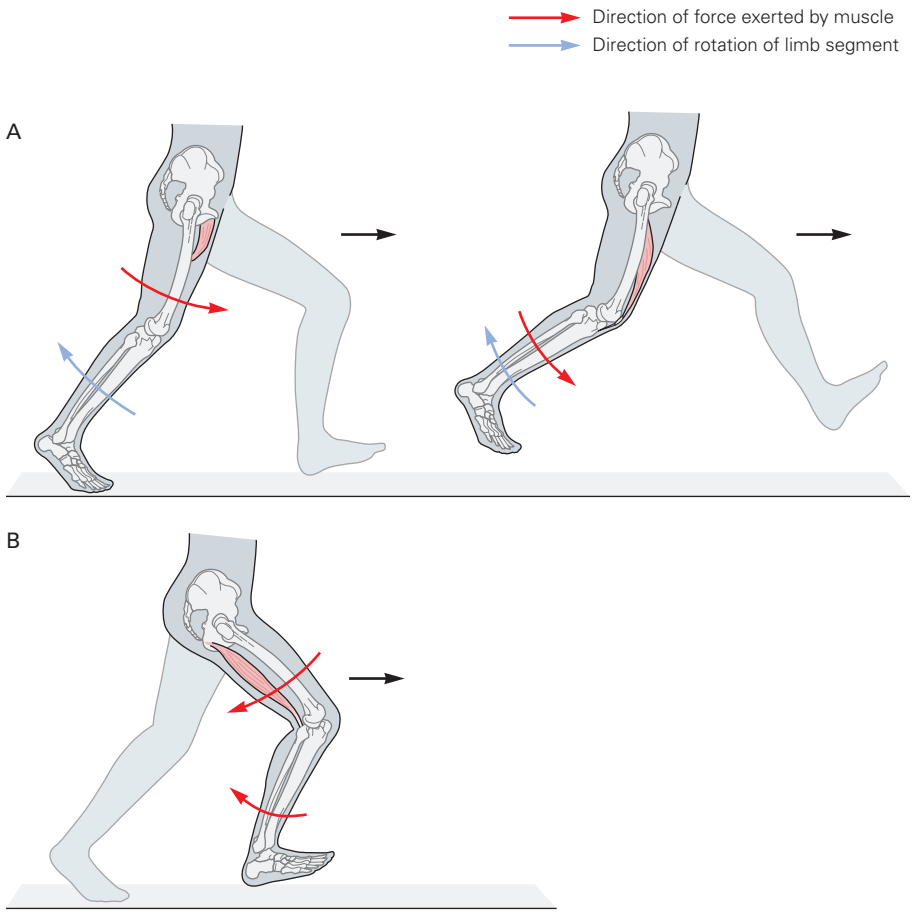

Figure 31–16 A single muscle can influence the motion about many joints.

A. Muscles that cross one joint can accelerate an adjacent body segment. For example, at the beginning of the swing phase while running, the hip flexor muscles are activated to accelerate the thigh forward (**red arrow**). This action causes the lower leg to rotate backward (**blue arrow**) and the knee joint to flex. To control the knee joint flexion during the first part of the swing phase, the knee extensor muscles are activated and undergo a lengthening contraction to accelerate the lower leg forward (**red arrow**) while it continues to rotate backward (**blue arrow**).

B. Many muscles cross more than one joint to exert an effect on more than one body segment. For example, the hamstring muscles of the leg accelerate the hip in the direction of extension and the knee in the direction of flexion (**red arrows**). During running, at the end of the swing phase, the hamstring muscles are activated and undergo lengthening contractions to control the forward rotation of the leg (hip flexion and knee extension). This strategy is more economical than activating individual muscles at the hip and knee joints to control the forward rotation of the leg.

those experienced by thigh muscles during the swing phase of running (Figure 31–16A).

Muscles that span more than one joint can be used to control these motion-dependent interactions between body parts. At the end of the swing phase in running, activation of the hamstring muscles causes both the thigh and lower leg to accelerate backward (Figure 31–16B). If a hip extensor muscle is used to accelerate the thigh backward instead of the hamstring muscles, the lower leg would accelerate forward, requiring activation of a knee flexor muscle to control the unwanted lower leg motion so that the foot could be placed on the ground. Use of the two-joint hamstring muscles is a more economical strategy, but one that can subject the hamstrings to high stresses during fast movements, such as sprinting. The control of such motion-dependent interactions often involves lengthening contractions, which maximize muscle stiffness and the ability of muscle to resist changes in length.

For most movements, the nervous system must establish rigid connections between some body parts for two reasons. First, as expressed in Newton's law of action and reaction, a reaction force must provide a foundation for the acceleration of a body part. For example, in a reaching movement performed by a person standing upright, the ground must provide a reaction force against the feet. The muscle actions that produce the arm movement exert forces that are transmitted through the body to the feet and are opposed by the ground. Different substrates provide different amounts of reaction force, which is why ice or sand can influence movement capabilities.

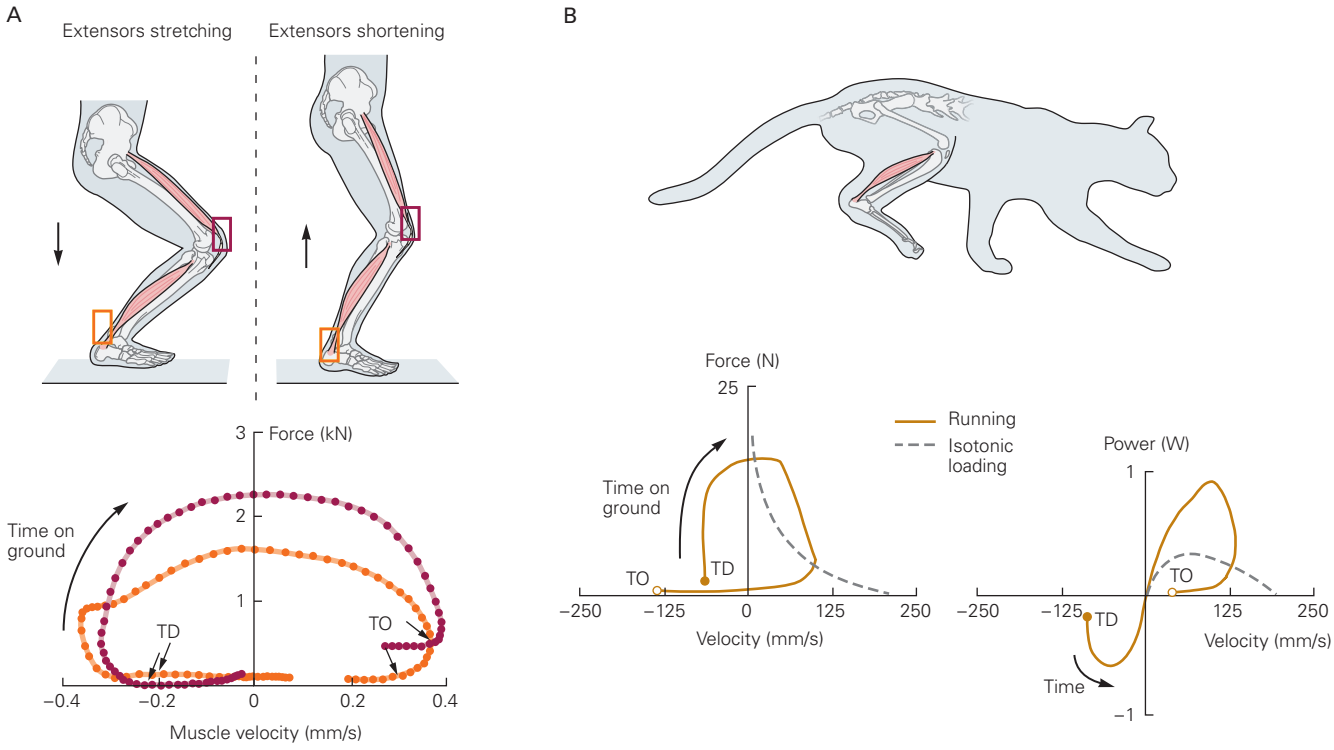

Figure 31–17 **An initial phase of negative work augments subsequent positive work performed by the muscle.** (Reproduced, with permission, from Finni, Komi, and Lepola 2000. Copyright © 2000, Springer-Verlag; Gregor et al. 1988.)

A. The force in the Achilles tendon (**orange**) and patellar tendon (**purple**) vary during the ground-contact phase of two-legged hopping. The feet contact the ground at touchdown (**TD**) and leave the ground at toe-off (**TO**). For approximately the first half of the movement, the quadriceps and triceps surae muscles lengthen, performing negative work (negative velocity). The muscles perform positive work when they shorten (positive velocity). The sites of force transducer measurements are indicated by rectangles.

B. The force exerted by the soleus muscle of a cat running at moderate speed varies from the instant the paw touches the ground (**TD**) until it leaves the ground (**TO**). The force exerted by the muscle during the shortening contraction (positive velocity) is greater than the peak forces measured when the muscle contracts maximally against various constant loads (isotonic loading). Negative velocity reflects a lengthening contraction in the soleus muscle. The power produced by the soleus muscle of the cat during running is greater than that produced in an isolated-muscle experiment (**dashed line**). The phase of negative power corresponds to the lengthening contraction just after the paw is placed on the ground (TD), when the muscle performs negative work.

Second, uncertain conditions are usually accommodated by stiffening the joints through concurrent activation of the muscles that produce force in opposite directions. Coactivation of opposing muscles occurs often when a support surface is unsteady, when the body might experience an unexpected perturbation, or when lifting a heavy load. Because coactivation increases the energetic cost of performing a task, one characteristic of skilled performance is the ability to accomplish a task with minimal activation of muscles that produce opposing actions.

Muscle Work Depends on the Pattern of Activation

Limb muscles in healthy young adults are active 10% to 20% of the time during waking hours. For much of this time, the muscles perform constant-length (*isometric*) contractions to maintain a variety of static body postures. In contrast, muscle length has to change during a movement so that the muscle can perform work to displace body parts. A muscle performs positive work and produces power during a shortening contraction, whereas it performs negative work and absorbs power during a lengthening contraction. The capacity of muscle to do positive work establishes performance capabilities, such as the maximal height that can be jumped.

The nervous system can augment the positive work capacity of muscle by commanding a brief period of negative work before performing positive work. This activation sequence, the *stretch–shorten cycle,* occurs in many movements. When a person jumps in place on two feet, for example, the support phase involves an initial stretch (lengthening) and subsequent shortening of the ankle extensor and knee extensor muscles (Figure 31–17A). The forces in the Achilles and patellar tendons increase during the stretch of the lengthening contraction and reach a maximum at the onset of the shortening phase. As a result, the muscles can perform more positive work and produce more power during the shortening contraction (Figure 31–17B).

Although negative work involves an increase in the length of the muscle, the length of the fascicles in the muscle often remains relatively constant, which indicates that the connective tissue structures are stretched prior to the shortening contraction. Thus, the capacity of the muscle to perform more positive work comes from strain energy that can be stored in the elastic elements of muscle and tendon during the stretch phase and released during the subsequent shortening phase. More strain energy can be stored in long tendons, but short tendons are more advantageous when the movement requires the rapid release of strain energy.

Highlights

1. The basic functional unit for the control of movement by the nervous system is the motor unit, which comprises a motor neuron and the muscle fibers it innervates.
2. The force exerted by a muscle depends in part on the number and properties of the motor units that are activated and the rates at which they discharge action potentials. The key motor unit properties include contraction speed, maximal force, and fatigability, all of which can be altered by physical activity. Motor unit properties vary continuously across the population that innervates each muscle; that is, there are not distinct types of motor units. Due to technological advances, it is becoming possible to characterize the adaptations exhibited by populations of motor units in response to different types of changes in physical activity.
3. Motor units tend to be activated in a stereotypical order that is highly correlated with motor neuron size. The rate at which motor units are recruited during a voluntary contraction increases with contraction speed.
4. The rate at which a motor unit discharges action potentials in response to a given synaptic input can be modulated by descending inputs from the brain stem. The modulatory input is likely critical for establishing the level of excitation in spinal pathways, but this has been difficult to demonstrate in humans.
5. Except at low muscle forces, variation in discharge rate has a greater influence on muscle force than does the number of activated motor units. Moreover, the variability in discharge rate of the motor unit population influences the level of fine motor control.
6. The sarcomere is the smallest element of muscle to include a complete set of contractile proteins. A transient connection between the contractile proteins myosin and actin, known as the cross-bridge cycle, enables muscle to exert a force. The organization of the sarcomeres within a muscle varies substantially and, in addition to motor unit activity, has a major effect on the contractile properties of the muscle.
7. For a given arrangement of sarcomeres, the force a muscle can exert depends on the activation of the cross bridges by Ca^{2+}, the amount of overlap between the thick and thin filaments, and the velocity of the moving filaments. Sarcomere force during lengthening contractions is augmented by a Ca^{2+}-mediated increase in titin stiffness. The force

produced by activated sarcomeres depends on the interactions of three filaments: actin, myosin, and titin.

8. Most of the force generated by activated sarcomeres is transmitted laterally through a network of noncontractile proteins that maintains the alignment of the thick and thin filaments.
9. The functional capability of a muscle depends on the torque that it can exert, which is influenced both by its contractile properties and by the location of its attachments on the skeleton relative to the joint that it spans.
10. To perform a movement, the nervous system activates multiple muscles and controls the torque exerted about the involved joints. The nervous system can vary the magnitude and direction of a movement by altering the amount of motor unit activity, and hence muscle torque, relative to the load acting on the body.
11. Although muscle exerts only a pulling force on the skeleton, it can do so whether the activated muscle shortens or is lengthened by a load torque that exceeds the muscle torque. The force capacity of muscle is greater during lengthening contractions. Motor unit activity differs during shortening and lengthening contractions, but little is known about how the synaptic inputs to motor neurons differ during these two types of contractions.
12. Faster movements elicit motion-dependent interactions between body parts that produce unwanted accelerations. These actions must be controlled by the nervous system to produce an intended movement.
13. The nervous system must coordinate the activity of multiple muscles to provide a mechanical link between moving body parts and the required support from the surroundings. The muscles engaged for each action, such as grasping, reaching, running, and walking, are organized into a few sets that exhibit a stereotypical pattern of activation, but it is not known why particular patterns are preferred.
14. The patterns of muscle activity vary substantially between movements and often include strategies that augment the work capacity of muscles. The patterns can be modified by experience, but little is known about the locus of the adaptations other than that both spinal and supraspinal pathways are involved.

Roger M. Enoka

Selected Reading

Booth FW. 2015. Muscle adaptation to exercise: new Saltin's paradigms. Scand J Med Sci Sports Suppl 4:49–52.

Duchateau J, Enoka RM. 2011. Human motor unit recordings: origins and insights into the integrated motor system. Brain Res 1409:42–62.

Enoka RM. 2015. *Neuromechanics of Human Movement*. 5th ed. Champaign, IL: Human Kinetics.

Farina D, Negro F, Muceli S, Enoka RM. 2016. Principles of motor unit physiology evolve with advances in technology. Physiology 31:83–94.

Gordon AM, Regnier M, Homsher E. 2001. Skeletal and cardiac muscle contractile activation: tropomyosin "rocks and rolls." News Physiol Sci 16:49–55.

Heckman CJ, Enoka RM. 2012. Motor unit. Compr Physiol 2:2629–2682.

Herzog W, Schappacher G, DuVall M, Leonard TR, Herzog JA. 2016. Residual force enhancement following eccentric contractions: a new mechanism involving titin. Physiology 31:300–312.

Hunter SK, Pereira HM, Keenan KG. 2016. The aging neuromuscular system and motor performance. J Appl Physiol 121:982–995.

Huxley AF. 2000. Mechanics and models of the myosin motor. Philos Trans R Soc Lond B Biol Sci 355:433–440.

Lieber RL, Ward SR. 2011. Skeletal muscle design to meet functional demands. Philos Trans R Soc Lond B Biol Sci 366:1466–1476.

Merletti R, Muceli S. 2020. Tutorial. Surface EMG detection in space and time: best practices. J Electromyogr Kinesiol 49:102363.

Narici M, Franchi M, Maganaris C. 2016. Muscle structural assembly and functional consequences. J Exp Biol 219:276–284.

References

Alexander RM, Ker RF. 1990. The architecture of leg muscles. In: JM Winters, SL-Y Woo (eds). *Multiple Muscle Systems: Biomechanics and Movement Organization*, pp. 568–577. New York: Springer-Verlag.

Azizi E, Roberts TJ. 2012. Geared up to stretch: pennate muscle behavior during active lengthening. J Exp Biol 217:376–381.

Bloom W, Fawcett DW. 1975. *A Textbook of Histology.* 10th ed. Philadelphia, PA: Saunders.

Botterman BR, Iwamoto GA, Gonyea WJ. 1986. Gradation of isometric tension by different activation rates in motor units of cat flexor carpi radialis muscle. J Neurophysiol 56:494–506.

Bottinelli R, Canepari M, Pellegrino MA, Reggiani C. 1996. Force-velocity properties of human skeletal muscle fibres: myosin heavy chain isoform and temperature dependence. J Physiol 495:573–586.

Del Vecchio A, Negro F, Felici F, Farina D. 2017. Associations between motor unit action potential parameters and surface EMG features. J Appl Physiol 123:835–843.

Desmedt JE, Godaux E. 1977. Ballistic contractions in man: characteristic recruitment pattern of single motor units of the tibialis anterior muscle. J Physiol 264:673–693.

Duchateau J, Enoka RM. 2016. Neural control of lengthening contractions. J Exp Biol 219:197–204.
Enoka RM, Duchateau J. 2016. Translating muscle fatigue to human performance. Med Sci Sport Exerc 48:2228–2238.
Enoka RM, Duchateau J. 2017. Rate coding and the control of muscle force. Cold Spring Harb Perspect Med 27:1–12.
Enoka RM, Fuglevand AJ. 2001. Motor unit physiology: some unresolved issues. Muscle Nerve 24:4–17.
Erim Z, De Luca CJ, Mineo K, Aoki T. 1996. Rank-ordered regulation of motor units. Muscle Nerve 19:563–573.
Farina D, Merletti R, Enoka RM. 2014. The extraction of neural strategies from the surface EMG: an update. J Appl Physiol 117:1215–1230.
Finni T, Komi PV, Lepola V. 2000. In vivo human triceps surae and quadriceps muscle function in a squat jump and counter movement jump. Eur J Appl Physiol 83:416–426.
Fuglevand AJ, Macefield VG, Bigland-Ritchie B. 1999. Force-frequency and fatigue properties of motor units in muscles that control digits of the human hand. J Neurophysiol 81:1718–1729.
Gordon AM, Regnier M, Homsher R. 2001. Skeletal and cardiac muscle contractile activation: tropomyosin "rocks and rolls." News Physiol Sci 16:49–55.
Gregor RJ, Roy RR, Whiting WC, Lovely RG, Hodgson JA, Edgerton VR. 1988. Mechanical output of the cat soleus during treadmill locomotion: in vivo vs in situ characteristics. J Biomech 21:721–732.
Heckman CJ, Mottram C, Quinlan K, Theiss R, Schuster J. 2009. Motoneuron excitability: the importance of neuromodulatory inputs. Clin Neurophysiol. 120:2040–2054.
Henneman E, Somjen G, Carpenter DO. 1965. Functional significance of cell size in spinal motoneurons. J Neurophysiol 28:560–580.
Hepple RT, Rice CL. 2016. Innervation and neuromuscular control in ageing skeletal muscle. J Physiol 594:1965–1978.
Huxley AF, Simmons RM. 1971. Proposed mechanism of force generation in striated muscle. Nature 233:533–538.
Kubo K, Miyazaki D, Shimoju S, Tsunoda N. 2015. Relationship between elastic properties of tendon structures and performance in long distance runners. Eur J Appl Physiol 115:1725–1733.
Lai A, Schache AG, Lin YC, Pandy MG. 2014. Tendon elastic strain energy in the human ankle plantar-flexors and its role with increased running speed. J Exp Biol 217:3159–3168.
Lieber RL, Fridén J. 2000. Functional and clinical significance of skeletal muscle architecture. Muscle Nerve 23:1647–1666.
Lieber RL, Ward SR. 2011. Skeletal muscle design to meet functional demands. Philos Trans R Soc Lond B Biol Sci 366:1466–1476.
Liddell EGT, Sherrington CS. 1925. Recruitment and some other factors of reflex inhibition. Proc R Soc Lond B Biol Sci 97:488–518.
Maas H, Finni T. 2018. Mechanical coupling between muscle-tendon units reduces peak stresses. Exerc Sport Sci Rev 46:26–33.
Macefield VG, Fuglevand AJ, Bigland-Ritchie B. 1996. Contractile properties of single motor units in human toe extensors assessed by intraneural motor axon stimulation. J Neurophysiol 75:2509–2519.
Milner-Brown HS, Stein RB, Yemm R. 1973. The orderly recruitment of human motor units during voluntary isometric contraction. J Physiol 230:359–370.
Moritz CT, Barry BK, Pascoe MA, Enoka RM. 2005. Discharge rate variability influences the variation in force fluctuations across the working range of a hand muscle. J Neurophysiol 93:2449–2459.
O'Connor SM, Cheng EJ, Young KW, Ward SR, Lieber RL. 2016. Quantification of sarcomere length distribution in whole muscle frozen sections. J Exp Biol 219:1432–1436.
Overduin SA, d'Avella A, Roh J, Carmena JM, Bizzi E. 2015. Representation of muscle synergies in the primate brain. J Neurosci 35:12615–12624.
Palmisano MG, Bremner SN, Homberger TA, et al. 2015. Skeletal muscle intermediate filaments form a stress-transmitting and stress-signalling network. J Cell Sci 128: 219–224.
Person RS, Kudina LP. 1972. Discharge frequency and discharge pattern of human motor units during voluntary contraction of muscle. Electroencephalogr Clin Neurophysiol 32:471–483.
Sawicki GS, Robertson BD, Azizi E, Roberts TJ. 2015. Timing matters: tuning the mechanics of a muscle-tendon unit by adjusting stimulation phase during cyclic contractions. J Exp Biol 218:3150–3159.
Schache AG, Dorn TW, Williams GP, Brown NA, Pandy MG. 2014. Lower-limb muscular strategies for increasing running speed. J Orthop Sports Phys Ther 44:813–824.
Sherrington CS. 1925. Remarks on some aspects of reflex inhibition. Proc R Soc Lond B Biol Sci 97:519–545.
Trappe S, Costill D, Gallagher P, et al. 2009. Exercise in space: human skeletal muscle after 6 months aboard the International Space Station. J Appl Physiol 106:1159–1168.
Trappe S, Luden N, Minchev K, Raue U, Jemiolo B, Trappe TA. 2015. Skeletal muscle signature of a champion sprint runner. J Appl Physiol 118:1460–1466.
Van Cutsem M, Duchateau J, Hainaut K. 1998. Changes in single motor unit behaviour contribute to the increase in contraction speed after dynamic training in humans. J Physiol 513:295–305.
Van Cutsem M, Feiereisen P, Duchateau J, Hainaut K. 1997. Mechanical properties and behaviour of motor units in the tibialis anterior during voluntary contractions. Can J Appl Physiol 22:585–597.
Ward SR, Eng CM Smallwood LH, Lieber RL. 2009. Are current measurements of lower extremity muscle architecture accurate? Clin Orthop Rel Res 467:1074–1082.

32

Sensory-Motor Integration in the Spinal Cord

DURING PURPOSEFUL MOVEMENTS the central nervous system uses information from a vast array of sensory receptors to ensure that the pattern of muscle activity suits the purpose. Without this sensory information, movements tend to be imprecise, and tasks requiring fine coordination in the hands, such as buttoning one's shirt, are difficult. The sensory-motor integration that makes the ongoing regulation of movement possible takes place at many levels of the nervous system, but the spinal cord has a special role because of the close coupling in the cord between sensory input and the motor output to the muscles.

Charles Sherrington was among the first to recognize the importance of sensory information in regulating movements. In 1906, he proposed that simple

reflexes—stereotyped movements elicited by activation of receptors in skin or muscle—are the basic units for movement. He also emphasized that all parts of the nervous system are connected and that no part is ever capable of activation without affecting or being affected by other parts. In his words, the simple reflex is a convenient if not a probable fiction.

Laboratory studies of reflexes in animals from the 1950s and onward demonstrated that descending motor pathways and afferent sensory pathways converge on common interneurons in the spinal cord. Later research in intact animals and in humans engaged in normal behavior confirmed that the neural circuitries in the spinal cord take part in conveying and shaping the motor command to the muscles by integrating descending motor commands and sensory feedback signals. Nevertheless, the idea of simple reflexes is convenient for understanding the principles of organization of sensory-motor integration in the spinal cord and of how sensory input to different spinal circuits contributes to movement control.

In this chapter, we explain the principles underlying sensory-motor integration in the spinal cord and describe how this integration regulates movement. For this purpose, we must first have a thorough knowledge of how reflex pathways in the spinal cord are organized.

Reflex Pathways in the Spinal Cord Produce Coordinated Patterns of Muscle Contraction

The sensory stimuli that activate spinal reflex pathways act outside the spinal cord, on receptors in muscles, joints, and skin. By contrast, the neural circuitry responsible for the motor response is entirely contained within the spinal cord. The interneurons in the reflex pathways and the resulting reflexes have traditionally been classified based on the sensory modality and type of sensory fiber that activates the interneurons. As we shall see, this classification is inconsistent with the significant convergence of multiple modalities on common interneurons, but as a starting point, it is still useful to distinguish reflex pathways based on whether the principal sensory input originates from muscle or skin.

The Stretch Reflex Acts to Resist the Lengthening of a Muscle

The simplest and certainly the most studied spinal reflex is the *stretch reflex*, a reflex muscle contraction elicited by lengthening of the muscle. Stretch reflexes were originally thought to be an intrinsic property of muscles. Early in the 20th century, however, Liddell and Sherrington showed that the stretch reflex could be abolished by cutting either the dorsal or ventral root, thus establishing that these reflexes require sensory input from muscle to spinal cord and a return path to muscle (Figure 32–1A).

We now know that the receptor that senses the change of length is the muscle spindle (Box 32–1) and that the type Ia sensory axon from this receptor makes direct excitatory connections with motor neurons. (The classification of sensory fibers from muscle is discussed in Box 32–2.) The afferent axon also connects to interneurons that inhibit the motor neurons innervating antagonist muscles, an arrangement called reciprocal innervation. This inhibition prevents muscle contractions that might otherwise resist the movements produced by the stretch reflexes.

Sherrington developed an experimental model for investigating spinal circuitry that is especially valuable in the study of stretch reflexes. He conducted his experiments on cats whose brain stems had been surgically transected at the level of the midbrain, between the superior and inferior colliculi. This is referred to as a *decerebrate preparation.* The effect of this procedure is to disconnect the rest of the brain from the spinal cord, thus blocking sensations of pain as well as interrupting normal modulation of reflexes by higher brain centers. A decerebrate animal has stereotyped and usually heightened stretch reflexes, making it easier to examine the factors controlling their expression.

Without control by higher brain centers, descending pathways from the brain stem powerfully facilitate the neuronal circuits involved in the stretch reflexes of extensor muscles. This results in a dramatic increase in tone of the extensor muscle that sometimes can suffice to support the animal in a standing position. In normal animals and humans, owing to the balance between facilitation and inhibition, stretch reflexes are weaker and considerably more variable in strength than those in decerebrate animals.

Neuronal Networks in the Spinal Cord Contribute to the Coordination of Reflex Responses

The Stretch Reflex Involves a Monosynaptic Pathway

The neural circuit responsible for the stretch reflex was one of the first reflex pathways to be examined in detail. The physiological basis of this reflex was examined by measuring the latency of the response in

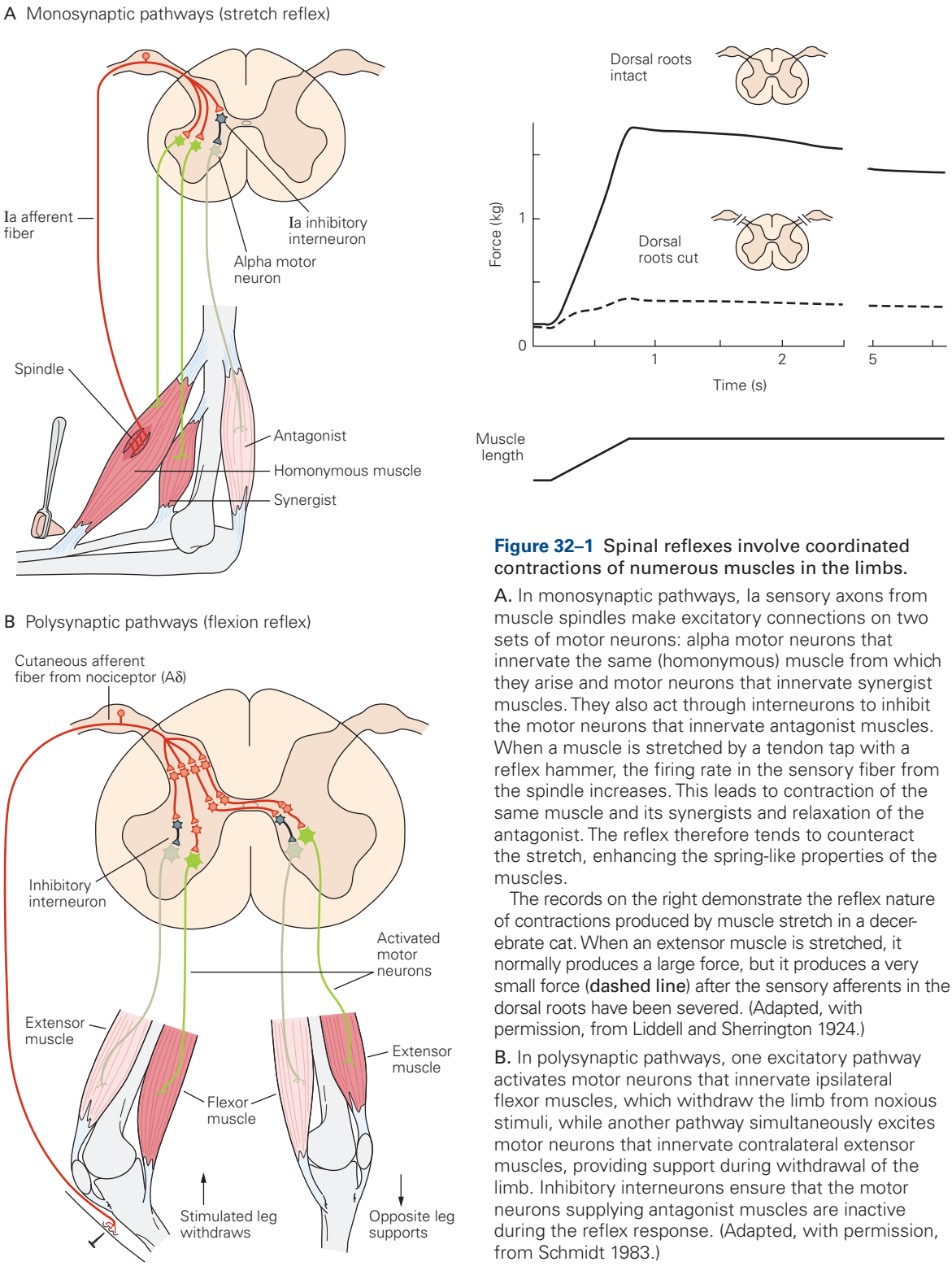

Figure 32–1 Spinal reflexes involve coordinated contractions of numerous muscles in the limbs.

A. In monosynaptic pathways, Ia sensory axons from muscle spindles make excitatory connections on two sets of motor neurons: alpha motor neurons that innervate the same (homonymous) muscle from which they arise and motor neurons that innervate synergist muscles. They also act through interneurons to inhibit the motor neurons that innervate antagonist muscles. When a muscle is stretched by a tendon tap with a reflex hammer, the firing rate in the sensory fiber from the spindle increases. This leads to contraction of the same muscle and its synergists and relaxation of the antagonist. The reflex therefore tends to counteract the stretch, enhancing the spring-like properties of the muscles.

The records on the right demonstrate the reflex nature of contractions produced by muscle stretch in a decerebrate cat. When an extensor muscle is stretched, it normally produces a large force, but it produces a very small force (**dashed line**) after the sensory afferents in the dorsal roots have been severed. (Adapted, with permission, from Liddell and Sherrington 1924.)

B. In polysynaptic pathways, one excitatory pathway activates motor neurons that innervate ipsilateral flexor muscles, which withdraw the limb from noxious stimuli, while another pathway simultaneously excites motor neurons that innervate contralateral extensor muscles, providing support during withdrawal of the limb. Inhibitory interneurons ensure that the motor neurons supplying antagonist muscles are inactive during the reflex response. (Adapted, with permission, from Schmidt 1983.)

Box 32–1 Muscle Spindles

Muscle spindles are small encapsulated sensory receptors that have a spindle-like or fusiform shape and are located within the fleshy part of a muscle. Their main function is to signal changes in the length of the muscle within which they reside. Changes in length of muscles are closely associated with changes in the angles of the joints that the muscles cross. Thus, muscle spindles are used by the central nervous system to sense relative positions of the body segments.

Each spindle has three main components: (1) a group of specialized *intrafusal* muscle fibers with noncontractile central regions; (2) sensory fibers that terminate on the central regions of the intrafusal fibers; and (3) motor axons that terminate on the contractile polar regions of the intrafusal fibers (Figure 32–2A,B).

When the intrafusal fibers are stretched, often referred to as "loading the spindle," the sensory axon endings are also stretched and increase their firing rate. Because muscle spindles are arranged in parallel with the *extrafusal* muscle fibers that make up the main body of the muscle, the intrafusal fibers change in length as the whole muscle changes. Thus, when a muscle is stretched, activity in the sensory axons of muscle spindles increases. When a muscle shortens, the spindle is unloaded and the activity decreases.

The intrafusal muscle fibers are innervated by *gamma* motor neurons, which have small-diameter myelinated axons, whereas the extrafusal muscle fibers are innervated by *alpha* motor neurons, with large-diameter myelinated axons. Activation of gamma motor neurons causes shortening of the polar regions of the intrafusal fibers. This in turn stretches the central region from both ends, leading to an increase in firing rate of the sensory axons or to a greater likelihood that the axons will fire in response to stretch of the muscle. Thus, the gamma motor neurons adjust the sensitivity of the muscle spindles. Contraction of the intrafusal muscle fibers does not contribute significantly to the force of muscle contraction.

The structure and functional behavior of muscle spindles is considerably more complex than this simple description depicts. As a muscle is stretched, the change in length has two phases: a dynamic phase, the period during which length is changing, and a static or steady-state phase, when the muscle has stabilized at a new length. Structural specializations within each component of the muscle spindle enable the sensory axons to signal aspects of each phase separately.

The intrafusal muscle fibers include nuclear bag fibers and nuclear chain fibers. The bag fibers can be classified as dynamic or static. A typical spindle has two or three bag fibers and a variable number of chain fibers, usually about five. Furthermore, the intrafusal fibers receive two types of sensory endings. A single Ia (large diameter) axon spirals around the central region of all intrafusal muscle fibers and serves as the *primary sensory ending* (Figure 32–2B). A variable number of type II (medium diameter) axons spiral around the static bag and chain fibers near their central regions and serve as *secondary sensory endings*.

The gamma motor neurons can also be divided into two classes: Dynamic gamma motor neurons innervate the dynamic bag fibers, whereas the static gamma motor neurons innervate the static bag fibers and the chain fibers.

This duality of structure is reflected in a duality of function. The tonic discharge of both primary and secondary sensory endings signals the steady-state length of the muscle. The primary sensory endings are, in addition, highly sensitive to the velocity of stretch, allowing them to provide information about the speed of movements. Because they are highly sensitive to small changes, the primary endings rapidly provide information about sudden unexpected changes in length, which can be used to generate quick corrective reactions.

Increases in the firing rate of dynamic gamma motor neurons increase the dynamic sensitivity of primary sensory endings but have no influence on secondary sensory endings. Increases in the firing rate of static gamma motor neurons increase the tonic level of activity in both primary and secondary sensory endings, decrease the dynamic sensitivity of primary endings (Figure 32–2C), and can prevent the silencing of primary endings when a muscle is released from stretch. Thus, the central nervous system can independently adjust the dynamic and static sensitivity of the different sensory endings in muscle spindles.

ventral roots to electrical stimulation of dorsal roots. When the Ia sensory axons innervating the muscle spindles were selectively activated, the reflex latency through the spinal cord was less than 1 ms. This demonstrated that the Ia fibers make direct connections on the alpha motor neurons because the delay at a single synapse is typically 0.5 ms to 0.9 ms (Figure 32–3B). In humans, an analog of the monosynaptic stretch reflex, the Hoffmann reflex, may be elicited by electrical stimulation of peripheral nerves (Box 32–3).

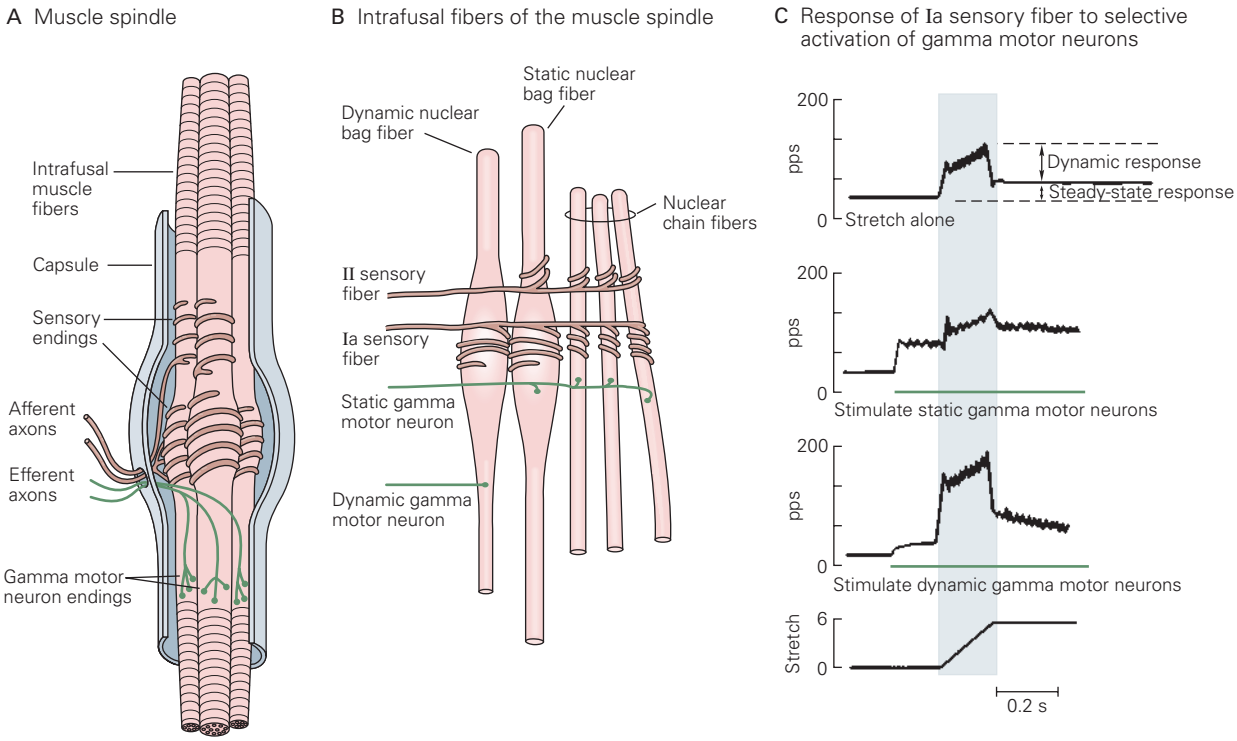

Figure 32–2 The muscle spindle detects changes in muscle length.

A. The main components of the muscle spindle are intrafusal muscle fibers, sensory axon endings, and motor axon endings. The intrafusal fibers are specialized muscle fibers with central regions that are not contractile. Gamma motor neurons innervate the contractile polar regions of the intrafusal fibers. Contraction of the polar regions pulls on the central regions of the intrafusal fiber from both ends. The sensory endings spiral around the central regions of the intrafusal fibers and are responsive to stretch of these fibers. (Adapted, with permission, from Hulliger 1984. Copyright © Springer-Verlag 1984.)

B. The muscle spindle contains three types of intrafusal fibers: dynamic nuclear bag, static nuclear bag, and nuclear chain fibers. A single Ia sensory axon innervates all three types of fibers, forming a primary sensory ending. Type II sensory axons innervate the nuclear chain fibers and static bag fibers, forming a secondary sensory ending. Two types of motor neurons innervate different intrafusal fibers. Dynamic gamma motor neurons innervate only dynamic bag fibers; static gamma motor neurons innervate various combinations of chain and static bag fibers. (Adapted, with permission, from Boyd 1980. Copyright © 1980. Published by Elsevier Ltd.)

C. Selective stimulation of the two types of gamma motor neurons has different effects on the firing of the Ia sensory fibers from the spindle. Without gamma stimulation, the Ia fiber shows a small dynamic response to muscle stretch and a modest increase in steady-state firing. When a static gamma motor neuron is stimulated, the steady-state response of the Ia fiber increases but the dynamic response decreases. When a dynamic gamma motor neuron is stimulated, the dynamic response of the Ia fiber is markedly enhanced, but the steady-state response gradually returns to its original level. (Adapted, with permission, from Brown and Matthews 1966.)

The pattern of connections of Ia fibers to motor neurons can be shown directly by intracellular recording. Ia fibers from a given muscle excite not only the motor neurons innervating that same (*homonymous*) muscle but also the motor neurons innervating other (*heteronymous*) muscles with a similar mechanical action.

Lorne Mendell and Elwood Henneman used a computer enhancement technique called *spike-triggered averaging* to determine the extent to which the action

Box 32–2 Classification of Sensory Fibers From Muscle

Sensory fibers are classified according to their diameter. Axons with larger diameters conduct action potentials more rapidly than those with smaller diameters (Chapters 9 and 18). Because each class of sensory receptors is innervated by fibers with diameters within a restricted range, this method of classification distinguishes to some extent the fibers that arise from different types of receptor organs. The main groups of sensory fibers from muscle are listed in Table 32–1.

The organization of reflex pathways in the spinal cord has been established primarily by electrically stimulating the sensory fibers and recording evoked responses in different classes of neurons in the spinal cord. This method of activation has three advantages over natural stimulation. The timing of afferent input can be precisely established; the responses evoked in motor neurons and other neurons by different classes of sensory fibers can be assessed by grading the strength of the electrical stimulus; and certain classes of receptors can be selectively activated.

The strength of the electrical stimulus required to activate a sensory fiber is measured relative to the strength required to activate the fibers with the largest diameter because these fibers have the lowest threshold for electrical activation. The thresholds of most type I fibers usually range from one to two times that of the largest fibers (with Ia fibers having, on average, a slightly lower threshold than Ib fibers). For most type II fibers, the threshold is 2 to 5 times higher, whereas types III and IV have thresholds in the range of 10 to 50 times that of the largest sensory fibers.

Table 32–1 Classification of Sensory Fibers From Muscle

Type	Axon	Receptor	Sensitivity to
Ia	12–20 μm myelinated	Primary spindle ending	Muscle length and rate of change of length
Ib	12–20 μm myelinated	Golgi tendon organ	Muscle tension
II	6–12 μm myelinated	Secondary spindle ending	Muscle length (little rate sensitivity)
II	6–12 μm myelinated	Nonspindle endings	Deep pressure
III	2–6 μm myelinated	Free nerve endings	Pain, chemical stimuli, and temperature (important for physiological responses to exercise)
IV	0.5–2 μm nonmyelinated	Free nerve endings	Pain, chemical stimuli, and temperature

potentials in single Ia fibers are transmitted to a population of spinal motor neurons. They found that individual Ia axons make excitatory synapses with all homonymous motor neurons innervating the medial gastrocnemius of the cat. This widespread divergence effectively amplifies the signals of individual Ia fibers, leading to a strong excitatory drive to the muscle from which they originate (*autogenic excitation*).

The Ia axons in reflex pathways also provide excitatory inputs to many of the motor neurons innervating synergist muscles (up to 60% of the motor neurons of some synergists) (Figure 32–1A). Although widespread, these connections are not as strong as the connections to homonymous motor neurons.

The Ia fibers also send inhibitory signals via the *Ia inhibitory interneurons* to the alpha motor neurons innervating antagonistic muscles. This disynaptic inhibitory pathway is the basis for reciprocal innervation: When a muscle is stretched, its antagonists relax.

Gamma Motor Neurons Adjust the Sensitivity of Muscle Spindles

Activity of muscle spindles may be modulated by changing the level of activity in the gamma motor neurons, which innervate the intrafusal muscle fibers of muscle spindles (Box 32–1). This function of gamma motor neurons, often referred to as the fusimotor

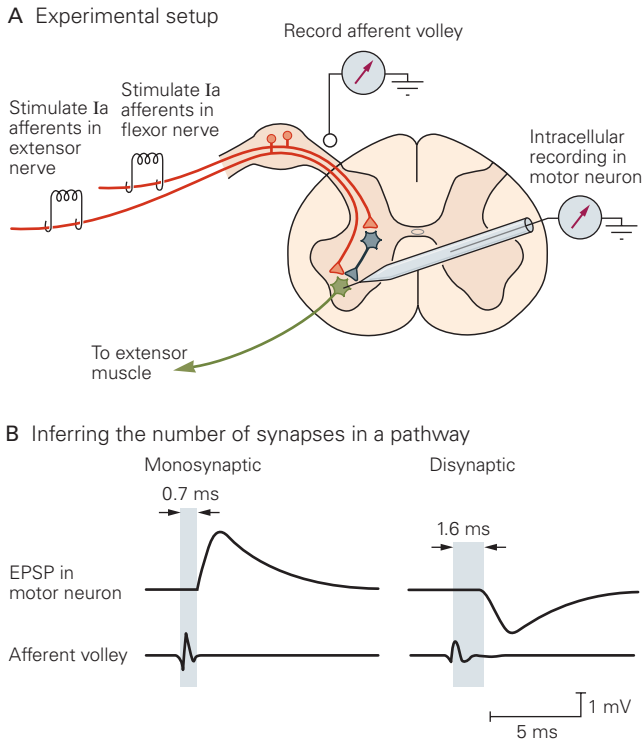

Figure 32–3 The number of synapses in a reflex pathway can be inferred from intracellular recordings.

A. An intracellular recording electrode is inserted into the cell body of a spinal motor neuron that innervates an extensor muscle. Stimulation of Ia sensory fibers from flexor or extensor muscles produces a volley of action potentials at the dorsal root.

B. *Left:* When Ia fibers from an extensor muscle are stimulated, the latency between the recording of the afferent volley and the excitatory postsynaptic potential (EPSP) in the motor neuron is only 0.7 ms, approximately equal to the duration of signal transmission across a single synapse. Thus, it can be inferred that the excitatory action of the stretch reflex pathway is monosynaptic. *Right:* When Ia fibers from an antagonist flexor muscle are stimulated, the latency between the recording of the afferent volley and the inhibitory postsynaptic potential in the motor neuron is 1.6 ms, approximately twice the duration of signal transmission across a single synapse. Thus, it can be inferred that the inhibitory action of the stretch reflex pathway is disynaptic.

system, can be demonstrated by selectively stimulating the alpha and gamma motor neurons under experimental conditions.

When only alpha motor neurons are stimulated, the firing of the Ia fiber from the muscle spindle pauses during contraction of the muscle because the muscle is shortening and therefore unloading (slackening) the spindle. However, if gamma motor neurons are activated at the same time as alpha motor neurons, the pause is eliminated. The contraction of the intrafusal fibers by the gamma motor neurons keeps the spindle under tension, thus maintaining the firing rate of the Ia fibers within an optimal range for signaling changes in length, whatever the actual length of the muscle (Figure 32–5). This *alpha-gamma co-activation* is recruited for many voluntary movements because it stabilizes the sensitivity of the muscle spindles.

In addition to the axons of gamma motor neurons, collaterals of alpha motor neuron axons sometimes innervate the intrafusal fibers. Axons that innervate both intrafusal and extrafusal muscle fibers are referred to as *beta* axons. Beta axon collaterals provide the equivalent of alpha-gamma coactivation. Beta innervation in spindles exists in both cats and humans, although it is unquantified for most muscles.

The forced linkage of extrafusal and intrafusal contraction by the beta fusimotor system highlights the importance of the independent fusimotor system (the gamma motor neurons). Indeed, in lower vertebrates, such as amphibians, beta efferents are the only source of intrafusal innervation. Mammals have evolved a mechanism that frees muscle spindles from complete dependence on the behavior of their parent muscles. In principle, this uncoupling allows greater flexibility in controlling spindle sensitivity for different types of motor tasks.

This conclusion is supported by recordings in spindle sensory axons during a variety of natural movements in cats. The amount and type of activity in gamma motor neurons are set at steady levels, which vary according to the specific task or context. In general, activity levels in both static and dynamic gamma motor neurons (Figure 32–2B) are set at progressively higher levels as the speed and difficulty of the movement increase. Unpredictable conditions, such as when the cat is picked up or handled, lead to marked increases in activity in dynamic gamma motor neurons and thus increased spindle responsiveness when muscles are stretched. When an animal is performing a difficult task, such as walking across a narrow beam, both static and dynamic gamma activation are at high levels (Figure 32–6).

Thus, the nervous system uses the fusimotor system to fine-tune muscle spindles so that the ensemble output of the spindles provides information most appropriate for a task. The task conditions under which independent control of alpha and gamma motor neurons occurs in humans have not yet been clearly established.

The Stretch Reflex Also Involves Polysynaptic Pathways

The monosynaptic Ia pathway is not the only spinal reflex pathway activated when a muscle is stretched. Type II sensory fibers from muscle spindles are also activated. These discharge tonically depending on

Box 32–3 The Hoffmann Reflex

The characteristics of the monosynaptic connections from Ia sensory fibers to spinal motor neurons in humans can be studied using an important technique introduced in the 1950s and based on early work by Paul Hoffmann. This technique involves electrically stimulating the Ia sensory fibers in a peripheral nerve and recording the reflex electromyogram (EMG) response in the homonymous muscle. The response is known as the *Hoffmann reflex*, or H-reflex.

The H-reflex is readily measured in the soleus muscle, an ankle extensor. The Ia fibers from the soleus and its synergists are excited by an electrode placed above the tibial nerve behind the knee (Figure 32–4A). The response recorded from the soleus muscle depends on stimulus strength. At low stimulus strengths, a pure H-reflex is evoked, for the threshold for activation of the Ia fibers is lower than the threshold for motor axons. Increasing the stimulus strength excites the motor axons innervating the soleus, producing two successive responses.

The first results from direct activation of the motor axons, and the second is the H-reflex evoked by stimulation of the Ia fibers (Figure 32–4B). These two components of the evoked EMG are called the M-wave and H-wave. The H-wave occurs later because it results from signals that travel to the spinal cord, across a synapse, and back again to the muscle. The M-wave, in contrast, results from direct stimulation of the motor axon innervating the muscle.

As the stimulus strength is increased still further, the M-wave continues to become larger and the H-wave progressively declines (Figure 32–4C). The decline in the H-wave amplitude occurs because action potentials in the motor axons propagate toward the cell body (antidromic conduction) and cancel reflexively evoked action potentials in the same motor axons. At very high stimulus strengths, only the M-wave persists.

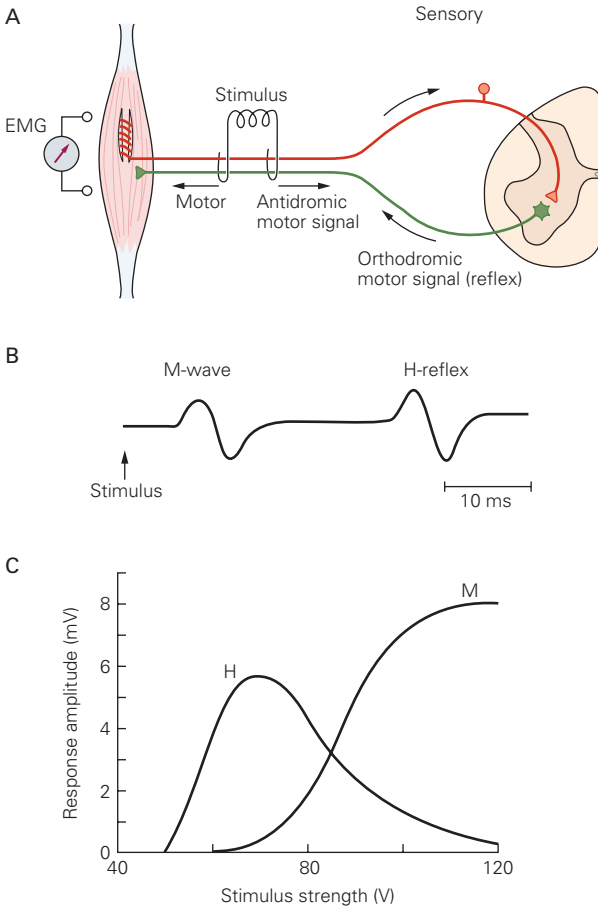

Figure 32–4 The Hoffmann reflex.

A. The Hoffmann reflex (H-reflex) is evoked by electrically stimulating Ia sensory fibers from muscle spindles. The sensory fibers excite alpha motor neurons, which in turn activate the muscle. When a mixed nerve is used, the motor neurons axons may also be activated directly.

B. At intermediate stimulus strengths, an M-wave precedes the H-wave (H-reflex) in the electromyogram (EMG).

C. As the stimulus strength increases, the orthodromic motor neuron spikes generated reflexively by the spindle sensory fibers are obliterated by antidromic spikes initiated by the electrical stimulus in the same motor axons. (Adapted, with permission, from Schieppati 1987. Copyright © 1987. Published by Elsevier Ltd.)

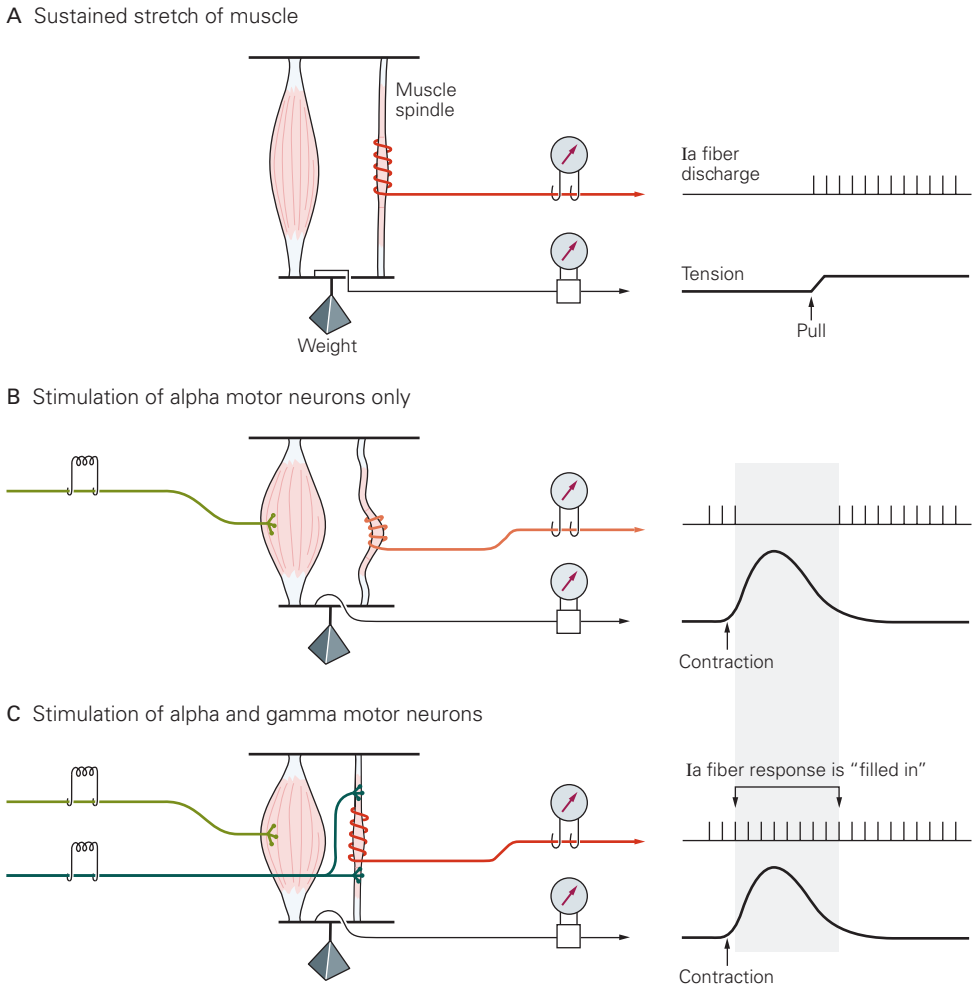

Figure 32–5 Activation of gamma motor neurons during active muscle contraction maintains muscle spindle sensitivity to muscle length. (Adapted, with permission, from Hunt and Kuffler 1951.)

A. Sustained tension elicits steady firing in the Ia sensory fiber from the muscle spindle (the two muscle fibers are shown separately for illustration only).

B. A characteristic pause occurs in the discharge of the Ia fiber when the alpha motor neuron is stimulated, causing a brief contraction of the muscle. The Ia fiber stops firing because the spindle is unloaded by the contraction.

C. Gamma motor neurons innervate the contractile polar regions of the intrafusal fibers of muscle spindles (see Figure 32–2A). If a gamma motor neuron is stimulated at the same time as the alpha motor neuron, the spindle is not unloaded during the contraction. As a result, the pause in discharge of the Ia sensory fiber that occurs when only the alpha motor neuron is stimulated is "filled in" by the response of the fiber to stimulation of the gamma motor neuron.

muscle length and gamma motor neuron activity (Box 32–1) and connect to different populations of excitatory and inhibitory interneurons in the spinal cord.

Some of the interneurons project directly to the spinal motor neurons, whereas others have more indirect connections. Because of the slower conduction velocity of type II sensory fibers and the signal relay through interneurons, the muscular responses elicited by group II fibers are smaller, more variable, and delayed compared to the monosynaptic stretch reflex. Some of the interneurons activated by group II fibers send axons across the midline of the spinal cord and give rise to crossed reflexes. Such connections that cross the midline are important for coordination of bilateral muscle activity in functional motor tasks.

Golgi Tendon Organs Provide Force-Sensitive Feedback to the Spinal Cord

Stimulation of Golgi tendon organs or their Ib sensory fibers in passive animals produces disynaptic inhibition of homonymous motor neurons (*autogenic*

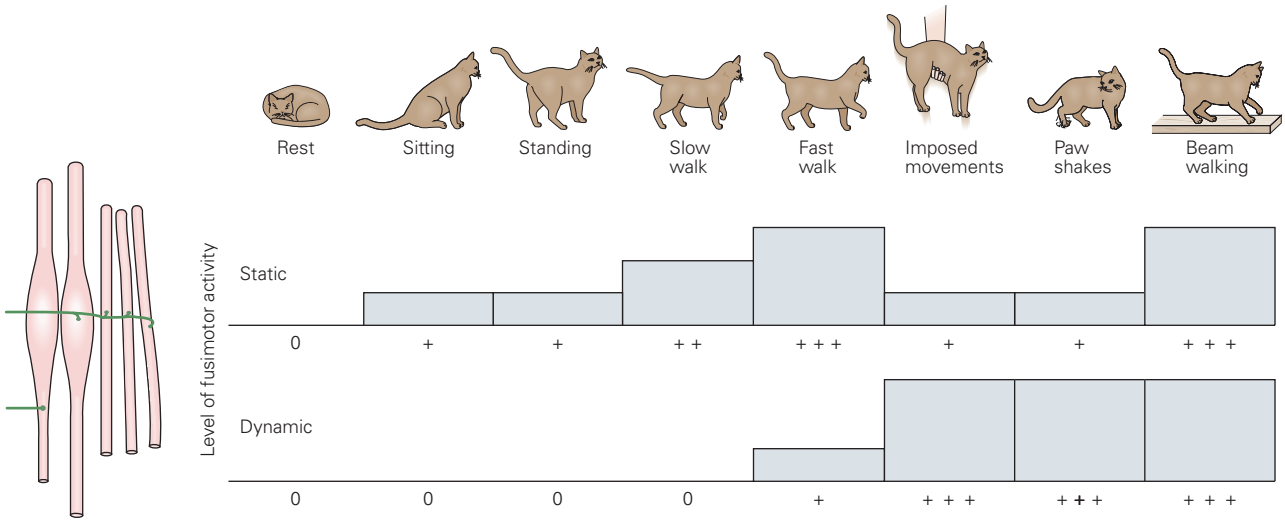

Figure 32–6 The level of activity in the fusimotor system varies with the type of behavior. Only static gamma motor neurons are active during activities in which muscle length changes slowly and predictably. Dynamic gamma motor neurons are activated during behaviors in which muscle length may change rapidly and unpredictably. (Adapted, with permission, from Prochazka et al. 1988.)

inhibition) and excitation of antagonist motor neurons (reciprocal excitation). Thus, these effects are the exact opposite of the responses evoked by muscle stretch or stimulation of Ia sensory axons.

This autogenic inhibition is mediated by *Ib inhibitory interneurons.* These inhibiting interneurons receive their principal input from Golgi tendon organs, sensory receptors that signal the tension in a muscle (Box 32–4), and they make inhibitory connections with homonymous motor neurons. However, stimulation of the Ib sensory fibers from tendon organs in active animals does not always inhibit homonymous motor neurons. Indeed, as we shall see later, stimulation of tendon organs may in certain conditions excite homonymous motor neurons.

One reason that the reflex actions of the sensory axons from tendon organs are complex in natural situations is that the Ib inhibitory interneurons also receive input from the muscle spindles, cutaneous receptors, and joint receptors (Figure 32–8A). In addition, they receive both excitatory and inhibitory input from various descending pathways.

Golgi tendon organs were first thought to have a protective function, preventing damage to muscle. It was assumed that they always inhibited homonymous motor neurons and that they fired only when tension in the muscle was high. We now know that these receptors signal minute changes in muscle tension, thus providing the nervous system with precise information about the state of a muscle's contraction.

The convergent sensory input from tendon organs, cutaneous receptors, and joint receptors to the Ib inhibitory interneurons (Figure 32–8A) may allow for precise spinal control of muscle force in activities such as grasping a delicate object. Additional input from cutaneous receptors may facilitate activity in the Ib inhibitory interneurons when the hand reaches an object, thus reducing the level of muscle contraction and permitting a soft grasp.

As is the case with the Ia fibers from muscle spindles, the Ib fibers from tendon organs form widespread connections with motor neurons that innervate muscles acting at different joints. Therefore, the connections of the sensory fibers from tendon organs with the Ib inhibitory interneurons are part of spinal networks that regulate movements of whole limbs.

Cutaneous Reflexes Produce Complex Movements That Serve Protective and Postural Functions

Most reflex pathways involve interneurons. One such reflex pathway is that of the flexion-withdrawal reflex, in which a limb is quickly withdrawn from a painful stimulus. Flexion-withdrawal is a protective reflex in which a discrete stimulus causes all the flexor muscles in that limb to contract coordinately. We know that this is a spinal reflex because it persists after complete transection of the spinal cord.

The sensory signal of the flexion-withdrawal reflex activates divergent polysynaptic reflex pathways. One

Box 32–4 Golgi Tendon Organs

Golgi tendon organs are slender encapsulated structures approximately 1 mm long and 0.1 mm in diameter located at the junction between skeletal muscle fibers and tendon. Each capsule encloses several braided collagen fibers connected in series to a group of muscle fibers.

Each tendon organ is innervated by a single Ib axon that branches into many fine endings inside the capsule; these endings become intertwined with the collagen fascicles (Figure 32–7A).

Stretching of the tendon organ straightens the collagen fibers, thus compressing the Ib nerve endings and causing them to fire. Because the nerve endings are so closely associated with the collagen fibers, even very small stretches of the tendons can compress the nerve endings.

Whereas muscle spindles are most sensitive to changes in length of a muscle, tendon organs are most sensitive to changes in muscle tension. Contraction of the muscle fibers connected to the collagen fiber bundle containing the receptor is a particularly potent stimulus to a tendon organ. The tendon organs are thus readily activated during normal movements. This has been demonstrated by recordings from single Ib axons in humans making voluntary finger movements and in cats walking normally.

Studies in anesthetized animal preparations have shown that the average level of activity in the population of tendon organs in a muscle is a good index of the total force in a contracting muscle (Figure 32–7B). This close agreement between firing frequency, and force is consistent with the view that the tendon organs continuously measure the force in a contracting muscle.

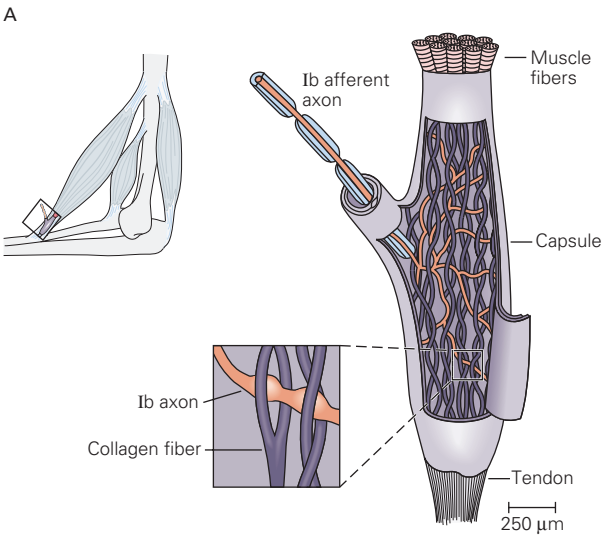

Figure 32–7A When the Golgi tendon organ is stretched (usually because of contraction of the muscle), the Ib afferent axon is compressed by collagen fibers (see enlargement) and its rate of firing increases. (Adapted, with permission, from Schmidt 1983; inset adapted, with permission, from Swett and Schoultz 1975.)

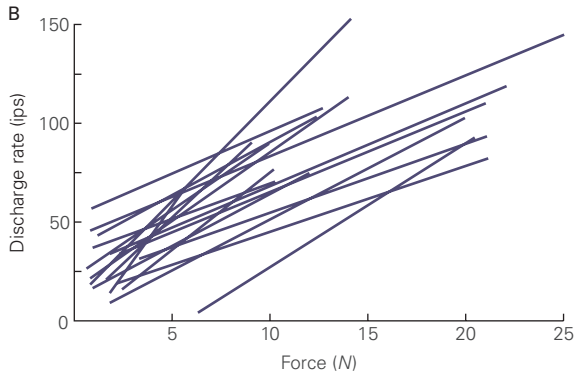

Figure 32–7B The discharge rate of a population of Golgi tendon organs signals the force in a muscle. Linear regression lines show the relationship between discharge rate and force for Golgi tendon organs of the soleus muscle of the cat. (Adapted, with permission, from Crago, Houk, and Rymer 1982.)

excites motor neurons that innervate flexor muscles of the stimulated limb, whereas another inhibits motor neurons that innervate the limb's extensor muscles (Figure 32–1B). This reflex can produce an opposite effect in the contralateral limb, that is, excitation of extensor motor neurons and inhibition of flexor motor neurons. This *crossed-extension reflex* serves to enhance postural support during withdrawal of a foot from a painful stimulus. Activation of the extensor muscles in the opposite leg counteracts the increased load caused by lifting the stimulated limb. Thus, flexion-withdrawal is a complete, albeit simple, motor act.

Although flexion reflexes are relatively stereotyped, both the spatial extent and the force of muscle contraction depend on stimulus intensity. Touching a stove that is slightly hot may produce moderately

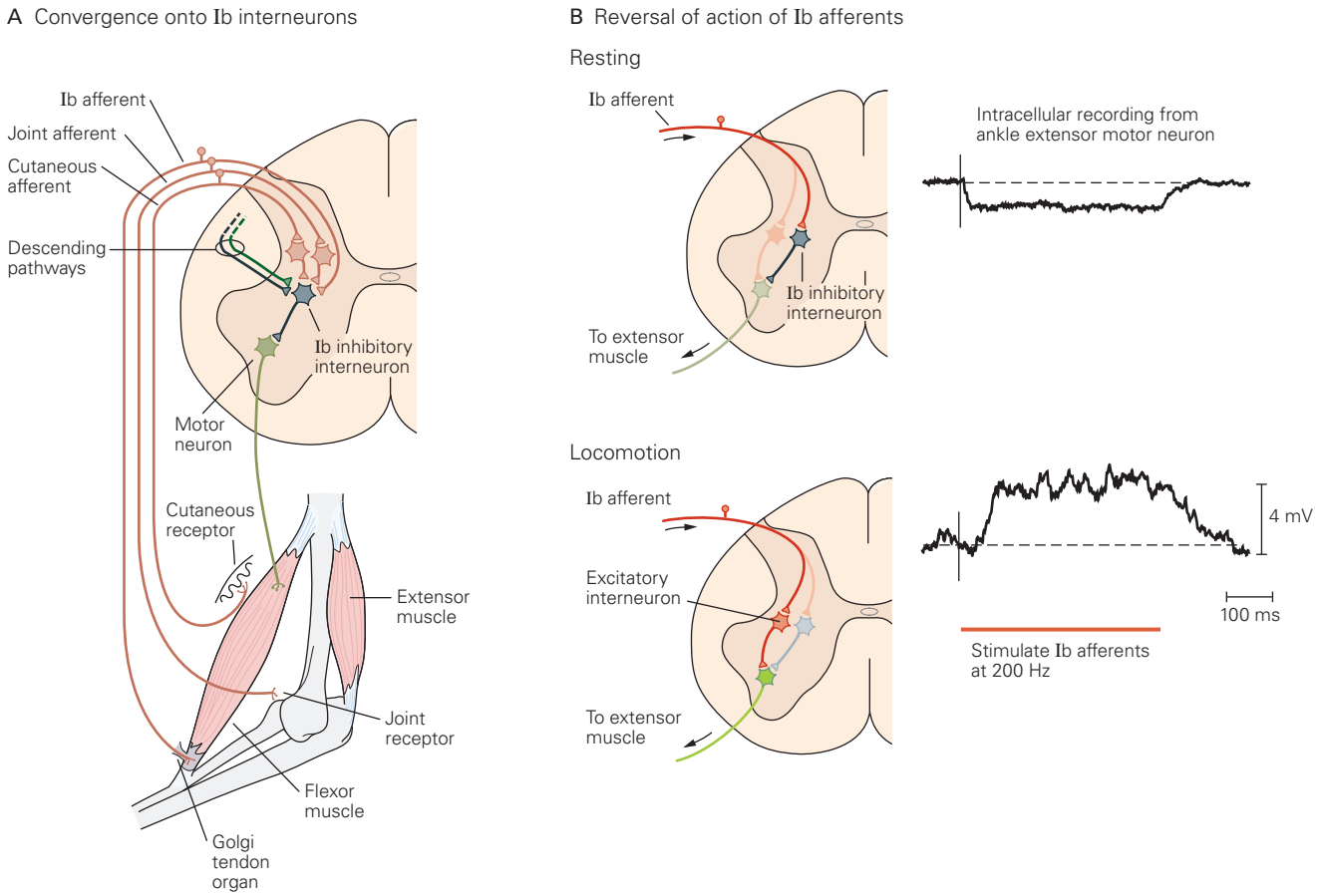

Figure 32–8 The reflex actions of Ib sensory fibers from Golgi tendon organs are modulated during locomotion.

A. The Ib inhibitory interneuron receives input from tendon organs, muscle spindles (not shown), joint and cutaneous receptors, and descending pathways.

B. The action of Ib sensory fibers on extensor motor neurons is reversed from inhibition to excitation when walking is initiated. When the animal is resting, stimulation of Ib fibers from the ankle extensor muscle inhibits ankle extensor motor neurons through Ib inhibitory interneurons, as shown by the hyperpolarization in the record. During walking, the Ib inhibitory interneurons are inhibited while excitatory interneurons that receive input from Ib sensory fibers are facilitated by the command system for walking, thus opening a Ib excitatory pathway from the Golgi tendon organs to motor neurons.

fast withdrawal only at the wrist and elbow, whereas touching a very hot stove invariably leads to a forceful contraction at all joints, leading to rapid withdrawal of the entire limb. The duration of the reflex usually increases with stimulus intensity, and the contractions produced in a flexion reflex always outlast the stimulus.

Because of the similarity of the flexion-withdrawal reflex to stepping, it was once thought that the flexion reflex is important in producing contractions of flexor muscles during walking. We now know, however, that a major component of the neural control system for walking is a set of intrinsic spinal circuits that do not require sensory stimuli (Chapter 33). Nevertheless, in mammals, the intrinsic spinal circuits that control walking share many of the interneurons involved in flexion reflexes.

Convergence of Sensory Inputs on Interneurons Increases the Flexibility of Reflex Contributions to Movement

The Ib inhibitory interneuron is not the only interneuron that receives convergent input from many different sensory modalities. An enormous diversity of sensory information converges on interneurons in the spinal cord, enabling them to integrate information from muscle, joints, and skin.

Interneurons activated by groups I and II sensory fibers have received special attention. It was thought

for some time that excitatory and inhibitory interneurons activated by group II fibers could be distinguished from those activated by group Ib afferents, but it is now believed that this distinction has to be abandoned and that groups I and II fibers converge on common populations of interneurons that integrate force and length information from the active muscle and thereby help coordinate muscle activity according to the length of the muscle, its activity level, and the external load.

Sensory Feedback and Descending Motor Commands Interact at Common Spinal Neurons to Produce Voluntary Movements

As pointed out by Michael Foster in his 1879 physiology textbook, it must be an "economy to the body" that the will should make use of the networks in the spinal cord to generate coordinated movements "rather than it should have recourse to an apparatus of its own of a similar kind." Research in the subsequent 140 years has confirmed this conjecture.

The first evidence came from intracellular recordings of synaptic potentials elicited in cat spinal motor neurons by combined and separate stimulation of sensory fibers and descending pathways. When separate stimuli are reduced in intensity to just below threshold for evoking a synaptic potential, combining the stimulations at appropriate intervals makes the synaptic potential reappear. This provides evidence of convergence of the sensory fibers and the descending pathways onto common interneurons in the reflex pathway (see Figure 13–14). Direct recordings from spinal interneurons have confirmed this, as have noninvasive Hoffmann reflex tests in human subjects (Figure 32–9).

Direct evidence that sensory feedback helps to shape voluntary motor commands through spinal reflex networks in humans comes from experiments in which sensory activity in length- and force-sensitive afferents has suddenly been reduced or abolished. This can be done by suddenly unloading or shortening a muscle during a voluntary contraction. The short latency of the consequent reduction in muscle activity can only be explained by sensory activity through a reflex pathway that directly contributes to the muscle activity.

Muscle Spindle Sensory Afferent Activity Reinforces Central Commands for Movements Through the Ia Monosynaptic Reflex Pathway

Stretch reflex pathways can contribute to the regulation of motor neurons during voluntary movements and during maintenance of posture because they form closed feedback loops. For example, stretching a muscle increases activity in spindle sensory afferents, leading to muscle contraction and consequent shortening of the muscle. Muscle shortening in turn leads to decreased activity in spindle afferents, reduction of muscle contraction, and lengthening of the muscle.

The stretch reflex loop thus acts continuously—the output of the system, a change in muscle length, becomes the input—tending to keep the muscle close to a desired or reference length. The stretch reflex pathway is a negative feedback system, or *servomechanism*, because it tends to counteract or reduce deviations from the reference value of the regulated variable.

In 1963, Ragnar Granit proposed that the reference value in voluntary movements is set by descending signals that act on both alpha and gamma motor neurons. The rate of firing of alpha motor neurons is set to produce the desired shortening of the muscle, and the rate of firing of gamma motor neurons is set to produce an equivalent shortening of the intrafusal fibers of the muscle spindle. If the shortening of the whole muscle is less than what is required by a task, as when the load is greater than anticipated, the sensory fibers increase their firing rate because the contracting intrafusal fibers are stretched (loaded) by the relatively greater length of the whole muscle. If shortening is greater than necessary, the sensory fibers decrease their firing rate because the intrafusal fibers are relatively slackened (unloaded) (Figure 32–10A).

In theory, this mechanism could permit the nervous system to produce movements of a given distance without having to know in advance the actual load or weight being moved. In practice, however, the stretch reflex pathways do not have sufficient control over motor neurons to overcome large unexpected loads. This is immediately obvious if we consider what happens when we attempt to lift a heavy suitcase that we believe to be empty. Automatic compensation for the greater-than-anticipated load does not occur. Instead, we have to pause briefly to plan a new movement with much greater muscle activation.

Strong evidence that alpha and gamma motor neurons are co-activated during voluntary human movement comes from direct measurements of the activity of the sensory fibers from muscle spindles. In the late 1960s, Åke Vallbo and Karl-Erik Hagbarth developed microneurography, a technique for recording from the largest afferent fibers in peripheral nerves. Vallbo later found that during slow movements of the fingers the large-diameter Ia fibers from spindles in the contracting muscles increase their rate of firing even when the muscle shortens as it contracts (Figure 32–10B). This occurs because the gamma motor neurons, which have

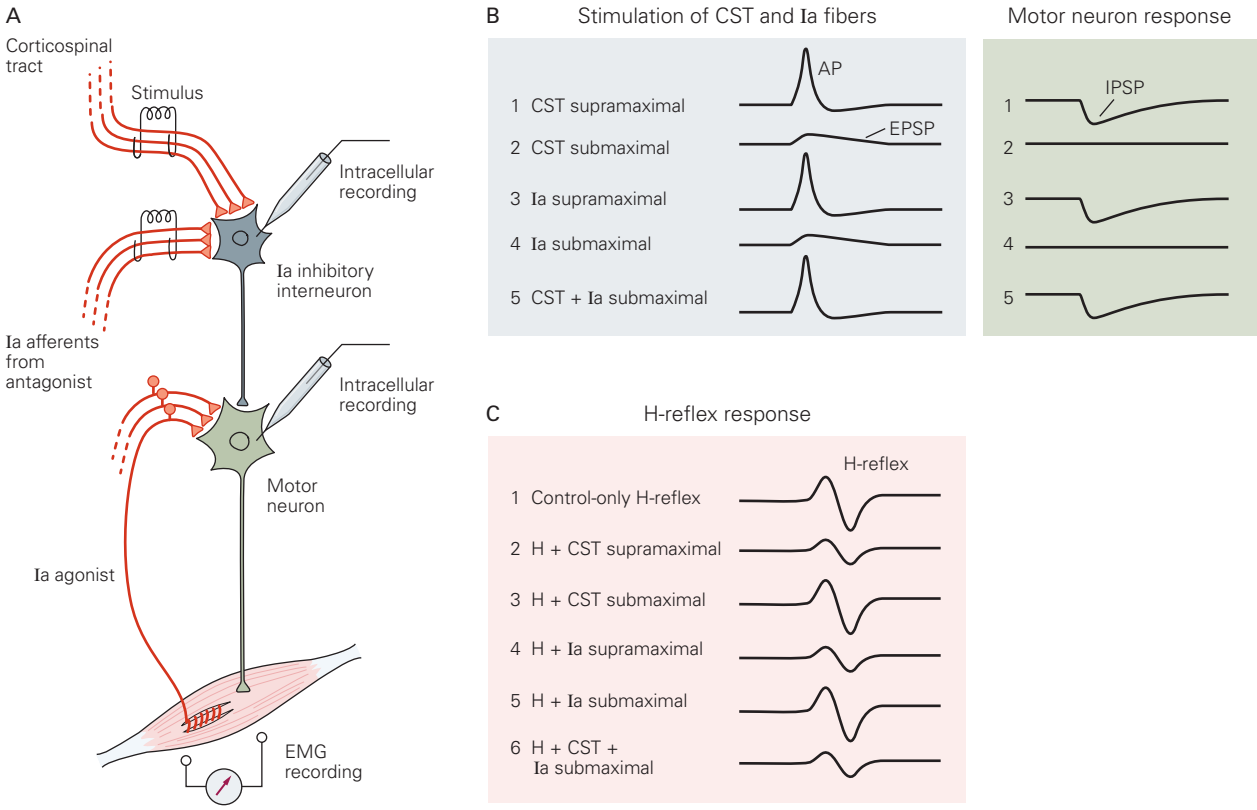

Figure 32–9 The spatial summation technique demonstrates how signals from descending inputs and spinal networks are integrated. This technique was introduced originally for investigation of spinal circuits in the cat in the 1950s, but it is also the basis of later investigations of the human spinal mechanisms of motor control. It relies on the spatial summation of synaptic inputs (see Figure 13–14), as illustrated here using the reciprocal Ia inhibitory pathway and corticospinal tract (**CST**).

A. The diagram shows the experimental setups for testing for convergence of excitatory reciprocal Ia and corticospinal pathways onto Ia inhibitory interneurons in the spinal cord.

B. In acute experiments on the cat spinal cord, supramaximal stimuli were applied separately to corticospinal fiber tracts (**1**) and Ia axons (**3**); each stimulus elicited an inhibitory postsynaptic potential (**IPSP**) in the motor neuron. Next, the intensities of the two stimuli were reduced to just submaximal levels, at which point each pathway failed to elicit an IPSP in the motor neuron (**2**, **4**). Then, when the two sets of submaximal stimuli were paired, they elicited an IPSP in the motor neuron (**5**), leading to the conclusion that the two input pathways converge on the same interneurons. This was confirmed by direct recording from a Ia inhibitory interneuron. (**AP**, action potential).

C. In humans, direct intracellular recording from interneurons and motor neurons is not possible, but recording of H-reflexes (Box 32–4, Figure 32–4) and transcutaneous stimulation of the corticospinal tract have provided indirect evidence for convergence similar to that demonstrated in cats (see part **B**). The electromyogram (**EMG**) record of the H-reflex provides a measure of the excitability of the spinal motor neurons (**1**). When the CST and antagonist Ia fibers were stimulated separately at supramaximal levels, the H-reflex amplitude was diminished due to the compound IPSPs elicited in the motor neurons (**2**, **4**). Next, the stimuli to these two excitatory pathways to the inhibitory interneurons were reduced until neither stimulus alone elicited a reduction in amplitude of the H-reflex (**3**, **5**). Then, the two submaximal stimuli were timed to produce synchronous subthreshold excitatory postsynaptic potentials (**EPSPs**) in the inhibitory interneurons (**6**). Because this protocol caused suppression of the H-reflex, one may conclude that the CST and Ia afferents converge on the same Ia inhibitory interneurons.

direct excitatory connections with spindles, are coactivated with alpha motor neurons.

Furthermore, when subjects attempt to make slow movements at a constant velocity, the firing of the Ia fibers mirrors the small deviations in velocity in the trajectory of the movements (sometimes the muscle shortens quickly and at other times more slowly). When the velocity of flexion increases transiently, the rate of firing in the fibers decreases because the muscle is shortening more rapidly and therefore exerts less tension on the intrafusal fibers. When the velocity decreases, firing increases because the muscle is

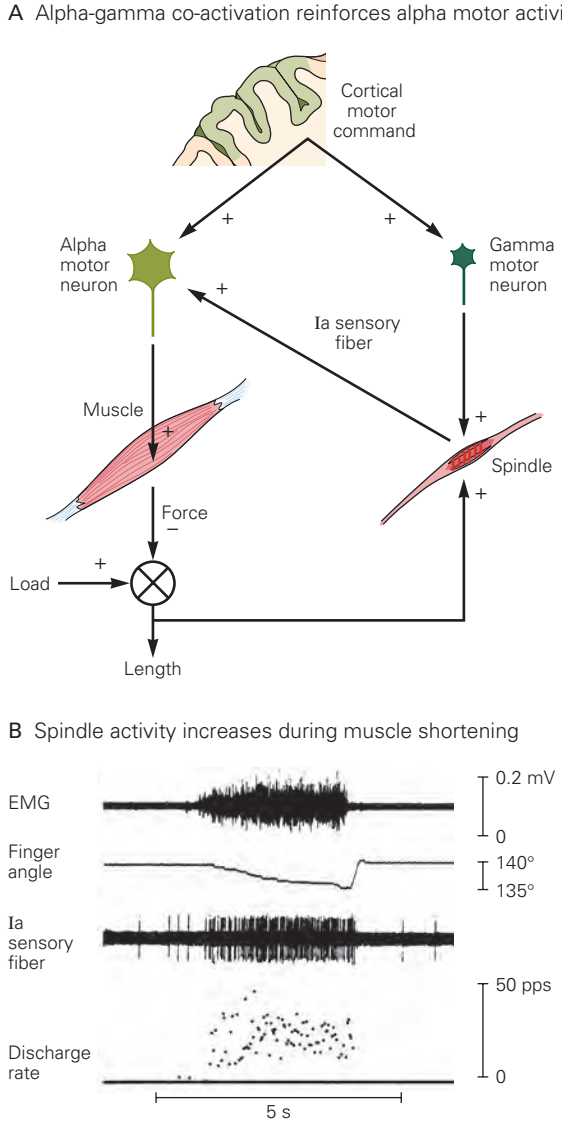

Figure 32–10 Co-activation of alpha and gamma motor neurons.

A. Co-activation of alpha and gamma motor neurons by a cortical motor command allows feedback from muscle spindles to reinforce activation in the alpha motor neurons. Any disturbance during a movement alters the length of the muscle and thus changes the activity in the sensory fibers from the spindles. The changed spindle input to the alpha motor neuron compensates for the disturbance.

B. The discharge rate in the Ia sensory fiber from a spindle increases during slow flexion of a finger. This increase depends on alpha-gamma co-activation. If the gamma motor neurons were not active, the spindle would slacken, and its discharge rate would decrease as the muscle shortened. (**EMG**, electromyogram; **PPS**, pulses/s) (Adapted, with permission, from Vallbo 1981.)

shortening more slowly, and therefore, the relative tension on the intrafusal fibers increases. This information can be used by the nervous system to compensate for irregularities in the movement trajectory by exciting the alpha motor neurons.

Modulation of Ia inhibitory Interneurons and Renshaw Cells by Descending Inputs Coordinate Muscle Activity at Joints

Reciprocal innervation is useful not only in stretch reflexes but also in voluntary movements. Relaxation of the antagonist muscle during a movement enhances speed and efficiency because the muscles that act as prime movers are not working against the contraction of opposing muscles.

The Ia inhibitory interneurons receive inputs from collaterals of the axons of neurons in the motor cortex that make direct excitatory connections with spinal motor neurons. This organizational feature simplifies the control of voluntary movements, because higher centers do not have to send separate commands to the opposing muscles.

It is sometimes advantageous to contract both the prime mover and the antagonist at the same time. Such *co-contraction* has the effect of stiffening the joint and is most useful when precision and joint stabilization are critical. An example of this phenomenon is the co-contraction of flexor and extensor muscles of the elbow immediately before catching a ball. The Ia inhibitory interneurons receive both excitatory and inhibitory signals from all of the major descending pathways (Figure 32–11A). By changing the balance of excitatory and inhibitory inputs onto these interneurons, supraspinal centers can modulate reciprocal inhibition of muscles and enable co-contraction, thus controlling the relative amount of joint stiffness to meet the requirements of the motor act.

The activity of spinal motor neurons is also regulated by another important class of inhibitory interneurons, the *Renshaw cells.* Excited by collaterals of the axons of motor neurons and receiving significant synaptic input from descending pathways, Renshaw cells make inhibitory synaptic connections with several populations of motor neurons, including the motor neurons that excite them, as well as Ia inhibitory interneurons (Figure 32–11B). The connections with motor neurons form a negative feedback system that regulates the firing rate of the motor neurons, whereas the connections with the Ia inhibitory interneurons regulate the strength of inhibition of antagonistic motor neurons, for instance in relation to co-contraction of antagonists. The distribution of projections from Renshaw

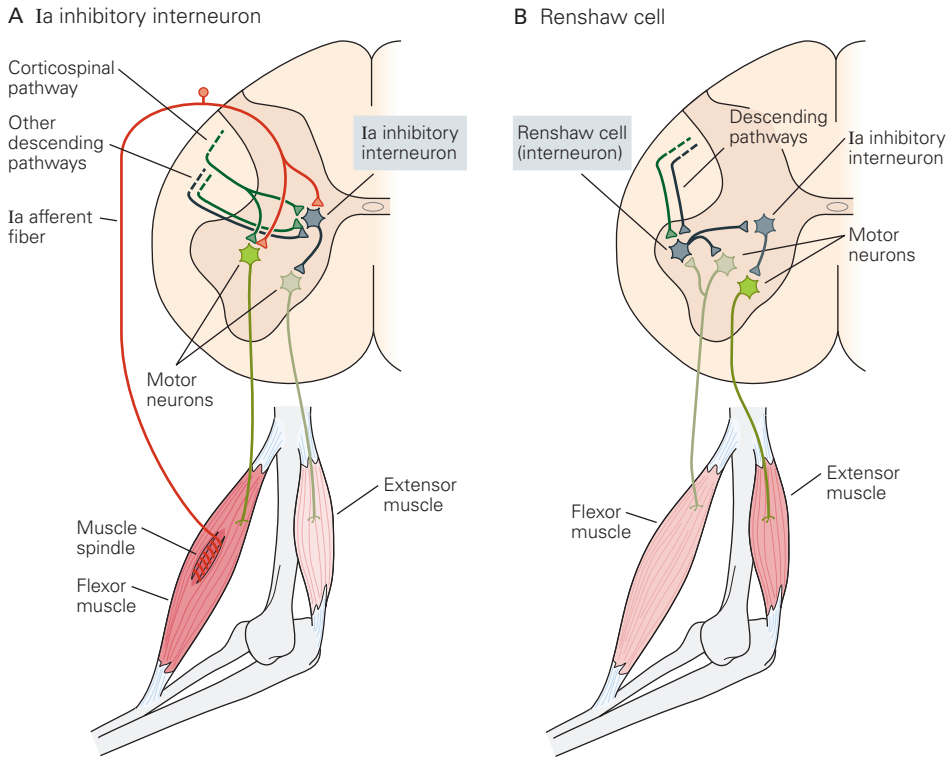

Figure 32–11 Inhibitory spinal interneurons coordinate reflex actions.

A. The Ia inhibitory interneuron regulates contraction in antagonist muscles in stretch reflex circuits through its divergent contacts with motor neurons. In addition, the interneuron receives excitatory and inhibitory inputs from corticospinal and other descending pathways. A change in the balance of these supraspinal signals allows the interneuron to coordinate co-contractions in antagonist muscles at a joint.

B. The Renshaw cell produces recurrent inhibition of motor neurons. These interneurons are excited by collaterals from motor neurons and inhibit those same motor neurons. This negative feedback system regulates motor neuron excitability and stabilizes firing rates. Renshaw cells also send collaterals to synergist motor neurons (not shown) and Ia inhibitory interneurons that synapse on antagonist motor neurons. Thus, descending inputs that modulate the excitability of the Renshaw cells adjust the excitability of all the motor neurons that control movement around a joint.

cells to different motor nuclei also facilitate that muscle activity is coordinated in functional synergies during movement.

Transmission in Reflex Pathways May Be Facilitated or Inhibited by Descending Motor Commands

As we have seen, in an animal at rest, the Ib sensory fibers from extensor muscles have an inhibitory effect on homonymous motor neurons. During locomotion, they produce an excitatory effect on those same motor neurons because transmission in the disynaptic inhibitory pathway is depressed (Figure 32–8B), while at the same time transmission through excitatory interneurons is facilitated.

This phenomenon, called *state-dependent reflex reversal*, illustrates how transmission in spinal circuit is regulated by descending motor commands to meet the changing requirements during movement. By favoring transmission through excitatory pathways from the load-sensitive Golgi tendon organs, the descending motor commands ensure that feedback from the active muscles automatically facilitates the activation of the muscles, thereby greatly simplifying the task for supraspinal centers.

State-dependent reflex reversal has also been demonstrated in humans. Stimulation of skin and muscle afferents from the foot produces facilitation of muscles that lift the foot early in the swing phase, but suppresses activity of the same muscles late in the swing phase. Both effects make good functional sense. Early in the swing phase, positive feedback from the foot will help to lift the foot over an obstacle, whereas suppression of the same muscles in late swing will help to lower the foot quickly to the ground so that the obstacle may be passed using the opposite leg first.

Descending Inputs Modulate Sensory Input to the Spinal Cord by Changing the Synaptic Efficiency of Primary Sensory Fibers

In the 1950s and early 1960s, John C. Eccles and his collaborators demonstrated that monosynaptic excitatory postsynaptic potentials (EPSPs) elicited in cat spinal motor neurons by stimulation of Ia sensory fibers become smaller when other Ia fibers are stimulated. This led to the discovery in the spinal cord of several groups of GABAergic inhibitory interneurons that exert presynaptic inhibition of primary sensory neurons (Figure 32–12). Some interneurons inhibit mainly Ia sensory axons, whereas others inhibit mainly Ib axons or sensory fibers from skin.

The principal mechanism responsible for sensory inhibition is a depolarization of the primary terminal caused by an inward Cl^- current when GABAergic receptors on the terminal are activated. This depolarization inactivates some of the Na^+ channels in the terminal, so the action potentials that reach the synapse are reduced in size. The effect of this is that release of neurotransmitter from the sensory afferent is diminished.

When tested by stimulation of peripheral afferents, presynaptic inhibition is widespread in the spinal cord and affects primary afferents from all muscles in a limb. However, similar to other interneurons, the neurons responsible for presynaptic inhibition are also controlled by descending pathways, making possible a much more focused modulation of presynaptic inhibition in relation to movement. Presynaptic inhibition at the synapse of Ia axons with motor neurons of the muscles that are activated as part of a movement is reduced at the onset of movement. In contrast, presynaptic inhibition of Ia axons on motor neurons connected to inactive muscles is increased. One example of this selective modulation is increased presynaptic inhibition of Ia axons at their synapse with antagonist motor neurons, which explains part of the reduction of stretch reflexes in antagonist muscles at the onset of agonist contraction. In this way, the nervous system takes advantage of the widespread connectivity of Ia axons, using presynaptic inhibition to shape activity in the Ia afferent network to facilitate activation of specific muscles.

Presynaptic inhibition provides a mechanism by which the nervous system can reduce sensory feedback predicted by the motor command, while allowing unexpected feedback access to the spinal motor circuit and the rest of the nervous system. In line with this function, presynaptic inhibition of Ia sensory axons from muscle spindles generally increases during

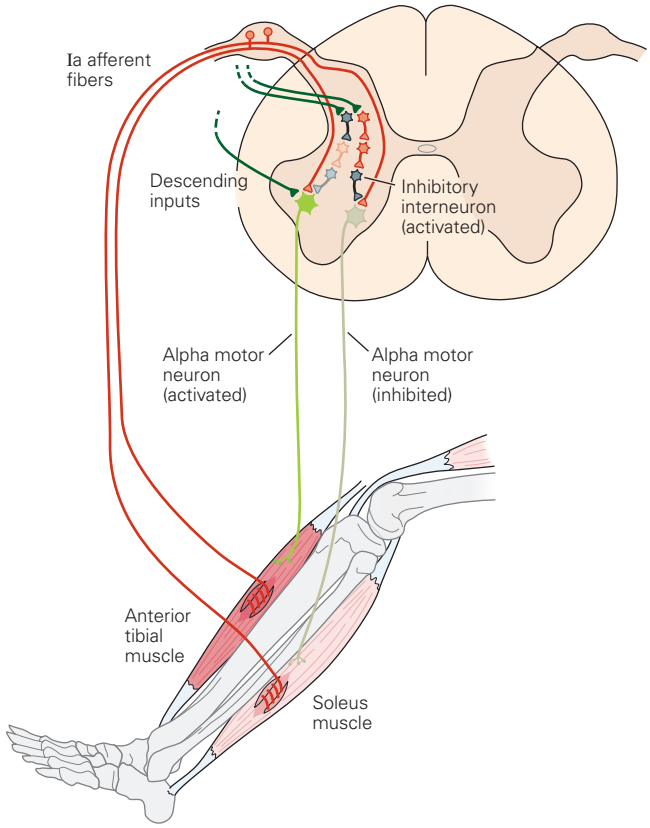

Figure 32–12 **Selective modulation of primary sensory axon terminals by descending presynaptic inhibitory inputs contributes to generation of coordinated limb movements.** Inhibitory interneurons (**blue**) activated by descending inputs can have either pre- or postsynaptic effects. Some interneurons releasing the inhibitory neurotransmitter γ-aminobutyric acid (GABA) form axo-axonic synapses with the primary sensory fibers. The principal inhibitory mechanism involves activation of GABAergic receptors on the terminals of the presynaptic Ia sensory axons, resulting in depolarization of the terminals and reduced transmitter release. Such presynaptic inhibition is widely distributed in the spinal cord. Stimulation of Ia sensory fibers from one flexor muscle may elicit presynaptic inhibition of both flexor and extensor Ia axon terminals on motor neurons innervating muscles throughout the limb. However, several different populations of interneurons mediating presynaptic inhibition exist, which allows a very specific regulation of presynaptic inhibition in relation to voluntary movements. Interaction of sensory inputs with descending motor commands in the corticospinal tract may thus *decrease* presynaptic inhibition of Ia axon terminals on agonist motor neurons (eg, anterior tibial motor neurons) and at the same time *increase* presynaptic inhibition of Ia terminals on antagonist motor neurons (eg, soleus motor neurons). Regulation of presynaptic inhibition may thus simultaneously facilitate the sensory feedback to the activation of agonist motor neurons and at the same time diminish the risk that stretch of the antagonist muscles will elicit a stretch reflex that would counteract the movement.

movements that are highly predictable, such as walking and running.

Finally, presynaptic inhibition may help stabilize the execution of movements by preventing excessive sensory feedback and associated self-reinforcing oscillatory activity.

Part of the Descending Command for Voluntary Movements Is Conveyed Through Spinal Interneurons

In cats as well as most other vertebrates, the corticospinal tract has no direct connections to spinal motor neurons; all the descending commands have to be channeled through spinal interneurons that are also part of reflex pathways. Humans and Old World monkeys are the only species in which corticospinal neurons make direct connections with the spinal motor neurons in the ventral horn of the spinal cord. Even in these species, a considerable fraction of the corticospinal tract fibers terminate in the intermediate nucleus on spinal interneurons, and the corticospinal fibers that terminate on motor neurons also have collaterals that synapse on interneurons. A considerable part of each descending command for movement in the corticospinal tract therefore has to be conveyed through spinal interneurons—and integrated with sensory activity—before reaching the motor neurons.

Propriospinal Neurons in the C3–C4 Segments Mediate Part of the Corticospinal Command for Movement of the Upper Limb

In the 1970s, Anders Lundberg and his collaborators demonstrated that a group of neurons in the C3–C4 spinal segments of the cat spinal cord send their axons to motor neurons located in more caudal cervical segments (Figure 32–13). Since the neurons in the C3–C4 segments project to motor neurons that innervate a range of forelimb muscles controlling different joints, and receive input from both skin and muscles throughout the forelimb, they are named *propriospinal neurons*. In addition to sensory input from skin and muscle afferents, the C3–C4 propriospinal neurons are activated by collaterals from the corticospinal tract and thereby relay disynaptic excitation from the motor cortex to the spinal motor neurons.

Subsequent experiments by Bror Alstermark in Sweden and Tadashi Isa in Japan have confirmed that similar propriospinal neurons also exist in the C3–C4 segments of the monkey spinal cord and are involved in mediating at least part of the motor command for reaching. Noninvasive experiments have also provided indirect evidence of the existence of C3–C4 propriospinal neurons in the human spinal cord. With the evolution of direct monosynaptic corticomotor connections in monkeys and humans, the corticospinal transmission through this disynaptic pathway may have become less important.

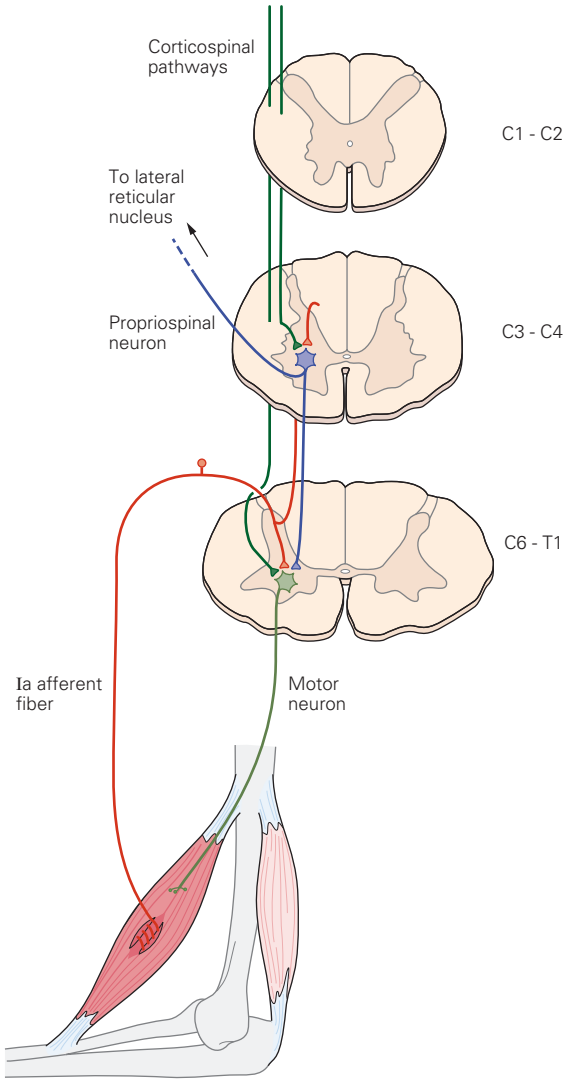

Figure 32–13 **Propriospinal neurons in spinal segments C3–C4 mediate part of the descending motor command to cervical motor neurons.** Some corticospinal fibers (**green**) send collaterals to propriospinal neurons in the C3–C4 segments (**blue**). These C3–C4 propriospinal neurons project to motor neurons located in more caudal cervical segments. They also receive excitatory input from muscle afferents and send collaterals to the lateral reticular nucleus.

Lumbar interneurons that receive input from groups I and II sensory axons from muscle also receive significant input from descending motor tracts and provide excitatory projections to spinal motor neurons. These interneurons thus convey part of the indirect motor command for voluntary movements to the spinal motor neurons that control leg muscles and may be a lumbar equivalent of the C3–C4 propriospinal neurons in the cervical spinal cord.

Neurons in Spinal Reflex Pathways Are Activated Prior to Movement

Synaptic transmission in spinal reflex pathways may change in response to the intention to move, independent of movement. Intracellular recordings from active monkeys have demonstrated that the intention to make a movement modifies activity in interneurons in the spinal cord and alters transmission in spinal reflex pathways. Similarly, in human subjects who have been prevented from contracting a muscle (by injection of lidocaine into the peripheral nerve supplying the muscle), the voluntary effort to contract the muscle still changes transmission in reflex pathways as if the movement had actually taken place.

In both humans and monkeys, spinal interneurons also change their activity well in advance of the actual movement. For example, in human subjects, Hoffmann reflexes elicited in a muscle that is about to be activated are facilitated fully 50 ms prior to the onset of contraction and remain facilitated throughout the movement. Conversely, reflexes in the antagonist muscles are suppressed. The suppression of stretch reflexes in the antagonist muscle prior to the onset of movement is an efficient way of preventing the antagonist from being reflexively activated when it is stretched at the onset of the agonist contraction.

Transmission in spinal reflex pathways can also be modified in connection with higher cognitive functions. Two examples are (1) an increase in the tendon jerk reflex in the soleus muscle of a human subject imagining pressing a foot pedal and (2) modulation of the Hoffmann reflex in arm and leg muscles while a subject observes grasping and walking movements, respectively.

Proprioceptive Reflexes Play an Important Role in Regulating Both Voluntary and Automatic Movements

All movements activate receptors in muscles, joints, and skin. Sensory signals generated by the body's own movements were termed *proprioceptive* by Sherrington, who proposed that they control important aspects of normal movements. A good example is the Hering-Breuer reflex, which regulates the amplitude of inspiration. Stretch receptors in the lungs are activated during inspiration, and the Hering-Breuer reflex eventually triggers the transition from inspiration to expiration when the lungs are expanded.

A similar situation exists in the walking systems of many animals; sensory signals generated near the end of the stance phase initiate the onset of the swing phase (Chapter 33). Proprioceptive signals can also contribute to the regulation of motor activity during voluntary movements, as shown in studies of individuals with sensory neuropathy of the arms. These patients display abnormal reaching movements and have difficulty in positioning the limb accurately because the lack of proprioception results in a failure to compensate for the complex inertial properties of the human arm.

Therefore, a primary function of proprioceptive reflexes in regulating voluntary movements is to adjust the motor output according to the changing biomechanical state of the body and limbs. This adjustment ensures a coordinated pattern of motor activity during an evolving movement and compensates for the intrinsic variability of motor output.

Spinal Reflex Pathways Undergo Long-Term Changes

Transmission in spinal reflex pathways is modulated not only to suit the immediate requirements of the movement but also to adapt the motor command to the motor experience of the individual. For example, transmission in the reciprocal Ia inhibitory pathway shows a gradual change when subjects improve their ability in coordinating agonist and antagonist contraction. Inactivity following long periods of bedrest or immobilization also results in changes in stretch reflexes and H-reflexes. Conversely, the soleus stretch reflex is low in highly trained ballet dancers and varies among different kinds of athletes.

Extensive studies of humans, monkeys, and rats by Jonathan Wolpaw and his colleagues have found that stretch reflexes can be operantly conditioned to either increase or decrease. The mechanisms underlying these changes are complex and involve alterations at multiple sites including changes in the properties of motor neurons. A general prerequisite for these changes is that corticospinal control of the spinal motor circuits must be intact.

Damage to the Central Nervous System Produces Characteristic Alterations in Reflex Responses

Stretch reflexes are routinely used in clinical examinations of patients with neurological disorders. They are typically elicited by sharply tapping the tendon of a muscle with a reflex hammer. Although the responses are often called tendon reflexes or tendon jerks, the receptor that is stimulated, the muscle spindle, actually lies in the muscle rather than the tendon. Only the primary sensory fibers in the spindle participate in the tendon reflex, for these are selectively activated by a rapid stretch of the muscle produced by the tendon tap.

Measuring alterations in the strength of the stretch reflex can assist in the diagnosis of certain conditions and in localizing injury or disease in the central nervous system. Absent or hypoactive stretch reflexes often indicate a disorder of one or more of the components of the peripheral reflex pathway: sensory or motor axons, the cell bodies of motor neurons, or the muscle itself (Chapter 57). Nevertheless, because the excitability of motor neurons is dependent on descending excitatory and inhibitory signals, absent or hypoactive stretch reflexes can also result from lesions of the central nervous system. Hyperactive stretch reflexes, conversely, always indicate that the lesion is in the central nervous system.

Interruption of Descending Pathways to the Spinal Cord Frequently Produces Spasticity

The force with which a muscle resists being lengthened depends on the muscle's intrinsic elasticity, or stiffness. Because a muscle has elastic elements in series and parallel that resist lengthening, it behaves like a spring (Chapter 31). In addition, connective tissue in and around the muscle may also contribute to its stiffness. These elastic elements may be pathologically altered following brain and spinal cord injury and thereby cause contractures and abnormal joint positions. However, there is also a neural contribution to the resistance of a muscle to stretch; the feedback loop inherent in the stretch reflex pathway acts to resist lengthening of the muscle.

Spasticity is characterized by hyperactive tendon jerks and an increase in resistance to rapid stretching of the muscle. Slow movement of a joint elicits only passive resistance, which is caused by the elastic properties of the joint, tendon, muscle, and connective tissues. As the speed of the stretch is increased, resistance to the stretch rises progressively. This phasic relation is what characterizes spasticity; an active reflex contraction occurs only during a rapid stretch, and when the muscle is held in a lengthened position, the reflex contraction subsides.

Spasticity is seen following lesion of descending motor pathways caused by stroke, injuries of the brain or spinal cord, and degenerative diseases such as multiple sclerosis. It is also seen in individuals with brain damage that occurs before, during, or shortly after birth, resulting in *cerebral palsy*.

Spasticity is not seen immediately following lesions of descending pathways, but develops over days, weeks, and even months. This parallels plastic changes at multiple sites in the stretch reflex circuitry. Sensory group Ia axons release more transmitter substance when active, and the alpha motor neurons change their intrinsic properties and their morphology (dendritic sprouting and denervation hypersensitivity) so that they become more excitable. Changes in excitatory and inhibitory interneurons that project to the motor neurons also take place and probably contribute to the increased excitability.

Whatever the precise mechanisms that produce spasticity, the effect is a strong facilitation of transmission in the monosynaptic reflex pathway. It is not the only reflex pathway affected by lesions of descending motor pathways. Pathways involving group I/II interneurons and sensory fibers from skin are also affected and exhibit the symptomatology observed in patients with central motor lesions. In the clinic, spasticity is therefore used in a broader sense and does not only relate to stretch reflex hyperexcitability. It is still debated whether reflex hyperexcitability contributes to the movement disorder following lesion of descending pathways or whether it may be a pertinent adaptation that helps to activate the muscles when descending input is diminished.

Lesion of the Spinal Cord in Humans Leads to a Period of Spinal Shock Followed by Hyperreflexia

Damage to the spinal cord can cause large changes in the strength of spinal reflexes. Each year, approximately 11,000 Americans sustain spinal cord injuries, and many more suffer from strokes. More than half of these injuries produce permanent disability, including impairment of motor and sensory functions and loss of voluntary bowel and bladder control. Approximately 250,000 people in the United States today have some permanent disability from spinal cord injury.

When the spinal cord is completely transected, there is usually a period immediately after the injury when all spinal reflexes below the level of the

transection are reduced or completely suppressed, a condition known as *spinal shock*. During the course of weeks and months, spinal reflexes gradually return, often greatly exaggerated. For example, a light touch to the skin of the foot may elicit strong flexion withdrawal of the leg.

Highlights

1. Reflexes are coordinated, involuntary motor responses initiated by a stimulus applied to peripheral receptors.
2. Many groups of interneurons in spinal reflex pathways are also involved in producing complex movements such as walking and transmitting voluntary commands from the brain.
3. Some components of reflex responses, particularly those involving the limbs, are mediated by supraspinal centers, such as brain stem nuclei, the cerebellum, and the motor cortex.
4. Reflexes are smoothly integrated into centrally generated motor commands because of the convergence of sensory signals onto spinal and supraspinal interneuronal systems involved in initiating movements. Establishing the details of these integrative events is one of the major challenges of contemporary research on sensory-motor integration in the spinal cord.
5. Because of the role of supraspinal centers in spinal reflex pathways, injury to or disease of the central nervous system often results in significant alterations in the strength of spinal reflexes. The pattern of changes provides an important aid to diagnosis of patients with neurological disorders.

Jens Bo Nielsen
Thomas M. Jessell

Selected Reading

Alstermark B, Isa T. 2012. Circuits for skilled reaching and grasping. Annu Rev Neurosci 35:559–578.

Baldissera F, Hultborn H, Illert M. 1981. Integration in spinal neuronal systems. In: JM Brookhart, VB Mountcastle, VB Brooks, SR Geiger (eds). *Handbook of Physiology: The Nervous System,* pp. 509–595. Bethesda, MD: American Physiological Society.

Boyd IA. 1980. The isolated mammalian muscle spindle. Trends Neurosci 3:258–265.

Fetz EE, Perlmutter SI, Orut Y. 2000. Functions of spinal interneurons during movement. Curr Opin Neurobiol 10:699–707.

Jankowska E. 1992. Interneuronal relay in spinal pathways from proprioceptors. Prog Neurobiol 38:335–378.

Nielsen JB. 2016. Human spinal motor control. Annu Rev Neurosci 39:81–101.

Pierrot-Deseilligny E, Burke D. 2005. *The Circuitry of the Human Spinal Cord. Its Role in Motor Control and Movement Disorders*. Cambridge: Cambridge Univ. Press.

Prochazka A. 1996. Proprioceptive feedback and movement regulation. In: L Rowell, JT Sheperd (eds). *Handbook of Physiology: Regulation and Integration of Multiple Systems*, pp. 89–127. New York: American Physiological Society.

Windhorst U. 2007. Muscle proprioceptive feedback and spinal networks. Brain Res Bull 73:155–202.

Wolpaw JR. 2007. Spinal cord plasticity in acquisition and maintenance of motor skills. Acta Physiol (Oxf) 189:155–169.

References

Appenteng K, Prochazka A. 1984. Tendon organ firing during active muscle lengthening in normal cats. J Physiol (Lond) 353:81–92.

Brown MC, Matthews PBC. 1966. On the sub-division of the efferent fibres to muscle spindles into static and dynamic fusimotor fibres. In: BL Andrew (ed). *Control and Innervation of Skeletal Muscle,* pp. 18–31. Dundee, Scotland: University of St. Andrews.

Crago A, Houk JC, Rymer WZ. 1982. Sampling of total muscle force by tendon organs. J Neurophysiol 47:1069–1083.

Gossard JP, Brownstone RM, Barajon I, Hultborn H. 1994. Transmission in a locomotor-related group Ib pathway from hind limb extensor muscles in the cat. Exp Brain Res 98:213–228.

Granit R. 1970. *Basis of Motor Control.* London: Academic.

Hagbarth KE, Kunesch EJ, Nordin M, Schmidt R, Wallin EU. 1986. Gamma loop contributing to maximal voluntary contractions in man. J Physiol (Lond) 380:575–591.

Hoffmann P. 1922. *Untersuchungen über die Eigenreflexe (Sehnenreflexe) menschlicher Muskeln.* Berlin: Springer.

Hulliger M. 1984. The mammalian muscle spindle and its central control. Rev Physiol Biochem Pharmacol 101:1–110.

Hunt CC, Kuffler SW. 1951. Stretch receptor discharges during muscle contraction. J Physiol (Lond) 113:298–315.

Liddell EGT, Sherrington C. 1924. Reflexes in response to stretch (myotatic reflexes). Proc R Soc Lond B Biol Sci 96:212–242.

Marsden CD, Merton PA, Morton HB. 1981. Human postural responses. Brain 104:513–534.

Matthews PBC. 1972. *Muscle Receptors.* London: Edward Arnold.

Mendell LM, Henneman E. 1971. Terminals of single Ia fibers: location, density, and distribution within a pool of 300 homonymous motoneurons. J Neurophysiol 34:171–187.

Pearson KG, Collins DF. 1993. Reversal of the influence of group Ib afferents from plantaris on activity in model gastrocnemius activity during locomotor activity. J Neurophysiol 70:1009–1017.

Prochazka A, Hulliger M, Trend P, Dürmüller N. 1988. Dynamic and static fusimotor set in various behavioural contexts. In: P Hnik, T Soukup, R Vejsada, J Zelena (eds). *Mechanoreceptors: Development, Structure and Function*, pp. 417–430. New York: Plenum.

Schieppati M. 1987. The Hoffmann reflex: a means of assessing spinal reflex excitability and its descending control in man. Prog Neurobiol 28:345–376.

Schmidt RF. 1983. Motor systems. In: RF Schmidt, G Thews (eds), MA Biederman-Thorson (transl). *Human Physiology*, pp. 81–110. Berlin: Springer.

Sherrington CS. 1906. *Integrative Actions of the Nervous System.* New Haven, CT: Yale Univ. Press.

Swett JE, Schoultz TW. 1975. Mechanical transduction in the Golgi tendon organ: a hypothesis. Arch Ital Biol 113:374–382.

Vallbo ÅB. 1981. Basic patterns of muscle spindle discharge in man. In: A Taylor, A Prochazka (eds). *Muscle Receptors and Movement*, pp. 263–275. London: Macmillan.

Vallbo ÅB, Hagbarth KE, Torebjörk HE, Wallin BG. 1979. Somatosensory, proprioceptive, and sympathetic activity in human peripheral nerves. Physiol Rev 59:919–957.

Wickens DD. 1938. The transference of conditioned excitation and conditioned inhibition form one muscle group to the antagonist muscle group. J Exp Psychol 22:101–123.

33

Locomotion

Locomotion is one of the most fundamental of animal behaviors and is common to all members of the animal kingdom. As one might expect of such an essential behavior, the neural mechanisms responsible for the basic alternating rhythmicity that underlies locomotion are highly conserved throughout the animal kingdom, from invertebrates to vertebrates, and from the early vertebrates to primates. However, while the basic locomotor-generating circuits have been conserved, the evolution of limbs, and then of ever more complex patterns of behavior, has resulted in the development of progressively more complex spinal and supraspinal circuits (Figure 33–1).

Scientists have been intrigued with the neural mechanisms of locomotion since the beginning of the 20th century, when pioneering work by Charles Sherrington and Thomas Graham Brown showed that the isolated spinal cord of the cat is able to generate the basic aspects of locomotor activity and subsequently that this capacity was intrinsic to the spinal cord. Throughout the 20th century, major advances were made in detailing both the rhythm- and pattern-producing capacities of the spinal cord, leading ultimately to the groundbreaking concept of a central pattern generator for locomotion in the spinal cord. This single concept, more than any other, has driven research into the mechanisms underlying locomotor control since the 1970s, allowing a detailed electrophysiological examination of the neuronal mechanisms involved in the control of locomotion that is not possible for most other motor acts.

Most research throughout the 20th century on the spinal mechanisms mediating locomotion was performed on the cat, which remains an important model

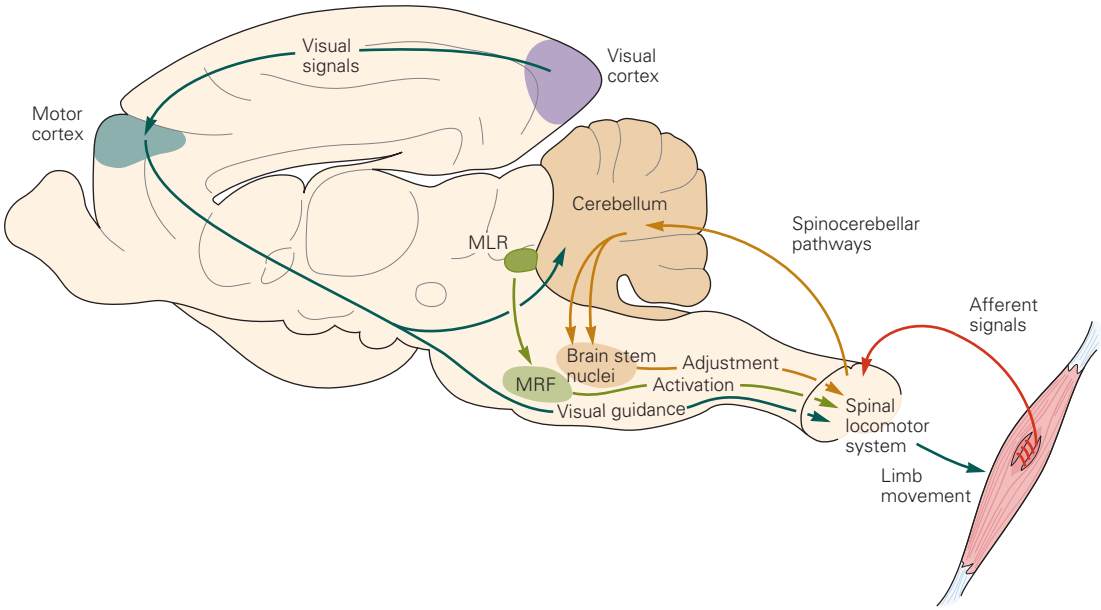

Figure 33–1 The locomotor system. Multiple regions of the central nervous system interact to initiate and regulate locomotion. Locomotor networks in the spinal cord—the central pattern generators (CPGs)—generate the precise timing and patterning of locomotion. Proprioceptive sensory feedback modulates the activity of the locomotor CPG. The initiation of locomotion is mediated by neurons in the mesencephalic locomotor region (**MLR**) that project to neurons in the medial reticular formation (**MRF**) in the lower brain stem, which in turn project to the spinal cord. Descending fibers from the vestibular nuclei, pontomedullary reticular formation, and the red nucleus (**brain stem nuclei**) maintain equilibrium and modulate the ongoing locomotor activity. Cortical activity from the posterior parietal cortex (not illustrated) and the motor cortex is involved in the planning and execution of visually guided locomotion, while the basal ganglia (not illustrated) and cerebellum are important for the selection and coordination of locomotor activity.

for studying many aspects of locomotor control. However, the complexity of the spinal circuits in mammals led to the search for simpler preparations that would allow a better understanding of the synaptic connectivity and neuronal properties responsible for the generation of locomotion. This search led to the development of the lamprey and the tadpole models (Box 33–1; Figures 33–2 and 33–3). Experiments using these species have led to a detailed understanding of the neuronal circuits responsible for generating swimming. Influential work on understanding the processes underlying locomotion has also come from other experimental models, including mouse, rat, turtle, salamander, and zebrafish.

More recently, the development of molecular-genetic techniques has provided a powerful tool to probe the spinal circuits responsible for locomotion in preparations as diverse as zebrafish and mouse. These techniques have allowed researchers to explore more thoroughly both the neuronal circuits in the mammalian spinal cord responsible for rhythmic, alternating patterns of activity that define over-ground locomotion and those responsible for swimming.

The rhythmic pattern of activity is only one element of the complex locomotor behavior observed in most vertebrates, especially mammals, which have evolved to allow them to move quickly and elegantly. This flexibility is provided via feedback and feedforward modification of the locomotor patterns generated by spinal networks.

Feedback information from the body and limbs in the form of cutaneous and proprioceptive inputs is important for regulating aspects of the locomotor cycle, including bending of the body, stride length, and the force produced during propulsion. This information is equally critical in assuring that animals can rapidly and efficiently react to unexpected perturbations in the environment, such as when hitting a branch during walking or stepping on an unstable surface.

Feedforward information from supraspinal systems modifies activity according to the goals of the animal and the environment in which it moves. Information from defined structures in the brain stem is important for both the initiation of locomotion and for regulating general aspects of locomotor activity, including the speed of locomotion, level of muscle activity, and interlimb coupling in animals with limbs. Information from cortical structures

Box 33–1 Preparations Used to Study the Neuronal Control of Locomotion

The neuronal control of locomotion is studied experimentally in diverse vertebrate species that produce swimming or over-ground locomotion, or both. The prevailing experimental models used for studying swimming are the lamprey, the tadpole, and the zebrafish; for over-ground locomotion, the cat, rat, or mouse; and for both swimming and locomotion, the turtle, salamander, and frog.

Semi-intact preparations—in which influences from parts of the brain, all supraspinal inputs, and/or afferent inputs to the spinal cord have been removed—are also commonly used in studies of the neuronal control of locomotion in vertebrates (Figure 33–2A). Finally, in vitro preparations of the spinal cord or of the brain stem and spinal cord from young animals or adult and anoxia-resistant animals are extensively used for circuit analysis (Figure 33–2C).

Intact Preparations Are Used to Study the Behavioral Output

In intact preparations, locomotion is studied either during walking over ground or on a motorized treadmill. Chronic electromyographic (EMG) recordings of limb muscles, coupled with video recordings of the movement, reveal details of the rhythm of locomotion, the pattern of muscle or joint activation, and interlimb coordination (Figure 33–2B). Such studies allow researchers to understand how normal locomotion behavior is expressed.

These behavioral studies are often combined with experimental manipulations that modify the supraspinal or afferent control of locomotion. Such experiments may use electrical stimulation or surgical ablation of circumscribed areas in the central nervous system, genetic inactivation or activation of defined populations of nerve cells, or perturbation of the afferent input to the spinal cord using genetic techniques or electrical stimulation. Finally, single-cell activity in the brain can be recorded from identified populations of neurons and correlated with specific aspects of the locomotor behavior (eg, speed, postural adjustments, gait modifications, flexor-extensor muscle activity). Cells are identified by their anatomical location, their projection pattern, transmitter content, and molecular markers.

Semi-intact Preparations Are Commonly Used to Study the Central Control of Locomotion in the Absence of Cortical Influence or Sensory Feedback

Decerebrate Preparations

In the decerebrate preparation, the brain stem is completely transected at the level of the midbrain (Figure 33–2A), disconnecting rostral brain centers, including the cortex, basal ganglia, and thalamus, from locomotor-initiating centers in the brain stem and spinal cord. These preparations allow investigation of the role of cerebellum and brain stem structures in controlling locomotion in the absence of influence from higher brain centers.

Locomotion is generally evoked by electrical stimulation of locomotor regions in the brain stem, as described in the text. To increase recording stability, the animals are often paralyzed by blocking transmission at the neuromuscular junction. When locomotion is initiated in such an immobilized preparation, often referred to as *fictive locomotion*, the motor nerves to flexors and extensor muscles discharge (recorded as an electroneurogram), but no movement takes place.

Spinal Preparations

In spinal preparations, the spinal cord is completely transected, generally at the lower thoracic level, thus isolating the spinal segments that control the hindlimb musculature from the rest of the central nervous system (Figure 33–2A). This procedure allows investigations of the spinal locomotor circuits without any influence from supraspinal structures.

Two types of spinal preparation are used: acute spinal preparations, in which studies are performed immediately after the spinalization, and chronic spinal preparations, in which the animals are allowed to recover from the surgery and are then studied over a period of time.

In acute spinal preparations, locomotion is frequently induced chemically, either by intravenous administration of drugs that stimulate monoaminergic and/or serotonergic receptors or by local application of glutamatergic receptor agonists. These drugs increase the excitability in the spinal locomotor circuits,

(continued)

contributes primarily to the planning and execution of locomotion in situations in which vision is used to make anticipatory modifications of gait. Finally, two structures with no direct spinal connections, the basal ganglia and the cerebellum, contribute to the selection of locomotor activity and to its coordination (Figure 33–1).

The way in which all of these structures interact and permit diverse modes of locomotion is the subject of this chapter.

Box 33–1 Preparations Used to Study the Neuronal Control of Locomotion (continued)

mimicking the locomotor-initiating drive from the brain stem. Alternatively, locomotion is induced electrically, by stimulation of the dorsal roots or dorsal columns. Acute spinal preparations are often paralyzed in order to increase recording stability from motor neurons and interneurons in the spinal cord, as well as to discriminate between central and peripheral effects.

In chronic spinal preparations, animals are studied for weeks or months after transection, often with the aim of finding better ways to improve the locomotor capability after spinal cord injury. In both young and adult cats and in young rodents, the hindlimb locomotor capability can often return following training but with no further treatment. In all animals, the locomotor capability is improved dramatically by drug treatments that activate the spinal central pattern generator. Electromyographic activity, together with behavioral measures, can be recorded before and after transection (Figure 33–2B).

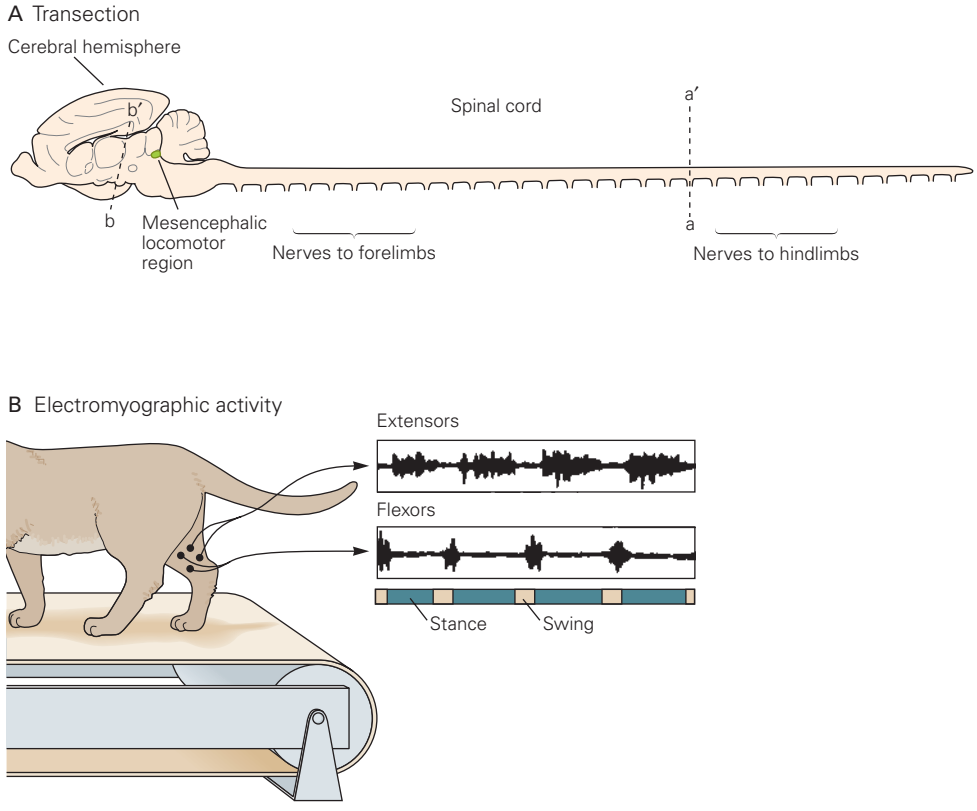

Figure 33–2 Selected animal models used to study locomotor control systems.

A. Schematic of the cat cerebral hemispheres, brain stem, and spinal cord showing the level of transection for spinalization (a′-a) and decerebration (b′-b). Decerebration isolates the brain stem and spinal cord from the cerebral hemispheres. Transection at a′-a isolates the lumbar spinal cord from all descending inputs.

B. The electromyogram can be used to record locomotor activity during actual movement in intact, decerebrate, or spinal animals.

Locomotion Requires the Production of a Precise and Coordinated Pattern of Muscle Activation

Locomotion requires the production of activity in many muscles that need to be coordinated in a precise rhythm and pattern. The rhythm defines the frequency of the cyclic activity, whereas the pattern defines the spatiotemporal activation of muscle groups within a cycle. In swimming animals, such as the lamprey or the tadpole, locomotion is expressed as a traveling

In Vitro Preparations Are Used to Study Central Organization of Networks

With in vitro preparations, the spinal cord or brain stem is removed from the animal and placed in a bath that is perfused with artificial cerebrospinal fluid (rodent, lamprey, and turtle) (Figure 33–2C). Alternatively, the brain stem and spinal cord are left in situ in the animal that is paralyzed or immobilized and kept in vitro (tadpole and zebrafish) (Figure 33–2D).

In all cases, no rhythmic afferent inputs occur in the cord, and motor activity is recorded in peripheral nerves or, more often, in the ventral roots where the motor neurons have their axons leaving the spinal cord.

Locomotion is induced chemically, either by application of glutamatergic or serotonergic receptor agonists or a combination of both, or electrically by stimulating the brain stem or peripheral afferents. Rhythm and pattern generation, circuit connectivity, cellular properties of interneurons and motor neurons, and circuit neuromodulation are studied with conventional electrophysiological methods, imaging, and anatomical tracing, or with molecular genetic methods that allow manipulation and recording of identified populations of neurons.

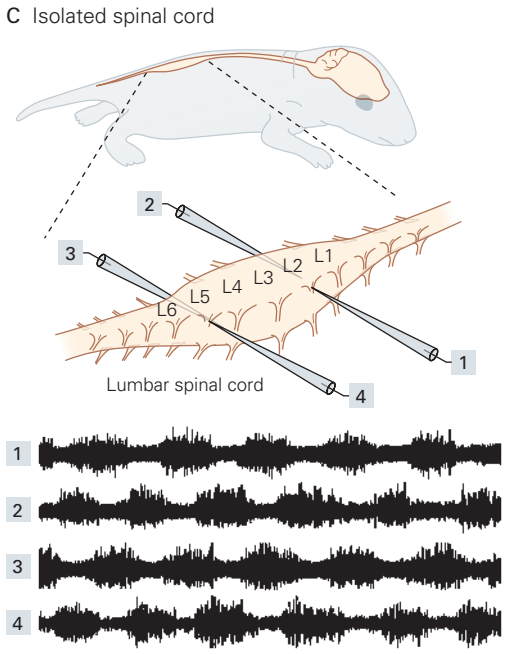

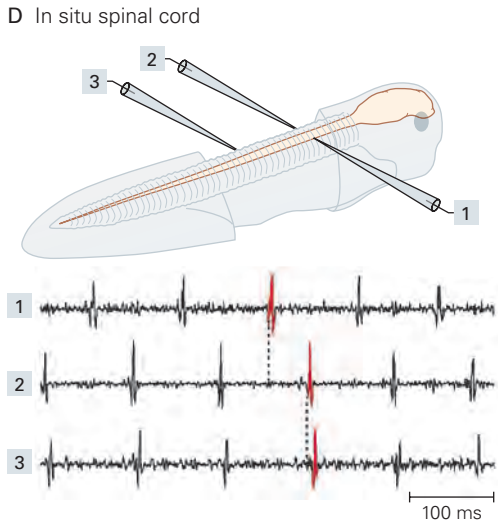

C. The isolated lumbar (L1–L6) spinal cord from a newborn rat or mouse. Motor activity is recorded in flexor-related L2 ventral roots and extensor-related L5 ventral roots on either side of the cord. Locomotor-like activity is induced by application of *N*-methyl-D-aspartate (NMDA) and serotonin (5-hydroxytryptamine, 5-HT) to the bathing solution. Flexor-extensor alternation is seen as out-of-phase activity between L2 and L5 ventral roots on the same side of the cord (**1** and **4**; **2** and **3**), and left–right alternations are seen as out-of-phase activity between L2–L2 and L5–L5 ventral roots on either side of the cord (**1** and **2**; **3** and **4**). (Adapted, with permission, from Kiehn et al. 1999; data from O Kiehn.)

D. In vitro tadpole preparation, in which the spinal cord remains in situ, showing ventral root recordings on the right side (**1**) and on the left side (**2** and **3**). side of the spinal cord. The swimming rhythm in the nervous system of the paralyzed animal was induced by a brief stimulation of the skin on the head. (Data from L Picton and KT Silar.)

wave of activity (Figure 33–3A) that propagates from rostral to caudal body segments during forward progression. This pattern can be recorded as an electromyogram (EMG) during locomotion in the intact animal (Figure 33–3B) and as an electroneurogram in the isolated spinal cord (Figure 33–3C). Activity in more caudal roots occurs later than that in more rostral roots, and the activity on each side of the body is reciprocal.

In limbed animals, the pattern of muscle activity is more complex and serves to support the body as well

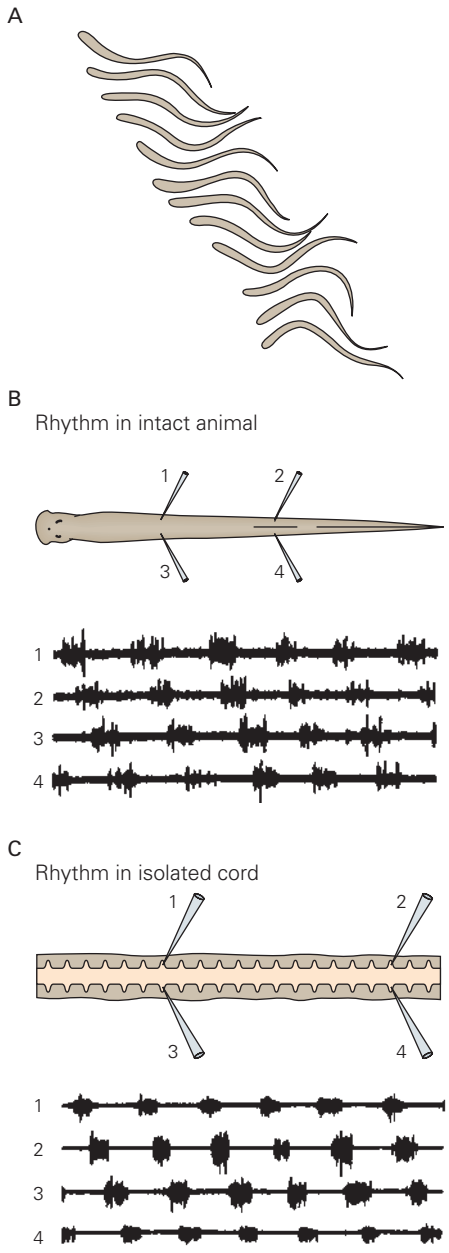

Figure 33–3 Lamprey swimming. The lamprey swims by means of a wave of muscle contractions traveling down one side of the body 180° out of phase with a similar traveling wave on the opposite side (**A**). This pattern is evident in electromyogram recordings from four locations along the animal during normal swimming (**B**). A similar pattern is recorded from four ventral roots in an isolated cord (**C**). (Data from S Grillner.)

as to transport it forward. The general unit of measure of locomotion in limbed vertebrates is the *step cycle*, which is defined as the time between any two successive events (eg, foot or paw contact of a given limb). The step cycle is divided into a *swing* phase, when the foot is off the ground and being transferred forward, and a *stance* phase, when the foot is in contact with the ground and propelling the body forward. Based on measures of changes in joint angle, each of these phases can be further divided into a period of flexion (F) followed by an initial period of extension (E_1) during swing and two additional periods of extension (E_2 and E_3) during stance (Figure 33–4A; see below).

Muscles within a single limb must be activated and coordinated in a precise spatiotemporal pattern (Figure 33–4B) so that the relative time of activation of different muscles, the duration of their activity, and the magnitude of that activity are coordinated to meet the demands of the environment (*intralimb coordination*).

In the hindlimb, swing is initiated by flexion of the knee produced by activation of muscles such as the semitendinosus, followed shortly by activation of hip and ankle flexors (the F phase). The hip flexors continue to contract throughout swing, but the activity in the knee and ankle flexors is arrested as the leg extends in preparation for contact with the support surface (the E_1 phase). Activity in most extensor muscles begins at this stage, before the foot contacts the ground. This preparatory prestance phase signifies that the extensor muscle activity is centrally programmed and not simply the result of afferent feedback arising from contact of the foot with the ground.

Stance begins with contact of the foot or paw with the ground. During early stance (the E_2 phase), the knee and ankle joints flex due to the acceptance of the weight of the body, causing extensor muscles to lengthen at the same time they are contracting strongly (eccentric contraction). The spring-like yielding of these muscles as weight is accepted allows the body to move smoothly over the foot and is essential for establishing an efficient gait. During late stance (the E_3 phase), the hip, knee, and ankle all extend as the extensor muscles provide a propulsive force to move the body forward.

There is also a requirement for *interlimb coordination*, the precise coupling between different limbs. The coupling between the four legs in quadrupeds, for example, can vary quite substantially, dependent on both the speed of locomotion and the adopted gait (a walk, pace, trot, gallop, or bound). This is particularly true of the pattern of coupling between muscles of limbs of the same side (homolateral limbs) and for the diagonal limbs. The relation between limbs can be characterized by the phase difference, with 0 reflecting limbs that move together in phase and 0.5 limbs that move fully out of phase (ie, in opposite directions). During walking, activity between the homolateral limbs varies by a phase value of 0.25, and three legs are always in contact

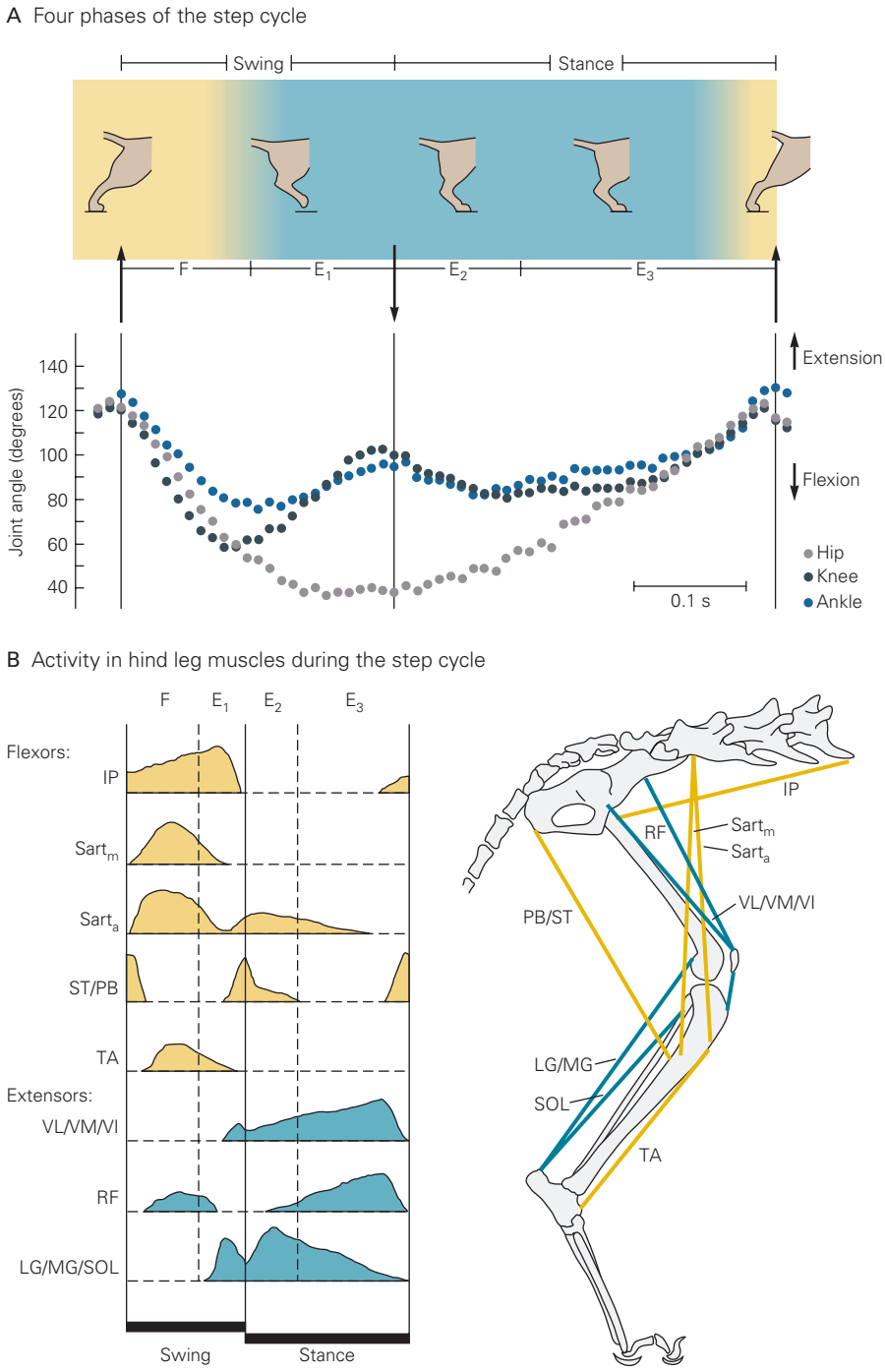

Figure 33–4 Stepping is produced by complex patterns of contractions in leg muscles.

A. The step cycle is divided into four phases. The flexion (**F**) and first extension (E_1) phases occur during the swing phase, when the foot is off the ground, whereas second extension (E_2) and third extension (E_3) occur during the stance phase, when the foot contacts the ground. E_2 is characterized by flexion at the knee and ankle as the leg begins to bear the animal's weight. The contracting knee and ankle extensor muscles lengthen during this phase. (Adapted, with permission, from Engberg and Lundberg 1969.)

B. Profiles of electrical activity in some of the hind leg flexor (**yellow**) and extensor (**blue**) muscles in the cat during stepping. Although flexor and extensor muscles are generally active during the swing and stance phases, respectively, the overall pattern of activity is complex in both timing and amplitude. (Muscles: **IP**, iliopsoas; **LG** and **MG**, lateral and medial gastrocnemius; **PB**, posterior biceps; **RF**, rectus femoris; **$Sart_m$** and **$Sart_a$**, medial and anterior sartorius; **SOL**, soleus; **ST**, semitendinosus; **TA**, tibialis anterior; **VL**, **VM**, and **VI**, vastus lateralis, medialis, and intermedius.)

with the ground. During a trot, the diagonal limbs (eg, the left hindlimb and the right forelimb) are in phase, and the phase difference between homolateral limbs is 0.5. Phase relationships between limbs of the same girdle (ie, the forelimbs or hindlimbs) are more stable during gaits produced by activation of alternating limbs, such as a walk or trot (generally out of phase by 0.5 cycle), compared to synchronous locomotion like a gallop or bound (generally in-phase).

The appropriate generation of the intra- and interlimb coordination of activity and the adaptation of these patterns of activity according to circumstance is one of the major functions of the central nervous system during locomotion.

The Motor Pattern of Stepping Is Organized at the Spinal Level

While the entire nervous system is necessary for an animal to produce a rich behavioral repertory, the spinal cord is sufficient to generate both the rhythm underlying locomotion as well as much of the specific pattern of muscle activity required for intra- and interlimb coordination.

At the beginning of the 20th century, Graham Brown showed that the isolated spinal cord had the intrinsic capacity to generate a rudimentary alternating locomotor pattern around the ankle joint in the absence of sensory inputs to the spinal cord (Figure 33–5). He proposed that locomotor networks controlling flexor and extensor activity in the spinal cord were organized as half-centers such that when half of the circuit was active it would inhibit the other half. The center would be released from inhibition through some sort of synaptic or neuronal fatigue.

This ground-breaking observation was mostly ignored until the mid-1960s and early 1970s, when there began a period of intense study of the mechanisms by which the spinal cord could generate a rhythmical pattern of activity. Initial studies showed that stimulation of sensory fibers in spinal cats treated with L-DOPA (a precursor of the monoamine transmitters dopamine and norepinephrine) and nialamide (a drug that prolongs the action of L-DOPA) could produce short sequences of rhythmic activity in flexor and extensor motor neurons. It was further found that groups of interneurons in the spinal cord were activated in a reciprocal flexor and extensor pattern. This organizational feature was consistent with Graham Brown's theory that mutually inhibiting half-centers produced the alternating burst activity in flexor and extensor motor neurons.

In the half-center model, the spinal cord produces only the locomotor rhythm, while the pattern is sculpted by afferent feedback caused by the movement. However, this view was changed by experiments that demonstrated that a well-organized locomotor pattern could be observed in decerebrate and spinal cats walking on a treadmill after section of the dorsal roots, thus removing the afferent feedback (Figure 33–6A,B). Later experiments in chronic spinal cats in which rhythmic afferent feedback was abolished by preventing movement (Figure 33–6C) showed that spinal circuits were not only able to intrinsically produce a locomotor rhythm but could also produce some of

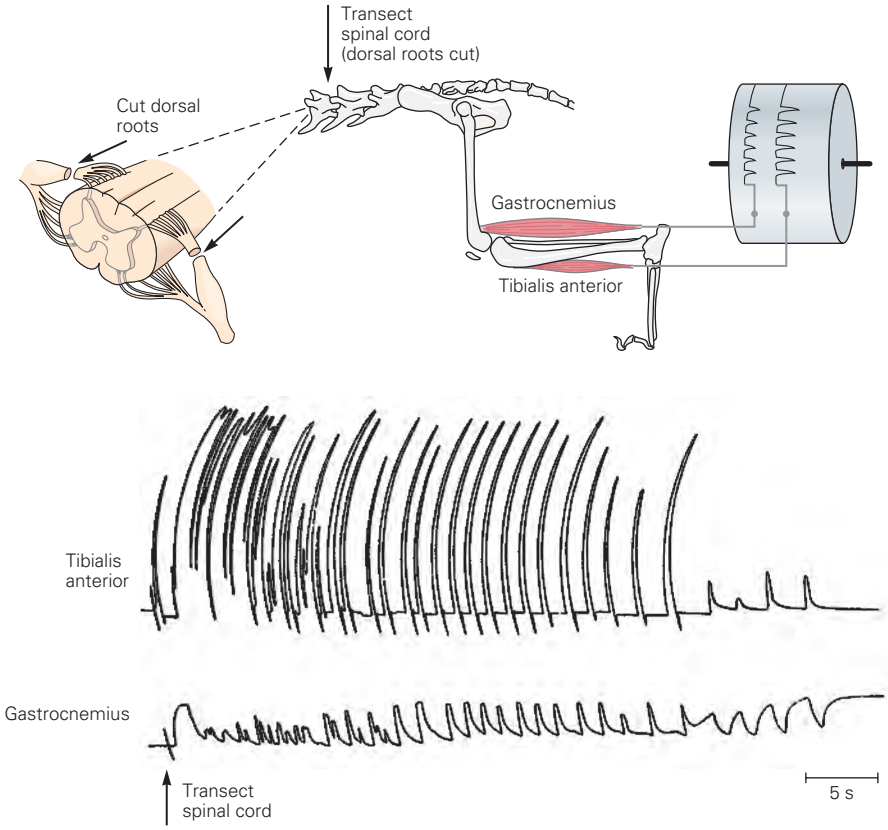

Figure 33–5 Rhythmic stepping is generated by spinal networks. The existence of intrinsic spinal networks was first demonstrated in 1911 by Thomas Graham Brown who developed an experimental preparation in which the dorsal roots were cut so that sensory information from the limb could not reach the spinal cord. The lower figure shows an original record from Graham Brown's study. Rhythmic alternating contractions of an ankle flexor (tibialis anterior) and an ankle extensor (gastrocnemius) are generated by the isolated spinal cord and persist for some time after the transection.

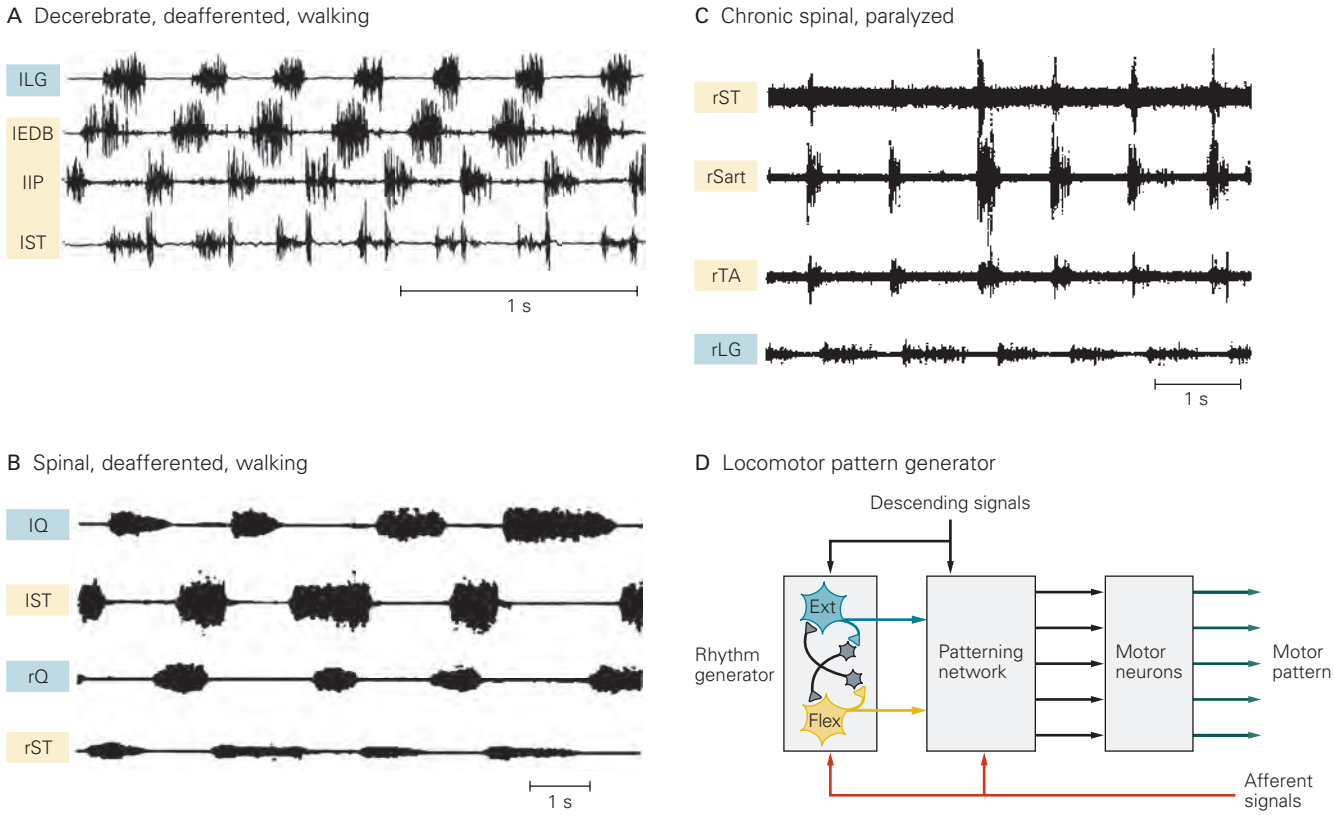

Figure 33–6 Spinal circuits generate both a rhythm and a pattern.

A. Even after removal of all sensory input to the spinal cord by cutting the dorsal roots, a decerebrate cat walking on a treadmill exhibits a complex motor pattern that is not just a simple alternation of flexor and extensor activity. (Abbreviations: **I**, left; **EDB**, extensor digitorum brevis; **LG**, lateral gastrocnemius; **IP**, iliopsoas; **ST**, semitendinosus.) (Adapted, with permission, from Grillner and Zangger 1984.)

B. Intravenous injection of L-DOPA and nialamide produces a well-organized locomotor pattern in an acute spinal cat with the dorsal roots cut. (Abbreviation: **I**, left; **Q**, quadriceps; **r**, right.) (Adapted with permission from Grillner and Zangger 1979. Copyright © 1979 Springer Nature.)

C. Fictive locomotion in a chronic spinal paralyzed cat, demonstrating the typical pattern of activity in the semitendinosus, tibialis anterior (**TA**), lateral gastrocnemius (**LG**), and sartorius (**Sart**) muscles in intact cats. (**l**, left; **r**, right.) (Adapted from Pearson and Rossignol 1991.)

D. Conceptual model of a spinal locomotor central pattern generator (CPG) based on studies in decerebrate cats. The CPG model is formed of separate rhythm- and pattern-generating layers. Each of these layers can be modified by descending inputs and peripheral afferent information. (Adapted from Rybak et al. 2006.)

the spatiotemporal details of the pattern of activity observed in the intact cat (Figure 33–6C).

These observations led to the important concept of a *central pattern generator* (CPG) that can generate both the rhythm and the pattern, independent of sensory inputs. Subsequent experiments led to the idea that separate components of the CPG are responsible for generating the underlying rhythm of locomotion within a limb and the spatiotemporal pattern of muscle action in the limb (Figure 33–6D). This notion was based on the observation that changes in rhythm and pattern can be influenced independently. Other studies have led to the concept that the CPG is modular, allowing independent control of activity around different joints.

Experiments in a variety of species have suggested that there are probably separate CPGs for each limb. For example, experiments using split belts, in which either the fore- and hindlimbs or the left and right limbs walk on separate treadmill belts, show that animals can independently modify step cycle duration in each pair of limbs. This organization would allow relatively simple descending commands to modify the coupling between each CPG and so to alter the pattern of the gait.

CPGs have now been identified and analyzed in many rhythmic motor systems, including those

controlling over-ground locomotion, swimming, flying, respiration, and swallowing, in both invertebrates and vertebrates. In all vertebrates except higher primates and humans, a prominent locomotor pattern can be observed immediately after spinal transection when the spinal cord below the transection is activated with neuroactive drugs that function as a substitute for the descending drive that normally activates the spinal locomotor networks (Box 33–1).

The Spinal Circuits Responsible for Locomotion Can Be Modified by Experience

Lesion of the spinal cord in otherwise intact adult mammals leads to paralysis. In the absence of any further intervention, such animals will regain only minimal locomotion. However, when quadrupedal animals with complete lesions of the thoracic spinal cord are trained daily, they regain a remarkable ability to use their hindlimbs to walk on a treadmill.

A similar improvement in locomotion can also be obtained from the application of noradrenergic agonists. Indeed, recordings of hindlimb joint angles and EMG activity from these animals show that the spinal cord isolated from all descending systems can generate most of the coordinating features in the hindlimb that are observed in intact animals. This training effect is believed to occur because of an activity-dependent reorganization of both internal spinal circuits and the modification of synaptic inputs from peripheral afferents that is specific to the training regimen. Indeed, cats can be trained specifically to either support their weight or to walk, without a transfer of motor skills between the two behaviors.

Spinal Locomotor Networks Are Organized Into Rhythm- and Pattern-Generation Circuits

The question of how the spinal cord generates the complex activity underlying locomotion has been one of intense study that has followed three complementary paths. The earliest experiments directed at this issue were performed in the cat and provided important information on the functional characteristics of different interneuronal populations. However, the complex nature of the mammalian spinal cord led researchers to identify models with fewer neurons in the spinal cord, such as the turtle and two aquatic preparations, the tadpole and the lamprey (Box 33–1). These latter two models have provided an excellent window into the organization of the spinal circuits involved in swimming and a foundation for studying rhythm and pattern generation in limbed animals. Last, the development of important molecular-genetic models in the mouse and the zebrafish has provided additional insights not available by more traditional methods.

The Swimming Central Pattern Generator

The lamprey—a jawless fish—swims like an eel with a wave of left–right bending traveling from front to back (Figure 33–3A). The spinal cord is made up of about 100 spinal segments, each containing neurons that can generate the rhythm and produce alternation between the two sides of the body. The rhythm is generated by interconnected glutamatergic excitatory neurons endowed with active membrane properties supporting rhythm generation. These glutamatergic neurons, which are the kernel in the swimming network, excite commissural inhibitory neurons, local inhibitory neurons, and motor neurons on the same side of the cord (Figure 33–7A).

The commissural interneurons, whose axons cross the midline, inhibit the contralateral interneurons involved in generating the alternating rhythm as well as contralateral motor neurons (Figure 33–7A). Cellular mechanisms contribute to phase switching in the network (Box 33–2). For example, Ca^{2+} entry triggered by bursting in glutamatergic neurons activates their calcium-activated K^+ channels. The opening of these channels hyperpolarizes the cells and enables termination of the burst. The termination of bursting on one side activates the other side by the commissural interneurons, thus allowing the contralateral rhythm-generating interneurons and motor neurons to become active. To enable coordination along the body, the segmental networks are connected through long-distance descending projections of excitatory and inhibitory neurons. This basic organization of interconnected excitatory neurons, inhibitory commissural neurons, and a rostrocaudal connectivity gradient for intersegmental coordination is also found in the tadpole and is possibly common to other swimming species.

Molecular and genetic approaches have expanded our understanding of the functional organization of CPGs in fish and identified two groups of glutamatergic interneurons—a group of commissural neurons and a group of ipsilaterally projecting neurons—that are involved in rhythm generation but at different speeds of locomotion. In adult zebrafish, the rhythm-generating circuit is composed of three functional classes of excitatory neurons that drive slow, intermediate, and fast pools of motor neurons that are selectively recruited as the speed of swimming increases.

The Quadrupedal Central Pattern Generator

The CPG controlling quadrupedal locomotion has added organizational complexity compared to the swimming CPG since it must generate both the rhythm and the pattern that involves the sequential flexor-extensor alternation of muscles around different joints within a limb (Figure 33–4B), as well as left–right coordination and coordination between the forelimbs and hindlimbs. Circuits controlling the forelimb are located in the cervical enlargement, whereas circuits controlling the hindlimb are located in the lower thoracic and lumbar spinal cord.

As in the CPG that generates rhythmical swimming activity, glutamatergic excitatory interneurons are involved in quadrupedal rhythm generation. Using advanced mouse genetics together with a molecular code that builds on expression of gene-regulating transcription factors that differentiate spinal neurons into classes with specific projection and transmitter phenotypes (Box 33–3), it has now been shown that the core of the rhythm-generating circuits in rodents includes two nonoverlapping groups of molecularly distinct glutamatergic neurons (Shox2^{ON} and Hb9; Figure 33–7B1).

The flexor (f) and extensor (e) rhythm-generating (R) circuits, which are connected by reciprocal inhibition (Figure 33–7B), drive other neurons in the locomotor network into rhythmicity and provide the rhythmic excitation for motor neurons (Figure 33–7B). As has been observed in the swimming CPG, ionic channels are also likely to contribute to rhythm generation and phase switching in the quadrupedal CPG.

The Flexor and Extensor Coordination Circuit

Flexor and extensor activity must be coordinated around joints (eg, hip-knee-ankle-toe in the hindlimb) to control the limb movement in a precise manner. Accordingly, the flexor-extensor alternation around the different joints is not simultaneous but has a sequential pattern, which suggests that multiple flexor-extensor alternating circuits are needed to time muscle actions in a limb. The basic flexor-extensor alternation circuits are organized in flexor and extensor modules composed of inhibitory and excitatory interneurons that are one synapse away from the flexor and extensor motor neurons they control (Figure 33–7B,B1).

Inhibitory and excitatory neurons in the module provide alternating inhibition and excitation of motor neurons. The reciprocally connected inhibitory Ia interneurons (Chapter 32) are part of the flexor and extensor modules providing the direct motor neuron inhibition in a reciprocal fashion (rIa in Figure 33–7B1). The rIas belong to the molecularly defined inhibitory V1 and V2b neurons (Figure 33–7B1). The excitatory neurons that directly excite motor neurons during locomotion are likely to belong to multiple classes of neurons in the spinal cord, including V2a-Shox2^{ON} and the dI3 neurons (Figure 33–7B1).

In this basic scheme, the flexor-extensor modules are driven by flexor (fR in Figure 33–7B1) and extensor rhythm-generating circuits (eR in Figure 33–7B1), which themselves are reciprocally connected via inhibitory neurons (Figure 33–7B), resulting in their out-of-phase activity.

Left–Right Coordination

Left–right alternation, for both swimming and overground locomotion, depends on crossed inhibition produced in two ways: directly by inhibitory commissural neurons or indirectly by excitatory commissural neurons, each of which acts on premotor inhibitory neurons (Figure 33–7B2). This dual inhibitory system has a counterpart in one specific neuronal population, the V0 commissural neurons (Figure 33–7B2). Ablation of V0 neurons results in loss of left–right alternation at all speeds of locomotion. The inhibitory dorsal class of V0 neurons ($V0_D$), which makes up about half of the V0 population, controls alternating locomotion during walking, whereas the excitatory ventral class of V0 neurons ($V0_V$), which makes up the remaining half of V0 neurons, controls alternating locomotion during trot. The dual system thus serves a speed-dependent role in coordinating alternating gaits (walk and trot). Separate excitatory non-V0 commissural neurons—possibly the ventral V3 neurons (Box 33–3)—are responsible for synchrony in gaits such as bound and gallop (Figure 33–7B2).

The dual-mode left–right alternating pathways are driven directly by the rhythm-generating neurons or indirectly by other non–rhythm-generating excitatory neurons, including the V2a-Shox2^{Off} neurons that are recruited at high speeds of locomotion and synaptically connect to the $V0_V$ neurons. The left–right synchronous pathways are active at higher speeds of locomotion when the alternating system is suppressed or less active.

The speed-dependent changes in the left–right alternation circuits in the rodent are an example of functional reorganization of the vertebrate locomotor network needed to produce diverse motor outputs. Similar dynamic circuit reorganization has also been demonstrated in zebrafish and in studies of rhythmic networks in invertebrates, such as the stomatogastric ganglion controlling gut movements in crustaceans, where different functional networks emerge from a common CPG network.

A Swimming CPG: Rhythm and left–right coordination circuits

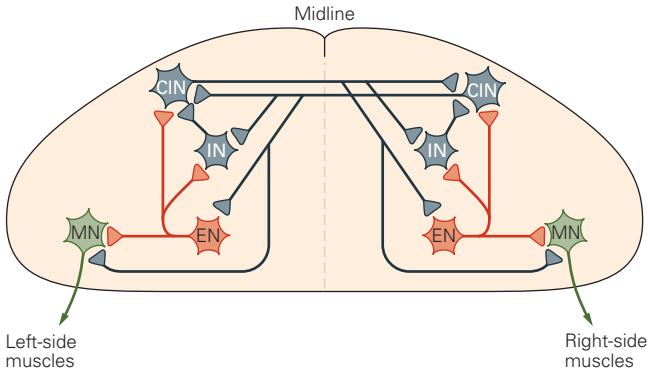

B Quadrupedal CPG

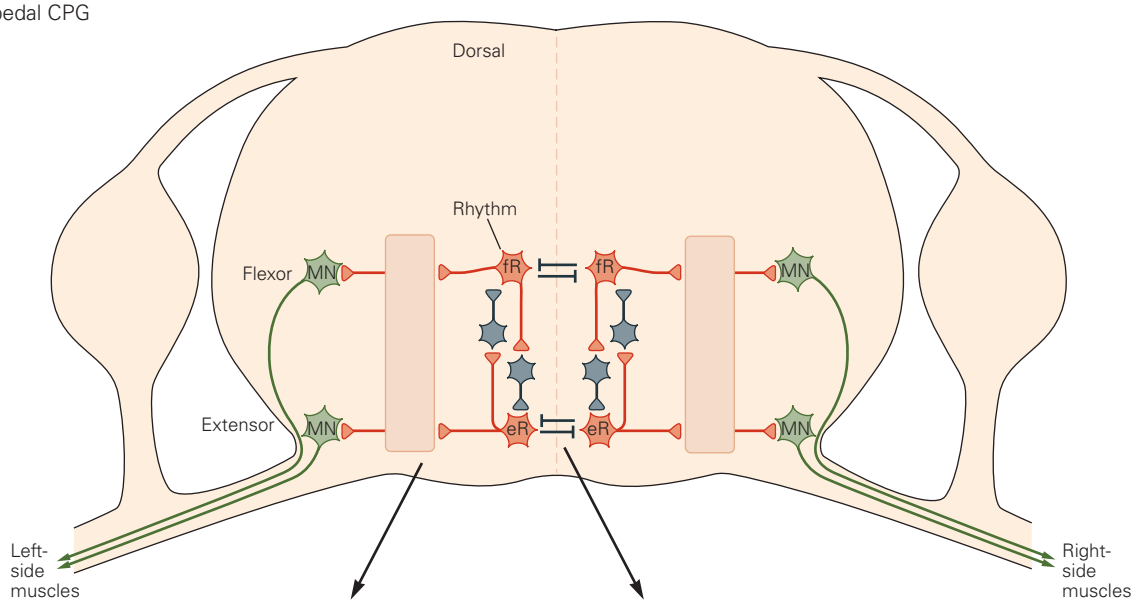

1 Flexor and extensor coordination

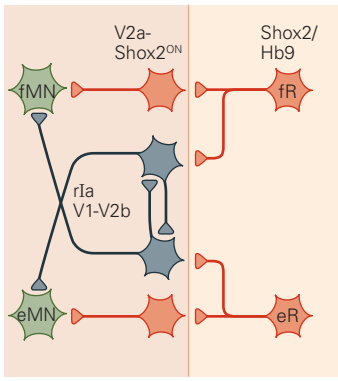

2 Left–right coordination

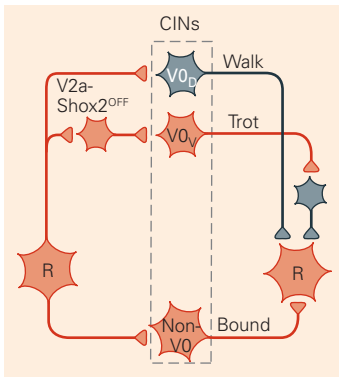

Interlimb Coordination

The organization of the networks that couple fore- and hindlimbs is not known in detail, but experiments using both lesion and genetic ablation suggest that these pathways involve both inhibitory and excitatory intersegmental connections.

Somatosensory Inputs From Moving Limbs Modulate Locomotion

Even though the CPG can produce the precise timing and phasing of the muscle activity needed to walk, this central pattern is normally modulated by sensory signals from the moving limbs. Two types of sensory input modulate the CPG activity: proprioceptive information generated by the active movement of the limb and tactile information generated when the moving limb meets an obstacle in the surrounding environment.

Proprioception Regulates the Timing and Amplitude of Stepping

One of the clearest indications that somatosensory signals from moving limbs regulate the locomotor cycle is that the rate of locomotion in spinal and decerebrate cats matches the speed of the motorized treadmill belt on which they walk. As the stepping rate increases, the stance phase becomes shorter while the swing phase remains relatively constant.

This observation suggests that some form of sensory input from the moving limb signals the end of the stance phase and thus leads to the initiation of the swing phase. The sensory information from the moving limb is generated by proprioceptors in the muscles and joints. These proprioceptors include stretch-sensitive muscle spindles in the hip and force-sensitive Golgi tendon organs in the ankle that are particularly important for facilitating locomotor phase transition.

The influence from the hip was noticed already by Sherrington, who showed that rapid extension at the hip joint leads to contractions in the hip flexor muscles of chronic spinal cats and dogs. More recent studies have found that preventing hip extension in a limb suppresses stepping in that limb, whereas rhythmically moving the hip in an immobilized cat can entrain the locomotor rhythm; that is, the stretching of the hip muscles causes the timing of the motor output to match the rhythm of the externally imposed movements (Figure 33–8A). The stretching also activates flexor muscle spindles and mimics the lengthening that occurs at the end of the stance phase, thus inhibiting extensor activity and facilitating activation of the flexor rhythm-generating circuits in the spinal cord (Figure 33–8B).

Activation of sensory fibers from Golgi tendon organs and muscle spindles in ankle extensor muscles prolongs the stance phase, often delaying the onset of

Figure 33–7 (Opposite) Spinal locomotor networks are organized into rhythm- and pattern-generation circuits with distinct cellular identities.

A. Circuit diagram of swimming central pattern generator (**CPG**) in the lamprey. Rhythm-generating circuits include excitatory interneurons (**EN**) that drive motor neurons (**MN**), inhibitory commissural interneurons (**CIN**) whose axons project to the other half of the cord, and local inhibitory interneurons (**IN**) with axons projecting on the same side of the cord. A single neuron in the diagram represents multiple neurons in the animal. **Gray neurons**, inhibitory; **red neurons**, excitatory. The vertical **dashed line** indicates the midline. (Data from Grillner 2006.)

B. General circuit diagram for limbed locomotion. Rhythm-generating circuits (**fR** and **eR**) composed of excitatory neurons on either side of the spinal cord drive flexor and extensor muscles on the same side through a pattern-generating layer (empty box). Rhythm-generating flexor (**fR**) and extensor (**eR**) neurons are reciprocally connected via inhibitory neurons and are connected across the midline via commissural interneurons (not shown) that mediate left–right coordination. The diagram shows one spinal segment. (Abbreviation: **MN**, motor neurons.) (Data from Kiehn 2016.)

B1. Flexor and extensor alternation is controlled at multiple levels in the locomotor network. One synapse away from flexor (**f**) and extensor (**e**) motor neurons (**MN**) are Ia-inhibitory interneurons, which reciprocally innervate antagonist motor neurons and each other (Chapter 32). The rIa neurons belong to two major groups of molecularly defined inhibitory neurons, V1 and V2b, in the ventral spinal cord. Excitatory neurons with different molecular markers (including V2a-Shox2^{ON}) provide premotor rhythmic excitation of motor neurons. Rhythm-generating Shox2^{ON} or Hb9 neurons (**fR** and **eR**) drive both inhibitory and excitatory premotor neurons. (Data from Kiehn 2016.)

B2. Rhythm-generating circuits drive left–right coordinating circuits composed of a dual inhibitory pathway involved in alternation and a single excitatory pathway involved in synchrony. The dual inhibitory pathway is composed of inhibitory $V0_D$ commissural neurons that directly inhibit rhythm generation on the other side and excitatory $V0_V$ commissural neurons that indirectly inhibit locomotor networks on the other side. The inhibitory $V0_D$ commissural neuron pathway controls the alternating gait walk. A population of V2a excitatory neurons is part of the left–right alternating circuit and connects to $V0_V$ commissural neurons. This pathway controls the alternating gait trot. Rhythm-generation circuits also drive a left–right synchronizing circuit possibly involved in bound, composed of non-V0 neurons. Only the projections from the left to the right side are shown. (Data from Kiehn 2016.)

Box 33–2 Neuronal Ion Channels Contribute to Central Pattern Generator Function

Neuronal membrane properties make an important contribution to the function of the central pattern generator (CPG). Neurons have a variety of K^+, Na^+, and Ca^{2+} channels that determine their activity and response to synaptic inputs. Studies of CPGs in diverse experimental models have shown that ion channels may be important for promoting rhythmicity, through bursting properties, or patterning, through ion channels that affect phase transitions or the rate of neuronal discharge.

Bursting and Plateau Properties Amplify Cellular Responses

Membrane properties that produce bursting allow cells to produce sustained oscillations in the absence of synaptic inputs. These properties are either intrinsic, as in cells in the sinusoidal node in the heart, or conditional, dependent on the presence of certain neurotransmitters. In some small motor CPGs (such as the pyloric network in the stomatogastric ganglion, which controls rhythmic movements in the gut of crustaceans), intrinsic bursting properties are essential for generating the rhythm.

Conditional bursting triggered by glutaminergic activation of *N*-methyl-D-aspartate (NMDA) receptors has been described in spinal cord interneurons and motor neurons in lamprey, rodents, and amphibians. In the lamprey, bursting due to NMDA receptor activation plays a role in generating swimming. In mammals, it is as yet uncertain whether NMDA receptor–induced bursting is essential for rhythm generation, although it may facilitate excitatory synaptic inputs in the circuit.

Plateau potential is another membrane property that may cause a neuron's membrane potential to jump to a depolarized state that will support action potential firing without further increase in the excitatory drive. Plateau properties amplify and prolong the effect of synaptic excitatory inputs and may promote rhythm generation and motor output. Plateau properties are generated by activation of slowly inactivating L-type Ca^{2+} channels or slowly inactivating Na^+ channels. These channels have been found in vertebrate interneurons and motor neurons. The expression of plateau properties mediated by L-type Ca^{2+} channels in motor neurons is controlled by neuromodulatory neurotransmitters, such as serotonin and norepinephrine. The slowly inactivating Na^+ channels are generally not regulated by neurotransmitters. Blockage of these channels decreases rhythm generation.

Phase Transitions May Be Regulated by Voltage-Gated Ion Channel Activation

Reciprocal inhibition between neurons is a common design in locomotor circuits; ion channels activated in the subthreshold spike range may enhance or delay phase transitions by such inhibition. Three types of voltage-gated channels are involved: a transient low threshold Ca^{2+} channel, cation-nonselective permeable hyperpolarization-activated cyclic nucleotide-gated (HCN) channels, and transient K^+ channels.

The transient low-threshold Ca^{2+} channels are inactivated at membrane potentials around rest. Transient inhibitory synaptic inputs remove the inactivation. When released from synaptic inhibition, activation of low-threshold Ca^{2+} channels will cause a short-lasting rebound excitation before the channels inactivate again. In the lamprey, spinal cord activation of metabotropic $GABA_B$ receptors depresses low-threshold Ca^{2+} channels involved in producing the swimming motor pattern. The suppression leads to a longer hyperpolarized phase and therefore to a slower alternation between antagonistic muscles, a possible mechanism for the slowing of swimming seen following $GABA_B$ receptor activation.

HCN channels are found in many CPG neurons and motor neurons and may help neurons escape from inhibition. They are activated by hyperpolarization, such as occurs during synaptic inhibition. Their activation depolarizes the cell, counteracting the hyperpolarization. Finally, the kinetics of their activation and deactivation are slow, so they stay open for some time after the hyperpolarization is released. The channel kinetics affect the integrative properties of the cell in two important ways. First, the depolarization caused by the channel opening limits the effect of sustained inhibitory inputs and helps the cell escape from inhibition. Second, the slow closing following synaptic inhibition leads to a rebound excitation promoting the next burst.

Voltage-gated A-type transient K^+ channels are usually inactivated at resting membrane potential. Hyperpolarization removes the resting inactivation, and subsequent depolarization will cause a transient activation of the channel. Their activation will therefore delay the onset of the next burst.

Regulation of Spiking Controls How Much Cells Are Activated

A number of different ion channels play a role in regulating the firing rate of a cell. Activation and inactivation kinetics of Na^+ channels are factors. Other important channels are sodium- and calcium-activated K^+ channels. The effect of activation of these K^+ channels is often seen as a slow after-hyperpolarization following an action potential or a train of action potentials. Activation of these channels therefore causes spike train adaptation and postactivation inhibition, which contribute to burst termination.

Box 33–3 Molecular-Genetics Combined With Anatomical, Electrophysiological, and Behavioral Analyses Are Used to Unravel the Locomotor Network Organization

To unravel the functional organization of the large neuronal networks in the spinal cord, researchers have used molecular-genetic–driven network analysis to take advantage of a molecular code that determines the spatial layout of the spinal locomotor networks.

It has been well documented that motor neurons develop and differentiate according to a genetic code expressed in the embryonic spinal cord (Chapter 45). This feature extends also to the development of spinal interneurons, which can be identified by different transcription factors (Table 33–1). The cardinal classes of interneuronal types belong to dorsally located interneurons (dI1–dI6) and ventrally located interneurons (V0–V3), with further subdivision within these categories (eg, $V0_D$ and $V0_V$, V2a-Shox2^{Off}, V2a-Shox^{On}) where a combination of transcription factors defines these subtypes (Table 33–1). Each group of interneurons has specific transmitter content and characteristic axonal projection patterns.

The ability to manipulate these specific interneuron types gives an unparalleled opportunity to examine the functional contribution of specific subsets of interneurons in the mouse or zebrafish that is not possible in species such as the cat. The molecular code of the spinal cord neurons is used to mark cells with a marker protein such as green fluorescent protein or for the expression of proteins that allow for cell type-specific ablation or activation/inactivation of cells types. Such studies have ascribed specific locomotor functions to the dI3, V0–V3, and Hb9 cells, all molecularly differentiated classes of neurons (Table 33–1).

Table 33–1 Developmental Molecular Codes Specify the Identity of Spinal Neurons in the Spinal Cord

Postmitotic transcription factors	Neuron type	Transmitters
Islt1/Tlx3	dI3	Glutamate
Pax2/7	$V0_D$	GABA/glycine
Evx1	$V0_V$	Glutamate
Evx1/Pitx2	$V0_C$	Acetylcholine
Evx1/Pitx2	$V0_D$	Glutamate
En1	V1	GABA/glycine
Chx10	V2a-Shox2^{Off}	Glutamate
Chx10/Shox2	V2a-Shox2^{ON}	Glutamate
GATA2/3	V2b	GABA/glycine
Sox1	V2c	GABA/glycine
Shox2	V2d	Glutamate
Hb9/Islt1-2	MN	Acetylcholine
Hb9	Hb9	Glutamate
Sim1	$V3_D$	Glutamate
Sim1	$V3_V$	Glutamate

Chx10, Ceh-10 homeodomain-containing homolog; Evx1, even skipped homeobox 1; En1, engrailed 1; GABA, γ-aminobutyric acid; GATA2/3, gata protein; Hb9, homeobox 9; Islt1-2, ISL1-2 transcription factor; Pax, paired box gene; Pitx2, paired-like homeodomain transcription factor 2; Sim1, single-minded homolog 1; MN, motor neuron; Shox2, Short stature homeobox 2; Sox1, SRY box-containing gene 1; Tlx1/3, T cell leukemia, homeobox 1/3.
Source: Adapted from Jessell 2000, Goulding 2009, Dougherty et al. 2013.

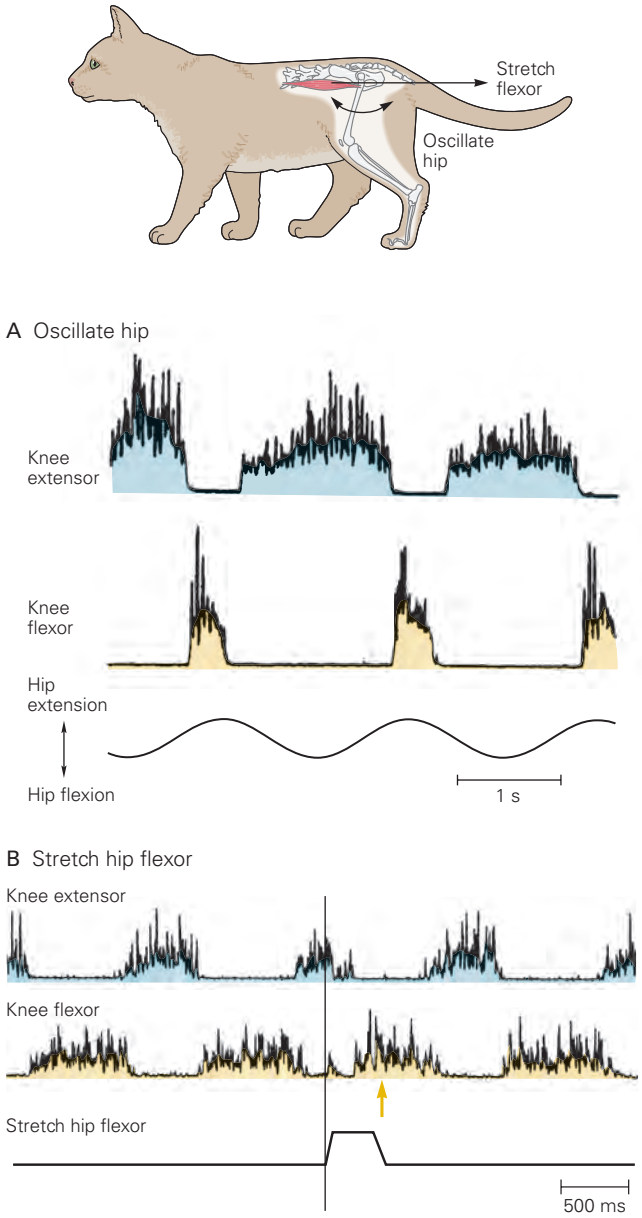

Figure 33–8 Hip extension initiates the transition from stance to swing phase of walking.

A. In an immobilized decerebrate cat, passive oscillating movement around the hip joint initiates and entrains the fictive locomotor pattern in knee extensor and flexor motor neurons. The flexor electromyogram (EMG) bursts correspond to the swing phase and are generated when the hip is extended. (Adapted, with permission, from Kriellaars et al. 1994.)

B. In a walking decerebrate cat, stretching of the hip flexor muscle (iliopsoas) inhibits knee extensor EMG activity, allowing knee flexor activity to begin earlier. The **arrow** in the knee flexor record indicates when activity in the muscle would have begun had the hip flexor muscle not been stretched. Activation of sensory fibers from muscle spindles in the hip flexor muscle is responsible for this effect. (Adapted, with permission, from Hiebert et al. 1996.)

the swing phase until the stimulus has ended (Figure 33–9A). Sensory fibers from both types of receptors are active during stance, with the intensity of the signal from the Golgi tendon organs being strongly related to the load carried by the leg. Golgi tendon organs have inhibitory actions on ankle extensor motor neurons when the body is at rest (Chapter 32) but an excitatory action during walking. This reversal of the sign of the reflex is caused by inhibition of inhibitory interneuron pathways together with a release of excitatory pathways during locomotion. The functional consequence of this reflex reversal during locomotion is that the swing phase is not initiated until the extensor muscles are unloaded and the forces exerted by these muscles are low, as signaled by a decrease in activity from the Golgi tendon organs near the end of stance.

In sum, proprioceptive signals from the ankle extensor muscles and hip flexor muscles work synergistically to facilitate the stance-to-swing phase transition. In the late stance phase, when the limb is unloaded, as inhibitory signals from Golgi tendon organs wane, their effects on extensor rhythm generation declines, while at the same time the activity in muscle afferents around the hip joint is increased, facilitating activity in flexor rhythm generation.

At least three excitatory pathways transmit sensory information from extensor muscles to extensor motor neurons during walking: a monosynaptic pathway from primary muscle spindles (group Ia afferents), a disynaptic pathway from primary muscle spindles and Golgi tendon organs (group Ia and Ib afferents), and a polysynaptic pathway from primary muscle spindles and Golgi tendon organs that includes interneurons in the extensor rhythm generator (Figure 33–9B). These pathways all contribute to phase transition from stance to swing when the ankle is unloaded and maintain extensors in stance phase when the ankle is loaded.

In addition to regulating the transition from stance to swing, proprioceptive information from muscle spindles and Golgi tendon organs contributes significantly to the generation of burst activity in extensor motor neurons. Reducing this sensory input in cats diminishes the level of extensor activity by more than half; in humans, it has been estimated that up to 30% of the activity of ankle extensor motor neurons is caused by feedback from the extensor muscles.

Mechanoreceptors in the Skin Allow Stepping to Adjust to Unexpected Obstacles

Mechanoreceptors in the skin, including some nociceptors, have a powerful influence on the CPG for

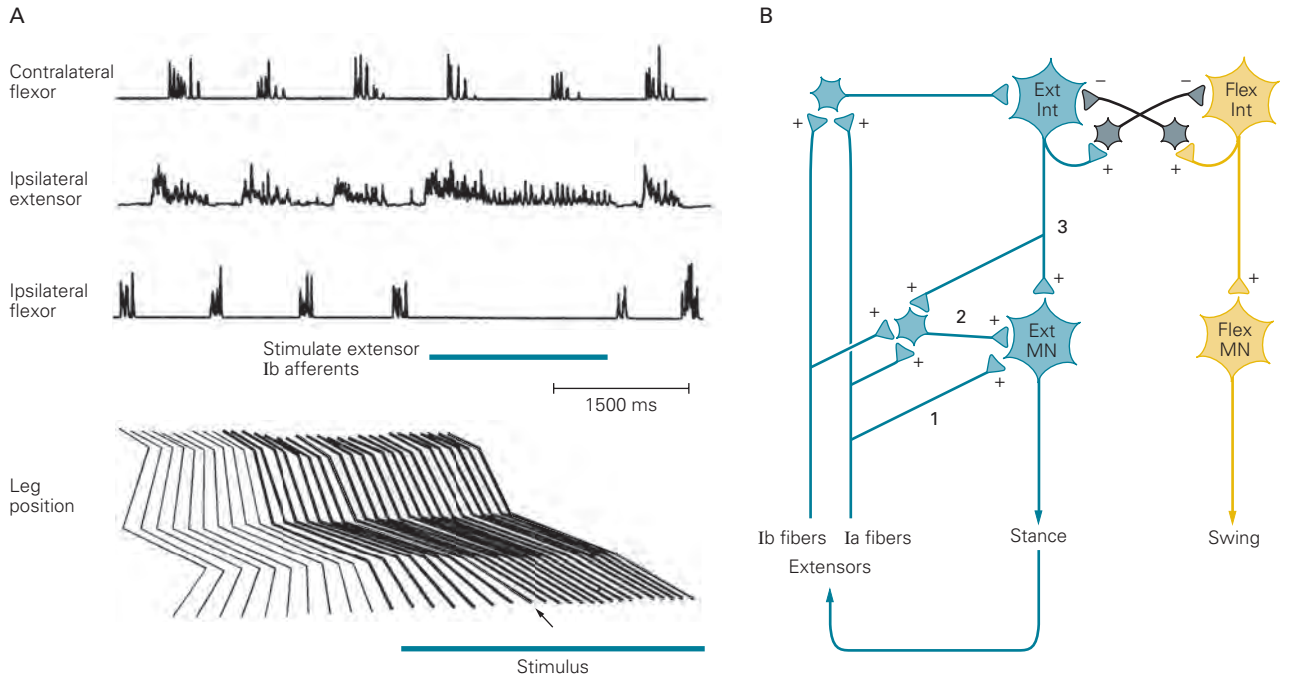

Figure 33–9 The swing phase of walking is initiated by sensory feedback from extensor muscles.

A. In a decerebrate cat, electrical stimulation of group I sensory fibers from ankle extensor muscles inhibits the electromyogram burst in ipsilateral flexors and prolongs the burst in the ipsilateral extensors during walking. The timing of contralateral flexor activity is not altered. Stimulating group I fibers from ankle extensors prevents initiation of the swing phase, as can be seen in the position of the leg during the time the fibers were stimulated. The **arrow** shows the point at which the swing phase would normally have occurred had the ankle extensor afferents not been stimulated. (Adapted, with permission, from Whelan, Hiebert, and Pearson 1995. Copyright © Springer-Verlag 1995.)

B. Mutually inhibiting groups of extensor (**Ext**) and flexor (**Flex**) interneurons (**Int**) constitute a rhythm generator in the afferent pathway regulating the stance phase. Feedback from extensor muscles increases the level of activity in extensor motor neurons (**MN**) during the stance phase and maintains extensor activity when the extensor muscles are loaded. The feedback is relayed through three excitatory (**+**) pathways: (**1**) monosynaptic connections from Ia fibers to extensor motor neurons; (**2**) disynaptic connections from Ia and Ib fibers to extensor motor neurons; and (**3**) polysynaptic excitatory pathways that act through the extensor rhythm generator to maintain the extensor motor neurons active in stance phase.

walking. One important function of these receptors is to detect obstacles and adjust stepping movements to avoid them. A well-studied example is the corrective reaction to stumbling in cats.

A mild mechanical stimulus applied to the dorsal part of the paw during the swing phase produces excitation of flexor motor neurons and inhibition of extensor motor neurons, leading to rapid flexion of the paw away from the stimulus and elevation of the leg in an attempt to step over the object. Because this corrective response is readily observed in spinal cats, it must be produced to a large extent by circuits entirely contained within the spinal cord.

One of the interesting features of the corrective reaction is that corrective flexion movements are produced only if the paw is stimulated during the swing phase. An identical stimulus applied during the stance phase produces the opposite response—excitation of extensor muscles that reinforces the ongoing extensor activity. This extensor action is appropriate; if a flexion reflex were produced during the stance phase, the animal might collapse because it is being supported by the limb. This is an example of a phase-dependent reflex reversal. The same stimulus can excite one group of motor neurons during one phase of locomotion while activating the antagonist motor neurons during another phase.

Supraspinal Structures Are Responsible for Initiation and Adaptive Control of Stepping

Although the basic motor patterns for locomotion are generated in the spinal cord, the initiation, selection, and planning of locomotion require activation

of supraspinal structures, including the brain stem, the basal ganglia, cerebellum, and cerebral cortex. Supraspinal regulation of stepping provides a number of behavioral modifications that cannot be mediated by spinal circuits alone. These include the voluntary initiation of locomotion and the regulation of speed; postural regulation, including weight support, balance, and interlimb coordination; and the planning and execution of anticipatory modifications of gait, particularly visually guided modifications.

Midbrain Nuclei Initiate and Maintain Locomotion and Control Speed

The locomotor networks in the spinal cord require a command or start signal from supraspinal regions to initiate and maintain their activity. The major neuronal structure involved in the initiation in vertebrates is a region in the midbrain called the mesencephalic locomotor region (MLR). The MLR was first identified in cats as a unitary region localized in or around the cuneiform nucleus, just below the inferior colliculus. Tonic electrical stimulation in this area in the resting animal increased postural tonus so that the animal stood up and then started to walk. As the intensity of stimulation rose, the speed of locomotion increased and alternating gaits switched to synchronous gaits such as gallop or bound (Figure 33–10).

Later studies with electrical stimulation confirmed the presence of the MLR in all vertebrates, suggesting that the MLR is evolutionarily conserved from the oldest vertebrates to humans. These studies have pointed to two midbrain structures as part of the MLR (Figure 33–11A): the cuneiform nucleus (CNF) and the more ventrally located pedunculopontine nucleus (PPN) (Figure 33–11A). These two nuclei differ in the types of neurons they contain.

Long-range projection neurons in the CNF are excitatory and use glutamate as their neurotransmitter, whereas those in the PPN are both glutamatergic and cholinergic. In both nuclei, the excitatory neurons are intermingled with local GABAergic interneurons. Electrical stimulation has, however, been unable to determine which nucleus or which types of neurons are involved in the initiation of locomotion and speed control. However, the use of selective activation and inactivation of neurotransmitter-specific CNF and PPN neurons suggests that the two nuclei play specific roles in speed control and gait selection of locomotion (Figure 33–11B). Glutamatergic neurons in both PPN and CNF are sufficient for supporting alternating locomotion at slower speeds, such as walking and trot, while glutamatergic neurons in the CNF are necessary for high-speed locomotion, such as gallop and bound, characteristic of escape locomotion. Expression of these gaits is dependent on the stimulation frequency, possibly reflecting the effect of firing frequency in the intact animal.

The role of cholinergic PPN neurons for locomotion is less well understood. In mammals, they do not seem to have a strong role in maintaining locomotion.

These roles of glutamatergic CNF and PPN neurons in locomotor control may also be reflected in the different inputs. PPN neurons receive strong input from the basal ganglia, specifically the substantia nigra pars reticulata, globus pallidus pars interna, and subthalamic nucleus, as well as from sensorimotor and frontal cortex. Additionally, the PPN receives sensorimotor information from many nuclei in the midbrain and brain stem. The nucleus may therefore serve as a hub for integrating information from many brain structures, possibly leading to the release of slower exploratory locomotion. In contrast, the input to neurons in CNF is much more restricted and arises principally from structures that may be involved in escape responses. The MLR is therefore composed of two regions that act together to select context-dependent locomotor behavior.

Another brain area that evokes locomotion when stimulated is the subthalamic (or diencephalic) locomotor region (to be distinguished from the subthalamic nucleus). This region includes nuclei in the dorsal and lateral hypothalamus involved in various homeostatic features such as regulating feeding. Neurons in these areas project to neurons in the reticular formation and bypass the PPN and CNF, suggesting a parallel pathway for initiating locomotion, possibly driven by the need to find food.

Midbrain Nuclei That Initiate Locomotion Project to Brain Stem Neurons

The excitatory signals from CNF and PPN are relayed indirectly to the spinal cord by way of neurons in the brain stem reticular formation, which provide the final command signal to the locomotor networks in the spinal cord. The identity of these neurons is only partly known. In general terms, two transmitter-defined pathways are involved: glutamatergic and serotonergic.

The glutamatergic locomotor pathways probably have multiple origins in the brain stem reticular formation, forming parallel descending pathways. They project directly or indirectly via a chain of intersegmental (propriospinal) glutamatergic interneurons to locomotor neurons in the spinal cord (Figure 33–10A). Reticulospinal neurons also participate in regulating

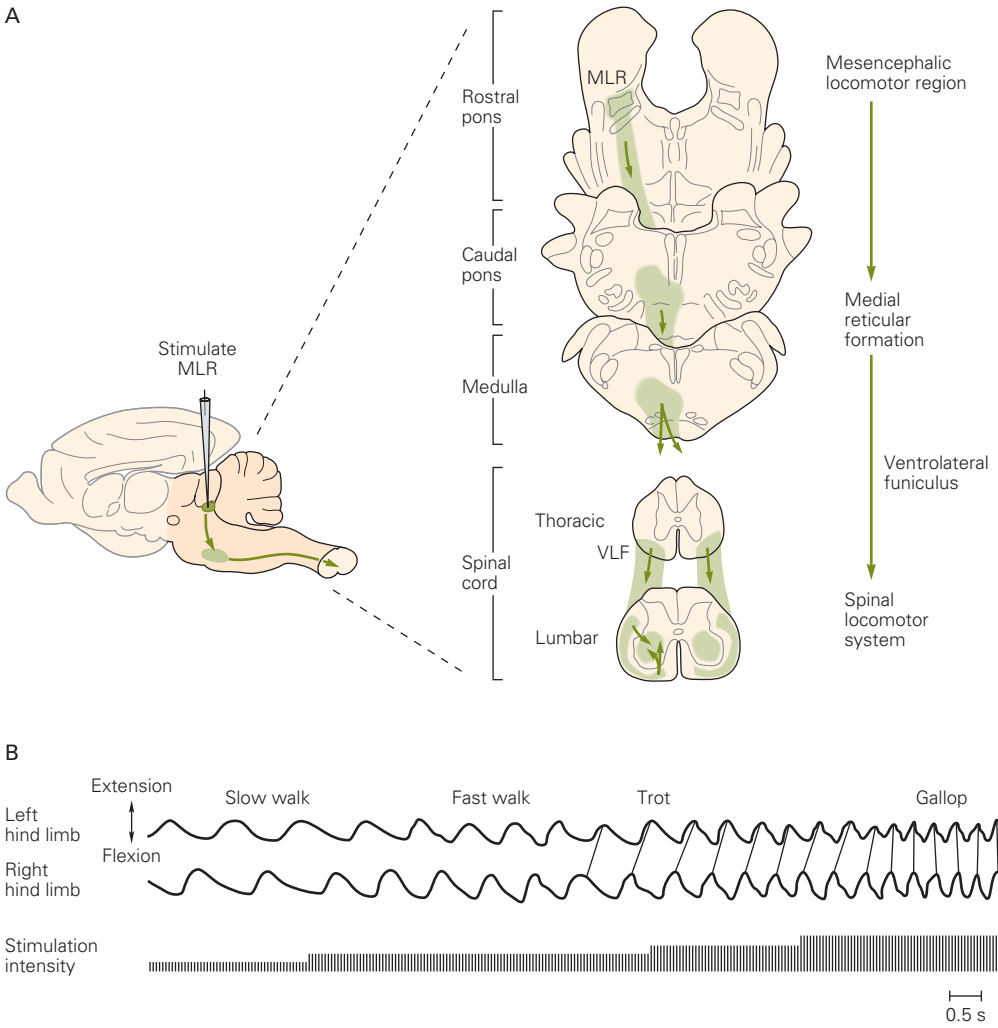

Figure 33–10 The mesencephalic locomotor region initiates locomotion.

A. Electrical stimulation of the mesencephalic locomotor region (MLR) in the cat initiates locomotion by activating neurons in the medial reticular formation whose axons descend in the ventrolateral funiculus (VLF) to the spinal locomotor system.

B. When the strength of electrical stimulation of the MLR in a decerebrate cat walking on a treadmill is gradually increased, the gait and rate of stepping change from slow walking to trotting and finally to galloping. As the cat progresses from trotting to galloping, the hind limbs shift from alternating to in-phase activity. (Adapted from Shik et al. 1966.)

the postural activity that is needed for the animal to locomote (see later discussion).

Evidence for the existence of a serotonergic locomotor pathway in mammals is restricted to experiments in rats that have shown the involvement of serotonergic neurons in the caudal brain stem. The mechanisms by which the final command signals from the brain stem to the spinal cord activate the spinal locomotor networks, maintain their activity, and allow the expression of different gaits are unknown.

The episodic nature of locomotion indicates that the initiating signals may be complemented by stop commands to allow for sudden locomotor arrest. Such signals have been found in *Xenopus* tadpole, in which head contact with obstacles activates GABAergic descending pathways that immediately terminate swimming. Likewise, in decerebrate cats, tonic electrical stimulation of the medullary and caudal pontine reticular formation leads to a general motor inhibition. Studies in mice have identified a restricted contingent of V2a neurons in the reticular formation that mediate an immediate arrest of ongoing locomotor activity. Such "V2a stop neurons" send a behaviorally relevant stop signal via descending projections to inhibitory

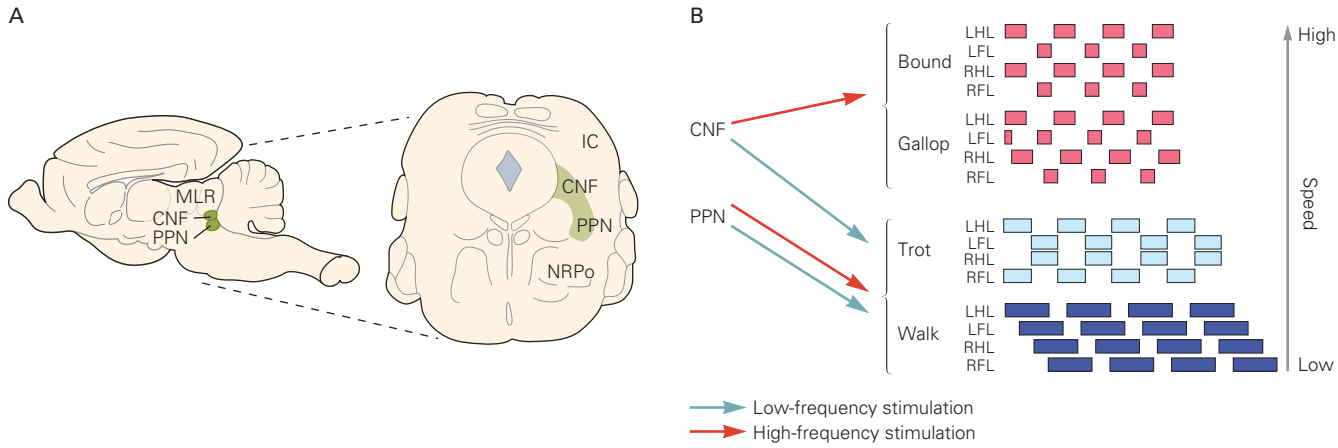

Figure 33–11 The mesencephalic locomotor region is composed of dual midbrain glutamatergic nuclei that control initiation of locomotion, speed and gait regulation, and context-dependent selection of locomotion.

A. *Left*: The site of the localization of mesencephalic locomotor region (**MLR**) in the midbrain of the mouse. *Right:* Transverse section shows that the MLR is composed of the cuneiform nucleus (**CNF**) and the pedunculopontine nucleus (**PPN**) in the midbrain, lateral to the cerebral aqueduct, and dorsal to the nucleus reticularis pontis oralis (**NRPo**). Glutamatergic, GABAergic, and cholinergic neurons are intermingled in the CNF and PPN. (Abbreviation: **IC**, inferior colliculus).

B. Effect in mice of optical stimulation of glutamatergic cells in the CNF or PPN that have been transfected with the light-sensitive channel, channelrhodopsin 2. Stimulation at low and high frequencies in the PPN leads only to alternating gaits—walking and trotting. Low-frequency simulation in the CNF likewise results only in slow, exploratory locomotion, while high-frequency stimulation evokes the synchronous gaits gallop and bound corresponding to escape locomotion.

The different types of gaits are shown as idealized diagrams from low to high speeds of locomotion. Filled boxes represent the stance phase; open spaces the swing phase. Walk is characterized by periods of support by three or four feet simultaneously. Trot is characterized by simultaneous activity in the diagonal fore and hindlimbs. Gallop is characterized by the forelimbs moving slightly out of phase and hind limbs being almost in phase. Bound is characterized by hind limbs and forelimbs moving simultaneously and forelimb and hindlimb out of phase. (Abbreviations: **LFL**, left forelimb; **LHL**, left hindlimb; **RFL**, right forelimb; **RHL**, right hindlimb.) (Adapted from data in Caggiano et al. 2018.)

interneurons in the ventral lumbar spinal cord that inhibits rhythm generation. A similar stop signal arrests swimming in the lamprey.

The Brain Stem Nuclei Regulate Posture During Locomotion

An important aspect of locomotor control is the regulation of posture. This general term encompasses several types of behavior, including the production of the postural support on which locomotion is superimposed, the control of balance, the regulation of interlimb coordination in quadrupeds, and the modification of muscle tonus required to adapt to locomotion on slopes or during turning. In addition, anticipatory changes in posture precede changes in voluntary gait modifications, and compensatory changes in posture follow unexpected perturbations. These functions are largely subserved by two descending systems originating from the brain stem: the vestibulospinal tract (VST), originating in the lateral vestibular nucleus (LVN), and the reticulospinal tract (RST), originating in the pontomedullary reticular formation (PMRF). Both pathways are phylogenetically old and found in all vertebrates.

Lesions of the LVN, the PMRF, or their descending axons in the spinal cord lead to a loss of weight support and the control of equilibrium, expressed as a crouched gait and swaying of the hindquarters to one side or the other. Lesions of these nuclei are also followed by large changes in the interlimb coordination between the fore- and hindlimbs. Likewise, tonic electrical or chemical stimulation of the pons and the medulla modulates the level of muscle tonus in the limbs and can either facilitate or suppress locomotion depending on the exact site stimulated (Figure 33–12).

Activity in the VST and RST, together with activity in the rubrospinal tract, which originates from the red nucleus, also phasically modifies the level of muscle tonus during each step. Weak electrical stimulation of any of these three structures produces phase-dependent modulation of locomotor activity. Brief activation of these pathways with short trains of stimuli produces

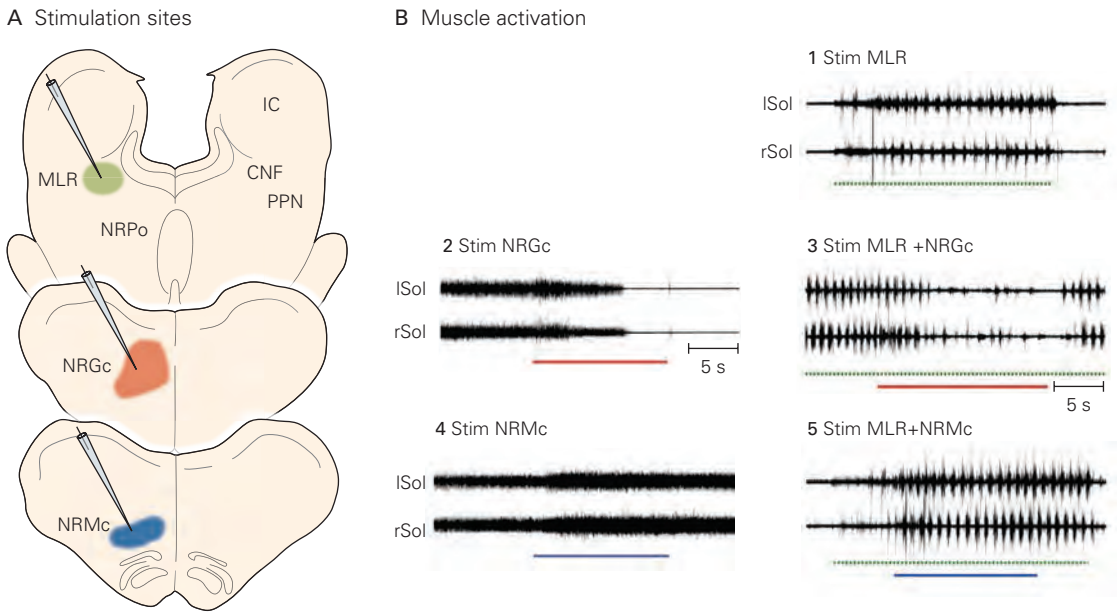

Figure 33–12 Locomotor activity is modified by the level of postural tone. (Adapted, with permission, from Takakusaki et al. 2016.)

A. Transverse sections of the brain stem of the cat at three different rostrocaudal levels. Colored areas indicate the regions stimulated during the trials shown in part **B**. (Abbreviations: **CNF**, cuneiform nucleus; **IC**, inferior colliculus; **MLR**, mesencephalic locomotor region; **NRPo**, nucleus reticularis pontis oralis; **NRGc**, nucleus reticularis gigantocellularis; **NRMc**, nucleus reticularis magnocellularis; **PPN**, pedunculopontine nucleus.)

B. Effects of stimulating the different regions of the brain stem indicated in part **A** in the decerebrate cat.

1. Stimulation of the MLR (CNF/PPN) (**green bar**) produces rhythmic activation in the left and right hindlimb extensor soleus muscles (**Sol**).

2. Tonic stimulation of the NRGc (**red bar**) in the medulla results in a loss of muscle tone in the extensor muscles.

3. Stimulation of the NRGc during CNF-induced locomotion reduces muscle tone and thereby inhibits locomotion.

4. Tonic stimulation of the NRMc (**blue bar**) in the ventral medulla produces an increase in muscle tone.

5. Stimulation of the NRMc during MLR stimulation results in increased vigor of locomotion.

transient changes in the amplitude of the muscle bursts but rarely produces any changes in the timing of the step cycle. Activation of the LVN primarily enhances responses in ipsilateral extensor muscles during their natural period of activity in the stance phase. In contrast, stimulation of the red nucleus generally produces transient increases in activity in contralateral flexor muscles, again during their natural period of activity in the swing phase.

Stimulation of the PMRF produces more complex and widespread responses that may modify activity in flexor muscles during the swing phase and in extensor muscles during the stance phase across all four limbs in a coordinated pattern (Figure 33–13). In flexor muscles, activity is generally facilitated by PMRF stimulation, but in extensor muscles, it may be facilitated or suppressed depending on the exact site stimulated. This phase-dependent nature of the responses is thought to be mediated by activation of interneurons in the spinal CPG. Stimulation of these three structures at higher strengths, or with longer trains, may produce changes in the timing of the step cycle as well as in the magnitude of EMG activity.

During locomotion, neurons within the LVN, PMRF, and red nucleus are phasically modulated at the frequency of the step cycle. Neurons in the LVN are generally activated in phase with ipsilateral extensor muscles, whereas neurons in the red nucleus are generally active during the contralateral swing phase. Neurons in the PMRF have more complicated periods of activity and may discharge in relation to ipsilateral or contralateral flexor or extensor muscles.

Brain stem structures also contribute to more complex activities during locomotion. For example, the red nucleus contributes to the complex modifications in muscle activity required for precise modifications of

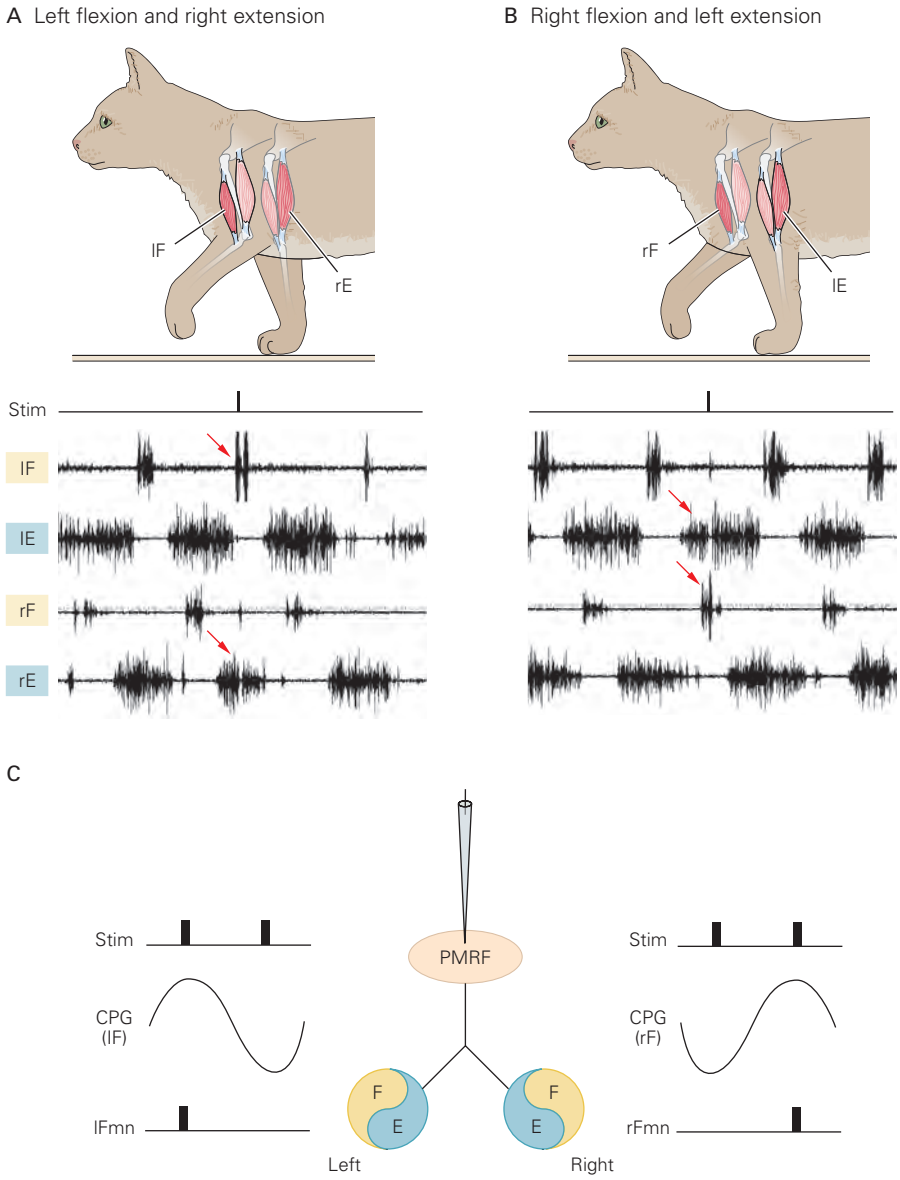

Figure 33–13 Microstimulation of the pontomedullary reticular formation (PMRF) produces phase-dependent responses in flexor and extensor muscles. (Data from T. Drew.)

A. Stimulation of the left PMRF during the swing phase of the left limb produces a transient increase in the electromyogram activity of the left flexor muscles (**IF**) and a simultaneous decrease in activity in the right extensor muscles (**rE**) (**red arrows**). There is little stimulus-evoked activity in the left extensor (**lE**) or right flexor (**rF**) muscles, which are inactive at this phase of the step cycle.

B. Stimulation at the same location in the PMRF during the swing phase of the right limb produces the inverse responses.

C. The phase-dependent nature of the responses is likely determined by the cyclical nature of the level of excitability in interneurons that are part of the locomotor central pattern generator (**CPG**). Responses are gated by activity in the flexor (**F**) and extensor (**E**) parts of the locomotor CPG. When the first stimulation arrives, flexor interneurons in the left CPG (**lF**) are active, whereas those in the right CPG (**rF**) are inactive. The stimulation therefore produces a response only in the left flexor motor neurons (**lFmn**). When the second stimulation arrives, flexor interneurons in the right CPG (**rF**) are active, whereas those on the left side are inactive, and therefore, the stimulation elicits a response only in the flexor motor neurons on the right (**rFmn**).

gait (see below). In a complementary manner, the widespread effects of the PMRF on multiple limbs allow it to produce the coordinated changes in postural activity that accompany gait modifications. The coordination between gait modifications and postural activity is assured by the strong connections from the motor cortex to the PMRF in the same manner as for discrete voluntary movements (Chapter 34). The PMRF also contributes to the compensatory changes in posture that occur as a consequence of perturbations. In this situation, it forms part of a spino-bulbo-spinal reflex that contributes to the widespread postural responses that follow the immediate spinal reflexes activated by a sudden perturbation.

Visually Guided Locomotion Involves the Motor Cortex

Walking is most often guided by vision, and the motor cortex is largely essential for visually guided movement, especially when gait must be modified to ensure precise control over limb trajectory and foot placement. In mammals, lesions of the motor cortex do not

prevent animals from walking on a smooth floor, but they severely impair "precision locomotion," which requires a high degree of visuomotor coordination, such as walking on the rungs of a horizontal ladder, stepping over a series of barriers, and stepping over single objects placed on a treadmill belt.

Experiments in intact cats trained to step over obstacles attached to a moving treadmill belt show that precision locomotion is associated with considerable modulation of the activity of numerous neurons in the motor cortex (Figure 33–14). Other neurons in the motor cortex show a more discrete pattern of activity and are activated sequentially during different parts of the swing phase. The activity of these cortical neurons correlates with the periods of modified muscle activity required to produce the gait modifications in a similar manner to what occurs during reaching (see Figure 34–21). Such subpopulations of neurons may serve to modify the activity of the groups of synergistic muscles required to produce flexible changes in limb trajectory.

Many of these cortical neurons project directly to the spinal cord (corticospinal neurons) and thus may regulate the activity of spinal interneurons, including those within the CPG, thereby adapting the timing and magnitude of motor activity to a specific locomotor task. Brief trains of electrical stimulation applied to either the motor cortex or the corticospinal tract in normal walking cats produce transient responses in the contralateral limb in a phase-dependent manner, similar to that produced by activity in various brain stem structures. However, in contrast to the situation

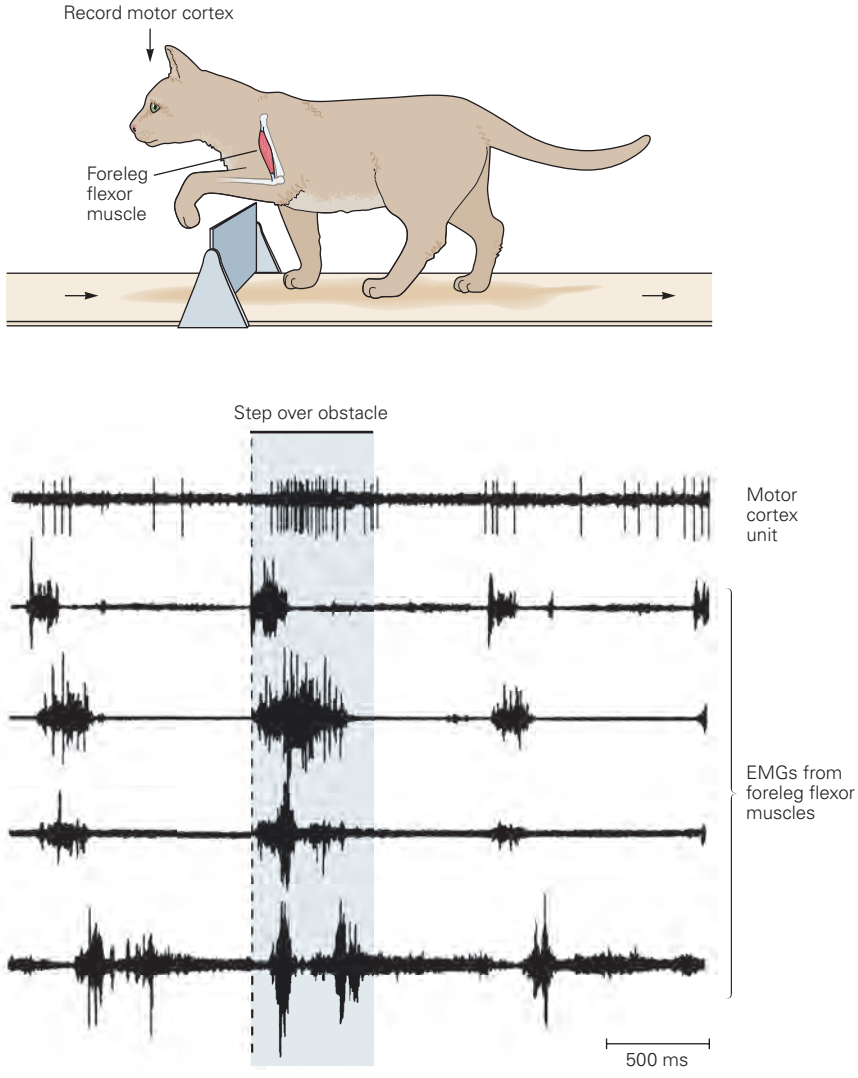

Figure 33–14 Stepping movements are adapted by the motor cortex in response to visual inputs. When a cat steps over a visible object fixed to a treadmill, neurons in the motor cortex increase in activity. This increase in cortical activity is associated with enhanced activity in foreleg muscles, as seen in the electromyograms (**EMG**). (Adapted, with permission, from Drew 1988.)

observed with brain stem structures, increasing the duration of the stimulation train applied to the motor cortex frequently results in a reset of the locomotor rhythm, characterized as an interruption of the ongoing step cycle and the initiation of a new step cycle. This suggests that in mammals the corticospinal tract has privileged access to the rhythm generator of the CPG.

Planning of Locomotion Involves the Posterior Parietal Cortex

When humans and animals approach an obstacle in their pathway, they must adjust their walking pattern to move around the obstacle or step over it. Planning of these adjustments begins two or three steps before the obstacle is reached. Recent experiments suggest that the posterior parietal cortex (PPC) is particularly involved in planning gait modifications. Lesions in this region cause walking cats to misplace the positioning of their paws as they approach an obstacle and increase the probability that one or more legs contact the obstacle as they step over it.

In contrast to what is observed in the motor cortex, recordings in PPC show that many neurons increase their activity in advance of the step over the obstacle. Moreover, many cells in the PPC discharge similarly regardless of which leg is first to step over the obstacle (Figure 33–15A,B). Such cells may provide an estimation of the position of the body with respect to objects in the environment (Figure 33–15B), allowing animals to modify gait as they approach the obstacle. The manner in which the PPC interacts with other cortical and subcortical structures generally considered to be involved in motor planning is unknown. However, recent work shows that the premotor cortex also makes an important contribution to planning visually guided gait modifications (Figure 33–15C) and may be implicated in the transformation of a global signal providing information concerning obstacle location to the muscle-based signal necessary for the execution of the step over the obstacle.

Visual information about the size and location of an obstacle is also stored in working memory, a form of short-term memory (Chapter 52). This information is used to ensure that gait modifications in the hindlimb are coordinated with those of the forelimb and is necessary because the obstacle is no longer within the visual field by the time the hindlimbs are stepping over it. The neurobiological mechanisms underlying this form of working memory remain to be established, but the persistence of the memory appears to depend, at least in part, on neuronal systems in the PPC. With bilateral lesions or cooling of the medial PPC, the memory is completely abolished (Figure 33–16A). Complementing this observation is the finding that the activity of some neurons in the PPC is elevated during a step over an obstacle, as well as throughout the time the animal straddles the obstacle (Figure 33–16B). This activity could represent the working memory of key features of the obstacle such as height.

The Cerebellum Regulates the Timing and Intensity of Descending Signals

Damage to the cerebellum results in marked abnormalities in locomotor movements, including the need for a widened base of support, impaired coordination of joints, and abnormal coupling between limbs during stepping. These symptoms, which are characteristic of *ataxia* (Chapter 37), indicate that the cerebellum contributes importantly to the regulation of locomotion.

A major function of the cerebellum is to correct movement based on a comparison of the motor signals sent to the spinal cord and the movement produced by that motor command (Chapter 37). In the context of locomotion, the motor signal is generated by neurons in the motor cortex and brain stem nuclei. Information about the movement comes from the ascending spinocerebellar pathways. For the hind legs of the cat, these are the dorsal and ventral spinocerebellar tracts. Neurons in the dorsal spinocerebellar tract (DSCT neurons) are strongly activated by numerous leg proprioceptors and thus provide the cerebellum with detailed information about the mechanical state of the hind legs. In contrast, neurons in the ventral tract (VSCT neurons) are activated primarily by interneurons in the CPG, thus providing the cerebellum with information about the state of the spinal locomotor network.

During locomotion, the motor command (the central efference copy), the movement (the afference copy, via the DSCT), and the state of the spinal networks (the spinal efference copy, via the VSCT) are integrated within the cerebellum and expressed as changes in the pattern of rhythmical discharge of Purkinje cells in the cerebellar cortex and neurons in the deep cerebellar nuclei. These signals from the deep cerebellar nuclei are then sent to the motor cortex and the various brain stem nuclei where they modulate descending signals to the spinal cord to correct any motor errors.

Behavioral experiments show that the cerebellum also plays an important role in the adaptation of gait. For example, when subjects walk on a split treadmill,

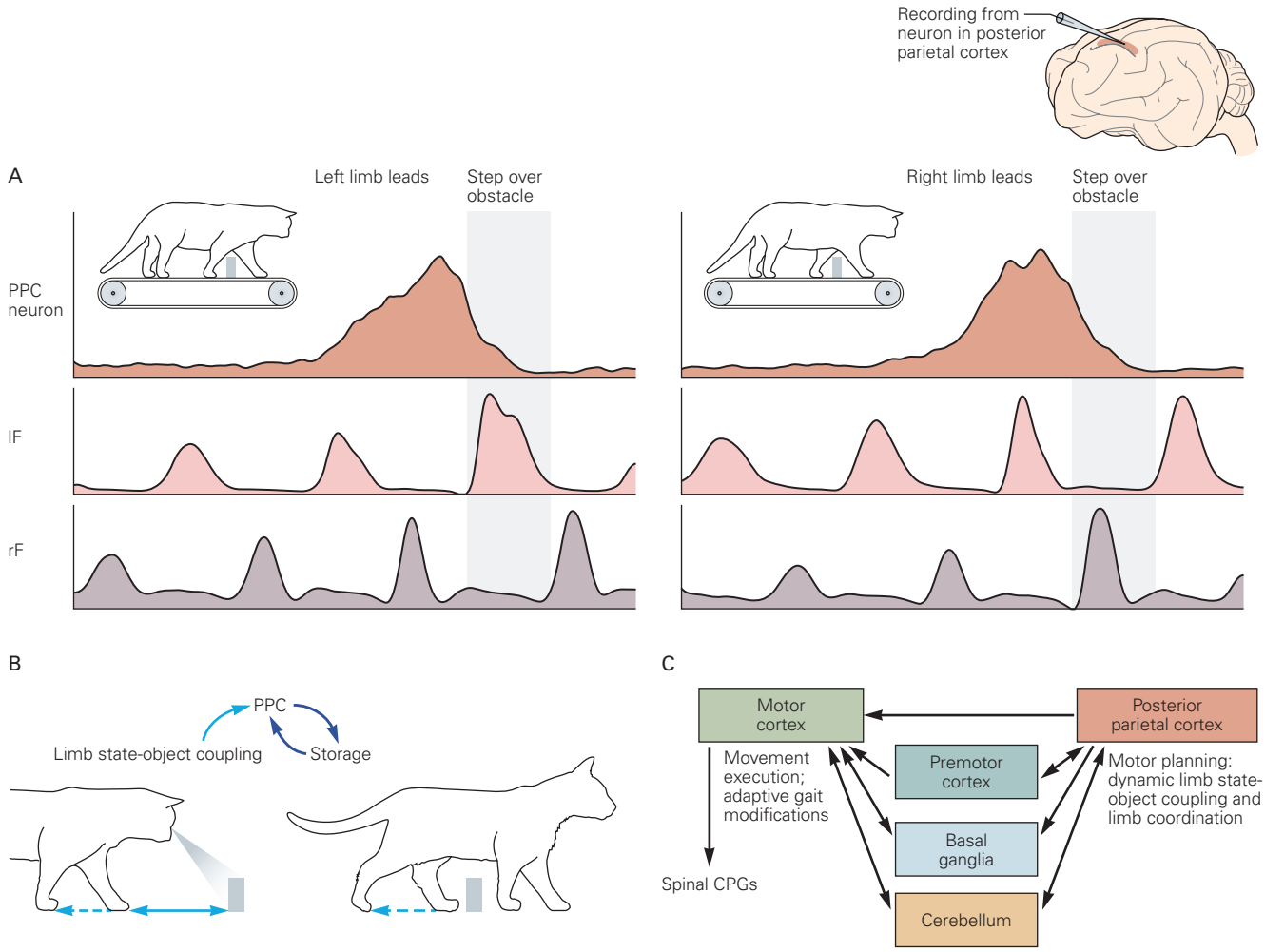

Figure 33–15 Neurons in the posterior parietal cortex (PPC) are involved in planning voluntary gait modifications.

A. Activity of a PPC neuron in the right cortex during a step over the obstacle when the left or right forelimb is the first to step over the obstacle. In each situation, the cell in the PPC discharges two to three steps in advance of the step over the obstacle.

B. The observation that PPC neurons discharge independent of which limb is the first to step over the obstacle suggests a global function of PPC in the planning of locomotion. In a general scheme, the PPC neurons are involved in the estimation of the relative location of an object with respect to the body (limb state–object coupling [**double arrow**]) and storage information in the PPC for later retrieval.

C. The PPC does not act alone in planning gait modifications. It is part of a cortical and subcortical network that includes, among other structures, the premotor cortex, the basal ganglia, and the cerebellum. Connections exist between each of these structures as well as between each of them and the motor cortex, which is responsible for the execution of the gait modification. (Abbreviation: **CPG**, central pattern generator.) (Adapted, with permission, from Drew and Marigold 2015.)

so that each leg walks at a different speed, they initially show a very asymmetric gait before adapting over time to a more asymmetric one. When the two treadmill belts are reset to the same speed, they again show an asymmetric gait, demonstrating that the experimental condition had produced adaptation (see Figure 30–13). Patients with damage to the cerebellum are not able to adapt to this condition.

The Basal Ganglia Modify Cortical and Brain Stem Circuits

The basal ganglia are found in all vertebrates from the oldest vertebrates to primates and probably contribute to the selection of different motor patterns. The importance of the basal ganglia to the control of locomotion is clearly demonstrated by the deficits in

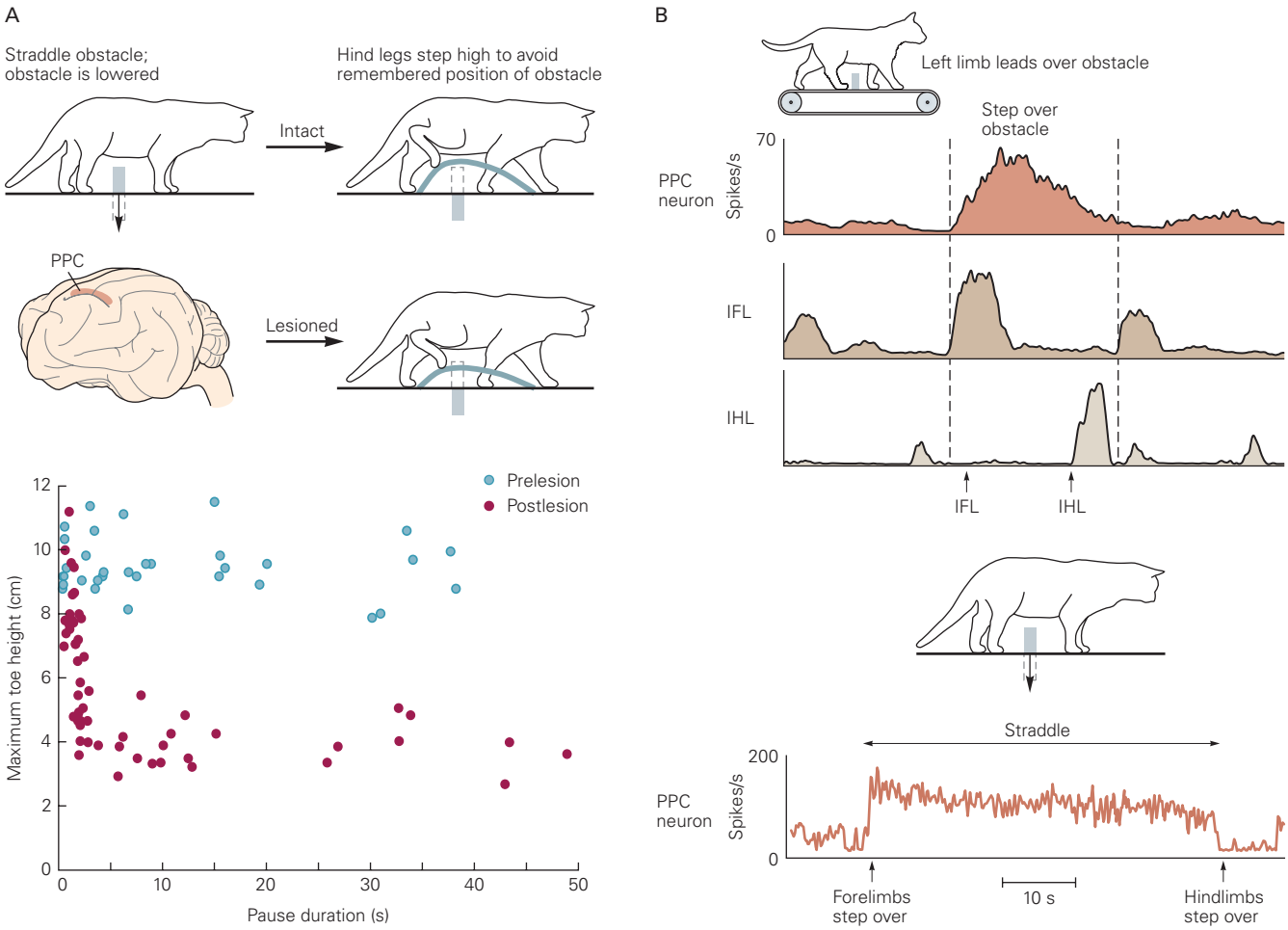

Figure 33–16 The posterior parietal cortex (PPC) is involved in maintaining an estimate of an obstacle in working memory during locomotion.

A. **Upper figure:** Normal animals were trained to walk forward, step over an obstacle, and then pause. While the animal paused, the obstacle was removed. When walking resumed, the hind legs stepped high to avoid the remembered obstacle. This memory lasted for more than 30 seconds. The trajectory of the hindlimbs was scaled appropriately for the height of the obstacle and for the relative position of the hind paws. Bilateral lesions of the PPC led to an impairment in the memory, making it impossible for the animal to pass the obstacle without hitting it. **Lower figure:** Following the lesion, animals stored the memory for only 1 to 2 seconds, and the maximum height of the toe was insufficient to clear the obstacle and was significantly lower than in the prelesion condition. (Adapted from McVea and Pearson 2009.)

B. **Upper figure:** Neurons recorded in an intact animal in the PPC on the right side discharged in the period between the passage of the left forelimb (**IFL**) and hindlimb (**IHL**) over an obstacle (represented by electromyogram activity from representative flexor muscles in each limb). This discharge may be used to coordinate the movement of the hindlimb with that of the forelimb during the visually guided gait modification. **Lower figure:** When the cat steps over an obstacle and pauses, as in part **A**, cells in the PPC show a maintained discharge that could provide the neural representation of the working memory. (Adapted, with permission, from Lajoie et al. 2010.)

locomotion observed in patients with Parkinson disease, which disrupts the normal functioning of the basal ganglia due to degradation of their dopaminergic inputs from the substantia nigra (Chapter 38).

Such patients show a characteristic slow, shuffling gait and, in later stages of the disease, can also show "freezing" of gait. Patients with Parkinson disease also show problems with balance during locomotion and with the anticipatory postural adjustments that occur at the initiation of a gait pattern. These deficits suggest that the basal ganglia contribute to the initiation, regulation, and modification of gait patterns. This regulation is mediated by the two major projections of the basal ganglia to the brain stem pathways and cortical structures.

The basal ganglia influence brain stem activity through their projections to the PPN. The PPN receives

inhibitory inputs from GABAergic inhibitory neurons in the substantia nigra pars reticulata (SNr) as well as from the globus pallidus pars interna (GPi); it also receives glutamatergic input from neurons in the subthalamic nucleus (STN). Decreased inhibitory input and increased glutamatergic input to PPN from the basal ganglia are thought to promote activity in PPN and favor exploratory locomotion. The STN and GPi are major targets of deep brain stimulation for improvement of motor symptoms such as rigidity and reduced mobility in patients with Parkinson disease.

The basal ganglia influence cortical activity by means of its connections via the thalamus to different parts of the frontal cortex, including the supplementary motor regions. These connections allow the basal ganglia to exert a modulatory effect on visually guided locomotion, possibly by selecting the appropriate motor patterns required in different behavioral situations.

Computational Neuroscience Provides Insights Into Locomotor Circuits

While functional studies have revealed much about the organization of the locomotor networks, their overall complexity makes it difficult to capture the integrative function of synaptic and cellular properties of the circuit. Computational network modeling, however, allows one to simulate the circuit activity and to investigate the dynamic interactions between the circuit elements. Computational models can be developed at many levels: to study the ionic basis of neural activity within a given circuit, to study the connectivity between different groups of neurons in a particular circuit, or to better understand the interactions between different structures in the locomotor network. Computational models at each of these levels have been developed to study rhythm and pattern generation in both invertebrates and vertebrates and in the latter, ranging from the lamprey to mammals. As in other domains, approaches combining experimental manipulation and computational modeling are likely to increase in the coming years and have the potential to advance our understanding of the complex systems and interconnections between structures that are required to produce the full locomotor repertoire.

Neuronal Control of Human Locomotion Is Similar to That of Quadrupeds

By necessity, most of our understanding of the neural mechanisms underlying the control of locomotion comes from experiments on quadrupedal animals. Nonetheless, the available evidence suggests that all the major principles concerning the origin and regulation of walking in quadrupeds also pertain to locomotion in humans. Although the issue of whether CPGs exist in humans remains contentious, several observations are compatible with the view that CPGs are important for human locomotion.

For example, observations of some patients with spinal cord injury parallel the findings from studies of spinal cats. Striking cases of patients with nearly complete transection of the spinal cord have shown uncontrollable, spontaneous, rhythmic movements of the legs when the hips were extended. This behavior closely parallels the rhythmic stepping movements in chronic spinal cats. Moreover, tonic electrical stimulation of the spinal cord below the injury can evoke locomotor-like activity, as in other mammals.

Parallels between human and quadrupedal walking have also been found in patients trained after spinal cord injury. Daily training combined with drug treatments restores stepping in spinal cats and improves stepping in patients with chronic spinal injuries. People with severe spinal cord injury who have been exposed to both treadmill-induced stepping and drug treatments similar to those that have been shown to activate the CPG in cats have demonstrated dramatic improvements in the ability to produce locomotion (Box 33–4). These results suggest that CPGs are present in humans and share functional similarities with CPGs found in other vertebrates.

Compelling evidence for the existence of spinal CPGs in humans also comes from studies in human infants who make rhythmic stepping movements immediately after birth if held upright and moved over a horizontal surface. This strongly suggests that some of the basic neuronal circuits for locomotion are innate and present at birth when descending control systems are not well developed. Because stepping can also occur in infants who lack cerebral hemispheres (*anencephaly*), these circuits must be located at or below the brain stem, perhaps entirely within the spinal cord.

During the first year of life, as automatic stepping is transformed into functional walking, these basic circuits are thought to be brought under supraspinal control. In particular, the stepping pattern gradually develops from a more primitive flexion-extension pattern that generates little effective forward movement to the mature pattern of complex movements. It is plausible, based on studies of cats, that this adaptation reflects maturation of descending systems that originate in the motor cortex and brain stem nuclei and are modulated by the cerebellum.

Box 33–4 Rehabilitative Training Improves Walking After Spinal Cord Injury in Humans

According to the World Health Organization, between 250,000 and 500,000 people worldwide incur spinal cords injuries annually. For many, this results in permanent loss of sensation, movement, and autonomic function. The devastating loss of functional abilities, together with the enormous cost of treatment and care, creates an urgent need for effective methods to repair the injured spinal cord and to facilitate functional recovery.

Over the past decades, progress has been made in animal research aimed at preventing secondary damage after injury, repairing the axons of lesioned neurons in the spinal cord, and promoting the regeneration of severed axons through and beyond the site of injury. In many instances, the regeneration of axons has been associated with modest recovery of locomotor function. However, none of the regeneration strategies has reached the point where they can be confidently used in humans with spinal cord injury.

Thus, rehabilitative training is the preferred treatment for people with spinal cord injury. One especially successful technique for enhancing walking in patients with partial damage to the spinal cord is repetitive, weight-supported stepping on a treadmill (Figure 33–17). This technique is based on the observation that spinal cats and rodents can be trained to step with their hind legs on a moving treadmill.

For humans, partial support of the body weight through a harness system is critical to the success of training; presumably, it facilitates the training of spinal cord circuits by reducing the requirements for supraspinal control of posture and balance.

Although the neural basis for the improvement in locomotor function with treadmill training has not been established, it is thought to depend on synaptic plasticity in local spinal circuits as well as successful transmission of at least some command signals from the brain through preserved descending pathways if the spinal cord injury is only partial.

Locomotor training is sometimes combined with other treatments. These include different types of medication designed to reduce spasticity, seen as involuntary muscle contractions, and facilitation of activity in spinal circuits by electrical transcutaneous activation of spinal circuits and/or activation of corticospinal pathways by transcranial magnetic stimulation.

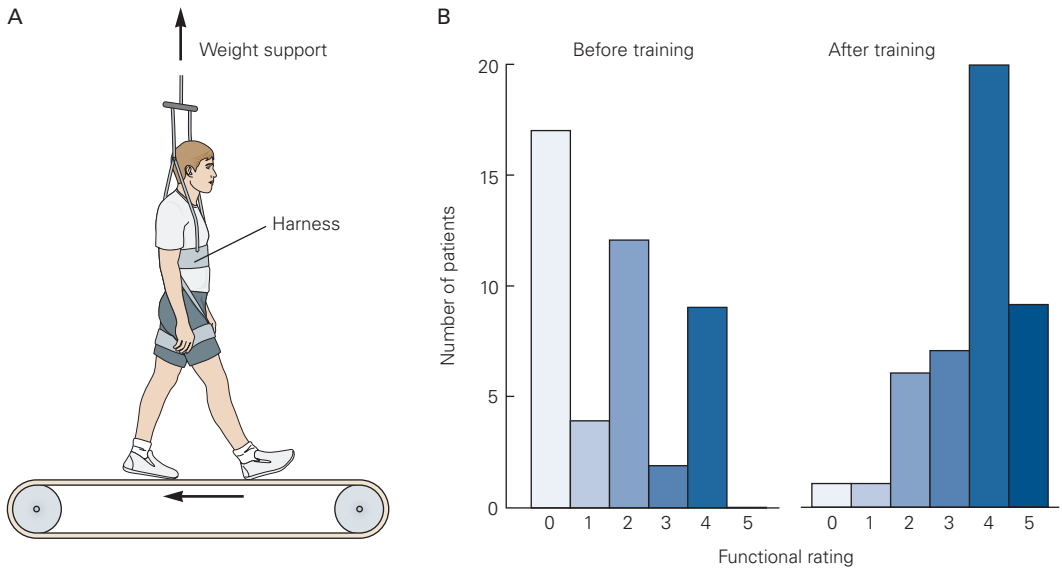

Figure 33–17 Treadmill training improves locomotor function in patients with partial spinal cord injury.

A. The patient is partially supported on a moving treadmill by a harness, and stepping movements are assisted by therapists.

B. Locomotor function improvement in 44 patients with chronic spinal cord injury after daily training lasting from 3 to 20 weeks. The functional rating ranges from 0 (unable to stand or walk) to 5 (walking without devices for more than five steps). (Adapted, with permission, from Wernig et al. 1995. Copyright © 2006, John Wiley and Sons.)

At the cortical level, stroke involving the motor cortex or damage to the corticospinal tracts leads to deficits in locomotion, as in cats. However, the deficits in humans are much stronger than in cats or even nonhuman primates, suggesting that the motor cortex in humans plays a more important role in locomotion than in other mammals. Studies using transcranial magnetic stimulation (TMS) to modulate motor cortical activity also show that the motor cortex contributes importantly to the control of human locomotion. TMS parameters that result in cortical inactivation, for example, produce a decrease in the level of muscle activity during locomotion. In contrast, TMS parameters that activate the motor cortex improve the recovery of locomotion following incomplete spinal cord injury.

Imaging studies, together with high-resolution electroencephalogram recordings, show changes in the activity of several cortical regions, including the motor cortex, premotor cortex, and PPC, during locomotion and particularly during imagined locomotion over obstacles. Imaging studies have also shown increased activity during locomotion in those parts of the midbrain shown to be important for the initiation and speed control of locomotion in animals. Similarly, neurons in the pedunculopontine nucleus can be affected in Parkinson disease, contributing to the severe gait disturbances seen in the late phase of the disease.

Highlights

1. Locomotion is a highly conserved behavior that is essential for the survival of the species. Our understanding of the neuronal mechanisms involved in the generation and control of locomotion came initially from the study of phylogenetically older animals, such as the lamprey and the tadpole. More recently, in mammals, with their more complex nervous systems, the organization of the different neural pathways involved in the generation and regulation of locomotion has also been determined in significant detail.
2. The spinal cord, in isolation from descending and rhythmical peripheral afferent inputs, can generate a complex locomotor pattern that contains elements of the rhythms and patterns observed in intact animals. The circuits responsible for producing this activity are referred to as central pattern generators (CPGs). Activity in spinal circuits can be modified by experience.
3. The basic components of CPGs controlling swimming are excitatory rhythm-generating neurons together with commissural inhibitory neurons responsible for left–right alternation. This organizational principle is also found in CPGs controlling limbed movements with the addition of flexor-extensor pattern-generating circuits and additional commissural neuronal networks. The circuits in the locomotor networks have a modular organization with distinct transmitter and molecular codes for the constituent neurons. Descending command signals act on these circuit elements to produce the diverse aspects of locomotor behavior.
4. Ionic membrane properties in interneurons and motor neurons contribute to rhythm and pattern generation. Cell-specific manipulation of these properties will enable a precise understanding of their relative contributions to locomotor production.
5. Peripheral afferent inputs modulate the function of spinal locomotor circuits. Proprioceptive sensors are used to stabilize phase transitions between stance and swing (and vice versa), whereas input from exteroceptors is used to modify limb activity in response to unexpected perturbations.
6. Circuits that are involved in initiating locomotion, controlling speed of locomotion, and selecting gaits are localized in the midbrain and encompass excitatory neurons in the pedunculopontine and cuneiform nuclei. These excitatory nuclei serve diverse roles in controlling either slow explorative locomotion or the full range of speeds and gaits including fast escape locomotion. Molecular-genetically driven cell-specific approaches allow unparalleled access to the organization of these pathways in the brain stem and how they integrate with spinal locomotor networks.
7. Activity in the three main structures in the brain stem with axons that descend to the spinal cord (the pontomedullary reticular formation, the lateral vestibular nucleus, and the red nucleus) contributes to the control of posture and interlimb coordination. Signals from these structures modify the level of muscle activity in a structure-specific manner.
8. The motor cortex provides precise control of muscle activity patterns to allow animals to make visually guided anticipatory adjustments of their gait. The signal from the motor cortex is integrated into the ongoing rhythm.
9. The posterior parietal cortex (PPC) is part of a network that contributes to the advanced planning

of gait based on visual information. PPC neurons estimate the relative location of objects with respect to the body and retain information in working memory to facilitate coordination of the limbs. The contribution of other cortical and subcortical areas to locomotor planning remains little studied.

10. Inputs from the cerebellum and the basal ganglia are used to correct motor errors and select the appropriate patterns of motor activity. The contribution of the basal ganglia to the control of locomotion is complex and is only now being determined.
11. The available evidence suggests that the neural control mechanisms determined from experiments in animals are also used to control locomotion in humans, including the existence of a CPG. Major advances remain to be made in understanding the mechanisms of spinal and supraspinal influences on human locomotor control.
12. Recent technological advances now give us an unparalleled opportunity to investigate the control mechanisms underlying locomotion. Molecular and genetic advances provide the ability to manipulate behavior at both the cellular and systems level and allow detailed study of the contributions of brain stem and spinal circuits to the initiation and regulation of locomotion. Advances in multineuronal recording techniques in animals, as well as the development of high-resolution recordings of human brain activity, will facilitate our understanding of the contribution of cortical structures to the control of locomotion.

Trevor Drew
Ole Kiehn

Suggested Reading

Armstrong DM. 1988. The supraspinal control of mammalian locomotion. J Physiol 405:1–37.

Brown T. 1911. The intrinsic factors in the act of progression in mammals. Proc R Soc B 84:308–319.

Drew T, Andujar JE, Lajoie K, Yakovenko S. 2008. Cortical mechanisms involved in visuomotor coordination during precision walking. Brain Res Rev 57:199–211.

Grillner S. 2006. Biological pattern generation: the cellular and computational logic of networks in motion. Neuron 52:751–766.

Jankowska E. 2008. Spinal interneuronal networks in the cat: elementary components. Brain Res Rev 57:46–55.

Kiehn O. 2016. Decoding the organization of spinal circuits that control locomotion. Nat Rev Neurosci 17:224–238.

Orlovsky G, Deliagina TG, Grillner S. 1999. *Neuronal Control of Locomotion: From Mollusc to Man*. Oxford: Oxford Univ. Press.

Pearson KG. 2008. Role of sensory feedback in the control of stance duration in walking cats. Brain Res Rev 57:222–227.

Rossignol S. 1996. Neural control of stereotypic limb movements. Supplement 29. In: *Handbook of Physiology, Exercise: Regulation and Integration of Multiple Systems*. New York: Wiley-Blackwell.

Sherrington CS. 1913. Further observations on the production of reflex stepping by combination of reflex excitation with reflex inhibition. J Physiol 47:196–214.

Takakusaki K, Chiba R, Nozu T, Okumura T. 2016. Brainstem control of locomotion and muscle tone with special reference to the role of the mesopontine tegmentum and medullary reticulospinal systems. J Neural Transm (Vienna) 123:695–729.

References

Ampatzis K, Song J, Ausborn J, El Manira A. 2014. Separate microcircuit modules of distinct v2a interneurons and motoneurons control the speed of locomotion. Neuron 83:934–943.

Bouvier J, Caggiano V, Leiras R, et al. 2015. Descending command neurons in the brain stem that halt locomotion. Cell 163:1191–1203.

Brocard F, Tazerart S, Vinay L. 2010. Do pacemakers drive the central pattern generator for locomotion in mammals? Neuroscientist 16:139–155.

Buchanan JT, Grillner S. 1987. Newly identified "glutamate interneurons" and their role in locomotion in the lamprey spinal cord. Science 236:312–314.

Butt SJ, Kiehn O. 2003. Functional identification of interneurons responsible for left-right coordination of hindlimbs in mammals. Neuron 38:953–963.

Caggiano V, Leiras R, Goni-Erro H, et al. 2018. Midbrain circuits that set locomotor speed and gait selection. Nature 553:455–460.

Capelli P, Pivetta C, Soledad Esposito M, Arber S. 2017. Locomotor speed control circuits in the caudal brainstem. Nature 551:373–377.

Choi JT, Bouyer LJ, Nielsen JB. 2015. Disruption of locomotor adaptation with repetitive transcranial magnetic stimulation over the motor cortex. Cereb Cortex 25:1981–1986.

Conway BA, Hultborn H, Kiehn O. 1987. Proprioceptive input resets central locomotor rhythm in the spinal cat. Exp Brain Res 68:643–656.

Crone SA, Quinlan KA, Zagoraiou L, et al. 2008. Genetic ablation of V2a ipsilateral interneurons disrupts left-right locomotor coordination in mammalian spinal cord. Neuron 60:70–83.

Dougherty KJ, Zagoraiou L, Satoh D, et al. 2013. Locomotor rhythm generation linked to the output of spinal shox2 excitatory interneurons. Neuron 80:920–933.

Drew T. 1988. Motor cortical cell discharge during voluntary gait modification. Brain Res 457:181–187.
Drew T. 1991. Functional organization within the medullary reticular formation of the intact unanesthetized cat. III. Microstimulation during locomotion. J Neurophysiol 66:919–938.
Drew T, Dubuc R, Rossignol S. 1986. Discharge patterns of reticulospinal and other reticular neurons in chronic, unrestrained cats walking on a treadmill. J Neurophysiol 55:375–401.
Drew T, Marigold DS. 2015. Taking the next step: cortical contributions to the control of locomotion. Curr Opin Neurobiol 33C:25–33.
Dubuc R, Brocard F, Antri M, et al. 2008. Initiation of locomotion in lampreys. Brain Res Rev 57:172–182.
Edgerton VR, Leon RD, Harkema SJ, et al. 2001. Retraining the injured spinal cord. J Physiol 533:15–22.
Engberg I, Lundberg A. 1969. An electromyographic analysis of muscular activity in the hindlimb of the cat during unrestrained locomotion. Acta Physiol Scand 75:614–630.
Forssberg H. 1985. Ontogeny of human locomotor control. I. Infant stepping, supported locomotion and transition to independent locomotion. Exp Brain Res 57:480–493.
Goulding M. 2009. Circuits controlling vertebrate locomotion: moving in a new direction. Nat Rev Neurosci 10:507–518.
Grillner S. 2006. Biological pattern generation: the cellular and computational logic of networks in motion. Neuron 52:751–766.
Grillner S. 1981. Control of locomotion in bipeds, tetrapods, and fish. In: V Brooks (ed). *Handbook of Physiology.* Rockville, MD: American Physiological Society.
Grillner S, Jessell TM. 2009. Measured motion: searching for simplicity in spinal locomotor networks. Curr Opin Neurobiol 19:572–586.
Grillner S, Rossignol S. 1978. On the initiation of the swing phase of locomotion in chronic spinal cats. Brain Res 146:269–277.
Grillner S, Zangger P. 1979. On the central generation of locomotion in the low spinal cat. Exp Brain Res 34:241–261.
Grillner S, Zangger P. 1984. The effect of dorsal root transection on the efferent motor pattern in the cat's hindlimb during locomotion. Acta Physiol Scand 120:393–405.
Hagglund M, Borgius L, Dougherty KJ, Kiehn O. 2010. Activation of groups of excitatory neurons in the mammalian spinal cord or hindbrain evokes locomotion. Nat Neurosci 13:246–252.
Harris-Warrick RM. 2011. Neuromodulation and flexibility in central pattern generator networks. Curr Opin Neurobiol 21:685–692.
Hiebert GW, Whelan PJ, Prochazka A, Pearson KG. 1996. Contribution of hind limb flexor muscle afferents to the timing of phase transitions in the cat step cycle. J Neurophysiol 75:1126–1137.
Hounsgaard J, Hultborn H, Kiehn O. 1986. Transmitter-controlled properties of alpha-motoneurones causing long-lasting motor discharge to brief excitatory inputs. Prog Brain Res 64:39–49.
Hultborn H, Nielsen JB. 2007. Spinal control of locomotion—from cat to man. Acta Physiol (Oxf) 189:111–121.
Jessell TM. 2000. Neuronal specification in the spinal cord: inductive signals and transcriptional codes. Nat Rev Genet 1:20–29.
Jordan LM, Liu J, Hedlund PB, Akay T, Pearson KG. 2008. Descending command systems for the initiation of locomotion in mammals. Brain Res Rev 57:183–191.
Juvin L, Gratsch S, Trillaud-Doppia E, Gariepy JF, Buschges A, Dubuc R. 2016. A specific population of reticulospinal neurons controls the termination of locomotion. Cell Rep 15:2377–2386.
Kiehn O. 2006. Locomotor circuits in the mammalian spinal cord. Annu Rev Neurosci 29:279–306.
Kiehn O, Sillar KT, Kjaerulff O, McDearmid JR. 1999. Effects of noradrenaline on locomotor rhythm-generating networks in the isolated neonatal rat spinal cord. J Neurophysiol 82:741–746.
Kriellaars DJ, Brownstone RM, Noga BR, Jordan LM. 1994. Mechanical entrainment of fictive locomotion in the decerebrate cat. J Neurophysiol 71:2074–2086.
Lajoie K, Andujar JE, Pearson K, Drew T. 2010. Neurons in area 5 of the posterior parietal cortex in the cat contribute to interlimb coordination during visually guided locomotion: a role in working memory. J Neurophysiol 103:2234–2254.
Lanuza GM, Gosgnach S, Pierani A, Jessell TM, Goulding M. 2004. Genetic identification of spinal interneurons that coordinate left-right locomotor activity necessary for walking movements. Neuron 42:375–386.
McCrea DA, Rybak IA. 2007. Modeling the mammalian locomotor CPG: insights from mistakes and perturbations. Prog Brain Res 165:235–253.
McLean DL, Masino MA, Koh IY, Lindquist WB, Fetcho JR. 2008. Continuous shifts in the active set of spinal interneurons during changes in locomotor speed. Nat Neurosci 11:1419–1429.
McVea DA, Pearson KG. 2009. Object avoidance during locomotion. Adv Exp Med Biol 629:293–315.
Pearson KG, Rossignol S. 1991. Fictive motor patterns in chronic spinal cats. J Neurophysiol 66:1874–1887.
Picton LD, Sillar KT. 2016. Mechanisms underlying the endogenous dopaminergic inhibition of spinal locomotor circuit function in Xenopus tadpoles. Sci Rep 6:35749.
Rossignol S, Frigon A. 2011. Recovery of locomotion after spinal cord injury: some facts and mechanisms. Annu Rev Neurosci 34:413–440.
Rybak IA, Stecina K, Shevtsova NA, McCrea DA. 2006. Modelling spinal circuitry involved in locomotor pattern generation: insights from the effects of afferent stimulation. J Physiol 577:641–658.
Ryczko D, Dubuc R. 2013. The multifunctional mesencephalic locomotor region. Curr Pharm Des 19:4448–4470.
Shik M, Severin F, Orlovskii G. 1966. [Control of walking and running by means of electric stimulation of the midbrain]. Biofizika 11:659–666. [article in Russian]
Soffe SR, Roberts A, Li WC. 2009. Defining the excitatory neurons that drive the locomotor rhythm in a simple

vertebrate: insights into the origin of reticulospinal control. J Physiol 587:4829–4844.
Talpalar AE, Bouvier J, Borgius L, Fortin G, Pierani A, Kiehn O. 2013. Dual-mode operation of neuronal networks involved in left-right alternation. Nature 500:85–88.
Talpalar AE, Endo T, Low P, et al. 2011. Identification of minimal neuronal networks involved in flexor-extensor alternation in the mammalian spinal cord. Neuron 71: 1071–1084.
Wernig A, Muller S, Nanassy A, Cagol E. 1995. Laufband therapy based on 'rules of spinal locomotion' is effective in spinal cord injured persons. Eur J Neurosci 7:823–829.
Whelan PJ, Hiebert GW, Pearson KG. 1995. Stimulation of the group I extensor afferents prolongs the stance phase in walking cats. Exp Brain Res 103:20–30.
Yang JF, Mitton M, Musselman KE, Patrick SK, Tajino J. 2015. Characteristics of the developing human locomotor system: similarities to other mammals. Dev Psychobiol 57:397–408.
Zagoraiou L, Akay T, Martin JF, Brownstone RM, Jessell TM, Miles GB. 2009. A cluster of cholinergic premotor interneurons modulates mouse locomotor activity. Neuron 64:645–662.
Zhang J, Lanuza GM, Britz O, et al. 2014. V1 and v2b interneurons secure the alternating flexor-extensor motor activity mice require for limbed locomotion. Neuron 82:138–150.
Zhang Y, Narayan S, Geiman E, et al. 2008. V3 spinal neurons establish a robust and balanced locomotor rhythm during walking. Neuron 60:84–96.

34

Voluntary Movement: Motor Cortices

In this chapter, we describe how the cerebral cortex uses sensory information from the external world to guide motor actions that allow the individual to interact with the surrounding environment. We begin with a general description of what we mean by the term voluntary movement and some theoretical frameworks for understanding its control, followed by the basic anatomy of the cortical circuits involved in voluntary motor behavior. We then consider how information related to the body, external space, and behavioral goals is combined and processed in parietal cortical regions. This is followed by a discussion of the

role of premotor cortical regions in selecting and planning motor actions. Finally, we examine the role played by the primary motor cortex in motor execution.

Voluntary Movement Is the Physical Manifestation of an Intention to Act

Animals, including humans, have a nervous system not just so that they can sense their world or think about it, but primarily to interact with it to survive and reproduce. Understanding how purposeful actions are achieved is one of the great challenges in neuroscience. We focus here on the cerebral cortical control of voluntary motor behavior, in particular voluntary arm and hand movements in primates.

In contrast to stereotypical fixed-latency reflexive responses that are automatically triggered by incoming sensory stimuli (Chapter 32), voluntary movements are purposeful, intentional, and context-dependent, and are typically accompanied, at least in humans, by a sense of "ownership" of the actions, the sense that the actions have been willfully caused by the individual. Decisions to act are often made without an external trigger stimulus. Moreover, the continuous flux of events and conditions in the world presents changing opportunities for action, and thus voluntary action involves choices between alternatives, including the choice not to act. Finally, the same object or event can evoke different actions at different times, depending on the current context.

Throughout evolution, these features of voluntary behavior have become increasingly prominent in higher primates, especially in humans, indicating that the neural circuits controlling voluntary behavior in primates are adaptive. In particular, evolution has resulted in an increasing degree of dissociation of the physical properties of sensory inputs from their behavioral salience to the individual. Adaptation of the control circuits also enhances the repertoire of voluntary motor actions available to a species by allowing individuals to remember and learn from prior experience, to predict the future outcomes of different action choices, and to adopt new strategies and find new solutions to attain their desired goals. Volitional self-control over how, when, and even whether to act endows primate voluntary behavior with much of its richness and flexibility and prevents behavior from becoming impulsive, compulsive, or even harmful.

Voluntary behavior is the physical manifestation of an individual's intention to act on the environment, usually to achieve a goal immediately or at some point in the future. This may require single nonstereotypical movements or sequences of actions tailored to current conditions and to the longer-term objectives of the individual. The ability to use fingers, hands, and arms independent of locomotion further helps primates, and especially humans, exploit their environment. Most animals must search their environment for food when hungry. In contrast, humans can "forage" by using their hands to cook a meal or simply enter a few numbers on a cellphone to order food for delivery. Because large areas of the cerebral cortex are implicated in various aspects of voluntary motor control, the study of the cortical control of voluntary movement provides important insights into the purposive functional organization of the cerebral cortex as a whole.

Theoretical Frameworks Help Interpret Behavior and the Neural Basis of Voluntary Control

The neural processes by which individuals acquire information about their environment and the relationship of their body to it, decide how to interact with the environment to achieve short- or long-term goals, and organize and execute the voluntary movement(s) that will fulfill their goals are traditionally partitioned into three analytic components: Perceptual mechanisms generate an internal representation of the external world and the individual within it, cognitive processes use this internal model of the world to select a course of action to interact with its environment, and the chosen plan of action is then relayed to the motor systems for implementation. This serial view of the brain's overall functional organization has long dominated neuroscience; this textbook, for example, has separate sections dedicated to perception, cognition, and movement.

The brain must transform a goal into motor commands that realize the goal. For example, taking a sip of coffee requires the brain to convert visual information about the coffee cup and somatic information about the current posture and motion of your arm and hand into a pattern of muscle contractions that moves your hand to the cup, grasps it, and then lifts it to your mouth. Many behavioral and modeling studies suggest that this could be accomplished by a series of transformations of sensorimotor coordinates that convert the retinal image of the cup into motor commands (Figure 34–1A).

Variants of this sensorimotor transformation model have guided the design and interpretation of many studies on the control of voluntary arm movements. Neural recording studies, including many that will be described here, have found possible neural correlates of the motor parameters and sensorimotor transformations presumed to underlie movement

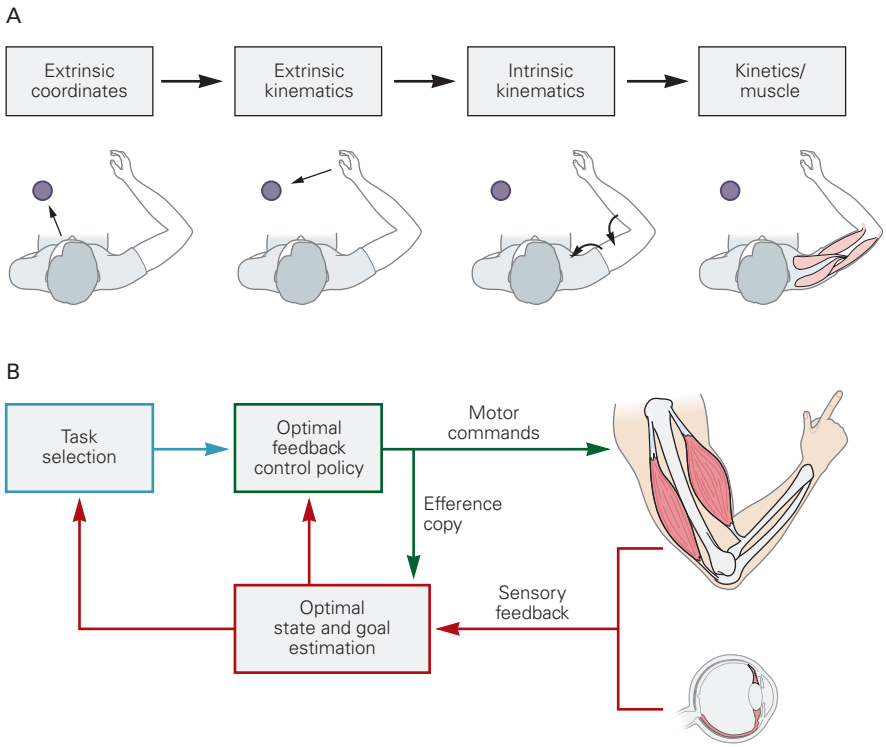

Figure 34–1 Theoretical frameworks for interpreting neural processing during voluntary motor actions.

A. The concept of sensorimotor transformations addresses the basic problem that tasks such as reaching to a visual target require the brain and spinal cord to convert sensory information about the spatial location of the target, initially represented in retinal coordinates, into patterns of muscle activity to move the limb to the target object. It is assumed that this sensorimotor transformation involves the use of intermediary representations—representation of the location of the target object relative to the body, the spatiotemporal trajectory of the hand (extrinsic kinematics), and motion of the joints (intrinsic kinematics) necessary to reach and grasp the object—before generating the patterns of neural activity that specify the causal forces (kinetics) or muscle activity.

B. Optimal feedback control recognizes three key processes for control. Optimal state and goal estimation (**red box**) integrates sensory feedback from various modalities along with an efference copy of motor commands to estimate the present position and motion of the body and objects in the world. Task selection (**blue box**) involves processes that identify behavioral goals based on internal desires and information about the state of the body and the world. Control policy (**green box**) determines the feedback gains, operations, and processes necessary to generate motor commands to control movement.

planning and execution. This conceptual framework is an example of a *representational model* of brain function. Just as the activity of neurons in primary sensory areas appears to encode specific physical properties of stimuli, the sensorimotor transformation model assumes that the activity of neurons in the motor system explicitly encodes or represents specific properties and parameters of the intended movement.

However, the sensorimotor transformation model has important limitations. Among them, the parameters and coordinate systems typically used in such models were imported from physics and engineering, rather than derived from the physiological properties of biological sensors and effectors. Furthermore, the model places all emphasis on strictly serial feedforward computations and relegates feedback circuits primarily to the detection and correction of performance errors after they are committed. The model also requires that every temporal detail of a movement be explicitly calculated before the motor system can generate any motor commands. Another limitation is its rigidity; it assumes that the same sequence of computations controls every movement in every context. Finally, this approach has not addressed how the proposed sensorimotor transformations could be implemented by neurons.

In recent years, theoretical studies of the motor system have been moving away from strictly representational models to more dynamical causal models. This approach begins with the premise that the functional architecture of motor control circuits evolved to generate movements, not to represent their parameters.

These circuit properties were acquired by evolutionary changes in neural circuitry and by experience-dependent adaptive processes during postnatal development that produce the patterns of synaptic connectivity within the neural circuits that are necessary to generate the desired movements. Spinal and supraspinal motor circuits ensure that spinal motor neurons generate the appropriate muscle contraction signals across task conditions without relying on computational formalisms such as coordinate transformations.

One such theoretical framework is optimal feedback control (Figure 34–1B; and see Chapter 30). There are many different forms of optimal control, and each captures important aspects of control. Optimal feedback control, as the name implies, emphasizes the importance of feedback signals for the planning and control of movements. It is optimal in the sense that it emphasizes the importance of the behavioral goal and the current context in determining how best to plan and control movements. This flexibility can explain how human motor performance can be both highly variable and yet successful.

The optimal feedback control framework also divides the control of voluntary movements into three key processes: state estimation, task selection, and control policy (Figure 34–1B). State estimation involves forward internal models that use efference copies of motor commands and external sensory feedback to provide the best estimate of the present state of the body and the environment (Chapter 30). Task selection involves the neural processes by which the brain chooses a behavioral goal in the current context and what motor action(s) might best attain that goal. This selection can be based on the sensory evidence supporting alternative actions and alternate options to attain the goal, and on other factors that influence the optimal response such as motivational state, task urgency, preferences, relative benefits versus risks, the mechanical properties of the body and environment, and even the biomechanical costs of different action choices. Finally, the control policy provides the set of rules and computations that establish how to generate the motor commands to attain the behavioral goal given the present state of the body and the environment. Importantly, the control policy process in optimal feedback control is not a series of pure feedforward computations to calculate every instantaneous detail of a desired movement trajectory and associated muscle activity patterns before movement onset. Instead, it involves context- and time-dependent adjustments to feedback circuit gains that allow the spatiotemporal form of muscle activity to emerge dynamically in real time as part of the control process underlying movement generation.

The sensorimotor transformation and optimal feedback control models are not mutually incompatible hypotheses. Optimal feedback control explains certain features of motor behavior but is largely agnostic as to the neural implementation for control. It assumes that motor circuits are dynamical systems that attain desired goals under varying task constraints. As a result, a given neuron may contribute to sensorimotor control in different task conditions, but its activity may not correspond to a specific movement parameter in a definable coordinate framework. In contrast, sensorimotor transformation models do not fully explain how real-time movement control is implemented by motor circuits, but emphasize the need to convert information from sensory signals to motor commands.

Even if the neural control system is dynamical, the system it controls—the musculoskeletal plant—is a physical object that must obey the universal physical laws of motion. Thus, neural activity should show correlations with those physical parameters and laws that will help to infer how those neurons are contributing to voluntary motor control, even if they are not attempting to encode those terms. Indeed, experimental tasks that dissociate different types of movement-related information have revealed important differences in how neural activity in different cortical motor regions correlates with different movement properties and different aspects of movement planning and execution. Finally, we can impose arbitrary volitional control on how we move. For example, we can choose to make an unobstructed reaching movement efficiently along a straight path to the target or whimsically along a complex curved path even though there is no obstacle to avoid and the movement is energetically costly. The experimental challenge is to reveal how the brain can implement this willful control with neurons and neural circuits.

Many Frontal and Parietal Cortical Regions Are Involved in Voluntary Control

Here we describe the regions of frontal and parietal cortex that convert sensory inputs into motor commands to produce voluntary movement. We then examine the neural circuits involved in the voluntary control of arm and hand movements that are prominent components of the motor repertory of primates. We focus on studies in the rhesus monkey (*Macaca mulatta*), as much of our knowledge of the cortical control of the arm and hand comes from this species and the neural circuity underlying human voluntary control appears to have a similar organization. Many other neural structures, including the prefrontal cortex, the basal ganglia, and

cerebellum, also play critical roles in the global organization of goal-directed voluntary behavior (Chapters 37 and 38).

Several different nomenclatures have been used in partitioning the precentral, postcentral, and parietal cortex, based on regional differences in cytoarchitectonic and myeloarchitectonic details, cortico-cortical connectivity, the distribution of different marker molecules, and regional differences in neural response properties. Here we will use some of the more widely accepted terminology without describing approximate homologies among the various nomenclatures.

Based on the pioneering cytoarchitectonic studies of humans by Brodmann, the different lobes of the monkey's cerebral cortex were divided into smaller regions, including two in precentral cortex (areas 4 and 6), four in the postcentral cortex (areas 1, 2, 3a, and 3b), and at least two in the superior and inferior parietal cortex (areas 5 and 7). While these cytoarchitectonic divisions persist in the literature, subsequent anatomical and functional studies have radically changed the view of how the precentral and parietal cortices are organized (Figure 34–2).

Current maps usually place the *primary motor cortex* (M1), the cortical region most directly involved in motor execution in primates, in Brodmann's area 4. Brodmann's area 6 is now typically divided into five or six functional areas that are principally involved in different aspects of the planning and control of motor actions of different parts of the body. Arm-control regions include the *dorsal premotor cortex* (PMd) and *predorsal premotor cortex* (pre-PMd), in the caudal and rostral parts of the dorsal convexity of lateral area 6, respectively. Hand-control regions include the *ventral premotor cortex* (PMv), found on the ventral convexity of area 6, which has been further divided into two or three smaller subregions. A variety of functions related to motor selection, sequencing, and initiation have been found in medial premotor cortical regions. These include a region on the medial surface of the cortical hemisphere that was originally called the secondary motor cortex by Woolsey and colleagues, who discovered it, but is now called the *supplementary motor area*. This region is in turn split into two regions, a *supplementary motor area proper* (SMA) in the caudal part and a *presupplementary motor area* (pre-SMA) in the rostral part. Outside of Brodmann's area 6, three additional motor areas, the dorsal, ventral, and rostral cingulate motor areas (CMAd, CMAv, and CMAr, respectively), are also involved in motor selection but have not been as well studied as more lateral premotor areas.

The *primary somatosensory cortex* (S-I; including areas 1, 2, 3a, and 3b) is located in the anterior postcentral gyrus. It processes cutaneous and muscle mechanoreceptor signals from the periphery and transmits that information to other parietal and precentral cortical regions (Chapter 19). Like area 6, Brodmann's parietal areas 5 and 7 are now divided into several regions within and adjacent to the intraparietal sulcus (IPS), each of which integrates various types of sensory information about the body or spatial goals for voluntary motor control. These include parietal lobe areas PE and PEc on the rostral or superior bank, and PF, PFG, PG, and OPT on the caudal, inferior bank. Areas inside the IPS include the anterior, lateral, medial, and ventral intraparietal areas (AIP, LIP, MIP, and VIP, respectively) as well as intraparietal area PEip and higher visual area V6A.

These precentral, postcentral, and parietal cortical regions are interconnected by complex patterns of reciprocal, convergent, and divergent projections. The SMA, PMd, and PMv have somatotopically organized reciprocal connections not only with M1 but also with each other. Both the SMA and M1 receive somatotopically organized input from S-I and the dorsorostral parietal cortex, whereas PMd and PMv are reciprocally connected with progressively more caudal, medial, and lateral parts of the parietal cortex. These somatosensory and parietal inputs provide the primary motor and caudal premotor regions with sensory information related to behavioral goals, target objects, and the position and motion of the body that is used to plan and guide motor acts.

In contrast, pre-SMA and pre-PMd project to SMA and PMd but do not project to M1 and are only weakly connected with the parietal lobe. They instead have reciprocal connections with prefrontal cortex and so may impose more arbitrary context-dependent control over voluntary behavior. Prefrontal cortex is also connected with other premotor cortical regions.

The control of hand and arm motor actions is implemented by partially segregated parallel circuits distributed across several parietal and precentral motor areas. Hand motor function is generally supported by frontoparietal circuits that are located more laterally, notably AIP and PMv. In contrast, proximal arm motor function is supported by circuits that are more medial, notably parietal areas PE and MIP and precentral areas PMd, SMA, and pre-SMA.

Descending Motor Commands Are Principally Transmitted by the Corticospinal Tract

Older textbooks often referred to the primary motor cortex (M1) as the "final common path." Other

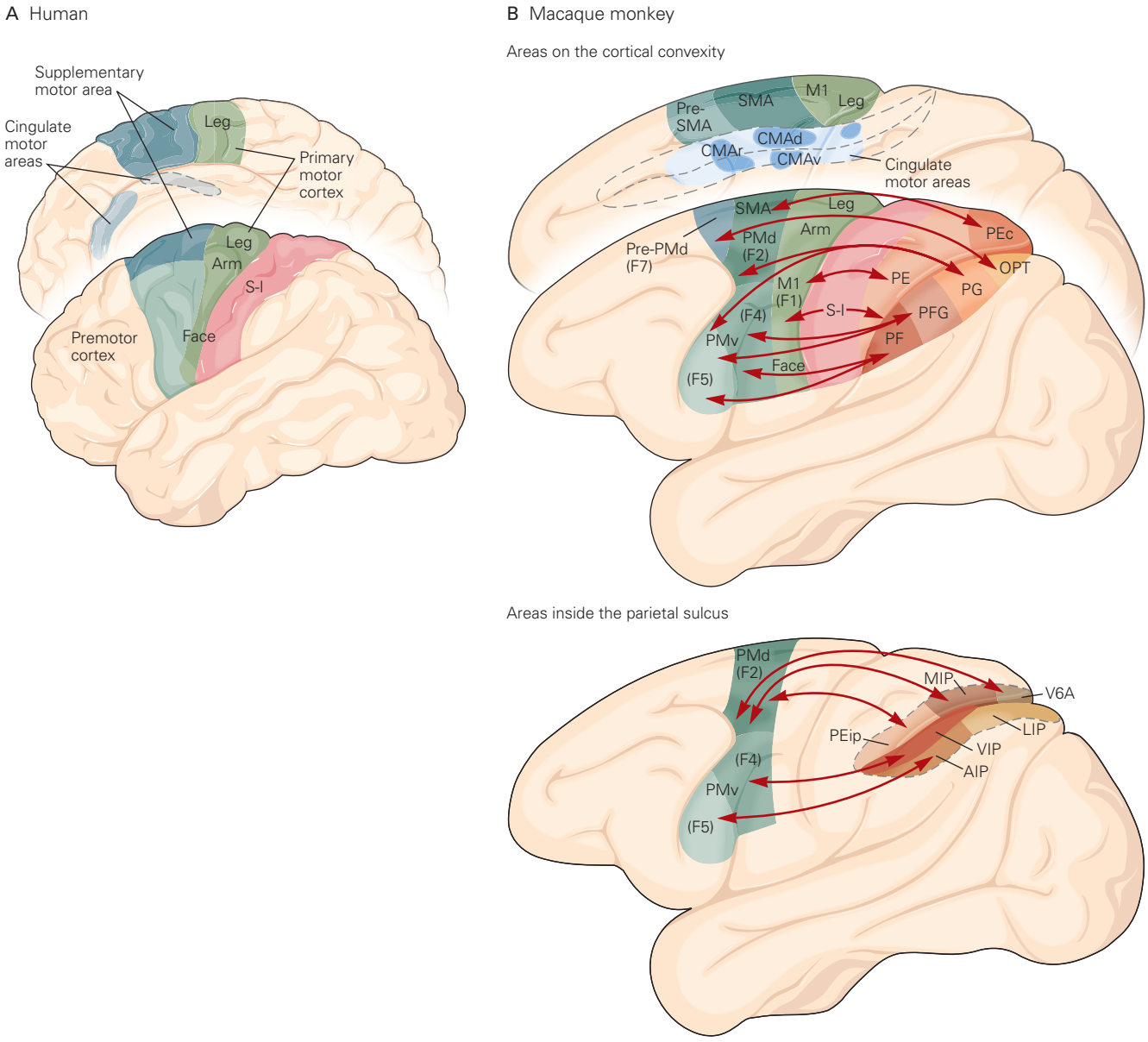

Figure 34–2 **Parietal and frontal motor areas that support voluntary control.** For illustration purposes, the intraparietal sulcus is opened in the bottom panel. The parietal areas are designated in Constantin von Economo's terminology by the letter **P** (parietal), followed by letters instead of numbers to indicate the cytoarchitectonically different areas. Areas PF and PFG roughly correspond to Brodmann's area 7b, and areas PG and OPT to Brodmann's area 7a. Areas inside the intraparietal sulcus include the anterior, lateral, medial, and ventral intraparietal areas (**AIP**, **LIP**, **MIP**, **VIP**, respectively), as well as the PE intraparietal area (**PEip**) and visual area 6A (**V6A**). **Arrows** show the patterns of the principal reciprocal connections between functionally related parietal and frontal motor areas. (Abbreviations: **CMAr**, rostral cingulate motor area; **CMAv**, ventral cingulate motor area; **CMd**, dorsal cingulate motor area; **F**, frontal; **M1**, primary motor cortex; **OPT**, occipito-parieto-temporal; **P**, parietal; **PE**, **PF**, and **PFG** are parietal areas according to the nomenclature of von Economo; **PMd**, dorsal premotor cortex; **PMv**, ventral premotor cortex; **Pre-PMd**, predorsal premotor cortex; **S-I**, primary somatosensory cortex; **SMA**, supplemental motor area.)

cortical motor areas were thought to influence voluntary movements via their projections to M1, which then formulated the descending motor command that was transmitted to the spinal cord. This is not correct.

Several cortical motor regions outside of M1 project to subcortical areas of the brain as well as to the spinal cord in parallel with the descending projections from M1. The key descending pathway for

voluntary control is the *pyramidal tract*, which originates in cortical layer V in a number of precentral and parietal areas. The pyramidal tract contains axons that terminate in brain stem motor structures (the *corticobulbar tract*) and axons that project down to the spinal cord (*corticospinal tract*). Precentral areas include not only M1 but also SMA, PMd, PMv, and the cingulate motor areas (Figure 34–3). Descending fibers from S-I and parietal areas, including PE and PFG, also travel in the pyramidal tract. The pre-SMA and pre-PMd do not send axons directly to the spinal cord; instead, their descending outputs reach the spinal cord indirectly through projections to other subcortical structures.

Most corticospinal tract axons originating in one hemisphere cross to the other side of the midline (decussate) at the pyramid in the caudal medulla, and from there project to the spinal cord itself, forming the lateral corticospinal tract. A small portion does not decussate and forms the ventral corticospinal tract. Many corticospinal axons in primates, and virtually all corticospinal axons in other mammals, terminate only on spinal interneurons and exert their influence on voluntary movement indirectly through spinal interneuronal and reflex pathways. In monkeys, all corticospinal axons from premotor cortical areas and many from M1 terminate on interneurons in the spinal intermediate zone, whereas postcentral and parietal areas target interneurons in the dorsal horn. The terminal endings of a sizeable portion of the corticospinal axons arising from M1 in primates, but not other mammals, arborize at their targets and synapse directly on spinal alpha motor neurons that in turn innervate muscles; these M1 neurons with direct monosynaptic projections to spinal motor neurons are called *corticomotoneuronal cells*.

Any voluntary arm movement can have destabilizing effects on the rest of the body due to mechanical interactions between body segments. Thus, control of voluntary arm movements requires coordination with neural circuits responsible for the control of posture and balance. This is mediated by descending projections from cortical motor areas to the reticular formation, which in turn project to the spinal cord via the reticulospinal tract (Chapters 33 and 36).

Imposing a Delay Period Before the Onset of Movement Isolates the Neural Activity Associated With Planning From That Associated With Executing the Action

Voluntary movement requires the intervention of a number of neural processes between the arrival of salient sensory inputs and the initiation of an appropriate motor response. With the development in the 1960s of single-cell recording in the cerebral cortex of awake animals, tasks that experimentally manipulate different attributes of movements have been used to study every cortical area involved in the control of arm and hand movements to try to identify neural correlates of the presumed control processes in each area.

In "reaction-time" tasks, animals make a prespecified response when they detect a particular stimulus, such as reaching to a target when it appears (Figure 34–4A). The stimulus informs the animal both what movement to make and when to make it. However, reaction times in such tasks are typically short, often less than 300 ms, and most or all putative planning stages leading up to the initiation of the movement are accomplished within that brief time. This makes it very difficult to discern what kinds of information are represented in the activity of the neurons at each given moment and thus to what processes they are contributing (Figure 34–4B).

However, a critical feature of voluntary behavior is that movement initiation is not obligatory the instant an intention to act is formed. This volitional control over the timing of movement has been exploited by so-called "instructed-delay" motor tasks (Figure 34–4A), in which an instructional cue informs the animal about specific aspects of an impending movement such as the location of a target, but the animal must withhold the response until a delayed stimulus signals when to make the movement. This protocol allows researchers to dissociate in time the neural processes associated with the early stages of planning the intended act from those that are directly coupled in real time to the initiation and control of the movement.

As expected, neurons in all the movement-related cortical areas discharge prior to and during movement execution in reaction-time tasks (Figure 34–4B), and their activity correlates systematically with different properties of movements, such as their direction, velocity, spatial trajectory, and causal forces and muscle activity. Critically, however, many neurons in the same areas also signal information about an intended motor act during an instructed-delay period long before its initiation (Figure 34–4B). Thus, even though planning and execution are distinct serial stages in voluntary motor control, they are not implemented by distinct neural populations in different cortical areas. Moreover, even a well-trained monkey will occasionally make the wrong movement in response to an instructional cue. In those trials, the activity during the delay period generally predicts the erroneous motor response that the monkey will eventually make. This is compelling evidence that the activity is a neural correlate of the monkey's motor intentions, not a passive sensory response to the instructional cues.

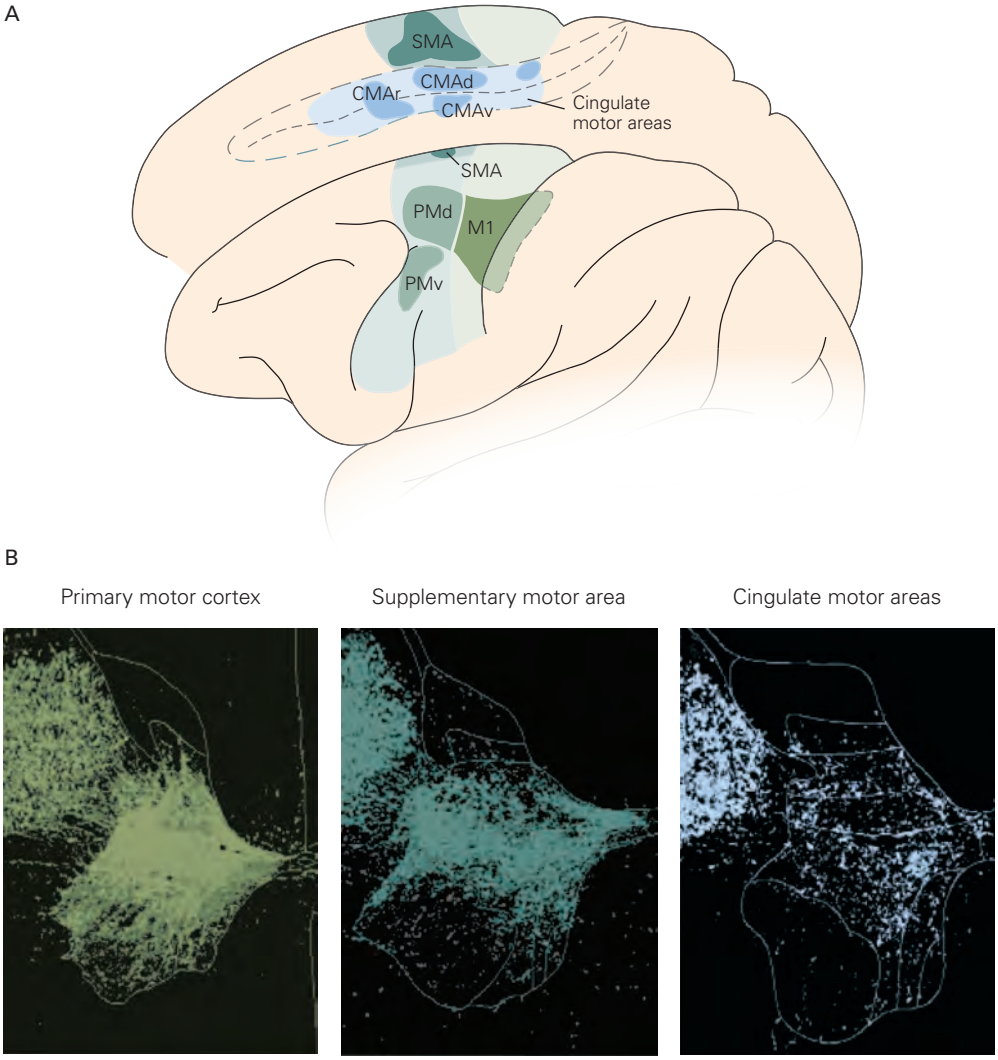

Figure 34–3 Cortical origins of the corticospinal tract. (Reproduced, with permission, from Dum and Strick 2002. Copyright © 2002 Elsevier Science Inc.)

A. Corticospinal neurons that modulate muscle activity in the contralateral arm and hand originate in the parts of the primary motor cortex (**M1**) motor map and many subdivisions of the premotor cortex (**PMd**, **PMv**, **SMA**) that are related to arm and hand movements (indicated by the darker zones). The axons from these areas project into the spinal cord cervical enlargement (see part **B**). Corticospinal fibers projecting to the leg, trunk, and other somatotopic parts of the brain stem and spinal motor system originate in the other parts of the motor and premotor cortex, indicated by the lighter zones. (Abbreviations: **CMAd**, dorsal cingulate motor area; **CMAr**, rostral cingulate motor area; **CMAv**, ventral cingulate motor area; **M1**, primary motor cortex; **PMd**, dorsal premotor cortex; **PMv**, ventral premotor cortex; **SMA**, supplementary motor area.)

B. Transverse sections of the spinal cord at the level of the cervical enlargement in monkeys after injection of the anterograde tracer horseradish peroxidase into different arm-related cortical motor regions to label the distribution of corticospinal axons arising from each cortical region. The corticospinal axons from the primary motor cortex (*left*), supplementary motor area (*middle*), and cingulate motor areas (*right*) all terminate on interneuronal networks in the intermediate laminae (V–VIII) of the spinal cord. Only the primary motor cortex contains corticospinal neurons (corticomotoneuronal cells) whose axons terminate directly on spinal motor neurons in the most ventral and lateral part of the spinal ventral horn (Rexed's lamina IX). Rexed's laminae I to IX of the dorsal and ventral horns are shown in faint outline in each section. The dense cluster of labeled axons adjacent to the dorsal horn (*upper left*) in each section are corticospinal axons descending in the dorsolateral funiculus, before entering the spinal intermediate and ventral laminae.

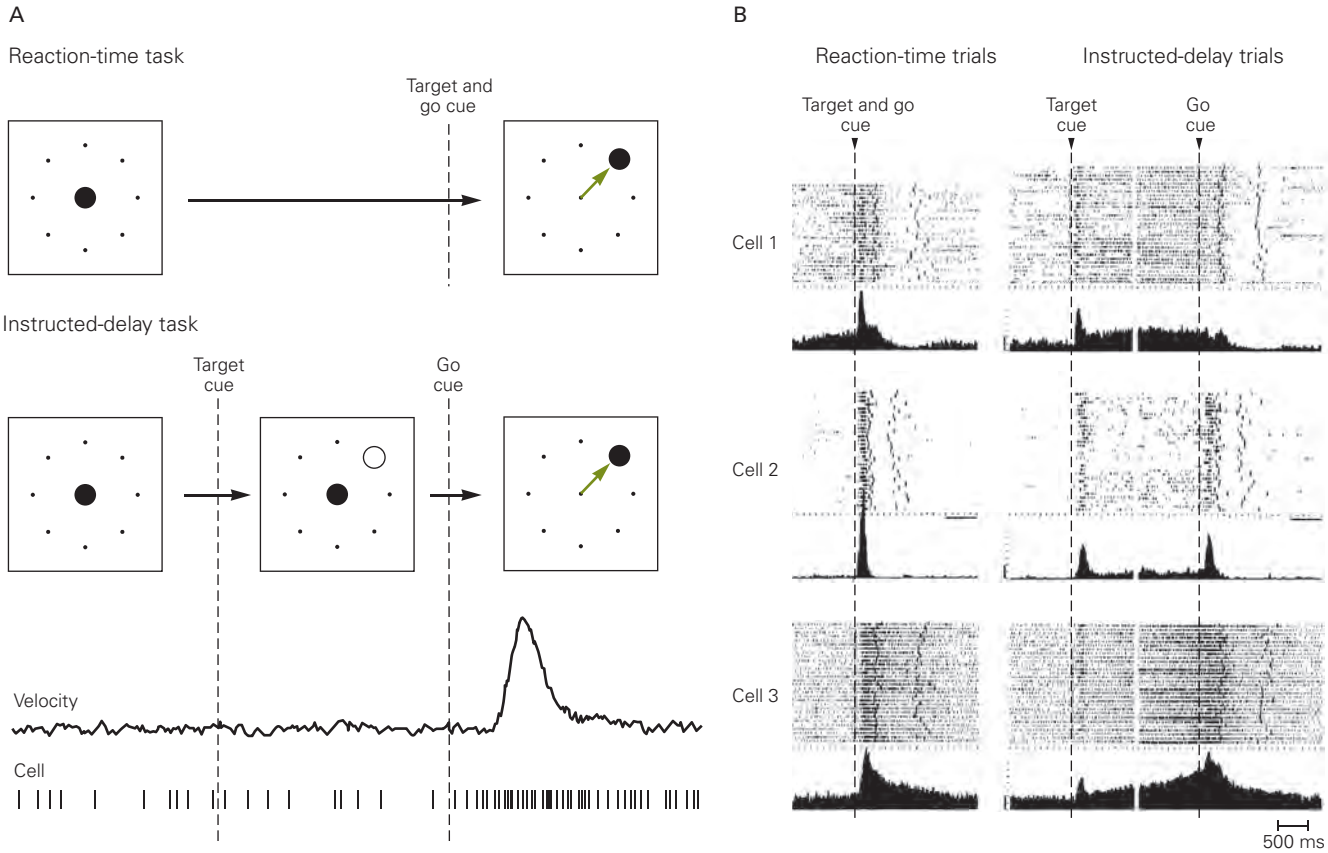

Figure 34–4 Neural processes related to movement planning and movement execution can be dissociated in time. (Reproduced, with permission, from Crammond and Kalaska 2000.)

A. In a *reaction-time task*, a sensory cue instructs the subject both where to move (target cue) and when to move (go cue). All neural operations required to plan and initiate the execution of the movement are performed in the brief time between the appearance of the cue and the onset of movement. In an *instructed-delay task*, an initial cue tells the subject where to move, and only later is the go cue given. The knowledge provided by the first cue permits the subject to plan the upcoming movement. Any changes in activity that occur after the first cue but before the second are presumed to be neural correlates of the planning stage.

B. Movement planning and execution are not completely segregated at the level of single neurons or neural populations in a given cortical area. Raster plots and cumulative histograms show the responses of three premotor cortex neurons to movements in each cell's preferred direction during reaction-time trials and instructed-delay trials. In the raster plots, each row represents activity in a single trial. The thin tics in each raster row represent action potentials, and the two thicker tics show the onset and end of movement. In reaction-time trials, the monkey does not know in which direction to move until the target appears. In contrast, in instructed-delay trials, an initial cue informs the monkey where the target lies well in advance of the appearance of a second signal to initiate the movement. During the delay period, activity in many premotor cells shows directionally tuned changes that signal the direction of the impending delayed movement. The activity in cell 1 appears to be strictly related to the planning phase of the task, for there is no execution-related activity after the go signal in the instructed-delay task. The other two cells show different degrees of activity related to both planning and execution.

Parietal Cortex Provides Information About the World and the Body for State Estimation to Plan and Execute Motor Actions

Sensory information is essential for selecting appropriate and effective actions. Before drinking from a cup, the brain uses visual input to identify which object is the cup, where it is located relative to the body, and its physical properties such as size, shape, and handle orientation. In addition, information about the current posture and motion of the arm and hand is provided by integrating proprioceptive signals from the limb with efference copies of motor commands (Chapter 30). Finally, cutaneous signals are critical when interacting manually with objects, such as grasping and lifting the cup.

Several lines of evidence implicate the parietal cortex as a key brain region in sensory processing for motor action. The parietal lobe, especially PE, PEip, and MIP,

receives strong somatic sensory inputs about body posture and movement from S-I. Several parietal regions along and within the IPS are major components of the dorsal visual pathway, which processes visuospatial information about objects that guides arm and hand movements while reaching to, grasping, and manipulating them. The parietal lobe is also reciprocally interconnected with precentral cortical motor areas to provide the precentral cortex with signals for the sensory guidance of movement and to receive efference copies of motor commands from those same precentral areas. Finally, human subjects with lesions of the posterior parietal cortex often demonstrate specific impairments in using sensory information to guide motor action (Box 34–1).

The Parietal Cortex Links Sensory Information to Motor Actions

We experience the space that surrounds us as a single unified environment within which objects have specific locations relative to each other and to ourselves. Classical neurology suggested that the parietal lobe constructed a unified multimodal neural representation of the world by integration of inputs from different sensory modalities. This single map of space was assumed to provide all the information necessary both for spatial perception and for the sensory guidance of movement, and so was shared by the different motor circuits that controlled different parts of the body, such as the eyes, arm, and hand.

However, the idea that the parietal cortex contains a single topographically organized representation of space is incorrect. Instead, the posterior parietal cortex contains several distinct functional areas that work in parallel and receive different combinations of sensory and motor inputs related to the guidance of movement of different effectors, such as the eyes, arm, and hand. Neurons in these areas are often multimodal, with both visual and somatic sensory receptive fields, and also discharge preferentially prior to and during movements of a specific effector. Each functional area is connected to frontal motor regions involved in control of the same effectors. Finally, each region is not topographically organized in the familiar sense of a faithful point-to-point representation of surrounding space, but rather comprises a complex mixture of neurons with different sensory inputs that may contribute to the multisensory integration required to guide motor actions with the environment.

Body Position and Motion Are Represented in Several Areas of Posterior Parietal Cortex

The S-I and adjacent superior parietal cortex regions PE, MIP, and PEip are a major source of proprioceptive and tactile sensory information about the position and motion of body parts. Neurons in S-I areas 1 and 2

Box 34–1 Lesion Studies of Posterior Parietal Cortex Lead to Deficits in the Use of Sensory Information to Guide Action

Naturally occurring or experimentally induced lesions have long been used to infer the roles of different neural structures. However, the effects of lesions must always be interpreted with caution. It is often incorrect to conclude that the function perturbed by an insult to a part of the motor system resides uniquely in the damaged structure or that the injured neurons explicitly perform that function. Furthermore, the adverse effects of lesions can be masked or altered by compensatory mechanisms in remaining, intact structures. Nevertheless, lesion experiments have been fundamental in differentiating the functional roles of brain regions.

Behavioral studies by Goodale, Milner, Rossetti, and others on patients with parietal cortical damage have led to the conclusion that a primary function of the parietal lobe is to extract sensory information about the external world and one's own body for the planning and guidance of movements. Such studies have shown that patients with lesions of certain parts of the parietal lobe suffer specific deficits in the ability to direct their arm and hand accurately to the spatial location of objects and to shape the orientation and grip aperture of the hand prior to grasping it.

They have also shown a particularly severe deficit in the ability to make rapid adjustments to their ongoing reach and grasping actions in response to unexpected changes in the location or orientation of the target object. This visual guidance of action is provided by visual signals that are routed through the dorsal visual stream and may operate in parallel with and independently of perceptual processes evoked by the visual inputs that are routed simultaneously through the ventral visual stream in the temporal lobe. For instance, whereas our visual perception of the size and orientation of objects can be deceived by certain perceptual illusions, the motor system often behaves as if it is not fooled and makes accurate movements.

typically respond to tactile input from a limited part of the contralateral body or to movements of one or a few adjacent joints in specific directions.

In contrast, many PE and MIP neurons discharge during passive and active movements of multiple joints. Some cells also respond during combined movements of multiple body parts, including bilateral movements of both arms. Many PE and MIP neurons also have large tactile receptive fields whose responses are modulated by context during limb movement or posture. For instance, a neuron with a tactile receptive field that covers the entire glabrous (palmar) surface of the hand may only respond to physical contact with an object when the hand is close to the body and not when it touches the object with the arm fully extended.

These findings indicate that while area 1 and 2 neurons encode the positions and movements of specific body parts, superior parietal neurons integrate information on the positions of individual joints as well as the positions of limb segments with respect to the body. This integration creates a neural "body schema" that provides information on where the arm is located with respect to the body and how different arm segments are positioned and moving with respect to one another. This body schema is critical for selecting how to attain behavioral goals and for ongoing control of movement.

For instance, a key requirement for efficient reaching is knowledge of where the arm is before and during the reach. Monkeys with experimental lesions in Brodmann's area 2 and the adjacent superior parietal lobule (area 5 or PE) show deficits in reaching to and manipulating objects under proprioceptive and tactile guidance without vision. Human patients with similar lesions show the same deficit, without the spatial neglect that is a common consequence of more lateral lesions in the inferior parietal lobe.

Spatial Goals Are Represented in Several Areas of Posterior Parietal Cortex

Functional areas within the IPS are strongly implicated in the processing of spatial, especially visual, information relevant to action. Each of these areas has unique ways of representing objects and spatial goals relative to the body and contributes to controlling motor actions of different parts of the body. For instance, many neurons in the lateral intraparietal area (LIP) receive visual input from extrastriate cortical areas. Their receptive fields are fixed in retinal coordinates and shift to new spatial locations whenever the monkey changes its direction of gaze. Neural responses also often increase when the animal attends to a stimulus within the receptive field even without looking at it, and they often discharge prior to a saccade that is directed toward a visual stimulus in their receptive field (Figure 34–5A; and see Chapter 35).

Several parietal regions are preferentially implicated in the control of arm and hand movements. For instance, the most medial regions of the superior parietal cortex, areas V6A and PEc, receive input from extrastriate visual areas V2 and V3. Many V6A and PEc neurons have visual receptive fields in retinal coordinates, but their activity is also frequently modulated by the direction of gaze, the current arm posture, and the direction of reaching movements.

The ventral intraparietal area (VIP) in the fundus of the IPS receives inputs from two components of the dorsal visual stream, the medial temporal cortex and medial superior temporal cortex, which are involved in the analysis of optic flow and visual motion. Many VIP neurons respond to visual stimuli and somatosensory stimuli with receptive fields on the face or head and, in some cases, on the arm or trunk. Neural activity is in head-centered coordinates, as somatosensory and visual information remains in register even if the eyes move to fixate different spatial locations (Figure 34–5B). Some VIP neurons respond to both visual and tactile stimuli moving in the same direction, whereas others are strongly activated by visual stimuli that move toward their tactile receptive field but only if the path of motion will eventually intersect the tactile receptive field. These neurons may allow the monkeys to link the location and motion of objects in their immediate peripersonal space with different parts of their body.

Another area of parietal cortex related to reaching is the parietal reach region (PRR). The PRR likely corresponds to the medial intraparietal cortex (MIP) and adjacent arm-control parts of the superior and inferior parietal cortex. The activity of many PRR neurons varies with the location of reach targets relative to the hand. However, this signal is not fixed to the current location of the hand or target but rather on the current direction of gaze (Figure 34–5C). Each time the monkey looks in a different direction, the reach-related activity of PRR neurons changes, even if the location of the target and hand and the required reach trajectory do not change. In contrast, the reach-related activity of many neurons in areas PE and PEip is less related to gaze and more strongly related to the current hand position and arm posture. PE and PEip neurons thus provide a more stable signal about the location of the reach target relative to the current position of the hand compared to PRR.

Finally, neurons in the anterior intraparietal area (AIP) are primarily implicated in object grasping and manipulation by movements of the hand. Many AIP neurons are preferentially active while reaching for

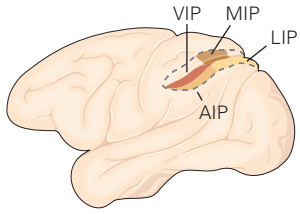

A Lateral intraparietal area (LIP)

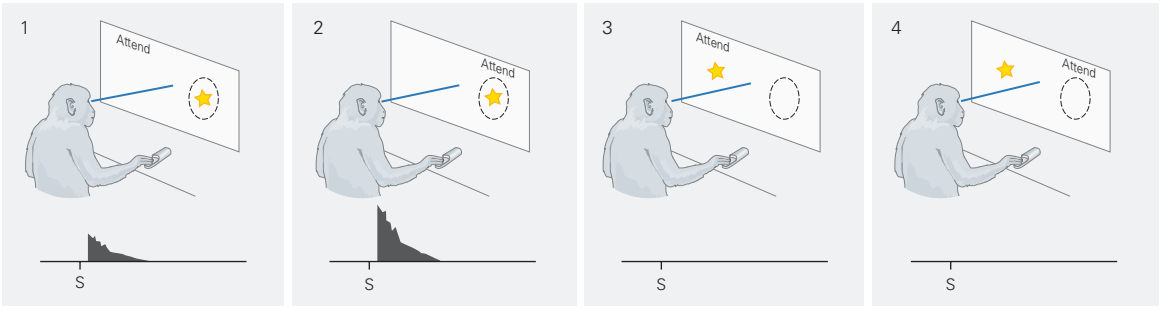

Receptive field characteristics

Retina-centered, attention sensitive

B Ventral intraparietal area (VIP)

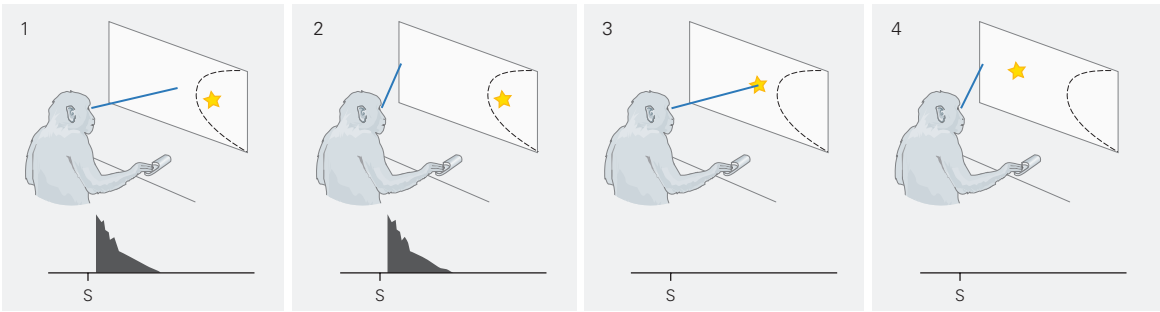

Head-centered

C Medial intraparietal area (MIP)

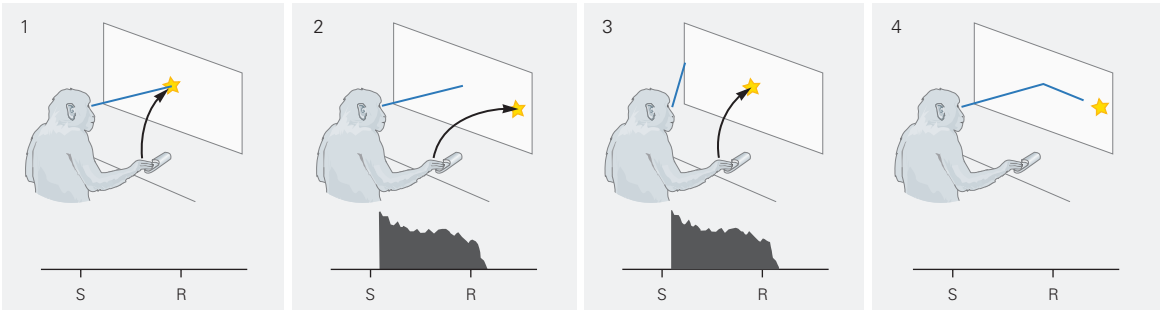

Retina-centered direction of reach; preparation to reach

D Anterior intraparietal area (AIP)

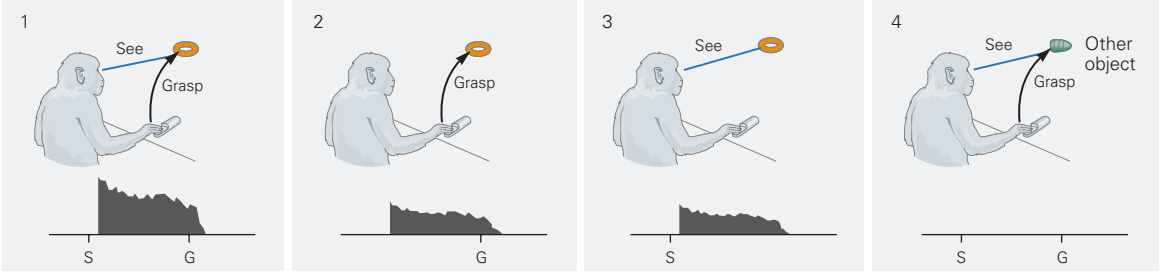

Retina-centered, object-specific viewing, grasping

and grasping objects of particular shapes, sizes, and spatial orientations, and often even while viewing those objects before grasping them (Figure 34–5D). There is a broad range of neural response properties, from neurons that respond almost exclusively to visual input about the objects but not to the grasping actions to neurons that discharge only during the hand movements themselves even in the dark. This suggests that the AIP contains neural circuits that begin to transform visual information about the physical properties of an object that are relevant to how it could be handled—what James Gibson has called the object's *affordances*—into appropriate hand actions (Chapter 56).

A fascinating discovery about the parietal cortex is that the receptive fields of neurons can be altered by individual experience, such as tool use. Monkeys were trained to retrieve food pellets that were out of normal reach of the arm and hand by using a rake-shaped tool. Many VIP neurons normally respond to visual objects when they are either located near the current position of the hand or anywhere within reach with the arm. After training, their visual receptive fields transiently expand to incorporate the tool when the monkey grasps it, as if the distal end of the tool had become a functional extension of the monkey's own hand and arm (Figure 34–6).

Internally Generated Feedback May Influence Parietal Cortex Activity

The delays involved in the transmission of visual and somatic feedback about arm movements from the periphery to cortical circuits can lead to oscillations or even instabilities in real-time sensorimotor control. One theoretical solution to this problem is to use a forward internal model to make predictive estimates of body motion based on internal efference copies of outgoing motor commands as well as from slower peripheral feedback signals (Chapter 30).

Several lines of evidence suggest that parietal cortex circuits, along with the cerebellum (Chapter 37), may implement a similar solution. Many reach-related neurons in PE, MIP, and PRR are active not only in response to passive sensory inputs but also before the onset of movement and during the instructed-delay period of delayed-reaching tasks. These responses suggest that these neurons process centrally generated signals about motor intentions prior to movement onset. This premovement activity is often interpreted as evidence that the parietal cortex generates feedforward signals that contribute to the early planning of movements. However, an alternate interpretation is that the premovement activity is driven by an efference copy of the motor command for the intended movement that is transmitted into the parietal cortex via its reciprocal connections with precentral motor areas. This combination of peripheral sensory inputs and central efference copies could permit some parietal reach-related circuits to compute a continuously updated estimate of the current state of the arm and its position relative to the behavioral goal. This estimate could be used to make rapid corrections for errors in ongoing arm movements.

Whether the parietal circuits are primarily involved in the formation of a subject's motor intentions or in

Figure 34–5 (Opposite) Neurons in the parietal cortex of the monkey are selective for the location of objects in the visual field relative to particular parts of the body. Each histogram represents the firing rate of a representative neuron as a function of time following presentation of a stimulus. In each diagram, the line emanating from the eyes indicates where the monkey is looking.

A. Neurons in the lateral intraparietal area have *retina-centered* receptive fields. The strength of the visual response depends on whether the monkey is paying attention to the stimulus (**S**). The neuron fires when a light is flashed inside its receptive field (**dotted circle**) (**1**). The response is more robust if the monkey is instructed to attend to the location of the stimulus (**2**). The neuron does not fire if the stimulus is presented outside the receptive field, regardless of where attention is directed (**3**, **4**).

B. In the ventral intraparietal area, some neurons have *head-centered* receptive fields. This is determined by keeping the head in a fixed position while the monkey is instructed to shift its gaze to various locations. This neuron fires when a light appears to the right of the midline of the head (**1**, **2**). It does not fire when the light appears at another location relative to the head, such as the midline or to the left. (**3**, **4**). The critical contrast is between situations 1 and 4. The retinal location of the light is the same in both (slightly to the right of the fixation point), yet the neuron fires in 1, when the stimulus is to the right of the head, but not in 4, when the stimulus is to the left of the head.

C. In the medial intraparietal area, neurons are selective for the retina-centered direction of the reach (**R**) and fire when the monkey is preparing to reach for a visual target. This neuron fires when the monkey reaches for a target to the right of where he is looking (**2**, **3**). It does not fire when he reaches for a target at which he is looking (**1**) or when he moves only his eyes to the target at the right (**4**). The physical direction of the reach is not a factor in the neuron's firing: It is the same in 1 and 3, and yet, the neuron fires only in 3.

D. In the anterior intraparietal area, neurons are selective for objects of particular shapes and fire when the monkey is looking at or preparing to grasp (**G**) an object. This neuron fires when the monkey is viewing a ring (**3**) or making a memory-guided reach to it in the dark (**2**). It fires especially strongly when the monkey is grasping the ring under visual guidance (**1**). It does not fire during viewing or grasping of other objects (**4**).

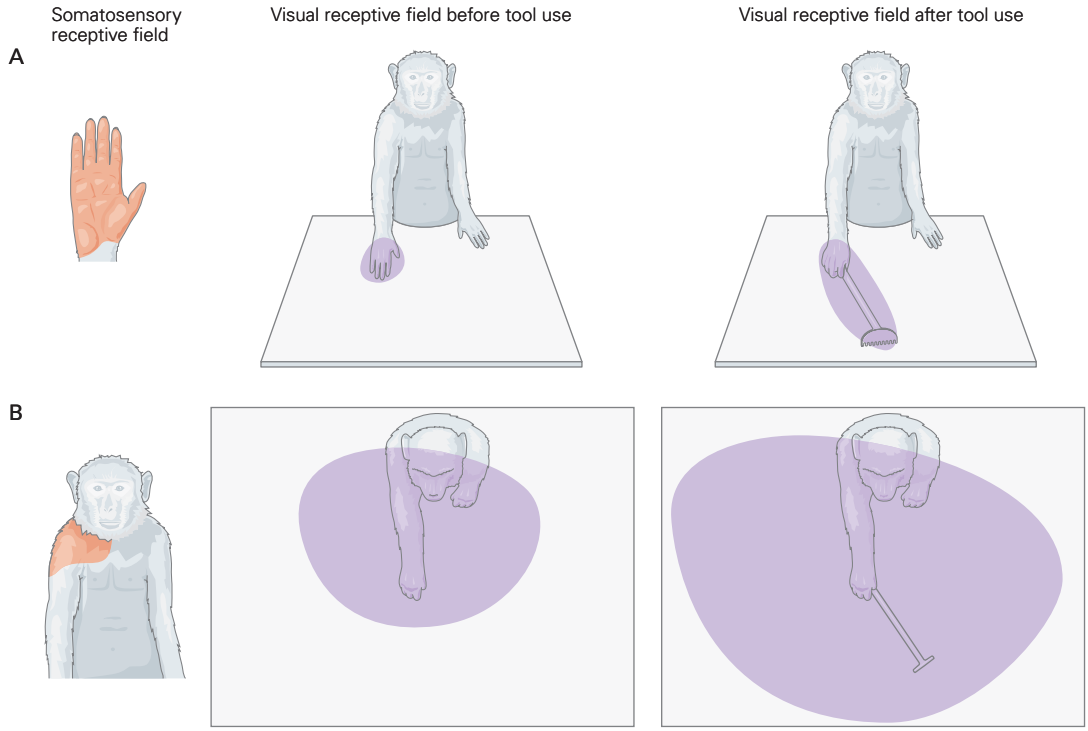

Figure 34–6 Some neurons in the parietal cortex of the monkey have receptive fields that dynamically expand once a tool is grasped. (Adapted from Maravita and Iriki, 2004. Copyright © 2003 Published by Elsevier Ltd.)

A. The **orange** area on the hand (*left*) indicates the somatosensory receptive field for a neuron. The **purple** area (*middle*) indicates the neuron's visual receptive field (vRF) region around the hand. The vRF is anchored to the hand and changes spatial location whenever the monkey moves its arm. The vRF expands when the monkey grasps a rake after it has learned how to use the rake to reach for objects in the workspace (*right*).

B. A single neuron that has a shoulder-centered bimodal somatosensory (**orange**) and visual (**purple**) receptive field is illustrated. The vRF for this neuron (*middle*) is larger than the one shown in part **A**, possibly reflecting the potential workspace related to whole-arm function. The vRF also expands to incorporate the extended workspace permitted by use of a rake (*right*).

state estimation will depend on the origin of its premovement activity. If it is mainly generated within the parietal cortex itself, this will strongly implicate the parietal cortex in the planning of intended movements. In contrast, if it is primarily driven by an efference copy relayed from precentral motor areas, this would strongly implicate the parietal circuits in state estimation, including predicting how the arm should move in response to the motor command.

Premotor Cortex Supports Motor Selection and Planning

As outlined at the beginning of this chapter, a decision to act in a particular way in a given situation is shaped by many factors, including sensory information about objects, events, and opportunities for action from the environment, body position and motion, internal motivational states, prior experiences, reward preferences, and learned arbitrary rules and strategies linking sensory inputs to motor actions. There can be many reasons why you want to drink some coffee, and that desire can be fulfilled by actions ranging from simply reaching out to your full coffee cup to making coffee at home or going to a café.

Frontal premotor cortical regions just rostral to M1 play an important role in early movement planning or task-selection processes. Many neurons in those areas, such as the PMd neurons shown in Figure 34–4, generate activity during instructed-delay tasks that reflect the motor intentions of the monkey and even the factors that influenced those action choices. The different premotor cortical regions are presumed to make different but overlapping contributions to motor selection and planning. For instance, the lateral premotor

cortex, including PMd and PMv, have traditionally been implicated in actions initiated and guided by external sensory inputs. In contrast, medial premotor areas, including SMA, pre-SMA, and CMA, have been implicated in the control of self-initiated movements as well as the suppression of actions. However, the distinction between their respective contributions is not absolute.

Medial Premotor Cortex Is Involved in the Contextual Control of Voluntary Actions

Clinton Woolsey's pioneering electrical stimulation studies showed that, in addition to the motor map in M1, the medial wall of the frontal cortex contains an array of neurons that also regulate body movements. This medial motor map, now called the supplementary motor area (SMA), includes the entire contralateral body but is coarser than the detailed map in M1, as described later. Strong stimulus currents are required to evoke movements, which are often complex actions such as postural adjustments or stepping and climbing and can involve both sides of the body. Today, there is agreement that this region contains two areas that have distinct cytoarchitectonic characteristics, axonal connections, and functional properties: a more caudal SMA proper and a more rostral presupplementary motor area (pre-SMA), which we will collectively call the supplementary motor cortex (SMC).

The SMC has been implicated in many aspects of voluntary behavior, although its contribution remains controversial. Several lines of evidence support a role in self-initiated behavior. In humans, electrical stimulation of SMC below the threshold for movement initiation can evoke an introspective sense of an urge to move that does not arise during M1 stimulation. Lesions of SMC produce problems initiating desired movements or suppressing undesirable movements (Box 34–2). Moreover, recordings of slow cortical potentials at the surface of the skull during the execution of self-paced movements show that the initial potential arises in the frontal cortex as much as 0.8 to 1.0 second before the onset of movement. This signal, named the *readiness*

Box 34–2 Lesions of Premotor Cortex Lead to Impairments in the Selection, Initiation, and Suppression of Voluntary Behavior

Lesions of the supplementary motor area (SMA) and presupplementary motor area (pre-SMA) and the prefrontal areas connected with them produce deficits in the initiation and suppression of movements. Initiation deficits manifest themselves as loss of self-initiated arm movements, even though the patient can move when adequately prompted. This deficit can involve movement of parts of the body (*akinesia*) contralateral to the region and speech (*mutism*).

Deficits in movement suppression, in contrast, include the inability to suppress behaviors that are socially inappropriate. These include compulsive grasping of an object when the hand touches it (*forced grasping*), irrepressible reaching and searching movements aimed at an object that has been presented visually (*groping movements*), and impulsive arm and hand movements to grab nearby objects and even people without conscious awareness of the intention to do so (*alien-hand* or *anarchic-hand syndrome*).

Another striking syndrome is *utilization behavior*, in which a patient compulsively grabs and uses objects without consideration of need or the social context. Examples are picking up and putting on multiple pairs of glasses or reaching for and eating food when the patient is not hungry or when the food is clearly part of someone else's meal.

These deficits in the initiation and suppression of actions may represent opposite facets of the same functional role for SMA and especially pre-SMA in the conditional or context-dependent control of voluntary behavior.

Lesions affecting premotor cortex also lead to impairments in the selection of motor actions. For example, when a normal monkey sees a tasty food treat behind a small transparent barrier, it readily reaches around the barrier to grasp it. However, after a large premotor cortex lesion, the monkey may persistently try to reach directly toward the treat and so repeatedly strikes the barrier with its hand, rather than making a detour around the barrier.

More focal lesions or inactivation of the ventral premotor cortex perturbs the ability to use visual information about an object to shape the hand appropriately for the object's size, shape, and orientation before grasping it. Focal lesions of the dorsal premotor cortex affect the ability to learn and recall arbitrary sensorimotor mappings or conditional stimulus–response associations, whereas supplementary motor cortex lesions impede the ability to learn and recall temporal sequences of movement.

potential, has its peak in the cortex centered in SMC. Because it occurs well before movement, the readiness potential has been widely interpreted as evidence that neural activity in this region is involved in forming the intention to move, not just in executing movement.

Neurons in both SMA and pre-SMA discharge before and during voluntary movements. Unlike M1 neurons, the activity of most SMA neurons is less tightly coupled to particular actions of a body part and appears instead to be associated with more complex, coordinated motor acts of the hand, arm, head, or trunk. Compared to SMA neurons, pre-SMA neurons often begin to discharge much earlier in advance of movement onset and are less tightly coupled to the execution of movements.

The SMC has been implicated in the so-called *executive control* of behavior, such as operations required to switch between different actions, plans, and strategies. For example, in monkeys, some SMC neurons discharge strongly when a subject is presented with a cue instructing it to change movement targets or to suppress a previously intended movement. The SMC may therefore contain a system that can override motor plans when they are no longer appropriate.

The SMC has also been implicated in the organization and execution of movement sequences. Some SMC neurons discharge before the start of a particular sequence of three movements but not before a different sequence of the same three movements (Figure 34–7). Other neurons discharge only when a particular movement occurs in a specific position in a sequence or when a particular pair of consecutive movements occurs regardless of their position in the sequence. In contrast, some other SMC neurons discharge only when the monkey makes the movement that occurs in a particular ordinal position of a sequence (eg, only the third) irrespective of its nature or how many movements remain to be executed in the sequence.

These seemingly disparate functions may reflect a more general role of the SMC in *contextual control* of voluntary behavior. Contextual control involves selecting and executing those actions deemed appropriate on the basis of different combinations of internal and external cues as well as withholding inappropriate actions in

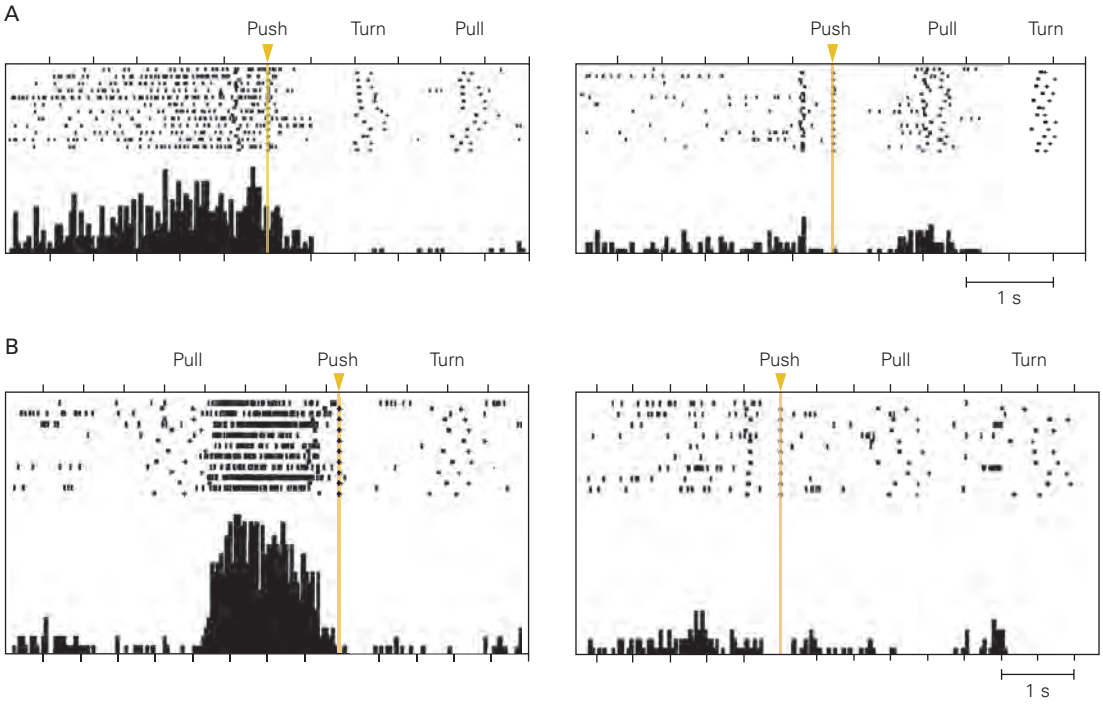

Figure 34–7 Some neurons in the supplementary motor complex of monkeys encode a specific sequence of motor acts. (Adapted, with permission, from Tanji 2001. Copyright © 2001 by Annual Reviews.)

A. A neuron discharges selectively during the waiting period before the first movement of the memorized sequence push-turn-pull (*left*). When the sequence is push-pull-turn (*right*), the cell remains relatively silent, even though the first movement in both sequences is the same (push). Triangles at the top of each raster plot indicate the start of the push movement.

B. Records of a neuron whose activity increases selectively during the interval between completion of one motor act, a pull, and the initiation of another act, a push. The cell is not active when a push is the first movement in the sequence or when pull is followed by turn.

a specific environmental or social context. It also can involve organizing the sequence of actions required to achieve a particular goal. Contextual control likely also involves contributions from other neural circuits such as regions of the prefrontal cortex and the basal ganglia.

The cingulate motor areas (CMA) may also contribute to the contextual control of behavior. CMA appears to be involved in selecting alternate actions following motor errors or in response to changing reward contingencies. For example, monkeys were trained to push or turn a handle in response to a noninstructive trigger signal. Initially, the monkeys received a large reward if they made the same movement (pushing or turning the handle) in sequential trials. After several trials, the reward size began to decrease. If the monkeys then switched to the other movement, the reward size returned to maximum once that movement was repeated for several trials. The best strategy for the monkeys, therefore, was to switch between repetitions of either pushing or turning the handle as soon as they detected a reduction in reward size.

In this task, some neurons in the rostral CMA responded during the interval between the reception of reward and the start of the next trial. On trials with a reduced reward, task-related activity in these neurons did not change when the monkeys made the same movement in the next trial; their activity only changed when the monkeys switched to the other movement in the next trial. Importantly, those same neurons did not show the same response change when a visual cue instructed the monkeys to change movements in the next trial. This suggests that these rostral CMA neurons were preferentially involved in the voluntary decision to switch and move to the alternate goal based on action outcomes (reward size), but not by visual instructions to switch.

Dorsal Premotor Cortex Is Involved in Planning Sensory-Guided Movement of the Arm

Some of the first neural evidence that the lateral premotor cortex, including PMd and PMv, plays a crucial role in the selection and planning of sensory-guided motor actions came from recording studies by Ed Evarts, Steven Wise, and colleagues in the 1980s. These studies showed that many premotor neurons emitted brief short-latency discharge bursts in response to instructional cues that signaled specific movements, or sustained activity during the instructed-delay period between the appearance of the instructional cue and a second cue that permitted the instructed movement (Figure 34–4).

This activity reflects information about the intended act, including the spatial location of the target, the direction of arm movement, and other movement attributes. Importantly, PMd delay-period activity can reflect the intention to reach to a particular location with either the contralateral or ipsilateral arm, even though the biomechanical details of the two arm movements are very different. This suggests that PMd activity can signal the intention to generate a motor act independent of the effector used to generate the action, in an extrinsic spatial coordinate framework consistent with a prediction of the sensorimotor coordinate transformation model of motor planning. Imaging studies have likewise found evidence for an extrinsic spatial representation of finger-tapping sequences made with either hand in human premotor cortex.

Selection of an appropriate action from among multiple alternatives is a critical aspect of voluntary control. Delay-period activity in PMd can reflect that process. For example, in one experiment, recordings were made from PMd neurons in monkeys during a task in which the animals first received two colored spatial cues that identified two potential targets for reaching in opposite directions. After a memorized-delay period, a new centrally-located color cue informed the monkeys which of the spatial cues was the correct target. Following the first instruction, neural activity in PMd signaled both potential-reaching movements, but immediately after the second instruction, activity in PMd signaled only the monkeys' reaching choice (Figure 34–8A). This showed that PMd can prepare multiple potential motor actions prior to the final decision about which action to take. Subsequent studies suggest that this might be limited to no more than three to four simultaneous potential actions. Reach-related neurons in parietal area PRR also contribute to the preparation for two potential motor actions before the final action decision is made (Figure 34–8B), revealing how this process is distributed across multiple arm movement–related cortical neural populations.

PMd neurons can also signal a deliberate decision not to move. Many PMd neurons generate directionally tuned activity during an instructed-delay period when a colored visual cue at a target location instructs a monkey to reach to the target, but decrease their activity when a different colored cue at the same location instructs the monkey to refrain from reaching to it. This differential activity is an unequivocal signal, seconds before the action is executed, about the monkey's intention to reach in a particular direction or not to move in response to an instructional cue (Figure 34–9). Interestingly, many neurons in the parietal area PE/MIP studied in the same task continue to generate directionally tuned activity during the delay period even after the instructional cue to withhold

Figure 34–8 Activity of reach-related cortical neurons in monkeys during a target selection task reflects potential movements to different targets as well as the chosen direction of reach.

A. The three-dimensional colored surface depicts the mean level of activity of a population of dorsal premotor cortex (**PMd**) neurons with respect to baseline in a task in which a monkey must choose one of two color-coded reach targets in each trial. Cells are sorted along one axis (labeled "cells") based on their preferred movement direction (neurons located at the **red** and **blue circles** prefer movements at 45° and 215°, respectively). Diagrams beside the neural response profile display the stimuli presented to the monkey at different times during the trial. **Red** and **blue** cues provide information about potential actions; **green** cues guide the monkeys through different stages of each trial but provide no information about what reach to make. Shortly after the start of each trial, two potential reach targets (**blue** and **red** spatial cues) appear in opposite locations relative to the starting position of the arm (**green circle**) for 500 ms and then disappear. After a memorized delay period, the color of the starting circle changes to either **red** or **blue** (color cue), indicating to the monkey which is the correct target, in this case at 45°. After a further delay period, the go signal (**green circles** at all eight possible target locations) instructs the monkey to begin reaching to its chosen target. During the period of target uncertainty between the appearance of the two spatial cues and the central color cue, PMd neurons that prefer the two potential reach movements (**red** and **blue circles**) are simultaneously activated, whereas neurons that prefer other movements are inactive or suppressed, so that the entire PMd population encodes the two potential reach actions. As soon as the color cue appears to identify the correct target, the PMd neural activity changes rapidly to signal the reach movement chosen by the monkey. Had the color cue designated the target at 215°, the neurons preferring that target (**blue circle**) would increase their activity, and the neurons preferring the target at 45° (**red circle**) would decrease their activity (not shown). (Reproduced, with permission, from Cisek and Kalaska 2010. Copyright © 2010 by Annual Reviews.)

B. In a second study of neural activity in the parietal reach region (**PRR**), the format of data is the same as in part **A**. In this study, the monkey is presented with a single spatial cue that instructs it to prepare to reach either to the cue's location (**PD**) or in the opposite direction (**OD**). After a random memorized delay period, a color cue specifies whether the reach should be to the remembered location of the spatial cue (**green**; PD) or in the OD (**blue**). PRR neural activity is sorted according to the preferred movement direction of each neuron, as in part **A**. Population activity initially specifies the spatial cue location but then reflects both potential movement directions during the remainder of the memorized delay period. Shortly after the color cue appears, the activity quickly shifts to reflect the chosen reach direction, either the PD or OD. (Reproduced, with permission, from Klaes et al. 2011. Copyright © 2011 Elsevier Inc.)

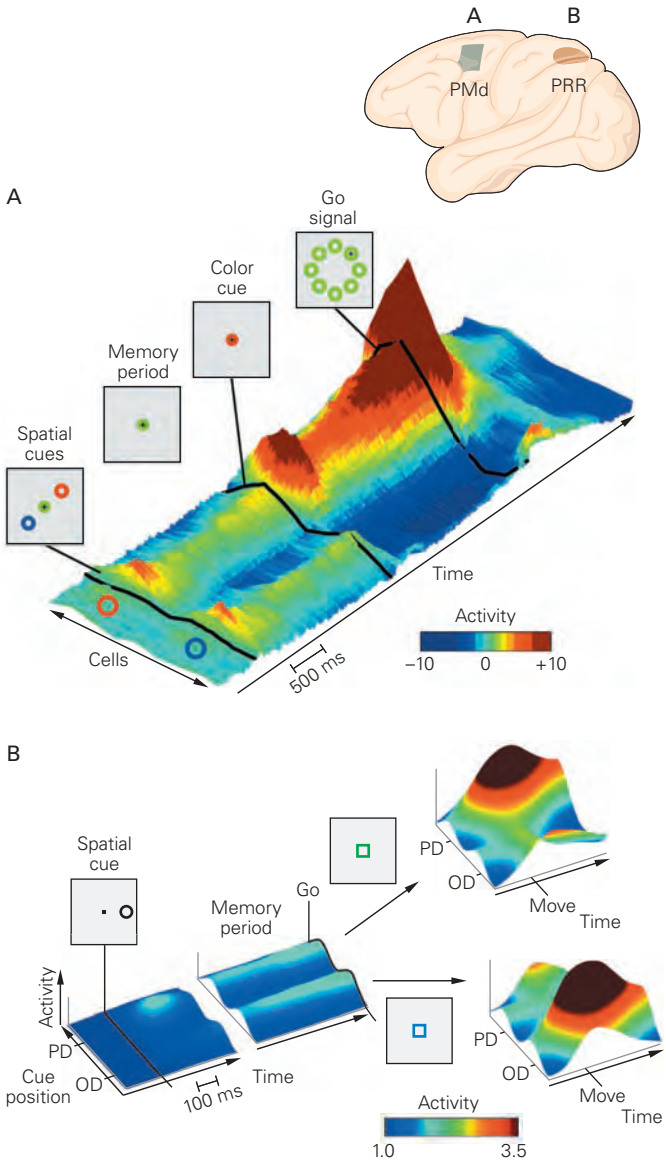

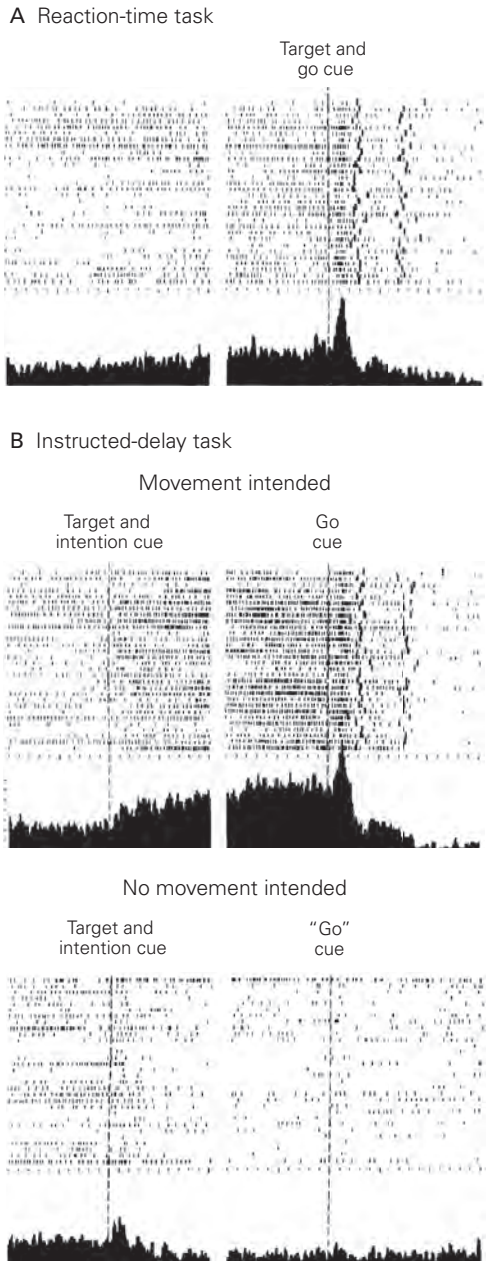

Figure 34–9 Decisions about response choices are evident in the activity of premotor cortex neurons in the monkey. (Reproduced, with permission, from Crammond and Kalaska 2000.)

A. In a reaction-time task (reaching), a cell exhibits gradually increasing tonic firing while waiting for the appearance of a target. When the target appears (go cue), the cell generates a directionally tuned response.

B. In an instructed-delay task, when a monkey is shown the target and instructed to move once the go cue appears, the cell generates a strong directionally tuned signal for the duration of the delay period before the go cue (top). When the monkey is shown the target and instructed not to move when the go cue appears, the cell's activity decreases (bottom).

reaching, suggesting that the parietal cortex retains a representation of potential actions that ultimately are not executed.

Many neurons in premotor cortex also discharge during movement execution. Given this close proximity of planning- and execution-related activity, even at the level of individual neurons, a major question is why planning-related neural activity does not immediately initiate a movement. What prevents the movement from being executed prematurely? It does not appear that planning-related activity simply fails to exceed a minimum threshold required to initiate the movement or that there is a separate overt braking mechanism that must be released to allow the movement to begin.

A different way to interpret neural processing during the planning and execution of reaching that might provide answers to such questions comes from a dynamical-systems perspective. The idea is that cortical motor circuits form a dynamical system whose distributed activity patterns evolve in time as a function of their initial state, input signals, and stochastic neural response variability ("noise"). Activity patterns during different stages of planning and execution thus reflect different states of the network, including a specific state during the delay period that can prepare the movement but not activate muscles (Figure 34–10). The overall similarity of the population-level activity patterns during repetitions of the same movement shows that the entire population undergoes a coordinated pattern of co-modulation of activity during the planning and execution of the movement, determined by the synaptic connectivity within the neural circuit.

Dorsal Premotor Cortex Is Involved in Applying Rules (Associations) That Govern Behavior

Behavior is often guided by arbitrary rules that link specific symbolic cues to particular actions. When driving your car, you must perform different actions depending on whether a traffic light is green, amber, or red. In monkeys that have learned to associate arbitrary cues with specific movements, many cells in premotor areas respond selectively to specific cues. For instance, in order to select the correct target in the two-target study in Figure 34–8, the monkeys had to apply a rule that mapped color to target location provided by the two sequential instructional cues.

The PMd is implicated in the acquisition of new movement-related associations or rules. In one experiment, recordings from PMd neurons were made while the monkeys learned the association between four unfamiliar visual cues and four different movement

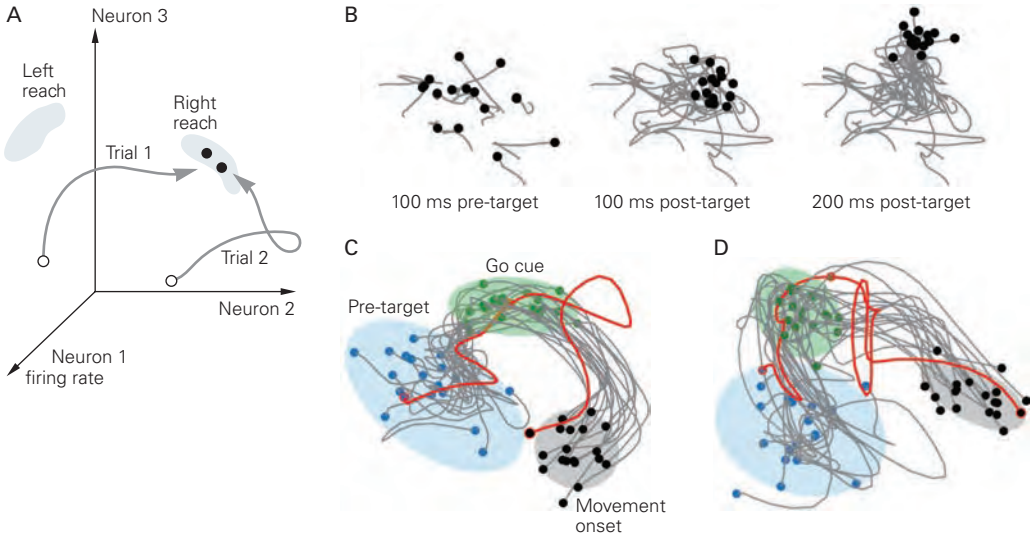

Figure 34–10 **The time-varying neural activity in the dorsal premotor cortex of monkeys during different stages of the planning and execution of a movement can be viewed as transitions between different activation states.** (Adapted, with permission, from Churchland MM et al. 2010. Stimulus onset quenches neural variability: a widespread cortical phenomenon. Nat Neurosci 13:369-378. Copyright © Springer Nature.)

A. A schematic illustration of how the simultaneous activity of neurons can be viewed as a trajectory through a multi-neuron activity "state space." The time-varying activity level of three simultaneously recorded neurons is represented along three axes, which defines a three-neuron state space. A specific plan (reach left or reach right) requires different combinations of preparatory firing rates for the three neurons (**gray zones**). Prior to the formation of the intention to move left or right, the baseline activity of the three neurons occupies a region in state space that is associated with holding the arm in its current position (**open circles**, for two different trials). When an instruction appears to make a reach to the right, the combined activity of the three neurons changes in a coordinated fashion, creating time-varying "neural trajectories" (**gray arrows**) that converge on the region of state space that is associated with generating a rightward movement (**filled circles** within the "right reach" gray zone).

B. Projection of the simultaneous activity of a large population of dorsal premotor cortex (PMd) neurons onto a two-dimensional state space shortly before (pre-target) and after (post-target) the appearance of a reach target cue in a task in which the reach movement must be delayed until a subsequent go cue is presented. **Gray lines** show the temporal evolution of the neural trajectories during the earliest part of movement preparation from 200 ms before target cue until the specified pre- or post-target time (**black dots**) in 15 different trials to the same target location. Neural activity initially meanders randomly within the region of state space associated with the starting posture of the arm (*left*). It then begins to converge onto a smaller region of the state space shortly after the reach target instruction appears (*center*) and begins to evolve along the neural trajectory associated with entering the preparatory state for the reach (*right*).

C. A more complete illustration of the neural trajectories recorded during 18 different repeated trials to the same target in this delayed reaching task from the initial pre-target postural state to the onset of movement. **Blue dots** indicate activity while holding the arm in the starting posture 100 ms before appearance of the target instruction onset. Once the target instruction appears, the neural trajectories evolve toward a region of state space associated with the preparatory activity state during the delay period (**green zone**), where it dwells until a go cue appears that allows the monkey to initiate the withheld movement (**green dots**). While in this reach-preparatory part of the state space during the delay period, the arm stays at the start position because PMd activity in that part of state space is not capable of activating muscles (ie, it is "output-null"). When the go cue appears, the neural trajectories unfold toward a different region of state space associated with the initiation of the intended reach movement (**gray zone** and **black dots**). The neural activity can only cause the muscle activity for the intended movement when it enters this "output-potent" zone of state space. The trial-to-trial variability of the neural trajectories can account for intertrial variability in movement kinematics and reaction times. One outlier trial (**red**) had a long reaction time and followed a more complex and time-consuming neural trajectory from the **green** to the **gray** zone. The output-null preparatory (**green**) and output-potent movement-initiation (**gray**) zones for reaches to different target locations occupy different regions of the total population state space distinct from those associated with this reach target.

D. Data are for the same target location as in part **C** but were recorded on a different day. The neural trajectory structure is fundamentally similar for the same movements between recording sessions. Differences in the overall pattern of activity can be explained by interday differences in the activity of individual neurons and differences in the composition of the recorded neural population between sessions.

directions. Although the monkeys' choices were initially random, they learned the rules within a few dozen trials. The monkeys made an arm movement in response to each cue; during the early "guessing" phase of learning, the activity of many PMd neurons was weak but gradually increased in strength and directional tuning as the monkeys learned which cue signaled which movement. Other neurons showed a reciprocal decline in activity as the rules were acquired. These changes in activity during learning reflected both the movement choices and the rising level of knowledge of the rules linking cues with actions.

The nature of the rule can also have a strong effect on neural responses. In monkeys that have been trained to choose between several possible movements based on a spatial rule (a visual cue's location) or a semantic rule (a cue's arbitrarily designated meaning independent of its location), many prefrontal and PMd neurons are preferentially active when the animal chooses a movement using one rule but not the other. This shows that the neural activity is related not just to a particular cue or action but also to the association between them.

Premotor areas are involved in the implementation of even abstract rules. For example, monkeys were trained in a task that required two decisions, one perceptual and the other behavioral, that had no prior association. In each trial, the monkeys first had to decide whether two sequentially presented visual images were the same or different (a *match/nonmatch perceptual decision*). In some trials, a *rule cue* presented at the same time as the sample visual image instructed the monkeys to move their hand if the two images were identical and to refrain from moving if they differed (a *go/no-go motor decision*); in other trials, the rule was reversed—move if the images differ and do not move if they match. Neural activity in PMd after the test visual images were presented was correlated more strongly to the motor decision than the perceptual decision in each trial, but both decisions were expressed in PMd. More strikingly, PMd activity was also correlated with the match/non-match *behavioral rule* during the delay period between the two visual images that guided the motor decision after the test image appeared (Figure 34–11). These results suggest that PMd has a major role in applying rules that govern the appropriateness of a behavior and in making behavioral decisions according to the prevailing rules. Neural recordings in prefrontal cortex during the same task (not shown) found a strong representation of the physical identity of the visual images, but weaker and later correlates of the behavioral rule and the motor decision than in PMd.

Ventral Premotor Cortex Is Involved in Planning Motor Actions of the Hand

The most lateral part of the premotor cortex, area PMv, is reciprocally connected with parietal cortex areas AIP, PF, and PFG and the secondary somatosensory area. Electrical stimulation shows that PMv contains extensively overlapping circuits that control hand and mouth movements.

Like AIP neurons, many PMv neurons appear to contribute to the control of hand actions based on the physical affordances offered by target objects. These neurons tend to fire preferentially during certain stereotypical hand actions, such as grasping, holding, tearing, or manipulating objects. Many neurons discharge only if the monkey uses a specific type of grip, such as a precision grip, whole-hand prehension, or finger prehension (Figure 34–12). Precision grip is the type most often represented. Some PMv neurons discharge throughout the entire action, while others discharge selectively at particular stages of one type of prehension, such as during the opening or closing of the fingers.

Another striking property of PMv neurons is that their discharge often correlates with the goal of a motor act and not with the individual movements forming it. Thus, many PMv neurons discharge when grasping an object is executed with effectors as different as the right hand, the left hand, and even the mouth. Conversely, a PMv neuron may be active when an index finger is flexed to grasp an object but not when the animal flexes the same finger to scratch itself.

Premotor Cortex May Contribute to Perceptual Decisions That Guide Motor Actions

A series of studies provide evidence that cortical motor areas not only represent the sensory information that guides voluntary movements but also express the neural operations necessary to make and act on perceptual decisions. Monkeys were trained to discriminate the difference in frequency between two brief vibratory stimuli applied to one finger and separated in time by a few seconds. The animals had to decide whether the frequency of the second stimulus was higher or lower than the first and to report their perceptual decision by reaching out to push one of two buttons with the other hand.

The decision-making process in this task can be conceived as a chain of neural operations: (1) encode the first stimulus frequency (f1) when it is presented; (2) maintain a representation of f1 in working memory during the interval between the two stimuli; (3) encode the second stimulus frequency (f2) when it is

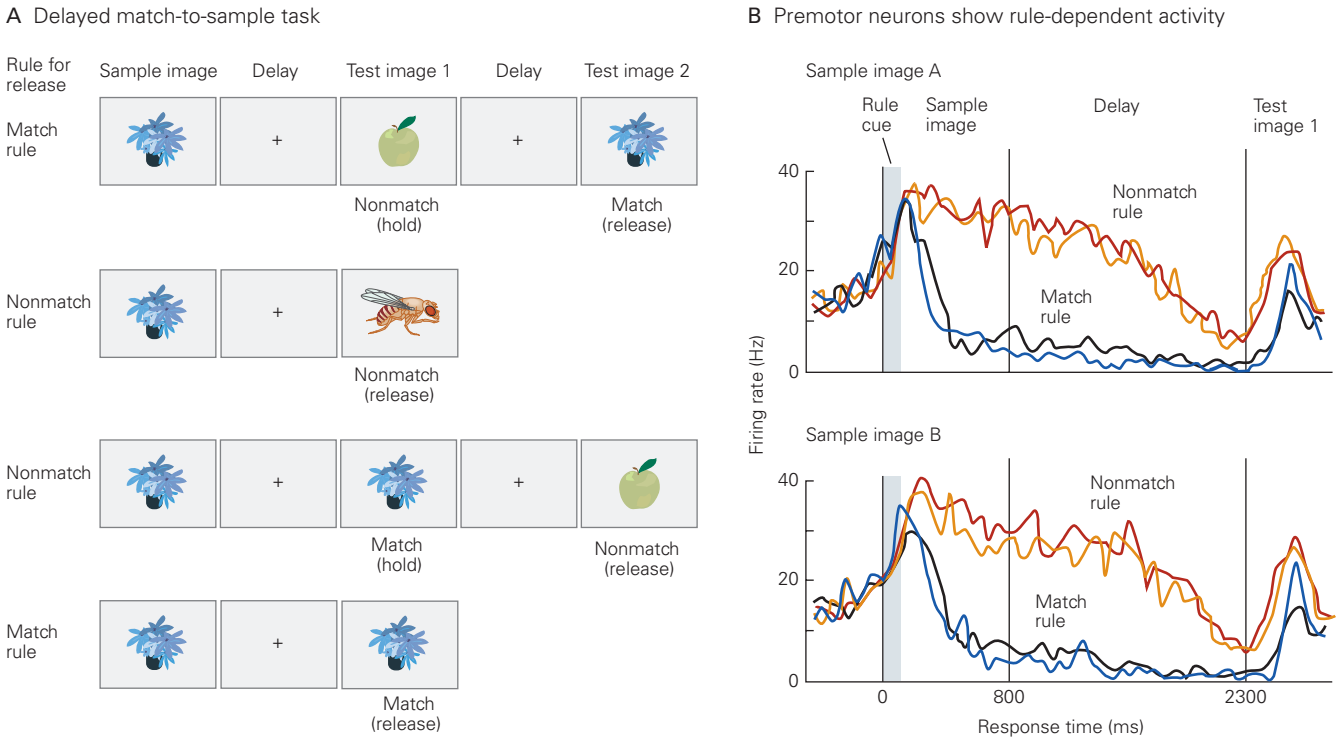

Figure 34–11 **Premotor cortex neurons in the monkey choose particular voluntary behaviors based on decisional rules.** (Reproduced, with permission, from Wallis and Miller 2003.)

A. A monkey must make a decision about whether to release a lever or keep holding it based on two prior decisions: a perceptual choice, whether a test image is the same as or different from a sample image presented earlier, and a behavioral choice, whether the current rule is to release the lever when the test image is the same as the sample (match rule) or when it is different (nonmatch rule). The monkey is informed of the behavioral rule that applies in each trial by a rule cue, such as an auditory tone or juice drops, which is presented for 100 ms at the same time as the onset of the sample image at the start of the trial.

B. A neuron in the dorsal premotor cortex has a higher discharge rate whenever the nonmatch rule is in effect during the delay between the presentation of the first and second images. The responses to two different sample images (upper and lower plots) were recorded from the same cell, indicating that the rule-dependent activity is not altered by changing the images. Nor, as shown by the pairs of curves associated with each rule, does activity depend on the type of rule cue (auditory tone or juice drops). (Tone cue trials: **orange** and **blue curves**; juice cue trials: **red** and **black curves**). Other dorsal premotor cortex cells (not shown) respond preferentially to the match rule over the nonmatch rule. The differential activity of the neuron up to presentation of the test image reflects the rule that will guide the animal's motor response to the test image, not the physical properties of the visual stimuli or the motor response.

presented; (4) compare f2 to the memory trace of f1; (5) decide whether the frequency of f2 is higher or lower than that of f1; and finally, (6) use that decision to choose the appropriate movement of the other hand. Everything prior to the last step would appear to fall entirely within the domain of sensory discriminative processing.

While the monkeys performed the task, neurons in the primary (S-I) and secondary (S-II) somatosensory cortices encoded the frequencies of the stimuli while they were presented. During the interval between f1 and f2, there was no sustained activity in S-I representing the memorized f1 and only a transient representation in S-II, which vanished before f2 was presented.

Strikingly, however, the activity of many neurons in the prefrontal cortex, SMC, and PMv scaled with the frequencies of f1 and f2 while they were being delivered. Furthermore, some prefrontal and premotor neurons showed sustained activity proportional to the frequency of f1 during the delay period between f1 and f2. Most remarkably, many neurons in those areas, especially in PMv, encoded the *difference* in frequency between f2 and f1 independently of their actual frequencies when f2 was delivered (Figure 34–13). This centrally generated signal is appropriate to mediate the perceptual discrimination that determines which button to push. Neurons that encoded the f2–f1 difference were absent in S-I and were far more common in SMC and PMv than in S-II.

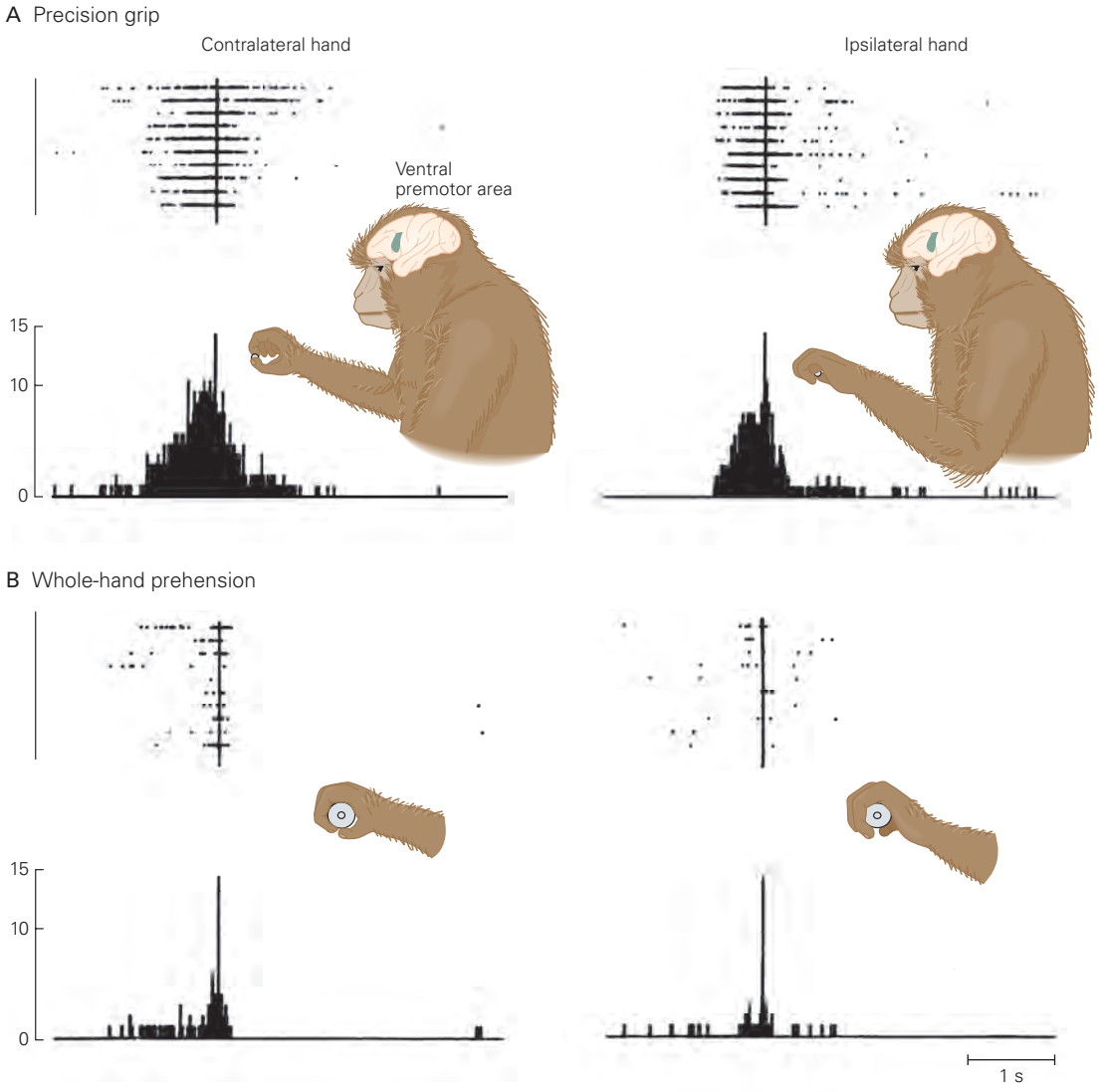

Figure 34–12 Some neurons in the ventral premotor cortex of a monkey discharge selectively during one type of grasping. This neuron discharges vigorously during a precision grip with the thumb and index finger of either the right or the left hand but very weakly during whole-hand prehension with either hand. Raster plots and histograms are aligned (**vertical line**) with the moment the monkey touches the food (**A**) or grasps the handle (**B**). (Reproduced, with permission, from Rizzolatti et al. 1988. Copyright © Springer-Verlag 1988.)

Several Cortical Motor Areas Are Active When the Motor Actions of Others Are Being Observed

Some premotor and parietal areas can be activated when no overt action is intended, such as when an individual is asked to imagine performing a certain motor act. This phenomenon, termed *motor imagery*, has been demonstrated in humans using functional brain imaging. The neural activity evoked by motor imagery presumably reflects brain mechanisms associated with motor planning and preparation that have been disassociated from its overt execution.

A second condition in which cortical motor circuits are activated without intending overt action is when an individual observes another individual performing motor acts that are part of her own motor repertoire. The control of behavior and social interaction depends greatly on the ability to recognize and understand what others are doing and why they are doing it. Such understanding could result from a high-order visual perceptual analysis of the nature of the observed behavior and by drawing inferences about the motivation and purpose of the behavior based on

one's own experience. An alternative explanation is the *direct-matching hypothesis*, the idea that observation of the actions of others activates motor circuits in the observer that control similar motor actions. According to this hypothesis, empathetic activation of motor circuits could provide a link between the observed actions and the observer's stored knowledge of the nature, motives, and consequences of similar actions that they had performed in the past.

Striking evidence in support of the direct-matching hypothesis was provided by the discovery of a remarkable population of neurons called mirror neurons, first in PMv and later in the parietal AIP of monkeys. Mirror neurons discharge both when the monkey actively grasps and manipulates objects and when it observes similar actions performed by another monkey or the experimenter (Figure 34–14). Mirror neurons typically do not respond when a monkey simply observes a potential target object or when it observes mimed arm and hand actions without a target object. Some parietal mirror neurons can even differentiate the ultimate goal of similar observed actions, such as grasping and picking up food to eat it versus putting it into a cup.

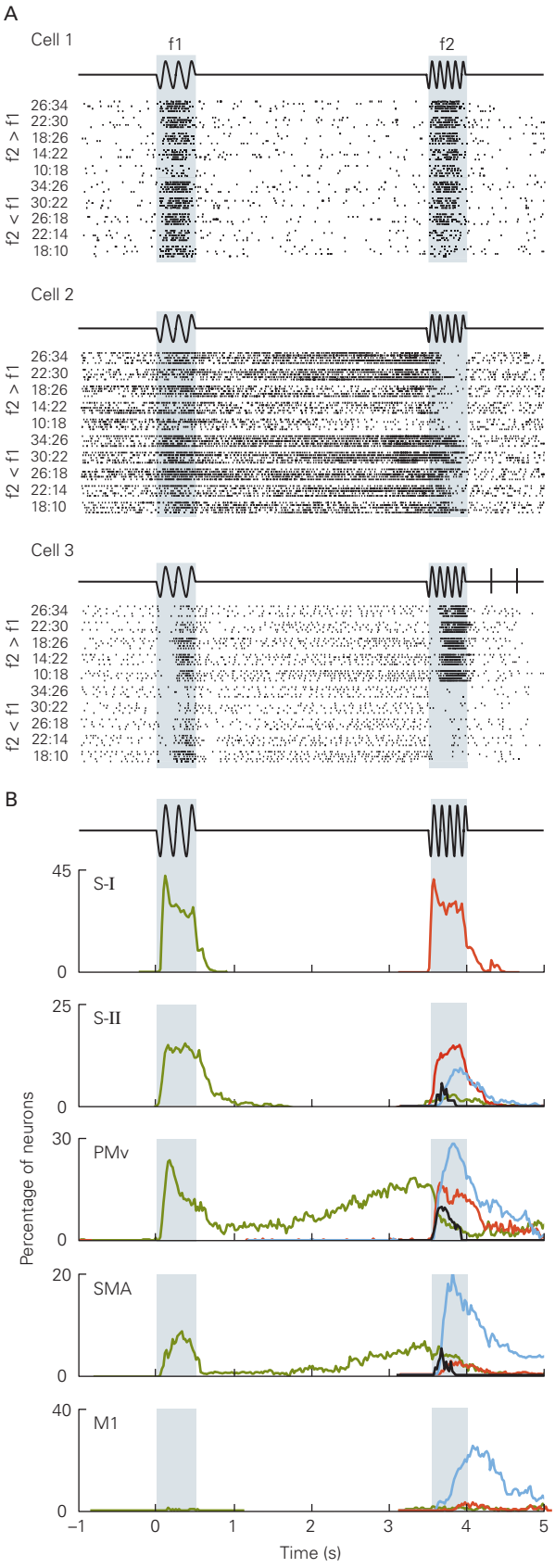

Figure 34–13 (Right) Neural activity in ventral premotor cortex in monkeys expresses the operations required to choose a motor response based on sensory information. (Adapted, with permission, from Romo, Hernández, and Zainos 2004. Copyright © 2004 Cell Press.)

A. These records of three neurons in the ventral premotor cortex of a monkey were made while the animal performed a task in which it had to decide whether the second of two vibration stimuli (**f1** and **f2**, applied to the index finger of one hand) was of higher or lower frequency than the first. The choice was signaled by pushing one of two buttons with the nonstimulated hand. The frequencies of f1 and f2 are indicated by the numbers on the left of each set of raster plots. Cell 1 encoded the frequencies of both f1 and f2 while the stimuli were being presented but was not active at any other time. This response profile resembles that of many neurons in the primary somatosensory cortex. Cell 2 encoded the frequency of f1 and sustained its response during the delay period. During the presentation of f2, the neuron's response was enhanced when f1 was higher than f2 and suppressed when it was lower. Cell 3 responded to f1 during stimulation and was weakly active during the delay period. However, during exposure to f2, the cell's activity robustly signaled the difference f2–f1 independently of the specific frequencies f1 and f2.

B. Histograms show the percentage of neurons in different cortical areas whose activity correlated at each instant with different parameters during the tactile discrimination task. **Green** shows the correlation with f1, **red** the correlation with f2, **black** the interaction between f1and f2, and **blue** the correlation with the difference between f2–f1. (Abbreviations: **M1**, primary motor cortex; **PMv**, ventral premotor cortex; **S-I**, primary somatosensory cortex; **S-II**, secondary somatosensory cortex; **SMA**, supplementary motor area.)

Neural-recording and brain-imaging studies show that humans are also endowed with a mirror-like mechanism to match observed actions with actions encoded in their motor system. This activity arises in various areas of cortex, including the rostral inferior parietal lobule, IPS, PMv, and posterior sector of the inferior frontal gyrus.

Cortical motor circuits appear to be involved in understanding and predicting the outcomes of observed events. In one experiment, PMd neurons implicated in the selection of reaching targets using visual cues (Figure 34–8) also discharged when monkeys simply watched the same cues and cursor motions on the monitor while an unseen party performed the task. The monkeys received a free juice reward when the cursor moved to the correct target but not if it moved to the wrong target. The monkeys began to lick the juice tube shortly after the cursor started to move to the correct target well before the juice was actually delivered, but quickly removed their mouth from the tube when the cursor moved toward the wrong target. This behavior showed that the monkeys correctly interpreted what they saw and accurately predicted its consequences.

Remarkably, the activity of most of the task-related PMd neurons was strikingly similar whether the monkeys used visual cues to plan and make arm movements or simply observed the visual events and predicted their outcome. Those neurons stopped responding during observation if no reward was delivered after correct trials or if the animal was sated and not interested in drinking juice. This showed that the neurons were not simply responding to the sensory inputs, but instead were processing the observed sensory events to predict their ultimate outcome for the monkey, namely the likelihood of a free juice reward.

This activation in connection with passive observation supports the idea that activation of premotor

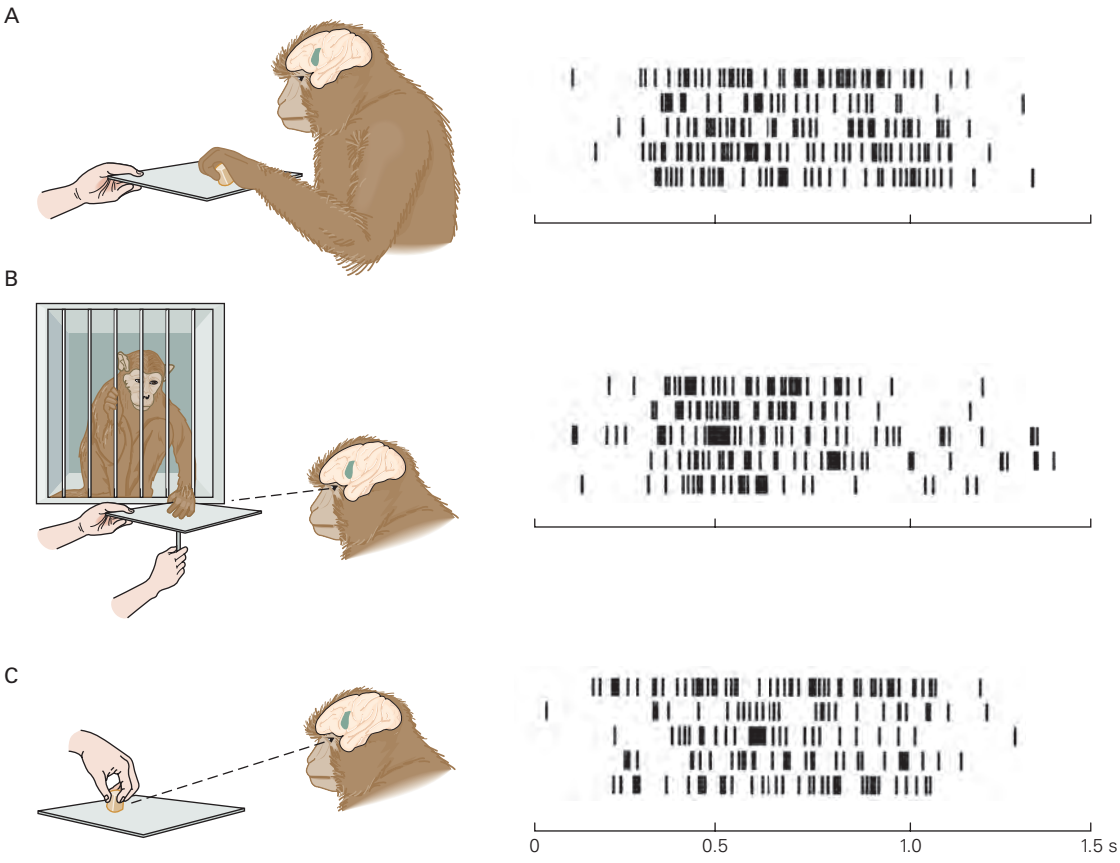

Figure 34–14 A mirror neuron in the ventral premotor cortex (area F5) of a monkey. (Reproduced, with permission, from Rizzolatti et al. 1996. Copyright © 1996 Elsevier Science B.V.)

A. The neuron is active when the monkey grasps an object.

B. The same neuron is also excited when the monkey observes another monkey grasping the object.

C. The neuron is similarly activated when the monkey observes the human experimenter grasping the object.

Time zero in the cell activity rasters corresponds approximately to the time of presentation of the object to grasp (panel A) or the onset of the observed grasping actions (panels B and C).

circuits in nonmotor contexts may contribute to understanding the nature and consequences of observed events in the environment. It has also been implicated in the ability of human subjects to learn new motor skills simply by observing a skilled person perform the same actions. Moreover, dysfunction of the mirror-neuron system in young children may contribute to some of the symptoms of autism.

Many Aspects of Voluntary Control Are Distributed Across Parietal and Premotor Cortex

While we have described the roles of premotor areas in parietal and precentral cortex separately, it must be emphasized that major sensorimotor control processes are shared across multiple cortical regions via their reciprocal interconnections.

For instance, the neural processes that link the physical affordances of target objects to appropriate hand actions are distributed across parietal area AIP, premotor area PMv, and M1, with visuospatial aspects of the process more prominent in AIP and motor components more prevalent in precentral cortex (Figure 34–15). Likewise, as already noted, neural correlates of reach target selection in PRR (Figure 34–8B) strikingly resemble those reported in PMd (Figure 34–8A).

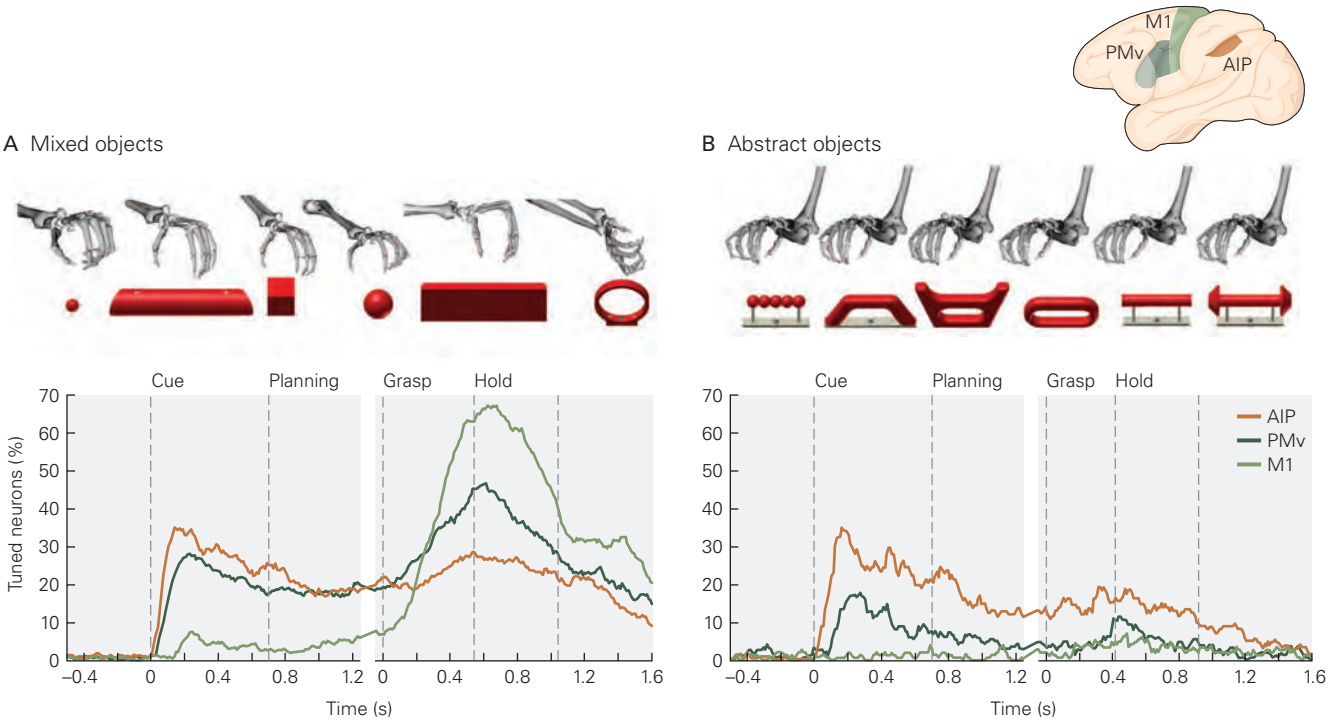

Figure 34–15 Visuomotor processing of object shape is distributed across several cortical areas in the monkey. (Reproduced, with permission, from Schaffelhofer and Scherberger 2016.)

A. A set of "mixed" objects elicit different visual responses and require different motor responses to grasp them. The plots show the percentages of neurons in the anterior intraparietal areas (**AIP**; **orange**), ventral premotor cortex (**PMv**; F5; **dark green**), and primary motor cortex (**M1**; **light green**) that significantly modulated their response as a function of object identity across time. Monkeys were first shown the object to grasp (cue and planning periods) and then allowed to reach to, grasp, and hold the object (grasp and hold periods). The proportion of neurons that varied their activity across object types (tuned neurons) during the cue and planning periods was greatest in AIP and least in M1, indicating that sensitivity to object visual shape was most prominent in AIP. During motor action (grasp and hold periods), the reverse pattern was observed, with many neurons in PMv and especially M1 displaying a strong dependence on the different grasping actions required to hold onto the different objects.

B. A set of "abstract" objects elicit different visual responses but require similar motor responses to grasp them. As with the "mixed" object set, many AIP neurons varied their activity as a function of object shape during the cue and planning periods, but fewer PMv and almost no M1 neurons showed sensitivity to observed object shape. During motor action (grasp and hold periods), very few PMv and M1 neurons showed any difference in activity as a function of the shape of the different objects, all of which required the same grasping action.

The Primary Motor Cortex Plays an Important Role in Motor Execution

Once an individual has decided on a behavioral goal, motor commands must then be communicated to muscles to move the body. The complexity of this problem cannot be underestimated as it requires precise control of the spatiotemporal patterns of activity of large numbers of muscles acting across many joints to achieve the behavioral goal, while also accounting for the complex, nonlinear mechanical properties of the musculoskeletal system and forces and loads imposed by the environment. These detailed patterns of muscle activity are coordinated by spinal motor neurons and interneuronal circuits (Chapter 32). However, the primary motor cortex (M1) plays an important role in generating the motor commands that control that spinal activity, including essential information necessary to select and control the timing and magnitude of muscle activity.

The Primary Motor Cortex Includes a Detailed Map of the Motor Periphery

The idea that a local region of the cerebral cortex contains a motor map of the body dedicated to voluntary motor control dates back to the work of the English neurologist John Hughlings Jackson in the middle of the 19th century. He reached this conclusion while treating patients with epileptic seizures that were characterized by recurring spasmodic involuntary movements that sometimes resembled fragments of purposive voluntary actions and that progressed systematically to include different parts of the body during each seizure episode (Chapter 58). Later in the 19th century, improved anesthesia and aseptic surgical techniques allowed direct experimental study of the cerebral cortex in experimental animals. Using those new methods, Gustav Fritsch and Eduard Hitzig in Berlin and David Ferrier in England showed that electrical stimulation of the surface of a limited area of cortex in different anesthetized mammalian species evoked movements of parts of the contralateral body. In monkeys, the electric currents needed to evoke movements were lowest in a narrow strip along the rostral bank of the central sulcus, the same region now called primary motor cortex.

Their experiments demonstrated that within this strip of tissue stimulation of adjacent sites evoked movements in adjacent body parts, starting with the foot, leg, and tail medially, and proceeding to the trunk, arm, hand, face, mouth, and tongue more laterally. When they lesioned a cortical site at which stimulation had evoked movements of a part of the body, movement of that body part was perturbed or lost after the animal recovered from surgery. These early experiments showed that the motor cortex contains an orderly motor map of major parts of the contralateral body and that the integrity of the motor map is necessary for voluntary control of the corresponding body parts. Studies in the first half of the 20th century on many species by Clinton Woolsey and on humans undergoing surgery by Wilder Penfield demonstrated that the general topographic organization of the rostral bank of the central sulcus is conserved across many species (Figure 34–16). One important observation was that the motor map is not an exact point-to-point reproduction of the body's anatomical form. Instead, the most finely controlled body parts, such as the fingers, face, and mouth, are represented by disproportionately large areas, reflecting the larger number of neurons needed for fine motor control.

Today the best-studied regions of the map are those parts controlling the arm and hand and reveal far more complexity than conveyed in the classic diagrams shown in Figure 34–16A,B. First, neurons controlling the muscles of the digits, hand, and distal arm tend to be concentrated within a central zone, whereas those controlling more proximal arm muscles are located in a horseshoe-shaped ring around the central core (Figure 34–16C). Second, stimulation sites overlap extensively, allowing control of muscles acting across different joints; conversely, each muscle can be activated by stimulating many sites dispersed across the arm/hand motor map. Finally, local horizontal axonal connections link different sites across the motor map, likely allowing coordination of activity across the map during the formation of motor commands.

Some Neurons in the Primary Motor Cortex Project Directly to Spinal Motor Neurons

As already noted, while many corticospinal axons in primates terminate only on spinal interneurons, others also synapse directly onto spinal motor neurons. These corticomotoneuronal (CM) cells are found only in the most caudal part of M1 that lies within the anterior bank of the central sulcus. There is extensive overlap in the distribution of the CM cells that project to the spinal motor neuron pools innervating different muscles (Figure 34–17A).

CM cells are very rare or absent in nonprimate species and become a progressively larger component of the corticospinal tract in primate phylogeny from prosimians to monkeys, great apes, and humans. In monkeys, more CM cells project to the motor pools for muscles of the digits, hand, and wrist than to

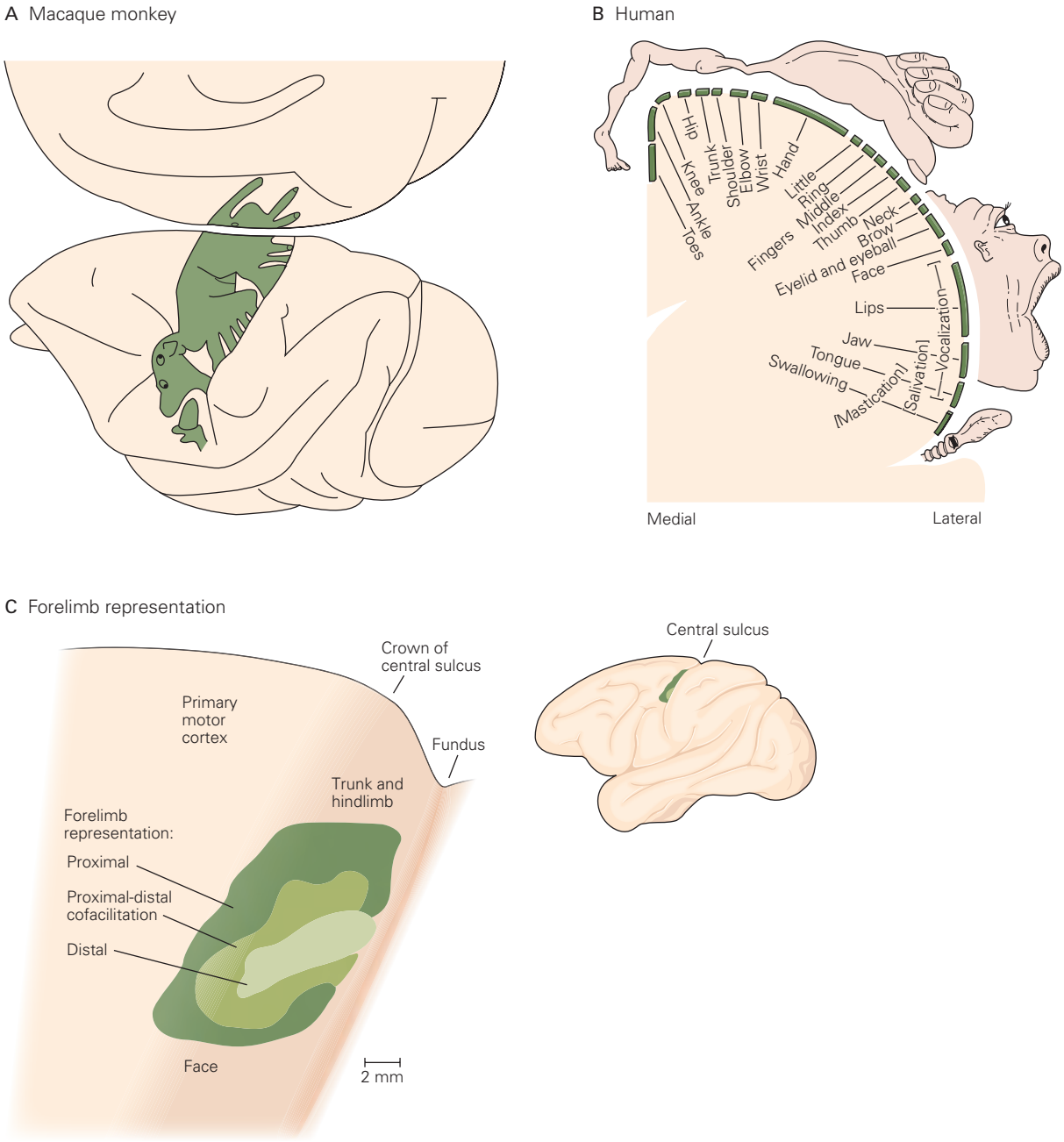

Figure 34–16 **The motor cortex contains a topographic map of motor output to different parts of the body.**

A. Studies by Clinton Woolsey and colleagues confirmed that the representation of different body parts in the monkey follows an orderly plan. Motor output to the foot and leg is medial, whereas the arm, face, and mouth areas are more lateral. The areas of cortex controlling the foot, hand, and mouth are much larger than the regions controlling other parts of the body.

B. Wilder Penfield and colleagues showed that the human motor cortex motor map has the same general mediolateral organization as in the monkey. However, the areas controlling the hand and mouth are even larger than in monkeys, whereas the area controlling the foot is much smaller. Penfield emphasized that this cartoon illustrated the relative size of the representation of each body part in the motor map; he did not claim that each body part was controlled by a single separate part of the motor map.

C. The arm motor map in monkeys has a concentric, horseshoe-shaped organization. Neurons that control the distal arm (digits and wrist) are concentrated in a central core (**pale green**) surrounded by neurons that control the proximal arm (elbow and shoulder; **dark green**). The neuron populations that control the distal and proximal parts of the arm overlap extensively in a zone of proximal-distal co-facilitation (**intermediate green**). (Reproduced, with permission, from Park et al. 2001. Copyright © 2001 Society for Neuroscience.)

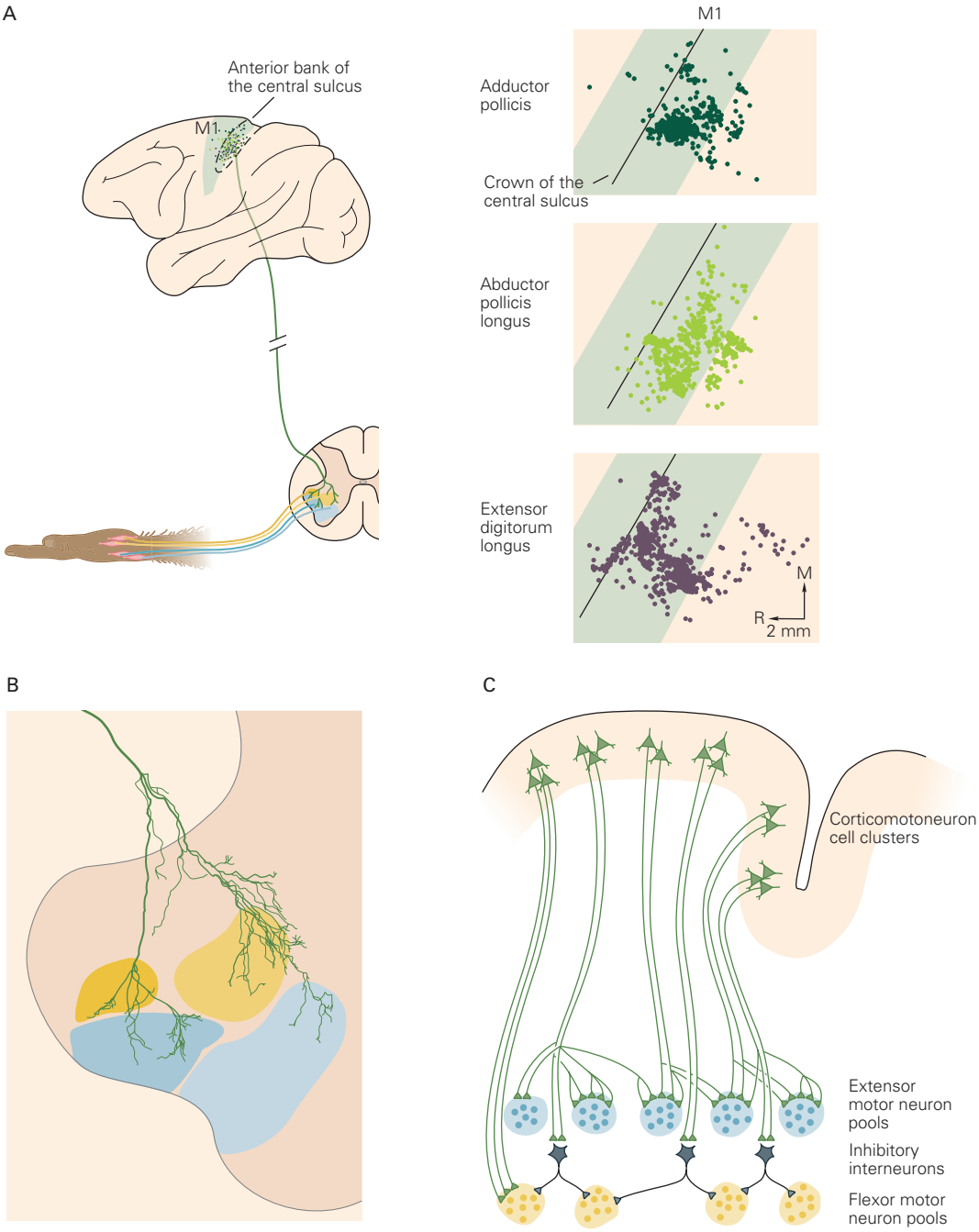

Figure 34–17 **Corticomotoneuronal cells activate complex muscle patterns through divergent connections with spinal motor neurons that innervate different arm muscles.**

A. Corticomotoneuronal (CM) cells, which project monosynaptically to spinal motor neurons, are located almost exclusively within the anterior bank of the central sulcus in the caudal part of the primary motor cortex (**M1**). The CM cells that control a single hand muscle are widely distributed throughout the arm motor map, and there is extensive overlap of the distribution of neurons projecting to different hand muscles. The distributions of the cell bodies of CM cells that project to the spinal motor pools that innervate the adductor pollicis, abductor pollicis longus, and extensor digitorum communis (shown on the right) illustrate this pattern of wide distribution and extensive overlap of CM cells projecting to different muscles. (Abbreviations: **M**, medial; **R**, rostral.) (Reproduced, with permission, from Rathelot and Strick 2006.)

B. A single CM axon terminal is shown arborized in the ventral horn of one segment of the spinal cord. It forms synapses with the spinal motor neuron pools of four different intrinsic hand muscles (**yellow** and **blue** zones), as well as with surrounding interneuronal networks. Each axon has several such terminal arborizations distributed along several spinal segments. (Reproduced, with permission, from Shinoda, Yokota, and Futami 1981.)

C. Different colonies of CM cells in the primary motor cortex terminate on different combinations of spinal interneuron networks and spinal motor pools, thus activating different combinations of agonist and antagonist muscles. Many other corticospinal axons terminate only on spinal interneurons (not shown). The figure shows CM projections largely onto extensor motor neuron pools. Flexor motor pools receive similar complex projections (not shown). (Adapted, with permission, from Cheney, Fetz, and Palmer 1985.)

those for more proximal parts of the arm. The terminal of a CM cell axon often branches and terminates on spinal motor neurons for several different agonist muscles and can also influence the contractile activity of still more muscles through synapses on spinal interneurons (Figure 34–17B,C). This termination pattern is organized to produce coordinated patterns of activity in a *muscle field* of agonist and antagonist muscles. Most frequently, a CM cell axon directly excites the spinal motor neurons for several agonist muscles and indirectly suppresses the activity of some antagonist muscles through spinal inhibitory interneurons (Figure 34–17C). The fact that CM cells are more prominent in humans than in other species may be one of the reasons why lesions of M1 in humans have a more profound effect on voluntary motor control compared to other mammals (Box 34–3).

The complexity of the motor map in M1—as revealed by short trains of electrical stimuli and anatomical and neurophysiological studies of direct and indirect M1 descending outputs targeting single muscles and small muscle groups—shows how motor commands from M1 to the spinal motor apparatus are able to control movements of every part of the body, with special focus on the fingers, hand, arm, face, and mouth in primates.

Activity in the Primary Motor Cortex Reflects Many Spatial and Temporal Features of Motor Output

As already noted, a given action such as reaching for an object can be described on many levels, ranging from the hand's spatial trajectory and velocity to its joint-centered causal forces and muscle activity (Figure 34–1A). Representational models assume that the motor system directly plans and controls specific parameters of movement. They predict that different neural populations encode the intended movement in a parameter space (ie, hand or joint motion or joint muscular torque) and perform the transformations between them. Dynamical models predict that neural circuits control movements through changes in their activation state from its current state to the desired final state. As their activity changes across time, correlates of various parameters and properties of the intended movement can be observed in the activity

Box 34–3 Lesions in Primary Motor Cortex Lead to Impairments in Motor Execution

The effects of primary motor cortex (M1) lesions differ across species. Large lesions in cats do not cause paralysis; the animals can move and walk on a flat open surface. However, they have severe difficulties using visual information to navigate within a complex environment, avoid obstacles, or climb the rungs of a ladder. In cats, the pyramidal tract neurons in M1 are much more strongly activated when an animal must modify its normal stepping motion to clear an obstacle under visual guidance than during normal unimpeded locomotion over a flat, featureless surface (Chapter 33).

Large M1 lesions in monkeys have more drastic consequences, including initial paralysis and usually the permanent loss of independent movements of the thumb and fingers. Monkeys nevertheless recover some ability to make clumsy movements of the hands and arms and to walk and climb.

More focal lesions of M1 typically result in muscle weakness, slowing and imprecision of movements, and discoordination of multi-joint motions, perhaps as a result of selective perturbations of the control circuitry for specific muscles or muscle groups. Lesions limited to part of the motor map, such as the contralateral arm, leg, or face, lead to paralysis of that body part. There is diminished use of the affected body part, and movements of the distal extremities are much more affected than those of the proximal arm and trunk.

The severity of the deficits also depends on the level of required skill. Control of fine motor skills, such as independent movements of the fingers and hand and precision grip, is abolished. Any residual control of the fingers and the hand is usually reduced to clumsy, claw-like, synchronous flexion and extension motions of all fingers, not unlike the unskilled grasps of young infants. Remaining motor functions, such as postural activity, locomotion, reaching, and grasping objects with the whole hand, are often clumsy.

In humans, large motor cortex lesions are particularly devastating, resulting in severe motor deficits or complete paralysis of affected body parts, usually with limited potential for recovery. This presumably reflects the increased importance in humans of descending signals from M1 onto spinal interneuronal circuits and spinal motor neurons and a diminished capacity of other cortical and subcortical motor structures to compensate for the loss of those descending M1 signals.

of single neurons and neural populations. However, the activity of most neurons reflects a combination of parameters that does not correspond to any identifiable parameter in any specific coordinate framework.

Despite their different assumptions, both perspectives suggest that one can infer the possible contribution of different neurons and different neural structures to motor control by studying how their activity correlates with different parameters of movements. The activity of M1 neurons has been intensively studied since the 1960s to try to reveal, for instance, whether M1 generates a high-level signal about the hand motion or a lower-level kinetic signal more related to the causal forces and muscle activity.

Knowledge about the nature of the control signals generated by M1 also helps to clarify the role of other motor structures, notably the spinal cord. If M1 encodes specific information about muscle activity patterns, less computational processing would be necessary at the spinal level. In contrast, if M1 mainly encodes higher-level information about the intended movement, the spinal cord would have to perform the processes that convert this global signal into detailed patterns of muscle activity.

However, one of the major experimental challenges in identifying how M1 controls movement is the fact that virtually all movement-related parameters are intercorrelated through the laws of motion. As a consequence, a particular muscular force (kinetics) will cause a specific motion (kinematics) given an initial condition (posture, movement) of the body. As a result, if one recorded neural activity while a monkey makes reaching movements in different directions, a neuron that theoretically signals the spatial direction of movement will also inevitably show a correlation with the direction of causal forces. Likewise, the contractile activity of a muscle will co-vary systematically with the spatial direction of movement even though it is clearly generating the causal forces. Unless the task design adequately dissociates these different classes of parameters, it will yield ambiguous information about the functional role of each neuron.

Edward Evarts was the first to examine this issue in the 1960s, in pioneering single-neuron recordings in monkeys while they made simple flexion/extension movements of the wrist. Using a system of pulleys and weights, he applied a load to the wrist of the monkey that pulled the wrist in either the direction of flexion or extension in different trials. This required the monkey to alter the level of wrist muscle activity to compensate for the load while making the movements. As a result, the kinematics (direction and amplitude) of wrist movements remained constant, but the kinetics (forces and muscle activity) changed with the load.

Using a microelectrode, he located single neurons in the M1 motor map that modulated their activity when the monkey made movements of the wrist without the external load. In some neurons, their discharge increased during wrist flexion (*preferred movement direction*) and was suppressed during extension, whereas others displayed the opposite pattern. This movement-related activity typically began 50 to 150 ms before the onset of agonist muscle activity, supporting a causal link between M1 neural activity and movement. When a load was applied, many M1 neurons increased their activity when the load resisted movement in their preferred direction and decreased activity when the load assisted the movement (Figure 34–18). These changes in neural activity paralleled the changes in muscle activity required to compensate for the external load.

Subsequent studies have confirmed that the activity of many M1 neurons varies systematically with the magnitude of muscle force output. This is best shown in tasks in which monkeys generate isometric forces against immovable objects that prevent movement. The activity of many M1 neurons, including CM cells, varies with the direction and level of static isometric output forces generated across a single joint, such as the wrist or elbow, as well as during precise pinches using the thumb and index finger (Figure 34–19A). At least over part of the tested range, these responses vary linearly with the level of static force.

Most natural behaviors involve multi-joint, multi-muscle actions. For instance, reaching movements of the arm in different directions requires different patterns of coordinated motions at the shoulder and elbow. Proximal limb muscle activity during reaching shows a roughly cosine pattern of activity with maximal activity in a specific movement direction, its preferred movement direction, that gradually diminishes as the angle between the desired direction of reach and the muscle's preferred direction increases (Figure 34–20A). Like the proximal arm muscles, single neurons related to shoulder and elbow movements respond in a continuously graded fashion during movements in different reach directions centered on a preferred direction of maximal activity (Figure 34–20B). Different neurons have different preferred directions that cover the entire directional continuum around the circle, and during any given movement, neurons with a wide range of preferred directions discharge at different rates.

As Ed Evarts had shown in single-joint tasks, much of the M1 activity during reaching is closely related to the causal kinetics. For instance, in monkeys trained to make reaching movements in eight directions while compensating for external loads that pulled the arm in different directions, the reach-related activity of both

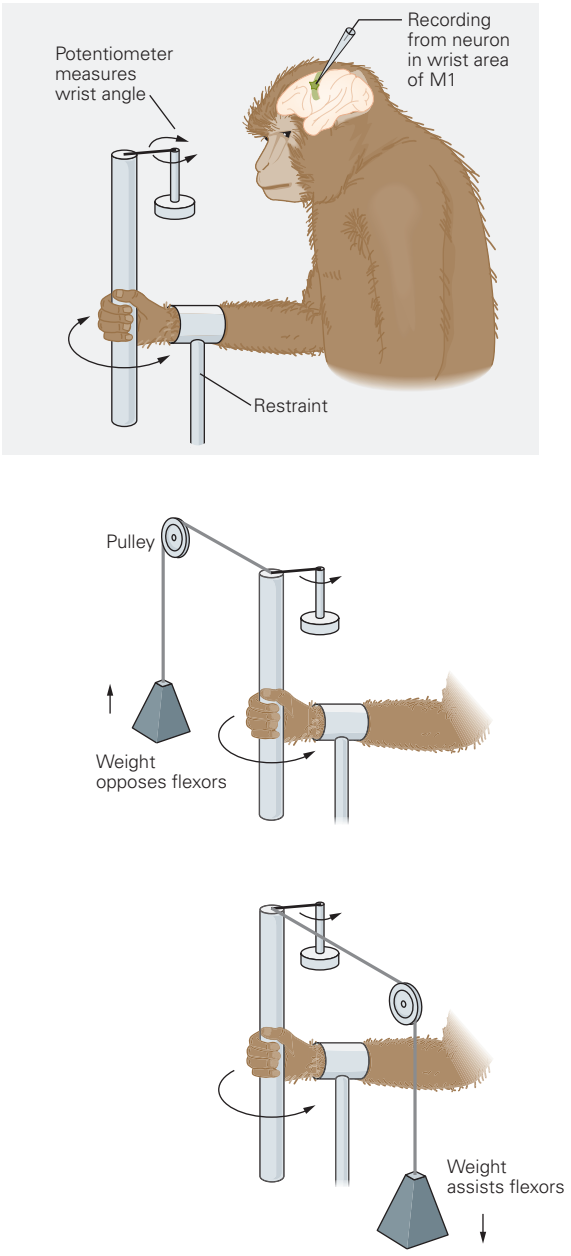

Figure 34–18 Activity of a motor cortex neuron correlates with changes in the direction and amplitude of muscle forces during wrist movements. The records are from an M1 neuron with an axon that projected down the pyramidal tract. The monkey flexes its wrist under three load conditions. When no load is applied to the wrist, the neuron fires before and during flexion (**A**). When a load opposing flexion is applied, the activity of the flexor muscles and the neuron increases (**B**). When a load assisting wrist flexion is applied, the flexor muscles and neuron fall silent (**C**). In all three conditions, the wrist displacement is the same, but the neural activity changes as the loads and compensatory muscle activity change. Thus, the activity of this motor cortex neuron is better related to the direction and level of forces and to muscle activity exerted during the movement than to the direction of wrist displacement. (Adapted from Evarts 1968.)

proximal-arm muscles and many M1 neurons changed systematically with the direction of the external loads and the corresponding corrective forces that the monkeys had to generate for each reach direction. Both muscle and neural activity increased when the load resisted movements in their preferred directions and decreased when the loads assisted those movements. In addition, when a monkey uses its whole arm to exert constant isometric force levels in different directions at the hand, the activity of many M1 neurons varies

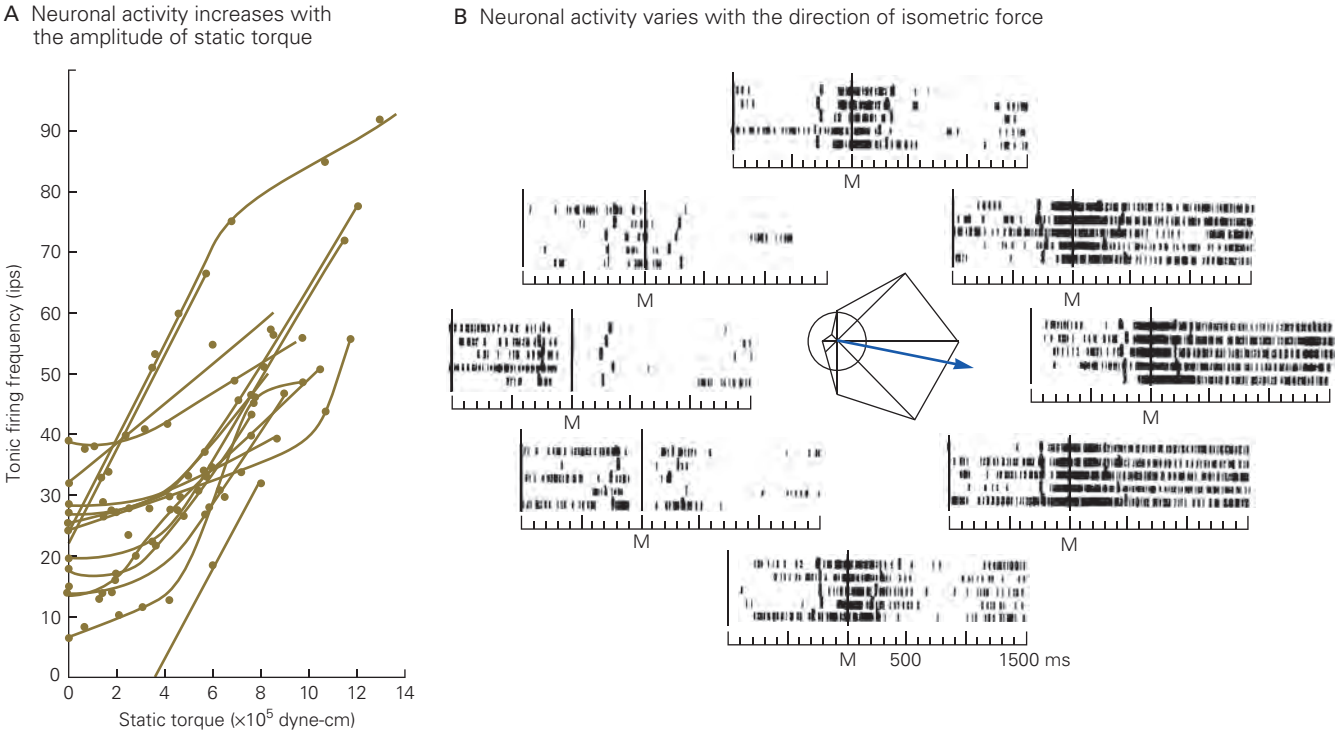

Figure 34–19 Activity in many primary motor cortex neurons correlates with the level and direction of force exerted in an isometric action.

A. The activity of many primary motor cortex neurons increases with the amplitude of static torque generated across a single joint. The plot shows the tonic firing rates of several different corticomotoneuronal cells at different levels of static torque exerted in the direction of wrist extension. Other motor cortex neurons show increasing activity with torque exerted in the direction of wrist flexion, and so would show response functions with the opposite slope (not shown). (Reproduced, with permission, from Fetz and Cheney 1980.)

B. When a monkey uses its whole arm to push on an immovable handle in its hand, the activity of some primary motor cortex neurons varies with the direction of isometric forces. Each of the eight raster plots shows the activity of the same primary motor cortex neuron during five repeated force ramps in one direction. Each row shows the pattern of spikes during a single trial of the task. The position of each raster of activity corresponds to the direction in which the monkey is generating isometric forces on the handle. The onset of the force ramp is indicated by the vertical line labeled **M**. The **thick ticks** on the left of that line in each row indicate when the target appeared on a computer monitor, telling the monkey the direction in which it should push on the handle. The central polar plot illustrates the directional tuning function of the neuron as a function of the direction of isometric forces. (Reproduced, with permission, from Sergio and Kalaska 2003.)

systematically with force direction, and the directional tuning curves for isometric force resemble those for activity during reaching movements (Figure 34–19B).

The complex and nonlinear properties of multisegmented limbs present a major control problem for the motor system. For instance, one can make reaching movements with similar hand trajectories but different arm geometries that require changes in the causal joint-centered torques and muscle activity. In one experiment, when monkeys made horizontal reaching movements along the same planar spatial hand trajectories while holding the arm in different spatial orientations (ie, elbow raised versus lowered), the activity of proximal-arm muscles and many M1 neurons showed corresponding changes in the strength and directional tuning of their reach-related activity. This indicates that the M1 neurons generate signals that take into account the changes in intrinsic limb biomechanics during the reaching movements.

Similarly, arm movements toward or away from the body require much larger angular motion at the shoulder and elbow joints compared to movements to the right or left. In contrast, muscular torques tend to be larger for movements to the right and left. Both of these factors influence the amount of muscle activity required to move the limb, which can be quantified by a single term, joint muscular power (joint angular velocity multiplied by net muscular torque about that joint). With the limb in the horizontal plane, joint power is greatest for movements away from the body and slightly to the left,

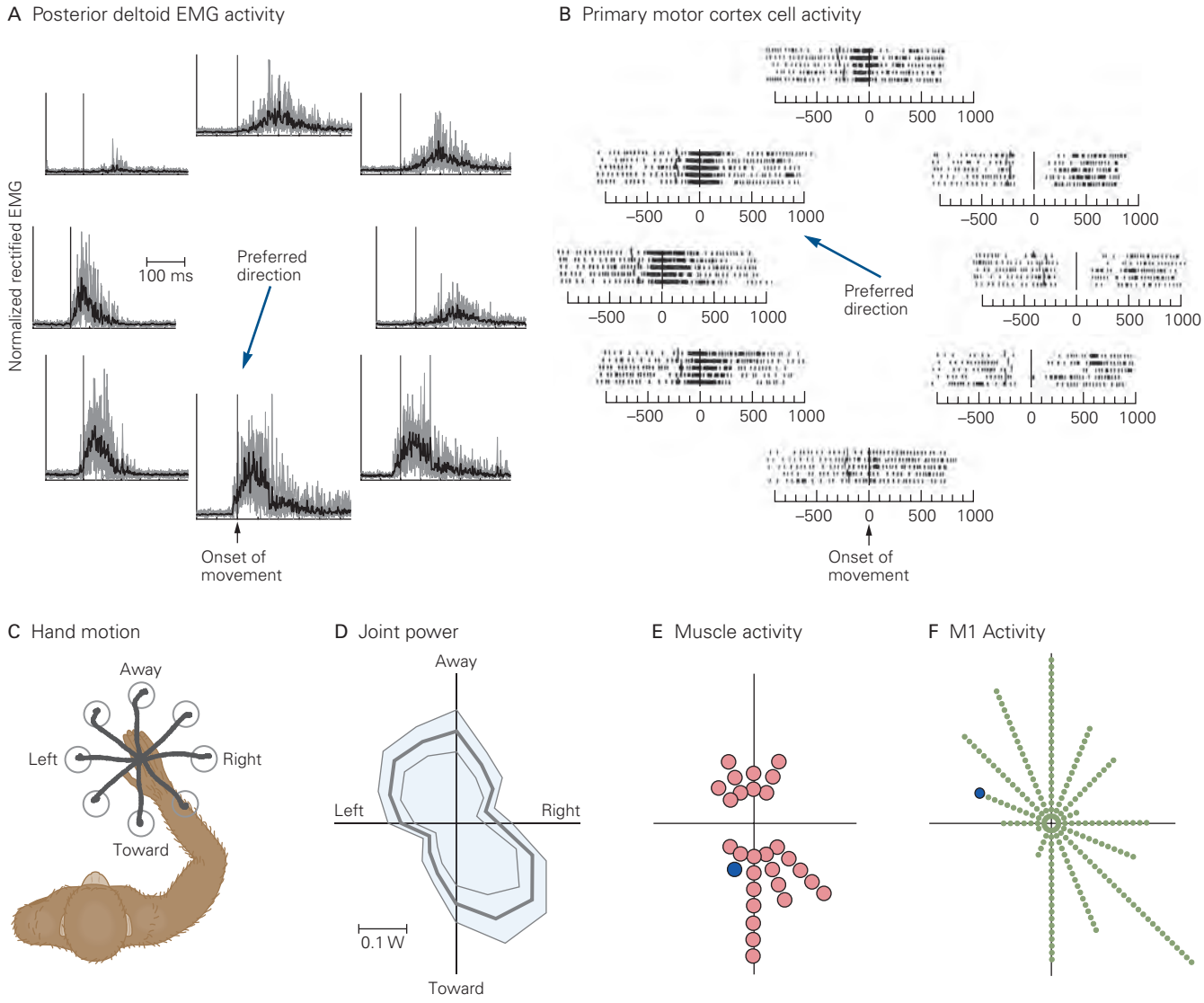

Figure 34–20 Limb muscles and primary motor cortical neurons are broadly tuned to the direction of reaching.

A. Plots show the activity of posterior deltoid of the right arm, a shoulder extensor, during arm movements in eight directions (see panel C) (central panel displays mean hand trajectories). The muscle is initially maximally active for movements at 270° (towards the body, preferred direction = 250°) and diminishes for movements in other directions. **Black lines** denote the mean activity of the muscle across multiple trials, and data are aligned on movement onset (**vertical thin line**). (Abbreviation: **EMG**, electromyography.)

B. Raster plots show the firing pattern of a single primary motor cortex neuron during whole-arm movements in eight directions. The neuron discharges at the maximal rate for movements near 135° and 180° and at lesser intensities for movements in other directions. The cell's lowest firing rate is for movements opposite the cell's preferred direction. Each row of **thin tics** in each raster plot represents the activity in a single trial, aligned at the time of movement onset (time 0); **thick tics**, time of target appearance. (Reproduced, with permission, from Georgopoulos et al. 1982. Copyright © 1982 Society for Neuroscience.)

C. Hand trajectories when reaching from a central position in the horizontal plane.

D. Peak joint power (joint muscular torques multiplied by joint velocity) for movements performed in different spatial directions (shoulder and elbow power added together). A large amount of power is required to reach away from the body and to the upper left and to reach toward the body and to the lower right. (Right X-axis is at 0°.)

E. Preferred directions of proximal-limb muscles tend to be for movements that require greater muscular power, reflecting the obvious link between muscle use and the physical requirements of the motor task. Each **dot** represents an individual muscle binned into 22.5° sectors; the **blue dot** represents the preferred direction of the muscle displayed in panel **A**.

F. Distribution of preferred directions of neurons in primary motor cortex (**M1**). Each **dot** represents an individual neuron, and the **blue dot** represents the preferred direction of the neuron displayed in panel **B**. (Adapted, with permission, from Scott et al. 2001.)

and toward the body and to the right (Figure 34–20C,D). This bias in the physics of limb movement leads to a bias in the preferred directions of shoulder and elbow muscles, which tend to be maximally active in these same directions (Figure 34–20E). Correspondingly, the distribution of preferred directions of neurons in M1 also parallels this bias, with neurons tending to have preferred directions either away and slightly to the left or toward and to the right (Figure 34–20F). Thus, the physics of the limb dictates the pattern of muscle activity needed to generate movement, and this in turn is reflected in the pattern of neural activity in M1.

The impact of limb physics on M1 activity extends to the level of muscle-related signals. The activity of some single M1 neurons, including CM cells, can be correlated with specific components of the contraction patterns of different muscles during such diverse tasks as isometric force generation, precision pinching of objects between the thumb and index finger, and complex reaching and grasping actions (Figure 34–21). These findings highlight how M1 contributes to the specification of muscle activity patterns for motor actions, including onset times and magnitudes. Nevertheless, the final pattern of muscle activity will only be generated by the spinal motor neurons since they alone take into account the additional influence of other descending supraspinal inputs and local spinal interneuronal processes.

All the studies described so far related the activity of single M1 neurons to motor output. However, voluntary motor control is implemented by the simultaneous coordinated activity of many neurons throughout the motor system. Their activity is noisy, varying stochastically between repetitions of the same movement. Furthermore, their broad symmetrical movement-related tuning curves introduce a high level of uncertainty as to what the limb should do in response to the ambiguous signal generated by each neuron.

A simple computational approach was developed to extract a unique signal about each reaching movement by pooling the heterogeneous single-neuron activity of the recorded M1 population. The activity of each neuron is represented by a vector pointing in its preferred direction; the length of the vector varies as a function of its mean discharge rate during reaches in each direction. This vector notation implies that an increase in the activity of a given M1 neuron evokes changes in activity in the spinal motor apparatus and muscles that causes the arm to move along a path corresponding to the neuron's task-related preferred direction; the strength of that single-neuron influence varies systematically with the difference between the neuron's preferred direction and the desired movement (Chapter 39, Figure 39–6). When the reach-related

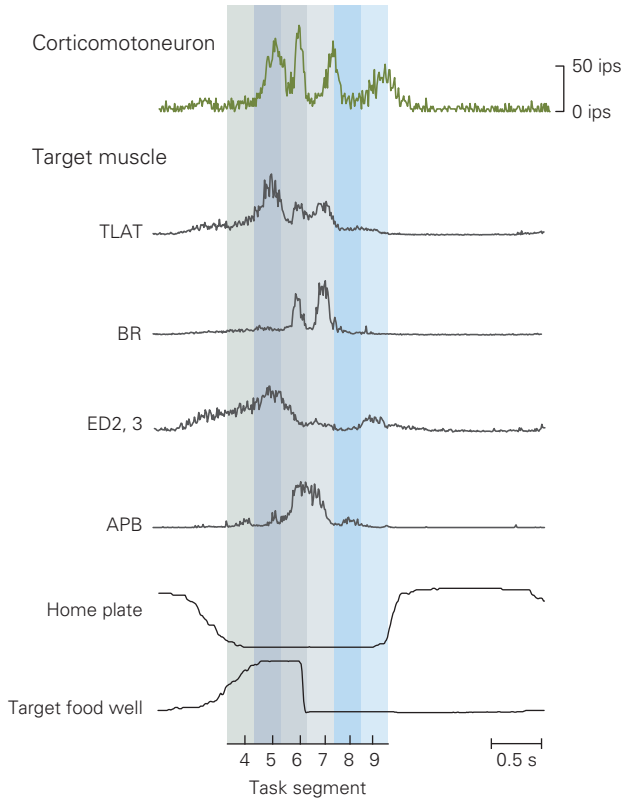

Figure 34–21 The activity of some primary motor cortex neurons can be correlated with particular patterns of muscle activity. Bursts of activity in a single corticomotoneuron during a reach-and-grasp movement to retrieve food pellets from a small well are correlated with bursts of contractile activity in several of its target muscles at different times during the movement. (Abbreviations: **APB**, abductor pollicis brevis; **BR**, brachioradialis; **ED2, 3**, extensor digitorum 2, 3; **ips**, impulses per second;**TLAT**, lateral triceps.) (Reproduced, with permission, from Griffin et al. 2008.)

activity of about 250 M1 neurons was represented by variable-length vectors for each of the eight reach directions and summed, the direction of the net resultant *population vectors* varied systematically with the actual reach directions (Figure 34–22A).

The novel insights of this analysis were that the control of a given reach movement involves coordinated changes in the activity of M1 neurons distributed throughout the M1 arm motor map and that their pooled activity clearly distinguishes the unique identity of each of the reach actions generated by the eight different distributed patterns of population activity. Subsequent studies demonstrated that "instantaneous" population vectors extracted from the pooled activity of large populations of M1 neurons during sequential 20-ms time bins from the start to the end of movement predicted the continually changing trajectory of the

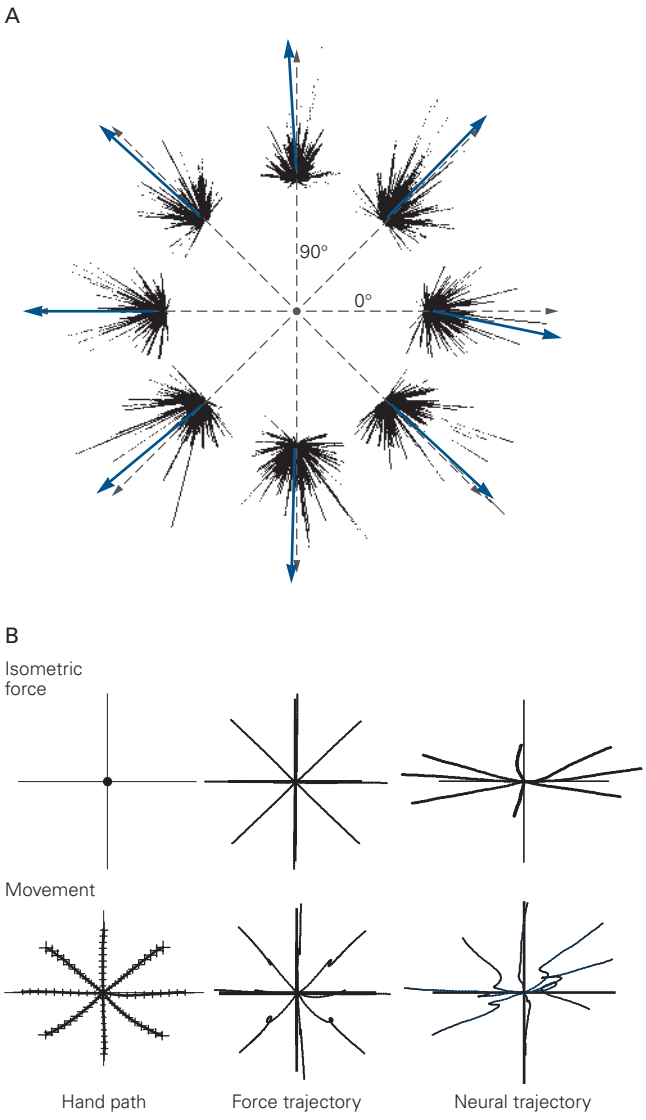

Figure 34–22 Population codes relate M1 activity to different properties of movement.

A. The eight single-neuron vector clusters (**thin black lines**) and the population vectors (**blue arrows**) represent the activity of the same population of cells during reaching movements in eight different directions. Each single-neuron vector points in the neuron's preferred movement direction, and its length is proportional to the discharge of the neuron during that movement. The population vectors were calculated by vectorial addition of all the single-cell vectors in each cluster; **dashed arrows** represent the direction of movement of the arm. (Reproduced, with permission, from Georgopoulos et al. 1983.)

B. Comparison of hand kinematics and kinetics and neural population activity in an isometric task and when moving a handle with a large mass. Force and neural trajectories were generated by linking sequences of 20-ms output force vectors or neural population vectors tip-to-tail for each direction of force or movement output. (Reproduced, with permission, from Sergio et al. 2005.)

arm motions 100 to 150 ms into the future while monkeys made reaching movements or traced spirals on a computer monitor. This showed that the simple vector notation could be used to extract from the activity of populations of neurons a signal about intended motor output even on a moment-to-moment basis. These findings were anticipated by a prescient study in 1970 by Donald Humphrey and colleagues, who showed that the appropriately summed activity of three to five M1 neurons was better correlated to the temporal patterns of motor output during single-joint movements than was the signal of any of the single neurons.

Subsequent studies used the population-vector decoder algorithm to provide further insight into neural processing in M1. In one study, the activity of proximal arm–related M1 neurons was recorded while monkeys performed two tasks (Figure 34–22B). In the first task, they generated isometric force ramps in eight different spatial directions uniformly distributed at 45° intervals in a horizontal plane against a rigid handle that they held in their hand, without arm movements. A 20-ms population-vector decoder was used to extract the net directional bias of the pooled activity of many M1 neurons, and the result showed that these pooled signals varied systematically with the direction of output forces throughout the duration of the force-ramp generation, even though there were no movements. However, unlike the actual uniformly distributed directions of the forces generated by the monkey at the hand, the decoded population-vector signals were skewed toward the *x*-axis. This showed that the M1 activity reflected the nonlinear relationship between causal shoulder muscle torques and measured isometric forces at the hand resulting from the complex biomechanical properties of the arm (see Figure 34–20).

In the second task, the monkeys made reaching movements of the arm in the same eight directions to move a heavy handle. This required an initial accelerative force in the direction of movement and then a transient reversal of the direction of forces to decelerate the movement of their arm and the mass as it approached the target. The decoded M1 population-vector signals in this task varied dramatically through time. They were directed initially toward the target but then transiently reversed just before the peak of hand velocity. This showed once again that the M1 activity was more closely correlated with the time course of causal forces generating the reaching movements, including their transient directional reversal, than to the uninterrupted motion of the hand toward the target. They also found that correlates of the forces to generate reaching were strongest in M1, weaker in PMd, and largely absent in PE/MIP. This indicated that, unlike M1,

reach-related neurons in area PE/MIP generated a reliable signal about stable arm postures and the kinematics of arm movements independent of the underlying causal forces and muscle activity.

Finally, one study has shown that reliable signals about the time-varying activity of proximal-arm muscles during reaching movements can be extracted from the activity of a population of simultaneously recorded M1 neurons. Another study found that the pooled activity of M1 neurons that fire selectively in connection with either shoulder or elbow movements can predict the changes in onset times and levels of contractile activity of the shoulder or elbow muscles during reaches in different directions.

These studies showed that the pooled activity of many M1 neurons is a rich and reliable source of signals about different time-varying attributes of whole-arm movements. This provided an important conceptual foundation for the development of more sophisticated decoder algorithms in brain–machine interfaces that make use of the movement-related information available in the simultaneous activity of many M1 neurons to allow subjects to control the actions of neuroprosthetic devices by covert modulations of M1 neuron activity without overt limb movements (Chapter 39).

Primary Motor Cortical Activity Also Reflects Higher-Order Features of Movement

Activity in M1 is not correlated only with causal forces and muscle activity. Many studies, beginning with those of Ed Evarts, that have attempted to dissociate kinematic from kinetic properties of motor outputs have found that the activity of some M1 neurons varies with the direction of movement but is only weakly influenced or not influenced at all by changes in output forces. Such neurons appear to preferentially signal the kinematic aspects of limb motion.

Changes in behavioral task can influence the relationship between M1 activity and motor output. One study has highlighted how contextual changes in an isometric force task altered the coding of force magnitude by M1 neurons. Either the order of forces or the range of expected forces results in changes in the activity in M1. They suggested that M1 neurons could dynamically adjust their relationship to output forces to optimize precision of control as a function of the range of forces that would be encountered in a given context. Another study found that many CM neurons may discharge intensely when monkeys performed precisely controlled force tasks with low force levels but are relatively inactive when the monkeys generate powerful contractions of the same muscles to make brisk, back-and-forth movements of the handle. Likewise, a study demonstrated that CM cells in M1 could be very active when monkeys generated a precision-pinch grip of the thumb and index finger with relatively low force output, but were much less active or nearly silent when the animals generated much larger forces with a power grip involving the entire hand.

Still another study has shown that some M1 neurons that respond to loads applied to the limb during postural control can lose this load sensitivity as soon as the monkey makes a reaching movement to another spatial target, and vice versa. That is, those neurons can reflect output forces during postural control, but reflect only kinematics during movement. This change in the cell's response occurs quite abruptly, about 150 ms before the onset of movement. Importantly, any neurons that are sensitive to loads during both posture and movement will retain the same motor field across behaviors; that is, if the neuron responds only to shoulder flexor loads during postural control, it will respond only to shoulder flexor loads during reaching.

Even a simple change in the metrics of limb movement can have a large influence on M1 activity. In a study of monkeys making slow or fast reaching movements in different directions from a central target to peripheral targets, proximal limb muscles displayed relatively simple scaling of their activity patterns, reflecting increased forces for faster and longer reaches. In contrast, M1 neurons displayed a broad range of changes in their activity patterns that rarely paralleled the pattern of changes observed for muscles.

Activity in neurons can also correlate with higher-level features of movement such as the nature of an upcoming motor action. This was demonstrated in a study in which monkeys were trained to make wrist movements to three targets in a row starting from one extreme, stopping at a central position, and then finishing at the other extreme. Visual cues instructed the monkeys when to make each movement. Because the task used a predictable sequence of wrist movements, the monkeys knew before the visual cues appeared what would be the next direction of movement. While many M1 neurons signaled the current wrist posture or the direction of each movement while they were being performed, some M1 neurons reliably signaled the next movement in the sequence before the visual cue appeared. Many subsequent studies have confirmed that M1 neurons can signal impending intended movements, although these planning-like signals are not as prominent in M1 as in premotor cortical areas.

In summary, neural recording studies have revealed a diverse range of response properties within

and across movement-related cortical areas, with stronger correlations to causal movement kinetics in M1 and to higher-order motor parameters in premotor and parietal cortex. However, these experimental findings have not yet led to a single unifying hypothesis about how cortical motor circuits control voluntary movements. Part of this uncertainty may result from inadequacies in experimental task design.

Representational motor-control models have interpreted these complex results as evidence of the transformations between different levels of representation of intended movements performed by neural populations distributed across different cortical motor areas. In contrast, nonrepresentational motor-control models such as optimal feedback control argue that these same results can only be interpreted as evidence of when and where neural correlates of different motor output parameters emerge in the dynamical activity distributed across cortical motor areas but do not shed much insight into the underlying neural computations. This illustrates the experimental challenges still confronting researchers as they try to reverse engineer the cortical motor circuitry to reveal its internal computational organization.

Sensory Feedback Is Transmitted Rapidly to the Primary Motor Cortex and Other Cortical Regions

Postcentral and posterior parietal cortex provide much of the sensory information related to the position and motion of the body and the location of spatial goals that is important in voluntary motor control, although the cerebellum is likely another important source (Chapter 37).

The type of afferent information transmitted to M1 differs between the proximal and distal portions of the limb. Afferent input from cutaneous and muscle sensory neurons is equally prevalent for hand-related neurons, reflecting the importance for both sources of sensory feedback when grasping and manipulating objects with the hand. Muscle afferents provide the major source of feedback from the proximal limb. Information from muscles is more prevalent in the rostral M1, whereas cutaneous input is more common in the caudal M1. Muscle afferent feedback to M1 is surprisingly rapid as it takes as little as 20 ms for M1 neurons to respond following a mechanical disturbance to the limb. Analogous to reaching, neural activity is broadly tuned to the direction of the mechanical disturbance.

Sensory feedback supports our ability to make rapid goal-directed corrections for motor errors that arise during movement planning and execution or are caused by unexpected disturbances of the limb. When a perturbing mechanical load is applied to the limb, the motor system generates a multipeaked compensatory electromyographic response, beginning with a short-latency stretch response (20–40 ms after the perturbation), followed by a long-latency response (50–100 ms) and then a so-called "voluntary" response (≥100 ms). The short latency of the initial response indicates that it is generated at the spinal level. The response is relatively small and stereotyped, and its intensity scales with the magnitude of the applied load. In contrast, motor corrections beginning in the long-latency epoch (50–100 ms) are modulated by a broad range of factors necessary to attain a behavioral goal, including the physics of the limb and environment, the presence of obstacles in the environment, the urgency of the goal, and properties of the target, including alternate goals. These context-dependent features suggest the long-latency feedback epoch is an adaptive process in which the control policy (ie, feedback gains) is adjusted based on the behavioral goal, as predicted by the optimal feedback control model.

The ability of the motor system to rapidly generate these goal-directed long-latency motor responses is supported by a transcortical feedback pathway. Neural activity across frontoparietal circuits responds rapidly to mechanical disturbances to a limb, and the pattern of activity across the cortex depends on the behavioral context. Perturbation-related activity is observed in all cortical regions beginning at approximately 20 ms after the disturbance even if the monkey is distracted by watching a movie and does not have to respond to the disturbance (Figure 34–23A,B). If the monkey is actively maintaining its hand at a spatial goal, there is an immediate increase in the neural response in parietal area PE following the disturbance, followed shortly thereafter by changes in activity in other cortical regions (Figure 34–23A,B). If the disturbance is a cue that instructs the monkey to move to another spatial target, then M1 activity reflects the need for a more vigorous response if the disturbance knocks the hand away from the target compared to knocking the hand into the target (Figure 34–23C). In contrast, perturbation-related activity in PE remains similar regardless of target location.

The Primary Motor Cortex Is Dynamic and Adaptable

One of the most remarkable properties of the brain is the adaptability of its circuitry to changes in the environment—the capacity to learn from experience and to store the acquired knowledge as memories. When human subjects practice a motor skill, performance improves.

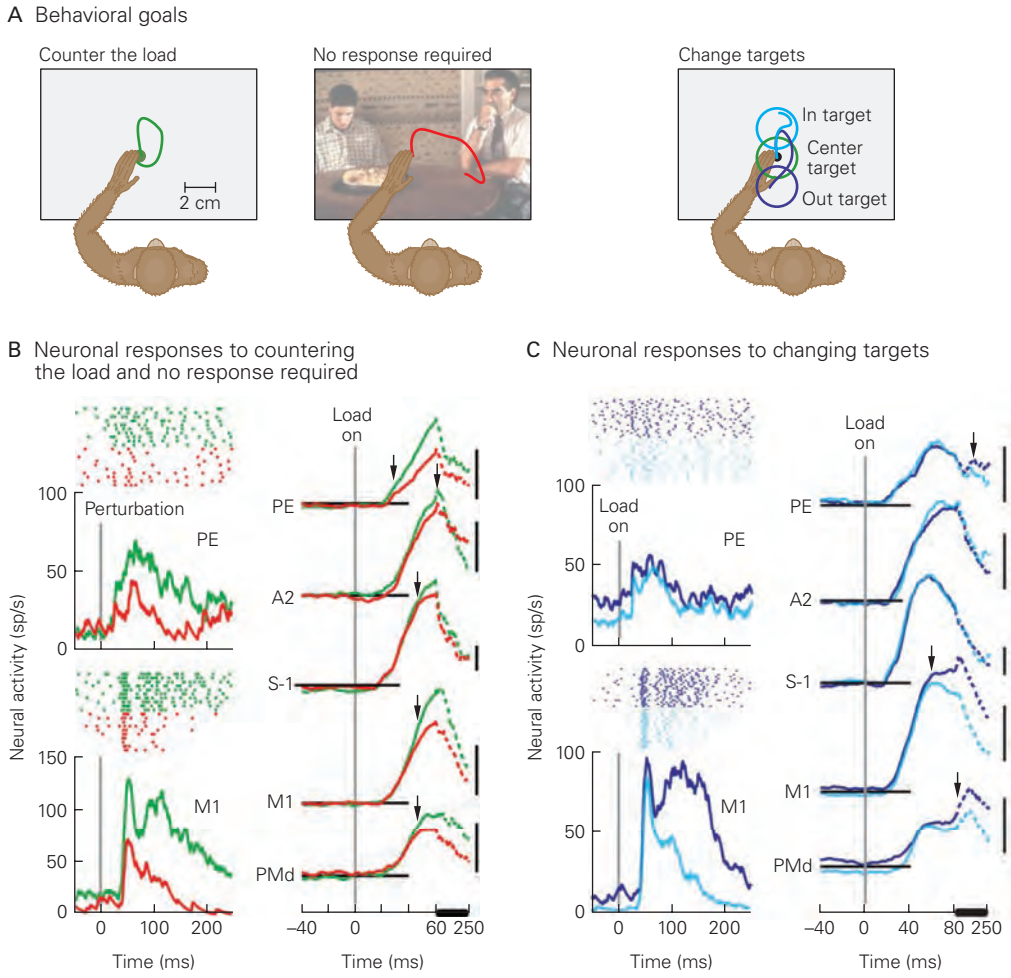

Figure 34–23 **Changes in behavioral goals alter rapid sensory feedback to parietal and frontal motor cortices.** (Reproduced, with permission, from Omrani et al. 2016. Part A photo is from the film American Pie and is reproduced, with permission, from Universal Studios. © 1999, Universal Pictures, All Rights Reserved.)

A. In the experiment described here, the responses of cortical regions to mechanical loads randomly applied to the arm are compared. In the *left* panel, motor corrections return the hand to the spatial goal following the disturbance (**green hand trajectory**). In the *middle* panel, the monkey watches a movie and does not have to respond to the disturbance, leading to the hand remaining to the right following the disturbance (**red hand trajectory**). In the *right* panel, the monkey places its hand at a central start target, and one of two other targets is also presented. The disturbance applied to the limb is a cue for the monkey to move to this second target with its position being either in the direction of the disturbance (**cyan** "in target" trajectory) or away from the disturbance (**blue** "out target" trajectory).

B. *Left:* Response of a neuron in PE and in M1 when a mechanical load was applied to the limb and the monkey had to counter the load and return the hand to a spatial target (**green**) or was not required to respond to the disturbance (**red**). *Right:* Population signals in each cortical region in response to perturbations. Note how all cortical areas show an increase in activity approximately 20 ms after the applied load. **Arrows** denote when activity was different when the monkey had to respond to the disturbance (**green curve**) as compared to not being required to respond to the disturbance (**red curve**). Note that PE is the first to show a difference in activity between the two conditions. Other cortical areas show changes at 40 ms or later. **A2** is a subregion of S-I. (For B and C: Vertical scale bars, 20/spikes/s); Activity between 60–250 ms (**thick horizontal line**) compressed for visualization purposes.)

C. *Left:* Responses of single neurons in PE and M1 when a mechanical load was a cue and instructed the monkey to move to another target. The disturbance either pushed the hand toward the target (**cyan**) or away from it (**blue**). *Right:* Population signals based on perturbation-related activity in each cortical region for the "in target" and "out target" conditions. The initial responses are similar for both "in target" and "out target" disturbances across all cortical areas, and **arrows** denote when there is a difference in activity between conditions. M1 is the first to display an increase in activity for the "out target" disturbance just prior to changes in muscle activity moving the hand to the spatial target.

Motor experience can also modify the motor map. In monkeys trained to use precise movements of the thumb, index finger, and wrist to extract treats from a small well, the area of the motor map in which intracortical microstimulation (ICMS) could evoke movements at these joints was larger than before training (Figure 34–24). If a monkey did not practice the task for a lengthy period, its skill level decreased, as did the cortical area from which the trained movements could be elicited by ICMS. Similar modifications of the

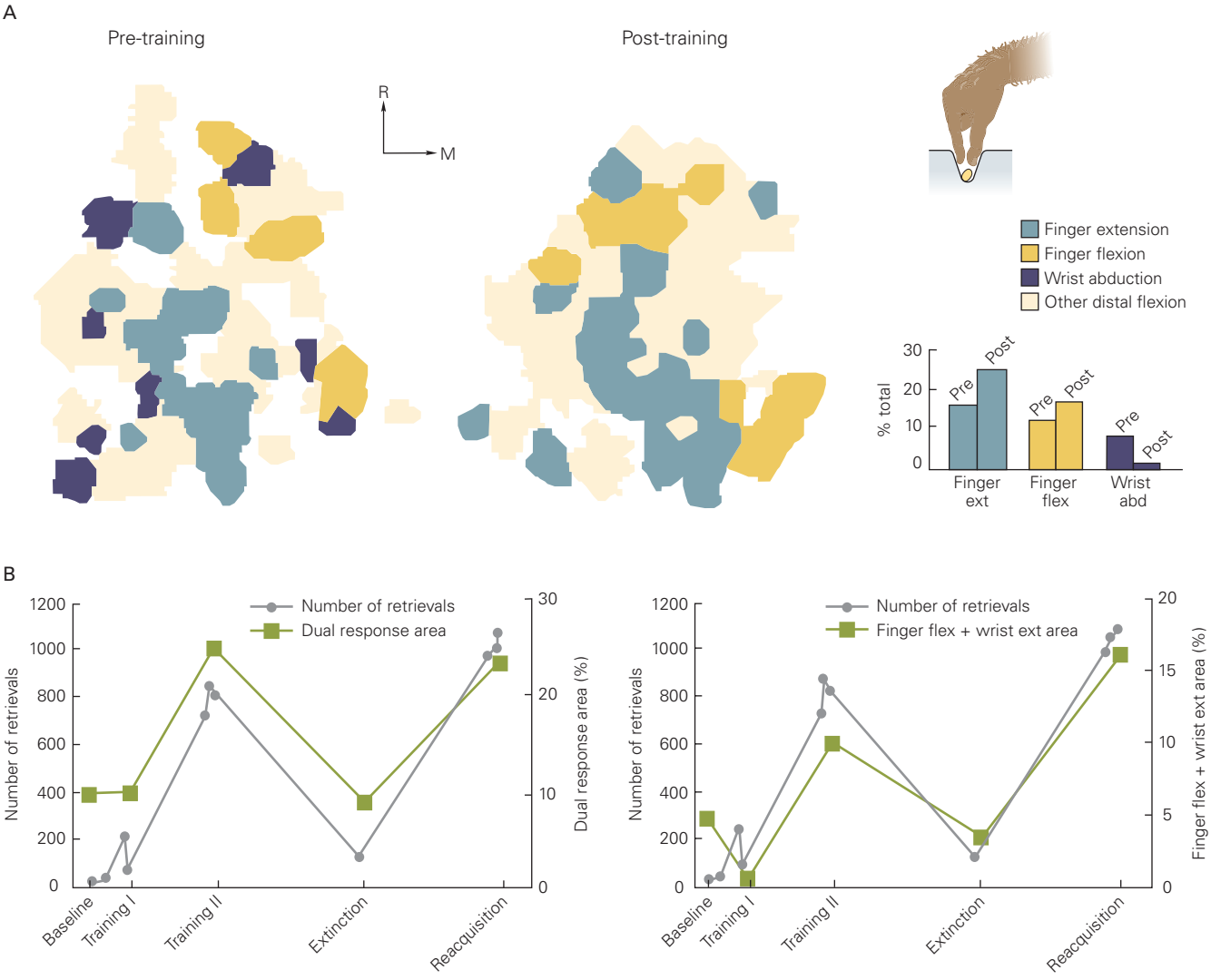

Figure 34–24 Learning a motor skill changes the organization of the M1 motor map. (Reproduced, with permission, from Nudo et al. 1996. Copyright © 1996 Society for Neuroscience.)

A. Motor maps for the hand in a monkey before and after training on retrieval of treats from a small well. Before training, areas of the motor map that generate index finger and wrist movements occupy less than half of a monkey's motor map. After training, the area from which the trained movements can be evoked by intracortical microstimulation expands substantially. The area of the map from which one could elicit individuated movements such as finger extension and flexion has expanded considerably, while the areas controlling wrist abduction, which this monkey used less in the new skill, became less prominent. (Abbreviations: **M**, medial; **R**, rostral.)

B. The areas of the motor output map parallel the level of performance (number of successful pellet retrievals) during acquisition of the motor skill and extinction (due to lack of practice). Two areas were tested: a "dual response" area (*left plot*), from which any combination of finger and wrist motions could be evoked, and an area from which the specific combination of finger flexion and wrist extension could be evoked (*right plot*). Both areas increased as the monkey's skill improved with practice and decreased as the monkey's skill was extinguished through lack of practice. These data are from a different monkey than the one in part **A** but trained for same task.

cortical representation of practiced actions in humans have been demonstrated by functional imaging and transcranial magnetic stimulation.

At least some of the processes contributing to these changes to the motor map are local to M1 itself. One of the mechanisms contributing to the cortical reorganization underlying improved reach-to-grasp performance in rodents involves changes in synaptic strength similar to long-term potentiation and depression within the local horizontal connections linking different parts of the arm motor map. It has been shown that spike-triggered ICMS could cause specific alterations to the M1 motor output map even without specific training. For instance, one study first identified two different cortical sites (A and B) that caused contractions of different muscles (muscle A and muscle B, respectively) when electrically stimulated. They then recorded the activity of a neuron at site A; whenever that neuron fired, they stimulated site B. Within a day or two of this ICMS conditioning at site B, electrical stimulation of site A was able to cause simultaneous contractions of both muscles A and B. The change likely resulted from a spike-timing dependent increase in synaptic strength that was limited to the horizontal cortical projection from site A to site B. Electromyographic responses elicited by ICMS at a third site that did not receive similar conditioning did not change, confirming that the effect was not generalized.

Motor adaptation to visual or mechanical disturbances has been studied extensively in human subjects (Chapter 30). Neural-recording studies have demonstrated that these alterations lead to changes in the activity of M1 neurons in monkeys as the animals adapt to the perturbations. For instance, when monkeys make reaching movements in a predictable external force field that pushes on the arm in a direction perpendicular to the direction of movement, their initially curved reach trajectories get straighter. As this adaptation evolves, large increases gradually arise in the activity of M1 cells whose preferred directional tuning is opposite to the applied force field. The magnitude of such adaptation-dependent changes in activity diminishes progressively as the angle between the force direction and cell preferred direction increases, following a cosine-like function. This shows that the adaptive changes were specific to the neurons that would make the greatest contribution to compensate for the external force field.

Another example of selective changes in M1 activity during motor learning comes from a visuomotor learning study in which visual feedback from a computer monitor is rotated 90° clockwise such that movements of a monkey's arm to the right result in downward movement of the cursor. Initially, the monkeys make arm movements in the original direction aimed at the visual target location, with corrections made online after movement onset. However, with practice, the monkeys begin to move in a new direction rotated counterclockwise to the visual target so that the cursor moves directly to the target. When training occurs for only one direction, learning generalizes poorly to other directions, suggesting that the adaptive changes occur only in neurons that evoke the adapted movement. The tuning curves of neurons with preferred directions near the learned direction were altered during training, whereas neurons with other preferred directions were not affected by the training. This confirmed that the adaptation was local, consistent with the findings of the force-field adaptation study, and explained why adaptation to the visuomotor rotation in one direction generalized poorly to other directions.

Motor-error signals in the precentral cortex also play an important role in trial-by-trial motor adaptation based on feedback learning. In one study with monkeys, an adjustable prism was used to displace the apparent location of the reach target in the environment. Visual feedback of the target and arm were blocked during the reaching movements, leading to systematic errors in touching the target. The monkeys were allowed to see visual feedback of the position of the hand relative to the target for a brief period of time at the end of movement (Figure 34–25). Activity in M1 and PMd during that brief period of visual feedback after movement reflected the direction of reach end-point errors and could be involved in adapting reaching movements to correct these errors. To test that hypothesis, ICMS was then used in M1 and PMd to simulate those error responses and showed that the monkeys began to make adaptive changes in their reaching movements to compensate for the simulated errors even though no reaching error was actually made.

Some motor skills are relatively easy to learn, such as compensation for a visuomotor rotation. Others, however, are very difficult to learn. Recent studies examined this discrepancy by first measuring the activity of a population of M1 neurons as the monkey moved a cursor on a computer screen using a brain–machine interface and a neural activity decoder. This population-level mapping between M1 activity and cursor motion was then altered by changing the association between the directional tuning of each neuron and cursor motion in the decoder. When the altered decoder mapping retained the normal co-modulation structure of neural activity, as would be the case for instance if the mapping between the activity of all

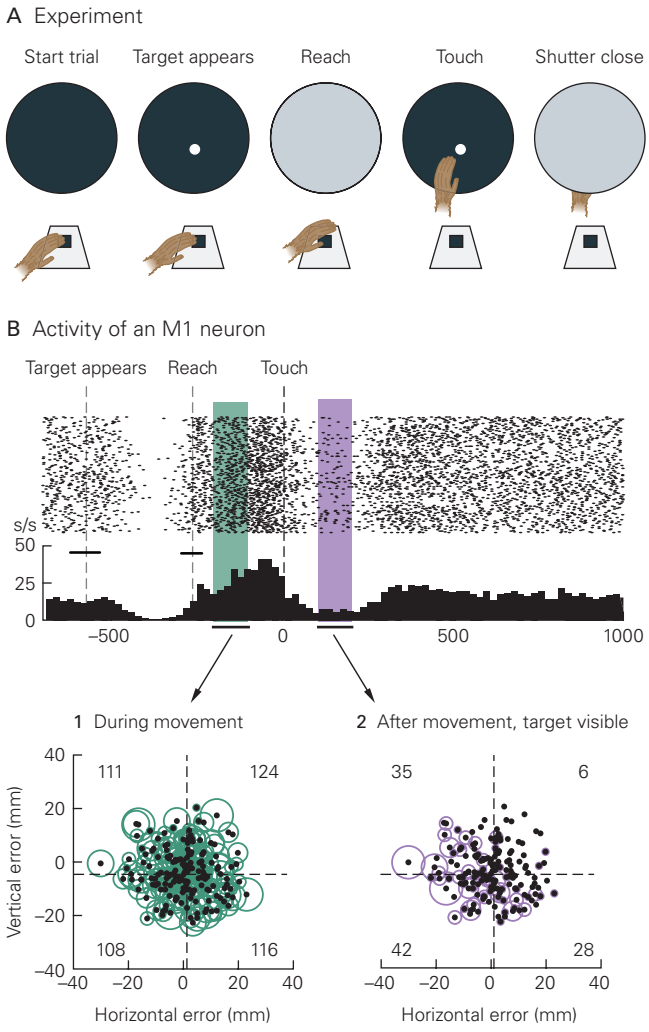

Figure 34–25 (right) **Error signals in the primary motor cortex drive adaptation.** After a movement is complete, M1 activity reflects the error between the spatial target and final hand position. (Reproduced, with permission, from Inoue, Uchimura, and Kitazawa 2016. Copyright © 2016 Elsevier Inc.)

A. Monkeys made reaching movements to spatial targets on a touch screen. On each trial, adjustable prism goggles shifted the viewed position of the spatial target by a variable amount during the movement, while a shutter blocked vision of the monkey's hand and the target. Feedback of the final hand position was only provided for 300 ms after contact with the touch screen at the end of movement.

B. Top: Discharge response of a typical M1 neuron. Raster plots and spike-timing histograms are aligned with the initial screen contact (touch).

1. Distribution of reach endpoint errors (**black dots**) where the origin represents the center of the target. **Diameters of green circles** denote the firing rate of the neuron during each movement (**green bar** in **B**); the firing rates were unrelated to the subsequent endpoint error. The numbers in each quadrant indicate the summed spike activity during movements that ended in the corresponding quadrant; they are all nearly equal.

2. Same as in part **B** except **purple circles** denote firing rate 100 to 200 ms after movement while the monkey can see its hand while touching the screen (**purple bar** in part **B**). The circles and spike counts show that the firing rate is greatest for endpoint errors down and to the left relative to the position of the target (0,0), revealing that that the neural activity during this postmovement period is strongly modulated by visual feedback of reach endpoint error.

neurons and cursor motions was rotated clockwise by 45°, the monkeys showed significant adaptation to the perturbation within a few hundred trials during a single recording session. In contrast, when the perturbation required the monkeys to learn a more complex "unnatural" remapping, for instance, random clockwise and counterclockwise rotations of the apparent directional tuning of neurons by different amounts, the monkeys showed little ability to recover proficient cursor control over several hundred trials in a single recording session. Importantly, another study found that monkeys could eventually master an "unnatural" change in an M1 neural activity decoder mapping if they could practice with the same altered decoder over several days, indicating that they could learn a new neural co-modulation structure if allowed enough experience with it. These studies reinforce how neural circuits in these cortical motor regions are critical for motor skill learning.

The studies just described used brain–machine interfaces and neural decoders to explore how single neurons and neural populations contribute to motor skill learning. This technology promises to be an increasingly important research tool for developing new insights into the neural mechanisms of voluntary motor control and motor skill learning (Chapter 39).

Highlights

1. Voluntary motor behavior implements an individual's intentional choice or decision to move within, and to interact physically with objects in, the environment. A hallmark of human motor action is the breadth of skills we possess and, when highly practiced, the ease and automaticity of these actions.
2. Voluntary motor control has long been separated into two stages—planning and execution—that

can be dissociated in time. Neural recording studies have found correlates of these two stages differentially distributed across many movement-related cortical areas.

3. The overall computational problem that the motor system must resolve to control voluntary movement is to convert sensory information about the current state of the world and the body into plans for action and ultimately into patterns of muscle activity that generate the causal forces required to execute the desired movement(s), while avoiding or correcting for errors.
4. Representational models of voluntary motor control such as the sensorimotor coordinate transformation hypothesis assume that the motor system directly plans and controls specific features or parameters of intended movements. Single neurons and neural populations express those parameters in their activity and perform definable computations to effect the transformations between the controlled movement parameters in corresponding coordinate frameworks.
5. Dynamical systems models of voluntary motor control, in contrast, assume that motor circuits find empirical solutions for the computations underlying the planning and execution of movements by evolutionary and individual adaptive processes. One recent theory, optimal feedback control, proposes that planning and execution of voluntary movements involve three functional processes, namely, state estimation, task selection, and a control policy. Single neurons and neural populations contribute to voluntary motor control by participating in the computations underlying these three processes.
6. Distributed frontoparietal circuits in cerebral cortex play a pivotal role in voluntary control. There are substantial reciprocal axonal interconnections between frontal and parietal cortical regions, partially segregated based on body part (eg, hand, arm, eye). Frontal motor and parietal cortical regions both directly influence spinal processing through the corticospinal tract and indirectly through brain stem descending pathways.
7. Posterior parietal cortex plays a prominent role in identifying potential goals and objects in the environment, state estimation of the body, and sensory guidance of motor actions. Important sources of sensory signals are transmitted from visual cortex through the dorsal visual pathway and from primary somatosensory cortex. Behavioral goals and objects are represented in many parietal subregions, but how they are represented (relative to the orientation of the eye, head, or arm) varies across subregions. The presence of multiple representations provides a rich basis for defining the movement-relevant properties and the locations of objects in the world and relative to the body that can be used to select and guide movement.
8. Premotor and prefrontal cortices play a prominent role in task selection and motor planning. The dorsal and ventral premotor regions are often implicated when external sensory information plays a dominant role in selecting motor actions. In contrast, more medial premotor regions, such as the supplementary and cingulate motor areas, may play a more dominant role when internal desires are more critical in selecting and initiating a motor action. However, this dichotomy is not absolute, and multiple premotor and prefrontal cortical areas all contribute to the control of voluntary behavior in a broad range of contexts and conditions.
9. Primary motor cortex in primates has a representation of the entire body along its mediolateral axis, with larger cortical territories associated with the hand and face relative to other body parts. This cortical region also provides a large component of the corticospinal tract and has projections to both interneurons and alpha motor neurons in the spinal cord.
10. Neural activity that reflects the causal forces and the spatiotemporal features of muscle activity necessary to move the limb is particularly prominent in the primary motor cortex and can be rapidly altered to correct movement errors or to compensate for displacements of the limb away from the desired movement if the limb is perturbed. However, neural activity in primary motor cortex can also show more complex properties, reflecting changes based on the behavioral context, performance goals and constraints, and features such as movement kinematics. These properties of primary motor cortex activity may reflect the formation of a task-specific control policy within the motor system.
11. Although parietal, premotor, and primary motor cortical regions play prominent roles in state estimation, motor planning, and motor execution, respectively, they are not uniquely responsible for any one aspect; they are instead distributed to some degree across most or all of these cortical regions.
12. The cortical motor system is adaptive and can undergo changes in its functional architecture to adapt to long-term changes in the physical

properties of the world and the body, as well as acquire, retain, and recall new motor skills.

13. New technologies such as large-scale multi-neuron recording and imaging methods, enhanced multi-neuron activity decoding algorithms, and optogenetic control of the activity of specific neural populations will lead to deeper insights into the functional architecture of cortical motor circuits.

Stephen H. Scott
John F. Kalaska

Selected Reading

Battaglia-Mayer A, Babicola L, Satta E. 2016. Parieto-frontal gradients and domains underlying eye and hand operations in the action space. Neuroscience 334:76–92.

Cisek P, Kalaska JF. 2010. Neural mechanisms for interacting with a world full of action choices. Annu Rev Neurosci 33:269–298.

Dum RP, Strick PL. 2002. Motor areas in the frontal lobe of the primate. Physiol Behav 77:677–682.

Hikosaka O, Isoda M. 2010. Switching from automatic to controlled behaviour: cortico-basal ganglia mechanism. Trends Cogn Sci 14:154–161.

Lemon RN. 2008 Descending pathways in motor control. Ann Rev Neurosci 31:195–218.

Passingham RE, Bengtsson SL, Lau HC. 2010. Medial frontal cortex: from self-generated action to reflection on one's own performance. Trends Cogn Sci 14:16–21.

Scott SH. 2004. Optimal feedback control and the neural basis of volitional motor control. Nat Rev Neurosci 5:532–546.

References

Batista AP, Buneo CA, Snyder LH, Andersen RA. 1999. Reach plans in eye-centered coordinates. Science 285:257–260.

Cheney PD, Fetz EE, Palmer SS. 1985. Patterns of facilitation and suppression of antagonist forelimb muscles from motor cortex sites in the awake monkey. J Neurophysiol 53:805–820.

Cherian A, Krucoff MO, Miller LE. 2011. Motor cortical prediction of EMG: evidence that a kinetic brain-machine interface may be robust across altered movement dynamics. J Neurophysiol 106:564–575.

Churchland MM, Shenoy KV. 2006. Temporal complexity and heterogeneity of single-neuron activity in premotor and motor cortex. J Neurophysiol 97:4235–4257.

Cisek P, Crammond DJ, Kalaska JF. 2003. Neural activity in primary motor and dorsal premotor cortex in reaching tasks with the contralateral versus ipsilateral arm. J Neurophysiol 89:922–942.

Cisek P, Kalaska JF. 2004. Neural correlates of mental rehearsal in dorsal premotor cortex. Nature 431:993–996.

Crammond DJ, Kalaska JF. 2000. Prior information in motor and premotor cortex: activity in the delay period and effect on pre-movement activity. J Neurophysiol 84:986–1005.

Duhamel JR, Colby CL, Goldberg ME. 1998. Ventral intraparietal area of the macaque: congruent visual and somatic response properties. J Neurophysiol 79:126–136.

Evarts EV. 1968. Relation of pyramidal tract activity to force exerted during voluntary movement. J Neurophysiol 31:14–27.

Evarts E, Tanji J. 1976. Reflex and intended responses in motor cortex pyramidal tract neurons of monkey. J Neurophysiol 39:1069–1080.

Fetz EE, Cheney PD. 1980. Postspike facilitation of forelimb muscle activity by primate corticomotoneuronal cells. J Neurophysiol 44:751–772.

Ganguly K, Carmena JM. 2009. Emergence of a stable cortical map for neuroprosthetic control. PLoS Biol. 7:e1000153.

Georgopoulos AP, Caminiti R, Kalaska JF, Massey JT. 1983. Spatial coding of movement: a hypothesis concerning the coding of movement direction by motor cortical populations. Exp Brain Res 49(Suppl 7):327–336.

Georgopoulos AP, Kalaska, JF, Caminiti R, Massey JT. 1982. On the relations between the direction of two-dimensional arm movements and cell discharge in primate motor cortex. J Neurosci 2:1527–1537.

Georgopoulos AP, Kettner RE, Schwartz AB. 1988. Primate motor cortex and free arm movements to visual targets in three-dimensional space. II. Coding of the direction of movement by a neuronal population. J Neurosci 8:2928–2937.

Goodale MA, Milner AD. 1992. Separate visual pathways for perception and action. Trends Neurosci 15:20–25.

Griffin DM, Hudson HM, Belhaj-Saïf A, McKiernan BJ, Cheney PD. 2008. Do corticomotoneuronal cells predict target muscle EMG activity? J Neurophysiol 99:1169–1186.

Heming EA, Lillicrap TP, Omrani M, Herter TM, Pruszynski JA, Scott SH. 2016. Primary motor cortex neurons classified in a postural task predict muscle activation patterns in a reaching task. J Neurophysiol 115:2021–2032.

Hepp-Reymond MC, Kirkpatrick-Tanner M, Gabernet L, Qi Hx, Weber B. 1999. Context-dependent force coding in motor and premotor cortical areas. Exp Brain Res 128:123–133.

Humphrey DR, Tanji J. 1991. What features of voluntary motor control are encoded in the neuronal discharge of different cortical areas? In: DR Humphrey, H-J Freund (eds). *Motor Control: Concepts and Issues*, pp 413–443. New York: Wiley.

Hwang EJ, Bailey PM, Andersen RA. 2013. Volitional control of neural activity relies on the natural motor repertoire. Curr Biol 23:353–361.

Inoue M, Uchimura M, Kitazawa S. 2016. Error signals in motor cortices drive adaptation in reaching. Neuron 90:1114–1126.

Kalaska JF, Cohen DA, Hyde ML, Prud'Homme M. 1989. A comparison of movement direction-related versus load direction-related activity in primate motor cortex, using a two-dimensional reaching task. J Neurosci 9:2080–2102.

Kaufman MT, Churchland MM, Ryu SI, Shenoy KV. 2014. Cortical activity in the null space: permitting preparation without movement. Nat Neurosci 17:440–448.

Klaes C, Westendorff S, Chakrabarti S, Gail A. 2011. Choosing goals, not rules: deciding among rule-based action plans. Neuron 70:536–548.

Kurtzer I, Herter TM, Scott SH. 2005. Random change in cortical load representation suggests distinct control of posture and movement. Nat Neurosci 8:498–504.

Maravita A, Iriki A. 2004. Tools for the body (schema). Trends Cogn Sci 8:79–86.

Moritz CT, Perlmutter SI, Fetz EE. 2008. Direct control of paralysed muscles by cortical neurons. Nature 456:639–642.

Muir RB, Lemon RN. 1983. Corticospinal neurons with a special role in precision grip. Brain Res 261:312–316.

Murata A, Wen W, Asama H. 2016. The body and objects represented in the ventral stream of the parieto-premotor network. Neurosci Res 104:4–15.

Nachev P, Kennard C, Husain M. 2008. Functional role of the supplementary and pre-supplementary motor areas. Nat Rev Neurosci 9:856–869.

Nudo RJ, Milliken GW, Jenkins WM, Merzenich MM. 1996. Use-dependent alterations of movement representations in primary motor cortex of adult squirrel monkeys. J Neurosci 16:785–807.

Omrani M, Murnaghan CD, Pruszynski JA, Scott SH. 2016. Distributed task-specific processing of somatosensory feedback for voluntary motor control. eLife 5:e13141.

Park MC, Belhaj-Saïf A, Gordon M, Cheney PD. 2001. Consistent features in the forelimb representation of primary motor cortex in rhesus macaques. J Neurosci 21:2784–2792.

Paz R, Vaadia E. 2004. Learning-induced improvement in encoding and decoding of specific movement directions by neurons in the primary motor cortex. PLoS Biol 2:E45.

Pruszynski JA, Kurtzer I, Nashed JY, Omrani M, Brouwer B, Scott SH. 2011. Primary motor cortex underlies multijoint integration for fast feedback control. Nature 478: 387–390.

Rathelot JA, Strick PL. 2006. Muscle representation in the macaque motor cortex: an anatomical perspective. Proc Natl Acad Sci U S A 103:8257–8262.

Rizzolatti G, Camarda R, Fogassi L, Gentilucci M, Luppino G, Matelli M. 1988. Functional organization of inferior area 6 in the macaque monkey. II. Area F5 and the control of distal movement. Exp Brain Res 71:491–507.

Rizzolatti G, Fadiga L, Gallese V, Fogassi L. 1996. Premotor cortex and the recognition of motor actions. Cogn Brain Res 3:131–141.

Romo R, Hernández A, Zainos A. 2004. Neuronal correlates of a perceptual decision in ventral premotor cortex. Neuron 41:165–173.

Rozzi S, Calzavara R, Belmalih A, et al. 2006. Cortical connections of the inferior parietal cortical convexity of the macaque monkey. Cereb Cortex 16:1389–1417.

Sadtler PT, Quick KM, Golub MD, et al. 2014. Neural constraints on learning. Nature 512:423–426.

Schaffelhofer S, Scherberger H. 2016. Object vision to hand action in macaque parietal, premotor, and motor cortices. eLife 5:e15278.

Schwartz AB. 1994. Direct cortical representation of drawing. Science 265:540–542.

Scott SH, Cluff T, Lowrey CR, Takei T. 2015. Feedback control during voluntary motor actions. Curr Opin Neurobiol 33:85–94.

Scott SH, Gribble P, Graham K, Cabel DW. 2001. Dissociation between hand motion and population vectors from neural activity in motor cortex. Nature 413:161–165.

Sergio LE, Hamel-Pâquet C, Kalaska JF. 2005. Motor cortex neural correlates of output kinematics and kinetics during isometric-force and arm-reaching tasks. J Neurophysiol 94:2353–2378.

Sergio LE, Kalaska JF. 2003. Systematic changes in motor cortex cell activity with arm posture during directional isometric force generation. J Neurophysiol 89:212–228.

Shenoy KV, Sahani M, Churchland M. 2013. Cortical control of arm movements: a dynamical systems perspective. Annu Rev Neurosci 36:337–359.

Shima K, Tanji J. 1998. Role of cingulate motor area cells in voluntary movement selection based on reward. Science 282:1335–1338.

Shinoda Y, Yokota J, Futami T. 1981. Divergent projections of individual corticospinal axons to motoneurons of multiple muscles in the monkey. Neurosci Lett 23:7–12.

Sommer MA, Wurtz RH. 2008. Brain circuits for the internal monitoring of movements. Ann Rev Neurosci 31:317–338.

Strick PL. 1983. The influence of motor preparation on the response of cerebellar neurons to limb displacements. J Neurosci 3:2007–2020.

Tanji J. 2001. Sequential organization of multiple movements: involvement of cortical motor areas. Ann Rev Neurosci 24:631–651.

Thach WT. 1978. Correlation of neural discharge with pattern and force of muscular activity, joint position, and direction of intended next arm movement in motor cortex and cerebellum. J Neurophysiol 41:654–676.

Wallis JD, Miller EK. 2003. From rule to response: neuronal processes in the premotor and prefrontal cortex. J Neurophysiol 90:1790–1806.

35

The Control of Gaze

In preceding chapters, we learned about the motor systems that control the movements of the body in space. In this and the next chapter, we consider the motor systems that control our gaze, balance, and posture as we move through the world around us. In examining these motor systems, we will focus on three biological challenges that these systems resolve: How do we visually explore our environment quickly and efficiently? How do we compensate for planned and unplanned movements of the head? How do we stay upright?

In this chapter, we describe the oculomotor system and how it uses visual information to guide eye movements. It is one of the simplest motor systems, requiring the coordination of only the 12 evolutionarily old muscles that move the two eyes. In humans and other primates, the primary objective of the oculomotor system is to control the position of the fovea, the central point in the retina that has the highest density of photoreceptors and thus the sharpest vision. The fovea is less than 1 mm in diameter and covers less than 1% of the visual field. When we want to examine an object, we must move its image onto the fovea (Chapter 22).

The Eye Is Moved by the Six Extraocular Muscles

Eye Movements Rotate the Eye in the Orbit

To a good approximation, the eye is a sphere that sits in a socket, the orbit. Eye movements are simply rotations of the eye in the orbit. The eye's orientation can be defined by three axes of rotation—horizontal, vertical, and torsional—that intersect at the center of the eyeball, and eye movements are described as rotations

around these axes. Horizontal and vertical eye movements change the line of sight by redirecting the fovea; torsional eye movements rotate the eye around the line of sight but do not change where the eyes are looking.

Horizontal rotation of the eye away from the nose is called *abduction*, and rotation toward the nose is *adduction* (Figure 35–1A). Vertical movements are referred to as *elevation* (upward rotation) and *depression* (downward rotation). Finally, torsional movements include *intorsion* (rotation of the top of the cornea toward the nose) and *extorsion* (rotation away from the nose).

Most eye movements are conjugate; that is, both eyes move in the same direction. These eye movements are called *version* movements. For example, during gaze to the right, the right eye abducts and the left eye adducts. Similarly, if the right eye extorts, the left eye intorts. When you change your gaze from far to near, the eyes move in opposite directions—both eyes adduct. These movements are called *vergence* movements.

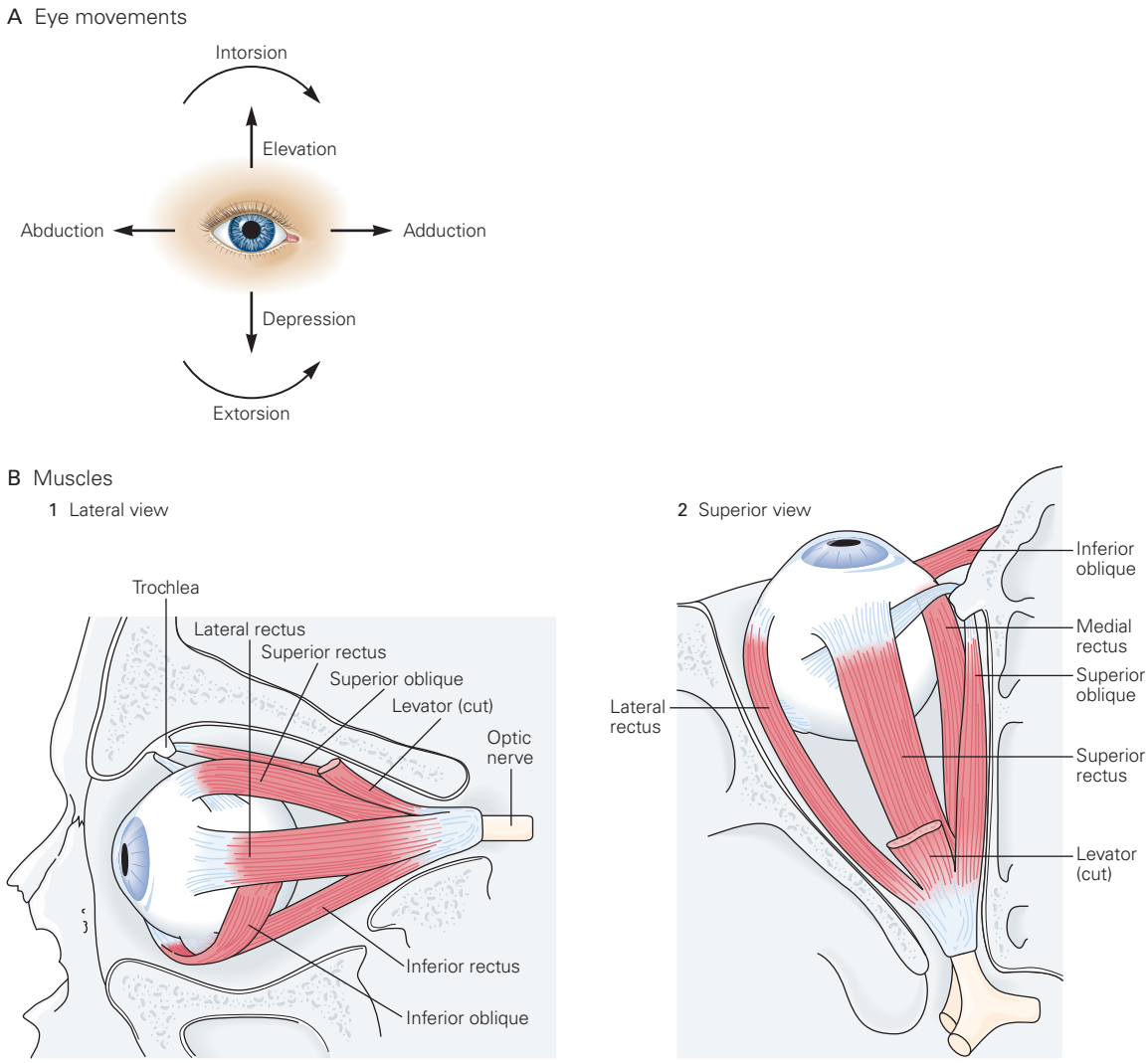

Figure 35–1 The different actions of eye movements and the muscles that control them.

A. View of the left eye and the three dimensions of eye movement.

B. 1. Lateral view of the left eye with the orbital wall cut away. Each rectus muscle inserts in front of the equator of the globe so that contraction rotates the cornea toward the muscle. Conversely, the oblique muscles insert behind the equator, and contraction rotates the cornea away from the insertion. The superior oblique tendon passes through the trochlea, a bony pulley on the nasal side of the orbit, before it inserts on the globe. The levator muscle of the upper eyelid raises the lid. 2. Superior view of the left eye with the roof of the orbit and the levator muscle cut away. The superior rectus passes over the superior oblique and inserts in front of it on the globe.

The Six Extraocular Muscles Form Three Agonist–Antagonist Pairs

Each eye is rotated by six extraocular muscles arranged in three agonist–antagonist pairs (Figure 35–1B). The four rectus muscles (lateral, medial, superior, and inferior) share a common origin, the annulus of Zinn, at the apex of the orbit. They insert on the surface of the eye, or sclera, anterior to the center of the eye, so the superior rectus elevates the eye and the inferior rectus depresses it. The origin of the inferior oblique muscle is on the medial wall of the orbit; the superior oblique muscle's tendon passes through the trochlea, or pulley, before inserting on the globe, so that its effective origin is also on the anteromedial wall of the orbit. The oblique muscles insert posterior to the center of the eye, so the superior oblique depresses the eye and the inferior oblique elevates it.

Each muscle has a dual insertion. The part of the muscle farthest from the eye inserts on a soft-tissue pulley through which the rest of the muscle passes on its way to the eye. When the extraocular muscles contract, they not only rotate the eye but also change their pulling directions as a result of these pulleys.

The actions of the extraocular muscles are determined by their geometry and by the position of the eye in the orbit. The medial and lateral recti rotate the eye horizontally; the medial rectus adducts, whereas the lateral rectus abducts. The superior and inferior recti and the obliques rotate the eye both vertically and torsionally. The superior rectus and inferior oblique elevate the eye, and the inferior rectus and superior oblique depress it. The superior rectus and superior oblique intort the eye, whereas the inferior rectus and inferior oblique extort it.

The superior and inferior recti and the obliques are often called the cyclovertical muscles because they produce both vertical and torsional eye rotation. The relative amounts of each rotation depend on eye position. The superior and inferior recti exert their maximal vertical action when the eye is abducted, that is, when the line of sight is parallel to the muscles' pulling directions, while the oblique muscles exert their maximal vertical action when the eye is adducted (Figure 35–2).

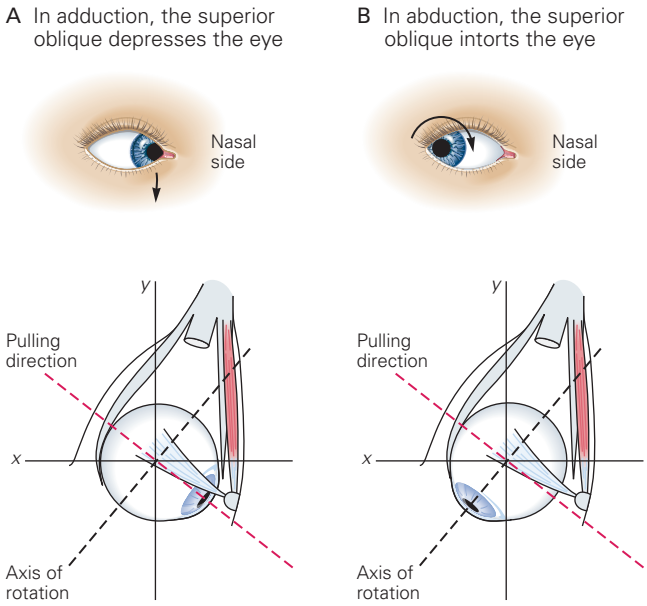

Figure 35–2 The effect of orbital position on the action of the superior oblique muscle.

A. When the eye is adducted (looking toward the nose), contraction of the superior oblique depresses the eye.

B. When the eye is abducted (looking away from the nose), contraction of the superior oblique intorts the eye.

Movements of the Two Eyes Are Coordinated

Humans and other frontal-eyed animals have binocular vision—the fields of vision of the two eyes overlap. This facilitates stereopsis, the ability to perceive a visual scene in three dimensions, as well as depth perception. At the same time, binocular vision requires precise coordination of the movements of the two eyes so that both foveae are always directed at the target of interest. For most eye movements, both eyes must move by the same amount and in the same direction. This is accomplished, in large part, through the pairing of eye muscles in the two eyes.

Just as each eye muscle is paired with its antagonist in the same orbit (eg, the medial and lateral recti), it is also paired with the muscle that moves the opposite eye in the same direction. For example, coupling of the left lateral rectus and right medial rectus moves both eyes to the left during a leftward saccade. The orientations of the vertical muscles are such that each pair consists of one rectus muscle and one oblique muscle. For example, the left superior rectus and the right inferior oblique both move the eyes upward in left gaze, while the right inferior rectus and the left superior oblique both move the eyes downward in right gaze (Table 35–1).

The Extraocular Muscles Are Controlled by Three Cranial Nerves

The extraocular muscles are innervated by groups of motor neurons whose cell bodies are clustered in the three oculomotor nuclei in the brain stem (Figure 35–3).

Table 35–1 Vertical Muscle Action in Adduction and Abduction

Muscle	Action in adduction	Action in abduction
Superior rectus	Intorsion	Elevation
Inferior rectus	Extorsion	Depression
Superior oblique	Depression	Intorsion
Inferior oblique	Elevation	Extorsion

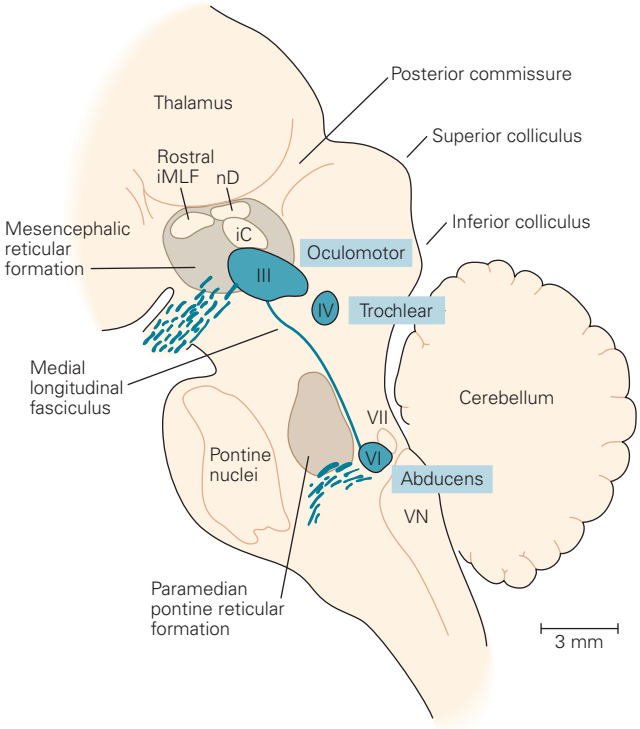

Figure 35–3 The oculomotor nuclei in the brain stem. The nuclei are shown in a parasagittal section through the thalamus, pons, midbrain, and cerebellum of a rhesus monkey. The oculomotor nucleus (cranial nerve III) lies in the midbrain at the level of the mesencephalic reticular formation; the trochlear nucleus (nerve IV) is slightly caudal; and the abducens nucleus (nerve VI) lies in the pons at the level of the paramedian pontine reticular formation, adjacent to the fasciculus of the facial nerve (VII). Compare with Figure 40–5. (Abbreviations: **iC**, interstitial nucleus of Cajal; **iMLF**, interstitial nucleus of the medial longitudinal fasciculus; **nD**, nucleus of Darkshevich; **VN**, vestibular nuclei.) (Adapted from Henn, Hepp, and Büttner-Ennever 1982.)

The lateral rectus is innervated by the abducens nerve (cranial nerve VI), whose nucleus lies in the pons in the floor of the fourth ventricle. The superior oblique muscle is innervated by the trochlear nerve (cranial nerve IV), whose nucleus is located in the contralateral midbrain at the level of the inferior colliculus. (The trochlear nerve gets its name from the trochlea, the bony pulley through which the superior oblique muscle travels.)

All the other extraocular muscles—the medial, inferior, and superior recti, and the inferior oblique—are innervated by the oculomotor nerve (cranial nerve III), whose nucleus lies in the midbrain at the level of the superior colliculus. Superior rectus axons cross the midline and join the contralateral oculomotor nerve. Thus, both superior rectus and superior oblique motor neurons innervate their respective muscles on the opposite side. The oculomotor nerve also contains fibers that innervate the levator muscle of the upper eyelid. Cell bodies of axons innervating both eyelids are located in the central caudal nucleus, a single midline structure within the oculomotor complex. Finally, traveling with the oculomotor nerve are parasympathetic fibers that innervate the iris sphincter muscle, which constricts the pupil, and the ciliary muscles that adjust the curvature of the lens to focus the eye during vergence movements from far to near, the process of accomodation.

The pupil and eyelid also have sympathetic innervation, which originates in the intermediolateral cell column of the ipsilateral upper thoracic spinal cord. Fibers of these neurons synapse on cells in the superior cervical ganglion in the upper neck. Axons of these postganglionic cells travel along the carotid artery to the cavernous sinus and then into the orbit. Sympathetic pupillary fibers innervate the iris dilator muscle, causing the pupil to dilate and thus providing the pupillary component of the so-called "fight or flight" response. Sympathetic fibers also innervate Müller's muscle, a secondary elevator of the upper eyelid. The sympathetic control of pupillary dilatation and lid elevation is responsible for the "wide-eyed" look of excitement and sympathetic overload.

The best way to understand the actions of the extraocular muscles is to consider the eye movements that remain after a lesion of a specific nerve (Box 35–1).

The force generated by an extraocular muscle is determined both by the firing rate of the motor neurons and the number of motor units recruited. Like the motor units for skeletal muscle (Chapter 31), eye motor units are recruited in a fixed sequence. For example, as the eye moves laterally, the number of active abducens neurons and their individual firing rates both increase, thereby increasing the strength of lateral rectus contraction.

Box 35–1 Extraocular Muscle or Nerve Lesions

Patients with lesions of the extraocular muscles or their nerves complain of double vision (diplopia) because the images of the object of gaze no longer fall on the corresponding retinal locations in both eyes. Lesions of each nerve produce characteristic symptoms that depend on which extraocular muscles are affected. In general, double vision increases when the patient tries to look in the direction of the weak muscle.

Abducens Nerve

A lesion of the abducens nerve (VI) causes weakness of the lateral rectus. When the lesion is complete, the eye cannot abduct beyond the midline, such that a horizontal diplopia increases when the subject looks in the direction of the affected eye.

Trochlear Nerve

A left trochlear nerve (IV) lesion affects both torsional and vertical eye movements by weakening the superior oblique muscle (Figure 35–4). Vertical misalignment in superior oblique paresis is also affected by the position of the head. A tilt to one side, such that the ear moves toward the shoulder, induces a small torsion of the eye in the opposite direction, known as ocular counter-roll. For example, when the head tilts to the left, the left eye is ordinarily intorted by the left superior rectus and left superior oblique, while the right eye is extorted by the right inferior rectus and right inferior oblique. In the left eye, the elevation action of the superior rectus is canceled by the depression action of the superior oblique, so the eye only rotates about the line of sight. When the head tilts to the right, the inferior oblique and inferior rectus extort the left eye and the superior oblique and the superior rectus relax.

With paresis of the left superior oblique, the elevating action of the superior rectus is unopposed when the head tilts to the left such that the left eye moves further upward. In contrast, tilting the head to the right relaxes the superior rectus and superior oblique (Figure 35–4D). Thus, patients with trochlear nerve lesions often prefer to keep their heads tilted away from the affected eye because this reduces the misalignment and can eliminate diplopia.

Oculomotor Nerve

A lesion of the oculomotor nerve (III) has complex effects because this nerve innervates multiple muscles. A complete lesion spares only the lateral rectus and superior oblique muscles. Thus, the paretic eye is typically deviated downward and abducted at rest and cannot move medially or upward. Downward movement is also affected because the inferior rectus muscle is weak; because the eye is abducted, the primary action of the intact superior oblique is intorsion rather than depression.

Because the fibers that control lid elevation, accommodation, and pupillary constriction travel in the oculomotor nerve, damage to this nerve also results in drooping of the eyelid (ptosis), blurred vision for near objects, and pupillary dilation (mydriasis). Although sympathetic innervation is still intact with an oculomotor nerve lesion, the ptosis is essentially complete, since Müller's muscle contributes less to elevation of the upper eyelid than does the levator muscle of the upper eyelid.

Sympathetic Oculomotor Nerves

Sympathetic fibers innervating the eye arise from the thoracic spinal cord, traverse the apex of the lung, and ascend to the eye on the outside of the carotid artery. Interruption of the sympathetic pathways to the eye leads to Horner syndrome, which includes a partial ipsilateral ptosis owing to weakness of Müller's muscle and a relative constriction (miosis) of the ipsilateral pupil. The pupillary asymmetry is most pronounced in low light because the normal pupil is able to dilate but the pupil affected by Horner syndrome is not.

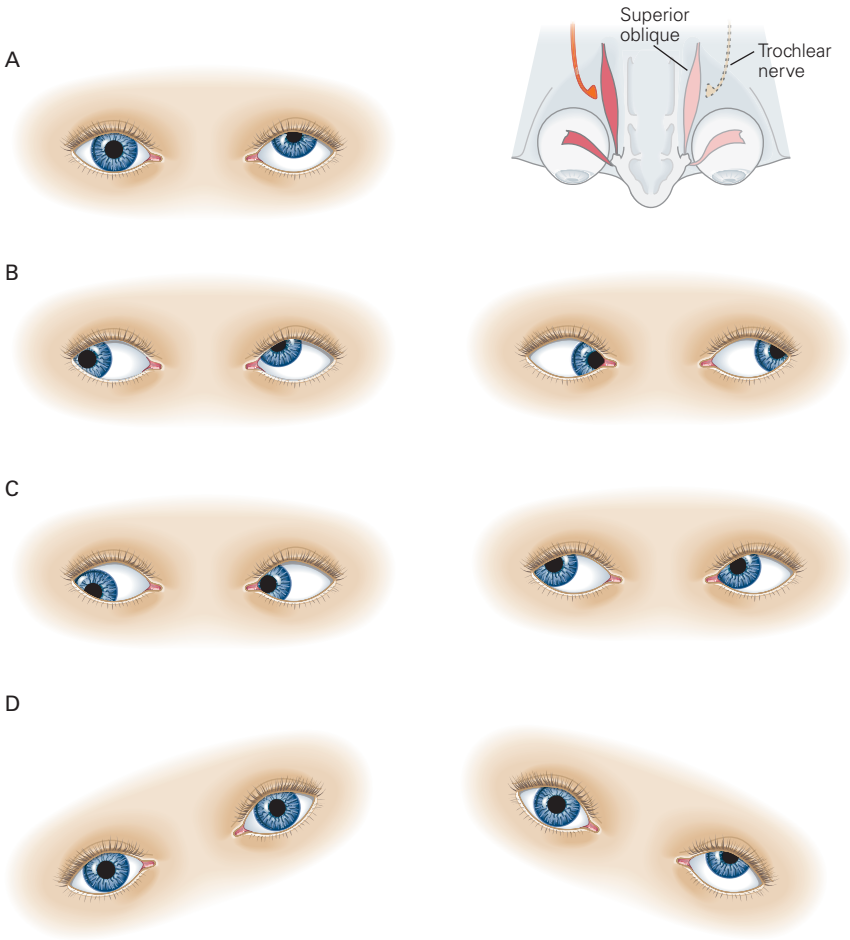

Figure 35–4 Effect of a left trochlear nerve palsy. The trochlear nerve innervates the superior oblique muscle, which inserts behind the equator of the eye. It depresses the eye when it is adducted and intorts the eye when it is abducted.

A. Hypertropia, a permanent upward deviation of the eye, can be seen when a patient is looking straight ahead. The right eye is in the center of the orbit, but the affected left eye is slightly above the right eye.

B. The hypertropia is worse when the eye is adducted because the unopposed inferior oblique pushes the eye higher (*left*). The condition is improved when the eye is abducted (*right*) because the superior oblique contributes less to depression than to intorsion.

C. When the patient looks to the right, the hypertropia is worse on downward gaze (*left*) than it is on upward gaze (*right*).

D. The hypertropia is improved by head tilt to the right (*left*) and worsened by tilt to the left (*right*). The ocular counter-rolling reflex induces intorsion of the left eye on leftward head tilt and extorsion of the eye on rightward head tilt (Chapter 27). With leftward head tilt, intorsion requires increased activity of the superior rectus, whose elevating activity is unopposed by the weak superior oblique, causing increased hypertropia. With rightward head tilt and extorsion of the left eye, the unopposed superior rectus muscle is less active, and the hypertropia decreases.

Six Neuronal Control Systems Keep the Eyes on Target

The oculomotor nuclei are the final common targets for all types of eye movements generated by higher brain networks. Hermann Helmholtz and other 19th-century psychophysicists appreciated that analysis of eye movements was essential for understanding visual perception, but they assumed that all eye movements were smooth. In 1890, Edwin Landott discovered that during reading the eyes do not move smoothly along a line of text but make fast intermittent movements called saccades (French, jerks), each followed by a short pause.

By 1902, Raymond Dodge outlined five distinct types of eye movement that direct the fovea to a visual target and keep it there. All of these eye movements share an effector pathway originating in the three oculomotor nuclei in the brain stem.

- Saccadic eye movements shift the fovea rapidly to a new visual target.
- Smooth-pursuit movements keep the image of a moving target on the fovea.
- Vergence movements move the eyes in opposite directions so that the image of an object of interest is positioned on both foveae regardless of its distance.
- Vestibulo-ocular reflexes stabilize images on the retina during brief head movements.
- Optokinetic movements stabilize images during sustained head rotation or translation.

A sixth system, the fixation system, holds the eye stationary during intent gaze when the head is not moving by actively suppressing eye movement. The optokinetic and vestibular systems are discussed in Chapter 27. We consider the other four systems here.

An Active Fixation System Holds the Fovea on a Stationary Target

Vision is most accurate when the eyes are still. The gaze system actively prevents the eyes from moving when we examine an object of interest. It is not as active in suppressing movement when we are doing something that does not require vision, such as mental arithmetic. Patients with disorders of the fixation system—for example, patients with irrepressible saccadic eye movements (opsoclonus)—have poor vision not because their visual acuity is deficient but because they cannot hold their eyes still enough for the visual system to work correctly.

The Saccadic System Points the Fovea Toward Objects of Interest

Our eyes explore the world in a series of very quick saccades that move the fovea from one fixation point to another (Chapter 25) (Figure 35–5). Saccades allow us to scan the environment quickly and to read. Highly stereotyped, they have a standard waveform with a single smooth increase and decrease of eye velocity. Saccades are also extremely fast, occurring within a fraction of a second at angular speeds up to 900° per second (Figure 35–6A). The velocity of a saccade is determined only by its size. We can voluntarily change

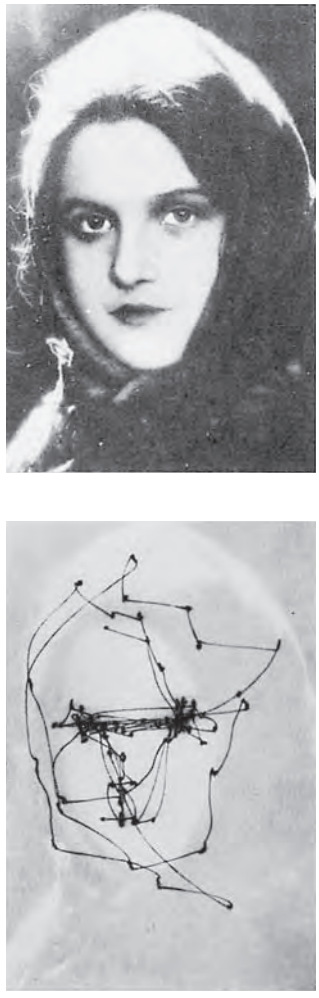

Figure 35–5 Eye movements track the outline of an object of attention. An observer looks at a picture of a woman for 1 minute. The resulting eye positions are then superimposed on the picture. As shown here, the observer concentrated on certain features of the face, lingering over the woman's eyes and mouth (*fixations*) and spending less time over intermediate positions. The rapid movements between fixation points are ***saccades.*** (Reproduced, with permission, from Yarbus 1967.)

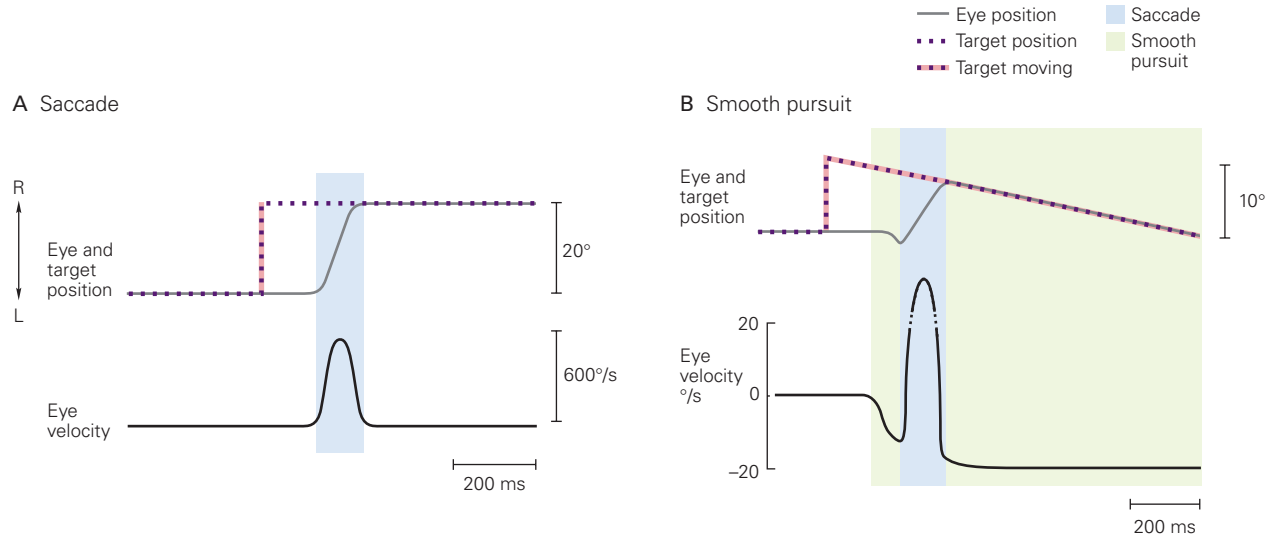

Figure 35–6 Saccadic and smooth-pursuit eye movements. Eye position, target position, and eye velocity are plotted against time.

A. *The human saccade*. At the beginning of the plot, the eye is on the target (the traces representing eye and target positions are superimposed). Suddenly, the target jumps to the right, and within 200 ms, the eye moves to bring the target back to the fovea. Note the smooth, symmetric velocity profile. Because eye movements are rotations of the eye in the orbit, they are described by the angle of rotation. Similarly, objects in the visual field are described by the angle of arc they subtend at the eye. Viewed at arm's length, a thumb subtends an angle of approximately 1°. A saccade from one edge of the thumb to the other therefore traverses 1° of arc. (Abbreviations: **L**, left; **R**, right.)

B. *Human smooth pursuit*. In this example, the subject is asked to make a saccade to a target that jumps away from the center of gaze and then slowly moves back to center. The first movement seen in the position and velocity traces is a smooth-pursuit movement in the same direction as the target movement. The eye briefly moves *away* from the target before a saccade is initiated because the latency of the pursuit system is shorter than that of the saccade system. The smooth-pursuit system is activated by the target moving back toward the center of gaze, the saccade adjusts the eye's position to catch the target, and thereafter, smooth pursuit keeps the eye on the target. The recording of saccade velocity is clipped so that the movement can be shown on the scale of the pursuit movement, an order of magnitude slower than the saccade.

the amplitude and direction of saccades but not their speed, although fatigue, drugs, or pathological states can slow saccades.

Ordinarily, there is no time for visual feedback to modify the course of a saccade as it is being made; instead, corrections to the direction and/or amplitude of movement are made over the course of successive saccades. Accurate saccades can be made not only to visual targets but also to sounds, tactile stimuli, memories of locations in space, and even verbal commands (eg, "look left").

When a saccade is made, the activity of neurons in higher brain centers that control gaze specify only a desired change in eye position (eg, 20° to the right of current gaze, usually based on a target location in the visual field). For the eye movement to be made, this location signal must be transformed into signals for the eye muscles that execute the desired velocity and change in eye position. We can illustrate how the gaze system generates eye movements by considering the activity of an oculomotor neuron during a saccade (Figure 35–7A). To move the eye quickly to a new position in the orbit and keep it there, two passive forces must be overcome: the elastic force of the orbital tissues, which tends to restore the eye to a central position, and a velocity-dependent viscous force that opposes rapid movement. Thus, the motor signal for an eye movement must include both a position component to counter the elastic force and a velocity component to overcome orbital viscosity and move the eye quickly to the new position.

This eye position and velocity information are coded by the discharge frequencies of oculomotor neurons. When a saccade is made, the firing rate of a neuron rises rapidly as eye velocity increases; this is called the *saccadic pulse* (Figure 35–7B). The frequency of this pulse determines the speed of the saccade, whereas the length of the pulse controls the duration of the saccade and thus its amplitude. When the saccade is completed and the eye has reached its goal, there must be a new level of tonic input to the eye muscles that is appropriate for the elastic restoring force at that orbital position. This difference in the tonic firing rate between before and after the saccade is called the *saccadic step* (Figure 35–7B). If the size of the step is not properly matched to

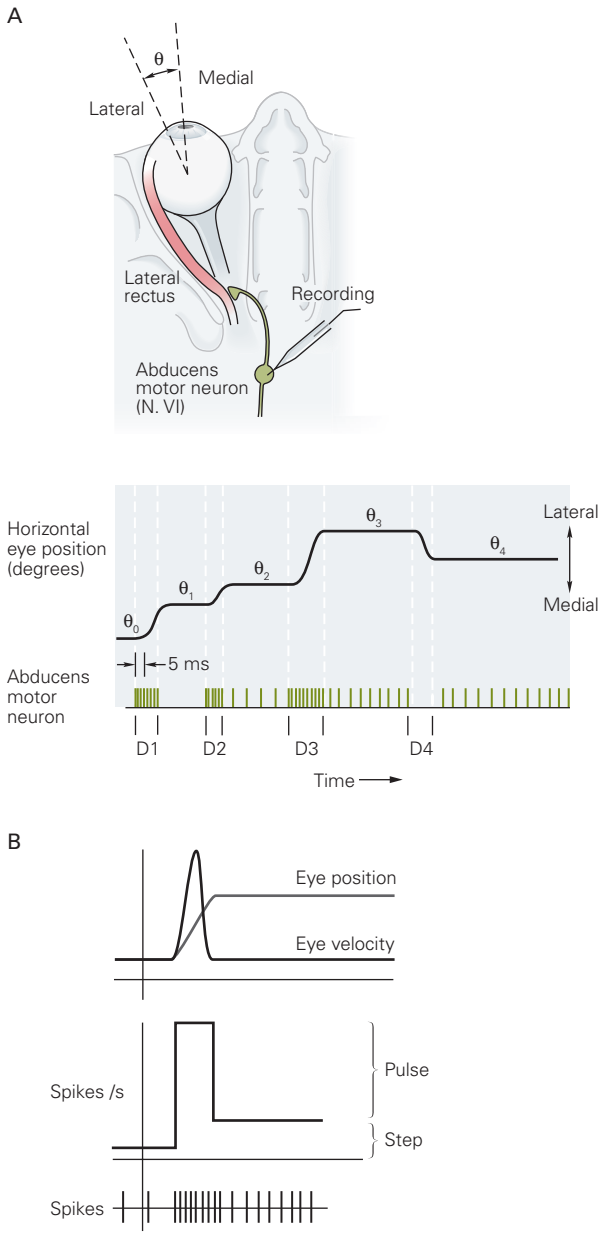

Figure 35–7 Oculomotor neurons signal eye position and velocity.

A. The record is from an abducens neuron of a monkey. When the eye is positioned in the medial side of the orbit, the cell is silent (**position** θ_0). As the monkey makes a lateral saccade, there is a burst of firing (**D1**), but in the new position (θ_1), the eye is still too far medial for the cell to discharge continually. During the next saccade, there is a burst (**D2**), and at the new position (θ_2), there is a tonic position-related discharge. Before and during the next saccade (**D3**), there is again a pulse of activity and a higher tonic discharge when the eye is at the new position (θ_3). When the eye makes a medial movement, there is a period of silence during the saccade (**D4**) even though the eye ends up at a position (θ_4) associated with a tonic discharge. (Adapted from Fuchs and Luschei 1970.)

B. Saccades are associated with a step of activity, which signals the change in eye position, and a pulse of activity, which signals eye velocity. The neural activity corresponding to eye position and velocity is illustrated both as a train of individual spikes and as an estimate of the instantaneous firing rate (spikes per second).

the pulse, then the eye drifts away from the target after the saccade. As described later, the pulse and step are generated by different brain stem structures.

The Motor Circuits for Saccades Lie in the Brain Stem

Horizontal Saccades Are Generated in the Pontine Reticular Formation

The neuronal signal for horizontal saccades originates in the paramedian pontine reticular formation, adjacent to the abducens nucleus to which it projects (Figure 35–8A). The paramedian pontine reticular formation contains a family of *burst neurons* that gives rise to the saccadic pulse. These cells fire at a high frequency just before and during ipsiversive saccades (toward the same side as the discharging neurons), and their activity resembles the pulse component of oculomotor neuron discharge (Figure 35–7B).

There are several types of burst neurons (Figure 35–8B). Medium-lead excitatory burst neurons make direct excitatory connections to motor neurons and interneurons in the ipsilateral abducens nucleus.

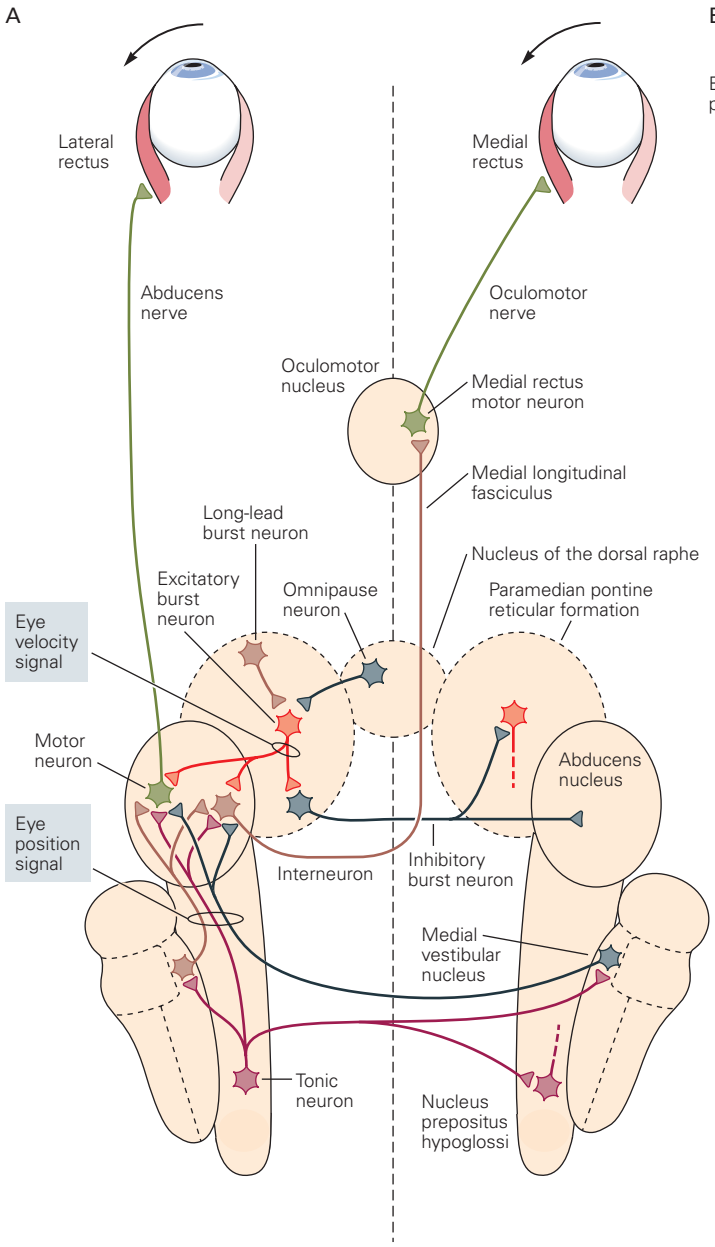

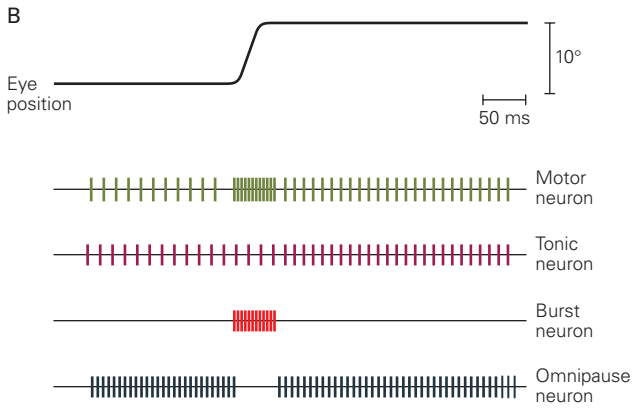

Figure 35–8 The brain stem motor circuit for horizontal saccades.

A. *Eye velocity component.* Long-lead burst neurons relay signals from higher centers to the excitatory burst neurons. The eye velocity component arises from excitatory burst neurons in the paramedian pontine reticular formation that synapse on motor neurons and interneurons in the abducens nucleus. The abducens motor neurons project to the ipsilateral lateral rectus muscles, while the interneurons project to the contralateral medial rectus motor neurons by axons that cross the midline and ascend in the medial longitudinal fasciculus. Excitatory burst neurons also drive ipsilateral inhibitory burst neurons that inhibit contralateral abducens motor neurons and excitatory burst neurons.

Eye position component. This component arises from a neural integrator comprising neurons distributed throughout the medial vestibular nuclei and nucleus prepositus hypoglossi on both sides of the brain stem. These neurons receive velocity signals from excitatory burst neurons and integrate this velocity signal to a position signal. The position signal excites the ipsilateral abducens neurons and inhibits the contralateral abducens neurons. (**Gray** neurons are inhibitory; all other neurons are excitatory. The vertical **dashed line** indicates the midline of the brain stem.)

B. Different neurons provide different information for a horizontal saccade. The motor neuron provides both position and velocity signals. The tonic neuron (nucleus prepositus hypoglossi) signals only eye position. The excitatory burst neuron (paramedian pontine reticular formation) signals only eye velocity. The omnipause neuron discharges at a high rate except immediately before, during, and just after the saccade.

Long-lead burst neurons drive the medium-lead burst cells and receive excitatory input from higher centers. Inhibitory burst neurons suppress the activity of contralateral abducens neurons and contralateral excitatory burst neurons and are themselves excited by medium-lead burst neurons.

A second class of pontine cells, *omnipause neurons*, fires continuously except around the time of a saccade; firing ceases shortly before and during all saccades (Figure 35–8B). Omnipause neurons are located in the nucleus of the dorsal raphe in the midline (Figure 35–8A). They are GABAergic (γ-aminobutyric acid) inhibitory neurons that project to contralateral pontine and mesencephalic burst neurons. Electrical stimulation of omnipause neurons arrests a saccade, which resumes when the stimulation stops. Making a saccade requires simultaneous excitation of burst neurons and inhibition of omnipause cells; this provides the system

with additional stability, such that unwanted saccades are infrequent.

If the motor neurons received signals from only the burst cells, the eyes would drift back to the starting position after a saccade, because there would be no new position signal to hold the eyes against elastic restorative forces. The appropriate tonic innervation is required to keep the eye at the new orbital position. This tonic position signal, the saccadic step, can be generated from the velocity burst signal by the neural equivalent of the mathematical process of integration. Velocity can be computed by differentiating position with respect to time; conversely, position can be computed by integrating velocity with respect to time.

For horizontal eye movements, neural integration of the velocity signal is performed by the medial vestibular nucleus and nucleus prepositus hypoglossi (Figure 35–8A) in conjunction with the flocculus of the cerebellum. As expected, animals with lesions of these areas make normal horizontal saccades, but the eyes drift back to a middle position after a saccade. Moreover, integration of the horizontal saccadic burst requires coordination of the bilateral nuclei prepositi hypoglossi and medial vestibular nuclei through commissural connections. Thus, a midline lesion of these connections also causes failure of the neural integrator.

Medium-lead burst neurons in the paramedian pontine reticular formation and neurons of the medial vestibular nucleus and nucleus prepositus hypoglossi project to the ipsilateral abducens nucleus and deliver respectively the pulse and step components of the motor signal. Two populations of neurons in the abducens nucleus receive this signal. One is a group of motor neurons that innervate the ipsilateral lateral rectus muscle. The second group consists of interneurons whose axons cross the midline and ascend in the medial longitudinal fasciculus to the motor neurons for the contralateral medial rectus, which lie in the oculomotor nucleus (Figure 35–8A).

Thus, medial rectus motor neurons do not receive the pulse and step signals directly. This arrangement allows for precise coordination of corresponding movements of both eyes during horizontal saccades and other conjugate eye movements. The susceptibility of the medial longitudinal fasciculus to strokes and multiple sclerosis make it clinically important.

Several cerebellar structures play an important role in the calibration of the saccade motor signal. First, the oculomotor portion of the dorsal vermis, acting through the caudal fastigial nucleus, controls the duration of the pulse and thus the accuracy of the saccade. The fastigial nucleus increases saccade velocity at the beginning of contraversive saccades and contributes to braking ipsiversive saccades to end the saccade. Second, the flocculus and paraflocculus of the vestibulocerebellum calibrate the neural integrator to ensure that the step is properly matched to the pulse, in order to hold the eyes at the new position after each saccade.

Vertical Saccades Are Generated in the Mesencephalic Reticular Formation

The burst neurons responsible for vertical saccades are found in the rostral interstitial nucleus of the medial longitudinal fasciculus in the mesencephalic reticular formation (Figure 35–3). Vertical and torsional neural integration are performed in the nearby interstitial nucleus of Cajal. The pontine and mesencephalic systems participate together in the generation of oblique saccades, which have both horizontal and vertical components.

Purely vertical saccades require activity on both sides of the mesencephalic reticular formation, and communication between the two sides occurs via the posterior commissure. There are not separate omnipause neurons for horizontal and vertical saccades; pontine omnipause cells inhibit both pontine and mesencephalic burst neurons.

Brain Stem Lesions Result in Characteristic Deficits in Eye Movements

We can now understand how different brain stem lesions cause characteristic syndromes. Lesions that include the paramedian pontine reticular formation result in paralysis of ipsiversive horizontal gaze of both eyes but spare contraversive and vertical saccades. A lesion of the abducens nucleus has a similar effect, as both abducens motor neurons and interneurons are affected. Lesions that include the midbrain gaze centers cause paralysis of vertical gaze. Certain neurological disorders cause degeneration of burst neurons and impair their function, leading to a progressive slowing of saccades.

Lesions of the medial longitudinal fasciculus disconnect the medial rectus motor neurons from the abducens interneurons (Figure 35–8A). Thus, during conjugate horizontal eye movements, such as saccades and pursuit, the abducting eye moves normally but adduction of the other eye is impeded. Despite this paralysis in version movements, the medial rectus typically acts normally in vergence movements because the motor neurons for vergence lie in the midbrain, as will be discussed later. This syndrome, called an *internuclear ophthalmoplegia*, is a consequence of a brain stem stroke or demyelinating diseases such as multiple sclerosis.

A lesion of the cerebellar fastigial nucleus causes ipsiversive saccades to overshoot their targets (*hypermetric* saccades), due to failure of normal termination of the saccadic burst. Contraversive saccades undershoot their targets (*hypometric* saccades). Correspondingly, damage to the oculomotor vermis disinhibits the fastigial nucleus and causes hypometric ipsiversive saccades. This may be due to an additional failure to compensate for the position-dependent passive forces of the orbital tissues.

Saccades Are Controlled by the Cerebral Cortex Through the Superior Colliculus

The pontine and mesencephalic burst circuits provide the motor signals necessary to drive the extraocular muscles for saccades. However, among higher mammals, eye movements are ultimately driven by cognitive behavior. The decision of when and where to make a saccade that is behaviorally important is usually made in the cerebral cortex. A network of cortical and subcortical areas controls the saccadic system through the superior colliculus (Figure 35–9).

The Superior Colliculus Integrates Visual and Motor Information into Oculomotor Signals for the Brain Stem

The superior colliculus in the midbrain is a major visuomotor integration region, the mammalian homolog of the optic tectum in nonmammalian vertebrates. It can be divided into two functional regions: the superficial layers and the intermediate and deep layers.

The three superficial layers receive both direct input from the retina and a projection from the striate

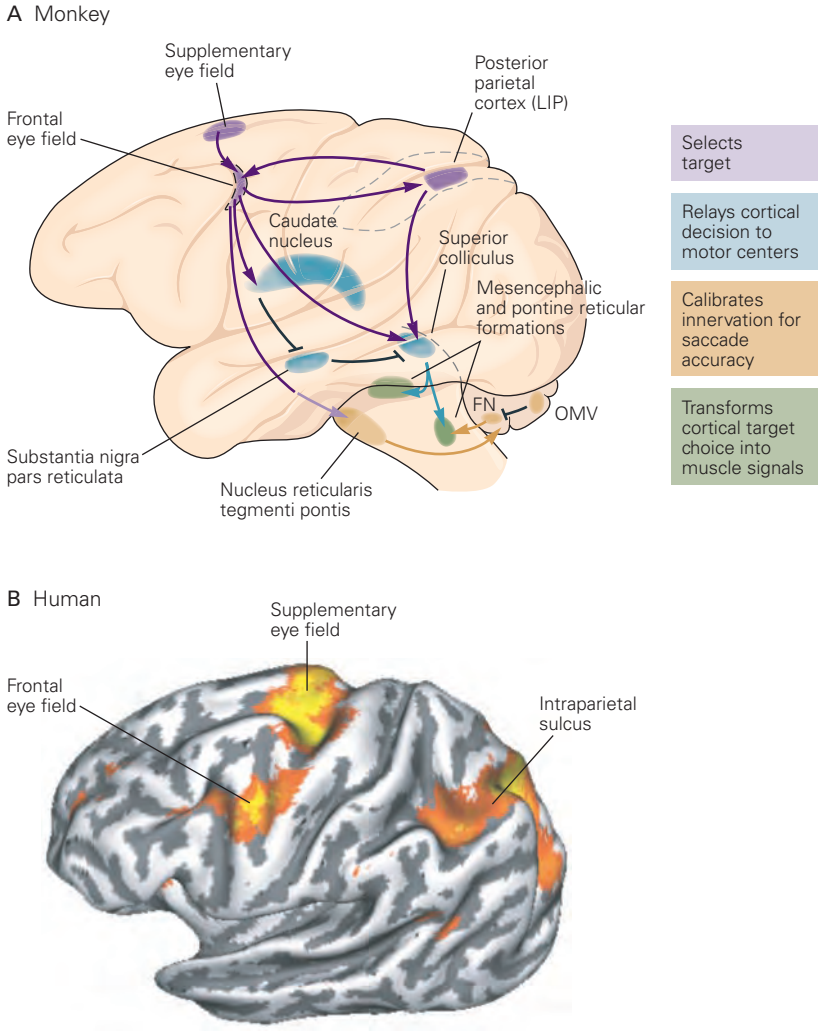

Figure 35–9 Cortical pathways for saccades.

A. In the monkey, the saccade generator in the brain stem receives a command from the superior colliculus. That command is relayed through the pontine and mesencephalic burst circuits, providing the motor signals that drive the extraocular muscles for saccades. The colliculus receives direct excitatory projections from the frontal eye fields and the lateral intraparietal area (**LIP**) and an inhibitory projection from the substantia nigra. The substantia nigra is suppressed by the caudate nucleus, which in turn is excited by the frontal eye fields. Thus, the frontal eye fields directly excite the colliculus and indirectly release it from suppression by the substantia nigra by exciting the caudate nucleus, which inhibits the substantia nigra. The oculomotor vermis (**OMV**) of the cerebellum, acting through the fastigial nucleus (**FN**), calibrates the burst to keep saccades accurate.

B. This lateral scan of a human brain shows areas of cortex activated during saccades. (Adapted from Curtis and Connolly 2008.)

cortex representing the entire contralateral visual hemifield. Neurons in the superficial layers respond to visual stimuli. In monkeys, the responses of half of these vision-related neurons are quantitatively enhanced when an animal prepares to make a saccade to a stimulus in the cell's receptive field. This enhancement is specific for saccades. If the monkey attends to the stimulus without making a saccade to it—for example, by making a hand movement in response to a brightness change—the neuron's response is not augmented. Neurons in the superficial layers of the superior colliculus are functionally arranged in a retinotopic map of the visual field in which representation of the visual field closest to the fovea occupies the largest area (Figure 35–10).

Neuronal activity in the two intermediate and deep layers is primarily related to oculomotor actions. The movement-related neurons in these layers receive visual information from the prestriate, middle temporal, and parietal cortices and motor information from the frontal eye field. The intermediate and deep layers also contain somatotopic, tonotopic, and retinotopic maps of sensory inputs, all in register with one another. For example, the image of a bird will excite a vision-related neuron, whereas the bird's chirp will excite an adjacent audition-related neuron, and both will excite a bimodal neuron. Polymodal spatial maps enable us to shift our eyes toward auditory or somatosensory stimuli as well as visual ones.

Much of the early research describing the sensory responsiveness of neurons in the intermediate layer was done in anesthetized animals. To understand how the brain generates movement, however, the activity of neurons needs to be studied in alert, active animals. Edward Evarts pioneered this approach in studies of the skeletomotor system, after which it was extended to the oculomotor system.

One of the earliest cellular studies in active animals revealed that individual movement-related neurons in the superior colliculus selectively discharge before saccades of specific amplitudes and directions, just as individual vision-related neurons in the superior colliculus respond to stimuli at specific distances and directions from the fovea (Figure 35–11A). The movement-related neurons form a map of potential eye movements that is in register with the visuotopic and tonotopic arrays of sensory inputs, so that the neurons that control eye movements to a particular target are found in the same region as the cells excited by the sounds and image of that target. Each movement-related neuron in the superior colliculus has a *movement field*, a region of the visual field that is the target for saccades controlled by that neuron. There is a map of movement fields in the intermediate layers that is in register with the map of visual receptive fields in the overlying superficial layers. Each movement neuron discharges before a saccade to the center of the overlying visual receptive field. A map of saccades evoked by electrical stimulation of the intermediate layers resembles the visual map.

Movement fields are large, so each superior colliculus cell fires before a wide range of saccades, although each cell fires most intensely before saccades of a specific direction and amplitude. A large population of cells is thus active before each saccade, and eye movement is encoded by the entire ensemble of these broadly tuned cells. Because each cell makes only a small contribution to the direction and amplitude of the movement, any variability or noise in the discharge of a given cell is minimized. Similar population coding is found in many sensory systems (Chapter 17) and the skeletal motor system (Chapter 34).

Activity in the superficial and intermediate layers of the superior colliculus can occur independently: Sensory activity in the superficial layers does not always lead to motor output, and motor output can occur without sensory activity in the superficial layers. In fact, the neurons in the superficial layers do not provide a large projection directly to the intermediate

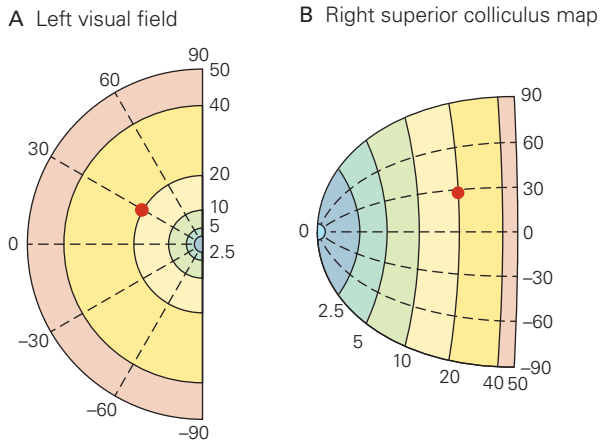

Figure 35–10 Neurons in the superior colliculus are organized in a retinotopic map.

A. Map of the left visual field in polar coordinates. **Dashed lines** represent the angle and **solid lines** the eccentricity.

B. Spatial map of neurons in the superior colliculus represented in polar coordinates of the visual field. In the nucleus, more neurons represent the part of the visual field close to the fovea and fewer neurons represent the periphery. For example, a stimulus appearing at 20° eccentricity and 30° elevation in the visual field (**red dot**) will excite neurons at the location of the red dot on the collicular map. (Reproduced, with permission, from Quaia et al. 1998.)

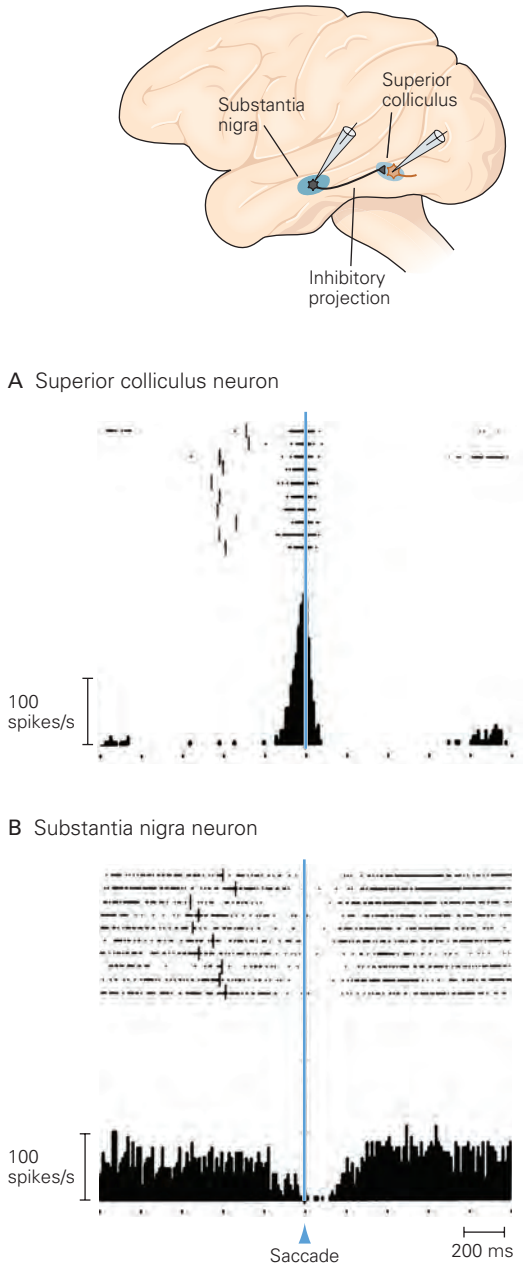

Figure 35–11 Neurons in the superior colliculus and substantia nigra are active around the time of a saccade. (Reproduced, with permission, from Hikosaka and Wurtz 1989.)

A. A neuron recorded from the region in the superior colliculus from which the neuron in B could be excited antidromically fires in a burst immediately before the saccade. Raster plots of activity in successive trials of the same task are summed to form the histogram below. The small vertical lines in the raster indicate target appearance. The trials are aligned at the beginning of the saccade (**blue line**).

B. A neuron in the substantia nigra pars reticulata is tonically active, becomes quiet just before the saccade, and resumes activity after the saccade. This type of neuron inhibits neurons in the intermediate layers of the superior colliculus.

layers. Instead, their axons terminate on neurons in the pulvinar and lateral posterior nuclei of the thalamus, which relay the signals from the superficial layers of the superior colliculus to cortical regions that project back to the intermediate layers.

Lesions of a small part of the colliculus affect the latency, accuracy, and velocity of saccades. Destruction of the entire colliculus renders a monkey unable to make any contraversive saccades, although with time, this ability is recovered.

The Rostral Superior Colliculus Facilitates Visual Fixation

The most rostral portion of the superior colliculus receives inputs from the fovea and the foveal representation in primary visual cortex (V1). Neurons in the intermediate layers in this region discharge strongly during active visual fixation and before small saccades to the contralateral visual field. Because the neurons are active during visual fixation, this area of the superior colliculus is often called the fixation zone.

Neurons here inhibit the movement-related neurons in the more caudal parts of the colliculus and also project directly to the nucleus of the dorsal raphe, where they inhibit saccade generation by exciting the omnipause neurons. With lesions in the fixation zone, an animal is more likely to make saccades to distracting stimuli.

The Basal Ganglia and Two Regions of Cerebral Cortex Control the Superior Colliculus

The superior colliculus receives a powerful GABAergic inhibitory projection from neurons in the substantia nigra, which fire spontaneously with high frequency. This discharge is suppressed at the time of voluntary eye movements to the contralateral visual field (Figure 35–11B) by inhibitory input from neurons in the caudate nucleus, which fire before saccades to the contralateral visual field.

The superior colliculus is controlled by two regions of the cerebral cortex that have overlapping but distinct functions: the lateral intraparietal area of the posterior parietal cortex (part of Brodmann's area 7) and the frontal eye field (part of Brodmann's area 8). Each of these areas contributes to the generation of saccades and the control of visual attention.

Perception of attended objects in the visual field is better than perception of unattended objects, as measured either by a subject's reaction time to an object suddenly appearing in the visual field or by the subject's ability to perceive a stimulus that is just barely

noticeable. Saccadic eye movements and visual attention are closely intertwined (Figure 35–5).

The lateral intraparietal area in the monkey is important in the generation of both visual attention and saccades. The role of this area in the processing of eye movements is best illustrated by a memory-guided saccade. To demonstrate this saccade, a monkey first fixates a spot of light. An object (the stimulus) appears in the receptive field of a neuron and then disappears; then the spot of light is extinguished. After a delay, the monkey must make a saccade to the former location of the vanished object. Neurons in the lateral intraparietal area respond from the moment the object appears and continue firing after the object has vanished and throughout the delay until the saccade begins (Figure 35–12A), but their activity can be also dissociated from saccade planning. If the monkey is planning a saccade to a target outside the receptive field of a neuron and a distractor appears in the field during the delay period, the neuron responds as vigorously to the distractor as it does to the target of a saccade (Figure 35–12B).

Lesioning of a monkey's posterior parietal cortex, which includes the lateral intraparietal area, increases the latency of saccades and reduces their accuracy. Such a lesion also produces selective neglect: A monkey with a unilateral parietal lesion preferentially attends to stimuli in the ipsilateral visual hemifield. In humans as well, parietal lesions—especially right parietal lesions—initially cause dramatic attentional deficits. Patients act as if the objects in the neglected field do not exist, and they have difficulty making eye movements into that field (Chapter 59).

Patients with Balint syndrome, which is usually the result of bilateral lesions of the posterior parietal

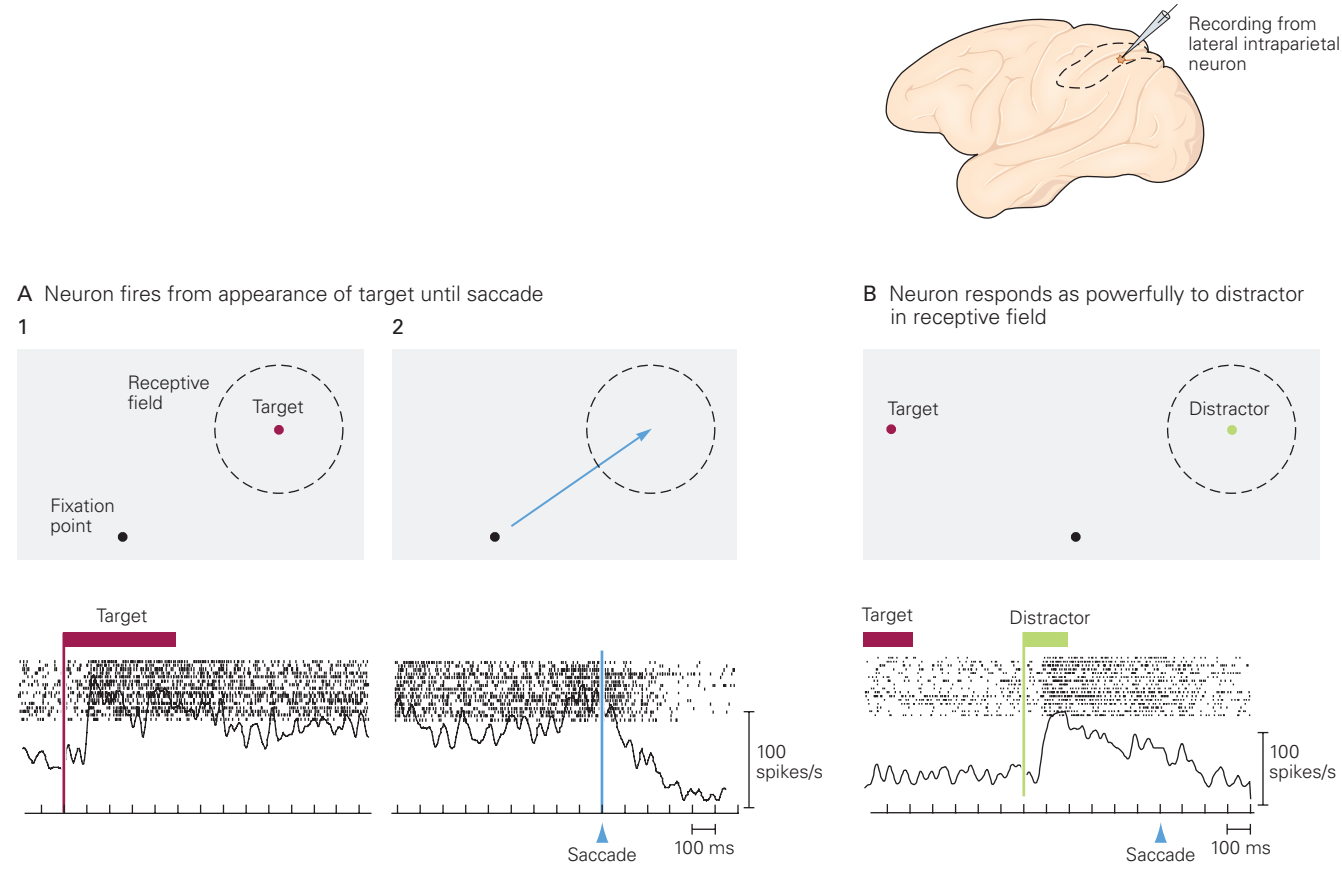

Figure 35–12 A parietal neuron is active before memory-guided saccades. Traces are aligned at events indicated by vertical lines. (Adapted, with permission, from Powell and Goldberg 2000.)

A. The monkey plans a saccade from a fixation point to a target in the receptive field of a neuron in the lateral intraparietal cortex. The neuron responds to the appearance of the target (**1**). It continues to fire after the target has disappeared but before the signal to make the saccade and stops firing after the onset of the saccade (**2**).

B. The monkey plans a saccade to a target outside the receptive field. The neuron responds initially to a distractor in the receptive field as strongly as it did to the target of a saccade.

and prestriate cortex, tend to see and describe only one object at a time in their visual environment. These patients make few saccades, as if they are unable to shift the focus of their attention from the fovea, and can therefore describe only a foveal target. Even after these patients have recovered from most of their deficits, their saccades are delayed and inaccurate.

Compared to the neurons in the parietal cortex, neurons in the frontal eye field are more closely associated with saccades. Three different types of neurons in the frontal eye field discharge before saccades.

Visual neurons respond to visual stimuli, and half of these neurons respond more vigorously to stimuli that are the targets of saccades (Figure 35–13A). Activity in these cells is not enhanced when an animal responds to the stimulus without making a saccade to it. Likewise, these cells are not activated before saccades that are made without visual targets; monkeys can be trained to make saccades of a specific direction and amplitude in total darkness.

Movement-related neurons fire before and during saccades to their movement fields. Unlike the movement-related cells in the superior colliculus, which fire before all saccades, movement-related neurons of the frontal eye field fire only before saccades that are relevant to the monkey's behavior (Figure 35–13B). These neurons, especially those whose receptive fields lie in the visual periphery, project more strongly to the superior colliculus than do the visual neurons.

Visuomovement neurons have both visual and movement-related activity and discharge most strongly before visually guided saccades. Electrical stimulation of the frontal eye field evokes saccades to the movement fields of the stimulated cells. Bilateral stimulation of the frontal eye field evokes vertical saccades.

Movement-related neurons in frontal eye field control the superior colliculus through two pathways. They excite the superior colliculus directly and they release it from the inhibitory influence of the substantia nigra by exciting the caudate nucleus, which in turn inhibits the nigra (Figure 35–9A). The frontal eye field also projects to the pontine and mesencephalic reticular formations, although not directly to the burst cells.

Two other cortical regions besides LIP that have inputs to the frontal eye field are thought to be important in the cognitive aspects of saccades. The supplementary eye field at the most rostral part of the supplementary motor area contains neurons that encode spatial information other than the direction of the desired eye movement. For example, a neuron in the left supplementary eye field that ordinarily fires before rightward eye movements will fire before a leftward saccade if that saccade is to the right side of the target. The dorsolateral prefrontal cortex has neurons that discharge when a monkey makes a saccade to a remembered target. The activity commences with the appearance of the stimulus and continues throughout the interval during which the monkey must remember the location of the target.

We can now understand the effects of lesions of these regions on the generation of saccades. Lesions of the superior colliculus in monkeys produce only transient damage to the saccade system because the projection from the frontal eye field to the brain stem remains intact. Animals can likewise recover from cortical lesions if the superior colliculus is intact. However, when both the frontal eye field and the colliculus are damaged, the ability to make saccades is permanently compromised. The predominant effect of a parietal lesion is an attentional deficit. After recovery, however, the system can function normally because the frontal eye field signals are sufficient to suppress the substantia nigra and stimulate the colliculus.

Damage to the frontal eye field alone causes more subtle deficits. Lesions of the frontal eye field in monkeys cause transient contralateral neglect and paresis of contraversive gaze, which recover rapidly. The latter deficit may reflect the loss of frontal eye field control of the substantia nigra; this loss of control means that the constant inhibitory input from the substantia nigra to the colliculus does not get suppressed, and the colliculus is unable to generate any saccades. Eventually the system adapts, and the colliculus responds to the remaining parietal signal. After recovery, the animals have no trouble producing saccades to targets in the visual field but have great difficulty with memory-guided saccades. Bilateral lesions of both the frontal eye fields and the superior colliculus render monkeys unable to make saccades at all.

Humans with lesions of the frontal cortex have difficulty suppressing unwanted saccades to attended stimuli. This is easily shown by asking subjects to make an eye movement away from a stimulus, the "anti-saccades task." For example, if a stimulus appears on the left, the subject should make a saccade of the same size to the right. To do this, the subject must attend to the stimulus, without turning the eyes toward it, and use its location to calculate the desired saccade to the opposite direction. Patients with frontal lesions have great difficulty suppressing the unwanted saccade to the stimulus.

As we have seen, neurons in the lateral intraparietal area of monkeys are active when the animal attends to a visual stimulus whether or not the animal makes a saccade to the stimulus. In the absence of frontal eye field signals, this undifferentiated signal is the only one to reach the superior colliculus. In humans, the failure to suppress a saccade is therefore to be expected

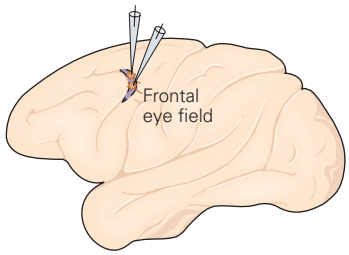

A Visual neuron responds to the stimulus and not to movement

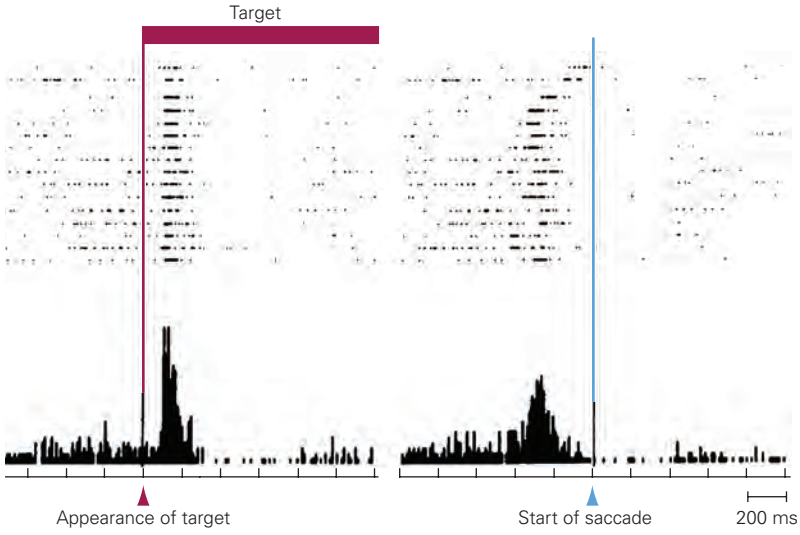

B Movement-related neuron responds before movement but not to stimulus

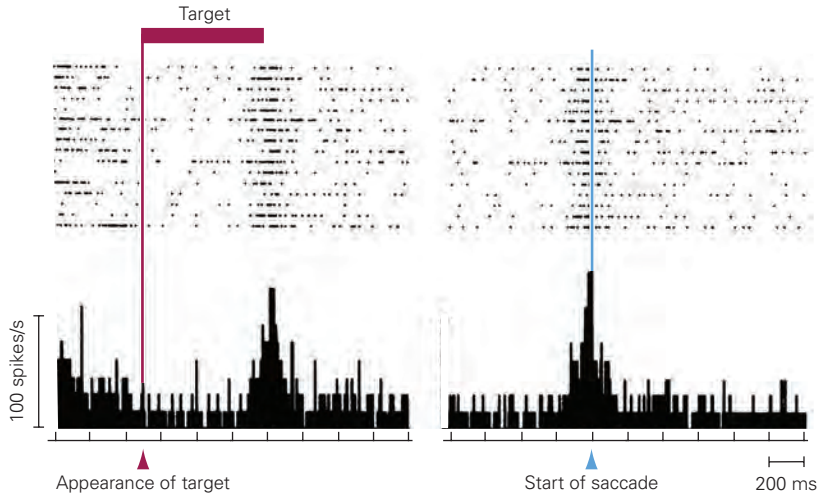

Figure 35–13 Visual and movement-related neurons in the frontal eye field. (Reproduced, with permission, from Bruce and Goldberg 1985.)

A. Activity of a visual neuron in the frontal eye field as a monkey makes a saccade to a target in its visual field. Raster plots of activity in successive trials of the same task are summed to form the histogram below. In the record on the left, the individual trials are aligned at the appearance of the stimulus. A burst of firing is closely time-locked to the stimulus. In the record on the right, the trials are aligned at the beginning of the saccade. Activity is not well aligned with the beginning of the saccade and stops before the saccade itself commences.

B. Activity of a movement-related neuron in the frontal eye field. The records of each trial are aligned as in part **A**. The cell does not respond to appearance of the saccade target (*left*) but is active at the time of the saccade (*right*).

if the superior colliculus responds to a parietal signal that generates attention to the stimulus without the frontal-nigral control that normally prevents saccades in response to parietal signals.

The Control of Saccades Can Be Modified by Experience

Quantitative study of the neural control of movement is possible because the discharge rate of a motor neuron has a predictable effect on a movement. For example, a certain frequency of firing in the abducens motor neuron has a predictable effect on eye position and velocity.

This relationship can change if disease damages an oculomotor nerve or causes an eye muscle to become weak, although the brain can compensate to some degree for such changes. Guntram Kommerell described a case that dramatically illustrates this point. A diabetic patient had an acute partial abducens nerve lesion affecting one eye and a retinal hemorrhage in the other. Because of the poor vision in the eye with a normal abducens nerve, he ordinarily used the eye with the newly weakened lateral rectus muscle. After a few days, the eye recovered the ability to make fairly accurate eye movements. When the weak eye was patched and the subject attempted to make a saccade with the visually poor eye, the saccade overshot the target. This implies that in order to compensate for the weakness of the visually normal eye the brain increased the neural signal to both eyes, resulting in too large a signal to the eye with normal motor input. This change in the motor response depends on the fastigial nucleus and vermis of the cerebellum (Figure 35–9A) and results from the visual system signaling that the preceding eye movement was inaccurate.

Some Rapid Gaze Shifts Require Coordinated Head and Eye Movements

So far, we have described how the eyes are moved when the head is still. When we look around, however, our head is moving as well. Head and eye movements must be coordinated to direct the fovea to a target.

Because the head has a much greater inertia than the eyes, a small shift in gaze drives the fovea to its target before the head begins to move. A small gaze shift usually consists of a saccade followed by a small head movement during which the vestibulo-ocular reflex moves the eyes back to the center of the orbit in the new head position (Figure 35–14). For larger gaze shifts, the eyes and the head move simultaneously in the same direction. Because the vestibulo-ocular reflex ordinarily moves the eyes in the direction opposite that of the head, the reflex must be temporarily suppressed.

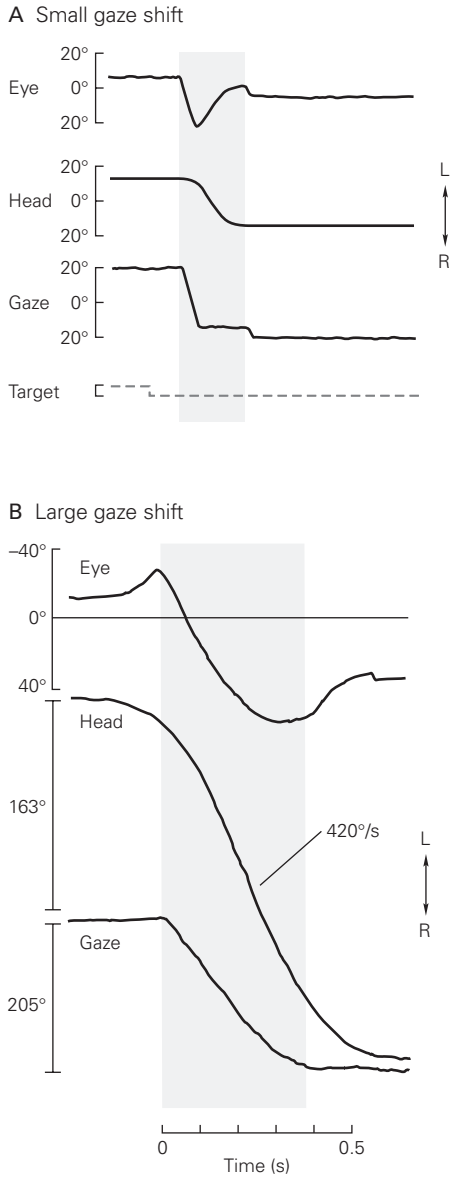

Figure 35–14 Directing the fovea to an object when the head is moving requires coordinated head and eye movements.

A. For a small gaze shift, the eye and head move in sequence. The eye begins to move 300 ms after the target appears. Near the end of the eye movement, the head begins to move as well. The eye then rotates back to the center of the orbit to compensate for the head movement. The gaze record is the sum of eye and head movements. (Abbreviations: **L**, left; **R**, right.) (Reproduced, with permission, from Zee 1977.)

B. For a large gaze shift, the eye and head move in the same direction simultaneously. Near the end of the gaze shift, the vestibulo-ocular reflex returns, the eye begins to compensate for head movement as in part **A**, and gaze becomes still. (Reproduced, with permission, from Laurutis and Robinson 1986.)

The Smooth-Pursuit System Keeps Moving Targets on the Fovea

The smooth-pursuit system holds the image of a moving target on the fovea by calculating how fast the target is moving and moving the eyes at the same speed. Smooth-pursuit movements have a maximum angular velocity of approximately 100° per second, much slower than saccades. Drugs, fatigue, alcohol, and even distraction degrade the quality of these movements.

Smooth pursuit and saccades have very different central control systems. This is best seen when a target jumps away from the center of gaze and then slowly moves back toward it. A smooth-pursuit movement is initiated first because the smooth-pursuit system has a shorter latency and responds to target motion on the peripheral retina as well as on the fovea. The task of the smooth-pursuit system differs from that of the saccade system. Instead of driving the eyes as rapidly as possible to a point in space, it must match the velocity of the eyes to that of a target in space. Therefore, as the target moves back toward the center of gaze, the smooth-pursuit system briefly moves the eye away from the target before the saccade is initiated (Figure 35–6B). The subsequent saccade then brings the eye to the target. Neurons that signal eye velocity for smooth pursuit are found in the medial vestibular nucleus and the nucleus prepositus hypoglossi. They receive projections from the flocculus of the cerebellum and project to the abducens nucleus as well as the oculomotor nuclei in the midbrain.

Neurons in both the flocculus and vermis transmit an eye-velocity signal that correlates with smooth pursuit. These areas receive signals from the cerebral cortex relayed by the dorsolateral pontine nucleus (Figure 35–15). Thus, lesions in the dorsolateral pons disrupt ipsiversive smooth pursuit.

There are two major cortical inputs to the smooth-pursuit system in monkeys. One arises from motion-sensitive regions in the superior temporal sulcus and the middle temporal and medial superior temporal areas. The other arises from the frontal eye field.

The middle temporal and medial superior temporal areas were named because of their position in sulcus-free cortex of the owl monkey, a New World monkey. In humans and Old World monkeys, these areas lie in the superior temporal sulcus, at the junction between the occipital and parietal lobes. Neurons in both the middle temporal and medial superior temporal areas calculate the velocity of the target. When the eye accelerates to match the target's speed, the rate of the target's motion across the retina decreases. As the speed of the retinal image decreases, neurons in the middle temporal area, whose activity signals retinal-image motion, stop firing, even though the target continues to move in space. Neurons in the medial superior temporal area continue to fire even if the target disappears briefly. These neurons have access to a process that adds the speeds of the moving eye and the target moving on the retina to compute the speed of the target in space.

Lesions of either the middle temporal or medial superior temporal area disrupt the ability of a subject to respond to targets moving in regions of the visual field represented in the damaged cortical area. Lesions of the latter area also diminish smooth-pursuit movements toward the side of the lesion, no matter where the target lies on the retina.

The two motion-selective areas provide the sensory information to guide pursuit movements but may not be able to initiate them. Electrical stimulation of either area does not initiate smooth pursuit but can affect pursuit movement, accelerating ipsiversive pursuit and slowing contraversive pursuit. The frontal eye field may

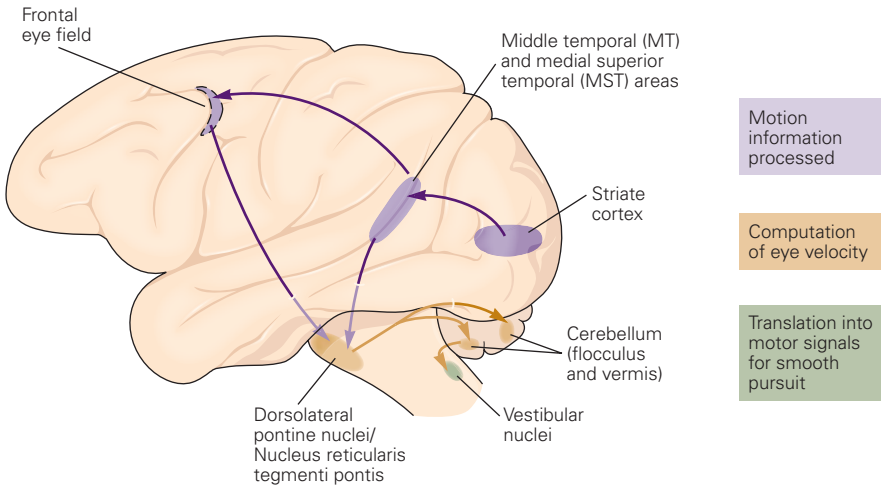

Figure 35–15 Cortical pathways for smooth-pursuit eye movements in the monkey. The cerebral cortex processes information about motion in the visual field and sends it to the oculomotor neurons via the dorsolateral pontine nuclei, the vermis and flocculus of the cerebellum, and the vestibular nuclei. The initiation signal for smooth pursuit may originate in part from the frontal eye field.

be more important for initiating pursuit. This area has neurons that fire in association with ipsiversive smooth pursuit. Electrical stimulation of the frontal eye field initiates ipsiversive pursuit, whereas lesions of this area diminish but do not eliminate smooth pursuit.

In humans, disruption of the pursuit pathway anywhere along its course, including lesions at the level of cortical, cerebellar, and brain stem areas, prevents adequate smooth-pursuit eye movements. Instead, moving targets are tracked using a combination of defective smooth-pursuit movements (the velocity is less than that of the target) and small saccades. Patients with brain stem and cerebellar lesions cannot pursue targets moving toward the side of the lesion.

Patients with parietal deficits that include the motion-sensitive areas have two different types of deficit. The first is a directional deficit that resembles that of monkeys with lesions of the medial superior temporal area: targets moving toward the side of the lesion cannot be tracked. The second is a retinotopic deficit that resembles the deficit of monkeys with lesions of the middle temporal area: There is an impairment of smooth pursuit of a stimulus limited to the visual hemifield opposite the lesion, regardless of the direction of motion.

The Vergence System Aligns the Eyes to Look at Targets at Different Depths

The smooth-pursuit and saccade systems produce conjugate eye movements: Both eyes move in the same direction and at the same speed. In contrast, the vergence system produces disconjugate movements of the eyes. When we look at an object that is close to us, our eyes *converge* or rotate toward each other; when we look at an object that is farther away, they *diverge* or rotate away from each other (Figure 35–16). These disconjugate movements ensure that the image of the object falls on the foveae of both retinas. Whereas the visual system uses slight differences in left and right retinal positions, or *retinal disparity*, to create a

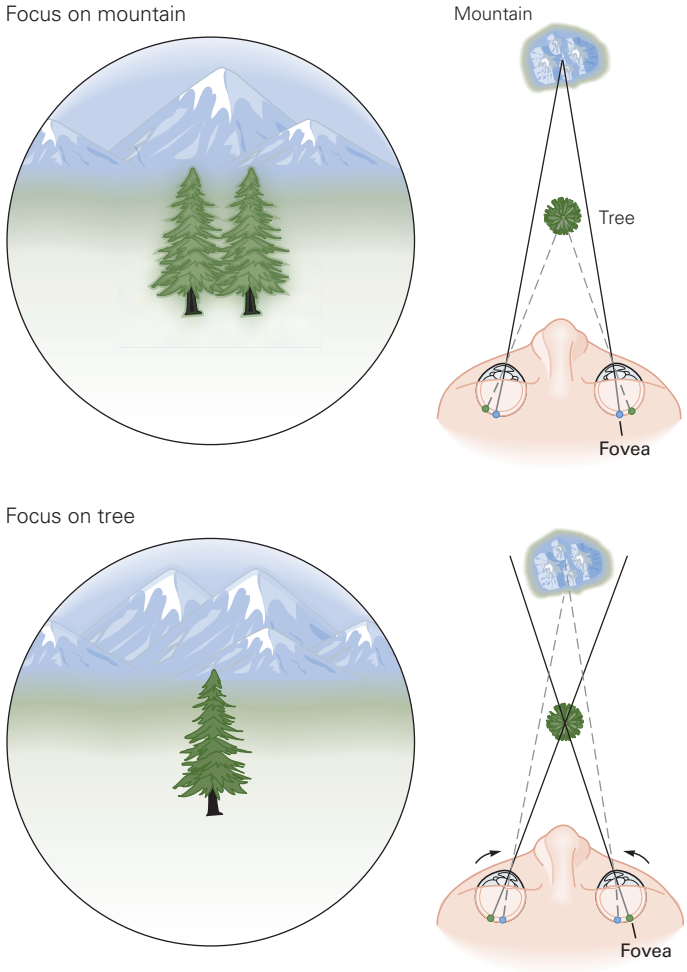

Figure 35–16 Vergence movements. When the eyes focus on a distant mountain, images of the mountain lie on the foveae, while those of the tree in the forefront occupy different retinal positions, yielding the percept of a double image. When the viewer looks instead at the tree, the vergence system must rotate each eye inward. Now the tree's image occupies similar positions on both foveae and is seen as one object, but the mountain's images occupy different locations on the retinas and appear double. (Reproduced, with permission, from F.A. Miles.)

sense of depth, vergence movements eliminate retinal disparity at the fovea.

Vergence is a function of the horizontal rectus muscles only, because the two eyes are horizontally, not vertically, displaced. Convergence of the eyes for near-field viewing is accomplished by simultaneously increasing the tone of the medial recti muscles and decreasing the tone of the lateral recti muscles to converge the eyes. Conversely, distance viewing is accomplished by reducing the tone of the medial rectus and increasing the tone of the lateral rectus.

At any given time, the entire visual field is not in focus on the retina. When we look at something nearby, distant objects are blurred. When we look at something far away, near objects are blurred. When we wish to focus on an object in a closer plane in the visual field, the oculomotor system contracts the ciliary muscle, thereby changing the radius of curvature of the lens. This process is called *accommodation.* With age, accommodation declines owing to increased rigidity of the lens; reading glasses are then needed to focus images at short distances.

Accommodation and vergence are linked. Accommodation is elicited by the blurring of an image, and whenever accommodation occurs, the eyes also converge. Conversely, retinal disparity induces vergence, and whenever the eyes converge, accommodation also takes place. At the same time, the pupils transiently constrict to increase the depth of field of the focus. The linked phenomena of accommodation, vergence, and pupillary constriction comprise the *near response.* Accommodation and vergence are controlled by midbrain neurons in the region of the oculomotor nucleus. Neurons in this region discharge during vergence, accommodation, or both.

Highlights

1. The oculomotor system provides a valuable window into the nervous system for both the clinician and the scientist. Patients with oculomotor deficits may experience alarming symptoms such as double vision that quickly send them to seek medical help. A physician with a thorough knowledge of the oculomotor system can describe and diagnose most oculomotor deficits at the bedside and localize the site of the lesion within the brain based on the neuroanatomy and neurophysiology of eye movements.
2. The purpose of eye movements is to rotate the eye in the orbit in order to direct the fovea, the area of the retina with best acuity, to the point of greatest interest in the visual scene and then to keep the image steady.
3. Six muscles work together to move each eye. These eye muscles are yoked in three pairs. The lateral rectus abducts the eye horizontally, and the medial rectus adducts it. The cyclovertical eye muscles move the eye both vertically and torsionally.
4. Motor neurons for the extraocular muscles lie in three brainstem nuclei. The abducens nucleus in the pons contains the neurons for the lateral rectus. The other oculomotor neurons are in the midbrain: The trochlear nucleus contains superior oblique neurons, and the oculomotor nucleus has the motor neurons for the medial, superior, and inferior rectus muscles and the inferior oblique muscle. Neurons that constrict the pupil and those that elevate the eyelid also lie in the oculomotor nucleus.
5. There are six different types of eye movements, with different control systems: (1) Saccades shift the fovea rapidly to a new visual target. (2) Smooth-pursuit movements keep the image of a moving object on the fovea. (3) Vergence movements rotate the eyes in opposite directions so that the image of an object of interest is positioned on both foveae regardless of its distance. (4) Vestibulo-ocular reflexes hold images still on the retina during brief, rapid head movements. (5) Optokinetic movements hold images stationary during sustained or slow head movements. (6) Fixation is an active process that keeps the eye still during intent gaze when the head is not moving.
6. The firing pattern of eye muscle neurons combines independent signals that code eye position and velocity. The neurons that generate the velocity signal for horizontal saccades lie in the paramedian pontine reticular formation, and this velocity signal is integrated in the medial vestibular nucleus and nucleus prepositus hypoglossi to provide the position signal.
7. The mesencephalic reticular formation provides the position and velocity signals for vertical and torsional eye movements as well as vergence eye movements.
8. Presaccadic burst neurons in the superior colliculus project a desired displacement signal to the reticular formation. These neurons are inhibited by a GABAergic projection from the substantia nigra and excited by projections from the frontal eye field and the posterior parietal cortex. A motor signal from the frontal eye field excites the caudate nucleus, which then inhibits the substantia nigra, allowing a saccade to occur.
9. The posterior parietal cortex projects an attentional signal to the superior colliculus that does not distinguish between attention and movement.

10. Most large gaze shifts involve head movements as well as eye movements. Because the eye moves faster than the head, it typically reaches the target first. The vestibulo-ocular reflex maintains the eye on target by driving the eye with a velocity opposite to that of the head movement.
11. The cerebellum calibrates eye movements based on visual feedback and mediates the learning process that keeps them accurate over time.
12. Smooth pursuit is driven by a network that includes the medial vestibular nucleus, the flocculus of the cerebellum, the dorsolateral pontine nucleus, and two motion-selective areas that are found in the superior temporal sulcus of some monkeys—the middle temporal and medial superior temporal areas. Homologous areas in the human brain are located at the parieto-occipital junction. The pursuit area of the frontal eye fields initiates smooth-pursuit movements.
13. Although the motor programming of eye movements is well understood, the great bulk of physiological research in this field was done with a monkey making a directed saccade to a spot of light. The neural mechanisms underlying the free choice of saccade targets as we explore the visual world are poorly understood. This question, lying at the intersection of cognition and motor control, is one of the great unknowns in neuroscience and will be at the center of oculomotor research in the future.

Michael E. Goldberg
Mark F. Walker

Selected Reading

Bisley JW, Goldberg ME. 2010. Attention, intention, and priority in the parietal lobe. Annu Rev Neurosci 33:1–21.

Krauzlis RJ, Goffart L, Hafed ZM. 2017. Neuronal control of fixation and fixational eye movements. Philos Trans R Soc Lond B Biol Sci 372:20160205.

Leigh RJ, Zee DS. 2015. *The Neurology of Eye Movements,* 6th ed. Philadelphia: FA Davis.

Lisberger SG. Visual guidance of smooth-pursuit eye movements: sensation, action, and what happens in between. Neuron 2010:477–491.

Sparks D. 2002. The brainstem control of saccadic eye movements. Nat Rev Neurosci 3:952–964.

Wurtz RH, Joiner WM, Berman RA. 2011. Neuronal mechanisms for visual stability: progress and problems. Philos Trans R Soc Lond B Biol Sci 366:492–503.

Yarbus AL. 1967. *Eye Movements and Vision.* New York: Plenum.

References

Andersen RA, Asanuma C, Essick G, Siegel RM. 1990. Corticocortical connections of anatomically and physiologically defined subdivisions within the inferior parietal lobule. J Comp Neurol 296:65–113.

Andersen RA, Cui H. 2009. Intention, action planning, and decision making in parietal-frontal circuits. Neuron 63:568–583.

Barnes GR. 2008. Cognitive processes involved in smooth pursuit eye movements. Brain Cogn 68:309–326.

Bisley JW, Goldberg ME. 2006. Neural correlates of attention and distractibility in the lateral intraparietal area. J Neurophysiol 95:1696–1717.

Bruce CJ, Goldberg ME. 1985. Primate frontal eye fields. I. Single neurons discharging before saccades. J Neurophysiol 53:603–635.

Büttner-Ennever JA, Büttner U, Cohen B, Baumgartner G. 1982. Vertical gaze paralysis and the rostral interstitial nucleus of the medial longitudinal fasciculus. Brain 105:125–149.

Büttner-Ennever JA, Cohen B, Pause M, Fries W. 1988. Raphe nucleus of the pons containing omnipause neurons of the oculomotor system in the monkey, and its homologue in man. J Comp Neurol 267:307–321.

Cannon SC, Robinson DA. 1987. Loss of the neural integrator of the oculomotor system from brain stem lesions in monkey. J Neurophysiol 57:1383–1409.

Cohen B, Henn V. 1972. Unit activity in the pontine reticular formation associated with eye movements. Brain Res 46:403–410.

Colby CL, Duhamel J-R, Goldberg ME. 1996. Visual, presaccadic and cognitive activation of single neurons in monkey lateral intraparietal area. J Neurophysiol 76:2841–2852.

Cumming BG, Judge SJ. 1986. Disparity-induced and blur-induced convergence eye movement and accommodation in the monkey. J Neurophysiol 55:896–914.

Curtis CE, Connolly JD. 2008. Saccade preparation signals in the human frontal and parietal cortices. J Neurophysiol 99:133–145.

Dash S, Thier P. 2014. Cerebellum-dependent motor learning: lessons from adaptation of eye movements in primates. Prog Brain Res 210:121–155.

Demer JL, Miller JM, Poukens V, Vinters HV, Glasgow BJ. 1995. Evidence for fibromuscular pulleys of the recti extraocular muscles. Invest Ophthalmol Vis Sci 36:1125–1136.

Duhamel J-R, Colby CL, Goldberg ME. 1992. The updating of the representation of visual space in parietal cortex by intended eye movements. Science 255:90–92.

Dürsteler MR, Wurtz RH, Newsome WT. 1987. Directional pursuit deficits following lesions of the foveal representation within the superior temporal sulcus of the macaque monkey. J Neurophysiol 57:1262–1287.

Fuchs AF, Luschei ES. 1970. Firing patterns of abducens neurons of alert monkeys in relationship to horizontal eye movement. J Neurophysiol 33:382–392.

Funahashi S, Bruce CJ, Goldman-Rakic PS. 1989. Mnemonic coding of visual space in the monkey's dorsolateral prefrontal cortex. J Neurophysiol 61:331–349.

Gottlieb JP, MacAvoy MG, Bruce CJ. 1994. Neural responses related to smooth-pursuit eye movements and their correspondence with electrically elicited smooth eye movements in the primate frontal eye field. J Neurophysiol 74:1634–1653.

Hécaen J, de Ajuriaguerra J. 1954. Balint's syndrome (psychic paralysis of visual fixation). Brain 77:373–400.

Henn V, Hepp K, Büttner-Ennever JA. 1982. The primate oculomotor system. II. Premotor system. A synthesis of anatomical, physiological, and clinical data. Hum Neurobiol 12:87–95.

Highstein SM, Baker R. 1978. Excitatory termination of abducens internuclear neurons on medial rectus motoneurons: relationship to syndrome of internuclear ophthalmoplegia. J Neurophysiol 41:1647–1661.

Hikosaka O, Wurtz RH. 1983. Visual and oculomotor functions of monkey substantia nigra pars reticulata. IV. Relation of substantia nigra to superior colliculus. J Neurophysiol 49:1285–1301.

Hikosaka O, Sakamoto M, Usui S. 1989. Functional properties of monkey caudate neurons. I. Activities related to saccadic eye movements. J Neurophysiol 61:780–798.

Hikosaka O, Wurtz RH. 1989. The basal ganglia. Rev Oculomotor Res 3: 257–281.

Huk A, Dougherty R, Heeger D. 2002. Retinotopy and functional subdivision of human areas MT and MST. J Neurosci 22:7195–7205.

Keller EL. 1974. Participation of medial pontine reticular formation in eye movement generation in monkey. J Neurophysiol 37:316–332.

Laurutis VP, Robinson DA. 1986. The vestibular reflex during human saccadic eye movements. J Physiol (Lond) 373: 209–233.

Luschei ES, Fuchs AF. 1972. Activity of brain stem neurons during eye movements of alert monkeys. J Neurophysiol 35:445–461.

Lynch JC, Graybiel AM, Lobeck LJ. 1985. The differential projection of two cytoarchitectonic subregions of the inferior parietal lobule of macaque upon the deep layers of the superior colliculus. J Comp Neurol 235:241–254.

McFarland JL, Fuchs AF. 1992. Discharge patterns in nucleus prepositus hypoglossi and adjacent medial vestibular nucleus during horizontal eye movement in behaving macaques. J Neurophysiol 68:319–332.

Munoz DP, Wurtz RH. 1993. Fixation cells in monkey superior colliculus. I. Characteristics of cell discharge. J Neurophysiol 70:559–575.

Mustari MJ, Fuchs AF, Wallman J. 1988. Response properties of dorsolateral pontine units during smooth pursuit in the rhesus macaque. J Neurophysiol 60:664–686.

Newsome WT, Wurtz RH, Komatsu H. 1988. Relation of cortical areas MT and MST to pursuit eye movements. II. Differentiation of retinal from extraretinal inputs. J Neurophysiol 60:604–620.

Olson CR, Gettner SN. 1995. Object-centered direction selectivity in the macaque supplementary eye field. Science 269:985–988.

Powell KD, Goldberg ME. 2000. Response of neurons in the lateral intraparietal area to a distractor flashed during the delay period of a memory-guided saccade. J Neurophysiol 84:301–310.

Quaia C, Aizawa H, Optican LM, Wurtz RH. 1998. Reversible inactivation of monkey superior colliculus. II. Maps of saccadic deficits. J Neurophysiol 79:2097–2110.

Quaia C, Lefevre P, Optican LM. 1999. Model of the control of saccades by superior colliculus and cerebellum. J Neurophysiol 82:999–1018.

Ramat S, Leigh RJ, Zee DS, Optican LM. 2007. What clinical disorders tell us about the neural control of saccadic eye movements. Brain 130:10–35.

Rao HM, Mayo JP, Sommer MA. 2016. Circuits for presaccadic visual remapping. J Neurophysiol 116:2624–2636.

Raybourn MS, Keller EL. 1977. Colliculo-reticular organization in primate oculomotor system. J Neurophysiol 269:985–988.

Robinson DA. 1970. Oculomotor unit behavior in the monkey. J Neurophysiol 33:393–404.

Schall JD. 1995. Neural basis of saccade target selection. Rev Neurosci 6:63–85.

Schiller PH, Koerner F. 1971. Discharge characteristics of single units in superior colliculus of the alert rhesus monkey. J Neurophysiol 34:920–936.

Schiller PH, True SD, Conway JL. 1980. Deficits in eye movements following frontal eye field and superior colliculus ablations. J Neurophysiol 44:1175–1189.

Scudder C, Kaneko C, Fuchs A. 2002. The brainstem burst generator for saccadic eye movements—a modern synthesis. Exp Brain Res 142:439–462.

Segraves MA, Goldberg ME. 1987. Functional properties of corticotectal neurons in the monkey's frontal eye field. J Neurophysiol 58:1387–1419.

Silver MA, Kastner S. 2009. Topographic maps in human frontal and parietal cortex. Trends Cogn Sci (Regul Ed) 13: 488–495.

Strupp M, Kremmyda O, Adamczyk C, et al. 2014. Central ocular motor disorders, including gaze palsy and nystagmus. J Neurol 261:S542–S558.

Stuphorn V, Brown JW, Schall JD. 2010. Role of supplementary eye field in saccade initiation: executive, not direct, control. J Neurophysiol 103:801–816.

Takagi M, Zee DS, Tamargo RJ. 1998. Effects of lesions of the oculomotor vermis on eye movements in primate: saccades. J Neurophysiol 80:1911–1931.

von Noorden GK, Campos EC. 2002. *Binocular Vision and Ocular Motility: Theory and Management of Strabismus,* 6th ed. St. Louis, MO: Mosby.

Wurtz RH, Goldberg ME. 1972. Activity of superior colliculus in behaving monkey. III. Cells discharging before eye movements. J Neurophysiol 35:575–586.

Xu-Wilson M, Chen-Harris H, Zee DS, Shadmehr R. 2009. Cerebellar contributions to adaptive control of saccades in humans. J Neurosci 29:12930–12939.

Zee DS. 1977. Disorders of eye-head coordination. In B Brooks, FJ Bajandas (Eds.), *Eye Movements*, Plenum Press, New York, 1977, pp. 9–40.

36

Posture

The control of posture involves two interrelated goals, equilibrium (balance) and orientation, crucial for most tasks of daily living. Balance control maintains the body in stable equilibrium to avoid falls. Orientation aligns the body segments with respect to each other and to the world, such as maintaining the head vertical. Both balance and orientation use several different types of control: automatic postural responses, anticipatory postural adjustments, postural sway in stance, sensory integration for a body schema, orientation to vertical, and dynamic stability during gait.

To appreciate the complexity of maintaining balance and orientation, imagine that you are waiting tables on a tour boat. You have a tray full of drinks to be delivered to a table on the other side of the rolling deck. Even as your mind is occupied with remembering customer orders, unconscious but complex sensorimotor processes for controlling postural orientation and balance allow you to move about in an efficient and coordinated manner without falling. As you cross the rolling deck, your brain rapidly integrates and interprets sensory information and adjusts motor output to maintain your balance and the upright orientation of your head and trunk, as well as stabilize the arm supporting the tray of full glasses. Sudden

unexpected motions of the boat evoke automatic postural responses that prevent falls. Before you reach out to place a glass on the table, your nervous system makes anticipatory postural adjustments to maintain your balance.

Somatosensory, vestibular, and visual information are integrated to provide a coherent sense of the position and velocity of the body in space with respect to the support surface, gravity, and visual environment. Since the surface is unstable and vision is not providing earth-stable information, your dependence on vestibular information is greater than usual. Your head is kept stable while your trunk motions and walking pattern adjust for disequilibrium caused by the moving surface. You notice that both your voluntary tasks and your balance control deteriorate when trying to attend to both goals.

Equilibrium and Orientation Underlie Posture Control

Postural equilibrium refers to the ability to actively stabilize the upper body by resisting external forces acting on the body. Although the dominant external force affecting equilibrium on earth is gravity, other inertial forces and external perturbations must also be resisted. Depending on the particular task or behavior, different sets of muscles are activated in response to or in anticipation of disturbance to equilibrium.

Postural orientation refers to the ability to actively align body segments, such as the trunk and head, with respect to each other and to the environment. Depending on the particular task or behavior, body segments may be aligned with respect to gravitational vertical, visual vertical, or the support surface. For example, when skiing downhill, the head may be oriented to gravitational and inertial vertical, but not to the visual or support surface references that are inclined.

The biomechanical requirements of postural control depend on anatomy and postural orientation and thus vary among species. Nevertheless, in a variety of species, the control mechanisms for postural equilibrium and orientation have many common features. The sensorimotor mechanisms for postural control are quite similar in humans and quadrupedal mammals even though their habitual stance is different.

Postural Equilibrium Controls the Body's Center of Mass

With many segments linked by joints, the body is mechanically unstable. To maintain balance, the nervous system must control the position and motion of the body's *center of mass* as well as the body's rotation about it. The center of mass is a point that represents the average position of the body's total mass. In the standing adult, for example, the center of mass is located about 2 cm in front of the second lumbar vertebra; in a young child, it is higher. The location of the center of mass is not fixed but depends on postural orientation. For example, when you flex at the hips while standing, the center of mass moves from a location inside the body to a position outside the body.

Although gravity pulls on all body segments, the net effect on body equilibrium acts through the body's center of mass. The force due to gravity is opposed by the forces between the feet and the ground. Each point on the surface will generate a force on the foot. All the forces acting between the foot and the ground can be summed to yield a single force vector termed the *ground reaction force*. This origin of the ground reaction force vector on the surface is the point at which the rotational effect of all the forces on the feet are balanced and is termed the *center of pressure* (Box 36–1).

Maintaining balance while standing requires keeping the downward projection of the center of mass within the base of support, an imaginary area defined by those parts of the body in contact with the environment. For example, the two feet or one foot of a standing human define a *base of support* (Box 36–1). However, when a standing person leans against a wall or is supported by crutches, the base of support extends from the ground under the feet to the contact point between the body and the wall or crutches. Because the body is always in motion, even during stable stance, the body's center of mass continually moves about with respect to the base of support. Postural instability is determined by how fast the center of mass is accelerating toward and beyond the boundary of its base of support and how close the downward projection of the body's center of mass is to the boundary.

Upright stance requires two actions: (1) maintaining support against gravity by keeping the center of mass at some height and joints stable and (2) maintaining balance by controlling the trajectory of the center of mass in the horizontal plane. Balance and antigravity support are controlled separately by the nervous system and may be differentially affected in certain pathological conditions. For example, antigravity support can be excessive when spasticity is present after a stroke or insufficient in the hypotonia of cerebral palsy, although balance control may be preserved. Alternatively, in vestibular disorders, antigravity support can be normal, although balance control is disordered.

Box 36–1 Center of Pressure

The center of pressure (CoP) is defined as the origin of the *ground reaction force* vector on the support surface. For the body to be in static equilibrium, that is, to remain motionless, the force caused by gravity and the ground reaction force must be equal and opposite, and the CoP must be directly under the center of mass (CoM) (Figure 36–1A). Misalignment of the CoM and CoP causes motion of the CoM. For example, if the CoM projection onto the base of support is to the right of the CoP, the body will sway to the right until the CoP moves to the right to move the CoM back over the base of support.

However, standing is never truly static. While the body is in motion (postural sway), CoM and CoP are not aligned and dynamic equilibrium must maintain balance (Figure 36–1B). In fact, when the body is unsupported, CoP and CoM are continually in motion and are rarely aligned, although when averaged over time during quiet stance, they are coincident. The sway of the body during quiet stance can be described by the trajectory of either CoM or CoP over time, such as sway path, area, velocity, and frequency.

In more dynamic situations like walking, running, turning, and jumping, stability can be achieved even when the CoM briefly goes outside the base of support. For example, when standing on one leg or on a narrow beam, momentum from rotating the hips, arms, and other body parts or movement of the CoP can be used to change the direction of the ground reaction force to return the body CoM over its base of support to maintain stability (Figure 36–1B). If the CoM is outside the base of support and heading away from it, subjects may need to take a step or grab a stable object to change the base of support and avoid a fall.

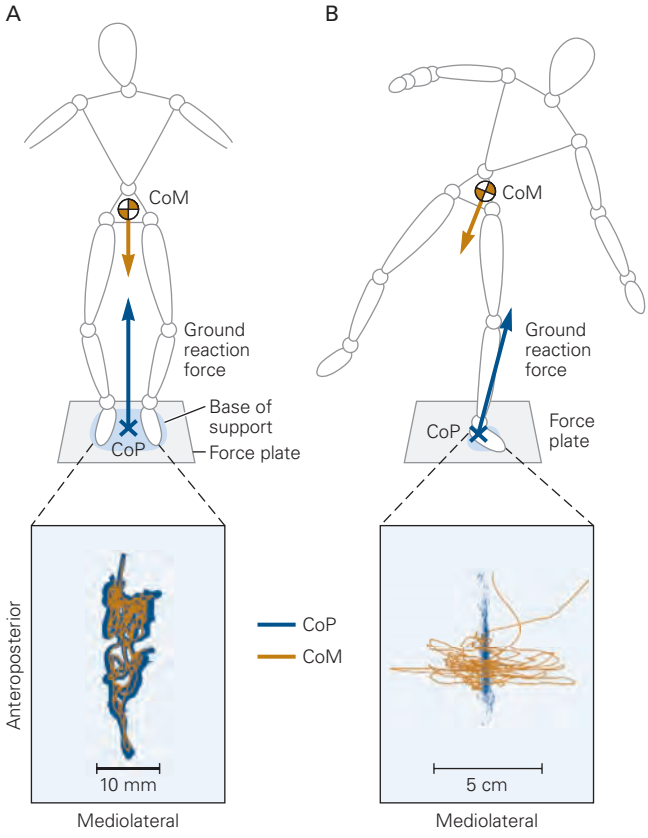

Figure 36–1 The center of mass is controlled by moving the center of pressure.

A. The force caused by gravity passes through the center of mass (**CoM**) in the trunk. The surface exerts an upward force against each foot, such that the ground reaction force vector originates at the center of pressure (**CoP**) on the support surface. **Below:** Even when the feet remain in place, the CoP (**blue displacement**) and CoM (**gold displacement**) are always in motion as we sway. During normal standing on two feet, the projection of the CoM of the body remains within the base of support (**light blue rectangle** around the feet in contact with the ground) for equilibrium. The base of support of the standing human is defined by contact of the feet on the support surface.

B. In a dynamic situation, such as standing on one leg on a narrow beam, equilibrium can be maintained even when the body CoM displacements (**gold displacements**) go outside of the base of support for brief periods. Strategies such as counter-rotation of the lower and upper body can tilt the ground reaction force so that it accelerates the body CoM back over its base of support. (Adapted, with permission, from Otten 1999. Permission conveyed through Copyright Clearance Center, Inc.)

Antigravity support, or "postural tone," is provided by the tonic activation of muscles that generate force against the ground to keep the trunk and limbs extended and the center of mass at the appropriate height. In humans, much of the support against gravity is provided by passive bone-on-bone forces in joints such as the knees, which can be fully extended during stance, and in stretched ligaments such as those at the front of the hips. Nevertheless, antigravity support in humans also requires active tonic muscle contraction, for example, in ankle, trunk, and neck extensors. Postural tone, however, should not be considered a static state of muscle activation, as can be seen in pathologies such as decerebrate rigidity or the rigidity of parkinsonism. Normal postural tone is constantly changing, as a "wave" or "reed in the wind," to accommodate changes in postural alignment, voluntary movements, and task requirements.

Postural tone is not sufficient, however, for maintaining balance. Both bipeds and quadrupeds are inherently unstable, and their bodies sway during quiet stance. Actively contracted muscles exhibit a spring-like stiffness that helps to resist body sway, but muscle stiffness alone is insufficient for maintaining balance. Even stiffening of the limbs through muscle cocontraction is not sufficient for balance control. Instead, complex patterns of muscle activation produce direction-specific forces to control the body's center of mass. Body sway caused by even subtle movements, such as the motion of the chest during breathing, is actively counteracted by alterations in postural tone.

Postural Orientation Anticipates Disturbances to Balance

Postural orientation is the manner in which body parts are aligned with respect to each other and to the environment. Animals arrange their bodies to accomplish specific tasks efficiently. Although this postural orientation interacts with balance control, the two systems can act independently. For example, soccer goalies may orient their body to intercept a ball by sacrificing the goal of maintaining balance. In contrast, a patient with Parkinson disease or thoracic kyphosis may use an inefficient, flexed postural alignment to maintain effective control of balance while standing.

The energy needed to maintain body position over a period of time can influence postural orientation. In humans, for example, the upright orientation of the trunk with respect to gravity minimizes the forces and thus the energy required to hold the body's center of mass over the base of support. Task requirements also affect postural orientation. For some tasks, it is important to stabilize the arrangement of the body in space, whereas for others, it is necessary to stabilize one body part with respect to another. When walking while carrying a full glass, for example, it is important to stabilize the hand against gravity to prevent spillage. In contrast, when walking while reading a cell phone, the hand must be stabilized with respect to the head and eyes to maintain visual acuity.

Subjects may adopt a particular postural orientation to optimize the accuracy of sensory signals regarding body motion. For example, when standing and walking inside a ship, in which the surface and visual references may be unstable, information about earth vertical is derived primarily from vestibular inputs. A person often aligns his head with respect to gravitational vertical when balancing on an unstable surface because the perception of vertical is most accurate when the head is upright and stable.

Anticipatory alterations of habitual body orientation can minimize the effect of a possible disturbance. For example, people often lean in the direction of an anticipated external force, or they flex their knees, widen their stance, and extend their arms when anticipating that stability will be compromised.

Postural Responses and Anticipatory Postural Adjustments Use Stereotyped Strategies and Synergies

When a sudden disturbance causes the body to sway, various postural motor strategies are used to maintain the center of mass within the base of support. In one strategy, the base of support remains fixed relative to the support surface: While the feet remain in place, the body rotates about the ankles back to the upright position (Figure 36–2A). In other strategies, the base of support is moved or enlarged, for example, by taking a step or by grabbing a support with the hand (Figure 36–2B).

Older views of motor control focused on trunk and proximal limb muscles as the main postural effectors. Recent behavioral studies show that any group of muscles from the neck and trunk, legs and arms, or feet and hands can act as postural muscles depending on the body parts in contact with the environment and the biomechanical requirements of equilibrium.

When studying the posture control system, scientists disrupt balance in a controlled manner to determine the subject's automatic postural response. This response is described by the ground reaction force vector, the motion of the center of pressure, and movements of parts of the body. The electrical activity

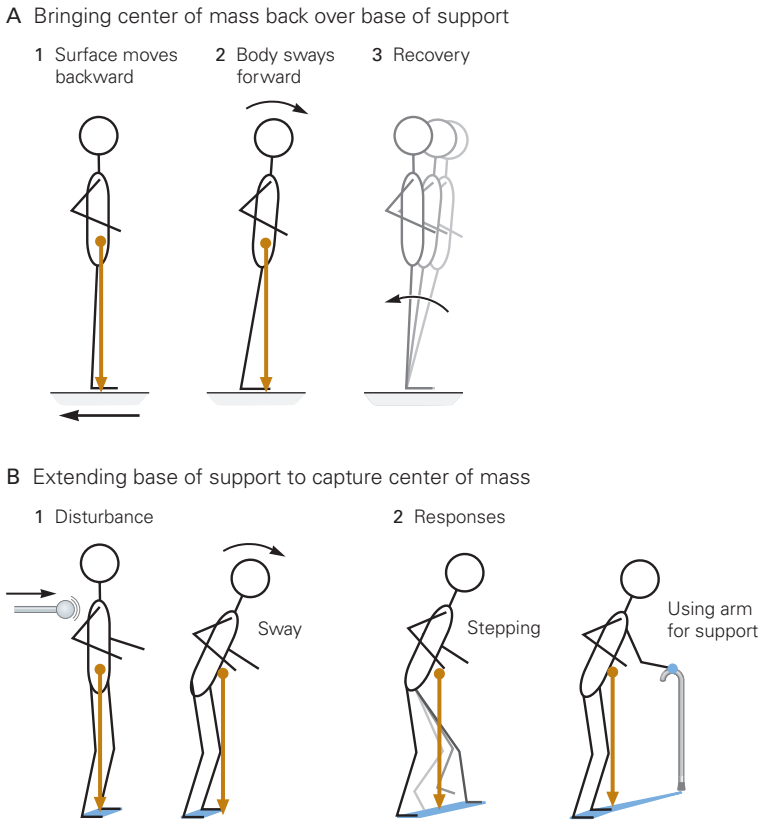

Figure 36–2 Automatic postural responses keep the center of mass within the base of support.

A. One postural strategy for regaining balance is to bring the center of mass back to its origin over the base of support. When the platform on which a subject is standing is suddenly moved backward, the body sways forward and the projection of the center of mass moves toward the toes. During recovery, the body actively exerts force into the surface about the ankles, bringing the center of mass back to the original position over the feet.

B. An alternative postural strategy enlarges the base of support to keep the center of mass within the base. A disturbance causes the subject to sway forward and the center of mass moves toward the boundary of the base of support (**blue area** on the ground). The base can be enlarged in two ways: taking a step and placing the foot in front of the center of mass to decelerate the body's motion, or grabbing a support and thereby extending the base to include the contact point between the hand and support.

of many muscles is recorded by electromyography (EMG), which reflects the firing of alpha motor neurons that innervate skeletal muscle and thus provides a window into the nervous system's output for balance control. The combination of all these measurements allows investigators to infer the active neural processes underlying balance control.

Automatic Postural Responses Compensate for Sudden Disturbances

An automatic postural response to a sudden disturbance is not a simple stretch reflex but rather the synergistic activation of a group of muscles in a characteristic sequence with the goal of maintaining equilibrium. That is, the recruitment of a muscle for a postural response serves the requirements of equilibrium and is not a reflexive change in the muscle's length caused by the disturbance. For example, when the surface under a person is rotated in the toes-up direction, the ankle extensor (gastrocnemius) is lengthened and a small stretch reflex may occur. However, the postural response for balance recruits the antagonist ankle flexor (tibialis anterior), which itself is shortened by the surface rotation, while suppressing the stretch response in the gastrocnemius. In contrast, when the platform is moved backward, the gastrocnemius is again lengthened but now it is recruited for the postural response, as evidenced by a second burst of EMG activity after the stretch reflex. Thus, the initial change in length of a muscle induced by perturbation does not determine whether that muscle is recruited for postural control, and stretch reflexes are not the basis for postural control. In fact, monosynaptic stretch reflexes are too weak to move the body center of mass effectively, and very often, the postural muscles activated to recover equilibrium have not been stretched.

Automatic postural responses to sudden disturbances have characteristic temporal and spatial features. A postural response in muscles must be recruited rapidly following the onset of a disturbance. Sudden movement of the support surface under a standing cat evokes EMG activity within 40 to 60 ms (Figure 36–3). Humans have longer latencies of postural response (90–120 ms in the ankle muscles); the increased delay is attributed to the larger body size of humans and thus

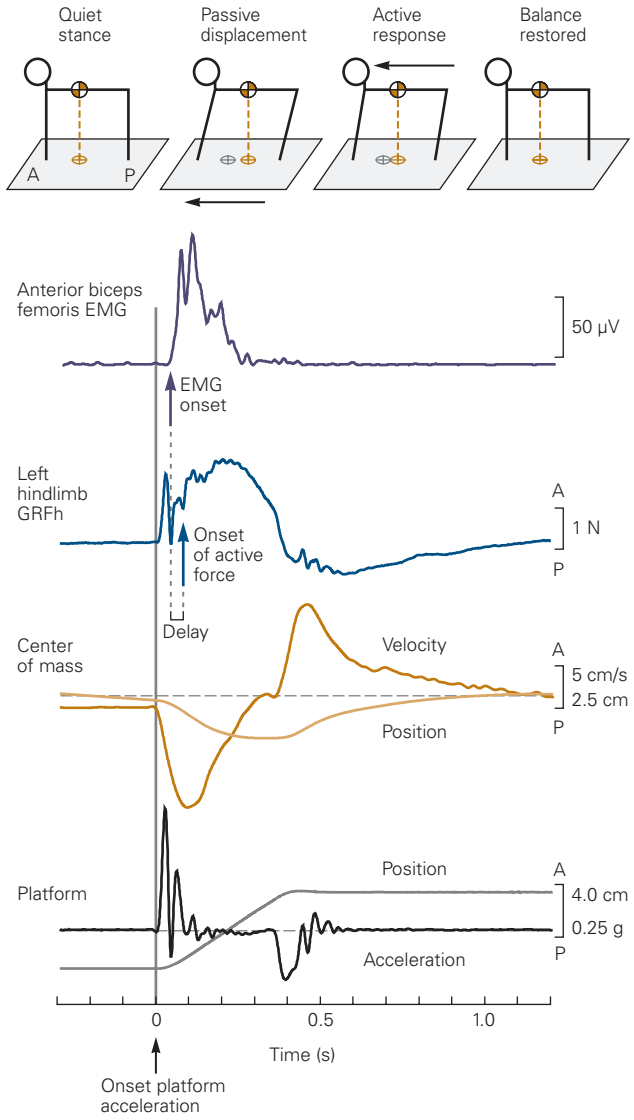

Figure 36–3 **Automatic postural responses have stereotypical temporal characteristics.** Electromyographic (**EMG**) activity has a characteristic latency. Anterior motion of the platform evokes an EMG response in the hip extensor muscle (anterior biceps femoris) of a cat approximately 40 ms after the onset of platform acceleration (100 ms in a human). This latency is stereotyped and repeatable across subjects and is approximately four times as long as that of the monosynaptic stretch reflex. As the platform moves, the paws are carried forward and the trunk remains behind owing to inertia, causing the center of mass to move backward with increasing velocity with respect to the platform. The velocity of the center of mass peaks and then decreases as the horizontal component of the ground reaction force (**GRFh**) increases following muscle activation. The delay of approximately 30 ms between the onset of EMG activity and the onset of the active response reflects excitation–contraction coupling and musculoskeletal compliance. The automatic postural response extends the hind limb, propelling the trunk forward and restoring the position of the center of mass with respect to the paws. (Abbreviations: **A**, anterior; **P**, posterior.) (Data from J. Macpherson.)

the greater signal conduction distances from sensory receptors to the central nervous system and thence to leg muscles. The latency of automatic postural responses is shorter than voluntary reaction time but longer than the monosynaptic stretch reflex.

Postural responses involving a change in support base, such as stepping, have even longer latencies than those that occur when the feet remain in place. The longer time presumably affords greater flexibility in the commands transmitted by long loops through the cortex; for example, the choice of foot to begin the step, the direction of the step, and the path of the step around obstacles.

Activation of postural muscles results in contraction and the development of force in the muscles, leading to torque (rotational force) at the joints. The net result is an active response, the ground reaction force (Box 36–1), that restores the center of mass to its original position over the base of support (Figure 36–3). The delay between EMG activation and the active response, approximately 30 ms in the cat and 50 ms in humans, reflects the excitation–contraction coupling time of each muscle as well as the compliance of the musculoskeletal system.

The amplitude of EMG activity in a particular muscle depends on both the speed and direction of postural disturbance. The amplitude increases as the speed of a movable platform under a standing human or cat increases, and it varies in a monotonic fashion as the direction of platform motion is varied systematically. Each muscle responds to a limited set of perturbation directions with a characteristic tuning curve (Figure 36–4).

Although individual muscles have unique directional tuning curves, muscles are not activated independently but instead are activated together in *synergies*, with characteristic time delays. The muscles within a synergy receive a common command signal during postural responses. In this way, the many muscles of the body are controlled by just a few signals, reducing the time needed to compute the appropriate postural response (Box 36–2).

The set of muscles recruited in a postural response to a disturbance depends on the body's initial stance. The same disturbance elicits very different postural responses in someone standing unaided, standing while grasping a stable support, or crouching on all four limbs. For example, forward sway activates muscles in the back of the legs and trunk during upright free stance. When the subject is holding onto a stable support, muscles of the arms rather than those of the legs are activated first. When the subject is crouched on toes and fingers, like a cat, muscles in the front of the legs and in the arms are activated (Figure 36–6A).

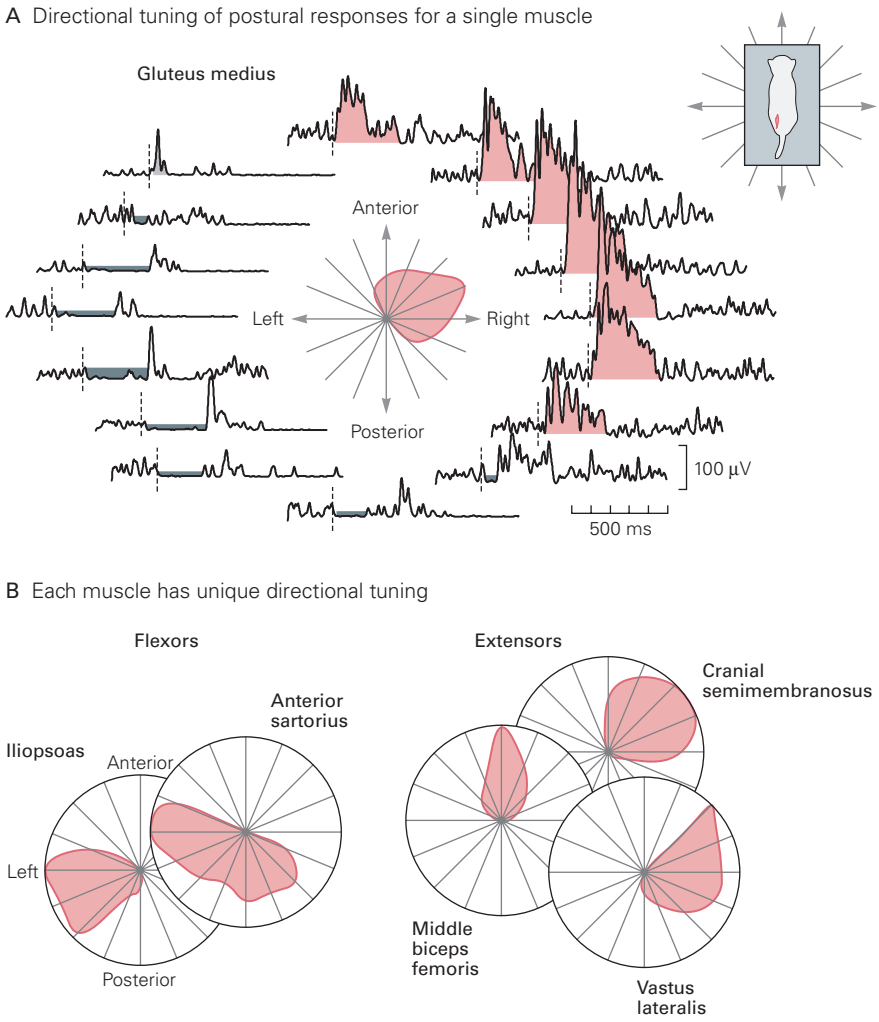

Figure 36–4 Automatic postural responses have stereotypical directional characteristics. (Adapted from Macpherson 1988.)

A. The gluteus medius muscle in the cat, a hip extensor and abductor, responds to a range of directions of motion in the horizontal plane. The electromyographic (EMG) records shown here are from a cat standing on a platform that was moved in the horizontal plane in each of 16 evenly spaced directions. The gluteus medius muscle of the left hind limb was activated by motion in several directions (**pink**) and inhibited in the remaining directions (**gray**). The **dashed vertical lines** indicate the onset of platform acceleration. In the center is a polar plot of the amplitude of EMG activity versus the direction of motion during the automatic postural response; it represents a directional tuning curve for the muscle. EMG amplitude was computed from the area under the curve during the first 80 ms of the response.

B. Every muscle has a characteristic directional tuning curve that differs from that of other muscles, even if they have similar actions. The middle biceps femoris and cranial semimembranosus, for example, are both extensors of the hip.

Because postural responses are influenced by recent experience, they adapt only gradually to new biomechanical conditions. When forward sway is induced by backward motion of a platform on which a subject is standing, the posterior muscles of the ankle, knee, and hip are activated in sequence beginning 90 ms after the platform starts moving. This postural response, the *ankle strategy*, restores balance primarily by rotating the body about the ankle joints. However, when forward sway is induced by backward motion of a narrow beam, it is impossible to use surface torque alone to recover equilibrium and the anterior muscles of the hip and trunk are activated. This postural response, the *hip strategy*, restores the body's center of mass by bending forward at the hip joints and counterrotating at the ankles (Figure 36–6B).

When a subject moves from standing on a wide platform to a narrow beam, she or he persists in using the ankle strategy in the first few trials. This strategy does not work when standing on the beam, and the subject falls. Over several trials, the subject will gradually switch to using the hip strategy. Similarly, moving from the beam back to the platform requires several trials to adapt the postural response back to the ankle strategy (Figure 36–6C).

Although sensory stimulation changes immediately after subjects move from the beam to the floor, the postural response adjusts gradually as it is tuned for optimal behavior by trial and error. If postural responses were simple reflexes, they would change immediately upon a change in sensory drive. Trial-to-trial changes in postural behavior generally occur at the subconscious level (implicit learning) and involve updating of the body schema and internal model of the world within the right parietal cortex. This body schema is dynamic, as it is constantly updated based on experience.

Postural responses not only improve with practice, but the improvements are retained, a sign of motor

Box 36–2 Synergistic Activation of Muscles

Coordinated movements require precise control of the many joints and muscles in the body. Maintaining control is biomechanically complex, in part because different combinations of joint rotations and muscle activations can achieve the same goal. Such redundancy confers great flexibility, for example, in modifying stepping patterns to negotiate obstacles in our path, but comes at the cost of increased complexity in the brain's computation of movement trajectories and forces.

Many factors must be included in the computation of movement commands, including the effect of external forces such as gravity and the forces that one body segment exerts on another during motion. All these factors come into play when the brain computes postural responses to sudden disturbances, but with the added constraint of a time limit on computation: Responses must occur within a certain time or balance will be lost.

It has long been believed that the brain simplifies the control of movement by grouping control variables, for example, activating several muscles together. Using mathematical techniques that parse complex data into a small number of components, one can determine that only four synergies are needed to account for the vast majority of activation patterns of 13 muscles of the human leg and trunk during automatic postural responses to many directions of platform motion (Figure 36–5). Activation of each synergy produces a unique direction of force against the ground, suggesting that postural control is based on task-related variables such as the force between foot and ground rather than the contraction force of individual muscles.

Like the arrangement of notes in a musical chord, each muscle synergy specifies the timing and amplitude of activation for a particular muscle together with others. Just as one note belongs to several different chords, each muscle belongs to more than one synergy. When several chords are played simultaneously, the chord structure is no longer evident in the multitude of notes. Similarly, when several synergies are activated concurrently, the observed muscle pattern gives the appearance of unstructured complexity, but a particular muscle's activation is the result of the systematic addition of synergy commands. Concurrent activation of synergies simplifies the neural command signals for movement as only a few central commands are required instead of a separate command for each muscle, while allowing flexibility and adaptability to postural control.

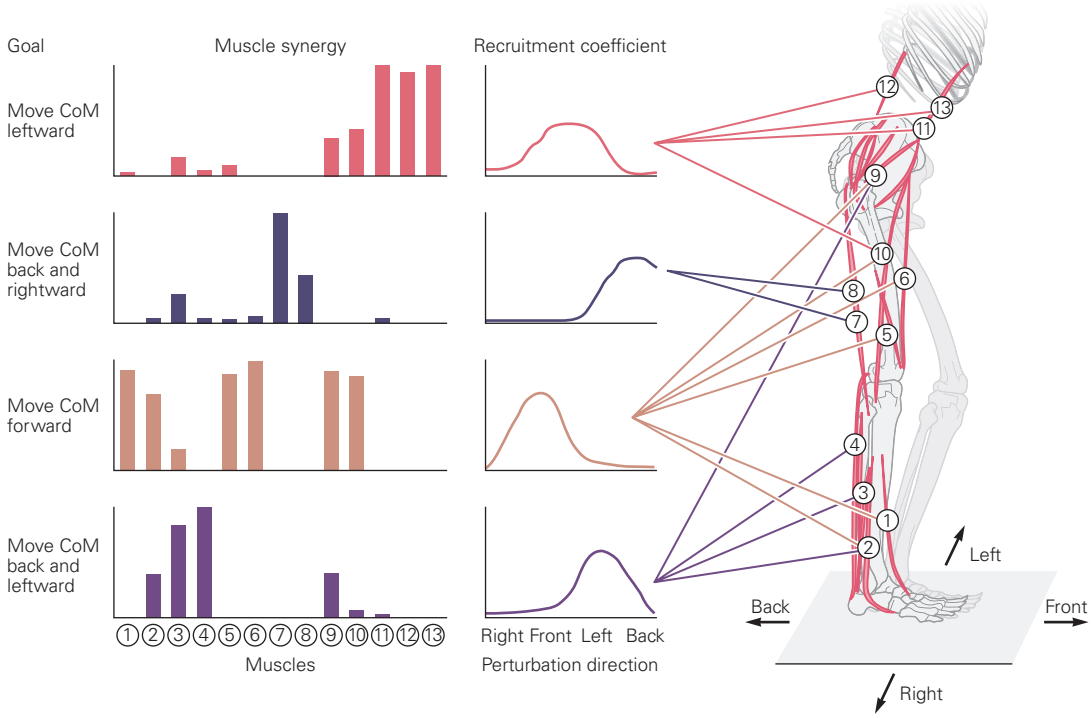

Figure 36–5 Postural commands activate synergies rather than individual muscles. Synergistic activation of several muscles allows movement goals to be translated into specific muscle activity patterns. Each muscle synergy activates a group of muscles in a fixed proportion (**colored bars**) to produce the mechanical output needed to achieve a postural goal. The height of each bar represents the relative amount of activation, or weighting, for each muscle (1–13). Each synergy is activated more or less at particular times during a behavior driven by central commands and sensory drive (recruitment function). For example, different postural synergies are activated for different directions of falling. (Abbreviation: **CoM**, center of mass.) (Reproduced, with permission, from L. Ting.)

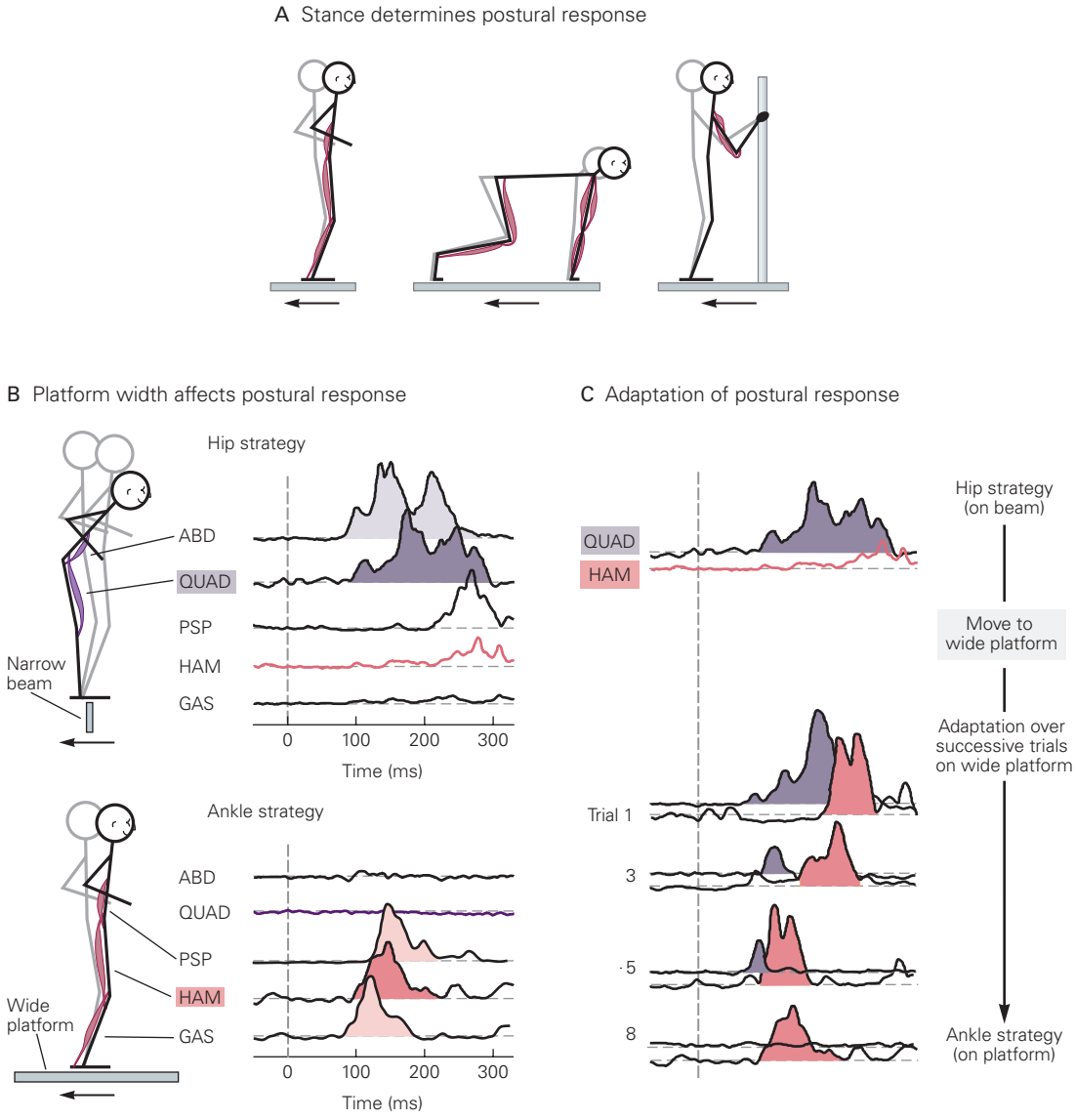

Figure 36–6 Automatic postural responses change with biomechanical conditions.

A. The backward movement of a platform activates different groups of muscles depending on initial stance. **Gray stick figures** show initial positions (upright unsupported, quadrupedal, or upright supported). The muscles activated in each postural response are shown in **red**. (Adapted, with permission, from Dunbar et al. 1986.)

B. When a subject stands on a narrow beam that is abruptly moved backward, the anterior muscles—abdominals (**ABD**) and quadriceps (**QUAD**)—are recruited to flex the trunk and extend the ankles, moving the hips backward (the hip strategy). When the subject instead stands on a wide platform that is moved backward, his posterior muscles—paraspinals (**PSP**), hamstrings (**HAM**), and gastrocnemius (**GAS**)—are activated to bring the body back to the erect position by rotating at the ankles (the ankle strategy). Muscles representative of different postural responses are highlighted in color. **Dashed vertical lines** in the plots indicate onset of platform (or beam) acceleration.

C. Postural strategy adapts after the subject moves from the narrow beam onto the wide platform. On the beam, the quadriceps are activated and the hamstrings are silent; after adaptation to the wide platform, the reverse is observed. The transition from quadriceps to hamstrings activation occurs over a series of trials; the activity in the quadriceps gradually decreases in amplitude, whereas the hamstrings are activated earlier and earlier until, by trial 8, quadriceps activity disappears altogether. Ankle and trunk muscles show similar patterns of adaptation. (B. and C, adapted, with permission, from Horak and Nashner 1986.)

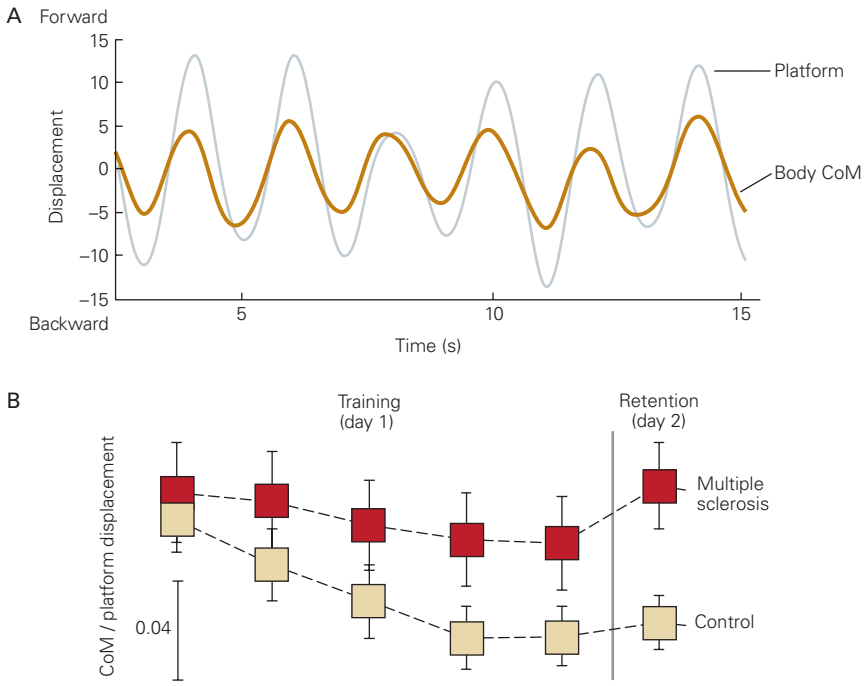

Figure 36–7 Postural responses can be learned and retained with practice.

A. Displacement of body center mass (**CoM**, **gold oscillation**) in response to forward and backward platform oscillations of varying amplitudes (**gray**) as a healthy subject learns to reduce postural instability.

B. Displacement of the body CoM by forward–backward surface oscillations is reduced across training sessions on day 1, and this improvement is retained on day 2 in healthy control subjects. People with multiple sclerosis also learn to reduce CoM displacements but do not retain this improvement the next day. The mean and standard error of group changes in gain (CoM/surface displacement) are compared. (Adapted, with permission, from Gera et al. 2016.)

learning. For example, when subjects practice standing on an oscillating surface, they gradually learn to decrease the extent of the displacement of their center of mass, and much of this improvement is retained the next day (Figure 36–7). Patients with neurological disorders, such as multiple sclerosis or Parkinson disease, who have significantly impaired postural responses can often learn to improve their postural control with practice, although they may need more practice than normal to retain the improvements (Figure 36–7).

Anticipatory Postural Adjustments Compensate for Voluntary Movement

Voluntary movements can also destabilize postural orientation and equilibrium. For example, rapidly lifting the arms forward while standing produces forces that extend the hips, flex the knees, and dorsiflex the ankles, moving the body's center of mass forward relative to the feet. The nervous system has advance knowledge of the effects of voluntary movement on postural alignment and stability and activates anticipatory postural adjustments, often in advance of the primary movement (Figure 36–8A).

Anticipatory postural adjustments are specific to biomechanical conditions. When a freely standing subject rapidly pulls on a handle fixed to the wall, the leg muscles (gastrocnemius and hamstrings) are activated before the arm muscles (Figure 36–8B). When the subject performs the same pull while his shoulders are propped against a rigid bar, no anticipatory leg muscle activity occurs because the nervous system relies on the support of the bar to prevent the body from moving forward. When the handle is pulled in response to an external cue, the arm muscles are activated faster in the supported condition than in the freestanding condition. Thus, voluntary arm muscle activation is normally delayed when the task requires active postural stability.

Another common preparatory postural adjustment occurs when one begins to walk. The center of mass is accelerated forward and laterally by the unweighting of one leg. This postural adjustment appears to be independent of the stepping program that underlies ongoing locomotion (Chapter 33). Similarly, a forward shift of the center of mass precedes the act of standing on the toes. A subject is unable to remain standing on his toes if he simply activates the calf muscles without moving his center of mass forward; he rises onto his toes only momentarily before gravity restores a flat-footed stance. Moving the center of mass forward over the toes before activating the calf muscles aligns it over the anticipated base of support and thus stabilizes the toe stance.

Postural equilibrium during voluntary movement requires control not only of the position and motion of the body's center of mass but also of the angular momentum about the center of mass. A diver can

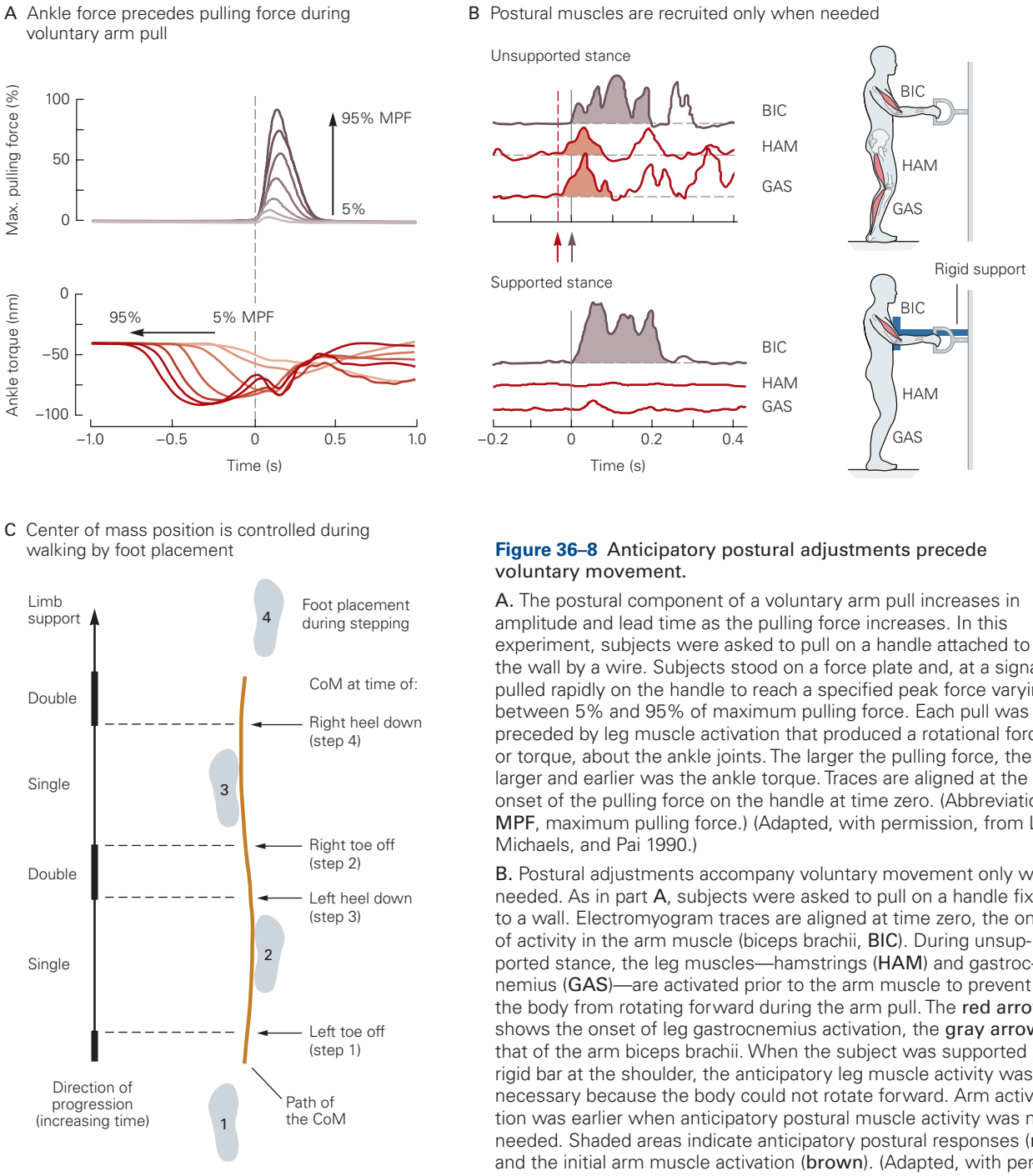

Figure 36–8 Anticipatory postural adjustments precede voluntary movement.

A. The postural component of a voluntary arm pull increases in amplitude and lead time as the pulling force increases. In this experiment, subjects were asked to pull on a handle attached to the wall by a wire. Subjects stood on a force plate and, at a signal, pulled rapidly on the handle to reach a specified peak force varying between 5% and 95% of maximum pulling force. Each pull was preceded by leg muscle activation that produced a rotational force, or torque, about the ankle joints. The larger the pulling force, the larger and earlier was the ankle torque. Traces are aligned at the onset of the pulling force on the handle at time zero. (Abbreviation: **MPF**, maximum pulling force.) (Adapted, with permission, from Lee, Michaels, and Pai 1990.)

B. Postural adjustments accompany voluntary movement only when needed. As in part **A**, subjects were asked to pull on a handle fixed to a wall. Electromyogram traces are aligned at time zero, the onset of activity in the arm muscle (biceps brachii, **BIC**). During unsupported stance, the leg muscles—hamstrings (**HAM**) and gastrocnemius (**GAS**)—are activated prior to the arm muscle to prevent the body from rotating forward during the arm pull. The **red arrow** shows the onset of leg gastrocnemius activation, the **gray arrow** that of the arm biceps brachii. When the subject was supported by a rigid bar at the shoulder, the anticipatory leg muscle activity was not necessary because the body could not rotate forward. Arm activation was earlier when anticipatory postural muscle activity was not needed. Shaded areas indicate anticipatory postural responses (**red**) and the initial arm muscle activation (**brown**). (Adapted, with permission, from Cordo and Nashner 1982.)

C. During walking, the trajectory of the center of mass (CoM) is controlled by foot placement. The body's center of mass is between the feet, moving forward and from side to side as the subject walks forward. When the body is supported by only one leg (single support phase), the CoM is outside the base of support and moves toward the lifting limb. People do not fall while walking because the placement of the foot on the next step decelerates the CoM and propels it back toward the midline. (Adapted from MacKinnon and Winter 1993.)

perform elaborate rolls and twists of the body about the center of mass while airborne, although the trajectory of his center of mass is fixed once he leaves the board. During voluntary movements, postural adjustments control the body's angular momentum by anticipating rotational forces.

Posture Control Is Integrated With Locomotion

During walking and running, the body is in a constant state of falling as the center of mass moves forward and laterally toward the leg that is in the swing phase (Figure 36–8C). During walking, the center of mass is within the base of support only when both feet are on the ground, the double stance phase, which is only one-third of a gait cycle. When one foot is supporting the body, the center of mass moves forward in front of the foot, always medial to the base of support.

Falling is prevented during walking and running by moving the base of support forward and laterally under the falling center of mass. Postural equilibrium during gait relies on the placement of each step to control the speed and trajectory of the center of mass. The nervous system plans foot placement several steps in advance using visual information about the terrain and surrounding environment.

The main postural challenge during walking is controlling the center of mass of the upper body over the moving legs, especially in the lateral direction. Excessive lateral displacement of the trunk and excessive lateral foot placement variability are signs of postural instability during locomotion. Patients with abnormal postural stability during gait may nevertheless exhibit normal automatic and anticipatory postural adjustments, postural sway in stance under different sensory conditions, and orientation to vertical, suggesting that postural control and gait have different nervous system circuits.

Somatosensory, Vestibular, and Visual Information Must Be Integrated and Interpreted to Maintain Posture

Because information about motion from any one sensory system may be ambiguous, multiple modalities must be integrated in postural centers to determine what orientation and motion of the body are appropriate. The influence of any one modality on the postural control system varies according to the task and biomechanical conditions.

According to prevailing theory, sensory modalities are integrated to form an internal representation of the body housed within the parietal cortex that the nervous system uses to plan and execute motor behaviors. Over time, this internal representation must adapt to changes associated with early development, aging, and injury.

Somatosensory Signals Are Important for Timing and Direction of Automatic Postural Responses

Many types of somatosensory fibers trigger and shape the automatic postural response. The largest fibers, those in group I (12–20 μm in diameter), appear to be essential for normal response latencies. The longer latency, slower rise time, and lower amplitude of the EMG response following destruction of the group I fibers reflect a loss of acceleration information encoded by muscle spindle primary receptors (Figure 36–9A). The largest and most rapidly conducting sensory fibers are the Ia afferents from muscle spindles and Ib afferents from Golgi tendon organs, as well as some fibers from cutaneous mechanoreceptors (Chapter 18). Group I fibers provide rapid information about the biomechanics of the body including responses to muscle stretch, muscle force, and directionally specific pressure on the foot soles. However, group II fibers from muscle spindles and cutaneous receptors may also play a role in shaping automatic postural responses. Although they may be too slow to generate the earliest part of the response, they likely encode center of mass velocity and position.

Both proprioceptive and cutaneous inputs provide cues about postural orientation. During upright stance, for example, muscles lengthen and shorten as the body sways under the force of gravity, generating proprioceptive signals related to load, muscle length, and velocity of stretch. Joint receptors may detect compressive forces on the joints, whereas cutaneous receptors in the sole of the foot respond to motion of the center of pressure and to changes in ground reaction force angle as the body sways. Pressure receptors near the kidneys are sensitive to gravity (somatic graviception) and are used by the nervous system to help detect upright or tilted postures. All of these signals contribute to the neural map of the position of body segments with respect to each other and the platform surface and may contribute to the neural computation of center of mass motion.

The large-diameter, fast somatosensory fibers from muscle spindles are critical for maintaining balance during stance. When these axons die, as occurs in some forms of peripheral neuropathy, automatic postural responses to movement of a platform are delayed, retarding the ground reaction force. As a

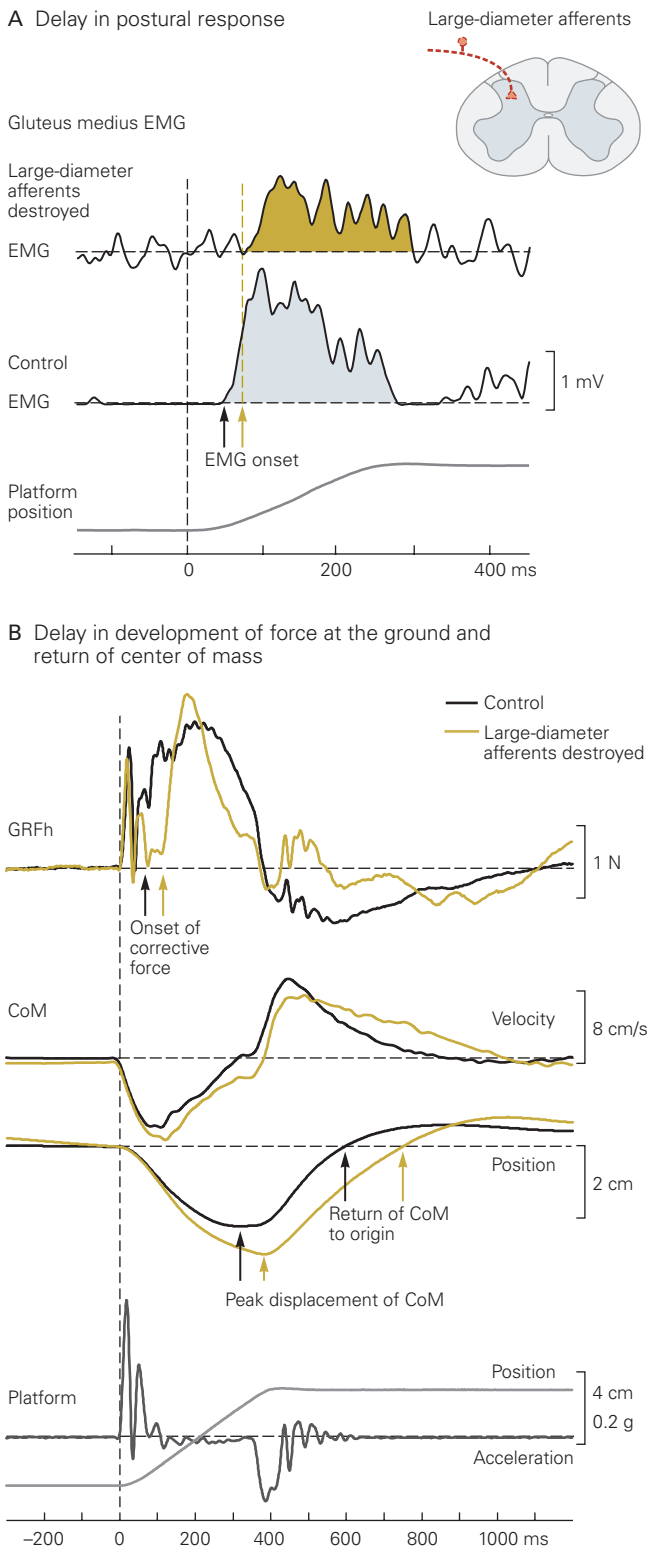

result, the center of mass moves faster and farther from the initial position and takes longer to return (Figure 36–9). Because it is more likely that the center of mass will move outside the base of support, balance is precarious and a fall may occur. Accordingly, individuals with large-fiber peripheral neuropathy in the legs experience ataxia and difficulties with balance.

Vestibular Information Is Important for Balance on Unstable Surfaces and During Head Movements

The otolithic organs of the vestibular apparatus provide information about the direction of gravity, whereas the semicircular canals measure the velocity of head rotation (Chapter 27). Vestibular information thus informs the nervous system about how much the body is tilted with respect to gravity as well as whether it is swaying forward, backward, or sideways.

Somatosensory and vestibular information about the gravitational angle of the body is combined to orient the body with respect to gravity and other inertial forces. To maintain balance while riding a bike in a circular path at high speed, for example, the body and bike must be oriented with respect to a combination of gravitational and centripetal forces (Figure 36–10A).

Unlike somatosensory inputs, vestibular signals are not essential for the normal timing of balance reactions. Instead, they influence the directional tuning of a postural response by providing information about the orientation of the body relative to gravity. In humans and experimental animals lacking functional vestibular afferent pathways, the postural response to *angular* motion or tilt of the support surface is opposite to the

Figure 36–9 (Left) **Loss of large-diameter somatosensory fibers delays automatic postural responses.** Electromyograms (**EMGs**) of postural responses to horizontal motion of a moveable platform were recorded in a cat before and after destruction of the large-diameter (group I) somatosensory fibers throughout the body by vitamin B_6 intoxication. Motor neurons and muscle strength are not affected by the loss of the somatosensory fibers, but afferent information about muscle length and force is diminished. (Reproduced, with permission, from J. Macpherson.)

A. The postural response in the gluteus medius evoked by horizontal motion of the support platform is significantly delayed after destruction of group I fibers. This delay of approximately 20 ms induces ataxia and difficulty in maintaining balance.

B. Destruction of group I fibers delays activation of the hind limb. This delay slows the restoration of the center of mass (**CoM**) and the recovery of balance following platform displacement. The delay in onset of the horizontal component of the ground reaction force (**GRFh**) results in a greater peak displacement of the CoM and a delay in its return to its origin relative to the paws.

A Orienting to gravito-inertial force

B Orienting to rotating visual field

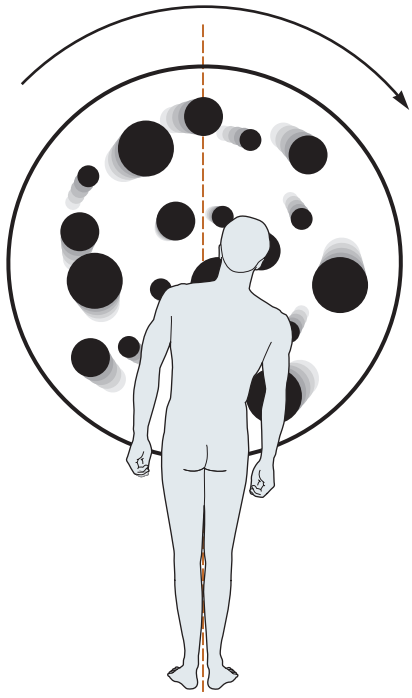

Figure 36–10 The postural system orients the body to various external reference frames.

A. When traveling at high speed along a curved path, a cyclist orients to the gravito-inertial force (angle A), the vector sum of the force caused by gravity and the centripetal force caused by acceleration along the curved path. (Used, with permission, from Joseph Daniel, Story Arts Media, LLC. Previously published in McMahon and Bonner 1983.)

B. The postural system can interpret rightward rotation of objects occupying a large region of the visual field as the body tilting to the left. In compensation for this illusion of motion, the subject tilts to the right, adopting a new postural vertical orientation that is driven by the visual system. The **red dashed line** indicates gravitational vertical. (Adapted, with permission, from Brandt, Paulus, and Straube 1986.)

normal response. Rather than resisting the tilt, subjects lacking vestibular signals do the opposite and accentuate the tilt through their own muscular activity. In contrast, the response to horizontal translation motion of a platform has the appropriate directional tuning and latency, even in the acute stage prior to vestibular compensation.

Why does the absence of vestibular signals cause difficulty with tilt but not with linear motion? The answer lies in how the nervous system determines the direction of vertical. Gravity is the main force that causes the body to fall. As the support surface tilts, healthy subjects orient to gravity using vestibular information to remain upright. In contrast, subjects without vestibular function use somatosensory inputs to orient themselves to the support surface and consequently fall downhill as the surface tilts. During linear motion, however, gravitational and surface vertical are collinear, and somatosensory signals are sufficient to compute the correct postural response. Although visual inputs also provide a vertical reference, visual processing is too slow to participate in the automatic postural response to rapid tilt, especially soon after the loss of vestibular function.

Without vestibular information, the response to linear motion of the support surface is larger than normal (*hypermetria*), leading to overbalancing and instability. Hypermetria is a major cause of ataxia when vestibular information is lost. Vestibular hypermetria may result from reduced cerebellar inhibition of the motor system, for the loss of vestibular inputs reduces the drive to the inhibitory Purkinje cells.

Humans and cats are quite ataxic immediately after loss of the vestibular apparatus. The head and trunk show marked instability, stance and gait are broad-based, and walking follows a weaving path with frequent falling. Instability is especially great on turning the head, probably because trunk motion cannot be distinguished from head motion using somatosensory information alone. Cats and humans lacking vestibular inputs produce motor output that results in them actively pushing themselves toward the side of

a voluntary head turn, likely because somatosensory inputs that encode trunk and head motion are misinterpreted in the absence of vestibular inputs. The postural system erroneously senses that the body is falling to the side away from the head tilt and generates a response in the opposite direction, resulting in imbalance.

Immediately following vestibular loss, neck muscles are abnormally activated during ordinary movements and often the head and trunk are moved together as a unit. After several months, routine movement becomes more normal through vestibular compensation, which may involve greater reliance on the remaining sensory information. However, more challenging tasks are hampered by a residual hypermetria, stiffness in head–trunk control, and instability, especially when visual and somatosensory information is unavailable for postural orientation. Vestibular information is critical for balance when visual information is reduced and the support surface is not stable, for example, at night on a sandy beach or on a boat deck.

Visual Inputs Provide the Postural System With Orientation and Motion Information

Vision reduces body sway when standing still and provides stabilizing cues, especially when a new balancing task is attempted or balance is precarious. Skaters and dancers maintain stability while spinning by fixing their gaze on a point in the visual field. However, visual processing is too slow to significantly affect the postural response to a sudden and unexpected disturbance of balance. Vision does play an important role in anticipatory postural adjustments during voluntary movements, such as planning where to place the feet when walking over obstacles.

Vision can have a powerful influence on postural orientation, evident when watching a movie scene filmed from the perspective of a moving viewer and projected on a large screen. Simulated rides in a roller coaster or airplane can induce strong sensations of motion along with activation of postural muscles. An illusion of movement is induced when sufficiently large regions of the visual field are stimulated, as when a large disk in front of a standing subject is rotated. The subject responds to this illusion by tilting his body; clockwise rotation of the visual field is interpreted by the postural system as the body falling to the left, to which the subject compensates by leaning to the right (Figure 36–10B). The rate and direction of optic flow—the flow of images across the retina as people move about—provide clues about body orientation and movement.

Information From a Single Sensory Modality Can Be Ambiguous

Any one sensory modality alone may provide ambiguous information about postural orientation and body motion. The visual system, for example, cannot distinguish self-motion from object motion. We have all experienced the fleeting sensation while sitting in a stationary vehicle of not knowing whether we are moving or the adjacent vehicle is moving.

Vestibular information can also be ambiguous for two reasons. First, vestibular receptors are located in the head and therefore provide information about acceleration of the head but not about the rest of the body. The postural control system cannot use vestibular information alone to distinguish between the head tilting on a stationary trunk and the whole body tilting by rotation at the ankles, both of which activate the semicircular canals and otolith organs. Additional information from somatosensory receptors is required to resolve this ambiguity. The otolith organs also cannot distinguish between acceleration owing to gravity and linear acceleration of the head. Tilting to the left, for example, can produce the same otolithic stimulation as acceleration of the body to the right (Figure 36–11).

Studies suggest that there are neural circuits that can disambiguate the head-tilt component of a linear acceleration by using a combination of canal and otolith inputs. Output from this circuit may allow the postural system to determine the orientation of gravity relative to the head regardless of head position and motion. The distinction between tilt and linear motion is especially important while standing on an unstable or a tilting surface.

Somatosensory inputs may also provide ambiguous information about body orientation and motion. When we stand upright, mechanoreceptors in the soles of our feet and proprioceptors in muscles and joints signal the motion of our body relative to the support surface. But somatosensory inputs alone cannot distinguish between body and surface motion, for example, whether ankle flexion stems from forward body sway or tilting of the surface. Our common experience is that the ground beneath us is stable and that somatosensory inputs reflect movements of the body's center of mass as we sway. But surfaces may move relative to the earth, such as a boat's deck, or may be pliant under our weight, like a soft or spongy surface. Therefore, somatosensory information must be integrated with vestibular and visual inputs to give the nervous system an accurate picture of the stability and inclination of the support surface and of our body's relationship to earth vertical.

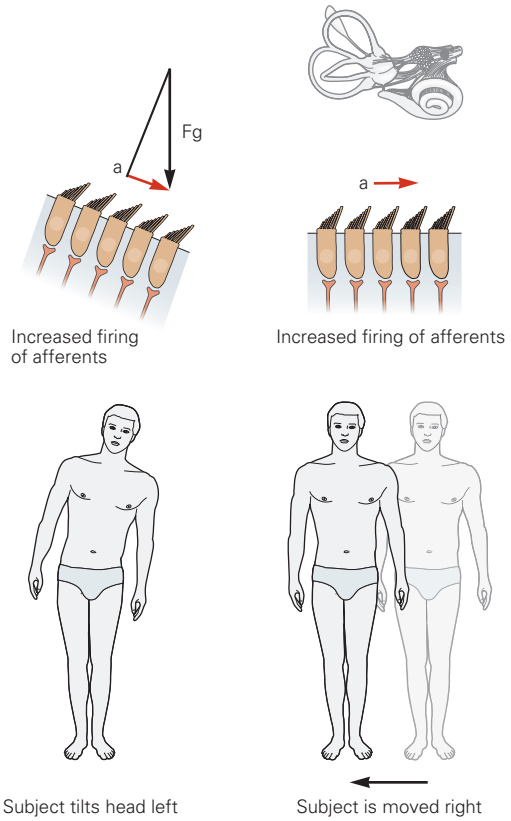

Figure 36–11 Vestibular inputs regarding body posture and motion can be ambiguous. The postural system cannot distinguish between tilt and linear acceleration of the body based on otolith inputs alone. The mechanoreceptors of the vestibular system are hair bundles that bend in response to shearing forces, thus changing the firing rate of the tonically active sensory afferents. The same shearing force can result from tilting of the head (*left*), which exposes the hair cells to a portion of the acceleration (**a**) owing to gravity (**Fg**), or from horizontal linear acceleration of the body (*right*).

The Postural Control System Uses a Body Schema That Incorporates Internal Models for Balance

Because of the mechanical complexity of the body, with its many skeletal segments and muscles, the nervous system requires a detailed representation of the body and its interaction with the environment. To execute the simple movement of raising your hand and touching your nose with your index finger while your eyes are closed, your nervous system must know the characteristics (length, mass, and connections) of each segment of the arm, the shoulder, and head as well as the orientation of your arm with respect to the gravity vector and your nose. Thus, information from multiple sensory systems is integrated into a central representation of the body, often called the body schema.

The body schema for postural control, as developed by Viktor Gurfinkel, is not simply a sensory map like the somatotopic representation of the skin in primary sensory cortex. Instead, it incorporates internal models of the body's relationship with the environment. The body schema is used to compute appropriate anticipatory and automatic postural reactions to maintain balance and postural orientation. A simplified example of such an internal model is one in which the body is represented as a single segment hinged at the foot (Figure 36–12A). The internal model generates an estimate of the orientation of the foot in space, which also serves as an estimate of the orientation of the support surface, a variable that cannot be directly sensed.

Henry Head, a neurologist working in the early part of the 20th century, described the body schema as a dynamic system in which both spatial and temporal features are continually updated, a concept that remains current. To allow adequate planning of movement strategies, the body schema must incorporate not only the relationship of body segments to space and to each other but also the mass and inertia of each segment and an estimate of the external forces acting on the body including gravity.

The body schema integrates sensory information from the somatosensory, vestibular, and visual systems to orient the body to vertical. Even in the dark, people can accurately reorient a projected line to a vertical position (visual vertical) and they can reorient themselves to vertical when sitting on a tilting swing (gravitational vertical). Visual vertical and gravitational vertical are independent of each other. Patients with asymmetrical vestibular function show abnormal visual vertical but normal gravitational vertical, whereas patients with hemi-neglect from stroke show abnormal gravitational vertical but normal visual vertical.

Another component of the body schema is a model of the sensory information expected as a result of a movement. Disorientation or motion sickness may result when the actual sensory information received by the nervous system does not match the expected sensory information, as in the microgravity environment of space flight. With continued exposure to the new environment, however, the model is gradually updated until expected and actual sensory information agree and the person is no longer spatially disoriented.

The internal model for balance control must be continually updated, both in the short term, as we use experience to improve our balance strategies, and in the long term, as we age and our bodies change in shape and size. One way the body schema is updated is by changing the relative sensitivity or weighting of each sensory system.

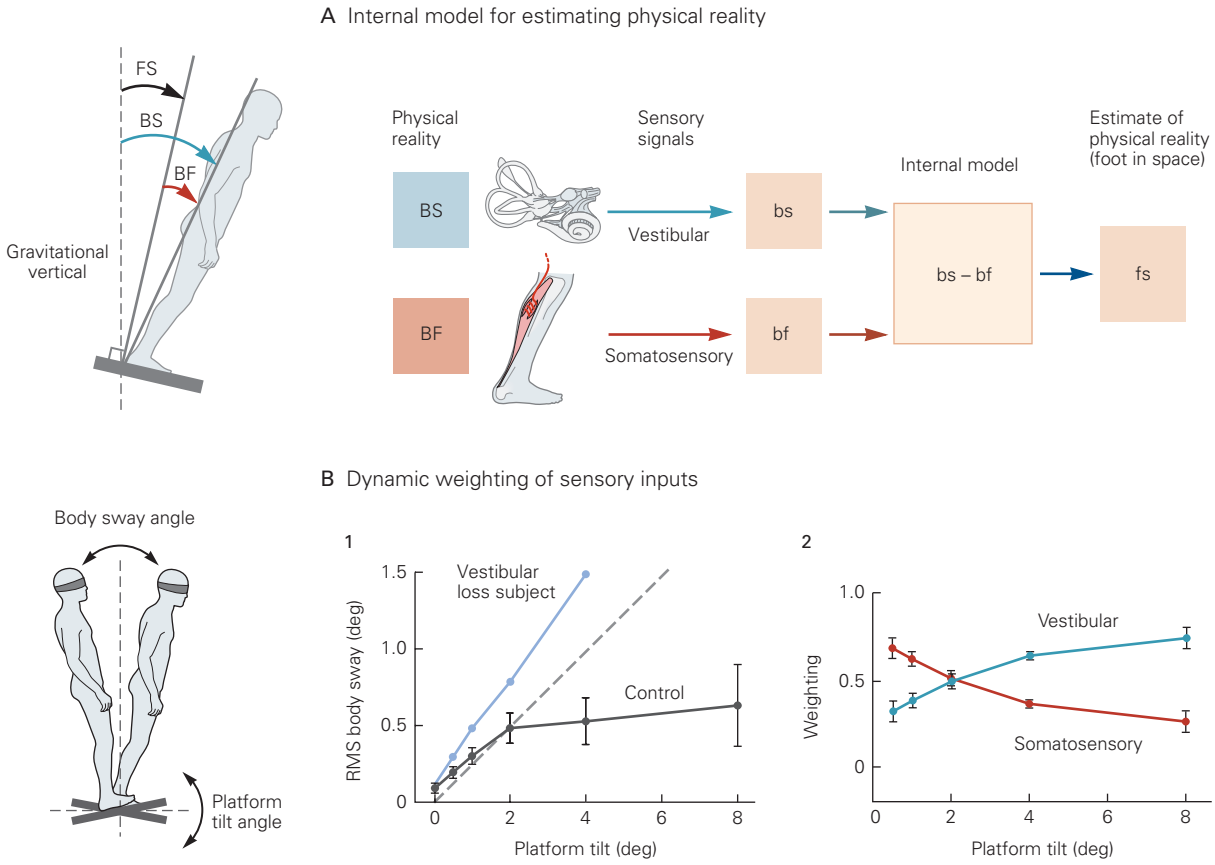

Figure 36–12 Many types of sensory signals are integrated and weighted in an internal model that optimizes balance and orientation. (Adapted from Peterka 2002.)

A. The simple example of a person standing on a tilted surface illustrates how the nervous system might estimate physical variables that are not sensed directly. The physical variables are body tilt with respect to earth vertical or body-in-space (**BS**), and body angle relative to the foot (**BF**). The angle of the foot in space (**FS**) is simply the difference BS – BF. The neural estimate of body in space (**bs**) comes from vestibular and other receptors that detect tilt of the body relative to gravity. The neural estimate of body angle to foot (**bf**) comes from somatosensory signals related to ankle joint angle. The internal model for estimating physical reality, bs – bf, produces a neural estimate of the foot in space (**fs**). Such estimates of the physical world are continually updated based on experience.

B. Sensory information is weighted dynamically to maintain balance and orientation under varying conditions. The figure illustrates findings from an experiment in which human subjects stood blindfolded on a platform that slowly rotated continuously in the toes-up or toes-down direction at amplitudes of up to 8° (peak to peak). **1.** Comparison of body sway during surface oscillations in a subject with loss of vestibular function and a group of control subjects. Body-sway angle is measured relative to gravitational vertical during platform tilt and expressed as root mean square (**RMS**) sway in degrees. The **dashed line** represents equal platform and body sway; for example, for a platform tilt of 4°, an equal amount of body sway is 1° RMS. In control subjects, the body and platform sway are equal for small platform tilts up to 2°, suggesting that people normally use somatosensory signals to remain perpendicular to the platform (minimizing changes in ankle angle). With larger platform tilts, body sway does not increase much beyond 0.5° RMS. In contrast, subjects with vestibular loss sway even more than the platform (1.5° RMS of body tilt at 4° of platform tilt) and cannot remain standing at platform tilts above 4°. Thus, when both vestibular and visual signals are absent, a person attempts to maintain his position only relative to the support surface and has difficulty maintaining balance as that surface moves. **2.** In control subjects, as platform tilt increases, the influence of somatosensory input decreases with increasing platform tilt while the influence of vestibular input increases. At larger tilt angles, the greater influence of vestibular input minimizes the degree of body sway away from gravitational vertical.

Control of Posture Is Task Dependent

The senses and muscles used to control posture vary, depending on task constraints and requirements. For example, when vestibular and somatosensory information is altered while working on a space station, vision is used to orient the body to tasks, and the goal of postural equilibrium changes from preventing falls due to gravity to preventing unintended collision with objects due to inertia. A healthy nervous system very quickly adapts to changing tasks, goals, and environments by modifying its relative dependence upon different sensory information and by using different sets of muscles to optimize achieving the goals of both posture control and voluntary movements.

Task Requirements Determine the Role of Each Sensory System in Postural Equilibrium and Orientation

The postural control system must be able to change the weighting of different sensory modalities to accommodate changes in the environment and movement goals. Subjects standing on a firm stable surface tend to rely primarily on somatosensory information for postural orientation. When the support surface is unstable, subjects depend more on vestibular and visual information. However, even when the support surface is not stable, light touch with a fingertip on a stable object is more effective than vision in maintaining postural orientation and balance. Vestibular information is particularly critical when visual and somatosensory information is ambiguous or absent, such as when skiing downhill or walking below deck on a ship.

The changeable weighting of individual sensory modalities was demonstrated in an experiment in which subjects were blindfolded and asked to stand quietly on a surface with a tilt that slowly oscillated by varying amounts, up to 8° in magnitude. For tilts of less than 2°, all subjects sway with the platform, suggesting that they use somatosensory information to orient their body to the support surface (Figure 36–12B). At larger tilts, healthy subjects attenuate their sway and orient their posture more with respect to gravitational vertical than to the surface, as they rely more on vestibular information so they stop increasing body sway. Thus, relative sensory weighting changes in control subjects such that somatosensory weight is highest with a stable platform and vestibular weight is highest when standing on an unstable surface, such as with large surface tilts (Figure 36–12B2). In contrast, patients who have lost vestibular function persist in swaying along with the platform and subsequently fall during large surface tilts. This behavior is consistent with the patients' inappropriate automatic postural response to platform tilts.

Studies such as these suggest that when people are standing on moving or unstable surfaces, the weighting of vestibular and visual information increases, whereas that of somatosensory information decreases. Any sensory modality may dominate at a particular time, depending on the conditions of postural support and the specific motor behavior to be performed.

Control of Posture Is Distributed in the Nervous System

Postural orientation and balance are achieved through the dynamic and context-dependent interplay among all levels of the central nervous system, from the spinal cord to cerebral cortex. The major areas of the brain involved in postural control are shown in Figure 36–13. Signals from specific areas in all lobes of the cerebral cortex converge and are integrated to determine appropriate outputs from motor cortical areas to subcortical structures. The basal ganglia, cerebellum, and pedunculopontine nucleus then send outputs to the brain stem. Ultimately, inputs from these varied sources result in activation of the reticulospinal and vestibulospinal pathways, which descend to the spinal cord where they contact interneurons and spinal motor neurons for postural control.

Afferent inputs from visual, vestibular, and somatosensory sources are integrated along the neuraxis, including the vestibular nuclei and right parietal cortex, to inform the internal model of body orientation and balance. This internal model is continually updated by the cerebellum based on error signals between expected and actual sensory feedback following motor commands.

Spinal Cord Circuits Are Sufficient for Maintaining Antigravity Support but Not Balance

Adult cats with complete spinal transection at the thoracic level can, with experience, support the weight of their hindquarters with fairly normal hind limb and trunk postural orientation, but they have little control of balance. These animals do not exhibit normal postural responses in their hind limbs when the support surface moves. Their response to horizontal motion consists of small, random, and highly variable bursts of activity in extensor muscles, and postural activity in flexor muscles is completely absent. Active balance is absent despite the fact that extensors and flexors can

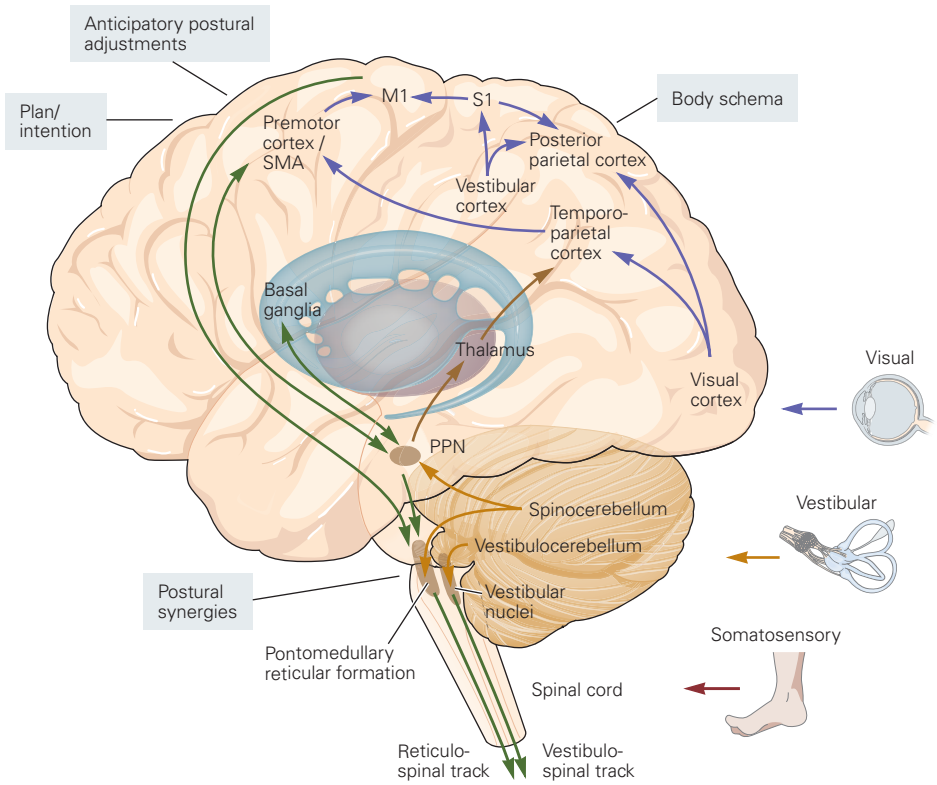

Figure 36–13 Many parts of the nervous system control posture. Areas of frontal, parietal, temporal, and occipital cortex, as well as the basal ganglia, cerebellum, and pendunculopontine nucleus (**PPN**), provide inputs to the recticulospinal and vestibulospinal pathways descending to spinal motor neurons. Afferent inputs from the visual, vestibular, and somatosensory systems are integrated in the brainstem and cortex to update the body schema and inform future postural commands. (Abbreviations: **M1**, primary motor cortex; **S1**, primary somatosensory cortex; **SMA**, supplementary motor area.) (Adapted from Beristain 2016.)

be recruited for other movements such as stepping on a treadmill, suggesting that unlike locomotion, postural muscle activation requires supraspinal control.

An adult cat with a spinal transection can stand independently for only short periods of time and within a narrow range of stability; head turns in particular cause the animal to lose balance. What stability there is likely results from the broad base of support afforded by quadrupedal stance, the stiffness of the tonically contracting hind limb extensors that support the weight of the hindquarters, and active compensation by forelimbs that continue to produce postural responses. Humans with spinal cord injuries have various amounts of antigravity muscle tonus but lack automatic postural responses below the level of the lesion. These results emphasize that antigravity support and balance control are distinct mechanisms and that the control of balance requires the involvement of supraspinal circuits.

The Brain Stem and Cerebellum Integrate Sensory Signals for Posture

If spinal circuits alone are not capable of producing automatic postural responses, what supraspinal centers are responsible for these responses? Although the answer to this question remains unknown, good candidates include the brain stem and cerebellum, which are highly interconnected and work together to modulate the descending commands to spinal motor centers of the limbs and trunk. These regions have the input–output structure that would be expected of centers for postural control.

Muscle synergies for automatic postural responses may be organized in the brain stem, perhaps the reticular formation. However, adaptation of postural synergies to changes in the environment and task demands may require the cerebellum.

Two regions of the cerebellum influence orientation and balance: the vestibulocerebellum (nodulus, uvula, and fastigial nucleus) and the spinocerebellum (anterior lobe and interpositus nucleus). These regions are interconnected with the vestibular nuclei and reticular formation of the pons and medulla (see Figure 37–4). Lesions of the brain stem and vestibulocerebellum produce a variety of deficits in head and trunk control including a tendency to tilt from vertical, even with eyes open, suggesting a deficit in the internal representation of postural orientation. Lesions of the spinocerebellum result in excessive postural sway that is worse with the eyes closed, ataxia during walking, and hypermetric postural responses, suggesting

deficits in balance corrections. Certain regions in the pons and medulla facilitate or depress extensor tonus and could be involved in antigravity support.

The brain stem and cerebellum are sites of integration of sensory inputs, perhaps generating the internal model of body orientation and balance. Vestibular and visual inputs are distributed to brain stem centers (Chapters 25 and 27) and the vestibulocerebellum. The spinocerebellum receives signals from rapidly conducting proprioceptive and cutaneous fibers. More slowly conducting somatosensory fibers project to the vestibular nuclei and reticular formation.

Two major descending systems carry signals from the brain stem and cerebellum to the spinal cord and could trigger automatic postural responses for balance and orientation. The medial and lateral vestibulospinal tracts originate from the vestibular nuclei, and the medial and lateral reticulospinal tracts originate from the reticular formation of the pons and medulla (see Figure 37–5). Lesions of these tracts result in profound ataxia and postural instability. In contrast, lesions of the corticospinal and rubrospinal tracts have minimal effect on balance even though they produce profound disturbance of voluntary limb movements.

The Spinocerebellum and Basal Ganglia Are Important in Adaptation of Posture

Patients with spinocerebellar disorders such as alcoholic anterior-lobe syndrome and basal ganglia deficits such as Parkinson disease experience postural difficulties. Studies suggest that the spinocerebellum and basal ganglia play complementary roles in adapting postural responses to changing conditions.

The spinocerebellum is where the amplitude of postural responses is adapted based on experience. The basal ganglia are important for quickly adjusting the postural set when conditions suddenly change. Both the spinocerebellum and the basal ganglia regulate muscle tone and force for voluntary postural adjustments. They are not necessary, however, for triggering or constructing the basic postural patterns.

Patients with disorders of the spinocerebellum have difficulty modifying the magnitude of balance adjustments with practice, over the course of repeated trials, but can readily adapt postural responses immediately after a change in conditions based on sensory feedback. For example, a patient standing on a movable platform scales the size of postural responses appropriately when platform velocity is increased with each trial. These postural adjustments rely on velocity information, which is encoded by somatosensory inputs at the beginning of platform movement.

In contrast, patients with cerebellar disorders cannot scale the size of postural responses based on feedforward control using the anticipated amplitude of postural displacements. Because the amplitude of platform movement is not known until the platform has stopped moving, well after the initial postural response is complete, a subject cannot use feedback from the trial at hand to guide the response but must instead use his experience from previous trials to inform his response in a subsequent trial of the same amplitude. Whereas a healthy subject does this quite readily, a patient with spinocerebellar disorders is unable to efficiently adapt his postural responses based on recent experience (Figure 36–14A).

A healthy subject standing on a moveable platform is able to scale muscle activity during sudden backward motion of the platform to counteract the forward sway induced by the perturbation. A subject with spinocerebellar disease always overresponds, although the timing of muscle activation is normal (Figure 36–14B). As a result, this individual returns beyond the upright position and oscillates back and forth. Reminiscent of the hypermetria observed immediately after labyrinthectomy, cerebellar hypermetria may also result from loss of Purkinje cell inhibition on spinal motor centers.

A patient with Parkinson disease can, with sufficient practice, gradually modify his postural responses but has difficulty changing responses when conditions change suddenly. Such postural inflexibility is seen when initial posture changes. For example, when a normal subject switches from standing upright to sitting on a stool on a movable platform, the pattern of his automatic postural response to backward movement of the platform changes immediately. Because leg muscle activity is no longer necessary after the switch from standing to sitting, this component ceases to be recruited.

In contrast, a patient with Parkinson disease employs the same muscle activation pattern for both sitting and standing (Figure 36–15). L-DOPA replacement therapy does not improve the patient's ability to switch postural set. With repetition of trials in the seated posture, however, the leg muscle activity eventually disappears, showing that enough experience permits adaptation of postural responses. A patient with Parkinson disease also has difficulty when instructed to increase or decrease the magnitude of a postural response, a difficulty that is consistent with the inability to change cognitive sets quickly.

Patients with Parkinson disease have problems with postural tone and force generation in addition to

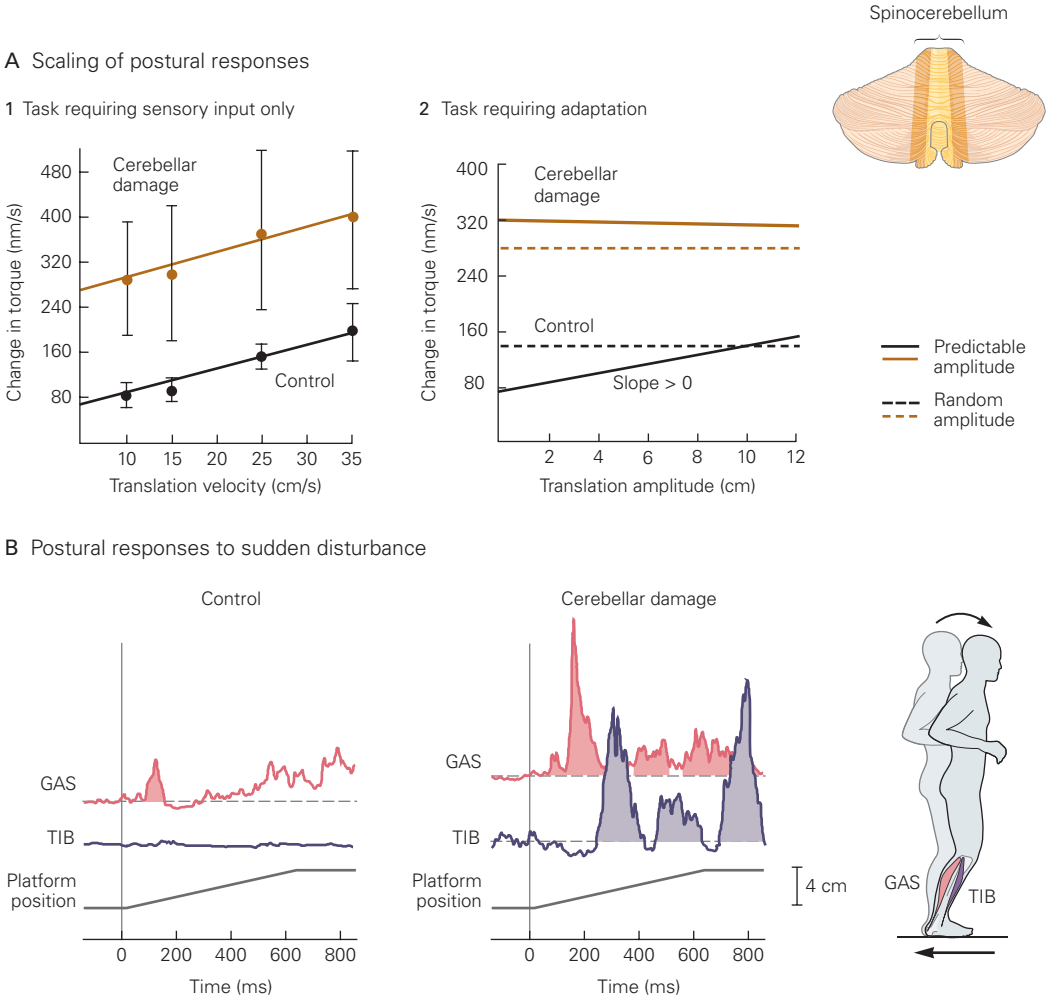

Figure 36–14 **The spinocerebellum has a role in adapting postural responses to changing conditions and in scaling postural responses to anticipated postural disturbances.** The spinocerebellum is important for adapting postural responses based on experience. Patients with a spinocerebellar disorder are able to use immediate sensory input, but not experience, to adjust automatic postural responses. (Adapted, with permission, from Horak and Diener 1994.)

A. 1. In this experiment, subjects stand on a platform that is moved horizontally; the velocity is increased on each trial. Maintaining balance requires scaling responses to the velocity of the platform using sensory feedback. The adjustments in a subject with a spinocerebellar disorder have the same regression coefficient (slope) as those of a control subject, even though in each trial the responses are larger and more variable than those of the control subject. **2.** When subjects are required to anticipate and adapt to platform translation, the postural adjustments in the spinocerebellar subject are compromised. When translation amplitude is random, responses are large, as if the subject expects a large translation. When trials with the same amplitude are repeated, a control subject learns to predict the amplitude of the disturbance and adjust his response. In contrast, a spinocerebellar subject shows no improvement in performance; he cannot use his experience in one trial to adjust his responses in subsequent trials. All responses are large, as if the subject always expects the large translation.

B. In this experiment, subjects stand on a platform that is moved backward (6 cm amplitude at 10 cm/s). In a control subject, the onset of movement evokes a small burst of activity in the gastrocnemius (**GAS**), an ankle extensor. In a subject with damage to the anterior lobe of the cerebellum, the muscle responses are overly large, with bursts of activity alternating between the gastrocnemius and its antagonist, the tibialis anterior (**TIB**).

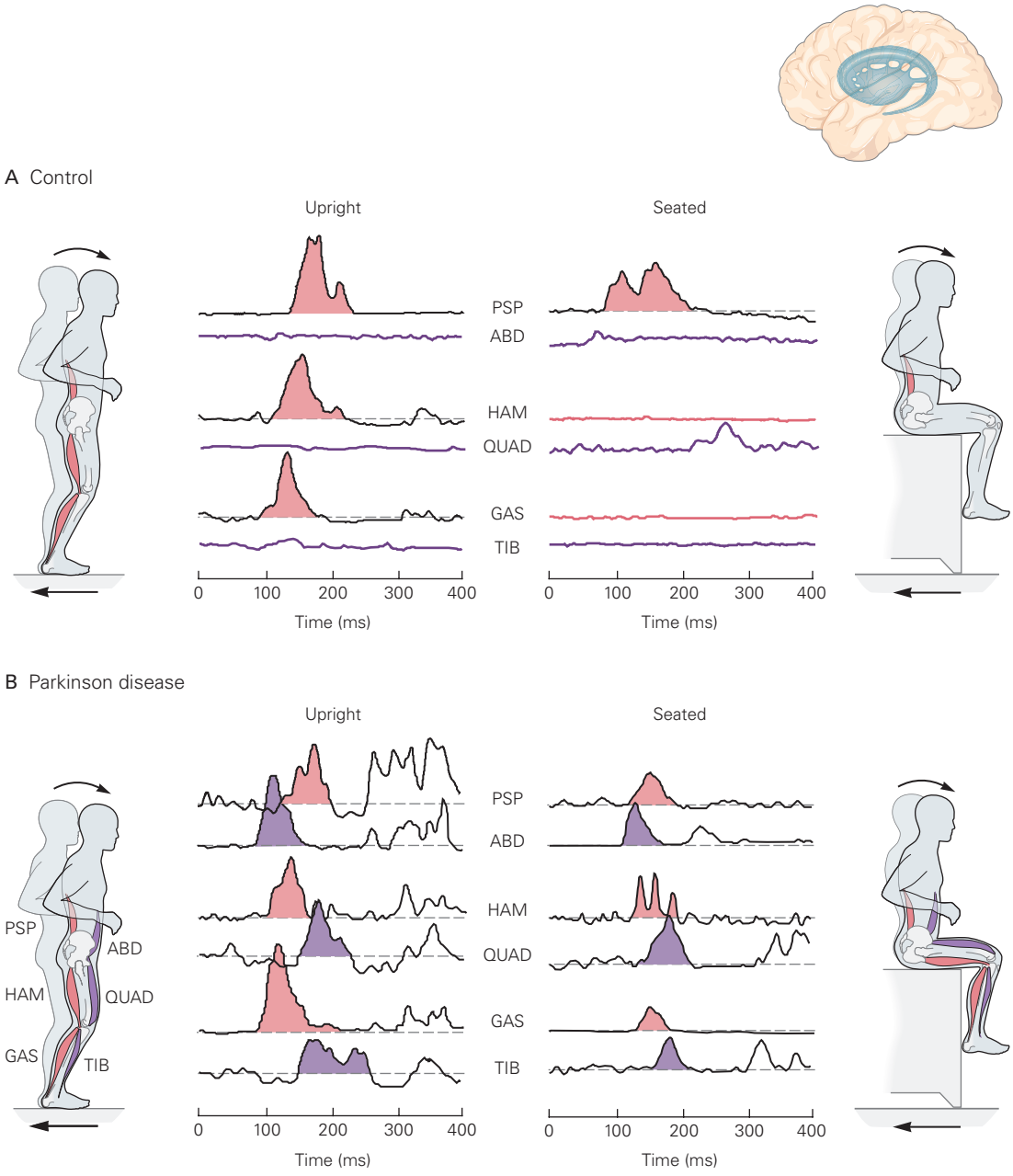

Figure 36–15 **The basal ganglia are important for adapting postural responses to a sudden change in initial conditions.** (Adapted, with permission, from Horak, Nutt, and Nashner 1992.)

A. When a normal subject switches from upright stance to sitting, he immediately modifies his response to backward movement of the support platform. The postural response to movement while seated does not involve the leg muscles—the gastrocnemius (**GAS**) and hamstrings (**HAM**)—but does activate the paraspinal muscles (**PSP**) and with shorter latency than in the response to movement while standing. (Abbreviations: **ABD**, abdominals; **QUAD**, quadriceps; **TIB**, tibialis anterior.)

B. A patient with Parkinson disease does not suppress the leg muscle response in the first trial after switching from standing to sitting. The postural response of this subject is similar for both initial positions: Antagonist muscles (**purple**) are activated along with agonists (**pink**).

an inability to adapt to changing conditions. The disease's bradykinesia (slowness of movement) is reflected in slow development of force in postural responses, and its rigidity is manifested in co-contraction. L-DOPA replacement greatly improves a patient's ability to generate not only forceful voluntary movements but also the accompanying postural adjustments, such as rising onto the toes and gait. However, neither the automatic postural response to an unexpected disturbance nor postural adaptation is improved by L-DOPA, suggesting that these functions involve the nondopaminergic pathways affected by Parkinson disease.

Cerebral Cortex Centers Contribute to Postural Control

Several areas of cerebral cortex influence postural orientation and equilibrium, including both anticipatory and automatic postural responses. Most voluntary movements, which are initiated in the cerebral cortex, require postural adjustments that must be integrated with the primary goal of the movement in both timing and amplitude. Where this integration occurs is not clear.

The cerebral cortex is more involved in anticipatory postural adjustments than in automatic postural reactions. However, recent electroencephalographic studies show that areas of cerebral cortex are activated by anticipation of a postural disturbance before an automatic postural response is initiated. This finding is consistent with the idea that the cortex optimizes balance control as part of motor planning.

The supplementary motor area and temporoparietal cortex have both been implicated in postural control. The supplementary motor area, anterior to the motor cortex, is likely involved with anticipatory postural adjustments that accompany voluntary movements. The temporoparietal cortex appears to integrate sensory information and may comprise internal models for perception of body verticality. Lesions of insular cortex can impair perception of the visual vertical, whereas lesions of superior parietal cortex impair perception of the postural vertical, and either of these defects may impair balance when standing on an unstable support.

Sensorimotor cortex receives somatosensory inputs signaling balance disturbances and postural responses. However, this region is not essential for automatic postural adjustments. Lesioning the motor cortex in cats impairs lifting of the forelimb in response to a light touch during stance but does not abolish the accompanying postural adjustment in the contralateral forelimb. Although the sensorimotor cortex is not responsible for postural adjustments, it may have a role in the process.

Behavioral studies, too, have implicated cortical processes in postural control. Control of posture, like control of voluntary movement, requires attention. When subjects must press a button following a visual or auditory cue while also maintaining balance, their reaction time increases with the difficulty of the task (balancing on one foot versus sitting, for example). Moreover, when subjects try to perform a cognitive task while actively maintaining posture, the performance of either or both can degrade. For example, when a subject is asked to count backward by threes while standing on one foot, both the cognitive task and postural adjustment deteriorate. The timing of automatic postural responses to unexpected disturbances is little affected by cognitive interference.

Balance control is also influenced by emotional state, thus implicating the limbic system in posture control. Fear of falling, for example, can increase postural tone and stiffness, reduce sway area, increase sway velocity, and alter balancing strategies in response to disturbances.

Finally, balance control is also influenced by attentional ability and demands, thus implicating the frontoparietal attention network. There is evidence of competition for central processing resources in dual task conditions, where a person must maintain balance and perform a concurrent cognitive task. Both postural control and cognitive performance may be impaired in dual-task conditions as compared to single-task conditions assessing either postural or cognitive performance in isolation. As cognitive demands increase, responses to postural perturbations are smaller in amplitude and occur at longer latency. However, when necessary, healthy individuals prioritize postural control over the cognitive task and demonstrate decreasing cognitive performance as postural demands increase. In contrast, individuals with nervous system disorders such as Parkinson disease may not prioritize postural control in dual-task situations and may be at increased risk for falls in dual-task situations.

Although the roles of specific areas of cerebral cortex in postural control are largely undefined, there is no doubt that the cortex is important for learning new, complex postural strategies. The cortex must be involved in the amazing improvement in balance and postural orientation of athletes and dancers who use cognitive information and advice from coaches. In fact, the cerebral cortex is involved in postural control each time we consciously maintain our balance while walking across a slippery floor, standing on a moving bus, or waiting tables on a rocking ship.

Highlights

1. The two goals of posture are balance and orientation. Balance control maintains the body in stable equilibrium to avoid falls. Postural orientation aligns the body segments with respect to each other and to the world, such as maintaining the head vertical.
2. A sudden displacement of the body center of mass while standing triggers ankle, hip, and/or stepping strategies to return the center of mass within the base of foot support.
3. Postural responses are fast and automatic, but adapt quickly to changes in environmental context, intention, and conditions. Postural responses can also be improved with practice.
4. Activation of centrally organized muscle synergies is used to control balance. This synergy organization simplifies the neural control so only a few central commands are required, instead of a separate command for each muscle, while allowing flexibility and adaptability for postural control.
5. Somatosensory, vestibular, and visual sensory modalities are integrated to form an internal representation of the body that the nervous system uses for postural orientation and balance control. Somatosensory signals trigger the fastest, largest postural responses and are most critical for control of postural sway in standing. Vestibular signals are particularly critical when standing on an unstable surface, when it is difficult to use somatosensory information for postural orientation. Visual inputs provide spatial orientation and motion information.
6. The body center of mass is often outside of the base of foot support during walking and running so balance is provided by adjusting foot placement and lateral trunk stability to control the center of mass with respect to the changing base of support.
7. The vestibulocerebellum and the spinocerebellum are interconnected with the vestibular nuclei and reticular formation of the brainstem for control of balance and postural orientation.
8. The basal ganglia are important for control of axial postural tone, adapting postural response strategies based on initial conditions, and anticipatory postural control. The cerebellum is important for adapting the magnitude of balance responses with practice, over the course of repeated trials, and for scaling the size of postural responses.
9. Posture control involves many brain areas from the brainstem to the frontal cortex, but the specific circuits involved in different types of posture control (automatic postural responses, anticipatory postural adjustments, body sway in stance, sensory integration for a body schema and verticality) have yet to be determined.

Fay B. Horak
Gammon M. Earhart

Suggested Reading

Chiba R, Takakusaki K, Ota J, Yozu A, Haga N. 2016. Human upright posture control models based on multisensory inputs; in fast and slow dynamics. Neurosci Res 104:96–104.

Cullen KE. 2016. Physiology of central pathways. In: JM Furman, T Lempert (eds). *Handbook of Clinical Neurology*, vol 137, pp 17–40. New York: Elsevier.

Dietz V. 1992. Human neuronal control of automatic functional movements—interaction between central programs and afferent input. Physiol Rev 72:33–69.

Horak FB. 2006. Postural orientation and equilibrium: what do we need to know about neural control of balance to prevent falls? Age Ageing 35(Suppl 2):ii7–ii11.

Horak FB, Macpherson JM. 1996. Postural orientation and equilibrium. In: LB Rowell, JT Shepherd (eds). *Handbook of Physiology, Section 12, Exercise: Regulation and Integration of Multiple Systems*, pp. 255–292. New York: Oxford Univ. Press.

Macpherson JM, Deliagina TG, Orlovsky GN. 1997. Control of body orientation and equilibrium in vertebrates. In: PSG Stein, S Grillner, AI Selverston, DG Stuart (eds). *Neurons Networks and Motor Behavior*, pp. 257–267. Cambridge, MA: MIT Press.

Massion J. 1994. Postural control system. Curr Opin Neurobiol 4:877–887.

Woollacott M, Shumway-Cook A. 2002. Attention and the control of posture and gait: a review of an emerging area of research. Gait Posture 16:1–14.

References

Beristain X. 2016. Gait. In: Salardini A, Biller J (eds). *The Hospital Neurology Book*. Beijing, China: McGraw-Hill Education.

Brandt T, Paulus W, Straube A. 1986. Vision and posture. In: W Bles, T Brandt (eds). *Disorders of Posture and Gait*, pp. 157–175. Amsterdam: Elsevier.

Cavallari P, Bolzoni F, Burttinit C, Esposti R. 2016. The organization and control of intra-limb anticipatory postural adjustments and their role in movement performance. Front Hum Neurosci 10:525.

Cordo PJ, Nashner LM. 1982. Properties of postural adjustments associated with rapid arm movements. J Neurophysiol 47:287–302.

Darriot J, Mohsen J, Cullen K. 2015. Rapid adaptation of multisensory integration in vestibular pathways. Front Syst Neurosci 16:1–5.

De Havas J, Gomi H, Haggard P. 2017. Experimental investigations of control principles of involuntary movement: a comprehensive review of the Kohnstamm phenomenon. Exp Brain Res 235:1953–1997.

Dunbar DC, Horak FB, Macpherson JM, Rushmer DS. 1986. Neural control of quadrupedal and bipedal stance: implications for the evolution of erect posture. Am J Phys Anthropol 69:93–105.

Gera G, Fling BW, Van Ooteghem K, Cameron M, Frank JS, Horak FB. 2016. Postural motor learning deficits in people with MS in spatial but not temporal control of center of mass. Neurorehabil Neural Repair 30:722–730.

Gurfinkel VS, Levick YS. 1991. Perceptual and automatic aspects of the postural body scheme. In: J Paillard (ed). *Brain and Space*, pp. 147–162. Oxford: Oxford Univ. Press.

Hof AL, Curtze C. 2016. A stricter condition for standing balance after unexpected perturbations. J Biomech 49:580–585.

Horak FB, Diener HC. 1994. Cerebellar control of postural scaling and central set in stance. J Neurophysiol 72:479–493.

Horak FB, Nashner LM. 1986. Central programming of postural movements: adaptation to altered support-surface configurations. J Neurophysiol 55:1369–1381.

Horak FB, Nutt J, Nashner LM. 1992. Postural inflexibility in parkinsonian subjects. J Neurol Sci 111:46–58.

Inglis JT, Horak FB, Shupert CL, Jones-Rycewicz C. 1994. The importance of somatosensory information in triggering and scaling automatic postural responses in humans. Exp Brain Res 101:159–164.

Jacobs JV, Horak FB. 2007. Cortical control of postural responses. J Neural Transm 114:1339–1348.

Jahn K, Deutschländer A, Stephan T, Strupp M, Wiesmann M, Brandt T. 2004. Brain activation patterns during imagined stance and locomotion in functional magnetic resonance imaging. Neuroimage 22:1722–1731.

Lee WA, Michaels CF, Pai YC. 1990. The organization of torque and EMG activity during bilateral handle pulls by standing humans. Exp Brain Res 82:304–314.

MacKinnon CD, Winter DA. 1993. Control of whole body balance in the frontal plane during human walking. J Biomech 26:633–644.

Macpherson JM. 1988. Strategies that simplify the control of quadrupedal stance. 2. Electromyographic activity. J Neurophysiol 60:218–231.

Macpherson JM, Everaert DG, Stapley PJ, Ting LH. 2007. Bilateral vestibular loss in cats leads to active destabilization of balance during pitch and roll rotations of the support surface. J Neurophysiol 97:4357–4367.

Macpherson JM, Fung J. 1999. Weight support and balance during perturbed stance in the chronic spinal cat. J Neurophysiol 82:3066–3081.

Maki BE, McIlroy WE. 1997. The role of limb movements in maintaining upright stance: the "change-in-support" strategy. Phys Ther 77:488–507.

Maurer C, Mergner T, Peterka RJ. 2006. Multisensory control of human upright stance. Exp Brain Res 171:231–250.

McMahon TA, Bonner JT. 1983. *On Size and Life*. New York: W.H. Freeman.

Mittelstaedt H. 1998. Origin and processing of postural information. Neurosci Biobehav Rev 22:473–478.

Otten W. 1999. Balancing on a narrow ridge: biomechanics and control. Phil Trans R Soc Lond B 354:869–875.

Peterka RJ. 2002. Sensorimotor integration in human postural control. J Neurophysiol 88:1097–1118.

Peterson DS, Horak FB. 2016. Neural control of walking in people with Parkinsonism. Physiology 3:95–107.

Rousseaux M, Honore J, Saj A. 2014. Body representations and brain damage. Neurophysiol Clin 44:59–67.

Stapley PJ, Ting LH, Kuifu C, Everaert DG, Macpherson JM. 2006. Bilateral vestibular loss leads to active destabilization of balance during voluntary head turns in the standing cat. J Neurophysiol 95:3783–3797.

Takakusaki K. 2017. Functional neuroanatomy for posture and gait control. J Mov Disord 10:1–17.

Ting LH, Chiel HJ, Trumbower RD, et al. 2015. Neuromechanical principles underlying movement modularity and their implications for rehabilitation. Neuron 86:38–54.

37

The Cerebellum

The cerebellum constitutes only 10% of the total volume of the brain but contains more than one-half of its neurons. The cerebellar cortex comprises a series of highly regular, repeating units, each of which contains the same basic microcircuit. Different regions of the cerebellum receive projections from distinct brain and spinal structures and then project back to the brain. The similarity of the architecture and physiology in all regions of the cerebellum implies that different regions of the cerebellum perform similar computational operations on different inputs.

The symptoms of cerebellar damage in humans and experimental animals provide compelling evidence that the cerebellum participates in the control of movement. The symptoms, in addition to being diagnostic for clinicians, thus help define the possible roles of the cerebellum in controlling behavior.

Several fundamental principles define our understanding of the physiological function of the cerebellum. First, the cerebellum acts in advance of sensory feedback arising from movement, thus providing feedforward control of muscular contractions. Second, to achieve such control, the cerebellum relies on internal models of the body to process and compare sensory inputs with copies of motor commands. Third, the cerebellum plays a special role in motor and perceptual timing. Fourth, the cerebellum is critical for adapting

and learning motor skills. Finally, the primate cerebellum has extensive connectivity to nonmotor areas of the cerebral cortex, suggesting it performs similar functions in the performance and learning of motor and nonmotor behaviors.

Damage of the Cerebellum Causes Distinctive Symptoms and Signs

Damage Results in Characteristic Abnormalities of Movement and Posture

Disorders that involve the cerebellum typically disrupt normal movement patterns, demonstrating the cerebellum's critical role in movement. Patients describe a loss of the automatic, unconscious nature of most movements. In the early 20th century, Gordon Holmes recorded the self-report of a man with a lesion of his right cerebellar hemisphere: "movements of my left arm are done subconsciously, but I have to think out each movement of the right arm. I come to a dead stop in turning and have to think before I start again."

This has been interpreted as an interruption in the automatic level of processing by cerebellar inputs and outputs. With a malfunctioning cerebellum, it seems that the cerebral cortex needs to play a more active role in programming the details of motor actions. Importantly, individuals with cerebellar damage do not experience the paralysis that can be associated with cerebral cortical damage. Instead, they show characteristic abnormalities in voluntary movement, walking, and posture that have provided important clues about cerebellar function.

The most prominent symptom of cerebellar disorders is *ataxia*, or lack of coordination of movement. Ataxia is a generic term used to describe the collective motor features associated with cerebellar damage. People with cerebellar disorders make movements that qualitatively appear jerky, irregular, and highly variable. *Limb ataxia* during reaching is characterized by curved hand paths that are *dysmetric* in that they over- or undershoot the intended target and oscillate (Figure 37–1A). Patients often break a movement down into components, presumably in an effort to simplify control of multi-joint movements (*decomposition of movement*). Yet this may not be effective. For example, patients often have difficulty holding the shoulder steady while moving the elbow, a deficit thought to be due to poor predictions of how the movement at the elbow mechanically affects the shoulder (Figure 37–1B). If prediction fails, then patients are forced to try to steady the shoulder using time-delayed feedback, which is less effective.

At the end of reaching movements, there can be marked oscillation as the hand approaches the target. This *action* (or *intention*) *tremor* is the result of a series of erroneous, overshooting attempts to correct the movement. It largely disappears when the eyes are shut, suggesting that it is driven by time-delayed visual feedback of the movement. Finally, patients show abnormalities in the rate and regularity of repeated movements, a sign referred to as *dysdiadochokinesia* (Greek, impaired alternating movement) that can be readily demonstrated when a patient attempts to perform rapid alternating movements (Figure 37–1C).

People with cerebellar damage also exhibit *gait ataxia* and poor balance. When walking, they take steps that are irregularly timed and placed. They have difficulty shifting their weight from one foot to the other, which can lead to falling. The trunk oscillates when they are unsupported in sitting, standing, and during walking, particularly as they start, stop, or turn. A wide stepping pattern with feet spread apart is common and is thought to be a compensatory measure to improve stability.

Other signs that are commonly observed with cerebellar dysfunction can also occur with damage to other brain regions. People with cerebellar damage often have slurred speech with irregular timing (dysarthria); repetitive to-and-fro movements of the eyes with a slow and fast phase (nystagmus); and reduced resistance to passive limb displacements (hypotonia), which is thought to be related to so-called "pendular reflexes" often observed in cerebellar patients. In patients with cerebellar disease, the leg may oscillate like a pendulum many times after a knee jerk produced by a tap on the patellar tendon with a reflex hammer, instead of coming to rest immediately.

Damage Affects Specific Sensory and Cognitive Abilities

It is now known that cerebellar damage affects proprioceptive abilities (the sense of limb position and movement), but only during active movement. Proprioceptive acuity—the sense of the position and movement of the limbs—is normally more precise for active movements than for passive movements. Cerebellar patients show normal proprioceptive acuity when they have to judge which of two passive movements is larger. However, their proprioceptive acuity is worse than that of healthy individuals when they move a limb actively. One interpretation of these findings is that the cerebellum normally helps to predict how active movements will unfold, which would be important for movement coordination and for perceiving where the limbs are during active movements.

Damage to the cerebellum also affects cognitive processes, although these deficits are less obvious compared to the pronounced disturbances of sensory–motor function. Some of the earliest studies implicating the cerebellum in a range of cognitive tasks involved functional imaging to study the brain activity during behavior in healthy individuals. For example, in a study using positron emission tomography to image the brain activity of subjects during silent reading, reading aloud, and speech, areas of the cerebellum involved in the control of mouth movements were more active when subjects read aloud than when they read silently. Surprisingly, however, cerebellar activation was more pronounced in a task with greater cognitive load, when subjects were asked to name a verb associated with a noun; a subject might respond with "bark" if he or she saw the word "dog." Compared with simply reading aloud, the word-association task produced a pronounced increase in activity within the right lateral cerebellum. Consistent with this finding, a patient with damage in the right cerebellum could not learn a word-association task.

By now, many studies have revealed clear deficits in executive function, visual spatial cognition, language, and emotional processing after cerebellar damage. There appears to be some regional specificity within the cerebellum for different types of cognitive function. Damage to the midline cerebellum or *vermis* seems to be related to emotional or affective dysregulation, likely due to its interconnectivity with limbic structures. Damage to the right cerebellar hemisphere is related to language and verbal dysfunction, presumably because this hemisphere is interconnected with the left cerebral cortical hemisphere. Likewise, damage to the left cerebellar hemisphere is related to visuospatial dysfunction, probably because this hemisphere is interconnected with the right cerebral cortical hemisphere. Additionally, studies that examine cognitive dysfunction produce variable results; patients perform normally in one study but not another. Some studies show that cognitive deficits are most pronounced when patients are tested shortly after damage to the cerebellum and that compensations at the level of cerebral cortex might gradually make up for

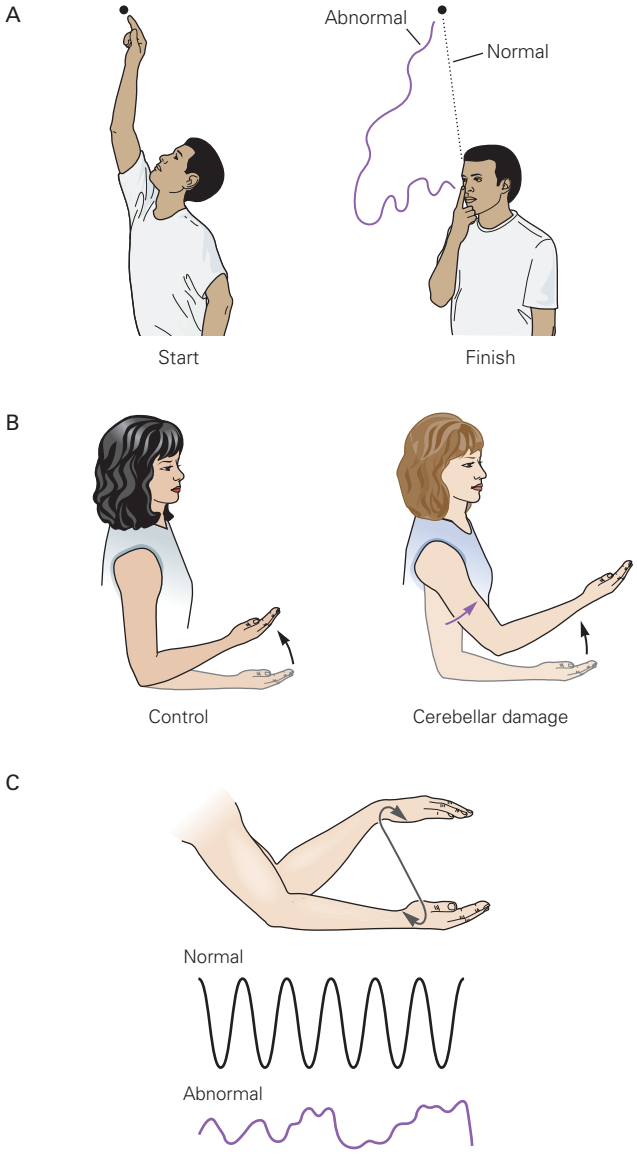

Figure 37–1 (Left) Typical defects observed in cerebellar diseases.

A. A cerebellar patient moving his arm from a raised position to touch the tip of his nose exhibits inaccuracy in range and direction (dysmetria) and moves his shoulder and elbow separately (decomposition of movement). Tremor increases as the finger approaches the nose.

B. Failure of compensation for interaction torques can account for cerebellar ataxia. Subjects flex their elbows while keeping their shoulder stable. In both the control subject and the cerebellar patient, the net elbow torque is large because the elbow is moved. In the control subject, there is relatively little net shoulder torque because the interaction torques are automatically cancelled by muscle torques. In the cerebellar patient, this compensation fails; the muscle torques are present but are inappropriate to cancel the interaction torques. As a result, the patient cannot flex her elbow without causing a large perturbation of her shoulder position. (Adapted, with permission, from Bastian, Zackowski, and Thach 2000.)

C. A subject was asked to alternately pronate and supinate the forearm while flexing and extending at the elbow as rapidly as possible. Position traces of the hand and forearm show the normal pattern of alternating movements and the irregular pattern (dysdiadochokinesia) typical of cerebellar disorder.

cerebellar loss of function. However, cognitive deficits may be more robust and long lasting when cerebellar damage is acquired in childhood.

Thus, cognitive deficits arising from cerebellar damage sometimes can be difficult to characterize. What is clear is that the motor dysfunction after cerebellar loss is more obvious than cognitive dysfunction. It may be that cortical regions of motor control are less able to compensate for losses of cerebellar motor control compared to cortical compensation for impairment of cerebellar computations involved in cognitive processes.

The Cerebellum Indirectly Controls Movement Through Other Brain Structures

Understanding the anatomy of the cerebellum and how it interacts with different brain structures is vital to understanding its function. In this section, we consider the general anatomy of the cerebellum as well as its inputs and outputs.

The Cerebellum Is a Large Subcortical Brain Structure

The cerebellum occupies most of the posterior cranial fossa. It is composed of an outer mantle of gray matter (the cerebellar cortex), internal white matter, and three pairs of deep nuclei: the fastigial nucleus, the interposed nucleus (itself composed of the emboliform and globose nuclei), and the dentate nucleus (Figure 37–2A). The surface of the cerebellum is highly convoluted, with many parallel folds or folia (Latin, leaves).

Two deep transverse fissures divide the cerebellum into three lobes. The primary fissure on the dorsal surface separates the anterior and posterior lobes, which together form the body of the cerebellum (Figure 37–2A). The posterolateral fissure on the ventral surface separates the body of the cerebellum from the smaller flocculonodular lobe (Figure 37–2B). Each lobe extends across the cerebellum from the midline to the most lateral tip. In the orthogonal, anterior-posterior direction, two longitudinal furrows separate three regions: the midline vermis (Latin, worm) and the two cerebellar hemispheres, each split into intermediate and lateral regions (Figure 37–2D).

The cerebellum is connected to the dorsal aspect of the brain stem by three symmetrical pairs of peduncles: the inferior cerebellar peduncle (also called the restiform body), the middle cerebellar peduncle (or brachium pontis), and the superior cerebellar peduncle (or brachium conjunctivum). Most of the output axons of the cerebellum arise from the deep nuclei and project through the superior cerebellar peduncle to other brain areas. The main exception is a group of Purkinje cells in the flocculonodular lobe that project to vestibular nuclei in the brain stem.

The Cerebellum Connects With the Cerebral Cortex Through Recurrent Loops

Many parts of the cerebellum form recurrent loops with the cerebral cortex. The cerebral cortex projects to the lateral cerebellum through relays in the pontine nuclei. In turn, the lateral cerebellum projects back to the cerebral cortex through relays in the thalamus. Peter Strick and his colleagues used viruses for transneuronal tracing in nonhuman primates to show that this recurrent circuit is organized as a series of parallel closed loops, where a given part of the cerebellum connects reciprocally with a specific part of the cerebral cortex (Figure 37–3A). Through these reciprocal connections, the cerebellum interacts with vast regions of the neocortex, including substantial connections to motor, prefrontal, and posterior parietal regions. More recently, Strick's group also demonstrated disynaptic connections between the cerebellum and basal ganglia in nonhuman primates.

The resting state connectivity between the cerebellum and cerebral cortex in humans was studied using fMRI scans of 1,000 subjects. Correlations in activity in different regions of the brain were assessed at low frequencies, measured by blood flow while subjects were at rest. They found that different regions of the cerebellum are functionally connected with cerebral cortical regions across the entire cerebral cortex (Figure 37–3C). Taken together, these studies demonstrate the vast impact the cerebellum could have on many aspects of brain function.

Different Movements Are Controlled by Functional Longitudinal Zones

The cerebellum can be broadly divided into three areas that have distinctive roles in different kinds of movements: the vestibulocerebellum, spinocerebellum, and cerebrocerebellum (Figure 37–4).

The *vestibulocerebellum* consists of the flocculonodular lobe and is the most primitive part of the cerebellum. It receives vestibular and visual inputs, projects to the vestibular nuclei in the brain stem, and participates in balance, other vestibular reflexes, and eye movements. It receives information from the semicircular canals and the otolith organs, which sense the head's motion and its position relative to gravity. Most of this

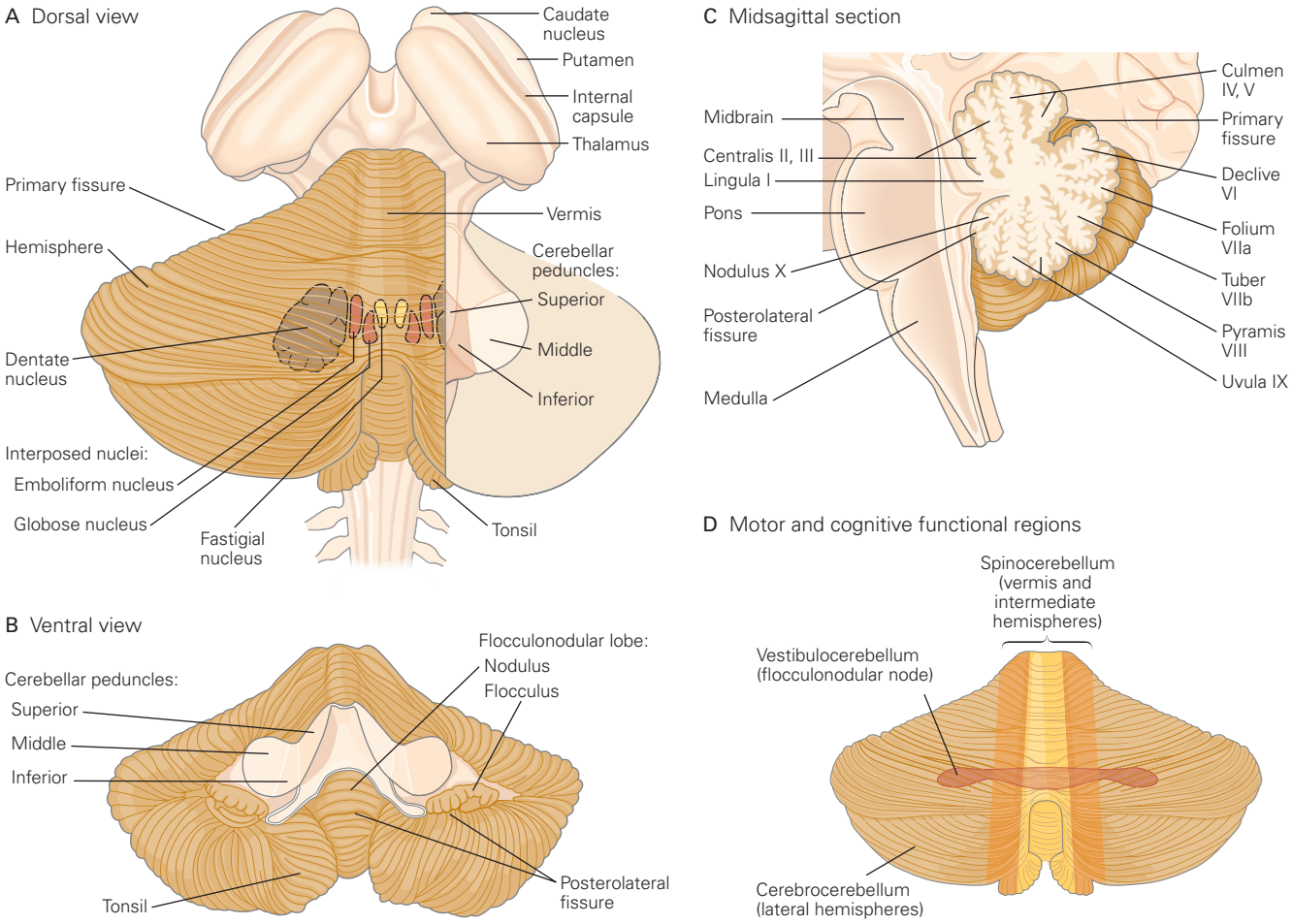

Figure 37–2 Gross features of the cerebellum. (Adapted, with permission, from Nieuwenhuys, Voogd, and van Huijzen 1988.)

A. Part of the right hemisphere has been cut away to reveal the underlying cerebellar peduncles.

B. The cerebellum is shown detached from the brain stem.

C. A midsagittal section through the brain stem and cerebellum shows the branching structure of the cerebellum. The cerebellar lobules are labeled with their Latin names and Larsell's Roman numeral designations. (Reproduced, with permission, from Larsell and Jansen 1972.)

D. Functional regions of the cerebellum.

vestibular input arises from the vestibular nuclei in the brain stem. The vestibulocerebellum also receives visual input, from both the pretectal nuclei that lie deep in the midbrain beneath the superior colliculus and the primary and secondary visual cortex through the pontine and pretectal nuclei.

The vestibulocerebellum is unique in that its output bypasses the deep cerebellar nuclei and proceeds directly to the vestibular nuclei in the brain stem. Purkinje cells in the midline parts of the vestibulocerebellum project to the lateral vestibular nucleus to modulate the lateral and medial vestibulospinal tracts, which predominantly control axial muscles and limb extensors to assure balance during stance and gait (Figure 37–5A). Disruption of these projections through lesions or disease impairs equilibrium.

The most striking deficits following lesions of the lateral vestibulocerebellum are in smooth-pursuit eye movement toward the side of the lesion. A patient with a lesion of the left lateral vestibulocerebellum can smoothly track a target that is moving to the right, but only poorly tracks motion to the left, using saccades predominantly (Figure 37–6A). These patients can have normal vestibulo-ocular reflex responses to head rotations but cannot suppress the reflex by fixating an object that rotates with the head (Figure 37–6B). These deficits occur commonly if the lateral

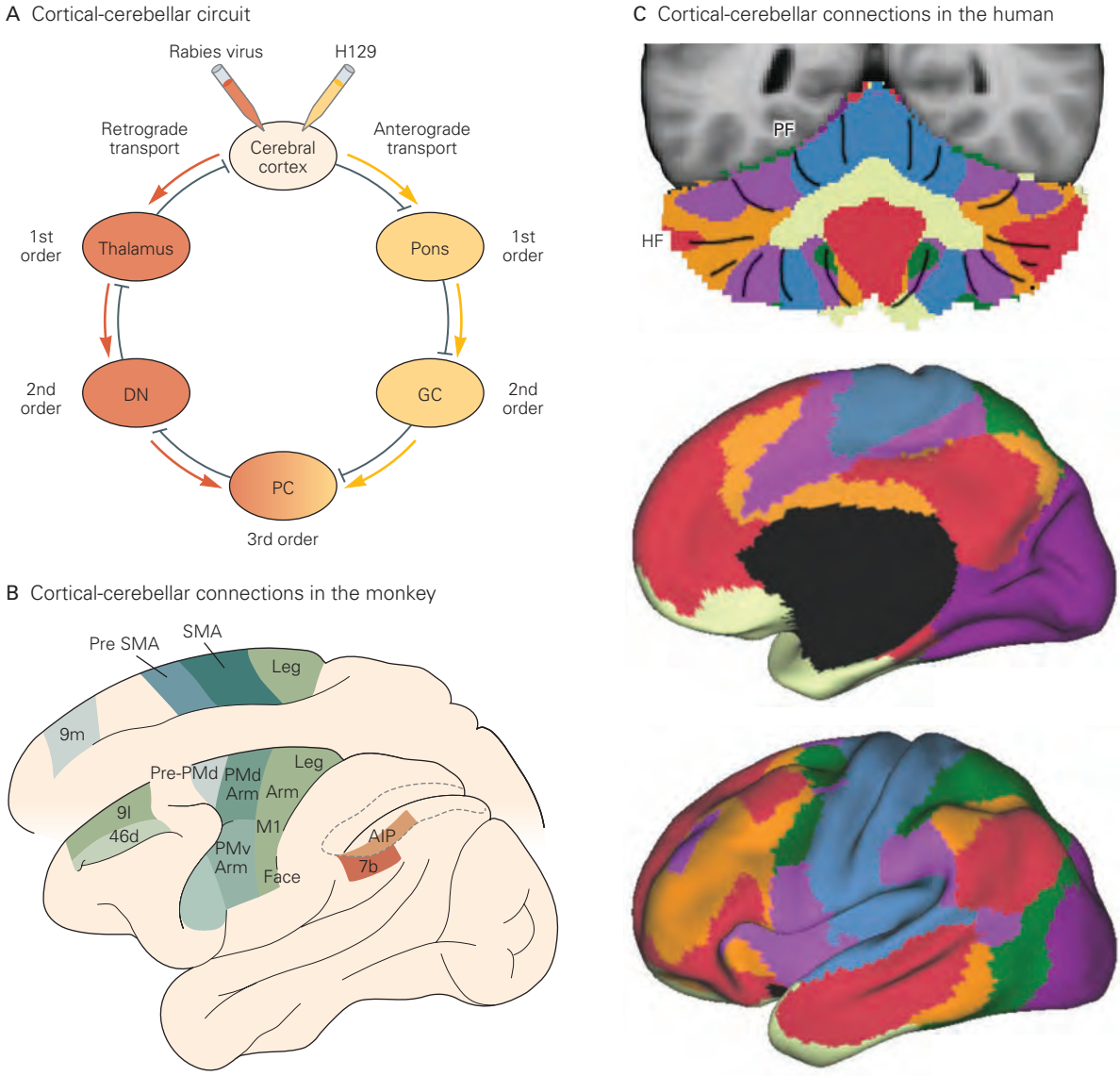

Figure 37–3 **The cerebellum connects to many areas of cerebral cortex.** (Parts A and B adapted, with permission, from Bostan, Dum, and Strick 2013. Copyright © 2013 Elsevier Ltd. part C adapted, with permission, from Buckner et al. 2011. Copyright © 2011 American Physiological Society.)

A. The cortical-cerebellar circuit in monkeys was traced with fluorescence-labeled transsynaptic viruses that can move in an anterograde or retrograde direction. Injection into the cerebral cortex of a retrograde virus, such as rabies virus, will label neurons that project to it and, by crossing synapses, can label second- and possibly higher-order neurons in a pathway. These are shown here in **red** as first-order (thalamus), second-order (deep nucleus), and third-order neurons (Purkinje cells). Injection into the cerebral cortex of an anterograde virus, such as the H129 strain of herpes simplex virus, will label neurons that are targets of the cerebral cortex. These are shown here in **yellow** as first-order (pons), second-order (granule cells), and third-order neurons (Purkinje cells). (Abbreviations: **DN**, dentate nuclei; **GC**, granule cell; **H129**, strain of herpes simplex virus; **PC**, Purkinje cell rabies virus.)

B. Areas of the cerebral cortex connected to the cerebellum. The numbers refer to cytoarchitectonic areas. (Abbreviations: **AIP**, anterior intraparietal area; **M1**, face, arm, and leg areas of the primary motor cortex; **PMd arm**, arm area of the dorsal premotor area; **PMv arm**, arm area of the ventral premotor area; **PrePMd**, predorsal premotor area; **PreSMA**, presupplementary motor area; **SMA arm**, arm area of the supplementary motor area.)

C. Color-coded coronal section of the human cerebellum (**top**) and lateral and medial views of the human cerebral cortex (**bottom**) created from resting state functional connectivity maps (based on functional magnetic resonance imaging scans of 1,000 subjects). Colors correspond to cerebellar and cerebral areas that are connected. Note that the cerebellum is functionally connected with nearly all cerebral areas. (Abbreviations: **HF**, horizontal fissure; **PF**, primary fissure.)

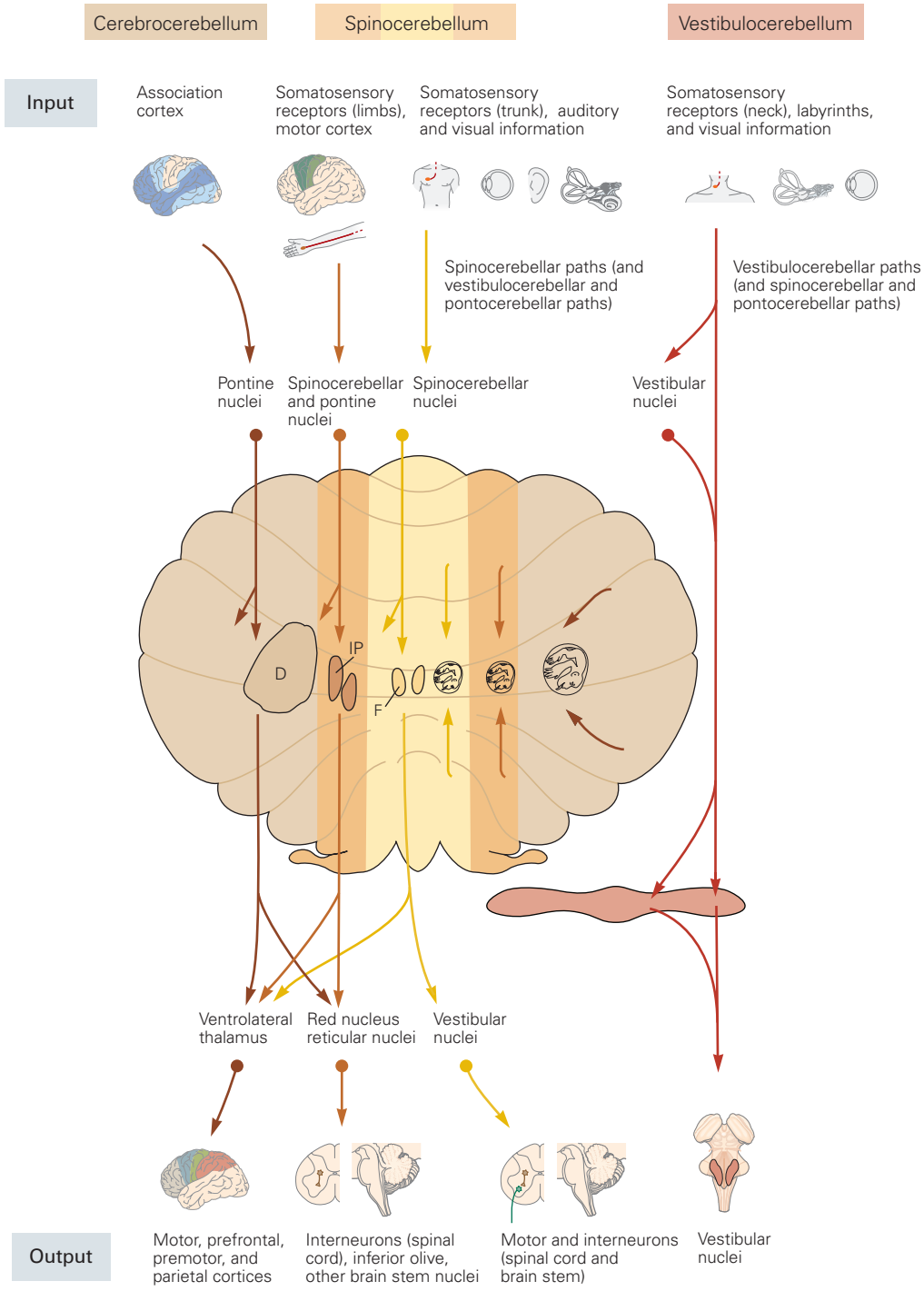

Figure 37–4 **The three functional regions of the cerebellum have different inputs and different output targets.** The cerebellum is shown unfolded, and **arrows** indicate the inputs and outputs of the different functional areas. The body maps in the deep nuclei are based on anatomical tracing and single-cell recordings in nonhuman primates. (Abbreviations: **D**, dentate nucleus; **F**, fastigial nucleus; **IP**, interposed nucleus.) (Adapted, with permission, from Brooks and Thach 1981).

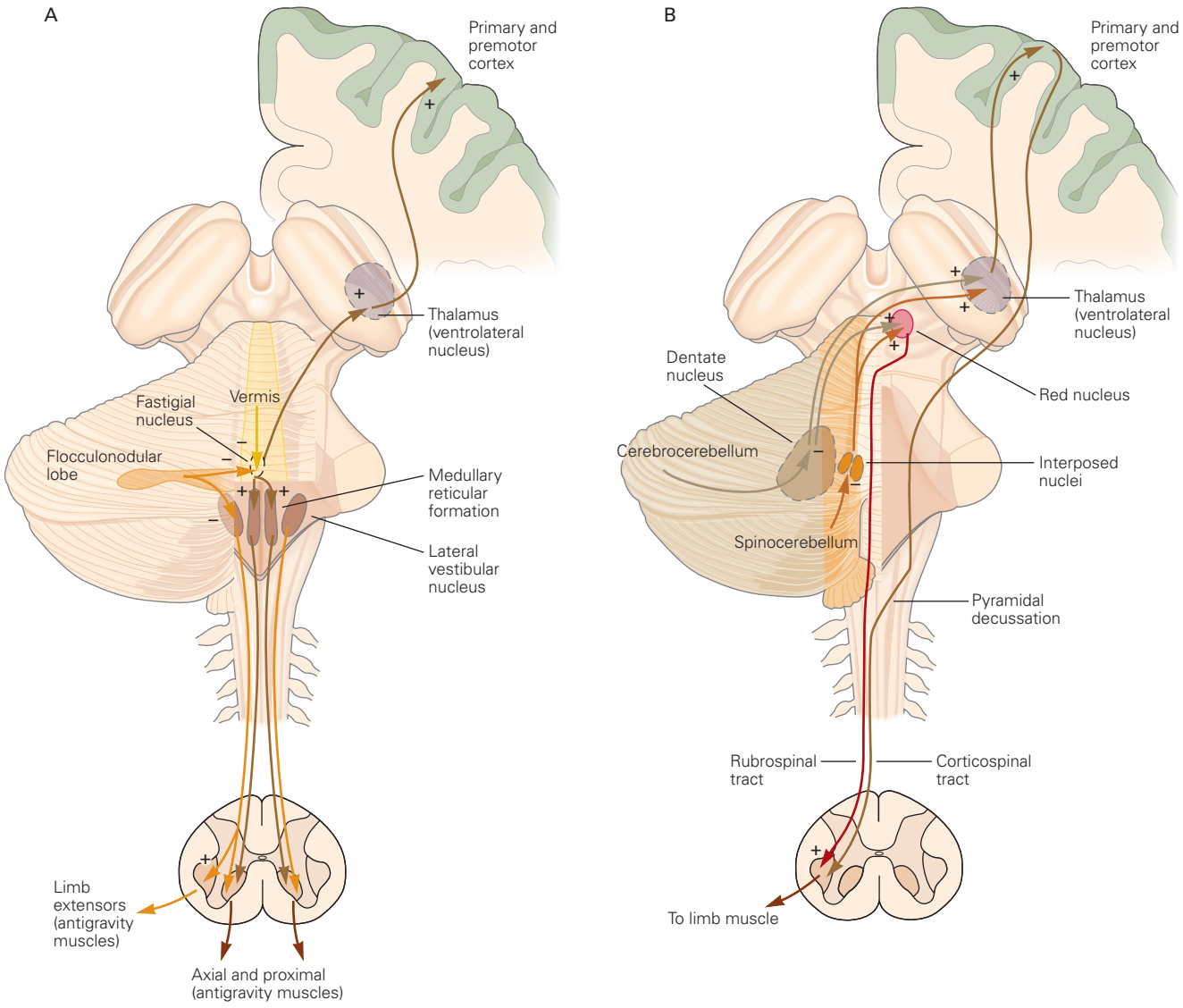

Figure 37–5 Input and output pathways of the cerebellum.

A. Nuclei in the vestibulocerebellum and the vermis control proximal muscles and limb extensors. The vestibulocerebellum (flocculonodular lobe) receives input from the vestibular labyrinth and projects directly to the vestibular nuclei. The vermis receives input from the neck and trunk, the vestibular labyrinth, and retinal and extraocular muscles. Its output is focused on the ventromedial descending systems of the brain stem, mainly the reticulospinal and vestibulospinal tracts and the corticospinal fibers acting on medial motor neurons. The oculomotor connections of the vestibular nuclei have been omitted for clarity.

B. Nuclei in the intermediate and lateral parts of the cerebellar hemispheres control limb and axial muscles. The intermediate part of each hemisphere (spinocerebellum) receives sensory information from the limbs and controls the dorsolateral descending systems (rubrospinal and corticospinal tracts) acting on the ipsilateral limbs. The lateral area of each hemisphere (cerebrocerebellum) receives cortical input via the pontine nuclei and influences the motor and premotor cortices via the ventrolateral nucleus of the thalamus, and directly influences the red nucleus.

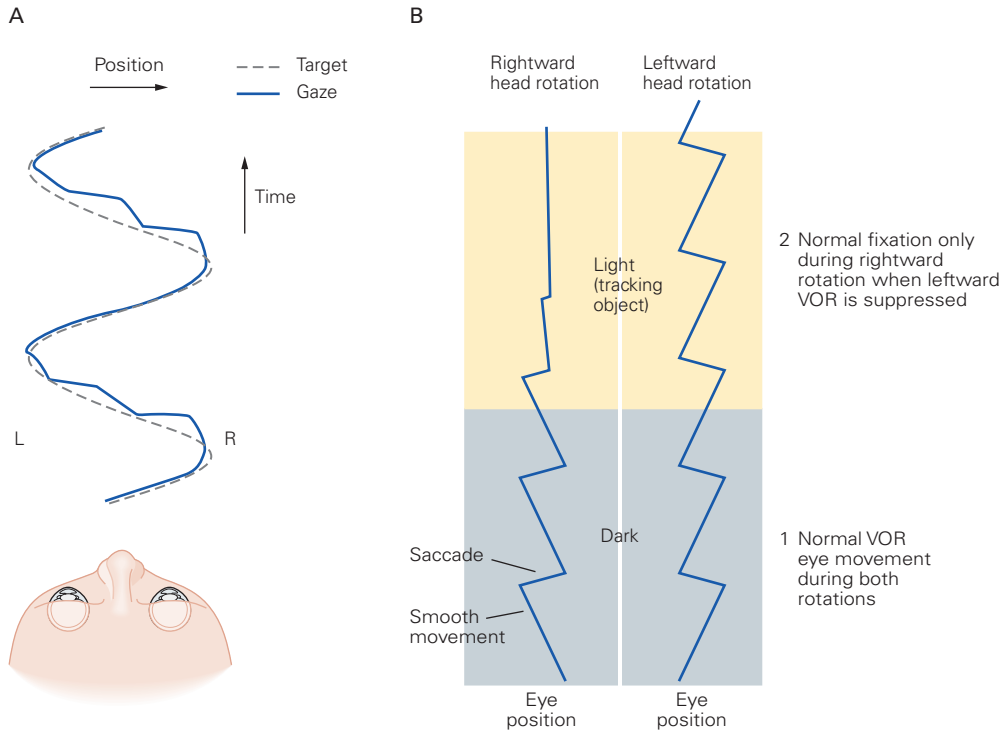

Figure 37–6 Lesions in the vestibulocerebellum have large effects on smooth-pursuit eye movements.

A. Sinusoidal target motion is tracked with smooth-pursuit eye movements as the target moves from left (**L**) to right (**R**). With a lesion of the left vestibulocerebellum, smooth pursuit is punctuated by saccades when the target moves from right to left.

B. In the same patient, responses to vestibular stimulation are normal, whereas object fixation is disrupted during leftward rotation. The traces on the left and right show the eye movements evoked by rightward and leftward head rotation experienced in separate sessions. In each session the patient sat in a chair that rotated continuously in one direction, first in the dark then in the light while fixating on a target that moves along with him. (**1**) In the dark, the eyes show a normal vestibulo-ocular reflex (**VOR**) during rotation in both directions: The eyes move smoothly in the direction opposite to the head's rotation, then reset with saccades in the direction of head rotation. (**2**) In the light, the eye position during rightward head rotation is normal: Fixation on the target is excellent and the vestibulo-ocular reflex is suppressed. During leftward head rotation, however, the subject is unable to fixate on the object and the vestibulo-ocular reflex cannot be suppressed.

vestibulocerebellum is compressed by an acoustic neuroma, a benign tumor that grows on the eighth cranial nerve as it courses directly beneath the lateral vestibulocerebellum.

The *spinocerebellum* is composed of the vermis and intermediate parts of the cerebellar hemispheres (Figure 37–4). It is so named because it receives extensive input from the spinal cord via the dorsal and ventral spinocerebellar tracts. These pathways convey information about touch, pressure, and limb position as well as the spiking activity of spinal interneurons. Thus, these inputs provide the cerebellum with varied information about the changing state of the organism and its environment.

The vermis receives visual, auditory, and vestibular input as well as somatic sensory input from the head and proximal parts of the body. It projects by way of the fastigial nucleus to cortical and brain stem regions that give rise to the medial descending systems controlling proximal muscles of the body and limbs (Figure 37–5A). The vermis governs posture and locomotion as well as eye movements. For example, lesions of the oculomotor region of the vermis cause saccadic eye movements that overshoot their target, much as patients with cerebellar damage make arm movements that overshoot their target.

The adjacent intermediate parts of the hemispheres also receive somatosensory input from the limbs. Neurons here project to the interposed nucleus, which provides inputs to lateral corticospinal and rubrospinal systems on the contralateral side of the brain and controls the more distal muscles of the limbs and digits (Figure 37–5B). Because corticospinal and rubrospinal systems cross the midline as they descend to the spinal cord, cerebellar lesions disrupt ipsilateral limb movements.

The *cerebrocerebellum* comprises the lateral parts of the hemispheres (Figure 37–4). These areas are phylogenetically the most recent and are much larger relative to the rest of the cerebellum in humans and apes than in monkeys and cats. Almost all of the inputs to and outputs from this region involve connections with the cerebral cortex. The output is transmitted through the dentate nucleus, which projects via the thalamus to contralateral motor, premotor, parietal, and prefrontal cortices. The dentate nucleus also projects to the contralateral red nucleus. The lateral hemispheres have many functions but seem to participate most extensively in planning and executing movement. They also have a role in cognitive functions unconnected with motor planning, such as visuospatial and language processes. There is now some correlative evidence implicating the cerebellar hemispheres in aspects of schizophrenia (Chapter 60), dystonia (Chapter 38), and autism (Chapter 62).

Two important principles of cerebellar function have emerged from recordings of the action potentials of single neurons in the cerebellar cortex and deep cerebellar nuclei during arm movements, along with controlled, temporary inactivation of specific cerebellar regions.

First, neurons in these areas discharge vigorously in relation to voluntary movements. Cerebellar output is related to the direction and speed of movement. The deep nuclei are organized into somatotopic maps of different limbs and joints, as in the motor cortex, although the organization of the cerebellar cortex has been characterized as "fractured somatotopy" with multiple disconnected and partial maps. Moreover, the interval between the onset of modulation of the firing of cerebellar neurons and movement is remarkably similar to that for neurons in the motor cortex. This result emphasizes the cerebellum's participation in recurrent circuits that operate synchronously with the cerebral cortex.

Second, the cerebellum provides feedforward control of muscle contractions to regulate the timing of movements. Rather than awaiting sensory feedback, cerebellar output anticipates the muscular contractions that will be needed to bring a movement smoothly, accurately, and quickly to its desired endpoint. Failure of these mechanisms causes the intention tremor of cerebellar disorders. For example, a rapid single-joint movement is initiated by the contraction of an agonist muscle and terminated by an appropriately timed contraction of the antagonist. The contraction of the antagonist starts early in the movement, well before there has been time for sensory feedback to reach the brain, and therefore must be programmed as part of the movement. When the dentate and interposed nuclei are experimentally inactivated, however, contraction of the antagonist muscle is delayed until the limb has overshot its target. The programmed anticipatory contraction of the antagonist in normal movements is replaced by a correction driven by sensory feedback. This correction is itself dysmetric and results in another error, necessitating a new adjustment (Figure 37–7).

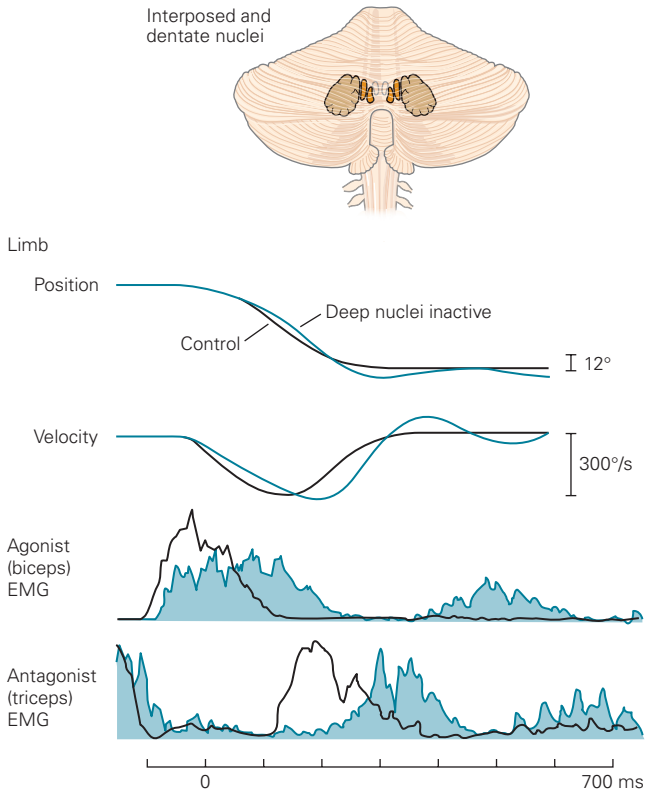

Figure 37–7 **The interposed and dentate nuclei are involved in the precise timing of agonist and antagonist activation during rapid movements.** The interposed (medial) and dentate (lateral) nuclei are highlighted in the drawing of the cerebellum. The records of limb movement show how a monkey normally makes a rapid elbow flexion limb movement and attempts to make the same movement when the interposed and dentate nuclei are inactivated by cooling. The electromyographic (EMG) traces show limb position and velocity and EMG responses of the biceps and triceps muscles. When the deep nuclei are inactivated, activation of the agonist (biceps) becomes slower and more prolonged. Activation of the antagonist (triceps), which is needed to stop the movement at the correct location, is likewise delayed and protracted so that the initial movement overshoots its appropriate extent. Delays in successive phases of the movement produce oscillations similar to the terminal tremor seen in patients with cerebellar damage.

The Cerebellar Cortex Comprises Repeating Functional Units Having the Same Basic Microcircuit

The cellular organization of the microcircuit in the cerebellar cortex is striking, and one of the premises of cerebellar research has been that the details of the microcircuit are an important clue to how the cerebellum works. In this section, we describe three major features of the microcircuit.

The Cerebellar Cortex Is Organized Into Three Functionally Specialized Layers

The three layers of the cerebellar cortex contain distinct kinds of neurons and are functionally specialized (Figure 37–8).

The deepest, or *granular layer*, is the input layer. It contains a vast number of granule cells, estimated at 100 billion, which appear in histological sections as small, densely packed, darkly stained nuclei. The granular layer also contains a few larger Golgi cells and, in some cerebellar regions, a smattering of other neurons such as cells of Lugaro, unipolar brush cells, and chandelier cells. The mossy fibers, one of the two principal afferent inputs to the cerebellum, terminate in this layer. The bulbous terminals of the mossy fibers excite granule cells and Golgi neurons in synaptic complexes called *cerebellar glomeruli* (Figure 37–8). As we will see later when discussing recurrent circuits in the cerebellum, Golgi cells inhibit granule cells.

The middle or *Purkinje cell layer* is the output layer of the cerebellar cortex. This layer consists of a single sheet of Purkinje cell bodies, each 50 to 80 μm in diameter. The fan-like dendritic trees of Purkinje cells extend upward into the molecular layer where they receive inputs from the second major type of afferent to the cerebellum, the climbing fibers, as well as from granule cells and inhibitory interneurons. Purkinje cell axons conduct the entire output of the cerebellar cortex, projecting to the deep nuclei in the underlying white matter or to the vestibular nuclei in the brain stem, where they release the inhibitory transmitter GABA (γ-aminobutyric acid).

The outermost or *molecular layer* contains the spatially polarized dendrites of Purkinje cells, which extend approximately 1 to 3 mm in the anterior-posterior direction but occupy only a very narrow territory in the medial-lateral direction. The molecular layer contains the cell bodies and dendrites of two types of "molecular layer interneurons," the stellate and basket cells, both of which inhibit Purkinje cells. It also contains the axons of the granule cells, called the *parallel fibers* because they run parallel to the long axis of the folia (Figure 37–8). Parallel fibers run perpendicular to the dendritic trees of the Purkinje cells and thus have the potential to form a few synapses with each of a large number of Purkinje cells.

The Climbing-Fiber and Mossy-Fiber Afferent Systems Encode and Process Information Differently

The two main types of afferent fibers in the cerebellum, the mossy fibers and climbing fibers, probably mediate different functions. Both form excitatory synapses with neurons in the deep cerebellar nuclei and in the cerebellar cortex. However, they terminate in different layers of the cerebellar cortex, affect Purkinje cells through very different patterns of synaptic convergence and divergence, and produce different electrical events in the Purkinje cells.

Climbing fibers originate in the inferior olivary nucleus in the brain stem and convey sensory information to the cerebellum from both the periphery and the cerebral cortex. The climbing fiber is so named because each one wraps around the proximal dendrites of a Purkinje neuron like a vine on a tree, making numerous synaptic contacts (Figure 37–9). Each Purkinje neuron receives synaptic input from only a single climbing fiber, but each climbing fiber contacts 1 to 10 Purkinje cells that are arranged topographically along a parasagittal strip in the cerebellar cortex. Indeed, the axons from clusters of related olivary neurons terminate in thin parasagittal strips that extend across several folia, and the Purkinje cells from one strip converge on a common group of neurons in the deep nuclei.

Climbing fibers have an unusually powerful influence on the electrical activity of Purkinje cells. Each action potential in a climbing fiber generates a protracted, voltage-gated Ca^{2+} conductance in the soma and dendrites of the postsynaptic Purkinje cell. This results in prolonged depolarization that produces an electrical event called a "complex spike": an initial large-amplitude action potential followed by a high-frequency burst of smaller-amplitude action potentials (Figure 37–9). Whether these smaller spikes are transmitted down the Purkinje cell's axon is not clear. In awake animals, complex spikes occur spontaneously at low rates, usually around one per second. Specific sensory or motor events cause one or two complex spikes that occur at precise times in relation to those events.

Mossy fibers originate from cell bodies in the spinal cord and brain stem. They carry sensory information from the periphery as well as both sensory information and corollary discharges that report the current movement command (Chapter 30) from the cerebral cortex

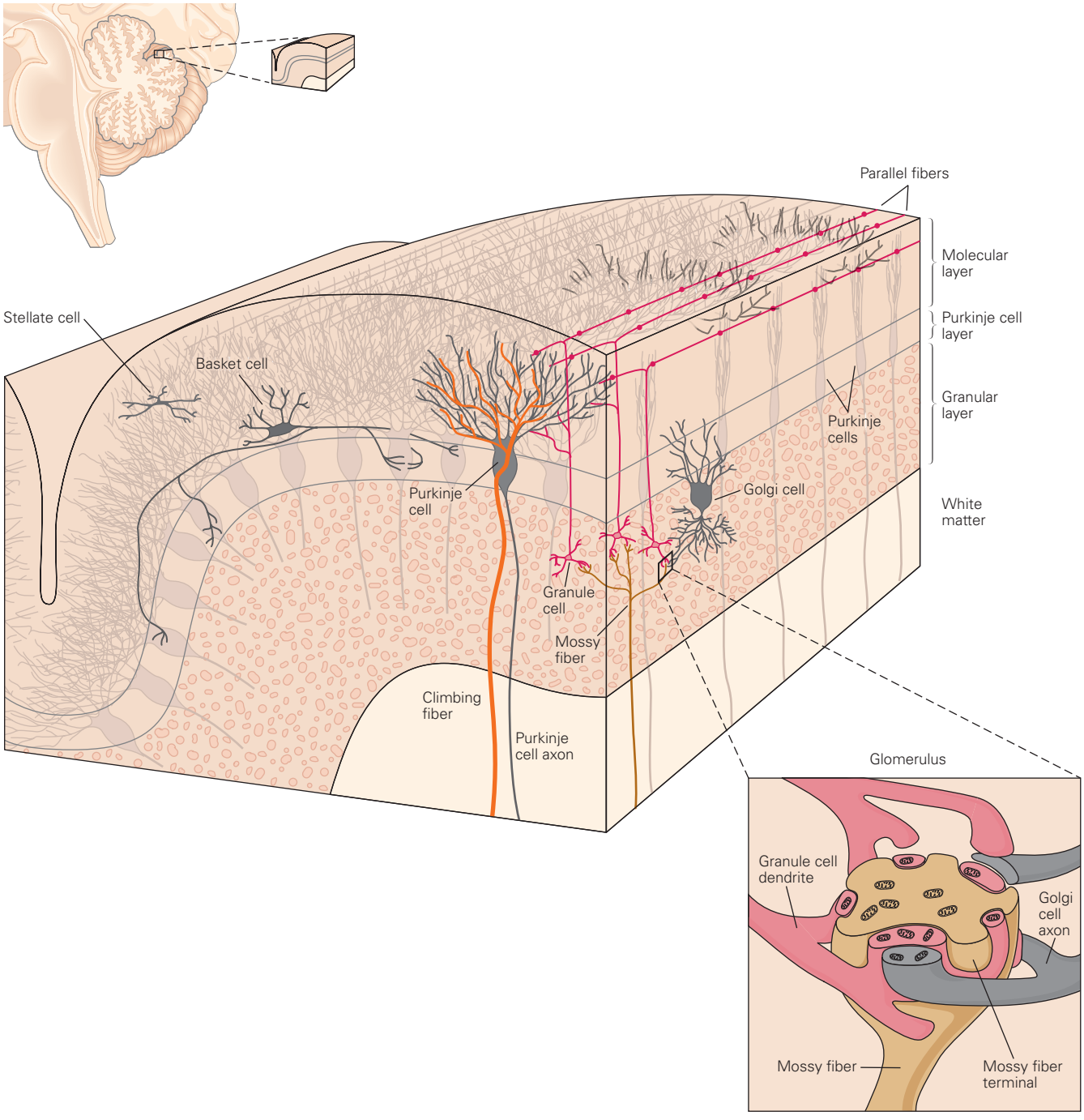

Figure 37–8 The cerebellar cortex contains five main types of neurons organized into three layers. A vertical section of a single cerebellar folium illustrates the general organization of the cerebellar cortex. The detail of a cerebellar glomerulus in the granular layer is also shown. A glomerulus is the synaptic complex formed by the bulbous axon terminal of a mossy fiber and the dendrites of several Golgi and granule cells. Mitochondria are present in all of the structures in the glomerulus, consistent with their high metabolic activity.

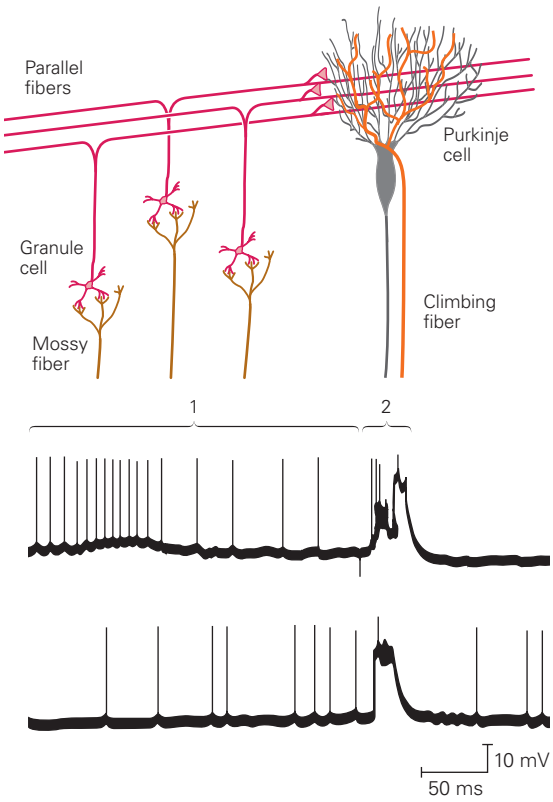

Figure 37–9 Simple and complex spikes recorded intracellularly from a cerebellar Purkinje cell. Simple spikes are produced by mossy-fiber input (**1**), whereas complex spikes are evoked by climbing-fiber synapses (**2**). (Reproduced, with permission, from Martinez, Crill, and Kennedy 1971.)

via the pontine nuclei. Mossy fibers affect Purkinje cells via multisynaptic pathways that have intriguing patterns of convergence and divergence. Individual mossy fibers, acting through granule cells and parallel fibers, have a tiny influence on Purkinje cell output, but collectively, the whole population of mossy fibers has massive effects on cerebellar output.

Mossy fibers form excitatory synapses on the dendrites of granule cells in the granular layer (Figure 37–8). Each granule cell has three to five short dendrites, and each dendrite receives contacts from a single mossy fiber. Due to this paucity of inputs, the spatial integration by a granule cell of its different mossy fiber synapses is not extensive; however, the cell can be the site of convergence of mossy fibers from multiple sensory modalities and motor corollary discharge. The next synaptic relay, between the granule cell axons and Purkinje cells, distributes information with very wide divergence and convergence. The parallel fibers allow each mossy fiber to influence a large number of Purkinje cells, and each Purkinje cell is contacted potentially by axons from somewhere between 200,000 and 1 million granule cells. Importantly, in response to changing conditions there seems to be tremendous potential for adaptation of cerebellar output at the synapses between parallel fibers and Purkinje cells. It appears that only a small fraction of these synapses are active at any given time.

Parallel fibers produce brief, small excitatory potentials in Purkinje cells (Figure 37–9). These potentials converge in the cell body and spread to the initial segment of the axon where they generate conventional action potentials called "simple spikes" that propagate down the axon. In awake animals, Purkinje cells emit a steady stream of simple spikes, with spontaneous firing rates as high as 100 per second even when an animal is sitting quietly. Purkinje cells fire at rates as high as several hundred spikes per second during active eye, arm, and face movements.

The climbing-fiber and mossy-fiber/parallel-fiber systems seem to be specialized for transmission of different kinds of information. Climbing fibers cause complex spikes that seem specialized for event detection. Although complex spikes occur only infrequently, synchronous firing in multiple climbing fibers enables them to signal important events. Synchrony seems to arise partly because signaling between many neurons in the inferior olivary nucleus occurs electrotonically (at gap-junction channels). In contrast, the high firing rates of the simple spikes in Purkinje cells can be modulated up or down in a graded way by mossy-fiber inputs, and thereby encode the magnitude and duration of peripheral stimuli or centrally generated behaviors.

The Cerebellar Microcircuit Architecture Suggests a Canonical Computation

The cerebellar microcircuit is replicated many times across the surface of the cerebellar cortex. This repeating architecture and pattern of convergence and divergence has led to the suggestion that since every such module has the same architecture and pattern of convergence and divergence, the cerebellar cortex performs the same basic "canonical" computation on all of its inputs, and that it potentially transforms cerebellar inputs in a similar way for all cerebellar output systems. Inspection of a diagram of the cerebellar microcircuit (Figure 37–10) reveals a number of different computational components. One general feature is the existence of parallel excitatory and inhibitory pathways to the Purkinje cells or deep cerebellar nuclei. The other general feature is the prevalence of recurrent loops.

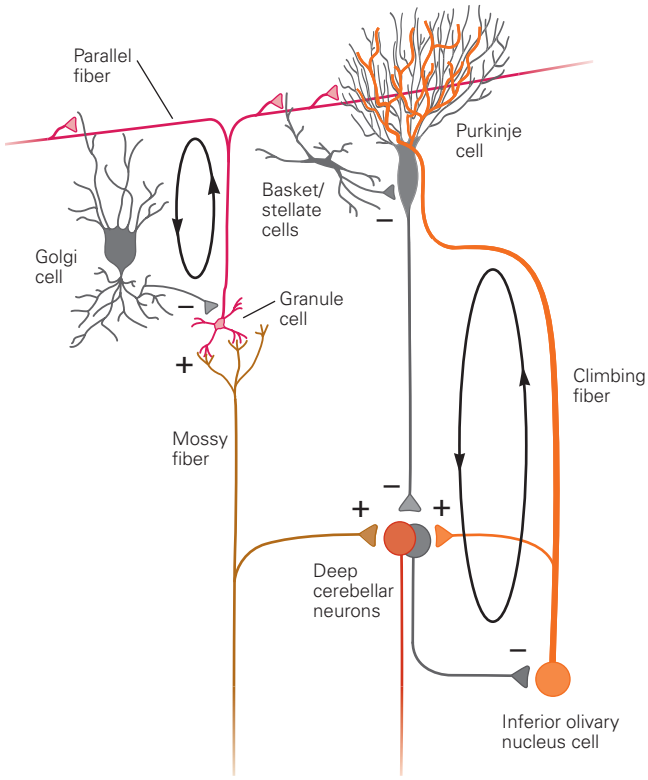

Figure 37–10 Synaptic organization of the cerebellar microcircuit. Excitation and inhibition converge both in the cerebellar cortex and in the deep nuclei. Recurrent loops involve Golgi cells within the cerebellar cortex and the inferior olive outside the cerebellum. (Adapted, with permission, from Raymond, Lisberger, and Mauk 1996. Copyright © 1996 AAAS.)

Parallel Feedforward Excitatory and Inhibitory Pathways

The excitatory inputs relayed from mossy fibers to granule cells to Purkinje cells work in parallel with feedforward inhibitory inputs through the two molecular layer interneurons, the stellate and basket cells. Both of these interneurons receive inputs from parallel fibers and inhibit Purkinje cells, but they have quite different architectures.

The short axons of stellate cells contact the nearby dendrites of Purkinje cells. Thus, a stellate cell acts locally in the sense that it and the Purkinje cell it inhibits are excited by the same parallel fibers. In contrast, a basket cell acts more widely. Its axon runs perpendicular to the parallel fibers (Figure 37–8) and creates flanks of inhibition on Purkinje cells that receive input from parallel fibers other than those that excite the basket cell. Stellate cells affect Purkinje cells via synapses that are on distal dendrites, whereas basket cells make powerful synapses on the cell body of Purkinje cells and seem to be positioned for a powerful influence on Purkinje cell simple spiking. Remarkably, even 60 years after the architecture of the cerebellar microcircuit was described, the functional role of molecular layer interneurons remains a mystery.

Convergence of excitatory and inhibitory pathways is a predominant feature also in the deep cerebellar nuclei. Here, inhibitory inputs from Purkinje cells converge with excitatory inputs from axon collaterals of mossy and climbing fibers (Figure 37–10). Thus, a mossy fiber affects target neurons in the deep nuclei in two ways: directly by excitatory synapses and indirectly by pathways through the cerebellar cortex and the inhibitory Purkinje cells. Neurons of the deep cerebellar nuclei are active spontaneously even in the absence of synaptic inputs, so the inhibitory output of the Purkinje cells both modulates this intrinsic activity and sculpts the excitatory signals transmitted from mossy fibers to the deep nuclei. In almost all parts of the cerebellum, collaterals from climbing fibers to the deep cerebellar nuclei create the opportunity for a similar interaction of excitatory and inhibitory inputs.

Recurrent Loops

An important recurrent loop is contained entirely within the cerebellar cortex and employs Golgi cells to sculpt the activity of the granule cells, the input elements in the cerebellar cortex. Golgi cells receive a few large excitatory inputs from mossy fibers, many smaller excitatory inputs from parallel fibers, and inhibitory inputs from neighboring Golgi cells. The GABAergic terminals from Golgi cells inhibit granule cells (Figure 37–10) and thereby regulate the activity of granule cells and the signals conveyed by the parallel fibers. This loop is evidence that important processing may occur within the granular layer. It may shorten the duration of bursts in granule cells, limiting the magnitude of the excitatory response of granule cells to their mossy fiber inputs, or could ensure that the granule cells respond only when a certain number of their mossy fiber inputs are active.

A second recurrent loop provides Purkinje cells with a way to regulate their own climbing fiber inputs (Figure 37–10). Purkinje cells inhibit GABAergic inhibitory neurons in the deep cerebellar nuclei that project to the inferior olive. When the simple-spike firing of a group of Purkinje cells decreases, the activity of these inhibitory interneurons increases, leading to decreases in the excitability of neurons in the inferior olive. The decreased excitability of the inferior olive reduces both the probability of action potentials in climbing fibers that project to the original group of Purkinje cells and the duration of each burst of climbing fiber action

potentials. In the section on cerebellar learning, we will see how this recurrent loop could allow the cerebellar cortex to control the inputs that cause adaptive changes in the synapses on its Purkinje cells.

The Cerebellum Is Hypothesized to Perform Several General Computational Functions

We know that the cerebellum is important for motor control and some nonmotor functions. Even though we do not yet know how the cerebellar circuit controls these functions, we are able to identity aspects of the control that seem to be particularly "cerebellar." These include reliable feedforward control, internal control of timing, integration of sensory inputs with corollary discharge, and state estimation through internal models.

The Cerebellum Contributes to Feedforward Sensorimotor Control

Sensory feedback is by its nature delayed. Therefore, when a movement is initiated there is a period of time before any useful sensory feedback is received about the movement. We saw earlier that cerebellar damage causes movement disorders that appear to result from out-of-date sensory feedback. If so, it is reasonable to assume that the cerebellum regulates and coordinates movement by preprogramming and coordinating commands for muscular contraction prior to the arrival of useful sensory feedback. The cerebellar output anticipates the muscular contractions that will be needed to bring a movement smoothly, accurately, and quickly to the desired endpoint, and uses sensory feedback mainly to monitor and improve its own performance.

Like neurons in the motor cortex, cerebellar neurons are activated before movement. Still, lesion studies and the symptoms in human motor disorders imply that the cerebellum and motor cortex play very different roles in movement. Lesions of the cerebellum disrupt the accuracy and coordination of voluntary movement, while lesions of the cerebral cortex largely prevent movement.

In addition, the pattern of cerebellar activity, not simply the rate of activity, conveys information for movement control. This is illustrated in mouse models of cerebellar disease. Deletion of certain ion channels produces excessive variability of Purkinje cell simple-spike firing patterns, which seems to lead to ataxia. This suggests that the regularity of cerebellar activity must be closely regulated to achieve normal movement.

The Cerebellum Incorporates an Internal Model of the Motor Apparatus

To program the correct muscle contractions for a smooth, accurate arm movement, the cerebellum needs to have some information about the physical configuration of the arm. Thus, it needs to create and maintain what are called "internal models" of the motor apparatus (Chapter 30). Internal models allow the cerebellum to perform a computation that helps the brain make good estimates of the exact muscle forces needed to move an arm in a desired manner.

An accurate *inverse dynamic* model of the arm, for example, can process sensory data about the current posture of the arm and automatically generate a sequence of properly timed and scaled commands to move the hand to a new desired position. An accurate *forward dynamic* model does the opposite: It processes a copy of a motor command and makes a prediction about the upcoming kinematics (ie, position and speed) of the arm movement. Recordings of the output of the cerebellum have provided evidence compatible with the idea that the cerebellum contains both types of models and that they are used to program both arm and eye movements.

One reason that the cerebellum may need these types of models for motor control is because of the complexities associated with moving linked segments of the body. Consider the mechanics of making a simple arm movement. Because of the mechanics of the arm and the momentum it develops when moving, movement of the forearm alone causes inertial forces that passively move the upper arm. If a subject wants to flex or extend the elbow without simultaneously moving the shoulder, then muscles acting at the shoulder must contract to prevent its movement. These stabilizing contractions of the shoulder joint occur almost perfectly in healthy subjects but not in patients with cerebellar damage, who experience difficulty controlling the inertial interactions among multiple segments of a limb (Figure 37–1B). As a result, patients exhibit greater inaccuracy of multi-joint versus single-joint movements.

In conclusion, the cerebellum uses internal models to allow it to preprogram a sequence of muscle contractions that will generate smooth, accurate movement. It also anticipates the forces that result from the mechanical properties of a moving limb. We do not yet know what these internal models look like in terms of the activity of cerebellar neurons, the circuits that operate as internal models, or how the cerebellar output is transformed into muscle forces. However, given that the properties of the limbs change throughout life, we can be confident that the cerebellum's learning capabilities

are involved in adapting these internal models to help generate the most proficient movements.

The Cerebellum Integrates Sensory Inputs and Corollary Discharge

Sensory signals converge in the cerebellum with motor signals that are called a corollary discharge (or efference copy) because they report commands that are being sent to motor nerves at the same time. For example, some neurons in the dorsal spinocerebellar tract relay inputs from sensory afferents in the spinal cord and transmit sensory signals to the cerebellum. In contrast, the neurons in the spinal cord that give rise to the axons in the ventral spinocerebellar tract receive the same afferent and descending inputs as do spinal motor neurons, and they transmit the final motor command back to the cerebellum. The interaction of sensory signals and corollary discharge allows comparison of the plans for a movement with the sensory consequences. This comparison occurs to some degree at Purkinje cells, but we now know that at least some granule cells receive converging sensory and corollary discharge inputs and could perform the comparison.

Internal models and corollary discharge together provide one possible explanation of the role of the cerebellum in movement. To be able to program accurate movements the cerebellum must be able to estimate the state of the motor system through sensory feedback and knowledge of prior motor activity. Next, it must combine information on the state of the motor system with the goals of the next movement and use internal models of the effector to help create commands for muscle forces that will generate an accurate and efficient movement. During the movement, the cerebellum must monitor movement performance through sensory feedback. Current thinking is that much of this is done by an internal model that converts corollary discharge into predictions of the sensory feedback. The cerebellum then compares real and predicted sensory feedback to determine a sensory prediction error and uses the sensory prediction error to guide corrective movements and learning.

Using a paradigm that required monkeys to ignore the sensory signals caused by their own movement, Kathy Cullen and colleagues have identified a neural correlate of a sensory prediction error in the deep cerebellar nuclei. Specifically, they studied the vestibular sensory signals that result from an animal's active head movements. They showed that the brain attenuates or even eliminates the vestibular sensory signals caused by one's own active head movement in order to better detect unpredictable vestibular signals due to the environment. However, when the head is effectively made heavier by adding resistance via a mechanical device, the vestibular sensory signals no longer match the predicted sensory signals that normally would attenuate the vestibular input. They showed that the cerebellum adjusts its predictions of the vestibular input to account for the changes in head movement caused by resistance due to the mechanical device. After some practice, the predicted and actual self-generated sensory inputs again match, and neurons in the deep cerebellar nucleus return to being unresponsive to vestibular inputs. Cerebellum-dependent learning is described in detail later in this chapter.

The Cerebellum Contributes to Timing Control

The cerebellum seems to have a role in movement timing that goes well beyond its role in regulating the timing of contractions in different muscles (Figure 37–7). When patients with cerebellar lesions attempt to make regular tapping movements with their hands or fingers, the rhythm is irregular and the motions vary in duration and force.

Based on a theoretical model of how tapping movements are generated, Richard Ivry and Steven Keele inferred that medial cerebellar lesions interfere only with accurate execution of the response, whereas lateral cerebellar lesions interfere with the timing of serial events. Such timing defects are not limited to motor events. They also affect the patient's ability to judge elapsed time in purely mental or cognitive tasks, as in the ability to distinguish whether one tone is longer or shorter than another or whether the speed of one moving object is greater or less than that of another. We will see in our discussion of motor learning that the cerebellum is critical for learning the timing of motor acts.

The Cerebellum Participates in Motor Skill Learning

In the early 1970s, on the basis of mathematical modeling of cerebellar function and the cerebellar microcircuit, David Marr and James Albus independently suggested that the cerebellum might be involved in learning motor skills. Along with Masao Ito, they proposed that the climbing-fiber input to Purkinje cells causes changes at the synapses that relay mossy fiber input signals from parallel fibers to Purkinje cells. According to their theory, the synaptic plasticity would lead to changes in simple-spike firing, and these changes would cause behavioral learning. Subsequent experimental evidence has supported and extended this theory of cerebellar motor learning.

Climbing-Fiber Activity Changes the Synaptic Efficacy of Parallel Fibers

Climbing fibers can selectively induce *long-term depression* in the synapses between parallel fibers and Purkinje cells that are activated concurrently with the climbing fibers. Many studies in brain slices and cultured Purkinje cells have found that concurrent stimulation of climbing fibers and parallel fibers depresses the Purkinje cell responses to subsequent stimulation of the same parallel fibers. The depression is selective for the parallel fibers that were activated in conjunction with the climbing-fiber input and does not appear in synapses from parallel fibers that had not been stimulated along with climbing fibers (Figure 37–11A). The resulting depression can last for minutes to hours.

Many studies in a variety of motor learning systems have recorded activity in Purkinje cells that is consistent with the predictions of the cerebellar learning theory. For example, if an unexpected resistance is applied to a well-practiced arm movement, extra muscle tension will be required to move. Climbing fiber activity can signal error until the unexpected resistance is learned. They presumably depress the synaptic

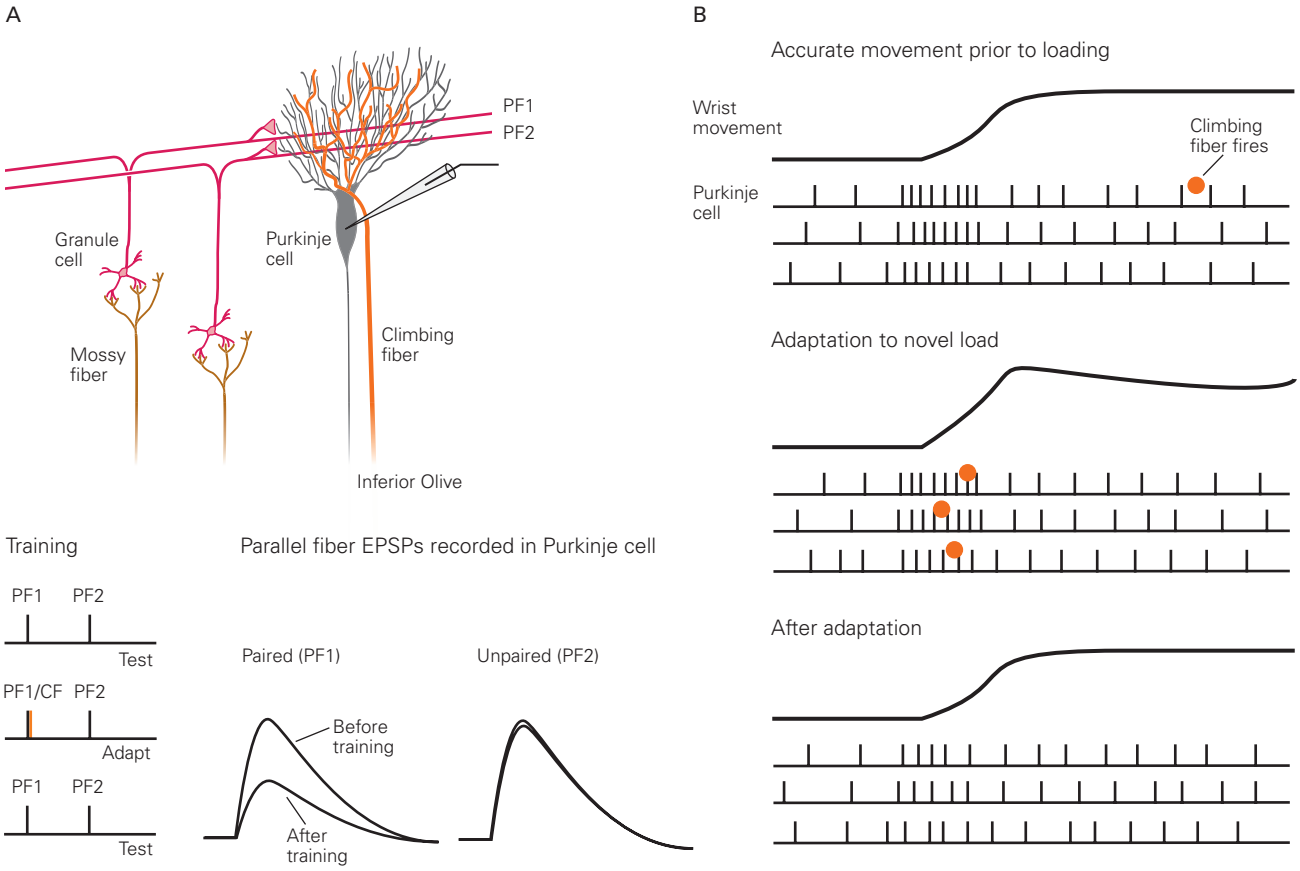

Figure 37–11 Long-term depression of the synaptic input from parallel fibers to Purkinje cells is one plausible mechanism for cerebellar learning.

A. Two different groups of parallel fibers and the presynaptic climbing fibers are electrically stimulated in vitro. Repeated stimulation of one set of parallel fibers (**PF1**) at the same time as the climbing fibers produces a long-term reduction in the responses of those parallel fibers to later stimulation. The responses of a second set of parallel fibers (**PF2**) are not depressed because they are not stimulated simultaneously with the presynaptic climbing fibers. (Abbreviations: **CF**, climbing fiber; **EPSP**, excitatory postsynaptic potential.) (Adapted from Ito et al. 1982.)

B. Top: An accurate wrist movement by a monkey is accompanied by a burst of simple spikes in a Purkinje cell, followed later by discharge of a single climbing fiber in one trial. **Middle:** When the monkey must make the same movement against a novel resistance (adaptation), climbing-fiber activity occurs during movement in every trial and the movement itself overshoots the target. **Bottom:** After adaptation, the frequency of simple spikes during movement is quite attenuated, and the climbing fiber is not active during movement or later. This is the sequence of events expected if long-term depression in the cerebellar cortex plays a role in learning. Climbing fiber activity is usually low (1/s) but increases during adaptation to a novel load. (Adapted, with permission, from Gilbert and Thach 1977.)

strength of parallel fibers involved in generating those errors, namely those that drove Purkinje simple-spike firing at the time of the climbing-fiber activity (Figure 37–11B). With successive movements, the parallel-fiber inputs conveying the flawed central command are increasingly suppressed, a more appropriate pattern of simple-spike activity emerges, and eventually movement errors disappear, along with the climbing-fiber error signal. Although this kind of result is consistent with the theory of cerebellar learning, it stops short of proving that the neural and behavioral learning was caused by long-term depression of the synapses from parallel fibers onto Purkinje cells.

The Cerebellum Is Necessary for Motor Learning in Several Different Movement Systems

The cerebellum is involved in learning a wide variety of movements, ranging from limb and eye movements to walking. In each movement system, motor learning operates to improve the feedforward control of movement. Errors render motor control transiently dependent on sensory feedback, and motor learning restores the ideal situation where performance is accurate without relying on sensory feedback.

Adaptation of limb movements that rely on eye–hand coordination can be demonstrated by having people wear prisms that deflect the light path sideways. When a person plays darts while wearing prism goggles that displace the entire visual field to the left, the initial dart throw lands to the left side of the target by an amount proportional to the strength of the prisms. The subject gradually adapts to the distortion through practice; within 10 to 30 throws, the darts land on target (Figure 37–12). When the prisms are removed, the adaptation persists, and the darts hit to the right of the target by roughly the same distance as the initial prism-induced error. Patients with a damaged cerebellar cortex or inferior olive are severely impaired or unable to adapt at all in this test.

Classical conditioning of the eye-blink response also depends on an intact cerebellum. In this form of associative learning, a puff of air is directed at the cornea, causing the eye to blink at the end of a neutral stimulus such as a tone. If the tone and the puff are paired repeatedly with a fixed duration of the tone, then the brain learns the tone's predictive power and the tone alone is sufficient to cause a blink. Michael Mauk and his colleagues have shown that the brain also can learn about the timing of the stimulus so that the eye blink occurs at the right time. It is even possible to learn to blink at different times in response to tones of different frequencies.

All forms of conjugate eye movement require the cerebellum for correct performance, and each form is subject to motor learning that involves the cerebellum. For example, the vestibulo-ocular reflex normally keeps the eyes fixed on a target when the head is rotated (Chapter 27). Motion of the head in one direction is sensed by the vestibular labyrinth, which initiates eye movements in the opposite direction to prevent visual images from slipping across the retina. When humans and experimental animals wear glasses that change the size of a visual scene, the vestibulo-ocular reflex initially fails to keep images stable on the retina because the amplitude of the reflex is inappropriate to the new conditions. After the glasses have been worn continuously for several days, however, the size of the reflex becomes progressively reduced (for miniaturizing glasses) or increased (for magnifying glasses) (Figure 37–13A). These changes are required to prevent images from slipping across the retina because magnified (or miniaturized) images also move faster (or slower). The performance of the baseline vestibulo-ocular reflex does not depend heavily on the cerebellum, but its adaptation does and can be blocked in experimental animals by lesions of the lateral part of the vestibulocerebellum called the floccular complex.

Saccadic eye movements also depend on the integrity of Purkinje cells in the oculomotor vermis in lobules V, VI, and VII of the vermis (Figure 37–2C). These cells discharge prior to and during saccades, and lesions of the vermis cause saccades to become hypermetric, much as we see in the arm movements of cerebellar patients. The outputs from neurons of the vermis concerned with saccades are transmitted through a very small region of the caudal fastigial nucleus to the saccade generator in the reticular formation.

The same Purkinje cells participate in a form of motor learning called saccadic adaptation. This adaptation is demonstrated by having a monkey fixate on a target straight ahead and then displaying a new target at an eccentric location. During the saccade to the new target, the experimenter moves the new target to a more eccentric location. Initially, the subject needs to make a second saccade to fixate on the target. Gradually, over several hundred trials, the first saccade grows in amplitude so that it brings the eye directly to the final location of the target (Figure 37–13B). Recordings during saccadic adaptation have revealed that climbing fiber inputs to the Purkinje cells in the oculomotor vermis signal saccadic errors during learning, and the simple-spike firing rate of the same cells adapts gradually along with the monkey's eye movements. Thus, the oculomotor vermis is a likely site for motor learning of the amplitude of saccadic eye movements. The story

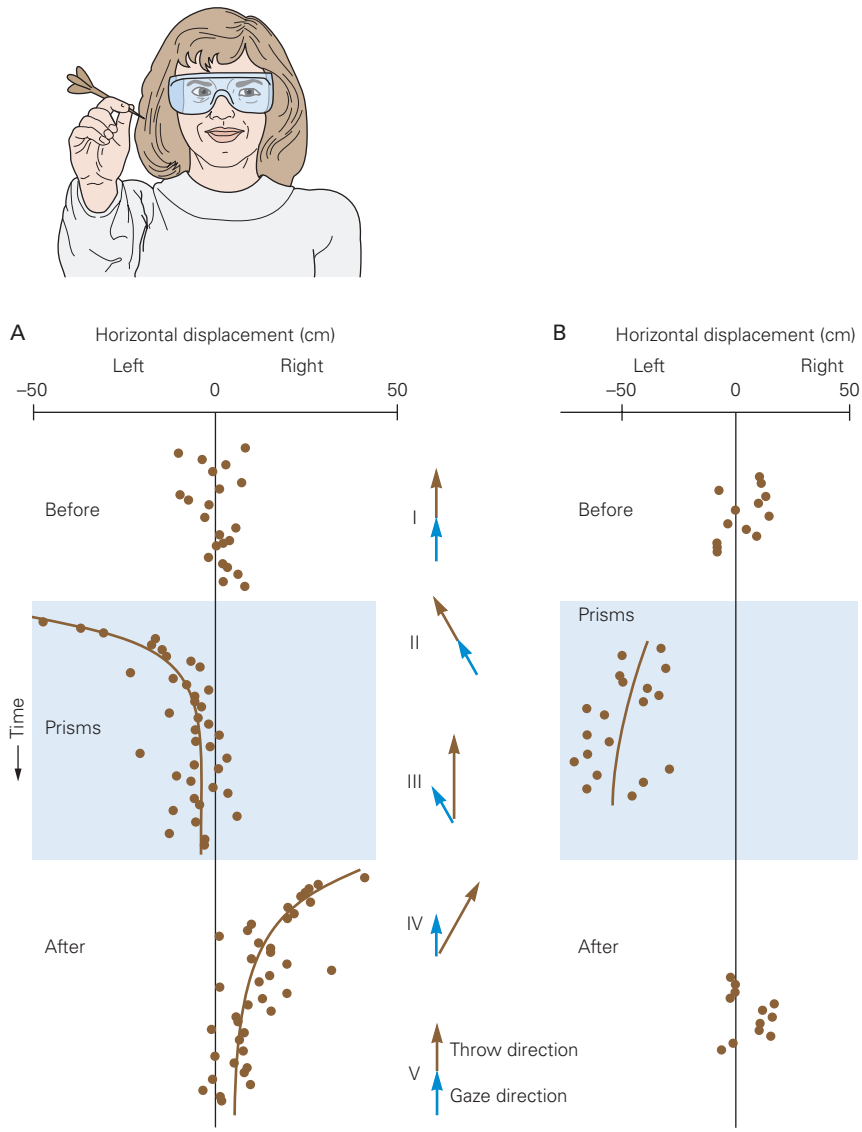

Figure 37–12 Adjustment of eye–hand coordination to a change in optical conditions. The subject wears prism goggles that bend the optic path to her right. She must look to her left along the bent light path to see the target directly ahead. (Adapted, with permission, from Martin et al. 1996).

A. Without prisms, the subject throws with good accuracy (**I**). The first hit after the prisms have been put in place is displaced left of center because the hand throws where the eyes are directed. Thereafter, hits trend rightward toward the target, away from where the eyes are looking (**II**). After removal of the prisms, the subject fixes her gaze in the center of the target; the first throw hits to the right of center, away from where the eyes are directed. Thereafter, hits trend toward the target (**III**). Immediately after removing the prisms, the subject directs her gaze toward the target; her adapted throw is to the right of the direction of gaze and to the right of the target (**IV**). After recovery from adaptation, she again looks at and throws toward the target (**V**). Data during and after prism use have been fit with exponential curves. Gaze and throw directions are indicated by the **blue** and **brown arrows**, respectively, on the *right*. The inferred gaze direction assumes that the subject is fixating the target.

B. Adaptation fails in a patient with unilateral infarctions in the territory of the posterior inferior cerebellar artery that affect the inferior cerebellar peduncle and inferior lateral posterior cerebellar cortex.

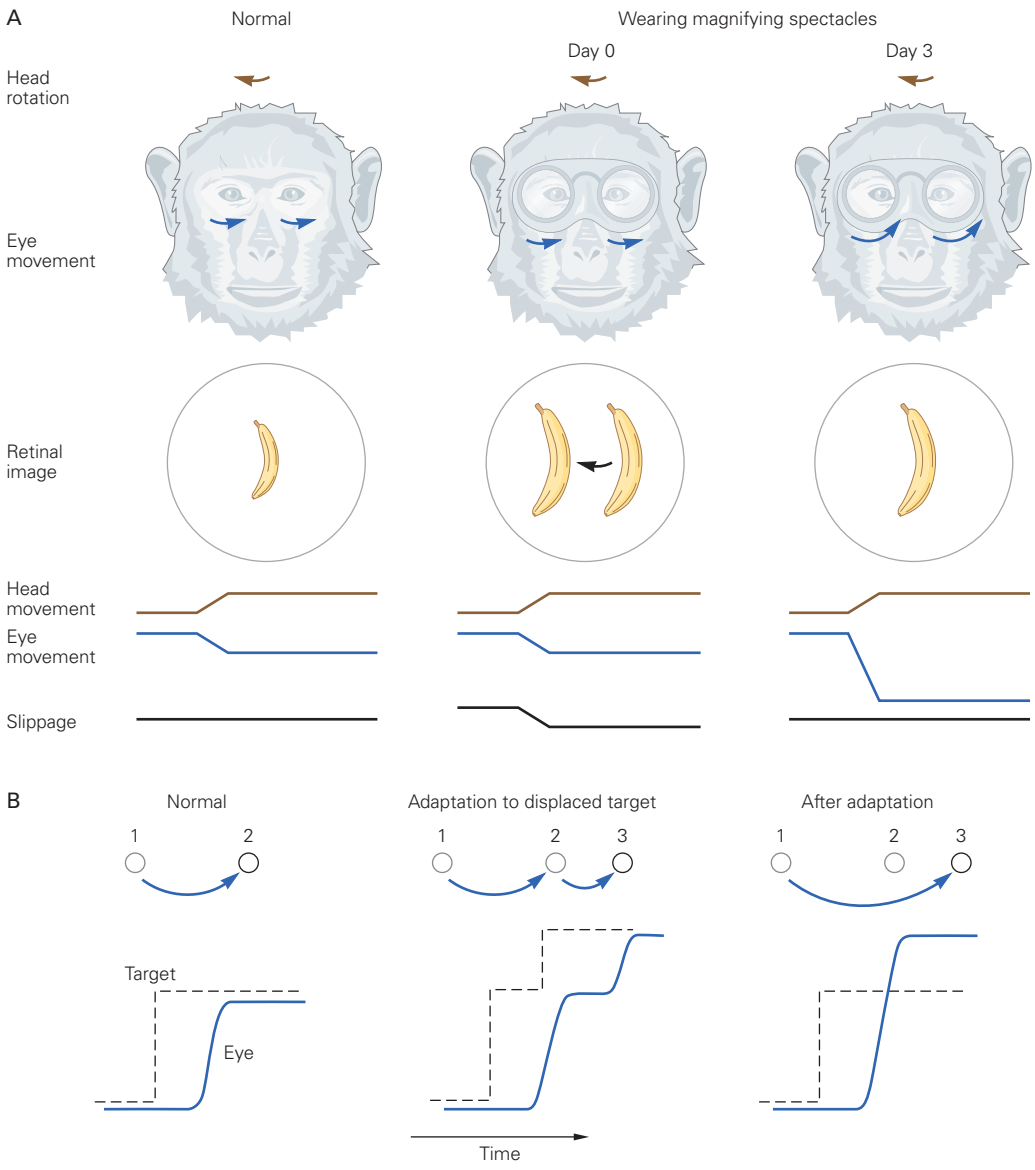

Figure 37–13 Cerebellar learning in the vestibulo-ocular reflex and in saccadic eye movements.

A. Motor learning in the vestibulo-ocular reflex of a monkey wearing magnifying spectacles. The columns show normal conditions before learning, the situation when the monkey first dons the spectacles (day 0), and after complete adaptation (day 3). Eye movements are normally equal and opposite to head turns, and the banana stays stable in the retina during head turns. With the spectacles on, the banana appears larger; when the head turns, the vestibulo-ocular reflex is too small and the banana's image slips across the retina. After adaptation, the eye movements are large enough that the image of the banana again remains stable on the retina during head turns. (Adapted, with permission, from Lisberger 1988.)

B. Motor learning in saccadic eye movements. The columns show saccades under normal conditions, on the first adaptation trial, and after full adaptation. Normally, the saccade responds to a change in target position by bringing the eye almost perfectly to the new target position. During adaptation, the target moves to a new position during the initial saccade, requiring a second saccade to bring the eye to the new, final target position. After adaptation, the original target position evokes a larger saccade that is appropriate to bring the eye to the new target position, even though the target does not move.

is very similar for smooth-pursuit eye movements, except that the relevant part of the cerebellum is the floccular complex, using the same Purkinje cells that participate in adaptation of the vestibulo-ocular reflex.

Finally, learning of new walking patterns has been studied in cerebellar patients using a split-belt treadmill that requires one leg to move faster than the other. Cerebellar damage does not impair the ability to use feedback to immediately change the walking pattern when the two belt speeds differ: Patients can lengthen the time that they stand on the slower treadmill belt and shorten the time that they stand on the faster treadmill belt. However, cerebellar patients cannot learn over hundreds of steps to make their walking pattern symmetric, whereas healthy individuals can (see Figure 30–14).

Learning Occurs at Several Sites in the Cerebellum

We know now that there are many sites of synaptic and cellular plasticity in the cerebellar microcircuit. Almost every synapse that has been studied undergoes either potentiation or depression, and the theory of cerebellar learning has been broadened accordingly. Detailed analyses of the role of cerebellar circuits in motor learning have been conducted in several motor systems: adaptation of multiple kinds of eye movements, classical conditioning of the eye blink, and motor learning in arm movements.

In today's broadened theory of cerebellar learning, learning occurs not only in the cerebellar cortex, as postulated by Marr, Albus, and Ito, but also in the deep cerebellar nuclei (Figure 37–14). Our understanding of learning in the cerebellar cortex is based partly on long-term depression of the synapses from parallel fibers to Purkinje cells, but many other synapses are characterized by plasticity, and they also probably participate. Available evidence is still compatible with the long-standing idea that inputs from climbing fibers provide the primary instructive signals that lead to changes in synaptic strength within the cerebellar cortex, but now there is room for the possibility of other instructive signals as well. Learning probably results from coordinated synaptic plasticity at multiple sites rather than from changes at a single site.

Studies of classical conditioning of the eye blink and adaptation of the vestibulo-ocular reflex provide strong evidence that learning occurs in both the cerebellar cortex and the deep cerebellar nuclei. Further, considerable evidence suggests that learning may occur first in the cerebellar cortex and then be transferred to the deep cerebellar nuclei. At least for eye blink conditioning, the cerebellar cortex may play a special role in learning timing.

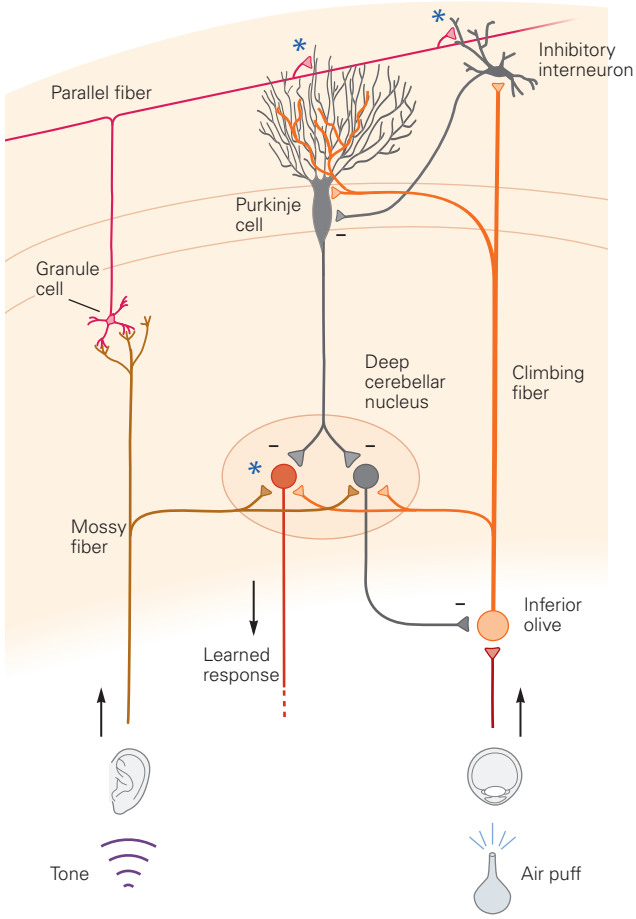

Figure 37–14 Learning in the cerebellar microcircuit can occur in the cerebellar cortex and the deep cerebellar nuclei. The diagram is based on classical conditioning of blinking, which is driven by pairing a tone (so-called conditioned stimulus carried by mossy fibers) and an air puff (the unconditioned stimulus carried by climbing fibers). Learning occurs at the parallel fiber–Purkinje cell synapses when the climbing fiber and parallel fibers are active together. Learning also occurs at the mossy-fiber synapse onto the deep cerebellar nuclei. (Sites of learning are denoted by **asterisks**.) While this example diagrams a classical conditioning paradigm, plasticity occurs at the same sites during adaptation of the vestibulo-ocular reflex when head turns are associated with image motion on the retina (Chapter 27). (Adapted, with permission, from Carey and Lisberger 2002.)

As discussed earlier, the cerebellum makes use of internal models to ensure smooth and accurate movement in advance of any guidance by sensory feedback. Synaptic changes that lead to circuit learning could be the mechanisms that create and maintain accurate internal models. One important function of learning in the cerebellum may be the continuous tuning of

internal models. Cerebellar internal models may use sensory feedback to adjust synaptic and cellular function so that motor commands produce movements that are rapid, accurate, and smooth. Thus, the cerebellum appears to be the learning machine envisioned by the earliest investigators, but its learning capabilities may be greater and more widely dispersed than originally imagined and may affect all cerebellar contributions to behavior.

Highlights

1. The cerebellum plays a critical role in movement. Damage to the cerebellum leads to profound movement incoordination called ataxia, which affects all movements ranging from eye and limb movements to balance and walking. Cerebellar damage also leads to some sensory deficits but only during active movement.
2. The cerebellum also plays a role in cognitive and emotional behavior. Deficits in these domains are less immediately obvious after cerebellar damage but appear with formalized testing. There is probably a common mechanism for deficits across both motor and nonmotor domains, but the mechanism is not yet understood.
3. The cerebellum acts through its connections to other brain structures. Its inputs come indirectly from wide regions of the cerebral cortex, as well as from the brainstem and spinal cord. Cerebellar outputs project to the vestibular nuclei, the brainstem reticular formation, and the red nucleus and via the thalamus to wide regions of the cerebral cortex.
4. Reciprocal connections between the cerebellum and the cerebral cortex include sensory and motor cortices as well as wide regions of the parietal and prefrontal cortices. Cerebrocerebellar connections are organized as a series of parallel, closed, recurrent loops, where a given region of the cerebral cortex makes both efferent and afferent connections with a given part of the cerebellum.
5. The circuit of the cerebellar cortex is highly stereotyped, suggesting a common computational mechanism for its interactions with other brain regions. It includes an input granular layer where mossy fibers synapse on granule cells and Golgi cells provide inhibitory feedback; an inhibitory Purkinje cell layer, with the sole output neurons of the cerebellar cortex; and a molecular layer where Purkinje cell dendrites and inhibitory interneurons receive inputs from the parallel fibers that emerge from the axons of granule cells.
6. The climbing-fiber and mossy-fiber inputs to the cerebellum are very different anatomically. Each Purkinje cell receives many synaptic contacts from a single climbing fiber but can be influenced via granule cells by a huge number of mossy fibers. Climbing fibers fire at very low frequencies and cause unitary "complex spikes" in Purkinje cells. Mossy fibers cause "simple spikes" that can discharge at very high rates. It is thought that the interplay between these inputs is essential for learning.
7. Theories of cerebellar motor control emphasize several general principles. The cerebellum is important for generating reliable feedforward action before there has been time for useful sensory feedback to occur. It plays a key role in the internal control of timing. The cerebellum relies on computations that combine sensory inputs with corollary discharge reporting the movement that was commanded. Internal models of the motor effector organs and the world allow the cerebellum to estimate the state of the motor system and guide accurate feedforward actions.
8. Learning and adaptation of movement are fundamental functions of the cerebellum. Cerebellar learning requires feedback about movement errors and updates movement on a trial-by-trial basis. There are many sites of synaptic plasticity in the cerebellum, and current evidence for motor learning systems supports at least two sites of learning in the cerebellum. One site involves long-term depression of the synapses from parallel fibers to Purkinje cells, guided by errors signaled by climbing-fiber inputs. The other site is in the deep cerebellar nuclei. It is likely that the same learning mechanism is used for cognitive and emotional processing.

Amy J. Bastian
Stephen G. Lisberger

Selected Reading

Bodranghien F, Bastian A, Casali C, et al. 2016. Consensus paper: revisiting the symptoms and signs of cerebellar syndrome. Cerebellum 15:369–391.

Bostan AC, Dum RP, Strick PL. 2013. Cerebellar networks with the cerebral cortex and basal ganglia. Trends Cogn Sci 17:241–254.

Boyden ES, Katoh A, Raymond JL. 2004. Cerebellum-dependent learning: the role of multiple plasticity mechanisms. Annu Rev Neurosci 27:581–609.
Ito M. 1984. *The Cerebellum and Neural Control*. New York: Raven.
Raymond JL, Lisberger SG, Mauk MD. 1996. The cerebellum: a neuronal learning machine? Science 272:1126–1131.
Stoodley CJ, Schmahmann JD. 2010. Evidence for topographic organization in the cerebellum of motor control versus cognitive and affective processing. Cortex 46:831–844.

References

Adamaszek M, D'Agata F, Ferrucci R, et al. 2017. Consensus paper: cerebellum and emotion. Cerebellum 16:552–576.
Adrian ED. 1943. Afferent areas in the cerebellum connected with the limbs. Brain 66:289–315.
Albus JS. 1971. A theory of cerebellar function. Math Biosci 10:25–61.
Arshavsky YI, Berkenblit MB, Fukson OI, Gelfand IM, Orlovsky GN. 1972. Recordings of neurones of the dorsal spinocerebellar tract during evoked locomotion. Brain Res 43:272–275.
Arshavsky YI, Berkenblit MB, Fukson OI, Gelfand IM, Orlovsky GN. 1972. Origin of modulation in neurones of the ventral spinocerebellar tract during locomotion. Brain Res 43:276–279.
Bastian AJ, Martin TA, Keating JG, Thach WT. 1996. Cerebellar ataxia: abnormal control of interaction torques across multiple joints. J Neurophysiol 176:492–509.
Bastian AJ, Zackowski KM, Thach WT. 2000. Cerebellar ataxia: torque deficiency or torque mismatch between joints? J Neurophys 83:3019–3030.
Bhanpuri NH, Okamura AM, Bastian AJ. 2013. Predictive modeling by the cerebellum improves proprioception. J Neurosci 33:14301–14306.
Brooks VB, Thach WT. 1981. Cerebellar control of posture and movement. In *Handbook of Physiology, The Nervous System*, Sect. I, Vol. 2, ed. V. B. Brooks, pp. 877–46. Bethesda: Am Physiol Soc.
Brooks JX, Carriot J, Cullen KE. 2015. Learning to expect the unexpected: rapid updating in primate cerebellum during voluntary self-motion. Nat Neurosci 18:1310–1317.
Buckner RL, Krienen FM, Castellanos A, Diaz JC, Yeo BT. 2011 The organization of the human cerebellum estimated by intrinsic functional connectivity. J Neurophysiol 106:2322–2345.
Courchesne E, Yeung-Courchesne R, Press GA, Hesselink JR, Jernigan TL. 1988. Hypoplasia of cerebellar vermal lobules VI and VII in autism. N Engl J Med 318:1349–1354.
Carey MR, Lisberger SG. 2002. Embarrassed but not depressed: some eye opening lessons for cerebellar learning. Neuron 35: 223–226.
Eccles JC, Ito M, Szentagothai J. 1967. *The Cerebellum as a Neuronal Machine*. New York: Springer.
Fiez JA, Petersen SE, Cheney MK, Raichle ME. 1992. Impaired non-motor learning and error detection associated with cerebellar damage. Brain 115:155–178.
Flament D, Hore J. 1986. Movement and electromyographic disorders associated with cerebellar dysmetria. J Neurophysiol 55:1221–1233.
Gao Z, van Beugen BJ, De Zeeuw CI. 2012. Distributed synergistic plasticity and cerebellar learning. Nat Rev Neurosci 13:619–635.
Ghasia FF, Meng H, Angelaki DE. 2008. Neural correlates of forward and inverse models for eye movements: evidence from three-dimensional kinematics. J Neurosci 28:5082–5087.
Gilbert PFC, Thach WT. 1977. Purkinje cell activity during motor learning. Brain Res 128:309–328.
Groenewegen HJ, Voogd J. 1977. The parasagittal zonation within the olivocerebellar projection. I. Climbing fiber distribution in the vermis of cat cerebellum. J Comp Neurol 174:417–488.
Heck DH, Thach WT, Keating JG. 2007. On-beam synchrony in the cerebellum as the mechanism for the timing and coordination of movement. Proc Natl Acad Sci U S A 104:7658–7663.
Hore J, Flament D. 1986. Evidence that a disordered servo-like mechanism contributes to tremor in movements during cerebellar dysfunction. J Neurophysiol 56:123–136.
Ito M, Sakurai M, Tongroach P. 1982. Climbing fibre induced depression of both mossy fibre responsiveness and glutamate sensitivity of cerebellar Purkinje cells. J Physiol Lond 324:113–134.
Ivry RB, Keele SW. 1989. Timing functions of the cerebellum. J Cogn Neurosci 1:136–152.
Jansen J, Brodal A (eds). 1954. *Aspects of Cerebellar Anatomy*. Oslo: Grundt Tanum.
Kelly RM, Strick PL. 2003. Cerebellar loops with motor cortex and prefrontal cortex of a nonhuman primate. J Neurosci 23:8432–8444.
Kim SG, Ugurbil K, Strick PL. 1994. Activation of a cerebellar output nucleus during cognitive processing. Science 265:949–951.
Larsell O, Jansen J. 1972. *The Comparative Anatomy and Histology of the Cerebellum: The Human Cerebellum, Cerebellar Connection and Cerebellar Cortex*, pp. 111–119. Minneapolis, MN: Univ. of Minnesota Press.
Lisberger SG. 1988. The neural basis for motor learning in the vestibulo-ocular reflex in monkeys. Trends in Neurosci 11:147–152.
Lisberger SG. 1994. Neural basis for motor learning in the vestibulo-ocular reflex of primates. III. Computational and behavioral analysis of the sites of learning. J Neurophysiol 72:974–998.
Lisberger SG, Fuchs AF. 1978. Role of primate flocculus during rapid behavioral modification of vestibulo-ocular reflex. I. Purkinje cell activity during visually guided horizontal smooth-pursuit eye movements and passive head rotation. J Neurophysiol 41:733–763.
Marr D. 1969. A theory of cerebellar cortex. J Physiol 202:437–470.
Martin TA, Keating JG, Goodkin HP, Bastian AJ, Thach WT. 1996. Throwing while looking through prisms. I. Focal olivocerebellar lesions impair adaptation. Brain 119:1183–1198.

Martinez FE, Crill WE, Kennedy TT. 1971. Electrogenesis of cerebellar Purkinje cell responses in cats. J Neurophysiol 34:348–356.

McCormick DA, Thompson RF. 1984. Cerebellum: essential involvement in the classically conditioned eyelid response. Science 223:296–299.

Medina JF, Lisberger SG. 2008. Links from complex spikes to local plasticity and motor learning in the cerebellum of awake-behaving monkeys. Nat Neurosci 11:1185–1192.

Nieuwenhuys R, Voogd J, van Huijzen C. 1981. The human central nervous system: a synopsis and atlas. Springer.

Nieuwenhuys R, Voogd J, van Huijzen Chr. 1988. The Human Central Nervous System: A Synopsis and Atlas, 3rd rev. ed. Berlin: Springer.

Ohyama T, Nores WL, Medina JF, Riusech FA, Mauk MD. 2006. Learning-induced plasticity in deep cerebellar nucleus. J Neurosci 26:12656–12663.

Pasalar S, Roitman AV, Durfee WK, Ebner TJ. 2006. Force field effects on cerebellar Purkinje cell discharge with implications for internal models. Nat Neurosci 9:1404–1411.

Robinson DA. 1976. Adaptive gain control of vestibuloocular reflex by the cerebellum. J Neurophysiol 39:954–969.

Strata P, Montarolo PG. 1982. Functional aspects of the inferior olive. Arch Ital Biol 120:321–329.

Strick PL, Dum RP, Fiez JA. 2009. Cerebellum and nonmotor function. Annu Rev Neurosci 32:413–434.

Thach WT. 1968. Discharge of Purkinje and cerebellar nuclear neurons during rapidly alternating arm movements in the monkey. J Neurophysiol 31:785–797.

Tseng YW, Diedrichsen J, Krakauer JW, Shadmehr R, Bastian AJ. 2007. Sensory prediction errors drive cerebellum-dependent adaptation of reaching. J Neurophysiol 98:54–62.

Yeo CH, Hardiman MJ, Glickstein M. 1984. Discrete lesions of the cerebellar cortex abolish the classically conditioned nictitating membrane response of the rabbit. Behav Brain Res 13:261–266.

38

The Basal Ganglia

Highlights

The traditional view that the basal ganglia play a role in movement arises primarily because diseases of the basal ganglia, such as Parkinson and Huntington disease, are associated with prominent disturbances of movement, and from the belief that basal ganglia neurons send their output exclusively to the motor cortex by way of the thalamus. However, we now know that the basal ganglia also project to wide areas of the brain stem and via the thalamus to nonmotor areas of the cerebral cortex and limbic system, thereby providing a mechanism whereby they contribute to a wide variety of cognitive, motivational, and affective operations. This understanding also explains why diseases of the basal ganglia are frequently associated with complex cognitive, motivational, and affective dysfunction in addition to the better-known motor disturbances.

This chapter provides a perspective on the fundamental contributions of the basal ganglia (Figure 38–1) to overall brain function. Recent advances in the fields of artificial neural networks and robotics emphasize that behavioral function is an emergent property of signal processing in physically connected networks (Chapter 5). Thus, how components of networks are connected and how their input signals are transformed into output signals impose important constraints on final behavioral outputs. We first describe the principal anatomical and physiological features of the basal ganglia network and consider the constraints these might impose on their function. We consider the extent to which the basal ganglia have been conserved during vertebrate brain evolution and, based on these insights, review evidence suggesting that the basal ganglia's normal functions are to select between incompatible behaviors and to mediate reinforcement learning. We conclude by examining important insights into how the system can malfunction in some of the major diseases involving the basal ganglia.

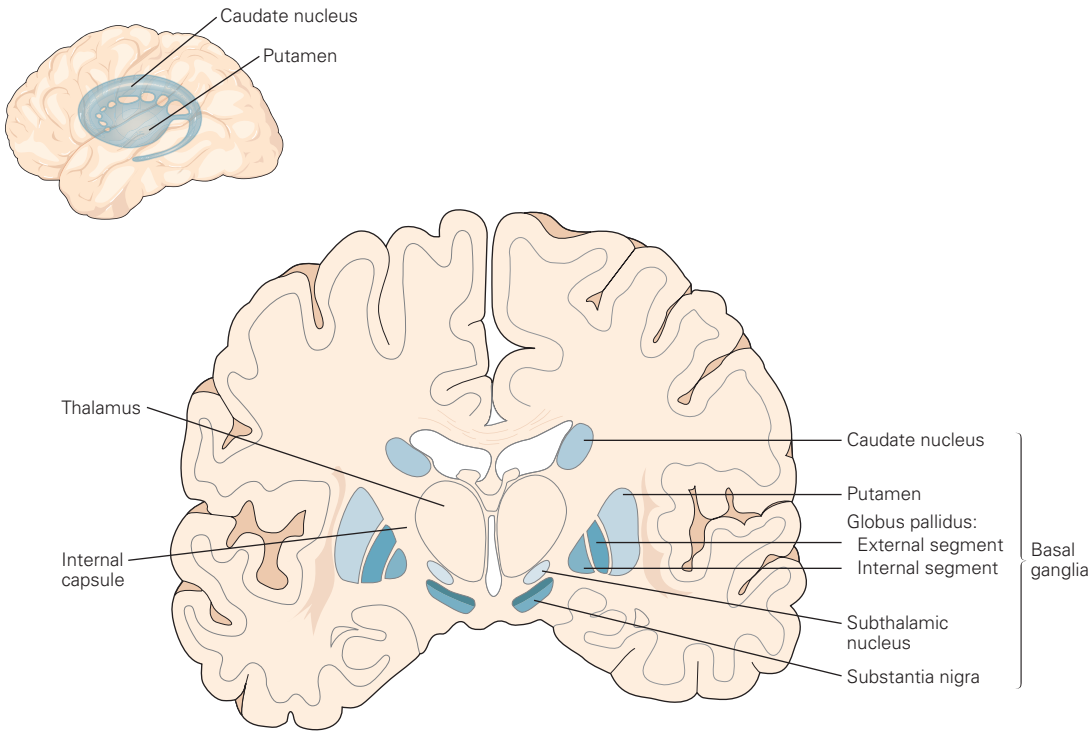

Figure 38–1 The basal ganglia and surrounding structures. The nuclei of the basal ganglia are identified on the right in this coronal section of a human brain. (Adapted from Nieuwenhuys, Voogd, and van Huijzen 1981.)

The Basal Ganglia Network Consists of Three Principal Input Nuclei, Two Main Output Nuclei, and One Intrinsic Nucleus

The striatum (a collective term for the caudate nucleus and putamen; see Figure 38–1), subthalamic nucleus, and substantia nigra pars compacta/ventral tegmental area are the three major input nuclei of the basal ganglia, receiving signals directly and indirectly from structures distributed throughout the neuraxis (Figure 38–2).

The Striatum, Subthalamic Nucleus, and Substantia Nigra Pars Compacta/Ventral Tegmental Area Are the Three Principal Input Nuclei of the Basal Ganglia

The striatum is the largest nucleus of the basal ganglia. It receives direct input from most regions of the cerebral cortex and limbic structures, including the amygdala and hippocampus. Important input from sensorimotor and motivational regions of the brain stem is relayed indirectly via the thalamus. In rodents, the number of contacts received in the striatum from the cerebral cortex and thalamus are approximately equivalent. Finally, important modulatory input to the striatum comes from the substantia nigra pars compacta (dopamine), midbrain raphe (serotonin), and pedunculopontine nucleus (acetylcholine).

The striatum is subdivided functionally on the basis of the organization of input connections, principally the topographically organized afferents from the cerebral cortex. Limbic, associative, and sensorimotor territories are generally recognized along a ventromedial-dorsolateral continuum. This diversity of input shows that the basal ganglia receive signals from brain regions involved in different motivational, emotional, cognitive, and sensorimotor processes, implying that whatever the basal ganglia are doing, they are doing it for a wide range of brain processes.

An additional architectural feature of the striatum suggests that the basal ganglia are performing more or less the same operations on their inputs from functionally diverse afferent structures. Specifically, within each of the striatum's functional territories, the cellular architecture is remarkably similar. In all regions, inhibitory γ-aminobutyric acid (GABA)-ergic medium spiny neurons are the principal cell type (>90% of all neurons). In addition, in all functionally defined regions, the medium spiny neurons are separated into two populations according to the relative expression of neuroactive peptides (substance P and dynorphin versus enkephalin) or the expression of D_1 and D_2 dopamine receptors, which are thought to positively and negatively modulate cyclic adenosine monophosphate signaling in these neurons. These populations contribute differentially to different efferent projections of the striatum. In addition to these long-range inhibitory connections to other basal ganglia nuclei, medium spiny neurons also send local collaterals to adjacent cells. Colocalized GABAergic and peptidergic neurotransmission provides local mutually inhibitory and excitatory influences. The remaining 5% to 10% of neurons in the striatum are purely GABAergic and cholinergic interneurons, which can be distinguished according to neurochemical, electrophysiological, and in some cases morphological characteristics. The fact that this local cellular architecture is present in all functional regions suggests that neurons in the striatum are applying the same or similar computations on functionally diverse afferent pathways.

The subthalamic nucleus has traditionally been considered an important internal relay in the "indirect output pathway" from the striatum to the basal ganglia output nuclei (see below). It is now also recognized as a second important input nucleus of the basal

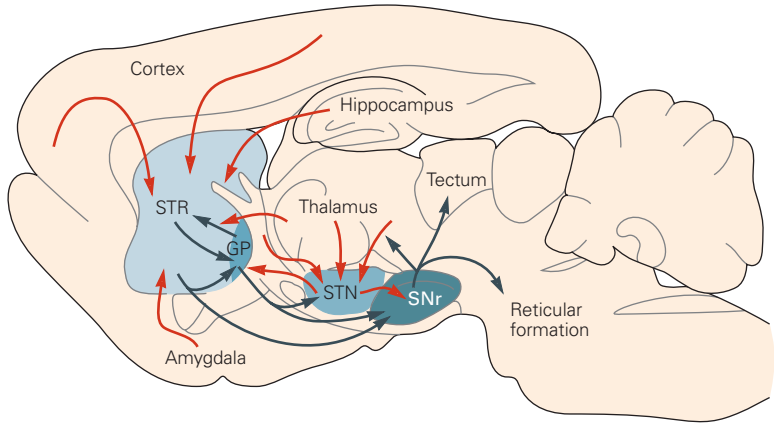

Figure 38–2 The principal input, intrinsic, and output connections of the mammalian basal ganglia. The main input nuclei are the striatum (**STR**), subthalamic nucleus (**STN**), and substantia nigra pars compacta (not shown). They receive input directly from the thalamus, cerebral cortex, and limbic structures (amygdala and hippocampus). The main output nuclei are the substantia nigra pars reticulata (**SNr**) and internal globus pallidus/entopeduncular nucleus (not shown). The external globus pallidus (**GP**) is classified as an intrinsic nucleus as most of its connections are with other basal ganglia nuclei. Structures are shown on a sagittal schematic of the rodent brain. **Red** and **dark gray arrows** denote excitatory and inhibitory connections, respectively.

ganglia. Topographically organized inputs derive not only from large parts of frontal cortex, but also from various thalamic and brain stem structures. The subthalamic nucleus is the only component of the basal ganglia that has excitatory (glutamatergic) output connections. These project to both output nuclei and to the intrinsic external globus pallidus.

The substantia nigra pars compacta/ventral tegmental area contain an important population of dopaminergic neurons. These neurons represent the third major input station of the basal ganglia and give rise to the nigrostriatal and mesolimbic/mesocortical dopamine projections. They receive significant afferent connections from other basal ganglia nuclei (the striatum, globus pallidus, and subthalamus), but also from many structures in the brain stem (eg, superior colliculus, rostromedial tegmental region, raphe nuclei, pedunculopontine nucleus, and parabrachial area). Other afferent connections are from the frontal cortex and the amygdala. This pattern of connectivity is important because it suggests the most important direct influence over the dopaminergic neurons arises from evolutionarily ancient parts of the brain (see below).

Individual dopaminergic neurons have highly branching axons that project into extensive regions of not only the other basal ganglia nuclei but also external structures (eg, frontal cortex, septal area, amygdala, habenula). This suggests that their important modulatory signals are widely broadcast throughout targeted structures. The highest concentration of dopaminergic terminals is found in the striatum, where synaptic and nonsynaptic contacts are formed with both medium spiny cells and interneurons. The existence of nonsynaptic contacts gives rise to what has been called *volume transmission*. This occurs when neurotransmitters diffuse through the brain's extracellular fluid from release points that may be remote from targeted cells. Consequently, volume transmission typically has a longer time course than synaptic neurotransmission. Deployment of volume transmission in targeted structures is further evidence for the idea that the effects of dopamine in targeted structures are widely broadcast and spatially imprecise. Variable proportions of GABAergic neurons (substantia nigra and the ventral tegmental area) and glutamatergic neurons (ventral tegmental area) contribute to local processing in these structures.

The Substantia Nigra Pars Reticulata and the Internal Globus Pallidus Are the Two Principal Output Nuclei of the Basal Ganglia

The internal globus pallidus/entopeduncular nucleus is one of the two principal output nuclei. It receives inputs from other basal ganglia nuclei and projects to external targets in the thalamus and brain stem. GABAergic input from the striatum and external globus pallidus are inhibitory, while input from the subthalamic nucleus is glutamatergic and excitatory. Neurons of the internal globus pallidus are themselves GABAergic and have high levels of tonic activity. Under normal circumstances, this imposes powerful inhibitory effects on targets in the thalamus, lateral habenula, and brain stem.

The substantia nigra pars reticulata is the second principal output nucleus. It also receives afferents from other basal ganglia nuclei and provides efferent connections to the thalamus and brain stem. Inhibitory (GABAergic) inputs come from the striatum and globus pallidus (external) and excitatory input from the subthalamus. Pars reticulata neurons are also GABAergic and impose strong inhibitory control over parts of the thalamus and brain stem, including the superior colliculus, pedunculopontine nucleus, and parts of the midbrain and medullary reticular formation.

The External Globus Pallidus Is Mostly an Intrinsic Structure of the Basal Ganglia

Most connections of the globus pallidus are with other basal ganglia nuclei, including inhibitory (GABAergic) input from the striatum and excitatory (glutamatergic) input from the subthalamus, and the globus pallidus provides inhibitory efferent connections to all the basal ganglia's input and output nuclei. This pattern of connections suggests that that the external globus pallidus is an essential regulator of internal basal ganglia activity.

Having described the core components of the basal ganglia, we will now consider in more detail how they are connected, first with each other and then with external structures in the brain.

The Internal Circuitry of the Basal Ganglia Regulates How the Components Interact

The Traditional Model of the Basal Ganglia Emphasizes Direct and Indirect Pathways

An influential interpretation of the intrinsic circuitry of the basal ganglia was proposed in the late 1980s by Roger Albin and colleagues (Figure 38–3A). In their scheme, signals originating in the cerebral cortex are distributed to two populations of medium spiny output neurons in the striatum.

Neurons containing substance P and a preponderance of D_1 dopamine receptors make direct inhibitory

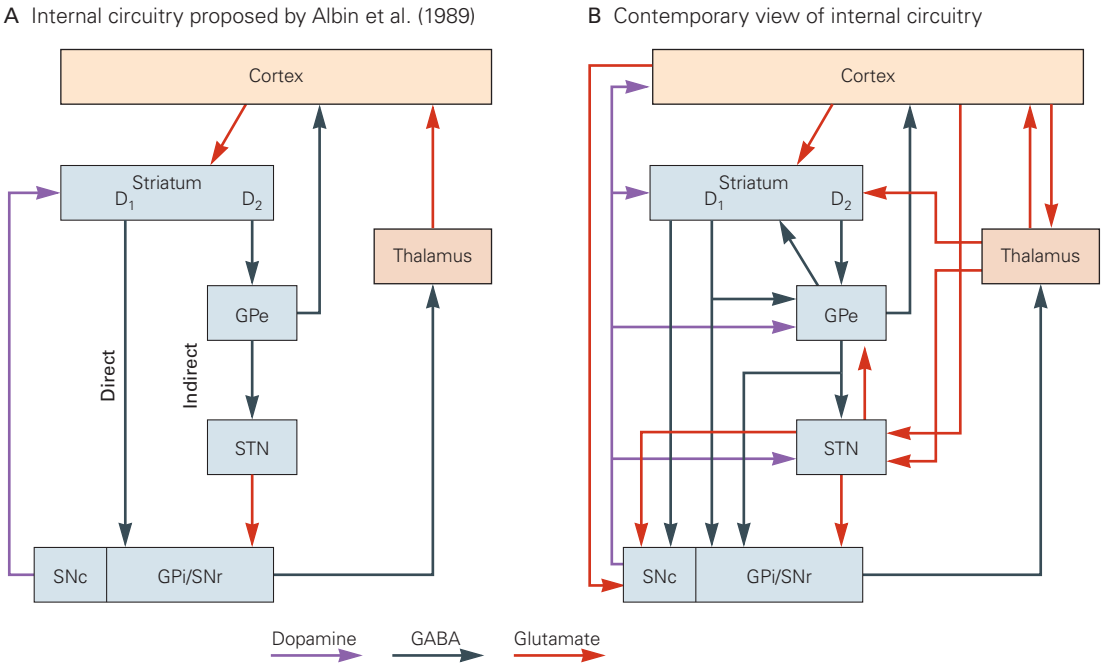

Figure 38–3 Intrinsic connections within the basal ganglia.

A. The influential proposal by Roger Albin and colleagues (1989) is presented, where output of the basal ganglia is determined by the balance between a *direct pathway* from the striatum to the output nuclei (internal globus pallidus [**Gpi**] and substantial nigra pars reticulata [**SNr**]), which promotes behavior, and an *indirect pathway* from the striatum to the output nuclei via relays in the external globus pallidus (**GPe**) and subthalamic nucleus (**STN**), which suppresses behavior. The balance between the direct and indirect projections was thought to be regulated by afferent dopaminergic signals from substantia nigra pars compacta (**SNc**) acting on differentially distributed D_1 and D_2 dopamine receptors.

B. More recent anatomical investigations have revealed a rather more complex organization where the transformations of basal ganglia inputs that generate outputs are less easy to predict.

contact with the basal ganglia output nuclei—the direct pathway. In contrast, striatal neurons containing enkephalin and expressing mainly D_2 dopamine receptors make excitatory contact with the output nuclei via relays in the globus pallidus and subthalamus—the indirect pathway. Basal ganglia output was thought to reflect a cortically determined balance between these inhibitory and excitatory projections terminating on the two output structures (the internal globus pallidus and substantia nigra pars reticulata). In this model, a behavior would be promoted when the direct pathway was dominant and inhibited when the indirect pathway was dominant.

Detailed Anatomical Analyses Reveal a More Complex Organization

Recent anatomical observations show that the internal circuitry of the basal ganglia is more complex than originally envisaged (Figure 38–3B). The main findings have been that: (1) medium spiny neurons of the direct pathway also provide collateral input to the globus pallidus; (2) globus pallidus neurons also make direct contact with the output nuclei in addition to the traditional indirect connections to the subthalamus—often with branching collaterals to all three structures; (3) the globus pallidus also projects back to the striatum and to structures outside the basal ganglia; (4) the subthalamic nucleus also projects back to the external globus pallidus, in addition to the feedforward connections to the two basal ganglia output nuclei; and (5) major inputs to the subthalamic nucleus originate from both cortical and subcortical structures external to the basal ganglia. Consequently, the subthalamus is now considered a major input structure of the basal ganglia (see above), rather than a simple relay in the intrinsic indirect projection. A modern appreciation of this complex organization within the basal ganglia suggests it is no longer possible to intuit how a particular input might be transformed by the basal ganglia to generate a specific output. For this reason, computational modeling of the internal circuitry of the basal ganglia has become increasingly important.

Although the overall pattern of intrinsic circuitry is complex (Figure 38–3B), connections between components of the basal ganglia are topographically ordered

throughout. Some of these projections are comparatively focused (eg, the striatonigral projection), while others are more diffuse (eg, the subthalamonigral projection). Significant reductions in the comparative numbers of neurons in afferent structures, the striatum, and the output nuclei suggest a dramatic compression of information as it is processed within the basal ganglia.

Basal Ganglia Connections With External Structures Are Characterized by Reentrant Loops

Inputs Define Functional Territories in the Basal Ganglia

The functional status of inputs to the striatum from the cerebral cortex, limbic structures, and thalamus provides the rationale for classifying functional territories within the basal ganglia nuclei (limbic, associative, and sensorimotor). However, the manner in which the afferent projections make contact with neurons of the basal ganglia nuclei suggests important functional differences. For example, axons arriving in the striatum from the cerebral cortex and central lateral thalamic nucleus appear to make few contacts with many striatal neurons. In contrast, inputs from other regions, principally the parafascicular thalamic nucleus, have axons that make many contacts with fewer individual striatal neurons. Afferent connections to the subthalamic nucleus, at least from cerebral cortex, are also topographically organized according to the limbic, associative, and sensorimotor classification. However, there is no evidence of the same kind of precise topographical input from external structures to SNc and VTA dopamine neurons in the ventral midbrain.

Output Neurons Project to the External Structures That Provide Input

Basal ganglia output neurons project to regions of the thalamus (the intralaminar and ventromedial nuclei) that project back to basal ganglia input nuclei as well as to those regions of cortex that provided the original inputs to the striatum. Similarly, outputs from the basal ganglia to the brain stem tend to target those regions that provide input to the striatum via the thalamic midline and intralaminar nuclei. Importantly, projections from the basal ganglia output nuclei to the thalamus and brain stem are also topographically ordered.

Finally, many output projections of the basal ganglia are extensively collateralized, thereby simultaneously contacting targets in the thalamus, midbrain, and hindbrain. An example of the functional consequences of this organization is that a subset of neurons in the substantia nigra pars reticulata associated with oral behavior can simultaneously influence the activity in the specific regions of the thalamus/cortex, midbrain, and hindbrain that interact during the production of oral behavior.

Reentrant Loops Are a Cardinal Principle of Basal Ganglia Circuitry

Spatial topographies associated with input projections, intrinsic connections, and outputs of the basal ganglia provided the basis for the influential organizational principle suggested by Garrett Alexander and colleagues in 1989. Connections between the cerebral cortex and basal ganglia can be viewed as a series of reentrant parallel projecting, partly segregated, cortico-striato-nigro-thalamo-cortical loops or channels (Figure 38–4). Thus, an important component of the projections from different functional areas of cerebral cortex (eg, limbic, associative, sensorimotor) makes exclusive contact with specific regions of the basal ganglia input nuclei. This regional separation is maintained in forward projections throughout the internal circuitry. Focused output signals from functional territories represented in the basal ganglia output nuclei are returned, via appropriate thalamic relays, to the cortical regions providing the original input signals.

The concept of parallel projecting reentrant loops through the basal ganglia has been extended to their connections with sensorimotor and motivational structures in the brain stem, including the superior colliculus, periaqueductal gray, pedunculopontine, and parabrachial nuclei. This implies that the reentrant loop architecture through the basal ganglia must have predated the evolutionary expansion of the cerebral cortex. An important difference is that for the cortical loops the thalamic relay is on the output side of the loop, whereas for the subcortical loops, the thalamic relay is on the input side (Figure 38–5). Further work will be required to test whether projections from different brain stem structures, as they pass through the thalamic and basal ganglia relays, are functionally distinct channels.

In summary, the partially segregated reentrant loop organization is one of the dominant features characterizing the connections between the basal ganglia and external structures. This pattern of connections provides important clues as to the role played by the basal ganglia nuclei in overall brain function. However, at

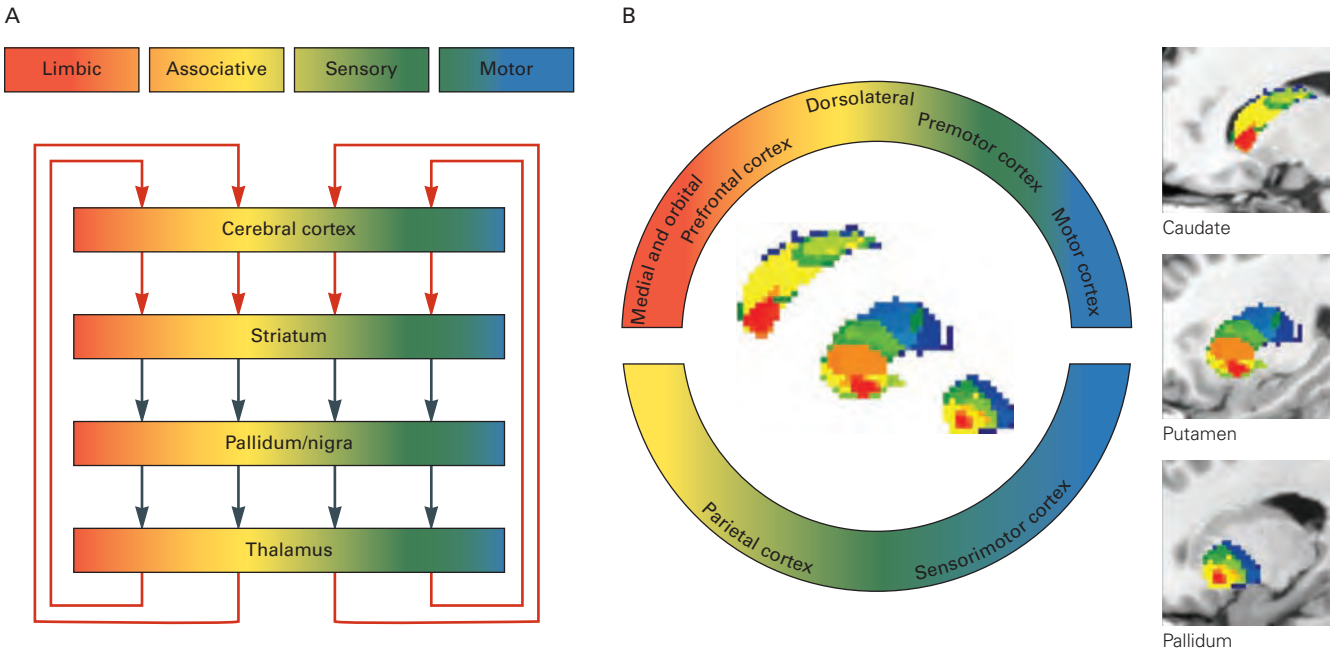

Figure 38–4 Connections between the basal ganglia and cerebral cortex.

A. The connections between the cerebral cortex and basal ganglia can be viewed as a series of parallel projecting, largely segregated loops or channels. Functional territories represented at the level of cerebral cortex are maintained throughout the basal ganglia nuclei and thalamic relays. However, for each loop, the relay points in the cortex, basal ganglia, and thalamus offer opportunities for activity inside the loop to be modified by signals from outside the loop. **Red** and **dark gray arrows** represent excitatory and inhibitory connections, respectively.

B. Spatially segregated rostral-caudal gradient of human frontal cortical connectivity in caudate, putamen, and pallidum. The color-coded ring denotes regions of cerebral cortex in the sagittal plane. (Reproduced, with permission, from Draganski et al. 2008. Copyright © 2008 Society for Neuroscience.)

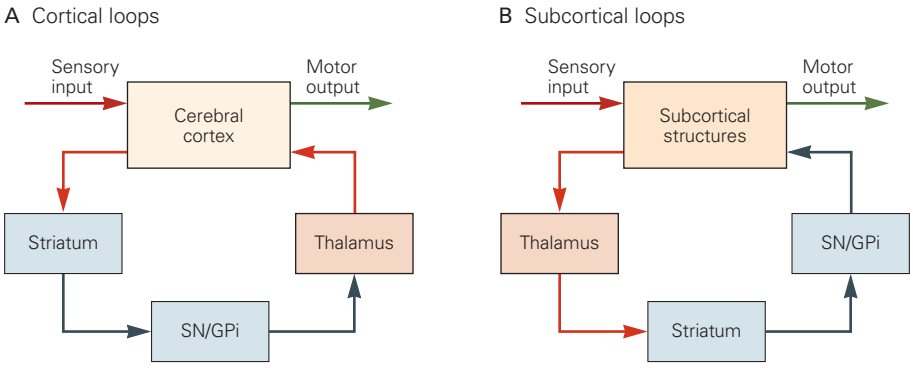

Figure 38–5 Cortical and subcortical sensorimotor loops through the basal ganglia.

A. For cortical loops, the position of the thalamic relay is on the return arm of the loop.

B. In the case of all subcortical loops, the position of the thalamic relay is on the input side of the loop. **Red** indicates predominantly excitatory regions and connections, while **dark gray** indicates inhibitory regions and connections. (Abbreviations: **SN/GPi**, substantia nigra/globus pallidus; **Thal**, thalamus.)

this point, it is important not to think of the reentrant loop architecture as comprising a series of independent and isolated functional channels. At each node or relay point in the loop (eg, in the cortex, the input nuclei, the output nuclei, and the thalamus), there is the opportunity for information flow within the loop to be modified by information from outside the loop (see the section on reinforcement learning below).

At the beginning of this chapter, we stated that behavior is an emergent property of signal processing within a neural network. Having specified the systems-level network of the basal ganglia, we now consider the signals that are being processed within this system.

Physiological Signals Provide Further Clues to Function in the Basal Ganglia

The Striatum and Subthalamic Nucleus Receive Signals Mainly from the Cerebral Cortex, Thalamus, and Ventral Midbrain

Signals received by the striatum from the cerebral cortex and thalamus are conveyed by excitatory glutamatergic neurotransmission. These fast, phasically active excitatory inputs are mediated predominantly by α-amino-3-hydroxy-5-methyl-4-isoxazolepropionic acid (AMPA) and kainate receptors when the medium spiny neurons are near resting potential; *N*-methyl-D-aspartate (NMDA) receptors play a greater role when the neurons are depolarized. Glutamatergic inputs from both cerebral cortex and thalamus also impinge on striatal interneurons.

It is important to appreciate that these signals come from external structures that are simultaneously generating a wide range of behavioral options. Since these options could not all be expressed at the same time, these inputs to the basal ganglia are thought to be in competition with each other. Another important signal to the striatum is an efference copy of the output activity from the external structures that generate behavioral responses. For example, the sensorimotor territories of the dorsolateral striatum receive collateral fibers from motor cortex axons that send signals to the spinal cord.

The effects of dopaminergic inputs from the ventral midbrain on striatal neuronal activity are complicated, with many conflicting results. In part, this is due to the problem of evoking normal patterns of input activity in slice and anaesthetized preparations. However, recent developments in optogenetic technology in alert, active animals have enabled investigators both to record and manipulate dopamine signals to the striatum in a temporally controlled manner. Consequently, current evidence suggests dopamine can increase signal-to-noise ratios in the striatum, enhancing the effects of strong external inputs while suppressing weak ones. There is further evidence that dopamine can increase the excitability of medium spiny neurons in the direct pathways while at the same time decreasing the excitability of those in the indirect pathway.

Finally, dopamine input is necessary for both long-term potentiation and long-term depression of glutamatergic inputs to striatal medium spiny neurons from both cortex and thalamus. This latter point is of great significance for the role played by the basal ganglia in reinforcement learning (see below). Dopamine can also influence the activity of GABAergic and cholinergic interneurons. Although anatomically significant, much less is known about the role(s) of serotoninergic inputs to the basal ganglia.

The main external sources of input to the striatum also provide parallel inputs to the subthalamic nucleus. The subthalamus therefore receives phasic excitatory (glutamatergic) signals from the cerebral cortex, thalamus, and brain stem. Following cortical activation, short-latency excitatory effects in the subthalamus are thought to be mediated via these "hyperdirect" connections, whereas longer-latency suppressive effects are more likely to come from indirect inhibitory inputs from other basal ganglia nuclei, principally the external globus pallidus. The subthalamus receives short-latency excitatory sensory input from the brain stem (eg, the superior colliculus); it is also influenced by dopaminergic, serotonergic, and cholinergic modulatory inputs.

Ventral Midbrain Dopamine Neurons Receive Input From External Structures and Other Basal Ganglia Nuclei

Afferent signals to the dopaminergic neurons in the ventral midbrain come from a wide variety of autonomic, sensory, and motor areas and operate over a range of time scales. For example, laterally located neurons in the substantia nigra receive short-latency excitatory inputs from cortical and subcortical sensorimotor regions, while more medially positioned neurons receive both short-latency sensory signals and autonomic-related inputs from the hypothalamus over longer time scales.

Important inhibitory control over dopaminergic neurons is exercised by GABAergic neurons, both local and distant from areas like the rostromedial tegmentum. However, the densest inputs to the dopaminergic neurons are inhibitory inputs from the striatum and

globus pallidus and excitatory signals from the subthalamic nucleus. The midbrain raphe nuclei provide important modulatory serotonergic input, while both the pedunculopontine nucleus and lateral dorsal tegmental nucleus provide cholinergic and glutamatergic inputs. An important functional question concerning the wide range of afferent signals to dopaminergic neurons is whether dopamine performs a highly integrative role or performs an essential function that is accessed by numerous different systems at different times.

Disinhibition Is the Final Expression of Basal Ganglia Output

The basal ganglia exercise influence over external structures by the fundamental processes of inhibition and disinhibition (Figure 38–6). GABAergic neurons in the basal ganglia output nuclei typically have high tonic firing rates (40–80 Hz). This activity ensures that target regions of the thalamus and brain stem are maintained under a tight and constant inhibitory control.

Focused excitatory inputs from external structures to the striatum can impose focused suppression (mediated via direct pathway GABAergic inhibitory connections) on subpopulations of output nuclei neurons. This focused reduction of inhibitory output effectively releases or disinhibits targeted regions in the thalamus (eg, ventromedial nucleus) and brain stem (eg, superior colliculus) from normal inhibitory control. This sudden release from tonic inhibition allows activity in the targeted region to influence behavioral output, which in the case of the midbrain superior colliculus is to elicit saccadic eye movements.

The patterns of signaling within the basal ganglia architecture provide important insights into what the overall functional properties of these networks might be (see below). Further constraints on the likely core functions of the basal ganglia also become apparent when considering the evolutionary history of the vertebrate brain.

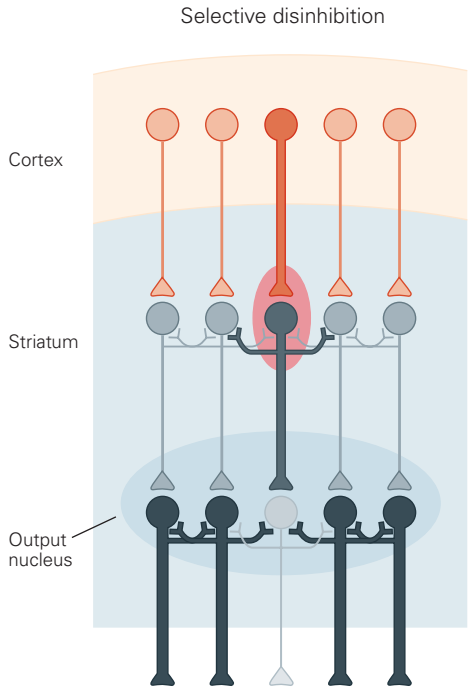

Figure 38–6 The diagram illustrates the principle of selection operating at the level of the basal ganglia output nuclei. Throughout the figure, the relative levels of activity within the competing channels are represented by the thickness of projections, and for clarity, the indirect pathway and the return connections of the loops via the thalamus have been omitted. One of the competing inputs to the striatum (the middle one) is more active than its competitors. Relative activities in the direct inhibitory pathways (shown here) differentially suppress activity in the different channels within the output nuclei. Because output nuclei neurons are also inhibitory and tonically active, the selected channel will be the one with the strongest inhibitory input from the striatum. Tonic inhibitory output is maintained on the nonselected channels. This selective disinhibitory mechanism operating at the level of the output nuclei means that selection will be an emergent property of the entire reentrant network. Disinhibition of selected external targets will allow them to direct movement, while nonselected targets remain inhibited and unable to influence behavior. **Red**, excitatory; **gray**, inhibitory.

Throughout Vertebrate Evolution, the Basal Ganglia Have Been Highly Conserved

Detailed comparisons between the mammalian basal ganglia and those found in phylogenetically ancient vertebrates (eg, the lamprey) have found striking similarities in their individual components, internal organization, inputs from external structures (the cortex/pallium and thalamus), and the efferent projections of their output nuclei. For example, both direct and indirect pathways from striatal medium spiny neurons have been observed in the lamprey. Similarly, tonically active GABAergic output neurons are present in the lamprey internal globus pallidus and substantia nigra pars reticulata. The neurotransmitters and membrane properties of basal ganglia neurons are also remarkably similar in evolutionarily ancient and modern species.

This high degree of morphological and neurochemical conservation implies that the architecture and operation of basal ganglia circuits have been retained for more than 500 million years. The basal ganglia are therefore an essential component of brain architecture

that is shared by all vertebrate species. Bearing in mind that a function emerges from specific patterns of signals being processed in specific neural networks, the conservation of basal ganglia architecture across vertebrate species places an additional important constraint on their overall function. Whatever computational problems the basal ganglia evolved to solve in evolutionarily ancient species, the same problems are likely to have remained unchanged and to confront all vertebrate species, including humans.

Thus far, we have identified features of basal ganglia morphology, connectional architecture, signal processing, and evolution that provide potential insights as to the role of the basal ganglia in overall brain function. Thus, proposed functions must be consistent with the predominant looped architecture that connects external structures with the basal ganglia and with an internal circuitry that is shared across the limbic, associative, and sensorimotor territories of the basal ganglia nuclei, and they must be shared by all vertebrate species. With these constraints in mind, we now consider functional properties that could be supported by the basal ganglia.

Action Selection Is a Recurring Theme in Basal Ganglia Research

Despite numerous suggestions that the basal ganglia are involved in a wide range of functions, including perception, learning, memory, attention, many aspects of motor function, and even analgesia and seizure suppression, evidence is accumulating that these nuclei have an underlying role in a variety of selection processes. Thus, throughout the prodigious literature on the basal ganglia there are recurring references to the involvement of these nuclei in the essential brain functions of action selection and reinforcement learning. In this and the next section we will evaluate the extent to which these core processes are consistent with the functional constraints identified above.

All Vertebrates Face the Challenge of Choosing One Behavior From Several Competing Options

Vertebrates are multifunctional organisms: They have to maintain energy and fluid balances, defend against harm, and engage in reproductive activities. Different areas of the brain operate in parallel to deliver these essential functions but must share limited motor resources. Sherrington's "final common motor path" means it is impossible to talk and drink at the same time. Thus, a fundamental selection problem, continually faced by all vertebrates, is determining which functional system should be allowed to direct behavioral output at any point in time. This is a problem that has not changed materially over the course of 500 million years of evolutionary history. What has changed over this time are the behavioral options that have evolved in different species to implement the core functions of survival and reproduction. Consequently, there has to be a system in the vertebrate brain that can adjudicate between the motivational systems that simultaneously compete for behavioral expression.

A similar selection problem also arises within vertebrate multimodal sensory systems. The visual, auditory, olfactory, and tactile systems are continually faced with multiple external stimuli, each one of which could drive a movement incompatible with one specified by others (eg, orienting/approach, avoidance/escape). It is therefore imperative to select a stimulus that will become the focus of attention and direct movement. The problem is which stimulus should be given access to the motor systems at any one time. Selective attention provides an effective solution to this problem, making it an essential feature of vertebrate brain function.

In summary, despite great evolutionary changes in the range, power, and sophistication of the sensory, motivational, cognitive, and motor systems that compete for behavioral expression in different species, the fundamental computational problems of selection have remained unaltered. And, if the basal ganglia provide a generic solution to the problems of selection, a high degree of structural and functional conservation within vertebrate brain evolution would be expected.

Selection Is Required for Motivational, Affective, Cognitive, and Sensorimotor Processing

In his *Principles of Psychology* (1890), William James observed, "Selection is the very keel on which our mental ship is built." In this statement, he is telling us that the neural systems of motivation, emotion, cognition, perception, and motor performance, at some stage, need to consult a mechanism that can select between parallel processed but incompatible options (Figure 38–7). It is therefore significant that intrinsic circuits in the basal ganglia nuclei are similar across the limbic, associative, and sensorimotor territories.

Such repetition within the basal ganglia circuitry suggests that the same or similar computational processes are applied to inputs from very different functional origins. This duplicated circuitry would therefore be in a position to resolve competitions between high-level motivational goals in the limbic territories;

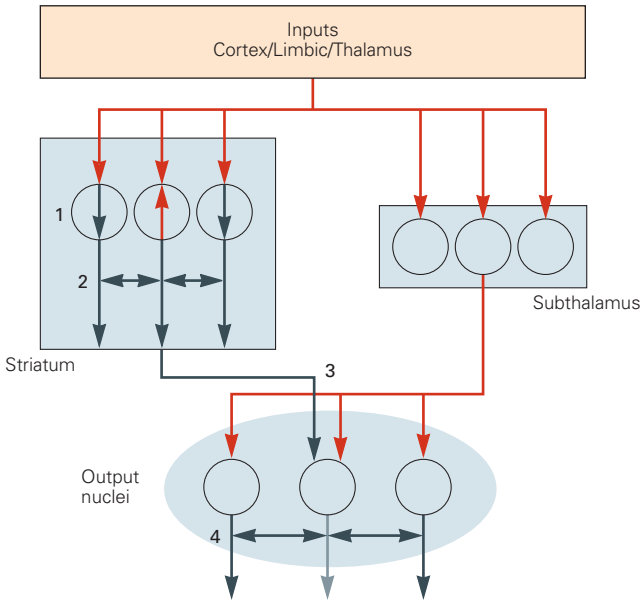

Figure 38–7 Cooperative mechanisms in the basal ganglia that would promote selection.

1. Because cortical and some thalamic inputs make comparatively few contacts with individual striatal neurons, a large population of sufficiently synchronized excitatory inputs is required to depolarize the membrane of a medium spiny neuron to an "up" state sufficient for it to fire action potentials. This mechanism can be seen as an input filter to exclude weak or less biologically significant competitors. The **internal arrows** in striatal neurons denote "up" (**red**) and "down" (**gray**) states.

2. Local GABAergic and peptidergic inhibitory collaterals between striatal spiny neurons and longer-range inhibitory effects of interneurons should cause highly activated striatal elements to suppress activity in adjacent more weakly activated channels.

3. The combination of focused inhibition from the striatum with the more diffuse excitation from the subthalamus would both decrease the activity in selected channels and increase activity in nonselected channels in the basal ganglia output nuclei. The output from just one of the striatal and subthalamic neurons has been illustrated to make this point.

4. Local inhibitory collaterals between output nuclei neurons should further sharpen the difference between inhibited and noninhibited channels.

competitions between incompatible cognitive representations in the central associative territories; and competitions between incompatible sensory and motor options resolved in the lateral sensorimotor regions.

The Neural Architecture of the Basal Ganglia Is Configured to Make Selections

At various times during the past 40 years, and more so recently, it has been argued that the principle function of the basal ganglia is to select between competing and incompatible behavioral options. It has now been recognized that many aspects of the basal ganglia architecture are consistent with this view (Figure 38–6). The parallel loops originating from and returning to diverse cortical and subcortical functional systems can be viewed as the basic substrate for selection.

The phasic excitatory input signals from the cerebral cortex and thalamus to the different functional territories of the striatum can be seen to carry signals representing the behavioral options competing for expression. To ensure that all options could in principle be assessed against all others, there needs to be a "common currency." This term refers to the parameter according to which qualitatively different functional options can be compared for the purpose of selection. This parameter would be represented by the relative magnitudes of input signals to the striatum, thereby providing each competitor with a measure of relative biological importance or salience. In principle, it should be necessary only for the basal ganglia to appreciate which option is most salient in terms of the common currency.

Processing within the parallel projecting internal architecture (Figure 38–6) would ensure that channels associated with the most salient input activity would cause focused inhibition at the level of the output nuclei (the winning options), while at the same time maintaining or increasing the tonic inhibitory activity in output channels returning to regions specifying weaker (losing) options. Experiments that have recorded neural activity in basal ganglia output nuclei in active animals describe populations of task-sensitive neurons whose activity is reduced or paused prior to movement (the winning option). Conversely, there is a separate, often larger population whose high level of tonic activity is further increased or at least maintained (the losing options). The returning signals within the disinhibited channel(s) are necessary to permit the structures providing the strongest motivational, cognitive, or sensorimotor inputs to access the shared motor resources. Importantly, the maintained or increased levels of inhibitory efferent signals within nonselected channels would prevent the output of nonselected target structures from distorting the selected option's input to the motor system. Thus, this model of the basal ganglia works by keeping all potential behavioral options under tight inhibitory control and selectively removing the inhibition from the option proving the most salient input.

A central-selection control architecture, similar to the systems-level architecture of the basal ganglia just described, was used successfully to select actions for

an autonomous mobile robot. Subsequently, it was confirmed that a biologically constrained computer simulation of basal ganglia architecture could do likewise. This work with artificial agents is important because it confirms that selection is indeed an emergent property of systems-level basal ganglia circuitry. The next question is: If the overall architecture can select, are there mechanisms within the basal ganglia that would support or facilitate this function?

Intrinsic Mechanisms in the Basal Ganglia Promote Selection

At each of the major relay points within each of the reentrant loops passing though the basal ganglia (external structures, input nuclei, intrinsic nuclei, output nuclei, and the thalamus), signals flowing within the parallel channels can be subjected to influences originating outside the loop. The selection model outlined above requires features within the internal circuitry of the basal ganglia that permit different channels to interact competitively with each other. Several of these can be identified (Figure 38–7). Together, these mechanisms can be viewed as a cooperative sequence of processes, each of which would facilitate the overall goal of selection. In addition, there is substantial evidence that the relative activity of direct and indirect striatal projection pathways is critical for action selection. The traditional and widely accepted view is that the relative activity in the direct and indirect pathways determines whether or not an animal will perform a particular movement. For example, recent optogenetic stimulation of direct pathway neurons leads to more movement, while optogenetic stimulation of indirect pathway neurons leads to less movement. However, an alternative view for which there is increasing evidence is that simultaneous activity in both pathways is critical for the process of selecting what to do. Here, the idea is that the direct pathway conveys signals representing the most salient options, while the indirect pathway is important for inhibiting the competing weaker options. The latter idea is consistent with the now repeated observations that both projection pathways are concurrently active during movement initiation and that specific patterns of activity in each pathway are associated with different movements.

Selection Function of the Basal Ganglia Questioned

Despite the wide appeal of the selection hypothesis of basal ganglia function, it is by no means universally accepted. Indeed, arguments against it have been voiced based on different studies, the results of which are considered incompatible with the selection model. For example, it has been reported that lesions or suppression of neural activity in motor territories of the internal globus pallidus failed to alter the reaction time between a sensory cue and the triggered movement.

These results could indicate that the basal ganglia are mainly involved in selecting and executing actions that are self-paced, or memory-driven, rather than cue-driven. However, a possibility not considered by these studies is that for well-practiced tasks it is likely that the sensory regions of the basal ganglia will be the most important. This is because such tasks can be performed under stimulus–response habitual control, where selection of the stimulus that triggers the response would be the critical selection. Thus, a failure to disrupt sensory cue selection in such tasks following experimental disruption of the relevant sensory region of basal ganglia would be far stronger evidence against the selection model.

Another recent study claims that in some tasks action choice is already clear in cortical activity even before it reaches the basal ganglia and that the basal ganglia activity is mainly related to reinforcing the commitment to perform the action. This study, and many others like it, base their claims on recordings from afferent structures showing that the neurons are coding the selected stimulus/action/motor program prior to relevant neural responses recorded from within the basal ganglia. An alternative interpretation of these data would be that recordings from all afferent structures that provide competing inputs to the basal ganglia will have shorter latencies than related signals recorded from within the basal ganglia. If in these experiments afferent recordings were from the structure proving the most salient of the competing inputs, then it will be coding for the ultimately selected option *before* it has been selected by basal ganglia.

Other findings are that recordings in the basal ganglia correlate with metrics of movement (eg, speed) and that dopamine signals in the striatum can affect the probability and also the vigor of movement. It is sometimes argued that these results are more indicative of the basal ganglia helping to commit to movement and determining the parameters of movement rather than simply selecting what to do. At least two alternative views could explain why recorded activity in the basal ganglia correlates with movement metrics. First, as mentioned above, one of the significant inputs to the striatum is an efference copy of signals relayed to the motor plant. It would be strange if these signals did not contain information about movement metrics. Second, at this point, it is probably wise to recognize

that actions are multidimensional and, as they are learned, require selections about not only *what* to do but also *where* to do it, *when* to do it, and *how* to do it.

The fact that correlates of these various properties of action can be recorded within the basal ganglia nuclei should not necessarily be surprising. Recent studies suggest that *what* and *where* options may arrive to the basal ganglia via glutamatergic input, for example, from the cortex, while *when* options may be modulated by dopaminergic inputs. One of the reasons we know that actions comprise these different dimensions is that each of them can be independently manipulated by reinforcement learning. It is to that topic, which is likely to be an inherent property of a selection architecture, that we now turn.

Reinforcement Learning Is an Inherent Property of a Selection Architecture

The basal ganglia have long been associated with fundamental processes of reinforcement learning. In his famous Law of Effect, first published in his book *Animal Intelligence* (1911), Edward Lee Thorndike proposed that "any act which in a given situation produces satisfaction becomes associated with that situation so that when the situation recurs the act is more likely than before to recur also." Using contemporary language, Thorndike is stating that in a given context an action that has been associated with reward is more likely to be selected in the future when the same or similar contexts are encountered.

Stated in this way, reinforcement learning can be seen as a process for biasing action selection; consequently, it would be expected to operate by modulating activity in the mechanism(s) responsible for selection. How would a reinforcer (reward or punishment) bias selection in the basal ganglia architecture described above? Theoretically, competition between the options represented in the reentrant loops could be biased by sensitizing a reward-related loop at any of its relay points (cortex, input nuclei, globus pallidus, output nuclei, and thalamus). Here, we present just two examples where there is good evidence that reward operating at different nodes within the basal ganglia's reentrant loop circuitry can bias selection (Figure 38–8).

Intrinsic Reinforcement Is Mediated by Phasic Dopamine Signaling Within the Basal Ganglia Nuclei

The popular view of reinforcement in the basal ganglia is that action selection is biased by a dopamine teaching signal that adjusts the sensitivity of intrinsic circuitry so that responses to inputs associated with unpredicted rewards are enhanced (Figure 38–8A). In this model, therefore, the process of reinforcement learning is intrinsic to the basal ganglia nuclei. However, as we have seen above, dopaminergic neurons have highly divergent axons that terminate in wide areas of targeted nuclei. Add to this the problem of volume transmission and the fact that dopaminergic neurons often respond together as a population to relevant events and the problem of how to reinforce only those elements associated with reward or punishment immediately becomes apparent.

It is thought that this issue is addressed by invoking the concept of a decaying eligibility trace. That is, spiking activity in the population of neurons associated with an action that leads to reward is thought to alter the state specifically of those neurons, making them receptive to later widely broadcast reward-related reinforcement signals. There is evidence that this process operates within the basal ganglia. Thus, in most contemporary models, competing behavioral options are represented by specific neurons, the activity of which can be reinforced by phasic increases or decreases in afferent dopamine signals.

Because behavioral experiments have established that unpredicted reward rather than reward per se is critical for learning, the phasic response properties of dopaminergic neurons have captured the imagination of both the biological and computational neuroscience communities. The powerful combination of biological experimentation and computational analyses now indicates clearly that the phasic activity of midbrain dopaminergic neurons provides a teaching signal for reinforcement learning.

While recording from dopaminergic neurons in the ventral midbrain, most studies presented subjects (usually monkeys) either with rewards or neutral stimuli that predicted rewards. The results of these experiments showed that the phasic dopamine responses evoked by unexpected rewards, or the onset of stimuli that predict them, had short response latencies (~100 ms from stimulus onset) and short durations (again ~100 ms). The magnitude of these responses was shown to be influenced by a range of factors including the size, reliability, and extent the reward would be delayed. Importantly, when a neutral stimulus predicted reward (as in traditional Pavlovian conditioning), the phasic dopamine response transferred from the reward to the predicting stimulus. Alternatively, if a reward was predicted but not delivered, the dopaminergic neurons paused briefly at the time the reward would have been delivered. A particularly exciting

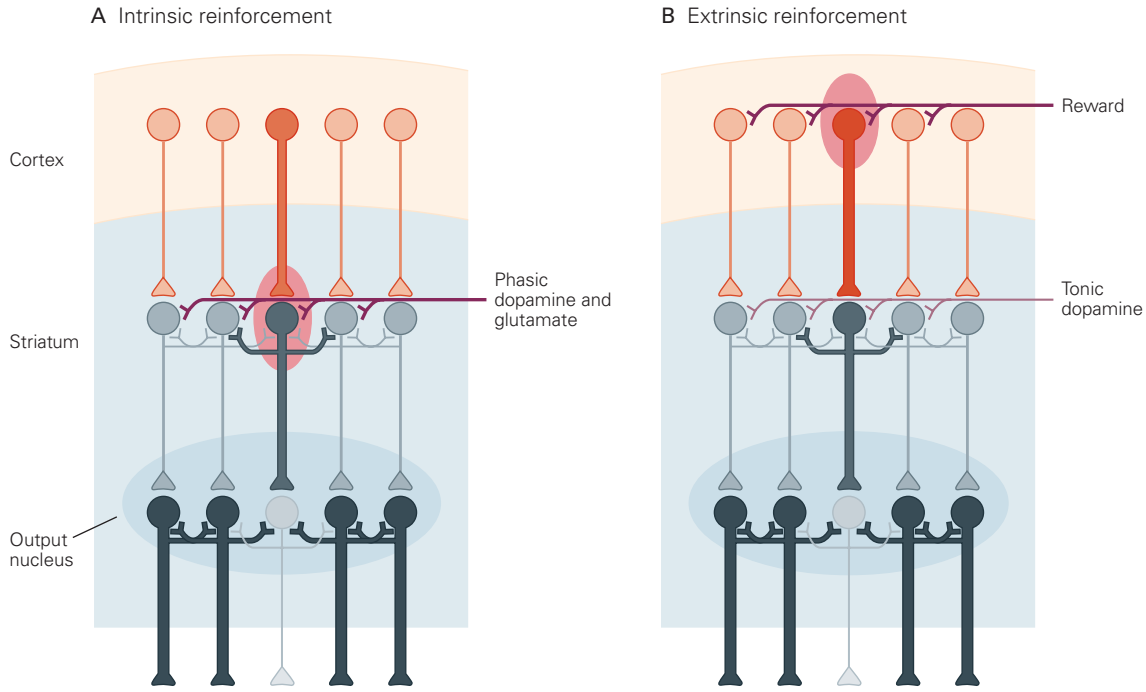

Figure 38–8 **Two separate reinforcement mechanisms can bias selection within the reentrant parallel-loop architecture of the basal ganglia.** (Return connections of the loops via the thalamus have been omitted for clarity.)

A. Intrinsic reinforcement (**red oval**) involves the selective sensitization of corticostriatal neurotransmission (indicated by the relative thickness of striatal projection neurons in different channels). Transmission in recently active (selected) channel(s) is reinforced by the combined phasic release of dopamine and glutamate evoked by an unpredicted biologically salient sensory event (eg, reward). Nonactive channels lack the eligibility trace required for dopamine reinforcement at the synapse. The resulting selective plasticity would cause reinforced versions of recent behavioral output to be preferentially reselected, thereby establishing an association between action and outcome.

B. Recent investigations demonstrate that an association with reward (**red oval**) can potentiate processing in structures providing afferent signals to the striatum. Insofar as selection by the basal ganglia is determined in part by the relative strength of inputs to the striatum (the common currency), reward-related modulation of afferent signals would effectively bias selection to favor reward-related inputs. Again, the thickness of projections in the figure denotes relative levels of activation.

finding was that these responses resembled the reward prediction error term in a machine learning reinforcement algorithm. It was therefore widely concluded that phasic dopamine responses could be operating as the brain's teaching signal in reinforcement learning.

With the advent of optogenetic methodology, it has now been established beyond reasonable doubt that phasic dopamine responses can signal both positive and negative reward prediction errors and that these responses correspondingly increase and decrease the probability that prior behavior will be selected. It is thought that phasic dopamine acts by strengthening inputs onto direct pathway neurons in the striatum and weakening inputs onto indirect pathway neurons. Consequently, there is evidence that direct pathway activity can lead animals to do more of a certain action, while indirect pathway activity would lead animals not to do an action.

However, the roles of these pathways may be more complex than this simple dichotomy. In accordance with the different action dimensions outlined above (*what*, *where*, *when*, and *how*), activity in both the direct and indirect pathways can reinforce or discourage faster or slower movements, depending on which movements lead to reward in that context. Furthermore, the effects of optogenetic self-stimulation of these pathways on action reinforcement seem to be different between the associative (dorsomedial) and sensorimotor (dorsolateral) domains of the striatum. This could be consistent with different dopamine signals observed in the ventral tegmental area, which projects more medially in the striatum, compared to those in the substantia nigra pars compacta, which projects more laterally. The latter has a higher proportion of dopaminergic neurons that respond to stimulus salience and preferentially respond when the animal

initiates self-paced movements (eg, pressing a lever for food whenever it wants, rather than when a sensory cue is presented).

Nonetheless, a wealth of experimental data indicates that phasic dopamine-evoked neural plasticity in the basal ganglia can bias future behavioral selections according to the value of the predicted outcome. This conclusion is consistent with the view that the basal ganglia operate as a generic selection mechanism that can support reinforcement learning.

Extrinsic Reinforcement Could Bias Selection by Operating in Afferent Structures

A second, less widely acknowledged mechanism for biasing selection within the reentrant loop architecture is by modulation of the input salience of competing behavioral options that previously have been associated with a reinforcer—reward or punishment (Figure 38–8B). Since the relative magnitudes of input saliences in competing channels are the common currency by which competing options are judged, reinforcement-induced boosting of a particular channel's input to a selection mechanism would increase the probability of that option being selected in the future.

Evidence in the literature indicates that when a particular stimulus is associated with reward, its representation is enhanced in many of the afferent structures projecting to the basal ganglia. The origin of the reinforcement signals that modulate processing in the input structures is currently unknown. However, the pretuning of basal ganglia inputs by association with reward implies that options associated with high-value outcomes would have a correspondingly higher probability of being selected. Continual updating of input saliences by reward and punishment would bias selections in such a way that the acquisition of reward (or avoidance of punishment) would be maximized in the long term. Finally, it is probably the reward-related tuning of afferent input to the ventral midbrain that enables dopaminergic neurons to accurately report reward prediction errors.

In summary, it is likely that reinforcement learning will be an additional inherent property of a selection architecture. The synaptic relay points at various locations around the parallel reentrant loop architecture provide ample opportunity for the activity in specific loops to be modulated by reward and punishment. There is now good evidence that selection bias can be achieved by reward via a mechanism involving the widespread release of dopamine within the basal ganglia. Reinforcement selectivity is likely to be achieved via some form of eligibility mechanism. A second possibility is that the relative salience of behavioral options can be modulated by reward and punishment acting directly within the structures that provide input to the basal ganglia.

Behavioral Selection in the Basal Ganglia Is Under Goal-Directed and Habitual Control

Over the past decades, it has become apparent that actions can be learned and then selected based on goal-directed or habitual control. Initially, as we learn to perform particular actions to obtain specific outcomes, these actions are goal-directed, and their performance is highly sensitive to changes in the expected value of the outcome or to changes in the contingency between the action and the outcome. With repetition and consolidation, actions can become not only more efficient but also more automatic, controlled by a stimulus–response type circuit.

In the case of habits, performance becomes less sensitive to changes in the outcome value or changes in contingency between action and the outcome, but rather is controlled by the salience of antecedent stimuli or contexts. Interestingly, shifts from goal-directed to habitual behaviors can be produced not only by extended training, but also by different schedules of reinforcement. Thus, the formation of habits is favored when rewards are delivered according to random time intervals, while goal-directed control is favored when rewards are delivered after a random number of actions.

Different cortical-basal ganglia loops seem to support the learning and performance of goal-directed actions versus habits. The acquisition of goal-directed actions appears to rely on the associative cortical-basal ganglia circuit involving the dorsomedial or associative striatum, the prelimbic cortex, the mediodorsal thalamus, the orbitofrontal cortex, and the amygdala. On the other hand, the formation of habits depends upon circuits coursing through the dorsolateral or sensorimotor striatum, infralimbic cortex, and the central amygdala.

It has been shown that since these two fundamental modes of behavioral control operate through different reentrant loops it has been possible to cause shifts between them through specific manipulations within the basal ganglia. Thus, damage to or inactivation of the associative territories effectively blocks goal-directed control while leaving automatic habitual control relatively unimpaired. Conversely, disruption of the sensorimotor basal ganglia causes habitual performance to switch back to goal-directed control.

Finally, efficient habits, where known stimuli or circumstances trigger a particular response, are very helpful in everyday life such as tying one's shoelaces or locking the front door. However, we also encounter circumstances that cause us to reevaluate our actions. Shifting between goal-directed actions and habits allows us to act flexibly in the environment, and inability to do so may underlie distorted behaviors observed in addiction and other behavioral and neurological disorders of the basal ganglia. It is to this topic that we now turn.

Diseases of the Basal Ganglia May Involve Disorders of Selection

The focus of this chapter has been how the functional architecture of the basal ganglia and their evolutionary history have determined their role in overall brain function. One of the motivations for this exercise that we all have is an intrinsic scientific interest in trying to understand something we currently do not. However, there is another important reason to better understand how the basal ganglia operate. In humans, basal ganglia dysfunction is associated with numerous debilitating conditions including Parkinson disease, Huntington disease, Tourette syndrome, schizophrenia, attention deficit disorder, obsessive-compulsive disorder, and many addictions. Numerous studies have attempted to shed light on how basal ganglia dysfunction leads to the symptoms that characterize these disorders. This effort can only be helped if we have a better understanding of what a complicated system like the basal ganglia is trying to do when it is operating normally.

A Selection Mechanism Is Likely to Be Vulnerable to Several Potential Malfunctions

Thus far, we have considered the theoretical and empirical evidence supporting the idea that the looped circuitry of the basal ganglia acts as a generic selection mechanism within which reinforcement learning operates to maximize reward and minimize punishment. If action selection and reinforcement learning are the normal functions of the basal ganglia, it should be possible to interpret many of the human basal ganglia–related disorders in terms of selection or reinforcement malfunctions.

Normal selection requires that the selected option is disinhibited at the level of basal ganglia output, while inhibition of nonselected or losing options is maintained or increased (Figure 38–9A). An obvious failure in such a system would be if none of the options were able to achieve sufficient disinhibition to reach a

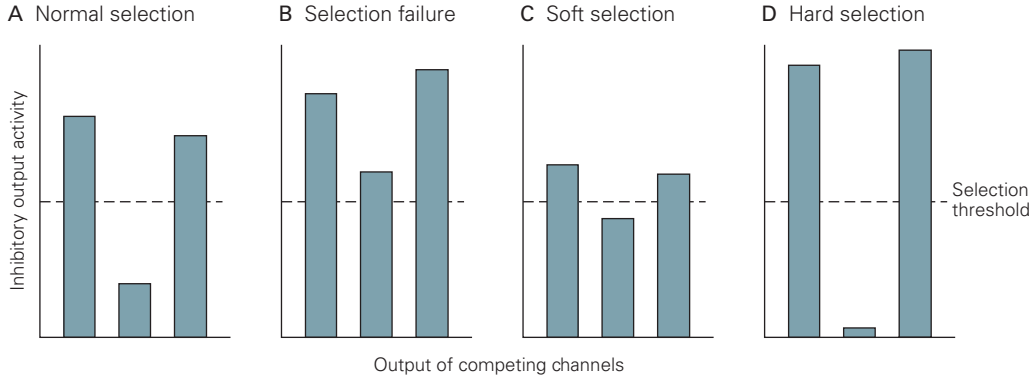

Figure 38–9 Potential disorders of behavior selection.

A. Normal selection within the basal ganglia is characterized by a reduction in inhibition of selected channels below a proposed selection threshold (central channel) while maintaining or increasing inhibition of nonselected channels (left and right channels). Consequently, the disinhibited target structure is able to initiate the action it controls, while the nonselected targets are maintained under inhibitory control.

B. Insufficient reduction in tonic inhibition of all channels means no target structure would be sufficiently disinhibited. This circumstance could explain the akinesia in Parkinson disease.

C. A failure to adequately disinhibit the selected channel or suppress disinhibitory activity in competing channels would cause current selections to be vulnerable to interruption. This disorder could account for the inability to maintain a train of thought and easy distraction by nonattended events in schizophrenia and attention deficit hyperactivity disorder.

D. One channel may become pathologically dominant either through abnormal disinhibition of the selected channel or excessive tonic inhibition of competing channels. This would make the relevant option easy to select and highly resistant to interruption. Hard selections may explain obsessive-compulsive disorder and addictive behaviors.

critical selection threshold (Figure 38–9B). However, a further important point when thinking about selection malfunctions is to appreciate that output inhibition and disinhibition are likely to be continuously variable rather than discrete on/off states. In that case, the difference between the disinhibited and inhibited channels would determine how "hard" or "soft" the selection is. When the difference is large (Figure 38–9D), competing options are likely to find the current selection is resistant to interruption—a larger than normal input salience would be required to cause the system to switch selections. Conversely, when the difference is small (Figure 38–9C), it would be comparatively easy for a competing option to initiate a selection switch.

Support for these ideas comes from behavioral observations showing that at the beginning of task learning there is frequently easy switching between strategies. However, as the task becomes well learned, the system becomes increasingly resistant to alternative strategies. Appreciation of the concepts of hard and soft selection could therefore play an important role when thinking about how a selection mechanism might become dysfunctional in the context of basal ganglia diseases.

Parkinson Disease Can Be Viewed in Part as a Failure to Select Sensorimotor Options

The cardinal symptoms of Parkinson disease are akinesia (difficulties in initiating movement), bradykinesia (initiated movements are slow), and rigidity (stiffness and resistance to passive movement). Tremor is often but not always present. The principal neurological deficit responsible for the motor symptoms of Parkinson disease is thought to be the progressive degeneration of dopaminergic neurotransmission in the basal ganglia.

A consequence of this loss of dopamine is increased tonic and oscillatory activity in the recordings from basal ganglia output nuclei. Since the output of the basal ganglia is GABAergic and inhibitory, in Parkinson disease, targeted structures are receiving high and uneven levels of inhibitory input. This condition impairs the normal selective (disinhibitory) function of the basal ganglia; movements are difficult to select and, when possible, are slow to execute.

Parkinson disease is, however, more nuanced than this. Over much of this progressive condition, the loss of dopaminergic transmission differentially affects the sensorimotor territories of the basal ganglia, leaving the limbic and associative territories comparatively unaffected. As discussed in the section on goal-directed and habitual control, the sensorimotor territories of the basal ganglia play an essential role in selecting habitual actions. Perhaps, therefore, it is not surprising that many of the motor features of Parkinson disease can be interpreted in terms of a loss of automatic habits. While patients can do things, they are trapped in the slower, serial, and voluntary mode of goal-directed control. In the future, it will be interesting to see if subtle losses of habitual control can be detected before clinical symptoms appear, thereby acting as an early marker for the condition.

Huntington Disease May Reflect a Functional Imbalance Between the Direct and Indirect Pathways

Huntington disease is a genetically transmitted disorder, the initial symptoms of which are subtle changes in mood, personality, cognition, and physical skills. The abnormal movements are characterized by jerky, random, and uncontrollable movements called chorea. The disease is associated with neuronal degeneration. Damage in the early stage is most evident in the striatal medium spiny neurons, but later spreads to other regions of the nervous system.

Observations that neuronal degeneration is evident in limbic, associative, and sensorimotor territories of the striatum would explain why the disease is characterized by disturbances of affect, cognition, and sensorimotor function. Also noteworthy is that the most vulnerable neurons are those in the striatum that project to the external globus pallidus (the indirect pathway) rather than the neurons that project directly to the basal ganglia output nuclei. At the level of the output nuclei, this disturbance would tip the balance in favor of the striatal projection responsible for disinhibition. Consequently, the symptoms of Huntington disease could reflect interference with expression of the selected affective, cognitive, and sensorimotor behaviors by competitors not being sufficiently suppressed.

Schizophrenia May Be Associated With a General Failure to Suppress Nonselected Options

Schizophrenic psychosis is a condition in which there are also disturbances of affect, cognition, and sensorimotor function. Typical symptoms include delusions (false beliefs not based in reality), hallucinations (hearing or seeing things that do not exist), disorganized thinking (inferred from disorganized speech), and abnormal motor behavior (unpredictable agitation, stereotypy, and failure to concentrate on the matter in hand). The disease is progressive, and in later stages, negative symptoms characterized by flattened affect, social withdrawal, absence of thought, and reduced motor behavior become evident (Chapter 60).

Understanding the neurobiological basis of schizophrenia has been complicated by many inconsistent experimental procedures, high variability in symptoms, the side effects of medications, substance abuse, and variability in response to treatments. There is, however, a consistent link between schizophrenia and the basal ganglia insofar as a major class of antipsychotic drugs acts to suppress dopaminergic neurotransmission. In terms of simple regional density of axon terminals and postsynaptic dopamine receptors, dopaminergic transmission within the basal ganglia is likely to be influenced most profoundly by dopamine-related pharmacological therapies. Moreover, there is evidence that dopamine dysregulation in the basal ganglia is intrinsic to the pathology of schizophrenia rather than a medication side effect; predates the psychosis; and is a risk factor for the illness. The implication here is that schizophrenia is associated with a net excess of dopaminergic transmission in the basal ganglia.

So how might dysregulation of this form distort the normal functions of selection and reinforcement? First, the observation that schizophrenia is characterized by disturbances of affect, cognition, and sensorimotor behavior again suggests that the neurobiological substrate will be present in each of the basal ganglia's functional territories. Second, a recurrent theme is that with the positive symptoms there seems to be too much of everything—intense emotional intrusions, too many ideas out of control, spontaneous sensory experiences, too many distracting stimuli, and unpredictable motor agitation. One way of unifying this confusing array of symptoms is to assume that they represent a similar basic fault playing out in different functional territories of the basal ganglia. Here, the basic fault could be a failure on the part of the mechanism responsible for suppressing the impact of competing but nonselected options. Consequently, in all functional territories, the currently selected option would be pathologically vulnerable to interruption (Figure 38–9C).

Attention Deficit Hyperactivity Disorder and Tourette Syndrome May Also Be Characterized by Intrusions of Nonselected Options

Further examples of hyperactive conditions that have been linked to basal ganglia dysfunction may also be due to a faulty selection mechanism where the system in each case is vulnerable to intrusions. Attention deficit hyperactivity disorder (ADHD), like schizophrenia, could in part be the result of a failure in the mechanism responsible for suppressing nonselected sensory options, thereby making it difficult to maintain a focus of attention. Alternatively, the impulsive aspects of the condition could reflect a malfunction in the neural systems that generate behavioral options based on the value of likely consequences. In this situation, options driven by immediately desired sensory events would take precedence over competing representations of disadvantageous longer-term consequences.

In the case of Tourette syndrome, converging evidence indicates that the involuntary behavioral intrusions (verbal and motor tics) are associated with aberrant activity in the cortical–basal ganglia–thalamic loops. In animal models, similar motor tics can be evoked by blocking inhibitory neurotransmission in local areas of the sensorimotor striatum. Were the disease state also to cause a similar failure of inhibition or inappropriate excitation in parts of the striatum not engaged by the current selection, disruptive motor intrusions might be expected. Furthermore, were the locus of the excessive excitation to remain constant and the motor characteristics of the intrusion to be repeated, it is likely that the mechanism for establishing automatic habits would be engaged, thereby further enhancing the automatic involuntary nature of the intrusion.

Obsessive-Compulsive Disorder Reflects the Presence of Pathologically Dominant Options

Persons with obsessive-compulsive disorder compulsively repeat specific actions (hand washing, counting things, checking things) or have particular thoughts repeatedly come to mind uninvited (obsessions). Studies using functional neuroimaging when the symptoms are present consistently report abnormal activation at various locations within the cortical-striatum-thalamus-cortical loops.

In terms of a selection mechanism dysfunction, the symptoms of obsessive-compulsive disorder would be expected when, for whatever reason, the input salience of relevant functional channels would be abnormally dominant, thereby making it difficult for competing options to interrupt or cause behavioral or attentional switching (hard selection). The fact that the obsessional and compulsive options are dominant behaviors that have been learned suggests that the fault responsible for obsessive-compulsive disorder may lie with the reinforcement mechanism capable of adjusting input salience. Of course, such a fault could be of genetic and/or environmental origin.

Addictions Are Associated With Disorders of Reinforcement Mechanisms and Habitual Goals

Addiction to drugs and other behaviors (eg, gambling, sex, eating) represents a dramatic dysregulation of

motivational selections. This is caused by an exaggerated salience of addiction-related stimuli, binge indulgence, and withdrawal anxiety. When addictions are being acquired, changes in dopaminergic and opioid peptide transmission in the basal ganglia have been reported.

Insofar as these transmission systems have been linked with fundamental mechanisms of reinforcement, it might be expected that the selective reinforcement of addiction-related stimuli would lead to observed increases in the ability of these stimuli to capture behavior. Alternatively, the increases in negative emotional states and stress-like responses experienced during withdrawal have been associated with reductions in dopamine function. In the limbic territories of the basal ganglia, such reductions are typically associated with negative reinforcement.

A final point to note is that if addiction-associated stimuli can automatically trigger the motivation/goal to indulge (ie, an automatic stimulus–goal association), a similar kind of mechanism may be operating in the limbic territories as is currently assigned to stimulus–response habits in the sensorimotor territories. Thus, if in the case of drug addiction the goal of drug acquisition may be correctly described as a stimulus-driven habit, the practicalities of obtaining the drug can be highly goal directed (eg, robbing a convenience store, phoning the dealer) and not at all habitual.

From the above sections, it can be seen that interpreting disorders of the basal ganglia in terms of dysregulations of selection and reinforcement does not require implausible intellectual contortions. Indeed, this could be regarded as further support for the view that the systems-level function of the basal ganglia is to operate as a generic selection mechanism. Moreover, having an overriding conceptual framework based on potential disorders of normal function has an important advantage for guiding future research. Instead of fishing in the brains of patients and animal models for clues of what might have gone wrong, one is hunting within a specified network for a malfunction that would be expected to produce the observed disorder.

Highlights

1. The basal ganglia are an interconnected group of nuclei located at the base of the forebrain and midbrain. There are three major input structures (the striatum, the subthalamic nucleus, and the dopamine cells of substantia nigra) and two major output structures (the internal globus pallidus and substantia nigra pars reticulata).
2. Input structures receive projections from most regions of the cerebral cortex, limbic system, and brain stem, many via relays in the thalamus. Inputs to the striatum and subthalamus are topographically organized.
3. The spatial topography is maintained throughout the intrinsic basal ganglia connections, as well as in projections back to the cortex, limbic system, and brain stem structures. Thus, an essential feature of systems-level basal ganglia architecture can be viewed as a series of reentrant loops.
4. The striatum was thought to be connected to the output nuclei via direct and indirect pathways. However, recent anatomical evidence suggests a more complex internal architecture.
5. Phasic excitatory input to the basal ganglia is mediated by the neurotransmitter glutamate. Tonic inhibitory output from the basal ganglia is mediated by the neurotransmitter GABA. The reentrant loops keep afferent structures under strong inhibitory control. For any task, the tonic inhibitory firing of some output neurons pauses, while for others, it is maintained or increased.
6. Basal ganglia architecture appeared at the outset of vertebrate evolution and has been highly conserved throughout. This suggests that the computational problems they solve are likely to be problems faced by all vertebrate species.
7. The internal microarchitecture of the intrinsic basal ganglia nuclei is largely the same throughout their motivational, affective, cognitive, and sensorimotor territories. This suggests that the same basal ganglia algorithm is applied to all general classes of brain function.
8. A recurring theme within the basal ganglia literature is their involvement in action selection and reinforcement learning.
9. The selection hypothesis is supported by the following: (1) Selection is a generic problem faced by all vertebrates. (2) A selection algorithm common to all basal ganglia territories could resolve competitions between incompatible motivational, affective, cognitive, and sensorimotor options. (3) Many intrinsic processes could support a selection function. (4) Selective removal of output inhibition within a multiple reentrant looped architecture is necessarily a selection process. (5) Computational models of basal ganglia architecture effectively select the actions of multifunctional robots.
10. Abundant evidence indicates that the basal ganglia are an essential substrate for reinforcement

learning where selections are biased by the valence/value of past outcomes.

11. The multidimensional aspects of action (what, where, when, and how to do something) can be independently modified by reinforcement learning. It will be important to determine whether these different aspects of action are learned within the same or different functional territories of the basal ganglia.
12. Recent optogenetic investigations have confirmed that phasic dopamine signaling can act as a training signal for reinforcement learning.
13. Within the reentrant looped architecture, future selections can be biased not only within the basal ganglia by dopamine but also at synapses in external afferent structures and the thalamic relays.
14. Reinforcement learning can bias selections on the basis of outcome value (goal-directed), or by operating on an acquired automatic stimulus–response association (habit). Goal-directed and habitual selections are made in different functional territories of the basal ganglia.
15. Insofar as diseases of the basal ganglia in humans can be interpreted as selection malfunctions, additional support is provided for the idea that the basal ganglia operate as a generic selection module.

Peter Redgrave
Rui M. Costa

Suggested Reading

Cui G, Jun SB, Jin X, et al. 2013. Concurrent activation of striatal direct and indirect pathways during action initiation. Nature 494:238–242.

da Silva JA, Tecuapetla F, Paixão V, Costa RM. 2018. Dopamine neuron activity before action initiation gates and invigorates future movements. Nature 554:244–248.

Grillner S, Robertson B, Stephenson-Jones M. 2013. The evolutionary origin of the vertebrate basal ganglia and its role in action selection. J Physiol 591:5425–5431.

Hikosaka O, Ghazizadeh A, Griggs W, Amita H. 2018. Parallel basal ganglia circuits for decision making. J Neural Transm (Vienna) 125:515–529.

Kravitz AV, Freeze BS, Parker PR, et al. 2010. Regulation of parkinsonian motor behaviours by optogenetic control of basal ganglia circuitry. Nature 466:622–626.

Redgrave P, Prescott T, Gurney KN. 1999. The basal ganglia: a vertebrate solution to the selection problem? Neuroscience 89:1009–1023.

Redgrave P, Rodriguez M, Smith Y, et al. 2010. Goal-directed and habitual control in the basal ganglia: implications for Parkinson's disease. Nat Rev Neurosci 11:760–772.

Saunders A, Oldenburg IA, Berezovskii VK, et al. 2015. A direct GABAergic output from the basal ganglia to frontal cortex. Nature 521:85–89.

Yin HH, Knowlton BJ. 2006. The role of the basal ganglia in habit formation. Nat Rev Neurosci 7:464–476.

Yttri EA, Dudman JT. 2016. Opponent and bidirectional control of movement velocity in the basal ganglia. Nature 533:402–406.

References

Albin RL, Mink JW. 2006. Recent advances in Tourette syndrome research. Trends Neurosci 29:175–182.

Albin RL, Young AB, Penney JB. 1989. The functional anatomy of basal ganglia disorders. Trends Neurosci 12:366–375.

Alexander GE, Crutcher MD, Delong MR. 1990. Functional architecture of basal ganglia circuits: neural substrates of parallel processing. Trends Neurosci 13:226–271.

Arbuthnott GW, Wickens J. 2007. Space, time and dopamine. Trends Neurosci 30:62–69.

Carmona S, Proal E, Hoekzema EA, et al. 2009. Ventro-striatal reductions underpin symptoms of hyperactivity and impulsivity in attention-deficit/hyperactivity disorder. Biol Psychiatry 66:972–977.

Chevalier G, Deniau JM. 1990. Disinhibition as a basic process in the expression of striatal functions. Trends Neurosci 13:277–281.

DeLong MR, Wichmann T. 2007. Circuits and circuit disorders of the basal ganglia. Arch Neurol 64:20–24.

Deniau JM, Mailly P, Maurice N, Charpier S. 2007. The pars reticulata of the substantia nigra: a window to basal ganglia output. In: JM Tepper. ED Abercrombie, JP Bolam (eds). *Gaba and the Basal Ganglia: From Molecules to Systems*. Prog Brain Res 160:151–172.

Desmurget M, Turner RS. 2010. Motor sequences and the basal ganglia: kinematics, not habits. J Neurosci 30:7685–7690.

Draganski B, Kherif F, Klöppel S, et al. 2008. Evidence for segregated and integrative connectivity patterns in the human basal ganglia. J Neurosci 28:7138–7152.

Fan D, Rossi MA, Yin HH. 2012. Mechanisms of action selection and timing in substantia nigra neurons. J Neurosci 32:5534–5548.

Gerfen CR, Surmeier DJ. 2011. Modulation of striatal projection systems by dopamine. Ann Rev Neurosci 34:441–466.

Gerfen CR, Wilson CJ. 1996. The basal ganglia. In: LW Swanson, A Bjorklund, T Hokfelt (eds). *Handbook of Chemical Neuroanatomy, Vol 12: Integrated Systems of the CNS, Part III*, pp. 371–468. Amsterdam: Elsevier.

Graybiel AM. 2008. Habits, rituals, and the evaluative brain. Ann Rev Neurosci 31:359–387.

Hikosaka O. 2007. Basal ganglia mechanisms of reward-oriented eye movement. Ann NY Acad Sci 1104:229–249.

Howes OD, Kapur S. 2009. The dopamine hypothesis of schizophrenia: version III—the final common pathway. Schizophr Bull 353:549–562.

Humphries MD, Stewart RD, Gurney KN. 2006. A physiologically plausible model of action selection and oscillatory activity in the basal ganglia. J Neurosci 26:12921–12942.

Kelly RM, Strick PL. 2004. Macro-architecture of basal ganglia loops with the cerebral cortex: use of rabies virus to reveal multisynaptic circuits. Prog Brain Res 143: 449–459.

Klaus A, Martins GJ, Paixao VB, Zhou P, Paninski L, Costa RM. 2017. The spatiotemporal organization of the striatum encodes action space. Neuron 95:1171–1180.

Koob GF, Volkow ND. 2016. Neurobiology of addiction: a neurocircuitry analysis. Lancet Psychiatry 38:760–773.

MacDonald AW, Schulz SC. 2009. What we know: findings that every theory of schizophrenia should explain. Schizophr Bull 3:493–508.

Matsuda W, Furuta T, Nakamura KC, et al. 2009. Single nigrostriatal dopaminergic neurons form widely spread and highly dense axonal arborizations in the neostriatum. J Neurosci 29:444–453.

Matsumoto M, Takada M. 2013. Distinct representations of cognitive and motivational signals in midbrain dopamine neurons. Neuron 79:1–14.

McHaffie JG, Stanford TR, Stein BE, Coizet V, Redgrave P. 2005. Subcortical loops through the basal ganglia. Trends Neurosci 28:401–407.

Mink JW. 1996. The basal ganglia: focused selection and inhibition of competing motor programs. Prog Neurobiol 50:381–425.

Minski M. 1986. *The Society of Mind*. London: Heinemann Ltd.

Nambu A. 2011. Somatotopic organization of the primate basal ganglia. Front Neuroanat 5:26.

Nambu A, Tokuno H, Takada M. 2002. Functional significance of the cortico-subthalamo-pallidal 'hyperdirect' pathway. Neurosci Res 43:111–117.

Nasser HM, Calu DJ, Schoenbaum G, Sharpe MJ. 2017. The dopamine prediction error: contributions to associative models of reward learning. Front Psychol 8:244.

Nieuwenhuys R, Voogd J, van Huijzen C. 1981. *The Human Central Nervous System: A Synopsis and Atlas*, 2nd ed. Berlin: Springer.

Piron C, Kase D, Topalidou M, et al. 2016. The globus pallidus pars interna in goal-oriented and routine behaviors: resolving a long-standing paradox. Mov Disord 31:1146–1154.

Plotkin JL, Surmeier DJ. 2015. Corticostriatal synaptic adaptations in Huntington's disease. Curr Opin Neurobiol 33:53–62.

Redgrave P, Gurney KN. 2006. The short-latency dopamine signal: a role in discovering novel actions? Nat Rev Neurosci 7:967–975.

Reiner AJ. 2010. The conservative evolution of the vertebrate basal ganglia. In: H Steiner, KY Tseng (eds). *Handbook of Basal Ganglia Structure and Function*, pp. 29–62. Burlington, MA: Academic Press

Reiner A, Jiao Y, DelMar N, Laverghetta AV, Lei WL. 2003. Differential morphology of pyramidal tract-type and intratelencephalically projecting-type corticostriatal neurons and their intrastriatal terminals in rats. J Comp Neurol 457:420–440.

Schultz W. 2007. Multiple dopamine functions at different time courses. Annu Rev Neurosci 30:259–288.

Silberberg G, Bolam JP. 2015. Local and afferent synaptic pathways in the striatal microcircuitry. Curr Opin Neurobiol 33:182–187.

Smith Y, Galvan A, Ellender TJ, et al. 2014. The thalamostriatal system in normal and diseased states. Front Syst Neurosci 8:5.

Surmeier DJ, Plotkin J, Shen W. 2009. Dopamine and synaptic plasticity in dorsal striatal circuits controlling action selection. Curr Opin Neurobiol 19:621–628.

Tecuapetla F, Jin X, Lima SQ, Costa RM. 2016. Complementary contributions of striatal projection pathways to action initiation and execution. Cell 166:703–715.

Thorndike EL. 1911. *Animal Intelligence*. New York: Macmillan.

van den Heuvel OA, van Wingen G, Soriano-Mas C, et al. 2016. Brain circuitry of compulsivity. Eur Neuropsychopharmacol 26:810–827.

Watabe-Uchida M, Zhu LS, Ogawa SK, Vamanrao A, Uchida N. 2012. Whole-brain mapping of direct inputs to midbrain dopamine neurons. Neuron 74:858–873.

Yael D, Vinner E, Bar-Gad I. 2015. Pathophysiology of tic disorders. Mov Disord 30:1171–1178.

Yin HH, Knowlton BJ. 2006. The role of the basal ganglia in habit formation. Nat Rev Neurosci 7:464–476.

39

Brain–Machine Interfaces

Understanding the normal function of the nervous system is central to understanding dysfunction caused by disease or injury and designing therapies. Such treatments include pharmacological agents, surgical interventions, and, increasingly, electronic medical devices. These medical devices fill an important gap between largely molecularly targeted and systemic medications and largely anatomically targeted and focal surgical lesions.

In this chapter, we focus on medical devices that measure or alter electrophysiological activity at the level of populations of neurons. These devices are referred to as brain–machine interfaces (BMIs), brain–computer interfaces, or neural prostheses. We use the term BMI to refer to all such devices because there is no standard distinction among them. BMIs can be organized into four broad categories: those that restore lost sensory capabilities, those that restore lost motor capabilities, those that regulate pathological neural activity, and those that restore lost brain processing capabilities.

BMIs can help people perform "activities of daily living," such as feeding oneself, physically dressing and grooming oneself, maintaining continence, and walking. A type of BMI that we will discuss extensively in this chapter converts electrical activity from neurons in the brain into signals that control prosthetic devices to help people with paralysis. By understanding how neuroscience and neuroengineering work together to create current BMIs, we can more clearly envision how many neurological diseases and injuries can be treated with medical devices.

BMIs Measure and Modulate Neural Activity to Help Restore Lost Capabilities

Cochlear Implants and Retinal Prostheses Can Restore Lost Sensory Capabilities

One of the earliest and most widely used BMIs is the cochlear implant. People with profound deafness can benefit from restoration of even some audition. Since the 1970s, several hundred thousand people who have a peripheral cause of deafness that leaves the cochlear nerve and central auditory pathways intact have received cochlear implants. These systems have restored considerable hearing and spoken language, even to children with congenital deafness who have learned to perceive speech using cochlear implants.

Cochlear implants operate by capturing sounds with a microphone that resides outside the skin and sending these signals to a receiver surgically implanted under the skin near the ear. After conversion (encoding) to appropriate spatial-temporal signal patterns, these signals electrically stimulate spiral ganglion cells in the cochlear modiolus (Chapter 26). In turn, signals from the activated cochlear cells are transmitted through the auditory nerve to the brain stem and higher auditory areas where, ideally, the neural signals are interpreted as the sounds captured by the microphone.

Another example of a BMI is a retinal prosthesis. Blindness can be caused by diseases such as retinitis pigmentosa, an inherited retinal degenerative disease. At present, there is no cure and no approved medical therapy to slow or reverse the disease. Retinal prostheses currently enable patients to recognize large letters and locate the position of objects. They operate by capturing images with a camera and sending these signals to a receiver positioned within the eye. After conversion to appropriate spatial-temporal patterns, these electrical signals stimulate retinal ganglion cells in the retina through dozens of electrodes. In turn, these cells send their signals through the optic nerve to the thalamus and higher visual areas where, ideally, the afferent signals are interpreted as the image captured by the camera.

Motor and Communication BMIs Can Restore Lost Motor Capabilities

BMIs are also being developed to assist paralyzed people and amputees by restoring lost motor and communication function. This is the central topic of this chapter. First, electrical neural activity in one or more brain areas is measured using penetrating multielectrode arrays placed, for example, in the arm and hand region of the primary motor cortex, dorsal and ventral premotor cortex, and/or intraparietal cortex (particularly the parietal reach region and medial intraparietal area) (Figure 39–1).

Second, an arm movement is attempted but cannot be made in the case of people with paralysis. Action potentials and *local field potentials* are measured during these attempts. With 100 electrodes placed in the primary motor cortex and another 100 in the dorsal premotor cortex, for example, action potentials from approximately 200 neurons and local field potentials from 200 electrodes are measured. Local field potentials are lower-frequency signals recorded on the same electrodes as the action potentials and believed to arise from local synaptic currents of many neurons near the electrode tips. Together, these neural signals contain considerable information about how the person wishes to move her arm.

Third, the relationship between neural activity and attempted movements is characterized. This relationship makes it possible to predict the desired movement from new neural activity, a statistical procedure we refer to as *neural decoding*. Fourth, the BMI is then operated in its normal mode where neural activity is measured in real time and desired movements are decoded from the neural activity by a computer. The decoded movements can be used to guide prosthetic devices, such as a cursor on a computer screen or a robotic arm. It is also possible to electrically stimulate muscles in a paralyzed limb to enact the decoded movements, a procedure known as *functional electrical stimulation*. Many other prosthetic devices can be envisioned as we increasingly interact with the world around us electronically (eg, smart phones, automobiles, and everyday objects that are embedded with electronics so that they can send and receive data—known as the "internet of things").

Finally, because the person can see the prosthetic device, she can alter her neural activity by thinking different thoughts on a moment-by-moment basis so as to guide the prosthetic device more accurately. This closed-loop feedback control system can make use of nonvisual sensory modalities as well, including delivering pressure and position information from electronic sensors wrapped on or embedded in a prosthetic arm. Such surrogate sensory information can be transformed into electrical stimulation patterns that are delivered to proprioceptive and somatosensory cortex.

The BMIs described above include motor and communication BMIs. Motor BMIs aim to provide natural control of a robotic limb or a paralyzed limb. In the case of upper-limb prostheses, this involves the

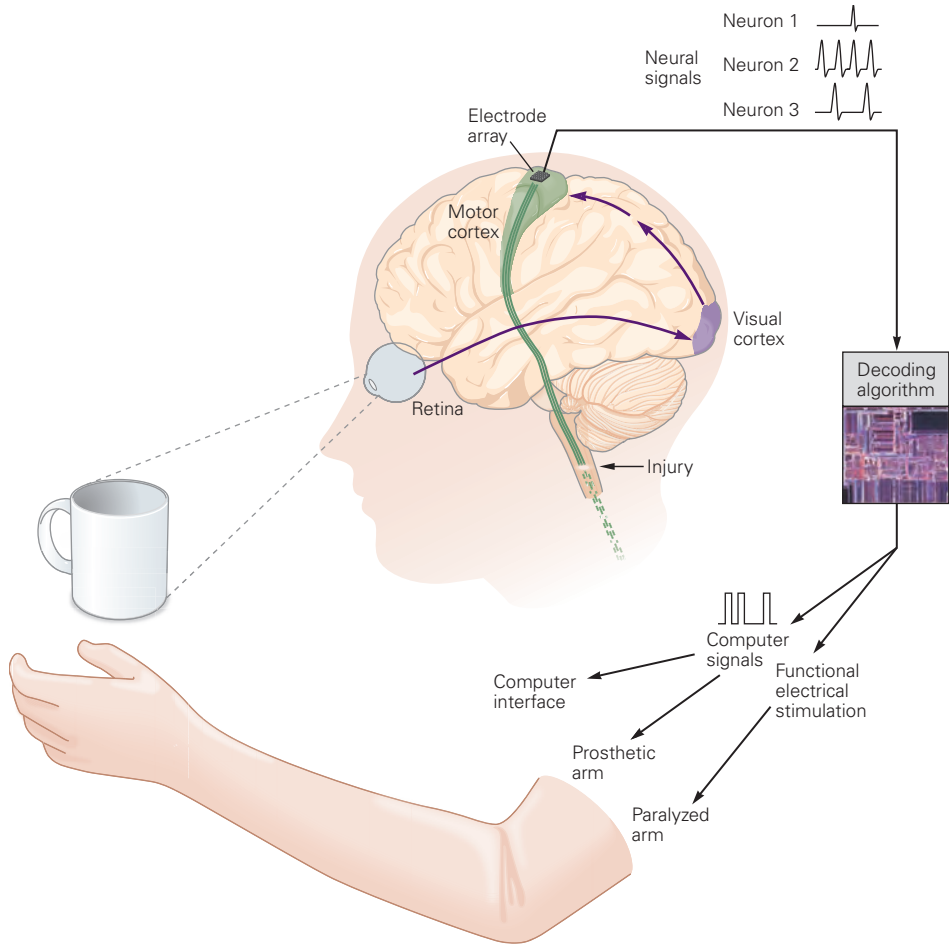

Figure 39–1 Concept of motor and communication brain–machine interfaces. One or more electrode arrays are implanted in brain regions such as the primary motor cortex, dorsal and ventral premotor cortex, or intraparietal cortex. They record action potentials from tens to hundreds of neurons and local field potentials. The recorded neural activity is then converted by a decoding algorithm into (1) computer commands for controlling a computer interface or a prosthetic (robotic) arm, or (2) stimulation patterns for functional electrical stimulation of muscles in a paralyzed arm.

precise movement of the arm along a desired path and with a desired speed profile. Such control is indeed an ambitious ultimate goal, but even intermediate steps toward this goal could improve quality of life by restoring some lost motor function and improving the patient's ability to carry out "activities of daily living." For example, numerous people with tetraplegia could benefit from being able to feed themselves.

Communication BMIs are designed to provide a fast and accurate interface with a plethora of electronic devices. The ability to move a computer cursor around an on-screen keyboard allows a patient to type commands for computers, smart phones, voice synthesizers, smart homes, and the "internet of things." Ideally, communication BMIs would allow for a communication rate at which most people speak or type. Such BMIs would benefit people with amyotrophic lateral sclerosis (ALS), who often become "locked in" and unable to communicate with the outside world through any movements. Communication BMIs would also benefit people with other neurodegenerative diseases that severely compromise the quality of movement and speech, as well as those with upper spinal cord injury. The ability to reliably type several words per minute is a meaningful improvement in quality of life for many patients.

Motor and communication BMIs build on basic neuroscientific research in voluntary movement (Chapter 34). The design and development of BMIs have so far depended on laboratory animal research, largely with nonhuman primates; recently, however, pilot clinical trials with humans with paralysis have begun.

Pathological Neural Activity Can Be Regulated by Deep Brain Stimulation and Antiseizure BMIs

BMIs have been developed to help people with disorders involving pathological neural activity in the brain, such as Parkinson disease and epilepsy. People with Parkinson disease benefit by having hand and arm tremor reduced. At present, there is no cure for Parkinson disease, and many people become resistant to pharmacological treatments. A deep brain stimulator (DBS) can help these people by delivering electrical pulses to targeted areas in the brain to disrupt the aberrant neural activity.

DBS is controlled by a neurostimulator implanted in the chest, with wires to stimulating electrodes in deep brain nuclei (eg, the subthalamic nucleus). The nuclei are continuously stimulated with these electrodes in order to alter the aberrant neural activity. This method can often greatly reduce Parkinson disease–related tremor for years. A DBS applied to different brain areas can also help people with essential tremor, dystonia, chronic pain, major depression, and obsessive-compulsive disorder.

Millions of people experiencing epileptic seizures are currently treated with antiseizure medications or neurosurgery, both of which often result in incomplete or impermanent seizure reduction. Antiseizure BMIs have shown considerable promise for further improving quality of life. These fully implanted BMIs operate by continuously monitoring neural activity in a brain region determined to be involved with seizures. They identify unusual activity that is predictive of seizure onset and then respond within milliseconds to disrupt this activity by electrically stimulating the same or a different brain region. This closed-loop response can be fast enough that seizure symptoms are not felt and seizures do not occur.

Replacement Part BMIs Can Restore Lost Brain Processing Capabilities

BMIs are capable of restoring more than lost sensory or motor capabilities. They are, in principle, capable of restoring internal brain processing. Of the four categories of BMIs, this is the most futuristic. An example is a "replacement part" BMI. The central idea is that if enough is known about the function of a brain region, and if this region is damaged by disease or injury, then it may be possible to replace this brain region.

Once the normal input activity to a brain region is measured (see next section), the function of the lost brain region could then be modeled in electronic hardware and software, and the output from this substitute processing center would then be delivered to the next brain region as though no injury had occurred. This would involve, for example, reading out neural activity with electrodes, mimicking the brain region's computational functions with low-power microelectronic circuits, and then writing in electrical neural activity with stimulating electrodes.

This procedure might also be used to initiate and guide neural plasticity. A replacement part BMI that is currently being investigated focuses on restoring memory by replacing parts of the hippocampus that are damaged due to injury or disease. Another potential application would be to restore the lost functionality of a brain region damaged by stroke.

These systems represent the natural evolution of the BMI concept, a so-called "platform technology" because a large number of systems can be envisioned by mixing and matching various write-in, computational, and read-out components. The number of neurological diseases and injuries that BMIs should be able to help address ought to increase as our understanding of the functions of the nervous system and the sophistication of the technology continue to grow.

Measuring and Modulating Neural Activity Rely on Advanced Neurotechnology

Measuring and modulating neural activity involves four broad areas of electronic technologies applied to the nervous system (so-called neurotechnology). The first area is the type of neural sensor; artificial neural sensors are designed with different levels of invasiveness and spatial resolution (Figure 39–2). Sensors that are external to the body, such as an *electroencephalogram* (EEG) cap, have been used extensively in recent decades. The EEG measures signals from many small metal disks (electrodes) applied to the surface of the scalp across the head. Each electrode detects average activity from a large number of neurons beneath it.

More recently, implantable electrode-array techniques, such as subdural *electrocorticography* (ECoG) and finely spaced micro-ECoG electrodes, have been used. Since ECoG electrodes are on the surface of the brain and are thus much closer to neurons than EEG electrodes, ECoG has higher spatial and temporal resolution and thus provides more information with which to control BMIs.

Most recently, arrays of *penetrating intracortical electrodes*, which we focus on in this chapter, have been used. The intracortical electrode arrays are made of silicon or other materials and coated with biocompatible materials. The arrays are implanted on the surface of the brain, with the electrode tips penetrating 1 to 2 mm

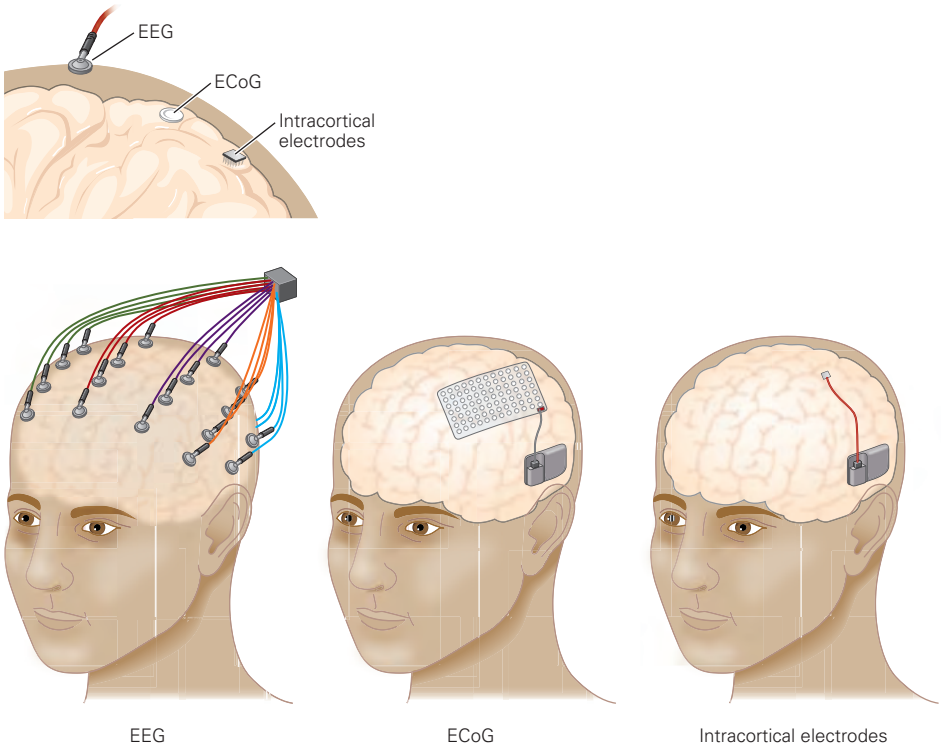

Figure 39–2 Brain–machine interfaces use different types of neural sensors. Electrical neural signals can be measured with various techniques ranging from electroencephalography (**EEG**) electrodes on the surface of the skin, to electrocorticography (**ECoG**) electrodes on the surface of the brain, to intracortical electrodes implanted in the outer 1 to 2 mm of cortex. The signals that can be measured range from the average of many neurons, to averages across fewer neurons, and finally to action potentials from individual neurons. (Adapted, with permission, from Blabe et al. 2015.)

into the cortex. They have the ability to record action potentials from individual neurons, as well as local field potentials from small clusters of neurons near each electrode tip. The electrodes are able to record high-fidelity signals because they are inserted into the brain, bringing the electrode tips within micrometers of neurons. This is beneficial for BMI performance because individual neurons are the fundamental information-encoding units in the nervous system, and action potentials are the fundamental units of the digital code that carries information from the input to the output region of a neuron. Moreover, intracortical electrodes can deliver electrical microstimulation to either disrupt neural activity (eg, DBS) or write in surrogate information (eg, proprioceptive or somatosensory information).

The second area of neurotechnology is scaling up the number of neurons measured at the same time. While one neuron contains some information about a person's intended movement, tens to hundreds of neurons are needed to move a BMI more naturally, and even more neurons are needed to approach naturalistic levels of motor function. Although it is possible to place electrode arrays in many areas across the brain, thereby gaining more information from multiple areas, a key challenge is to measure activity from thousands of neurons within each individual brain area. Many efforts are underway to achieve this goal, including use of electrode arrays with many tiny shafts, each with hundreds of electrode contacts along its length; many tiny electrodes that are not physically wired together, but are instead inserted into the brain as stand-alone islands that transmit data outside of the head and receive power wirelessly; and optical imaging technologies that can capture the activity of hundreds or more neurons by detecting how each neuron's fluorescence changes over time.

The third area is low-power electronics for signal acquisition, wireless data communications, and wireless powering. In contrast to the BMI systems described above, which implant a passive electrode array in which each electrode is wired to the outside world by a connector passing through the skin, future BMIs will be fully implanted like DBS systems. Electronic circuits are needed to amplify neural signals, digitize them, process them (eg, to detect when

an action potential occurred or to estimate local field potential power), and transmit this information to a nearby receiver incorporated into a prosthetic arm, for example. Power consumption must be minimized for two reasons. First, the more power is consumed, the more power a battery or a wireless charging system would need to provide. Batteries would therefore need to be larger and replaced more often, and delivering power wirelessly is challenging. Second, using power generates heat, and the brain can only tolerate a small temperature increase before there are deleterious effects. These trade-offs are similar to those of smart phones, which represent the current best technology available for low-power electronics.

The final area is so-called supervisory systems. Software running on electronic hardware is at the heart of BMIs. Some software implements the mathematical operations of the neural decoding, while other software must tend to aspects of the BMI's overall operation. For example, the supervisory software should monitor whether or not a person wishes to use the prosthesis (eg, if the person is sleeping); if neural signals have changed, thereby requiring recalibration of the decoder; and overall BMI performance and safety.

Having discussed the range of different BMIs and neurotechnologies being developed, in the rest of this chapter we focus on motor and communication BMIs. We first describe different types of decoding algorithms and how they work. We then describe recent progress in BMI development toward assisting paralyzed people and amputees. Next, we consider how sensory feedback can improve BMI performance and how BMIs can be used as an experimental paradigm to address basic scientific questions about brain function. Finally, we conclude with a cautionary note about ethical issues that can arise with BMIs.

BMIs Leverage the Activity of Many Neurons to Decode Movements

Various aspects of movement—including position, velocity, acceleration, and force—are encoded in the activity of neurons throughout the motor system (Chapter 34). Even though our understanding of movement encoding in the motor system is incomplete, there is usually a reliable relationship between aspects of movement and neural activity. This reliable relationship allows us to estimate the desired movement from neural activity, a key component of a BMI.

To study movement encoding, one typically considers the activity of an individual neuron across repeated movements (referred to as "trials") to the same target. The activity of the neuron can be averaged across many trials to create a spike histogram for each target (Figure 39–3A). By comparing the spike histograms for different targets, one can characterize how the neuron's activity varies with the movement produced. One can also assess using the spike histograms whether the neuron is more involved in movement preparation or movement execution.

In contrast, estimating a subject's desired movement from neural activity (referred to as movement *decoding*) needs to be performed on an individual trial while the neural activity is being recorded. The activity of a single neuron cannot unambiguously provide such information. Thus, the BMI must monitor the activity of many neurons on a single trial (Figure 39–3B) rather than one neuron on many trials. A desired movement can be decoded from the neural activity associated with either preparation or execution of the movement. Whereas preparation activity is related to the movement goal execution activity is related to the moment-by-moment details of movement (Chapter 34).

Millions of neurons across multiple brain areas work together to produce a movement as simple as reaching for a cup. Yet in many BMIs, desired movements can be decoded reasonably accurately from the activity of dozens of neurons recorded from a single brain area. Although this may seem surprising, the fact is that the motor system has a great deal of redundancy—many neurons carry similar information about a desired movement (Chapter 34). This is reasonable because millions of neurons are involved in controlling the contractions of dozens of muscles. Thus, most of the neurons in regions of dorsal premotor cortex and primary motor cortex controlling arm movement are informative about most arm movements.

When decoding a movement, the activity of one neuron provides only incomplete information about the movement, whereas the activity of many neurons can provide substantially more accurate information about the movement. This is true for activity associated with both movement preparation and execution. There are two reasons why using multiple neurons is helpful for decoding. First, a typical neuron alone cannot unambiguously determine the intended movement direction. Consider a neuron whose activity (during either preparation or execution) is related to movement direction via a cosine function, known as a *tuning curve* (Figure 39–4A). If this neuron fires at 30 spikes per second, the intended movement direction could be either 120° or 240°. However, by recording from a second neuron whose tuning curve is different from that of the first neuron, the movement direction can be

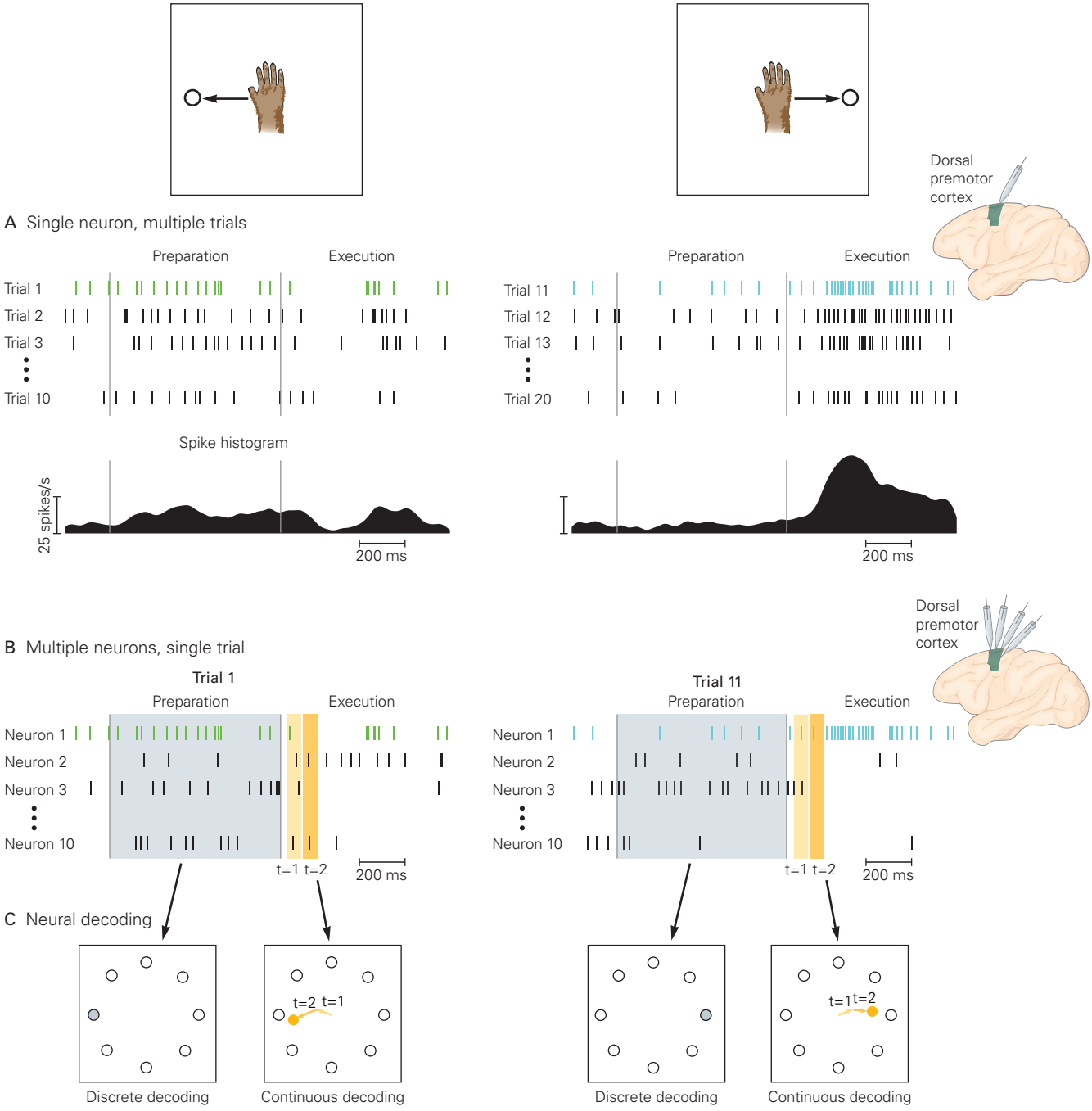

Figure 39–3 **Movement encoding uses the activity of individual neurons averaged across experimental trials, whereas movement decoding uses the activity of many neurons on individual experimental trials.**

A. Activity of one neuron recorded in the dorsal premotor cortex of a monkey preparing and executing leftward arm movements (*left*) and rightward arm movements (*right*). Characterizing the movement encoding of a neuron involves determining how the activity of the neuron on repeated leftward or rightward movements (each row of spike trains) relates to aspects of arm movement. **Below** is the spike histogram for this neuron for leftward and rightward movements, obtained by averaging neural activity across trials. This neuron shows a greater level of preparation activity for leftward movements and a greater level of execution activity for rightward movements. Many neurons in the dorsal premotor cortex and primary motor cortex show movement-related activity in both the preparation and execution epochs like the neuron shown.

B. Neural activity for many neurons recorded in the dorsal premotor cortex for one leftward movement (*left*) and one rightward movement (*right*). The spike trains for neuron 1 correspond to those shown in part **A**. Spike counts are taken during the preparation epoch, typically in a large time bin of 100 ms or longer to estimate movement goal. In contrast, spike counts are taken during the execution epoch typically in many smaller time bins, each lasting tens of milliseconds. Using such short time bins provides the temporal resolution needed to estimate the moment-by-moment details of the movement.

C. Neural decoding involves extracting movement information from many neurons on a single experimental trial. In the subject's workspace, there are eight possible targets (**circles**). Discrete decoding (see Figure 39–5) extracts the target location; the estimated target is filled in with **gray**. In contrast, continuous decoding (see Figure 39–6) extracts the moment-by-moment details of the movement; the **orange dot** represents the estimated position at one moment in time.

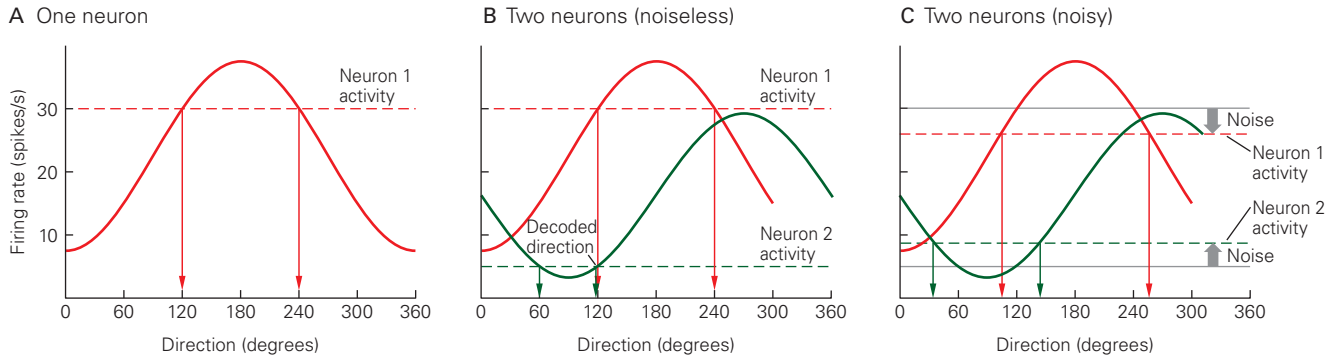

Figure 39–4 More than one neuron is needed for accurate movement decoding.

A. The tuning curve of one neuron defines how the neuron's activity varies with movement direction. If this neuron shows activity of 30 spikes/s, it could correspond to movement in the 120° or 240° direction.

B. A second neuron (**green**) with a different tuning curve shows activity of 5 spikes/s, which could correspond to movement in the 60° or 120° direction. The only movement direction consistent with the activity of both neurons is 120°, which is determined to be the decoded direction.

C. Because neural activity is "noisy" (represented as a vertical displacement of the dashed lines), it is usually not possible to conclusively determine the movement direction from the activity of two neurons. Here, no one movement direction is consistent with the activity of both neurons.

more accurately determined. If the second neuron fires at 5 spikes per second, corresponding to a movement in either the 60° or 120° direction, the only movement direction that is consistent between the two neurons is 120° (Figure 39–4B). Thus, by recording from these two neurons simultaneously, the intended reach direction can be determined more accurately than by recording from one neuron. (However, two neurons do not necessarily provide a perfect estimate of the intended reach direction due to noise, as described next.)

The second reason why decoding a movement from the activity of several neurons gives greater accuracy is because a neuron's activity level usually varies across repeated movements in the same direction. This variability is typically referred to as spiking "noise." Let us say that due to spiking noise the first neuron fires at slightly less than 30 spikes per second and the second neuron fires at slightly more than 5 spikes per second (Figure 39–4C). Under these conditions, no single movement direction is consistent with the activity level of both neurons. Instead, a compromise must be made between the two neurons to determine a movement direction that is as consistent as possible with their activities. By extending this concept to more than two neurons, the movement direction can be decoded even more accurately as the number of neurons increases.

Decoding Algorithms Estimate Intended Movements From Neural Activity

Movement decoders are a central component of BMIs. There are two types of BMI decoders: discrete and continuous (Figure 39–3C). A *discrete decoder* estimates one of several possible movement goals. Each of these movement goals could correspond to a letter on a keyboard. A discrete decoder solves a classification problem in statistics and can be applied to either preparation activity or execution activity. A *continuous decoder* estimates the moment-by-moment details of a movement trajectory. This is important, for example, for reaching around obstacles or turning a steering wheel. A continuous decoder solves a regression problem in statistics and is usually applied to execution activity rather than preparation activity because the moment-by-moment details of a movement can be more accurately estimated from execution activity (Chapter 34).

Motor BMIs must produce movement trajectories as accurately as possible to achieve the desired movement and typically use a continuous decoder to do this. In contrast, communication BMIs are concerned with enabling the individual to transmit information as rapidly as possible. Thus, the speed and accuracy with which movement goals (or keys on a keyboard) can be selected are of primary importance. Communication BMIs can use a discrete decoder to directly select a desired key on a keyboard or a continuous decoder to continuously guide the cursor to the desired key, where only the key eventually struck actually contributes to information conveyance. This seemingly subtle distinction has implications that influence the type of neural activity required and therefore the brain area that is targeted, as well as the type of decoder that is used.

Neural decoding involves two phases: calibration and ongoing use. In the calibration phase, the relationship between neural activity and movement is characterized by a statistical model. This can be achieved by recording neural activity while a paralyzed person attempts to move, imagines moving, or passively observes movements of a computer cursor or robotic limb. Once the relationship has been defined, the statistical model can then be used to decode new observed neural activity (ongoing use phase). The goal during the ongoing use phase is to find the movement that is most consistent with the observed neural activity (Figure 39–4B,C).

Discrete Decoders Estimate Movement Goals

We first define a population activity space, where each axis represents the firing rate of one neuron. On each trial (ie, movement repetition), we can measure the firing rate of each neuron during a specified period, and together they yield one point in the population activity space. Across many trials, involving multiple movement goals, there will be a scatter of points in the population activity space. If the neural activity is related to the movement goal, then the points will be separated in the population activity space according to the movement goal (Figure 39–5A). During the calibration phase, *decision boundaries* that partition the population activity space into different regions are determined by a statistical model. Each region corresponds to one movement goal.

During the ongoing use phase, we measure new neural activity for which the movement goal is unknown (Figure 39–5B). The decoded movement goal is determined by the region in which the neural activity lies. For example, if the neural activity lies within the region corresponding to the leftward target, then the discrete decoder would guess that the subject intended to move to the leftward target on that trial. It is possible that the subject intended to move to the rightward target, even though the recorded activity lies within the region corresponding to the leftward target. In this case, the discrete decoder would incorrectly estimate the subject's intended movement goal. Decoding accuracy typically increases with an increasing number of simultaneously recorded neurons.

Continuous Decoders Estimate Moment-by-Moment Details of Movements

Arm position, velocity, acceleration, force, and other aspects of arm movement can be decoded using the methods described here with varying levels of accuracy. For concreteness, we will discuss decoding movement velocity because it is one of the quantities most strongly reflected in the activity of motor cortical

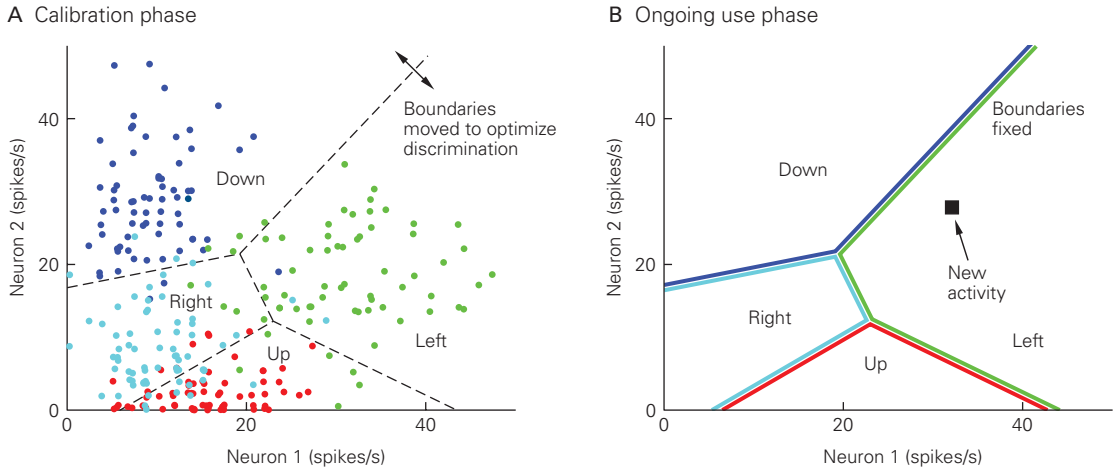

Figure 39–5 Discrete decoding.

A. Calibration phase. A population activity space is shown for two neurons, where each axis represents the firing rate of one neuron. On each trial (ie, movement repetition), the activity of the two neurons together defines one point in the population activity space. Each point is colored by the movement goal, which is known during the calibration phase. Decision boundaries (**dashed lines**) are determined by a statistical model to optimize discrimination among the movement goals. The decision boundaries define a region in the population activity space for each movement goal.

B. Ongoing use phase. During this phase, the decision boundaries are fixed. If we record new neural activity (**square**) for which the movement goal is unknown, the movement goal is determined by the region in which the neural activity lies. In this case, the neural activity lies in the region corresponding to the leftward target, so the decoder would guess that the subject intended to move to the leftward target.

neurons and is the starting point for the design of most BMI systems.

Consider a population of neurons whose level of activity indicates the movement velocity (ie, speed and direction). During the calibration phase, a "pushing vector" is determined for each neuron (Figure 39–6A). A pushing vector indicates how a neuron's activity influences movement velocity. Various continuous decoding algorithms differ in how they determine the pushing vectors. One of the earliest decoding algorithms, the population vector algorithm (PVA), assigns each neuron's pushing vector to point along the neuron's preferred direction (see Figure 34–22A). A neuron's preferred direction is defined as the direction of movement for which the neuron shows the highest level of activity (ie, peak of curves in Figure 39–4). Much of the pioneering work on BMIs used the PVA. However, the PVA does not take into account the properties of the spiking noise (ie, its variance and covariance across neurons), which influences the accuracy of the decoded movements. A more accurate decoder, the optimal linear estimator (OLE), incorporates the properties of the spiking noise to determine the pushing vectors.

During the ongoing use phase, the pushing vectors are each scaled by the number of spikes emitted by the corresponding neuron at each time step (Figure 39–6B). At each time step, the decoded movement is the vector sum of the scaled pushing vectors across all neurons. The decoded movement represents a change in position during one time step (ie, velocity). The BMI cursor (or limb) position (Figure 39–6C) is then updated according to the decoded movement.

To further improve decoding accuracy, the estimation of velocity at each time step should take into account not only current neural activity (as illustrated in Figure 39–6), but also neural activity in the recent past. The rationale is that movement velocity (and other kinematic variables) changes gradually over time, and so neural activity in the recent past should be informative about the movement velocity. This can be achieved by temporally smoothing the neural activity before applying a PVA or OLE or by using a Kalman filter to define a statistical model describing how movement velocity (or other kinematic variables) changes smoothly over time. With a Kalman filter, the estimated velocity is a combination of the scaled pushing vectors at the current time step (as in Figure 39–6B) and the estimated velocity at the previous time step. Indeed, continuous decoding algorithms that take into account neural activity in the recent past have been shown to provide higher decoding accuracy than those that do not. The Kalman filter and its extensions are widely used in BMIs and among the most accurate continuous decoding algorithms available.

Increases in Performance and Capabilities of Motor and Communication BMIs Enable Clinical Translation

Patients with paralysis wish to perform activities of daily living. For people with ALS or upper spinal cord injury who are unable to speak or to move their arms, the most desired tasks are often the ability to communicate, to move a prosthetic (robotic) arm, or to move the paralyzed arm by stimulating the musculature. Having described how neural signals can be read out from motor areas of the brain and how these electrical signals can be decoded to arrive at BMI control signals, we now describe recent progress toward restoring these abilities.

The majority of laboratory studies are carried out in able-bodied nonhuman primates, although paralysis is sometimes transiently induced in important control experiments. Three types of experimental paradigms are in broad use, differing in the exact way in which arm behavior is instructed and visual feedback is provided during BMI calibration and ongoing use. Setting

Figure 39–6 (Opposite) Continuous decoding.

A. During the calibration phase, a pushing vector is determined for each of 97 neurons. Each vector represents one neuron and indicates how one spike from that neuron drives a change in position per time step (ie, velocity). Thus, the units of the plot are millimeters per spike during one time step. Different neurons can have pushing vectors of different magnitudes and directions.

B. During ongoing use, spikes are recorded from the same neurons as in panel A during movement execution. At each time step, the new length of an arrow is obtained by starting with its previous length in panel A and scaling it by the number of spikes produced by the neuron of the same color during that time step. If a neuron does not fire, there is no arrow for that neuron during that time step. The decoded movement (**black arrow**) is the vector sum of the scaled pushing vectors, representing a change in position during one time step (ie, velocity). For a given neuron, the direction of its scaled pushing vectors is the same across all time steps. However, the magnitudes of the scaled pushing vectors can change from one time step to the next depending on the level of activity of that neuron.

C. The decoded movements from panel B are used to update the position of a computer cursor (**orange dot**), robotic limb, or paralyzed limb at each time step.

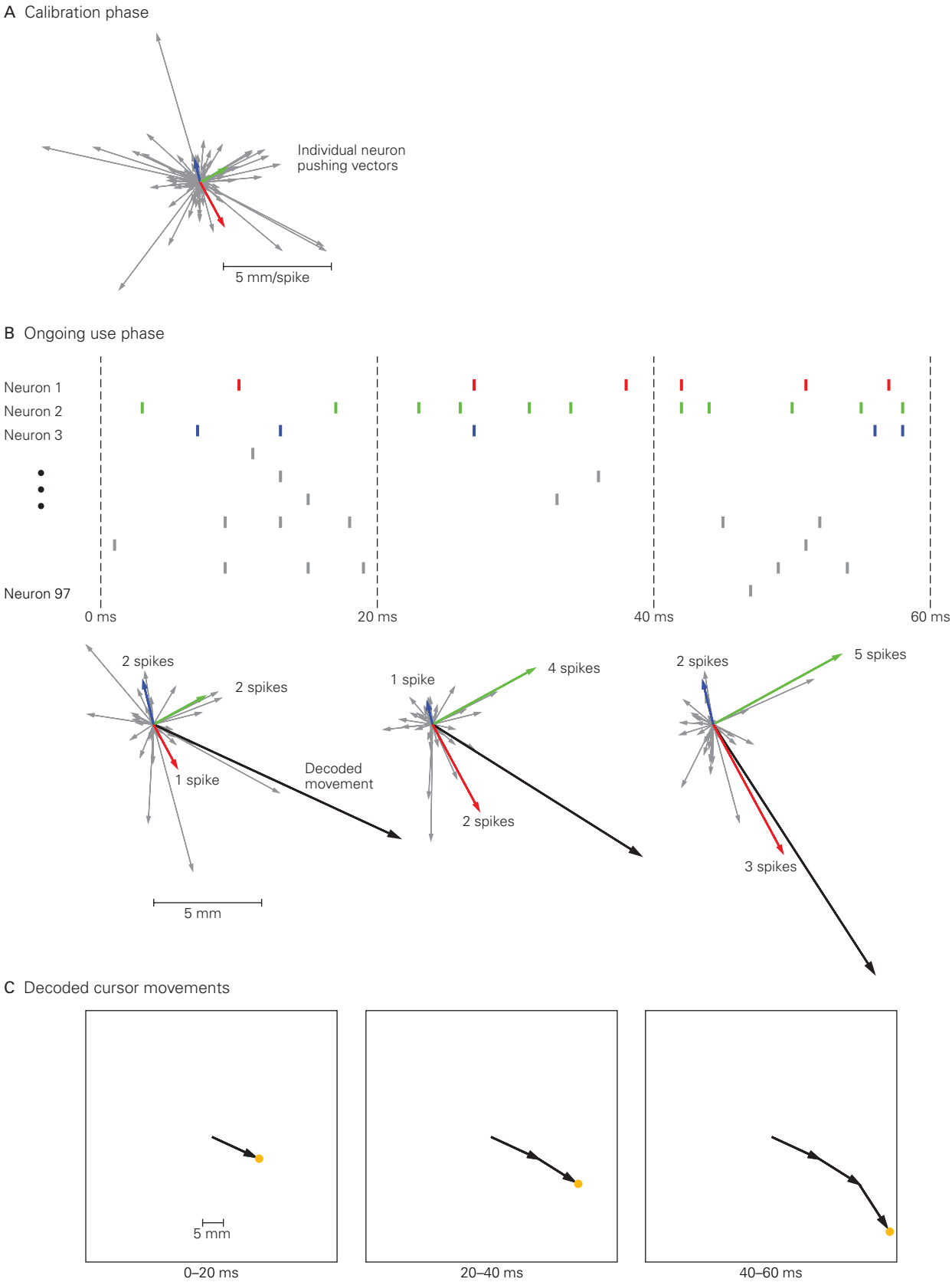
A Calibration phase
Individual neuron pushing vectors
5 mm/spike
B Ongoing use phase
Neuron 1
Neuron 2
Neuron 3
Neuron 97
0 ms
20 ms
40 ms
60 ms
2 spikes
2 spikes
1 spike
Decoded movement
5 mm
1 spike
4 spikes
2 spikes
2 spikes
5 spikes
3 spikes
C Decoded cursor movements
5 mm
0–20 ms
20–40 ms
40–60 ms

these differences aside, we focus below on how BMIs function and perform. We also highlight recent pilot clinical trials with people with paralysis.

Subjects Can Type Messages Using Communication BMIs

To investigate how quickly and accurately a communication BMI employing a discrete decoder and preparation activity can operate, monkeys were trained to fixate and touch central targets and prepare to reach to a peripheral target that could appear at one of several different locations on a computer screen. Spikes were recorded using electrodes implanted in the premotor cortex. The number of spikes occurring during a particular time window during the preparation epoch was used to predict where the monkey was preparing to reach (Figure 39–7A). If the decoded target matched the peripheral target, a liquid reward was provided to indicate a successful trial.

By varying the duration of the period in which spike counts are taken and the number of possible targets, it was possible to assess the speed and accuracy of target selections (Figure 39–7B). Decoding accuracy tended to increase with the period in which spike counts are taken because spiking noise is more easily averaged out in longer periods.

An important metric for efficient communication is information transfer rate (ITR), which measures how much information can be conveyed per unit time. A basic unit of information is a bit, which is specified by a binary value (0 or 1). For example, with three bits of information, one can specify which of $2^3 = 8$ possible targets or keys to press. Thus, the metric for ITR is bits per second (bps). ITR increases with the period in which spike counts are taken, then declines. The reason is that ITR takes into account both how accurately and how quickly each target is selected. Beyond some point of diminishing returns of a longer period, accuracy fails to increase rapidly enough to overcome the slowdown in target-selection rate accompanying a longer period.

Overall performance (ITR) increases with the number of possible targets, despite a decrease in decoding accuracy, because each correct target selection conveys more information. Fast and accurate communication

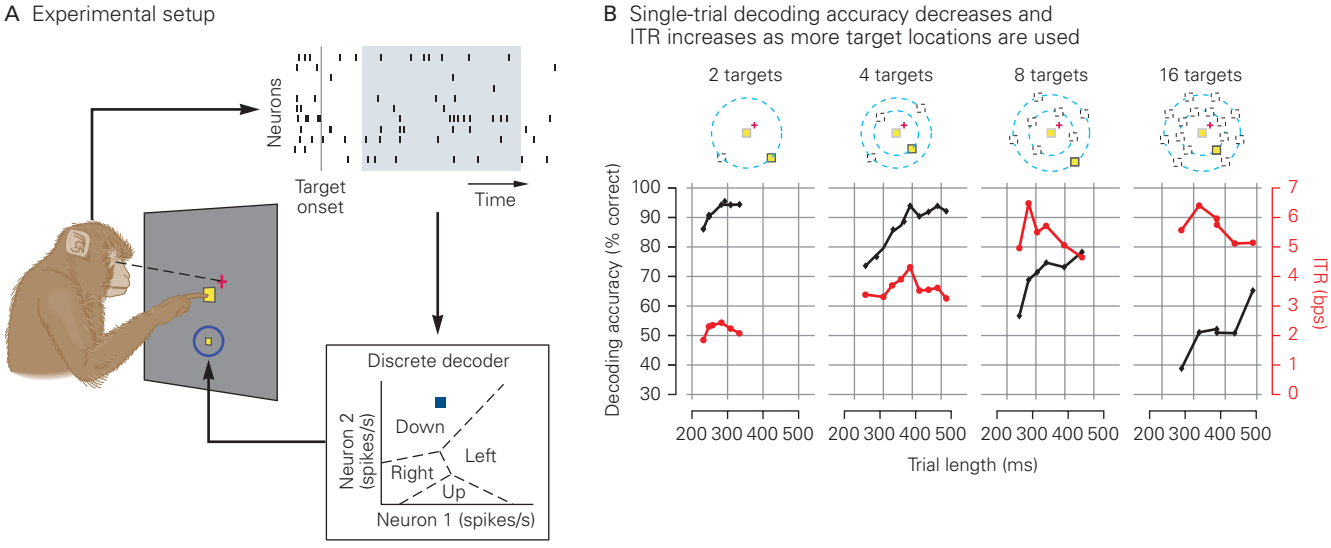

Figure 39–7 A communication brain–machine interface can control a computer cursor using a discrete decoder based on neural activity during the preparation epoch.

A. After a monkey touched a central target (**large yellow square**) and fixated a central point (**red +**), a peripheral target (**small yellow square**) appeared and the monkey prepared to reach to it. Spike counts were taken during the preparation epoch and fed into a discrete decoder. The duration of the period in which spike counts are taken (ie, width of **light blue** shading) affects decoding performance and information transfer rate (**ITR**) (see panel **B**). Based on the spike counts (**blue square**), the discrete decoder guessed the target the monkey was preparing to reach to.

B. Decoding accuracy (**black**) and information transfer rate (**ITR, bits/s; red**) are shown for different trial lengths and numbers of targets. Trial length was equal to the duration of the period in which spike counts were taken (varied during the experiment) plus 190 ms (fixed during the experiment). The latter provided time for visual information of the peripheral target to reach the premotor cortex (150 ms), plus the time to decode the target location from neural activity and render the decoded target location on the screen (40 ms). (Adapted, with permission, from Santhanam et al. 2006.)

has been demonstrated in BMIs with this design based on a discrete decoder applied to preparatory activity. The ITR of this BMI is approximately 6.5 bps, which corresponds to approximately two to three targets per second with greater than 90% accuracy.

Recent studies have also investigated how quickly and accurately a communication BMI employing a continuous decoder and execution activity can operate. Two different types of continuous decoders were evaluated: a standard Kalman filter decoding movement velocity (V-KF) and a recalibrated feedback intention-trained Kalman filter (ReFIT-KF). The V-KF was calibrated using the neural activity recorded during actual arm movements (ie, open-loop control). The ReFIT-KF incorporated the closed-loop nature of BMIs into decoder calibration by assuming that the user desired to move the cursor straight to the target at each time step.

To assess performance, both types of decoders were used in closed-loop BMI control (Figure 39–8A). Monkeys were required to move a computer cursor from a central location to eight peripheral locations and back. A gold standard for performance evaluation was established by having the monkeys also perform the same task using arm movements. The ReFIT-KF outperformed the V-KF in several ways: Cursor movements using ReFIT-KF were straighter, producing less movement away from a straight line to the target; cursor movements were faster, approaching the speed of arm movements (Figure 39–8B); and there were fewer (potentially frustrating) long trials.

Given its performance benefits, the ReFIT-KF is being used in clinical trials by people with paralysis (Figure 39–8C). Spiking activity was recorded using a 96-channel electrode array implanted in the hand control area of the left motor cortex. Signals were filtered to extract action potentials and high-frequency local field potentials, which were decoded to provide "point-and-click" control of the BMI-controlled cursor. The subject was seated in front of a computer monitor and was asked, "How did you encourage your sons to practice music?" By attempting to move her right hand, the computer cursor moved across the screen and stopped over the desired letter. By attempting to squeeze her left hand, the letter beneath the cursor was selected, much like clicking a mouse button.

BMI performance in the clinical trials was assessed by measuring the number of intended characters subjects were able to type (Figure 39–8D). Subjects were able to demonstrate that the letters they typed were intended by using the delete key to erase occasional mistakes. These clinical tests showed that it is possible to type at a rate of many words per minute using a BMI.

Subjects Can Reach and Grasp Objects Using BMI-Directed Prosthetic Arms

Patients with paralysis would like to pick up objects, feed themselves, and generally interact physically with the world. Motor BMIs with prosthetic limbs aim to restore this lost motor functionality. As before, neural activity is decoded from the brain but is now routed to a robotic arm where the wrist is moved in three dimensions (x, y, and z) and the hand is moved in an additional dimension (grip angle, ranging from an open hand to a closed hand).

In one test of a robotic arm, a patient with paralysis was able to use her neural activity to direct the robotic arm to reach out, grab a bottle of liquid, and bring it to her mouth (Figure 39–9). The three-dimensional reaches and gripping were slower and less accurate than natural arm and hand movements. Importantly, this demonstrated that the same BMI paradigm originally developed with animals, including measuring and decoding signals from motor cortex, works in people even years after the onset of neural degeneration or the time of neural injury.

BMI devices directing prosthetic arms and hands are now able to do more than just control three-dimensional movement or open and close the hand. They can also orient the hand and grasp, manipulate, and carry objects. A person with paralysis was able to move a prosthetic limb with 10 degrees of freedom to grasp objects of different shapes and sizes and move them from one place to another (Figure 39–10). Completion times for grasping and moving objects were considerably slower than natural arm movements, but the results are encouraging. These studies illustrate the existing capabilities of prosthetic arms and also the potential for even greater capabilities in the future.

Subjects Can Reach and Grasp Objects Using BMI-Directed Stimulation of Paralyzed Arms

An alternative to using a robotic arm is to restore lost motor function to the biological arm. Arm paralysis results from the loss of neural signaling from the spinal cord and brain, but the muscles themselves are often still intact and can be made to contract by electrical stimulation. This capacity underlies functional electrical stimulation (FES), which sends electrical signals via internal or external electrodes to a set of muscle groups. By shaping and timing the electrical signals sent to the different muscle groups, FES is able to move the arm and hand in a coordinated fashion to pick up objects.

Laboratory studies in monkeys have demonstrated that this basic approach is viable in principle.

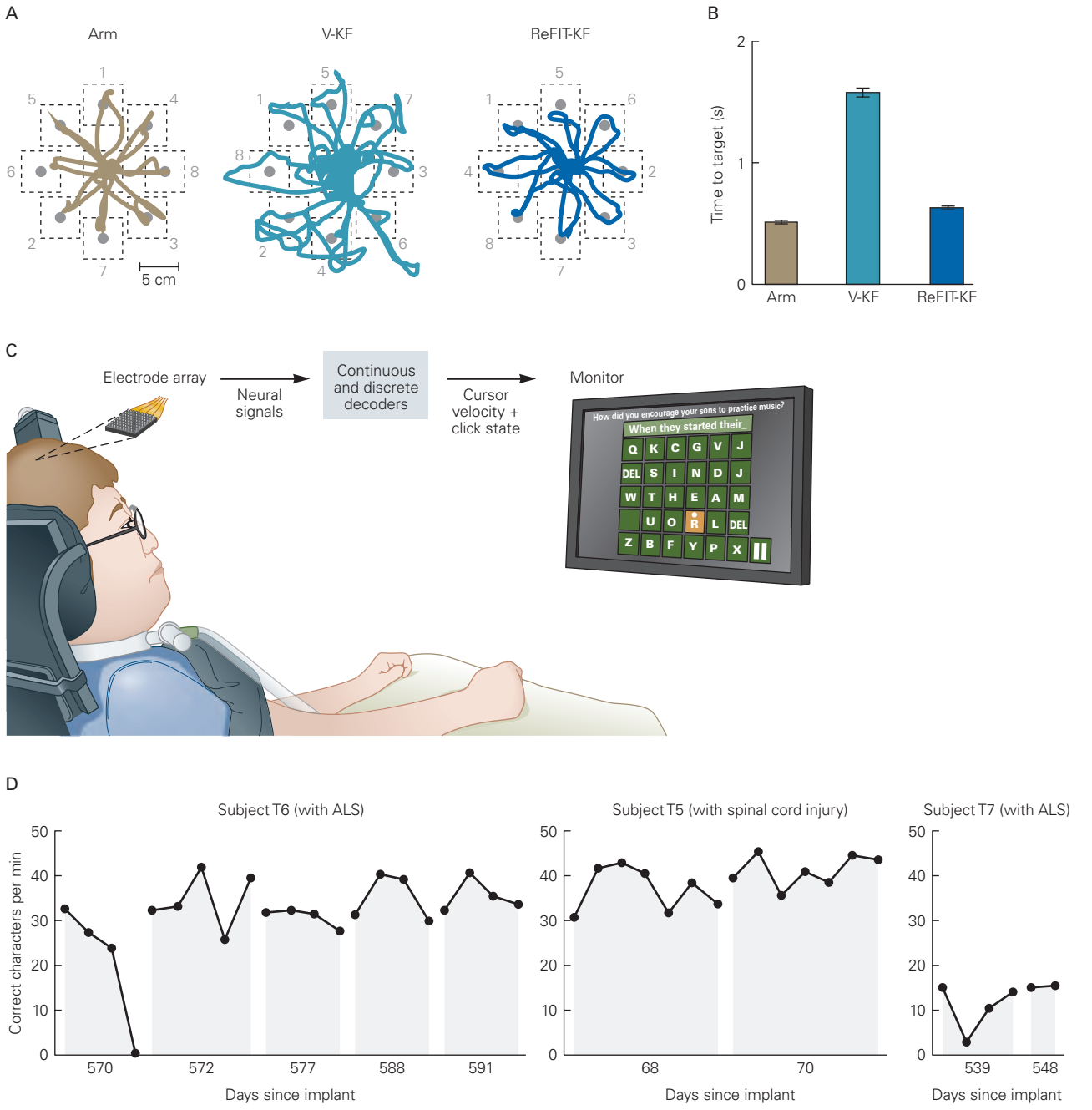

Figure 39–8 A communication brain–machine interface (BMI) can control a computer cursor using a continuous decoder based on neural activity during the execution epoch.

A. Comparison of cursor control by a monkey using its arm, a standard decoder that estimates velocity (BMI with Kalman filter decoding movement velocity [**V-KF**]), and a feedback intention-trained decoder (BMI with recalibrated feedback intention-trained Kalman filter [**ReFIT-KF**]). Traces show cursor movements to and from targets alternating in the sequence indicated by the numbers shown. Traces are continuous for the duration of all reaches. (Adapted, with permission, from Gilja et al. 2012.)

B. Time required to move the cursor between the central location and a peripheral location on successful trials (mean ± standard error of the mean). (Adapted, with permission, from Gilja et al. 2012.)

C. Pilot clinical trial participant T6 (53-year-old female with amyotrophic later sclerosis [**ALS**]) using a BMI to type the answer to a question. (Adapted, with permission, from Pandarinath et al. 2017.)

D. Performance in a typing task for three clinical trial participants. Performance can be sustained across days or even years after array implantation. (Adapted, with permission, from Pandarinath et al. 2017.)

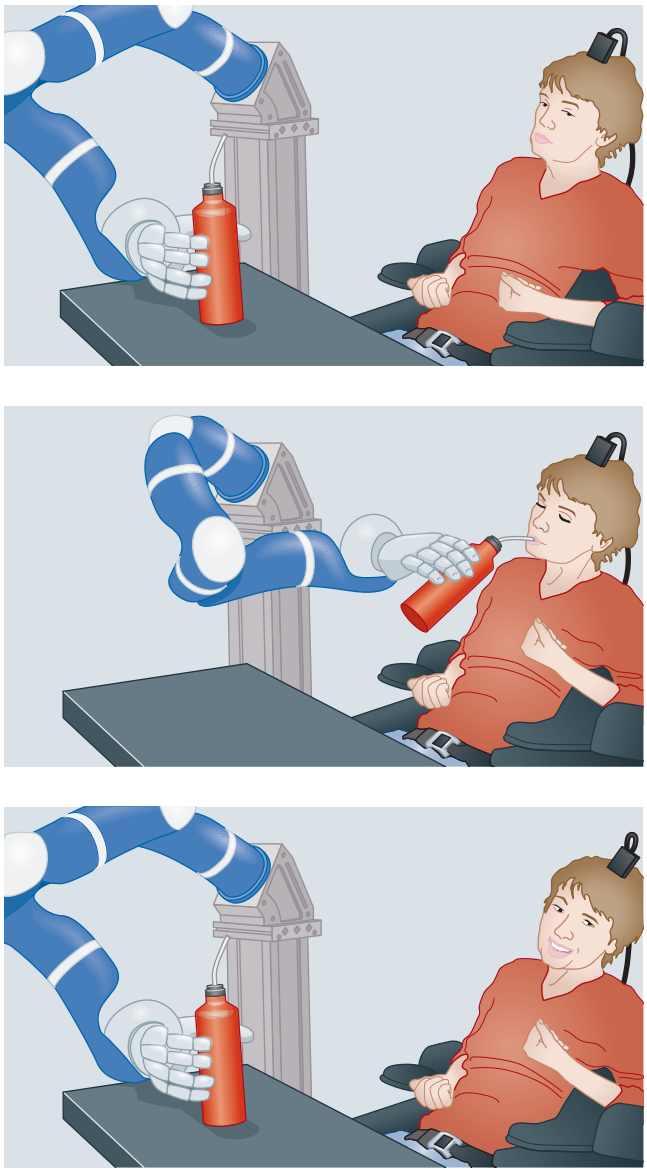

Figure 39–9 A subject with paralysis drinks from a bottle using a robotic arm controlled by a motor brain–machine interface using a continuous decoder. Three sequential images from the first successful trial show the subject using the robotic arm to grasp the bottle, bring it to her mouth and drink coffee through a straw, and place the bottle back on the table. (Adapted from Hochberg et al. 2012.)

It is implemented by calibrating a continuous decoder to predict the intended activity of each of several of the muscles, transiently paralyzed with a nerve block. These predictions are then used to control the intensity of stimulation of the same paralyzed muscles, which in turn controls motor outputs such as a grip angle and force. This process in effect bypasses the spinal cord and restores some semblance of voluntary control of the paralyzed arm and hand. Similar results have recently been demonstrated in patients with paralysis using either externally applied or fully implanted state-of-the-art FES electrodes. Intracortically recorded signals from motor cortex were decoded to restore movement via FES in a person with upper spinal cord injury (Figure 39–11). The subject was able to achieve control of different wrist and hand motions, including finger movements, and perform various activities of daily living.

Subjects Can Use Sensory Feedback Delivered by Cortical Stimulation During BMI Control

During arm movements, we rely on multiple sources of sensory feedback to guide the arm along a desired path or to a desired goal. These sources include visual, proprioceptive, and somatosensory feedback. However, in most current BMI systems, the user receives only visual feedback about the movements of the computer cursor or robotic limb. In patients with normal motor output pathways but lacking proprioception, arm movements are substantially less accurate than in healthy individuals, both in terms of movement direction and extent. Furthermore, in tests of BMI cursor control in healthy nonhuman primate subjects, the arm continues to provide proprioceptive feedback even though arm movements are not required to move the cursor. BMI cursor control is more accurate when the arm is passively moved together with the BMI cursor along the same path, rather than along a different path. This demonstrates the importance of "correct" proprioceptive feedback. Based on these two lines of evidence, it is perhaps not surprising that BMI-directed movements relying solely on visual feedback are slower and less accurate than normal arm movements. This has motivated recent attempts to demonstrate how providing surrogate (ie, artificial) proprioceptive or somatosensory feedback can improve BMI performance.

Several studies have attempted to write in sensory information by stimulating the brain using cortical electrical microstimulation. Laboratory animals can discriminate current pulses of different frequencies and amplitudes, and this ability can be utilized to provide proprioceptive or somatosensory information in BMIs by using different pulse frequencies to encode different physical locations (akin to proprioception) or different textures (akin to somatic sensation). Electrical microstimulation in the primary somatosensory cortex can be used by nonhuman primates to control a cursor on a moment-by-moment basis without vision. In these subjects, the use of electrical microstimulation

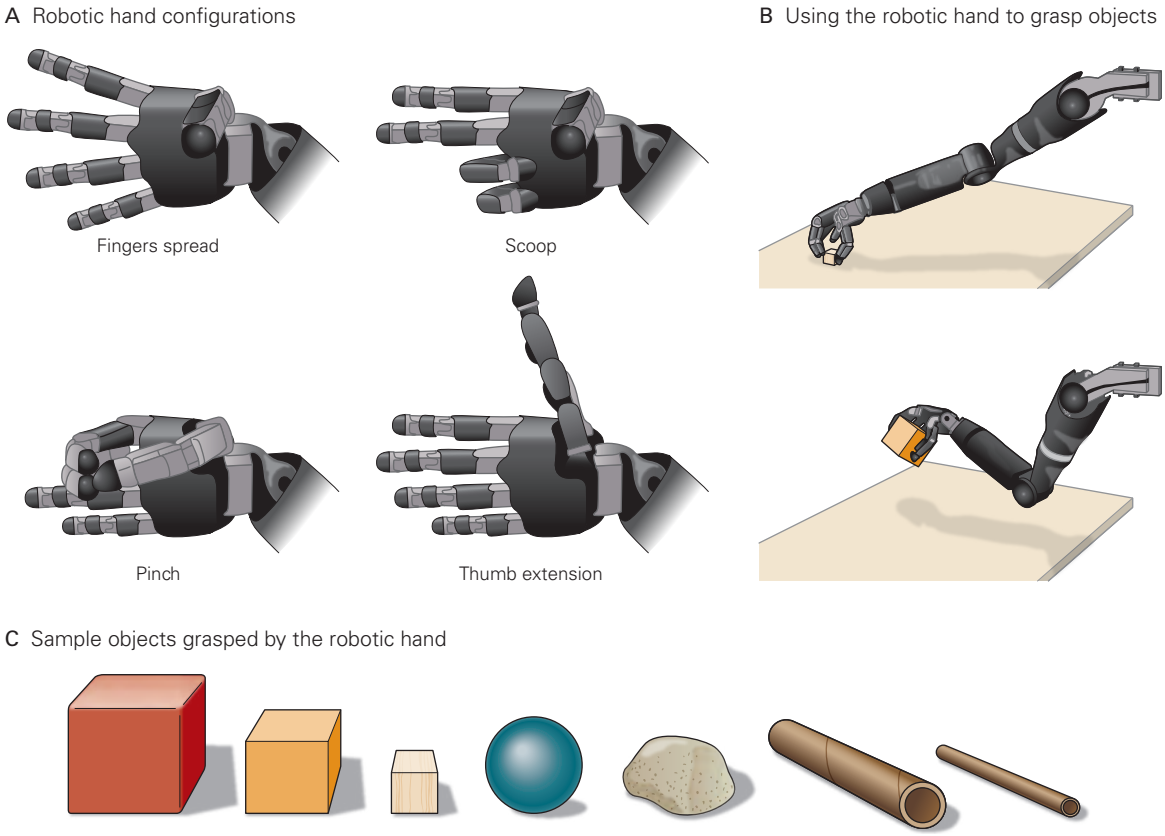

Figure 39–10 A motor brain–machine interface (BMI) can control a prosthetic arm with 10 degrees of freedom.

A. Examples of different hand configurations directed by the BMI. The 10 degrees of freedom are three-dimensional arm translation, three-dimensional wrist orientation, and four-dimensional hand shaping.

B. A subject uses the prosthetic arm to pick up an object and move it.

C. Objects of different shapes and sizes are used to test the generalization ability of the BMI. (Adapted from Wodlinger et al. 2015.)

and visual feedback together led to more accurate movements than either type of sensory feedback alone.

Furthermore, electrical microstimulation in the primary somatosensory cortex can also be used to provide tactile information. Nonhuman primates moved a BMI-directed cursor under visual feedback to hit different visual targets, each of which elicited a different stimulation frequency. Subjects learned to use differences in the stimulation feedback to distinguish the rewarded target from the unrewarded targets. This demonstrates that electrical microstimulation can also be used to provide somatosensory feedback during BMI control.

Finally, surrogate somatosensory information was delivered via electrical microstimulation to a person with paralysis and compromised sensory afferents. The person reported naturalistic sensations at different locations of his hand and fingers corresponding to different locations of stimulation in the primary somatosensory cortex.

BMIs Can Be Used to Advance Basic Neuroscience

BMIs are becoming an increasingly important experimental tool for addressing basic scientific questions about brain function. For example, cochlear implants have provided insight into how the brain processes sounds and speech, how the development of these mechanisms is shaped by language acquisition, and how neural plasticity allows the brain to interpret a few channels of stimulation carrying impoverished auditory information. Similarly, motor and communication BMIs are helping to elucidate the neural mechanisms underlying sensorimotor control. Such scientific findings can then be used to refine the design of BMIs.

The key benefit of BMIs for basic science is that they can simplify the brain's input and output interface with the outside world, without simplifying the complexities of brain processing that one wishes to study.

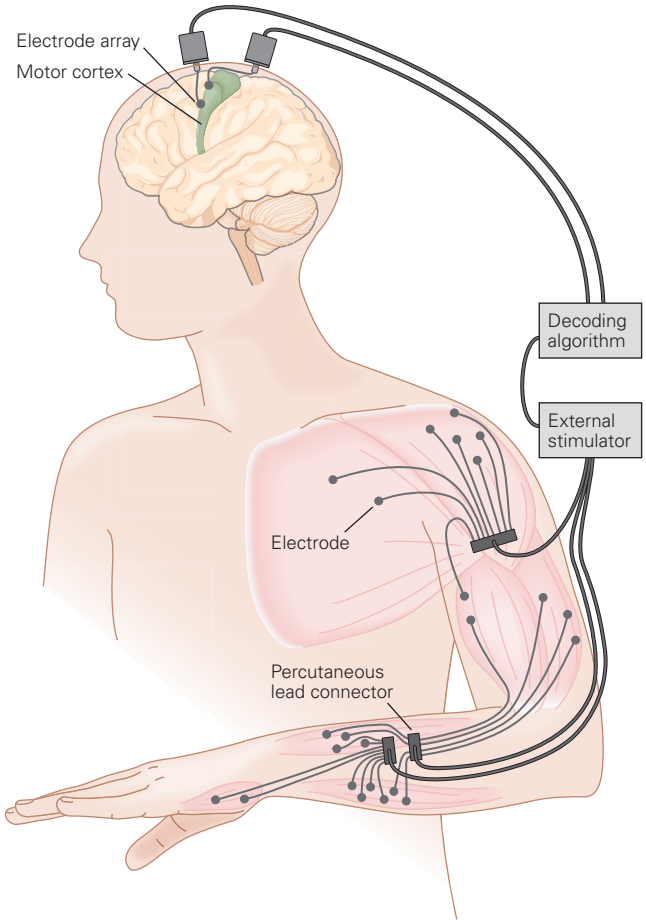

Figure 39–11 A motor brain–machine interface (BMI) can control the muscles of a paralyzed arm using a continuous decoder and functional electrical stimulation. Neural activity recorded in the motor cortex is decoded into command signals that control the stimulation of deltoid, pectoralis major, biceps, triceps, forearm, and hand muscles. This enables cortical control of whole-arm movements and grasping. Muscle stimulation is performed through percutaneous intramuscular fine-wire electrodes. (Adapted, with permission, from Ajiboye et al. 2017. Copyright © 2017 Elsevier Ltd.)

To illustrate this point, consider the output interface of the brain for controlling arm movements. Thousands of neurons from the motor cortex and other brain areas send signals down the spinal cord and to the arm, where they activate muscles that move the arm. Understanding how the brain controls arm movement is challenging because one can typically record from only a small fraction of the output neurons that send signals down the spinal cord, the relationship between the activity of the output neurons and arm movements is unknown, and the arm has nonlinear dynamics that are difficult to measure. Furthermore, it is usually difficult to determine which recorded neurons are output neurons.

One way to ease this difficulty is to use a BMI. Because of the way a BMI is constructed, only those neurons that are recorded can directly affect the movement of the cursor or robotic limb. Neurons throughout the brain are still involved, but they can influence the cursor movements only indirectly through the recorded neurons. Thus, in contrast to arm and eye movement studies, one can record from the entire set of output neurons in a BMI, and BMI-directed movements can be causally attributed to specific changes in the activity of the recorded neurons. Furthermore, the mapping between the activity of the recorded neurons and cursor movement is defined by the experimenter, so it is fully known. This mapping can be defined to be simple and can be easily altered by the experimenter during an experiment. In essence, a BMI defines a simplified sensorimotor loop, whose components are more concretely defined and more easily manipulated than for arm or eye movements.

These advantages of BMIs allow for studies of brain function that are currently difficult to perform using arm or eye movements. For example, one class of studies involves using BMIs to study how the brain learns. The BMI mapping defines which population activity patterns will allow the subject to successfully move the BMI-directed cursor to hit visual targets. By defining the BMI mapping appropriately, the experimenter can challenge the subject's brain to produce novel neural activity patterns.

A recent study explored what types of activity patterns are easier and more difficult for the brain to generate. They found that it was easier for subjects to learn new associations between existing activity patterns and cursor movements than to generate novel activity patterns. This finding has implications for our ability to learn everyday skills. A second class of studies involves asking how the activity of neurons that directly control movement differ from those that do not directly control movement. In a BMI, one can choose to use only a subset of the recorded neurons (the output neurons) for controlling movements. At the same time, other neurons (the nonoutput neurons) can be passively monitored without being used for controlling movements. Comparing the activity of output and nonoutput neurons can provide insight into how a network of neurons internally processes information and relays only some of that information to other networks.

Using this paradigm, a recent study recorded neural activity simultaneously in the primary cortex and striatum and designated a subset of the M1 neurons as the output neurons for controlling the BMI. They found that, during BMI learning, M1 neurons that were most relevant for behavior (the output neurons) preferentially increased their coordination with the striatum, which is known to play an important role during natural behavior (Chapter 38). Identifying output versus nonoutput neurons in a study using arm or eye movements would be challenging.

BMIs Raise New Neuroethics Considerations

A growing number of biomedical ethics considerations centered on the brain have arisen from the dramatic expansion in our understanding of neuroscience and our capabilities with neurotechnology. These advances are driven by society's curiosity about the functioning of the brain, the least-well understood organ in the body, as well as the desire to address the massive unmet need of those suffering from neurological disease and injury. The use of BMIs raises new ethical questions for four principal reasons.

First, recording high-fidelity signals (ie, spike trains) involves risk, including the risks associated with initial implantation of the electrodes as well as possible biological (immunological or infectious) responses during the lifetime of the electrodes and the associated implanted electronics. Electrodes implanted for long periods currently have functional lifetimes on the order of many months to a few years, during which time glial scar tissue can form around the electrodes and electrode materials can fail. Efforts to increase the functional lifetime of electrodes range from nanoscale flexible electrodes made with new materials to mitigating immunological responses, as is done with cardiac stents.

For these reasons, patients considering receiving implanted recording technologies will need to evaluate the risks and benefits of a BMI, as is the case for all medical interventions. It is important for patients to have options, as each person has personal preferences involving willingness to undergo surgery, desire for functional restoration and outcome, and cosmesis—be it while deliberating cancer treatment or BMI treatment. BMIs based on different neural sensors (Figure 39–2) have different risks and benefits.

Second, because BMIs can read out movement information from the brain at fine temporal resolution, it seems plausible that they will be able to read out more personal and private types of information as well. Future neuroethics questions that may arise as the technology becomes more sophisticated include whether it is acceptable, even with patient consent, to read out memories that may otherwise be lost to Alzheimer disease; promote long-term memory consolidation by recording fleeting short-term memories and playing them back directly into the brain; read out subconscious fears or emotional states to assist desensitization psychotherapy; or read out potential intended movements, including speech, that would not naturally be enacted.

Third, intracortical write-in BMIs, similar to DBS systems currently used to reduce tremor, may one day evoke naturalistic spatial-temporal activity patterns across large populations of neurons. In the extreme it may not be possible for a person to distinguish self-produced and volitional neural activity patterns from artificial or surrogate patterns. Although there are numerous therapeutic and beneficial reasons for embracing this technology, such as reducing tremor or averting an epileptic seizure, more dubious uses can be envisioned such as commandeering a person's motor, sensory, decision making, or emotional valence circuits.

Finally, ethical questions also involve the limits within which BMIs should operate. Current BMIs focus on restoring lost function, but it is possible for BMIs to be made to enhance function beyond natural levels. This is as familiar as prescribing a pair of glasses that confer better than normal vision, or overprescribing a pain medication, which can cause euphoria that is often addictive. Should BMIs be allowed, if and when it becomes technically possible,

to move a robotic arm faster and more accurately than a native arm? Should continuous neural recordings from BMIs, covering hours, days, or weeks, be saved for future analysis, and are the security and privacy issues the same or different from personal genomics data? Should BMIs with preset content be available for purchase, for example, to skip a grade of mathematics in high school? Should an able-bodied person be able to elect to receive an implanted motor BMI? While the safe and ethical limits of such sensory, motor, and cognitive BMI treatments might seem readily apparent, society continues to wrestle with these same questions concerning other currently available medical treatments. These include steroids that enhance musculature, energy drinks (eg, caffeine) that enhance alertness, and elective plastic surgery that alters appearance.

Although many of these ideas and questions may appear far-fetched at present, as mechanisms of brain function and dysfunction continue to be revealed, BMI systems could build on these discoveries and create even more daunting ethical quandaries. But equally important is the immediate need to help people suffering from profound neurological disease and injury through restorative BMIs. In order to achieve the right balance, it is imperative that physicians, scientists, and engineers proceed in close conversation and partnership with ethicists, government oversight agencies, and patient advocacy groups.

Highlights

1. Brain–machine interfaces (BMIs) are medical devices that read out and/or alter electrophysiological activity at the level of populations of neurons. BMIs can help to restore lost sensory, motor, or brain processing capabilities, as well as regulate pathological neural activity.
2. BMIs can help to restore lost sensory capabilities by stimulating neurons to convey sensory information to the brain. Examples include cochlear implants to restore audition or retinal prostheses to restore vision.
3. BMIs can help to restore lost motor capabilities by measuring the activity from many individual neurons, converting this neural information into control signals, and guiding a paralyzed limb, robotic limb, or computer cursor.
4. Whereas motor BMIs aim to provide control of a robotic limb or paralyzed limb, communication BMIs aim to provide a fast and accurate interface with a computer or other electronic devices.
5. BMIs can help to regulate pathological neural activity by measuring neural activity, processing the neural activity, and subsequently stimulating neurons. Examples include deep brain stimulators and antiseizure systems.
6. Neural signals can be measured using different technologies, including electroencephalography, electrocorticography, and intracortical electrodes. Intracortical electrodes record the activity of neurons near the electrode tip and can also be used to deliver electrical stimulation.
7. To study movement encoding, one usually considers the activity of an individual neuron across many experimental trials. In contrast, for movement decoding, one needs to consider the activity of many neurons across an individual experimental trial.
8. A discrete decoder estimates one of several possible movement goals from neural population activity. In contrast, a continuous decoder estimates the moment-by-moment details of a movement from neural population activity.
9. The field is making substantial progress in increasing the performance of BMIs, measured in terms of the speed and accuracy of the estimated movements. It is now possible to move a computer cursor in a way that approaches the speed and accuracy of arm movements.
10. In addition to controlling computer cursors, BMIs can also guide a robotic limb or a paralyzed limb using functional electrical stimulation. Developments from preclinical experiments with able-bodied, nonhuman primates have subsequently been tested in clinical trials with paralyzed people.
11. Future advances of BMI will depend, in part, on developments in neurotechnology. These include advances in hardware (eg, neural sensors and low-power electronics), software (eg, supervisory systems), and statistical methods (eg, decoding algorithms).
12. An important direction for improving BMI performance is to provide the user with additional forms of sensory feedback in addition to visual feedback. An area of current investigation uses stimulation of neurons to provide surrogate sensory feedback, representing somatosensation and proprioception, during ongoing use.
13. Beyond helping paralyzed patients and amputees, BMI is being increasingly used as a tool for understanding brain function. BMIs simplify the brain's input and output interfaces and allow the experimenter to define a causal relationship between neural activity and movement.

14. BMIs raise new neuroethics questions, which need to be considered together with the benefits provided by BMIs to people with injury or disease.

Krishna V. Shenoy
Byron M. Yu

Selected Reading

Andersen RA, Hwang EJ, Mulliken GH. 2010. Cognitive neural prosthetics. Annu Rev Psychol 61:169–190.

Donoghue JP, Nurmikko A, Black M, Hochberg LR. 2007. Assistive technology and robotic control using motor cortex ensemble-based neural interface systems in humans with tetraplegia. J Physiol 579:603–611.

Fetz EE. 2007. Volitional control of neural activity: implications for brain-computer interfaces. J Physiol 579:571–579.

Green AM, Kalaska JF. 2011. Learning to move machines with the mind. Trends Neurosci 34:61–75.

Hatsopoulos NG, Donoghue JP. 2009. The science of neural interface systems. Annu Rev Neurosci 32:249–266.

Kao JC, Stavisky SD, Sussillo D, Nuyujukian P, Shenoy KV. 2014. Information systems opportunities in brain-machine interface decoders. Proc IEEE 102:666–682.

Nicolelis MAL, Lebedev MA. 2009. Principles of neural ensemble physiology underlying the operation of brain-machine interfaces. Nat Rev Neurosci 10:530–540.

Schwartz AB. 2016. Movement: how the brain communicates with the world. Cell 164:1122–1135.

Shenoy KV, Carmena JM. 2014. Combining decoder design and neural adaptation in brain-machine interfaces. Neuron 84:665–680.

References

Aflalo T, Kellis S, Klaes C, et al. 2015. Decoding motor imagery from the posterior parietal cortex of a tetraplegic human. Science 348:906–910.

Ajiboye AB, Willett FR, Young DR, et al. 2017. Restoration of reaching and grasping movements through brain-controlled muscle stimulation in a person with tetraplegia: a proof-of-concept demonstration. Lancet 389:1821–1830.

Anumanchipalli GK, Chartier J, Chang EF. 2019. Speech synthesis from neural decoding of spoken sentences. Nature 568:493–498.

Blabe CH, Gilja V, Chestek CA, Shenoy KV, Anderson KD, Henderson JM. 2015. Assessment of brain-machine interfaces from the perspective of people with paralysis. J Neural Eng 12:043002.

Bouton CE, Shaikhouni A, Annetta NV, et al. 2016. Restoring cortical control of functional movement in a human with quadriplegia. Nature 533:247–250.

Carmena JM, Lebedev MA, Crist RE, et al. 2003. Learning to control a brain-machine interface for reaching and grasping by primates. PLoS Biol 1:E42.

Chapin JK, Moxon KA, Markowitz RS, Nicolelis MA. 1999. Real-time control of a robot arm using simultaneously recorded neurons in the motor cortex. Nat Neurosci 2:664–670.

Collinger JL, Wodlinger B, Downey JE, et al. 2013. High-performance neuroprosthetic control by an individual with tetraplegia. Lancet 381:557–564.

Dadarlat MC, O'Dohert JE, Sabes PN. 2015. A learning-based approach to artificial sensory feedback leads to optimal integration. Nat Neurosci 18:138–144.

Ethier C, Oby ER, Bauman MJ, Miller LE. 2012. Restoration of grasp following paralysis through brain-controlled stimulation of muscles. Nature 485:368–371.

Fetz EE. 1969. Operant conditioning of cortical unit activity. Science 163:955–958.

Flesher SN, Collinger JL, Foldes ST, et al. 2016. Intracortical microstimulation of human somatosensory cortex. Sci Transl Med 8:361ra141.

Ganguly K, Carmena JM. 2009. Emergence of a stable cortical map for neuroprosthetic control. PLoS Biol 7:e1000153.

Gilja V, Nuyujukian P, Chestek CA, et al. 2012. A high-performance neural prosthesis enabled by control algorithm design. Nat Neurosci 15:1752–1757.

Gilja V, Pandarinath C, Blabe CH, et al. 2015. Clinical translation of a high-performance neural prosthesis. Nat Med 21:1142–1145.

Golub MD, Chase SM, Batista AP, Yu BM. 2016. Brain-computer interfaces for dissecting cognitive processes underlying sensorimotor control. Curr Opin Neurobiol 37:53–58.

Hochberg LR, Bacher D, Jarosiewicz B, et al. 2012. Reach and grasp by people with tetraplegia using a neurally controlled robotic arm. Nature 485:372–375.

Hochberg LR, Serruya MD, Friehs GM, et al. 2006. Neuronal ensemble control of prosthetic devices by a human with tetraplegia. Nature 442:164–171.

Humphrey DR, Schmidt EM, Thompson WD. 1970. Predicting measures of motor performance from multiple cortical spike trains. Science 170:758–762.

Jackson A, Mavoori J, Fetz EE. 2006. Long-term motor cortex plasticity induced by an electronic neural implant. Nature 444:56–60.

Jarosiewicz B, Sarma AA, Bacher D, et al. 2015. Virtual typing by people with tetraplegia using a self-calibrating intracortical brain-computer interface. Sci Transl Med 7:313ra179.

Kennedy PR, Bakay RA. 1998. Restoration of neural output from a paralyzed patient by a direct brain connection. Neuroreport 9:1707–1711.

Kim SP, Simeral JD, Hochberg LR, Donoghue JP, Black MJ. 2008. Neural control of computer cursor velocity by decoding motor cortical spiking activity in humans with tetraplegia. J Neural Eng 5:455–476.

Koralek AC, Costa RM, Carmena JM. 2013. Temporally precise cell-specific coherence develops in corticostriatal networks during learning. Neuron 79:865–872.

McFarland DJ, Sarnacki WA, Wolpaw JR. 2010. Electroencephalographic (EEG) control of three-dimensional movement. J Neural Eng 7:036007.

Moritz CT, Perlmutter SI, Fetz EE. 2008. Direct control of paralysed muscles by cortical neurons. Nature 456:639–642.

Musallam S, Corneil BD, Greger B, Scherberger H, Andersen RA. 2004. Cognitive control signals for neural prosthetics. Science 305:258–262.

O'Doherty JE, Lebedev MA, Ifft PJ, et al. 2011. Active tactile exploration using a brain-machine-brain interface. Nature 479:228–231.

Pandarinath C, Nuyujukian P, Blabe CH, et al. 2017. High performance communication by people with paralysis using an intracortical brain-computer interface. eLife 6:e18554.

Sadtler PT, Quick KM, Golub MD, et al. 2014. Neural constraints on learning. Nature 512:423–426.

Santhanam G, Ryu SI, Yu BM, Afshar A, Shenoy KV. 2006. A high-performance brain-computer interface. Nature 442:195–198.

Schalk G, Miller KJ, Anderson NR, et al. 2008. Two-dimensional movement control using electrocorticographic signals in humans. J Neural Eng 5:75–84.

Serruya MD, Hatsopoulos NG, Paninski L, Fellows MR, Donoghue JP. 2002. Instant neural control of a movement signal. Nature 416:141–142.

Shenoy KV, Meeker D, Cao S, et al. 2003. Neural prosthetic control signals from plan activity. Neuroreport 14:591–596.

Stavisky SD, Willett FR, Wilson GH, Murphy BA, Rezaii P, Avansino DT, et al. 2019. Neural ensemble dynamics in dorsal motor cortex during speech in people with paralysis. eLife;8:e46015.

Suminski AJ, Tkach DC, Fagg AH, Hatsopoulos NG. 2010. Incorporating feedback from multiple sensory modalities enhances brain-machine interface control. J Neurosci 30:16777–16787.

Taylor DM, Tillery SIH, Schwartz AB. 2002. Direct cortical control of 3d neuroprosthetic devices. Science 296:1829–1832.

Velliste M, Perel S, Spalding MC, Whitford AS, Schwartz AB. 2008. Cortical control of a prosthetic arm for self-feeding. Nature 453:1098–1101.

Wessberg J, Stambaugh CR, Kralik JD, et al. 2000. Real-time prediction of hand trajectory by ensembles of cortical neurons in primates. Nature 408:361–365.

Wodlinger B, Downey JE, Tyler-Kabara EC, Schwartz AB, Boninger ML, Collinger JL. 2015. Ten-dimensional anthropomorphic arm control in a human brain-machine interface: difficulties, solutions, and limitations. J Neural Eng 12:016011.

This page intentionally left blank

Part VI

Preceding Page

Embracing couple mourning someone's death, perhaps buried in a nearby funerary urn. (Mali, Djenné style. Inland Delta of the Niger River, 13th–15th centuries AD. University of Iowa Stanley Museum of Art, The Stanley Collection of African Art. X1986.451.)

VI The Biology of Emotion, Motivation, and Homeostasis

Emotional and homeostatic behaviors all involve the coordination of one or more somatic, autonomic, hormonal, or cognitive processes. Subcortical brain regions concerned with a range of functions—including feeding, drinking, heart rate, breathing, temperature regulation, sleep, sex, and facial expressions—play a critical role in this coordination. Subcortical brain regions are bidirectionally connected with cortical brain areas, providing a means for reperesentations of internal state variables (eg, visceral information) to influence cognitive operations, such as subjective feelings, decision-making, and attention, and for cognitive functions to regulate or extinguish neural representations in subcortical brain areas that help coordinate behavior reflecting emotional states.

Our consideration of these systems begins with the brain stem, a structure critical for wakefulness and conscious attention on the one hand and sleep on the other. The significance of this small region of the brain—located between the spinal cord and the diencephalon—is disproportionate to its size. Damage to the brain stem can profoundly affect motor and sensory processes because it contains all of the ascending tracts that bring sensory information from the surface of the body to the cerebral cortex and all of the descending tracts from the cerebral cortex that deliver motor commands to the spinal cord. Finally, the brain stem contains neurons that control respiration and heartbeat as well as nuclei that give rise to most of the cranial nerves that innervate the head and neck.

Six neurochemical modulatory systems in the brain stem modulate sensory, motor, and arousal systems. The dopaminergic pathways that connect the midbrain to the limbic system and cortex are particularly important, because they are involved in processing stimuli and events in relation to reinforcement expectation, and therefore contribute to motivational state and learning. Addictive drugs such as nicotine, alcohol, opiates, and cocaine are thought to produce their actions by co-opting the same neural pathways that positively reinforce behaviors essential for survival. Other modulatory transmitters

regulate sleep and wakefulness, in part by controlling information flow between the thalamus and cortex. Disorders of electrical excitation in corticothalamic circuits can result in seizures and epilepsy.

Rostral to the brain stem lies the hypothalamus, which functions to maintain the stability of the internal environment by keeping physiological variables within the limits favorable to vital bodily processes. Homeostatic processes in the nervous system have profound consequences for behavior that have intrigued many of the founders of modern physiology, including Claude Bernard, Walter B. Cannon, and Walter Hess. Neurons controlling the internal environment are concentrated in the hypothalamus, a small area of the diencephalon that comprises less than 1% of the total brain volume. The hypothalamus, with closely linked structures in the brain stem and limbic system, acts directly on the internal environment, through its control of the endocrine system and autonomic nervous system, to achieve goal-directed behavior. It acts indirectly through its connections to higher brain regions to modulate emotional and motivational states. In addition to influencing motivated behaviors, the hypothalamus, together with the brain stem below and the cerebral cortex above, maintains a general state of arousal, which ranges from excitement and vigilance to drowsiness and stupor.

The neurobiological investigation of emotion has relied on experiments that define emotions in terms of specific measures ranging from subjective reports of feelings in humans, to approach or defensive behaviors, to physiological responses such as autonomic reactivity. Charles Darwin observed in his seminal book *The Expression of the Emotions in Man and Animals* that many emotions are conserved across species, making clear the relevance of studying emotions by using animal models to probe neural mechansisms. In experimental frameworks, emotional states are thereby considered to be central brain states that can cause coordinated behavioral, physiological, and cognitive responses across species.

In recent years, much work on emotion has focused on the amygdala, which can orchestrate different responses via its connections to the cortex, hypothalamus, and brain stem. Lesions of the amygdala in humans impair fear learning and expression, as well as fear recognition in others, due to decreased allocation of attention to features of faces that communicate fear. Symptoms in a variety of psychiatric disorders—ranging from addiction to anxiety to social deficits—likely involve amygdala dysfunction. However, the amygdala is only one component of a larger set of brain regions that includes parts of the hypothalamus, the brain stem, and cortical areas also responsible for coordinating emotional responses. In particular, the medial and ventral prefrontal cortex and amygdala are closely interconnected. Dynamic processing within and between these structures likely subserves many functions beyond coordinated emotional behavior, including extinction, the cognitive regulation of emotional

states, interactions between social and emotional domains, and the influence of the amgydalar representations on decision-making and subjective feelings.

Part Editors: C. Daniel Salzman and John D. Koester

Part VI

This page intentionally left blank

40

The Brain Stem

In primitive vertebrates—reptiles, amphibians, and fish—the forebrain is only a small part of the brain and is devoted mainly to olfactory processing and to the integration of autonomic and endocrine function with the basic behaviors necessary for survival. These basic behaviors include feeding, drinking, sexual reproduction, sleep, and emergency responses. Although we are accustomed to thinking that the forebrain orchestrates most human behaviors, many complex responses, such as feeding—the coordination of chewing, licking, and swallowing—are actually made up of relatively simple, stereotypic motor responses governed by ensembles of neurons in the brain stem.

The importance of this pattern of organization in human behavior is clear from observing infants born without a forebrain (hydranencephaly). Hydranencephalic infants are surprisingly difficult to distinguish from normal babies. They cry, smile, suckle, and move their eyes, face, arms, and legs. As these sad cases illustrate, the brain stem can organize virtually all of the behavior of the newborn.

In this chapter, we describe the functional anatomy of the brain stem, particularly the cranial nerves, as well as the ensembles of local circuit neurons that organize the simple behaviors of the face and head. Finally, we consider the modulatory functions of nuclei in the brain stem that adjust the sensitivity of sensory, motor, and arousal systems.

The brain stem is the rostral continuation of the spinal cord, and its motor and sensory components are similar in structure to those of the spinal cord. But the portions of the brain stem that control the cranial nerves are much more complex than the corresponding parts of the spinal cord that control the spinal nerves because cranial nerves mediate more complex behaviors. The core of the brain stem, the *reticular formation*, is homologous to the intermediate gray matter of the spinal cord but is also more complex. Like the spinal cord, the reticular formation contains ensembles of local-circuit interneurons that generate motor and autonomic patterns and coordinate reflexes and simple behaviors. In addition, the brain stem contains glutamatergic and GABAergic circuitry that regulates arousal, wake–sleep cycles, breathing, and other vital functions, as well as monoaminergic modulatory neurons that act to optimize the functions of the nervous system.

The Cranial Nerves Are Homologous to the Spinal Nerves

Because the spinal nerves reach only as high as the first cervical vertebra, the cranial nerves provide the somatic and visceral, sensory and motor innervation for the head. Two cranial nerves, the glossopharyngeal and vagus nerves, also supply visceral sensory and motor innervation of the neck, chest, and most of the abdominal organs with the exception of the pelvis. In addition, some cranial nerves are associated with specialized functions, such as vision or hearing, that go beyond the sensory and motor plan of the spinal cord.

Assessment of the cranial nerves is an important part of the neurological examination because abnormalities of function can pinpoint a site in the brain stem that has been damaged. Therefore, it is important to know the origins of the cranial nerves, their intracranial course, and where they exit from the skull.

The cranial nerves are traditionally numbered I through XII in rostrocaudal sequence. Cranial nerves I and II enter at the base of the forebrain. The other cranial nerves arise from the brain stem at characteristic locations (Figure 40–1). All but one exit from the ventral surface of the brain stem (Figure 40–2). The exception is the trochlear (IV) nerve, which leaves the midbrain from its dorsal surface just behind the inferior colliculus and wraps around the lateral surface of the brain stem to join the other cranial nerves concerned with eye movements. The cranial nerves with sensory functions (V, VII, VIII, IX, and X) have associated sensory ganglia that operate much as dorsal root ganglia do for spinal nerves. These ganglia are located along the course of individual nerves as they enter the skull.

The olfactory (I) nerve, which is associated with the forebrain, is described in detail in Chapter 29; the optic (II) nerve, which is associated with the diencephalon, is described in Chapters 21 and 22. The spinal accessory (XI) nerve can be considered a cranial nerve anatomically but actually is a spinal nerve originating from the higher cervical motor rootlets. It runs up into the skull before exiting through the jugular foramen to innervate the trapezius and sternocleidomastoid muscles in the neck.

Cranial Nerves Mediate the Sensory and Motor Functions of the Face and Head and the Autonomic Functions of the Body

Three ocular motor nerves control movements of the eyes. The *abducens (VI) nerve* has the simplest action; it contracts the lateral rectus muscle to move the globe laterally. The *trochlear (IV) nerve* also innervates a single muscle, the superior oblique, which both depresses the eye and rotates it inward depending on the eye's position. The *oculomotor (III) nerve* supplies all of the other muscles of the orbit, including the retractor of the lid. It also provides the parasympathetic innervation responsible for pupillary constriction in response to light and accommodation of the lens for near vision. The ocular motor system is considered in detail in Chapter 35.

The *trigeminal (V) nerve* is a mixed nerve (containing both sensory and motor axons) that leaves the brain stem in two roots. The motor root innervates the muscles of mastication (the masseter, temporalis, and pterygoids) and a few muscles of the palate (tensor veli palatini), inner ear (tensor tympani), and upper neck (mylohyoid and anterior belly of the digastric muscle). The sensory fibers arise from neurons in the trigeminal ganglion, located at the floor of the skull in the middle cranial fossa.

Three branches emerge from the trigeminal ganglion. The *ophthalmic division* (V_1) runs with the ocular motor nerves through the superior orbital fissure (Figure 40–2A) to innervate the orbit, nose, and forehead and scalp back to the vertex of the skull (Figure 40–3). Some fibers from this division also innervate

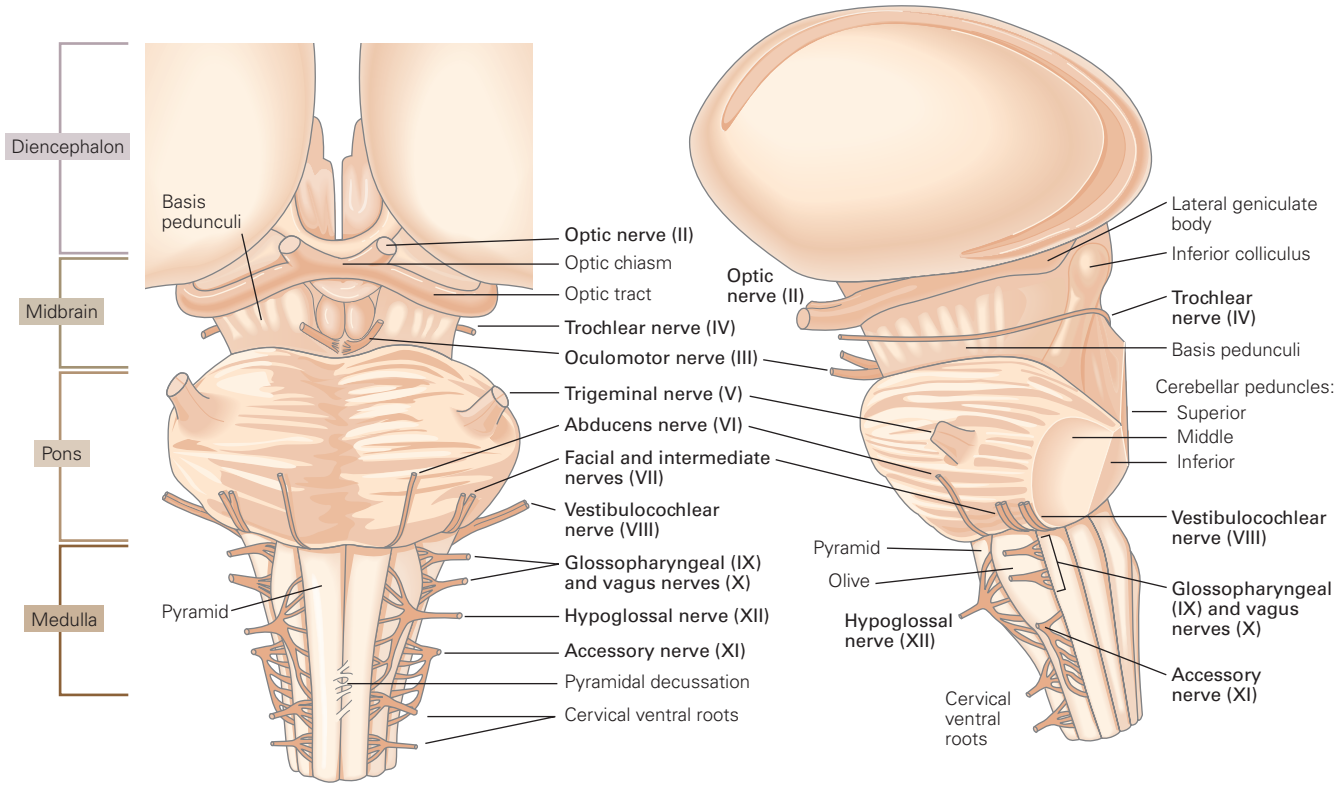

Figure 40–1 The origins of cranial nerves in the brain stem (ventral and lateral views). The olfactory (I) nerve is not shown because it terminates in the olfactory bulb in the forebrain. All of the cranial nerves except one emerge from the ventral surface of the brain; the trochlear (IV) nerve originates from the dorsal surface of the midbrain.

the meninges and blood vessels of the anterior and middle intracranial fossas. The *maxillary division* (V_2) runs through the round foramen of the sphenoid bone to innervate the skin over the cheek and the upper portion of the oral cavity. The *mandibular division* (V_3), which also contains the motor axons of the trigeminal nerve, leaves the skull through the oval foramen of the sphenoid bone. It innervates the skin over the jaw, the area above the ear, and the lower part of the oral cavity, including the tongue.

Complete trigeminal sensory loss results in numbness of the entire face and the inside of the mouth. One-sided trigeminal motor weakness does not cause much weakness of jaw closure because the muscles of mastication on either side are sufficient to close the jaw. Nevertheless, the jaw tends to deviate toward the side of the lesion when the mouth is opened because the internal pterygoid muscle on the opposite side, when unopposed, pulls the jaw toward the weak side.

The *facial (VII) nerve* is also a mixed nerve. Its motor root innervates the muscles of facial expression as well as the stapedius muscle in the inner ear, stylohyoid muscle, and posterior belly of the digastric muscle in the upper neck. The sensory root runs as a separate bundle, the intermediate nerve, through the internal auditory canal and arises from neurons in the geniculate ganglion, located near the middle ear. Distal to the geniculate ganglion, the sensory fibers diverge from the motor branch. Some innervate skin of the external auditory canal while others form the chorda tympani, which joins the lingual nerve and conveys taste sensation from the anterior two-thirds of the tongue. The *autonomic component* of the facial nerve includes parasympathetic fibers that travel through the motor root to the sphenopalatine and submandibular ganglia, which innervate lacrimal and salivary glands (except the parotid gland) and the cerebral vasculature.

The facial nerve may suffer isolated injury in Bell palsy, a common complication of certain viral infections. Early on, the patient may complain mainly of the face pulling toward the unaffected side because of the weakness of the muscles on the side of the lesion. Later, the ipsilateral corner of the mouth droops, food falls out of the mouth, and the eyelids no longer close on that side. Loss of blinking may result in drying

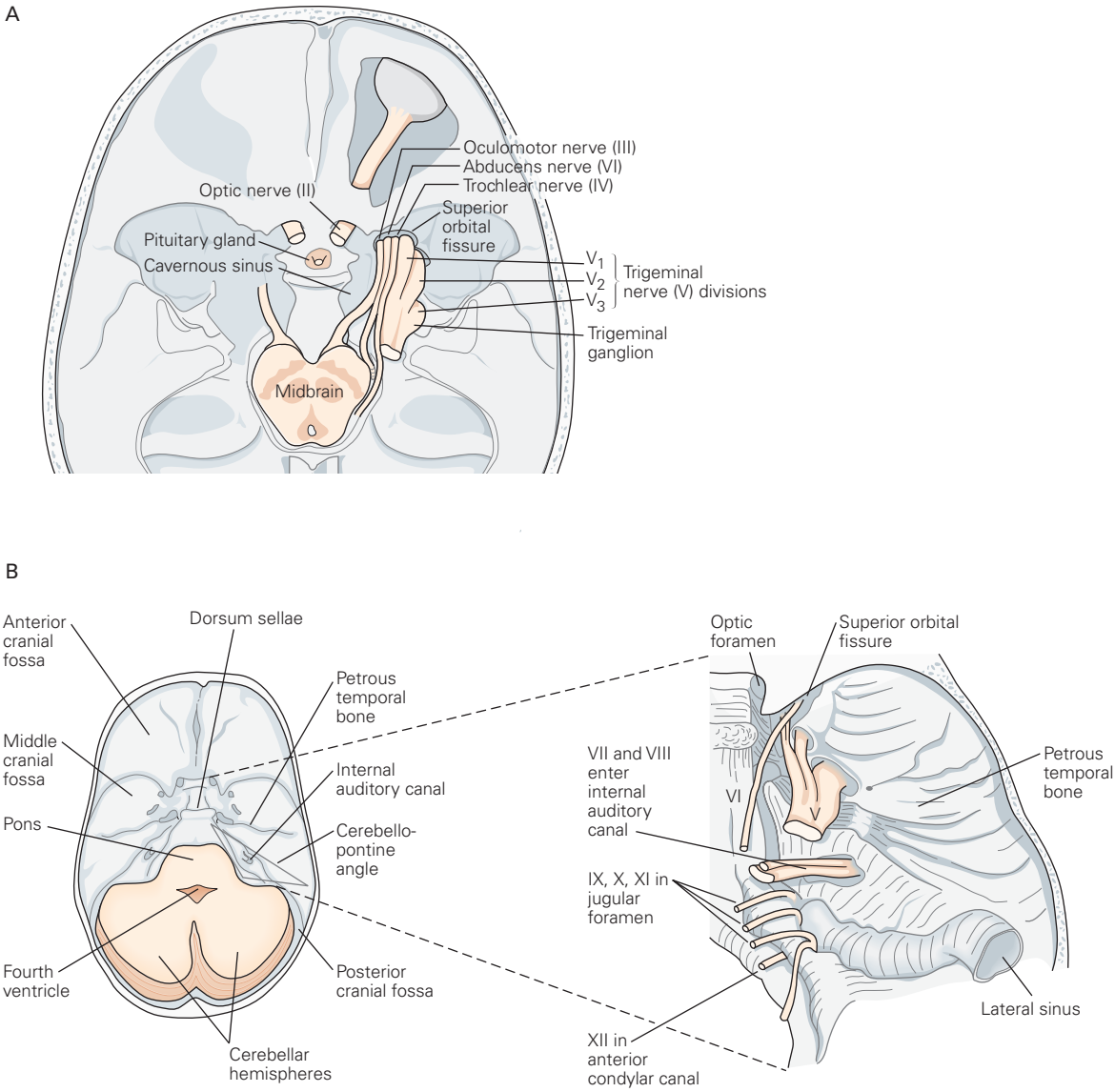

Figure 40–2 The cranial nerves exit the skull in groups.

A. Cranial nerves II, III, IV, V, and VI exit the skull near the pituitary fossa. The optic (**II**) nerve enters the optic foramen, but the oculomotor (**III**), trochlear (**IV**), and abducens (**VI**) nerves, and the first division of the trigeminal (**V**) nerve leave through the superior orbital fissure. The second and third divisions of the trigeminal nerve exit through the round and oval foramina, respectively.

B. In the posterior fossa, the facial (**VII**) and vestibulocochlear (**VIII**) nerves exit through the internal auditory canal, whereas the glossopharyngeal (**IX**), vagus (**X**), and accessory (**XI**) nerves leave through the jugular foramen. The hypoglossal nerve (**XII**) has its own foramen.

and injury to the cornea. The patient may complain that sound has a booming quality in the ipsilateral ear because the stapedius muscle fails to tense the ossicles in response to a loud sound (the stapedial reflex). Taste may also be lost on the anterior two-thirds of the tongue on the ipsilateral side. If the Bell palsy is caused by a herpes zoster infection of the geniculate ganglion, small blisters may form in the outer ear canal, the ganglion's cutaneous sensory field.

The *vestibulocochlear (VIII) nerve* contains two main bundles of sensory axons from two ganglia. Fibers from the vestibular ganglion relay sensation of angular and linear acceleration from the semicircular canals, utricle, and saccule in the inner ear. Fibers from the cochlear ganglion relay information from the cochlea concerning sound. A vestibular schwannoma, one of the most common intracranial tumors, may form along the vestibular component of cranial nerve VIII

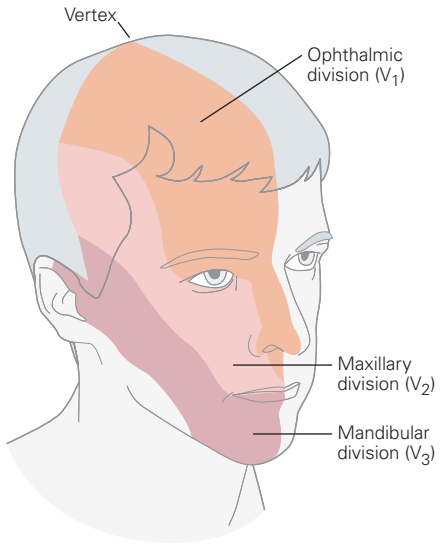

Figure 40–3 The three sensory divisions of the trigeminal (V) nerve innervate the face and scalp. The V_2 and V_3 divisions also innervate the upper and lower parts of the oral cavity, including the tongue. The C2 cervical root innervates the back of the head. The area around the ear is innervated by branches of the VII and X nerve.

as it runs within the internal auditory meatus. Most patients complain only about hearing loss, as the brain is usually able to adapt to the gradual loss of vestibular input from one side.

The *glossopharyngeal (IX) nerve* and *vagus (X) nerve* are mixed nerves and provide parasympathetic autonomic input to thoracic and visceral organs. These closely related nerves transmit sensory information from the pharynx and upper airway as well as taste from the posterior third of the tongue and oral cavity. The glossopharyngeal nerve transmits visceral information from the neck (for example, information on blood oxygen and carbon dioxide from the carotid body, and arterial pressure from the carotid sinus), whereas the vagus nerve transmits visceral information from the thoracic and abdominal organs except for the distal colon and pelvic organs. Both nerves include parasympathetic motor fibers. The glossopharyngeal nerve provides parasympathetic control of the parotid salivary gland, whereas the vagus nerve innervates the rest of the internal organs of the neck, thorax, and abdomen. The glossopharyngeal nerve innervates only one muscle of the palate, the stylopharyngeus, which raises and dilates the pharynx. The remaining striated muscles of the larynx and pharynx are under control of the vagus nerve.

The vagal sensory neurons innervate the length of the gastrointestinal tract and thus are able to regulate multiple postprandial functions. One excellent example is the role of vagal afferents in regulating food intake following a meal. Cholecystokinin (CCK) is an endogenous peptide secreted by duodenal enteroendocrine cells during meals, which helps to induce satiety. CCK acts (at least in part) via action on vagal afferents in the gut, stimulating a feeling of fullness. Exogenous electrical stimulation of the vagus nerve is now being used clinically to treat a wide variety of conditions including obesity, intractable epilepsy, and even depression. However, the neuroanatomic and molecular mechanisms underlying these effects remain poorly understood. Similarly, bariatric surgery remains one of the most widely used and effective strategies to combat obesity. Some studies have suggested that surgical alterations in the responsiveness of vagal afferents to gut signals may contribute to the sustained weight loss following these surgeries.

Because many of the functions of nerves IX and X are bilateral and partially overlapping, unilateral injury of nerve IX may be difficult to detect. Patients with unilateral cranial nerve X injury are hoarse, because one vocal cord is paralyzed, and they may have some difficulty swallowing. Examination of the oropharynx shows weakness and numbness of the palate on one side.

The *spinal accessory (XI) nerve* is purely motor and originates from motor neurons in the upper cervical spinal cord. It innervates the trapezius and sternocleidomastoid muscles on the same side of the body. Because the mechanical effect of the sternocleidomastoid is to turn the head toward the opposite side, an injury of the left nerve causes weakness in turning the head to the right. A lesion of the cerebral cortex on the left will cause weakness of voluntary muscles on the entire right side of the body except for the sternocleidomastoid; instead, the ipsilateral sternocleidomastoid will be weak (because the left cerebral cortex is concerned with muscles that interact with the right side of the world, and the left sternocleidomastoid turns the head to the right).

The *hypoglossal (XII) nerve* is also purely motor, innervating the muscles of the tongue. When the nerve is injured, for example during surgery for head and neck cancer, the tongue atrophies on that side. The muscle fibers exhibit twitches of muscle fascicles (fasciculations), which may be seen clearly through the thin mucosa of the tongue.

Cranial Nerves Leave the Skull in Groups and Often Are Injured Together

In assessing dysfunction of the cranial nerves, it is important to determine whether the injury is within

the brain or further along the course of the nerve. As cranial nerves leave the skull in groups through specific foramina, damage at these locations can affect several nerves.

The cranial nerves concerned with orbital sensation and movement of the eyes—the oculomotor, trochlear, and abducens nerves, as well as the ophthalmic division of the trigeminal nerve—are gathered together in the *cavernous sinus*, along the lateral margins of the sella turcica, and then exit the skull through the *superior orbital fissure* adjacent to the optic foramen (Figure 40–2A). Tumors in this region, such as those arising from the pituitary gland, often make their presence known first by pressure on these nerves or the adjacent optic chiasm.

Cranial nerves VII and VIII exit the brain stem at the *cerebellopontine angle*, the lateral corner of the brain stem at the juncture of the pons, medulla, and cerebellum (Figure 40–2B), and then leave the skull through the internal auditory meatus. A common tumor of the cerebellopontine angle is the vestibular schwannoma (sometimes erroneously called an "acoustic neuroma"), which derives from Schwann cells in the vestibular component of nerve VIII. A large tumor of the cerebellopontine angle may not only impair the function of nerves VII and VIII but may also press on nerve V near its site of emergence from the middle cerebellar peduncle, causing facial numbness, or compress the cerebellum or its peduncles on the same side, causing ipsilateral clumsiness.

The lower cranial nerves (IX, X, and XI) exit through the *jugular foramen* (Figure 40–2B) and are vulnerable to compression by tumors at that site. Nerve XII leaves the skull through its own (hypoglossal) foramen and is generally not affected by tumors located in the adjacent jugular foramen, unless the tumor becomes quite large. If a tumor involves nerves IX and X, but nerve XI is spared, it is generally within or near the brain stem rather than near the jugular foramen.

The Organization of the Cranial Nerve Nuclei Follows the Same Basic Plan as the Sensory and Motor Areas of the Spinal Cord

Cranial nerve nuclei are organized in rostrocaudal columns that are homologous to the sensory and motor laminae of the spinal cord (Chapters 18 and 31). This pattern is best understood from the developmental plan of the caudal neural tube that gives rise to the brain stem and spinal cord.

The transverse axis of the embryonic caudal neural tube is subdivided into alar (dorsal) and basal (ventral) plates by the sulcus limitans, a longitudinal groove along the lateral walls of the central canal, fourth ventricle, and cerebral aqueduct (Figure 40–4). The alar plate forms the sensory components of the dorsal horn of the spinal cord, whereas the basal plate forms the motor components of the ventral horn. The intermediate gray matter is made up primarily of the interneurons that coordinate spinal reflexes and motor responses.

The brain stem shares this basic plan. As the central canal of the spinal cord opens into the fourth ventricle, the walls of the neural tube are splayed outward

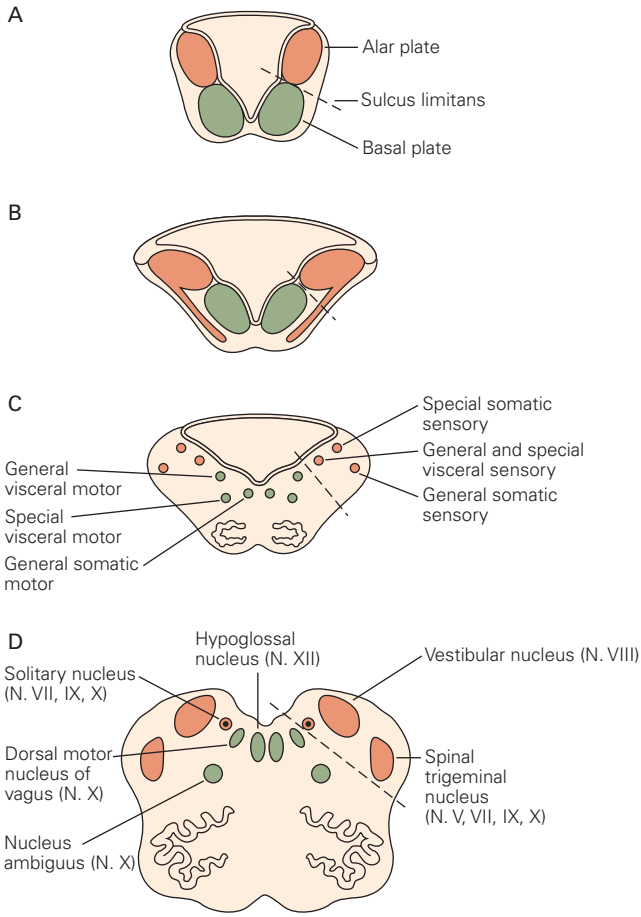

Figure 40–4 The developmental plan of the brain stem is the same general plan as that of the spinal cord.

A. The neural tube is divided into a dorsal sensory portion (the alar plate) and a ventral motor portion (the basal plate) by a longitudinal groove, the sulcus limitans.

B–D. During development, the sensory and motor cell groups migrate into their adult positions but largely retain their relative locations. In maturity (part **D**), the sulcus limitans (**dashed line**) is still recognizable in the walls of the fourth ventricle and the cerebral aqueduct, demarcating the border between dorsal sensory (**orange**) and ventral motor (**green**) structures. The section in part D is from the rostral medulla.

so that the dorsal sensory structures (derived from the alar plate) are displaced laterally, whereas the ventral motor structures (derived from the basal plate) remain more medial. The nuclei of the brain stem are divided into *general nuclei*, which serve functions similar to those of the spinal cord laminae, and *special nuclei*, which serve functions unique to the head, such as hearing, balance, taste, and control of the musculature related to the jaw, face, oropharynx, and larynx.

Embryonic Cranial Nerve Nuclei Have a Segmental Organization

Although the columns of sensory and motor nuclei in the adult hindbrain are organized rostrocaudally, the arrangement of neurons at each level derives from a strikingly segmental pattern in the early embryo. Before neurons appear, the future hindbrain region of the neural plate becomes subdivided into a series of eight segments of approximately equal size, known as *rhombomeres* (Figure 40–5A).

Each rhombomere develops a similar set of differentiated neurons, as if the developing hindbrain is made up of series of modules. Pairs of rhombomeres are associated with specific sets of muscles derived from the embryonic branchial arches (eg, rhombomeres 2 and 3 with the muscles of mastication and 4 and 5 with the muscles of facial expression) (Figure 40–5A). The even-numbered rhombomeres differentiate ahead of the odd-numbered ones. Rhombomeres 2, 4, and 6 form the branchial motor nuclei of the trigeminal, facial, and glossopharyngeal nerves, respectively. Later, rhombomeres 3, 5, and 7 contribute motor neurons to these nuclei, again respectively; in each case, the axons of individual motor neurons from odd-numbered rhombomeres extend rostrally as they join those of their even-numbered neighbors.

At this developmental stage, each of these nuclei is composed of homologous neurons derived from two adjacent segments. This early transverse segmental organization changes later in development, as rhombomere boundaries disappear and the dorsolateral migration of the cell bodies aligns the cells into rostrocaudal columns. Ultimately, some somatic and parasympathetic motor neurons migrate into the ventrolateral tegmentum; for example, the migration of the facial motor neurons of rhombomere 4 around the abducens nucleus generates the internal genu of the facial nerve (Figure 40–5A). Furthermore, neural crest cells from each rhombomere migrate into the corresponding branchial arches where they provide sensory and autonomic ganglion cells, as well as positional cues for the development of the arch muscles.

Adult Cranial Nerve Nuclei Have a Columnar Organization

Overall, the brain stem nuclei on each side are organized in six rostrocaudal columns, three of sensory nuclei and three of motor nuclei (Figure 40–6). These are considered later, in dorsolateral to ventromedial sequence. Although the columns are discontinuous along the rostrocaudal axis of the brain stem, nuclei with similar functions (sensory or motor, somatic or visceral) have similar dorsolateral-ventromedial positions at each level of the brain stem.

Within each motor nucleus, motor neurons for an individual muscle are also arranged in a cigar-shaped longitudinal column. Thus, each motor nucleus in cross section forms a mosaic map of the territory that is innervated. For example, in a cross section through the facial nucleus, the clusters of neurons that innervate the different facial muscles form a topographic map of the face.

General Somatic Sensory Column

The general somatic sensory column occupies the most lateral region of the alar plate and includes the trigeminal sensory nuclei (N. V). The *spinal trigeminal nucleus* is a continuation of the dorsal-most laminae of the spinal dorsal horn (Figure 40–5A) and is sometimes called the medullary dorsal horn. Along its outer surface lies the spinal trigeminal tract, a direct continuation of Lissauer's tract of the spinal cord (Chapter 20), thus allowing some cervical sensory fibers to reach the trigeminal nuclei and some trigeminal sensory axons to reach the dorsal horn in upper cervical segments. This arrangement allows dorsal horn sensory neurons to have a range of inputs that are much broader than that of individual spinal or trigeminal segments and ensures the integration of trigeminal and upper cervical sensory maps.

The spinal trigeminal nucleus receives sensory axons from the trigeminal ganglion (N. V) and from all cranial nerve sensory ganglia concerned with pain and temperature in the head, including geniculate ganglion (N. VII) neurons that relay information from the external auditory meatus, petrosal ganglion (N. IX) cells that convey information from the posterior part of the palate and tonsillar fossa, and nodose ganglion (N. X) axons that relay information from the posterior wall of the pharynx. The spinal trigeminal nucleus thus represents the entire oral cavity as well as the surface of the face.

The somatotopic organization of the afferent fibers in the spinal trigeminal nucleus is inverted: The forehead

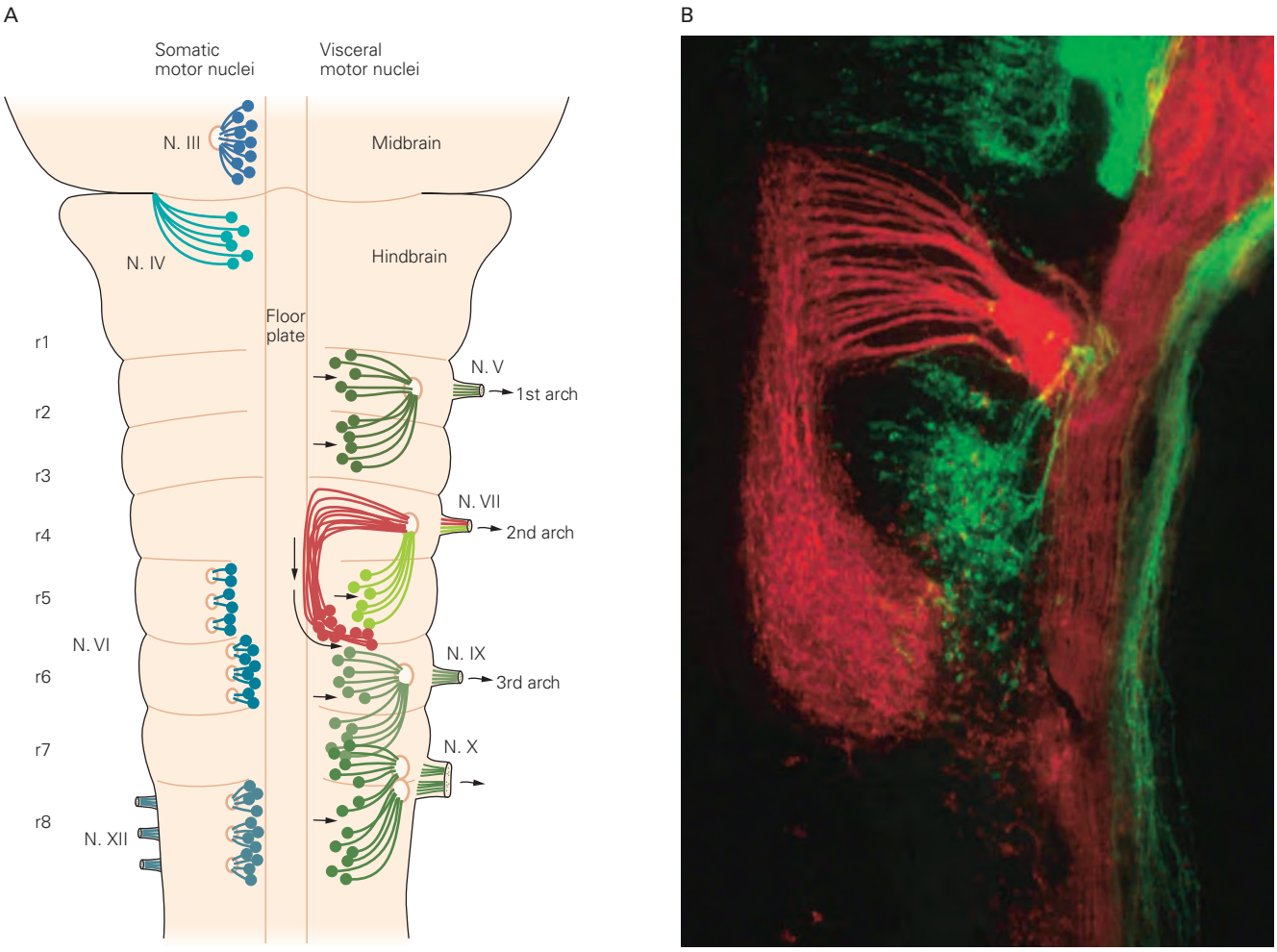

Figure 40–5 Embryonic cranial nerve nuclei are organized segmentally.

A. In the developing hindbrain (seen here from the ventral side), special and general visceral motor neurons (represented on the right side of the brain stem) form in each hindbrain segment (rhombomere) except rhombomere 1 (**r1**). Each special visceral motor nucleus comprises neurons in two rhombomeres: the trigeminal motor nucleus is formed by neurons in r2 and r3, the facial nucleus by neurons in r4 and r5, the glossopharyngeal nucleus by neurons in r6 and r7, and the motor nuclei of the vagus by neurons in r7 and r8. Axons of neurons in each of these nuclei course laterally within the brain, leaving the brain through exit points in the lateral neuroepithelium (of r2, r4, r6, and r7) and running together outside the brain to form the respective cranial motor nerves (V, VII, IX, X). The trigeminal (**V**) nerve innervates muscles in the 1st branchial arch, the facial (**VII**) nerve innervates muscles in the 2nd branchial arch, and the glossopharyngeal (**IX**) nerve innervates muscles in the 3rd branchial arch.

All of the visceral motor neurons (various shades of **green**, represented on the right side of the brain stem) develop initially next to the floor plate at the ventral midline; after extending their axons toward their respective exit points, the cell bodies then migrate laterally (**arrows**). Exceptions are the facial motor neurons formed in r4 (**red**); the cell bodies, after extending their axons toward the exit point, migrate caudally to the axial level of r6 before migrating laterally. General visceral (parasympathetic) motor neurons associated with nerve VII (**light green**) take a more conventional course (see panel **B**).

General somatic motor nuclei (**various shades of blue**, represented on the left side of the brain stem) are formed in r1 (trochlear nucleus), r5 and r6 (abducens nucleus), and r8 (hypoglossal nucleus). The cell bodies of these neurons remain close to their place of birth, next to the floor plate. The axons of abducens and hypoglossal neurons exit the brain directly ventrally, without coursing laterally. The axons of trochlear neurons (**light blue**) extend laterally and dorsally within the brain until, caudal to the inferior colliculus, they turn medially, decussate just behind the inferior colliculus, and exit near the midline of the opposite side.

B. The brain stem of a mouse embryo in which fluorescent dyes label different populations of cranial nerve VII motor neurons. A red-fluorescing dye fills the cell bodies of facial motor neurons via retrograde transport from the motor root of the facial nerve. These neurons develop initially in r4 and then migrate posteriorly, alongside the floor plate, to r6 (see **red** neurons in part **A**). A green-fluorescing dye fills the cell bodies of general visceral motor neurons in r5 (see **light green** neurons in part **A**) via retrograde transport from the root of the intermediate nerve (sensory and preganglionic general visceral motor axons). (Micrograph reproduced, with permission, from Dr. Ian McKay.)

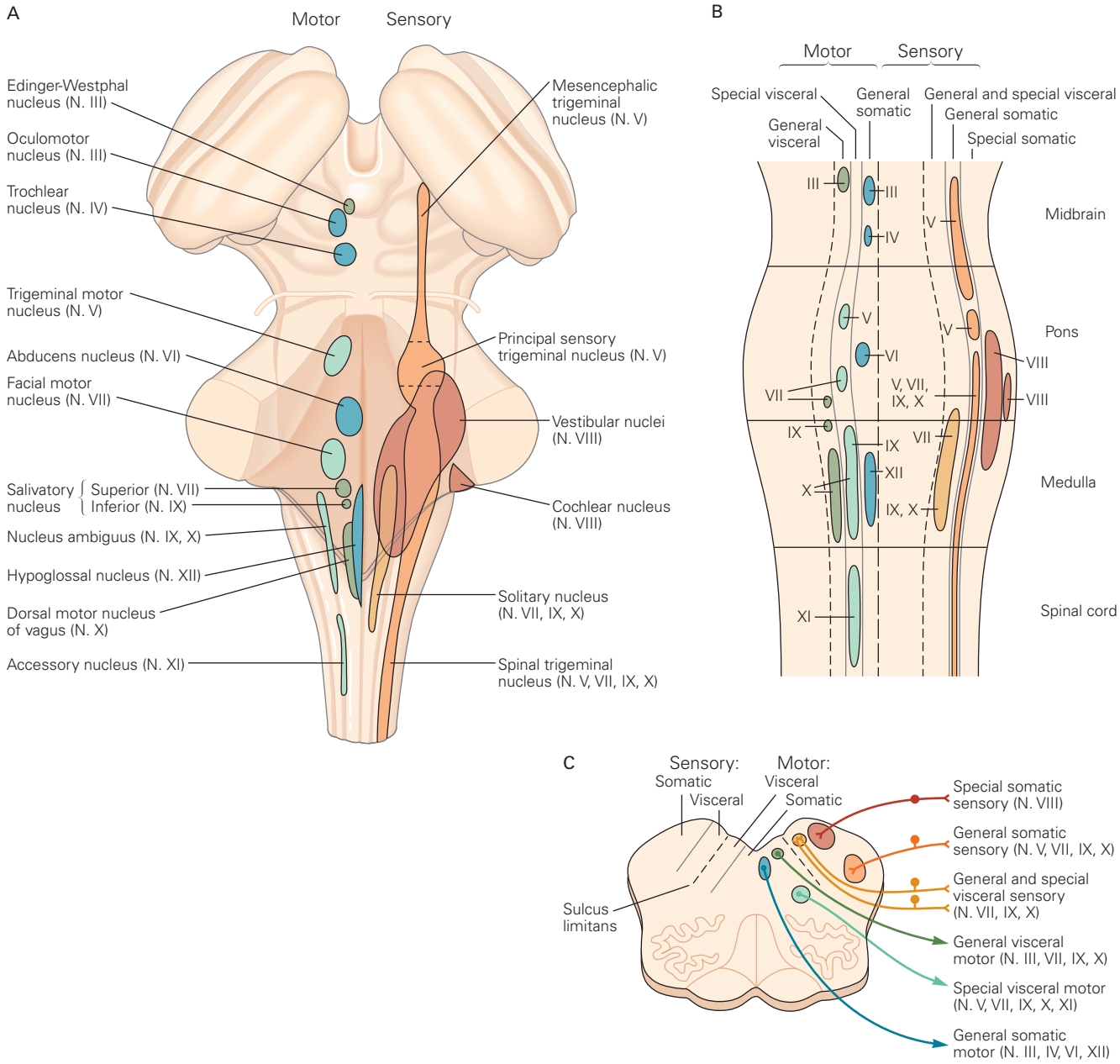

Figure 40–6 Adult cranial nerve nuclei are organized in six functional columns on the rostrocaudal axis of the brain stem.

A. This dorsal view of the human brain stem shows the location of the cranial nerve sensory nuclei (*right*) and motor nuclei (*left*).

B. A schematic view of the functional organization of the cranial nerve nuclei makes it clearer that they form motor and sensory columns.

C. The medial-lateral arrangement of the cranial nerve nuclei is shown in a cross section at the level of the medulla (compare with Figure 40–4D).

is represented ventrally and the oral region dorsally, with the tongue extending medially toward the taste region of the nucleus of the solitary tract, with which it shares some afferent information concerning food texture and temperature. Axons from the spinal trigeminal nucleus descend on the same side of the brain stem into the cervical spinal cord, where they cross the midline in the anterior commissure with spinothalamic axons and join the opposite spinothalamic tract. (For this reason, upper cervical spinal cord injury may cause facial numbness.) The trigeminothalamic axons then ascend back through the brain stem in close association with the spinothalamic tract, providing inputs to brain stem nuclei for reflex motor and autonomic responses in addition to carrying pain and temperature information to the thalamus.

The *principal sensory trigeminal nucleus* lies in the mid-pons just lateral to the trigeminal motor nucleus. It receives the axons of neurons in the trigeminal ganglion concerned with position sense and fine touch discrimination, the same types of sensory information carried from the rest of the body by the dorsal columns. The axons from this nucleus are bundled just medial to those from the dorsal column nuclei in the medial lemniscus, through which they ascend to the ventroposterior medial thalamus.

The *mesencephalic trigeminal nucleus*, located at the midbrain level in the lateral surface of the periaqueductal gray matter, relays mechanosensory information from the muscles of mastication and the periodontal ligaments. The large cells of this nucleus are not central neurons but primary sensory ganglion cells that derive from the neural crest and, unlike their relatives in the trigeminal ganglion, migrate into the brain during development. The central branches of the axons of these pseudo-unipolar cells contact motor neurons in the trigeminal motor nucleus, providing monosynaptic feedback to the jaw musculature, critical for rapid and precise control of chewing movements.

Special Somatic Sensory Column

The special somatic sensory column has inputs from the acoustic and vestibular nerves and develops from the intermediate region of the alar plate. The *cochlear nuclei* (N. VIII), which lie at the lateral margin of the brain stem at the pontomedullary junction, receive afferent fibers from the spiral ganglion of the cochlea. The output of the cochlear nuclei is relayed through the pons to the superior olivary and trapezoid nuclei and bilaterally on to the inferior colliculus (Chapter 28). The *vestibular nuclei* (N. VIII) are more complex. They include four distinct cell groups that relay information from the vestibular ganglion to various motor sites in the brain stem, cerebellum, and spinal cord concerned with maintaining balance and coordination of eye and head movements (Chapter 27).

Visceral Sensory Column

The visceral sensory column is concerned with special visceral information (taste) and general visceral information from the facial (VII), glossopharyngeal (IX), and vagus nerves (X). It is derived from the most medial tier of neurons in the alar plate. All of the afferent axons from these sources terminate in the *nucleus of the solitary tract*. The solitary tract is analogous to the spinal trigeminal tract or Lissauer's tract, bundling afferents from different cranial nerves as they course rostrocaudally along the length of the nucleus. As a result, sensory information from different regions of the viscera produces a unified map of the internal body in the nucleus.

Special visceral afferents from the anterior two-thirds of the tongue travel to the nucleus of the solitary tract through the chorda tympani branch of the facial nerve, whereas those from the posterior parts of the tongue and oral cavity arrive through the glossopharyngeal and vagus nerves. These afferents terminate in roughly somatotopic fashion in the anterior third of the nucleus of the solitary tract (or solitary nucleus). General visceral afferents are relayed through the glossopharyngeal and vagus nerves. Those from the rest of the gastrointestinal tract (down to the transverse colon) terminate in the middle portion of the solitary nucleus in topographic order, whereas those from the cardiovascular and respiratory systems terminate in the caudal and lateral portions.

The solitary nucleus projects directly to parasympathetic and sympathetic preganglionic motor neurons in the medulla and spinal cord that mediate various autonomic reflexes, as well as to parts of the reticular formation that coordinate autonomic and respiratory responses. Most ascending projections from the solitary nucleus that carry information from the viscera to the forebrain are relayed through the parabrachial nucleus in the pons, although some reach the forebrain directly. Together, the solitary and parabrachial nuclei supply visceral sensory information to the hypothalamus, basal forebrain, amygdala, thalamus, and cerebral cortex.

General Visceral Motor Column

All motor neurons initially develop adjacent to the floor plate, a longitudinal strip of non-neuronal cells

at the ventral midline of the neural tube (Chapter 45). Neurons fated to become the three types of brain stem motor neurons migrate dorsolaterally, settling in three distinct rostrocaudal columns. The neurons that form the general visceral motor column take up a position along the most lateral region of the basal plate, just medial to the sulcus limitans. During development, the parasympathetic motor neurons destined to join the superior salivatory nucleus (part of the facial nerve) and nucleus ambiguus (part of the vagus nerve) migrate ventrolaterally, leaving behind axons that ascend medially before turning laterally to exit the brain stem, in a course similar to the facial motor neurons.

The *Edinger-Westphal nucleus* (N. III) lies in the midline separating the somatic oculomotor neurons just below the floor of the cerebral aqueduct. It contains preganglionic neurons that control pupillary constriction and lens accommodation through the ciliary ganglion.

The *superior salivatory nucleus* (N. VII) lies just dorsal to the facial motor nucleus and comprises parasympathetic preganglionic neurons that innervate the sublingual and submandibular salivary glands and the lacrimal glands and intracranial circulation through the sphenopalatine and submandibular parasympathetic ganglia.

Parasympathetic preganglionic neurons associated with the gastrointestinal tract form a column at the level of the medulla just dorsal to the hypoglossal nucleus and ventral to the nucleus of the solitary tract. At the most rostral end of this column is the *inferior salivatory nucleus* (N. IX) comprising the preganglionic neurons that innervate the parotid gland through the otic ganglion. The rest of this column constitutes the *dorsal motor vagal nucleus* (N. X). Most of the preganglionic neurons in this nucleus innervate the gastrointestinal tract below the diaphragm; a few are cardiomotor neurons.

The *nucleus ambiguus* (N. X) runs the rostrocaudal length of the ventrolateral medulla and contains parasympathetic preganglionic neurons that innervate thoracic organs, including the esophagus, heart, and respiratory system, as well as special visceral motor neurons that innervate the striated muscle of the larynx and pharynx, and neurons that generate respiratory motor patterns (see later in chapter). The parasympathetic preganglionic neurons are organized in topographic fashion, with the esophagus represented most rostrally and dorsally.

Special Visceral Motor Column

The special visceral motor column includes motor nuclei that innervate muscles derived from the branchial (pharyngeal) arches. Because these arches are homologous to the gills in fish, the muscles are considered special visceral muscles, even though they are striated. During development, these cell groups migrate to an intermediate position in the basal plate and are eventually located ventrolaterally in the tegmentum.

The *trigeminal motor nucleus* (N. V) lies at midpontine levels and innervates the muscles of mastication. Nearby in separate clusters are located the *accessory trigeminal nuclei* that innervate the tensor tympani, tensor veli palatini, and mylohyoid muscles, and the anterior belly of the digastric muscle.

The *facial motor nucleus* (N. VII) lies caudal to the trigeminal motor nucleus at the level of the caudal pons and innervates the muscles of facial expression. During development, facial motor neurons migrate medially and rostrally around the medial margin of the abducens nucleus before turning laterally, ventrally, and caudally toward their definitive position at the pontomedullary junction (Figure 40–5A). This sinuous course that the axons leave behind forms the *internal genu of the facial nerve*. The adjacent *accessory facial motor nuclei* innervate the stylohyoid and stapedius muscles and the posterior belly of the digastric muscle.

The nucleus ambiguus contains branchial motor neurons with axons that run in the glossopharyngeal and vagus nerves. These neurons innervate the striated muscles of the larynx and pharynx. During development, these motor neurons migrate into the ventrolateral medulla, and as a consequence, their axons run dorsomedially toward the dorsal motor vagal nucleus, then turn sharply within the medulla to exit laterally, similar to the course of the facial motor axons.

General Somatic Motor Column

The neurons of the somatic motor column migrate the least during development, remaining close to the ventral midline. The *oculomotor nucleus* (N. III) lies at the midbrain level; it consists of five rostrocaudal columns of motor neurons innervating the medial, superior, and inferior rectus muscles, the inferior oblique muscle, and the levator of the eyelids. The motor neurons for the medial and inferior rectus and inferior oblique muscles are on the side of the brain stem from which the nerve exits, whereas those for the superior rectus are on the opposite side. The levator motor neurons are bilateral.

The *trochlear nucleus* (N. IV), which innervates the trochlear muscle, lies at the midbrain/rostral pontine level on the side of the brain stem opposite from

which the nerve exits. The *abducens nucleus* (N. VI), which innervates the lateral rectus muscle, is located at the midpontine level. The *hypoglossal nucleus* (N. XII) in the medulla consists of several columns of neurons, each of which innervates a single muscle of the tongue.

The Organization of the Brain Stem Differs From the Spinal Cord in Three Important Ways

One major difference between the organization of the brain stem and that of the spinal cord is that many long ascending and descending sensory tracts that run along the outside of the spinal cord are incorporated within the interior of the brain stem. Thus, the ascending sensory tracts (the medial lemniscus and spinothalamic tract) run through the reticular formation of the brain stem, as do the auditory, vestibular, and visceral sensory pathways.

A second major difference is that in the brain stem, the cerebellum and its associated pathways form additional structures that are superimposed on the basic plan of the spinal cord. Fibers of the cerebellar tracts and nuclei are bundled with those of the pyramidal and extrapyramidal motor systems to form a large ventral portion of the brain stem. Thus, from the midbrain to the medulla, the brain stem is divided into a dorsal portion, the tegmentum, which follows the basic segmental plan of the spinal cord, and a ventral portion, which contains the structures associated with the cerebellum and the descending motor pathways. At the level of the midbrain, the ventral (motor) portion includes the cerebral peduncles, substantia nigra, and red nuclei. The base of the pons includes the pontine nuclei, corticospinal tract, and middle cerebellar peduncle. In the medulla, the ventral motor structures include the pyramidal tracts and inferior olivary nuclei.

A third major difference is that, although the hindbrain is segmented into rhombomeres during development, there is no clear repeating pattern in the adult brain. In contrast, the spinal cord is not segmented during development, but the final pattern consists of repeating segments. The prominent ladder-like arrays of ventral root axons and dorsal root ganglia suggest that segmentation is imposed by a polarizing effect of the adjacent body segments, or somites into which they migrate—in each somite, the rostral part attracts axonal growth cones and neural crest cells, whereas the caudal part is repulsive. In the head, such patterning is lacking as the cranial mesoderm is not segmented into somites but rather develops under the influence of the rhombomeres.

Neuronal Ensembles in the Brain Stem Reticular Formation Coordinate Reflexes and Simple Behaviors Necessary for Homeostasis and Survival

In the 19th century, Charles Darwin pointed out in his book *The Expression of the Emotions in Man and Animals* that the muscles of facial expression are activated in similar patterns in all mammals during similar emotional situations (fear, anger, disgust, happiness). He hypothesized that the patterns of facial expression must be deeply embedded in the organization of the brain stem. We now recognize that a wide range of reflexes and simple, repetitive, coordinated behaviors, such as facial emotional expression, breathing, and eating, are controlled by neurons in the brain stem reticular formation called *pattern generators*, which produce stereotyped innate responses. Impairment of cranial nerve reflexes and motor patterns in patients with neurological disease can indicate the precise site of brain stem damage.

Cranial Nerve Reflexes Involve Mono- and Polysynaptic Brain Stem Relays

The responses of the pupils to light (*pupillary light reflexes*) are determined by the balance between sympathetic tone in the pupillodilator muscles and parasympathetic tone in the pupilloconstrictor muscles of the iris. Sympathetic tone is maintained by postganglionic neurons in the superior cervical ganglion, which in turn are innervated by preganglionic neurons in the first and second thoracic spinal segments. Parasympathetic tone is supplied by postganglionic ciliary ganglion cells under the control of preganglionic neurons in the Edinger-Westphal nucleus and adjacent areas of the midbrain.

Light impinging on the retina activates a special class of retinal ganglion cells that act as brightness detectors. These cells receive inputs from photopigment-containing rod and cone cells, but they also have their own photopigment, melanopsin, which allows them to respond to light even when the rods and cones have degenerated. These cells send their axons through the optic nerve, chiasm, and tract to the olivary pretectal nucleus, where they terminate on neurons whose axons project to preganglionic neurons in the Edinger-Westphal nucleus (Figure 40–7). Thus, injury to the dorsal midbrain in the region of the posterior commissure can prevent pupillary light responses (midposition, fixed pupils), whereas injury to the oculomotor nerve eliminates parasympathetic tone to that pupil (fixed and dilated pupil). The melanopsin-containing

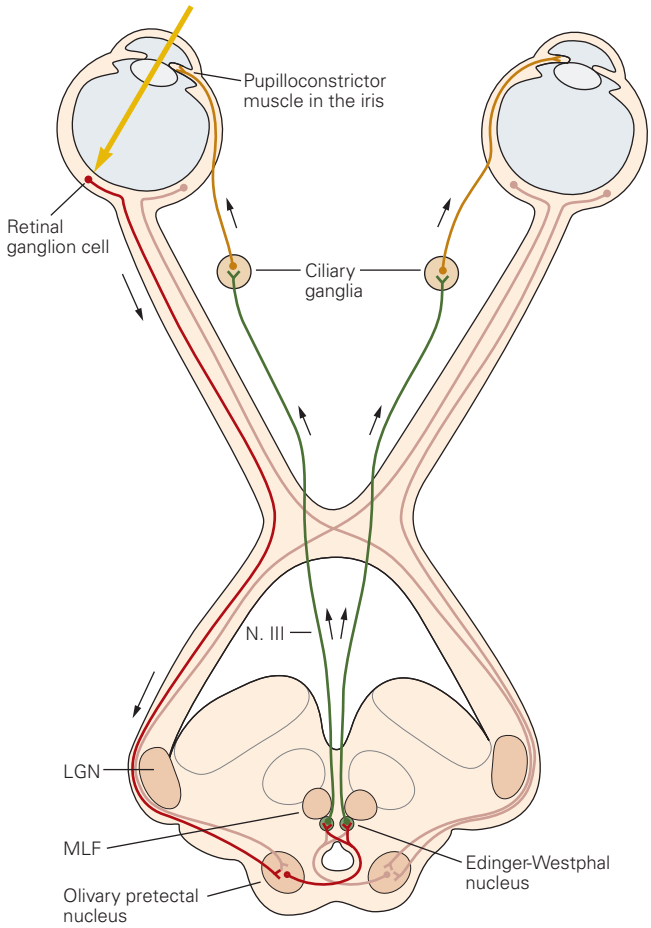

Figure 40–7 The pupillary response to light is mediated by parasympathetic innervation of the iris. Retinal ganglion cells that contain the photopigment melanopsin act as luminance detectors, sending their axons through the optic tract to the olivary pretectal nucleus, at the junction of the midbrain and the thalamus. Neurons in this nucleus project through the posterior commissure to parasympathetic preganglionic neurons in and around the Edinger-Westphal nucleus. The axons of the preganglionic cells exit with the oculomotor (III) nerve and contact ciliary ganglion cells, which control the pupilloconstrictor muscle in the iris. (Abbreviations: LGN, lateral geniculate nucleus; MLF, medial longitudinal fasciculus.)

retinal ganglion cells also project to the suprachiasmatic nucleus of the hypothalamus, where they entrain circadian rhythms to the day–night cycle (Chapter 44).

Vestibulo-ocular reflexes stabilize the image on the retina during head movement by rotating the eyeballs counter to the rotation of the head. These reflexes are activated by pathways from the vestibular ganglion and nerve to the medial, superior, and lateral vestibular nuclei, and from there to neurons in the reticular formation and ocular motor nuclei that coordinate eye movements. The reflex movements are seen most clearly in comatose patients, in whom turning the head will elicit counter-rotational movements of the eyes (so-called doll's eye movements). Damage to these pathways in the pons impairs these movements.

The *corneal reflex* involves closure of both eyelids as well as upward turning of the eyes (Bell phenomenon) when the cornea is gently stimulated (eg, with a wisp of cotton). The sensory axons from the first division of the trigeminal nerve terminate in the spinal trigeminal nucleus, which relays the sensory signals to pattern generator neurons in the reticular formation adjacent to the facial motor nucleus. The pattern generator neurons provide bilateral inputs to the motor neurons that protect the cornea from damage by causing the orbicularis oculi muscle to close the eyelid and the oculomotor nuclei to roll the eyes upward and back in the orbit. Because the output of the pattern generator is bilateral, damage along the sensory pathway prevents the reflex in both eyes, whereas damage to the facial nerve prevents closure on the same side only.

The *stapedial reflex* contracts the stapedius muscle in response to a loud sound, thus damping movement of the ossicles. The sensory pathway is through the cochlear nerve and nucleus to the reticular formation adjacent to the facial motor nucleus and from there to the stapedial motor neurons, which run in the facial nerve. As described earlier, in patients with injury to the facial nerve (eg, Bell palsy), the stapedial reflex is impaired, and the patient complains that sounds in that ear have a "booming" quality (hyperacusis).

A variety of gastrointestinal reflexes are controlled by multisynaptic brain stem relays. For example, the tasting of food causes neurons in the solitary nucleus that project to the reticular formation adjacent to the motor facial and dorsal motor vagal nuclei to stimulate the preganglionic salivary neurons. The contact of food in the mouth can also elicit gastric contractions and acid secretion, presumably through inputs from the solitary nucleus directly to parasympathetic preganglionic gastric neurons in the dorsal motor vagal nucleus. In patients who have had Bell palsy, the damaged VII nerve parasympathetic axons may regrow aberrantly so that salivary axons reach the lacrimal gland in error, causing tasty food to initiate reflex tearing (crocodile tears).

The *gag reflex* protects the airway in response to stimulation of the posterior oropharynx. The afferent sensory fibers in the glossopharyngeal and vagus nerves terminate in the spinal trigeminal nucleus, whose axons project to the reticular formation adjacent to the nucleus ambiguus. Branchial motor neurons in the nucleus ambiguus innervate the posterior pharyngeal muscles, resulting in elevation of the

palate, constriction of pharyngeal muscles (to expel the offending stimulus), and closure of the airway. Loss of the gag reflex on one side of the throat indicates injury to the medulla or to cranial nerve X on that side (cranial nerve IX has such a small territory of sensory and motor innervations in the pharynx that transection of this nerve does not cause a noticeable deficit).

Pattern Generators Coordinate More Complex Stereotypic Behaviors

As Darwin proposed, pools of pattern generator neurons in the reticular formation adjacent to the facial nucleus control facial emotional expression through stereotypic patterns of contraction of facial muscles simultaneously on the two sides of the face. Pattern generator neurons on each side of the brain stem project to the facial motor neurons on both sides of the brain, so that spontaneous facial expressions are virtually always symmetric. Even patients who have had major strokes in the cerebral hemispheres and cannot voluntarily move the contralateral orofacial muscles still tend to smile symmetrically when they hear a joke and can raise their eyebrows symmetrically, both of which are initiated by facial pattern generators.

Similarly, orofacial movements involved in eating are produced by pattern generator neurons in the reticular formation near the cranial motor nuclei that mediate the behaviors. Licking movements are organized in the reticular formation near the hypoglossal nucleus, chewing movements near the trigeminal motor nucleus, sucking movements near the facial and ambiguus nuclei, and swallowing near the nucleus ambiguus. Not surprisingly, neurons in these reticular areas are closely interconnected with each other and receive inputs from the part of the nucleus of the solitary tract concerned with taste and from the part of the spinal trigeminal nucleus concerned with tongue and oral sensation, as well as from neurons in the adjacent reticular formation that respond to more complex combinations of taste, texture, and temperature of food. As a result, even a decerebrate rat is able to make appropriate choices of which foods to swallow and which to reject.

Vomiting is another example of a coordinated response mediated by pattern generator neurons. Toxic substances in the blood stream can be detected by nerve cells in the area postrema, a small region adjacent to the nucleus of the solitary tract along the floor of the fourth ventricle. Unlike most of the brain, which is protected by a blood–brain barrier, the area postrema contains fenestrated capillaries that allow its neurons to sample the contents of the blood stream. These neurons, when they detect a toxin, activate a pool of neurons in the ventrolateral medulla that control a pattern of responses that clears the digestive tract of any poisonous substances. These responses include reversal of peristalsis in the stomach and esophagus, increased abdominal muscle contraction, and activation of the same motor patterns used in the gag reflex to clear the oropharynx of unwanted material.

A variety of responses organized by the brain stem require coordination of cranial motor patterns with autonomic and sometimes endocrine responses. A good example is the *baroreceptor reflex*, which ensures an adequate blood flow to the brain (Chapter 41). The nucleus of the solitary tract receives information about stretch of the aortic arch through the vagus (X) nerve and stretch of the carotid sinus through the glossopharyngeal (IX) nerve. This information is relayed to neurons in the ventrolateral medulla that produce a coordinated response that protects the brain against a fall in blood pressure.

Reduced stretch of the aortic arch and carotid sinus reduces drive to the parasympathetic preganglionic cardiac-vagal neurons in the nucleus ambiguus, resulting in reduced vagal tone and increased heart rate. Simultaneously, increased firing of neurons in the rostral ventrolateral medulla drives sympathetic preganglionic vasoconstrictor and cardioaccelerator neurons. This combination of increased cardiac output and increased vascular resistance elevates blood pressure. Meanwhile, other neurons in the ventrolateral medulla increase the firing of hypothalamic neurons that secrete vasopressin from their terminals in the posterior pituitary gland. Vasopressin also has a direct vasoconstrictor effect, and it maintains blood volume by reducing water excretion through the kidney.

Control of Breathing Provides an Example of How Pattern Generators Are Integrated Into More Complex Behaviors

One of the most important functions of the brain stem is control of breathing. The brain stem automatically generates breathing movements beginning in utero at 11 to 13 weeks of gestation in humans, and continues nonstop from birth until death. This behavior does not require any conscious effort, and in fact, it is rare for us to even think about the need to breathe. The primary purpose of breathing is to ventilate the lungs to control blood levels of oxygen, carbon dioxide, and hydrogen ions (pH). (These are often measured together clinically and referred to as "blood gases.") Breathing movements involve contraction of the diaphragm, activated by the phrenic nerve. The diaphragm is assisted

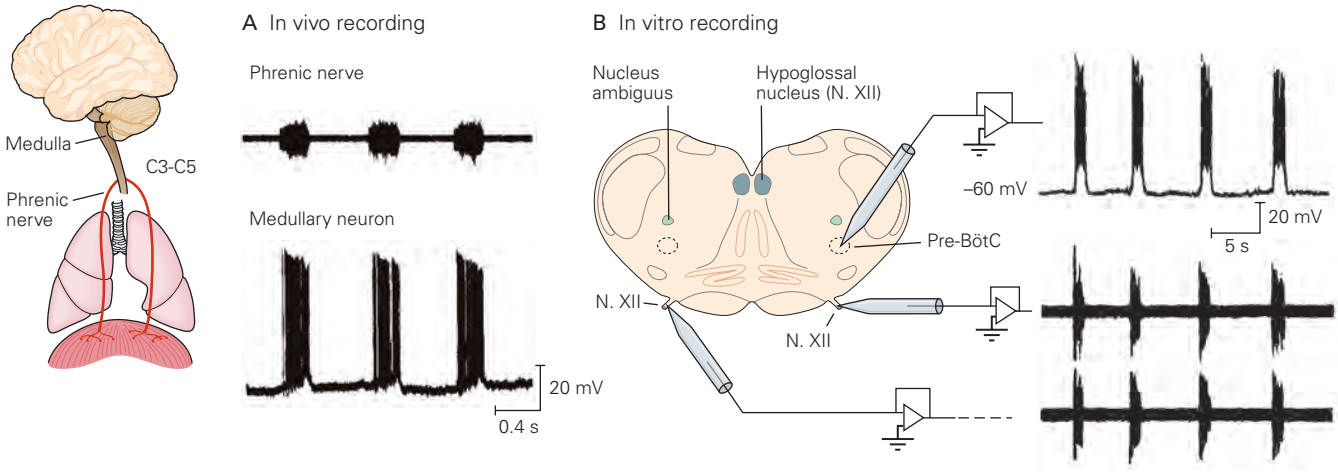

Figure 40–8 Rhythmic breathing is generated within the medulla.

A. Rhythmic activity in the phrenic motor nerve of a guinea pig causes contraction of the diaphragm. The firing of the phrenic nerve is phase-locked to bursts of firing by neurons in the medulla. The activity in a single medullary neuron, recorded intracellularly, is shown. (Reproduced, with permission, from Richerson and Getting 1987. Copyright © 1987. Published by Elsevier B.V.)

B. Similar rhythmic firing can be recorded in vitro from accessory respiratory nerves, such as the hypoglossal (**XII**) nerve. The minimal tissue necessary to support this rhythm is a slice about 0.5 mm thick at the level of the rostral medulla. Neurons in the pre-Bötzinger complex (**Pre-BötC**) near the nucleus ambiguus fire bursts that are phase-locked to the motor rhythm. (Reproduced, with permission, from Smith et al. 1991. Copyright © 1991 AAAS.)

when necessary by accessory muscles of respiration, including the intercostal muscles, pharyngeal muscles (to change airway diameter), some neck muscles (which help expand the chest), the tongue protruder muscles (to open the airway), and even some facial muscles (which flare the nares).

Respiratory activity can be generated by the medulla even when it is isolated from the rest of the nervous system. Many medullary neurons have patterns of firing that correlate with inspiration or expiration (Figure 40–8A). Some have more refined patterns, such as firing only during early inspiration or late inspiration. These respiratory neurons are concentrated in two regions, the dorsal and ventral respiratory groups.

The *dorsal respiratory group* is located bilaterally in and around the ventrolateral part of the nucleus of the solitary tract. Neurons in this group receive respiratory sensory input, including afferents from stretch receptors in the lungs and peripheral chemoreceptors, and participate in such reflex actions as limitation of lung inflation at high volume (the Hering-Breuer reflex) and the ventilatory response to low oxygen (*hypoxia*). The *ventral respiratory group*, a column of neurons in and around the nucleus ambiguus, coordinates respiratory motor output. Some of these neurons are motor neurons with axons that leave the brain through the vagus nerve and innervate accessory muscles of respiration or premotor neurons that innervate the phrenic motor nucleus, whereas others form a pattern generator, the *pre-Bötzinger complex*, that generates respiratory rhythm.

The intrinsic rhythmicity of the pre-Bötzinger complex is so resilient that, even in a transverse brain slice from the rostral medulla, neurons in the pre-Bötzinger complex are able independently to generate a respiratory rhythm that can be recorded in the rootlets of the hypoglossal (XII) nerve that emerge from the ventral surface of the slices (Figure 40–8B). Acute destruction of this cell group in an intact animal results in inability to maintain a normal respiratory rhythm.

The most important inputs to the respiratory pattern generator come from chemoreceptors that sense oxygen and carbon dioxide. Under normal conditions, ventilation is primarily regulated by the levels of CO_2 rather than O_2 (Figure 40–9A). However, breathing is also strongly stimulated if O_2 becomes sufficiently low, such as at high altitude or in people with lung disease. The peripheral chemoreceptors in the carotid and aortic bodies normally respond primarily to a decrease in blood oxygen, but during hypoxia, they also become more sensitive to elevated levels of CO_2 (*hypercapnia*). Afferent fibers from the carotid sinus nerve travel in the glossopharyngeal nerve and activate neurons in the dorsal respiratory group.

The response to hypercapnia is largely driven by *central chemoreceptors* in the brain stem that sense the

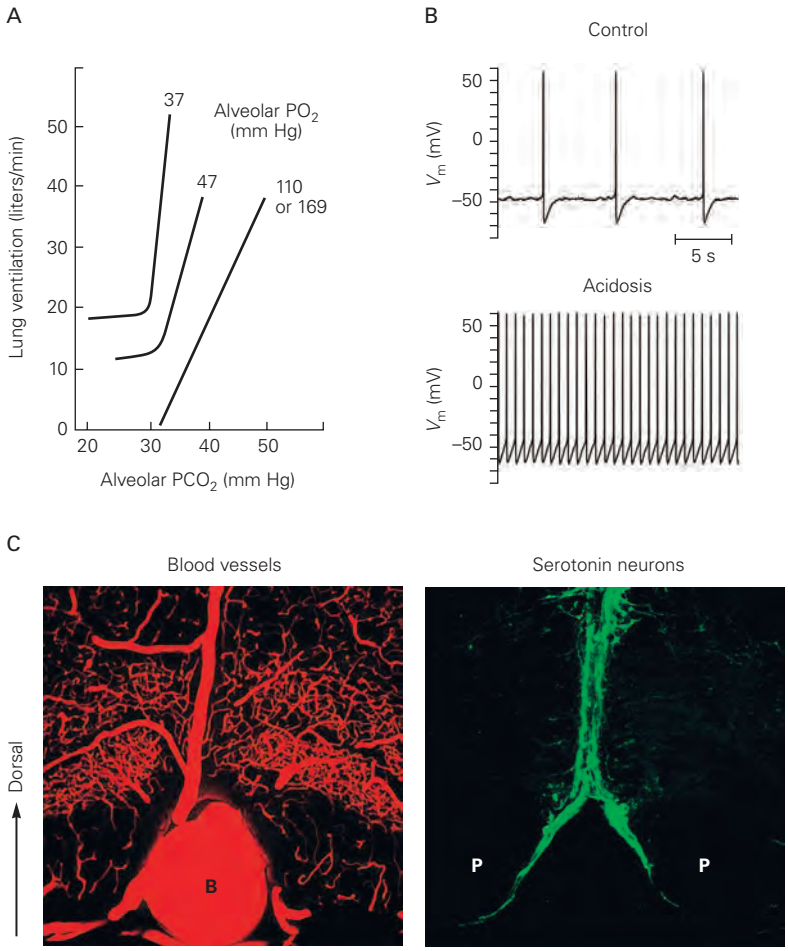

Figure 40–9 Respiratory motor output is regulated by carbon dioxide in the blood.

A. Lung ventilation (determined by the rate and depth of breathing) in humans is steeply dependent on the partial pressure of carbon dioxide (PCO_2) at normal levels of the partial pressure of oxygen (PO_2) (>100 mm Hg). When PO_2 drops to very low values (<50 mm Hg), breathing is stimulated directly and also becomes more sensitive to an increase in PCO_2 (seen here as an increase in the slope of the curves for alveolar PO_2 of 37 and 47 mm Hg). (Reproduced, with permission, from Nielsen and Smith 1952.)

B. Central chemoreceptors in the medulla control ventilatory motor output to maintain normal blood CO_2. The firing rate of serotonergic neurons within the raphe nuclei of the medulla increases when elevated PCO_2 causes a pH decrease. The records shown here are from in vitro recordings of a neuron in the raphe nuclei of a rat at two different levels of pH (7.4, control, and 7.2, acidosis). (Reproduced, with permission, from Wang et al. 2002.)

C. Serotonergic neurons are closely associated with large arteries in the ventral medulla where they can monitor local changes in PCO_2. Two images of the same transverse section of the rat medulla show blood vessels after injection of a red fluorescent dye into the arterial system (*left*) and green antibody staining for tryptophan hydroxylase, the enzyme that synthesizes serotonin (*right*). The basilar artery (**B**) is on the ventral surface of the medulla between the pyramidal tracts (**P**). (Reproduced, with permission, from Bradley et al. 2002. Copyright © 2002 Springer Nature.)

accompanying decrease in pH. The most sensitive area for this is along the ventral surface of the medulla lateral to the pyramidal tract. This region contains at least two sets of neurons that respond to elevated CO_2. Glutamatergic neurons in the retrotrapezoid nucleus in the rostral ventrolateral medulla, near the facial motor nucleus, are highly sensitive to CO_2 levels. Absence of these neurons, due to a mutation in the phox2b transcription factor required for their development, causes congenital central hypoventilation syndrome, in which there is failure to breathe adequately, particularly during sleep. In addition, serotonergic neurons in the rostral ventrolateral medulla, like retrotrapezoid neurons, lie along penetrating arteries and are sensitive to acidosis (Figure 40–9B,C). Genetic deletion of these neurons reduces the ventilatory response to hypercapnia, especially during sleep. Recent studies demonstrate that a serotonin 5-HT_{2A} agonist can restore arousal responses to CO_2, suggesting that the serotonergic neurons play a modulatory role, increasing the sensitivity of the CO_2 reflexes during hypercapnia, and that this may be especially important during sleep.

The motor pattern generated by the respiratory system is remarkably stable in healthy people, but a variety of diseases can alter these patterns. One of the most common and easily recognized patterns is Cheyne-Stokes respiration, which is characterized by repeated cycles of gradually increasing then decreasing ventilation, alternating with cessation of breathing (apnea). This periodic breathing is seen, for example, in congenital central hypoventilation syndrome, where the central neurons are not sufficiently sensitive to rising CO_2, particularly during sleep. By the time they begin to respond, CO_2 levels may already be quite high. This causes hyperventilation, which reduces CO_2 levels below the threshold where breathing is required. The result is a period of apnea, until the CO_2 levels again become quite high (Figure 40–10).

A similar pattern is seen in people who have cardiac or pulmonary disease that increases the time it takes for the change in alveolar CO_2 to register with the medulla. Cheyne-Stokes respiration often occurs in hospitalized patients with marginal cardiac or respiratory reserve when they fall asleep, thus reducing

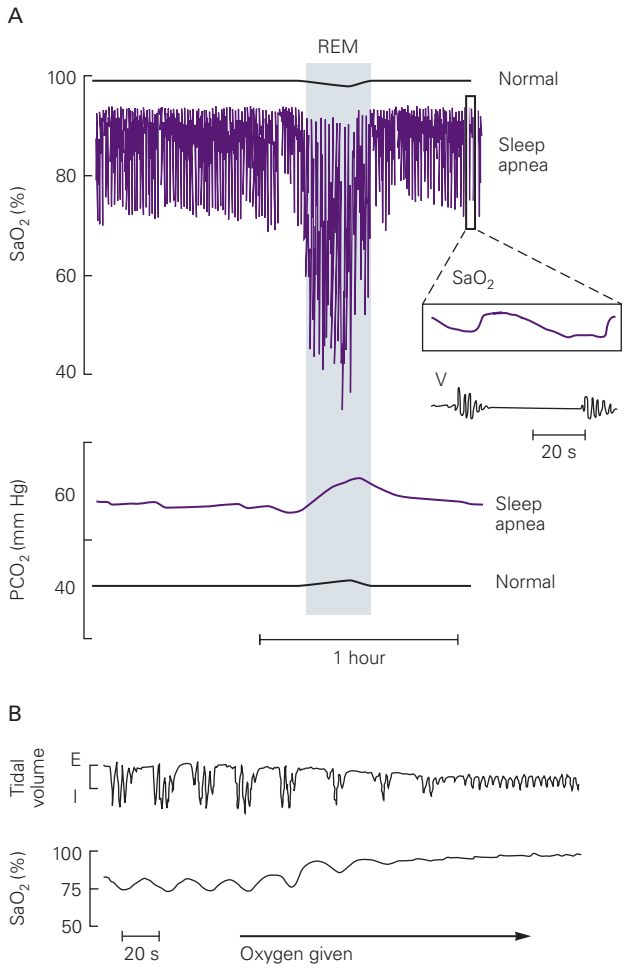

Figure 40–10 Respiratory motor patterns can become unstable during sleep.

A. Sleep apnea (cessation of breathing) is a common problem that often goes undetected. The records here show blood oxygen saturation (SaO_2) and CO_2 partial pressure (PCO_2) during sleep in a healthy person and a patient with obstructive sleep apnea. In the healthy person, SaO_2 remains near 100%, and PCO_2 remains near 40 mm Hg during both rapid eye movement (REM) and non-REM sleep. In the patient with sleep apnea, reduced muscle tone (hypotonia) during sleep leads to collapse of the upper airway, resulting in obstruction and apnea. Repetitive apnea at the rate of approximately once per minute causes the patient's SaO_2 to fall repetitively and dramatically. (The inset shows a period of approximately 80 seconds on an expanded scale. Ventilation [V] begins at the nadir of the SaO_2 and again ceases when the blood oxygen increases.) During non-REM sleep, the patient's PCO_2 increases to near 60 mm Hg. During REM sleep, the SaO_2 and PCO_2 become even more abnormal, as worsening airway hypotonia causes greater obstruction. Many people with sleep apnea wake up repeatedly during the night because of the apnea, but the arousals are too brief for them to be aware that their sleep is interrupted. (Adapted, with permission, from Grunstein and Sullivan 1990.)

B. Breathing in most normal individuals becomes unstable during sleep at high altitudes. The upper trace shows an example of a Cheyne-Stokes breathing pattern in a healthy person, during the first night after arriving at an altitude of 17,700 feet, where the low partial pressure of oxygen in the air reduces the blood SaO_2 to approximately 75% to 80%. Repeated cycles of waxing and waning ventilation are separated by periods of apnea. Administration of supplemental oxygen results in a rapid return to a normal respiratory pattern. This abnormal pattern disappears in most people after they have acclimated to the altitude. (Reproduced, with permission, from Lahiri et al. 1984.)

other behavioral drives for respiration. Although not dangerous in itself, it can indicate that there is a serious underlying cardiorespiratory problem that needs to be corrected.

Other inputs to the respiratory pattern generator come from the circuitry mediating particular behaviors, as breathing must be coordinated with many motor actions that share the same muscles. To accomplish this coordination, respiratory neurons in the medulla receive input from neuronal networks concerned with vocalization, swallowing, sniffing, vomiting, and pain. For example, the ventral respiratory group is connected with a part of the parabrachial complex in the pons termed the *pontine respiratory group* or *pneumotaxic center*. These pontine neurons coordinate breathing with behaviors such as chewing and swallowing. They can cause holding of the breath at full inspiration (called *apneusis*), which is required during eating and drinking. The reserve of air in the lungs permits a cough, if necessary, to expel any food or drink that may enter the airway. Other neurons in the intertrigeminal zone, between the motor and principal sensory trigeminal nuclei, receive facial and upper airway sensory inputs and project to the ventrolateral medulla to temporarily stop breathing to protect against accidental inspiration of dust or water.

Voluntary motor pathways can take over the control of breathing during talking, eating, singing, swimming, or playing a wind instrument. Descending inputs cause hyperventilation at the onset of exercise, in anticipation of an increase in oxygen demand. In fact, this leads to a sustained drop in blood CO_2 during exercise—the opposite of what would be expected for a negative feedback control system. Other descending inputs from the limbic system produce hyperventilation in connection with pain or anxiety and, in some people, may be responsible for causing spontaneous panic attacks, characterized by hyperventilation and a feeling of suffocation. These various descending inputs allow efficient integration of breathing with

other behaviors, but they ultimately must yield to the need to maintain blood gas homeostasis, as even a small increase in CO_2 produces severe air hunger or *dyspnea*. Thus, the respiratory control system is a fascinating example of a brain stem pattern generator that must be sufficiently stable to ensure survival yet flexible enough to accommodate a wide variety of behaviors.

Monoaminergic Neurons in the Brain Stem Modulate Sensory, Motor, Autonomic, and Behavioral Functions

In addition to containing the primary sensory and motor nuclei of the cranial nerves and the reflex and pattern generator mechanisms that control basic behaviors, the brain stem also contains a set of modulatory cell groups. In a groundbreaking series of experiments in the 1970s, Hans Kuypers used the newly discovered method of retrograde transport of axonal tracers to identify the cell groups in the brain stem and diencephalon that contribute to modulation of spinal cord sensory and motor systems and those that send inputs directly to the cerebral cortex. To a surprising extent, these two sets of experiments, starting at opposite ends of the neuraxis, identified a common substrate whose role it is to modulate circuitry at other levels of the nervous system, almost as if it were an "autonomic system" for the brain.

These cell groups have direct connections to the forebrain, brain stem, and spinal cord that regulate the overall level of function of their targets. Like the way serotonergic neurons set the overall sensitivity of CO_2 reflexes, brain stem monoaminergic modulatory systems adjust the overall responsiveness of a wide variety of sensory systems by means of projections to sensory neurons in the spinal cord and brain stem, including nociceptive systems. Descending projections from these modulatory systems also control motor tone, which is critical for adjusting posture and gait as well as initiating finer movements. Ascending inputs to the forebrain control overall arousal as well as responses to rewarding situations. While these modulatory systems are not sufficient to accomplish motor, sensory, or cognitive tasks on their own, their ability to adjust the responsiveness of these systems plays an enormously influential role in overall behavior.

Many Modulatory Systems Use Monoamines as Neurotransmitters

The monoaminergic systems use decarboxylated derivatives of the cyclic amino acids tyrosine, tryptophan, and histidine as neurotransmitters. They were among the first in the brain to be identified and mapped due to the property that some of them possess to fluoresce when exposed to formaldehyde. In the 1960s, Dahlstrom and Fuxe used this property to identify serotonergic, noradrenergic, and dopaminergic cell groups in the brain stem. In the 1970s, with the development of immunohistochemical methods able to map the enzymes that synthesize monoamines, other investigators mapped neurons containing epinephrine and histamine.

The cell groups of these modulatory systems in general were unlike earlier identified nuclei in the brain. Rather than forming compact clusters of cell bodies, the monoaminergic cell groups tended to form columns that extended longitudinally through the brain stem and hypothalamus (see Figure 40–6). The monoamine systems were therefore designated with letters and numbers, to avoid confusion with other systems of nomenclature for the brain (Figure 40–11).

The first cell groups identified by Dahlstrom and Fuxe were simply identified alphabetically as the "A" cell groups, and then numbered sequentially from caudal to rostral. It was later determined that the A1–A7 cell groups produce norepinephrine and the A8–A14 groups produce dopamine. The A1, A3, and A5 designations were applied to neurons located in the ventrolateral corner of the medullary and pontine tegmentum (the A3 group was quite small and the term is no longer used), while the A2, A4, A6, and A7 names were applied to cell groups located more dorsally, similar to the columns of motor neurons in the brain stem (Figure 40–11A). The A1 and A2 groups, located among the neurons of the nucleus ambiguus and the nucleus of the solitary tract (respectively), are mainly concerned with autonomic functions. Together, they modulate hypothalamic and brain stem systems that regulate the autonomic nervous system. The noradrenergic A4–A7 cell groups have widespread influence over sensory and motor systems, ranging from the cerebral cortex to the spinal cord, and provide important modulation of arousal and wakefulness.

The dopaminergic systems (Figure 40–11E) include the A8–A10 cell groups, located in the midbrain in and near the substantia nigra, that modulate motor systems as well as forebrain mechanisms of reward and motivation. The A11 and A13 dopaminergic neurons, in the dorsal hypothalamus, provide input to sensory, motor, and autonomic systems in the brain stem and spinal cord. The A12, A14, and A15 neurons have a neuroendocrine role, including release of dopamine as a pituitary release-inhibiting hormone for prolactin secretion. The A16 cell group modulates olfactory inputs, and the A17 neurons in the retina modulate vision.

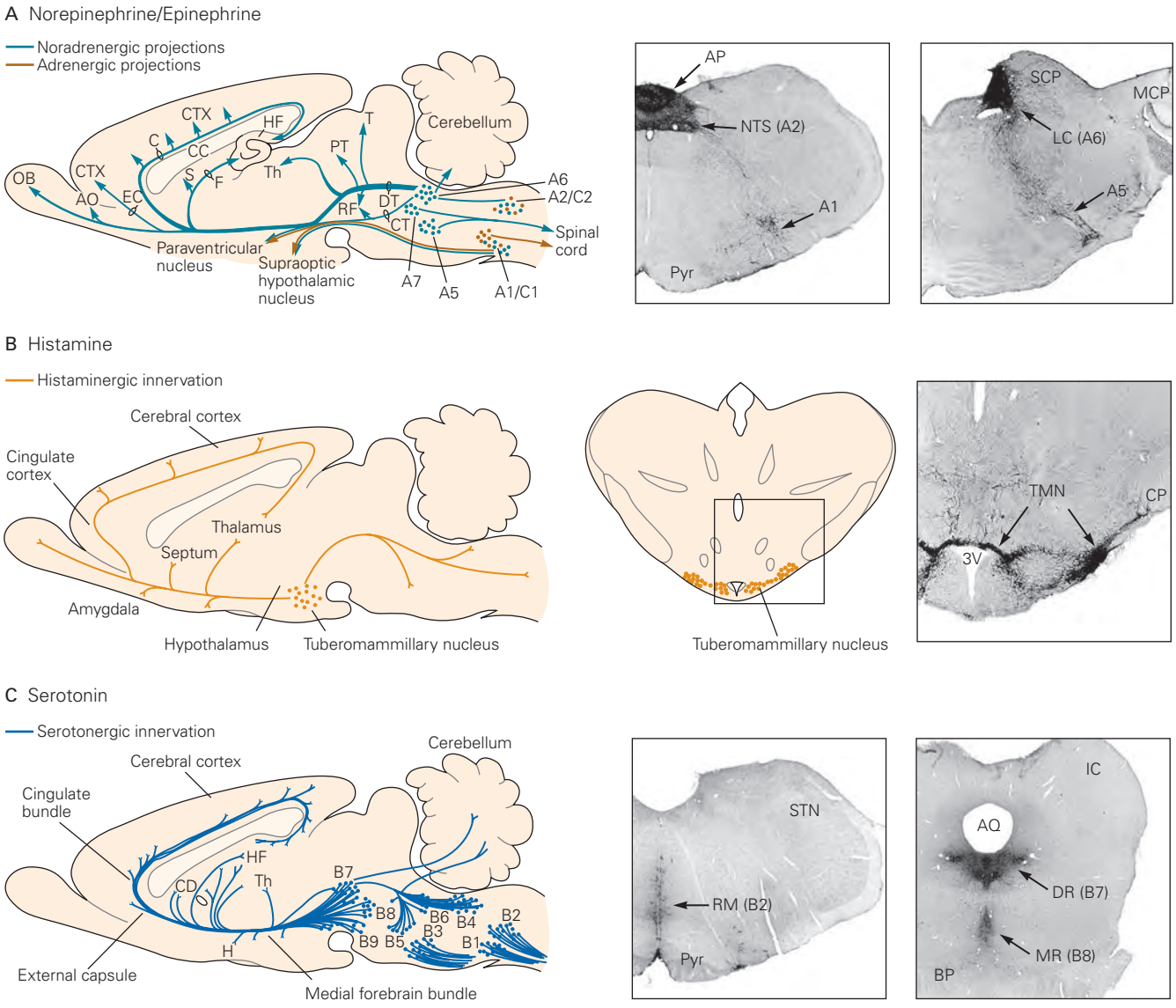

Figure 40–11 Locations and projections of monoaminergic and cholinergic neurons in the rat brain. (Abbreviations: **3V**, third ventricle; **AC**, anterior commissure; **AP**, area postrema; **AQ**, Sylvian aqueduct; **ARC**, arcuate nucleus; **BM**, nucleus basalis of Meynert; **BP**, brachium pontis; **CD**, caudate; **CP**, cerebral peduncle; **DBh**, horizontal limb of the diagonal band; **DR**, dorsal raphe; **FX**, fornix; **IC,** inferior colliculus; **LC**, locus ceruleus; **LDT**, laterodorsal tegmental nucleus; **MCP**, middle cerebellar peduncle; **MGN**, medial geniculate nucleus; **MR**, median raphe; **MS**, medial septum; **MTT**, mammillothalamic tract; **NTS**, nucleus tractus solitarius; **OC**, optic chiasm; **PPT**, pedunculopontine tegmental nucleus; **PUT**, putamen; **Pyr**, pyramidal tract; **RM**, raphe magnus; **SC**, superior colliculus; **SCP**, superior cerebellar peduncle; **SN**, substantia nigra; **STN**, spinal trigeminal nucleus; **TMN**, tuberomammillary nucleus; **VTA**, ventral tegmental area.)

A. Noradrenergic neurons (A groups) and adrenergic neurons (C groups) are located in the medulla and pons. The A2 and C2 groups in the dorsal medulla are part of the nucleus of the solitary tract. The A1 and C1 groups in the ventral medulla are located near the nucleus ambiguus. Both groups project to the hypothalamus; some C1 neurons project to sympathetic preganglionic neurons in the spinal cord and control cardiovascular and endocrine functions. The A5, A6 (locus ceruleus), and A7 cell groups in the pons project to the spinal cord and modulate autonomic reflexes and pain sensation. The locus ceruleus also projects rostrally to the forebrain and plays an important role in arousal and attention.

B. All histaminergic neurons are located in the posterior lateral hypothalamus, mostly within the tuberomammillary nucleus. These neurons project to virtually every part of the neuraxis and play a major role in arousal.

C. Serotonergic neurons (B groups) are found within the medulla, pons, and midbrain, mostly near the midline in the raphe nuclei. Those within the medulla (the B1–B4 groups corresponding to the raphe magnus, raphe obscurus, and raphe pallidus) project throughout the medulla and spinal cord and modulate afferent pain signals, thermoregulation, cardiovascular control, and breathing. Those within the pons and midbrain (the B5–B9 groups in the raphe pontis, median raphe, and dorsal raphe) project throughout the forebrain and contribute to arousal, mood, and cognition.

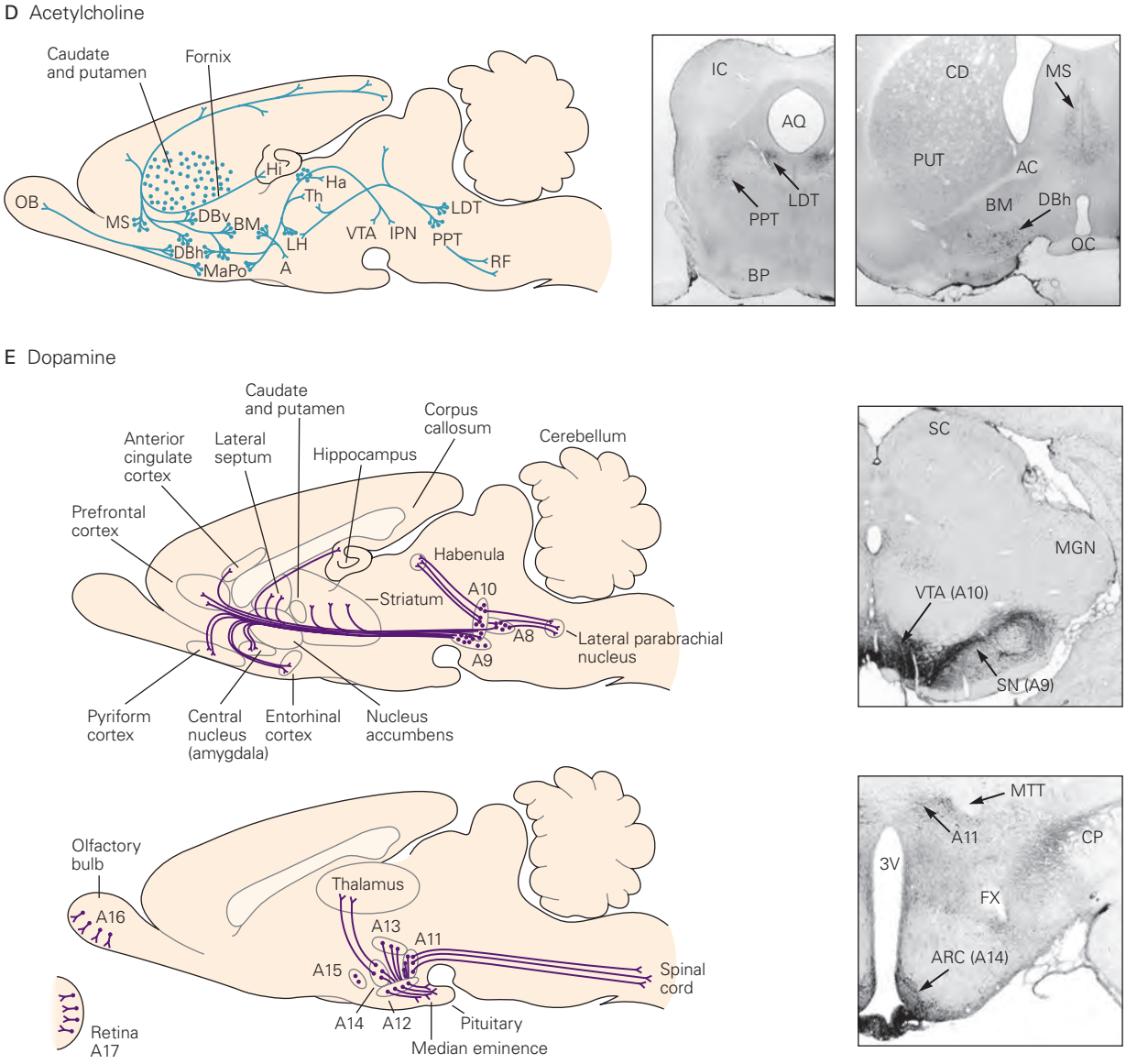

Figure 40–11 (*Continued*) **D.** Cholinergic neurons (sometimes called Ch groups) are located in the pons, midbrain, and basal forebrain. Those in the pons and midbrain (mesopontine groups) are divided into a ventrolateral cluster (pedunculopontine nucleus) and the dorsomedial cluster (laterodorsal tegmental nucleus). The mesopontine cholinergic neurons project to the brain stem reticular formation and the thalamus. Those in the basal forebrain are divided into the medial septum, the nuclei of the vertical and horizontal limbs of the diagonal band, and the nucleus basalis of Meynert. These neurons project throughout the cerebral cortex, hippocampus, and amygdala. Both groups play an important role in arousal, and the basal forebrain groups are also involved in more selective attention.

E. Dopaminergic neurons are located in the midbrain and hypothalamus. The dopaminergic cell groups were originally included with the noradrenergic cell groups and are still labeled as A groups (A8–A17). The A8 group is in the midbrain dorsally adjacent to the substantia nigra. The A9 cell group constitutes the substantia nigra pars compacta. These two groups of neurons project to the striatum and play an important role in initiation of movement. The A10 group is located in the ventral tegmental area just medial to the substantia nigra. These cells project to the frontal and temporal cortex and limbic structures of the basal forebrain and play a role in emotion and memory. The A11 and A13 cell groups in the zona incerta of the hypothalamus project to the lower brain stem and spinal cord and regulate sympathetic preganglionic neurons. The A12, A14, and A15 cell groups are components of the neuroendocrine system. Some of them inhibit release of prolactin into the hypophysial portal circulation, and others control gonadotrophin secretion. Dopaminergic neurons are also found in the olfactory bulb (A16) and the retina (A17).

The B cell groups, which had a slightly different color of fluorescence, were found to produce serotonin. They are associated with the midline raphe cell groups in the pons and medulla (Figure 40–11C). The B1–B4 cell groups in the medulla mainly provide descending modulation of sensory, motor, and autonomic neurons in the brain stem and spinal cord. The B5–B7 neurons in the pons mainly provide serotonergic innervation of the thalamus, hypothalamus, and cerebral cortex. The functions of serotonin in modulating these targets can be quite complex to decipher, mainly because there are at least 14 different serotonin receptors, and different ones can be expressed by different cell types in a target area.

A few years after the A and B cell groups were named, immunohistochemical studies demonstrated that some medullary neurons have the enzymes to make dopamine and norepinephrine but do not fluoresce. These neurons, named cell groups C1–C3, were found to process these other catecholamines to adrenalin, or epinephrine. They are closely related to the A1–A3 cell groups in the medulla (Figure 40–11A).

Histaminergic cell groups are mainly found in the tuberomammillary nucleus and adjacent areas of the posterior hypothalamus (near the mammillary body) and are named E1–E5 (Figure 40–11B). They are the sole source of histaminergic actions in the entire brain, from the cerebral cortex to the spinal cord, and are involved in a variety of arousal responses.

Although cholinergic neurons are not, strictly speaking, monoaminergic, some of them also participate in modulatory systems, and these have been numbered Ch1–Ch6 (Figure 40–11D). This classification system did not include the many other cholinergic neurons in the nervous system, such as motor neurons or striatal interneurons, and is not used much anymore. Rather, scientists refer to the cholinergic neurons by their location, eg, the pedunculopontine (Ch6) and laterodorsal tegmental (Ch5) neurons in the pons, which project widely from the cerebral cortex to the medulla, and the basal forebrain (Ch1–Ch4) groups, which project to the cerebral cortex, hippocampus, and amygdala.

Monoaminergic Neurons Share Many Cellular Properties

Neurons that use monoamines as neurotransmitters have many similar electrophysiological properties. For example, most continue to fire spontaneous action potentials in a highly regular pattern when isolated from their synaptic inputs in brain slice preparations. Their action potentials typically are followed by a slow membrane depolarization that leads to the next spike (Figure 40–12). The spontaneous regular firing pattern of monoaminergic neurons is regulated by intrinsic pacemaker currents (Chapter 10). Tonic firing in vivo may be important for ensuring continuous delivery of monoamines to targets. For example, the basal ganglia depend on continuous exposure to dopamine from the neurons of the substantia nigra to facilitate motor responses.

The properties of monoaminergic neurons are suited to their unique and widespread modulatory roles in brain function. Indeed, some axon terminals of monoaminergic cells do not even form conventional synaptic connections, instead releasing neurotransmitter diffusely to many targets at once. Most

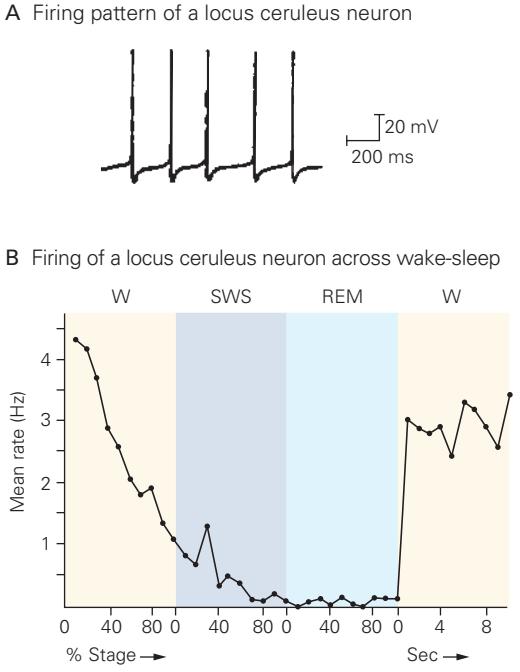

Figure 40–12 Monoaminergic neurons have similar firing patterns across the wake–sleep cycle.

A. When monoaminergic neurons are isolated from synaptic input, they fire spontaneously at a regular rate. This recording is from a noradrenergic neuron in the locus ceruleus. Action potentials are followed by a characteristic afterhyperpolarization followed by a slow depolarization to the next spike, producing a pacemaker-like activity (Chapter 10). Serotonergic and histaminergic neurons exhibit similar spontaneous activity.

B. All three monoaminergic cell types show similar patterns of firing across the wake–sleep cycle. The plot shows that a locus ceruleus neuron in a rat fires fastest when the animal is awake (**W**), slows down as wakefulness wanes and during slow-wave sleep (**SWS**), and almost completely ceases to fire during rapid eye movement (**REM**) sleep. (Adapted, with permission from Aston-Jones and Bloom 1981. © Society for Neuroscience.)

monoaminergic neurotransmission occurs by means of metabotropic synaptic actions through G protein–coupled receptors. Many monoaminergic neurons co-release neuropeptides, which have slow effects through other G protein–coupled receptors. Thus, although some monoaminergic synaptic actions involve fast synaptic mechanisms (Chapter 13), many involve slower metabotropic and neuromodulatory pathways as well (Chapter 14).

Autonomic Regulation and Breathing Are Modulated by Monoaminergic Pathways

Neurons in the adrenergic C1 group in the rostral ventrolateral medulla play a key role in maintaining resting vascular tone as well as adjusting vasomotor tone necessitated by various behaviors. For example, an upright posture disinhibits neurons in the rostral ventrolateral medulla that directly innervate the sympathetic preganglionic vasomotor neurons, thus increasing vasomotor tone to prevent a drop in blood pressure (the baroreceptor reflex). Neurons in the noradrenergic A5 group in the pons inhibit the sympathetic preganglionic neurons and play a role in depressor reflexes (eg, the fall in blood pressure in response to deep pain).

Serotonin regulates many different autonomic functions including gastrointestinal peristalsis, thermoregulation, cardiovascular control, and breathing. Electrical stimulation of serotonergic neurons within the medullary raphe nuclei increases heart rate and blood pressure. Serotonergic neurons in the medulla also project to neurons in the medulla and spinal cord that regulate breathing, as described earlier.

The role of serotonergic neurons as CO_2 receptors may explain why defects in the serotonergic system have been linked to sudden infant death syndrome (SIDS) (Figure 40–13A). SIDS is the leading cause of postneonatal mortality in the Western world, responsible for six infant deaths every day in the United States. A widely held theory holds that some SIDS cases are due to defective CO_2 chemoreception, breathing, and arousal. A relatively high number of serotonergic neurons are found in the raphe nuclei of infants who die of SIDS, but these have an immature morphology, and they are associated with relatively low serotonin levels and low serotonergic receptor densities.

A plausible neurobiological mechanism for SIDS is that a defect in development of serotonergic neurons leads to reduced ability to detect a rise in partial pressure of CO_2 when airflow is obstructed during sleep, thus blunting the normal protective response, which includes arousal and increased ventilation (Figure 40–13C). Infants sleeping face down would be unable to arouse sufficiently to change position when bedding blocks the airway. The Back to Sleep campaign, which encourages parents to place infants on their backs when put down to sleep, has reduced the incidence of SIDS by 50%.

Pain Perception Is Modulated by Monoamine Antinociceptive Pathways

Although pain is necessary for an animal to minimize injury, continued pain following an injury may be maladaptive (eg, if the pain prevents vigorous escape from

Figure 40–13 (Opposite) Serotonergic neurons have a role in the response to a rise in CO_2 levels as well as sudden infant death syndrome.

A. Serotonergic neurons in the medulla are central respiratory chemoreceptors that are thought to stimulate breathing in response to an increase in arterial blood PCO_2 (partial pressure of CO_2). The dendrites of these neurons wrap around large arteries and are stimulated by an increase in PCO_2 (see Figure 40–9C). They project to and excite motor neurons in the medulla and spinal cord that control breathing.

B. Serotonergic neurons in the midbrain are also PCO_2 sensors. Shown here is the increase in firing rate of a serotonergic neuron from the dorsal raphe nucleus in response to an increase in PCO_2 (monitored by the resultant decrease in external pH). This increase in firing rate may sensitize ascending arousal pathways from the parabrachial nucleus, which also receives input from other CO_2 sensory pathways. This important response prevents suffocation during sleep when the airway is obstructed. (Reproduced, with permission, from Richerson 2004. Copyright © 2004 Springer Nature.)

C. Sudden infant death syndrome (SIDS).

1. *Triple risk hypothesis of SIDS*. Infants are at risk to die from SIDS when three conditions coincide. First, the infant must be vulnerable because of an underlying abnormality of the brain stem, such as a genetic predisposition or an environmental insult (eg, exposure to cigarette smoke). Second, the baby must be in the stage of development (usually 2–6 months of age) when it may be difficult to change position to escape suffocation. Third, there also must be an exogenous stressor (eg, lying face down in a pillow). (Reproduced, with permission from, Filiano and Kinney 1994. © 1994 S. Karger AG.)

2. *Proposed mechanism of SIDS*. The combination of abnormal serotonergic neurons (eg, from exposure to cigarette smoke) and postnatal immaturity of neurons involved in respiratory control leads to the inability to respond effectively to airway obstruction (eg, from lying face down in a crib). The infant then does not wake up and turn its head or breathe faster, either of which would correct the problem. As a result, blood oxygenation decreases severely (hypoxia) while blood CO_2 rises (hypercapnia).

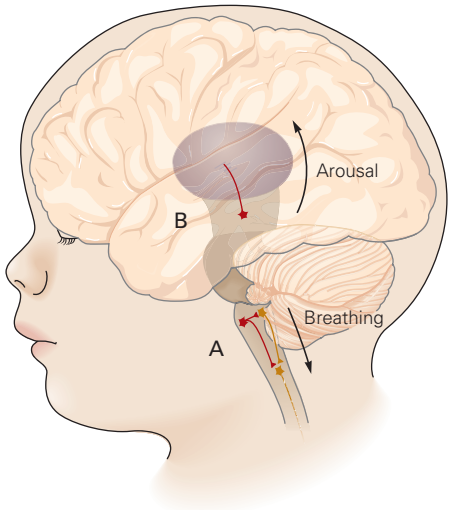

A Serotonergic neurons

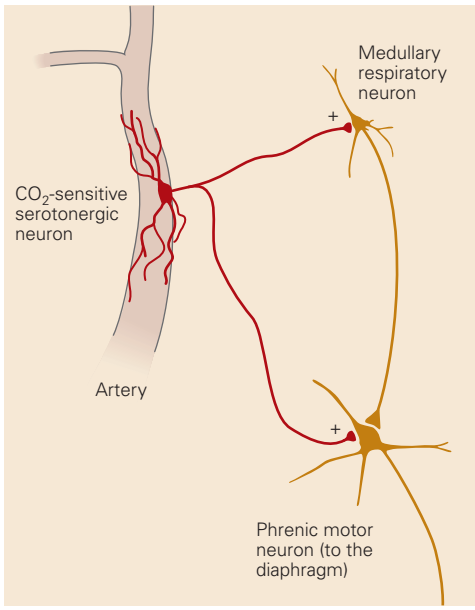

B

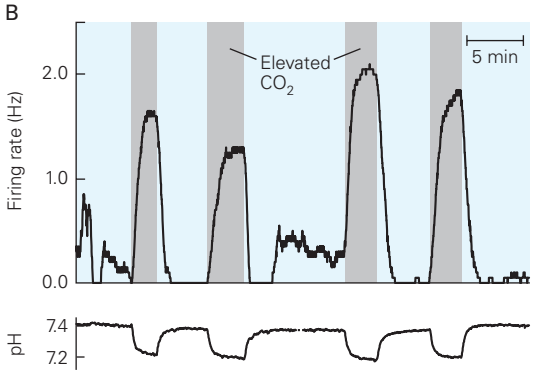

C Sudden Infant Death Syndrome

1 Triple risk hypothesis

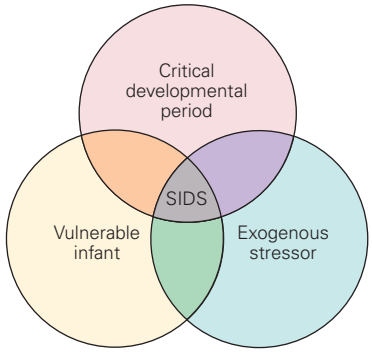

2 Proposed mechanism

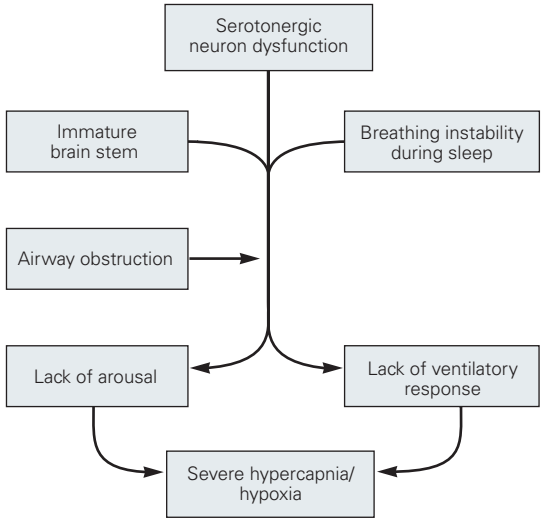

a predator). The monoaminergic systems include important descending projections to the dorsal horn of the spinal cord that modulate pain perception (Chapter 20).

The noradrenergic inputs to the spinal cord originate from the pontine cell groups A5–A7, with the locus ceruleus (A6) providing most of the input to the dorsal horn. Similarly, the serotonergic raphe nuclei in the medulla, particularly the nucleus raphe magnus, project to the dorsal horn where they modulate the processing of information about noxious stimuli. Direct application of serotonin to dorsal horn neurons inhibits their response to noxious stimuli, and intrathecal administration of serotonin attenuates the defensive withdrawal of the paw evoked by noxious stimuli. In addition, intrathecal administration of antagonists of serotonin receptors blocks the pain inhibition evoked by stimulation of the raphe nuclei.

Insight into the role of serotonin in pain processing has been used in treating migraine headaches. In particular, the triptan agonists of 5-HT_{1D} receptors have been found to be therapeutically effective. One of the possible mechanisms of action of this family of tryptamine-based drugs includes presynaptic inhibition of pain afferents from the meninges, preventing sensitization of central neurons. Drugs that block monoamine reuptake, including both traditional antidepressants and selective serotonin reuptake inhibitors, are effective in limiting pain in patients with chronic pain and migraine headaches.

Motor Activity Is Facilitated by Monoaminergic Pathways

The dopaminergic system is critical for normal motor performance. A massive projection ascends from the substantia nigra pars compacta to the striatum, where dopaminergic fibers act on striatal neuron receptors to release inhibition of motor responses (Chapter 38).

Patients with Parkinson disease in whom midbrain dopaminergic neurons have degenerated have trouble initiating movement and difficulty sustaining movements. Such patients speak softly, write with small letters, and take small steps. Conversely, drugs that facilitate dopaminergic transmission in the striatum can result in unintended behaviors, ranging from motor tics (small muscle twitches), to chorea (large-scale, jerky limb movements), to complex cognitive behaviors (such as compulsive gambling or sexual activity).

As first shown by Sten Grillner, serotonergic neurons play an important role in modulating motor programs. Drugs that activate serotonin receptors can induce hyperactivity, myoclonus, tremor, and rigidity, all of which are part of the "serotonin syndrome." Increases in the firing of raphe neurons have been observed in animals during repetitive motor activities such as feeding, grooming, locomotion, and deep breathing. Conversely, the firing of both serotonergic raphe and noradrenergic locus ceruleus neurons practically ceases during the atonia and lack of movement that occur during rapid eye movement (REM) sleep.

Noradrenergic cell groups in the pons also send extensive projections to motor cell groups. This modulatory input acts on presynaptic β- and α_1-adrenergic receptors to facilitate excitatory inputs to motor neurons (Chapter 31). The sum of these effects is to facilitate motor neuron responses in stereotypic and repetitive behaviors such as rhythmic chewing, swimming, or locomotion. Conversely, increased β-adrenergic activation during stress can exaggerate motor responses and produce tremor. Drugs that block β-adrenergic receptors are used clinically to reduce certain types of tremor and are often taken by musicians prior to performances to minimize tremulousness.

Ascending Monoaminergic Projections Modulate Forebrain Systems for Motivation and Reward

The forebrain is continuously bombarded with sensory information and must determine which stimuli deserve attention. It must also decide which of many available behaviors should receive priority, based in part on experience—which behaviors have achieved rewarding outcomes in the past. The ascending monoaminergic systems play key roles in modulating all of these choices.

As noted earlier, dopaminergic inputs to the striatum adjust the likelihood that a specific motor pattern or even a cognitive pattern will be expressed. Low dopamine levels reduce output from the direct pathway striatal neurons (which release behaviors) and increase activity of indirect pathway striatal neurons (which inhibit behavior). Dopamine also has been linked to reward-based learning. Rewards are objects or events for which an animal will work (Chapter 42) and are useful in positively reinforcing behavior. Activity of dopaminergic neurons increases when a reward (such as food or juice) is unexpectedly given. But after animals are trained to expect a reward following a conditioned stimulus, the activity of the neurons increases immediately after the conditioned stimulus rather than after the reward. This pattern of activity indicates that dopaminergic neurons provide a reward-prediction error signal, an important element in reinforcement learning. The importance of dopamine in learning is also supported by observations that lesions of dopaminergic systems prevent reward-based learning.

The same dopaminergic pathways that are important for reward and learning are involved in addiction to many drugs of abuse (Chapter 43)

Noradrenergic neurons of the locus ceruleus play an important role in attention. These neurons have a low baseline level of activity in drowsy monkeys. In alert, attentive monkeys the cells have two firing patterns. In the *phasic mode*, the baseline activity of the neurons is low to moderate, but there are bursts of firing just before the monkey responds to stimuli to which it has been attentive. This pattern of activity is thought to facilitate selective attention to a stimulus that is about to initiate a behavior. In contrast, in the *tonic mode*, the baseline level of activity is elevated and does not change in response to external stimuli. This mode of firing may promote the search for a new behavioral and attentional goal when the current task is no longer rewarding (Figure 40–14).

Many monoaminergic neurons also participate in regulating overall arousal (Figure 40–15). The noradrenergic locus ceruleus, serotonergic dorsal and median raphe nuclei, dopaminergic A10 neurons, and histaminergic tuberomammillary neurons innervate the thalamus, hypothalamus, basal forebrain, and cerebral cortex. All of these systems have the property of firing fastest during wakefulness, slowing down during slow wave (or non-REM) sleep, and grinding to a halt during REM sleep.

Stimulation of noradrenergic neurons in the locus ceruleus or histaminergic cells in the tuberomammillary nucleus increases electroencephalogram (EEG) arousal, indicating that these systems play an important role in cortical and behavioral arousal. However, lesions restricted to one or even a combination of monoaminergic cell groups do not cause profound loss of wakefulness, suggesting that the various cell groups

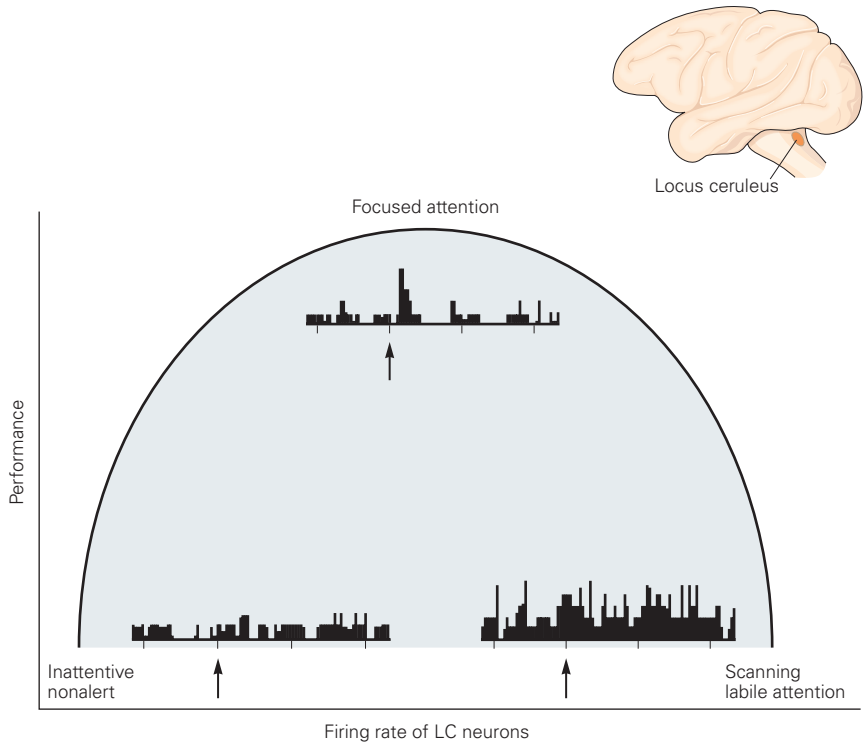

Figure 40–14 Locus ceruleus (LC) neurons exhibit different patterns of activity with different levels of attentiveness and task performance. The inverted U curve shows the relationship between a monkey's performance on a target detection task and the level of locus ceruleus activity. Histograms show the responses of LC neurons to presentation of the target during different levels of task performance. Performance is poor at low levels of LC activity because the animals are not alert. Performance is optimal when baseline activity is moderate and phasic activation follows presentation of the target. Performance is also poor when baseline activity is high because the higher baseline is incompatible with focusing on the assigned task. The tonic mode (with high baseline activity) might be optimal for tasks (or contexts) that require behavioral flexibility instead of focused attention. If so, the LC could regulate the balance between focused and flexible behavior. (Adapted, with permission, from Aston-Jones, Rajkowski, and Cohen 1999. Copyright © 1999 Society of Biological Psychiatry. Published by Elsevier Inc.)

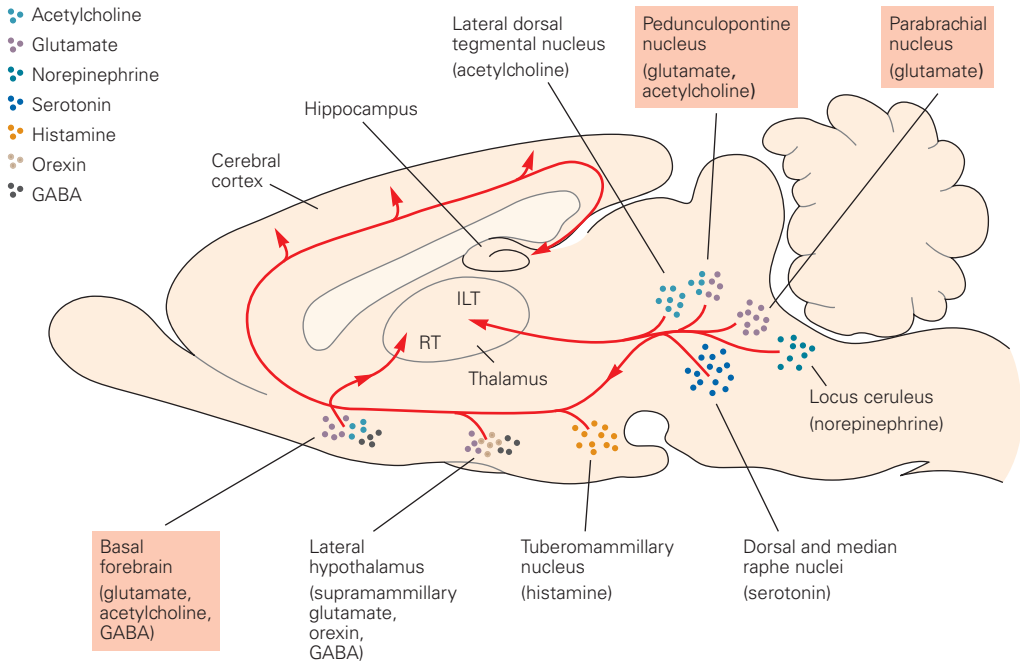

Figure 40–15 Major cell groups in the ascending arousal system. Neurons using the neurotransmitters norepinephrine, serotonin, dopamine, histamine, and acetylcholine have widespread forebrain projections. Although they all contribute to arousal by modulating various brain functions, ablation of any one of these cell groups has little effect on the waking state, suggesting that none of them are essential for maintaining a waking state. On the other hand, extensive damage to glutamatergic neurons in the parabrachial and pedunculopontine nuclei or to the GABAergic, glutamatergic, and cholinergic neurons in the basal forebrain (**orange boxes**) can cause a profound and prolonged coma. Thus, the parabrachial–pedunculopontine–basal forebrain–cortical pathway appears to be the only one that is essential to maintaining a waking state. (Abbreviations: **GABA**, γ-aminobutyric acid; **ILT**, intralaminar thalamic nuclei; **LC**, locus ceruleus; **RT**, reticular nucleus of the thalamus.)

probably have overlapping and at least partly redundant roles in sleep/wake regulation. The monoaminergic pathways modulate specific cellular properties of postsynaptic neurons in the thalamus and cerebral cortex, enhancing alertness and interaction with environmental stimuli.

Monoaminergic and Cholinergic Neurons Maintain Arousal by Modulating Forebrain Neurons

The monoaminergic and cholinergic neurons induce arousal by activating cortical neurons both directly and indirectly. They do this in part by modulating the activity of neurons in the brain stem, hypothalamus, basal forebrain, and thalamus that activate the cerebral cortex.

Both noradrenergic and serotonergic neurons innervate the parabrachial complex, a glutamatergic cell group that is critical for maintaining a waking forebrain. Noradrenergic inputs also activate histaminergic and orexin neurons in the lateral hypothalamus as well as cholinergic and GABAergic neurons in the basal forebrain, all of which project directly to the cerebral cortex. The parabrachial, histaminergic, orexin, and cholinergic basal forebrain neurons all excite cortical pyramidal cells, whereas the GABAergic basal forebrain neurons inhibit cortical inhibitory interneurons, thus disinhibiting the cortical pyramidal cells. The net effect of these inputs is to make the cortical pyramidal neurons more responsive to incoming sensory and cognitive inputs.

Parabrachial, noradrenergic, serotonergic, histaminergic, and cholinergic inputs also innervate the thalamus and modulate its ability to transmit sensory information to the cerebral cortex. Thalamic relay neurons fire in rhythmic bursts during sleep (Chapter 44) but fire single spikes related to incoming sensory stimuli during wakefulness. The firing pattern of thalamic and cortical neurons changes from burst mode to single-spike mode when the cells are depolarized following application of acetylcholine, norepinephrine,

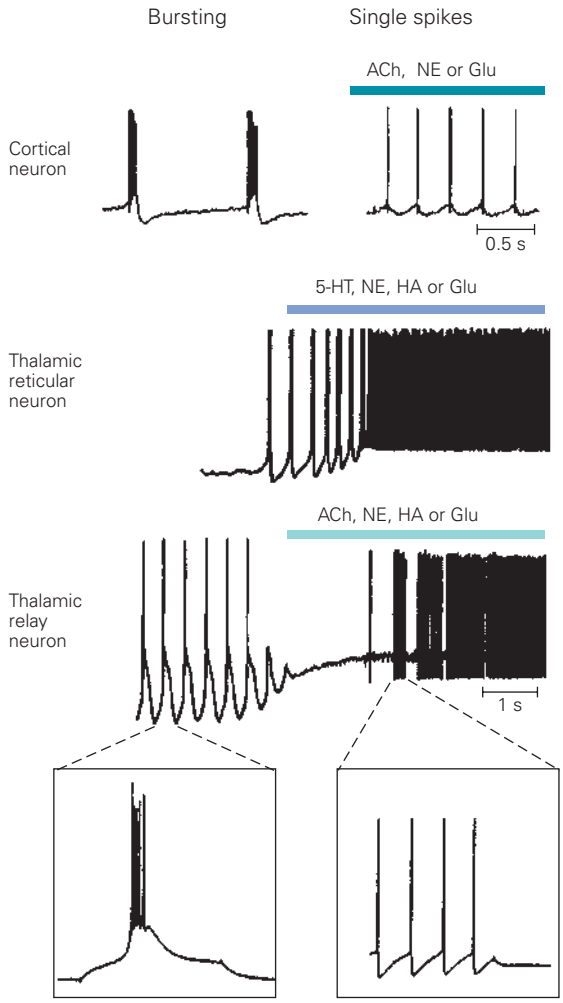

Figure 40–16 Monoaminergic and cholinergic systems modulate the activity of thalamic and cortical neurons to maintain arousal. The firing patterns of cortical and thalamic neurons are converted from burst mode to single-spike mode by the action of acetylcholine or monoamines. Recordings are from neurons in brain slices. Thalamic and cortical neurons have limited ability to convey information when firing in rhythmic bursts. However, when in single-spike mode, their firing activity reflects the inputs they receive. Therefore, the monoaminergic and cholinergic arousal systems keep open the lines of communication necessary for cortical information processing. (Reproduced, with permission, from Steriade, McCormick, and Sejnowski 1993. Copyright © 1993 AAAS.)

serotonin, or histamine (Figure 40–16). Thus, the monoaminergic neurons that participate in the ascending arousal system regulate cortical activity in part by altering the firing of thalamic neurons.

Many pharmacological agents that target monoaminergic and cholinergic systems influence arousal. For example, antihistamines cause drowsiness, serotonin reuptake blockers decrease the amount of REM sleep, and nicotine is a powerful stimulant. In addition, arousal is induced by amphetamines, cocaine, and other drugs that block dopamine reuptake; mice lacking the dopamine transporter are insensitive to such drugs.

Patients with Parkinson disease, who lose dopaminergic neurons in the substantia nigra, also lose noradrenergic neurons in the locus ceruleus and tend to be abnormally sleepy during the day. Some drugs used to treat Parkinson disease activate the D_2 dopamine receptor on presynaptic terminals of the remaining dopaminergic arousal neurons, which results in presynaptic inhibition, thus reducing dopamine release. As a result, although these drugs may make the movement disorder better (through their effects on postsynaptic D_2 receptors on neurons in the striatum), the inhibitory effect on remaining dopaminergic cells in the arousal system may exacerbate daytime sleepiness.

Highlights

1. The plan for the brain stem and the cranial nerves unfolds early in development, as neurons assemble into clusters that come, in time, to assume their functional organization. Building on the basic plan of the spinal cord, motor and sensory neurons concerned with the face, head, neck, and internal viscera form into discrete nuclei with specific functions and territories of innervation.
2. Neurons in the reticular formation surrounding these cranial nerve nuclei develop into ensembles of neurons that can generate patterns of autonomic and motor responses that subserve simple, stereotyped, coordinated functions, ranging from facial expression to feeding and breathing. These behavior patterns are sufficiently complex and flexible to represent the entire behavioral repertory of a newborn baby.
3. As the forebrain develops and exerts its control over these brain stem pattern generators, a variety of more complex responses and ultimately volitional control of behavior evolve.
4. Even a skilled actor, however, finds it difficult to produce the facial expressions associated with specific emotions unless he recreates the emotional states internally, thereby triggering the prepatterned facial expressions associated with those feeling states. Thus, some of the most complex human emotions and behaviors are played out unconsciously by means of stereotypic patterns of motor and autonomic responses in the brain stem.

5. The brain stem also contains a series of cell groups that have long-ranging and diffuse projections. Their targets range from the cognitive and behavioral systems in the cerebral cortex, to hypothalamic and brain stem autonomic control areas, to sensory and motor control systems in the spinal cord. Many of the neurons that participate in these modulatory systems, which set the tone for more specific sensory, motor, behavioral, and autonomic outputs, use monoamines as neuromodulators.
6. As a result of the diffuseness of these modulatory pathways and the multiplicity of receptors that they employ, a large portion of all central nervous system–active drugs act on these pathways. Unfortunately, many of the off-target effects of these drugs are due to the diffuseness of these pathways and their use of the same neurotransmitters and receptors at multiple locations. A challenge for the future of central nervous system pharmacology will be to develop drugs more highly selective for the targeted functions that require modulation.

Clifford B. Saper
Joel K. Elmquist

Selected Reading

Feldman JL, Del Negro CA, Gray PA. 2013. Understanding the rhythm of breathing: so near and yet so far. Ann Rev Physiol 75:423–452.

Gautron L, Elmquist JK, Williams KW. 2015. Neural control of energy balance: translating circuits to therapies. Cell 161:133–145.

Guyenet PG, Bayliss DA. 2015. Control of breathing and CO_2 homeostasis. Neuron 87:94–961.

Hodges MR, Richerson GB. 2010. Medullary serotonin neurons and their roles in central respiratory chemoreception. Respir Physiol Neurobiol 173:256–263.

Llorca-Torralba M, Borges G, Neto F, Mico JA, Berrocoso E. 2016. Noradrenergic locus coeruleus pathways in pain modulation. Neuroscience 338:93–113.

Plum F, Posner JB, Saper CB, Schiff ND. 2007. *Plum and Posner's Diagnosis of Stupor and Coma*, 4th ed. Philadelphia: Davis.

Saper CB. 2002. The central autonomic nervous system: conscious visceral perception and autonomic pattern generation. Annu Rev Neurosci 25:433–469.

Saper CB, Stornetta RL. 2014. Central autonomic system. In: G Paxinos (ed). *The Rat Nervous System*, 4th ed., pp. 627–671. San Diego: Elsevier.

Schultz W. 2016. Dopamine reward prediction-error signalling: a two-component response. Nat Rev Neurosci 17:183–195.

Sohn JW, Elmquist JK, Williams KW. 2013. Neuronal circuits that regulate feeding behaviour and metabolism. Trends Neurosci 36:504–512.

References

Aston-Jones G, Cohen JD. 2005. An integrative theory of locus coeruleus-norepinephrine function: adaptive gain and optimal performance. Annu Rev Neurosci 28:403–450.

Aston-Jones G, Rajkowski J, Cohen J. 1999. Role of locus coeruleus in attention and behavioral flexibility. Biol Psychiatry 46:1309–1320.

Aston-Jones G, Bloom FE. 1981. Activity of norepinephrine-containing locus ceruleus neurons in behaving rats anticipates fluctuations in the sleep-wake cycle. J Neurosci 1:876–886.

Bieger D, Hopkins DA. 1987. Viscerotropic representation of the upper alimentary tract in the medulla oblongata in the rat: the nucleus ambiguus. J Comp Neurol 262:546–562.

Blessing WW, Li Y-W. 1989. Inhibitory vasomotor neurons in the caudal ventrolateral region of the medulla oblongata. Prog Brain Res 81:83–97.

Bouret S, Richmond BJ. 2015. Sensitivity of locus coeruleus neurons to reward value for goal-directed attention. J Neurosci 35:4005–4014.

Bradley SR, Pieribone VA, Wang W, Severson CA, Jacobs RA, Richerson GB. 2002. Chemosensitive serotonergic neurons are closely associated with large medullary arteries. Nat Neurosci 5:401–402.

Bruinstroop E, Cano G, Vanderhorst VG, et al. 2012. Spinal projections of the A5, A6 (locus coeruleus), and A7 noradrenergic cell groups in rats. J Comp Neurol 520:1985–2001.

Chang RB, Strochlic DE, Williams EK, Umans BD, Liberles SD. 2015. Vagal sensory neuron subtypes that differentially control breathing. Cell 161:622–633.

Filiano JJ, Kinney HC. 1994. A perspective on neuropathologic findings in victims of the sudden infant death syndrome: the triple-risk model. Biol Neonate 65:194–197.

Gray PA, Janczewski WA, Mellen N, McCrimmon DR, Feldman JL. 2001. Normal breathing requires pre-Bötzinger complex neurokinin-1 receptor-expressing neurons. Nat Neurosci 4:927–930.

Grunstein RR, Sullivan CE. 1990. Neural control of respiration during sleep. In: MJ Thorpy (ed). *Handbook of Sleep Disorders*. New York: Marcel Dekker.

Jenny AB, Saper CB. 1987. Organization of the facial nucleus and cortico-facial projection in the monkey: a reconsideration of the upper motor neuron facial palsy. Neurol 37:930–939.

Lahiri S, Maret K, Sherpa M, Peters R Jr. 1984. Sleep and periodic breathing at high altitude: Sherpa natives vs. sojourners. In: J West, S lahiri (eds). *High Altitude and Man*, pp. 73–90. Bethesda: American Physiological Society.

Morecraft RJ, Louie JL, Herrick JL, Stilwell-Morecraft KS. 2001. Cortical innervation of the facial nucleus in the non-human primate: a new interpretation of the effects of

stroke and related subtotal brain trauma on the muscles of facial expression. Brain 124(Pt 1):176–208.

Mulkey DK, Stornetta RL, Weston MC, et al. 2004. Respiratory control by ventral surface chemoreceptor neurons in rats. Nat Neurosci 7:1360–1369.

Nielson M, Smith H. 1952. Studies on the regulation of respiration in acute hypoxia; with an appendix on respiratory control during prolonged hypoxia. Acta Physiol Scan 24:293–313.

Richerson GB. 2004. Serotonergic neurons as carbon dioxide sensors that maintain pH homeostasis. Nat Rev Neurosci 5:449–461.

Richerson GB, Getting PA. 1987. Maintenance of complex neural function during perfusion of the mammalian brain. Brain Res 409:128–132.

Rinaman L, Card JP, Schwaber JS, Miselis RR. 1989. Ultrastructural demonstration of a gastric monosynaptic vagal circuit in the nucleus of the solitary tract in rat. J Neurosci 9:1985–1996.

Smith JC, Ellenberger HH, Ballanyi K, Richter DW, Feldman JL. 1991. Pre-Bötzinger complex: a brain stem region that may generate respiratory rhythm in mammals. Science 254:726–729.

Steriade M, McCormick DA, Sejnowski TJ. 1993. Thalamocortical oscillations in the sleeping and aroused brain. Science 262:679–685.

Wang W, Bradley SR, Richerson GB. 2002. Quantification of the response of rat medullary raphe neurons to independent change in pH and PCO_2. J Physiol 540:951–970.

Williams EK, Chang RB, Strochlic DE, Umans BE, Lowell BB, Liberles SD. 2016. Sensory neurons that detect stretch and nutrients in the digestive system. Cell 166:209–221.

41

The Hypothalamus: Autonomic, Hormonal, and Behavioral Control of Survival

THE SURVIVAL OF AN INDIVIDUAL requires tight control of body temperature, water balance, and blood pressure, together with sufficient food intake and appropriate regulation of sleep/wakefulness

cycles. Survival of a species requires that individuals be fertile, mate, and nurture their offspring, and that aggression toward others be appropriate and adaptive. Neurons in the hypothalamus control all of these key survival activities.

As we shall learn in this chapter, the hypothalamus together with interconnected areas of the brain responds to bodily and emotional challenges by recruiting appropriate behavioral and physiological responses. Coordination of these activities ensures constancy of the internal environment, a process known as homeostasis. The hypothalamus acts on three major systems: the autonomic motor system, the neuroendocrine system, and neural pathways that mediate motivated behavior.

The autonomic motor system is distinct from the somatic motor system, which controls skeletal muscle. Whereas somatic motor neurons regulate contractions of striated muscles (Chapter 31), autonomic motor neurons regulate blood vessels, the heart, the skin, and visceral organs through synapses upon smooth and cardiac muscle cells, upon glands cells that serve endocrine and exocrine functions, and upon metabolic targets such as adipocytes. The neuroendocrine system works differently, by secreting several peptide hormones from the pituitary, the "master gland," located just beneath the hypothalamus. These pituitary hormones control water retention by the kidney, parturition, lactation, somatic growth, gamete development, and also the release of nonpeptide hormones from three downstream glands—the gonads, adrenal cortex, and thyroid.

Although largely involuntary, autonomic and neuroendocrine responses are tightly integrated with voluntary behavior executed by the somatic motor system. Running, climbing, and lifting exemplify voluntary actions that have metabolic, cardiovascular, and thermoregulatory consequences. These needs are automatically met by the autonomic and neuroendocrine systems through changes in cardiorespiratory drive, cardiac output, regional blood flow, heat dissipation, and fuel mobilization. Such compensatory changes are implemented primarily by feedforward central commands, supplemented by reflexes activated by sensory feedback. Similarly, emotional states evoke autonomic and neuroendocrine responses. Feelings of fear, anger, happiness, and sadness have characteristic autonomic and hormonal manifestations.

In this chapter, we first explore the concept of homeostasis and the general means by which it is achieved. We then discuss the anatomical and functional organization of the hypothalamus and its two "involuntary" motor arms—the autonomic and neuroendocrine systems. After that, we focus in depth on three classic examples of hypothalamic homeostatic control—regulation of body temperature, of water balance and its related deficiency drive, thirst, and of energy balance and its drive, hunger. We conclude by examining sexually dimorphic regions of the hypothalamus and their role in regulating sexual behavior, aggression, and parenting. Additional discussion of sleep cycles and regulation of circadian rhythms can be found in Chapter 44.

Homeostasis Keeps Physiological Parameters Within a Narrow Range and Is Essential for Survival

In the mid-19th century, the French physiologist and founder of experimental medicine Claude Bernard drew attention to the stability of the body's internal environment over a broad range of behavioral states and external conditions. "The internal environment (*le milieu interior*)," he wrote, "is a necessary condition for a free life." Building on this idea, in the 1930s, the American physiologist Walter B. Cannon introduced the concept of homeostasis to describe the mechanisms that maintain the constancy of composition of the bodily fluids, body temperature, blood pressure, and other physiological variables—all of which are necessary for survival.

Homeostatic mechanisms are highly adaptive because they greatly extend the range of conditions that can be tolerated. For example, during exercise, many parameters can increase dramatically—cardiac output by 4- to 5-fold, oxygen and fuel consumption by 5- to 10-fold, and heat production to a similar degree. In the absence of compensatory responses, blood pressure would increase in proportion to cardiac output, rupturing blood vessels; circulating fuels would fall to critically low levels, starving cells of energy; and hyperthermia would denature cell proteins. Indeed, the capacity of homeostasis is remarkable, making it possible for animals to survive at high latitudes where seasonal temperatures can fluctuate by 70°C and for humans to run 251 km in the sands of the extremely hot Sahara Desert (Marathon des Sables). Homeostatic mechanisms greatly extend the range of habitats, activities, and traumas that can be survived.

Homeostasis requires negative sensory feedback from the body. The concept of feedback loops evolved from the discovery of sensors that detect critical physiological variables and then couple them with behavioral, autonomic, and neuroendocrine motor outputs. Drawing upon the engineering principle of negative feedback control, this led to the concept that

physiological "set points" help control key parameters like body temperature, blood osmolarity, blood pressure, and body fat content.

Set point models are appealing because thermostats are so effective in maintaining room temperature at a targeted set point and, by analogy, physiological variables like body temperature are likewise tightly controlled. In such models, a "set point" exists for a parameter, 37°C in the case of body temperature, and at any given moment, the real level of the parameter is assessed and compared with the targeted set point through feedback and error detection (Figure 41–1A). Any deviation above or below triggers counteracting corrective responses—if too hot, cutaneous vasodilatation, sweating, and a dip in the pool; if too cold, vasoconstriction, thermogenesis, shivering, and the donning of a sweater. For regulation of body temperature, the set point and detection of error were historically seen as emergent properties of neurons in the preoptic area of the hypothalamus (POA).

Over time, the set point model required revision because intensive investigation failed to uncover any molecular or neuronal bases for encoding set points and performing error detection. In addition, "set point–like" regulation can, in principle, be achieved without a set point, feedback, or error detection—the so-called "settling point" model (Figure 41–1B). Consider the changing level of a lake. When rainfall is excessive, its level rises; the rivers draining the lake rise and their flow increases. The converse is true when rainfall is low. The changing flow of the rivers draining the lake thus maintains its level near a settling point without requiring an idealized set point, feedback, or error detection. While aspects of the settling point model have appeal, it too is incomplete because homeostatic processes clearly receive important feedback

A Set point model

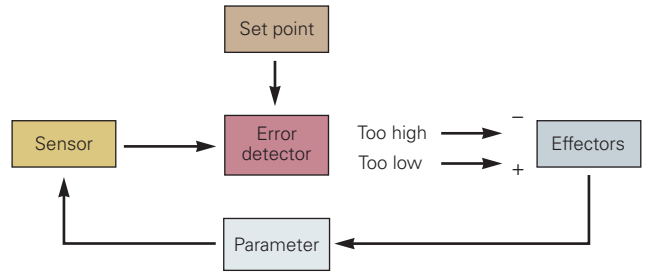

B Settling point model

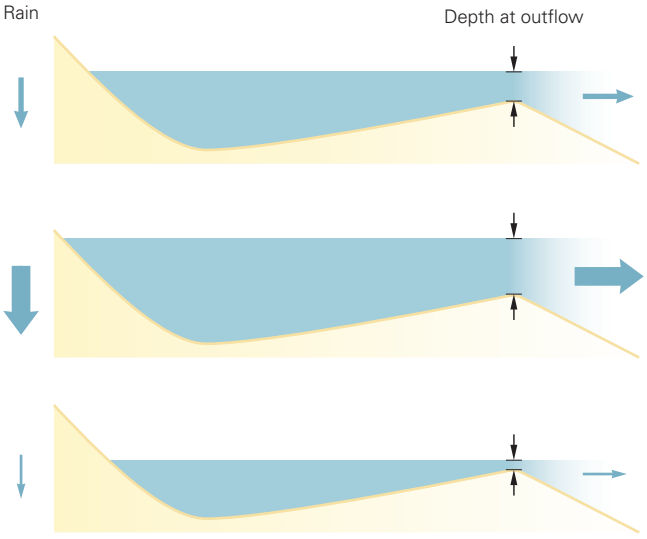

C Combined model: settling point of multiple afferent/efferent loops

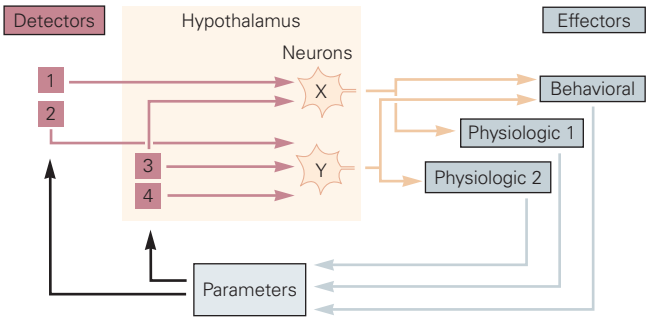

Figure 41–1 (Left) Set points, settling points, and homeostasis.

A. The set point view was inspired by engineering principles. As with a thermostat, constancy is achieved by providing feedback on the existing level of a parameter, determining how it compares to an idealized set point, and then instituting corrective measures to return the parameter to the set point. While popular for many years, it has fallen out of favor as years of research have failed to uncover molecular and neural bases for encoding set points and performing error detection.

B. The settling point model was inspired by observations that many systems achieve constancy in the absence of any feedback or error detection. In this example, the level of outflow of water from a lake is proportional to the depth of the lake. When it rains, the increase or decrease in the level of the lake causes more or less water to flow out of the lake. The level of the lake remains fairly constant without a set point or error detection. A related example is regulation of body weight. Increased food intake leads to increased body weight. As body weight increases, the energy cost of carrying and sustaining that increased weight goes up. Because of this, body weight too should have its settling point. (Reproduced, with permission, from Speakman et al. 2011.)

C. In this model the concepts of feedback in part **A** and settling point in part **B** are combined. The apparent set point is in fact the settling point, an emergent property of multiple feedback-informed afferent/efferent loops.

regarding disturbances, and this feedback produces vital responses that hasten recovery. As we shall see, temperature, osmolarity, and body fat are directly or indirectly "sensed," and this affects the activity of neurons in the hypothalamus that generate counteracting responses.

Most physiologists today have adopted a "distributed settling point" model that incorporates strong feedback control of multiple sensory/effector loops (Figure 41–1C). With body temperature, for example, there is no single specific set point and no location in the brain where a single set point is encoded and error detection takes place; in short, there is no thermostat. Instead, there are multiple temperature detectors located in different sites (skin, core, and brain), and each is coupled through neuronal pathways that traverse the preoptic area on their way to different body temperature effectors (cutaneous blood vessels, sweat glands, brown fat metabolism, shivering and behavioral pathways). When engaged, each of these effectors impact body temperature. The apparent set point for body temperature is in fact the emergent settling point that results from the combined activities of the multiple feedback-informed afferent/efferent loops. As we will see later, this nuanced model also applies to regulation of blood pressure, blood osmolarity, and body fat.

The Hypothalamus Coordinates Homeostatic Regulation

The hypothalamus integrates the status of physiological parameters with outputs to behavioral, autonomic, and neuroendocrine motor systems and thereby regulates six vital physiological functions (Table 41–1). The hypothalamus lies at the base of the brain immediately above the pituitary gland (Figure 41–2). It is bounded anteriorly (rostrally) by the diagonal band of Broca; dorsally by the anterior commissure, the bed nuclei of the stria terminalis, the zona incerta, and thalamus; and posteriorly (caudally) by the ventral tegmental area and interpeduncular nucleus.

The Hypothalamus Is Commonly Divided Into Three Rostrocaudal Regions

Regions of the hypothalamus are named according to their location and appearance in Nissl-stained sections. The hypothalamus is divided, rostral to caudal, into three regions. (1) The *preoptic hypothalamus* lies above the optic chiasm and contains neurons that control water balance and thirst, temperature, sleep, sexual behavior, and circadian rhythms. (2) The *tuberal hypothalamus* lies above the pituitary and contains neurons controlling pituitary hormone secretion, autonomic outflow, and various behaviors including hunger, sexual behavior, and aggression. (3) The *posterior hypothalamus* includes the posterior and mammillary nuclei, as well as histaminergic neurons in the tuberomammillary nucleus that affect arousal. The functions of other neurons in the posterior hypothalamus areas are less well defined.

The *lateral hypothalamic area* (LHA) spans from the middle to the caudal hypothalamus. It is linked more closely to reward pathways and arousal than to maintenance of homeostasis and specific survival behaviors. Indeed, it is heavily connected with the nucleus accumbens and ventral tegmental area, two areas involved in reward (Chapter 43), and contains neurons that project extensively throughout the cortex. Lastly, LHA neurons expressing the neuropeptide orexin (hypocretin) play a critical role in stabilizing wakefulness (Chapter 44).

Table 41–1 The Hypothalamus Integrates Behavioral (Somatomotor), Autonomic, and Neuroendocrine Responses Involved in Six Vital Functions

1. *Blood pressure and electrolyte composition*. The hypothalamus regulates thirst, salt appetite, and drinking behavior; autonomic control of vasomotor tone; and the release of hormones such as vasopressin (via the paraventricular nucleus).
2. *Energy metabolism*. The hypothalamus regulates hunger and feeding behavior, the autonomic control of digestion, and the release of hormones such as glucocorticoids, growth hormone, and thyroid-stimulating hormone (via the arcuate and paraventricular nuclei).
3. *Reproductive (sexual and parental) behaviors*. The hypothalamus controls autonomic modulation of the reproductive organs and endocrine regulation of the gonads (via the medial preoptic, ventromedial, and ventral premammillary nuclei).
4. *Body temperature*. The hypothalamus influences thermoregulatory behavior (seeking a warmer or cooler environment), controls autonomic body heat conservation/loss mechanisms, and controls secretion of hormones that influence metabolic rate (via the preoptic region).
5. *Defensive behavior*. The hypothalamus regulates the stress response and fight-or-flight response to threats in the environment such as predators (via the paraventricular, anterior hypothalamic, and dorsal premammillary nuclei, and the lateral hypothalamic area).
6. *Sleep–wake cycle*. The hypothalamus regulates the sleep–wake cycle (via a circadian clock in the suprachiasmatic nucleus) and levels of arousal when awake (via the lateral hypothalamic area and tuberomammillary nucleus).

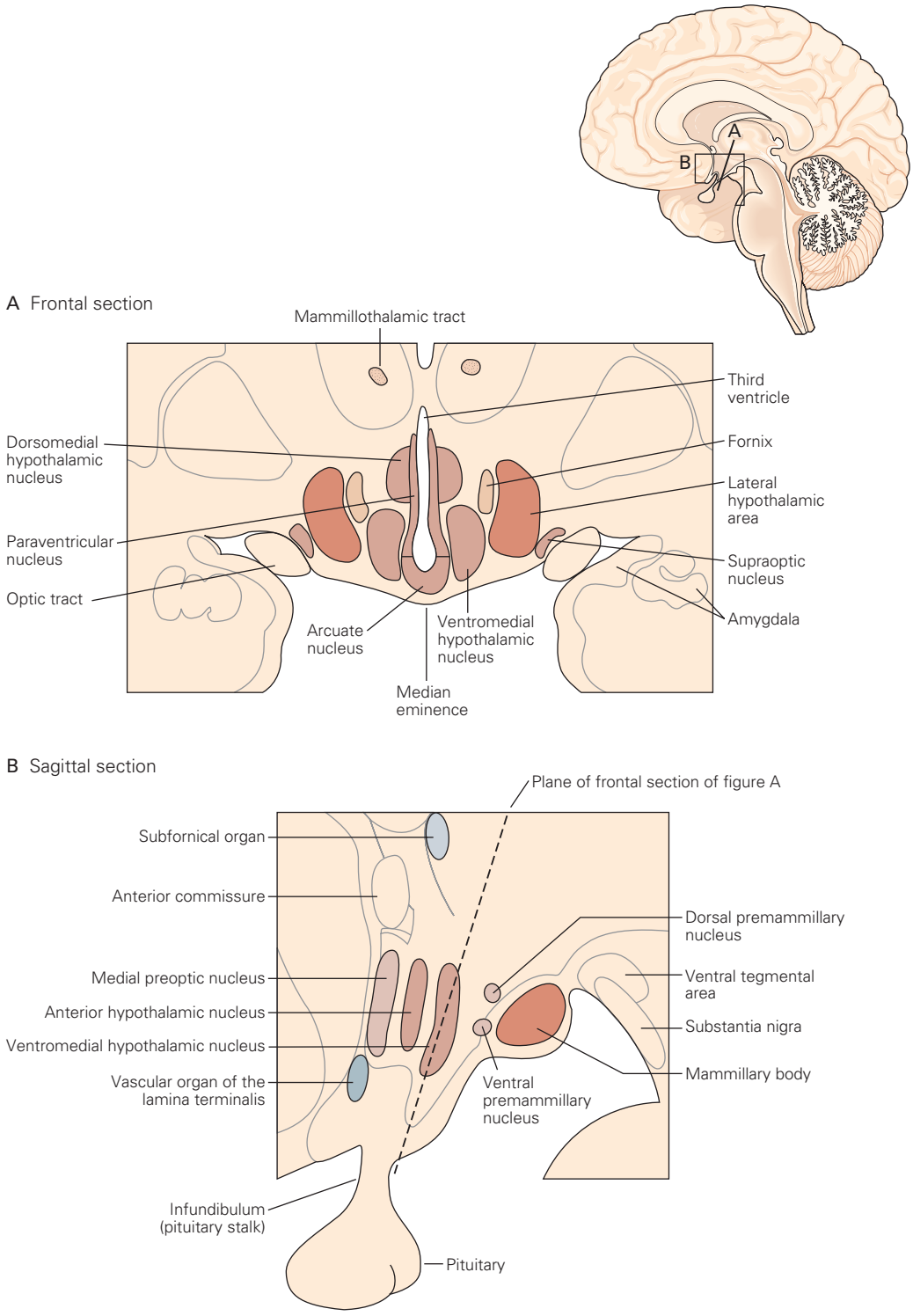

Figure 41–2 The structure of the hypothalamus.

A. Frontal view of the hypothalamus (section along plane A shown in the sagittal view of the brain, upper right). The third ventricle is in the midline; the paraventricular, dorsomedial, and arcuate nuclei adjacent to the ventricle form the neuroendocrine motor zone and periventricular region at this level. The ventromedial nucleus is part of the medial column of hypothalamic nuclei, and the lateral hypothalamic area is the lateral zone component represented in the part of the hypothalamus shown here.

B. Sagittal (rostrocaudal) view of the medial column of hypothalamic nuclei, showing the adjacent (caudal) substantia nigra and ventral tegmental area of the midbrain. The functional significance of key hypothalamic nuclei is summarized in Table 41–1.

Modality-Specific Hypothalamic Neurons Link Interoceptive Sensory Feedback With Outputs That Control Adaptive Behaviors and Physiological Responses

General principles of hypothalamic function have emerged over several decades. Neurons in the periphery and brain respond when parameters under homeostatic control are disturbed. Such neurons can respond directly to the stimulus or indirectly to changes in hormones and other factors that track the regulated parameter. This sensory information is then relayed to functionally appropriate regulatory neurons in a particular site (or sites) within the hypothalamus. Once the information is integrated by hypothalamic neurons, the results are then conveyed downstream to motor circuits that control specific behaviors and physiological responses. The result is a coordinated corrective response (eg, warmth-seeking plus heat production and retention, thirst plus water retention by the kidney, or hunger plus decreased energy expenditure).

Our understanding of the functions of hypothalamic neurons has been refined recently using optogenetic and chemogenetic techniques in active animals. By selectively activating subsets of hypothalamic neurons, one can evoke specific behaviors and physiological responses, even when the need is totally absent. Key regulatory neurons for body temperature are located in the median preoptic nucleus (MnPO). Water balance is regulated by neurons in three sites—the MnPO, the vascular organ of the lamina terminalis (OVLT), and the subfornical organ (SFO)—and energy balance by neurons in the arcuate nucleus (Figure 41–2A).

Modality-Specific Hypothalamic Neurons Also Receive Descending Feedforward Input Regarding Anticipated Homeostatic Challenges

In addition to input from sensory signals that provide important feedback regarding the status of the body, key regulatory neurons in the hypothalamus receive "top-down" feedforward inputs from neurons that anticipate future homeostatic challenges. For example, when food-deprived animals detect cues that predict the availability of food, there is a rapid drop in the firing of hunger-promoting neurons in the arcuate nucleus even before food is ingested. Such top-down feedforward control prepares the body for anticipated homeostatic challenges. In addition, such rapid regulation, by countering an aversive state represented by high activity in deficiency-driven neurons, could be important for motivating deficiency-based behaviors such as thirst and hunger (discussed below).

Next, we examine two effectors arms of the hypothalamus—the autonomic motor system and the neuroendocrine system.

The Autonomic System Links the Brain to Physiological Responses

Although the autonomic motor system implements many of the physiological responses initiated by the hypothalamus, the autonomic system is also regulated by circuits in the brain stem and spinal cord (Chapter 40). As a consequence, autonomic functions vary in their dependence on the hypothalamus. For example, micturition is largely independent of the hypothalamus, while blood pressure regulation depends heavily on circuits in the brain stem but can also be modulated by the hypothalamus. In contrast, thermogenesis by brown adipose tissue is largely subservient to the hypothalamus.

Visceral Motor Neurons in the Autonomic System Are Organized Into Ganglia

Unlike the somatic motor system, in which motor neurons are located in the ventral spinal cord and brain stem, the cell bodies of autonomic motor neurons are found in enlargements of peripheral nerves called ganglia.[1] The autonomic motor neurons innervate secretory epithelial cells in glands, smooth and cardiac muscle, and adipose tissue.

Efforts to understand the principles of organization of autonomic ganglia began in 1880 in England with the work of Walter Gaskell and were later continued by John N. Langley. They stimulated autonomic nerves and observed the responses of end organs (eg, vasoconstriction, piloerection, sweating, pupillary constriction). They used nicotine to block signals from individual ganglia to test interactions between ganglia. Langley proposed that specific chemical substances must be released by preganglionic neurons of the autonomic ganglia and that these substances act by binding to receptors on the postganglionic neurons, which target the end organs. These ideas set the stage for the later investigations of chemical synaptic transmission.

[1]The peripheral nerves also have sensory ganglia, located on the dorsal roots of the spinal cord and on five of the cranial nerves: trigeminal (V), facial (VII), vestibulocochlear (VIII), glossopharyngeal (IX), and vagus (X) (Chapter 40).

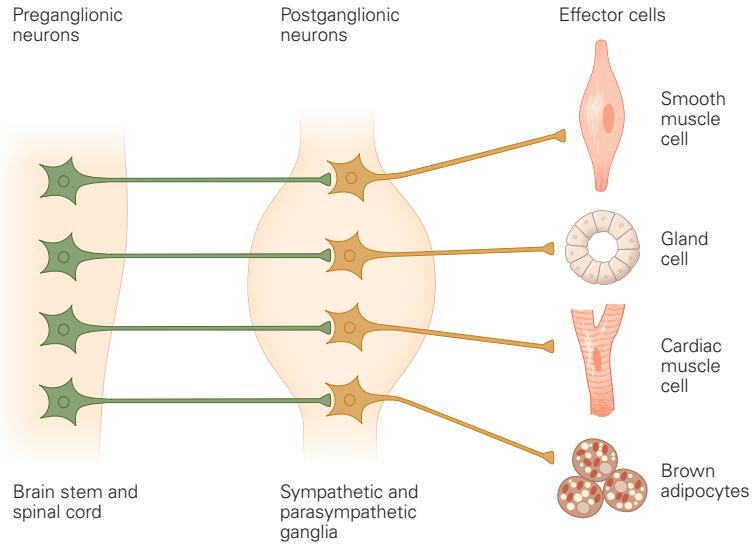

Figure 41–3 Distinct cell types in peripheral autonomic pathways selectively control target cells with different phenotypes. Autonomic motor neurons lie outside the central nervous system in ganglia controlled by preganglionic neurons in the spinal cord and brain stem. These downstream neurons within parasympathetic and sympathetic ganglia regulate three types of effector cells: smooth muscle, gland cells, and cardiac muscle. Additionally, downstream neurons found only in sympathetic ganglia selectively control brown adipocytes and immune cells in lymphoid tissue. This figure illustrates the three basic cell types—preganglionic neurons, downstream ganglionic neurons, and different target effector cells—that control function.

Langley also distinguished the autonomic and somatic motor systems and in so doing, created much of our current nomenclature.

The autonomic system is divided into three divisions: sympathetic, parasympathetic, and enteric. All neurons in sympathetic and parasympathetic ganglia are controlled by *preganglionic neurons* whose cell bodies are located in the spinal cord and brain stem. The preganglionic neurons synthesize and release the neurotransmitter acetylcholine (ACh), which acts on nicotinic ACh receptors on *postganglionic neurons*, producing fast excitatory postsynaptic potentials and initiating action potentials that propagate to synapses with effector cells in *end organs* (Figure 41–3). The sympathetic and parasympathetic systems are differentiated by five criteria:

1. The segmental organization of their preganglionic neurons in the spinal cord and brain stem
2. The peripheral locations of their ganglia
3. The types and locations of end organs they innervate
4. The effects they produce on end organs
5. The neurotransmitters employed by their postganglionic neurons

Preganglionic Neurons Are Localized in Three Regions Along the Brain Stem and Spinal Cord

The parasympathetic pathways arise from a cranial nerve zone in the brain stem and a second zone in sacral segments of the spinal cord (Figure 41–4). These parasympathetic zones surround a sympathetic zone that extends continuously in thoracic and lumbar segments of the cord.

The cranial parasympathetic pathways arise from preganglionic neurons in the general visceral motor nuclei of four cranial nerves: the oculomotor (N. III) in the midbrain and the facial (N. VII), glossopharyngeal (N. IX), and vagus (N. X) in the medulla. The cranial parasympathetic nuclei are described in Chapter 40 together with the mixed cranial nerves (eg, the facial, glossopharyngeal, and vagus). The spinal parasympathetic pathway originates in preganglionic neurons in sacral segments S2–S4. Their cell bodies are located in intermediate regions of the gray matter, and their axons project in peripheral nerves through the ventral roots.

The sympathetic preganglionic cell column extends between the cervical and lumbosacral enlargements of the spinal cord, corresponding to the first thoracic segment and third lumbar segment (Figure 41–4). Most of the cell bodies of sympathetic preganglionic neurons are located in the intermediolateral cell column; others are found in the central autonomic area surrounding the central canal and in a band connecting the central area with the intermediolateral cell column. The axons of preganglionic sympathetic neurons project from the spinal cord through the nearest ventral root and then run with small connecting nerves known as rami communicantes before terminating on postganglionic cells in the paravertebral sympathetic chain (Figure 41–5).

Sympathetic Ganglia Project to Many Targets Throughout the Body

The sympathetic motor system regulates systemic physiological parameters such as blood pressure and body temperature by influencing target cells within virtually every tissue throughout the body (Figure 41–4).

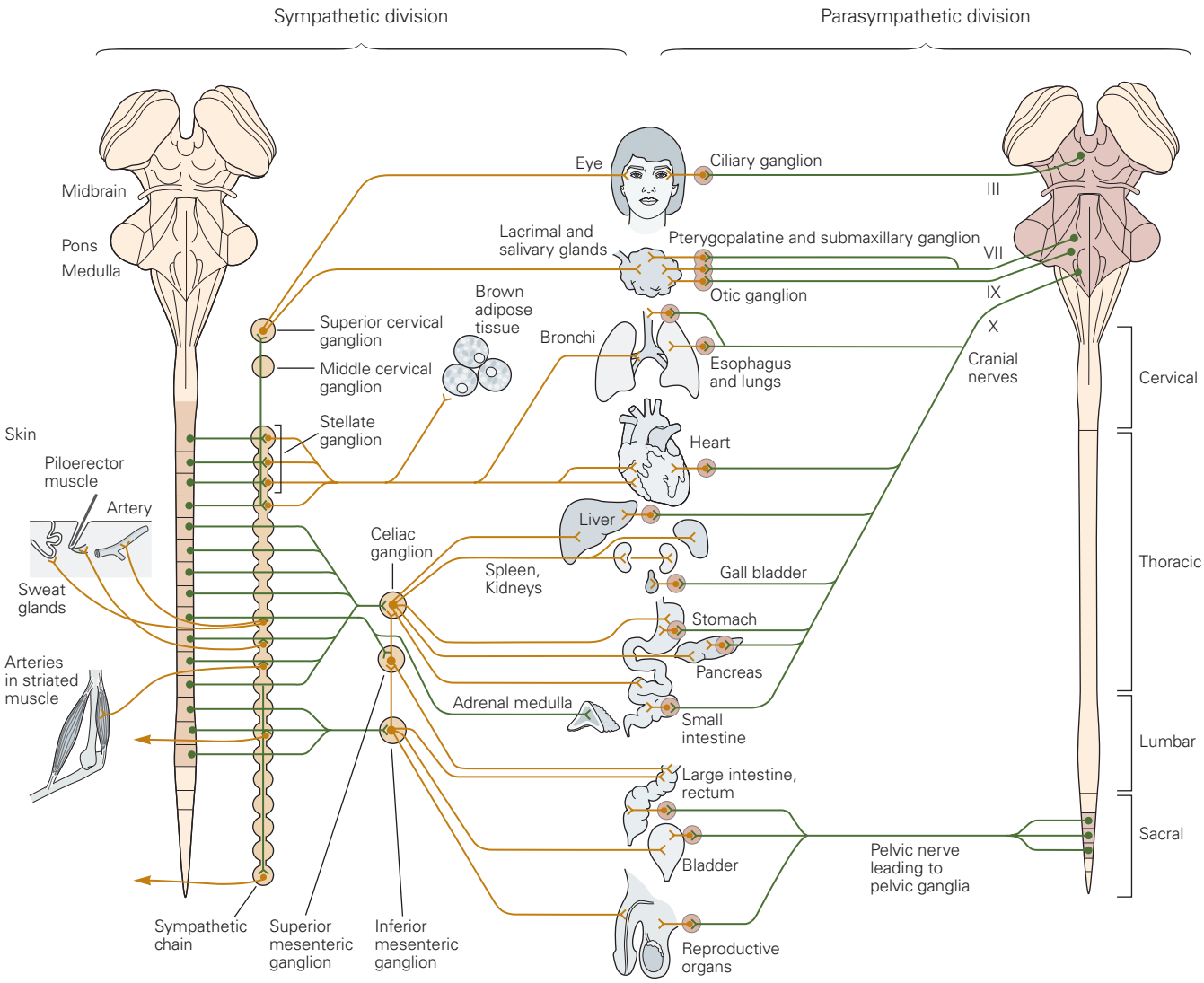

Figure 41–4 Sympathetic and parasympathetic divisions of the autonomic motor system. The sympathetic ganglia lie close to the spinal column and supply virtually every tissue in the body. Some tissues, such as skeletal muscle, are regulated only indirectly through their arterial blood supply. The parasympathetic ganglia are located near their targets, which do not include the skin or skeletal muscle.

This regulation depends on synaptic input from the spinal cord and from supraspinal structures that control the activity of the preganglionic neurons.

Important groups of supraspinal neurons that excite preganglionic sympathetic activity are located in the rostral ventrolateral medulla, the raphe pallidus in the brain stem, and the paraventricular nucleus in the hypothalamus. Preganglionic neurons integrate these descending inputs along with local segmental sensory inputs and form synapses with neurons in paravertebral and prevertebral sympathetic ganglia (Figure 41–5).

Ganglionic neurons in turn form synapses with a variety of end organs, including blood vessels, heart, bronchial airways, piloerector muscles, brown fat, and salivary and sweat glands. Sympathetic neurons also regulate immune function through projections to primary lymphoid tissue in the bone marrow and thymus and to secondary lymphoid cells in the spleen. A subset of preganglionic neurons synapse on chromaffin cells in the medulla of the adrenal gland (Figure 41–5), which secrete epinephrine (adrenaline) and norepinephrine (noradrenaline) into the circulation as hormones to act on distant targets.

The paravertebral and prevertebral sympathetic ganglia differ in both location and organization. Paravertebral ganglia are distributed segmentally,

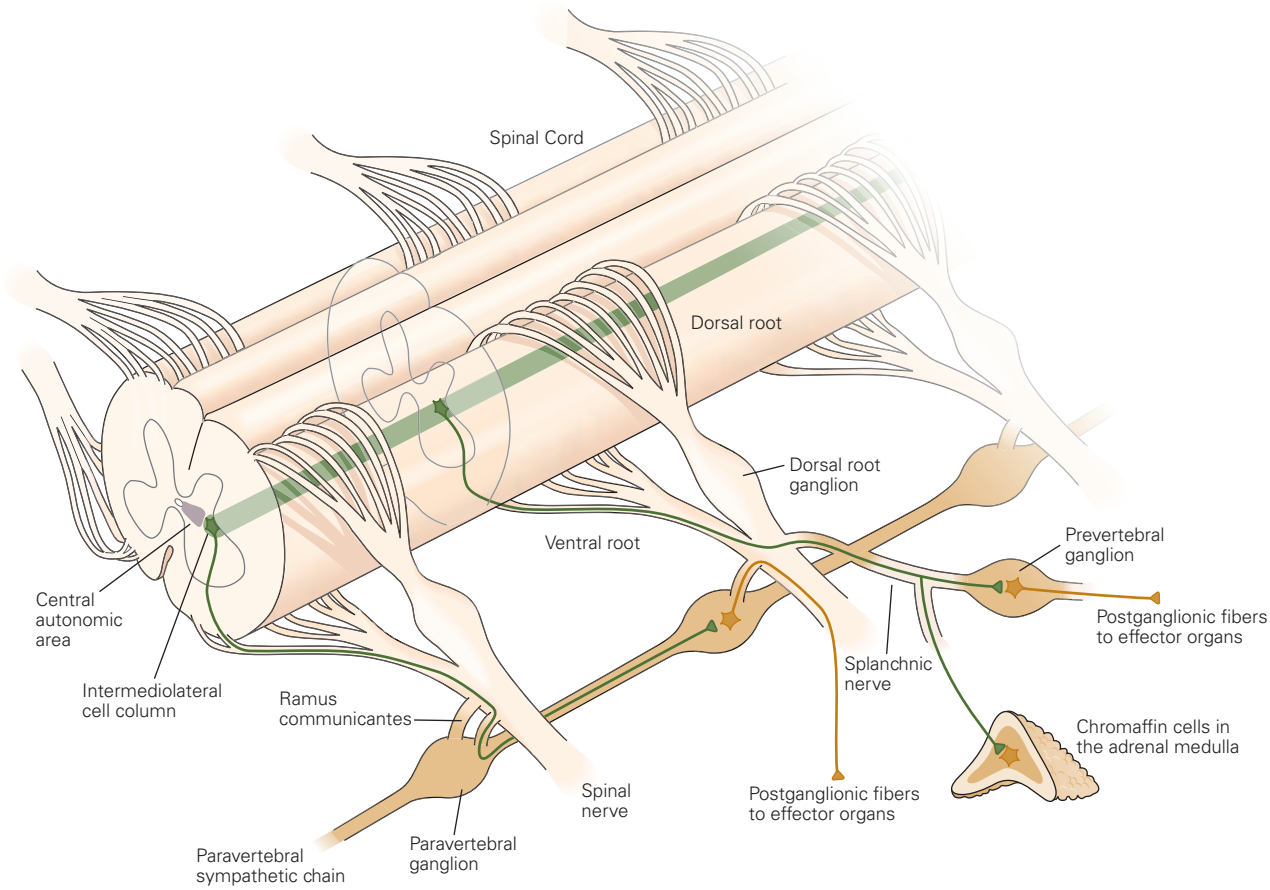

Figure 41–5 The sympathetic outflow is organized into groups of paravertebral and prevertebral ganglia. The axons of preganglionic cells in the spinal cord reach postganglionic neurons by way of ventral roots and the paravertebral sympathetic chain. The axons either form synapses on postganglionic neurons in paravertebral ganglia or project out of the chain into splanchnic nerves. Preganglionic axons in the splanchnic nerves form synapses with postganglionic neurons in prevertebral ganglia and with chromaffin cells in the adrenal medulla.

extending bilaterally as two chains from the first cervical segment to the last sacral segment. The chains lie lateral to the vertebral column at its ventral margin and generally contain one ganglion per segment (Figures 41–4 and 41–5). Two important exceptions are the superior cervical and stellate ganglia. The superior cervical ganglion is a coalescence of several cervical ganglia and supplies sympathetic innervation to the entire head, including the cerebral vasculature. The stellate ganglion, which innervates the heart and lungs, is a coalescence of ganglia from lower cervical segments and the first thoracic segment. These sympathetic pathways have an orderly somatotopic relation to one another from their segmental origin in preganglionic neurons to their terminus in peripheral targets.

The prevertebral ganglia are midline structures that lie close to the arteries for which they are named (Figures 41–4 and 41–5). In addition to sending sympathetic signals to visceral organs in the abdomen and pelvis, these ganglia also receive sensory feedback from their end organs.

Parasympathetic Ganglia Innervate Single Organs

In contrast to sympathetic ganglia, which regulate many targets and lie some distance from their targets close to the spinal cord, parasympathetic ganglia generally innervate single end organs and lie near to or within the end organs they regulate (Figure 41–4). In addition, the parasympathetic system does not influence lymphoid tissue, skin, or skeletal muscle except in the head, where it regulates vascular beds in the jaw, lip, and tongue.

The cranial and sacral parasympathetic ganglia innervate different targets. The cranial outflow includes four ganglia in the head (Chapter 40). The oculomotor

(III) nerve projects to the ciliary ganglion, which controls pupillary size and focus by innervating the iris and ciliary muscles. The facial (VII) nerve and a small component of the glossopharyngeal (IX) nerve project to the pterygopalatine (or sphenopalatine) ganglion, which promotes production of tears by the lacrimal glands and mucus by the nasal and palatine glands. Cranial nerve IX and a small component of nerve VII project to the otic ganglion. Its postganglionic neurons innervate the parotid, the largest salivary gland. Nerve VII also projects to the submandibular ganglion, which controls secretion of saliva by the submaxillary and sublingual glands.

The vagus (X) nerve projects broadly to parasympathetic ganglia in the heart, lungs, liver, gallbladder, and pancreas. It also projects to the stomach, small intestine, and more rostral segments of the gastrointestinal tract. The caudal parasympathetic outflow supplies the large intestine, rectum, bladder, and reproductive organs.

The Enteric Ganglia Regulate the Gastrointestinal Tract

The entire gastrointestinal tract, from the esophagus to the rectum—and including the pancreas and gallbladder—is controlled by the system of enteric ganglia. This system, by far the largest and most complex division of the autonomic nervous system, contains as many as 100 million neurons.

The enteric system has been studied most extensively in the small intestine of the guinea pig. Its activity is coordinated by two interconnected plexuses, small islands of interconnected neurons. The myenteric plexus controls smooth muscle movements of the gastrointestinal tract; the submucous plexus controls mucosal function (Figure 41–6). Working together, this distributed network of ganglia coordinates the orderly peristaltic propulsion of gastrointestinal contents and controls the secretions of the stomach and intestines and other components of digestion. In addition, the enteric system regulates local blood flow and also immune function in Peyer's patches. The enteric system is modulated by external inputs from sympathetic prevertebral ganglia and from parasympathetic components of the vagus nerve.

Unlike the sympathetic and parasympathetic divisions of the autonomic system, the enteric plexus contains interneurons and sensory neurons in addition to motor neurons. This intrinsic neural circuitry can maintain the basic functions of the gut even after the splanchnic sympathetic and vagal parasympathetic pathways are cut. Through splanchnic nerves and the afferent portion of the vagus nerve, the gastrointestinal tract also sends sensory information about the physiological status of the tract to the spinal cord and brain stem.

Acetylcholine and Norepinephrine Are the Principal Transmitters of Autonomic Motor Neurons

All preganglionic neurons in the sympathetic and parasympathetic systems use ACh as their excitatory neurotransmitter, activating ionotropic nicotinic ACh receptors on ganglionic neurons. These receptors resemble those at the neuromuscular junction in having nonselective cation pores, but they are encoded by different genes.

Activation of the ganglionic neurons triggers action potentials that propagate to postganglionic synapses with end organs in the periphery. At these end organ synapses, parasympathetic neurons release ACh, which activates muscarinic G protein–coupled receptors; sympathetic neurons release norepinephrine, which activates α- and β-adrenergic G protein–coupled receptors. The postsynaptic action can be either excitatory or inhibitory, depending on the type of target cell and its receptors (Table 41–2). Notable exceptions to this organization are the sympathetic postganglionic neurons that control sweat glands. They assume a cholinergic phenotype after birth.

In addition to acting on different receptors in different postsynaptic cells, one transmitter can activate different receptor types in the same postsynaptic cell. This principle was first discovered in sympathetic ganglia where ACh activates both nicotinic and muscarinic postsynaptic receptors to produce both a fast and slow excitatory postsynaptic potential (Figure 41–7A and Chapter 14). In some cases, one transmitter can activate both a postsynaptic receptor as well as a receptor on the presynaptic terminals from which the transmitter was released. Such presynaptic responses can cause either presynaptic inhibition or presynaptic facilitation (Figure 41–7B and Chapter 15). This specialization of synaptic transmission in sympathetic and parasympathetic neurons leads to functional diversity in the regulation of end organ function.

Cholinergic and adrenergic synaptic transmission in the peripheral autonomic motor system is often modulated by the co-release of various neuropeptides, nitric oxide, or adenosine triphosphate, which by activating multiple receptor types further contribute to functional diversity (Table 41–2 and Figure 41–7C). The motor responses elicited in end organs depend on the identity of the postganglionic neurotransmitters and the pre- and postsynaptic receptors

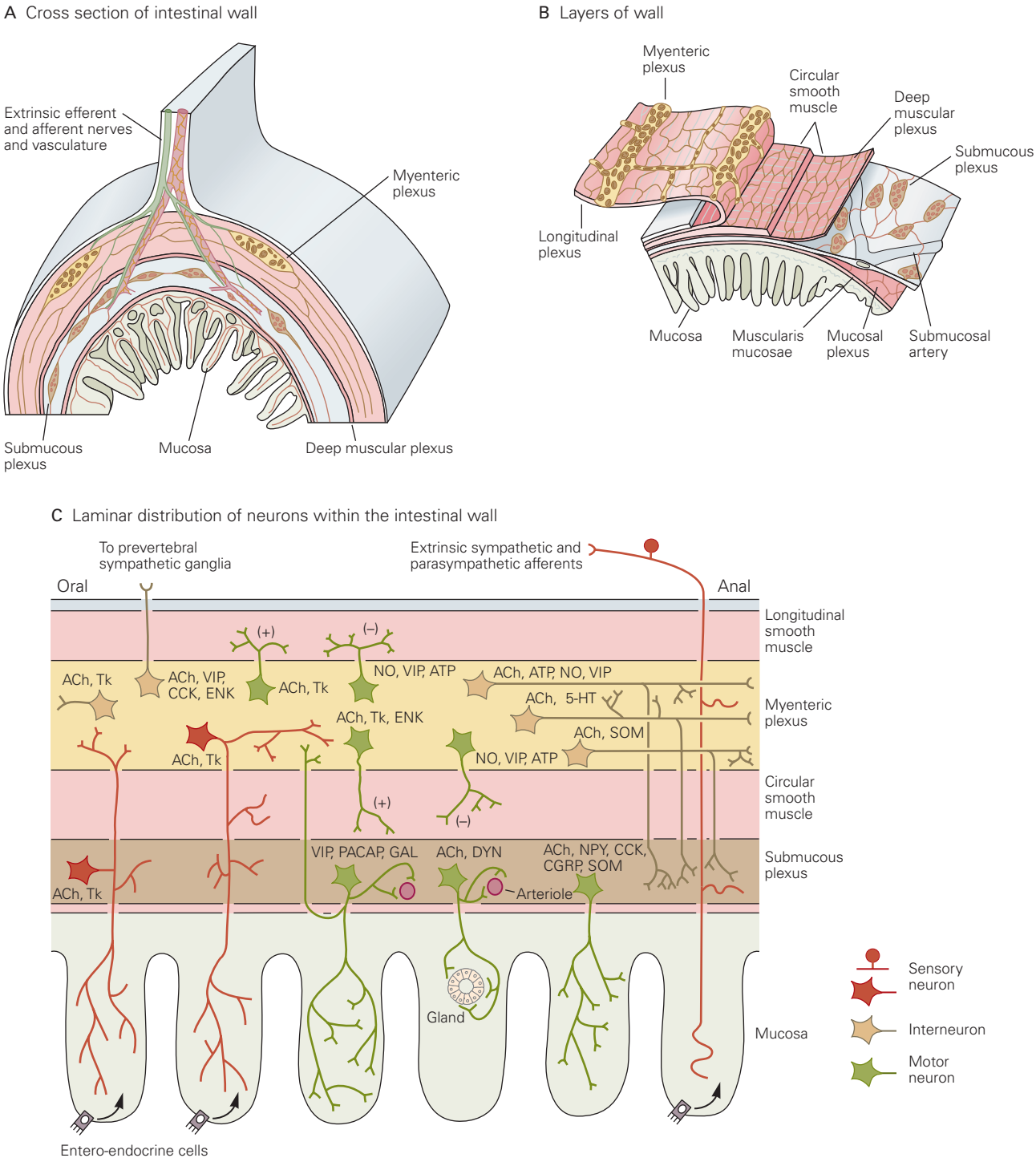

Figure 41–6 Organization of the enteric plexuses in the guinea pig. The myenteric plexus and submucous plexus lie between the layers of intestinal wall (**A** and **B**). At least 14 types of neurons have been identified within the enteric system based on morphology, chemical coding, and functional properties (**C**). Four sets of motor neurons provide excitatory (+) and inhibitory (–) inputs to two smooth muscle layers. Three additional groups of motor neurons control secretions from the mucosa and produce vasodilation. The network also includes two major classes of intrinsic sensory neurons. (Abbreviations: **ACh**, acetylcholine; **ATP**, adenosine triphosphate; **CCK**, cholecystokinin; **CGRP**, calcitonin gene-related polypeptide; **DYN**, dynorphin; **ENK**, enkephalin; **GAL**, galanin; **NO**, nitric oxide; **NPY**, neuropeptide Y; **PACAP**, pituitary adenylate cyclase-activating peptide; **SOM**, somatostatin; **Tk**, tachykinin; **VIP**, vasoactive intestinal peptide; **5-HT**, serotonin.) (Parts A and B adapted, with permission, from Furness and Costa 1980; part C reproduced, with permission, from Furness et al. 2004. Copyright © 2004 Elsevier Ltd.)

Table 41–2 Autonomic Neurotransmitters and Their Receptors

Transmitter	Receptor	Responses
Norepinephrine	α_1	Stimulates smooth muscle contraction in arteries, urethra, gastrointestinal tract, iris (pupillary dilation), uterine contractions during pregnancy, ejaculation; glycogenolysis in liver; glandular secretion (salivary glands, lacrimal glands).
	α_2	Presynaptic inhibition of transmitter release from sympathetic and parasympathetic nerve terminals; stimulates contraction in some arterial smooth muscle.
	β_1	Increases heart rate and strength of contraction.
	β_2	Relaxes smooth muscle in airways and gastrointestinal tract; stimulates glycogenolysis in liver.
	β_3	Stimulates lipolysis in white adipocytes and thermogenesis in brown adipocytes; inhibits bladder contraction.
Acetylcholine	Nicotinic	Fast EPSP in autonomic ganglion cells.
	Muscarinic: M_1, M_2, M_3	Glandular secretion; ocular circular muscle (pupillary constriction); ciliary muscles (focus of lens); stimulates endothelial production of NO and vasodilation; slows EPSPs in sympathetic neurons; slows heart rate; presynaptic inhibition at cholinergic nerve terminals; bladder contraction; salivary gland secretion.
Neuropeptide Y	Y_1, Y_2	Stimulates arterial contraction and potentiates responses mediated by α_1-adrenergic receptors; presynaptic inhibition of transmitter release from some postganglionic sympathetic nerve terminals.
NO	Diffuses through membranes; often acts to stimulate intracellular soluble guanylate cyclase	Vasodilation, penile erection, urethral relaxation.
Vasoactive intestinal peptide	VIPAC1, VIPAC2	Glandular secretion and dilation of blood vessels supplying glands.
ATP	P_{2X}, P_{2Y}	Fast and slow excitation of smooth muscle in bladder, vas deferens, and arteries.

ATP, adenosine triphosphate; EPSP, excitatory postsynaptic potential; NO, nitric oxide.

at the postganglionic synapse. For example, ACh and vasoactive intestinal peptide (VIP) are frequently co-released from neurons that control glandular secretion (Figure 41–7C). In salivary glands, the two transmitters act directly to evoke secretion. In addition, VIP causes dilation of the blood vessels supplying the gland. Because cotransmitters can be released in varying proportions that depend on the frequency of presynaptic firing, different patterns of activity can regulate the volume of secretions, their protein and water content, and their viscosity. This regulation operates both through a direct effect on the gland cells and through indirect effects on the glandular blood flow that provides the water contained in secretions.

Understanding the pharmacology of these receptors and the second-messenger signaling pathways they control is important in the treatment of numerous medical conditions, including hypertension, heart failure, asthma, emphysema, allergies, sexual dysfunction, and incontinence.

Autonomic Responses Involve Cooperation Between the Autonomic Divisions

To survive, animals and humans must have "fight-or-flight" responses in order to stand and fight a predator or run away and live to see another day. Walter Cannon, in addition to introducing the concept of

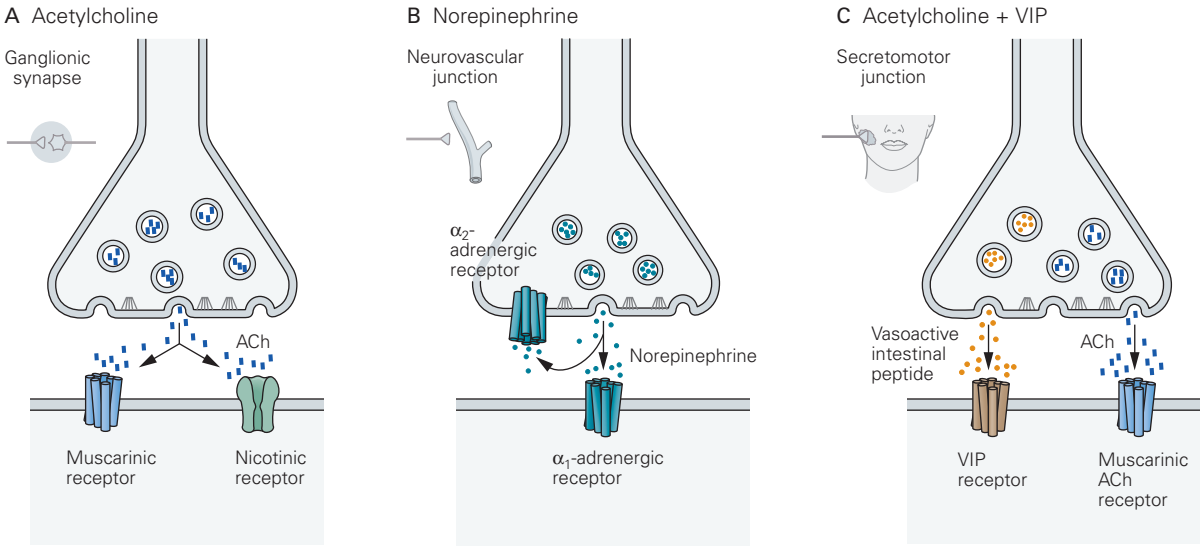

Figure 41–7 Synaptic transmission in the peripheral autonomic system.

A. In sympathetic ganglia, acetylcholine (**ACh**) can activate both nicotinic and muscarinic receptors to produce fast and slow postsynaptic potentials, respectively.

B. At neurovascular junctions, norepinephrine can simultaneously activate postsynaptic α_1-adrenergic receptors to produce vasoconstriction and presynaptic α_2-adrenergic receptors to inhibit further transmitter release.

C. Cotransmission involves the co-activation of more than one type of receptor by more than one transmitter. Parasympathetic postganglionic nerve terminals in the salivary glands release both ACh and vasoactive intestinal peptide (**VIP**) to control secretion. At some autonomic synapses with end organs, three or more receptor types are activated.

homeostasis, also appreciated that this fight-or-flight response is a critical sympathetic function.

Two important ideas underlie this insight. First, the sympathetic and parasympathetic systems play complementary, even antagonistic, roles; the sympathetic system promotes arousal, defense, and escape, whereas the parasympathetic system promotes eating and procreation. Second, actions of the sympathetic system are relatively diffuse; they influence all parts of the body and once turned on can persist for some time. These ideas are behind the popular notion of the "adrenaline rush" produced by excitement, as by a roller coaster ride.

We now know that extreme sympathetic responses such as "fight-or-flight" can have long-term pathological consequences resulting in the syndrome known as post-traumatic stress disorder (Chapter 61). This disorder was first recognized in soldiers during World War I, when it was referred to as "shell shock." A variety of life-threatening experiences, ranging from sexual abuse and domestic violence to aircraft disasters, can also induce post-traumatic stress disorder, which affects millions of people in the United States alone.

Because the fight-or-flight model assumes antagonistic roles for the sympathetic and parasympathetic systems, Cannon's model led to an overemphasis on the extremes of autonomic behavior. Actually, during everyday life, the different divisions of the autonomic system are tightly integrated. In addition, we now know that the sympathetic system is less diffusely organized than first envisioned by Cannon. Even within the sympathetic division, subsets of neurons control specific targets, and these pathways can be activated independently.

As in the somatic motor system, reflexes in the autonomic motor system are elicited through sensory pathways and are hierarchically organized. An important feature of this organization is that it allows for coordination between the different divisions of the autonomic system. The interplay between different systems in simple autonomic behaviors is analogous to the role of antagonist muscles in locomotion. To walk, one must alternately contract antagonist muscles that flex and extend a joint. Similarly, the sympathetic and parasympathetic systems are often partners in the regulation of end organs. In most cases, ranging from the simplest reflexes to more complex behaviors, all three peripheral divisions of the autonomic system work together. We illustrate this organization with two examples: control of the bladder (micturition reflex) and regulation of blood pressure.

Bladder Control

The micturition reflex is an example of a physiological cycle resulting from coordination between sympathetic and parasympathetic systems. In this cycle, the bladder is emptied by the parasympathetic pathway, which contracts the bladder and relaxes the urethra. The sympathetic system allows the bladder to fill by stimulating the urethra and inhibiting the parasympathetic pathway, thus inhibiting the reflex for bladder emptying. The sensory feedback required for this behavior is integrated with the motor outflow at both spinal and supraspinal levels (Figure 41–8).

Spinal components of the reflex are most influential during the storage phase of the micturition cycle, when sympathetic and somatic motor effects predominate. When the bladder is full, its distension triggers a sensory signal sufficient to activate the pontine micturition center (PMC). Descending signals from the PMC then increase parasympathetic outflow. Somatic control of the external urinary sphincter, which consists of striated muscle, contributes to both phases of the micturition cycle and is a voluntary behavior that originates through forebrain mechanisms (Figure 41–8). Patients with spinal cord injuries at the cervical or thoracic levels retain the reflex but not voluntary control of urination, because the connections between the bladder and the pons are severed.

Blood Pressure Regulation

The baroreceptor reflex is one of the simplest mechanisms for regulating blood pressure and further illustrates coordinated homeostatic control by antagonist sympathetic and parasympathetic pathways. It prevents orthostatic hypotension and fainting by compensating for rapid hydrostatic effects produced by changes in posture. When a recumbent person stands up, the sudden elevation of the head above the heart causes a transient decrease of cerebral blood pressure that is rapidly sensed by baroreceptors in the carotid sinus in the neck (Figure 41–9). Other important pressure sensors are located in the aortic arch and in the pulmonary circulation.

When neurons in the ventrolateral medulla detect the decrease in afferent baroreceptor activity produced by low blood pressure, they produce a reflexive suppression of parasympathetic activity to the heart and stimulation of sympathetic activity to the heart and vascular system. These changes in autonomic tone restore blood pressure by increasing heart rate, the strength of cardiac contractions, and the overall vascular resistance to blood flow through arterial vasoconstriction.

Under the converse condition of elevated arterial pressure, the increase in baroreceptor activity enhances parasympathetic inhibition of the heart and decreases sympathetic stimulation of cardiac function and vascular resistance. In general, the parasympathetic component of the baroreceptor reflex has a more rapid onset and is briefer than the sympathetic component. Consequently, parasympathetic activity is critical for the rapid response of baroreceptor reflexes but less important than sympathetic activity for long-term blood pressure regulation.

Visceral Sensory Information Is Relayed to the Brain Stem and Higher Brain Structures

Visceral sensory information reaches the brain mainly through two cranial nerves (IX and X), which end in caudal segments of the nucleus of the solitary tract (NTS), and through the abdominal splanchnic nerves, which end in the spinal cord (Chapter 40). The splanchnic information is transmitted to the brain through the spinothalamic tract (Chapter 4), which branches out along the way and also sends afferents to the NTS and lateral parabrachial nucleus.

The NTS relays sensory information in two different directions. First, it projects to networks in the brain stem and spinal cord that control and coordinate autonomic reflexes (as we saw for the baroreceptor reflex). In this way, visceral sensory signals relayed through the NTS regulate vagal motor control of the heart and gastrointestinal tract directly. Some neurons in the NTS project to neurons in the ventrolateral medullary reticular formation that control blood pressure by differentially regulating blood flow in particular vascular beds (Figure 41–9). Second, the NTS sends ascending projections to the forebrain, relaying visceral information to higher structures (Figure 41–10A). These higher structures, including the hypothalamus, use this information to coordinate autonomic, neuroendocrine, and behavioral responses.

Visceral sensory information is relayed from the NTS to the forebrain via direct and indirect projections (Figure 41–10A). The major indirect pathway involves the lateral parabrachial nucleus, which receives afferents from the NTS and sends efferents to higher structures, including the amygdala, hypothalamus, bed nucleus of the stria terminalis, insular cortex, and infralimbic/prelimbic cortex. The direct projections from the NTS target many of these same forebrain sites. The rostral NTS is an important part of the afferent taste pathway (Chapter 29). Information

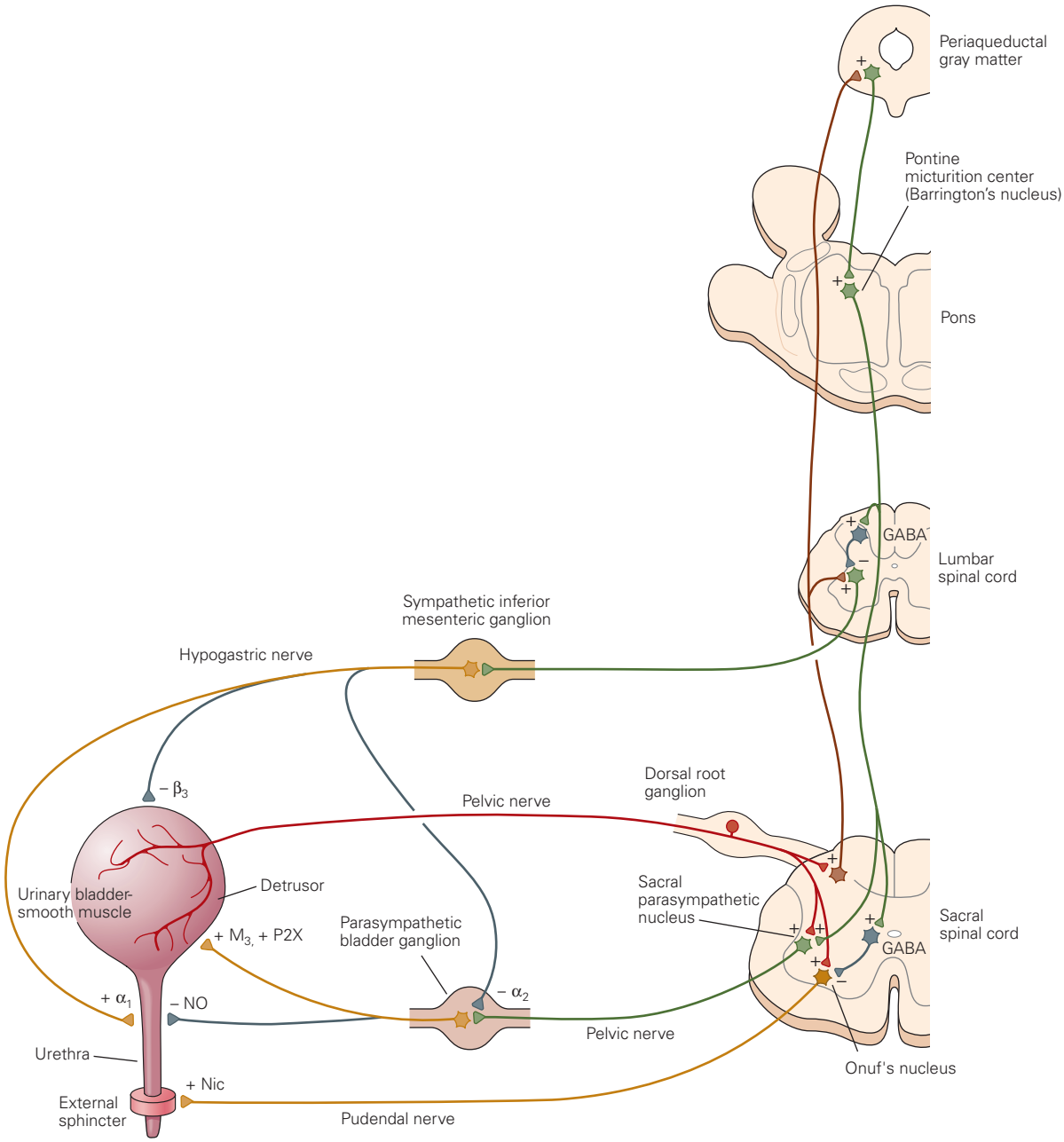

Figure 41–8 **The micturition reflex requires interplay between the parasympathetic and sympathetic divisions of the autonomic system.** (Adapted from DeGroat, Booth, and Yoshimura 1993.)

When bladder volume is low, urinary outflow is inhibited because activity in the sympathetic pathway is greater than activity in the parasympathetic pathway. Mild distension of the detrusor (storage portion of the bladder) initiates a low level of sensory activity, which reflexively activates spinal preganglionic neurons. The resulting low level of preganglionic activity is effectively transmitted and amplified by the sympathetic inferior mesenteric ganglion but filtered out by the parasympathetic bladder ganglion because of differences in patterns of synaptic convergence in the two ganglia. The resulting predominance of sympathetic tone keeps the detrusor relaxed and the urethra constricted. Sympathetic postganglionic fibers also reduce parasympathetic activity by inhibiting preganglionic release of acetylcholine. In addition to their effects on the autonomic outflow, the sensory signals are sufficient to keep the external urinary sphincter closed.

When filling causes the bladder to reach a critical volume, the associated increase in sensory activity reaches a threshold that allows impulses to pass through the pontine micturition center (Barrington's nucleus). Descending activity from this nucleus then further excites the parasympathetic outflow. The resulting increase in parasympathetic preganglionic firing promotes summation of fast excitatory postsynaptic potentials and initiation of postsynaptic action potentials in the bladder ganglion as it switches to its "on" state. During the emptying process, descending pathways also inhibit the sympathetic and somatic outflows through inhibitory spinal interneurons. Inhibition of somatic motor neurons in Onuf's nucleus causes relaxation and opening of the external sphincter. In this figure, the sacral spinal cord is enlarged relative to the other slices.

(Abbreviations: α_1, alpha-1 adrenergic receptor, α_2, alpha-2 adrenergic receptor, β_3, beta-3 adrenergic receptor, **GABA**, γ-aminobutyric acid; M_3, muscarinic ACh receptor 3; **nic**, nicotinic receptor; **NO**, nitric oxide; **P2X**, purinergic receptor.)

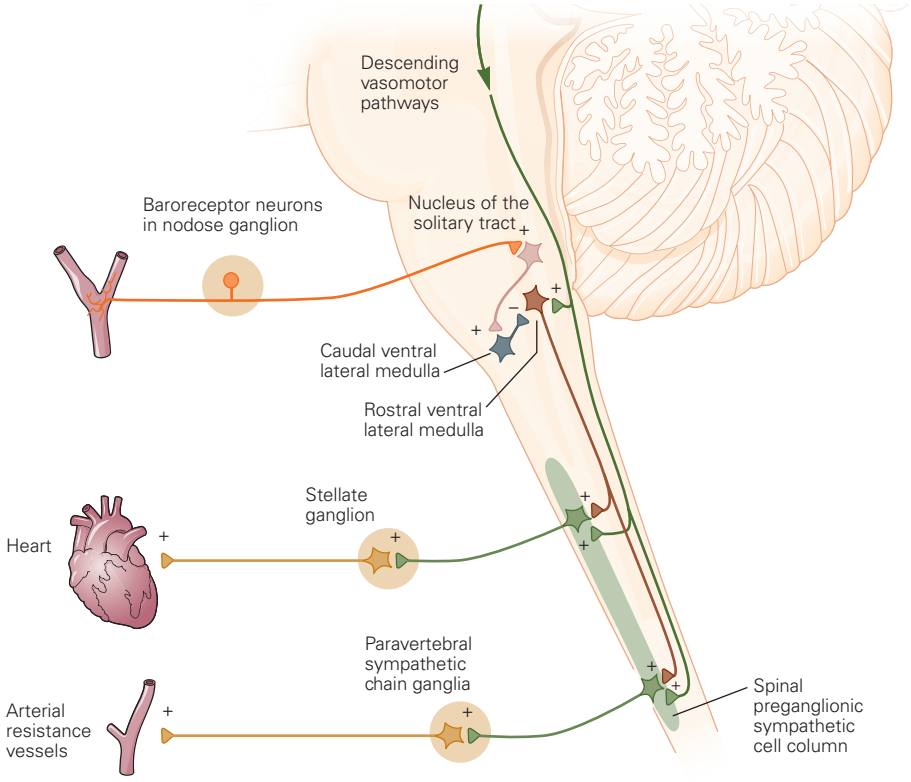

Figure 41–9 The baroreceptor reflex behaves as a negative feedback loop with gain. Arterial blood pressure is sensed by baroreceptors, a type of stretch receptor neuron, in the carotid sinus near the base of the brain. After integration in the medulla, this information provides negative feedback control of the cardiovascular system. The sympathetic component of the circuit includes outputs that stimulate the heart's pumping capacity (cardiac output) by increasing heart rate and the strength of contractions. In addition, sympathetic stimulation causes arteries to contract, which raises the hydraulic resistance to blood flow. Together, the effects of increased cardiac output and increased vascular resistance raise mean arterial blood pressure. Inhibitory projections from the caudal to the rostral ventral lateral medulla create negative feedback so that an increase in blood pressure inhibits sympathetic activity, whereas a decrease raises sympathetic activity. Although omitted for simplicity, parasympathetic neurons in the cardiac ganglion also contribute to the reflex by creating an inhibitory cardiac input that is functionally antagonistic to the sympathetic pathway (Figure 41–10). During baroreceptor reflexes, parasympathetic activity within the heart is therefore increased by hypertension and reduced by hypotension.

in this pathway is relayed via the medial parabrachial nucleus to the taste area of insular cortex.

Central Control of Autonomic Function Can Involve the Periaqueductal Gray, Medial Prefrontal Cortex, and Amygdala

The periaqueductal gray, which surrounds the cerebral aqueduct in the midbrain, receives inputs from most parts of the central autonomic network and projects to the medullary reticular formation to initiate integrated behavioral and autonomic responses. For example, in the defensive "fight-or-flight" response, the periaqueductal gray helps redirect blood flow from the digestive system to the hind limbs, thus enhancing running (Figure 41–10B).

The medial prefrontal cerebral cortex is a visceral sensory-motor region. It includes two functional areas that interact with each other: the rostral insular cortex and the rostromedial tip of the cingulate gyrus (also referred to as the infralimbic and prelimbic areas). Stimulation here can produce a variety of autonomic effects including contractions of the stomach and changes in blood pressure. These visceral sensory and motor areas of cortex send descending projections to the parts of the central autonomic network in the brain stem discussed above.

Finally, visceral regions of cortex, along with many subcortical parts of the central autonomic

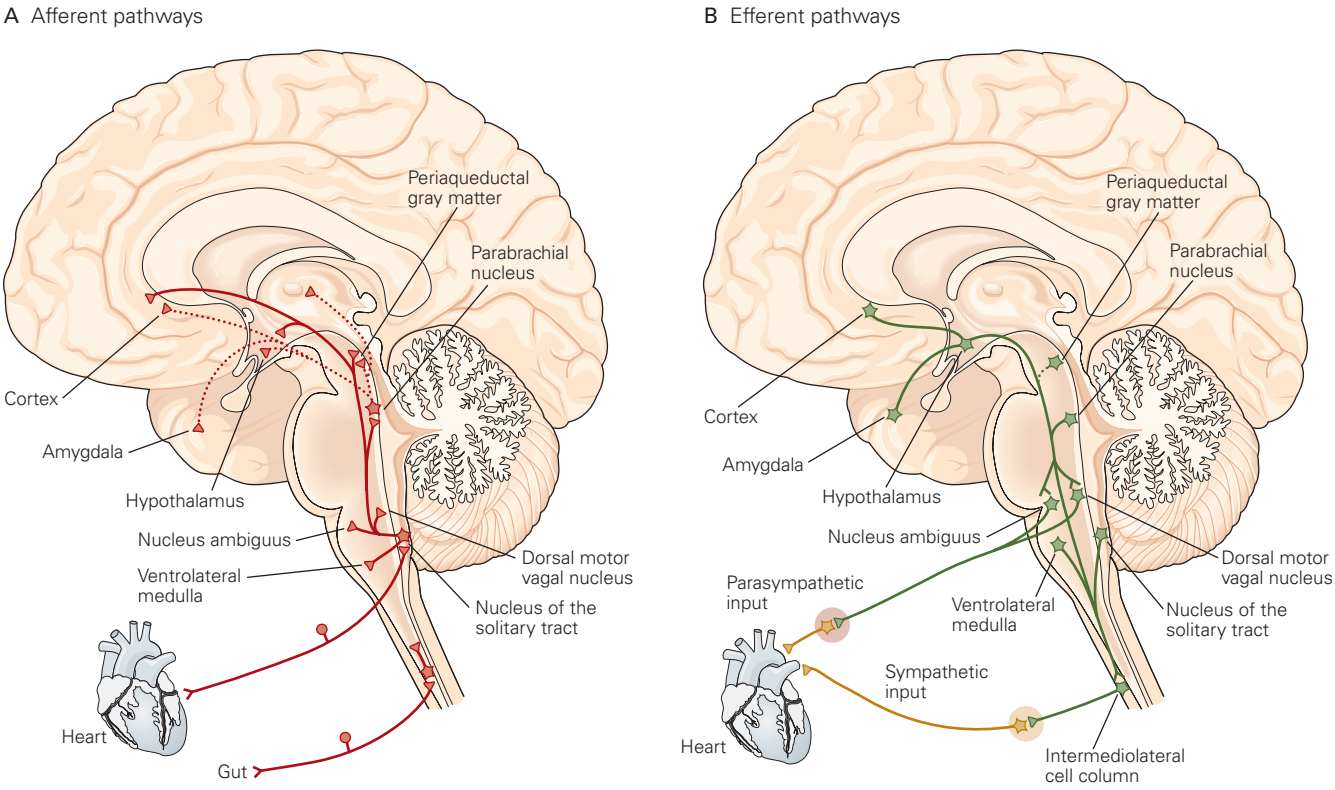

Figure 41–10 **The central autonomic network.** Nearly all of the cell groups illustrated here are interconnected with one another, forming the central autonomic network.

A. Visceral information (**solid lines**) is distributed to the brain from the nucleus of the solitary tract and from ascending spinal pathways activated by the splanchnic nerves (from the gut, for example). The nucleus of the solitary tract distributes this information to preganglionic parasympathetic neurons (the dorsal motor vagal nucleus and nucleus ambiguus), to regions of the ventrolateral medulla that coordinate autonomic and respiratory reflexes, and to more rostral parts of the central autonomic network in the pons (parabrachial nucleus), midbrain (periaqueductal gray), and forebrain. The parabrachial nucleus also projects to many of the more rostral components of the central autonomic network, including visceral and gustatory nuclei of the thalamus (**dotted lines**). Other pathways from the spinal cord (not shown) also transmit visceral information to many parts of the central autonomic network, including the nucleus of the solitary tract, parabrachial nucleus, periaqueductal gray, hypothalamus, amygdala, and cortex. The spinal cord also projects to the main somatosensory nucleus of the thalamus (ventral posterolateral nucleus).

B. All of the efferent pathways shown here (except perhaps for the periaqueductal gray) project directly to autonomic preganglionic neurons. In the hypothalamus, the descending division of the paraventricular nucleus and three cell clusters in the lateral zone project heavily to both parasympathetic and sympathetic preganglionic neurons. Other pathways (not shown) arise from certain monoaminergic cell groups in the brain stem, including noradrenergic neurons in the A5 region and serotonergic neurons in the raphe nuclei.

network, interact with the amygdala. Complex pathways between certain amygdalar cell groups underlie certain conditioned emotional responses—learned associations between specific stimuli and behaviors with accompanying autonomic responses. When a rat learns that a mild electric shock follows an auditory cue, the auditory cue alone comes to produce the elevated heart rate and freezing that was originally elicited by the shock alone (Chapters 42 and 53). Such learned responses are prevented by selective lesions of the amygdalar region, which projects to the hypothalamus and lower brain stem parts of the central autonomic network.

The Neuroendocrine System Links the Brain to Physiological Responses Through Hormones

Another effector arm of the hypothalamus is the neuroendocrine system, which controls secretion of hormones by the pituitary gland. The pituitary has two functionally and anatomically distinct subdivisions,

the anterior and posterior pituitary. The posterior pituitary is an extension of the brain and contains hormone-secreting axon terminals of hypothalamic neurons. These terminals secrete vasopressin or oxytocin directly into the systemic circulation. The anterior pituitary, on the other hand, is entirely nonneuronal and is composed of five types of endocrine cells. Hormone secretion from these cells is controlled by stimulatory and inhibitory factors released by hypothalamic neurons into a specialized circulatory system that carries blood from the base of the brain (median eminence) to the anterior pituitary.

Hypothalamic Axon Terminals in the Posterior Pituitary Release Oxytocin and Vasopressin Directly Into the Blood

Large neurons in the paraventricular and supraoptic nuclei form the magnocellular component of the neuroendocrine motor system of the hypothalamus (Figure 41–11). The magnocellular neurons send their axons through the hypothalamo-hypophysial tract to the posterior pituitary, or *neurohypophysis* (Figure 41–12). Approximately one-half of these neurons synthesize and secrete vasopressin (the antidiuretic hormone) into the general circulation; the other half synthesize and secrete oxytocin, a structurally similar hormone. Both hormones circulate to organs, where vasopressin controls blood pressure and water reabsorption by the kidney and oxytocin controls uterine smooth muscle and milk release.

Vasopressin and oxytocin are nine-amino acid peptide hormones. Like other peptide hormones, they are synthesized in the cell body as larger prohormones (Chapter 16) and then cleaved within Golgi transport vesicles before traveling down the axon to release sites in the posterior pituitary. The genes for these peptides have similar sequences and probably arose by duplication.

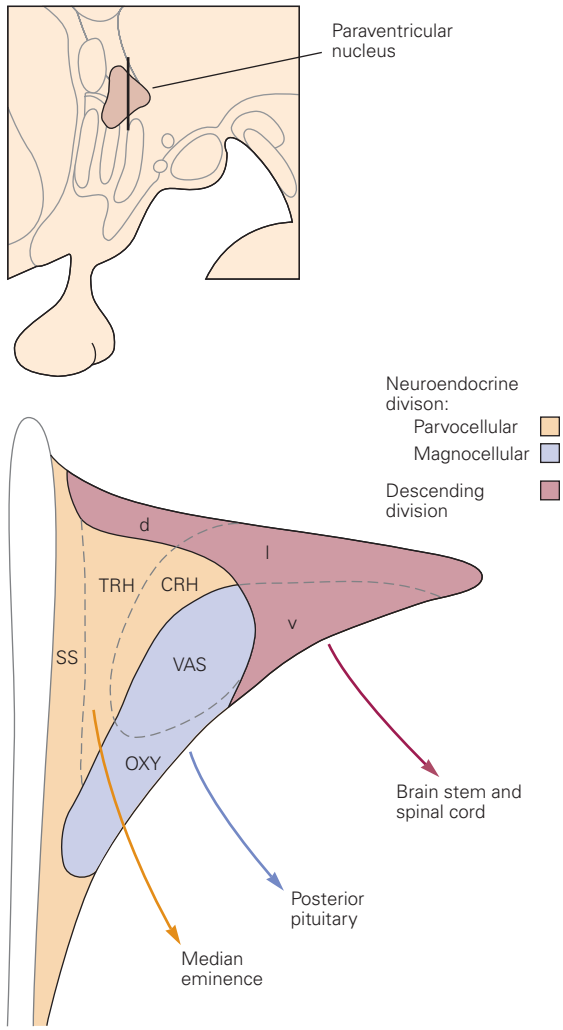

Figure 41–11 **The paraventricular nucleus in the hypothalamus is a microcosm of neuroendocrine, autonomic, and sensory-motor integration.** The three structural-functional divisions of the paraventricular nucleus are shown. The *magnocellular neuroendocrine division* comprises two distinct although partly interdigitated pools of neurons that normally release vasopressin (**VAS**) or oxytocin (**OXY**). Their axons course through the internal zone of the median eminence and terminate in the posterior pituitary. Two other populations of magnocellular vasopressin and oxytocin neurons lie in the supraoptic nucleus along the base of the brain.

The *parvocellular neuroendocrine division* includes three major, separate (although partly interdigitated) pools of neurons that control anterior pituitary hormone secretion. Their axons end in the external zone of the median eminence, where they release their peptide neurotransmitters—somatostatin (**SS**), growth hormone-inhibiting hormone (GIH), thyrotropin-releasing hormone (**TRH**), or corticotropin-releasing hormone (**CRH**)—into the hypophysial portal veins.

The *descending division* has three parts—dorsal (**d**), lateral (**l**), and ventral (**v**)—each comprising topographically organized conventional neurons that project to the brain stem and spinal cord. Their axons terminate in many parts of the central autonomic network in the brain stem (Figure 41–10), the marginal zone (lamina I) of the dorsal horn of the spinal cord and spinal trigeminal nucleus, and a number of regions in the brain stem reticular formation and periaqueductal gray matter. The descending division modulates autonomic outflow (and inflow), the inflow of nociceptive information, and eating and drinking behaviors. Appropriate integration of magnocellular neuroendocrine, parvocellular neuroendocrine, autonomic, and behavioral responses is mediated primarily by external inputs rather than by interneurons or extensive recurrent axon collaterals of projection neurons. Circulating steroid and thyroid hormones also produce selective effects on particular types of neurons in the paraventricular nucleus.

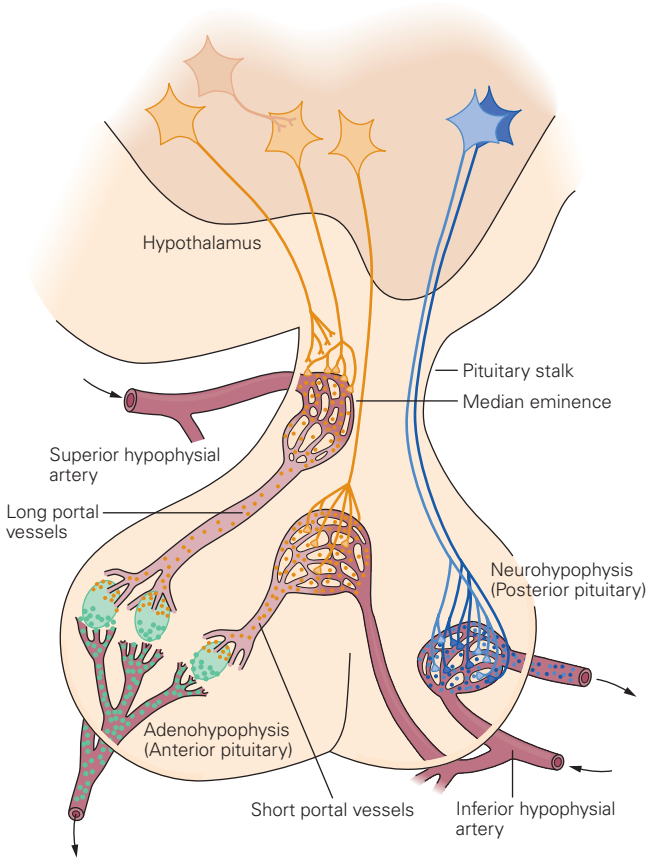

Figure 41–12 The hypothalamus controls the pituitary gland both directly and indirectly through neuroendocrine neurons. Neurons in the magnocellular neuroendocrine system (**blue**) send their axons directly to the posterior pituitary (neurohypophysis) where they release the peptides vasopressin and oxytocin into the general circulation. Neurons in the parvocellular neuroendocrine system (**yellow**) send their axons to the hypophysial portal system in the median eminence and pituitary stalk. Portal veins transport hypothalamic hormones (peptides and dopamine) to the anterior pituitary (adenohypophysis) where they increase the release of hormones from five classic types of endocrine cells (Figure 41–11). The output of neuroendocrine neurons is regulated in large part by inputs from other regions of the brain. (Adapted from Reichlin 1978, and Gay 1972.)

Endocrine Cells in the Anterior Pituitary Secrete Hormones in Response to Specific Factors Released by Hypothalamic Neurons

In the 1950s, Geoffrey Harris proposed that the anterior pituitary, or *adenohypophysis*, is regulated indirectly by the hypothalamus. He showed that the hypophysial portal veins, which carry blood from the hypothalamic median eminence to the anterior pituitary, transport factors released from hypothalamic neurons that control anterior pituitary hormone secretion (Figure 41–12). In the 1970s, Andrew Schally, Roger Guillemin, and Wylie Vale determined the structure of a group of hypothalamic peptide hormones that control pituitary hormone secretion from the five classic endocrine cell types in the anterior pituitary. These hormones, which are released into the median eminence by hypothalamic neurons, fall into two classes: releasing hormones and release-inhibiting hormones. Only one anterior pituitary hormone, prolactin, is under predominantly inhibitory control (mediated by dopamine).

The *parvocellular neuroendocrine motor zone* of the hypothalamus is centered along the wall of the third ventricle (Figure 41–2A) and contains neurons that project to and release their hormones into the median eminence. The parvocellular neurons releasing *gonadotropin-releasing hormone* (GnRH) are atypical in that they are scattered in a continuum extending from the medial septum through to the mediobasal hypothalamus. They are controlled by upstream neurons that release *kisspeptin*. The remaining parvocellular neuroendocrine neurons lie within the paraventricular and arcuate nuclei and the short periventricular region between them (Figures 41–2 and 41–11).

Distinct pools of neurons in and around the paraventricular nucleus release *corticotropin-releasing hormone* (CRH), *thyrotropin-releasing hormone* (TRH), or *somatostatin* (or growth hormone release-inhibiting hormone) (Figure 41–11). The CRH neurons control the release of anterior pituitary adrenocorticotropic hormone (ACTH), which in turn controls the release of cortisol (glucocorticoids) from the adrenal cortex. Thus, this pool of CRH neurons is the "final common pathway" for all centrally mediated glucocorticoid stress hormonal responses. The arcuate nucleus contains two pools of parvocellular neuroendocrine neurons. One group releases *growth hormone–releasing hormone* (GHRH) and the other dopamine, which inhibits prolactin secretion. Some of the dopaminergic neurons are distributed dorsally as far as the paraventricular nucleus.

The axons of all these parvocellular neuroendocrine neurons travel in the hypothalamo-hypophysial tract and end in the specialized proximal end of the pituitary stalk, the median eminence (Figure 41–12). There, in a region of capillary loops in the external zone of the median eminence, the axon terminals release the various hypophysiotropic factors. While the median eminence is within the brain, it is considered outside the blood–brain barrier. This is due to the fenestrated nature of the median eminence

Table 41–3 Hypothalamic Substances That Release or Inhibit the Release of Anterior Pituitary Hormones

Hypothalamic substance	Anterior pituitary hormone
Releasing:	
Thyrotropin-releasing hormone (TRH)	Thyrotropin (TSH), prolactin (PRL)
Corticotropin-releasing hormone (CRH)	Adrenocorticotropin (ACTH), β-lipotropin
Gonadotropin-releasing hormone (GnRH)	Luteinizing hormone (LH), follicle-stimulating hormone (FSH)
Growth hormone–releasing hormone (GHRH or GRH)	Growth hormone (GH)
Inhibiting:	
Prolactin release-inhibiting hormone (PIH), dopamine	Prolactin
Growth hormone release-inhibiting hormone (GIH or GHRIH; somatostatin)	Growth hormone, thyrotropin

capillaries, which allow diffusion of the hypophysiotropic factors into the portal circulation. The median eminence capillary loops are the proximal end of the hypophysial portal system of veins that carry the factors to the anterior pituitary, where they act on cognate receptors on the five types of endocrine cells (Figure 41–12 and Table 41–3).

Dedicated Hypothalamic Systems Control Specific Homeostatic Parameters

Body Temperature Is Controlled by Neurons in the Median Preoptic Nucleus

Body Temperature Reflects the Balance Between Heat Production and Loss

The body generates heat through all of its exothermic biochemical reactions and ion fluxes. These processes can be greatly increased above a baseline level, the resting metabolic rate, by exercise and shivering (both of which increase skeletal muscle heat production), by the digestion and assimilation of food (the so-called thermic effect of food), and by sympathetic stimulation of thermogenic activity in brown adipose tissue (Box 41–1).

The body loses heat by radiation, convection, conduction (if immersed in cool water), and endothermic evaporation of either sweat from the skin or moisture from the respiratory tract (a process augmented in some species by panting). The defensive reaction to cold, in addition to producing heat, involves sympathetically mediated cutaneous vasoconstriction and piloerection (goose bumps). By sending less blood to the skin, vasoconstriction conserves core temperature. Piloerection helps insulate the skin by creating a layer of motionless air near the skin's surface. Conversely, defenses against overheating include inhibition of sympathetic pathways that activate cutaneous vasodilation and brown adipose tissue. Voluntary behavioral responses like taking a swim or putting on a sweater play a particularly important role in thermoregulation.

Box 41–1 Brown Adipose Tissue, Bioenergetics, and Sympathetically Driven Thermogenesis

Brown adipose tissue is a remarkably specialized heat-producing tissue that is especially abundant in newborns and small mammals, but is also found in adult humans. It has a rich blood supply for delivery of fuel and oxygen and for removal of heat and is densely innervated by postganglionic sympathetic nerves. Brown adipocytes, the producers of heat, are found in concentrated deposits in and around the core and also as isolated cells within larger white adipose tissue depots.

Sympathetic stimulation of β-adrenergic receptors activates uncoupling protein-1 (UCP1), a mitochondrial proton transport protein that is unique to brown adipocytes. When activated, UCP1 "leaks" protons across the mitochondrial inner membrane into the mitochondrial matrix, down the proton electrochemical gradient. This uncouples mitochondrial respiration from adenosine triphosphate (ADP) availability, greatly increasing fuel oxidation and, importantly, the production of heat.

Exercise and shivering, on the other hand, increase heat production by using adenosine triphosphate (ATP) to perform work. The resulting increase in ADP activates proton transport into mitochondria via ATP synthase, which then increases coupled mitochondrial respiration, fuel oxidation, and ultimately the production of heat.

They usually begin before the onset of physiologic responses. Like thirst/drinking and hunger/eating, activities generated in response to cold or hot challenges are motivated behaviors.

Body Temperature Is Detected at Multiple Sites

Core temperature is held relatively constant. At the shell, on the other hand, temperature fluctuates extensively because the shell is adjacent to the external environment, it has a high surface-to-mass ratio (in the case of limbs favoring heat loss over heat production), and thermal challenges dramatically affect its supply of warm blood (decreased when heat needs to be conserved; increased when heat needs to be lost).

Most primary afferents that detect temperature have their cell bodies in the spinal dorsal root ganglia. Neurons that detect noxious temperatures are part of the pain pathway (Chapter 20). Their function is to limit local tissue damage by promoting withdrawal as opposed to regulating body temperature. Neurons that respond to innocuous temperatures are often called thermoreceptors. Some thermoreceptor neurons have their endings in the skin, just below the epidermis, and these respond to shell temperature. They are predominantly, but not entirely, cold-responsive. Other thermoreceptor neurons have their endings in and around the large organs and respond to core temperature. They are also largely, but not entirely, cold-responsive. The fibers for the deep-tissue thermoreceptor neurons travel in the splanchnic nerves and, like the thermoreceptor neurons in the shell, have their cell bodies in the dorsal root ganglia. In addition, some also travel in the vagal afferent nerve. Finally, there are warm-sensing neurons in the hypothalamic medial preoptic area.

The molecular sensors utilized by thermoreceptor neurons for detecting changes in temperature are a subset of excitatory transient receptor potential (TRP) channels. Different TRP channels respond to different ranges of temperatures (Chapter 20). Recent studies have implicated specific TRP channel types in various forms of sensing innocuous temperature in the three sites mentioned above: TRMP8 channels mediate cold-sensing by shell thermoreceptor neurons, and TRPM2 channels mediate warm-sensing both by somatosensory thermoreceptor neurons and by neurons in the hypothalamic preoptic area.

Multiple Thermoreceptor/Thermoeffector Loops Control Temperature

Involuntary thermal regulation is controlled by a multisensor, multieffector thermoregulatory system. Thermal information from the shell and the viscera ascends via primary afferents whose cell bodies are in the dorsal root ganglia. They project to second-order neurons in the dorsal horn of the spinal cord. These neurons project via the spinothalamic tract to the lateral parabrachial nucleus where neurons relay cold-sensing and warm-sensing information to neurons in the hypothalamic MnPO. Activation of the cold-sensing or warm-sensing afferent pathways induces appropriate physiological responses aimed at increasing or decreasing body temperature.

The neurons in the MnPO that indirectly respond to cold and warmth send efferent signals via relays through the medial preoptic area, dorsomedial hypothalamus, and raphe pallidus in the ventral medulla, and from there on to the sympathetic preganglionic neurons in the intermediolateral nucleus of the spinal cord. These latter neurons excite postganglionic sympathetic neurons that project to blood vessels, sweat glands, and arrector muscles of hair follicles to control cutaneous blood flow, sweating, and piloerection, respectively, as well as to brown adipose tissue to control thermogenesis. In addition, cold causes shivering when gamma motor neurons in the ventral horn of the spinal cord are activated by excitatory neurons in the raphe pallidus (Chapter 32). The resultant contraction of intrafusal muscle fibers within muscle spindles activates IA afferents from the spindles to alpha motor neurons. This proprioceptive feedback increases activity of alpha motor neurons, as well as their propensity to undergo rhythmic bursts of activity, causing increased muscle tone and frank shivering.

The neural pathways controlling voluntary thermoregulatory behaviors involve the same thermoreceptor pathways. Stimulation of warm-sensitive neurons in and around the MnPO evokes dramatic cold-seeking behavior, decreases heat production, and increases heat loss. The conscious perception of body temperature relies upon the same first-order thermoreceptor neurons, but the afferent pathway diverges to activate second-order neurons in the dorsal horn, which project directly or indirectly to neurons in the ventromedial nucleus of the thalamus. These thalamic neurons project to the insular cortex.

From the above discussion, it is clear that there is neither a set point for body temperature nor a "thermostat" that maintains it at 37°C. Instead, as mentioned earlier, an apparent set point for body temperature emerges as a settling point controlled by multiple sensorymotor feedback loops containing thermoreceptors and thermoeffectors. It is a major achievement of evolution that this multicomponent afferent/efferent system is

so effective in keeping the temperature of the body core remarkably constant.

Dysregulation of Circuits Controlling Temperature Causes Fever

In the past, when the set point view of thermoregulation was dominant, fever was thought to be caused by raising the body temperature set point—a view that still persists in major medical textbooks. Based on the advances described above, fever is now thought to arise through modulation of the afferent/efferent loops, particularly as they traverse the hypothalamic preoptic area. Prostaglandin E2, generated by the action of inflammatory cytokines on endothelial cells in the preoptic area, inhibits warm-activated GABAergic neurons in the MnPO, thus disinhibiting the effector pathways that promote cutaneous vasoconstriction, brown adipose tissue thermogenesis, and shivering. Nonsteroidal anti-inflammatory drugs, such as aspirin, ibuprofen, and acetaminophen, reduce fever by inhibiting hypothalamic generation of prostaglandin E2.

Water Balance and the Related Thirst Drive Are Controlled by Neurons in the Vascular Organ of the Lamina Terminalis, Median Preoptic Nucleus, and Subfornical Organ

Changes in Blood Osmolarity Cause Cells to Shrink or Swell

Driven by osmosis, water moves freely across cell membranes. This has a number of important consequences. First, because of its large size, the intracellular compartment contains two-thirds of the body's water. Second, if blood osmolarity changes from its normal value (~290 mOsm/kg)—because water is gained by drinking or lost by renal excretion and by sweating, or because solutes have been added by eating (or by drinking, eg, sea water—1000 mOsm/kg)—water will move and the osmolarity of all compartments will equilibrate, including the intracellular one.

Because the intracellular content of osmotically active molecules is relatively fixed over the short term, increases in blood osmolarity cause cells to shrink, and conversely, decreases cause cells to swell. This is particularly dangerous for the brain because it is encased by the rigid skull. With extreme hyperosmolarity (too little water), the brain shrinks, pulling away from the skull and tearing blood vessels. With hypo-osmolarity (too much water), the brain swells, causing cerebral edema, seizures, and coma. To prevent such incidents, the brain acts to maintain normal osmolarity. It does this by detecting changes in osmolarity and then regulating the motivation to drink (thirst) and the kidney's capacity to excrete water.

Osmolarity Is Affected When Water Is Lost or Gained and When Food Is Ingested

Water is gained by drinking and, to a small degree, by the oxidation of fuel (fuel + $O_2 \rightarrow CO_2 + H_2O$). It is lost in a number of ways—by breathing (dry air in, humidified air out), via the gastrointestinal tract (especially when diarrhea is present), by sweating, and by urination. Eating also increases blood osmolarity by moving water from the blood to the gut to aid digestion and by adding solutes to the bloodstream as food is broken down and absorbed.

Because of these effects, there are significant interactions between neural systems that control hunger and thirst. For example, eating is such a significant osmotic challenge that dehydration and its associated hyperosmolarity strongly suppress hunger (dehydration-induced anorexia). Conversely, the act of eating itself, even in an individual with normal water content, rapidly stimulates thirst so as to mitigate the anticipated, eating-induced increase in osmolarity.

Vasopressin Released From the Posterior Pituitary Regulates Renal Water Excretion

The ability of the kidney to excrete water is tightly controlled by vasopressin. When it is absent, humans can excrete up to approximately 900 mL/h of urine, and when it is at maximal levels, humans excrete as little as approximately 15 mL/h. Vasopressin decreases water excretion by increasing its reabsorption from urine by the kidney.

Osmolarity Is Detected by Osmoreceptor Neurons

The brain maintains water balance by monitoring sensory input from osmoreceptors—sensory neurons that respond to osmolarity—which reflects the body's state of hydration. Osmoreceptor neurons are found in the periphery and on neurons in and around the hypothalamus. The central osmoreceptors monitor systemic osmolarity, while the peripheral osmoreceptors monitor osmolarity in and around the gut and related structures.

Peripheral Osmoreceptors Allow Changes in Systemic Osmolarity to Be Anticipated

Sensory information about peripheral osmolarity enables the brain to make preemptive changes in thirst

and vasopressin secretion that anticipate and mitigate future shifts in systemic osmolarity, such as the decrease that occurs with drinking or the increase that occurs with eating. Such regulation serves to prevent overshooting normal osmolarity, which would otherwise occur when previously ingested water, which has not yet affected systemic osmolarity, is slowly absorbed from the gut. Indeed, when a dehydrated, hyperosmolar individual ingests water, thirst and vasopressin secretion rapidly decrease, well before systemic osmolarity falls. The identity of peripheral osmoreceptors is unknown.

Central Osmoreceptors and the Afferent/Efferent Circuits Control Water Balance

Three nuclei in the lamina terminalis, which forms the anterior wall of the third ventricle, play a key role in detecting and in responding to disturbances in systemic osmolarity (Figure 41–13). From ventral to dorsal, they are the OVLT, the MnPO, and the SFO. The OVLT and SFO are circumventricular organs, and like the previously discussed median eminence, they lie outside the blood–brain barrier. Because of this, neurons in these two nuclei can rapidly detect changes in blood osmolarity as well as blood-borne circulating factors that are unable to cross the blood–brain barrier (an important example being angiotensin II).

Consistent with this arrangement, osmoreceptor neurons in the OVLT and SFO make extensive connections to neurons in the MnPO. While MnPO neurons themselves do not directly sense osmolarity, they are indirectly responsive to osmolarity via relays from the OVLT and SFO. While all neurons in the OVLT and SFO appear to be dedicated to the regulation of water balance, some neurons in the MnPO are involved in regulation of body temperature (as noted earlier), cardiovascular function, and sleep. Regulation of water balance or body temperature is carried out by subsets of modality-specific neurons in the MnPO.

Neurons from all three lamina terminalis nuclei send dense excitatory projections to secretory vasopressin neurons in the paraventricular hypothalamic nucleus (PVH) and supraoptic nucleus. As described below, these three lamina terminalis nuclei are also able to cause thirst.

Central osmoreceptors, and probably also peripheral osmoreceptors, detect changes in osmolarity by

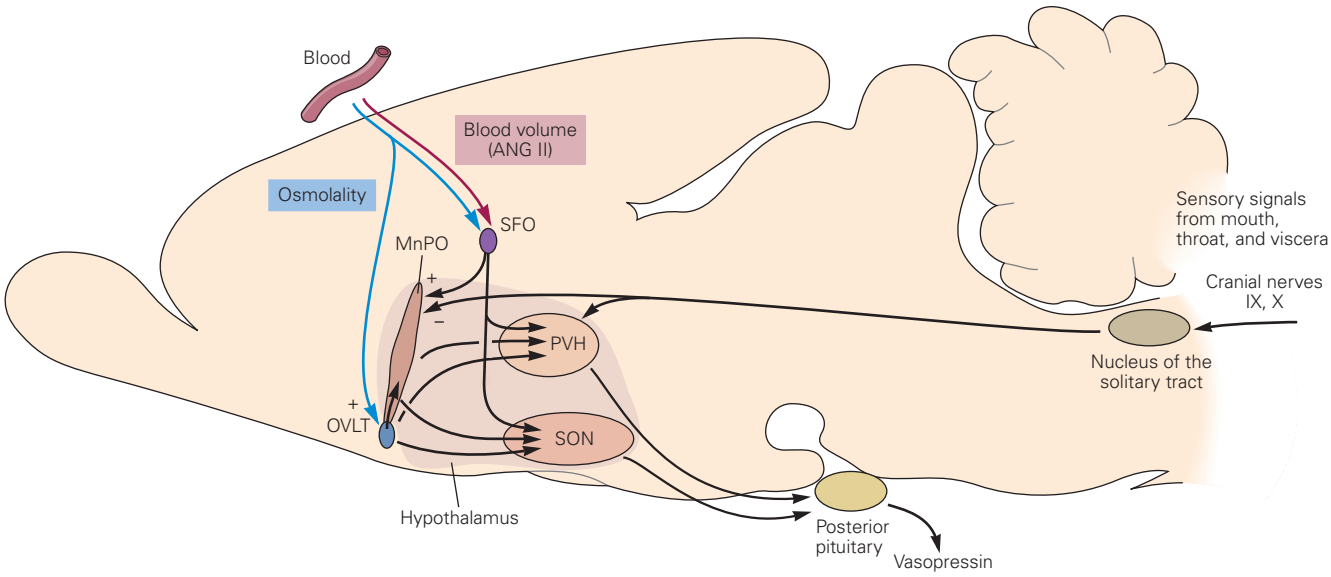

Figure 41–13 Neural and endocrine components combine to regulate fluid balance. The circuitry is shown in a sagittal section through the rat brain. Information from baroreceptors in the circulatory system and from sensory receptors in the mouth, throat, and viscera is conveyed to the nucleus of the solitary tract and neighboring structures in the caudal brain stem through the glossopharyngeal (**IX**) and vagal (**X**) nerves. The hormone angiotensin II (**ANG II**) provides the brain with an additional signal concerning low blood volume. Circulating angiotensin II is sensed by receptors in the subfornical organ (**SFO**); SFO neurons project to the median preoptic area (**MnPO**), paraventricular nucleus of the hypothalamus (**PVH**), supraoptic nucleus (**SON**), and the vascular organ of the lamina terminalis (**OVLT**). The osmolality of the blood is sensed by receptors in and near the OVLT that project to the MnPO, PVH, and SON. Neurosecretory cells in the PVH and SON nuclei trigger release of vasopressin from the posterior pituitary, thus decreasing water excretion by the kidney. (Adapted, with permission, from Swanson 2000.)

responding to changes in cell volume. Shrinking or swelling, which increases or decreases, respectively, their cation permeability, causes increases or decreases in firing rate.

Decreased intravascular volume—for example, that due to acute blood loss—also potently stimulates thirst and vasopressin secretion. Low blood volume is detected by the kidney, which increases its secretion of renin. Renin is a protease that converts circulating angiotensinogen to *angiotensin I* (ANG I). ANG I is then further cleaved by angiotensin-converting enzyme in the lung, generating *angiotensin II* (ANG II). ANG II excites SFO neurons that directly, and also via a relay in the MnPO, drive vasopressin neurons and presumptive thirst neurons.

Thirst Is Controlled by Neurons in the OVLT, MnPO, and SFO

As with vasopressin secretion, all three lamina terminalis structures participate in generating the motivational state of thirst, the desire to seek and ingest water. Lesion of all three structures completely blocks dehydration- and ANG II–induced thirst, as well as secretion of vasopressin. Electrical stimulation of these structures, on the other hand, elicits drinking. Activation of excitatory glutamatergic neurons in the SFO and MnPO induces intense drinking in an otherwise water-satiated mouse within seconds.

Thus, excitatory neurons in the SFO and MnPO, and likely also in the OVLT, have a remarkable capacity to induce thirst. Importantly, the behavior induced is specific—only water drinking occurs. Notably, the excitatory SFO neurons driving this behavior are the same subset of SFO neurons that are activated by dehydration and that express ANG II receptors. The downstream pathway by which these neurons stimulate thirst is presently unknown.

The activity of both the thirst neurons in the SFO and vasopressin neurons in the SON and PVH decreases or increases rapidly in response to sensory cues, such as drinking or eating, respectively, that anticipate future homeostatic disturbances. This rapid regulation occurs independent of any changes in systemic osmolarity and is therefore independent of feedback; hence, it is an example of feedforward control. The likely function of this feedforward regulation is to anticipate disturbances, institute preemptive corrective actions, and thus greatly reduce or eliminate their impact.

In summary, years of research have led to a clear model. Dehydration (water deficiency) increases the activity of neurons in the SFO and OVLT, and in the MnPO via relays from the SFO and OVLT, and this increase in activity enhances thirst and vasopressin secretion. As we shall see, a similar general system, but with different neural structures, controls caloric deficiency–based regulation of hunger and energy metabolism.

Energy Balance and the Related Hunger Drive Are Controlled by Neurons in the Arcuate Nucleus

As with temperature and water balance, energy balance is regulated by feedback signals from the body that modulate activity of key hypothalamic neurons, which then initiate adaptive changes in both physiology and behavior. Regulation of energy balance differs, however, in important ways.

First, the feedback signals monitored are numerous and, in many cases, only very indirectly related to the key parameter, energy balance. Examples of this feedback include neural and hormonal signals from the gut, leptin from adipocytes, insulin from pancreatic beta cells, and metabolite levels in the blood. This is in striking contrast to the single, directly sensed signals monitored for thermoregulation and water balance. Second, energy can be stored as fat. The amount of energy that can be accumulated is remarkably high, so high that the energy needs of a starving person can be met for more than a month. Heat and water, in contrast, are not stored. Thus, organisms have an "energy buffer" that allows survival during prolonged deficiency.

Third, since storage has benefits, regulation of energy balance, as opposed to temperature and water balance, is asymmetric in that low energy stores are defended against very aggressively, while high stores are defended against only very weakly—hence the high prevalence of obesity in societies with calorically dense, palatable food. Fourth, energy storage can be a liability—when excessive, it promotes diseases such as obesity, diabetes, heart disease, and cancer. Finally, in circuits regulating energy balance, neuropeptides play a remarkably important role.

Fat Is Stored When Intake of Energy Exceeds Expenditure

Consistent with the first law of thermodynamics, the calories that are stored as fat equal the number of calories ingested minus calories expended. While there is only one way to gain energy—by eating—there are many ways to expend energy.

Most energy is expended by biochemical reactions that are required for basic life functions. As these processes are constantly in operation, such "obligatory energy expenditure" is fixed and not regulated. Two other types of energy expenditure, however,

are dramatically different; one is voluntary physical activity, while the other is involuntary, resulting from sympathetic stimulation of brown adipose tissue and shivering. Sympathetically controlled energy expenditure, often referred to as adaptive thermogenesis, is controlled by the brain. Its function is to respond to perturbations in temperature and in energy stores.

The Intake and Expenditure of Energy Are Usually Matched

For most individuals, body fat stores are relatively constant over time. Thus, calories ingested roughly equal calories expended. A simple calculation demonstrates this point. An average middle-aged person expends 3,392 kcal per day (kcal corresponds to the common term "calorie"). Over the course of a year, this typical person gains 350 g of fat (which equates to 9 kcal of fat per day). Thus, on average, 9 kcal extra must have been consumed per day to account for this gain. This is the amount of energy found in 4% of a typical candy bar or expended by walking about 150 meters. Thus, the mismatch between intake and expenditure (9 kcal) is tiny—only 0.27% of total energy expenditure.

Such close matching is the result of powerful homeostatic mechanisms that use feedback from the body to regulate intake and expenditure. As is true for regulation of temperature and osmolarity, the constancy of body weight, and the close matching between intake and expenditure, is unrelated to any specific "set point." Instead, this remarkable control is the emergent settling point of multiple afferent/efferent feedback loops.

Obesity Is Caused by Genes and Recent Lifestyle Changes

Dysregulation of the above-mentioned afferent/efferent feedback loops results in obesity. While some cases of obesity are due to known mutations in genes required for homeostatic regulation, most are of undetermined cause. Of these, many are likely due to multiple mutations, many of which are uncharacterized. Because the incidence of obesity in Western societies has increased greatly in recent years, too fast to be due to new mutations, changes in diet and physical activity must also play an important role. Homeostatic systems that evolved to achieve energy balance in hunter-gatherers are likely overwhelmed by abundant, palatable, calorically dense food.

But even in our modern obesogenic environment, there are still large variations in fat stores: Only 41% to 70% of interindividual variation in fat stores can be attributed to genetic factors. Thus, genetic predisposition and environment together cause obesity. Of interest, many of the predisposing genetic loci identified to date involve genes that affect brain function.

Multiple Afferent Signals Control Appetite

The major afferent signals affecting energy balance can be divided into two major categories. (1) Short-term signals from cells that line the gastrointestinal tract report the status of food in the gut. All but one of these signals increase with eating and function to terminate meals; the exception is ghrelin, which increases with fasting and stimulates hunger. (2) Longer-term signals report the status of energy reserves (ie, fat stores). These include the pancreatic hormone insulin and the adipocyte hormone leptin, both of which are released in proportion to fat stores. Their levels, especially that of leptin, inform the brain whether fat stores are adequate (Figure 41–14A).

Signals From the Gut Trigger Meal Termination. During eating, as food enters the stomach and intestine, physical distention increases firing of stretch-sensitive vagal afferents. In addition, chemodetection of food by intestinal endocrine cells stimulates secretion of hormones such as cholecystokinin (CCK), glucagon-like peptide-1 (GLP-1), and peptide YY (PYY). These responses have three primary functions.

First, they cause contraction of the pyloric sphincter, a valve between the stomach and intestine. This limits further passage of food, preventing the small intestine from being overloaded. Second, the intestinal hormones stimulate secretion of bile and enzymes into the intestinal lumen to aid digestion. Third, the vagal afferents and the intestinal hormones decrease subsequent food intake, bringing about meal termination (satiation). The intestinal hormones accomplish this primarily by stimulating local vagal afferent terminals, which in turn excite neurons in the caudal region of the NTS.

Two of these hormones, GLP-1 and PYY, may also directly stimulate neurons in the brain. The activated neurons in the NTS project directly, or via a relay in the lateral parabrachial nucleus, to neurons in the forebrain, including the amygdala and hypothalamus. Neurons in the lateral parabrachial nucleus that express calcitonin gene-related polypeptide (CGRP) are one such important relay involved in satiation. These circuits then bring about meal termination.

When food is absorbed, the increase in blood glucose stimulates β-cells to release insulin and the hormone amylin. Amylin then excites neurons in the area postrema (a circumventricular organ outside the blood–brain barrier, located just above the NTS).

Circulating amylin increases within minutes following a meal, decreasing subsequent food intake.

Ghrelin is released by endocrine cells in the stomach. Unlike the factors described above, its secretion is high before eating and falls during the meal. It may play a role in meal initiation. Indeed, ghrelin is the only known systemic factor that increases hunger and thus eating. It excites neurons in a number of sites, including agouti-related peptide neurons in the arcuate nucleus (see below). The physiological significance of ghrelin is unclear because deletion of its gene does not appear to affect hunger.

Blood Glucose and Insulin Affect Appetite. Glucose is sensed by neurons in the periphery, hindbrain, and hypothalamus. Although glucose sensing does not appear to play a role in the day-to-day regulation of energy balance, the detection of and response to dangerously low blood glucose levels (*glucopenia*) is an important function of the brain. Two adaptive responses are initiated: (1) intense glucoprivic hunger, due at least in part to indirect activation of agouti-related peptide neurons, and (2) secretion of glucagon, epinephrine, and corticosteroids, which stimulate hepatic glucose production. The hormonal responses are caused by increases in sympathetic outflow as well as activation of the CRH pathway associated with stress (Chapter 61). Amino acids also can be sensed and, consequently, regulate energy balance and dietary choice—the latter to ensure ingestion of sufficient quantity and quality of protein.

Insulin, on the other hand, is thought to signal an increase in fat stores. Insulin's primary function is to control blood glucose, the stimulus for its secretion. Insulin lowers blood glucose by driving it into muscle and fat cells and by decreasing its production by the liver. As fat stores increase, its ability to do this is decreased (a phenomenon called insulin resistance). Thus, higher fat stores increase basal and meal-stimulated insulin secretion in an effort to overcome resistance and normalize glucose. The fat store–mediated increase in insulin levels inhibits neurons in the hypothalamus, especially the arcuate nucleus, which is thought to decrease hunger.

The Fat Cell Hormone Leptin Signals the Brain About Fat Stores and Affects Hunger and Energy Expenditure. In 1949, scientists at the Jackson Laboratory in Maine noted the appearance of "some very plump young mice." This obesity was due to a genetic mutation, which they named *obese* (*ob*). Sixteen years later, they identified another obesity mutation, *diabetes* (*db*). The extreme obesity of *ob/ob* and *db/db* mice results from intense hyperphagia and reduced brown fat thermogenesis. Based on a series of parabiosis experiments, Douglas Coleman proposed that *ob/ob* mice lack a circulating satiety factor and that *db/db* mice lack its receptor.

In a tour-de-force positional cloning effort led by Jeffrey Friedman and Rudolph Leibel, the *ob* gene was localized on a small region on chromosome 6. Friedman and his lab then homed in on and identified the *ob* gene. Renamed the *leptin* gene, it encodes leptin, a 167-amino acid protein secreted by adipocytes in proportion to the size of fat stores. Treating *ob/ob* mice with leptin cures their obesity. The *db* gene was identified a few years later, and as predicted by Coleman, it turned out to encode leptin's receptor and was found to be expressed by neurons in the hypothalamus. It is an interleukin-6–type class I cytokine receptor that produces its antiobesity effects by activating the JAK2/STAT3 signaling pathway.

Much has been learned subsequently about leptin. First, humans with a genetic deficiency of leptin or its receptor, like the mutant mice, are massively obese; hence, leptin's function is highly conserved, and such mutations are extremely rare. Second, humans with common forms of obesity have very high circulating levels of leptin, a by-product of their increased fat stores. This finding initially led to the view, later questioned, that "garden variety" obesity is caused by resistance to leptin action. Third, starvation, which reduces fat stores, drastically decreases leptin levels. This reduction is of interest because fasting causes many adaptive responses that are also seen in mice and humans that lack leptin: hunger, low energy expenditure, decreased fertility, and other altered neuroendocrine responses. Indeed, restoration of normal leptin levels in fasted individuals reverses or ameliorates many of fasting's effects. Thus, leptin's primary function is to signal, when its levels are low, that fat stores are inadequate.

These low leptin levels then bring about key adaptive responses such as increased hunger, decreased sympathetically mediated thermogenesis (to conserve limited fuel stores), decreased fertility (to prevent pregnancy when its demands cannot be met), and others. According to this view, leptin's dynamic range for signaling extends from the very low levels seen with fasting, signaling that fat stores are too low, to the levels found in well-fed, nonobese individuals, signaling that fat stores are sufficient. Levels above this may produce some effect to restrain obesity, but this effect, if present, is remarkably weak. Thus, the defense of energy balance is asymmetric—strong against low stores, weak against high stores. A corollary of this is that obese individuals do not have leptin resistance;

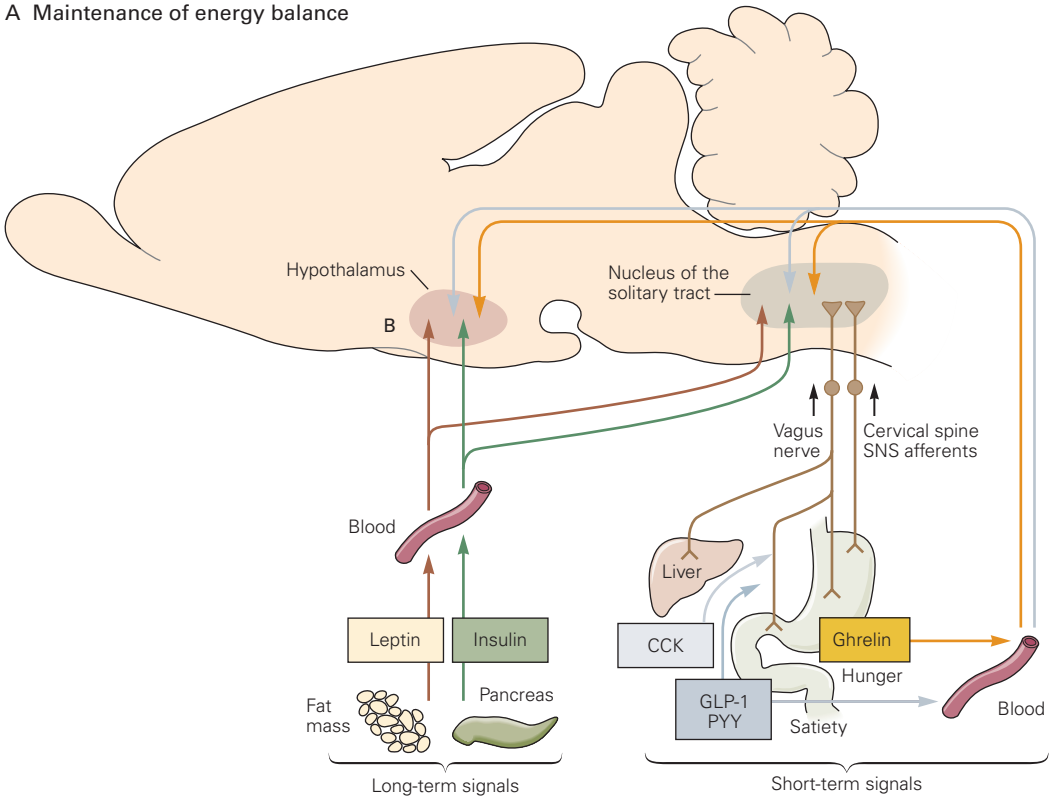
A Maintenance of energy balance
Hypothalamus
B
Nucleus of the solitary tract
Vagus nerve
Cervical spine SNS afferents
Blood
Liver
Leptin
Insulin
CCK
Ghrelin
Hunger
GLP-1 PYY
Satiety
Blood
Fat mass
Pancreas
Long-term signals
Short-term signals

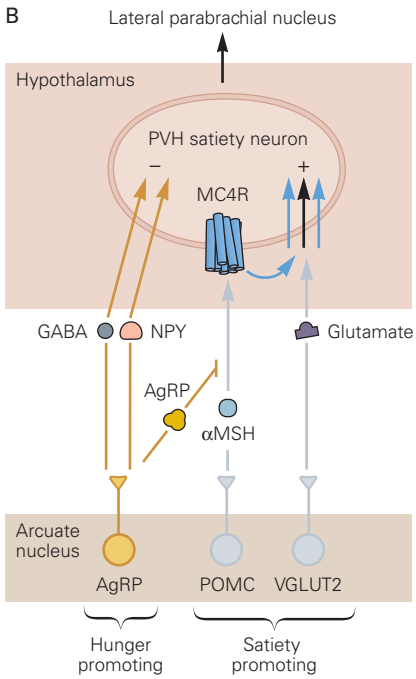
B
Lateral parabrachial nucleus
Hypothalamus
PVH satiety neuron
–
+
MC4R
GABA
NPY
Glutamate
AgRP
αMSH
Arcuate nucleus
AgRP
POMC
VGLUT2
Hunger promoting
Satiety promoting

rather, they simply have leptin levels that exceed the maximally effective concentration.

POMC, AgRP, and MC4R Neurons Are Key Nodes in the Afferent/Efferent Loop

Neuron-specific manipulation technologies have revealed two antagonistic populations of neurons in the arcuate nucleus that control energy balance: one expresses agouti-related peptide (AgRP) and the other the precursor polypeptide proopiomelanocortin (POMC) (Figure 41–14B). POMC neurons decrease hunger and stimulate sympathetically driven energy expenditure; AgRP neurons do the opposite. POMC neurons release the processed peptide α-melanocyte-stimulating hormone (αMSH), which activates the melanocortin-4 receptor (MC4R), a G protein–coupled receptor.

The downstream MC4R-expressing neurons that control hunger lie within the PVH. When these MC4R neurons are excited by αMSH released from POMC afferents, hunger is decreased. The PVH-MC4R "satiety neurons" are glutamatergic; they decrease hunger via their excitatory projections to the lateral parabrachial nucleus.

The MC4R-expressing neurons that control energy expenditure are sympathetic preganglionic neurons in the spinal cord. POMC neurons project to these sites, in addition to the PVH, increasing sympathetically driven energy expenditure.

The AgRP neurons increase hunger in part by opposing the actions of POMC neurons (Figure 41–14B). They release three factors: AgRP, an inverse agonist of MC4R, and neuropeptide Y and γ-aminobutyric acid (GABA), two inhibitory transmitters. The AgRP neurons project to and inhibit the PVH-MC4R satiety neurons and directly inhibit POMC neurons. In addition, different subsets of arcuate AgRP neurons project to other sites, including the lateral hypothalamus and the bed nucleus of the stria terminalis. These sites, when inhibited by AgRP inputs, can also stimulate hunger.

A third group of neurons in the arcuate nucleus express VGLUT2, release glutamate, and act in parallel with POMC neurons to induce satiety (Figure 41–14B). Like POMC neurons, and opposite to AgRP neurons, they excite the PVH-MC4R satiety neurons. αMSH/MC4R signaling in PVH-MC4R neurons causes satiety by two mechanisms: by directly activating the PVH-MC4R satiety neurons and by upregulating excitatory transmission from the VGLUT2 neurons to the PVH-MC4R neurons via postsynaptic facilitation.

The importance of the POMC, AgRP, and PVH-MC4R satiety neurons in regulating food intake is supported by a number of compelling findings. First, fasting activates AgRP neurons and inhibits POMC neurons, while feeding or leptin treatment does the opposite. The downstream PVH-MC4R satiety neurons are inhibited by fasting and excited by feeding. Second, genetic deficiency of the POMC protein or MC4R causes massive obesity. Third, genetic ablation of AgRP neurons in mice causes starvation, while stimulation of AgRP neurons rapidly brings about extreme hyperphagia, even in mice that are calorically replete and otherwise sated. Finally, several findings implicate the PVH-MC4R satiety neurons as an important

Figure 41–14 (Opposite) Neural and endocrine components combine to regulate energy balance.

A. *Short-term signals*. During meals, cholecystokinin (**CCK**) from the intestinal tract stimulates sensory fibers of the vagus nerve, thus promoting satiation (meal termination). Glucagon-like peptide-1 (**GLP-1**) and peptide YY (**PYY**), also released by the intestinal tract, appear to work on both sensory fibers of the vagus and neurons in the brain. The vagal sensory fibers, along with sympathetic fibers from the gut and orosensory information, converge in the nucleus of the solitary tract (NTS). Prior to mealtime, release of ghrelin from the stomach peaks, providing a blood-borne signal to neurons in the brain. Whereas CCK promotes satiety, ghrelin promotes eating.

Long-term signals. Leptin and insulin are among the humoral signals that inform the brain about the status of the fat stores. Leptin is produced in fat-storing cells, whereas insulin is produced in the pancreas. Both hormones are sensed by receptors in the arcuate nucleus of the hypothalamus as well as by receptors in the NTS. Leptin and insulin reduce food intake and increase energy expenditure. (Abbreviation: **SNS**, sympathetic nervous system.)

B. Neurons in the arcuate nucleus that synthesize agouti-related peptide (**AgRP**), proopiomelanocortin (**POMC**), and vesicular glutamate transporter 2 (**VGLUT2**) project to the paraventricular nucleus of the hypothalamus (**PVH**) where they control hunger and satiety. Satiety-promoting POMC neurons release the processed POMC peptide, α-melanocyte stimulating hormone (**αMSH**), which binds to melanocortin-4 receptors (**MC4R**) on neurons in the PVH. Activation of these neurons causes satiety. In contrast, the hunger-promoting AgRP neurons release two inhibitory transmitters, γ-aminobutyric acid (**GABA**) and neuropeptide Y (**NPY**), and the MC4R antagonist AgRP. Their combined effect is to inhibit the MC4R-expressing neurons, causing hunger. The MC4R-expressing neurons also receive direct excitatory input from another population of arcuate neurons, VGLUT2 neurons, which also promote satiety. The binding of αMSH to MC4R causes satiety by two mechanisms: by directly activating the PVH-MC4R neurons and by upregulating excitatory transmission from the arcuate VGLUT2 neurons to the PVH-MC4R neurons (**blue arrows**). Finally, PVH-MC4R neurons project to the lateral parabrachial nucleus where they promote satiety.

downstream target of AgRP and POMC neurons. Most notable are the development of marked hyperphagia and obesity in mice genetically engineered to lack MC4R neurons in the PVH and the induction of intense feeding following optogenetic stimulation of AgRP terminals in the PVH, which inhibits the satiety neurons.

Surprisingly, environmental cues that predict future ingestion of food induce inhibition of AgRP neurons. Indeed, in fasted mice, which have high AgRP neuron activity, presentation of food alone without ingestion decreases AgRP neuron firing. This is roughly analogous to rapid, feedforward inhibition of vasopressin secretion and thirst neuron activity (mentioned previously). Thus, in addition to receiving strong bottom-up feedback signals from the body, the hunger-promoting AgRP neurons also receive top-down feedforward information from the environment. The function of this input is not yet clear, but it could serve as an anticipatory signal to limit future ingestion of excessive calories, or as discussed below, it could serve as a reward-related signal to motivate feeding.

Finally, the complete pathway accounting for regulation of hunger by the AgRP and POMC neuron → PVH pathway is presently unknown. It is likely that, via relays through a number of synapses, it affects neuronal activity in pathways controlling reward as well as perception. This is the case because, in the fasted state, food and cues predictive of food are both more rewarding and much more likely to become the focus of attention. How specificity for a given goal—in this case food—is retained as neural information flows from the highly specific deficiency-regulated homeostatic neurons in the hypothalamus to the "nonspecific" reward and perception pathways in the accumbens and cortex is one of the great mysteries of motivated behaviors such as hunger and thirst. The solution could provide clues for disorders of motivated behavior like drug addiction.

Psychological Concepts Are Used to Explain Motivational Drives Such as Hunger

In a simplified stimulus–response view of behavior, one might assume that neural detection of water or energy deficiency (the stimulus) is hardwired to motor pathways for drinking or eating (the response), and thus analogous to the knee-jerk stretch reflex (Chapter 3). However, this cannot be the case because the responses that can be employed to obtain food, all motivated by the deficiency stimulus, are remarkably varied and complex—to such a degree that they could not be hardwired. Indeed, animals can complete an infinite number of complex operant learning tasks to obtain water or food rewards.

The challenge to understanding motivational drive is to devise a model that accounts for the ability of deprivation states to induce behavior that is remarkably varied and complex, while remaining completely specific for one goal. Two compelling theories are relevant. According to *incentive motivation theory*, deficiency increases the reward value of food and water. *Drive reduction theory* posits that deficiency generates an aversive state, the resolution of which is thought to motivate behavior. Notably, these two views are not mutually exclusive and may in some ways be two sides of the same coin.

Incentive Motivation: Fasting Increases the Reward Value of Food. The incentive motivation theory is the work of theorists over many years, most recently refined by Frederick Toates and Kent Berridge. Consider eating and the hunger drive. Briefly, food is viewed as inherently rewarding. Through learned associations, cues and tasks related to obtaining food also become rewarding; in this way, varied and complex behavioral responses are learned (Figure 41–15A).

The theory posits that the deprivation state increases the reward value of food and of the related cues and tasks (ie, their incentive salience). Thus, during fasting, the reward value is increased, and all food and cues and tasks related to food are extremely rewarding. After a meal, the reward value is decreased, and only the most inherently palatable foods, for example, ice cream, are still sufficiently rewarding to be eaten. The task of neuroscientists is to determine how deprivation increases reward value. Experimental activation of AgRP neurons in an otherwise sated mouse dramatically increases the reward value of food—remarkably, the reward value of food is increased to the same extremely high level seen with fasting.

Drive Reduction: Activity of AgRP Hunger Neurons Can Be Aversive. As we know from personal experience, the behavioral states created by dehydration and caloric deficiency, namely thirst and hunger, are unpleasant. It was originally proposed many years ago that reduction of these states, which relieves this discomfort, is rewarding and hence motivates drinking and feeding. Recently, Scott Sternson's group has provided compelling new support for a modified version of this model (Figure 41–15B). Using a behavioral conditioning paradigm such as the place preference test, they discovered that optogenetic activation of AgRP neurons in sated mice was aversive. When the same mice were then studied in a food-deprived state (which is associated with

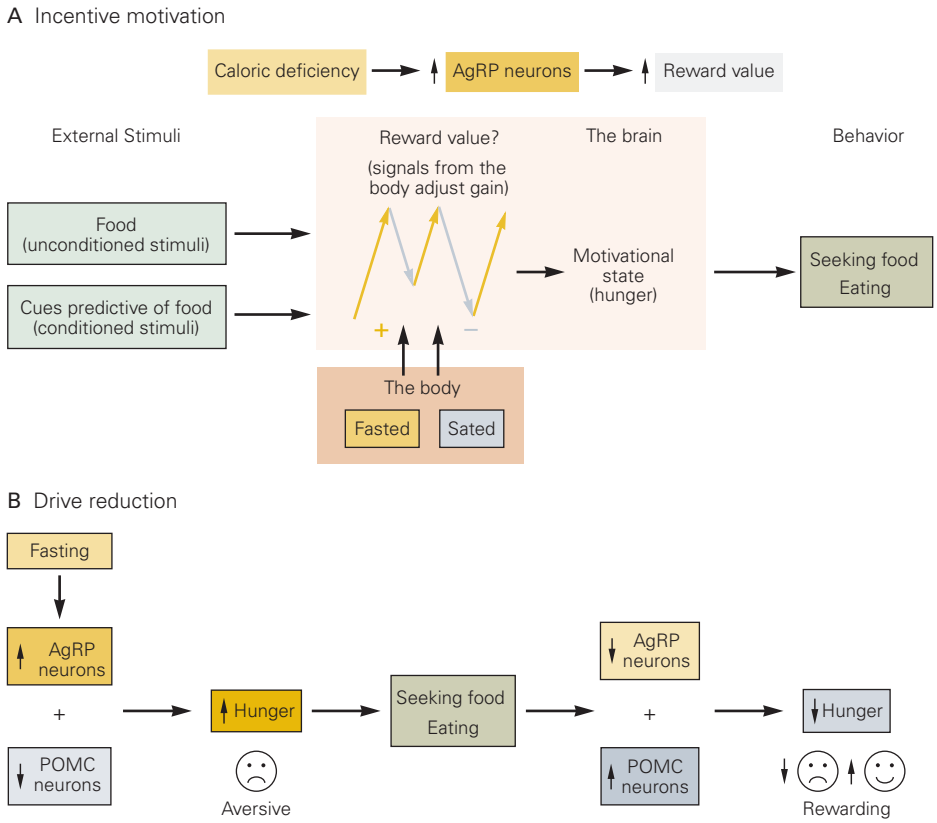

Figure 41–15 Two theories of how fasting promotes eating.

A. *Incentive motivation.* Food is inherently rewarding, and different foods have different reward values (lettuce–low, ice cream–high). Through learned associations, cues that predict food become rewarding. The fed (sated) versus fasted state sets the gain determining how rewarding food and food cues are. Fasting greatly increases while the sated state decreases reward value.

B. *Drive reduction.* The feeling of hunger is aversive. Eating reduces this aversive state. Consistent with this theory, experimental stimulation of hunger-promoting agouti-related peptide (**AgRP**) neurons is aversive, while stimulation of satiety-promoting paraventricular nucleus of the hypothalamus melanocortin-4 receptors (**MC4R**) neurons (which are downstream of the AgRP and proopiomelanocortin [**POMC**] neurons) in an otherwise hungry mouse creates a pleasant feeling.

increased AgRP neuron activity), they engaged in behaviors that in the earlier conditioning had lowered AgRP neuron activity—in short, they acted as if motivated to turn off the AgRP neuron–induced aversive state. Similar results were obtained with thirst neurons in the SFO.

In further support of this view, optogenetic activation of downstream PVH-MC4R satiety neurons in calorically deprived mice, but not in sated mice, is emotionally positive (ie, the mice like it). Thus, causing satiety when otherwise hungry is pleasant. In total, these findings provide strong evidence for the view that homeostatic deficiency is unpleasant, that the aversive state is caused by activation of deficiency-responsive homeostatic neurons, and that when afflicted by the deficiency-induced aversive state animals engage in behaviors that they associate with relief.

This model provides an explanation for why dieting is so difficult. It generates an aversive, unpleasant state that can only be relieved by eating. Finally, the rapid reduction in AgRP neuron activity in response to sensory cues that predict food, and the alleviation of the aversive state that this should cause, could function as a rewarding "teaching signal" that motivates pursuit of the goal (food).

Sexually Dimorphic Regions in the Hypothalamus Control Sex, Aggression, and Parenting

Now we turn to behaviors that are not homeostatic, but are controlled by the hypothalamus, involve integration between sensory cues and signals from the body (ie, gonadal steroids), and are critical for survival of the species.

Males and females differ in their sexual, aggressive, and parenting behaviors. These differences are especially notable in animals, for example in mice, where they are clearly hardwired (ie, require no prior training). These differences include mounting and lordosis by males and females, respectively; territorial-related behaviors such as marking and aggression by males; and the tendency toward nurturing in females versus aggressive behavior in males when dealing with the young. The latent capacity for these sexually dimorphic behaviors is the product of sex steroid action on the brain during embryogenesis (Chapter 51). Full actualization of adult sex-specific behaviors also requires adult levels of gonadal steroids. Sex chromosome–specific genes, other than *Sry*, which causes male sex determination, as well as genes that are imprinted in a sexually dimorphic way, also subtly modulate sex-specific behaviors independent of gonadal steroids. Ultimately, the behaviors themselves are triggered by cues from the environment, such as pheromones.

Two regions of the hypothalamus are critically involved in the control of these behaviors, the POA and the ventral lateral aspect of the ventromedial hypothalamic nucleus (vlVMH). Both sites are sexually dimorphic: The POA contains more neurons in males, and the vlVMH contains more progesterone-expressing neurons in females. These sites are heavily interconnected, and they receive strong input from two other sexually dimorphic areas outside the hypothalamus: the medial division of the posteromedial bed nucleus of the stria terminalis (BNSTmpm) and medial amygdala (MeA).

Sexual Behavior and Aggression Are Controlled by the Preoptic Hypothalamic Area and a Subarea of the Ventromedial Hypothalamic Nucleus

Brain lesion studies have demonstrated that the sexually dimorphic brain regions—the accessory olfactory bulb, BNSTmpm, MeA, and particularly POA and vlVMH—play important roles in sex-specific behaviors. Neurons in these regions are highly interconnected, are downstream of pathways involved in detecting and responding to pheromones (BNSTmpm and MeA), express sex hormone receptors, and, with the exception of neurons in the vlVMH, also express aromatase (Figure 41–16). Neurons in both the POA and vlVMH send strong projections to the lateral periaqueductal gray area, which is thought to mediate and coordinate the motor and autonomic aspects of sexual and aggressive behavior.

The vlVMH plays a critical role in controlling sexually dimorphic behaviors. Firing rates of vlVMH neurons in male mice increase during mating or periods of aggression toward a male intruder. Stimulation of these neurons triggers intense attack behavior toward intruder males and toward atypical targets for male aggression such as castrated males, females, or even rubber gloves! Silencing these neurons eliminates aggressive behavior toward male intruders.

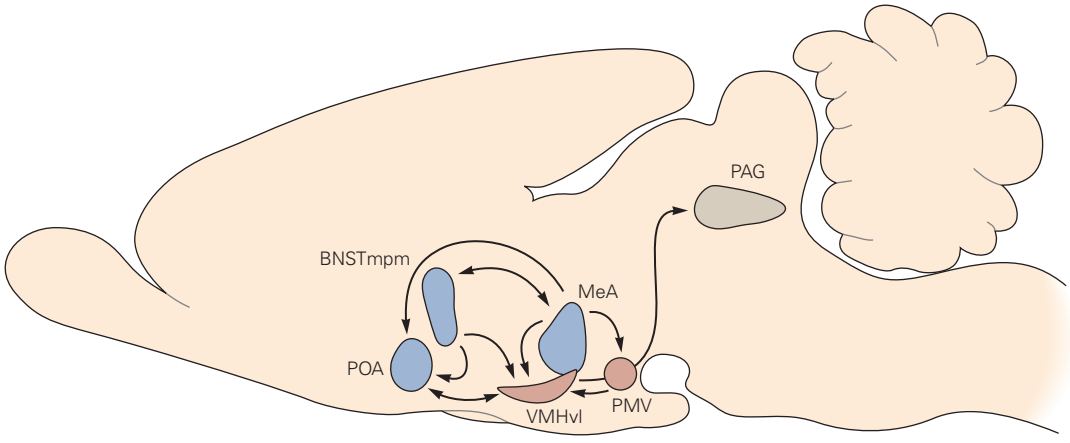

Figure 41–16 Sexually dimorphic neural structures comprise highly interconnected behavioral circuits. Hypothalamic and amygdalar nuclei that regulate sexually dimorphic behaviors are extensively interconnected. These areas process pheromonal information, and subsets of adult neurons within each of these regions express sex hormone receptors; neurons within some of these regions (**blue**) also express aromatase. (Abbreviations: **BNSTmpm**, medial division of the posteromedial bed nucleus of the stria terminalis; **MeA**, medial amygdala; **PAG**, periaqueductal gray; **PMV**, ventral premammillary nucleus; **POA**, preoptic hypothalamus; **VMHvl**, ventrolateral component of the ventromedial hypothalamus.) (Reproduced, with permission, from Yang and Shah 2014. Copyright © 2014 Elsevier Inc.)

Furthermore, stimulation of a subset of vlVMH neurons that express estrogen receptor evokes either sexual behavior (mounting) or aggression, depending on the number of neurons activated and their degree of activation: Lower levels of activation induce mounting, whereas higher levels induce aggression. Consistent with these results, genetic ablation of related progesterone receptor–expressing vlVMH neurons causes loss of both sexual behavior and aggression in males and loss of sexual behavior in females. Thus, it is clear that sex neurons in the vlVMH-expressing steroid receptors play a critical role in driving sexual behavior in males and females and aggression in males.

Parental Behavior Is Controlled by the Preoptic Hypothalamic Area

Nurturing parental behavior is key to the survival of one's offspring. Male rodents demonstrate strikingly different patterns of behavior. Males can be nurturing or hostile to offspring, even to the point of infanticide, depending on whether they view the offspring as their own or those of another male. Female mice, on the other hand, are generally nurturing.

Social interaction between mouse pups and appropriately receptive adult female and male mice, but not hostile adult male mice, induces activity in subsets of galanin-expressing neurons in the POA. These offspring-activated neurons are largely distinct from POA neurons activated by mating. Genetic ablation of galanin-expressing POA neurons prevents nurturing parental behavior, even to the point of inducing uncharacteristic aggression in females toward their offspring. On the other hand, stimulation of these galanin-positive neurons in males, which are normally extremely hostile to unrelated pups, decreases aggression and induces nurturing pup grooming. Thus, neurons in the POA, in addition to controlling sexual behavior itself, also play a role in ensuring survival of the fruit of sexual behavior.

Highlights

1. The hypothalamus and the autonomic and neuroendocrine motor systems coordinate and control body homeostasis by inducing adaptive behaviors; by controlling glands, smooth muscle, cardiac muscle, and adipocytes; and by releasing hormones from the pituitary gland.
2. Homeostatic control of body temperature, fluid and electrolyte balance, and blood pressure allows organisms to function under harsh environmental conditions.
3. Feedback loops that sense temperature, osmolarity, blood pressure, and body fat are essential for homeostatic control. The combined action of multiple feedback-informed sensory-afferent/efferent-effector control loops results in emergent settling points.
4. Modality-specific hypothalamic neurons link specific interoceptive sensory feedback with outputs that control adaptive behaviors and physiologic responses. In addition to feedback, these modality-specific neurons also receive feedforward information regarding future anticipated homeostatic challenges.
5. The autonomic motor system contains neurons located in sympathetic, parasympathetic, and enteric ganglia located near the spinal column or embedded within peripheral targets. Functional subsets of autonomic neurons selectively innervate effector tissues comprised of smooth muscle, cardiac muscle, glandular epithelia, and adipocytes.
6. Sympathetic neurons are activated in response to exercise and stress. Parasympathetic and sympathetic neurons generally have antagonistic functions, but often act in concert. The enteric system coordinates peristaltic contractions of the gastrointestinal tract with mucosal function and local blood flow.
7. Preganglionic neurons that control the sympathetic and parasympathetic outflows are located in the spinal cord and brain stem.
8. Acetylcholine, norepinephrine, and neuropeptide cotransmitters act as synaptic signaling molecules in the autonomic motor system. Excitatory fast synaptic transmission in autonomic ganglia is mediated by acetylcholine acting on nicotinic receptors. G protein–coupled receptors in ganglia mediate additional pre- and postsynaptic excitatory and inhibitory effects. G protein–coupled receptors mediate transmitter actions at autonomic neuroeffector junctions.
9. The neuroendocrine system links the hypothalamus, via the pituitary gland, to various physiologic responses in the body. The posterior pituitary contains hypothalamic axon terminals that release two neurohormones into the blood: Vasopressin stimulates water reabsorption by the kidney, while oxytocin controls uterine contraction and milk release. The anterior pituitary contains endocrine cells that secrete hormones in response to factors released by hypothalamic neurons. These anterior pituitary hormones control the thyroid gland, glucocorticoid secretion

by the adrenal cortex, sex steroid secretion by the gonads, lactation, and linear growth.

10. Body temperature is detected in multiple sites including the periphery, in and around major organs, and in the brain. Constancy of body temperature is maintained by multiple thermoreceptor-afferent/thermoeffector-efferent control loops.
11. Some neurons in the lamina terminalis are activated by both dehydration and loss of intravascular volume. Key parameters sensed in these deficiency states include osmolarity and angiotensin II levels, respectively. When these neurons are activated, they cause thirst and release of vasopressin from the posterior pituitary. Vasopressin release is also rapidly regulated in a feedforward fashion by cues that anticipate future disturbances in osmolarity.
12. Energy balance involves short-term and long-term feedback signals. Short-term signals from the gut mediate satiation, which terminates meals. CCK, released by intestinal endocrine cells, plays a key role in satiation. A key long-term signal is leptin, which is secreted by adipocytes in proportion to the amount of fat stores. When fat stores are low, the consequent low levels of leptin signal the brain to induce a hunger state and to decrease energy expenditure, resulting in replenished fat stores.
13. Leptin is more effective in defending against low fat stores than in resisting obesity.
14. POMC-, AgRP-, and MC4R-expressing neurons in the hypothalamus are key nodes in the afferent/efferent loop controlling energy balance. Neurons that signal satiety are activated by satiety-promoting POMC neurons and inhibited by hunger-promoting AgRP neurons.
15. How specificity for a given goal (eg, food) is retained as neural information flows from the highly specific deficiency-regulated homeostatic neurons in the hypothalamus to the "nonspecific" reward and perception pathways in the accumbens and cortex is one of the great mysteries of motivated behaviors such as hunger and thirst. Solving this could provide clues for disorders of motivated behavior like drug addiction.
16. Leptin regulates hunger and energy expenditure in part by activating POMC neurons and inhibiting AgRP neurons. Hunger-promoting AgRP neurons are also rapidly regulated in a feedforward fashion by cues that anticipate future changes in energy balance.
17. Motivational drives such as hunger have been explained by two mechanisms: The deficiency state (starvation) increases the reward value of food, or deficiency generates an aversive state, the resolution of which motivates behavior.
18. Sexually dimorphic regions in the hypothalamus control sexual behavior and aggression. Neural activity in the sexually dimorphic preoptic area controls parental behavior. Full actualization of adult sex-specific behaviors also requires adult levels of gonadal steroids.

Bradford B. Lowell
Larry W. Swanson
John P. Horn

Selected Reading

Andermann ML, Lowell BB. 2017. Towards a wiring diagram understanding of appetite control. Neuron 95:757–778.

Berridge KC. 2004. Motivation concepts in behavioral neuroscience. Physiol Behav 81:179–209.

Bourque CW. 2008. Central mechanisms of osmosensation and systemic osmoregulation. Nat Rev Neurosci 9:519–531.

Clarke IJ. 2015. Hypothalamus as an endocrine organ. Compr Physiol 5:217–253.

Dulac C, O'Connell LA, Wu Z. 2014. Neural control of maternal and paternal behaviors. Science 345:765–770.

Guyenet PG. 2006. The sympathetic control of blood pressure. Nat Rev Neurosci 7:335–346.

Jænig, W. 2006. *The Integrative Action of the Autonomic Nervous System*. Cambridge, England: Cambridge Univ. Press.

Leib DE, Zimmerman CA, Knight ZA. 2016. Thirst. Curr Biol 26:R1260–R1265.

Morrison SF. 2016. Central control of body temperature. F1000Res 5:F1000.

Morton GJ, Meek TH, Schwartz MW. 2014. Neurobiology of food intake in health and disease. Nat Rev Neurosci 15:367–378.

Romanovsky AA. 2007. Thermoregulation: some concepts have changed. Functional architecture of the thermoregulatory system. Am J Physiol Regul Integr Comp Physiol 292:R37–R46.

Rosenbaum M, Leibel RL. 2014. 20 years of leptin: role of leptin in energy homeostasis in humans. J Endocrinol 223:T83–T96.

Yang CF, Shah NM. 2014. Representing sex in the brain, one module at a time. Neuron 82:261–278.

References

Ahima RS, Prabakaran D, Mantzoros C, et al. 1996. Role of leptin in the neuroendocrine response to fasting. Nature 382:250–252.

Aponte Y, Atasoy D, Sternson SM. 2011. AGRP neurons are sufficient to orchestrate feeding behavior rapidly and without training. Nat Neurosci 14:351–355.

Balthasar N, Dalgaard LT, Lee CE, et al. 2005. Divergence of melanocortin pathways in the control of food intake and energy expenditure. Cell 123:493–505.

Berthoud HR, Neuhuber WL. 2000. Functional and chemical anatomy of the afferent vagal system. Auton Neurosci 85:1-17.

Betley JN, Xu S, Cao ZF, et al. 2015. Neurons for hunger and thirst transmit a negative-valence teaching signal. Nature 521:180–185.

Brookes SJ, Spencer NJ, Costa M, Zagorodnyuk VP. 2013. Extrinsic primary afferent signalling in the gut. Nat Rev Gastroenterol Hepatol 10:286–296.

Burnstock G. 2013. Cotransmission in the autonomic nervous system. Handb Clin Neurol 117:23–35.

Campos CA, Bowen AJ, Schwartz MW, Palmiter RD. 2016. Parabrachial CGRP neurons control meal termination. Cell Metab 23:811–820.

Chambers AP, Sandoval DA, Seeley RJ. 2013. Integration of satiety signals by the central nervous system. Curr Biol 23:R379–R388.

Chen Y, Lin YC, Kuo TW, Knight ZA. 2015. Sensory detection of food rapidly modulates arcuate feeding circuits. Cell 160:829–841.

Coleman DL. 2010. A historical perspective on leptin. Nat Med 16:1097–1099.

DeGroat WC, Booth AM, Yoshimura N. 1993. Neurophysiology of micturition and its modification in animal models of human disease. In: CA Maggi (ed). *Nervous Control of the Urogenital System*, pp. 227–348. Chur, Switzerland: Harwood Academic Publishers.

Fenselau H, Campbell JN, Verstegen AM, et al. 2017. A rapidly acting glutamatergic ARC→PVH satiety circuit postsynaptically regulated by α-MSH. Nat Neurosci 20: 42–51.

Furness JB. 2012. The enteric nervous system and neurogastroenterology. Nat Rev Gastroenterol Hepatol 9: 286–294.

Furness JB, Costa M. 1980. Types of nerves in the enteric nervous system. Neurosci 5:1–20.

Furness JB, Jones C, Nurgali K, Clerc N. 2004. Intrinsic primary afferent neurons and nerve circuits within the intestine. Prog Neurobiol 72:143–164.

Garfield AS, Li C, Madara JC, et al. 2015. A neural basis for melanocortin-4 receptor-regulated appetite. Nat Neurosci 18:863–871.

Gay VL. 1972. The hypothalamus: physiology and clinical use of releasing factors. Fertil Steril 23:50–63.

Gibbins IL. 1995. Chemical neuroanatomy of sympathetic ganglia. In: E McLachlan (ed). *Autonomic Ganglia*, pp. 73–122. Luxembourg: Harwood Academic Publishers.

Huszar D, Lynch CA, Fairchild-Huntress V, et al. 1997. Targeted disruption of the melanocortin-4 receptor results in obesity in mice. Cell 88:131–141.

Ingalls AM, Dickie MM, Snell GD. 1950. Obese, a new mutation in the house mouse. J Hered 41:317–318.

Krashes MJ, Koda S, Ye C, et al. 2011. Rapid, reversible activation of AgRP neurons drives feeding behavior in mice. J Clin Invest 121:1424–1428.

Krashes MJ, Lowell BB, Garfield AS. 2016. Melanocortin-4 receptor-regulated energy homeostasis. Nat Neurosci 19:206–219.

Lechner SG, Markworth S, Poole K, et al. 2011. The molecular and cellular identity of peripheral osmoreceptors. Neuron 69:332–344.

Lee H, Kim DW, Remedios R, et al. 2014. Scalable control of mounting and attack by Esr1+ neurons in the ventromedial hypothalamus. Nature 509:627–632.

Lin D, Boyle MP, Dollar P, et al. 2011. Functional identification of an aggression locus in the mouse hypothalamus. Nature 470:221–226.

Locke AE, Kahali B, Berndt SI, et al. 2015. Genetic studies of body mass index yield new insights for obesity biology. Nature 518:197–206.

Lowell BB, Spiegelman BM. 2000. Towards a molecular understanding of adaptive thermogenesis. Nature 404:652–660.

Luquet S, Perez FA, Hnasko TS, Palmiter RD. 2005. NPY/AgRP neurons are essential for feeding in adult mice but can be ablated in neonates. Science 310:683–685.

Mandelblat-Cerf Y, Kim A, Burgess CR, et al. 2017. Bidirectional anticipation of future osmotic challenges by vasopressin neurons. Neuron 93:57–65.

Mandelblat-Cerf Y, Ramesh RN, Burgess CR, et al. 2015. Arcuate hypothalamic AgRP and putative POMC neurons show opposite changes in spiking across multiple timescales. Elife 4:e07122.

McKinley MJ, Yao ST, Uschakov A, McAllen RM, Rundgren M, Martelli D. 2015. The median preoptic nucleus: front and centre for the regulation of body fluid, sodium, temperature, sleep and cardiovascular homeostasis. Acta Physiol (Oxf) 214:8–32.

Mountjoy KG, Robbins LS, Mortrud MT, Cone RD. 1992. The cloning of a family of genes that encode the melanocortin receptors. Science 257:1248–1251.

Myers MG Jr, Leibel RL, Seeley RJ, Schwartz MW. 2010. Obesity and leptin resistance: distinguishing cause from effect. Trends Endocrinol Metab 21:643–651.

Nakamura K, Morrison SF. 2011. Central efferent pathways for cold-defensive and febrile shivering. J Physiol 589:3641–3658.

Oka Y, Ye M, Zuker CS. 2015. Thirst driving and suppressing signals encoded by distinct neural populations in the brain. Nature 520:349–352.

Powley TL, Phillips RJ. 2004. Gastric satiation is volumetric, intestinal satiation is nutritive. Physiol Behav 82:69–74.

Reichlin S. 1978. The hypothalamus: introduction. Res Publ Assoc Res Nerv Ment Dis 56:1–14.

Romanovsky AA. 2014. Skin temperature: its role in thermoregulation. Acta Physiol (Oxf) 210:498–507.

Rossi J, Balthasar N, Olson D, et al. 2011. Melanocortin-4 receptors expressed by cholinergic neurons regulate energy balance and glucose homeostasis. Cell Metab 13:195–204.

Saper CB. 2002. The central autonomic nervous system: conscious visceral perception and autonomic pattern generation. Annu Rev Neurosci 25:433–469.

Saper CB, Romanovsky AA, Scammell TE. 2012. Neural circuitry engaged by prostaglandins during the sickness syndrome. Nat Neurosci 15:1088–1095.

Shah BP, Vong L, Olson DP, et al. 2014. MC4R-expressing glutamatergic neurons in the paraventricular hypothalamus regulate feeding and are synaptically connected to the parabrachial nucleus. Proc Natl Acad Sci U S A 111:13193–13198.

Song K, Wang H, Kamm GB, et al. 2016. The TRPM2 channel is a hypothalamic heat sensor that limits fever and can drive hypothermia. Science 353:1393–1398.

Speakman JR, Levitsky DA, Allison DB, et al. 2011. Set points, settling points and some alternative models: theoretical options to understand how genes and environments combine to regulate body adiposity. Dis Model Mech 4:733–745.

Stricker EM, Hoffmann ML. 2007. Presystemic signals in the control of thirst, salt appetite, and vasopressin secretion. Physiol Behav 91:404–412.

Swanson LW. 2000. Cerebral hemisphere regulation of motivated behavior. Brain Res 886:113–164.

Tan CH, McNaughton PA. 2016. The TRPM2 ion channel is required for sensitivity to warmth. Nature 536:460–463.

Tan CL, Cooke EK, Leib DE, et al. 2016. Warm-sensitive neurons that control body temperature. Cell 167:47–59 e15.

Tanaka M, Owens NC, Nagashima K, Kanosue K, McAllen RM. 2006. Reflex activation of rat fusimotor neurons by body surface cooling, and its dependence on the medullary raphe. J Physiol 572:569–583.

Toates F 1986. *Motivational Systems*. New York: Cambridge University Press.

Williams EK, Chang RB, Strochlic DE, Umans BD, Lowell BB, Liberles SD. 2016. Sensory neurons that detect stretch and nutrients in the digestive system. Cell 166:209–221.

Wong LC, Wang L, D'Amour JA, et al. 2016. Effective modulation of male aggression through lateral septum to medial hypothalamus projection. Curr Biol 26:593–604.

Wu Z, Autry AE, Bergan JF, Watabe-Uchida M, Dulac CG. 2014. Galanin neurons in the medial preoptic area govern parental behaviour. Nature 509:325–330.

Yang CF, Chiang MC, Gray DC, et al. 2013. Sexually dimorphic neurons in the ventromedial hypothalamus govern mating in both sexes and aggression in males. Cell 153:896–909.

Zhang Y, Proenca R, Maffei M, Barone M, Leopold L, Friedman JM. 1994. Positional cloning of the mouse obese gene and its human homologue. Nature 372:425–432.

Zimmerman CA, Lin YC, Leib DE, et al. 2016. Thirst neurons anticipate the homeostatic consequences of eating and drinking. Nature 537:680–684.

42

Emotion

Elation, compassion, sadness, fear, and anger are commonly considered examples of emotions. These states have an enormous impact on our behavior and well-being. But what exactly is an emotion? Distinguishing different emotion states is difficult and requires an account of the environmentally or internally generated challenge an organism faces as well as its physiological responses. For example, before we can conclude that a rat is in a state of fear, we need to know that the rat is evaluating a specific threatening stimulus (a predator in its environment) and is mounting an adaptive response, such as high arousal and freezing.

Emotions are often represented along two dimensions: valence (ie, pleasantness to unpleasantness) and intensity (ie, low to high arousal), called "core affect" in many psychological theories. However, emotions can also be grouped into categories, such as categories of basic emotions (happiness, fear, anger, disgust, sadness) and categories of more complex emotions that help regulate social or moral behaviors (eg, shame, guilt, embarrassment, pride, jealousy). There is considerable debate about whether all the categories that are in common usage (like the ones just mentioned) will correspond to scientifically useful categories in a future neuroscience of emotion.

Within experimental contexts, the term *emotion* is used in several different ways, often related to the ways in which emotion is measured (Box 42–1). In everyday conversation, most people use the term "emotion" synonymously with "conscious experience of emotion" or "feeling," and most psychological studies in humans have focused on this sense of "emotion" as well. Most research in animals has focused instead on specific behavioral or physiological responses, in good part because it is impossible to obtain verbal reports in animal studies. Yet emotions have been conserved throughout the evolution of species, as Charles Darwin first observed in his seminal book, *The Expression of the Emotions in Man and Animals.* The empirical approach we describe in this chapter thus considers emotions as central brain states that can be studied in humans as well as many other animals, provided that we distinguish between emotions and feelings.

Emotion states typically cause a broad range of physiological responses that occur when the brain

Box 42–1 Ways of Measuring Emotion

Measures Commonly Used in Humans

Psychophysiology. Psychophysiology uses several measures to assay the physiological parameters associated with emotional states. These measures include autonomic responses (Chapter 41) as well as some somatic responses. The most commonly used measure is the galvanic skin response (also known as the skin conductance response), a measure of sympathetic autonomic arousal derived from the sweatiness of the palms of the hands. Other measures include heart rate, heart rate variability, blood pressure, respiration, pupil dilation, facial electromyography (EMG), and the startle response (see below). Some of these measures mostly correlate with basic dimensions of emotion, such as valence (eg, the

Table 42–1 Common Questionnaires Used to Assess Fear in Human Emotion Studies

Questionnaire	Type of fear questions
Fear Survey Schedule II	Probes an individual's level of fear across a range of different objects and situations that commonly evoke fear
Fear of Negative Evaluation Scale	Measures fear of being evaluated negatively by others
Social Avoidance and Distress Scale	Measures fear of social situations
Anxiety Sensitivity Index	Measures fear of experiencing different bodily sensations and feelings
Beck Anxiety Inventory	Measures fear and panic-related symptoms experienced over the prior week
Albany Panic and Phobia Questionnaire	Has the subject estimate the amount of fear they would experience in different situations
Fear Questionnaire	Measures the degree of avoidance due to fear
PANAS-X Fear (general)	Measures how much, in general, a person feels fear-related affective states
PANAS-X Fear (moment)	Measures how much, during the present moment, a person feels fear-related affective states

PANAS, Positive and Negative Affect Schedule.

detects certain environmental situations. These physiological responses are relatively automatic, yet depend on context, and occur within the brain as well as throughout the body. In the brain, they involve changes in arousal levels and in cognitive functions such as attention, memory processing, and decision making. Somatic responses involve endocrine, autonomic, and musculoskeletal systems (Chapter 41). In sum, emotions are neurobiological states that cause coordinated behavioral and cognitive responses triggered by the brain. This can occur when an individual detects a significant stimulus (positively or negatively charged) or has a specific thought or memory that leads to an endogenously generated emotion state.

Some stimuli—objects, animals, or situations—trigger emotions without the organism having to learn anything about those stimuli. Such stimuli have innately reinforcing qualities and are called unconditioned stimuli; examples are a painful shock or a disgusting taste. However, the vast majority of stimuli acquire their emotional significance through associative learning.

When an individual detects an emotionally significant stimulus, three physiological systems are engaged: the endocrine glands, the autonomic motor system, and the musculoskeletal system (Figure 42–1). The endocrine system is responsible for the secretion and regulation of hormones into the bloodstream that affect bodily tissues and the brain. The autonomic system mediates changes in the various physiological control systems of the body: the cardiovascular system, the visceral organs, and the tissues in the body cavity (Chapter 41). The skeletal motor system mediates

magnitude of the startle response) or arousal (eg, the galvanic skin response), whereas others (eg, facial EMG) can provide more fine-grained information about emotions. Facial expression has been used extensively but has no simple relationship to specific emotions.

Subjective ratings. Subjective ratings are often used in human studies and include categorical and continuous ratings (Table 42–1). These ratings can range along emotion dimensions, such as valence (pleasantness/unpleasantness), or the intensity of specific emotions. Subjective ratings necessarily depend on culture-specific words and concepts for emotions.

Experience sampling. Psychologists use experience sampling to quantify the emotions that people actually experience in everyday life. Participants might have their cell phone sound an alarm every few hours, and they then have to stop whatever activity they are doing and fill out a brief questionnaire about what they are feeling at the moment. In this way, a plot of the data can characterize how people's emotions change throughout the day or over longer periods. It turns out that we are actually fairly good at predicting what emotion people will feel next, from knowing how they currently feel.

Hormonal measures. Hormonal responses to emotional states are typically slower than psychophysiological measures. Emotion researchers measure a variety of hormones to assay emotional states over these lengthy periods. Relatively undifferentiated arousal responses are used to evaluate stress. The stress hormone cortisol (Chapter 61) is easily measured from people's saliva.

Specific experimental probes. Several specific behavioral and physiological assays are used to probe emotions with specific stimuli. These assays generally fall within the field of psychophysiology. A common measure is the amplitude of a subject's eyeblink (or other startle reflexes) when a loud sound is presented. This is potentiated when the subject is in a negatively valenced emotional state. Potentiation of the startle reflex is often used to assay the level of anxiety in people, and the same measure has also been validated in animals.

Measures Commonly Used in Nonhuman Animals

Innate behavioral responses. Animals often exhibit stereotyped behaviors as a consequence of certain emotional states. Observing and scoring the behavior is one method of measuring emotional behaviors. Such behaviors can include approaching a stimulus that is rewarding or that promises reward in the future (a positively valenced emotional state), as well as avoiding or defending against threatening stimuli (a negatively valenced emotional state). In addition, analysis of facial expressions can be utilized in many animal model systems, and has even been used for mice.

Psychophysiology and specific experimental probes. As in the case of humans, animal studies can use several psychophysiological measures (eg, heart rate, respiratory rate, galvanic skin response, pupil diameter, startle). In addition, specific behavioral assays have been developed in animals, often derived from initial observations of their innate behavioral responses. Behaviors such as freezing, attacking, exploring, approaching, and hiding can be measured in response to well-controlled experimental stimuli that are designed to induce certain emotional states. The correspondence between human and animal behaviors, which Charles Darwin originally noted in his 1872 book *The Expression of the Emotions in Man and Animals*, provides powerful animal models for investigating human emotions and their pathology.

overt behaviors such as freezing, fight-or-flight, and particular facial expressions. Together, these three systems control the physiological expression of emotion states in the body.

We begin this chapter with a discussion of the historical antecedents of modern research on the neuroscience of emotion. We then describe the neural circuits and cellular mechanisms that underlie the most thoroughly studied emotion, fear, and in so doing, we will focus on the amygdala. However, it is important to note that there does not appear to be any single brain structure that participates in only one emotion. For instance, the amygdala, which has been known to participate in negatively valenced emotions, also plays a central role in positively valenced emotions: Distinct populations of neurons within the amygdala process positively valenced versus negatively valenced stimuli. We briefly review how emotion states can be changed through extinction and regulation and how emotion interacts with other cognitive processes. We conclude with a survey on the relevance of emotion research to understanding psychiatric disorders.

The Modern Search for the Neural Circuitry of Emotion Began in the Late 19th Century

The modern attempt to understand emotions began in 1890 when William James, the founder of American psychology, asked: What is the nature of fear? Do we run from the bear because we are afraid, or are we afraid because we run? James proposed that the conscious

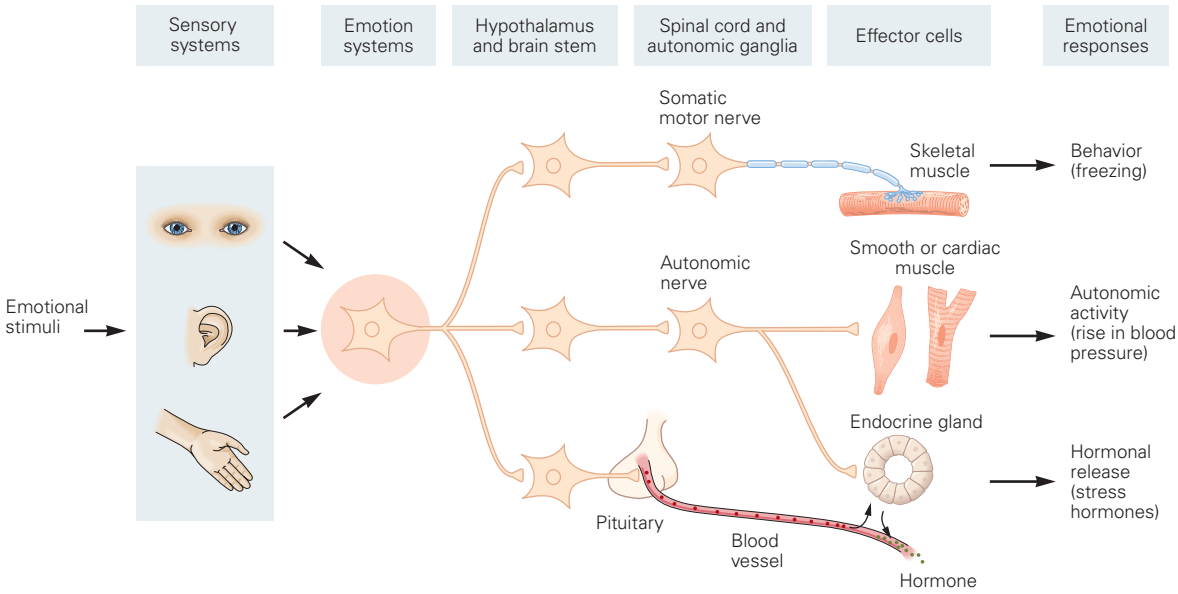

Figure 42–1 Neural control of emotional responses to external stimuli. External stimuli processed by sensory systems converge on "emotion systems" (eg, the amygdala). If the stimuli are emotionally salient, the emotion systems are activated, and their outputs are relayed to hypothalamic and brain stem regions that control physiological responses, including skeletomuscular action, autonomic nervous system activity, and hormonal release. The figure shows some responses associated with fear. It omits many of the complexities of emotion (eg, the effects of emotion states on cognition).

feeling of fear is a consequence of the bodily changes that occur during the act of running away—we feel afraid because we run. James's *peripheral feedback theory* drew on the knowledge of the brain at the time, namely, that the cortex had areas devoted to movement and sensation (Figure 42–2). Little was known at that time about specific areas of the brain responsible for emotion and feeling, but James's view is still debated to this day.

At the turn of the 20th century, researchers found that animals were still capable of emotional responses after the complete removal of the cerebral hemispheres, demonstrating that some aspects of emotion are mediated by subcortical regions. The fact that electrical stimulation of the hypothalamus could elicit autonomic responses similar to those that occur during emotional responses in an intact animal suggested to Walter B. Cannon that the hypothalamus might be a key region in the control of fight-or-flight responses and other emotions.

In the 1920s, Cannon showed that transection of the brain above the level of the hypothalamus (by means of a cut that separates the cortex, thalamus, and anterior hypothalamus from the posterior hypothalamus and lower brain areas) left an animal still capable of showing rage. By contrast, a transection below the hypothalamus, which left only the brain stem and the spinal cord, eliminated the coordinated reactions of natural rage. This clearly implicated the hypothalamus in organizing emotional reactions. Cannon called the hypothalamically mediated reactions "sham rage" because these animals lacked input from cortical areas, which he assumed were critical for the emotional experience of "real" rage (Figure 42–3).

Cannon and his student Phillip Bard proposed an influential theory of emotion centered on the hypothalamus and thalamus. According to their theory, sensory information processed in the thalamus is sent both to the hypothalamus and to the cerebral cortex. The projections to the hypothalamus were thought to produce emotional responses (through connections to the brain stem and spinal cord), while the projections to the cerebral cortex were thought to produce conscious feelings (Figure 42–2). This theory implied that the hypothalamus is responsible for the brain's evaluation of the emotional significance of external stimuli and that emotional reactions depend on this appraisal.

In 1937, James Papez extended the Cannon-Bard theory. Like Cannon and Bard, Papez proposed that sensory information from the thalamus is sent to both the hypothalamus and the cerebral cortex. The descending connections to the brain stem and spinal cord give rise to emotional responses, and the ascending connections to the cerebral cortex give rise to feelings. But Papez

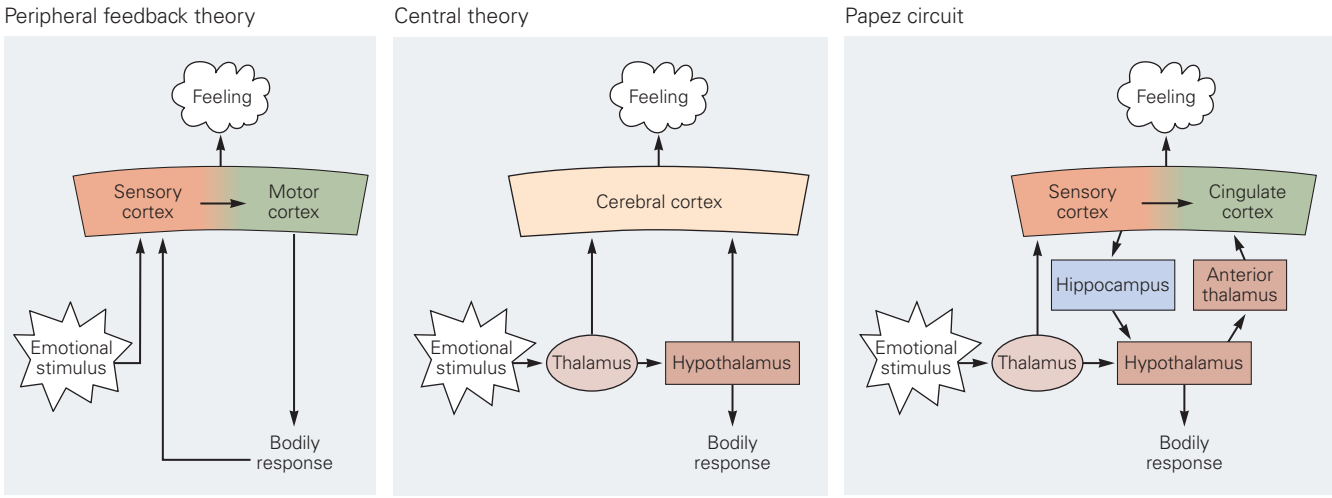

Figure 42–2 Early theories of the emotional brain. (Adapted, with permission, from LeDoux 1996.)

William James's peripheral feedback theory. James proposed that information about emotionally competent stimuli is processed in sensory systems and transmitted to the motor cortex to produce responses in the body. Feedback signals to the cortex convey sensory information about the body responses. The cortical processing of this sensory feedback is the "feeling," according to James.

The Cannon-Bard central theory. Walter Cannon and Philip Bard proposed that emotions are explained by processes within the central nervous system. In their model, sensory information is transmitted to the thalamus where it is then relayed to both the hypothalamus and the cerebral cortex. The hypothalamus evaluates the emotional qualities of the stimulus, and its descending connections to the brain stem and spinal cord give rise to somatic responses, while the thalamocortical pathways give rise to conscious feelings.

The Papez circuit. James Papez refined the Cannon-Bard theory by adding additional anatomical specificity. He proposed that the cingulate cortex is the cortical region that receives hypothalamic output in the creation of feelings. The outputs of the hypothalamus reach the cingulate via the anterior thalamus, and the outputs of the cingulate reach the hypothalamus via the hippocampus.

went on to expand the neural circuitry of feelings considerably beyond the Cannon-Bard theory by interposing a new set of structures between the hypothalamus and the cerebral cortex. He argued that signals from the hypothalamus go first to the anterior thalamus and then to the cingulate cortex, where signals from the hypothalamus and sensory cortex converge. This convergence accounts for the conscious experience of feeling in Papez's theory. The sensory cortex then projects to both the cingulate cortex and the hippocampus, which in turn makes connections with the mammillary bodies of the hypothalamus, thus completing the loop (Figure 42–2).

The hypothalamus is currently receiving intense interest in studies of emotion in animals, particularly in experiments using optogenetics to manipulate the activity of precise cell populations. These studies have shown that specific populations in the mouse ventromedial hypothalamus are necessary and sufficient for defensive emotion states. Thus the hypothalamus does not merely orchestrate emotional behaviors, but is part of the neural circuitry that constitutes the emotion state itself. The role of the hypothalamus in emotion is much less studied in humans, in part because functional magnetic resonance imaging (fMRI) does not have the spatial resolution to investigate specific hypothalamic nuclei, let alone neuronal subpopulations within them.

In the late 1930s, Heinrich Klüver and Paul Bucy removed the temporal lobes of monkeys bilaterally, thus lesioning all temporal cortex as well as subcortical structures like the amygdala and hippocampus, and found a variety of psychological disturbances, including alterations in feeding habits (the monkeys put inedible objects in their mouth) and sexual behavior (they attempted to have sex with inappropriate partners, like members of other species). In addition, the monkeys had a striking lack of concern for previously feared objects (eg, humans and snakes). This remarkable set of findings came to be known as the Klüver-Bucy syndrome and already suggested that the amygdala might be important for emotion (although it was not the only structure lesioned in these experiments).

Building on the Cannon-Bard and Papez models and the findings of Klüver and Bucy, Paul MacLean suggested in 1950 that emotion is the product of the "visceral brain." According to MacLean, the visceral brain includes the various cortical areas that had long been referred to as the limbic lobe, so named by Paul

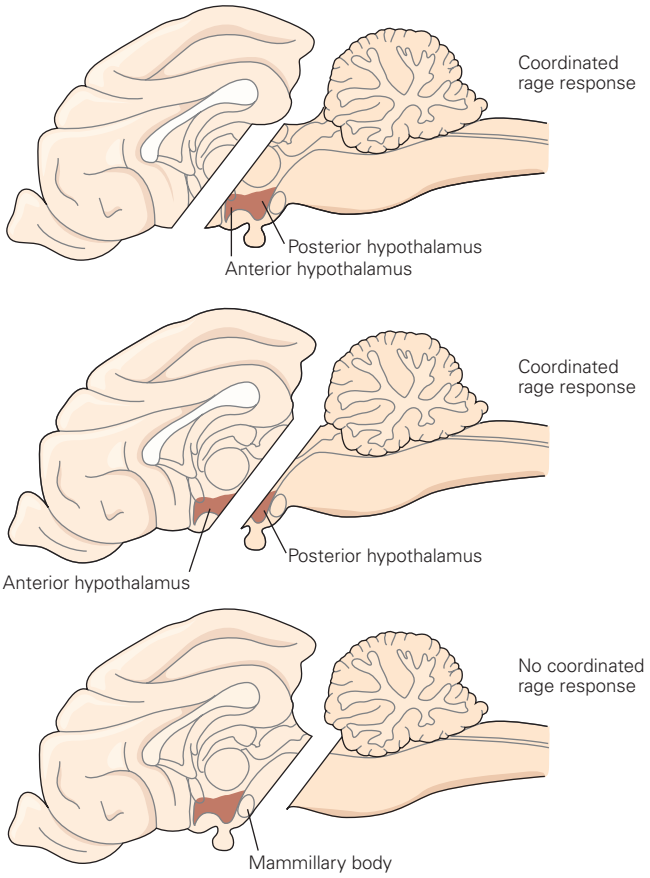

Figure 42–3 Sham rage. An animal exhibits sham rage following transection of the forebrain and the disconnection of everything above the transection (**top**) or transection at the level of the anterior hypothalamus and the disconnection of everything above it (**middle**). Only isolated elements of rage can be elicited if the posterior hypothalamus also is disconnected (**bottom**). This work derives from historical lesion studies in animals. More recent work suggests a more complex picture, in which the hypothalamus is intimately involved in creating the emotion state itself, not merely its behavioral expression.

Broca because these areas form a rim (Latin *limbus*) in the medial wall of the hemispheres. The visceral brain was later renamed the *limbic system*. The limbic system includes the various cortical areas that make up Broca's limbic lobe (especially medial areas of the temporal and frontal lobes) and the subcortical regions connected with these cortical areas, such as the amygdala and hypothalamus (Figure 42–4).

MacLean intended his theory to be an elaboration of Papez's ideas. Indeed, many areas of MacLean's limbic system are parts of the Papez circuit. However, MacLean did not share Papez's view that the cingulate cortex was the seat of feelings. Instead, he thought of the hippocampus as the part of the brain where the external world (represented in sensory regions of the lateral cortex) converged with the internal world (represented in the medial cortex and hypothalamus), allowing internal signals to give emotional weight to external stimuli and thereby to conscious feelings. For MacLean, the hippocampus was involved both in the expression of emotional responses in the body and in the conscious experience of feelings.

Subsequent findings raised problems for MacLean's limbic system theory. In 1957, it was found that damage to the hippocampus, the keystone of the limbic system, produced deficits in converting short- to long-term memory, a function that is distinct from emotions. In addition, animals with damage to the hippocampus are able to express emotions, and humans with hippocampal lesions appear to express and feel emotions normally. In general, damage to areas of the limbic system did not have the expected effects on emotional behavior.

Several of MacLean's other ideas on emotion are nevertheless still relevant. MacLean thought that emotional responses are essential for survival and therefore involve relatively primitive circuits that have been conserved in evolution, an idea already proposed by Charles Darwin almost a century earlier. This notion is key to an evolutionary perspective of emotion. It is now clear that emotions are processed by many subcortical and cortical regions and that the limbic system is by no means the primary system for emotion. Nonetheless, one component of the original limbic system, the amygdala, has received the most attention in studies of both humans and animals. Today, the role of the amygdala in learned fear is probably the best worked-out example of emotion processing in a specific brain structure, and therefore, we consider it next.

The Amygdala Has Been Implicated in Both Learned and Innate Fear

In Pavlovian fear conditioning, an association is learned between an unconditioned stimulus (US) (eg, electric shock) and a conditioned stimulus (CS) (eg, a tone) that predicts the US. For example, if an animal is presented with an emotionally neutral CS (a tone) for several seconds and then shocked during the final second of the CS, especially if this pairing of tone and shock is repeated several times, presentation of the tone alone will elicit defensive freezing and associated changes in autonomic and endocrine activity. In addition, many defensive reflexes, such as eyeblink and startle, will be facilitated by the tone alone.

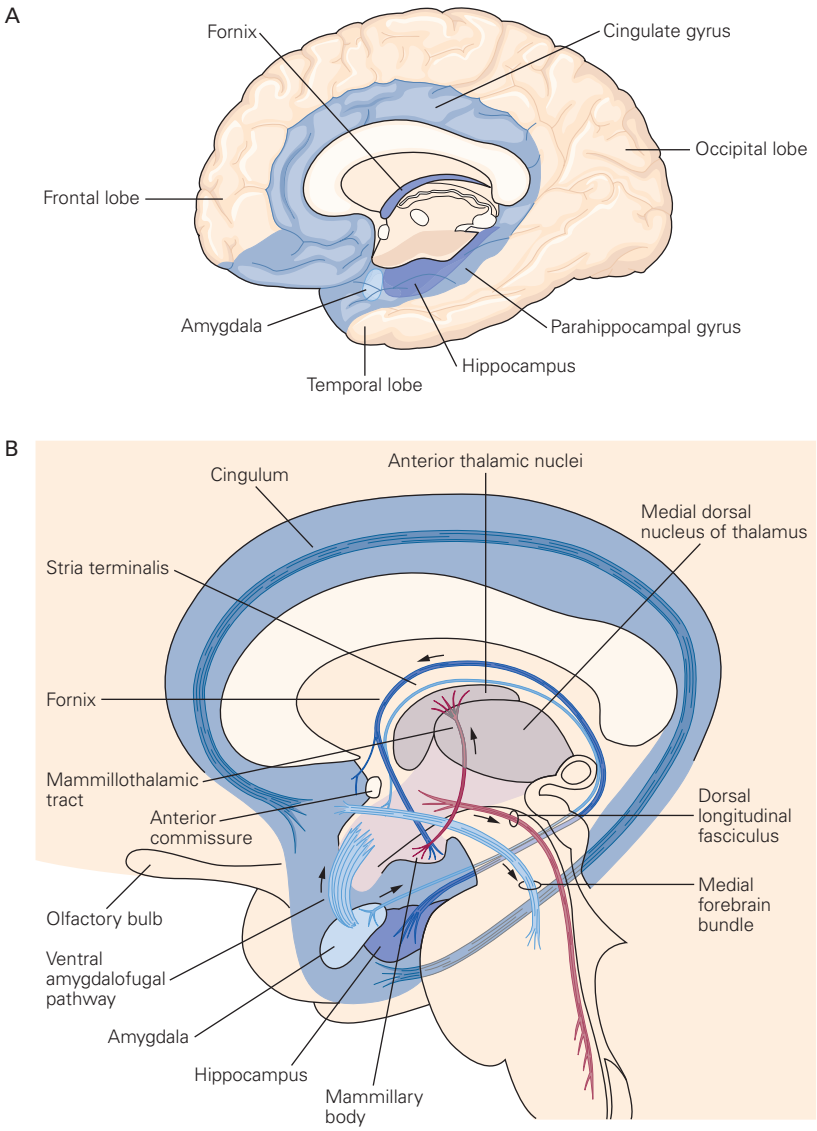

Figure 42–4 The limbic system consists of the limbic lobe and deep-lying structures. (Adapted, with permission, from Nieuwenhuys et al. 1988.)

A. This medial view of the brain shows the prefrontal limbic cortex and the limbic lobe. The limbic lobe consists of primitive cortical tissue (**blue**) that encircles the upper brain stem as well as underlying cortical structures (hippocampus and amygdala).

B. Interconnections of the deep-lying structures included in the limbic system. The **arrows** indicate the predominant direction of neural activity in each tract, although these tracts are typically bidirectional.

Research in many laboratories has established that the amygdala is necessary for Pavlovian fear conditioning: Animals with amygdala damage fail to learn the association between the CS and the US and thus do not express fear when the CS is later presented alone.

The amygdala consists of approximately 12 nuclei, but the lateral and central nuclei are especially important in fear conditioning (Figure 42–5). Damage to either nucleus, but not to other regions, prevents fear conditioning. The lateral nucleus of the amygdala receives most sensory input (but the medial nucleus receives olfactory input), including sensory information about the CS (eg, a tone) from both the thalamus and the cortex. The cellular and molecular mechanisms within the amygdala that underlie learned fear, especially in the lateral nucleus, have been elucidated in great detail. The findings support the view that the lateral nucleus is a site of memory storage in fear conditioning. Neurons in the central nucleus, by contrast, mediate outputs to brain stem areas involved in the control of defensive behaviors and associated autonomic and humoral responses (Chapter 41). The lateral and central nuclei are connected by way of several local circuits within the amygdala, including connections with the basal and intercalated masses. The actual circuitry for Pavlovian learning is thus considerably more complex than what is indicated by Figure 42–5, involving multiple relays among amygdala regions.

Sensory inputs reach the lateral nucleus from the thalamus both directly and indirectly. Much as

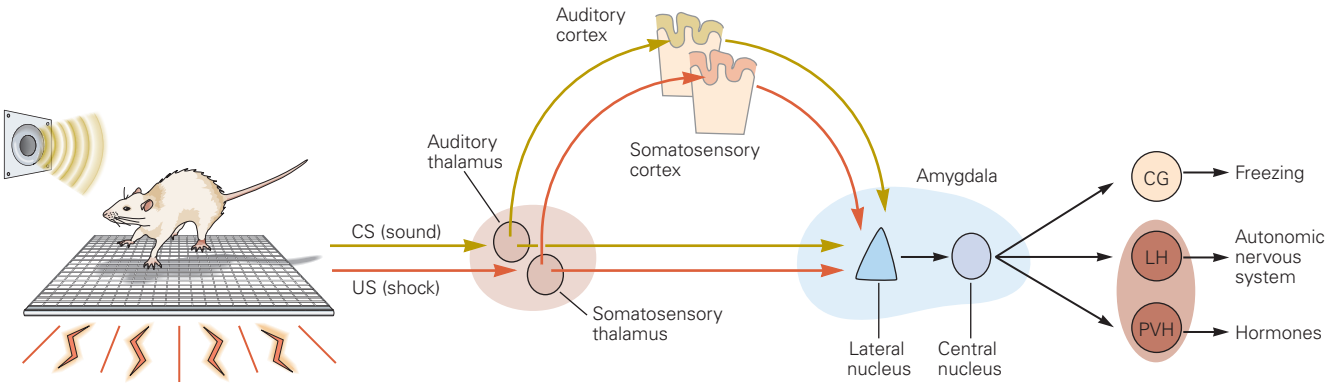

Figure 42–5 Neural circuits engaged during fear conditioning. The conditioned stimulus (**CS**) and unconditioned stimulus (**US**) are relayed to the lateral nucleus of the amygdala from the auditory and somatosensory regions of the thalamus and cerebral cortex. Convergence of the CS and US pathways in the lateral nucleus is believed to underlie the synaptic changes that mediate learning. The lateral nucleus communicates with the central nucleus both directly and through intra-amygdala pathways (not shown) involving the basal and intercalated nuclei. The central nucleus relays these signals to regions that control various motor responses, including the central gray region (**CG**), which controls freezing behavior; the lateral hypothalamus (**LH**), which controls autonomic responses; and the paraventricular hypothalamus (**PVH**), which controls stress hormone secretion by the pituitary–adrenal axis. (Adapted from Medina et al. 2002.)

predicted by the Cannon-Bard hypothesis, sensory signals from thalamic relay nuclei are conveyed to sensory areas of cerebral cortex. As a result, the amygdala and cortex are activated simultaneously. However, the amygdala is able to respond to an auditory danger cue before the cortex can fully process the stimulus information. This scheme is well worked out only for auditory fear conditioning in rodents, and it remains unclear how it applies to other cases, such as visually evoked fear in humans.

The lateral nucleus is thought to be a site of synaptic change during fear conditioning. The CS and US signals converge on neurons in the lateral nucleus; when the CS and US are paired, the effectiveness of the CS in eliciting action potentials is enhanced. This basic mechanism for a form of associative learning is similar to cellular mechanisms that underlie declarative memory in the hippocampus as well (Chapter 54). In particular, the synaptic plasticity found in the hippocampus has also been demonstrated in specific central amygdala circuits. The central amygdala thus does not simply drive motor outputs but is also part of the circuitry through which fear associations are formed and stored, very likely by transmitting information about the CS and US from the lateral nucleus. Neural plasticity likely also occurs in the basal and accessory basal nuclei during fear learning. As with the hypothalamus, recent work in rodents using tools such as optogenetics to manipulate specific subpopulations of amygdala neurons has begun to dissect this circuitry in further detail.

The emotional charge of a stimulus is evaluated by the amygdala together with other brain structures, such as the prefrontal cortex. If this system detects danger, it orchestrates the expression of behavioral and physiological responses by way of connections from the central amygdala and parts of prefrontal cortex to the hypothalamus and brain stem. For example, freezing behavior is mediated by connections from the central nucleus to the ventral periaqueductal gray region. In addition, the basal and accessory basal nuclei of the amygdala send projections to many parts of the cerebral cortex, including the prefrontal, rhinal, and sensory cortices; these pathways provide a means for neural representations in the amygdala to influence cognitive functions. For example, through its widespread projections to cortical areas, the amygdala can modulate attention, perception, memory, and decision making. Its connections with the modulatory dopaminergic, noradrenergic, serotonergic, and cholinergic nuclei that project to cortical areas also influence cognitive processing (Chapter 40). Given these very widespread connections and functional effects, the amygdala is well situated to implement one of the key features of an emotion: its coordinated and multicomponent responses.

The Amygdala Has Been Implicated in Innate Fear in Animals

Although the majority of stimuli acquire their emotional significance through learning, especially in

humans, many animals also rely on innate (unconditioned) signals in the detection of threats, mates, food, and so forth. For example, rodents exhibit freezing and other defensive behaviors when fox urine is detected. Recent studies have made considerable progress in uncovering the circuits underlying this innate fear.

In mammals, sensory signals of unconditioned threats involving predator or conspecific odors are transmitted from the vomeronasal component of the olfactory system (Chapter 29) to the medial amygdala. This stands in contrast to auditory and visual threats, which as noted above are processed via the lateral amygdala. Outputs of the medial amygdala reach the ventromedial hypothalamus, which connects with the premammillary hypothalamic nucleus. In contrast to learned fear, which depends on the ventral periaqueductal gray region, unconditioned fear responses depend on inputs from the hypothalamus to the dorsal periaqueductal gray region. There are other subcortical systems specialized for processing specific innate threats; for instance, the mouse superior colliculus is involved in detecting aerial predators, such as a hawk flying overhead.

It is difficult to study unconditioned emotional responses in humans because the possibility of learning begins right at birth and cannot be experimentally controlled, and because there appear to be large individual differences. For instance, it is thought that threat-related stimuli such as snakes and spiders may be innately fear-inducing stimuli for those people with phobias toward these animals but not for people who keep them as pets. These large individual differences, and the relative roles of innate and learned fear, are important topics for understanding psychiatric illnesses such as anxiety disorders.

The Amygdala Is Important for Fear in Humans

The basic findings from animal studies regarding the role of the amygdala in emotion have been confirmed in studies of humans. Patients with damage to the amygdala fail to show fear conditioning when presented with a neutral CS paired with a US (electric shock or loud noise). In normal human subjects, activity in the amygdala increases during CS–US pairing, as measured with fMRI.

Studies of rare human patients with bilateral amygdala lesions have led to the surprising finding of a dissociation in fear reactions to exteroceptive and interoceptive stimuli (Figure 42–6). Not only do such patients fail to show any autonomic fear reactions to exteroceptive stimuli, to either the CS or the US, but they also appear to lack any conscious experience of fear, as evidenced either from behavioral observation or through subjective verbal report on a questionnaire. In one study, such a patient was confronted with snakes and spiders in an exotic pet store, with monsters in a haunted house, and with autobiographical recollections of highly traumatic personal events (eg, being threatened with death by another person). In none of these instances was there any evidence of fear, and the patient reported feeling no fear at all (even though the patient was able to feel other emotions). These findings argue that the amygdala is necessary for the induction and experience of fear in humans.

By striking contrast, the very same patients with amygdala lesions report intense panic when they are made to feel as though they are suffocating (an interoceptive fear cue, achieved by inhaling carbon dioxide, which lowers blood pH). The dissociation of fear reactions to exteroceptive and interoceptive stimuli supports the idea that there are multiple fear systems in the human brain and that the amygdala cannot be the only structure essential for all forms of fear. Ongoing work is providing more insight, such as mapping out the specific amygdala nuclei that are damaged in these patients and which nuclei are responsible for what types of deficits. This level of resolution is standard in animal studies of the amygdala but has been difficult to achieve in humans, since the amygdala lesions cannot be made experimentally but instead must rely on rare patients that reflect accidents of nature. Equally important, there are theoretical frameworks for how to subdivide the different types of fear. For example, fear can be mapped onto a dimension of threat imminence, which may cover a range from threats that are very far away (perhaps evoking mild anxiety, and engaging monitoring and attention), to threats that are more proximal (evoking fear, and engaging responses such as freezing), to threats that are about to cause death (evoking panic, and engaging defensive behaviors). Eventually, we will need to have a more fine-grained mapping between brain systems and varieties of emotion that incorporates all of these details.

Certain forms of fear learning are relatively unique to humans. For example, simply telling a human subject that the CS may be followed by a shock is enough to allow the CS to elicit fear responses. The CS elicits characteristic autonomic responses even though it was never associated with the delivery of the shock. Humans can also be conditioned by allowing them to observe someone else being conditioned—the observer learns to fear the CS even though the CS or US was never directly presented to the observing subject. Some other animals also are able to learn fear through such observational learning, although this seems to be more rare than is the case in humans. One form of learning that is ubiquitous in humans appears to be unique to our species: active pedagogy, whereby another person teaches somebody that a stimulus is dangerous. While learning what to avoid

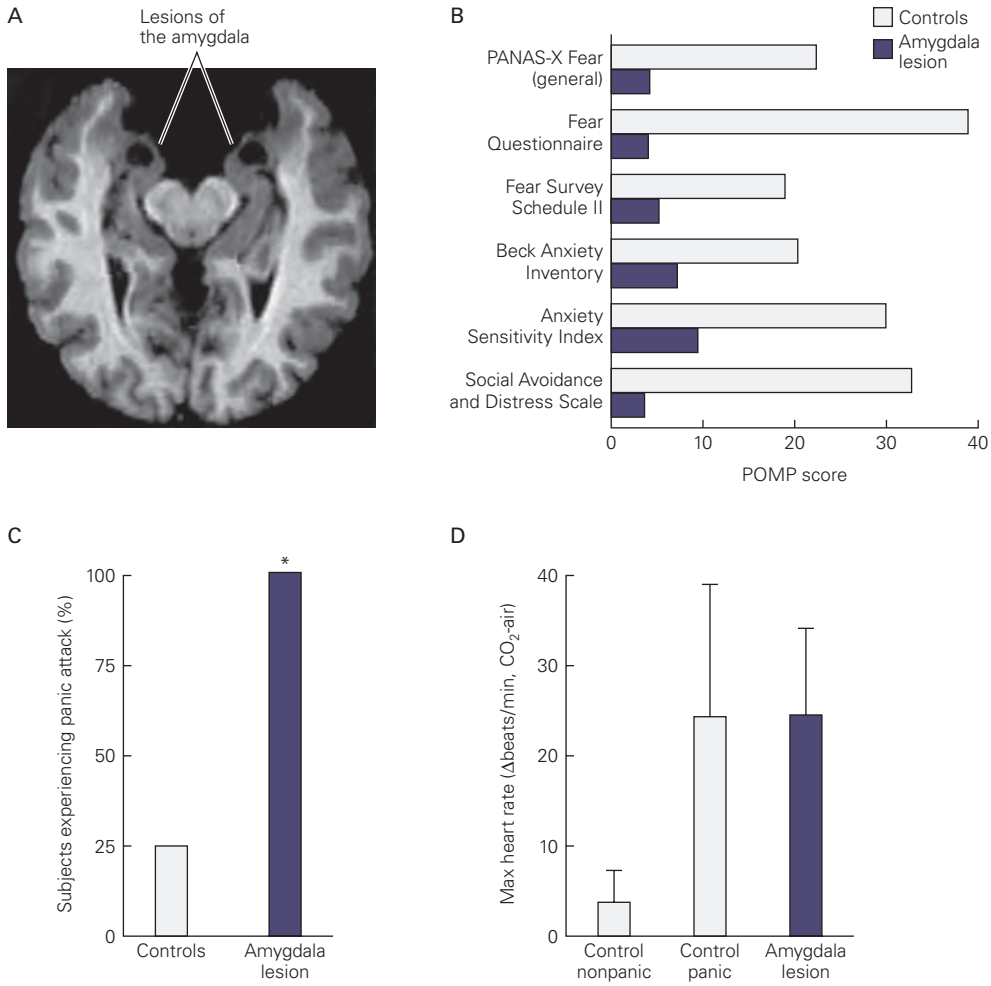

Figure 42–6 In humans, the amygdala is necessary for fear responses to external, but not internal, stimuli.

A. Magnetic resonance imaging scan of a subject's brain with bilateral amygdala lesions. Lesions were relatively restricted to the entire amygdala, a very rare lesion in humans.

B. The subject with bilateral amygdala lesions, S.M., did not report feeling fear for any of the questionnaire-based measures normally used to assess fear and anxiety (percentage of maximum score possible [POMP]). This was consistent with other findings: She did not exhibit fear when watching horror movies, when confronted with large spiders and snakes, or when visiting a haunted house during Halloween. These findings show that the human amygdala is necessary for inducing fear in response to these external stimuli. (Abbreviation: PANAS, Positive and Negative Affect Schedule.)

C. By contrast, a study of S.M. and two other subjects with bilateral amygdala lesions found that they exhibited strong panic when given an internal stimulus. They were asked to inhale carbon dioxide (CO_2), which produces a feeling of suffocation. This caused all three patients with amygdala lesions and 3 out of 12 of the control subjects with intact amygdalae to experience panic attacks.

D. Change from baseline in maximum heart rate during CO_2 inhalation relative to air trials. Both the amygdala lesion patients (n = 2) and the control subjects who panicked (n = 3) had higher increases in heart rate than the control subjects who did not panic (n = 9). (Mean ± standard error of the mean.) (Adapted, with permission from Feinstein et al 2011, 2013.)

and what to approach in the world is a large part of development in the young of all species, active teaching about the significance of stimuli has not been found in any species other than humans so far (learning through passive observation is more common).

The emotional learning and memory capacities of the human amygdala fall into the category of *implicit learning* and memory, which includes forms of memory such as the unconscious recall of perceptual and motor skills (Chapter 53). In situations of danger, however, the hippocampus and other components of the medial temporal lobe system that participate in *explicit learning* and memory (the conscious recall of people, places, and things) will be recruited as well and will encode aspects

of the learning episode. As a result, the learned indicators of danger can also be recalled consciously, at least in humans and probably in some other species as well.

Studies of patients with bilateral damage to the amygdala or hippocampus illustrate the separate contributions of these structures to implicit and explicit memory for emotional events, respectively. Patients with damage to the amygdala show no conditioned skin-conductance responses to a CS (suggesting no implicit emotional learning) but have normal declarative memory of the conditioning experience (indicating intact explicit learning). By contrast, patients with hippocampal damage show normal conditioned skin-conductance responses to the CS (suggesting intact implicit emotional learning) but have no conscious memory of the conditioning experience (indicating impaired explicit learning).

Amygdala function is altered in a number of psychiatric disorders in humans, especially disorders of fear and anxiety (Chapter 61). In addition, the amygdala plays an important role in processing cues related to addictive drugs (Chapter 43). In all of these cases, the amygdala is but one component of a distributed neural network that includes other cortical and subcortical regions. For instance, declarative memory for highly emotional events involves interactions between the amygdala and hippocampus; motivational consequences of Pavlovian conditioning involve interactions between the amygdala and the ventral striatum; and learning that a previously dangerous stimulus is now safe involves interactions between the amygdala and the prefrontal cortex. An important future direction will be to go beyond examining each component in isolation in order to better understand how emotions are processed by complex multicomponent networks of brain regions. This level of analysis is common in studies of human emotion using fMRI (see below).

The Amygdala's Role Extends to Positive Emotions

Although most work on the neural basis of emotion during the past half century has focused on aversive responses, especially fear, other studies have shown that the amygdala is also involved in positive emotions, in particular the processing of rewards. In monkeys and rodents, the amygdala participates in associating neutral stimuli with rewards (appetitive Pavlovian conditioning), just as it participates in associating neutral stimuli with punishments, and there appear to be distinct populations of neurons that encode rewards and punishments in the amygdala. This is broadly similar to findings from the rodent hypothalamus, where neurons involved in defense and in mating are also close together and only modern molecular techniques can test their independent roles.

Studies in nonhuman primates and rodents have investigated a suggestion first made by Larry Weiskrantz that the amygdala represents stimulus reward as well as punishment. For example, in a recent study, monkeys were trained to associate abstract visual images with rewarding or aversive USs. The meaning was then reversed (eg, by pairing an aversive outcome with a visual image that had previously been associated with a reward). In this way, it was possible to distinguish the role of the amygdala in representing visual information from its role in representing the reinforcement (a rewarding or aversive stimulus) predicted by a visual image. Changes in the type of reinforcement associated with an image modulated neural activity in the amygdala, and the modulation occurred rapidly enough to account for behavioral learning.

Subsequent studies using modern molecular and genetic techniques have demonstrated that distinct circuitry within the amygdala mediates a neural representation of rewarding USs, as well as rewarding experiences. The activation of a neural representation of an appetitive US in the amygdala is sufficient to induce innate valenced physiological responses as well as appetitive learning. Moreover, reactivation of neurons activated earlier by an enjoyable experience appears to be sufficient to elicit positive emotions. These findings are consistent with a growing number of functional imaging studies in humans that have shown that the amygdala is involved in emotions quite broadly. For example, the human amygdala is activated when subjects observe pictures of stimuli associated with food, sex, and money or when people make decisions based on the reward value of stimuli.

Emotional Responses Can Be Updated Through Extinction and Regulation

Once conditioned fear has been learned, it can be extinguished by later experiencing that the CS is now safe, for instance, by repeatedly presenting the CS without any US pairing. The circuitry underlying fear extinction has been studied in detail as it is highly relevant to psychiatric illnesses such as post-traumatic stress disorder (PTSD). Projections from the prefrontal cortex to the amygdala are required to override the conditioned fear in the amygdala. While conditioned fear responses decline during extinction, they are never completely erased, as demonstrated by the phenomenon of reinstatement, where fear can suddenly reappear.

Cognitive therapies for changing emotion states have also been studied, primarily in humans. For instance, a focused effort to increase or decrease the intensity of an emotion like fear has some effect on the emotion state. Indeed, neuroimaging studies have found that people can, to some degree, change their amygdala activation to fear-inducing stimuli just by how they think about those stimuli. Emotion regulation is a complex phenomenon, since there are multiple strategies for changing the emotion, ranging from just suppressing the motor behaviors to better control over how we evaluate a situation. These multiple sources of emotion regulation, especially in humans, highlight the fact that emotions must often be adjusted in keeping with complex social norms.

Emotion Can Influence Cognitive Processes

As evidenced in the above examples, emotion interacts with many other aspects of cognition, including memory, decision making, and attention. We discussed above an example of nondeclarative emotional memory, Pavlovian fear conditioning, but emotions can also influence declarative memory. Projections from the amygdala to the hippocampus can influence how learning is encoded and consolidated into long-term declarative memory. This accounts for why we remember best those events in our lives that are the most emotional, such as weddings and funerals.

Emotion has complex effects on decision making, as one might expect, since the subjective evaluation of such variables as risk, effort, and value is modulated by emotion. For instance, different choices with the same objective risk can elicit different behavioral decisions depending on whether they are framed as a win or a loss. For example, subjects typically prefer a sure gain of $5 to a 50% chance of winning $10, but prefer a 50% chance of losing $10 to a sure loss of $5. Interestingly, fMRI studies have revealed that such framing modulates amygdala activation. There is greater amygdala activation in the "win" frame when subjects choose a sure amount over a risky gamble, and greater amygdala activation in the "loss" frame when subjects choose the gamble over the sure amount. Thus, value representations in the amygdala are not rigidly associated with stimuli but are modulated by context-dependent evaluation.

Because emotionally relevant stimuli are highly salient to an organism's self-interest, they typically capture attention. For instance, people tend to orient toward, and look at, emotionally relevant visual stimuli, even when those stimuli are presented under conditions where they cannot be consciously perceived. One intriguing finding is that patients with bilateral amygdala lesions are impaired not only in their experience and expression of fear, as described above, but also in their recognition of fear in other people. One such patient, a woman called S.M., was selectively impaired in recognizing fear from facial expressions. This impairment in turn appears to result from a more basic impairment in allocating visual attention to those regions of the face that normally signal fear. S.M. does not spontaneously fixate on the eye region of the face when she looks at facial expressions and therefore does not process detailed visual information from wide eyes that would normally contribute to the recognition of fear when one is looking at a fearful face (Figure 42–7).

These findings suggest an important role for the amygdala in attention and highlight the possibility that apparently specific deficits for certain emotions (like fear) might arise from more basic attentional or motivational effects. There is ongoing debate about the precise role of the human amygdala in attentional aspects of emotion processing: Some studies argue that it comes into play even for nonconscious threat-related stimuli and in a very automatic fashion; other studies argue that the amygdala requires more elaborated and conscious processing once attention has already been allocated. Single-neuron recordings from the human amygdala support the latter view, whereas some fMRI studies support the former view. All of the findings from human lesion studies will need to be more finely dissected; some recent work on patients who have damage only to specific amygdala subnuclei is yielding further insights.

Many Other Brain Areas Contribute to Emotional Processing

As seen in the case of conditioned and unconditioned fear, the amygdala contributes to emotional processing as part of a larger circuit, or set of circuits, that includes regions of the hypothalamus and brain stem, eg, the periaqueductal gray region in the brain stem. Cortical areas are also important components of this circuit.

A number of human studies have implicated the ventral region of the anterior cingulate cortex, the insular cortex, and the ventromedial prefrontal cortex in various aspects of emotional processing. The medial prefrontal cortex and amygdala are closely connected with one another, and neurons in these brain regions show complex responses that encode information about many emotional and cognitive variables. These findings contribute to an emerging picture of a dynamic neural substrate for emotion states: Individual states are not the outcome of a single structure or specific neurons, but are more

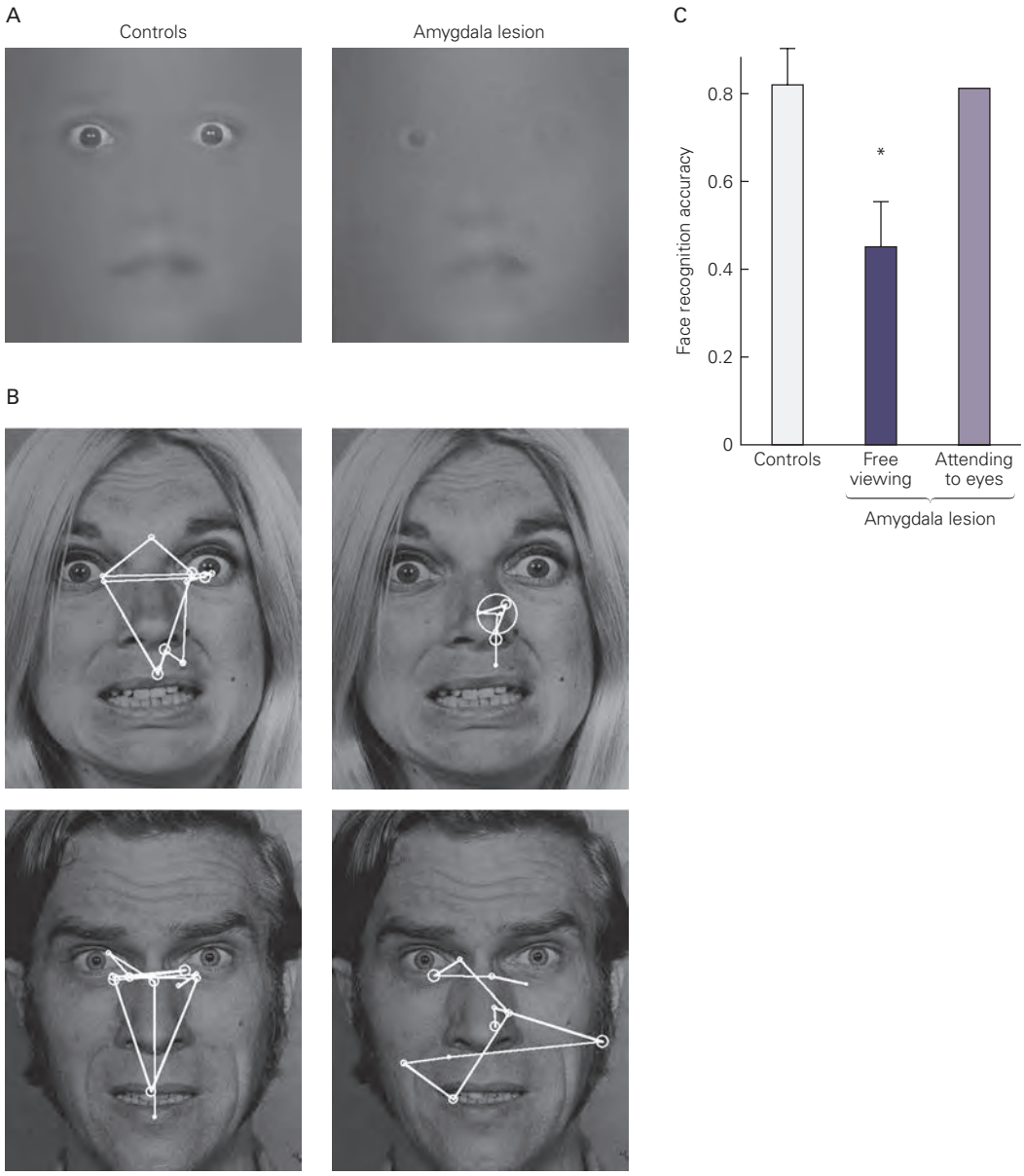

Figure 42–7 **Bilateral amygdala lesions impair the recognition of fear in the facial expressions of others.** This impairment may be due to abnormal processing of information from the face. (Reproduced, with permission, from Adolphs et al. 2005.)

A. S.M. made significantly less use of information from the eye region of faces when judging emotion. These images show the regions of the face from which control subjects (*left*) or S.M. (*right*) were able to recognize fear. The results were obtained by showing subjects many trials with only small parts of the face revealed. All those trials in which subjects were able to recognize fear could then be summed to produce an image like this, which shows the regions of the face that viewers make use of in order to discriminate fearful from happy faces (these particular parts of the face allow viewers to tell apart fearful from happy faces, whereas other parts do not help with this discrimination).

B. While looking at whole faces, S.M. (*right*) exhibited abnormal face gaze (indicated by **white lines**), making far fewer fixations to the eyes than did controls (*left*). This shows that S.M. failed to attend to and hence process visual information from the eye region. This deficit was observed across all emotions, but was most important for fear recognition because wide eyes normally predict fear.

C. S.M. showed poor ability to recognize fear when freely observing whole faces (**free viewing**), but her performance improved remarkably when instructed to look at the eyes (**attending to eyes**). This result shows that the role of the amygdala in processing fearful expressions involves directing attention onto features that are particularly significant (the eyes), rather than the downstream process of interpreting the sensory input.

flexibly assembled over a distributed population of multifunction neurons.

Some emotions are associated with social interaction and range from empathy and pride to embarrassment and guilt. Like the primary emotions such as fear, pleasure, or sadness, these social emotions produce various bodily changes and behaviors and can be experienced consciously as distinct feelings. This class of emotions may depend especially on cortical regions in the prefrontal cortex.

Studies of patients with neurological disease and focal brain lesions have advanced the understanding of the neural circuitry of emotions (Box 42–2). For example, damage to some sectors of the prefrontal cortex markedly impairs social emotions and related feelings. In addition, these patients show marked changes in social behavior that resemble the behavior of patients with developmental sociopathic personalities. Patients with damage to some sectors of the prefrontal cortex are unable to hold jobs, cannot maintain stable social relationships, are prone to violate social conventions, and cannot maintain financial independence. It is common for family ties and friendships to break after the onset of this condition. Recent studies reveal that, under controlled experimental conditions, the moral judgments of these patients can also be flawed.

Patients with medial and ventral frontal lobe damage, unlike patients with more dorsal or lateral frontal lobe damage, do not have motor defects such as limb paralysis or speech defects and thus may appear at first to be neurologically normal. Their perceptual abilities, attention, learning, recall, language, and motor abilities often show no signs of disturbance. Some patients have IQ scores in the superior range.

Box 42–2 Lesion Studies of Emotion

Examination of patients with focal lesions complements neuroimaging studies of the neural correlates of emotions. In addition to studies of the amygdala, lesion studies have provided insights into the role of several other brain regions in processing emotions.

One of the most famous set of studies harks back to the accident of Phineas Gage, who in 1848 suffered an injury to his ventromedial prefrontal cortex. Gage was working on constructing a railway in Vermont and was tamping gunpowder into a hole with a long metal rod, called a tamping iron. By accident, he struck a spark in the rock and the gunpowder exploded, shooting the tamping iron straight through his head.

Amazingly, Gage lived for many years after this horrible accident, but he was a changed person with notable changes in his social and emotional behavior. This was the first evidence that parts of the prefrontal cortex played a role in emotions. Since Gage, several patients with damage centered on the ventromedial prefrontal cortex have been described. These patients have poor insight and decision-making abilities and tend to have blunted or unusual emotional responses, especially for social emotions.

Unlike normal individuals, patients with these frontal lesions do not exhibit changes in heart rate or degree of palm sweating when shown pictures that have emotional content, although they can describe the pictures flawlessly. Likewise, patients with frontal lesions do not show skin conductance changes, a sign of sympathetic activation, during the period that precedes making risky and disadvantageous decisions, suggesting that their emotional memory is not engaged during that critical period. Also unlike normal subjects, these patients fail in tasks in which they have to make a decision under conditions of uncertainty, and in which reward and punishment are important factors.

Several brain regions are also more specifically involved in feelings. Damage to the right somatosensory cortex (primary and secondary somatosensory cortices and insula) impairs social feelings such as empathy. Consistent with this finding, patients with lesions in the right somatosensory cortex fail to guess accurately the feelings behind the facial expressions of other individuals. This ability to read faces is not impaired in patients with comparable lesions of the *left* somatosensory cortex, indicating that the right cerebral hemisphere is dominant in the processing of at least some feelings. Body sensations such as pain and itch remain intact, as do feelings of basic emotions such as fear, joy, and sadness.

On the other hand, damage to the human insular cortex, especially on the left, can suspend addictive behaviors, such as smoking. This suggests that the insular cortices play a role in associating external cues with internal states such as pleasure and desire. Interestingly, complete bilateral damage to the human insular cortices, as caused by herpes simplex encephalitis, does not eliminate emotional feelings or body sensations, suggesting that the somatosensory cortices and subcortical nuclei in the hypothalamus and brain stem are also involved in generating feeling states.

For these reasons, they sometimes attempt to return to their work and social activities after their initial recovery from brain damage. Only when they start to interact with others are their defects noticed.

In the prefrontal cortex, the ventromedial sector is particularly important for such interactions. In most patients with impaired social emotions, this sector is damaged bilaterally, although damage restricted to the right side can be sufficient to cause impairments. The critical region encompasses Brodmann's areas 12, 11, 10, 25, and 32, which receive extensive projections from the dorsolateral and dorsomedial sectors of the prefrontal cortex. Some of these areas project extensively to subcortical areas related to emotions: the amygdala, the hypothalamus, and the periaqueductal gray region in the brain stem.

Interestingly, when asked about punishment, reward, or responsibility, adult patients with damage to the ventromedial prefrontal cortex often respond as if they still have the basic knowledge of the rules, but their actions indicate that they fail to use them in real-life situations. This dissociation suggests that their behavioral defects are not caused by a loss of factual knowledge but rather by impairment of the brain's assignment of motivational value to factors that normally exert control over behavior. In some respects, this dissociation is similar to the dissociation between explicit and implicit emotional learning vis-à-vis the hippocampus and the amygdala. An interesting hypothesis arising from these dissociations is that one might find greater deficits following lesions to emotion-related structures, like the amygdala or ventromedial prefrontal cortex, in other species, or in children, in whom explicit behavioral control has not yet evolved or developed to the degree that it has in adults. There is some support for this idea: Lesions to these structures early in life can result in more severe deficits in emotional and social behaviors than if the lesions are sustained in adulthood (a pattern opposite to that of most other lesions, which show better recovery of function the earlier the onset). These findings also suggest hypotheses for neural dysfunction that may contribute to the emotional difficulties seen in developmental psychiatric disorders, such as autism.

The above lesion studies have been complemented by controlled experimental studies using fMRI, which provide further insight into mechanisms. Functional imaging of value-based decision making in healthy human subjects shows that the ventromedial prefrontal cortex is activated during the period before making a choice. That same region is activated also just by the administration of punishment and reward, supporting the notion that the emotional significance of anticipated punishments and rewards is computed as part of the mechanism that guides this kind of decision making. Punishment and reward are frequently featured in experiments involving economic and moral decisions, and such decision making prominently involves many of the same structures that are also involved in processing emotions.

The prefrontal cortex, especially areas in the ventromedial sector, operates in parallel with the amygdala. During an emotional response, ventromedial areas govern the attention accorded to certain stimuli, influence the content retrieved from memory, and help shape mental plans for responding to the triggering stimulus. By influencing attention, both the amygdala and the ventromedial prefrontal cortex are also likely to alter cognitive processes, for example, by speeding up or slowing down the flow of sensory representations (Chapter 17).

Functional Neuroimaging Is Contributing to Our Understanding of Emotion in Humans

Neuroimaging studies of emotions typically use fMRI. These studies have contributed to our understanding of emotion in three important ways. First, they have begun to dissociate and experimentally manipulate specific aspects of emotion, such as feelings, value, or concepts of emotions. These studies are beginning to show how all these different aspects can be coordinated by activity in different brain regions.

Second, fMRI studies on emotion have been accumulating at an ever-increasing pace, and much of the data from such studies are now widely available. This provides the opportunity for meta-analyses of many studies, avoiding the limitations that may be inherent in any one study in isolation. For instance, some meta-analyses have confirmed the role of the ventromedial prefrontal cortex in representing value for many different kinds of stimuli, including food and money. Other meta-analyses have suggested that specific basic emotions (eg, fear, anger, or happiness) activate a widely distributed and overlapping set of brain regions, confirming the view that no brain structure is responsible for a single emotion.

Finally, fMRI studies have begun to use novel methods in their analyses. For example, the pattern of activation seen across many voxels in a brain region, rather than the mean level of activation in that region, is used to train powerful machine-learning algorithms to classify emotion states. This approach is demonstrating that it is possible to decode specific emotion states from distributed patterns of brain activation.

Functional Imaging Has Identified Neural Correlates of Feelings

Conscious experiences of an emotion are generally referred to as feelings. Evidence for the neural correlates of feelings comes primarily from functional imaging studies of humans and from neuropsychological testing of patients with specific brain lesions. A main challenge for these studies is in dissociating the conscious experience of the emotion from other aspects of the emotion, such as the elicitation of physiological responses, since these tend to occur contemporaneously. Another challenge is how to connect such studies with studies of emotion in animals, where we have no agreed-upon dependent measures to assay what they consciously experience.

One early functional imaging study used positron emission tomography to test the idea that feelings are correlated with activity in those cortical and subcortical somatosensory regions that specifically receive inputs related to the internal environment—the viscera, endocrine glands, and musculoskeletal system. Healthy subjects were asked to recall personal episodes and to attempt to reexperience as closely as possible the emotions that accompanied those events. Activity changed in many regions known to represent and regulate body states, such as the insular cortex, secondary somatosensory cortex (S-II), cingulate cortex, hypothalamus, and upper brain stem. These results support the idea that at least a part of the neural substrate for feelings involves brain regions that regulate and represent bodily states, a finding that bears some resemblance to the hypothesis of William James mentioned earlier, that feelings are based on an awareness of bodily reactions.

The importance of both cortical and subcortical structures in processing feelings is also borne out by more recent fMRI studies. One such study examined the feeling of fear induced by anticipation of electrical shock (Figure 42–8). In this study, subjects lay in the scanner while they saw a game on a video screen in which a virtual predator (a red dot) gets closer to the subject. Once the predator caught them, they could receive a painful electric shock to the hand. The anxiety produced when the predator was some distance away was associated with activation of the medial prefrontal cortex; as the predator closed in, the periaqueductal gray became activated, and this was correlated with reports by the subjects of a feeling of dread. This finding supports a role for the medial prefrontal cortex in planning and anticipation related to a distant threat and a role for the periaqueductal gray in mounting the defensive responses required for coping with an immediate threat.

Another brain region of interest in relation to feelings is the subgenual sector of the anterior cingulate cortex (Brodmann's area 25), which has been found in neuroimaging studies to be activated when subjects are experiencing sadness. This region is of special interest because it is also differentially activated in patients with bipolar depression, and it appears thinned in structural MRI scans of patients with chronic depression. Direct electrical stimulation of this brain region (deep brain stimulation) can dramatically improve the mood of some patients with severe depression.

Emotion Is Related to Homeostasis

While it seems clear that no brain region is specialized for any specific emotion, it is even doubtful that there are any brain regions specialized for emotions in general. It may be that all brain regions involved in emotions also carry out other functions. In fact, those nonemotional functions may give us clues about how emotions evolved and, indeed, may be the basic building blocks through which emotion states are assembled.

For example, sectors of the human insular cortex that are activated during recall of feelings are also activated during the conscious sensation of pain and temperature. The insular cortex receives homeostatic information (about temperature and pain, changes in blood pH, carbon dioxide, and oxygen) through pathways that originate in peripheral nerve fibers. These afferent fibers include, for example, the C and Aδ fibers that form synapses with neurons in lamina I of the posterior horn of the spinal cord or the pars caudalis of the trigeminal nerve nucleus in the brain stem. The pathways from lamina I and the trigeminal nucleus project to brain stem nuclei (nucleus of the solitary tract and parabrachial nucleus) and from there to the thalamus and on to the insular cortex. The identification of this functional system is further support for the idea that signals in the afferent somatosensory pathways play a role in the processing of feelings.

Moreover, in patients with pure autonomic failure, a disease in which visceral afferent information is severely compromised, functional imaging studies reveal a blunting of emotional processes *and* attenuation of activity in the somatosensory areas that contribute to feelings. Like other feelings, social feelings engage the insular cortices and the primary and secondary somatosensory cortices (S-I and S-II), as has been found in functional neuroimaging experiments evaluating empathy for pain and, separately, admiration and compassion.

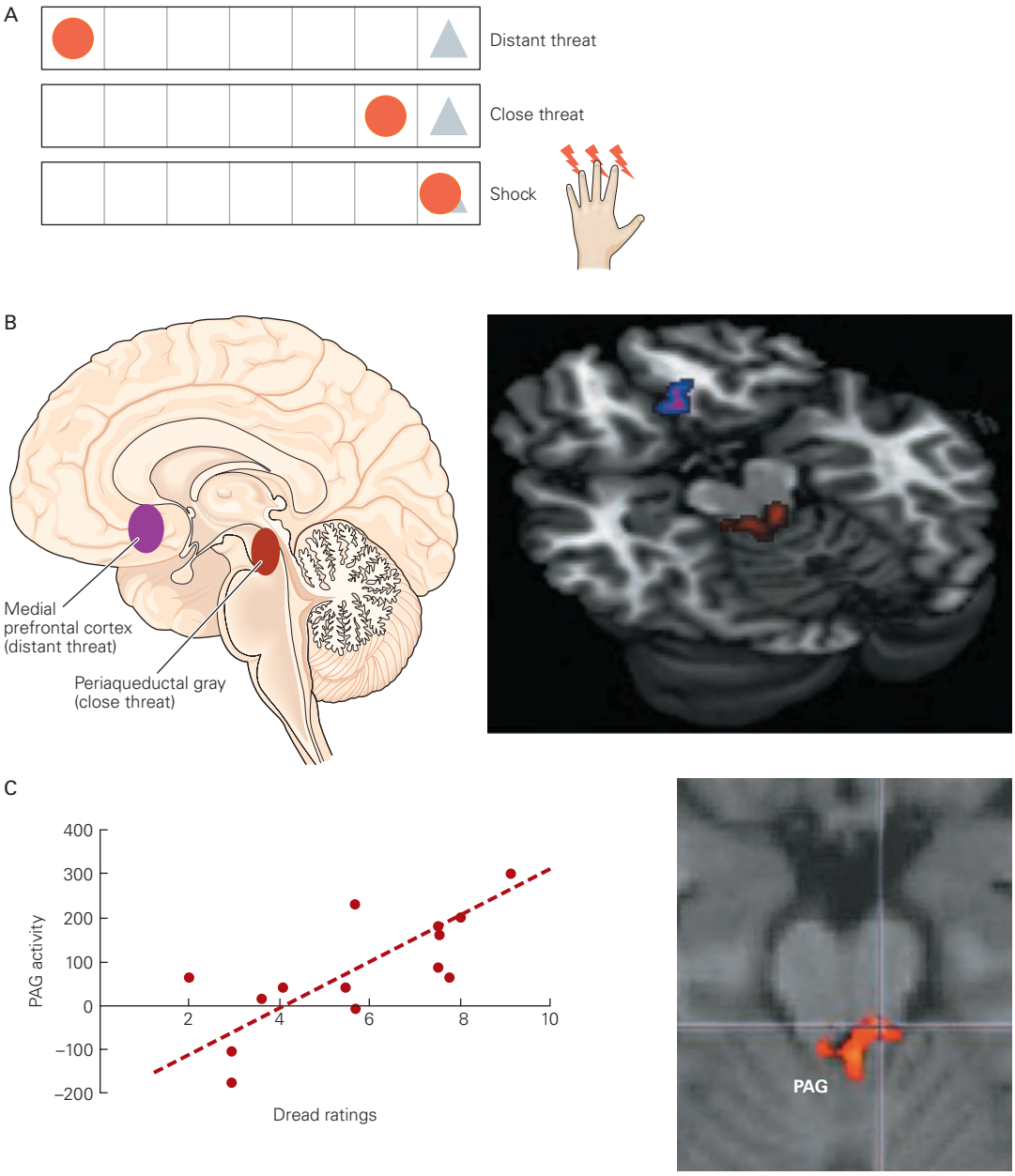

Figure 42–8 Both cortical and subcortical regions come into play during emotion states. Results are from a functional magnetic resonance imaging study in which a subject lies in the scanner while watching a virtual predator (**red dot**) move around on the screen and get closer to a subject (**blue triangle**, representing the actual research participant). (Reproduced, with permission, from Mobbs et al. 2007. Copyright © 2007 AAAS.)

A. Once the predator catches up to the subject, there is a chance that a real and painful electric shock will be delivered to the hand.

B. When the predator gets closer to the subject, activity in the prefrontal cortex and periaqueductal gray matter increases. Notably, this pattern of neural activation shifts such that a distant predator elicits greater activity in the medial prefrontal cortex, whereas a predator close by elicits more activity in the periaqueductal gray.

C. Activation of the periaqueductal gray (**PAG**) is correlated with the subjective sense of dread measured by ratings that subjects gave while in the scanner.

Using these data as support, some influential modern theories build on William James's original hypothesis and propose that the feeling of all emotions is grounded in the brain's representation of bodily homeostasis. As in the case of the amygdala's role in both positive and negative emotions, the insula's role in processing both interoceptive and emotional information is still compatible with the possibility that these processes are distinct. That is, different populations of neurons within these structures may be involved in processing different emotions. Therefore, fMRI may not provide the level of resolution needed to elucidate distinct yet anatomically intermingled neuronal populations, and cellular techniques in animal models may be required.

Although most neuroscience research thus far has focused on negatively valenced emotions, the neural circuitry for positively valenced emotions is being elucidated in studies in both humans and animals. These studies consistently implicate the medial prefrontal cortex in computing the subjective value of rewards, as well as the nucleus accumbens and other nuclei of the basal ganglia in processing the hedonic component (or pleasure) of positive emotions. A growing number of functional imaging studies in humans—especially in the fields of neuroeconomics and social neuroscience—links the role of these structures in emotion processing to their role in value-based decision making and social behavior.

Highlights

1. In the overall physiology of regulating the body and behavior of organisms, emotion states carry out functions intermediate to those of the simpler processes of reflexes and homeostatic regulation, on the one hand, and those of cognitive processes and deliberate behavior on the other. Emotions are more flexible, context-dependent, and controlled than are simple reflexes, but less flexible, context-dependent, and controlled than deliberate behavior. Emotions evolved to produce behavior in response to recurring environmental and internal challenges that are too varied for reflexes, but sufficiently stereotyped that they do not require the full flexibility of cognition.
2. Emotion states need to be carefully distinguished from the conscious experience of emotion (feelings) and also from the concepts and words that we have in everyday language to describe emotions. For example, a hissing cat's behavior is caused by an emotion state, but whether the cat consciously feels afraid is unclear. The cat probably has no concept, and certainly no words, with which to think about the emotion. Human subjects who recognize fear while observing a facial expression are attributing fear to another person and are thinking about a particular emotion, but are not themselves necessarily in a state of fear or experiencing fear. It is a major challenge in designing experiments, especially in humans, to independently control and manipulate these different components of emotion.
3. Emotions coordinate integrated changes in many organismal parameters, including effects on somatic behavior, autonomic and endocrine responses, and cognition. We do not yet understand how this coordination arises, although it is probably achieved through a combination of hierarchical control (through brain regions that function as "command centers" of sorts) and distributed dynamics. Understanding how this is accomplished in biological organisms will also inform how we might engineer robots that exhibit emotional behaviors in the future.
4. Different specific emotions can be thought of categorically (eg, happiness, fear, anger) or dimensionally (in terms of arousal and valence or other dimensional frameworks). It is likely that many of the categories for which we have words in a particular language (like the examples just given) will need to be revised once we have a more scientific understanding. New analytic methods applied to data acquired using fMRI, including methods that take into account the spatial and temporal patterns of brain activity and utilize powerful machine-learning algorithms, may provide new insights into how the brain mediates a broad range of emotions.
5. In humans, emotions can be regulated by several mechanisms. Thus, we have some control over how we feel and some control over how we express emotional behaviors, for instance, through facial expressions. Nonhuman animals do not have this same level of control, and so their emotional behaviors will generally be honest signals of their emotion state, whereas humans often engage in strategic deception.
6. Fear is probably the emotion whose neurobiology is best understood. It depends on the amygdala, in both animals and humans. However, some data suggest that certain types of fear, such as the panic of suffocating induced by inhaling carbon dioxide, are independent of the amygdala. Indeed, we now know that the amygdala is part of a distributed

brain system, and therefore, many other brain regions also participate in processing fear. Increasingly, modern studies use sophisticated genetic and cellular techniques to image and to causally manipulate brain function, allowing us to understand the necessary and sufficient roles of multiple brain structures in mediating different emotional behaviors.

7. The ventral and medial prefrontal cortex is intimately involved in emotion and connected with the amygdala. Social emotions, reward representations, and emotion regulation and extinction all involve specific sectors of prefrontal cortex. This region of the brain, together with the insula, may also be the most important for our conscious experience of emotions, an aspect of emotion that remains the most challenging to study.

C. Daniel Salzman
Ralph Adolphs

Selected Reading

Amaral DG and Adolphs R (eds). 2016. *Living Without an Amygdala*. New York: Guilford Press.

Anderson, DJ, Adolphs R. 2018. *The Neuroscience of Emotion in People and Animals: A New Synthesis*. Princeton University Press.

Bechara A, Tranel D, Damasio H, Adolphs R, Rockland C, Damasio AR. 1995. A double dissociation of conditioning and declarative knowledge relative to the amygdala and hippocampus in humans. Science 269:1115–1118.

Craig AD. 2002. How do you feel? Interoception: the sense of the physiological condition of the body. Nat Rev Neurosci 3:655–666.

Damasio AR. 1994. *Descartes's Error: Emotion, Reason, and the Human Brain*. New York: Penguin Books.

Darwin, C. 1872/1965. *The Expression of the Emotions in Man and Animals*. Chicago: Univ of Chicago Press.

Dolan RJ. 2002. Emotion, cognition, and behavior. Science 298:1191–1194.

Feinstein JS, Adolphs R, Damasio A, Tranel D. 2011. The human amygdala and the induction and experience of fear. Curr Biol 21:34–38.

Feinstein JS, Buzza C, Hurlemann R, et al. 2013. Fear and panic in humans with bilateral amygdala damage. Nat Neurosci 16:270–272.

Feldman Barrett L, Adolphs R, Marsella S, Martinez AM, Pollack SD. 2019. Emotional expressions reconsidered: challenges to inferring emotion from human facial movements. Psychol Sci Public Interest 20:1–68.

McGaugh JL. 2003. *Memory and Emotions: The Making of Lasting Memories*. New York: Columbia Univ Press.

Salzman CD, Fusi S. 2010. Emotion, cognition, and mental state representation in amygdala and prefrontal cortex. Ann Rev Neurosci 33:173–202.

Thornton MA, Tamir DI. 2017. Mental models accurately predict emotion transitions. Proc Natl Acad Sci U S A 114:5982–5987.

Whalen PJ, Phelps EA. 2009. *The Human Amygdala*. New York: Guilford Press.

References

Adolphs R, Gosselin F, Buchanan T, Tranel D, Schyns P, Damasio A. 2005. A mechanism for impaired fear recognition in amygdala damage. Nature 433:68–72.

Anderson SW, Bechara A, Damasio H, Tranel D, Damasio AR. 1999. Impairment of social and moral behavior related to early damage in human prefrontal cortex. Nat Neurosci 2:1032–1037.

Berridge KC, Kringelbach ML. 2013. Neuroscience of affect: brain mechanisms of pleasure and displeasure. Curr Opin Neurobiol 23:294–303.

Cahill L, McGaugh JL. 1998. Mechanisms of emotional arousal and lasting declarative memory. Trends Neurosci 21:294–299.

Clithero JA, Rangel A. 2014. Informatic parcellation of the network involved in the computation of subjective value. Soc Cogn and Affect Neurosci 9:1289–1302.

Damasio AR, Grabowski TJ, Bechara A, et al. 2000. Feeling emotions: subcortical and cortical brain activity during the experience of self-generated emotions. Nat Neurosci 3:1049–1056.

Damasio H, Grabowski T, Frank R, Galaburda AM, Damasio AR. 1994. The return of Phineas Gage: clues about the brain from the skull of a famous patient. Science 264:1102–1105.

De Martino B, Kumaran D, Seymour B, Dolan RJ. 2006. Frames, biases, and rational decision-making in the human brain. Science 313:684-687.

Gore F, Schwartz EC, Brangers BC, et al. 2015. Neural representations of unconditioned stimuli in basolateral amygdala mediate innate and learned responses. Cell 162:132–145.

Holland PC, Gallagher M. 2004. Amygdala-frontal interactions and reward expectancy. Curr Opin Neurobiol 14:148–155.

Jin J, Gottfried JA, Mohanty A. 2015. Human amygdala represents the complete spectrum of subjective valence. J Neurosci 35:15145–15156.

LeDoux, JE. 1996. *The Emotional Brain*. 1996. New York: Simon & Schuster.

LeDoux JE. 2000. Emotion circuits in the brain. Annu Rev Neurosci 23:155–184.

Lin D, Boyle MP, Dollar P, Lee H, Perona P, Anderson DJ. 2011. Functional identification of an aggression locus in the mouse hypothalamus. Nature 470:221–226.

MacLean PD. 1990. *The Triune Brain in Evolution*. New York: Plenum.

Mayberg HS, Lozano AM, Voon V, et al. 2005. Deep brain stimulation for treatment-resistant depression. Neuron 45:651–660.

Medina JF, Repa CJ, Mauk MD, LeDoux JE. 2002. Parallels between cerebellum- and amygdala-dependent conditioning. Nat Rev Neurosci 3:122–131.

Mobbs D, Petrovic P, Marchant JL, et al. 2007. When fear is near: threat imminence elicits prefrontal-periaqueductal gray shifts in humans. Science 317:1079–1083.

Nieuwenhuys R, Voogd J, van Huijzen Chr. 1988. *The Human Central Nervous System: A Synopsis and Atlas*, 3rd ed. Berlin: Springer-Verlag.

Ochsner KN, Gross JJ. 2005. The cognitive control of emotions. Trends Cogn Sci 9:242–249.

Paton JJ, Belova MA, Morrison SE, Salzman CD. 2006. The primate amygdala represents the positive and negative value of visual stimuli during learning. Nature 439:865–870.

Pessoa L, Adolphs R. 2010. Emotion processing and the amygdala: from a "low road" to "many roads" of evaluating biological significance. Nat Neurosci 11:773–782.

Phelps EA. 2006. Emotion and cognition: insights from studies of the human amygdala. Annu Rev Psychol 57:27–53.

Rauch SL, Shin LM, Phelps EA. 2006. Neurocircuitry models of posttraumatic stress disorder and extinction: human neuroimaging research—past, present, and future. Biol Psychiat 60:376–382.

Redondo RL, Kim J, Arons AL, Ramirez S, Liu X, Tonegawa S. 2014. Bidirectional switch of the valence associated with a hippocampal contextual memory engram. Nature 513:426–430.

Saez A, Rigotti M, Ostojic S, Fusi S, Salzman CD. 2015 Abstract context representations in primate amygdala and prefrontal cortex. Neuron 87:869–881.

Weiskrantz L. 1956. Behavioral changes associated with ablation of the amygdaloid complex in monkeys. J Comp Physiol Psychol 49:381–391.

43

Motivation, Reward, and Addictive States

Motivational States Influence Goal-Directed Behavior

One day a cheetah, taking refuge from the mid-day sun in the shade of a tree, views a distant antelope with apparent indifference. Later in the afternoon, the sighting of the antelope provokes immediate orienting and stalking behavior. The stimulus is the same, but the behavioral responses are very different. What has changed is the motivational state of the animal.

Motivational states influence attentiveness, goal selection, investment of effort in the pursuit of goals, and responsiveness to stimuli. They thus drive approach, avoidance, and action selection. This chapter focuses on the neurobiological basis of motivational states related to rewards and the manner in which reward-related brain circuits are implicated in mechanisms underlying drug addiction.

Both Internal and External Stimuli Contribute to Motivational States

Motivational states reflect one's desires, and desires can be influenced by physiological status as well as by stimuli that predict future rewarding and aversive events. Motivational states thus depend on both internal and external variables. Internal variables include physiological signals concerning hunger or thirst, as well as variables related to the circadian clock. For example, the frequency and duration of foraging vary with the time of day, the time since an animal has last eaten, and whether, if female, she is lactating.

Other internal variables are related to cognitive processes. In the game of blackjack, for instance, being dealt the same card in different hands can cause a player to go bust or make 21, leading to very different emotional responses and adjustments in subsequent decision making and action selection. The differential meaning of the same stimulus (a particular card) is made possible by the cognitive understanding of the rules of the game of blackjack. The cognitive understanding of

a rule is an internal variable. Similarly, different social situations often elicit distinct behavioral responses to the same stimulus, such as whether one chugs wine at a college party or sips it at a formal dinner.

External variables also influence motivational states. These variables include *rewarding incentive stimuli.* For example, when a dehydrated cheetah comes across a watering hole during a search for antelopes, the sight of the water may serve as an incentive stimulus, tipping the balance between hunger and thirst and driving the animal to interrupt its quest for food to drink. However, an internal variable—the state of the cheetah's hydration—can also lead to a different reward value being assigned to the same sensory stimulus, the watering hole. Even innately rewarding stimuli, such as a sweet tastant that normally elicits pleasure, can in some circumstances become unpleasurable. Chocolate cake may be innately rewarding to chocolate lovers, but satiation to the chocolate—which involves modulation of an internal variable—can decrease the reward value of this stimulus and thereby affect motivational state.

Rewards Can Meet Both Regulatory and Nonregulatory Needs on Short and Long Timescales

Feeding, drinking, and thermoregulatory behaviors and their underlying motivational states typically arise in response to (or anticipation of) a physiological imbalance. In these cases, actions acquire rewards in a relatively short timescale. In contrast, some motivational states serve biological imperatives other than short-term physiological homeostasis. More complex long-term goals, such as finding and sustaining a love partner or achieving an educational or professional goal, require goal-oriented actions on longer timescales. Nonregulatory motivational states may resemble those arising from physiological signals, but motivated behaviors often involve sequences of actions in which not every action is immediately rewarded (except in the sense of making progress toward a longer-term goal).

In general, incentive stimuli, even stimuli that only signal progress toward a longer-term goal, can influence motivational states so that complex behavioral sequences are completed. A simple example of this concept is when a cheetah must stalk, chase, run down, and kill an antelope, and then drag the carcass to a refuge before beginning to feed. Of course, even the complexity of the actions involved in foraging and feeding is far simpler than the steps required of a student motivated to achieve a graduate degree and develop an academic career. Motivational states must be sustained across challenging circumstances in order to achieve such goals.

The Brain's Reward Circuitry Provides a Biological Substrate for Goal Selection

Rewards are objects, stimuli, or activities that have positive value. Rewards can incite an animal to switch from one behavior to another or to resist interruption of ongoing action. For example, a rat that encounters a seed while scouting the environment may cease exploring in order to eat the seed or carry it to a safer place; while nibbling the seed, the rat will resist the efforts of another rat to steal the food from its paws. If seeds are made available only at a particular location and time, the rat will go to that location as the expected moment of reward delivery approaches.

Much contemporary work in neuroscience is directed at elucidating the neural systems that process different types of rewards. These systems must link the initial sensory representation of a reward to different behaviors that respond to physiological needs and environmental challenges and opportunities. Pathologies such as addiction can highjack these reward systems, resulting in maladaptive behavior (discussed in the latter part of this chapter).

Goal-directed behaviors entail the assessment of risks, costs, and benefits. Straying from the herd may offer an antelope better opportunities for foraging but only at the risk of becoming an easier target for a lurking cheetah. Attacking the venturesome antelope offers the cheetah an easier promise of a meal but at the risk that energetic and hydromineral resources will be depleted needlessly if the antelope gets away. Thus, the neural mechanisms responsible for goal selection must weigh the costs and benefits of different behaviors that might attain a specific goal.

In 1954, James Olds and Peter Milner reported their work on the neural pathways responsible for reward-related behaviors. These classic studies employed electrical brain stimulation as a goal. Rats and other vertebrates ranging from goldfish to humans will work for electrical stimulation of certain brain regions. The avidity and persistence of this self-stimulation are remarkable. Rats will cross electrified grids, run uphill while leaping over hurdles, or press a lever for hours on end in order to trigger the electrical stimulation. The phenomenon that leads the animal to work for self-stimulation is called *brain stimulation reward* (Figure 43–1A). Brain stimulation, therefore, elicits a motivational state, a strong drive to perform an action (eg, lever pressing) that will deliver further stimulation.

Although brain stimulation reward is an artificial goal, it mimics some of the properties of natural goal objects. For example, brain stimulation can compete with, summate with, or substitute for other reward-predictive stimuli to induce motivational states that

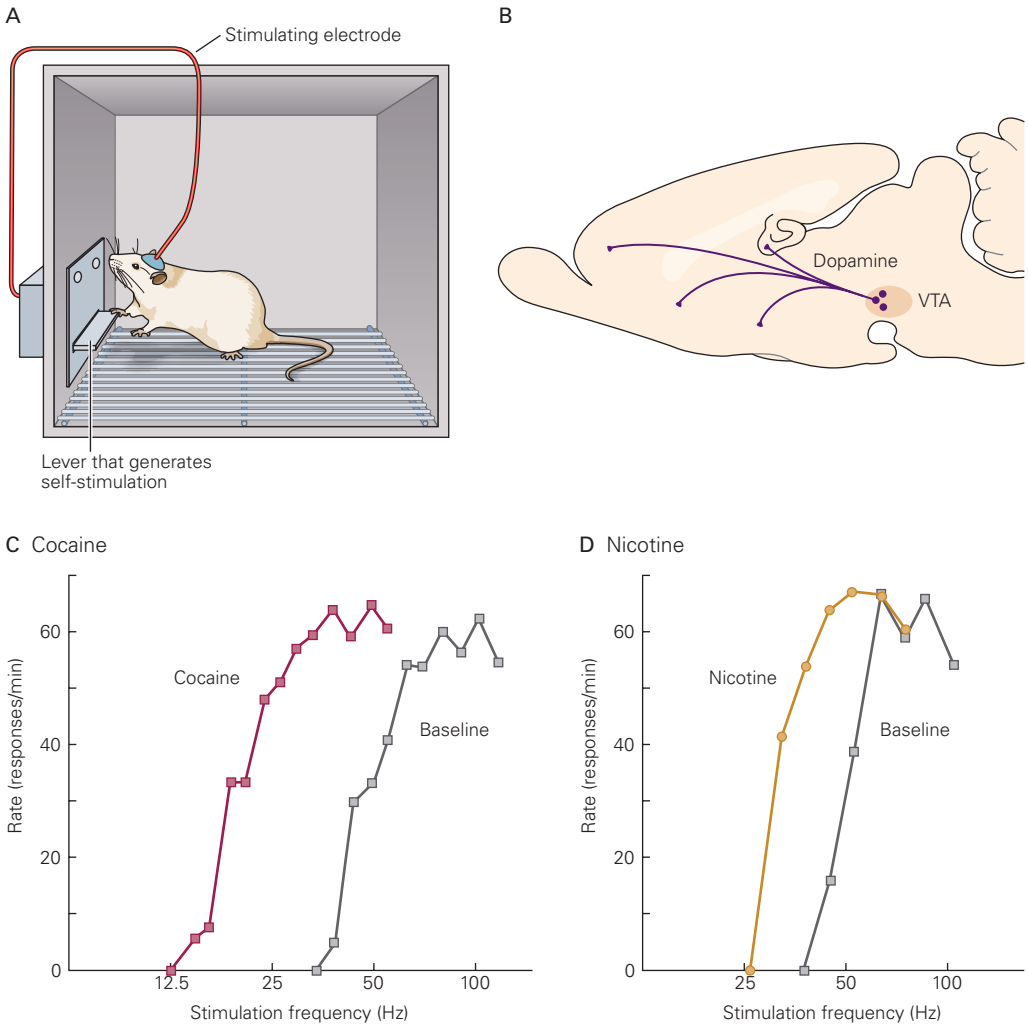

Figure 43–1 Intracranial self-stimulation recruits reward circuitry and dopaminergic neural pathways.

A. Classic testing apparatus for self-stimulation experiments. In this example, an electrode is implanted in a brain region of a rodent. Lever pressing by the rodent triggers electrical stimulation of that brain area.

B. Brain structures that produce self-stimulation behavior typically activate dopaminergic pathways emanating from the ventral tegmental area (VTA), among other pathways.

C–D. Cocaine and nicotine affect the rate of electrical self-stimulation. The rate at which the animal presses the stimulation lever increases with increases in the frequency of the self-stimulation current. In the presence of the drugs, animals press the lever at lower stimulation frequencies, indicating that the drugs augment the effects of the electrical stimulation.

drive goal-directed behaviors. The circuitry that mediates brain stimulation reward is broadly distributed. Rewarding effects can be produced by electrical stimulation of sites at all levels of the brain, from the olfactory bulb to the nucleus of the solitary tract.

Particularly effective sites lie along the course of the medial forebrain bundle and along longitudinally oriented fiber bundles coursing near the midline of the brain stem. Stimulation of either of these pathways results in activation of dopaminergic neurons in the ventral tegmental area of the midbrain. These neurons project to several areas of the brain, including the nucleus accumbens (the major component of the ventral striatum), the ventromedial portion of the head of the caudate nucleus (in the dorsal striatum), the basal forebrain, and regions of the prefrontal cortex (Figure 43–1B).

Activation of dopaminergic neurons in the ventral tegmental area plays a crucial role in brain stimulation reward. The effects of this activation are strengthened

by increases in dopaminergic synaptic transmission and weakened by decreases. These dopaminergic neurons are excited by glutamatergic cells in the prefrontal cortex and amygdala as well as from cholinergic cells in the laterodorsal tegmental and pedunculopontine nuclei of the hindbrain, and are inhibited by local GABAergic cells within or just caudal to the ventral tegmental area. Brain stimulation is thought to activate dopaminergic neurons in the ventral tegmental area in part through the activation of these hindbrain cholinergic neurons. Blockade of this cholinergic input reduces the rewarding effects of the electrical stimulation. While most attention has focused on dopamine pathways in mediating brain stimulation reward, it is important to emphasize the involvement of non-dopaminergic pathways as well.

The strength of brain stimulation reward is indicated by the finding that starving rats provided with brief daily access to food will forego eating to press a lever for brain stimulation. The heedless pursuit of an artificial goal to the detriment of a biological need is one of many parallels between self-stimulation and drug abuse. Indeed, drugs of abuse augment the rewarding effects of activation of dopaminergic pathways with brain stimulation (Figure 43–1C,D). Lower frequencies of stimulating currents accompanied by cocaine or nicotine administration—both of which enhance dopaminergic neurotransmission through different mechanisms—produce a rate of lever pressing equivalent to that obtained during self-stimulation at higher stimulating currents in the absence of these drugs. These results indicate that cocaine and nicotine amplify the effects of neuronal activation elicited by microstimulation.

Dopamine May Act as a Learning Signal

An earlier view of the function of dopamine was that it conveyed "hedonic signals" in the brain and that, in humans, it was directly responsible for subjective pleasure. From this point of view, addiction would reflect the habitual choice of short-term pleasure despite a host of long-term life problems that emerge. In fact, however, new research indicates that the hedonic principle cannot easily explain the persistence of drug use by addicted persons as negative consequences mount.

The effects of dopamine have proven to be far more complex than was first thought. Dopamine can be released by aversive as well as by rewarding stimuli, and the short latency component of a dopamine neuron's response may not be related to the rewarding or aversive qualities of a stimulus at all. Moreover, rodents lacking dopamine—rats in which dopamine is depleted by 6-hydroxydopamine and mice genetically engineered so that they cannot produce dopamine—continue to exhibit hedonic responses to sucrose. Dopamine delivery itself is not currently considered to produce hedonic qualities. Instead, the degree to which a particular sensory stimulus is rewarding is thought to be processed by a broad network of brain areas, spanning sensory cortices of different modalities, association cortex, prefrontal cortex (in particular, orbitofrontal regions), and many subcortical areas such as the amygdala, hippocampus, nucleus accumbens, and ventral pallidum.

Many of the brain areas whose activity is modulated by reward anticipation or receipt receive dopaminergic input. What information do dopaminergic neurons transmit to these brain areas? Wolfram Schultz and his colleagues discovered that dopaminergic neurons often have a complex and changing pattern of responses to rewards during learning. In one experiment, Schultz trained monkeys to expect juice at a fixed interval after a visual or auditory cue. Before the monkeys learned the predictive cues, the appearance of the juice was unexpected and produced a transient increase in firing above basal levels by ventral tegmental area dopaminergic neurons. As the monkeys learned that certain cues predict the juice, the timing of the firing changed. The neurons no longer fired in response to presentation of the juice—the reward—but earlier, in response to a predictive visual or auditory cue. If a cue was presented but the reward was withheld, firing paused at the time the reward would have been presented. In contrast, if a reward exceeded expectation or was unexpected, because it appeared without a prior cue, firing was enhanced (Figure 43–2).

These observations suggest that dopamine release in the forebrain serves not as a pleasure signal but as a *prediction error* signal. A burst of dopamine would signify a reward or reward-related stimulus that had not been predicted; pauses would signify that the predicted reward is less than expected or absent. If a reward is just as expected based on environmental cues, dopaminergic neurons would maintain their tonic (baseline) firing rates. Alterations in dopamine release are thus thought to modify future responses to stimuli to maximize the likelihood of obtaining rewards and to minimize fruitless pursuits. For natural rewards, like the sweet juice consumed by the monkeys in Schultz's experiments, once the environmental cues for a reward are learned, dopaminergic neuron firing returns toward baseline levels. Schultz has interpreted this to mean that as long as nothing changes in the environment, there is nothing more to learn and therefore no need to alter behavioral responses.

Experiments using functional magnetic resonance imaging in humans have provided further evidence

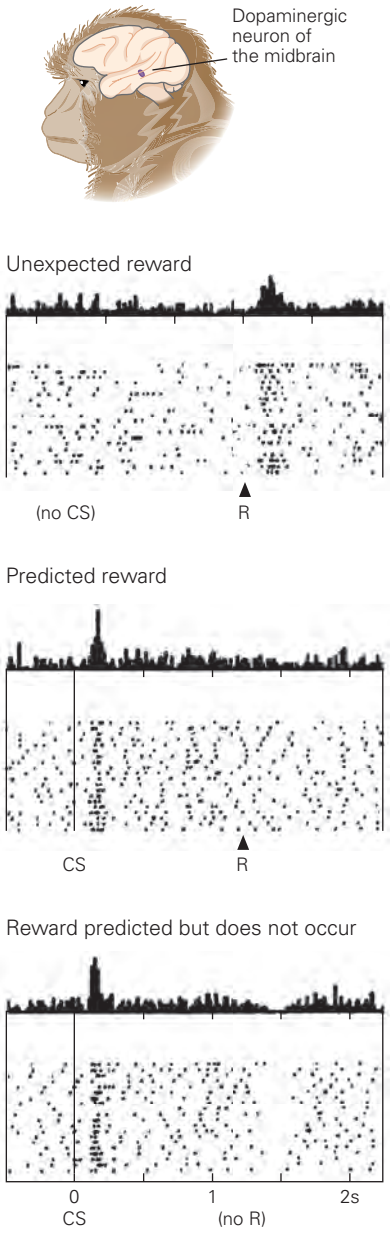

Figure 43–2 Dopaminergic neurons report an error in reward prediction. Graphs show firing rates recorded from midbrain dopaminergic neurons in awake, active monkeys. **Top:** A drop of sweet liquid is delivered without warning to a monkey. The unexpected reward (**R**) elicits a response in the neurons. The reward can thus be construed as a positive error in reward prediction. **Middle:** The monkey has been trained that a conditioned stimulus (**CS**) predicts a reward. In this record, the reward occurs according to the prediction and does not elicit a response in the neurons because there is no error in the prediction of reward. The neurons are activated by the first appearance of a predicting stimulus but not by the reward. **Bottom:** A conditioned stimulus predicts a reward that fails to occur. The dopaminergic neurons show a decrease in firing at the time the reward would have occurred. (Reproduced, with permission, from Schultz, Dayan, and Montague 1997. Copyright © 1997 AAAS.)

that dopaminergic agonists and antagonists modulate reward learning and the blood oxygen level–dependent (BOLD) signal in the nucleus accumbens. However, in some experiments, mice that lack a dopamine synthesis gene can still learn where to find a sugar or cocaine reward, suggesting that dopamine is not required for all forms of reward learning. In addition, rodents who receive amphetamines to elevate presynaptic dopamine levels over a more extended time interval exhibit enhanced "wanting" behavior (ie, increased responding in the presence of a Pavlovian cue predicting sucrose reward).

These considerations have led some investigators to suggest that dopamine has a broader role than simply driving reinforcement learning by providing prediction-error signals. Indeed, several recent studies have demonstrated considerable variation in the response properties of different subpopulations of midbrain dopaminergic neurons. Some neurons are activated by both rewarding and aversive stimuli, while others are activated preferentially by one of the two types of stimuli, and still others show opposite responses (activated by rewards and suppressed by aversive stimuli). There is some evidence that these neuronal differences are related to differences in afferent inputs and efferent projections between subpopulations of dopaminergic neurons. Understanding the precise role of this complex mixture of dopamine signals—in learning, in driving goal-directed behavior, and especially in more complex forms of learning that involve longer timescales of sequences of actions to acquire distant rewards—remains an active area of investigation.

Unlike natural rewards, addictive drugs cause dopamine release in the reward circuitry no matter how often they are consumed, and the magnitude of this release is often greater than that seen with natural rewards—dopamine is released even when the drug no longer produces subjective pleasure. To the brain, consumption of addictive drugs might always signal "better than expected" and in this way would continue to influence behavior to maximize drug seeking and drug taking. If this idea is correct, it might explain why drug seeking and consumption become compulsive and why the life of the addicted person becomes focused increasingly on drug taking at the expense of all other pursuits.

Drug Addiction Is a Pathological Reward State

Drug addiction is a chronic and sometimes fatal syndrome characterized by compulsive drug seeking and consumption despite serious negative consequences such as medical illness and inability to function in the

family, workplace, or society. Many drug addicts are aware of the destructive nature of their addiction but are unable to alter their addictive behavior despite numerous attempts at treatment.

An interesting feature of drug addiction is that only a minute fraction of all chemical substances can cause the syndrome. These so-called drugs of abuse do not share a common chemical structure, and they produce their effects by binding to different protein targets in the brain. Rather, these diverse substances can each cause a similar behavioral syndrome of addiction because their actions converge on the brain circuits that control reward and motivation (Figure 43–3).

Advances in understanding these actions have come about in large part based on studies of laboratory animals that self-administer the same drugs that cause addiction in humans. In fact, when animals are given free and unlimited access to these drugs, a subset will lose control over drug consumption—which becomes increasingly involuntary—at the expense of eating and sleeping, and some will even die by overdose. Drug self-administration and other animal models of addiction (Box 43–1) have made it possible to study both the neural circuitry through which drugs of abuse act to produce their initial rewarding effects and the molecular and cellular adaptations that drugs induce in this circuitry after repeated exposures cause an addiction-like syndrome. Over the past decade, these studies in animals, together with brain imaging studies in human addicts, have provided an increasingly complete view of the addiction process.

All Drugs of Abuse Target Neurotransmitter Receptors, Transporters, or Ion Channels

A great deal is known about the initial interactions of addictive drugs with the nervous system. Virtually all of the proteins with which such drugs interact have been cloned and characterized (Table 43–1).

Each class of drug of abuse produces a different range of acute behavioral effects, consistent with the fact that each class acts on different targets and that these targets have distinct patterns of expression throughout the nervous system and peripheral tissues. Cocaine and other psychostimulants are activating and can cause cardiac side effects because their targets

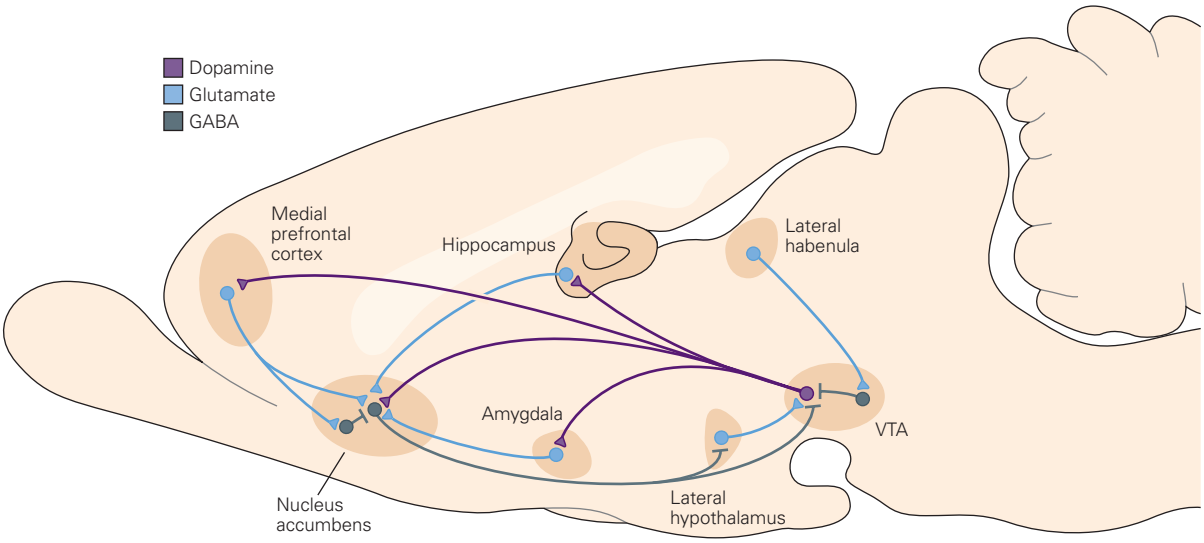

Figure 43–3 Brain reward circuits. A schematic drawing of the major dopaminergic, glutamatergic, and γ-aminobutyric acid (GABA)-ergic connections to and from the ventral tegmental area (VTA) and nucleus accumbens (NAc) in the rodent brain. The primary reward circuit includes dopaminergic projections from the VTA to the NAc. The VTA projections release dopamine in response to reward-related stimuli (and in some cases aversion-related stimuli). There are also GABAergic projections from the NAc to the VTA, with some in a direct pathway innervating the VTA and some in an indirect pathway innervating the VTA via intervening GABAergic neurons in the ventral pallidum (not shown). The NAc also contains numerous types of interneurons. The NAc receives dense innervation from glutamatergic monosynaptic circuits from the medial prefrontal cortex, hippocampus, lateral habenula, and amygdala, among other regions. The VTA receives such inputs from the amygdala and prefrontal cortex and from several brain stem nuclei that use the transmitter acetylcholine (not shown). It also receives the peptidergic terminals of neurons in the lateral hypothalamus as well as other inputs. These various inputs control aspects of reward-related perception and memory. (Adapted from Russo and Nestler 2013.)

Box 43–1 Animal Models of Drug Addiction

Several animal models have played an important role in understanding how addictive drugs produce reward acutely and an addiction-like syndrome after repeated exposures.

Drug Self-administration

The reinforcing effects of a drug can be demonstrated in experiments in which animals perform a task (eg, press a lever) to receive an intravenous drug injection. In addition to studying acquisition of this behavior, scientists assess how hard an animal will work to deliver the drug by use of progressive ratio procedures, where each successive drug dose requires an increasing number of lever presses.

Animals reach a so-called break point when they stop self-administering the drug. After weeks or months of withdrawal from or extinction of drug self-administration, animals display a relapse-like behavior: They will press the stimulation lever, which no longer delivers the drug, in response to a test dose of the drug, cues associated previously with the drug (a light or tone), or stress. These various self-administration behaviors are considered the best-validated models of human addiction.

Conditioned Place Preference

Animals learn to associate a particular environment with passive exposure to drugs. For example, a rodent will spend more time on the side of a box where it was given cocaine than on the side where it received saline. This paradigm offers an indirect measure of potency of a drug reward and demonstrates the strong cue-conditioned effects of addictive drugs.

Locomotor Sensitization

All drugs of abuse stimulate locomotion in rodents upon initial drug exposure, with increasing locomotor activation seen after repeated drug doses. Since the neural circuitry that mediates locomotor responses to drugs of abuse partly overlaps with the circuitry that mediates reward and addiction, locomotor sensitization provides a model with which to study plasticity in this circuitry during a course of chronic drug exposure.

Intracranial Self-Stimulation

Animals will work (eg, press a lever) to deliver electrical current into parts of the brain's reward circuitry (see Figure 43–1). Drugs of abuse reduce the stimulation threshold for such self-stimulation, meaning that in the presence of drug animals will work for stimulation frequencies that have no effect under control conditions.

(monoamine transporters) are expressed in peripheral nerves that innervate the heart. In contrast, opiates are sedatives and potent analgesics because their targets (opioid receptors) are expressed in sleep and pain centers.

Nevertheless, all drugs of abuse acutely induce reward and reinforcement, and this shared action reflects the fact that the drugs, despite their very different initial targets, induce some common functional effects on the brain's reward circuitry (Figure 43–4). The best established of these shared initial effects is increased dopaminergic neurotransmission in the nucleus accumbens, albeit via different mechanisms. For example, cocaine produces this effect by blocking dopamine reuptake transporters located on the terminals of the ventral tegmental neurons, whereas opiates activate ventral tegmental area dopamine neuron cell bodies by inhibiting nearby GABAergic interneurons.

Opiates also produce reward through dopamine-independent actions (eg, by activating opioid receptors on nucleus accumbens neurons themselves). All other drugs of abuse act through a combination of dopamine-dependent and -independent mechanisms (eg, activation of endogenous opioid and cannabinoid signaling) to produce some of the same functional effects on nucleus accumbens neurons. Importantly, by increasing dopaminergic neurotransmission, all such drugs also produce some of the same functional effects mediated by activation of dopamine receptors on the many other projection targets of ventral tegmental dopamine neurons (Figure 43–3), actions that are also instrumental in reward and in initiating some of the deleterious actions of repeated drug exposure.

Repeated Exposure to a Drug of Abuse Induces Lasting Behavioral Adaptations

The acute rewarding actions of drugs of abuse do not account for addiction. Rather, addiction is mediated by the brain's adaptations to the repeated exposure to such acute actions. Two main questions in the field

Table 43–1 Major Classes of Addictive Drugs

Class	Source	Molecular target	Examples
Opiates	Opium poppy	μ opioid receptor (agonist)[1]	Morphine, methadone, oxycodone, heroin, many others
Psychomotor stimulants	Coca leaf Synthetic[2] Synthetic	Dopamine transporter (antagonist)[3]	Cocaine Amphetamines Methamphetamine
Cannabinoids	Cannabis	CB1 cannabinoid receptors (agonist)	Marijuana
Nicotine	Tobacco	Nicotinic acetylcholine receptor (agonist)	Tobacco
Ethyl alcohol	Fermentation	$GABA_A$ receptor (agonist), NMDA-type glutamate receptor (antagonist), and multiple other targets	Various beverages
Phencyclidine-like drugs	Synthetic	NMDA-type glutamate receptor (antagonist)	Phencyclidine (PCP, angel dust)
Sedative/hypnotics	Synthetic	$GABA_A$ receptor (positive allosteric modulator)	Barbiturates, benzodiazepines
Inhalants	Varied	Unknown	Glues, gasoline, nitrous oxide, others

[1]The signaling pathways induced by μ receptor activation differ between opiates, differences that might be related to different addiction liabilities. Additionally, most opiates activate the δ opioid receptor, although the action at μ receptors is most important for reward and addiction.
[2]The original synthesis of amphetamine was based on the natural plant product ephedrine.
[3]While cocaine is an antagonist of the transporter, amphetamine and methamphetamine act differently: They are substrates for the transporter and, once in the nerve terminal cytoplasm, act to stimulate dopamine release.
GABA, γ-aminobutyric acid; **NMDA**, *N*-methyl-D-aspartate.
Note: Caffeine can produce mild physical dependence but does not result in compulsive use. Some illegal drugs that are abused can be harmful but do not generally produce addiction; these include the hallucinogens lysergic acid diethylamide (LSD), mescaline, psilocybin, and 3,4-methylenedioxymethamphetamine (MDMA), popularly known as ecstasy.

remain: What specific adaptations mediate the behavioral syndrome of addiction, and why are some individuals more likely to become addicted?

We know—in both animals and humans—that roughly 50% of the risk for addiction across all drugs of abuse is genetic, but the specific genes that confer risk remain largely unknown. As for most other common chronic conditions, the genetic risk for addiction is highly complex, reflecting the combined actions of hundreds of genetic variations, each of which has a very small effect. The other 50% of the risk, while incompletely understood, involves a host of environmental factors including early life stress, stress throughout life, and peer pressure.

Historically, the adaptations induced by repeated drug exposure have been described by a series of pharmacological terms. *Tolerance* refers to the diminishing effect of a drug after repeated administration at the same dose or to the need for an increase in dose to produce the same effect. *Sensitization*, also known as reverse tolerance, occurs when repeated administration of the same drug dose elicits escalating effects. *Dependence* is defined as an adaptive state that develops in response to repeated drug administration and is unmasked during *withdrawal*, which occurs when drug taking stops. The symptoms of withdrawal vary from drug to drug and include effects opposite to a drug's acute actions. Tolerance, sensitization, and dependence/withdrawal are seen with many drugs that are not addicting. For instance, two drugs used to treat hypertension, the β-adrenergic antagonist propranolol and the α_2-adrenergic agonist clonidine, produce strong dependence as evidenced by severe hypertension upon their sudden withdrawal.

Drugs of abuse are unique in causing tolerance, sensitization, and dependence/withdrawal in reward- and motivation-related behaviors, and these behaviors contribute to the syndrome of addiction. Reward tolerance, which can be viewed as homeostatic suppression of endogenous reward mechanisms in response to repeated drug exposure, is one factor leading to escalating patterns of drug use. Motivational dependence, which is manifested as negative emotional (eg, depression- and anxiety-like) symptoms seen during early drug withdrawal and also mediated by

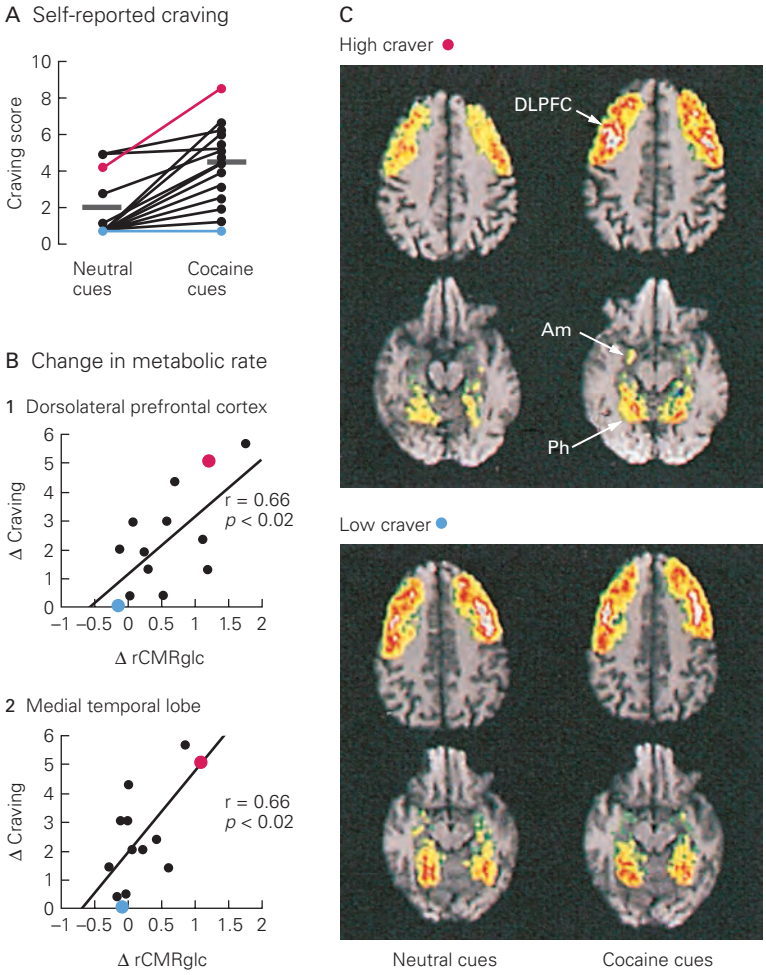

Figure 43–4 Positron emission tomography (PET) imaging reveals neural correlates of cue-induced cocaine craving. (Adapted, with permission, from Grant et al. 1996.)

A. Subjects were shown neutral or cocaine-related cues and asked, "How do you rate your craving or urge for cocaine on a scale of 1–10?" The mean craving score (**horizontal bar**) is significantly higher for exposure to cocaine-related cues than for exposure to neutral stimuli, even though the magnitude of the response across individuals varies considerably. Two subjects, identified by **red** and **blue dots**, represent high-level and low-level craving, respectively.

B. Changes in self-reported craving are correlated with changes in metabolic rate in the dorsolateral prefrontal cortex and medial temporal lobe during exposure to cocaine-related cues. The abscissa plots the difference in metabolic rate between the two sessions (activity with cocaine cues minus activity with neutral cues). Metabolic rate is measured as the regional cerebral metabolic rate for glucose (**rCMRglc**). The ordinate plots the difference between the average of the responses to the question, "Do you have a craving or urge for cocaine?" in separate sessions with neutral and cocaine-related cues. (Each session lasted 30 minutes, and in each session, the question was asked three times.)

C. When subjects report a craving for cocaine, metabolic activity increases in the dorsolateral prefrontal cortex (**DLPFC**) and in two medial temporal lobe structures, the amygdala (**Am**) and parahippocampal gyrus (**Ph**). Pseudocolored PET images of metabolic activity are spatially aligned with high-resolution structural magnetic resonance images. Metabolic rate markedly increased in the amygdala and parahippocampal gyrus in one subject who reported a large increase in craving during presentation of cocaine-related cues (**red dots** in parts **A** and **B**). This effect is not evident in a subject who reported no increase in craving while exposed to the cocaine-related cues (**blue dots** in parts **A** and **B**). Metabolic activity outside the dorsolateral prefrontal cortex and medial temporal lobe is not shown.

suppressed endogenous reward mechanisms, is a leading factor in driving the return to drug use, or *relapse*. Reward sensitization, which typically occurs after longer withdrawal periods, can trigger relapse in response to exposure to the drug itself or to drug-associated cues (eg, being with people or in a place where drug was previously used).

Interestingly, a given drug can produce all of these adaptations—tolerance, sensitization, and dependence—simultaneously, due to different acute effects of the drug; this phenomenon emphasizes the involvement of multiple cell types and circuits in mediating a drug's global actions. The key challenge for neuroscientists is to identify the changes in specific types of neurons and glia—and in their consequent contributions to circuit function—that are induced by repeated drug exposure and that mediate the behavioral features that define a state of addiction.

Lasting Molecular Adaptations Are Induced in Brain Reward Regions by Repeated Drug Exposure

An extensive literature shows that repeated exposure to a drug of abuse in animal models alters the levels of many neurotransmitters and neurotrophic factors, their receptors and intracellular signaling pathways, and transcriptional regulatory proteins throughout the brain's reward circuitry. Most of these changes cannot be studied in living patients—only a small number of neurotransmitters and receptors can be assessed in patients with brain imaging—although studies of postmortem human brain tissue are being used increasingly to validate findings from animal models. Most of the reported research has focused on the ventral tegmental area and nucleus accumbens, although an increasing number of studies are examining other parts of the reward circuitry.

The most robust experimental findings are available for psychostimulants and opiates, probably because the changes induced by these drugs are larger in magnitude than those of other drugs of abuse. This likely reflects the greater inherent addictiveness of psychostimulants and opiates: With equivalent exposures, a larger fraction of people will become addicted to these drugs as compared with other classes of abused substances. Nevertheless, given the dominant public health consequences of alcohol, nicotine, and marijuana addictions, more attention should be given to these drugs.

Below, we summarize this large literature by focusing on a small number of drug-induced adaptations that have been linked causally to specific behavioral features of addiction in animal models. As will be clear in the next section, the present research focus is on relating these and many other molecular changes to synaptic and circuit adaptations also implicated in addiction.

Upregulation of the cAMP-CREB Pathway

Several drugs of abuse activate G_i protein–linked receptors, such as the D_2 dopamine receptor; the μ, δ, and κ opioid receptors; and the CB1 cannabinoid receptor. This means that, to a certain extent, many drugs of abuse will activate G_i protein–linked signaling pathways, with effects such as inhibition of adenylyl cyclase (Chapter 14), in the nucleus accumbens and other target neurons.

Work over the past two decades has established that, after repeated exposure, the affected neurons adapt to this sustained suppression of the cyclic adenosine monophosphate (cAMP) pathway by upregulating it, including induction of certain isoforms of adenylyl cyclase and protein kinase A. Repeated drug exposure likewise induces upregulation of the transcription factor CREB, which is normally activated by the cAMP pathway. Such upregulation of the cAMP-CREB pathway can be seen as a molecular mechanism of tolerance and dependence: It restores normal activity of these pathways despite the presence of a drug (tolerance and dependence), and when the drug is removed, the upregulated pathway is unopposed, causing abnormally high activity of the pathway (withdrawal) (Figure 43–5). Indeed, upregulation of the cAMP-CREB pathway in nucleus accumbens neurons has been shown to mediate both reward tolerance and motivational dependence and withdrawal in animal models.

Induction of ΔFosB

ΔFosB is a member of the Fos family of transcription factors. It is a truncated product of the *FosB* gene generated through alternative splicing. In contrast to all other members of the Fos family, which are induced rapidly and transiently in response to many perturbations in neural activity or cell signaling, ΔFosB is induced only slightly by initial presentation of stimuli. However, with repeated drug exposure, ΔFosB accumulates in neurons because of its unusual stability, unique among all Fos family proteins.

This phenomenon occurs within neurons of the nucleus accumbens and several other brain reward areas after repeated exposure to virtually any drug of abuse, including cocaine and other psychomotor stimulants, opiates, nicotine, ethanol, cannabinoids, and phencyclidine. Recent studies involving the selective

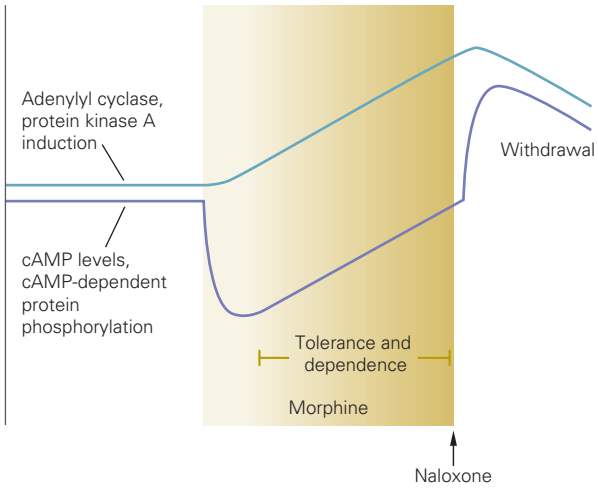

Figure 43–5 Upregulation of the cAMP-CREB pathway is a molecular mechanism underlying drug tolerance and dependence. Morphine or other μ opioid receptor agonists acutely inhibit the functional activity of the cyclic adenosine monophosphate (**cAMP**) pathway in brain reward neurons, as indicated, for example, by cellular levels of cAMP or protein kinase A (PKA)–dependent phosphorylation of substrates such as CREB. With continued drug exposure (**shading**), functional activity of the cAMP-CREB pathway is gradually upregulated and increases far above control levels upon removal of the drug (eg, by administration of the μ opioid receptor antagonist naloxone). These changes in the functional state of the cAMP-CREB pathway are mediated via the induction of adenylyl cyclase and PKA and activation of PKA substrates such as CREB in response to repeated drug administration. Induction of these proteins accounts for the gradual recovery in the functional activity of the cAMP-CREB pathway seen during chronic drug exposure (tolerance and dependence) and for the elevated activity of the cAMP-CREB pathway seen upon removal of the drug (withdrawal). First demonstrated for opiate drugs, similar regulation is seen in response to several other types of drugs of abuse. (Reproduced, with permission, from Nestler et al. 2020.)

expression or knockdown of ΔFosB in the nucleus accumbens of adult mice have provided direct evidence that induction of ΔFosB mediates reward sensitization, including increased drug self-administration and relapse. This is yet another example of a common adaptation to drugs of abuse that contributes to aspects of addiction shared across numerous drugs of abuse.

CREB and ΔFosB are two of many transcription factors implicated in drug addiction. Ongoing research is focused on characterizing the chromatin regulatory mechanisms through which these factors cooperate to regulate the expression of specific genes in the affected neurons and glia. Work is also underway to understand how these target genes drive their associated behavioral abnormalities via altered expression of proteins involved in synaptic, cell, and circuit function (Figure 43–6).

Lasting Cellular and Circuit Adaptations Mediate Aspects of the Drug-Addicted State

Repeated exposure to a drug of abuse can alter a neural circuit in two major ways. One mechanism, referred to as whole-cell or homeostatic plasticity, involves altering the intrinsic excitability of a nerve cell that will ultimately alter functioning of the larger circuit of which it is a part. It is easy to imagine how whole-cell plasticity in neurons within the brain's reward circuitry might mediate aspects of reward tolerance, sensitization, and dependence and withdrawal.

The other mechanism is synaptic plasticity, where connections between particular neurons are either strengthened or weakened. These synapse-specific adaptations could mediate the features of addiction that involve maladaptive memories, such as memories of the association of drug exposure with a host of environmental cues. This pathological learning and memory can increasingly focus an individual on the drug at the expense of natural rewards. Most attention in the field to date has concentrated on synaptic plasticity.

Synaptic Plasticity

As discussed elsewhere in this book, two major forms of synaptic plasticity have been described at glutamatergic synapses: *long-term depression* (LTD) and *long-term potentiation* (LTP). Over the past two decades, the molecular basis of both adaptations has been established, with distinct mechanisms underlying each of several distinct subtypes of LTD and LTP that occur throughout the nervous system. We now know that several types of drugs of abuse, in particular psychomotor stimulants and opiates, cause LTD- and LTP-like changes at particular classes of glutamatergic synapses in the brain's reward circuitry, with most work to date focused on the ventral tegmental area and nucleus accumbens.

Changes in the nucleus accumbens show interesting time-dependent adaptations as a function of drug withdrawal. At early withdrawal points (hours to days), glutamatergic synapses on neurons of the nucleus accumbens display LTD-like changes, which evolve into LTP-like changes after longer periods of withdrawal (weeks to months). Drug-induced LTD- and LTP-like adaptations in the nucleus accumbens involve morphological changes similar to those in other brain regions (mostly the hippocampus and cerebral cortex) where LTD and LTP occur in association with morphological changes in individual dendritic spines. During early withdrawal, LTD-like responses occur coincidently with increased numbers of

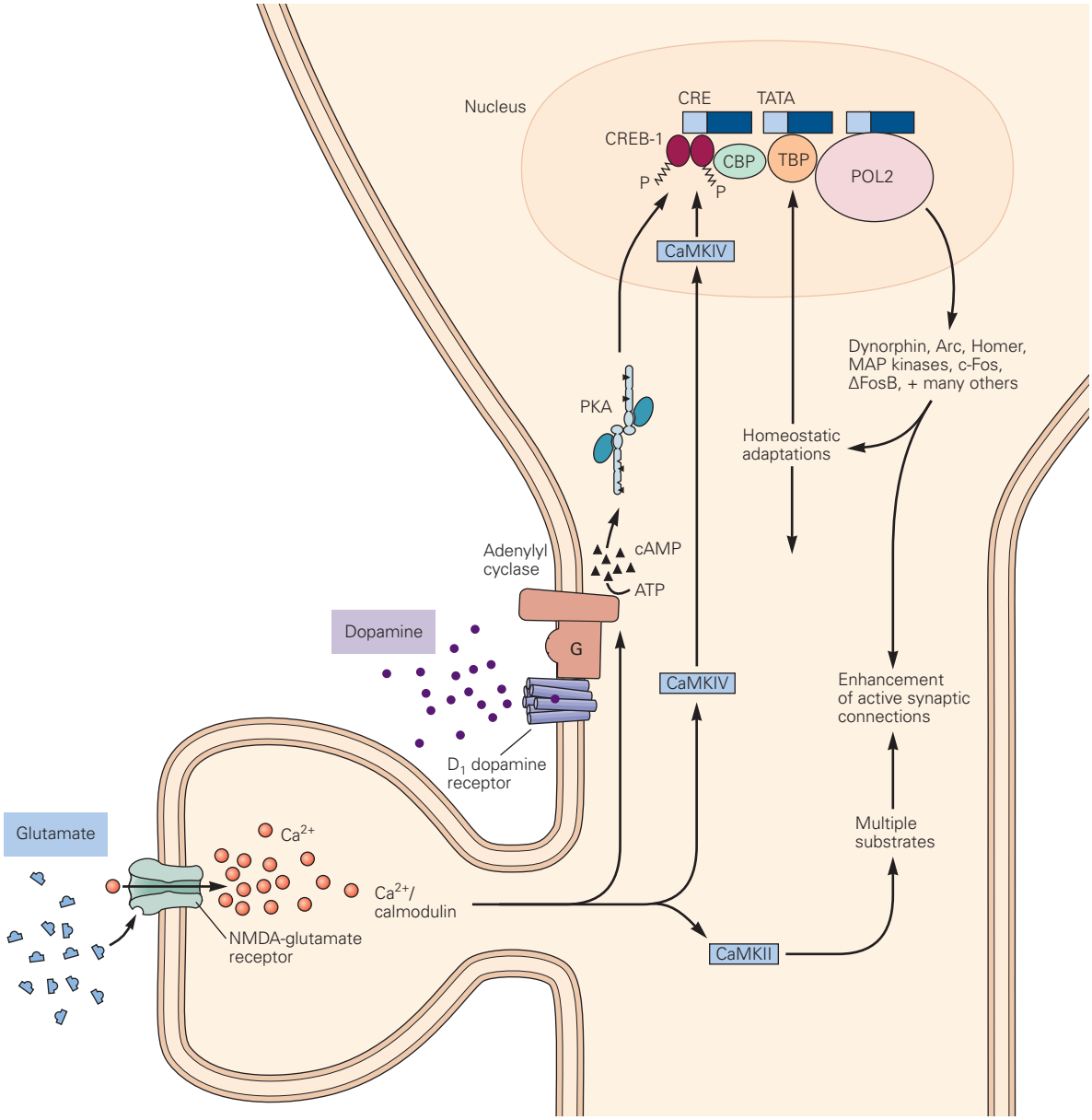

Figure 43–6 Dopamine- and glutamate-activated intracellular signaling pathways implicated in drug addiction. NMDA-type glutamate receptors permit Ca^{2+} entry, which binds calmodulin. The Ca^{2+}/calmodulin complex activates two types of Ca^{2+}/calmodulin-dependent protein kinases, CaMKII in the cytoplasm and CaMKIV in the cell nucleus. Certain dopamine receptors activate a stimulatory G protein that in turn activates adenylyl cyclase to produce cyclic adenosine monophosphate (**cAMP**). The cAMP-dependent protein kinase A (**PKA**) catalytic subunit can enter the nucleus. Once activated in the nucleus, both PKA and CaMKIV phosphorylate and thus activate cAMP response element binding protein (**CREB**). CREB recruits CREB-binding protein (**CBP**) and many other chromatin regulatory proteins and thereby activates the RNA polymerase II–dependent transcription of many genes, giving rise to proteins that can alter cellular function. Arc and Homer are localized in synaptic regions; mitogen-activated protein (**MAP**) kinases are protein kinases that control numerous cellular processes; Fos and ΔFosB are transcription factors; and dynorphin is a type of endogenous opioid peptide. These proteins are thought to contribute both to homeostatic responses to excessive dopamine stimulation and to the morphological and functional changes in synapses associated with memory formation. (Abbreviations: **ATP**, adenosine triphosphate; **NMDA**, *N*-methyl-D-aspartate; **POL 2**, RNA polymerase 2; **TBP**, TATA binding protein.)

immature, thin dendritic spines, whereas during later withdrawal, LTP-like responses occur coincidently with increased numbers of mature, mushroom-shaped spines. These findings suggest that repeated drug use weakens certain glutamatergic synapses with nucleus accumbens neurons via the induction of so-called *silent synapses* (Chapter 54), with a subset of these synapses strengthening during prolonged withdrawal.

These advances now define several ongoing lines of investigation. We need to understand which particular glutamatergic connections are affected and how those changes contribute to behavioral features of addiction. We need to define the molecular basis of this time-dependent synaptic plasticity, which is mediated in part through transcriptional mechanisms and altered expression levels of a host of proteins, including glutamate receptors, postsynaptic density proteins, proteins that regulate the actin cytoskeleton, and so on (Figure 43–6). In addition, we need to examine drug-induced glutamatergic synaptic plasticity at the several other reward-related brain regions that become corrupted in an addicted state, beyond the ventral tegmental area and nucleus accumbens. Finally, we need to understand how repeated exposure to drugs of abuse also corrupts inhibitory GABAergic synaptic transmission throughout this circuitry.

Whole-Cell Plasticity

As with synaptic plasticity, most examples of drug-induced whole-cell plasticity involve the ventral tegmental area and nucleus accumbens. For example, repeated cocaine exposure increases the intrinsic excitability of nucleus accumbens neurons, which contributes to reward tolerance. This adaptation is due in part to a decrease in expression of specific types of K^+ channels mediated by CREB, thus linking molecular-transcriptional adaptations to altered neural activity and an addiction-related behavioral abnormality. Repeated opiate exposure also increases the intrinsic excitability of dopaminergic neurons in the ventral tegmental area, but in a manner that impedes dopaminergic transmission to the nucleus accumbens. As with repeated cocaine exposure, this adaptation too is mediated by suppression of certain K^+ channels and contributes to reward tolerance.

Circuit Plasticity

Advanced tools are making it possible for the first time to track the activity of specific nerve cell types in the brain in awake, active animals and to experimentally manipulate the activity of those cells and study the behavioral consequences (Chapter 5). This is enabling scientists to define the precise ensembles of neurons within a given brain region that are affected by drug exposure over the life cycle of addiction—from initial drug exposure to compulsive drug consumption to withdrawal and relapse—and to provide causal evidence for the involvement of those neurons and the microcircuits within which they function. This work is beginning to define the distinct roles that various glutamatergic projections to the nucleus accumbens—from the prefrontal cortex, hippocampus, amygdala, and thalamus—play in controlling different cell types in the nucleus accumbens and the broader reward circuitry and in producing distinct addiction-related behavioral abnormalities.

While we have focused exclusively in this chapter on the effects of acute and chronic actions of drugs of abuse on the neural control of behavior, we realize that this is an oversimplification. As discussed in Chapter 7, neuronal function is intricately controlled by a host of nonneural cells in the brain, including astroglia, microglia, oligodendrocytes, and endothelial cells. There is growing evidence that each of these cell types is affected both directly and indirectly by drugs of abuse and that these nonneuronal actions also affect the long-term behavioral consequences of drug exposure. Integrating such actions with the neuronal effects of drugs of abuse will be required to achieve a comprehensive understanding of addiction.

Natural Addictions Share Biological Mechanisms With Drug Addictions

As previously indicated, the brain's reward circuitry evolved to motivate individuals to pursue natural rewards such as food, sex, and social interactions. Just as drug-addicted individuals display compulsive consumption of drugs of abuse, some people exhibit compulsive consumption of nondrug rewards (eg, compulsive overeating, shopping, gambling, video gaming, and sex), with behavioral consequences very similar to those observed in drug addiction. An interesting question for the field is whether these so-called "natural addictions" are mediated by some of the same molecular, cellular, and circuit adaptations that underlie drug addiction.

It is possible that these normal pleasurable behaviors excessively activate reward mechanisms in certain individuals who are particularly susceptible due to genetic or nongenetic factors. As with drugs, such activation may result in profound alterations in motivation that promote the repetition of initially rewarding behavior, despite the impact of negative consequences

associated with the resulting compulsive behavior. It is far more difficult to study the neurobiological basis of natural addictions because of limitations in animal models (imagine a mouse model of compulsive shopping!), although progress is being made in developing such paradigms. In any event, brain imaging studies in humans support the notion that addictions to both drugs and behavioral rewards are associated with similar dysregulation of the brain's reward circuitry (Figure 43–3).

Highlights

1. Motivational states drive behaviors that either seek rewards or defend against or avoid aversive stimuli. Motivational states themselves are determined by a variety of internal and external variables. Internal variables include both physiological states and cognitive states. External variables include stimuli that possess innately rewarding or aversive properties, although the motivational significance of these properties may be modified by internal variables.
2. Rewards are desirable objects, stimuli, or actions. Rewards tend to elicit motivational states that drive approach behaviors. Rewards can meet regulatory needs on a short timescale, but can also result from complex sequences of behavior that achieve a long-term goal.
3. Key components of reward-related circuitry in the brain include dopaminergic neurons and brain areas targeted by dopaminergic neurons, such as the nucleus accumbens, ventral pallidum, amygdala, hippocampus, and parts of the prefrontal cortex. However, dopamine itself does not account for hedonic experiences.
4. Many dopaminergic neurons exhibit physiological response properties that suggest they communicate a prediction-error signal, with enhanced activity occurring when something better than expected occurs. This type of signal could play a critical role in different forms of reinforcement learning, learning that links stimuli or actions to rewards. However, recent studies have revealed more response heterogeneity in dopaminergic neurons than previously appreciated, including responses to aversive stimuli. This heterogeneity and its complex effects on neural circuit function remain active areas of investigation.
5. Drug addiction can be defined as the compulsive seeking and taking of a drug despite negative consequences to one's physical health or occupational and social functioning. The risk for addiction is roughly 50% genetic, with many hundreds of genes, each of which contributes a very small effect to this heritability. Important nongenetic risk factors include a history of adverse life events.
6. Drugs of abuse compose only a very small fraction of known chemical compounds. These drugs are chemically diverse, with each type acting initially on a distinct protein target. Nevertheless, the drugs can induce a common behavioral syndrome because their actions at these targets converge in producing similar functional effects on midbrain dopaminergic neurons or their projection regions such as the nucleus accumbens.
7. Addiction requires repeated exposure to a drug of abuse. Such repeated exposure is often accompanied by tolerance, sensitization, and dependence/withdrawal. While many nonabused drugs can produce tolerance and dependence/withdrawal, drugs of abuse are unique in their ability to produce these adaptations as well as sensitization in motivational and reward states.
8. The adaptations underlying drug addiction are mediated in part through lasting changes in gene expression, which result in altered intrinsic activity of neurons as well as structural and functional alterations in their synaptic contacts within the brain's reward circuitry.
9. An important goal of current research is to understand how a myriad of molecular changes summate to underlie specific changes in neural and synaptic function. Likewise, it will be important to understand how these neural and synaptic changes combine to alter the functioning of the brain's larger reward-related circuitry, so as to mediate specific behavioral abnormalities that define an addicted state.
10. This delineation of molecular, cellular, and circuit mechanisms of addiction will require increased attention to the specific cell types (neuronal and nonneuronal) in which certain drug-induced adaptations occur and to the specific microcircuits within the reward pathways affected by those adaptations.
11. A subset of individuals show addiction-like behavioral abnormalities to nondrug rewards, such as food, gambling, and sex. Evidence suggests that such so-called natural addictions are mediated by the same brain circuitry involved in drug addiction, with some common molecular and cellular abnormalities implicated as well.
12. These considerations highlight the need to learn more about the precise molecular, cellular, and

circuit bases of drug addiction. Nonetheless, our evolving understanding of the brain's reward circuitry and how individual synapses and cells in that circuitry are altered by drug exposure in a way that corrupts circuit function and usurps normal systems of reward and associative memory provides a compelling notion of what happens in the addicted brain.

Eric J. Nestler
C. Daniel Salzman

Selected Reading

Berridge KC, Robinson TE. 2016. Liking, wanting, incentive-sensitization theory of addiction. Am Psychologist 71: 670–679.

Di Chiara G. 1998. A motivational learning hypothesis of the role of mesolimbic dopamine in compulsive drug use. J Psychopharmacol 12:54–67.

Hyman SE, Malenka RC, Nestler EJ. 2006. Neural mechanisms of addiction: the role of reward-related learning and memory. Annu Rev Neurosci 29:565–598.

Olds J, Milner PM. 1954. Positive reinforcement produced by electrical stimulation of septal area and other regions of rat brain. J Comp Physiol Psych 47:419–427.

Schultz W. 2015. Neuronal reward and decision signals: from theories to data. Physiol Rev 95:853–951.

Wise RA, Koob GF. 2014. The development and maintenance of drug addiction. Neuropsychopharmacology 39:254–262.

References

Bevilacqua L, Goldman D. 2013. Genetics of impulsive behavior. Philos Trans R Soc Lond B Biol Sci 368:20120380.

Calipari ES, Bagot RC, Purushothaman I, et al. 2016. In vivo imaging identifies temporal signature of D1 and D2 medium spiny neurons in cocaine reward. Proc Natl Acad Sci U S A 113:2726–2731.

Carlezon WA Jr, Chartoff EH. 2007. Intracranial self-stimulation (ICSS) in rodents to study the neurobiology of motivation. Nat Protoc 2:2987–2995.

Dong Y. 2016. Silent synapse-based circuitry remodeling in drug addiction. Int J Neuropsychopharmacol 19:pyv136.

Everitt BJ, Belin D, Economidou D, Pelloux Y, Dalley JW, Robbins TW. 2008. Review. Neural mechanisms underlying the vulnerability to develop compulsive drug-seeking habits and addiction. Philos Trans R Soc Lond B Biol Sci 363:3125–3135.

Gipson CD, Kupchik YM, Kalivas PW. 2014. Rapid, transient synaptic plasticity in addiction. Neuropharmacology 76 Pt B:276–286.

Goldstein RZ, Volkow ND. 2011. Dysfunction of the prefrontal cortex in addiction: neuroimaging findings and clinical implications. Nat Rev Neurosci 12:652–669.

Grant S, London ED, Newlin DB, et al. 1996. Activation of memory circuits during cue-elicited cocaine cravings. Proc Natl Acad Sci U S A 93:12040–12045.

Loweth JA, Tseng KY, Wolf ME. 2014. Adaptations in AMPA receptor transmission in the nucleus accumbens contributing to incubation of cocaine craving. Neuropharmacology 76 Pt B:287–300.

Lüscher C, Malenka RC. 2011. Drug-evoked synaptic plasticity in addiction: from molecular changes to circuit remodeling. Neuron 69:650–663.

Matsumoto M, Hikosaka O. 2009. Two types of dopamine neuron distinctly convey positive and negative motivational signals. Nature 459:837–841.

Nestler EJ, Kenny PJ, Russo SJ, Schaefer A. 2020. *Molecular Neuropharmacology: A Foundation for Clinical Neuroscience*, 4th ed. New York: McGraw-Hill.

Pessiglione M, Seymour B, Flandin G, Dolan RJ, Frith CD. 2006. Dopamine-dependent prediction errors underpin reward-seeking behavior in humans. Nature 442: 1042–1045.

Polter AM, Kauer JA. 2014. Stress and VTA synapses: implications for addiction and depression. Eur J Neurosci 39:1179–1188.

Robbins TW, Clark L. 2015. Behavioral addictions. Curr Opin Neurobiol 30:66–72.

Robinson TE, Kolb B. 2004. Structural plasticity associated with exposure to drugs of abuse. Neuropharmacology 47(Suppl 1):33–46.

Robison AJ, Nestler EJ. 2011. Transcriptional and epigenetic mechanisms of addiction. Nat Rev Neurosci 12:623–637.

Russo SJ, Nestler EJ. 2013. The brain reward circuitry in mood disorders. Nat Rev Neurosci 14:609–625.

Schmidt HD, McGinty JF, West AE, Sadri-Vakili G. 2013. Epigenetics and psychostimulant addiction. Cold Spring Harb Perspect Med 3:a012047.

Schultz W, Dayan P, Montague PR. 1997. A neural substrate of prediction and reward. Science 275:1593–1599.

Scofield MD, Kalivas PW. 2014. Astrocytic dysfunction and addiction: consequences of impaired glutamate homeostasis. Neuroscientist 20:610–622.

Stuber GD, Britt JP, Bonci A. 2012. Optogenetic modulation of neural circuits that underlie reward seeking. Biol Psychiatry 71:1061–1067.

Volkow ND, Morales M. 2015. The brain on drugs: from reward to addiction. Cell 162:712–725.

44

Sleep and Wakefulness

Sleep is a remarkable state. It consumes fully a third of our lives—approximately 25 years in the average lifetime—yet we know little about what happens in the brain during this daily excursion. Perhaps even more surprising, the exact functions of sleep and of dreaming, one of the more noteworthy components of sleep, are still unknown.

Although the psychological content of dreams has been a rich subject of speculation from Plato and Aristotle to Sigmund Freud, we still do not understand whether dreams carry deep personal meaning, as Freud hypothesized, or represent the brain "throwing out its trash," the bits and pieces of daily experience that are not worth retaining, as Francis Crick speculated. One function of sleep may be to allow synaptic remodeling and consolidation of memory traces reflecting the day's experiences, but the role of dreaming in this process remains a subject of intense debate.

When studying sleep and wakefulness, researchers typically use a polysomnogram, which consists of three physiological measures: brain activity measured by an electroencephalogram (EEG) (see Figure 58–1), eye movements recorded by an electro-oculogram (EOG), and muscle tone measured by an electromyogram (EMG) (Figure 44–1B). In clinical polysomnograms, respiration is also measured, as breathing during sleep is disrupted in many patients with sleep disorders.

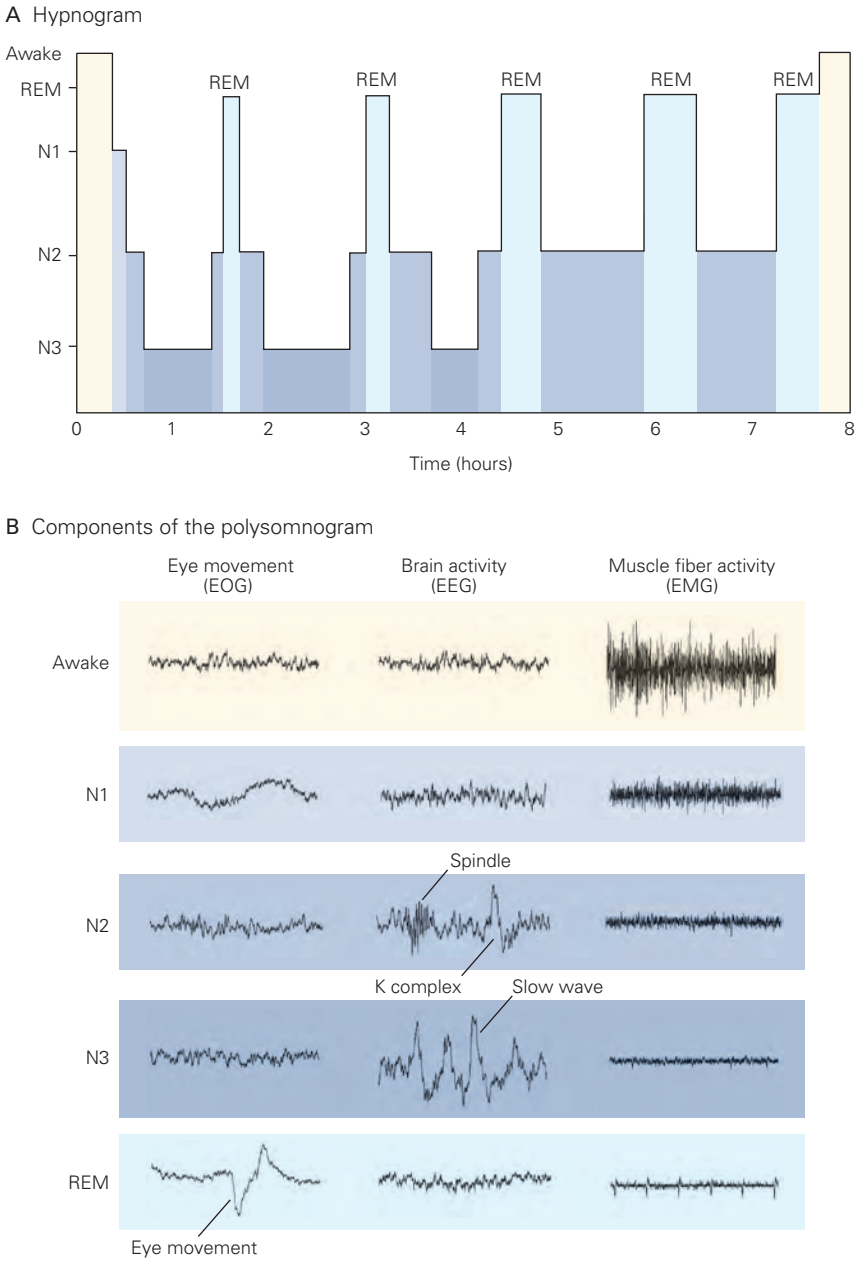

Figure 44–1 Electrophysiological patterns of wakefulness and sleep.

A. A hypnogram or graph showing the progression of sleep stages over a typical night in a healthy young person. Periods of rapid eye movement (**REM**) sleep alternate with non-REM sleep about every 90 minutes. An individual typically progresses from the awake state into light non-REM sleep (N1) then progressively deeper non-REM sleep (N2, N3), then back to lighter non-REM sleep before the first period of REM sleep occurs (**light blue bars**). As the night progresses, the individual spends less time in the deepest stage of non-REM sleep, and the duration of REM sleep periods increases.

B. The records show the components of the polysomnogram used to distinguish sleep stages. The electro-oculogram (**EOG**) records eye movements from electrodes on either side of the eyes. The electroencephalogram (**EEG**) records cortical field potentials from the scalp; the electromyogram (**EMG**) records muscle fiber firing through the skin. During the awake state, the EOG shows voluntary eye movements, the EEG shows fast low-amplitude activity, and the EMG shows variable muscle tone. Stage N1 sleep is characterized by a slight slowing of EEG frequencies and slow roving eye movements, with less EMG activity; stage N2 is characterized by bursts of 12- to 14-Hz activity called sleep spindles and high-voltage slow waves called K-complexes; stage N3 is dominated by high-voltage slow waves. During REM sleep, the EEG is similar to that of the awake state. Rapid eye movements can be seen on the EOG, but the EMG is so silent that contamination by tiny electrocardiogram signals can sometimes be seen (as in the illustrated case).

During wakefulness, the EEG is characterized by mainly high-frequency, low-voltage activity, indicative of the unique activity of individual cortical neurons; the EOG shows frequent eye movements; and the EMG shows moderate and variable muscle tone. During quiet wakefulness, with eyes closed, rhythmic EEG waves in the alpha range (8–13 Hz) are common, particularly over the occipital region. For most of the sleep period, the EEG shows slower activity, but periodically during the night, there are shifts into a sleep state with a faster, lower-voltage EEG, loss of muscle tone, and rapid eye movements called rapid eye movement (REM) sleep. The entire period of slow EEG activity, from light drowsiness to deep sleep, is referred to as non-REM sleep and is divided into three stages, N1 to N3 (Figure 44–1).

Sleep Consists of Alternating Periods of REM Sleep and Non-REM Sleep

As an individual becomes drowsy and transitions into light non-REM sleep (stage N1), the EEG slows and shows waves in the theta range (4–7 Hz) (Figure 44–1B).

Consciousness begins to fade during stage N1, but the individual may still be awakened by minimal stimulation. Stage N2 often contains some slow EEG activity in the theta and delta range (0.5–4 Hz) as well as *sleep spindles*, 10- to 16-Hz waxing and waning EEG oscillations lasting 1 to 2 seconds, typically with a gradual onset and offset so the EEG waves resemble an old-fashioned spindle tapered at both ends. The EEG also may show large, single slow waves called *K-complexes* (Figure 44–1B). During stage N3, the EEG shows abundant, very slow EEG delta activity. During stages N2 and N3, people are generally unconscious of the world around them as the slow cortical activity disrupts information processing. Across all stages of non-REM sleep, eye movements are absent, muscle tone is low, breathing is slow and regular, and body temperature falls.

Slow EEG activity and sleep spindles arise, respectively, from cortico-cortical and cortico-thalamic electrophysiological interactions. During non-REM sleep, the membrane potential of cortical pyramidal neurons fluctuates between *Up states* (when they are depolarized and fire) and *Down states* (when they are hyperpolarized and silent). These slow oscillations in membrane potential, which occur even in an isolated cortical slab, correlate with slow waves in the EEG. During stage N2 sleep, spindles arise from an interaction of neurons in the reticular nucleus of the thalamus and thalamocortical relay neurons. Thalamocortical neurons are generally hyperpolarized and inactive during non-REM sleep, but inhibition from the reticular thalamic neurons can result in the opening of low-threshold Ca^{2+} channels, which drive a burst of Na^{+} spikes in the thalamocortical neurons. The thalamocortical neurons then excite and recruit more reticular neurons, initiating the next cycle of the sleep spindle. This pattern of inhibition and excitation repeats about every 100 ms, and after several cycles, the spindle activity wanes as the reticular neurons become less responsive (Figure 44–2).

After about 90 minutes of sleep, people usually enter the stage known as REM sleep, a period in which dreams are often vivid and sometimes bizarre. REM sleep was discovered in 1953 when Eugene Aserinsky and Nathaniel Kleitman observed that across a night of sleep, adults have several episodes of jerky conjugate eye movements, and when awakened from this state, about three-fourths of subjects reported dreams with visual imagery.

Muscle tone is extremely low during REM sleep, owing to inhibition of motor neurons by descending pathways from the brain stem. This paralysis affects nearly all motor neurons except those that support respiration, eye movements, and a few other functions such as sphincter control. As discussed later in this chapter, this inhibition of motor neurons is crucial as it prevents the physical enactment of dreams.

During REM sleep, the body undergoes many additional physiological changes. Body temperature falls during non-REM sleep, and it can fall further during REM sleep as the generation and retention of heat are minimal. Autonomic regulation is altered such that heart rate and blood pressure can vary wildly. In addition, men experience penile erections and women experience physiological signs of sexual arousal during REM sleep.

Across the night, episodes of non-REM sleep alternate with REM sleep, and each of these sleep cycles takes about 90 minutes. Sleep in a healthy young adult usually begins with a rapid descent into stage N3 non-REM sleep, followed by lighter non-REM sleep and then some REM sleep, and with each cycle, non-REM sleep becomes lighter and the periods of REM sleep become longer (Figure 44–1A). At the end of the sleep period, people often wake spontaneously from an episode of REM sleep.

The Ascending Arousal System Promotes Wakefulness

Modern perspectives of the neural basis of sleep and wakefulness go back about 100 years to the concepts derived by the neurologist and neuropathologist Baron Constantin von Economo. Around World War I, he observed an unusual type of encephalitis, believed to be a viral infection of the brain that specifically attacked the sleep–wake control circuitry. In most cases, patients had "encephalitis lethargica," sleeping 20 or more hours per day. When they awoke, they were generally cogent, but they would stay awake only long enough to eat and then go right back to sleep. This intense sleepiness would persist for many months before improving. But in patients who died during this interval, von Economo found focal damage to the brain, at the junction of the midbrain and diencephalon, leading him to hypothesize that the upper brain stem and posterior hypothalamus contain critical circuitry that activates the forebrain, producing a normal wakeful state.

Other patients afflicted in the same epidemic had just the opposite problem: unrelenting severe insomnia. They would be restless and, despite feeling sleepy, unable to fall asleep. Eventually, they would fall into a fitful sleep for only a few hours each day, but would waken without feeling refreshed. In post mortem examinations of these patients, von Economo found

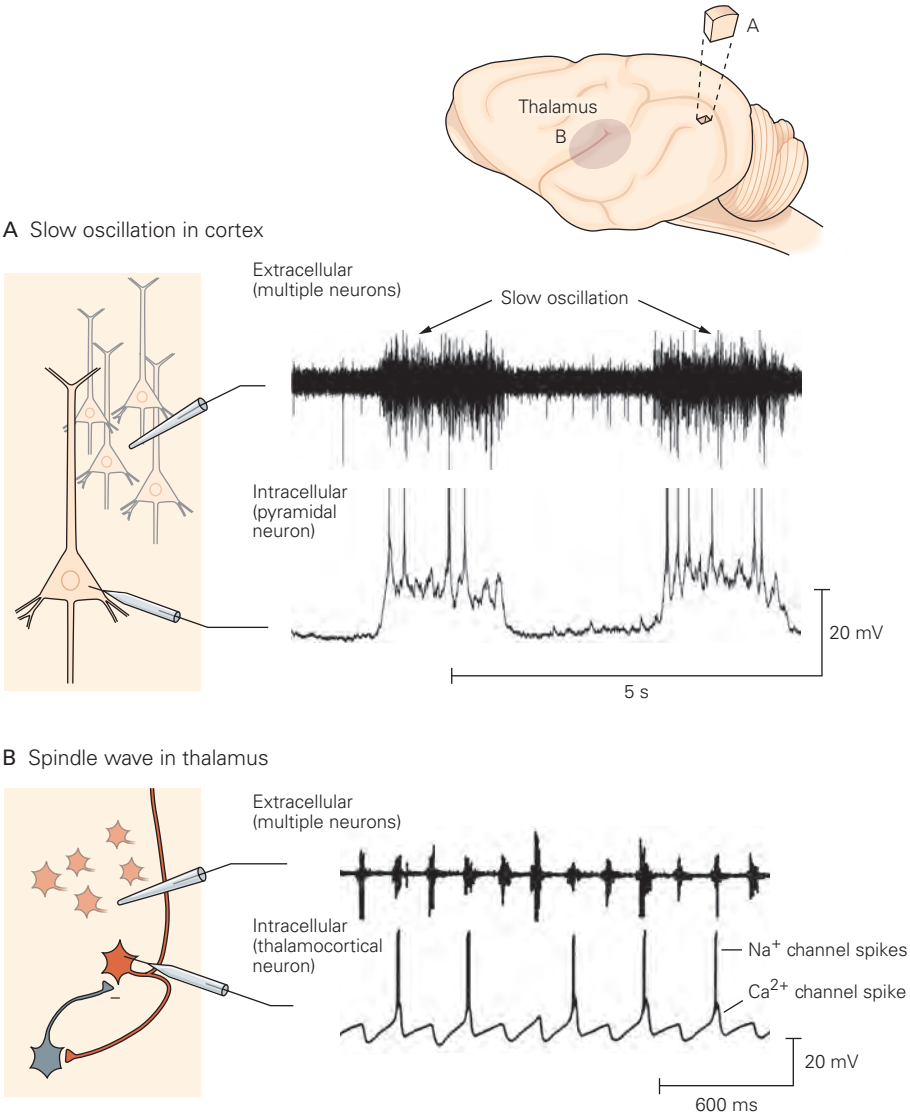

Figure 44–2 Cellular mechanisms of electroencephalogram rhythms during sleep.

A. The slow oscillation that underlies the slow waves of the EEG during non-REM sleep is generated within the cerebral cortex by intrinsic massively recurrent excitatory and inhibitory connections. Slow waves will continue even in an isolated cortical slab. Intracellular recordings from such neurons during slow oscillations show rhythmic down states when the individual neurons are hyperpolarized and do not fire, alternating with up states when the membrane potential is more depolarized and the neurons fire multiple action potentials. This synchronous firing produces waves of dendritic potentials, which appear as slow waves in the EEG. (Data from Dr. David McCormick.)

B. Similarly, in a thalamic slice, recurrent circuitry generates spindle waves. A burst of spikes in reticular nucleus neurons (**gray**) hyperpolarizes thalamocortical relay neurons (**red**) sufficiently to de-inactivate low-threshold (T-type) Ca^{2+} channels. As the hyperpolarization wanes, these Ca^{2+} channels open and the resultant Ca^{2+} current depolarizes the relay neuron, producing a brief burst of Na^+ channel spikes on top of a Ca^{2+} channel spike plateau. Meanwhile, as the burst in the relay cell continues, its excitatory output generates a T-type Ca^{2+} channel spike in the reticular neuron, which drives another burst of Na^+ spikes. The resultant volley of feedback inhibition to the relay cells initiates a new burst cycle. This firing pattern recurs 12 to 14 times per second, and the resulting waves of thalamocortical action potentials reaching the cortex produce sleep spindles in the EEG. The upper trace shows action potentials from a local population of relay cells. The lower trace shows inhibitory postsynaptic potentials and spike bursts from an individual relay cell; on this slow time base, each upstroke in the intracellular record represents a burst of up to six action potentials. As the trace shows, individual relay neurons do not reach spike threshold during every cycle of the spindle wave. As a result, the amplitude of the extracellular spike activity varies from cycle to cycle, depending on which neurons happen to fire and their distances from the extracellular electrode tip. However, each burst of thalamic firing would produce a volley of excitatory postsynaptic potentials in the cortex, resulting in an electroencephalogram wave, time-locked to the thalamic firing. (Reproduced, with permission, from Bal, von Krosigk, and McCormick 1995. Copyright © 1995 The Physiological Society.)

lesions in the anterior hypothalamus. He proposed that neurons in this area are important for inhibiting the brain stem arousal system to allow sleep. Modern studies have shown a system of wake–sleep circuitry in the brain that is remarkably close to von Economo's model.

The Ascending Arousal System in the Brain Stem and Hypothalamus Innervates the Forebrain

The composition of the ascending arousal system has been debated since von Economo's time. In the late 1940s and early 1950s, lesion studies confirmed that damage to the upper midbrain reticular formation could cause coma, whereas electrical stimulation of this region could arouse animals. The location and nature of the wake-promoting neurons were unknown.

In the succeeding decades, it became clear that these lesions damaged the axons of neurons in the upper brain stem that project to the forebrain, including noradrenergic neurons in the locus ceruleus, serotonergic neurons in the dorsal and median raphe, and midbrain dopaminergic neurons (Chapter 40). The axons of other neurons in the posterior hypothalamus, including those producing histamine and orexin, also join this pathway, which splits into two bundles, with some projections innervating the thalamus and others the hypothalamus, basal forebrain, and cerebral cortex (Figure 44–3).

Neurons contributing to all of these ascending pathways fire fastest during the awake state but much slower during sleep, suggesting that they are wake-promoting. However, although many monoamine antagonists cause sleepiness, and lesions of the

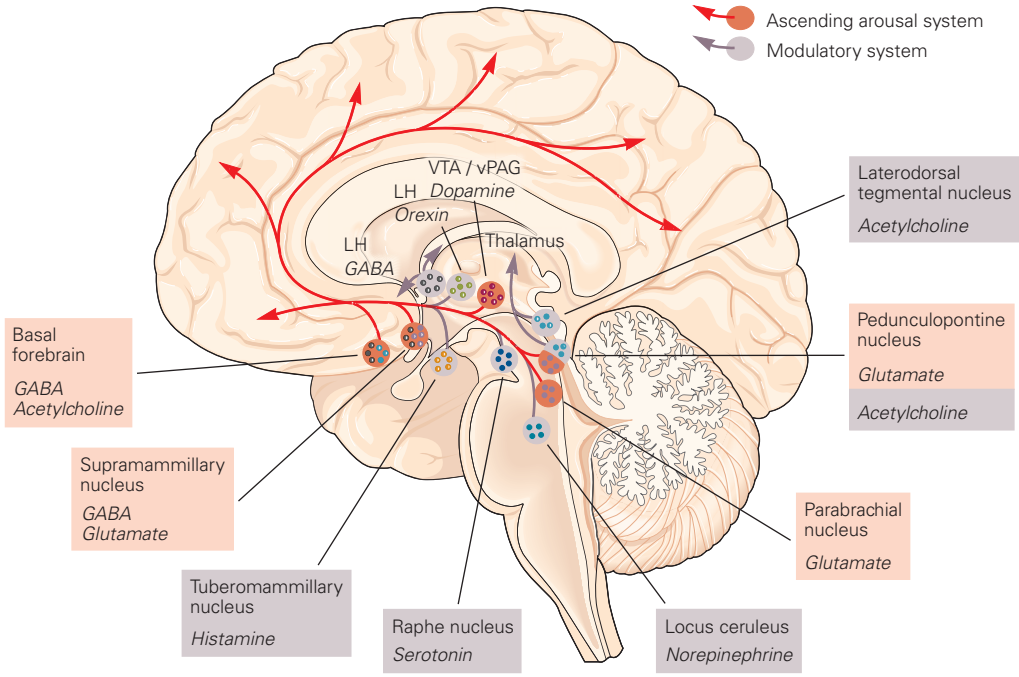

Figure 44–3 The ascending arousal system. The ascending arousal system comprises primarily axons from glutamatergic neurons in the parabrachial and pedunculopontine tegmental nuclei and cholinergic and GABAergic (**dark gray**) neurons in the basal forebrain. Lesions of either the parabrachial and pedunculopontine nuclei or the basal forebrain cause coma. Of somewhat lesser importance are dopaminergic neurons in the ventral tegmental area (**VTA**) and ventral periaqueductal gray (**vPAG**) matter and glutamatergic and GABAergic neurons in the supramammillary nucleus, where lesions can increase sleep by about 20%. In addition, populations of modulatory neurons can strongly promote wakefulness when stimulated, but when damaged cause minimal changes in wake–sleep amounts. These include the monoaminergic neurons in the noradrenergic locus ceruleus, the serotonergic dorsal and median raphe nuclei, and the histaminergic tuberomammillary nucleus; the cholinergic neurons in the pedunculopontine and lateral dorsal tegmental nuclei; and the orexinergic neurons in the lateral hypothalamus (**LH**). All of these neurons send their axons through the hypothalamus and basal forebrain directly to the cerebral cortex, where their net effect is to increase cortical arousal. Many of the modulatory pathways also activate the thalamus, enabling thalamic transmission of sensory information to the cerebral cortex. GABAergic neurons in the lateral hypothalamus also promote wakefulness by inhibiting neurons in the ventrolateral preoptic area and reticular nucleus of the thalamus that oppose wakefulness.

monoaminergic cell groups impair the ability to stay awake under adverse conditions, such lesions have little lasting effect on the amount or timing of wake or sleep.

Lesions of the orexinergic neurons in the lateral hypothalamus cause narcolepsy, a condition in which sleep–wake states are present in normal amounts but are unstable, as discussed later. In fact, of all of the monoaminergic cell groups that are thought to contribute to arousal, only lesions of the dopaminergic neurons near the dorsal raphe nucleus cause small but long-lasting reductions in arousal, resulting in about a 20% increase in total sleep time. Interestingly, the ability of drugs such as amphetamine or modafinil to promote wakefulness appears to depend upon their ability to block dopamine reuptake, as mice with deletions of the dopamine transporter do not respond to these drugs.

Because lesions of the ascending monoaminergic and orexinergic pathways have little if any effect on the total amount of wakefulness, recent work has emphasized the role of glutamatergic, cholinergic, and GABAergic neurons in maintaining wakefulness. Lesions of glutamatergic neurons in the dorsolateral rostral pons, including the parabrachial nucleus and adjacent pedunculopontine tegmental nucleus, cause a comatose state from which the animals cannot be awakened. Lesions confined to the thalamus impair the content of consciousness but have relatively little effect on wake–sleep cycles. On the other hand, lesions of the posterior lateral hypothalamus cause profound sleepiness, which cannot be accounted for by damage to the orexinergic or histaminergic neurons in this region. Glutamatergic neurons in the supramammillary region, which activate the cortex, and GABAergic neurons in the lateral hypothalamus that inhibit sleep-promoting circuits, may account for this arousal effect. Finally, large bilateral lesions of the basal forebrain also can produce coma, similar to lesions of the dorsolateral pons. Optogenetic or chemogenetic activation of cholinergic, GABAergic, or glutamatergic neurons in the basal forebrain indicates that neurons of all three types may produce arousal.

Thus, the current view of the ascending arousal system is that the crucial components are glutamatergic neurons in the dorsolateral pons, supramammillary hypothalamus, and basal forebrain; cholinergic neurons in the dorsolateral pons and basal forebrain; and GABAergic neurons in the lateral hypothalamus and basal forebrain. These are likely to be augmented by modulatory pathways containing orexin and monoamines, needed to allow full and sustained wakefulness particularly under adverse conditions (Figure 44–3).

Damage to the Ascending Arousal System Causes Coma

Consciousness depends upon the activity of the cerebral hemispheres during the awake state. Hence, loss of consciousness occurs when there is injury to the ascending arousal system or to both cerebral hemispheres, or there is a severe metabolic derangement (eg, low blood sugar, inadequate oxygenation, various forms of drug intoxication) that affects both the arousal system and its cortical targets. A patient who cannot be awakened, even by vigorous stimulation, is said to be in a coma. Those who can be partially awakened by such stimuli are said to be stuporous or obtunded.

The clinical approach to a comatose or obtunded patient is first to determine if there is injury to the ascending arousal system. Because of the proximity of the arousal pathways to those that control eye movement and pupillary responses, as well as respiration and some motor responses (Chapter 40), clinicians examine these brain stem functions carefully. If these functions are intact, it is likely that the problem is due to a metabolic condition, which can be assessed by various blood and spinal fluid tests. In addition, a computed tomographic (CT) scan of the brain is needed to look for pathology affecting both cerebral hemispheres (eg, a large tumor or blood clot).

Circuits Composed of Mutually Inhibitory Neurons Control Transitions From Wake to Sleep and From Non-REM to REM Sleep

In contrast to coma, sleep is a temporary, reversible loss of consciousness produced by specific brain circuitry that inhibits the ascending arousal system. Neurons in the ventrolateral preoptic nucleus contain the inhibitory neurotransmitters GABA and galanin and project extensively to most parts of the ascending arousal system. These preoptic neurons fire slowest during wakefulness, increase their firing as animals fall asleep, and fire fastest during deep sleep after a period of sleep deprivation.

Similarly, GABAergic neurons in the nearby median preoptic nucleus also promote sleep and project to some components of the arousal system. Lesions of these preoptic neurons result in fragmented sleep and cause animals to lose as much as half of their total sleep. Of clinical relevance, elderly people often have fragmented sleep, and those with the most fragmented sleep show the greatest loss of the sleep-promoting ventrolateral preoptic galanin neurons in postmortem examination. In addition, a population of GABAergic neurons in the parafacial zone, a region near the facial

nerve as it courses through the brain stem, inhibits the parabrachial nucleus. Lesions of the parafacial zone also result in loss of up to half of total sleep time.

Interestingly, the ventrolateral preoptic neurons receive inhibitory inputs from neurons throughout the arousal system. Mutually inhibitory connections between the ventrolateral preoptic neurons and the arousal system result in a neural circuit with properties similar to an electrical flip-flop switch, in which each side of the circuit turns the other off. Such a circuit produces rapid and full transitions between two states. Although it may sometimes appear that it takes a long time to fall asleep, the actual transitions from wake to sleep, or vice versa, are generally quick, taking only a few seconds to a few minutes. In fact, most animals spend nearly their entire day clearly awake or asleep, with very little time spent in transitions. These rapid transitions are behaviorally adaptive as an animal would be vulnerable in an intermediate, drowsy state. A neural flip-flop switch prevents this situation because when either side of the switch gains advantage over the other, the circuit produces a rapid and complete transition in state (Figure 44–4).

REM sleep is generated by a network of brain stem neurons centered in the pons. The fast EEG rhythms and dream activity of REM sleep are thought to be driven by coordinated activity of glutamatergic neurons in the subceruleus region (ventral to the locus ceruleus in the pons) plus cholinergic and glutamatergic neurons in the parabrachial and pedunculopontine tegmental nucleus that innervate the basal forebrain and thalamus. Other glutamatergic subceruleus neurons produce the paralysis of REM sleep via projections to the ventromedial medulla and spinal cord, where they activate GABAergic and glycinergic neurons that deeply hyperpolarize motor neurons.

The subceruleus area in turn receives input from a population of GABAergic neurons in and just lateral to the periaqueductal gray matter, where the cerebral aqueduct opens into the fourth ventricle. These neurons are most active during wake and non-REM sleep, and they inhibit the subceruleus neurons, preventing entry into REM sleep. Conversely, GABAergic neurons in the subceruleus area also project back to the ventrolateral periaqueductal gray region. The mutual inhibition between the two populations of neurons may form another flip-flop switch that promotes rapid and complete transitions into and out of REM sleep.

Interestingly, the noradrenergic locus ceruleus and serotonergic dorsal raphe nucleus innervate and inhibit the subceruleus region. Thus, REM sleep is often reduced when people take antidepressants that increase brain levels of serotonin or norepinephrine. In addition, as these monoaminergic neurons are active during wakefulness, they prevent direct transitions from wake into REM sleep (Figure 44–5).

Sleep Is Regulated by Homeostatic and Circadian Drives

The circadian regulation of sleep obeys a 24-hour biological clock (described later), whereas the homeostatic drive for sleep gradually accumulates during the awake state. After a period of sleep deprivation, much of the lost sleep is recovered over the next few nights, which in younger people may involve deeper and longer periods of stage N3 non-REM sleep.

REM sleep is also recovered after REM deprivation; rebound REM sleep can include especially intense dreams, long periods of REM sleep, and occasional breakthrough of REM sleep phenomena into wakefulness, such as dream-like hallucinations or brief paralysis when falling asleep or waking up. Rebound sleep on a weekend is commonly enriched in REM sleep in people who wake up early to an alarm clock on workdays and miss out on the last portion of sleep, which is mainly REM sleep.

The Homeostatic Pressure for Sleep Depends on Humoral Factors

Humoral factors circulating in the brain signal the homeostatic pressure for non-REM sleep. The brain is metabolically quite active during wakefulness and uses ATP, but with sustained periods of wakefulness, ATP is dephosphorylated to adenosine, which acts as a local neuromodulator in the extracellular environment. Adenosine type 1 receptors are inhibitory receptors that are expressed on wake-promoting neurons and in many other parts of the brain, so higher adenosine levels may produce sleepiness by inhibiting these neurons. In addition, adenosine can excite neurons via adenosine type 2a receptors; these receptors are common in the shell of the nucleus accumbens and may cause sleepiness by means of projections to the hypothalamus that activate the ventrolateral preoptic neurons.

The pressure for sleep can be measured by the time it takes an individual to fall asleep if given the opportunity in a comfortable environment. This approach is used by sleep clinicians in the Multiple Sleep Latency Test, in which an individual is given 20-minute intervals to try to fall asleep in a comfortable, quiet bed every 2 hours beginning at 9 am, for five sleep opportunities. An individual who is well rested generally

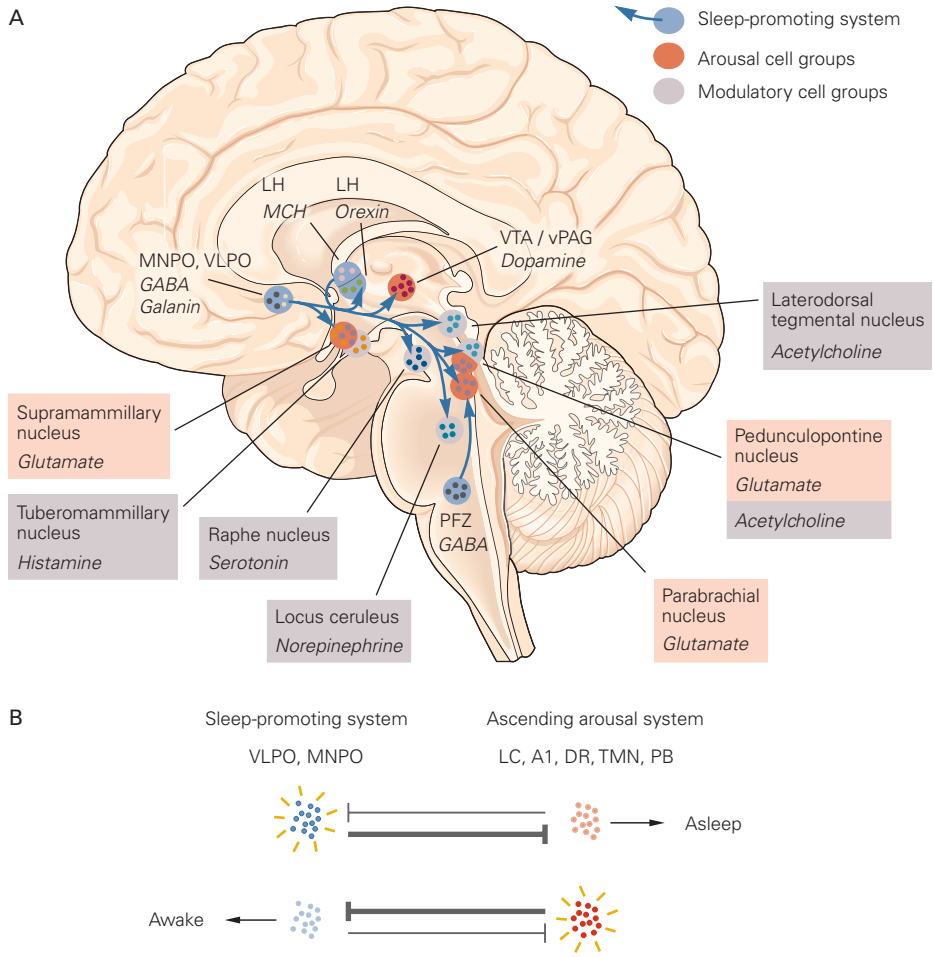

Figure 44–4 Sleep-promoting pathways.

A. The components of the ascending arousal system (Figure 44–3) receive inhibitory, largely GABAergic inputs from sleep-promoting neurons. Neurons in the ventrolateral and median preoptic nuclei (**VLPO, MNPO**) innervate the entire arousal-promoting system, while those in the parafacial zone (**PFZ**) innervate mainly the parabrachial area. Many of the VLPO neurons also contain galanin (GAL), an inhibitory peptide. Neurons in the lateral hypothalamus (**LH**) that release melanin-concentrating hormone (**MCH**) may promote REM sleep by inhibiting both nearby orexinergic neurons as well as neurons in the periaqueductal gray matter that prevent REM sleep (see Figure 44–5). (Abbreviations: **vPAG**, ventral periaqueductal gray; **VTA**, ventral tegmental area.)

B. The flip-flop switch relationship of the ventrolateral and median preoptic nuclei and the mutually inhibitory components of the ascending arousal system (**LC**, locus ceruleus; **A1**, noradrenergic neurons; **DR**, dorsal raphe; **TMN**, tuberomammillary nucleus; **PB**, parabrachial nucleus). When activated, the sleep-promoting neurons inhibit the components of the ascending arousal system. However, the sleep-promoting cell groups are also inhibited by the arousal system. The net effect is that the individual spends most time fully awake or asleep while minimizing time in transitional states.

takes at least 15 to 20 minutes to fall asleep, but a very sleepy person can easily fall asleep within a few minutes in each nap. Another test of sleep pressure is the Psychomotor Vigilance Task. The subject is told to watch a small lamp and press a button as soon as they see the light turned on. The light then turns on at random times over a 5- to 10-minute test period; sleepy subjects are inattentive and intermittently are slow or completely fail to respond to the light stimulus.

Circadian Rhythms Are Controlled by a Biological Clock in the Suprachiasmatic Nucleus

Circadian rhythms are roughly 24-hour physiological rhythms that synchronize the internal state of an animal with the external daily environment and anticipate various physiologic demands that occur on a daily basis. In humans, circadian wake-promoting signals during the day counterbalance the rising homeostatic

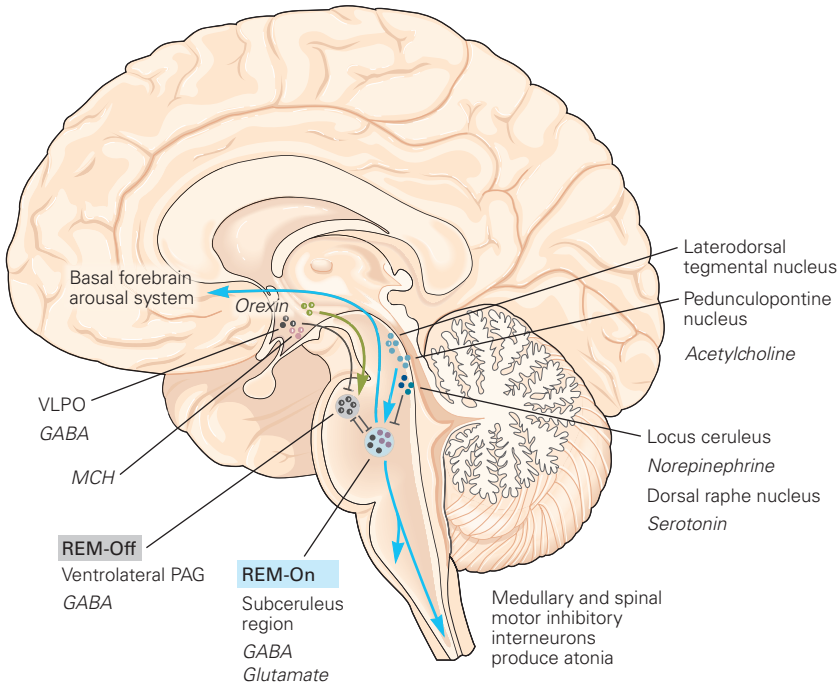

Figure 44–5 The REM sleep switch. Brain stem neurons are essential for controlling the transitions between non–rapid eye movement (**REM**) and REM sleep. REM sleep is generated by a population of neurons in the rostral pons, just ventral to the laterodorsal tegmental nucleus and locus ceruleus, in what is called the sublaterodorsal area in rodents and the subceruleus region in humans. These glutamatergic neurons project to other parts of the brain stem, where they initiate the motor and autonomic manifestations of REM sleep, and to the forebrain, where they mediate behavioral and electroencephalographic components of REM sleep. The descending projection activates inhibitory interneurons in the medulla and spinal cord that profoundly hyperpolarize motor neurons and prevent the individual from acting out his or her dreams. These REM-on neurons are inhibited by GABAergic neurons in the ventrolateral periaqueductal gray matter and adjacent pontine reticular formation, while the latter are themselves inhibited by neurons in the REM-on region, thus forming a flip-flop switch (see Figure 44–4B). These REM-off neurons are under the control of forebrain neurons, including neurons that release the excitatory orexin neuropeptides, neurons in the ventrolateral preoptic nucleus (**VLPO**) that release the inhibitory signaling molecules γ-aminobutyric acid (**GABA**) and galanin, and hypothalamic neurons that release the inhibitory neuropeptide melanin-concentrating hormone (**MCH**). In addition, modulatory neurons in the locus ceruleus and dorsal raphe inhibit the REM generator, whereas cholinergic neurons in the pedunculopontine and laterodorsal tegmental nuclei promote REM sleep. This model explains many clinical observations, such as the fact that cholinergic agonist drugs promote REM sleep, whereas drugs such as antidepressants that increase monoamine levels suppress REM sleep. Loss of orexinergic neurons can cause abrupt onset of REM sleep, whereas loss of REM-on neurons in the sublaterodorsal area abolishes atonia during REM sleep. Thus, individuals with this condition act out their dreams (*REM sleep behavior disorder*).

sleep pressure. The circadian wake-promoting signal dips slightly in the mid-afternoon, when many people take a nap or siesta. Around the habitual bedtime, this circadian waking influence rapidly collapses, the homeostatic drive for sleep is unopposed, and sleep ensues. In the hour or two before the customary waking time, circadian promotion of sleep occurs to ensure an adequate amount of sleep, since homeostatic sleep pressure is low late in the sleep period (Figure 44–6A).

Circadian rhythms are driven by a small group of GABAergic neurons in the suprachiasmatic nucleus located in the hypothalamus just above the optic chiasm. The 24-hour rhythm of activity in this biological clock is driven by a set of "clock genes," which undergo a transcriptional-translational cycle with an approximately 24-hour period. The positive limb of the loop consists of two proteins, BMAL1 and CLOCK, which dimerize and form a transcription factor that binds to the E-box motif, which is found in the promoter region of hundreds of genes that undergo daily cycles in their expression. Among those genes whose expression is increased by BMAL1 and CLOCK are the *Period* and *Cryptochrome* genes. Their protein products also dimerize, form a complex with casein kinase 1 delta or epsilon, and are translocated to the nucleus of the cell, where they cause BMAL1 and CLOCK to dissociate

A Wake–sleep cycle with light cues

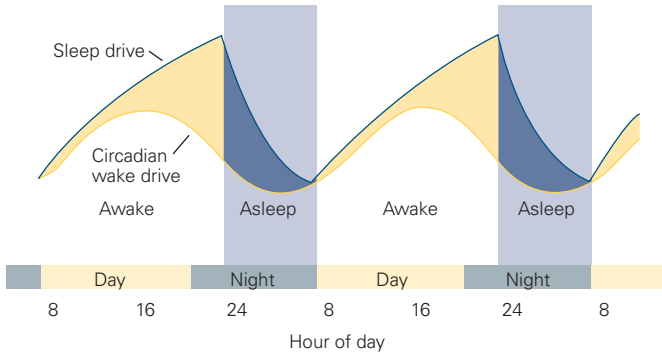

B Genetic clock of the wake–sleep cycle

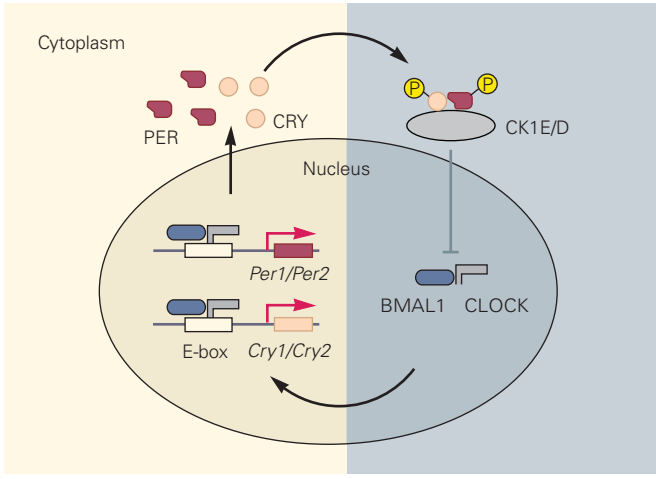

C Wake–sleep cycle without light cues

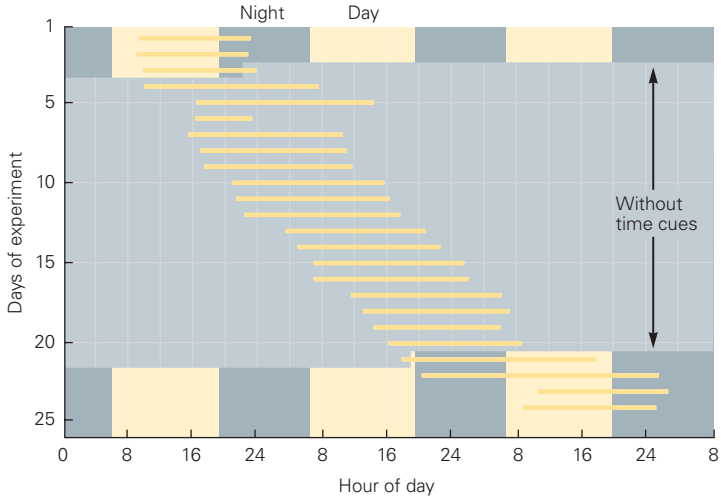

Figure 44–6 The circadian drive for wakefulness interacts with the homeostatic drive for sleep to shape wake–sleep cycles.

A. Sleep drive builds up gradually over the course of a long period of wakefulness, whereas the circadian drive for wakefulness varies on a 24-hour cycle, regardless of previous sleep. The peak of this circadian wake cycle occurs in the hours before bed, as the homeostatic sleep drive is rising, whereas the low point occurs in the hours just before the habitual time of awakening, when the homeostatic drive for sleep is ebbing.

B. The 24-hour rhythm in mammalian cells is regulated by a set of proteins that form a transcriptional-translational loop. BMAL1 and CLOCK form a dimer that binds to the E-box motif found on many genes that have circadian rhythms of transcription. Among these are the *Period 1* and *2* genes (*Per1, Per2*) and the *Cryptochrome 1* and *2* genes (*Cry1, Cry2*). Their products dimerize and form a complex with casein-1 kinase epsilon or delta (**CK1E/D**). The complex translocates to the nucleus, where it inhibits the dimerization of BMAL1 and CLOCK, causing it to fall off the E-box. This reduces the transcription of *Period* and *Cryptochrome* genes; as PER and CRY proteins are degraded, BMAL1 and CLOCK dimerize once more, and the cycle repeats.

C. Circadian rhythms regulate the timing of sleep and wake. The plot shows the wake cycles (**yellow bars**) of an individual who initially lives under regular lighting conditions for 3 days and then lives in a dimly lit environment with no time cues for 18 days. The individual maintains daily cycles of about 25.2 hours, drifting an entire day over this period. Blind people who cannot relay light signals to the suprachiasmatic nucleus (see Figure 44–7) often live continuously like this, a condition called non–24-hour wake–sleep disorder.

from the E-box, reducing transcription of many genes, including themselves. This results in a fall in Period and Cryptochrome proteins until BMAL1 and CLOCK can once more dimerize, restarting the cycle. In addition to this core loop, additional genetic side loops modulate the period of the circadian clock (Figure 44–6B).

This daily gene cycle functions in almost all cells in the body, including those in the brain, and it is essential for driving a wide range of circadian rhythms, from secretion of hormones and digestive enzymes to readying the liver for metabolic processing of food and the cardiovascular system for the active period of the day. When removed from the body and placed in a culture dish, most cells in the body rapidly fall out of synchrony, as the individual cellular clock cycles vary between cells by as much as an hour or two from the 24-hour mean. However, when neurons of the suprachiasmatic nucleus are cultured they continue to communicate with one another and thereby synchronize their cellular rhythms. This coordinated activity by suprachiasmatic neurons results in a close to 24-hour rhythm; the average period in humans who are placed in a continuous dim light environment is 24.1 hours, resulting in a slow drift in circadian rhythms (Figure 44–6C).

The suprachiasmatic nucleus exerts control over all of the other body clocks by regulating body temperature as well as autonomic, endocrine, and behavioral functions. Interestingly, although the daily rhythm in body temperature can adjust the timing of rhythms in many organs, the rhythm of the suprachiasmatic nucleus itself is highly resistant to changes in temperature, so its fundamental pacemaking is unaltered. In the end, the circadian timing of the brain and body runs on suprachiasmatic time.

Still, the suprachiasmatic clock must be entrained to the external world. If it were not, each person with a 24.1-hour cycle would progressively wake up six minutes later each day than the day before and would be unable to adjust to seasonal variations in sunrise and sunset. To avoid this situation, the suprachiasmatic nucleus receives direct inputs from a special class of retinal ganglion cells that signal light levels, rather than participating in image formation. Like all retinal ganglion cells, these neurons receive inputs from rods and cones, but they also contain melanopsin, a photopigment that makes them intrinsically photosensitive and hence they function as luminance detectors. In addition to entraining internal circadian rhythms to the ambient light cycle, these cells also regulate other non–image-forming visual functions such as the pupillary light reflex and the feeling of pain that can occur when one looks into bright lights.

Some individuals have unusually short circadian periods due to mutations in clock genes or their regulatory elements. For example, individuals with *familial advanced sleep-phase syndrome* prefer to go to bed early in the evening and cannot sleep past 3 or 4 am. In families with this disorder, mutations in the genes coding for Period or Casein kinase-1 delta result in more rapid cycling of the clock.

Blind people in whom the melanopsin-containing neurons are damaged lack visual input to their suprachiasmatic nucleus, often resulting in *non–24-hour sleep–wake rhythm disorder*. Because most people have an intrinsic cycle longer than 24 hours, circadian rhythms in these individuals drift, becoming a few minutes later each day, so that most of the time they are out of synch with the rest of the world. They lack the ability to entrain to external light–dark conditions because the suprachiasmatic nucleus lacks the crucial resetting signal from the retina. This problem is most common in people who have lost their eyes (eg, due to trauma or infection), but it is not seen in blind people in whom the melanopsin-containing neurons are intact (eg, blindness due to degeneration of rods and cones, or problems with the cornea or lens) and who also retain their pupillary light reflexes.

In contrast to light, which is signaled by the melanopsin neurons, the hormone melatonin signals darkness. Melatonin is made by the pineal gland, and the suprachiasmatic neurons time its release through communication with neurons in the paraventricular nucleus of the hypothalamus that activate sympathetic innervation of the pineal gland. Neurons in the suprachiasmatic nucleus contain melatonin receptors, which reinforce circadian rhythms. Similarly, exogenous melatonin or melatonin agonists can entrain circadian rhythms, promoting sleep by regularizing sleep onset. This treatment approach is particularly useful in entraining circadian rhythms in individuals with non–24-hour sleep–wake rhythm disorder.

Circadian Control of Sleep Depends on Hypothalamic Relays

The suprachiasmatic nucleus is most active during the daily light period in all mammalian species. While humans are diurnal (awake during the day and asleep during the night), nocturnal mammals have the opposite activity cycle. How can such opposite behavioral patterns be set by the suprachiasmatic nucleus if it is most active during the light period?

The answer appears to lie in a series of relays interposed between the suprachiasmatic nucleus and the wake–sleep control circuitry, which give the circadian

timing system flexibility in meeting the needs of the individual. The suprachiasmatic neurons are GABAergic, and they send the bulk of their output to an adjacent region called the subparaventricular zone. This area in the anterior hypothalamus contains mostly GABAergic neurons that fire in antiphase to the suprachiasmatic nucleus, ie, are most active at night. The targets of the subparaventricular zone largely overlap those of the suprachiasmatic nucleus, including parts of the paraventricular, dorsomedial, ventromedial, and lateral hypothalamus that regulate various physiological and behavioral systems. Presumably, then, the timing of a particular physiological or behavioral function would depend upon the relationships of these two antiphase circadian inputs to their target neurons.

One crucial target of the subparaventricular zone is the dorsomedial nucleus of the hypothalamus, which regulates a number of circadian behaviors, including the wake–sleep cycle. Lesions of the dorsomedial nucleus severely disrupt circadian rhythms of sleep, feeding, locomotor activity, and corticosteroid secretion. The dorsomedial nucleus is thought to promote wakefulness via GABAergic projections to the ventrolateral preoptic nucleus and glutamatergic projections to the lateral hypothalamus (Figure 44–7).

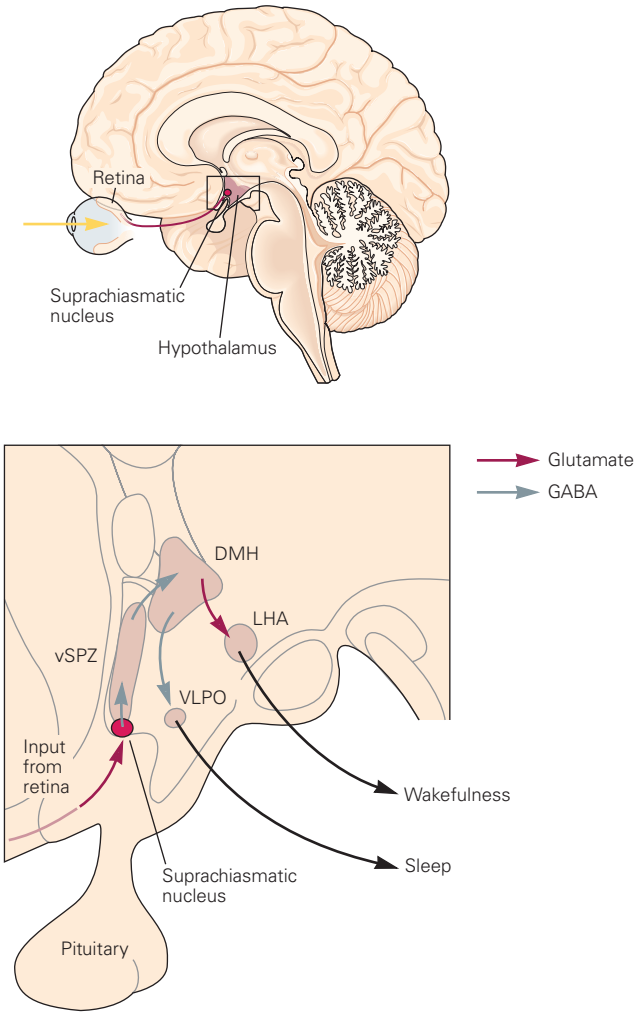

Figure 44–7 **Neurons in the suprachiasmatic nucleus provide a master clock for wake–sleep.** Retinal inputs signaling light activate the suprachiasmatic nucleus (**upper figure**), which then drives the wake–sleep cycle through a series of relays in the hypothalamus (**lower figure**). The sagittal section through the hypothalamus shows the suprachiasmatic nucleus projecting to neurons in the ventral subparaventricular zone (**vSPZ**), which in turn project to the dorsomedial nucleus of the hypothalamus (**DMH**). The DMH contains glutamatergic neurons that excite orexinergic and glutamatergic neurons in the lateral hypothalamic area (**LHA**), causing wakefulness. GABAergic neurons in the DMH inhibit the ventrolateral preoptic nucleus (**VLPO**), turning off the sleep-promoting system. Animals with DMH lesions fail to show circadian rhythms of wake–sleep and sleep about an hour more per day.

Sleep Loss Impairs Cognition and Memory

When people are sleepy, they often have impaired vigilance, working memory, judgement, and insight. Some of the attentional problems may be caused by *microsleeps*, brief periods of slower cortical activity. For example, subjects who rarely miss stimuli on the Psychomotor Vigilance Task when well rested may miss over 20% of the visual stimuli when sleepy. In addition to these global lapses in cortical function, sleepiness can also produce *local sleep* with slow EEG waves in focal cortical areas. Executive function is often the first thing to fail with sleepiness, and sleep-deprived people show reduced metabolism and focal slowing in the frontal cortex in EEGs.

While sleepiness impairs cognition, sleep itself helps consolidate memories. When subjects are taught a simple motor task, such as pressing buttons in a predetermined sequence, they become more efficient with practice. Robert Stickgold and colleagues found that if the training is in the morning, and the subjects are tested 12 hours later in the evening (without intervening sleep), they perform at about the same level as when they stopped their training. However, if they are tested the next morning after a night of sleep, they usually perform better than on the day of training. Subjects who are trained in the evening still perform better 12 hours later if they have had a chance to sleep overnight but not if they remained awake. Improvement of certain types of memory consolidation (eg, memory for a visual perception task) is correlated with the amount of REM sleep, while other types (eg, memory for a finger-tapping sequence task) correlate with stage N2 non-REM sleep.

These studies suggest that in each stage of sleep the cerebral cortex undergoes synaptic reorganization to consolidate the memory of specific types of salient information. Conversely, this memory consolidation is lost when subjects are deprived of sleep or have fragmented sleep. A related theory, proposed by Giulio Tononi and Chiara Cirelli, is that rebalancing of synaptic strengths based on recent experience (synaptic homeostasis) occurs during sleep. The size of many excitatory synapses is increased during learning, requiring that some excitatory inputs be reduced to avoid overexciting the target neuron. Tononi and Cirelli found that the size of smaller synapses in motor and sensory cortex is reduced during sleep, resulting in strong inputs being strengthened while competing weaker ones are removed.

Diseases that cause sleep loss or that wake people from sleep can impair cognition. For example, *obstructive sleep apnea* can severely fragment sleep, resulting in daytime sleepiness, inattention, and other cognitive impairments. Fragmented sleep is also common in Alzheimer disease. Alzheimer patients tend to have fewer neurons in the ventrolateral preoptic nucleus, and the extent of neuronal loss correlates with their degree of sleep fragmentation. Whether treating sleep fragmentation can improve cognition in Alzheimer patients remains to be determined.

Sleep Changes With Age

Sleep changes with age in striking and characteristic ways. As every new parent quickly learns, the lengthy sleep time of a newborn is distributed almost randomly throughout the day. Although the EEG rhythms in newborns are not as well formed as those of older children or adults, more than 50% (8–9 hours per day) of that sleep is spent in a state much like REM sleep.

Sleep recordings from a premature infant exhibit an even higher percentage of REM-like sleep, indicating that in utero the fetus spends a large fraction of the day in a brain-activated but movement-inhibited state. As neuronal activity influences the development of functional circuits in the brain (Chapters 48 and 49), it is reasonable to think that the spontaneous activity of the immature brain during sleep facilitates the development of neural circuits.

By approximately 4 months of age, the average baby begins to show diurnal rhythms that are synchronized with day and night, much to the relief of weary parents. The total duration of sleep gradually declines, and by 5 years of age, the child may sleep 11 hours each night plus a nap, and 10 hours of sleep is typical around age 10. At these early ages, sleep is deep; stage N3 is prominent, with an abundance of delta waves in the EEG. As a result, children are not easily wakened by environmental stimuli.

With age, sleep becomes lighter and more fragmented. The percentage of time spent in stage N3 sleep drops across adulthood, and by the age of 50 to 60, it is not unusual for N3 to fade entirely, especially in men. This shift toward lighter stages of non-REM sleep results in two to three times as many spontaneous awakenings and more easily disrupted sleep. Many sleep disorders, including insomnia and sleep apnea, become more prevalent with age, and insomnia is common, often due to waking in response to neural signals to empty the bladder or due to discomfort from menopausal symptoms or from arthritis and other diseases. Why this change occurs with age is unclear; homeostatic sleep pressure appears normal, but the neural mechanisms for producing deep non-REM sleep may be less effective.

Disruptions in Sleep Circuitry Contribute to Many Sleep Disorders

Insomnia May Be Caused by Incomplete Inhibition of the Arousal System

Insomnia is one of the most common problems in all of medicine, yet the underlying neurobiology remains a mystery. Insomnia is defined as difficulty falling asleep or trouble staying asleep, so that function the next day is impaired. Positron emission tomography studies in patients with chronic insomnia demonstrate unusual activation of brain arousal systems during sleep, and the EEG often shows persistence of high-frequency activity (15–30 Hz) that is usually seen only during wake.

In addition, rats exposed to acute stress show high-frequency EEG activity during sleep, as well as simultaneous activity in neurons of the ventrolateral preoptic nucleus and components of the arousal system, such as the locus ceruleus and histamine neurons. This simultaneous activation can produce a unique state in which the EEG shows slow waves consistent with sleep along with high-frequency activity consistent with the awake state; this may explain why some patients appear asleep on the polysomnogram recording but they may feel awake.

Clinically, insomnia is often treated with cognitive behavioral therapy that is aimed at reducing the hyperarousal and improving sleep habits. Some patients may be treated with benzodiazepines and

related drugs that potentiate GABA transmission and, therefore, may help reduce activity in arousal-promoting brain regions. Other patients derive benefit from drugs that block the arousal system more directly, such as antihistamines.

Sleep Apnea Fragments Sleep and Impairs Cognition

Sleep apnea is one of the most common sleep disorders, affecting about 5% of adults and children. Patients with *obstructive sleep apnea* have repeated episodes of airway obstruction that force the individual to briefly awaken from sleep to resume breathing. During sleep, muscle tone falls, and in people with small airways, relaxation of airway dilator muscles such as the genioglossus (which normally acts to pull the tongue forward) results in collapse of the airway. This causes a brief period of no air flow, and consequently, blood levels of carbon dioxide rise while oxygen levels fall, activating chemosensory systems in the medulla that increase respiratory effort.

These chemosensory systems also activate neurons in the parabrachial nucleus that promote awakening, which results in a further increase in muscle tone that reopens the airway. These airway obstructions can occur hundreds of times per night, but the arousals are usually so brief that the individual may not remember them in the morning. Many people with obstructive sleep apnea do not feel rested in the morning; they feel sleepy all day and they have difficulty with a wide variety of cognitive tasks, especially those that require vigilance or learning.

Clinicians often treat sleep apnea with a *continuous positive airway pressure (CPAP) device* that delivers mildly pressurized air via the nose to inflate and open the airway during sleep. Sleep apnea can also be treated with upper airway surgery to remove obstructions such as large tonsils, a dental device to move the tongue forward, or weight loss to reduce adipose tissue in the neck. Treated patients often feel more alert and have better cognitive function, although there may be some residual cognitive impairment, possibly due to neuronal injury from repeated episodes of low oxygen saturation or hypoxia (Figure 44–8).

Narcolepsy Is Caused by a Loss of Orexinergic Neurons

Narcolepsy was first described in the late 1800s, but the underlying cause, a deficiency in a single

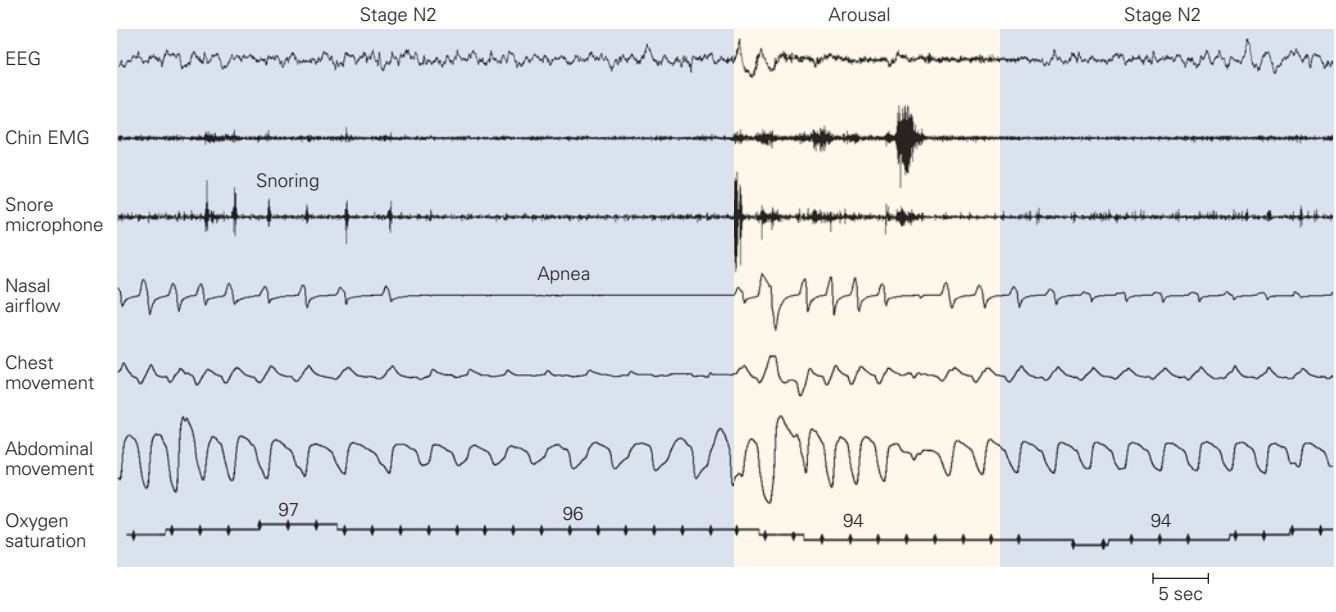

Figure 44–8 An episode of sleep apnea. At the start of this polysomnogram, an individual is in stage N2 sleep. Some snoring is detected, but nasal airflow is good and oxygen saturation is normal. The individual then experiences an obstructive apnea with no nasal airflow; nevertheless, respiratory effort persists (shown by the abdominal movement). The apnea is terminated by a brief awakening (low-voltage fast electroencephalogram [EEG]), accompanied by a loud snore, increased electromyographic activity, intensified respiratory effort, and opening of the airway. Oxygen saturation drops by about 3%, reaching its nadir about 15 seconds after the apnea finishes, as it takes time for blood to get from the lungs to the fingertip where oxygen saturation is measured.

neurotransmitter, has become clear only in the last two decades. Narcolepsy typically begins in the teen years as moderate to severe sleepiness every day, even with ample amounts of sleep at night. People with narcolepsy can easily fall asleep in class, while driving, or during other activities when sleep might be embarrassing or dangerous. Unlike sleep apnea, their sleep is restorative, and they often feel much more alert after a 15- to 20-minute nap.

In addition, in people with narcolepsy, elements of REM sleep often occur during wakefulness. For example, at night, while falling asleep or waking up, an individual with narcolepsy might find himself unable to move (*sleep paralysis*) or may have vivid dream-like hallucinations (*hypnagogic or hypnopompic hallucinations*) superimposed on wakefulness. Even more mysteriously, during the day, when surprised with a good joke or by unexpectedly seeing a friend, a person with narcolepsy can develop *cataplexy*, emotionally triggered muscle weakness that is similar to the paralysis of REM sleep. Mild cataplexy can cause weakness of the face and neck, but when severe, the individual can lose all muscle control, collapse to the ground, and be unable to move for 1 to 2 minutes.

Narcolepsy remained mysterious until the late 1990s when a new family of peptide neurotransmitters, orexins (also known as hypocretins), was discovered. There are two orexin peptides, derived from the same mRNA precursor, and they are found only in cells in the posterior lateral hypothalamus. It was soon found that loss of orexin signaling in animals or humans could reproduce the entire narcolepsy phenotype. People with narcolepsy show a highly selective loss of more than 90% of their orexin neurons, while other types of hypothalamic neurons are spared. This cell loss is probably due to an autoimmune attack as it is linked to genes that affect immune function and has been triggered by seasonal influenza epidemics and use of a certain influenza vaccine. Recently, researchers discovered that people with narcolepsy have immune cells (T lymphocytes) that target the orexin neuropeptides (Figure 44–9).

Orexinergic neurons promote wakefulness and suppress REM sleep, in part by activating monoaminergic neurons in the locus ceruleus and dorsal raphe as well as REM-off GABAergic neurons in the periaqueductal gray matter, all of which inhibit the REM sleep generating neurons in the pons. Thus, people and animals with loss of orexinergic neurons have great difficulty remaining awake for long periods, and REM sleep is disinhibited, such that REM sleep (or components of REM sleep, such as motor atonia during

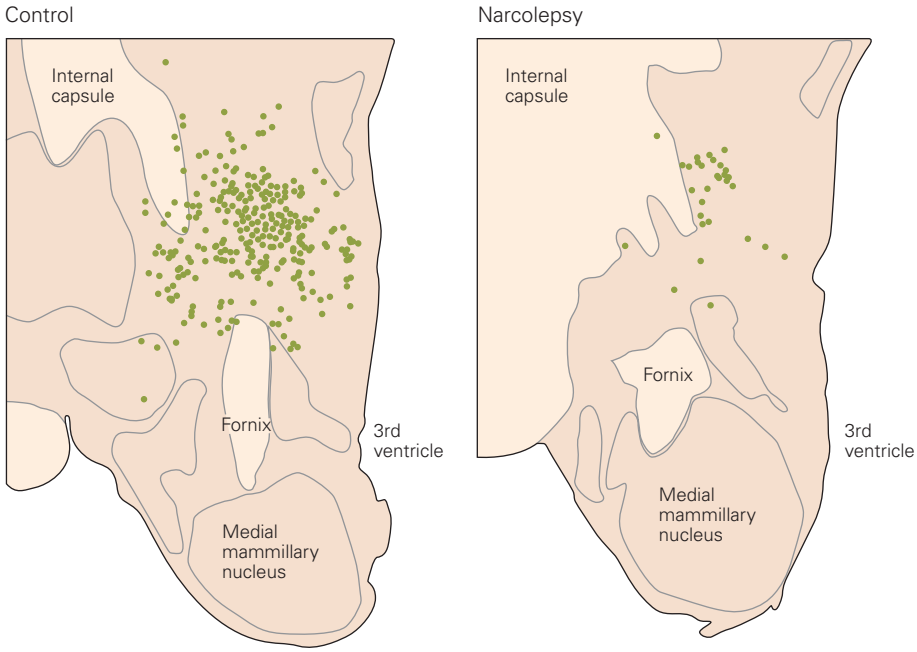

Figure 44–9 Narcolepsy is associated with a loss of hypothalamic neurons that produce the orexin neuropeptides. A dramatic loss of orexinergic neurons (**green dots**) is evident in these drawings of sections through the brain at the level of the mammillary bodies in an individual with narcolepsy (*right*) compared to a normal brain (*left*). (Reproduced, with permission, from Crocker et al. 2005. Copyright © 2005 American Academy of Neurology.)

wakefulness, or cataplexy) breaks through at inappropriate times during the day.

In terms of sleep circuitry, loss of orexinergic neurons can be considered to destabilize both the wake–sleep and the REM/non-REM switches in the brain. Thus, patients with narcolepsy can easily doze off during the day but also spontaneously wake from sleep more frequently at night. The dysregulation of REM sleep is also apparent on the Multiple Sleep Latency Test; healthy individuals almost never experience REM sleep during the day as it is under tight circadian control, but patients with narcolepsy often experience REM sleep during daytime naps.

The absence of orexin signaling also explains the mysterious symptom of cataplexy. Evidence from mice lacking orexins suggests that pleasant experiences turn on neurons in the prefrontal cortex and amygdala that can activate the brain stem pathways that trigger REM sleep paralysis. This influence is normally opposed by the orexin system, so that one may feel slightly "weak with laughter." When orexin signaling is absent, full-blown paralysis can occur.

Narcolepsy is treated with medications and behavioral approaches. Sleepiness can be substantially attenuated with wake-promoting medications such as amphetamine and modafinil. One to two strategically timed naps during the day are often helpful and can improve alertness for a couple of hours. Cataplexy often responds well to antidepressants such as serotonin or norepinephrine reuptake inhibitors, as these drugs strongly suppress REM sleep. Sodium oxybate taken during the night enhances deep sleep, and through an unknown mechanism, it helps consolidate wakefulness and reduce cataplexy during the day.

REM Sleep Behavior Disorder Is Caused by Failure of REM Sleep Paralysis Circuits

REM sleep behavior disorder—the loss of paralysis during REM sleep in some older adults—is the direct opposite of cataplexy. The lack of paralytic inhibition permits the patients to act out their dreams. The individual often calls out and may grab or violently punch or kick; injuries from hitting nearby furniture or the bed partner are not unusual. These dramatic movements typically awaken the patient, who can then recall a dream about fighting off an attacker in a way that closely matches the actual movements.

REM sleep behavior disorder was first identified in 1986 by Mahowald and Schenck. Ten years later, they reported that 40% of their original cohort of 19 patients had developed Parkinson disease or a related neurodegenerative disorder with deposition of alpha-synuclein, such as Lewy body dementia or multiple system atrophy. Subsequent studies have shown that about half of patients with REM sleep behavior disorder develop a synucleinopathy by 12 to 14 years after onset, and nearly all by 25 years. It is now thought that the synucleinopathy begins in the brain stem and early on damages the subceruleus neurons that normally drive REM sleep paralysis. If this relationship is confirmed, the diagnosis of REM sleep behavior disorder may identify individuals with nascent synucleinopathies who could be treated with drugs, not yet developed, that slow the neurodegeneration.

Restless Legs Syndrome and Periodic Limb Movement Disorder Disrupt Sleep

Restless legs syndrome occurs in about 10% of the population and is characterized by an irresistible urge to move the legs, usually accompanied by an annoying internal discomfort like "ants in the pants." This restless sensation typically occurs in the evening and first half of the night and often makes it hard to fall asleep. The sensation is much worse with rest and improves by moving the legs in bed or walking about.

Many people suffering from restless legs syndrome also experience *periodic limb movement disorder*, in which the legs and sometimes arms flex in a stereotyped way every 20 to 40 seconds during non-REM sleep. These leg movements fragment sleep and can produce daytime sleepiness. Iron deficiency is a common cause of restless legs, and treatment with iron can be very helpful. Genome-wide association studies have found genes common to both conditions, but the underlying pathophysiology is not yet understood. Patients with both disorders often improve with low doses of a D_2 dopamine agonist, the antiepileptic drug pregabalin, or an opiate drug.

Non-REM Parasomnias Include Sleepwalking, Sleep Talking, and Night Terrors

Parasomnias are unusual behaviors that occur during either REM or non-REM sleep. Non-REM parasomnias are common in children and include sleepwalking, sleep talking, confusional arousals, bed-wetting, and night terrors. About 15% of young adolescents have some sleepwalking, but this usually fades over time, so only about 1% of adults regularly sleepwalk.

The non-REM parasomnias typically begin with a sudden arousal from stage N3 sleep, which can occur spontaneously or be triggered by a noise or airway obstruction from sleep apnea. These are not full arousals, as for the first minute or two, the EEG still shows

the slow EEG delta waves typical of stage N3 sleep even as the child walks, dresses, or eats. Over time, the EEG changes to the pattern typical of wakefulness and eventually the individual wakes up. Sleepwalkers or talkers often have no memory of these events, so that reports from the family are necessary to make the diagnosis. Bed-wetting (enuresis) may also occur during deep non-REM sleep in some children.

Night terrors also occur in stage N3 sleep and are common in children age 2 to 5. The child often sits up and cries as if in great fear, sometimes with dilated pupils and a fast heart rate. During the episode, the child is inconsolable; attempts to calm or wake the child may only cause the screams and fearful behavior to worsen. Like sleep walking, but in contrast to ordinary nightmares, the child usually does not remember the night terror, and the events are typically much more difficult for the parent than the child.

The underlying cause of non-REM parasomnias is unknown. They are usually managed by ensuring adequate sleep to reduce pressure for deep non-REM sleep, reducing stress, and treating underlying sleep disorders such as sleep apnea that might trigger arousals from sleep. Fluid restriction in the evening may help with enuresis. Most children outgrow non-REM parasomnias as their N3 sleep decreases in late adolescence. Drugs that reduce the amount of N3 sleep, such as tricyclic antidepressants, are sometimes used as well. As with REM sleep behavior disorder, people can be seriously hurt sleepwalking if they fall down stairs or trip over furniture, and it is important to make the bedroom layout safe. The amount of time spent in stage N3 sleep is high in individuals with high homeostatic sleep pressure, so getting adequate sleep is also helpful.

Sleep Has Many Functions

Although there has been remarkable progress in our understanding of the brain circuitry that regulates sleep and wakefulness, we still understand relatively little about the actual functions of sleep. For an activity that occupies one-third of the life of humans, and much more in some other species, we have very little understanding of sleep's purposes. Allan Rechtschaffen, who first systematized the stages of sleep (and was an author of this chapter in earlier editions of this book), once said that if sleep did not have a vital function it would be the biggest mistake that evolution ever made. He found that rats would die of overwhelming infection and hypothermia if chronically deprived of sleep. However, the methods for keeping animals continuously awake were stressful, and it is unclear whether the consequences observed were due to loss of sleep or continuous stress. Indeed, it is not clear if prolonged sleep loss and stress can be dissociated.

One proposed function of sleep suggests that a period of brain inactivity is needed to permit metabolic recovery of the brain. The role of adenosine as a sleep-promoting humoral factor is based on the rundown of adenosine triphosphate (ATP) stores to adenosine during the awake period. Another idea is that sleep may permit the body to reconstitute injured tissue and replenish energy stores, but there is little evidence that sleep deprivation impairs any of these processes.

A recent hypothesis has been raised by the observation that during sleep the extracellular space in the brain expands, thus permitting the cerebrospinal fluid to "clean out" undesirable molecules that should not be allowed to build up extracellularly. The waking brain has very little extracellular space, largely due to ion fluxes to and from neurons during synaptic communication. These fluxes establish an osmotic gradient that drives most fluid in the brain into cells. During sleep, neurons and glia may shrink as that fluid moves back into the extracellular space. Among the molecules that may be washed out from the extracellular space during sleep are beta-amyloid peptides. In mice engineered to produce high levels of human beta-amyloid, sleep deprivation reduces the clearance of beta-amyloid from the extracellular space in the brain, thus accelerating its deposition in the plaques that are characteristic of Alzheimer disease (Chapter 64). Because buildup of beta-amyloid peptide in the brain is thought to be an early step in Alzheimer disease, work is now underway to determine whether poor sleep may predispose people to this disease.

In addition to these biochemical functions, sleep also promotes memory formation. As described earlier, the synaptic homeostasis model suggests that synapses are rebalanced during sleep, although it is not clear why this process would require sleep. A more basic need may be to provide a time for synapses to consolidate new memory traces. During the waking state, experience can modify synaptic strength on the fly by such processes as protein phosphorylation, insertion of premade receptors into the postsynaptic membrane, or translation of mRNA in the dendrites into new protein. But some portion of the synaptic remodeling that underlies memory formation requires nuclear-dependent transcription of new mRNA. Because synaptic sites on dendrites may be a millimeter from the nucleus or even more in some neurons, time is required for messenger molecules that are produced at the synapse to reach the nucleus and alter transcription and then for

the resulting mRNA to be transported back to the dendrite where it can result in new protein synthesis. This process may require a time when these messengers are not competing with new incoming signals to complete their work in stabilizing memories.

One thing about sleep is certain: It is required for normal brain function, and inadequate sleep, as defined by an increased tendency to fall asleep during the day, is associated with impaired cognitive function. Medical training programs are now being redesigned to reduce the risk of interns and residents making critical medical decisions while sleep deprived. Similar approaches to school start times, drowsy driving, and other aspects of our society could potentially improve productivity and save many lives.

Highlights

1. Sleep involves distinct changes in the electroencephalogram (EEG), electromyogram (EMG), and electro-oculogram (EOG) that are recorded on a polysomnogram. These changes can be used to divide sleep into rapid eye movement (REM) sleep—during which the EEG is similar to wake, but the body has such low muscle tone that it is essentially paralyzed—and three stages of non-REM sleep (N1–N3), with low to high amounts of slow waves in the EEG.
2. During the night, sleep alternates between periods of non-REM sleep followed by bouts of REM sleep, with the entire cycle taking about 90 minutes. Over the course of a night, non-REM sleep becomes progressively lighter, while REM sleep bouts become longer.
3. The waking state is actively produced by an ascending arousal network. The key neurons required to drive wakefulness are glutamatergic neurons in the parabrachial and pedunculopontine tegmental nuclei, dopaminergic neurons in the midbrain, glutamatergic neurons in the supramammillary nucleus, and GABAergic and cholinergic neurons in the basal forebrain that directly innervate the cerebral cortex. Modulatory cell groups, using mainly monoamines such as norepinephrine, serotonin, and histamine as neurotransmitters, can drive arousal under appropriate conditions, but unlike the main pathways, lesions of these cell groups do not impair baseline wakefulness.
4. During sleep, the ascending arousal system is inhibited by GABAergic neurons in the ventrolateral preoptic nuclei and the parafacial zone. Conversely, during wake, the ventrolateral preoptic neurons are inhibited by neurons in the ascending arousal system. These mutually antagonistic pathways produce a neural circuit resembling an electrical flip-flop switch, which favors rapid and complete transitions between sleep and wakefulness. Similarly, populations of mutually inhibitory neurons in the caudal midbrain and pons govern transitions between REM and non-REM sleep. Monoamine neurotransmitters, such as serotonin and norepinephrine, also act on these switching neurons and prevent transitions into REM sleep during wakefulness. Orexin neurons in the lateral hypothalamus activate REM sleep-suppressing neurons, preventing transitions from wake into REM sleep.
5. Sleep is regulated by a homeostatic drive to sleep, so that the longer one is awake, the more intense the drive, and the more sleep is required to satisfy the need to sleep. There is also a circadian influence on sleep that inhibits sleep during the day but promotes it at night, especially during the latter part of the night, when homeostatic sleep drive wanes. The circadian cycle is synchronized with the outside world by light signals from the retina to the brain's master circadian clock in the suprachiasmatic nucleus. The suprachiasmatic nucleus then activates hypothalamic pathways that regulate wake–sleep states, as well as many other behaviors, hormonal cycles, and physiological adjustments.
6. Sleep needs change throughout development, from about 16 hours per day in a newborn to about 8 hours per day in a healthy young adult. However, sleep-promoting mechanisms weaken with aging, and so individuals over 70 years old have more fragmented sleep and sleep about an hour less per day.
7. Sleep apnea is a condition in which the airway collapses due to reduced muscle tone during sleep. This impaired breathing causes frequent awakenings and can impair cognition. Restoring airway patency with continuous positive airway pressure (CPAP) can overcome this problem.
8. Insomnia may be caused by hyperactivation of the arousal system, and it is best treated with cognitive behavioral therapy.
9. Narcolepsy is caused by selective loss of the orexin (also called hypocretin) neurons in the hypothalamus. The orexin neuropeptides normally promote wake and regulate REM sleep, and loss of orexin signaling results in chronic daytime sleepiness and poor control of REM sleep.

Specifically, people with narcolepsy may quickly transition into REM sleep after dozing off, and they can have fragments of REM sleep, such as cataplexy and hypnogogic hallucinations, during wake. Narcolepsy is usually treated with medications that promote wake and suppress REM sleep.

10. REM sleep behavior disorder is due to loss of atonia during REM sleep, causing patients to act out their dreams. REM sleep behavior disorder is usually an early manifestation of either Parkinson disease or Lewy body dementia.
11. Restless legs syndrome is a genetically influenced disorder in which people feel that they have to move their legs. This makes them very uncomfortable when awake, and they can have periodic leg movements during sleep that disrupt sleep.
12. Sleepwalking and related parasomnias usually occur in young children during deep (stage N3) non-REM sleep. They are best managed by ensuring adequate, good-quality sleep.
13. Sleep loss impairs the ability to maintain sustained attention and clouds judgment. The reasons for this are not understood. Theories about the brain requiring down time to recharge its metabolic status or to allow it to flush out unwanted products from the extracellular space have received attention, but it is unclear whether this accounts for the penalty paid due to lack of sleep. One attractive theory for the function of sleep is that it may be required for synaptic remodeling that is necessary for certain types of learning.

Clifford B. Saper
Thomas E. Scammell

Selected Reading

Buhr ED, Takahashi JS. 2013. Molecular components of the mammalian circadian clock. Handb Exp Pharmacol 217:3–27.

Kryger MH, Roth T, Dement WC. 2017. *Principles and Practice of Sleep Medicine*, 6th ed. Philadelphia: Elsevier.

Saper CB. 2013. The central circadian timing system. Curr Opin Neurobiol 23:747–751.

Saper CB, Fuller PM, Pedersen NP, Lu J, Scammell TE. 2010. Sleep state switches. Neuron 68:1023–1042.

Scammell TE, Arrigoni E, Lipton JO. 2017. Neural circuitry of wakefulness and sleep. Neuron 93:747–765.

References

Achermann P, Borbely AA. 2003. Mathematical models of sleep regulation. Front Biosci 8:683–693.

Anaclet C, Pedersen NP, Ferrari LL, et al. 2015. Basal forebrain control of wakefulness and cortical rhythms. Nat Commun 6:8744.

Aschoff J. 1965. Circadian rhythms in man. Science 148: 1427–1432.

Aserinsky E, Kleitman N. 1953. Regularly occurring periods of eye motility and concomitant phenomena during sleep. Science 118:273–274.

Bal T, von Krosigk M, McCormick DA. 1995. Synaptic and membrane mechanisms underlying synchronized oscillations in the ferret lateral geniculate nucleus *in vitro*. J Physiol 483:641–663.

Boeve BF. 2013. Idiopathic REM sleep behaviour disorder in the development of Parkinson's disease. Lancet Neurol 12:469–482.

Buyssee DJ, Germain A, Hall M, Monk TH, Nofzinger EA. 2011. A neurobiological model of insomnia. Drug Discov Today Dis Models 8:124–137.

Chemelli RM, Willie JT, Sinton CM, et al. 1999. Narcolepsy in orexin knockout mice: molecular genetics of sleep regulation. Cell 98:437–451.

Crocker A, Espana RA, Papadopoulou M, et al. 2005. Concomitant loss of dynorphin, NARP, and orexin in narcolepsy. Neurology 65:1184–1188.

Dement W, Kleitman N. 1957. Cyclic variations in EEG during sleep and their relation to eye movements, body motility, and dreaming. Electroencephalogr Clin Neurophysiol Suppl 9:673–690.

de Vivo L, Bellesi M, Marshall W, et al. 2017. Ultrastructural evidence for synaptic scaling across the wake/sleep cycle. Science 355:507–510.

Dijk DJ, Czeisler CA. 1995. Contribution of circadian pacemaker and sleep homeostat to sleep propensity, sleep structure, electroencephalographic slow waves, and sleep spindle activity in humans. J Neurosci 15:3526–3538.

Fuller PM, Sherman D, Pedersen NP, Saper CB, Lu J. 2011. Reassessment of the structural basis of the ascending arousal system. J Comp Neurol 519:933–956.

Lim AS, Ellison BA, Wang JL, et al. 2014. Sleep is related to neuron numbers in the ventrolateral preoptic/intermediate nucleus in older adults with and without Alzheimer's disease. Brain 137:2847–2861.

Lin L, Faraco J, Li R, et al. 1999. The sleep disorder canine narcolepsy is caused by a mutation in the hypocretin (orexin) receptor 2 gene. Cell 98:365–376.

Lu J, Sherman D, Devor M, Saper CB. 2006. A putative flip-flop switch for control of REM sleep. Nature 41:589–594.

Mahowald MW, Schenck CH. 2005. Insights from studying human sleep disorders. Nature 437:1279–1285.

McCormick DA, Bal T. 1997. Sleep and arousal: thalamocortical mechanisms. Annu Rev Neurosci 20:185–215.

Moruzzi G, Magoun HW. 1949. Brain stem reticular formation and activation of the EEG. Electroencephalogr Clin Neurophysiol Suppl 1:455–473.

Peyron C, Faraco J, Rogers W, et al. 2000. A mutation in a case of early onset narcolepsy and a generalized absence of hypocretin peptides in human narcoleptic brains. Nat Med 6:991–997.

Saper CB, Scammell TE, Lu J. 2005. Hypothalamic regulation of sleep and circadian rhythms. Nature 437:1257–1263.

Stickgold R. 2005. Sleep-dependent memory consolidation. Nature 437:1272–1278.

Tononi G, Cirelli C. 2014. Sleep and the price of plasticity: from synaptic and cellular homeostasis to memory consolidation and integration. Neuron 81:12–34.

Xie L, Kang H, Xu Q, et al. 2013. Sleep drives metabolite clearance from the adult brain. Science 342:373–377.

Xu M, Chung S, Zhang S, et al. 2015 Basal forebrain circuit for sleep-wake control. Nat Neurosci 18:1641–1647.

This page intentionally left blank

Part VII

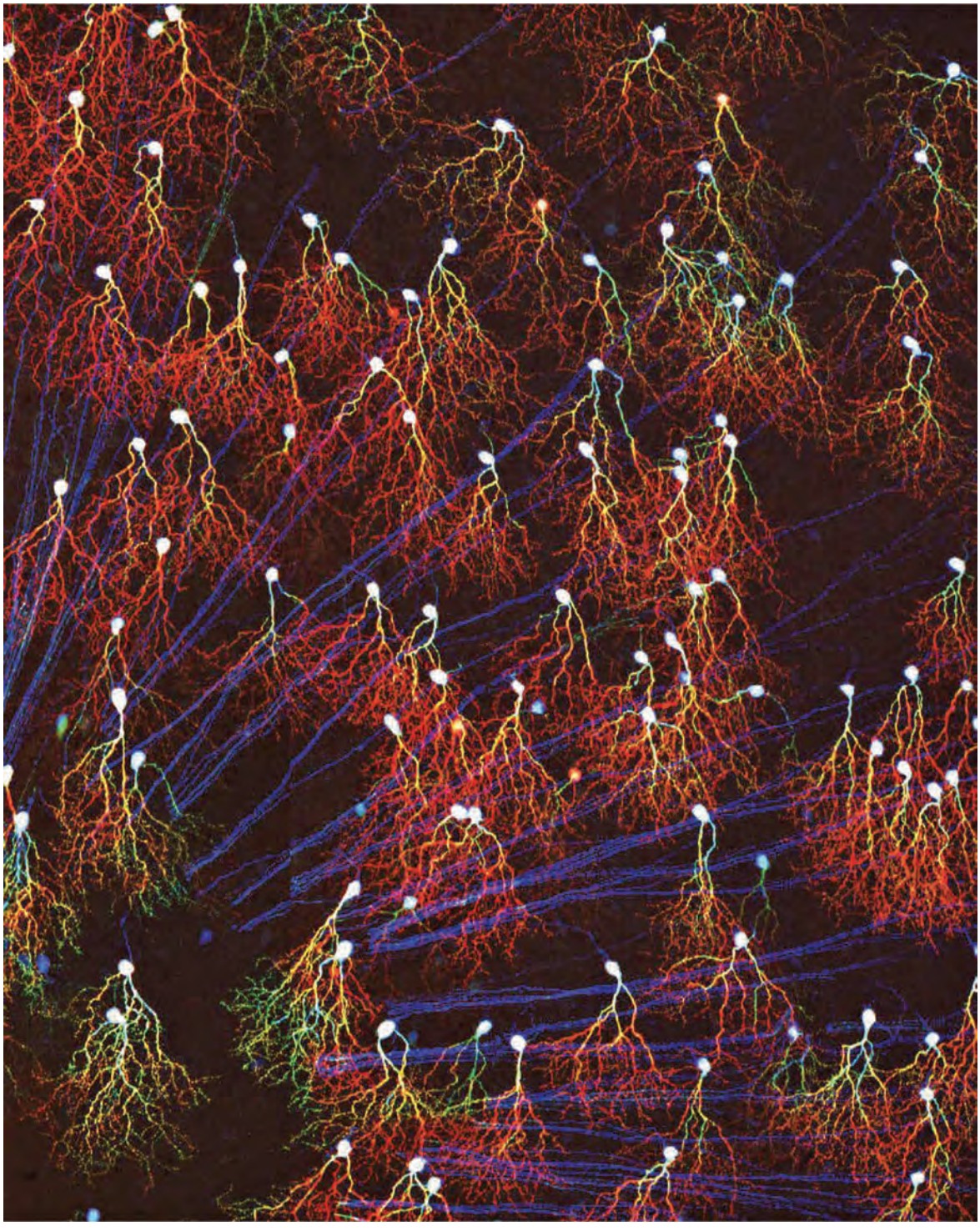

Preceding Page

Transgenic labeling of a single type of retinal ganglion cell in the mouse retina. Colors represent depth through the retina, with axons at the surface in blue and the deepest dendrites in red. Incompletely understood guidance mechanisms result in J-RGC dendrites "pointing" ventrally, resulting in their preferential response to ventral motion. J-RGC axons are guided to the optic nerve through which they travel to the rest of the brain. (Reproduced, with permission, from Jinyue Liu and Joshua Sanes. Reproduced, with permission, from Journal of Neuroscience. Cover of issue 37(50), December 13, 2017; for Liu J, Sanes JR. 2017. Cellular and molecular analysis of dendritic morphogenesis in a retinal cell type that senses color contrast and ventral motion. J Neurosci 37:12247–12262.)

VII Development and the Emergence of Behavior

THE INNUMERABLE BEHAVIORS controlled by the mature nervous system—our thoughts, perceptions, decisions, emotions, and actions—depend on precise patterns of synaptic connectivity among the billions of neurons in our brain and spinal cord. These connections form during embryonic and early postnatal life but can then be remodeled throughout life. In this section, we describe how the nervous system develops and matures.

The history of developmental neurobiology is long and illustrious. Nearly 150 years ago, Santiago Ramón y Cajal undertook a comprehensive series of anatomical studies on the structure and organization of the nervous system and then set out to probe its development. The only method available to him was light microscopic analysis of fixed tissue, but from his observations, he deduced many developmental principles that are still recognized as correct. During the first half of the 20th century, other anatomists followed in his footsteps. Progress then accelerated as new methods became available—first electrophysiology and electron microscopy and, more recently, molecular biology, genetics, and live imaging. We now know a great deal about molecules that determine how nerve cells acquire their identities, how they extend axons to target cells, and how these axons choose appropriate synaptic partners once they have arrived at their destinations.

It is useful to divide the numerous steps that compose neural development into three epochs, which are conceptually distinct even though they overlap temporally to some extent. The first, beginning at the earliest stages of embryogenesis, leads to the generation and differentiation of neurons and glia. One can think of this epoch as devoted to producing the components from which neural circuits will be assembled: the hardware. These steps depend on the expression of particular genes at particular times and places. Some of the molecules that control these spatial and temporal patterns are transcription factors that act at the level of DNA to regulate gene expression. They act within the differentiating cells and are therefore called cell-autonomous factors. Other factors, called cell non-autonomous, include cell surface and secreted molecules that arise from other cells.

They act by binding to receptors on the differentiating cells and generating signals that regulate the activity of the cell-autonomous transcriptional programs. The interaction of these intrinsic and extrinsic factors is critical for the proper differentiation of each nerve cell.

A second epoch encompasses the steps by which neurons wire up: the migration of their somata to appropriate places, the guidance of axons to their targets, and the formation of synaptic connections. The complexity of the wiring problem is staggering—axons of many neuronal types must navigate, often over long distances, and then choose among a hundred or more potential synaptic partners. Nonetheless, progress has been encouraging. A major factor has been the ability to address the problem through the analysis of simple and genetically accessible organisms such as the fruit fly *Drosophila* and the nematode worm *Caenorhabditis elegans*. It turns out that many of the key molecules that control the formation of the nervous system are conserved in organisms separated by millions of years of evolution. Thus, despite the great diversity of animal forms, the developmental programs that govern body plan and neural connectivity are conserved throughout phylogeny.

In the third epoch, the genetically determined patterns of connectivity (the hardware) are molded by activity and experience (the software). Unfortunately for investigators, these steps in mammals are shared to a very limited degree with invertebrates and lower vertebrates. A newly hatched bird or fly is not remarkably different in its behavioral repertoire from its adult self, but no one could say that about a person. This is largely because our nervous system is something of a rough draft at birth. The hardwired circuits that lay out its basic plan are modified over a prolonged postnatal period by experience, acting via neural activity. In this way, the experience of each individual can leave indelible imprints on his or her nervous system and the cognitive abilities of the brain can be enhanced by learning. These processes act in all mammals, and neuroscientists now use mice to probe the mechanisms that underlie them—but they are especially prominent and prolonged in humans. It may be that the prolonged period during which experience can sculpt the human nervous system is the most important single factor in making its capabilities unique among all species.

As our understanding of development increases, it is increasingly informing neurology and psychiatry. Many genes that regulate the first two epochs have now been implicated as susceptibility factors for, or even causes of, some neurodegenerative and behavioral disorders. Thus, studies of neural development are beginning to provide insights into the etiology of neurological diseases and to suggest rational strategies for restoring neural connections and function after disease or traumatic injury. More recently, as we learn about the cellular and molecular changes that underlie experience-dependent remodeling, we can hope to understand how, for example, the plasticity that is so evident during early life can be recruited in adults to

improve rehabilitative therapy after injury, stroke, or neurodegenerative disease. Moreover, there is increasing reason to believe that some behavioral disorders, such as autism or schizophrenia, may result in part from defects in the experience-dependent tuning of neural circuits during early postnatal life.

Part VII summarizes these epochs in a sequential manner. Beginning with the early stages of neural development, we concentrate on the factors that control the diversity and survival of nerve cells, guide axons, and regulate the formation of synapses. We then explain how interactions with the environment, both social and physical, modify or consolidate the neural connections formed during early development. Finally, we examine ways in which developmental processes can be harnessed in adults and how factors such as steroid hormones mold the brain, affecting sexual and gender identity. The last steps—changes that occur as the brain ages—are covered in Section IX (Chapter 64).

Part Editor: Joshua R. Sanes

Part VII

This page intentionally left blank

45

Patterning the Nervous System

A vast array of neurons and glial cells is produced during development of the vertebrate nervous system. Different types of neurons develop in discrete anatomical positions, acquire varied morphological forms, and establish connections with specific populations of target cells. Their diversity is far greater than that of cells in any other organ of the body. The retina, for example, has dozens of types of interneurons, and the spinal cord has more than a hundred types of motor neurons. At present, the true number of neuronal types in the mammalian central nervous system remains unknown, but it is surely more than a thousand. The number of glial types is even less clear; unexpected heterogeneity is being discovered in what was thought, until recently, to be rather homogeneous classes of astrocytes and oligodendrocytes.

The diversity of neuronal types underlies the impressive computational properties of the mammalian nervous system. Yet, as we describe in this chapter and those that follow, the developmental principles that drive the differentiation of the nervous system are begged and borrowed from those used to direct the development in other tissues. In one sense, the development of the nervous system merely represents an elaborate example of the basic challenge that pervades

all of developmental biology: how to convert a single cell, the fertilized egg, into the highly differentiated cell types that characterize the mature organism. Only at later stages, as the neurons form complex circuits and experience modifies their connections, do principles of neural development diverge from those in other organs.

Early developmental principles are conserved not only among tissues but also across species and phyla. Indeed, much of what we know about the cellular and molecular bases of neural development in vertebrates comes from genetic studies of so-called simple organisms, most notably the fruit fly *Drosophila melanogaster* and the worm *Caenorhabditis elegans.* Nevertheless, because a main goal of studying neural development is to explain how the assembly of the nervous system underlies both human behavior and brain disorders, our description of the rules and principles of nervous system development focus primarily on vertebrate organisms.

The Neural Tube Arises From the Ectoderm

The vertebrate embryo arises from the fertilized egg. Cell divisions initially form a ball of cells, called the morula, which then hollows out to form the blastula. Next, infoldings and growth generate the gastrula, a structure with polarity (dorsal-ventral and anterior-posterior) and three layers of cells—the endoderm, mesoderm, and ectoderm (Figure 45–1A).

The *endoderm* is the innermost germ layer that later gives rise to the gut, as well as to the lungs, pancreas, and liver. The *mesoderm* is the middle germ layer that gives rise to muscle, connective tissues, and much of the vascular system. The *ectoderm* is the outermost layer. Most of the ectoderm gives rise to the skin, but a narrow central strip flattens out to become the *neural plate* (Figure 45–1B). It is from the neural plate that the central and peripheral nervous systems arise.

Soon after the neural plate forms, it begins to invaginate, forming the *neural groove.* The folds then deepen and eventually separate from the rest of the ectoderm to form the *neural tube*, through a process called neurulation (Figure 45–1C,D). The caudal region of the neural tube gives rise to the spinal cord, whereas the rostral region becomes the brain. As the neural tube closes, cells at its junction with the overlying ectoderm are set aside to become the neural crest, which eventually gives rise to the autonomic and sensory nervous systems, as well as several non-neural cell types (Figure 45–1E).

Secreted Signals Promote Neural Cell Fate

As with other organs, the emergence of the nervous system is the culmination of a complex molecular program that involves the tightly orchestrated expression of specific genes. For the nervous system, the first step is the formation of the neural plate from a restricted region of the ectoderm. This step reflects the outcome of an early choice that ectodermal cells have to make: whether to become neural or epidermal cells. This decision has been the subject of intense study for nearly 100 years.

Much of this work has focused on a search for signals that control the fate of ectodermal cells. We now know that two major classes of proteins work together to promote the differentiation of an ectodermal cell into a neural cell. The first are *inductive factors,* signaling molecules that are secreted by nearby cells. Some of these factors are freely diffusible and exert their actions at a distance, but others are tethered to the cell surface and act locally. The second are surface receptors that enable cells to respond to inductive factors. Activation of these receptors triggers the expression of genes encoding intracellular proteins—transcription factors, enzymes, and cytoskeletal proteins—that push ectodermal cells along the pathway to becoming neural cells.

The ability of a cell to respond to inductive signals, termed its *competence,* depends on the exact repertoire of receptors, transduction molecules, and transcription factors that it expresses. Thus, a cell's fate is determined not only by the signals to which it is exposed—a consequence of when and where it finds itself in the embryo—but also by the profile of genes it expresses as a consequence of its prior developmental history. We will see in subsequent chapters that the interaction of localized inductive signals and intrinsic cell responsiveness is evident at virtually every step throughout neural development.

Development of the Neural Plate Is Induced by Signals From the Organizer Region

The discovery that specific signals are responsible for triggering the formation of the neural plate was the first major advance in understanding the mechanisms that pattern the nervous system. In 1924, Hans Spemann and Hilde Mangold made the remarkable observation that the differentiation of the neural plate from uncommitted ectoderm depends on signals secreted by a specialized group of cells they called the *organizer region.*

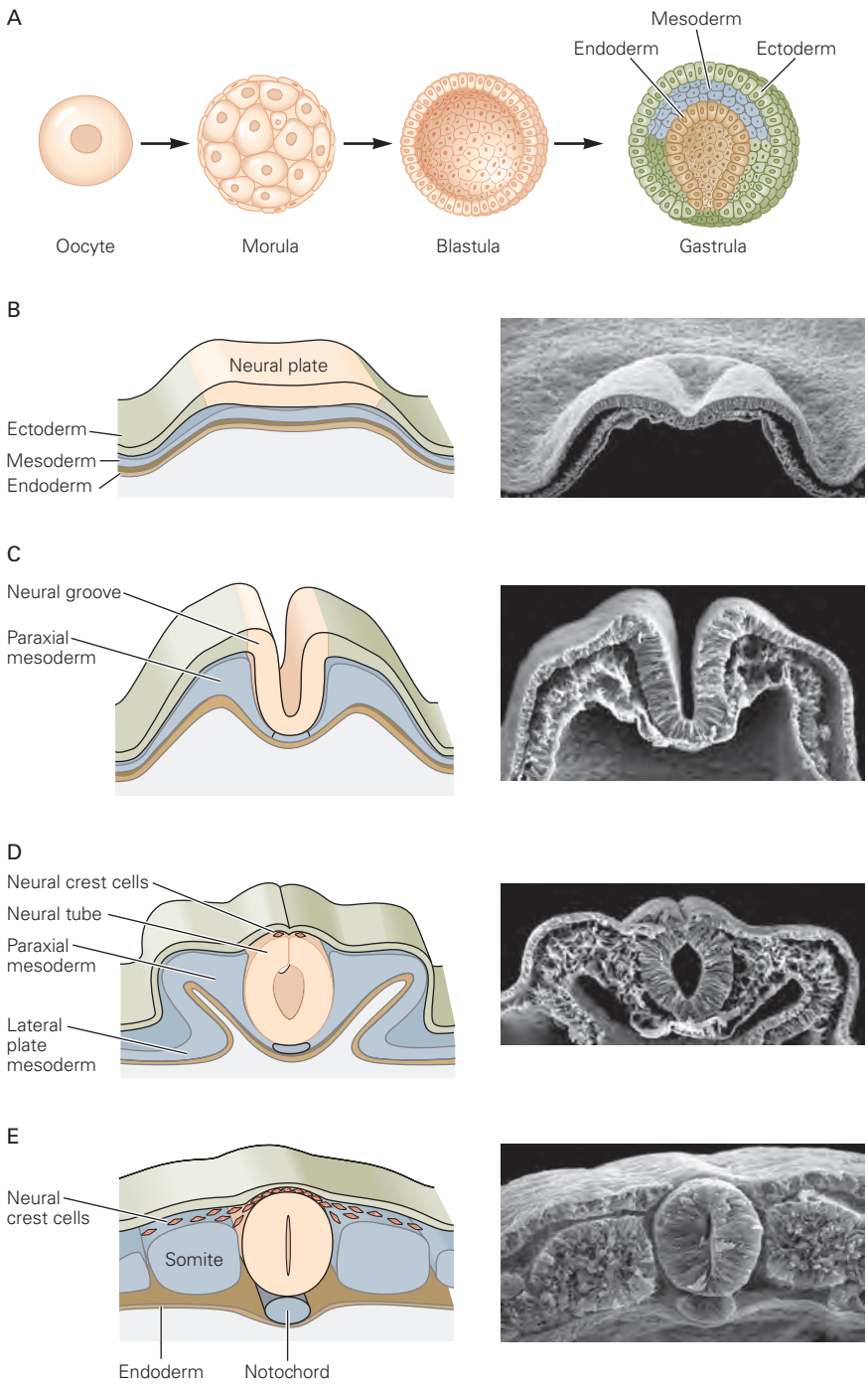

Figure 45–1 The neural plate folds to form the neural tube. (Scanning electron micrographs of chick neural tube reproduced, with permission, from G. Schoenwolf.)

A. Following fertilization of the egg by sperm, cell divisions give rise successively to the morula, blastula, and gastrula. Three germ cell layers—the ectoderm, mesoderm, and endoderm—form during gastrulation.

B. A strip of ectoderm becomes the neural plate, the precursor of the central and peripheral nervous systems.

C. The neural plate buckles at its midline to form the neural groove.

D. Closure of the dorsal neural folds forms the neural tube.

E. The neural tube lies over the notochord and is flanked by somites, an ovoid group of mesodermal cells that give rise to muscle and cartilage. Cells at the junction between the neural tube and overlying ectoderm are set aside to become the neural crest.

Their experiments involved transplanting small pieces of tissue from one amphibian embryo to another. Most telling were transplantations of the dorsal lip of the blastopore, which is destined to form the dorsal mesoderm, from its normal dorsal position to the ventral side of a host embryo. The dorsal lip lies underneath the dorsal ectoderm, a region that normally gives rise to dorsal epidermis, including the neural plate (Figure 45–2). They grafted the tissue from a pigmented embryo into unpigmented host, allowing them to distinguish the position and fate of donor and host cells.

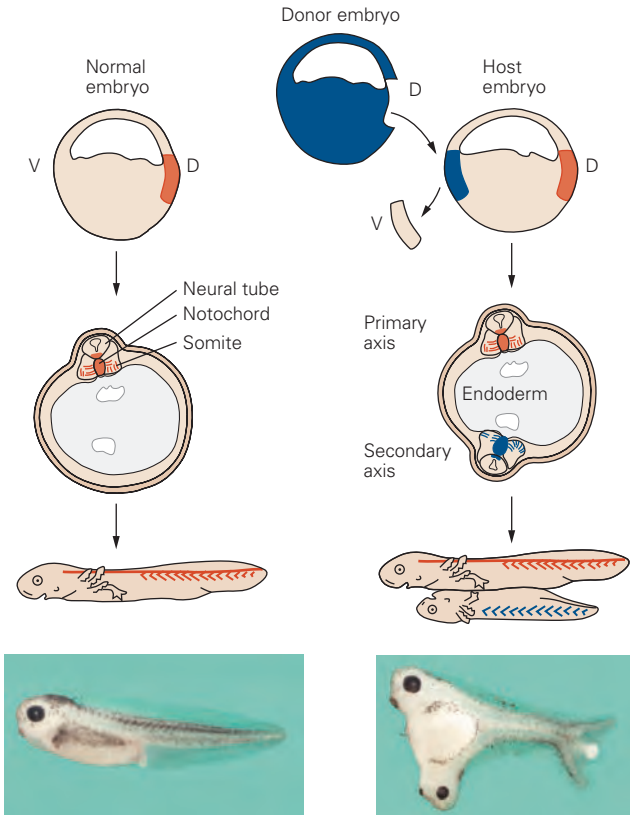

Figure 45–2 Signals from the organizer region induce a second neural tube. (Micrographs reproduced, with permission, from Eduardo de Robertis.)

Left: In the normal frog, embryo cells from the organizer region (the dorsal blastopore lip) populate the notochord, floor plate, and somites. *Right:* Spemann and Mangold grafted the dorsal blastopore lip from an early gastrula stage embryo into a region of a host embryo that normally gives rise to the ventral epidermis. Signals from grafted cells induce a second embryonic axis, which includes a virtually complete neural tube. The donor tissue was from a pigmented embryo, whereas the host tissue was unpigmented, permitting the fate of grafted cells to be monitored by their color. Grafted cells themselves contribute only to the notochord, floor plate, and somites of the host embryo. As the embryo matures, the secondary neural tube develops into a complete nervous system. In the *Xenopus* embryo shown in the micrograph, the second neural axis was induced by injection of an antagonist of bone morphogenetic protein (BMP), in effect substituting for the organizer signal (Figure 45–3). The primary neural axis is also apparent. (Abbreviations: **D**, dorsal; **V**, ventral.)

Spemann and Mangold found that transplanted cells from the dorsal lip of the blastopore followed their normal developmental program, generating midline mesoderm tissue such as the somites and notochord. But the transplanted cells also caused a striking change in the fate of the neighboring ventral ectodermal cells of the host embryo. Host ectodermal cells were induced to form a virtually complete copy of the nervous system (Figure 45–2). They therefore called the donor tissue the *organizer*. Spemann and Mangold went on to show that the dorsal lip of the blastopore was the only tissue that possessed this "organizing" effect.

These pioneering studies also demonstrated that "induction" plays a critical role in neural development. Induction is a process by which cells of one tissue direct the development of neighboring cells at a region where the two come into proximity. The importance is that it provides a mechanism by which signals from one tissue can lead to subdivision of a second tissue. In this case, the mesoderm induces one part of the ectoderm to become the neural plate, and eventually the nervous system, while the remainder goes on to become epithelium, and eventually skin. The new juxtaposition thereby formed could, in principle, set the stage for a cascade of subsequent inductions and subdivisions. Indeed, we will see that many aspects of neural tube patterning are now known to depend on signals secreted by local organizing centers through actions similar in principle to that of the classical organizer region.

Neural Induction Is Mediated by Peptide Growth Factors and Their Inhibitors

For decades after Spemann and Mangold's pioneering studies, identification of the neural inducer constituted a Holy Grail of developmental biology. The search was marked by little success until the 1980s, when the advent of molecular biology and the availability of better markers of early neural tissue led to breakthroughs in our understanding of neural induction and its chemical mediators.

The first advance came from a simple finding: When the early ectoderm is dissociated into single isolated cells, effectively preventing cell-to-cell signaling, the cells readily acquire neural properties in the absence of added factors (Figure 45–3A). The surprising implication of this finding was that the "default" fate of ectodermal cells is neural differentiation and that this fate is prevented by signaling among ectodermal cells. In this model, the long sought-after "inducer" is actually a "de-repressor": It prevents ectoderm from repressing neural fate.

These ideas immediately raised two further questions. What ectodermal signal represses neural differentiation, and what does organizer tissue provide to overcome the effects of the repressor? Studies of neural induction in frogs and chicks have now provided answers to these questions.

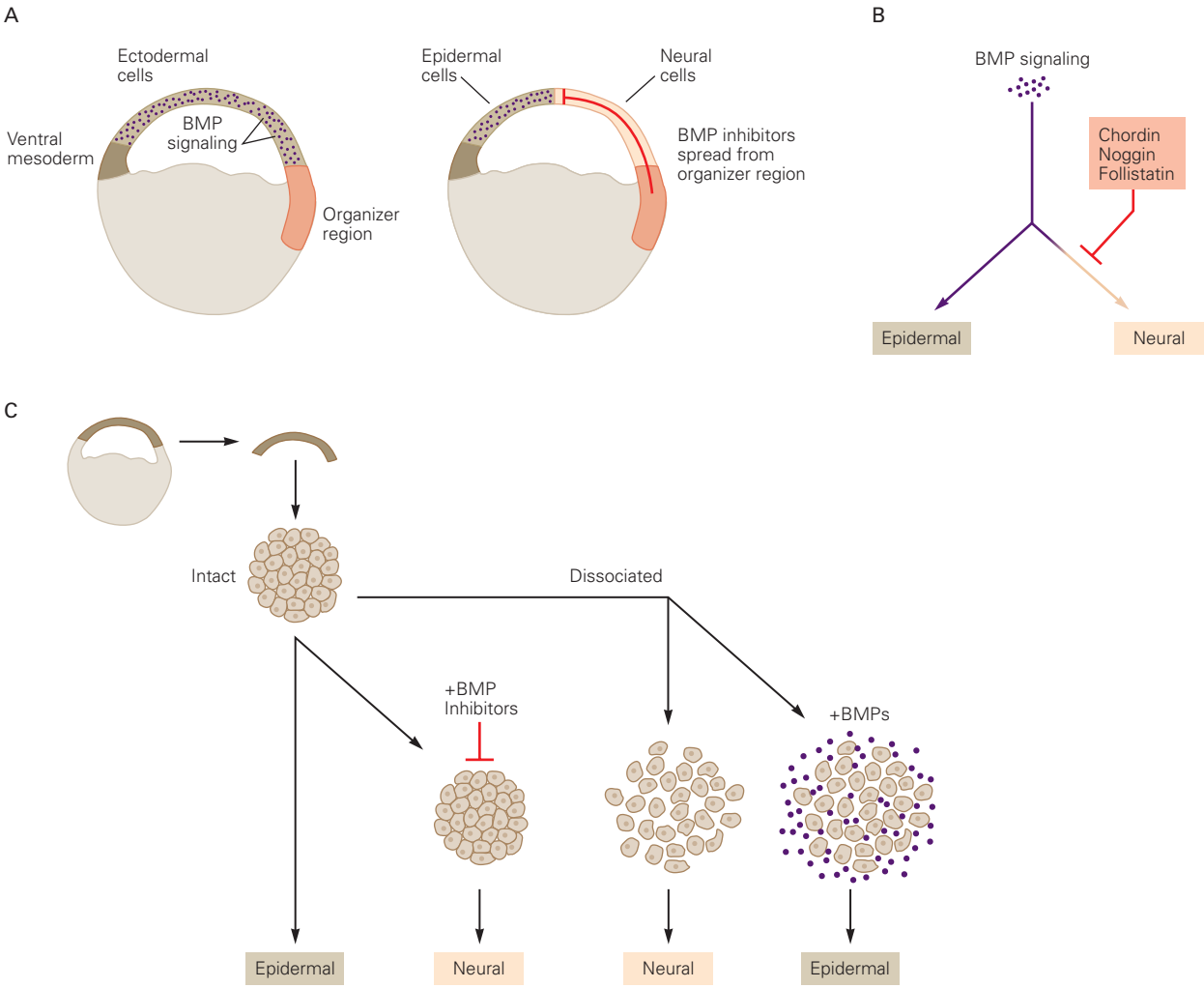

Figure 45–3 Inhibition of bone morphogenetic protein (BMP) signaling initiates neural induction.

A. In *Xenopus* frog embryos, signals from the organizer region (**red line**) spread through the ectoderm to induce neural tissue. Ectodermal tissue that is beyond the range of organizer signals gives rise to epidermis.

B. BMP inhibitors secreted from the organizer region (including noggin, follistatin, and chordin) bind to BMPs and block the ability of ectodermal cells to acquire an epidermal fate, thus promoting neural character.

C. Ectodermal cells acquire neural or epidermal character depending on the presence or absence of BMP signaling. When ectodermal cell aggregates are exposed to BMP signaling, they differentiate into epidermal tissue. When BMP signaling is blocked, either by dissociating ectodermal tissue into single cells or by addition of BMP inhibitors to ectodermal cell aggregates, the cells differentiate into neural tissue.

In the absence of signals from the organizer, ectodermal cells synthesize and secrete *bone morphogenetic proteins* (BMPs), members of a large family of transforming growth factor β (TGFβ)-related proteins. The BMPs, acting through serine/threonine kinase class receptors on ectodermal cells, suppress the potential for neural differentiation and promote epidermal differentiation (Figure 43–3B). Key evidence for the role of BMPs as neural repressors came from experiments in which a truncated version of a BMP receptor, which blocks BMP signaling, was found to trigger the differentiation of neural tissue in the *Xenopus* frog embryo. Conversely, exposure of ectodermal cells to BMP signaling promoted differentiation as epidermal cells (Figure 45–3C).

The identification of BMPs as suppressors of neuronal differentiation in turn suggested that the

organizer might induce neural differentiation in ectodermal cells by secreting factors that antagonize BMP signaling. Direct support for this idea came from the finding that cells of the organizer region express many secreted proteins that act as BMP antagonists. These proteins include noggin, chordin, follistatin, and even some variant BMP proteins. Each of these proteins has the ability to induce ectodermal cells to differentiate into neural tissue (Figure 45–3B). Thus, there is no single neural inducer. In fact, multiple classes of proteins are required for induction, as shown by the later finding that the exposure of ectodermal cells to fibroblast growth factors (FGFs) is also a necessary step in neural differentiation.

Together, these studies provided a molecular explanation of the cellular phenomenon of neural induction. Although many details of the pathway remain to be clarified and some mechanistic differences among species remain perplexing, a key chapter in neural development has now been brought to a satisfying conclusion nearly a century after the organizer was discovered by Spemann and Mangold.

Rostrocaudal Patterning of the Neural Tube Involves Signaling Gradients and Secondary Organizing Centers

As soon as cells of the neural plate have been induced, they begin to acquire regional characteristics that mark the first steps in dividing the nervous system into regions such as forebrain, midbrain, hindbrain, and spinal cord. The subdivision is directed by a series of secreted inductive factors and follows the same basic principles of neural induction. Neural plate cells in different regions of the neural tube respond to these inductive signals by expressing distinct transcription factors that gradually constrain the developmental potential of cells in each local domain. In this way, neurons in different positions acquire functional differences. Signaling occurs along both the rostrocaudal and the dorsoventral axes of the neural tube. We begin by describing rostrocaudal patterning and then return to dorsoventral patterning.

The Neural Tube Becomes Regionalized Early in Development

After the neural tube forms, cells divide rapidly, but rates of proliferation are not uniform. Individual regions of the neural epithelium expand at different rates and begin to form the specialized parts of the mature central nervous system. Differences in the rate of proliferation of cells in rostral regions of the neural tube result in the formation of three brain vesicles: the forebrain (or prosencephalic) vesicle, the midbrain (or mesencephalic) vesicle, and the hindbrain (or rhombencephalic) vesicle (Figure 45–4A).

At this early three-vesicle stage, the neural tube flexes twice: once at the *cervical flexure,* at the junction of the spinal cord and hindbrain, and once at the *cephalic flexure,* at the junction of the hindbrain and midbrain. A third flexure, the *pontine flexure,* forms later, and later still, the cervical flexure straightens out and becomes indistinct (Figure 45–4D). The cephalic flexure remains prominent throughout development, and its persistence is the reason why the orientation of the longitudinal axis of the forebrain deviates from that of the brain stem and spinal cord.

As the neural tube develops, two of the primary embryonic vesicles divide further, thus forming five vesicles (Figure 45–4B,C). The forebrain vesicle divides to form the telencephalon, which will give rise to the cortex, hippocampus, and basal ganglia, and the diencephalon, which will give rise to the thalamus, hypothalamus, and retina. The mesencephalon, which does not divide further, gives rise to the inferior and superior colliculi and other midbrain structures. The hindbrain vesicle divides to form the metencephalon, which will give rise to the pons and cerebellum, and the myelencephalon, which will give rise to the medulla. Together with the spinal cord, these divisions make up the major functional regions of the mature central nervous system (see Chapter 4). The progressive subdivision of the neural tube into these functional domains is regulated by a variety of secreted signals.

Signals From the Mesoderm and Endoderm Define the Rostrocaudal Pattern of the Neural Plate

It was originally believed that the organizer, as defined by Spemann and Mangold, was uniform in character, and therefore induced an initially uniform neural plate. Subsequent studies showed, however, that the organizer is regionally specialized and secretes factors that initiate the rostrocaudal patterning of the neural plate almost as soon as induction commences. One important class of factors comprises the Wnt proteins (an acronym based on their founding family members, the *Drosophila W*ingless protein and the mammalian Int1 proto-oncogene protein). Others include retinoic acid and FGFs. They are produced by mesodermal cells of the organizer as well as nearby paraxial mesoderm.

The net level of Wnt signaling activity is low at rostral levels of the neural plate and increases

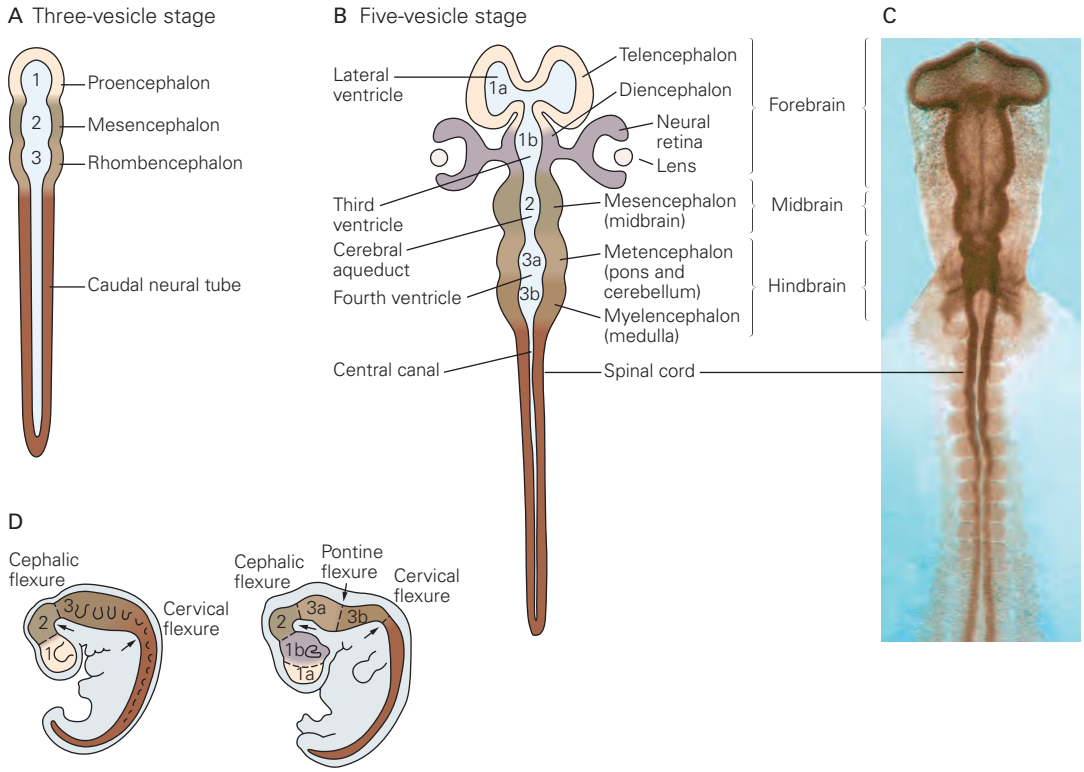

Figure 45–4 Sequential stages of neural tube development.

A. At early stages of neural tube development, there are three brain vesicles, which will form the prosencephalon (forebrain), mesencephalon (midbrain), and rhombencephalon (hindbrain).

B. Further division within the prosencephalon and rhombencephalon generate additional vesicles. The prosencephalon splits to form the telencephalon and diencephalon, and the rhombencephalon splits to form the metencephalon and the myelencephalon.

C. Top-down view of the neural tube of a chick embryo at the five-vesicle stage. (Reproduced, with permission, from G. Schoenwolf.)

D. The neural tube bends at borders between vesicles, forming the cephalic, pontine, and cervical flexures.

progressively in the caudal direction. This activity gradient arises because the mesoderm adjacent to the caudal region of the neural plate expresses high levels of Wnt. Sharpening this gradient, tissue that underlies the rostral region of the neural plate is a source of secreted proteins that inhibit Wnt signaling, much as BMP inhibitors attenuate BMP signaling at an earlier stage. Thus, cells at progressively more caudal positions along the neural plate are exposed to increasing levels of Wnt activity and acquire a more caudal regional character, spanning the entire range from forebrain to midbrain to hindbrain and finally to spinal cord (Figure 45–5A). These results suggest that an anterior character is the "default" state for neural tissue, with signals such as Wnt imposing a posterior character. Indeed, when ectodermal cells are induced to become neural by application of BMP inhibitors, they differentiate into cells characteristic of anterior structures.

Signals From Organizing Centers Within the Neural Tube Pattern the Forebrain, Midbrain, and Hindbrain

The early influence of mesodermal and endodermal tissues on rostrocaudal neural pattern is further refined by signals from specialized cell groups in the neural tube itself. One that has been studied in particular detail is called the *isthmic organizer*, which forms at the boundary of the hindbrain and midbrain (Figure 45–5B). The isthmic organizer serves a key role in patterning these two domains of the neural tube as well as in specifying the neuronal types within them. Dopaminergic neurons of the substantia nigra and ventral tegmental area are generated in the midbrain, just rostral to the isthmic organizer, whereas serotonergic neurons of the raphe nuclei are generated just caudal to the isthmic organizer, within the hindbrain. As an illustration of how these secondary neural signaling

centers impose neural pattern, we describe the origin and signaling activities of the isthmic organizer.

The rostrocaudal positional character of the neural plate stems from the expression of homeodomain transcription factors, the homeodomain being a section of the protein that binds to a specific DNA sequence in regulatory regions of genes, leading to changes in the gene's transcription. Cells in forebrain and midbrain domains of the neural plate express Otx2, whereas cells in the hindbrain domain express Gbx2, both of which are homeodomain transcription factors. The point of transition between Otx2 and Gbx2 expression is located at the midbrain–hindbrain boundary (Figure 45–5B) and marks the position at which the isthmic organizer will emerge after neural tube closure. At this boundary, other transcription factors are expressed, notably En1 (an Engrailed class transcription factor).

These transcription factors in turn control the expression of two signaling factors, Wnt1 and FGF8, by cells of the isthmic organizer. Wnt1 is involved in the proliferation of cells in the midbrain–hindbrain domain and in the maintenance of FGF8 expression. The spread of FGF8 from the isthmic organizer into the midbrain domain marked by Otx2 expression induces differentiation of dopaminergic neurons, whereas its spread into the hindbrain domain marked by Gbx2 expression triggers the differentiation of serotonergic neurons (Figure 45–5C).

The roles of FGF8 and Wnt1 in signaling from the *isthmic organizer* illustrate an important economy in early neural patterning. The early actions of inductive signals impose discrete domains of transcription factor expression, and these transcriptional domains then allow cells to interpret the actions of the same secreted factor in different ways, producing different neuronal subtypes. In this way, a relatively small number of secreted factors—FGFs, BMPs, hedgehog proteins, Wnt proteins, and retinoic acid—are used in different regions and at different times to program the vast diversity of neuronal cell types generated within the central and peripheral nervous systems.

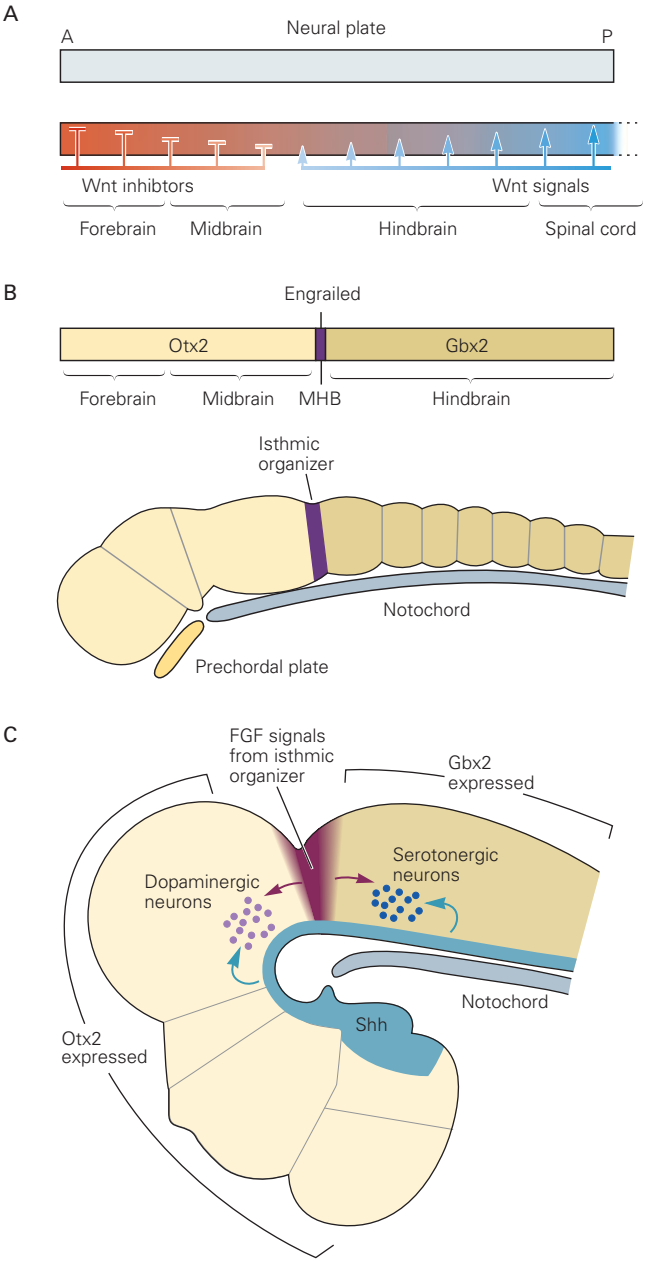

Figure 45–5 (Left) Early anteroposterior patterning signals establish distinct transcription factor domains and define the position of the midbrain–hindbrain boundary region.

A. The anteroposterior pattern of the neural plate is established by exposure of neural cells to a gradient of Wnt signals. Anterior (**A**) regions of the neural plate are exposed to Wnt inhibitors secreted from the endoderm and thus perceive only low levels of Wnt activity. Progressively more posterior (**P**) regions of the neural plate are exposed to high levels of Wnt signaling from the paraxial mesoderm and to lower levels of Wnt inhibitors.

B. In response to this Wnt signaling gradient and other signals, cells in anterior and posterior regions of the neural plate begin to express different transcription factors: Otx2 at anterior levels and Gbx2 at more posterior levels. The intersection of these two transcription factor domains marks the region of the midbrain–hindbrain boundary (**MHB**), where Engrailed transcription factors are expressed. The neural tube then forms segments anterior and posterior to the MHB.

C. Fibroblast growth factor (**FGF**) signals from the isthmic organizer act in concert with sonic hedgehog (**Shh**) signals from the ventral midline to specify the identity and position of dopaminergic and serotonergic neurons. The distinct fates of these two classes of neurons result from the expression of Otx2 in the midbrain and Gbx2 in the hindbrain.

(Adapted, with permission, from Wurst and Bally-Cuif 2001. Copyright © 2001 Springer Nature.)

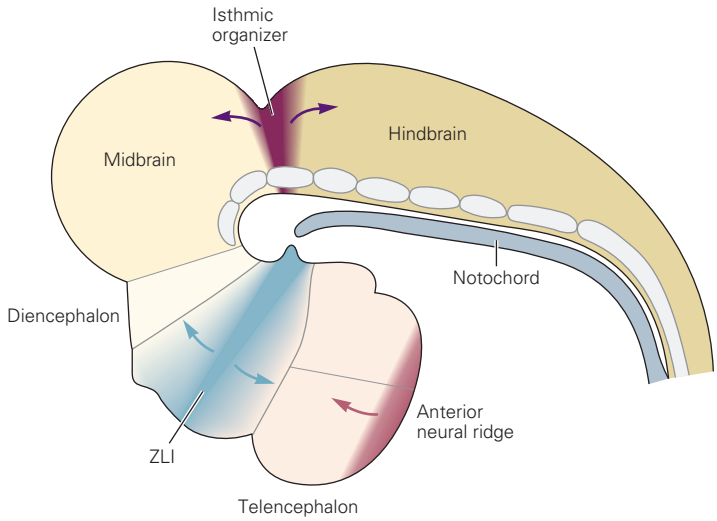

Figure 45–6 Local signaling centers in the developing neural tube. This side view of the neural tube at a later stage shows the positions of three key signaling centers that pattern the neural tube along the anterior-posterior axis: the anterior neural ridge, the zona limitans intrathalamica (**ZLI**) at the boundary between the rostral and caudal forebrain (diencephalon), and the isthmic organizer, the boundary of the midbrain and hindbrain. The ZLI is a source of sonic hedgehog, and the isthmic organizer and anterior neural ridge are sources of fibroblast growth factor (see Figure 45–5).

Other cell groups serve similar roles in subdividing the neural tube into domains. For example, at the very rostral margin of the neural tube, a specialized group of cells, called the *anterior neural ridge*, secretes FGF that patterns the telencephalon (Figure 45–6). More caudally is a restricted region called the *zona limitans intrathalamica*, which appears as a pair of horn-like spurs within the diencephalon. Zona limitans intrathalamica cells secrete the protein sonic hedgehog (Shh), which patterns nearby cells that give rise to the nuclei of the thalamus. FGFs and Shh are described in detail below in the context of their prominent role in patterning the cortex and spinal cord, respectively.

Repressive Interactions Divide the Hindbrain Into Segments

An important next step in patterning the neural tube along the rostrocaudal axis is the subdivision of the forebrain and hindbrain into segments, compartmental units that are arrayed along the rostrocaudal axis. These units are called *prosomeres* in the forebrain and *rhombomeres* in the hindbrain.

We use the formation of rhombomeres 3 and 4 (of 7 total) to illustrate the mechanisms leading to segmentation (Figure 45–7). An initial morphogen gradient leads to expression of two distinct transcription factors in this region—*krox20* in what will become rhombomere 3, endowing these cells with a rhombomere 3 identity, and *hoxb1* in what will become rhombomere 4, endowing these cells with a rhombomere 4 identity. Cells near the border express both factors and therefore have an uncertain identity. However, these two factors inhibit each other's expression, so eventually the identity of each cell is fixed.

The problem is that some cells are trapped within the wrong rhombomere. This intermingling is rectified in several ways, one of which is a second inhibitory interaction, this one of a markedly different type. Krox20 and Hoxb1 induce the expression of cell surface recognition and signaling molecules called EphA4 and ephrinB3, respectively. These two proteins bind to each other, leading to transmission of a repulsive signal that separates the cells. We will see below that this repulsion is also key to later decisions that axons make as they grow to their targets. In the hindbrain, before neurons form, it sharpens the borders between rhombomeres. More broadly, rhombomere segregation provides another example of a general theme in neural development: that inductive or adhesive interactions combine with repressive or inhibitory ones to pattern the nervous system.

Dorsoventral Patterning of the Neural Tube Involves Similar Mechanisms at Different Rostrocaudal Levels

As the neural epithelium acquires its rostrocaudal character, cells located at different positions along its dorsoventral axis also begin to acquire distinct identities. Together, patterning along the rostrocaudal and dorsoventral axes divides the neural tube into a three-dimensional grid of molecularly distinct cell types, leading eventually to generation of the various neuronal and glial cell types that distinguish one part of the nervous system from another.

In contrast to the diversity of signals and organizing centers responsible for rostrocaudal patterning of developing neurons, there is a striking consistency in

the strategies and principles that establish dorsoventral pattern. We focus initially on the mechanisms of dorsoventral patterning at caudal levels of the neural tube that give rise to the spinal cord and then describe how similar strategies are used to pattern the forebrain.

Neurons in the spinal cord serve two major functions. They relay cutaneous sensory input to higher centers in the brain, and they transform sensory input into motor output. The neuronal circuits that mediate these functions are segregated anatomically. Circuits involved in the processing of cutaneous sensory information are located in the dorsal half of the spinal cord, whereas those involved in the control of motor output are mainly located in the ventral half of the spinal cord.

The neurons that form these circuits are generated at different positions along the dorsoventral axis of the spinal cord in a patterning process that begins with the establishment of distinct progenitor cell types. Motor neurons are generated close to the ventral midline, and most of the interneuron classes that control motor output are generated just dorsal to the position at which motor neurons appear (Figure 45–8). The dorsal half of the neural tube generates projection neurons and local circuit interneurons that process incoming sensory information.

How are the position and identity of spinal neurons established? The dorsoventral patterning of the neural tube is initiated by signals from mesodermal and ectodermal cells that lie close to the ventral and dorsal poles of the neural tube and is perpetuated by signals from two midline neural organizing centers. Ventral patterning signals are initially provided by the notochord, a mesodermal cell group that lies immediately under the ventral neural tube (Figure 45–1). This signaling activity is transferred to the floor plate, a specialized glial cell group that sits at the ventral midline of the neural tube itself. Similarly, dorsal signals are provided initially by cells of the epidermal ectoderm that span the dorsal midline of the neural tube, and subsequently by the roof plate, a glial cell group embedded at the dorsal midline of the neural tube (Figure 45–8).

Thus, neural patterning is initiated through a process of *homogenetic* induction, in which like begets like: Notochord signals induce the floor plate, which

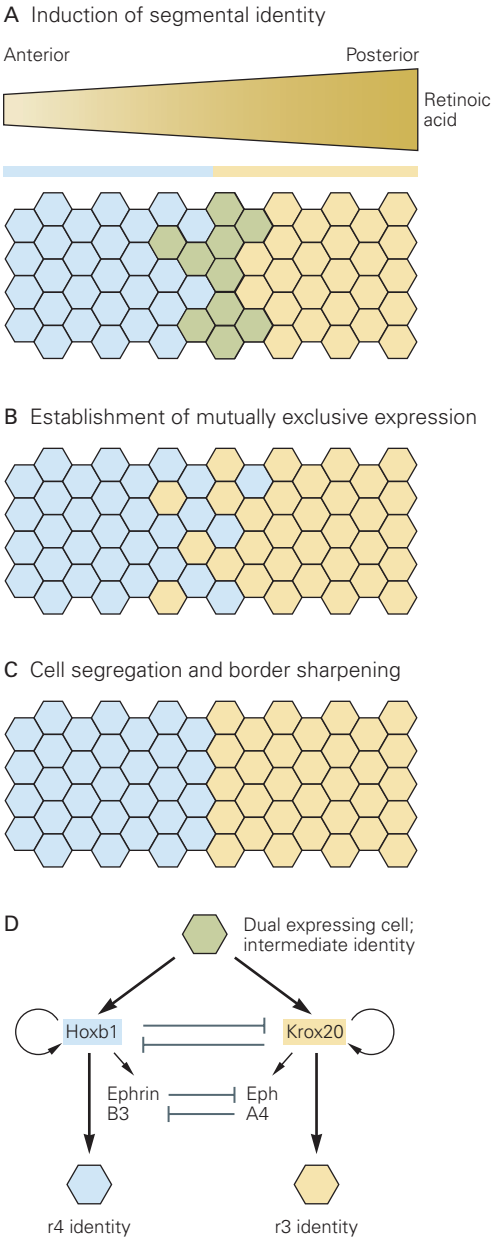

Figure 45–7 (Left) **Repressive interactions divide the hindbrain into rhombomeres.** The sharp border between hindbrain rhombomeres 3 and 4 forms in several steps. (Adapted, with permission, from Addison and Wilkinson 2016. Copyright © 2016 Elsevier Inc.)

A. A gradient of retinoic acid upregulates expression of *hoxb1* in anterior cells (**blue**) and *krox20* in posterior cells (**yellow**), with some cells at the prospective border expressing both genes (**green**).

B. Hoxb1 expression and Krox20 expression become mutually exclusive, thus endowing each cell with a unique molecular identity.

C. Cells trapped in the wrong domain migrate to sharpen the border.

D. Inhibitory interactions underlying border formation. Hoxb1 and Krox20 repress each other's expression in individual cells, so a modest imbalance in level leads to exclusive expression of one factor. Krox20 then upregulates EphA4 in r3 cells, whereas ephrinB3 is upregulated in r4 cells. EphA4 and ephrinB3 repel each other, driving migration of isolated cells and sharpening the segment border.

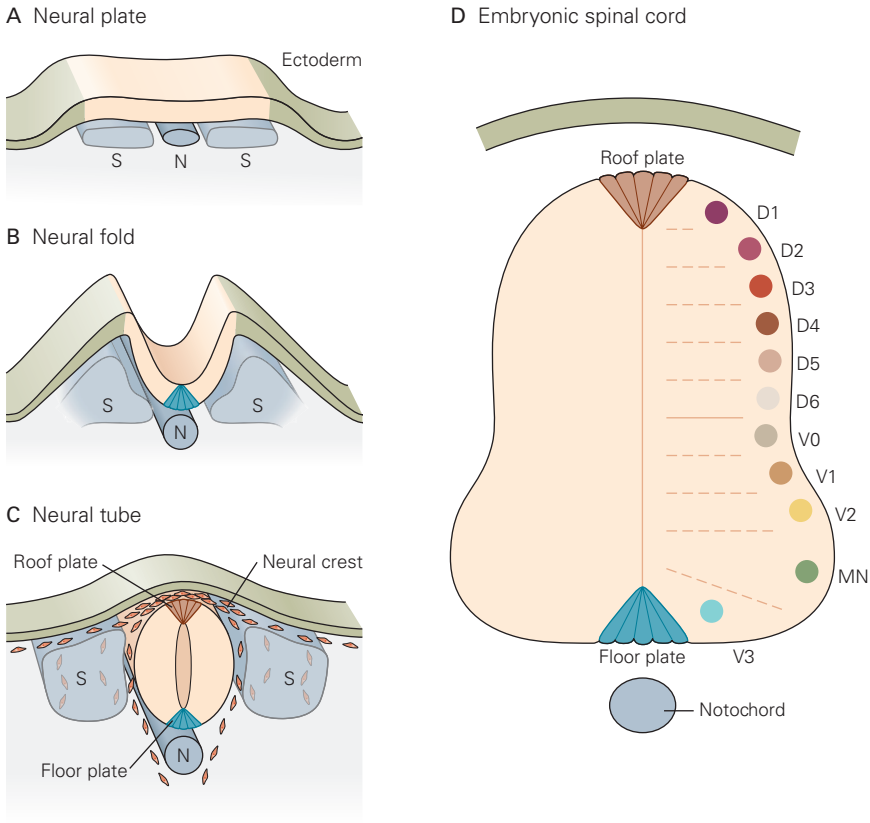

Figure 45–8 Distinct precursor populations form along the dorsoventral axis of the developing spinal cord.

A. The neural plate is generated from ectodermal cells that overlie the notochord (**N**) and the future somites (**S**). It is flanked by the epidermal ectoderm. (See also Figure 45–1)

B. The neural plate folds dorsally at its midline to form the neural fold. Floor plate cells (**blue**) differentiate at the ventral midline of the neural tube.

C. The neural tube forms by fusion of the dorsal tips of the neural folds. Roof plate cells form at the dorsal midline of the neural tube. Neural crest cells migrate from the neural tube into and past the somites before populating the sensory and sympathetic ganglia.

D. Distinct classes of neurons are generated at different dorsoventral positions in the embryonic spinal cord. Ventral interneurons (**V0–V3**) and motor neurons (**MN**) differentiate from progenitor domains in the ventral spinal cord. Six classes of early dorsal interneurons (**D1–D6**) develop in the dorsal half of the spinal cord. (Adapted from Goulding et al. 2002.)

induces ventral neurons, and signals from ectoderm induce the roof plate, which induces dorsal neurons. This strategy ensures that inductive signals are positioned appropriately to control neural cell fate and pattern over a prolonged period of development, as tissues grow and cells move.

The Ventral Neural Tube Is Patterned by Sonic Hedgehog Protein Secreted from the Notochord and Floor Plate

Within the ventral half of the neural tube, the identity and position of developing motor neurons and local interneurons depend on the inductive activity of the Shh protein, which is secreted by the notochord and subsequently by the floor plate. Shh is a member of a family of secreted proteins related to the *Drosophila* hedgehog protein, which had been discovered earlier and shown to control many aspects of embryonic development.

Shh signaling is necessary for the induction of each of the neuronal classes generated in the ventral half of the spinal cord. How can a single inductive signal specify the fate of at least half a dozen neuronal classes? The answer lies in the ability of Shh to act as a morphogen—a signal that can direct different cell fates at different concentration thresholds. The secretion of Shh from the notochord and floor plate establishes a ventral-to-dorsal gradient of Shh protein activity in the ventral neural tube, such that progenitor cells occupying different dorsoventral positions within the neural epithelium are exposed to small (two- to three-fold) differences in ambient Shh signaling activity. Different levels of Shh signaling activity direct progenitor cells in different ventral domains to differentiation as motor neurons and interneurons (Figure 45–9A).

These findings raise two additional questions. How is the spread of Shh protein within the ventral neural epithelium controlled in such a precise manner? And how are small differences in Shh signaling activity converted into all-or-none decisions about the identity of progenitor cells in the ventral neural tube?

Active Shh protein is synthesized from a larger precursor protein, cleaved through an unusual autocatalytic process that involves a serine protease-like activity resident within the carboxy terminus of the precursor protein. Cleavage generates an amino

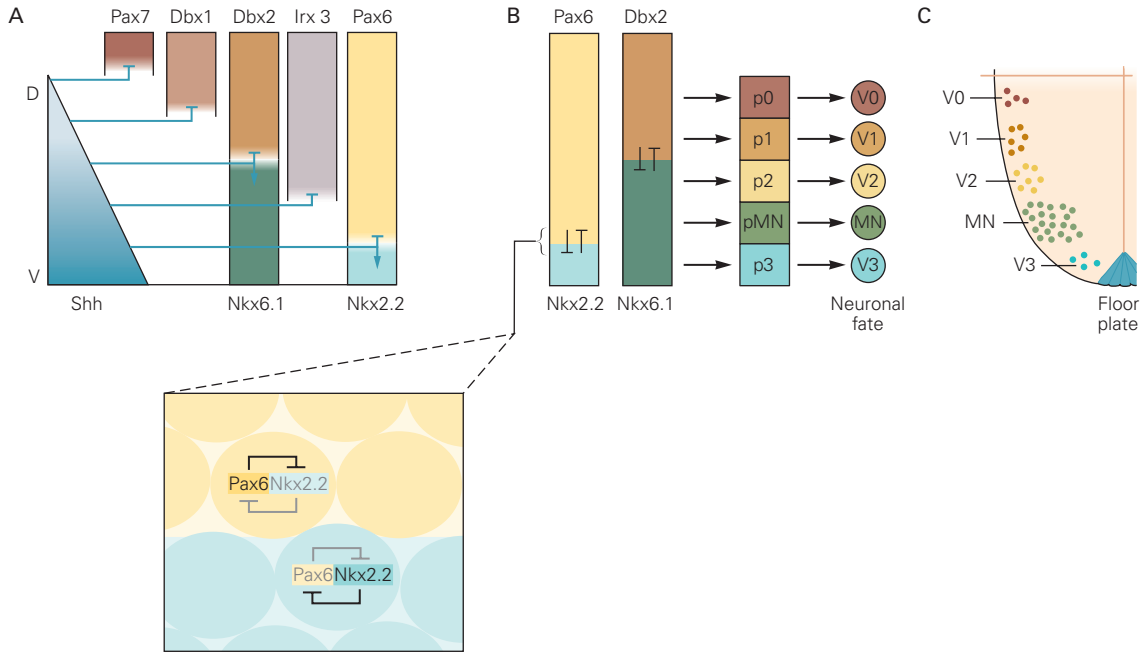

Figure 45–9 A sonic hedgehog signaling gradient controls neuronal identity and pattern in the ventral spinal cord.

A. A ventral-to-dorsal (**V–D**) gradient of sonic hedgehog (**Shh**) signaling establishes dorsoventral domains of homeodomain protein expression in progenitor cells within the ventral half of the neural tube. At each concentration, a different homeodomain transcription factor (Pax7, Dbx1, Dbx2, Irx3, or Pax6) is repressed, with Pax7 the most sensitive and Pax6 the least sensitive to repression. Other homeodomain transcription factors (Nkx6.1 and Nkx2.2) are induced at different Shh levels. The homeodomain proteins that abut a common progenitor domain boundary have similar Shh concentration thresholds for repression and activation. Graded Shh signaling generates a corresponding gradient of Gli transcription factor activity (not shown).

B. Cross-repression between transcription factors induced or repressed by Shh/Gli signaling specifies different neuronal classes. For example, Pax6 and Nkx2.2, and Dbx2 and Nkx6.1, act in a cell-autonomous manner to repress each other's expression (inset), conferring cell identity to progenitor cells in an unambiguous manner. The sequential influence of graded Shh and Gli signaling, together with homeodomain transcriptional cross-repression, establishes five cardinal progenitor domains.

C. The postmitotic neurons that emerge from these domains give rise to the five major classes of ventral neurons: the interneurons **V0–V3** and motor neurons (**MN**).

terminal protein fragment that possesses all of the signaling activity of Shh. During cleavage, the active amino terminal fragment is modified covalently by the addition of a cholesterol molecule. Following Shh secretion, this lipophilic anchor tethers most of the protein to the surface of notochord and floor plate cells. Nevertheless, a small fraction of the anchored protein is released from the cell surface and transferred from cell to cell within the ventral neural epithelium. In reality, the molecular machinery that ensures the formation of a long-distance gradient of extracellular Shh protein is more complex, involving specialized transmembrane proteins that promote the release of Shh from the floor plate, as well as proteins that regulate Shh protein transfer between cells.

How does the gradient of Shh protein within the ventral neural tube direct progenitor cells along different pathways of differentiation? Shh signaling is initiated by its interaction with a transmembrane receptor complex that consists of a ligand-binding subunit called *patched* and a signal-transducing subunit called *smoothened* (named for the corresponding *Drosophila* genes). The binding of Shh to patched relieves its inhibition of smoothened and so activates an intracellular signaling pathway that involves several protein kinase enzymes, transport proteins, and most important, the Gli proteins, a class of zinc finger transcription factors.

In the absence of Shh, the Gli proteins are proteolytically processed into transcriptional repressors that prevent the activation of Shh target genes. Activation of the Shh signaling pathway inhibits this proteolytic processing, with the result that transcriptional activator forms of Gli predominate, thus directing the expression of Shh target genes. In this way, an extracellular gradient of Shh protein is converted into a nuclear gradient of Gli activator proteins. The ratio of

Gli repressor and activator proteins at different dorsoventral positions determines which target genes are activated.

What genes are activated by Shh-Gli signaling, and how do they participate in the specification of ventral neuronal subtypes? The major Gli targets are genes encoding yet more transcription factors. One major class of Gli targets encodes homeodomain proteins, transcription factors that contain a conserved DNA-binding motif termed a *homeobox*. A second major class of target genes encodes proteins with a basic helix-loop-helix DNA-binding motif. Some homeodomain and basic helix-loop-helix proteins are repressed and others activated by Shh signaling, each at a particular concentration threshold. In this way, cells in the ventral neural tube are allocated to one of five cardinal progenitor domains, each marked by its own transcription factor profile (Figure 45–9B,C).

The transcription factors that define adjacent progenitor domains repress each other's expression. Thus, although a cell may initially express several transcription factors that could direct the cell along different pathways of differentiation, a minor imbalance in the starting concentration of the two factors is rapidly amplified through repression, and only one of these proteins is stably expressed. This winner-take-all strategy of transcriptional repression sharpens the boundaries of progenitor domains and ensures that an initial gradient of Shh and Gli activity will resolve itself into clear distinctions in transcription factor profile. The transcription factors that specify a ventral progenitor domain then direct the expression of downstream genes that commit progenitor cells to a particular postmitotic neuronal identity. Thus, studies of Shh signaling have not only revealed the logic of ventral neuronal patterning but also demonstrated that the fate of a neuron is determined in part by the actions of transcriptional repressors rather than activators. This principle operates in many other tissues and organisms.

Although originally studied in the context of neural development, defects in Shh signaling have now been implicated in a wide variety of human diseases. Mutations in human Shh pathway genes result in defects in the development of ventral forebrain structures (holoprosencephaly), as well as neurological defects such as spina bifida, limb deformities, and certain cancers.

The Dorsal Neural Tube Is Patterned by Bone Morphogenetic Proteins

A signaling strategy based on graded morphogen levels activating sets of transcriptional programs has also been found to determine the patterning of cell types in the dorsal spinal cord. The differentiation of roof plate cells at the dorsal midline of the neural tube is triggered by BMP signals from epidermal cells that initially border the neural plate and later flank the dorsal neural tube.

After the neural tube has closed, roof plate cells themselves begin to express BMP as well as Wnt proteins. Wnt proteins promote the proliferation of progenitor cells in the dorsal neural tube. BMP proteins induce the differentiation of neural crest cells at the very dorsal margin of the neural tube and later induce generation of diverse populations of sensory relay neurons that settle in the dorsal spinal cord.

Dorsoventral Patterning Mechanisms Are Conserved Along the Rostrocaudal Extent of the Neural Tube

The strategies used to establish dorsoventral pattern in the spinal cord also control cell identity and pattern along the dorsoventral axis of the hindbrain and midbrain, as well as throughout much of the forebrain.

In the mesencephalic region of the neural tube, Shh signals from the floor plate act in concert with the rostrocaudal patterning signals discussed earlier to specify dopaminergic neurons of the substantia nigra and ventral tegmental area as well as serotonergic neurons of the raphe nuclei (see Figure 45–5C). In the forebrain, Shh signals from the ventral midline and BMP signals from the dorsal midline act in combination to establish different regional domains. Shh signaling from the ventral midline sets up early progenitor domains that later produce neurons of the basal ganglia and some cortical interneurons, whereas BMP signaling from the dorsal midline is involved in establishing early neocortical character.

Local Signals Determine Functional Subclasses of Neurons

To this point, we have seen how a uniform group of neural precursor cells, the neural plate, is progressively partitioned into discrete rostrocaudal and dorsoventral domains within the neural tube, largely by morphogen-dependent differential expression of different sets of transcriptional regulators. The next question is how cells within these domains go on to generate the extraordinary diversity of neuronal types that characterize the vertebrate central nervous system. We address that question by focusing on development of the motor neuron.

Motor neurons can be distinguished from all other classes of neurons in the central nervous system by the simple fact that they have axons that extend into the periphery. Viewed in this light, motor neurons represent a coherent and distinct class. But motor neuron types can be distinguished by their position within the central nervous system as well as by the target cells they innervate. The primary job of most motor neurons is to innervate skeletal muscles, of which there are approximately 600 in a typical mammal. From this, it follows that there must be an equal number of motor neuron types.

In this section, we discuss the developmental mechanisms that direct the differentiation of these different functional subclasses. The details of motor neuron development are also important for understanding the basis of neurological disorders that affect these neurons, including spinal muscular atrophy and amyotrophic lateral sclerosis (Lou Gehrig disease). In both diseases, some motor neuron types are highly vulnerable whereas others are relatively resilient. Similar principles drive the diversification of other neuronal classes into distinct types.

Rostrocaudal Position Is a Major Determinant of Motor Neuron Subtype

Motor neurons are generated along much of the rostrocaudal axis of the neural tube, from the midbrain to the spinal cord. Distinct motor neuron types develop at each rostrocaudal level (Figure 45–10), suggesting that one goal of the patterning signals that establish rostrocaudal positional identity within the neural tube is to make motor neurons different.

One major class of genes involved in specifying motor neuron types is the *Hox* gene family. Their name reflects the fact that they were the first transcription factors found that contain a homeodomain, a DNA binding domain now known to be present in many transcription factors that regulate developmental processes in organisms as diverse as yeast, plants, and mammals. For example, the *Otx* and *Gbx* genes discussed above contain homeodomains. The mammalian *Hox* gene family is especially large, containing 39 genes organized in four chromosomal clusters. These genes derive from an ancestral *Hox* complex that also gave rise to the *HOM-C* gene complex in *Drosophila*, where they were initially discovered and analyzed (Figure 45–11).

Members of the vertebrate *Hox* gene family are expressed in overlapping domains along the rostrocaudal axis of the developing midbrain, hindbrain, and spinal cord. As in *Drosophila*, the position of an individual *Hox* gene within its cluster predicts its rostrocaudal domain of expression within the neural tube. In most but not all cases, *Hox* genes located at more 3′ positions within the chromosomal cluster are expressed in more rostral domains, within the midbrain and hindbrain, whereas genes at more 5′ positions are expressed in progressively more caudal positions within the spinal cord (Figures 45–10 and 45–11). This spatial array of *Hox* gene expression determines many aspects of neuronal diversity.

Genetic studies, mostly in mice, have revealed how *Hox* genes control motor neuron identity in the hindbrain and spinal cord. We saw above that Hox genes contribute to formation of the rhombomeres, the fundamental cellular building blocks of the hindbrain. Later, the same genes help to determine the identity of motor neurons within rhombomeres. For example, *Hoxb1* is expressed at high levels in rhombomere 4, the domain that gives rise to facial motor neurons, but is absent from rhombomere 2, the domain that gives rise to trigeminal motor neurons (Figure 45–10).

In the mouse, mutations that eliminate the activity of *Hoxb1* change the fate of cells in rhombomere 4; there is a switch in the identity and connectivity of the motor neurons that emerge from this domain. In the absence of *Hoxb1* function, cells in rhombomere 4 generate motor neurons that innervate trigeminal rather than facial targets, that is, the motor neuron subtype normally generated within rhombomere 2 (Figure 45–12). Many additional studies have confirmed the general principle that motor neuron identity in the hindbrain is controlled by the spatial distribution of *Hox* gene expression.

The control of spinal motor neuron identity is more complicated. Spinal motor neurons are clustered within longitudinal columns that occupy discrete segmental positions, in register with their peripheral targets. Motor neurons that innervate forelimb and hindlimb muscles are found in the lateral motor columns at cervical and lumbar levels of the spinal cord, respectively. In contrast, motor neurons that innervate sympathetic neuronal targets are found within the preganglionic motor column at thoracic levels of the spinal cord. Within the lateral motor columns, motor neurons that innervate a single limb muscle are clustered together into discrete groups, termed *motor pools*. Because each limb in higher vertebrates contains more than 50 different muscle groups, a corresponding number of motor pools are required.

The identity of motor neurons in the spinal cord is controlled by the coordinate activity of *Hox* genes found at more 5′ positions within the chromosomal *Hox* clusters. For example, the spatial domains of expression and activity of Hox6 and Hox9 proteins establish the identities of motor neurons in the

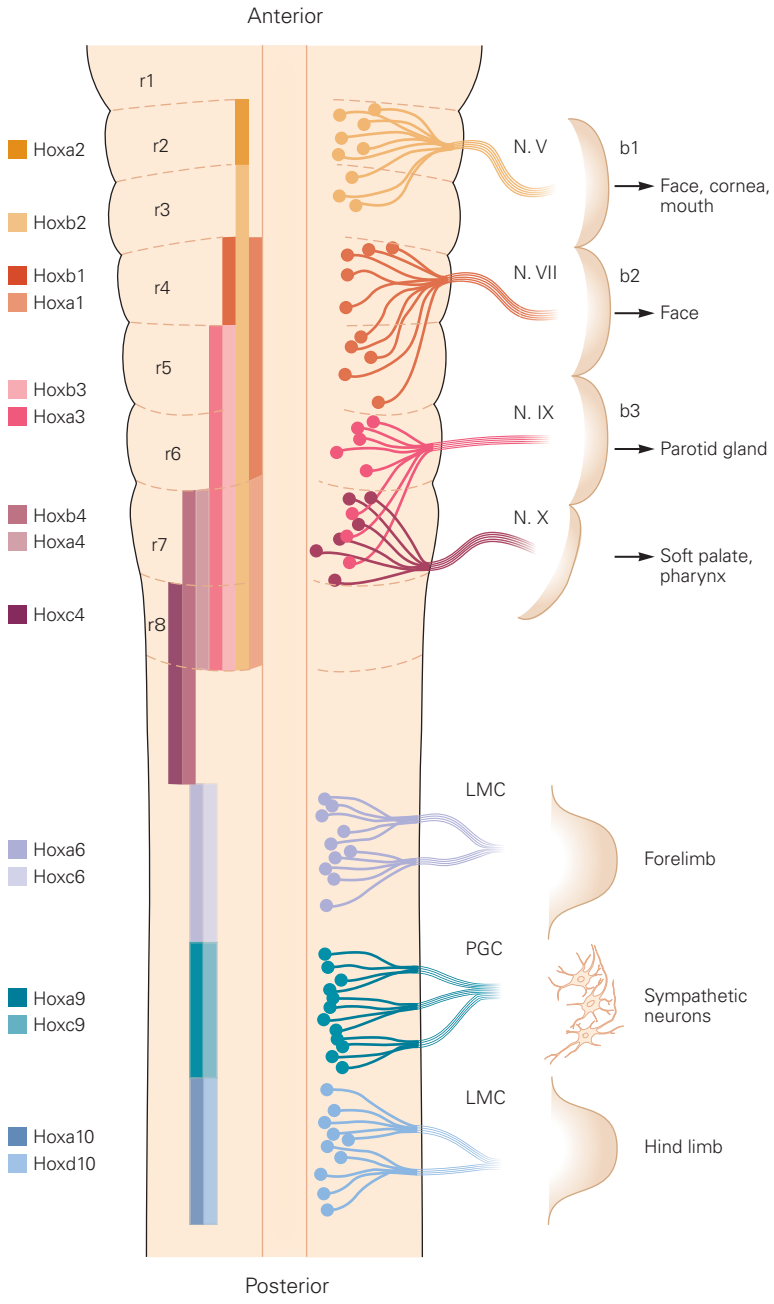

Figure 45–10 The anteroposterior profile of *Hox* gene expression determines the subtype of motor neurons in the hindbrain and spinal cord. Different Hox proteins are expressed in discrete but partially overlapping rostrocaudal domains of the hindbrain and spinal cord. The position of *Hox* genes on the four mammalian chromosomal clusters roughly corresponds to their domain of expression along the anteroposterior axis of the neural tube.

At hindbrain levels, motor neurons sending axons into cranial nerves V (trigeminal), VII (facial), IX (glossopharyngeal), and X (vagus) are depicted. These cranial motor nerves project to peripheral targets in the branchial arches **b1–b3**. The hindbrain rhombomeres (**r1–r8**) and Hox profiles are shown on the left.

At spinal levels, motor neurons that send axons to the forelimb and hind limb are contained within the lateral motor columns (**LMC**), located at brachial and lumbar levels of the spinal cord, respectively. Preganglionic autonomic motor neurons (**PGC**) destined to innervate sympathetic ganglion targets are generated at thoracic levels. (Adapted, with permission, from Kiecker and Lumsden 2005. Copyright © 2005 Springer Nature.)

brachial lateral motor column and the preganglionic motor column. Hox6 proteins specify brachial lateral motor column identity, whereas Hox9 proteins specify preganglionic motor column identity. Motor neurons at the boundary of the forelimb and thoracic regions acquire an unambiguous columnar identity because the Hox6 and Hox9 proteins are mutually repressive (Figure 45–13A), similar to the transcriptional cross-repression that occurs in the dorsoventral patterning of the spinal cord.

Local Signals and Transcriptional Circuits Further Diversify Motor Neuron Subtypes

How do motor neurons within the lateral motor columns develop more refined identities, directing their axons to specific limb muscles? Once again, *Hox* genes control this stage of motor neuron diversification. We illustrate this function of Hox proteins by considering the pathway that generates the distinct divisional and pool identities of neurons within the brachial lateral

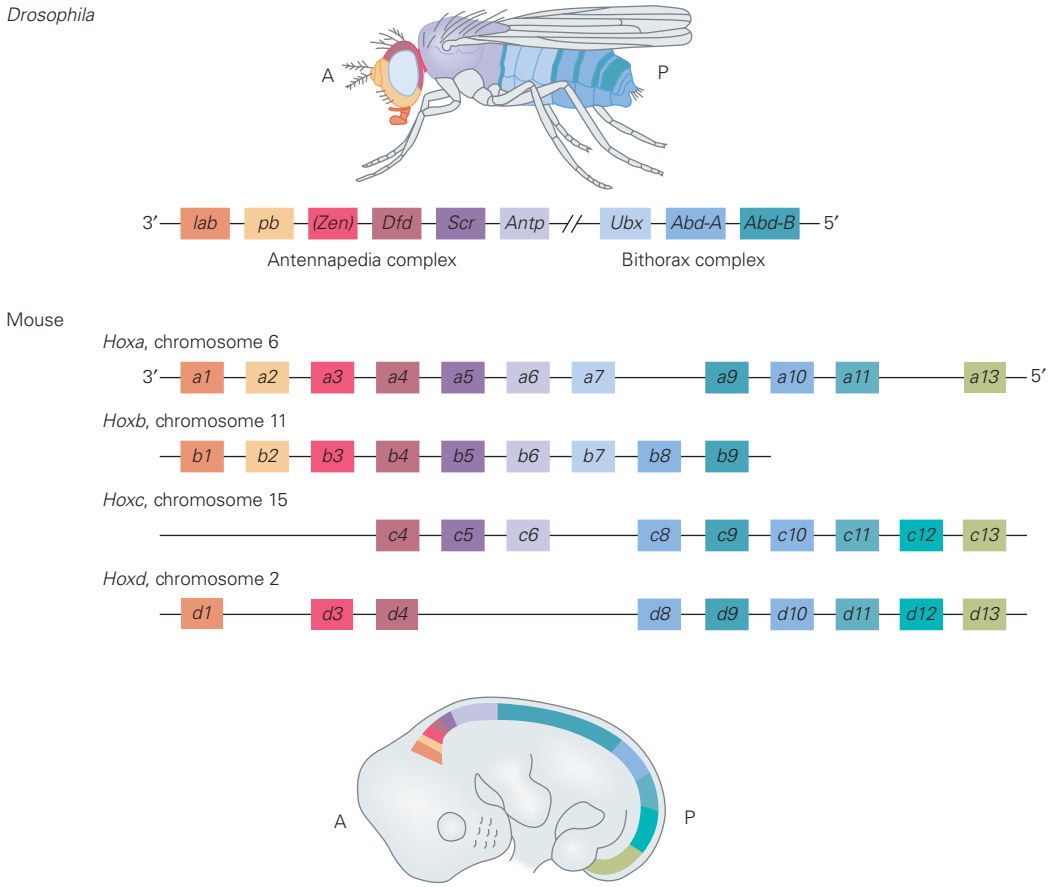

Figure 45–11 The clustered organization of *Hox* genes is conserved from flies to vertebrates. The diagram shows the chromosomal arrangement of *Hox* genes in the mouse and *HOM-C* genes in *Drosophila*. Insects have one ancestral *Hox* gene cluster, whereas higher vertebrates such as birds and mammals have four duplicate *Hox* gene clusters. The position of a given *Hox* or *HOM-C* gene on the chromosomal cluster is typically related to the position on the anteroposterior body axis where the gene is expressed. (Adapted, with permission, from Wolpert et al. 1998. Permission conveyed through Copyright Clearance Center, Inc.)

motor column that innervate the muscles of the forelimb (Figure 45–13A).

Repressive interactions between Hox proteins expressed by the neurons in different lateral motor columns ensure that neurons that populate different motor pools express distinct profiles of Hox protein expression. These Hox profiles direct the expression of downstream transcription factors as well as the axonal surface receptors that enable motor axons to respond to local cues within the limb that guide them to specific muscle targets. For example, the expression of Hox6 proteins activates a retinoic acid signaling pathway that directs the expression of two homeodomain transcription factors, Is11 and Lhx1. These factors in turn assign motor neurons to two divisional classes and determine the pattern of expression of the ephrin receptors that guide motor axons in the limb. The axons of motor neurons in these two divisions project into the ventral and dorsal halves of the limb mesenchyme under the control of ephrin signaling (Figure 45–14).

Not all motor neuron columns are determined by Hox protein activity, however. The median motor column is generated at all segmental levels of the spinal cord in register with axial muscles. Development of median motor column cells is controlled by Wnt4/5 signals secreted from the ventral midline of the spinal cord and by the expression of the homeodomain proteins Lhx3 and Lhx4, which render neurons in this column immune to the segmental patterning actions of Hox proteins.

Thus, in both the hindbrain and spinal cord, the point-to-point connectivity of motor neurons with specific muscles emerges through tightly orchestrated programs of homeodomain protein expression and activity. In vertebrates, these genes have evolved to

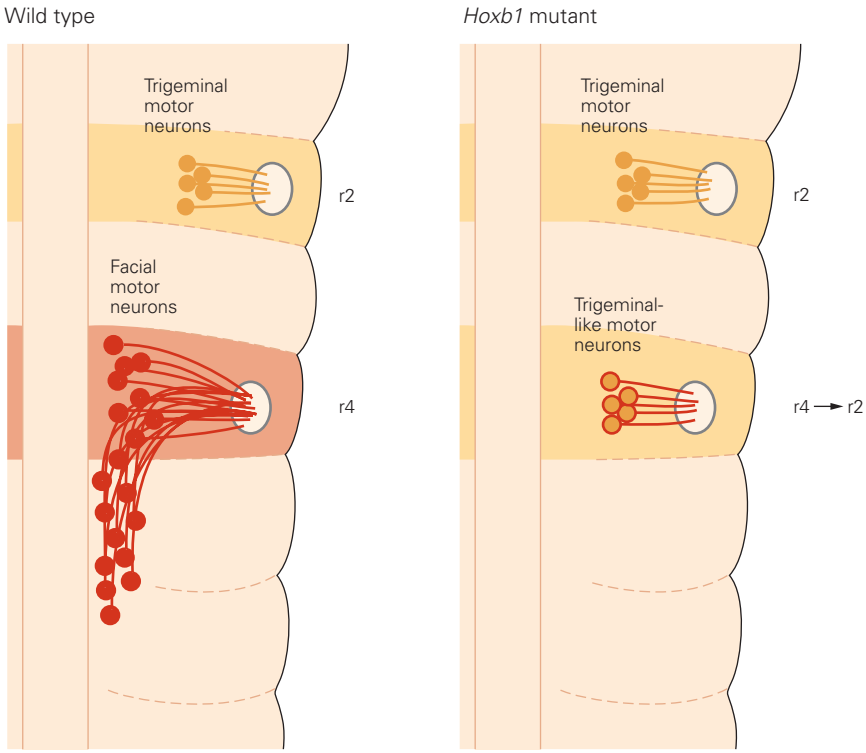

Figure 45–12 The mouse *Hoxb1* gene controls the identity and projection of hindbrain motor neurons. *Hoxb1* is normally expressed at highest levels by cells in rhombomere r4. In wild-type mice, trigeminal motor neurons are generated in rhombomere r2, and their cell bodies migrate laterally before projecting their axons out of the hindbrain at the r2 level. In contrast, the cell bodies of facial motor neurons generated in rhombomere r4 migrate caudally yet project their axons out of the hindbrain at the r4 level. In mouse *Hoxb1* mutants, motor neurons generated in rhombomere r4 migrate laterally instead of caudally, acquiring the features of r2 level trigeminal motor neurons. **Ellipses** indicate axonal exit points. (Adapted, with permission, from Struder et al. 1996. Copyright © 1996 Springer Nature.)

direct neuron subtype and connectivity as well the basic body plan.

The Developing Forebrain Is Patterned by Intrinsic and Extrinsic Influences

Neurons in the mammalian forebrain form circuits that mediate emotional behaviors, perception, and cognition and participate in the storage and retrieval of memories. Much like the hindbrain, the embryonic forebrain is initially divided along its rostrocaudal axis into transversely organized domains called *prosomeres*. Prosomeres 1 to 3 develop into the caudal part of the diencephalon, from which the thalamus emerges. Prosomeres 4 to 6 give rise to the rostral diencephalon and telencephalon. The ventral region of the rostral diencephalon gives rise to the hypothalamus and basal ganglia, whereas the telencephalon gives rise to the neocortex and hippocampus.

Inductive Signals and Transcription Factor Gradients Establish Regional Differentiation

Finally, we turn to the patterning of the neocortex itself, asking whether the developmental mechanisms and principles that govern the development of other regions of the central nervous system also control the emergence of cortical areas specialized for particular sensory, motor, and cognitive functions.

From the time of Brodmann's classical anatomical description at the beginning of the 20th century, we have known that the cerebral cortex is subdivided into many different areas. Recent studies of cortical development have begun to provide insight into the signaling mechanisms that establish somatosensory, auditory, and visual areas.

There is now evidence for the existence of a cortical "protomap," a basic plan in which different cortical areas are established early in development before inputs from other brain regions can influence development. This view is supported by studies of transcription factor expression in the developing neocortex. Two homeodomain transcription factors, Pax6 and Emx2, are expressed in complementary anteroposterior gradients in the ventricular zone of the developing neocortex—high levels of Pax6 at anterior levels and high levels of Emx2 at posterior levels. These early patterns are established in part by a local rostral source of FGF signals, which promote Pax6 and repress Emx2 expression (Figure 45–15A). As is the case in the hindbrain, the distinct spatial domains of expression of Pax6 and Emx2 are sharpened by cross-repressive interactions between the two transcription factors.

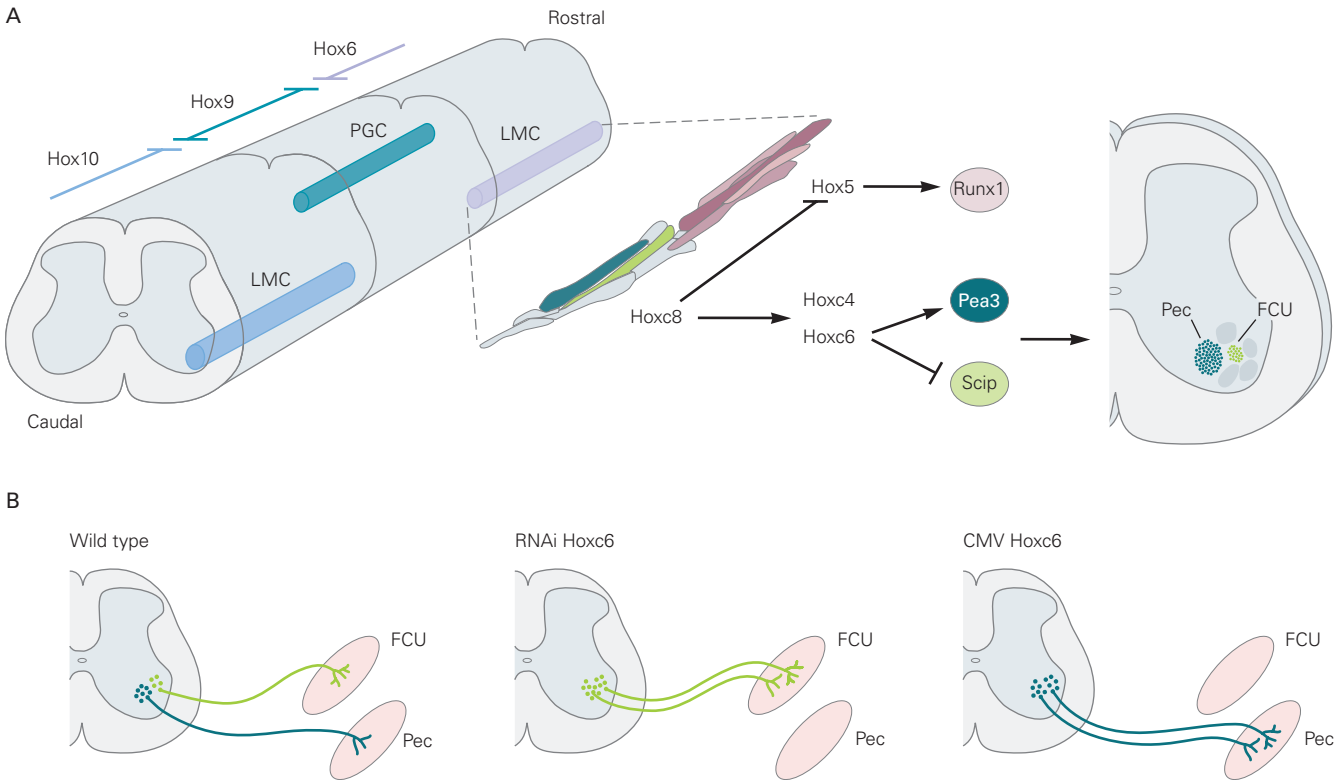

Figure 45–13 Hox proteins control the identity of neurons in motor columns and pools. (Adapted, with permission, from Dasen et al. 2005.)

A. Hox6, Hox9, and Hox10 proteins are expressed in motor neurons at distinct rostrocaudal levels of the spinal cord and direct motor neuron identity and peripheral target connectivity. Hox6 activities control the identity of cells in the brachial lateral motor column (**LMC**), Hox9 controls the identity of cells in the preganglionic column (**PGC**), and Hox10 controls the identity of cells in the lumbar column (**LMC**). Cross-repressive interactions between Hox6, Hox9, and Hox10 proteins refine Hox profiles, and Hox activator functions define LMC and PGC identities. A more complex Hox transcriptional network controls motor pool identity and connectivity. Hox genes determine the rostrocaudal position of motor pools within the LMC. Hoxc8 is required in caudal LMC neurons to generate the motor pools for the pectoralis (**Pec**) and flexor carpi ulnaris (**FCU**) muscles; these neurons express the transcription factors Pea3 and Scip, respectively. The patterns of Hox expression in the Pec and FCU pools are established through a transcriptional network that appears to be driven largely by Hox cross-repressive interactions.

B. Changing the Hox code within motor pools changes the pattern of muscle connectivity. Alterations in the profile of Hox6 expression determine the expression of Pea3 and Scip and control the projection of motor axons to the Pec or FCU muscles. RNA interference (**RNAi**) knock-down of Hox6 suppresses innervation of the Pec muscle so that motor axons innervate the FCU muscle only. Ectopic expression of Hoxc6 driven by a cytomegalovirus (**CMV**) promoter represses connectivity with FCU, so that motor axons innervate only the Pec muscle.

The spatial distribution of Pax6 and Emx2 helps to establish the initial regional pattern of the neocortex. In mice lacking Emx2 activity, there is an expansion of rostral neocortex—the motor and somatosensory areas—at the expense of the more caudal auditory and visual areas. Conversely, in mice lacking Pax6 activity, visual and auditory areas are expanded at the expense of motor and somatosensory areas (Figure 45–15B).

Thus, as in the spinal cord, hindbrain, and midbrain, early neocortical patterns are established through the interplay between local inductive signals and gradients of transcription factor expression. How these gradients specify discrete functional areas in the neocortex remains unclear. Unlike segmentation in the hindbrain, where transcription factors precisely specify rhombomeres, transcriptional markers of individual neocortical areas have not yet been identified.

Afferent Inputs Also Contribute to Regionalization

In the adult neocortex, different functional areas can be distinguished by differences in the layering pattern of neurons—the cytoarchitecture of the areas—and by their neuronal connections. One striking instance of

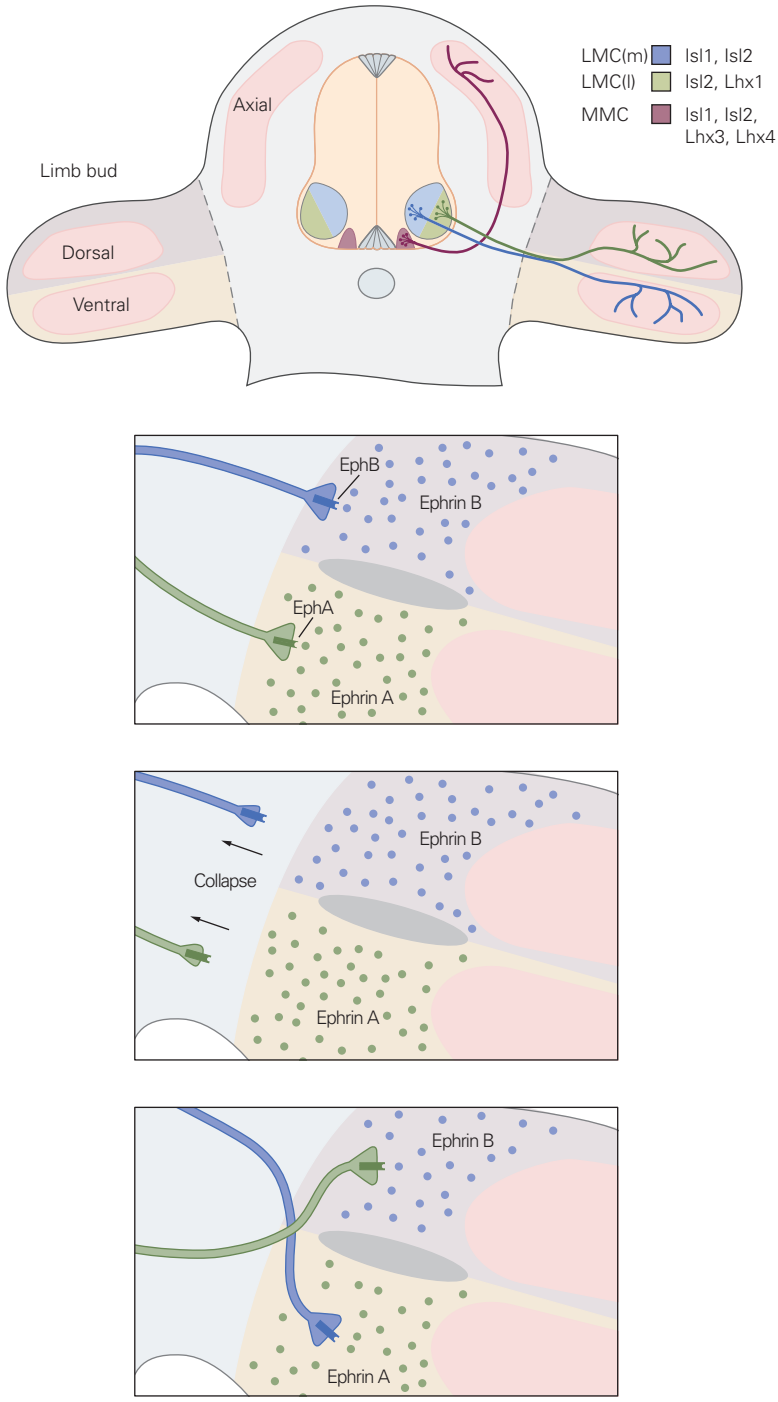

Figure 45–14 **The axons of lateral motor column neurons are guided into the limb by ephrin class tyrosine kinase receptors.** Motor neurons in the medial and lateral divisions of the lateral motor column (**LMC**) project axons into the ventral and dorsal halves of the limb mesenchyme, respectively. The profile of expression of LIM class homeodomain proteins regulates this dorsoventral projection. The LIM homeodomain protein Isl1 expressed by medial LMC neurons directs a high level of expression of EphB receptors, such that as the axons of these cells enter the limb, they are prevented from projecting dorsally by the high level of repellant ephrin B ligands expressed by cells of the dorsal limb mesenchyme. These axons therefore project into the ventral limb mesenchyme. Conversely, the LIM homeodomain protein Lhx1 expressed by lateral LMC neurons directs a high level of expression of EphA receptors, such that as the axons of these cells enter the limb, they are prevented from projecting ventrally by the high level of repellant ephrin A ligands expressed by cells of the ventral limb mesenchyme. These axons therefore project into the dorsal limb mesenchyme. Eph and ephrin signaling is discussed in greater detail in Chapter 47. (Abbreviation: **MMC**, medial motor column.)

regional distinctiveness in cell pattern is a grid-like array of neurons and glial cells termed "barrels" in the primary somatosensory cortex of rodents. Each cortical barrel receives somatosensory information from a single whisker on the snout, and the regular array of cortical barrels reflects the somatotopic organization of afferent information from the body surface, culminating in the projection of thalamic efferents to specific cortical barrels (Figure 45–16A).

Cortical barrels are evident soon after birth, and their development depends on a critical period of afferent input from the periphery; their formation is disrupted if the whisker field in the skin is eliminated during this critical period. Strikingly, if prospective

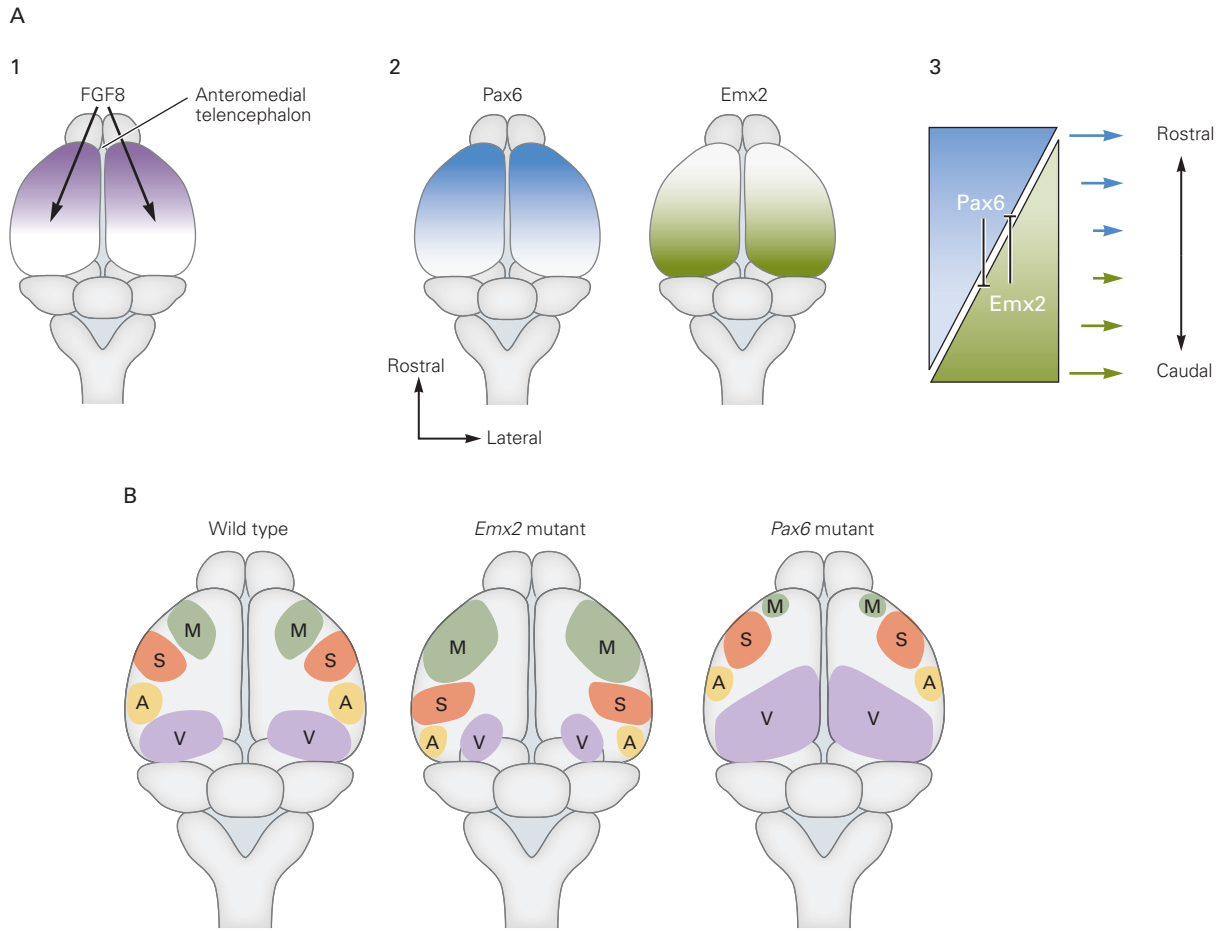

Figure 45–15 Anteroposterior gradients of expression of transcription factors establish discrete functional areas along the anteroposterior axis of the developing forebrain. (Adapted from Hamasaki et al. 2004.)

A. (**1**) FGF8 signals from the anteromedial telencephalon establish the rostrocaudal pattern of the cerebral cortex. (**2**) A top-down view of the developing cerebral cortex in the mouse shows inverse rostrocaudal gradients of the transcription factors Pax6 and Emx2. (**3**) These two transcription factors mutually repress each other's expression.

B. Different functional areas develop at different rostrocaudal positions. Motor areas develop in the anterior region (**M**) and visual areas in more posterior regions (**V**). Genetic elimination of Emx2 function results in expansion of the motor areas and contraction in auditory (**A**) and visual areas. Conversely, elimination of Pax6 function results in an expansion of the visual areas and a contraction of motor and auditory areas. (Abbreviation: **S**, somatosensory areas.)

visual cortical tissue is transplanted into the somatosensory cortex around the time of birth, barrels form in the transplanted tissue with a pattern that closely resembles that of the normal somatosensory barrel field (Figure 45–16B). Together, these findings demonstrate that afferent input superimposes aspects of neocortical patterning on the basic features of the protomap.

The nature of the input to different cortical areas influences neural function as well as cytoarchitecture. This can be shown by monitoring physiological and behavioral responses after rerouting afferent pathways of one sensory modality to a region of neocortex that normally processes a different modality. In animals in which retinal inputs are rerouted into the auditory pathway, the primary auditory cortex contains a systematic representation of visual space rather than of sound frequency (Figure 45–17). When these animals are trained to discriminate a visual from an auditory cue, they perceive a cue as visual when the rewired auditory cortex is activated by vision.

Thus, brain pathways and neocortical regions are established through genetic programs during early development but later depend on afferent inputs for their specialized anatomical, physiological, and behavioral functions.

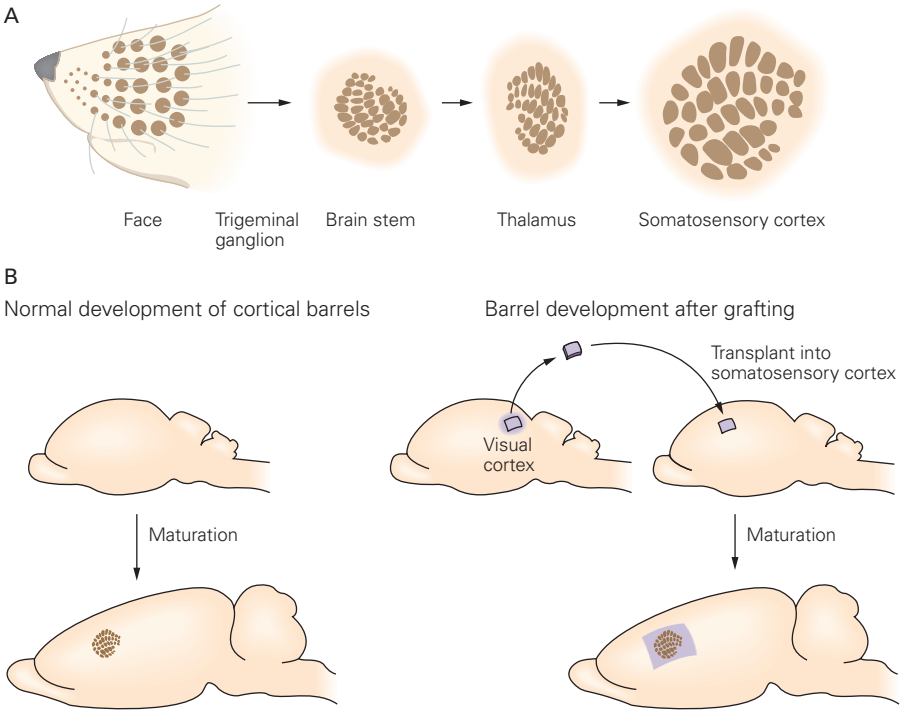

Figure 45–16 Sensory input regulates the organization of "barrels" in the developing somatosensory cortex in rodents. (Adapted from Schlaggar and O'Leary 1991.)

A. The barrel area of the rodent somatosensory cortex forms a somatotopic representation of the rows of whiskers on the animal's snout. Similar representations of the whisker field are present upstream—in the brain stem and in the thalamic nuclei that relay somatosensory inputs from the face to the cortex.

B. A barrel-like cellular organization is induced in developing visual cortex tissue that was grafted at an early postnatal stage into the somatosensory cortex.

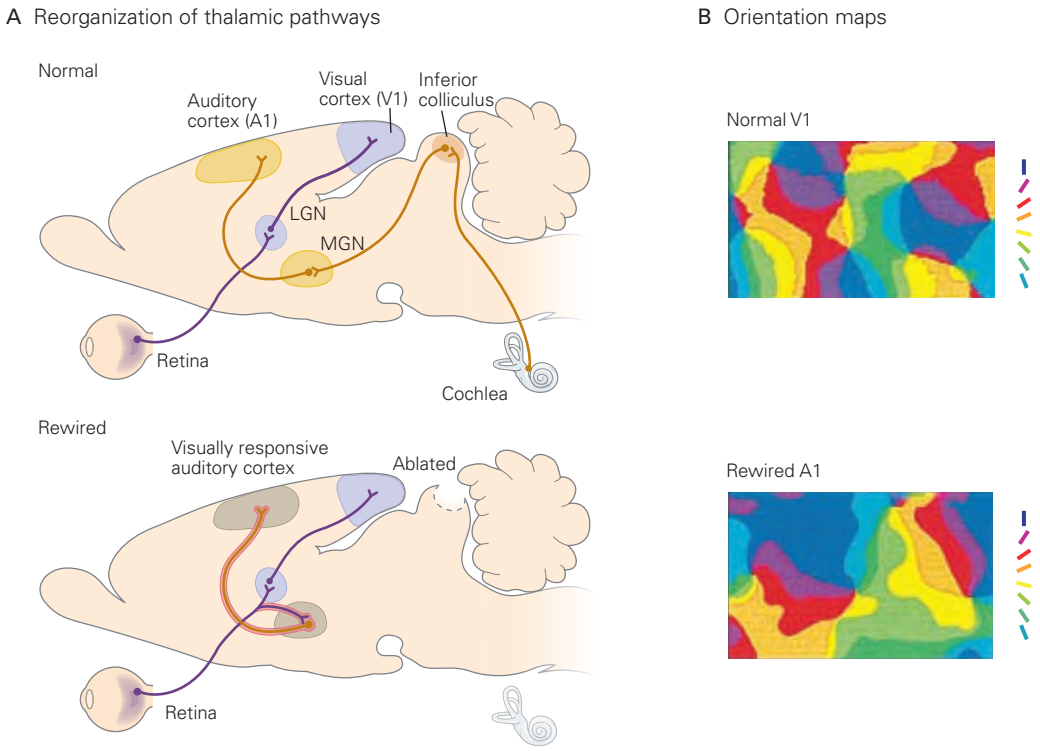

Figure 45–17 Rerouting thalamocortical input can recruit cortical areas for new sensory functions. (Adapted, with permission, from Sharma, Angelucci, and Sur 2000. Copyright © 2000 Springer Nature.)

A. The visual pathway consists of afferent fibers from the retina that innervate the lateral geniculate nucleus (**LGN**) and superior colliculus. Axons from the LGN project to the primary visual cortex (**V1**). The auditory pathway projects from the cochlear nucleus (not shown) to the inferior colliculus, and then to the medial geniculate nucleus (**MGN**) and on to the primary auditory cortex (**A1**). Ablating the inferior colliculus in neonatal ferrets causes retinal afferents to innervate the MGN. As a consequence, the auditory cortex is reprogrammed to process visual information.

B. Visual orientation maps similar to those seen in normal V1 cortex are observed in rewired A1 auditory cortex of ferrets using optical imaging of intrinsic signals. The different colors represent different receptor field orientations (see bars at right). The pattern of activity in rewired A1 resembles that of normal V1.

Highlights

1. The early vertebrate embryo consists of three layers of cells—ectoderm, mesoderm, and endoderm. The entire nervous system arises from the ectoderm, and more specifically from a central strip of ectoderm called the neural plate.
2. Formation of neural plate within the ectoderm occurs by a process called induction, in which underlying mesodermal cells secrete soluble factors that induce a neural program of gene expression in neighboring ectodermal cells. Induction involves a "de-repression" mechanism in which mesoderm-derived soluble factors prevent ectoderm-derived bone morphogenetic proteins (BMPs; members of the transforming growth factor β family) from suppressing the neural fate.
3. Following induction, the neural plate invaginates from the ectoderm to form a neural tube. The tube gives rise to the central nervous system, while cells at the border between neural tube and ectoderm form neural crest, which migrates through the embryo to form the sensory and autonomic ganglia of the peripheral nervous system.
4. As soon as the neural tube forms, it begins to become regionalized. Regionalization along the anterior-posterior axis leads to a series of subdivisions. The anterior region becomes the brain, and the posterior region becomes the spinal cord. Divisions of the prospective brain generate the forebrain, midbrain, and hindbrain. The forebrain divides further to form the telencephalon, from which cortex, hippocampus, and basal ganglia arise; and the diencephalon, which gives rise to thalamus, hypothalamus, and retina. The hindbrain divides to form the pons and cerebellum anteriorly and the medulla posteriorly.
5. Anterior-posterior patterning is established by gradients of Wnt signaling, which arise from selective production of Wnts posteriorly and selective production of Wnt inhibitors anteriorly.
6. Subdivisions along the anteroposterior axis are established by groups of cells called organizing centers at defined positions within the neural tube. The organizing centers secrete factors that pattern neighboring regions of the neural tube and specify neuronal types within them. For example, the isthmic organizer at the boundary of the hindbrain and midbrain secretes Wnts and fibroblast growth factors (FGFs). They act differentially in anterior and posterior regions because the earlier patterning events led to expression of different transcription factors by cells in these regions.
7. Still later, further subdivisions form segments called prosomeres in the forebrain and rhombomeres in the hindbrain, with differential expression of transcription factors leading to generation of distinct neural types in each.
8. In both the hindbrain and the spinal cord, motor neurons acquire distinct properties according to their anterior-posterior position, differentiating into the groups that innervate distinct muscles. Differential expression of transcription factors called Hox proteins is particularly important in diversification of motor neurons. They act with other transcription and soluble factors to divide motor neurons into columns and pools, with each pool destined to innervate a specific muscle.
9. The neural tube is also patterned along the dorsoventral axis. Similar to anterior-posterior regionalization, patterning results from gradients of morphogens. The most important are sonic hedgehog (Shh), which forms a ventral high–dorsal low gradient, and BMPs, which form a dorsal high–ventral low gradient. Different levels of Shh and BMPs induce different transcription factors, which in turn lead to generation of different cell types.
10. Regionalization of the cerebral cortex into motor, sensory, and association areas also begins with gradients of morphogens that induce differential expression of transcription factors, leading to establishment of a "protomap" of area identity. Interactions among areas along with input from subcortical regions refine the protomap to form definitive cortical areas.
11. Several general principles explain many aspects of early neural development: (a) Inductive interactions lead to subdivision of a uniform set of cells into discrete areas. (b) A small set of soluble factors such as FGFs, BMPs, and Wnts are used multiple times at multiple stages to regionalize the nervous system. (c) Varying levels of these factors lead to expression of different transcription factors, which in turn generate different neural cell types. (d) Repressive interactions between cells expressing different transcription factors sharpen boundaries along both anteroposterior and dorsoventral axes.
12. Until recently, studies on early stages of neural development have been restricted to experimental animals. Recent advances now enable neuroscientists to recapitulate some of these processes using cultured human cells. It should therefore

soon be possible to learn whether there are critical early differences between humans and other species that contribute to the complexity of the human brain and to human brain disorders.

Joshua R. Sanes
Thomas M. Jessell

Selected Reading

Anderson C, Stern CD. 2016. Organizers in development. Curr Top Dev Biol 117:435–454.

Catela C, Shin MM, Dasen JS. 2015. Assembly and function of spinal circuits for motor control. Annu Rev Cell Dev Biol 31:669–698.

Dessaud E, McMahon AP, Briscoe J. 2008. Pattern formation in the vertebrate neural tube: a sonic hedgehog morphogen-regulated transcriptional network. Development 135: 2489–2503.

Goulding M. 2009. Circuits controlling vertebrate locomotion: moving in a new direction. Nat Rev Neurosci 10:507–518.

Hamburger V. 1988. *The Heritage of Experimental Embryology. Hans Spemann and the Organizer.* New York: Oxford Univ. Press.

Kiecker C, Lumsden A. 2012. The role of organizers in patterning the nervous system. Annu Rev Neurosci 35:347–367.

Ozair MZ, Kintner C, Brivanlou AH. 2013. Neural induction and early patterning in vertebrates. Wiley Interdiscip Rev Dev Biol 2:479–498.

Rakic P. 2002. Evolving concepts of cortical radial and areal specification. Prog Brain Res 136:265–280.

Sur M, Rubenstein JL. 2005. Patterning and plasticity of the cerebral cortex. Science 310:805–810.

References

Addison M, Wilkinson DG. 2016. Segment identity and cell segregation in the vertebrate hindbrain. Curr Top Dev Biol 117:581–596.

Bell E, Wingate RJ, Lumsden A. 1999. Homeotic transformation of rhombomere identity after localized Hoxb1 misexpression. Science 284:2168–2171.

Cholfin JA, Rubenstein JL. 2007. Patterning of frontal cortex subdivisions by Fgf17. Proc Natl Acad Sci U S A 104:7652–7657.

Dasen JS. 2017. Master or servant? Emerging roles for motor neuron subtypes in the construction and evolution of locomotor circuits. Curr Opin Neurobiol 42:25–32.

Dasen JS, Tice BC, Brenner-Morton S, Jessell TM. 2005. A Hox regulatory network establishes motor neuron pool identity and target-muscle connectivity. Cell 123:477–491.

Goulding M, Lanuza G, Sapir T, Narayan S. 2002. The formation of sensorimotor circuits. Curr Opin Neurobiol 12:505–515.

Hamasaki T, Leingartner A, Ringstedt T, O'Leary DD. 2004. EMX2 regulates sizes and positioning of the primary sensory and motor areas in neocortex by direct specification of cortical progenitors. Neuron 43:359–372.

Horng S, Sur M. 2006. Visual activity and cortical rewiring: activity-dependent plasticity of cortical networks. Prog Brain Res 157:3–11.

Ille F, Atanasoski S, Falkm S, et al. 2007. Wnt/BMP signal integration regulates the balance between proliferation and differentiation of neuroepithelial cells in the dorsal spinal cord. Dev Biol 304:394–408.

Kiecker C, Lumsden A. 2005. Compartments and their boundaries in vertebrate brain development. Nat Rev Neurosci 6:553–564.

Levine AJ, Brivanlou AH. 2007. Proposal of a model of mammalian neural induction. Dev Biol 308:247–256.

Lim Y, Golden JA. 2007. Patterning the developing diencephalon. Brain Res Rev 53:17–26.

Liu A, Niswander LA. 2005. Bone morphogenetic protein signalling and vertebrate nervous system development. Nat Rev Neurosci 6:945–954.

Lupo G, Harris WA, Lewis KE. 2006. Mechanisms of ventral patterning in the vertebrate nervous system. Nat Rev Neurosci 7:103–114.

Mallamaci A, Stoykova A. 2006. Gene networks controlling early cerebral cortex arealization. Eur J Neurosci 23:847–856.

Nordstrom U, Maier E, Jessell TM, Edlund T. 2006. An early role for WNT signaling in specifying neural patterns of Cdx and Hox gene expression and motor neuron subtype identity. PLoS Biol 4:1438–1452.

Rash BG, Grove EA. 2006. Area and layer patterning in the developing cerebral cortex. Curr Opin Neurobiol 16:25–34.

Schlaggar BL, O'Leary DDM. 1991. Potential of visual cortex to develop an array of functional units unique to somatosensory cortex. Science 252:1556–1560.

Sharma J, Angelucci A, Sur M. 2000. Induction of visual orientation modules in auditory cortex. Nature 404:841–847.

Song MR, Pfaff SL. 2005. Hox genes: the instructors working at motor pools. Cell 123:363–365.

Stamataki D, Ulloa F, Tsoni SV, Mynett A, Briscoe J. 2005. A gradient of Gli activity mediates graded Sonic Hedgehog signaling in the neural tube. Genes Dev 19:626–641.

Struder M, Lumsden A, Ariza-McNaughton L, Bradley A, Krumlauf R. 1996. Altered segmental identity and abnormal migration of motor neurons in mice lacking *Hoxb-1*. Nature 384:630–634.

von Melchner L, Pallas SL, Sur M. 2000. Visual behaviour mediated by retinal projections directed to the auditory pathway. Nature 404:871–876.

Wolpert L, Beddington R, Brockes J, Jessell TM, Lawrence PA, Meyerowitz E. 1998. *Principles of Development*. New York: Oxford Univ Press.

Wolpert L, Smith J, Jessell T, Lawrence P, Robertson E, Meyerowitz E. 2006. *Principles of Development*, 3rd ed. New York: Oxford Univ. Press.

Wurst W, Bally-Cuif L. 2001. Neural plate patterning: upstream and downstream of the isthmic organizer. Nat Rev Neurosci 2:99–108.

46

Differentiation and Survival of Nerve Cells

In the preceding chapter, we described how local inductive signals pattern the neural tube and establish the early regional subdivisions of the nervous system—the spinal cord, hindbrain, midbrain, and forebrain. Here, we turn to the issue of how progenitor cells within these regions differentiate into neurons and glial cells, the two major cell types of the nervous system. The mature brain comprises billions of nerve cells and a similar number of glial cells arranged in complex patterns, yet its precursor, the neural plate, initially contains only a few hundred cells arranged in a simple columnar epithelium. From this observation alone, it should be apparent that the generation of neural cells and their delivery to appropriate sites must be carefully regulated.

We begin by discussing some of the molecules that specify neuronal and glial cell fates. The basic mechanisms of neurogenesis endow cells with common neuronal properties, features that are largely independent of the region of the nervous system in which they are generated or the specific functions they perform. We also describe mechanisms by which developing neurons become specialized, for example by acquiring the machinery to synthesize specific neurotransmitters.

We next discuss how neurons are delivered from their sites of origin to their final destinations. A common theme is that neurons are frequently "born"—that is, become postmitotic—far from where they end up, for example, in the layers of the cerebral cortex or the ganglia of the peripheral nervous system. Such distances necessitate elaborate migratory mechanisms, which differ among neuronal types.

After the identity and functional properties of the neuron have begun to emerge, additional

developmental processes determine whether the neuron will live or die. Remarkably, approximately half of the neurons generated in the mammalian nervous system are lost through programmed cell death. We examine the factors that regulate the survival of neurons and the possible benefits of widespread neuronal loss. Finally, we describe a core biochemical pathway in nerve cells destined for elimination.

The Proliferation of Neural Progenitor Cells Involves Symmetric and Asymmetric Cell Divisions

Histologists in the late 19th century showed that neural epithelial cells close to the ventricular lumen of the embryonic brain exhibit features of mitosis. We now know that the proliferative zones surrounding the ventricles are the major sites for the production of neural cells in the central nervous system. Moreover, newborn cells in the proliferative zones often become committed to neuronal or glial fates before migrating from these zones.

At early stages of embryonic development, most progenitor cells in the ventricular zone of the neural tube proliferate rapidly. Many of these early neural progenitors have the properties of stem cells: They can generate additional copies of themselves, a process called *self-renewal*, and also give rise to differentiated neurons and glial cells. In a later chapter, we will describe the more recent discovery that stem cells resembling those of embryos also exist in the adult brain and may be harnessed for therapeutic purposes (Chapter 50).

As with other types of stem cells, neural progenitor cells undergo stereotyped programs of cell division. One mode of cell division is symmetric: Neural stem cells divide to produce two stem cells, and in this way expand the population of proliferative progenitor cells. This mode predominates at the earliest times, as the neuroepithelium expands. A second mode is asymmetric: The progenitor produces one differentiated daughter and another daughter that retains its stem cell–like properties. This mode retains but does not amplify the stem cell population. A third mode leads to production of two differentiated daughters. In this symmetric mode, the stem cell population is depleted. All three modes have been found in the embryonic cerebral cortex in vivo and in cortical cells grown in tissue culture (Figure 46–1).

The incidence of symmetric and asymmetric cell division is influenced by signals in the local environment of the dividing cell, making it possible to control the probability of self-renewal or differentiation. Environmental factors can influence the outcome of progenitor cell divisions in two fundamental ways. They can act in an "instructive" manner, biasing the outcome of the division process and causing the stem cell to adopt one fate at the expense of others. Or they can act in a "selective" manner, permitting the survival and maturation of only certain cell progeny.

Radial Glial Cells Serve as Neural Progenitors and Structural Scaffolds

Radial glial cells are the earliest morphologically distinguishable cell type to appear within the primitive neural epithelium. Their cell bodies are located in the ventricular zone, and their long process extends to the pial surface. As the brain thickens, the processes of radial glial cells remain attached to the ventricular and pial surfaces. After the generation of neurons is complete, many radial glial cells differentiate into astrocytes. The elongated shape of the radial glial cell places it in a favorable position to serve as a scaffold for the migration of neurons that emerge from the ventricular zone (Figure 46–2).

The ventricular zone was once thought to contain two major cell types: radial glial cells and a set of neuroepithelial progenitors that serve as the primary source of neurons. More recently, this classical view has changed dramatically. Once symmetric divisions of stem cells have expanded the neuroepithelium, these cells give rise to radial glial cells. The radial glial cells serve as progenitor cells that generate both neurons and astrocytes in addition to their role in neuronal migration (Figure 46–2). Labeling of radial glial cells with fluorescent dyes or viruses shows that their clonal progeny include both neuronal and radial glial cells. These findings indicate that radial glial cells are able to undergo both asymmetric and self-renewing cell division and serve as a major source of postmitotic neurons as well as astrocytes.

The Generation of Neurons and Glial Cells Is Regulated by Delta-Notch Signaling and Basic Helix-Loop-Helix Transcription Factors

How do radial glial cells make the decision to self-renew, generate neurons, or give rise to mature astrocytes? The answer to this question involves an evolutionarily conserved signaling system.

In flies and vertebrates, neural fate is regulated by a cell-surface signaling system, comprised of the

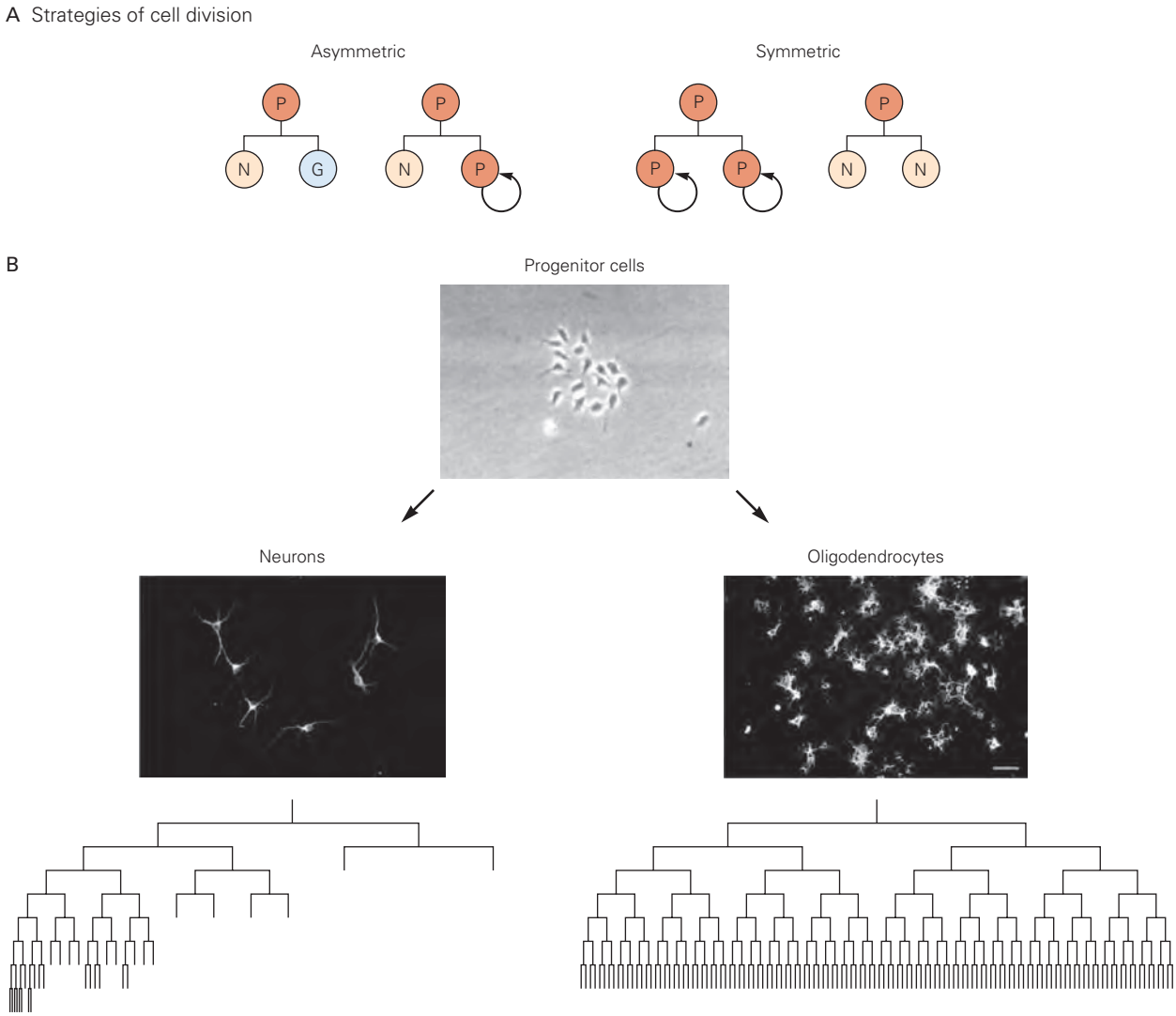

Figure 46–1 Neural progenitor cells have different modes of division.

A. Asymmetric and symmetric modes of cell division. A progenitor cell (P) can undergo asymmetric division to generate a neuron (N) and a glial cell (G), or a neuron and another progenitor. This mode of division contributes to the generation of neurons at early stages of development and of glial cells at later stages, typical of many regions of the central nervous system. Progenitor cells can also undergo symmetric division to generate two additional progenitor cells or two postmitotic neurons.

B. Time-lapse cinematography captures the divisions and differentiation of isolated cortical progenitor cells in the rodent. Lineage diagrams illustrate cells that undergo predominantly asymmetric division, giving rise to neurons, or symmetric division, giving rise to oligodendrocytes. (Adapted, with permission, from Qian et al. 1998. Permission conveyed through Copyright Clearance Center, Inc.)

transmembrane ligand Delta and its receptor Notch. This signaling system was revealed in genetic studies in *Drosophila*. Neurons emerge from within a larger cluster of ectodermal cells, called a *proneural region*, all of which have the potential to generate neurons. Yet within the proneural region, only certain cells form neurons; the others become epidermal support cells.

Delta and Notch are initially expressed at similar levels by all proneural cells (Figure 46–3A). With time, however, Notch activity is enhanced in one cell and suppressed in its neighbor. The cell in which Notch activity is highest loses the potential to form a neuron and acquires an alternative fate. The binding of Delta to Notch results in proteolytic cleavage of the Notch cytoplasmic domain, which then enters the nucleus.

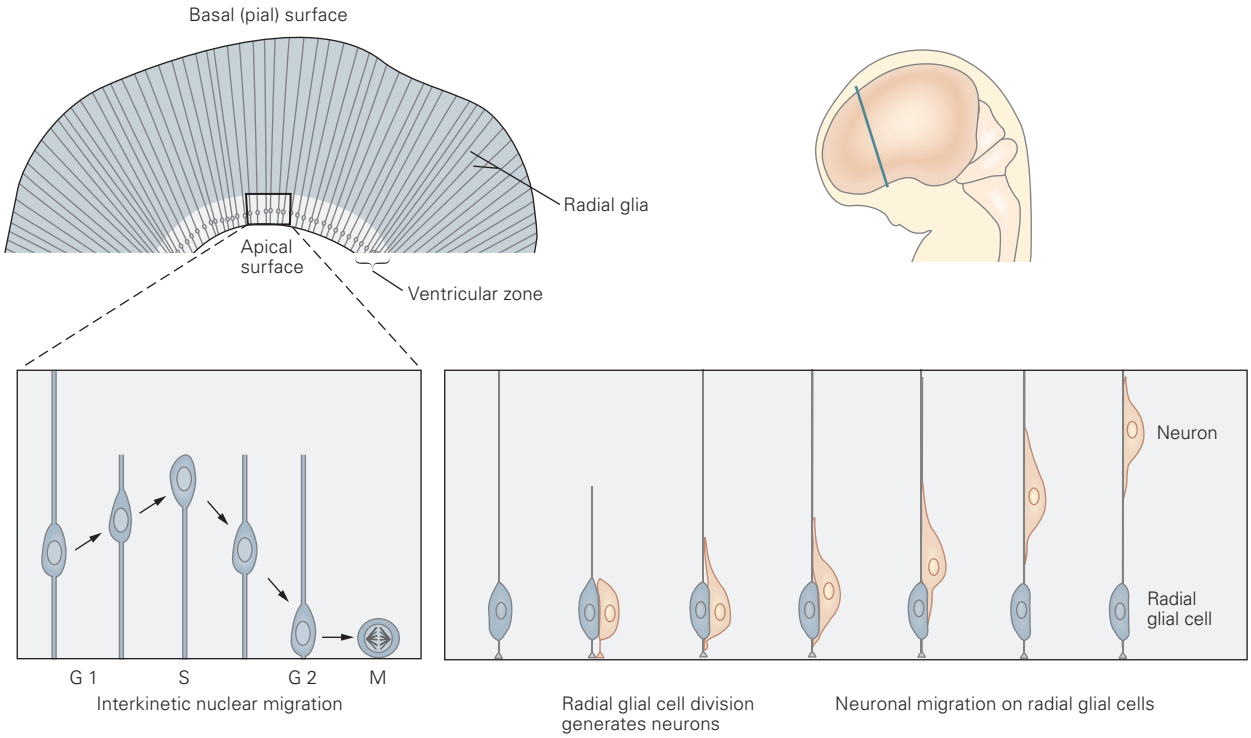

Figure 46–2 **Radial glial cells serve as precursors to neurons in the central nervous system and also provide a scaffold for radial neuronal migration.** The nuclei of progenitor cells in the ventricular zone of the developing cerebral cortex migrate along the apical-basal axis as they progress through the cell cycle. *Left*: During the G1 phase, the nuclei rise from the inner (apical) surface of the ventricular zone. During the S phase, they reside in the outer (basal) third of the ventricular zone. During the G2 phase, they migrate apically, and mitosis (**M**) occurs when the nuclei reach the ventricular surface. *Right*: During cell division, radial glial cells give rise to postmitotic neurons that migrate away from the ventricular zone using radial glial cells as a guide.

There, it functions as a transcription factor, regulating the activity of a cascade of other transcription factors of the basic helix-loop-helix (bHLH) family. The bHLH transcription factors suppress the ability of the cell to become a neuron and reduce the level of expression of the ligand Delta (Figure 46–3B,C).

The initial difference in Notch levels between cells may be small and in some cases stochastic (random). Through this feedback pathway, however, these initial minor differences are amplified to generate all-or-none differences in the status of Notch activation and, consequently, the fates of the two cells. This basic logic of Delta-Notch and bHLH signaling has been conserved in vertebrate and invertebrate neural tissues.

How does Notch signaling regulate neuronal and glial production in mammals? At early stages in the development of the mammalian cortex, Notch signaling promotes the generation of radial glial cells by activating members of the Hes family of bHLH transcriptional repressors. Two of these proteins, Hes1 and Hes5, appear to maintain radial glial cell character by activating the expression of an ErbB class tyrosine kinase receptor for neuregulin, a secreted signal that promotes radial glial cell identity. The Notch ligand Delta1 as well as neuregulin are expressed by newly generated cortical neurons; thus, the radial glial cells depend on feedback signals from their neuronal progeny for continued production.

At later stages of cortical development, Notch signaling continues to activate Hes proteins, but a change in the intracellular response pathway results in astrocyte differentiation. At this stage, the Hes proteins work by activating a transcription factor, STAT3, which recruits the serine-threonine kinase JAK2, a potent inducer of astrocyte differentiation. STAT3 also activates expression of astrocyte-specific genes such as the glial-fibrillary acidic protein (GFAP).

The generation of oligodendrocytes, the second major class of glial cells in the central nervous system, follows many of the principles that control neuron

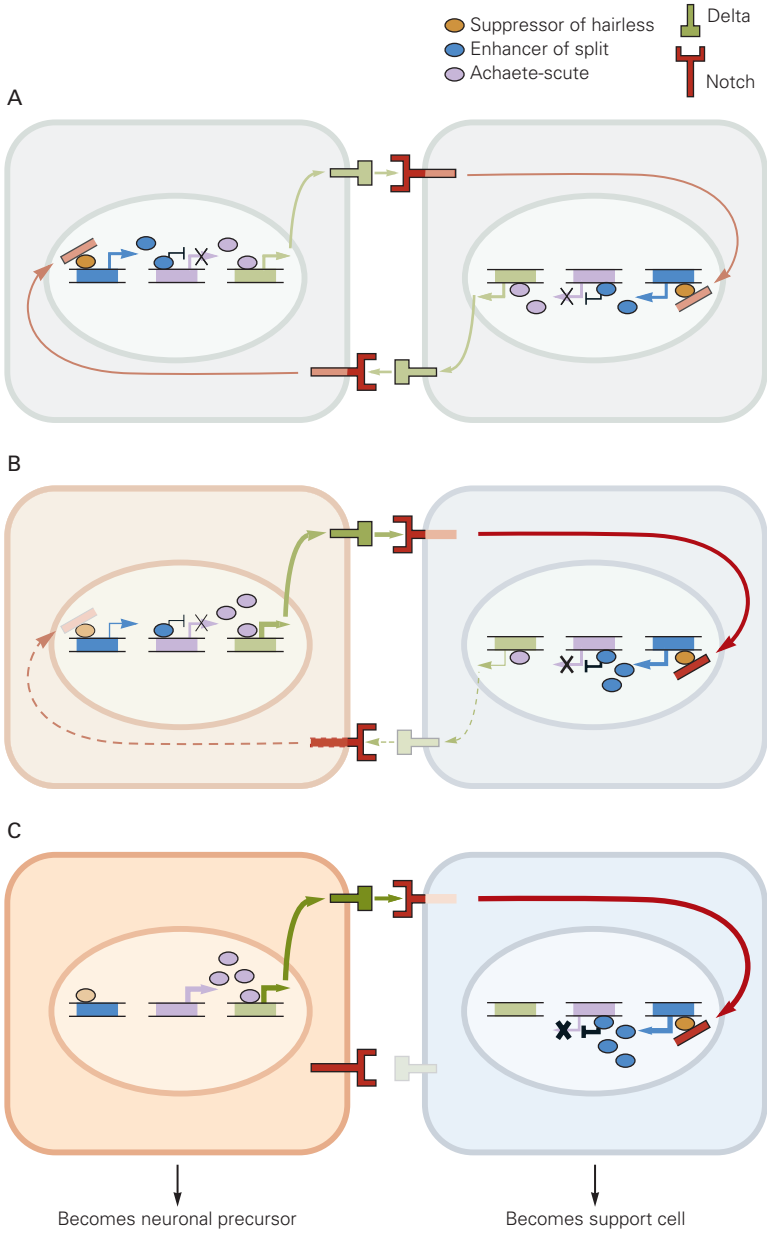

Figure 46–3 Delta binds the receptor Notch and determines neuronal fate.

A. At the onset of the interaction between two cells, Delta engages the receptor Notch. Delta and Notch are expressed at similar levels in each cell, and thus their initial signaling strength is equal.

B. A small imbalance in the strength of Delta-Notch signaling breaks the symmetry of the interaction. In this example, the left cell provides a slightly greater Delta signal, thus activating Notch signaling in the right cell to a greater extent. On binding by Delta, the cytoplasmic domain of Notch is cleaved to form a proteolytic fragment called Notch-Intra, which enters the nucleus of the cell and initiates a basic helix-loop-helix (bHLH) transcriptional cascade that regulates the level of Delta expression. Notch-Intra forms a transcriptional complex with a bHLH protein, suppressor of hairless, which binds to and activates the gene encoding a second bHLH protein, enhancer of split. Once activated, enhancer of split binds to and represses expression of the gene encoding a third bHLH protein, achaete-scute. Achaete-scute activity promotes expression of Delta. Thus, by repressing achaete-scute, enhancer of split decreases transcriptional activation of the Delta gene and production of Delta protein. This diminishes the ability of the cell on the right to activate Notch signaling in the left cell.

C. Once the level of Notch signaling in the left cell has been reduced, suppressor of hairless no longer activates enhancer of split, and the level of expression of achaete-scute increases, resulting in enhanced expression of Delta and further activation of Notch signaling in the right cell. In this way, a small initial imbalance in Delta-Notch signaling is rapidly amplified into a marked asymmetry in the level of Notch activation in the two cells. In the mammalian central nervous system, cells with high levels of Notch activation are diverted from neuronal fates, whereas cells with low levels of Notch activation become neurons.

and astrocyte production (Figure 46–4). Notch signaling regulates the expression of two bHLH transcription factors, Olig1 and Olig2, which have essential roles in the production of embryonic and postnatal oligodendrocytes.

Additional mechanisms exist to ensure that the effects of Notch signals are avoided in cells destined to become neurons. One involves a cytoplasmic protein called Numb. The key role of Numb in neurogenesis was first shown in *Drosophila*, where it determines the neuronal fate of daughter cells of asymmetrically dividing progenitors. In the mammalian cortex, Numb is preferentially localized in neuronal daughters and antagonizes Notch signaling. Loss of Numb activity causes progenitor cells to proliferate extensively. The inhibition of Notch signaling results in the expression of several proneural bHLH transcription factors, notably Mash1, neurogenin-1, and neurogenin-2. Neurogenins promote neuronal production by activating downstream

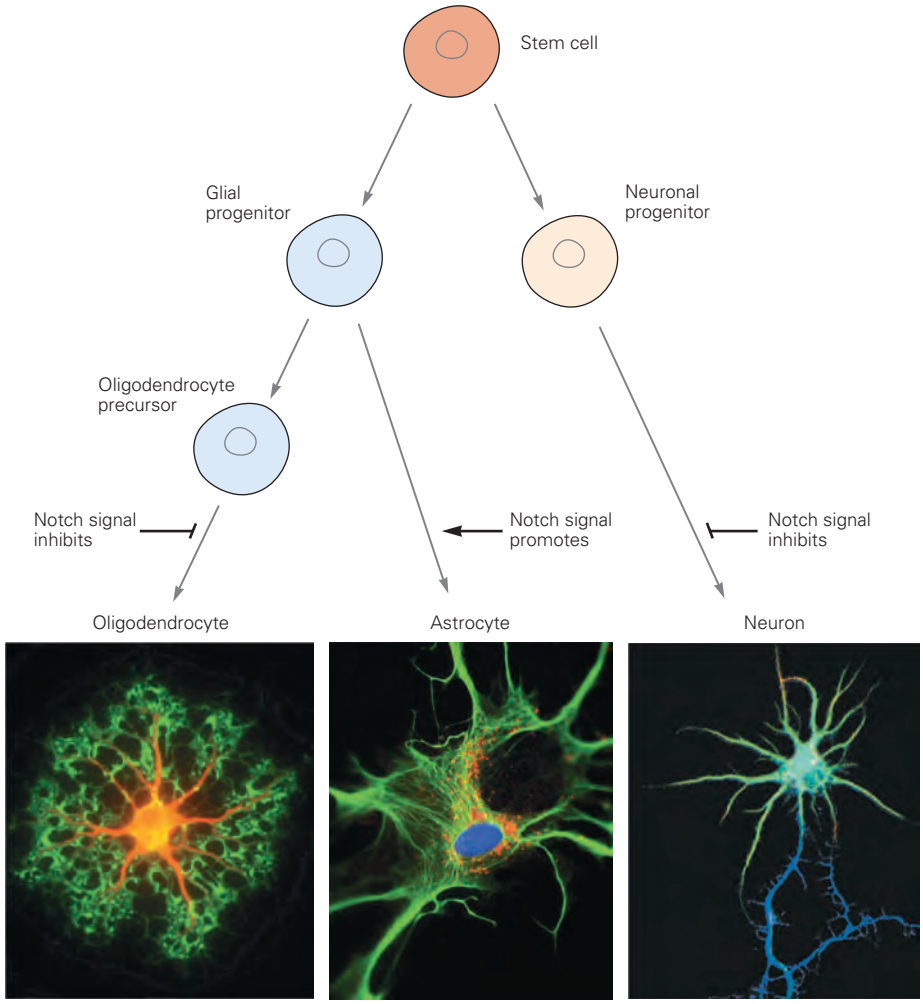

Figure 46–4 Notch signaling regulates the fate of cells in the developing cerebral cortex. Notch signaling has several roles in cell differentiation in the developing cerebral cortex. Activation of Notch signaling in glial progenitor cells results in differentiation of the cells as astrocytes and inhibits differentiation as oligodendrocytes (left pathway). Notch signaling also inhibits progenitor cells from differentiating into neurons (right pathway). (Photo of oligodendrocyte reproduced, with permission, from David H. Rowitch; photo of astrocyte reproduced, with permission, from SAASTA on behalf of photographers Edward Nyatia and Dirk Michael Lang; photo of neuron reproduced, with permission, from Masatoshi Takeichi.)

bHLH proteins such as neuroD, and they block the formation of astrocytes by inhibiting JAK and STAT signaling.

Although Delta-Notch signaling and bHLH transcription factor activators lie at the heart of the decision to produce neurons or glial cells, several additional transcriptional pathways augment this core molecular program. One important transcription factor, REST/NRSF, represses the expression of neuronal genes in neural progenitors and glial cells. REST/NRSF is rapidly degraded as neurons differentiate, permitting the expression of neurogenic bHLH factors and other neuronal genes. Homeodomain transcription factors of the SoxB class also play an important role in maintaining neural progenitors by blocking neurogenic bHLH protein activity. The differentiation of neurons therefore requires the avoidance of REST/NRSF and SoxB protein activity.

The Layers of the Cerebral Cortex Are Established by Sequential Addition of Newborn Neurons

The ventricular zone in the most anterior portion of the mammalian neural tube gives rise to the cerebral cortex in a series of steps. Cells from the ventricular zone, which is on the apical edge of the neuroepithelium, initially migrate basally to form a subventricular zone, which houses a set of progenitor cells with a more restricted set of fates. Next to form is an intermediate zone, through which newly formed neurons migrate, and a preplate, which houses the earliest-born neurons. Additional neurons migrate to form a layer called the cortical plate, which lies within the preplate. The cortical plate thereby divides the preplate into an apical subplate and a basal marginal zone (Figure 46–5A).

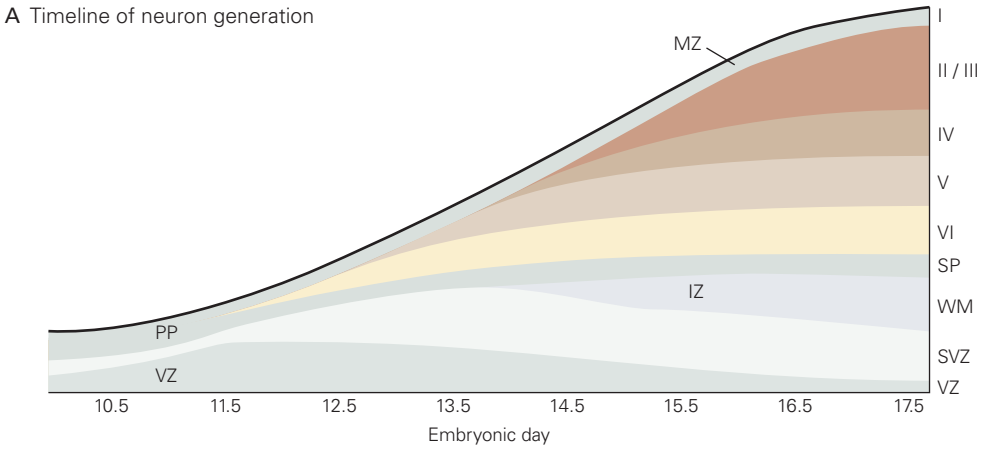
A Timeline of neuron generation
MZ
I
II / III
IV
V
VI
SP
IZ
WM
PP
SVZ
VZ
VZ
10.5
11.5
12.5
13.5
14.5
15.5
16.5
17.5
Embryonic day

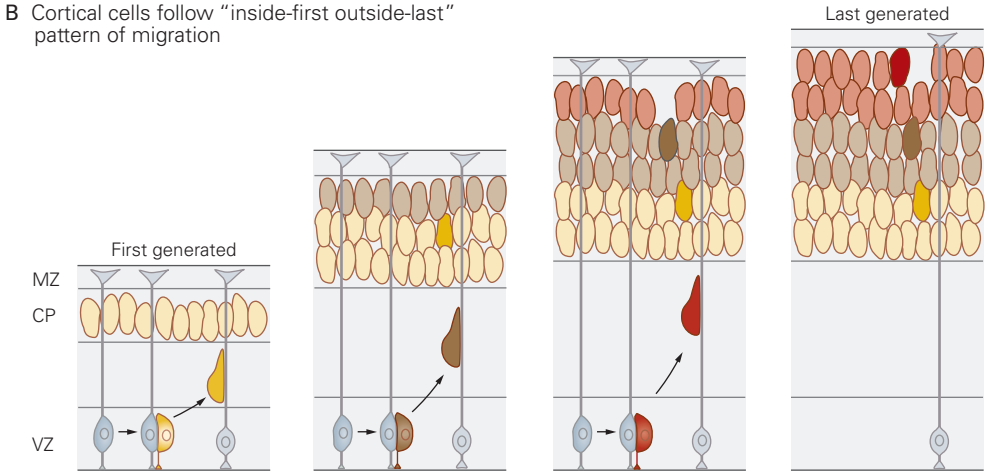
B Cortical cells follow "inside-first outside-last" pattern of migration
Last generated
First generated
MZ
CP
VZ

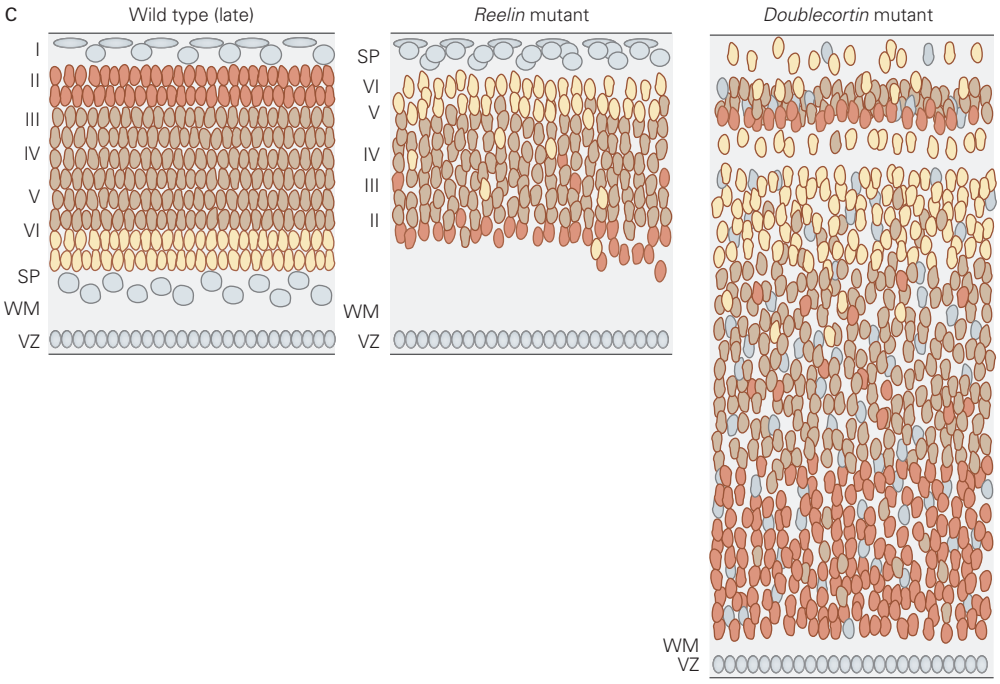
C
Wild type (late)
Reelin mutant
Doublecortin mutant
I
II
III
IV
V
VI
SP
WM
VZ
SP
VI
V
IV
III
II
WM
VZ
WM
VZ

Once within the cortical plate, neurons become organized into well-defined layers. The layer in which a neuron settles is correlated precisely with the neuron's *birthday*, a term that refers to the time at which a dividing precursor cell undergoes its final round of cell division and gives rise to a postmitotic neuron. Cells that migrate from the ventricular and subventricular zones and leave the cell cycle at early stages give rise to neurons that settle in the deepest layers of the cortex. Cells that exit the cell cycle at progressively later stages migrate over longer distances and pass earlier-born neurons before settling in more superficial layers of the cortex. Thus, the layering of neurons in the cerebral cortex follows an inside-first, outside-last rule (Figure 46–5B).

Neurons Migrate Long Distances From Their Site of Origin to Their Final Position

The migration of neurons from the cortical ventricular zone to the cortical plate follows a process termed *radial migration.* In this mode, the neurons move along the long unbranched processes of radial glial cells to reach their destinations. In contrast, interneurons enter the cortex from subcortical sites by a process called *tangential migration*. We discuss these modes in turn and then describe a third migratory strategy, *free migration*, which predominates in the peripheral nervous system.

Excitatory Cortical Neurons Migrate Radially Along Glial Guides

Classical anatomical studies of cortical development in the 1970s provided evidence that neurons generated in the ventricular zone migrate to their settling position along a pathway of radial glial fibers. Radial glial cells serve as the primary scaffold for radial neuronal migration. Their cell bodies are located close to the ventricular surface and give rise to elongated fibers that span the width of the developing cerebral wall. Each radial glial cell has one basal end-foot at the apical surface of the ventricular zone and processes that terminate in multiple end-feet at the pial surface (Figure 46–6). Radial glial scaffolds are especially important in the development of the primate cortex, where neurons are required to migrate over long distances as the cortex expands. A single radial glial cell scaffold can support the migration of up to 30 generations of cortical neurons before eventually differentiating into an astrocyte.

What forces and molecules power neuronal migration on radial glial cells? After a neuron leaves the cell cycle, its leading process wraps around the shaft of the radial glial cell and its nucleus translocates within the cytoplasm of the leading process. Although the leading process of the migrating neuron extends slowly and steadily, the nucleus moves in an intermittent, stepwise manner because of complex rearrangements of the cytoskeleton. A microtubular lattice forms a cage around the nucleus; movement of the nucleus depends on a centrosome-like structure, termed a *basal body*, from which a system of microtubules projects into the leading process, providing tracks along which the nucleus moves (Figure 46–7A).

Neuronal migration along radial glia also involves adhesive interactions between cells. Adhesive receptors such as integrins promote neuronal extension on radial glial cells. The migration of neurons along glial fibers is nevertheless different from the extension of axons driven by growth cones (Chapter 47). In neuronal migration, the leading process is devoid of the structured actin filaments that typify growth cones and more closely resembles an extending dendrite, an inference made first by Santiago Ramón y Cajal.

Disruption in the migratory and settling programs of cortical neurons underlies much human cortical pathology (Figure 46–5C). For example, in lissencephaly

Figure 46–5 (Opposite) **The migration of neurons within the embryonic cerebral cortex leads to layered cortical organization.** (Adapted from Olsen and Walsh 2002.)

A. This temporal sequence of neurogenesis is for the mouse cerebral cortex. Neurons begin to accumulate in the cortical plate during the last 5 days of embryonic development. Within the cortical plate, neurons populate the deep layers before settling in the superficial layers. (Abbreviations: **IZ**, intermediate zone; **MZ**, marginal zone; **PP**, preplate; **SP**, subplate; **SVZ**, subventricular zone; **VZ**, ventricular zone; **WM**, white matter.)

B. During normal cortical development, neurons use radial glial cells as migratory scaffolds as they enter the cortical plate. As they approach the pial surface, neurons stop migrating and detach from radial glial cells. This orderly inside-out pattern of neuronal migration results in the formation of six neuronal layers in the mature cerebral cortex, arranged between the white matter and subplate. (Abbreviation: **CP**, cortical plate.)

C. In the mouse mutant *reeler,* which lacks functional reelin protein, the layering of neurons in the cortical plate is severely disrupted and partially inverted. In addition, the entire cortical plate develops beneath the subplate. In *doublecortin* mutants, the cortex is thickened, neurons lose their characteristic layered identity, and some layers contain fewer neurons. A similar disruption is observed in *Lis1* mutants, which underlies certain forms of human lissencephaly.

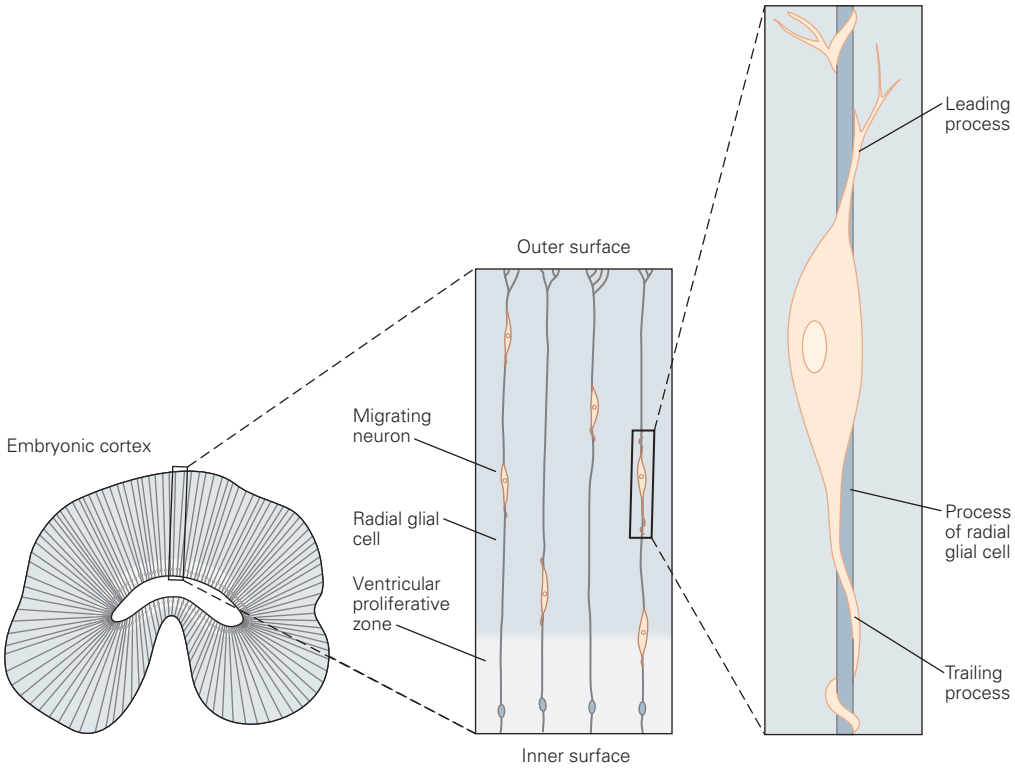

Figure 46–6 Neurons migrate along radial glial cells. After their generation from radial glial cells, newly generated neurons in the embryonic cerebral cortex extend a leading process that wraps around the shaft of the radial glial cell, thus using the radial glial cells as scaffolds during their migration from the ventricular zone to the pial surface of cortex.

(Greek, smooth brain, referring to the characteristic smoothing of the cortical surface in patients with the disorder), neurons leave the ventricular zone but fail to complete their migration into the cortical plate. As a result, the mature cortex is typically reduced from six to four neuronal layers, and the arrangement of neurons in each remaining layer is disordered. Occasionally, lissencephaly is accompanied by the presence of an additional group of neurons in the subcortical white matter. Patients with lissencephalies from mutations in the *Lis1* and *doublecortin* genes often suffer severe intellectual disability and intractable epilepsy. The Lis1 and doublecortin proteins have been localized to microtubules, suggesting that they are involved in microtubule-dependent nuclear movement, although their precise functions in neuronal migration remain unclear.

Mutations that disrupt the reelin signaling pathway disrupt the final stage of neuronal migration through the cortical subplate. The reelin protein is secreted from the Cajal-Retzius cells, a class of neurons found in the preplate and marginal zone. Signals from these cells are crucial for the migration of cortical neurons. In mice lacking functional reelin, neurons fail to detach from their radial glial scaffolds and pile up underneath the cortical plate, disobeying the inside-out migratory rule. As a consequence, the normal layering of cell types is partially inverted and the marginal zone is lost. Reelin acts through cell-surface receptors that include the ApoE receptor 2 and the very-low-density lipoprotein receptor. The binding of reelin to these receptors activates an intracellular protein, Dab1, which transduces reelin signals. Not surprisingly, the loss of proteins that transduce reelin signals produces similar migratory phenotypes.

Cortical Interneurons Arise Subcortically and Migrate Tangentially to Cortex

Progenitor cells in the cortical ventricular zone were initially believed to give rise to all cortical neurons. However, as better molecular labels for distinct neuronal types became available, it was found that interneurons arise in the ventricular zone of subcortical structures. Most of them originate in regions of the ventral telencephalon called the ganglionic eminences (Figure 46–8).

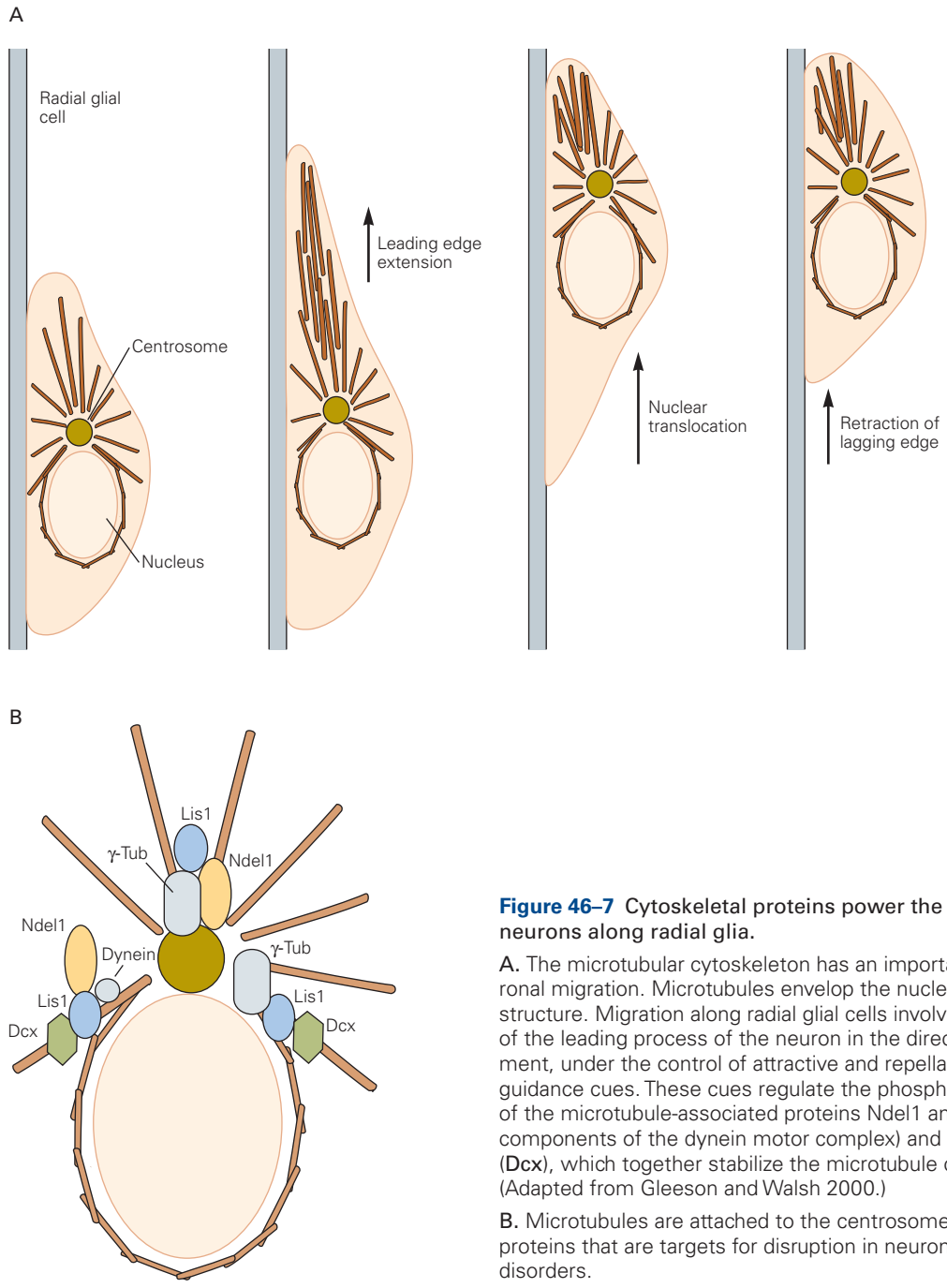

Figure 46–7 Cytoskeletal proteins power the migration of neurons along radial glia.

A. The microtubular cytoskeleton has an important role in neuronal migration. Microtubules envelop the nucleus in a cage-like structure. Migration along radial glial cells involves elongation of the leading process of the neuron in the direction of movement, under the control of attractive and repellant extracellular guidance cues. These cues regulate the phosphorylation status of the microtubule-associated proteins Ndel1 and Lis1 (two components of the dynein motor complex) and of doublecortin (**Dcx**), which together stabilize the microtubule cytoskeleton. (Adapted from Gleeson and Walsh 2000.)

B. Microtubules are attached to the centrosome by a series of proteins that are targets for disruption in neuronal migration disorders.

The medial and central eminences generate most cortical interneurons, which migrate dorsally from their sites of origin to enter the cortex. Some enter through the intermediate zone, while others enter through the marginal zone (Figure 46–5A). Once they reach particular anterior-posterior and mediolateral positions, they switch to a radial mode of migration to travel the final distance to appropriate layers. Distinct populations of neurons generated in the ganglionic eminences migrate at different times and through different routes, contributing to the diversity of the interneuronal population. Precise relationships between time and place of origin, migratory route, and ultimate fate remain to be determined.

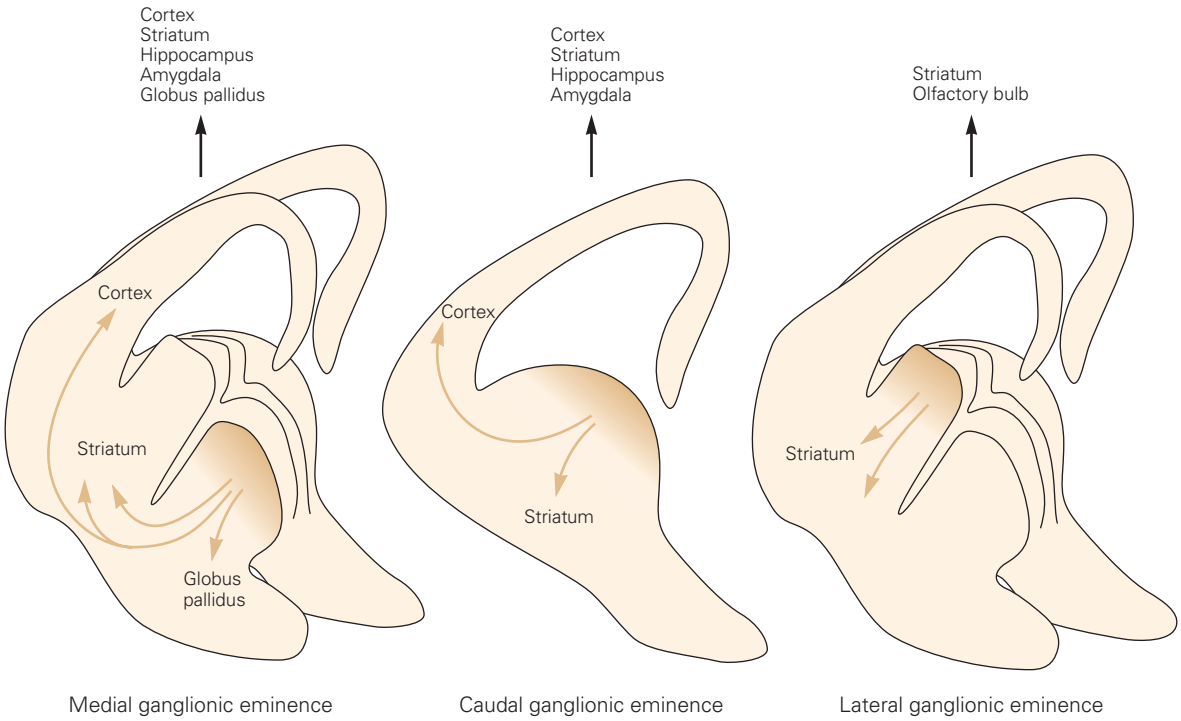

Figure 46–8 Forebrain interneurons are generated in the ventral telencephalon and migrate tangentially to the cerebral cortex. Neurons generated in the ganglionic eminences migrate to and settle in many regions of the forebrain, where they differentiate into interneurons. Cortical interneurons arise from medial and caudal ganglionic eminences. Other cells generated in these regions migrate in other directions, populating the hippocampus, striatum, globus pallidus, and amygdala with interneurons. The lateral ganglionic eminence generates cells that migrate to the striatum and the olfactory bulb. Cells migrating to the bulb use neighboring migrating cells as substrates for migration, a process called chain migration. (Adapted, with permission, from Bandler, Mayer, and Fishell 2017. Copyright © 2017 Elsevier Ltd.)

Nonetheless, it is now clear that cortical neurons originate from two sources: excitatory neurons from the cortical ventricular zone and interneurons from the ganglionic eminences.

Interneurons in other forebrain structures also arise from the ganglionic eminences, as well as a few other subcortical sites such as the preoptic area. Cells migrating caudally from the medial and caudal eminences populate the hippocampus, while cells migrating ventrolaterally from these regions populate the basal ganglia. In contrast, neurons generated in the lateral ganglionic eminence migrate rostrally and contribute the periglomerular and granule interneurons of the olfactory bulb. In this rostral migratory stream, neurons use neighboring neurons as substrates for migration (chain migration). In the adult brain, neurons that follow the rostral migratory stream originate instead in the subventricular zone of the striatum.

Transcription factors control the character of ganglionic eminence neurons. The homeodomain proteins Dlx1 and Dlx2 are expressed by cells in the ganglionic eminences. In mice lacking Dlx1 and Dlx2 activity, the resultant perturbation of neuronal migration leads to a profound reduction in the number of GABAergic interneurons in the cortex. Other transcription factors are responsible for differences among ganglionic eminences. For example, Nkx2.1 is selectively expressed by cells in the medial ganglionic eminence. In its absence, interneurons generated in this region take on characteristics of those normally generated in the lateral and caudal ganglionic eminences. Yet other transcription factors specify the distinct characteristics of subpopulations of neurons within each ganglionic eminence.

One of the main features that these transcription factors specify is the migratory path that the newborn interneurons take. A host of soluble and cell surface factors produced by cells in and near the ganglionic eminences provide repulsive cues that lead to expulsion of cells from the ventricular zone, so-called motogenic (movement-promoting) cues that speed their migration and attractive cues that direct them to their targets. These factors include slits, semaphorins, and ephrins, all of which we will encounter in Chapter 47 as molecules that guide axons to their targets.

Neural Crest Cell Migration in the Peripheral Nervous System Does Not Rely on Scaffolding

The peripheral nervous system derives from neural crest stem cells, a small group of neuroepithelial cells at the boundary of the neural tube and epidermal ectoderm. Soon after their induction, neural crest cells are transformed from epithelial to mesenchymal cells and begin to detach from the neural tube. They then migrate to many sites throughout the body (Figure 46–9). Neural crest cell migration does not rely on scaffolding (ie, radial glial cells or preexisting axon tracts) and thus is called free migration. This form of neuronal migration requires significant cytoarchitectural and cell adhesive changes and differs from most of the migratory events in the central nervous system.

Neural crest migration is promoted and guided by several families of secreted factors. For example, bone morphogenetic proteins (BMPs), which are critical for neural crest induction at an earlier stage (Chapter 45), are required for neural crest migration at later stages. Exposure of neural epithelial cells to BMPs triggers molecular changes that convert epithelial cells to a mesenchymal state, causing them to delaminate from the neural tube and migrate into the periphery. BMPs trigger changes in neural crest cells by inducing expression of transcription factors, notably the zinc finger proteins snail, slug, and twist, which have a conserved role in promoting epithelial-to-mesenchymal transitions. These transcription factors direct expression of proteins that regulate the properties of the cytoskeleton as well as enzymes that degrade extracellular matrix proteins. These enzymes give neural crest cells the ability to break down the basement membrane surrounding the epithelium of the neural tube, permitting them to embark on their migratory journey into the periphery.

As neural crest cells begin to delaminate, their expression of cell adhesion molecules changes. Alterations in expression of adhesive proteins, notably cadherins, permit neural crest cells to loosen their adhesive contacts with neural tube cells and begin the delamination process. Neural crest cells also begin to express integrins, receptors for extracellular matrix proteins such as laminins and collagens that are found along peripheral migratory paths.

The first structures encountered by migrating neural crest cells are somites, epithelial cells that later give rise to muscle and cartilage. Neural crest cells pass through the anterior half of each somite but avoid the posterior half (Figure 46–9A). The rostral channeling of migratory neural crest cells is imposed by ephrin B proteins, which are concentrated in the posterior half of each somite. Ephrins provide a repellant signal that interacts with EphB class tyrosine kinase receptors on neural crest cells to prevent their invasion. Neural crest cells that remain within the anterior sclerotome of the somite differentiate into sensory neurons of the dorsal root ganglia; those that migrate around the dorsal region of the somite approach the skin and give rise to melanocytes.

Differentiation of the neural crest into its various derivatives depends on complex interactions between the distinct cues that cells receive along their journey and intrinsic predispositions that vary along the rostrocaudal axis. Development of sensory neurons is initiated at the time the cells emigrate from the neural tube. The cells are exposed to signals from the dorsal neural tube and somites that induce expression of neurogenin, a transcription factor of the bHLH family, which in turn promotes a sensory fate. Subsequent influences diversify the neurons into multiple sensory types, such as nociceptive and proprioceptive neurons (Figure 46–10). In contrast, those neural crest cells that follow a more medial and ventral migratory path are exposed to BMPs secreted from the dorsal aorta. They express the bHLH factor Mash1, which leads to their differentiation into sympathetic neurons.

Structural and Molecular Innovations Underlie the Expansion of the Human Cerebral Cortex

No mice or monkeys are reading this book. This is in large part because the human brain is different from that of even our closest relatives, both qualitatively and quantitatively. Yet most studies of mammalian neural development have been carried out on mice, whose brain contains approximately 1,000-fold fewer neurons than those of the human brain and 100-fold fewer than the best-studied nonhuman primate, the rhesus macaque. Recently, however, new methods are making it possible to elucidate some of the molecular and structural features that lead to the expansion of the human brain and particularly the human cerebral cortex.

Classical anatomical studies made clear that the primate cortex has not only a far larger size and thickness than that of rodents but also more discrete areas and more layers (Figure 46–11A). In addition, the packing density of neurons is higher in primates than in mice, so the difference in neuronal number is greater than would be expected from size alone. One main contributor to the expansion in primates is a large pool of neuronal progenitors. Many of these progenitors are a second type of radial glial cell, called the outer radial

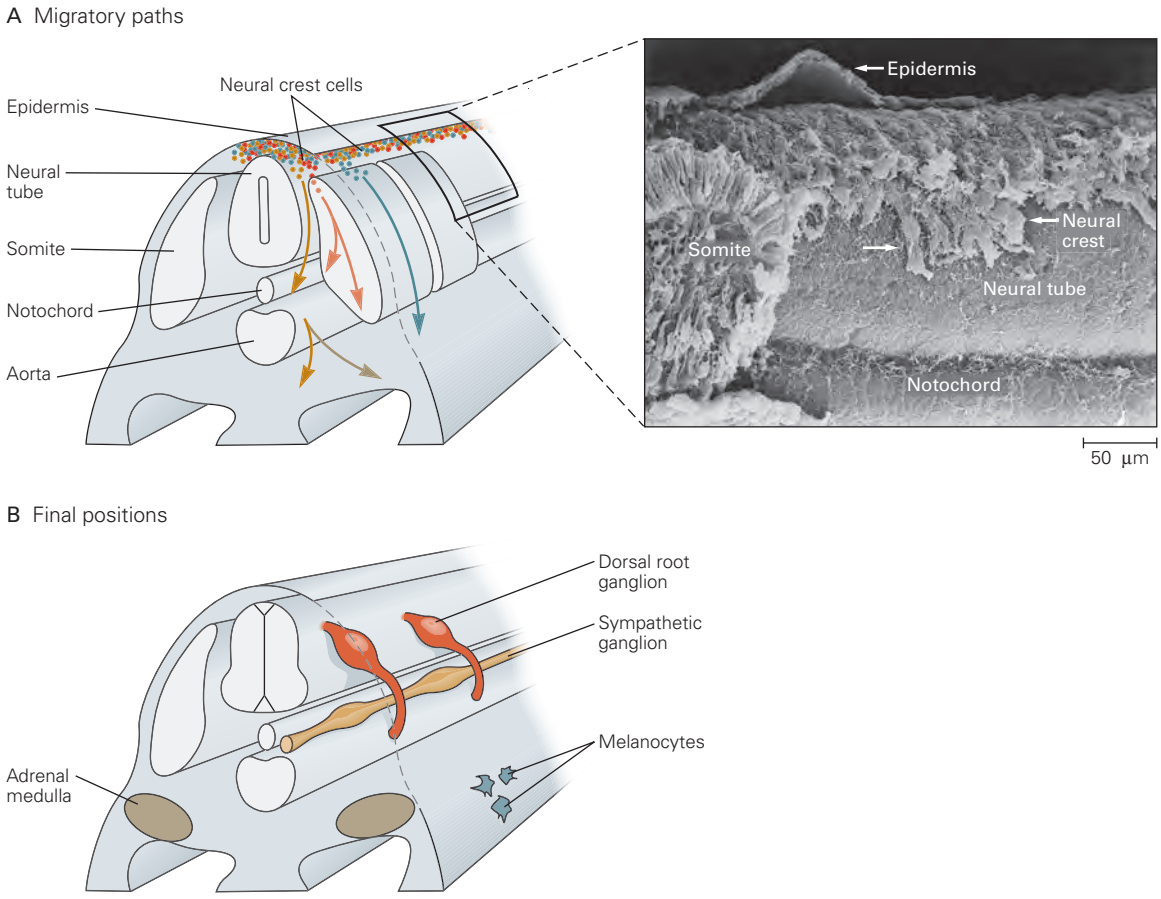

Figure 46–9 Neural crest cell migration in the peripheral nervous system.

A. A cross section through the middle part of the trunk of a chick embryo shows the main pathways of neural crest cells. Some cells migrate along a superficial pathway, just beneath the ectoderm, and differentiate into pigment cells of the skin. Others migrate along a deeper pathway that takes them through the somites, where they coalesce to form dorsal root sensory ganglia. Still others migrate between the neural tube and somites, past the dorsal aorta. These cells differentiate into sympathetic ganglia and adrenal medulla. The scanning electron micrograph shows neural crest cells migrating away from the dorsal surface of the neural tube of a chick embryo. (Micrograph reproduced, with permission, from K. Tosney.)

B. Neural crest cells reach their final settling positions where they complete differentiation.

glial cell to distinguish it from the canonical or inner radial glia described above. Outer radial glia, unlike inner radial glia, lack contact with the ventricular surface and exhibit molecular differences from inner radial glia. However, they are capable of generating neurons and serving as a migratory guide. The massive increase in their number in primates, and particularly humans, provides a partial explanation for the increase in the number of neurons in the human cerebral cortex.

How can human-specific developmental features be analyzed experimentally? New methods of molecular analysis are making it possible to compare the proteins, transcripts, and genes of humans with those of our close relatives, resulting in the discovery of intriguing specializations. However, hypotheses derived from these findings are difficult to test: Most of the developmental studies we describe in these chapters cannot be performed on humans, and even nonhuman primates are difficult subjects for developmental analysis. A possible solution is the recently devised "organoid" culture system.

Cells from adult skin can be reprogrammed to become multipotential progenitors called induced pluripotent stem cells (iPSCs) by methods that we will discuss in Chapter 50. When placed into culture under carefully controlled conditions and allowed to expand in three dimensions (quite unlike conventional two-dimensional cultures), they proliferate and self-organize into structures that resemble the developing forebrain and exhibit species-specific features

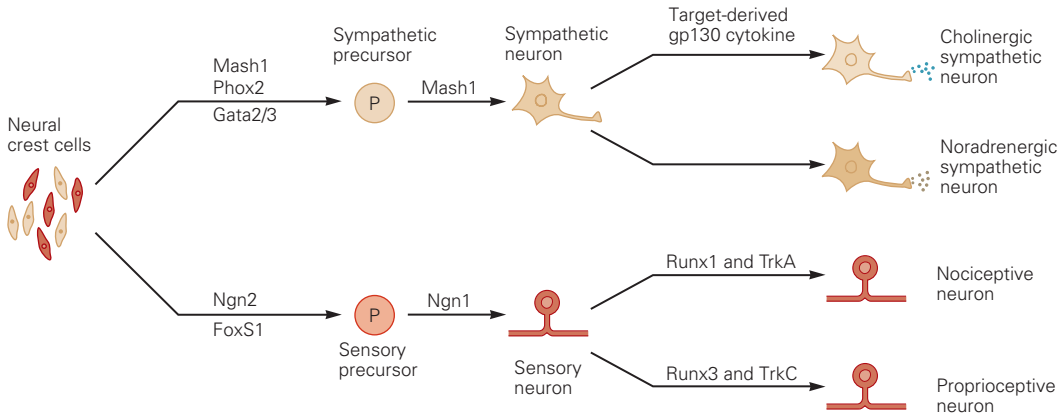

Figure 46–10 **Neural crest cells differentiate into sympathetic and sensory neurons.** The neuronal fates of trunk neural crest cells are controlled by transcription factor expression. Expression of the basic helix-loop-helix (bHLH) protein Mash1 directs neural crest cells along a sympathetic neuronal pathway. Sympathetic neurons can acquire noradrenergic or cholinergic transmitter phenotypes depending on the target cells they innervate and the level of gp130 cytokine signaling (see Figure 46–13). Two bHLH proteins, neurogenin-1 and -2, direct neural crest cells along a sensory neuronal pathway. Sensory neurons that express the transcription factor Runx1 and the tyrosine kinase receptor TrkA become nociceptors; those that express Runx3 and TrkC become proprioceptors. (Abbreviations: **Ngn-1**, neurogenin-1; **Ngn-2**, neurogenin-2.)

(Figure 46–11B). Most notably, organoids from human cells contain a bilayered, large subventricular zone with numerous outer radial glia, whereas organoids from mouse cells contain a smaller subventricular zone containing predominately conventional or inner radial glia. These organoids can be used to elucidate the development of at least some early aspects of human cortical development.

Additional applications abound. One is to obtain iPSCs from patients with brain disorders. Organoids derived from such patients have features that may lead to cortical malformations such as lissencephaly (see Figure 46–5). The hope is that these organoids can be used to elucidate disease mechanisms and eventually test therapies. A second application is to compare organoids derived from chimpanzee and human iPSCs. This comparison provides a novel means of investigating the most recent evolutionary innovations that separate us from our closest living relatives.

Intrinsic Programs and Extrinsic Factors Determine the Neurotransmitter Phenotypes of Neurons

Neurons continue to develop after they have migrated to their final position, and no aspect of their later differentiation is more important than the choice of chemical neurotransmitter. Neurons that populate the brain use two major neurotransmitters: The amino acid L-glutamate is the major excitatory transmitter, whereas γ-aminobutyric acid (GABA) is the major inhibitory transmitter. Some spinal cord neurons use another amino acid, glycine, as their inhibitory transmitter. In the peripheral nervous system, sensory neurons use glutamate, motor neurons use acetylcholine, and autonomic neurons use acetylcholine or norepinephrine. Smaller numbers of neurons use other transmitters, such as serotonin and dopamine. The choice of neurotransmitter determines which postsynaptic cells a neuron can talk to and what it can say.

Neurotransmitter Choice Is a Core Component of Transcriptional Programs of Neuronal Differentiation

Distinct molecular programs are used to establish neurotransmitter phenotype in different brain regions and neuronal classes. We shall illustrate the general strategy for assignment of amino acid neurotransmitter phenotypes by focusing on neurons in the cerebral cortex and cerebellum.

The cerebral cortex contains glutamatergic pyramidal neurons that are generated within the cortical plate and rely on the bHLH factors neurogenin-1 and neurogenin-2 for their differentiation. In contrast, as discussed earlier in the chapter (see Figure 46–8), most GABAergic inhibitory interneurons migrate into the cortex from the ganglionic eminences; their inhibitory transmitter character is specified by the bHLH protein

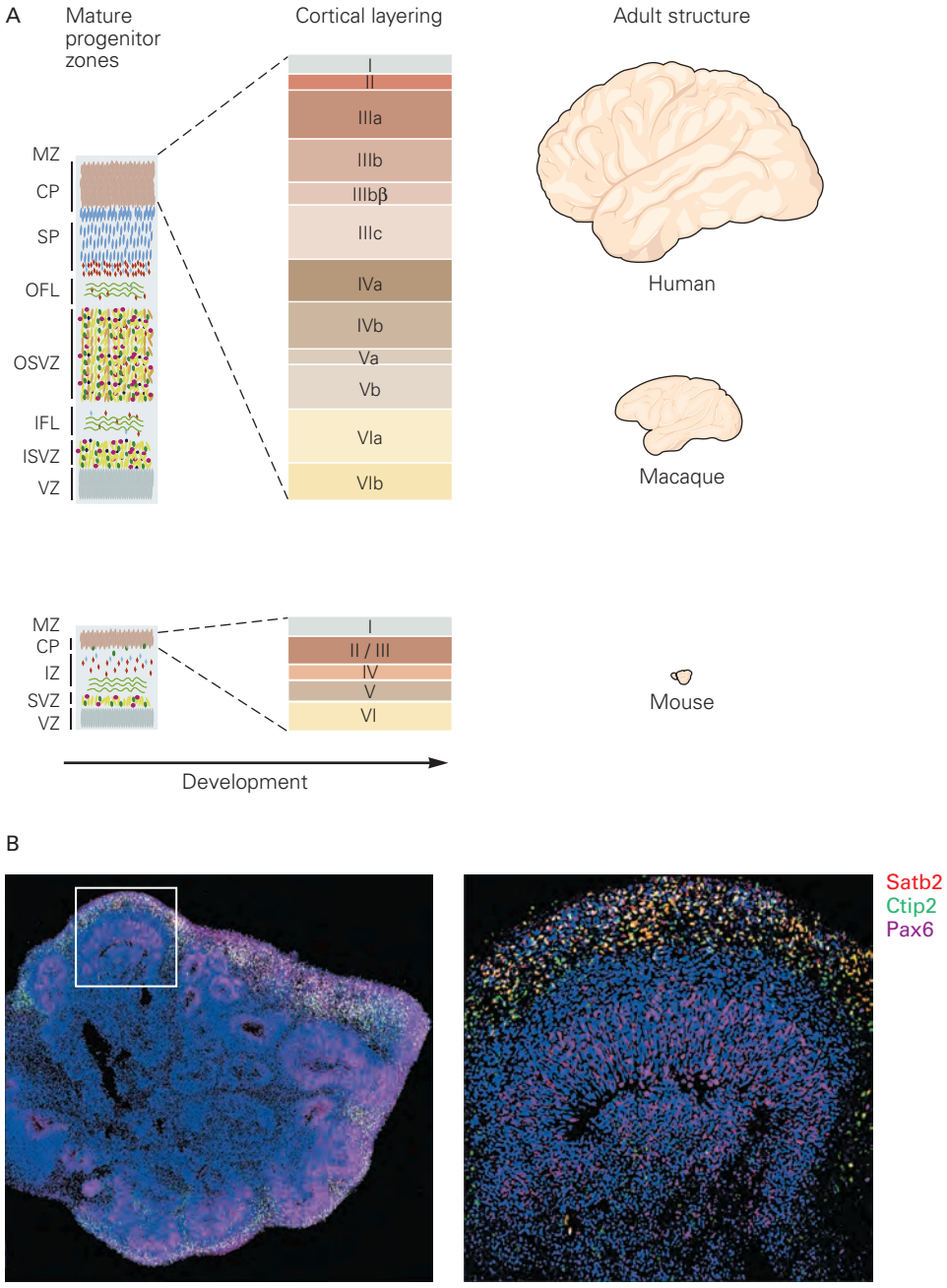

Figure 46–11 Expansion of the proliferative zones contributes to cortical specialization in humans and other primates.

A. The size of the neuroepithelium is initially small in both rodents and humans, but their relative size differs dramatically as development proceeds, owing to increased self-renewal rates and larger numbers of progenitors in humans. The primate subventricular zone is greatly enlarged compared to the mouse and becomes subdivided into inner and outer regions, which contain large populations of radial glial cells, both of which generate neurons. In mice, nearly all radial glial cells are of the inner type. (Abbreviations: **CP**, cortical plate; **IFL**, inner fiber layer; **ISVZ**, inner subventricular zone; **IZ**, intermediate zone; **MZ**, marginal zone; **OFL**, outer fiberlayer; **OSVZ**, outer subventricular zone; **SP**, subplate; **SVZ**, subventricular zone; **VZ**, ventricular zone.) (Adapted, with permission, from Giandomenico and Lancaster 2017.)

B. Section through an organoid generated from human induced pluripotent stem cells. The area between the white lines is enlarged in the micrograph on the right. The section was stained with antibodies to transcription factors (Satb2, Ctip2, and Pax6) selectively expressed in specific layers in human cortex, demonstrating that a layered cortical structure develops in the organoid. (Micrographs reproduced, with permission, from P. Arlotta.)

Mash1 (Figure 46–12A) as well as by the Dlx1 and Dlx2 proteins.

Similarly, the cerebellum contains several different classes of inhibitory neurons (Purkinje, Golgi, basket, and stellate neurons) and two major classes of excitatory neurons (granule neurons and large cerebellar nucleus neurons). These inhibitory and excitatory neurons have different origins; GABAergic neurons derive from the ventricular zone, whereas glutamatergic neurons migrate into the cerebellum from the rhombic lip. The generation of GABAergic and glutamatergic neurons is controlled by two different bHLH transcription factors, Ptf1a for inhibitory and Math-1 for excitatory neurons (Figure 46–12B). These bHLH factors are expressed by neuroepithelial cells but not by mature neurons, implying that differentiation into glutamatergic and GABAergic neurons is initiated prior to neuronal generation.

Transcriptional programs also determine the transmitter phenotype in the peripheral nervous system. For example, BMPs promote noradrenergic neuronal differentiation by inducing the expression of a variety of transcription factors that include the bHLH protein Mash1, the homeodomain protein Phox2, and the zinc finger protein Gata2. In contrast, Runx proteins are determinants of the glutamatergic phenotype of sensory neurons (Figure 46–10).

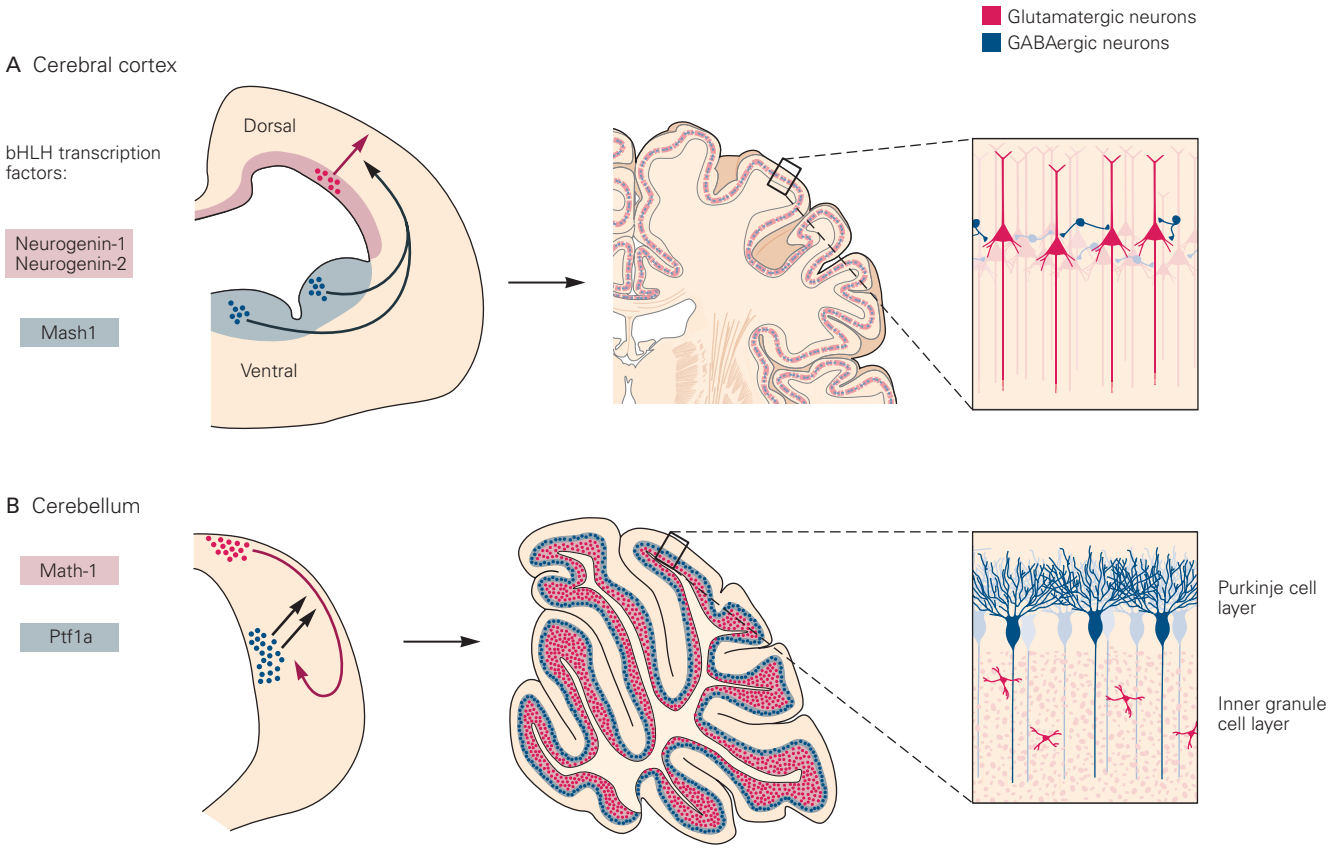

Figure 46–12 The neurotransmitter phenotype of central neurons is controlled by basic helix-loop-helix transcription factors.

A. GABAergic and glutamatergic neurons in the cerebral cortex are generated in different proliferative zones and are specified by different basic helix-loop-helix (**bHLH**) transcription factors. Glutamatergic pyramidal neurons derive from the cortical ventricular zone, and their differentiation depends on the activities of neurogenin-1 and -2. The differentiation of GABAergic interneurons in the ganglionic eminences of the ventral telencephalon depends on the bHLH protein Mash1. These neurons migrate dorsally to supply the cerebral cortex with most of its inhibitory interneurons.

B. GABAergic and glutamatergic neurons in the developing cerebellum also derive from different proliferative zones and are specified by different bHLH transcription factors. Glutamatergic granule cells migrate into the cerebellum from the rhombic lip, settle in the inner granular layer, and are specified by the bHLH protein Math-1. GABAergic Purkinje neurons migrate from the deep cerebellar proliferative zone, settle in the Purkinje cell layer, and are specified by the bHLH protein Ptf1a.

Signals From Synaptic Inputs and Targets Can Influence the Transmitter Phenotypes of Neurons

Because neurotransmitter phenotype is a core neuronal property, it was long thought that transmitter properties were fixed at the earliest stage of neuronal differentiation. This view was challenged by studies showing that the migratory pathway of a neural crest cell exposes the cell to environmental signals that have a critical role in determining its transmitter phenotype.

Most sympathetic neurons use norepinephrine as their primary transmitter. However, those that innervate the exocrine sweat glands in the footpads use acetylcholine, and even these neurons express norepinephrine when they first innervate the sweat glands of the skin. Only after their axons have contacted the sweat glands do they stop synthesizing norepinephrine and start producing acetylcholine.

When the sweat glands from the footpad of a newborn rat are transplanted into a region that is normally innervated by noradrenergic sympathetic neurons, the synaptic neurons acquire cholinergic transmitter properties, indicating that cells of the sweat gland secrete factors that induce cholinergic properties in sympathetic neurons.

Several secreted factors trigger the switch from a noradrenergic to cholinergic phenotype in sympathetic neurons. The sweat gland secretes a cocktail of interleukin-6–like cytokines, notably cardiotrophin-1, leukemia inhibitory factor, and ciliary neurotrophic factor. Several aspects of neuronal metabolism that are linked to transmitter synthesis and release are controlled by these factors. The neurons stop producing the large dense-core granules characteristic of noradrenergic neurons and start making the small electron-translucent vesicles typical of cholinergic neurons (Figure 46–13).

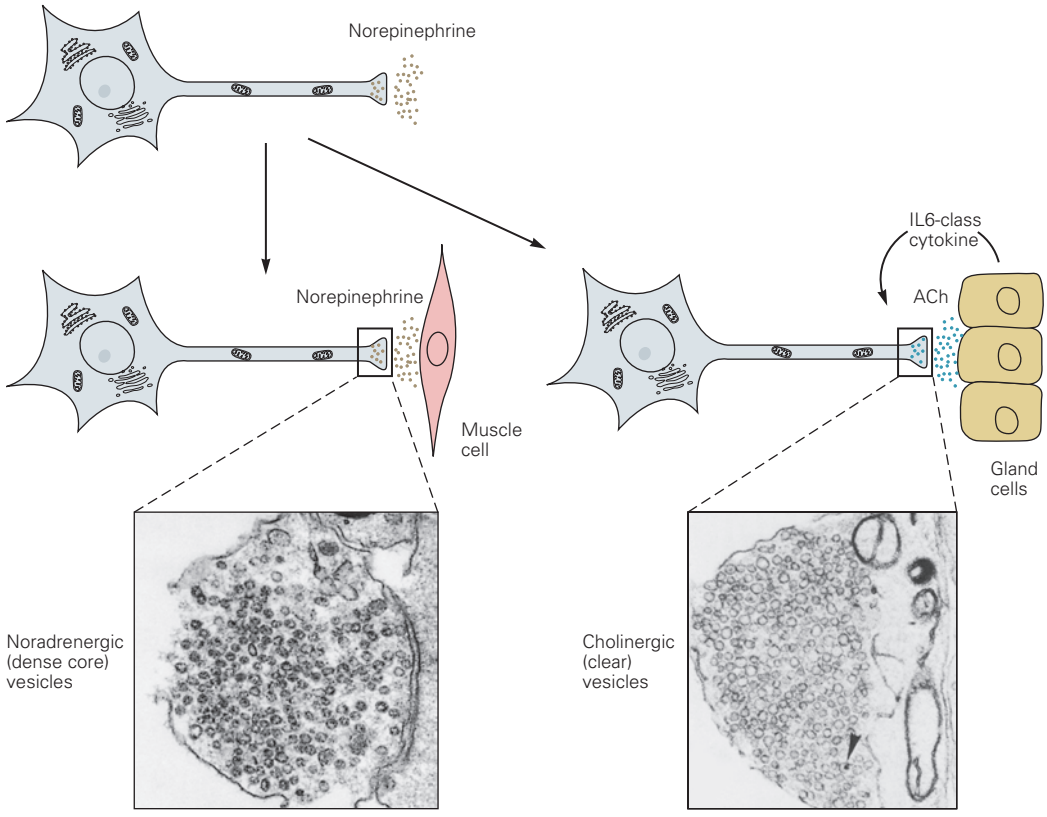

Figure 46–13 **The target of sympathetic neurons determines neurotransmitter phenotype.** Sympathetic neurons are initially specified with a noradrenergic transmitter phenotype. Most sympathetic neurons, including those that innervate cardiac muscle cells, retain this transmitter phenotype, and their terminals are packed with the dense-core vesicles in which norepinephrine is stored. But the sympathetic neurons that innervate sweat gland targets are induced to switch to a cholinergic transmitter phenotype; their terminals become filled with the small clear vesicles in which acetylcholine (**ACh**) is stored. Sweat gland cells direct the switch by secreting members of the interleukin cytokine family. Several members of this family, including leukemia inhibitory factor and ciliary neurotrophic factor, are potent inducers of cholinergic phenotype in sympathetic neurons grown in cell culture. (Abbreviation: **IL6**, interleukin-6.) (Micrographs reproduced, with permission, from S. Landis.)

More recently, evidence has accumulated that the transmitter phenotype of central neurons can also be influenced by signals including hormones and electrical activity. When the spontaneous activity of embryonic amphibian neurons is increased, some motor neurons can be respecified to synthesize and use the inhibitory neurotransmitter GABA instead of or in addition to acetylcholine. Conversely, when activity is decreased, some inhibitory neurons switch to using the excitatory neurotransmitter glutamate along with or instead of GABA. Postsynaptic partners typically express new receptors that correspond to the transmitter being released onto them. These switches occur without overall respecification of the neuron and are best viewed as homeostatic responses aimed at keeping the overall activity of the system in a narrow range.

Although such transmitter switches in central neurons are likely to occur only rarely under natural conditions, activity-dependent neurotransmitter plasticity may be a more common phenomenon in the adult nervous system. For example, changes in the light cycle where rodents are housed can lead to reciprocal changes in the numbers of neurons that use dopamine and somatostatin as neuromodulators in areas of the brain responsible for maintaining a circadian rhythm. In this and other cases, neurotransmitter switching has measurable consequences on the behavior of the animal, suggesting that this process, along with less drastic synaptic changes discussed in Chapter 49, are employed by the brain as responses to novel environments.

The Survival of a Neuron Is Regulated by Neurotrophic Signals From the Neuron's Target

One of the more surprising findings in developmental neuroscience is that a large fraction of the neurons generated in the embryonic nervous system end up dying later in embryonic development. Equally surprising, we now know that the potential for cell death is preprogrammed in most animal cells, including neurons. Thus, decisions about life and death are aspects of a neuron's fate.

The Neurotrophic Factor Hypothesis Was Confirmed by the Discovery of Nerve Growth Factor

The target of a neuron is a key source of factors essential for the neuron's survival. The critical role of target cells in neuronal survival was discovered in studies of the dorsal root ganglia.

In the 1930s, Samuel Detwiler and Viktor Hamburger discovered that the number of sensory neurons in embryos is increased by transplantation of an additional limb bud into the target field and decreased if the limb target is removed. At the time, these findings were thought to reflect an influence of the limb on the proliferation and subsequent differentiation of sensory neuron precursors. In the 1940s, however, Rita Levi-Montalcini made the startling observation that the death of neurons is not simply a consequence of pathology or experimental manipulation, but rather occurs during the normal program of embryonic development. Levi-Montalcini and Hamburger went on to show that removal of a limb leads to the excessive death of sensory neurons rather than a decrease in their production.

These early discoveries on the life and death of sensory neurons were quickly extended to neurons in the central nervous system. Hamburger found that approximately half of all motor neurons generated in the spinal cord die during embryonic development. Moreover, in experiments similar to those performed on sensory ganglia, Hamburger discovered that motor neuron death could be increased by removing a limb and reduced by adding an additional limb (Figure 46–14A,B). These findings indicate that signals from target cells are critical for the survival of neurons within the central as well as peripheral nervous system. In some cases, manipulating synaptic activity affects the extent of death, perhaps by modulating the types or amount of signals that the target cell produces (Figure 46–14C). We now know that the phenomenon of neuronal overproduction, followed by a phase of neuronal death, occurs in most regions of the vertebrate nervous system.

The early discoveries of Levi-Montalcini and Hamburger laid the foundations for the *neurotrophic factor hypothesis.* The core of this hypothesis is that cells at or near the target of a neuron secrete small amounts of an essential nutrient or trophic factor and that the uptake of this factor by nerve terminals is needed for the survival of the neuron (Figure 46–15). This hypothesis was dramatically confirmed in the 1970s when Levi-Montalcini and Stanley Cohen purified the protein we now know as nerve growth factor (NGF) and showed that this protein is made by target cells and supports the survival of sensory and sympathetic neurons in vitro. Moreover, neutralizing antibodies directed against NGF were found to cause a profound loss of sympathetic and sensory neurons in vivo.

Neurotrophins Are the Best-Studied Neurotrophic Factors

The discovery of NGF prompted a search for additional neurotrophic factors. Today, we know of over a

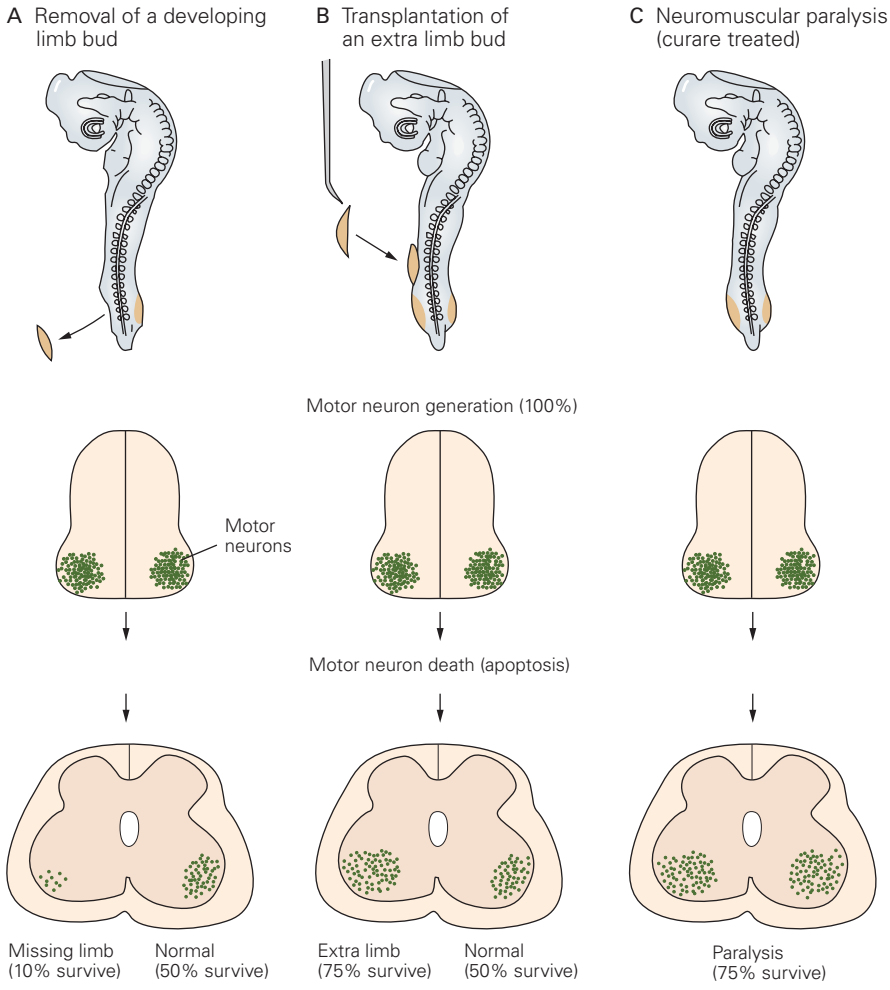

Figure 46–14 **The survival of motor neurons depends on signals provided by their muscle targets.** The role of the muscle target in motor neuron survival was demonstrated by Viktor Hamburger in a classic series of experiments performed on the chick embryo. (Adapted from Purves and Lichtman 1985.)

A. A limb bud was removed from a 2.5-day-old chick embryo soon after the arrival of motor nerves. A section of the lumbar spinal cord 1 week later reveals few surviving motor neurons on the deprived side of the spinal cord. The number of motor neurons on the contralateral side with an intact limb is normal.

B. An extra limb bud was grafted adjacent to a host limb prior to the normal period of motor neuron death. A section of the lumbar spinal cord 2 weeks later shows an increased number of limb motor neurons on the side with the extra limb.

C. Blockade of nerve-muscle activity with the toxin curare, which blocks acetylcholine receptors, rescues many motor neurons that would otherwise die. Curare may act by enhancing the release of trophic factors from inactive muscle.

dozen secreted factors that promote neuronal survival. The best-studied are related to NGF and are called the neurotrophin family.

There are four main neurotrophins: NGF itself, brain-derived neurotrophic factor (BDNF), and neurotrophins-3 and -4 (NT-3 and NT-4). Other classes of proteins that promote neuronal survival include members of the transforming growth factor β family, the interleukin-6–related cytokines, fibroblast growth factors, and even certain inductive signals we encountered earlier (BMPs and hedgehogs). Other neurotrophic factors, notably members of the glial cell line–derived neurotrophic factor (GDNF) family, are responsible for the survival of different types of sensory and sympathetic neurons (Figure 46–16).

Neurotrophins interact with two major classes of receptors, the Trk receptors and p75. Neurotrophins promote cell survival through activation of Trk receptors. The Trk family comprises three membrane-spanning tyrosine kinases named TrkA, TrkB, and TrkC, each of which exists as a dimer (Figure 46–17).

Much is now known about the intracellular signaling pathways activated by binding of neurotrophins to Trks. As with other tyrosine kinase receptors, the binding of neurotrophins to Trk receptors leads to dimerization of the Trk proteins. Dimerization results in phosphorylation of specific tyrosine residues in the activation loop of the kinase domain. This phosphorylation leads to a conformational change in the receptor and to phosphorylation of tyrosine residues that serve as docking sites for adaptor proteins. The adaptors then trigger production of second messengers that both promote the survival of neurons and trigger their maturation. These divergent biological responses involve different intracellular signaling pathways: neuronal differentiation largely via the mitogen-activated protein kinase (MAPK) enzymatic pathways and survival largely via the phosphatidylinositol-3 kinase pathway (Figure 46–18).

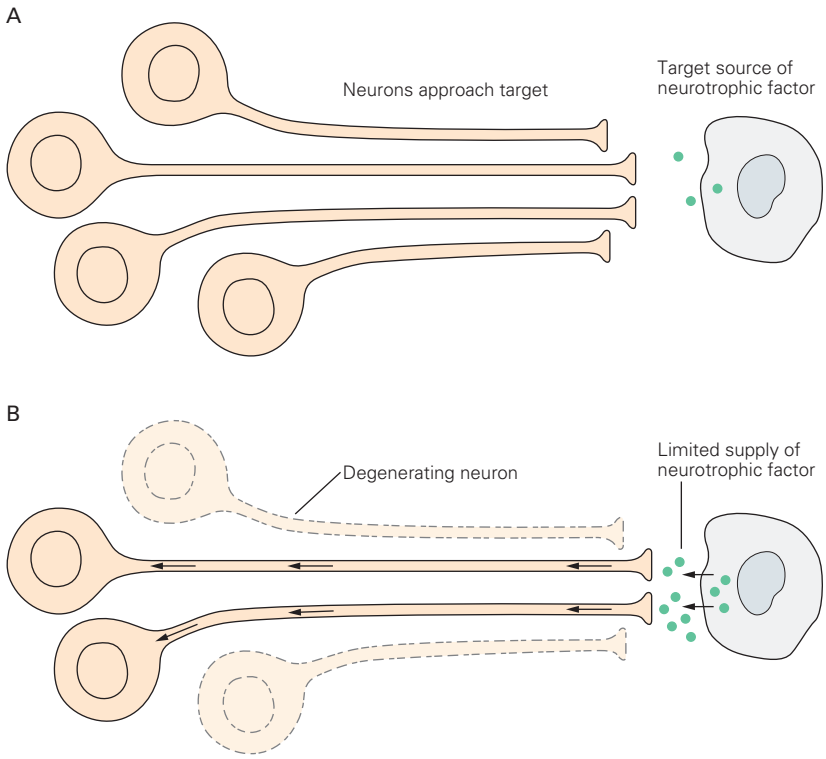

Figure 46–15 The neurotrophic factor hypothesis.

A. Neurons extend their axons to target cells, which secrete low levels of neurotrophic factors. (For simplicity, only one target cell is shown.) The neurotrophic factor binds to specific receptors and is internalized and transported to the cell body, where it promotes neuronal survival.

B. Neurons that fail to receive adequate amounts of neurotrophic factor die through a program of cell death termed apoptosis.

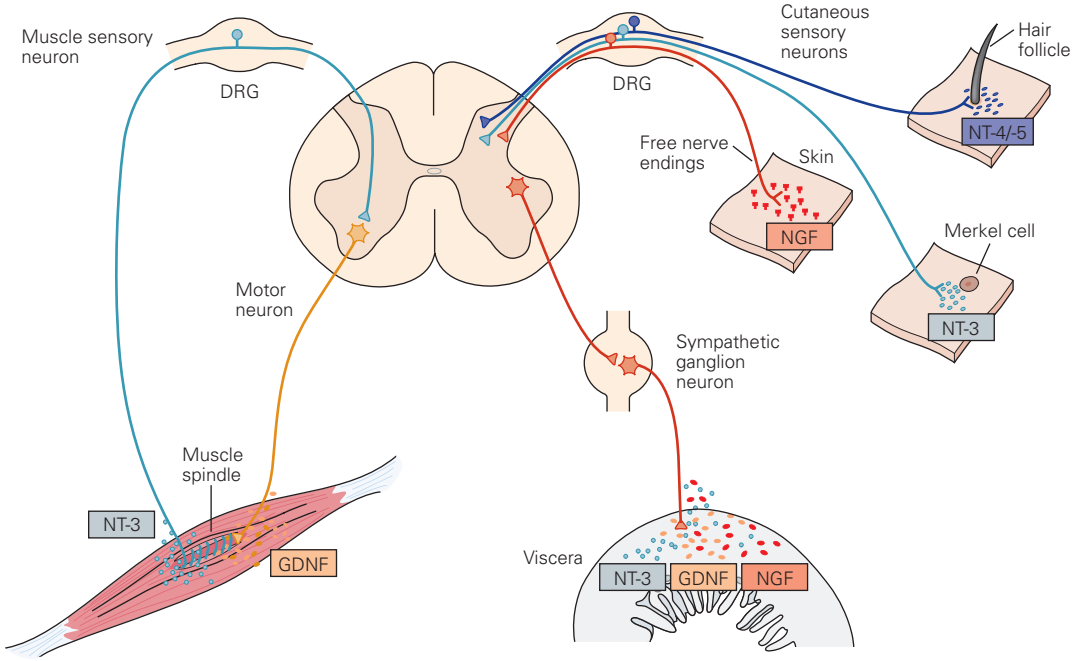

Figure 46–16 Particular neurotrophic factors promote the survival of distinct populations of dorsal root ganglion neurons. Proprioceptive sensory neurons that innervate muscle spindles depend on neurotrophin-3 (**NT-3**); nociceptive neurons that innervate skin depend on nerve growth factor (**NGF**) and neurturin; mechanoreceptive neurons that innervate Merkel cells depend on NT-3; and those that innervate hair follicles depend on neurotrophin-4 and -5 (**NT-4/-5**) and brain-derived neurotrophic factor. Motor neurons depend on glial cell line–derived neurotrophic factor (**GDNF**) and other factors. Sympathetic neurons depend on NGF, NT-3, and GDNF. (Adapted from Reichardt and Fariñas 1997.)

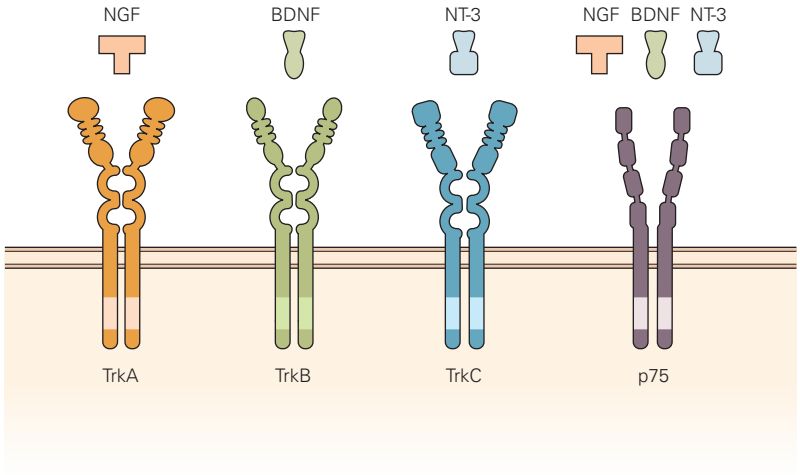

Figure 46–17 **Neurotrophins and their receptors.** Each of the three main neurotrophins interacts with a different transmembrane tyrosine kinase receptor (**Trk**). In addition, all three neurotrophins can bind to the low-affinity neurotrophin receptor p75. (Abbreviations: **BDNF**, brain-derived neurotrophic factor; **NGF**, nerve growth factor; **NT-3**, neurotrophin-3.) A fourth neurotrophin, NT-4, is not shown. (Adapted from Reichardt and Fariñas 1997.)

In contrast to the specificity of Trk receptor interactions, all neurotrophins bind the receptor p75 (Figure 46–17). In some cases, p75 works along with Trk receptors, tuning the affinity and specificity of Trks for their neurotrophin ligands and thereby contributing to neuronal survival. However, p75 leads a double life. It can also bind unprocessed precursors of neurotrophins, called proneurotrophins, and it can associate with other membrane receptors called sortilins. Binding of proneurotrophins to the p75/sortilin complex promotes neuronal death. Receptor p75 is a member of the tumor necrosis factor (TNF) receptor family and promotes cell death by activating proteases of the caspase family, which we discuss below.

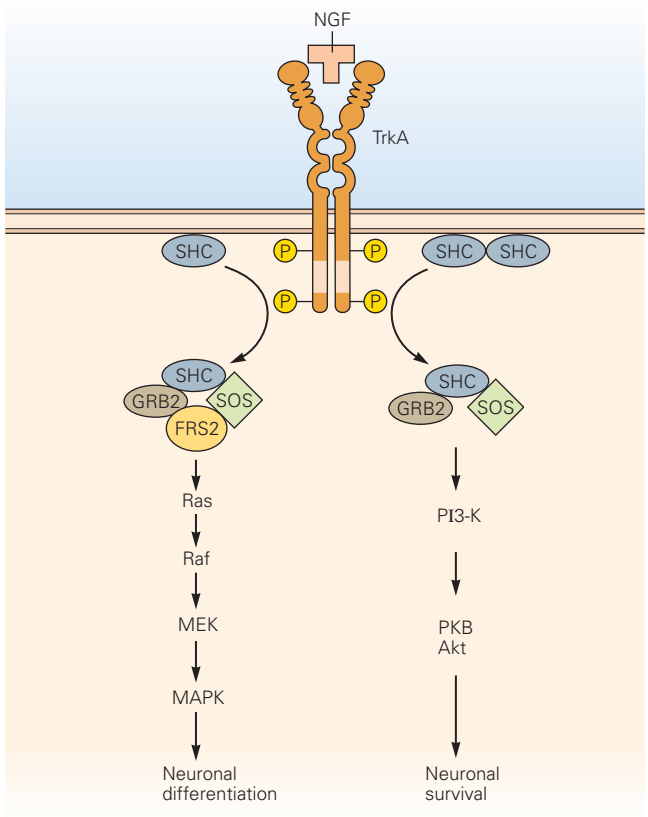

Figure 46–18 **Binding of nerve growth factor to the TrkA receptor activates alternative intracellular signaling pathways.** The binding of nerve growth factor (**NGF**) induces dimerization of the TrkA receptor, which triggers its phosphorylation at many different residues. Phosphorylation of TrkA results in the recruitment of the adaptor proteins SHC, GRB2, and SOS. The additional recruitment of FRS2 to this complex (*left*) activates a Ras kinase signaling pathway that promotes neuronal differentiation. In the absence of FRS2 (*right*), the complex activates a phosphatidylinositol-3 kinase (**PI3-K**) pathway that promotes neuronal survival. (Abbreviations: **Akt/PKB**, protein kinase B; **MAPK**, mitogen-activated protein kinase; **MEK**, mitogen-activated/ERK kinase; **P**, phosphate.)

Neurotrophin signaling is relayed from the axon terminal to the cell body of the neuron through a process that involves internalization of a complex of neurotrophin bound to Trk receptors. The retrograde transport of this complex occurs in a class of endocytotic vesicles called signaling endosomes. The transport of these vesicles brings activated Trk receptors into cellular compartments able to activate signaling pathways and transcriptional programs essential for neuronal survival, maturation, and synaptic differentiation.

The picture is more complex for neurons in the central nervous system. The survival of motor neurons, for example, is not dependent on a single neurotrophic factor. Instead, different classes of motor neurons require neurotrophins, GDNF, and interleukin-6–like proteins expressed by muscles or peripheral glial cells. The survival of these neuronal classes depends on the exposure of axons to local neurotrophic factors.

Neurotrophic Factors Suppress a Latent Cell Death Program

Neurotrophic factors were once believed to promote the survival of neural cells by stimulating their metabolism in beneficial ways, hence their name. It is now evident, however, that neurotrophic factors suppress a latent death program present in all cells of the body, including neurons.

This biochemical pathway can be considered a suicide program. Once it is activated, cells die by apoptosis (Greek, falling away): They round up, form blebs, condense their chromatin, and fragment their nuclei. Apoptotic cell deaths are distinguishable from necrosis, which typically results from acute traumatic injury and involves rapid lysis of cell membranes without activation of the cell death program.

The first clue that deprivation of neurotrophic factors kills neurons by unleashing an active biochemical program emerged from studies that assessed neuronal survival after inhibition of RNA and protein synthesis. Exposure of sympathetic neurons to protein synthesis inhibitors was found to prevent the death of sympathetic neurons triggered by removal of NGF. These results sparked the idea that neurons have the ability to synthesize proteins that are lethal and that NGF prevents their synthesis, thereby suppressing an endogenous cell death program.

Key insights into the biochemical nature of the endogenous cell death program emerged from genetic studies of the nematode *Caenorhabditis elegans*. During the development of *C. elegans*, a precise number of cells is generated and a fixed number of these cells die—the same number from embryo to embryo. The findings prompted a screen for genes that block or enhance cell death, which led to the identification of the cell death (*ced*) genes. Two of these genes, *ced-3* and *ced-4*, are needed for the death of neurons; in their absence, every one of the cells destined to die instead survives. A third gene, *ced-9*, is needed for survival and works by antagonizing the activities of *ced-3* and *ced-4* (Figure 46–19). Thus, in the absence of *ced-9*, many additional cells die, even though these deaths still depend on *ced-3* and *ced-4* activity.

The cell death pathway in *C. elegans* has been conserved in mammals. Similar proteins and pathways control the apoptotic death of central and peripheral neurons, indeed of all developing cells. The worm *ced-9* gene encodes a protein that is related to members of the mammalian Bcl-2 family, which protect

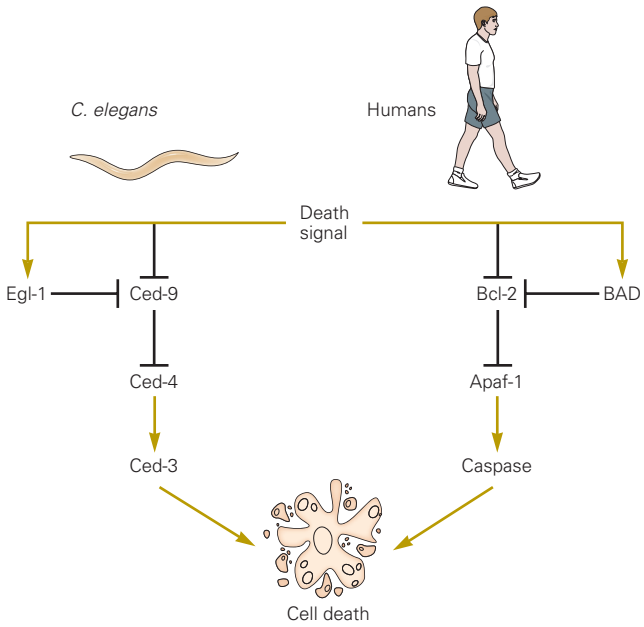

Figure 46–19 Neurons and other cells express a conserved death program. Different cellular insults trigger a genetic cascade that involves a series of death effector genes. These death genes and pathways have been conserved in the evolution of species from worms to humans. The core death pathway activates a set of proteolytic enzymes, the caspases. Caspases cleave many downstream and essential protein substrates (see Figure 46–20), resulting in the death of cells by a process termed *apoptosis*. Genetic analysis of the worm *Caenorhabditis elegans* indicates that the Ced-9 protein acts upstream and inhibits the activity of Ced-4 and Ced-3, two proteins that promote cell death. Many vertebrate homologs of Ced-9, the Bcl-2 family of proteins, have been identified. Some of these proteins, such as Bcl-2 itself, inhibit cell death, but others promote cell death by antagonizing the actions of Bcl-2. The Bcl-2 class proteins act upstream of Apaf-1 (a vertebrate homolog of Ced-4) and the caspases (vertebrate homologs of Ced-3).

lymphocytes and other cells from apoptotic death. The worm *ced-3* gene encodes a protein closely related to a class of mammalian cysteine proteases called caspases. The worm *ced-4* gene encodes a protein that is functionally related to a mammalian protein called apoptosis activating factor-1 (Apaf-1).

The mammalian apoptotic cell death pathway works in a way that resembles the worm pathway (Figure 46–20). The morphological and histochemical changes that accompany the apoptosis of mammalian cells result from the activation of caspases, which cleave specific aspartic acid residues within cellular

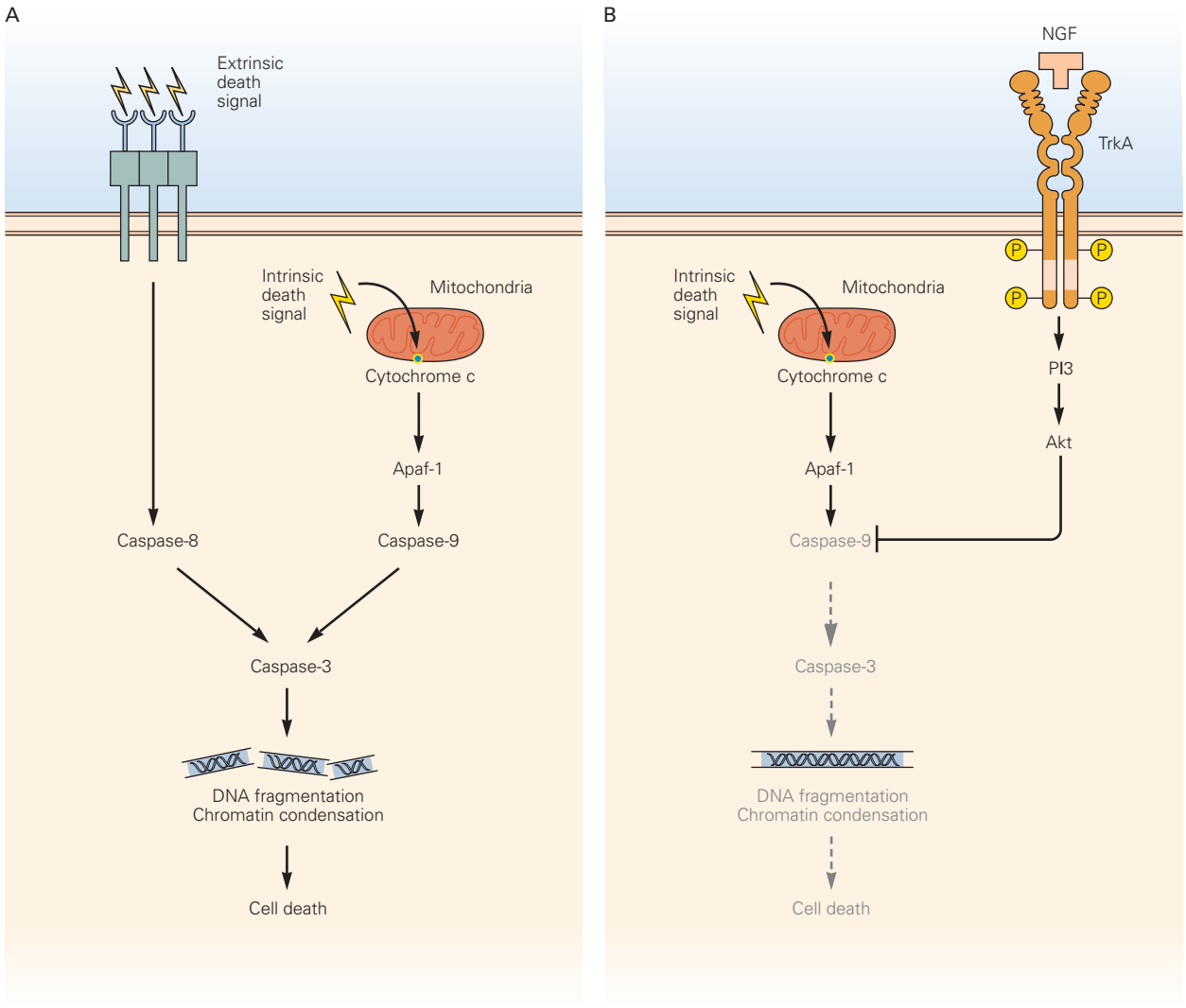

Figure 46–20 **Neurotrophic factors suppress caspase activation and cell death.** (Adapted from Jesenberger and Jentsch 2002.)

A. Two types of pathways trigger cell death: extrinsic activation of surface membrane death receptors and intrinsic activation of a mitochondrial pathway. Both pathways result in activation of caspases such as caspase-8 and caspase-9, which initiate a proteolytic cleavage cascade that converges at the level of caspase-3 activation. Cleavage of the caspase precursor removes the caspase prodomain and produces a proteolytically active enzyme conformation.

The extrinsic pathway involves activation of death receptors by ligands such as tumor necrosis factor receptor 1 or Fas/CD95. The intrinsic pathway involves stress-induced signals such as DNA damage that initiate the release of cytochrome c from the mitochondrial intermembrane space. Cytochrome c binds to Apaf-1 and recruits and activates caspase-9.

B. Binding of neurotrophins to Trk receptors recruits the PI3 kinase pathway and Akt and suppresses the cell death pathway by inhibiting caspase-9. This pathway is inhibited in developing neurons by neurotrophic factors, explaining why withdrawal of these factors leads to apoptosis. (Abbreviations: **NGF**, nerve growth factor; **P**, phosphate.)

proteins. Two classes of caspases regulate apoptotic death: the initiator and effector caspases. Initiator caspases (caspase-8, -9, and -10) cleave and activate effector caspases. Effector caspases (caspase-3 and -7) cleave other protein substrates, thus triggering the apoptotic process. Perhaps 1% of all proteins in the cell serve as substrates for effector caspases. Their cleavage contributes to neuronal apoptosis through many pathways: by activation of proteolytic cascades, inactivation of repair, DNA cleavage, mitochondrial permeabilization, and initiation of phagocytosis.

The survival of mammalian neurons depends on the balance between antiapoptotic and proapoptotic members of the Bcl-2 family of proteins. Some Bcl-2 proteins such as BAX and BAK increase the permeability of the mitochondrial outer membranes, causing the release of proapoptotic proteins such as cytochrome *c* into the cytosol. The release of cytochrome *c* induces Apaf-1 to bind and activate caspase-9, leading to the cleavage and activation of effector caspases. The binding of neurotrophic factors to their tyrosine kinase receptors is thought to lead to the phosphorylation of protein substrates that promote Bcl-2–like activities (Figure 46–20B). Thus, withdrawal of neurotrophic factors from neurons changes the balance from antiapoptotic to proapoptotic members of the Bcl-2 family, which triggers the neuron's demise.

The caspase cell death program can also be activated by many cellular insults, including DNA damage and anoxia. The activation of cell-surface death receptors such as Fas by extracellular ligands results in the activation of caspase-8 or -10 as well as the recruitment of death effector proteins such as FADD. Recruitment of an initiator caspase to the Fas-FADD complex then leads to activation of effector caspases. Because many neurodegenerative disorders result in apoptotic death, pharmacological strategies to inhibit caspases are under investigation.

Highlights

1. Stem cells near the ventricular surface of the neural tube divide to expand the neuroepithelium. Further divisions then generate the neurons and glia of the central nervous system as well as radial glia.
2. Processes of radial glia extend from the ventricular to the pial surface. Radial glial cells continue dividing to form neurons and astrocytes. In the cortex, they also serve as a scaffold on which newborn excitatory neurons migrate to appropriate layers.
3. The choice between neuronal and glial fate is determined by signals from ligands of the Delta family to receptors of the Notch family on neighboring cells. Initially, cells express both Notch and Delta. Activation of Notch leads to a glial fate, downregulating Delta, which in turn attenuates Notch activity on the neighbors, promoting their differentiation into neurons.
4. As cortical principal (excitatory) neurons migrate along radial glia, they form cortical layers in an inside-out sequence (layer 6 forms before layer 5, and so on). Disruptions of migration are among the causes of intellectual disability and epilepsy.
5. Unlike excitatory neurons, forebrain interneurons arise subcortically in ganglionic eminences and then migrate tangentially into the cortex, basal ganglia, and other forebrain structures.
6. Neural crest cells migrate from their source at the dorsal tip of the neural tube through somites and mesenchyme to form sensory and autonomic neurons and glia, as well as several nonneural cell types.
7. For principal neurons, interneurons, and peripheral neurons, intrinsic differences and cues encountered along the migratory path interact to induce expression of distinct combinations of transcription factors. The transcriptional programs then lead to diversification of the developing neurons into multiple classes and types.
8. The greater complexity of the primate, and particularly the human brain compared to those of lower mammals is due in part to a larger pool of neuronal progenitors, including a second type of radial glial cell.
9. A recent advance in the ability to study the human brain is the discovery that complex neuronal ensembles called cerebral organoids can be generated from stem cells. Although they fail to acquire characteristics of the mature cortex, they enable analysis of some aspects of early brain development and its disorders and may be useful in testing possible therapeutics.
10. The neurotransmitters that neurons use are determined as part of the transcriptional program that endows each neuronal type with its defining characteristics. However, extrinsic factors, including patterns of electric activity and hormonal milieu, can lead to transmitter switching in some cases.
11. The nervous system generates up to twice as many neurons as survive in adulthood. The excess is eliminated by a cell death program that is conserved from invertebrates to humans.

12. Trophic factors play a crucial role in determining which neurons within a population live or die. They control survival by holding the cell death program in check. In some cases, neurons appear to compete for a limited supply of neurotrophic factors; the cell death program is activated in those that lose the competition.
13. Multiple trophic factors are produced in the body, with each controlling the fate of only some neuronal types. The best-studied, called neurotrophins (nerve growth factor, brain-derived neurotrophic factor, neurotrophin-3, and neurotrophin-4), bind to and activate kinases called Trk receptors.

Joshua R. Sanes
Thomas M. Jessell

Selected Reading

Di Lullo E, Kriegstein AR. 2017. The use of brain organoids to investigate neural development and disease. Nat Rev Neurosci 18:573–584.

Gleeson JG, Walsh CA. 2000. Neuronal migration disorders: from genetic diseases to developmental mechanisms. Trends Neurosci 23:352–359.

Lodato S, Arlotta P. 2015. Generating neuronal diversity in the mammalian cerebral cortex. Annu Rev Cell Dev Biol 31:699–720.

Spitzer NC. 2017. Neurotransmitter switching in the developing and adult brain. Annu Rev Neurosci 40:1–19.

Wamsley B, Fishell G. 2017. Genetic and activity-dependent mechanisms underlying interneuron diversity. Nat Rev Neurosci 18:299–309.

Wilsch-Bräuninger M, Florio M, Huttner WB. 2016. Neocortex expansion in development and evolution—from cell biology to single genes. Curr Opin Neurobiol 39:122–132.

References

Anderson DJ. 1997. Cellular and molecular biology of neural crest cell lineage determination. Trends Genet 13:276–280.

Bandler RC, Mayer C, Fishell G. 2017. Cortical interneuron specification: the juncture of genes, time and geometry. Curr Opin Neurobiol 42:17–24.

Bershteyn M, Nowakowski TJ, Pollen AA, et al. 2017. Human iPSC-derived cerebral organoids model cellular features of lissencephaly and reveal prolonged mitosis of outer radial glia. Cell Stem Cell 20:435–449.

Costa RO, Perestrelo T, Almeida RD. 2018. PROneurotrophins and CONSequences. Mol Neurobiol 55:2934–2951.

Detwiler SR. 1936. *Neuroembryology: An Experimental Study.* New York: Macmillan.

Doupe AJ, Landis SC, Patterson PH. 1985. Environmental influences in the development of neural crest derivatives: glucocorticoids, growth factors, and chromaffin cell plasticity. J Neurosci 5:2119–2142.

Duband JL. 2006. Neural crest delamination and migration: integrating regulations of cell interactions, locomotion, survival and fate. Adv Exp Med Biol 589:45–77.

Florio M, Borrell V, Huttner WB. 2017. Human-specific genomic signatures of neocortical expansion. Curr Opin Neurobiol 42:33–44.

Furshpan EJ, Potter DD, Landis SC. 1982. On the transmitter repertoire of sympathetic neurons in culture. Harvey Lect 76:149–191.

Giandomenico SL, Lancaster MA. 2017. Probing human brain evolution and development in organoids. Curr Opin Cell Biol 44:36–43.

Gray GE, Sanes JR. 1992. Lineage of radial glia in the chicken optic tectum. Development 114:271–283.

Guo J, Anton ES. 2014. Decision making during interneuron migration in the developing cerebral cortex. Trends Cell Biol 24:342–351.

Hamburger V. 1975. Cell death in the development of the lateral motor column of the chick embryo. J Comp Neurol 160:535–546.

Hamburger V, Levi-Montalcini R. 1949. Proliferation differentiation and degeneration in the spinal ganglia of the chick embryo under normal and experimental conditions. J Exp Zool 111:457–501.

Hoshino M. 2006. Molecular machinery governing GABAergic neuron specification in the cerebellum. Cerebellum 5: 193–198.

Howard MJ. 2005. Mechanisms and perspectives on differentiation of autonomic neurons. Dev Biol 277:271–286.

Jesenberger V, Jentsch S. 2002. Deadly encounter: ubiquitin meets apoptosis. Nat Rev Mol Cell Biol 3:112–121.

Lancaster MA, Renner M, Martin CA, et al. 2013. Cerebral organoids model human brain development and microcephaly. Nature 501:373–379.

Landis SC. 1980. Developmental changes in the neurotransmitter properties of dissociated sympathetic neurons: a cytochemical study of the effects of medium. Dev Biol 77:349–361.

Le Douarin NM. 1998. Cell line segregation during peripheral nervous system ontogeny. Science 231:1515–1522.

Nowakowski TJ, Pollen AA, Sandoval-Espinosa C, Kriegstein AR. 2016. Transformation of the radial glia scaffold demarcates two stages of human cerebral cortex development. Neuron 91:1219–1227.

Olson EC, Walsh CA. 2002. Smooth, rough and upside-down neocortical development. Curr Opin Genet Dev 12:320–327.

Oppenheim RW. 1981. Neuronal cell death and some related regressive phenomena during neurogenesis: a selective

historical review and progress report. In: WM Cowan (ed). *Studies in Developmental Neurobiology: Essays in Honor of Viktor Hamburger,* pp. 74–133. New York: Oxford Univ. Press.

Purves D, Lichtman JW. 1985. *Principles of Neural Development*. Sunderland, MA: Sinauer.

Qian X, Goderie SK, Shen Q, Stern JH, Temple S. 1998. Intrinsic programs of patterned cell lineages in isolated vertebrate CNS ventricular zone cells. Development 125:3143–3152.

Reichardt LF. 2006. Neurotrophin-regulated signaling pathways. Philos Trans R Soc Lond B Biol Sci 361:1545–1564.

Reichardt LF, Fariñas I. 1997. Neurotrophic factors and their receptors: roles in neuronal development and function. In: MW Cowan, TM Jessell, L Zipursky (eds). *Molecular Approaches to Neural Development*, pp. 220–263. New York: Oxford Univ. Press.

Sánchez-Alcañiz JA, Haege S, Mueller W. 2011. Cxcr7 controls neuronal migration by regulating chemokine responsiveness. Neuron 69:77–90.

Shah NM, Groves AK, Anderson DJ. 1996. Alternative neural crest cell fates are instructively promoted by TGF beta superfamily members. Cell 85:331–343.

Sun Y, Nadal-Vicens M, Misono S, et al. 2001. Neurogenin promotes neurogenesis and inhibits glial differentiation by independent mechanisms. Cell 104:365–376.

Wang Y, Li G, Stanco A, et al. 2011. CXCR4 and CXCR7 have distinct functions in regulating interneuron migration. Neuron 69:61–76.

Zeng H, Sanes JR. 2017. Neuronal cell-type classification: challenges, opportunities and the path forward. Nat Rev Neurosci 18:530–546.

47

The Growth and Guidance of Axons

In the two preceding chapters, we saw how neurons are generated in appropriate numbers, at correct times, and in the right places. These early developmental steps set the stage for later events that direct neurons to form functional connections with target cells. To form connections, neurons have to extend long processes—axons and dendrites—which permit connectivity with postsynaptic cells and synaptic input from other neurons. In this chapter, we examine how neurons elaborate axons and dendrites and how axons are guided to their targets.

We begin the chapter by discussing how certain neuronal processes become axons and others dendrites. We then describe the growing axon, which may have to travel a long distance and ignore many inappropriate neuronal partners before terminating in just the right region and recognizing its correct synaptic targets. We consider the strategies by which the axon overcomes these challenges. Finally, we illustrate general features of axonal guidance by describing the development of two well-studied axonal pathways: one that conveys visual information from the retina to the brain and another that conveys cutaneous sensory information from the spinal cord to the brain.

Differences Between Axons and Dendrites Emerge Early in Development

The processes of neurons vary enormously in their length, thickness, branching pattern, and molecular architecture. Nonetheless, most neuronal processes fit into one of two functional categories: axons and dendrites. More than a century ago, Santiago Ramón y Cajal hypothesized that this distinction underlies the ability of neurons to transmit information in a particular direction, an idea he formalized as the law of dynamic polarization. Cajal wrote that "the transmission of the nerve impulse is always from the dendritic branches and the cell body to the axon." In the decades before electrophysiological methods were up to the task, this law provided a means of analyzing neural circuits histologically. Although exceptions have been found, Ramón y Cajal's law remains a basic principle

that relates structure to function in the nervous system and highlights the importance of knowing how neurons acquire their polarized form.

Progress in understanding how neuronal polarization occurs comes in large part from studies of neurons taken from the rodent brain and grown in tissue culture. Hippocampal neurons grown in isolation develop processes reminiscent of those seen in vivo: a single, long, cylindrical axon and several shorter, tapered dendrites (Figure 47–1A). As cytoskeletal and synaptic proteins are differentially targeted to these components, axons and dendrites acquire distinctive molecular profiles. For example, a particular form of the Tau protein is localized in axons and the MAP2 protein in dendrites (Figure 47–1B)

Cultured neurons are especially useful for developmental studies because they initially show no obvious sign of polarization and acquire their specialized features gradually in a stereotyped sequence of cellular steps. This sequence begins with extension of several short processes, each equivalent to the others. Soon thereafter, one process is established as an axon and the remaining processes acquire dendritic features (Figure 47–1A).

How does this occur? Cytoskeletal proteins that maintain elongated processes and drive growth are central to this process. If the actin filaments in an early neurite are destabilized, the cytoskeleton becomes reconfigured in a way that commits the neurite to becoming the axon; secondarily, the remaining neurites react by becoming dendrites. If the nascent axon is removed, one of the remaining neurites quickly assumes an axonal character. This sequence suggests that axonal specification is a key event in neuronal polarization and that signals from newly formed axons both suppress the generation of additional axons and promote dendrite formation.

The nature of the axonally derived signal that represses other axons is not known, but some insight into signals that control cytoskeletal arrangements has come from the study of a group of proteins encoded by the *Par* complex genes. As first shown in the nematode worm *Caenorhabditis elegans*, Par proteins are involved in diverse aspects of cytoskeletal reorganization, including the polarization of neuronal processes. Mammalian forebrain neurons lacking *Par3*, *Par4*, *Par6*, or relatives of *Par1* grow multiple processes that are intermediate in length between axons and dendrites and bear markers of both processes (Figure 47–1B).

Although neurons grown in culture are similar to those in the brain, they are deprived of key extrinsic cues and signals. Cultured neurons become randomly arranged with respect to each other, whereas in many regions of the developing brain, neurons line up in rows, with their dendrites pointing in the same direction (Figure 47–2A). As the neurons migrate to their destinations (Chapter 46), axons and dendrites often grow as extensions of their trailing and leading processes, respectively. This difference in vivo and in vitro implies that extrinsic signals regulate the polarization machinery. In the developing brain, the local release of semaphorins and other axonal guidance factors, discussed later in the chapter, may help to orient dendrites (Figure 47–2C). The job of the Par protein complex is to link these extracellular signals to the cellular machinery that rearranges the cytoskeleton, a process achieved in part through the regulation of proteins that modify actin or tubulin function. In fact, both the Tau protein in axons and the MAP2 protein in dendrites associate with and affect microtubules. Cytoskeletal differences also contribute to other mechanisms that amplify distinctions between axons and dendrites, such as polarized trafficking of molecules and generation of a specialized initial segment in axons.

If local signals are needed to polarize neurons in the brain, how is polarity established in the uniform environment of a tissue culture? One possible explanation is that minor variations in the intensity of signaling within a neuron, or in signals from its immediate environment, will activate Par proteins in one small domain of the neuron, triggering the nearest cell process to become an axon. If, by happenstance, one process grows slightly faster than its neighbors or encounters an environment that speeds neurite extension (Figure 47–2B), its chances of becoming an axon increase markedly. Presumably, this proto-axonal process emits signals that decrease the chance of other processes following suit, forcing them to become dendrites.

Dendrites Are Patterned by Intrinsic and Extrinsic Factors

Once polarization occurs, dendrites grow and mature, acquiring the structural features that distinguish them from axons. Nascent dendrites form branched arbors, with their branches generally being more numerous and closer to the cell body than those of axons. In addition, small protrusions called spines extend from the distal branches of many dendrites. Finally, some dendritic branches are retracted or "pruned" to give the arbor its final and definitive shape (Figure 47–3).

Although the core features of dendrite formation are common to many neurons, there is striking variation in their number, shape, and branching pattern among neuronal types. Indeed, the shape of dendritic arbors is one of the main ways in which neurons can

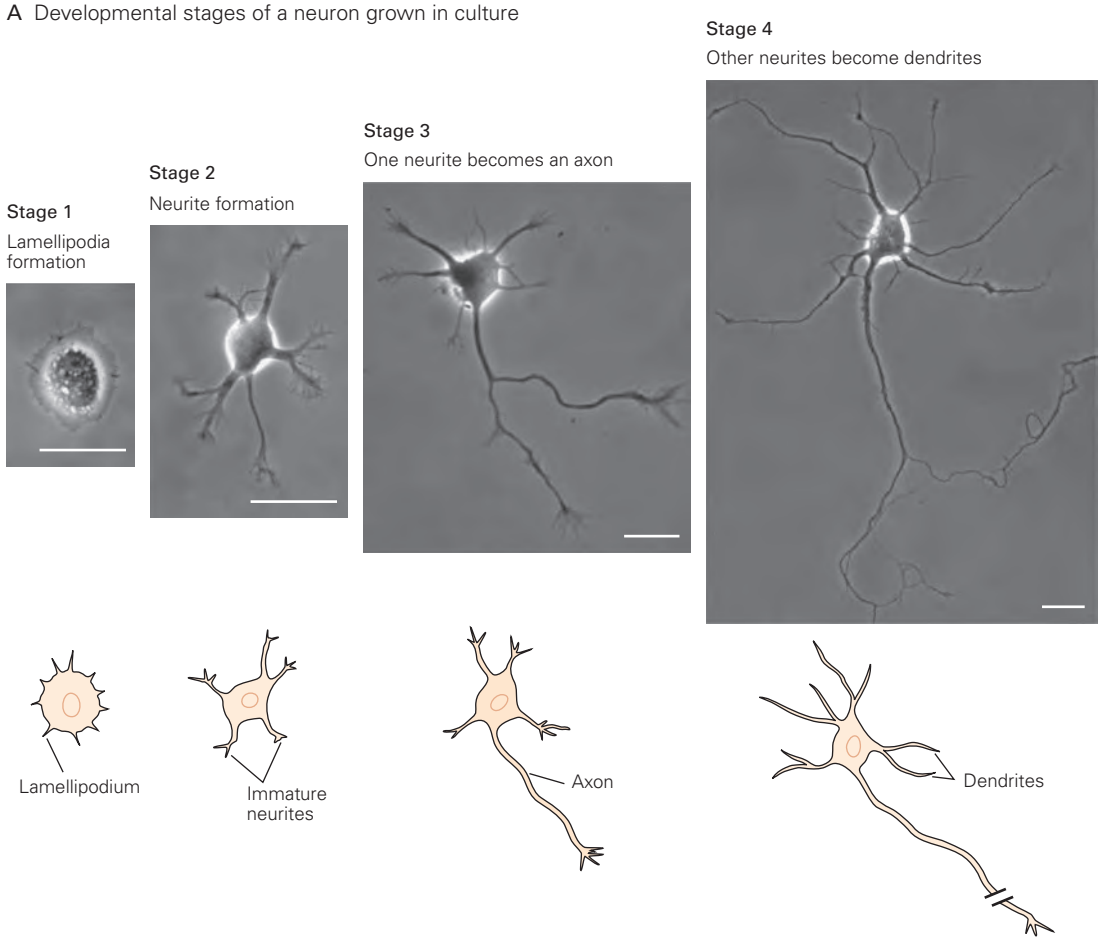

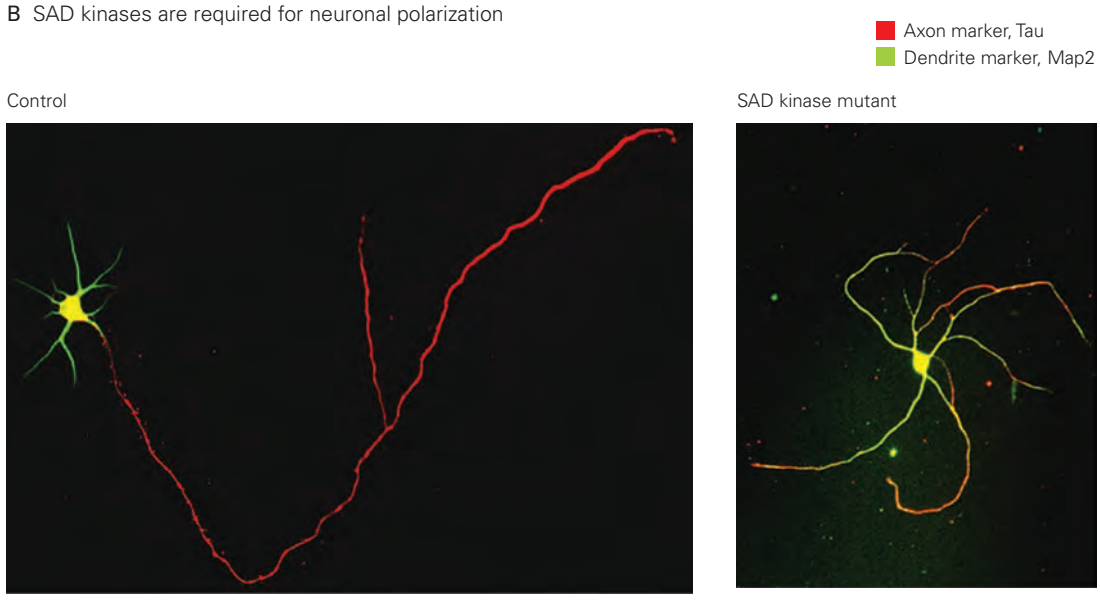

Figure 47–1 The differentiation of axons and dendrites marks the emergence of neuronal polarity.

A. Four stages in the polarization of a hippocampal neuron grown in tissue culture. (Adapted, with permission, from Kaech and Banker 2006. Copyright © 2007 Springer Nature.)

B. Hippocampal neurons grown in culture possess multiple short, thick dendrites that are enriched in the microtubule-associated protein MAP2. They also possess a single long axon that is marked by a dephosphorylated form of the microtubule-associated protein tau (*left*). A cultured neuron isolated from a mutant mouse lacks expression of a *Par* family gene (SAD kinase). The neuron generates neurites that express both tau and MAP2, markers of axons and dendrites, respectively. The length and diameter of these neurites are intermediate in size between those of axons and dendrites (*right*). (Reproduced, with permission, from Kishi et al. 2005.)

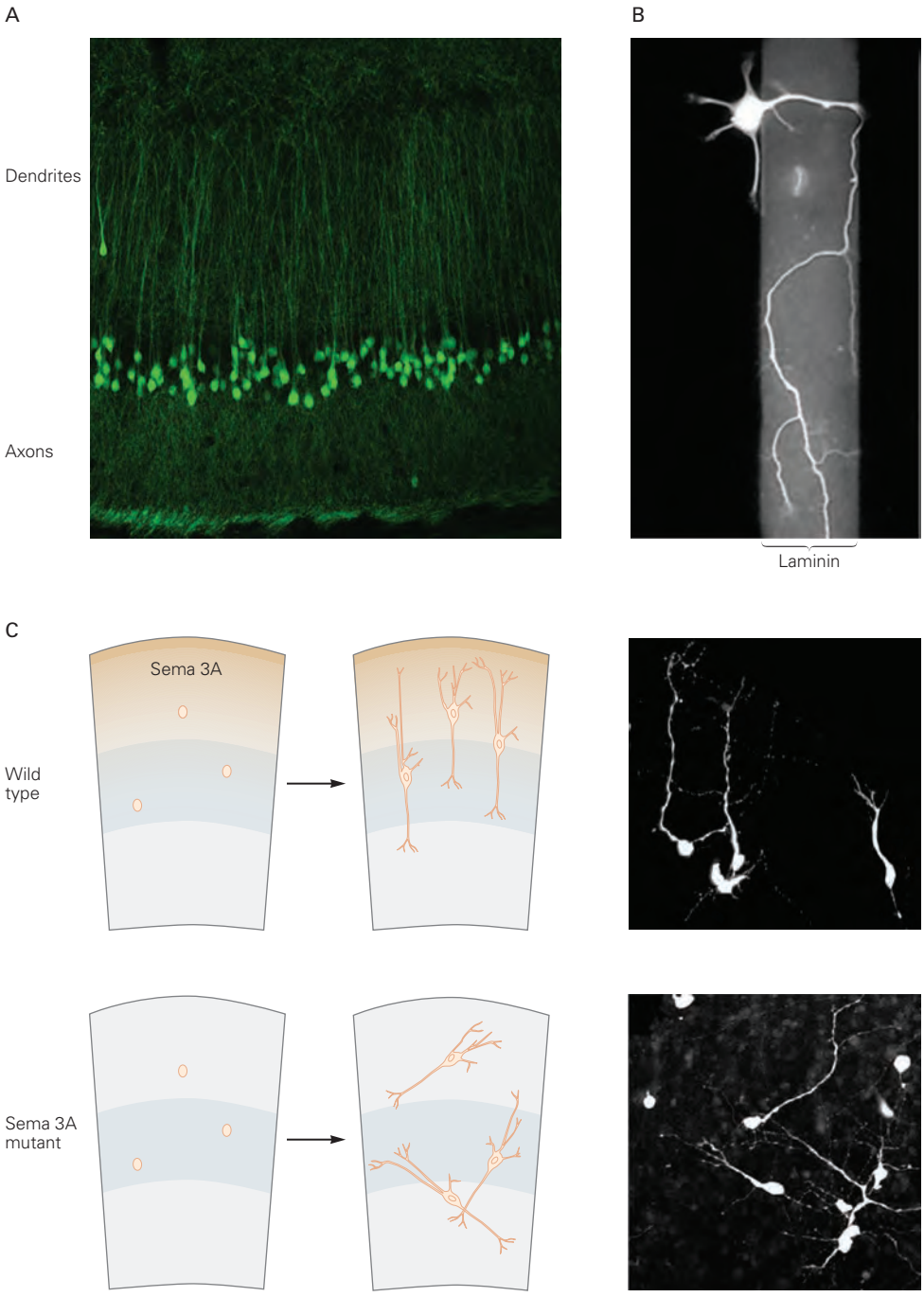

Figure 47–2 Extracellular factors determine whether neuronal processes become axons or dendrites.

A. Cortical pyramidal neurons in vivo display a common axonal and dendritic orientation.

B. Neurons growing on laminin acquire polarity. When a cortical neuron extends a process from a less attractive substrate onto laminin, the process grows faster and usually becomes an axon. (Image reproduced, with permission, from Paul Letourneau.)

C. In the developing neocortex, semaphorin-3A (**Sema 3A**) is secreted by cells near the pial surface. Semaphorin-3A is an attractant for growing dendrites, helping to establish neuronal polarity and orientation. The parallel orientation of cortical pyramidal neurons is disrupted in mutant mice lacking functional semaphorin-3A. (Reproduced, with permission, from Polleux, Morrow, and Ghosh 2000. Copyright © 2000 Springer Nature.)

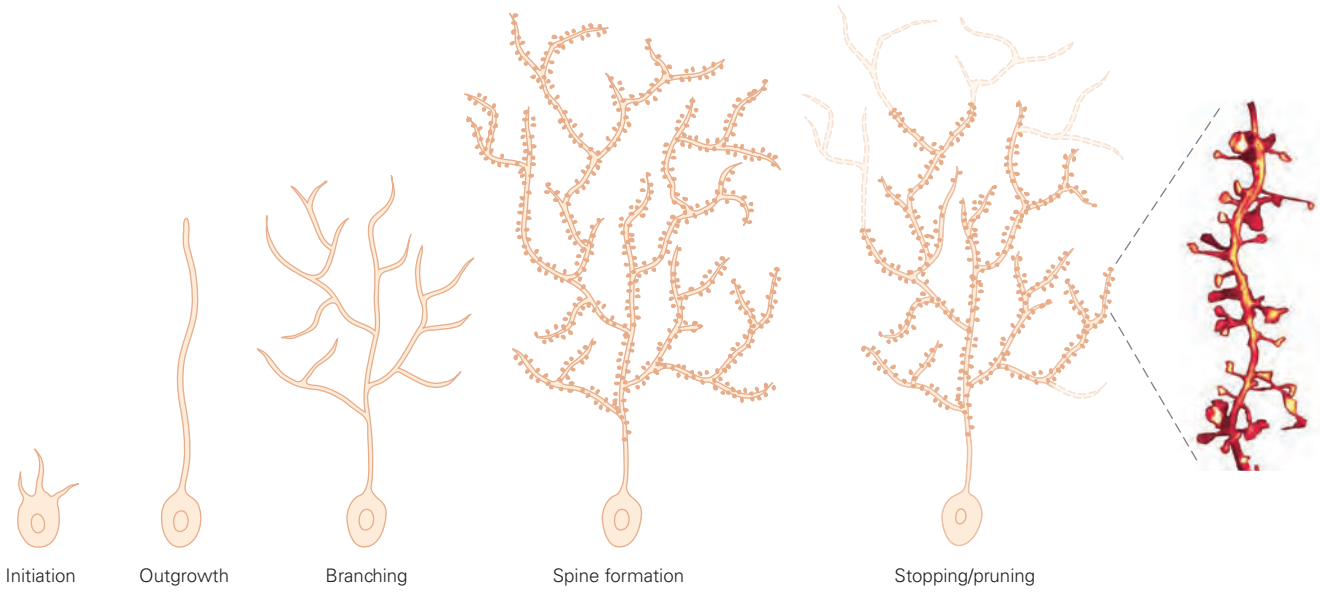

Figure 47–3 Dendritic branching develops in a series of steps. The outgrowth of dendrites involves the formation of elaborate branches from which spines develop. Certain branches and spines are later pruned to achieve the mature pattern of dendrite arborization. (Image of spines at right reproduced, with permission, from Stefan W. Hell.)

be classified. Cerebellar Purkinje cells can be distinguished from granule cells, spinal motor neurons, and hippocampal pyramidal neurons simply by looking at the pattern of their dendrites. These variations are critical for the distinct functions of different neuronal types. For example, the size of a dendritic arbor and the density of its branches are main determinants of the number of synapses it receives.

How is dendritic pattern established? Neurons must have intrinsic information about their shape because the patterns in tissue culture are strikingly reminiscent of those in vivo (Figure 47–4). The transcriptional programs that specify neuronal subtype (Chapter 46) presumably also encode information about neuronal shape. In both invertebrates and vertebrates, some transcription factors are selectively expressed by specific neuronal types and appear to be devoted to controlling the size, shape, and complexity of their dendritic arbors. They do so by coordinating the expression of downstream genes, including those encoding components of the cytoskeletal apparatus and membrane proteins that mediate interactions with neighboring cells.

A second mechanism for establishing the pattern of dendritic arbors is the recognition of one dendrite by others of the same cell. In some neurons, dendrites are spaced evenly with respect to each other, an arrangement that allows them to sample inputs efficiently without major gaps or clumps (Figure 47–5A). In many cases, this process, called self-avoidance, occurs through a mechanism in which branches belonging to the same neuron repel each other. Several cell-surface adhesion molecules have now been found that mediate self-avoidance by interacting in a way that results in repulsion (Figure 47–5D). Although it seems counterintuitive that an adhesive interaction between adjacent membranes would lead to repulsion rather than attachment, the consequences of most intercellular interactions are determined by the signaling they initiate rather than by adhesion per se, as we will see later in this chapter.

The dendrites of neighboring neurons also provide cues. In many cases, the dendrites of a particular neuron type cover a surface with minimal overlap, a spacing pattern called *tiling* (Figure 47–5B). The tiling of dendrites is conceptually related to self-avoidance, but in tiling, the inhibitory dendritic interactions are among neurons of a particular type, whereas in self-avoidance, they are among sibling dendrites of a single neuron. Tiling allows each class of neuron to receive information from the entire surface or area it innervates. Tiling of a region by the dendrites of one class of neuron also avoids the confusion that could arise if the dendrites of many different neurons occupied the same area.

A particularly interesting situation is one in which dendrites engage in self-avoidance but synapse on the dendrites of other cells of the same type. In this situation, dendrites face the challenging task of distinguishing nominally identical dendrites from dendrites of

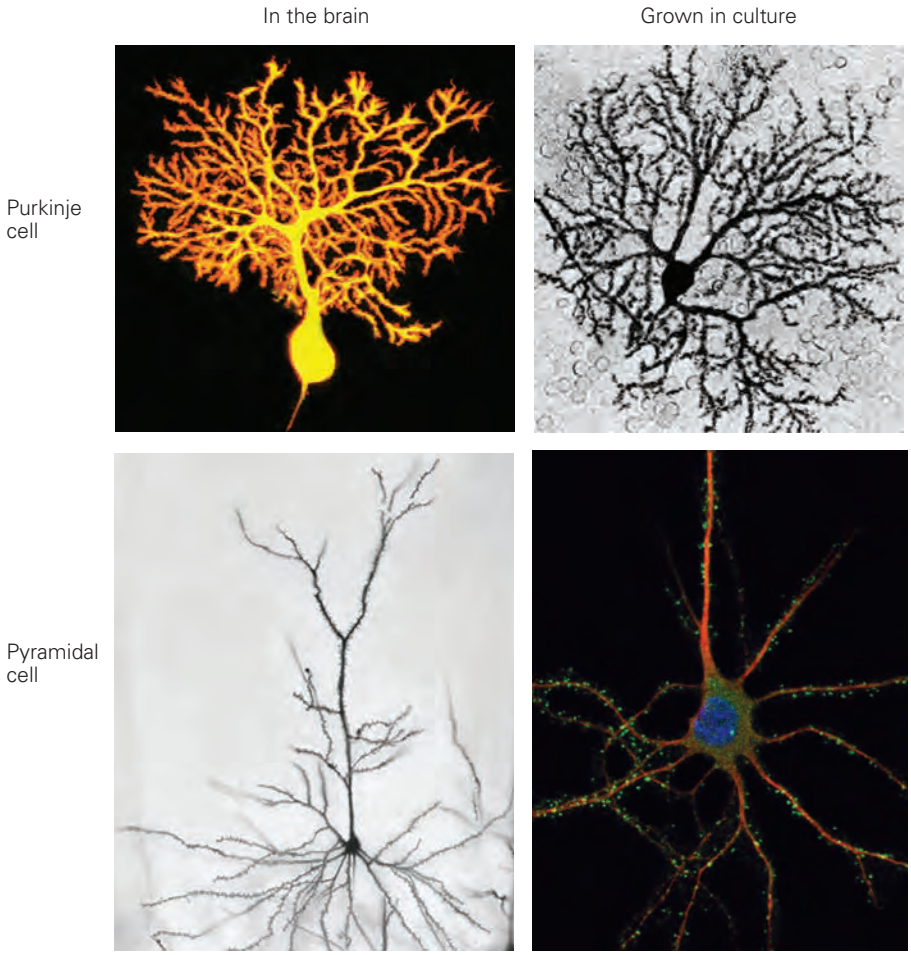

Figure 47–4 The morphologies of neurons are preserved in dissociated cell culture. Cerebellar Purkinje neurons and hippocampal pyramidal neurons have distinctive patterns of dendritic branching. These basic patterns are recapitulated when these two classes of neurons are isolated and grown in dissociated cell culture. (Image upper left: Dr. David Becker; upper right reproduced, with permission, from Yoshio Hirabayashi; lower left reproduced, with permission, from Terry E. Robinson; lower right reproduced, with permission, from Kelsey Martin.)

nominally identical cells (Figure 47–5C). Two groups of molecules have been identified that mediate this self-/non–self-discrimination: clustered protocadherins in mammals and DS-CAMs in *Drosophila*. Although they are unrelated structurally, they share several features (Figure 47–5D).

First, both are encoded by large, complex genes that generate large numbers of isoforms. *Drosophila* Dscam1 encodes around 38,000 distinct proteins through alternative splicing, and the clustered protocadherins encode around 60 proteins that can assemble into thousands of distinct multimers. Second, nearly all of the isoforms bind homophilically; for example, protocadherin γa1 on the surface of one dendrite binds well to protocadherin γa1 on a neighboring membrane, but poorly if at all to other isoforms. Third, in ways that remain incompletely understood, each neuron within a population expresses a random subset of all possible Dscam1 or protocadherin isoforms. Given the large number of isoforms, it is unlikely that individual neurons express identical sets of isoforms on their cell surface. The upshot is that dendrites of each neuron in a population bind homophilically to sibling dendrites, leading to repulsion and self-avoidance, whereas they bind poorly to dendrites of neighboring neurons, enabling other recognition systems to foster synaptogenesis.

Together, the mechanisms we have described, and many others, establish an overall arborization pattern through a combination of intrinsic and extracellular mechanisms. For dendrites, the extrinsic patterning signals determine neuronal morphology. For axons, which we consider next, the signals guide the axons to their targets.

The Growth Cone Is a Sensory Transducer and a Motor Structure

Once an axon forms, it begins to grow toward its synaptic target. The key neuronal element responsible for axonal growth is a specialized structure at the tip of the axon called the *growth cone.* Both axons and dendrites

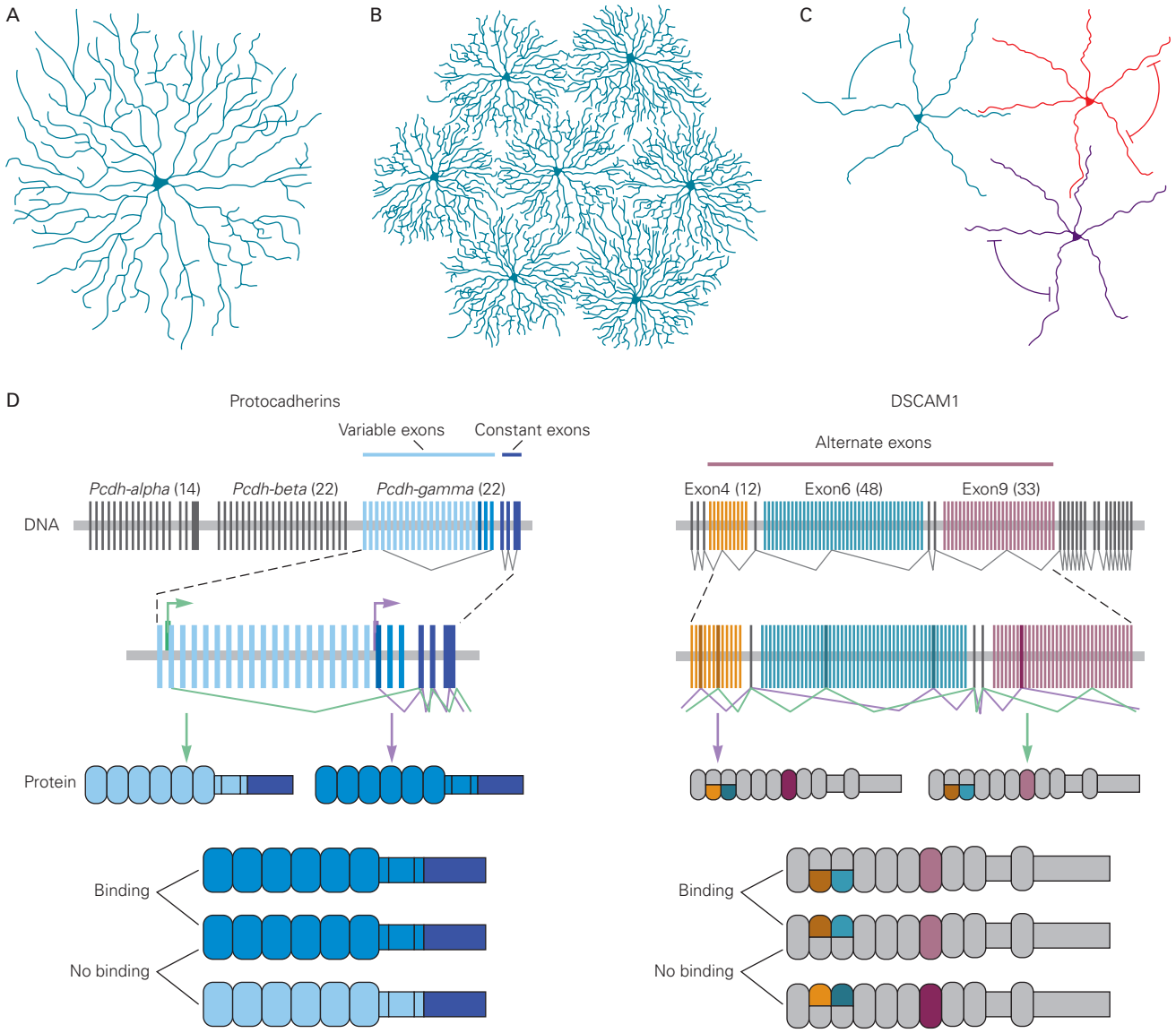

Figure 47–5 Interactions among dendritic branches pattern dendritic arbors.

A. Self-avoidance among sibling dendrites leads to even spacing of branches, minimizing gaps and clumps. In retinal starburst amacrine cells, self-avoidance fails when gamma protocadherins are lost.

B. Tiling of dendrites is conceptually similar to self-avoidance but applies to groups of neurons. It ensures that neighboring neurons of a single type cover territory efficiently.

C. Self-/non-self–discrimination allows sibling dendrites to avoid each other while interacting freely with dendrites of other neurons of the same type.

D. Generation of numerous adhesion molecules from a single genomic complex by promoter choice at the mouse clustered protocadherin (**Pcdh**) locus (*left*) and by alternative splicing at the *Drosophila* DSCAM1 locus (*right*).

use growth cones for elongation, but those linked to axons have been studied more intensively.

Ramón y Cajal discovered the growth cone and had the key insight that it was responsible for axonal pathfinding. With static images alone for inspiration (Figure 47–6A), he envisioned the growth cone to be "endowed with exquisite chemical sensitivity, rapid ameboid movements and a certain motive force, thanks to which it is able to proceed forward and overcome obstacles met in its way . . . until it reaches its destination."

Many studies over the past century have confirmed Ramón y Cajal's intuition. We now know

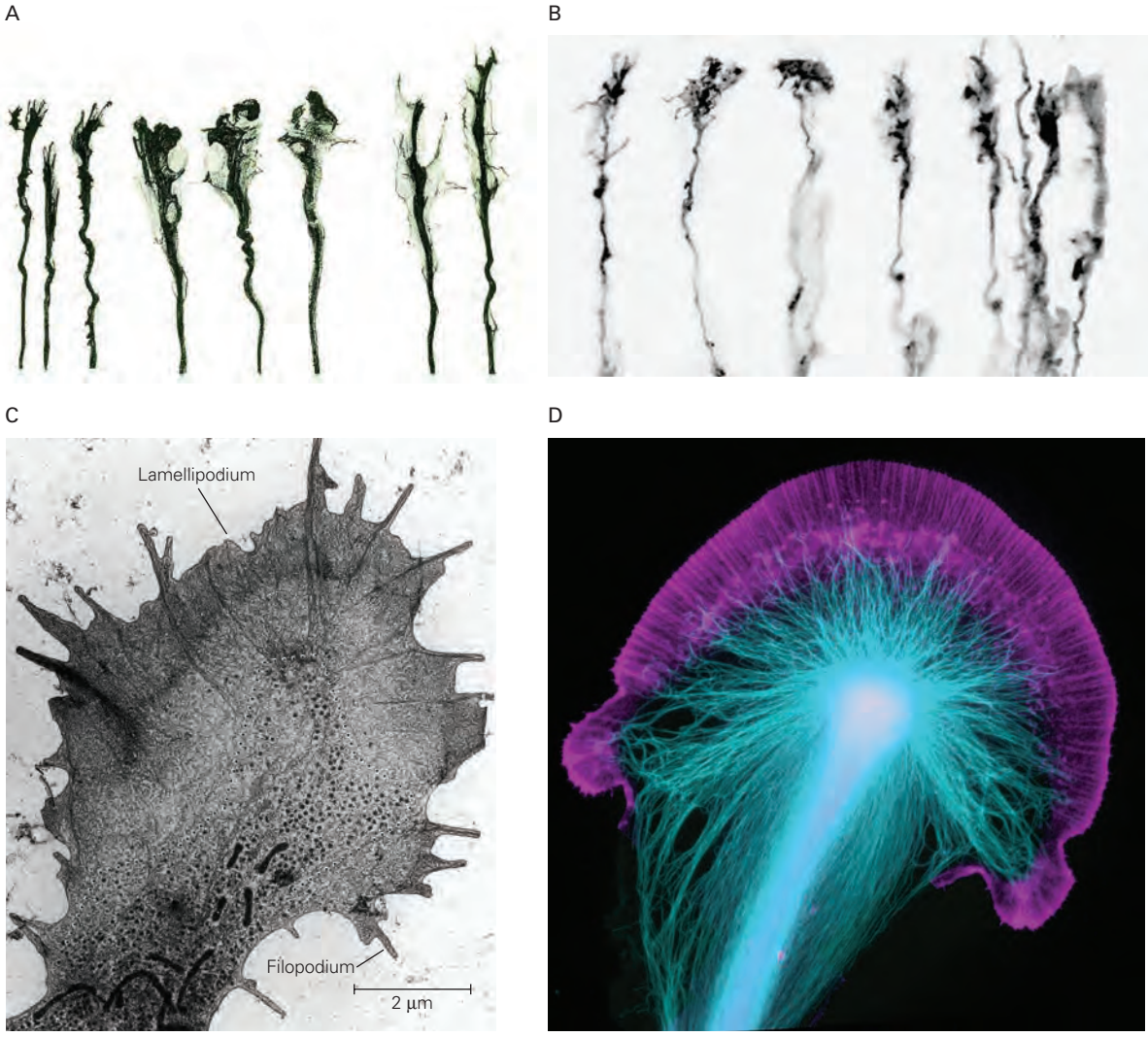

Figure 47–6 Neuronal growth cones.

A. Drawings of growth cones by Santiago Ramón y Cajal, who discovered these cellular structures and inferred their function.

B. Growth cones visualized in dye-labeled retinal ganglion neurons in the mouse. Note the similarities with Cajal's drawings. (Reproduced, with permission, from Carol Mason and Pierre Godement.)

C. The three main domains of the growth cone—filopodia, lamellipodia, and a central core—are shown by whole-mount scanning electron microscopy. (Reproduced, with permission, from Bridgman and Dailey 1989. Permission conveyed through Copyright Clearance Center, Inc.)

D. The growth cone of a neuron from *Aplysia* in which actin and tubulin have been visualized. Actin (**purple**) is concentrated in lamellipodia and filopodia, whereas tubulin and microtubules (**aquamarine**) are concentrated in the central core. (Reproduced, with permission, from Paul Forscher and Dylan Burnette.)

that the growth cone is both a sensory structure that receives directional cues from the environment and a motor structure whose activity drives axon elongation. Ramón y Cajal also pondered "what mysterious forces precede the appearance of these processes . . . promote their growth and ramification . . . and finally establish those protoplasmic kisses . . . which seem to constitute the final ecstasy of an epic love story." In more modern and prosaic terms, we now know that the growth cone guides the axon by transducing positive and negative cues into signals that regulate the cytoskeleton, thereby determining the course and rate of axonal growth toward its targets, where it will form synapses.

Growth cones have three main compartments. Their *central core* is rich in microtubules, mitochondria, and other organelles. Long slender extensions called

filopodia project from the body of the growth cone. Between the filopodia lie *lamellipodia*, which are also motile and give the growth cone its characteristic ruffled appearance (Figure 47–6C,D).

Growth cones sense environmental signals through their filopodia: rod-like, actin-rich, membrane-limited structures that are highly motile. Their surface membranes bear receptors for the molecules that serve as directional cues for the axon. Their length—tens of micrometers in some cases—permits the filopodia to sample environments far in advance of the central core of the growth core. Their rapid movements permit them to compile a detailed inventory of the environment, and their flexibility permits them to navigate around cells and other obstacles.

When filopodia encounter signals in the environment, the growth cone is stimulated to advance, retract, or turn. Several motors power these orienting behaviors. One source of power is the movement of actin along myosin, an interaction similar to the one that powers the contraction of skeletal muscle fibers, although the actin and myosin of neurons are different from those in muscle. The assembly of actin monomers into polymeric filaments also contributes a propulsive force for filopodial extension. As the actin filaments are constantly depolymerized at the base of filopodia, the balance of polymerization and depolymerization enables the filopodia to move forward without becoming longer. Depolymerization slows during periods of growth cone advance, leading to greater net forward motion. The movement of membranes along the substrate provides yet another source of forward motion.

The contribution of each type of molecular motor to the advance of the growth cone is likely to vary from one situation to another. Nevertheless, the final step involves the flow of microtubules from the central core of the growth cone into the newly extended tip, thus moving the growth cone ahead and leaving in its wake a new segment of axon. New lamellipodia and filopodia form in the advancing growth cone and the cycle repeats (Figure 47–7).

Accurate pathfinding can occur only if the growth cone's motor action is linked to its sensory function. Therefore, it is crucial that the recognition proteins on the filopodia are signal-inducing receptors and not merely binding moieties that mediate adhesion. The binding of a ligand to its receptor affects growth in diverse ways. In some cases, it engages the cytoskeleton directly, through the intracellular domain of receptors (Figure 47–7). Integrin receptors couple to actin in growth cones when they bind molecules associated with the surface of adjoining cells or the extracellular matrix, thereby influencing motility.

Of equal if not greater importance is the ability of ligand binding to stimulate the formation, accumulation, and even breakdown of soluble intracellular molecules that function as second messengers. These second messengers affect the organization of the cytoskeleton, and in this way regulate the direction and rate of movement of the growth cone.

One important second messenger is calcium. The calcium concentration in growth cones is regulated by the activation of receptors on filopodia, and this affects the organization of the cytoskeleton, which in turn modulates motility. Growth cone motility is optimal within a narrow range of calcium concentrations, called a *set point*. Activation of filopodia on one side of the growth cone leads to a concentration gradient of calcium across the growth cone, providing a possible basis for changes in the direction of growth.

Other second messengers that link receptors and motor molecules include cyclic nucleotides, which modulate the activity of enzymes such as protein kinases, protein phosphatases, and rho-family guanosine triphosphatases (GTPases). In turn, these messengers and enzymes regulate the activity of proteins that regulate the polymerization and depolymerization of actin filaments, thereby promoting or inhibiting axonal extension.

The critical role of intracellular signals in growth cone motility and orientation can be demonstrated using embryonic neurons grown in culture. Application of growth factors to one side of a growth cone activates receptors locally and leads to extension and turning of the growth cone toward the source of the signal. In essence, the factor attracts the growth cone. Yet when cyclic adenosine monophosphate (cAMP) levels in the neuron are decreased, the same stimulus acts as a repellent and the growth cone turns away from the signal (Figure 47–8A). Other repulsive factors can become attractive when levels of the second messenger cyclic guanosine 3′,5′-monophosphate (cGMP) are raised.

Recently, another mechanism for coupling guidance molecules to growth cone behavior has come to light. It was long thought that all neuronal protein synthesis occurs in the cell body, but we now know that growth cones (as well as some dendrites) contain the machinery for protein synthesis, including a subset of messenger RNAs. Initial evidence that these molecules play an important role came from experiments in which axons were severed from their parent cell body. The growth cones continued to advance for a few hours; they could be stimulated to turn toward or away from local depots of guidance molecules, and these behaviors were abolished by inhibitors of protein

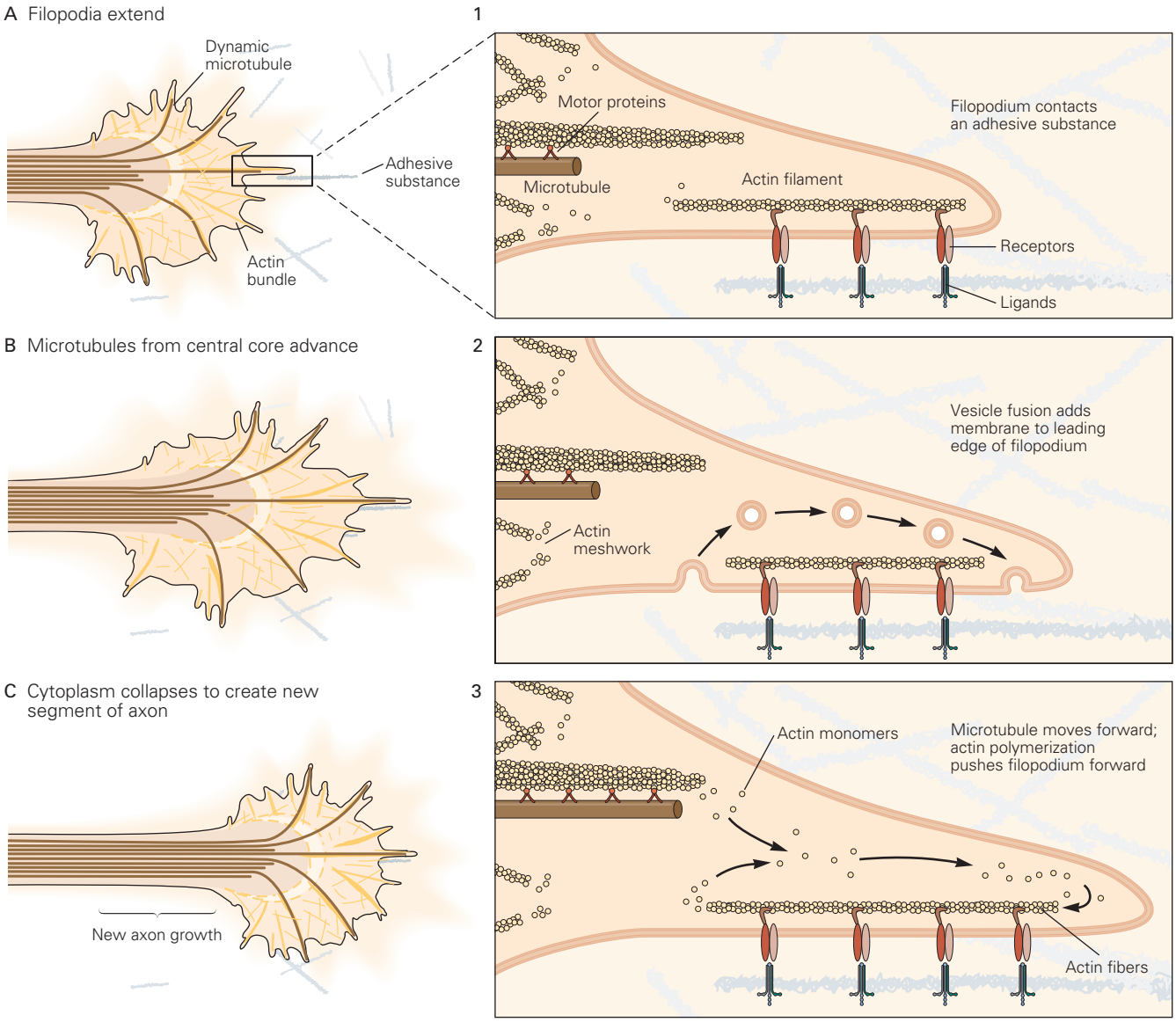

Figure 47–7 **The growth cone advances under the control of cellular motors.** (Adapted, with permission, from Heidemann 1996. Copyright © 1996 Academic Press Inc.)

A. A filopodium contacts an adhesive cue and contracts, thus pulling the growth cone forward (**1**). Actin filaments assemble at the leading edge of a filopodium and disassemble at the trailing edge, interacting with myosin along the way (**2**). Actin polymerization pushes the filopodium forward (**3**). Force generated by the retrograde flow of actin pushes the filopodium forward. Exocytosis adds membrane to the leading edge of the filopodium and supplies new adhesion receptors to maintain traction. Membrane is recovered at the back of the filopodium. The actin polymer is linked to adhesion molecules on the plasma membrane.

B. The combined action of these motors creates an actin-depleted space that is filled by the advance of microtubules from the central core.

C. Individual microtubules condense to form a thick bundle, and the cytoplasm collapses around them to create a new segment of axonal shaft.

synthesis. The local protein synthesis is regulated by second messengers produced in response to activation of guidance receptors on the growth cones (Figure 47–8). This mechanism leads to synthesis of new motor proteins precisely when and where they are needed. Thus, the growth cone has many strategies and mechanisms for integrating molecular signals to direct the axon in specific directions.

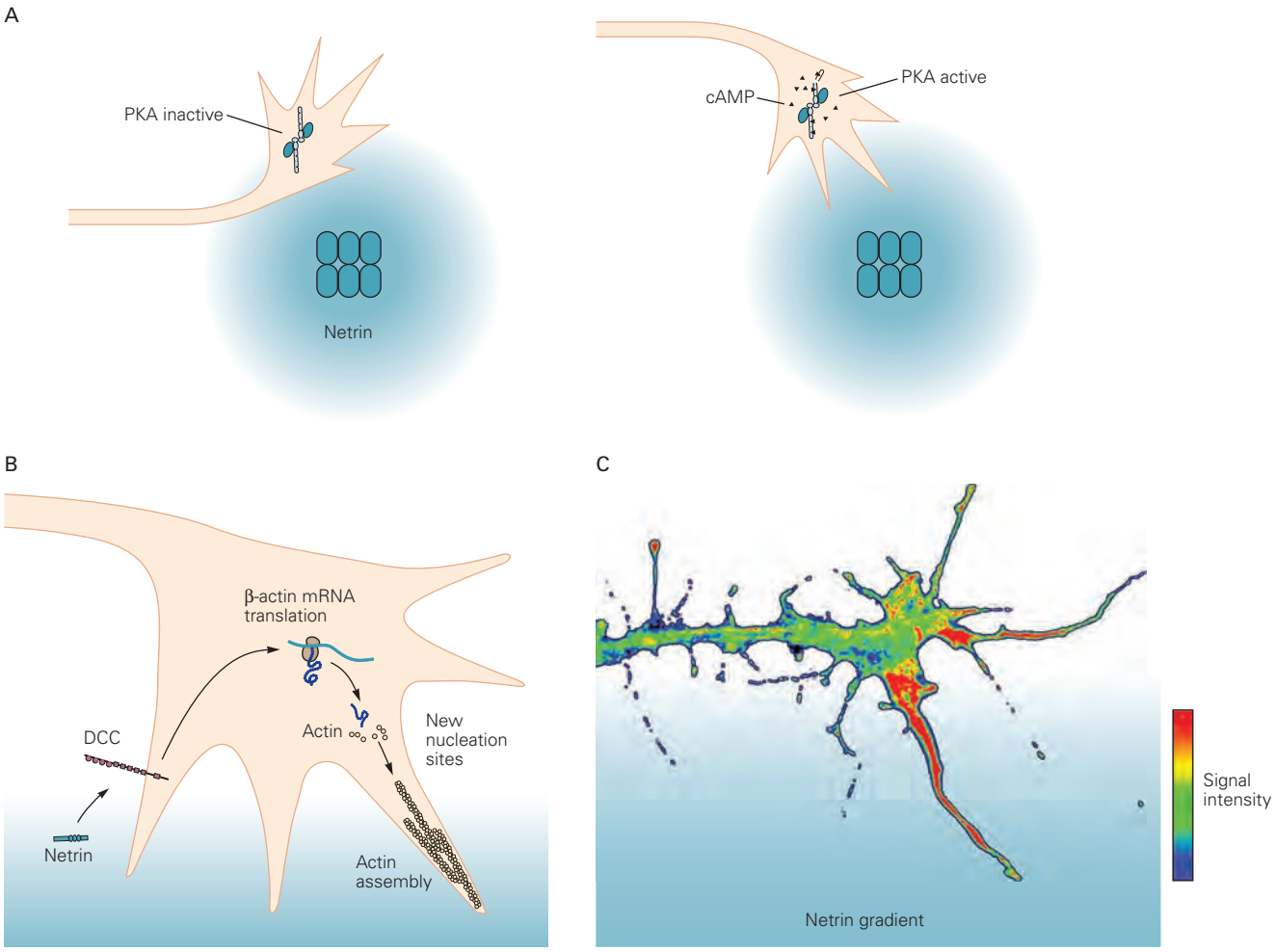

Figure 47–8 Changes in the level of intracellular regulatory proteins can determine whether the same extrinsic cue attracts or repels the growth cone.

A. The state of protein kinase A (**PKA**) activity can alter the growth cone's response to an extracellular orienting factor, in this instance, the protein netrin. When PKA activity and intracellular cyclic adenosine monophosphate (**cAMP**) levels are low, the growth cone is repelled by netrin. When PKA activity is high, the resulting elevation in intracellular cAMP causes the growth cone to be attracted to a local source of netrin. (Adapted, with permission, from Ming et al. 1997.)

B. Netrin activation of growth cone receptors (deleted in colon cancer, **DCC**) leads to local synthesis of actin, which leads to turning.

C. Immunohistochemical analysis of a growth cone showing local synthesis of actin in response to local application of netrin. (Reproduced, with permission, from Christine Holt. Adapted, with permission, from Leung et al. 2006.)

Molecular Cues Guide Axons to Their Targets

For much of the 20th century, a debate raged between advocates of two very different views of how growth cones navigate embryonic terrains to reach their targets. A molecular view of axonal guidance was first articulated at the turn of the 20th century by the physiologist J. N. Langley. But by the 1930s, many eminent biologists, including Paul Weiss, believed that axonal outgrowth was essentially random and that appropriate connections persisted largely because of productive, matching patterns of electrical activity in the axon and its target cell.

In our molecular age, Weiss's ideas may seem simplistic, but they were not unreasonable at the time. In tissue culture, axons grow preferentially along mechanical discontinuities (scratches and bumps on a cover slip), and embryonic nerve trunks often align themselves with solid supports (blood vessels or cartilage). It seemed logical to Weiss that mechanical guidance, called *stereotropism*, could account for axonal patterning. Today, we are quite comfortable with the

idea that electrical signals can be used to change the way current flows in a computer without the need to resolder connections. Likewise, patterns of activity and experience can strengthen or weaken neural connections without requiring the formation of new axonal pathways. Then why not consider that congruent activity, called *resonance* by Weiss, is involved in establishing appropriate connections?

Today, few scientists believe that stereotaxis or resonance is a crucial force in initial patterning of neuronal circuits. The tipping point that shifted opinion in favor of the molecular view was an experiment performed with frogs and other amphibia in the 1940s by Roger Sperry (ironically, a student of Weiss). Sperry manipulated the information carried from the eye to the brain by the axons of retinal ganglion cells. These axons terminate in their target areas—the lateral geniculate body in the thalamus and the superior colliculus (called optic tectum in lower vertebrates) in the midbrain—in such a way that an orderly retinotopic map of the visual field is created.

Because of the optics of the eye, the visual image on the retina is an inversion of the visual field. The retinal ganglion cells reinvert the image by the pattern in which their axons terminate in the optic tectum, the main visual center in the brain of frogs (Figure 47–9A). If the optic nerve is cut, the animal is blinded. In lower vertebrates, cut retinal axons can reestablish projections to the tectum, whereupon vision is restored. This is not the case in mammals, as we will discuss in Chapter 50.

Sperry's key experiment was to sever the optic nerve in a frog and then rotate the eye in its socket by 180° before regeneration of the nerve. Remarkably, the frog exhibited orderly responses to visual input, but the behavior was wrong. When the frog was presented with a fly on the ground, it jumped up, and when offered a fly above its head, it struck downward (Figure 47–9B). Importantly, the animal never learned to correct its mistakes. Sperry suggested—and later verified with anatomical and physiological methods—that the retinal axons had reinnervated their original tectal targets, even though these connections provided the brain with erroneous spatial information that led to aberrant behavior. The inference of these experiments was that recognition between axons and their targets relied on molecular matching rather than functional validation and refinement of random connections.

But Weiss's ideas are by no means obsolete. Indeed, we now recognize that the activity of neural circuits can play a crucial role in shaping connectivity. The current view is that molecular matching predominates during embryonic development and that activity and experience modify circuits after they have formed. In this chapter and the next, we describe the molecular cues that guide the formation of neural connections, and then in Chapter 49, we examine the role of activity and experience in the fine-tuning of synaptic connections.

Sperry's conjecture, often called the *chemospecificity hypothesis*, prompted developmental neurobiologists to search for axonal and synaptic "recognition molecules." Success was limited for the first few decades, in part because these molecules are present in small amounts and on discrete subsets of neurons and there were no effective methods for isolating rare molecules from complex tissues. Eventually advances in biochemical and molecular-biological methods made this task more feasible, and many proteins involved in the guidance of axons to their targets have now been discovered. These proteins typically consist of paired ligands and receptors: The ligands are presented by cells along the pathway an axon follows and the receptors by the growth cone itself.

In the most general terms, guidance cues can be presented on cell surfaces, in the extracellular matrix, or in soluble form. As described above (Figure 47–8), they interact with receptors embedded in the growth cone membrane to promote or inhibit outgrowth of the axon. Most receptors have an extracellular domain that selectively binds the cognate ligand and an intracellular domain that couples to the cytoskeleton, either directly or through intermediates such as second messengers. The ligands can speed or slow growth. Ligands presented to one side of the growth cone can result in local activation or inhibition, leading to turning. In this way, the local distribution of environmental cues determines the pathway of the advancing growth cone.

As a result of these recent discoveries, axon guidance—a process that appeared mysterious years ago—can now be viewed as the orderly consequence of protein–protein interactions that instruct the growth cone to grow, turn, branch, or stop (Figures 47–10, 11). This limited set of instructions is sufficient, when presented with spatial precision, to choreograph growth cone behaviors with exquisite subtlety. Axonal guidance can therefore be explained by describing how and where ligands are presented and how the growth cone integrates this information to generate an orderly response. In the rest of the chapter, we illustrate lessons learned by describing the journeys of two types of axons: those of retinal ganglion neurons and those of a particular class of sensory relay neurons in the spinal cord.

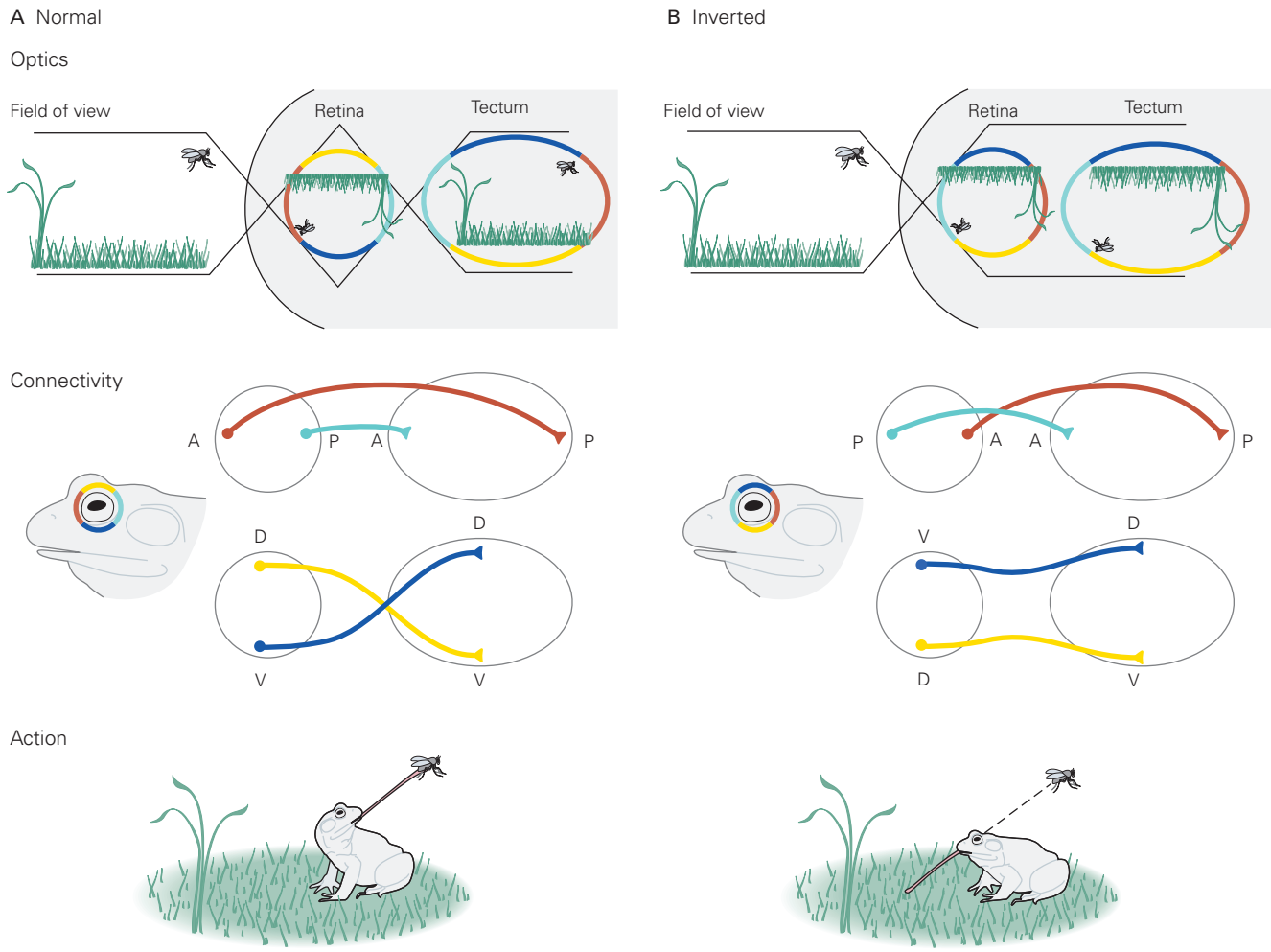

Figure 47–9 Roger Sperry's classical experiments on regeneration in the visual system provided evidence for chemoaffinity in the wiring of connections.

A. In the visual system of the frog, the lens projects an inverted visual image onto the retina and the optic nerve then transfers the image, with an additional inversion, to the optic tectum. The spatial arrangement of retinal inputs to the tectum allows for this transfer. Neurons in the anterior retina project axons to the posterior tectum, while neurons in the posterior retina project to the anterior tectum. Similarly, neurons in the dorsal retina project to the ventral tectum, and neurons in the ventral retina project to the dorsal tectum. As a result, visually guided behaviors (here catching a fly) are accurate. (Abbreviations: **A**, anterior; **D**, dorsal; **P**, posterior; **V**, ventral.)

B. If the optic nerve is cut and the eye is surgically rotated in its socket before the nerve regenerates, visually guided behavior is aberrant. When a fly is presented overhead, the frog perceives it as below, and vice versa. The inversion of behavioral reflexes results from the connection of regenerating retinal axons to their original targets, even though these connections now transfer an inverted, inappropriate map of the world into the brain.

The Growth of Retinal Ganglion Axons Is Oriented in a Series of Discrete Steps

Sperry's experiment implied the existence of axon guidance cues but did not reveal where they were or how they worked. For a time, one prominent view was that recognition occurred mostly at or near the target and that mechanical forces or long-range chemotactic factors sufficed to get axons to the vicinity of the target.

We now know that axons reach distant targets in a series of discrete steps, making frequent decisions at closely spaced intervals along their route. To illustrate this point, we shall trace in greater detail the path that Sperry was trying to understand, that of a retinal axon growing to the optic tectum.

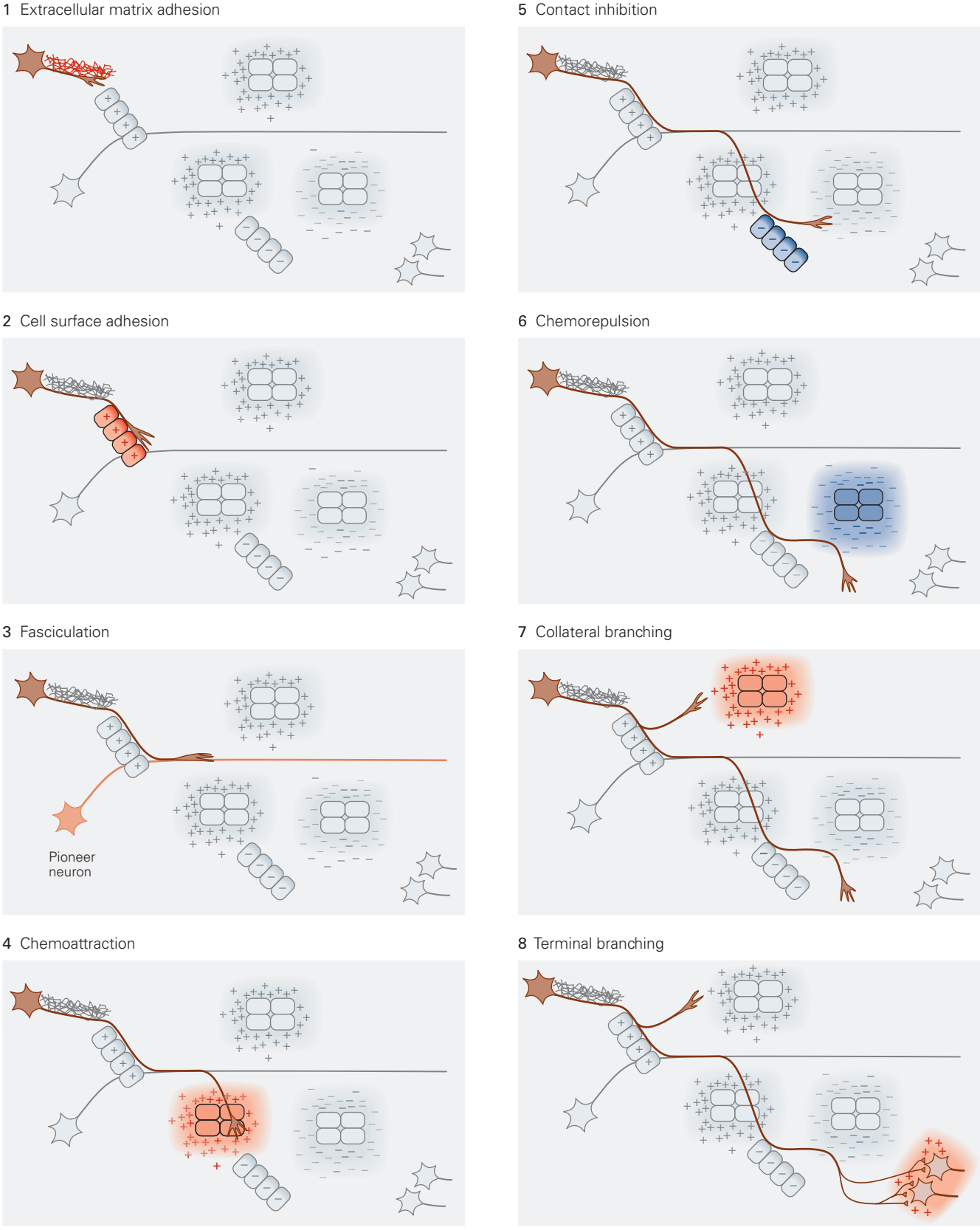

Figure 47–10 Extracellular cues use a variety of mechanisms to guide growth cones. The axon can interact with growth-promoting molecules in the extracellular matrix (**1**). It can interact with adhesive cell-surface molecules on neural cells (**2**). The growing axon can encounter another axon from a "pioneer" neuron and track along it, a process termed *fasciculation* (**3**). Soluble chemical signals can attract the growing axon to its cellular source (**4**). Intermediate target cells that express cell-surface repellent cues can cause the axon to turn away (**5**). Soluble chemical signals can repel the growing axon (**6**). Extracellular signals also lead to formation of collaterals from axon shafts (**7**) or branching of the growing axon (**8**).

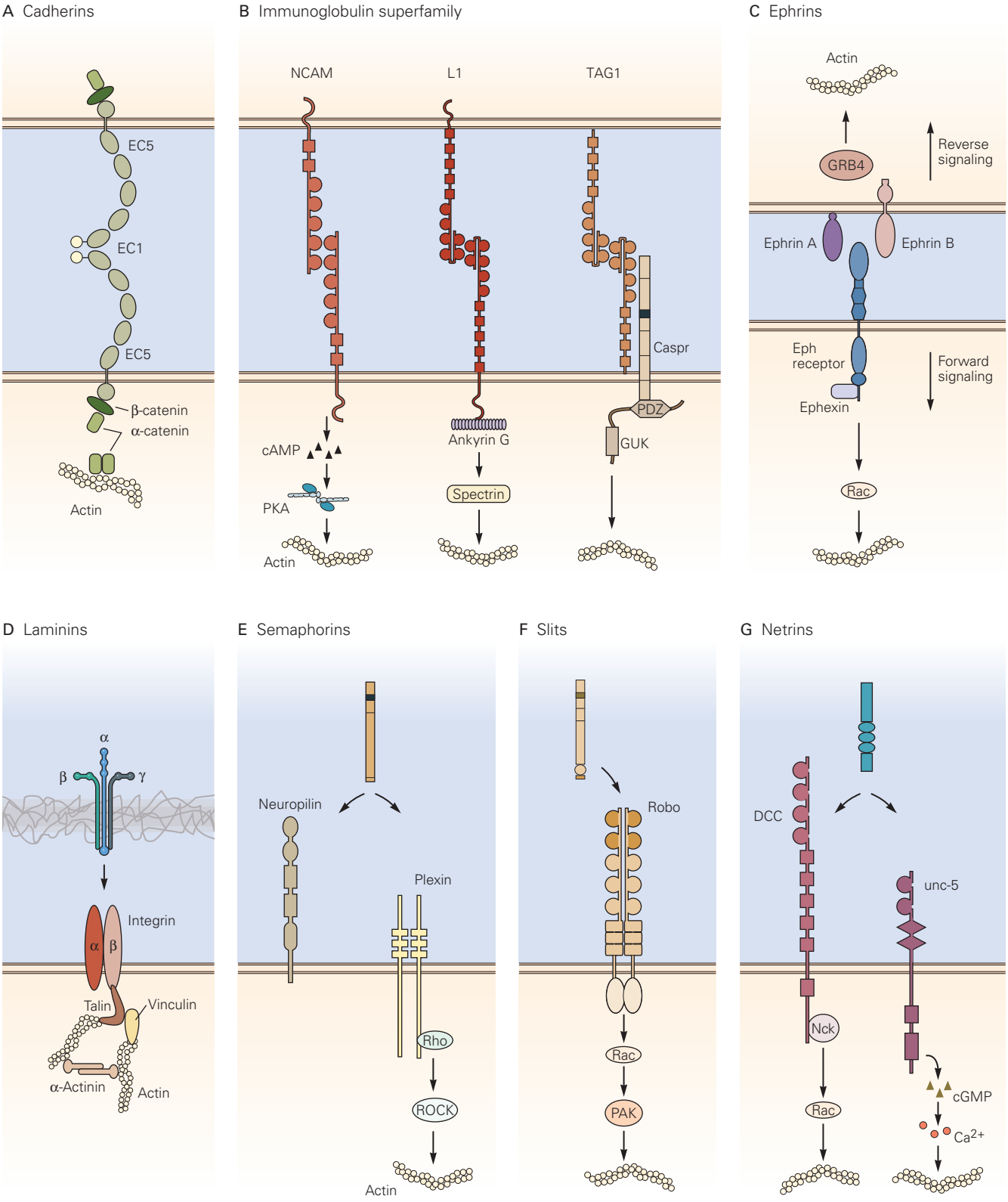
A Cadherins
EC5
EC1
EC5
β-catenin
α-catenin
Actin
B Immunoglobulin superfamily
NCAM
L1
TAG1
Caspr
PDZ
GUK
cAMP
PKA
Actin
Ankyrin G
Spectrin
Actin
C Ephrins
Actin
GRB4
Reverse signaling
Ephrin A
Ephrin B
Eph receptor
Ephexin
Forward signaling
Rac
D Laminins
α
β
γ
Integrin
α
β
Talin
Vinculin
α-Actinin
Actin
E Semaphorins
Neuropilin
Plexin
Rho
ROCK
Actin
F Slits
Robo
Rac
PAK
G Netrins
DCC
unc-5
Nck
Rac
cGMP
Ca2+

Growth Cones Diverge at the Optic Chiasm

The first task of the axon of a retinal ganglion cell is to leave the retina. As it enters the optic fiber layer, it extends along the basal lamina and glial end-feet at the retina's edge. The growth of the axon is oriented from the outset, indicating that it can read directional cues in the environment. As it approaches the center of the retina, it comes under the influence of attractants emanating from the optic nerve head (the junction of the optic nerve with the retina proper), which guide it into the optic stalk. It then follows the optic nerve toward the brain (Figure 47–12).

The first axons to travel this route follow the cells of the optic stalk, the rudiment of the neural tube that connects the retina to the diencephalon from which it arose. These "pioneer" axons then serve as scaffolds for later-arriving axons, which are able to extend accurately simply by following their predecessors (see "fasciculation" in Figure 47–10). Once they reach the optic chiasm, however, the retinal axons must make a choice. Axons that arise from neurons in the nasal hemiretina of each eye cross the chiasm and proceed to the opposite side of the brain, whereas those from the temporal half are deflected as they reach the chiasm and so stay on the same side of the brain (Figure 47–13A).

This divergence in trajectory reflects the differential responses of axons from the nasal and temporal hemiretinas to guidance cues presented by midline chiasm cells. Some retinal axons contact and traverse chiasm cells, whereas others are inhibited by these cells and deflected away, thus remaining on the ipsilateral side. One of the key molecules presented by chiasm cells is a membrane-bound repellent of the ephrin-B family (Figure 47–13B), which also figures in later steps of retinal ganglion cell axon guidance.

The fraction of temporal retinal axons that project ipsilaterally varies among species: few in lower vertebrates, some in rodents, and many in humans. These differences reflect placement of the eyes. In many animals, the eyes point to the sides and monitor different parts of the visual world, so that information from the two eyes need not be combined. In humans, both eyes look forward and sample largely overlapping regions of the visual world, so coordination of visual input is essential.

After crossing the optic chiasm, retinal axons assemble in the optic tract along the ventral surface of the diencephalon. Axons then leave the tract at different points. In most vertebrate species, the tectum of the midbrain (called the superior colliculus in mammals) is the major target of retinal axons, but a small number of axons project to the lateral geniculate nucleus of the thalamus. In humans, however, most axons project to the lateral geniculate, a sizable number reach the

Figure 47–11 (Opposite) Diverse molecular families control the growth and guidance of developing axons.

A. A large family of classical cadherins promote cell and axonal adhesion, primarily through homophilic interactions between cadherin molecules on adjacent neurons. Adhesive interactions are mediated through interactions of the extracellular EC1 domains. Cadherins transduce adhesive interactions though their cytoplasmic interactions with catenins, which link cadherins to the actin cytoskeleton.

B. A diverse array of immunoglobulin superfamily proteins are expressed in the nervous system and mediate adhesive interactions. The three examples shown here, NCAM, L1, and TAG1, can bind both homophilically and heterophilically to promote axon outgrowth and adhesion. These proteins contain both immunoglobulin domains (**circles**) and fibronectin type III domains (**squares**). Homophilic interactions typically involve amino terminal immunoglobulin domains. Different immunoglobulin adhesion molecules interact with the cytoskeleton via diverse cytoplasmic mediators, only a few of which are shown here.

C. Different ephrin proteins bind to Eph class tyrosine kinase receptors. Class A ephrins are linked to the surface membrane through a glycosyl phosphatidylinositol tether, whereas class B ephrins are transmembrane proteins. Class A ephrins typically bind class A Eph kinases, and class B ephrins typically bind class B Eph kinases. Forward Eph signaling usually elicits repellant or inhibitory responses in receptive cells, whereas reverse ephrin signaling can elicit adhesive or inhibitory responses. Ephrin-Eph signaling involves many different cytoplasmic mediators.

D. Laminin proteins are components of the extracellular matrix and promote cell adhesion and axon extension through interactions with integrin receptors. Integrins mediate adhesion and axon growth through interactions with the cytoskeleton via many intermediary proteins.

E. Semaphorin proteins can promote or inhibit axonal growth through interaction with a diverse array of plexin and neuropilin receptors, which transduce signals via Rho class GTPases and downstream kinases.

F. Slit proteins typically mediate repellant responses through interaction with Robo class receptors, which influence axonal growth via intermediary GTPases such as Rac.

G. The secreted or extracellular matrix–associated netrin proteins mediate both chemoattractant and chemorepellent responses. Attractant responses are mediated through interaction with **DCC** (deleted in colorectal cancer) receptors, whereas repellent responses involve interactions with DCC and unc-5 coreceptors. Netrin receptors signal via GTPases and cyclic guanosine monophosphate (**cGMP**) cascades.

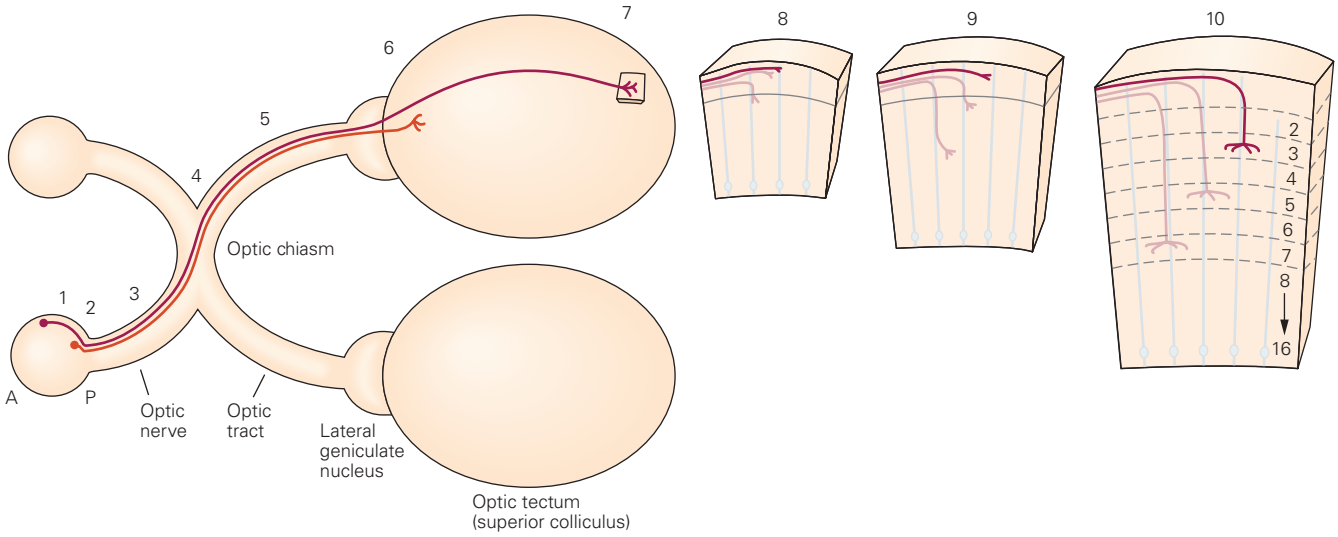

Figure 47–12 The axons of retinal ganglion cells grow to the optic tectum in discrete steps. Two neurons that carry information from the nasal half of the retina are shown. The axon of one crosses the optic chiasm to reach the contralateral optic tectum. The axon of the other also crosses the optic chiasm but projects to the lateral geniculate nucleus. The numbers indicate important landmarks on the axon's journey. The growing axon is directed toward the optic nerve head (the junction of the nerve with the retina) (**1**), enters into the optic nerve (**2**), extends through the optic nerve (**3**), swerves to remain ipsilateral (not shown) or crosses to the contralateral side at the optic chiasm (**4**), extends through the optic tract (**5**), enters into the optic tectum or lateral geniculate nucleus (not shown) (**6**), navigates to an appropriate rostrocaudal and dorsoventral position on the tectum (**7**), turns to enter the neuropil (descends in chicks as shown here; ascends in mammals) (**8**), stops at an appropriate layer where a rudimentary terminal arbor is formed (**9**), and finally is remodeled (**10**). (Abbreviations: **A**, anterior; **P**, posterior).

colliculus, and small numbers project to the pulvinar, superchiasmatic nucleus, and pretectal nuclei. Within these targets, different retinal axons project to different regions. As Sperry showed, the retinal axons form a precise retinotopic map on the tectal surface. Similar maps form in other areas innervated by retinal axons such as the lateral geniculate nucleus.

Having reached an appropriate position within the tectum, retinal axons need to find an appropriate synaptic partner. To achieve this last leg of their journey, retinal axons turn and dive into the tectal neuropil (Figure 47–12), descending (or, in mammals, ascending) along the surface of radial glial cells, which provide a scaffold for radial axonal growth. Although radial glial cells span the entire extent of the neuroepithelium, each retinal axon confines its synaptic terminals to a single layer. The dendrites of many postsynaptic cells extend through multiple layers and form synapses along their entire length, but retinal inputs are restricted to a small fraction of the target neuron's dendritic tree. These organizational features imply that layer-specific cues arrest axonal elongation and trigger arborization.

The problem of long-distance axon navigation is therefore solved by dividing the journey into short segments in which intermediate targets guide the axons along the path to their final targets. Some intermediate targets, such as the optic chiasm, are "decision" regions where axons diverge.

Reliance on intermediate targets is an effective solution to the problem of long-distance axonal navigation but is not the only one. In some cases, the first axons reach their targets when the embryo is small and the distance to be covered is short. These "pioneer" axons respond to molecular cues embedded in cells or the extracellular matrix along their way. The first axons to exit the retina fall within this class. Axons that appear later, when distances are longer and obstacles more numerous, can reach their targets by following the pioneers. Yet another guidance mechanism is a molecular gradient. Indeed, as we will see, gradients of cell-surface molecules in the tectum inform axons about their proper termination zone.

Gradients of Ephrins Provide Inhibitory Signals in the Brain

So far, we have seen how retinal axons reach the tectum by responding to a series of discrete directional cues. However, these choices during growth do not account

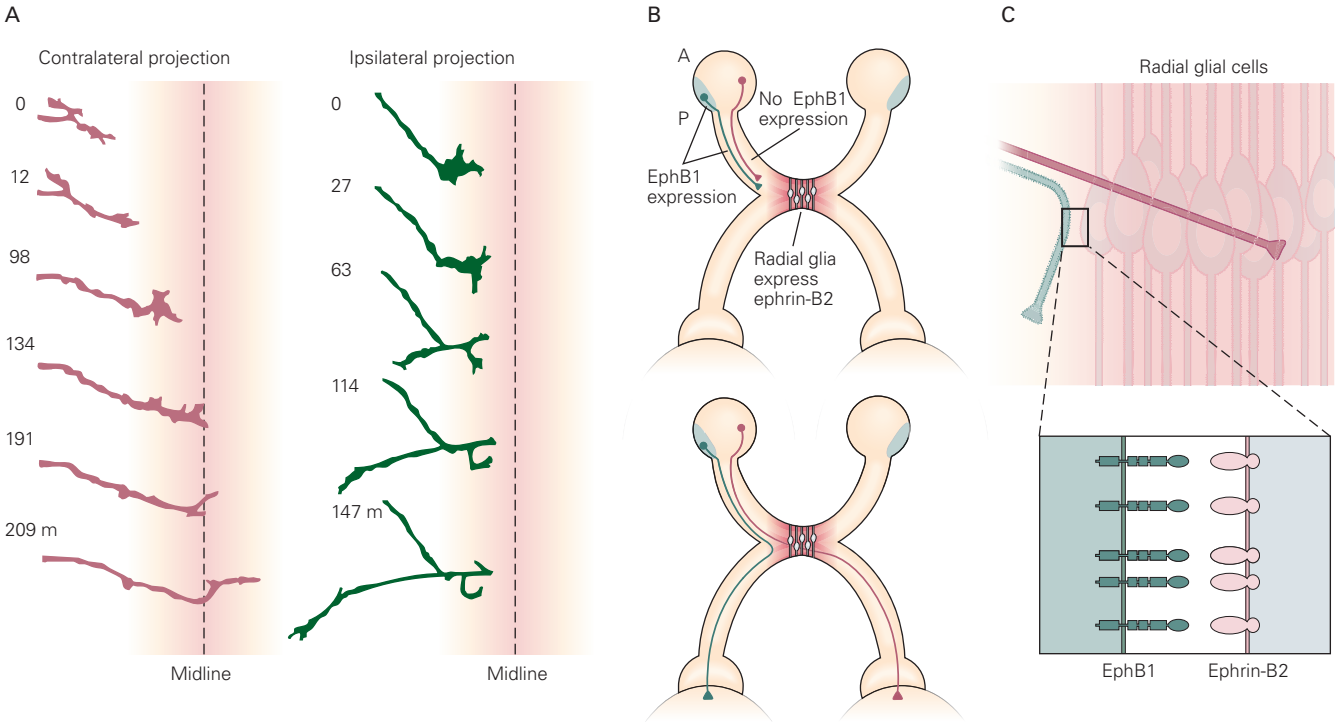

Figure 47–13 Axons of retinal ganglion neurons diverge as they reach the optic chiasm.

A. A time lapse series shows axons approaching the midline. Axons that arise from the nasal hemiretina cross the optic chiasm and project to the contralateral tectum (*left*). In contrast, axons from the temporal hemiretina reach the chiasm but fail to cross and thus project toward the ipsilateral tectum (*right*). (Reproduced, with permission, from Godement, Wang, and Mason 1994.)

B. The axons of neurons from the temporal hemiretina, which express the tyrosine kinase receptor EphB1, encounter ephrin-B2 expressed by midline radial glial cells at the optic chiasm and so are prevented from crossing the midline. The axons of nasal hemiretina neurons, which lack EphB1 receptors, are unaffected by the presence of ephrin-B2 and cross to the contralateral side. (Abbreviations: **A**, anterior; **P**, posterior.)

C. Higher-power view illustrating the trajectories of retinal ganglion cell axons at the chiasm.

for the smoothly graded connections implied by Sperry's analysis of the retinotopic map in the tectum. The quest for the hypothetical "map molecules" became a major focus for developmental neurobiologists, and so we describe it in some detail.

A key breakthrough in the quest for these molecules came with the development of bioassays in which explants from defined portions of the retina were laid on substrates of tectal membrane fragments. The membrane fragments were taken from defined anteroposterior portions of the tectum and arranged in alternating stripes. Axons from the temporal (posterior) hemiretina were found to grow preferentially on membranes from anterior tectum, a preference similar to that exhibited in vivo (Figure 47–14). This preference was found to result from the presence of inhibitory factors in posterior membranes rather than from attractive or adhesive substances in anterior membranes. This observation was one of the first to demonstrate the role of inhibitory or repellent substances in axon guidance.

This stripe assay permitted the characterization of an inhibitory cue, present in membranes from the posterior but not the anterior tectum. Independently, molecular biologists identified a family of receptor tyrosine kinases, the Eph kinases, and a large family of membrane-associated ligands, the ephrins. Both receptors and ligands are divided into A and B subfamilies. The ephrin-A proteins bind and activate EphA kinases; conversely, ephrin-B proteins bind and activate EphB kinases (Figure 47–11C).

The two lines of research converged when the tectal inhibitory cue was identified as ephrin-A5. We now know that the Eph kinases and ephrins serve many functions in neural and nonneural tissues and that each class of proteins can serve as ligands or receptors, depending on cellular context. In the developing

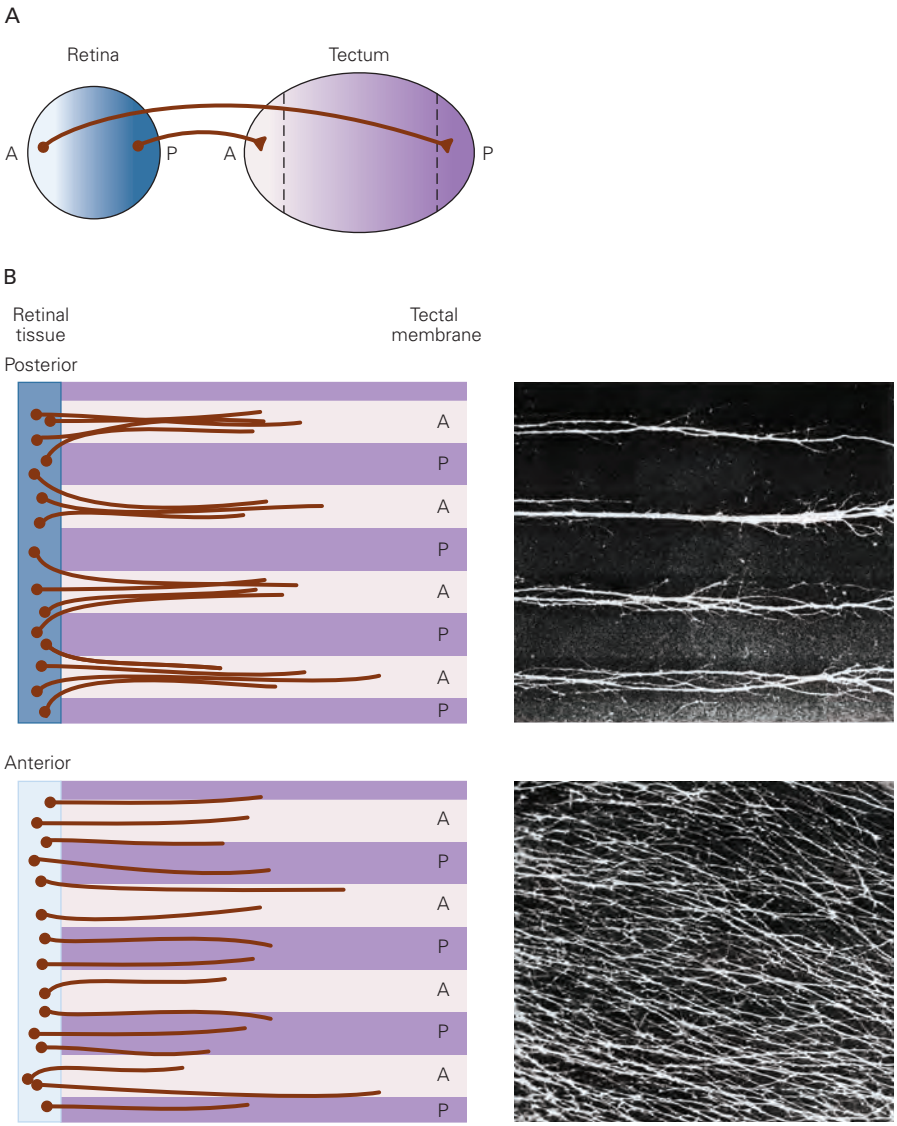

Figure 47–14 Repellent signals guide developing retinal axons in vitro.

A. Retinal ganglion axons from the posterior (temporal) hemiretina project into the anterior developing tectum. Conversely, axons from the anterior (nasal) hemiretina project into the posterior tectum.

B. Fragments of membrane were taken from specified anteroposterior portions of the tectum and arranged in alternating strips. Axons from explants of posterior retina grow selectively on the fragments from anterior tectum. The preferential growth of axons on anterior membrane results from an inhibitory cue in the posterior membrane. In contrast, axons from anterior retina grow on both anterior and posterior tectal membrane fragments. (Abbreviations: A, anterior; P, posterior.) (Adapted, with permission, from Walter, Henke-Fahle, and Bonhoeffer 1987.)

nervous system, these proteins comprise a major group of repellent signals.

Ephrin–Eph interactions account in large part for formation of the retinotopic map in the tectum. Levels of ephrin-A2 and ephrin-A5 in the tectum as well as levels of the Eph receptors in the retina are graded along the anteroposterior axis. These gradients run in the same direction. Ephrin-A concentrations run from posterior-high to anterior-low in tectum, while Eph A concentrations run from posterior-high to anterior-low in retina (Figure 47–15A). Such counter-gradients account, at least in part, for topographic mapping. Axons from posterior retinal ganglion cells with high levels of EphA receptors are repelled most strongly by the high level of ephrin-A in the posterior tectum and thus are confined to the anterior tectum. The less sensitive axons from the anterior retina are able to penetrate further into the posterior domain of the tectum. Ephrin-A2 and ephrin-A5 are therefore strong candidates for chemospecificity factors of the type postulated by Sperry.

The crucial role of the interaction of ephrins and Eph kinases in the formation of retinotopic maps has been confirmed in vivo. Overexpression of ephrin-A2 in the developing optic tectum of chick embryos generates small patches of cells in the rostral tectum that are abnormally rich in ephrin-A2. Temporal retinal axons, which normally avoid the ephrin-rich caudal tectum, also avoid these patches in the rostral tectum, and they terminate in abnormal positions. In contrast, nasal retinal axons, which normally grow toward the

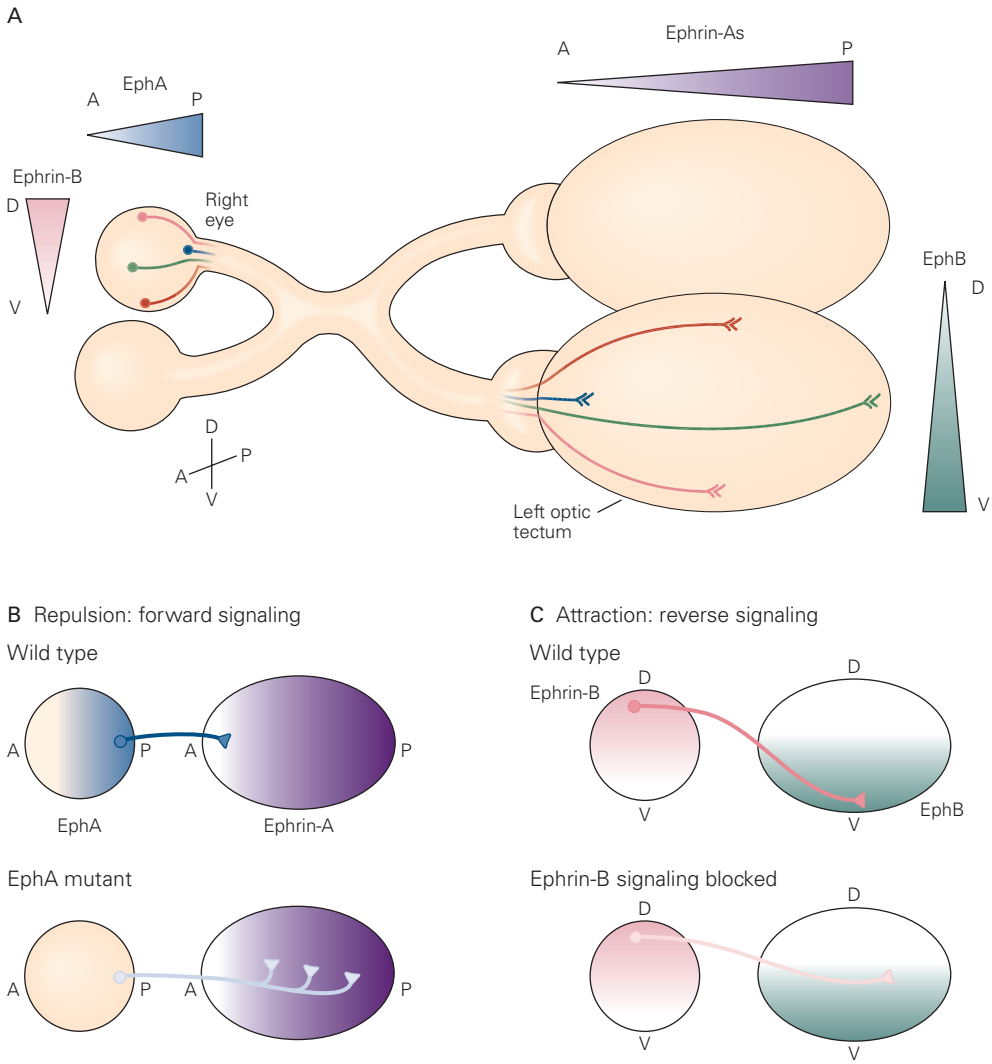

Figure 47–15 The formation of retinotopic maps in vivo depends on ephrin-Eph kinase signaling.

A. In the retina, EphA receptors are expressed in an anteroposterior (**A-P**) gradient, and ephrin-B is expressed in a dorsoventral (**D-V**) gradient. In the tectum, ephrin-A receptors are distributed in an anteroposterior gradient and EphB in a dorsoventral gradient.

B. Expression of EphA in retinal axons that derive from neurons in the posterior (temporal) retina directs axon growth to the anterior tectum through avoidance of ephrin-A proteins. In EphA mutant mice, posterior retinal axons are able to project to a more posterior domain within the tectum.

C. EphB signaling directs the projection of dorsal retinal axons to the ventral tectum. Blocking ephrin-B signaling with soluble EphB protein causes dorsal axons to project to an abnormally dorsal domain within the tectum.

caudal tectum, are not perturbed by encounters with excess ephrin-A.

Conversely, in mice with targeted mutations in the relevant *ephA* or *ephrin-A* genes, some posterior retinal axons terminate in inappropriately posterior tectal regions (Figure 47–15B). Anterior retinal axons, which naturally express low levels of EphA proteins, project normally in these mutants. In mice lacking both ephrin-A proteins, these deficits are more severe than with either single mutant. Thus, the interaction of ephrin-A with EphA receptors is crucial for the targeting of retinal axons in the tectum. These ephrin/EphA pairs possess the properties of the recognition molecules that Sperry predicted were necessary to direct

topographic mapping along the anteroposterior axis of the tectum.

Of course, the retinal map also has a dorsoventral axis. Ephrin/EphB pairs are involved in establishing order along this axis. Just as ephrin-A and EphA are graded along the anteroposterior axis, ephrin-B and EphB are graded along the dorsoventral axis, and manipulation of ephrin-B and EphB levels affects dorsoventral mapping (Figure 47–15C). Thus, at a simple level, the retinotopic map is arranged in rectangular coordinates with ephrin-A/EphA and ephrin-B/EphB labeling the anteroposterior and dorsoventral axes, respectively.

Although this simple view is satisfying, the reality is more complex. First, EphB kinases are expressed in the tectum as well as in the retina, and ephrins-A are expressed in the retina as well as in the tectum. Thus, so-called "*cis*" interactions (Eph and ephrin on the same cell) as well as "*trans*" interactions (Eph on growth cone, ephrin on target cell) may be involved. Second, both ligands and receptors are present at multiple points along the optic pathway and play multiple roles. As we have seen, ephrin-B/EphB interactions affect not only dorsoventral mapping but also the decision of an axon to cross to the contralateral side at the optic chiasm. Finally, in developing visual circuits, more precise spatial mapping of retinal inputs is regulated by patterns of neural activity, as discussed in the next two chapters. Nonetheless, we now have the outline of a molecular strategy for the initial formation of topographic projections from the eye to the brain.

Axons From Some Spinal Neurons Are Guided Across the Midline

One of the fundamental features of the central nervous system is the need to coordinate activity on both sides of the body. To accomplish this task, certain axons need to project to the opposite side.

We have seen one example of axonal crossing in the optic chiasm. Another example that has been studied in detail is the axonal crossing of *commissural neurons* that convey sensory information from the spinal cord to the brain at the ventral midline of the spinal cord across the floor plate. After crossing, axons turn abruptly and grow up toward the brain. This simple trajectory raises several questions. How do these axons reach the ventral midline? How do they cross the midline, and after crossing, how do they *ignore* cues that axons on the other side are using to get to the midline? In other words, why do they turn toward the brain instead of crossing back?

Netrins Direct Developing Commissural Axons Across the Midline

Many of the neurons that send axons across the ventral midline are generated in the dorsal half of the spinal cord. The first task for these axons is to reach the ventral midline. Ramón y Cajal considered the possibility that chemotactic factors emitted by targets could attract axons, but this idea lay dormant for nearly a century. We now know that such factors do exist, and one of them, the protein netrin-1, is expressed by cells of the floor plate as well as by progenitors along the ventral midline. When presented in culture, netrin attracts commissural axons; when mice are deprived of netrin-1 function, axons fail to reach the floor plate (Figure 47–16). It may act as both a secreted factor (chemotaxis) and a membrane guidance molecule (haptotaxis) to guide the axons of commissural neurons to the floor plate.

The netrin protein is structurally related to the protein product of *unc-6*, a gene shown to regulate axon guidance in the nematode *Clostridia elegans.* Two other *C. elegans* genes, *unc-5* and *unc-40*, encode receptors for the unc-6 protein. Vertebrate netrin receptors are related to the unc-5 and unc-40 receptors. The unc-5H proteins are homologs of unc-5, and DCC (deleted in colorectal cancer) are related to unc-40 (see Figure 47–11G). These receptors are members of the immunoglobulin superfamily, and their functions have been remarkably conserved throughout animal evolution (Figure 47–17). This conservation supports the use of simple and genetically accessible invertebrates to unravel developmental complexities. In no area has this approach been more fruitful than in the analysis of axon guidance. Dozens of genes that affect this process were first identified and cloned in *Drosophila* and *C. elegans* and then shown to play important and related roles in mammals.

Chemoattractant and Chemorepellent Factors Pattern the Midline

Other signaling systems work with netrins to guide commissural axons. One group consists of bone morphogenetic proteins, which are secreted by the roof plate. They act as repellents, directing commissural axons ventrally as they begin their journey. Additional factors from the floor plate, such as the hedgehog proteins initially involved in patterning the spinal cord (Chapter 45), may collaborate with netrins at a later stage, serving as axonal attractants.

Once commissural axons reach the midline, they find themselves exposed to the highest available levels

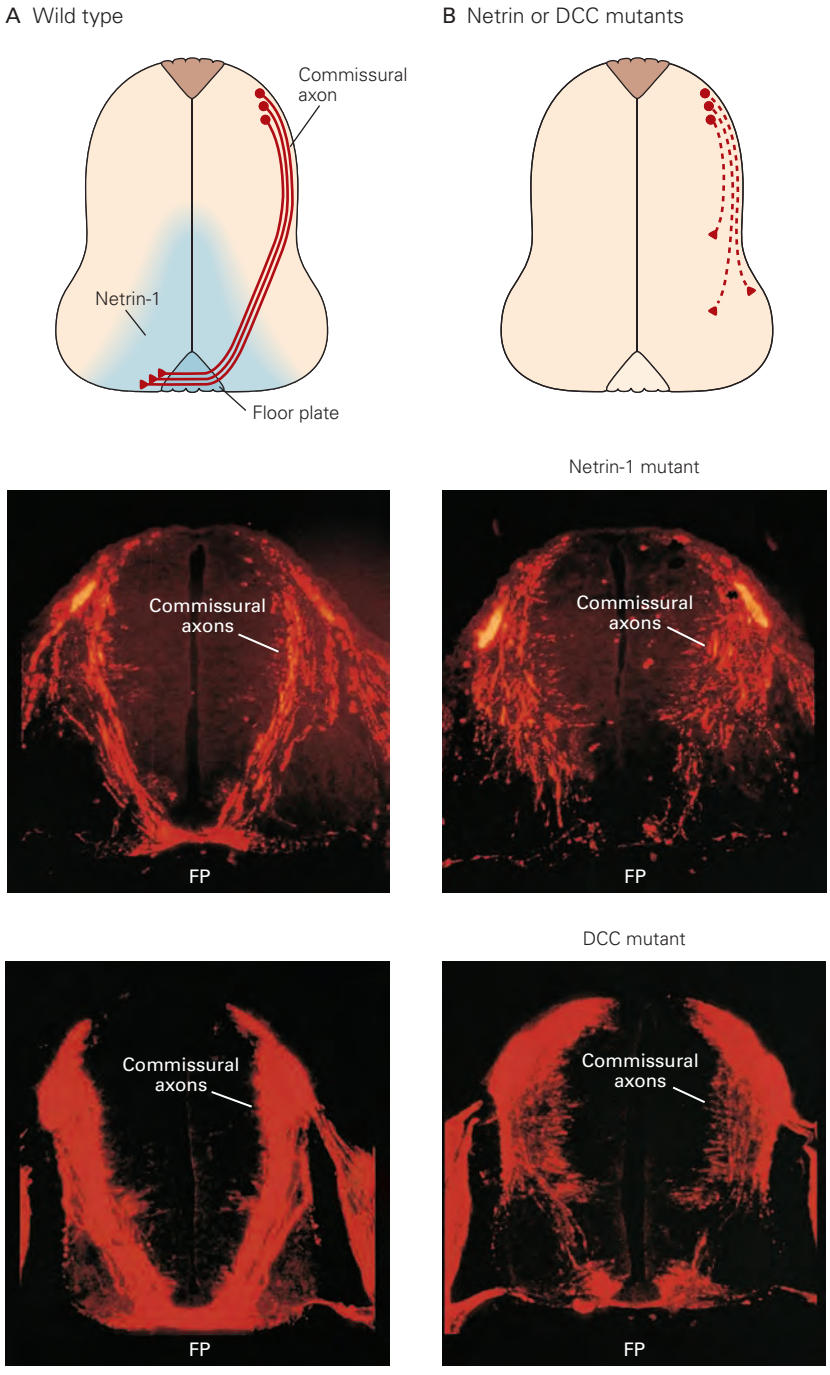

Figure 47–16 Netrin signaling attracts the axons of spinal commissural neurons to the floor plate. (Micrographs reproduced, with permission, from Marc Tessier-Lavigne.)

A. Netrin-1 is generated by floor plate cells and ventral neural progenitors. It attracts the axons of commissural neurons to the floor plate (**FP**) at the ventral midline of the spinal cord.

B. Most commissural axons fail to reach the floor plate when netrin or deleted in colorectal cancer (**DCC**) proteins are eliminated.

of netrin-1 and sonic hedgehog. Yet this netrin-rich environment does not keep the axons at the midline indefinitely. Instead they cross to the other side of the spinal cord, even while their contralateral counterparts are navigating up the netrin chemoattractant gradient.

This puzzling behavior is explained by the fact that growth cones change their responsiveness to attractive and repellent signals as a consequence of exposure to floor plate signals. This switch illustrates an important property of intermediate targets involved in axon guidance. Factors presented by intermediate targets not only guide the growth of axons but also change the sensitivity of the growth cone, preparing it for the next leg of its journey.

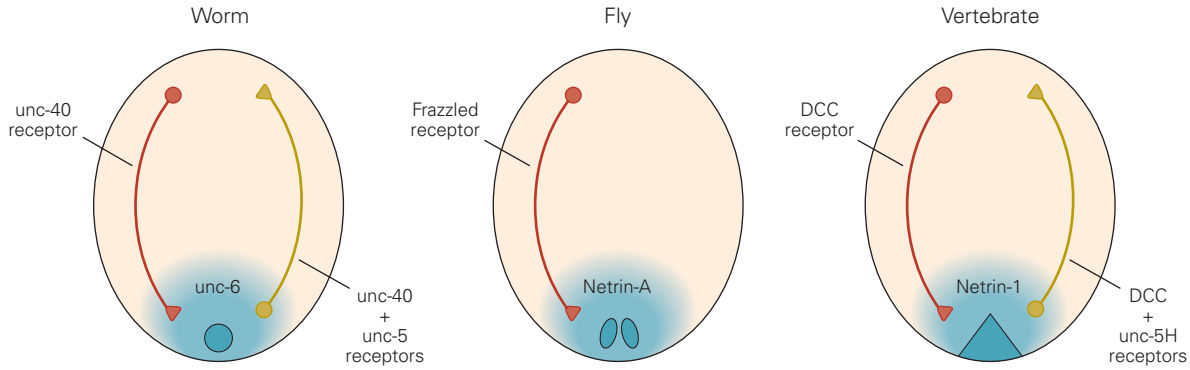

Figure 47–17 **The expression and activity of netrins have been conserved throughout evolution.** Netrins are secreted by ventral midline cells in worms, flies, and vertebrates and interact with receptors on cells or axons that migrate or extend along the dorsoventral axis. The netrin receptors unc-40 (worm), frazzled (fly), and deleted in colorectal cancer (**DCC**) (vertebrate) mediate netrin's attractant activity, whereas unc-5 class receptors mediate its repellent activity.

Once axons arrive at the floor plate, they become sensitive to Slit, a chemorepellent signal secreted by floor plate cells (Figure 47–18). Before commissural axons reach the floor plate, the Robo proteins that serve as Slit receptors are kept inactive by expression of a related protein, Rig-1. As axons reach the floor plate, levels of Rig-1 on their surface decline, unleashing Robo activity and causing axons to respond to the repellant actions of Slit. This repellent action propels growth cones *down* the Slit gradient into the contralateral side

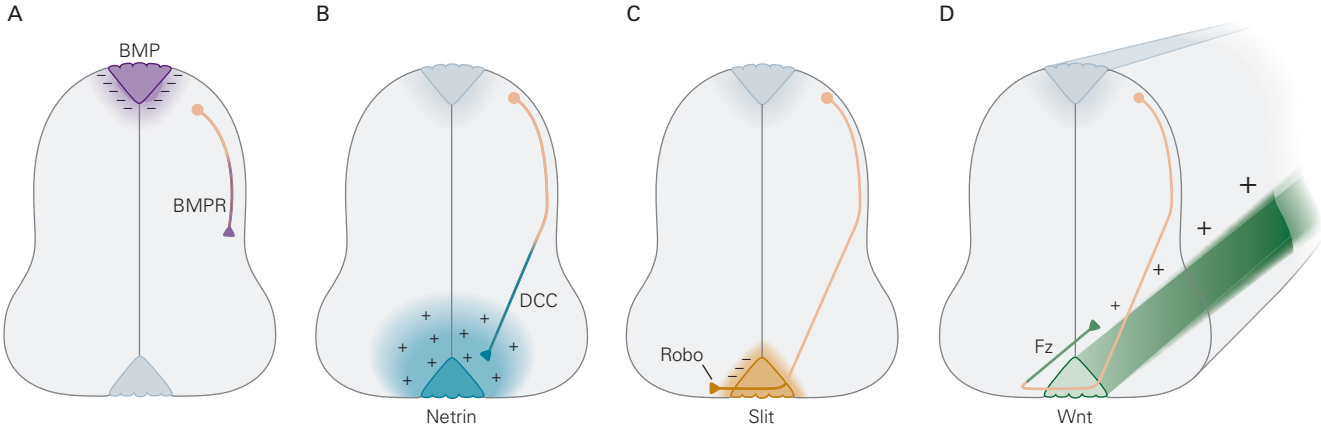

Figure 47–18 **Guidance cues expressed by roof plate and floor plate cells guide commissural axons in the developing spinal cord.**

A. Bone morphogenetic proteins (**BMP**) secreted by roof plate cells interact with BMP receptors (**BMPR**) on commissural axons to direct the axons away from the roof plate.

B. Netrin expressed by floor plate cells attracts deleted in colorectal cancer (**DCC**)-expressing commissural axons to the ventral midline of the spinal cord. Sonic hedgehog has also been implicated in the ventral guidance of commissural axons.

C. Slit proteins secreted by floor plate cells interact with Robo receptors on commissural axons to prevent these axons from recrossing the midline. Prior to crossing, but not after, commissural axons express robo3 (Rig-1) in addition to robo1 and robo2. The Rig-1 protein inactivates the Robo receptors, preventing the axons from responding to the repellent effects of Slits as they approach the ventral midline.

D. After commissural axons cross the midline, Wnt proteins secreted from floor plate cells and distributed in a rostrocaudal gradient interact with frizzled (**Fz**) proteins on the commissural axons, guiding the axons toward the brain.

of the spinal cord. In addition, activated Robo forms a complex with DCC, rendering these Netrin receptors incapable of responding to their ligand. The decreased sensitivity of growth cones to the attractive properties of the floor plate helps to account for the transient influence of floor plate signals on axons.

Finally, once axons have left the floor plate, they turn rostrally toward their eventual synaptic targets in the brain. A rostrocaudal gradient of Wnt proteins expressed by floor plate cells appears to direct axon growth rostrally at the ventral midline (Figure 47–18D). Thus, different cues guide commissural axons during distinct phases of their overall trajectory. This same process is presumably played out for hundreds and even thousands of classes of neurons to establish the mature pattern of brain wiring.

Highlights

1. As neurons extend processes, one generally becomes an axon and the others become dendrites. This process is called polarization. The two types of processes differ in structure and molecular architecture as well as function.
2. Cell types differ markedly in the shape, size, and branching patterns of their dendrites. Type-specific dendritic features arise both from intrinsic differences in transcriptional programs among types and from extrinsic influences on the developing dendrites.
3. Interactions among dendrites are critical for dendritic patterning. Repellent interactions among the dendrites of a single cell, a process called self-avoidance, leads to even coverage of an area, with minimal gaps or clumps. Repellent actions between dendrites of neighboring cells, a process called tiling, minimizes overlap of dendritic fields. In some cases, dendrites avoid other dendrites from their own neuron but interact with dendrites of nominally identical neighboring cells. This process is called self-/non–self-discrimination.
4. Growth cones at the tips of axons serve as both sensory and motor elements to guide axons to their destinations. Cytoskeletal elements of the growth cone, including actin and myosin, propel the growth.
5. Receptors on the growth cone recognize and bind ligands in the environment through which the axon is extending, guiding the growth. These interactions lead to generation of their second messengers that mediate growth, turning and stopping of the growth cone, and branching of the axon.
6. Some growth cones contain protein synthetic machinery including messenger RNAs. In these cases, receptors can promote local synthesis of specific proteins that mediate growth or turning.
7. Ligand–receptor pairs include several key families of molecules including cadherins, Slits and their Robo receptors, semaphorins and their plexin receptors, and ephrins and their Eph kinase receptors.
8. The growth of an axon to a distant target is broken into discrete shorter steps. At each step, molecules on the surface of or secreted by neighboring structures guide the axon. They can also lead to alterations in the growth cone's complement of receptors, allowing it to respond to different sets of cues at the subsequent stage.
9. Roger Sperry proposed a chemospecificity hypothesis to explain the specific growth of axons from different parts of the retina to different parts of the optic tectum (superior colliculus), forming an orderly retinotopic map. The ephrins and their receptors, the Eph kinases, are key molecules that guide map formation. They are graded in expression along the retina and tectum and act in large part by repelling axons from incorrect positions rather than attracting them to correct positions.
10. Both attractive and repellent molecules guide axons across midline structures, a process called decussation. Evolutionarily conserved signals include Slits, netrins, and Wnts. Mutations in genes that encode these ligands and receptors can result in developmental neurological disorders.

Joshua R. Sanes

Selected Reading

Bentley M, Banker G. 2016. The cellular mechanisms that maintain neuronal polarity. Nat Rev Neurosci 17:611–622.

Cang J, Feldheim DA. 2013. Developmental mechanisms of topographic map formation and alignment. Annu Rev Neurosci 36:51–77.

Dong X, Shen K, Bülow HE. 2015. Intrinsic and extrinsic mechanisms of dendritic morphogenesis. Annu Rev Physiol 77:271–300.

Herrera E, Erskine L, Morenilla-Palao C. 2017. Guidance of retinal axons in mammals. Semin Cell Dev Biol pii: S1084-9521.

Jung H, Gkogkas CG, Sonenberg N, Holt CE. 2014. Remote control of gene function by local translation. Cell 157:26–40.

Lai Wing Sun K, Correia JP, Kennedy TE. 2011. Netrins: versatile extracellular cues with diverse functions. Development 138:2153–2169.

Lefebvre JL, Sanes JR, Kay JN. 2015. Development of dendritic form and function. Annu Rev Cell Dev Biol 31:741–777.

Tojima T, Hines JH, Henley JR, Kamiguchi H. 2011. Second messengers and membrane trafficking direct and organize growth cone steering. Nat Rev Neurosci 12:191–203.

Zhang C, Kolodkin AL, Wong RO, James RE. 2017. Establishing wiring specificity in visual system circuits: from the retina to the brain. Annu Rev Neurosci 40:395–424.

Zipursky SL, Grueber WB. 2013. The molecular basis of self-avoidance. Annu Rev Neurosci 36:547–568.

References

Barnes AP, Lilley BN, Pan YA, et al. 2007. LKB1 and SAD kinases define a pathway required for the polarization of cortical neurons. Cell 129:549–563.

Bridgman PC, Dailey ME. 1989. The organization of myosin and actin in rapid frozen nerve growth cones. J Cell Biol 108:95–109.

Campbell DS, Holt CE. 2001. Chemotropic responses of retinal growth cones mediated by rapid local protein synthesis and degradation. Neuron 32:1013–1026.

Fazeli A, Dickinson SL, Hermiston ML, et al. 1997. Phenotype of mice lacking functional Deleted in colorectal cancer (Dcc) gene. Nature 386:796–804.

Forscher P, Smith SJ. 1988. Actions of cytochalasins on the organization of actin filaments and microtubules in a neuronal growth cone. J Cell Biol 107:1505–1516.

Frisen J, Yates PA, McLaughlin T, Friedman GC, O'Leary DD, Barbacid M. 1998. Ephrin-A5 (AL-1/RAGS) is essential for proper retinal axon guidance and topographic mapping in the mammalian visual system. Neuron 20:235–243.

Godement P, Wang LC, Mason CA. 1994. Retinal axon divergence in the optic chiasm: dynamics of growth cone behavior at the midline. J Neurosci 14:7024–7039.

Grueber WB, Jan LY, Jan YN. 2003. Different levels of the homeodomain protein cut regulate distinct dendrite branching patterns of *Drosophila* multidendritic neurons. Cell 112:805–818.

Harrison RG. 1959. The outgrowth of the nerve fiber as a mode of protoplasmic movement. J Exp Zool 142:5–73.

Heidemann SR. 1996. Cytoplasmic mechanisms of axonal and dendritic growth in neurons. Int Rev Cytol 165:235–296.

Kaech S, Banker G. 2006. Culturing hippocampal neurons. Nat Protoc 1:2406–2415.

Kalil K, Dent EW. 2014. Branch management: mechanisms of axon branching in the developing vertebrate CNS. Nat Rev Neurosci 15:7–18.

Kapfhammer JP, Grunewald BE, Raper JA. 1986. The selective inhibition of growth cone extension by specific neurites in culture. J Neurosci 6:2527–2534.

Keino-Masu K, Hinck L, Leonardo ED, Chan SS, Culotti JG, Tessier-Lavigne M. 1996. Deleted in colorectal cancer (DCC) encodes a netrin receptor. Cell 87:75–85.

Kidd T, Brose K, Mitchell KJ, et al. 1998. Roundabout controls axon crossing of the CNS midline and defines a novel subfamily of evolutionarily conserved guidance receptors. Cell 92:205–215.

Kishi M, Pan YA, Crump JG, Sanes JR. 2005. Mammalian SAD kinases are required for neuronal polarization. Science 307:929–932.

Lefebvre JL, Kostadinov D, Chen WV, Maniatis T, Sanes JR. 2012. Protocadherins mediate dendritic self-avoidance in the mammalian nervous system. Nature 488:517–521.

Letourneau PC. 1979. Cell-substratum adhesion of neurite growth cones, and its role in neurite elongation. Exp Cell Res 124:127–138.

Leung K-M, van Horck FPG, Lin AC, Allison R, Standart N, Holt CE. 2006. Asymmetrical beta-actin mRNA translation in growth cones mediates attractive turning to netrin-1. Nat Neurosci 9:1247–1256.

Ming GL, Song HJ, Berninger B, Holt CE, Tessier-Lavigne M, Poo MM. 1997. cAMP-dependent growth cone guidance by netrin-1. Neuron 19:1225–1235.

Polleux F, Morrow T, Ghosh A. 2000. Semaphorin 3A is a chemoattractant for cortical apical dendrites. Nature 404:567–573.

Serafini T, Colamarino SA, Leonardo ED, et al. 1996. Netrin-1 is required for commissural axon guidance in the developing vertebrate nervous system. Cell 87:1001–1014.

Shigeoka T, Jung H, Jung J, et al. 2016. Dynamic axonal translation in developing and mature visual circuits. Cell 166:181–192.

Sperry RW. 1943. Visuomotor coordination in the newt (*Triturus viridescens*) after regeneration of the optic nerve. J Compar Neurol 79:33–55.

Sperry RW. 1945. Restoration of vision after crossing of optic nerves and after contralateral transplantation of eye. J Neurophysiol 8:17–28.

Thu CA, Chen WV, Rubinstein R, et al. 2014. Single-cell identity generated by combinatorial homophilic interactions between α, β, and γ protocadherins. Cell 158:1045–1059.

Walter J, Henke-Fahle S, Bonhoeffer F. 1987. Avoidance of posterior tectal membranes by temporal retinal axons. Development 101:909–913.

Wang L, Marquardt T. 2013. What axons tell each other: axon-axon signaling in nerve and circuit assembly. Curr Opin Neurobiol 23:974–982.

Weiss P. 1941. Nerve patterns: the mechanics of nerve growth. Growth 5:163–203. Suppl.

Zhang XH, Poo MM. 2002. Localized synaptic potentiation by BDNF requires local protein synthesis in the developing axon. Neuron 36:675–688.

48

Formation and Elimination of Synapses

So far, we have examined three stages in the development of the mammalian nervous system: the formation and patterning of the neural tube, the generation and differentiation of neurons and glia, and the growth and guidance of axons. One additional step must occur before the brain becomes functional: the formation of synapses. Only when synapses are formed and functional can the brain go about the business of processing information.

Three key processes drive synapse formation. First, axons make choices among many potential postsynaptic partners. By forming synaptic connections only on particular target cells, neurons assemble functional circuits that can process information. In many cases, synapses are even formed at specific sites on the postsynaptic cell; some types of axons form synapses on dendrites, others on cell bodies, and yet others on axons or nerve terminals. Although cellular and subcellular specificity are evident throughout the brain, the general features of synapse formation can be illustrated with a few well-studied examples.

Second, after cell–cell contacts have formed, the portion of the axon that contacts the target cell differentiates into a presynaptic nerve terminal, and the domain of the target cell contacted by the axon differentiates into a specialized postsynaptic apparatus. Precise coordination of pre- and postsynaptic differentiation depends on interactions between the axon and its target cell. Much of what we know about these interactions comes from studies of the neuromuscular junction, the synapse between motor neurons and skeletal muscle fibers. The simplicity of this synapse made it a favorable system to probe the structural and electrophysiological principles of chemical synapses (Chapter 12), and this simplicity has also helped in the analysis of developing synapses. We will use the neuromuscular synapse to illustrate key features of

synaptic development and then apply insights from this peripheral synapse to examine synapses that form in the brain.

Finally, once formed, synapses mature, often undergoing major rearrangements. One striking aspect of the rearrangement is that as some synapses grow and strengthen, many others are eliminated. Like neuronal cell death (Chapter 46), synapse elimination at first glance is a puzzling and seemingly wasteful step in neural development. It is increasingly clear, however, that it plays a key role in refining initial patterns of connectivity. We will discuss the main features of synaptic rearrangement at the neuromuscular junction, where it has been studied intensively, as well as at synapses between neurons, where it also is prominent.

Synapse formation stands at an interesting crossroads in the sequence of events that assemble the nervous system. The initial steps in this process appear to be largely "hardwired" by molecular programs. However, as soon as synapses form, the nervous system begins to function, and the activity of neural circuits plays a critical role in subsequent development. Indeed, the information-processing capacity of the nervous system is refined through its use, most dramatically in early postnatal life but also into adulthood. In this sense, the nervous system continues to develop throughout life. We will consider this interplay of molecular programs and neural activity as we describe synapse formation and rearrangement. This discussion will be a useful prelude to Chapter 49, in which we discuss how genes and the environment—nature and nurture—interact to customize nervous systems early in postnatal life.

Neurons Recognize Specific Synaptic Targets

Once axons reach their designated target areas, they must choose appropriate synaptic partners from the many potential targets within easy reach. Although synapse formation is a highly selective process at both cellular and subcellular levels, few of the molecules that confer synaptic specificity have been identified.

The specificity of synaptic connections is particularly evident when intertwined axons select subsets of target cells. In these cases, axon guidance and selective synapse formation can be distinguished. The first report of such specificity came more than 100 years ago when J. N. Langley, studying the autonomic nervous system, proposed the first version of a chemospecificity hypothesis (see Chapter 46). Langley observed that autonomic preganglionic neurons are generated at distinct rostrocaudal levels of the spinal cord. Their axons enter sympathetic ganglia together but form synapses with different postsynaptic neurons that innervate distinct targets. Using behavioral assays as a guide, Langley inferred that the axons of preganglionic neurons located in the rostral spinal cord form synapses on ganglion neurons that project their axons to relatively rostral targets such as the eye, whereas neurons that derive from more caudal regions of the spinal cord synapse on ganglion neurons that project to caudal targets such as the ear (Figure 48–1A). He then showed that similar patterns were reestablished after the preganglionic axons were severed and allowed to regenerate, leading him to postulate that some sort of molecular recognition was responsible (Figure 48–1B).

Electrophysiological studies later confirmed Langley's intuition about the specificity of synaptic connections in these ganglia. Moreover, this selectivity is apparent from early stages of innervation, even though specific types of postsynaptic neurons are interspersed within the ganglion. The reestablishment of selectivity in adults after nerve damage shows that specificity does not emerge through peculiarities of embryonic timing or neuronal positioning.

Recognition Molecules Promote Selective Synapse Formation in the Visual System

To illustrate the idea of target specificity in more detail, we will first consider retinal ganglion cells. These neurons differ in their response properties—some ganglion neurons respond to increases in light level (ON cells), others to decreases (OFF cells), others to moving objects, and still others to light of a particular color. The axons of all ganglion cells run through the optic nerve, forming parallel axonal pathways from the retina to the brain.

The response properties of each class of ganglion cell depend on the synaptic inputs they receive from amacrine and bipolar interneurons, which in turn receive synapses from light-sensitive photoreceptors. All of the synapses from bipolar and amacrine cells onto ganglion cell dendrites occur in a narrow zone of the retina called the inner plexiform layer. Axons and dendrites therefore have the daunting task of recognizing their correct partners within a large crowd of inappropriate bystanders.

One important contributor to synaptic matchmaking in the inner plexiform layer is its division into sublayers. The processes of each amacrine and bipolar cell type, as well as the dendrites of each functionally distinct ganglion cell type, branch and synapse in just one or a few of approximately 10 sublayers. For example, the dendrites of ON and OFF cells are restricted to inner and outer portions of the plexiform layer,

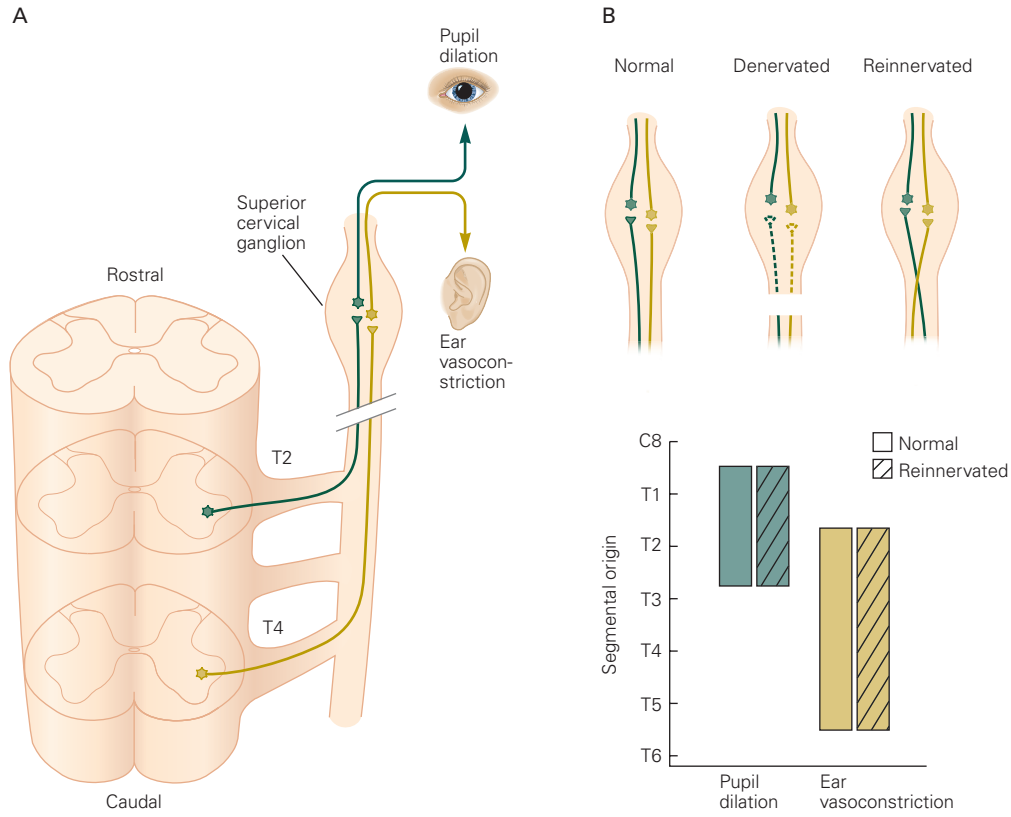

Figure 48–1 Preganglionic motor neurons regenerate selective connections with their sympathetic neuronal targets.

A. Preganglionic motor neurons arise from different levels of the thoracic spinal cord. Axons that arise from rostrally located thoracic neurons innervate superior cervical ganglion neurons that project to rostral targets, including the intrinsic eye muscles. Axons that arise from neurons at caudal levels of the thoracic spinal cord innervate ganglion neurons that project to more caudal targets, such as the blood vessels of the ear. These two classes of ganglion neurons are intermingled in the ganglion, which suggested to J. N. Langley that preganglionic axons from different thoracic levels selectively form synapses with ganglion neurons that terminate in specific peripheral targets.

B. After nerve damage in adults, similar segment-specific patterns of connectivity form during reinnervation, supporting the notion that synapse formation is selective. (Adapted from Njå and Purves 1977.)

respectively, and therefore receive synapses from different interneurons; particular types of ON and OFF cells have narrower restrictions within these zones (Figure 48–2). This layer-specific arborization of pre- and postsynaptic processes restricts the choice of synaptic partners to which they have ready access. Similar lamina-specific connections are found in many other regions of the brain and spinal cord. For example, in the cerebral cortex, distinct populations of axons confine their dendritic arbors and synapses to just one or two of the six main layers.

Laminar specificity does not, however, completely account for the wiring of the retina. As the number of retinal cell types—currently estimated at around 130 in mice—greatly exceeds the number of plexiform sublayers, the processes of many cell types arborize within each sublayer. Anatomical and physiological studies have shown that connectivity is specific even within individual sublayers. Moreover, patterns of connectivity appear to be largely, although not entirely, "hardwired," occurring before visual experience has a chance to affect circuitry. Thus, there must be molecules that restrict axons and dendrites to specific sublayers, as well as molecules that distinguish synaptic partners within a sublayer.

One clue to the basis of both laminar and intralaminar synaptic specificity in the retina comes from the finding that specific types of interneurons and ganglion neurons express different classes of recognition molecules of the immunoglobulin and cadherin families (Chapter 47). Thus, the processes of cells that express a particular recognition molecule are confined

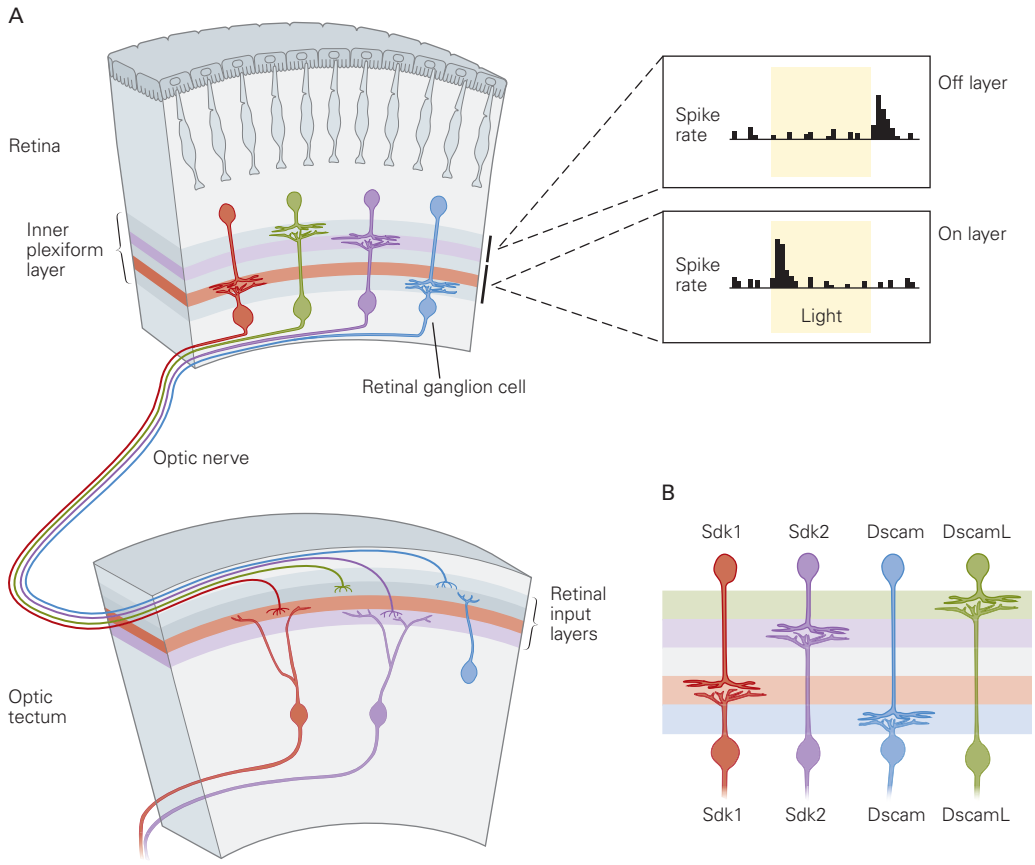

Figure 48–2 Retinal ganglion neurons form layer-specific synapses. (Reproduced, with permission, from Sanes and Yamagata 2009.)

A. The dendrites of retinal ganglion neurons receive input from the processes of retinal interneurons (amacrine and bipolar cells) in the inner plexiform layer, which is subdivided into at least 10 sublaminae. Specific subsets of interneurons and ganglion cells often arborize and synapse in just one layer. These lamina-specific connections determine which aspects of visual stimuli (their onset or offset) activate each type of retinal ganglion cell. The responses of OFF and ON retinal ganglion cells are shown on the right.

B. Immunoglobulin superfamily adhesion molecules (Sdk1, Sdk2, Dscam, and DscamL) are expressed by different subsets of amacrine and retinal ganglion neurons in the developing chick embryo. Amacrine neurons that express one of these four proteins form synapses with retinal ganglion cells that express the same protein. Manipulating Sdk or Dscam expression alters these patterns of lamina-specific arborization.

to one or a few plexiform sublayers (Figure 48–2B). Many of these proteins promote homophilic interactions; that is, they bind to the same protein on other cell surfaces. The roles of several recognition molecules have now been assessed in chick and mouse retina, either by removing them during development or by implanting them into neurons that do not normally express them. Results of these so-called "loss-of-function" and "gain-of-function" experiments hint at the existence of a complex code of recognition molecules that promotes specific connectivity within a target region. In mice, for example, two cadherins direct bipolar interneurons to appropriate sublayers, while Sidekick 2, a member of the immunoglobulin superfamily, is required for interneurons to choose among ganglion cells with dendrites in one particular sublayer.

Sensory Receptors Promote Targeting of Olfactory Neurons

A different type of specificity is evident in the olfactory system. Each olfactory sensory neuron in the nasal epithelium expresses just one of approximately 1,000 types of odorant receptors. Neurons expressing one receptor are randomly distributed across a large sector of the epithelium, yet all of their axons converge on the dendrites of just a few target neurons in the olfactory

bulb, forming synapse-rich glomeruli (Figure 48–3A). When an individual olfactory receptor is deleted, the axons that normally express the receptor reach the olfactory bulb but fail to converge into specific glomeruli or to terminate on the appropriate postsynaptic cells (Figure 48–3B). Conversely, when neurons are forced to express a different odorant receptor, their axons form glomeruli at a different position within the olfactory bulb (Figure 48–3C).

Together, these experiments suggest that olfactory receptors not only determine a neuron's responsiveness to specific odorants but also help the axon to form appropriate synapses on target neurons. Initially, it was suspected that specific olfactory receptors served not only as odor detectors but also as recognition molecules. More recent studies provide evidence for a different mechanism: that second messengers generated from activation of the olfactory receptors influence the expression of recognition molecules that match olfactory axons with appropriate targets in the olfactory bulb.

The matching occurs in two steps. First, intrinsic differences in the abilities of olfactory receptors to stimulate formation of the second messenger cyclic adenosine monophosphate lead to differential expression of guidance molecules in embryos, generating a coarse matching of olfactory neurons and olfactory bulb targets along the anterior-posterior axis. Second, selective expression of recognition molecules by four groups of olfactory sensory neurons targets them to corresponding domains along the dorsoventral axis of the olfactory bulb.

Thus, an early phase of molecular recognition generates a coarse map of nose-to-brain connectivity by activity-independent mechanisms (Figure 48–4A). Then, postnatally, odorant receptors are activated by odorants, and because of developmental changes in

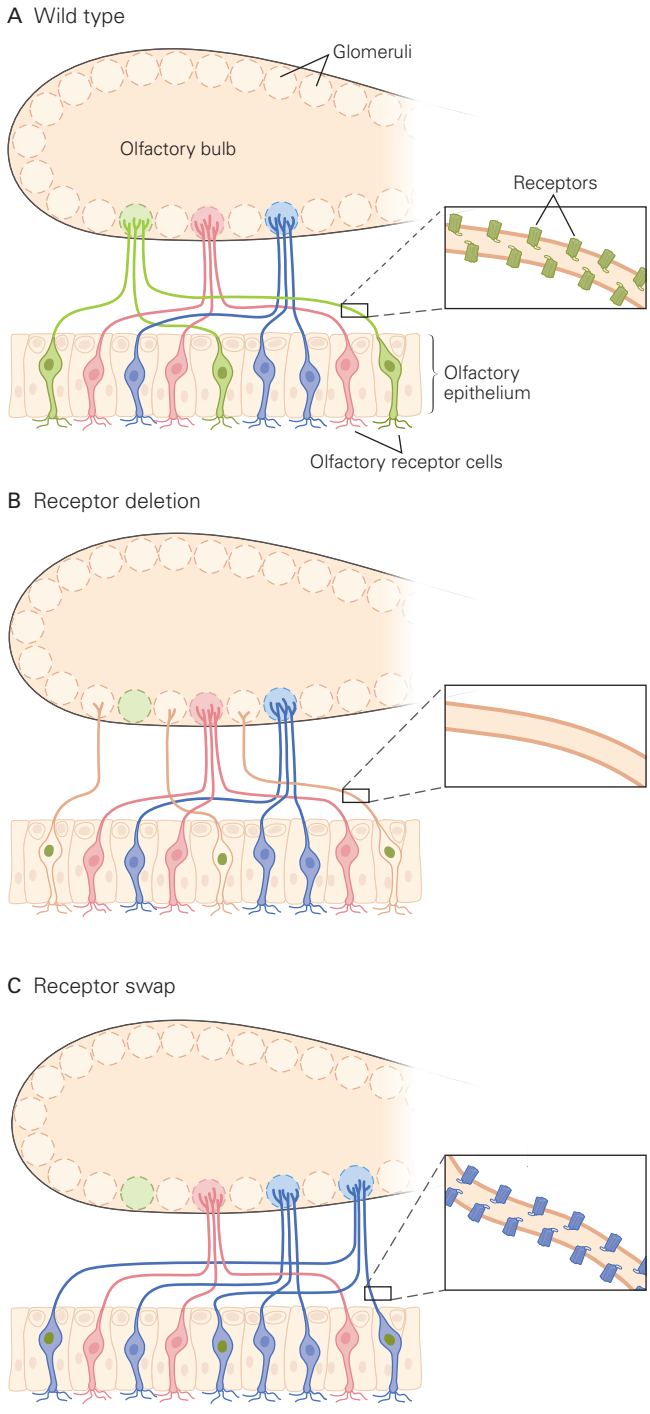

Figure 48–3 (Right) Odorant receptors influence the targeting of sensory axons to discrete glomeruli in the olfactory bulb. (Adapted, with permission, from Sanes and Yamagata 2009.)

A. Each olfactory receptor neuron expresses one of approximately 1,000 possible odorant receptors. Neurons expressing the same receptor are distributed sparsely throughout the olfactory epithelium of the nose. The axons of these neurons form synapses with target neurons in a single glomerulus in the olfactory bulb.

B. In mouse mutants in which an odorant receptor gene has been deleted, the sensory neurons that would have expressed the gene send their axons to other glomeruli, in part because these neurons now express other receptors.

C. When one odorant receptor gene replaces another in a set of sensory neurons, their axons project improperly.

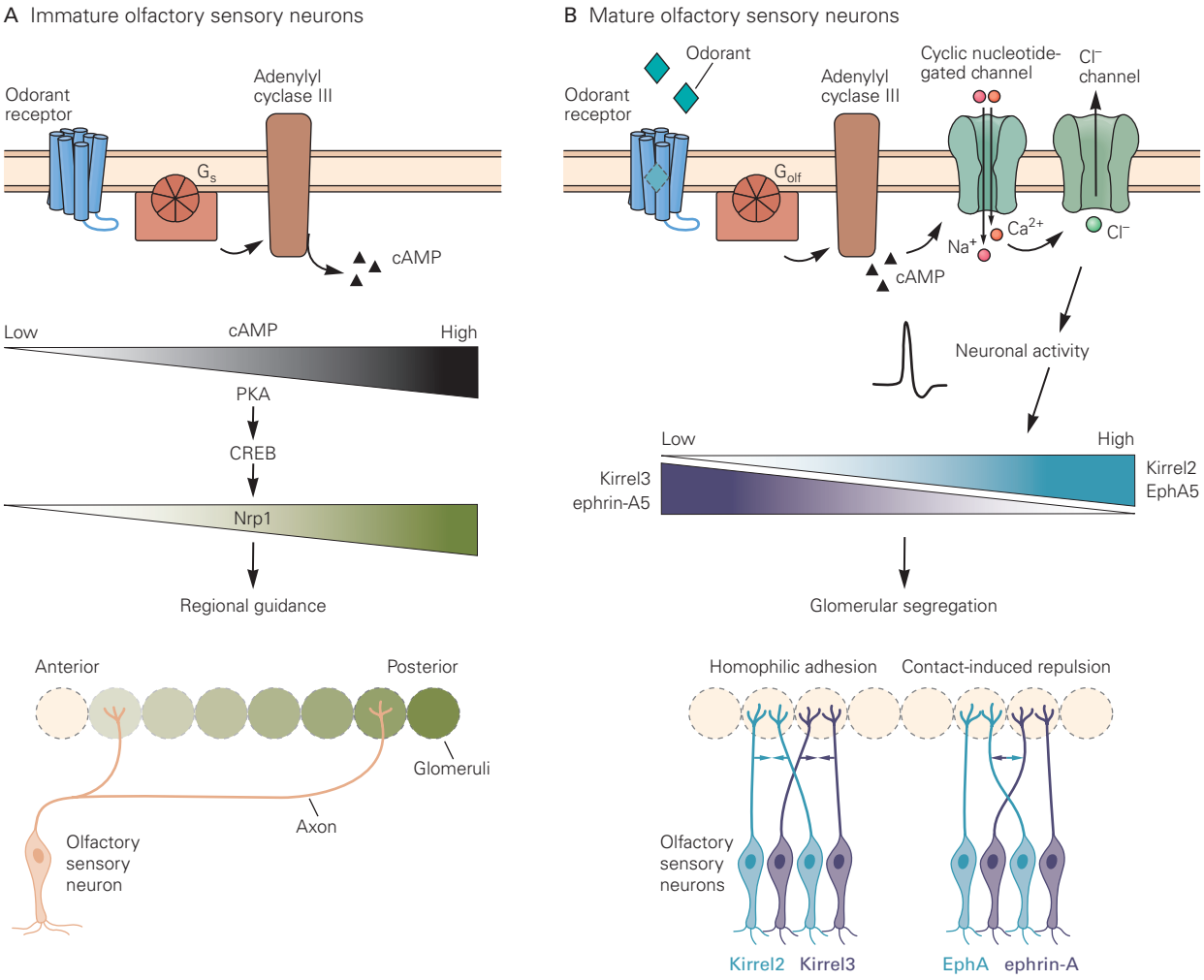

Figure 48–4 Odorant receptors promote specific connections in the olfactory bulb by controlling expression of guidance and recognition molecules. Activation of olfactory receptors in olfactory sensory neurons leads to activation of adenylyl cyclase and production of the second messenger cyclic adenosine monophosphate (**cAMP**).

A. Prenatally, prior to olfaction, the receptors are spontaneously active. Different receptor types exhibit different levels of spontaneous activity and therefore generate different levels of cAMP, which in turn induce distinct, graded levels of axon guidance molecules such as neuropilins and semaphorins. These guidance molecules mediate interactions among axons that guide them to appropriate regions of the olfactory bulb. (Abbreviations: **CREB**, cAMP response element-binding protein; **Nrp1**, neuropilin1; **PKA**, protein kinase A.)

B. Postnatally, olfactory receptors are activated by odorant molecules. This olfactory activity also generates distinct levels of cAMP in each type of odorant receptor neuron, but now the second messenger acts through ion channels to induce new sets of guidance molecules such as kirrels and ephrins. These molecules mediate interactions that segregate axonal terminals into glomeruli. Thus, successive phases of receptor activity, the first spontaneous and the second evoked by odorants, act together to map olfactory sensory axons of different types onto different glomeruli.

intracellular signaling, this activation leads to induction of a second set of recognition molecules. These molecules lead to convergence of axons onto glomeruli, thus refining the projection by an activity-dependent mechanism (Figure 48–4B). Segregation of axons first to particular regions and then to particular glomeruli occurs via both adhesive and repulsive interactions.

Different Synaptic Inputs Are Directed to Discrete Domains of the Postsynaptic Cell

Nerve terminals not only discriminate among candidate targets but also terminate on a specific portion of the target neuron. In the cerebral cortex and hippocampus, for example, axons arriving in layered structures

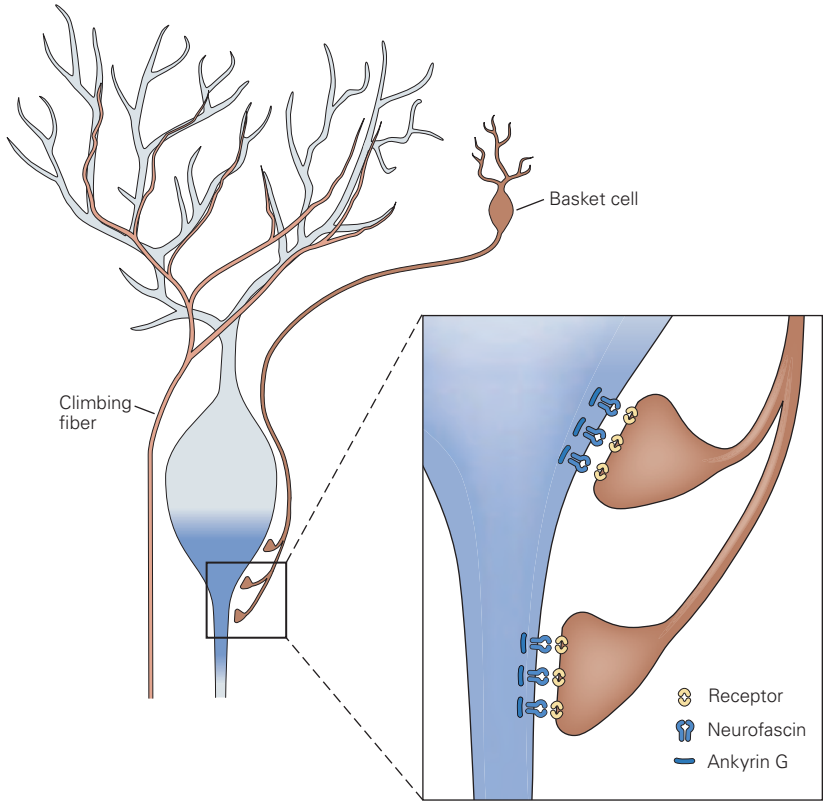

Figure 48–5 The axons of inhibitory interneurons in the cerebellum terminate on a distinct region of the cerebellar Purkinje cell. Many neurons form synapses on cerebellar Purkinje neurons, each selecting a distinct domain on the Purkinje cell. The axons of inhibitory basket cells form most of their synapses on the axon hillock and initial segment. Basket cells select these domains by recognizing neurofascin, a cell surface immunoglobulin superfamily adhesion molecule that is anchored to the initial segment of the axon by ankyrin G. When the localization of neurofascin is perturbed, basket cell axons fail to restrict synapse formation to the initial segment. (Adapted from Huang 2006.)

often confine their terminals to one layer, even if the dendritic tree of the postsynaptic cell traverses numerous layers. In the cerebellum, the axons of different types of neurons terminate on distinct domains of the Purkinje neurons. Granule cell axons contact distal dendritic spines, climbing fiber axons contact proximal dendritic shafts, and basket cell axons contact the axon hillock and initial segment (Figure 48–5).

Such specificity presumably relies on molecular cues on the postsynaptic cell surface. For Purkinje neurons of the cerebellum, one such cue is neurofascin, an adhesion molecule of the immunoglobulin superfamily. Neurofascin is present at high levels on the axonal initial segment, thus directing basket cells to form axons selectively on this axonal domain. Adhesion molecules can therefore also serve as recognition molecules for particular domains of a neuron. Since individual neurons can form synapses with several classes of pre- and postsynaptic cells, it follows that each neuronal subtype must express a variety of synaptic recognition molecules.

Neural Activity Sharpens Synaptic Specificity

So far, we have emphasized the role of recognition molecules in the initial formation of synapses. Once synapses form, however, neural activity within the circuit plays a critical role in refining synaptic patterns. For example, as described above, guidance of olfactory neurons to the olfactory bulb includes an initial activity-independent crude mapping followed by an activity-dependent phase in which the projection is refined.

A similar biphasic pattern has been studied in detail in the visual system. Retinal ganglion cells project to the optic tectum (superior colliculus), where interactions between ephrins and Eph kinases result in formation of a crude retinotopic map of retinal axons on the tectal surface (Chapter 47). Activity-dependent processes then sculpt the axonal arbors of retinal ganglion cells. The axons initially form broad diffuse arbors, which gradually become denser but more focused, sharpening the tectal map (Figure 48–6). This refinement is inhibited when the activity of synapses is blocked. The molecular mechanisms of this activity-dependent refinement are largely unknown. As in the olfactory system, an attractive idea is that the level and pattern of neuronal activity regulate the expression of recognition molecules.

These examples from the olfactory and visual systems illustrate a widespread phenomenon: Molecular cues initially control synapse specificity, but once the circuit begins to function, specificity is sharpened

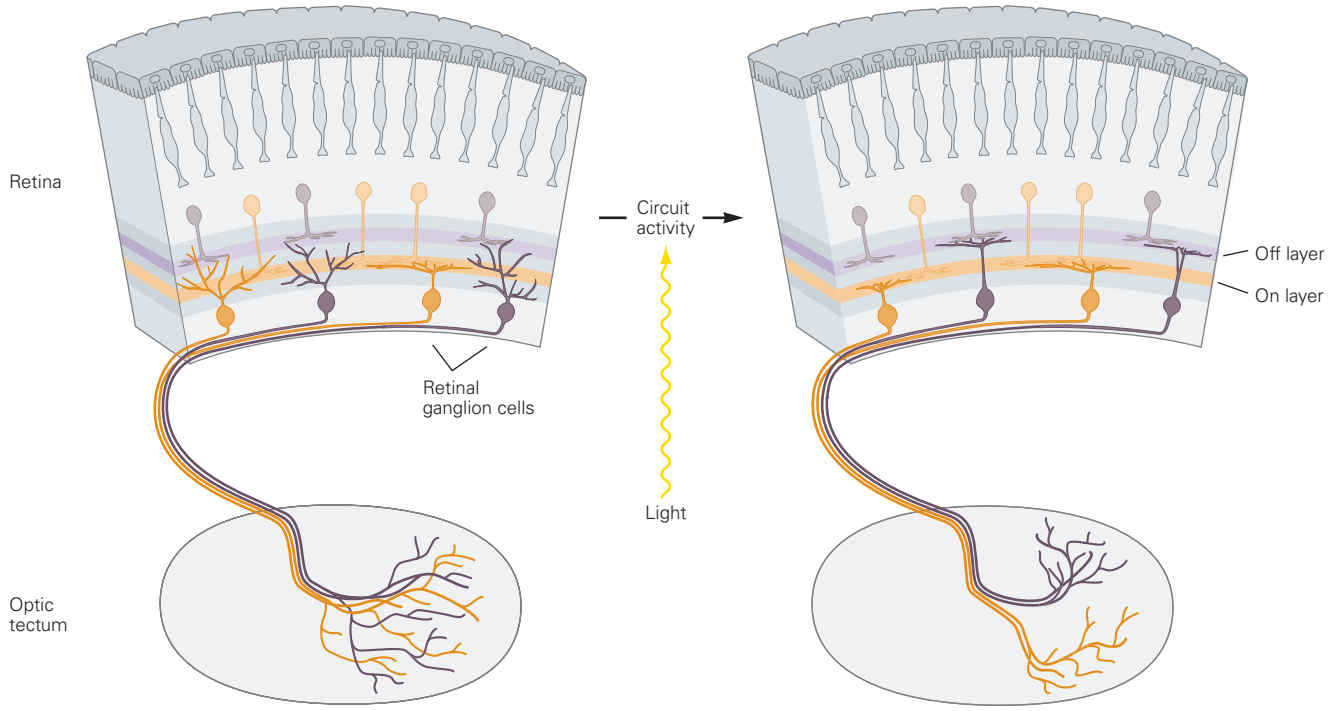

Figure 48–6 Electrical activity refines the specificity of synaptic connections of retinal ganglion cells. Some retinal ganglion cells initially form dendritic arbors that are limited to specific sublaminae in the inner plexiform layer of the retina, whereas others initially form diffuse arbors that are later pruned to form large specific patterns. Similarly, the axonal arbors of retinal ganglion cells initially innervate a large region of their target fields in the superior colliculus. This expansive axonal arbor is then refined so as to concentrate many branches in a small region. Abolishing electrical activity in retinal ganglion cells decreases the remodeling of dendritic and axonal arbors.

through neural activity. In the visual system, sharpening involves loss of synapses. We will return to this process of synapse elimination at the end of this chapter and consider its consequences for behavior in the next chapter.

In a few cases, neural activity promotes specificity in a different way, by turning an inappropriate target into an appropriate one. This mechanism has been most clearly demonstrated in skeletal muscle, where mammalian muscle fibers can be divided into several categories according to their contractile characteristics (Chapter 31). Muscle fibers of particular types express genes for distinctive isoforms of the main contractile proteins, such as myosins and troponins.

Few muscles are composed exclusively of a single type of fiber; most have fibers of all types. Yet the branches of an individual motor axon innervate muscle fibers of a single type, even in "mixed" muscles in which fibers of different types are intermingled (Figure 48–7A). This pattern implies a remarkable degree of synaptic specificity. However, matching does not always come about through recognition in the motor axon of the appropriate type of muscle fiber. The motor axon can also convert the target muscle fiber to an appropriate type. When a muscle is denervated at birth, before the properties of its fibers are fixed, a nerve that normally innervates a slow muscle can be redirected to innervate a muscle destined to become fast, and vice versa. Under these conditions, the contractile properties of the muscle are partially transformed in a direction imposed by the firing properties of the motor nerve (Figure 48–7B,C).

Different patterns of neural activity in fast and slow motor neurons are responsible for the switch in muscle properties. Most strikingly, direct electrical stimulation of a muscle with patterns normally evoked by slow or fast nerves leads to changes that are nearly as dramatic as those produced by cross-innervation (Figure 48–7D). Although activity-based conversion of the type observed at the neuromuscular junction is unlikely to be a major contributor to synaptic specificity in the central nervous system, it is likely that central axons modify the properties of their synaptic targets, contributing to the diversification of neuronal subtypes and refining connectivity imposed by recognition molecules.

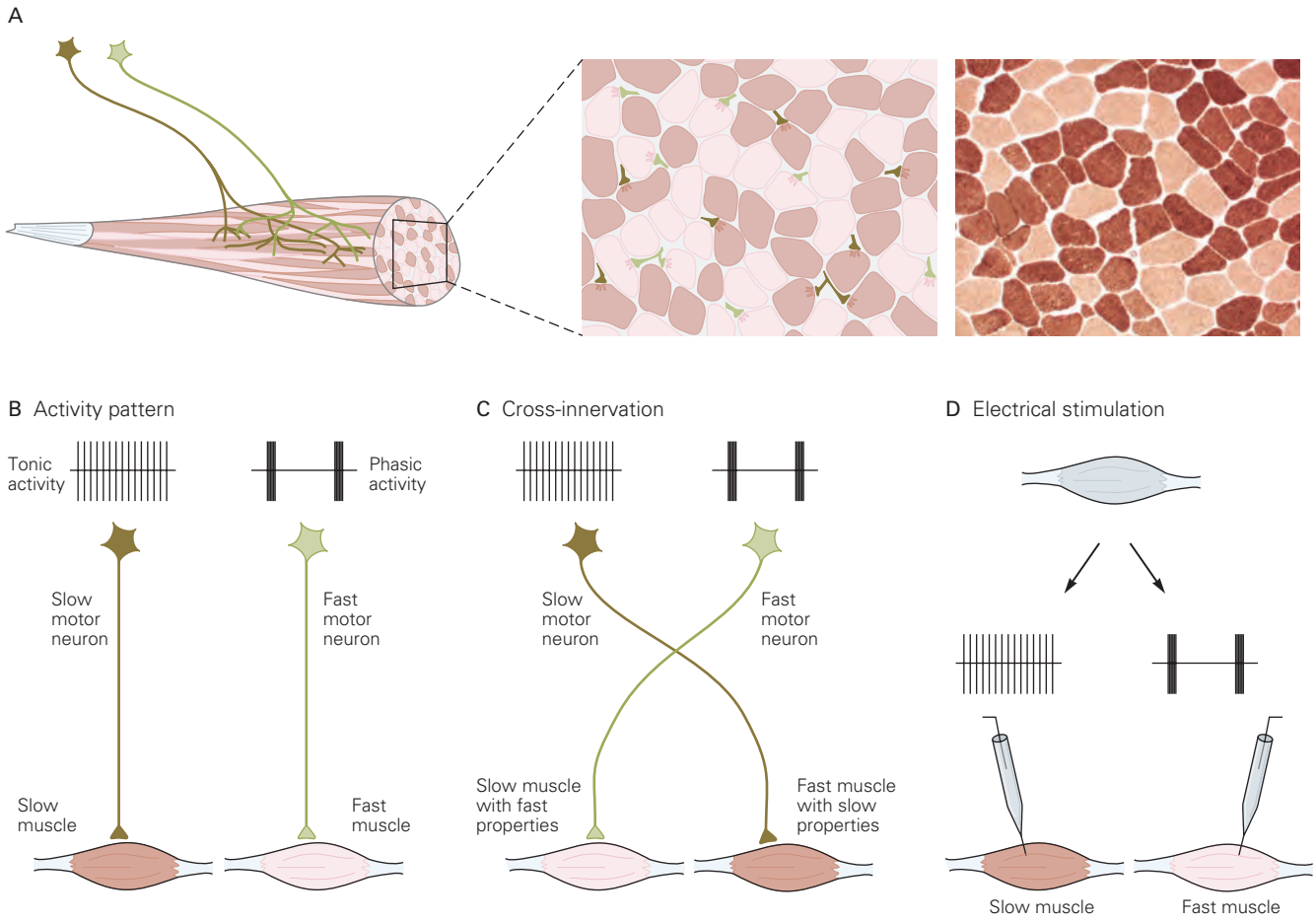

Figure 48–7 The pattern of motor neuron activity can change the biochemical and functional properties of skeletal muscle cells.

A. Muscle fibers have characteristic metabolic, molecular, and electrical properties that identify them as "slow" (tonic) or "fast" (phasic) types. The micrograph on the right shows a section of muscle tissue with histochemical staining for myosin ATPase. The middle sketch shows a section through the muscle, in which motor neurons (**green** and **brown**) form synapses on a single type of muscle fiber. (Photo on right reproduced, with permission, from Arthur P. Hays.)

B. Motor neurons that connect with fast and slow muscle fibers (fast and slow motor neurons) exhibit distinct patterns of electrical activity: steady low-frequency (tonic) firing for slow fibers and intermittent high-frequency bursts (phasic) for fast fibers.

C. Cross-innervation experiments showed that some property of the motor neuron helps to determine whether muscle fibers are fast or slow. Cross-innervation was achieved by surgically rerouting fast axons to slow muscle and vice versa. Although the properties of the motor neurons are little changed, the properties of the muscle change profoundly. For example, fast motor neurons induce fast properties in the slow muscle. (Adapted, with permission, from Salmons and Sreter 1976.)

D. The effects of innervation by fast and slow nerves on muscle are mediated in part by their distinct patterns of activity. Stimulation of a fast muscle in a slow tonic pattern converts the muscle into a slow type. Conversely, fast phasic stimulation of a slow muscle can convert it to a faster type.

Principles of Synaptic Differentiation Are Revealed at the Neuromuscular Junction

The neuromuscular junction comprises three types of cells: a motor neuron, a muscle fiber, and Schwann cells. All three types are highly differentiated in the region of the synapse.

The process of synapse formation is initiated when a motor axon, guided by the multiple factors described in Chapter 47, reaches a developing skeletal muscle and approaches an immature muscle fiber. Contact is made, and the process of synaptic differentiation gets underway. As the growth cone begins its transformation into a nerve terminal, the portion of the muscle

surface opposite the nerve terminal begins to acquire its own specializations. As development proceeds, synaptic components are added and structural signs of synaptic differentiation become apparent in the pre- and postsynaptic cells and in the synaptic cleft. Eventually, the neuromuscular junction acquires its mature and complex form (Figure 48–8).

Three general features of neuromuscular junction development have provided clues about the molecular mechanisms that underlie synapse formation. First, nerve and muscle organize each other's differentiation. In principle, the precise apposition of pre- and postsynaptic specializations might be explained by independent programming of nerve and muscle properties. However, in muscle cells cultured alone, acetylcholine (ACh) receptors are generally distributed uniformly on the surface, although some are clustered as in mature postsynaptic membranes. Yet, when motor neurons are added to the cultures, they extend neurites that contact the muscle cells more or less randomly, instead of seeking out the ACh receptor clusters. New receptor clusters appear precisely at the points of contact with the presynaptic neurites, while preexisting uninnervated clusters eventually disperse (Figure 48–9). Thus, factors on or released by motor axons exert a profound influence on the synaptic organization of the muscle cell.

Likewise, muscles signal retrogradely to motor nerve terminals. When motor neurons in culture extend neurites, they assemble and transport synaptic vesicles, some of which form aggregates similar to those found in nerve terminals. When the neurites contact muscle cells, new vesicle clusters form opposite the muscle membrane, and most of the preexisting clusters disperse.

These studies also revealed a second feature of neuromuscular development: that motor neurons and muscle cells can synthesize and arrange most synaptic components without each other's help. Uninnervated myotubes can synthesize functional ACh receptors and gather them into high-density aggregates. Likewise, motor axons can form synaptic vesicles and cluster them into varicosities in the absence of muscle. In fact, vesicles in growth cones can synthesize and release ACh in response to electrical stimulation, before the growth cone has reached its target cells. Thus, the developmental signals that pass between nerve and muscle do not induce wholesale changes in cell properties; rather, they assure that components of the pre- and postsynaptic machinery are organized at the correct time and in the right places. It is useful therefore to think of the intercellular signals that control synaptogenesis as organizers rather than inducers.

A third key feature of neuromuscular junction development is that new synaptic components are added in several distinct steps. The newly formed synapse is not simply a prototype of a fully developed synapse. Although nerve and muscle membrane form close contacts at early stages of synaptogenesis, only later does the synaptic cleft widen and the basal lamina appear. Similarly, ACh receptors accumulate in the postsynaptic membrane before acetylcholinesterase accumulates in the synaptic cleft, and the postsynaptic membrane acquires junctional folds only after the nerve terminal has matured. Several different axons innervate each myotube around the time of birth, but during early postnatal life, all but one axon withdraws.

This elaborate sequence is not orchestrated by the simple act of contact between nerve and muscle. Instead, multiple signals pass between the cells—the nerve sends a signal to the muscle that triggers the first steps in postsynaptic differentiation, at which point the muscle sends a signal that triggers the initial steps of nerve terminal differentiation. The nerve then sends further signals to the muscle, and this interaction continues.

We now consider retrograde (from muscle to nerve) and anterograde (from nerve to muscle) organizers in more detail.

Differentiation of Motor Nerve Terminals Is Organized by Muscle Fibers

Soon after the growth cone of a motor axon contacts a developing myotube, a rudimentary form of neurotransmission begins. The axon releases ACh in vesicular packets, the transmitter binds to receptors, and the myotube responds with depolarization and weak contraction.

The onset of transmission at the new synapse reflects the intrinsic capabilities of each synaptic partner. Nevertheless, these intrinsic capabilities cannot readily explain the marked increase in the rate of transmitter release that occurs after nerve-muscle contact is made, nor can they explain the accumulation of synaptic vesicles and the assembly of active zones in the small portion of the motor axon that contacts the muscle surface. These developmental steps require signals from muscle to nerve.

A clue to the source of these signals came from studies on the reinnervation of adult muscle. Although axotomy leaves muscle fibers denervated and leads to insertion of ACh receptors in nonsynaptic regions, the postsynaptic apparatus remains largely intact. It is still recognizable by its synaptic nuclei, junctional folds, and the ACh receptors, which remain far more densely

A Development stages

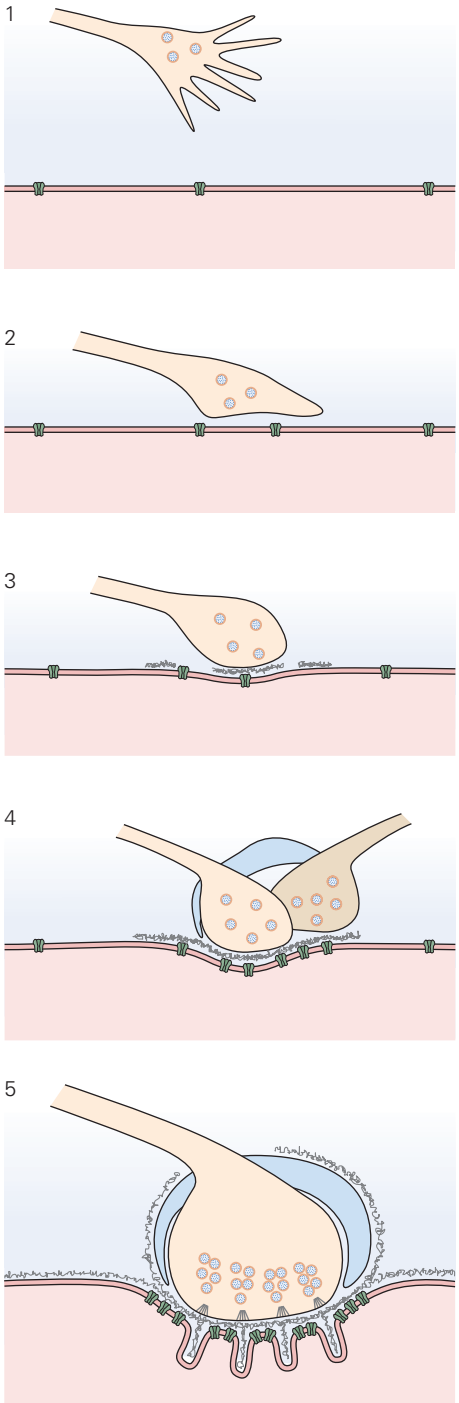

B Mature neuromuscular junction

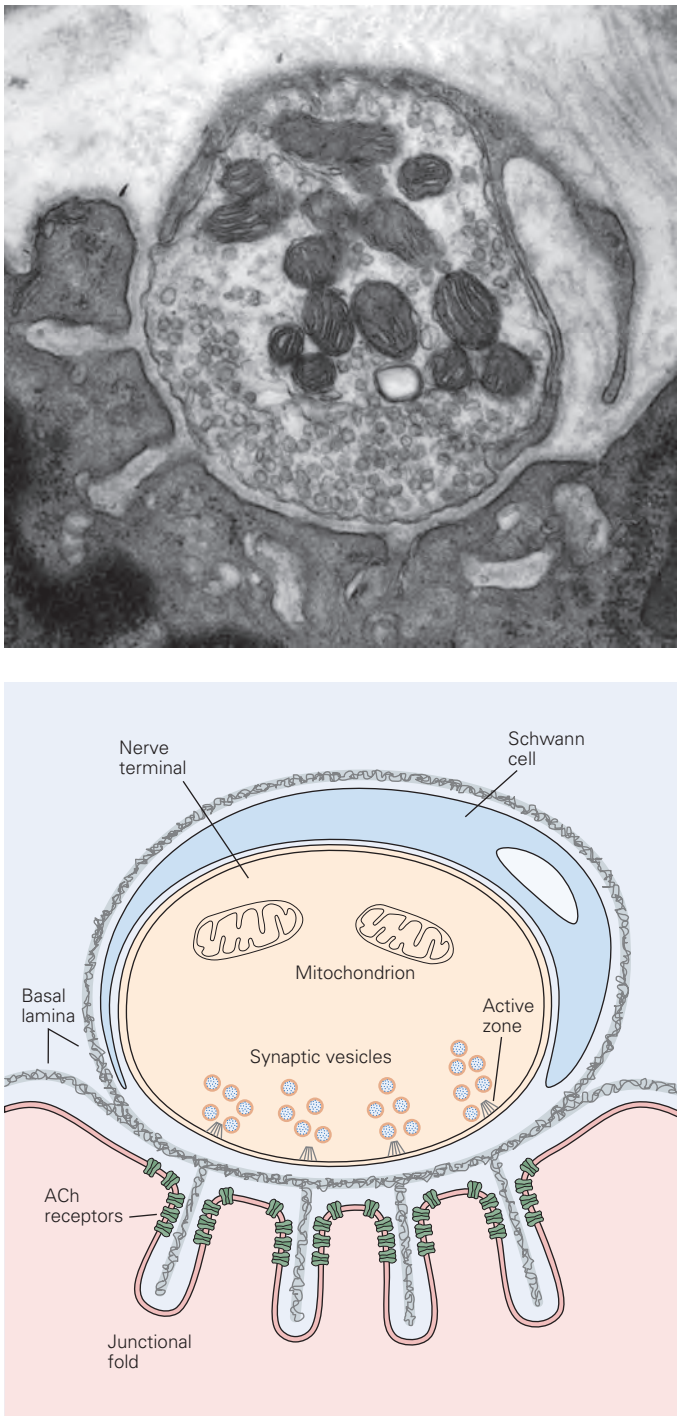

Figure 48–8 The neuromuscular junction develops in sequential stages.

A. A growth cone approaches a newly fused myotube (**1**) and forms a morphologically unspecialized but functional contact (**2**). The nerve terminal accumulates synaptic vesicles and a basal lamina forms in the synaptic cleft (**3**). As the muscle matures, multiple axons converge on a single site (**4**). Finally, all axons but one are eliminated and the surviving terminal matures (**5**). As the synapse matures, acetylcholine (**ACh**) receptors become concentrated in the postsynaptic membrane and depleted from the extrasynaptic membrane. (Adapted, with permission, from Hall and Sanes 1993.)

B. At the mature neuromuscular junction, pre- and postsynaptic membranes are separated by a synaptic cleft that contains basal lamina and extracellular matrix proteins. Vesicles are clustered at presynaptic release sites, transmitter receptors are clustered in the postsynaptic membrane, and nerve terminals are coated by Schwann cell processes. (Micrograph reproduced, with permission, from T. Gillingwater.)

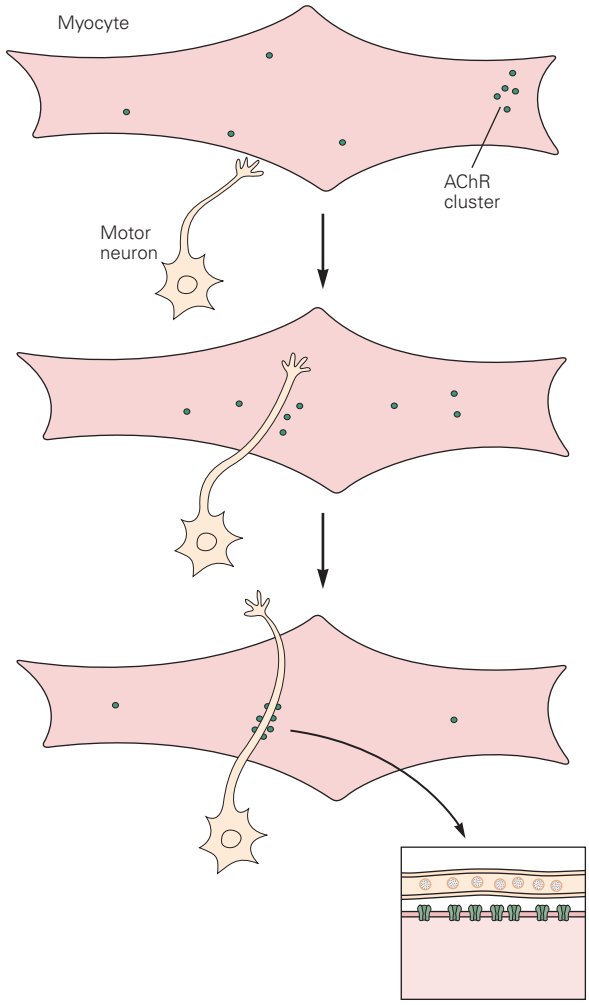

Figure 48–9 Nerve and muscle cells express synaptic components, but synaptic organization requires cell interactions. Acetylcholine receptors (AChR) are synthesized by muscle cells cultured without neurons. Many receptors are diffusely distributed, but some form high-density aggregates similar to those found in the postsynaptic membrane of the neuromuscular junction. When neurons first contact muscle, they do not restrict themselves to the receptor-rich aggregates. Instead, new receptor aggregates form at sites of neurite-muscle contact, and many of the preexisting clusters disperse. Similarly, motor axons contain synaptic vesicles that cluster at sites of neurite contact with muscle cells. (Adapted, with permission, from Anderson and Cohen 1977; Lupa, Gordon, and Hall 1990.)

packed in synaptic areas than in extrasynaptic areas of the cell. Damaged peripheral axons regenerate readily (unlike those in the central nervous system) and form new neuromuscular junctions that look and perform much like the original ones.

A century ago, Fernando Tello-Muñóz, a student of Santiago Ramón y Cajal, noted that the new junctions form at preexisting synaptic sites on the denervated muscle fibers even though the postsynaptic specializations occupy only 0.1% of the muscle fiber surface (Figure 48–10A). Later, electron microscopy showed that specialization in the axon occurs only in the terminals that contact the muscle. For example, active zones form directly opposite the mouths of the postsynaptic junctional folds. This striking example of subcellular specificity implies that motor axons recognize signals associated with the postsynaptic apparatus.

When regenerating axons reach a muscle fiber, they encounter the basal lamina of the synaptic cleft. To explore the significance of this association, muscles were damaged in vivo in a way that killed the muscle fibers but left their basal lamina intact. The necrotic fibers were phagocytized, leaving behind basal lamina sheaths on which synaptic sites were readily recognizable. At the same time that the muscle was damaged, the nerve was cut and allowed to regenerate. Under these conditions, motor axons reinnervated the empty basal lamina sheaths, contacting synaptic sites as precisely as they would have if muscle fibers were present. Moreover, nerve terminals developed at these sites and active zones even formed opposite struts of basal lamina that once lined junctional folds. These observations implied that components of the basal lamina organize presynaptic specialization (Figure 48–10B).

Several such molecular organizers have now been identified. Among the best studied are isoforms of the protein laminin. Laminins are major components of all basal laminae and promote axon outgrowth in many neuronal types. They are heterotrimers of α, β, and γ chains, comprising a family of five α, four β, and three γ chains (Chapter 47). Muscle fibers synthesize multiple laminin isoforms and incorporate them into the basal lamina. Laminin-211, a heterotrimer containing the $\alpha 2$, $\beta 1$, and $\gamma 1$ chains, is the major laminin in the basal lamina, and its absence leads to severe muscular dystrophy. In the synaptic cleft, however, isoforms bearing the $\beta 2$ chain predominate (Figure 48–11A), and nerve terminals fail to differentiate fully in mutant mice that lack the $\beta 2$ laminin (Figure 48–11B). The $\beta 2$ laminins appear to act by binding to voltage-sensitive calcium channels that reside in the axon terminal membrane, where they couple activity to transmitter release. Laminins act on the extracellular domain of the channels, whereas the intracellular segment recruits or stabilizes other components of the release apparatus.

The finding that presynaptic differentiation is only partially compromised in the absence of laminins indicated that additional muscle-derived organizers of axonal specialization must exist. Several have now been identified, including members of the fibroblast

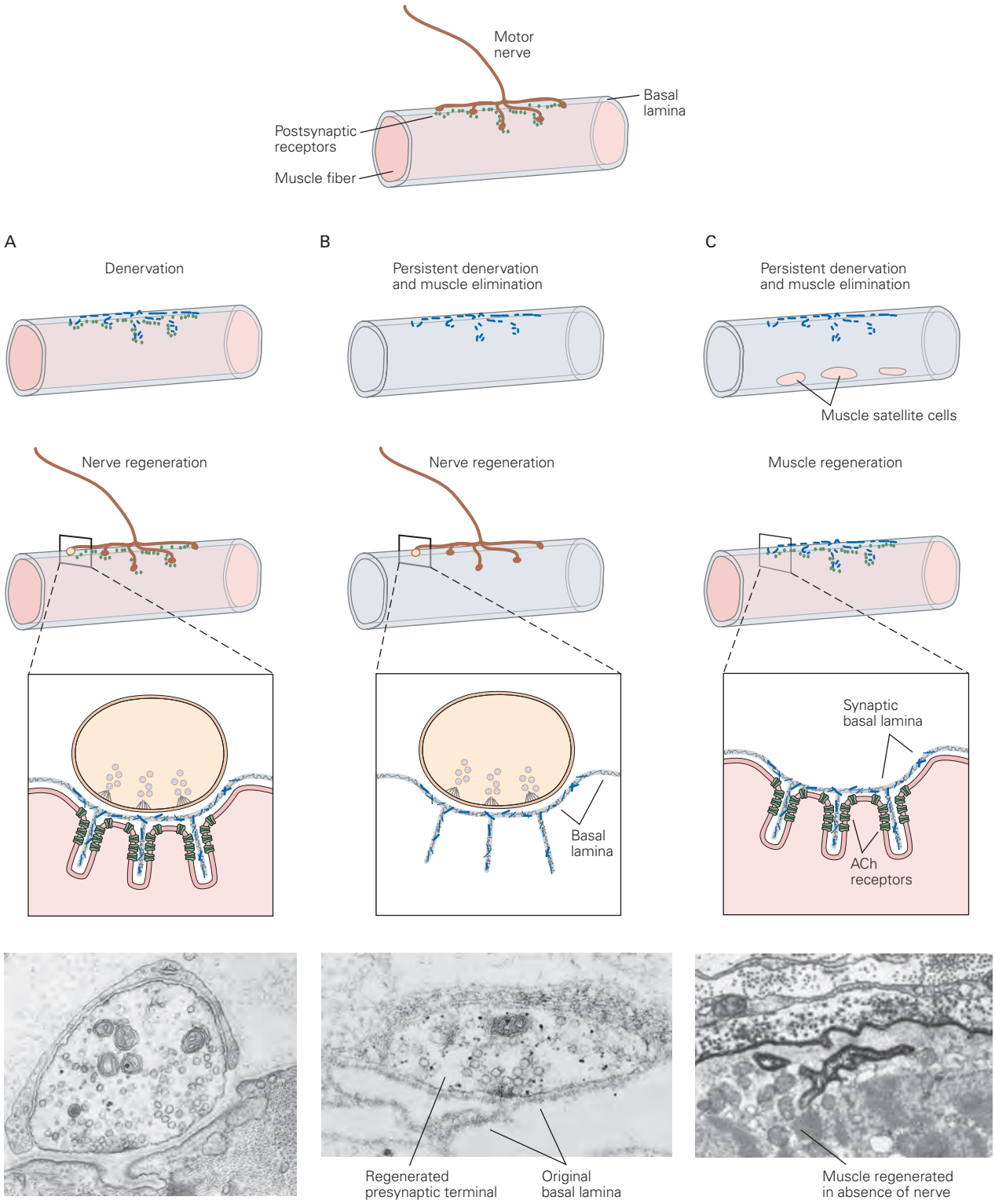

Figure 48–10 Synaptic portions of basal lamina contain proteins that organize developing and regenerating nerve terminals.

A. Damaged motor axons regenerate and form new neuromuscular junctions. Nearly all of the new synapses form at the original synaptic sites. (Micrograph reproduced, with permission, from Glicksman and Sanes 1983.)

B. A strong preference for innervation at original synaptic sites persists even after the muscle fibers have been removed, leaving behind basal lamina "ghosts." Regenerated axons develop synaptic specialization on contact with the original synaptic sites on the basal lamina. (Micrograph reproduced, with permission, from Glicksman and Sanes 1983.)

C. Following denervation of a skeletal muscle fiber and elimination of mature muscle fibers, muscle satellite cells proliferate and differentiate to form new myofibers. The expression of acetylcholine (ACh) receptors on the regenerated myofiber surface is concentrated in the synaptic areas of basal lamina, even when reinnervation is prevented. (Micrograph reproduced, with permission, from Burden, Sargent, and McMahan 1979.)

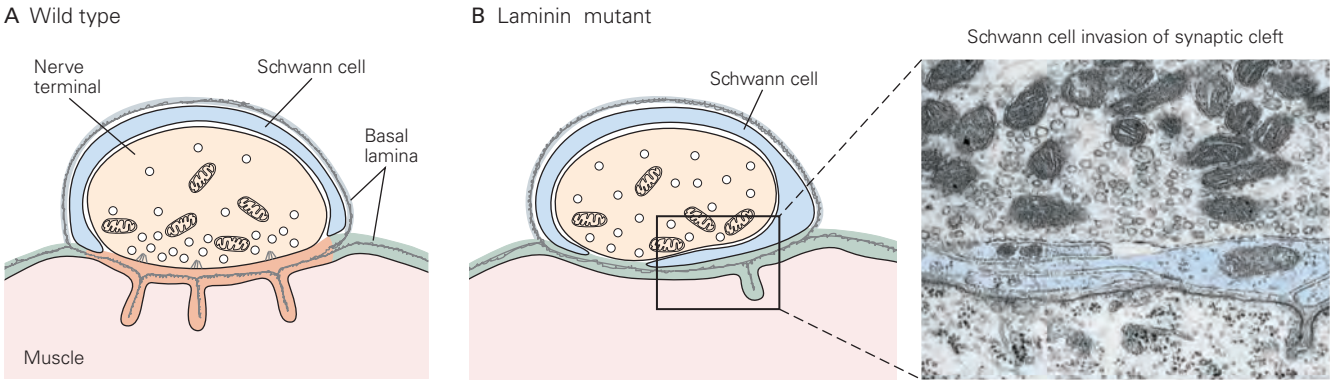

Figure 48–11 Different laminin isoforms are localized at synaptic and extrasynaptic areas of the basal lamina.

A. Different laminin isoforms are found in synaptic (**brown**) and extrasynaptic (**green**) areas of basal lamina. Isoforms, containing the β2 chain, are concentrated in the synaptic areas.

B. Maturation of neuromuscular junctions is impaired in mice lacking β2 laminins. These mutants have few active zones, and the synaptic cleft is invaded by Schwann cell processes (**blue**). (Micrograph reproduced, with permission, from Noakes et al. 1995.)

growth factor and collagen IV families, as well as a muscle membrane-associated protein, LRP4, that we will soon encounter again in the context of postsynaptic differentiation. Thus target-derived proteins from multiple families collaborate to organize the presynaptic nerve terminal.

Differentiation of the Postsynaptic Muscle Membrane Is Organized by the Motor Nerve

Soon after myoblasts fuse to form myotubes, the genes that encode ACh receptor subunits are activated. Receptor subunits are synthesized, assembled into pentamers in the endoplasmic reticulum, and inserted into the plasma membrane. As noted above, some receptors spontaneously form aggregates, but the majority are distributed throughout the membrane at a low density, approximately 1,000 per μm^2.

Once synapse formation is complete, however, the distribution of the receptors changes drastically. The receptors become concentrated at the synaptic sites of the membrane (to a density up to 10,000 per μm^2) and depleted in the nonsynaptic membrane (reduced to 10 per μm^2 or less). This thousand-fold difference in ACh receptor density occurs within a few tens of micrometers from the edge of the nerve terminal.

Appreciation of the critical role of the nerve in the redistribution of ACh receptors inspired a search for factors that might promote their clustering. This quest led to the discovery of a proteoglycan, agrin. Agrin is synthesized by motor neurons, transported down the axon, released from nerve terminals, and incorporated into the synaptic cleft (Figure 48–12A,B). Some agrin isoforms are also made by muscle cells, but the neuronal isoforms are about a thousand-fold more active in aggregating ACh receptors.

The phenotype of mutant mice lacking agrin shows that agrin has a central role in the organization of ACh receptors. Agrin mutants have grossly perturbed neuromuscular junctions and die at birth. The number, size, and density of ACh receptor aggregates are severely reduced in these mice (Figure 48–12C). Other components of the postsynaptic apparatus—including cytoskeletal, membrane, and basal lamina proteins—are also reduced. Interestingly, the differentiation of presynaptic elements is also perturbed. However, the defects in the presynaptic element do not result directly from lack of agrin in the motor neuron, but rather indirectly from the failure of the disorganized postsynaptic apparatus to generate signals for presynaptic specialization.

How does agrin work? Agrin's major receptor is a complex of a muscle-specific tyrosine kinase called MuSK (muscle-specific trk-related receptor with a kringle domain) and a coreceptor subunit called LRP4 (Figure 48–12A). MuSK and LRP4 are normally concentrated at synaptic sites in the muscle membrane, and muscles of mutant mice lacking MuSK or LRP4 do not have ACh receptor clusters (Figure 48–12C). Myotubes generated in vitro from these mutants express normal levels of ACh receptors, but these receptors cannot be clustered by agrin. Binding of agrin to the MuSK/LRP4 complex initiates a chain of events that ends in receptor clustering. Key events are agrin-induced activation of MuSK's kinase activity; autophosphorylation of the MuSK intracellular domain; recruitment of

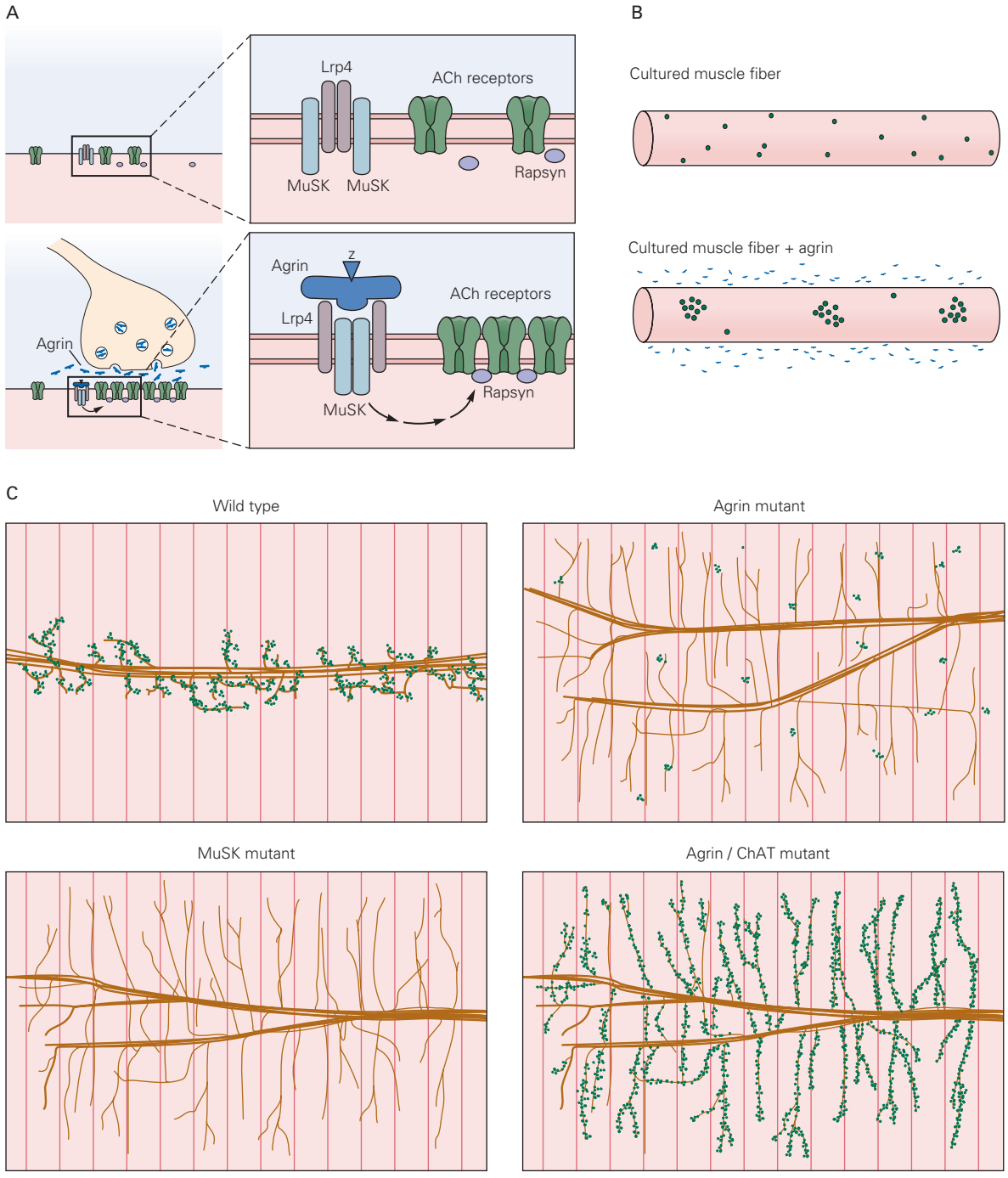

Figure 48–12 Agrin induces aggregation of acetylcholine (ACh) receptors at synaptic sites.

A. Agrin is a large (~400 kDa) extracellular matrix proteoglycan. Alternative splicing includes a "z" exon that confers the ability to cluster ACh receptors. When released by a nerve terminal, agrin binds Lrp4 on the muscle membrane, activating the membrane-associated receptor tyrosine kinase MuSK and triggering an intracellular cascade that results in ACh receptor clustering. Key intracellular signaling molecules are Dok7, Crk, and CrkL. These signal to rapsyn, a cytoplasmic ACh receptor–associated protein, which physically interacts with and clusters the ACh receptors. (Adapted, with permission, from DeChiara et al. 1996.)

B. Few ACh receptor clusters form on myofibers grown in culture under control conditions, but addition of agrin induces ACh receptor clustering. (Adapted, with permission, from Misgeld et al. 2005.)

C. Muscles from wild-type neonatal mice and from three mutant types. Muscles were labeled for ACh receptors (**green**) and motor axons (**brown**). In wild-type mice, ACh receptor clusters have formed under each nerve terminal by birth, whereas in agrin mutants, most clusters have dispersed. ACh receptor clusters are also absent in MuSK, Dok7, and rapsyn mutant mice. When the genes for agrin and **ChAT** (choline acetyltransferase) are mutated, clusters of ACh receptors remain, indicating that agrin works by counteracting receptor dispersion mediated by ACh. All mutant conditions also show axonal abnormalities, reflecting defects in retrograde signaling to the motor axon. (Abbreviation: **MuSK**, muscle-specific trk-related receptor with a kringle domain.) (Adapted, with permission, from Gautam et al. 1996.)

adaptor proteins Dok-7, Crk, and CrkL; and strengthening of an interaction between a cytoplasmic protein rapsyn and the ACh receptors. Rapsyn may be the final element in the sequence: It binds directly to the ACh receptors and can induce their aggregation in vitro. In mice lacking rapsyn, muscles form normally and ACh receptors accumulate in normal numbers but fail to aggregate at the synaptic sites on the membrane. Accordingly, muscles of mutant mice lacking Dok7 or rapsyn resemble those lacking MuSK or LRP4: They synthesize ACh receptors but do not have ACh receptor clusters.

Thus, an extracellular protein (agrin), transmembrane proteins (MuSK and LRP4), adaptor proteins (Dok-7, Crk, and CrkL), and a cytoskeletal protein (rapsyn) form a chain that links commands from the motor axon to ACh receptor clustering in the muscle membrane.

Nevertheless, postsynaptic differentiation can occur in the absence of agrin signaling. This capacity was apparent in early studies on cultured muscle (see Figure 48–9) and is also seen in vivo: ACh receptor clusters form initially but then disperse in agrin mutants (Figure 48–12C). Clustering also occurs in muscles that lack innervation entirely. Thus, the signaling pathway that initiates postsynaptic differentiation can be activated without agrin, but agrin is required to maintain clustering of ACh receptors.

The role of agrin is perhaps best understood in terms of the requirement that pre- and postsynaptic specializations be perfectly aligned. ACh receptor aggregates persist in uninnervated muscles but disappear in agrin mutant muscles, suggesting that axons sculpt the postsynaptic membrane through the combined action of agrin and a dispersal factor. One major dispersal factor is ACh itself; clustering persists in mutants that lack both agrin and ACh (Figure 48–12C). Thus, agrin may render ACh receptors immune to the declustering effects of ACh. Through a combination of positive and negative factors, the motor neuron ensures that the patches of postsynaptic membrane contacted by axon branches are rich in ACh receptors.

The Nerve Regulates Transcription of Acetylcholine Receptor Genes

Along with redistribution of ACh receptors in the plane of the membrane, the motor nerve orchestrates the transcriptional program responsible for expression of ACh receptor genes in muscle. To understand this aspect of transcriptional control, it is important to appreciate the geometry of the muscle.

Individual muscle fibers are often more than a centimeter long and contain hundreds of nuclei along their length. Most nuclei are far from the synapse, but a few are clustered beneath the synaptic membrane, so that their transcribed and translated products do not have far to go to reach the synapse. In newly formed myotubes, most nuclei express genes encoding ACh receptor subunits. In adult muscles, however, only synaptic nuclei express ACh receptor genes; nonsynaptic nuclei do not. Two processes contribute to this transformation.

First, as synapses begin to form, expression of the ACh receptor subunit genes is increased in synaptic nuclei (Figure 48–13). Signals acting through MuSK are needed for this specialization. Second, around the time of birth, ACh receptor gene expression shuts down in nonsynaptic nuclei. This change reflects a repressive effect of the nerve, as originally shown by studies of denervated muscle. When muscle fibers are denervated, as happens when the motor nerve is damaged, the density of ACh receptors in the postsynaptic membrane increases markedly, a phenomenon termed *denervation supersensitivity.*

This repressive effect of the nerve is mediated by electrical activation of the muscle. Under normal conditions, the nerve keeps the muscle electrically active, and fewer ACh receptors are synthesized in active muscle than in inactive muscle. Indeed, direct stimulation of denervated muscle through implanted electrodes decreases ACh receptor expression, preventing or reversing the effect of denervation (Figure 48–13B). Conversely, when nerve activity is blocked by application of a local anesthetic, the number of ACh receptors throughout the muscle fiber increases, even though the synapse is intact.

In essence, then, the nerve uses ACh to repress expression of ACh receptor genes extrasynaptically. Current that passes through the channel of the receptor leads to an action potential that propagates along the entire muscle fiber. This depolarization opens voltage-dependent Ca^{2+} channels, leading to an influx of Ca^{2+}, which activates a signal transduction cascade that reaches nonsynaptic nuclei and regulates transcription of ACh receptor genes. Thus, the same voltage changes that produce muscle contraction over a period of milliseconds also regulate transcription of ACh receptor genes over a period of days.

The increase in transcription of ACh receptor genes in nuclei beneath the synapse, along with the decrease in nuclei distant from synapses, leads to localization of ACh receptor mRNA and thus preferential synthesis and insertion of ACh receptors near synaptic sites. This local synthesis is reminiscent of that seen

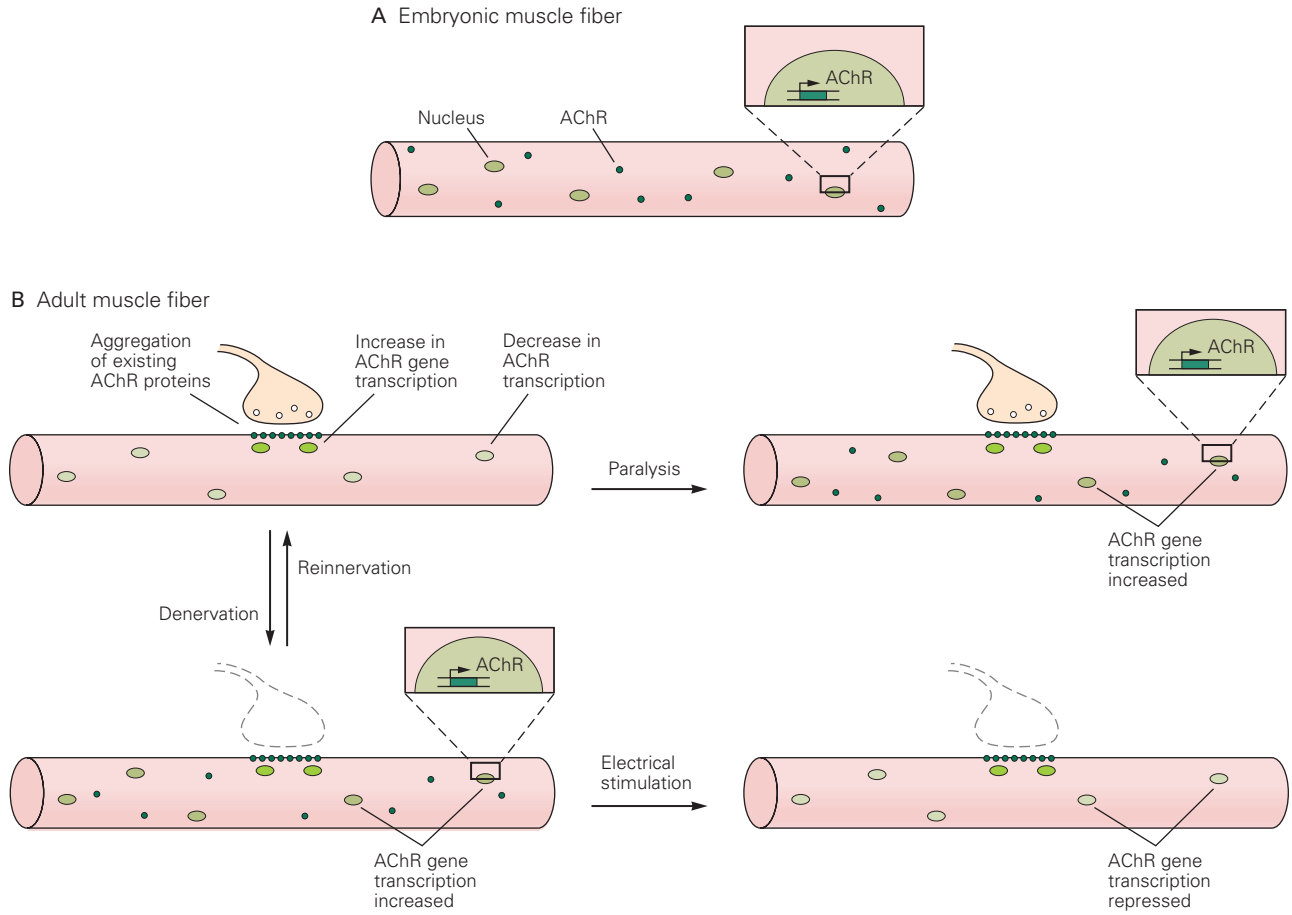

Figure 48–13 Clustering of acetylcholine (ACh) receptors at the neuromuscular junction results from transcriptional regulation and local protein trafficking.

A. ACh receptors (**AChR**) are distributed diffusely on the surface of embryonic myotubes.

B. After the muscle is innervated by a motor axon, the number of receptors in extrasynaptic regions decreases, whereas receptor density at the synapse increases. This reflects the aggregation of preexisting receptors and enhanced expression of ACh receptor genes in nuclei that lie directly beneath the nerve terminal. In addition, the transcription of receptor genes is repressed in nuclei in extrasynaptic regions. Electrical activity in muscle represses ACh gene expression in nonsynaptic nuclei, leading to a lower density of ACh receptors in these regions. The nuclei at synaptic sites are immune to this repressive effect. Following denervation, ACh receptor gene expression is upregulated in extrasynaptic nuclei, although not to the high level attained by synaptic nuclei. Paralysis mimics the effect of denervation, whereas electrical stimulation of denervated muscle mimics the influence of the nerve and decreases the density of ACh receptors in the extrasynaptic membrane.

at postsynaptic sites on dendritic spines in the brain. Local synthesis in muscle is advantageous since ACh receptors synthesized near the ends of fibers would never reach the synapse without degradation.

Many components of the postsynaptic apparatus are regulated in ways similar to those we have described for ACh receptors—their aggregation depends on agrin and MuSK, and their transcription is enhanced in synaptic nuclei and repressed in extrasynaptic nuclei by electrical activity. Thus, synaptic components have tailor-made regulatory mechanisms, but many of these components are regulated in parallel.

The Neuromuscular Junction Matures in a Series of Steps

The adult neuromuscular junction is dramatically different in its molecular architecture, shape, size, and functional properties from the simple nerve-muscle contact that initiates neurotransmission in the embryo. Maturation of the nerve terminal, the postsynaptic membrane, and the intervening synaptic cleft occurs in a complex series of steps. We illustrate this stepwise synaptic construction with a continued focus on the development of ACh receptors.

As we have seen, ACh receptors aggregate in the plane of the membrane as the neuromuscular junction begins to form, and receptor gene transcription is enhanced in postsynaptic nuclei. A few days later, activity begins to decrease the level of extrasynaptic receptors. These transcriptional changes are soon followed by changes in the stability of the receptors. In embryonic muscle, ACh receptors are turned over rapidly (with a half-life of approximately 1 day) in both synaptic and extrasynaptic regions. In contrast, in adult muscle, the receptors are relatively stable (with a half-life of approximately 2 weeks). The metabolic stabilization of ACh receptors helps concentrate them at synaptic sites and stabilize the postsynaptic apparatus.

Yet another alteration is in the composition of the ACh receptors. In the embryo, ACh receptors are composed of α-, β-, δ-, and γ-subunits. During the first few postnatal days, the γ gene is turned off and a closely related gene called ε is activated. As a result, new ACh receptors inserted in the membrane are composed of α-, β-, δ-, and ε-subunits. This altered subunit composition tunes the receptor in a way that is suited to its mature function. However, although it occurs at the same time as the metabolic stabilization, the two changes are not causally linked.

These molecular changes in the ACh receptors are accompanied by changes in their distribution (Figure 48–14). Soon after birth, junctional folds begin to form in the postsynaptic membrane and ACh receptors become concentrated at the crests of the folds, along with rapsyn, whereas other membrane and cytoskeletal proteins are localized in the depths of the folds. The initial aggregate of ACh receptors appears to have a plaque-like appearance. Perforations that undergo fusion and fission eventually transform the dense plaque into a pretzel shape that follows the branches of the nerve ending. New receptor-associated cytoskeletal proteins are added to the aggregate, presumably to drive the geometric changes. Finally, the postsynaptic membrane enlarges and eventually contains many more ACh receptors than were present in the initial cluster. Each of these changes occurs while the synapse is functional, suggesting that ongoing activity plays an important role in synaptic maturation.

Central Synapses and Neuromuscular Junctions Develop in Similar Ways

Synapses in the central nervous system are structurally and functionally similar to neuromuscular junctions in many ways. Presynaptically, most of the major protein components of synaptic vesicles are identical at both types of synapses. Likewise, the mechanisms of transmitter release differ only quantitatively, not qualitatively. Postsynaptically, neurotransmitter receptors are concentrated beneath the nerve terminal and associated with "clustering" proteins.

These parallels extend to synaptic development. Studies of cultured neurons have shown that the cellular logic of synapse formation is conserved between neuromuscular junctions and central synapses. At both synaptic types, pre- and postsynaptic elements regulate each other's differentiation by organizing synaptic components rather than by inducing their expression, and synapses develop in a progressive series of steps (Figure 48–15). The molecular details differ, however. Neuromuscular organizing molecules such as agrin and laminins do not play key roles at central synapses, suggesting that other synaptic organizers are involved. Recently, some of these organizing molecules have been identified.

Neurotransmitter Receptors Become Localized at Central Synapses

The concentration of neurotransmitter receptors in the postsynaptic membrane is a feature shared by many synapses. In the brain, receptors for glutamate, glycine, γ-aminobutyric acid (GABA), and other neurotransmitters are concentrated in patches of membrane aligned with nerve terminals that contain the corresponding transmitter.

The processes by which these receptors become localized may be similar to those at the neuromuscular junction. In cultures of dissociated hippocampal neurons, for example, both glutamatergic and GABAergic nerve terminals appear to stimulate clustering of appropriate receptors in the postsynaptic membrane. Moreover, nerves can induce expression of genes encoding glutamate receptors in central neurons, much as occurs for ACh receptors in muscle. Finally, electrical activity also regulates expression of neurotransmitter receptors in neurons.

In forming receptor clusters, central neurons face an obvious challenge that myotubes do not: They are contacted by axon terminals from distinct classes of neurons that use different neurotransmitters (Figure 48–16A). Thus, the nerve terminal probably has an instructive role in the clustering of receptors. In cultures of hippocampal neurons, glutamatergic and GABAergic axons terminate on adjacent regions of the same dendrite. Initially, glutamate and GABA receptors are dispersed, but soon, each type becomes selectively clustered beneath terminals that release that neurotransmitter. This observation implies the existence of multiple clustering signals with parallel pathways of signal transduction.

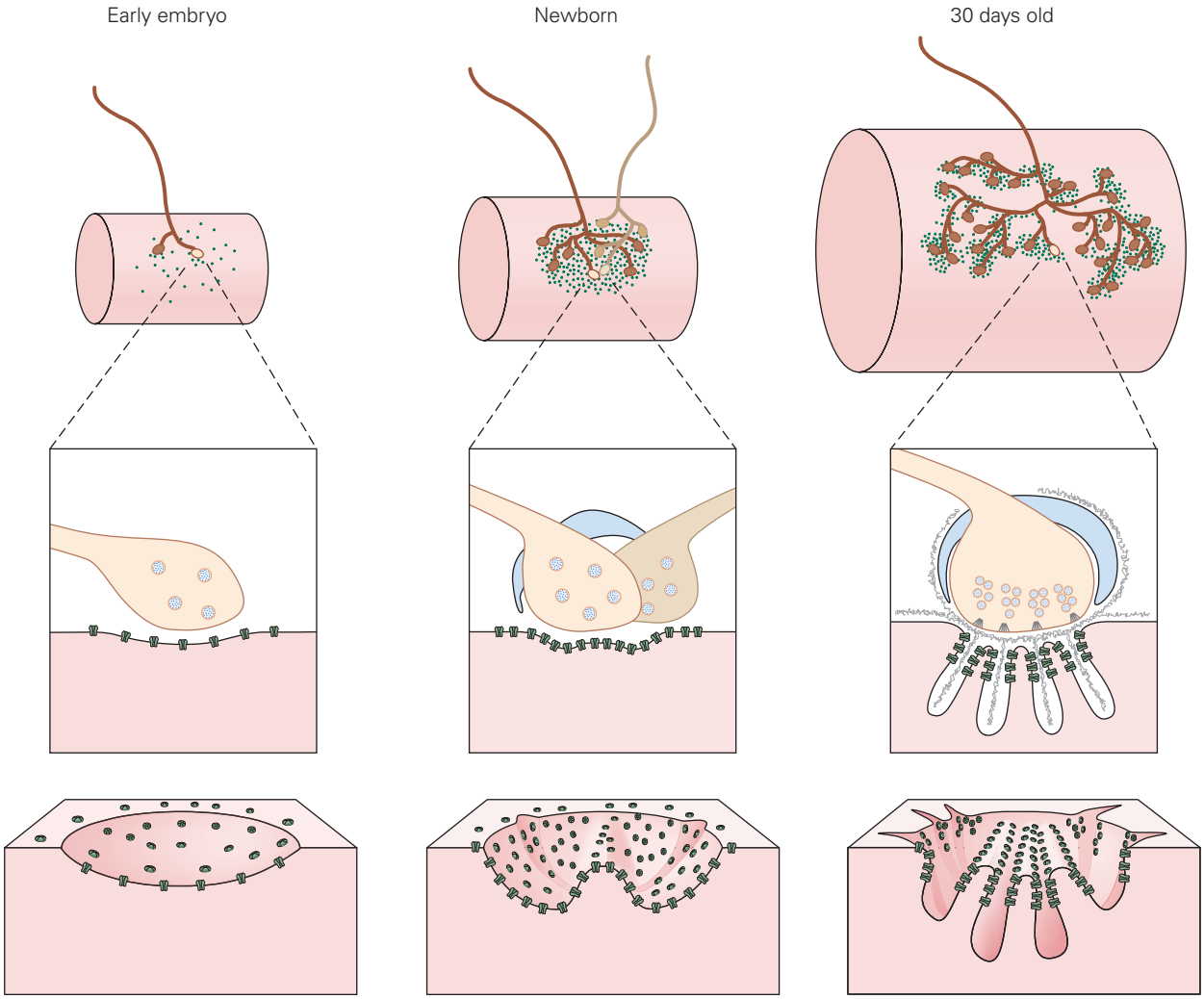

Figure 48–14 **The postsynaptic membrane at the neuromuscular junction matures in stages.** During early embryogenesis, ACh receptors exist as loose aggregates. Later, these aggregates condense into a plaque-like structure. After birth, the dense cluster opens up as the nerve develops multiple terminals. These axon branches expand in an intercalary fashion as the muscle grows, and the plaque indents to form a gutter, which then invaginates to form folds. Receptors are concentrated at the crests of the folds. (Adapted, with permission, from Sanes and Lichtman 2001.)

At the neuromuscular junction, rapsyn binds to the intracellular domain of ACh receptors and clusters them. Several proteins have been found to play similar roles at central synapses. One, gephyrin, is highly concentrated in the synaptic densities at glycinergic and some GABAergic synapses (Figure 48–16A). Gephyrin is not structurally related to rapsyn but has the same function: It links the receptors to the underlying cytoskeleton. In nonneural cells, glycine receptors cluster when gephyrin is co-expressed; conversely, clusters fail to form at inhibitory synapses in gephyrin-deficient mutant mice (Figure 48–16B). Similarly, a class of proteins that share conserved segments called PDZ domains—the prototypes being PSD-95 or SAP-90—facilitate clustering of *N*-methyl-D-aspartate (NMDA)-type glutamate receptors and their associated proteins. Other PDZ-containing proteins interact with α-amino-3-hydroxy-5-methylisoxazole-4-propionate acid (AMPA), kainate, and metabotropic types of glutamate receptors.

Synaptic Organizing Molecules Pattern Central Nerve Terminals

Although central synapses and neuromuscular junctions share many features, their synaptic clefts differ

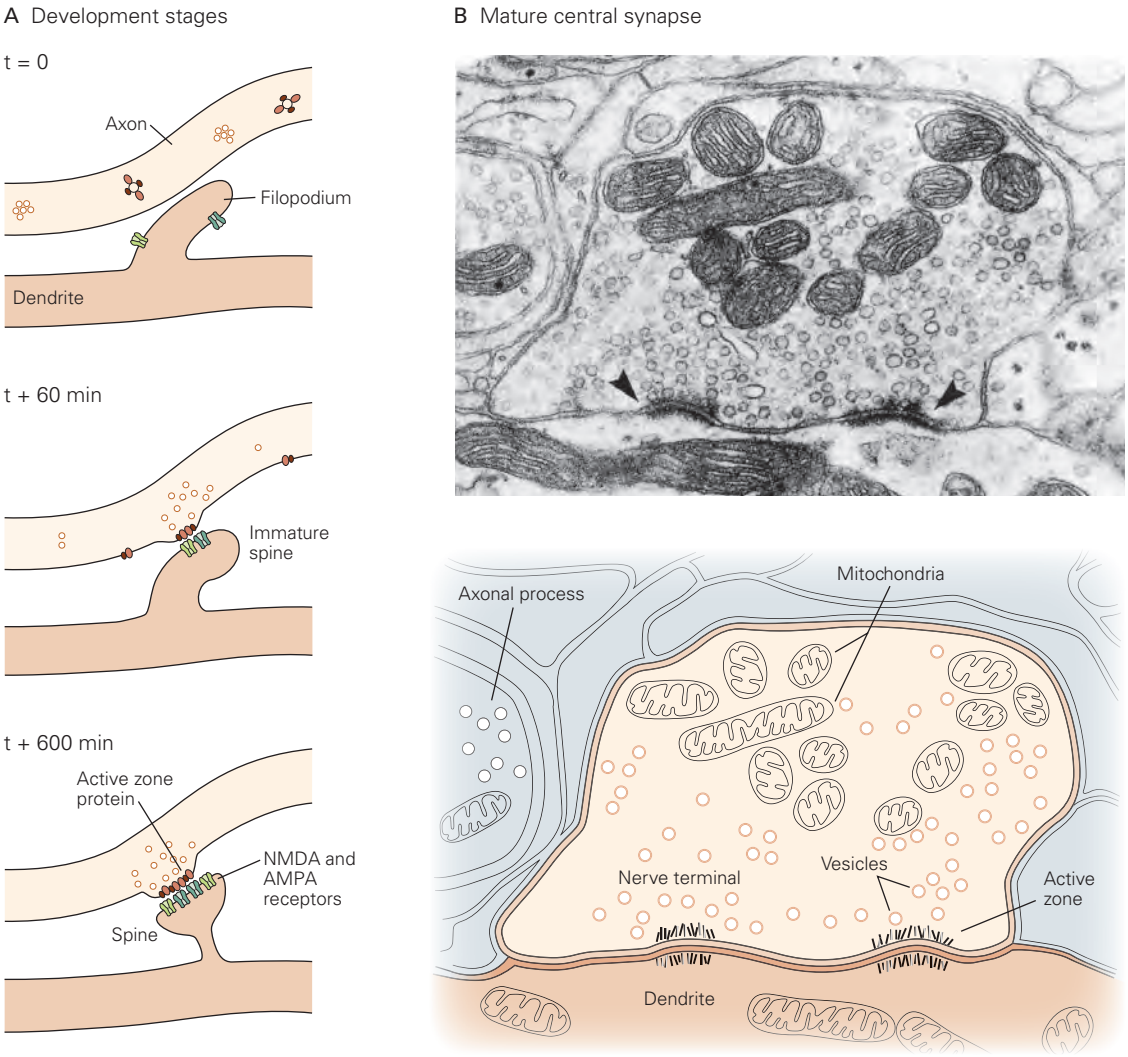

Figure 48–15 Ultrastructure of a synapse in the mammalian central nervous system.

A. Initial contact between an axon and a filopodium on a developing dendrite leads to a stable dendritic spine and an axodendritic synapse. This entire process can take as little as 60 minutes. (Abbreviations: **AMPA**, α-amino-3-hydroxy-5-methylisoxazole-4-propionate acid; **NMDA**, *N*-methyl-D-aspartate.)

B. In a mature interneuron synapse in the cerebellum, synaptic vesicles in the nerve terminal are clustered at active zones (**arrows**) directly opposite receptor-rich patches of postsynaptic membrane. (Reproduced, with permission, from J.E. Heuser and T.S. Reese.)

dramatically. Whereas muscle fibers are ensheathed by a basal lamina that has a distinctive molecular structure at the neuromuscular junction, central neurons do not have a prominent basal lamina. Instead, formation of central synapses is regulated in large part by molecules embedded in the pre- and postsynaptic membranes.

Several interacting pairs of membrane proteins have now been found that link the pre- and postsynaptic membranes and also organize synaptic differentiation as synapses form. Perhaps the best studied are a set of proteins called neurexins, which are enriched in presynaptic membranes, and their partners, the neuroligins, which are concentrated in postsynaptic membranes (Figure 48–17A). There are three neurexin and four neuroligin genes in the mammalian genome. The ability of neurexins and neuroligins to promote synaptic differentiation was first revealed by culturing neurons

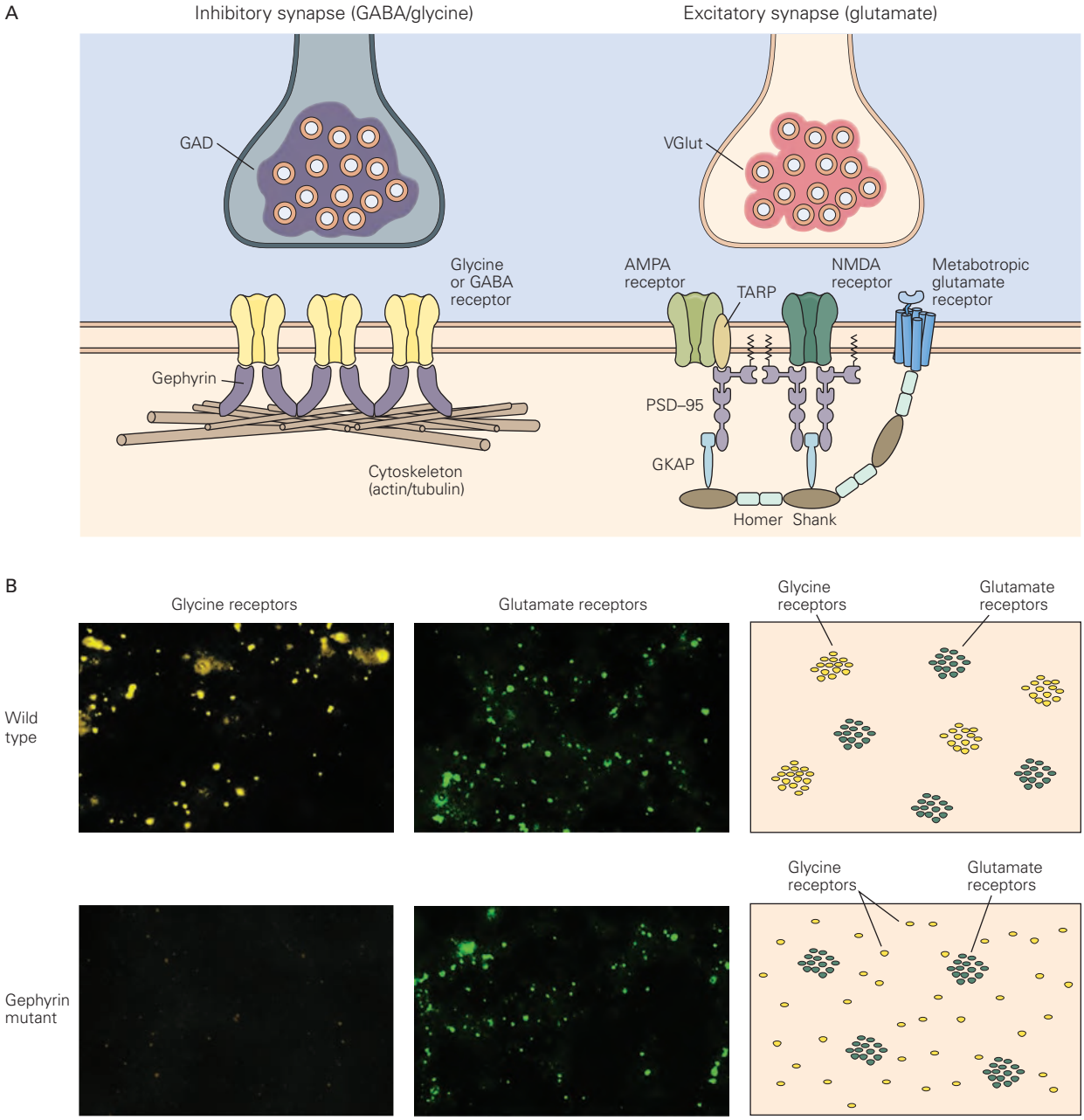

Figure 48–16 Localization of neurotransmitter receptors in central neurons.

A. Glutamate receptors are localized at excitatory synapses, and γ-aminobutyric acid (**GABA**) and glycine receptors are localized at inhibitory synapses. The receptors are linked to the cytoskeleton by adaptor proteins. Glycine receptors are linked to microtubules by gephyrin (*left*), and *N*-methyl-D-aspartate (**NMDA**)-type glutamate receptors are linked to each other and to the cytoskeleton by PSD-95–related molecules (*right*). The PSD family of molecules contains PDZ domains that interact with a variety of synaptic proteins to assemble signaling complexes. Other PDZ-containing proteins interact with α-amino-3-hydroxy-5-methylisoxazole-4-propionate acid (**AMPA**)-type and metabotropic glutamate receptors (see Chapter 13). (Abbreviations: **GAD**, glutamate decarboxylase; **GKAP**, Guanylate-kinase-associated protein; **TARP**, transmembrane AMPA receptor regulatory proteins; **VGlut**, vesicular glutamate transporter.)

B. In gephyrin mutant mice, glycine receptors do not cluster at synaptic sites on spinal motor neurons, and the animals show spasticity and hyperreflexia. In the same neurons, glutamate receptor clusters are unaffected. (Adapted, with permission, from Feng et al. 1998.)

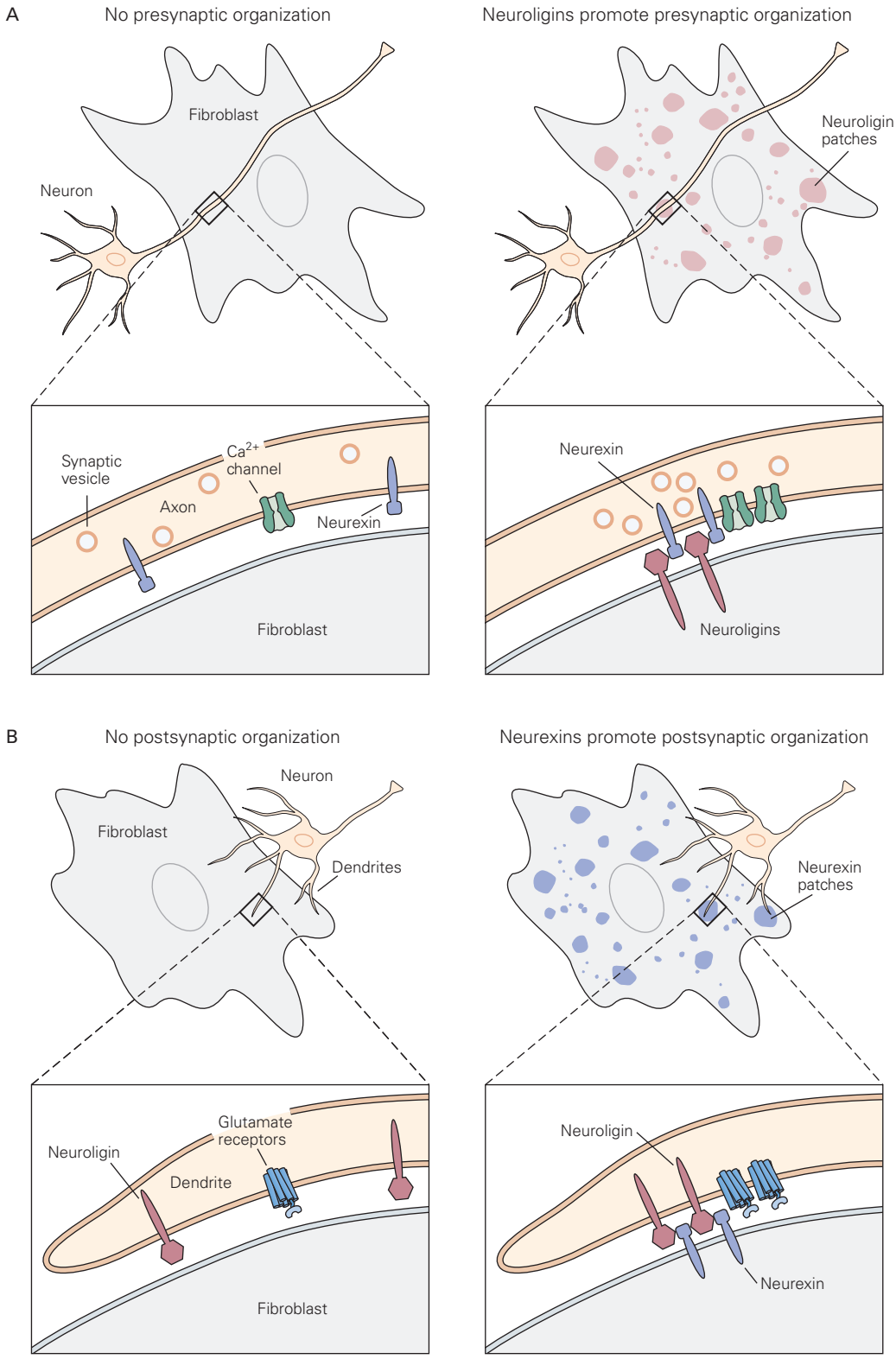

Figure 48–17 Synaptic organizers such as neurexins and neuroligins promote differentiation of central synapses.

A. When brain neurons are cultured with fibroblast cells that express neuroligin, those segments of the axon that contact these cells form presynaptic specializations, marked by clustered neurexin, Ca^{2+} channels, and synaptic vesicles.

B. Similarly, when neurons are cultured with cells that express neurexin, dendrites that contact these cells accumulate aggregates of glutamate receptors, accompanied by scaffolding molecules (not shown) and clustered neuroligins. Neurons grown with control cells fail to form such pre- and postsynaptic specializations.

with nonneural cells engineered to express one or the other. In culture, synaptic vesicles form clusters at sites of contact with the neuroligin-expressing cells, and they are capable of releasing neurotransmitter when stimulated (Figure 48–17A). Conversely, neurotransmitter receptors in dendrites aggregate at sites that contact nonneural cells engineered to express neurexins (Figure 48–17B). Thus, neurexin–neuroligin interactions facilitate precise apposition of pre- and postsynaptic specializations.

How do neurexins and neuroligins work? Part of the answer is that their carboxy terminal tails bind to PDZ domains in proteins such as PSD-95 (Figure 48–16). Indeed, a remarkable number of proteins in both pre- and postsynaptic membranes have PDZ domain-binding motifs, notably adhesion molecules, neurotransmitter receptors, and ion channels. Moreover, many cytoplasmic proteins that possess PDZ domains are present in nerve terminals and beneath the postsynaptic membrane. Thus, PDZ-containing proteins can serve as scaffolding molecules that link key components on both sides of the synapse. Interactions of proteins such as neurexins and neuroligins may provide a means of coupling the intercellular interactions required for synaptic recognition to the intracellular interactions required to cluster synaptic components within the cell membrane.

Although neurexin–neuroligin interactions promote synaptic differentiation in culture, mice lacking neurexins or neuroligins form synapses in vivo. However, the synapses that form in the mutants are defective, with the nature and severity of the defects varying among synaptic types. Thus, the primary role of these synaptic organizers may be to specify the properties of particular synapses. For example, neuroligin1 is concentrated in the postsynaptic membrane of excitatory synapses, and levels of glutamate receptors are reduced at excitatory synapses in neuroligin1 mutants. Conversely, neuroligin2 is concentrated at inhibitory synapses and plays a critical role in patterning the inhibitory postsynaptic membrane.

Additional complexity in the tuning of central synapses by neurexins arises from the fact that they bind to multiple postsynaptic organizing molecules in addition to the neuroligins (Figure 48–18). Moreover, thousands of neurexin isoforms are generated from each neurexin gene as a result of differences in promoter choice (generating α and β forms) and alternative splicing at multiple sites. Different neurexin isoforms are differentially expressed by neurons and have different affinities for the various neurexin ligands. Neuroligins are also alternatively spliced and differentially expressed and thus are likely to have multiple presynaptic partners.

More recently, other synaptic organizing molecules have been found; they include protein tyrosine phosphatases and leucine-rich repeat proteins as well as members of the fibroblast growth factor (FGF) and

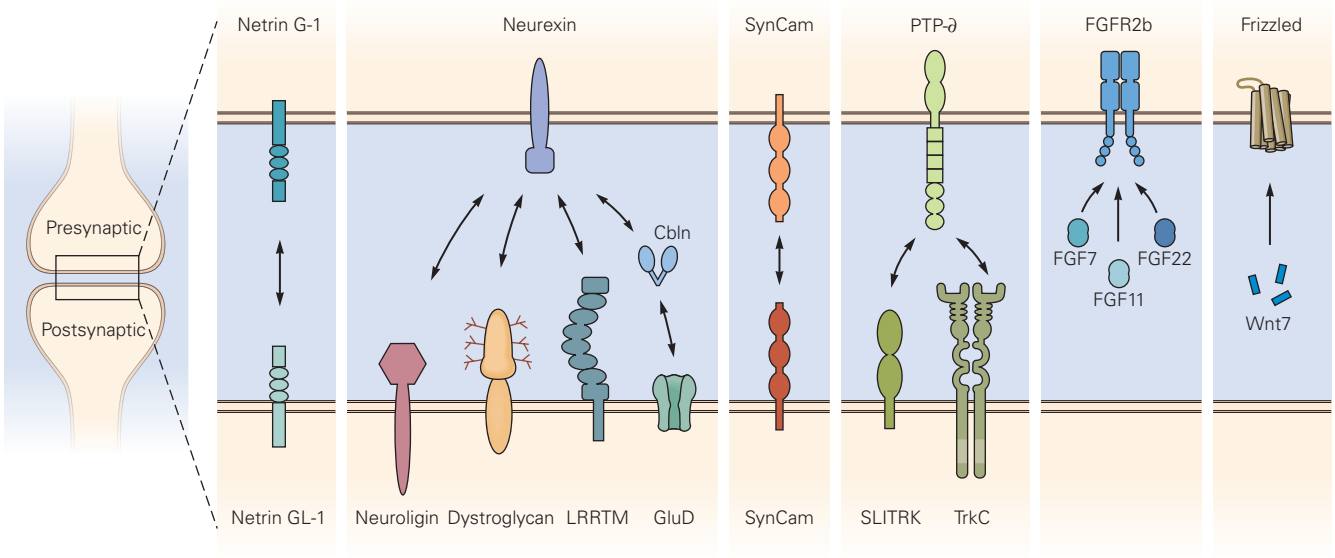

Figure 48–18 **Numerous macromolecular complexes link pre- and postsynaptic membranes at central synapses.** The figure shows some of the many transsynaptic proteins that interact at synaptic sites. Some bias synapse formation in favor of appropriate partners, whereas others act to regulate the properties of the synapse; some may do both.

Wnt families of secreted morphogens and their receptors (Figure 48–18). They are present at specific subsets of synapses and play distinct roles. For example, similar to neuroligin1 and neuroligin2, FGF22 and FGF7 are localized to and promote differentiation of excitatory and inhibitory synapses, respectively. Some of these organizing proteins may act in parallel with neurexins, while others may act as initial organizers, with neuroligins and neurexins consolidating the synapses at a later time and specifying their particular properties.

Together, these results suggest that central synapses are not patterned by master organizers akin to agrin, MuSK, LRP4, and laminins. Indeed, loss of no single central organizer studied to date is lethal in the manner observed for agrin, MuSK, LRP4, and laminin mutants. Instead, the enormous variety of neuronal and synaptic types in the central nervous system and their wide range of functional properties arise from a multitude of organizers that act combinatorially and in cell type–specific ways. Consistent with this view, genetic variation in many central organizers and synaptic recognition molecules, including neurexins, neuroligins, cadherins, and contactins, has been associated with behavioral perturbations in experimental animals and with behavioral disorders, including autism, in humans (Chapter 62).

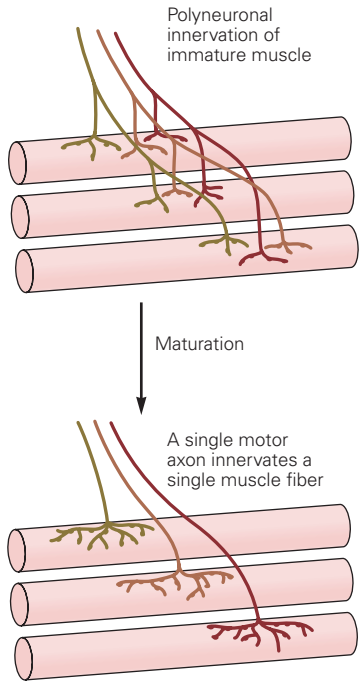

Figure 48–19 Some neuromuscular synapses are eliminated after birth. Early in the development of the neuromuscular junction, each muscle fiber is innervated by several motor axons. After birth, all motor axons but one withdraw from each fiber, and the surviving axon becomes more elaborate. Synapse elimination occurs without any overall loss of axons—axons that "lose" at some muscle fibers "win" at others. Central synapses are also subject to elimination.

Some Synapses Are Eliminated After Birth

In adult mammals, each muscle fiber bears only a single synapse. However, this is not the case in the embryo. At intermediate stages of development, several axons converge on each myotube and form synapses at a common site. Soon after birth, all inputs but one are eliminated.

The process of synapse elimination is not a manifestation of neuronal death. Indeed, it generally occurs long after the period of naturally occurring cell death (Chapter 46). Each motor axon withdraws branches from some muscle fibers but strengthens its connections with others, thus focusing its increasing capacity for transmitter release on a decreasing number of targets. Moreover, axonal elimination is not targeted to defective synapses; all inputs to a neonatal myotube are morphologically and electrically similar, and each can activate the postsynaptic cell (Figure 48–19).

What is the purpose of the transient stage of polyneuronal innervation? One possibility is that it ensures that each muscle fiber is innervated. A second is that it allows all axons to capture an appropriate set of target cells. A third, intriguing idea is that synapse elimination provides a means by which activity can change the strength of specific synaptic connections. We will explore this idea in Chapter 49.

Like synapse formation, synapse elimination results from intercellular interactions. Every muscle fiber ends up with exactly one input: None have zero, and very few have more than one. It is difficult to imagine how this could occur without feedback from the muscle cell. Moreover, the axons that remain after partial denervation at birth have a larger number of synapses than they did initially. Thus, synapse elimination appears to be a competitive process.

What drives the competition, and what is the reward? There is good evidence that neural activity plays a role: Paralysis of muscle reduces synapse elimination, whereas direct stimulation enhances it. These findings showed that activity was involved but did not reveal how the outcome was determined, because all axons were stimulated or paralyzed together. Because the essence of the competitive process is that some synapses gain territory at the expense of others, differential activity among axons may be a determinant

of axon winners and losers. Changing the activity of only a subset of axons in a living animal has been a technical challenge, but genetic approaches have made this possible in mice. In fact, when the activity of one of the inputs to a muscle fiber is decreased, that axon is highly likely to withdraw.

If the more active axon wins the competition, there is a new problem. Because all synapses made by an axon have the same activity pattern, one might predict that the least active axon in the muscle would eventually lose all of its synapses and the most active would retain all of its synapses. Yet this does not happen. Instead, all axons win at some sites and lose at others, so that every axon ends up innervating a substantial number of muscle fibers.

One possible resolution to this paradox is that the outcome of competition may not depend on the number of synaptic potentials from the winning axon at a synapse but rather on the total amount of synaptic input that the axon provides to the muscle—a product of the number of impulses and the amount of transmitter released per impulse. In this case, an axon that loses at several synapses might redistribute its resources (eg, synaptic vesicles) so that the remaining terminals would be strengthened and more likely to win at their synapses. Conversely, an axon that wins many competitions might find itself with insufficient vesicles to generate large synaptic potentials and thus would eventually lose to competitors at some synapses. Accordingly, the number of muscle fibers innervated by individual axons would vary much more among axons than is actually observed.

If activity drives the competition, what is the object of the competition? One idea is that the mechanisms are similar to those that determine whether neurons live or die. The muscle might produce limited amounts of a trophic substance for which the axons compete. As the winner grows, it either deprives the loser of its sustenance or gains enough strength to mount an attack that results in removal of its competitor. Alternatively, the muscle might release a toxic or punitive factor. In these scenarios, although the muscle does contribute a factor in the competition, the outcome is entirely dependent on differences between axons. These differences could be related to activity. The more active axon might be better able to take up trophic factor or resist a toxin. Such positive and negative competitive interactions have been demonstrated at nerve-muscle synapses in culture, although not in vivo.

Nevertheless, the muscle could play a selective role in synapse elimination rather than just providing a broadly distributed signal. For example, the more active axon might trigger a signal from the muscle fiber that strengthens its adhesive interactions with the synaptic cleft, whereas the less active axon might elicit a signal that weakens those interactions.

The complexity of the brain makes direct demonstration of synapse elimination problematic, but electrophysiological evidence from many parts of the central nervous system indicates that synapse elimination is widespread. In autonomic ganglia and cerebellar Purkinje cells, synapse elimination has been documented directly and its rules seem similar to those found at neuromuscular junctions. Individual axons withdraw from some postsynaptic cells while simultaneously increasing the size of the synapses they form with other neurons.

Glial Cells Regulate Both Formation and Elimination of Synapses

Classical studies of synapse formation and maturation focused, logically enough, on the pre- and postsynaptic partners. More recently, however, there has been a growing appreciation of the role played by a third type of cell: the glial cells that cap nerve terminals. Schwann cells are the glia at neuromuscular junctions, and astrocytes are the glia at central synapses. Both have been implicated in synapse formation and maturation.

The most penetrating analyses were performed by the late Ben Barres and his colleagues. They devised methods to culture neurons in defined media and in the complete absence of nonneuronal cells. Using this system, they found that neurons formed few synapses when cultured in isolation but many when astrocytes were present (Figure 48–20). The astrocytes provide multiple signals to neurons. Some, such as thrombospondin, promote postsynaptic maturation, whereas others, such as cholesterol, promote presynaptic maturation.

Another glial type, the microglial cell, also plays critical roles. Microglia are relatives of macrophages and monocytes in other tissues, sharing their ability to eliminate dead cells or debris. Initially thought to be primarily involved in the brain's response to damage, they have now been found to phagocytose synaptic terminals during the period of synapse elimination. True to their phagocytic origins, they use the complex system of complement factors, initially studied in the context of immunity, to target terminals; the targeting is activity dependent, providing a possible mechanism for the activity dependence of synapse elimination (Figure 48–21). An intriguing possibility is that dysregulation of microglial pruning contributes to synaptic loss in neurodegenerative diseases such as Alzheimer disease and schizophrenia (see Chapters 60 and 64).

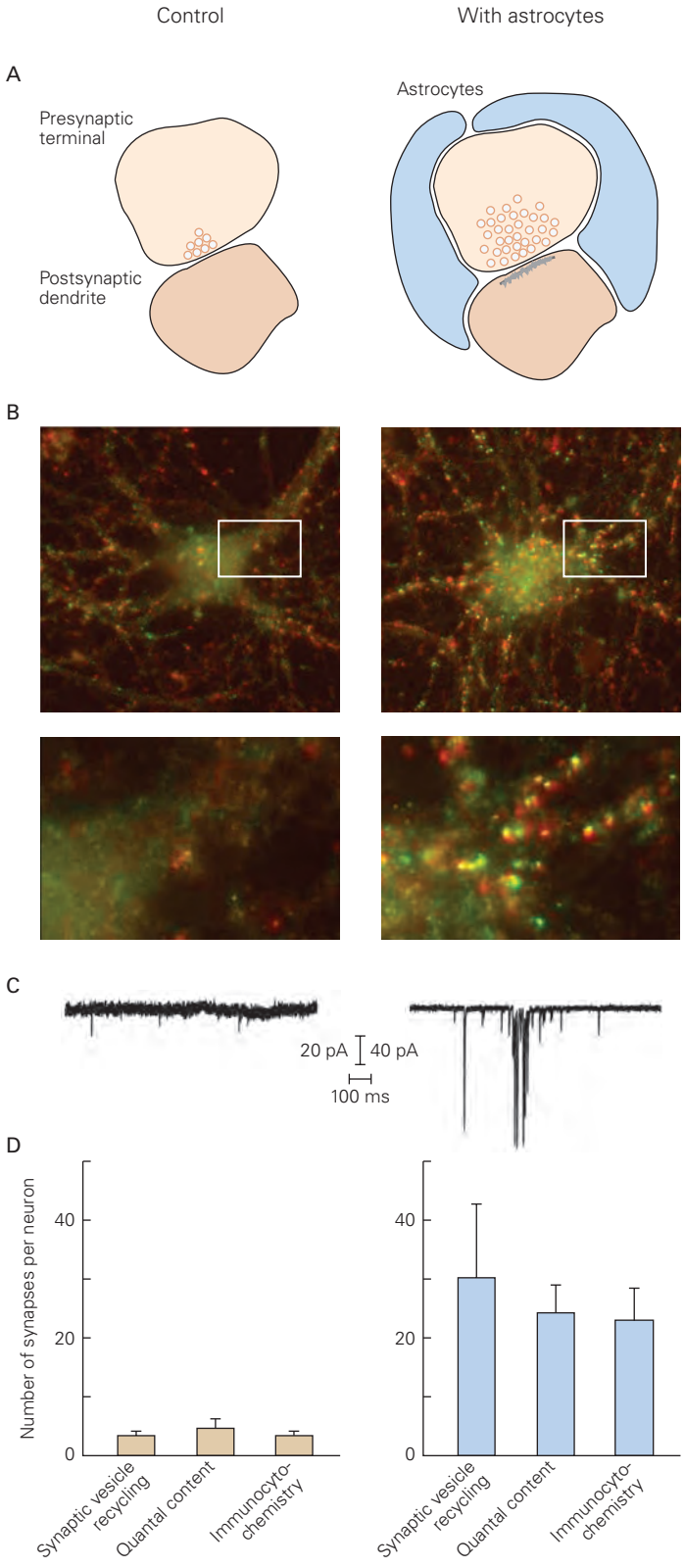

Figure 48–20 Signals from astrocytes promote synapse formation.

A. Astrocytes promote the maturation of both pre- and postsynaptic elements of the synapse.

B. Neurons cultured with astrocytes form more synapses, as assessed by expression of synaptic proteins (**yellow dots**). (Reproduced, with permission, from Ben A. Barres.)

C. Retinal neurons cultured with astrocytes form a greater number of synapses, as shown by increased transmitter release.

D. Synapse formation is enhanced in the presence of astrocytes by three measures.

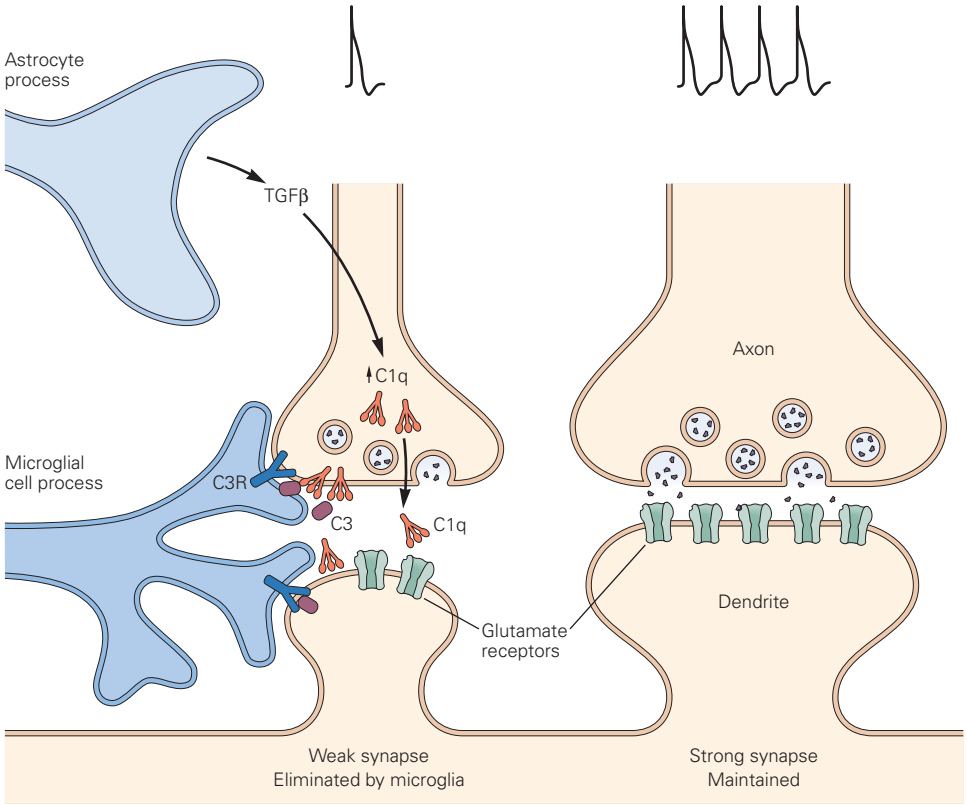

Figure 48–21 Microglia prune synapses, contributing to synapse elimination. Microglia engulf weak synapses. The engulfment is stimulated by complement components such as C1q, which tags the inactive terminal and marks it for removal by a process involving interaction of C3 with the complement receptor C3R on the microglia. Astrocytes play a role by secreting transforming growth factor β (TGFβ), which promotes production of C1q. (Adapted, with permission, from Allen 2014. Permission conveyed through Copyright Clearance Center, Inc.)

The roles of glia in synaptic development are only beginning to be worked out, and the assignments of astrocytes and microglia to synapse formation and elimination are clearly oversimplifications. Both glial types are involved in both processes, and Schwann cells may play both roles at the neuromuscular junction. Moreover, a complex set of signals passes between astrocytes and microglia, and between neurons and glia, all of which contribute to development and are at risk of going awry in brain disorders.

Highlights

1. Elaborate guidance mechanisms bring axons to appropriate target areas, but within those areas they still need to choose synaptic partners, often from among many neuronal types. Multiple mechanisms guide these choices.
2. Matching cell-surface recognition molecules on pre- and postsynaptic partners provide one prevalent mechanism for synaptic specificity. They include members of the cadherin, immunoglobulin, and leucine-rich repeat protein superfamilies. Individual members are selectively expressed by subsets of neurons and exhibit selective binding. Often, the binding is homophilic, biasing connectivity in favor of partners expressing the same molecule.
3. Other mechanisms promoting specificity include selective interactions among axons, the ability of some axons to convert their targets to the appropriate types, and selective elimination of inappropriate contacts.
4. At present, it remains unknown how many molecular species are required to wire up neural circuits in the mammalian brain. At one time, it seemed that molecular complexity might need to approach the complexity of circuits, but it is more likely that a few hundred recognition molecules will suffice, given their combinatorial use, as well as deployment of the same gene at multiple times and in multiple regions.

5. Spatial constraints that enhance specificity include restriction of axons and dendrites to particular laminae within a target region—thereby restricting their choice of partners—and restriction of synapses of particular types to defined domains on the target cell surface.
6. Some specificity mechanisms do not require the partners to be electrically active, but in many cases, activity-dependent mechanisms sharpen specificity. Activity can be spontaneous, early in development, or driven by experience at later stages.
7. The skeletal neuromuscular junction, at which the axon of a motor neuron synapses on a muscle fiber, has been a favored preparation for working out principles of synaptic development. A key finding is that multiple interactions between the synaptic partners are required for the formation, maturation, and maintenance of the synapse.
8. Motor neurons and muscle fibers can express genes encoding pre- and postsynaptic components, respectively, in each other's absence, but they exert profound influences on the levels and distribution of these components in their partners. Thus, signals between synaptic partners are best viewed as organizers rather than inducers.
9. At the neuromuscular junction, a layer of basal lamina occupies the synaptic cleft between the motor nerve terminal and the postsynaptic membrane. Nerve and muscle secrete signaling molecules into the cleft, where they become stabilized and organize differentiation.
10. A key nerve-derived organizer of postsynaptic differentiation is agrin. It acts through the receptors MuSK and LRP4 to cluster acetylcholine receptors and other postsynaptic components beneath the nerve terminal. Nerve-evoked activity also affects postsynaptic differentiation by modulating expression of postsynaptic components. Key muscle-derived organizers of presynaptic differentiation include members of the laminin and fibroblast growth factor families.
11. Central synapses develop in ways similar to those discovered at the neuromuscular junction. Many central synaptic organizers have now been discovered, including neuroligins, neurexins, protein tyrosine phosphatases, leucine-rich repeat proteins, and numerous others.
12. Many of the synapses that form initially in both the peripheral and central nervous systems are subsequently eliminated, generally by competitive, activity-dependent mechanisms. The consequence is that as circuits mature, the number of inputs a neuron receives may decrease dramatically, but the size and strength of the remaining inputs increase even more dramatically.
13. Along with pre- and postsynaptic partners, glial cells play key roles at the synapse. In particular, both astrocytes and microglial cells receive signals from and send signals to developing synaptic partners, with these signals contributing to synapse formation, maturation, maintenance, and elimination.

Joshua R. Sanes

Selected Reading

Allen NJ, Lyons DA. 2018. Glia as architects of central nervous system formation and function. Science 362:181–185.

Baier H. 2013. Synaptic laminae in the visual system: molecular mechanisms forming layers of perception. Annu Rev Cell Dev Biol 29:385–416.

Darabid H, Perez-Gonzalez AP, Robitaille R. 2014. Neuromuscular synaptogenesis: coordinating partners with multiple functions. Nat Rev Neurosci 15:703–718.

Hirano S, Takeichi M. 2012. Cadherins in brain morphogenesis and wiring. Physiol Rev 92:597–634.

Krueger-Burg D, Papadopoulos T, Brose N. 2017. Organizers of inhibitory synapses come of age. Curr Opin Neurobiol 45:66–77.

Nishizumi H, Sakano H. 2015. Developmental regulation of neural map formation in the mouse olfactory system. Dev Neurobiol 75:594–607.

Südhof TC. 2017. Synaptic neurexin complexes: a molecular code for the logic of neural circuits. Cell 171:745–769.

Takahashi H, Craig AM. 2013. Protein tyrosine phosphatases PTPδ, PTPσ, and LAR: presynaptic hubs for synapse organization. Trends Neurosci 36:522–534.

Thion MS, Ginhoux F, Garel S. 2018. Microglia and early brain development: an intimate journey. Science 362:185–189.

Yogev S, Shen K. 2014. Cellular and molecular mechanisms of synaptic specificity. Annu Rev Cell Dev Biol 30:417–437.

References

Allen NJ. 2014. Astrocyte regulation of synaptic behavior. Annu Rev Cell Dev Biol. 30:439–463.

Anderson, MJ, Cohen MW. 1977. Nerve-induced and spontaneous redistribution of acetylcholine receptors on cultured muscle cells. J Physiol 268:757–773.

Ango F, di Cristo G, Higashiyama H, Bennett V, Wu P, Huang ZJ. 2004. Ankyrin-based subcellular gradient of

neurofascin, an immunoglobulin family protein, directs GABAergic innervation at Purkinje axon initial segment. Cell 119:257–272.

Buller AJ, Eccles JC, Eccles RM. 1960. Interactions between motoneurons and muscles in respect of the characteristic speeds of their responses. J Physiol 150:417–439.

Burden SJ, Sargent PB, McMahan UJ. 1979. Acetylcholine receptors in regenerating muscle accumulate at original synaptic sites in the absence of the nerve. J Cell Biol 82:412–425.

Christopherson KS, Ullian EM, Stokes CC, et al. 2005. Thrombospondins are astrocyte-secreted proteins that promote CNS synaptogenesis. Cell 120:421–433.

DeChiara TM, Bowen DC, Valenzuela DM, et al. 1996. The receptor tyrosine kinase MuSK is required for neuromuscular junction formation in vivo. Cell 85:501–512.

Duan X, Krishnaswamy A, De la Huerta I, Sanes JR. 2014. Type II cadherins guide assembly of a direction-selective retinal circuit. Cell 158:793–807.

Feng G, Tintrup H, Kirsch J, et al. 1998. Dual requirement for gephyrin in glycine receptor clustering and molybdoenzyme activity. Science 282:1321–1324.

Fox MA, Sanes JR, Borza DB, et al. 2007. Distinct target-derived signals organize formation, maturation, and maintenance of motor nerve terminals. Cell 129:179–193.

Gautam M, Noakes PG, Moscoso L, et al. 1996. Defective neuromuscular synaptogenesis in agrin-deficient mutant mice. Cell 85:525–535.

Glicksman MA, Sanes JR. 1983. Differentiation of motor nerve terminals formed in the absence of muscle fibres. J Neurocytol 12:661–671.

Graf ER, Zhang X, Jin SX, Linhoff MW, Craig AM. 2004. Neurexins induce differentiation of GABA and glutamate postsynaptic specializations via neuroligins. Cell 119:1013–1026.

Hall ZW, Sanes JR. 1993. Synaptic structure and development: the neuromuscular junction. Cell 72:99–121. Suppl.

Huang ZJ. 2006. Subcellular organization of GABAergic synapses: role of ankyrins and L1 cell adhesion molecules. Nat Neurosci 9:163–166.

Imai T, Suzuki M, Sakano H. 2006. Odorant receptor-derived cAMP signals direct axonal targeting. Science 314:657–661.

Krishnaswamy A, Yamagata M, Duan X, Hong YK, Sanes JR. 2015. Sidekick 2 directs formation of a retinal circuit that detects differential motion. Nature 2524:466–470.

Lupa MT, Gordon H, Hall ZW. 1990. A specific effect of muscle cells on the distribution of presynaptic proteins in neurites and its absence in a C2 muscle cell variant. Dev Biol 142:31–43.

Misgeld T, Kummer TT, Lichtman JW, Sanes JR. 2005. Agrin promotes synaptic differentiation by counteracting an inhibitory effect of neurotransmitter. Proc Natl Acad Sci U S A 102:11088–11093.

Nishimune H, Sanes JR, Carlson SS. 2004. A synaptic laminin-calcium channel interaction organizes active zones in motor nerve terminals. Nature 432:580–587.

Nja A, Purves D. 1977. Re-innervation of guinea-pig superior cervical ganglion cells by preganglionic fibres arising from different levels of the spinal cord. J Physiol 272:633–651.

Noakes PG, Gautam M, Mudd J, Sanes JR, Merlie JP. 1995. Aberrant differentiation of neuromuscular junctions in mice lacking s-laminin/laminin beta 2. Nature 374:258–262.

Salmons S, Sreter FA. 1976. Significance of impulse activity in the transformation of skeletal muscle type. Nature 263:30–34.

Sanes JR, Lichtman JW. 2001. Induction, assembly, maturation and maintenance of a postsynaptic apparatus. Nat Rev Neurosci 2:791–805.

Sanes JR, Yamagata M. 2009. Many paths to synaptic specificity. Annu Rev Cell Dev Biol 25:161–195.

Schafer DP, Lehrman EK, Kautzman AG, et al. 2012. Microglia sculpt postnatal neural circuits in an activity and complement-dependent manner. Neuron 74:691–705.

Scheiffele P, Fan J, Choih J, Fetter R, Serafini T. 2000. Neuroligin expressed in nonneuronal cells triggers presynaptic development in contacting axons. Cell 101:657–669.

Serizawa S, Miyamichi K, Takeuchi H, Yamagishi Y, Suzuki M, Sakano H. 2006. A neuronal identity code for the odorant receptor-specific and activity-dependent axon sorting. Cell 127:1057–1069.

Terauchi A, Johnson-Venkatesh EM, Toth AB, Javed D, Sutton MA, Umemori H. 2010. Distinct FGFs promote differentiation of excitatory and inhibitory synapses. Nature 465:783–787.

Uezu A, Kanak DJ, Bradshaw TW, et al. 2016. Identification of an elaborate complex mediating postsynaptic inhibition. Science 353:1123–1129.

Vaughn JE. 1989. Fine structure of synaptogenesis in the vertebrate central nervous system. Synapse 3:255–285.

Yamagata M, Sanes JR. 2012. Expanding the Ig superfamily code for laminar specificity in retina: expression and role of contactins. J Neurosci 32:14402–14414.

Yumoto N, Kim N, Burden SJ. 2012. Lrp4 is a retrograde signal for presynaptic differentiation at neuromuscular synapses. Nature 489:438–442.

49

Experience and the Refinement of Synaptic Connections

The human nervous system is functional at birth—newborn babies can see, hear, breathe, and suckle. However, the capabilities of human infants are quite rudimentary compared to those of other species. Wildebeest calves can stand and run within minutes of birth, and many birds can fly shortly after they hatch from their eggs. In contrast, a human baby cannot lift its head until it is 2 months old, cannot bring food to its mouth until it is 6 months old, and cannot survive without parental care for a decade.

What accounts for the delayed maturation of our motor, perceptual, and cognitive abilities? One main factor is that the embryonic connectivity of the nervous system, discussed in Chapters 45 through 48, is only a "rough draft" of the neural circuits that exist in our adult selves. Embryonic circuits are refined by sensory stimulation—our experiences. This two-part sequence—genetically determined connectivity followed by experience-dependent reorganization—is a common feature of mammalian neural development, but in humans, the second phase is especially prolonged.

At first glance, this delay in human neural development might seem dysfunctional. It does exact a toll,

but it also provides an advantage. Because our mental abilities are shaped largely by experience, we gain the ability to custom fit our nervous systems to our individual bodies and unique environments. It has been argued that it is not just the large size of the human brain but also its experience-dependent maturation that makes our mental capabilities superior to those of other species.

The plasticity of the nervous system in response to experience endures throughout life. Nevertheless, periods of heightened susceptibility to modification, known as *sensitive periods*, occur at particular times in development. In some cases, the adverse effects of deprivation or atypical experience during circumscribed periods in early life cannot easily be reversed by providing appropriate experience at a later age. Such periods are referred to as *critical periods*. As we shall see, new discoveries are blurring the distinction between sensitive and critical periods, so we will use the term "critical periods" to refer to both.

Behavioral observations have helped us appreciate critical periods. Imprinting, a form of learning in birds, is one of the most striking illustrations of a lifelong behavior established during a critical period. Just after hatching, birds become indelibly attached, or imprinted, to a prominent moving object in their environment and follow it around. This is typically their mother, but it could be an experimenter who is near the newborn chick. The process of imprinting is important for the protection of the hatchling. Although the attachment is acquired rapidly and persists, imprinting can only occur during a critical period soon after hatching—in some species, only a few hours.

In humans, critical periods are evident in the ways children acquire the capacities to perceive the world around them, learn a language, or form social relationships. A 5-year-old child can quickly and effortlessly learn a second language, whereas a 15-year-old adolescent may become fluent but is likely to speak with an accent, even if he lives to be 90 years old. Likewise, deaf children fitted with a cochlear implant during the first 3 to 4 years of life generally acquire and understand spoken language well, whereas neither production nor understanding may ever be normal following implantation at later ages. Such critical periods demonstrate that experience-dependent neural development is concentrated in, although certainly not confined to, early postnatal life.

We begin this chapter by examining the evidence that early experience shapes a range of human mental capacities, from our ability to make sense of what we see to our ability to engage in appropriate social interactions. The neural basis of these experiential effects has been analyzed in numerous parts of the brains of experimental animals, including the auditory, somatosensory, motor, and visual systems. Here, rather than surveying multiple systems, we will focus primarily on the visual system because research on this system has provided a particularly rich understanding of how experience shapes neural circuitry. We will see that experience is needed to refine patterns of synaptic connections and to stabilize these patterns once they have formed. Finally, we will consider recent evidence that critical periods in many systems are less restrictive than once thought and, in some cases, can be extended or even "reopened."

Understanding critical periods in childhood and the extent to which they can be reopened in adulthood has many important practical consequences. First, much educational policy is based on the idea that early experience is crucial, so it is important to know exactly when a particular form of enrichment will be optimally beneficial. Second, medical treatment of many childhood conditions, such as congenital cataracts or deafness, is now predicated on the idea that early intervention is imperative if long-lasting deficits are to be avoided. Third, there is increasing suspicion that some behavioral disorders, such as autism, may be caused by impairment of reorganization of neural circuits during critical periods. Finally, the possibility of reopening critical periods in adulthood is leading to new therapeutic approaches to neural insults, such as stroke, that previously were thought to have irreversible consequences.

Development of Human Mental Function Is Influenced by Early Experience

Early Experience Has Lifelong Effects on Social Behaviors

One of the first indications that early social and perceptual experiences have irreversible consequences for human development came from studies of children who had been deprived of these experiences early in life. In rare cases, children abandoned in the wild and later returned to human society have also been studied. As might be expected, these children were socially maladjusted, but surprisingly, the defects proved to persist throughout life.

In the 1940s, the psychoanalyst René Spitz provided more systematic evidence that early interactions with other humans are essential for normal social development. Spitz compared the development of infants raised in a foundling home with the development

of infants raised in a nursing home attached to a women's prison. Both institutions were clean and both provided adequate food and medical care. The babies in the prison nursing home were all cared for by their mothers, who, although in prison and away from their families, tended to shower affection on their infants in the limited time allotted to them each day. In contrast, infants in the foundling home were cared for by nurses, each of whom was responsible for several babies. As a result, children in the foundling home had far less contact with other humans than did those in the prison's nursing home.

The two institutions also differed in another respect. In the prison nursing home, the cribs were open, so that the infants could readily watch other activities in the ward; they could see other babies play and observe the staff go about their business. In the foundling home, the bars of the cribs were covered by sheets that prevented the infants from seeing outside. In reality, the babies in the foundling home were living under conditions of severe sensory and social deprivation.

Infants at the two institutions were followed through their early years. At the end of the first 4 months, the infants in the foundling home fared better on several developmental tests than those in the prison nursing home, suggesting that intrinsic factors did not favor the infants in the prison nursing home. But by the end of the first year, the motor and intellectual performance of the children in the foundling home had fallen far below that of children in the prison nursing home. Many of the children in the foundling home had developed a syndrome that Spitz called *hospitalism* and is now sometimes called *anaclitic depression*. These children were withdrawn and displayed little curiosity or gaiety. Moreover, their defects extended beyond emotional and cognitive signs. They were especially prone to infection, implying that the brain exerts complex controls over the immune system as well as behavior. By their second and third years, children in the prison nursing home were similar to children raised in normal families at home—they were agile, had a vocabulary of hundreds of words, and spoke in sentences. In contrast, the development of children in the foundling home was still further delayed—many were unable to walk or to speak more than a few words.

More recent studies of other similarly deprived children have confirmed these conclusions and shown that the defects are long-lasting. Longitudinal studies of orphans who were raised for several years in large impersonal institutions with little or no personal care, then adopted by caring families, have been especially revealing. Despite every effort of the adoptive parents, many of the children were never able to develop appropriate, caring relationships with family members or peers (Figure 49–1A). More recent imaging studies have revealed defects in brain structure correlated with, and presumably due to, this deprivation (Figure 49–1B).

As compelling as these observations are, it is difficult to derive definitive conclusions from them. An influential set of studies that extended the analysis of social behavior to monkeys was carried out in the 1960s by two psychologists, Harry and Margaret Harlow. The Harlows reared newborn monkeys in isolation for 6 to 12 months, depriving them of contact with their mothers, other monkeys, or people. At the end of this period, the monkeys were physically healthy but behaviorally devastated. They crouched in a corner of their cage and rocked back and forth like autistic children (Figure 49–1C). They did not interact with other monkeys, nor did they fight, play, or show any sexual interest. Thus, a 6-month period of social isolation during the first 18 months of life produced persistent and serious disturbances in behavior. By comparison, isolation of an older animal for a comparable period was found to be without such drastic consequences. These results confirmed, under controlled conditions, the critical influence of early experience on later behavior. For ethical reasons, these studies would not be possible today.

Development of Visual Perception Requires Visual Experience

The dramatic dependence of the brain on experience and the ability of that experience to shape perception is evident in people born with cataracts. Cataracts are opacities of the lens that interfere with the optics of the eye but not directly with the nervous system; they are easily removed surgically. In the 1930s, it became apparent that patients who had congenital binocular cataracts removed after the age of 10 years experienced permanent deficits in visual acuity and had difficulties perceiving shape and form. In contrast, when cataracts that develop in adults are removed decades after they form, normal vision returns immediately.

Likewise, children with *strabismus* (crossed eyes) do not have normal depth perception (*stereopsis*), an ability that requires the two eyes to focus on the same location at the same time. They can acquire this ability if their eyes are aligned surgically during the first few years of life, but not if surgery occurs later in adolescence. As a result of these observations, congenital cataracts are now usually removed, and strabismus is corrected surgically, in early childhood. Over the

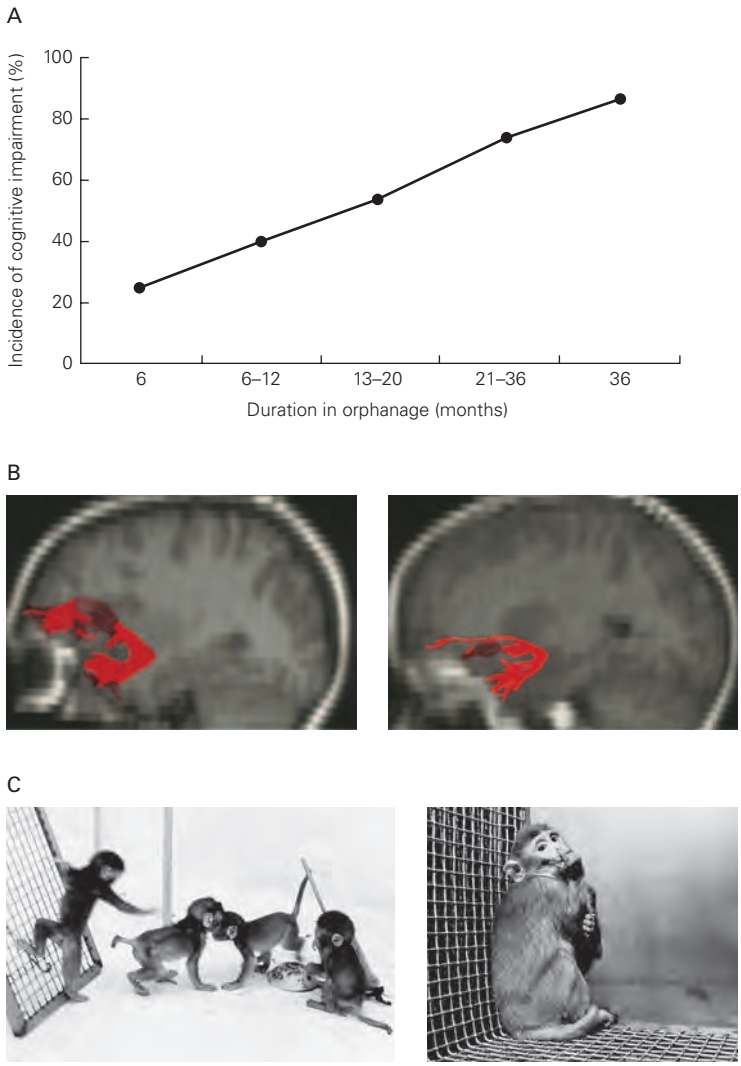

Figure 49–1 Early social deprivation has a profound impact on later brain structure and behavior.

A. Neurocognitive dysfunction is evident in children raised under conditions of social deprivation in orphanages. The incidence of cognitive impairment increases with the duration of stay in the orphanage. (Adapted from Behen et al. 2008.)

B. Diffusion tensor magnetic resonance imaging (MRI) scans show a well-developed and robust uncinate fasciculus (**red region**) in a normal child (*left*), whereas in a socially deprived child (*right*), it is thin and poorly organized. (Reproduced, with permission, from Eluvathingal et al. 2006. Copyright © 2006 by the AAP.)

C. Early social interactions impact later social behavior patterns. Monkeys reared in the presence of their siblings acquire social skills that permit effective interactions in later life (*left*). A monkey reared in isolation never acquires the capacity to interact with others and remains secluded and isolated in later life (*right*). (Source: Harry F. Harlow. Used with permission.)

past five decades, researchers have elucidated structural and physiological underpinnings of these critical periods.

Development of Binocular Circuits in the Visual Cortex Depends on Postnatal Activity

Because sensory experience of the world is transformed into patterns of electrical activity in the brain, one might imagine that electrical signals in neural circuits affect the brain's circuitry. But is this true? And if it is true, what changes occur, and how does activity trigger them?

Our most detailed understanding of these links comes from studies of the neural circuits that mediate binocular vision. The key figures in the early phases of this work were David Hubel and Torsten Wiesel. Following their pioneering studies on the structural and functional organization of the visual cortex in cats and monkeys (Chapter 23), they undertook another set of studies on how experience affects the circuits they had delineated.

Visual Experience Affects the Structure and Function of the Visual Cortex

In one influential study, Hubel and Wiesel raised a monkey from birth to 6 months of age with one eyelid sutured shut, thus depriving the animal of vision in that eye. When the sutures were removed, it became clear that the animal was blind in the deprived eye, a condition called *amblyopia*. They then performed electrophysiological recordings from cells along the visual

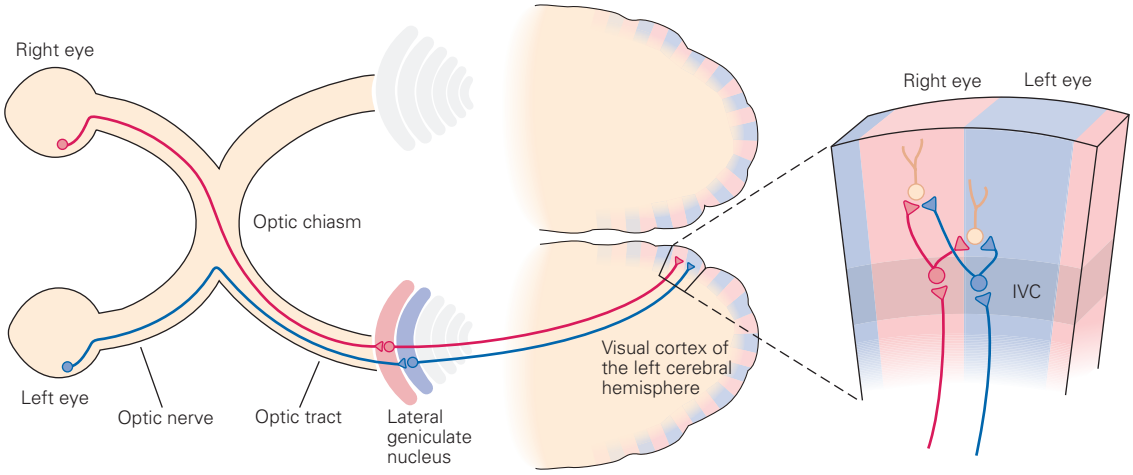

Figure 49–2 Afferent pathways from the two eyes project to discrete columns of neurons in the visual cortex. Retinal ganglion neurons from each eye send axons to separate layers of the lateral geniculate nucleus. The axons of neurons in this nucleus project to neurons in layer IVC of the primary visual cortex, which is organized in alternating sets of ocular dominance columns; each column receives input from only one eye. The axons of the neurons in layer IVC project to neurons in adjacent columns as well as to neurons in the upper and lower layers of the same column. As a result, most neurons in the upper and lower layers of the cortex receive information from both eyes.

pathway to determine where the defect arose (Figure 49–2). They found that retinal ganglion cells in the deprived eye, as well as neurons in the lateral geniculate nucleus that receive input from the deprived eye, responded well to visual stimuli and had essentially normal receptive fields.

In contrast, cells in the visual cortex were fundamentally altered. In the cortex of normal animals, most neurons are responsive to binocular input. In animals that had been monocularly deprived for the first 6 months, most cortical neurons did not respond to signals from the deprived eye (Figure 49–3). The few cortical cells that were responsive were not sufficient for visual perception. Not only had the deprived eye lost its ability to drive most cortical neurons, but little recovery ever occurred: The loss was permanent and irreversible.

Hubel and Wiesel went on to test the effects of visual deprivation imposed for shorter periods and at different ages. They obtained three types of results, depending on the timing and duration of the deprivation. First, monocular deprivation for a few weeks shortly after birth led to loss of cortical responses from the deprived eye that was reversible after the eye had been opened, especially if the opposite eye was then closed to encourage use of the initially deprived eye. Second, monocular deprivation for a few weeks during the next several weeks also resulted in a substantial loss of cortical responsiveness to signals from the deprived eye, but in this case, the effects were irreversible. Finally, deprivation in adults, even for periods of many months, had no effect on the responses of cortical cells to signals from the deprived eye or on visual perception. These results demonstrated that the cortical connections that control visual perception are established within a critical period of early development.

Are there anatomical correlates of these functional defects? To address this question, we need to recall three basic facts about the anatomy of the visual cortex (Figure 49–2). First, inputs from the two eyes remain segregated in the lateral geniculate nucleus. Second, the geniculate inputs carrying information from the two eyes to the cortex terminate in alternating columns, termed *ocular dominance columns*. Third, lateral geniculate axons terminate on neurons in layer IVC of the primary visual cortex; convergence of input from the two eyes on a common target cell occurs at the next stage of the pathway, in cells above and below layer IVC.

To examine whether the architecture of ocular dominance columns depends on visual experience early in postnatal life, Hubel and Wiesel deprived newborn animals of vision in one eye and then injected a labeled amino acid into the normal eye. The injected label was incorporated into proteins in retinal ganglion cell bodies, transported along the retinal axons to the lateral geniculate nucleus, transferred to geniculate neurons, and then transported to the synaptic terminals of these axons in the primary visual cortex. After closure of one eye, the columnar array of synaptic terminals relaying input from the deprived eye was reduced, whereas the columnar array of terminals relaying input from the

normal eye was expanded (Figure 49–4). Thus, sensory deprivation early in life alters the structure of the cerebral cortex.

How are these striking anatomical changes brought about? Does sensory deprivation alter ocular dominance columns after they have been established, or does it interfere with their formation? A columnar organization of the visual cortex is already evident by birth in monkeys, although the mature pattern is not achieved until several weeks after birth (Figure 49–5). Only at this time do the terminals of fibers from the lateral geniculate nucleus become completely segregated in the cortex. Because the inputs are partially but not completely segregated at the time visual deprivation exerts its effects, we can conclude that the deprivation perturbs the ability of the inputs to acquire their mature pattern. We shall return to the question of what leads to the initial, experience-independent phases of segregation in a later section of this chapter.

Patterns of Electrical Activity Organize Binocular Circuits

How does activity lead to maturation of ocular dominance columns? The crucial factor may be the

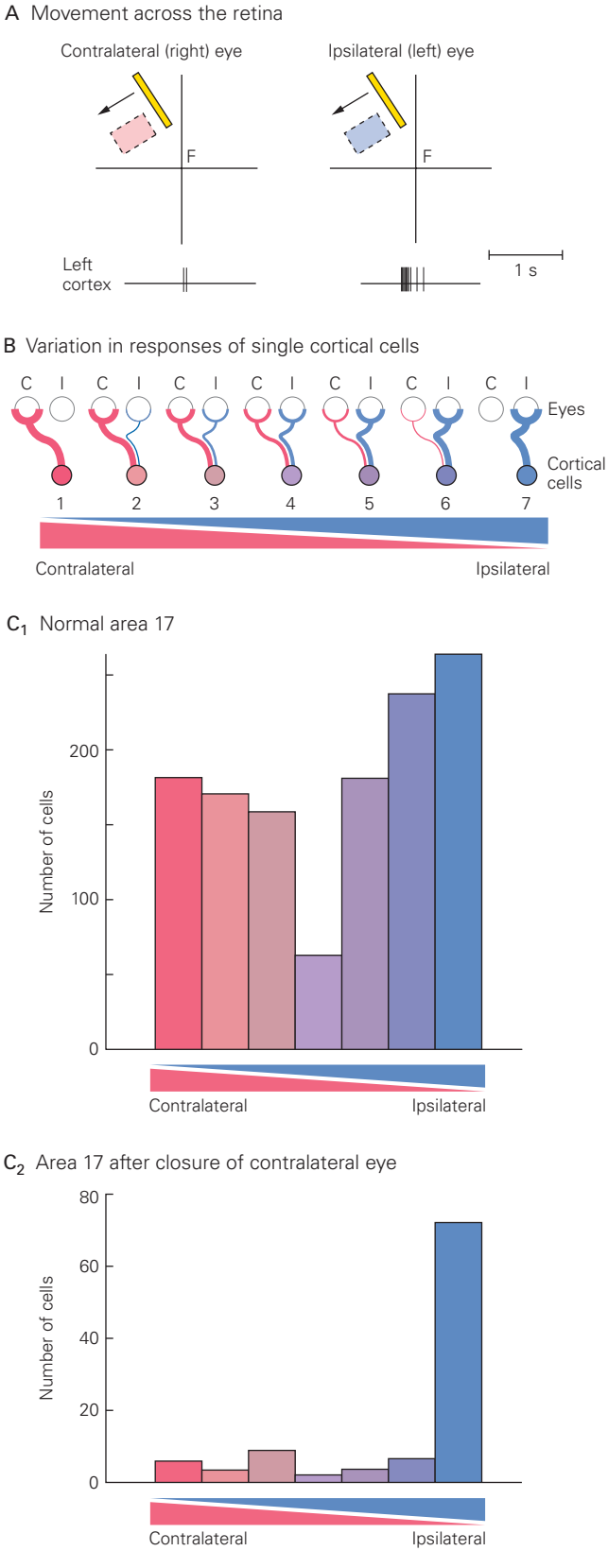

Figure 49–3 (Right) Responses of neurons in the primary visual cortex of a monkey to visual stimuli. (Adapted from Hubel and Wiesel 1977.)

A. A diagonal bar of light is moved leftward across the visual field, traversing the receptive fields of a binocularly responsive cell in area 17 of visual cortex. Receptive fields measured through the right and left eye are drawn separately. The receptive fields of the two cells are similar in orientation, position, shape, and size, and respond to the same form of stimulus. Recordings (below) show that the cortical neuron responds more effectively to input from the ipsilateral eye. (Abbreviation: **F**, fixation point.)

B. The responses of individual cortical neurons in area 17 can be classified into seven groups. Neurons receiving input only from the contralateral eye (**C**) fall into group 1, whereas neurons that receive input only from the ipsilateral eye (**I**) fall into group 7. Other neurons receive inputs from both eyes, but the input from one eye may influence the neuron much more than the other (groups 2 and 6), or the differences may be slight (groups 3 and 5). Some neurons respond equally to input from both eyes (group 4). According to these criteria, the cortical neuron shown in part A falls into group 6.

C. Responsiveness of neurons in area 17 to stimulation of one or the other eye. **1.** The responses of more than 1,000 neurons in area 17 in the left hemisphere of normal adult and juvenile monkeys. Neurons in layer IV that normally receive only monocular input have been excluded. **2.** The responses of neurons in the left hemisphere of a monkey in which the contralateral (right) eye was closed from the age of 2 weeks to 18 months and then reopened. Most neurons respond only to stimulation of the ipsilateral eye.

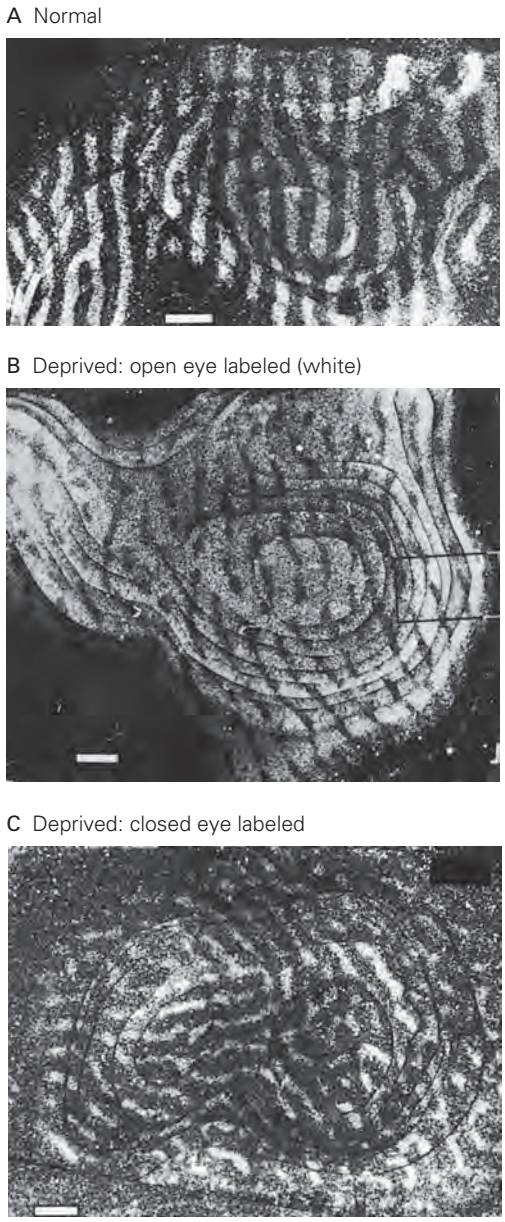

Figure 49–4 Visual deprivation of one eye during a critical period of development reduces the width of the ocular dominance columns for that eye. (Scale bars = 1 mm) (Adapted, with permission, from Hubel, Wiesel, and LeVay 1977.)

A. A tangential section through area 17 of the right hemisphere of a normal adult monkey, 10 days after one eye was injected with a radiolabeled amino acid. Radioactivity is localized in stripes (**white**) in layer IVC of the visual cortex, indicating sites of termination of the axons from the lateral geniculate nucleus that carry input from the injected eye. The alternating unlabeled (**dark**) stripes indicate sites of termination of the axons carrying signals from the uninjected eye. Labeled and unlabeled stripes are of equal width.

B. A comparable section through the visual cortex of an 18-month-old monkey whose right eye had been surgically closed at 2 weeks of age. Label was injected into the left (open) eye. The wider (**white**) stripes are the labeled terminals of afferent axons carrying signals from the open eye; the narrow (**dark**) stripes are terminals of axons with input from the closed eye.

C. A section comparable to that in part B from an 18-month-old animal whose right eye had been shut at 2 weeks. Label was injected into the closed eye, giving rise to narrow (**white**) stripes of labeled axon terminals and wide (**dark**) stripes of unlabeled terminals.

differences in the proportion of inputs from each eye that converge on common target cells at birth. If by chance the fibers conveying input from one eye are initially more numerous in one local region of cortex, those axons may have an advantage, leading to further segregation.

How might this occur? An attractive idea, based on a theory first proposed in the 1940s by Donald Hebb, is that synaptic connections are strengthened when pre- and postsynaptic elements are active together. In the case of binocular interactions, neighboring axons from the same eye tend to fire in synchrony because they are activated by the same visual stimulus at any instant. The synchronization of their firing means that they cooperate in the depolarization and excitation of a target cell. This cooperative action maintains the viability of those synaptic contacts at the expense of the noncooperating synapses.

Cooperative activity could also promote branching of axons and thus create the opportunity for the formation of additional synaptic connections with cells in the target region. At the same time, the strengthening of synaptic contacts made by the axons of one eye will impede the growth of synaptic inputs from the opposite eye. In this sense, fibers from the two eyes may be said to compete for a target cell. Together,

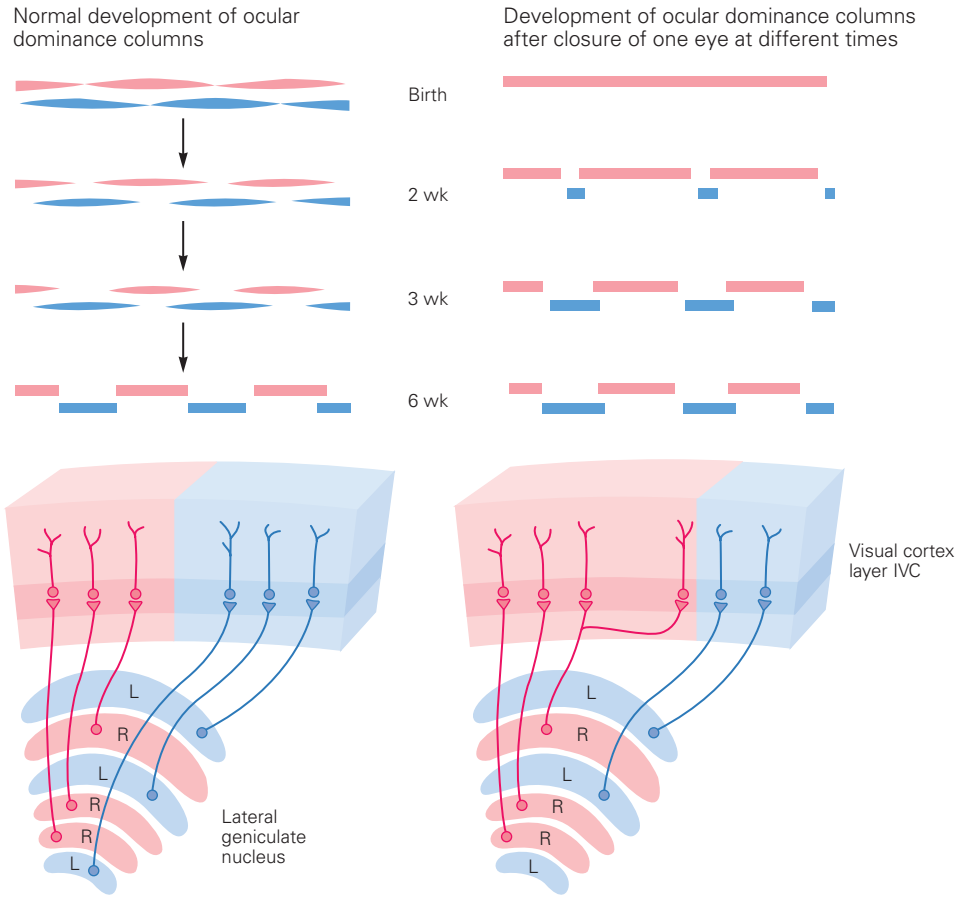

Figure 49–5 The effects of eye closure on the formation of ocular dominance columns. The top diagrams show the gradual segregation of the terminals of lateral geniculate afferents in layer IVC of the visual cortex under normal conditions (*left*) and when one eye is deprived of stimulation (*right*). **Blue domains** represent the areas of termination of inputs from one eye, **red domains** those of the other eye. The lengths of the domains represent the density of the terminals at each point along layer IVC. For clarity, the columns are shown here as one above the other, whereas in reality, they are side by side in the cortex. During normal development, layer IVC is gradually divided into alternating sites of input from each eye. The consequences of depriving sight in one eye depend on the timing of eye closure. Closure at birth leads to dominance by the open eye (**red**) because at this point little segregation has occurred. Closure at 2, 3, and 6 weeks has a progressively weaker effect on the formation of ocular dominance columns because the columns become more segregated with time. (Abbreviations: **L**, left; **R**, right.) (Adapted, with permission, from Hubel, Wiesel, and LeVay 1977.)

cooperation and competition between axons ensure that two populations of afferent fibers will eventually innervate distinct regions of the primary visual cortex with little local overlap.

Competition and cooperation are not simply the outcome of neural activity per se or of differences in absolute levels of activity among axons. Instead, they appear to depend on precise temporal patterns of activity in the competing (or cooperating) axons. The principle was dramatically illustrated by Hubel and Wiesel in a set of studies that examined stereoscopic vision—the perception of depth. The brain normally computes depth perception by comparing the disparity in retinal images between the two eyes. When the eyes are improperly aligned, this comparison cannot be made and stereoscopy is impossible. Such misalignments occur in children who are "cross-eyed," or strabismic. As noted above, this condition can be surgically repaired, but unless the surgery occurs during the first few years of life, the children forever remain incapable of stereoscopy.

Hubel and Wiesel examined the impact of strabismus on the organization of the visual system in cats. To render cats strabismic, the tendon of an extraocular muscle was severed in kittens. Both eyes remained fully functional but misaligned. Inputs from the two eyes that converged on a binocular cell in the visual cortex now carried information about different stimuli

in slightly different parts of the visual field. As a result, cortical cells became monocular, driven by input from one eye or the other but not both (Figure 49–6). Conversely, cortical neurons remained binocularly responsive following binocular visual deprivation, leading to a decrease but not an imbalance in activity arising from the two eyes. These findings suggested to Hubel and Wiesel that disruption of the synchrony of inputs led to competition rather than cooperation, so that cortical cells came to be dominated by one eye, presumably the one that had dominated at the outset.

These physiological studies led investigators to test whether pharmacological blockade of electrical activity in retinal ganglion cells could affect neural connectivity in the visual system. Activity was blocked by injecting both eyes with tetrodotoxin, a toxin that selectively blocks voltage-sensitive Na^+ channels. Signals from the two eyes were generated separately by direct electric stimulation of the bilateral optic nerves. In kittens, ocular dominance columns are not established if activity in retinal ganglion neurons is blocked before the critical period of development. When the two optic nerves were stimulated synchronously, ocular dominance columns still failed to form. Only when the optic nerves were stimulated asynchronously were ocular dominance columns established.

If the development of ocular dominance columns indeed depends on competition between fibers from the two eyes, might it be possible to induce the formation of columns where they normally are not present, simply by establishing competition between two sets of axons? This radical possibility was tested in frogs, where retinal ganglion neurons from each eye project only to the contralateral side of the brain. In normal frogs, afferent fibers from the two eyes do not compete for the same cells, so there is no columnar segregation of afferent inputs. To generate competition, a third eye was transplanted early in larval development into a region of the frog's head near one of the normal eyes. The retinal ganglion neurons of the extra eye extended axons to the contralateral optic tectum. Remarkably, axon terminals from the transplanted and normal eyes segregated, generating a pattern of alternating columns (Figure 49–7).

This finding provided dramatic support for the idea that competition between afferent axons for the same population of target neurons drives their segregation into distinct target territories. The columnar segregation of retinal inputs in the frog brain is dependent on synaptic activity, presumably at the synapses between retinal axons and tectal neurons. Thus, neural activity has powerful roles in fine-tuning visual circuits.

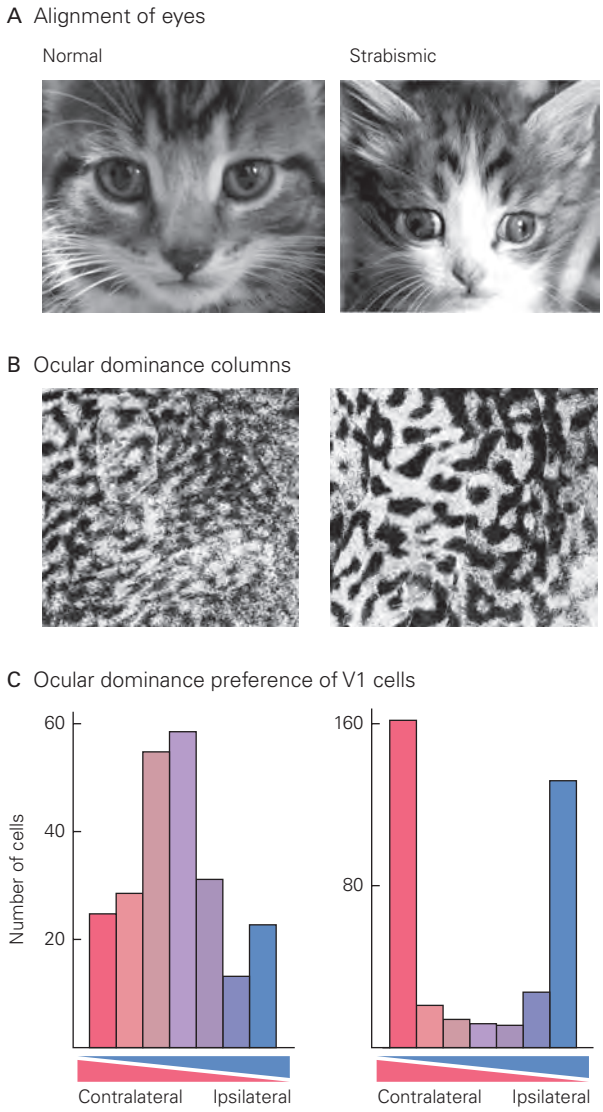

Figure 49–6 Inducing strabismus in kittens impairs the formation of binocular response regions in the primary visual cortex.

A. The eyes of strabismic cats are misaligned. (Photos [*left*] Steve Richardson/Alamy Stock Photo and [*right*] reproduced with permission from Van Sluyters and Levitt 1980.)

B. In strabismic animals, left and right eye domains are more sharply defined, an indication of the paucity of binocular regions. (Reproduced, with permission, from Löwel 1994. Copyright © 1994 Society for Neuroscience.)

C. Strabismic animals have fewer binocularly tuned neurons in the visual cortex. (Reproduced, with permission, from Hubel and Wiesel 1965.)

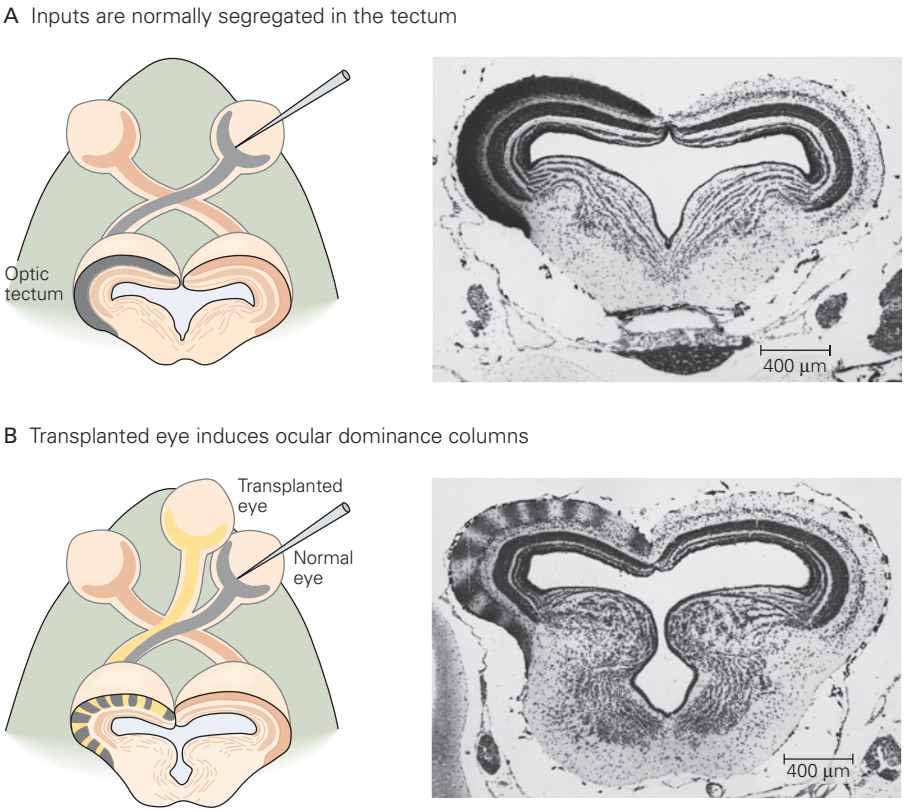

Figure 49–7 Ocular dominance columns can be experimentally induced in a frog by transplantation of a third eye. (Adapted, with permission, from Constantine-Paton and Law 1978. Copyright © 1978 AAAS.)

A. Three days before the transplant, the right eye was injected with a radiolabeled amino acid. The autoradiograph in a coronal section of the hindbrain shows the entire superficial neuropil of the left optic lobe filled with silver grains, indicating the region occupied by synaptic terminals from the labeled (contralateral) eye.

B. Some time after a third eye was transplanted near the normal right eye, the right eye was injected with a radiolabeled amino acid. The autoradiograph shows that the left optic lobe receives inputs from both the labeled eye and the transplanted eye. The normally continuous synaptic zone of the contralateral eye has become divided into alternating dark and light zones that indicate the sites of inputs from each eye.

Reorganization of Visual Circuits During a Critical Period Involves Alterations in Synaptic Connections

The pioneering work of Hubel, Wiesel, and their colleagues showed that early experience is required for the emergence of normal structure and function in the visual cortex. However, the cellular and molecular mechanisms that underlie the critical period remained mysterious. In recent years, many investigators have begun addressing these issues. Much of their work has involved the use of mice, because mice are more amenable to mechanistic analysis than the cats and monkeys studied by Hubel, Wiesel, and their disciples.

Cortical Reorganization Depends on Changes in Both Excitation and Inhibition

Unlike cats and monkeys, most of the mouse visual cortex receives only contralateral input and its binocular region is not divided into ocular dominance columns. Nonetheless, the small binocular region contains a mixture of monocularly and binocularly driven neurons, and closure of the contralateral eye during the critical period for ocular dominance markedly shifts the preference of binocular neurons to inputs from the ipsilateral eye (Figure 49–8).

What converts this early loss of input into a permanent alteration of functional capability? One idea is that thalamic axons carrying information from the deprived eye lose their ability to activate cortical neurons. However, although a decrease in efficacy of the thalamocortical synapse may contribute to this effect, this is not the whole story. Each thalamic axon carries input from only one eye (Figure 49–2). Because loss of responsiveness to the deprived eye occurs only if the other eye remains active, one might imagine that the earliest changes would occur at the first site where inputs from the two eyes have the opportunity to interact. Consistent with this idea, the first physiological changes are not observed in layer IV neurons, each of which receives input from only one eye. Rather, they occur in the binocular neurons of layers II/III and V, which receive convergent input from both right eye– and left eye– driven monocular layer IV neurons. This implies that the loss of cortical responsiveness to the deprived eye results from a circuit alteration rather than from a simple loss of input.

Several possible cellular mechanisms have been proposed to account for these changes in circuitry.

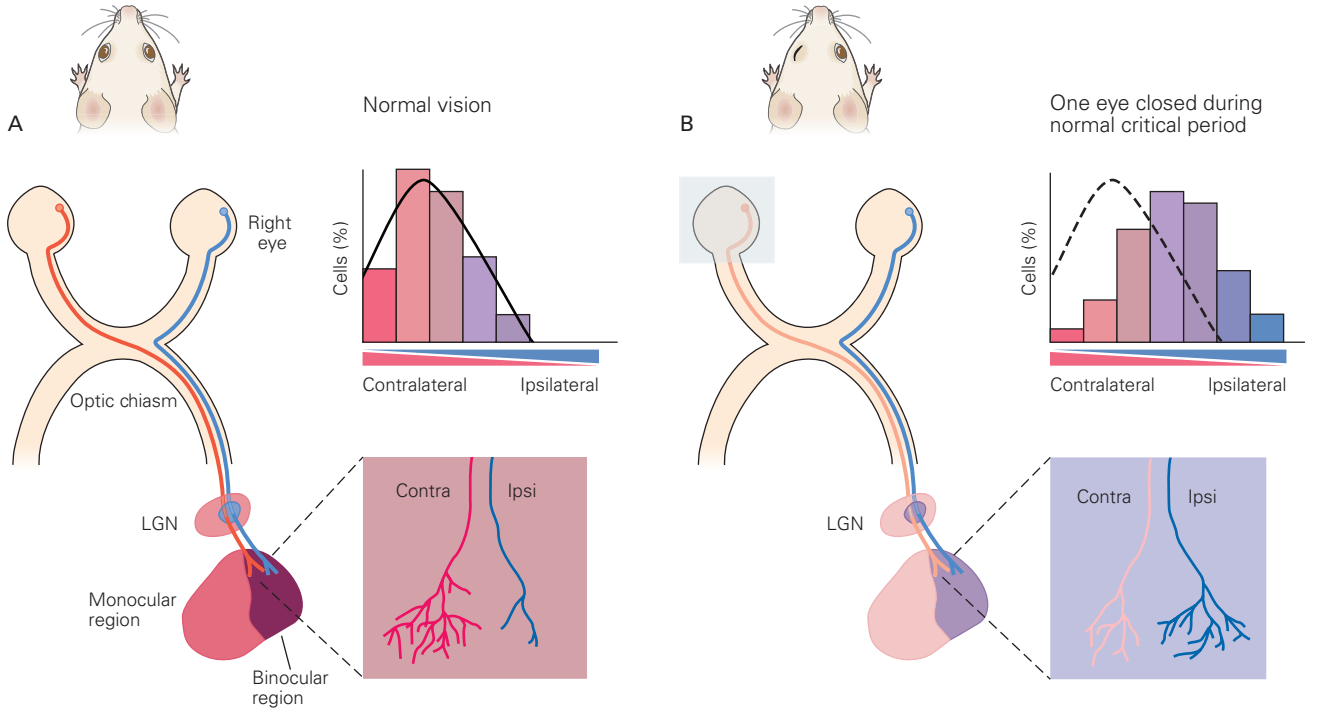

Figure 49–8 A critical period for ocular dominance plasticity is evident in mice. (Adapted, with permission, from Hensch 2005.)

A. The visual cortex in mice contains a small region that receives thalamic (lateral geniculate nucleus [**LGN**]) inputs from both eyes. In this binocular region, most neurons are predominantly responsive to contralateral eye input, fewer respond to binocular inputs, and very few respond to ipsilateral eye input only.

B. When the contralateral eye has been closed during the normal critical period and then reopened, inputs from that eye are underrepresented, and many more neurons respond to binocular or ipsilateral eye input. Eye closure before or after the time of the normal critical period does not elicit the same shift in responsiveness.

First, excitatory synapses within the primary visual cortex may weaken because of the decreased input from the closed eye, perhaps through long-term depression (LTD) (Chapter 53). Second, excitatory synapses carrying input from the open eye may become stronger. Third, the strength of inhibitory synapses may be altered, leading to a net decrease in the level of excitation of cortical neurons by inputs from the closed eye or a net increase in excitation from the open eye. Fourth, neuromodulation within the cortex may tune the circuit in more subtle ways, altering the balance between excitation and inhibition.

Careful analysis of neurons in mouse cortex has provided insight into roles played by some of these mechanisms. During the first few days after closing one eye, responses to input from the closed eye are greatly weakened, with no major effect on inputs from the open eye. The weakening results from a process like LTD or a closely related phenomenon called spike timing–dependent plasticity (STDP). Then, over the following few days, responses to inputs from the open eye become stronger. The increase results from a combination of synaptic changes called long-term potentiation and homeostatic plasticity. Homeostatic plasticity is a circuit mechanism that endeavors to maintain a steady level of input to neurons. In this case, loss of excitatory drive from the closed eye leads to a compensatory increase in excitatory drive from the open eye.

Further studies demonstrated that inhibitory interneurons have an important role in the timing of the critical period. Maturation of inhibitory input onto visual cortical neurons coincides with the beginning of the critical period. Moreover, manipulations that lead to earlier development of γ-aminobutyric acid (GABA) signaling result in advancing the critical period (Figure 49–9). Conversely, delaying GABA signaling delays the period in which monocular deprivation enhances the preference for ipsilateral eye input (Figure 49–9). Together these results and others suggest that a sufficient level of inhibitory input plays a critical role in "gating" the opening of the critical period, whereas excitatory mechanisms may play a more prominent role in enacting the alterations that occur during the critical period.

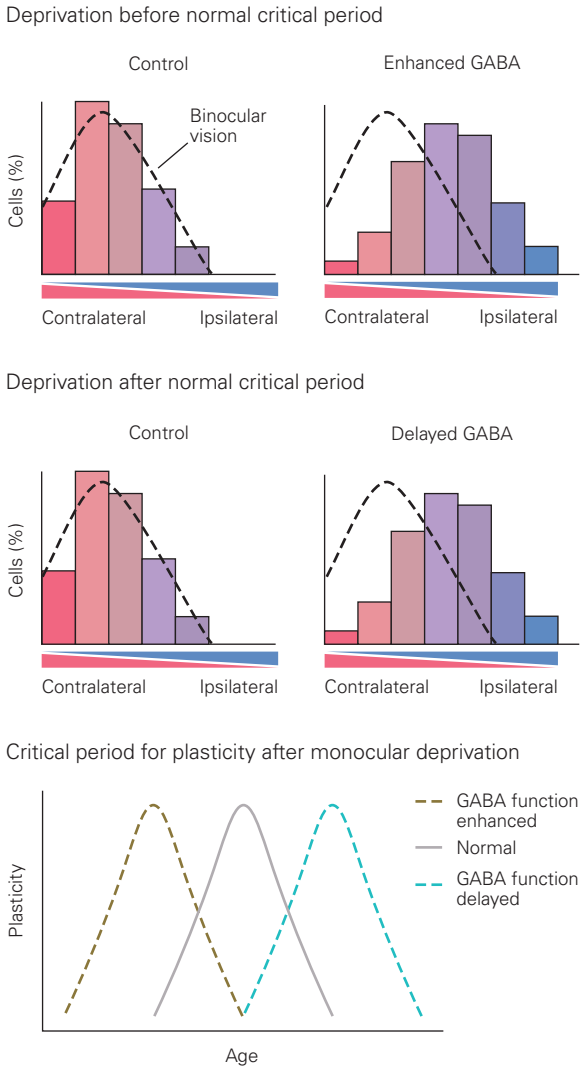

Figure 49–9 The timing of the critical period for ocular dominance plasticity in mice is sensitive to the level of GABAergic neurotransmission. Altering the status of γ-aminobutyric acid (GABA) synthesis and signaling shifts the period in which monocular deprivation can change the response properties of neurons in the visual cortex. Enhancing GABA signaling (through administration of benzodiazepines) shifts the critical period for monocular deprivation to an earlier developmental time. In contrast, delaying GABA signaling (by reducing GABA synthesis genetically and then administering benzodiazepines at a later time) shifts the critical period for monocular deprivation to a later developmental time. (Adapted from Hensch et al. 1998.)

Synaptic Structures Are Altered During the Critical Period

Many studies have sought structural changes that correlate with the altered responsiveness of the visual cortex to input from the closed and open eyes. Particular attention has been paid to dendritic spines as potential sites of plasticity.

Spines are small protrusions from the dendrites of many cortical neurons on which excitatory synapses form. They are dynamic structures, and their appearance and loss are thought to reflect the formation and elimination of synapses. Spine motility is especially marked during early postnatal development, and increases in spine dynamics and number have been associated with changes in behavior.

Striking alterations in the motility and number of dendritic spines on neurons in the mouse visual cortex are observed following closure of one eye. Two days after eye closure in young mice, the motility and turnover of dendritic spines on neurons in the visual cortex increases, suggesting that synaptic connections are beginning to rearrange (Figure 49–10). A few days later, the number of spines begins to change; the number of spines on the apical dendrites of pyramidal neurons decreases initially, but after longer periods of deprivation increases again.

These alterations in spine motility and number can be correlated with three known features of the critical period. First, rather than occurring in layer IV, the changes occur primarily in superficial and deep layers of the cortex, where binocular cells lie. Second, they occur only in the portion of the visual cortex that normally receives binocular input. Third, they fail to occur following eye closure in adult mice (Figure 49–10).

Together, these results support a linkage of spine dynamics with critical period plasticity. According to one model, spine motility may result from the imbalance of inputs to binocular neurons from the open and closed eyes, and it may reflect the first stages in synaptic rearrangement. In turn, the loss of spines, and presumably of synapses, corresponds in time and space to the loss of input from the closed eye and may provide a structural basis for the permanence of this loss. The later growth of new spines occurs as or after responsiveness to the open eye increases and may underlie the adaptive rearrangement that permits the cortex to make the best use of the input available to it.

Thalamic Inputs Are Remodeled During the Critical Period

How are local changes in spines related to the large-scale structural changes in ocular dominance columns

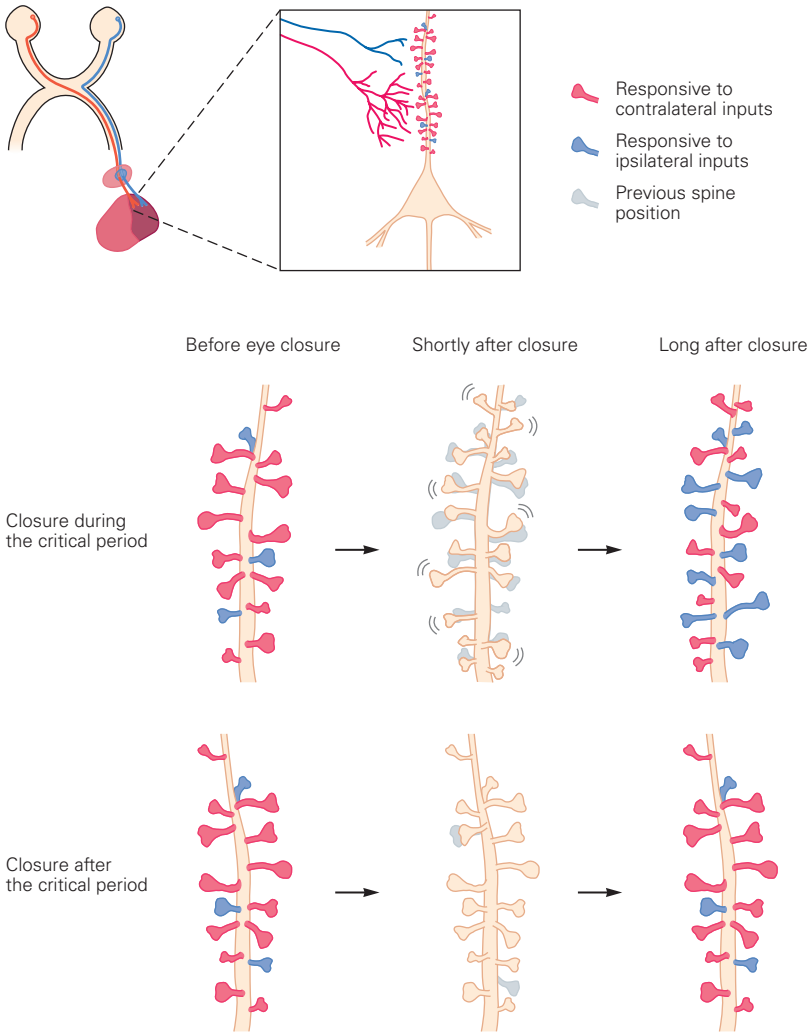

Figure 49–10 The motility of dendritic spines in the mouse visual cortex changes after one eye is closed. The dendrites of pyramidal neurons in the visual cortex have many spines, the density of which remains comparatively constant under normal conditions. Closure of one eye (contralateral in this example) during the critical period for binocular development enhances the motility of dendritic spines and, over time, results in an increase in the proportion of spines that receive synaptic input from the open eye. Similar changes in spine motility are not observed if the eye is closed after the critical period. (Adapted from Oray, Majewska, and Sur 2004.)

shown in Figure 49–4? When developing axons from the lateral geniculate nucleus first reach the cortex, the terminal endings of several neurons overlap extensively. Each fiber extends a few branches over an area of the visual cortex that spans several future ocular dominance columns. As the cortex matures, axons retract some branches, expand others, and even form new branches (Figure 49–11A).

With time, each geniculate neuron becomes connected almost exclusively to a group of neighboring cortical neurons within a single column. The arbors become segregated into columns through the pruning or retraction of certain axons and the sprouting of others. This dual process of axon retraction and sprouting occurs widely throughout the nervous system during development.

What happens after one eye is closed? Axons from a closed eye are at a disadvantage, and a greater than normal proportion retract. At the same time, axons from the open eye sprout new terminals at sites vacated by fibers that would otherwise convey input from the closed eye (Figure 49–11B). If an animal is deprived of the use of one eye early during the critical period of axonal segregation, the normal processes of axon retraction and outgrowth are perturbed. In contrast, if an animal is deprived of the use of one eye after the ocular dominance columns are almost fully segregated, axons conveying input from the open eye actually sprout collaterals in regions of the cortex that they had vacated earlier (see Figure 49–5).

Initially, it was believed that rearrangements of thalamocortical axons in monocularly deprived animals caused the changes in cortical responsiveness to the open and closed eyes. We now know, through electrophysiological recording and imaging of spines, that physiological changes and synaptic alterations

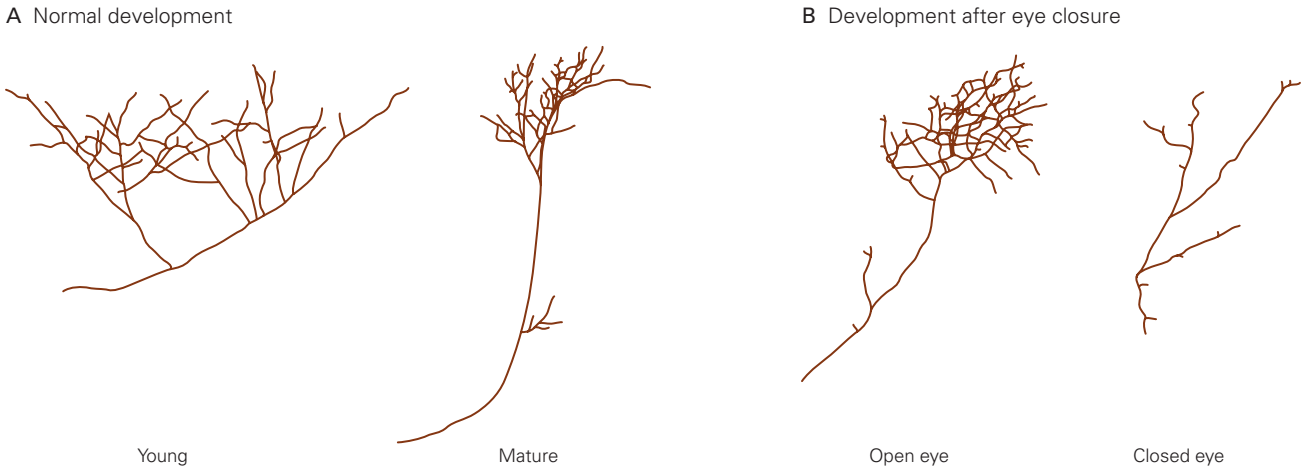

Figure 49–11 The branching of thalamocortical fibers in the visual cortex of kittens changes after the closure of an eye. (Adapted, with permission, from Antonini and Stryker 1993. Copyright © 1993 AAAS.)

A. During normal postnatal development, the axons of lateral geniculate nucleus cells branch widely in the visual cortex. The branching eventually becomes confined to a small region.

B. After one eye is closed, the terminal arbors of neurons in the pathway from that eye are dramatically smaller compared to those of the open eye.

precede the large-scale axonal rearrangements. So rather than causing the physiological changes, axonal remodeling may contribute to making these changes enduring and irreversible. The question then becomes: How do alterations in synaptic structure and function within the cortex lead to alterations in the input?

One idea is that synaptic activity regulates the secretion of neurotrophic factors by cortical neurons. Such factors may then regulate survival of some neurons at the expense of others (Chapter 46) or promote the expansion of some axonal arbors at the expense of others. One such factor, brain-derived neurotrophic factor (BDNF) is synthesized and secreted by cortical neurons, and administering excess BDNF or interfering with its receptor trkB modifies the formation of ocular dominance columns. Nevertheless, interpreting the actions of BDNF is not straightforward. BDNF and trkB signaling affect the cortex in many ways, including enhancing the growth of thalamocortical axons. BDNF can also speed the maturation of inhibitory circuits, which, as noted above, can influence plasticity. It remains unclear whether BDNF is a specific catalyst of the competition that preferentially promotes expansion of some arbors.

Synaptic Stabilization Contributes to Closing the Critical Period

A hallmark of critical periods is that the interval in which experience affects the development of neural circuits is limited. What brings this period of heightened plasticity to a close?

Since synapses and circuits are labile during critical periods, investigators have sought developmental changes in cortex that could lead to stabilization. One parameter is the state of myelination of axons, which occurs around the time the critical period closes. Formation of myelin creates physical barriers to sprouting and axonal growth. Moreover, as discussed in detail in Chapter 50, myelin contains factors such as Nogo and myelin-associated glycoprotein that actively inhibit growth of axons. In mutant mice lacking Nogo or one of its receptors, NogoR, the critical period remains open into adulthood, suggesting that the appearance of these receptors normally contributes to closing the critical period (Figure 49–12).

Another possible agent of closure is the perineuronal net, a web of glycosaminoglycans that wraps certain classes of inhibitory neurons. These nets form around the time that the critical period closes. Infusion of the enzyme chondroitinase, which digests perineuronal nets, maintains plasticity. Thus, critical periods may close once molecular barriers to synaptic growth and rearrangement come into play.

Additional agents of closure may be intrinsic to the neurons. In Chapter 50, we will see that neuronal growth programs decrease with age, and in Chapter 51, we will describe epigenetic mechanisms that "lock in" experience-dependent patterns of gene expression established in early postnatal life.

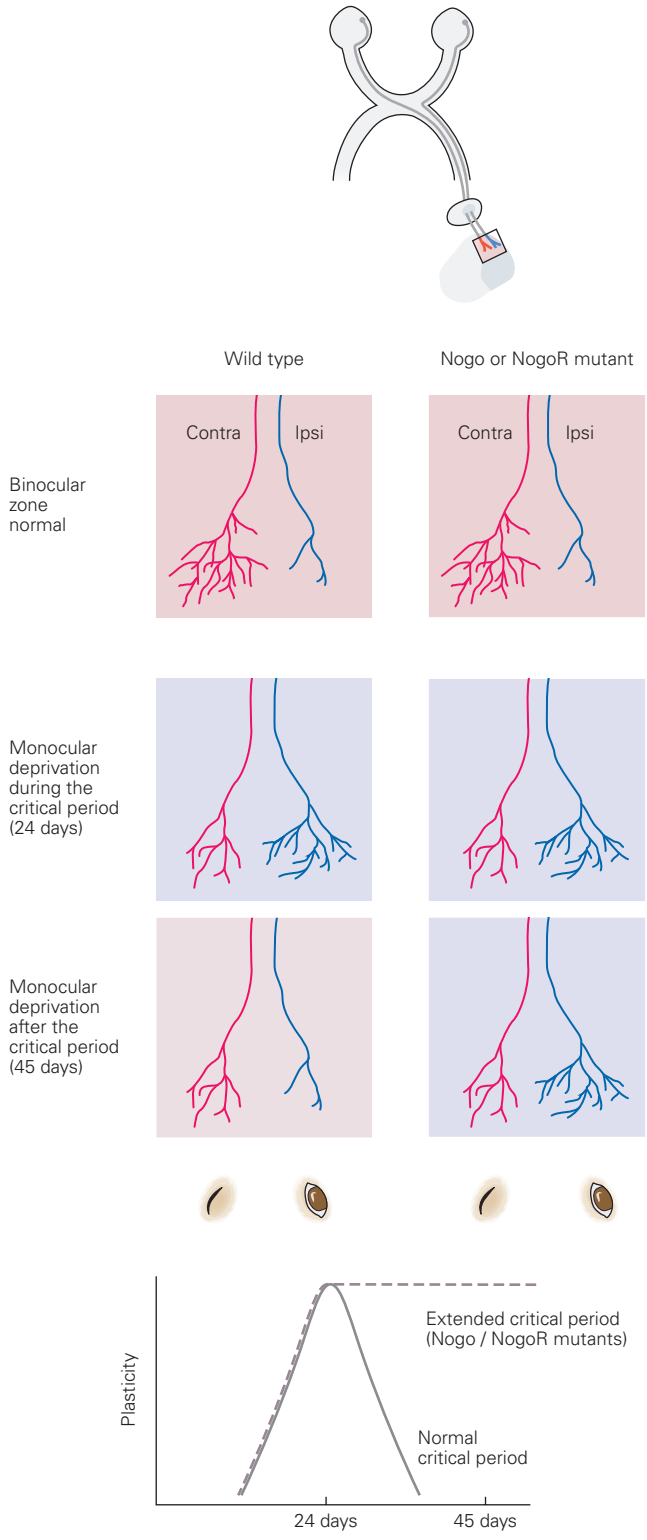

Why should there be an end to critical periods? Would it not be advantageous for the brain to maintain its ability to remodel into adulthood? Perhaps not—the ability of our brain to adapt to variations in sensory input, to gradual physical growth (eg, increases in the distance between the eyes affecting binocular correspondence), and to various congenital disorders is a valuable asset. At an extreme, if one eye is lost, it is advantageous to devote all available cortical real estate to the remaining eye. However, one would not want wholesale reorganization, possibly accompanied by loss of skills and memories, if vision through one eye were lost temporarily in adulthood due to disease or injury. So, enhancing plasticity during a critical period may represent an adaptive compromise between flexibility and stability.

Experience-Independent Spontaneous Neural Activity Leads to Early Circuit Refinement

As noted above, the segregation of visual cortex into ocular dominance columns in cats and monkeys begins before the onset of visual experience. What drives this early phase of segregation? One possibility is that axons from the ipsilateral and contralateral eyes bear different molecular labels that lead to their association. A similar mechanism occurs in the formation of the olfactory projection (Chapter 48). However, no such molecule or mechanism has yet been discovered in the visual projection. Instead segregation appears to rely on spontaneous activity, which not only occurs prior to sensory input but also exhibits striking patterning. This mechanism was initially discovered in studies of the lateral geniculate nucleus, whose neurons provide visual input to the visual cortex.

The arbors of retinal ganglion cells from the two eyes are segregated into alternating layers in the lateral geniculate nucleus, much as the projections from this nucleus are segregated in alternating ocular dominance

Figure 49–12 (Left) The critical period for monocular deprivation is extended in mice lacking Nogo signaling. The drawings show arborization patterns of thalamocortical axons carrying signals from contralateral and ipsilateral eyes to the binocular zone in visual cortex. Monocular deprivation during the critical period results in a shift in ocular preference in neurons in the binocular zone in both wild-type mice and mice mutant for Nogo or the Nogo receptor (**NogoR**). After the normal critical period (at 45 days), the shift in ocular preference continues in mice with mutant Nogo-A or the Nogo receptor but not in wild-type mice. The plot shows that elimination of Nogo signaling prevents closure of the critical period. (Adapted from McGee et al. 2005.)

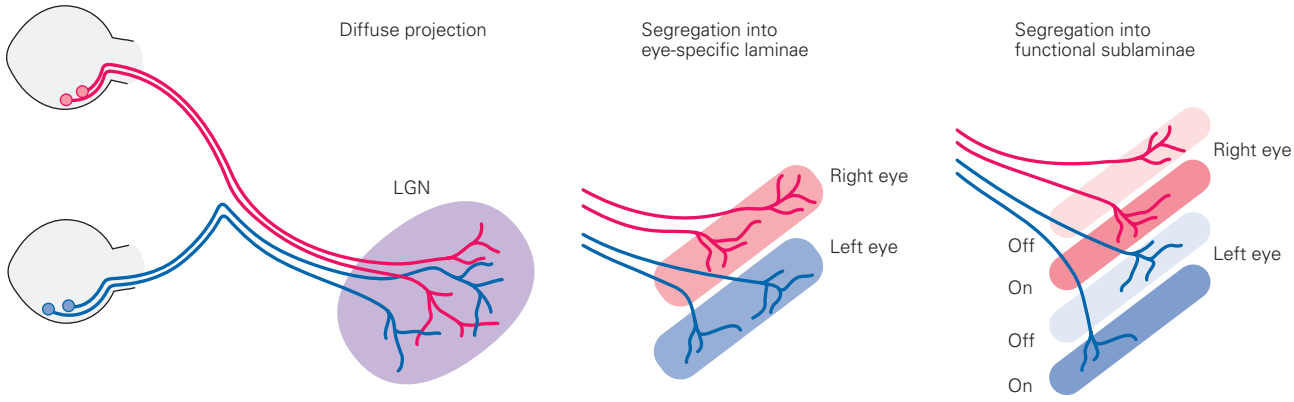

Figure 49–13 **The terminals of retinal ganglion cells in the lateral geniculate nucleus (LGN) become segregated during normal development.** At early stages of development, the terminals of axons from each eye intermingle, but at later stages, they segregate into separate layers of the nucleus. In some species, axons from one eye even segregate into functionally specialized sublayers (on and off layers in ferrets). (Adapted, with permission, from Sanes and Yamagata 1999.)

columns in the visual cortex (Figure 49–13). In both structures, individual axons at first form terminals in multiple domains (layers in the geniculate nucleus, columns in the cortex). Later, the terminals become segregated by a process of refinement. The refinement involves both growth of terminal arbors in the "appropriate" layer and elimination of terminals from the inappropriate layer (Chapter 48).

As in the cortex, application of tetrodotoxin to the optic nerves disrupts the segregation of the inputs from each eye, indicating that activity is essential for segregation. In contrast to cortex, however, segregation of inputs is complete before the onset of visual experience—prior to birth in monkeys and postnatally but prior to eye opening in mice. Thus, vision cannot drive the neural activity essential for segregation.

It turns out that the axons of retinal ganglion neurons are spontaneously active in utero, well before the eyes open. Neighboring ganglion cells fire in synchronous bursts that last a few seconds, followed by silent periods that may last for minutes. Sampling the activity of retinal ganglion neurons across the entire retina revealed that these bursts propagate across much of the retina in a wave-like manner (Figure 49–14). This pattern of ganglion cell activity appears to be coordinated by excitatory inputs from amacrine cells in the overlying layer of the retina (Chapter 22).

The spontaneous, synchronous firing of a select group of ganglion neurons excites a local group of neurons in the lateral geniculate nucleus. Such synchronized activity appears to strengthen these synapses at the expense of other nearby synapses, perhaps by a Hebbian mechanism similar to that posited for experience-dependent refinement. This does not mean that visually evoked activity has no role in sculpting the retinogeniculate pathway. At a later stage, other aspects of refinement, such as spatial rearrangement of synapses along the axon, are regulated by visual experience.

The discovery that spontaneous activity can lead to circuit refinement provides a likely explanation for the initial segregation of inputs to the visual cortex. More generally, the parsing of activity-dependent circuit refinement into two phases, the first dependent on spontaneous activity and the second on sensory input, now appears to be a general theme in the development of brain circuits that begin refinement before they have the chance to respond to environmental stimulation.

Activity-Dependent Refinement of Connections Is a General Feature of Brain Circuitry

We have seen that neural activity is critical for segregating axons from the two retinas into distinct layers in the lateral geniculate nucleus and then into distinct columns in the visual cortex. Is this developmental role of activity a special case, or does activity also affect maturation elsewhere in the visual system, and even in other parts of the brain? Studies of many systems show that activity-dependent control of refinement is a general property of neural circuits in the mammalian brain.

Many Aspects of Visual System Development Are Activity-Dependent

One well-studied example of activity-dependent development in the visual system is the sharpening

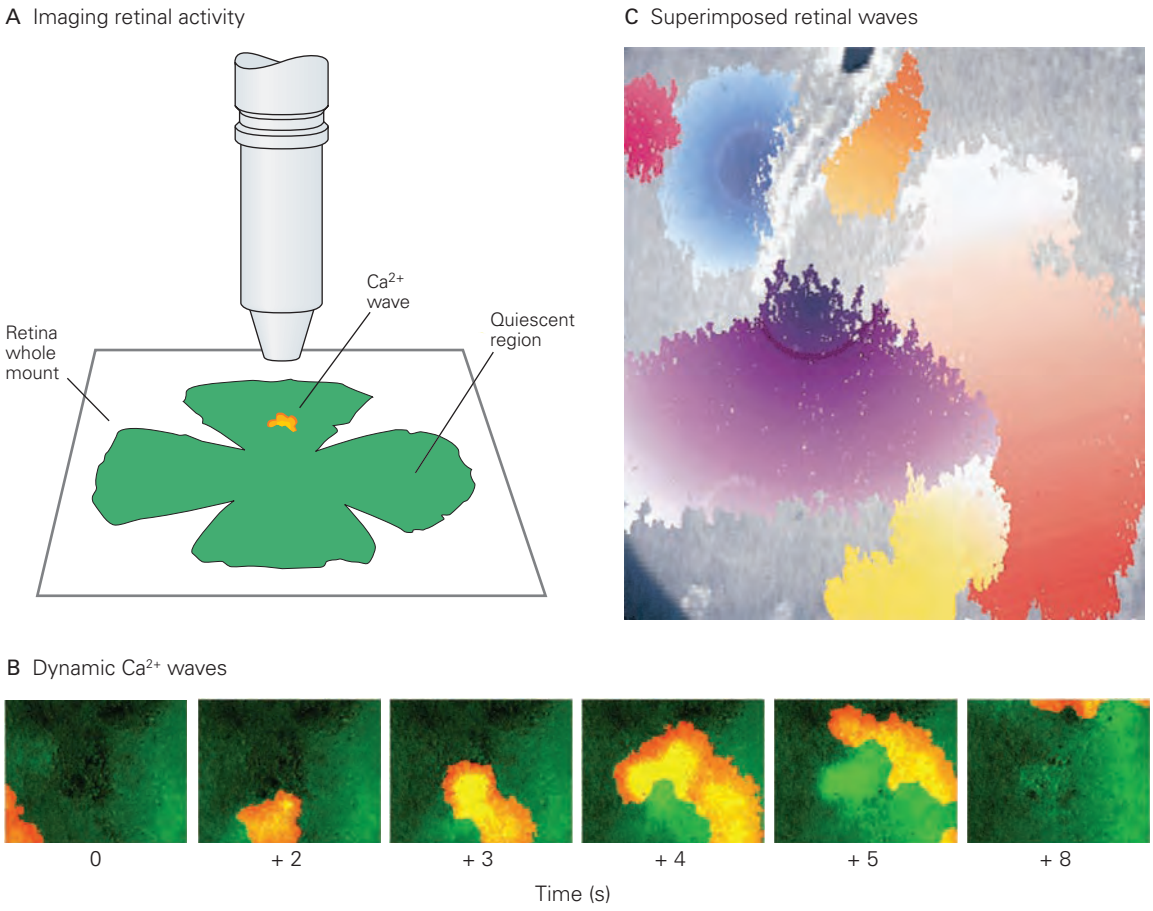

Figure 49–14 Correlated waves of neural activity in the developing retina.

A. Microscopic visualization of the activity of retinal ganglion neurons in a flat-mounted preparation of mammalian retina. Spontaneous waves of neural activity are visualized by monitoring Ca^{2+} transients (**yellow domain**) after loading of cells with dyes that change their fluorescent emission spectrum in response to changes in intracellular Ca^{2+} concentration.

B. These still images from a movie sequence show the propagation of one Ca^{2+} activity focus (**yellow domain**) across the retina. Images were taken 1 second apart. Many cells within the activity focus are activated synchronously. (Reproduced, with permission, from Blankenship et al. 2009. Copyright © 2009 Elsevier Inc.)

C. Retinal activity waves recorded over time are superimposed in this image. Discrete waves are indicated in different colors; the origin of a wave is indicated by a darker hue. These waves originate in different retinal foci and spread in distinct, unpredictable directions. (Reproduced, with permission, from Meister et al. 1991. Copyright © 1991 AAAS.)

of the topographic distribution of retinal ganglion cell axons onto their central targets, a topic we introduced in Chapter 47. In vertebrates, molecular cues such as ephrins guide axons from the retina to appropriate sites in the optic tectum (called the superior colliculus in mammals—see Figure 47–11), but they are not sufficient to form the refined visual map.

Histological and physiological studies have found that the map formed initially in the superior colliculus/optic tectum is coarse and that individual retinal ganglion cell axons have large, overlapping arbors. These axonal arbors are later pruned to their mature size, resulting in a more restricted and precise field of termination. If retinal activity is inhibited, only the initial coarse map forms.

Is it the pattern of activity or activity itself that is important in visual map formation? Put another way, is activity simply a precondition for refinement, or does it have an organizing role, determining exactly which axons win or lose the competition? Many experiments show that the latter idea is closer to the truth.

In one study, the accuracy of the retinotectal map was assessed in fish raised in a tank illuminated only by brief flashes from a strobe light. A control group was raised in a normal laboratory environment. The total light intensity presented to the fish was similar

under both conditions, but the resulting pattern was very different. In control fish, the images fell haphazardly on various parts of the retina as the fish swam around their tanks. This input produces local synchronous activity of the sort generated by the waves of spontaneous activity described above—neighboring ganglion cells tend to fire together, but there is little correlation with the firing patterns of distant ganglion cells. In these fish, the map becomes precise. In contrast, stroboscopic illumination synchronously activates nearly all of the ganglion cells, and in these fish, the retinotectal map remains coarse.

Presumably, the tectum determines which retinal axons are near neighbors by judging which ones fire in synchrony, much as activity patterns in the lateral geniculate nucleus or visual cortex determine which axons carry signals from the same eye. This information is then used to refine the topographic map, through mechanisms similar to those in the cortex. When all of the axons fire in synchrony, the tectum cannot determine which axons are neighbors; refinement fails, and the map remains coarse.

Sensory Modalities Are Coordinated During a Critical Period

Our experience of the world is shaped by synthesizing sensory input from multiple modalities. For example, our mental image of where an object is with respect to our body is the same whether we localize it by touch, sound, or sight. For each modality, information is mapped in an orderly way within relevant brain areas, much like the retinotopic maps in the optic tectum and visual cortex. Multimodal localization requires that these maps, which are formed independently during development, be brought into register. This aspect of refinement occurs during critical periods.

Studies on barn owls have provided insight into how auditory and visual maps are coordinated during a critical period. During the day, owls use vision to localize their prey—mice or other small rodents—but at night, they rely on auditory cues, and at dusk, both sensory channels are used. The localization of sound must be precise if owls are to succeed in finding prey, and it is intuitively obvious that the visual and auditory cues for the same location need to be consistent.

Auditory localization in owls, as in people, results from the presence of neurons that vary in their sensitivity to sounds sensed by the two ears. For example, sounds arising from a source to the left arrive slightly sooner at the left ear than at the right ear and are slightly louder in the left ear. These discrepancies help us determine the point in horizontal space from which a sound arises (Chapter 28). Computation of the temporal difference in the arrival of sounds at the two ears is particularly crucial. The difference is only a few tens of microseconds, as expected from calculations based upon the speed of sound and the width of the head. Remarkably, the auditory system is sensitive to these extremely short interaural time differences (ITDs) and can calculate prey position from them (Figure 49–15). Moreover, many auditory neurons in the optic tectum

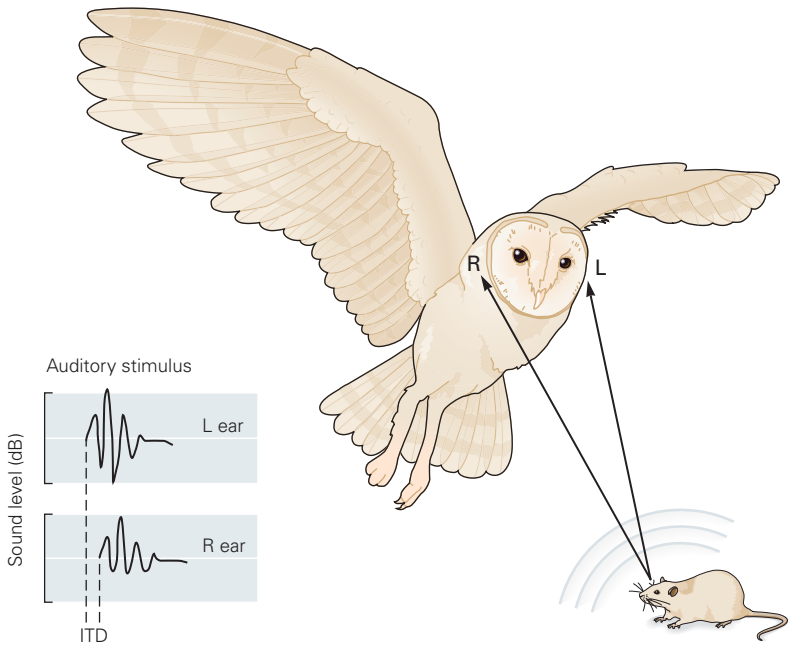

Figure 49–15 The barn owl uses interaural time differences to localize its prey. Sound waves generated by movements of a mouse are received by the owl's left and right ears. As the prey emits noise, the difference in the time of arrival of auditory stimuli at the two ears—the interaural time difference (ITD)—is used to calculate the precise position of the prey target. (Reproduced, with permission, from Knudsen 2002. Copyright © 2002 Springer Nature.)

with receptive fields centered on a particular location are also tuned to ITDs that correspond to sounds emitted from that same point in space. The registration is imprecise at early stages but becomes progressively more precise during early adolescence as a consequence of the animal's experience.

Crucial insight into how this registration occurs came from experiments in which prisms were mounted over the eyes of young owls. The prisms shifted the retinal image horizontally so that the visual map in the tectum reflected a world systematically displaced from its "actual" orientation. This change abruptly disrupted the correspondence between visual and auditory receptive fields. Over the next several weeks, however, the ITD to which tectal neurons responded optimally, ie, their auditory receptive field, changed until the visual and auditory maps came back into register (Figure 49–16). Thus, the visual map instructs the auditory map.

Further experiments showed that this reorganization resulted from rewiring of connections between two deeper auditory nuclei (Figure 49–17). When prism goggles were placed on young owls, changes in ITD tuning were fully adaptive in that the animals compensated completely for the effects of the prisms. In contrast, goggles placed on mature owls (older than 7 months of age) had little effect. Thus, reorganization of this auditory projection occurs optimally during a critical juvenile period.

Different Functions and Brain Regions Have Different Critical Periods of Development

Not all brain circuits are stabilized at the same time. Even within the visual cortex, the critical periods for organization of inputs differ among layers in both mice

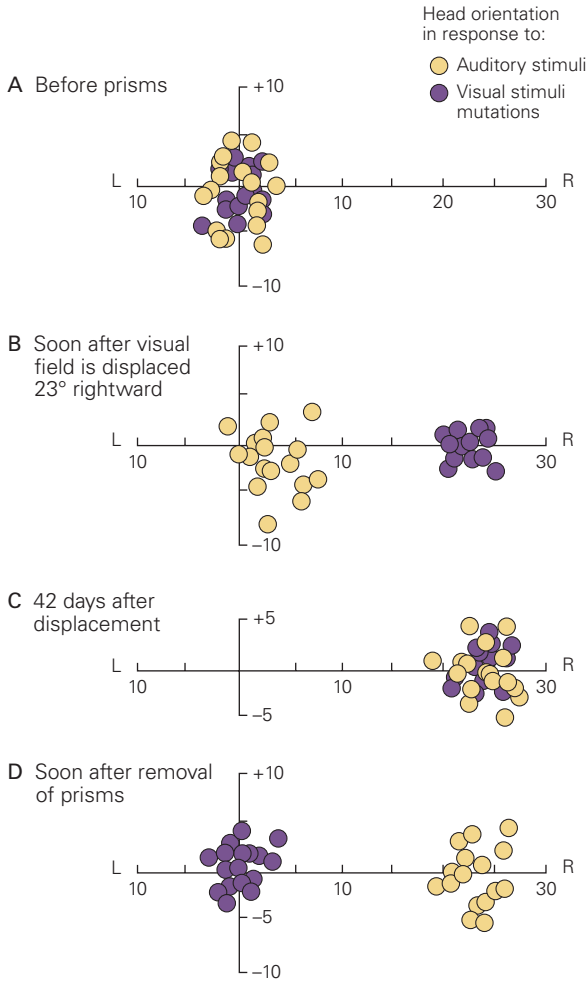

Figure 49–16 (Right) **Reorganization of sensory maps in the optic tectum of owls after systematic displacement of the retinal image.** The retinal image in adolescent owls can be displaced by prism goggles, which shift images from 5° to 30°. (Adapted, with permission, from Knudsen 2002. Copyright © 2002 Springer Nature.)

A. Before application of the prisms, the visual and auditory neural maps coincide.

B. The prism goggles displace the retinal image by 23°. Consequently, the neural and auditory maps are out of alignment.

C. The two brain maps are once again congruent 42 days after prism application because the auditory map has shifted to realign with the visual map.

D. Soon after the prisms are removed, the visual map reverts to its original position, but the auditory map remains in its shifted position.

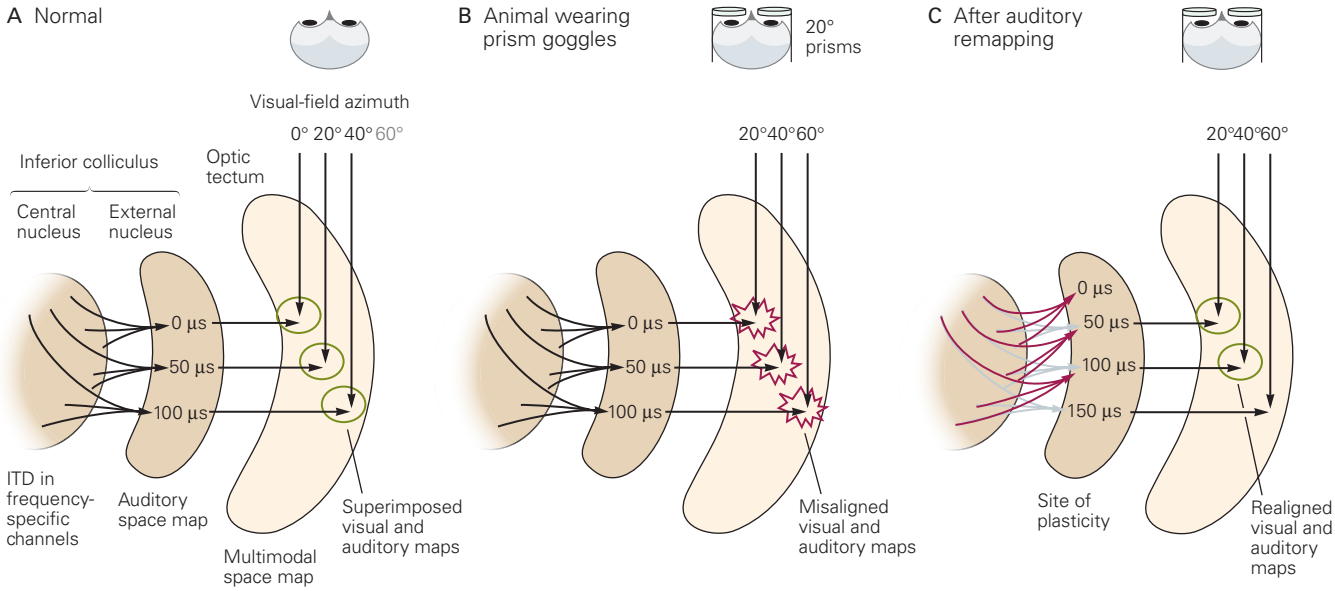

Figure 49–17 The effect of prism experience on information flow in the midbrain auditory localization pathway in the barn owl. (Adapted from Knudsen 2002.)

A. The auditory pathway in a normal owl. The interaural time difference (ITD) is measured and mapped in frequency-specific channels in the brain stem. This information ascends to the inferior colliculus, where a neural map of auditory space is created. The map is conveyed to the optic tectum where it merges with a map of visual space.

B. After an owl is fitted with prism goggles, the visual and auditory space maps in the optic tectum become misaligned.

C. After reorganization of auditory maps, the visual and auditory maps are once again in alignment.

and monkeys. As an example, the neural connections in layer IVC of the visual cortex of the monkey are not affected by monocular deprivation by the time the animal is 2 months old. In contrast, connections in the upper and lower layers continue to be influenced by sensory experience (or lack of it) for almost the entire first year after birth. Critical periods for other features of the visual system, such as orientation tuning, occur at different developmental stages (Figure 49–18A).

The timing of critical periods also varies between brain regions (Figure 49–18B). The adverse consequences of sensory deprivation for the primary sensory regions of the brain are generally fully realized early in postnatal development. In contrast, social experience can affect the intracortical connections over a much longer period. These differences may explain why certain types of learning are optimal at particular stages of development. For example, certain cognitive capacities—language, music, and mathematics—usually must be acquired well before puberty if they are to develop at all. In addition, insults to the brain at specific early stages of postnatal life may selectively affect the development of certain perceptual abilities and behavior.

Critical Periods Can Be Reopened in Adulthood

By definition, critical periods are limited in time. Nevertheless, they are less sharply defined than originally thought. Extending or reopening critical periods in adulthood could increase brain plasticity and make it possible to facilitate recovery from strokes and other insults that impair discrete regions of the nervous system.

Some of the first evidence for plasticity in the adult cortex came from studies by Merzenich and colleagues on the representation of the fingers of monkeys in the somatosensory cortex. Recordings of neuronal receptive fields in normal adult animals showed that each digit is mapped in an orderly way on the cortical surface, with abrupt discontinuities between areas responding to different digits (Figure 49–19A). Amputation of a digit left the cortical representation of that digit initially unresponsive, but after several months, areas serving the neighboring digits filled in the gap (Figure 49–19B). Much as happens in the visual cortex following monocular deprivation, the somatosensory map was readjusted so that the cortex could devote

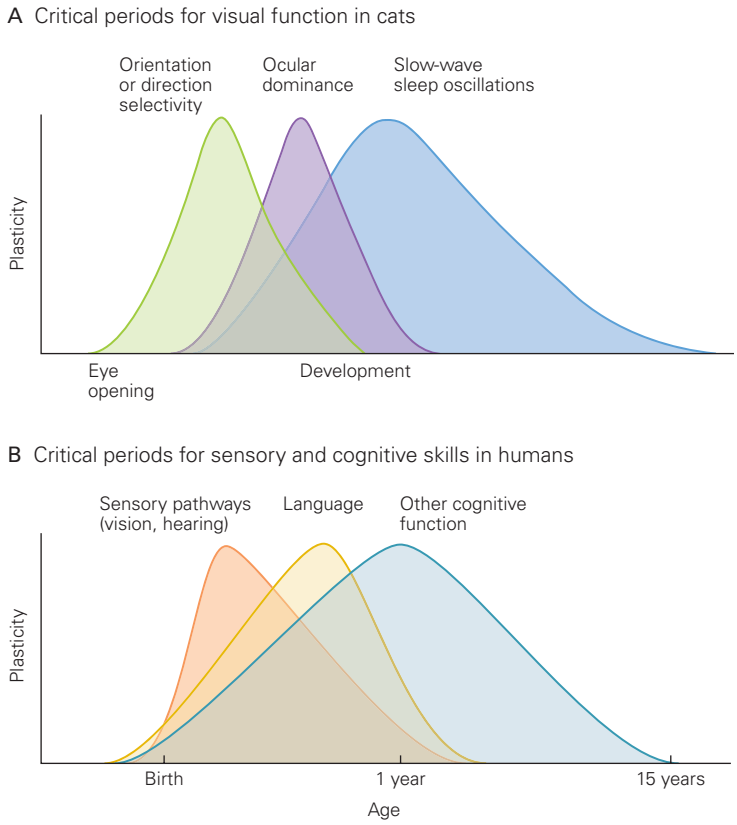

Figure 49–18 The timing of critical periods varies with brain function. (Reproduced, with permission, from Hensch 2005. Copyright © 2005 Springer Nature.)

A. In cats, the critical periods for development of orientation or direction selectivity in visual neurons occur earlier than those for establishment of ocular dominance and slow-wave sleep oscillation.

B. In humans, the timing of periods for development of sensory processing, language, and cognitive functions varies.

most of its resources to useful inputs. Conversely, when two fingers were sutured together so they received coincident input, a swath of cortex on both sides of the border between the two digit areas eventually became responsive to both areas (Figure 49–19C). This result suggests that, as in the visual system, borders may result from competition and can be blurred when competition declines. What was most surprising was that these effects occurred in adulthood, long after all known critical periods had closed.

In the years since Merzenich's studies, evidence has accumulated that critical periods can be reopened in many systems. We illustrate this principle by returning to two areas in which critical periods have been well mapped, the optic tectum in the owl and the visual cortex in the mouse.

Visual and Auditory Maps Can Be Aligned in Adults

In initial studies of the matching of auditory and visual maps in owls, realignment following displacement of the visual field with prism goggles was largely restricted to an early sensitive period (Figures 49–16 and 49–17). However, three strategies dramatically enhance binaural tuning plasticity in adult owls.

First, when adult owls that had worn goggles as adolescents are refitted with the goggles, the auditory map again shifts to align with the new visual map (Figure 49–20A). In contrast, in adult owls that had not worn the goggles as adolescents, the use of goggles has little effect on the organization of the auditory map. Thus, the events of map rearrangement during the normal critical period must leave a neural trace that permits rearrangement later in life. In fact, in the owls that wore prisms in early life, axons to auditory nuclei that were normally pruned were maintained, providing a structural basis for the reorganization in adulthood.

A second method for inducing late plasticity is to displace the retinal image in small steps by having the owl wear a series of prism spectacles of progressively increasing strength. Under these conditions, adjustment of the auditory map is typically three- to fourfold greater than the response to a single large displacement of the retinal image (Figure 49–20B).

The third technique is to allow owls to hunt live prey. In earlier experiments, animals were housed and fed under standard laboratory conditions. However, when adult prism-wearing owls are allowed to capture live mice under low light conditions for 10 weeks, they exhibit far greater plasticity of binaural tuning

than owls fed dead mice (Figure 49–19C), albeit less than that exhibited by juvenile owls that did not hunt. The finding that hunting increases the plasticity of binaural tuning in adult owls dramatically demonstrates that behavioral context affects the ability of the nervous system to reorganize. Whether this effect results from increased sensory information, attention, arousal, motivation, or reward needs to be resolved.

Binocular Circuits Can Be Remodeled in Adults

As the body of observations on monocular deprivation grew, it became apparent that some plasticity persisted beyond the classical critical period in cats, rats, and mice. In mice, for example, modest shifts in ocular dominance occur even when one eye is deprived of vision at 2 or 3 months of age. By 4 months of age, however, monocular deprivation has no detectable effect.

Over the past decade, several interventions have been discovered that enhance the extent of ocular dominance plasticity in young adults and even enable substantial plasticity in older animals. Some are noninvasive: Environmental enrichment, social interaction (via group housing), visual stimulation, and exercise all increase the magnitude and speed of changes that occur following monocular deprivation in adults. A second group of interventions targets mechanisms that appear to affect the timing of the normal critical period. As noted above, treating the cortex with chondroitinase to disrupt perineuronal nets or interference with the inhibitory effects of myelin on axonal growth can both extend and reopen the critical period. Remarkably, transplantation of immature inhibitory interneurons into the visual cortex also reopens the critical period even in 6-month-old mice.

How can we reconcile the strong evidence for critical periods with the newer evidence for reorganization

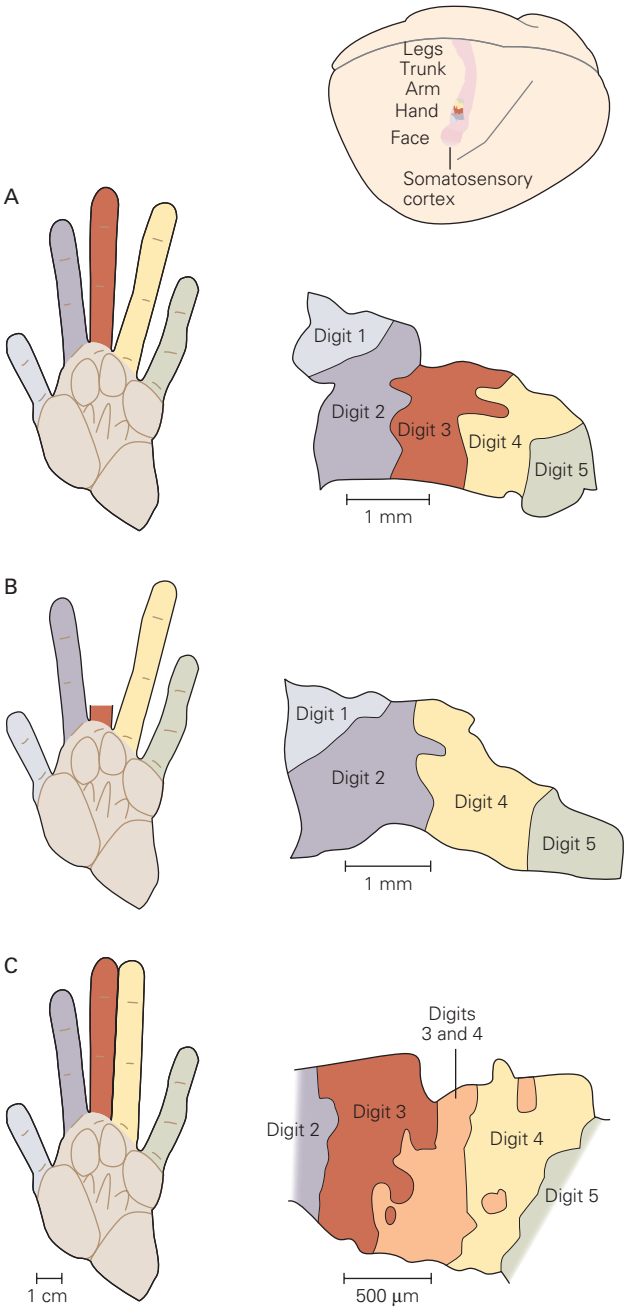

Figure 49–19 (Left) Representation of digits in somatosensory cortex can be remapped in adult monkeys. (Adapted, with permission, from Merzenich et al. 1984 and Allard et al. 1991.)

A. Lightly touching specific spots on the digits (*left*) elicits responses from neurons in somatosensory cortex (*right*), revealing orderly topographic maps of each digit on the cortical surface. Abrupt discontinuities distinguish regions serving adjacent digits.

B. Following amputation of a digit, the cortical region it previously supplied is left unresponsive. Several months later, axons from the adjacent digits (2 and 4) have formed synaptic connections in the unresponsive area.

C. After digits 3 and 4 have been sutured together, they received simultaneous sensory stimulation, and cortical regions at the border between areas representing the digits become responsive to both.

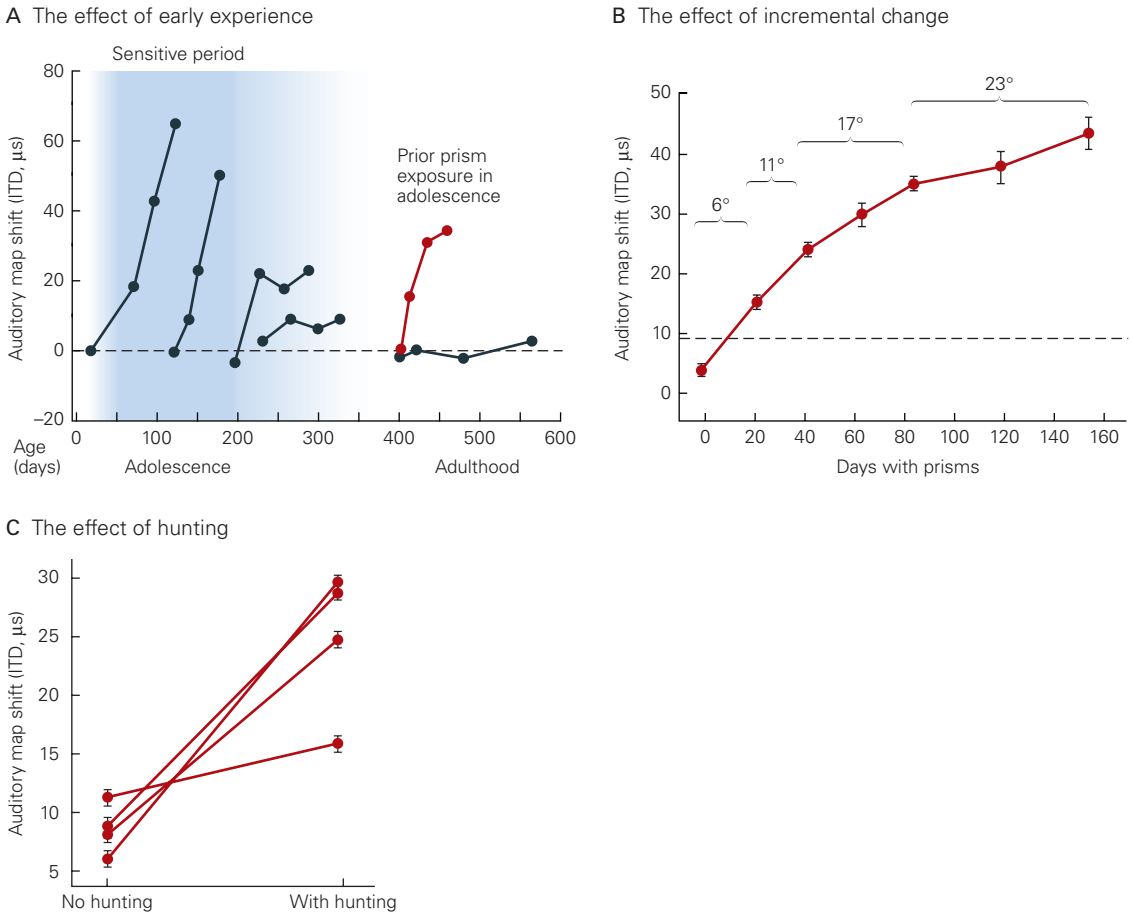

Figure 49–20 Different behavioral conditions have different effects on the realignment of visual and auditory neural maps in the mature barn owl.

A. The remodeling of the auditory maps that results from wearing prism goggles for a brief period during adolescence leaves a neural trace that can be reactivated in the adult. When these birds are fitted with the goggles as adults, the auditory map is still able to realign with the visual map. (Abbreviation: ITD, interaural time difference.) (Reproduced, with permission, from Knudsen 2002. Copyright © 2002 Springer Nature.)

B. When an animal is fitted with a series of prisms, each of which produces a small displacement in the visual image, the auditory map is successfully brought into alignment. The dotted line shows the extent of realignment if the animal is fitted with a 23° prism on day 0. (Reproduced, with permission, from Linkenhoker and Knudsen 2002. Copyright © 2002 Springer Nature.)

C. If an adult owl has the opportunity to hunt live prey while wearing prism goggles, auditory remapping occurs, perhaps because of enhanced motivation to sharpen perception. (Reproduced, with permission, from Bergan et al. 2005. Copyright © 2005 Society for Neuroscience.)

of circuitry in adults? The plasticity observed in adults is modest and slow compared to that seen during the critical period, and its mechanisms differ in some respects from those for earlier deprivation. These differences result from two factors. First, from early postnatal life into adolescence, the molecular environment in the brain is conducive to axonal growth, and cellular mechanisms are optimal for promoting the formation, strengthening, weakening, and elimination of synapses. Under these conditions, circuits can readily change in response to experience. Conversely, in mature circuits, molecular and structural elements promote stability and impede plasticity. Second, in a developing circuit, no particular pattern of connectivity is firmly entrenched, so there is less to overcome. The connections specified by genetic determinants are less precise, and the connections themselves are relatively weak. The patterns of neural activity that result from experience sharpen and even realign these patterns of connectivity.

In sum, experience during critical periods has a potent effect on circuits because the cellular and molecular conditions are optimal for plasticity and because the instructed pattern of connectivity does not have

to compete with a long-existing pattern. These differences help explain the special behavioral, pharmacological, or genetic interventions needed to stimulate plasticity in adults.

Highlights

1. Although the nervous system is malleable throughout life, plasticity is particularly great during restricted intervals in early postnatal life called critical periods. Alterations that occur during these periods are nearly irreversible.
2. Critical periods vary in time among brain areas and tasks. For example, children with strabismus (crossed eyes) will never have good stereoscopic vision unless their eyes are brought into alignment during the first few postnatal years, and people cannot learn a new language without an accent after their early teens.
3. The richest understanding of critical periods comes from studies initiated by Hubel and Wiesel on how input from the two eyes is integrated in the cortex. They deprived one eye of vision for varying periods in young cats or monkeys. In normal animals, most neurons in visual cortex are binocularly responsive, but following monocular deprivation for a brief period in early postnatal life, most cortical cells permanently lost responsiveness to input from the once-closed eye. Responses in the eye itself and the lateral geniculate nucleus were nearly normal, pinpointing the cortex as the site of change. Much longer deprivation in adulthood had little effect.
4. A structural basis for the loss of binocularity was seen in the alternating pattern of ocular dominance columns, within which neurons are dominated by input from one eye or the other. Following monocular deprivation during the critical period, columns representing the open eye expanded at the expense of those representing the closed eye. This form of plasticity may be designed to optimize the use of cortical space for each individual at each time period—for example, subtly shifting binocular interactions as the head grows and the eyes become further apart.
5. The binocular interaction reflects competition between the two sets of inputs, since vision and symmetrical columns are retained following binocular deprivation. Many lines of evidence indicate that the competition depends on patterns of activity arising in the two eyes, with inputs from each eye being more synchronous with each other than with inputs from the other eye. Postnatally, synchrony is driven by visual experience. Prenatally or prior to eye opening, patterned spontaneous activity in the two eyes accounts for the synchrony.
6. Cellular mechanisms underlying the effects of monocular deprivation have been studied in greatest detail in mice. Following monocular deprivation, input from the closed eye is weakened rapidly by a process akin to long-term depression (LTD). Shortly thereafter, input from the other eye is strengthened, partly by a compensatory mechanism called homeostatic plasticity. Structural remodeling of thalamic axons and cortical dendrites occurs later.
7. Maturation of inhibitory interneurons is a main determinant of when the critical period opens. The end of the critical period is marked by the formation of myelin and proteoglycan-rich perineuronal structures that hamper structural remodeling.
8. Although plasticity of binocular interactions was initially believed to be confined to early postnatal life, it is now apparent that critical periods can be "reopened" to some extent in adults. In some cases, this can be done by altering the animal's environment or the way in which the altered experience is delivered. Critical periods can also be reopened by manipulating some of the factors that normally close them in adolescence.
9. Plasticity in adulthood is modest in magnitude and difficult to trigger compared to early postnatal critical periods. Nonetheless, reopening of critical periods could, if properly controlled, enable reorganization to compensate for losses incurred from injuries, disease, and early maladaptive experience.
10. Critical periods occur during development of numerous systems, such as formation of orderly maps of auditory, somatosensory, and visual input onto relevant sensory cortices. Many of the principles and mechanisms that characterize the plasticity of binocular interactions also regulate these critical periods, including roles of spontaneous and experience-dependent activity, competition, alterations in excitatory and inhibitory synapses, and selective growth and pruning of inputs to achieve appropriate patterns of adult connectivity.
11. The existence of critical periods demonstrates that the brain's ability to remodel declines precipitously in adulthood. This seems disadvantageous but may represent a useful adaptation, allowing each brain to adapt to its environment

as it develops, but then buffering it against excessive change later, perhaps even enabling skills and memories to persist. If this is the case, therapies based on reopening critical periods in adults may come at a cost.

Joshua R. Sanes

Selected Reading

Espinosa JS, Stryker MP. 2012. Development and plasticity of the primary visual cortex. Neuron 75:230–249.

Harlow HF. 1958. The nature of love. Am Psychol 13: 673–685.

Hensch TK, Quinlan EM. 2018. Critical periods in amblyopia. Vis Neurosci 35:E014.

Hübener M, Bonhoeffer T. 2014. Neuronal plasticity: beyond the critical period. Cell 159:727–737.

Knudsen EI. 2002. Instructed learning in the auditory localization pathway of the barn owl. Nature 417:322–328.

Leighton AH, Lohmann C. 2016. The wiring of developing sensory circuits: from patterned spontaneous activity to synaptic plasticity mechanisms. Front Neural Circuits 10:71.

Thompson A, Gribizis A, Chen C, Crair MC. 2017. Activity-dependent development of visual receptive fields. Curr Opin Neurobiol 42:136–143.

Wiesel TN. 1982. Postnatal development of the visual cortex and the influence of environment. Nature 299:583–591.

References

Allard T, Clark SA, Jenkins WM, Merzenich MM. 1991. Reorganization of somatosensory area 3b representations in adult owl monkeys after digital syndactyly. J Neurophysiol 66:1048–1058.

Antonini A, Stryker MP. 1993. Rapid remodeling of axonal arbors in the visual cortex. Science 260:1819–1812.

Behen ME, Helder E, Rothermel R, Solomon K, Chugani HT. 2008. Incidence of specific absolute neurocognitive impairment in globally intact children with histories of early severe deprivation. Child Neuropsychol 14: 453–469.

Bergan JF, Ro P, Ro D, Knudsen EI. 2005. Hunting increases adaptive auditory map plasticity in adult barn owls. J Neurosci 25:9816–9820.

Blankenship A, Ford K, Johnson J, et al. 2009. Synaptic and extrasynaptic factors governing glutamatergic retinal waves. Neuron 62:230–241.

Buonomano DV, Merzenich MM. 1998. Cortical plasticity: from synapses to maps. Annu Rev Neurosci 21:149–186.

Constantine-Paton M, Law MI. 1978. Eye-specific termination bands in tecta of three-eyed frogs. Science 202:639–641.

Davis MF, Figueroa Velez DX, et al. 2015. Inhibitory neuron transplantation into adult visual cortex creates a new critical period that rescues impaired vision. Neuron 86:1055–1066.

Eluvathingal TJ, Chugani HT, Behen ME, et al. 2006. Abnormal brain connectivity in children after early severe socioemotional deprivation: a diffusion tensor imaging study. Pediatrics 117:2093–2100.

Galli L, Maffei L. 1988. Spontaneous impulse activity of rat retinal ganglion cells in prenatal life. Science 242: 90–91.

Hebb DO. 1949. *Organization of Behavior: A Neuropsychological Theory*. New York: Wiley.

Hensch TK. 2005. Critical period plasticity in local cortical circuits. Nat Rev Neurosci 6:877–888.

Hensch TK, Fagiolini M, Mataga N, Stryker MP, Baekkeskov S, Kash SF. 1998. Local GABA circuit control of experience-dependent plasticity in developing visual cortex. Science 282:1504–1508.

Hofer S, Mrsic-Flogel T, Bonhoeffer T, Hubener M. 2009. Experience leaves a lasting structural trace in cortical circuits. Nature 457:313–317.

Hong YK, Park S, Litvina EY, Morales J, Sanes JR, Chen C. 2014. Refinement of the retinogeniculate synapse by bouton clustering. Neuron 84:332–339.

Hubel DH, Wiesel TN. 1965. Binocular interaction in striate cortex of kittens reared with artificial squint. J Neurophysiol 28:1041–1059.

Hubel DH, Wiesel TN. 1977. Ferrier lecture: functional architecture of macaque monkey visual cortex. Proc R Soc Lond B Biol Sci 198:1–59.

Hubel DH, Wiesel TN, LeVay S. 1977. Plasticity of ocular dominance columns in monkey striate cortex. Philos Trans R Soc Lond B Biol Sci 278:377–409.

Khibnik LA, Cho KK, Bear MF. 2010. Relative contribution of feed forward excitatory connections to expression of ocular dominance plasticity in layer 4 of visual cortex. Neuron 66:493–500.

Kral A, Sharma A. 2012. Developmental neuroplasticity after cochlear implantation. Trends Neurosci 35:111–122.

Linkenhoker BA, Knudsen EI. 2002 Incremental training increases the plasticity of the auditory space map in adult barn owls. Nature 419:293–296.

Löwel S. 1994. Ocular dominance column development: strabismus changes the spacing of adjacent columns in cat visual cortex. J Neurosci 14:7451–7468.

McGee AW, Yang Y, Fischer QS, Daw NW, Strittmatter SM. 2005. Experience-driven plasticity of visual cortex limited by myelin and Nogo receptor. Science 309:2222–2226.

Meister M, Wong ROL, Baylor DA, Shatz CJ. 1991. Synchronous bursts of action potentials in ganglion cells of the developing mammalian retina. Science 252:939–943.

Merzenich MM, Nelson RJ, Stryker MP, Cynader MS, Schoppmann A, Zook JM. 1984. Somatosensory cortical map changes following digit amputation in adult monkeys. J Comp Neurol 224:591–605.

Nelson CA 3rd, Zeanah CH, Fox NA, Marshall PJ, Smyke AT, Guthrie D. 2007. Cognitive recovery in socially deprived young children: the Bucharest Early Intervention Project. Science 318:1937–1940.

Oray S, Majewska A, Sur M. 2004. Dendritic spine dynamics are regulated by monocular deprivation and extracellular matrix degradation. Neuron 44:1021–1030.

Pizzorusso T, Medini P, Berardi N, Chierzi S, Fawcett JW, Maffei L. 2002. Reactivation of ocular dominance plasticity in the adult visual cortex. Science 298:1248–1251.

Rakic P. 1981. Development of visual centers in the primate brain depends on binocular competition before birth. Science 214:928–931.

Sanes JR, Yamagata M. 1999. Formation of lamina-specific synaptic connections. Curr Opin Neurobiol 9:79–87.

Shatz CJ, Stryker MP. 1988. Prenatal tetrodotoxin infusion blocks segregation of retino-geniculate afferents. Science 242:87–89.

Van Sluyters RC, Levitt FB. 1980. Experimental strabismus in the kitten. J Neurophysiol 43:686–699.

Zhang J, Ackman JB, Xu HP, Crair MC. 2011. Visual map development depends on the temporal pattern of binocular activity in mice. Nat Neurosci 15:298–307.

50

Repairing the Damaged Brain

For much of its history, neurology has been a discipline of outstanding diagnostic rigor but little therapeutic efficacy. Simply put, neurologists have been renowned for their ability to localize lesions with great precision but until recently have had little to offer in terms of treatment. This situation is now changing.

Advances in our understanding of the structure, function, and chemistry of the brain's neurons, glial cells, and synapses have led to new ideas for treatment. Many of these are now in clinical trials, and some are already available to patients. Developmental neuroscience is emerging as a major contributor to this sea change for three main reasons. First, efforts to preserve or replace neurons lost to damage or disease rely on recent advances in our understanding of the mechanisms that control the generation and death of nerve cells in embryos (Chapters 45 and 46). Second, efforts to improve the regeneration of neural pathways following injury draw heavily on what we have learned about the growth of axons and the formation of synapses (Chapters 47 and 48). Third, there is increasing evidence that some devastating brain disorders, such as autism and schizophrenia, are the result of disturbances in the formation of neural circuits in embryonic or early postnatal life. Accordingly, studies of normal development provide an essential foundation for discovering precisely what has gone wrong in disease.

In this chapter, we focus on the first two of these issues: how neuroscientists hope to augment the limited ability of neurons to recover normal function. We shall begin by describing how axons degenerate following the separation of the axon and its terminals from the cell body. The regeneration of severed axons is robust in the peripheral nervous system of mammals and in the central nervous system of lower vertebrates, but very poor in the central nervous system of

mammals. Many investigators have sought the reasons for these differences in the hope that understanding them will lead to methods for augmenting recovery of the human brain and spinal cord following injury. Indeed, we shall see that several differences in regenerative capacity of mammalian neurons have been discovered, each of which has opened promising new approaches to therapy.

We shall then consider an even more dire consequence of neural injury: the death of neurons. The inability of the adult brain to form new neurons has been a central dogma of neuroscience since the pioneering neuroanatomist Santiago Ramón y Cajal asserted that in the injured central nervous system, "Everything may die, nothing may be regenerated." This pessimistic view dominated neurology for most of the last century despite the fact that Ramón y Cajal added, "It is for the science of the future to change, if possible, this harsh decree." Remarkably, in the past few decades, evidence has accumulated that neurogenesis does occur in certain regions of the adult mammalian brain. This discovery has helped accelerate the pace of research on ways to stimulate neurogenesis and to replace neurons following injury. More than a century later, neuroscientists are finally beginning to reverse Cajal's "harsh decree."

Damage to the Axon Affects Both the Neuron and Neighboring Cells

Because many neurons have very long axons and cell bodies of modest size, most injuries to the central or peripheral nervous system involve damage to axons. Transection of the axon, either by cutting or by crushing, is called *axotomy*, and its consequences are numerous.

Axon Degeneration Is an Active Process

Axotomy divides the axon in two: a proximal segment that remains attached to the cell body and a distal segment that has lost this crucial attachment. Axotomy dooms the distal segment of the axon because energy supplies dwindle during a short-lived latent period. Soon the alterations become irreversible. Synaptic transmission fails at severed nerve terminals, and calcium levels increase within the axon. The calcium activates proteases, initiating a program of cytoskeletal disassembly and degradation, and physical degeneration of the axon ensues. Once the denervation begins, its progression is relatively rapid and inexorably proceeds to completion (Figure 50–1). This degenerative response is the first step in an elaborate constellation

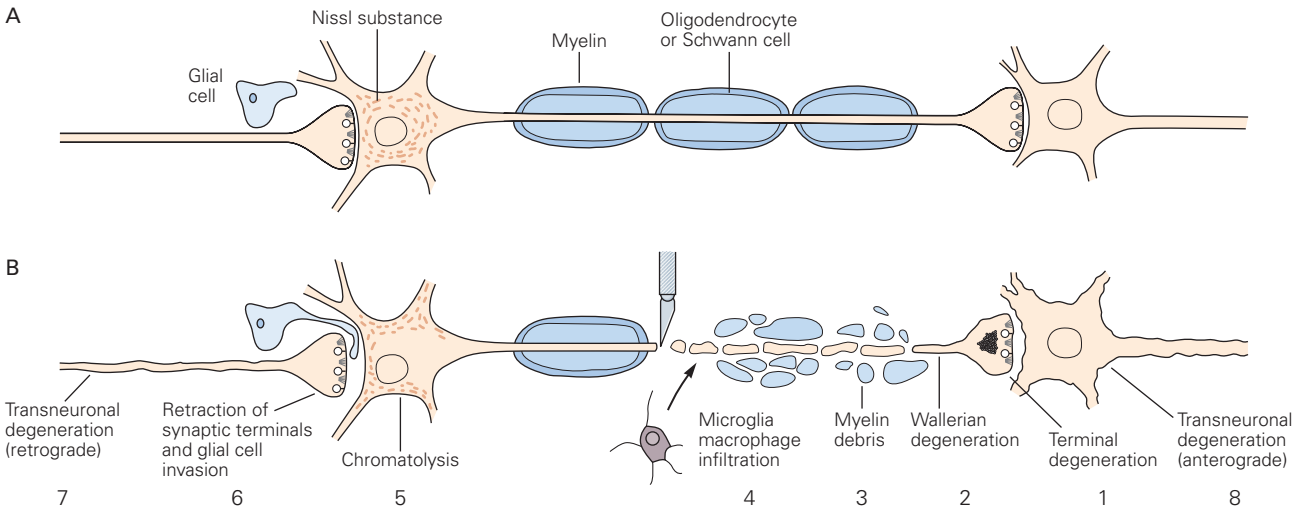

Figure 50–1 Axotomy affects the injured neuron and its synaptic partners.

A. A normal neuron with an intact functional axon wrapped by myelinating cells contacts a postsynaptic neuron. The neuron's cell body is itself a postsynaptic target.

B. After axotomy, the nerve terminals of the injured neuron begin to degenerate (**1**). The distal axonal stump separates from the parental cell body, becomes irregular, and undergoes Wallerian degeneration (**2**). Myelin begins to fragment (**3**) and the lesion site is invaded by phagocytic cells (**4**). The cell body of the damaged neuron undergoes chromatolysis: The cell body swells and the nucleus moves to an eccentric position (**5**). Synaptic terminals that contact the damaged neuron withdraw and the synaptic site is invaded by glial cell processes (**6**). The injured neuron's inputs (**7**) and targets (**8**) can atrophy and degenerate.

of changes, called *Wallerian degeneration*, that were initially described in 1850 by Augustus Waller.

The degeneration of transected axons was long thought to be a passive process, the consequence of separation from the cell body, where most of the cell's proteins are synthesized. Lacking a source of new protein, the distal stump was thought to simply wither away. But the discovery and analysis in mice of a spontaneously occurring mutation called *Wlds* (Wallerian degeneration slow) challenged this view (Figure 50–2). In *Wlds* mutant mice, the distal stumps of peripheral nerves persist for several weeks after transection, about 10-fold longer than in normal mice. This remarkable finding suggested that degeneration is not a passive consequence of separation from the cell body, but is rather an actively regulated response.

Analysis of the *Wlds* mutant mice led to insights into the nature of this regulation. The mutation led to formation of a mutant form of nicotinamide mononucleotide adenyltransferase 1 (NMNAT1), an enzyme involved in biosynthesis of a metabolic cofactor, nicotinamide adenine dinucleotide (NAD). A related enzyme, NMNAT2, which is normally present in the axon, becomes quite unstable and breaks down rapidly following axotomy, leading to loss of NAD, which is critical for maintenance of energy homeostasis in the axon. Although normal NMNAT1 is confined to the nucleus, the mutant *Wlds* form mislocalizes to the axon, where it substitutes for NMNAT2 to prolong axonal survival. Surprisingly, a main way that both the wild type and *Wlds* forms of NMNAT maintain NAD levels is not by synthesizing it but by inhibiting another protein, SARM1, that breaks down NAD. Thus, loss of SARM protects damaged axons, whereas activation of SARM1 leads to degeneration (Figure 50–3A). Several other proteins modulate this core pathway (Figure 50–3B).

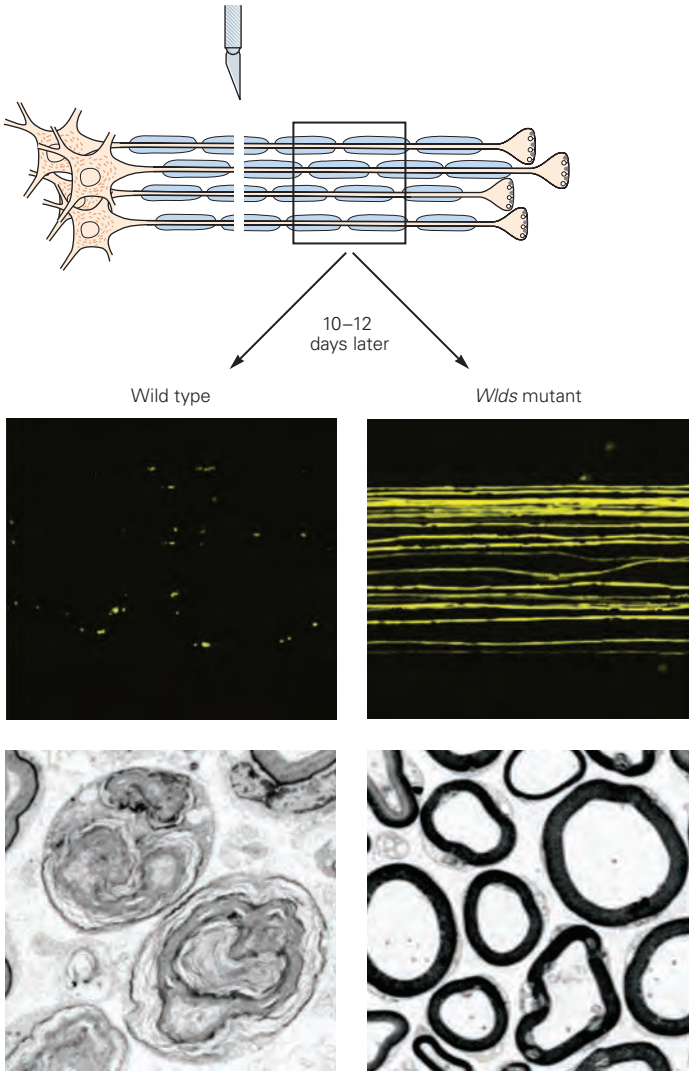

Figure 50–2 Axonal degeneration is delayed in *Wlds* mutant mice. In wild type animals, axons in the distal stump degenerate rapidly after sectioning of a peripheral nerve, as shown by disrupted axonal fragments (**yellow**) and the lack of myelinated axonal profiles at the electron micrographic level. In *Wlds* mutant mice the distal portion of severed axons persists for a long time. (Confocal micrographs reproduced, with permission, from Beirowski et al. 2004. Copyright © 2004 Elsevier B.V.; electron micrographs reproduced, with permission, from Mack TGA, Reiner M, Beirowski B, et al. 2001. Copyright © 2001 Springer Nature.)

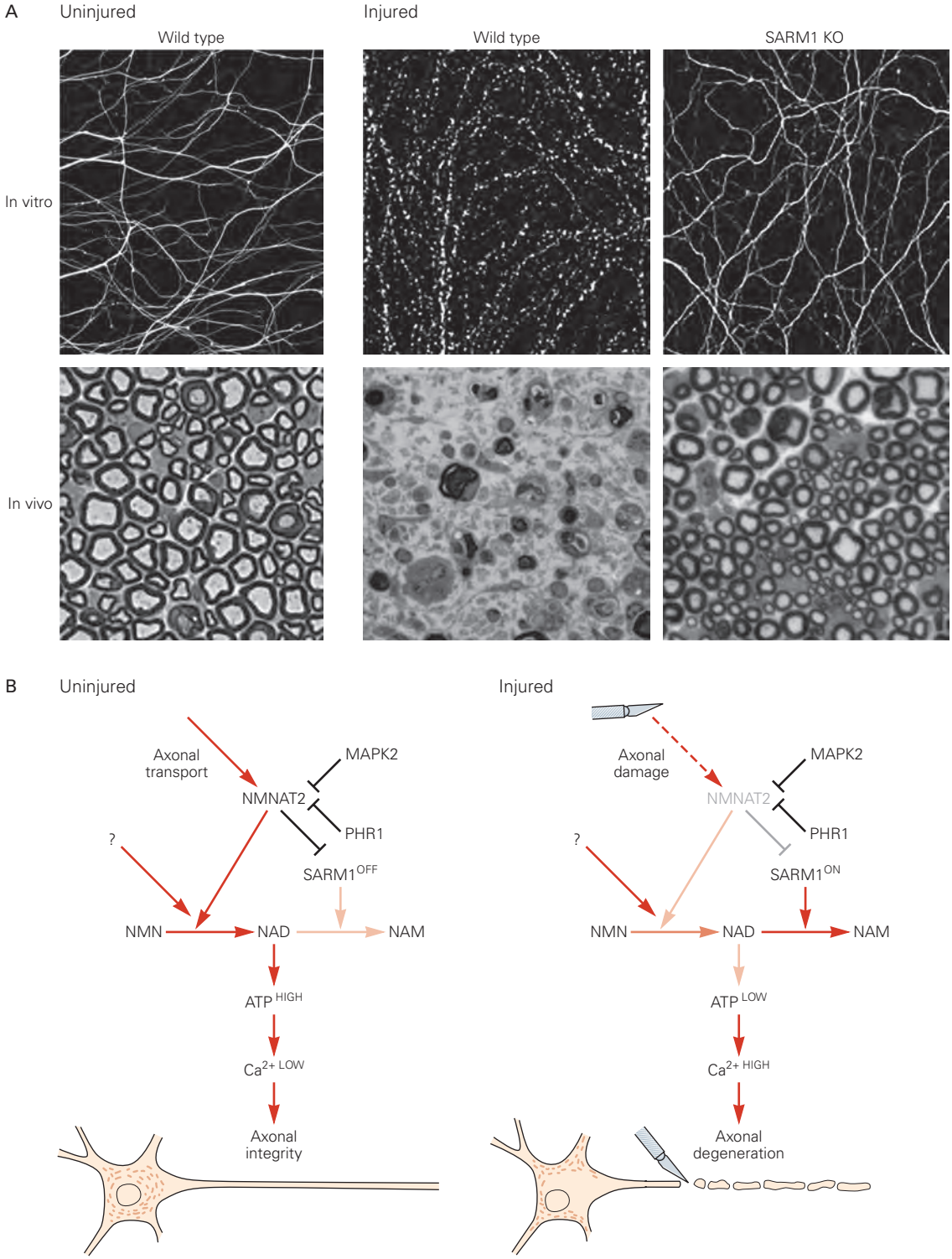

Figure 50–3 A core pathway regulates axon degeneration following axotomy in mice.

A. Damage to neurites in vitro leads to degeneration of the portions separated from the cell body. Likewise, axotomy in vivo leads to Wallerian degeneration, as shown by loss of myelin profiles in the cross section. Both in vitro and in vivo axons are spared if the *SARM1* gene is deleted. (From Gerdts et al. 2013.)

B. NMNAT2, closely related to the mutant *Wlds* protein, is normally present in axons. It can generate nicotinamide adenine dinucleotide (**NAD**) and inhibit SARM1, which degrades NAD. High NAD levels are required for energy metabolism, keeping adenosine triphosphate (**ATP**) levels high and calcium levels low in the axon. Following axotomy, NMNAT2 levels decrease rapidly, disinhibiting SARM1. NAD levels fall, ATP is depleted, calcium levels rise, calcium-dependent proteases are activated, and the axon is degraded. Kinases (MAPK) and a ubiquitin ligase (Phr1) regulate the pathway.

Together, these exciting new discoveries provide an answer to the question of why, following axotomy, the distal stump degenerates while the proximal stump is preserved. The conventional explanation that the distal stump is deprived of nutrients normally delivered from the cell body is incomplete. Instead, a signaling pathway in the axon senses damage and rapidly triggers degeneration. In this scenario, the key element supplied by the axon is NMNAT2. Its breakdown following axotomy disinhibits SARM1 and, perhaps in parallel with activation of factors that stimulate SARM1, triggers the loss of NAD, leading to the energy crisis that results in Wallerian degeneration.

These recent discoveries may be useful in devising treatments for neurological disorders in which axonal degeneration is prominent and generally precedes neuronal death. A fatal disease of motor neurons, amyotrophic lateral sclerosis, falls into this category. Other possibilities include some forms of spinal muscular atrophy, Parkinson disease, and even Alzheimer disease. Axon degeneration that occurs in these diseases, as well as after metabolic, toxic, or inflammatory insults, resembles the degeneration that follows acute trauma and may be regulated in similar ways. Thus, while methods for saving transected distal axons are unlikely to be useful clinically for treating patients who have suffered traumatic injury, the same techniques could be useful in treating neurodegenerative diseases.

Even though the proximal portion of the axon remains attached to the cell body, it too suffers. And in some cases, the neuron itself dies by apoptosis, probably because axotomy isolates the cell body from its supply of target-derived trophic factors. Even when this does not occur, the cell body often undergoes a series of cellular and biochemical changes called the *chromatolytic reaction:* The cell body swells, the nucleus moves to an eccentric position, and the rough endoplasmic reticulum becomes fragmented (Figure 50–1B). Chromatolysis is accompanied by other metabolic changes, including an increase in protein and RNA synthesis as well as a change in the pattern of genes that the neuron expresses. These changes are reversed if regeneration is successful.

Axotomy Leads to Reactive Responses in Nearby Cells

Axotomy sets in motion a cascade of responses in numerous types of neighboring cells. Among the most important responses are those of the glial cells that ensheath the distal nerve segment. One is fragmentation of the myelin sheath, which is then removed by phagocytes. This process is rapid in the peripheral nervous system, where the myelin-producing Schwann cells break the myelin into small fragments and engulf it. Schwann cells, which then divide, secrete factors that recruit macrophages from the blood stream. The macrophages in turn assist the Schwann cells in disposing of debris. Schwann cells also produce growth factors that promote axon regeneration, a point to which we will return later.

In contrast, in the central nervous system, the myelin-forming oligodendrocytes have little or no ability to dispose of myelin, and removal of debris depends on resident phagocytic cells called *microglia*. This difference in cellular properties may help explain the observation that Wallerian degeneration proceeds to completion much more slowly in the central nervous system.

Axotomy also affects both the synaptic inputs to and the synaptic targets of the injured neuron. When axotomy disrupts the major inputs to a cell—as happens in denervated muscle, or to neurons in the lateral geniculate nucleus when the optic nerve is cut—the consequences are severe. Usually the target atrophies and sometimes dies. When targets are only partially denervated, their responses are more limited. In addition, axotomy affects presynaptic neurons. In many instances, synaptic terminals withdraw from the cell body or dendrites of chromatolytic neurons and are replaced by the processes of glial cells—Schwann cells in the periphery and microglia or astrocytes in the central nervous system. This process, called *synaptic stripping*, depresses synaptic activity and can impair functional recovery.

Although the mechanism of synaptic stripping remains unclear, two possibilities have been suggested. One is that postsynaptic injury causes axon terminals to lose their adhesiveness to synaptic sites so that they are subsequently wrapped by glia. The other is that glia initiate the process of synaptic stripping in response to factors released from the injured neuron or to changes in its cell surface. Whatever the trigger, the activation of microglia and astrocytes by axotomy clearly contributes to the stripping process. In addition, biochemically altered astrocytes, called reactive astrocytes, contribute to formation of a *glial scar* near sites of injury.

As a result of these transsynaptic effects, neuronal degeneration can propagate through a circuit in both anterograde and retrograde directions. For example, a denervated neuron that becomes severely atrophic can fail to activate its target, which in turn becomes atrophic. Likewise, when synaptic stripping

prevents an afferent neuron from obtaining sufficient sustenance from its target cell, the afferent neuron's inputs are placed at risk. Such chain reactions help to explain how injury in one area in the central nervous system eventually affects regions far from the site of the injury.

Central Axons Regenerate Poorly After Injury

Central and peripheral nerves differ substantially in their ability to regenerate after injury. Peripheral nerves can often be repaired following injury. Although the distal segments of peripheral axons degenerate, connective tissue elements surrounding the distal stump generally survive.

Axonal sprouts grow from the proximal stump, enter the distal stump, and grow along the nerve toward its targets (Figure 50–4). The mechanisms that drive this process are related to those that guide embryonic axons. Chemotropic factors secreted by Schwann cells attract axons to the distal stump, adhesive molecules within the distal stump promote axon growth along cell membranes and extracellular matrices, and inhibitory molecules in the perineural sheath prevent regenerating axons from going astray.

Once regenerated peripheral axons reach their targets, they are able to form new functional nerve endings. Motor axons form new neuromuscular junctions; autonomic axons successfully reinnervate glands, blood vessels, and viscera; and sensory axons reinnervate muscle spindles. Finally, those axons that lost their myelin sheaths are remyelinated, and chromatolytic cell bodies regain their original appearance. Thus, in all three divisions of the peripheral nervous system—motor, sensory, and autonomic—the effects of axotomy are reversible. Peripheral regeneration is not perfect, however. In the motor system, recovery of strength may be substantial, but recovery of fine movements is usually impaired. Some motor axons never find their targets, some form synapses on inappropriate muscles, and some motor neurons die. Nevertheless, the regenerative capacities in the peripheral nervous system are impressive.

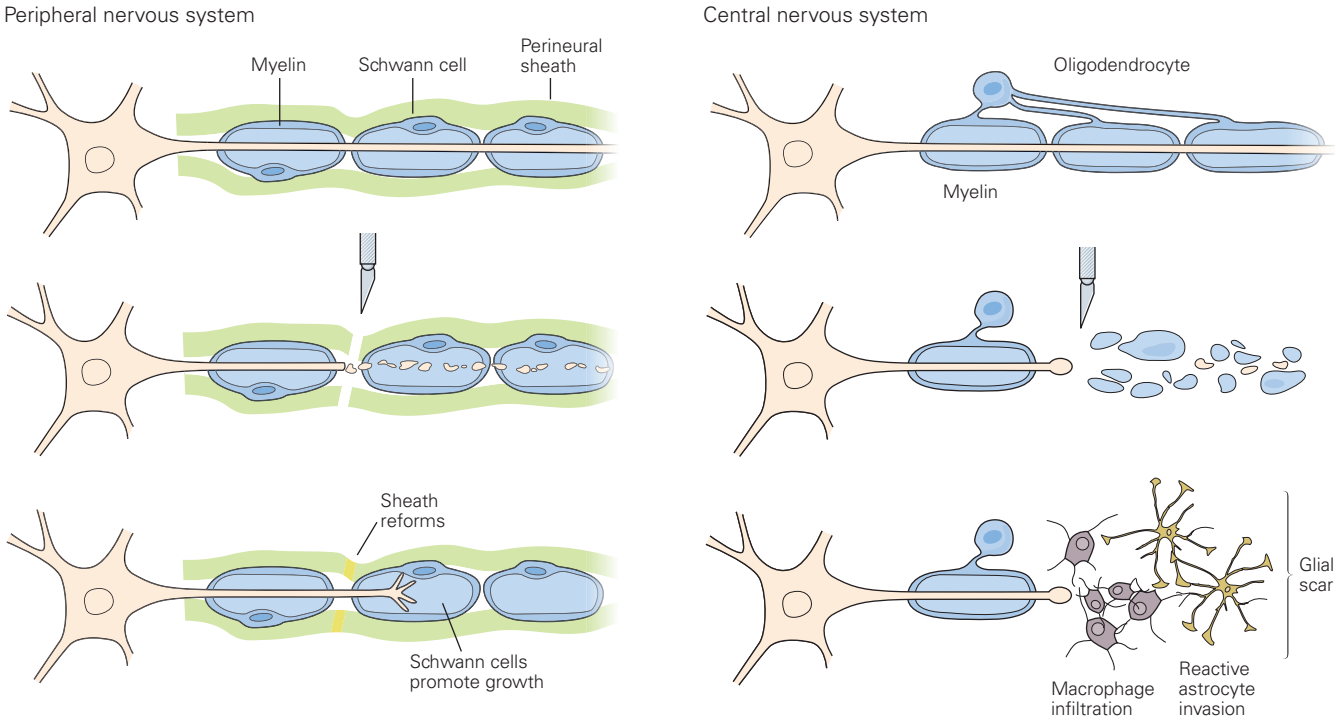

Figure 50–4 Axons in the periphery regenerate better than those in the central nervous system. After sectioning of a peripheral nerve, the perineural sheath reforms rapidly and Schwann cells in the distal stump promote axonal growth by producing trophic and attractant factors and expressing high levels of adhesive proteins. After sectioning of an axona in the central nervous system, the distal segment disintegrates and myelin fragments. In addition, reactive astrocytes and macrophages are attracted to the lesion site. This complex cellular milieu, termed a *glial scar*, inhibits axonal regeneration.

In contrast, regeneration after injury is poor in the central nervous system (Figure 50–4). The proximal stumps of damaged axons can form short sprouts, but these soon stall and form swollen endings called "retraction bulbs", which fail to progress. Long-distance regeneration is rare. The failure of central regeneration is what led to the long-standing belief that injuries to the brain and spinal cord are largely irreversible and that therapy must be restricted to rehabilitative measures.

For some time, neurobiologists have been seeking the reasons why regenerative capacity in the central and peripheral nervous systems differs so dramatically. The goal of this work has been to identify the crucial barriers to regeneration so that they can be overcome. These studies have begun to bear fruit, and there is now cautious optimism that the injured human brain and spinal cord have a regenerative capacity that can eventually be exploited.

Before discussing these new developments, it is helpful to consider the problem of neural regeneration in a broader biological context. Is it the ability of peripheral axons to regenerate that is unusual, or the inability of central axons to do so? It is in fact the latter. Obviously, central axons grow well during development. More surprisingly, axons in immature mammals can also regenerate following transection in the brain or spinal cord. Moreover, regeneration is robust in the adult central nervous systems of lower vertebrates such as fish and frogs, as exemplified by the studies of Roger Sperry on restoration of vision following damage to the optic nerve (Chapter 47).

So why have mature mammals lost this seemingly important capacity for repair? The answer may lie in what the mammalian brain *can* do peerlessly, which is to remodel its basic wiring diagram in accordance with experience during critical periods in early postnatal life, so that each individual's brain is optimized to deal with the changes and challenges of internal and external worlds (Chapter 49). Once remodeling has occurred, it must be stabilized. Although it is obviously useful to reassign cortical space to one eye if the other is blinded in childhood, we would not want our cortical connections similarly rearranged in response to a brief period of unusual illumination or darkness. Maintaining constancy in the face of small perturbations in connectivity may therefore have the unavoidable consequence of limiting the ability of central connections to regenerate in response to injury. In this view, our limited regenerative capacity is a Faustian bargain in which we have sacrificed recuperative power to ensure the maintenance of precisely wired circuits that underlie our superior intellectual capacity.

Therapeutic Interventions May Promote Regeneration of Injured Central Neurons

In seeking reasons for the poor regeneration of central axons, one critical question is whether it reflects an inability of neurons themselves to grow or an inability of the environment to support axonal growth. This issue was addressed by Albert Aguayo and his colleagues in the early 1980s. They inserted segments of a central nerve trunk into a peripheral nerve, and segments of a peripheral nerve into the brain or spinal cord, to find out how axons would respond when confronted with a novel environment.

As expected, axons in the grafts, which were separated from their somata, promptly degenerated, leaving "distal stumps" containing glia, support cells, and extracellular matrix. What was striking was the behavior of axons near the translocated segments. Spinal axons that regenerated poorly following spinal cord injury grew several centimeters into the peripheral graft (Figure 50–5). Similarly, retinal axons, which regenerated poorly following damage to the optic nerve, grew long distances into a peripheral graft placed in their path.

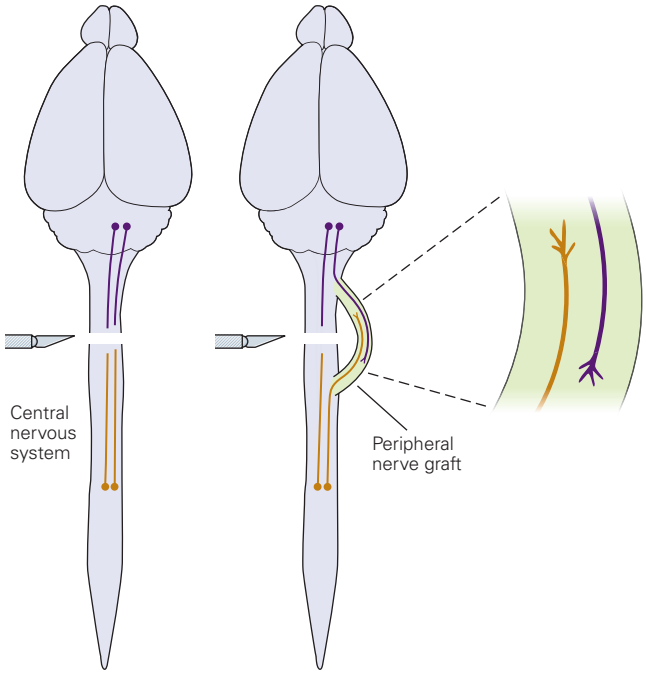

Figure 50–5 A transplanted peripheral nerve provides a favorable environment for the regeneration of central axons. *Left*: After sectioning of the spinal cord, ascending and descending axons fail to cross the lesion site. *Right*: Insertion of a peripheral nerve graft that bypasses the lesion site promotes regeneration of both ascending and descending axons. (Adapted from David and Aguayo 1981.)

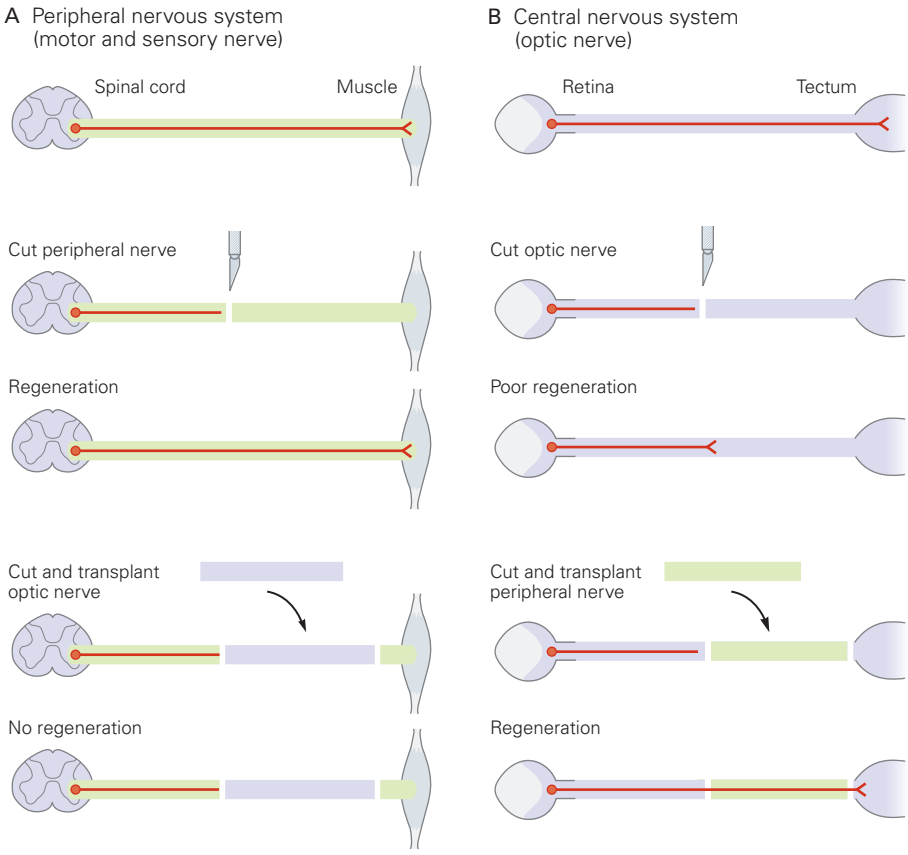

Figure 50–6 Peripheral and central nerves differ in their ability to support axonal regeneration.

A. In the peripheral nervous system, severed axons regrow past the site of injury. Insertion of a segment of optic nerve into a peripheral nerve suppresses the ability of the peripheral nerve to regenerate.

B. In the central nervous system, severed axons typically fail to regrow past the site of injury. Insertion of a section of peripheral nerve into a central nerve tract promotes regeneration.

Conversely, peripheral axons regenerated well through their own distal nerve trunk, but fared poorly when paired with a severed optic nerve (Figure 50–6).

Aguayo extended these studies to show that axons from multiple regions, including the olfactory bulb, brain stem, and mesencephalon, could all regenerate long distances if provided with a suitable environment. Even an optimal environment cannot fully restore the growth potential of central axons for reasons we will discuss in a later section. Nevertheless, these pioneering experiments focused attention on components of the central environment that inhibit regenerative ability and motivated an intensive search for the molecular culprits.

Environmental Factors Support the Regeneration of Injured Axons

In probing the differences between peripheral and central growth environments, initial searches were influenced by the results of experiments performed by Ramón y Cajal's student Francisco Tello nearly a century before Aguayo's studies. Tello transplanted segments of peripheral nerves into the brains of experimental animals and found that injured central axons grew toward the implants, whereas they barely grew when implants were not available.

This result implied that peripheral cells provide growth-promoting factors to the injured areas, factors normally absent from the brain. Ramón y Cajal reasoned that central nerve pathways lacked "substances able to sustain and invigorate the indolent and scanty growth" similar to those provided by peripheral pathways. Numerous studies over the succeeding century identified constituents of peripheral nerves that are potent promoters of neurite outgrowth. These include components of Schwann cell basal laminae, such as laminin, and cell adhesion molecules of the immunoglobulin superfamily. In addition, cells in denervated

distal nerve stumps begin to produce neurotrophins and other trophic molecules of the sort described in Chapter 46. Together, these molecules nourish neurons and guide growing axons in the embryonic nervous system, so it makes sense that they also promote the regrowth of axons. By contrast, central neuronal tissue is a poor source of these molecules, containing little laminin and low levels of trophic molecules. Thus, in the embryo, both central and peripheral nervous systems provide environments that promote axon outgrowth. But only the peripheral environment retains this capacity in adulthood or is able to regain it effectively following injury.

The practical implications of this view are that supplementing the central environment with growth-promoting molecules might improve regeneration. To this end, investigators have infused neurotrophins into areas of injury or inserted fibers rich in extracellular matrix molecules such as laminin to serve as scaffold for axonal growth. In some attempts, Schwann cells themselves, or cells engineered to secrete trophic factors, have been grafted into sites of injury. In many of these cases, injured axons grow more extensively than they do under control conditions. Yet regeneration remains limited, with axons generally failing to extend long distances. More important, functional recovery is minimal.

Components of Myelin Inhibit Neurite Outgrowth

What accounts for such disappointingly limited regeneration? One part of the explanation is that the environment encountered by severed central axons is not only poor in growth-promoting factors but also rich in growth-inhibiting factors, some of which are derived from myelin. In culture, fragments of central but not peripheral myelin potently inhibit neurite outgrowth from co-cultured central or peripheral neurons. Conversely, sprouting of spinal axon collaterals following injury is enhanced in rats treated to prevent myelin formation in the spinal cord (Figure 50–7).

These findings implied that although both central and peripheral environments might contain a supply of growth-promoting elements, central nerves also contain inhibitory components. The fact that myelin inhibits neurite growth may seem peculiar, but not if we consider that myelination normally occurs postnatally, after axon extension is largely complete.

Searches for the inhibitory components of central myelin turned up an embarrassment of riches. Several classes of molecules that occur at higher levels in central myelin compared to peripheral myelin are able to inhibit neurite outgrowth when presented to cultured neurons. The first to be discovered was identified when an antibody generated against myelin proteins proved

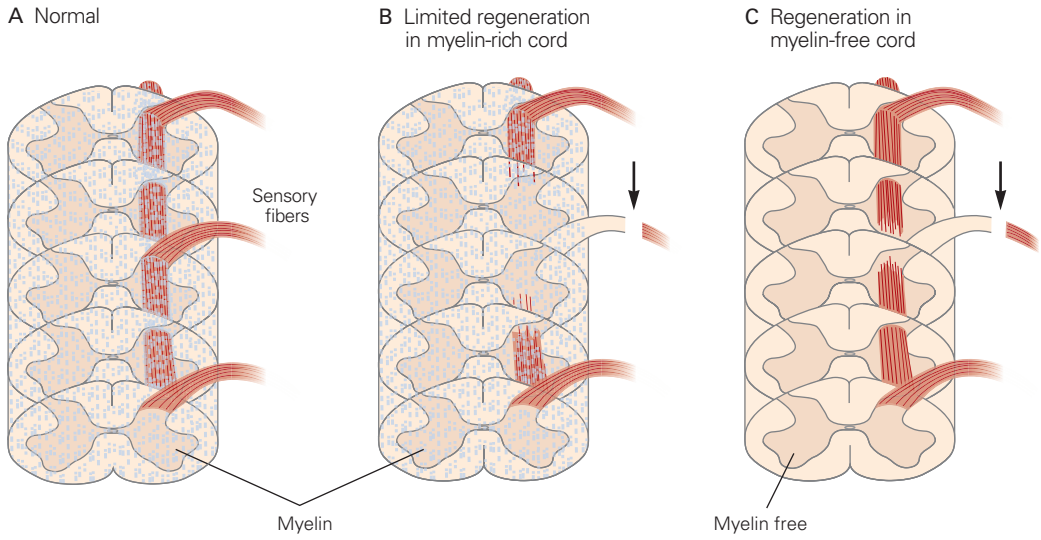

Figure 50–7 Myelin inhibits regeneration of central axons. (Adapted, with permission, from Schwegler, Schwab, and Kapfhammer 1995.)

A. Sensory fibers normally extend rostrally in a myelin-rich spinal cord.

B. Right dorsal root fibers were sectioned in 2-week-old normal rats. Regeneration of the fibers was assessed histochemically 20 days later. The central branches of the sectioned axons degenerated, leaving a portion of the spinal cord denervated. Little regeneration occurred in the myelin-rich cord.

C. Some littermates received local x-irradiation to block myelination. In these animals, sensory fibers that entered the cord through neighboring uninjured roots sprouted new collaterals following denervation.

to be capable of partially neutralizing myelin's ability to inhibit neurite outgrowth. Use of this antibody to isolate the corresponding antigen yielded the protein now called Nogo. Two other proteins, myelin-associated glycoprotein (MAG) and oligodendrocyte-myelin glycoprotein (OMgp), initially isolated as major components of myelin, have also been found to inhibit the growth of some neuronal types.

Intriguingly, Nogo, MAG, and OMgp bind to common membrane receptors, NogoR and PirB (Figure 50–8). NogoR, as well as related receptors such as LINGO that have been implicated in growth inhibition, all interact with the neurotrophin receptor p75 (Chapter 46). This interaction converts p75 from a growth-promoting to a growth-inhibiting receptor. Perhaps because there are so many growth inhibitory factors and receptors, regeneration of central axons is not greatly enhanced in mutant mice lacking any one of them. However, many of the inhibitory components trigger the same intracellular signaling pathway in which RhoA is activated, thereby stimulating Rho kinase (ROCK); ROCK in turn leads to the collapse of growth cones and blocks actin and tubulin polymerization required for neurite growth. Current studies are

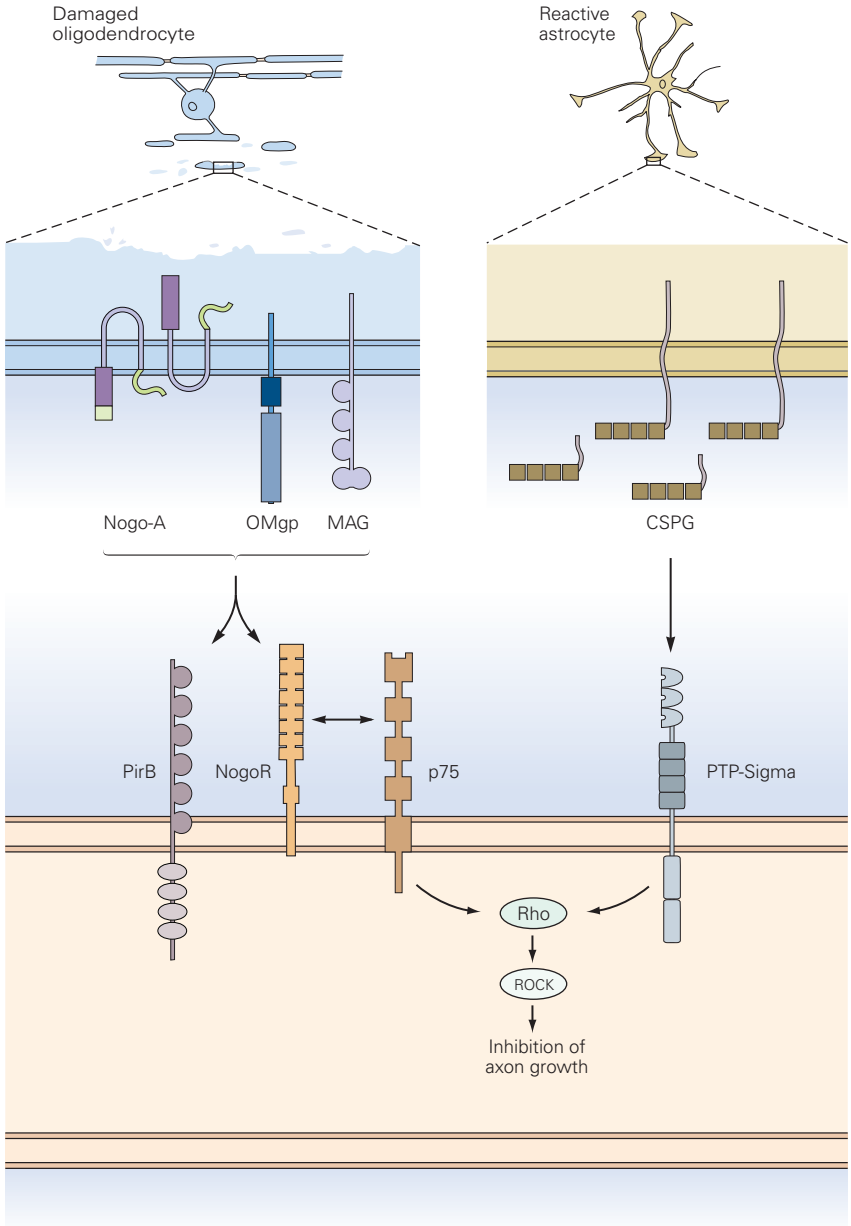

Figure 50–8 Myelin and glial scar components that inhibit regeneration of central axons. (Adapted from Yiu and He 2006.)

Left: Myelin contains the proteins Nogo-A, oligodendrocyte-myelin glycoprotein (**OMgp**), and myelin-associated glycoprotein (**MAG**). All three proteins are exposed when myelin breaks down. They can bind to the receptor protein NogoR, which can associate with the neurotrophin receptor p75, as well as an immunoglobulin-like receptor protein PirB. Inactivation of PirB results in a modest enhancement of corticospinal axon regeneration. *Right:* Chondroitin sulphate proteoglycans (**CSPG**) are major components of the glial scar and are thought to suppress axon regeneration through interaction with the receptor tyrosine phosphatase PTP-sigma, which activates intracellular mediators such as Rho and ROCK.

exploring whether interference with that shared pathway might neutralize the impact of many inhibitors in one fell swoop.

Injury-Induced Scarring Hinders Axonal Regeneration

Myelin debris is not the only source of growth-inhibiting material in the injured brain or spinal cord. As noted earlier, astrocytes become activated and proliferate following injury, acquiring features of reactive astrocytes that generate scar tissue at sites of injury. Scarring is an adaptive response that helps to limit the size of the injury, reestablish the blood-brain barrier, and reduce inflammation.

But the scar itself hinders regeneration in two ways: through mechanical interference with axon growth and through growth-inhibiting effects of proteins produced by cells within the scar. Chief among these inhibitors are a class of chondroitin sulfate proteoglycans (CSPG) that are produced in abundance by reactive astrocytes and directly inhibit axon extension by interaction with tyrosine phosphatase receptors on axons (Figure 50–8). Attention has therefore focused on ways of dissolving the glial scar by infusion of an enzyme called *chondroitinase*, which breaks down the sugar chains on CSPG. This treatment promotes axon regeneration and functional recovery in animals. Drugs that reduce inflammation and decrease scarring, notably prednisolone, are also beneficial if administered shortly after injury, before the scar forms.

An Intrinsic Growth Program Promotes Regeneration

So far, we have emphasized differences between the local environments of peripheral and central axons. However, environmental differences cannot completely account for the poor regeneration of central axons. Even though they can regenerate in peripheral nerves, central axons grow much less well than peripheral axons when navigating the same path. Thus, adult central axons may be less capable than peripheral axons of regeneration.

In support of this idea, experiments in tissue culture have shown that the growth potential of central neurons decreases with age, whereas mature peripheral neurons extend axons robustly in a favorable environment. One potential explanation for this difference is variation in the expression of proteins thought to be critical for optimal axon elongation. One example is the 43 kDa growth-associated protein, or GAP-43. This protein is expressed at high levels in embryonic central and peripheral neurons. In peripheral neurons, the level remains high in maturity and increases even more following axotomy, whereas in central neurons, its expression decreases as development proceeds. Transcription factors required to coordinate axonal growth programs are also expressed at high levels during development, and then are downregulated in maturity.

Is this reduced ability of central axons to regenerate reversible? Hope is provided by two sets of studies. One involves what has been called a "conditioning lesion." Recall that primary sensory neurons in dorsal root ganglia have a bifurcated axon, with a peripheral branch that extends to skin, muscle, or other targets, and a central branch that enters the spinal cord. The peripheral branch regenerates well following injury, whereas the central branch regenerates poorly. However, the central branch will regenerate successfully if the peripheral branch is damaged several days before the central branch is damaged (Figure 50–9). Somehow, prior injury or conditioning lesion activates an axonal growth program.

One component of the growth program responsible for regeneration of the central branch appears to be cyclic adenosine monophosphate (cAMP). This second-messenger molecule activates enzymes that in turn promote neurite outgrowth. Levels of cAMP are high when neurons initially form circuits; they decline postnatally in central but not peripheral neurons. In some instances, increased supplies of cAMP or proteins normally activated by cAMP can promote regeneration of central axons following injury. Accordingly, drugs that increase cAMP levels or activate targets of cAMP are being actively considered as therapeutic agents to be administered following spinal cord injury.

A second group of investigations has manipulated developmentally regulated intrinsic factors to restore regenerative ability in adults. For example, injury sometimes leads to formation of cytokines such as ciliary neurotrophic factors (CNTFs) that promote growth by activating a signaling pathway involving molecules called JAK and STAT that travel to the nucleus and regulate a growth program. In adults, however, the pathway is inhibited by a protein called suppressor of cytokine signaling 3 (SOCS3). Deletion of the *SOCS3* gene in mice relieves the inhibition and augments the ability of cytokines to promote regeneration of injured axons (Figure 50–10A).

Similarly, a signaling pathway involving the kinase mammalian target or rapamycin (mTOR) regulates energy metabolism, promoting an anabolic growth-promoting state required for axon regeneration. However, mTOR is downregulated as central neurons

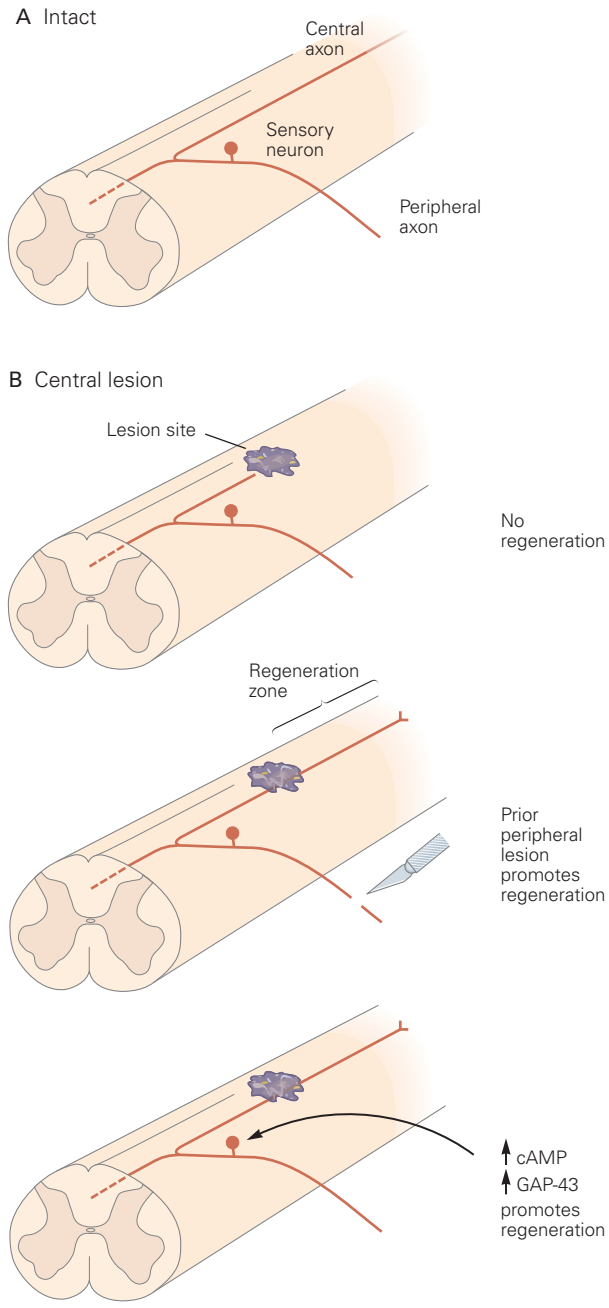

Figure 50–9 A conditioning lesion promotes regeneration of the central branch of a primary sensory neuron axon. After lesions of the spinal cord, there is little regeneration of the central branch beyond the injury site. However, if the peripheral branch of the axon is sectioned before the central branch is damaged, the latter will grow beyond the lesion site. The impact of such a "conditioning lesion" can be mimicked by elevating levels of cyclic adenosine monophosphate (**cAMP**) or of the growth-associated protein GAP-43 in the peripheral branch.

mature and is further inhibited by a phosphatase called PTEN. Analogous to SOCS3 and JAK/STAT signaling, deletion of the *PTEN* gene in mice promotes axonal regrowth following injury to the optic nerve or spinal cord (Figure 50–10B). Moreover, loss of SOCS3 and PTEN stimulates regeneration significantly more than loss of either one. Although their multiple roles make it unlikely that either SOCS3 or PTEN is a useful target for therapy, the signaling pathways they regulate provide multiple starting points for designing drugs that could augment regeneration.

Formation of New Connections by Intact Axons Can Lead to Recovery of Function Following Injury

So far, we have discussed interventions designed to enhance the limited regenerative capacity of injured central axons. An alternative strategy focuses on the significant, although incomplete, functional recovery that can occur following injury even without appreciable regeneration of cut axons. If the basis for this limited recovery of function can be understood, it may be possible to enhance it.

A rearrangement of existing connections in response to injury may contribute to recovery of function. We have learned that axotomy leads to changes in both the inputs to and the targets of the injured neuron. Although many of these changes are detrimental to function, some are beneficial. In particular, the central nervous system can, following injury, spontaneously undergo adaptive reorganization that helps it regain function. For example, after transection of the descending corticospinal pathway, which occurs with many traumatic injuries of the spinal cord, the cortex can no longer transmit commands to motor neurons below the site of the lesion. Over several weeks, however, intact corticospinal axons rostral to the lesion begin to sprout new terminal branches and form synapses on spinal interneurons whose axons extend around the lesion, thereby forming an intraspinal detour that contributes to limited recovery of function (Figure 50–11).

Similar instances of functional reorganization have been demonstrated in the motor cortex and brain stem. These compensatory responses attest to the latent plasticity of the nervous system. The ability of the nervous system to rewire itself is most vigorous during the critical periods of early postnatal life but can be revived by traumatic events in adulthood (Chapter 49).

How can the rewiring ability of the central nervous system be improved? It is possible that some of the beneficial effects of grafts in experimental animals reflect reorganization of intact axons rather than regeneration of transected axons. As the nervous system's

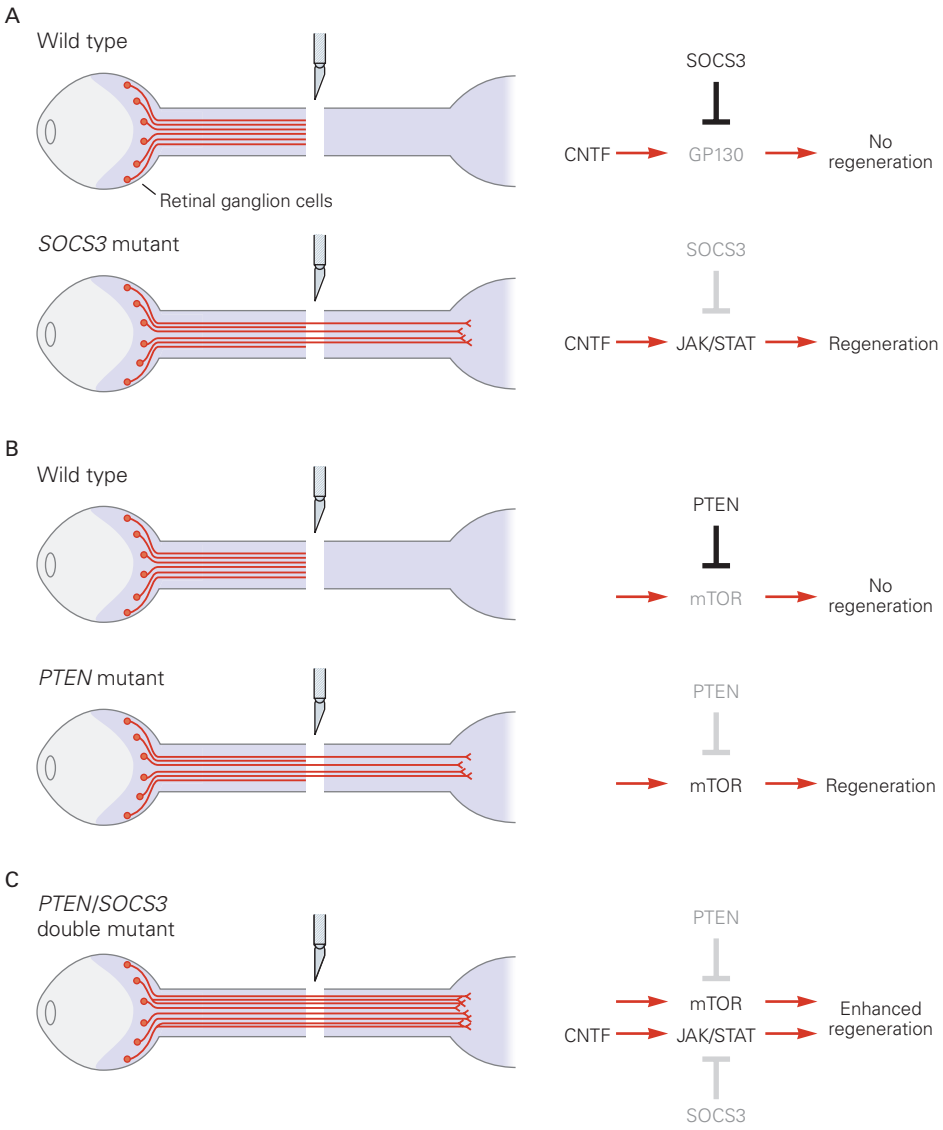

Figure 50–10 Signaling pathways that regulate axon regeneration in the optic nerve.

A. The regeneration of retinal ganglion cell axons in the optic nerve is normally constrained by neuronal expression of several genes. One encodes SOCS3, which blocks the ability of ciliary neurotrophic factor (**CNTF**) to bind its receptor GP130 and thus blocks CNTF from promoting regeneration. In *SOCS3* mutant mice, ambient levels of CNTF are sufficient to improve optic nerve regeneration. Elimination of GP130 as well as SOCS3 blocks the capacity for regeneration. Addition of extra CNTF enhances the capacity for regeneration in *SOCS3* mutant mice.

B. Another gene encodes PTEN, which blocks signaling through the mammalian target of rapamycin (**mTOR**) pathway, which regulates energy metabolism. Accordingly, regeneration is enhanced in *PTEN* mutant mice.

C. Because *SOCS3* and *PTEN* regulate different growth-promoting signals, mutant mice lacking both genes exhibit greater regenerative ability than either single mutant. (Adapted from Smith et al. 2009.)

plasticity becomes better understood, therapeutic strategies that promote specific changes in circuitry may become possible. Perhaps most promising is an approach in which cellular or molecular interventions that promote growth are combined with behavioral therapies that result in circuit rewiring.

Neurons in the Injured Brain Die but New Ones Can Be Born

The failure to grow a new axon is by no means the worst fate that can befall an injured neuron. For many neurons, axotomy leads to the death of the cell. Efforts

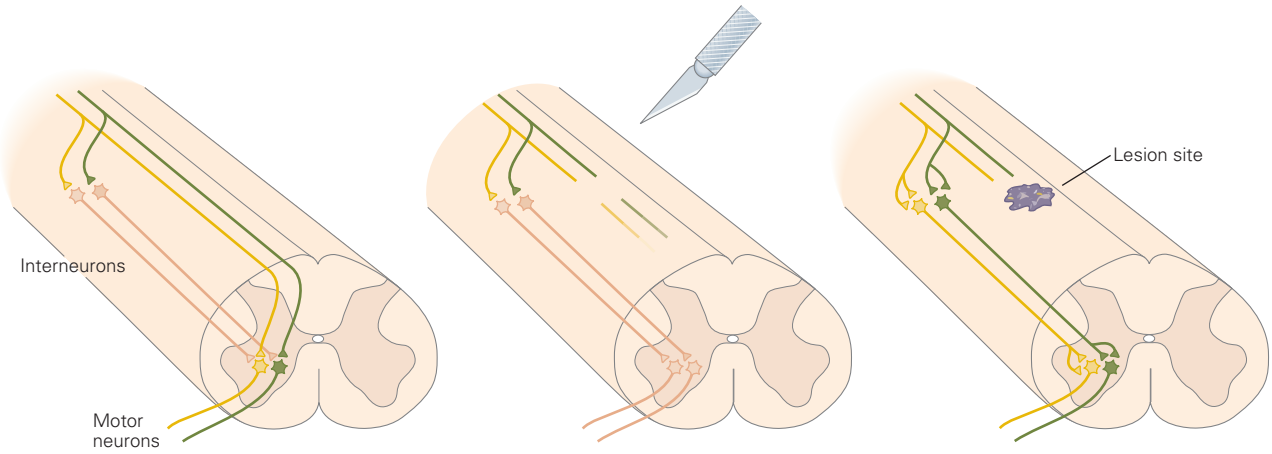

Figure 50–11 Function can be recovered after spinal cord injury through reorganization of spinal circuits. Severed corticospinal axons can reestablish connections with motor neurons by sprouting axon collaterals that innervate propriospinal interneurons whose axons bypass the lesion and contact motor neurons located caudal to the lesion site. (Adapted from Bareyre et al. 2004.)

to improve recovery following injury therefore need to consider survival of neurons and not simply the regrowth of axons. Since neuronal death is a frequent consequence of other neural insults, such as stroke and neurodegenerative disease, improved ways of retaining or replacing neurons would have broad utility.

The loss of cells following injury is not unique to the nervous system, although in other tissues, new cells are often effective at repairing damage. This regenerative capacity is most dramatic in the hematopoietic system, where a few stem cells can repopulate the entire adaptive immune system. In contrast, it has long been believed that the generation of neurons is complete by birth. Because of this, approaches to regeneration have often focused on finding ways to spare neurons that would otherwise die.

This traditional view has changed, prompted initially by Joseph Altman's discovery in the 1960s that neurogenesis continues into adulthood in some parts of the mammalian brain. Since this finding challenged fundamental tenets of prevailing dogma, the idea that new neurons could form in postnatal rodents was met with skepticism for three decades.

Eventually, however, the application of better cell labeling technologies amply supported Altman's conclusion and showed that it also applies to nonhuman primates and even, in a limited way, to humans. We are now confident that new neurons are added to the dentate gyrus of the hippocampus and to the olfactory bulb throughout life, although the rate of addition declines with age. Some of the newborn cells in the dentate gyrus of the adult hippocampus die soon after they are born and others become glial cells, but a substantial minority differentiate into granule cells that are indistinguishable from those born at embryonic stages (Figure 50–12). New neurons are also added to the adult olfactory bulb. They are generated near the surface of the lateral ventricles, far from the bulb itself, and then migrate to their destination (Figure 50–13). In both cases, the new neurons extend processes, form synapses, and become integrated into functional circuits. Thus, neurons born at embryonic stages are gradually replaced by later-born neurons, so that the total number of neurons in these regions of the brain is maintained.

The properties of neurons born in mature animals are not completely understood, but they appear able to recapitulate many of the properties of neurons that arise in the embryo. When the generation of new neurons in the adult is prevented, certain behaviors mediated by the olfactory bulb and hippocampus are degraded. Conversely, some behavioral alterations are accompanied by alterations in the tempo of adult neurogenesis. Adult neurogenesis can be decreased in animal models of depression and chronic stress, whereas enrichment of the habitat of an animal or an increase in the physical activity of otherwise sedentary rodents can increase the generation of new neurons.

What cells give rise to adult-born neurons? The principle that embryonic neurons and glia arise from multipotential progenitors also applies to neurons born in adults. Stem cells are the source of neurons in the adult as well as the embryo. They are likely derived from radial glia, which also serve as a source of

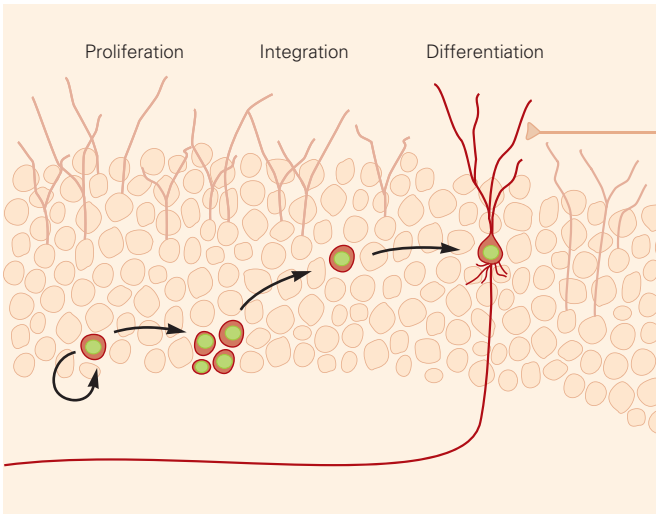

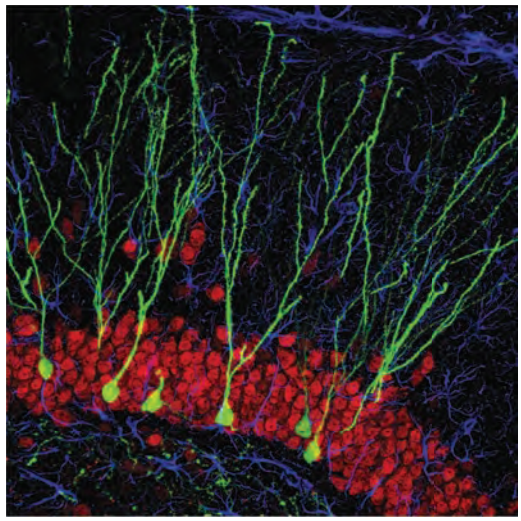

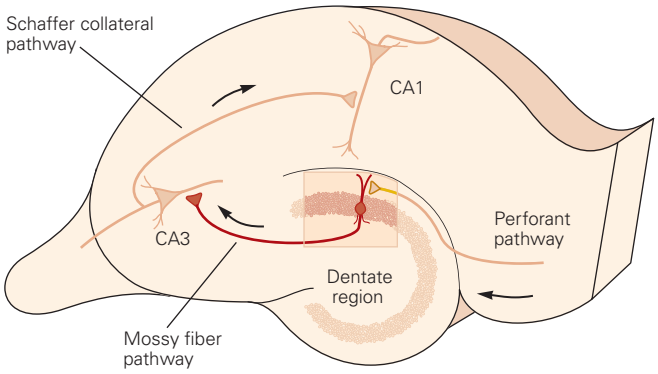

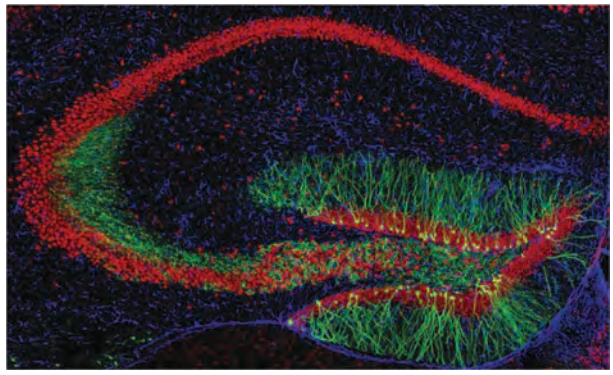

Figure 50–12 Neurons born in the germinal zone of the dentate gyrus in adult rodents are integrated into hippocampal circuits. The diagrams on the left show the pathways of neuronal differentiation and integration into dentate gyrus circuits. The images on the right show newly generated neurons and their dendritic arbors labeled with a virus expressing green fluorescence protein. (Micrographs reproduced, with permission, from F. Gage.)

neurons during embryonic development (Chapter 46). A subset of these cells exit the cell cycle during gestation, become quiescent, and take up residence near the ventricular surface. In adulthood, they are activated, reenter the cell cycle, and give rise to neurons.

Although so far adult neurogenesis has not been directly linked to repair of damaged tissue, its discovery has influenced research on recovery from injury in two important ways. First, the findings that endogenously generated neurons can differentiate and extend processes through the thicket of adult neuropil, and can be integrated into functional circuits, led researchers to test the idea that the same could be true for transplanted neurons or precursors. Second, since neural precursors can be induced to divide and differentiate, strategies designed to augment this innate ability are now being considered, with the goal of producing neurons in large enough numbers to replace those lost to injury or neurodegenerative disease. As we describe below, these ideas have progressed over the past few decades from science fiction to efforts that are tantalizingly close to clinical tests.

Therapeutic Interventions May Retain or Replace Injured Central Neurons

Transplantation of Neurons or Their Progenitors Can Replace Lost Neurons

For many years, neurologists have transplanted developing neurons into experimental animals to see if the new neurons could reverse the effects of injury or disease. These attempts have had promising results in a few cases.

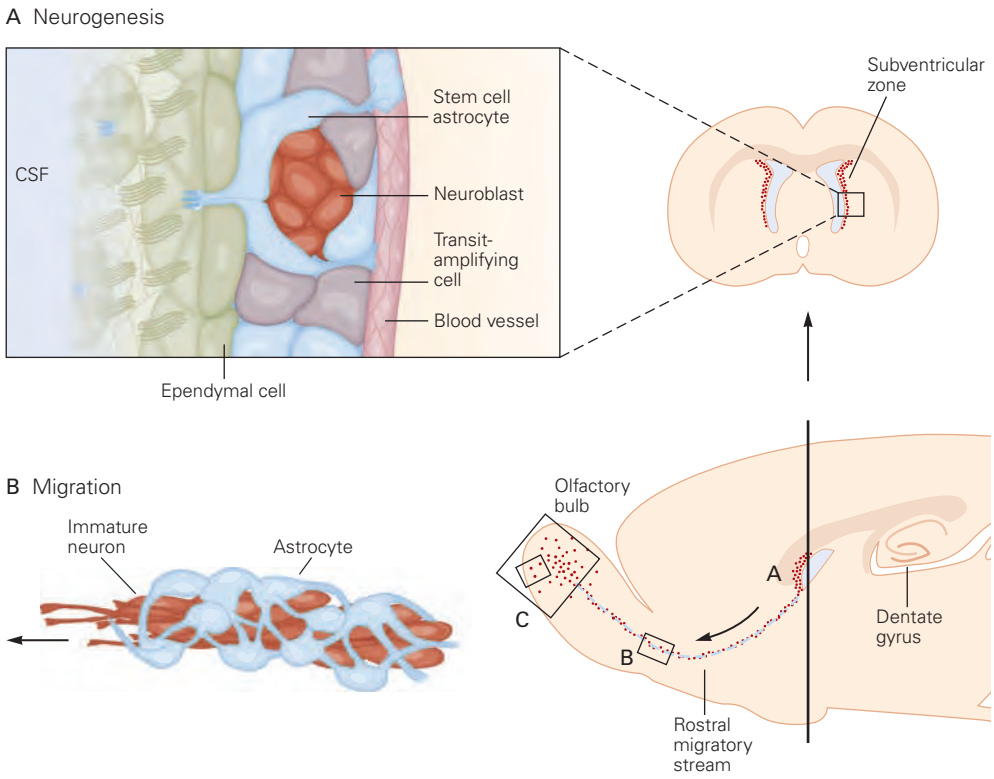

Figure 50–13 The origin and fate of neurons born in the adult ventricular zone. (Adapted from Tavazoie et al. 2008.)

A. Neuroblasts develop in an orderly progression from astrocytic stem cells via a population of cells within a local niche close to blood vessels in the subventricular zone. (Abbreviation: **CSF**, cerebrospinal fluid.)

B. Neuroblasts differentiate into immature neurons that migrate to the olfactory bulb using astrocytes as guides. They crawl along each other in a process called chain migration.

C. On arrival in the olfactory bulb, immature neurons differentiate into granule cells and periglomerular cells, two classes of olfactory bulb interneurons. (Image reproduced, with permission, from A. Mizrahi.)

One is to replace dopaminergic cells that die in Parkinson disease. When transplanted into the striatum, these neurons release dopamine onto their targets without the need to grow long axons or form elaborate synapses (Figure 50–14). Another is to transplant immature inhibitory interneurons from the ganglionic eminences in which they are produced (Chapter 46) to the cortex, where they mature and form synapses. By enhancing inhibition, these neurons attenuate the manifestations of disorders in which insufficient inhibitory drive plays a role, such as epilepsy and anxiety.

Unfortunately, application of these methods to human patients has been fraught with difficulties. One is the difficulty of obtaining and growing developing neurons in sufficient numbers and with sufficient purity. Second, it has been challenging to modify neurons by introducing new genes so as to improve their chances of functioning in a new environment. Third, in many cases, the grafted neurons are already too mature

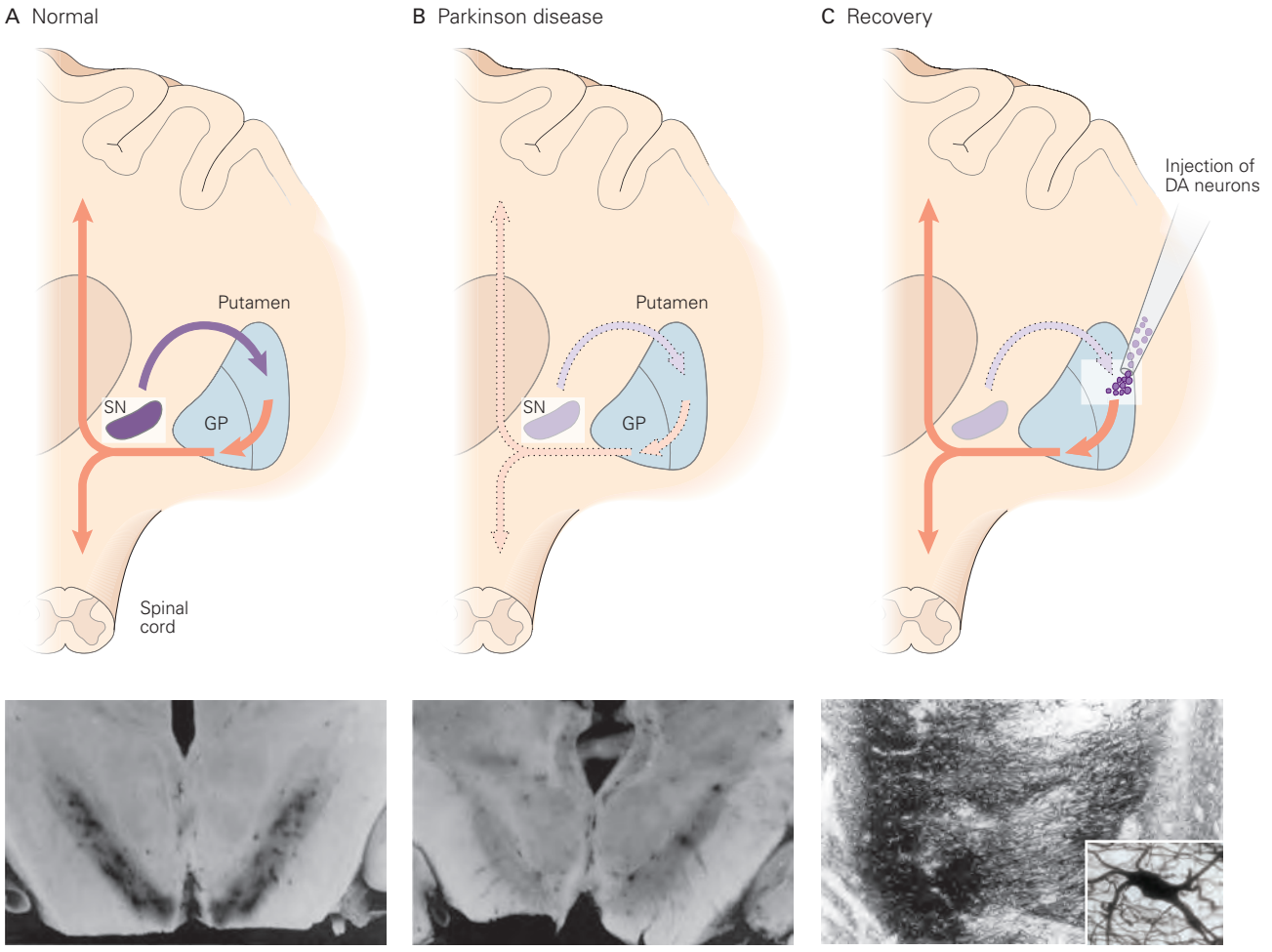

Figure 50–14 Loss of dopaminergic (DA) neurons in Parkinson disease can be treated by grafting embryonic cells into the putamen.

A. In the healthy brain, dopaminergic projections from the substantia nigra (**SN**) innervate the putamen, which in turn activates neurons in the globus pallidus (**GP**). Pallidal outputs to the brain and spinal cord facilitate movement. The image below shows melanin-rich dopaminergic neurons in human substantia nigra.

B. In Parkinson disease, the loss of dopaminergic neurons in the substantia nigra deprives the putamen–globus pallidus pathways of their drive. The image beneath the diagram shows the virtual absence of melanin-rich dopaminergic neurons in the substantia nigra of an individual with Parkinson disease.

C. Direct injection of embryonic dopaminergic neurons into the putamen reactivates the globus pallidus output pathways. The image below shows tyrosine hydroxylase expression in the cell bodies and axons of embryonic mesencephalic dopaminergic neurons grafted into the putamen of a human patient. (Image reproduced, with permission, from Kordower and Sortwell 2000. Copyright © 2000. Published by Elsevier B.V.)

to differentiate properly or to integrate effectively into functional circuits.

These obstacles can be overcome by transplanting neural precursors into the adult brain where they can go on to differentiate into neurons in a hospitable environment. Several classes of precursors have been transplanted successfully, including neural stem cells and committed precursors. Some initial success has been obtained with embryonic stem (ES) cells. These cells are derived from early blastocyst stage embryos and can give rise to all cells of the body. Because they can divide indefinitely in culture, large numbers of cells can be generated, induced to differentiate, and then engrafted.

More recently, this technology has been enhanced by the molecular reprogramming of skin fibroblast cells to create induced pluripotent stem (iPS) cells (Figure 50–15). These cells have a distinct advantage over ES cells; embryos are not required for their production, effectively bypassing a minefield of practical, political, and ethical concerns that have hindered research using human ES cells. Another advantage of iPS cells is that they can be generated from an individual patient's own skin cells, neatly avoiding issues of immunological incompatibility. It is also possible to genetically modify the iPS cells in culture by repairing a defective gene before transplantation.

Because ES and iPS cells have the potential to generate any cell type, it is essential that their differentiation be guided along specific pathways in culture before they are transplanted. Methods for generating specific classes of neural precursors, neurons, and glial cells from ES and iPS cells have now been devised (Figure 50–15).

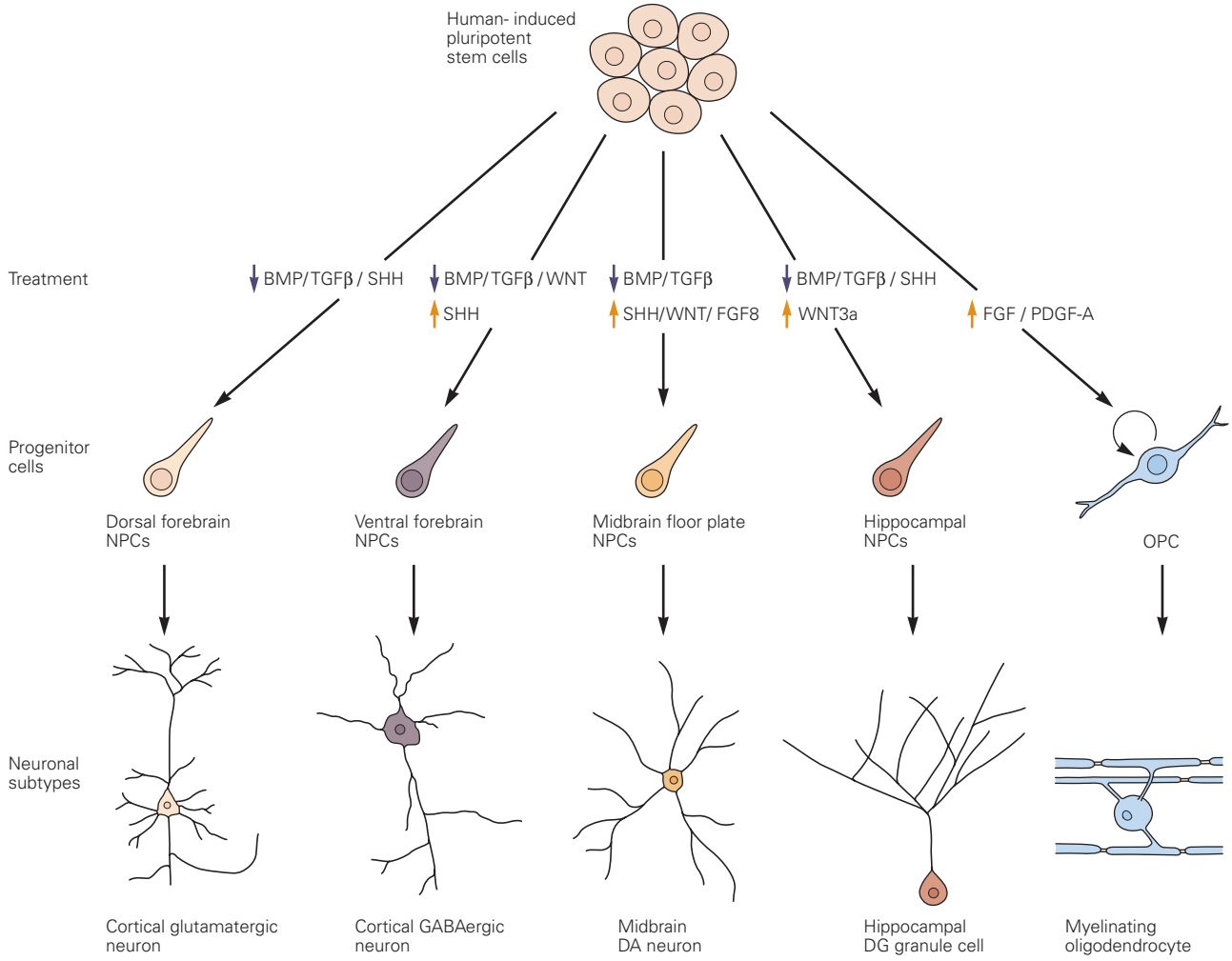

Figure 50–15 Induced pluripotent stem cells can be reprogrammed to generate precursors of many neuronal and glial types. The precursors can then be transplanted into the brain or spinal cord, where cells complete their differentiation and integrate into functional circuits. (Abbreviations: **DA**, dopamine; **DG**, dentate gyrus; **NPC**, neural progenitor cell; **OPC**, oligodendrocyte progenitor cell.) (Adapted, with permission, from Wen et al. 2016. Copyright © 2016 Elsevier Ltd.)

For example, it is possible to generate neurons that possess many or all of the properties of the spinal motor neurons that are lost in amyotrophic lateral sclerosis (Figure 50–16) or to generate the dopaminergic neurons lost from the striatum in Parkinson disease and then to engraft such neurons into the spinal cord or brain.

Although many hurdles need to be overcome, clinical trials using ES and iPS cell-derived neurons are underway. In addition, these cells are being used in chemical screens to identify compounds that counteract the cellular defects that underlie human neurodegenerative disease.

Stimulation of Neurogenesis in Regions of Injury May Contribute to Restoring Function

What if, following injury in adults, endogenous neuronal precursors could be stimulated to produce neurons capable of replacing those that have been lost? Two sets of recent findings suggest that this idea is not so far-fetched.

First, precursors capable of forming neurons in culture have been isolated from many parts of the adult nervous system, including the cerebral cortex and spinal cord, even though neurogenesis in adults is ordinarily confined to the olfactory bulb and hippocampus. This diversion of cell fate led to the idea that neurogenesis in the adult occurs in only a few sites, because only they contain appropriate permissive or stimulatory factors. This hypothesis has spurred a search for such factors, in the hope that they could be used to render a larger range of sites capable of supporting neurogenesis.

Second, in a few cases, the generation of new neurons can be stimulated by traumatic or ischemic injury (akin to stroke), even in areas such as the cerebral cortex

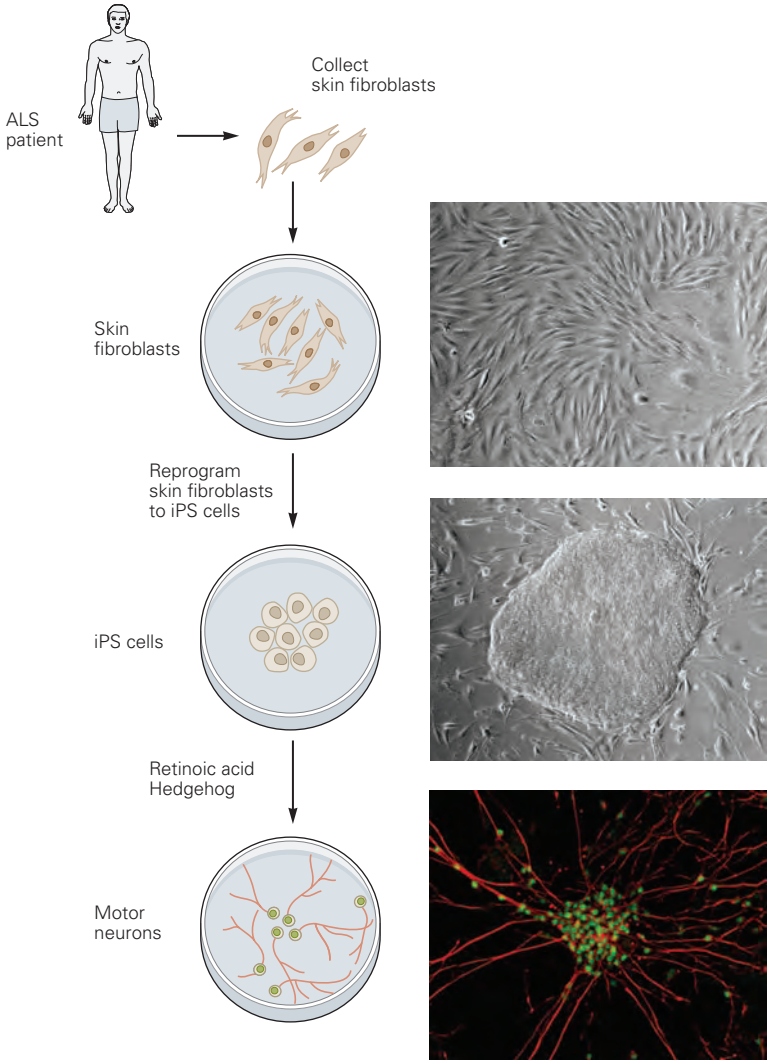

Figure 50–16 **Induced pluripotent stem cells derived from an individual with amyotrophic lateral sclerosis (ALS) can differentiate into spinal motor neurons.** Fibroblasts from the skin of a patient with ALS were used to generate induced pluripotent stem (**iPS**) cells, which were then directed to a motor neuron fate (see Figure 50–15). These cells can be used to analyze mechanisms that underlie motor neuron loss in ALS. The images at right show (from top to bottom) cultured fibroblasts, an iPS cell clump, and differentiated motor neurons expressing characteristic nuclear transcription factors (**green**) and axonal proteins (**red**). (Micrographs reproduced, with permission, from C. Henderson, H. Wichterle, G. Croft, and M. Weygandt.)

or spinal cord in which neurogenesis normally fails to occur. The fact that recovery after stroke and injury is poor demonstrates that spontaneous compensatory neurogenesis, if it occurs in humans, is insufficient for tissue repair. However, injury-induced neurogenesis has been enhanced in experimental animals in several ways. In one, administration of growth factors promotes neuronal production from progenitors grown in culture. In another, glial cells that retain the capacity to divide, such as Müller glia in the retina or astrocytes in the cortex, are reprogrammed to differentiate into neurons. If such interventions could be adapted to humans, the range of neurons subject to replacement would be greatly increased.

Transplantation of Nonneuronal Cells or Their Progenitors Can Improve Neuronal Function

Cells other than neurons are lost after brain injury. Among the most profound losses are those of oligodendrocytes, the cells that form the myelin sheath around central axons. The stripping of myelin continues long after traumatic injury and contributes to progressive loss of function of axons that may not have been injured directly.

Although the adult brain and spinal cord are capable of generating new oligodendrocytes and replacing lost myelin, this production is insufficient to restore function in many cases. Since several common neurological diseases, most notably multiple sclerosis, are accompanied by a profound state of demyelination, there is strong interest in providing the nervous system with additional oligodendrocyte precursors in order to augment remyelination.

Neural stem cells, multipotential progenitors, ES cells, and iPS cells can give rise not only to neurons but also to nonneural cells, including oligodendrocytes and their direct precursors. Indeed, at present, human ES cells are being channeled into oligodendrocyte progenitor cells and implanted into injured spinal cords of experimental animals. Transplanted cells that differentiate into oligodendrocytes enhance remyelination and substantially improve the locomotor ability of experimental animals (Figure 50–17).

Restoration of Function Is the Aim of Regenerative Therapies

We need to bear in mind that efforts to replace central neurons or to enhance the regeneration of their axons

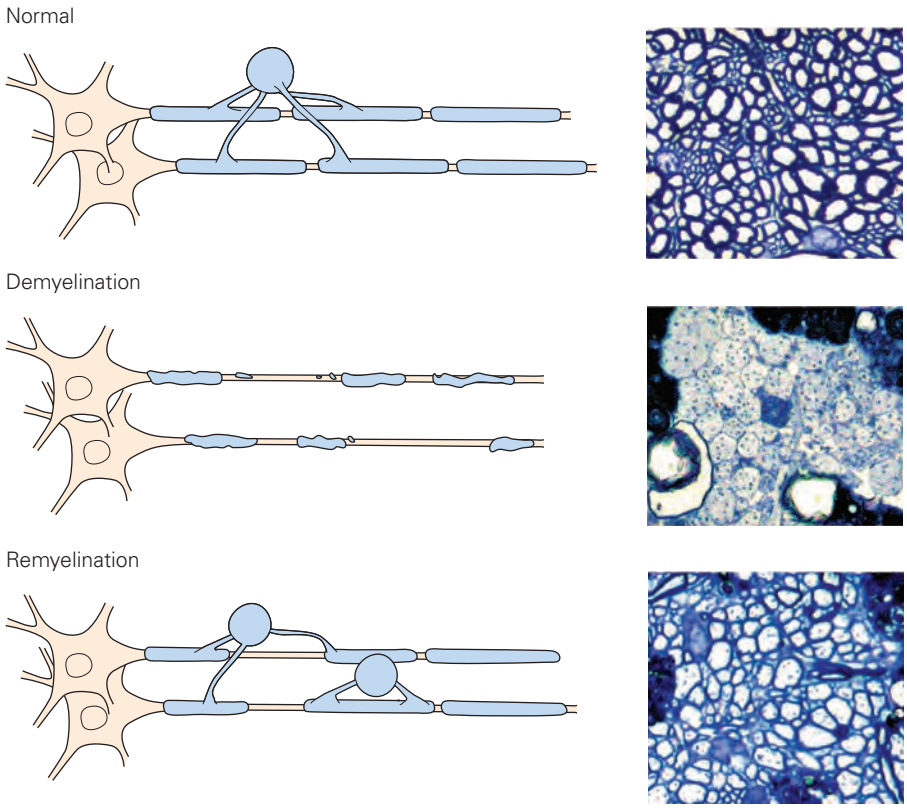

Figure 50–17 Restoration of myelination in the central nervous system by transplanted oligodendrocyte stem cells. In rodents with demyelinated axons, grafts of oligodendrocyte precursor cells can restore myelination to near normal. Sections through central nerve tracts are shown in the images at right. (Adapted, with permission, from Franklin and ffrench-Constant 2008. Copyright © 2008 Springer Nature.)

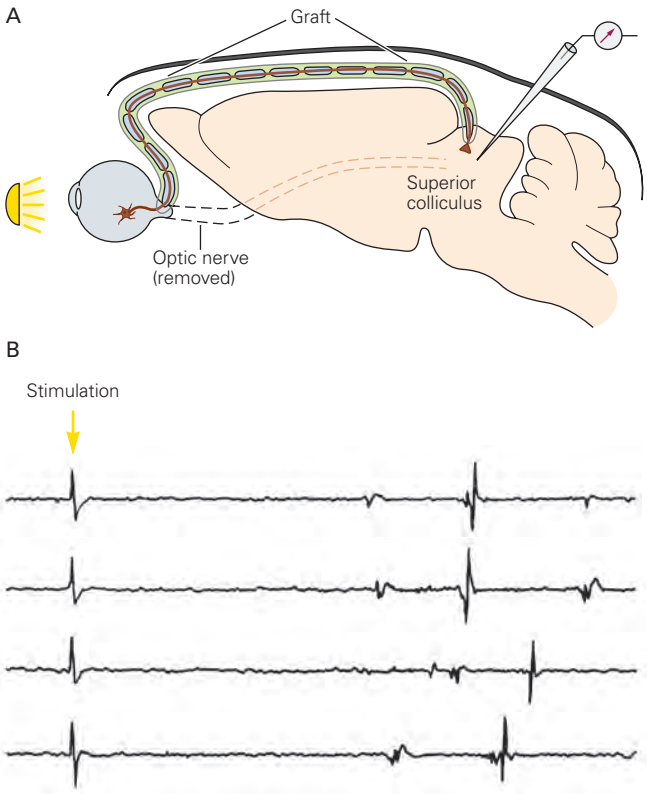

Figure 50–18 Regenerated retinal ganglion axons in the optic nerve can form functional synapses. (Adapted, with permission, from Keirstead et al. 1989. Copyright © 1989 AAAS.)

A. A segment of optic nerve in an adult rat was removed, and a segment of sciatic nerve was grafted in its place. The other end of the sciatic nerve was attached to the superior colliculus. Some retinal ganglion cell axons regenerated through the sciatic nerve and entered the superior colliculus.

B. Once the axons of the retinal ganglion neurons had regenerated, recordings were made from the superior colliculus. Flashes of light delivered to the eye elicited action potentials in collicular neurons, demonstrating that at least some regenerated axons had formed functional synapses.

would be of little use if these axons were unable to form functional synapses with their target cells. The same fundamental questions asked about axon regeneration in adults therefore apply to synaptogenesis: Can it happen, and if not, why not?

It has been difficult to address these questions because axonal regeneration following experimentally induced injury is usually so poor that the axons never reach appropriate target fields. However, several of the studies discussed earlier in this chapter offer hope that synapse formation is possible within the dense adult neuropil. In fact, axon branches that regenerate following injury can form synapses on nearby targets. For example, Aguayo and his colleagues found that retinal axons were able to regrow into the superior colliculus when they were channeled through a peripheral nerve that had been grafted into the optic nerve (Figure 50–18A). Remarkably, some collicular neurons fired action potentials when the eye was illuminated, showing that functional synaptic connections had been reestablished (Figure 50–18B). More recent studies have promoted regeneration of severed axons by enhancing their intrinsic growth programs, as described above, and observed some restoration of function.

Likewise, neurons that arise endogenously or are implanted by investigators can form and receive synapses. Thus, there is reason to believe that if injured axons can be induced to regenerate, or new neurons supplied to replace lost ones, they will wire up in ways that help restore lost functions and behaviors.

Highlights

1. When axons are transected, the distal segment degenerates, a process called Wallerian degeneration. The proximal segment and cell body also undergo changes, as do the injured neuron's synaptic inputs and targets.
2. It was long thought that Wallerian degeneration was a passive and inevitable consequence of the distal segment being deprived of sustenance from the cell body, but it is not known to be an active, regulated process. Genes called *NMNAT* and *SARM1* are key components of a core signaling pathway that controls the process. Intervention in the pathway can slow or even halt degeneration.
3. Axons can regenerate and form new synapses following injury, but in mammals, regeneration is far more widespread and effective in peripheral axons than in central axons.

4. A key factor in the differential response of peripheral and central axons is that the environment confronting injured central axons is poor at supporting growth. It both lacks nutritive factors present in the pathway of peripheral nerves and contains growth-inhibitory factors absent from peripheral nerves.
5. Structures that inhibit regeneration include myelin fragments that persist following Wallerian degeneration and astrocytes that form glial scars at injury sites. Inhibitory factors in myelin include Nogo and myelin-associated glycoprotein. Inhibitory factors secreted by astrocytes include chondroitin sulfate proteoglycans.
6. Central regeneration is also hindered by intrinsic decreased ability of adult central neurons to grow, due to downregulation of growth programs active during development. Interventions that restore or disinhibit growth pathways, such as JAK/STAT and mTOR signaling, enable regeneration.
7. However, it is important to note that the failure of regeneration following injury may be related to the stabilization of connections that occurs at the end of critical periods. For example, myelination, which occurs largely at the end of a critical period, may have the secondary effect of preventing further, large-scale rearrangement of synaptic connections. Thus, caution will be needed to ensure that treatments aimed at fostering recovery following injury do not end up promoting formation of maladaptive circuits.
8. Another approach for restoring function following damage is to harness the ability of intact axons to form new connections, generating adaptive circuits that can compensate to some extent for those lost to injury.
9. The traditional view that all neurogenesis occurs during or shortly after gestation has now been modified by the discovery that new neurons are born throughout life in a few brain areas. These neurons arise from resident stem cells and can integrate into functional circuits.
10. Cells capable of forming new neurons are also present in many other areas of the brain and spinal cord but remain quiescent. Attempts to activate them by providing growth factors or introducing growth-promoting genes (transcriptional reprogramming) could harness their potential following injury or in neurodegenerative disease.
11. Another approach to neuronal replacement is to implant developing neurons. Although fetal neurons are sometimes used for this purpose in experimental animals, a more useful source may be neurons derived from ES or iPS cells. They can be grown in large quantities, genetically modified if necessary, and treated to differentiate into specific neuronal types. Clinical studies using this approach are now beginning.

Joshua R. Sanes

Selected Reading

Benowitz LI, He Z, Goldberg JL. 2017. Reaching the brain: advances in optic nerve regeneration. Exp Neurol 287:365–373.

Dell'Anno MT, Strittmatter SM. 2017. Rewiring the spinal cord: direct and indirect strategies. Neurosci Lett 652: 625–634.

Gerdts J, Summers DW, Milbrandt J, DiAntonio A. 2016. Axon self-destruction: new links among SARM1, MAPKs, and NAD+ metabolism. Neuron 89:449–460.

He Z, Jin Y. 2016. Intrinsic control of axon regeneration. Neuron 90:437–451.

Magnusson JP, Frisén J. 2016. Stars from the darkest night: unlocking the neurogenic potential of astrocytes in different brain regions. Development 143:1075–1086.

McComish SF, Caldwell MA. 2018. Generation of defined neural populations from pluripotent stem cells. Philos Trans R Soc Lond B Biol Sci 373:pii: 20170214.

Zhao C, Deng W, Gage FH. 2008. Mechanisms and functional implications of adult neurogenesis. Cell 132:645–660.

References

Alilain WJ, Horn KP, Hu H, Dick TE, Silver J. 2011. Functional regeneration of respiratory pathways after spinal cord injury. Nature 475:196–200.

Altman J. 1969. Autoradiographic and histological studies of postnatal neurogenesis. IV. Cell proliferation and migration in the anterior forebrain, with special reference to persisting neurogenesis in the olfactory bulb. J Comp Neurol 137:433–457.

Altman J, Das GD. 1965. Autoradiographic and histological evidence of postnatal hippocampal neurogenesis in rats. J Comp Neurol 124:319–335.

Bareyre FM, Kerschensteiner M, Raineteau O, Mettenleiter TC, Weinmann O, Schwab ME. 2004. The injured spinal cord spontaneously forms a new intraspinal circuit in adult rats. Nat Neurosci 7:269–277.

Bei F, Lee HHC, Liu X, et al. 2016. Restoration of visual function by enhancing conduction in regenerated axons. Cell 164:219–232.

Beirowski B, Berek L, Adalbert R, et al. 2004. Quantitative and qualitative analysis of Wallerian degeneration using restricted axonal labelling in YFP-H mice. J Neurosci Methods 134:23–35.

Bradbury EJ, McMahon SB. 2006. Spinal cord repair strategies: why do they work? Nat Rev Neurosci 7:644–653.

Bradbury EJ, Moon LD, Popat RJ, et al. 2002. Chondroitinase ABC promotes functional recovery after spinal cord injury. Nature 416:636–640.

Caroni P, Schwab ME. 1988. Antibody against myelin-associated inhibitor of neurite growth neutralizes nonpermissive substrate properties of CNS white matter. Neuron 1:85–96.

Conforti L, Gilley J, Coleman MP. 2014. Wallerian degeneration: an emerging axon death pathway linking injury and disease. Nat Rev Neurosci 15:394–409.

David S, Aguayo AJ. 1981. Axonal elongation into peripheral nervous system "bridges" after central nervous system injury in adult rats. Science 214:931–933.

Dimos JT, Rodolfa KT, Niakan KK, et al. 2008. Induced pluripotent stem cells generated from patients with ALS can be differentiated into motor neurons. Science 321:1218–1221.

Duan X, Qiao M, Bei F, Kim IJ, He Z, Sanes JR. 2015. Subtype-specific regeneration of retinal ganglion cells following axotomy: effects of osteopontin and mTOR signaling. Neuron 85:1244–1256.

Essuman K, Summers DW, Sasaki Y, Mao X, DiAntonio A, Milbrandt J. 2017. The SARM1 toll/interleukin-1 receptor domain possesses intrinsic NAD+ cleavage activity that promotes pathological axonal degeneration. Neuron 93:1334–1343.

Ferri A, Sanes JR, Coleman MP, Cunningham JM, Kato AC. 2003. Inhibiting axon degeneration and synapse loss attenuates apoptosis and disease progression in a mouse model of motoneuron disease. Curr Biol 13:669–673.

Franklin RJ, ffrench-Constant C. 2008. Remyelination in the CNS: from biology to therapy. Nat Rev Neurosci 9:839–855.

Galtrey CM, Fawcett JW. 2007. The role of chondroitin sulfate proteoglycans in regeneration and plasticity in the central nervous system. Brain Res Rev 54:1–18.

Gerdts J, Brace EJ, Sasaki Y, DiAntonio A, Milbrandt J. 2015. SARM1 activation triggers axon degeneration locally via NAD^+ destruction. Science 348:453–457.

Gerdts J, Summers DW, Sasaki Y, DiAntonio A, Milbrandt J. 2013. Sarm1-mediated axon degeneration requires both SAM and TIR interactions. J Neurosci 33:13569–13580.

Goldman SA, Kuypers NJ. 2015. How to make an oligodendrocyte. Development 142:3983-3995.

Guo Z, Zhang L, Wu Z, Chen Y, Wang F, Chen G. 2014. In vivo direct reprogramming of reactive glial cells into functional neurons after brain injury and in an Alzheimer's disease model. Cell Stem Cell 14:188–202.

Imayoshi I, Sakamoto M, Ohtsuka T. 2008. Roles of continuous neurogenesis in the structural and functional integrity of the adult forebrain. Nat Neurosci 10:1153–1161.

Jorstad NL, Wilken MS, Grimes WN, et al. 2017. Stimulation of functional neuronal regeneration from Müller glia in adult mice. Nature 548:103–107.

Keirstead HS, Nistor G, Bernal G, et al. 2005. Human embryonic stem cell-derived oligodendrocyte progenitor cell transplants remyelinate and restore locomotion after spinal cord injury. J Neurosci 25:4694–4705.

Keirstead SA, Rasminsky M, Fukuda Y, Carter DA, Aguayo AJ, Vidal-Sanz M. 1989. Electrophysiologic responses in hamster superior colliculus evoked by regenerating retinal axons. Science 246:255–257.

Kordower J, Sortwell C. 2000. Neuropathology of fetal nigra transplants for Parkinson's disease. Prog Brain Res 127:333–344.

Lim DA, Alvarez-Buylla A. 2016. The adult ventricular-subventricular zone (V-SVZ) and olfactory bulb (OB) Neurogenesis. Cold Spring Harb Perspect Biol 8:pii: a018820.

Lois C, Alvarez-Buylla A. 1994. Long-distance neuronal migration in the adult mammalian brain. Science 264: 1145–1148.

Mack TGA, Reiner M, Beirowski B, et al. 2001. Wallerian degeneration of injured axons and synapses is delayed by a Ube4b/Nmnat chimeric gene. Nat Neurosci 4:1199–1206.

Magavi SS, Leavitt BR, Macklis JD. 2000. Induction of neurogenesis in the neocortex of adult mice. Nature 405:951–955.

Magnusson JP, Göritz C, Tatarishvili J, et al. 2014. A latent neurogenic program in astrocytes regulated by Notch signaling in the mouse. Science 346:237–241.

Maier IC, Schwab ME. 2006. Sprouting, regeneration and circuit formation in the injured spinal cord: factors and activity. Philos Trans R Soc Lond B Biol Sci 361:1611–1634.

Osterloh JM, Yang J, Rooney TM, et al. 2012. dSarm/Sarm1 is required for activation of an injury-induced axon death pathway. Science 337:481–484.

Schwab ME, Thoenen H. 1985. Dissociated neurons regenerate into sciatic but not optic nerve explants in culture irrespective of neurotrophic factors. J Neurosci 5:2415–2423.

Schwegler G, Schwab ME, Kapfhammer JP. 1995. Increased collateral sprouting of primary afferents in the myelin-free spinal cord. J Neurosci 15:2756–2767.

Smith PD, Sun F, Park KK, et al. 2009. SOCS3 deletion promotes optic nerve regeneration in vivo. Neuron 64:617–623.

Sohur US, Emsley JG, Mitchell BD, Macklis JD. 2006. Adult neurogenesis and cellular brain repair with neural progenitors, precursors and stem cells. Philos Trans R Soc Lond B Biol Sci 361:1477–1497.

Southwell DG, Nicholas CR, Basbaum AI, et al. 2014. Interneurons from embryonic development to cell-based therapy. Science 344:1240622.

Takahashi K, Tanabe K, Ohnuki M, et al. 2007. Induction of pluripotent stem cells from adult human fibroblasts by defined factors. Cell 131:861–872.

Takahashi K, Yamanaka S. 2006. Induction of pluripotent stem cells from mouse embryonic and adult fibroblast cultures by defined factors. Cell 126:663–676.

Tavazoie M, Van der Verken L, Silva-Vargas V, et al. 2008. A specialized vascular niche for adult neural stem cells. Cell Stem Cell 3:279–288.

Thuret S, Moon LD, Gage FH. 2006. Therapeutic interventions after spinal cord injury. Nat Rev Neurosci 7: 628–643.

Torper O, Ottosson DR, Pereira M, et al. 2015. In vivo reprogramming of striatal NG2 glia into functional neurons that integrate into local host circuitry. Cell Rep 12:474–481.

Wen Z, Christian KM, Song H, Ming GL. 2016. Modeling psychiatric disorders with patient-derived iPSCs. Curr Opin Neurobiol 36:118–127.

Wernig M, Zhao JP, Pruszak J, et al. 2008. Neurons derived from reprogrammed fibroblasts functionally integrate into the fetal brain and improve symptoms of rats with Parkinson's disease. Proc Natl Acad Sci U S A 105:5856–5861.

Winkler C, Kirik D, Bjorklund A. 2005. Cell transplantation in Parkinson's disease: how can we make it work? Trends Neurosci 28:86–92.

Yiu G, He Z. 2006. Glial inhibition of CNS axon regeneration. Nat Rev Neurosci 7:617–627.

Zhou FQ, Snider WD. 2006. Intracellular control of developmental and regenerative axon growth. Philos Trans R Soc Lond B Biol Sci 361:1575–1592.

51

Sexual Differentiation of the Nervous System

Few words are more loaded with meaning than the word "sex." Sexual activity is a biological imperative and a major human preoccupation. The physical differences between men and women that underlie partner recognition and reproduction are obvious to all of us, and their developmental origins are well understood. In contrast, our understanding of behavioral differences between the sexes is primitive. In many cases, their very existence remains controversial, and the origins of those that have been clearly demonstrated remain unclear.

In this chapter, we first briefly summarize the embryological basis of sexual differentiation. We then discuss at greater length the behavioral differences between the two sexes, focusing on those differences or dimorphisms for which some neurobiological basis has been found. These dimorphisms include physiological responses (erection, lactation), drives (maternal behavior), and even more complex behaviors (gender identity). In analyzing these dimorphisms, we will discuss three issues.

First, what are the genetic origins of sexual differences? Human males and females have a complement of 23 chromosomal pairs, and only one differs between the sexes. Females have a pair of X chromosomes (and are therefore XX), whereas males have one copy of the X chromosome paired with a Y chromosome (XY). The other 22 chromosome pairs, called *autosomes*, are shared between males and females. We will see that the initial genetic determinants arise from a single gene on the Y chromosome, while later ones arise indirectly from sex-specific patterns of expression imposed upon other genes as development proceeds.

Second, how are sexual differences initiated by the Y chromosome translated into differences between the brains of men and women? We will see that key intermediates are the sex hormones, a set of steroids that

includes testosterone and estrogens. These hormones act during embryogenesis as well as postnatally, first organizing the physical development of both genitalia and brain regions, and later activating particular physiological and behavioral responses. Hormonal regulation is especially complex because the nervous system, which is profoundly influenced by sex steroids, also controls their synthesis. This feedback loop may help to explain how the external environment, including social and cultural factors, can ultimately shape sexual dimorphism at a neural level.

Third, what are the crucial neural differences that underlie sexually dimorphic behaviors? Clear physical and molecular differences between the brains of men and women have been found. These differences reflect differences in neural circuitry between the sexes, and in a few cases, these distinctions in connectivity are directly related to behavioral differences. In other cases, however, sexually dimorphic behaviors appear to result from differential usage of the same basic circuits.

Before proceeding, we must define two words that are commonly used in many ways and sometimes confused with each other: *sex* and *gender.* As a descriptor of biological differences between men and women, the word *sex* is used in three ways. First, *anatomical sex* refers to overt differences including the differences in the external genitalia as well as other sexual characteristics such as the distribution of body hair. *Gonadal sex* refers to the presence of male or female gonads, the testes or ovaries. Finally, *chromosomal sex* refers to the distribution of the sex chromosomes between females (XX) and males (XY).

Whereas *sex* is a biological term, *gender* encompasses the collection of social behaviors and mental states that typically differ between males and females. *Gender role* is the set of behaviors and social mannerisms that is typically distributed in a sexually dimorphic fashion within the population. Toy preferences in children as well as distinctive attire are some examples of gender roles that can distinguish males from females. *Gender identity* is the feeling of belonging to the category of the male or female sex. Importantly, gender identity is distinct from *sexual orientation*, the erotic responsiveness displayed toward members of one or the other sex.

Are gender and sexual orientation genetically determined? Or are they social constructs molded by cultural expectations and personal experience? As the examples in this chapter will illustrate, we are still far from untangling the contributions of genes and environment to these complex phenomena. However, our recognition that genes and experience interact to shape neural circuits gives us a more realistic framework with which to answer this question compared to our predecessors, who were constrained by the simplistic view that genes and experience acted in mutually exclusive ways.

Genes and Hormones Determine Physical Differences Between Males and Females

Chromosomal Sex Directs the Gonadal Differentiation of the Embryo

Sex determination is the embryonic process whereby chromosomal sex directs the differentiation of the gonadal sex of the animal. Surprisingly, this process differs in fundamental ways within the animal kingdom and even among vertebrates. In most mammals, including humans, however, an XY genotype drives differentiation of the embryonic gonad into testes, whereas an XX genotype leads to ovarian differentiation. Hormones produced by the testes and ovaries subsequently direct sexual differentiation of the nervous system and the rest of the body.

It is the presence of the Y chromosome rather than the lack of a second X chromosome that is the crucial determinant of male differentiation. This was first evident in rare individuals born with two or even three X chromosomes in addition to a Y chromosome (XXY or XXXY). These individuals are men who exhibit male-typical traits. In fact, female cells do not have two active X chromosomes. Early in embryogenesis, one of the two X chromosomes in each female cell is chosen at random for inactivation, and the genes on it are rendered transcriptionally silent. Thus, both male and female cells have a single active X chromosome, and male cells also have a Y chromosome.

The sex-determining activity of the Y chromosome is encoded by the gene *SRY* (sex-determining region on Y) whose activity is required for masculinization of the embryonic gonads (Figure 51–1). Inactivation or deletion of *SRY* leads to complete sex reversal: Individuals are chromosomally male (XY) but externally indistinguishable from females. Conversely, in rare instances, *SRY* translocates to another chromosome (to the X chromosome or an autosome) during spermatogenesis. Such sperm can fertilize eggs to produce individuals who are chromosomally female (XX) but externally male. However, such XX sex-reversed men are infertile, as many of the genes required for sperm function are located on the Y chromosome.

How does *SRY* instruct the undifferentiated gonads to develop into testes? The female differentiation

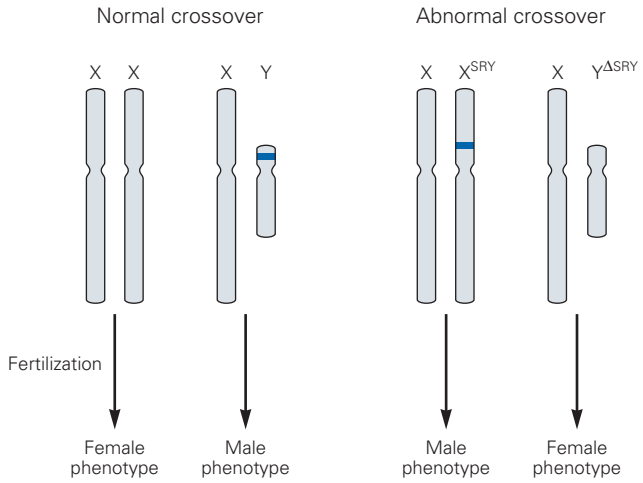

Figure 51–1 The role of the *SRY* gene in sex determination in humans. *SRY*, the sex-determining locus (**blue domain**), resides on the nonhomologous region of the short arm of the Y chromosome. The presence of *SRY* is determinative for male differentiation in many mammals, including primates and most rodents. Normally X- or Y-bearing sperm fertilize an oocyte to generate XX females or XY males, and the resulting phenotypic sex is concordant for the chromosomal sex. Rarely, *SRY* translocates to the X chromosome or an autosome (not shown). In such cases, XX^{SRY} offspring are phenotypically male, whereas $XY^{\Delta SRY}$ offspring (the Δ indicating a gene deletion) are phenotypically female. (Adapted from Wilhelm, Palmer, and Koopman 2007.)

program appears to be the default mode; patterning genes prime the body and gonads to develop along female-specific pathways. The *SRY* gene encodes a transcription factor that regulates expression of genes, some of which prevent execution of the default program and initiate the process of male gonadal differentiation. One of the best-studied targets of the SRY transcription factor is another transcription factor, SOX9, which is required for differentiation of the testes. Thus, SRY initiates a cascade of inductive interactions that ultimately lead to male-specific gonad development.

Gonads Synthesize Hormones That Promote Sexual Differentiation

The chromosomal complement of the embryo directs sexual differentiation of the gonads, and in turn, the gonads determine the sex-specific features of all organs of the body, including the nervous system. They do this by secreting hormones. Gonadal hormones have two major roles. Their developmental role is traditionally referred to as *organizational* because the early effects of hormones on the brain and the rest of the body lead to major, generally irreversible, aspects of cell and tissue differentiation. Later, some of the same hormones trigger physiological or behavioral responses. These influences, generally termed *activational*, are reversible.

One example of an organizational role of gonadal hormones is seen in the differentiation of structures that connect the gonads to the external genitalia. In males, the Wolffian duct gives rise to the vas deferens, the seminal vesicles, and the epididymis. In females, the Müllerian duct differentiates into the oviduct, the uterus, and the vagina (Figure 51–2). Initially, both female (XX) and male (XY) embryos possess Wolffian and Müllerian ducts. In males, the developing testes secrete a protein hormone, the Müllerian inhibiting substance (MIS), and a steroid hormone, testosterone. MIS leads to a regression of the Müllerian duct, and testosterone induces the Wolffian duct to differentiate into its mature derivatives. In females, the absence of MIS permits the Müllerian duct to differentiate into its adult derivatives, and the absence of circulating testosterone causes the Wolffian duct to resorb. Thus, the Y chromosome overrides a female default program to generate male gonads, which in turn secrete hormones that override a female default program of genital differentiation.

The action of MIS is largely confined to embryos, but steroid hormones exert effects throughout life—that is, they also have activational roles at later stages. All of the steroid hormones derive from cholesterol (Figure 51–3). The sex steroids can be divided into androgens, which generally promote male characteristics, and the estrogens plus progesterone that promote female characteristics. The testes produce mostly the androgen testosterone, while the ovaries produce mostly progesterone and an estrogen, 17-β-estradiol. The menstrual cycle is a good example of the activational function of estrogen and progesterone.

A glance at the metabolic relationships among steroid hormones (Figure 51–3) reveals a surprise. The female hormone progesterone is the precursor of the male hormone testosterone, and testosterone is the direct precursor of the female hormone 17-β-estradiol. Thus, the enzymes that convert one hormone to the other control not only the level of the hormone but also the "sign" (male or female) of the hormonal effect. Aromatase, the enzyme that converts testosterone to estradiol, is present at high levels in the ovaries but not in the testes. Differential expression of aromatase is the reason for sexual dimorphism in circulating testosterone and estrogen. Aromatase is also expressed in various regions of the brain (Figure 51–4A), and many of the effects of testosterone on neurons are thought to occur after its conversion to estrogen. Testosterone

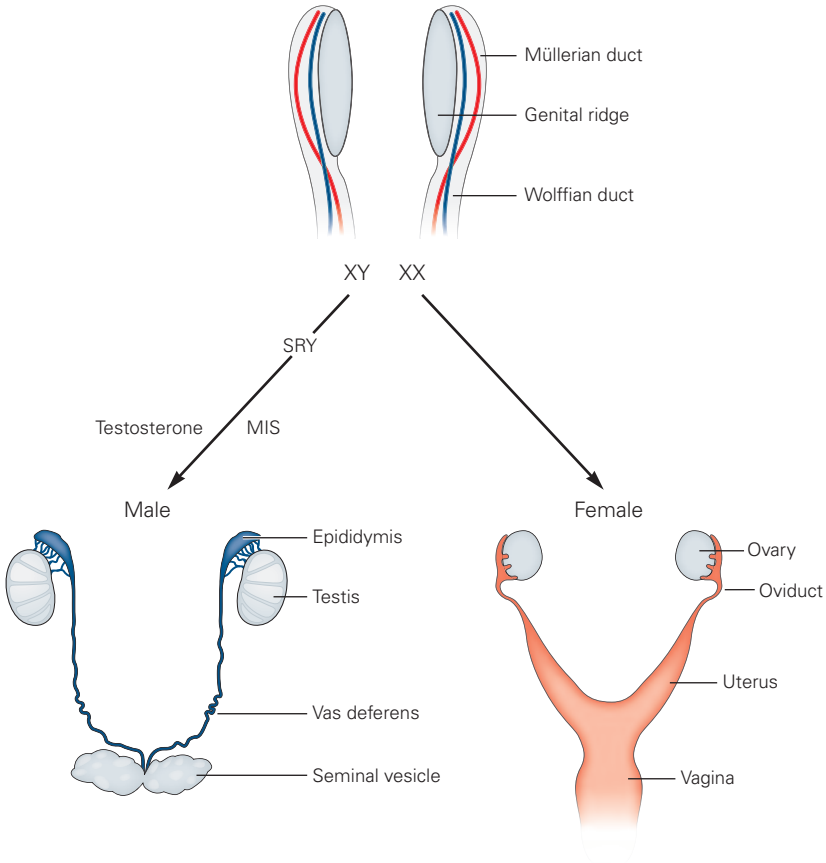

Figure 51–2 Sexual differentiation of the internal genitalia. Embryos of both sexes develop bilateral genital ridges (the gonadal anlagen) that can differentiate into either testes or ovaries; Müllerian ducts, which can differentiate into oviducts, the uterus, and the upper vagina; and Wolffian ducts, which can differentiate into the epididymis, the vas deferens, and the seminal vesicles. In XY embryos, the expression of the *SRY* gene in the genital ridge induces differentiation of this tissue into testes and of the Wolffian ducts into the rest of the male internal genitalia, while the Müllerian ducts are resorbed. In XX embryos, the *absence* of *SRY* permits the genital ridges to develop into ovaries and the Müllerian ducts to differentiate into the rest of the female internal genitalia; in the absence of circulating testosterone, the Wolffian ducts degenerate. (Abbreviation: **MIS**, Müllerian inhibiting substance.) (Adapted, with permission, from Wilhelm, Palmer, and Koopman 2007.)

is also converted by the enzyme 5α-reductase into another androgenic steroid, 5α-dihydrotestosterone (DHT), in various target tissues, including the external genitalia. In these tissues, DHT is responsible for induction of secondary male characteristics such as facial and body hair and growth of the prostate. Later in life, DHT is the culprit in male pattern baldness.

Disorders of Steroid Hormone Biosynthesis Affect Sexual Differentiation

As one can imagine, mutations in genes encoding enzymes involved in steroid hormone biosynthesis have far-reaching consequences. The resulting phenotypes dramatically illustrate both the organizational and activational effects of steroid hormones, as well as the difficulty of neatly distinguishing the two. Here, we describe three disorders (Table 51–1).

The first, congenital adrenal hyperplasia (CAH), is a genetic deficiency in the synthesis of corticosteroids by the adrenal glands that results in overproduction of testosterone and related androgens. This condition is autosomal recessive and occurs once in 10,000 to 15,000 live births. In girls born with CAH, excess androgens lead to some masculinization of the external genitalia, a process called *virilization*. Virilization clearly reflects the organizational roles of steroids. This condition can be diagnosed at birth and resolved by surgical intervention. Treatment with corticosteroids reduces testosterone levels, permitting these females to undergo puberty and become fertile.

A second genetic disorder, 5α-reductase II deficiency, can also affect sexual differentiation. In male fetuses, 5α-reductase II is expressed at high levels in the precursor of the external genitalia, where it converts circulating testosterone into DHT. The high local concentrations of DHT virilize the external genitalia. Clinical 5α-reductase II deficiency is inherited in an autosomal recessive manner, and males present at birth with ambiguous (under-virilized) or overtly feminized external genitalia. In many instances, therefore, chromosomally male patients (XY) with this condition are mistakenly raised as females until puberty, at which time the large increase in circulating testosterone virilizes the body hair, musculature, and, most dramatically, the external genitalia.

The critical role of steroid receptors in controlling sexual differentiation is well illustrated by patients

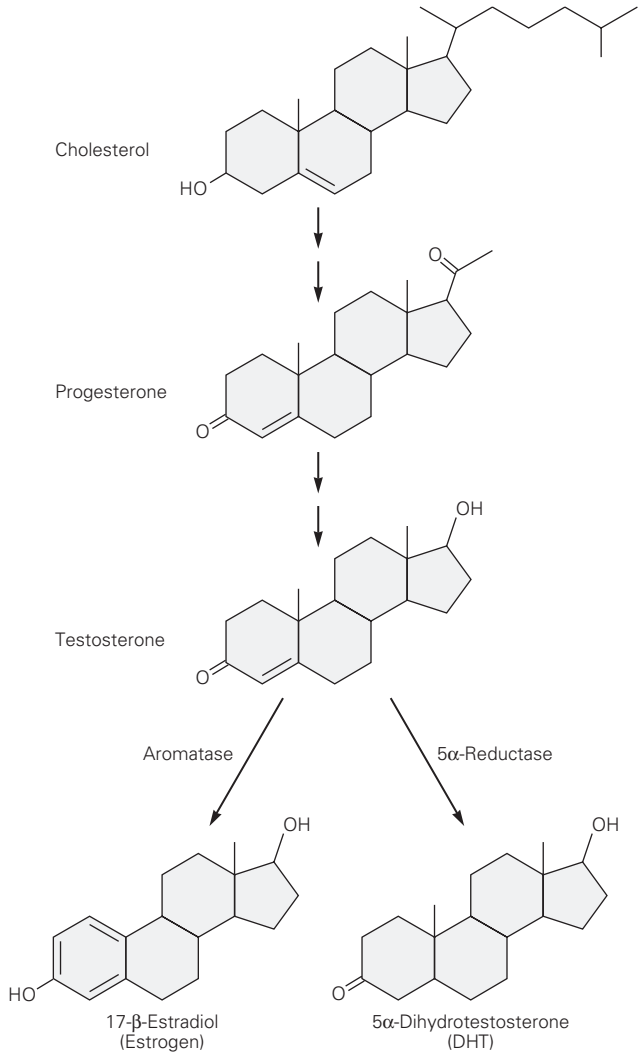

Figure 51–3 Steroid hormone biosynthesis. Cholesterol is the precursor of all steroid hormones and is converted via a series of enzymatic reactions into progesterone and testosterone. Testosterone or related androgens are obligate precursors of all estrogens in the body, a conversion that is catalyzed by aromatase. The expression of 5α-reductase in target tissues converts testosterone into dihydrotestosterone, an androgen.

with a third disorder, complete androgen insensitivity syndrome (CAIS). Testosterone, estrogen, and progesterone are hydrophobic molecules that are able to diffuse across cell membranes, enter the bloodstream, enter cells in many organs, and bind to intracellular ligand-specific receptors. The receptors for these hormones are encoded by distinct but homologous genes.

A single gene encodes a receptor that binds the androgens testosterone and DHT. The androgen receptor binds DHT approximately three-fold more tightly than testosterone, accounting for the greater potency of DHT. There is also a single receptor for progesterone (progesterone receptor), whereas two genes encode receptors that bind estrogens (estrogen receptors α and β). These steroid hormone receptors are present in many tissues of the body, including the brain (Figure 51–4B).

These receptor proteins are transcription factors that bind specific sites in the genome and modulate transcription of target genes. They contain several signature motifs, including a hormone-binding domain, a DNA-binding domain, and a domain that modulates the transcriptional activity of target genes (Figure 51–5A). Hormones activate the transcriptional activity by binding to the receptor. In the absence of ligand, the receptors bind to protein complexes that sequester them in the cytoplasm. Upon binding of ligand, the receptors dissociate from the complex and enter the nucleus, where they dimerize and bind to specific sequence elements in the promoter and enhancer regions of target genes, modulating their transcription (Figure 51–5B).

Patients with CAIS are chromosomally XY but carry a loss-of-function allele of the X-linked androgen receptor that abolishes cellular responses to testosterone and DHT. Because the pathway of sex determination via *SRY* remains functional, these patients have testes. However, because of deficient androgen signaling, the Wolffian ducts do not develop, the testes fail to descend, and the external genitalia are feminized. In adulthood, most of these patients opt for surgical removal of the testes and hormonal supplementation appropriate for females.

Sexual Differentiation of the Nervous System Generates Sexually Dimorphic Behaviors

Sex-specific behaviors occur because the nervous system differs between males and females. These differences arise from a combination of genetic factors, such as signaling pathways initiated by sex determination, as well as environmental factors, such as social experience. In many cases, both genetic and environmental inputs act through the steroid hormone system to sculpt the nervous system. Many instances of sexual dimorphism have been documented, including differences in the numbers and size of neurons in particular structures, differences in gene expression in various neuronal groups, and differences in the pattern and number of connections. Here, we examine a few cases in which studies in experimental animals have provided insights. In later sections, we ask whether similar

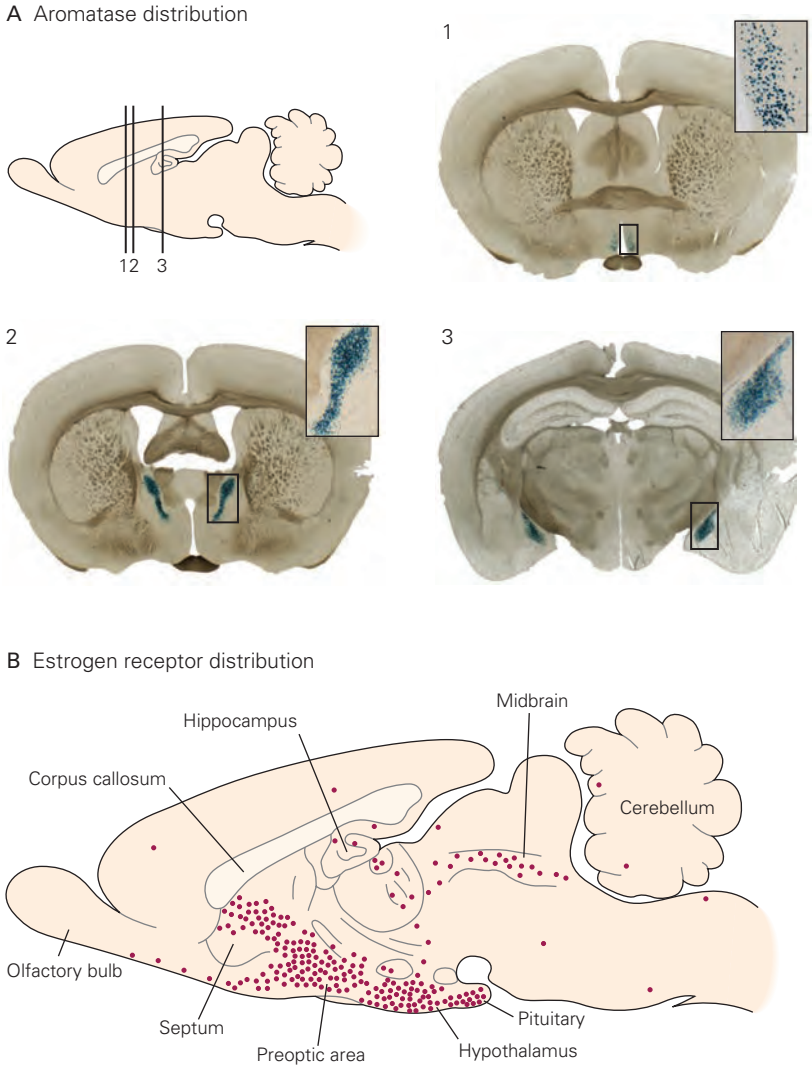

Figure 51–4 Aromatase and estrogen receptors are expressed in specific regions of the brain.

A. The enzyme aromatase catalyzes the conversion of testosterone into estrogen (Figure 51–3) and is expressed in discrete neuronal populations in the brain. The distribution of aromatase-expressing neurons labeled with a reporter protein (**blue**) in transgenic mice is shown here in three coronal planes of the brain: in neurons in the preoptic hypothalamus (**1**), in the bed nucleus of the stria terminalis (BNST) (**2**), and in the medial amygdala (**3**). These areas contain sexually dimorphic neurons that regulate sexual behavior, aggression, and maternal behaviors. (Adapted, with permission, from Wu et al. 2009.)

B. This midsagittal section of an adult rat brain shows binding of estrogen to cells in various hypothalamic regions, including the sexually dimorphic preoptic area. Additional estrogen binding is seen in the septum, hippocampus, pituitary, and midbrain. Other, more lateral areas such as the amygdala (not shown) also contain estrogen receptors.

Table 51–1 Three Clinical Syndromes That Highlight the Role of Androgens in Masculinization in Humans

	Complete androgen insensitivity syndrome (CAIS)	**5α-Reductase II deficiency**	**Congenital adrenal hyperplasia (CAH)**
Chromosomal sex	XY	XY	XX
Molecular basis	Nonfunctional androgen receptor, leading to inability to respond to circulating androgens	Nonfunctional 5α-reductase II, leading to deficit in conversion of testosterone to 5α-dihydrotestosterone (DHT) in target tissues	Defect in corticosteroid synthesis, leading to increase in circulating androgens from the adrenals
Gonad	Testis	Testis	Ovary
Wolffian derivatives	Vestigial	Present	Absent
Müllerian derivatives	Absent	Absent	Present
External genitalia			
At birth	Feminized	Variably feminized	Variably virilized
After puberty	Feminized	Masculinized	Feminized
Gender identity	Female	Female or male	Female or male
Sexual partner preference	Male	Female or male	Female or male

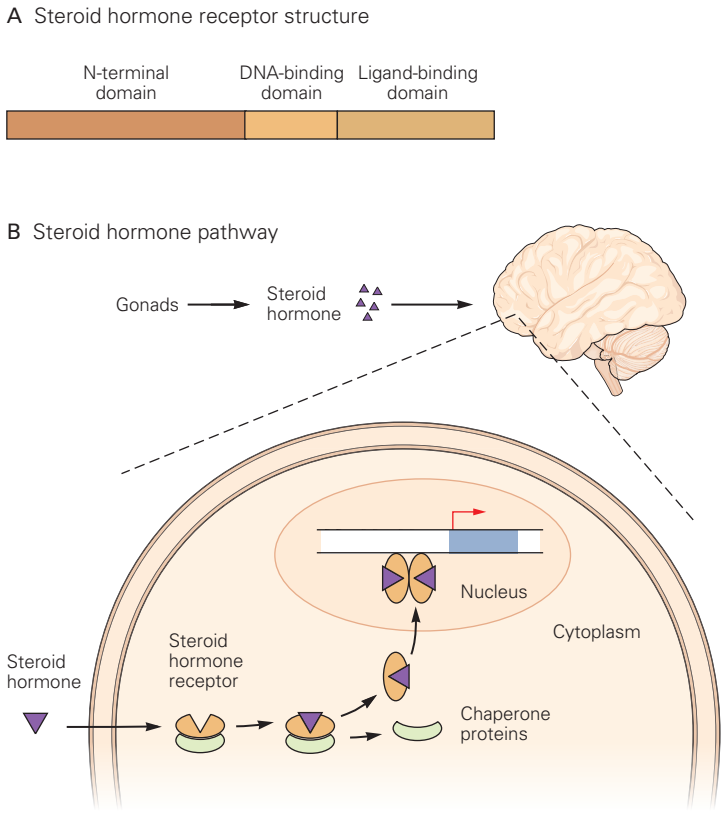

Figure 51–5 Steroid hormone receptors and their mechanism of action.

A. The canonical receptors for steroid hormones are ligand-activated transcription factors. These receptors have an N-terminal domain, which contains a transcriptional transactivator domain; a central DNA-binding domain; and a C-terminal ligand-binding domain, which may contain an additional transcriptional transactivator domain.

B. Sex steroid hormones are hydrophobic and enter the circulation by diffusing across the plasma membrane of steroidogenic cells in the gonads. They enter target cells in distant tissues such as the brain by passing through the plasma membrane and bind their cognate receptors. The steroid hormone receptor typically exists in a multiprotein complex with chaperone proteins in the cytoplasm of hormone-responsive cells. Ligand-binding promotes dissociation of the receptor from the chaperone complex and translocation into the nucleus. In the nucleus, the receptor is thought to bind to hormone response elements as a homodimer to modulate transcription of target genes. (Adapted from Wierman 2007.)

mechanisms underlie sexually dimorphic behaviors in humans.

However, before proceeding, we note that the ways in which chromosomal mechanisms of sex determination are linked to the cellular processes of sexual differentiation in the central nervous system vary widely among species. In insects, sex differences in behavior are independent of hormonal secretion from the gonads, and instead rely exclusively on a sex determination pathway within individual neurons. This mode of sexual differentiation of the brain and behavior is particularly well understood in the fruit fly, where it has been demonstrated that the sex determination cascade initiates expression of a transcription factor, fruitless (Fru), that specifies much of the repertoire of male sexual behaviors (Box 51–1).

Erectile Function Is Controlled by a Sexually Dimorphic Circuit in the Spinal Cord

The lumbar spinal cord of many mammals, including humans, contains a sexually dimorphic motor center, the spinal nucleus of the bulbocavernosus (SNB). Motor neurons in the SNB innervate the bulbocavernosus muscle, which plays an important part in penile reflexes in males and vaginal movements in females.

In adult rats, the male SNB contains many more motor neurons than the female SNB. In addition, male SNB motor neurons are larger in size and have larger dendritic arbors, with a corresponding increase in the number of synapses they receive. Like the SNB motor neurons, the bulbocavernosus muscle is larger in males than females; it is completely absent in the females of some mammalian species. SNB motor neurons also innervate the levator ani muscle, which is involved in copulatory behavior and is also larger in males than females.

How do these differences arise? Initially, the circuit is not sexually dimorphic. At birth, male and female rats have similar numbers of neurons in the SNB and similar numbers of fibers in the bulbocavernosus and levator ani muscles. In females, however, many motor neurons in the SNB and many fibers in the bulbocavernosus and levator ani muscles die in early postnatal life. Thus, this sexual dimorphism arises not by male-specific generation of cells, but rather by female-specific cell death (Figure 51–7A).

Perinatal injections of testosterone or DHT can rescue a significant number of the dying neurons and muscle fibers in the female rat. Conversely, treatment of male pups with an androgen receptor antagonist increases the number of dying neurons and muscle fibers. So at a deeper level, we see that the dimorphism results from male-specific preservation of motor neurons and muscle fibers that would die in the absence of hormone.

Where does testosterone act to establish this structural dimorphism? Is it primarily a survival factor for the motor neurons, with muscle fibers dying secondarily because they lose their innervation? Or does testosterone act on muscles, which then provide a trophic factor to support the survival of SNB motor neurons? This issue has been examined in rats carrying a mutation of the androgen receptor (*tfm* allele) that reduces binding of ligand to 10% of normal. The receptor resides on the X chromosome, so all males that carry a mutant gene on their one and only X chromosome are feminized and sterile. For female heterozygotes, the situation is more complicated. As described earlier, one of the X chromosomes is randomly inactivated in each XX female.

Female heterozygotes are therefore mosaics: Some cells express a functional androgen receptor allele, others the mutated allele. Each muscle fiber has many nuclei, so most bulbocavernosus muscle fibers in the heterozygous female express functional androgen receptors. Motor neurons have a single nucleus, however, so each neuron is either normal or receptor-deficient. If androgen receptors were required in the neuron, one would expect only receptor-expressing SNB motor neurons to survive, whereas if receptors were required only in muscles, one would expect surviving motor neurons to be a mixture of wild type and mutant.

In fact, the latter situation occurs, indicating that survival of SNB motor neurons does not depend on a neuron-autonomous function of the androgen receptor. Rather, these neurons receive a trophic cue from the androgen-dependent bulbocavernosus and the levator ani muscles (Figure 51–7A). These cues may include the ciliary neurotrophic factor (CNTF) or a related molecule, because mutant male mice lacking a CNTF receptor exhibit a decreased number of SNB motor neurons, typical of females.

Male and female SNB motor neurons also differ in size. Androgens determine the differences in number and size of these neurons in different ways. Studies of *tfm* mutants showed that androgens exert an organizational effect during early postnatal life through a direct effect on muscle. Low levels of androgens during this critical period lead to an irreversible reduction in the number of SNB motor neurons. Later, androgens act directly on SNB motor neurons to increase the extent of their dendritic arbors. A loss of circulating testosterone, such as that occurring after castration, leads to a dramatic pruning of dendritic arbors; injection of supplemental testosterone to a castrated male rat can restore this dendritic branching pattern (Figure 51–7B). This effect persists in adulthood and is reversible, so it can be viewed as an activational influence. Thus, androgens can exert diverse effects, even on a single neuronal type.

Song Production in Birds Is Controlled by Sexually Dimorphic Circuits in the Forebrain

Several species of songbirds learn species-specific vocalizations that are used for courtship rituals and territorial marking (Chapter 55). A set of interconnected brain nuclei controls the learning and production of birdsong (Figure 51–8A). In some songbird species, both sexes sing and the structure of the song circuit is similar in males and females. In other species, such as zebra finches and canaries, males alone sing. In these species, several song-related nuclei are significantly larger in the male than in the female.

The development of sexual dimorphism in song circuitry has been studied in detail in the zebra finch. The robust nucleus of the archistriatum (RA) in the adult male zebra finch contains five times as many neurons as the same nucleus in females. In addition, the afferent projections to RA exhibit a striking sexual dimorphism—only in males does the RA receive input from high vocal centers (HVCs) (Figure 51–8B). These sex differences in cell number and connectivity of RA are not evident until after hatching, when in females a large number of RA neurons die and in males the axons of HVC neurons enter the RA nucleus.

These sexually dimorphic anatomical features are regulated by steroid hormones. When females are supplied with estrogen (or an aromatizable androgen such as testosterone) after hatching, the number of neurons in the RA and the termination pattern in the nucleus are similar to that of the male. However, early hormone administration to young females is not sufficient to masculinize the song nuclei to a size comparable to that of adult males, nor is it sufficient to induce singing in females. To achieve these functions, female birds that receive testosterone or estradiol after hatching must also receive testosterone or dihydrotestosterone (but not estrogen) as adults. Thus, steroids play both organizational and activational roles in this system as well.

Box 51–1 Genetic and Neural Control of Mating Behavior in the Fruit Fly

In the presence of a female fruit fly, the adult male fly engages in a series of essentially stereotyped routines that usually culminate in copulation (Figure 51–6A). This elaborate male courtship ritual is encoded by a cascade of gene transcription within the brain and peripheral sensory organs that masculinizes the underlying neural circuitry.

Sex determination in the fly does not depend on gonadal hormones as it does in vertebrates. Instead, it occurs cell autonomously throughout the body. In other words, sexual differentiation of the brain and the rest of the body is independent of gonadal sex. The male-specific Y chromosome of fruit flies does not bear a sex-determining locus. Instead, sex is determined by the ratio of X chromosome number to autosome number (X:A). A ratio of 1 is determinative for female differentiation, whereas a ratio of 0.5 drives male differentiation.

The X:A ratio sets into motion a cascade of gene transcription and alternative splicing programs that leads to the expression of sex-specific splice forms of two genes, *doublesex* (*dsx*) and *fruitless* (*fru*). The *dsx* gene encodes a transcription factor that is essential for sexual differentiation of the nervous system and the rest of the body, with the sex-specific splice variants responsible for male- and female-typical development.

The *fru* gene encodes a set of putative transcription factors that are generated by multiple promoters and alternative splicing. In males, one particular mRNA (fru^M) is translated into functional proteins. In female flies, alternative splicing results in the absence of such proteins.

Males carrying a genetically modified *fru* allele that can only be spliced in the female-specific manner (fru^F) have essentially normal, *dsx*-dependent sexual differentiation. These fru^F males therefore resemble wild type males externally. However, the loss of Fru^M in these animals abolishes male courtship behavior directed toward females. These data indicate that Fru^M is required for male courtship and copulation.

Conversely, transgenic female flies carrying a fru^M allele exhibit male mating behavior toward wild type females, indicating that fru^M is sufficient to inhibit female sexual responses and promote male mating.

Intriguingly, fru^F males do not court females and, like wild type females, do not reject mating attempts by wild type males or fru^M females. Similarly, fru^M females attempt to mate with both fru^M and wild type females. These data suggest that fru^M may also specify sexual partner preference, which in the case of wild type males would be directed to females.

In wild type females without fru^M, the neural pathways are wired such that these flies exhibit sexually receptive behaviors toward males. When groups of fru^F males (or fru^M females) are housed together, they court each other vigorously, often forming long chains of flies attempting copulation.

To build the circuitry underlying male courtship rituals, fru^M appears to initiate cell-autonomous male-typical differentiation of the neurons in which it is expressed. This leads to overt neuroanatomic dimorphism in cell number or projections of many classes of neurons (Figure 51–6B). Some neurons that express fru^M are not distributed in dimorphic patterns. In these neurons, fru^M may regulate the expression of particular classes of genes whose products drive a male-specific program of physiology and function.

Are neurons that express fru^M required for male courtship behavior? When synaptic transmission is genetically blocked in these neurons in adult males, all components of courtship behavior are abolished. Importantly, these males continue to exhibit normal movement, flight, and other behaviors in response to visual and olfactory stimuli. These findings demonstrate that fru^M appears to be expressed in a neural circuit that is essential for and dedicated to male fly courtship.

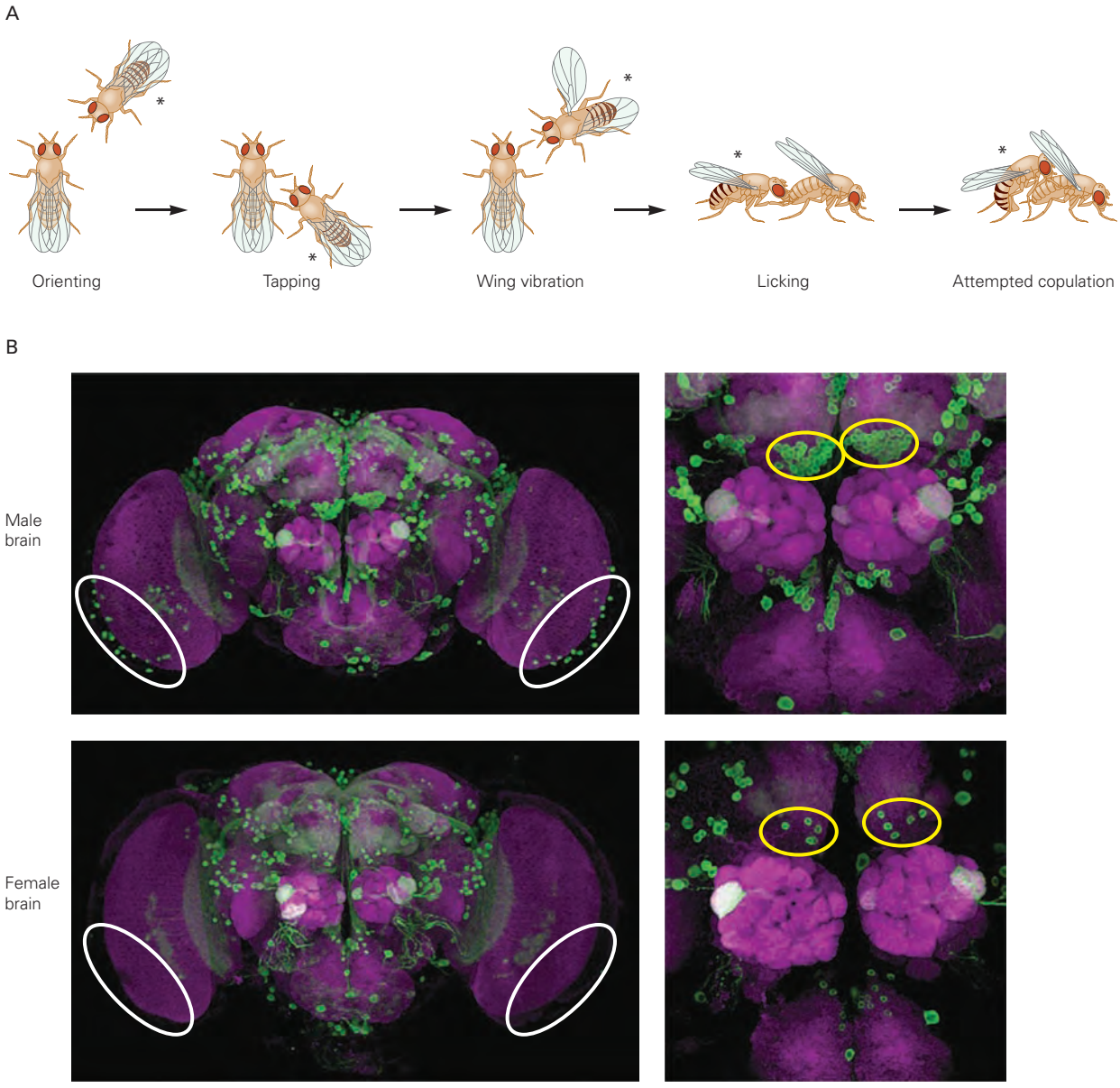

Figure 51–6 Control of male courtship in the fruit fly *Drosophila melanogaster.*

A. Male flies (labeled with **asterisk**) engage in a stereotyped sequence of behavioral routines that culminate in attempted copulation. The male fly orients toward the female and then taps her with his forelegs. This is followed by wing extension in the male and a species-specific pattern of wing vibrations that is commonly referred to as the fly courtship song. If the female fly is sexually receptive, she slows down and permits the male to lick her genitalia. The female then opens her vaginal plates in order to allow the male to initiate copulation. All steps in the male mating ritual require the expression of a sex-specific splice variant of the *fruitless* (*fru*) gene. (Adapted, with permission, from Greenspan and Ferveur 2000.)

B. The *fru* gene encodes a male-specific splice variant that is necessary and sufficient to drive most steps in the male fly courtship ritual. *Fru* expression is visualized using a fluorescent reporter protein (**green**) in transgenic flies. Neuronal clusters that express *Fru* are present in comparable numbers in the central nervous system of both male and female flies. However, there are regional sex differences in *Fru* expression. A cluster of *Fru*-expressing neurons is present in the male optic lobes (in the area within the **white ellipses**) but absent in the corresponding regions in the female brain. The two male antennal lobe regions (areas within **yellow ellipses**) contain about 30 neurons each, whereas each female region has only four to five neurons. (Adapted, with permission, from Kimura et al. 2005.)

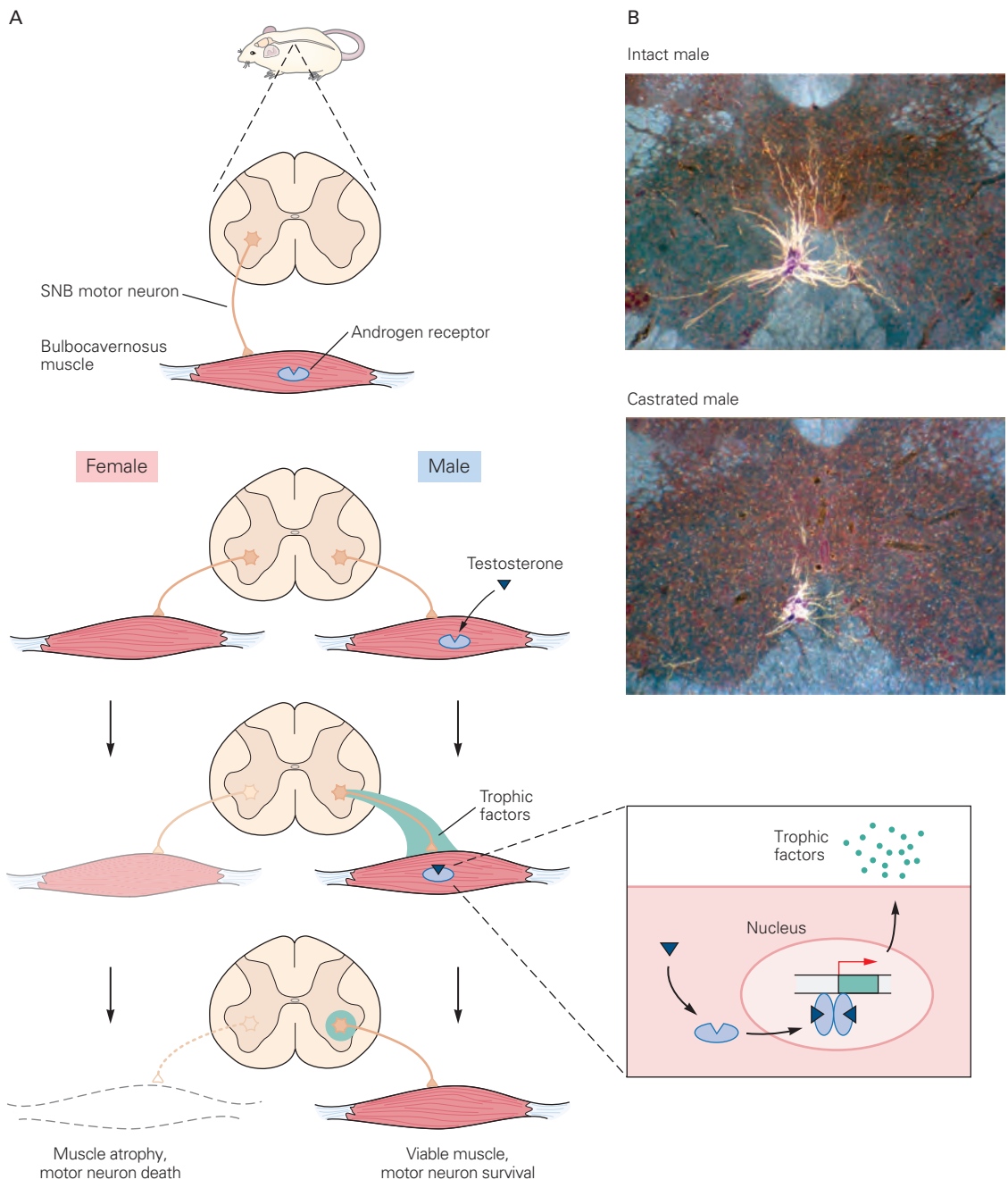

Figure 51–7 Sexual dimorphism in the spinal nucleus of the bulbocavernosus muscle in the rat.

A. The spinal nucleus of the bulbocavernosus (**SNB**) is found in the male lumbar spinal cord but is greatly reduced in the female. The motor neurons of the nucleus are present in both sexes at birth, but the lack of circulating testosterone in females leads to death of the SNB neurons and their target muscles. It is thought that testosterone in the male circulation promotes the survival of the target muscles, which express the androgen receptor. In response to testosterone, the muscles provide trophic support to the innervating SNB neurons. This muscle-derived survival factor is likely to be ciliary neurotrophic factor or a related member of the cytokine family. Thus, testosterone acts on muscle cells to control the sexual differentiation of SNB neurons. (Reproduced, with permission, from Morris, Jordan, and Breedlove 2004. Copyright © 2004 Springer Nature.)

B. Dendritic branching of SNB neurons is regulated by circulating testosterone in adult male rats. In males, the dendrites arborize extensively within the spinal cord (**upper photo**). The fact that the arbors are pruned in adult castrated male rats (**lower photo**) is evidence that this dendritic branching depends on androgens. The spinal cord is shown in transverse section, and the SNB neurons and their dendrites are labeled by a retrograde tracer injected into target muscles. (From Cooke and Woolley 2005. Reproduced, with permission from D. Sengelaub.)

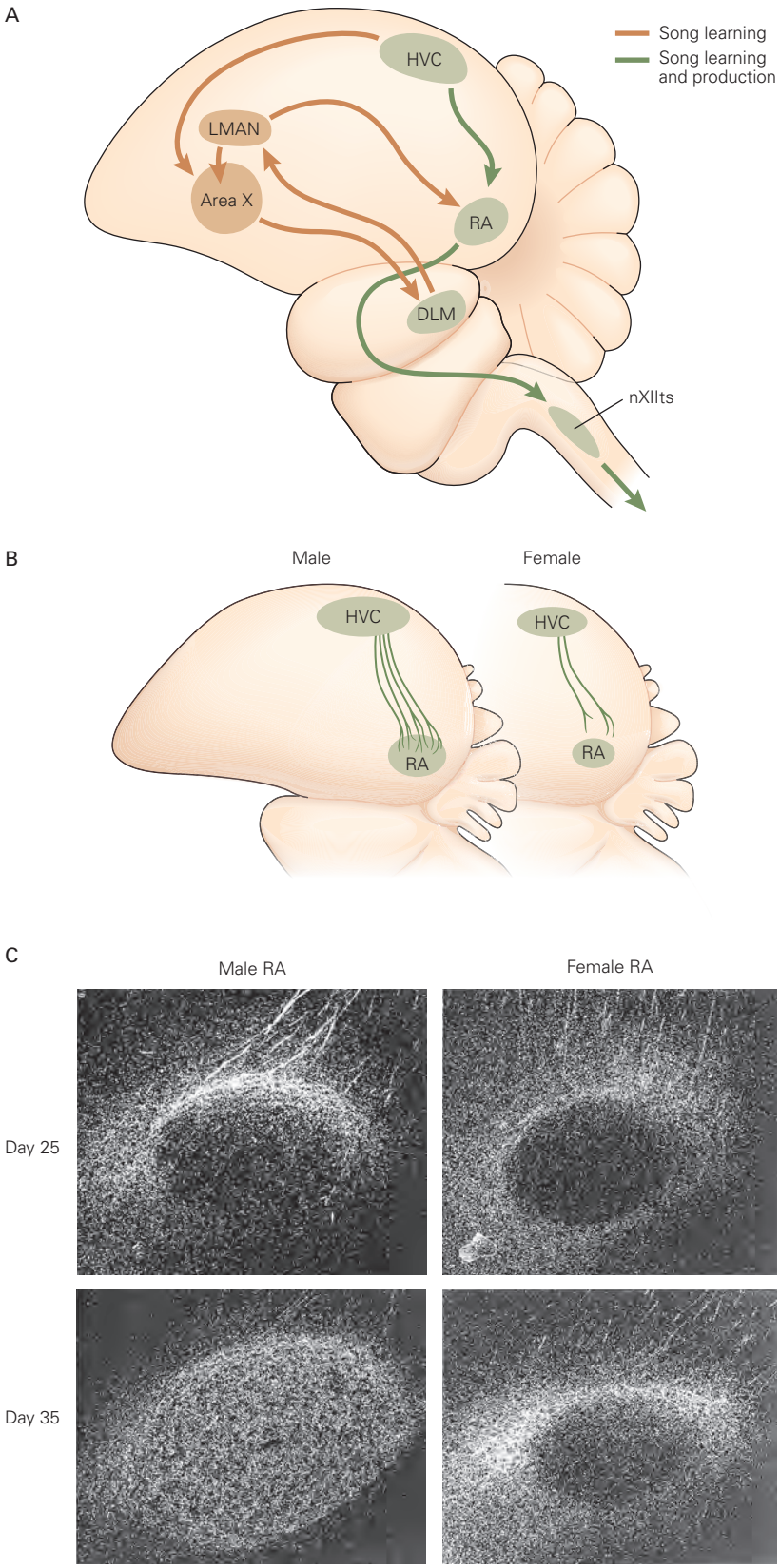

Figure 51–8 Sexual dimorphism in the avian song circuit.

A. Songbirds have a dedicated neural circuit for song production and learning, with distinct components contributing to learning or production. Many of these components are sexually dimorphic in songbirds in which only one sex sings. For example, in zebra finches, only the male sings, and the male high vocal center (**HVC**), robust nucleus of the archistriatum (**RA**), lateral magnocellular nucleus of the anterior neostriatum (**LMAN**), and area X are larger in volume and contain more neurons than the comparable regions in the female. (Abbreviations: **DLM**, medial nucleus of the dorsolateral thalamus; **nXIIts**, hypoglossal nucleus.) (Reproduced, with permission, from Brainard and Doupe 2002. Copyright © 2002 Springer Nature.)

B. In the male, the axons of HVC neurons terminate on neurons in the RA nucleus, whereas in females, the axons terminate in a zone surrounding the nucleus. The sexual dimorphism in cell number and connectivity of these regions is regulated by estrogen. (Reproduced, with permission, from Morris, Jordan, and Breedlove 2004. Copyright © 2004 Springer Nature.)

C. The pattern of termination of the axons of HVC neurons in the RA nucleus varies in males and females at different ages after hatching. (Reproduced, with permission, from Konishi and Akutagawa 1985. Copyright © 1985 Springer Nature.)

Mating Behavior in Mammals Is Controlled by a Sexually Dimorphic Neural Circuit in the Hypothalamus

In many mammalian species, the preoptic region of the hypothalamus and a reciprocally connected region, the bed nucleus of the stria terminalis (BNST), play important roles in sexually dimorphic mating behaviors (Chapter 41; Figure 51–4). In male rodents and monkeys, these areas are activated during mating behavior; surgical lesions that ablate the preoptic region or the BNST result in deficits in male sexual behavior in male rodents and, in the case of preoptic lesions, disinhibit female-type sexual receptivity in males.

Both the preoptic hypothalamus and the BNST are sexually dimorphic, containing more neurons in males compared to females. The sexually dimorphic nucleus of the preoptic area (SDN-POA) also contains significantly more neurons in the male. A male-specific perinatal surge of testosterone promotes survival of neurons in the SDN-POA and BNST, whereas in females, these same cells gradually die off in the early postnatal period. This development is similar to that in the sexually dimorphic nuclei of the rodent spinal cord and the songbird brain, suggesting that androgen control is a common mechanism for production of sex differences in the size of neuronal populations.

Curiously, the ability of brain testosterone to promote the survival of neurons is likely to be exerted via aromatization into estrogen and subsequent activation of the estrogen receptors (see Figures 51–3 and 51–4). How then is the neonatal female brain shielded from the effects of circulating estrogen? In newborn females, there is very little estrogen in the circulation, and the small amount present is easily sequestered by binding to α-fetoprotein, a serum protein. This explains why female mice lacking α-fetoprotein exhibit male-typical behaviors and reduced female-typical sexual receptivity. In this case, then, structural sexual dimorphism does not result from differential effects of androgens and estrogens, but rather from sex differences in the level of hormone available to the target tissue.

Environmental Cues Regulate Sexually Dimorphic Behaviors

Sex-specific behaviors are usually initiated in response to sensory cues in the environment. There are many such cues, and different species use distinct sensory modalities to elicit similar responses. Courtship rituals can be triggered by species-specific vocalizations, visual signals, odors, and even, in the case of weakly electric fish, by electric discharges. Recent genetic and molecular studies have led to significant insight into how sensory experience controls some of these behaviors in rodents. Here, we discuss two examples: the regulation of partner choice by pheromones and the regulation of maternal behavior by experience during infancy.

Pheromones Control Partner Choice in Mice

Many animals rely on their sense of smell to move about, obtain food, and avoid predators. They also rely on pheromones—chemicals that are produced by an animal to affect the behavior of another member of the species. In rodents, pheromones can trigger many sexually dimorphic behaviors, including mate choice and aggression.

Pheromones are detected by neurons in two distinct sensory tissues in the vertebrate nose: the main olfactory epithelium (MOE) and the vomeronasal organ (VNO) (Figure 51–9A). It is thought that sensory neurons in the MOE detect volatile odors, whereas those in the VNO detect nonvolatile chemosensory cues. Removal of the olfactory bulb, the only synaptic target of neurons in the MOE and the VNO, abolishes mating as well as aggression in mice and other rodents. These and other studies indicate an essential role for olfactory stimulation in initiating mating and fighting.

Genetically engineered disruption of pheromone responsiveness in the MOE or VNO reveals that these sensory tissues have a surprisingly complex role in the mating behavior of mice. A functional MOE is essential to trigger male sexual behavior, and an intact VNO is required for sex discrimination and directing the male to mate with females.

Key to these experiments is the fact that olfactory neurons in the MOE and the VNO use different signal transduction cascades to convert olfactory input into electrical responses. The cation channel Trpc2 appears essential for pheromone-evoked signaling in VNO neurons; it is not expressed in MOE neurons, which use a different signal transduction apparatus. Thus, mice lacking the gene *trpc2* have a nonfunctional VNO and an intact MOE. Mating behavior directed to animals of the opposite sex appears unaltered in *trpc2* mutant males as well as females.

However, both male and female *trpc2* mutants often exhibit male sexual behavior with members of either sex. For example, *trpc2* mutant females mate with females in a manner seemingly indistinguishable from wild type males, except of course the females cannot ejaculate. These and other findings suggest that the VNO is used to discriminate among sexual partners.

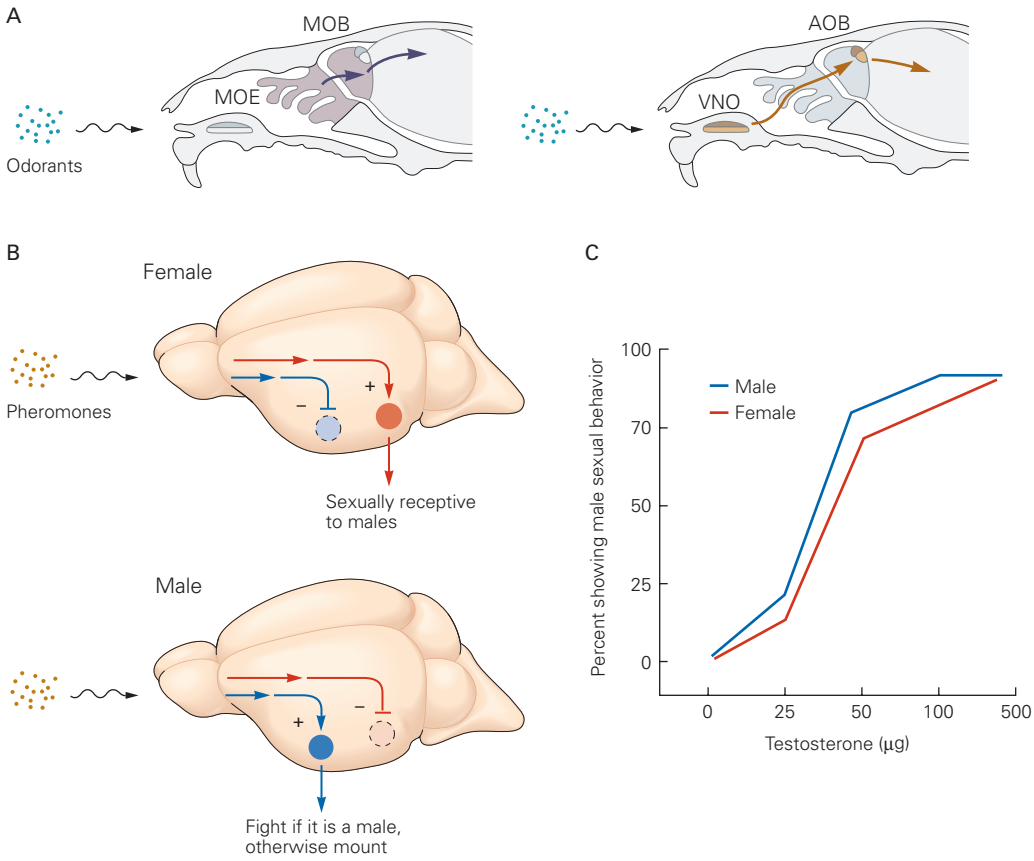

Figure 51–9 Pheromonal and hormonal control of sexually dimorphic behavior in mice.

A. Odorants are detected by sensory neurons in the main olfactory epithelium (**MOE**), which projects to the main olfactory bulb (**MOB**), and by neurons in the vomeronasal organ (**VNO**), which projects to the accessory olfactory bulb (**AOB**). Many of the central connections of the MOE and VNO pathway are anatomically segregated. (Adapted, with permission, from Dulac and Wagner 2006.)

B. Female mice possess the neural circuitry that can activate either male (**blue**) or female (**red**) mating behaviors. In wild type females, pheromones activate female mating behavior and inhibit male-type mating. By contrast, in males, pheromones activate a circuitry that will initiate fights with males and mating with females. (Adapted, with permission, from Kimchi, Xu, and Dulac 2007.)

C. Testosterone activates male sexual behavior in male and female mice. The data are from a study in which the gonads of male and female mice were surgically removed in adulthood. None of the animals exhibited male sexual behavior with wild type females following surgery. After administration of testosterone, mating behavior was restored in castrated males, and females displayed male sexual behavior. This effect was dose-dependent; at the highest dose, male and female mice exhibited comparable levels of male-type mating behavior toward wild type females. (Adapted, with permission, from Edwards and Burge 1971. Copyright © 1971 Springer Nature.)

When the VNO is inactivated, animals can no longer distinguish between males and females, and mutants therefore exhibit male sexual behavior toward members of both sexes. Similarly, adult wild type females treated with testosterone also exhibit male sexual behavior toward females (Figure 51–9C).

One implication of these studies is that female mice possess the neural circuitry for male sexual behavior (Figure 51–9B). Activation of this neural circuit is inhibited in wild type females by sensory input from the VNO and by the lack of testosterone. Removal of the VNO or administration of testosterone activates male sexual behavior in females. Male pattern mating behavior has been observed in females of many species, indicating that the findings in mice are likely to be of general relevance. Thus, neural pathways for male sexual behavior appear to be present in both sexes. Similarly, the female-typical behavior of male rats following hypothalamic lesions suggests that the neural pathway for female sexual behavior also exists in the

male brain. In such cases, it is the differential regulation of these circuits that underlies the sexually dimorphic expression of male and female sexual behaviors.

Early Experience Modifies Later Maternal Behavior

The preoptic area of the hypothalamus and the BNST are also important for another set of sexually dimorphic behaviors in females. Nursing rodents are good mothers, building a nest for their litter, crouching over the pups to keep them warm, and returning the pups to the nest when they happen to crawl away. Surgical lesioning or experimental stimulation of the preoptic region abolishes or activates these maternal behaviors, respectively.

Studies of these behaviors have shed light on variations among individual females and how these differences exert lifelong effects on behavior of the offspring. Female lab rats exhibit distinct, stable forms of maternal care: Some lick and groom (LG) their pups frequently (high-LG mothers), whereas others lick and groom less frequently (low-LG mothers). Female offspring of high-LG mothers display high-LG activity when they themselves become mothers compared to female offspring of low-LG mothers (Figure 51–10). Moreover, pups of high-LG mothers show less anxiety-like behaviors in stressful conditions than do the pups of low-LG mothers.

These results suggested that levels of licking and grooming behavior and stress responses are genetically determined. However, studies by Michael Meaney and his colleagues provide an alternative explanation. When female rat pups are transferred from

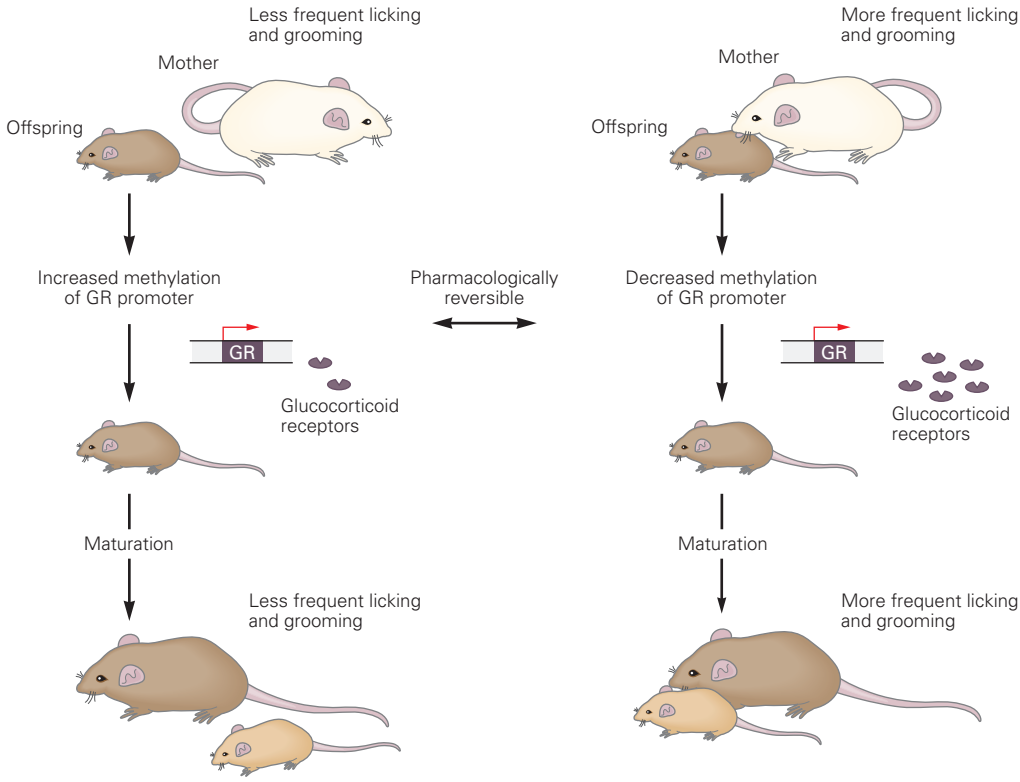

Figure 51–10 Epigenetic regulation of maternal behavior in rats. In a common lab rat strain, different mothers lick and groom their pups at low or high frequencies, resulting in distinct epigenetic modifications at the glucocorticoid receptor (**GR**) promoter. Mothers that lick and groom at high frequency raise progeny with low levels of DNA methylation at the GR promoter, resulting in higher levels of GR expression in the hippocampus. Females raised by these mothers exhibit higher frequencies of licking and grooming behavior with their own pups. Mothers that lick and groom at low frequency raise progeny with high DNA methylation levels at the GR promoter and lower levels of hippocampal GR expression. Females nursed by these mothers subsequently exhibit similar low levels of licking and grooming of their pups. Pharmacological reversal of the epigenetic modifications at the GR promoter results in a corresponding change in both GR expression and maternal behavior. (Adapted from Sapolsky 2004.)

their mother to a foster mother at birth, their maternal behavior and stress responses as adults resemble those of their foster mother rather than those of their biological mother. Thus, experience in infancy can lead to lifelong behavioral patterns. Because these patterns impact maternal behavior, their influence can endure over many generations.

How does brief and early experience lead to such long-lasting changes? One mechanism involves a covalent modification of the genome. Stress responses are coordinated by glucocorticoids acting on glucocorticoid receptors in the hippocampus. Throughout life, tactile stimulation, including grooming, leads to transcriptional activation of the glucocorticoid receptor gene, which ultimately leads to reduced release of hypothalamic hormones that trigger stress responses. Tactile stimulation during early life also regulates the glucocorticoid receptor gene in a second way. A key site in the glucocorticoid receptor gene is methylated by the enzyme DNA methyltransferase, leading to gene inactivation. Initially, gene methylation occurs in all pups, but pups reared by high-LG mothers are selectively demethylated. Thus, in animals reared by high-LG mothers, the effects of adult experience are potentiated. This is an example of epigenetic modification by which genes can be turned on or off more or less permanently. These animals exhibit blunted behavioral responses to stressful stimuli later in life.

What are the biological links between early experience and behavioral variation? A peptide hormone, oxytocin, plays a major role. Classic work showed that oxytocin regulates provision of milk by the mother, which occurs via reflex ejection in response to suckling (milk let-down). Oxytocin is synthesized by neurons in the hypothalamus and released into the general circulation through their projections in the posterior pituitary. It elicits smooth muscle contraction in the mammary gland, resulting in milk ejection. Oxytocin release from the pituitary is controlled by suckling, which provides a sensory stimulus that is conveyed to the hypothalamus by spinal afferent nerves.

Oxytocin and a related polypeptide hormone vasopressin also play important roles in regulating maternal bonding and other social behaviors (Chapter 2). In these cases, experience appears to modulate behaviors by affecting both release of oxytocin and levels of the oxytocin receptor in specific brain areas. In both rats and voles, individual differences in the care females provide their offspring correlate with variations in oxytocin receptor level in specific brain areas. Especially noteworthy is that oxytocin receptor levels in several regions are higher in female offspring reared by high-LG mothers than in female progeny of low LG-mothers. Thus, sensory stimulation may affect activity of these polypeptide hormone systems, which in turn regulate maternal and other social behaviors.

A Set of Core Mechanisms Underlies Many Sexual Dimorphisms in the Brain and Spinal Cord

In the previous few sections, we described neural circuits that regulate several sexually dimorphic behaviors. Can we discern any common themes?

A variety of sexually dimorphic neural circuits, or wiring diagrams, can in principle generate sex differences in behavior (Figure 51–11). Although it is challenging to trace the chain of causality from genetic factors to dimorphic circuits to sex-specific behaviors, there are a few general possibilities. In one, a neural circuit, from sensory input to motor output, might be unique to one sex. In fact, this alternative is seldom encountered. Most behaviors are shared between the sexes, and even behaviors such as feeding, maternal retrieval of a pup by the scruff of its neck, or biting (during territorial scuffles between males) all call upon similar jaw movements. Consistent with this commonality, it appears that most sexual dimorphisms in behavior arise from sex differences in key neuronal populations within common circuits. The activity and connectivity of these populations alter behavioral output in a male- or female-typical manner.

Estrogen can act not only during development but also in adults to periodically reconfigure presynaptic connectivity within a hypothalamic neural circuit, ensuring that female mice only mate when they are ovulating and fertile. These studies paint a picture of dynamic neural circuits in the female brain: Wiring diagrams are plastic and responsive to hormonal changes across the estrous cycle, which is analogous to the menstrual cycle in humans. Similarly, estrogen also exerts cycle-related effects on dendritic spine plasticity in other brain regions, although the behavioral consequences in these instances are less well understood.

Another recurring theme in the developing brain is that masculinization is controlled by estrogen during the organizational phase. This control has profound enduring effects on social behaviors in adult life. Testosterone (which is aromatized into estrogen) or estrogen treatment of neonatal rodent females masculinizes the brain. As adults, these females are no longer sexually receptive to males, and in fact display male-typical social interactions, albeit at reduced intensity. Providing testosterone to these females, to mimic adult levels of testosterone in males, boosts the intensity of social behaviors, including territorial aggression (the propensity of animals to fight over territory or mates),

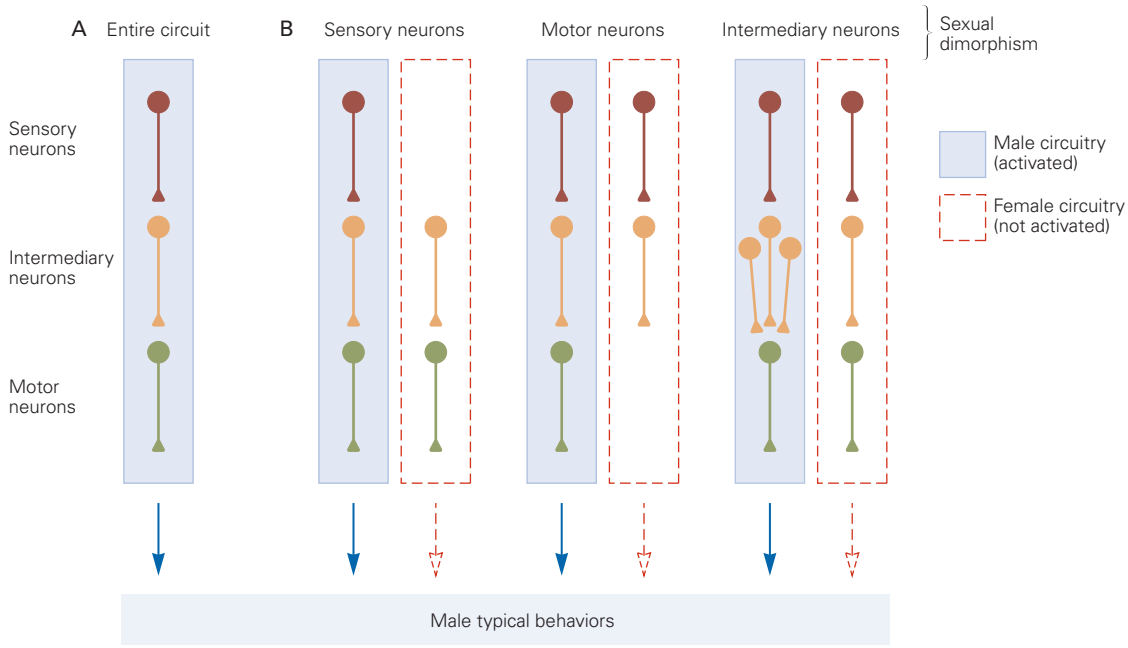

Figure 51–11 Possible circuit configurations that underlie sex differences in behavior. Neural circuit diagrams can be configured to generate sex differences in behaviors. Although it is possible to envision a neural circuit entirely exclusive to one or the other sex, most behaviors are shared between the sexes, and the current consensus is that sex differences in behavior or physiology reflect sexual dimorphisms in key neuronal populations embedded within an otherwise shared neural circuit. Such sexual dimorphisms have been found at the level of sensory neurons, motor neurons (as discussed for spinal nucleus of the bulbocavernosus neurons), or neurons interposed between sensory and motor pathways (such as the BNST and the sexually dimorphic nucleus of the preoptic area).

to male-typical levels. Thus, the perinatal surge of testosterone acts largely via aromatization into estrogens to masculinize the brain, whereas in adult life, both testosterone and estrogen facilitate the display of male-typical social interactions (Figure 51–12A).

These findings imply that male mice lacking androgen receptor exclusively in the nervous system should not only have male genitalia but also exhibit male patterns of social behavior, albeit at reduced intensity. This has in fact been borne out nicely by genetic engineering studies in mice; such mutant male mice indeed appear indistinguishable externally from control males, but they exhibit male-type sexual and aggressive behaviors with diminished intensity. However, there is growing evidence that the developmental control of masculinization of the brain by estrogen has shifted during evolution such that testosterone may be the predominant masculinizing agent in primates, including humans.

How do the actions of the limited number of sex hormones modulate the display of a large array of complex social interactions such as courtship vocalizations (similar to songbirds, many animals, including mice, vocalize as part of their mating ritual), sexual behavior, marking (the propensity of animals of many species to claim territory with pheromones secreted in bodily fluids), and aggression? As described earlier in this chapter, sex hormones bind to cognate receptors to modulate gene expression in target cells. These steroids are available at different times, amounts, and places in the brain of the two sexes. Accordingly, sex hormone–regulated genes are expressed in sexually dimorphic patterns that are also different for different brain regions. These genes regulate differentiation and adult function of neural circuits along male- or female-typical lines (Figure 51–12B).

Experimental inactivation of such sex hormone–regulated genes reveals that individual genes influence only a subset of the sexually dimorphic social interactions without altering the entire behavioral program of males and females. Thus, an additional emerging theme is that sex hormones control differentiation and function of neural circuits in a modular manner, with different sex hormone–regulated genes acting in distinct neuronal populations to regulate separate aspects of male- or female-typical behaviors. In short, there is no single neuronal population that governs

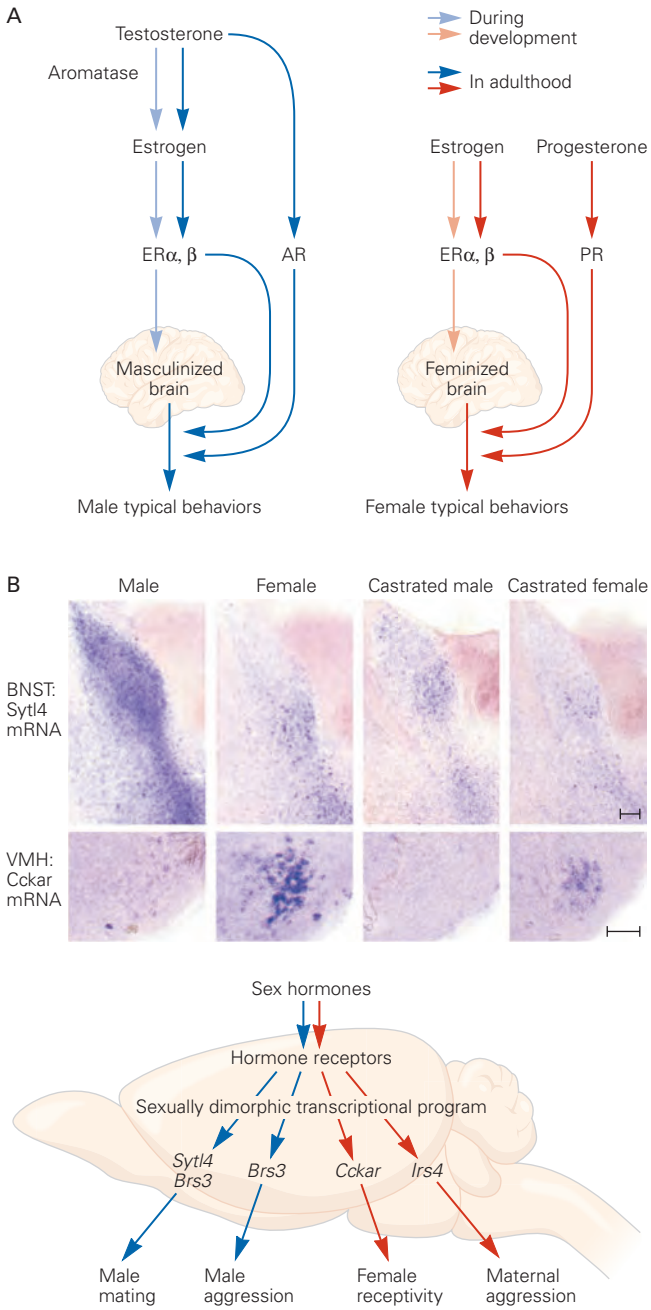

Figure 51–12 Mechanisms whereby sex hormones influence development and function of the nervous system.

A. Masculinization of the nervous systems occurs in at least two distinct steps: a developmental organizational phase largely controlled by estrogen signaling and a postpubertal activational phase controlled by estrogen and testosterone signaling via their cognate hormone receptors to regulate gene expression. (Abbreviations: **AR**, androgen receptor; **ER**, estrogen receptor; **PR**, progesterone receptor.)

B. Histological images show sexually dimorphic expression patterns of *Sytl4* mRNA in the bed nucleus of the stria terminalis (**BNST**) and *Cckar* in the ventromedial hypothalamus (**VMH**) of adult mice. Expression of these genes is clearly different in unmanipulated males and females and dramatically altered upon experimental removal of sex hormones from the circulation following castration in adult life. Both the BNST and VMH regulate mating and aggression in the two sexes.

Current thinking about how sex hormones regulate sex differences in behavior is illustrated in the diagram below. Molecular studies have identified many genes, such as *Sytl4* and *Cckar*, whose expression is sexually dimorphic in the adult brain and controlled by sex hormones. Many such genes, when experimentally mutated in mice via genetic engineering, regulate distinct components of sexually dimorphic behaviors but not the entire repertory of social interactions. In other words, sex hormones control sexually dimorphic behaviors in a modular genetic manner. (Reproduced, with permission, from Xu et al. 2012.)

gender-typical behaviors; rather, the neural control of distinct behaviors is distributed across multiple different neuronal populations.

This modular control of sexually dimorphic behaviors fits well with our thinking that most circuits are shared between the males and females and that sex differences in behavior arise from key neural populations that alter circuit function in a male- or female-typical fashion. It seems likely that neurons exhibiting sexually dimorphic molecular or anatomical features represent such key neuronal populations.

The Human Brain Is Sexually Dimorphic

Are sex differences between the brains of male and female mammals also present in humans, and if so, might they be functionally important? Early studies

revealed that a few structures are markedly larger in men. These include Onuf's nucleus in the spinal cord, the homolog of the SNB in rodents (Figure 51–7); the BNST, implicated in rodent mating behavior (Figure 51–4); and the interstitial nucleus of the anterior hypothalamus 3 (INAH3), related to the rodent SDN-POA discussed earlier (Figure 51–13).

Advances in high-resolution magnetic resonance imaging (MRI) and histology have uncovered more subtle structural and molecular dimorphisms in the

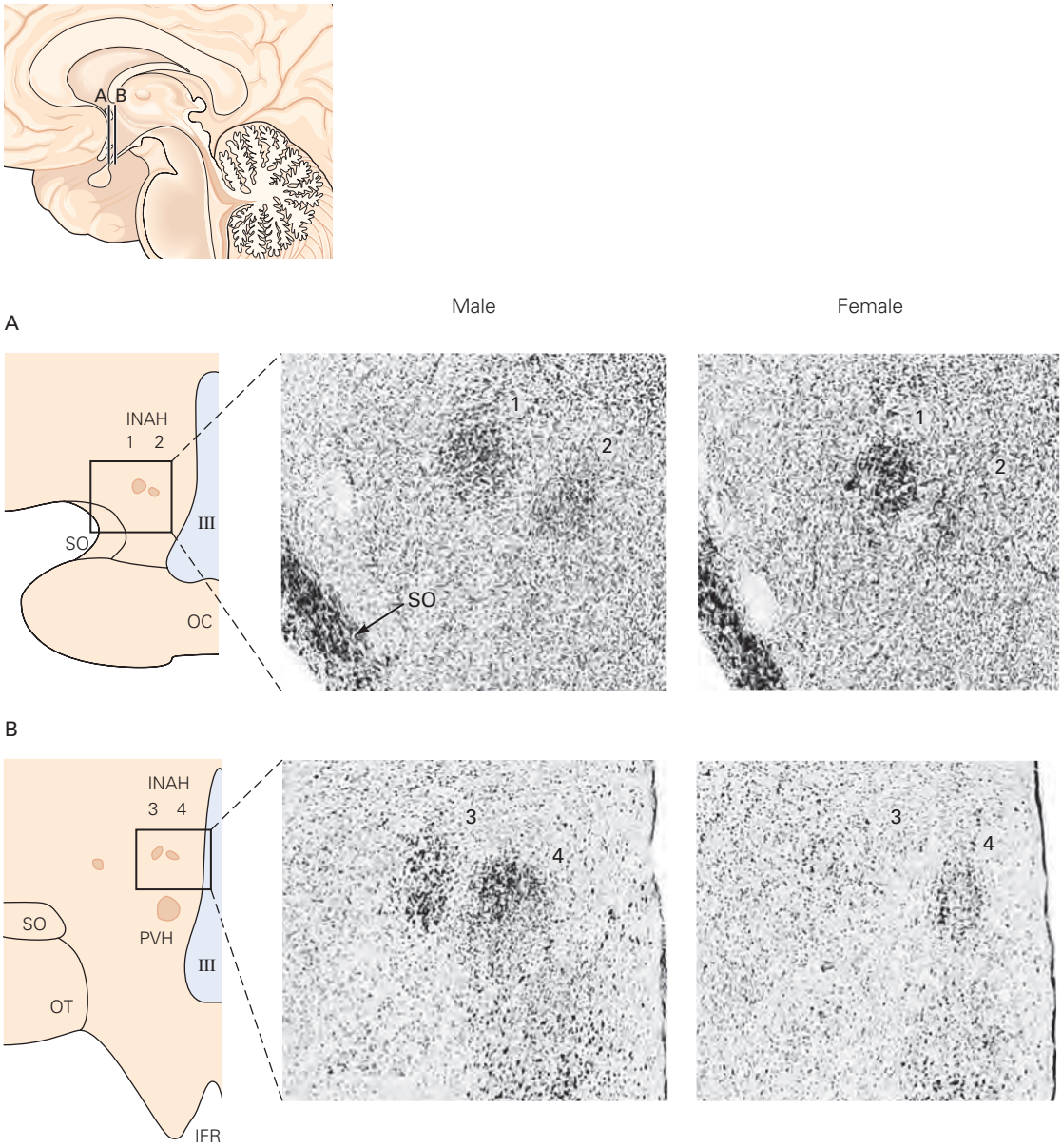

Figure 51–13 Sexual dimorphism in the interstitial nucleus of the anterior hypothalamus (INAH) 3 in the human brain. The human hypothalamus contains four small, discrete neuronal clusters, INAH1 to INAH4. The photomicrographs show these nuclei in adult male and female brains. While INAH1, INAH2, and INAH4 appear similar in men and women, INAH3 is significantly larger in men. The section in part **A** is 0.8 mm anterior to the section in part **B**. (Abbreviations: **IFR**, infundibular recess; **III**, third ventricle; **OC**, optic chiasm; **OT**, optic tract; **PVH**, paraventricular nucleus of the hypothalamus; **SO**, supraoptic nucleus.) (Adapted, with permission, from Gorski 1988.)

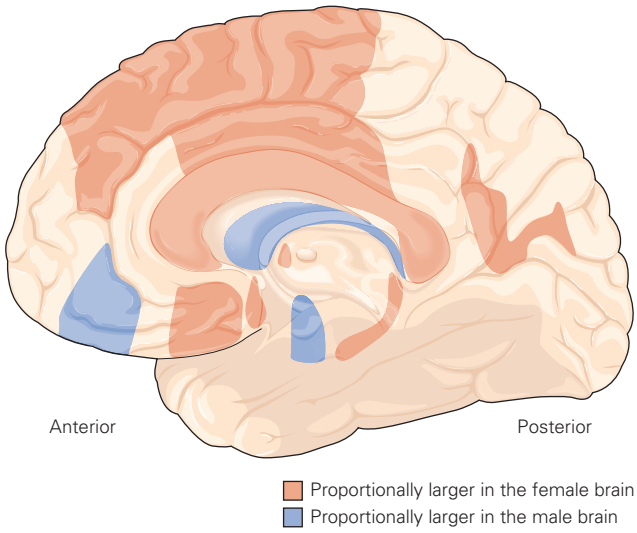

Figure 51–14 Sexual dimorphism is widespread in the adult human brain. A magnetic resonance imaging study measured the volume of many brain regions in adult men and women. The volume of each region was normalized to the size of the cerebrum for both sexes. Sex differences were significant in many regions, including several cortical areas that likely mediate cognitive functions. (Adapted, with permission, from Cahill 2006. Copyright © 2006 Springer Nature.)

central nervous system. For example, structures such as the fronto-orbital cortex and several gyri—including the precentral, superior frontal, and lingual gyri—occupy a significantly larger volume in adult women compared to a cohort of adult men (Figure 51–14). Moreover, the frontomedial cortex, amygdala, and angular gyrus volumes are larger in men compared to women. Thus, there are likely to be many sexual dimorphisms in the human brain.

Sexual Dimorphisms in Humans May Arise From Hormonal Action or Experience

What remains unclear is how these brain dimorphisms arise and how they relate to behavior. They might arise early from the organizational effects of hormones or later as a result of experience. Sex differences arising before or soon after birth could underlie behavioral differences, whereas those that arise later in life might be results of dimorphic experiences. Answers to these questions are fairly clear in a few cases. For example, studies of the development of neural circuits responsible for penile erection and lactation in rodents translate readily to humans.

Two recent observations suggest that enduring effects of experience on behavior first studied in animals (Figure 51–10) are also relevant to humans. First, as discussed in Chapter 49, children raised for lengthy periods in orphanages with little individual care have long-lasting defects in a variety of social behaviors. Even years after placement in foster homes, these children have on average lower levels of oxytocin and vasopressin in their serum than children raised with biological parents. Second, people who have suffered abuse as children often grow up to be poor parents. Postmortem studies have shown that adults who had been abused as children exhibited greater promoter methylation of their glucocorticoid receptor genes than adults in control populations. Although these studies are new and require replication, they provide tantalizing hints at the biological mechanisms that underlie the lifelong effects of early parental care.

Dimorphic Structures in the Brain Correlate with Gender Identity and Sexual Orientation

In contrast to progress in mapping the biological bases of some relatively simple sexually dimorphic behaviors in people, differences in sexual partner preference and gender identity remain poorly understood. Little progress has been made in relating sex differences in cognitive functions to structural differences in the brain, in part because the very existence of cognitive differences remains a matter of controversy; if they exist at all, they are small and represent differences in means between highly variable male and female populations. On the other hand, several lines of evidence have connected clear differences in gender identity and sexual orientation to dimorphic structures in the brain.

Early insight into this issue came from observation of people with single-gene mutations that dissociate anatomical sex from gonadal and chromosomal sex, such as CAIS, CAH, and 5α-reductase deficiency (Table 51–1). For example, girls with CAH experience an excess of testosterone during fetal life; the disorder is generally diagnosed at birth and corrected. Nevertheless, the early exposure to androgens is correlated with subsequent changes in gender-related behaviors. On average, girls with CAH tend to have toy preferences and engage in play typical of boys of equivalent age. There is also a small but significant increase in the incidence of homosexual and bisexual orientation in females treated for CAH as children, and a significant proportion of these females also express the desire to live as men, consistent with a change in gender identity. These findings suggest that early organizational effects of steroids affect gender-specific behaviors independent of chromosomal and anatomical sex.

In 5α-reductase II deficiency and CAIS, many of the affected males show completely feminized

external genitalia and are mistakenly raised as females until puberty. Thereafter, their histories diverge. In 5α-reductase II deficiency, the symptoms arise from a defect in testosterone processing largely confined to the developing external genitalia. At puberty, the large increase in circulating testosterone virilizes the body hair, musculature, and most dramatically, the external genitalia. At this stage, many but not all patients choose to adopt a male gender. In CAIS, in contrast, defects arise from a body-wide defect in the androgen receptor. These patients commonly seek medical advice after they fail to menstruate at puberty. Concordant with their feminized external phenotype, most CAIS patients express a female gender identity and a sexual preference for men. They opt for surgical removal of the testes and hormonal supplementation appropriate for females.

What accounts for the different outcomes? Among many possibilities, one is that the dramatic change in behavior in 5α-reductase II patients at puberty results from the effects of testosterone acting on the brain. In CAIS patients, these effects do not occur because androgen receptors are absent from the brain. Clearly, however, this explanation does not rule out social and cultural upbringing as important factors in determining gender identity and sexual orientation.

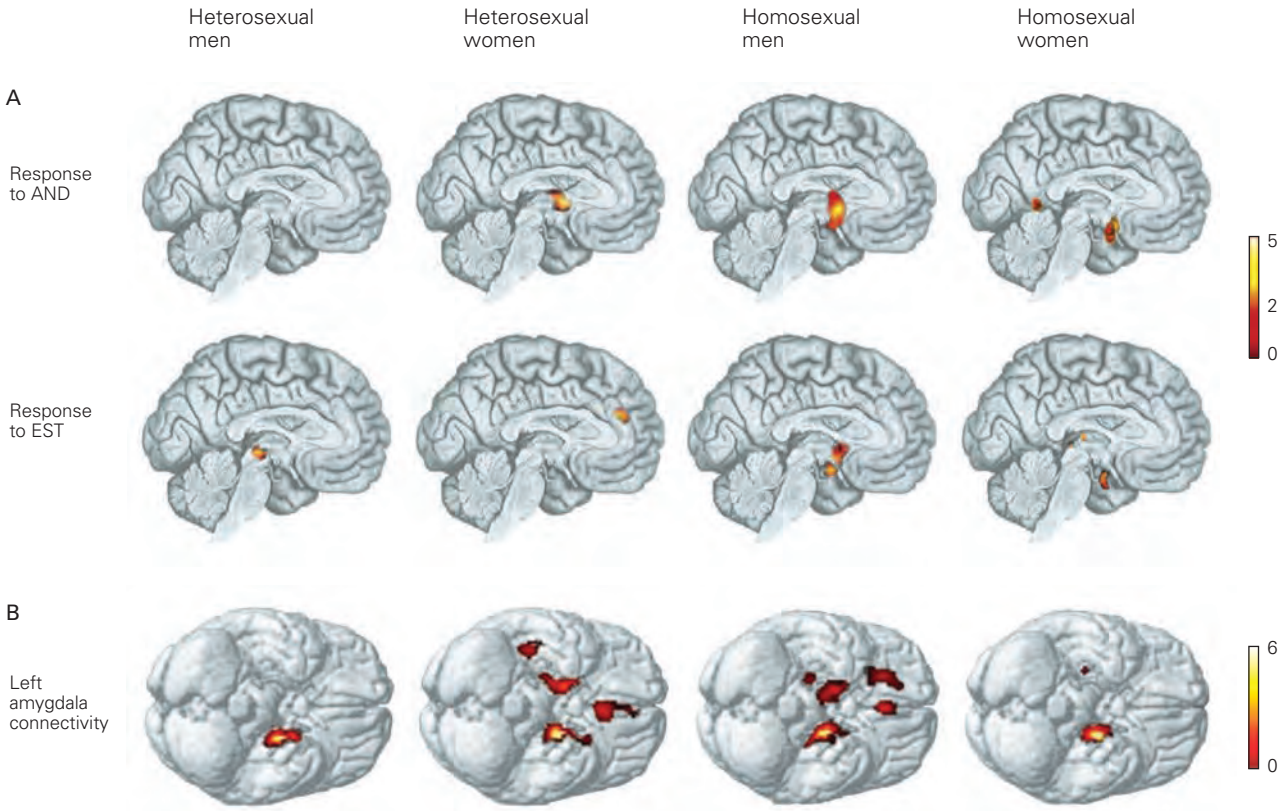

Figure 51–15 Some sexually dimorphic patterns of olfactory activation in the brain correlate with sexual orientation.

A. Positron emission tomography imaging was used to identify brain regions that were activated when subjects sniffed androstadienone (**AND**) or estratetraenol (**EST**) compared to nonodorous air. AND activated several hypothalamic centers in the brains of heterosexual women but not men, whereas EST activated several hypothalamic centers in heterosexual males but not females. Patterns of activation in the hypothalamus of homosexual men were similar to those of heterosexual women in response to AND, whereas similar patterns of activation were found in heterosexual men and homosexual women in response to EST. The color calibration on the right shows the level of putative neural activity. Because the same brain sections were selected to compare, the figure does not illustrate maximal activation for each condition. (Adapted, with permission, from Berglund, Lindstrom, and Savic 2006; Savic, Berglund, and Lindstrom 2005.)

B. Heterosexual and homosexual subjects were scanned while breathing unscented air, and a measure of covariance was used to estimate connectivity among regions. In heterosexual women and homosexual men, the left amygdala was strongly connected to the right amygdala, whereas connectivity remained local in heterosexual men and homosexual women. (Adapted, with permission, from Savic and Lindstrom 2008.)

A second set of studies probing the biology of sexual orientation assessed responses to pheromones. Pheromone perception in humans is quite different from that of mice and is likely a less important sense. Humans do not have a functional VNO, and most of the genes implicated in pheromone reception in the mouse VNO, such as *trpc2* and those encoding VNO receptors, are absent or nonfunctional in the human genome. To the extent that humans do sense pheromones, they appear to use the main olfactory epithelium and bulb. Chemicals that appear to be human pheromones include androstadienone (AND), an odorous androgenic metabolite, and estratetraenol (EST), an odorous estrogenic metabolite. AND is present at 10-fold higher concentrations in male sweat compared to female sweat, whereas EST is present in the urine of pregnant women. Both compounds can produce sexual arousal—AND in heterosexual women and EST in heterosexual men—even at concentrations so low that there is no conscious olfactory perception.

Brain areas activated by AND and EST have been identified by positron emission tomography (PET) imaging. When AND is presented, certain hypothalamic nuclei are activated in heterosexual women but not heterosexual men, whereas when EST is presented, adjacent regions containing clusters of nuclei are activated in men but not in women (Figure 51–15A). In homosexual men and women, there is a reversal of hypothalamic activation: AND but not EST activates hypothalamic centers in homosexual men, and conversely, EST but not AND activates those areas in lesbian women. Heterosexual and homosexual brains therefore appear to process olfactory sensory information in different ways.

Do sexually dimorphic structures in homosexual brains correlate with anatomical sex or sexual orientation? Imaging studies have provided support for the view that the brains of homosexual men resemble those of heterosexual woman and that the brains of homosexual women resemble those of heterosexual men (Figure 51–15B). Moreover, the volume of the sexually dimorphic BNST is small in male-to-female transsexuals compared to men, whereas female-to-male transsexuals appear to have a larger BNST compared to women (Figure 51–16). It is not clear, however, whether the structural dimorphism in these individuals is a consequence or a cause of gender identity or sexual orientation.

The male mouse counterpart of the human BNST plays a critical role in recognizing the sex of *other* mice and guides subsequent social interactions, such as aggression with males and mating with females. Thus, a region linked to gender identity in the human brain plays an important role in sex recognition in rodents.

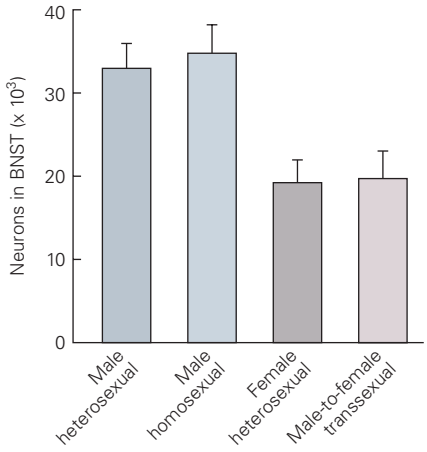

Figure 51–16 Sexual dimorphism in the bed nucleus of the stria terminalis (BNST) in humans. The nucleus has significantly more neurons in men compared to women regardless of male sexual orientation. Similar to women, male-to-female transsexuals have fewer neurons than men. In the one female-to-male transsexual brain available for postmortem analysis (not shown in the bar graph), the number of neurons is well within the normal range for men. (Adapted, with permission, from Kruijver et al. 2000.)

As is the case with the sexual dimorphism of the mouse BNST discussed earlier, hormonal influences are also thought to underlie the dimorphism of the human BNST.

If prenatal influences do lead to dissociation of sex from gender, are those influences genetic? Other than the rare syndromes described earlier, attempts to find genetic bases for sexual orientation or gender identity have not been productive. Claimed genetic contributions are small and claims of associations with specific genomic loci have not been replicated. Thus, while the current weight of evidence favors some contribution of early, even prenatal, factors in these processes, their cause and relative importance remain unknown.

Highlights

1. In humans and many other mammals, the sex determination pathway directs differentiation of the bipotential gonad into testes in males and ovaries in females. The *SRY* gene on the Y chromosome directs the gonad to form testes, whereas the absence of *SRY* enables the gonad to differentiate into ovaries.
2. Sex steroid hormones produced by the gonads—testosterone by testes and estrogens, and progesterone by ovaries—drive sexual differentiation of both the nervous system and the rest of the body.

3. Sex hormones act early during a critical window in development to irreversibly organize neural substrates for behavior in a sexually dimorphic manner, whereas in adult life, these hormones act acutely and reversibly to activate sex-typical physiological and behavioral responses.
4. During the critical window, testes produce a transient surge of testosterone that masculinizes the developing bipotential nervous system. By contrast, the ovaries are quiescent during this period, and it is thought that the absence of sex hormones enables the nervous system in this period to differentiate along a female-typical pathway.
5. Many of the actions of testosterone that masculinize the nervous system occur following its conversion to estrogen locally at the site of action. There is evidence to suggest that in humans and other primates testosterone also acts directly via its cognate hormone receptor to effect masculinization of the neural substrates of behavior.
6. Sex hormones control sexual differentiation of neural pathways by utilizing cellular processes such as apoptosis, neurite extension, and synapse formation that are employed widely during other developmental events.
7. Sex hormones bind to cognate hormone receptors that modulate gene expression. Such genes in turn regulate the cellular processes that result in sex differences in neuronal number, connectivity, and physiology.
8. Many neuronal populations that are sexually dimorphic by morphological and other criteria have been identified in the vertebrate brain over the past few decades. Functional studies show that these regions influence some, but not all, sexually dimorphic behaviors.
9. Recent molecular studies have identified many sex hormone–regulated genes whose expression patterns are sexually dimorphic. These genes as well as the neurons they are expressed in regulate sexually dimorphic social behaviors in a modular manner. In other words, individual genes and the neuronal populations that express them modulate one or a few sexually dimorphic behaviors so that the control of these behaviors is distributed among many different neuronal groups.
10. Such sexually dimorphic neuronal populations are likely embedded within neural circuits found in both sexes, and they are thought to guide behavior along male- or female-typical patterns.
11. Both sensory stimuli and past experience profoundly regulate the display of sexually dimorphic behaviors. In some cases, the influence of past experience can extend across the life span of the animal.
12. Pheromones guide choice of sexual partner in rodents. There is evidence from imaging studies that men and women may also show sexually dimorphic neural responses to male and female pheromones and that these responses can align with sexual orientation; in these cases, however, it is unclear if the neural responses are learned responses based on past experience.
13. There are many sex differences between the brains of men and women, and in some instances, these sex differences align with gender in adult life rather than gender assigned at birth. In these cases, it is not clear whether the sex differences causally reflect gender identity or are a result of it. These issues are difficult to disentangle at present.

Nirao M. Shah
Joshua R. Sanes

Selected Reading

Arnold AP. 2004. Sex chromosomes and brain gender. Nat Rev Neurosci 5:701–708.

Bayless DW, Shah NM. 2016. Genetic dissection of neural circuits underlying sexually dimorphic social behaviours. Philos Trans R Soc Lond B Biol Sci 371:20150109.

Byne W. 2006. Developmental endocrine influences on gender identity: implications for management of disorders of sex development. Mt Sinai J Med 73:950–959.

Cahill L. 2006. Why sex matters for neuroscience. Nat Rev Neurosci 7:477–484.

Curley JP, Jensen CL, Mashoodh R, Champagne FA. 2010. Social influences on neurobiology and behavior: epigenetic effects during development. Psychoneuroendocrinology 36:352–371.

Dulac C, Wagner S. 2006. Genetic analysis of brain circuits underlying pheromone signaling. Annu Rev Genet 40:449–467.

Hines M. 2006. Prenatal testosterone and gender-related behavior. Eur J Endocrinol 155:S115–S121.

Kohl J, Dulac C. 2018. Neural control of parental behaviors. Curr Opin Neurobiol 49:116–122.

Morris JA, Jordan CL, Breedlove SM. 2004. Sexual differentiation of the vertebrate nervous system. Nat Neurosci 7:1034–1039.

Swaab DF. 2004. Sexual differentiation of the human brain: relevance for gender identity, transsexualism and sexual orientation. Gynecol Endocrinol 19:301–312.
Wilhelm D, Palmer S, Koopman P. 2007. Sex determination and gonadal development in mammals. Physiol Rev 87:1–28.
Yang CF, Shah NM. 2014. Representing sex in the brain, one module at a time. Neuron 82:261–278.

References

Bakker J, De Mees C, Douhard Q, et al. 2006. Alpha-fetoprotein protects the developing female mouse brain from masculinization and defeminization by estrogens. Nat Neurosci 9:220–226.
Bayless DW, Yang T, Mason MM, et al. 2019. Limbic neurons shape sex recognition and social behavior in sexually naïve males. Cell 176:1190–1205.
Berglund H, Lindstrom P, Savic I. 2006. Brain response to putative pheromones in lesbian women. Proc Natl Acad Sci U S A 103:8269–8274.
Brainard MS, Doupe AJ. 2002. What songbirds teach us about learning. Nature 417:351–358.
Byne W, Lasco MS, Kemether E, et al. 2000. The interstitial nuclei of the human anterior hypothalamus: an investigation of sexual variation in volume and cell size, number and density. Brain Res 856:254–258.
Cohen-Kettenis PT. 2005. Gender change in 46, XY persons with 5α-reductase-2 deficiency and 17β-hydroxysteroid dehydrogenase-3 deficiency. Arch Sex Behav 34:399–410.
Cooke BM, Woolley CS. 2005. Gonadal hormone modulation of dendrites in the mammalian CNS. J Neurobiol 64: 34–46.
Demir E, Dickson BJ. 2005. *Fruitless* splicing specifies male courtship behavior in *Drosophila*. Cell 121:785–794.
Edwards DA, Burge KG. 1971. Early androgen treatment and male and female sexual behavior in mice. Horm Behav 2:49–58.
Forger NG, de Vries GJ. 2010. Cell death and sexual differentiation of behavior: worms, flies, and mammals. Curr Opin Neurobiol 20:776–783.
Goldstein LA, Kurz EM, Sengelaub DR. 1990. Androgen regulation of dendritic growth and retraction in the development of a sexually dimorphic spinal nucleus. J Neurosci 10:935–946.
Gorski RA. 1988. Hormone-induced sex differences in hypothalamic structure. Bull Tokyo Metropol Inst Neurosci 16 (Suppl 3):67–90.
Gorski RA. 1988. Sexual differentiation of the brain: mechanisms and implications for neuroscience. In: SS Easter Jr, KF Barald, BM Carlson (eds). *From Message to Mind: Directions in Developmental Neurobiology*, pp. 256–271. Sunderland, MA: Sinauer.
Gorski RA, Harlan RE, Jacobsen CD, Shryne JE, Southam AM. 1980. Evidence for the existence of a sexually dimorphic nucleus in the preoptic area of the rat. J Comp Neurol 193:529–539.
Greenspan RJ, Ferveur JF. 2000. Courtship in *Drosophila*. Annu Rev Genet 34:205–232.
Inoue S, Yang R, Tantry A, et al. 2019. Periodic remodeling in a neural circuit governs timing of female sexual behavior. Cell 179:1393–1408.
Juntti SA, Tollkuhn J, Wu MV, et al. 2010. The androgen receptor governs the execution, but not programming, of male sexual and territorial behaviors. Neuron 66:260–272.
Kimchi T, Xu J, Dulac C. 2007. A functional circuit underlying male sexual behavior in the female mouse brain. Nature 448:1009–1014.
Kimura K, Ote M, Tazawa T, Yamamoto D. 2005. *Fruitless* specifies sexually dimorphic neural circuitry in the *Drosophila* brain. Nature 438:229–233.
Kohl J, Babayan BM, Rubinstein ND, et al. 2018. Functional circuit architecture underlying parental behaviour. Nature 556:326–331.
Konishi M, Akutagawa E. 1985. Neuronal growth, atrophy and death in a sexually dimorphic song nucleus in the zebra finch brain. Nature 315:145–147.
Koopman P, Gubbay J, Vivian N, Goodfellow P, Lovell-Badge R. 1991. Male development of chromosomally female mice transgenic for *Sry*. Nature 351:117–121.
Kruijver FP, Zhou JN, Pool CW, Hofman MA, Gooren LJ, Swaab DF. 2000. Male-to-female transsexuals have female neuron numbers in a limbic nucleus. J Clin Endocrinol Metab 85:2034–2041.
Långström N, Rahman Q, Carlström E, Lichtenstein P. 2010. Genetic and environmental effects on same-sex sexual behavior: a population study of twins in Sweden. Arch Sex Behav 39:75–80.
Lee H, Kim DW, Remedios R, et al. 2014. Scalable control of mounting and attack by Esr1+ neurons in the ventromedial hypothalamus. Nature 509:627–632.
LeVay S. 1991. A difference in hypothalamic structure between heterosexual and homosexual men. Science 253:1034–1037.
Leypold BG, Yu CR, Leinders-Zufall T, Kim MM, Zufall F, Axel R. 2002. Altered sexual and social behaviors in *trp2* mutant mice. Proc Natl Acad Sci U S A 99:6376–6381.
Liu YC, Salamone JD, Sachs BD. 1997. Lesions in medial preoptic area and bed nucleus of stria terminalis: differential effects on copulatory behavior and noncontact erection in male rats. J Neurosci 17:5245–5253.
Mandiyan VS, Coats JK, Shah NM. 2005. Deficits in sexual and aggressive behaviors in *Cnga2* mutant mice. Nat Neurosci 8:1660–1662.
Manoli DS, Foss M, Villella A, Taylor BJ, Hall JC, Baker BS. 2005. Male-specific *fruitless* specifies the neural substrates of *Drosophila* courtship behaviour. Nature 436:395–400.
McCarthy MM, Arnold AP. 2011. Reframing sexual differentiation of the brain. Nat Neurosci 14:677–683.
McGowan PO, Sasaki A, D'Alessio AC, et al. 2009. Epigenetic regulation of the glucocorticoid receptor in human brain associates with childhood abuse. Nat Neurosci 12:342–348.
Nottebohm F, Arnold AP. 1976. Sexual dimorphism in vocal control areas of the songbird brain. Science 194:211–213.
Ohno S, Geller LN, Lai EV. 1974. TFM mutation and masculinization versus feminization of the mouse central nervous system. Cell 3:235–242.

Sapolsky RM. 2004. Mothering style and methylation. Nat Neurosci 7:791–792.
Savic I, Berglund H, Gulyas B, Roland P. 2001. Smelling of odorous sex hormone-like compounds causes sex-differentiated hypothalamic activations in humans. Neuron 31:661–668.
Savic I, Berglund H, Lindstrom P. 2005. Brain response to putative pheromones in homosexual men. Proc Natl Acad Sci U S A 102:7356–7361.
Savic I, Lindstrom P. 2008. PET and MRI show differences in cerebral asymmetry and functional connectivity between homo- and heterosexual subjects. Proc Natl Acad Sci U S A 105:9403–9408.
Sekido R, Lovell-Badge R. 2009. Sex determination and *SRY*: down to a wink and a nudge? Trends Genet 25:19–29.
Shah NM, Pisapia DJ, Maniatis S, Mendelsohn MM, Nemes A, Axel R. 2004. Visualizing sexual dimorphism in the brain. Neuron 43:313–319.
Stockinger P, Kvitsiani D, Rotkopf S, Tirian L, Dickson BJ. 2005. Neural circuitry that governs *Drosophila* male courtship behavior. Cell 121:795–807.
Stowers L, Holy TE, Meister M, Dulac C, Koentges G. 2002. Loss of sex discrimination and male-male aggression in mice deficient for TRP2. Science 295:1493–1500.
Unger EK, Burke KJ Jr, Yang CF, Bender KJ, Fuller PM, Shah NM. 2015. Medial amygdalar aromatase neurons regulate aggression in both sexes. Cell Rep 10:453–462.
Weaver IC, Cervoni N, Champagne FA, et al. 2004. Epigenetic programming by maternal behavior. Nat Neurosci 7:847–854.
Wei YC, Wang SR, Jiao ZL, et al. 2018. Medial preoptic area in mice is capable of mediating sexually dimorphic behaviors regardless of gender. Nat Commun 9:279.
Wierman ME. 2007. Sex steroid effects at target tissues: mechanisms of action. Adv Physiol Educ 31:26–33.
Wu MV, Manoli DS, Fraser EJ, et al. 2009. Estrogen masculinizes neural pathways and sex-specific behaviors. Cell 139:61–72.
Wu Z, Autry AE, Bergan JF, Watabe-Uchida M, Dulac CG. 2014. Galanin neurons in the medial preoptic area govern parental behaviour. Nature 509:325–330.
Xu X, Coats JK, Yang CF, et al. 2012. Modular genetic control of sexually dimorphic behaviors. Cell 148:596–607.
Yang CF, Chiang MC, Gray DC, et al. 2013. Sexually dimorphic neurons in the ventromedial hypothalamus govern mating in both sexes and aggression in males. Cell 153:896–909.
Yang T, Yang CF, Chizari MD, et al. 2017. Social control of hypothalamus-mediated male aggression. Neuron 95:955–970.
Zhang J, Webb DM. 2003. Evolutionary deterioration of the vomeronasal pheromone transduction pathway in catarrhine primates. Proc Natl Acad Sci U S A 100:8337–8341.
Zhang TY, Meaney MJ. 2010. Epigenetics and the environmental regulation of the genome and its function. Annu Rev Psychol 61:439–466.

Part VIII

Preceding Page

Tingarri Men and Initiates at Marabindinya. In this painting by the Aboriginal Australian artist, Anatjari Tjampitjinpa, Tingarri instructors are depicted as concentric circles and their young initiates are shown as horseshoe shapes along the boundaries. The background of the painting depicts the sandhill country of the central Australian desert. Such symbolic representations recall the neural representations of episodic memories, consisting of events taking place in space and time, encoded in the firing of grid cells and place cells in the entorhinal cortex and hippocampus, respectively.

VIII Learning, Memory, Language and Cognition

Motor and sensory functions take up less than one-half of the cerebral cortex in humans. The rest of the cortex is occupied by the association areas, which coordinate events arising in the motor and sensory centers. Three association areas—the prefrontal, parietal-temporal-occipital, and limbic—are involved in cognitive behavior: speaking, thinking, feeling, perceiving, planning skilled movements, learning, memory, decision-making, and consciousness.

Most of the early evidence relating cognitive functions to the association areas came from clinical studies of brain-damaged patients. Thus, the study of language in patients with aphasia yielded important information about how human mental processes are distributed in the two hemispheres of the brain and how they develop. More refined analyses have come from human imaging studies using functional magnetic resonance imaging (fMRI) and other methods.

Deeper insights into the neural circuitry and cellular mechanisms giving rise to cognitive processes have come from electrophysiological recordings and genetic-based manipulations, including cell type–specific gene deletions and cell type–specific optogenetic excitation or inhibition in experimental animals, particularly in rodents. Such studies can evaluate the relative contribution of specific genes, neurons, and synaptic connections to specific types of behavior.

So far in this book, we have considered neural mechanisms associated with basic functions of the brain, including primary sensory perception, movement, and homeostatic control. In this part and the next, we begin to consider the more complex, higher-order brain functions mentioned earlier, the realm of cognitive neural science. The aim of this merger of neurophysiology, anatomy, developmental biology, cell and molecular biology, theory, and cognitive psychology is to ultimately provide an understanding of the neural mechanisms of the mind.

Until the latter part of the 20th century, the study of higher mental function was approached through behavioral observations gleaned from brain-damaged patients and animals with experimental lesions. In the first part of the 20th century, to avoid untestable

concepts and hypotheses, psychology became rigidly concerned with behaviors defined strictly in terms of observable stimuli and responses. Orthodox behaviorists thought it unproductive to deal with consciousness, feeling, attention, or even motivation. By concentrating only on observable actions, behaviorists asked: What can an organism do, and how does it do it? Indeed, careful quantitative analysis of stimuli and responses has contributed greatly to our understanding of the acquisition and use of "implicit" knowledge of perceptual and motor skills. However, humans and other higher animals also have "explicit" knowledge of facts and events. They have knowledge of space, rules, and relations—what Edward Tolman termed *cognitive maps*. Animals can choose a newly available route to a goal without ever learning the sensory-response association, and humans can reason deliberatively from what they know to imagine something unknown. Indeed, that is what makes neural science possible—in fact, all of science and the humanities.

Thus, we also need to ask: What does the animal know about the world, and how does it come to know it? How is that knowledge represented in the brain? Does explicit knowledge differ from implicit knowledge? And how can such knowledge be communicated to others and enable us to make rational decisions based on past experience? Much, perhaps most, knowledge is unconscious a great deal of the time. We need to know the nature of the unconscious processes, the systems that mediate them, and their influence on the nature of conscious mental activity. Finally, we need to know about the highest realms of conscious knowledge, the knowledge of oneself as an individual, a thinking and feeling human being.

The modern effort to understand the neural mechanisms of higher mental functions began at the end of the 19th century when Pierre Broca and Carl Wernicke discovered regions of the cerebral cortex responsible for the production and comprehension of language. Throughout the 20th century, studies of patients with brain damage resulting from accidents, war, and disease led to an expansion of knowledge of the roles of specific brain areas responsible for cognitive functions, including attention, intention (planning), reasoning, and learning and memory. However, it was only in the past 20 to 30 years, based in part on new technological approaches, that our understanding of cognitive processes advanced from anatomical localization to an understanding of how neural activity in specific brain regions underlies such processes.

In Part VIII, we explore such questions of cognitive brain science. Chapter 52 introduces basic mechanisms of human learning and memory, focusing on the use of fMRI and behavioral studies to elucidate the role of different brain regions in implicit and explicit memory. In Chapter 53, we discuss the cellular and molecular mechanisms responsible for implicit memory storage, focusing on studies in invertebrates and vertebrates that have elucidated the role of synaptic plasticity in implicit memory storage. In Chapter 54, we

expand on the theme of synaptic plasticity, this time for the storage of explicit memory by the hippocampus and related brain regions. We further consider how the synaptic connectivity between the entorhinal cortex and hippocampus enables us to perceive and remember our spatial location in a given environment. Next, in Chapter 55, we focus on the neural mechanisms underlying language, a uniquely human function that enables us to communicate our store of knowledge to others, including brain circuits necessary for speaking and perceiving the spoken word. Finally, in Chapter 56, we examine how the brain enables us to use our knowledge to make rational decisions. Viewed through the lens of decision-making, the distinction between the apparently separate processes of knowledge and know-how can be seen as a unified function, one that provides a basis for understanding how consciousness may emerge from brain activity. Achieving a full understanding of the neural mechanisms that enable us to maintain a rich set of memories of our past experiences over a lifetime, to communicate those memories to others, and to use them to make informed, conscious decisions is perhaps one of the most daunting challenges in all of science.

Part Editors: Eric R. Kandel and Steven A. Siegelbaum

Part VIII

This page intentionally left blank

52

Learning and Memory

In his masterful novel *One Hundred Years of Solitude*, Gabriel Garcia Márquez describes a strange plague that invades a tiny village and robs people of their memories. The villagers first lose personal recollections, then the names and functions of common objects. To combat the plague, one man places written labels on every object in his home. But he soon realizes the futility of this strategy, because the plague eventually destroys even his knowledge of words and letters.

This fictional incident reminds us of how important learning and memory are in everyday life. Learning refers to a change in behavior that results from acquiring knowledge about the world, and memory refers to the processes by which that knowledge is encoded, stored, and later retrieved. Marquez's story challenges us to imagine life without the ability to learn and remember. We would forget people and places we once knew, and no longer be able to use and understand language or execute motor skills we had once learned; we would not recall the happiest or saddest moments of our lives and would even lose our sense of personal identity. Learning and memory are essential to the full functioning and independent survival of people and animals.

In 1861, Pierre Paul Broca discovered that damage to the posterior portion of the left frontal lobe (Broca's area) produces a specific deficit in language. Soon thereafter, it became clear that other mental functions, such as perception and voluntary movement, are also mediated by discrete parts of the brain (Chapter 1). This naturally led to the question: Are there discrete neural systems concerned with memory? If so, is there a "memory center," or is memory processing widely distributed throughout the brain?

Contrary to the prevalent view that cognitive functions are localized in the brain, many students of learning doubted that memory is localized. In fact, until the middle of the 20th century, many psychologists doubted that memory is a discrete function, independent of perception, language, or movement. One reason for the persistent doubt is that memory storage involves many different parts of the brain. We now appreciate, however, that these regions are not all equally important. There are several fundamentally different types of memory, and certain regions of the brain are much more important for encoding some types of memory than for others.

During the past several decades, researchers have made significant progress in the analysis and understanding of learning and memory. In this chapter, we focus on studies of normal human memory behavior, its perturbations following brain lesions due to injury or surgery, and measurements of brain activity during learning and memory recall using functional magnetic resonance imaging (fMRI) and extracellular electrophysiological recordings. These studies have yielded three major insights.

First, there are several forms of learning and memory. Each form of learning and memory has distinctive cognitive and computational properties and is supported by different brain systems. Second, memory involves encoding, storage, retrieval, and consolidation. Finally, imperfections and errors in remembering can provide clues about the nature and function of learning and memory and the fundamental role that memory plays in guiding behavior and planning for the future.

Memory can be classified along two dimensions: (1) the time course of storage and (2) the nature of the information stored. In this chapter, we consider the time course of storage. In the next two chapters, we focus on the cellular, molecular, and circuit-based mechanisms of different forms of learning and memory, based largely on studies of animal models.

Short-Term and Long-Term Memory Involve Different Neural Systems

Short-Term Memory Maintains Transient Representations of Information Relevant to Immediate Goals

When we reflect on the nature of memory, we usually think of the long-term memory that William James referred to as "memory proper" or "secondary memory." That is, we think of memory as "the knowledge of a former state of mind after it has already once dropped from consciousness." This knowledge depends on the formation of a memory trace that is durable, in which the representation persists even when its content has been out of conscious awareness for a long period.

Not all forms of memory, however, constitute "former states of mind." In fact, the ability to store information depends on a form of short-term memory, called working memory, which maintains current, albeit transient, representations of goal-relevant knowledge. In humans, working memory consists of at least two subsystems—one for verbal information and another for visuospatial information. The functioning of these two subsystems is coordinated by a third system called the *executive control processes*. Executive control processes are thought to allocate attentional resources to the verbal and visuospatial subsystems and to monitor, manipulate, and update stored representations.

We use the verbal subsystem when we attempt to keep speech-based (phonological) information in conscious awareness, as when we mentally rehearse a password before entering it. The verbal subsystem consists of two interactive components: a store that represents phonological knowledge and a rehearsal mechanism that keeps these representations active while we need them. Phonological storage depends on posterior parietal cortices, and rehearsal partially depends on articulatory processes in Broca's area.

The visuospatial subsystem of working memory retains mental images of visual objects and of the location of objects in space. The rehearsal of spatial and object information is thought to involve modulation of this information in the parietal, inferior temporal, and occipital cortices by the frontal and premotor cortices.

Single-cell recordings in nonhuman primates indicate that, over a period of seconds, some prefrontal neurons maintain spatial representations, others maintain object representations, and still others represent the integration of spatial and object knowledge. Although neurons concerned with working memory of objects tend to lie in the ventrolateral prefrontal cortex and those concerned with spatial knowledge tend to lie in the dorsolateral prefrontal cortex, all three classes of neurons are found in both prefrontal subregions (Figure 52–1).

Thus, working memory involves activation of representations of information stored in specialized cortical regions that vary based on the content of the information, as well as activation of general control mechanisms in prefrontal cortex. Prefrontal control signals in working memory are further dependent on interaction with the striatum and ascending dopaminergic inputs from the midbrain.

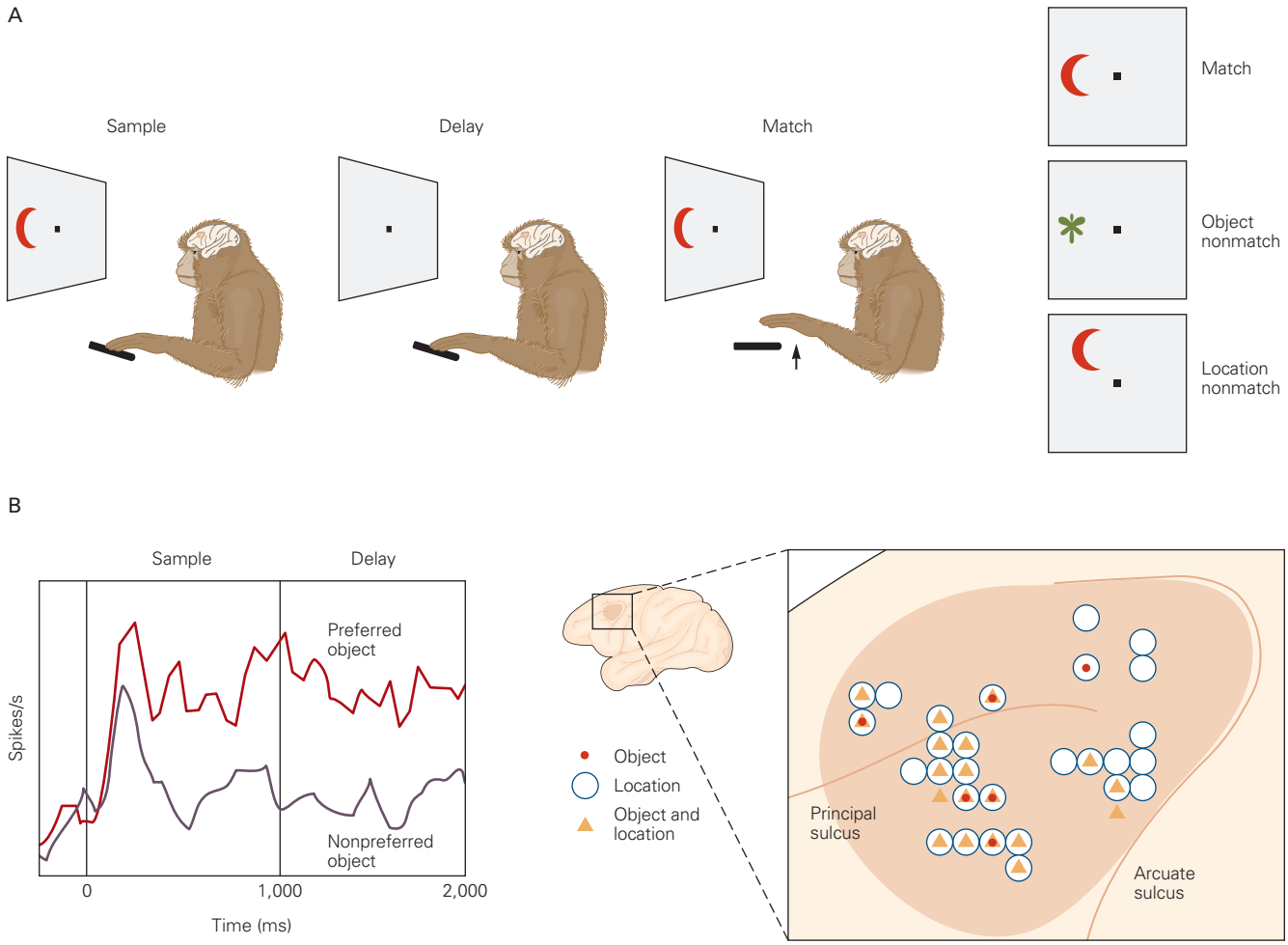

Figure 52–1 **The prefrontal cortex maintains a working memory.** (Adapted, with permission, from Rainer, Asaad, and Miller 1998.)

A. The role of prefrontal cortex in maintaining information in working memory is often assessed in monkeys using electrophysiological methods in conjunction with a delayed-match-to-sample (DMS) task. In this type of task, each trial begins when the monkey grabs a response lever and visually fixates a small target at the center of a computer screen. An initial visual stimulus (the sample) is briefly presented and must be held in working memory until the next stimulus (the match) appears. In the task illustrated here, the monkey was required to remember the sample ("what") and its location ("where") and release the lever only in response to stimuli that matched on both dimensions.

B. Neural firing rates in the lateral prefrontal cortex of a monkey during the delay period are often maintained above baseline and represent responses to the type of stimulus (what), the location (where), and the integration of the two (what and where). As shown, at left is the activity of a prefrontal neuron in response to a preferred object (to which the neuron responds robustly) and to a nonpreferred object (to which the neuron responds minimally). Activity is robust both when the monkey looks at the preferred object (sample) and during the delay. In the sketch at right, the symbols represent recording sites where neurons maintained each type of information (what, where, and what and where). Typically, several types of neurons were found at one site; hence, many symbols overlap and some symbols indicate more than one neuron.

Information Stored in Short-Term Memory Is Selectively Transferred to Long-Term Memory

In the mid-1950s, startling new evidence about the neural basis of long-term memory emerged from the study of patients who had undergone bilateral removal of the hippocampus and neighboring regions in the medial temporal lobe as treatment for epilepsy. The first and best-studied case was a patient called H.M. studied by the psychologist Brenda Milner and the surgeon William Scoville. (After H.M. died on December 2, 2008, his full name, Henry Molaison, was revealed to the world.)

H.M. had suffered for a number of years from untreatable temporal lobe epilepsy caused by brain

damage sustained at age 7 years in a bicycle accident. As an adult, his seizures rendered him unable to work or lead a normal life, and at the age of 27, he underwent surgery. Scoville removed the brain regions thought to be responsible for the seizures, including the hippocampal formation, the amygdala, and parts of the multimodal association area of the temporal cortex bilaterally (Figure 52–2). After the surgery, H.M.'s seizures were better controlled, but he was left with a devastating memory deficit (or amnesia). What was so remarkable about H.M.'s deficit was its specificity.

He still had normal working memory, for seconds or minutes, indicating that the medial temporal lobe is not necessary for transient memory. He also had long-term memory for events that had occurred before the operation. For example, he remembered his name, the job he had held, and childhood events. In addition, he retained a command of language, including his vocabulary, indicating that semantic memory—factual knowledge about people, places, and things—was preserved. His IQ remained unchanged, in the range of bright-normal.

What H.M. now lacked, and lacked dramatically, was the ability to transfer new information into long-term memory, a deficit termed anterograde amnesia. He was unable to retain for lengthy periods information about people, places, or objects that he had just encountered. Asked to remember a new telephone number, H.M. could repeat it immediately for seconds to minutes because of his intact working memory. But when distracted, even briefly, he forgot the number. H.M. could not recognize people he met after surgery, even when he met them again and again. For several years, he saw Milner every month, yet each time she entered the room, he reacted as though he had never seen her before. H.M. is not unique. All patients with extensive bilateral lesions of the limbic association areas of the medial temporal lobe show similar long-term memory deficits.

H.M. is a historic case because his deficit provided the first clear link between memory and the medial temporal lobe, including the hippocampus. Subsequent studies by Larry Squire and others of patients with brain damage more limited to the hippocampus confirmed its central role in memory. The observation that H.M. and others with medial temporal lobe damage had a profound deficit in the formation of new memories while the retrieval of old memories remained largely intact suggested that memories must be transferred over time from the hippocampus and medial temporal lobe to other brain structures. These studies gave rise to four central questions that continue to drive memory research to this day: First, what is the functional role of the medial temporal lobe memory system? Second, what are the roles of different subregions within this system? Third, how do these subregions work together with other brain circuits to support different forms of memory? Fourth, where are hippocampal-dependent memories ultimately stored?

The Medial Temporal Lobe Is Critical for Episodic Long-Term Memory

A crucial finding about H.M. was that formation of long-term memory was impaired only for certain types of information. H.M. and other patients with damage to the medial temporal lobe were able to form and retain certain types of durable memories just as well as healthy subjects.

For example, H.M. learned to draw the outlines of a star while looking at the star and his hand in a mirror (Figure 52–3). Like healthy subjects learning to remap hand–eye coordination, H.M. initially made many mistakes, but after several days of training, his performance was error-free and comparable to that of healthy subjects. Nevertheless, he did not consciously remember having performed the task.

Long-term memory formation in amnesic patients is not limited to motor skills. These patients retain simple reflexive learning, including habituation, sensitization, and some forms of conditioning (to be discussed later in this chapter). Furthermore, they are able to improve their performance on certain perceptual and conceptual tasks. For example, they do well with a form of memory called priming, in which perception of a word or object or access to the meaning of a word or object is improved by prior exposure. Thus, when shown only the first few letters of previously studied words, a subject with amnesia is able to generate the same number of studied words as normal subjects, even though the amnesic patient has no conscious memory of having recently encountered the words (Figure 52–4).

This pattern of selectively impaired performance in patients with amnesia raised questions about how to classify these different forms of memory: What are the key features that distinguish between memories that survive medial temporal lobe damage and those that do not? Early theories by Squire and colleagues suggested that a critical factor may be conscious awareness—damage to the medial temporal lobe appears to impair forms of memory that can be accessed consciously and can be reported on or expressed in words, while leaving intact forms of memory that cannot. For this reason, memories that depend on the medial temporal

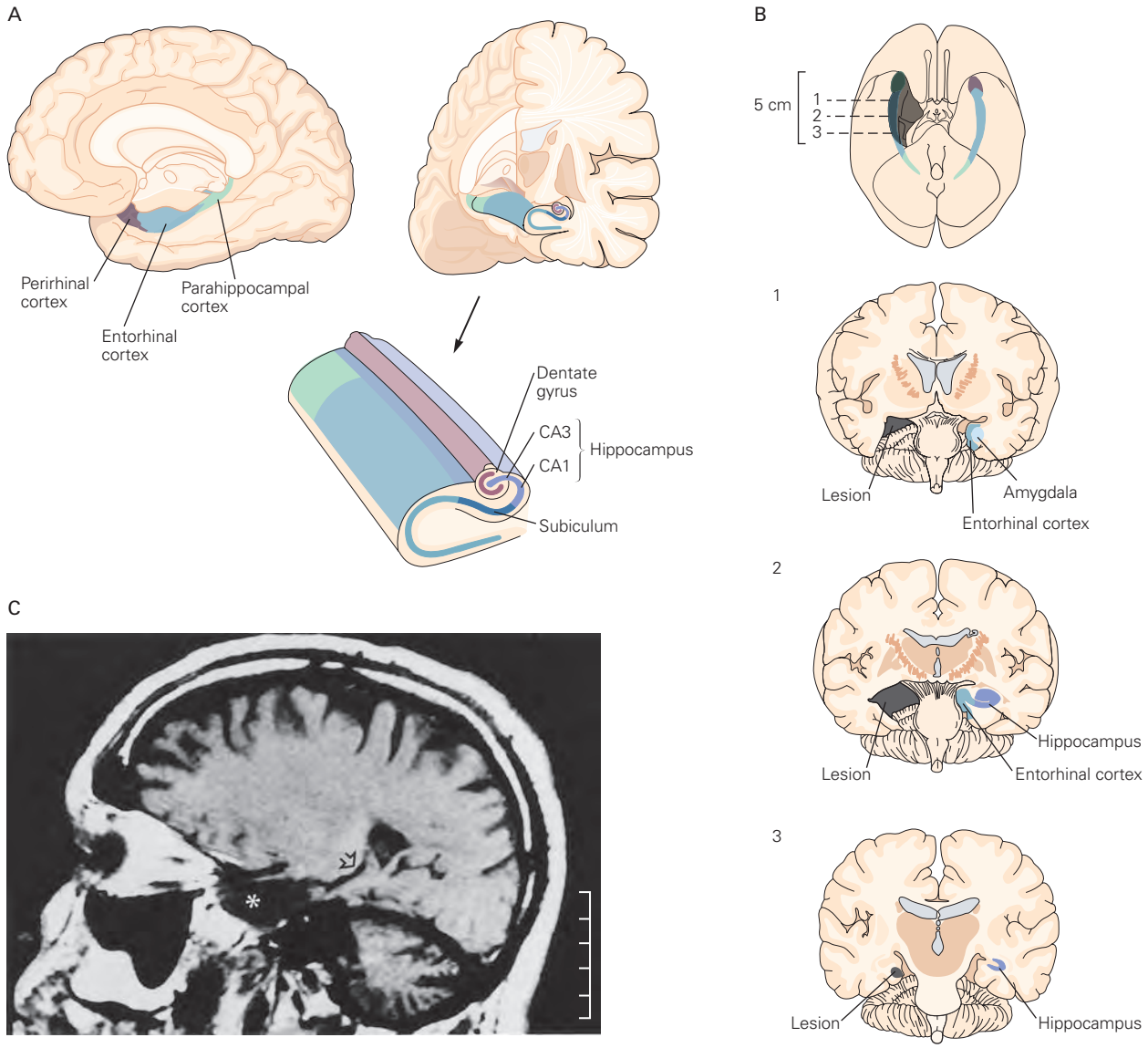

Figure 52–2 The medial temporal lobe and memory storage.

A. The key components of the medial temporal lobe important for memory storage.

B. The areas of temporal lobe resected (**gray shading**) in the patient known as H.M., viewed from the ventral surface of the brain (left hemisphere is on the right side of the image). Surgery was a bilateral, single-stage procedure, but to illustrate the structures that were removed from the left hemisphere (right side of the image), the left hemisphere is shown here intact. The longitudinal extent of the lesion is shown in a ventral view of the brain (top). Cross sections 1 through 3 show the estimated extent of areas of the brain removed from H.M. (Adapted, with permission, from Corkin et al. 1997.)

C. Magnetic resonance image (MRI) scan of a parasagittal section from the left side of H.M.'s brain. The calibration bar at the right of the panel has 1-cm increments. The **asterisk** in the central area of the scan indicates the resected portion of the anterior temporal lobes. The nearby **arrowhead** points to the remaining portion of the intraventricular portion of the hippocampal formation. Approximately 2 cm of preserved hippocampal formation is visible bilaterally. Note also the substantial degeneration in the enlarged folial spaces of the cerebellum. (Adapted, with permission, from Corkin et al. 1997.)

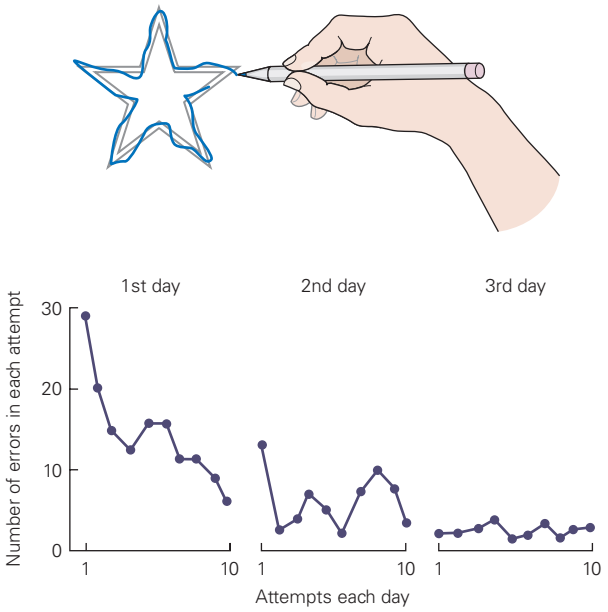

Figure 52–3 The amnesic patient H.M. could learn skilled movements. He was taught to trace between two outlines of a star while viewing his hand in a mirror. The graph plots the number of times, during each attempt, that he strayed outside the outlines as he drew the star. As with healthy subjects, H.M. improved considerably with repeated attempts despite the fact that he had no recollection of performing the task. (Reproduced, with permission, from Blakemore 1977.)

lobe are often referred to as *explicit* (or *declarative*) memory. Explicit memory can be further classified into episodic memory (the memory of personal experiences or autobiographical memory) and semantic memory (memory for facts). *Episodic memory* refers to our ability to remember rich details of moments in time, including information about what happened, when, and where. For example, episodic memory is used to recall that we saw the first flowers of spring yesterday or that we heard Beethoven's "Moonlight Sonata" several months ago. *Semantic memory* is used to recall the meanings of words or concepts, among other facts.

Cognitive psychologists found a similar distinction between different forms of memory in healthy subjects by using tasks that differ in how memories are expressed. One type is a nonconscious form of memory that is evident in the performance of a task. This form of memory is often referred to as *implicit* memory (also referred to as *nondeclarative* or procedural memory). Implicit memory is typically manifested in an automatic manner, with little conscious processing on the part of the subject. Different forms give rise to priming, skill learning, habit memory, and conditioning (Figure 52–5). Explicit memory is considered to be highly flexible; multiple pieces of information can be associated under different circumstances. Implicit memory, however, is tightly connected to the original conditions under which the learning occurred.

The terms "explicit memory" and "implicit memory" are used to describe two broad forms of memory that differ in their hallmark behavioral characteristics and in their neural underpinnings. These forms of memory can be acquired in parallel. For example, one might form an explicit memory of how good a bakery smelled upon entering it yesterday, while at the same time, one might develop an automatic conditioned response of increased salivation upon viewing a picture of the bakery. Moreover, we now believe that these forms of memory, while distinct, normally interact to support behavior, although the precise

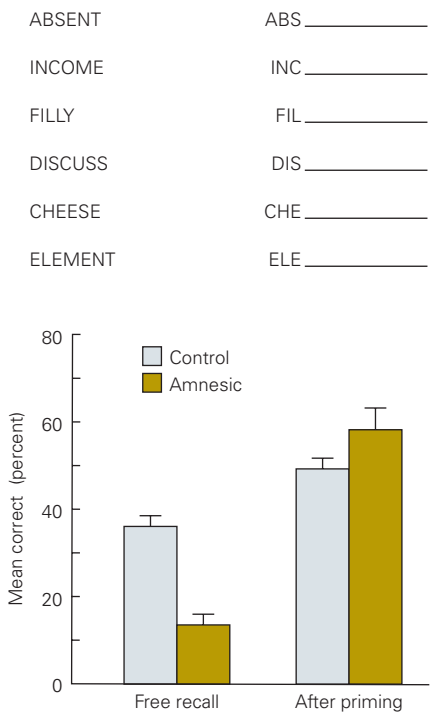

Figure 52–4 Amnesic subjects differ in their ability to recall words under two conditions. Subjects were presented with common words and then asked to recall the words. Amnesic patients did not do well on this test during free recall. However, when subjects were given the first three letters of a word that had been presented and instructed to form the first word that came to mind (word completion), the amnesic subjects performed as well as normal subjects. The baseline guessing rate in the word completion condition for words not previously presented was 9%. (Adapted from Squire 1987.)

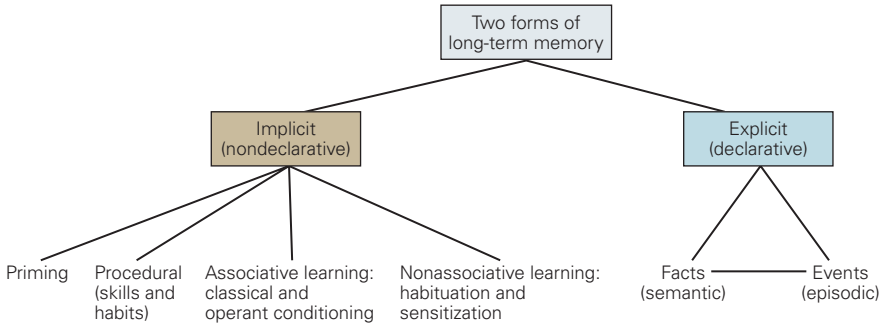

Figure 52–5 Long-term memory is commonly classified as either explicit (the memory is reported verbally) or implicit (the memory is expressed through behavior without conscious awareness).

nature and extent of their interactions are a topic of ongoing investigation.

There are also ongoing debates about the role of conscious awareness in memory and about whether it is indeed a necessary feature of memories supported by the medial temporal lobe. These debates are driven by a growing body of work showing that the same medial temporal circuits necessary for explicit memory are also necessary for some forms of implicit memory (as described below). Indeed, although episodic memory is typically assessed by asking subjects to report the content of their memory, it remains unknown whether conscious accessibility is an integral feature of the memories themselves. Nonetheless, the distinction between implicit and explicit memory played an important historical role in differentiating forms of memory and still offers a productive framework for considering the neural bases of memory. Thus, we use the terms "explicit memory" and "implicit memory" here to distinguish these two forms of memory and the classes of subjective experience and behaviors that they are based on. In the following sections, we focus on episodic memory, which has been the target of a great deal of cognitive neuroscience research in both amnesic patients and healthy individuals.

Episodic Memory Processing Involves Encoding, Storage, Retrieval, and Consolidation

Episodic memory has been studied extensively and offers a window into understanding how the brain builds, stores, and retrieves details about episodes in our lives. We now know that the brain does not have a single long-term store of episodic memories. Instead, the storage of any item of knowledge is widely distributed among many brain regions that process different aspects of the content of the memory and can be accessed independently (by visual, verbal, or other sensory clues). Second, episodic memory is mediated by at least four related but distinct types of processing: encoding, storage, consolidation, and retrieval.

Encoding is the process by which new information is initially acquired and processed during the formation of a new memory. The extent of this processing is critically important for determining how well the learned material will be remembered. For a memory to persist and be well remembered, the incoming information must undergo what the psychologists Fergus Craik and Robert Lockhart called "deep" encoding. This is accomplished by attending to the information and associating it with memories that were already established. Memory encoding is also stronger when one is motivated to remember, whether because the information has particular emotional or behavioral relevance (eg, a memory for a particularly delicious meal on an enjoyable first date) or whether the information itself is neutral but is associated with something meaningful (eg, remembering the location of that restaurant).

Storage refers to the neural mechanisms and sites by which the newly acquired information is retained as a lasting memory over time. One of the remarkable features about long-term storage is that it seems to have an almost unlimited capacity. In contrast, working memory storage is very limited; psychologists believe that human working memory can hold only a few pieces of information at any one time.

Consolidation is the process that transforms temporarily stored and still labile information into a more stable form. As we shall learn in the next two chapters, consolidation involves expression of genes and protein synthesis that give rise to structural changes at synapses.

Finally, *retrieval* is the process by which stored information is recalled. It involves bringing back to mind different kinds of information that are stored in different sites. Retrieval of memory is much like perception; it is a constructive process and therefore subject to distortion much as perception is subject to illusions (Box 52–1). When a memory is retrieved, it becomes active again, providing an opportunity for an old memory to be encoded again. Because retrieval is constructive, re-encoding of a retrieved memory can differ from the original memory. For example,

Box 52–1 Episodic Memories Are Subject to Change During Recall

How accurate is episodic memory? This question was explored by the psychologist Frederic Bartlett in a series of studies in the 1930s in which subjects were asked to read stories and then retell them. The recalled stories were shorter and more coherent than the original stories, reflecting reconstruction and condensation of the original.

The subjects were unaware that they were editing the original stories and often felt more certain about the edited parts than about the unedited parts of the retold stories. They were not confabulating; they were merely interpreting the original material so that it made sense on recall.

Observations such as these demonstrate that episodic memory is malleable. Moreover, the fact that people incorporate later edits into their original memories leads us to believe that episodic memory is a constructive process in the sense that individuals perceive the environment from the standpoint of a specific point in space as well as a specific point in their own history. Much like sensory perception, episodic memory is not a passive recording of the external world but an active process in which incoming bottom-up sensory information is shaped by top-down signals, representing prior experience, along the afferent pathways. Likewise, once information is stored, recall is not an exact copy of the information stored. Past experiences are used in the present as cues that help the brain reconstruct a past event. During recall, we use a variety of cognitive strategies, including comparison, inference, shrewd guessing, and supposition, to generate a memory that seems coherent to us, that is consistent with other memories, and that is consistent with our "memory of the memory."

re-encoding can include information from the old memory together with the new context in which it was retrieved. This re-encoding allows memories of separate moments in time to be connected in memory, but it also opens the door to errors in memory, as discussed later in the chapter.

Retrieval of information is most efficient when a retrieval cue reminds individuals of the episodic nature of the events linking the elements of the encoded experience. For example, in a classic behavioral experiment, Craig Barclay and colleagues asked some subjects to encode sentences such as "The man lifted the piano." On a later retrieval test, "something heavy" was a more effective cue for recalling piano than "something with a nice sound." Other subjects, however, encoded the sentence "The man tuned the piano." For them, "something with a nice sound" was a more effective retrieval cue for piano than "something heavy" as it reflected better the initial experience. Retrieval, particularly of explicit memories, also is partially dependent on working memory.

Episodic Memory Involves Interactions Between the Medial Temporal Lobe and Association Cortices

Although studies of amnesic patients during the past few decades have refined our understanding of various types of memory, medial temporal lobe damage affects all four operations of memory—encoding, storage, consolidation, and retrieval—and thus it is often difficult to discern how the medial temporal lobe contributes to each. fMRI allows us to scan brain activity in the process of building new memories or retrieving existing memories, and thus to identify specific regions that are active during different processes (Chapter 6).

A common method for studying encoding with fMRI is the *subsequent memory paradigm*. In a typical subsequent memory task, a human subject views a series of stimuli (eg, words or pictures) one at a time while being scanned with fMRI, often while engaged in a cover task (eg, determining whether the pictures are in color or black and white). A subject's memory for the stimuli is then tested outside of the scanner, allowing the researchers to sort all the encoding events into those that were later remembered compared to those that were later forgotten. fMRI scans show that remembered items, compared with forgotten items, are associated with greater activity in the hippocampus during encoding. This difference is also evident in simultaneous activity in other parts of the brain, including prefrontal, retrosplenial, and parietal cortices. Often, the activity of these regions covaries on a moment-to-moment basis with the activity in the hippocampus during memory encoding, suggesting that these regions are functionally connected (Figure 52–6).

These fMRI findings, together with findings from patients with amnesia, provide strong support for an

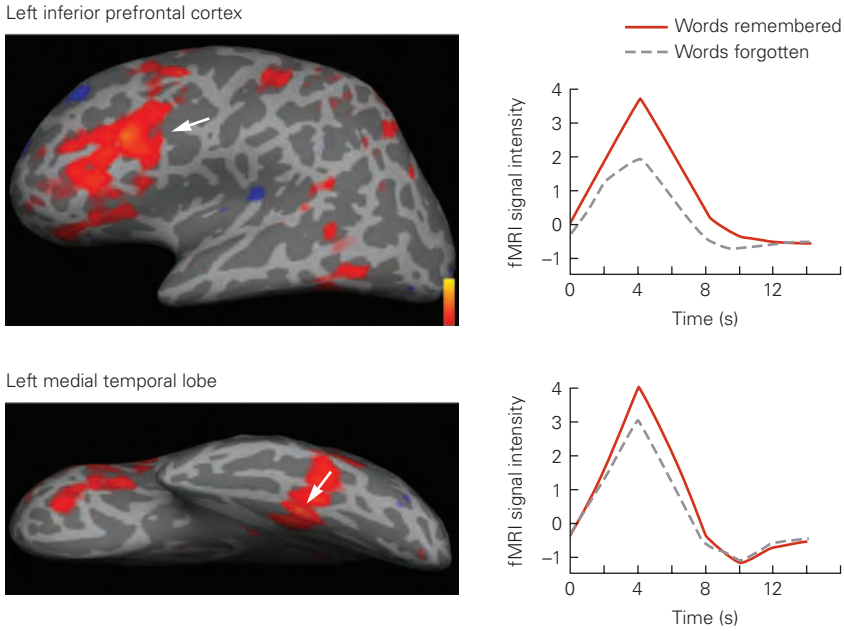

Figure 52–6 In the study illustrated here, neural activity during encoding of visual events (presentation of words) was measured using functional magnetic resonance imaging (fMRI). Subsequently, recall of the studied words was tested, and each word was classified as either remembered or forgotten. The scans taken during encoding were then sorted into two groups: those made during encoding of words that were later remembered and those made during encoding of words that were later forgotten. The activity in regions of the left prefrontal cortex and medial temporal lobe was greater during the encoding of words later remembered than those later forgotten (locations denoted by white arrows). At right are the observed fMRI responses in these regions for words later remembered and those later forgotten. (Adapted, with permission, from Wagner et al. 1998.)

important role of the hippocampus in encoding episodic memories. The fMRI findings also extend the findings from amnesic patients, showing that successful formation of episodic memories depends on interaction between frontoparietal networks and the medial temporal lobe. However, as the medial temporal lobe is a large structure, a key goal is to understand the role of its different subregions. Such information is being provided by higher-resolution fMRI studies that use more powerful brain scanning technologies. These studies reveal that distinct subregions within and outside the hippocampus contribute to different aspects of memory encoding. Thus, whereas some cortical areas surrounding the hippocampus are particularly important for object recognition (perirhinal cortex), others are important for encoding spatial context (parahippocampal cortex). These cortical regions provide strong (but indirect) inputs to the hippocampus proper, which is thought to bind together spatial and object information, forming a unified memory.

Interaction between the medial temporal lobe and widely separated cortical regions is also central in memory consolidation and retrieval. It was initially thought that the hippocampus was not important for retrieval, since patient H.M., whose medial temporal lobe was surgically removed, could still recall childhood memories. In fact, early observations suggested that H.M. could recall many of the experiences of his life up until several years before his operation. These observations of H.M. and other amnesic patients with damage to the medial temporal lobe suggested that old memories must be ultimately stored in various other cortical regions through interaction with the medial temporal lobe. However, even though patients with hippocampal damage like H.M. have some ability to recall older memories, there is evidence that the extent of memory recall may be impaired in these patients. Current thinking suggests that there is a distributed circuit for consolidation and retrieval involving several brain regions, with the hippocampus playing an essential role in the binding of associations during both encoding and retrieval. The cortical regions serve as the long-term repository of the separate elements of information that constitute a memory and in the controlled retrieval and reactivation of the content of the memory itself.

As with studies of encoding, studies of retrieval of episodic knowledge have implicated specific regions of association cortex, frontoparietal networks, and the medial temporal lobe. The retrieval of contextual or event details associated with an episodic memory also involves activity in the hippocampus, with medial temporal lobe retrieval processes facilitating the activation of neocortical representations that were present during encoding.

fMRI scans have a fairly limited time resolution due to the relatively slow time course of changes in blood flow associated with brain activity. To achieve higher temporal resolution of brain activity, researchers can record electrical activity from the human brain using extracellular electrodes. Such recordings are rare and possible only in human patients who are already

undergoing brain surgery for medical reasons, such as severe epilepsy, when electrode implantation is used to localize the site of seizure generation. In one study, intracranial electroencephalography (iEEG) signals were measured using subdural electrodes placed in the medial temporal lobe and other areas of cortex. A subject first learned associations between pairs of words and then had to retrieve memories of those associations. The retrieval of memories was associated with neural activity in the hippocampus, coupled with neural activity in temporal association cortex, a region involved in language and multisensory integration. This coupled neural activity was associated with a reactivation of cortical patterns that were initially observed when participants first memorized word pairs. This finding provides a link between the neural activity observed in the hippocampus during initial encoding of a memory and the later coupled activity in the temporal association cortex during retrieval. Related observations of reactivation of encoding patterns during retrieval have been reported in numerous human functional imaging studies, documenting the ubiquity of such effects. As with encoding of episodic memory, retrieval involves a complex interaction between the medial temporal lobe and distributed cortical regions, including frontoparietal networks and other high-level association areas.

Episodic Memory Contributes to Imagination and Goal-Directed Behavior

Memory enables us to use our past experience to predict future events, thus promoting adaptive behavior. Like retrieval of memories, imagination of future events involves construction of details from memory. The first report of a possible connection between memory and imagination came from the case study of patient K.C., as reported by Endel Tulving in 1985. Patient K.C. displayed typical and devastating amnesia as a result of damage to his hippocampus and medial temporal lobe. Similar to patient H.M., he had a complete lack of episodic memory while language and nonepisodic functions were unimpaired. Tulving's studies revealed further that such brain damage was associated with the loss of the ability to imagine events in the future. When asked what he would be doing the next day, K.C. was unable to provide details.

The importance of the hippocampus in imagining future events is also seen with fMRI studies. Such studies examined brain activity of healthy individuals, comparing activity when subjects were asked to remember an event from the past (eg, think of your birthday last year) with activity when they imagined events in the future (eg, imagine a beach vacation next summer). The subjects were asked to report any vivid details of the event that came to mind. The MRI scans showed a striking overlap in the network of brain regions that were active during memory retrieval and imagination of future events. This network included the hippocampus, prefrontal cortex, posterior cingulate cortex, retrosplenial cortex, and lateral parietal and temporal areas (Figure 52–7).

Further evidence supporting the view that episodic memory and hippocampal function are necessary for planning future behavior comes from a study on human performance of a spatial navigation task using virtual reality simulations. High-resolution fMRI and multivoxel pattern analysis (Chapter 6) showed that activity in the hippocampus was related to simulation of navigation goals. Moreover, hippocampal activity during planning covaried with goal-related activity in prefrontal, medial temporal, and medial parietal cortex (Figure 52–8).

Episodic memory encoding and storage are also influenced by the adaptive value of events. Alison Adcock and colleagues showed that the anticipation of a potential reward can enhance memory by eliciting coordinated activity between the medial temporal lobe and midbrain regions that are rich in dopamine neurons. Reward can also retroactively enhance memories. When human participants navigate a maze for a reward, they have better memory for neutral events that happened right before the reward. The ability to retroactively shape episodic memory based on outcomes is important because the relevance of a specific episode may only become known after the fact. Together with the role of episodic memory in constructing the retrieval of past events and in imagining and simulating future events, the findings on reward support the view that a major function of episodic memory is to guide adaptive behaviors.

The Hippocampus Supports Episodic Memory by Building Relational Associations

In addition to the broad role of the hippocampus in episodic memory, future thinking, and goal-directed behavior, studies of rodents first pointed to a role for the hippocampus in spatial navigation (Chapter 54), findings that were later supported by studies of nonhuman primates and humans. In rodents, single neurons in the hippocampus encode specific spatial information, and lesions of the hippocampus interfere with the animal's memory for spatial location. Functional imaging of the brain in healthy humans shows that activity increases in the right hippocampus when spatial information is recalled and in the left hippocampus when words,

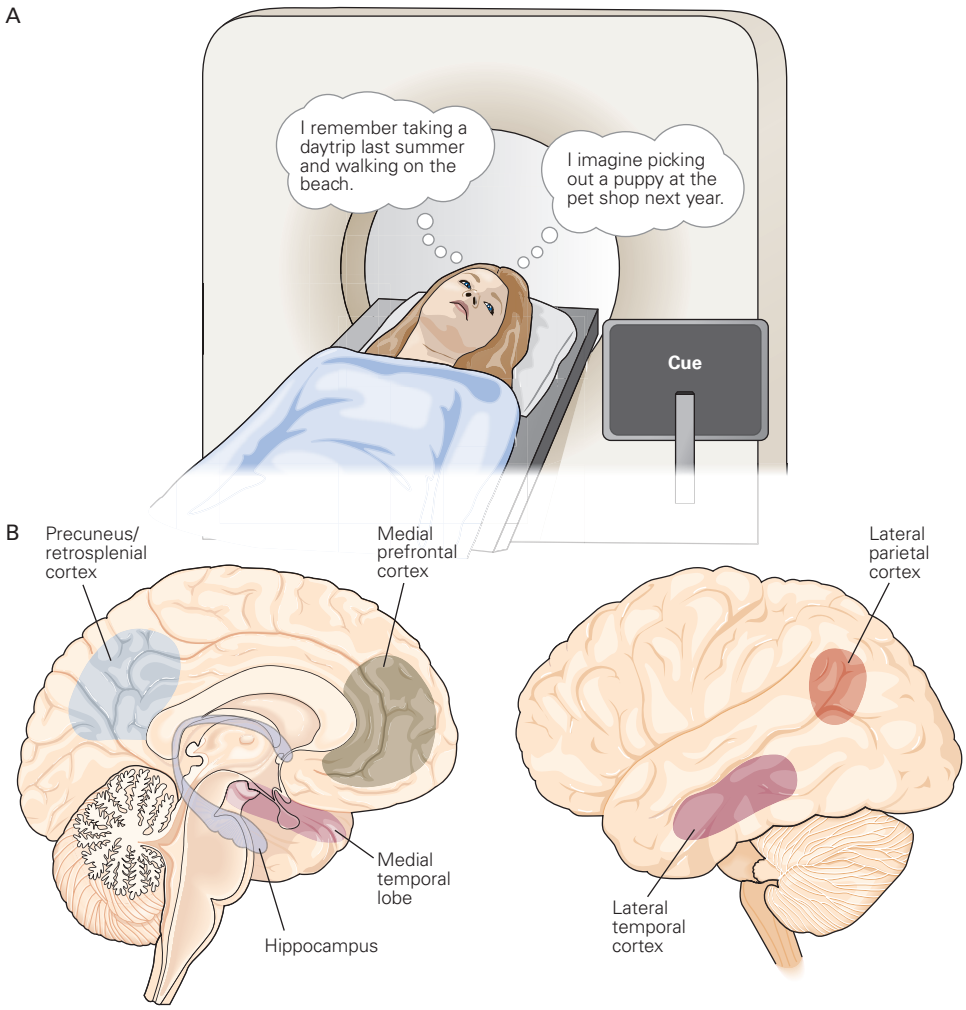

Figure 52–7 Brain regions supporting retrieval of memories for past events and imagination of future events. (Adapted, with permission, from Schacter, Addis, and Buckner 2007.)

A. Subjects were instructed to either remember a personally experienced event in their past or imagine a plausible event in their future while lying inside a functional magnetic resonance imaging scanner. Events are elicited by a cue word (eg, "beach" or "birthday"). Subjective ratings of event phenomenology (eg, vividness and emotionality of the episode) and detailed event descriptions are often obtained in an interview following the scanning in order to confirm that an episodic event was successfully generated.

B. The core brain system that mediates past and future thinking is consistently activated while remembering the past, when envisioning the future, and during related forms of mental simulation. Prominent components of this network include medial prefrontal regions, posterior regions in the medial and lateral parietal cortex (extending into the precuneus and retrosplenial cortex), the lateral temporal cortex, and the medial temporal lobe. Moreover, regions within this core brain system are functionally correlated with each other and with the hippocampus. This core brain system is thought to function adaptively to integrate information about relationships and associations from past experiences to construct mental simulations about possible future events.

objects, or people are recalled. These physiological findings are consistent with the clinical observation that lesions of the right hippocampus differentially give rise to problems with spatial orientation, whereas lesions of the left hippocampus differentially cause deficits in verbal memory.

The fact that the hippocampus supports spatial processing, semantic memory, and episodic memory raises questions about how the hippocampus contributes to such different behaviors. One compelling theory, proposed by Howard Eichenbaum and Neal Cohen, suggests that the hippocampus provides a general mechanism for forming and storing complex multimodal associations. According to this view, the hippocampus binds in memory the separate elements of experiences, encoding events as relational maps of

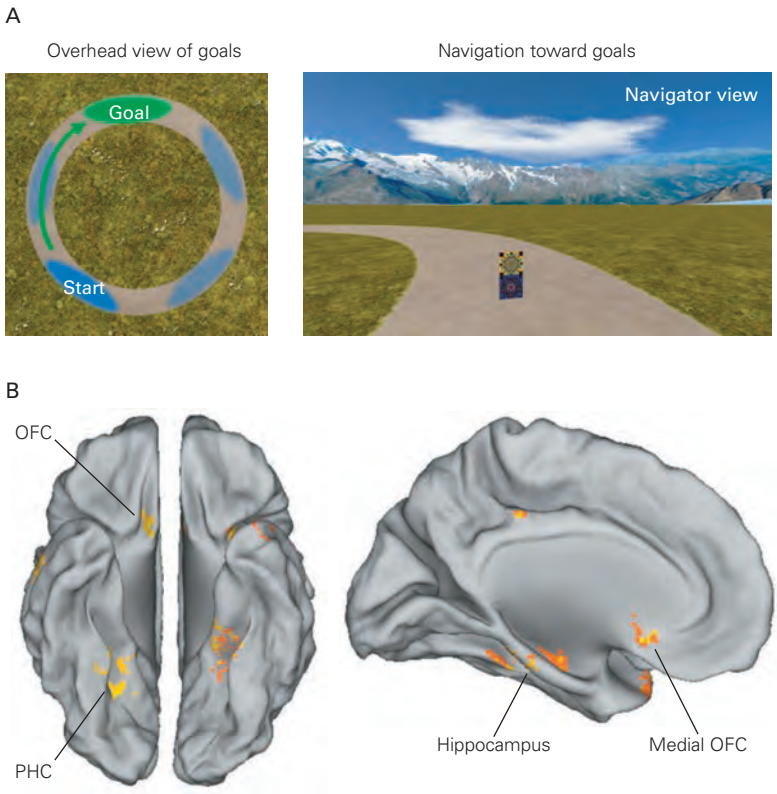

Figure 52–8 **Neural circuits supporting memory-based goal-directed navigation.** (Reproduced, with permission, from Brown et al. 2016.)

A. Human participants navigate to goals in a virtual reality environment while being scanned with functional magnetic resonance imaging. They first explore the space and learn where goals are located and then are tested on their ability to navigate to specific goals.

B. Navigational planning elicits goal-related activity in a core network including the hippocampus, medial temporal lobe, parahippocampal cortex (**PHC**), and orbitofrontal cortex (**OFC**).

items within spatial and temporal contexts, thus composing a "memory space" that can distinguish distinct episodes, or sequences of events, even when the same (or similar) events occur in different episodes (Figure 52–9). As discussed later in this chapter, the view that the hippocampus encodes relations offers insights into the mechanism by which memories are built and explains why, in some cases, the hippocampus may contribute to memory processes that are not consciously accessible but do encode relations.

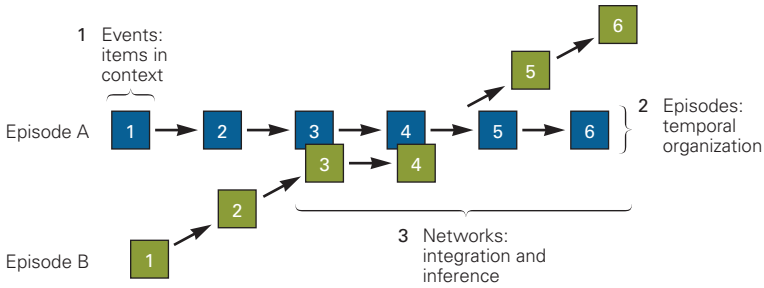

Figure 52–9 **The hippocampus supports relational processing underlying episodic memory.** A conceptual illustration of a memory space designating three key types of relational processing: events, episodes, and networks. The schematic illustrates processing of two distinct episodes (Episode A and Episode B), which have both distinct and overlapping elements. For example, the episodes might be two distinct visits to an Italian restaurant on separate evenings with the same friend. The evenings are experienced as distinct (different days, different weather, different moods), yet they share some overlap (the company of the same friend at the same restaurant). *Events* (**1**) are defined as items (objects, behaviors) that are associated with the context in which they occurred (denoted here as events 1 to 6 in each episode, such as the specific table you sat at, the food you ordered, etc.). *Episodes* (**2**) are defined in this view as the temporal organization of these events. While most of the items in each episode are unique, some of them overlap (here, items 3 and 4; in the example, your friend and the restaurant). Relational *networks* (**3**) are formed via associations between events and episodes by way of the overlapping events, supporting the capacity for links between indirectly related events. (Reproduced, with permission, from Eichenbaum and Cohen 2014. Copyright © 2014 Elsevier Inc.)

Implicit Memory Supports a Range of Behaviors in Humans and Animals

Just as there are many ways in which explicit memory guides behavior, there are also many ways in which nonexplicit forms of memory, those without conscious awareness, can influence behavior. Implicit memory refers to forms of knowledge that guide behavior without conscious awareness. Priming, for example, is the automatic influence of exposure to one cue on processing of a later cue.

Priming can be classified as conceptual or perceptual. *Conceptual priming* provides enhanced access to task-relevant semantic knowledge because that knowledge has been used before. It is correlated with decreased activity in left prefrontal regions that subserve initial retrieval of semantic knowledge. In contrast, *perceptual priming* occurs within a specific sensory modality and depends on cortical modules that operate on sensory information about the form and structure of words and objects.

Damage to unimodal sensory regions of cortex impairs modality-specific perceptual priming. For example, one patient with an extensive surgical lesion of the right occipital lobe failed to demonstrate visual priming for words but had normal explicit memory (Figure 52–10). This condition is the reverse of that found in amnesic patients such as H.M., suggesting that the neural mechanisms of priming are distinct from those for explicit memory. The fact that perceptual priming can be intact in patients with amnesia due to medial temporal damage further suggests that it is distinct from explicit memory.

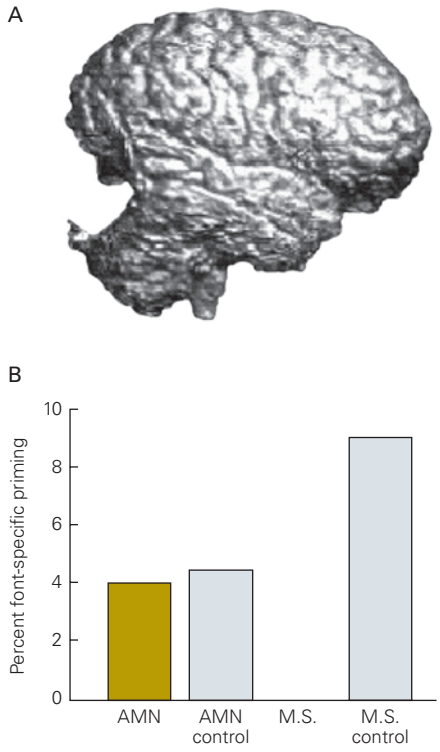

Figure 52–10 The right occipital cortex is required for visual priming for words. (Adapted from Vaidya et al. 1998.)

A. Structural magnetic resonance imaging depicts the near-complete removal of the right occipital cortex in a patient, M.S., who suffered pharmacologically intractable epilepsy with a right occipital cortical focus.

B. Font-specific priming is a form of visual priming in which the individual is better able to identify a briefly flashed word when the type font is identical to an earlier presentation, compared to identification when the font is different. Priming is measured as performance when the font is the same minus performance when the font is different. Font-specific priming is intact in amnesic patients (**AMN**) and their controls as well as in the controls for patient M.S., but not in M.S. himself. The patient M.S. has normal explicit memory, even for visual cues (data not shown), but lacks implicit memory for specific properties of visually presented words.

Different Forms of Implicit Memory Involve Different Neural Circuits

Other forms of implicit memory subserve the learning of habits and motor, perceptual, and cognitive skills and the formation and expression of conditioned responses. In general, these forms of implicit memory are characterized by incremental learning, which proceeds gradually with repetition and, in some cases, is driven by reinforcement.

The learning of habits, motor skills, and conditioned responses can take place independently of the medial temporal lobe system. For example, H.M. was able to acquire new visuomotor skills, like the mirror-tracing task (see Figure 52–3). Therefore, early theories posited that these forms of memory generally do not depend on the medial temporal lobe but, rather, depend on the basal ganglia and cerebellum (see Chapters 37 and 38). However, subsequent work suggested that this is not a general rule and that the medial temporal lobe is required for forms of implicit learning that store relational associations, even when such associations are learned through repetition and appear to take place without conscious awareness.

It is now thought that several kinds of incremental implicit learning involve the medial temporal lobes. For example, Turk-Browne and colleagues investigated implicit learning of regularities between visual cues, called statistical learning. In a typical statistical learning task, human subjects are presented with a

stream of sounds or images that follow a structured sequence or "grammar" of repetitions. Learning of the sequence is typically measured by a faster reaction time to repeated compared to nonrepeated sequences. At first glance, it would appear that statistical learning should not involve the medial temporal lobe: The learning is nonverbal, it does not require conscious thought and is therefore implicit, and it is assumed to reflect the accumulated computation of probabilistic relationships across multiple episodes, rather than the specific memory of one episode. Yet fMRI studies show that the hippocampus is active during statistical learning, and damage to the medial temporal lobe has been found to impair performance on this implicit task.

Statistical learning is an example of how learning takes place through repetition. New perceptual, motor, or cognitive abilities are also learned through repetition. With practice, performance becomes more accurate and faster, and these improvements generalize to learning novel information. Skill learning moves from a cognitive stage, where knowledge is represented explicitly and the learner must pay a great deal of attention to performance, to an autonomous stage, where the skill can be executed without much conscious attention. As an example, driving a car initially requires that one be consciously aware of each component of the skill, but after practice, one no longer attends to the individual components.

The learning of sensorimotor skills depends on numerous brain regions that vary with the specific associations being learned. As we learned in Chapter 38, these include the basal ganglia, cerebellum, and neocortex. Dysfunction of the basal ganglia in patients with Parkinson and Huntington disease impairs learning of motor skills. Patients with cerebellar lesions also have difficulties acquiring some motor skills. Functional imaging of healthy individuals during sensorimotor learning shows changes in the activity of the basal ganglia and cerebellum and their connectivity with cortical regions. Danielle Bassett and colleagues have used network-analysis algorithms applied to whole-brain fMRI data to characterize dynamic changes in network functional connectivity that take place during motor skill learning. Finally, skilled behavior can depend on structural changes in motor neocortex, as seen by the expansion of the cortical representation of the fingers in musicians (Chapter 53).

Habits emerge from the repeated association of cues or actions with rewarding outcomes. Habit learning in humans is studied with tasks that involve incremental learning of stimulus–reward associations. In a typical task, subjects perform a series of trials in which they are asked to choose among visual cues and receive trial-by-trial feedback on their choice. The relationship between the cues and the feedback varies probabilistically over the course of the task so that participants must keep updating their responses based on the feedback. Because learning takes place over numerous trials, explicit memory of any one specific trial may not be as useful for successful performance as the gradual accumulation of feedback-driven learning of stimulus–outcome associations.

fMRI studies demonstrate that incremental learning of stimulus–reward associations depends on the striatum, the area of the basal ganglia that receives input from neocortex, and its modulatory dopaminergic inputs. Patients with a loss of striatal dopamine, as occurs in Parkinson disease, are less effective at learning based on trial-by-trial reinforcement. These findings are consistent with other studies that indicate dopamine has an important role in modulating cortico-striatal circuitry for reinforcement learning (see Chapter 38).

At first glance, stimulus-reward learning appears to be precisely the sort of learning that does not depend on the medial temporal lobe: It is implicit rather than explicit, and it occurs gradually rather than through an explicit memory for a single event. Indeed, early theories posited that learning probabilistic stimulus–reward associations does not depend on the medial temporal lobe. However, subsequent work has revealed that the hippocampus does contribute to stimulus–reward learning under some circumstances, such as when the task demands learning of more complex stimulus–stimulus associations (Figure 52–11). The contribution of the hippocampus to implicit learning takes place via interactions with other cortical and subcortical circuits. fMRI studies show functional connectivity between the hippocampus and the striatum in support of learning across a variety of tasks. Interactions between the hippocampus and the striatum are sometimes competitive and sometimes cooperative, depending on the demands of the task.

Implicit Memory Can Be Associative or Nonassociative

Some forms of implicit memory have also been studied in nonhuman animals, and these animal studies have distinguished two types of implicit memory: nonassociative and associative. With nonassociative learning, an animal learns about the properties of a single stimulus. With associative learning, the animal learns about the relationship between two stimuli or between a stimulus and a behavior. We consider the cellular mechanisms of implicit memory in animals in the next chapter.

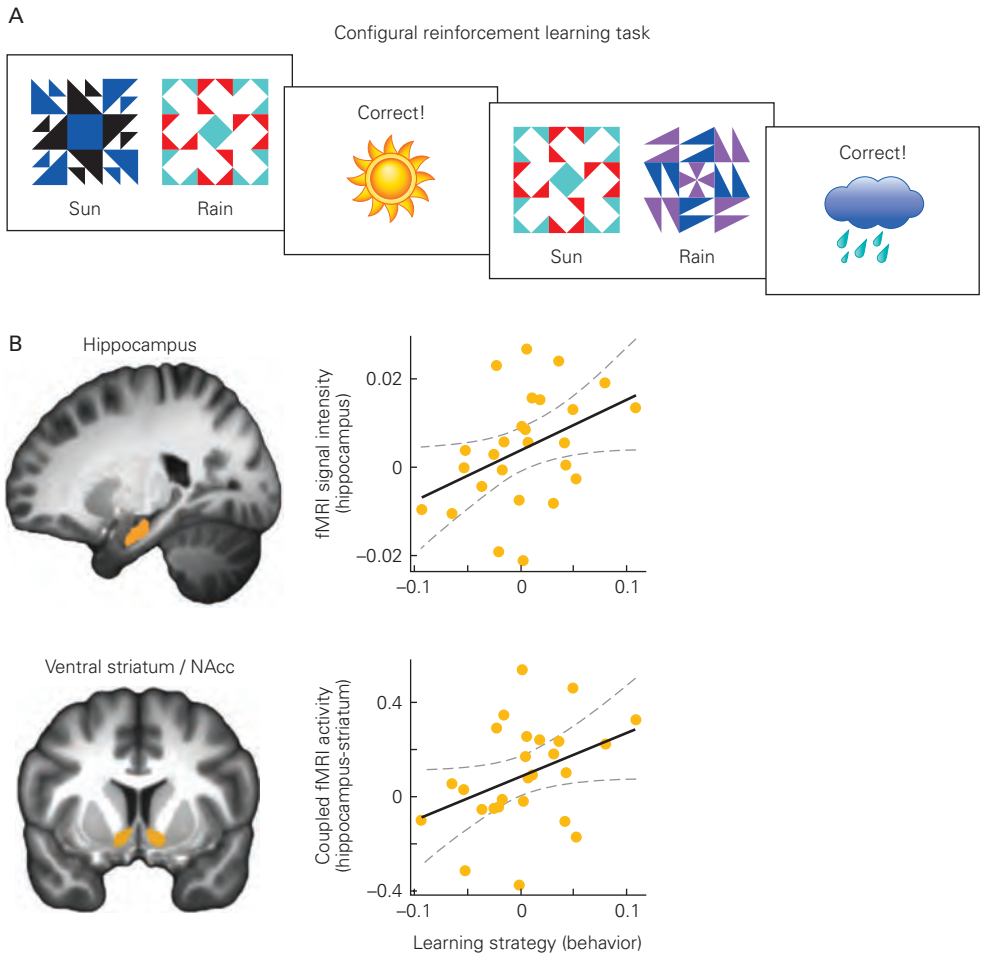

Figure 52–11 Learning stimulus–response associations involves both the striatum and the hippocampus. (Adapted, with permission, from Duncan et al. 2018.)

A. Participants use trial-by-trial reinforcement to learn to predict outcomes (rain or sun) based on cues (colorful shapes). The cues have a probabilistic relation to each weather outcome that the viewer learns by trial and error. The weather can be predicted based either on each individual cue or on the combined presentation of the two cues (their configuration). Reinforcement learning models can discern which strategy each subject uses.

B. The striatum is known to play a critical role in learning to update choices based on reinforcement. When subjects learn about the configuration, this same task also elicits activity in the hippocampus and increased coupling of activity in the hippocampus and the striatum. Scatter plots show that the extent to which subjects use a configural learning strategy correlates with blood oxygenation level–dependent activity in the hippocampus and with functional coupling between the hippocampus and the striatum. The images show activity in hippocampus and the nucleus accumbens (**NAcc**), a region in the ventral portion of the striatum that responds to rewarding stimuli. (Abbreviation: **fMRI**, functional magnetic resonance imaging.)

Nonassociative learning results when a subject is exposed once or repeatedly to a single type of stimulus. Two forms of nonassociative learning are common in everyday life: habituation and sensitization. Habituation is a decrease in a response that occurs when a benign stimulus is presented repeatedly. For example, most people in the United States are startled when they first hear the sound of a firecracker on Independence Day, but as the day progresses, they become accustomed to the noise and do not respond. Sensitization (or pseudo-conditioning) is an enhanced response to a wide variety of stimuli after the presentation of an intense or noxious stimulus. For example, an animal will respond more vigorously to a mild tactile stimulus after receiving a painful pinch. Moreover, a sensitizing stimulus can override the effects of habituation, a process called dishabituation. For example, after the startle response to a noise has been reduced by habituation,

one can restore the intensity of response to the noise by delivering a strong pinch.

With sensitization and dishabituation, the timing of stimuli is not important because no association between stimuli must be learned. In contrast, with two forms of associative learning, the timing of the stimuli to be associated is critical. Classical conditioning involves learning a relationship between two stimuli, whereas operant conditioning involves learning a relationship between the organism's behavior and the consequences of that behavior.

Classical conditioning was first described in the early 1900s by the Russian physiologist Ivan Pavlov. The essence of classical conditioning is the pairing of two stimuli: a conditioned stimulus and an unconditioned stimulus. The conditioned stimulus (CS), such as a light, a tone, or a touch, is chosen because it produces either no overt response or a weak response usually unrelated to the response that eventually will be learned. The unconditioned stimulus (US), such as food or a shock, is chosen because it normally produces a strong and consistent response (the unconditioned response), such as salivation or withdrawal of a limb. Unconditioned responses are innate; they are produced without learning. Repeated presentation of a CS followed by a US gradually elicits a new or different response called the conditioned response.

One way of explaining conditioning is that repeated pairing of the CS and US causes the CS to become an anticipatory signal for the US. With sufficient experience, an animal will respond to the CS as if it were anticipating the US. For example, if a light is followed repeatedly by the presentation of meat, eventually the sight of the light itself will make the animal salivate. Thus, classical conditioning is one way an animal learns to predict events.

The probability that an established conditioned response will occur decreases if the CS is repeatedly presented without the US. This process is known as extinction. If a light that has been paired with food is later repeatedly presented in the absence of food, it will gradually cease to evoke salivation. Extinction is an important adaptive mechanism; it would be maladaptive for an animal to continue to respond to cues that are no longer meaningful. The available evidence indicates that extinction is not the same as forgetting; instead, something new is learned—the CS now signals that the US will not occur.

For many years, psychologists thought that classical conditioning resulted as long as the CS preceded the US within a critical time interval. According to this view, each time a CS is followed by a US (reinforcing stimulus), a connection is strengthened between the internal representations of the stimulus and response or between the representations of one stimulus and another. The strength of the connection was thought to depend on the number of pairings of CS and US. A substantial body of evidence now indicates that classical conditioning cannot be adequately explained simply by the fact that two events or stimuli occur one after the other (Figure 52–12). Indeed, it would not be adaptive to depend solely on sequence. Rather, all animals capable of associative conditioning, from snails to humans, remember the salient relationship between associated events. Thus, classical conditioning, and perhaps all forms of associative learning, enables animals to distinguish events that reliably occur together from those that are only randomly associated.

Lesions in several regions of the brain affect classical conditioning. One well-studied example is conditioning of the protective eyeblink reflex, a form of motor learning. A puff of air to the eye naturally causes an eyeblink. A conditioned eyeblink can be established by pairing the puff with a tone that precedes the puff. Studies in rabbits indicate that the conditioned response (an eyeblink in response to a tone) is abolished by a lesion at either of two sites. Damage to the vermis of the cerebellum abolishes the conditioned response but does not affect the unconditioned response (eyeblink in response to a puff of air). Interestingly, neurons in the same area of the cerebellum show learning-dependent increases in activity that closely parallel the development of the conditioned behavior. A lesion in the interpositus nucleus, a deep cerebellar nucleus, also abolishes the conditioned eyeblink. Thus, both the vermis and the deep nuclei of the cerebellum play an important role in conditioning the eyeblink, and perhaps other simple forms of classical conditioning involving skeletal muscle movement.

Another well-studied example is fear conditioning, which depends on the amygdala. In fear conditioning, a neutral cue, such as a tone, is paired with an aversive outcome, such as a shock. This pairing leads to a conditioned fear response in which the neutral tone alone elicits a behavioral reaction, such as freezing. Fear conditioning depends on plasticity in the inputs to and connections between the subnuclei of the amygdala, particularly the basolateral amygdala, as we will discuss in the next chapter.

Operant Conditioning Involves Associating a Specific Behavior With a Reinforcing Event

A second major paradigm of associative learning, discovered by Edgar Thorndike and systematically studied by B. F. Skinner and others, is operant conditioning

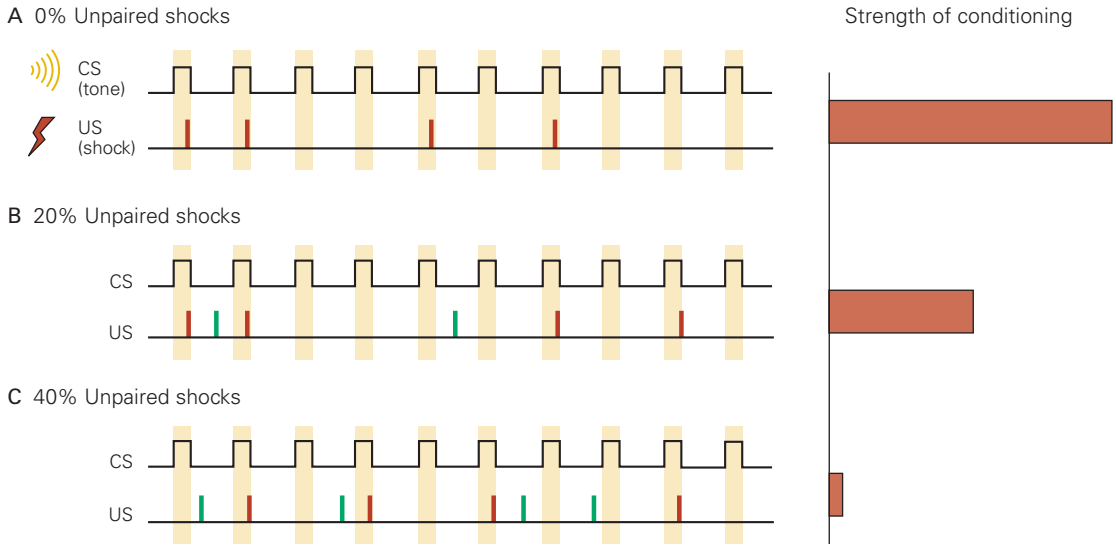

Figure 52–12 Classical conditioning depends on the degree of correlation of two stimuli. In this experiment with rats, a tone (the conditioned stimulus [**CS**]) was paired with an electric shock (the unconditioned stimulus [**US**]) in four out of 10 of the trials (**red ticks**). In some trial blocks, the shock was presented without the tone (**green ticks**). Suppression of lever-pressing to obtain food is a sign of freezing, a conditioned defensive response. The degree of conditioning was evaluated by determining how effective the tone alone was in suppressing lever-pressing to obtain food. (Adapted from Rescorla 1968.)

A. Maximal conditioning occurred when the US was presented only with the CS.

B–C. Little or no conditioning occurred when the shock was presented without the tone almost as often as with it (40%). Some conditioning occurred when the shock occurred without the tone 20% of the time.

(also called trial-and-error learning). In a typical laboratory example of operant conditioning, a hungry rat or pigeon is placed in a test chamber in which the animal is rewarded for a specific action. For example, the chamber may have a lever protruding from one wall. Because of previous learning, or through play and random activity, the animal will occasionally press the lever. If the animal promptly receives a positive reinforcer (eg, food) after pressing the lever, it will begin to press the lever more often than the spontaneous rate. The animal can be described as having learned that among its many behaviors (eg, grooming, rearing, and walking) one behavior is followed by food. With this information, the animal is likely to press the lever whenever it is hungry.

If we think of classical conditioning as the formation of a predictive relationship between two stimuli (the CS and the US), operant conditioning can be considered as the formation of a predictive relationship between an action and an outcome. Unlike classical conditioning, which tests the responsiveness of a reflex to a stimulus, operant conditioning tests behavior that occurs either spontaneously or without an identifiable stimulus. Thus, operant behaviors are said to be emitted rather than elicited. In general, actions that are rewarded tend to be repeated, whereas actions followed by aversive, although not necessarily painful, consequences tend not to be repeated. Many experimental psychologists think that this simple idea, called the law of effect, governs much voluntary behavior.

Operant and classical conditioning involve different kinds of association—an association between an action and a reward or between two stimuli, respectively. However, the laws of operant and classical conditioning are quite similar. For example, timing is critical in both. In operant conditioning, the reinforcer usually must closely follow the operant action. If the reinforcer is delayed too long, only weak conditioning occurs. Similarly, classical conditioning is generally poor if the interval between the CS and US is too long or if the US precedes the CS.

Associative Learning Is Constrained by the Biology of the Organism

Animals generally learn to associate stimuli that are relevant to their survival. For example, animals readily learn to avoid certain foods that have been followed by a negative reinforcement (eg, nausea produced by a poison), a phenomenon termed *taste aversion*.

Unlike most other forms of conditioning, taste aversion develops even when the unconditioned response (poison-induced nausea) occurs after a long delay, up to hours after the CS (specific taste). This makes biological sense because the ill effects of infected foods and naturally occurring toxins usually follow ingestion only after some delay. For most species, including humans, taste-aversion conditioning occurs only when certain tastes are associated with illness. Taste aversion develops poorly if a taste is followed by a painful stimulus that does not produce nausea. Also, animals do not develop an aversion to a visual or auditory stimulus that has been paired with nausea.

Errors and Imperfections in Memory Shed Light on Normal Memory Processes

Memory allows us to revisit our personal past; provides access to a vast network of facts, associations, and concepts; and supports learning and adaptive behavior. But memory is not perfect. We often forget events rapidly or gradually, sometimes distort the past, and occasionally remember events that we would prefer to forget. In the 1930s, the British psychologist Frederic Bartlett reported experiments in which people read and tried to remember complex stories. He showed that people often misremember many features of the stories, often distorting information based on their expectations of what should have happened. Forgetting and distortion can provide important insights into the workings of memory.

Memory's imperfections have been classified into seven basic categories, dubbed the "seven sins of memory": transience, absent-mindedness, blocking, misattribution, suggestibility, bias, and persistence. Here, we focus on six of these.

Absent-mindedness results from a lack of attention to immediate experience. Absent-mindedness during encoding is a likely source of common memory failures such as forgetting where one recently placed an object. Absent-mindedness also occurs when we forget to carry out a particular task such as picking up groceries on the way home from the office, even though we initially encoded the relevant information.

Blocking refers to a temporary inability to access information stored in memory. People often have partial awareness of a sought-after word or image but are nonetheless unable to recall the entire word accurately or completely. Sometimes, it feels like a blocked word is on "the tip of the tongue"—we are aware of the initial letter of the word, the number of syllables in it, or a like-sounding word. Determining which information is correct and which is incorrect requires a great deal of conscious effort.

Absent-mindedness and blocking are sins of omission: At a moment when we need to remember information, it is inaccessible. However, memory is also characterized by sins of commission, situations in which some form of memory is present but wrong.

Misattribution refers to the association of a memory with an incorrect time, place, or person. False recognition, a type of misattribution, occurs when individuals report that they "remember" items or events that never happened. Such false memories have been documented in controlled experiments where people claim to have seen or heard words or objects that had not been presented previously but are similar in meaning or appearance to what was actually presented. Studies using positron emission tomography imaging and fMRI have shown that many brain regions show similar levels of activity during both true and false recognition, which may be one reason why false memories sometimes feel like real ones.

Suggestibility refers to the tendency to incorporate new information into memory, usually as a result of leading questions or suggestions about what may have been experienced. Research using hypnotic suggestion indicates that various kinds of false memories can be implanted in highly suggestible individuals, such as remembering hearing loud noises at night. Studies with young adults have also shown that repeated suggestions about a childhood experience can produce memories of events that never occurred. These findings are important theoretically because they highlight that memory is not simply a "playback" of past experiences (Box 52–1). Despite these important theoretical and practical implications, next to nothing is known about the neural bases of suggestibility.

Bias refers to distortions and unconscious influences on memory that reflect one's general knowledge and beliefs. People often misremember the past to make it consistent with what they presently believe, know, or feel. This idea is consistent with the idea of "predictive coding" supported by studies showing that even low-level neural mechanisms of perception and sensation are shaped by expectations. The specific brain mechanisms by which expectations influence memory are not well understood.

Persistence refers to obsessive memory, constant remembering of information or events that we might want to forget. Neuroimaging studies have illuminated some neurobiological factors that contribute to persistent emotional memories. Some key results implicate the amygdala, the almond-shaped structure near the hippocampus long known to be involved in emotional

processing (Chapter 42). Studies indicate that the level of recall of emotional components of a story is correlated with the level of activity in the amygdala during presentation of the story. Related studies implicate the amygdala in the encoding and retrieval of emotionally charged experiences that can repeatedly intrude into consciousness.

Although persistence can be disabling, it also has adaptive value. The persistence of memories of disturbing experiences increases the likelihood that we will recall information about arousing or traumatic events at times when it may be crucial for survival.

Indeed, many memory imperfections may have adaptive value. False memories and suggestibility may both be related to one of the most basic adaptive functions of memory: the integration of experiences separated in time into a network of learned associations. For memory to play an important role in guiding future behavior, it must be flexible so that we can leverage past experiences to make inferences about future events even when the circumstances have changed. Similarly, although the various forms of forgetting (transience, absent-mindedness, and blocking) can be annoying, a memory system that automatically retains every detail of every experience could result in an overwhelming clutter of useless trivia. This is exactly what happened in the fascinating case of Shereshevski, a mnemonist studied by the Russian neuropsychologist Alexander Luria and described in the book *The Mind of a Mnemonist*. Shereshevski was filled with highly detailed memories of his past experiences but was unable to generalize or to think at an abstract level. A healthy memory system does not encode, store, and retrieve all the details of every experience. Thus, transience, absent-mindedness, and blocking allow us to avoid the unfortunate fate of Shereshevski.

Highlights

1. Different forms of learning and memory can be distinguished behaviorally and neurally. Working memory maintains goal-relevant information for short periods. Explicit (or declarative) memory involves two classes of knowledge: episodic memory, which represents personal experiences, and semantic memory, which represents general knowledge and facts. Implicit memory includes forms of perceptual and conceptual priming, as well as the learning of motor and perceptual skills, perceptual regularities, and reinforced habits.
2. Encoding, storage, retrieval, and consolidation of new explicit memories depend on interactions between specific regions within the neocortex and medial temporal lobe and specific hippocampal subregions. The initiation of long-term storage of explicit memory requires the temporal lobe system, as highlighted by studies of amnesic patients such as H.M. Consolidation processes stabilize stored representations, rendering explicit memories less dependent on the medial temporal lobe. Retrieval of explicit memories involves the medial temporal lobe, as well as frontoparietal networks that subserve attention and cognitive control.
3. Multiple processes interact to support memory-guided behavior. Retrieval of episodic memory guides the imagining of future events, which is important for making decisions about future choices and actions. Motivationally significant events are prioritized in memory through the enhancement of encoding, storage, and consolidation processes. Motivation also impacts retrieval, perhaps through different mechanisms of prioritization.
4. Implicit memory emerges automatically in the course of perceiving, thinking, and acting. It tends to be inflexible and expressed in the performance of tasks even without conscious awareness. Implicit memory involves a wide variety of brain regions and circuits, including cortical areas that support the specific perceptual, conceptual, or motor systems recruited to process a stimulus or perform a task, as well as the striatum and the amygdala. Implicit learning that involves the encoding of relational associations additionally involves the hippocampus.
5. Imperfections and errors in remembering provide telltale clues about learning and memory mechanisms. The past can be forgotten or distorted, indicating that memory is not a faithful record of all details of every experience. Retrieved memories are the result of a complex interplay among various brain regions and can be reshaped over time by multiple influences. Various forms of forgetting and distortion tell us much about the flexibility of memory that allows the brain to adapt to the physical and social environment.

Daphna Shohamy
Daniel L. Schacter
Anthony D. Wagner

Suggested Reading

Baddeley AD. 1986. *Working Memory*. Oxford: Oxford Univ. Press.

Eichenbaum H. 2017. Prefrontal-hippocampal interactions in episodic memory. Nat Rev Neurosci 18:547–558.

Eichenbaum H, Cohen NJ. 2001. *From Conditioning to Conscious Recollection: Memory Systems of the Brain*. Oxford: Oxford Univ. Press.

Kamin LJ. 1969. Predictability, surprise, attention, and conditioning. In: BA Campbell, RM Church (eds). *Punishment and Aversive Behavior*, pp. 279–296. New York: Appleton–Century–Crofts.

Kumaran D, Hassabis D, McClelland JL. 2016. What learning systems do intelligent agents need? Complementary learning systems theory updated. Trends Cog Sci 20:512–534.

Milner B, Squire LR, Kandel ER. 1998. Cognitive neuroscience and the study of memory. Neuron 20:445–468.

Schacter DL, Benoit RG, Szpunar KK. 2017. Episodic future thinking: mechanisms and functions. Curr Opin Behav Sci 17:41–50.

Shohamy D, Turk-Browne NB. 2013. Mechanisms for widespread hippocampal involvement in cognition. J Exp Psychol Gen 142:1159–1170.

Tulving E. 1983. *Elements of Episodic Memory*. Oxford: Oxford Univ. Press.

Yonelinas AP, Ranganath C, Ekstrom A, Wiltgen B. 2019. A contextual binding theory of episodic memory: systems consolidation reconsidered. Nat Rev Neurosci 20:364–375.

References

Adcock RA, Thangavel A, Whitfield-Gabrieli S, Knutson B, Gabrieli JD. 2006. Reward motivated learning: mesolimbic activation precedes memory formation. Neuron 50:507–517.

Bartlett FC. 1932. *Remembering: A Study in Experimental and Social Psychology*. Cambridge: Cambridge Univ. Press.

Blakemore C. 1977. *Mechanics of the Mind*. Cambridge: Cambridge Univ. Press.

Brewer JB, Zhao Z, Desmond JE, et al. 1998. Making memories: brain activity that predicts how well visual experience will be remembered. Science 281:1185–1187.

Brown TI, Carr VA, LaRocque KF, et al. 2016. Prospective representation of navigational goals in the human hippocampus. Science 352:1323–1326.

Corkin S. 2002. What's new with the amnesic patient H.M.? Nat Rev Neurosci 3:153–160.

Corkin S, Amaral DG, González RG, et al. 1997. H.M.'s medial temporal lobe lesion: findings from magnetic resonance imaging. J Neurosci 17:3964–3979.

Craik FIM, Lockhart RS. 1972. Levels of processing: a framework for memory research. J Verb Learn Verb Behav 11:671–684.

Duncan K, Doll BB, Daw ND, Shohamy D. 2018. More than the sum of its parts: a role for the hippocampus in configural reinforcement learning. Neuron 98:646–657.

Eichenbaum H, Cohen NJ. 2014. Can we reconcile the declarative memory and spatial navigation views on hippocampal function? Neuron 83:764–770.

Eldridge LL, Knowlton BJ, Furmanski CS, et al. 2000. Remembering episodes: a selective role for the hippocampus during retrieval. Nat Neurosci 3:1149–1152.

Hebb DO. 1966. *A Textbook of Psychology*. Philadelphia: Saunders.

Luria AR. 1968. *The Mind of a Mnemonist*. New York: Basic Books.

Naya Y, Yoshida M, Miyashita Y. 2001. Backward spreading of memory-related signal in the primate temporal cortex. Science 291:661–664.

Nyberg L, Habib R, McIntosh AR, Tulving E. 2000. Reactivation of encoding-related brain activity during memory retrieval. Proc Natl Acad Sci U S A 97:11120–11124.

Pavlov IP. 1927. *Conditioned Reflexes: Investigation of the Physiological Activity of the Cerebral Cortex*. GV Anrep (transl). London: Oxford Univ. Press.

Penfield W. 1958. Functional localization in temporal and deep sylvian areas. Res Publ Assoc Res Nerv Ment Dis 36:210–226.

Petrides M. 1994. Frontal lobes and behavior. Curr Opin Neurobiol 4:207–211.

Poldrack RA, Clark J, Pare-Blagoev EJ, et al. 2001. Interactive memory systems in the human brain. Nature 414:546–550.

Rainer G, Asaad WF, Miller EK. 1998. Memory fields of neurons in the primate prefrontal cortex. Proc Natl Acad Sci U S A 95:15008–15013.

Rescorla RA. 1968. Probability of shock in the presence and absence of CS in fear conditioning. J Comp Physiol Psychol 66:1–5.

Rescorla RA. 1988. Behavioral studies of Pavlovian conditioning. Annu Rev Neurosci 11:329–352.

Schacter DL. 2001. *The Seven Sins of Memory: How the Mind Forgets and Remembers*. Boston and New York: Houghton Mifflin.

Schacter DL, Addis DR. 2007. The cognitive neuroscience of constructive memory: remembering the past and imagining the future. Philos Trans Roy Soc B 362:773–786.

Schacter DL, Addis DR, Buckner RL. 2007. Remembering the past to imagine the future: the prospective brain. Nat Rev Neurosci 8:657–661.

Schacter DL, Guerin SA, St. Jacques PL. 2011. Memory distortion: an adaptive perspective. Trends Cog Sci 15:467–474.

Sestieri C, Shulman GL, Corbetta M. 2017. The contribution of the human posterior parietal cortex to episodic memory. Nat Rev Neurosci 18:183–192.

Shohamy D, Adcock RA. 2010. Dopamine and adaptive memory. Trends Cog Sci 14:464–472.

Skinner BF. 1938. *The Behavior of Organisms: An Experimental Analysis*. New York: Appleton–Century–Crofts.

Squire LR. 1987. *Memory and Brain*. New York: Oxford Univ. Press.

Thorndike EL. 1911. *Animal Intelligence: Experimental Studies*. New York: Macmillan.

Tomita H, Ohbayashi M, Nakahara K, et al. 1999. Top-down signal from prefrontal cortex in executive control of memory retrieval. Nature 401:699–703.

Tulving E, Schacter DL. 1990. Priming and human memory systems. Science 247:301–306.

Uncapher M, Wagner AD. 2009. Posterior parietal cortex and episodic encoding: insights from fMRI subsequent memory effects and dual attention theory. Neurobiol Learn Mem 91:139–154.

Vaidya CJ, Gabrieli JD, Verfaellie M, et al. 1998. Font-specific priming following global amnesia and occipital lobe damage. Neuropsychology 12:183–192.

Vaz AP Inati SK, Brunel N, Zaghloul KA. 2019. Coupled ripple oscillations between the medial temporal lobe and neocortex retrieve human memory. Science 363: 975–978.

Wagner AD. 2002. Cognitive control and episodic memory: contributions from prefrontal cortex. In: LR Squire, DL Schacter (eds). *Neuropsychology of Memory*, 3rd ed., pp. 174–192. New York: Guilford Press.

Wagner AD, Schacter DL, Rotte M, et al. 1998. Building memories: remembering and forgetting of verbal experiences as predicted by brain activity. Science 281:1188–1191.

Wheeler ME, Petersen SE, Buckner RL. 2000. Memory's echo: vivid remembering reactivates sensory-specific cortex. Proc Natl Acad Sci U S A 97:11125–11129.

Wimmer GE, Shohamy D. 2012. Preference by association: how memory mechanisms in the hippocampus bias decisions. Science 338:270–273.

53

Cellular Mechanisms of Implicit Memory Storage and the Biological Basis of Individuality

Throughout this book we have emphasized that all behavior is a function of the brain and that malfunctions of the brain produce characteristic disturbances of behavior. Behavior is also shaped by experience. How does experience act on the neural circuits of the brain to change behavior? How is new information acquired by the brain, and once acquired, how is it stored, retrieved, and remembered?

In the previous chapter, we saw that memory is not a single process but has at least two major forms. Implicit memory operates unconsciously and automatically, as in the memory for conditioned responses, habits, and perceptual and motor skills, whereas explicit memory operates consciously, as in the memory for people, places, and objects. The circuitry for long-term memory storage differs between explicit and implicit memory. Long-term storage of explicit memory begins in the hippocampus and the medial temporal lobe of the neocortex, whereas long-term storage of different types of implicit memory requires a family of neural structures: the neocortex for priming, the striatum for skills and habits, the amygdala for Pavlovian threat conditioning (also known as fear conditioning), the cerebellum for learned motor skills, and certain reflex pathways for nonassociative learning such as habituation and sensitization (Figure 53–1).

Over time, explicit memories are transferred to different regions of the neocortex. In addition, many cognitive, motor, and perceptual skills that we initially store as explicit memory ultimately become so ingrained with practice that they become stored as implicit memory. The transference from explicit to implicit memory and the difference between them is dramatically demonstrated in the case of the English musician and conductor Clive Waring, who in 1985 sustained a viral infection of his brain (herpes encephalitis) that affected

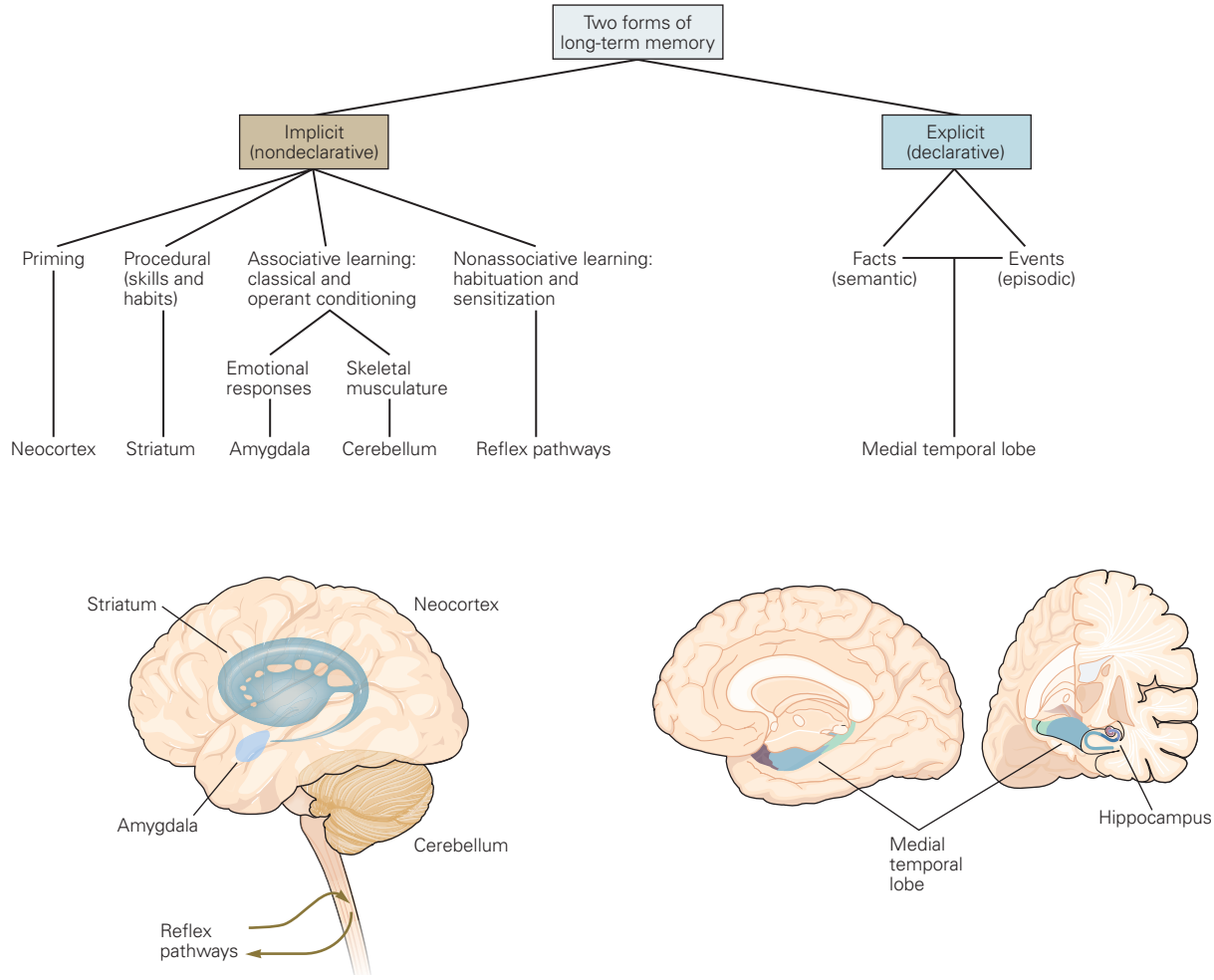

Figure 53–1 Two forms of long-term memory involve different brain systems. Implicit memory involves the neocortex, striatum, amygdala, cerebellum, and, in the simplest cases, the reflex pathways themselves. Explicit memory requires the medial temporal lobe and the hippocampus, as well as certain areas of neocortex (not shown).

the hippocampus and temporal cortex. Waring was left with a devastating loss of memory for events or people he had encountered even a minute or two earlier, but his ability to read music, play the piano, or conduct a chorale was unaffected. Once a performance was completed, however, he could not remember a thing about it.

Similarly, the abstract expressionist painter William de Kooning developed severe disturbances of explicit memory as a result of Alzheimer disease. As the disease progressed and his memory for people, places, and objects deteriorated, he nevertheless continued to produce important and interesting paintings. This aspect of his creative personality was relatively untouched.

In this chapter, we examine the cellular and molecular mechanisms that underlie implicit memory storage in invertebrate and vertebrate animals. We focus on learning about threats (sometimes called fear learning). Implicit memory for motor skills and habits in mammals involving the cerebellum and basal ganglia was considered in Chapters 37 and 38. In the next chapter, we examine the biology of explicit memory in mammals.

Storage of Implicit Memory Involves Changes in the Effectiveness of Synaptic Transmission

Studies of elementary forms of implicit learning—habituation, sensitization, and classical conditioning—provided the conceptual framework for investigating the neural mechanisms of memory storage. Such learning has been analyzed in simple invertebrates and in a variety of vertebrate behaviors, such as the flexion and

eye blink reflexes, and also defensive behaviors such as freezing. These simple forms of implicit memory involve changes in the effectiveness of the synaptic pathways that mediate the behavior.

Habituation Results From Presynaptic Depression of Synaptic Transmission

Habituation is the simplest form of implicit learning. It occurs, for example, when an animal learns to ignore a novel stimulus. An animal reacts to a new stimulus with a series of orienting responses. If the stimulus is neither beneficial nor harmful, the animal learns to ignore it after repeated exposure.

The physiological basis of this behavior was first investigated by Charles Sherrington while studying posture and locomotion in cats. Sherrington observed a decrease in the intensity of certain reflexes in response to repeated electrical stimulation of the motor pathways. He suggested that this decrease, which he called *habituation*, is caused by diminished synaptic effectiveness in the stimulated pathways.

Habituation was later investigated at the cellular level by Alden Spencer and Richard Thompson. They found close cellular and behavioral parallels between habituation of a spinal flexion reflex in cats (the withdrawal of a limb from a noxious stimulus) and habituation of more complex human behaviors. They showed that during habituation the strength of the input from local excitatory interneurons onto motor neurons in the spinal cord decreased, whereas the input to the same interneurons from sensory neurons innervating the skin was unchanged.

Because the organization of interneurons in the vertebrate spinal cord is quite complex, it was difficult to analyze further the cellular mechanisms of habituation in the flexion reflex. Progress required a simpler system. The marine mollusk *Aplysia californica*, which has a simple nervous system of about 20,000 central neurons, proved to be an excellent system for studying implicit forms of memory.

Aplysia has a repertory of defensive reflexes for withdrawing its respiratory gill and siphon, a small fleshy spout above the gill used to expel seawater and waste (Figure 53–2A). These reflexes are similar to the withdrawal reflex of the leg studied by Spencer and Thompson. Mild touching of the siphon elicits reflex withdrawal of both the siphon and gill. With repeated stimulation, these reflexes habituate. As we shall see, these responses can also be dishabituated, sensitized, and classically conditioned.

The neural circuit mediating the gill-withdrawal reflex in *Aplysia* has been studied in detail. Touching the siphon excites a population of mechanoreceptor sensory neurons that innervate the siphon. The release of glutamate from sensory neuron terminals generates fast excitatory postsynaptic potentials (EPSPs) in interneurons and motor cells. The EPSPs from the sensory cells and interneurons summate on motor cells both temporally and spatially, causing them to discharge strongly, thereby producing vigorous withdrawal of the gill. If the siphon is repeatedly touched, however, the monosynaptic EPSPs produced by sensory neurons in both interneurons and motor cells decrease progressively, paralleling the habituation of gill withdrawal. In addition, repeated stimulation also leads to a decrease in the strength of synaptic transmission from the excitatory interneurons to the motor neurons; the net result is that the reflex response diminishes (Figure 53–2B,C).

What reduces the effectiveness of synaptic transmission between the sensory neurons and their postsynaptic cells during repeated stimulation? Quantal analysis (Chapter 15) revealed that the amount of synaptic glutamate released from presynaptic terminals of sensory neurons decreases. That is, fewer synaptic vesicles are released with each action potential in the sensory neuron; the sensitivity of the postsynaptic glutamate receptors does not change. Because the reduction in transmission occurs in the activated pathway itself and does not require another modulatory cell, the reduction is referred to as *homosynaptic depression*. This depression lasts many minutes.

An enduring change in the functional strength of synaptic connections thus constitutes the cellular mechanism mediating short-term habituation. As change of this type occurs at several sites in the gill-withdrawal reflex circuit, *memory is distributed and stored throughout the circuit*. Depression of synaptic transmission by sensory neurons, interneurons, or both is a common mechanism underlying habituation of escape responses of crayfish and cockroaches as well as startle reflexes in vertebrates.

How long can the effectiveness of a synapse change last? In *Aplysia*, a single session of 10 stimuli leads to short-term habituation of the withdrawal reflex lasting minutes. Four sessions separated by periods ranging from several hours to 1 day produce long-term habituation, lasting as long as 3 weeks (Figure 53–3).

Anatomical studies indicate that long-term habituation is caused by a decrease in the number of synaptic contacts between sensory and motor neurons. In naïve animals, 90% of the sensory neurons make physiologically detectable connections with identified motor neurons. In contrast, in animals trained for

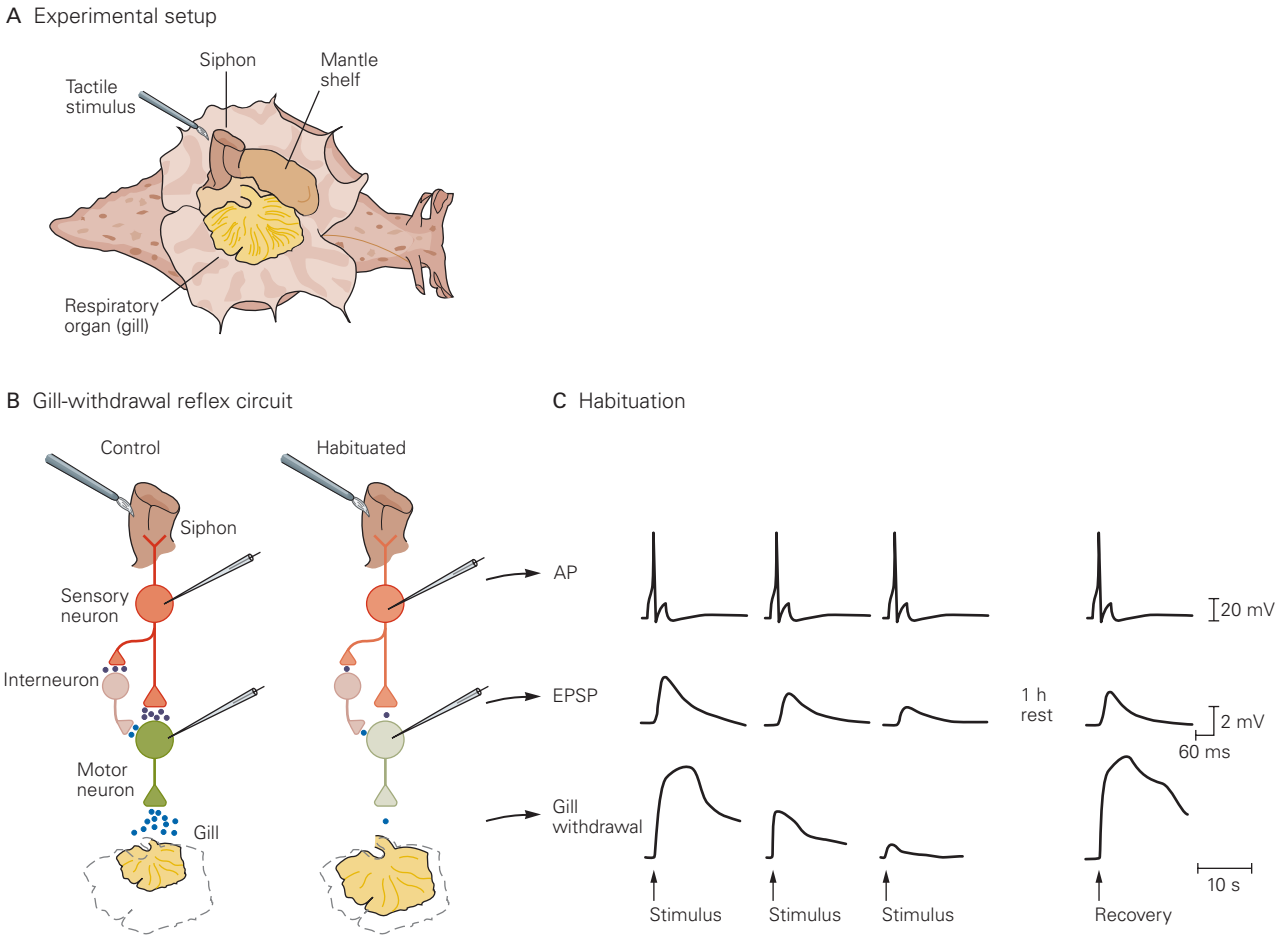

Figure 53–2 Short-term habituation of the gill-withdrawal reflex of the marine snail *Aplysia*.

A. A dorsal view of *Aplysia* illustrates the respiratory organ (gill) and the mantle shelf, which ends in the siphon, a fleshy spout used to expel seawater and waste. Touching the siphon elicits the gill-withdrawal reflex. Repeated stimulation leads to habituation.

B. Simplified diagrams of the gill-withdrawal reflex circuit and sites involved in habituation. Approximately 24 mechanoreceptor neurons in the abdominal ganglion innervate the siphon skin. These sensory cells make excitatory synapses onto a cluster of six motor neurons that innervate the gill, as well as on interneurons that modulate the firing of the motor neurons. (For simplicity, only one of each type of neuron is illustrated here.) Touching the siphon leads to withdrawal of the gill (**dashed outline** shows original gill size; **solid outline** shows maximal withdrawal).

C. Repeated stimulation of the siphon sensory neuron (**top traces**) leads to a progressive depression of synaptic transmission between the sensory and motor neurons. The size of the motor neuron excitatory postsynaptic potential (**EPSP**) gradually decreases despite no change in the presynaptic action potential (**AP**). In a separate experiment, repeated stimulation of the siphon results in a decrease in gill withdrawal (habituation). One hour after repetitive stimulation, both the EPSP and gill withdrawal have recovered. Habituation involves a decrease in transmitter release at many synaptic sites throughout the reflex circuit. (Adapted, with permission, from Pinsker et al. 1970; Castellucci and Kandel 1974.)

long-term habituation, the incidence of connections is reduced to 30%; the reduction in number of synapses persists for a week and does not fully recover even 3 weeks later (see Figure 53–9). As we shall see, the converse occurs with long-term sensitization, where synaptic transmission is associated with an *increase* in the number of synapses between sensory and motor neurons.

Not all classes of synapses are equally modifiable. In *Aplysia*, the strength of some synapses rarely changes, even with repeated activation. In synapses specifically involved in learning (such as the connections between sensory and motor neurons in the withdrawal reflex circuit), a relatively small amount of training can produce large and enduring changes in synaptic strength.

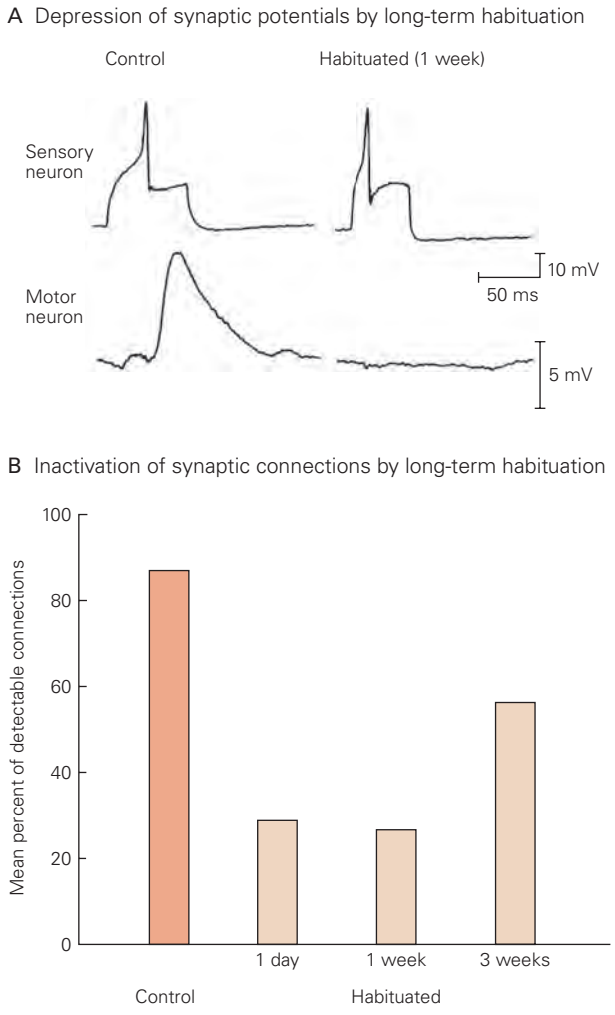

Figure 53–3 Long-term habituation of the gill-withdrawal reflex in *Aplysia.* (Adapted, with permission, from Castellucci, Carew, and Kandel 1978.)

A. Comparison of action potentials in sensory neurons and the postsynaptic potential in motor neurons in an untrained animal (control) and one that has been subjected to long-term habituation. In the habituated animal 1 week after training, no synaptic potential occurs in the motor neuron in response to the sensory neuron action potential.

B. After long-term habituation training, the mean percentage of sensory neurons making physiologically detectable connections with motor neurons is reduced even at 3 weeks.

Sensitization Involves Presynaptic Facilitation of Synaptic Transmission

The ability to recognize and respond to danger is necessary for survival. Not only snails and flies, but all animals, including humans, must distinguish predators from prey and hostile environments from safe ones. Because the ability to respond to threats is a universal requirement of survival, it has been conserved throughout evolution, allowing studies of invertebrates to shed light on neural mechanisms in mammals.

At the beginning of the 20th century, both Freud and Pavlov appreciated that anticipatory defensive responses to danger signals are biologically adaptive, a fact that likely accounts for the profound conservation of this capacity throughout vertebrates and invertebrates. In the laboratory, threat (fear) conditioning is typically studied by presenting a neutral stimulus, such as a tone, prior to the onset of an aversive stimulus, such as electrical shock. The two stimuli become associated such that the tone leads to the elicitation of defensive behaviors that protect against the harmful consequences predicted by the tone. Freud called this "signal anxiety," which prepares the individual for fight or flight when there is even the suggestion of external danger.

When an animal repeatedly encounters a harmless stimulus, its responsiveness to the stimulus habituates, as seen above. In contrast, when the animal confronts a *harmful* stimulus, it typically learns to respond more vigorously to a subsequent presentation of the same stimulus. Presentation of a harmful stimulus can even cause an animal to mount a defensive response to a subsequent *harmless* stimulus. As a result, defensive reflexes for withdrawal and escape become heightened. This enhancement of reflex responses is called *sensitization.*

Like habituation, sensitization can be transient or long lasting. A single shock to the tail of an *Aplysia* produces short-term sensitization of the gill-withdrawal reflex that lasts minutes; five or more shocks to the tail produce sensitization lasting days to weeks. Tail shock is also sufficient to overcome the effects of habituation and enhance a habituated gill-withdrawal reflex, a process termed *dishabituation*.

Sensitization and dishabituation result from an enhancement in synaptic transmission at several connections in the neural circuit of the gill-withdrawal reflex, including the connections made by sensory neurons with motor neurons and interneurons—the same synapses depressed by habituation (Figure 53–4A). Typically, modifiable synapses can be regulated bidirectionally, participate in more than one type of learning, and store more than one type of memory. The bidirectional synaptic changes that underlie habituation and sensitization are the result of different cellular mechanisms. In *Aplysia*, the same synapses that are weakened by habituation through a homosynaptic process can be strengthened by sensitization through a *heterosynaptic* process that depends on modulatory

interneurons activated by the harmful stimulus to the tail.

At least three groups of modulatory interneurons are involved in sensitization. The best studied use serotonin as a transmitter (Figure 53–4B). The serotonergic interneurons form synapses on many regions of the sensory neurons, including axo-axonic synapses on the presynaptic terminals of the sensory cells. After a single tail shock, the serotonin released from the interneurons binds to a receptor in the sensory neurons that is coupled to a stimulatory G protein that increases the activity of adenylyl cyclase. This action produces the second messenger cyclic adenosine monophosphate (cAMP), which in turn activates the cAMP-dependent protein kinase (PKA) (Chapter 14). Serotonin also activates a second type of G-protein–coupled receptor that leads to the hydrolysis of phospholipids and the activation of protein kinase C (PKC).

The protein phosphorylation mediated by PKA and PKC enhances the release of transmitter from sensory neurons through at least two mechanisms (Figure 53–4B). In one action, PKA phosphorylates a K^+ channel, causing it to close. This broadens the action potential and thus enhances the duration of Ca^{2+} influx through voltage-gated Ca^{2+} channels, which in turn enhances transmitter release. In a second action, protein phosphorylation through PKC enhances the functioning of the release machinery directly. Presynaptic facilitation in response to release of serotonin by a tail shock lasts for a period of many minutes. Repeated noxious stimuli can strengthen synaptic activity for days (by a mechanism we consider below).

Classical Threat Conditioning Involves Facilitation of Synaptic Transmission

Classical conditioning is a more complex form of learning. Rather than learning about the properties of one stimulus, as in habituation and sensitization, the animal learns to associate one type of stimulus with another. As described in Chapter 52, an initial weak conditioned stimulus (eg, the ringing of a bell) becomes highly effective in producing a response when paired with a strong unconditioned stimulus (eg, presentation of food). In reflexes that can be enhanced by both classical conditioning and sensitization, such as the defensive withdrawal reflexes of *Aplysia*, classical conditioning results in greater and longer-lasting enhancement.

Although aversive classical conditioning is traditionally referred to as fear conditioning, we will use the more neutral term *threat conditioning* to avoid the implication that animals have subjective states comparable to those that humans experience and label as "fear." This distinction is important because humans can respond to threats behaviorally and physiologically in the absence of any reported feeling of fear. This terminology allows the findings from research on implicit learning in all animals, from the simplest worm to humans, to be interpreted in an objective manner without invoking empirically unverifiable subjective fear states in animals.

For classical conditioning of the *Aplysia* gill-withdrawal reflex, a weak touch to the siphon serves as the conditioned stimulus while a strong shock to the tail serves as the unconditioned stimulus. When the gill-withdrawal reflex is classically conditioned, gill withdrawal in response to siphon stimulation alone is greatly enhanced. This enhancement is even more dramatic than the enhancement produced in an unpaired pathway by tail shock alone (sensitization). In classical conditioning, the timing of the conditioned and unconditioned stimuli is critical. To be effective, the conditioned stimulus (siphon touch) must *precede* (and thus predict) the unconditioned stimulus (tail shock), often within an interval of about 0.5 seconds.

The convergence in individual sensory neurons of the signals initiated by the conditioned and unconditioned stimuli is critical. Alone, a strong shock to the tail (unconditioned stimulus) will excite serotonergic interneurons that form synapses on presynaptic terminals of the siphon sensory neurons, resulting in presynaptic facilitation (Figure 53–5A). However, when the tail shock immediately follows a slight tap on the siphon (conditioned stimulus), the serotonin from the interneurons produces even greater presynaptic facilitation, a process termed *activity-dependent facilitation* (Figure 53–5B).

How does this work? During conditioning, the modulatory interneurons activated by tail shock release serotonin shortly *after* the action potential produced in the siphon sensory neurons by the tap on the siphon. The action potential triggers an influx of Ca^{2+} into the presynaptic terminals of the sensory neurons, and the Ca^{2+} binds to calmodulin, which in turn binds to the enzyme, adenylyl cyclase. This primes the adenylyl cyclase so that it responds more vigorously to the serotonin released following the tail shock. This in turn enhances the production of cAMP, which increases the amount of presynaptic facilitation. If the order of stimuli is reversed so that serotonin release precedes Ca^{2+} influx in the presynaptic sensory terminals, there is no potentiation and no classical conditioning.

Thus, the cellular mechanism of classical conditioning in the monosynaptic pathway of the withdrawal reflex is largely an elaboration of the mechanism of

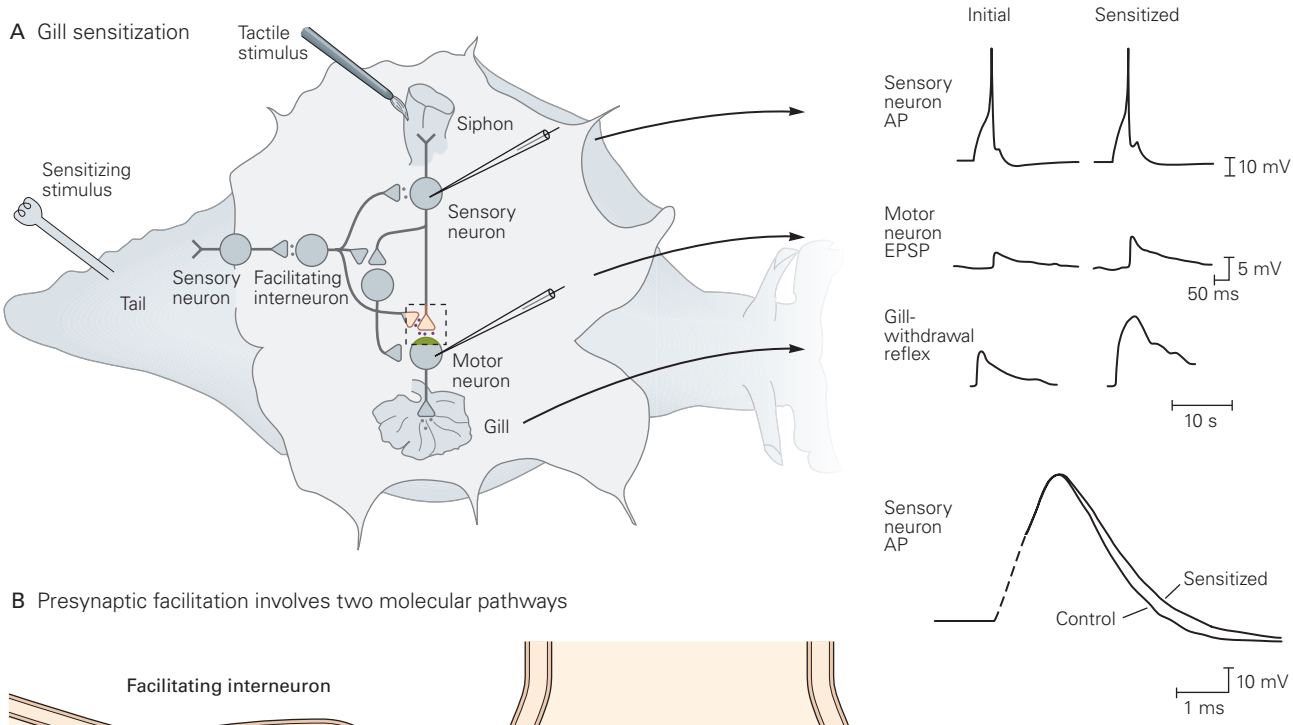
A Gill sensitization
Tactile stimulus
Siphon
Sensitizing stimulus
Sensory neuron
Facilitating interneuron
Tail
Sensory neuron
Motor neuron
Gill
Initial
Sensitized
Sensory neuron AP
10 mV
Motor neuron EPSP
5 mV
50 ms
Gill-withdrawal reflex
10 s
Sensory neuron AP
Sensitized
Control
10 mV
1 ms

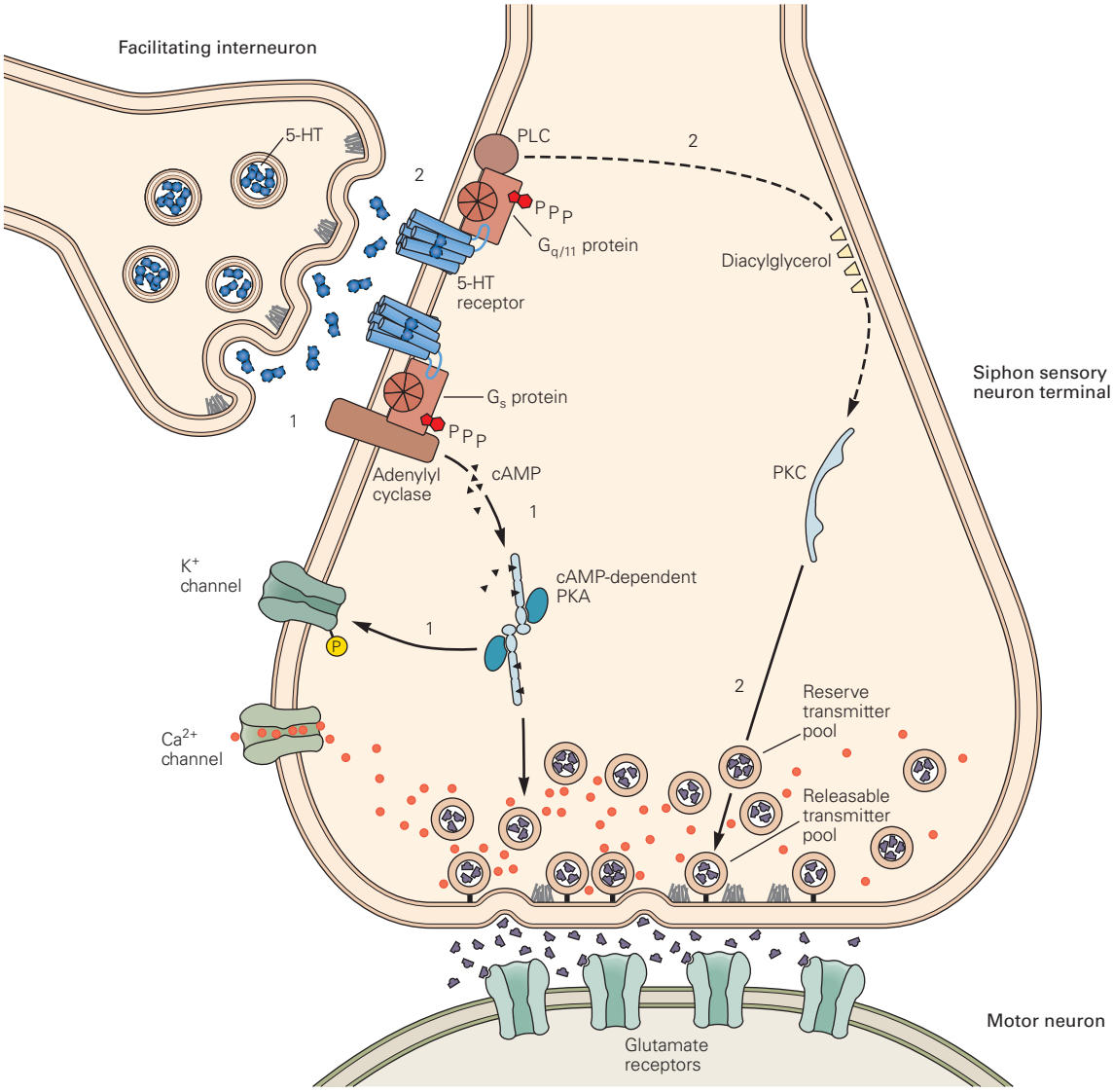
B Presynaptic facilitation involves two molecular pathways
Facilitating interneuron
5-HT
PLC
2
P P P
$G_{q/11}$ protein
5-HT receptor
Diacylglycerol
Siphon sensory neuron terminal
G_s protein
1
Adenylyl cyclase
cAMP
PKC
K^+ channel
cAMP-dependent PKA
P
Ca^{2+} channel
Reserve transmitter pool
Releasable transmitter pool
Glutamate receptors
Motor neuron

sensitization, with the added feature that the adenylyl cyclase serves as a *coincidence detector* in the presynaptic sensory neuron, recognizing the temporal order of the physiological responses to the tail shock (unconditioned stimulus) and the siphon tap (conditioned stimulus).

In addition to the presynaptic component of activity-dependent facilitation, a postsynaptic component is triggered by Ca^{2+} influx into the motor neuron when it is highly excited by the siphon sensory neurons. The properties of this postsynaptic mechanism are similar to those of long-term potentiation of synaptic transmission in the mammalian brain (discussed later in this chapter and in Chapters 13 and 54).

Long-Term Storage of Implicit Memory Involves Synaptic Changes Mediated by the cAMP-PKA-CREB Pathway

Cyclic AMP Signaling Has a Role in Long-Term Sensitization

In all forms of learning, practice makes perfect. Repeated experience converts short-term memory into a long-term form. In *Aplysia*, the form of long-term memory that has been most intensively studied is long-term sensitization. Like the short-term form, long-term sensitization of the gill-withdrawal reflex involves changes in the strength of connections at several synapses. But in addition, it also recruits the growth of new synaptic connections.

Five spaced training sessions (or repeated applications of serotonin) over approximately 1 hour produce long-term sensitization and long-term synaptic facilitation lasting 1 or more days. Spaced training over several days produces sensitization that persists for 1 or more weeks. Long-term sensitization, like the short-term form, requires protein phosphorylation that is dependent on increased levels of cAMP (Figure 53–6).

The conversion of short-term memory into long-term memory, called *consolidation*, requires synthesis of messenger RNAs and proteins in the neurons in the circuit. Thus, activation of specific gene expression is required for long-term memory. The transition from short-term to long-term memory depends on the prolonged rise in cAMP that follows repeated applications of serotonin. The increase in cAMP leads to prolonged activation of PKA, allowing the catalytic subunit of the kinase to translocate into the nucleus of the sensory neurons. It also leads indirectly to activation of a second protein kinase, the mitogen-activated protein kinase (MAPK), a kinase commonly associated with cellular growth (Chapter 14). Within the nucleus, the catalytic subunit of PKA phosphorylates and thereby activates the transcription factor CREB-1 (*c*AMP *r*esponse *e*lement *b*inding protein 1), which binds a promoter element called CRE (*c*AMP *r*ecognition *e*lement) (Figures 53–6 and 53–7).

To turn on gene transcription, phosphorylated CREB-1 recruits a transcriptional coactivator, CREB-binding protein (CBP), to the promoter region. CBP has two important properties that facilitate transcriptional activation: It recruits RNA polymerase II to the

Figure 53–4 (Opposite) Short-term sensitization of the gill-withdrawal reflex in *Aplysia*.

A. Sensitization of the gill-withdrawal reflex is produced by applying a noxious stimulus to another part of the body, such as the tail. A shock to the tail activates tail sensory neurons that excite facilitating (modulatory) interneurons, which form synapses on the cell body and terminals of the mechanoreceptor sensory neurons that innervate the siphon. Through these axo-axonic synapses, the modulatory interneurons enhance transmitter release from the siphon sensory neurons onto their postsynaptic gill motor neurons (presynaptic facilitation), thus enhancing gill withdrawal. Presynaptic facilitation results, in part, from a prolongation of the sensory neuron action potential (**AP**; **bottom traces**). (Abbreviation: **EPSP**, excitatory postsynaptic potential.) (Adapted, with permission, from Pinsker et al. 1970; Klein and Kandel 1980.)

B. Presynaptic facilitation in the sensory neuron is thought to occur by means of two biochemical pathways. The diagram shows details of the synaptic complex in the dashed box in part **A**.

Pathway 1: A facilitating interneuron releases serotonin (**5-HT**), which binds to metabotropic receptors in the sensory neuron terminal. This action engages a G protein (G_s), which in turn increases the activity of adenylyl cyclase. The adenylyl cyclase converts adenosine triphosphate to cyclic adenosine monophosphate (**cAMP**), which binds to the regulatory subunit of protein kinase A (**PKA**), thus activating its catalytic subunit. The catalytic subunit phosphorylates certain K^+ channels, thereby closing the channels and decreasing the outward K^+ current. This prolongs the action potential, thus increasing the influx of Ca^{2+} through voltage-gated Ca^{2+} channels and thereby augmenting transmitter release.

Pathway 2: Serotonin binds to a second class of metabotropic receptor that activates the $G_{q/11}$ class of G protein that enhances the activity of phospholipase C (**PLC**). The PLC activity leads to production of diacylglycerol, which activates protein kinase C (**PKC**). The PKC phosphorylates presynaptic proteins, resulting in the mobilization of vesicles containing glutamate from a reserve pool to a releasable pool at the active zone, thus increasing the efficiency of transmitter release.

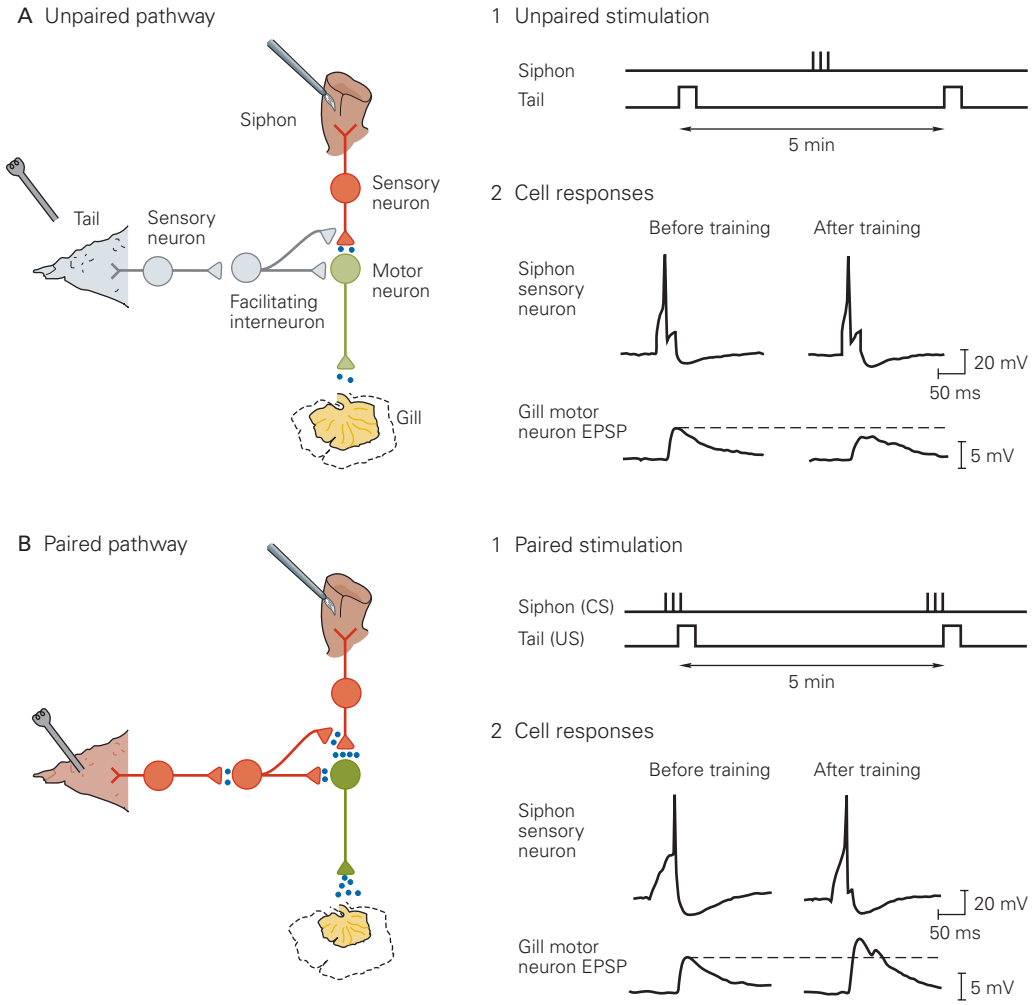

Figure 53–5 Classical conditioning of the gill-withdrawal reflex in *Aplysia*. (Adapted, with permission, from Hawkins et al. 1983.)

A. The siphon is stimulated by a light tap and the tail is shocked, but the two stimuli are not paired in time. The tail shock excites facilitatory interneurons that form synapses on the presynaptic terminals of sensory neurons innervating the mantle shelf and siphon. This is the mechanism of sensitization. **1.** The pattern of unpaired stimulation during training. **2.** Under these conditions, the size of the motor neuron test excitatory postsynaptic potential (**EPSP**) is only weakly facilitated by the tail shock. Often, as in this example, the EPSP actually decreases slightly despite the tail shock because repeated unpaired stimulation of the siphon leads to synaptic depression due to habituation.

B. The tail shock is paired in time with stimulation of the siphon. **1.** The siphon is touched (conditioned stimulus [**CS**]) immediately prior to shocking the tail (unconditioned stimulus [**US**]). As a result, the siphon sensory neurons are primed to be more responsive to input from the facilitatory interneurons in the unconditioned pathway. This is the mechanism of classical conditioning; it selectively amplifies the response of the conditioned pathway. **2.** Recordings of test EPSPs in an identified motor neuron produced by a siphon sensory neuron before training and 1 hour after training. After training with paired sensory input, the EPSP in the siphon motor neuron is considerably greater than either the EPSP before training or the EPSP following unpaired tail shock (shown in part **A2**). This synaptic amplification produces a more vigorous gill withdrawal.

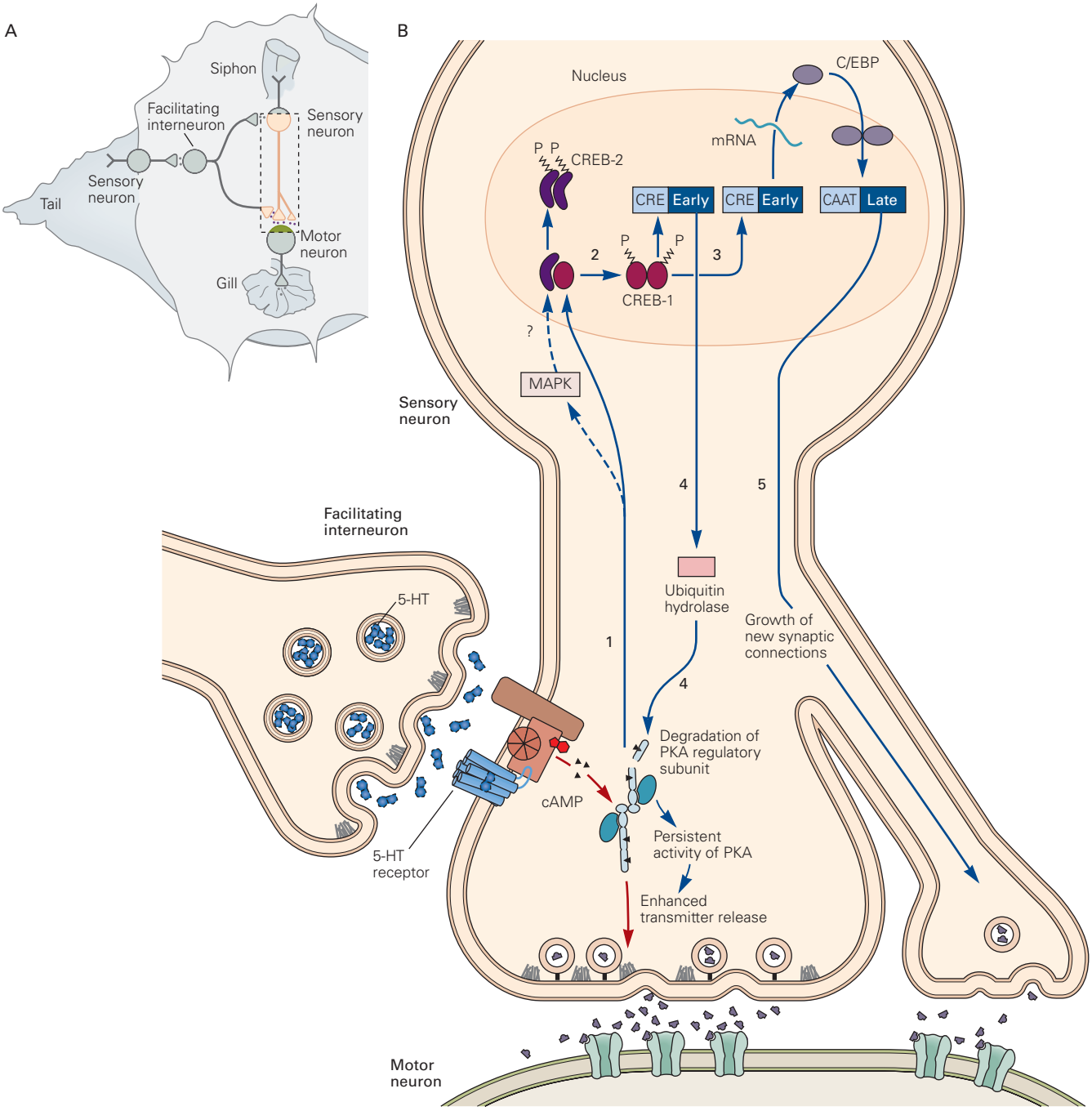

Figure 53–6 Long-term sensitization involves synaptic facilitation and the growth of new synaptic connections.

A. Long-term sensitization of the gill-withdrawal reflex of *Aplysia* involves long-lasting facilitation of transmitter release at the synapses between sensory and motor neurons.

B. Long-term sensitization of the gill-withdrawal reflex leads to persistent activity of protein kinase A (**PKA**), resulting in the growth of new synaptic connections. Repeated tail shock leads to more pronounced elevation of cyclic adenosine monophosphate (**cAMP**), producing long-term facilitation (lasting 1 or more days) that outlasts the increase in cAMP and recruits the synthesis of new proteins. This inductive mechanism is initiated by translocation of PKA to the nucleus (**pathway 1**), where PKA phosphorylates the transcriptional activator cAMP response element binding protein 1 (**CREB-1**) (**pathway 2**). CREB-1 binds cAMP regulatory elements (**CRE**) located in the upstream region of several cAMP-inducible genes, activating gene transcription (**pathway 3**). PKA also activates the mitogen-activated protein kinase (**MAPK**), which phosphorylates the transcriptional repressor cAMP response element binding protein 2 (**CREB-2**), thus removing its repressive action. One gene activated by CREB-1 encodes a ubiquitin hydrolase, a component of a specific ubiquitin proteasome that leads to the proteolytic cleavage of the regulatory subunit of PKA, resulting in persistent activity of PKA, even after cAMP has returned to its resting level (**pathway 4**). CREB-1 also activates the expression of the transcription factor C/EBP, which leads to expression of a set of unidentified proteins important for the growth of new synaptic connections (**pathway 5**).

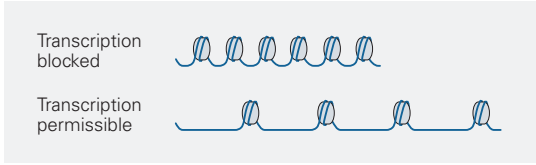

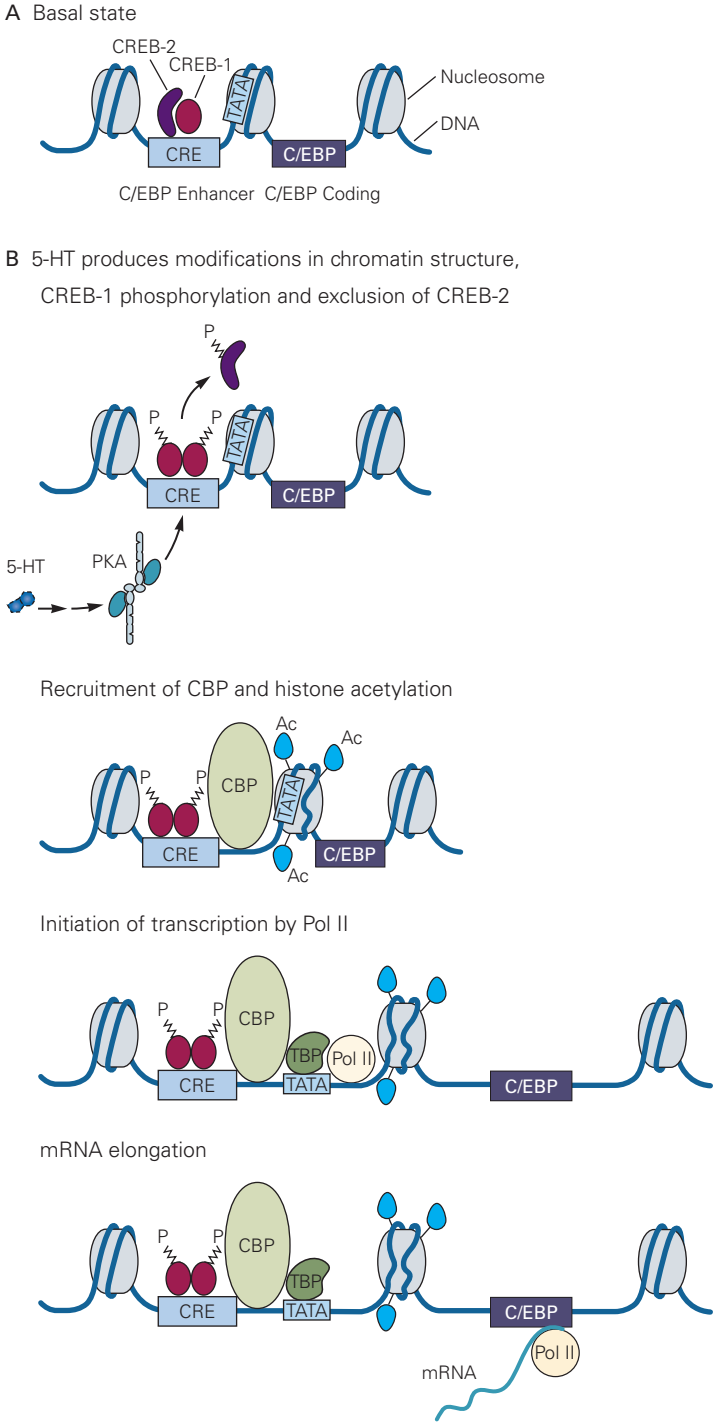

Figure 53–7 Regulation of histone acetylation by serotonin, CREB-1, and CBP.

A. Under basal conditions, the activator CREB-1 (here in complex with CREB-2) occupies the binding site for cAMP recognition element (**CRE**) within the promoter region of its target genes. In the example shown here, CREB-1 binds to the CRE within the C/EBP promoter. In the basal state, CREB-1 binding is not able to activate transcription because the TATA box, the core promoter region responsible for recruiting RNA polymerase II (**Pol II**) during transcription initiation, is inaccessible because the DNA is tightly bound to histone proteins in the nucleosome.

B. Serotonin (**5-HT**) activates protein kinase A (**PKA**), which phosphorylates CREB-1 and indirectly enhances CREB-2 phosphorylation by MAPK, causing CREB-2 to dissociate from the promoter. This allows CREB-1 to form a complex at the promoter with CREB binding protein (**CBP**). Activated CBP acetylates specific lysine residues of the histones, causing them to bind less tightly to DNA. Along with other changes in chromatin structure, acetylation facilitates the repositioning of the nucleosome that previously blocked access of the Pol II complex to the TATA box. This repositioning allows Pol II to be recruited to initiate transcription of the C/EBP gene. (Abbreviation: **TBP**, TATA binding protein.)

promoter, and it functions as an acetyltransferase, adding acetyl groups to certain lysine residues on its substrate proteins. One of the most important substrates of CBP are DNA-binding histone proteins, which are components of nucleosomes, the fundamental building blocks of chromatin. The histones contain a series of positively charged basic residues that strongly interact with the negatively charged phosphates of DNA. This interaction causes DNA to become tightly wrapped around the nucleosomes, much like string is wrapped around a spool, thereby preventing necessary transcription factors from accessing their gene targets.

The binding of CBP to CREB-1 leads to histone acetylation, which causes a number of important structural and functional changes at the level of the nucleosome. For example, acetylation neutralizes the positive charge of lysine residues in the histone tail domains, decreasing the affinity of histones for DNA. Also, specific classes of transcriptional activators can bind to acetylated histones and facilitate the repositioning of nucleosomes at the promoter region. Together, these and other types of chromatin modifications serve to regulate the accessibility of chromatin to the transcriptional machinery, and thus enhance the ability of a gene to be transcribed. This type of modification of DNA structure is termed *epigenetic* regulation. As we will see in Chapter 54, a mutation in the gene encoding CBP underlies Rubinstein-Taybi syndrome, a disorder associated with mental retardation.

The turning on of transcription by PKA also depends on its ability to indirectly activate the MAPK pathway (Chapter 14). MAPK phosphorylates the transcription factor CREB-2, relieving its inhibitory action on transcription (Figure 53–6B). The combined effects of CREB-1 activation and relief of CREB-2 repression induce a cascade of new gene expression important for learning and memory (Figure 53–7).

The presence of both a repressor (CREB-2) and an activator (CREB-1) of transcription at the first step in long-term facilitation suggests that the threshold for long-term memory storage can be regulated. Indeed, we see in everyday life that the ease with which short-term memory is transferred into long-term memory varies greatly with attention, mood, and social context.

The Role of Noncoding RNAs in the Regulation of Transcription

There are other targets of transcription and chromatin regulation in memory consolidation and reconsolidation besides messenger RNAs. Of particular interest are noncoding RNAs such as microRNAs (miRNAs), PIWI-interacting RNAs (piRNAs), and long noncoding RNAs. These are also targeted to specific genetic sites, and their expression in turn regulates transcriptional and posttranscriptional mechanisms.

Studies in *Aplysia* show that miRNAs and piRNAs are both regulated by neuronal activity and contribute to long-term facilitation. MicroRNAs are a class of conserved noncoding RNAs, 20 to 23 nucleotides in length, that contribute to transcriptional and posttranscriptional regulation of gene expression through a specific set of RNA–protein machinery. In *Aplysia*, the most abundant and conserved brain species of these miRNAs are present in sensory neurons, where one of them—miRNA-124—normally constrains serotonin-induced synaptic facilitation by inhibiting the translation of CREB-1 mRNA, suppressing levels of CREB-1 protein. Serotonin inhibits the synthesis of miRNA-124, thereby leading to the disinhibition of the translation of CREB-1 mRNA, enabling the initiation of CREB-1–mediated transcription. The piRNAs are 28 to 32 nucleotides in length, slightly longer than miRNAs, and bind to a protein called Piwi. Individual piRNAs promote the methylation of specific DNA sequences, thereby silencing the genes, providing another example of epigenetic regulation. One piRNA, piRNA-F, increases in response to serotonin, which leads to the methylation of the promoter of CREB-2, reducing CREB-2 gene transcription.

Thus, we see here an example of integrative action at the transcriptional level. Serotonin regulates both piRNA and microRNA in a coordinated fashion: Serotonin rapidly decreases levels of miRNA-124 and facilitates the activation of CREB-1, which begins the process of memory consolidation. After a delay, serotonin also increases levels of piRNA-F, resulting in the methylation and silencing of the promoter of the transcription repressor CREB-2. The decrease in CREB-2 increases the duration of action of CREB-1, thereby consolidating a stable form of long-term memory in the sensory neuron (Figure 53–8).

Two of the genes expressed in the wake of CREB-1 activation and the consequential alteration in chromatin structure are important in the early development of long-term facilitation. One is a gene for ubiquitin carboxyterminal hydrolase, the other a gene for a transcription factor, CAAT box enhancer binding protein (C/EBP), a component of a gene cascade necessary for synthesizing proteins needed for the growth of new synaptic connections (Figures 53–6 and 53–7).

The hydrolase facilitates ubiquitin-mediated protein degradation (Chapter 7) and helps enhance activation of PKA. PKA is made up of four subunits; two regulatory subunits inhibit two catalytic subunits (Chapter 14). With long-term training and the

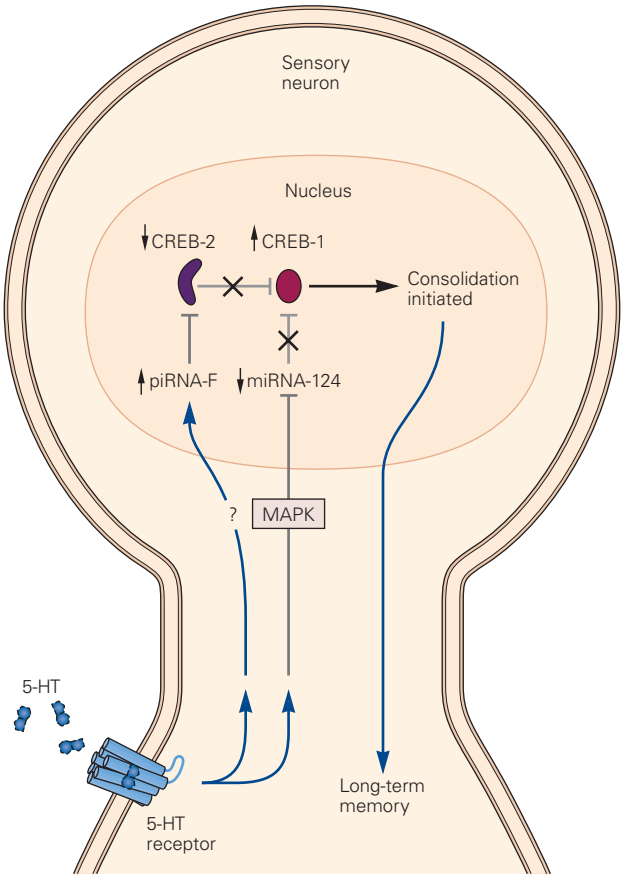

Figure 53–8 Small non-coding RNA molecules contribute to the memory consolidation switch. Long-term facilitation of the sensory to motor neuron synapses is consolidated through the action of two distinct classes of small noncoding RNA molecules. miRNA-124 normally acts to suppress levels of the CREB-1 transcription factor by binding to its mRNA and inhibiting its translation. Serotonin (**5-HT**) downregulates miRNA-124 levels through a mechanism requiring mitogen-activated protein kinase (**MAPK**). This enhances the levels of CREB-1, promoting activation of CREB-1–dependent transcription of gene products necessary for memory consolidation. In a complementary pathway, 5-HT enhances with a delay the synthesis of several piRNAs, including piRNA-F, which bind to the Piwi protein. The piRNA-F/Piwi complex leads to enhanced methylation of the *CREB-2* gene, resulting in long-lasting transcriptional repression of *CREB-2* and decreased levels of CREB-2 protein. Because CREB-2 normally inhibits the action of CREB-1, the increased levels of piRNA-F in response to 5-HT enhance and prolong CREB-1 activity, resulting in more effective memory consolidation.

induction of the hydrolase, approximately 25% of the regulatory subunits are degraded in the sensory neurons. As a result, free catalytic subunits can continue to phosphorylate proteins important for the enhancement of transmitter release and the strengthening of synaptic connections, including CREB-1, long after cAMP has returned to its resting level (Figure 53–6B). Formation of a constitutively active enzyme is therefore the simplest molecular mechanism for long-term memory. With repeated training, a second-messenger kinase critical for short-term facilitation can remain persistently active for up to 24 hours without requiring a continuous activating signal.

The second and more enduring consequence of CREB-1 activation is the activation of the transcription factor C/EBP. This transcription factor forms both a homodimer with itself and a heterodimer with another transcription factor called *activating factor*. Together, these factors act on downstream genes that trigger the growth of new synaptic connections that support long-term memory.

With long-term sensitization, the number of presynaptic terminals in the sensory neurons in the gill-withdrawal circuit doubles (Figure 53–9). The dendrites of the motor neurons also grow to accommodate the additional synaptic input. Thus, long-term structural changes in both post- and presynaptic cells increase the number of synapses. Long-term habituation, in contrast, leads to *pruning* of synaptic connections, as described above. Long-term disuse of functional connections between sensory and motor neurons reduces the number of terminals of each sensory neuron by one-third (Figure 53–9A).

Long-Term Synaptic Facilitation Is Synapse Specific

A typical pyramidal neuron in the mammalian brain makes 10,000 presynaptic connections with a wide range of target cells. It is therefore generally thought that long-term memory storage should be synapse specific—that is, only those synapses that actively participate in learning should be enhanced. However, the finding that long-term facilitation involves gene expression—which occurs in the nucleus, far removed from a neuron's synapses—raises some fundamental questions regarding information storage.

Is long-term memory storage indeed synapse specific, or do the gene products recruited during long-term memory storage alter the strength of every presynaptic terminal in a neuron? And if long-term memory is synapse specific, what are the cellular mechanisms that enable the products of gene transcription to selectively strengthen just some synapses and not others?

Kelsey Martin and her colleagues addressed these questions for long-term facilitation by using a cell culture system consisting of an isolated *Aplysia* sensory neuron with a bifurcated axon that makes separate synaptic contacts with two motor neurons. The sensory

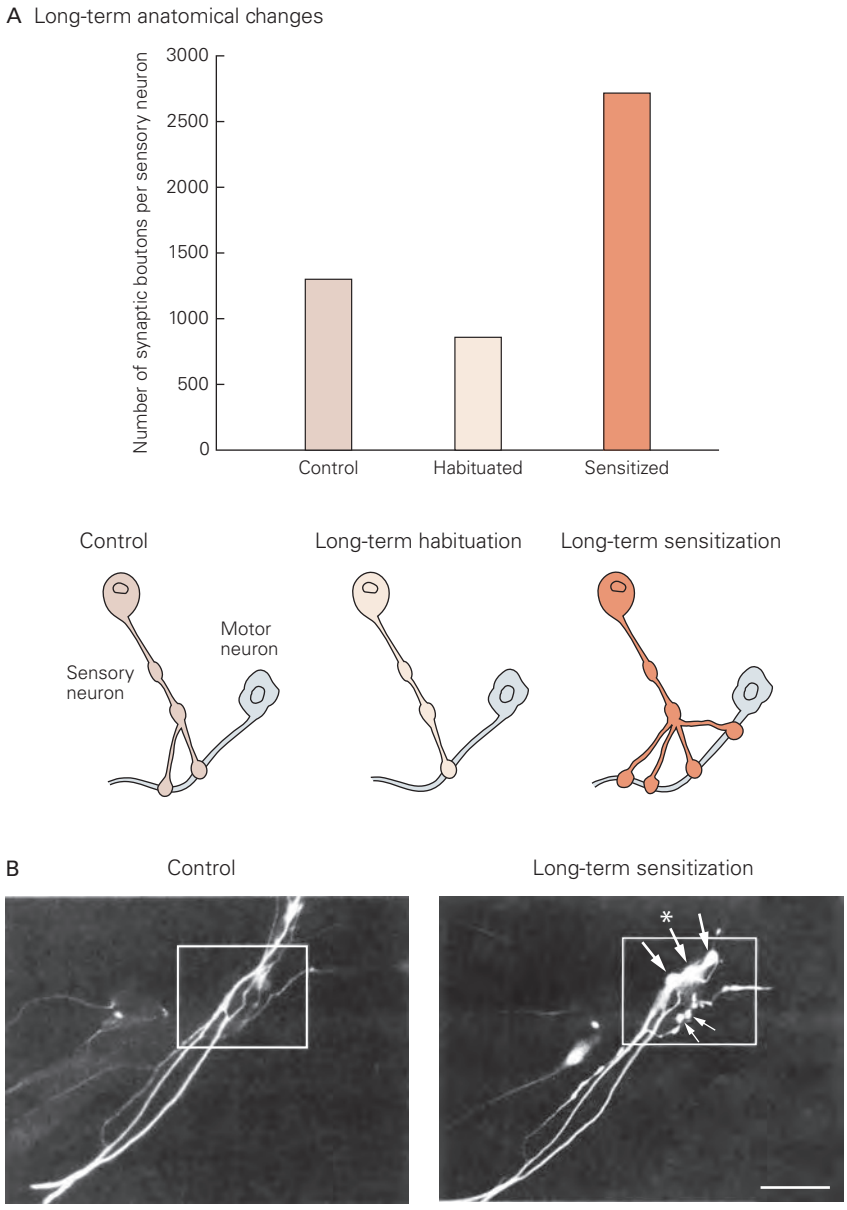

Figure 53–9 Long-term habituation and sensitization involve structural changes in the presynaptic terminals of sensory neurons.

A. Long-term habituation leads to a loss of synapses, and long-term sensitization leads to an increase in the number of synapses. When measured either 1 day (shown here) or 1 week after training, the number of presynaptic terminals relative to control levels is greater in sensitized animals and less in habituated animals. The drawings below the graph illustrate changes in the number of synaptic contacts. The swellings or varicosities on the sensory neuron processes are called synaptic boutons; they contain all the specialized structures necessary for transmitter release. (Adapted, with permission, from Bailey and Chen 1983. Copyright © 1983 AAAS.)

B. Fluorescence images of a sensory neuron axon contacting a motor neuron in culture before (*left*) and 1 day after (*right*) five brief exposures to serotonin. The resulting increase in varicosities simulates the synaptic changes associated with long-term sensitization. Prior to serotonin application, no presynaptic varicosities are visible in the outlined area (*left*). After serotonin, several new boutons are apparent (**arrows**), some of which contain a fully developed active zone (**asterisk**) or have small immature active zones. Scale bar = 50 µm. (Reproduced, with permission, from Glanzman, Kandel, and Schacher 1990.)

neuron terminals on one of the two motor neurons were activated by focal pulses of serotonin, thus mimicking the neural effects of a shock to the tail. When only one pulse of serotonin was applied, those synapses showed short-term facilitation. The synapses on the second motor neuron, which did not receive serotonin, showed no change in synaptic transmission.

When five pulses of serotonin were applied to the same synapses, those synapses displayed both short-term and long-term facilitation, and new synaptic connections were formed with the motor neuron. Although long-term facilitation and synaptic growth require gene transcription and protein synthesis, the synapses that did not receive serotonin showed no enhancement of synaptic transmission (Figure 53–10). Thus, both short-term and long-term synaptic facilitation are synapse specific and manifested only by those synapses that receive the modulatory serotonin signal.

But how are the nuclear products able to enhance transmission at only certain synapses and not others of the same neuron? Are the newly synthesized proteins somehow targeted to only those synapses that receive serotonin? Or are they shipped out to all synapses but used productively for the growth of new synaptic connections only at those synapses that have been marked by at least a single pulse of serotonin?

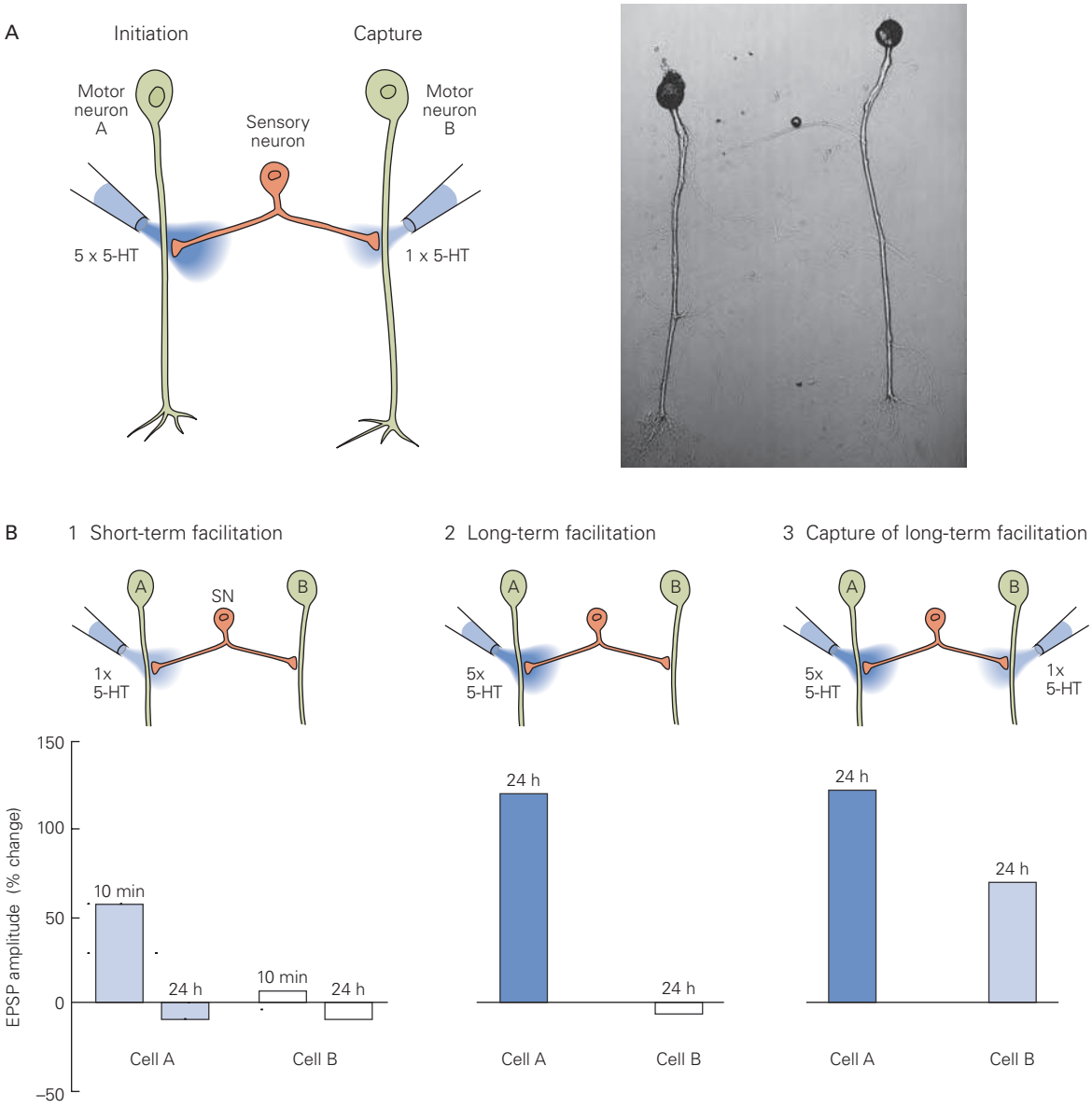

Figure 53–10 **The long-term facilitation of synaptic transmission is synapse specific.** (Adapted, with permission, from Martin et al. 1997.)

A. The experiment uses a single presynaptic sensory neuron that contacts two postsynaptic motor neurons A and B. The pipette on the left is used to apply five pulses of serotonin (**5-HT**) to a sensory neuron synapse with motor neuron A, initiating long-term facilitation at that synapse. The pipette on the right is used to apply one pulse of 5-HT to a sensory neuron synapse with motor neuron B, allowing this synapse to make use of (capture) new proteins produced in the cell body in response to the five pulses of 5-HT at the synapse with motor neuron A. The image at the right shows the actual appearance of the cells in culture.

B. 1. One pulse of 5-HT applied to the synapse with motor neuron A produces only short-term (10-minute) facilitation of the excitatory postsynaptic potential (**EPSP**) in the neuron. By 24 hours, the EPSP has returned to its normal size. There is no significant change in EPSP size in cell B. **2.** Application of five pulses of 5-HT to the synapses with cell A produces long-term (24-hour) facilitation of the EPSP in that cell but no change in the size of the EPSP in cell B. **3.** When five pulses of 5-HT onto the synapse with cell A are paired with a single pulse of 5-HT onto the synapses with cell B, cell B now displays long-term facilitation and an increase in EPSP size after 24 hours.

To test this question, Martin and her colleagues again selectively applied five pulses of serotonin to the synapses made by the sensory neuron onto one of the motor neurons. This time, however, the synapses with the second motor neuron were simultaneously activated by a single pulse of serotonin (which by itself produces only short-term synaptic facilitation lasting minutes). Under these conditions, the single pulse of serotonin was sufficient to induce long-term facilitation and growth of new synaptic connections at the contacts between the sensory neuron and the second motor neuron. Thus, application of the single pulse of serotonin onto the synapses at the second branch enabled those synapses to use the nuclear products produced in response to the five pulses of serotonin onto the synapses of the first branch, a process called *capture*.

These results suggest that newly synthesized gene products, both mRNAs and proteins, are delivered by fast axonal transport to all the synapses of a neuron but are functional only at synapses that have been marked by previous synaptic activity, that is, by presynaptic release of serotonin. Although one pulse of serotonin at a synapse is insufficient to turn on new gene expression in the cell body, it is sufficient to mark that synapse, allowing it to make use of new proteins generated in the cell body in response to five pulses of serotonin at another synapse. This idea, developed by Martin and her colleagues for *Aplysia* and independently by Frey and Morris for the hippocampus in rodents, is called *synaptic capture* or *synaptic tagging*.

These findings raise the question, what is the nature of the synaptic mark that allows the capture of the gene products for long-term facilitation? When an inhibitor of PKA was applied locally to the synapses receiving the single pulse of serotonin, those synapses could no longer capture the gene products produced in response to the five pulses of serotonin (Figure 53–11). This indicates that local phosphorylation by PKA is required for synaptic capture.

In the early 1980s, Oswald Steward discovered that ribosomes, the machinery for protein synthesis, are present at synapses as well as in the cell body. Martin examined the importance of local protein synthesis in long-term synaptic facilitation by applying a single pulse of serotonin together with an inhibitor of local protein synthesis onto one set of synapses while simultaneously applying five pulses of serotonin to a second set of synapses. Normally, long-term facilitation and synaptic growth would persist for up to 72 hours in response to synaptic capture. In the presence of the local protein synthesis inhibitor, synaptic capture still occurred, producing long-term synaptic facilitation at the synapses exposed to only one pulse of serotonin. However, the facilitation only lasted 24 hours. After 24 hours, synaptic growth and facilitation at these synapses collapsed, indicating that the maintenance of learning-induced synaptic growth requires new local protein synthesis at the synapse (Figure 53–11B).

Martin and her colleagues thus found that regulation of protein synthesis at the synapse plays a major role in controlling synaptic strength at the sensory-to-motor neuron connection in *Aplysia*. As we shall see in Chapter 54, local protein synthesis is also important for the later phases of long-term potentiation of synaptic strength in the hippocampus.

These findings indicate there are two distinct components of synaptic marking in *Aplysia*. The first component, lasting about 24 hours, initiates long-term synaptic plasticity and synaptic growth, requires transcription and translation in the nucleus, and recruits local PKA activity, but does not require local protein synthesis. The second component, which stabilizes the long-term synaptic change after 72 hours, requires local protein synthesis at the synapse. How might this local protein synthesis be regulated?

Maintaining Long-Term Synaptic Facilitation Requires a Prion-Like Protein Regulator of Local Protein Synthesis

The fact that mRNAs are translated at the synapse in response to marking of that synapse by one pulse of serotonin suggests that these mRNAs may initially be dormant and under the control of a regulator of translation recruited by serotonin. Translation of most mRNAs requires that transcripts contain a long tail of adenosine nucleotides at their 3′ end [poly(A) tail]. Joel Richter had earlier found that in *Xenopus* (frog) oocytes the maternal mRNAs only have a short tail of adenine nucleotides and thus are silent until activated by the cytoplasmic polyadenylation element binding protein (CPEB). CPEB binds to a site on mRNAs and recruits poly(A) polymerase, leading to the elongation of the poly(A) tail.

Kausik Si and his colleagues found that serotonin increases the local synthesis of a novel, neuron-specific isoform of CPEB in *Aplysia* sensory neuron terminals. The induction of CPEB is independent of transcription but requires new protein synthesis. Blocking CPEB locally at an activated synapse blocks the long-term maintenance of synaptic facilitation at the synapse but not its initiation and initial 24-hour maintenance.

How might CPEB stabilize the late phase of long-term facilitation? Most biological molecules have a relatively short half-life (hours to days), whereas memory

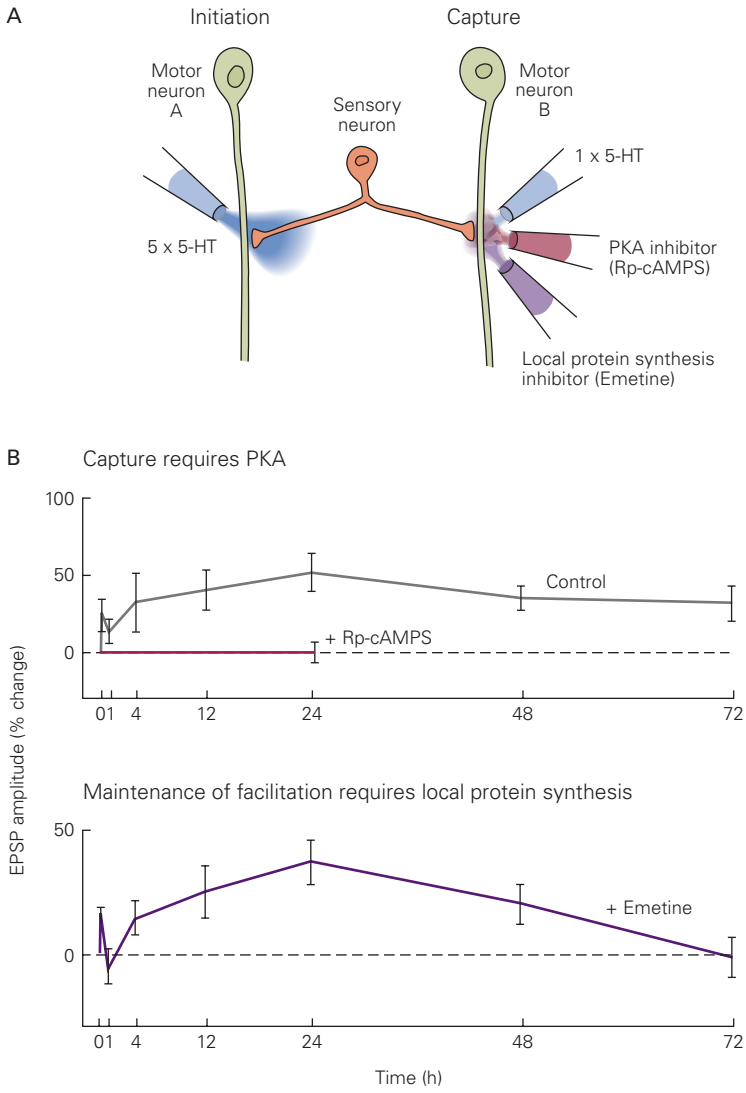

Figure 53–11 Long-term facilitation requires both cyclic adenosine monophosphate (cAMP)-dependent phosphorylation and local protein synthesis. (Adapted, with permission, from Casadio et al. 1999.)

A. Five pulses of serotonin (**5-HT**) are applied to the synapses on motor neuron A, and a single pulse is applied to those of cell B. Inhibitors of protein kinase A (**PKA**; Rp-cAMPS) or local protein synthesis (emetine) are applied to synapses on cell B.

B. Rp-cAMPS blocks the capture of long-term facilitation completely at the synapses on neuron B. Emetine has no effect on the capture of facilitation or the growth of new synaptic connections measured 24 hours after 5-HT application, but by 72 hours, it fully blocks synaptic enhancement. The outgrowth of new synaptic connections is retracted, and long-term facilitation decays after 1 day if capture is not maintained by local protein synthesis. (Abbreviations: **EPSP**, excitatory post-synaptic potential; **Rp-cAMPS**, Rp-diaster-eomer of adenosine cyclic 3′,5′-phosphorothioate.)

lasts days, weeks, or even years. How can learning-induced alterations in the molecular composition of a synapse be maintained for such a long time? Most hypotheses posit some type of self-sustained mechanism that modulates synaptic strength and structure.

Si and his colleagues made the surprising discovery that the neuronal isoform of *Aplysia* CPEB appears to have self-sustaining properties that resemble those of prion proteins. Prions were discovered by Stanley Prusiner, who demonstrated that these proteins were the causative agents of Creutzfeldt-Jakob disease, a devastating neurodegenerative human disease, and mad cow disease. Prion proteins can exist in two forms: a soluble form and an aggregated form that is capable of self-perpetuation. *Aplysia* CPEB also has two conformational states, a soluble form that is inactive and an aggregated form that is active. This switch depends on an N-terminal domain of CPEB that is rich in glutamine, similar to prion domains in other proteins.

In a naïve synapse, CPEB exists in the soluble, inactive state, and its resting level of expression is low. However, in response to serotonin, the local synthesis of CPEB increases until a threshold concentration is reached that switches CPEB to the aggregated, active state, which is then capable of activating the translation of dormant mRNAs. Once the active state is established, it becomes self-perpetuating by recruiting soluble CPEB to the aggregates, maintaining its ability to activate the translation of dormant mRNAs. Although dormant mRNAs are made in the cell body and distributed throughout the cell, they are translated only at synapses that have active CPEB aggregates.

Whereas conventional prion mechanisms are pathogenic—the aggregated state of most prion proteins causes cell death—the *Aplysia* CPEB is a new form of a prion-like protein, one whose aggregated state plays an important physiological function. The active self-perpetuating form of *Aplysia* CPEB maintains long-term molecular changes in a synapse that are necessary for the persistence of memory storage (Figure 53–12).

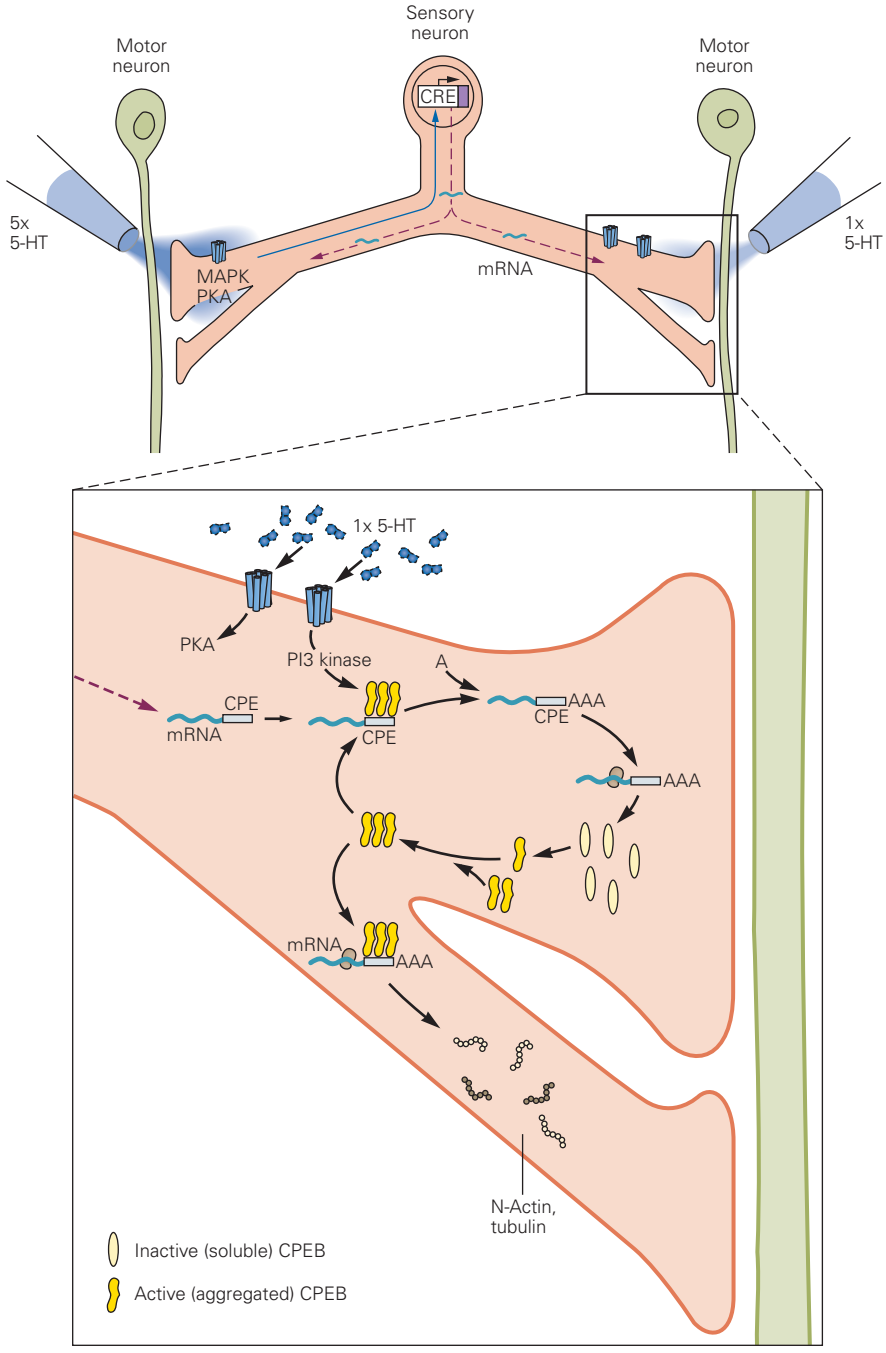

Figure 53–12 A self-perpetuating switch for protein synthesis at axon terminals in *Aplysia* maintains long-term synaptic facilitation. Five pulses of serotonin (**5-HT**) set up a signal that goes back to the nucleus to activate synthesis of mRNA. Newly transcribed mRNAs and newly synthesized proteins in the cell body are then sent to all terminals by fast axonal transport. However, only those terminals that have been marked by at least one pulse of serotonin can use the proteins to grow the new synapses needed for long-term facilitation. The marking of a terminal involves two substances: (1) protein kinase A (**PKA**), which is necessary for the immediate synaptic growth initiated by the proteins transported to the terminals, and (2) phosphoinositide 3 kinase (**PI3 kinase**), which initiates the local translation of mRNAs required to maintain synaptic growth and long-term facilitation past 24 hours. Some of the mRNAs at the terminals encode cytoplasmic polyadenylation element binding protein (**CPEB**), a regulator of local protein synthesis. In the basal state, CPEB is thought to exist in a largely inactive conformation as a soluble monomer that cannot bind to mRNAs. Through some as yet unspecified mechanism activated by serotonin and PI3 kinase, some copies of CPEB convert to an active conformation that forms aggregates. The aggregates function like prions in that they are able to recruit monomers to join the aggregate, thereby activating the monomers. The CPEB aggregates bind the cytoplasmic polyadenylation element (**CPE**) site of mRNAs. This binding recruits the poly(A) polymerase machinery and allows poly(A) tails of adenine nucleotides (**A**) to be added to dormant mRNAs. The polyadenylated mRNAs can now be recognized by ribosomes, allowing the translation of these mRNAs to several proteins. For example, in addition to CPEB, this leads to the local synthesis of N-actin and tubulin, which stabilize newly grown synaptic structures. (Model based on Bailey, Kandel, and Si 2004.)

Memory Stored in a Sensory-Motor Synapse Becomes Destabilized Following Retrieval but Can Be Restabilized

A variety of studies in mammals by Karim Nader and others have found that in its early stages long-term memory storage is dynamic and can be disrupted. In particular, a memory trace can become labile after retrieval and require an additional round of consolidation (so-called *reconsolidation*).

Until recently, it was unclear whether the same set of synapses involved in storing a memory are destabilized and restabilized following retrieval or whether, after synaptic reactivation following a memory, a new set of synapses is regulated. This question was examined for retrieval of long-term sensitization of the gill- and siphon-withdrawal reflex in *Aplysia*. These experiments revealed that a retrieved memory becomes labile as a result of ubiquitin-mediated protein degradation and is then reconsolidated by means new protein synthesis.

Does a similar reconsolidation mechanism occur at sensory-motor synapses that have undergone long-term facilitation? Indeed, when a synapse that has undergone long-term facilitation is reactivated by a brief burst of presynaptic action potentials, that synapse becomes destabilized through protein degradation and requires protein synthesis for restabilization. Such results suggest that reconsolidation of memory involves restabilization of synaptic facilitation at the same synapses at which the initial memory was stored.

Classical Threat Conditioning of Defensive Responses in Flies Also Uses the cAMP-PKA-CREB Pathway

Do the cellular mechanisms for implicit memory storage found in *Aplysia* have parallels in other animals? Studies on aversive learning indicate that the same mechanisms are also used to store memory in the fruit fly *Drosophila* and in rodents, indicating conserved mechanisms throughout Metazoan evolution. The fruit fly is particularly convenient for the study of implicit memory storage because its genome is easily manipulated and, as first demonstrated by Seymour Benzer and his colleagues, the fly can be classically conditioned. In a typical classical conditioning paradigm, an odor is paired with repeated electrical shocks to the feet. The extent of learning is then examined by allowing the flies to choose between two arms of a maze, where one arm contains the odor that had been paired with a shock and the other arm contains an unpaired odor. Following training, a large fraction of wild type flies avoids the arm with the conditioned odor. Several fly mutants have been identified that do not learn to avoid the conditioned odor. These learning-defective mutants have been given imaginatively descriptive names such as *dumb*, *dunce*, *rutabaga*, *amnesiac*, and *PKA-R1*. Of great interest, all of these mutants have defects in the cAMP cascade.

Olfactory conditioning depends on a region of the fly brain called the mushroom bodies. Neurons of the mushroom bodies, called Kenyon cells, receive olfactory input from the antennal lobes, structures similar to the olfactory lobes of the mammalian brain. The Kenyon cells also receive input from dopaminergic neurons that respond to aversive stimuli, such as a foot shock. The dopamine binds to a metabotropic receptor (encoded by the *dumb* gene) that activates a stimulatory G protein and a specific type of Ca^{2+}/calmodulin-dependent adenylyl cyclase (encoded by the *rutabaga* gene), similar to the cyclase involved in classical conditioning in *Aplysia*. The convergent action of dopamine released by the unconditioned stimulus (foot shock) and a rise in intracellular Ca^{2+} triggered by olfactory input leads to the synergistic activation of adenylyl cyclase, producing a large increase in cAMP.

Recent experiments have demonstrated that flies can be classically conditioned when an odorant is paired with direct stimulation of the dopaminergic neurons, bypassing the foot shock. In these experiments, the mammalian P2X receptor (an adenosine triphosphate [ATP]-gated cation channel) is expressed as a transgene in the dopaminergic neurons. The flies are then injected with a caged derivative of ATP. The dopaminergic neurons can then be excited to fire action potentials by shining light on the flies to release ATP from its cage and activate the P2X receptors. When the dopaminergic neurons are activated in this manner in the presence of an odor, the flies undergo aversive conditioning—they learn to avoid the odor. Thus, the unconditioned stimulus activates a dopamine signal that reinforces aversive conditioning, much as serotonin acts as an aversive reinforcement signal for learned defensive responses in *Aplysia.*

A reverse genetic approach has also been used to explore memory formation in *Drosophila.* In these experiments, various transgenes are placed under the control of a promoter that is heat sensitive. The heat sensitivity permits the gene to be turned on at will by elevating the temperature of the chamber housing the flies. This was done in mature animals to minimize any potential effect on the development of the brain. When the catalytic subunit of PKA was blocked by transient expression of an inhibitory transgene, flies were unable

to form short-term memory, indicating the importance of the cAMP signal transduction pathway for associative learning and short-term memory in *Drosophila.*

Long-term memory in *Drosophila* requires new protein synthesis just as in *Aplysia* and other animals. Knockout of a CREB activator gene selectively blocks long-term memory without interfering with short-term memory. Conversely, when the gene is overexpressed, a training procedure that ordinarily produces only short-term memory produces long-term memory.

As in *Aplysia*, certain forms of long-term memory in *Drosophila* also involve CPEB and may depend on prion-like behavior in this protein. Male flies learn to suppress their courtship behavior after exposure to unreceptive females. When the N-terminal domain of CPEB is deleted genetically, there is a loss of long-term courtship memory; the male fly fails to recognize the unreceptive female. This N-terminal domain is rich in glutamine residues and corresponds to the glutamine rich prion-like domain of CPEB in *Aplysia*. Thus several molecular mechanisms involved in implicit memory are conserved from *Aplysia* to flies, and as we will see next, this conservation extends to mammals.

Memory of Threat Learning in Mammals Involves the Amygdala

Research over the past several decades has resulted in a detailed understanding of the neural circuits for both innate and learned defensive responses to threats in mammals, often referred to as "fear learning." In particular, as we have noted in Chapter 42, both types of defensive responses crucially involve the amygdala, which participates in the detection and evaluation of a broad range of significant and potentially dangerous environmental stimuli. The amygdala-based defense system quickly learns about new dangers. It can associate a new neutral stimulus (conditioned stimulus) with a known threat (unconditioned stimulus) after a single paired exposure, and this learned association is often retained throughout life.

The amygdala receives information about threats directly from sensory systems. The input nucleus of the amygdala, the lateral nucleus, is the site of convergence for signals from both unconditioned and conditioned stimuli. Both signals are carried by a rapid pathway that goes directly from the thalamus to the amygdala and a slower indirect pathway that projects from the thalamus to sensory areas of neocortex and from there to the amygdala. These parallel pathways both contribute to conditioning (Figure 53–13). The amygdala also receives higher-order cognitive information by means of connections from cortical associational areas, especially medial cortical regions in the frontal and temporal lobes.

During Pavlovian conditioning, the strength of synaptic transmission is modified in the amygdala. In response to a tone, an extracellular electrophysiological signal proportional to the excitatory synaptic response is recorded in the lateral nucleus. Following pairing of the tone with a shock, the electrophysiological response to the tone is enhanced by an increase in synaptic transmission, which depends on the

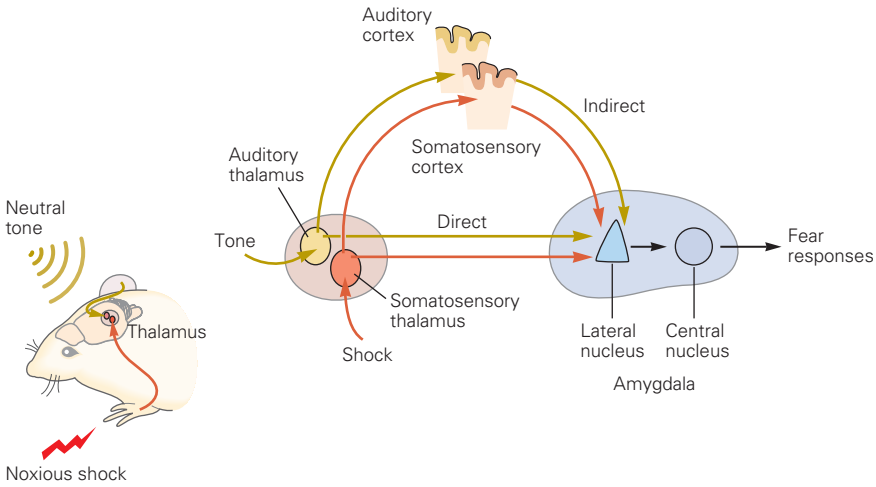

Figure 53–13 Threat learning engages parallel pathways from the thalamus to the amygdala. The signal for the conditioned stimulus, here a neutral tone, is carried by two pathways from the auditory thalamus to the lateral nucleus of the amygdala: by a direct pathway and by an indirect pathway via the auditory cortex. Similarly, the signal for the unconditioned stimulus, here a shock, is conveyed through parallel nociceptive pathways from the somatosensory part of the thalamus to the lateral nucleus, one a direct pathway and one an indirect pathway via the somatosensory cortex. The lateral nucleus in turn projects to the central nucleus, the output nucleus of the amygdala, which activates neural circuits that increase heart rate, produce other autonomic changes, and elicit defensive behaviors that constitute the defensive state. (Reproduced, with permission, from Kandel 2006.)

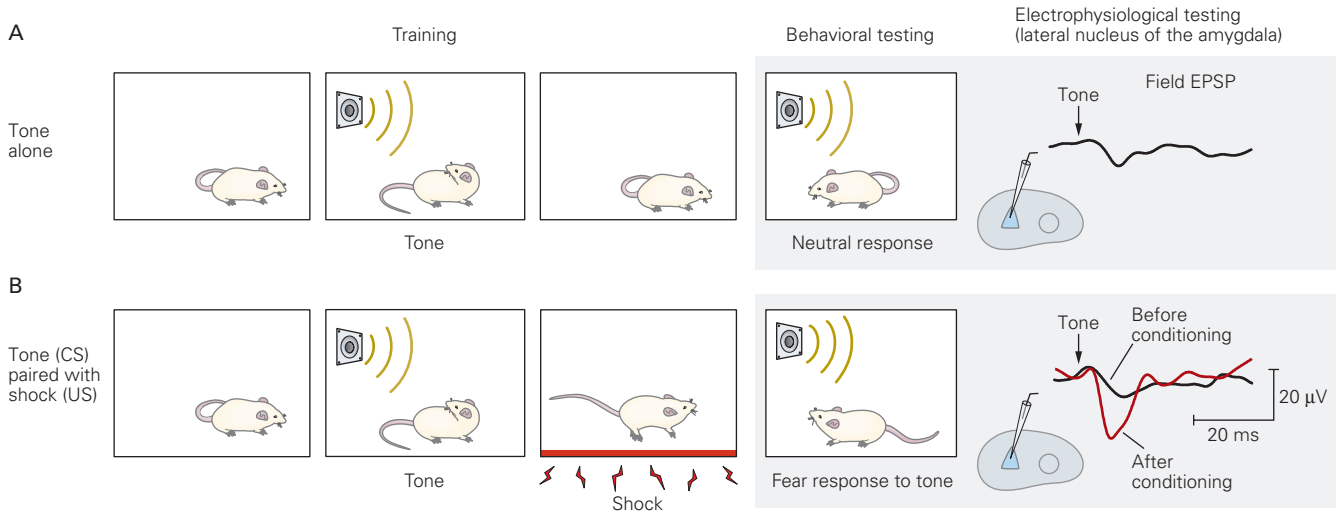

Figure 53–14 Threat learning produces correlated behavioral and electrophysiological changes.

A. An animal ordinarily ignores a neutral tone. The tone produces a small synaptic response in the amygdala recorded by an extracellular field electrode. This field excitatory postsynaptic potential (**field EPSP**) is generated by the small voltage drop between the recording electrode in the amygdala and a second electrode on the exterior of the brain as excitatory synaptic current enters the dendrites of a large population of amygdala neurons.

B. When the tone is presented immediately before a foot shock, the animal learns to associate the tone with the shock. As a result, the tone alone will elicit what the shock previously elicited: It causes the mouse to freeze, an instinctive defense response. After threat conditioning, the electrophysiological response in the lateral nucleus of the amygdala to the tone is greater than the response prior to conditioning. (Abbreviations: **CS**, conditioned stimulus; **US**, unconditioned stimulus.) (Reproduced, with permission, from Rogan et al. 2005.)

convergence of the tone (conditioned stimulus) and the shock (unconditioned stimulus) onto single neurons in the lateral amygdala (Figure 53–14).

It is generally thought that behavioral learning depends on synaptic plasticity. In an effort to understand how such plasticity might occur during learning in the lateral amygdala, researchers have studied *long-term potentiation* (LTP), a cellular model of plasticity. We initially discussed LTP in connection with excitatory synapse function in Chapter 13 and will examine it in detail in Chapter 54 in connection with explicit memory and the hippocampus. In brain slices that include the lateral amygdala, LTP can be induced by high-frequency tetanic stimulation of either the direct or indirect sensory pathways, which produces a long-lasting increase in the excitatory postsynaptic response to these inputs. This change results from a form of homosynaptic plasticity (Figure 53–15).

Long-term potentiation in the lateral nucleus of the amygdala is triggered by Ca^{2+} influx into the postsynaptic neurons in response to strong synaptic activity. The Ca^{2+} entry is mediated by the opening of both *N*-methyl-D-aspartate (NMDA)-type glutamate receptors and L-type voltage-gated Ca^{2+} channels in the postsynaptic cell. Because NMDA receptors are normally blocked by extracellular Mg^{2+}, they require a large synaptic input to generate enough postsynaptic depolarization to relieve this blockade (Chapter 13). L-type channels also require a strong depolarization to open. Thus, LTP is only generated in response to coincident synaptic activity. Calcium influx triggers a biochemical cascade that enhances synaptic transmission through both the insertion of additional α-amino-3-hydroxy-5-methyl-4-isoxazolepropionic acid (AMPA)-type glutamate receptors in the postsynaptic membrane and an increase in transmitter release from the presynaptic terminals. As in *Aplysia*, monoamine neurotransmitters, such as norepinephrine and dopamine, released during tetanic stimulation provide a heterosynaptic modulatory signal that contributes to the induction of LTP.

Studies in awake behaving rodents indicate that similar mechanisms contribute to the acquisition of Pavlovian threat conditioning. This form of learning requires postsynaptic NMDA receptors and voltage-gated calcium channels in the lateral amygdala, and it is enhanced by norepinephrine released in lateral amygdala from the locus ceruleus.

In addition, the size of the LTP elicited by electrical stimulation in slices of the amygdala from animals previously trained is less than that found in slices from untrained animals. Because there is an upper limit to the amount by which synapses can be

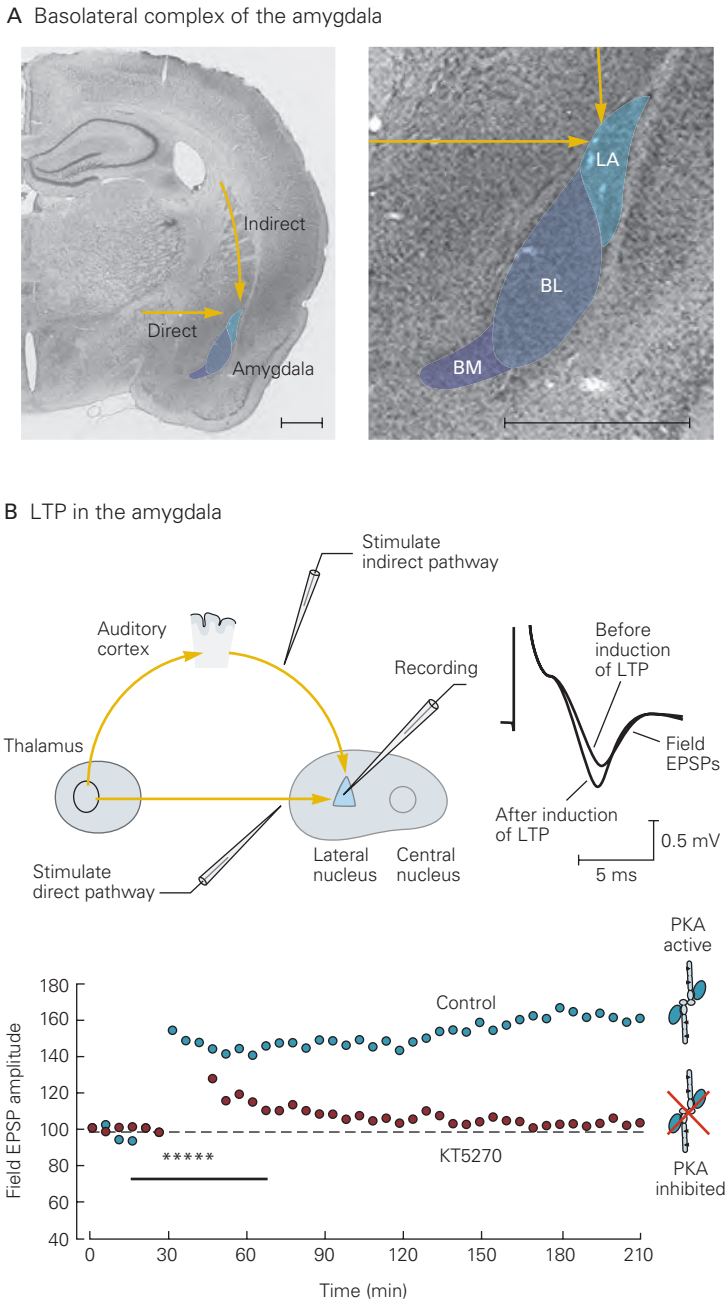

Figure 53–15 Long-term potentiation at synapses in the amygdala may mediate threat conditioning.

A. A coronal brain slice from a mouse shows the position of the amygdala. The enlargement shows three key input nuclei of the amygdala—lateral (**LA**), basolateral (**BL**), and basomedial (**BM**)—which together form the basolateral complex. These nuclei project to the central nucleus, which projects to the hypothalamus and brain stem. (Adapted, with permission, from Maren 1999. Copyright © 1999 Elsevier.)

B. High-frequency tetanic stimulation of the direct or indirect pathway from the thalamus to the lateral nucleus initiates long-term potentiation (**LTP**). The drawing shows the position of the extracellular voltage recording electrode in the lateral nucleus, and the positions of two stimulating electrodes used to activate either the direct pathway or indirect pathway. The plot shows the amplitude of the extracellular field excitatory postsynaptic potential (**EPSP**) in response to stimulation of the indirect cortical pathway during the time course of the experiment. When a pathway is stimulated at a low frequency (once every 30 seconds), the field EPSP is stable. However, when five trains of high-frequency tetanic stimulation are applied (**asterisks**), the response is enhanced for a period of hours. The facilitation depends on protein kinase A (**PKA**) and is compromised when the PKA inhibitor KT5720 is applied (the **bar**). Field EPSPs before and after induction of LTP are also shown. (Adapted, with permission, from Huang and Kandel 1998; Huang, Martin, and Kandel 2000.)

potentiated, this result is taken as evidence that threat conditioning recruits LTP, which precludes further LTP in response to electrical stimulation. Thus, artificially induced LTP and behaviorally induced LTP are closely related.

Two types of genetic experiments also strongly support the idea that an LTP-like phenomenon contributes to the cellular mechanism for storing the memory of a learned threat. First, genetic disruption of the GluN2B (NR2B) subunit of the NMDA receptor interferes both with threat conditioning and the induction of LTP in pathways that transmit the conditioned stimulus signal to the lateral amygdala. Moreover, this mutation affects only learned threats; it does not affect responses to unconditioned threats or routine synaptic transmission. Conversely, overexpression of the GluN2B subunit facilitates learning. Similarly, disruption of CREB signaling, a step downstream from Ca^{2+} influx, interferes with conditioning, whereas enhancement of CREB activity facilitates learning.

Does the LTP important for threat learning involve insertion of new AMPA receptors, as observed in brain slices? To address this question, researchers infected pyramidal neurons in the lateral nucleus with a genetically engineered virus that did not damage the neurons but caused them to express AMPA receptors tagged with a fluorescent label. Threat conditioning led to an increase in insertion of the tagged AMPA receptors into the cell membrane, similar to what is seen during experimentally induced LTP in brain slices. When a different virus was used to express a C-terminal portion of the AMPA receptor that competes with and prevents the insertion of endogenous AMPA receptors, memory for learned threat was substantially reduced, even though the virus infected only 10% to 20% of the neurons in the lateral nucleus. This surprising result suggests that LTP needs to be induced at nearly all activated synapses to effectively support threat learning.

One of the virtues of the Pavlovian paradigm is its amenability to experimental study due to the fact that specific stimuli are transmitted to the amygdala by known pathways. This has allowed experimenters to directly activate conditioned stimulus or unconditioned stimulus pathways, bypassing the normal sensory input. Such studies have provided convincing evidence implicating these pathways to the amygdala in threat learning.

Based on these findings, researchers explored whether threat learning could be induced when they paired an auditory conditioned stimulus (tone) with direct depolarization of lateral amygdala neurons, instead of using an external, pain-eliciting unconditioned shock stimulus to produce the depolarization via the unconditioned stimulus pathway to the lateral amygdala. To accomplish this, they used an optogenetic approach (Chapter 5). They injected a virus into the amygdala to express channelrhodopsin-2, a light-activated excitatory cation channel, in lateral amygdala neurons. Following pairing of the auditory stimulus with a light pulse that depolarized lateral amygdala cells, presentation of the tone alone elicited conditioned freezing. The amount of freezing was greater when norepinephrine was present, which is further evidence that modulatory pathways also have a role in synaptic facilitation in this circuit. Thus, an aversive shock itself is not necessary to induce threat learning. Rather, it is the association of a stimulus with activation of the lateral amygdala that is key.

Other studies demonstrated the possibility of artificially manipulating the amygdala to impair as well as to instantiate, threat memory. They first trained animals to associate a foot shock with optogenetic stimulation of auditory inputs to the amygdala. They then delivered a pattern of optogenetic stimulation that generated *long-term depression* (LTD) of the auditory input to the amygdala, a form of synaptic plasticity in which weak, repetitive stimulation decreases the strength of synaptic transmission. Induction of LTD was able to inactivate the memory of the shock. Then, using a pattern of optical stimulation that produced LTP of the same auditory input, they found that the memory of the shock could be reinstated. The findings that inactivation and reactivation of a memory could be engineered using LTD and LTP strengthened the possible causal link between synaptic strength and behavioral memory storage.

The persistence of the synaptic changes underlying the memory for a threat depend on gene expression and protein synthesis in the amygdala, much like long-term memory in *Aplysia* and *Drosophila*. Thus, cAMP-dependent protein kinase and MAPK activate the transcription factor CREB to initiate gene expression. The importance of CREB is underscored by the finding that different neurons in the lateral amygdala have varying levels of CREB expression prior to threat conditioning. Neurons that express a larger than average amount of CREB are selectively recruited during learning. Conversely, if neurons with a large resting level of CREB are selectively ablated after learning, memory is impaired.

While most of the work on the neural mechanisms of threat conditioning has involved the lateral nucleus of the amygdala, in recent years, evidence has accumulated that plasticity in the central nucleus is also important. The central nucleus receives direct and indirect inputs from the lateral nucleus and forms synaptic connections with neurons in the periaqueductal gray region in the midbrain, which projects to the brain stem to control a number of defensive reactions, including freezing behavior. Within a lateral cell group of the central nucleus, inhibitory cells called PKC delta neurons control the activity of the output neurons in the medial cell group that project to the periaqueductal gray.

Memory for threat conditioning in humans also involves the amygdala. Thus, in humans, damage to the amygdala impairs the implicit memory of threat conditioning but not the explicit memory of having been conditioned. Functional imaging studies have found that the amygdala is activated by threats even when the person is not aware of the presence of the threat because the stimulus was subliminal. Although human studies are limited in their ability to reveal neurobiological details, they demonstrate the relevance of the animal work for human psychopathology.

In summary, Pavlovian threat conditioning has emerged as one of the most useful experimental

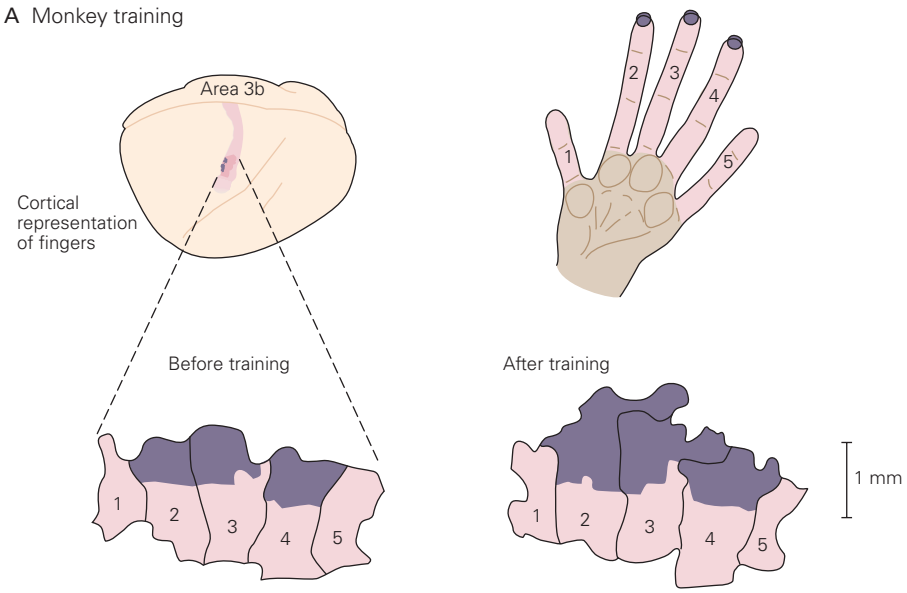

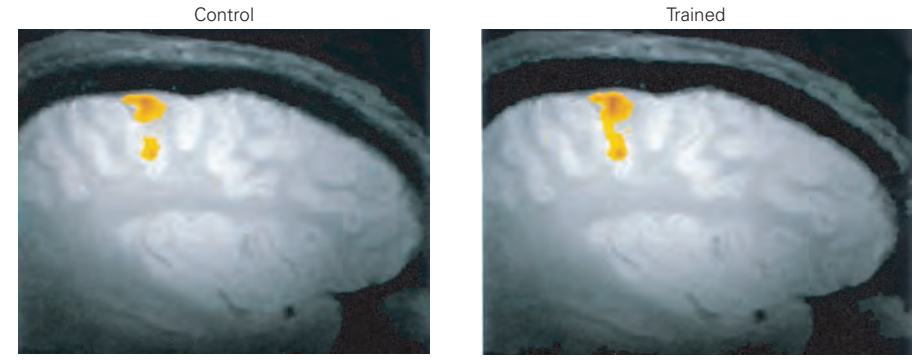

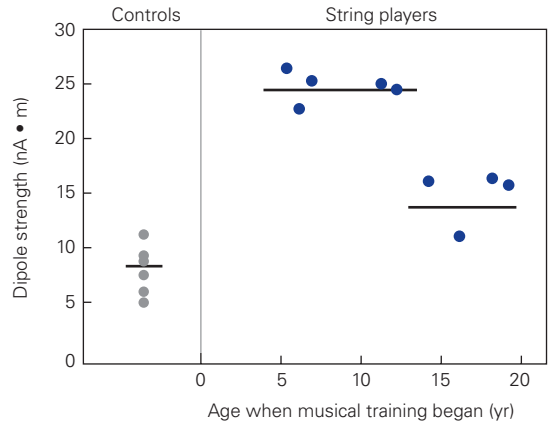

Figure 53–16 Training expands representation of inputs from the fingers in the cortex.

A. A monkey was trained for 1 hour per day to perform a task that required repeated use of the tips of fingers 2, 3, and occasionally 4. After training, the portion of area 3b of the somatosensory cortex representing the tips of the stimulated fingers (**dark color**) is substantially greater than normal (measured 3 months prior to training). (Adapted, with permission, from Jenkins et al. 1990.)

B. 1. A human subject trained to do a rapid sequence of finger movements will improve in accuracy and speed after 3 weeks of daily training (10–20 minutes each day). Functional magnetic resonance imaging scans of the primary motor cortex (based on local blood oxygenation level–dependent signals) after training show that the region activated in trained subjects (**orange region**) is larger than the region activated in untrained (controls). The control subjects received no training and performed unlearned finger movements using the same hand as control subjects. The change in cortical representation in trained subjects persisted for several months. (Reproduced, with permission, from Karni et al. 1998. Copyright © 1998 National Academy of Sciences.)

2. The size of the cortical representation of the fifth finger of the left hand is greater in string players than in nonmusicians. The graph plots the dipole strength obtained from magnetoencephalography, a measure of neural activity. The increase is most pronounced in musicians that began musical training before age 13. (Reproduced, with permission, from Elbert et al. 1995. Copyright © 1995 AAAS.)

models for studying associative learning and memory in the mammalian brain. In part, this is due to the fact that the behavioral paradigm has been applied successfully across diverse species, from flies to humans, and thus builds upon the earlier progress that invertebrate models have made.

Learning-Induced Changes in the Structure of the Brain Contribute to the Biological Basis of Individuality

To what extent do the anatomical alterations in synapses required for long-term memory storage alter the large-scale functional architecture of the mature brain? The answer is well illustrated by the fact that the maps of the body surface in the primary somatic sensory cortex differ among individuals in a manner that reflects their use of specific sensory pathways. This remarkable finding results from the expansion or retraction of the connections of sensory pathways in the cortex according to the specific experience of the individual (Chapter 49).

The reorganization of afferent inputs as a result of behavior is also evident at lower levels in the brain, specifically at the level of the dorsal column nuclei, which contain the first synapses of the somatic sensory system. Therefore, organizational changes probably occur throughout the somatic afferent pathway.

The process by which experience alters the maps of somatosensory inputs in the cortex is illustrated in an experiment in which adult monkeys were trained to use their middle three fingers at the expense of other fingers to obtain food. After several thousand trials of this behavior, the area of cortex devoted to the middle fingers expanded greatly (Figure 53–16A). Thus, practice may expand synaptic connections by strengthening the effectiveness of existing connections.

The normal development of somatosensory input to cortical neurons may depend on the level of activity in neighboring afferent axons. In one experiment using monkeys, the skin surfaces of two adjacent fingers were surgically connected so that the connected fingers were always used together, thus ensuring that their afferent somatosensory axons were normally coactivated. As a result, the normally sharp discontinuity between the zones in the somatosensory cortex that receive inputs from these digits was abolished. Thus, normal development of the boundaries of representation of adjacent fingers in the cortex may be guided not only genetically but also through experience. Fine tuning of cortical connections may depend on associative mechanisms such as LTP, similar to the role of cooperative activity in shaping the development of ocular dominance columns in the visual system (Chapter 49).

This plasticity is evident in humans as well. People trained to perform a task with their fingers show an expansion in the fMRI signal in the primary motor cortex during performance of the task (Figure 53–16B). Thomas Elbert explored the hand representation in the motor cortex of string instrument players. These musicians use their left hand for fingering the strings, manipulating the fingers in a highly individuated way. By contrast, the right hand, used for bowing, is used almost like a fist. The representation of the right hand in the cortex of string instrument players is the same as that of nonmusicians. But the representation of the left hand is greater than in nonmusicians and substantially more prominent in players who started to play their instrument prior to age 13 years (Figure 53–16B).

Because each of us is brought up in a somewhat different environment, experiencing different combinations of stimuli and developing motor skills in different ways, each individual's brain is uniquely modified. This distinctive modification of brain architecture, along with a unique genetic makeup, constitutes a biological basis for individuality.

Highlights

1. Many aspects of personality are guided by implicit memory. A great deal of what we experience—what we perceive, think, fantasize—is not directly controlled by conscious thought.
2. In mammals, both innate and learned defensive responses involve the amygdala. The amygdala-based defense system quickly learns about new dangers. It can associate a new neutral (conditioned) stimulus with a known threatening (unconditioned) stimulus on a single paired exposure, and this learned association is often retained throughout life.
3. During Pavlovian conditioning, the strength of synaptic transmission is modified in the lateral amygdala by pairing the conditioned and unconditioned stimuli. As a result, electrophysiological responses of neurons in the lateral amygdala are enhanced and behavioral learning occurs.
4. Many of the molecular mechanisms underlying threat conditioning in invertebrates also contribute to conditioning in mammals.
5. Damage to the human amygdala impairs implicit threat conditioning but does not affect the explicit memory of having been conditioned.

6. Habits are routines that are acquired gradually by repetition and are the result of a distinct form of implicit learning. As with all forms of implicit learning, habits are expressed in action alone, without conscious control, and independent of verbal reports.
7. As these arguments make clear, the empirical study of unconscious psychic processes was severely limited for many years by the lack of suitable experimental methods. Today, however, biology has a wide range of empirical methods that are providing cellular and molecular insights that are expanding our understanding of a wide range of mental activities.

Eric R. Kandel
Joseph LeDoux

Selected Reading

Alberini CM, Kandel ER. 2016. The regulation of transcription in memory consolidation. In: ER Kandel, Y Dudai, MR Mayford (eds). *Learning and Memory*, pp. 157–174. New York: Cold Spring Harbor Laboratory Press.

Bailey CH, Kandel ER, Harris KM. 2015. Structural components of synaptic plasticity and memory consolidation. Cold Spring Harb Perspect Biol 7:a021758.

Busto GU, Cervantes-Sandoval I, Davis RL. 2010. Olfactory learning in *Drosophila*. Physiology (Bethesda) 25:338–346.

Duvarci S, Pare D. 2014. Amygdala microcircuits controlling learned fear. Neuron 82:966–980.

Fanselow MS, Zelikowsky M, Perusini J, Barrera VR, Hersman S. 2014. Isomorphisms between psychological processes and neural mechanisms: from stimulus elements to genetic markers of activity. Neurobiol Learn Mem 108:5–13.

Hawkins RD, Kandel ER, Bailey CH. 2006. Molecular mechanisms of memory storage in *Aplysia*. Biol Bull 210: 174–191.

LeDoux JE. 2014. Coming to terms with fear. Proc Natl Acad Sci U S A 111:2871–2878.

LeDoux J. 2015. *Anxious: Using the Brain to Understand and Treat Fear and Anxiety*. New York: Viking.

LeDoux JE. 2019. *The Deep History of Ourselves: The Four-Billion Year History of How We Got Conscious Brains*. New York: Viking.

Nader K. 2016. Reconsolidation and the dynamic nature of memory. In: ER Kandel, Y Dudai, MR Mayford (eds). *Learning and Memory*, pp. 245–260. New York: Cold Spring Harbor Laboratory Press.

Phelps EA. 2006. Emotion and cognition: insights from studies of the human amygdala. Annu Rev Psychol 57: 27–53.

Tubon CT Jr, Yin JCP. 2008. CREB responsive transcription and memory formation. In: SM Dudek (ed). *Transcriptional Regulation by Neuronal Activity, Part III*, pp. 377–397. New York: Springer.

References

Bailey CH, Chen MC. 1983. Morphological basis of long-term habituation and sensitization in *Aplysia*. Science 220:91–93.

Bailey CH, Kandel ER, Si K. 2004. The persistence of long-term memory: a molecular approach to self-sustaining changes in learning-induced synaptic growth. Neuron 44:49–57.

Bear MF, Connors BW, Paradiso MA. 2001. *Neuroscience: Exploring the Brain,* 2nd ed. Chicago: Lippincott Williams & Wilkins.

Casadio A, Martin KC, Giustetto M, et al. 1999. A transient, neuron-wide form of CREB-mediated long-term facilitation can be stabilized at specific synapses by local protein synthesis. Cell 99:221–237.

Castellucci VF, Carew TJ, Kandel ER. 1978. Cellular analysis of long-term habituation of the gill-withdrawal reflex in *Aplysia californica*. Science 202:1306–1308.

Castellucci VF, Kandel ER. 1974. A quantal analysis of the synaptic depression underlying habituation of the gill-withdrawal reflex in *Aplysia*. Proc Natl Acad Sci U S A 71:5004–5008.

Claridge-Chang A, Roorda RD, Vrontou E, et al. 2009. Writing memories with light-addressable reinforcement circuitry. Cell 139:405–415.

Ehrlich DE, Josselyn SA. 2016. Plasticity-related genes in brain development and amygdala-dependent learning. Genes Brain Behav 15:125–143.

Eichenbaum H, Cohen NJ. 2001. *From Conditioning to Conscious Recollection: Memory Systems of the Brain.* Oxford: Oxford Univ. Press.

Elbert T, Pantev C, Wienbruch C, Rockstroh B, Taub E. 1995. Increased cortical representation of the fingers of the left hand in string players. Science 270:305–307.

Glanzman DL, Kandel ER, Schacher S. 1990. Target-dependent structural changes accompanying long-term synaptic facilitation in *Aplysia* neurons. Science 249:799–802.

Greco JA, Liberzon I. 2016. Neuroimaging of fear-associated learning. Neuropsychopharmacology 41:320–334.

Gründemann J, Lüthi A. 2015. Ensemble coding in amygdala circuits for associative learning. Curr Opin Neurobiol 35:200–206.

Guan Z, Giustetto M, Lomvardas S, et al. 2002. Integration of long-term–memory-related synaptic plasticity involves bidirectional regulation of gene expression and chromatin structure. Cell 111:483–493.

Hawkins RD, Abrams TW, Carew TJ, Kandel ER. 1983. A cellular mechanism of classical conditioning in *Aplysia:* activity-dependent amplification of presynaptic facilitation. Science 219:400–405.

Hegde AN, Inokuchi K, Pei W, et al. 1997. Ubiquitin C-terminal hydrolase is an immediate-early gene essential for long-term facilitation in *Aplysia*. Cell 89:115–126.

Herry C, Johansen JP. 2014. Encoding of fear learning and memory in distributed neuronal circuits. Nat Neurosci 17:1644–1654.

Huang YY, Kandel ER. 1998. Postsynaptic induction and PKA-dependent expression of LTP in the lateral amygdala. Neuron 21:169–178.

Huang YY, Martin KC, Kandel ER. 2000. Both protein kinase A and mitogen-activated protein kinase are required in the amygdala for the macromolecular synthesis-dependent late phase of long-term potentiation. J Neurosci 20:6317–6325.

Janak PH, Tye KM. 2015. From circuits to behaviour in the amygdala. Nature 517:284–292.

Jenkins WM, Merzenich MM, Ochs MT, Allard T, Guic-Robles E. 1990. Functional reorganization of primary somatosensory cortex in adult owl monkeys after behaviorally controlled tactile stimulation. J Neurophysiol 63:82–104.

Johansen JP, Diaz-Mataix L, Hamanaka H, et al. 2014. Hebbian and neuromodulatory mechanisms interact to trigger associative memory formation. Proc Natl Acad Sci U S A 111:E5584–E5592.

Kandel ER. 2001. The molecular biology of memory storage: a dialogue between genes and synapses. Science 294:1030–1038.

Kandel ER. 2006. *In Search of Memory: The Emergence of a New Science of Mind.* New York: Norton.

Karni A, Meyer G, Rey-Hipolito C, et al. 1998. The acquisition of skilled motor performance: fast and slow experience-driven changes in primary motor cortex. Proc Natl Acad Sci U S A 95:861–868.

Keleman K, Krüttner S, Alenius M, Dickson BJ. 2007. Function of the *Drosophila* CPEB protein Orb2 in long-term courtship memory. Nat Neurosci 10:1587–1593.

Klein M, Kandel ER. 1980. Mechanism of calcium current modulation underlying presynaptic facilitation and behavioral sensitization in *Aplysia*. Proc Natl Acad Sci U S A 77:6912–6916.

Krabbe S, Gründemann J, Lüthi A. 2018. Amygdala inhibitory circuits regulate associative fear conditioning. Biol Psychiatry 83:800–809.

Mahan AL, Ressler KJ. 2011. Fear conditioning, synaptic plasticity and the amygdala: implications for posttraumatic stress disorder. Trends Neurosci 35:24–35.

Maren S. 2017. Synapse-specific encoding of fear memory in the amygdala. Neuron 95:988–990.

Maren S. 1999. Long-term potentiation in the amygdala: a mechanism for emotional learning and memory. Trends Neurosci 22:561–567.

Martin KC, Casadio A, Zhu H, et al. 1997. Synapse-specific, long-term facilitation of *Aplysia* sensory to motor synapses: a function for local protein synthesis in memory storage. Cell 91:927–938.

Nabavi S, Fox R, Proulx CD, Lin JY, Tsien RY, Malinow R. 2014. Engineering a memory with LTD and LTP. Nature 511:348–352.

Pape HC, Pare D. 2010. Plastic synaptic networks of the amygdala for the acquisition, expression, and extinction of conditioned fear. Physiol Rev 90:419–463.

Pavlov IP. 1927. *Conditioned Reflexes: An Investigation of the Physiological Activity of the Cerebral Cortex*. GV Anrep (transl). Oxford: Oxford Univ. Press.

Pinsker H, Kupferman I, Castelucci V, Kandel ER. 1970. Habituation and dishabituation of the gill-withdrawal reflex in *Aplysia*. Science 167:1740–1742.

Rajasethupathy P, Antonov I, Sheridan R, et al. 2012. A role for neuronal piRNAs in the epigenetic control of memory-related synaptic plasticity. Cell 149:693–707.

Rogan MT, Leon KS, Perez DL, Kandel ER. 2005. Distinct neural signatures for safety and danger in the amygdala and striatum of the mouse. Neuron 46:309–320.

Sears RM, Fink AE, Wigestrand MB, Farb CR, de Lecea L, LeDoux JE. 2013. Orexin/hypocretin system modulates amygdala-dependent treat learning trough the locus coeruleus. Proc Natl Acad Sci U S A 110:20260–20265.

Sears RM, Schiff HC, LeDoux JE. 2014. Molecular mechanisms of threat learning in the lateral nucleus of the amygdala. Prog Mol Biol Transl Sci 122:263–304.

Si K, Giustetto M, Etkin A, et al. 2003. A neuronal isoform of CPEB regulates local protein synthesis and stabilizes synapse-specific long-term facilitation in *Aplysia*. Cell 115:893–904.

Si K, Lindquist S, Kandel ER. 2003. A neuronal isoform of the *Aplysia* CPEB has prion-like properties. Cell 115:879–891.

Spencer AW, Thompson RF, Nielson DR Jr. 1966. Response decrement of the flexion reflex in the acute spinal cat and transient restoration by strong stimuli. J Neurophysiol 29:240–252.

Squire LR, Kandel ER. 2008. *Memory: From Mind to Molecules*, 2nd ed. Greenwood Village: Roberts.

Yin JCP, Wallach JS, Del Vecchio M, et al. 1994. Induction of a dominant negative CREB transgene specifically blocks long-term memory in *Drosophila*. Cell 79:49–58.

54

The Hippocampus and the Neural Basis of Explicit Memory Storage

Explicit memory—the conscious recall of information about people, places, objects, and events—is what people commonly think of as memory. Sometimes called *declarative memory*, it binds our mental life together by allowing us to recall at will what we ate for breakfast, where we ate it, and with whom. It allows us to join what we did today with what we did yesterday or the week or month before that.

Two structures in the mammalian brain are particularly critical for encoding and storing explicit memory: the prefrontal cortex and the hippocampus (Chapter 52). The prefrontal cortex mediates working memory, which can be actively maintained for only very short periods and is then rapidly forgotten, such as a password that is remembered only until it is entered. Information in working memory can be stored elsewhere in the brain as long-term memory for periods ranging from days to weeks to years, and throughout a lifetime. Although long-term storage of explicit memory requires the hippocampus, the ultimate storage site for most declarative memory is thought to be the cerebral cortex.

In this chapter, we focus on the cellular, molecular, and network mechanisms of the hippocampus that underlie the long-term storage of explicit memory. Because the hippocampus receives its major input from a region of the cerebral cortex called the entorhinal cortex, an area that processes many forms of sensory input, we also consider how information from the entorhinal cortex is transformed by the hippocampus. In particular, we examine how neural activity in the entorhinal cortex and hippocampus contributes to

spatial memory by encoding a representation of an animal's location in its environment.

Explicit Memory in Mammals Involves Synaptic Plasticity in the Hippocampus

Unlike working memory, which is thought to be maintained by ongoing neural activity in the prefrontal cortex (Chapter 52), the long-term storage of information is thought to depend on long-lasting changes in the strength of connections among specific ensembles of neurons (neural assemblies) in the hippocampus that encode particular elements of memory.

The idea that memory storage involves long-lasting structural changes in the brain, first referred to as an "engram" by the German biologist Richard Semon in the early 20th century, dates back to the French philosopher Rene Descartes. In an attempt to locate an engram, the American psychologist Karl Lashley examined the effects of lesions in different regions of the neocortex on the ability of a rat to learn to navigate a maze. Since the performance in the maze seemed to be directly proportional to the size of the lesion, rather than its precise location, Lashley concluded that any memory trace must be distributed throughout the brain. Although it is now generally accepted that storage of an explicit memory is distributed throughout the neocortex, it is also clear that the process of storing memory requires the hippocampus, as demonstrated by the pioneering studies of Brenda Milner on patient H.M. (Chapter 52) and subsequent studies in animals with targeted lesions of the hippocampus. Thus, understanding how the brain stores explicit memory depends on an understanding of how the cortico-hippocampal circuit processes and stores information.

The nature of the basic mechanisms for memory storage was and remains the subject of much speculation and debate among psychologists and neuroscientists. One influential theory was proposed by the Canadian psychologist Donald Hebb, who suggested in 1949 that memory-encoding neural assemblies may be generated when synaptic connections are strengthened based on experience. According to *Hebb's rule*: "When an axon of cell A . . . excites cell B and repeatedly or persistently takes part in firing it, some growth process or metabolic change takes place in one or both cells so that A's efficiency as one of the cells firing B is increased." The key element of Hebb's rule is the requirement for coincidence of pre- and postsynaptic firing, and so the rule has sometimes been rephrased as "Cells that fire together, wire together." A similar Hebbian coincidence principle is thought to be involved in fine-tuning synaptic connections during the late stages of development (Chapter 49). Hebb's ideas were later refined by the theoretical neuroscientist David Marr, based on a consideration of the hippocampal circuit.

The hippocampus comprises a loop of connections that process multimodal sensory and spatial information from the superficial layers of the nearby entorhinal cortex. This information passes through multiple synapses before arriving at the hippocampal CA1 region, the major output area of the hippocampus. The critical importance of CA1 neurons in learning and memory is seen in the profound memory loss exhibited by patients with lesions in this region alone, an observation supported by numerous animal studies. Information from the entorhinal cortex reaches CA1 neurons along two excitatory pathways, one direct and one indirect.

In the indirect pathway, the axons of neurons in layer II of the entorhinal cortex project through the *perforant pathway* to excite the granule cells of the dentate gyrus (an area considered part of the hippocampus). Next, the axons of the granule cells project in the *mossy fiber pathway* to excite the pyramidal cells in the CA3 region of the hippocampus. Finally, axons of the CA3 neurons project through the *Schaffer collateral pathway* to make excitatory synapses on more proximal regions of the dendrites of the CA1 pyramidal cells (Figure 54–1). (Because of its three successive excitatory synaptic connections, the indirect pathway is often referred to as the *trisynaptic pathway*). Finally, CA1 pyramidal cells project back to the deep layers of entorhinal cortex and forward to the subiculum, another medial temporal lobe structure that connects the hippocampus with a wide diversity of brain regions.

In parallel with the indirect pathway, the entorhinal cortex also projects directly to CA3 and CA1 hippocampal regions. In the direct pathway to CA1, neurons in layer III of the entorhinal cortex send their axons through the *perforant pathway* to form excitatory synapses on the very distal regions of the apical dendrites of CA1 neurons (such projections are also called the *temporoammonic pathway*). Interactions between direct and indirect inputs at each stage of the hippocampal circuit are likely important for memory storage or recall, although the precise nature of these interactions remains to be determined.

In addition to the above pathways that link different stages of the hippocampal circuit, CA3 pyramidal neurons also make strong excitatory connections with one another. This self-excitation through recurrent collaterals is thought to contribute to associative aspects of memory storage and recall. Under pathological conditions, such self-excitation can lead to seizures.

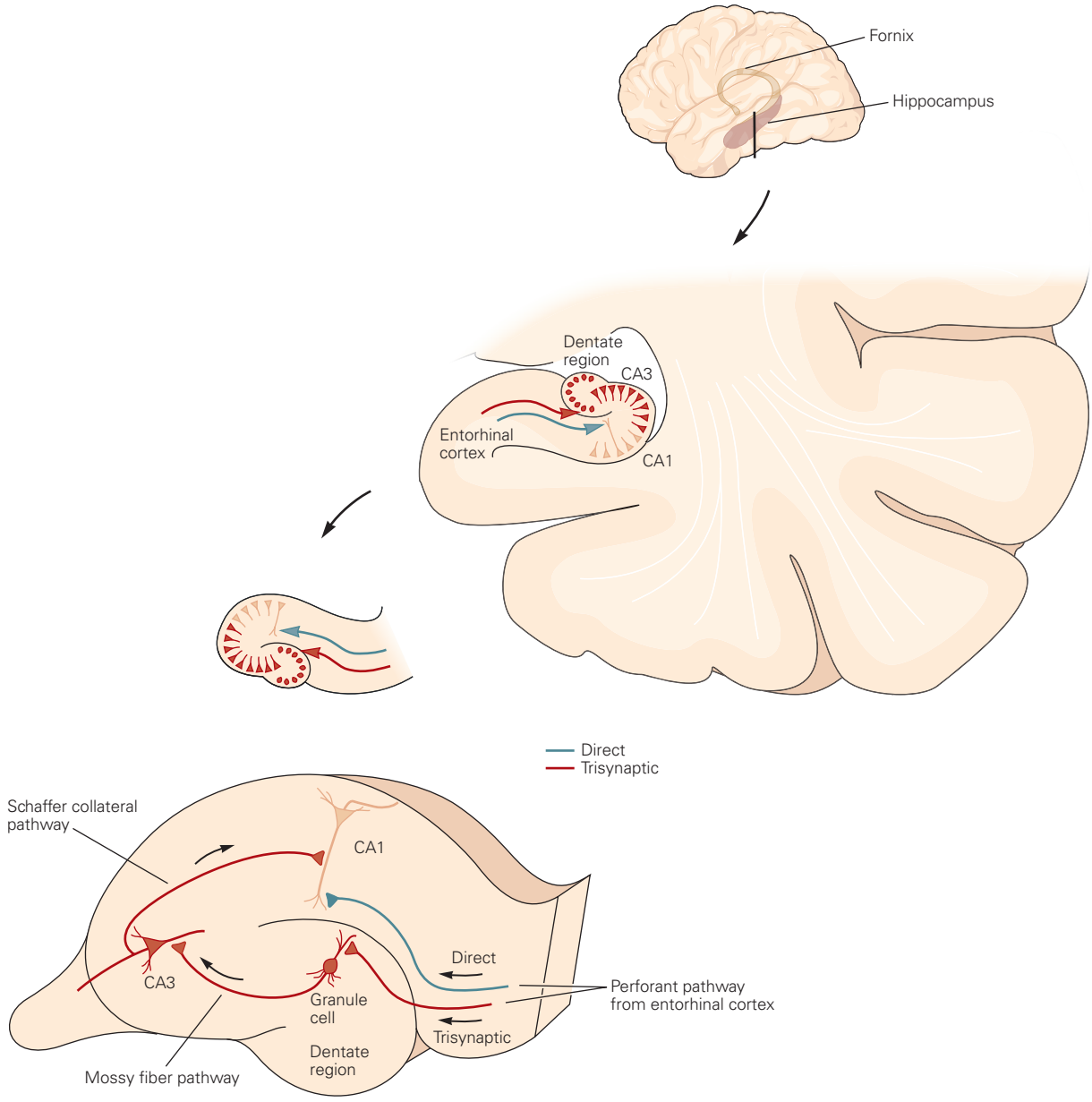

Figure 54–1 The cortico-hippocampal synaptic circuit is important for declarative memory. Information arrives in the hippocampus from the entorhinal cortex through the perforant pathways, which provide both direct and indirect input to pyramidal neurons in area CA1, the major output neurons of the hippocampus. (**Arrows** denote the direction of impulse flow.) The indirect *trisynaptic pathway* has three component connections. Neurons in layer II of the entorhinal cortex send their axons through the perforant path to make excitatory synapses onto the granule cells of the dentate gyrus. The granule cells project through the mossy fiber pathway and make excitatory synapses with the pyramidal cells in area CA3 of the hippocampus. The CA3 cells excite the pyramidal cells in CA1 by means of the Schaffer collateral pathway. In the *direct pathway*, neurons in layer III of the entorhinal cortex project through the perforant path to make excitatory synapses on the distal dendrites of CA3 and CA1 pyramidal neurons without inter vening synapses (shown only for CA1).

Finally, neurons in the relatively small CA2 region, located between CA3 and CA1, receive information from entorhinal cortex layer II through both a direct pathway and an indirect pathway via the dentate gyrus and CA3. The CA2 region also receives strong input from hypothalamic nuclei that release oxytocin and vasopressin, hormones important for social behavior. In turn, CA2 sends a strong output to CA1,

providing CA1 with a third source of excitatory input (in addition to the direct and trisynaptic routes from the entorhinal cortex).

Long-Term Potentiation at Distinct Hippocampal Pathways Is Essential for Explicit Memory Storage

How is information stored in the hippocampal circuit to provide a long-lasting memory trace? In 1973, Timothy Bliss and Terje Lømo discovered that a brief period of high-frequency synaptic stimulation causes a persistent increase in the amplitude of hippocampal excitatory postsynaptic potentials (EPSPs), a process termed *long-term potentiation* or LTP (Chapter 13). The enhancement in the EPSP, in turn, increases the probability that the postsynaptic cell will fire action potentials.

Bliss and Lømo examined the initial stage of the indirect hippocampal pathway—the synapses formed by the perforant pathway from entorhinal cortex layer II neurons with dentate gyrus granule neurons. Subsequent studies showed that brief high-frequency trains of stimulation can induce forms of LTP at nearly all excitatory synapses of this indirect pathway as well as at the direct perforant path synapses with CA3 and CA1 neurons (Figure 54–2). LTP can last for days or even weeks when induced in intact animals using implanted electrodes and can last several hours in isolated slices of hippocampus and in hippocampal neurons in cell culture.

Studies in the different hippocampal pathways have shown that LTP at different synapses is not a single process. Rather, it comprises a family of processes that strengthen synaptic transmission at different hippocampal synapses through distinct cellular and molecular mechanisms. Indeed, even at a single synapse, different forms of LTP can be induced by different patterns of synaptic activity, although these distinct processes share many important similarities.

All forms of LTP are induced by synaptic activity in the pathway that is being potentiated—that is, LTP is homosynaptic. In addition, LTP is synapse specific; only those synapses that are activated by the tetanic stimulation are potentiated. However, the various forms of LTP differ in their dependence on specific receptors and ion channels. In addition, different forms of LTP recruit different second-messenger signaling pathways that act at different synaptic sites. Some forms of LTP result from an enhancement of the postsynaptic response to the neurotransmitter glutamate, whereas other forms of LTP result from the enhancement of glutamate release from the presynaptic terminal, and still other forms of LTP engage both the presynaptic and postsynaptic neurons.

The similarities and differences in the mechanisms of different forms of LTP can be seen by comparing LTP at Schaffer collateral, mossy fiber, and direct entorhinal synapses. In all three pathways, synaptic transmission is persistently enhanced in response to a brief tetanic stimulation. However, the contribution of the *N*-methyl-D-aspartate (NMDA) receptor to the induction of LTP differs in the three pathways. At the Schaffer collateral synapses, the induction of LTP in response to a brief 100-Hz stimulation is completely blocked when the tetanus is applied in the presence of the NMDA receptor antagonist 2-amino-5-phosphonovaleric acid (AP5 or APV). In contrast, APV only partially inhibits the induction of LTP at the direct entorhinal synapses with CA1 neurons and has no effect on LTP at the mossy fiber synapses with CA3 pyramidal neurons (Figure 54–2).

Long-term potentiation in the mossy fiber pathway is largely presynaptic and is triggered by the large Ca^{2+} influx into the presynaptic terminals during the tetanus. The Ca^{2+} influx activates a calcium/calmodulin-dependent adenylyl cyclase, thereby increasing the production of cyclic adenosine monophosphate (cAMP) and activating protein kinase A (PKA; see Chapter 14). This leads to the phosphorylation of presynaptic vesicle proteins that enhance the release of glutamate from the mossy fiber terminals, resulting in an increase in the EPSP. Activity in the postsynaptic cell is not required for this form of LTP. Thus, unlike Hebbian plasticity, mossy fiber LTP is nonassociative.

In the Schaffer collateral pathway, however, LTP is associative, largely as a result of the properties of the NMDA receptors (Figure 54–3; see also Chapter 13). As is the case with most excitatory synapses in the brain, glutamate released from the Schaffer collateral terminals activates both α-amino-3-hydroxy-5-methyl-4-isoxazolepropionic acid (AMPA) and NMDA receptor-channels in the postsynaptic membrane of CA1 pyramidal neurons. However, unlike the AMPA receptors, activation of the NMDA receptors is associative because it requires simultaneous presynaptic and postsynaptic activity. This is because the pore of the NMDA receptor-channel is normally blocked by extracellular Mg^{2+} at typical negative resting potentials, which prevents these channels from conducting ions in response to glutamate. For the NMDA receptor-channel to function efficiently, the postsynaptic membrane must be depolarized sufficiently to expel the bound Mg^{2+} by electrostatic repulsion. In this manner, the NMDA receptor-channel acts as a coincidence detector: It is functional only when (1) the action potentials in the presynaptic neuron release glutamate that binds to the receptor *and* (2) the membrane of the postsynaptic

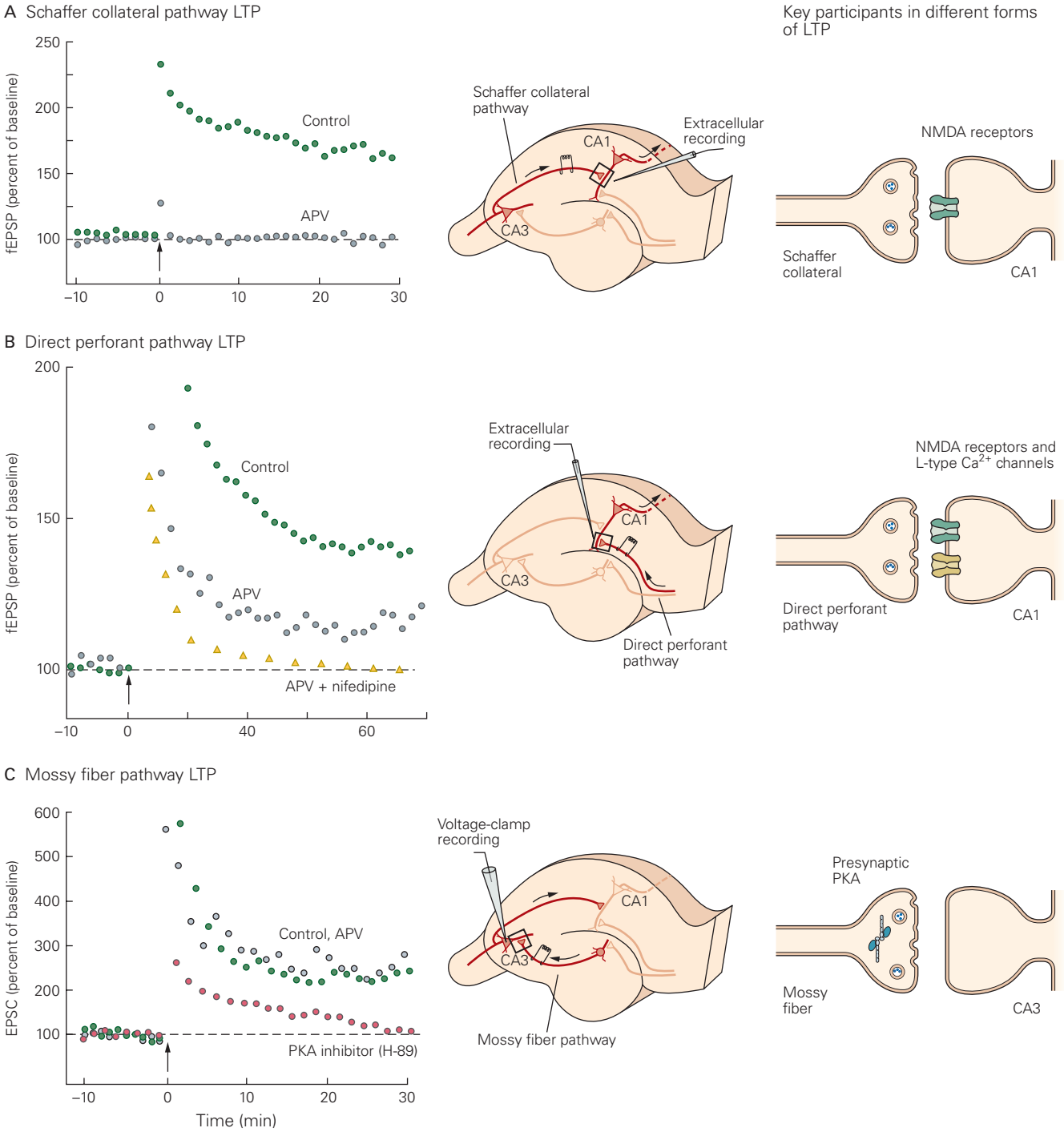

Figure 54–2 Different neural mechanisms underlie long-term potentiation at each of the three synapses in the trisynaptic pathway. Long-term potentiation (**LTP**) occurs at synapses throughout the hippocampus but depends to differing degrees on activation of *N*-methyl-D-aspartate (**NMDA**)-type glutamate receptors.

A. Tetanic stimulation of the Schaffer collateral fibers (at time 0 in the plot) induces LTP at the synapses between presynaptic CA3 pyramidal neurons and postsynaptic CA1 pyramidal neurons. The plot shows the size of the extracellular field excitatory postsynaptic potential (**fEPSP**) as a percentage of the baseline fEPSP prior to induction of LTP. At these synapses, LTP requires activation of the NMDA receptor-channels in the postsynaptic CA1 neurons as it is completely blocked when the tetanus is delivered in the presence of the NMDA receptor antagonist 2-amino-5-phosphonovaleric acid (**APV**). (Adapted from Morgan and Teyler 2001.)

B. Tetanic stimulation of the direct pathway from entorhinal cortex to CA1 neurons generates LTP of the fEPSP that depends partly on activation of the NMDA receptor-channels and partly on activation of L-type voltage-gated Ca^{2+} channels. It is therefore only partially blocked by APV. Addition of APV and nifedipine, a dihydropyridine that blocks L type channels, is needed to fully inhibit LTP.

C. Tetanic stimulation of the mossy fiber pathway induces LTP at the synapses with the pyramidal cells in the CA3 region. In this experiment, the excitatory postsynaptic current (**EPSC**) was measured under voltage-clamp conditions. This LTP does not require activation of the NMDA receptors and so is not blocked by APV. However, it does require activation of protein kinase A (**PKA**) and so is blocked by the kinase inhibitor H-89. (Reproduced, with permission, from Zalutsky and Nicoll 1990. Copyright © 1990 AAAS.)

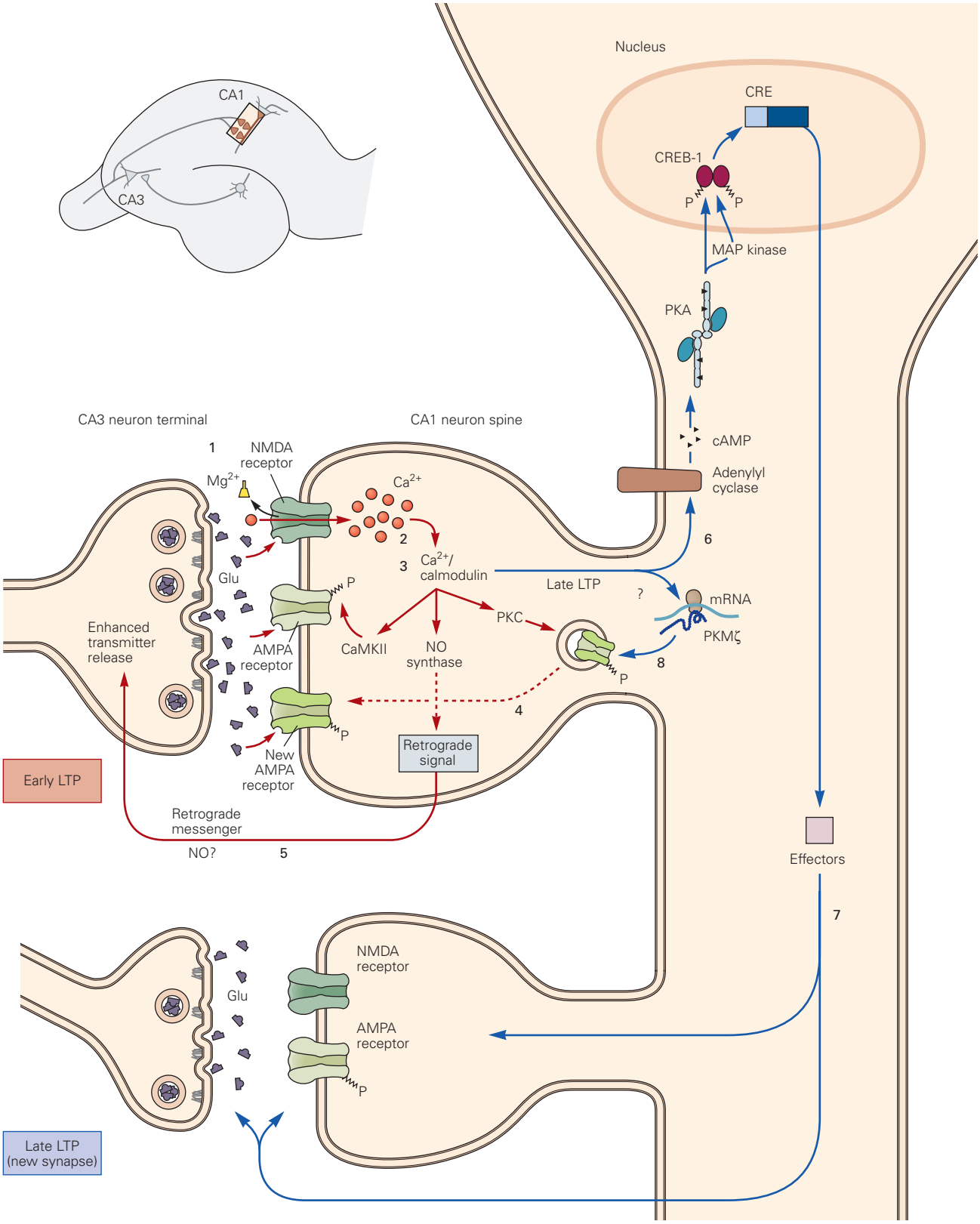
CA1
CA3
Nucleus
CRE
CREB-1
P
P
MAP kinase
PKA
cAMP
Adenylyl cyclase
CA3 neuron terminal
CA1 neuron spine
1
NMDA receptor
Mg^{2+}
Ca^{2+}
2
3
Ca^{2+}/ calmodulin
Glu
P
Late LTP
?
mRNA
PKC
PKMζ
Enhanced transmitter release
AMPA receptor
CaMKII
NO synthase
8
P
4
P
New AMPA receptor
Retrograde signal
Early LTP
Retrograde messenger
NO?
5
6
Effectors
7
Glu
NMDA receptor
AMPA receptor
P
Late LTP (new synapse)

cell is sufficiently depolarized by strong synaptic activity to relieve the Mg^{2+} block. Thus, the NMDA receptor is able to associate presynaptic and postsynaptic activity to recruit plasticity mechanisms that strengthen connections between pairs of cells, fulfilling Hebb's coincidence requirement for synaptic modification.

What are the functional consequences of the activation of NMDA receptors by strong synaptic excitation? Whereas most AMPA receptor-channels conduct only monovalent cations (Na^+ and K^+), the NMDA receptor-channels have a high permeability to Ca^{2+} (Chapter 13). Thus, the opening of these channels leads to a significant increase in the Ca^{2+}concentration in the postsynaptic cell. The increase in intracellular Ca^{2+} activates several downstream signaling pathways—including calcium/calmodulin–dependent protein kinase II (CaMKII), protein kinase C (PKC), and tyrosine kinases—that lead to changes that enhance the magnitude of the EPSP at Schaffer collateral synapses (Figure 54–3).

Different Molecular and Cellular Mechanisms Contribute to the Forms of Expression of Long-Term Potentiation

Neuroscientists often find it useful to distinguish between the *induction* of LTP (the biochemical reactions activated by the tetanic stimulation) and the *expression* of LTP (the long-term changes responsible for enhanced synaptic transmission). The mechanisms for the induction of LTP at the CA3-CA1 synapse are largely postsynaptic. Is the expression of LTP at this synapse caused by an increase in transmitter release, an increased postsynaptic response to a fixed amount of transmitter, or some combination of the two?

A number of lines of experiments suggest that the form of expression of LTP depends on the type of synapse and precise pattern of activity that induces LTP. In many cases, the expression of LTP in CA1 neurons in response to Ca^{2+} influx through NMDA receptor-channels depends on an increase in the response of the postsynaptic membrane to glutamate. But stronger patterns of stimulation can elicit forms of LTP at the same synapse whose expression depends on presynaptic events that enhance transmitter release.

One of the key pieces of evidence for a postsynaptic contribution to the expression of LTP at Schaffer collateral synapses comes from an examination of so-called "silent synapses." In some recordings from pairs of hippocampal pyramidal neurons, stimulation of an action potential in one neuron fails to elicit a response in the postsynaptic neuron when that neuron is at its resting potential (approximately –70 mV). This result is not surprising, as each hippocampal presynaptic neuron is connected to only a small number of other neurons. What *is* surprising is that in some neuronal pairs that appear unconnected when the postsynaptic membrane is initially at –70 mV, stimulation of the same presynaptic neuron is able to elicit a large excitatory postsynaptic current in the second neuron when the second neuron is depolarized under voltage clamp to +30 mV. In such neuronal pairs, the postsynaptic membrane appears to lack functional AMPA receptors so that the excitatory postsynaptic current (EPSC) is mediated solely by NMDA receptors-channels. As a result, there is no measurable EPSC when the membrane is held at the cell's resting potential (–70 mV) because of the strong Mg^{2+} block of these receptor-channels (the synapse is effectively silent). However, a large EPSC can be generated at +30 mV because the depolarization relieves the block (Figure 54–4).

The key finding from these experiments is seen following the induction of LTP using strong synaptic stimulation. Pairs of neurons initially connected solely by silent synapses now often exhibit large EPSPs at the

Figure 54–3 (Opposite) A model for the induction of long-term potentiation (LTP) at Schaffer collateral synapses. A single high-frequency tetanus induces early LTP. The large depolarization of the postsynaptic membrane (caused by strong activation of the α-amino-3-hydroxy-5-methyl-4-isoxazolepropionic acid [**AMPA**] receptors) relieves the Mg^{2+} blockade of the *N*-methyl-D-aspartate (**NMDA**) receptor-channels (**1**), allowing Ca^{2+}, Na^+, and K^+ to flow through these channels. The resulting increase of Ca^{2+} in the dendritic spine (**2**) triggers calcium-dependent kinases (**3**)—calcium/calmodulin–dependent kinase (**CaMKII**) and protein kinase C (**PKC**)—leading to induction of LTP. Second-messenger cascades activated during induction of LTP have two main effects on synaptic transmission. Phosphorylation through activation of protein kinases, including PKC, enhances current through the AMPA receptor-channels, in part by causing insertion of new receptors into the spine synapses (**4**). In addition, the postsynaptic cell releases retrograde messengers, such as nitric oxide (**NO**), that activate protein kinases in the presynaptic terminal to enhance subsequent transmitter release (**5**). Repeated bouts of tetanic stimulation induce late LTP. The prolonged increase in Ca^{2+} influx recruits adenylyl cyclase (**6**), which generates cyclic adenosine monophosphate (**cAMP**) that activates protein kinase A (**PKA**). This leads to the activation of MAP kinase, which translocates to the nucleus where it phosphorylates CREB-1. CREB-1 in turn activates transcription of targets (containing the CRE promoter) that are thought to lead to the growth of new synaptic connections (**7**). Repeated stimulation also activates translation of mRNA encoding PKMζ, a constitutively active isoform of PKC (**8**). This leads to a long-lasting increase in the number of AMPA receptors in the postsynaptic membrane.

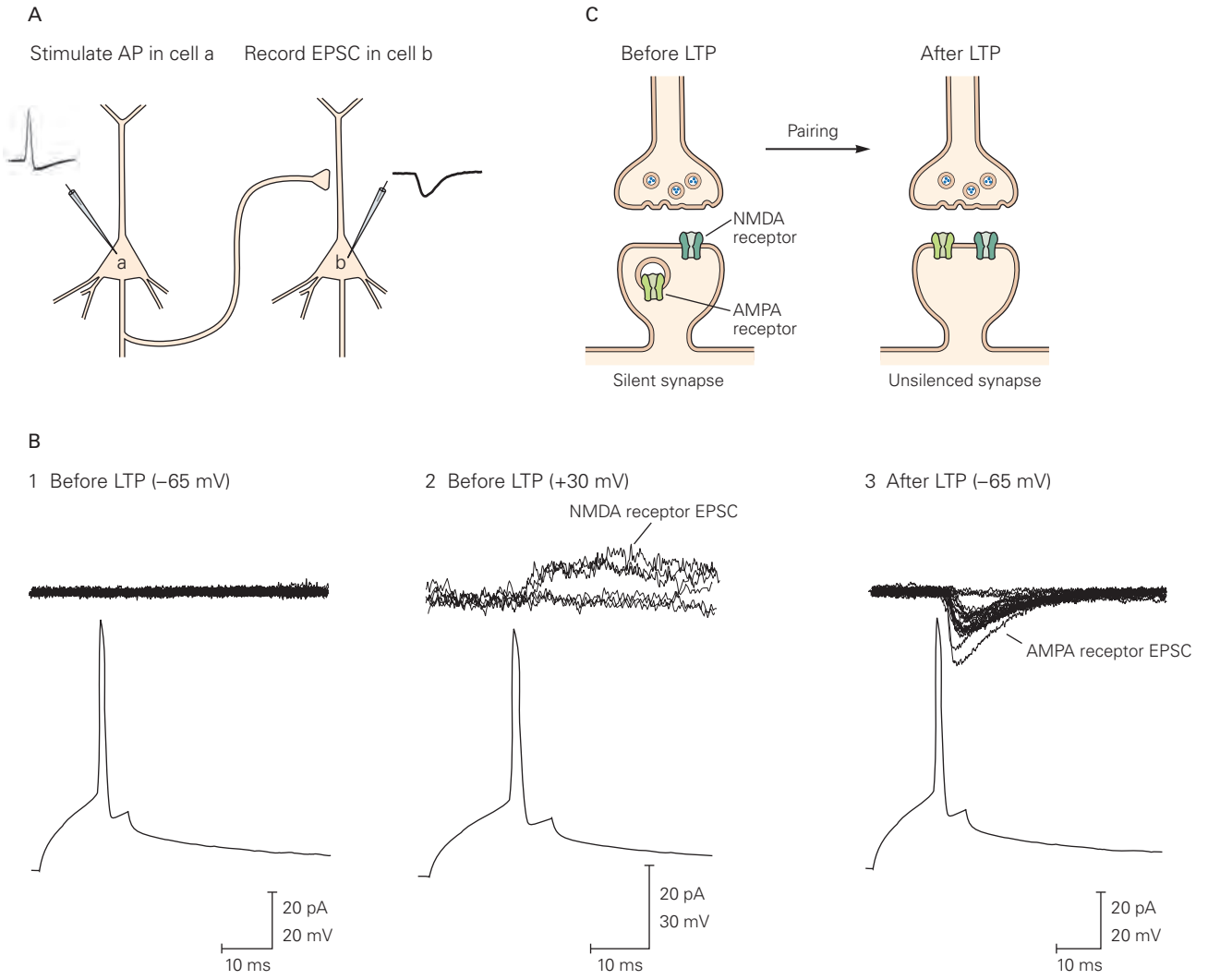

Figure 54–4 Adding α-amino-3-hydroxy-5-methyl-4-isoxazolepropionic acid (AMPA) receptors to silent synapses during long-term potentiation (LTP).

A. Intracellular recordings are obtained from a pair of hippocampal pyramidal neurons. An action potential (**AP**) is triggered in neuron *a* by a depolarizing current pulse, and the resultant excitatory postsynaptic current (**EPSC**) produced in neuron *b* is recorded under voltage-clamp conditions.

B. Before induction of LTP, there is no EPSC in cell *b* (top traces) in response to an action potential in cell *a* (bottom traces) when the membrane potential of neuron *b* is at its resting value of –65 mV (**1**). However, when neuron *b* is depolarized by the voltage clamp to +30 mV, the *N*-methyl-D-aspartate (**NMDA**) receptors are activated and slow EPSCs characteristic of these receptors are observed (**2**). LTP is then induced by pairing action potentials in neuron *a* with postsynaptic depolarization in neuron *b* to relieve the Mg^{2+} block of the NMDA receptors. After this pairing, fast EPSCs initiated by activation of AMPA receptors are seen in cell *b* (**3**). (Reproduced, with permission, from Montgomery, Pavlidis, and Madison 2001. Copyright © 2001 Cell Press.)

C. Mechanism of the unsilencing of silent synapses. Prior to LTP, the dendritic spine contacted by a presynaptic CA3 neuron contains only NMDA receptors. Following induction of LTP, intracellular vesicles containing AMPA receptors fuse with the plasma membrane at the synapse, adding AMPA receptors to the membrane.

negative resting potential, and these EPSPs are mediated by AMPA receptors. The simplest interpretation of this result is that LTP somehow recruits new functional AMPA receptors to the silent synapse membrane, a process Roberto Malinow refers to as "AMPAfication."

How does the induction of LTP increase the response of AMPA receptors? The strong synaptic stimulation used to induce LTP triggers glutamate release at both silent and nonsilent synapses on the same postsynaptic neuron. This leads to the opening

of a large number of AMPA receptor-channels at the nonsilent synapses, which in turn produces a large postsynaptic depolarization. The depolarization then propagates throughout the neuron, thus relieving Mg^{2+} block of the NMDA receptor-channels at both the nonsilent and silent synapses. At the silent synapses, the Ca^{2+} influx through the NMDA receptor-channels activates a biochemical cascade that ultimately leads to the insertion of clusters of AMPA receptors in the postsynaptic membrane. These newly inserted AMPA receptors are thought to come from a reserve pool stored in endosomal vesicles within dendritic spines, the site of all excitatory input to pyramidal neurons (Chapter 13). Calcium influx through the NMDA receptor-channels elevates spine Ca^{2+} levels, triggering a postsynaptic signaling cascade that leads to phosphorylation of the cytoplasmic tail of the vesicular AMPA receptors by PKC (Chapter 14), leading to their insertion in the postsynaptic membrane (Figure 54–3).

Because the induction of almost all forms of postsynaptic LTP requires Ca^{2+} influx into the postsynaptic cell, the finding that transmitter release is enhanced during some forms of LTP implies that the presynaptic cell must receive a signal from the postsynaptic cell that LTP has been induced. There is now evidence that calcium-activated second messengers in the postsynaptic cell, or perhaps Ca^{2+} itself, cause the postsynaptic cell to release one or more chemical messengers, including the gas nitric oxide, that diffuse to the presynaptic terminals to enhance transmitter release (Figure 54–3 and Chapter 14). Importantly, these diffusible retrograde signals appear to affect only those presynaptic terminals that have been activated by the tetanic stimulation, thereby preserving synapse specificity.

Long-Term Potentiation Has Early and Late Phases

Long-term potentiation has two phases, early and late, that provide a means of regulating the duration of the enhancement of synaptic transmission. The phase we have focused on up to now lasts for only 1 to 3 hours and is termed early LTP; this phase is typically induced by a single train of 100-Hz tetanic stimulation for 1 second. More prolonged periods of activity (using three or four trains of 100-Hz tetanic stimulation, each lasting 1 second) induce a late phase of LTP that can last 24 hours or even longer. Unlike early LTP, late LTP requires the synthesis of new proteins (Figure 54–5).

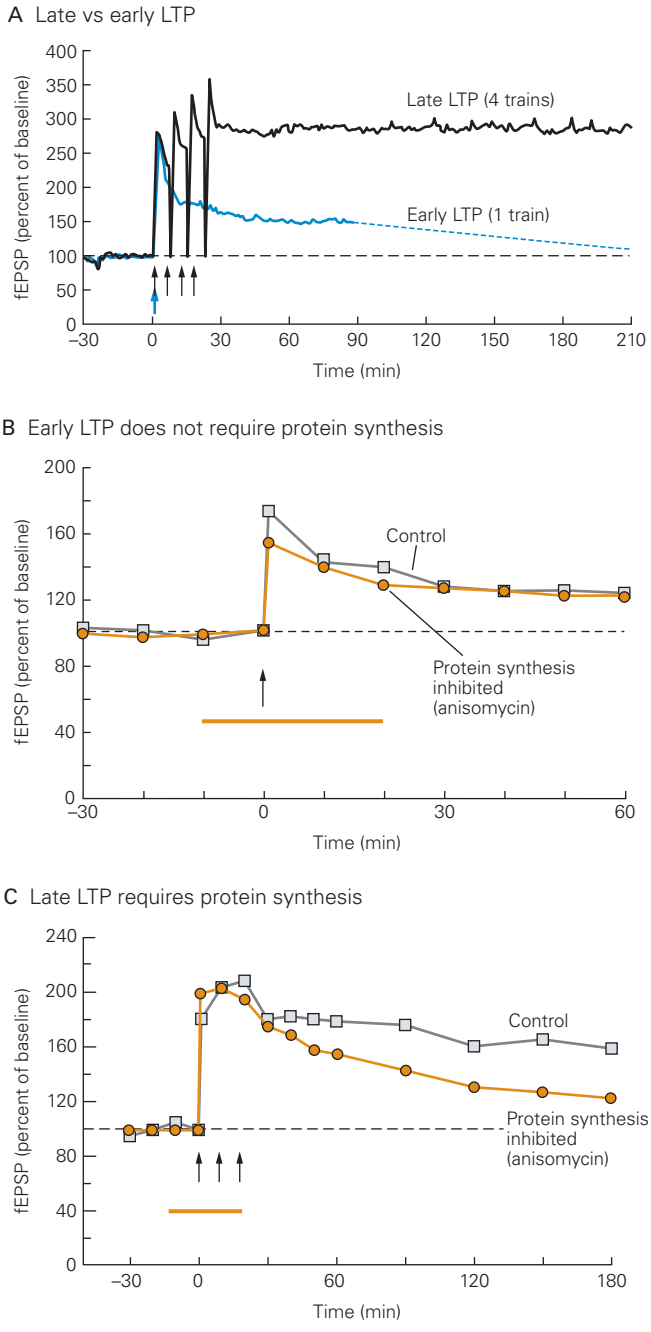

Figure 54–5 (Right) Long-term potentiation (LTP) in the CA1 region of the hippocampus has early and late phases.

A. Early LTP is induced by a single tetanus lasting 1 second at 100 Hz, whereas late LTP is induced by four tetani given 10 minutes apart. Early LTP of the field excitatory postsynaptic potential (**fEPSP**) lasts only 1 to 2 hours, whereas the late LTP lasts more than 8 hours (only the first 3.5 hours are shown).

B. Early LTP induced by one tetanus is not blocked by anisomycin (**bar**), an inhibitor of protein synthesis.

C. Late LTP, normally induced by three trains of stimulation, is blocked by anisomycin. (Three or four trains can be used to induce late LTP.) (Panels B and C reproduced, with permission, from Huang and Kandel 1994.)

Whereas the early phase of LTP is mediated by changes at existing synapses, late LTP is thought to result from the growth of new synaptic connections between pairs of co-activated neurons.

Although the mechanisms for early LTP in the Schaffer collateral and mossy fiber pathways are quite different, the mechanisms for late LTP in the two pathways appear similar (Figure 54–3). In both pathways, late LTP recruits the cAMP and PKA signaling pathway to activate by phosphorylation the cAMP response element binding protein (CREB) transcription factor, leading to the synthesis of new mRNAs and proteins. Like sensitization of the gill-withdrawal reflex in *Aplysia*, which also involves cAMP, PKA, and CREB (Chapter 53), late LTP in the Schaffer collateral pathway is synapse specific. When two independent sets of synapses in the same postsynaptic CA1 neuron are stimulated using two electrodes spaced some distance apart, the application of four trains of tetanic stimulation to one set of synapses induces late LTP only at the activated synapses; synaptic transmission is not altered at the second set of synapses that were not tetanized.

How can late LTP achieve synapse specificity given that transcription and most translation occurs in the cell body, such that newly synthesized proteins should be available to all synapses of a cell? To explain synapse specificity, Uwe Frey and Richard Morris proposed the synaptic capture hypothesis, in which synapses that are activated during the tetanus are tagged in some way, perhaps by protein phosphorylation, that enables them to make use of ("capture") the newly synthesized proteins. Frey and Morris tested this idea using the two-pathway protocol described above. They delivered four tetani to induce late LTP at one set of synapses with one electrode and delivered a single tetanus to a second set of synapses with the other electrode. Although a single tetanus on its own induces only early LTP, it is able to induce late LTP when delivered within 2–3 hours of the four tetani from the first electrode. This phenomenon is similar to the synapse-specific capture of long-term facilitation at the sensory-motor neuron synapses in *Aplysia* (Chapter 53).

According to Frey and Morris, the single train of tetanic stimulation, although not sufficient to induce new protein synthesis, is sufficient to tag the activated synapses, allowing them to capture the newly synthesized proteins produced in response to the prior delivery of the four trains of tetanic stimulation. The increased synaptic plasticity that this tagging mechanism affords, and its limitation to the period when newly synthesized proteins are around, may explain the recent finding that hippocampal cell assemblies that store memories of events closely spaced in time have a larger number of common neurons than do cell assemblies for events widely separated in time.

How can a few brief trains of synaptic stimulation produce such long-lasting increases in synaptic transmission? One mechanism proposed by John Lisman depends on the unique properties of CaMKII. After a brief exposure to Ca^{2+}, CaMKII can be converted to a calcium-independent state through its autophosphorylation at threonine-286 (Thr286). This ability to become persistently active in response to a transient Ca^{2+} stimulus has led to the suggestion that CaMKII may act as a simple molecular switch that can extend the duration of LTP following its initial activation.

Studies from Todd Sacktor have suggested that longer-lasting changes that maintain late LTP may depend on an atypical isoform of PKC termed PKMζ (PKM zeta). Most isoforms of PKC contain both a regulatory domain and a catalytic domain (Chapter 14). Binding of diacylglycerol, phospholipids, and Ca^{2+} to the regulatory domain relieves inhibitory domain binding to the catalytic domain, allowing PKC to phosphorylate its protein substrates. In contrast, PKMζ lacks a regulatory domain and so is constitutively active.

Levels of PKMζ in the hippocampus are normally low. Tetanic stimulation that induces LTP leads to an increase in synthesis of PKMζ through enhanced translation of its mRNA. Because this mRNA is present in the CA1 neuron dendrites, its translation can rapidly alter synaptic strength. Blockade of PKMζ with a peptide inhibitor during the tetanic stimulation blocks late LTP but not early LTP. If the blocker is applied several hours after LTP induction, the late LTP that had been established will be reversed. This result indicates that the maintenance of late LTP requires the ongoing activity of PKMζ to maintain the increase in AMPA receptors in the postsynaptic membrane (Figure 54–3). A second atypical PKC isoform may substitute for PKMζ under certain conditions, which may explain the surprising finding that genetic deletion of PKMζ has little effect on late LTP.

Constitutively active forms of protein kinases may not be the only mechanism for maintaining long-lasting synaptic changes in the hippocampus. Repeated stimulation may lead to the formation of new synaptic connections, just as long-term facilitation leads to the formation of new synapses during learning in *Aplysia*. In addition, long-lasting synaptic changes likely involve epigenetic changes in chromatin structure. During late LTP, phosphorylated CREB activates gene expression by recruiting the CREB binding protein (CBP), which acts as a histone acetylase, transferring an acetyl group to specific lysine residues on histone proteins, and thereby producing

long-lasting changes in gene expression. Mutations in CBP impair late LTP and learning and memory in mice. In humans, de novo mutations in the CBP gene underlie Rubinstein-Taybi syndrome, a developmental disorder associated with intellectual impairment. Other studies implicate a second epigenetic mechanism, DNA methylation, in long-lasting synaptic plasticity and learning and memory.

Spike-Timing-Dependent Plasticity Provides a More Natural Mechanism for Altering Synaptic Strength

Under most circumstances, hippocampal neurons do not produce the high-frequency trains of action potentials typically used to induce LTP experimentally. However, a form of LTP termed spike-timing-dependent plasticity (STDP) can be induced by a more natural pattern of activity in which a single presynaptic stimulus is paired with the firing of a single action potential in the postsynaptic cell at a relatively low frequency (eg, one pair per second over several seconds). However, the presynaptic cell must fire just before the postsynaptic cell. If instead the postsynaptic cell fires just before the EPSP, a long-lasting decrease in the size of the EPSP occurs. Such long-term depression of synaptic transmission represents a distinct form of synaptic plasticity from LTP and is described more fully below. If the postsynaptic action potential occurs more than a hundred milliseconds before or after the EPSP, the synaptic strength will not change.

The pairing rules of STDP thus follow Hebb's postulate and result in large part from the cooperative properties of the NMDA receptor-channel. If the postsynaptic spike occurs during the EPSP, it is able to relieve the Mg^{2+} blockade of the channel at a time when the NMDA receptor has been activated by the binding of glutamate. This leads to a large influx of Ca^{2+} through the receptor and the induction of STDP. However, if the postsynaptic action potential occurs prior to the presynaptic release of glutamate, any relief from the Mg^{2+} block will occur when the gate of the receptor-channel is closed (because of the absence of glutamate). As a result, there will be only a small influx of Ca^{2+} through the receptor that is insufficient to induce STDP.

Long-Term Potentiation in the Hippocampus Has Properties That Make It Useful as A Mechanism for Memory Storage

NMDA receptor–dependent LTP at the Schaffer collateral pathway and other hippocampal pathways has three properties with direct relevance to learning and memory (Figure 54–6). First, LTP in such pathways requires the near-simultaneous activation of a large number of afferent inputs, a feature called *cooperativity* (Figure 54–6). This requirement stems from the fact

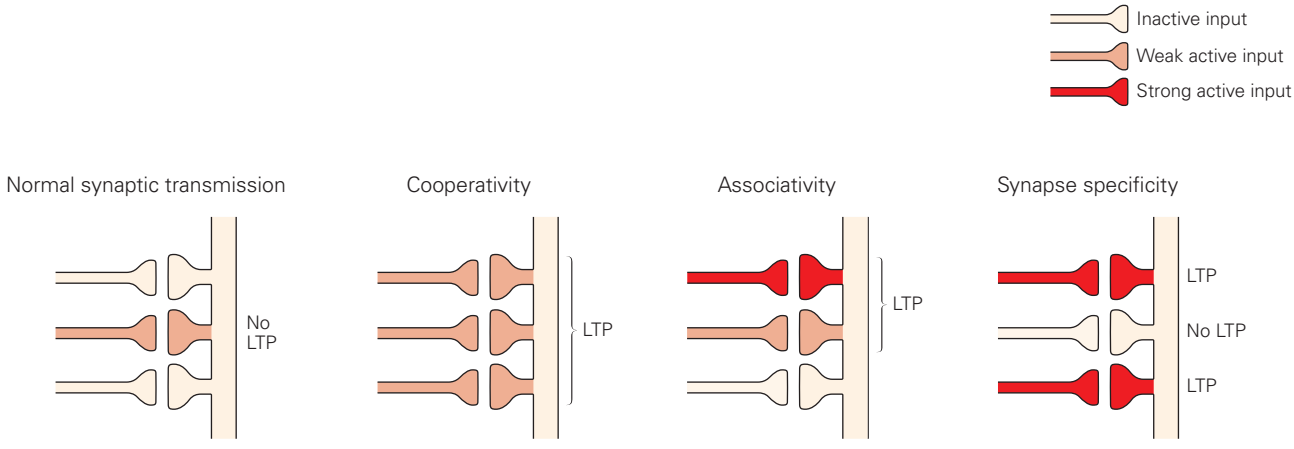

Figure 54–6 Long-term potentiation (LTP) in CA1 pyramidal neurons of the hippocampus shows cooperativity, associativity, and synapse specificity. With normal synaptic transmission, a single action potential in one or a few axons (weak input) leads to a small excitatory postsynaptic potential (EPSP) that is insufficient to expel Mg^{2+} from the *N*-methyl-D-aspartate (NMDA) receptor-channels and thus cannot induce LTP. This ensures that irrelevant stimuli are not remembered. The near-simultaneous activation of several weak inputs during strong activation (cooperativity) produces a suprathreshold EPSP that triggers an action potential, resulting in LTP in all pathways. Stimulation of strong and weak inputs together (associativity) causes LTP in both pathways. In this way, a weak input becomes significant when paired with a powerful one. An unstimulated synapse does not undergo LTP despite the strong stimulation of neighboring synapses. This ensures that memory is selectively stored at active synapses (synapse specificity).

that relief of Mg^{2+} block of the NMDA receptor-channel requires a large depolarization, which is achieved only when the postsynaptic cell receives input from a large number of presynaptic cells.

Second, LTP at synapses with NMDA receptor-channels is *associative.* A weak presynaptic input normally does not produce enough postsynaptic depolarization to induce LTP. However, if the weak input is paired with a strong input that produces a suprathreshold depolarization, the resulting large depolarization will propagate to the synapses with weak input, leading to relief of the Mg^{2+} blockade of the NMDA receptors and induction of LTP at those synapses.

Third, NMDA receptor-dependent LTP is *synapse specific.* If a particular synapse is not activated during a period of strong synaptic stimulation, the NMDA receptors at that site will not be able to bind glutamate and thus will not be activated despite the strong postsynaptic depolarization. As a result, that synapse will not undergo LTP.

Each of these three properties—cooperativity, associativity, and synapse specificity—underlies a key requirement of memory storage. Cooperativity ensures that only events of a high degree of significance, those that activate sufficient inputs, will result in memory storage. Associativity, like associative Pavlovian conditioning, allows an event (or conditioned stimulus) that has little significance in and of itself to be endowed with a higher degree of meaning if that event occurs just before or simultaneously with another more significant event (an unconditioned stimulus). In a network with strong recurrent connections, such as CA3, associative LTP enables a pattern of activity in one group of cells to become linked to a distinct pattern of activity in a separate, but partially overlapping, group of synaptically coupled cells. Such linkages of cell assemblies are thought to enable related events to become associated with one another and to be important for storing and recalling large varieties of experiences, as occurs with explicit memory. Finally, synapse specificity ensures that inputs that convey information not related to a particular event will not be strengthened. Synapse specificity is critical when large amounts of information must be stored in one network, because much more information can be stored in a cell through functional alterations at individual synapses than through blanket changes in a property of the cell, such as its excitability.

Spatial Memory Depends on Long-Term Potentiation

Long-term potentiation is an experimentally induced change in synaptic strength produced by strong direct stimulation of neural pathways. Does this or a related form of synaptic plasticity occur physiologically during explicit memory storage? If so, how important is it for explicit memory storage in the hippocampus?

To date, a large number of experimental approaches have shown that inhibiting LTP interferes with spatial memory. In one approach, a mouse is placed in a pool filled with an opaque fluid (the Morris water maze); to escape from the liquid, the mouse must swim to find a platform submerged in the fluid and completely hidden from view. The animal is released at random locations around the pool and initially encounters the platform by chance. However, in subsequent trials, the mouse quickly learns to locate the platform and then remembers its position based on spatial information—distal markings on the walls of the room in which the pool is located. This task requires the hippocampus. In a nonspatial, or cued, version of this test, the platform is raised above the water surface or marked with a flag so that it is visible, permitting the mouse to navigate directly to it using brain pathways that do not require the hippocampus.

When NMDA receptors are blocked by a pharmacological antagonist injected into the hippocampus immediately before an animal is trained to navigate the Morris water maze, the animal cannot remember the location of the hidden platform using spatial information but can find it in the version of the task with the visible marker. These experiments thus suggest that some mechanism involving NMDA receptors in the hippocampus, perhaps LTP, is involved in spatial learning. However, if the NMDA receptor blocker is injected into the hippocampus *after* an animal has learned a spatial memory task, it does not inhibit subsequent memory recall for that task. This is consistent with findings that NMDA receptors are required for the induction, but not the maintenance, of LTP.

More direct evidence correlating memory formation and LTP comes from experiments with mutant mice that have genetic lesions that interfere with LTP. One interesting mutation is produced by the genetic deletion of the NR1 subunit of the NMDA receptor. Neurons lacking this subunit fail to form functional NMDA receptors. Mice with a general deletion of the subunit die soon after birth, indicating the importance of these receptors for neural function. However, it is possible to generate lines of conditional mutant mice in which the NR1 deletion is restricted to CA1 pyramidal neurons and occurs only 1 or 2 weeks after birth (see Chapter 2, Figure 2–8, for a description of how this mouse line is generated). These mice survive into adulthood and show a loss of LTP in the Schaffer collateral pathway. Although this disruption is highly

localized, the mutant mice have a serious deficit in spatial memory (Figure 54–7).

In some cases, genetic changes can actually enhance both hippocampal LTP and spatial learning and memory. One of the first examples of such an enhancement comes from studies of a mutant mouse that overexpresses the NR2B subunit of the NMDA receptor. This subunit is normally present at hippocampal synapses in the early stages of development but is downregulated in adults. Receptors that include this subunit allow more Ca^{2+} influx than those without the subunit. In mutant mice that overexpress the NR2B subunit, LTP is enhanced, presumably because of an enhancement in Ca^{2+} influx. Importantly, learning and memory for several different tasks are also enhanced (Figure 54–8).

One concern with gene knockouts or transgene expression is that such mutations might lead to subtle developmental abnormalities. That is, changes in the size of LTP and spatial memory in the mutant animals could be the result of an early developmental alteration in the wiring of the hippocampal circuit rather than a change in the basic mechanisms of LTP. This possibility can be addressed by reversibly turning on and off a transgene that interferes with LTP.

Reversible gene expression has been used to explore the role of CaMKII, whose autophosphorylation properties and function in LTP were discussed earlier in this chapter (see also Chapter 2, Figure 2–9, for a description of the methodology). Mutation of the autophosphorylation Thr286 site to the negatively charged amino acid aspartate mimics the effect of autophosphorylation at Thr286 and converts the CaMKII to a calcium-independent form. Transgenic expression of this dominant mutation of CaMKII (CaMKII-Asp286) results in a systematic shift in the relation between the frequency of a tetanus and the resultant change in synaptic strength during long-term plasticity.

In the transgenic mice, tetanic stimulation at an intermediate frequency of 10 Hz, which normally induces a small amount of LTP, induces long-term depression of synaptic transmission in the Schaffer collateral pathway (Figure 54–9A). In contrast, the transgenic mice showed normal LTP to a 100-Hz tetanus. The defect in synaptic plasticity with 10-Hz stimulation is associated with an inability of the mutant mice to remember spatial tasks. However, the defects in the induction of LTP and in spatial memory can be fully extinguished when the mutant gene is switched off in the adult, showing that the memory defect is not due to a developmental abnormality (Figure 54–9).

These several experiments using restricted knockout and overexpression of the NMDA receptor and regulated overexpression of CaMKII-Asp286 make it clear that the molecular pathways important for LTP at Schaffer collateral synapses are also required for spatial memory. However, such results do not directly show that spatial learning and memory are actually associated with an enhancement in hippocampal synaptic transmission. Mark Bear and his colleagues addressed this question by monitoring the strength of synaptic transmission at the Schaffer collateral synapses in vivo in rats.

Recordings were made of synaptic strength using an array of extracellular electrodes to stimulate the Schaffer collateral inputs and another array to record the extracellular field EPSPs at various locations. Rats were then trained to avoid one side of a box through administration of a foot shock; the field EPSPs were remeasured after training, showing a small but significant increase in the amplitude of synaptic transmission at a subset of the recording electrodes. Does the increase in synaptic transmission during learning result from LTP or some other mechanism? Because the amount of LTP at a given synapse is finite, if learning does indeed recruit an LTP-like process, then the ability to induce LTP by tetanic stimulation after learning should be reduced. Indeed, Bear and his colleagues found that the magnitude of LTP is diminished at those recording sites where the behavioral training produced the greatest enhancement in the field EPSP. This result is similar to findings in the amygdala, where fear learning reduces the magnitude of LTP induced by subsequent tetanic stimulation.

If LTP-like changes take place during memory formation in the hippocampus, such changes would be expected only in a small subset of synapses, namely those that participate in the storage of the particular memory. Different memories probably correspond to different assemblies of cells with strengthened synaptic interconnections. If this is true, however, hippocampal memories should be vulnerable to disruption by manipulations that indiscriminately alter synaptic strength within the network as a whole. To test this idea, investigators induced LTP throughout the dentate gyrus *after* hippocampal-dependent spatial training in the water maze task. This protocol indeed impairs the animal's memory of the goal location in the water maze. Control animals that are given NMDA receptor antagonists after learning but prior to high-frequency stimulation exhibit normal spatial memory. These results indicate that the memory impairment was generated specifically as a consequence of the generation of indiscriminate LTP, which likely disrupts the specific pattern of strong and weak synapses that encode memory of the goal location.

A Action of Cre recombinase is restricted to CA1 region

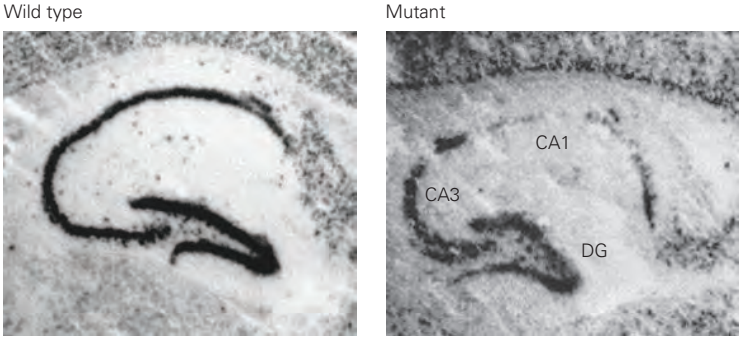

B Long-term potentiation

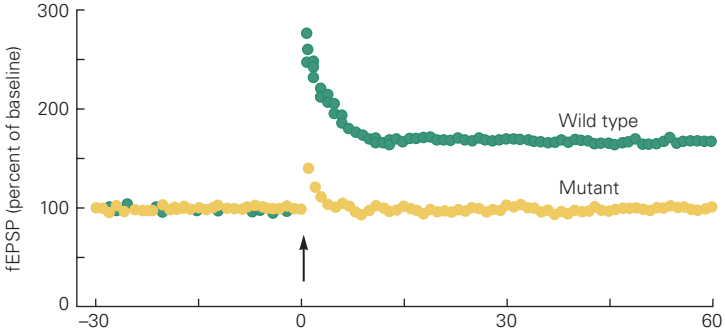

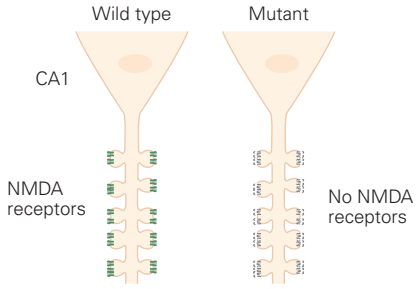

C Morris water maze learning

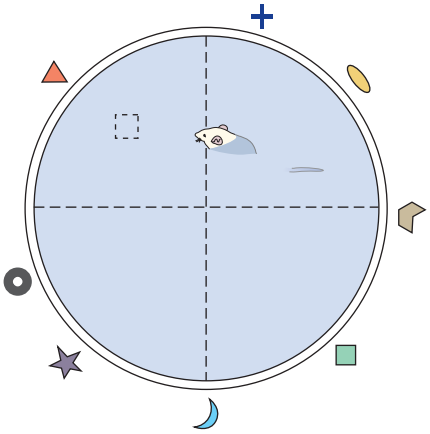

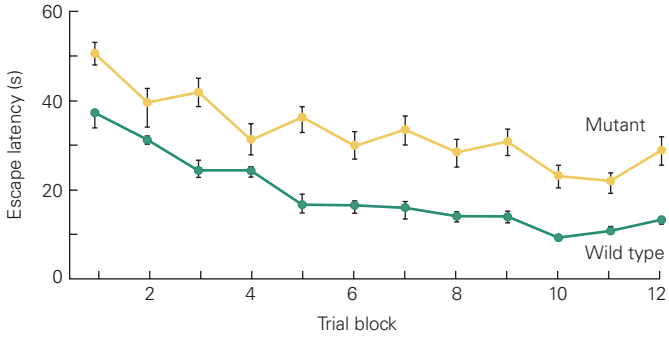

D Probe trial test of memory

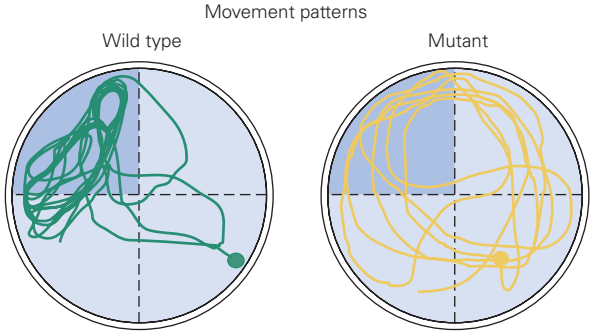

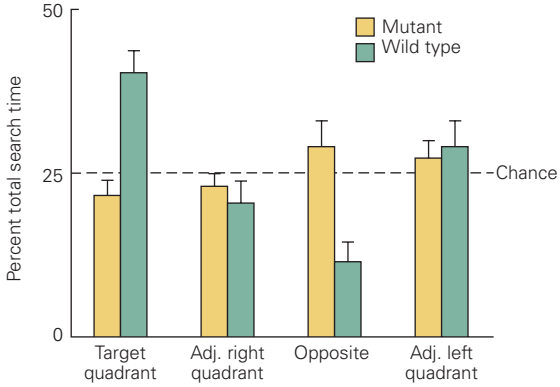

Finally, although most behavioral tests of LTP have used spatial learning tasks to assess memory, studies have also shown that NMDA receptors, and by inference LTP, are necessary for a variety of hippocampal-dependent explicit memories. When NMDA receptors in the CA1 area are blocked, mice are not able to master a nonspatial object recognition task, learn complex odor discrimination, or undergo the social transmission of a food preference, in which an animal learns to accept a novel food by observing a conspecific (another animal of its species) consume that same food. Thus, NMDA receptor–dependent LTP is likely required for many, if not all, forms of explicit memory in the hippocampus (most of which include a spatial recognition element).

Explicit Memory Storage Also Depends on Long-Term Depression of Synaptic Transmission

If synaptic connections could only be enhanced and never attenuated, synaptic transmission might rapidly saturate—the strength of the synaptic connections might reach a point beyond which further enhancement is not possible. Moreover, uniform synaptic strengthening may lead to a loss of memory specificity, with one memory interfering with another. Yet individuals are able to learn, store, and recall new memories throughout a lifetime. This paradox led to the suggestion that neurons must have mechanisms to downregulate synaptic function to counteract LTP.

Such an inhibitory mechanism, termed *long-term depression* (LTD), was first discovered in the cerebellum, where it is important for motor learning. Since then, LTD has also been characterized at a number of synapses within the hippocampus. Whereas LTP is typically induced by a brief high-frequency tetanus, LTD is induced by prolonged low-frequency synaptic stimulation (Figure 54–10A). As mentioned above, it can also be induced by a spike pairing protocol in which an EPSP is evoked *after* an action potential in the postsynaptic cell. This suggests a corollary to Hebb's learning rule: Active synapses that do not contribute to the firing of a cell are weakened. Like LTP, a number of molecular and synaptic mechanisms are engaged during the induction and expression of LTD.

Surprisingly, many forms of LTD require activation of the same receptors involved in LTP, namely the NMDA receptors (Figure 54–10A). How can activation of a single type of receptor produce both potentiation and depression? A key difference lies in the experimental protocols used to induce LTP or LTD. Compared to the high-frequency stimulation used to induce LTP, the low-frequency tetanus used to induce LTD produces a relatively modest postsynaptic depolarization and thus is much less effective at relieving the Mg^{2+} block of the NMDA receptors. As a result, any increase in Ca^{2+} concentration in the postsynaptic cell is much smaller than the increase observed during induction of LTP and therefore insufficient to activate CaMKII, the enzyme implicated in LTP. Rather, LTD may result from activation of the calcium-dependent phosphatase calcineurin, an enzyme complex that has a higher affinity for Ca^{2+} compared to that of CaMKII (Chapter 14).

Figure 54–7 (Opposite) Long-term potentiation (LTP) and spatial learning and memory are impaired in mice that lack the *N*-methyl-D-aspartate (NMDA) receptor in the CA1 region of the hippocampus. (Reproduced, with permission, from Tsien, Huerta, and Tonegawa 1996.)

A. A line of mice is bred in which the gene encoding the NR1 subunit of the NMDA receptor is selectively deleted in CA1 pyramidal neurons. In situ hybridization is used to detect mRNA for the NR1 subunit in hippocampal slices from wild type and mutant mice that contain two floxed NR1 alleles and express Cre recombinase under the control of the *CaMKIIα* promoter. Note that NR1 mRNA expression (**dark staining**) is greatly reduced in the CA1 region of the hippocampus but not in CA3 and the dentate gyrus (**DG**).

B. LTP at the CA1 Schaffer collateral synapses is abolished in these mice. Field excitatory postsynaptic potentials (**fEPSPs**) were recorded in response to Schaffer collateral stimulation. Tetanic stimulation at 100 Hz for 1 second (**arrow**) caused a large potentiation in wild type mice but failed to induce LTP in the NMDA receptor knockout (mutant) mice.

C. Mice that lack the NMDA receptor in CA1 pyramidal neurons have impaired spatial memory. A platform (**dashed square**) is submerged in an opaque fluid in a circular tank (a Morris water maze). To avoid remaining in the water, the mice have to find the platform using spatial (contextual) cues on the walls surrounding the tank and then climb onto the platform. The graph shows escape latency or the time required by mice to find the hidden platform in successive trials. The mutant mice display a longer escape latency in every block of trials (four trials per day) than do the wild type mice. Also, mutant mice do not reach the optimal performance attained by the control mice after 12 training days, even though they show some improvement with training.

D. After the mice have been trained in the Morris maze, the platform is taken away. In this probe trial, the wild type mice spend a disproportionate amount of time in the quadrant that formerly contained the platform (the target quadrant), indicating that they remember the location of the platform. Mutant mice spend an equal amount of time (25%) in all quadrants; that is, they perform at chance level, indicating deficient memory.

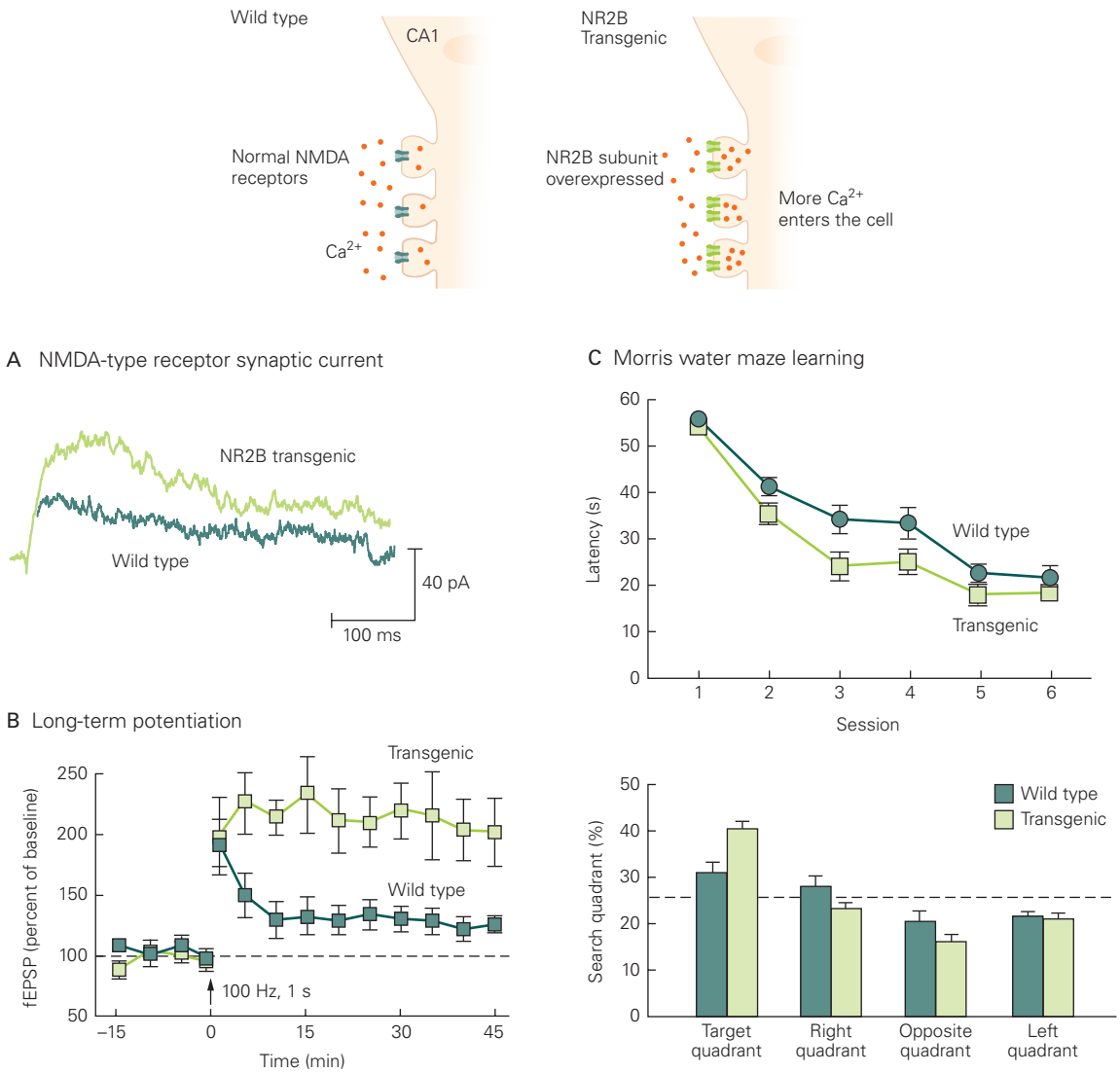

Figure 54–8 Learning and memory are enhanced in mice that overexpress a subunit of the *N*-methyl-D-aspartate (NMDA) glutamate receptor. (Reproduced, with permission, from Tang et al. 1999. Copyright © 1999 Springer Nature.)

A. The amplitude of the current generated by the NMDA receptors in response to a brief pulse of glutamate is enhanced and its time course prolonged in hippocampal neurons obtained from mice that contain a transgene that expresses higher levels of the receptor's NR2B subunit compared to wild type mice.

B. Long-term potentiation produced by tetanic stimulation of the Schaffer collateral synapses is greater in the transgenic mice than in wild type mice. (Abbreviation: **fEPSP**, field excitatory postsynaptic potential.)

C. Spatial learning is enhanced in the transgenic mice (**upper plot**). The rate of learning in a Morris water maze (the reduction in time to find the hidden platform, or escape latency) is faster in transgenic mice than in wild type mice. Spatial memory is also enhanced in the transgenic mice (**lower plot**). In the probe trial, the transgenic mice spend more time in the target quadrant, which previously contained the hidden platform, than do wild-type mice.

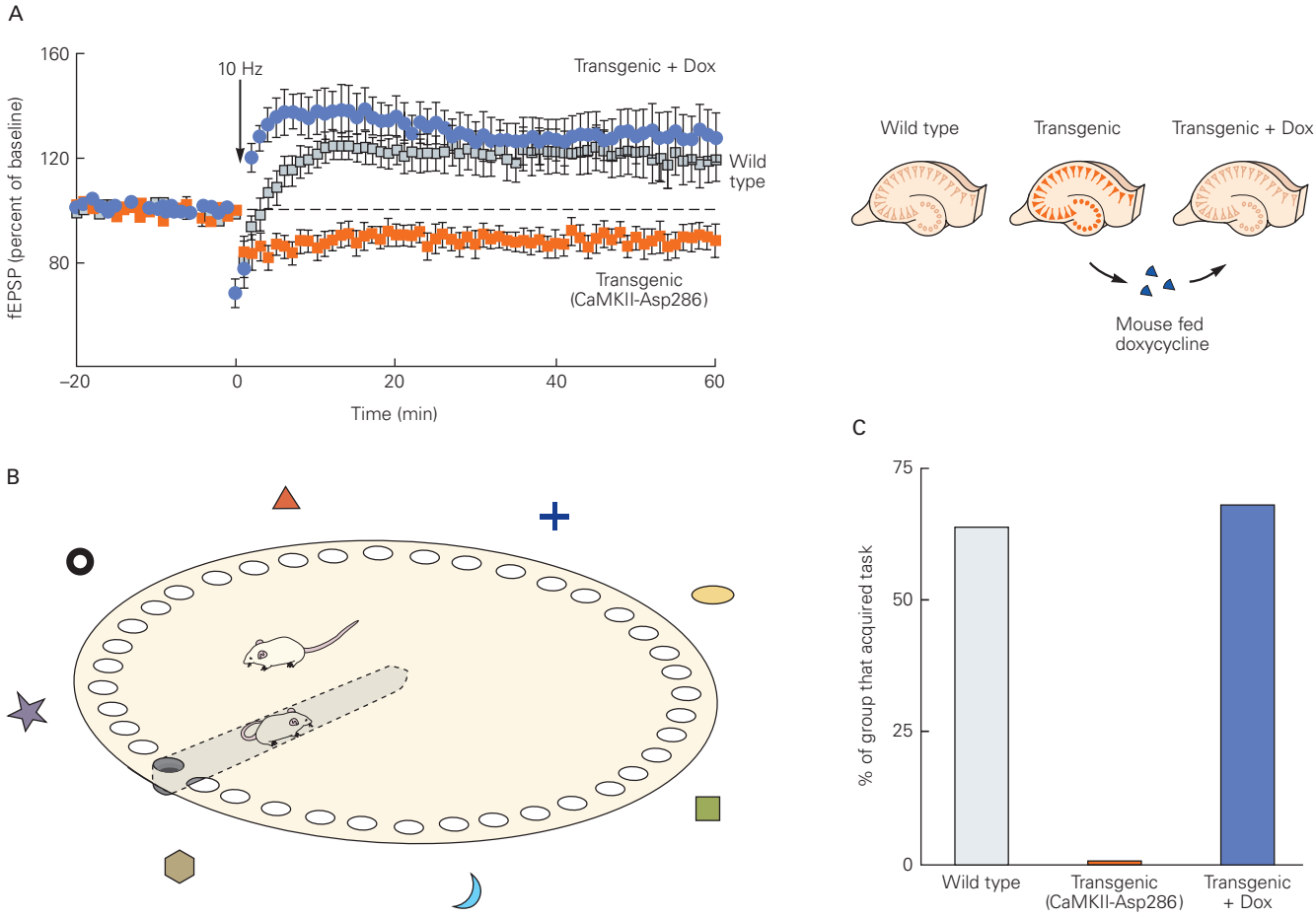

Figure 54–9 **Deficits in long-term potentiation (LTP) and spatial memory due to a transgene are reversible.** (Reproduced, with permission, from Mayford et al. 1996.)

A. An LTP deficit is seen in hippocampal slices from transgenic mice that overexpress CaMKII-Asp286 kinase, a constitutively active mutant form of CaMKII. Expression of this transgene is driven by a second transgene, the tTA bacterial transcription factor, which is inhibited by the antibiotic doxycycline (**Dox**) (see Chapter 2, Figure 2–9, for a complete description). Four groups of mice were tested: transgenic mice that were fed doxycycline, which blocks expression of the kinase; transgenic mice without doxycycline, in which the kinase is expressed; and wild type mice with and without doxycycline. In wild type mice, a 10-Hz tetanus induces LTP; doxycycline has no effect (data are not shown). In the transgenic mice, the tetanus fails to induce LTP but causes a small synaptic depression. In the transgenic mice that were fed doxycycline, the deficit in LTP is reversed. (Abbreviation: **fEPSP**, field excitatory postsynaptic potential.)

B. The effect of the kinase on spatial memory was tested in a Barnes maze. The maze consists of a platform with 40 holes, one of which leads to an escape tunnel that allows the mouse to exit the platform. The mouse is placed in the center of the platform. Mice do not like open, well-lit spaces and therefore try to escape from the platform by finding the hole that leads to the escape tunnel. The most efficient way of learning and remembering the location of the hole (and the only way of meeting the criteria set for the task by the experimenter) is for the mouse to use distinctive markings on the four walls as spatial cues, thus demonstrating hippocampal spatial memory.

C. Transgenic mice that receive doxycycline perform as well as wild type mice in learning the Barnes maze task (approximately 65% of animals learn the task), whereas transgenic mice without the doxycycline, which thus express CaMKII-Asp286, do not learn the task.

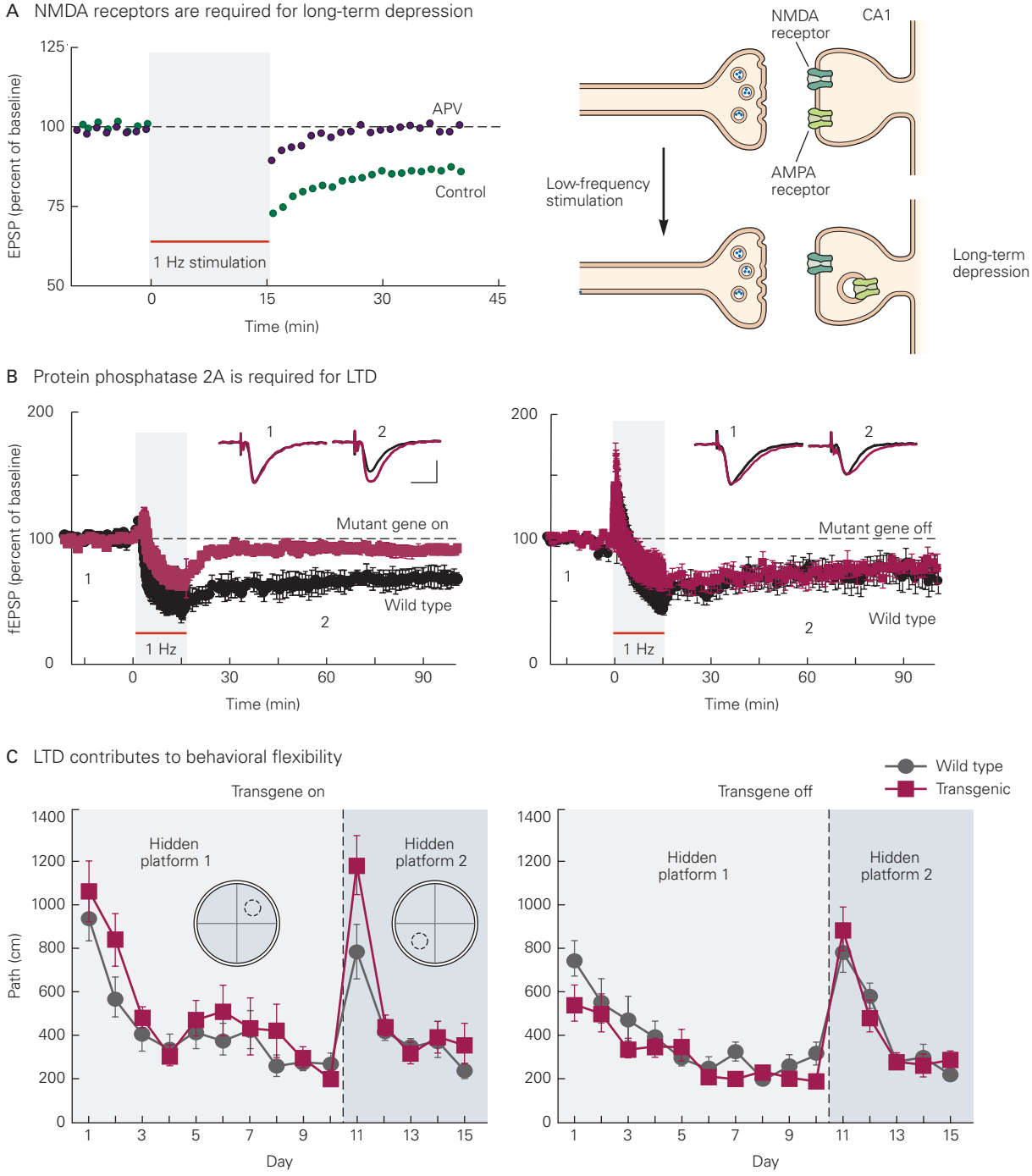

Figure 54–10 Long-term depression of synaptic transmission requires *N*-methyl-D-aspartate (NMDA) receptors and phosphatase activity.

A. Prolonged low-frequency stimulation (1 Hz for 15 minutes) of Schaffer collateral fibers produces a long-term decrease in the size of the field excitatory postsynaptic potential (**fEPSP**) in the hippocampal CA1 region, a decrease that outlasts the period of stimulation (control). Long-term depression (**LTD**) occurs when α-amino-3-hydroxy-5-methyl-4-isoxazolepropionic acid (**AMPA**) receptors are removed from the postsynaptic membrane by endocytosis; it is blocked when the NMDA receptors are blocked by the drug 2-amino-5-phosphonovaleric acid (**APV**). (Adapted from Dudek and Bear 1992.)

B. LTD requires protein dephosphorylation. The plots compare LTD in the hippocampal CA1 region of wild type mice and transgenic mice that express a protein that inhibits phosphoprotein phosphatase 2A. Transgene expression is under control of the tTA system. In the absence of doxycycline, the phosphatase inhibitor is expressed, and induction of LTD is inhibited (*left plot*). When expression of the phosphatase inhibitor is turned off by administering doxycycline, a normal-sized LTD is induced (*right plot*).

C. Inhibition of phosphatase 2A reduces behavioral flexibility. Transgenic mice expressing the phosphatase inhibitor learn the location of a submerged platform in the Morris maze at the same rate as wild-type mice (days 1–10). Thus, LTD is not necessary for learning the initial platform location. At the end of day 10, the platform is moved to a new hidden location and the mice are retested (days 11–15). Now the transgenic mice travel significantly longer paths to find the platform on the first day of retesting (day 11), indicating an impaired learning (reduced flexibility). When transgene expression is turned off with doxycycline, the transgenic mice display normal learning on all phases of the test. (Panels B and C reproduced, with permission, from Nicholls et al. 2008.)

Long-term depression may also depend on a surprising metabotropic action of the ionotropic NMDA receptor-channels. Glutamate binding, in addition to opening the receptor pore, is thought to trigger a conformational change in a cytoplasmic domain of the receptor that directly activates a downstream signaling cascade that increases the activity of phosphoprotein phosphatase 1 (PP1). Activation of PP1 or calcineurin eventually leads to changes in protein phosphorylation that promote endocytosis of AMPA receptors, resulting in a decrease in the size of an EPSP.

Distinctly different forms of LTD can be induced through the activation of G protein–coupled metabotropic glutamate receptors. Such forms of LTD depend on activation of mitogen-activated protein (MAP) kinase signaling pathways (Chapter 14) rather than activation of phosphatases. These types of LTD lead to a reduction in synaptic transmission through a decrease in glutamate release from presynaptic terminals as well as through alterations in the trafficking of AMPA receptors in the postsynaptic cells.

Much less is known about the behavioral role of LTD compared to that of LTP, but some insight has come from studies with mice using a transgene that expresses an inhibitor of protein phosphatase. LTD that depends on NMDA receptors is inhibited when the transgene is expressed but is normal when transgene expression is suppressed (Figure 54–10B). Transgene expression does not affect LTP or forms of LTD that involve metabotropic glutamate receptors. Mice that express the transgene show normal learning the first time they are tested in the Morris maze. However, when the same mice are retested after the hidden platform has been moved to a new location, they show a decreased ability to learn the new location and tend to persevere in searching for the platform near the previously learned location (Figure 54–10C). Thus, LTD may be necessary not only to prevent LTP saturation but also to enhance flexibility in memory storage and specificity in memory recall. Studies on fear conditioning suggest that LTD in the amygdala may be important for reversing learned fear.

Memory Is Stored in Cell Assemblies

While the cumulative evidence for a relationship between long-term synaptic plasticity and memory formation is strong, we know less about how specific cellular processes such as LTP enable memory formation. This reflects limitations in our knowledge of how neural circuits operate and how memories might be embedded in them. Theoretical models for memory storage in neural circuits can be traced to Hebb's concept of a cell assembly—a network of neurons that is activated whenever a function is executed; for example, each time a memory is recalled. Cells within an assembly are bound together by excitatory synaptic connections strengthened at the time the memory was formed.

Today, more than half a century later, Hebb's thoughts still form the framework for how the hippocampus mediates the storage and recall of memory, although experimental proof has been difficult to obtain. A proper test requires recording the activity of thousands of neurons simultaneously, in combination with the experimental excitation or inactivation of selected cell groups. Technological advances are now enabling such experiments. By and large, the results obtained so far confirm Hebb's cell assembly model and implicitly point to LTP as the mechanism for their formation.

In a telling study with mice, Susumu Tonegawa and his colleagues tested whether reactivation of neurons that participated in the storage of a specific memory is sufficient to trigger recall of that memory. The researchers first applied an electric shock to an animal as it explored a novel environment. Reexposure of the animal to the same environment a day or more later elicited a freezing response, indicating that the animal associated the environment or context (the conditioned stimulus) with the shock (the unconditioned stimulus). Using a genetic strategy, Tonegawa caused a subset of dentate gyrus granule neurons that were active during the fear conditioning to express the light-activated cation channel channelrhodopsin-2 (Figure 54–11). The conditioned animals were subsequently placed in a novel environment that did not resemble the conditioned environment and so did not elicit a fear response. However, light activation of the subset of granule cells that were active during fear conditioning was able to elicit a strong freezing response, even though the animals were in a nonthreatening environment. This supports the idea that memories are stored in cell assemblies and, more importantly, demonstrates that reactivation of these assemblies is sufficient to induce recall of an experience.

In a complementary experimental approach, a light-activated inhibitory Cl^- transporter was expressed in CA1 cells active at the time of fear conditioning. Later, the labeled cells were inactivated and the animals were placed again in the environment in which they received the shock. Under these conditions, the normal freezing behavior (ie, recall of the memory of fear conditioning) was blocked, suggesting that activity in the labeled CA1 cell population was necessary for memory retrieval. Taken together, these findings

suggest that reactivation of the specific cell assembly pattern that occurred during encoding is both necessary and sufficient for memory retrieval.

Perhaps the most direct test of the ensemble model is the creation of a false memory. Tonegawa and colleagues expressed channelrhodopsin in cells that were active during exploration of a novel environment (context A), except that no shock was delivered this time. At a later time, the labeled cells were reactivated using light stimulation as the mice explored a second novel environment (context B), this time in combination with an electric shock. When the animals were returned to the neutral context A, they froze, although they had never been shocked in this environment. This result indicates that the reactivation of the original engram of context A when paired with an aversive experience in context B is able to create a false memory, causing the animals to fear context A. Thus, it is possible to modify the behavioral significance of a neural representation (a pattern of neural firing in response to a given stimulus) by pairing the assembly with a new experience unrelated to the original experience.

Different Aspects of Explicit Memory Are Processed in Different Subregions of the Hippocampus

Explicit memory stores knowledge of facts (semantic memory), places (spatial memory), other individuals (social memory), and events (episodic memory). As discussed above, successful storage and recall of explicit

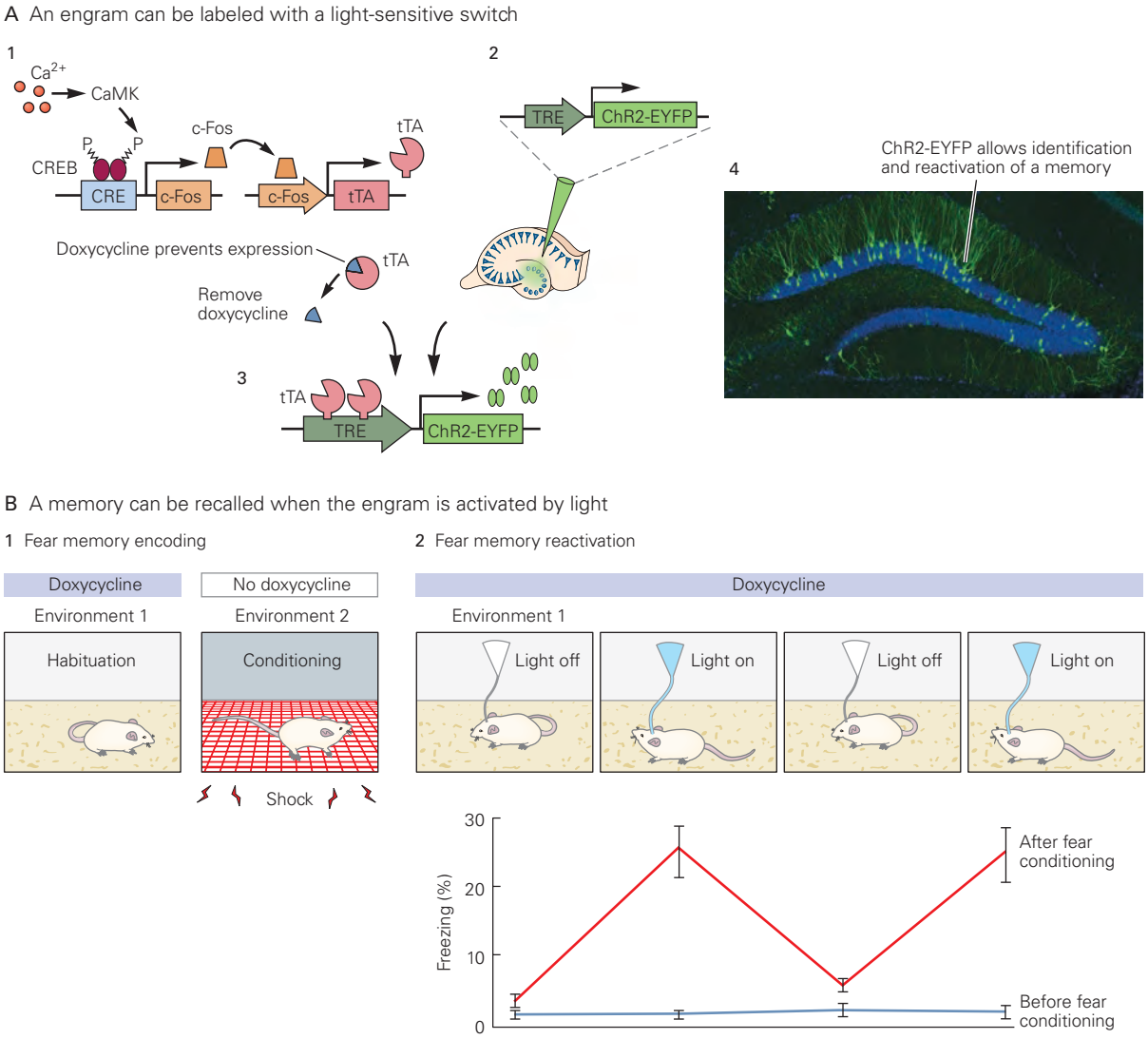

memory requires that patterns of activity be formed within local cell assemblies to avoid mix-up between memories. At the same time, an important psychological feature of hippocampal-dependent memory is that a few cues are usually enough to trigger the recall of a complex memory. How does the hippocampus perform all of these diverse functions? Do its subregions have specialized roles, or is memory a unitary function of the hippocampus? In at least some instances, it has been possible to assign key functions to specific areas of the hippocampus.

The Dentate Gyrus Is Important for Pattern Separation

How does the hippocampus store a different pattern of neural activity in response to every experience that needs to be remembered, including patterns that distinguish between two closely related environments? Contemporary ideas about how neural circuits accomplish this task, often referred to as *pattern separation*, dates to the theoretical work of David Marr in the late 1960s and early 1970s. In a landmark paper on the cerebellum, Marr suggested that the extensive divergence of mossy-fiber inputs onto an extraordinarily large number of cerebellar granule cells might allow for pattern separation in this system.

This idea of "expansion recoding," in which distinct firing patterns are formed through the projection of a limited number of inputs onto a larger population of synaptic target cells, was later applied by others to the hippocampus. They proposed that hippocampal pattern separation results from the divergence of entorhinal inputs onto a larger number of granule cells in the dentate gyrus. The findings of subsequent experimental studies are broadly in line with these theoretical suggestions: Neural activity patterns recorded in different environments differ more extensively in the dentate gyrus and CA3 than they do one synapse upstream in the entorhinal cortex. The dentate gyrus is also implicated in pattern separation by the fact that lesions or genetic manipulations targeted to this area impair the ability of rats and mice to discriminate between similar locations and contexts.

The dentate gyrus is the site of one of the most unexpected findings in neuroscience, the discovery that the birth of new neurons, or neurogenesis, is not limited to early stages of development. New neurons

Figure 54–11 (Opposite) Stimulating a neuronal assembly associated with a stored memory of fear conditioning elicits fear behavior. (Panels reproduced or redrawn, with permission, from Liu et al. 2012. Copyright © 2012 Springer Nature.)

A. *Experimental protocol*. 1. Exposure of a mouse to a new environment increases activity in a group of hippocampal neurons (cell assembly) that codes for the environment. The activity increases intracellular Ca^{2+}, which activates a CaM kinase signaling cascade, resulting in phosphorylation of the transcription factor CREB. Phosphorylated CREB increases expression of immediate early genes, including the c-Fos transcription factor. In the *c-fos-tTA* transgenic mouse line, c-Fos binds to the *c-fos* promoter of the transgene and thereby initiates expression of the transcription factor tTA. The antibiotic doxycycline is fed to mice, which binds to and inhibits tTA, until the day of the experiment. 2. The dentate gyrus of the same transgenic mice was previously injected with an adeno-associated virus that contains a DNA sequence encoding ChR2 fused to the fluorescent marker protein EYFP (ChR2-EYFP). The transcription of this sequence is under control of the TRE promoter, which requires tTA (without doxycycline) for expression. 3. Exposure of the mice to a novel environment (after removing doxycycline from the feed) leads to expression of tTA and subsequent expression of ChR2-EYFP in a subset of active dentate gyrus neurons. 4. The ChR2-EYFP remains expressed for several days in the neurons, as seen by the EYFP fluorescence signal in dentate gyrus granule cells in a hippocampal slice. (ChR2-EYPF in **green**, dentate gyrus cell body layer in **blue**.)

B. *Recall of a fear memory*. An optical fiber is implanted above the dentate gyrus. 1. During fear memory encoding, mice were first habituated in one environment while being fed doxycycline (which prevents expression of ChR2-EYFP). The mice were then taken off doxycycline and exposed to a new environment for a few minutes. This turns on gene transcription in the assembly of neurons that are active in the new environment, leading to prolonged expression of ChR2-EYFP in these cells. The mice were then given a series of footshocks while in the new environment to induce fear conditioning: The mice learn to associate the new environment with a fearful stimulus. The mice were then returned to their cage and put back on doxycycline. 2. During fear memory reactivation 5 days after conditioning, mice show a normal defensive freezing behavior when reintroduced to the environment where they received footshocks (not shown). However, when mice are exposed to the environment to which they were initially habituated (no associated foot shock), they normally recognize this as a neutral environment and do not exhibit defensive freezing. However, as the mice explore the neutral environment, delivery of blue light to activate ChR2-expressing neurons in the dentate gyrus causes the mice to freeze. This indicates that activation of the ensemble of ChR2-expressing neurons initially activated in the conditioning environment is sufficient to recall the fear memory associated with that environment. The experimental data show the freezing response in the neutral environment is much greater when light pulses are turned on compared to when the light is off (**red plot**; light delivery indicated in cartoon on top). Delivery of light pulses to an animal that had not undergone fear conditioning does not elicit freezing (**blue plot**).

continue to be born from precursor stem cells throughout adulthood and become incorporated into neural circuits. Nevertheless, adult neurogenesis is limited to granule neurons in two brain regions: inhibitory granule cells in the olfactory bulb and the excitatory granule neurons of the dentate gyrus. Recent experimental findings raise the possibility that newly born granule neurons in the adult are particularly important for pattern separation, even though they represent only a minor fraction of the total number of granule cells. Procedures that stimulate neurogenesis enhance the ability of a mouse to discriminate between closely related environments. Experimental silencing of all dentate gyrus granule neurons except those newly born in the adult does not seem to impair pattern separation, implying that it is the newborn neurons that are most essential to pattern separation. Although some uncertainties remain on the role of neurogenesis in pattern separation and memory encoding, methods that enhance neurogenesis are currently being explored as a means of treating different types of age-related memory loss.

The CA3 Region Is Important for Pattern Completion

A key feature of explicit memory is that a few cues are often sufficient to retrieve a complex stored memory. Marr suggested in a second landmark paper in 1971 that the recurrent excitatory connections of CA3 pyramidal cells might underlie this phenomenon. He proposed that when a memory is encoded, neuronal activity patterns are stored as changes in connections between active CA3 cells. During subsequent retrieval of the memory, the reactivation of a subset of this stored cell assembly would be sufficient to activate the entire original neural ensemble that encodes the memory because of the strong recurrent connections between the cells of the ensemble. This restoration is referred to as *pattern completion*.

The importance of LTP for pattern completion in the CA3 network is seen in studies with mice in which the NMDA glutamate receptor is selectively deleted from the CA3 neurons. These mice experience a selective loss of LTP at the recurrent synapses between CA3 neurons, with no change in LTP at the synapses between mossy fibers and CA3 neurons or at the Schaffer collateral synapses between CA3 and CA1 neurons. Despite this deficit, the mice show normal learning and memory for finding a submerged platform in a water maze using a complete set of spatial cues. However, when the mice are asked to find the platform with fewer spatial cues, their performance is impaired, indicating that LTP at the recurrent synapses between CA3 neurons is important for pattern completion.

The CA2 Region Encodes Social Memory

Studies comparing neuronal representations in the dentate gyrus and CA3 and CA1 areas have indicated that each region has a unique function in the storage and retrieval of hippocampal memory. Recent evidence suggests that the CA2 region plays a crucial role in social memory, the ability of an individual to recognize and remember other members of its own species (conspecifics). Genetic silencing of CA2 disrupts the ability of a mouse to remember encounters with other mice, but does not impair other forms of hippocampal-dependent memory, including memory of objects and places.

The CA2 region is also unique among hippocampal regions in having very high levels of receptors for the hormones oxytocin and vasopressin, important regulators of social behaviors. Selective stimulation of the vasopressin inputs to CA2 neurons can greatly prolong the duration of a social memory. Social memory also depends on CA1 neurons in the ventral region of the hippocampus, an area linked to emotional behavior, which receives important input from CA2.

A Spatial Map of the External World Is Formed in the Hippocampus

How do hippocampal neurons encode features of the external environment to form a memory of spatial locale, enabling an animal to navigate to a remembered goal? At the end of the 1940s, the cognitive psychologist Edward Tolman proposed that somewhere in the brain there must be representations of one's environment. He referred to these neural representations as cognitive maps. They were thought to form not only an internal map of space but also a mental database in which information is stored in relation to an animal's position in the environment, similar to the GPS coordinates of a photograph.

Tolman did not have the opportunity to determine whether a cognitive map actually existed in the brain, but in 1971, John O'Keefe and John Dostrovsky discovered that many cells in the CA1 and CA3 areas of the rat hippocampus fire selectively when an animal is located at a specific position in a specific environment. They called these cells "place cells" and the spatial location in the environment where the cells preferentially fired "place fields" (Figure 54–12A,B). When the animal enters a new environment, new place fields are formed within minutes and are stable for weeks to months.

Different place cells have different place fields, and collectively, they provide a map of the environment, in the sense that the combination of currently active cells is sufficient to read out precisely where the animal is in the environment. A place-cell map is not egocentric in its organization, like the neural maps for touch or vision on the surface of the cerebral cortex. Rather, it is allocentric (or geocentric); it is fixed with respect to a point in the outside world. Based on these properties, John O'Keefe and Lynn Nadel suggested in 1978 that place cells are part of the cognitive map that Tolman had in mind. The discovery of place cells provided the first evidence for an internal representation of the environment that allows an animal to navigate purposefully around the world.

Entorhinal Cortex Neurons Provide a Distinct Representation of Space

How is the hippocampal spatial map formed? What type of spatial information is carried by afferent connections from the entorhinal cortex to the hippocampal place cells? In 2005, a surprising discovery was made about the spatial representation formed by certain neurons in the medial entorhinal cortex, whose axons provide a major part of the perforant pathway input to the hippocampus. These neurons represent space in a manner very different from the hippocampal place cells. Instead of firing when the animal is in a unique location, like the place cells, these entorhinal neurons, termed *grid cells*, fire whenever the animal is at any of several regularly spaced positions forming a hexagonal grid-like array (Figure 54–12C). When the animal moves about in the environment, different grid cells become activated, such that the activity in the entire population of grid cells always represents the animal's current position.

The grid allows the animal to locate itself within a Cartesian-like external coordinate system that is independent of context, landmarks, or specific markings. A grid cell's firing pattern is expressed in all environments that an animal visits, including during complete darkness. The independence of grid-cell firing from visual input implies that intrinsic networks, as well as self-motion cues, may serve as sources of information to ensure that grid cells are activated systematically throughout the environment. The gridded spatial information conveyed by the entorhinal inputs is then transformed within the hippocampus into unique spatial locations represented by the firing of ensembles of place cells, but how this transformation occurs remains to be determined. Since grid cells were discovered in the medial entorhinal cortex of rats in 2005, they have been identified in mice, bats, monkeys, and humans. Recordings from flying bats have shown that grid cells and place cells represent locations in three-dimensional space, suggesting the generality of the cortico-hippocampal spatial navigation system. Finally, it has been proposed that grid cells in primates may encode positions in multiple sensory coordinate systems, including eye fixation coordinates.

Grid cells display a characteristic relation between their firing fields and anatomical organization (Figure 54–13). The x,y coordinates of a cell's grid fields—often called the phase of the grid—differ among cells at the same location of the medial entorhinal cortex. The x,y coordinates of two neighboring cells are often as different as those of widely separated grid cells. In contrast, the size of the individual grid fields and the spacing between them generally increase topographically from the dorsal to the ventral part of the medial entorhinal cortex, expanding from a typical grid spacing of 30 to 40 cm at the dorsal pole to several meters in some cells at the ventral pole (Figure 54–13A). The expansion is not linear but step-like, suggesting that the grid-cell network is modular.

Interestingly, a gradual expansion is seen also in the size of the place fields of hippocampal place cells along the dorsal to ventral axis of the hippocampus (Figure 54–13B). This is consistent with the known pattern of synaptic connectivity: Dorsal entorhinal cortex innervates dorsal hippocampus, whereas ventral entorhinal cortex innervates ventral hippocampus. The finding that place fields are larger in the ventral hippocampus is in accord with results suggesting that the dorsal hippocampus is more important for spatial memory, whereas the ventral hippocampus is more important for nonspatial memory, including social memory and emotional behavior.

Grid cells are not the only medial entorhinal cells with projections to the hippocampus. Others include *head direction cells*, which respond primarily to the direction that the animal is facing (Figure 54–14A). Such cells were originally discovered in the presubiculum, another region of the parahippocampal cortex, but they exist also in the medial entorhinal cortex. Many entorhinal head direction cells also have grid-like firing properties. Like grid cells, such head direction cells are active when an animal traverses the vertices of a triangular grid in a two-dimensional environment. However, within each grid field, these cells fire only if the animal is facing a certain direction. Head direction cells and conjunctive grid and head direction cells are thought to provide directional information to the entorhinal spatial map.

Intermingled among grid cells and head direction cells is yet another type of spatially modulated cell, the *border cell* (Figure 54–14B). The firing rate of a border

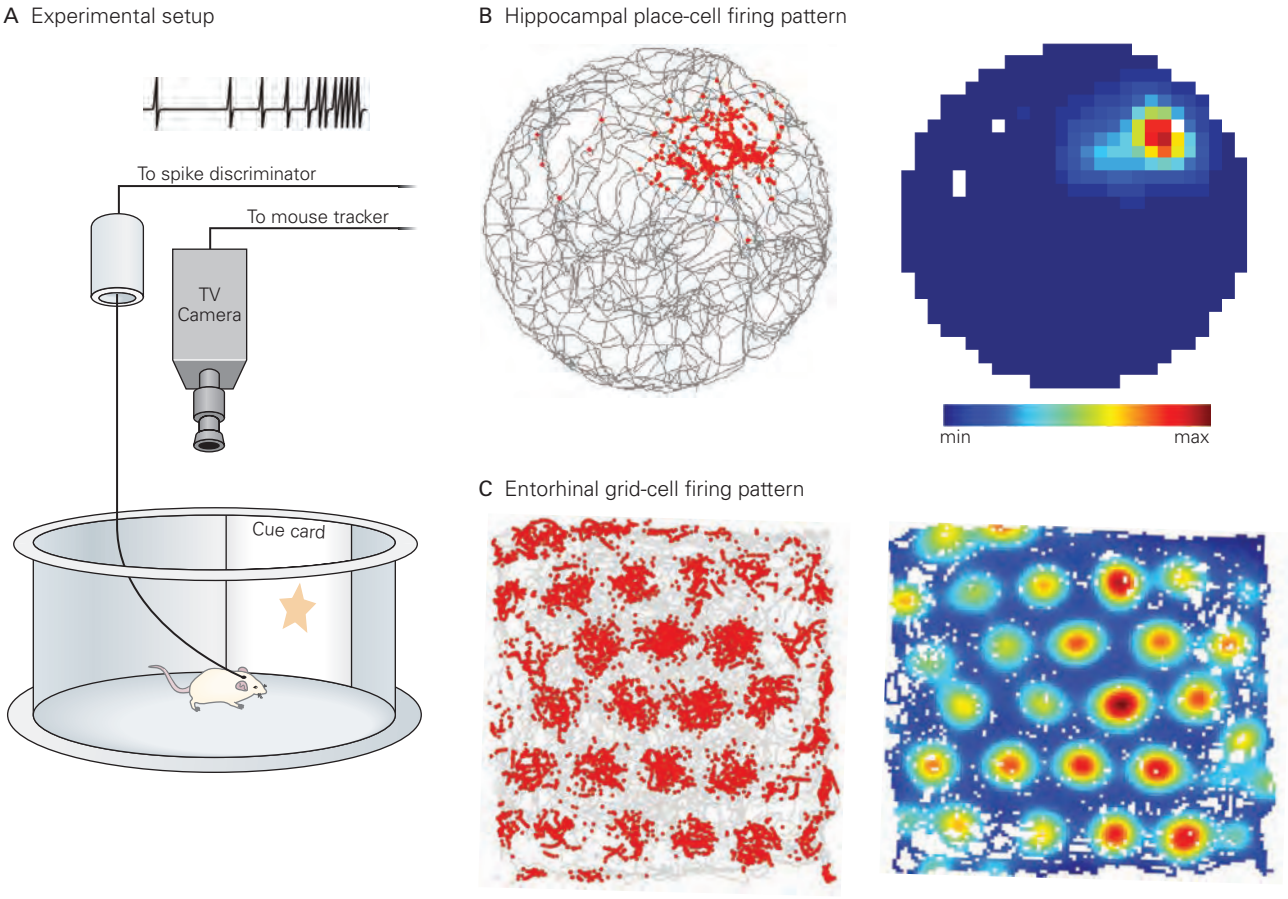

Figure 54–12 The firing patterns of cells in the hippocampus and medial entorhinal cortex signal the animal's location in its surroundings.

A. Electrodes implanted in the hippocampus of a mouse are attached to a recording cable, which is connected to an amplifier attached to a computer-based spike-discrimination program. The mouse is placed in an enclosure with an overhead TV camera that transmits to a device that detects the position of the mouse. The enclosure also contains a visual cue to orient the animal. Spikes in individual hippocampal pyramidal neurons ("place cells") are detected by a spike discrimination program. The firing rate of each cell is then plotted as a function of the animal's location in the cylinder. This information is visualized as a two-dimensional activity map for the cell, from which the cell's firing fields can be determined (shown in part **B**). (Adapted, with permission, from Muller, Kubie, and Ranck 1987. Copyright © 1987 Society for Neuroscience.)

B. Location-specific firing of a hippocampal place cell. A rat is running in a cylindrical enclosure similar to the one shown in part **A**. *Left*: The animal's path in the enclosure is shown in **gray**; firing locations of individual spikes are shown for a single place cell as **red dots**. *Right*: The firing rate of the same cell is color-coded (**blue** = low rate, **red** = high rate). In larger environments, place cells usually have more than one firing field but the fields have no apparent spatial relationship.

C. Spatial pattern of firing of an entorhinal grid cell in a rat during 30 minutes of foraging in a square enclosure 220 cm wide. The pattern shows typical periodic grid firing fields. *Left*: The trajectory of the rat is shown in **gray**; individual spike locations are shown as **red dots**. *Right*: Color-coded firing rate map for the grid cell to the left. Color coding as for the place cell in part **B**. (Adapted, with permission, from Stensola et al. 2012.)

cell increases whenever the animal approaches a local border of the environment, such as an edge or a wall. Border cells may help align the phase and orientation of grid cell firing to the local geometry of the environment. A similar role may be played by recently discovered object-vector cells—cells in medial entorhinal cortex that encode the animal's distance and direction relative to salient landmarks. A final entorhinal cell type is the *speed cell*. Speed cells fire proportionally to the running speed of the animal, irrespective of the animal's location or direction (Figure 54–14C). Together with head direction cells, speed cells can provide grid cells with information about the animal's instantaneous velocity, allowing the ensemble of active grid cells to be updated dynamically in accordance with a moving animal's changing location.

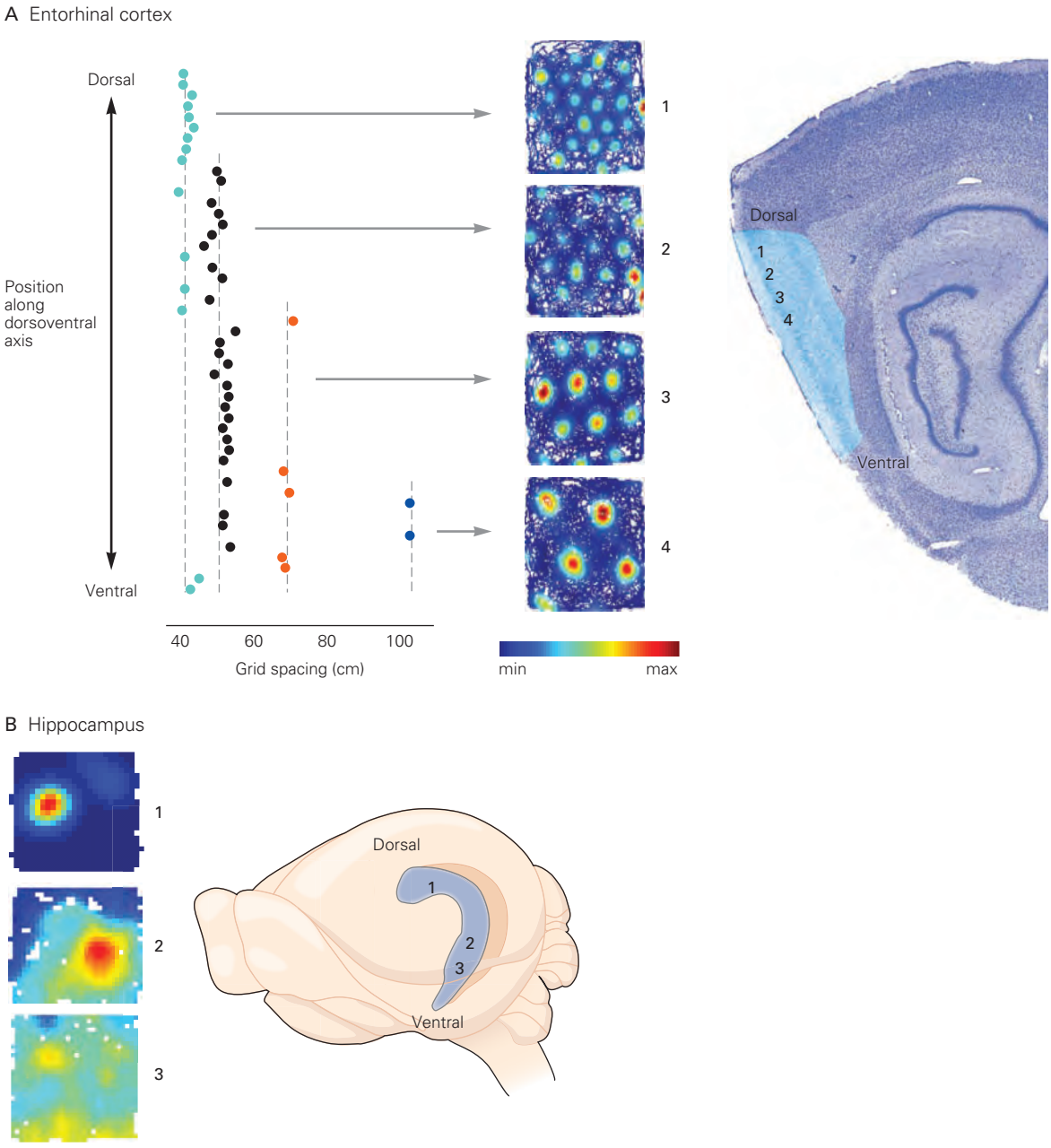

Figure 54–13 Grid fields and place fields expand in size as a function of neuronal location along the dorsoventral axis of the entorhinal cortex and hippocampus.

A. Topographical organization of grid scale in the entorhinal cortex. Grid spacing (distance between grid fields) was determined for 49 grid cells (colored dots) recorded in the same rat at successive dorsal to ventral levels in the medial entorhinal cortex (**green** area in the sagittal brain section on the right). **Dashed lines** indicate mean grid-spacing values, indicating that grid-spacing falls in one of four discrete modules, with points colored according to module. Firing rate maps for four of the cells are shown in the middle (similar to those of Figure 54–12C). Recording locations for these cells are indicated by numbers 1 to 4 to the right. (Adapted, with permission, from Stensola et al. 2012.)

B. Place fields from three different locations along the dorsoventral axis of the hippocampus. *Right*: Recording positions (numbers) in the hippocampal formation are shown at right. *Left*: Color-coded maps show the firing fields of each place cell at the recording locations. The field size expands in cells along the dorsoventral axis of the hippocampus. (Reproduced, with permission, from Kjelstrup et al. 2008.)

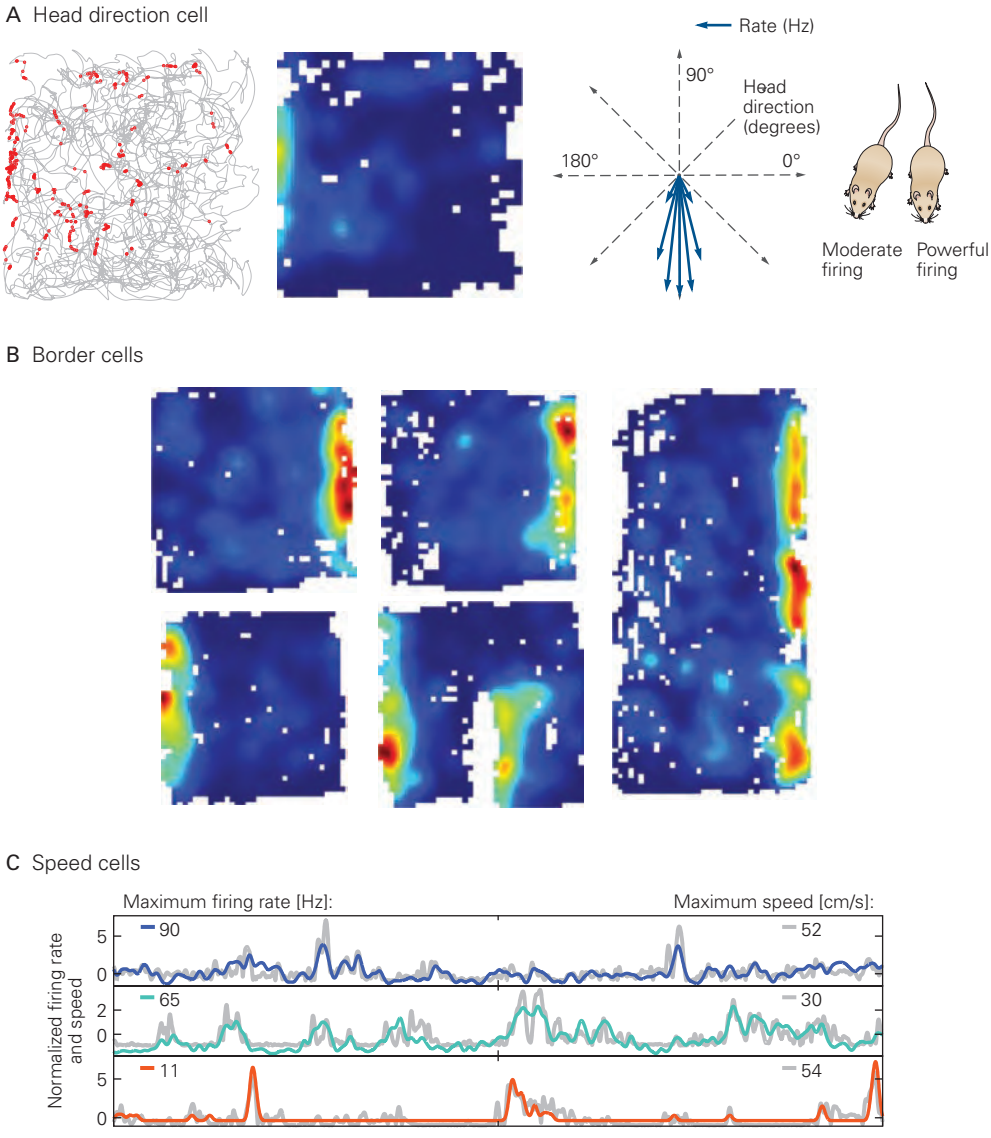

Figure 54–14 The medial entorhinal cortex contains several functional cell types tuned to distinct representations of an animal's navigation.

A. On the left is the trajectory of a rat exploring a 100-cm-wide square enclosure (**red dots** indicate firing locations). A color-coded firing rate map is also shown (color scale as in previous figures). Note that the cell's firing is scattered across the enclosure. The plot on the right shows the same cell's firing rate as a function of head direction, in polar coordinates. The cell fires selectively when the rat faces south, anywhere in the box. (Adapted, with permission, from Sargolini et al. 2006.)

B. Firing rate maps for a representative border cell in enclosures with different geometric shapes (**red** = high rate; **blue** = low rate). **Top row:** The firing field map follows the walls when the enclosure is stretched from a square (left and middle maps) to a rectangle (right map). **Bottom row:** The firing field of the same border cell in another environment. Introduction of a discrete wall (**white pixels**, right map) inside the square enclosure causes a new border field to appear to the right of the wall. (Reproduced, with permission, from Solstad et al. 2008.)

C. Speed cells. Traces show normalized firing rate (**colored traces**) and speed (**gray**) for seven representative entorhinal speed cells during 2 minutes of free foraging. Maximum values of firing rate and speed are indicated (left and right, respectively). Note high correspondence between speed and firing rate in these cells. (Reproduced, with permission, from Kropff et al. 2015.)

Taken together, these discoveries point to a network of functionally dedicated cells in the medial entorhinal cortex reminiscent of the feature detectors of the sensory cortices. The functional specificity of each cell type stems from the cell's representation of a specific feature of behavior. In this sense, the entorhinal cell types differ from cells in most other association cortices, which integrate information from many sources in ways that are not straightforward to decode.

What are the key differences between space-coding cells in the hippocampus and the medial entorhinal cortex? A striking property of all entorhinal cell types is the rigidity of their firing patterns. Ensembles of colocalized grid cells maintain the same intrinsic firing pattern regardless of context or environment. When a pair of grid cells has overlapping grid fields in one environment, their grid fields overlap also in other environments. If their grid fields are opposite, or "out of phase," they will be opposite in other environments as well. A similar rigidity is seen in head direction cells and border cells: Cells with similar orientation in one environment have similar orientations in other environments. Speed cells also maintain their unique tuning to running speed across environments. These findings suggest that the medial entorhinal cortex, or modules of this cortical circuit, may operate like a universal map of space that disregards the details of the environment. By doing so, the entorhinal map differs strongly from the place-cell map of the hippocampus.

The firing pattern of a hippocampal place cell is very sensitive to changes in the environment. The place fields of a given place cell in the hippocampus often switch to encode a completely different spatial locale when an animal's environment undergoes a major change, a process referred to as "remapping." Sometimes even minor changes in sensory or motivational inputs are sufficient to elicit remapping. The lack of correlation of hippocampal place maps for different environments (Figure 54–15) is thought to facilitate storage of discrete memories and minimize the risk that one memory will be confused with another, a process termed interference. For an explicit memory system like the hippocampus, with millions of events to be stored, this may be a huge advantage. For accurate and fast representation of an animal's position in space, as occurs in the medial entorhinal cortex, it may instead be beneficial to use a more stereotyped code that is less sensitive to environmental context or nonspatial sensory stimuli.

Place Cells Are Part of the Substrate for Spatial Memory

In addition to representing the animal's current location, place cells are thought to also store the memory of a location in position-related firing patterns that are evoked in the absence of the sensory inputs that originally elicited the firing. For example, as an animal sleeps after running repeated laps along a linear maze,

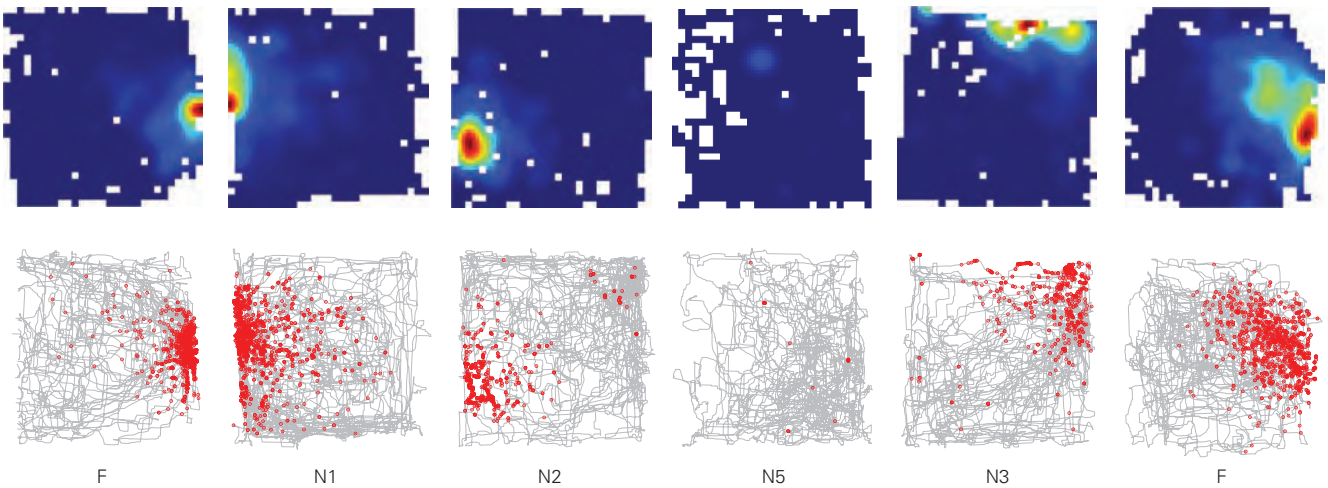

Figure 54–15 Place cells form independent maps for different environments. Rate maps showing firing patterns of a single hippocampal place cell in different square enclosures, each located in a different room. The rat was tested in one familiar (**F**) and 11 novel (**N**) rooms (recordings only shown for four of the novel rooms). The top row shows firing rate maps, whereas the bottom row shows trajectories of the animal's movement with firing locations in **red**. The cell was active only in some of the rooms (F, N1, N2, N3), where the firing locations were different. When the rat was returned to the familiar room at the end of the experiment, the cell's firing field had a similar location to the initial recording in the familiar room, indicating that a given cell's spatial firing pattern in the same environment is stable. (Adapted, with permission, from Alme et al. 2014.)

place cells spontaneously fire in the same order that they did in the maze, a phenomenon called "replay." Similarly, past trajectories and experiences may influence firing rates at particular locations in the environment. The ability of place cells to represent events and locations experienced in the past likely underlies the ability of the hippocampus to encode complex memories of events.

Once the firing pattern of a population of hippocampal neurons is formed for a given environment, how is it maintained? Because the place cells are the same hippocampal pyramidal neurons that undergo experimental LTP, a natural question is whether LTP is important. This question was addressed in experiments in mice in which LTP was disrupted.

In mice lacking the NR1 subunit of the NMDA receptor, hippocampal pyramidal neurons still fire in place fields despite the fact that LTP is blocked. Thus, this form of LTP is not required for the transformation of spatial sensory information into place fields. However, the place fields of the mutant mice are larger and fuzzier in outline than those in normal animals. In a second experiment with mutant mice, late LTP and long-term spatial memory were selectively disrupted by expression of a transgene that encodes a protein inhibitor of PKA. In these mice, place fields also form, but the firing patterns of individual cells are stable only for an hour or so (Figure 54–16). Thus, late LTP is required for long-term stabilization of place fields but not their formation.

To what degree do these maps of an animal's surroundings mediate explicit memory? In humans, explicit memory is defined as the conscious recall of facts about people, places, and objects. Although consciousness cannot be studied empirically in the mouse, selective attention, which is required for conscious recall, can be examined.

When mice are presented with different behavioral tasks, the long-term stability of place fields correlates strongly with the degree of attention required to

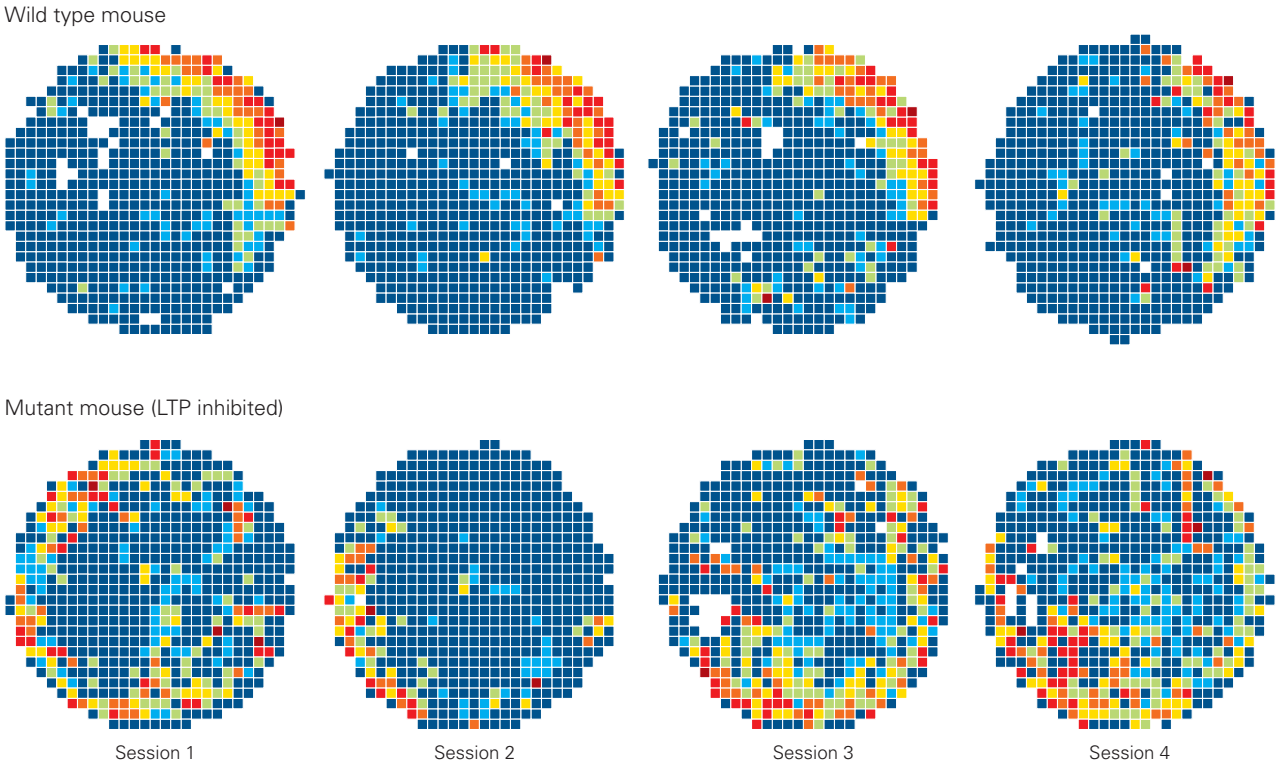

Figure 54–16 Disruption of long-term potentiation (LTP) degrades the stability of place field formation in the hippocampus. Color-coded firing rate maps (see Figure 54–12) show place fields recorded in four successive sessions from a single hippocampal pyramidal neuron in a wild type mouse and from a neuron in a mutant mouse that expresses the persistently active CaMKII (which inhibits the induction of LTP). Before each recording session, the animal is taken out of the enclosure and sometime later reintroduced into it. In each of the four sessions, the place field for the cell in the wild type animal is stable; the cell fires whenever the animal is in the upper right region of the enclosure. By contrast, the place field for the cell in the mutant mouse is unstable across the four sessions. (Reproduced, with permission, from Rotenberg et al. 1996.)

perform the task. When a mouse does not attend to the space it walks through, place fields form but are unstable after 3 to 6 hours. Animals with unstable place fields are unable to learn a spatial task. However, when a mouse is forced to attend to the space, for example, when trained to run to a specific location, the place fields are stable for days.

How does this attentional mechanism work? Studies in primates have shown the importance of the prefrontal cortex and the modulatory dopaminergic system during attention. Indeed, the formation of stable place fields in mice requires the activation of the dopamine D_1/D_5 type of receptor, which has been shown to enhance the formation of late LTP through production of cAMP and activation of PKA. These results suggest that long-term memory of a place field, rather than being a form of implicit memory that is stored and recalled without conscious effort, requires the animal to attend to its environment, as is the case for explicit memory in humans.

Disorders of Autobiographical Memory Result From Functional Perturbations in the Hippocampus

Our sense of identity is greatly dependent on our store of explicit autobiographical memories and our ability to recognize and navigate through familiar spatial environments. Neurological and psychiatric disorders that disrupt these abilities often occur as a result of changes in neural circuitry and plasticity mechanisms within the hippocampus and related regions in the temporal lobe.

There is now substantial evidence that the devastating memory loss associated with Alzheimer disease is associated with an accumulation of extracellular plaques of the protein fragment β-amyloid (Aβ) and intracellular neurofibrillary tangles of tau, a microtubule associated protein (Chapter 64). However, even before plaques and tangles are apparent, elevated levels of soluble Aβ and tau are thought to disrupt a number of cellular processes, particularly by reducing the magnitude of both early and late LTP at certain synapses. Mouse models of Alzheimer disease also show alterations in hippocampal place cell stability and population-level synchrony, which may contribute to memory loss and spatial disorientation. Changes in grid-cell function have also been observed in electrophysiological recordings in mouse disease models and in humans through functional magnetic resonance imaging studies. Although a number of preclinical studies have shown that agents that decrease levels of Aβ can rescue synaptic function and memory in rodents, so far these treatments have been less successful in treating patients with Alzheimer disease, perhaps because treatment must be initiated at early stages prior to irreversible synaptic changes.

Altered hippocampal function may also contribute to cognitive problems experienced by individuals with schizophrenia, including disturbances in working memory (Chapter 60). Recent studies using a genetic mouse model of schizophrenia report reduced synchrony between the hippocampus and prefrontal cortex associated with working memory. Furthermore, the place fields of place cells in the hippocampus CA1 region may be overly rigid in this mouse, suggesting that the ability of the hippocampus to distinguish different contexts may be impaired. Finally, a deficit in social memory in these mice has been linked to a reduction of parvalbumin-positive inhibitory neurons in the CA2 region; a similar loss of inhibitory neurons has been observed in postmortem brain tissue from individuals with schizophrenia and bipolar disorder.

Thus, studies of the hippocampus and related temporal lobe structures offer the great promise of providing fundamental insight into how explicit memories are stored and recalled and how functional alterations in these structures may contribute to neuropsychiatric disease. In turn, such insight may aid in the discovery of new treatments for these devastating disorders.

Highlights

1. Explicit memory has both a short-term component, termed working memory, and a long-term component. Both forms depend on the prefrontal cortex and hippocampus.
2. Long-term memory is thought to depend on activity-dependent long-term synaptic plasticity at synapses within the cortico-hippocampal circuit. A brief high-frequency train of tetanic stimulation leads to long-term potentiation (LTP) of excitatory synaptic transmission at each stage of the cortico-hippocampal circuit.
3. LTP at many synapses depends on calcium influx into the postsynaptic cell mediated by the *N*-methyl-D-aspartate (NMDA) type of glutamate receptor. This receptor acts as a coincidence detector: It requires both glutamate release and strong postsynaptic depolarization to conduct calcium.
4. The expression of LTP depends on either the insertion of the α-amino-3-hydroxy-5-methyl-4-isoxazolepropionic acid (AMPA) type of

glutamate receptors in the postsynaptic membrane or an increase in presynaptic glutamate release, depending on the type of synapse and intensity of tetanic stimulation.

5. LTP has both early and late phases. Early LTP depends on covalent modifications, whereas late LTP depends on new protein synthesis, gene transcription, and growth of new synaptic connections.
6. Pharmacological and genetic manipulations that disrupt LTP often lead to an impairment of long-term memory, indicating that LTP may provide an important cellular mechanism for memory storage.
7. Memories are stored by cell assemblies. LTP may be required for forming event-specific assemblies. Recall of memory may reflect reactivation of the same assemblies that were active during the original event.
8. The hippocampus encodes both spatial and nonspatial signals. Many hippocampal neurons act as place cells, firing action potentials when an animal visits a particular location in its environment.
9. The entorhinal cortex, the area of the cortex that provides most of the input to hippocampus, also encodes both nonspatial and spatial information. The medial portion of entorhinal cortex contains neurons, called grid cells, that fire when an animal crosses the vertices of a hexagonal grid-like lattice of spatial locales. Grid cells are organized into semi-independent semi-topographically organized modules with distinct grid frequencies. The entorhinal map also contains border cells, object-vector cells, head direction cells, and speed cells.
10. Within a grid-cell module, pairs of grid cells maintain firing relationships rigidly across environments and experiences, suggesting that grid cells form a universal map that is expressed similarly in all environments. In contrast, place cells in the hippocampus form maps that are plastic as they are completely uncorrelated between environments.
11. Neuropsychiatric disorders such as Alzheimer disease and schizophrenia have been associated with deficits in hippocampal and entorhinal synaptic function, place-cell properties, and learning and memory. Treatments aimed at restoring such function may yield new therapeutic approaches to disease.
12. Despite their clear differences, implicit (Chapter 53) and explicit memory storage rely on a common logic. Both activity-dependent presynaptic facilitation for storing implicit memory and associative long-term potentiation for storing explicit memory rely on the associative properties of specific proteins: Adenylyl cyclase activation in implicit memory requires neurotransmitter plus intracellular Ca^{2+}, whereas NMDA receptor activation in explicit memory requires glutamate plus postsynaptic depolarization. Such similarities indicate the fundamental importance of associative learning rules for memory storage.

Edvard I. Moser
May-Britt Moser
Steven A. Siegelbaum

Selected Reading

Basu J, Siegelbaum SA. 2015. The corticohippocampal circuit, synaptic plasticity, and memory. Cold Spring Harb Perspect Biol 7:a021733.

Bliss TV, Collingridge GL. 2013. Expression of NMDA receptor-dependent LTP in the hippocampus: bridging the divide. Mol Brain 6:5.

Frey U, Morris RG. 1991. Synaptic tagging and long-term potentiation. Nature 385:533–536.

Hafting T, Fyhn M, Molden S, Moser M-B, Moser EI. 2005. Microstructure of a spatial map in the entorhinal cortex. Nature 436:801–806.

Kessels HW, Malinow R. 2009. Synaptic AMPA receptor plasticity and behavior. Neuron 61:340–350.

Martin SJ, Grimwood PD, Morris RG. 2000. Synaptic plasticity and memory: an evaluation of the hypothesis. Annu Rev Neurosci 23:649–711.

Nicoll RA. 2017. A brief history of long-term potentiation. Neuron 93:281–290.

Rowland DC, Roudi Y, Moser MB, Moser EI. 2016. Ten years of grid cells. Annu Rev Neurosci 39:19–40.

Taube JS. 2007. The head direction signal: origins, and sensory-motor integration. Annu Rev Neurosci 30:181–207.

Tonegawa S, Pignatelli M, Roy DS, Ryan TJ. 2015. Memory engram storage and retrieval. Curr Opin Neurobiol 35: 101–109.

References

Abel T, Nguyen PV, Barad M, Deuel TAS, Kandel ER, Bourtchouladze R. 1997. Genetic demonstration of a role for PKA in the late phase of LTP and in hippocampal based long-term memory. Cell 88:615–626.

Alme CB, Miao C, Jezek K, Treves A, Moser EI, Moser M-B. 2014. Place cells in the hippocampus: eleven maps for eleven rooms. Proc Natl Acad Sci U S A 111:18428–18435.

Bliss TVP, Lømo T. 1973. Long-lasting potentiation of synaptic transmission in the dentate gyrus of the anesthetized rabbit following stimulation of the perforant path. J Physiol (Lond) 232:331–356.

Dudek SM, Bear MF. 1992. Homosynaptic long-term depression in area CA1 of hippocampus and effects of *N*-methyl-D-aspartate receptor blockade. Proc Natl Acad Sci U S A 89:4363–4367.

Fyhn M, Hafting T, Treves A, Moser M-B, Moser EI. 2007. Hippocampal remapping and grid realignment in entorhinal cortex. Nature 446:190–194.

Hebb DO. 1949. *The Organization of Behavior: A Neuropsychological Theory.* New York: Wiley.

Hitti FL, Siegelbaum SA. 2014. The hippocampal CA2 region is essential for social memory. Nature 508:88–92.

Høydal ØA, Skytøen ER, Andersson SO, Moser MB, Moser EI. 2019. Object-vector coding in the medial entorhinal cortex. Nature 568:400–404.

Huang Y-Y, Kandel ER. 1994. Recruitment of long-lasting and protein kinase A-dependent long-term potentiation in the CA1 region of hippocampus requires repeated tetanization. Learn Mem 1:74–82.

Kandel ER. 2001. The molecular biology of memory storage: a dialog between genes and synapses (Nobel Lecture). Biosci Rep 21:565–611.

Kjelstrup KB, Solstad T, Brun VH, et al. 2008. Finite scale of spatial representation in the hippocampus. Science 321:140–143.

Kropff E, Carmichael JE, Moser M-B, Moser EI. 2015. Speed cells in the medial entorhinal cortex. Nature 523:419–424.

Lisman J, Yasuda R, Raghavachari S. 2012. Mechanisms of CaMKII action in long-term potentiation. Nat Rev Neurosci 13:169–182.

Liu X, Ramirez S, Pang PT, et al. 2012. Optogenetic stimulation of a hippocampal engram activates fear memory recall. Nature 484:381–385.

Mayford M, Bach ME, Huang Y-Y, Wang L, Hawkins RD, Kandel ER. 1996. Control of memory formation through regulated expression of a CaMKII transgene. Science 274:1678–1683.

McHugh TJ, Blum KI, Tsien JZ, Tonegawa S, Wilson MA. 1996. Impaired hippocampal representation of space in CA1-specific NMDAR1 knockout mice. Cell 87:1339–1349.

McHugh TJ, Jones MW, Quinn JJ, et al. 2007. Dentate gyrus NMDA receptors mediate rapid pattern separation in the hippocampal network. Science 317:94–99.

Montgomery JM, Pavlidis P, Madison DV. 2001. Pair recordings reveal all-silent synaptic connections and the postsynaptic expression of long-term potentiation. Neuron 29:691–701.

Morgan SL, Teyler TJ. 2001. Electrical stimuli patterned after the theta-rhythm induce multiple forms of LTP. J Neurophysiol 86:1289–1296.

Muller RU, Kubie JL, Ranck JB Jr. 1987. Spatial firing patterns of hippocampal complex-spike cells in a fixed environment. J Neurosci 7:1935–1950.

Nakashiba T, Young JZ, McHugh TJ, Buhl DL, Tonegawa S. 2008. Transgenic inhibition of synaptic transmission reveals role of CA3 output in hippocampal learning. Science 319:1260–1264.

Nakazawa K, Quirk MC, Chitwood RA, et al. 2002. Requirement for hippocampal CA3 NMDA receptors in associative memory recall. Science 297:211–218.

Nicholls RE, Alarcon JM, Malleret G, et al. 2008. Transgenic mice lacking NMDAR-dependent LTD exhibit deficits in behavioral flexibility. Neuron 58:104–117.

O'Keefe J, Dostrovsky J. 1971. The hippocampus as a spatial map: preliminary evidence from unit activity in the freely-moving rat. Brain Res 34:171–175.

O'Keefe J, Nadel L. 1978. *The Hippocampus as a Cognitive Map*. Oxford: Clarendon Press.

Ramirez S, Liu X, Lin PA, et al. 2013. Creating a false memory in the hippocampus. Science 341:387–391.

Rotenberg A, Mayford M, Hawkins RD, Kandel ER, Muller RU. 1996. Mice expressing activated CaMKII lack low frequency LTP and do not form stable place cells in the CA1 region of the hippocampus. Cell 87:1351–1361.

Rumpel S, LeDoux J, Zador A, Malinow R. 2005. Postsynaptic receptor trafficking underlying a form of associative learning. Science 308:83–88.

Sacktor TC. 2011. How does PKMζ maintain long-term memory? Nat Rev Neurosci 12:9–15.

Sargolini F, Fyhn M, Hafting T, et al. 2006. Conjunctive representation of position, direction, and velocity in entorhinal cortex. Science 312:758–762.

Silva AJ, Stevens CF, Tonegawa S, Wang Y. 1992. Deficient hippocampal long-term potentiation in α-calcium-calmodulin kinase II mutant mice. Science 257:201–206.

Solstad T, Boccara CN, Kropff E, Moser M-B, Moser EI. 2008. Representation of geometric borders in the entorhinal cortex. Science 322:1865–1868.

Stensola H, Stensola T, Solstad T, Frøland K, Moser M-B, Moser EI. 2012. The entorhinal grid map is discretized. Nature 492:72–78.

Tang YP, Shimizu E, Dube GR, et al. 1999. Genetic enhancement of learning and memory in mice. Nature 401:63–69.

Taube JS, Muller RU, Ranck JB Jr. 1990. Head-direction cells recorded from the postsubiculum in freely moving rats. I. Description and quantitative analysis. J Neurosci 10:420–435.

Tsien JZ, Huerta PT, Tonegawa S. 1996. The essential role of hippocampal CA1 NMDA receptor-dependent synaptic plasticity in spatial memory. Cell 87:1327–1338.

Whitlock JR, Heynen AJ, Shuler MG, Bear MF. 2006. Learning induces long-term potentiation in the hippocampus. Science 313:1093–1097.

Zalutsky RA, Nicoll RA. 1990. Comparison of two forms of long-term potentiation in single hippocampal neurons. Science 248:1619–1624.

55

Language

Language is uniquely human and arguably our greatest skill and our highest achievement. Despite its complexity, all typically developing children master it by the age of 3. What causes this universal developmental phenomenon, and why are children so much better at acquiring a new language than adults? What brain systems are involved in mature language processing, and are these systems present at birth? How does brain damage produce the various disorders of language known as the aphasias?

For centuries, these questions about language and the brain have prompted vigorous debate among theorists. In the last decade, however, an explosion of information regarding language has taken us beyond the nature–nurture debates and beyond the standard view that a few specialized brain areas are responsible for language. Two factors have brought about this change.

First, functional brain imaging techniques such as positron emission tomography (PET), functional magnetic resonance imaging (fMRI), electroencephalography (EEG), and magnetoencephalography (MEG) have allowed us to examine activation patterns in the brain while a person carries out language tasks—naming objects or actions, listening to sounds or words, and detecting grammatical anomalies. The results of these studies reveal a far more complex picture than the one first proposed by Carl Wernicke in 1874. Moreover, structural

brain imaging techniques, such as diffusion tensor imaging (DTI), tractography, and quantitative magnetic resonance imaging (qMRI), have revealed a network of connections that link specialized language areas in the brain. These discoveries are taking us beyond previous, simpler views of the neural underpinnings of language processing and production that assumed involvement of only a few specific brain areas and connections.

Second, behavioral and brain studies of language acquisition show that infants begin to learn language earlier than previously thought, and in ways that had not been previously envisioned. Well before children produce their first words, they learn the sound patterns underlying the phonetic units, words, and phrase structure of the language they hear. Listening to language alters the infant brain early in development, and early language learning affects the brain for life.

Taken together, these advances are shaping a new view of the functional anatomy of language in the brain as a complex and dynamic network in the adult brain, one in which multiple, spatially distributed brain systems cooperate functionally via long-distance neural fascicles (axon fiber bundles). This mature network arises from the considerable brain structure and function in place at birth and develops in conjunction with powerful innate learning mechanisms responsive to linguistic experience. This new view of language encompasses not only its development and mature state, but also its dissolution when brain damage leads to aphasia.

Humans are not the only species to communicate. Passerine birds attract mates with songs, bees code the distance and direction to nectar by dancing, and monkeys signal a desire for sexual contact or fear at the approach of an enemy with coos and grunts. With language, we accomplish all of the above and more. We use language to provide information and express our emotions, to comment on the past and future, and to create fiction and poetry. Using sounds that have only an arbitrary association with the meanings they convey, we talk about anything and everything. No animal has a communication system that parallels human language either in form or in function. Language is the defining characteristic of humans, and living without it creates a totally different world, as patients with aphasia following a stroke experience so heartbreakingly.

Language Has Many Structural Levels: Phonemes, Morphemes, Words, and Sentences

What distinguishes language from other forms of communication? The key feature is a finite set of distinctive speech sounds or phonemes that can be combined with infinite possibilities. Phonemes are the building blocks of units of significance called morphemes. Each language has a distinctive set of phonemes and rules for combining them into morphemes and words. Words can be combined according to the rules of syntax into an infinite number of sentences.

Understanding language presents an interesting set of puzzles, ones that challenge supercomputers. The advent of virtual personal assistants such as Siri and Alexa, based on machine-learning algorithms, has allowed electronic devices to respond to select kinds of human utterances. However, we are still not conversing with computers. Fundamental advances will need to be made before humans can expect to have a conversation with a machine that resembles a conversation you can have with any 3-year-old. Machine-learning solutions do not accomplish their limited responses by mimicking human brain systems used for language, nor do they learn in the ways that human infants learn. Comparing machine-learning approaches (artificial intelligence) and human approaches is of theoretical and practical interest (Chapter 39) and is a hot topic for future research.

Language presents such a complex puzzle because it involves many functionally interconnected levels, starting at the most basic level with the sounds that distinguish words. For example, in English, the sounds /r/ and /1/ differentiate the words *rock* and *lock*. In Japanese, however, this sound change does not distinguish words because the /r/ and /l/ sounds are used interchangeably. Similarly, Spanish speakers distinguish between the words *pano* and *bano*, whereas English speakers treat the /p/ and /b/ sounds at the beginning of these words as the same sounds. Given that many languages use identical sounds but group them differently, children must discover how sounds are grouped to make meaningful distinctions in their language.

Phonetic units are subphonemic. As we have illustrated above with /r/ and /l/, these two sounds are both phonetic units, but their phonemic status differs in English and Japanese. In English, the two are phonemically distinct, meaning that they change the meaning of a word. In Japanese, /r/ and /l/ belong to the same phonemic category and are not distinct. Phonetic units are distinguished by subtle acoustic variations caused by the shape of the vocal tract called *formant frequencies* (Figure 55–1). The patterns and timing of formant frequencies distinguish words that differ in only one phonetic unit, such as the words *pat* and *bat*. In normal speech, formant changes occur very rapidly, on the order of milliseconds. The auditory system has to track these rapid changes in order for an individual

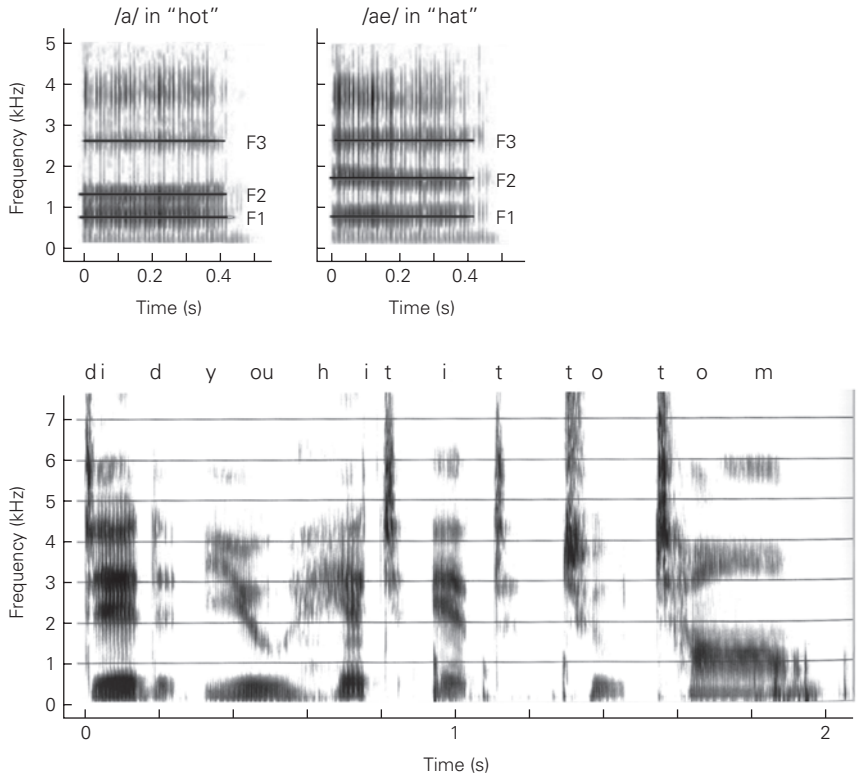

Figure 55–1 Formant frequencies. Formants are systematic variations in the concentration of energy at various sound frequencies and represent resonances of the vocal tract. They are shown here as a function of time in a spectrographic analysis of speech. The formant patterns for two simple vowels (/a/ and /ae/) spoken in isolation are distinguished by differences in formant 2 (F2). Formant patterns for the sentence "Did you hit it to Tom?" spoken slowly and clearly illustrate the rapid changes that underlie normal speech. (Data from Patricia Kuhl.)

to distinguish semantically different sounds and thus understand speech. Whereas in written language, spaces are customarily inserted between words, in speech, there are no acoustic breaks between words. Thus, speech requires a process that can detect words on the basis of something other than sounds bracketed by silence. Computers have a great deal of trouble recognizing words in the normal flow of speech.

Phonotactic rules specify how phonemes can be combined to form words. Both English and Polish use the phonemes /z/ and /b/, for example, but the combination /zb/ is not allowed in English, whereas in Polish, it is common (as in the name *Zbigniew*).

Morphemes are the smallest structural units of a language, best illustrated by prefixes and suffixes. In English, for example, the prefix *un* (meaning *not*) can be added to many adjectives to convey the opposite meaning (eg, *unimportant*). Suffixes often signal the tense or number of a word. For example, in English, we add *s* or *es* to indicate more than one of something (*pot* becomes *pots*, *bug* becomes *bugs*, or box becomes *boxes*). To indicate the tense of a regular verb, we add an ending to the word (eg, *play* can become *plays*, *playing*, and *played*). Irregular verbs do not follow the rule (eg, *go* becomes *went* rather than *goed* and *break* becomes *broke* rather than *breaked*). Every language has a different set of rules for altering the tense and number of a word.

Finally, to create language, words have to be strung together. *Syntax* specifies word and phrase order for a given language. In English, for example, sentences typically conform to a subject-verb-object order (eg, *He eats cake*), whereas in Japanese, it is typically subject-object-verb (eg, *Karewa keeki o tabenzasu*, literally *He cake eats*). Languages have systematic differences in the order of larger elements (noun phrases and verb phrases) of a sentence, and in the order of words within phrases, as illustrated by the difference between English and French noun phrases. In English, adjectives precede the noun (eg, *a very intelligent man*), whereas in French, most follow the noun (eg, *un homme tres intelligent*).

Language Acquisition in Children Follows a Universal Pattern

Regardless of culture, all children initially exhibit universal patterns of speech perception and production that do not depend on the specific language children hear (Figure 55–2). By the end of the first year, infants have learned through exposure to a specific language which phonetic units convey meaning in that language and to recognize likely words, even though they do not yet understand those words. By 12 months of age,

infants understand approximately 50 words and have begun to produce speech that resembles the native language. By the age of 3 years, children know approximately 1,000 words (by adulthood 70,000), create long adult-like sentences, and can carry on a conversation. Between 36 and 48 months, children respond to the differences between grammatical and ungrammatical sentences in an adult-like way, although tests using the most complex sentences indicate that the intricacies of grammar are not mastered until late childhood, between 7 and 10 years of age.

In the last half of the 20th century, debate on the nature and acquisition of language was ignited by a highly publicized exchange between a strong learning theorist and a strong nativist. In 1957, the behavioral psychologist B. F. Skinner proposed that language was acquired through learning. In his book *Verbal Behavior*, Skinner argued that language, like all animal behavior, was a learned behavior that developed in children as a function of external reinforcement and careful parental shaping. By Skinner's account, infants learn language as a rat learns to press a bar—through monitoring and management of reward contingencies. The nativist Noam Chomsky, writing a review of *Verbal Behavior*, took a very different position. Chomsky argued that traditional reinforcement learning has little to do with the ability of humans to acquire language. Instead, he proposed that every individual has an innate "language faculty" that includes a universal grammar and a universal phonetics; exposure to a specific language triggers a "selection" process for one language.

More recent studies of language acquisition in infants and children have clearly demonstrated that the kind of learning going on in infancy does not resemble that described by Skinner with its reliance on external shaping and reinforcement. At the same time, a nativist account such as Chomsky's, in which the language the infant hears triggers selection of one of several innate options, also does not capture the process.

The "Universalist" Infant Becomes Linguistically Specialized by Age 1

In the early 1970s, psychologist Peter Eimas showed that infants were especially good at hearing the acoustic changes that distinguish phonetic units in the world's languages. When speech sounds were acoustically varied in small equal steps to form a series ranging from one phonetic unit to another, say from /ba/ to /pa/, Eimas showed that infants could discern very slight acoustic changes at the locations in the series (the "boundary") where adults heard an abrupt change between the two phonetic categories, a phenomenon called *categorical perception.* Eimas demonstrated that infants could detect these slight acoustic changes at the phonetic boundary between two categories for phonetic units in languages they had never experienced, whereas adults have this ability only for phonetic units in languages in which they are fluent. Japanese people, for example, find it very difficult to hear the acoustic differences between the American English /r/ and /l/ sounds. Both are perceived as Japanese /r/, and as we have seen, Japanese speakers use the two sounds interchangeably when producing words.

Categorical perception was originally thought to occur only in humans, but in 1975, cognitive neuroscientists showed that it exists in nonhuman mammals such as chinchillas and monkeys. Since then, many studies have confirmed this result (as well as identifying species differences between mammals and birds). These studies suggest that the evolution of phonetic units was strongly influenced by preexisting auditory structures and capacities. Infants' ability to hear all possible differences in speech prepares them to learn any language; at birth, they are linguistic "universalists."

Speech production develops simultaneously with speech perception (Figure 55–2). All infants, regardless of culture, produce sounds that are universal. Infants "coo" with vowel-like sounds at 3 months of age and "babble" using consonant–vowel combinations at about 7 months of age. Toward the end of the first year, language-specific patterns of speech production begin to emerge in infants' spontaneous utterances. As children approach the age of 2 years, they begin to mimic the sound patterns of their native language. Chinese toddlers' utterances reflect the pitch, rhythm, and phonetic structure of Mandarin, and the utterances of British toddlers sound distinctly British. Infants develop an ability to imitate the sounds they hear others produce as early as 20 weeks of age. Very early in development, infants begin to master the subtle motor patterns required to produce their "mother tongue." Speech-motor patterns acquired in the earliest stages of language learning persist throughout life and influence the sounds, tempo, and rhythm of a second language learned later.

Right before the onset of first words, infants' abilities to discriminate native and nonnative phonetic units show a dramatic shift. At 6 months of age, infants can discriminate all phonetic units used in all languages, but by the end of the first year, they fail to discriminate phonetic changes that they successfully recognized 6 months earlier. At the same time, infants become significantly more adept at hearing native-language phonetic differences. For example, when American

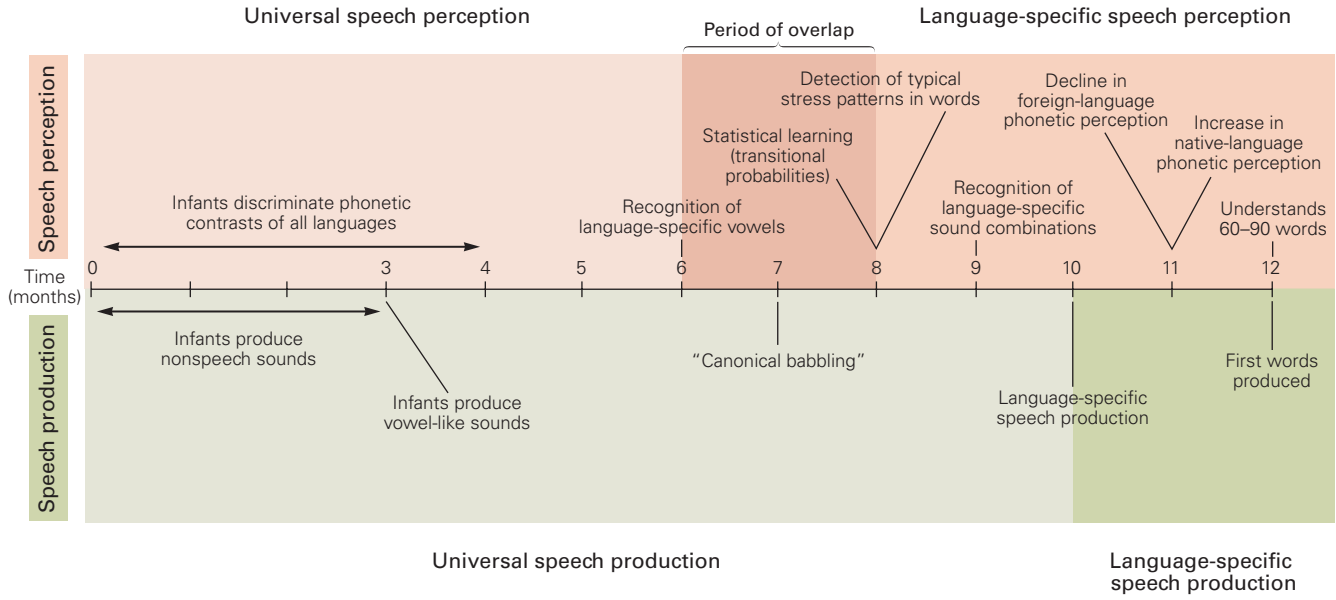

Figure 55–2 Language development progresses through a standard sequence in all children. Speech perception and production in children in various cultures initially follow a language-universal pattern. By the end of the first year of life, language-specific patterns emerge. Speech perception becomes language-specific before speech production. (Adapted, with permission, from Doupe and Kuhl 1999.)

and Japanese infants were tested between 6 and 12 months of age on the discrimination of the American English /r/ and /l/, American infants improved significantly between 8 and 10 months, whereas Japanese infants declined, suggesting that this is a sensitive period for phonetic learning. Moreover, infants' native-language discrimination ability at 7.5 months of age predicts the rate at which known words, sentence complexity, and mean length of utterance grow between 14 and 30 months.

If the second half of the first year is a sensitive period for speech learning, what happens when infants are exposed to a new language during this time? Do they learn? When American infants were exposed to Mandarin Chinese in the laboratory between 9 and 10 months of age, the infants learned if exposure occurred through interaction with a human being; infants exposed to the exact same material through television or audiotape with no live human interaction do not learn (Figure 55–3). When tested, the performance of the group exposed to live speakers was statistically indistinguishable from that of infants raised in Taiwan who had listened to Mandarin for 10 months. These results established that, at 9 months of age, the right kind of exposure to a foreign language permits phonetic learning, supporting the view that this is a sensitive period for such learning. The study also demonstrated, however, that social interaction plays a more significant role in learning than previously thought.

Further work showed that the degree to which infants track the eye movements of the tutor—watching what she is looking at as she names objects in the foreign language—correlates strongly with neural measures of phonetic and word learning after exposure to the new language, again implicating social brain areas in language learning.

An infant's ability to pick up social cues is essential to language learning, but what other skills promote learning during this critical period? Studies suggest that early exposure to speech induces an implicit learning process that increases native-language discrimination and reduces the infant's innate ability to hear distinctions between the phonetic units of all other languages. Infants are sensitive to the statistical properties of the language they hear. Distributional frequency patterns of sounds affect infants' speech learning by 6 months of age. Infants begin to organize speech sounds into categories based on *phonetic prototypes*, the most frequently occurring phonetic units in their language.

Six-month-old infants in the United States and Sweden were tested with prototypical English and Swedish vowels to examine whether infants discriminated acoustic variations in the vowels, like those that occur when different talkers produce them. By 6 months of age, the American and Swedish infants ignored

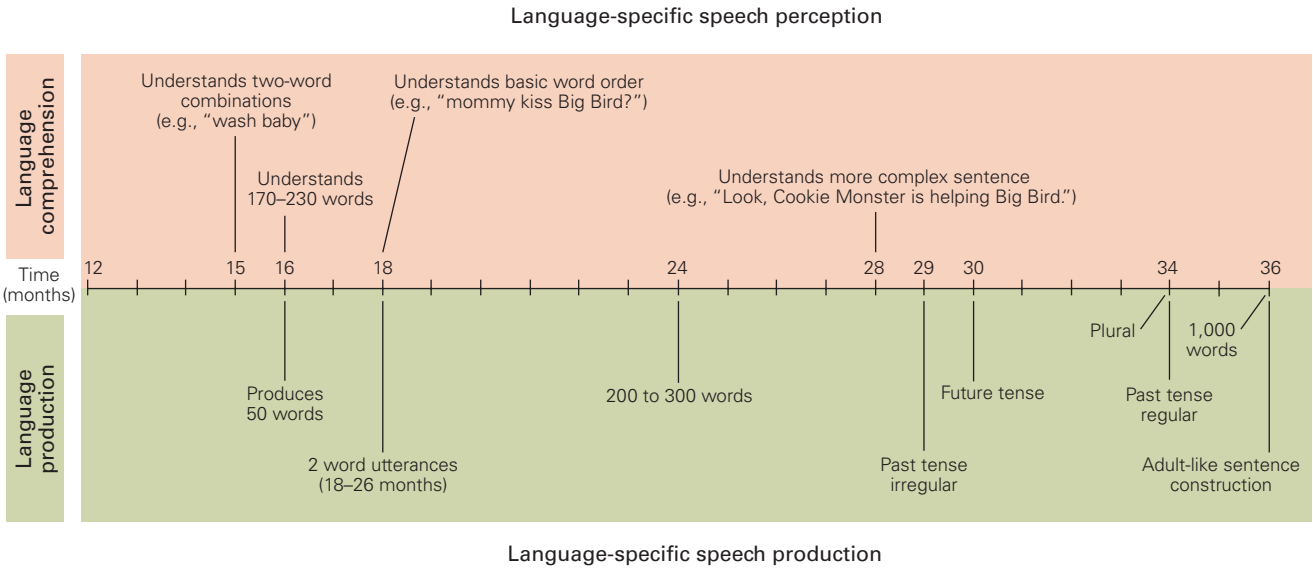

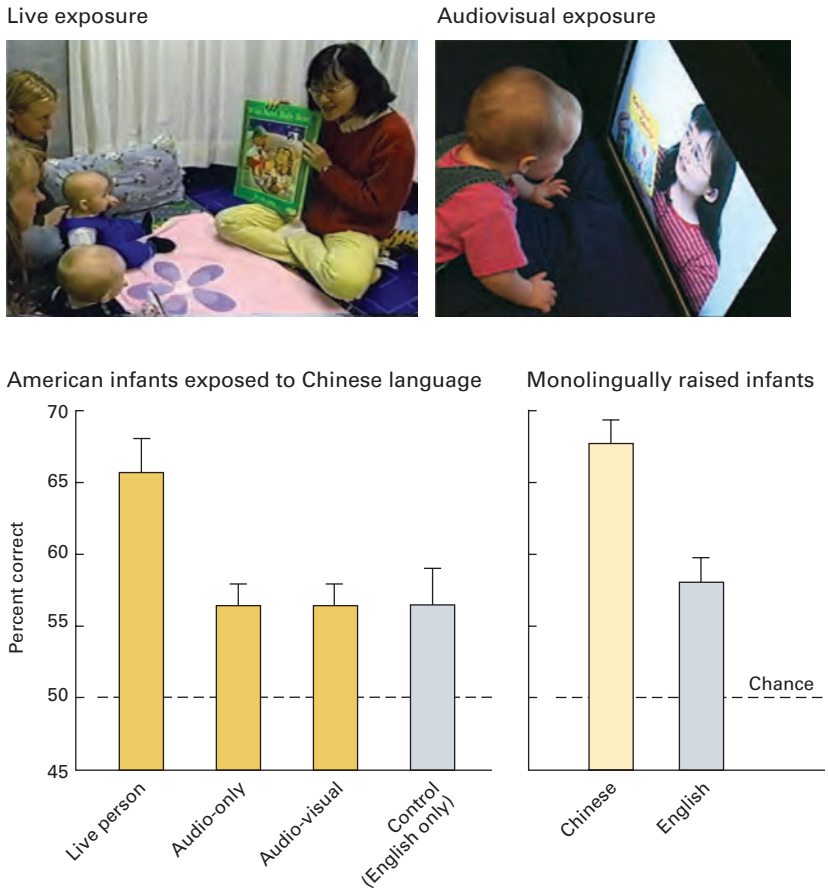

Figure 55–3 Infants can learn the phonemes of a nonnative language at 9 months of age. Three groups of American infants were exposed for the first time to a new language (Mandarin Chinese) in 12 25-minute sessions between the ages of 9 and 10.5 months. One group interacted with live native speakers of Mandarin; a second group was exposed to the identical material through television; and a third group heard tape recordings only. A control group had similar language sessions but heard only English. Performance on discrimination of Mandarin phonemes was tested in all groups after exposure (age 11 months). (Reproduced, with permission, from Kuhl, Tsao, and Liu 2003.)

Left. Only infants exposed to live Mandarin speakers discriminated the Mandarin phonemes. Infants exposed through TV or tapes showed no learning, and their performance was indistinguishable from that of control infants (who heard only English).

Right. The performance of American infants exposed to live Mandarin speakers was equivalent to that of monolingual Taiwanese infants of the same age who had experienced Mandarin from birth.

acoustic variations around native language prototypes but not with nonnative prototypes. Paul Iverson has shown that language experience alters the acoustic features to which speakers of different languages attend and distorts perception around category prototypes. This makes stimuli perceptually more similar to the prototype, which helps explain why 11-month-old Japanese infants fail to discriminate English /r/ and /1/ after experience with Japanese.

The Visual System Is Engaged in Language Production and Perception

Language is ordinarily communicated through an auditory-vocal channel, but deaf individuals communicate through a visual-manual channel. Natural signed languages, such as American Sign Language (Ameslan or ASL), are those invented by the deaf and vary across countries. Deaf infants "babble" with their hands at approximately the same time in development as hearing infants babble orally. Other developmental milestones, such as first words and two-word combinations, also occur on the developmental timetable of hearing infants.

Additional studies indicate that visual information of another kind, the face of the talker, is not only very helpful for communication but also affects the everyday perception of speech. We all experience the benefits of "lip reading" at noisy parties—watching speakers' mouths move helps us understand speech in a noisy environment. The most compelling laboratory demonstration that vision plays a role in everyday speech perception is the illusion that results when discrepant speech information is sent to the visual and auditory modalities. When subjects hear the syllable "ba" while watching a person pronounce "ga" they report hearing an intermediate articulation "da." Such demonstrations support the idea that speech categories are defined both auditorily and visually and that perception is governed by both sight and sound.

Prosodic Cues Are Learned as Early as In Utero

Long before infants recognize that things and events in the world have names, they memorize the global sound patterns typical in their language. Infants learn such prosodic cues as pitch, duration, and loudness changes. In English, for example, a strong/weak pattern of stress is typical—as in the words "BAby," "MOMmy," "TAble," and "BASEball"—whereas in some languages, a weak/strong pattern predominates. Six- and 9-month-old infants given a listening choice between words in English or Dutch show a listening preference for native-language words at the age of 9 months (but not at 6 months).

Prosodic cues can convey both linguistic information (differences in intonation and tone in languages such as Chinese) and paralinguistic information, such as the emotional state of the speaker. Even in utero fetuses learn prosodic cues by listening to their mother's speech. Certain sounds are transmitted through bone conduction to the womb; these are typically intense (above 80 dB), low-frequency sounds (particularly below 300 Hz, but as high as 1,000 Hz with some attenuation). Thus, the prosodic patterns of speech, including voice pitch and the stress and intonation patterns characteristic of a particular language and speaker, are transmitted to the fetus, while the sound patterns that convey phonetic units and words are greatly attenuated. At birth, infants demonstrate having learned this prosodic information by their preference for (1) the language spoken by their mothers during pregnancy, (2) their mother's voice over that of another female, and (3) stories with a distinct tempo and rhythm read out loud by the mother during the last 10 weeks of pregnancy.

Transitional Probabilities Help Distinguish Words in Continuous Speech

Seven- to 8-month-old infants learn to recognize words using the probability that one syllable will follow another. Such transitional probabilities between syllables within a word are high because the sequential order remains fixed. In the word *potato*, for example, the syllable "ta" always follows the syllable "po" (probability of 1.0). Between words, on the other hand, as between "hot" and "po" in the string *hot potato*, are much lower transitional probabilities.

Psychologist Jenny Saffran showed that infants treat phonetic units and syllables with high transitional probabilities as word-like units. In one experiment, infants heard 2-minute strings of pseudo-words, such as *tibudo*, *pabiku*, *golatu*, and *daropi*, without any acoustic breaks between them. They were then tested for recognition of these pseudo-words as well as new ones formed by combining the last syllable of one word with the two initial syllables of another word (such as *tudaro* formed from *golatu* and *daropi*). Infants recognized the original pseudo-words but not the new combinations they had not been previously exposed to, indicating that they used transitional probabilities to identify words.

These forms of learning clearly do not involve Skinnerian reinforcement. Caretakers do not manage the contingencies and gradually shape through reinforcement the statistical analyses performed by infants. Conversely, language learning by infants also

does not appear to reflect a process in which innately provided options are chosen based on language experience. Rather, infants learn language implicitly through detailed analysis of the patterns of statistical variation in the natural speech they hear and sophisticated analysis of information provided through social interaction (eg, eye gaze). The learning of these patterns in turn alters perception to favor the native language. In summary, both the statistical properties of language and the social cues provided during language interactions help infants learn. Language evolved to capitalize on the kinds of cues that infants are innately able to recognize. This mirrors the argument that the development of phonetic units was significantly influenced by the features of mammalian hearing, ensuring that infants would find it easy to discriminate phonemes, the fundamental units of meaning in language.

There Is a Critical Period for Language Learning

Children learn language more naturally and efficiently than adults, a paradox given that the cognitive skills of adults are superior. Why should this be the case?

Many consider language acquisition to be an example of a skill that is learned best during a critical period in development. Eric Lenneberg proposed that maturational factors at puberty cause a change in the neural mechanisms that control language acquisition. Evidence supporting this view comes from classic studies of Chinese and Korean immigrants to the United States who had been immersed in English at ages ranging from 3 to 39 years. When asked to identify errors in sentences containing grammatical mistakes, an easy task for native speakers, the responses of second-language learners declined with the age of arrival in the United States. A similar trend emerges when one compares individuals exposed to ASL from birth to those exposed between 5 and 12 years of age. Those exposed from birth were best at identifying errors in ASL, those exposed at age 5 were slightly poorer, and those exposed after the age of 12 years were substantially poorer.

What restricts our ability to learn a new language after puberty? Developmental studies suggest that prior learning plays a role. Learning a native language produces a neural commitment to detection of the acoustic patterns of that language, and this commitment interferes with later learning of a second language. Early exposure to language results in neural circuitry that is "tuned" to detect the phonetic units and prosodic patterns of that language. Neural commitment to native language enhances the ability to detect patterns based on those already learned (eg, phonetic learning supports word learning) but reduces the ability to detect patterns that do not conform. Learning the motor patterns required to speak a language also results in neural commitment. The motor patterns learned for one language (eg, lip rounding in French) can interfere with those required for pronunciation of a second language (eg, English) and thus can hinder efforts to pronounce the second language without an accent. Early in life, two or more languages can be easily learned because interference effects are minimal until neural patterns are well established.

Neurobiologist Takao Hensch has been working on identifying the chemical switches that open and close neurodevelopmental critical periods in learning, including those in animals and humans. Hensch has found that the neurotransmitter γ-aminobutyric acid (GABA) opens the critical period by inhibiting the firing of excitatory neurons, bringing them into balance with the firing of inhibitory neurons so as to create an excitatory–inhibitory (EI) balance. Studies testing this hypothesis in humans are difficult to conduct, but investigations on the infants of mothers who altered the EI balance of the fetus during pregnancy by taking psychotropic medications (serotonin reuptake inhibitors [SRIs]) for depression support the EI hypothesis. One of fluoxetine's off-target effects is to increase the sensitivity of some GABA receptors to GABA. When compared to infants of depressed mothers who were not exposed prenatally to SRIs and control mothers without depression or SRIs, infants exposed prenatally to SRIs showed an accelerated phonetic learning process, indicating that the well-established timing of the early transition in infants' phonetic perception can be altered.

We do not completely lose the ability later in life to learn a new language, but it is far more difficult. Regardless of the age at which learning begins, second-language learning is improved by a training regimen that mimics critical components of early learning—long periods of listening in a social context (immersion), the use of both auditory and visual information, and exposure to simplified and exaggerated speech resembling "parentese."

The "Parentese" Speaking Style Enhances Language Learning

Everyone agrees that when adults talk to their children they sound unusual. Discovered by linguists and anthropologists in the early 1960s as they listened to languages spoken around the world, "motherese" (or "parentese," as fathers produce it as well) is a special speaking style used when addressing infants and

young children. Parentese has a higher pitch, slower tempo, and exaggerated intonation contours, and is easily recognized. Compared to adult-directed speech, the pitch of the voice is increased on average by an octave both in males and in females. Phonetic units are spoken more clearly and are acoustically exaggerated, thus increasing the acoustic distinctiveness of phonetic units. Adults speaking to infants exaggerate just those features of speech that are critical to their native language. For example, when talking to their infants, Chinese mothers exaggerate the four tones in Mandarin that are critical to word meaning.

When given a choice, infants prefer listening to infant-directed rather than adult-directed speech. When infants are allowed to activate recordings of infant-directed or adult-directed speech by turning their head left or right, they will turn in whatever direction is required to turn on infant-directed speech.

Recent research by psychologists Nairan Ramirez-Esparza and Adrian Garcia-Sierra shows that the degree to which parentese is used in language spoken to infants at 11 and 14 months of age at home is strongly correlated with a child's language development by the age of 24 months and remains strongly correlated at the age of 36 months. This relationship holds for both monolingual and bilingual children. However, in bilingual children, early advances in the two languages differ depending on the language spoken in parentese. For example, Spanish-language parentese enhances a child's behavioral and neural responses to Spanish, but not English, and vice versa. Children raised in families in which the amount of language exposure and the use of parentese are low often show deficits in language and literacy by the time they enter school, and these deficits correlate with decreased functional activation in brain areas related to language.

Successful Bilingual Learning Depends on the Age at Which the Second Language Is Learned

How does the brain handle two languages? Behavioral data show that if exposure to two languages begins at birth, children reach the milestones of language at the same age as their monolingual peers—they coo, babble, and produce words at the benchmark ages seen in monolinguals. The idea that bilingual experience produces "confusion" has been debunked by studies that measure "conceptual" vocabulary, that is, word knowledge regardless of the language the child uses to express that knowledge. Older studies measured words in only one of the infants' two languages, and such word counts often showed decreased vocabulary when compared to monolinguals. Conceptual vocabulary scores show that bilingual children's vocabulary counts meet or exceed those of their monolingual peers.

Exposure to a second language after puberty shows limitations in the degree to which the new language can be learned. Whether subjects are tested on phonological rules, morphological endings, or syntax, the ability to learn a new language appears to decline every 2 years after the age of 7 years, indicating that acquisition of a second language after puberty is quite difficult.

Brain measures on bilingual infants reflect these behavioral data. Psychologist Naja Ferjan Ramirez used MEG to show that activation of the superior temporal area in 11-month-old infants exposed to two languages (English and Spanish) from birth is the same for the sounds of both languages and that brain responses to English sounds are equivalent to those of age-matched monolingual infants for English. Bilingual infants listening to speech also exhibit greater activation in the prefrontal cortex, a region mediating attention, when compared to monolingual infants; this finding is consistent with the fact that bilingual children (adults as well) demonstrate superior cognitive skills related to attention. Arguably, listening to two languages requires multiple shifts in attention to activate one language over another.

If a second language is acquired later in development, the age at which exposure occurs and the degree of eventual proficiency affect how the brain processes both languages. In "late" bilinguals (those who learned a second language after puberty), the second language and native language are processed in spatially separated areas in the language-sensitive left frontal region. In "early" bilinguals (those who acquired both languages as children), the two languages are processed in the same left frontal area.

A New Model for the Neural Basis of Language Has Emerged

Numerous Specialized Cortical Regions Contribute to Language Processing

The classical Wernicke-Geschwind neural model of language was based on the works of Broca (1861), Wernicke (1874), Lichtheim (1885), and Geschwind (1970). In the Wernicke-Geschwind model, acoustic cues contained in spoken words were processed in auditory pathways and relayed to Wernicke's area, where the meaning of a word was conveyed to higher brain structures. The arcuate fasciculus was assumed to

Table 55–1 Differential Diagnosis of the Main Types of Aphasia

Type of aphasia	Speech	Comprehension	Capacity for repetition	Other signs	Region affected
Broca	Nonfluent, effortful	Largely preserved for single words and grammatically simple sentences	Impaired	Right hemiparesis (arm > leg); patient aware of defect and can be depressed	Left posterior frontal cortex and underlying structures
Wernicke	Fluent, abundant, well articulated, melodic	Impaired	Impaired	No motor signs; patient can be anxious, agitated, euphoric, or paranoid	Left posterior superior and middle temporal cortex
Conduction	Fluent with some articulatory defects	Intact or largely preserved	Impaired	Often none; patient can have cortical sensory loss or weakness in right arm	Left superior temporal and supramarginal gyri
Global	Scant, nonfluent	Impaired	Impaired	Right hemiplegia	Massive left perisylvian lesion
Transcortical motor	Nonfluent, explosive	Intact or largely preserved	Intact or largely preserved	Sometimes right-sided weakness	Anterior or superior to Broca's area
Transcortical sensory	Fluent, scant	Impaired	Intact or largely preserved	No motor signs	Posterior or inferior to Wernicke's area

be a unidirectional pathway that brought information from Wernicke's area to Broca's area to enable speech production. Both Wernicke's and Broca's areas interacted with association areas. The Wernicke-Geschwind model formed the basis for a practical classification of the aphasias that clinical neurologists still use today (Table 55–1).

Advancements in basic and clinical neuroscience, the advent of more sophisticated functional brain imaging tools, advanced methods for structural brain imaging, and an increasing number of studies that combine brain and behavioral measures have resulted in the development of a new "dual-stream" model. In the dual-stream model, the processing of language is thought to involve large-scale networks that are composed of different brain areas, each with a specialized function, and the white matter tracts that connect them.

This dual-stream model of language processing is similar to the well-established "what" and "where" dual-stream model of the visual system. The existence of two cortical streams of auditory information processing was first postulated by Josef Rauschecker. Gregory Hickok and David Poeppel further elaborated the dual-stream model, and it has since been even further expanded upon by Angela Friederici as well as others studying the neurobiology of language. Figure 55–4 shows the basic components of the dual-stream model.

Compared to the classic Wernicke-Geschwind model, the dual-stream model comprises a larger number of cortical areas that are more widely distributed in the brain and adds critical connecting bidirectional pathways between specialized brain regions. These improvements in the model for language processing are due to advances in structural brain imaging techniques, such as DTI and diffusion-weighted imaging, which provide quantitative measures on a microscopic scale of the white matter in fascicles that connect various cortical areas and allow for the detailed delineation of neural tracts throughout the brain (tractography).

In the dual-stream model, initial spectrotemporal processing of auditory speech sounds is performed bilaterally in the auditory cortex. This information is then communicated to the posterior superior temporal gyrus bilaterally, where phonological-level processing occurs. Language processing then diverges into a dorsal "sensorimotor stream," which maps sound to articulation, and a ventral "sensory-conceptual" stream, which maps sound to meaning.

The bidirectional dorsal stream connects auditory speech information with motor plans that produce speech. The dorsal stream passes above the lateral ventricles and maps sounds onto articulatory representations, connecting regions of the inferior frontal lobe, premotor cortex, and insula (all involved in speech articulation) to the region that is classically recognized as Wernicke's area. It is considered to comprise two pathways: Dorsal pathway 1 connects the posterior

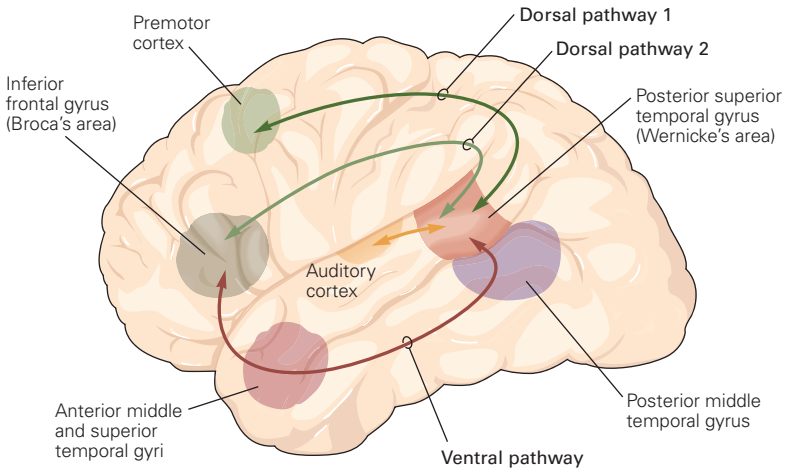

Figure 55–4 Dual-stream model of language processing. Temporal and spectral analyses of speech signals occur bilaterally in the auditory cortex followed by phonological analysis in the posterior superior temporal gyri (**yellow arrow**). Processing then diverges into two separate pathways: a dorsal stream that maps speech sounds to motor programs and a ventral stream that maps speech sounds to meaning. The dorsal pathway is strongly left hemisphere dominant and has segments that extend to the premotor cortex (dorsal pathway 1) and to the posterior inferior frontal cortex (dorsal pathway 2). The ventral pathway occurs bilaterally and extends to the anterior temporal lobe and the posterior inferior frontal cortex. (Adapted, with permission, from Hickok and Poeppel 2007, and Skeide and Friederici 2016.)

superior temporal gyrus to the premotor cortex, and dorsal pathway 2 connects the posterior superior temporal gyrus to Broca's area. Pathway 2 is involved in higher-order analysis of speech, such as discriminating subtle differences in meaning based on grammar and interpreting language using more complex concepts. The dorsal stream is strongly left hemisphere dominant. The arcuate fasciculus and the superior longitudinal fasciculus are white matter fiber tracts that mediate communication along the dorsal stream.

The ventral stream passes below the Sylvian fissure and is composed of regions of the superior and middle temporal lobes as well as regions of the posterior inferior frontal lobe. This stream conveys information for auditory comprehension, which requires transformation of the auditory signal to representations in a mental lexicon, a "brain-based dictionary" that links individual word forms to their semantic meaning. This stream comprises the inferior fronto-occipital fasciculus, the uncinate fasciculus, and the extreme fiber capsule system and is largely bilaterally represented.

The cortical brain regions included in the dual-stream model also interact with spatially distributed regions throughout both hemispheres of the brain that provide additional information crucial for language processing. These regions include the prefrontal cortex and cingulate cortices, which exert executive control and mediate attentional processes, respectively, as well as regions in the medial temporal, frontal, and parietal areas involved in memory retrieval.

The Neural Architecture for Language Develops Rapidly During Infancy

The study of language development in infancy requires a methodology that documents significant changes in behavior and links those changes to changes in brain function and morphology over time. Neuroimaging methods for the infant brain have improved substantially over the past decade, allowing for a detailed assessment of the progression of development of the specialized regions and structural connections required by the language network. For example, developmental neuroscientists have created models of the average infant brain and brain atlases for the infant brain at 3 and 6 months of age. These models indicate that brain structures essential to language processing in adulthood, such as the inferior frontal cortex, premotor cortex, and superior temporal gyrus, support speech processing in early infancy. Studies using DTI and tractography indicate that the arcuate fasciculus and the uncinate fasciculus connect language regions by 3 months of age.

The development of the neural substrates for language in 1- to 3-day-old infants has been studied in depth by Daniela Perani using fMRI and DTI. Perani's fMRI work reveals that listening to speech activates the infant superior temporal gyrus bilaterally and that in the left hemisphere this activation extends to the planum temporale, inferior frontal gyrus, and inferior parietal lobe. Perani's DTI studies of the same newborn infants demonstrate weak intrahemispheric connections, but strong connections between the hemispheres. Nevertheless, the ventral fiber tract connecting the ventral portion of the inferior frontal gyrus via the extreme fiber capsule system to the temporal cortex is evident in newborns and in both hemispheres. The dorsal pathway connecting the temporal cortex to the premotor cortex is also present in the newborns, although the dorsal tract that connects the temporal cortex to Broca's area in adults is not detectable in newborns. These early connections between sensory areas

and the premotor cortex are important because they may allow the sensory-to-motor mapping essential for the development of early imitation of the sounds and words of the language.

Jens Brauer and colleagues replicated these findings on the development of ventral and dorsal pathways in newborns, revealing the maturational primacy of the ventral connection linking temporal areas to the inferior frontal gyrus. Brauer also verified that the dorsal pathway connects the temporal and premotor cortex at birth and showed that the dorsal pathway to the inferior frontal gyrus develops later. Brauer used the same protocol with children 7 years of age and adults. In 7-year-olds, the dorsal pathway fully connects auditory areas and the inferior frontal gyrus, but in adults, it has more extensive and far-reaching connections.

EEG and MEG functional brain imaging studies on young infants as early as 2 months of age show that the inferior frontal and temporal cortices, implicated in both the classical and contemporary models of language processing, are activated bilaterally by speech—syllables, words, and sentences. This finding supports the hypothesis that left hemisphere specialization increases over time, with syllables showing dominant left hemisphere specialization at the end of the first year, words by the age of 2, and sentences in middle childhood.

EEG and MEG studies of young infants in which infants listen passively to native and nonnative syllables have produced results consistent with the behavioral transitions described earlier in this chapter. Several infant laboratories have shown that brain activity in response to speech, measured early in development, provides sensitive markers that predict language skills several years later. These studies hold promise for the eventual identification of brain measures in infants that indicate risk for developmental disabilities involving language, such as autism spectrum disorder, dyslexia, and specific language impairment. Early identification would allow earlier and more effective interventions for these impairments, improving outcomes for these children and their families.

Studies using functional MEG brain imaging of infants show that at 7 months of age, native and nonnative speech syllables activate not only superior temporal regions of the infant brain but also inferior frontal regions and the cerebellum, forging an association between speech patterns they hear and the motor plans they use to babble and imitate. By 12 months of age, language experience alters the patterns of activation in both sensory and motor brain regions.

Auditory activation becomes stronger for *native* sounds, indicating that brain areas have begun to become specialized for native language phonology. In contrast, motor activation in both Broca's area and the cerebellum is increased in response to *nonnative* sounds, because by 12 months infants have sufficient sensorimotor knowledge to imitate native sounds and some words and have linked stored auditory patterns (words like "cup" and "ball") to the motor plans necessary to produce them. But they cannot make the sensorimotor associations for foreign-language sounds and words because the necessary motor plans cannot be generated. Therefore, we see longer and more diffuse activation as infants struggle to create the motor plans for a sound or word they have never experienced. The importance of motor learning in language development is also shown by longitudinal whole-brain voxel-based morphometry studies of 7-month-old infants showing that gray matter concentrations in the cerebellum correlate with the number of words those infants can produce at 1 year of age.

Over the next 5 years, there is likely to be an explosive increase in brain studies focused on development of the language network. In a number of laboratories, these brain measures will be linked to behavioral measures, enabling the creation of models that delineate how language experience alters the infant brain to increase its specialization for the language or languages to which the child is exposed. The finding that the classic brain regions known to be part of the language network in adults—in particular, the left and right temporal cortices and the left inferior frontal cortex—are already activated by speech at birth recalls Chomsky's view of innate language capabilities.

The Left Hemisphere Is Dominant for Language

Current views of language processing agree that while the neural circuitry necessary for transforming speech sounds to meaning may be present in both hemispheres, the left hemisphere is more highly specialized for language processing. This left hemisphere dominance develops with maturation and learning.

Evidence from a variety of sources suggests that left hemisphere specialization for language develops rapidly in infancy. Word learning represents a case in point. Deborah Mills and her colleagues used event-related potentials to track development of the neural signals generated in response to words that children knew. Her studies showed that both age and language proficiency produce changes in the strength of the neural responses to known words, as well as a change in hemisphere dominance between 13 and 20 months of age. At the earliest age studied, known words activate a broad and bilaterally distributed

pattern across the brain. As infants approach 20 months and vocabulary grows, the activation pattern shifts to become left hemisphere dominant in the temporal and parietal regions. In late talkers, this shift is delayed to nearly 30 months. In 24-month-old children with autism, the degree to which this left hemisphere dominance is evident predicts children's linguistic, cognitive, and adaptive abilities at age 6.

Several studies show that immersion in a second language in adulthood produces growth in the superior longitudinal fasciculus, a white matter fiber tract that is important for language. Neuroscientist Ping Mamiya, collaborating with geneticist Evan Eichler, demonstrated, using DTI, that white matter integrity of the superior longitudinal fasciculus in the right hemisphere increased in Chinese college students in proportion to the number of days they spent in an English immersion class and decreased after immersion ended. Moreover, analysis of polymorphisms in the catechol-*O*-methyltransferase (*COMT*) gene showed an effect on this relationship—students with two of the variants demonstrated these changes, while students with the third variant showed no change in white matter properties with language experience.

There is great interest in brain studies investigating the selectivity of the brain mechanisms underlying language. Studies in the visual system by neuroscientist Nancy Kanwisher led to the suggestion that certain visual areas (the fusiform face area) are highly selective for particular stimuli, such as faces. Similar claims have been advanced for brain areas underlying speech analysis. For example, Kanwisher's group has proposed that Broca's area contains many subregions, each highly selective for particular levels of language. Additional studies on selectivity, particularly during development, will be the focus of future studies.

Helen Neville and Laura-Anne Pettito have shown that the left hemisphere is activated not only by auditory stimuli but also by visual stimuli that have linguistic significance. Deaf individuals process sign language in left hemisphere speech-processing regions. Such studies show that the language network processes linguistic information regardless of modality.

Prosody Engages Both Right and Left Hemispheres Depending on the Information Conveyed

Prosodic cues in language can be linguistic, conveying semantic meaning as tones do in Mandarin Chinese or Thai, as well as paralinguistic, expressing our attitudes and emotions. The pitch of the voice carries both kinds of information, and the brain's processing of each kind of information differs.

Emotional changes in pitch engage the right hemisphere, primarily the right frontal and temporal regions. Emotional information helps convey a speaker's mood and intentions, and this helps interpret sentence meaning. Patients with right hemisphere lesions often produce speech with inappropriate stress, timing, and intonation, and their speech sounds emotionally flat; they also frequently fail to interpret the emotional cues in others' speech.

Semantic changes in pitch involve a different pattern of brain activity, as demonstrated by neuroimaging studies. Jackson Grandour used a novel experimental design using Chinese syllables that carried either their native Chinese tone or the nonnative Thai tone. fMRI results for both Chinese and Thai speakers show higher activation in the left planum temporale for syllables carrying the native tone as opposed to nonnative tone (Figure 55–5). The right hemisphere did not show this double dissociation, supporting the view that language processing occurs in the left hemisphere even for auditory signals typically processed on the right.

Studies of the Aphasias Have Provided Insights into Language Processing

According to recent estimates, there are more than 795,000 strokes per year in the United States. Aphasia occurs in 21% to 38% of acute strokes and increases the probability of mortality and morbidity. In the past decade, the number of individuals with aphasia grew by more than 100,000 per year. Broca's aphasia, Wernicke's aphasia, and conduction aphasia compose the three classical models of clinical aphasia syndromes. Hickok and Poeppel describe each of these subtypes in the context of the dual-stream model. Accordingly, Broca's aphasia and conduction aphasia are due to sensorimotor integration problems related to damage to the dorsal stream of language processing, whereas Wernicke's aphasia, word deafness, and transcortical sensory aphasia are produced by damage to the ventral stream.

Broca's Aphasia Results From a Large Lesion in the Left Frontal Lobe

Broca's aphasia is a disorder of speech production, including impairments in grammatical processing, caused by lesions of the dorsal stream. When we speak, we rely on auditory patterns stored in the brain. Naming a cup when presented with coffee requires a

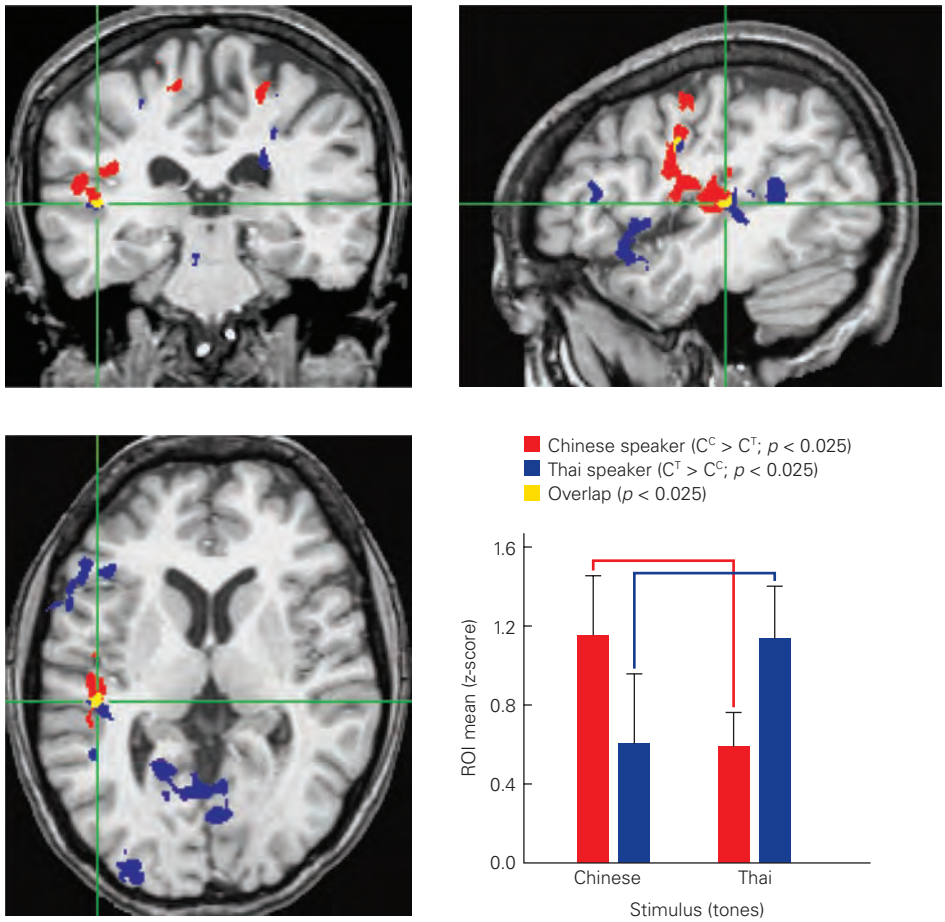

Figure 55–5 Brain activation for Chinese and Thai lexical tones revealed by functional magnetic resonance imaging. Language stimuli were composed of Chinese syllables superimposed with either Thai tones (C^T) or Chinese tones (C^C). Both native Chinese and native Thai speakers demonstrated a left hemisphere (**LH**) dominance when listening to their native tones. In the Chinese speakers, activation of the left hemisphere was stronger for Chinese tones, whereas in the Thai speakers, activation was stronger for Thai tones. Overlap for the two groups occurs in the left planum temporale and the ventral precentral gyrus. In the left planum temporale (**green crosshairs**), a double dissociation was found between tonal processing and language experience (bar charts). The right hemisphere (**RH**) did not show these effects. (*Top left*, coronal section; *top right*, sagittal section; *bottom left*, axial section.) (Abbreviation: **ROI**, region of interest.) (Adapted, with permission, from Xu et al. 2006. Copyright © 2005 Wiley-Liss, Inc.)

patient to connect the stored sensory pattern associated with the word "cup" to the motor plans required to hit that auditory target. With Broca's aphasia, the sensorymotor integration necessary for fluent speech production is damaged. Thus, speech is labored and slow, articulation is impaired, and the melodic intonation of normal speech is lacking (Table 55–2). Yet patients sometimes have considerable success at verbal communication because their selection of certain types of words, especially nouns, is often correct. By contrast, verbs and grammatical words such as prepositions and conjunctions are poorly selected or can be missing altogether. Another major sign of Broca's aphasia is a defect in the ability to repeat complex sentences.

Because most patients with Broca's aphasia give the impression of understanding conversational speech, the condition was initially thought to be a deficit of production only. But Broca's aphasics have difficulty comprehending sentences with meanings that depend mostly on grammar. Broca's aphasics can understand *The apple that the girl ate was green*, but have trouble understanding *The girl that the boy is chasing is tall*. This is because they can understand the first sentence without recourse to grammatical rules—girls eat apples but apples do not eat girls; apples can be green but girls cannot. However, they have difficulty with the second sentence because both girls and boys can be tall, and either can chase the other. To understand

Table 55–2 Examples of Spontaneous Speech Production and Repetition for the Primary Types of Aphasia

Type of aphasia	Spontaneous speech	Repetition
	Stimulus (Western Aphasia Battery picnic picture): What do you see in this picture?	Stimulus: "The pastry cook was elated."
Broca	"O, yea. Det's a boy an' a girl . . . an' . . . a . . . car . . . house . . . light po' (pole). Dog an' a . . . boat. 'N det's a . . . mm . . . a coffee, an' reading. Det's a mm . . . a . . . det's a boy . . . fishin'." (Elapsed time: 1 min 30 s)	"Elated."
Wernicke	"Ah, yes, it's, ah . . . several things. It's a girl . . . uncurl . . . on a boat. A dog . . . 'S is another dog . . . Uh-oh . . . long's . . . on a boat. The lady, it's a young lady. An' a man a They were eatin'. 'S be place there. This . . . a tree! A boat. No, this is a . . . It's a house. Over in here . . . a cake. An' it's, it's a lot of water. Ah, all right. I think I mentioned about that boat. I noticed a boat being there. I did mention that before. . . . Several things down, different things down . . . a bat . . . a cake . . . you have a . . ." (Elapsed time: 1 min 20 s)	"/I/ . . . no . . . In a fog."
Conduction	"Kay. I see a guy readin' a book. See a women /ka . . . he . . . /pourin' drink or something. An' they're sittin' under a tree. An' there's a . . . car behind that an' then there's a house behind th' car. An' on the other side, the guy's flyn' a /fait . . . fait/(kite). See a dog there an' a guy down on the bank. See a flag blowin' in the wind. Bunch of /hi . . . a . . . /trees in behind. An a sailboat on th' river, river . . . lake. 'N guess that's about all. . . . 'Basket there." (Elapsed time: 1 min 5 s)	"The baker was . . . What was that last word?" ("Let me repeat it: The pastry cook was elated.") "The baker-er was / vaskerin/ . . . uh . . ."
Global	(Grunt)	(No response)

the second sentence, it is necessary to analyze its grammatical structure, something that Broca's aphasics have difficulty doing.

Broca's aphasia results from damage to Broca's area (the left inferior frontal gyrus); the surrounding frontal fields; the underlying white matter, insula, and basal ganglia; and a small portion of the anterior superior temporal gyrus (Figure 55–6). A small sector of the insula, an island of cortex buried deep inside the cerebral hemisphere, can also be included among the neural correlates of Broca's aphasia. Broca's aphasics typically have no difficulty perceiving speech sounds or recognizing their own errors and no trouble in coming up with words. When damage is restricted to Broca's area alone or to its subjacent white matter, the result is the condition of Broca's area aphasia, a milder version of true Broca's aphasia, from which many patients are able to recover.

Wernicke's Aphasia Results From Damage to Left Posterior Temporal Lobe Structures

Wernicke's aphasics have difficulty comprehending the sentences uttered by others, and damage occurs in areas of the brain that subserve grammar, attention, and word meaning. Wernicke's aphasia can be caused by damage to different levels of the ventral stream, where auditory information is linked to word knowledge. It is usually caused by damage to the posterior section of the left auditory association cortex, although in severe cases, the middle temporal gyrus and white matter are involved (Figure 55–7).

Patients with Wernicke's aphasia can produce speech at a normal rate that sounds effortless, melodic, and quite unlike that of patients with Broca's aphasia. But speech can be unintelligible as well because Wernicke's aphasics often shift the order of individual sounds and sound clusters. These errors are called *phonemic paraphasias* (a paraphasia is substitution of an erroneous phoneme for the correct one). Even when individual sounds are normally produced, Wernicke's aphasics have great difficulty selecting words that accurately represent their intended meaning (known as a *verbal* or *semantic paraphasia*). For example, a patient might say *headman* when they mean president.

Conduction Aphasia Results From Damage to a Sector of Posterior Language Areas

Conduction aphasia, like Broca's aphasia, is thought to involve the dorsal stream. Speech production and auditory comprehension are less compromised than

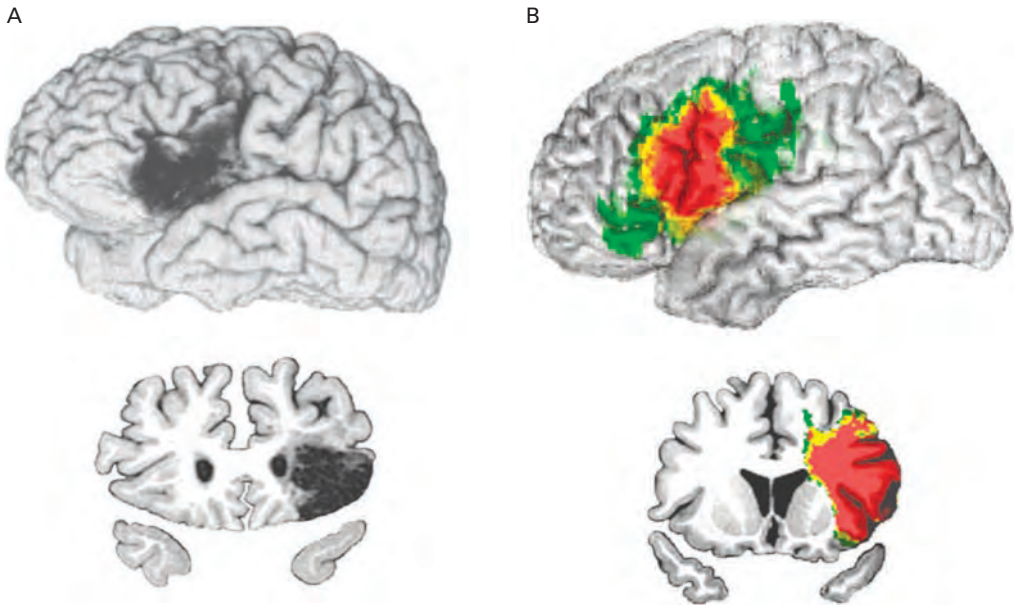

Figure 55–6 Sites of lesions in Broca's aphasia. (Images used with permission of Hanna and Antonio Damasio.)

A. Top: A three-dimensional magnetic resonance imaging (MRI) reconstruction of a lesion (infarction) in the left frontal operculum (**dark gray**) in a patient with Broca's aphasia. **Bottom:** A coronal MRI section of the same brain through the damaged area.

B. Top: A three-dimensional MRI overlap of lesions in 13 patients with Broca's aphasia (**red** indicates that lesions in five or more patients share the same pixels). **Bottom:** A coronal MRI section of the same composite brain image through the damaged area.

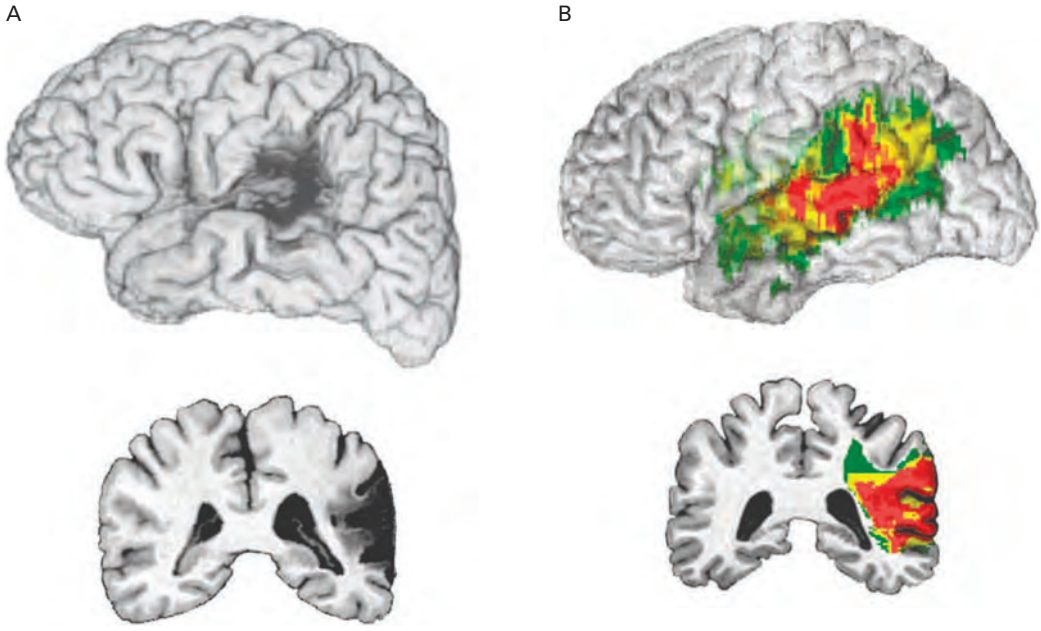

Figure 55–7 Sites of lesions in Wernicke's aphasia. (Images reproduced, with permission, from Hanna and Antonio Damasio.)

A. Top: Three-dimensional magnetic resonance imaging (MRI) reconstruction of a lesion (an infarction) in the left posterior and superior temporal cortex (**dark gray**) in a patient with Wernicke's aphasia. **Bottom:** Coronal MRI section of the same brain through the damaged area.

B. Top: Three-dimensional MRI overlap of lesions in 13 patients with Wernicke's aphasia obtained with the MAP-3 technique (**red** indicates that five or more lesions share the same pixels). **Bottom:** Coronal MRI section of the same composite brain image through the damaged area.

in the two other major aphasias, but patients cannot repeat sentences verbatim, cannot assemble phonemes effectively (and thus produce many phonemic paraphasias), and cannot easily name pictures and objects (Table 55–2).

Conduction aphasia is caused by damage to the left superior temporal gyrus and the inferior parietal lobe. The damage can extend to the left primary auditory cortex, the insula, and the underlying white matter. Large lesions in the Sylvian parietal temporal area, situated in the middle of the network of auditory and motor regions, are consistent with the idea that the damage occurs in the dorsal stream. Damage to left hemisphere auditory regions often produces speech production deficits, supporting the idea that sensory systems participate in speech production. Such lesions interrupt the interfaces linking auditory representations of words and the motor actions used to produce them. The damage compromises white matter (dorsal stream) and affects feedforward and feedback projections that interconnect areas of temporal, parietal, insular, and frontal cortex.

Global Aphasia Results From Widespread Damage to Several Language Centers

Patients with global aphasia are almost completely unable to comprehend language or formulate and repeat sentences, thus combining features of Broca's, Wernicke's, and conduction aphasias. Speech is reduced to a few words at best. The same word might be used repeatedly, appropriately or not, in a vain attempt to communicate an idea. Nondeliberate ("automatic") speech may be preserved, however. This includes stock expletives (which are used appropriately and with normal phonemic, phonetic, and inflectional structures), routines such as counting or reciting the days of the week, and the ability to sing previously learned melodies and their lyrics. Auditory comprehension is limited to a small number of words and idiomatic expressions.

Classic global aphasia involves damage to the inferior frontal and parietal cortices (as seen in Broca's aphasia), the auditory cortex and the insula (as seen in conduction aphasia), and the posterior superior temporal cortex (as seen in Wernicke's aphasia). Subcortical regions, such as the basal ganglia, are often affected as well. Such widespread damage is typically caused by a stroke in the region supplied by the middle cerebral artery. Weakness in the right side of the face and paralysis of the right limbs accompany classic global aphasia.

Transcortical Aphasias Result From Damage to Areas Near Broca's and Wernicke's Areas

Aphasias can be caused by damage not only to speech centers of the cortex but also to pathways that connect those components to the rest of the brain. Transcortical aphasia can be either motor or sensory. Patients with transcortical motor aphasia speak nonfluently, but they can repeat sentences, even very long sentences. Transcortical motor aphasia has been linked to damage to the left dorsolateral frontal area, a patch of association cortex anterior and superior to Broca's area, although there can be substantial damage to Broca's area itself. The left dorsolateral frontal cortex is involved in the allocation of attention and the maintenance of higher executive abilities, including the selection of words.

Transcortical motor aphasia can also be caused by damage to the left supplementary motor area, located high in the frontal lobe, directly in front of the primary motor cortex and buried mesially between the hemispheres. Electrical stimulation of the area in nonaphasic surgery patients causes the patients to make involuntary vocalizations or to be unable to speak, and functional neuroimaging studies have shown it to be activated during speech production. Thus, the supplementary motor area appears to contribute to the initiation of speech, whereas the dorsolateral frontal regions contribute to ongoing control of speech, particularly when the task is difficult.

Transcortical sensory aphasics have fluent speech, impaired comprehension, and great trouble naming things. These patients have deficits in semantic retrieval, without significant disruption of syntactic and phonological abilities.

Transcortical motor and sensory aphasias are caused by damage that spares the arcuate fasciculus and the dorsal stream. Transcortical aphasias are thus the complement of conduction aphasia, behaviorally and anatomically. Transcortical sensory aphasia appears to be caused by damage to the ventral stream, affecting parts of the junction of the temporal, parietal, and occipital lobes, which connect the perisylvian language areas with the parts of the brain responsible for word meaning.

Less Common Aphasias Implicate Additional Brain Areas Important for Language

Several other language-related regions in the cerebral cortex and subcortical structures, for example, the anterior temporal and inferotemporal cortex, have only recently become associated with language. Damage to the left temporal cortex causes severe and pure

naming defects—impairments of word retrieval without any accompanying grammatical, phonemic, or phonetic difficulty.

When the damage is confined to the left temporal pole, the patient has difficulty recalling the names of unique places and persons but not the names of common things. When the lesions involve the mid-temporal sector, the patient has difficulty recalling both unique and common names. Finally, damage to the left posterior inferotemporal sector causes a deficit in recalling words for particular types of items—tools and utensils—but not words for natural or unique things. Recall of words for actions or spatial relationships is not compromised (Figure 55–8).

The left temporal cortex contains neural systems that hold the key to retrieving words denoting various categories of things ("tools," "eating utensils"), but not words denoting actions ("walking," "riding a bicycle"). These findings were obtained not only from studies of patients with brain lesions resulting from

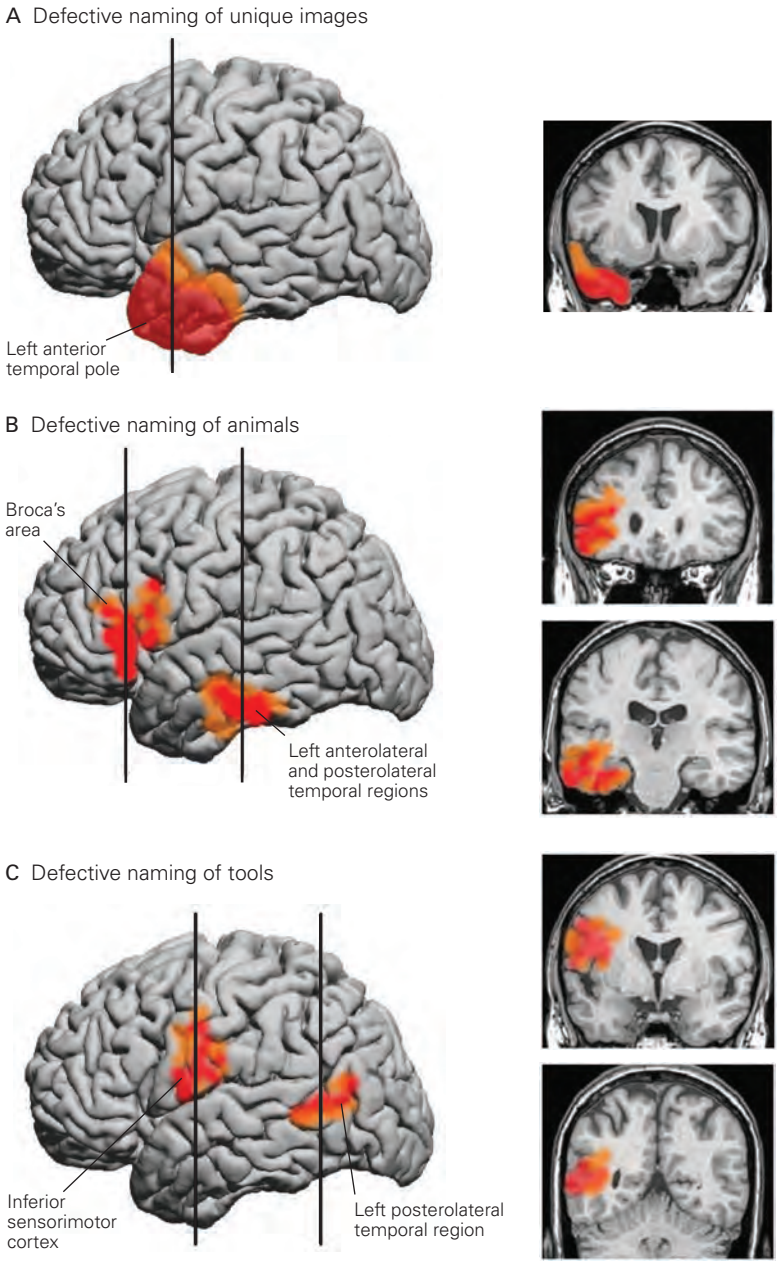

Figure 55–8 Regions of the brain other than Broca's and Wernicke's areas involved in language processing. Functional magnetic resonance imaging was used to study patients with selected brain lesions. (Images reproduced, with permission, from Hanna and Antonio Damasio.)

A. The region of maximal overlap of lesions associated with impaired naming of unique images, such as the face of a person, is the left anterior temporal pole.

B. The sites of maximal overlap of lesions associated with impaired naming of nonunique animals are the left anterolateral and posterolateral temporal regions as well as Broca's region.

C. The sites of maximal overlap of lesions associated with deficits in naming of tools are the left sensorimotor cortex and left posterolateral temporal cortex.

stroke, head injury, herpes encephalitis, and degenerative processes such as Alzheimer disease, but also from functional imaging studies of typical individuals and from electrical stimulation of these same areas of temporal cortex during surgery.

Areas of frontal cortex in the mesial surface of the left hemisphere, which include the supplementary motor area and the anterior cingulate region, play an important role in the initiation and continuation of speech. Damage in these areas impairs the initiation of movement (akinesia) and causes mutism, a complete absence of speech. In aphasic patients, the complete absence of speech is a rarity and is only seen during the very early stages of the condition. Patients with akinesia and mutism fail to communicate by words, gestures, or facial expression because the drive to communicate is impaired, not because the neural machinery of expression is damaged as in aphasia.

Damage to the left subcortical gray nuclei impairs grammatical processing in both speech and comprehension. The basal ganglia are closely interconnected with the frontal and parietal cortex and may have a role in assembling morphemes into words and words into sentences, just as they serve to assemble the components of a complex movement into a smooth action.

Highlights

1. Language exists at many levels, each of which has to be mastered during childhood—the elemental phonetic units (vowels and consonants) used to change the meaning of a word, the words themselves, word endings (morphemes) that change tense and pluralization, and the grammatical rules that allow words to be strung together to create sentences with meaning. By the age of 3, young children, regardless of the language(s) they are learning, have mastered all levels and can carry on a conversation with an adult. No artificially intelligent machine can yet duplicate this feat.
2. The learning strategies used by children to master language under 1 year of age are surprising. Language learning proceeds as infants (1) exploit the statistical properties of speech (distributional frequency patterns of sounds to detect relevant phonetic units and transitional probabilities between adjacent syllables to detect likely words), and (2) exploit the social context in which language occurs by following the eye movements of adults as they refer to objects and actions to learn word–object and word–action correspondences. At early ages, natural language learning requires a social context and social interaction. Infants' strategies are not well described by Skinnerian operant conditioning or by Chomsky's innate representation and selection based on experience. Instead, powerful implicit learning mechanisms that operate in social contexts vault infants forward from the very earliest months of life.
3. Infants' speech production and speech perception skills are "universal" at birth. In speech perception, infants discriminate all sounds used to distinguish words across all languages until the age of 6 months. By 12 months, discrimination for native-language sounds has dramatically increased, whereas discrimination of foreign-language sounds decreases. Production is initially universal as well and becomes language specific by the end of the first year. By the age of 3, infants know 1,000 words. Mastery of grammatical structure in complex sentences continues until the age of 10. Future work will advance the field by linking the detailed behavioral milestones that now exist to functional and structural brain measures to show how the brain's network for language is shaped as a function of language experience.
4. A new "dual-stream" model of language has emerged based on advances in functional neural imaging and structural brain imaging over the past decade. The new model bears similarities to the dual-stream model for the visual system. The dual-stream model for language goes beyond the classic Wernicke-Geschwind model by showing that numerous brain regions and the neural pathways that connect them support sound-to-meaning (ventral) and sound-to-articulation (dorsal) pathways. Refinement in the model will continue as additional studies show relationships between behavioral and brain measures. Future studies will integrate structural and functional brain measures, genetic measures, and behavioral assessments of language processing and of learning, including second language learning in adulthood.
5. Studies on the infant brain reveal a remarkably well-developed set of brain structures and pathways by 3 to 6 months of age. Structural DTI reveals a fully formed ventral pathway at birth and a dorsal pathway that links auditory areas to premotor, but not Broca's, area at birth. EEG and MEG brain imaging studies mirror the transition in phonetic perception between 6 and 12 months of age, a "critical period" for sound learning. MEG

brain scans at this period reveal the co-activation of auditory and motor centers when infants hear speech and show changes in both sensory and motor brain areas as a function of experience. The data indicate that dorsal pathways are sufficiently well formed in the first year to support sensory-to-motor connections and imitation learning during this period.

6. Hemispheric specialization generally increases with age and language experience, with initial representation of the areas and pathways represented bilaterally and dominance emerging with language experience. There are differences in the degree of lateralization, however, for various levels of language. The dorsal stream, which mediates auditory-motor representations of speech, is more left lateralized than the ventral stream, which mediates auditory-conceptual representations of words.
7. The classical aphasias—Broca's, Wernicke's, and conduction aphasia—are well described within the context of the dual-stream model of language. Broca's aphasia, with its emphasis on the inability to produce speech but relatively good speech understanding, is seen as a dorsal stream deficit, whereas Wernicke's aphasia, with its emphasis on speech comprehension deficits, is seen as a ventral stream deficit. Conduction aphasia, like Broca's, is viewed as caused by a dorsal stream deficit, with damage that encompasses auditory and motor regions. Future research on aphasia will benefit from additional studies of functional and structural damage that can be combined with detailed behavioral protocols.
8. Future studies will allow detailed comparisons between human and nonhuman brains to reveal the structures and pathways that are uniquely human and subserve language. Future work will also focus on the degree to which language structures in humans are selectively activated by speech as opposed to other complex auditory sounds and whether adult-level selectivity is present early in development.
9. Human language represents a unique aspect of human cognitive achievement. Understanding the brain systems that allow this cognitive feat in nearly all children, and especially the discovery of biomarkers that identify children who are at risk for developmental disorders of language, will advance brain science and be beneficial for society. Behavioral studies now allow us to connect the dots with regard to how early language experience is linked to advanced language development by the time children enter school. This may lead to language interventions that improve outcomes for all children.

Patricia K. Kuhl

Selected Reading

Brauer J, Anwander A, Perani D, Friederici AD. 2013. Dorsal and ventral pathways in language development. Brain Lang 127:289–295.

Buchsbaum BR, Baldo J, Okada K, et al. 2011. Conduction aphasia, sensory-motor integration, and phonological short-term memory—an aggregate analysis of lesion and fMRI data. Brain Lang 119:119–128.

Chomsky N. 1959. A review of B. F. Skinner's "Verbal Behavior." Language 35:26–58.

Damasio H, Tranel D, Grabowski TJ, Adolphs R, Damasio AR. 2004. Neural systems behind word and concept retrieval. Cognition 92:179–229.

Doupe A, Kuhl PK. 1999. Birdsong and human speech: common themes and mechanisms. Annu Rev Neurosci 22:567–631.

Gopnik A, Meltzoff AN, Kuhl PK. 2001. *The Scientist in the Crib: What Early Learning Tells Us About the Mind*. New York: HarperCollins.

Hickok G, Poeppel D. 2007. The cortical organization of speech processing. Nat Rev Neurosci 8:393–402.

Iverson P, Kuhl PK, Akahane-Yamada R, et al. 2003. A perceptual interference account of acquisition difficulties for non-native phonemes. Cognition 87:B47–B57.

Kuhl PK. 2004. Early language acquisition: cracking the speech code. Nat Rev Neurosci 5:831–843.

Kuhl PK, Rivera-Gaxiola M. 2008. Neural substrates of language acquisition. Annu Rev Neurosci 31:511–534.

Kuhl PK, Tsao F-M, Liu H-M. 2003. Foreign-language experience in infancy: effects of short-term exposure and social interaction on phonetic learning. Proc Natl Acad Sci U S A 100:9096–9101.

Kuhl PK, Williams KA, Lacerda F, Stevens KN, Lindblom B. 1992. Linguistic experience alters phonetic perception in infants by 6 months of age. Science 255:606–608.

Perani D, Saccuman MC, Scifo P, et al. 2011. Neural language networks at birth. Proc Natl Acad Sci U S A 108:16056–16061.

Pinker S. 1994. *The Language Instinct.* New York: William Morrow.

Skeide MA, Friederici AD. 2016. The ontogeny of the cortical language network. Nat Rev Neurosci 17:323–332.

References

Berwick RC, Friederici AD, Chomsky N, Bolhuis JJ. 2013. Evolution, brain, and the nature of language. Trends Cogn Sci 17:89–98.

Broca P. 1861. Remarques sur le siege de la faculte du langage articule, suivies d'une observation d'aphemie (perte de la parole). Bull Societe Anatomique de Paris 6:330–357.

Buchsbaum BR, Baldo J, Okada K, et al. 2011. Conduction aphasia, sensory-motor integration, and phonological short-term memory: an aggregate analysis of lesion and fMRI data. Brain Lang 119:119–128.

Burns TC, Yoshida KA, Hill K, Werker JF. 2007. The development of phonetic representation in bilingual and monolingual infants. App Psycholing 28:455–474.

Damasio AR, Damasio H. 1992. Brain and language. Sci Am 267:88–109.

Damasio AR, Tranel D. 1993. Nouns and verbs are retrieved with differently distributed neural systems. Proc Natl Acad Sci U S A 90:4957–4960.

Dronkers NF, Baldo JV. 2009. Language: aphasia. In: LR Squire (ed). *Encyclopedia of Neuroscience* (Vol. 5), pp. 343–348. Oxford: Academic Press.

Dubois J, Hertz-Pannier L, Dehaene-Lambertz G, Cointepas Y, Le Bihan D. 2006. Assessment of the early organization and maturation of infants' cerebral white matter fiber bundles: a feasibility study using quantitative diffusion tensor imaging and tractography. Neuroimage 30: 1121–1132.

Eimas PD, Siqueland ER, Jusczyk P, Vigorito J. 1971. Speech perception in infants. Science 171:303–306.

Fedorenko E, Duncan J, Kanwisher N. 2012. Language-selective and domain-general regions lie side by side within Broca's area. Curr Biol 22:2059–2062.

Ferjan Ramirez N, Ramirez RR, Clarke M, Taulu S, Kuhl PK. 2017. Speech discrimination in 11-month-old bilingual and monolingual infants: a magnetoencephalography study. Dev Sci 20:e12427.

Flege JE. 1995. Second language speech learning: theory, findings, and problems. In: W Strange (ed). *Speech Perception and Linguistic Experience*, pp. 233–277. Timonium, MD: York Press.

Flege JE, Yeni-Komshian GH, Liu S. 1999. Age constraints on second-language acquisition. J Mem Lang 41:78–104.

Friederici AD. 2009. Pathways to language: fiber tracts in the human brain. Trends Cog Sci 13:175–181.

Garcia-Sierra A, Ramirez-Esparza N, Kuhl PK. 2016. Relationships between quantity of language input and brain responses in bilingual and monolingual infants. Int J Psychophysiol 110:1–17.

Geschwind N. 1970. The organization of language and the brain. Science 170:940–944.

Golfinopoulos E, Tourville JA, Guenther FH. 2010. The integration of large-scale neural network modeling and functional brain imaging in speech motor control. Neuroimage 52:862–874.

Hickok G, Okada K, Serences JT. 2009. Area Spt in the human planum temporale supports sensory-motor integration for speech processing. J Neurophysiol 101:2725–2732.

Johnson J, Newport E. 1989. Critical period effects in second language learning: the influence of maturational state on the acquisition of English as a second language. Cognit Psychol 21:60–99.

Knudsen EI. 2004. Sensitive periods in the development of the brain and behavior. J Cogn Neurosci 16:1412–1425.

Kuhl PK. 2000. A new view of language acquisition. Proc Natl Acad Sci U S A 97:11850–11857.

Kuhl PK, Andruski J, Christovich I, et al. 1997. Cross-language analysis of phonetic units in language addressed to infants. Science 277:684–686.

Lenneberg E. 1967. *Biological Foundations of Language*. New York: Wiley.

Lesser RP, Arroyo S, Hart J, Gordon B. 1994. Use of subdural electrodes for the study of language functions. In: A Kertesz (ed). *Localization and Neuro-Imaging in Neuropsychology*, pp. 57–72. San Diego: Academic Press.

Liu H-M, Kuhl PK, Tsao F-M. 2003. An association between mothers' speech clarity and infants' speech discrimination skills. Dev Sci 6:Fl–F10.

Mamiya PC, Richards TL, Coe BP, Eichler EE, Kuhl PK. 2016. Brain white matter structure and COMT gene are linked to second-language learning in adults. Proc Natl Acad Sci U S A 113:7249–7254.

Mills DL, Coffey-Corina SA, Neville HJ. 1993. Language acquisition and cerebral specialization in 20-month-old infants. J Cogn Neurosci 5:317–334.

Miyawaki K, Jenkins JJ, Strange W, Liberman AM, Verbrugge R, Fujimura O. 1975. An effect of linguistic experience: the discrimination of /r/ and /l/ by native speakers of Japanese and English. Percept Psychophys 18:331–340.

Neville HJ, Coffey SA, Lawson D, Fischer A, Emmorey K, Bellugi U. 1997. Neural systems mediating American Sign Language: effects of sensory experience and age of acquisition. Brain Lang 57:285–308.

Newport EL, Aslin RN. 2004. Learning at a distance I. Statistical learning of non-adjacent dependencies. Cogn Psychol 48:127–162.

Peterson SE, Fox PT, Posner MI, Mintun M, Raichle ME. 1988. Positron emission tomographic studies of the cortical anatomy of single-word processing. Nature 331:585–589.

Petitto LA, Holowka S, Sergio LE, Levy B, Ostry DJ. 2004. Baby hands that move to the rhythm of language: hearing babies acquiring sign language babble silently on the hands. Cognition 93:43–73.

Poeppel D. 2014. The neuroanatomic and neurophysiological infrastructure for speech and language. Curr Opin Neurobiol 28:142–149.

Price CJ. 2012. A review and synthesis of the first 20 years of PET and fMRI studies of heard speech, spoken language and reading. Neuroimage 62:816–847.

Pulvermüller F, Fadiga L. 2010. Active perception: sensorimotor circuits as a cortical basis for language. Nat Rev Neurosci 11:351–360.

Raizada RD, Richards TL, Meltzoff A, Kuhl PK. 2008. Socioeconomic status predicts hemispheric specialisation of the left inferior frontal gyrus in young children. Neuroimage 40:1392–1401.

Ramirez-Esparza N, Garcia-Sierra A, Kuhl PK. 2014. Look who's talking: speech style and social context in language input are linked to concurrent and future speech development. Dev Sci 17:880–891.

Rauschecker JP. 2011. An expanded role for the dorsal auditory pathway in sensorimotor control and integration. Hear Res 271:16–25.

Saffran JR, Aslin RN, Newport EL. 1996. Statistical learning by 8-month old infants. Science 274:1926–1928.

Saur D, Kreher BW, Schnell S, et al. 2008. Ventral and dorsal pathways for language. Proc Natl Acad Sci U S A 105:18035–18040.

Silva-Pereyra J, Rivera-Gaxiola M, Kuhl PK. 2005. An event related brain potential study of sentence comprehension in preschoolers: semantic and morphosyntactic processing. Cogn Brain Res 23:247–258.

Skinner BF. 1957. *Verbal Behavior*. Acton, MA: Copley Publishing Group.

Tsao F-M, Liu H-M, Kuhl PK. 2004. Speech perception in infancy predicts language development in the second year of life: a longitudinal study. Child Dev 75: 1067–1084.

Weikum WM, Oberlander TF, Hensch TK, Werker JF. 2012. Prenatal exposure to antidepressants and depressed maternal mood alter trajectory of infant speech perception. Proc Natl Acad Sci U S A 109:17221–17227.

Weisleder A, Fernald A. 2013. Talking to children matters: early language experience strengthens processing and builds vocabulary. Psychol Sci 24:2143–2152.

Wernicke C. 1874. *Der Aphasische Symptomenkomplex: Eine Psychologische Studie auf Anatomischer Basis*. Breslau: Cohn und Weigert.

Xu Y, Gandour J, Talavage T, et al. 2006. Activation of the left planum temporale in pitch processing is shaped by language experience. Hum Brain Mapp 27:173–183.

Yeni-Komshian GH, Flege JE, Liu S. 2000. Pronunciation proficiency in the first and second languages of Korean–English bilinguals. Biling Lang Cogn 3:131–149.

Zatorre RJ, Gandour JT. 2008. Neural specializations for speech and pitch: moving beyond the dichotomies. Philos Trans R Soc Lond B Biol Sci 363:1087–1104.

Zhao TC, Kuhl PK. 2016. Musical intervention enhances infants' neural processing of temporal structure in music and speech. Proc Natl Acad Sci U S A 113:5212–5217.

56

Decision-Making and Consciousness

In the earlier chapters, we have seen how sensory input is transformed into neural activity that is then processed by the brain to give rise to immediate percepts and how those percepts can be stored as short- and long-term memories (Chapters 52–54). We have also examined in detail how movement is controlled by the spinal cord and brain. Here, we begin to consider one of the most challenging aspects of neuroscience: the transformation of sensory input to motor output through the higher-order cognitive process of decision-making. In doing so, we are afforded a glimpse of the building blocks of higher thought and consciousness.

Outside neuroscience, the term *cognitive* typically connotes some distinction from reflexes and dedicated routines, and yet as we shall see, neuroscience recognizes the rudiments of cognition in simple behaviors that display two types of flexibility—contingency and freedom from immediacy. Contingency means that a stimulus does not command or initiate an action in the way it does for a reflex. A stimulus might motivate a particular behavior, but the action may be delayed, pending additional information, or it may never occur. This freedom from immediacy of action means there are operations that transpire over time scales that are not immediately beholden to changes in the environment or the real-time demands of control of the body.

Both types of flexibility—contingency and time—are on display when we make decisions. Of course, not all decisions invoke cognition. Many behavioral routines—swimming, walking, feeding, and grooming—have branch points that may be called decisions, but they proceed in an orderly manner without much flexibility or control of tempo. They are governed mainly by the time steps of nervous transmission and are dedicated for the most part to particular input–output relationships. The point of drawing these distinctions is not to establish sharp boundaries around decision-making, but to help us focus on aspects of decisions that make them a model for cognition.

For present purposes, we will use the following definition: A decision is a commitment to a proposition, action, or plan based on evidence (sensory input),

prior knowledge (memory), and expected outcomes. The commitment is provisional. It does not necessitate behavior, and it can be modified. We can change our mind. The critical component is that some consideration of evidence leads to a change in the state of the organism that we liken to a provisional implementation of an action, strategy, or new mental process.

Such propositions can be represented as a plan of action: I decide to turn to the right, to leave safe shelter, to look for water, to choose a path least likely to encounter a predator, to approach a stranger, or to seek information in a book. The concept of a plan emphasizes freedom from immediacy. Moreover, not all plans come to fruition. Not all thought leads to action, but it is useful to conceive of thought as a type of plan of action. This view invites us to consider knowing as the result of directed—mostly nonconscious—interrogation, rather than an emergent property of neural representations.

Decision-making has been studied in simple organisms, notably worms, flies, bees, and leeches, as well as in mammals from mice to primates. Simpler organisms are appealing because they have smaller nervous systems, but they lack the behavioral repertory required to study decisions that entail forms of cognition. The hope is that the biological insights from these species will inform our understanding of the processes characterized in mammals, especially primates. This is a laudable goal because, to paraphrase Plato, decision-making offers our best shot at carving cognitive function at its joints—to identify the common principles that support its normal function and to elucidate their mechanisms so they may be repaired in disease.

In this chapter, we focus primarily on perceptual decisions made by primates in contrived settings. The principles extend naturally to reasoning from evidence and to value-based decisions concerning preference. In the last part of the chapter, we derive insights about broader aspects of cognition. Viewed through the lens of decision-making, brain states associated with knowing and being consciously aware may be closer to a neurobiological explanation than is commonly thought.

Perceptual Discriminations Require a Decision Rule

Until recently, decision-making was studied primarily by economists and political scientists. However, psychologists and neuroscientists working in the field of perception have been long concerned with decisions. Indeed, the simplest type of decision involves the detection of a weak stimulus, such as a dim light or a faint sound, odor, or touch. The decision a subject must make is whether or not the stimulus is present—yes or no. In the laboratory, there is no uncertainty about where and when the stimulus is likely to be present. Such experiments were therefore used to infer the fundamental sensitivities of a sensory system from behavior, a subfield of psychology known as psychophysics. Detection experiments played a role in inferring signal-to-noise properties of sensory neurons that transduce light touch, faint sounds, and dim lights. In the last case, such experiments provided evidence that the visual system is capable of detecting the dimmest of light, a single photon, subject to background noise of photoreceptors. In other words, it is as efficient as possible, given the laws of physics.

The psychophysical investigation of perception began with Ernst Weber and Gustav Fechner in the 19th century. They were interested in measuring the smallest detectable difference in intensity between two sensory stimuli. Such measurements can reveal fundamental principles of sensory processing without ever recording from a neuron. It turns out they also lay the foundation for the neuroscience of decision-making, because every yes/no answer is a choice based on the sensory evidence.

In Chapter 17, we learned how psychophysicists conceptualize the detection problem (Box 17–1). On any one trial, the state of the world is either stimulus present or stimulus absent. The decision is based on a sample of noisy evidence. If the stimulus is present, the evidence is a random sample drawn from the probability distribution of signal + noise. If the stimulus is absent, the evidence is a sample from the noise-only distribution (Figure 56–1A). The brain does not directly perceive a stimulus but receives a neural representation of the sample. As a result, some of the noise arises from the neural activity involved in forming this representation. It is the job of the brain to decide from which distribution the sample came, using information encoded in neural firing rates. However, the brain does not have access to the distributions, just the one sample involved in each given decision. It is the separation of these distributions—the degree that they do not overlap—that determines the discriminability of a stimulus from noise. The decision rule is to say "yes" if the evidence exceeds some criterion or threshold.

A Simple Decision Rule Is the Application of a Threshold to a Representation of the Evidence

The criterion instantiates the decision-maker's policy or strategy. If the criterion is lax—that is, the threshold

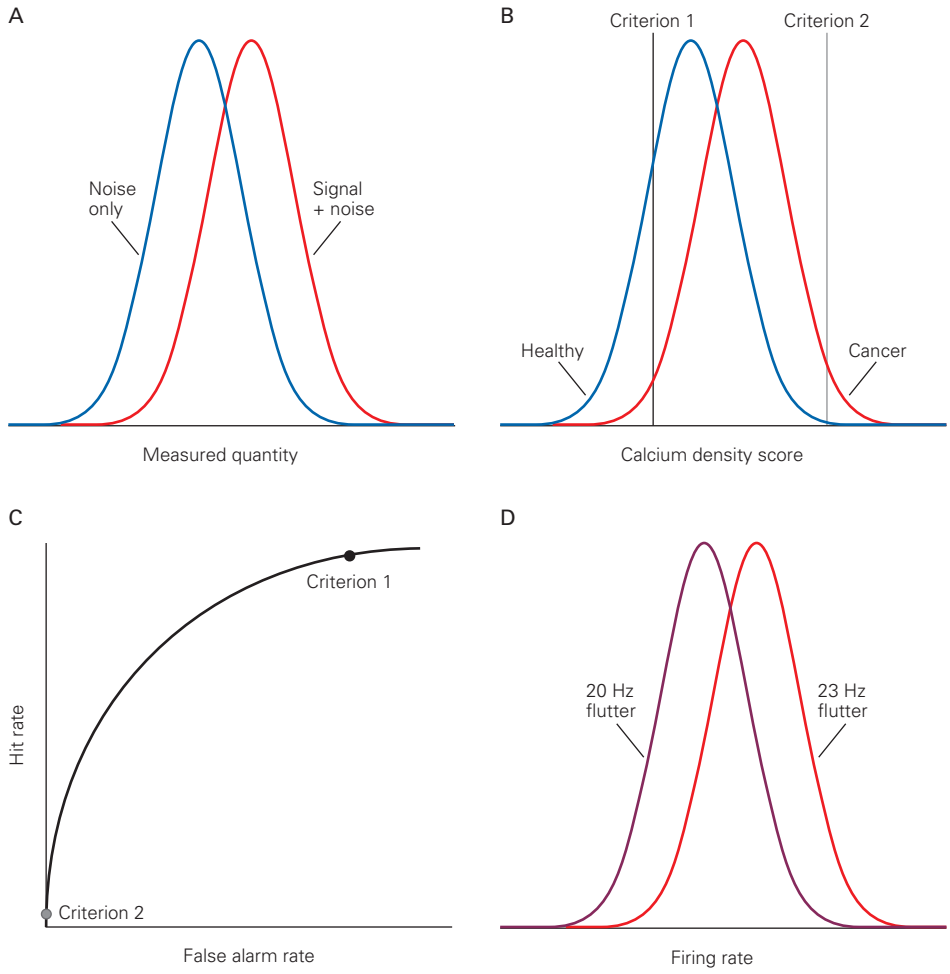

Figure 56–1 The framework of signal detection theory formalizes the relationship between evidence and decisions. In panels **A** through **C**, we consider simple yes–no decisions in which a decision-maker receives just one measurement.

A. The height of the curves represents the probability of observing a measurement on the x-axis (be it number of spikes per second, radioactive counts, or blood pressure) under two conditions: signal present or absent. In both cases, the measurement is variable, giving rise to the spread of possible values associated with the two conditions. If the signal is present, the decision-maker receives a random sample from the **Signal + noise** probability distribution (**red**). If the signal is absent, the decision-maker receives a sample from the **Noise only** probability distribution (**blue**). The decision arises by comparing the measure to a criterion, or threshold, and answering *yes* or *no*, signal is present or absent, if the value is greater or less than the criterion.

B. The criterion is an expression of policy, as illustrated in medical decision-making. Suppose the measure is derived from calcifications detected in a screening mammogram—a score combining number, density, and shape. The criterion 1 (**left line**) for interpreting the test as a positive or negative (breast cancer or not) is liberal. It leads to many false positives (83%), but very few women with cancer receive a negative result. Criterion 2 (**right line**) is conservative. It would miss many cases of cancer, but it would rarely render a positive result to a healthy person. That would make sense if a positive decision were rationale for a dangerous (or painful) procedure.

C. The receiver operating characteristic shows the combination of proportions of "yes" decisions that are correct (hit rate) and incorrect (false alarm rate) for all possible criteria. The liberal and conservative criteria are shown by the **black** and **gray** symbols, respectively.

D. The framework also applies to decisions between two alternatives. Here, the decision is whether a vibration applied to the index finger has a higher frequency than a vibration applied a few seconds before. The same depiction of overlapping distributions might conform to neural responses from some part of the brain that represents a sensory stimulus. For example, a neuron in the somatosensory cortex might respond over many individual trials with a higher average spike rate to vibratory stimulation of the finger at 23 Hz than stimulation at 20 Hz. However, the distributions overlap so that on any given presentation we cannot say with 100% certainty whether the vibration was at 20 Hz or 23 Hz based on the neuron's response.

is low—the decision-maker will rarely fail to detect the stimulus, but they will often respond "yes" on the trials when there was no stimulus because the background noise exceeds the threshold. This type of error is called a *false alarm*. If the criterion is more conservative—that is, the threshold is high—the decision-maker will rarely say "yes" when the stimulus is absent but will often say "no" when the stimulus is present. This type of error is called a *miss*. The appropriate criterion depends on the relative cost of the two types of errors and also on the design of the experiment. For example, if the stimulus is present on 90% of trials, then a lax criterion might be warranted since false alarms will be rare.

The policy ought to be influenced by a value or cost associated with making correct and incorrect decisions. For example, in medical diagnosis, it is often the case that a disease affects only a small fraction of the population, but a diagnostic test does not discriminate perfectly between people with and without the disease. We can illustrate this using the distribution of mammogram calcification scores. The scores are larger in women with breast cancer than in healthy women, but the range of values overlaps to an extent, implying that the test is not perfect (Figure 56–1B).

In this situation, a lax criterion might seem problematic because it would produce a large number of false alarms: patients who are healthy but told they might have a disease based on the test. However, it may well be the case that a miss is life threatening, whereas a false alarm leads to a stressful week as the patient awaits a more decisive test. In this situation, it is actually sensible to apply a lax criterion even if it leads to many false alarms. Alternatively, a false alarm may trigger a painful or risky procedure, in which case a more stringent criterion would be more appropriate. The medical analogy allows us to appreciate the strategic roles of the criterion setting. We praise and criticize decision-makers based on their policy, not on the noisy imperfections of the measurements.

The important point is that the criterion represents a decision rule, which instantiates knowledge about the problem and an attitude about the positive value associated with making correct choices (hits and correct rejections) and the negative value of making errors (misses and false alarms). Note that the application of different criteria does not change the fundamental characteristic of the evidence samples that is responsible for the accuracy of decisions. This is reflected by the overlap between the blue and red distributions, which does not change if a decision-maker adjusts her criterion. The curve in Figure 56–1C, termed the receiver operating characteristic (ROC), shows how changing the criterion affects the accuracy of the decision whether a stimulus (or cancer) is present or absent for all possible criteria. Each point on the curve is an ordered pair of the probability of a correct "yes" response (hits) versus an erroneous "yes" response (false alarms) associated with a given criterion (threshold). The ROC tells us something about the reliability of the measurement (ie, the separation between the two distributions) regardless of how the decision-maker uses it. The criterion tells us something about the decision-maker's policy. It bears on why two decision-makers receiving the same evidence might reach different decisions. Indeed, it is the policy, not the noise, that the decision-maker controls and for which she may be praised or criticized, that is, held responsible. We will think about this topic again when we discuss the trade-off between speed and accuracy.

The challenge for neuroscience is to relate the terms *signal*, *noise*, and *criterion* to neural representations of sensory information and operations upon those representations that result in a choice. We will develop these connections in subsequent sections. Here, we wish to seed an important insight about the term *noise* as it pertains to the neural representations of evidence. Decision-makers do not make the same decision even when confronting repetitions of identical facts or sensory stimuli. Some variability at some stage must creep into the process. The distinction between signal and noise need not devolve into scholastic arguments about chance and determinism. Any source of variance in the representation of the evidence is effectively noise if it is responsible for errors. If the brain did not distinguish such variability from the signal and thus made a mistake, we would be justified in construing this variability as unaccounted by the decision-maker.

Perceptual Decisions Involving Deliberation Mimic Aspects of Real-Life Decisions Involving Cognitive Faculties

The neural bases for more cognitive decisions have been examined by extending simple perceptual decisions in three ways: first, by moving beyond detection to a choice between two or more competing alternatives; second, by requiring the decision process to take time by involving consideration of many samples of evidence; and third, by considering decisions about matters involving values and preferences.

Vernon Mountcastle was the first to study perceptual decisions as a choice between two alternative interpretations of a sensory stimulus. He trained monkeys to make a categorical decision about the frequency of a fluttering pressure applied lightly to a fingertip (Figure 56–2). Since the *vibratory flutter* has an intensity that is easily detected, the decision is not

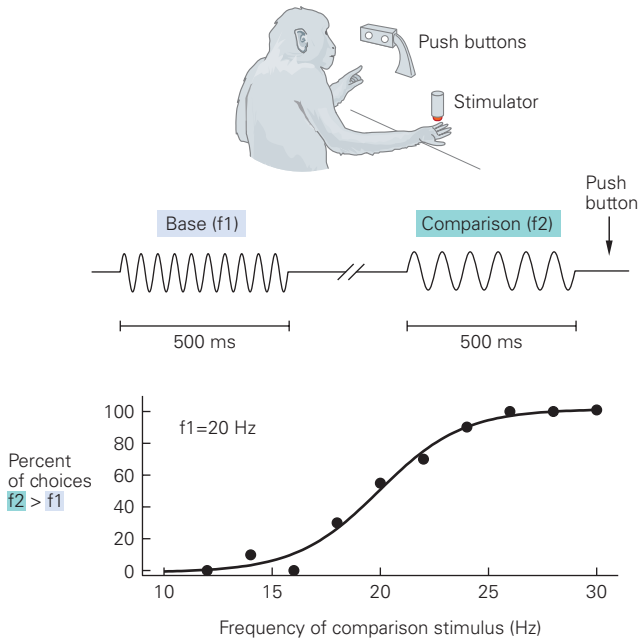

Figure 56–2 The discrimination of flutter-vibration frequency was the first perceptual decision studied in the central nervous system. A 20-Hz vibratory stimulus is applied to the finger on the right hand; following a delay period of several seconds, a second vibratory stimulus is applied. The monkey indicates whether the second vibration (**f2**) was at a higher or lower frequency than that of the first stimulus (**f1**) by pushing the left or right button with the other hand. The plots show that the proportion of trials in which the monkey decided that the comparison stimulus was greater than the reference depended on the magnitude and sign of the difference. With larger differences, the monkey almost always chose correctly, but when the difference was small, the choices were often incorrect. (Adapted from Romo and Salinas 2001.)

about whether the stimulus is present or absent but whether the vibration rate is fast or slow. On every trial of the experiment, the monkey experienced a reference frequency, f1, equal to 20 cycles per second (Hz). The pressure cycles are too fast to count; they feel more like a buzzing. The reference was then turned off, and after a few seconds, a second test stimulus, f2, was applied. The frequency of f2 was chosen from a range of values from 10 to 30 Hz. The monkey was rewarded for indicating whether the test frequency was higher or lower than the f1 reference.

We can represent the process conceptually using the same type of signal and noise distributions we drew for the detection problem (Figure 56–1D). Here, the "noise-only" distribution represents a quantity that is sampled in association with the 20-Hz reference, whereas the red distribution represents a quantity that is sampled in association with a test stimulus with a flutter frequency greater than 20 Hz. Mountcastle favored the idea that the brain obtained two samples of evidence—one accompanying the 20-Hz reference and the second from the test. The decision, higher or lower, could arise by evaluating the inequality—greater than or less than—or, equivalently, by subtracting the two samples and answering based on the sign of the difference. This was a terrific insight, but the neural recordings were out of step with the theory. Mountcastle's neural recordings explained the monkey's ability to detect vibratory stimulation as a function of intensity and frequency (Chapter 17)—a yes/no decision—but they were unable to explain the mechanism for the comparison between the two alternatives, whether f2 is greater or less than f1.

Two key elements were missing. First, to evaluate f2 versus f1, the brain needs a representation of frequency. Mountcastle found neurons in the somatosensory cortex and thalamus with firing rates that were phase-locked to frequencies of the flutter, and they could measure the reliability of this frequency locking, but they did not find neurons that were tuned to particular frequencies less than or greater than 20 Hz. Second, both representations need to be available at the same time in order to compare them. However, the neural responses to f1 lasted only as long as the flutter vibration. Mountcastle failed to observe neural responses that conveyed the representation of the reference frequency through the delay period up to the time that the test stimulus was presented. It was therefore impossible to study the neural operations corresponding to the decision process, which seemed to require some trace of the reference stimulus during analysis of the test.

These obstacles were overcome using a simpler task design and a different sensory modality. Inspired by Mountcastle, William Newsome trained monkeys to decide whether a field of dynamic random dots had a tendency to move in one direction or its opposite (eg, left or right). The random dot motion stimulus is constructed such that at one easy extreme all dots share the same direction of motion, say to the right. At the other easy extreme, all dots move to the left, and in between, the direction can be difficult to discern because many dots contribute only noise (Figure 56–3A).

Unlike the flutter vibration task, where a decision is rendered difficult by making the comparison frequencies more similar, the two directions of motion remain fixed and opposite for all levels of difficulty. The two directions were rendered less distinct by degrading the signal-to-noise ratio of the random dots. Each random dot appears only briefly, and then either reappears at a random location or at a displacement to support a consistent direction and speed. The probability of the latter (displacement) determines the motion

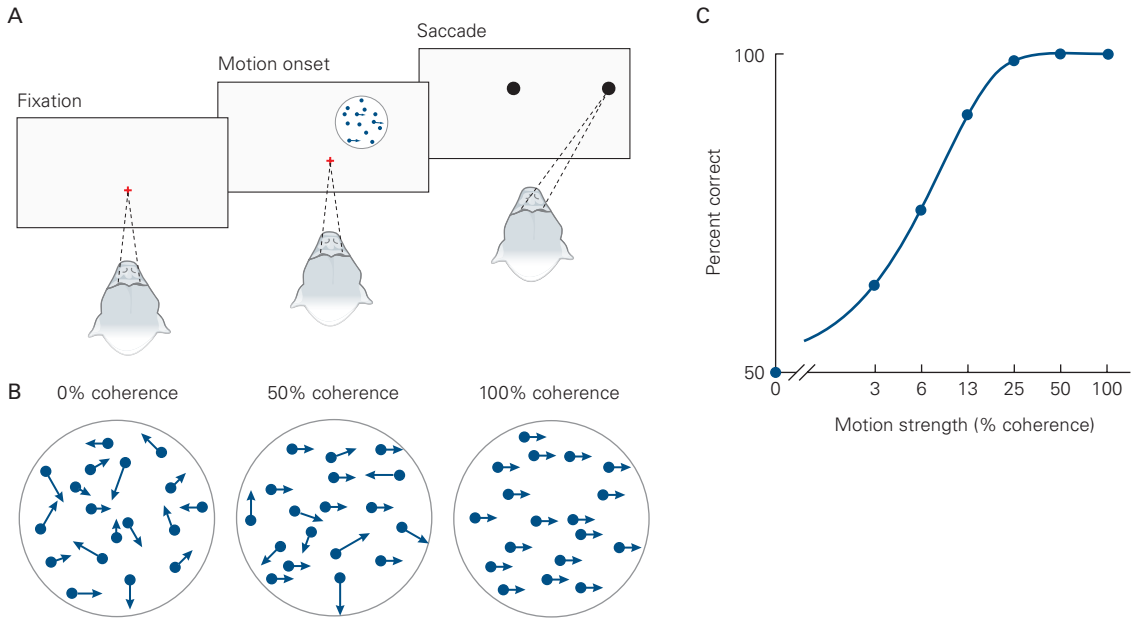

Figure 56–3 In the random dot motion discrimination task, the observer decides if the net motion of dots is in one direction or its opposite (eg, right or left).

A. The monkey maintains its gaze on a cross while viewing the random dot motion display. When the stimulus and fixation cross are extinguished, the monkey indicates its decision by shifting the gaze to the left or right choice targets and receives a reward if the decision is correct.

B. The difficulty of the decision is controlled by the coherence of dot motion. Each dot appears for only a few milliseconds at a random location and then reappears 40 ms later, either at a new random location or at a displacement consistent with a chosen speed and direction. The probability that a dot present at time t_1 undergoes displacement in the same direction at t_2 establishes the motion strength (% coherence). (Reproduced, with permission, from Britten et al. 1992. Copyright © 1992 Society for Neuroscience.)

C. The decision is more likely to be correct when the motion is stronger.

strength, which is commonly expressed on a 0 to 100 scale, termed the percentage coherence. At the most difficult extreme, 0% coherence, all dots are plotted at random locations in each successive frame, giving the appearance of dancing snowflakes with no dominant direction. At intermediate levels of difficulty, the dancing snowflakes give rise to a weak sense that the wind might be blowing them ever so slightly to the right or left. Any one dot is unlikely to be displaced more than once, so there is no feature to track.

This simple stimulus was originally developed by Anthony Movshon to promote a decision strategy that would benefit from integrating visual information across its spatial extent and as a function of time. Moreover, it satisfied another desideratum: The same neurons should inform the decision at all levels of difficulty. For a left versus right decision, direction-selective neurons in the visual cortex that are, say, sensitive to leftward motion emit signals that are relevant to the decision at all levels of difficulty. That would not be the case if difficulty were controlled by the angular difference between the two directions. Another advantage of this task over the vibration-flutter task is that there is only one stimulus presentation. There is no need to remember anything between a reference and a test stimulus. Finally, humans and monkeys perform this task at nearly identical levels. They answer perfectly for the strong-motion trials and make more errors when the strength of motion is reduced (Figure 56–3C). This establishes a platform for a quantitative reconciliation of decisions and neural activity. Is there a way to explain the likelihood that a decision will be accurate from measurements of the signal-to-noise ratio in the appropriate sensory neurons?

Neurons in Sensory Areas of the Cortex Supply the Noisy Samples of Evidence to Decision-Making

In higher mammals and primates, neurons that respond differentially to the direction of motion are first encountered in the primary visual cortex (area V1). They are a subset of the orientation-tuned simple

and complex cells discovered by Hubel and Wiesel (Chapter 22). These neurons project to a secondary visual cortical area, area MT.[1]

Area MT contains a complete map of the contralateral visual field, and almost all the neurons in area MT are direction selective. Neurons with similar direction preferences cluster together so that MT contains a map of both space and motion direction at each point in the visual field. Their receptive fields are larger than those of V1 neurons, and some manifest properties that are not evident in V1 (eg, pattern motion; Chapter 23), but most respond as if they integrate signals from V1 that share the same direction selectivity over a larger patch of the visual field. In Newsome's experiments, the random dot motion stimulus was contained in a circular aperture that matched the size of an MT neuron's receptive field. It was thus possible to measure the response of a neuron perfectly situated to convey evidence to the decision process on single trials.

It seemed possible that the neurons with receptive fields aligned to the random dot motion stimulus and a firing preference for one or the other direction under consideration might contribute the evidence used to make the decision. Indeed, we can begin to understand the monkey's perception of motion by applying the same signal-to-noise considerations to the MT neural responses. We consider two types of direction-selective neurons (Figure 56–4). One type responds better to rightward motion than to leftward motion, and it yields higher firing rates when the rightward motion is stronger. It also responds above baseline to the 0% coherence stimulus because the random noise contains all motion directions including leftward and rightward, and it yields lower firing rates (compared to 0% coherence) when the leftward motion is stronger (Figure 56–4B). The other type of neuron responds well to leftward motion. It exhibits the same pattern as the right-preferring type, only with the direction preferences reversed. The neural responses are noisy, so the firing rates on any trial or in any epoch may be conceptualized as a random draw from one of the distributions in Figure 56–4C. These distributions can be interpreted in two ways. The two curves might represent the possible firing rates of a rightward-preferring neuron when weak motion is to the right or left, respectively. They might also represent the possible firing rates of right- and left-preferring neurons, respectively, to the same weak rightward stimulus.

Because the responses of the two classes of neurons are available at the same time, we are able to characterize the evidence as the difference between the firing rates of the left- and right-preferring neurons. (The brain in fact relies on the difference between the averages from many left- and many right-preferring neurons.) We refer to such a quantity as a decision variable because the decision could be made by applying a criterion to this difference. Here, the criterion would be at zero. Thus, if the decision variable is positive, answer right; if it is negative, answer left.

Notice that when the stimulus is purely random (0% coherence), there is no correct answer. The monkey is rewarded randomly by the experimenter on a random half of the trials, and the monkey answers right and left with about equal probability. This is not because the monkey is guessing but because fluctuation in the random dot motion stimulus and the noisy firing rates of the right- and left-preferring neurons lead to variability in the evidence used to make the decision. This makes sense because the right- and left-preferring neurons respond equivalently to this type of stimulus. On some trials, the right-preferring neurons respond more than the left-preferring neurons, and the brain interprets this as evidence for rightward motion. On other trials, the left-preferring neurons respond more and the monkey chooses left.

Neuroscientists have been able to use a network of small populations of neurons to model the relation between the accuracy of an animal's choice versus motion strength, known as the *psychometric function*. The success of such models gives support to the idea that the signal and noise properties of cortical neurons can explain the fidelity of a perceptual decision, just as Mountcastle had hoped. This achievement was possible because of a clever experimental design that allowed the same neuron to participate in decisions across a wide range of difficulty. But are these neurons actually used to make the decision? Do they actually supply the noisy evidence that the monkey uses to make its decision?

We now know that they do. Because of the columnar organization of direction-selective neurons in area MT, it is possible to apply small currents through a microelectrode to excite a cluster of neurons sharing the same receptive field property. Newsome and colleagues placed the electrode in the middle of a cluster of neurons with receptive fields that were exactly aligned to the random dot motion stimulus. He reasoned that at weak stimulating currents the majority of stimulated

[1]The letters MT stand for middle temporal, a sulcus in the species of New World monkey in which the area was first discovered. This sulcus does not exist in Old World monkeys and humans, but the homologous area does, and it retains its original name. Area MT is sometimes referred to as area V5 (the fifth visual area) in humans. The name is unimportant, but the area is!

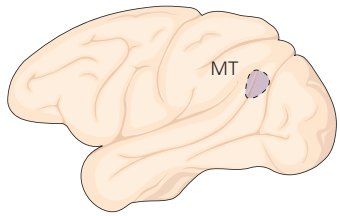

Figure 56–4 Neurons in area MT provide noisy evidence bearing on the direction of motion.

A. Responses from a right-preferring neuron during the discrimination task. The random dot movie is in the receptive field of the neuron. The panels in the left column of the 2 × 2 panel display show the neuron's responses to motion in its preferred direction, and panels in the right column show its responses to the nonpreferred direction. The panels in the top row show the neuron's responses to strongly coherent motion, and the bottom panels show the responses to weakly coherent motion. In each panel, the time of each action potential (spike) is represented by a small vertical tick mark. Each row of spikes in a panel shows the neuron's response to the motion stimulus in a single trial. (Adapted with permission from Mazurek et al. 2003.)

B. The mean firing rate varies as a function of motion strength. The neuron increases its firing rate above baseline even in response to the 0% coherence stimulus because the dynamic random dots contain all directions of motion, including the neuron's preferred direction. The firing rate then increases with stronger rightward motion. It decreases, relative to the response to 0% coherence, with stronger leftward motion. The responses of this right-preferring neuron to leftward motion are mirrored by the responses of a left-preferring neuron to rightward motion.

C. Probability distributions of the firing rates from left-preferring and right-preferring neurons to weak rightward motion. The right-preferring neuron tends to respond more, but the overlap of the distributions shows that it is possible for the left-preferring neuron to respond more than the right-preferring neuron on any given trial. These same considerations apply to the pooled signals from populations of right- and left-preferring neurons. The plot on the right shows the distribution of the difference between firing rates of the left-preferring neuron and the right-preferring neuron measured in response to the same stimulus over many trials. The decision is to choose right if this difference is positive and to choose left if it is negative. This rule would lead to correct rightward choices on 80% of the trials.

A Single trial responses from a right-preferring neuron

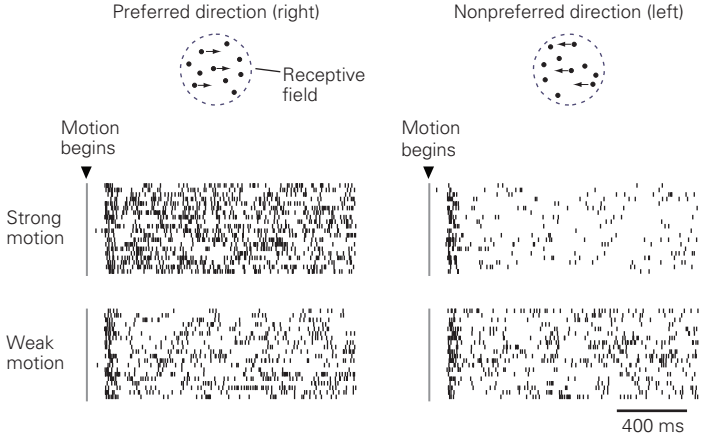

B Firing rate depends on motion strength and direction

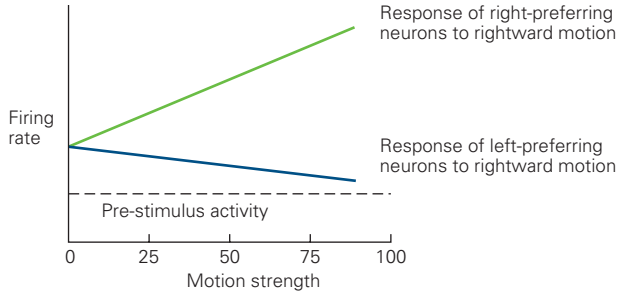

C Noisy evidence for left and right are conceptualized as random samples from probability distributions

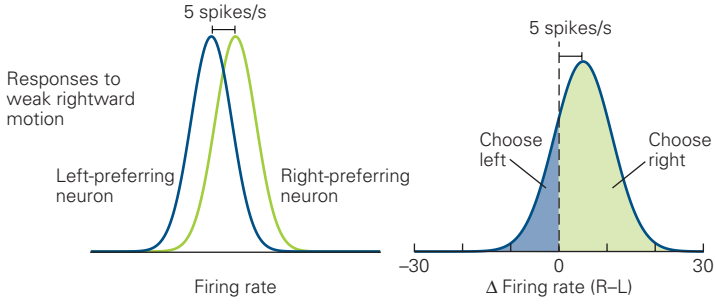

neurons were likely to share the same receptive field and the same direction preference. Newsome had the monkey decide between this direction and its opposite. For example, if these neurons preferred rightward motion, the weak currents caused the monkey to decide more often in favor of right (Figure 56–5).

We now refer to such weak stimulation, designed to affect a cluster of neurons within a 50- to 100μm radius, as *microstimulation*. Notably, microstimulation did not cause a hallucination of visual motion. It biased the monkey's decisions, which were guided mainly by the random dot motion stimulus. The monkey did not respond when the stimulus was not shown, and microstimulation did not affect the monkey's decisions when the random dots were presented at a location of the visual field outside the receptive field of the stimulated neurons. The microstimulation exerted its largest effect on choices when the motion strength was weakest. The stimulated neurons simply added a small amount of evidence for rightward motion, which is effectively evidence against leftward motion, as discussed below.

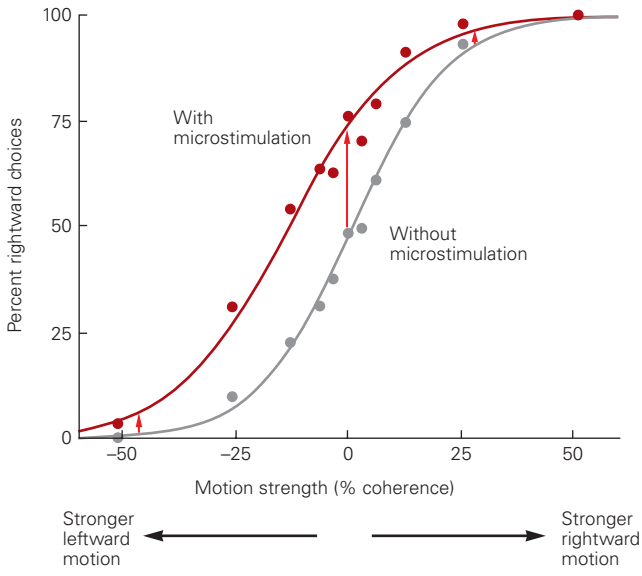

Figure 56–5 **Artificial activation of neurons that respond preferentially to rightward motion causes a monkey to decide that motion is rightward.** In the experiment, an electrode is placed in the middle of a patch of neurons in area MT that prefer the same direction of motion, say rightward. The random dot motion is shown in the receptive field of these neurons. A weak alternating current is applied on half of the trials during the presentation of the random dots movie. The amount of current activates about 200 to 400 neurons within 50 to 100 μm of the electrode tip. On trials with microstimulation, the monkey is more likely to choose the preferred direction of the simulated neurons. The effect is most pronounced when the decision is more difficult (**middle red arrow**). (Adapted, with permission, from Ditterich, Mazurek, and Shadlen 2003.)

The microstimulation experiment shows that the direction-selective neurons in area MT contribute evidence to the perceptual decision. However, the stimulated neurons do not necessarily need to affect the decision directly; they only have to participate in a neural circuit that lies in a causal chain. In addition, many more neurons in MT were not affected by the electrical stimulation but nonetheless responded to the same random dot patch in the same direction-selective manner. They are in other columns with receptive fields that are not centered on the stimulus but overlap it. If the electrode is moved to stimulate these neurons, they too cause the monkey to choose the preferred direction more often. These findings imply that in any one experiment the microstimulation only affects a small fraction of the neurons that contribute to the decision. Most respond at their usual firing rates to the random dot motion. The microstimulation only changes the total signal that the brain uses to make its decision by a small amount. No wonder the effect is only evident when the decision is difficult.

There is an important principle to be learned here. Had Newsome used only the easier conditions, the electrical stimulation would have yielded a null effect, and thus, the causal relationship between the neural activity and behavior would not have been established. The same pattern of effects has recently been established using techniques to turn neurons off. Silencing induces a bias in choices against the direction of the silenced neurons, but this too is only apparent on trials when the motion is difficult. Without evidence for sufficiency or necessity, a neuroscientist might conclude that the neurons in MT do not cause changes in perceptual decisions. This would be a mistake, notably one that is likely to be made in any experiment in which perturbations are restricted to a subset of the neurons involved in a computation. That is the rule, not the exception, for studies of higher cortical functions. It is only mitigated by studying behavior in conditions when a small difference to the total pool of neural signals might make a difference, as in the difficult (low signal-to-noise) regime employed in Newsome's experiments.

To summarize so far, the perceptual decision arises from a simple *decision rule*: the application of a criterion to the noisy evidence supplied by noisy direction-selective neurons in the visual cortex. We have characterized the noisy evidence as a single number: the difference in the mean firing rates from two opposing pools of direction-selective neurons. This account leaves out two important points: The operations that establish the decision variable must be carried out by neurons that receive information directly or indirectly from area MT, and these operations take time. As we will see, time is the key to understanding

decision-making, and it is also the factor that relates decision-making to higher cognitive function.

Accumulation of Evidence to a Threshold Explains the Speed Versus Accuracy Trade-Off

The decision rule considered so far is appropriate if the brain received only a brief snapshot of the motion, say for a tenth of a second. However, decision-making normally takes some time, so that when the viewing duration is longer, decisions tend to be more accurate. In fact, the strength of motion that is required to support 75% accuracy, termed the *sensory threshold*, decreases as a function of viewing duration. With more time, the decision-maker can achieve this level of accuracy with a weaker motion strength. Put another way, the sensitivity to weak motion improves as a function of viewing duration, t. Indeed, the sensitivity improves as a function of the square root of time ($\sqrt{t}$), which is the rate of improvement in the signal-to-noise ratio that one obtains by accumulating or averaging. The suggestion then is that the difference in firing rates of left- and right-preferring direction-selective neurons supplies the momentary evidence to another process that accumulates this noisy evidence as a function of time—in this case, two processes that accumulate evidence for left and right, respectively.

The accumulation of noisy evidence follows a path comprising random steps in both the positive and negative direction on top of a constant bias determined by the coherence and direction of the moving dots. This is termed a *biased random walk* or *drift plus diffusion* process (Figure 56–6). Because evidence for left is evidence against right (and vice versa), the two random walks are anticorrelated, albeit imperfectly so. The accumulations evolve with time and continue to do so until the stimulus is turned off or until one of the accumulations reaches an upper *stopping bound*, which determines the answer, left or right. Even the 0% coherence (pure noise) stimulus will reach a stopping bound eventually, but it is equally likely that the left or right accumulation will do so. When the random dot motion favors one direction, it is more likely that the corresponding accumulation determines the choice, and increasingly so with stronger motion. Such accumulations of noisy evidence are dynamic versions of the decision variable. The decision rule remains similar: Choose right if there is more evidence for right than left, and vice versa. The stopping bounds also explain another important feature of the decision—the time it takes to make it.

This simple idea thus explains the observed trade-off between the speed and accuracy of a decision. It specifies the exact relationship between the probability that each motion strength will lead to a correct choice and the amount of time that is taken, on average, to respond, termed the reaction time (Figure 56–6C). If the stopping bounds are close to the starting point of the accumulation, the decision will be based on very little evidence—fast but error prone. If the stopping bounds are further from the starting point, more accumulated evidence is needed to stop—slower but more likely to be correct. If the flow of information is cut off before either bound has been reached, the decision-maker may feel she has not yet reached an answer, but may nonetheless answer based on the accumulation that is closer to its stopping bound. This mechanism, termed *bounded evidence accumulation*, explains the effect of task difficulty on choice accuracy and the associated reaction times on a variety of perceptual tasks. It explains the degree of confidence that a decision-maker has in a decision and why such confidence depends on both the amount of evidence and deliberation time. It also explains the rate of improvement in accuracy when the experimenter controls viewing duration by $\sqrt{t}$, mentioned above, and it explains why this improvement saturates with longer viewing durations. The brain stops acquiring additional evidence when the accumulated evidence reaches a stopping bound.

Neurons in the Parietal and Prefrontal Association Cortex Represent a Decision Variable

Neurons in several parts of the brain, including the parietal and prefrontal cortices, change their firing rates to represent the accumulation of evidence—in the case of visual motion from area MT—bearing on the direction decision. The neurons that represent the accumulation differ from sensory neurons in two important ways. First, they can continue to respond for several seconds after a sensory stimulus has come and gone. Moreover, they seem to be capable of holding a firing rate at one level and then increasing or decreasing that level when new information arrives. This is exactly the type of feature one would like to see in a neuron that represents the accumulation of evidence. Second, such neurons tend to be associated with circuits that control the behavioral response that the monkey has learned to use to communicate its decision. Such neurons were first identified for their capacity to maintain persistent activity in the absence of a sensory stimulus or ongoing action. They were therefore thought to play a role in working (short-term) memory, planning an action, or maintaining attention at a location in the visual field (Figure 56–7).

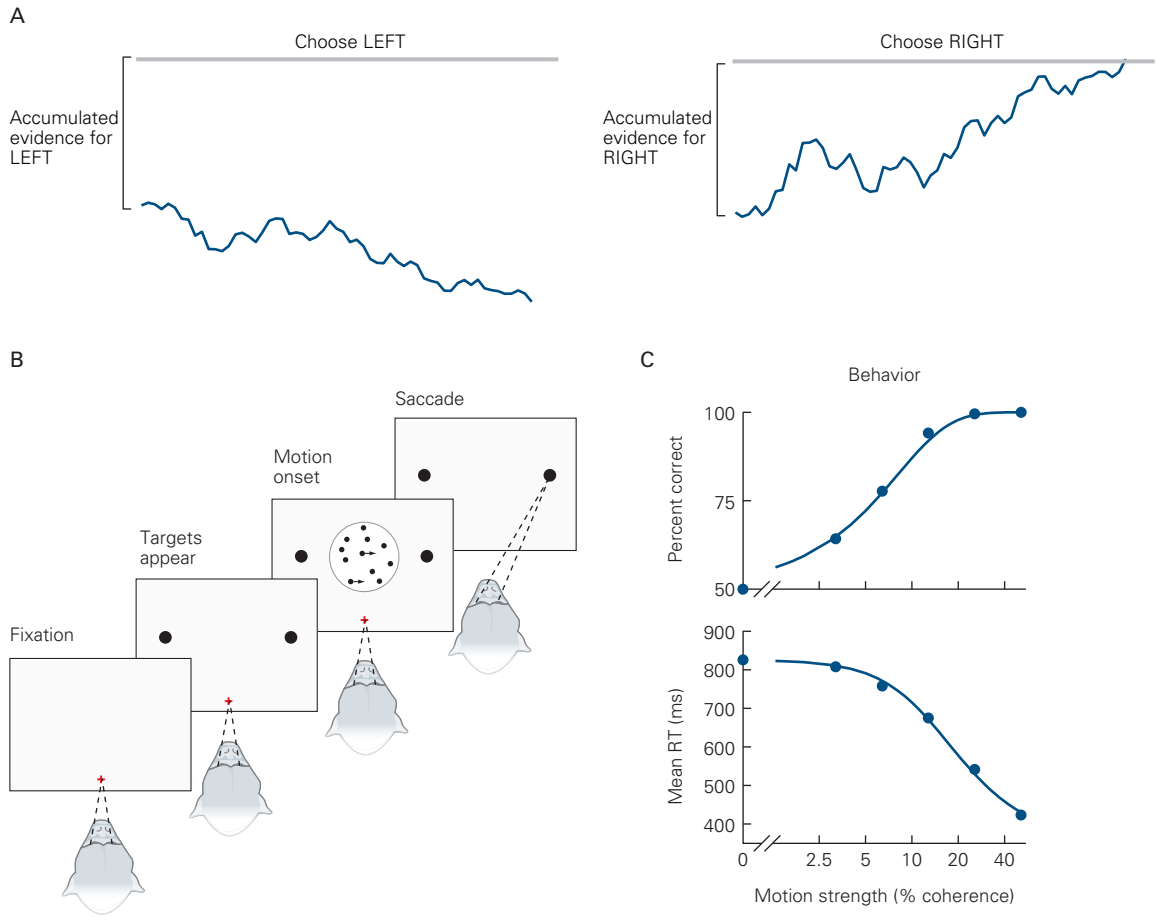

Figure 56–6 The speed and accuracy of a decision are explained by a process of evidence accumulation.

A. A decision and the time it takes to reach it are both explained by the accumulation of evidence, as a function of time, until there is sufficient evidence to terminate the decision in favor of one or the other choice. The cartoon illustrates a decision for rightward motion because the "choose right" accumulation was the first to reach the stopping bound (**thick gray lines**). Because the evidence is noisy, the accumulations resemble biased random walks, also known as drift-diffusion processes. For the decision between left and right motion, there are two accumulations. The one shown on the left accumulates evidence for left and against right. The one shown on the right accumulates evidence for right and against left. For this process, the bias (or drift rate) is the mean of the evidence samples depicted by the distribution of differences (right minus left) in Figure 56–4C. The process is a random walk because even if the motion is rightward, left-preferring neurons in area MT might respond more than right-preferring neurons at any instant. The two processes tend to evolve in an anticorrelated fashion because the random dot motion stimulus supplies the same noisy samples of evidence to both accumulations via the visual cortex. They are not perfectly anticorrelated because right- and left-preferring neurons introduce additional noise. Were the anticorrelation perfect (eg, if all the noise comes from the motion stimulus), the two processes could be represented by one accumulation that terminates at either an upper or lower stopping bound.

B. In a choice-reaction time task, the decision-maker reports a decision whenever ready with an answer. In this case, the monkey signals its choice by the direction of a saccade.

C. Graphs show a typical data set. In addition to the proportion of correct choices, the reaction time (**RT**), the time from onset of motion to the beginning of the eye movement response, also depends on the strength of motion. The total length of RT is the time to reach a decision, explained by the process in **A**, plus the time required to convey sensory information from the stimulus to the neurons that compute the decision and the time required to convert the decision to a motor response. (Adapted, with permission, from Gold and Shadlen 2007.)

It seemed possible that neurons whose activity represents a plan to act might also represent the formation of that plan during decision making. For example, if a monkey has learned to answer "rightward" by moving its hand to a target on a touch screen, the neurons of interest will tend to be active in association with that movement and they will decrease their activity if the monkey plans to reach to the opposite "leftward" target. Those neurons project to brain areas that command reach movements. If the monkey has learned to answer with an eye movement, the neurons that help to plan eye movements to the choice-target represent the decision variable. Such neurons have been studied extensively in the lateral intraparietal area (LIP). Indeed, these LIP neurons provided neuroscientists with the first view of a decision process as it unfolds in time.

Neurons that represent the evolving decision increase their firing rates gradually as the evidence mounts for one of the choices, and they decrease gradually when the evidence favors the other option (Figure 56–8). Their firing rates, plotted as a function of time, approximate a ramp: a baseline rate plus a constant multiplied by time, where the constant is proportional to the strength of the momentary evidence (eg, the average difference in the firing rates of the right- and left-preferring MT neurons). This captures the average firing rates across many trials, but it leaves out the critical point that the decision variable is an accumulation of both signal and noise. The signal is the mean of the difference. The noise is the variance—that is, the spread around the mean. The accumulated noise is obscured by the averaging in Figure 56–8, but it is apparent in the variability of firing rates across multiple decisions.

The responses start at a common level and evolve as the brain acquires more and more information, until something stops the process. A neural signature of the stopping rule is apparent in the responses aligned to the eye movement itself. The firing rate appears to reach the same level on trials that take as little as a few tenths of a second and trials that take as much as a full second. The level is achieved less than a tenth of a second before the eyes start to move. Of course, it takes less time to achieve this level if the firing rates are increasing at a rapid pace (eg, solid red trace in Figure 56–8). This suggests that the brain terminates the decision when the representation of accumulated evidence reaches a threshold. That is exactly what the bounded accumulation framework predicts. There appears to be no common level of activity in neurons that signal a rightward movement when the monkeys choose the opposite direction. Instead, another population of neurons that accumulate evidence for left (and against right) reaches their threshold and terminates the decision process when the monkey answers left (Figure 56–6A). The neurons that favor the right choice simply stop accumulating evidence at a time determined by the left choice neurons. This explains why the downward traces in Figure 56–8 do not reach a common level of activity around the time of the eye movement. It is not yet known where in the brain the threshold operation is applied. Computational theorists have proposed that a likely candidate is the striatum, a brain area involved in selecting between competing actions (Chapter 38), but there are many other candidate structures, including movement areas of the cortex and brainstem.

Area LIP is not the only part of the brain that represents the accumulation of evidence toward a decision, and LIP itself is not limited to making decisions about random dot motion. Many neurons in the parietal and prefrontal cortex exhibit persistent firing. In fact, the first brain areas shown to exhibit this type of activity were in the frontal lobe, rostral to the primary motor cortex, and some neurons with this property were found in the motor cortex itself. The persistent activity was thought to represent working memory for a location in space or a rule, category, or plan of action, as discussed in Chapter 52. But these neurons are also capable of representing graded levels of activity, suggesting a capacity to represent more analog quantities, like an evolving decision variable, the expected value of making an action, or working memory of a sensory quality, as we next consider.

Twenty years after Mountcastle published his studies of flutter-vibration discrimination, his student Ranulfo Romo rejuvenated this line of research by focusing on neurons in the prefrontal cortex, which had the kind of persistent activity we have been discussing. Romo modified the task. The monkeys were still presented with two vibrating stimuli, separated by a delay, and were required to decide whether the vibration frequency of the second stimulus (f2) was greater or less than the vibration frequency of the first stimulus (f1). However, instead of using the same 20-Hz reference stimulus on all trials, the flutter frequency was varied across trials. He found that many neurons in the prefrontal cortex respond in a graded and persistent manner to the frequency of the first flutter-vibration stimulus during the delay period while the monkey awaited the second stimulus. Some neurons increased their firing rate as a function of the vibration frequency of f1, while others were more active with lower frequencies. These persistent neural responses were not observed by Mountcastle in his original studies. There is evidence that a decision variable is constructed in the ventral premotor cortex, where neurons respond

to the difference, f2 – f1. This is challenging to study because the decision variable does not evolve over a long time scale. There is no need to acquire many samples of evidence. All that is needed is an estimate of f2 and the application of a threshold. The flutter-vibration task complements the motion decision task by demonstrating the diverse functions of persistent activity. In the motion task, the persistence supports the computation of the decision variable—the accumulated evidence bearing on the decision alternatives. In the flutter-vibration task, the persistent activity represents a sensory quality—the frequency of the reference stimulus—through a delay period.

Perceptual Decision-Making Is a Model for Reasoning From Samples of Evidence

Most of the decisions animals and humans make are not about weak or noisy sensory stimuli. They are about activities, purchases, propositions, and menu items. They are informed by knowledge and

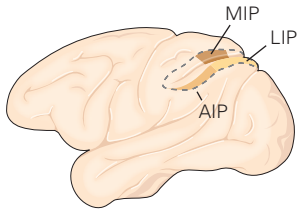

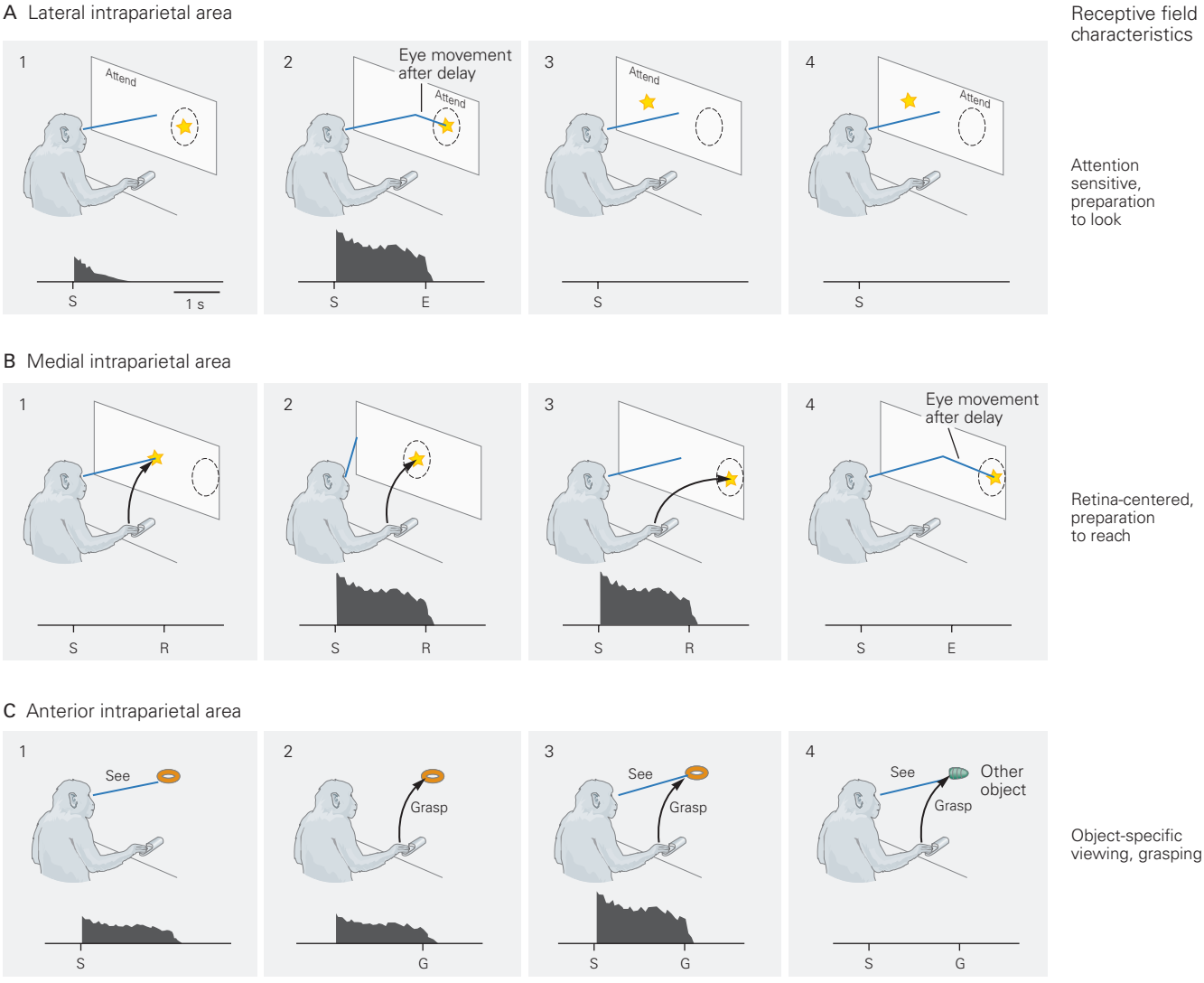

expectations derived from sources such as personal experience, books, friends, and spreadsheets. Some are based on internal (subjective) valuation or preference. Many involve reasoning from sources of evidence that may differ in reliability and that must be weighed against costs and benefits. To what extent do the neural mechanisms of perceptual decision-making apply to these other types of decisions?

Imagine the following scenario. As you leave your home in the morning, you realize that you will be outdoors from 4 to 5 pm and must decide whether to carry an umbrella. To make this interesting, assume this occurred before the age of the internet and accurate satellite weather prediction. You must decide based on yesterday's forecast of "possible chance of rain", the clear appearance of the sky at 7:00 am, a small drop in the barometric pressure compared to 1 hour before, and the observation that among a dozen pedestrians visible from your window only one seems to be carrying an umbrella. Let us assume further that you have experience with such decisions and have some sense of how reliable these indicators are. Finally, the cumbersomeness of carrying the umbrella is such that your decision boils down to a reasoned assessment of whether rain is more likely than not.

The right way to make this decision is to consider each of the indicators and ask how likely they would be if rain does or does not occur in the afternoon. These likelihoods are learned estimates of conditional probabilities, the probability of observing the indicator when it rains in the afternoon, and the probability of the same observation when it does not rain. For example, suppose through experience you have learned that the forecast, chance of rain, implies a 1 in 4 chance of rain. Then, the conditional probabilities are 1 in 4 and 3 in 4 that it will or will not rain, respectively, given the weather report. The ratio of these two probabilities is termed the likelihood ratio (LR), which is 1 in 3 in this case. If the LR is greater than 1, it favors rain, and if the LR is less than 1, it favors no rain. There is an LR for each of the four indicators. If the product of the four LRs is greater than 1, then you should carry the umbrella.

For reasons that will be clear in a moment, it is useful take logarithms of LRs, termed the log-likelihood ratio (logLR). This provides a more natural scale for belief, and it allows us to replace multiplication with addition [recall that $\log(xy)=\log(x)+\log(y)$]. To appreciate the scale, assume that the one passerby with an umbrella would be equally likely to carry the umbrella whether or not rain is a prospect. Both probabilities are 1 in 2. The LR is therefore 1, and the $\log(1)=0$, which corresponds to the intuition that this observation is uninformative. LRs greater than 1 have positive logarithms, and LRs less than 1 have negative logarithms, consistent with the way they bear on the prediction of rain.

Monkeys can be trained to perform a version of this weather prediction task. In the experiment depicted in

Figure 56–7 (Opposite) **Persistent neural activity maintains working memory, attention, and plans of action.** The monkey is asked to view a scene and respond to a visual stimulus (**S**) by either moving its eyes (**E**) or reaching (**R**) or grasping (**G**) with its hand. Each histogram represents the firing rate of a representative neuron as a function of time following presentation of the visual stimulus. The **dashed circles** show the *response fields*. This term is preferable to receptive and movement field because these neurons are neither purely sensory nor purely motor. The **blue line** shows where on the screen the monkey is asked to initially fixate its gaze.

A. Neurons in the lateral intraparietal area (**LIP**) fire when a monkey is preparing to make an eye movement to an object or when the monkey directs attention to the object's location. Most LIP neurons are not selective for object features such as shape and color. This neuron fires when the object is presented in the neuron's response field, which lies in the circled area to the right of where the monkey is looking (**1**). The neuron's firing is enhanced if the object is presented while the monkey's attention is directed to this location or if the monkey is asked to plan an eye movement to the location (**2**). The firing can persist for several seconds after the stimulus has been removed (**2**), thereby providing a potential mechanism for maintaining a short-term or working memory of its location. The neuron does not fire if an object is presented outside the neuron's response field (eg, to the left) (**3**) even if the monkey is asked to attend to the location of the neuron's response field (**4**). An object must appear there even if only briefly (**2**).

B. In the medial intraparietal area (**MIP**), neurons fire when the monkey is preparing to reach for a visual target. This neuron starts firing shortly after the appearance of a target in the response field of the neuron, in this case, a fixed angle to the right of where the monkey is looking, whether its gaze is on the left edge (**2**) or the center (**3**) of the screen, and it continues to fire as the monkey waits to reach. The neuron does not fire when the monkey reaches for a target at the center of its gaze (**1**) or when the monkey plans to shift its gaze to a target in the response field, without reaching (**4**). The physical direction of the reach is not a factor in the neuron's firing: It is the same in **1** and **2**, and yet the neuron fires only in **2**.

C. In the anterior intraparietal area (**AIP**), neurons fire when the monkey is looking at or preparing to grasp an object and are selective for objects of particular shapes. This neuron fires when the monkey is viewing a ring (**1**) or making a memory-guided reach to it in the dark (**2**). It fires especially strongly when the monkey is grasping the ring under visual guidance (**3**). It does not fire during viewing or grasping of other objects (**4**).

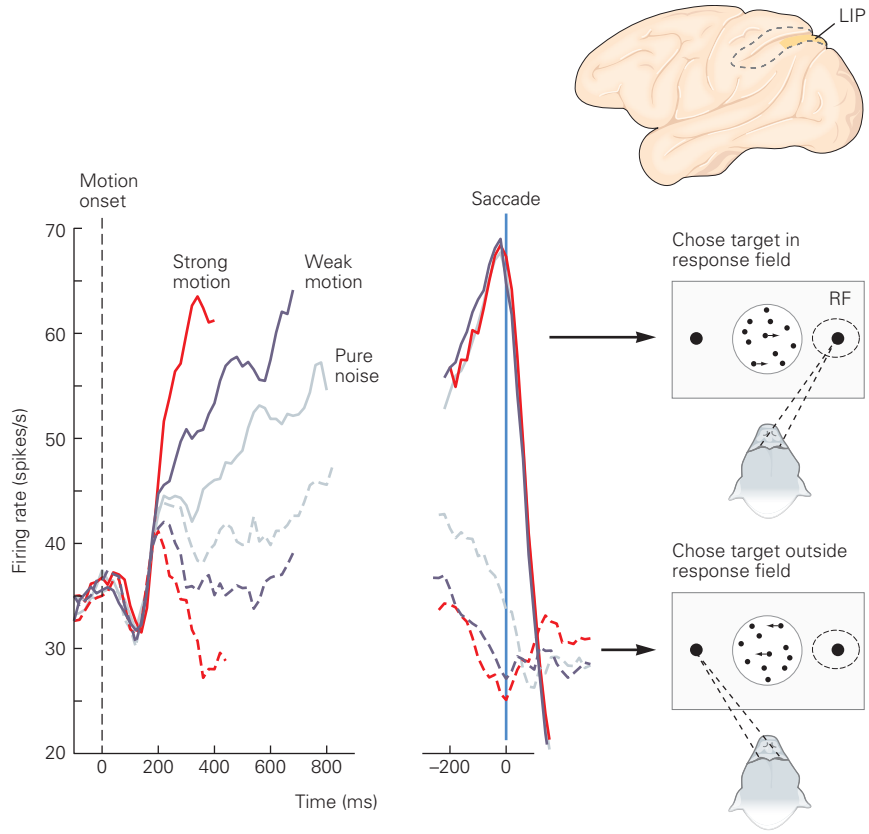

Figure 56–8 Neurons in the lateral intraparietal area (LIP) represent the accumulation of noisy evidence. These neural recordings were obtained while a monkey performed the reaction time version of the motion task. The traces are average firing rates from 55 neurons. The neurons were of the same type shown in Figure 56–7A.

The traces show average responses to three motion strengths: strong (**red**), weak (**purple**), and zero (pure noise, **gray**). The **solid traces** are from trials in which the monkey chose the target in the neuron's response field (**RF**; right choice). The **dashed traces** are from trials in which the monkey chose the target outside the neuron's response field (left choice). For the nonzero strengths, the direction of random dot motion was the direction the monkey chose (ie, only correct choices are shown). The responses in the plot on the left, which are aligned to the start of random dot motion, exhibit a gradual buildup of activity, leading to rightward choices, and a gradual decline in activity, leading to leftward choices. The rate of this buildup and decline reflects the strength and direction of motion. The responses on the right are to the same dot motion but are now aligned to the moment the monkey makes its eye movement (**saccade**) to indicate its choice and reveal its reaction time. The responses reach a common level just before the monkey makes its choice, consistent with the idea that a threshold applied to the firing rate establishes the termination of these trials. The responses do not reach a common level before leftward choices because these decisions were terminated when a separate population of neurons, with the left choice target in their response fields, reached a threshold firing rate. (Adapted, with permission, from Roitman and Shadlen 2002. Copyright © 2002 Society for Neuroscience.)

Figure 56–9, a monkey had to decide whether to look at a red or a green target, only one of which would lead to a reward. Before committing to red or green, the monkey was shown four shapes. Each served as an indicator about the location of the reward. The monkey had learned to associate predictive value with a total of 10 shapes, half of which favored reward at red, the other half at green. The shapes also differed in the reliability with which they predicted the reward location. The monkey learned to rely on these shapes rationally, making its decisions by combining evidence from each shape and by giving the more informative shapes more leverage on the choices.

While the monkeys made their decisions, neural activity was recorded from the same parietal area studied in the motion task. As before, the neurons responded in a way that revealed the formation of the decision for or against the choice target in their response field. When the red target was in the response field, the neuron assigned positive values

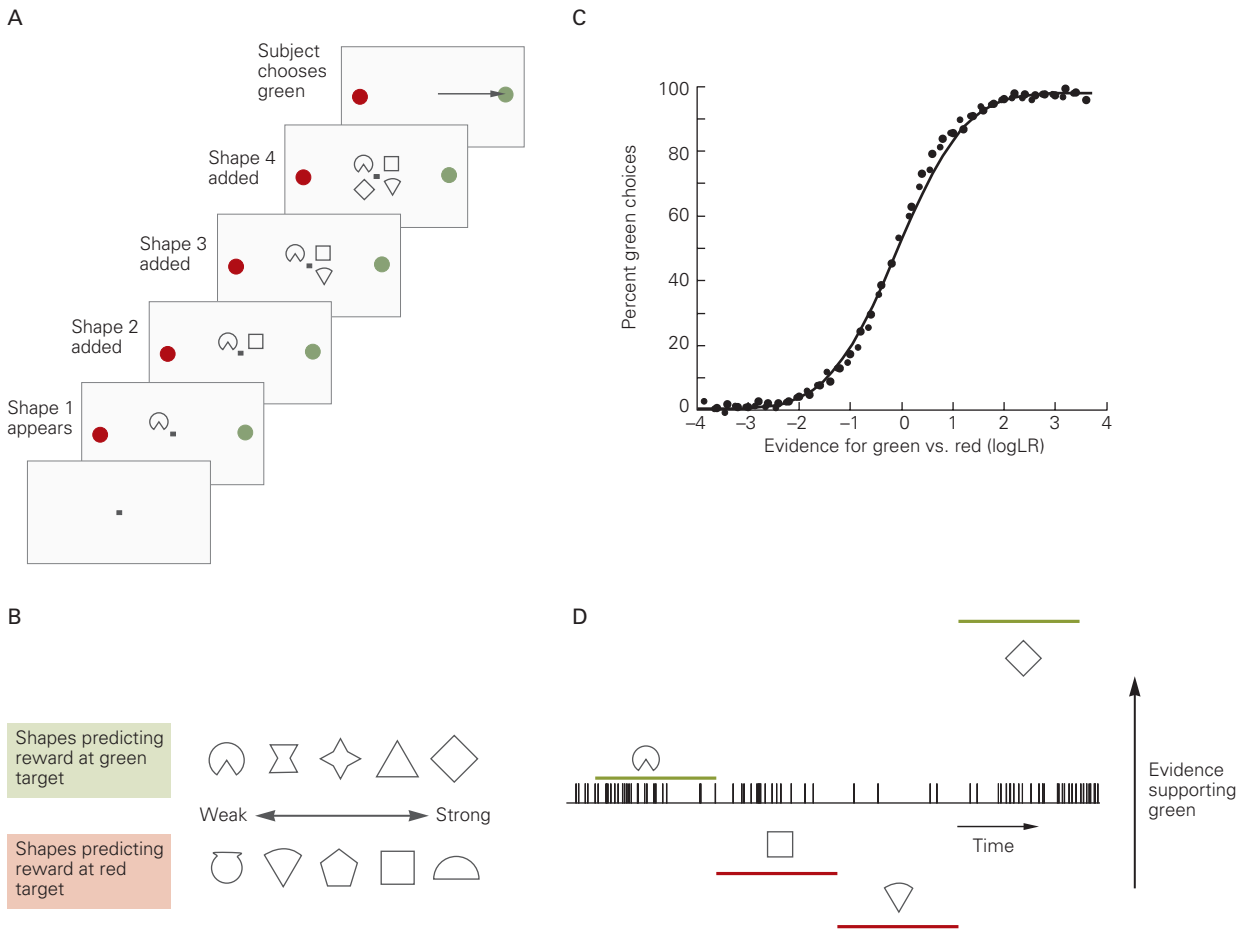

Figure 56–9 Evidence accumulation underlies probabilistic reasoning from evidentiary symbols.

A. A monkey was trained to make decisions based on a sequence of four shapes, drawn randomly with replacement from a set of 10. The shapes were added to the display sequentially every one-half second.

B. Each shape provides a different amount of evidence that a reward is associated with a red or green choice target. Some, like the diamond and semicircle, are highly reliable predictors that a reward will occur if the choice is for green or red, respectively. Others are less reliable predictors. The degree of reliability is quantified by the likelihood ratio or its logarithm. A good decision-maker should base the decision on the product of the likelihood ratios or the sum of their logarithms (**logLR**).

C. The monkey's decisions were guided by the probabilistic evidence from the four shapes. On trials in which the sum of the logLR from the four shapes strongly favored green, the monkey almost always chose green. When the sum was closer to 0, the monkey had to base its decision on weak evidence and chose less consistently. The pattern of choices demonstrates that the monkey assigned greater weight to the shapes that were more reliable (strong versus weak).

D. The same types of parietal neurons studied in the perceptual decision-making task represent the running sum of evidence bearing on the choice target in its response field. The spikes are shown from a single decision when the green target was in the neuron's response field. The **horizontal black line** below the spikes marks the neutral level of evidence for green versus red, such that the two choice targets are equally likely to be rewarded. The vertical position of the green or red lines associated with each successive presentation of an indicated shape show the cumulative evidence conferred by the shapes that the reward was at the green target. The first shape was weak evidence for green. The second and third shapes supplied mounting evidence against green (for red). Note the reduction in firing rate. The final shape provided strong evidence for green, such that the cumulative evidence from all the shapes favored green. Note the increase in firing rate. It is an example of a single neuron in the association cortex using persistent activity to compute quantities useful for decision-making. Based on the firing rates from many trials, it was shown that neurons encode the cumulative sum of the logarithm of the probability ratios—the logLR that a reward is associated with the choice target in the neuron's response field. (Adapted, with permission, from Yang and Shadlen 2007.)

to the red-favoring shapes and negative values to the green-favoring shapes. When the green target was in the response field, the signs were reversed. As shown in the example, the response changed discretely when each of the four shapes was presented, and it did so by an amount commensurate with the degree of reliability. In fact, the increment (or decrement) was proportional to the logLR assigned by the experimenter to the shape! The brain simply adds these logLRs to form a decision. And if the monkey is allowed to view as many shapes as it wants, it will typically stop when the accumulated evidence (in units of logLR) reaches a criterion level. The LIP neurons do the same thing they did in the motion decision. They produce firing rates that represent the cumulative sum of noisy increments and decrements.

By adding in units of logLR, the brain achieves reasoning from probabilistic cues in the way a statistician or actuary combines evidence from multiple sources. The experiment demonstrates that the mechanism used for perceptual decision-making is also at play in more complicated decisions that involve reasoning from more abstract sources of evidence. It speaks to the broader theme of this chapter: The study of decision-making offers insight into how the brain achieves a variety of cognitive functions.

Decisions About Preference Use Evidence About Value

Many, if not most, decisions made by humans and animals are expressions of preference, based on an assignment of value. In some instances, the value is innate. For example, most animals experience sweet as positive and bitter as negative (Chapter 29). In the vast majority of instances, however, value is learned through experience, or it is derived from reasoning based on other preferences. Unlike a decision about the direction of motion, a medical diagnosis, or the weather, a decision about which of a pair of items one prefers is not objectively right or wrong. It can only be said to be consistent or inconsistent with one's expression of value. In fact, our knowledge of a subject's valuation of an object may only be revealed to us by observing her choices.

Yet despite the qualitative difference between subjective and objective evidence, there are parallels between the neural mechanisms that support perceptual and value-based decisions. Decision-makers take more time to choose between items of similar value than items that differ substantially in value, and their choices are less consistent. In a typical experiment, the participant is asked to indicate the value of each item that they will later make choices about. For example, they might be asked how much they are willing to pay or they are asked to indicate a rating from highly undesirable through neutral to highly desirable. This procedure is typically repeated to provide a subjective value for each item to be used in the experiment.

The participant is then asked to decide between pairs of items. The difference in the subjective values communicated before the experiment provides an index of the difficulty of the decision between the items. It is analogous to motion coherence. A similar approach works with animals. For example, a monkey might demonstrate a preference for grape juice over apple juice, and then be asked to choose between a small volume of grape juice versus a large volume of apple juice. The decision is rendered more difficult by titrating the ratio of volumes to values that lead the monkey to choose either juice with equal tendency.

Two types of neurons associated with this type of value encoding have been identified. The first, typically located in the striatum, encodes the value associated with an action. The second, primarily in the orbitofrontal and cingulate cortex, appears to encode the value associated with specific items. Decisions about preference seem to arise from the same strategy that governs perceptual decisions. Just as a decision between left and right motion is guided by the difference in firing rates of left- and right-preferring sensory neurons, a decision between two items is based on the difference in activity of neurons encoding the values of each item. These neural representations are noisy, and this feature might explain why a decision-maker may make choices that are inconsistent with their values. It might also explain why decisions between items of similar value tend to take more time—a speed–consistency trade-off similar to the speed–accuracy trade-off discussed above.

The analogy to perceptual decision-making is appealing, but it misses the more interesting aspects of value-based decisions. As mentioned above, the value of most items is not given by biology but instead is learned. Further, there is no reason to assume that such value is monovalent. One may value an item differently, based on different qualities and considerations, and one or more of those qualities may dominate under different circumstances. Accordingly, the value of an item could appear to change simply by the occasion of its comparison to another item, which might invite emphasis on a more or less desirable aspect. Novelty, familiarity, and the value of exploration itself might also play a role in modifying a subjective valuation.

These considerations might contribute to the "noisy" representation of value that is thought to

explain inconsistencies and long decision times in preference choices. This type of noise belies processes that are far more complex than variability in random dot displays and the noisy spike rates of neurons. Such evaluative processes are likely to involve prospection and memory retrieval, which are only beginning to be understood at the neural level (Chapter 52). In the end, these processes must furnish samples of evidence bearing on the relative value of the items, and this evidence is either accumulated or evaluated individually against a criterion to halt the process with a decision.

Decision-Making Offers a Framework for Understanding Thought Processes, States of Knowing, and States of Awareness

States of knowledge have persistence. Even if they concern information derived from the senses, the knowledge of sensation generally outlasts the sensory activity itself. In this way, the state of knowledge resembles a perceptual decision—a commitment to a proposition about the object, based on sensory evidence. As we have seen, these states are often tied to possible behaviors rather than to the features of the sensory information. This is a position argued by many philosophers and the psychologist James J. Gibson.

This simple point can be made on empirical grounds. Persistent neural activity is not present in sensory areas of the brain unless a stimulus is unchanging and then only if the neurons do not adapt. Naturally, sensory neurons must change their response when the environment changes or the observer moves in the environment, whereas knowledge states persist through sensory changes and without a continuous stream of input. Indeed, persistent activity is apparent in areas of the brain that associate sources of information—from the senses and from memory—with circuits that organize behavior.

In the prefrontal cortex, persistent states represent plans of action, abstract rules, and strategies. In the parietal and temporal lobes, neural representations have the dual character of knowledge and the behavior that knowledge bears upon, such as making an eye movement or reaching, eating, or avoiding. The responses can resemble a spatial representation, as they do in area LIP, if the target of the projection is the eye movement system, but that is only because there is correspondence between space and action. A useful guide is to consider the source and target of the association. If the source is the visual cortex and the targets are premotor areas that control hand posture (eg, grip), as they do in the anterior intraparietal area (Figure 56–7C), the association area might convey knowledge about curvature, distance, convexity, and texture. One might be inclined to use terms borrowed from geometry to catalogue such knowledge, but it may be simpler to think about the repertory of hand shapes available to the organism. Importantly, the neurons in association cortex do not command an immediate action. They represent the possibility of acting in a certain way—an intention or provisional affordance (Box 56–1).

Let us defer for the moment the aspect of the knowledge state that includes conscious awareness and consider the simpler sense of knowledge as a state of possible utilization. Such preconscious ideation is probably the dominant state in which an animal interacts with the environment. It is arguably also the lion's share of human experience, although because we are not conscious of it, we underestimate its dominance. Two important insights emerge from this perspective. The first is that the correspondence between knowledge and neuronal activity lies at a level of brain organization between sensation and behavior. Although the flow of information from sensory epithelia (eg, the retina) through the primary cortical sensory areas is essential for perception, knowledge resulting from activity in higher brain regions has temporal flexibility and persistence not seen in lower brain regions—what the philosopher Maurice Merleau-Ponty termed the *temporal thickness of the present*.

The second insight is that the computation leading to a knowledge state has the structure of a decision—a provisional commitment to something approximating a possible selection from a submenu of the behavioral repertory. We might say that the parietal association neurons interrogate the sensory areas for evidence bearing on the possibility of a behavior: look there, reach there, posture the hand this way to grasp. Of course, neurons do not ask questions. Nevertheless, we can think of the circuits as if they scan the world looking for evidence bearing on a possible behavior. The type of information they can access is limited by functional and anatomical connectivity. The type of question is framed by the target of the projection, such as regions that control gaze, reaching, and grasping.

Sir Arthur Conan Doyle endowed Sherlock Holmes with the insight that the key to discovery was knowing where to look and what to look for. We acquire knowledge by controlling the brain's interrogation system. Some interrogations are automatic, whereas others are learned. An example of the former is a sudden change of brightness of an object in the visual field; it provides evidence bearing on the possibility of orienting the eyes or body toward it. An example

Box 56–1 Affordances, Perception, and Knowledge

James J. Gibson, known for his ecological theory of perception, referred to *affordances* as properties of objects and the environment. The term comes from the verb *afford*. An object affords possible behaviors, such as lifting, grabbing, filling, hiding in, drawing/writing upon (eg, parchment) or with (eg, a brush), or walking upon. The affordance refers to the potential behaviors of the animal. The same object, say a stone, could afford grasping, dropping, breaking (ie, used as a tool), throwing (as a missile weapon), or pinning (as a paperweight).

Gibson was widely criticized for claiming that perceptual processes picked up these affordances directly from the optical array, what he termed "direct perception." The term is commonly misunderstood as antithetical to computational accounts of information processing. By "direct perception," Gibson did not mean that there were no computations on the data received through the senses. He promoted the mathematical understanding of these operations. He meant that we do not perceive the intermediates.

We do perceive the parts of objects that are accidentally occluded by something in our line of sight, and we perceive the back of an opaque object that is occluded by its front. We do not perceive the outlines, the line art, and many other details, but that is not to say that they do not register on the retina and the visual cortex. Gibson held that representation of visual information is not a sufficient condition for perception. From the perspective of the neuroscience of decision-making, one might place emphasis on the representation of potential behavior—something like a provisional commitment to a plan.

Affordance still refers to a category of actions, but it is about the organization of the action (eg, throwing) or strategy, and also—but not necessarily—a quality of the object. The modifier, "provisional," emphasizes that the action may not actually ensue now or ever. This modifier would have been superfluous in Gibson's use of the term *affordance*, because an affordance was a property of the object (in his ecological framework) and therefore had a permanence independent of the perceiver.

of the latter draws on learning and foraging; we learn, through play and social interaction (eg, school), how to look for hidden items and how to explore in a goal-directed way.

The beautiful thing about this construction is that an answer to the question confers a kind of meaning. Even for such a mundane question like "Might I look there?," an affirmative answer—a decision to (possibly) look at an as yet undefined object in the periphery of one's visual field—confers a spatial knowledge about the item. Before we have looked directly at it to identify what it is, we know about its *thereness*. From the perspective of decision-making, the location of an object is not perceived because there is a neural activity in a map of the visual field. Rather, the location is perceived because some aspect of the visual field—a fleck of contrast, change in brightness, appearance or disappearance—answered the question above in the affirmative.

This way of thinking helps us understand the disease states known by the term *agnosia*, from the Greek word meaning "absence of knowledge." The classic example is visual hemineglect, which is caused by damage to the parietal lobe (Chapter 59). A patient with a right parietal lesion will ignore the left side of the visual field and also the left side of objects even when the entire object is in the right visual field (Figure 56–10; see also Figure 59–1). Unlike the left side blindness, called homonymous hemianopsia (or hemiblind), which accompanies damage to the right visual cortex (homonymous because it is the same regardless of which eye is used), the patient with a parietal lesion does not complain of an inability to see. She is unaware of the deficit, so much so that crossing a street is a major hazard.

A hemiblind patient with damage to the right visual cortex still expects to interrogate and receive information from the left visual field. When that patient receives no visual information, he knows to turn to face parallel to the street, thereby placing its contents in the intact right hemifield. In contrast, the patient with hemineglect does not interrogate the left hemifield in the first place. She does not perceive a lack of visual information because the apparatus to conduct the interrogation is not working. Like most deficits, there is enough redundancy in the brain (or the damage partial) that some visual capacities are present. In fact, when confronted with a single spot of light on a dark background, the same patient may report its presence accurately even in the affected hemifield.

There are other versions of hemineglect that involve an absence of knowledge of the body. For example, a patient with a right parietal injury may deny that her left arm is hers. She may recognize it as

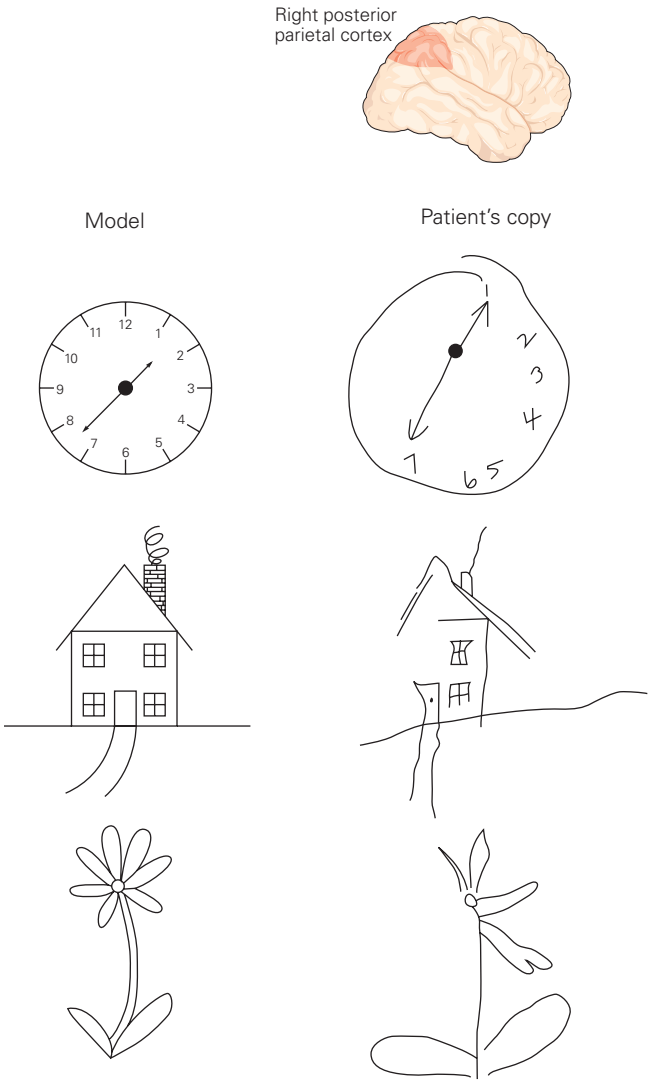

Figure 56–10 Damage to the parietal or temporal cortices results in agnosia, or deficits in knowing. After damage to the right parietal lobe, many patients are unaware of the left side of space or the left part of objects. The drawings on the right were made by patients with unilateral visual neglect following lesion of the right posterior parietal cortex. Agnosias can also be induced in healthy individuals by diverting attention (see Figure 25–8). (Reproduced, with permission, from Bloom F, Lazerson A. 1988. *Brain, Mind and Behavior*, 2nd ed., p. 300. New York: Freeman.)

an arm but deny that it is hers. When asked whose arm it is, she may express ignorance bordering on disinterest (personal experience). The syndrome is usually associated with some visual neglect as well and some weakness on the same side of the body suggestive of a more rostral and superior localization. Consider that the body's position is known to us partly through the somatosensory system, partly through the predicted consequences of our motor command, and partly through vision. The arm in particular is a common feature of our lower visual field. Indeed, we are accustomed to ignoring it.

These examples are the most common of the agnosias (which are thankfully rare). Other well-known examples involve problems in face recognition (prosopagnosia) and the perception of color (achromatopsia), both associated with lesions of the temporal lobe. The different types of agnosia have loose correspondence to the anatomical specializations we learned about in Chapter 24. In particular, the ventral extension of the central visual pathways into the temporal lobe is referred to as the "what" pathway, which contains circuits that are specialized for processing faces, objects, color, and semantic memory. The dorsal extension, which has been termed the "where" or "how" pathway, seems concerned with representations supporting localization.

An alternative formulation would characterize these streams in terms of associations with behaviorally relevant targets. For the dorsal stream, those are parietal areas with projections to motor systems that reach, look, or grasp. For the ventral stream, those are temporal lobe areas with projections to structures that guide foraging decisions to eat, avoid, hide, approach, mate, and communicate. The last few behaviors are social affordances conferred by color and facial identity/expression. With a small stretch of imagination, the organization of social affordances links to other functions of the temporal lobe (and temporal parietal junction) in humans. For example, these regions are associated with language comprehension and inference about what someone else is thinking. The former is associated with a devastating agnosia, known as Wernicke aphasia (Chapters 1 and 55); the latter is known as theory of mind and will be discussed below.

From the perspective of decision-making, perceiving, believing, and thinking have the character of a provisional commitment to a proposition. Brain states that correspond to a sense of knowing, be it perceiving or believing, share two important aspects with decision-making: an extended temporal profile that withstands changes in the sensory and motor streams (ie, a freedom from immediacy) and a propositional character captured by the term "affordance." Knowing is not solely about the information but is like the outcome of a decision to embrace a proposition: Might I do something, enact something, approach someone, or retain the possibility of trying the option I am not choosing now?

Two caveats deserve mention. This framework does not replace a computational account of

information processing, nor does it explain the neural mechanisms that support these computations. It mainly tells us about the level of brain organization that carries out these operations. For example, consider the search for the neurons that achieve knowledge about the color red, despite changes in the spectral content of the morning and evening light—a phenomenon known as *color constancy*. Instead of searching in sensory areas for neurons that respond selectively to red in this invariant way, one might look for neurons that guide the choice of ripe fruit. This does not obviate the computations required to recover the surface reflectance properties of the fruit's skin, despite variation in the spectral content of the illuminating light. The raw data for such computations are supplied by sensory neurons that lack color constancy and maintain temporal fidelity with changes in the environment. The knowledge state "red," however, is invariant to the illuminant and likely persistent. In animals that lack language, the knowledge state may not be dissociable from "ripe vegetation."

The second caveat is that we have not distinguished knowledge states that we are consciously aware of from those that we experience unconsciously. For example, as I make my way through the forest trying to find the creek that I hear burbling, my brain might consider locations of objects I pass that are graspable, attached to vegetation, and with color suggesting ripeness. I may be unaware of this consciously. Yet that evening in my search for food, I may return to this part of the forest, guided by these unconscious encounters. I may do this without knowing why, or the memory might pierce consciousness. All that has been said up to now could apply to conscious and nonconscious experience. We are now prepared to elucidate the difference.

Consciousness Can be Understood Through the Lens of Decision Making

Clearly, we are unaware of most of the operations that transpire in our brains, and this is true even for the processes that ultimately pierce consciousness. This is why Freud famously quipped that consciousness is overrated. Every thought that enters our awareness began as neural computation preceding the conscious awareness of that thought. Indeed, the sophistication of nonconscious mental processes, including those leading to "I've got it!" moments and the activities we perform while occupied by a phone call, involves decisions that transpire without conscious awareness.

It is difficult to study nonconscious processing because people deny experience of the process. Indeed, the term nonconscious experience seems like an oxymoron. The experimenter must find a way to prove that information processing has occurred despite the fact that the subject is unaware of it. In recent years, it has become possible to establish conditions whereby information is provided to a human subject that has a high likelihood of going unnoticed but is nonetheless able to influence behavior, thereby permitting scientific characterization of nonconscious mental processing (Chapter 59). This has encouraged neuroscientists to ask what it is about the neural activity that gives rise to the thoughts, perceptions, and movements that do reach conscious awareness. We will not review this vast topic here but instead share a pertinent insight: Viewed through the lens of decision-making, the problem of consciousness may be simpler than imagined.

Broadly speaking, two sets of phenomena fall under the heading consciousness. The first concerns levels of arousal. One is not conscious when one is asleep, under general anesthesia, comatose, or having a generalized seizure. One is fully conscious when awake, and there are levels of consciousness between these extremes. These states are associated with terms such as confusion, dissociation, stupor, and obtundation. Some alterations of consciousness are normal (eg, sleep), whereas others are induced by toxins (eg, alcohol), metabolic disturbances (eg, hypoglycemia), low oxygen, trauma (eg, concussion), or fever (eg, delirium).

The neuroscience underlying these states—and the transitions between them—is immensely important to medicine. We might classify this group of phenomena as neurology-consciousness. However, these topics are not what most people mean when they speak of the mystery of consciousness. This is partly because they are less mysterious but also because their characterization is more objective and the phenomena can be studied in animals. That said, there is much to be learned about the mechanisms responsible for sleep, awakening, anesthesia, and so forth. Much of the neuroscience is unfolding at a rapid pace (Chapter 44).

We will not say more about neurology-consciousness here, except to seed one useful insight. Imagine a mother and father sleeping comfortably in their bedroom as a storm ensues outdoors. There are also traffic sounds and even the occasional thunder. This scene goes on for some time, until the cry of a baby awakens the parents. This common occurrence tells us that the nonconscious brain is capable of processing sounds and deciding to become conscious. It decides, nonconsciously, that some sounds afford an opportunity for more sleep while others sound a call to nurture. This

decision is similar to the perceptual decisions considered earlier in this chapter. Both involve nonconscious processing of evidence. However, the commitment to awaken and parent is a decision to engage the environment consciously. This may be a touchstone between neurology-consciousness and the more intriguing consciousness that you are experiencing as you read these words (or so the authors hope).

When neuroscientists, psychologists, and philosophers ponder the mysteries of consciousness, they are referring to loftier themes than wakefulness. This loftier set of phenomena comprises awareness, imagery, volition, and agency. There is a subjective component to all conscious experience. The experience of conscious perception incorporates a sense that it is me that is beholding the content. It parallels the "me" in volition. It is not that my arm moved on its own; I made it move! We used the term deliberation earlier in this chapter to describe the thought process leading to a decision. Our use of the term was metaphorical. It describes a computation and a biological mechanism, but it does not require awareness. Actual deliberation implies conscious intention. We are aware of the steps of reasoning along the way. We could report, were we asked, about the evidence we relied upon—that is, the evidence we were consciously aware of during the decision and possibly some of the evidence we used nonconsciously were it accessible from memory to include in our report. Could the difference between conscious awareness of an item and nonconscious processing of that item be a mere matter of whether the brain has decided on the possibility of reporting? Could it be this simple?

Consider the following scenario. A psychologist concludes that a study participant has seen something nonconsciously because the item affected a subsequent behavior and the participant denies having seen it. Suppose the subsequent behavior involved reaching in the direction of the object. Based on what we know about decision-making, we would conclude that brain circuits like the ones discussed earlier received sufficient evidence to commit to the possibility of looking, reaching, and approaching, but there was insufficient evidence to commit to the possibility of reporting. Just as the brain entertains the possibility of looking, reaching, or grasping, it may also entertain the possibility of reporting. That is, reporting is also a *provisional affordance*.

Events afford the possibility of reporting, and this includes the nonconscious states of knowledge acquired through decision-making. Indeed, the event of having decided may be experienced consciously—the *aha* moment—by virtue of another decision to report. In the study scenario, the participant was not consciously aware of the item because her brain did not commit to a provisional report. The evidence did not satisfy a decision criterion like the termination bounds in the perceptual decision-making task considered earlier in the chapter.

This account provides a plausible explanation of the failure of the participant to report that she saw the item, but the mere entertaining of the possibility of reporting does not seem to explain the phenomenology of the perceptual experience itself, at least not at first glance. This explanation demands more careful consideration of the character of the report. Just as we attach states of spatial knowledge to configurations of the hand for reaching and grasping, we must consider the knowledge state that accompanies the affordance of reporting. Whether by language or gesture (eg, pointing), the report is a provisional communication with another agent or oneself (eg, in the future). It presumes knowledge about the mind of the receiver.

Cognitive scientists use the term *theory of mind* to refer to this type of knowledge or mental capacity. It can be demonstrated by asking someone to reason about the motivation behind another agent's actions, and it can be studied in animals and preverbal children by examining their reactions to another child or puppet. In one study protocol, two children witness a desired toy placed in a left or right container (Figure 62–2). The test child then witnesses the toy's displacement to the other container while the other child is absent. When that child returns, the experimenter assesses the test child's expectation of which container the returning child will open to find the toy. Children under 3 years old do not exhibit theory of mind by this assay. They think the returning child will open the container that contains the toy, not the one it was in before the transfer. Whether animals other than humans have theory of mind is controversial. We suspect there are inchoate forms of this capacity in the animal kingdom and in children under 3. When adults perform tasks that depend on theory of mind, the right temporal-parietal junction and superior temporal sulcus are active.

Theory of mind—in concert with narrative—has profound consequences for the knowledge state associated with the reporting affordance. Imagine a woman looking at a power drill resting on a table. She experiences the location of the drill, relative to her eyes and hand, as well as its texture and shape. It has a graspable surface that is partly in her line of sight and partly occluded (eg, the back). These are the knowledge states that arise through provisional commitments to look at, reach for, and grasp the drill. They are likely to involve neural activity similar to what is illustrated in Figure 56–7, and they are the outcome of simple decisions. The drill brings to mind other affordances

associated with its utility as a tool, its potential to make noise, and the potential danger posed by the sharp bit at one end. This is an elaborate, potentially rich collection of knowledge, but it could all be experienced nonconsciously. For example, if the woman were preoccupied with some other task, such as a phone conversation with her friend, she might nonetheless make use of these knowledge states.

But suppose there is a man on the other side of the table and suppose the woman—her brain, that is—has also reached a provisional commitment to report to the man about the drill between them. Consider the change to her knowledge state. The drill now has a presence not only in her visual field, relative to her gaze, her hand, and her repertory of actions, but also in the man's field of vision and his possible actions. The parts of the drill that are not in plain sight to her are known to be in the line of sight of the man. Indeed, her capacity for "theory of mind" also supplies knowledge that other parts of the drill are seen only by her and that the man could be experiencing those parts just as she experiences the parts that are not in her direct line of sight—that is, both preconsciously as occluded parts of the object and consciously as part of an object that could be seen directly from another vantage point. There is something about the drill that is at once private, public, and in the world—independent of either mind. The drill is there for the next person who enters the room, or an imagined person. The transformation of knowledge of the drill is from a collection of first-person experiences (eg, qualities and affordances) to a thing in the world that possesses an existence unto itself. It is conceivable that this state of knowledge is our conscious awareness of the world, or at least a part of it, for the knowledge state associated with a decision to report is further enriched by content of the report itself.

The report might be simple, like pointing to the location of a tool or a hiding spot, or it might involve narrative. In the case of the hiding spot, additional content might be conveyed to indicate that the enclosure affords safety from a predator or, alternatively, a predator's location. Many simple reports do not require narrative because items such as tools and enclosures persist and theory of mind presumes the affordance of a tool or a hiding place in another's mind, whereas events, which also afford the possibility of reporting, often require narrative because they are transient.

The knowledge state associated with narrative can incorporate history, simulation, prediction, etiology (eg, origin stories), purpose, and consequence. For the drill, narrative might enhance the knowledge state to include memory of the place of purchase, an episode in which it malfunctioned, and the mechanism of its detachable bit. Narrative allows us to reason in more complex environments than the scenarios considered earlier (eg, the umbrella example and the probabilistic reasoning task; Figure 56–9). We could not reason about science, medical diagnosis, and jurisprudence without origin stories, simulation, hypotheses, prospection, and counterfactuals. The evolutionary advantage of this capacity is obvious (at least for the time being, until it leads us to make the earth uninhabitable).

To summarize, the conscious awareness of an item might arise when the nonconscious brain reaches a decision to report the item to another mind. The intention is provisional in that no overt report—verbal or gesture—need occur, just as no eye movement need ensue for the parietal cortex to engage the possible intention of foveating. Just as the provisional intention to foveate corresponds to preconscious knowledge of the location of an as yet unidentified object in the periphery, the possibility of reporting to another agent (or self), about whom we have theory of mind, corresponds to the knowledge of an item in a way that satisfies most aspects of conscious awareness.

Naturally, our journey from perceptual decision-making through affordances to consciousness is at best incomplete. For example, it does not yet provide a satisfying account of what a conscious experience feels like. But it is a start, as it supplies a coarse explanation of why sensory information acquired through the eyes is experienced differently from auditory or somatosensory experiences, and it provides insight into the private aspects of perceptual awareness as well as our experience of objects as things in the world, independent of what they afford to the perceiver. These last features follow from the consideration of another agent's mind.

The view of consciousness from the perspective of decision-making is, if nothing else, simplifying. There is no reason to search for a special area of the brain that bestows consciousness, or a special neuron type, or a special ingredient in the representation of information (eg, an oscillation or synchronization), or a special mechanism. The mechanism might look like any other kind of provisional commitment—that is, a decision that confers a state of knowing but does not entail conscious awareness. Of course, brain activity itself is not conscious, just as the brain activity supporting a possible hand posture is not the hand posture itself. In this sense, the mechanism of consciousness is only different from other affordances because it involves reporting instead of reaching, looking toward, eating, drinking, hiding from, walking through, and mating. All are likely to involve decision formation and threshold detection.

Thus, by studying the neuroscience of decision-making, we are also studying the neuroscience of consciousness. There is still much to be learned about the mechanisms of the simplest decisions described in the first part of the chapter. For example, we do not know what sets the bounds and how thresholds are implemented in brain circuits. Nevertheless, answers to these and other fundamental questions are in the crosshairs of modern neuroscience, and therefore, so is human consciousness.

Highlights

1. A decision is a commitment to a proposition, action, or plan—among options—based on evidence, prior knowledge, and expected outcomes. The commitment does not necessitate immediate action or any behavior, and it may be modified.
2. Decision-making provides a window on the neuroscience of cognition. It models contingent behavior and mental operations that are free from the immediate demands of sensory processing and control of the body's musculature.
3. A decision is formed by applying a rule to the state of evidence bearing on the alternatives. A simple decision rule for choosing between two alternatives employs a criterion. If the evidence exceeds the criterion, then choose the alternative supported by the evidence; if not, choose the other alternative.
4. For certain perceptual decisions, the source of evidence and its neural representation are known.
5. The accuracy of many decisions is limited by considerations of the signal strength and its associated noise. For neural systems, this noise is attributed to the variable discharge of single neurons, hence the variable firing rate of small populations of neurons that represent the evidence.
6. Many decisions benefit from multiple samples of evidence, which are combined across time. Such decision processes take time and require neural representations that can hold and update the accumulated evidence (ie, the decision variable). Neurons in the prefrontal and parietal cortex, which are capable of holding and updating their firing rates, represent the evolving decision variable. These neurons are also involved in planning, attention, and working memory.
7. The speed–accuracy trade-off is controlled by setting a bound or threshold on the amount of evidence required to terminate a decision. It is an example of a policy that makes one decision-maker different from another.
8. Many decisions are about propositions, items, or goals that differ in value to the organism. Such value-based decisions depend on stored associations between items and valence.
9. The source of evidence for many decisions is memory and active interrogation of the environment—information seeking. These operations come into play when animals forage and explore, and when a jazz musician improvises.
10. Decision-making invites us to consider knowledge not as an emergent property of neural representations but the result of directed, mostly nonconscious interrogation of evidence bearing on propositions, plans, and affordances. The intention is provisional in that no overt action need ensue. Just as the provisional intention to foveate corresponds to preconscious knowledge of the location of an as yet unidentified object in the periphery, the possibility of reporting to another agent (or self), about whom we have theory of mind, corresponds to the knowledge of an item in the ways we are aware of it consciously.
11. Viewed through the lens of decision-making, conscious awareness of an item might arise when the nonconscious brain reaches a decision to report to another mind. The affordance has the quality of narrative, much like silent speech or the idea preceding its expression in language. It also imbues objects with a presence in the environment inhabited by other minds, hence independent of the mind of the perceiver. It confers private and public content to aspects of the object as perceived.

Michael N. Shadlen
Eric R. Kandel

Selected Reading

Clark A. 1997. *Being There: Putting brain, body, and world together again*. Cambridge, MA: MIT Press. 269 pp.

Dehaene S. 2014. *Consciousness and the Brain: Deciphering How the Brain Codes Our Thoughts*. New York: Viking.

Dennett D. 1991. *Consciousness Explained*. Boston: Little, Brown.

Donlea JM, Pimentel D, Talbot CB, et al. 2018. Recurrent circuitry for balancing sleep need and sleep. Neuron 97:378–389.e4.

Gibson JJ. 2015. *The Ecological Approach to Visual Perception*. Classic Edition. New York: Psychology Press.
Graziano MSA, Kastner S. 2011. Human consciousness and its relationship to social neuroscience: a novel hypothesis. Cogn Neurosci 2:98–113.
Green DM, Swets JA. 1966. *Signal Detection Theory and Psychophysics*. New York: John Wiley and Sons, Inc.
Kang YHR, Petzschner FH, Wolpert DM, Shadlen MN. 2017. Piercing of consciousness as a threshold-crossing operation. Curr Biol 27:2285–2295.
Laming DRJ. 1968. *Information Theory of Choice-Reaction Times*. New York: Academic Press.
Link SW. 1992. *The Wave Theory of Difference and Similarity*. Hillsdale, NJ: Lawrence Erlbaum Associates.
Luce RD. 1986. *Response Times: Their Role in Inferring Elementary Mental Organization*. New York: Oxford University Press.
Markkula G. 2015. Answering questions about consciousness by modeling perception as covert behavior. Front Psychol 6:803.
Merleau-Ponty M. 1962. *Phenomenology of Perception*. London: Routledge & Kegan Paul Ltd.
Rangel A, Camerer C, Montague PR. 2008. A framework for studying the neurobiology of value-based decision-making. Nat Rev Neurosci 9:545–556.
Saxe R, Baron-Cohen S. 2006. The neuroscience of theory of mind. Soc Neurosci 1:i–ix.
Shadlen MN, Newsome WT. 1994. Noise, neural codes and cortical organization. Curr Opin Neurobiol 4:569–579.
Vickers D. 1979. *Decision Processes in Visual Perception*. London: Academic Press.
Wimmer H, Perner J. 1983. Beliefs about beliefs: representation and constraining function of wrong beliefs in young children's understanding of deception. Cognition 13:103–128.

References

Albright TD, Desimone R, Gross CG. 1984. Columnar organization of directionally selective cells in visual area MT of macaques. J Neurophysiol 51:16–31.
Andersen RA, Gnadt JW. 1989. Posterior parietal cortex. Rev Oculomot Res 3:315–335.
Born RT, Bradley DC. 2005. Structure and function of visual area MT. Annu Rev Neurosci 28:157–189.
Brincat SL, Siegel M, von Nicolai C, Miller EK. 2018. Gradual progression from sensory to task-related processing in cerebral cortex. Proc Natl Acad Sci U S A 115:E7202-E7211.
Britten KH, Shadlen MN, Newsome WT, Movshon JA. 1992. The analysis of visual motion: a comparison of neuronal and psychophysical performance. J. Neurosci. 12: 4745–65.
Brody CD, Hernandez A, Zainos A, Romo R. 2003. Timing and neural encoding of somatosensory parametric working memory in macaque prefrontal cortex. Cereb Cortex 13:1196–1207.
Constantinidis C, Funahashi S, Lee D, et al. 2018. Persistent Spiking Activity Underlies Working Memory. J Neurosci 38:7020–7028.
Ditterich J, Mazurek M, Shadlen MN. 2003. Microstimulation of visual cortex affects the speed of perceptual decisions. Nat Neurosci 6:891–898.
Fetsch CR, Odean NN, Jeurissen D, El-Shamayleh Y, Horwitz GD, Shadlen MN. 2018. Focal optogenetic suppression in macaque area MT biases direction discrimination and decision confidence, but only transiently. Elife 7:e36523.
Funahashi S, Bruce C, Goldman-Rakic P. 1989. Mnemonic coding of visual space in the monkey's dorsolateral prefrontal cortex. J Neurophysiol 61:331–349.
Gnadt JW, Andersen RA. 1988. Memory related motor planning activity in posterior parietal cortex of monkey. Exp Brain Res 70:216–220.
Gold JI, Shadlen MN. 2007. The neural basis of decision making. Annu Rev Neurosci 30:535–574.
Kiani R, Hanks TD, Shadlen MN. 2008. Bounded integration in parietal cortex underlies decisions even when viewing duration is dictated by the environment. J Neurosci 28:3017–3029.
Kiani R, Shadlen MN. 2009. Representation of confidence associated with a decision by neurons in the parietal cortex. Science 324:759–764.
Mazurek ME, Roitman JD, Ditterich J, Shadlen MN. 2003. A role for neural integrators in perceptual decision making. Cereb Cortex 13:1257–1269.
Mountcastle VB, Steinmetz MA, Romo R. 1990. Frequency discrimination in the sense of flutter: psychophysical measurements correlated with postcentral events in behaving monkeys. J Neurosci 10:3032–3044.
Padoa-Schioppa C. 2011. Neurobiology of economic choice: a good-based model. Ann Rev Neurosci 34:333–359.
Padoa-Schioppa C, Assad JA. 2006. Neurons in the orbitofrontal cortex encode economic value. Nature 441:223–226.
Roitman JD, Shadlen MN. 2002. Response of neurons in the lateral intraparietal area during a combined visual discrimination reaction time task. J Neurosci 22:9475–9489.
Romo R, Salinas E. 2001. Touch and go: decision-making mechanisms in somatosensation. Annu Rev Neurosci 24:107–137.
Salzman CD, Britten KH, Newsome WT. 1990. Cortical microstimulation influences perceptual judgements of motion direction. Nature 346:174–177.
Snyder LH, Batista AP, Andersen RA. 1997. Coding of intention in the posterior parietal cortex. Nature 386:167–170.
Yang T, Shadlen MN. 2007. Probabilistic reasoning by neurons. Nature 447:1075–1080.

Part IX

Preceding Page

Bedroom at Arles by Vincent Van Gogh. Van Gogh wrote to his friend and fellow painter, Gaugin, that he had felt "my vision was strangely tired. Well, I rested for two and a half days, and then I got back to work. But not yet daring to go outside, I did . . . a no. 30 canvas of my bedroom with the whitewood furniture that you know. Ah, well, it amused me enormously doing this bare interior. With a simplicity à la Seurat. In flat tints, but coarsely brushed in full impasto, the walls pale lilac, the floor in a broken and faded red, the chairs and the bed chrome yellow, the pillows and the sheet very pale lemon green, the blanket blood-red, the dressing-table orange, the washbasin blue, the window green. I had wished to express *utter repose* with all these very different tones, you see, among which the only white is the little note given by the mirror with a black frame (to cram in the fourth pair of complementaries as well)." Van Gogh had psychotic episodes, but there is still debate about the cause—among the theories considered have been bipolar disorder, temporal lobe epilepsy, syphilis, schizophrenia, and even toxicity from the foxglove plant (a remedy for mental illness at the time) in combination with lead poisoning from his oil paints and the consumption of absinthe. (Van Gogh Museum, Amsterdam.)

IX Diseases of the Nervous System

> He remembered that during his epileptic fits, or rather immediately preceding them, he had always experienced a moment or two when his whole heart, and mind, and body seemed to wake up to vigour and light; when he became filled with joy and hope, and all his anxieties seemed to be swept away forever; these moments were but presentiments, as it were of the one final second (it was never more than a second) in which the fit came upon him. That second, of course, was inexpressible. When his attack was over, and the prince reflected on his symptoms, he used to say to himself: "These moments, short as they are, when I feel such extreme consciousness of myself, and consequently more of life than at other times, are due only to the disease—to the sudden rupture of normal conditions. Therefore they are not really a higher kind of life, but a lower." This reasoning, however, seemed to end in a paradox, and lead to the further consideration: —"What matter though it be only disease, an abnormal tension of the brain, if when I recall and analyze the moment, it seems to have been one of harmony and beauty in the highest degree—an instant of deepest sensation, overflowing with unbounded joy and rapture, ecstatic devotion, and completest life?" Vague though this sounds, it was perfectly comprehensible to Muishkin, though he knew that it was but a feeble expression of his sensations.*

WHAT, EXACTLY, IS THE NATURE OF THE RELATIONSHIP between the mind and the brain? Dostoevsky's own experience of epilepsy profoundly influenced his writing, and in this passage, he probes some of the most profound questions about human experience. Are our thoughts and moods simply transient combinations of chemicals and electrical signals? Do we have any influence over them? If not, can we be held responsible for our actions? What if some of our peak experiences are just happy chemical accidents? Or, as Prince Muishkin wonders, what if some of our peaks are happy accidents of disease? What, then, would it mean to "get better"? Individuals with bipolar disorder, for example, can have a very difficult time relinquishing the expansive feelings and creative energies that can accompany mania.

Although these profound questions are the purview of philosophers rather than neuroscientists, few circumstances bring the mind–brain relationship into question as sharply as becoming victim to a neurological or psychiatric disorder. The range of these conditions

*Dostoevsky F. *The Idiot*. Translated by Eva Martin. Project Gutenberg EBook, last updated May 13, 2017.

is very wide, from motor disturbances to epilepsy, schizophrenia, mood imbalances, cognitive disorders, neurodegeneration, and even aging. The more we learn, the more it becomes apparent that these diseases exert very broad effects that blur the boundaries between their classifications. So-called movement disorders such as Parkinson disease, for example, involve cognitive and affective changes; disorders of cognition such as autism or schizophrenia can have very physical manifestations.

Despite these somewhat fuzzy boundaries, each chapter in this section will examine the principles underlying each major class of disease from the perspective of neuroscience. The emphasis here is on molecular mechanisms, so far as they are currently understood. It is perhaps surprising that so many different disease conditions seem to converge on one physiological point: synaptic function. In autism and several psychiatric disorders, synaptic development goes awry; in epilepsy, abnormal ion channel activity disturbs the balance of synaptic input from excitatory and inhibitory neurons. Aging and neurodegenerative disorders bring about synaptic loss through gradual alterations in protein and RNA homeostasis that tax normal cellular functions.

This observation is offered to help give shape to the material you are about to encounter, but should not be used to oversimplify. Anyone tempted by reductionism would do well to engage with the works of great artists such as Dostoevsky and Van Gogh, who represent the complexities of human experience in all its anguish and glory.

Part Editor: Huda Y. Zoghbi

Part IX

57

Diseases of the Peripheral Nerve and Motor Unit

… to move things is all that mankind can do, for such the sole executant is muscle, whether in whispering a syllable or in felling a forest.

Charles Sherrington, 1924

A major task of the elaborate information processing that takes place in the brain is the contraction of skeletal muscles. The challenge of deciding when and how to move is, to a large degree, the driving force behind the evolution of the nervous system (Chapter 30).

In all but the most primitive animals, movement is generated by specialized muscle cells. There are three general types of muscles: Smooth muscle is used primarily for internal actions such as peristalsis and control of blood flow; cardiac muscle is used exclusively for pumping blood; and skeletal muscle is used primarily for moving bones. In this chapter, we examine a variety of neurological disorders in mammals that affect movement by altering either action potential conduction in a motor nerve, synaptic transmission from nerve to muscle, or muscle contraction itself.

In 1925, Charles Sherrington introduced the term *motor unit* to designate the basic unit of motor function—a motor neuron and the group of muscle fibers it innervates (Chapter 31). The number of muscle fibers innervated by a single motor neuron varies widely throughout the body depending on the dexterity of the movements being controlled and the mass of the body part to be moved. Thus, eye movements are finely controlled by motor units with fewer than 100 muscle

fibers, whereas in the leg, a single motor unit contains up to 1,000 muscle fibers. In each case, all the muscles innervated by a motor unit are of the same type. Moreover, motor units are recruited in a fixed order for both voluntary and reflex movements. The smallest motor units are the first to be recruited, joined later by larger units as muscle force increases.

The motor unit is a common target of disease. The distinguishing features of diseases of the motor unit vary depending on which functional component is primarily affected: (1) the cell body of the motor or sensory neuron, (2) the corresponding axons, (3) the neuromuscular junction (the synapse between the motor axon and muscle), or (4) the muscle fibers innervated by the motor neuron. Accordingly, disorders of the motor unit have traditionally been grouped into motor neuron diseases, peripheral neuropathies, disorders of the neuromuscular junction, and primary muscle diseases (myopathies) (Figure 57–1).

Patients with peripheral neuropathies experience weakness that arises from abnormal function of motor neurons or their axons, although problems with sensation can also occur since most peripheral neuropathies also involve sensory neurons. By contrast, in motor neuron diseases, the motor neurons and motor tracts in the spinal cord degenerate but sensory nerves are spared. In myopathies, weakness is caused by degeneration of the muscles with little or no change in motor neurons. In neuromuscular junction diseases, alterations in the neuromuscular synapse lead to weakness that may be intermittent. Clinical and laboratory studies usually distinguish disorders of peripheral nerves from those of the neuromuscular junction or muscle (Table 57–1).

Disorders of the Peripheral Nerve, Neuromuscular Junction, and Muscle Can Be Distinguished Clinically

When a peripheral nerve is cut, the muscles innervated by that nerve immediately become paralyzed and then waste progressively. Because the nerve carries sensory as well as motor fibers, sensation in the area innervated by the nerve is also lost and tendon reflexes are lost immediately. The term *atrophy* (literally, lack of nourishment) refers to the wasting away of a once-normal muscle; because of historical usage the term appears in the names of several diseases that are now regarded as neurogenic.

The main symptoms of the *myopathies* are due to weakness of skeletal muscle and often include difficulty in walking or lifting. Other less common symptoms include inability of the muscle to relax (myotonia), cramps, pain (myalgia), or the appearance in the urine of the heme-containing protein that gives muscle its red color (myoglobinuria). The *muscular dystrophies* are myopathies with special characteristics: The diseases are inherited, all symptoms are caused by weakness, the weakness becomes progressively more

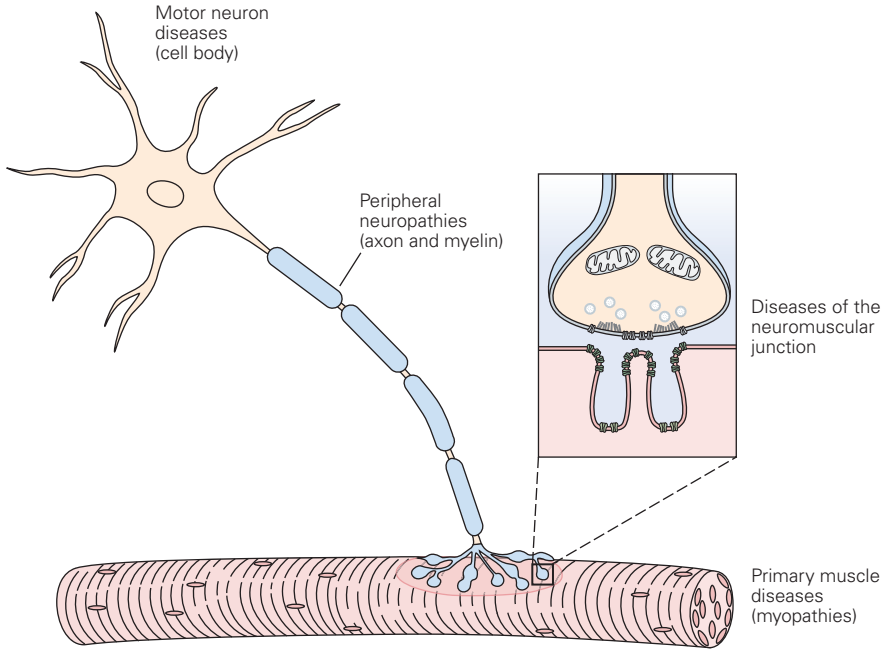

Figure 57–1 The four types of motor unit disorders. Motor unit disorders are categorized according to the part of the motor unit that is affected. Motor neuron diseases affect the cell body of the neuron, while peripheral neuropathies target the axon. Diseases of the neuromuscular junction affect the functioning of the synapse, and myopathies affect muscle fibers.

Table 57–1 Differential Diagnosis of Disorders of the Motor Unit

Finding	Nerve	Neuromuscular junction	Muscle
Clinical			
Weakness	++	+	++
Wasting	++	–	+
Fasciculations	+	–	–
Cramps	+	–	+/–
Sensory loss	+/–	–	–
Hyperreflexia, Babinski	+ (ALS)	–	–
Laboratory			
Elevated serum CPK	–	–	++
Elevated cerebrospinal fluid protein	+/–	–	–
Slowed nerve conduction	+	–	–
Response to repetitive stimulation	Normal	Decremental (MG) Incremental (LEMS)	Normal
Electromyography			
Fibrillation, fasciculation	++	–	+/–
Duration of potentials	Increased	Normal	Decreased
Amplitude of potentials	Increased	Normal	Decreased
Muscle Biopsy			
Isolated fiber atrophy	++	Normal	+/–
Grouped fiber atrophy	++	Normal	Normal
Muscle necrosis	Normal	Normal	++

ALS, amyotrophic lateral sclerosis; CPK, creatine phosphokinase; LEMS, Lambert-Eaton myasthenic syndrome; MG, myasthenia gravis.

severe, and signs of degeneration and regeneration are seen histologically.

Distinguishing neurogenic and myopathic diseases may be difficult because both are characterized by weakness of muscle. As a first approximation, weakness of the distal limbs most often indicates a neurogenic disorder, whereas proximal limb weakness signals a myopathy. The main clinical and laboratory features used for the differential diagnosis of diseases of the motor unit are listed in Table 57–1.

One test that is very helpful is needle electromyography (EMG), a clinical procedure in which a small needle is inserted into a muscle to record extracellularly the electrical activity of several neighboring motor units. Three specific measurements are important: spontaneous activity at rest, the number of motor units under voluntary control, and the duration and amplitude of action potentials in each motor unit. (Normal ranges of values have been established for the amplitude and duration of motor unit potentials; the amplitude is determined by the number of muscle fibers within the motor unit.)

In normal muscle, there is usually no activity outside the end-plate in the muscle at rest. During a weak voluntary contraction, a series of motor unit potentials is recorded as different motor units become recruited. In fully active normal muscles, these abundant potentials overlap in an interference pattern so that it is impossible to identify single potentials (Figure 57–2A).

In neurogenic disease, the partially denervated muscle is spontaneously active even at rest. The muscle may still contract in response to voluntary motor commands, but the number of motor units under voluntary control is smaller than normal because some motor axons have been lost. The loss of motor units is evident in the EMG during a maximal contraction, which shows a pattern of discrete motor unit potentials instead of the profuse interference pattern for normal muscles (Figure 57–2B). In recently denervated muscle, the EMG may also show spontaneous low-amplitude electrical potentials that correspond to the firing of a single muscle fiber, known as fibrillation potentials. As the neurogenic disease progresses, the amplitude and duration of individual motor unit potentials may increase because the remaining axons give off small branches that innervate the muscle fibers denervated

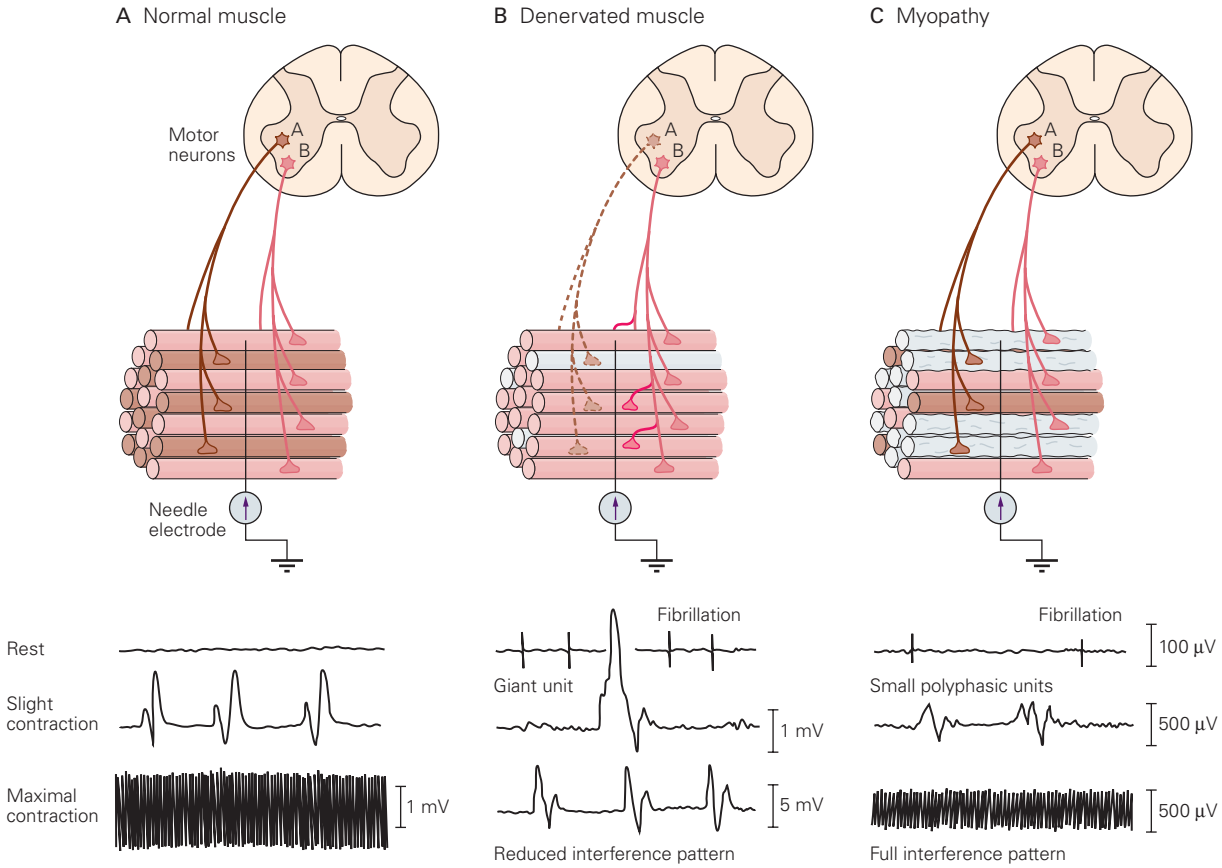

Figure 57–2 Electrical recording from skeletal muscle reveals different profiles in neuropathies and primary muscle diseases.

A. Typical activity in a normal muscle. The muscle fibers innervated by a single motor neuron are usually not adjacent to one another. When a motor unit potential is recorded by a needle electrode inserted into the muscle, the highly effective transmission at the neuromuscular junction ensures that each muscle fiber innervated by the same neuron will generate an action potential and contract in response to an action potential in the motor neuron. In the normal, resting muscle, there is no electrical activity recorded from muscle in the electromyogram (EMG). Slight activation of the muscle by a voluntary movement reveals characteristic extracellular electrical responses in muscle (motor unit potentials (MUPs)). Maximal muscle contraction produces a characteristic complex burst of electrical activity from muscle (the interference pattern).

B. When motor neurons are diseased, the number of motor units under voluntary control is reduced. The muscle fibers supplied by the degenerating motor neuron (cell A) become denervated and atrophic. However, the surviving neuron (cell B) sprouts axonal branches that reinnervate some of the denervated muscle fibers. Axons of the surviving motor neuron fire spontaneously even at rest, giving rise to fasciculations, another characteristic of motor neuron disease. Single denervated fibers also fire spontaneously, producing fibrillations (top trace). With loss of nerve input from motor neuron A and reinnervation of the denervated fibers by motor neuron B, activation of motor neuron B produces an enlarged MUP (giant motor unit). In this setting, there is simplification of the interference pattern.

C. When muscle is diseased (myopathy), the number of muscle fibers in each motor unit is reduced. Some muscle fibers innervated by the two motor neurons shrink and become nonfunctional. In the electromyogram, the motor unit potentials do not decrease in number but are smaller and of longer duration than normal and are polyphasic. Affected single muscle fibers sometimes contract spontaneously, producing fibrillation. When muscle is mildly activated, the MUPs show reduced amplitudes. After maximal muscle contraction, the interference pattern also shows a reduction in amplitude.

by the loss of other axons. Accordingly, surviving motor units contain more than the normal number of muscle fibers.

In myopathic diseases, there is no activity in the muscle at rest and no change in the number of motor units firing during a contraction. But because there are fewer surviving muscle fibers in each motor unit, the motor unit potentials are of longer duration and more complex, with alternating +/− polarity (polyphasic), and are smaller in amplitude (Figure 57–2C).

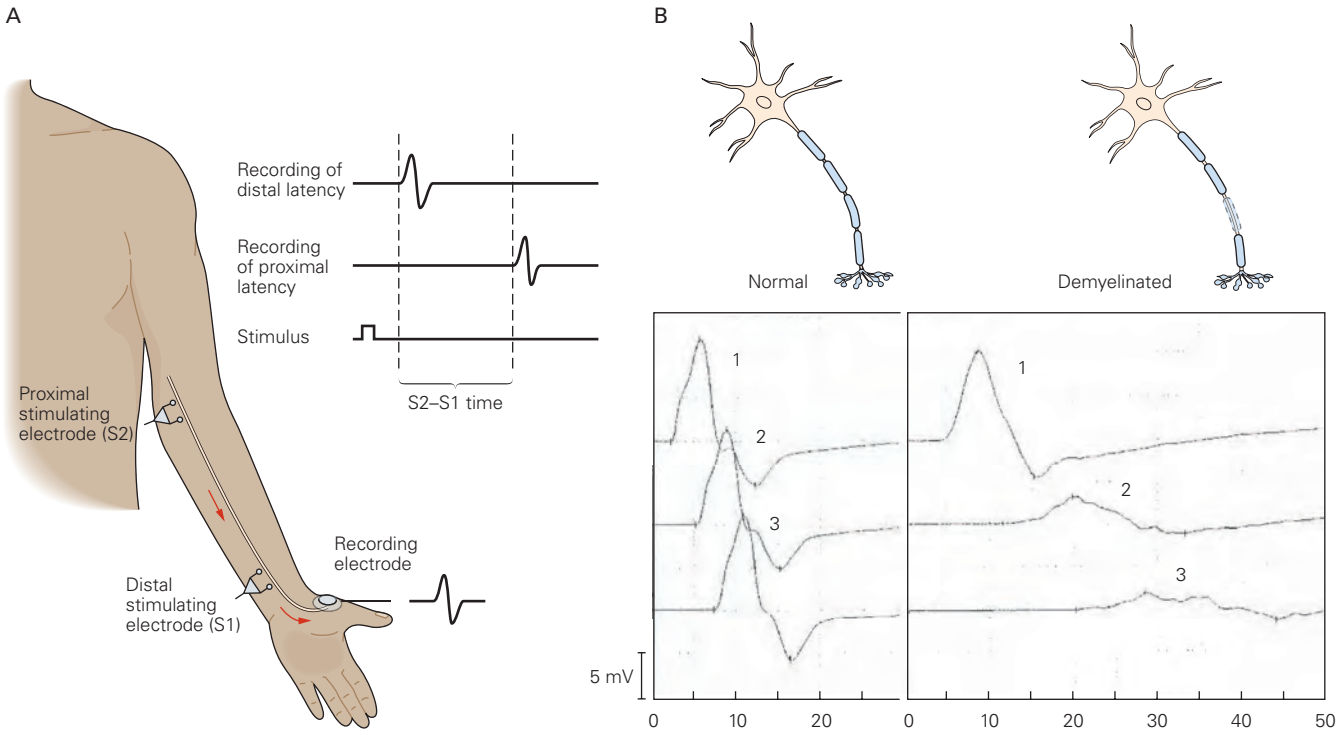

Figure 57–3 Motor nerve conduction velocity can be determined by recording the compound muscle action potential (CMAP) in response to electrical stimulation at different points along the nerve.

A. A shock is applied through a proximal surface stimulating electrode (**S2**) or through a distal stimulating electrode (**S1**), and the extracellular CMAP in the thumb is measured transcutaneously by the recording electrode. The time it takes the action potential to propagate from S2 to the muscle (t_{S2}) is the proximal latency; the time from S1 to the muscle (t_{S1}) is the distal latency. The distance between S1 and S2 divided by ($t_{S2} - t_{S1}$) gives the conduction velocity.

B. The waveforms of the thumb CMAPs elicited by stimulation of the motor nerve at the wrist (**1**), just below the elbow (**2**), and just above the elbow (**3**). In normal subjects (*left*), the waveforms are the same regardless of the site of stimulation. They are distinguished only by the longer time period required for the waveform to develop as the site of the stimulus is moved up the arm (away from the recording site). When the motor nerve is demyelinated between S1 and S2 but above the wrist, the CMAP is normal when stimulation occurs at the wrist (**1**) but delayed and desynchronized when stimulation is proximal to the nerve lesion (**2**, **3**). (Adapted, with permission, from Bromberg 2002.)

The conduction velocities of peripheral motor axons can also be measured through electrical stimulation and recording (see Figure 57–3). The conduction velocity of motor axons is slowed in demyelinating neuropathies but is normal in neuropathies without demyelination (axonal neuropathies).

Another test that helps to distinguish myopathic from neurogenic diseases is the measurement of serum enzyme activities. The sarcoplasm of muscle is rich in soluble enzymes that are normally found in low concentrations in the serum. In many muscle diseases, the concentration of these sarcoplasmic enzymes in serum is elevated, presumably because the diseases affect the integrity of surface membranes of the muscle, allowing the enzymes to leak into the bloodstream. The enzyme activity most commonly used for diagnosing myopathy is creatine kinase, an enzyme that phosphorylates creatine and is important in the energy metabolism of muscle.

Muscle histochemical appearance in a biopsy can also provide a useful diagnostic tool. Human muscle fibers are identified by histochemical reactions as type I or type II, which respectively are either aerobic (enriched for oxidative enzymes) or anaerobic (abundant glycolytic enzymes) (Chapter 31). All muscle fibers innervated by a single motor neuron are of the same histochemical type. However, the muscle fibers of one motor unit are normally interspersed among the muscle fibers of other motor units. In a cross section of healthy muscle, enzyme stains show that oxidative or glycolytic fibers are intermixed in a "checkerboard" pattern.

In chronic neurogenic diseases, the muscle innervated by a dying motor neuron becomes atrophic and some muscle fibers disappear. Axons of surviving neurons tend to sprout and reinnervate some of the adjacent remaining muscle fibers. Because the motor neuron determines the biochemical and thus histochemical properties of a muscle fiber, the reinnervated muscle fibers assume the histochemical properties of the innervating neuron. As a result, the fibers of a muscle in neurogenic disease become clustered by type (a pattern called fiber-type grouping).

If the disease is progressive and the neurons in the surviving motor units also become affected, atrophy occurs in groups of adjacent muscle fibers belonging to the same histochemical type, a process called group atrophy. In contrast, in myopathic diseases, the muscle fibers are affected in a more or less random fashion. Sometimes an inflammatory cellular response is evident, and sometimes there is prominent infiltration of the muscle by fat and connective tissue.

Fasciculations—visible twitches of muscle that can be seen as flickers under the skin—are often signs of neurogenic diseases. They result from involuntary but synchronous contractions of all muscle fibers in a motor unit. Fibrillations—spontaneous contractions within single muscle fibers—can also be signs of ongoing denervation of muscle. Fibrillations are not visible but can be recorded with an EMG. The electrical record of a fibrillation is a low-amplitude potential that reflects electrical activity in a single muscle cell. Electrophysiological studies suggest that fasciculations arise in the motor nerve terminal.

In diagnosing motor neuron disorders, clinicians have historically distinguished between so-called lower motor neurons and premotor neurons. Lower motor neurons are motor neurons of the spinal cord and brain stem that directly innervate skeletal muscles. Premotor neurons, also known as "upper" motor neurons, originate in the motor cortex and issue commands for movements to the lower motor neurons through their axons in the corticospinal (pyramidal) tract.

Diseases of upper motor neurons can be distinguished from those affecting lower motor neurons by distinct sets of symptoms. Disorders of lower motor neurons cause atrophy, fasciculations, decreased muscle tone, and loss of tendon reflexes, whereas disorders of upper motor neurons and their axons result in spasticity, overactive tendon reflexes, and abnormal plantar extensor reflex (the Babinski sign).

The primary symptom of disorders of the neuromuscular junction is weakness; in some neuromuscular junction diseases, this weakness is quite variable even over the course of a single day.

A Variety of Diseases Target Motor Neurons and Peripheral Nerves

Motor Neuron Diseases Do Not Affect Sensory Neurons (Amyotrophic Lateral Sclerosis)

The best-known disorder of motor neurons is amyotrophic lateral sclerosis (ALS; Lou Gehrig disease). "Amyotrophy" is another term for neurogenic atrophy of muscle; "lateral sclerosis" refers to the hardness felt when the pathologist examines the spinal cord at autopsy. This hardness results from the proliferation of astrocytes and scarring of the lateral columns of the spinal cord due to degeneration of the corticospinal tracts.

The symptoms of ALS usually start with painless weakness in a single arm or leg. Typically, the patient, often a man in his 40s or 50s, discovers that he has trouble in executing fine movements of the hands—typing, playing the piano, playing baseball, fingering coins, or working with tools. This focal weakness then spreads over 3 or 4 years to involve all four limbs, as well as the muscles of chewing, speaking, swallowing, and breathing.

Most cases of ALS involve both the upper and the lower motor neurons. Some motor neurons are spared, notably those supplying ocular muscles and those involved in voluntary control of bladder sphincters. The typical weakness of the hand is associated with wasting of the small muscles of the hands and feet and fasciculations of the muscles of the forearm and upper arm. These signs of lower motor neuron disease are often associated with hyperreflexia, an over-responsiveness in tendon reflexes characteristic of corticospinal upper motor neuron disease. The cause of most cases (90%) of ALS is not known; the disease is progressive and ultimately affects the muscles of respiration. There is no effective treatment for this fatal condition.

About 10% of cases are inherited in a dominant manner (Table 57–2). In North America, greater than 25% of inherited cases arise from mutations in the gene *C9orf72*. The offending genetic defect is an expansion in an intronic hexanucleotide repeat, from 30 or fewer in normal individuals to hundreds or even thousands in affected individuals. Besides giving rise to conventional ALS, mutations in *C9orf72* can also cause frontotemporal dementia. The toxicity of the mutant C9orf72 protein probably reflects both a reduction in total activity of the mutant protein and toxic effects of the intronic expansion. For example, the expanded intronic segments produce intranuclear deposits of RNA that likely sequester and inactivate important nuclear proteins. In addition, the expanded RNA is translated to

Table 57–2 Selected Amyotrophic Lateral Sclerosis Genes

				Proportion of ALS	
Gene	**Protein**	**Protein function**	**Mutations**	**Familial**	**Sporadic**
SOD1	Cu-Zn superoxide dismutase	Superoxide dismutase	>150	20%	2%
DCTN1	Dynactin subunit 1	Component of dynein motor complex	10	1%	<1%
ANG	Angiogenin	Ribonuclease	>10	<1%	<1%
TARDBP	TDP-43	RNA-binding protein	>40	5%	<1%
FUS	FUS	RNA-binding protein	>40	5%	<1%
VCP	Transitional endoplasmic reticulum ATPase	Ubiquitin segregase	5	1–2%	<1%
OPTN	Optineurin	Autophagy adaptor	1	4%	<1%
C9orf72	C9orf72	Possible guanine nucleotide exchange factor	Intronic GGGGCC	25%	10%
UBQLN2	Ubiquilin 2	Autophagy adaptor	5	<1%	<1%
SQSTM1	Sequestosome 1	Autophagy adaptor	10	<1%	?
FFN1	Profilin-1	Actin-binding protein	5	<1%	<1%
HNRNPA1	hnRNP A1	RNA-binding protein	3	<1%	<1%
MATR3	Matrin 3	RNA-binding protein	4	<1%	<1%
TUBA4A	Tubulin α-4A chain	Microtubule subunit	7	<1%	<1%
CHCHD10	Coiled-coil-helix-coiled-coil-helix domain-containing protein 10	Mitochondrial protein of unknown function	2	<1%	<1%
TBK1	Serine/threonine-protein kinase TBK1	Regulates autophagy and inflammation	10	1%	<1%

Source: Modified from Taylor, Brown, and Cleveland 2016.

produce peptides composed of repeated couplets of amino acids, such as poly-(glycine-proline) or poly-(proline-arginine); some of these are neurotoxic.

Two other genes commonly mutated in ALS are *SOD1* and *TDP43*. *SOD1* encodes the protein copper/zinc cytosolic superoxide dismutase, whereas *TDP43* encodes a 43-kD, RNA-interacting protein that is normally intranuclear but is mislocalized to the cytosol in most cases of ALS (both inherited and sporadic). Mutations in *SOD1* and several other ALS genes (eg, *ubiquilin-2*) destabilize the conformation of the protein product, promoting misfolding and causing adverse consequences to diverse subcellular processes and compartments. By contrast, mutations in *TDP43* and a few other ALS genes (eg, *FUS*) encoding RNA binding proteins act at the RNA level, impairing RNA homeostasis and perturbing critical processes such as surveillance of gene splicing. Infrequently, familial ALS is caused by mutations in genes encoding cytoskeletal proteins such as profilin-1, dynactin, or tubulin-A4.

Many studies suggest that mutant ALS-associated proteins tend to aggregate, particularly in membraneless organelles called stress granules that form in conditions of cellular distress. Several lines of investigation support the view that aggregates migrate and transmit pathology between adjacent cells, accounting for spread of the disease to different brain regions. Strikingly, mice that express high levels of defective SOD1 or profilin-1 proteins develop a lethal, adult-onset form of motor neuron disease, but mice expressing equivalently high levels of normal SOD1 or profilin-1 proteins do not. These findings are consistent with the concept that the defective protein has gained some sort of toxic function.

In the past 10 years, it has also become clear that motor neuron pathophysiology is modulated by the reactions of nonneural cells to degeneration in the motor neuron. Thus, in most cases of ALS, there are varying degrees of proliferation and activation of microglia, astrocytes, and some populations of lymphocytes, which may begin as compensatory responses but can eventually adversely affect the injured motor neurons. Genetic studies have underscored the importance of non–cell-autonomous factors, such as variants that reduce function of the microglial gene *TREM-2* and enhance the risk of developing not only ALS but also other neurodegenerative disorders (eg, Alzheimer disease).

Progressive bulbar palsy is a type of motor neuron disease in which damage is restricted to muscles innervated by cranial nerves, causing dysarthria (difficulty speaking) and dysphagia (difficulty swallowing). (The term "bulb" is used interchangeably with "pons," the structure at the base of the brain where motor neurons that innervate the face and swallowing muscles reside, and "palsy" means weakness). If only lower motor neurons are involved, the syndrome is called progressive spinal muscular atrophy.

Progressive spinal muscular atrophy is actually a developmental motor neuron disorder characterized by weakness, wasting, loss of reflexes, and fasciculations. Most cases arise in infancy and are caused by recessively inherited mutations in the gene encoding a protein called survival motor neuron (SMN). Survival in these cases is very short, although there are rare cases that begin in late childhood or even early adulthood and are associated with longer survival of many years. The SMN protein is implicated in trafficking RNA in and out of the nucleus and in the formation of complexes that are important in RNA splicing. The SMN locus on chromosome 5 in humans has two almost identical copies of the *SMN* gene: *SMN1* produces a full-length SMN protein, while alternative splicing of *SMN2* causes omission of the seventh exon in the gene, leading to expression of a small amount of full-length SMN and a shortened SMN. The clinical effect of the loss of full-length SMN from mutations at the main locus can be mitigated to some degree by the shortened SMN protein expressed by the *SMN2* gene (Figure 57–4A,B).

Two treatment strategies have achieved extraordinary benefits in spinal muscular atrophy. In one, small strings of approximately 20 nucleic acids (antisense oligonucleotides [ASO]s) are administered to alter splicing of the *SMN2* gene so that it produces higher levels of the full-length SMN protein (Figure 57-4A). This occurs because the ASO is targeted to bind to the SMN2 RNA and inhibit the action of the RNA binding protein hnRNPA1/A2 that normally leads the splicing machinery to skip exon 7. By blocking the binding of hnRNPA1/A2, the ASO blocks the inhibitory effect of hnRNPA1/A2 on splicing, promoting expression of full-length SMN protein (Figure 57–4B). It seems likely that ASOs will become powerful therapeutic tools with many applications. In this example, ASO is used to promote exon inclusion; as noted below in the discussion on muscle dystrophy, ASO can also be used to promote exon skipping. It can also be used in other paradigms to inhibit or enhance levels of target gene expression.

The second approach to treating spinal muscular atrophy has been to deliver the missing *SMN* gene to spinal motor neurons and muscle using high doses of intravenously infused adeno-associated virus carrying the *SMN1* gene. This, too, dramatically augments survival in infantile spinal muscular atrophy (Figure 57–4B).

ALS and its variants are restricted to motor neurons; they do not affect sensory neurons or autonomic neurons. The acute viral disease poliomyelitis is also confined to motor neurons. These diseases illustrate the individuality of nerve cells and the principle of selective vulnerability. The basis of this selectivity is, in general, not understood.

Diseases of Peripheral Nerves Affect Conduction of the Action Potential

Diseases of peripheral nerves may affect either axons or myelin. Because motor and sensory axons are bundled together in the same peripheral nerves, disorders of peripheral nerves usually affect both motor and sensory functions. Some patients with peripheral neuropathy report abnormal, frequently unpleasant, sensory experiences such as numbness, pins-and-needles prickling, or tingling. When these sensations occur spontaneously without an external sensory stimulus, they are called paresthesias.

Patients with paresthesias usually have impaired perception of cutaneous sensations (pain and temperature), often because the small fibers that carry these sensations are selectively affected. This is not always the case, however. Proprioceptive sensations (position and vibration) can be lost without loss of cutaneous sensation. Lack of pain perception may lead to injuries. The sensory deficits are more prominent distally (called a glove-and-stocking pattern), likely because the distal portions of the nerves are most remote from the cell body and therefore most susceptible to disorders that interfere with axonal transport of essential metabolites and proteins.

Peripheral neuropathy is first manifested by weakness that is usually distal. Tendon reflexes are usually

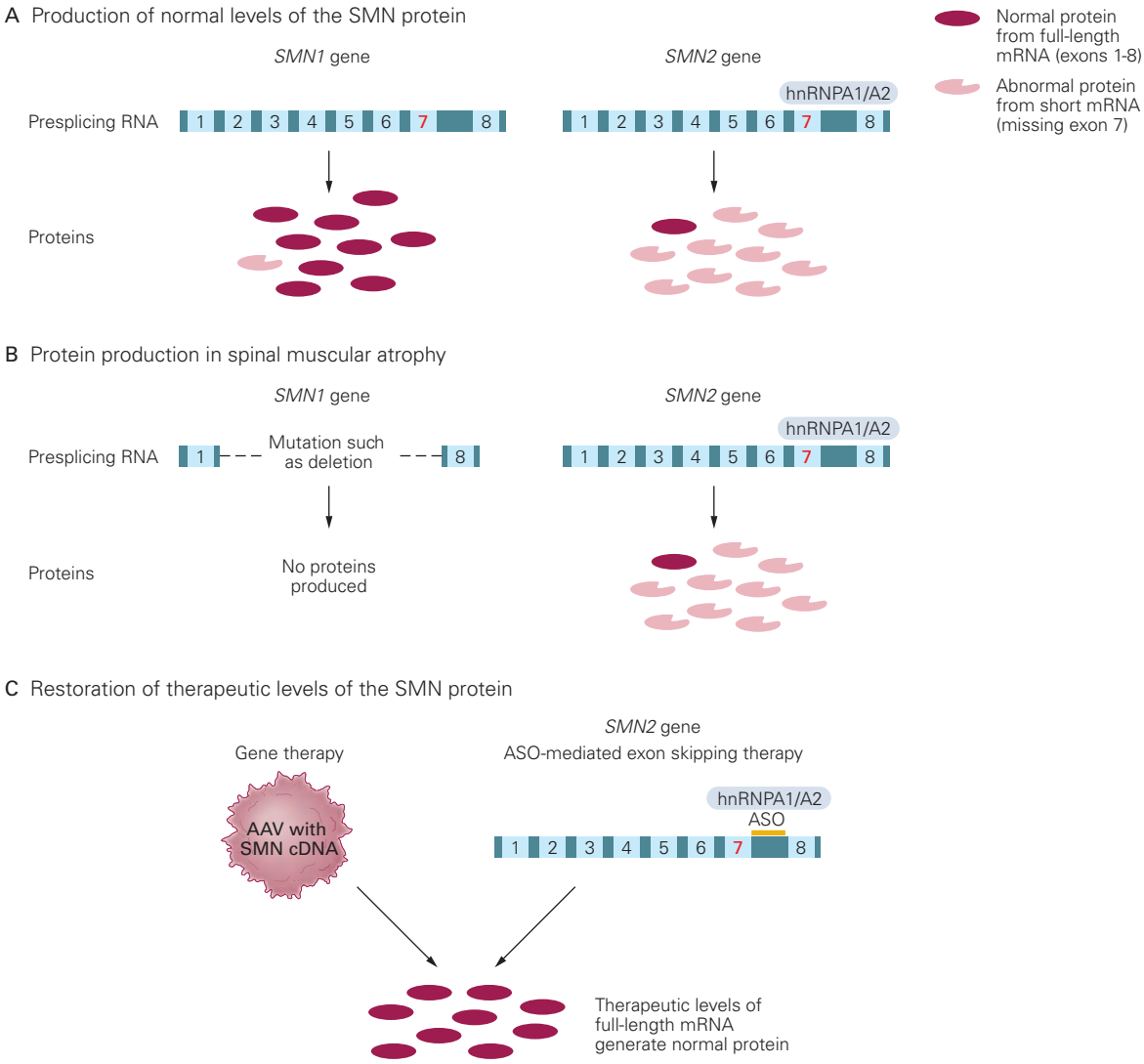

Figure 57–4 Spinal motor atrophy caused by defective survival motor neuron gene (*SMN1*) can be treated by gene replacement therapy or by manipulating splicing of *SMN2*.

A. Normally, most of the survival motor neuron (**SMN**) protein is produced from the *SMN1* gene, whose mRNA is spliced from eight exons. In normal circumstances, about 90% of the mRNA has all eight exons, yielding normal levels of the SMN protein. In the adjacent sister gene, *SMN2*, binding of the protein hnRNPA1/A2 to the *SMN2* transcript excludes exon 7; *SMN2* therefore makes a shortened SMN protein.

B. In spinal muscular atrophy, genetic lesions (commonly deletions) in *SMN1* lead to a marked reduction in levels of total SMN protein.

C. When SMN1 protein is absent, one therapeutic approach is to replace the missing *SMN1* gene using an adeno-associated viral vector (**AAV**) to deliver the missing gene to the central nervous system and muscle. An alternative approach is to deliver an antisense oligonucleotide (**ASO**) that blocks the effect of hnRNPA1/A2, thereby enhancing production of a full-length mRNA (with all eight exons) from *SMN2*. This restores SMN protein levels.

depressed or lost, fasciculation is seen only rarely, and wasting does not ensue unless the weakness has been present for many weeks.

Neuropathies may be either acute or chronic. The best-known acute neuropathy is Guillain-Barré syndrome. Most cases follow respiratory infection or infectious diarrhea, but the syndrome may occur without apparent preceding illness. The condition may be mild or so severe that mechanical ventilation is required. Cranial nerves may be affected, leading to paralysis of ocular, facial, and oropharyngeal muscles. The disorder is attributed to an autoimmune attack on peripheral nerves by circulating antibodies. It is therefore treated by removing the offending antibodies by

infusions of gamma globulin and plasmapheresis (a procedure in which blood is removed from a patient, cells are separated from the antibody-carrying plasma, and the cells alone are returned to the patient).

The chronic neuropathies vary from mild to incapacitating or even fatal conditions. There are many varieties, including genetic diseases (acute intermittent porphyria, Charcot-Marie-Tooth disease), metabolic disorders (diabetes, vitamin B_{12} deficiency), toxicities (lead), nutritional disorders (alcoholism, thiamine deficiency), carcinomas (especially carcinoma of the lung), and immunological disorders (plasma cell diseases, amyloidosis). Some chronic disorders, such as neuropathy due to vitamin B_{12} deficiency in pernicious anemia, are amenable to therapy.

In addition to being acute or chronic, neuropathies may be categorized as demyelinating (in which the myelin sheath breaks down) or axonal (in which the axon is affected). In demyelinating neuropathies, as might be expected from the role of the myelin sheath in saltatory conduction, conduction velocity is slowed. In axonal neuropathies, the myelin sheath is not affected and conduction velocity is normal.

Axonal and demyelinating neuropathies may lead to positive or negative symptoms and signs. The negative signs consist of weakness or paralysis, loss of tendon reflexes, and impaired sensation resulting from loss of motor and sensory nerves. The positive symptoms of peripheral neuropathies consist of paresthesias that arise from abnormal impulse activity in sensory fibers and either spontaneous activity of injured nerve fibers or electrical interaction (cross-talk) between abnormal axons, a process called ephaptic transmission to distinguish it from normal synaptic transmission. It is not known why damaged nerves become hyperexcitable. Even lightly tapping the site of injury can evoke a burst of painful sensations in the region over which the nerve is distributed.

Negative symptoms, which have been studied more thoroughly than positive symptoms, can be attributed to three basic mechanisms: conduction block, slowed conduction, and impaired ability to conduct impulses at higher frequencies. Conduction block was first recognized in 1876 when the German neurologist Wilhelm Erb observed that stimulation of an injured peripheral nerve below the site of injury evoked a muscle response, whereas stimulation above the site of injury produced no response. He deduced that the lesion blocked conduction of impulses of central origin, even when the segment of the nerve distal to the lesion was still functional. Later studies confirmed this conclusion by showing that selective application of diphtheria and other toxins produces conduction block by causing demyelination only at the site of application (Figure 57–5).

Why does demyelination produce nerve block, and how does it lead to slowing of conduction velocity? Conduction velocity is much more rapid in myelinated fibers than in unmyelinated axons for two reasons (Chapter 9). First, there is a direct relationship between conduction velocity and axon diameter, and myelinated axons tend to be larger in diameter. Second, membrane capacitance in the myelinated regions of the axon is lower than at the unmyelinated nodes of Ranvier, greatly speeding up the rate of depolarization and thus conduction. With demyelination, the spatial distribution of ion channels along the denuded axon is not optimal for supporting action potential propagation and may even cause a failure of conduction. When myelin is disrupted by disease, the action potentials in different axons of a nerve begin to conduct at slightly different velocities. As a result, the nerve loses its normal synchrony of conduction in response to a single stimulus. (Figure 57–2 shows how conduction velocities are measured in peripheral nerves.)

This slowing and loss of synchrony are thought to account for some of the early clinical signs of demyelinating neuropathy. For example, functions that normally depend on the arrival of synchronous bursts of neural activity, such as tendon reflexes and vibratory sensation, are lost soon after the onset of a chronic neuropathy. As demyelination becomes more severe, conduction becomes blocked. This block may be intermittent, occurring only at high frequencies of neural firing, or complete (Figure 57–3).

The Molecular Basis of Some Inherited Peripheral Neuropathies Has Been Defined

Myelin proteins are affected in a group of demyelinating hereditary peripheral neuropathies collectively termed Charcot-Marie-Tooth (CMT) disease. CMT is characterized by muscle weakness and wasting, loss of reflexes, and loss of sensation in the distal parts of the limbs. These symptoms appear in childhood or adolescence and are slowly progressive.

One form (type 1) has the features of a demyelinating neuropathy (Figure 57–5). Conduction in peripheral nerves is slow, with histological evidence of demyelination followed by remyelination. Sometimes, the remyelination leads to gross hypertrophy of the nerves. Type 1 disorders are inexorably progressive, without remissions or exacerbations. Another form (type 2) has normal nerve conduction velocity and is considered an axonal neuropathy without demyelination. Both types 1 and 2 are inherited as autosomal dominant diseases.

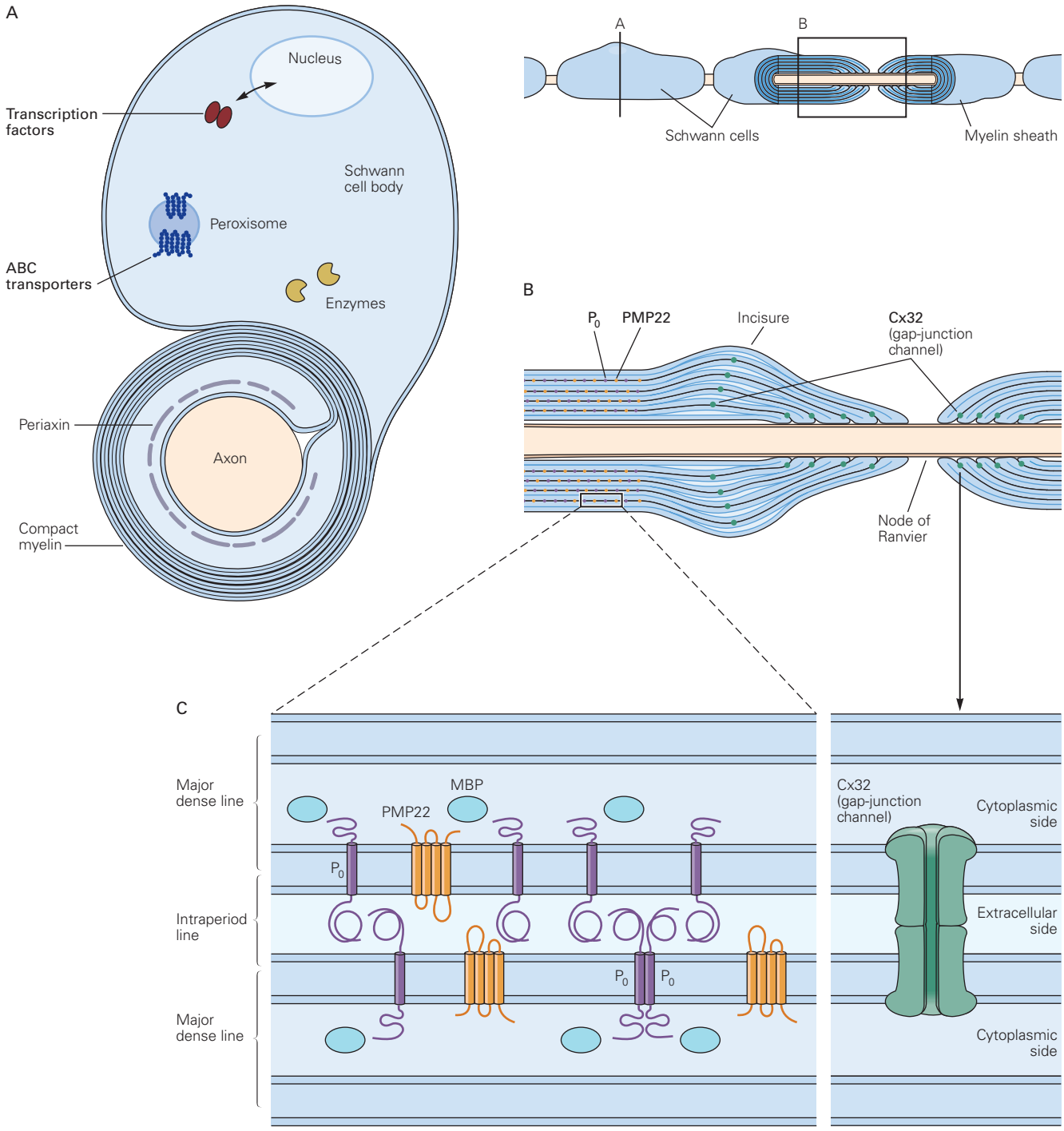

Figure 57–5 Gene defects in components of myelin cause demyelinating neuropathies.

A. Myelin production and function in the Schwann cell can be adversely affected by many genetic defects, including abnormalities in transcription factors, **ABC** (ATP-binding cassette) transporters in peroxisomes, and multiple proteins implicated in organizing myelin. Viewed microscopically at high power, the site of apposition of the intracellular faces of the Schwann cell membrane appears as a dense line, whereas the apposed extracellular faces are described as the "intraperiod line" (see part **C**). (Adapted from Lupski 1998.)

B. Peripheral axons are wrapped in multiple layers of thin sheaths of myelin that are processes of Schwann cells. The myelin is compact and tight except near the nodes of Ranvier and at focal sites described as "incisures" by Schmidt and Lanterman. Three myelin-associated proteins are defective in three different demyelinating neuropathies: P_0 (Dejerine-Sottas infantile neuropathy), peripheral myelin protein (**PMP22**) (Charcot-Marie-Tooth neuropathy type 1), and connexin-32 (**Cx32**) (X-linked Charcot-Marie-Tooth neuropathy). (Adapted from Lupski 1998.)

C. The rim of cytoplasm in which myelin basic protein (**MBP**) is located defines the major dense line, whereas the thin layer of residual extracellular space defines the intraperiod line. Mutations in PMP22 and P_0 genes adversely affect the organization of compact myelin. (Adapted, with permission, from Brown and Amato 2002.)

Type 1 disease is attributed to mutations on two different chromosomes (locus heterogeneity). The more common form (type 1A) is linked to chromosome 17, while the less common form (1B) is localized to chromosome 1. The genes at these loci have been directly implicated in myelin physiology (Figure 57–5). Type 1A involves a defect in peripheral myelin protein 22, and type 1B the myelin protein P_0. Moreover, an X-linked form of demyelinating neuropathy occurs because of mutations in the gene expressing connexin-32, a subunit of the gap-junction channels that interconnect myelin folds near the nodes of Ranvier (Figure 57–5B,C). Still other genes have been implicated in inherited demyelination.

Some of the genes and proteins implicated in axonal neuropathies are shown in Figure 57–6 and Table 57–3. Genes encoding the neurofilament light subunit and an axonal motor protein related to kinesin, which is important for transport along microtubules, are mutated in two types of axonal neuropathies. Defects in these genes are associated with peripheral neuropathies with prominent weakness. The mechanisms by which genes alter axonal function in other axonal neuropathies are less evident.

As noted above, a wide range of problems other than genetic mutations lead to peripheral neuropathies. Particularly striking are nerve defects associated with the presence of autoantibodies directed against ion channels in distal peripheral nerves. For example, some individuals with motor unit instability (cramps and fasciculations), as well as sustained or exaggerated muscle contractions caused by hyperexcitability of motor nerves, have serum antibodies directed against one or more axonal voltage-gated K^+ channels. The prevailing view is that binding of the autoantibodies to the channels reduces K^+ conductance and thereby depolarizes the axon, leading to augmented and sustained firing of the distal motor nerve and associated muscle contractions. Alterations in ion channel function underlie a variety of neurological disorders, as in acquired disorders of channels in the neuromuscular junction and inherited defects in voltage-gated channels in muscle (discussed below).

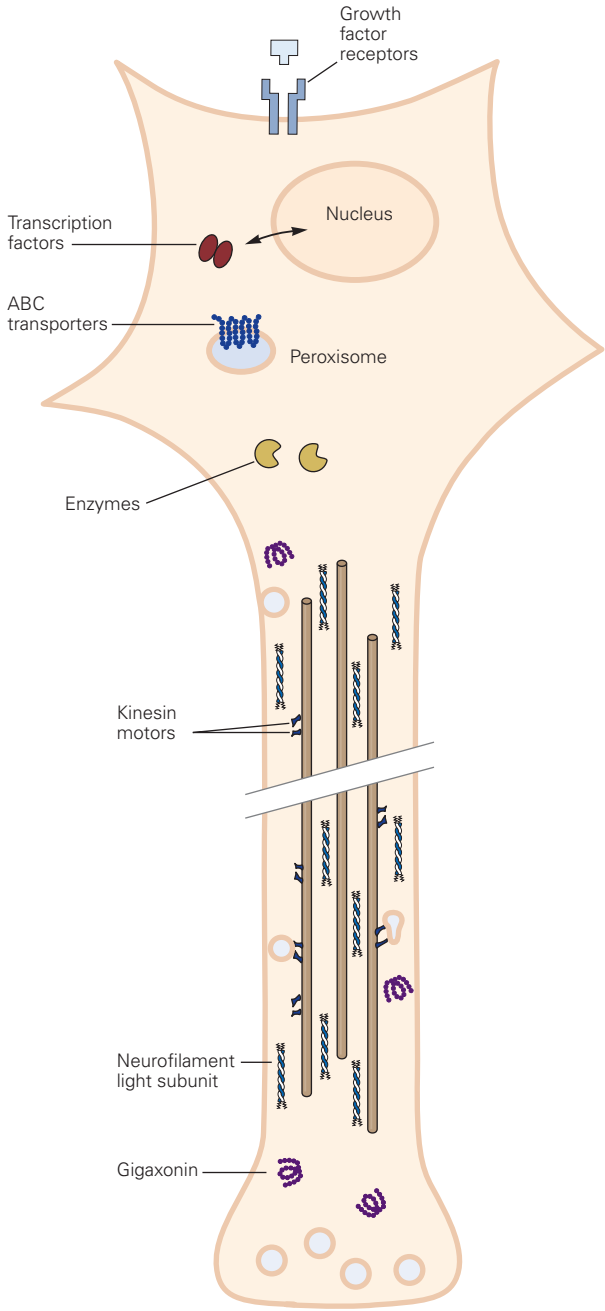

Figure 57–6 Gene defects that cause axonal neuropathies. These include defects in receptors for growth factors, ABC (ATP-binding cassette) transporters in peroxisomes, cytosolic enzymes, microtubule motor proteins like the kinesins, neurofilament proteins, and other structural proteins such as gigaxonin. (Adapted, with permission, from Brown and Amato 2002.)

Disorders of Synaptic Transmission at the Neuromuscular Junction Have Multiple Causes

Many diseases involve disruption of chemical transmission between neurons and their target cells. By analyzing such abnormalities, researchers have learned a great deal about the mechanisms underlying normal synaptic transmission as well as disorders caused by dysfunction at the synapse.

Table 57–3 Representative Peripheral Neuropathy Genes

Site of primary defect	Protein	Disease
Myelin	Proteolipid myelin protein 22	Charcot-Marie-Tooth disease (CMT)
	Proteolipid protein P_0	Infantile CMT (Dejerine-Sottas neuropathy)
	Connexin-32	X-linked CMT
Axon	Kinesin KIF1Bβ motor protein	Motor predominant neuropathy
	Heat shock protein 27	Motor predominant neuropathy
	Neurofilament light subunit	Motor predominant neuropathy
	Tyrosine kinase A receptor	Congenital sensory neuropathy
	ABC1 transporter	Tangier disease
	Transthyretin	Amyloid neuropathy

Diseases that disrupt transmission at the neuromuscular junction fall into two broad categories: those that affect the presynaptic terminal and those that primarily involve the postsynaptic membrane. In both categories, the most intensively studied cases are autoimmune and inherited defects in critical synaptic proteins.

Myasthenia Gravis Is the Best-Studied Example of a Neuromuscular Junction Disease

The most common and extensively studied disease affecting synaptic transmission is myasthenia gravis, a disorder at the neuromuscular junction in skeletal muscle. Myasthenia gravis (the term means severe weakness of muscle) has two major forms. The most prevalent is the autoimmune form. The second is congenital and heritable; it is not an autoimmune disorder and is heterogeneous. Fewer than 500 of these congenital cases have been identified, but they have provided information about the organization and function of the human neuromuscular junction. This form is discussed later in the chapter.

In autoimmune myasthenia gravis, antibodies are produced against components of the postsynaptic end-plate in muscle, such as the nicotinic acetylcholine (ACh) receptor and muscle-specific tyrosine kinase (MuSK). Anti–ACh receptor antibodies interfere with synaptic transmission by reducing the number of functional receptors or by impeding the interaction of ACh with its receptors. As a result, communication between the motor neuron and the skeletal muscle becomes weakened. This weakness always affects cranial muscles—eyelids, eye muscles, and oropharyngeal muscles—as well as limb muscles. Its severity of symptoms varies over the course of a single day, from day to day, or over longer periods (giving rise to periods of remission or exacerbation), making myasthenia gravis unlike most other diseases of muscle or nerve. The weakness is reversed by drugs that inhibit acetylcholinesterase, the enzyme that degrades ACh. As one example, when patients are asked to look upward in a sustained gaze, the eyelids tire after several seconds and droop downward (ptosis). Like decremental responses on EMG, this fatiguability and drooping reverse after treatment with inhibitors of acetylcholinesterase (Figure 57–7).

When a motor nerve is stimulated at rates of two to five stimuli per second, the amplitude of the compound

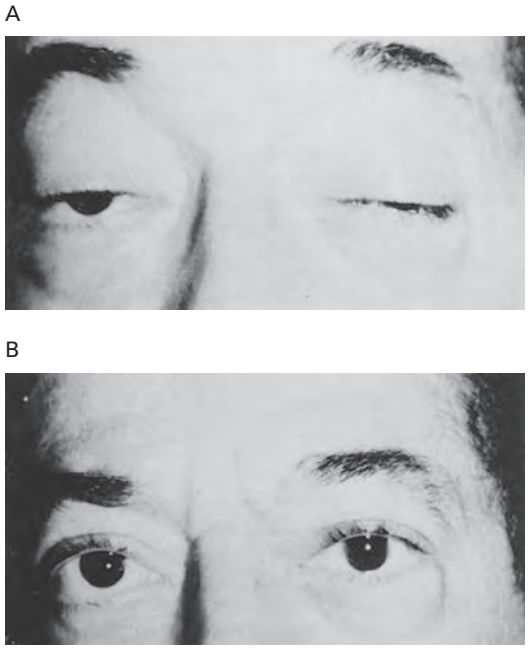

Figure 57–7 Myasthenia gravis often selectively affects the cranial muscles. (Reproduced, with permission, from Rowland, Hoefer, and Aranow 1960.)

A. Severe drooping of the eyelids, or ptosis, is characteristic of myasthenia gravis. This patient also could not move his eyes to look to either side.

B. One minute after an intravenous injection of 10 mg of edrophonium, an inhibitor of acetylcholinesterase, both eyes are open and can be moved freely.

action potential evoked in normal human muscle remains constant. In myasthenia gravis, the amplitude of the evoked compound action potential decreases rapidly. This pattern of decremental response of the compound muscle action potential to repetitive stimulation of the motor nerve mirrors the clinical symptom of fatiguability in myasthenia. Moreover, this abnormality resembles the pattern induced in normal muscle by d-tubocurarine (the active compound in curare), which blocks nicotinic ACh receptors and inhibits the action of ACh at the neuromuscular junction. Neostigmine (Prostigmin), which inhibits acetylcholinesterase and thus increases the duration of action of ACh at the neuromuscular junction, reverses the decrease in amplitude of evoked compound action potentials in myasthenic patients (Figure 57–8).

About 15% of adult patients with myasthenia have benign tumors of the thymus (thymomas). As the symptoms in myasthenic patients are often improved by removal of these tumors, some element of the thymoma may stimulate autoimmune pathology. Indeed, myasthenia gravis often affects people who have other autoimmune diseases, such as rheumatoid arthritis, systemic lupus erythematosus, or Graves disease (hyperthyroidism).

Normally, an action potential in a motor axon releases enough ACh from synaptic vesicles to induce a large excitatory end-plate potential with an amplitude of about 70 to 80 mV relative to the resting potential of –90 mV (Chapter 12). Thus, the normal end-plate potential is greater than the threshold needed to initiate an action potential, about –45 mV. In normal muscle, the difference between the threshold and the actual end-plate potential amplitude—the safety factor—is therefore quite large (Figure 57–8). In fact, in many muscles, the amount of ACh released during synaptic transmission can be reduced to as little as 25% of normal before it fails to initiate an action potential.

The density of ACh receptors is reduced over time in myasthenia. This reduces the probability that a molecule of ACh will find a receptor before it is hydrolyzed by the acetylcholinesterase. In addition, the geometry of the end-plate is also disturbed in myasthenia (Figure 57–9). The normal infolding at the junctional folds is reduced and the synaptic cleft is enlarged. These morphological changes increase the diffusion of

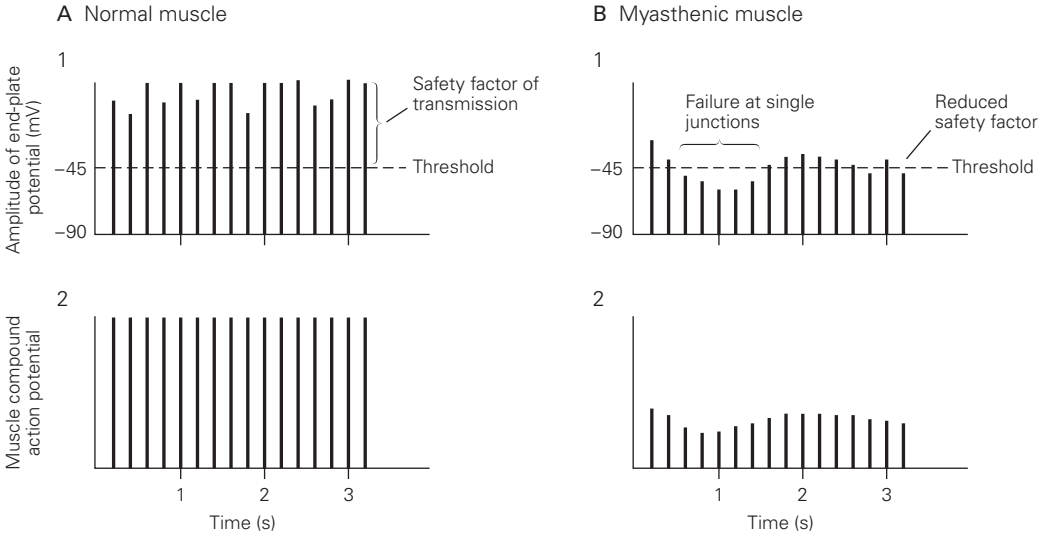

Figure 57–8 Synaptic transmission at the neuromuscular junction fails in myasthenia gravis. (Reproduced, with permission, from Lisak and Barchi 1982.)

A. In the normal neuromuscular junction, the amplitude of the end-plate potential is so large that all fluctuations in the efficiency of transmitter release occur well above the threshold for a muscle action potential. This results in a large safety factor for synaptic transmission (**1**). Therefore, during repetitive stimulation of the motor nerve, the amplitude of the compound action potentials, representing the contributions from all muscle fibers in which synaptic transmission is successful in triggering an action potential, is constant and invariant (**2**).

B. In the myasthenic neuromuscular junction, postsynaptic changes reduce the amplitude of the end-plate potential so that under optimal circumstances the end-plate potential may be just sufficient to produce a muscle action potential. Fluctuations in transmitter release that normally accompany repeated stimulation now cause the end-plate potential to drop below this threshold, leading to conduction failure at that junction (**1**). The amplitude of the compound action potentials in the muscle declines progressively and shows only a small and variable recovery (**2**).

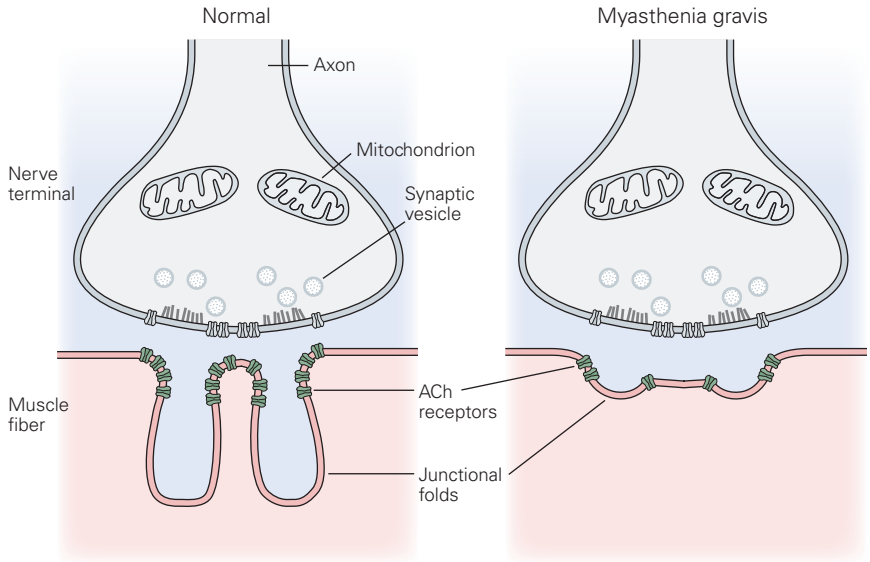

Figure 57–9 **Morphological abnormalities of the neuromuscular junction are characteristic of myasthenia gravis.** At the neuromuscular junction, acetylcholine (**ACh**) is released by exocytosis of synaptic vesicles at active zones in the nerve terminal. Acetylcholine flows across the synaptic cleft to reach ACh receptors that are concentrated at the peaks of junctional folds. Acetylcholinesterase in the cleft rapidly terminates transmission by hydrolyzing ACh. The myasthenic junction has reduced numbers of ACh receptors, simplified synaptic folds, a widened synaptic space, but a normal nerve terminal.

ACh away from the synaptic cleft and further reduce the probability of ACh interacting with the few remaining functional receptors. As a result, the amplitude of the end-plate potential is reduced to the point where it is barely above threshold (Figure 57–8).

Thus, in myasthenia, synaptic transmission is readily blocked even though the vesicles in the presynaptic terminals contain normal amounts of ACh and the process of transmitter release is intact. Both the physiological abnormality (the decremental response) and the clinical symptoms (muscle weakness) are partially reversed by drugs that inhibit acetylcholinesterase. This is because the released ACh molecules remain unhydrolyzed for a longer time, and this increases the probability that they will interact with receptors.

How do antibodies cause the symptoms of myasthenia? The antibodies do not simply occupy the ACh binding site. Rather, they appear to react with epitopes elsewhere on the receptor molecule. This increases the turnover of nicotinic ACh receptors, probably because myasthenic antibodies bind and cross-link the receptors, triggering their degradation (Figure 57–9). In addition, some myasthenic antibodies bind proteins of the complement cascade of the immune system, causing lysis of the postsynaptic membrane.

Despite the evidence documenting the primary role of antibodies against the nicotinic ACh receptor in myasthenia, about one-fifth of patients with myasthenia do not have these antibodies—including some who respond to anti-immune therapy like plasmapheresis. Instead, the majority of these patients have antibodies to other postsynaptic proteins, such as MuSK (*mu*scle-specific trk-related receptor with a *K*ringle domain) and lipoprotein-related protein 4 (LPR4), which is an activator of MuSK. MuSK is a muscle-specific receptor tyrosine kinase that interacts with another postsynaptic protein, agrin, to organize the nicotinic ACh receptors into clusters at the neuromuscular junction (Chapter 48); it appears to be functionally important both during development and in the adult. The anti-MuSK antibodies block some of the normal clustering of the nicotinic ACh receptors following the interaction of agrin with MuSK. Anti-LPR4 antibodies also block ACh receptor clustering.

Treatment of Myasthenia Is Based on the Physiological Effects and Autoimmune Pathogenesis of the Disease

Anticholinesterases, especially pyridostigmine, provide some symptomatic relief but do not alter the basic disease. Immunosuppressive therapies such as corticosteroids and azathioprine or related drugs suppress antibody synthesis. Intravenous infusions of pooled immunoglobulins reduce levels of the pathogenic autoantibodies and ameliorate symptoms, often within a few days. An analogous benefit is achieved by plasmapheresis, which involves filtering the plasma. Although the benefit of these interventions is short-lived, it may be sufficient to prepare a patient for thymectomy or to support the patient through more severe episodes.

There Are Two Distinct Congenital Forms of Myasthenia Gravis

In two distinct types of myasthenia, symptoms may be present from birth or shortly thereafter. In neonatal

myasthenia, the mother herself has autoimmune myasthenia that is transmitted passively to the newborn via the immune system. In congenital myasthenia, the infant has an inherited defect in some component of the neuromuscular junction, rather than an autoimmune disease, and thus does not have serum antibodies to the nicotinic ACh receptor or MuSK.

Congenital myasthenic syndromes fall into three broad groups based on the site of the defect in the neuromuscular synapse: presynaptic, synaptic cleft, and postsynaptic forms. Clinical features common to all three types include a positive family history, weakness with easy fatigability (present since infancy), drooping of the eyelids (ptosis), a decremental response to repetitive stimulation on EMG, and negative screening for anti-nicotinic ACh receptor antibodies. Subnormal development of the skeletal muscles reflects the fact that normal function at the neuromuscular synapse is required to maintain normal muscle bulk.

In one presynaptic form of congenital myasthenia, the enzyme choline acetyltransferase is absent or reduced in the distal motor terminal. This enzyme is essential for the synthesis of ACh from choline and acetyl-CoA (Chapter 16). In its absence, the synthesis of ACh is impaired. The result is weakness that usually begins in infancy or early childhood. In another presynaptic form of congenital myasthenia, the number of quanta of ACh released after an action potential is less than normal; the molecular basis for this defect is not known.

Congenital myasthenia may also result from the absence of acetylcholinesterase in the synaptic cleft. In this circumstance, end-plate potentials and miniature end-plate potentials are not small, as in autoimmune myasthenia, but are markedly prolonged, which may explain the repetitive response of the evoked muscle potential in those patients. Cytochemical studies indicate that ACh-esterase is absent from the basement membranes. At the same time, nicotinic ACh receptors are preserved.

The physiological consequence of ACh-esterase deficiency is sustained action of ACh on the end-plate and ultimately the development of an end-plate myopathy. This myopathy indicates that skeletal muscle can react adversely to excessive stimulation at the neuromuscular junction. In treating this disorder, it is critical to avoid using agents that inhibit ACh-esterase, which can increase the electrical firing at the end-plate and thereby exacerbate the muscle weakness.

The majority of congenital myasthenia cases are caused by primary mutations in the genes encoding different subunits of the ACh receptor. The *slow channel syndrome* is characterized by prominent limb weakness but little weakness of cranial muscles (the reverse of the pattern usually seen in autoimmune myasthenia, where muscles of the eyes and oropharynx are almost always affected). End-plate currents are slow to decay, and there is abnormal prolongation of channel opening. The mutations probably act both by increasing the affinity of the nicotinic ACh receptor for ACh, thereby prolonging the effects of this transmitter, and by directly slowing the channel closing rate. In some instances, quinidine is effective therapy for slow channel syndrome because it blocks the open receptor-channel. As with ACh-esterase mutations, end-plate function degenerates due to excessive postsynaptic stimulation, so anticholinesterase medications are potentially dangerous.

In the fast channel syndrome, a different set of mutations in one or more nicotinic ACh receptor subunits leads to an accelerated rate of channel closing and end-plate current decay. The fast channel syndrome may respond to either acetylcholinesterase inhibitors or 3,4-diaminopyridine. The latter blocks a presynaptic potassium conductance and thereby increases the probability of quantal release of ACh, probably by prolonging the action potential.

Lambert-Eaton Syndrome and Botulism Also Alter Neuromuscular Transmission

Some patients with cancer, especially small-cell cancer of the lung, have a syndrome of proximal limb weakness and a neuromuscular disorder with characteristics that are the opposite of those seen in myasthenia gravis. Instead of a decline in synaptic response to repetitive nerve stimulation, the amplitude of the evoked potential increases; that is, neuromuscular transmission is facilitated. Here, the first postsynaptic potential is abnormally small, but subsequent responses increase in amplitude so that the final summated potential is two to four times the amplitude of the first potential.

This disorder, *Lambert-Eaton syndrome*, is attributed to the action of antibodies against voltage-gated Ca^{2+} channels in the presynaptic terminals. It is thought that these antibodies react with the channels, degrading the channels as the antibody–antigen complex is internalized. Calcium channels similar to those of presynaptic terminals are found in cultured cells from the small-cell carcinoma of the lung; development of antibodies against these antigens in the tumor might be followed by pathogenic action against nerve terminals, another kind of molecular mimicry.

A facilitating neuromuscular block is also found in human botulism, as the botulinum toxin also impairs release of ACh from nerve terminals. Both botulism

and Lambert-Eaton syndrome are ameliorated by administration of calcium gluconate or guanidine, agents that promote the release of ACh. These drugs are less effective than immunosuppressive treatments for long-term control of Lambert-Eaton syndrome, which is chronic. Botulism, on the other hand, is transient, and if the patient is kept alive during the acute phase by treating symptoms, the disorder disappears in weeks as the infection is controlled and botulinum is inactivated.

Diseases of Skeletal Muscle Can Be Inherited or Acquired

The weakness seen in any myopathy is usually attributed to degeneration of muscle fibers. At first, the missing fibers are replaced by regeneration of new fibers. Ultimately, however, renewal cannot keep pace and fibers are progressively lost. This leads to the appearance of compound motor unit potentials of brief duration and reduced amplitude. The decreased number of functioning muscle fibers then accounts for the diminished strength, whether the skeletal muscle disease is inherited or acquired.

Dermatomyositis Exemplifies Acquired Myopathy

The prototype of an acquired myopathy is dermatomyositis, defined by two clinical features: rash and myopathy. The rash has a predilection for the face, chest, and extensor surfaces of joints, including the fingers. The myopathic weakness primarily affects proximal limb muscles. The rash and weakness usually appear simultaneously and become worse in a matter of weeks. The weakness may be mild or life-threatening.

This disorder affects children or adults. About 10% of adult patients have malignant tumors. Although the pathogenesis is not known, dermatomyositis is thought to be an autoimmune disorder of small intramuscular blood vessels.

Muscular Dystrophies Are the Most Common Inherited Myopathies

The best-known inherited muscle diseases are the muscular dystrophies; several major types are distinguished by clinical and genetic patterns (Table 57–4). Some types are characterized by weakness alone (Duchenne, facioscapulohumeral, and limb-girdle dystrophies); others (eg, the myotonic muscular dystrophies) have additional clinical features. Most are recessively inherited and begin in early childhood (Duchenne, Becker, and limb-girdle dystrophy); less frequently, the dystrophies are dominantly inherited (facioscapulohumeral or myotonic dystrophy). The cardinal trait of limb-girdle dystrophies is slowly progressive proximal weakness; in the myotonic muscular dystrophies, progressive weakness is accompanied by severe muscle stiffness.

Duchenne muscular dystrophy affects only males because it is transmitted as an X-linked recessive trait. It starts in early childhood and progresses relatively rapidly, so that patients are in wheelchairs by age 12 and usually die in their third decade. This dystrophy is caused by mutations that severely reduce levels of dystrophin, a skeletal muscle protein that apparently confers tensile strength to the muscle cell. In a related inherited muscle disorder, Becker muscular dystrophy, dystrophin is present but is either abnormal in size or reduced in quantity. Becker dystrophy is thus typically much milder, although there is considerable clinical variability according to how much dystrophin is retained; individuals with Becker dystrophy typically are able to walk well into adulthood, albeit with weakness of the proximal leg and arm muscles.

Dystrophin is encoded by the *DMD* gene, the second largest human gene, spanning about 2.5 million base pairs, or 1% of the X chromosome and 0.1% of the total human genome (Figure 57–10A). It contains at least 79 exons that encode a 14-kb mRNA. The inferred amino acid sequence of the dystrophin protein suggests a rod-like structure and a molecular weight of 427,000, with domains similar to those of two cytoskeletal proteins, alpha-actinin and spectrin. Dystrophin is localized to the inner surface of the plasma membrane. The amino terminus of dystrophin is linked to cytoskeletal actin, whereas the carboxy terminus is linked to the extracellular matrix by transmembrane proteins (Figure 57–11).

The majority of boys with Duchenne muscular dystrophy have a deletion in the *DMD* gene; about a third have point mutations. In either case, these mutations introduce premature stop codons in the mutant RNA transcripts that prevent synthesis of full-length dystrophin. Becker dystrophy is also caused by deletions and missense mutations, but the mutations do not introduce stop codons. The resulting dystrophin protein is nearly normal in length and can at least partially substitute for normal dystrophin (Figure 57–10B). Some boys with Duchenne dystrophy benefit from treatment with ASOs that cause skipping of specific mutant exons, generating a shortened but partially functional dystrophin protein (Figure 57–10C). Another promising approach is to deliver a form of the *DMD* gene to the muscle using adeno-associated virus. While the full-length *DMD* gene is too large to fit

Table 57–4 Representative Muscular Dystrophy Genes

Site of primary defect	Protein	Disease
Extracellular matrix	Collagen VI α1, α2, and α3	Bethlem myopathy
	Merosin laminin α2-subunit	Congenital myopathy
Transmembrane	α-Sarcoglycan	LGMD-2D
	β-Sarcoglycan	LGMD-2E
	χ-Sarcoglycan	LGMD-2C
	σ-Sarcoglycan	LGMD-2F
	Dysferlin	LGMD-2B, Miyoshi myopathy
	Caveolin-3	LGMD-1C, rippling muscle disease
	α7-Integrin	Congenital myopathy
	XK protein	McLeod syndrome
Submembrane	Dystrophin	Duchenne, Becker dystrophies
Sarcomere/myofibrils	Tropomyosin B	Nemaline rod myopathy
	Calpain	LGMD-2A
	Titin	Distal (Udd) dystrophy
	Nebulin	Nemaline rod myopathy
	Telethonin	LGMD-2G
	Skeletal muscle actin	Nemaline rod myopathy
	Troponin	Nemaline rod myopathy
Cytoplasm	Desmin	Desmin storage myopathy
	αβ-Crystallin	Distal myofibrillar myopathy
	Selenoprotein	Rigid spine syndrome
	Plectin	Epidermolysis bullosa simplex
Sarcoplasmic reticulum	Ryanodine receptor	Central core disease, malignant hyperthermia
	SERCA1	Brody myopathy
Nucleus	Emerin	Emery-Dreifuss dystrophy
	Lamin A/C	Emery-Dreifuss dystrophy
	Poly A binding protein, repeat	Oculopharyngeal dystrophy
Enzymes/miscellaneous	Myotonin kinase, CTG repeat	Myotonic dystrophy
	Zinc finger 9, CCTG repeat	Proximal myotonic dystrophy
	Epimerase	Inclusion body myositis
	Myotubularin	Myotubular myopathy
	Chorein	Chorea-acanthocytosis
Golgi apparatus	Fukutin	Fukuyama congenital dystrophy
	Fukutin-related peptide	Limb-girdle dystrophy
	POMT1	Congenital muscular dystrophy
	POMGnT1	Congenital muscular dystrophy

LGMD, limb-girdle muscular dystrophy.

within that virus, there is evidence that some truncated versions of dystrophin retain partial function; indeed, severely shortened dystrophins have been discovered in patients with very mild forms of Becker dystrophy. Packaging of genes encoding mini-dystrophins into the adeno-associated virus is feasible, permitting delivery to skeletal muscle and improvement of the dystrophic process (Figure 57–10C).

The discovery of the affected gene product in Duchenne muscular dystrophy by Louis Kunkel in the mid-1980s stimulated rapid discovery of numerous other novel muscle proteins, some with an intimate relationship to dystrophin. As a result, the primary genetic and protein defects underlying most major muscular dystrophies have now been identified (Figure 57–11). From these, several themes have emerged in our understanding of the biology of the muscular dystrophies.

First, and perhaps most important, is the concept that normal muscle requires a functional unit linking the contractile proteins through dystrophin to a complex of dystrophin-associated transmembrane proteins (sarcoglycans, β-dystroglycan) that, in turn, are linked to proteins at the membrane surface (eg, α-dystroglycan) and the extracellular matrix (eg, laminin). Disruption of this linked network due to a mutation in one of the proteins leads to reductions in levels of many of the proteins (Table 57–4).

Second, some of these proteins have attached sugar groups that are critical for binding the extracellular matrix proteins. Genetic defects in several of the intracellular Golgi proteins (fukutin, fukutin-related peptide, POMT1, POMTGn1) impair the deposition of the sugars (glycosylation) of the transmembrane proteins, often leading to aberrant muscle development and pronounced clinical pathology, not only in muscle but sometimes in the brain.

Third, the integrity of the extracellular matrix is essential for normal muscle function: Defects in extracellular matrix proteins (laminin α2 or α7-integrin) also cause muscular dystrophies.

Fourth, other proteins (eg, dysferlin), distinct from those complexed with dystrophin, mediate membrane repair after injury. Whereas dystrophin is important in maintaining the tensile strength and integrity of the muscle membrane, dysferlin and its binding partner caveolin-3 are central to generating rafts of vesicles that coalesce and heal breaches that occur in the muscle membrane.

It is of clinical interest that disorders due to defects in many of these proteins are less aggressive and more slowly disabling than those in Duchenne dystrophy. Defects in this diverse group of skeletal muscle proteins lead to the limb-girdle phenotype, characterized by slowly progressive proximal weakness of the arms and legs. Most are recessively inherited; mutations in both copies of a particular gene prevent expression of the normal protein product and lead to loss of function of that protein. Some limb-girdle genes are dominantly transmitted; mutations in only one copy of the gene in a pair can cause pathology. As in most primary muscle diseases, in the limb-girdle phenotype, weakness is prominent in the torso and in proximal muscles of the arms and legs. Why this pattern is so common is not known, especially since the affected proteins are expressed in both distal and proximal muscles. The pattern of degeneration most likely reflects muscle use. The proximal muscles are, on average, more subject to low-level but chronic contractile activity because they serve as antigravity muscles.

Myotonic dystrophy has several distinctive features including an autosomal inheritance pattern, weakness that is predominantly distal, involvement of nonmuscle tissues, and striking muscle stiffness (*myotonia*). The stiffness is induced by excessive electrical discharges of the muscle membrane associated with voluntary muscle contractions or percussion or electrical stimulation of the muscle. It is most intense within the first few movements after a period of rest and improves with continued muscular activity ("warm-up" phenomenon). Patients typically have difficulty relaxing the grip of a handshake for several seconds, opening the eyelids after forceful squinting, or moving their legs with the first few steps after rising from a chair. EMG demonstrates that the muscle cell membrane is electrically hyperexcitable in myotonic dystrophy; after a contraction, bursts of repetitive action potentials wax and wane in amplitude and frequency (20–100 Hz) over several seconds and thereby delay relaxation (Figure 57–12A). This sustained contraction is truly myogenic and independent of nerve supply because it persists after blockade of either the incoming motor nerve or neuromuscular transmission with agents such as curare.

The manifestations of myotonic dystrophy are not confined to muscles, however. Almost all patients have cataracts; affected men commonly have testicular atrophy and baldness and often develop cardiac conduction system defects that lead to irregularities in the heartbeat. The primary genetic defect is a dominantly transmitted expansion of a triplet of base pairs (CTG) in a noncoding region of a gene (myotonin kinase) on chromosome 19. RNA transcripts of the expanded CTG segments accumulate in the nucleus and alter splicing of several critical genes, including the ClC-1 Cl^- channel. Loss of function of this channel leads to

A The *DMD* gene

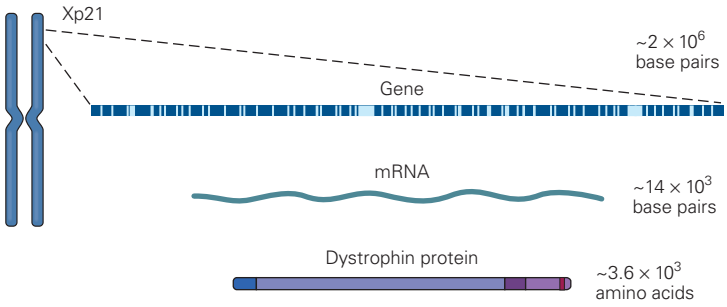

Normal dystrophin staining

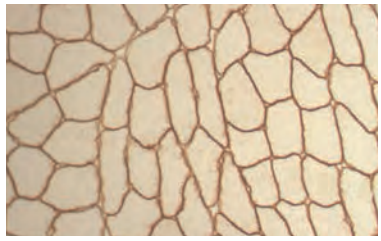

B Effects of deletion

1 Deletion of single exon results in severe (Duchenne) dystrophy

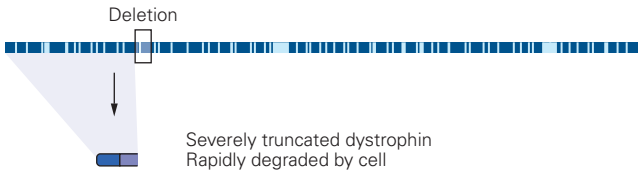

Dystrophin staining in Duchenne dystrophy

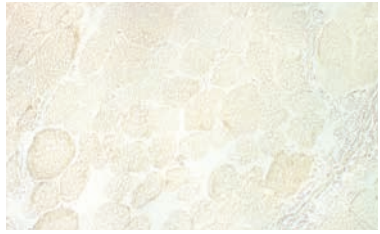

2 Deletion of four exons results in milder (Becker) dystrophy

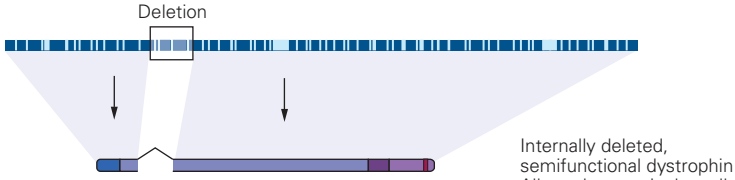

Dystrophin staining in Becker dystrophy

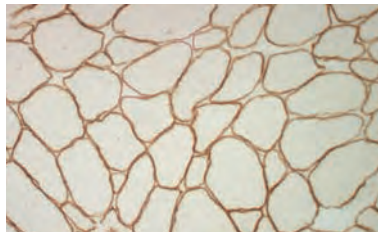

C Exon skipping and mini gene replacement therapies in Duchenne dystrophy

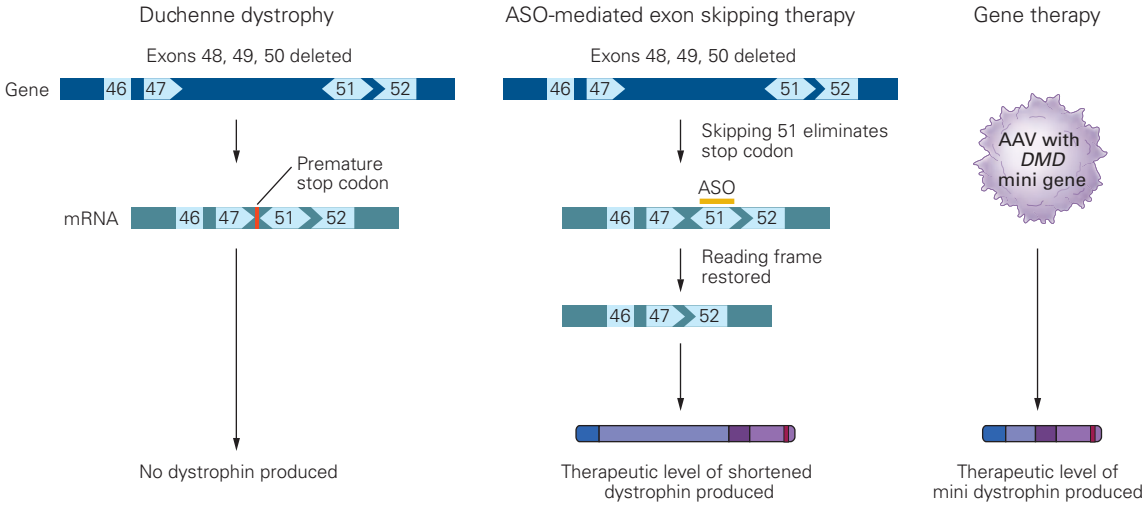

excessive electrical activity in skeletal muscle and, as a consequence, myotonia. As discussed below, direct mutations in the same Cl^- channel gene can lead to a similar abnormal pattern of muscle activity.

Some Inherited Diseases of Skeletal Muscle Arise From Genetic Defects in Voltage-Gated Ion Channels

The electrical excitability of skeletal muscle is essential to the rapid and nearly synchronous contraction of an entire muscle fiber. The depolarizing end-plate potential at the neuromuscular junction triggers an action potential that propagates longitudinally along the surface of the muscle fiber and radially inward along the transverse tubules, invaginations of the fiber membrane in apposition with the sarcoplasmic reticulum (Chapter 31).

Depolarization of the transverse tubules induces a conformational change in L-type voltage-gated Ca^{2+} channels that is directly transmitted to Ca^{2+} release channels (the ryanodine receptors) in the sarcoplasmic reticulum, causing the channels to open. The release of Ca^{2+} from the sarcoplasmic reticulum raises myoplasmic Ca^{2+} and thus activates adenosine triphosphate (ATP)-dependent movement of actin-myosin filaments.

Normally, one action potential is generated in a muscle fiber for each end-plate potential. Repolarization of the muscle action potential depends on inactivation of Na^+ channels and the opening of delayed-rectifier voltage-gated K^+ channels similar to those in axons. This repolarization is also augmented by Cl^- influx through the ClC-1 Cl^- channels. Inherited muscle diseases arise from mutations in any one of these channels.

The electrical coupling of the end-plate potential to depolarization of the transverse tubules is disrupted in several inherited diseases of muscle. These disorders reflect a variety of defects in excitability, ranging from complete failure of action potential generation to prolonged bursts of repetitive discharges in response to a single stimulus (Figure 57–12). The derangements of muscle fiber excitability are transient and result in periodic paralysis from reduced excitability or myotonia from hyperexcitability. Between episodes, muscle function is normal. These are rare diseases of skeletal muscle, with a prevalence of 1 per 100,000 or less. Inheritance is autosomal dominant, except for one form of myotonia.

Weakness may be so severe during an attack of periodic paralysis that a patient is bedridden for hours, unable to raise an arm or leg off the bed. Fortunately, during such attacks, the muscles of respiration and swallowing are spared, so life-threatening respiratory arrest does not occur; consciousness and sensation are also spared. Attack frequency varies from almost daily to only a few in a lifetime.

During an attack, the resting potential of affected muscles is depolarized from a normal value of –90 mV

Figure 57–10 (Opposite) Two forms of muscular dystrophy are caused by deletion mutations in the dystrophin gene. (After Hoffman and Kunkel 1989.)

A. The relative position of the *DMD* gene within the Xp21 region of the X chromosome. An enlargement of this locus shows the 79 exons (**light blue lines**) and introns (**dark blue lines**) defining the gene with about 2.0×10^6 base pairs. Transcription of the gene gives rise to mRNA (about 14×10^3 base pairs), and translation of this mRNA gives rise to the protein dystrophin (molecular weight 427,000).

B. A deletion that disrupts the reading frame results in the clinically severe Duchenne muscular dystrophy, whereas a deletion that preserves the reading frame usually results in the clinically milder Becker muscular dystrophy. In both cases, the gene is transcribed into mRNA and the exons flanking the deletion are spliced together. 1. If the borders of neighboring exons do not maintain the translational reading frame, then incorrect amino acids are inserted into the growing polypeptide chain until an abnormal stop codon is reached, causing premature termination of the protein. The truncated protein may be unstable, may fail to be localized in the membrane, or may fail to bind to glycoproteins. Functional dystrophin is then almost totally absent. 2. If the deletion preserves the reading frame, a dystrophin molecule is produced with an internal deletion but intact ends. Although the protein is smaller than normal and may be present in less than normal amounts, it can often suffice to preserve some muscle function.

C. One approach to correcting a deletion of the *DMD* gene is to induce formation of an mRNA transcript that skips one or more exons to restore the reading frame. For example, when there is a deletion of exons 48, 49, and 50, the splicing of exon 47 to exon 51 yields a transcript that is out of frame, in which a stop codon is introduced, preventing production of dystrophin. However, addition of an antisense oligonucleotide (**ASO**) that binds exon 51 and prevents its splicing will promote the in-frame splicing of exon 47 to exon 52. Although this transcript is slightly shorter than normal, as is the resulting dystrophin protein, the protein will nonetheless function well enough to ameliorate the muscle degeneration. Another therapeutic approach is to deliver a short form of the dystrophin gene (mini- or micro-dystrophin, ~30% of the full-length protein) to the muscle using adeno-associated virus (**AAV**); full-length dystrophin is too large to be delivered within the AAV.

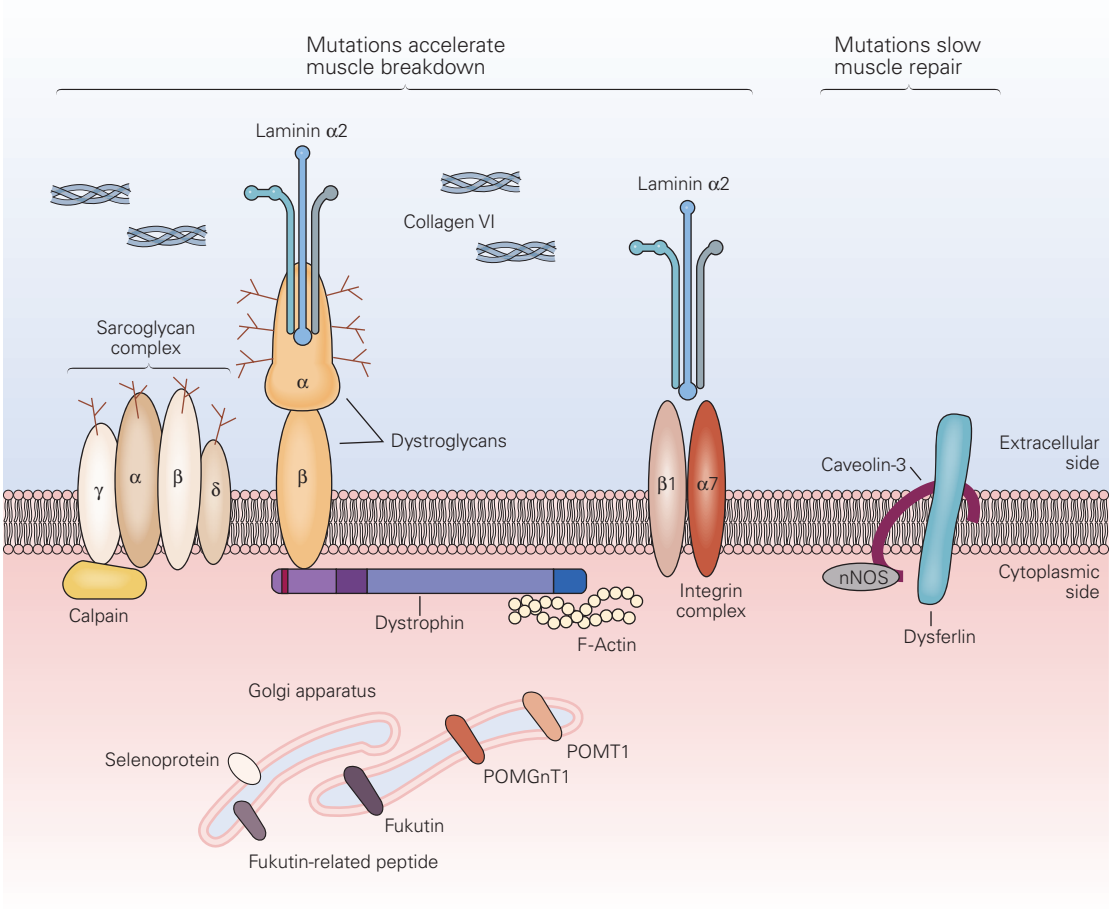

Figure 57–11 **In muscular dystrophy, mutated proteins either weaken the muscle cell membrane or slow its repair after injury.** For example, a deficiency of dystrophin, a submembrane protein, causes Duchenne muscular dystrophy. Dystrophin interacts with complexes of other membrane proteins that are mutated in other dystrophies, including the dystroglycans and the sarcoglycans, which are closely associated with extracellular proteins such as laminin α2 and collagen. Several other proteins mutated in different forms of muscular dystrophy are normally present in the Golgi apparatus, where they are essential for adding sugar groups to membrane proteins. These include **POMT1** (protein-O-mannosyl transferase 1), **POMGnT1** (protein-O-mannosyl α-,2-*N*-acetylglucosaminyl transferase), fukutin, fukutin-related peptide, and a selenoprotein. Dysferlin, which is mutated in still other dystrophies, is involved in the repair of skeletal muscle membrane after injury. (Adapted, with permission, from Brown and Mendell 2005.)

to about –60 mV. At this potential, most Na^+ channels are inactivated, rendering the muscle fiber chronically refractory and thus unable to generate action potentials. Recovery of strength occurs spontaneously and is associated with repolarization to a resting potential within a few millivolts of normal and recovery of excitability.

Two variants of periodic paralysis have been delineated. Hyperkalemic periodic paralysis attacks occur during periods of high venous K^+ (≥6.0 mM versus normal levels of 3.5–4.5 mM). Ingesting foods with high K^+ content such as bananas or fruit juice may trigger an attack. Conversely, hypokalemic periodic paralysis presents as episodic weakness in association with low blood K^+ (≤2.5 mM). Affected muscle is paradoxically depolarized in the setting of reduced extracellular K^+, which shifts the reversal potential for K^+ to more negative values. Both forms are inherited as autosomal dominant traits.

Hyperkalemic periodic paralysis is caused by missense mutations in a gene that encodes the pore-forming subunit of a voltage-gated Na^+ channel

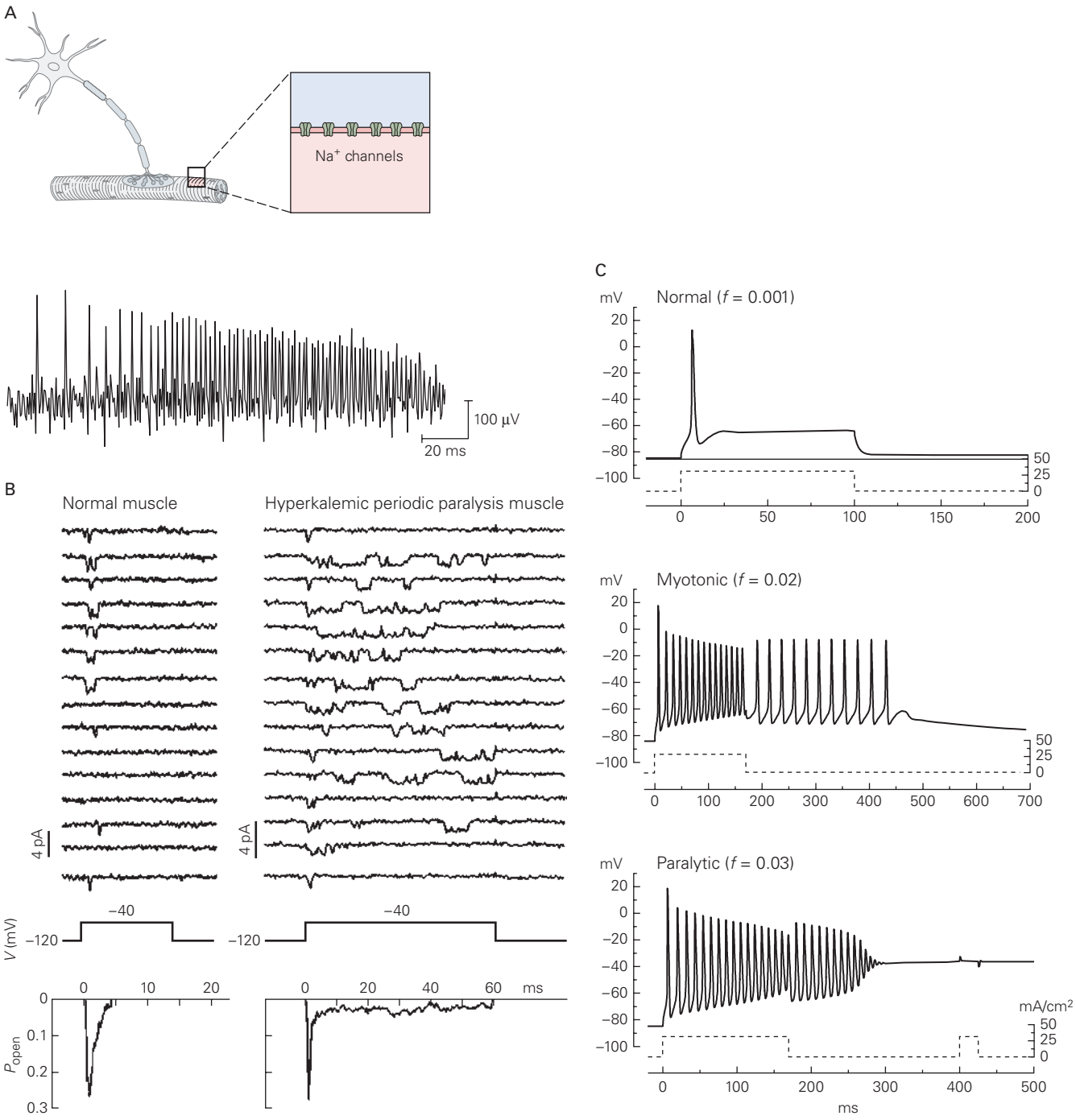

Figure 57–12 Myotonia or paralysis can result from genetically altered function in ion channels in skeletal muscle.

A. The electrical signature of myotonia (muscle stiffness) is a rapid burst of action potentials in response to a single stimulus. The action potentials, here shown in extracellular recordings, vary in amplitude and wax and wane in frequency. Such a burst may follow a voluntary muscle contraction or a mechanical stimulus, such as percussion of the muscle.

B. Cell-attached patch recordings from cultured human muscle cells. In normal muscle, the Na^+ channels open early and briefly in response to a 60 msec voltage-clamp depolarization from –120 mV to –40 mV. In muscle from patients with hyperkalemic periodic paralysis (defective M1592V Na^+ channel), the prolonged openings and reopenings indicate impaired inactivation. The probability of channel opening (obtained by averaging individual records) persists in the hyperkalemic muscle following inactivation. (Reproduced, with permission, from Cannon 1996.)

C. Even modest disruption of Na^+ channel inactivation is sufficient to produce bursts of myotonic discharges or depolarization-induced loss of excitability. These computer simulation records show muscle voltage in response to depolarizing current injection (**dashed line**). Among the total pool of mutant channels, a small fraction (*f*) fails to inactivate normally. In these simulations, *f* was varied from normal to values appropriate for myotonic or paralytic muscle. (Reproduced, with permission, from Cannon 1996.)

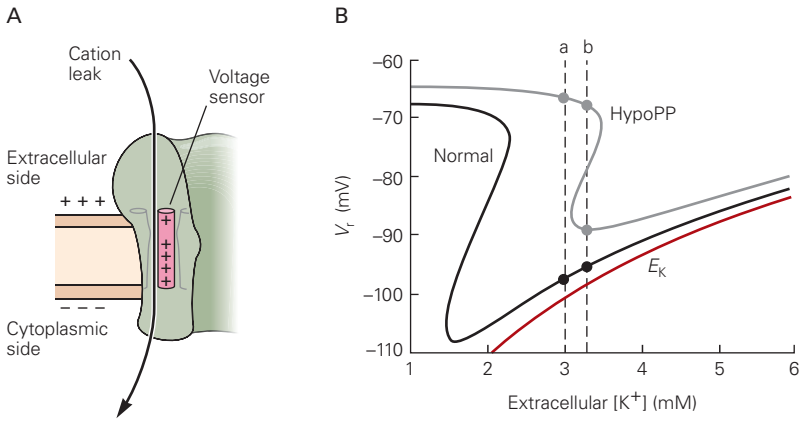

Figure 57–13 Hypokalemic periodic paralysis (HypoPP) is caused by leaky ion channels.

A. In HypoPP, missense mutations in the voltage-sensor domains create leaky Ca^{2+} or Na^+ channels that allow cation influx via an anomalous pathway separate from the channel pore.

B. Although this leak is small (~0.5% of the total resting membrane conductance), model simulations show that it causes an increased susceptibility to depolarization of resting potential (V_r), resulting in inexcitability and weakness as the external $[K^+]$ is lowered. This paradoxical depolarization of V_r diverges from the Nernst potential for K^+ (E_K) because of loss of the contribution from the inward rectifier K^+ channel in low $[K^+]$. Normally, this depolarization occurs only at extremely low $[K^+]$ (<2 mM) and is not seen in healthy people, but for patients with HypoPP, the cation leak shifts the depolarization point into the physiological range of $[K^+]$. For this simulation, in 3.3 mM $[K^+]$ (**line b**), excitability is preserved for normals (V_r = –95.6 mV), whereas HypoPP fibers may be excitable (V_r = –89 mV) or refractory and inexcitable (V_r = –67.7 mV). Reduction of $[K^+]$ to 3.0 mM (**line a**) results in complete loss of excitability for all HypoPP fibers (–66.3 mV) and retained excitability for normal fibers (V_r = –97.8 mV). (Adapted, with permission, from Cannon 2017.)

expressed in skeletal muscle. The resulting mutant Na^+ channels have inactivation defects. Subtle inactivation defects produce myotonia, whereas more pronounced defects result in chronic depolarization and loss of excitability with paralysis (Figure 57–12A–C). Hypokalemic paralysis is caused by missense mutations in the voltage-sensor domains of either Ca^{2+} channels or Na^+ channels in skeletal muscle. Disruption of the voltage-sensor domain allows an influx of ion current through an anomalous pathway, separate from the channel pore (Figure 57–13). This current "leak" in resting fibers produces a susceptibility to depolarization and loss of excitability in low extracellular K^+. A rare form of periodic paralysis that is characterized by weakness, developmental defects, and cardiac irritability is caused by primary mutations in an inwardly rectifying K^+ channel important for the resting potential (Figure 57–13).

In myotonia congenita, muscle stiffness is present from birth and is nonprogressive. Unlike myotonic dystrophy, there is no muscle wasting, permanent muscle weakness, or other organ involvement. Congenital myotonia is a consequence of mutations in the gene coding for the ClC-1 Cl^- channel in skeletal muscle membrane (Figure 57–14). The resultant decrease

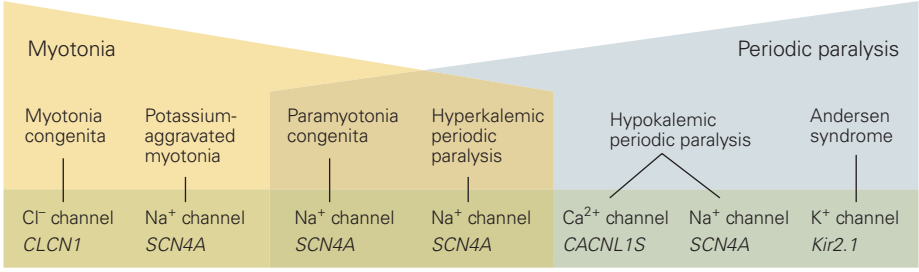

Figure 57–14 The myotonias and periodic paralyses are caused by mutations in genes that code for diverse voltage-gated ion channels in the skeletal muscle membrane. Some of these channel disorders are characterized only by myotonia, some by periodic paralysis without myotonia, and some by both myotonia and paralysis. Some clinical disorders (eg, hypokalemic periodic paralysis) can arise from defects in different channels in different individuals.

in Cl^- influx leads to membrane depolarization and repetitive firing. The disease is inherited as a dominant, semi-dominant, or recessive trait.

Highlights

1. Distinct disorders arise from pathology in different components of the motor unit. Pure motor diseases such as amyotrophic lateral sclerosis or spinal muscular atrophy are caused by loss of motor neurons, whereas combined motor and sensory features are present in most peripheral nerve disorders. These disorders usually spare eye movements and the eyelids.
2. Pure motor weakness, sometimes highly variable in severity over time, is also caused by disorders of the neuromuscular junction, which may begin early in life (congenital or neonatal myasthenia) or in childhood or adulthood (commonly autoimmune myasthenia gravis). The latter often involves eyelids and facial muscles.
3. Many forms of weakness are caused by mutations in genes that are important in skeletal muscle. These disorders usually become evident in infancy or childhood, involve the proximal more than the distal muscles, and progress relentlessly. Some (eg, Duchenne muscular dystrophy) also entail degeneration of cardiac muscle.
4. Inherited diseases of skeletal muscle with transient episodes of weakness (periodic paralysis) or involuntary after-contractions lasting seconds (myotonia) are caused by missense mutations in voltage-gated ion channels. During an episode of weakness, muscle fibers are depolarized and refractory from conducting action potentials. This intermittent failure to maintain the resting potential may arise from gain-of-function mutations in Na^+ channels, loss-of-function mutations in K^+ channels, or anomalous leakage currents in Na^+ or Ca^{2+} channels. Myotonia is a hyperexcitable state of skeletal muscle caused by Cl^- channel loss-of-function or Na^+ channel gain-of-function mutations.
5. Studies of the diseases of the peripheral nervous system show the powerful synergy between clinical and basic neuroscience. For most of the disorders inherited as Mendelian traits, molecular genetic analyses have led to the description of causative defects in muscle and nerve proteins, beginning only with the clinical data in affected families and DNA from family members.
6. Small animal models of many of these disorders, with precisely defined genetic defects, are proving invaluable for the analysis of mechanisms of disease pathogenesis and studies of new treatments. Combined with innovation in new biological therapies (gene therapy, gene silencing), these models have led to transformative successes in human trials (eg, spinal muscular atrophy).
7. In several of these disorders, a new generation of molecular therapies (eg, antisense oligonucleotides or viral-mediated gene delivery) that augment function of the mutant genes is substantially improving clinical outcomes.

Robert H. Brown
Stephen C. Cannon
Lewis P. Rowland

Selected Reading

Brown RH, Al-Chalabi A. 2017. Amyotrophic lateral sclerosis. N Engl J Med 377:162–172.

Cannon SC. 2015. Channelopathies of skeletal muscle excitability. Compr Physiol 5:761–790.

Engel AG, Shen X-M, Selcen D, et al. 2015. Congenital myasthenic syndromes: pathogenesis, diagnosis, and treatment. Lancet Neurol 14:420–434.

Fridman V, Reilly MM. 2015. Inherited neuropathies. Semin Neurol 35:407–423.

Gilhus NE, Verschuuren JJ. 2015 Myasthenia gravis: subgroup classification and therapeutic strategies. Lancet Neurol 14:1023–1036.

Ranum LP, Day JW. 2004. Pathogenic RNA repeats: an expanding role in genetic disease. Trends Genet 20:506–512.

References

Bromberg MB. 2002. Acute and chronic dysimmune polyneuropathies. In: WF Brown, CF Bolton, MJ Aminoff (eds). *Neuromuscular Function and Disease*, p. 1048, Fig. 58–2. New York: Elsevier Science.

Bromberg MB, Smith A, Gordon MD. 2002. Toward an efficient method to evaluate peripheral neuropathies. J Clin Neuromuscular Dis 3:172–182.

Brown RH Jr, Amato AA. 2002. Inherited peripheral neuropathies: classification, clinical features and review of molecular pathophysiology. In: WF Brown, CF Bolton, MJ Aminoff (eds). *Neuromuscular Function and Disease*, p. 624, Fig. 35–2. New York: Elsevier Science.

Brown RH, Mendell J. 2005. Muscular dystrophy. In: *Harrison's Principles of Internal Medicine*. New York: McGraw-Hill.

Cannon SC. 2010. Voltage-sensor mutations in channelopathies of skeletal muscle. J Physiol (Lond) 588:1887–1895.

Cannon SC. 1996. Ion channel defects and aberrant excitability in myotonia and periodic paralysis. Trends Neurosci 19:3–10.

Cannon SC. 2017. Sodium channelopathies of skeletal muscle. Handb Exp Pharm 246:309–330.

Cannon SC, Brown RH Jr, Corey DP. 1991. A sodium channel defect in hyperkalemic periodic paralysis: potassium-induced failure of inactivation. Neuron 64:619–626.

Cannon SC, Brown RH Jr, Corey DP. 1993. Theoretical reconstruction of myotonia and paralysis caused by incomplete inactivation of sodium channels. Biophys J 66:270–288.

Chamberlain JR, Chamberlain JS. 2017. Progress toward molecular therapy for Duchenne muscular dystrophy. Mol Ther 25:1125–1131.

Cull-Candy SG, Miledi R, Trautmann A. 1979. End-plate currents and acetylcholine noise at normal and myasthenic human endplates. J Physiol (Lond) 86:353–380.

Drachman DB. 1983. Myasthenia gravis: immunology of a receptor disorder. Trends Neurosci 6:446–451.

Finkel RS, Mercuri E, Darras BT, et al. 2017. Nusinersen versus sham control in infantile-onset spinal muscular atrophy. N Engl J Med 377:1723–1732.

Gilhus NE, Verschuuren JJ. 2015. Myasthenia gravis: subgroup classification and therapeutic strategies. Lancet Neurol 14:1023–1036.

Hoffman EP, Brown RH, Kunkel LM. 1987. Dystrophin: the protein product of the Duchenne muscular dystrophy locus. Cell 51:919–928.

Hoffman EP, Kunkel LM. 1989. Dystrophin in Duchenne/Becker muscular dystrophy. Neuron 2:1019–1029.

Lisak RP, Barchi RL. 1982. *Myasthenia Gravis*. Philadelphia: Saunders.

Lupski JR. 1998. Molecular genetics of peripheral neuropathies. In: JB Martin (ed). *Molecular Neurology*, pp. 239–256. New York: Scientific American.

Mendell JR, Al-Zaidy S, Shell R, et al. 2017. Single-dose gene-replacement therapy for spinal muscular atrophy. N Engl J Med 377:1713–1722.

Mendell JR, Goemans N, Lowes LP, et al. 2016. Longitudinal effect of etiplersen versus historical control on ambulation in Duchenne muscular dystrophy. Ann Neurol 79:257–271.

Milone M. 2017. Diagnosis and management of immune-mediated myopathies. Mayo Clin Proc 92:826–837.

Newsom-Davis J, Buckley C, Clover L, et al. 2003. Autoimmune disorders of neuronal potassium channels. Ann NY Acad Sci 998:202–210.

Patrick J, Lindstrom J. 1973. Autoimmune response to acetylcholine receptor. Science 180:871–872.

Rahimov F, Kunkel LM. 2013. Cellular and molecular mechanisms underlying muscular dystrophy. J Cell Biol 201:499–510.

Rosen DR, Siddique T, Patterson D, et al. 1993. Mutations in Cu/Zn superoxide dismutase gene are associated with familial amyotrophic lateral sclerosis. Nature 362:59–62.

Rowland LP, Hoefer PFA, Aranow H Jr. 1960. Myasthenic syndromes. Res Publ Assoc Res Nerv Ment Dis 38:548–600.

Taylor JP, Brown RH, Cleveland DW. 2016. Decoding ALS: from genes to mechanisms. Nature 539:197–206.

58

Seizures and Epilepsy

Until quite recently, the function and organization of the human cerebral cortex—the region of the brain concerned with perceptual, motor, and cognitive functions—has eluded both clinicians and neuroscientists. In the past, the analysis of brain function relied largely on observations of loss of brain functions resulting from brain damage and cell loss caused by strokes or trauma. These natural experiments provided much of the early evidence that distinct brain regions serve specific functions, or as the famous American neurologist C. Miller Fisher said, "We learn about the brain 'stroke by stroke.'" Observation of patients with seizures and epilepsy has been equally important in the study of brain function because the behavioral consequences of these disorders of neural *hyperactivity* inform clinicians how activation affects the brain regions from which they originate.

Temporary disruptions of brain function resulting from abnormal, excessive neuronal activity are called seizures, whereas the chronic condition of repeated seizures is called epilepsy. For centuries, understanding the neurological origins of seizures was confounded by the dramatic, and sometimes bizarre, behaviors associated with seizures. The chronic condition of epilepsy was widely associated with possession by evil spirits, yet seizures also were thought to be a sign of oracular, prescient, or special creative powers.

The Greeks in the time of Hippocrates (circa 400 BC) were aware that head injuries to one side of the brain could cause seizure activity on the opposite side of the body. In those earlier times, the diagnosis of epilepsy was probably much broader than the contemporary definition. Other causes of episodic unconsciousness, such as syncope as well as mass hysteria and

psychogenic seizures, were almost certainly attributed to epilepsy. Moreover, historical writings typically describe generalized convulsive seizures involving both cerebral hemispheres; thus, it is likely that seizures involving a very limited area of the brain were misdiagnosed or never diagnosed at all. Even today, it can be difficult for physicians to distinguish between episodic loss of consciousness and the various types of seizures. Nevertheless, as our ability to treat and even cure epilepsy continues to improve, these diagnostic distinctions take on increasing significance.

The early neurobiological analysis of epilepsy began with John Hughlings Jackson's work in London in the 1860s. Jackson realized that seizures need not involve loss of consciousness but could be associated with localized symptoms such as the jerking of an arm. His observation was the first formal recognition of what we now call partial (or focal) seizures. Jackson also observed patients whose seizures began with focal neurological symptoms, then progressed to convulsions with loss of consciousness by steadily involving adjacent regions in an orderly fashion (the so-called Jacksonian march). His observations gave rise to the concept of the motor homunculus (the anatomical map representing the body organization or "wiring diagram" over the cortical surface) long before functional organization was established using electrophysiological techniques (Chapter 4).

Another pioneering development that presaged modern therapy was the first surgical treatment for epilepsy in 1886 by the British neurosurgeon Victor Horsley. Horsley resected cerebral cortex adjacent to a depressed skull fracture and cured a patient with focal motor seizures. Related medical innovations include the first use of phenobarbital as an anticonvulsant in 1912 by Alfred Hauptmann, the development of electroencephalography by Hans Berger in 1929, and the discovery of the anticonvulsant properties of phenytoin (Dilantin) by Houston Merritt and Tracey Putnam in 1937. The birth of routine surgical treatment for epilepsy dates to the early 1950s, when Wilder Penfield and Herbert Jasper in Montreal stimulated the cortex and pinpointed the motor and sensory maps before removing the epileptic focus. As in any chronic disease, the physiological features of seizures are not the only consideration in the care and management of patients with epilepsy. Psychosocial factors are also extremely important. The diagnosis of epilepsy has consequences that can affect all aspects of everyday life, including educational opportunities, driving, and employment. Although many societal limitations imposed on epileptics are appropriate—most would agree that patients with epilepsy should not be commercial pilots—a diagnosis of epilepsy can result in inappropriately negative effects on educational opportunities and employment. To improve this situation, physicians have a duty to educate themselves and the public on the underlying science of epilepsy and its major comorbidities, including cognitive problems and depression.

Classification of Seizures and the Epilepsies Is Important for Pathogenesis and Treatment

Not all seizures are the same. Thus, the pathogenesis and classification of seizures must take into account their clinical characteristics as well as acquired and genetic factors in each patient. Seizures and the chronic condition of repetitive seizures (epilepsy) are common. Based on epidemiological studies in the United States, 1% to 3% of all individuals living to the age of 80 will be diagnosed with epilepsy. The highest incidence occurs in young children and the elderly.

In many respects, seizures represent a prototypic neurological disease in that the symptoms include both "positive" and "negative" sensory or motor manifestations. Examples of positive signs that can occur during a seizure include the perception of flashing lights or the jerking of an arm. Negative signs reflect impairments of normal brain function such as an impairment of consciousness and cognitive awareness or even transient blindness, speech arrest, or paralysis. These examples underscore a general feature of seizures: The signs and symptoms depend on the location and extent of brain regions that are affected. Finally, the manifestations of seizures result in part from synchronous activity triggered in surrounding tissue with normal cellular and network properties. The latter activity is particularly important in the spread of a seizure beyond its original boundaries—seizures quite literally hijack the normal functions of the brain.

Seizures Are Temporary Disruptions of Brain Function

Seizures have been classified clinically into two categories, focal or generalized, based on their onset (Table 58–1). This classification is conceptually simple, but because several terms have been used over the years to refer to the same condition, the binary nature may have been obscured. Nonetheless, this classification of seizures has proven extremely useful to clinicians, and anticonvulsant medications are targeted to one or the other type.

Table 58–1 International Classification of Seizures

Seizures
Focal onset
Aware versus impaired awareness
Motor versus nonmotor onset
Focal to bilateral tonic-clonic
Generalized onset
Motor
Tonic-clonic (formerly grand mal)
Other motor
Nonmotor (absence)
Unknown onset
Motor
Tonic-clonic
Other motor
Nonmotor
Unclassified

Source: Commission on Classification and Terminology of the International League Against Epilepsy, 2017.

Focal onset (also called partial) seizures originate in a small group of neurons (the seizure focus), and thus the symptoms depend on the location of the focus within the brain. Focal onset seizures can occur either without alteration of consciousness (often called simple partial) or with alteration of consciousness (often called complex partial). A typical focal onset seizure might begin with jerking in the right hand and progress to clonic movements (ie, jerks) of the entire right arm. If a focal onset seizure progresses further, the patient may lose consciousness, fall to the ground, rigidly extend all extremities (tonic phase), then have convulsive jerking in all extremities (clonic phase).

A focal onset seizure can be preceded by telltale symptoms called *auras*. Common auras include unprovoked and often vivid sensations such as a sense of fear, a rising feeling in the abdomen, or even a specific odor. The novelist Fyodor Dostoyevsky described his auras as a "feeling … so strong and sweet that for a few seconds of such bliss I would give ten or more years of my life, even my whole life perhaps." The aura is a product of electrical activity in the seizure focus and thus represents the earliest seizure manifestation. The time after a seizure but before the patient returns to his or her normal level of neurological function is called the post-ictal period.

Generalized onset seizures constitute the second main category. They begin without an aura or focal onset and involve both hemispheres from the onset. Thus, they are sometimes called primary generalized seizures to avoid confusion with seizures that secondarily generalize following a focal onset. Generalized onset seizures can be further divided into motor (convulsive) or nonmotor types depending on whether the seizure is associated with tonic-clonic movements.

The prototypic nonmotor generalized onset seizure is the *typical absence seizure* in children (formerly called petit mal). These seizures begin abruptly, usually last less than 10 seconds, are associated with staring and sudden cessation of all motor activity, and result in loss of awareness but not loss of posture. Patients appear as if in a trance, but the episodes are so brief that their occurrence can be missed by a casual observer. Unlike a focal onset seizure, there is no aura before the seizure or confusion after the seizure (the post-ictal period). Patients may exhibit mild motor manifestations such as eye blinking, but do not fall or have tonic-clonic movements. Typical absence seizures have very distinctive electrical characteristics on the electroencephalogram (EEG) known as a spike-and-wave pattern.

Some generalized onset seizures involve only abnormal (myoclonic, clonic, or tonic) movements or a sudden loss of motor tone (atonia). The most common motor type of generalized onset seizure is the tonic-clonic (formerly called *grand mal*) seizure. Such seizures begin abruptly, often with a grunt or cry, as tonic contraction of the diaphragm and thorax forces expiration. During the tonic phase, the patient may fall to the ground in a rigid posture with clenched jaw, lose bladder or bowel control, and become blue (cyanotic). The tonic phase typically lasts 30 seconds before evolving into clonic jerking of the extremities lasting 1 to 2 minutes. This active phase is followed by a post-ictal phase during which the patient is sleepy, disoriented, and may complain of headache and muscle soreness.

A generalized onset tonic-clonic seizure can be difficult to distinguish on purely clinical grounds from a focal seizure with a brief aura, which then rapidly progresses to a generalized tonic-clonic seizure. This distinction is not academic, as it can be vital to pinpointing the underlying cause and choosing the proper treatment. However, some seizures are simply difficult to classify because of undetermined onset.

Epilepsy Is a Chronic Condition of Recurrent Seizures

Recurrent seizures constitute the minimal criterion for the diagnosis of epilepsy. The oft-quoted clinical rule, "A single seizure does not epilepsy make," emphasizes this point, and even repeated seizures in response to a provocation such as alcohol withdrawal are not considered epilepsy. Various factors that contribute to a clinical pattern of recurrent seizures—the

underlying etiology of the seizures, the age of onset, or family history—are ignored in the classification scheme for seizures in Table 58–1. The classification of the epilepsies evolved primarily based on clinical observation rather than a precise cellular, molecular, or genetic understanding of the disorder. The factors influencing seizure type and severity can often be recognized as patterns of signs and symptoms, referred to as *epilepsy syndromes*. Such factors include the age of seizure onset, whether the seizures are inherited, and certain patterns on the EEG. The recognition of these syndromes has played a role in the recent discovery of single gene mutations as a cause of seizure disorders.

The primary variables in the classification of the epilepsies are whether or not a focal brain abnormality can be identified (localization-related versus generalized epilepsies) and whether there is an identifiable cause (symptomatic) or not (unknown, often called idiopathic). The great majority of adult-onset epilepsies are classified as symptomatic localization-related epilepsies. This category includes such causes as trauma, stroke, tumors, and infections. A large number of individuals have adult-onset epilepsies without a clearly defined cause.

Unfortunately, despite the usefulness of this classification scheme, many epilepsy syndromes do not fit neatly. One expects (and hopes) that this classification will be greatly refined as criteria include the underlying etiologies rather than just clinical phenotype.

The Electroencephalogram Represents the Collective Activity of Cortical Neurons

Because neurons are excitable cells, it should not be surprising that seizures result directly or indirectly from a change in the excitability of single neurons or groups of neurons. This view dominated early experimental studies of seizures. To study such effects, electrical recordings of brain activity can be made with intracellular or extracellular electrodes. Extracellular electrodes sense action potentials in nearby neurons and can detect the synchronized activity of ensembles of cells called *field potentials*.

At the slow time resolution of extracellular recording (hundreds of milliseconds to seconds), field potentials can appear as single transient changes called spikes. These spikes reflect action potentials in many neurons and should not be confused with spikes in recordings of single neurons, which are individual action potentials that last only 1 or 2 ms. The EEG thus represents a set of field potentials as recorded by multiple electrodes on the surface of the scalp (Figure 58–1).

Because the electrical activity originates in neurons in the underlying brain tissue, the waveform recorded by the surface electrode depends on the orientation and distance of the electrical source with respect to the electrode. The EEG signal is inevitably distorted by the filtering and attenuation caused by intervening layers of tissue and bone that act in the same way as resistors and capacitors in an electric circuit. Thus, the amplitude of EEG signals (measured in microvolts) is much smaller than the voltage changes in a single neuron (millivolts). High-frequency activity in single cells, such as action potentials, is filtered out by the EEG signal, which primarily reflects slower voltage changes across the cell membrane, such as synaptic potentials.

Although the EEG signal is a measure of the extracellular current caused by the summated electrical activity of many neurons, not all cells contribute equally to the EEG. The surface EEG reflects predominately the activity of cortical neurons in close proximity to each of the set of EEG electrodes on the scalp. Thus, deep structures such as the base of a cortical gyrus, mesial walls of the major lobes, hippocampus, thalamus, or brain stem do not contribute directly to the surface EEG. The contributions of individual nerve cells to the EEG are discussed in Box 58–1.

The surface EEG shows patterns of activity—characterized by the frequency and amplitude of the electrical activity—that correlate with various stages of sleep and wakefulness (Chapter 44) and with some pathophysiological processes such as seizures. The normal human EEG shows activity over the range of 1 to 30 Hz with amplitudes in the range of 20 to 100 μV. The observed frequencies have been divided into several groups: alpha (8–13 Hz), beta (13–30 Hz), delta (0.5–4 Hz), and theta (4–7 Hz).

Alpha waves of moderate amplitude are typical of relaxed wakefulness and are most prominent over parietal and occipital sites. During intense mental activity, beta waves of lower amplitude are more prominent in frontal areas and over other regions. Alerting relaxed subjects by asking them to open their eyes results in so-called desynchronization of the EEG with a reduction in alpha activity and an increase in beta activity (Figure 58–1B). Theta and delta waves are normal during drowsiness and early slow-wave sleep; if they are present during wakefulness, it is a sign of brain dysfunction.

As neuronal ensembles become synchronized, as when a subject relaxes or becomes drowsy, the summated currents become larger and can be seen as abrupt changes from the baseline activity. Such "paroxysmal" activity can be normal, eg, the episodes of high-amplitude activity (1–2 seconds, 7–15 Hz) that occur during sleep (sleep spindles). However, a sharp

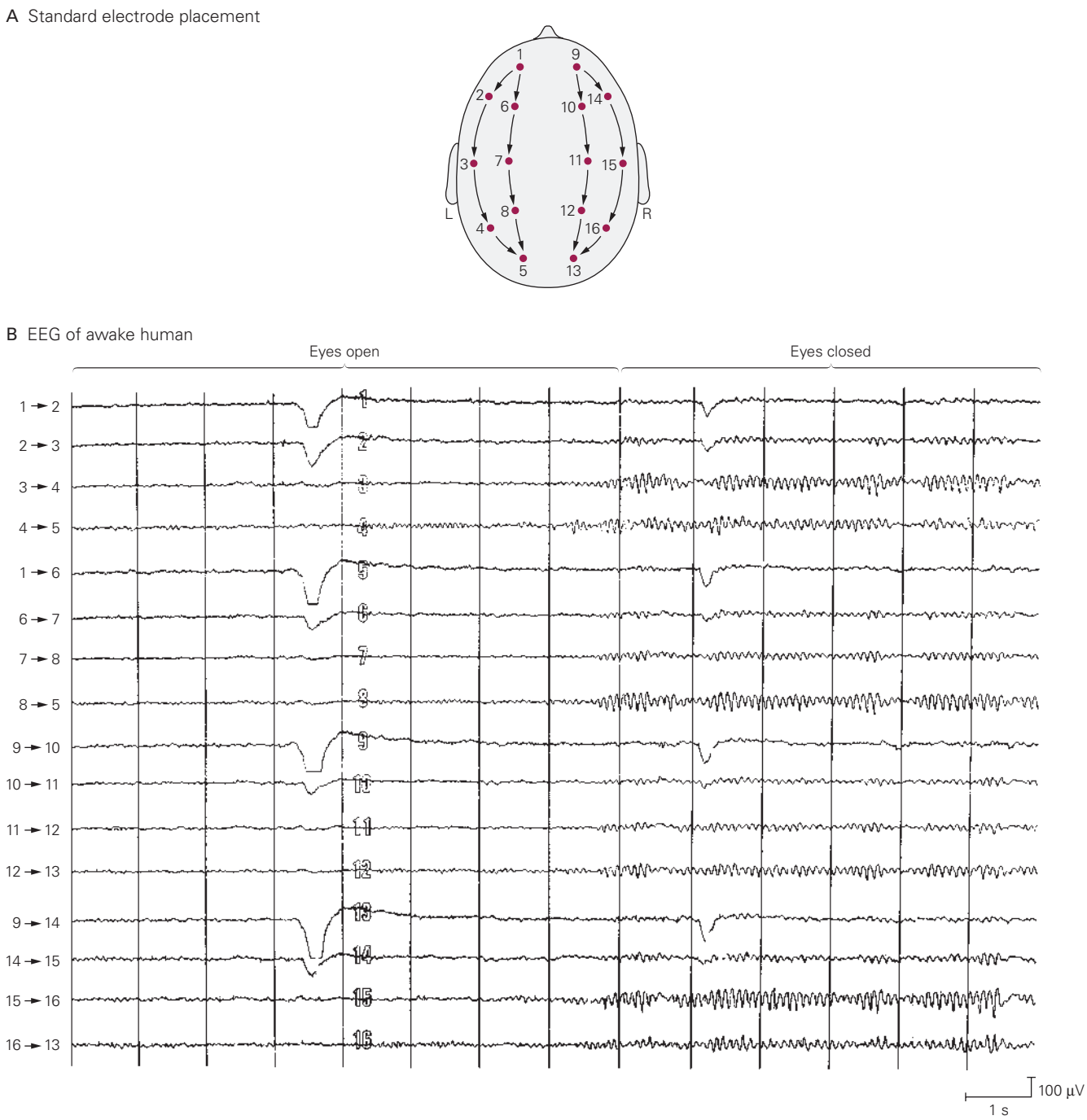

Figure 58–1 The normal electroencephalogram (EEG) in an awake human subject.

A. A standard set of placements (or montage) of electrodes on the surface of the scalp. The electrical response at each site reflects the activity between two of the electrodes.

B. At the beginning of the recording, the EEG shows low-voltage activity (~20 µV) over the surface of the scalp. The **vertical lines** are placed at 1-second intervals. During the first 8 seconds, the subject was resting quietly with eyes open, and then the subject was asked to close his eyes. With the eyes closed, larger-amplitude activity (8–10 Hz) develops over the occipital region (sites 3, 4, 8, 12, 15, and 16). This is the normal alpha rhythm characteristic of the relaxed, wakeful state. Slow large-amplitude artifacts occur at 3.5 seconds when the eyes blink and at 9 seconds when the eyes close.

Box 58–1 The Contribution of Individual Neurons to the Electroencephalogram

The contribution of the activity of single neurons to the electroencephalogram (EEG) can be understood by examining a simplified cortical circuit and some basic electrical principles. Pyramidal neurons are the major projection neurons in the cortex. The apical dendrites of these cells, which are oriented perpendicular to the cell surface, receive a variety of synaptic inputs. Thus, synaptic activity in the pyramidal cells is the principal source of EEG activity.

To understand the contribution of a single neuron to the EEG, consider the flow of charge produced by an excitatory postsynaptic potential (EPSP) on the apical dendrite of a cortical pyramidal neuron (Figure 58–2). Ionic current enters the dendrite at the site of generation of the EPSP, creating what is commonly called a current sink. It then must complete a loop by flowing down the dendrite and back out across the membrane at other sites, creating a current source.

The voltage signal created by a synaptic current is approximately predicted by Ohm's law ($V = IR$, where V is voltage, I is current, and R is resistance). Because the membrane resistance (R_m) is much larger than that of the salt solution that constitutes the extracellular medium (R_e), the voltage recorded across the membrane with an

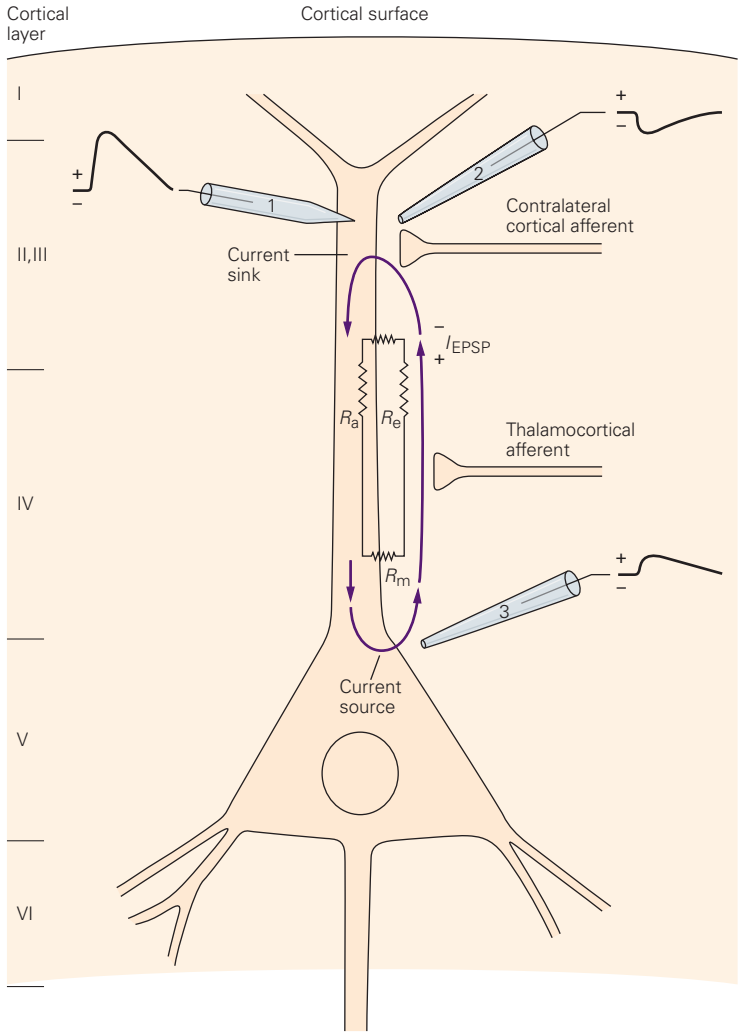

Figure 58–2 The pattern of electrical current flow for an excitatory postsynaptic potential (EPSP) initiated at the apical dendrite of a pyramidal neuron in the cerebral cortex. Activity is detected by three electrodes: an intracellular electrode inserted in the apical dendrite (**1**), an extracellular electrode positioned near the site of the EPSP in layer II of the cortex (**2**), and an extracellular electrode near the cell body in layer V (**3**). At the site of the EPSP (current sink), positive charge flows across the cell membrane (I_{EPSP}) into the cytoplasm, down the dendritic cytoplasm, and then completes the loop by exiting through the membrane near the cell body (current source). The potentials recorded by the extracellular electrodes at the sink and at the source have opposite polarity; the potentials recorded by the intracellular electrode have the same polarity regardless of the site. R_m, R_a, and R_e are the resistances of the membrane, cytoplasm, and extracellular space, respectively.

intracellular electrode (V_m) is also larger than the voltage at an extracellular electrode positioned near the current sink (V_e).

At the site of generation of an EPSP, the extracellular electrode detects the voltage change due to charge flowing away from the electrode into the cytoplasm as a negative voltage deflection. However, an extracellular electrode near the current source records a signal of opposite polarity (compare electrodes 1 and 3 in Figure 58–2). The situation is reversed if the site of the EPSP generation is on the basal segment of the apical dendrites.

In the cerebral cortex, excitatory axons from the contralateral hemisphere terminate primarily on dendrites in layers II and III, whereas thalamocortical axons terminate in layer IV (Figure 58–2). As a result, the activity measured by a surface EEG electrode will have opposite polarities for these two inputs even though the electrical event (membrane depolarization) is the same.

Similarly, the origin or polarity of cortical synaptic events cannot be unambiguously determined from surface EEG recordings alone. EPSPs in superficial layers and inhibitory postsynaptic potentials (IPSPs) in deeper layers both appear as upward (negative) potentials, whereas EPSPs in deeper layers and IPSPs in superficial layers have downward (positive) potentials (Figure 58–3).

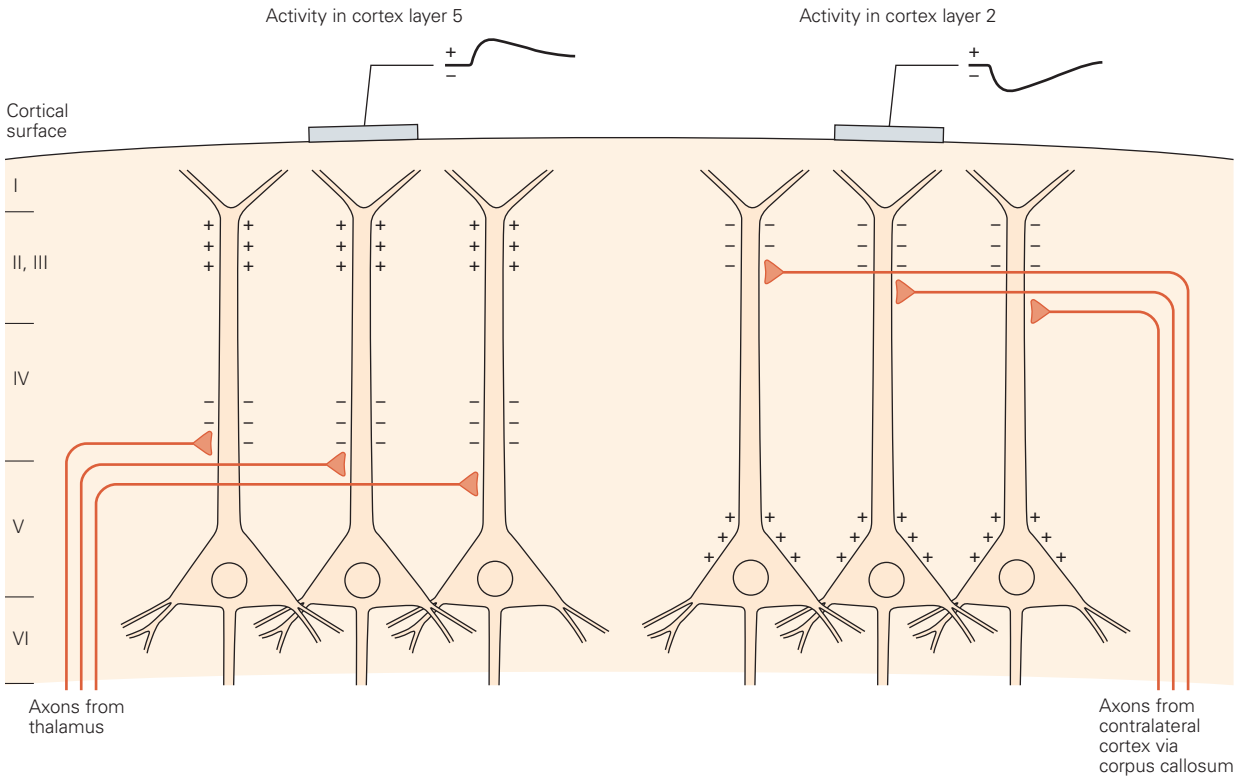

Figure 58–3 Surface electroencephalogram (EEG) recordings do not unambiguously indicate the polarity of synaptic events. The polarity of the surface EEG depends on the location of the synaptic activity within the cortex. A thalamocortical excitatory signal in layer V causes an upward voltage deflection at the surface EEG electrode because the electrode is nearer the current source. In contrast, an excitatory signal from the contralateral hemisphere in layer II causes a downward deflection because the electrode is nearer the sink.

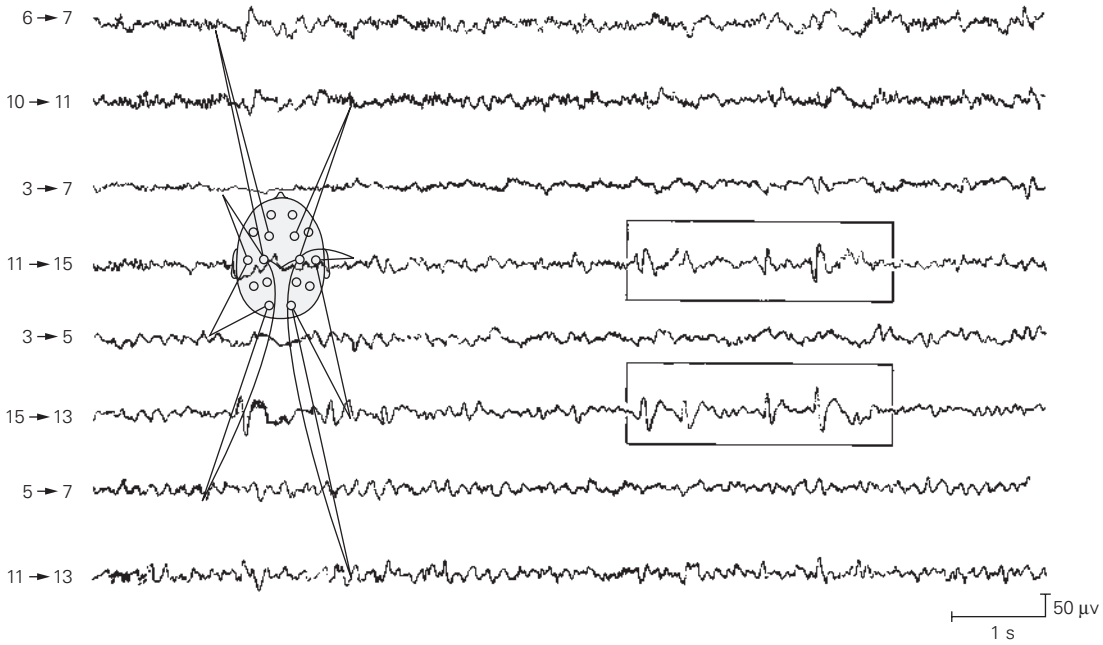

Figure 58–4 The electroencephalogram (EEG) can provide clues to the location of a seizure focus. Each trace represents the electrical activity between pairs of scalp electrodes as indicated in the electrode map. For example, electrode pairs 11–15 and 15–13 measure activity from the right temporal area. EEG activity in a patient with epilepsy shows sharp waves in the electrodes over the right temporal area (record enclosed in boxes). Such paroxysmal activity arises suddenly and disrupts the normal background EEG pattern. The focal abnormality may indicate that the seizure focus in this patient is in the right temporal lobe. Because the patient had no clinical seizures during the recording, these are interictal spikes (see Figure 58-7). (Adapted, with permission, from Lothman and Collins 1990.)

wave or EEG spike can also provide a clue to the location of a seizure focus in a patient with epilepsy (Figure 58–4). New recording and analytical methods such as spectral analysis of the EEG are increasingly being used to detect abnormal zones of synchrony (fast ripples) within a seizure focus.

Focal Onset Seizures Originate Within a Small Group of Neurons

Despite the variety of clinically defined seizures, important insights into the generation of seizure activity can largely be understood by comparing the electrographic patterns of focal onset seizures with those of generalized onset seizures.

The defining feature of focal onset seizures is that the abnormal electrical activity originates from a *seizure focus*. The seizure focus is considered to be nothing more than a small group of neurons, perhaps 1,000 or so, that have enhanced excitability and the ability to occasionally spread that activity to neighboring regions and thereby cause a seizure. The enhanced excitability (epileptiform activity) may result from many different factors such as altered cellular properties, glial dysfunction, or altered synaptic connections caused by a local scar, blood clot, or tumor. The development of a focal onset seizure can be arbitrarily divided into four phases: (1) the interictal period between seizures followed by (2) synchronization of activity within the seizure focus, (3) seizure spread, and finally, (4) secondary generalization. Phases 2 to 4 represent the ictal phase of the seizure. Different factors contribute to each phase.

Much of our knowledge about the electrical events during seizures comes from studies of animal models of focal onset seizures. A seizure is induced in an animal by focal electrical stimulation or by acute injection of a convulsant agent. This approach along with in vitro studies of tissue from these animal models has provided a good understanding of electrical events within the focus during a seizure as well as during the onset of the interictal period.

Neurons in a Seizure Focus Have Abnormal Bursting Activity

How does electrical activity in a single neuron or group of neurons lead to a focal onset seizure? Each neuron

within a seizure focus has a stereotypic and synchronized electrical response, the paroxysmal depolarizing shift, a depolarization that is sudden, large (20–40 mV), and long-lasting (50–200 ms), and that triggers a train of action potentials at its peak. The paroxysmal depolarizing shift is followed by an afterhyperpolarization (Figure 58–5A).

The paroxysmal depolarizing shift and afterhyperpolarization are shaped by the intrinsic membrane properties of the neuron (eg, voltage-gated Na^+, K^+, and Ca^{2+} channels) and by synaptic inputs from excitatory and inhibitory neurons (primarily glutamatergic and GABAergic, respectively). The depolarizing phase results primarily from activation of α-amino-3-hydroxy-5-methyl-4-isoxazolepropionic acid (AMPA)- and *N*-methyl-D-aspartate (NMDA)-type glutamate receptor-channels (Figure 58–5A), as well as voltage-gated Na^+ and Ca^{2+} channels. NMDA-type receptor-channels are particularly effective in enhancing excitability because depolarization relieves Mg^{2+} blockage of the channel. Removal of the blockage increases current through the channel, thus enhancing the depolarization and allowing additional Ca^{2+} to enter the neuron (Chapter 13).

The normal response of a cortical pyramidal neuron to excitatory input consists of an excitatory postsynaptic potential (EPSP) followed by an inhibitory postsynaptic potential (IPSP) (Figure 58–5B). Thus, the paroxysmal depolarizing shift can be viewed as a massive enhancement of these depolarizing and hyperpolarizing synaptic components. The afterhyperpolarization is generated by voltage-dependent and Ca^{2+}-dependent K^+ channels as well as by a γ-aminobutyric acid (GABA)-mediated Cl^- conductance (ionotropic $GABA_A$ receptors) and K^+conductance (metabotropic $GABA_B$ receptors) (Figure 58–5A). The Ca^{2+} influx through voltage-dependent Ca^{2+} channels and NMDA-type receptor-channels triggers the opening of calcium-activated channels, particularly K^+ channels. The afterhyperpolarization limits the duration of the paroxysmal depolarizing shift, and its gradual disappearance is the most important factor in the onset of a focal onset seizure, as discussed later.

Thus, it is not surprising that many convulsants act by enhancing excitation or blocking inhibition. Conversely, anticonvulsants can act by blocking excitation or enhancing inhibition. For example, the benzodiazepines diazepam (Valium) and lorazepam (Ativan) enhance $GABA_A$-mediated inhibition and are used in the emergency treatment of prolonged repetitive seizures. The anticonvulsants phenytoin (Dilantin) and carbamazepine (Tegretol) and several others reduce the opening of voltage-gated Na^+ channels that underlie the action potential. Molecular models of the Na^+ channel indicate that these drugs are more effective when the channel is in the open or activated state.

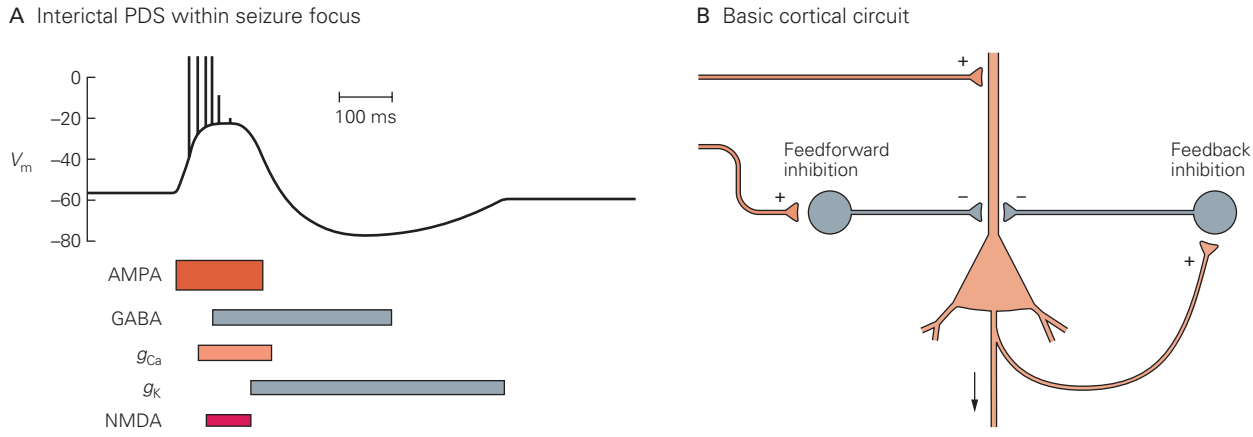

Figure 58–5 The conductances that underlie the paroxysmal depolarizing shift of a neuron in a seizure focus.

A. The paroxysmal depolarizing shift (**PDS**) is largely dependent on α-amino-3-hydroxy-5-methyl-4-isoxazolepropionic acid (**AMPA**)- and *N*-methyl-D-aspartate (**NMDA**)-type glutamate receptor-channels whose effectiveness is enhanced by the opening of voltage-gated Ca^{2+} channels (g_{Ca}). Following the depolarization, the cell is hyperpolarized by activation of γ-aminobutyric acid (**GABA**) receptors (both ionotropic $GABA_A$ and metabotropic $GABA_B$) as well as by voltage-gated and calcium-activated K^+ channels (g_K). (Adapted, with permission, from Lothman 1993a.)

B. Recurrent axon branches activate inhibitory neurons and cause feedback inhibition of the pyramidal neuron. Extrinsic excitatory inputs can also activate feedforward inhibition. The PDS represents exaggerated excitation in a seizure focus, whereas the inhibitory circuitry forms the basis of surround inhibition, important in restricting interictal activity to the seizure focus.

Thus, fittingly, the ability of these drugs to block Na^+ channels is enhanced by repetitive activity associated with seizures; that is, the greatest effect is in those neurons that need to be silenced the most.

The Breakdown of Surround Inhibition Leads to Synchronization

As long as the abnormal electrical activity is restricted to a small group of neurons, there are no clinical manifestations. The synchronization of neurons in a seizure focus is dependent not only on the intrinsic properties of each individual cell but also on the number and strength of connections between neurons. During the interictal period, the abnormal activity is confined to the seizure focus by inhibition of the surrounding tissue.

This "inhibitory surround," initially described by David Prince, is particularly dependent on feedforward and feedback inhibition by GABAergic inhibitory interneurons (Figure 58–6A). Although inhibitory circuits in the cerebral cortex are often represented by simple diagrams (Figure 58–6B), the morphology and connectivity of cortical inhibitory neurons are actually quite complex and a topic of continuing investigation with many new methods such as cell type–specific viral labeling and optogenetic stimulation.

During the development of a focal seizure, the excitation in the circuit overcomes the inhibitory

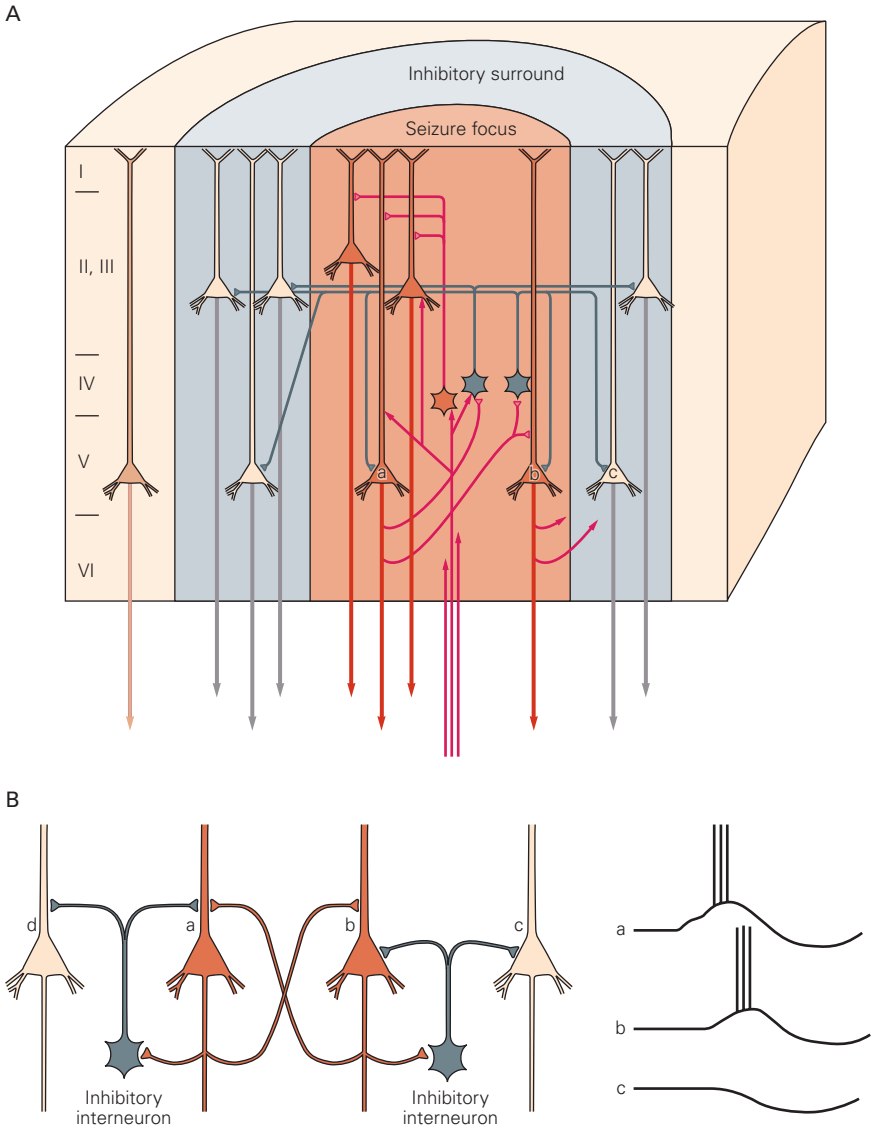

Figure 58–6 The spatial and temporal organization of a seizure focus depends on the interplay between excitation and inhibition of neurons in the focus.

A. The pyramidal cell *a* shows the typical electrical properties of neurons in a seizure focus (see part **B**). Excitation in cell *a* activates another pyramidal cell (*b*), and when many such cells fire synchronously, a spike is recorded on the electroencephalogram. However, cell *a* also activates γ-aminobutyric acid (GABA)-ergic inhibitory interneurons (**gray**). These interneurons can reduce the activity of cells *a* and *b* through feedback inhibition, thus limiting the seizure focus temporally, as well as prevent the firing of cells outside the focus, represented here by cell *c*. This latter phenomenon creates an inhibitory surround that acts to contain the hyperexcitability to the seizure focus during interictal periods. When extrinsic or intrinsic factors alter this balance of excitation and inhibition, the inhibitory surround begins to break down and the seizure activity spreads, leading to seizure generation. (Adapted, with permission, from Lothman and Collins 1990.)

B. The synaptic connections and activity patterns for cells *a*, *b*, and *c* shown in part **A**. Cells *a* and *b* (within the seizure focus) undergo a paroxysmal depolarizing shift, whereas cell *c* (in the inhibitory surround) is hyperpolarized due to input from GABAergic inhibitory interneurons.

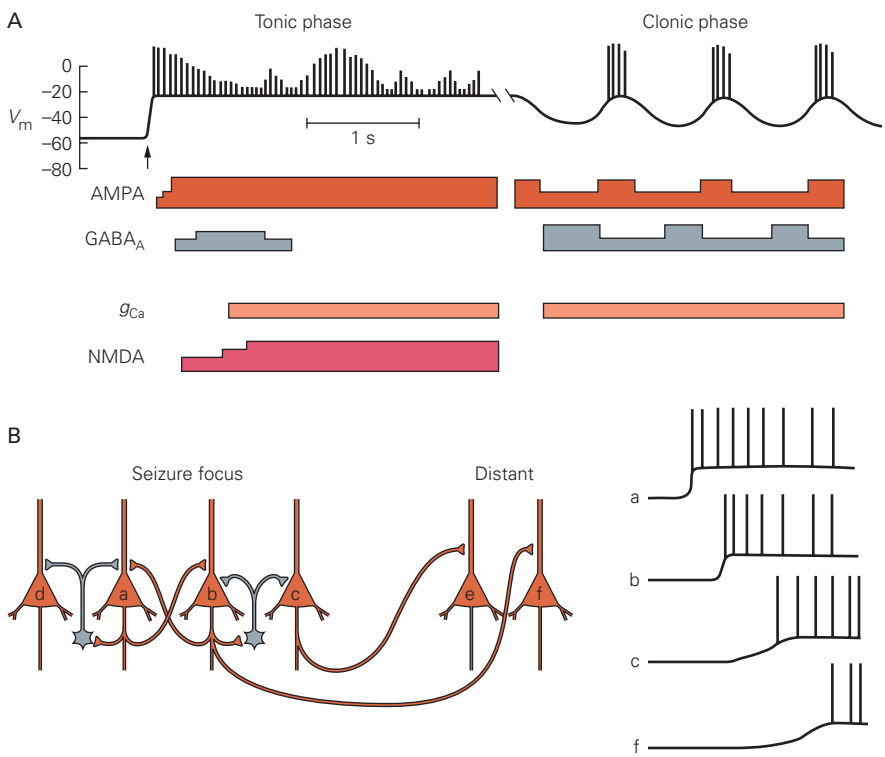

Figure 58–7 A focal onset seizure begins with the loss of the afterhyperpolarization and surround inhibition. (Adapted, with permission, from Lothman 1993a.)

A. With the onset of a seizure (**arrow**), neurons in the seizure focus depolarize as in the first phase of a paroxysmal depolarizing shift. However, unlike the interictal period, the depolarization persists for seconds or minutes. The γ-aminobutyric acid (**GABA**)-mediated inhibition fails, whereas excitatory activity in the α-amino-3-hydroxy-5-methyl-4-isoxazolepropionic acid (**AMPA**)- and *N*-methyl-D-aspartate (**NMDA**)-type glutamate receptors is functionally enhanced. This activity corresponds to the tonic phase of a secondarily generalized tonic-clonic seizure. As the GABA-mediated inhibition gradually returns, the neurons in the seizure focus enter a period of oscillation corresponding to the clonic phase.

B. As the surround inhibition breaks down, neurons in the seizure focus become synchronously excited and send trains of action potentials to distant neurons, thus spreading the abnormal activity from the focus. Compare this pattern of activity in cells *a* to *c* with that during the interictal period (Figure 58–6B).

surround, and the afterhyperpolarization in the neurons of the original focus gradually disappears. As a result, a nearly continuous high-frequency train of action potentials is generated, and the seizure begins to spread beyond the original focus (Figure 58–7).

An important factor in the spread of focal onset seizures appears to be that the intense firing of the pyramidal neurons results in a relative decrease in synaptic transmission from the inhibitory GABAergic interneurons, although the interneurons remain viable. Whether this decrease results from a presynaptic change in the release of GABA or a postsynaptic change in GABA receptors is still not understood and may not be the same in all cases. Other factors that may contribute to the loss of the inhibitory surround over time include changes in dendritic morphology, the density of receptors or channels, or a depolarizing shift in E_K caused by extracellular K^+ ion accumulation. Prolonged firing also transmits action potentials to distant sites in the brain, which in turn may trigger trains of action potentials in neurons that project back to neurons in the seizure focus (backpropagation). Reciprocal connections between the neocortex and thalamus may be particularly important in this regard.

Despite our understanding of such mechanisms, we still do not know what causes a seizure to occur at any particular moment. The inability to predict when a seizure will occur is perhaps the most debilitating aspect of epilepsy. New approaches to this dilemma are discussed in Box 58–2. Some patients learn to recognize the triggers most critical for them, such as sleep deprivation or stress, and thus adjust their lifestyle to avoid these circumstances. But in many individuals, seizures do not follow a predictable pattern.

In a few patients, sensory stimuli such as flashing lights can trigger seizures, suggesting that repeated excitation of some circuits causes a change in excitability. For example, NMDA-type glutamate receptor activity and GABAergic inhibition can undergo changes dependent on the frequency of firing of the presynaptic neuron. This provides one possible molecular mechanism for such changes in network excitability. On a longer time scale, circadian rhythms and hormonal patterns may also influence the likelihood

Box 58–2 New Approaches to Real-Time Seizure Detection and Prevention

Perhaps the most disabling aspect of seizures and epilepsy is the uncertainty of it all—when will the next seizure occur? As you can imagine, this impacts employment, driving, and recreation and often prevents the development of an individual's full potential. Patients with epilepsy sometimes have a brief warning or aura, but rarely do they have enough time to institute a therapeutic intervention such as a pill or an injection in order to abort the seizure.

Clinicians and epilepsy researchers have long recognized the importance of real-time seizure *detection* and real-time seizure *prevention* as a goal of therapy. Of course, acute detection must precede an acute treatment. However, in general, this approach has only been possible in patients undergoing EEG monitoring either with surface EEG electrodes or implanted electrodes. Several technologies are now emerging that allow new hope for detection, and thus enable efforts to abort or prevent an imminent seizure. Most are still in the experimental phase in animal models, but a few have reached clinical trials and even, in the case of vagal nerve stimulators, clinical practice. Seizure prevention can be imagined in two general ways: either altering the excitability of large regions of brain or somehow interrupting activity within a seizure focus. These two approaches can also be considered in engineering terms as open-loop or closed-loop strategies, respectively.

The first approach led to the development in 1997 of the vagal nerve stimulator, implanted in the neck and powered by a pacemaker-style battery (Figure 58–8). The

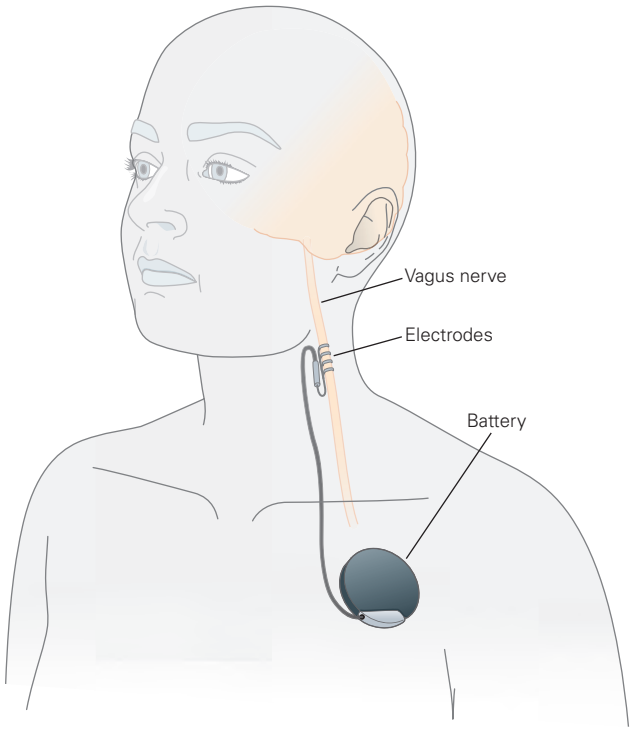

Figure 58–8 Vagal nerve stimulation. Schematic of placement of electrodes on the left vagus nerve powered by a battery implanted subcutaneously in the chest wall. The stimulation can be programmed at regular intervals (eg, every 30 seconds) and can also be activated on demand by placing a magnet over the chest. (Adapted from Stacey and Litt 2008.)

resulting chronic, intermittent stimulation of the vagus nerve has been effective in reducing seizure frequency in some patients. The patient can also activate the stimulator with a hand-held magnet during an aura to see if acute stimulation can prevent a seizure. The exact mechanism of seizure reduction by vagal nerve stimulation is still unclear, but presumably involves activation of the autonomic nervous system, and thus, this form of stimulation has limited specificity to particular brain regions.

Because many patients with intractable epilepsy have seizures that originate from one or more discrete foci in the brain, it would obviously be ideal to be able to detect abnormal activity within a seizure focus, and thus through some sort of feedback mechanism deliver a stimulus that would abort the spread of epileptiform activity from that focus. This goal has been an active area of investigation over the past decade, leading to a clinical trial the results of which were recently published. The device tested was a chronically implanted neurostimulator (RNS System, Neuropace) that directly stimulates the seizure focus when epileptiform activity is detected (Figure 58–9).

In this multicenter double-blinded trial, the device was implanted in patients with intractable focal onset seizures with one or two seizure foci. The patients were monitored for an average of 5 years. The device can be programmed by the clinician to match characteristics for each patient. The patients were randomized into two groups, responsive stimulation or sham stimulation groups, for the first 5 months, and then followed for up to 2 years. There was a 44% reduction in seizure frequency after 1 year and a 53% reduction after 2 years, suggestive of a progressive effect. The device was generally well tolerated. Thus, this approach has therapeutic potential for some patients and provides proof-of-concept evidence for closed-loop seizure detection and stimulation.

The RNS System uses electrical stimulation, but other strategies being studied in animals promise to refine methods of seizure prevention. These include neuronal stimulation or silencing using viral-mediated delivery of opto- or chemogenetic probes. In general, a replication-defective virus can be targeted to a specific cell type within a brain region. In the optogenetic approach, the virus is engineered to express ion channels or pumps that reduce neuron excitability when exposed to light. In the chemogenetic approach, a chemical is delivered systemically. This strategy has now been successfully employed in animal models of epilepsy.

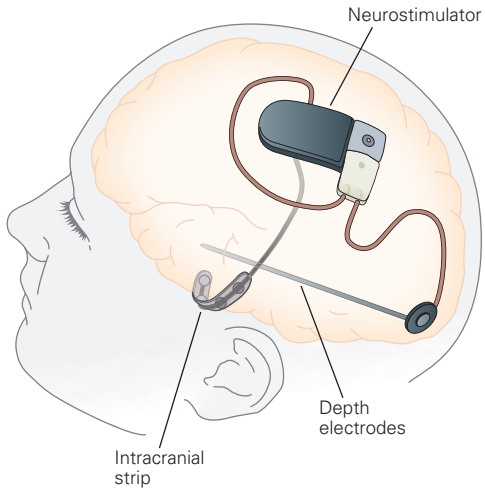

Figure 58–9 Closed-loop seizure detection and prevention. This schematic diagram of the closed-loop RNS System shows the intracranial strip and depth electrodes that detect seizure activity and subsequently deliver programmed stimulation to the seizure focus. (Adapted, with permission, from Heck et al. 2014.)

The optogenetic strategy is similar to the neurostimulator except that stimulation is delivered through a fiber optic light guide implanted near the seizure focus. The advantage of this approach is that the virus is engineered to deliver stimulation to a specific population of neurons. The chemogenetic approach has the advantage of noninvasive delivery of the chemical, but lacks the speed that can be achieved with optical or electrical stimulation. Even when optimized and tested in clinical trials, these invasive approaches are likely to be useful only in a subset of focal onset epilepsies that have stable and well-defined seizure foci. Thus, continuing and complementary efforts to understand the genetic mechanisms of epileptogenesis, as well as new technologies such as stem cell therapies, remain essential.

of seizures, as demonstrated by patients who have seizures only while sleeping (nocturnal epilepsy) or during their menstrual period (catamenial epilepsy). If we could develop continuous monitoring methods to predict the timing of seizure generation (Box 58–2), acute intervention to deliver a drug or change neural activity patterns to prevent seizures might become a therapeutic option. However, EEG studies reveal great variability between patients in pre-ictal patterns. Continuous chronic stimulation of neural circuits is another method of modifying the excitability of epileptic circuits. As an example of this approach, implanted vagal nerve stimulators have been modestly successful in treating pharmaco-resistant epilepsy that does not respond to other treatments.

The Spread of Seizure Activity Involves Normal Cortical Circuitry

If activity in the seizure focus is sufficiently intense, the electrical activity begins to spread to other brain regions. Spread of seizure activity from a focus generally follows the same axonal pathways as does normal cortical activity. Thus, thalamocortical, subcortical, and transcallosal pathways can all become involved in seizure spread. Seizure activity can propagate from a seizure focus to other areas of the same hemisphere or across the corpus callosum to involve the contralateral hemisphere (Figure 58–10). Once both hemispheres become involved, a focal onset seizure has become secondarily generalized. At this point, the patient generally experiences loss of consciousness. The spread of a partial seizure usually occurs rapidly over a few seconds, but can also evolve over many minutes. Rapid generalization is more likely if a focal onset seizure begins in the neocortex than if it begins in the limbic system (in particular, the hippocampus and amygdala).

An interesting unanswered question is what terminates a seizure. Remarkably, few mechanisms for the self-limiting return to the interictal state have been defined with certainty. One definite conclusion at this point is that termination is not due to cellular metabolic exhaustion, because under severe conditions clinical seizures may continue for hours (see below). During the initial 30 seconds or so of a focal onset seizure that secondarily generalizes, neurons in the involved areas undergo prolonged depolarization and fire continuously (due to loss of the afterhyperpolarization that normally follows a paroxysmal depolarizing shift). As the seizure evolves, the neurons begin to repolarize and the afterhyperpolarization reappears. The cycles of depolarization and repolarization correspond to the clonic phase of the seizure (Figure 58–7A).

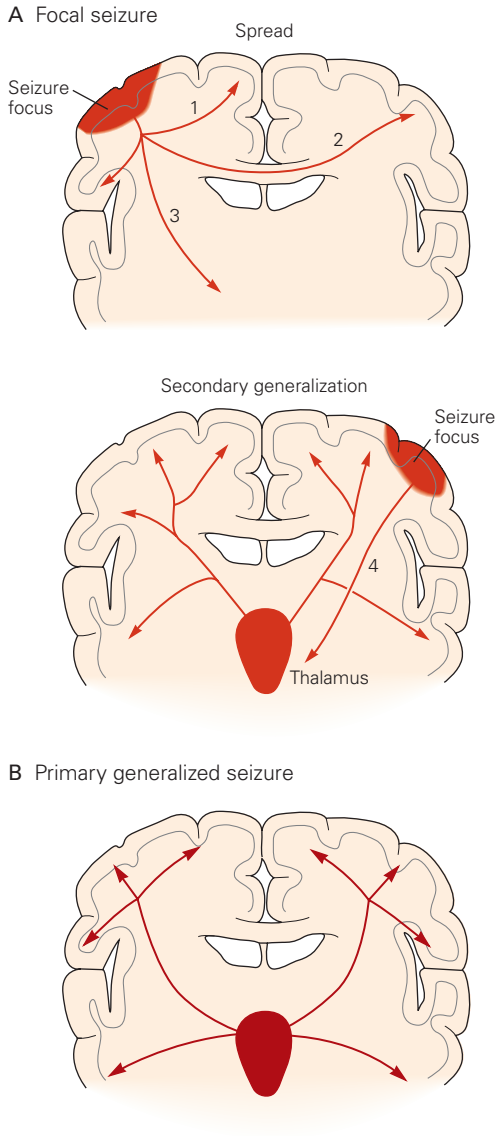

Figure 58–10 Focal and generalized onset seizures propagate via several pathways. (Adapted, with permission, from Lothman 1993b.)

A. Focal onset seizures can spread locally from a focus via intrahemispheric fibers (**1**) and more remotely to homotopic contralateral cortex (**2**) and subcortical centers (**3**). The secondary generalization of a focal onset seizure spreads to subcortical centers via projections to the thalamus (**4**). Widespread thalamocortical interconnections then contribute to rapid activation of both hemispheres.

B. In a generalized onset seizure, such as a typical absence seizure, interconnections between the thalamus and cortex are a major route of seizure propagation.

The seizure is often followed by a period of decreased electrical activity, the postictal period, which may be accompanied by symptoms of confusion, drowsiness, or even focal neurological deficits such as a hemiparesis (Todd paralysis). A neurological exam in the postictal period can lead to insights about the locus of the seizure focus when there is prolonged depression of one brain region or function, once other brain regions have regained normal function.

Generalized Onset Seizures Are Driven by Thalamocortical Circuits

Unlike the typical focal onset seizure, a generalized onset seizure abruptly disrupts normal brain activity in both cerebral hemispheres simultaneously. Generalized onset seizures and their associated epilepsies vary both in their manifestations and etiologies. Although the cellular mechanisms of generalized onset seizures differ in a number of interesting respects from those of focal onset or secondarily generalized seizures, a generalized onset seizure can be difficult to distinguish clinically or by EEG from a focal onset seizure that rapidly generalizes.

The most studied type of generalized onset seizure is the typical absence seizure (petit mal), whose characteristic EEG pattern (the 3-Hz spike-and-wave pattern in Figure 58–11A) was first recognized by Hans Berger in 1933. F. A. Gibbs recognized the relationship of this EEG pattern to typical absence seizures (he aptly described the pattern as "dart and dome") and attributed the mechanism to generalized cortical disturbance. The distinctive clinical features of typical absence seizures have a clear correlation with the EEG activity.

The typical absence seizure begins suddenly, lasts 10 to 30 seconds, and produces impaired awareness with only minor motor manifestations such as blinking or lip smacking. Unlike a focal onset seizure that secondarily generalizes, generalized onset seizures are not preceded by an aura or followed by postictal symptoms. The spike-wave EEG pattern can be seen in all cerebral areas abruptly and simultaneously and is immediately preceded and followed by normal background activity. Very brief (1–5 seconds) runs of 3-Hz EEG activity without apparent clinical symptoms are common in patients with absence seizures, but if frequent, they can affect their ability to carry out normal activities such as school performance.

In contrast to Gibbs's hypothesis of diffuse cortical hyperexcitability, Penfield and Jasper noted that the EEG in typical absence seizures is similar to rhythmic EEG activity in sleep, so-called sleep spindles (Chapter 44). They proposed a "centrencephalic" hypothesis in which generalization was attributed to rhythmic activity (pacing) by neuronal aggregates in the upper brain stem or thalamus that project diffusely to the cortex.

Research on animal models of generalized onset seizures and studies of the genetics of generalized epilepsy suggest that elements of both hypotheses are correct. In cats, parenteral injections of penicillin, a weak $GABA_A$ antagonist, produce behavioral unresponsiveness associated with an EEG pattern of bilateral synchronous slow waves (generalized penicillin epilepsy). During such a seizure, thalamic and cortical cells become synchronized through the same reciprocal thalamocortical connections that contribute to normal sleep spindles during slow-wave sleep.

Such seizures could in theory represent a form of diffuse hyperexcitability in the cortex. Recordings from individual cortical neurons show an increase in the rate of firing during a depolarizing burst that in turn produces a powerful GABAergic inhibitory feedback that hyperpolarizes the cell for approximately 200 ms after each burst (Figure 58–11C). This depolarization followed by inhibition differs fundamentally from the paroxysmal depolarizing shift in focal onset seizures in that GABAergic inhibition is preserved. In the typical absence seizure, the summated activity of the bursts produces the spike while the summated inhibition produces the wave of the spike-wave EEG pattern.

What are the properties of cells and networks that facilitate this generalized and synchronous activity? An early clue came from studies of the intrinsic bursting of thalamic relay neurons. Henrik Jahnsen and Rodolfo Llinas found that these neurons robustly express the T-type voltage-gated Ca^{2+} channel that is inactivated at the resting membrane potential but becomes available for activation when the cell is hyperpolarized (Chapter 10). A subsequent depolarization then transiently opens the Ca^{2+} channel (thus its name, T-type), and the Ca^{2+} influx generates low-threshold Ca^{2+} spikes. Consistent with the hypothesis that T-type channels contribute to absence seizures, certain anticonvulsant agents that block absence seizures, such as ethosuximide (Zarontin) and valproic acid (Depakote), also block T-type channels. T-type channels are encoded by three related genes (*Cav3.1*–*Cav3.3*), with *Cav3.1* the predominant type in the thalamus.

The circuitry of the thalamus seems ideally suited to the generation of generalized onset seizures. The pattern of thalamic neuron activity during sleep spindles suggests a reciprocal interaction between thalamic relay neurons and GABAergic interneurons in the thalamic reticular nucleus and perigeniculate nucleus (Figure 58–11B). Studies of thalamic brain slices by David McCormick and his colleagues indicate that

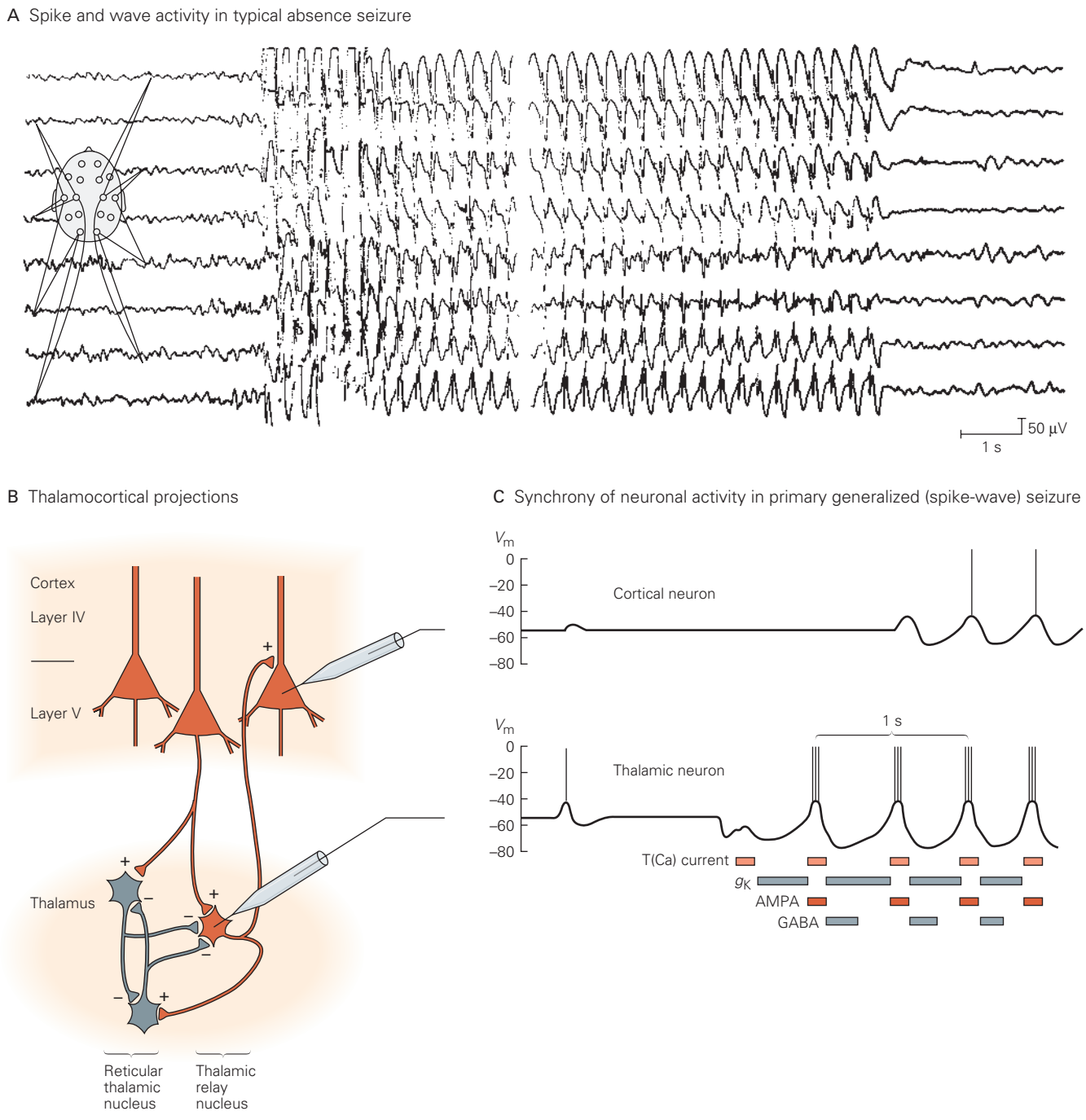

Figure 58–11 Generalized onset seizures have distinctive electroencephalogram (EEG) and single-neuron patterns.

A. This EEG from a 12-year-old patient with typical absence (petit mal) seizures shows the sudden onset of synchronous spikes at a frequency of 3 per second and wave activity lasting approximately 14 seconds. The seizure clinically manifested as a staring spell with occasional eye blinks. Unlike a focal onset seizure, there is no buildup of activity preceding the seizure and the electrical activity returns abruptly to the normal background level following the seizure. The discontinuity in the trace is due to removal of a 3-second period of recording. (Reproduced, with permission, from Lothman and Collins 1990.)

B. Thalamocortical connections that participate in the generation of sleep spindles (Chapter 44) are thought to be essential for the generation of generalized onset seizures. Pyramidal cells in the cortex are reciprocally connected by excitatory synapses with thalamic relay neurons. GABAergic inhibitory interneurons in the reticular thalamic nucleus are excited by pyramidal cells in the cortex and by thalamic relay neurons and inhibit the thalamic relay cells. The interneurons are also reciprocally connected.

C. Neuronal activity of cortical and thalamic neurons becomes synchronized during a generalized onset seizure. The depolarization is dependent on conductances in α-amino-3-hydroxy-5-methyl-4-isoxazolepropionic acid (**AMPA**)-type glutamate receptor-channels and T-type voltage-gated Ca^{2+} channels. The repolarization is due to γ-aminobutyric acid (**GABA**)-mediated inhibition as well as voltage- and calcium-dependent K^+ conductances (g_K). (Adapted, with permission, from Lothman 1993a.)

the interneurons hyperpolarize the relay neurons, thus removing the inactivation of T-type Ca^{2+} channels. This action leads to an oscillatory response: A rebound burst of action potentials following each IPSP to which the T-type Ca^{2+} channels contribute stimulates the GABAergic interneurons, resulting in another round of relay neuron rebound firing. The relay neurons also excite cortical neurons, manifested in the EEG by a "spindle." Both the T-type Ca^{2+} channel and the $GABA_B$ receptor-channel play an important role in the generation of this activity, which resembles human absence seizures (Chapter 44).

Mutations in voltage-gated Ca^{2+} channels have produced several mouse models of generalized epilepsy, including the so-called *totterer* mouse, which bears a mutation in the P/Q-type calcium channels involved in neurotransmitter release. Studies of these mutants by Jeffrey Noebels and his colleagues have revealed that the animals develop generalized onset seizures when they reach adolescence. EEGs in these animals show a paroxysmal spike-wave discharge and seizures that are characterized by an arrest of behavior and blockade by ethosuximide, similar to typical absence seizures in children. Thalamic neurons in these mice have elevated T-type Ca^{2+} channels that favor rebound bursting. Mutations of over 20 different genes for this phenotype have now been described in mice. Remarkably, many encode ion channel subunits or proteins involved in presynaptic transmitter release.

Locating the Seizure Focus Is Critical to the Surgical Treatment of Epilepsy

The pioneering studies of Wilder Penfield in Montreal in the early 1950s led to the recognition that removal of the temporal lobe in certain patients with focal onset seizures of hippocampal origin could reduce the number of seizures or even cure epilepsy. As surgical treatment for such patients became more common, it became clear that the surgical outcome is directly related to the adequacy of the resection. Thus, precise localization of the seizure focus in cases of focal onset seizures is essential. Electrical mapping of seizure foci originally relied on the surface EEG, which we have seen is biased toward particular sets of neurons in the cortex immediately adjacent to the skull. However, seizures intractable to conventional medical management often begin in deep structures that show little or no abnormality on the surface EEG at the onset of the seizure. Thus, the surface EEG is somewhat limited in identifying the location of the seizure focus.

The development of magnetic resonance imaging (MRI) markedly improved the noninvasive anatomical mapping of seizure foci. This technique is now routine in the evaluation of epilepsies involving the temporal lobe, but also shows increasing promise for identifying seizure foci in other locations. The scientific basis of anatomical mapping of seizure foci by MRI was the observation that a majority of patients with intractable focal onset seizures with impaired awareness have atrophy and cell loss in the mesial portions of the hippocampal formation. There is a dramatic loss of neurons within the hippocampus (mesial temporal sclerosis), changes in dendritic morphology of surviving cells, and collateral sprouting of some axons. The anatomical resolution of modern MRI machines has allowed a noninvasive, quantitative assessment of the size of the hippocampus in epilepsy patients. Loss of volume of the hippocampus on one or another side of the brain generally correlates well with the localization of seizure foci in the hippocampus as determined by functional criteria using implanted depth electrodes.

The typical patient with mesial temporal epilepsy has unilateral disease, which leads to shrinkage of the hippocampus on one side that can be associated with apparent dilatation of the temporal horn of the lateral ventricle. Such a case is illustrated in Box 58–3. However, in many patients, abnormalities cannot be detected using anatomical MRI; thus, nonanatomical (functional) imaging techniques (fMRI) are used as well (Chapter 6).

Functional neuroimaging takes advantage of the changes in cerebral metabolism and blood flow that occur in the seizure focus during the ictal and interictal periods. The electrical activity associated with a seizure places a large metabolic demand on brain tissue. During a focal onset seizure, there is an approximately three-fold increase in glucose and oxygen utilization. Between seizures, the seizure focus often shows decreased metabolism. Despite the increased metabolic demands, the brain is able to maintain normal adenosine triphosphate (ATP) levels during a focal onset seizure. On the other hand, the transient interruption of breathing during a generalized motor seizure causes a decrease in oxygen levels in the blood. This results in a drop in ATP concentration and an increase in anaerobic metabolism as indicated by rising lactate levels. This oxygen debt is quickly replenished in the postictal period, and no permanent damage to brain tissue results from a single generalized seizure.

Positron emission tomography (PET) scans of patients with focal onset seizures originating in the mesial temporal lobe frequently show interictal hypometabolism, with metabolic changes extending to the lateral temporal lobe, ipsilateral thalamus, basal ganglia, and frontal cortex. PET scans using nonhydrolyzable glucose analogs have been particularly helpful

Box 58–3 Surgical Treatment of Temporal Lobe Epilepsy

A 27-year-old woman had episodes of decreased responsiveness beginning at age 19. At first, she would stare off and appear confused during the episodes. Later, she developed an aura consisting of a feeling of fear. This fear was followed by altered consciousness, a wide-eyed stare, tightening of the left arm, and a scream that lasted for 14 to 20 seconds (Figure 58–12).

These spells were diagnosed as complex partial seizures. The seizures occurred several times a week despite treatment with several antiepileptic drugs. She was unable to work or drive due to frequent seizures. She had a history of meningitis at age 6 months, and throughout childhood she had experienced brief episodes of altered perception described as "like someone threw a switch."

Based on an evaluation summarized in Figures 58–13 and 58–14, a right amygdalohippocampectomy was performed. The patient was seizure-free following the operation and returned to full-time employment.

Figure 58–12 The patient is shown reading quietly in the period preceding the seizure (A), during the period when she reported a feeling of fear (B), and during the period when there was alteration of consciousness and an audible scream (C). (Reproduced, with permission, from Dr. Martin Salinsky.)

in identifying seizure foci in patients with normal MRI scans and in some early childhood epilepsies. Unfortunately, for unclear reasons, PET has been less reliable in localizing seizure foci in extratemporal areas such as the frontal lobe. An additional limitation is the expense of the PET scan and the short half-life of the isotopes (a nearby cyclotron is required). PET scanning can also be used to look for functional changes in neurotransmitter receptor binding and transport related to seizure activity.

A related technique that measures cerebral blood flow, single-photon emission computed tomography (SPECT), has been used more frequently than PET. SPECT does not have the resolution of PET but can be performed in the nuclear medicine department of many large hospitals. Injection of radioisotopes and SPECT imaging at the time of a seizure (ictal SPECT) reveal a pattern of hypermetabolism followed by hypometabolism in the seizure focus and surrounding tissue. Magnetoencephalography and functional MRI also offer further advantages in the mapping of seizure foci.

With rigorous selection of patients for epilepsy surgery, the cure rate for epilepsy with a well-defined

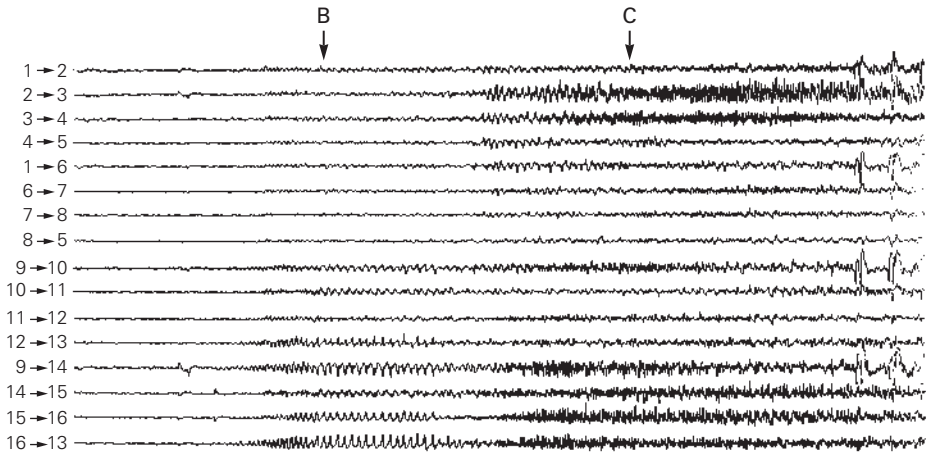

Figure 58–13 The electroencephalogram (EEG) at the time of the photographs in Figure 58–12. Low-amplitude background rhythms occur in the beginning (*left*). At the point when the patient reported fear (**B**), there is a buildup of EEG activity at the onset of a focal onset seizure with impaired awareness, but this activity is confined to the EEG electrodes over the right hemisphere (electrodes 9–16). At the point awareness is altered (**C**), the seizure activity has spread to the left hemisphere (electrodes 1–8). EEG spike-waves are particularly prominent in lead 9 over the right anterior temporal region. (Reproduced, with permission, from Dr. Martin Salinsky.)

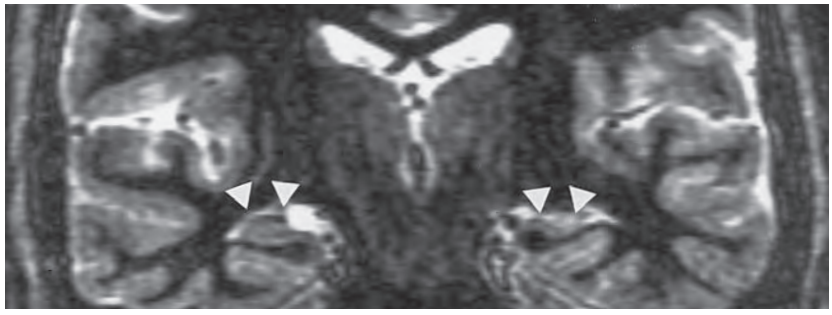

Figure 58–14 Enhanced magnetic resonance imaging reveals atrophy of the right hippocampus (arrows on the right) and a normal left hippocampus (arrows on the left). (Reproduced, with permission, from Dr. Martin Salinsky.)

seizure focus in the temporal lobe can approach 80%. Patients with complicating factors (eg, multiple foci) have lower success rates. However, even among these patients, the number and severity of seizures are usually reduced. Patients who have been "cured" of seizures may still experience cognitive problems such as memory loss and social problems such as adjustments to more independent living and limited employment opportunities. These factors emphasize the need for treatment as early in life as feasible.

Prolonged Seizures Can Cause Brain Damage

Repeated Convulsive Seizures Are a Medical Emergency

As noted above, brain tissue can compensate for the metabolic stress of a focal onset seizure or the transient decrease in oxygen delivery during a single generalized tonic-clonic seizure. In a generalized seizure, stimulation of the hypothalamus leads to massive

activation of the "stress" response of the sympathetic nervous system. The increased systemic blood pressure and serum glucose initially compensate for increased metabolic demand, but these homeostatic mechanisms fail during prolonged seizures. The resulting systemic metabolic derangements, including hypoxia, hypotension, hypoglycemia, and acidemia, lead to a reduction in high-energy phosphates (ATP and phosphocreatine) in the brain and thus can be devastating to brain tissue.

Systemic complications such as cardiac arrhythmias, pulmonary edema, hyperthermia, and muscle breakdown can also occur. The occurrence of repeated generalized seizures without return to full consciousness between seizures, called *status epilepticus*, is a true medical emergency. This condition requires aggressive seizure management and general medical support because 30 or more minutes of continuous convulsive seizures leads to brain injury or even death. Status epilepticus can involve nonconvulsive seizures for which the metabolic consequences are much less severe.

In addition to the dangers of status epilepticus, patients with poorly controlled seizures are also at risk for sudden death (sudden unexpected death in epilepsy [SUDEP]), the leading cause of death in patients with uncontrolled seizures. The underlying mechanisms for SUDEP are not completely understood, but recent studies by Richard Bagnall and colleagues as well as others suggest that cases of SUDEP have clinically relevant mutations in the genes implicated in cardiac arrhythmia and epilepsy. Such data support an association between SUDEP and cardiac arrhythmias or interruption of brain stem circuits involved in respiratory control. This topic is appropriately the focus of intense current investigation.

Excitotoxicity Underlies Seizure-Related Brain Damage

Repeated seizures can damage the brain independently of cardiopulmonary or systemic metabolic changes, suggesting that local factors in the brain can result in neuronal death. The immature brain appears particularly vulnerable to such damage, perhaps because of greater electrotonic coupling between neurons in the developing brain, less effective potassium buffering by immature glia, and decreased glucose transport across the blood–brain barrier.

In 1880, Wilhelm Sommer first noted the vulnerability of the hippocampus to such insults, with preferential loss of the pyramidal neurons in the CA1 and CA3 regions. This pattern has been duplicated in experimental animals by electrical stimulation of afferents to the hippocampus or by injection of excitatory amino acid analogs such as kainic acid. Interestingly, kainic acid causes local damage at the site of injection and also at the site of termination of afferents originating at the injection site.

These observations suggest that release of the excitatory transmitter glutamate during excessive stimulation such as a seizure can itself cause neuronal damage, a condition termed *excitotoxicity*. Because it has been difficult to detect increases in extracellular glutamate during status epilepticus, it appears that excitotoxicity results more from excessive stimulation of glutamate receptors than from tonic increases in extracellular glutamate. The histological appearance of acute excitotoxicity includes massive swelling of cell bodies and dendrites, the predominant locations of glutamate receptors and excitatory synapses.

Although the cellular and molecular mechanisms of excitotoxicity are still not fully understood, several features are clear. Overactivation of glutamate receptors leads to an excessive increase in intracellular Ca^{2+} that can activate a self-destructive cellular cascade involving calcium-dependent enzymes, such as phosphatases, proteases, and lipases. Lipid peroxidation can also cause production of free radicals that damage vital cellular proteins and lead to cell death. The role of mitochondria in Ca^{2+} homeostasis and in control of free radicals may also be important. The pattern of cell death was first thought to reflect necrosis due to the autolysis of critical cellular proteins. However, the activation of "death genes," characteristic of programmed cell death (apoptosis), may also be involved.

Seizure-related brain damage or excitotoxicity can be specific to certain types of cells in particular brain regions, perhaps due to protective factors, such as calcium-binding proteins in some cells and sensitizing factors, such as the expression of calcium-permeable glutamate receptors in other cells. For example, excitotoxicity induced in vitro by excessive activation of AMPA-type glutamate receptors preferentially affects interneurons that express AMPA-type receptors that have high Ca^{2+} permeability, providing a possible mechanism for their selective vulnerability.

Several outbreaks of "amnestic" shellfish poisoning provide a vivid example of the consequences of overactivation of glutamate receptors. Domoic acid, a glutamate analog not present in the brain, is a natural product of certain species of marine algae that flourish during appropriate ocean conditions. Domoic acid can be concentrated by filter feeders such as shellfish. Ingestion of domoic-contaminated shellfish sporadically causes outbreaks of neurological damage, including severe seizures and memory loss (amnesia).

The area most sensitive to damage is the hippocampus, providing further support for the excitotoxicity hypothesis and the critical role of the hippocampus in learning and memory.

The Factors Leading to Development of Epilepsy Are Poorly Understood

A single seizure does not warrant a diagnosis of epilepsy. Normal people can have a seizure under extenuating circumstances such as after drug ingestion or extreme sleep deprivation. Clinicians look for possible causes of seizures in such patients but usually do not begin treatment with anticonvulsants following a single seizure. Unfortunately, our understanding of what factors contribute to susceptibility to epilepsy is still rudimentary. However, progress on this front is increasing rapidly with the advent of experimental mutagenesis in animal models and clinical neurogenetics in patients including whole-exome sequencing.

Some forms of epilepsy have long been considered to result in part from a genetic predisposition. For example, infants with febrile seizures often have a family history of similar seizures. The role of genetics in epilepsy is supported by the existence of familial epileptic syndromes in humans as well as seizure-prone animal models with such exotic names as *Papio papio* (a baboon with photosensitive seizures), audiogenic mice (in which loud sounds induce seizures), and spontaneous single-locus mutations such as *reeler* and *totterer* mice (names alluding to the clinical manifestations of cerebellar mutations in these animals). Even with a genetic predisposition or a structural lesion, the evolution of the epileptic phenotype often involves maladaptive changes in brain structure and function.

Mutations in Ion Channels Are Among the Genetic Causes of Epilepsy

Recent studies have provided a wealth of new information concerning the molecular genetics of epilepsy. At present, more than 120 genes have been linked to an epileptic phenotype; approximately half of these were discovered in humans and the others in animals, mostly mice. The affected proteins include ion channel subunits, proteins involved in synaptic transmission such as transporters, vesicle proteins, synaptic receptors, and molecules involved in Ca^{2+} signaling. For example, seizures in the *totterer* mutant mouse are due to a spontaneous mutation in the gene that encodes the $Ca_V2.1$ or α_{1A}-subunit of the P/Q-type voltage-gated Ca^{2+} channel. That a mutation in these classes of proteins can cause epilepsy is perhaps not unexpected given the dependence of seizures on synaptic transmission and neuronal excitability.

Some of the other genes linked to epilepsy in mice have been more surprising, such as the genes for centromere BP-B, a DNA binding protein, and the sodium/hydrogen exchanger, which is affected in the slow-wave epilepsy mouse. A wide variety of human genes cause neurological disorders, of which epilepsy is only one manifestation. For example, Rett syndrome, a disease associated with intellectual disability, autism, and seizures, is caused by mutations in *MECP2* (methyl-CpG-binding protein-2), a regulator of gene transcription. Although the exact links are not known, it is clear that mutations in many different genes may result in epilepsy.

In most cases, genetic epilepsy syndromes in humans have complex rather than simple (Mendelian) inheritance patterns, suggesting the involvement of many, rather than single, genes. Nevertheless, a number of monogenic epilepsies have been identified in studies of families with epilepsy. Ortrud Steinlein and colleagues reported in 1995 that a mutation in the α4-subunit of the nicotinic acetylcholine receptor-channel is responsible for autosomal dominant nocturnal frontal lobe epilepsy (ADNFLE), the first example of an autosomal gene defect in human epilepsy. Subsequently, other voltage- and ligand-gated channel proteins have been identified as critical genes for epilepsy. Mutations in ion channel genes (channelopathies) constitute a major cause of known monogenic epilepsies (Figure 58–15). Many more genes are being discovered by clinical exome analysis for de novo mutations. The large number of genes for K^+ channels and the critical role of these channels in balancing excitation and inhibition are important reasons for the expanding epilepsy genome.

In voltage-gated channels, mutations largely involve the main pore-forming subunit(s), but there are also examples of epilepsy-causing mutations in regulatory subunits. When examined in vitro, the mutant channel proteins are most commonly associated with either reductions in the expression of the channel on the surface of the plasma membrane (due to reduced targeting to the membrane or premature degradation) or altered kinetics of the channels. It is straightforward to consider how changes in ion channel gating might affect the excitability of neurons and their synchronization during seizure generation. However, ion channel mutations may also affect neuronal development and thus exert their epileptogenic effects through a

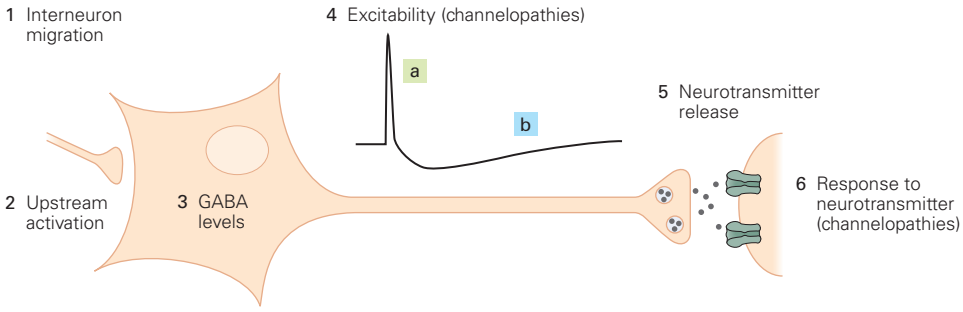

	Channel	Subunits affected	Epilepsy
a	Voltage-gated Na^+	Na_V 1.1, Na_V 1.2, β1	Generalized epilepsy with febrile seizures plus (GEFS+) Severe myoclonic epilepsy of infancy Benign infantile epilepsy
	Voltage-gated K^+	K_V 1.1	Temporal lobe epilepsy
	Ca^{2+}-activated K^+	Ca_V 1.1	Absence epilepsy
b	$GABA_A$ receptor	α1, β3, γ2	GEFS+ Juvenile myoclonic epilepsy Childhood absence epilepsy
	M-type K^+	KCNQ2/3	Benign neonatal epilepsy
	Voltage-gated Ca^{2+}	Ca_V 2.1	Absence epilepsy
	Cl^-	CLCN2	Juvenile myoclonic epilepsy

Figure 58–15 **Channelopathies are a major, but not the only, cause of monogenic human epilepsies.** The human epilepsy genes discovered so far can affect multiple phases of synaptic transmission including the migration of interneurons (**1**), upstream activation of interneurons (**2**), γ-aminobutyric acid (GABA) levels within interneurons (**3**), the excitability of excitatory and inhibitory neurons (**4**), the release of neurotransmitters (**5**), and the postsynaptic response to neurotransmitters (**6**). The inset shows that the impact of mutations in these genes on neuronal excitability can affect the shape of the action potential as well as the afterpotentials and synaptic events that follow. Mutations indicated near the spike (**a**) affect the repolarization of the action potential. Other mutations shown in (**b**) affect the afterhyperpolarization, synaptic conductances, or interspike interval.

secondary action on cell migration, network formation, or patterns of gene expression.

In the early days of research on epilepsy genes, it was widely expected that the genes would mostly underlie generalized epilepsies, based on the idea that a gene mutation (eg, in an ion channel) would be expected to affect most neurons. However, the very first autosomal dominant epilepsy gene discovered by Steinlein and colleagues caused a focal onset (frontal lobe) epilepsy, and another gives rise to seizures originating in the temporal lobe with an auditory aura. In retrospect, this should not be so surprising because channel subunits are rarely expressed uniformly in the brain, and some brain regions are more likely to generate seizures than other regions.

Timing of gene expression is also important. For example, *totterer* mice with mutations in the pore-forming $Ca_V2.1$ subunit of P/Q-type Ca^{2+} channels show spike-wave–type seizures that begin in the third postnatal week, presumably because N-type Ca^{2+} channels are the predominant functional isoform earlier in development, whereas P/Q-type Ca^{2+} channels predominate later. The neurological phenotype begins once the mutant channel is functionally required during development.

Moreover, one mutation can give rise to different epilepsy phenotypes, or different mutant genes can cause the same epilepsy phenotype. As an example of the latter, the ADNFLE syndrome, first discovered as a mutation in the α4-subunit of the nicotinic

ACh receptor, can also be caused by a mutation in the α2-subunit. But not all family members who carry this autosomal dominant mutation have epilepsy, indicating that even in this form of monogenic epilepsy other genes as well as nongenetic factors can influence the phenotype. The GEFS+ syndrome (generalized epilepsy with febrile seizures plus) is a good example of this heterogeneity. It is a childhood syndrome and can involve different seizure types in different family members. GEFS+ is seen in families with mutations in the genes for one of three different Na^+ channel subunits or one of two $GABA_A$ receptors. Family studies of generalized onset epilepsy suggest that seizure types may be heritable within families. These findings indicate that even monogenic epilepsies are likely modified by other genes, environmental influences, and even experience-dependent changes in synapses.

Altered cortical development may be a common cause of epilepsy. The increased resolution of MRI scans has revealed an unexpectedly large number of cortical malformations and localized areas of abnormal cortical folding in patients with epilepsy. Thus, mutations that disturb the normal formation of the cortex or network wiring are candidate genes for epilepsy. This idea is supported by the mapping of two X-linked cortical malformations with epileptic phenotypes: familial periventricular heterotopia and familial subcortical band heterotopia. The genes responsible for these two disorders that encode filamin A and doublecortin, respectively, are presumably important in neuronal migration. Small focal cortical dysplasias can function as seizure foci that give rise to partial and secondarily generalized seizures, whereas more extensive cortical malformations can cause a variety of seizure types and usually are associated with other neurological problems.

Another X-linked gene, *aristaless related homeobox* (*ARX*), is an example of a cell type–specific transcription factor altering migration, because it is expressed only in interneuron precursors. A particularly instructive example is the association of epilepsy with tuberous sclerosis complex (TSC), an autosomal dominant genetic disorder that results from the lack of the functional Tsc1-Tsc2 complex, leading to hyperactivity of the mammalian target of rapamycin (mTOR) complex 1 (mTORC1) signaling pathway. Early clinical trials of mTOR inhibitors as treatment for refractory epilepsy in these patients have been promising. Such examples provide hope for linking the underlying biology of epilepsy syndromes to clinically relevant treatments.

The epilepsy genome is rapidly expanding, driven by clinical exome sequencing and an appreciation of the biological pathways leading to neural network instability. Unfortunately, the vast majority of cases of epilepsy cannot yet be explained by even the recent surge in the identification of epilepsy genes. The identification of large numbers of patients through online registries may provide the population samples needed to evaluate susceptibility genes that underlie complex inheritance patterns.

The Genesis of Acquired Epilepsies Is a Maladaptive Response to Injury

Epilepsy often develops following a discrete cortical injury such as a penetrating head wound. This injury serves as the nidus for a seizure focus, leading at some later point to seizures. This has led to the idea that the early insult triggers a set of progressive physiological or anatomical changes that lead to chronic seizures. That is, the characteristic "silent" interval (usually months or years) between the insult and the onset of recurrent seizures may reflect progressive maladaptive molecular and cellular changes that might be amenable to therapeutic manipulation. Although an attractive hypothesis, a unified picture of this process has yet to emerge. The most promising evidence has come from studies of tissue removed from patients undergoing temporal lobectomy and rodent models of limbic seizures.

In one experimental model, hyperexcitability is induced by repeated stimulation of limbic structures, such as the amygdala or hippocampus. The initial stimulus is followed by an electrical response (the afterdischarge) that becomes more extensive and prolonged with repeated stimuli until a generalized seizure occurs. This process, called *kindling*, can be induced by electrical or chemical stimuli. Many investigators believe that kindling may contribute to the development of epilepsy in humans.

Kindling is thought to involve synaptic changes in the hippocampal formation that resemble those important in learning and memory (Chapters 53 and 54). These include short-term changes in excitability and persistent morphological changes, including generation of adult-born neurons, axonal sprouting, and synaptic reorganization. Rearrangements of synaptic connections have been observed in the dentate gyrus of patients with long-standing temporal lobe seizures as well as following kindling in experimental animals. In addition to axonal sprouting (Figure 58–16), changes include alterations in dendritic structure, control of transmitter release, and novel expression and alterations in subunit stoichiometry of ion channels and pumps.

The long-term changes that lead to epilepsy also are likely to involve specific patterns of gene

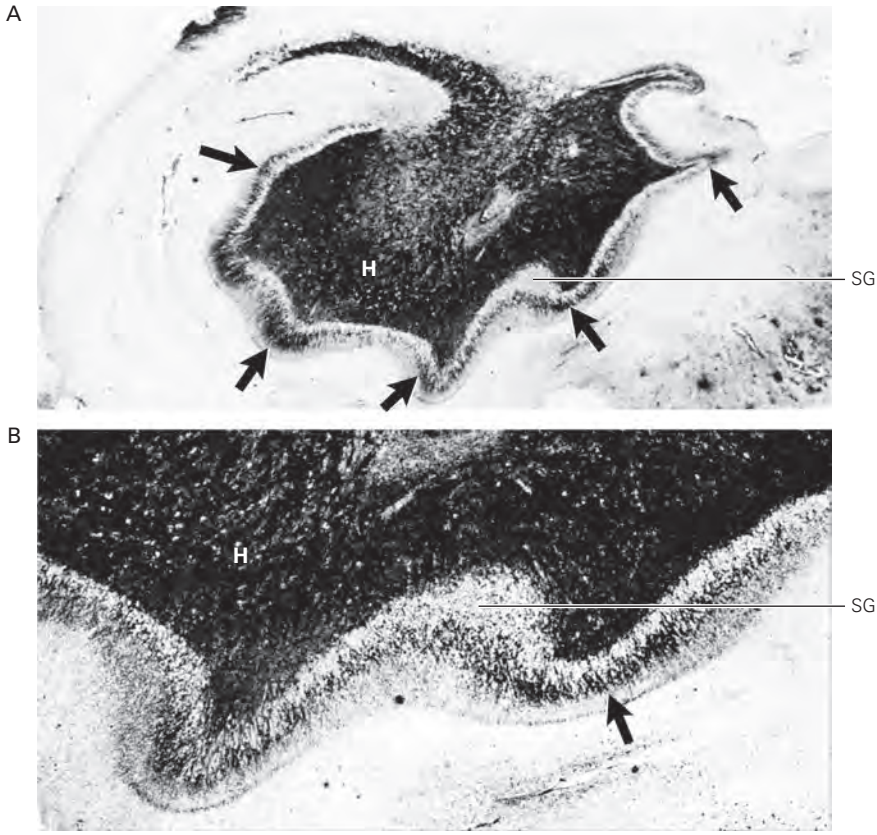

Figure 58–16 Mossy fiber synaptic reorganization (sprouting) in the human temporal lobe may cause hyperexcitability. (Reproduced, with permission, from Sutula et al. 1989. Copyright © 1989 American Neurological Association.)

A. Timm stain of a transverse section of hippocampus removed from a patient with epilepsy at the time of temporal lobectomy for control of epilepsy. The stain appears black in the axons of the dentate granule cells (mossy fibers) due to the presence of zinc in these axons. The mossy fibers normally pass through the dentate hilus (**H**) on their way to synapse on CA3 pyramidal cells. In the epileptic tissue shown here, stained fibers appear in the supragranular layer of the dentate gyrus (**SG, arrowheads**), which now contains not only the granule cell dendrites but also newly sprouted mossy fibers. These aberrant sprouts of mossy fibers form new recurrent excitatory synapses on dentate granule cells.

B. This high magnification of a segment of the supragranular layer shows the Timm-stained mossy fibers in greater detail.

expression. For example, the proto-oncogene c-*fos* and other immediate early genes as well as growth factors can be activated by seizures. Because many immediate early genes encode transcription factors that control other genes, the gene products that result from epileptiform activity could initiate changes that contribute to or suppress the development of epilepsy by altering such mechanisms as cell fate, axon targeting, dendritic outgrowth, and synapse formation.

Highlights

1. Seizures are one of the most dramatic examples of the collective electrical behavior of the mammalian brain. The distinctive clinical pattern of partial seizures and generalized seizures can be attributed to the distinctly different patterns of activity of cortical neurons.
2. Studies of focal onset seizures in animals reveal a series of events—from the activity of neurons in the seizure focus to synchronization and subsequent spread of epileptiform activity throughout the cortex. The gradual loss of GABAergic surround inhibition is critical to the early steps in this progression. In contrast, generalized onset seizures are thought to arise from activity in thalamocortical circuits, perhaps combined with a general abnormality in the membrane excitability of all cortical neurons.
3. The electroencephalogram (EEG) has long provided a window on the electrical activity of the cortex, both in normal phases of arousal and during abnormal activities such as seizures. The EEG

can be used to identify certain electrical activity patterns associated with seizures, but it provides limited insight into the pathophysiology of seizures. Several much more powerful and noninvasive approaches are now available to locate the focus of a partial seizure. This has led to the widespread and successful use of epilepsy surgery for selected patients, particularly those with complex partial seizures of hippocampal onset. The promise of invasive approaches to seizure detection and seizure prevention provides additional hope for improved control of seizures.

4. The increasing power of genetic, molecular, and modern cell-physiological approaches applied to the study of seizures and epilepsy also gives new hope that an understanding of these disruptions of normal brain activity will provide new therapeutic options for patients afflicted with epilepsy, as well as new insights into the function of the mammalian brain.
5. Further neurobiological studies of the progression from an acute seizure to the development of epilepsy should provide alternative strategies for treatment beyond the standard options of anticonvulsants or epilepsy surgery.

Gary Westbrook

Selected Reading

Cascino GD. 2004. Surgical treatment for epilepsy. Epilepsy Res 60:179–186.

Engel J. 1989. *Seizures and Epilepsy*. Philadelphia: Davis.

Kleen JK, Lowenstein DH. 2017. Progress in epilepsy: latest waves of discovery. JAMA Neurol 74:139–140.

Krook-Magnuson E, Soltesz I. 2015. Beyond the hammer and the scalpel: selective circuit control for the epilepsies. Nat Neurosci 18:331–338.

Krueger DA, Wilfong AA, Holland-Bouley K, et al. 2013. Everolimus treatment of refractory epilepsy in tuberous sclerosis complex. Ann Neurol 74:679–687.

Kullmann DM, Schorge S, Walker MC, Wykes RC. 2014. Gene therapy in epilepsy—is it time for clinical trials? Nat Rev Neurol 10:300–304.

Lennox WG, Lennox MA. 1960. *Epilepsy and Related Disorders*. Boston: Little, Brown.

Lennox WG, Mattson RH. 2003. Overview: idiopathic generalized epilepsies. *Epilepsia* 44(Suppl 2):2–6.

Lerche H, Shah M, Beck H, Noebels J, Johnston D, Vincent A. 2013. Ion channels in genetic and acquired forms of epilepsy. J Physiol 591:753–764.

Lowenstein DH. 2015. Decade in review-epilepsy: edging toward breakthroughs in epilepsy diagnostics and care. Nat Rev Neurol 11:616–617.

Maheshwari A, Noebels JL. 2014. Monogenic models of absence epilepsy: windows into the complex balance between inhibition and excitation in thalamocortical microcircuits. Prog Brain Res 213:223–252.

Noebels J. 2015. Pathway-driven discovery of epilepsy genes. Nat Neurosci 18:344–350.

Paz JT, Huguenard JR. 2015. Optogenetics and epilepsy: past, present and future. Epilepsy Curr 15:34–38.

Penfield W, Jasper H. 1954. *Epilepsy and the Functional Anatomy of the Human Brain*. Boston: Little, Brown.

Snowball A, Schorge S. 2015. Changing channels in pain and epilepsy: exploring ion channel gene therapy for disorders of neuronal hyperexcitability. FEBS Letters 589:1620–1624.

Stables JP, Bertram EH, White HS, et al. 2002. Models for epilepsy and epileptogenesis: report from the NIH workshop. Epilepsia 43:1410–1420.

Stafstrom CE, Carmant L. 2015. Seizures and epilepsy: an overview for neuroscientists. Cold Spring Harb Perspect Med 5:a022426.

References

Bagnall RD, Crompton DE, Petrovski S, et al. 2016. Exome-based analysis of cardiac arrhythmia, respiratory control and epilepsy genes in sudden unexpected death in epilepsy. Ann Neurol 79:522–534.

Berenyi A, Belluscio M, Mao D, Buzsaki G. 2012. Closed-loop control of epilepsy by transcranial electrical stimulation. Science 337:735–737.

Bergey GK, Morrell MJ, Mizrahi EM, et al. 2015. Long-term treatment with responsive brain stimulation in adults with refractory partial seizures. Neurology 84:810–817.

Biervert C, Schroeder BC, Kubisch C, et al. 1998. A potassium channel mutation in neonatal human epilepsy. Science 279:403–406.

Fisher RS, Cross JH, D'Souza C, et al. 2017. Instruction manual for the ILAE 2017 operational classification of seizure types. Epilepsia 58:531–542.

Gadhoumi K, Lina J-M, Mormann F, Gotman J. 2016. Seizure prediction for therapeutic devices: a review. J Neurosci Methods 260:270–282.

Haug K, Warnstedt M, Alekov AK, et al. 2003. Mutations in CLCN2 encoding a voltage-gated chloride channel are associated with idiopathic generalized epilepsies. Nat Genet 33:527–532.

Heck CN, King-Stephens D, Massey AD, et al. 2014. Two-year reduction in adults with medically intractable partial onset epilepsy treated with responsive neurostimulation: final results of the RNS system pivotal trial. Epilepsia 55:432–441.

Kätzel D, Nicholson E, Schorge S, Walker MC, Kullmann DM. 2013. Chemical-genetic attenuation of focal neocortical seizures. Nat Commun 5:3847.

Kramer MA, Eden UT, Kolaczyk E, et al. 2010. Coalescence and fragmentation of cortical networks during focal seizures. J Neurosci 30:10076–10085.

Lothman EW. 1993a. The neurobiology of epileptiform discharges. Am J EEG Technol 33:93–112.

Lothman EW. 1993b. Pathophysiology of seizures and epilepsy in the mature and immature brain: cells, synapses and circuits. In: WE Dodson, JM Pellock (eds). *Pediatric Epilepsy: Diagnosis and Therapy*, pp. 1–15. New York: Demos Publications.

Lothman EW, Collins RC. 1990. Seizures and epilepsy. In: AL Pearlman, RC Collins (eds). *Neurobiology of Disease*, pp. 276–298. New York: Oxford University Press.

Mulley JC, Scheffer IE, Harkin LA, Berkovic SF, Dibbens LM. 2005. Susceptibility genes for complex epilepsy. Hum Mol Genet 14:R243–R249.

Santhakumar V, Aradi S, Soltesz I. 2005. Role of mossy fiber sprouting and mossy cell loss in hyperexcitability: a network model of the dentate gyrus incorporating cell types and axonal topography. J Neurophysiol 93:437–463.

Spencer WA, Kandel ER. 1968. Cellular and integrative properties of the hippocampal pyramidal cell and the comparative electrophysiology of cortical neurons. Int J Neurol 6:266–296.

Stacey WC, Litt B. 2008. Technology insight: neuroengineering and epilepsy-designing devices for epilepsy control. Nat Clin Pract Neurol 4:190–201.

Steinlein OK, Mulley JC, Propping P, et al. 1995. A missense mutation in the neuronal nicotinic acetylcholine receptor alpha 4 subunit is associated with autosomal dominant nocturnal frontal lobe epilepsy. Nat Genet 11:201–203.

Sutula T, Cascino G, Cavazos J, Parada I, Ramirez L. 1989. Mossy fiber synaptic reorganization in the epileptic human temporal lobe. Ann Neurol 26:321–330.

Teitelbaum J, Zatorre RJ, Carpenter S, et al. 1990. Neurologic sequelae of domoic acid intoxication due to ingestion of contaminated mussels. N Engl J Med 322:1781–1787.

Tung JK, Berglund K, Gross RE. 2016. Optogenetic approaches for controlling seizure activity. Brain Stimul 9:801–810.

von Krosigk M, Bal T, McCormick DA. 1993. Cellular mechanisms of a synchronized oscillation in the thalamus. Science 261:361–364.

Walsh CA. 1999. Genetic malformations of the human cerebral cortex. Neuron 23:19–29.

Wiebe S, Blume WT, Girvin JP, Eliasziw M. 2001. Effectiveness and efficiency of surgery for temporal lobe epilepsy study. A randomized, controlled trial of surgery for temporal lobe epilepsy. N Engl J Med 14:211–216.

Winawer MR, Marini C, Grinton BE, et al. 2005. Familial clustering of seizure types within the idiopathic generalized epilepsies. Neurology 65:523–528.

Zhao M, Alleva R, Ma H, Daniel AGS, Schwartz TH. 2015. Optogenetic tools for modulating and probing the epileptic network. Epilepsy Res 116:15–26.

59

Disorders of Conscious and Unconscious Mental Processes

Although cognitive neuroscience emerged at the end of the 20th century as a major new discipline, a precise meaning of the term *cognition* remains elusive. The term is used in different ways in different contexts. At one extreme, the term *cognitive* in cognitive neuroscience connotes what was meant by the older term *information processing*. In this sense, cognition is simply what the brain does. When cognitive neuroscientists say that visual features or motor acts are *represented* by neural activity, they are using concepts from information processing. From this point of view, the language of cognition provides a bridge between descriptions of neural activity and behavior because the same terms can be applied in both domains.

At the other extreme, the term *cognition* refers to those higher-level processes fundamental to the formation of conscious experience. This is what is meant by the term *cognitive therapy*, an approach to treatment pioneered by Aaron Beck and Albert Ellis and developed from behavior therapy. Rather than trying to change a patient's behavior directly, cognitive therapy has the aim of changing the patient's attitudes and beliefs (Box 59–1).

In common parlance, the term *cognition* means thinking and reasoning, a usage closer to its Latin root *cognoscere* (getting to know or perceiving). Thus, the *Oxford English Dictionary* defines it as "the action or faculty of knowing." Indeed, we know the world by applying thinking and reasoning to the raw data of our senses.

This idea is implicit in our characterization of many kinds of disorders of cognition. After brain damage, some patients can no longer process the input supplied by the senses. This type of disorder was first delineated by Sigmund Freud, who called it agnosia, or loss of knowledge (Chapter 17). Agnosias can take many forms. A patient with visual agnosia can see perfectly well but is no longer able to recognize or make sense of what he sees. A patient with prosopagnosia has a specific problem recognizing faces. A patient with auditory agnosia might hear perfectly well but is unable to recognize spoken words.

Cognition is sometimes impaired from birth so that a person has difficulty in acquiring knowledge. This might lead to general mental retardation or, if the problem is more localized, to specific learning difficulties such as dyslexia (difficulty learning about written

Box 59–1 Cognitive Therapy

Dissatisfaction with psychological treatments based on Freud's theories of unconscious motivation intensified in the middle of the 20th century. Not only did these theories have no relevance to experimental psychology, but there was no empirical evidence that psychodynamic treatments actually worked.

The first form of alternative psychological therapy to emerge from laboratory studies is known as *behavior therapy*. The fundamental assumption of this approach is that maladaptive behavior is learned and can therefore be eliminated by applying the Pavlovian and Skinnerian principles of stimulus-response learning. So, for example, a child who has been attacked by a dog can become fearful of all dogs, but this fearful response can be extinguished if the child learns that the conditioned stimulus (the sight of a dog) is not followed by the unconditioned stimulus (being bitten).

Behavior therapy was shown to be quick and effective for phobias, but many mental disorders are better characterized in terms of maladaptive thinking rather than maladaptive behavior. In the 1960s, Aaron Beck and Albert Ellis initiated a new kind of therapy in which the principles of learning are used to change thoughts rather than behavior. This is known as *cognitive therapy* or *cognitive behavior therapy*.

This form of therapy has been particularly successful in the treatment of depression. Depression is typically associated with negative thoughts (eg, a person remembering only the bad things that have happened to him/her) and negative attitudes (eg, a person believing that he/she will never achieve his/her goals). Cognitive therapists teach their clients methods for reducing the frequency of negative thoughts and changing their negative attitudes into positive ones.

language) or autism (difficulty in learning about other minds). Finally, cognition can become dysfunctional so that the knowledge acquired about the world is false. These disorders of thinking lead to the sort of false perceptions (hallucinations) and false beliefs (delusions) associated with major mental illnesses such as schizophrenia.

Conscious and Unconscious Cognitive Processes Have Distinct Neural Correlates

Cognition—deriving knowledge through thinking and reasoning—is one of three components of consciousness (see Chapter 42 for discussion of the conscious aspects of emotions, often called feelings). The other two are emotion and will. It used to be taken for granted that thinking and reasoning were under conscious voluntary control and that cognition was not possible without consciousness. By the end of the 19th century, however, Freud developed a theory of unconscious mental processes and suggested that much human behavior is guided by internal processes of which we are not aware.

Of more direct importance for neuroscience was the idea of *unconscious inference*, originally proposed by Helmholtz. Helmholtz was the first to carry out quantitative psychophysical experiments and to measure the speed with which afferent signals in peripheral nerves are conducted. Prior to these experiments, sensory signals were assumed to arrive in the brain immediately (with the speed of light), but Helmholtz showed that nerve conduction was actually quite slow. He also noted that reaction times were even slower. These observations implied that a great deal of brain work intervened between sensory stimuli and conscious perception of an object. Helmholtz concluded that much of what goes on in the brain is not conscious and that what does enter consciousness (ie, what is perceived) depends on unconscious inferences. In other words, the brain uses evidence from the senses to decide on the most likely identity of the object that is causing activity in the sensory organs but does this without our awareness.

This view was extremely unpopular with Helmholtz's contemporaries and, indeed, still is today. Most people believe that consciousness is necessary for making inferences and that moral responsibility can be assigned only to decisions that are based on conscious inference. If inferences could be made without consciousness, there could be no ethical basis for praise or blame. Helmholtz's ideas about unconscious inferences were largely ignored.

Nevertheless, by the middle of the 20th century, evidence began to accumulate in favor of the idea that most cognitive processing never enters consciousness. After the development of electronic computers and the emergence of the study of artificial intelligence, researchers began to study how, and to what extent, machines could perceive the world beyond themselves.

It rapidly became clear that many perceptual processes that at first seem simple are actually very complex when defined as a set of computations.

Visual perception is the prime example. In the 1960s, almost no one realized how difficult it would be to build machines that could recognize the shape and appearance of objects, because it seems so easy for us. I look out of the window and I see buildings, trees, flowers, and people. I am not aware of any mental processes behind this perception; my awareness of all these objects seems instantaneous and direct. It turns out that teaching a machine how to work out which edges go with which object in a typical cluttered visual scene containing many overlapping objects is exceptionally difficult. The computational approach to vision revealed the underlying neural processes on which our seemingly effortless perception of the world depends. Similar processes underlie all sensory perception and especially the perception of sounds as speech. Most neuroscientists now believe that we are not conscious of cognitive processes, only our perceptions.

The evidence for unconscious cognitive processes comes not only from artificial intelligence studies but also studies of cognition in people with brain damage. The effects of unconscious processes on behavior can be demonstrated most strikingly in certain patients with "blind sight," a disorder first delineated in the 1970s by Lawrence Weiskrantz. These patients have lesions in the primary visual cortex and claim to see nothing in the part of the visual field served by the damaged area. Nevertheless, when asked to guess, they are able to detect simple visual properties such as movement or color far better than is expected by chance. Despite having no sensory-based perception of objects in the blind parts of the visual field, these patients do possess unconscious information about the objects, and this information is available to guide their behavior.

Another example is unilateral neglect caused by lesions in the right parietal lobe (Chapter 17). Patients with this disorder have normal vision, but they seem unware of objects on the left side of the space in front of them. Some patients even ignore the left side of individual objects. In one experiment by John Marshall and Peter Halligan, patients were shown two drawings of a house. The left side of one house was on fire (Figure 59–1). When asked if there were any differences between the houses, patients replied "no." But when asked which house they would prefer to live in, they chose the house that was not burning. This choice was thus made based on information that was not represented in consciousness. Blind sight and unilateral neglect are just two examples of the abundant empirical evidence for the existence of unconscious cognitive processes, evidence not available to us through introspection.

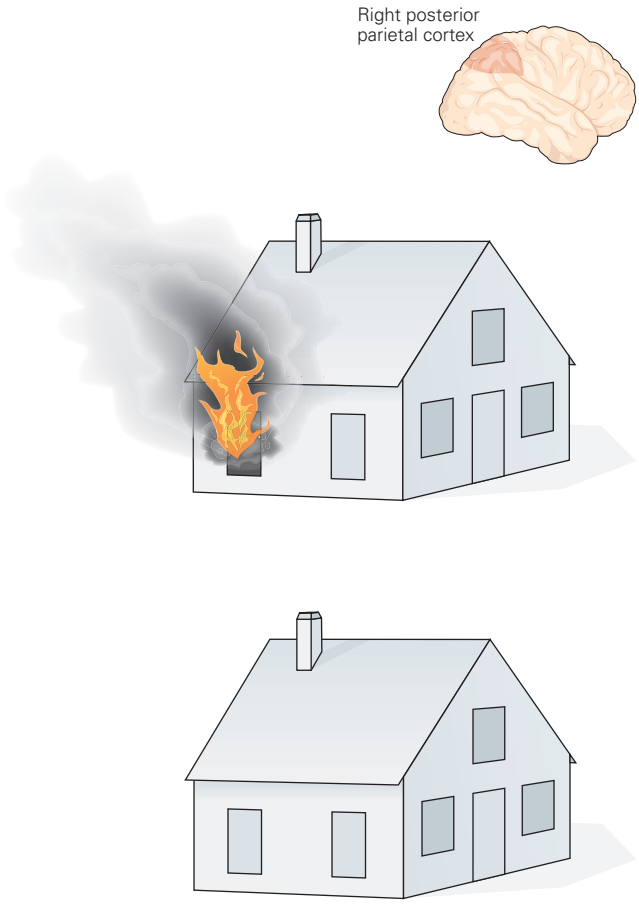

Figure 59–1 Unconscious processing in cases of spatial neglect. After damage to the right parietal lobe, many patients seem to be unaware of the left side of space (unilateral neglect syndrome). When such patients are shown the two drawings reproduced here, they say that the two houses look the same. However, they also say that they would prefer to live in the lower house, indicating that they have unconsciously processed the image of the fire in the other house. (Adapted from Marshall and Halligan 1988.)

Currently, one of the most exciting areas of investigation in neuroscience concerns the search for the *neural correlates of consciousness* initiated by Francis Crick and Christopher Koch. The aim is to demonstrate qualitative differences between the neural activity associated with conscious and unconscious cognitive processes. This research is important not only because it may give us answers to the difficult question of the function of consciousness but also because it is relevant to our understanding of many neurological and psychiatric disorders. The weird experiences

and delusional beliefs of patients with certain cognitive disorders were once dismissed as beyond understanding. Cognitive neuroscience provides us with a framework for understanding how these experiences and beliefs can arise from specific alterations in normal cognitive mechanisms.

Differences Between Conscious and Unconscious Processes in Perception Can Be Seen in Exaggerated Form After Brain Damage

The relationship between sensory stimulation and perception is far from direct. Perception can change without any change in sensory stimulation, as illustrated by ambiguous figures such as the Rubin figure and the Necker cube (Figure 59–2). Conversely, a big change in sensory stimulation can occur without the observer being aware of this change—the perception remains constant. A compelling example of this is change blindness.

To demonstrate change blindness, two versions of a complex scene are constructed. In one well-known example developed by Ron Rensink, the picture consists of a military transport plane standing on an airport runway. In one of the two versions, an engine is missing. If these two pictures are shown in alternation on a computer screen, but critically interspersed with a blank screen, it can take minutes to notice the difference even though it is immediately obvious when pointed out. (See Figure 25-8 for another example.)

In light of these phenomena, we can explore the neural activity associated with changes in perception when there is no change in sensory stimulation. Likewise, we can discover whether changes in sensory input are registered in the brain even if not represented in consciousness. We can ask whether there is some qualitative difference between the neural activity associated with conscious as opposed to unconscious processes.

Two important results have emerged from studies of the neural activity associated with specific types of conscious percepts. First, certain kinds of percepts are related to neural activity in specific areas of the brain. Those brain areas that are specialized for recognition of certain kinds of objects (eg, faces, words, landscapes) or for certain visual features (eg, color, motion) are more active when the object or the feature is consciously perceived (Figure 59–3). For example, when we perceive the faces in the Rubin figure, there is more activity in the area of the fusiform gyrus, which is specialized for the processing of faces.

This observation also applies to deviant perception (hallucinations). After degeneration of the peripheral visual system leading to blindness, some patients experience intermittent visual hallucinations (Charles Bonnet syndrome). These hallucinations vary from one patient to another: Some patients see colored patches, others see grid-like patterns, and some even see faces. Dominic ffytche found that these hallucinations are associated with increased activity in the secondary visual cortex, and the content of the hallucination is related to the specific locus of activity (Figure 59–4). Schizophrenic patients frequently experience complex auditory hallucinations, which usually have the form of voices talking to or about the patient. These

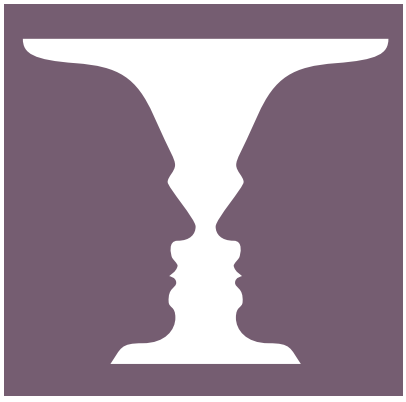

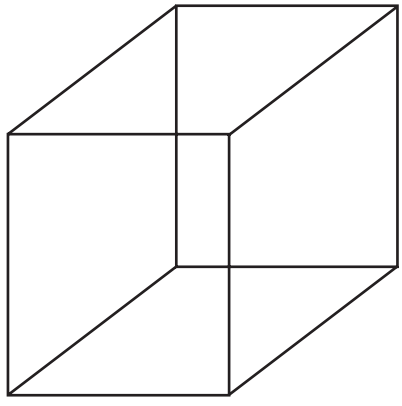

Figure 59–2 Ambiguous figures. If you stare at the figure on the left (the Rubin figure), you sometimes see a vase and sometimes two faces looking at each other. If you stare at the figure on the right (the Necker cube), you see a three-dimensional cube, but the front face of the cube is sometimes seen at the bottom left and sometimes at the top right. In each figure, the brain finds two equally good, but mutually exclusive, interpretations of what is there. Our conscious perception spontaneously alternates between these two interpretations.

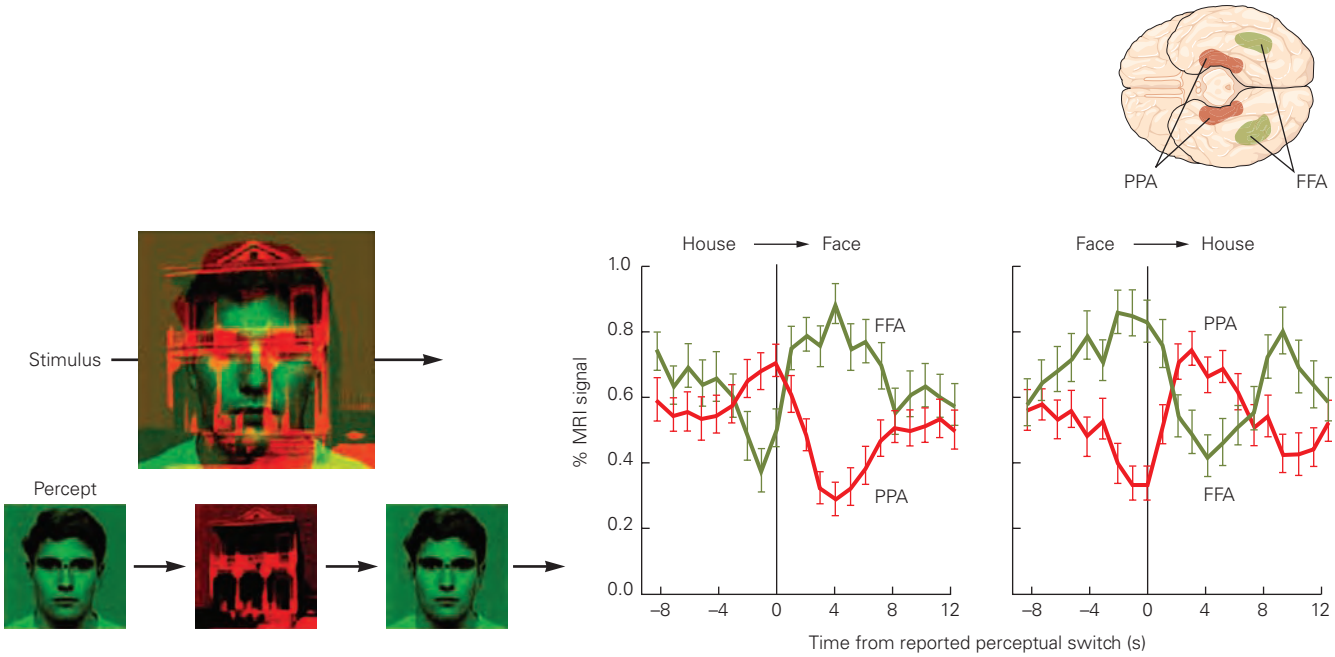

Figure 59–3 Neural activity associated with ambiguous visual information. An ambiguous stimulus was created by simultaneously presenting a face to one eye and a house to the other eye. Brain activity was measured while subjects observed these images. Subjects were instructed to press a button whenever a spontaneous switch in perception occurred (because of binocular rivalry). When the face is perceived (*left*), activity increases in the fusiform face area (**FFA**); when the house is perceived (*right*), activity increases in the parahippocampal place area (**PPA**). (Abbreviation: **MRI**, magnetic resonance imaging.) (Reproduced, with permission, from Tong et al. 1998. Copyright © 1998 by Cell Press.)

hallucinations are associated with activity in the auditory cortex.

These observations suggest that conscious experience may result from activity in certain cortical regions. This idea is difficult to test experimentally, but in the 1950s, the neurosurgeon Wilder Penfield found that electrical stimulation of the cortex in patients undergoing neurosurgery can generate a conscious experience. More recently, it has been found that transcranial magnetic stimulation of the cortex in the region of V5/MT can lead to seeing moving light flashes.

The second important conclusion drawn from studies that seek to correlate neural activity and specific percepts is that activity in a specialized area is necessary but not sufficient to yield conscious experience. For example, in the change blindness paradigm, subjects are often unaware of large changes in the picture they are viewing. If the change involves a face, activity is elicited in the fusiform gyrus whether or not the subject is aware of the change. But when the sensory change is also perceived consciously, there is, in addition, activity in the parietal and frontal cortices (Figure 59–5).

These observations are relevant to our understanding of unilateral neglect. Since objects on the left side still elicit neural activity in the visual cortex, it may be that the damage in the right parietal cortex simply prevents the formation of *conscious* representations of objects on the left side of space. Nevertheless, this sensory activity can support an unconscious inference in patients that they would not want to live in the house that is burning on the left side.

Stimuli that do not enter awareness can also elicit overt responses. A face with a fearful expression elicits a fear response in the autonomic nervous system, measured as an increase in skin conductance (galvanic response) because of sweating. This response occurs even if the face is immediately followed by another visual stimulus, such that the face is not consciously perceived. There may be an advantage to having a rapid but low-resolution system for recognizing dangerous things. We jump first; only later, on the basis of a slow, high-resolution system, are we able to identity the object that made us jump (Chapter 48). Damage in one or the other of these two recognition systems can explain certain otherwise puzzling neurological and psychiatric disorders.

Prosopagnosia is a perceptual disorder in which faces are no longer recognizable. The patient knows

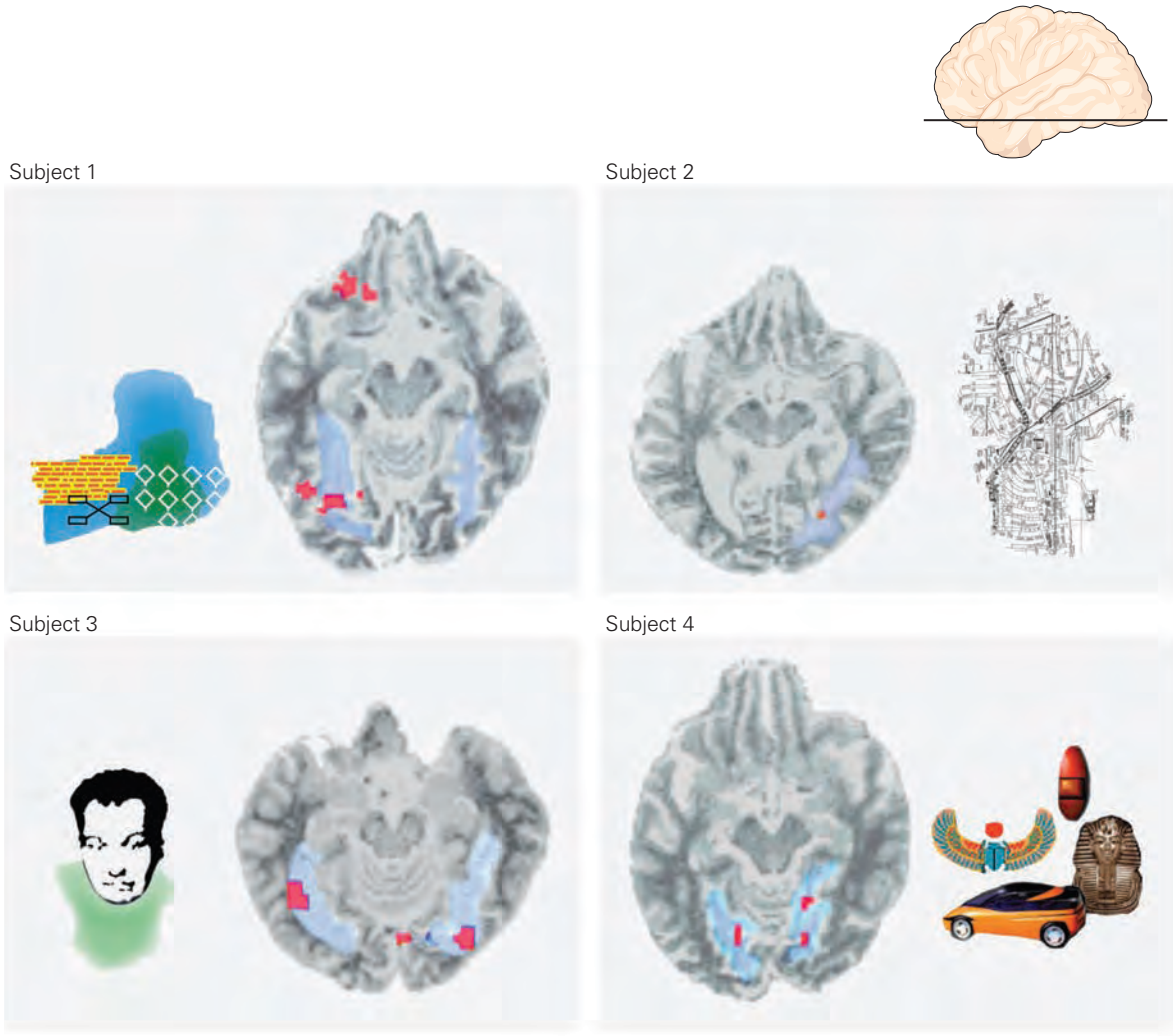

Figure 59–4 Neural activity associated with visual hallucinations. Some patients with damage to the retina experience visual hallucinations. The location of the neural activity and the content of the hallucination are related. The experience of colors, patterns, objects, or faces is associated with heightened activity (**red**) in specific regions of inferior temporal cortex. The **blue** area is the fusiform gyrus. (Reproduced, with permission, from ffytche et al. 1998. Copyright © 1998 Springer Nature.)

he is looking at a face but cannot recognize the face, even a beloved face known for years. The problem is specific to faces, since the patient may still be able to recognize the person from their clothes, gait, and voice. However, patients with prosopagnosia are able to identify faces unconsciously. They show autonomic responses to familiar faces and do better than chance when asked to guess whether or not a face shown to them belongs to a person who is familiar. In fact, their awareness of the autonomic (emotional) responses elicited by a face may enable them to judge familiarity.

Capgras syndrome, a delusion that is occasionally observed in schizophrenic patients and in some patients suffering from brain injury or dementia, produces a more unsettling experience. These patients firmly believe that someone close to them, usually a husband or wife, has been replaced by an impostor. They claim that the person, although similar if not identical in appearance, is in fact someone else. Often, this delusion is acted on with the demand that the impostor leave the house.

Hadyn Ellis and Andy Young have suggested that this bizarre delusion is the mirror phenomenon of prosopagnosia. According to this view, the circuitry for face recognition is intact, but the circuitry that mediates the emotional response to the face is not. As a result, patients recognize the person in front of them but, because the emotional response is lacking,

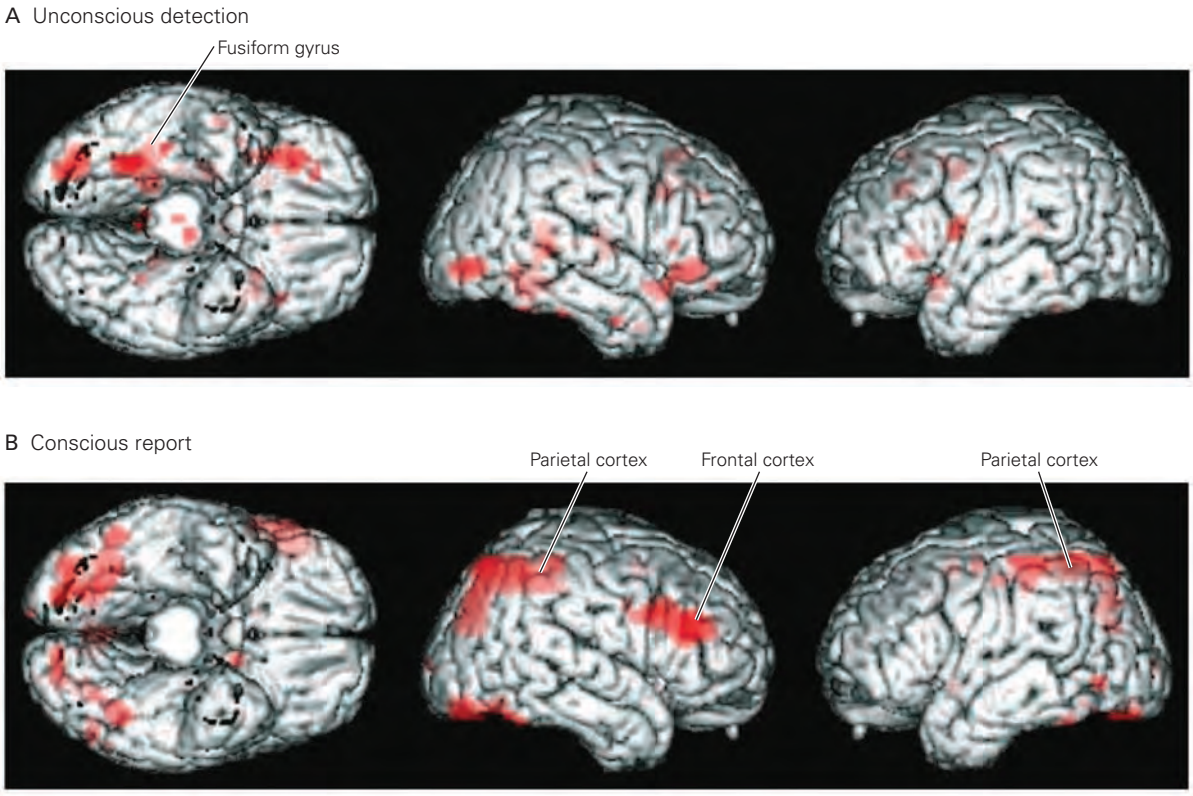

Figure 59–5 Brain activity with and without awareness. Activity in the fusiform face area increases when the face viewed by subjects changes, whether subjects are unaware of the change or conscious of it. When subjects are aware of the change, activity in parietal and frontal cortex also increases. (Reproduced, with permission, from Beck et al. 2001.)

feel that there is something fundamentally wrong. This account has been partially confirmed by the observation that these patients do not have normal autonomic responses to familiar faces.

This explanation implies that Capgras delusions are not the consequence of disordered thinking but of disordered experience. A patient sees the face of his wife without having the normal emotional response. The conclusion that this is not his wife but an impostor is a cognitive response to this abnormal experience, the mind's attempt to explain the experience.

The Control of Action Is Largely Unconscious

The sense that we are in control of our own actions is a major component of consciousness. But are we aware of all aspects of our own actions? David Milner and Mel Goodale studied a patient known as D.F. who demonstrates a striking lack of awareness of certain aspects of her own actions. As a result of damage to her inferior temporal lobe caused by carbon monoxide poisoning, D.F. suffers from *form agnosia*—she is unable to identify the shapes of things. She cannot distinguish a square from an oblong card and cannot describe the orientation of a slot. Yet when she picks up the oblong card to place it through the slot, she orients her hand and forms her grasp appropriately because of the unconscious operation of visuomotor circuits (Figure 59–6).

This sort of unconscious guidance is not unique to patients with brain damage. It is simply revealed more starkly in the case of D.F. because the system that normally brings visual information about shape into consciousness is impaired. Indeed, we can all make rapid and accurate grasping movements without being aware of the perceptual and motor information that is being used to control these movements. Sometimes, we are not even aware of having made the movement. This largely unconscious system for visually guided reaching and grasping is analogous to, and probably overlaps with, the rapid but poor-resolution system associated with fear responses.

Although we may not be aware of the perceptual and motor details of actions like reaching and grasping,

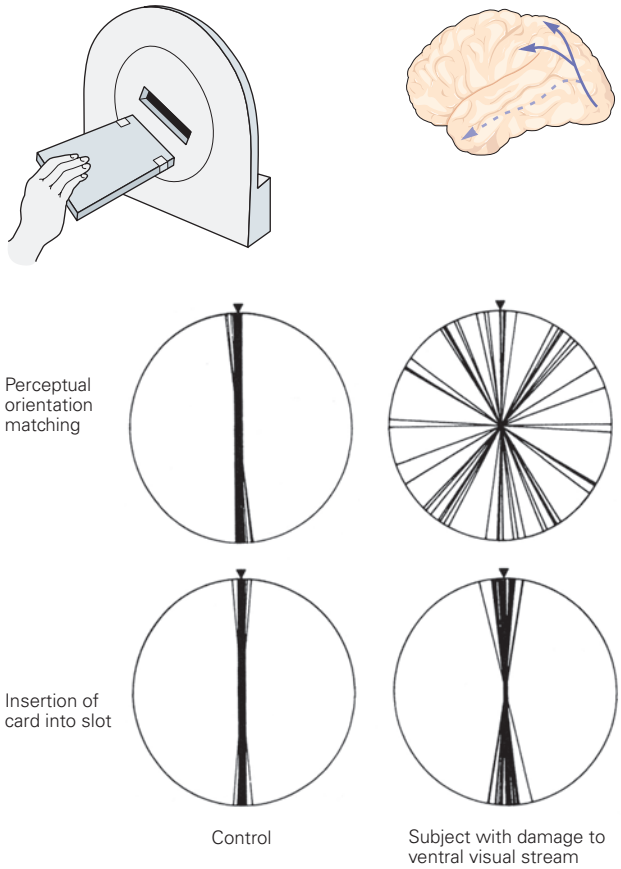

Figure 59–6 Action can be controlled by unconscious stimuli. A patient, D.F., with damage to the inferior temporal cortex, is unable to recognize objects based on their shape (form agnosia). She cannot align the tablet with the orientation of the slot (perceptual matching) because she is not consciously aware of the orientation of either the tablet or the slot. However, when she is asked to put the tablet through the slot in a quick movement, she orients her hand rapidly and accurately. Presumably, the movement is driven by visuomotor computations of which the subject is unaware. (Adapted, with permission, from Milner and Goodale 1995.)

we are vividly aware of being in control of some of our actions—we are aware of a difference between actions that we cause and those that happen involuntarily. Benjamin Libet studied the phenomenon of voluntary action in controlled experiments. He asked his subjects to lift a finger "whenever they felt the urge to do so" and to report the time at which they had this urge. His subjects had no difficulty in reliably reporting the time of this subjective experience. At the same time, Libet used electroencephalography to measure the "readiness potential," a change in brain activity that occurs up to 1 second before a subject makes any voluntary movement. The time at which subjects reported feeling the urge to lift a finger occurred hundreds of milliseconds *after* the beginning of this readiness potential. This result has generated much discussion among philosophers as well as neuroscientists concerning the existence of free will. If brain activity can *predict* an action before a person is aware of having the urge to perform that action, does this mean that our experience of freely willing actions is an illusion?

Although Libet's result has been widely replicated, the relevance of his experimental protocol for our understanding of free will remains controversial. Lifting one finger is not an action that we often perform. Actions usually have goals. For example, we might press a button in order to ring a bell. When our actions are followed by the goal we expect, we feel that we are in control of our actions. It is this subjective experience that gives us a sense of agency, of being the cause of events. Applying Libet's paradigm to such actions, Patrick Haggard discovered the phenomenon of "intentional binding." When a deliberate movement (pressing a button) is followed by its intended goal (hearing a tone), these events are experienced subjectively as bound together in time (Figure 59–7).

This temporal binding of our actions to their goals provides an empirical marker of our sense of agency, since a stronger sense of agency is associated with a greater degree of binding. If a movement occurs passively, caused for example by magnetic stimulation to the brain, then intentional binding is decreased; we actually perceive the time between movement and outcome as longer than the actual physical time.

Our sense of agency is closely linked to our belief in free will and to the idea that people can be held

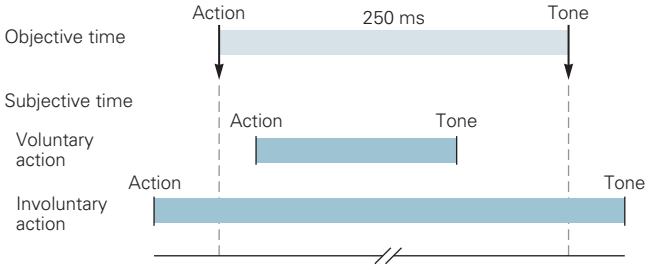

Figure 59–7 We experience our actions and their effects as bound together in time. When subjects are asked to press a button that triggers a sound 250 ms later, they experience their action and the sound as occurring closer together (subjective time) than they actually are (objective time). In contrast, when their finger moves involuntarily through trans cranial magnetic stimulation (TMS) of motor cortex, the movements and the sound are experienced as further apart compared to objective time. Temporal binding occurs only when the movement is intended and deliberate and thus is a marker of the experience of agency. (Based on Haggard, Clark, and Kalogeras 2002.)

responsible for their actions when these are performed deliberately. Intentional binding is increased when associated with outcomes that have moral consequences. It is reduced for actions that have been commanded by others, rather than performed freely. These results do not address the question of whether or not free will exists, but they suggest that our conscious experience of acting freely has a major role in creating social norms of responsibility. Such norms are critical for maintaining social cohesion.

Unconscious inference occurs in the motor domain as well as the sensory domain. Our experience of agency is created from two components: our prior expectations and the sensory consequences of the outcome of the action. We are surprised if the actual sensations do not match what we expect, as when we pick up an object that is much lighter than anticipated (Chapter 30). If the outcome confirms our expectations, however, we pay little attention to the actual sensory evidence—we experience what we expected to happen rather than what actually happened.

Pierre Fourneret and Marc Jeannerod asked subjects to draw a vertical line using a computer's mouse. The subjects could not see their hand and so could not see that the computer created a distortion in the line displayed on the screen. The striking result was that subjects were not aware that they had moved their hand at an angle of 10° to the left to produce the vertical line on the screen (Figure 59–8). This lack of awareness occurred for deviations of up to 15°. When subjects were instructed not to look at the screen but simply repeat the movement they had just made, they did not reproduce the deviant movement they had made but instead drew the straight-ahead movement that they believed they had made. It would seem that as long as the goal is realized (drawing a straightforward line), we experience the expected sensory feedback, not the actual sensory feedback.

This phenomenon helps us understand some otherwise bizarre experiences. For example, after the amputation of a limb, some patients may experience a phantom limb. They still experience the urge to move the missing limb, and they can select specific movements they want the missing limb to make. Their sensorimotor systems predict the proprioceptive sensations they would feel if they were to move an intact limb, and it is these predicted sensations that underlie the sensation of a moving phantom limb.

After a limb has been paralyzed due to stroke, some patients believe that they are still able to move the limb (anosognosia for hemiplegia). Here, again, such patients can select the movements they want to make and are aware of their expectations about the movement. Despite the lack of sensory evidence that follows their attempt to initiate the movement, they believe that the movement did occur.

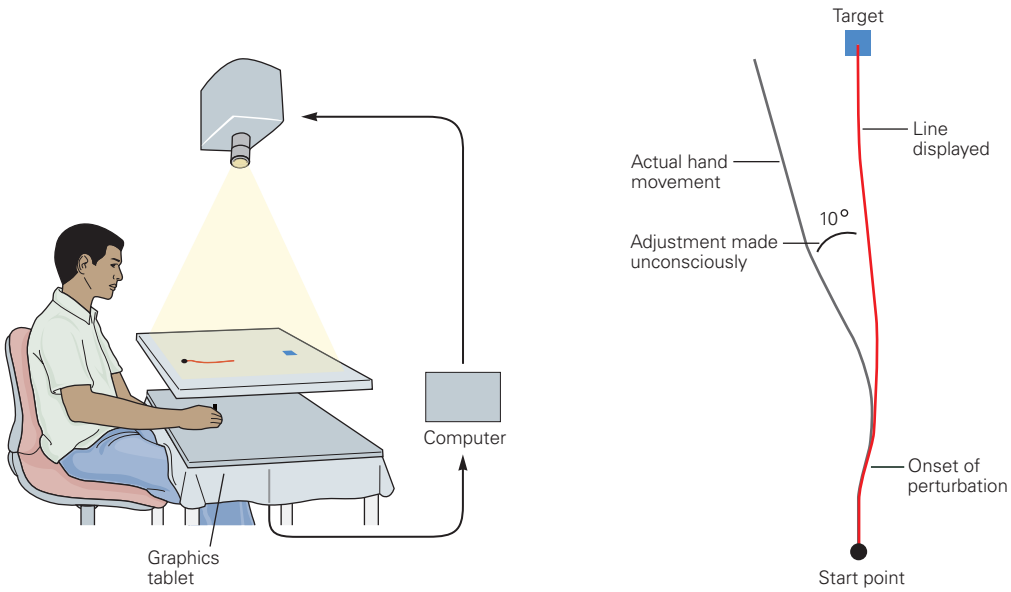

Figure 59–8 Actions can be modified unconsciously. Subjects are asked to draw a straight line with a computer mouse. They can see the line on the screen but not their hand movement. The computer is programmed to systematically distort the line displayed on the screen. In the result shown here, the subject had to move his hand 10° to the left to produce a vertical line on the screen. Subjects are not aware of making such adjustments. (Adapted, with permission, from Fourneret and Jeannerod 1998. Copyright © 1998 Elsevier Science Ltd.)

The Conscious Recall of Memories Is a Creative Process

For most of us, memory is the conscious imaginative reliving of a past experience. If we take no account of subjective experience (the behaviorist stance), however, memory is a process by which our past experience alters future behavior. Our behavior is often affected by past experience, but without conscious recall of the memory or awareness of the influence it is having on us. Once again, this type of experience is seen most strikingly in patients with damage to specific areas of the brain.

Some patients become densely amnesic after damage to the medial regions of the temporal lobe. They show no decline in intellect as measured by IQ tests but cannot remember anything for more than a few minutes. Although devastating, this memory impairment is actually rather circumscribed. The problem is largely manifested in *declarative memory*, and most severely in a type of declarative memory called *episodic memory*, the ability to recollect events in one's life (Chapter 54). *Procedural memory*, in which consciousness has a minor role (Chapter 53), remains intact. Thus, patients can still remember motor skills such as riding a bicycle and can often learn new motor skills at a normal rate. This selective effect of brain damage can lead to dramatic dissociations. A patient who has been learning some new skill every day for a week will deny ever having performed the task before. He is then surprised to find how skillful he has become.

A widely used protocol tests subjects' ability to recall lists of words they have memorized, a task that taps a form of declarative memory. In the recall phase, a subject is presented with a list of the words that were on the study list plus new words. An amnesic patient has great difficulty with this type of task and may misclassify most of the previously seen words as new since she cannot recall seeing them before. Nevertheless, the brain activity elicited by reading old words is different from that elicited by the new words: There is unconscious recognition of a difference, equivalent to that shown by patients with unilateral neglect or prosopagnosia. Normal subjects usually find this task easy, but they too will occasionally misclassify old words as new; as with amnesiacs, evoked brain responses in normal subjects register the distinction lost to conscious recall (Figure 59–9).

Occasionally, a subject misclassifies a new word as an old one. This misclassification amounts to a false memory. Such misclassifications are most likely to occur when the new word is semantically related to one or more of the old words. If the list of old words contained *big*, *great*, *huge*, then the new word *large* is likely to be identified as old. One explanation for this is that the perception of the new word *large* has been unconsciously primed by the previous presentation of the old words. Thus, the new word *large* is processed easily and quickly, and because the subject is aware of this, he concludes the word must be familiar and classifies it as old.

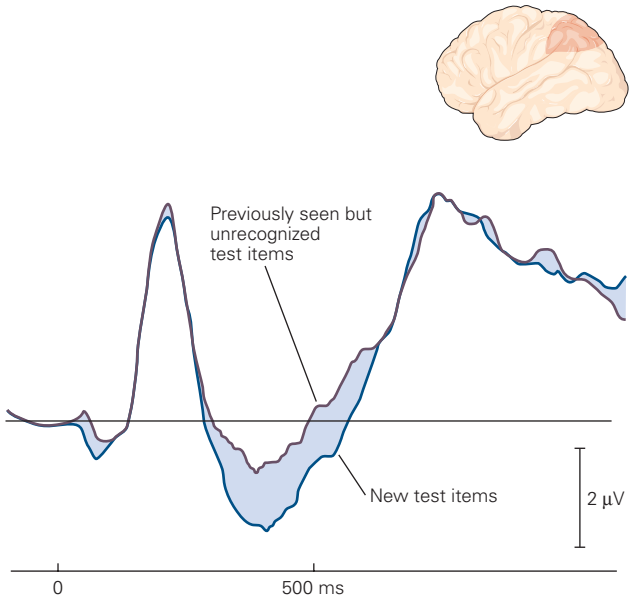

Figure 59–9 Brain activity shows the imprint of forgotten memories. Subjects were presented with a list of words, including some that had been presented earlier and some that were new. When asked to identify the words presented earlier, subjects correctly identified some of the old words but forgot others. Immediately after the visual presentation of a word, there is a brief fluctuation in the evoked potential in the brain. Evoked responses in the parietal region of the brain reflect whether or not the words had been seen before, even when subjects did not consciously recognize the words. The pattern produced by old words, whether recognized or not, is different from that produced by the new words. (Reproduced, with permission, from Rugg et al. 1998. Copyright © 1998 Springer Nature.)

This observation emphasizes that memory is a creative process. Our conscious memories are constructed from both conscious recall and unconscious knowledge. To guard against false memories, as with false percepts, we use our knowledge about the world to determine which memories are plausible.

In some patients, the process by which memories are screened can become dramatically disturbed. If asked what happened yesterday, most patients with amnesia will say that they cannot remember, but a few will give elaborate accounts that do not correspond to reality. Such false memories are called confabulations and can sometimes be extremely implausible. For example, one patient said that he had met Harold Wilson

(a former British Prime Minister) and discussed a building job they were both working on.

The creative mechanisms needed to reconstruct memories of past episodes are also involved when imagining events that might happen in the future. In amnesic patients with damage to the hippocampus, the ability to imagine new events is markedly impaired.

Behavioral Observation Needs to Be Supplemented With Subjective Reports

By the middle of the 20th century, it had become clear that the classic behaviorist approach was inadequate for the exploration of many psychological processes. Language acquisition, selective attention, and working memory cannot be understood in terms of relations between stimuli and responses, however complex the relationships postulated.

The demonstration that some cognitive processes are unconscious requires that we move even further from behaviorism. If we want to explore the whole range of conscious and unconscious cognitive processes, we will not be able to do so by focusing on overt behavior alone. We cannot assume that a subject making purposeful, goal-directed actions is necessarily aware of the stimuli eliciting the action or even of the action itself. We must supplement behavioral observations with subjective reports. We have to ask the subject, "Did you see the stimulus? Did you move your hand?"

One hundred years ago, introspection was the major method for obtaining data in psychology. How else could one study consciousness? But different schools of psychology obtained different results and, as John B. Watson emphasized, there seemed to be no objective way of deciding who was right. How can you independently confirm subjective experience? Thus, the method fell into disrepute. During the decades in which psychology was dominated by behaviorism, subjective reports were not considered an appropriate source of data. As a result, methods for recording subjective reports lag far behind methods for recording overt behavior. Regrettably, many studies of cognitive processes still do not require reports of subjective experience from subjects because of the long tradition of excluding such reports.

The one domain of psychology in which subjective reports continued to be used was psychophysics, the study of the relationship between sensation (physical energy) and perception (psychological experience) introduced by Fechner in 1860. Such studies give robust and reliable results and have created some of the few laws in psychology, such as Weber's law (the just-noticeable difference between two stimuli is proportional to the magnitude of the stimuli). In these studies, subjects are typically asked "Did you see the stimulus?" or "How confident are you that you saw the stimulus?"

Signal detection theory, developed in the 1950s, provides a robust methodology for measuring the ability to detect a stimulus (discriminability, d') independently of any reporting biases (Chapter 17). If your discriminability is high, then you will successfully detect small changes in the stimuli. More recently, there has been increasing interest in the second question, "How confident are you that you saw the stimulus?" Reporting one's confidence requires *metacognition*, the ability to reflect on our cognitive processes. This ability has an important role in the control of behavior. For example, if we realize that we are not performing some task very well, we might slow down and pay more attention to what we are doing.

The ability to reflect on our perception can be measured objectively. Likewise, the ability to reflect on the quality of our cognitive processes can also be assessed quantitatively. If your metacognitive accuracy is high, then you will successfully discriminate between your right and wrong answers. In other words, a correct detection will usually be associated with a high degree of confidence, whereas an incorrect detection will be associated with a low degree of confidence. However, your metacognitive accuracy need not be related to your signal detection ability. You could be good at detecting signals while at the same time poor at knowing whether your answers are likely to be right or wrong. In fact, patients with damage to anterior prefrontal cortex retain the ability to detect visual signals but show a marked deficit in metacognitive accuracy.

Verbal reports cannot, of course, be used in signal detection experiments with laboratory animals or preverbal infants. One alternative is to identify aspects of behaviors that reflect confidence. For example, if we are confident that we left our keys somewhere in the living room, we will spend more time looking there before we switch to the hall. Louise Goupil and Sid Kouider applied this insight to the study of metacognition in preverbal infants. The infants had to remember which of two boxes had contained a toy that was later removed without their knowledge. They spent more time searching inside the correct box. The infants were also more likely to ask an adult for help to open the correct box. These effects did not occur after long intervals. This behavior suggests that the infants had some insight into their current state of knowledge. They knew when they could no longer remember which was

the correct box. Similar experiments suggest that rats and monkeys also have some metacognitive abilities.

Verification of Subjective Reports Is Challenging

Reports of subjective experience, such as confidence, serve like a meter. Just as an electrical meter converts electrical resistance into the position of a pointer on a dial (reading 100 ohms), so a subject converts a light stimulus into the report of a color ("I see red"). But there is a critical way in which the meter is not like a person. The meter does not experience red and cannot communicate meaning. And, although the meter might be faulty, it can never pretend to see red when it is really seeing blue. Most of the time, we presume that subjective reports are true, that is, the subject is trying as far as possible to give an accurate description of his experience. But how can we be sure that we can rely on these subjective reports?

The problem of verifying subjective reports can partially be addressed with the use of brain imaging. Brain imaging studies have shown that neural activity occurs in localized areas of the brain during mental activity that is not associated with any overt behavior. The content of such mental activity, such as imagining or daydreaming, can be known only from the subject's reports.

If we scan a subject while he says he is imagining moving his hand, activity will be detected in many parts of the motor system. In most motor regions, this activity is less intense than the activity associated with an actual movement, but it is well above resting levels. Similarly, if a subject reports that she is imagining a face she has recently seen, activity can be detected in the fusiform gyrus, the "face recognition area" (Figure 59–10). In these examples, the location of the observed neural activity detected by the scanner

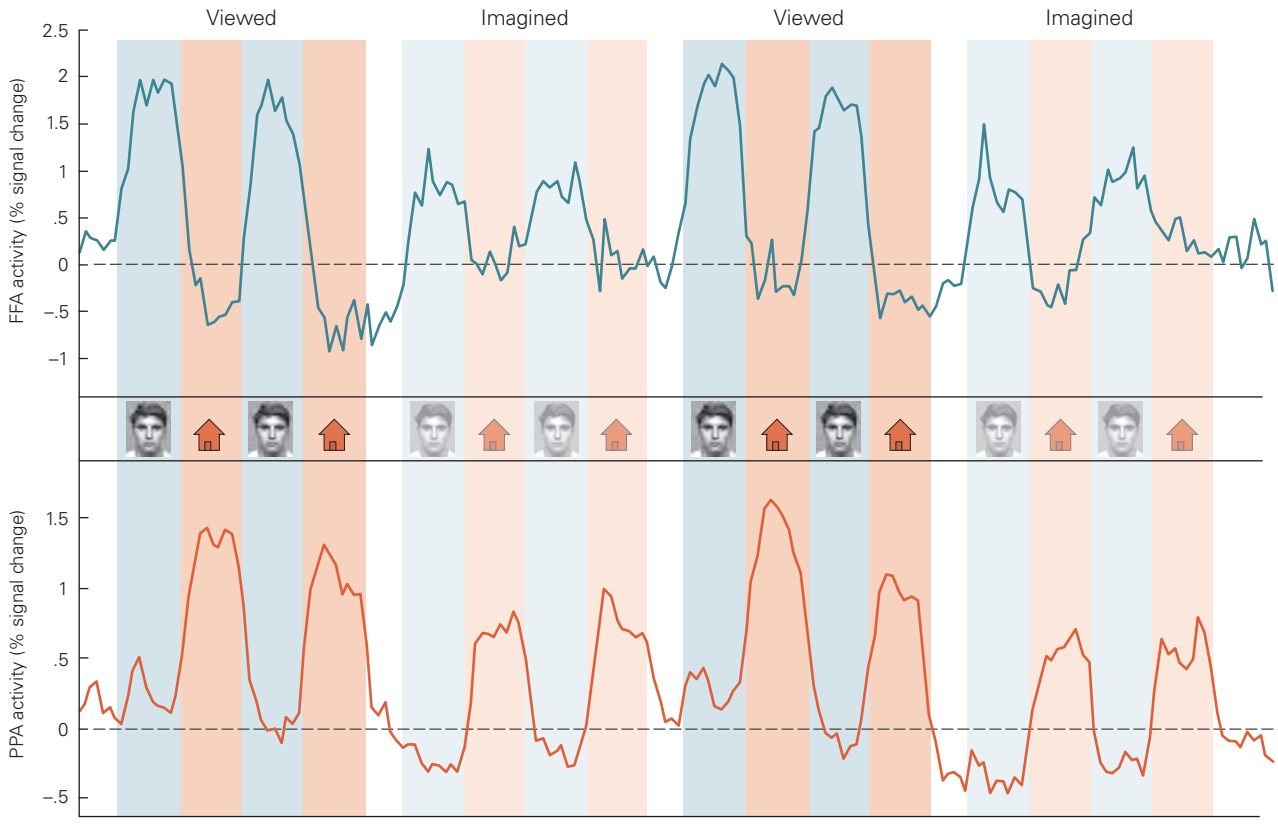

Figure 59–10 Imagining a face or a place correlates with activity in specific areas of the brain. Subjects were scanned while they viewed or imagined faces and houses. In the first block of trials, subjects alternately viewed a face or a house. When viewing a face, brain activity increases in the fusiform face area of the inferior temporal lobe (**FFA**). When viewing a house, brain activity increases in the parahippocampal place area of the inferior temporal cortex (**PPA**). In the next block of trials, subjects alternately *imagined* a face and a house. The same brain regions are active during both the imagining and direct viewing of faces and houses, although the activity is less pronounced during the imagined viewing. (Reproduced, with permission, from O'Craven and Kanwisher 2000. Copyright © 2000 MIT.)

provides independent confirmation of the content of the experience reported by the subject. The content of consciousness can, in certain limited cases, be inferred from patterns of neural activity.

Malingering and Hysteria Can Lead to Unreliable Subjective Reports

What if a subject reports seeing "blue" even though what they experienced was red? How could this arise, and what is the status of the subjective report in such cases?

Consider a patient who has become amnesic as a result of extensive damage to the medial temporal cortex. Shown a photograph of someone whom he sees every day on the ward, the patient denies ever having seen this person, even while physiological measurements (electroencephalogram or skin conductance) show a response to this photo (but not to photos of people he has not seen before). We conclude that conscious memory processes have been damaged while unconscious processes remain intact. This patient's subjective report is an accurate account of what he knows *consciously*, but it excludes those things he "knows" that have not entered consciousness.

Another patient, found wandering on the street, shows no evidence of brain damage but reports he cannot remember anything about himself or his history. When shown photographs of people from his past, he denies any knowledge of them, but at the same time, he shows physiological responses to the photos. In this case, because of the lack of detectable brain damage (and other features of the memory loss), we begin to wonder about the truthfulness of his statements. Perhaps the physiological responses indicate that he does consciously recognize people. Subsequently, the patient is identified by the police, and we discover that he is wanted for a serious crime committed in the neighboring county. Our doubts about the reliability of his reports increase. Finally, our suspicions are confirmed when he foolishly tells a fellow patient, "It's so easy to fool those clinical psychologists."

In this case, we have direct evidence that the patient was deliberately misleading others about himself. To deceive others, we must be conscious not only of our own mental state but also that of others. Is there some way we can test for deceit? One approach is to use a memory test of the kind discussed earlier. The patient studies a list of words. He is then shown a new list consisting of the words he has just studied and new words, and he must decide whether each word is old or new. A genuine amnesic would not recognize any of the words; he would have to guess, but through unconscious priming effects, he would perform better than chance. The malingering patient can recognize the old words but will have a strong tendency to deny that he has seen them before. Unless he is very sophisticated, he may perform worse than chance. It seems we should be able to distinguish between the genuine amnesic and the malingerer.

A third kind of patient also simulates amnesia (or some other disorder) but does so unconsciously and thus is not a malingerer. Such a case would be called hysterical or psychogenic amnesia. Like the malingerer, his performance on the recognition test is worse than chance. Nonetheless, he is not aware of his simulation. The same mechanism occurs in normal people who have been hypnotized and then told that they will have no memory for what has just happened. This phenomenon is sometimes referred to as a dissociated state: That part of the mind that records experiences and makes verbal reports has become dissociated from the part that is creating the simulation. Hysterical simulations can also create sensory loss, such as hysterical blindness, and motor disorders, such as hysterical paralysis or hysterical dystonia.

We are still a long way from understanding the cognitive processes or underlying physiology of these disorders. A key problem is how to distinguish hysteria from malingering. From the standpoint of conscious experience, the two disorders are quite different: The malingerer is aware that he is simulating, whereas the hysterical patient is not. Yet the patients' subjective reports and overt behavior in the two cases are very similar. Is there no measure that can distinguish between these different disorders? Perhaps the only way to demonstrate the critical distinction between these different states of consciousness is through neuroimaging studies.

Highlights

1. The study of mental disorders forces us to confront the conceptual gap between the mental and the physical. It is no longer possible to maintain that mental disorders have mental causes, whereas physical disorders have physical causes.
2. Cognitive neuroscience has had a major impact on our attempts to bridge this gap because its descriptive language, the language of information processing, can be applied simultaneously to psychological and neural processes. Information theory and the development of the computer hint at how science can address the question of how subjective experience can emerge from activity in a physical brain.

3. It is now clear that perception, action, and memory are the result of many parallel processes and that, although some of these processes support conscious experience, the majority occur below the level of awareness.
4. Striking abnormalities occur when some of these processes are damaged while others remain intact. One patient, D.F., with damage to the inferior temporal cortex, is no longer consciously aware of the shape of an object and hence cannot describe it or recognize what it is. She can nevertheless form her hand into the appropriate shape to pick up the object.
5. We have very little awareness of the details of our actions, but we are vividly aware of being in control (the sense of agency). In extreme cases, this sense of agency can become detached from the control of action. After limb amputation, many people experience having a phantom limb that they can move, and after a limb has been paralyzed due to a stroke, some patients believe that they can still move the limb.
6. Recollection of the past is not like replaying a video. Memory is a creative process based on imperfect recall filled out with general knowledge. Through loss of this creativity, patients with amnesia have difficulty with imagining the future as well as remembering the past.
7. Subjective experience is an important part of human life. When we make a decision, our choice is indicated by our behavior, but our confidence in that choice is a subjective experience. We can study such experiences through verbal report. Confidence in our choices is an example of *metacognition* (ie, the ability to reflect on our cognitive processes). Damage to the frontal cortex can impair metacognition, while leaving decision-making intact.
8. Verbal reports are not always reliable. People can fake memory loss in order to escape justice. Malingering of this kind is very difficult to detect, since it closely resembles disorders such as hysterical amnesia, in which the patient is not aware that he is simulating the disorder. The challenge for cognitive neuroscience is to distinguish these cases.

Christopher D. Frith

Selected Reading

Dehaene S. 2014. *Consciousness and the Brain: Deciphering How the Brain Codes Our Thoughts*. New York: Viking.

Frith CD. 2007. *Making Up the Mind: How the Brain Creates Our Mental World*. Oxford: Blackwell.

Gazzaniga MS (ed). 1995. *Cognitive Neuroscience: A Reader*. Oxford: Blackwell.

Marr D. 1982. *Vision: A Computational Investigation into the Human Representation and Processing of Visual Information*. San Francisco: Freeman.

McCarthy R, Warrington EK. 1990. *Cognitive Neuropsychology: A Clinical Introduction*. London, San Diego: Academic Press.

Sacks O. 1970. *The Man Who Mistook His Wife for a Hat and Other Clinical Tales*. New York: Touchstone.

References

Bauer RM. 1994. Autonomic recognition of names and faces in prosopagnosia: a neuropsychological application of the Guilty Knowledge test. Neuropsychology 22:457–469.

Beck DM, Rees G, Frith CD, Lavie N. 2001. Neural correlates of change and change blindness. Nat Neurosci 4:645–650.

Beck JS. 1995. *Cognitive Therapy: Basics and Beyond*. New York: Guilford Press.

Burgess PW, Baxter D, Rose M, Alderman N. 1986. Delusional paramnesic syndrome. In: PW Halligan, JC Marshall (eds). *Method in Madness*: *Case Studies in Cognitive Neuropsychiatry*, pp. 51–78. Hove, UK: Psychology Press.

Caspar EA, Christensen JF, Cleeremans A, Haggard P. 2016. Coercion changes the sense of agency in the human brain. Curr Biol 26:585–592.

Dierks T, Linden DE, Jandl M, et al. 1999. Activation of Heschl's gyrus during auditory hallucinations. Neuron 22:615–621.

Ellis HD, Young AW. 1990. Accounting for delusional misidentification. Br J Psychiatry 157:239–248.

ffytche DH, Howard RJ, Brammer MJ, David A, Woordruff P, Williams S. 1998. The anatomy of conscious vision: an fMRI study of visual hallucinations. Nat Neurosci 1:738–742.

Fleming SM, Ryu J, Golfinos JG, Blackmon KE. 2014. Domain-specific impairment in metacognitive accuracy following anterior prefrontal lesions. Brain 137:2811–2822.

Fotopoulou A, Tsakiris M, Haggard P, Vagopoulou A, Rudd A, Kopelman, M. 2008. The role of motor intention in motor awareness: an experimental study on anosognosia for hemiplegia. Brain 131:3432–3442.

Fourneret P, Jeannerod M. 1998. Limited conscious monitoring of motor performance in normal subjects. Neuropsychology 36:1133–1140.

Frith CD. 2011. Explaining delusions of control: the comparator model 20 years on. Conscious Cogn 21:52–54.

Frith CD. 2013. Action, agency and responsibility. Neuropsychologia 55:137–142.

Glinsky EL, Schacter DL. 1988. Long-term retention of computer learning in patients with memory disorders. Neuropsychology 26:173–178.

Goupil L, Romand-Monnier M, Kouider S. 2016. Infants ask for help when they know they don't know. Proc Natl Acad Sci U S A 113:3492–3496.

Haggard P, Clark S, Kalogeras J. 2002. Voluntary action and conscious awareness. Nat Neurosci 5:382–385.

Hassabis D, Kumaran D, Vann SD, Maguire EA. 2007. Patients with hippocampal amnesia cannot imagine new experiences. Proc Natl Acad Sci U S A 104:1726–1731.

Jacoby LL, Whitehouse K. 1989. An illusion of memory: false recognition influenced by unconscious perception. J Exp Psychol Gen 118:126–135.

Kopelman MD. 1995. The assessment of psychogenic amnesia. In: AD Baddeley, BA Wilson, FN Watts (eds). *Handbook of Memory Disorders*. New York: Wiley.

Libet B, Gleason CA, Wright EW, Pearl DK. 1983. Time of conscious intention to act in relation to onset of cerebral activity (readiness potential). The unconscious initiation of a freely voluntary act. Brain 106:623–642.

Maniscalco B, Lau H. 2011. A signal detection theoretic approach for estimating metacognitive sensitivity from confidence ratings. Conscious Cogn 21:422–430.

Marshall JC, Halligan PW. 1988. Blindsight and insight in visuo-spatial neglect. Nature 336:766–767.

Milner AD, Goodale MA. 1995. *The Visual Brain in Action*. Oxford: Oxford Univ. Press.

Moore J, Haggard P. 2008. Awareness of action: inference and prediction. Conscious Cogn 17:136–144.

Moretto G, Walsh E, Haggard P. 201 Experience of agency and sense of responsibility. Conscious Cogn 20:1847–1854.

O'Craven KM, Kanwisher N. 2000. Mental imagery of faces and places activates corresponding stimulus-specific brain regions. J Cogn Neurosci 12:1013–1023.

Öhman A, Soares JJ. 1994. "Unconscious anxiety": phobic responses to masked stimuli. J Abnorm Psychol 103:231–240.

Penfield W, Perot P. 1963. The brain's record of auditory and visual experience: a final summary and discussion. Brain 86:595–696.

Rensink RA, O'Regan JK, Clark JJ. 1997. To see or not to see: the need for attention to perceive changes in scenes. Psychol Sci 8:368–373.

Rugg MD, Mark RE, Walla P, Schloerscheidt AM, Birch CS, Allan K. 1998. Dissociation of the neural correlates of implicit and explicit memory. Nature 392:595–598.

Schurger A, Mylopoulos M, Rosenthal D. 2016. Neural antecedents of spontaneous voluntary movement: a new perspective. Trends Cogn Sci 20:77–79.

Shepherd J. 2012 Free will and consciousness: experimental studies. Conscious Cogn 21:915–927.

Smith CH, Oakley DA, Morton J. 2013. Increased response time of primed associates following an "episodic" hypnotic amnesia suggestion: a case of unconscious volition. Conscious Cogn 22:1305–1317.

Stewart L, Battelli L, Walsh V, Cowey A. 1999. Motion perception and perceptual learning studied by magnetic stimulation. Electroencephalogr Clin Neurophysiol Suppl 51:334.

Swets JA, Tanner WPJ, Birdsall TG. 1959. Decision processes in perception. Psychol Rev 68:301–340.

Tong F, Nakayama K, Vaughn JT, Kanwisher N. 1998. Binocular rivalry and visual awareness in human extrastriate cortex. Neuron 21:753–759.

Watson JB. 1930. *Behaviorism*. Chicago: Univ. of Chicago Press.

Weiskrantz L. 1986. *Blindsight*: *A Case Study and Its Implications*. Oxford: Oxford Univ. Press.

60

Disorders of Thought and Volition in Schizophrenia

In this chapter and the next, we examine disorders that affect perception, thought, mood, emotion, and motivation: schizophrenia, depression, bipolar disorder, and anxiety disorders. These have been challenging to understand, but recent progress in genetic analysis has begun to yield significant clues to their pathogenesis.

Mental illness has damaging effects on individuals, families, and society. The World Health Organization reports that mental illnesses, in the aggregate, constitute the leading cause of disability worldwide and are the leading risk factors for the 800,000 annual suicides reported by the World Health Organization. In addition, depression and anxiety disorders frequently co-occur with and worsen the outcomes of diabetes mellitus, coronary artery disease, stroke, and several other illnesses.

Medications such as antipsychotic drugs, lithium, and antidepressant drugs discovered during the mid-20th century made it possible to close large and often substandard mental hospitals; however, halfway houses and other less restrictive treatment settings did not materialize in sufficient numbers. As a result, many people with schizophrenia and severe bipolar disorder become homeless at some time in their lives, and in many countries, individuals with severe mental disorders compose a large fraction of prison populations.

In addition, although antipsychotic drugs, lithium, and antidepressant drugs have played important roles in controlling symptoms of mental disorders, significant limitations in treatment efficacy remain. For example, there are no effective treatments for the highly disabling cognitive impairments and deficit symptoms of schizophrenia. Even for symptoms that benefit from existing medications, such as hallucinations and delusions, residual symptoms remain and relapses are the rule. Because of significant scientific challenges posed by the human brain and limitations in animal models of mental disorders, there has been little advance in the efficacy of psychiatric drugs for more than 50 years. However, recent progress in human genetics and neural science has created significant opportunities to improve upon this unfortunate state of affairs.

Schizophrenia Is Characterized by Cognitive Impairments, Deficit Symptoms, and Psychotic Symptoms

In medicine, the understanding of a disease, and therefore its diagnosis, is ultimately based on identification of two features: (1) etiological factors (eg, microbes, toxins, or genetic risks) and (2) mechanism of pathogenesis (the processes by which etiologic agents produce disease). While human genetics and neural science are beginning to provide insights into the etiology and pathogenesis of disorders such as schizophrenia, bipolar disorder, and autism spectrum disorders, this research has not yet yielded objective diagnostic tests or biomarkers. As a result, psychiatric diagnoses still rely on a description of the patient's symptoms, the examiner's observations, and the course of the illness over time.

Schizophrenia is a very severe illness. Its symptoms can be divided into three clusters: (1) cognitive symptoms; (2) deficit, or negative, symptoms; and (3) psychotic symptoms. These symptom clusters exhibit different temporal patterns of onset—with cognitive impairments and deficit symptoms typically the earliest. The different timing of onset and the precise symptoms of each cluster are thought to result from the effects of developmental pathogenic mechanisms on different neural circuits and brain regions. As a result, existing treatments such as antipsychotic drugs, which act on one "downstream" aspect of the disease process, exert no beneficial effects on cognitive impairments or deficit symptoms.

At the beginning of the 20th century, Emil Kraepelin in Germany recognized that cognitive decline was a distinguishing feature of schizophrenia, because psychotic symptoms occur in a variety of psychiatric conditions. Indeed, Kraepelin's term for what later came to be called schizophrenia was *dementia praecox*, a term that highlighted the early onset of cognitive loss. Cognitive impairments in schizophrenia target working memory and executive function, declarative memory, verbal fluency, the ability to identify the emotions conveyed by facial expressions, and other aspects of social cognition. These impairments do not significantly improve with existing medications, but ongoing research shows promising, albeit still modest, benefits from psychological therapies aimed at cognitive remediation.

Deficit symptoms include blunted emotional responses, withdrawal from social interaction, impoverished content of thought and speech, and loss of motivation. Psychotic symptoms include hallucinations, delusions, and disordered thought such as loosening of association (Box 60–1). Psychotic symptoms of schizophrenia are responsive to antipsychotic drugs. These drugs also reduce psychotic symptoms that

Box 60–1 Thought Disorder

The structure of a psychotic person's speech may range from wandering to incoherence, a symptom commonly referred to as loosening of association. Other examples of schizophrenic speech include neologisms (idiosyncratically invented words), blocking (sudden spontaneous interruptions), or clanging (associations based on the sounds rather than the meanings of words, such as, "If you can make sense out of nonsense, well, have fun. I'm trying to make cents out of sense. I'm not making cents anymore. I have to make dollars.")

Examples of loosening of associations are:

"I'm supposed to be making a film but I don't know what is going to be the end of it. Jesus Christ is writing a book about me."

"I don't think they care for me because two million camels . . . 10 million taxis . . . Father Christmas on the rebound."

Question: "How does your head feel?" Answer: "My head, well that's the hardest part of the job. My memory is just as good as the next working man's. I tell you what my trouble is, I can't read. You can't learn anything if you can't read or write properly. You can't pick up a nice book, I don't just mean a sex book, a book about literature or about history or something like that. You can't pick up and read it and find things out for yourself."

Several types of loosening of association have been described (eg, derailment, incoherence, tangentiality, or loss of goal). However, it remains unclear whether these reflect disturbances in fundamentally different mechanisms or different manifestations of a common underlying disturbance, such as the inability to represent a "speech plan" to guide coherent speech. A disturbance of such a mechanism would be consistent with, and may parallel, impairment of control of other cognitive functions in schizophrenia, such as deficits in working memory.

occur in other neuropsychiatric disorders, including bipolar disorder, severe depression, and neurodegenerative disorders such as Parkinson disease, Huntington disease, and Alzheimer disease.

Schizophrenia Has a Characteristic Course of Illness With Onset During the Second and Third Decades of Life

Schizophrenia affects 0.25% to 0.75% of the population worldwide, with only modest regional differences. Males are more commonly affected than females, with the sex ratio estimated to be 3:2, and onset is often earlier in males. Schizophrenia typically begins during the late teen years or the early to mid-twenties. Enduring cognitive and deficit symptoms generally begin months and sometimes years prior to the onset of psychotic symptoms. This period is referred to as the ultra-high-risk state by some researchers and as the schizophrenia prodrome by others.

Individuals in this risk state generally have measurable declines in cognitive functioning accompanied by such symptoms as social isolation, suspiciousness, and decreased motivation to engage in school work or other tasks. Attenuated psychotic symptoms often follow, including transient and mild hallucinations. Not every teen with such symptoms progresses to develop the full spectrum of symptoms warranting a diagnosis of schizophrenia. A small fraction recovers; others develop serious psychiatric conditions other than schizophrenia. Antipsychotic medications do not appear to benefit individuals in the risk state, nor do they delay the onset of schizophrenia. However, talk therapies and therapies delivered via computer-based approaches aimed at cognitive remediation show promise in delaying the onset of psychosis.

The Psychotic Symptoms of Schizophrenia Tend to Be Episodic

Psychotic symptoms, including hallucinations and delusions, are the most dramatic manifestations of schizophrenia. Hallucinations are percepts that occur in the absence of appropriate sensory stimuli, and they may occur in any sensory modality. In schizophrenia, the most common hallucinations are auditory. Typically, an affected person hears voices, but noises and music are also common. Sometimes, the voices will carry on a dialog and frequently are experienced as derogatory or bullying. Occasionally, voices will issue commands to the affected individual that can create a high risk of harm to self or others.

Delusions are firm beliefs that have no realistic basis and are not explained by the patient's culture, nor are they amenable to change by argument or evidence. Delusions may be quite varied in form. For some affected individuals, reality is significantly distorted: The world is full of hidden signs meant only for the affected person (ideas of reference), or the person believes that he is being closely watched, followed, or persecuted (paranoid delusions). Others may experience bizarre delusions; for example, they may believe that someone is inserting thoughts into or extracting thoughts from their minds or that their close relatives have been replaced by aliens from another planet. In addition to the person's enduring cognitive impairments, psychotic episodes are frequently accompanied by disordered thought and odd patterns of speech (Box 60–1).

Psychotic symptoms may also occur in other neuropsychiatric disorders, such as bipolar disorder, major (unipolar) depression, various neurodegenerative disorders, and drug-induced states. However, these other conditions can usually be distinguished from schizophrenia by associated symptoms and age of onset. Once schizophrenia has become fully manifest, psychotic symptoms tend to be episodic. Periods of florid psychosis accompanied by markedly disordered thinking, emotion, and behavior are interspersed with periods in which psychotic symptoms are milder or even absent. Psychotic episodes typically require hospitalization; the severity and duration of such episodes are markedly shortened by antipsychotic drugs. First and second episodes of psychosis often respond fully to antipsychotic drugs, but cognitive impairments and deficit symptoms typically persist. After the first few psychotic relapses, people with schizophrenia typically suffer residual psychotic symptoms even between their acute relapses and suffer these symptoms despite treatment with antipsychotic drugs. Cognitive and social functioning typically continue to deteriorate over several years until they reach a plateau well below the person's premorbid level of functioning.

The Risk of Schizophrenia Is Highly Influenced by Genes

As early as 1930, Franz Kalman in Germany studied familial patterns of schizophrenia and concluded that genes contribute significantly. To separate genetic from environmental influences more clearly, Seymour Kety, David Rosenthal, and Paul Wender examined children who were adopted at or shortly after birth in Denmark. They found that the rate of schizophrenia in the biological family of the adoptee was much more strongly

predictive of schizophrenia than the rate of schizophrenia in the adoptive family.

Kety and his colleagues also observed that some of the biological relatives of adoptees with schizophrenia exhibited milder symptoms related to schizophrenia, such as social isolation, suspiciousness, eccentric beliefs, and magical thinking, but not frank hallucinations or delusions. Since Kety's time, it has been observed that such relatives may also exhibit cognitive impairments that are intermediate between unaffected individuals and those with schizophrenia. They also may exhibit thinning of the cerebral cortex observed by magnetic resonance imaging (MRI) that is also intermediate between healthy individuals and those with schizophrenia. (Cortical thinning in schizophrenia is discussed below.) Such individuals are now diagnosed with schizotypal disorder, which appears to be the milder end of the schizophrenia spectrum of psychotic disorders. The severity and nature of symptoms appear to be influenced by the individual's overall burden of risk-associated genetic variants as well as exposure to environmental risk factors.

Irving Gottesman's studies of extended pedigrees of Danish patients with schizophrenia supported the importance of genes. Gottesman noted the correlations between the risk of schizophrenia in relatives and the degree to which they shared DNA sequences with an affected person. He found a greater lifetime risk of schizophrenia among first-degree relatives (including parents, siblings, and children, who share 50% of DNA sequences with the patient) than among second-degree relatives (including aunts, uncles, nieces, nephews, and grandchildren, who share 25% of their DNA sequences). Even third-degree relatives (who share only 12.5% of the patient's DNA sequences) were at higher risk for schizophrenia than the approximately 1% of the general population at risk for this disease (Figure 60–1).

Based on the differences in levels of risk Gottesman measured in these pedigrees, he recognized that schizophrenia risk was not transmitted within families as Mendelian dominant or recessive traits (ie, it was not caused by a single genetic locus). He predicted correctly that schizophrenia is a polygenic trait, involving a large number of loci throughout the human genome. This genetic architecture underlies many human phenotypes, including disease phenotypes, and may involve many hundreds of loci within the genome. In polygenic traits, variants at each disease-associated locus contribute small, additive effects to the phenotype. Genetic risk variants act together with environmental factors to produce the schizophrenia phenotype.

In 2014, a large global consortium reported on a genome-wide association study of more than 35,000 individuals with schizophrenia. The study identified 108 genome-wide significant loci associated with schizophrenia that were distributed across the genome. The research continues, and the number of known loci is already greater than 250. Each of these loci represents a segment of DNA identified by a single

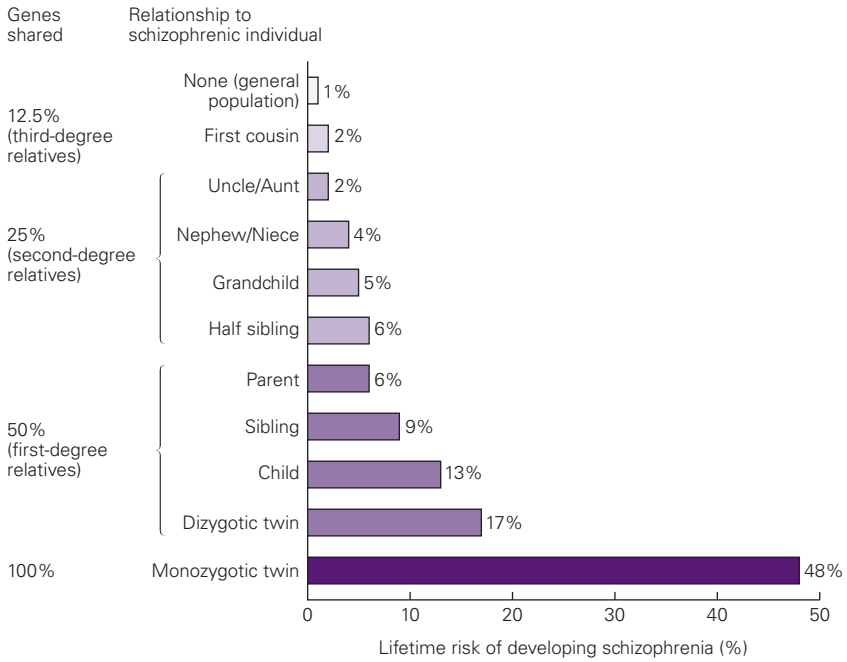

Figure 60–1 **The lifetime risk of schizophrenia increases as a function of genetic relatedness to a person with schizophrenia.** The risk of schizophrenia rises with genetic relatedness to an affected individual and, therefore, with increased sharing of DNA sequences. However, the pattern of segregation in families does not follow simple Mendelian ratios; rather, inheritance reflects genetic complexity. In addition, risk varies within categories of relatedness (first- and second-degree relatives), suggesting a role for unshared developmental or environmental effects. (Reproduced, with permission, from Gottesman 1991.)

nucleotide polymorphism that confers a small increment in risk (typically 5%–10%) for schizophrenia. The value of such allelic variants is as a tool to identify genes that play a role in the molecular mechanism of disease. In turn, the implicated genes help identify molecular pathways that can potentially be exploited in the development of therapeutic drugs.

In addition to the utility of genetics for discovering biological processes involved in disease, it can also contribute to the stratification of study populations in epidemiological and clinical studies. A person's risk of schizophrenia or other disorders can be estimated by calculating his or her total burden of common risk alleles for the condition. The result is a polygenic risk score, a measure that is increasingly being used to stratify populations by genetic susceptibility to schizophrenia in both clinical studies and in epidemiologic studies of environmental risk factors.

Environmental risk factors for schizophrenia that have been replicated across studies include nutrient deprivation in utero (notably in studies following famines), season of birth (winter and early spring birth), urban birth, and migration. The analysis of causal factors within such broad categories of exposure is likely to benefit from knowing who is susceptible. Moreover, clues to environmentally induced causal pathways may be found in the risk genotypes of those with schizophrenia who have had a particular exposure.

Given the lack of objective diagnostic tests, current diagnostic criteria, such as those within the fifth edition of the *Diagnostic and Statistical Manual of Mental Disorders*, are based on clinical observation and course of illness. As a result, individuals currently diagnosed with schizophrenia are highly heterogeneous. Polygenic risk scores can explain only a portion of the variance in schizophrenia cohorts, and the scores provide only probabilistic information. However, they represent the first objective tool that permits stratification of subjects diagnosed with schizophrenia. As such, the application of such scores may begin to diminish heterogeneity in clinical studies ranging from neuroimaging to neurophysiological studies to treatment trials.

Although almost all cases of schizophrenia reflect polygenic risks, as predicted by Gottesman, a small percentage of cases are highly influenced by the presence of a penetrant mutation that typically exerts pleiotropic effects, including intellectual disability, resulting in what is often called syndromic schizophrenia. Most of these penetrant mutations are copy number variants: deletions, duplications, or sometimes triplications of a particular segment of a chromosome.

The most common and best studied cause of syndromic schizophrenia is the 22q11.2 microdeletion, which accounts for approximately 1% of patients diagnosed with schizophrenia. The microdeletion typically occurs de novo and results in loss of one of two copies of 38 to 44 genes. As is typical for such copy number variations, those affected suffer from a complex of symptoms. The syndrome accompanying the 22q11.2 microdeletion, sometimes called velocardiofacial or DiGeorge syndrome, includes cognitive disability, cardiovascular defects, and facial dysmorphology. The penetrance of each of these symptoms and signs is independent of the others; thus, affected individuals have different combinations of phenotypes. Individuals with the 22q.11.2 microdeletion have a 25% to 40% risk of schizophrenia and a 20% risk of autism. Other syndromic forms of psychosis are similarly variable.

Syndromic forms of schizophrenia can provide important windows into the biology of psychosis, even if their similarities to common polygenic types of schizophrenia are still a matter of study. One powerful advantage of penetrant mutations is the ability to generate cellular and animal models in order to characterize their effects on brain structure and function. A second advantage is the ability to prospectively study individuals carrying these mutations. Studying syndromic schizophrenia, therefore, has the potential to reveal much about basic pathophysiological mechanisms. One important area of investigation is how copy number variations and other high-penetrance mutations that lead to psychosis manifest based on a person's genetic background, specifically the many common DNA variants that influence risk. To this point, recent findings suggest that the propensity in individuals carrying a copy number variation to develop psychotic symptoms may result from a strong interaction of the copy number variation with the person's polygenic background risk for schizophrenia, suggesting significant shared mechanisms between schizophrenia associated with single genetic mutations and that associated only with polygenic variants.

Schizophrenia Is Characterized by Abnormalities in Brain Structure and Function

Abnormalities in the structure and function of the brain have been identified in schizophrenia both by postmortem examination and by a variety of noninvasive technologies in living patients. The best replicated finding, both by postmortem study and by structural MRI, is loss of gray matter in prefrontal, temporal, and parietal regions of cerebral cortex (Figure 60–2) with counterbalancing increases in the size of the cerebral ventricles (Figure 60–3). Thinning of the cerebral cortex

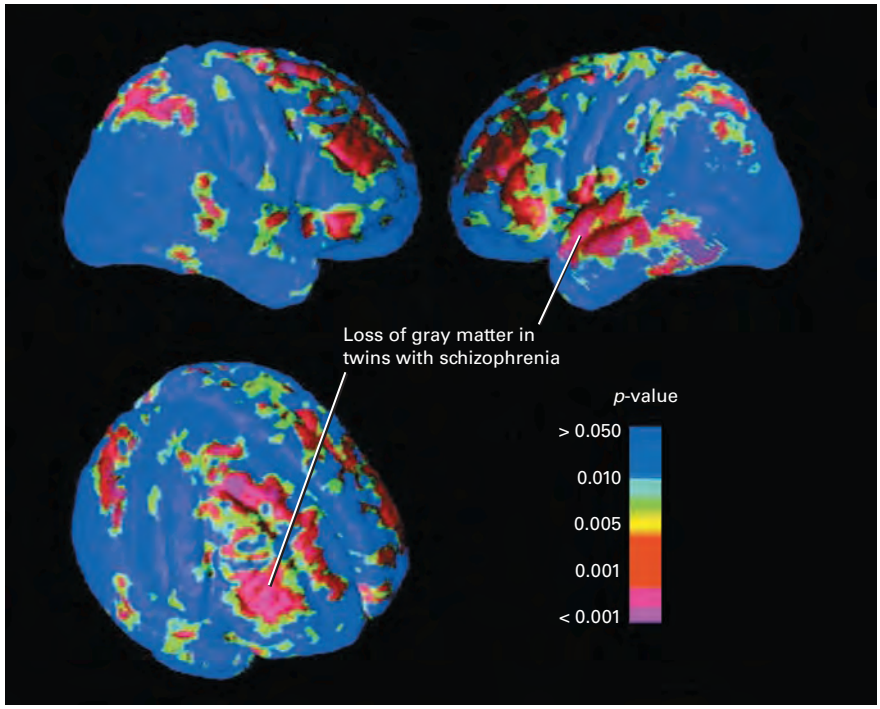

Figure 60–2 Gray matter loss in schizophrenia. Gray matter loss is well documented in schizophrenia. First-degree relatives who do not have a diagnosis of schizophrenia still often exhibit cortical gray matter loss intermediate between healthy individuals and those diagnosed with schizophrenia. Consistent with this, a study that examined losses of cortical gray matter in monozygotic and dizygotic twin pairs discordant for schizophrenia compared to healthy matched control twins found significant losses in those at genetic risk for schizophrenia but without the disease. Those members of twin pairs diagnosed with schizophrenia demonstrated additional, disease-specific cortical thinning in dorsolateral prefrontal, superior temporal, and superior parietal association areas. These additional defects appear to reflect the influence of nongenetic factors involved in pathogenesis (eg, developmental or environmental factors). The disease-specific gray matter loss correlates with the degree of cognitive impairment rather than with duration of illness or drug treatment. The images here show regional deficits in gray matter in monozygotic twins with schizophrenia relative to their healthy co-twins (n = 10 pairs) viewed from the right, left, and right oblique perspectives. Differences in twins are illustrated by the pseudocolor scale superimposed on cortical surface maps, with **pink** and **red** indicating the greatest statistical significance. (Reproduced, with permission, from Cannon et al. 2002.)

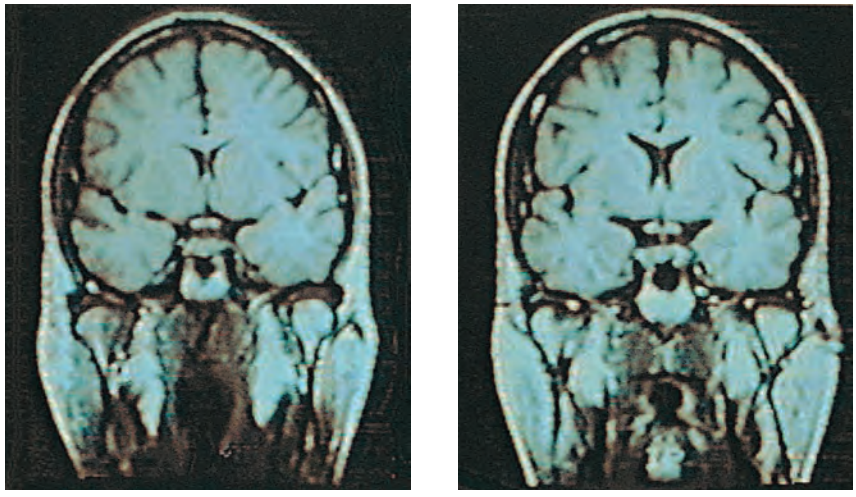

Unaffected twin | Schizophrenic twin

Figure 60–3 Enlargement of lateral ventricles in schizophrenia. Magnetic resonance imaging comparison of monozygotic twins discordant for schizophrenia. The affected member of the twin pair has the enlarged ventricles characteristic of schizophrenia. Because there is a wide range of normal ventricular volumes in the population, an unaffected monozygotic twin serves as a particularly appropriate control subject. Because monozygotic twins have identical genomes, this comparison also illustrates the role of nongenetic factors in schizophrenia.

is most pronounced in the dorsolateral prefrontal cortex, a brain region critical for working memory and thus cognitive control of thought, emotion, and behavior.

Loss of gray matter in the superior temporal gyrus, temporal pole, amygdala, and hippocampus in schizophrenia has also been correlated with impairments in cognition, recognition of emotions in others, and regulation of emotion in the affected person. Functional neuroimaging using positron emission tomography and functional MRI (fMRI) has demonstrated that patients' deficits in performing working memory tasks while being imaged are associated with decrements in the activation of dorsolateral prefrontal cortex, a brain region known to play a critical role in working memory (Figure 60–4).

There is also growing recognition that schizophrenia is characterized by disruptions in connectivity between brain regions (Figure 60–5). Anatomical connectivity can be measured by diffusion tensor imaging, which identifies major axon tracts as they course between brain regions. Functional connectivity between brain regions can be estimated physiologically by measuring the degree to which activity patterns in different brain regions correlate with each other, using such approaches as resting state fMRI and electrophysiology. Both imaging and physiological methods reveal that individuals with schizophrenia have deficits in the connections between brain regions. Weaker connections would likely impair cognition and complex behaviors.

Loss of Gray Matter in the Cerebral Cortex Appears to Result From Loss of Synaptic Contacts Rather Than Loss of Cells

Postmortem studies have examined the cellular abnormalities that underlie the gross anatomical findings and functional deficits in schizophrenia. These studies have revealed that gray matter loss in the prefrontal and temporal cortical regions is not the result of cell death but rather a reduction in dendritic processes. As a consequence, the packing density of cells in the cerebral cortex increases. More cells per unit volume and less total gray matter contribute to enlargement of the ventricular spaces.

A reduction in dendrites and dendritic spines on pyramidal neurons, the most common type of excitatory neuron in the neocortex (Figure 60–6), would likely signify a loss of synaptic contacts in affected brain regions in individuals with schizophrenia. The loss of synaptic connections could underlie abnormalities in long-range functional connectivity and failures to recruit prefrontal cortical regions during tasks that require working memory (Figures 60–4 and 60–5).

Abnormalities in Brain Development During Adolescence May Be Responsible for Schizophrenia

Schizophrenia exhibits a stereotypic onset between late adolescence and early adulthood, with cognitive decline and negative symptoms occurring months or years before the onset of psychosis. This timing suggests the pathogenesis of schizophrenia might involve abnormalities in the late stages of brain development during adolescence, when cognitive function, emotion regulation, and executive function normally mature.

Throughout development, neurons elaborate an excessively large number of synaptic connections. Generally, synapses are strengthened and preserved when they are utilized, while weak or inefficient synapses are eliminated through a process called pruning. The process of synaptic refinement, which involves both synaptogenesis and pruning, results in neural computations that are efficient and adapted to the environment. Experience-dependent synaptic refinement was first described in the visual cortex, where pruning of weak connections is necessary for the emergence of binocular vision (see Chapter 49). Synaptogenesis and pruning continue throughout life, making possible new learning and updating of older memories. However, superimposed on such local events are significant waves of synaptic pruning that are spatially specific and developmentally timed. The last such wave in human brain maturation occurs during adolescence and early adulthood, with pruning in the temporal and prefrontal association cortex. This late wave of pruning is followed by myelination of many axons in these areas of cortex.

In the early 1980s, Irwin Feinberg hypothesized that schizophrenia might result from abnormal and excessive synaptic pruning during adolescence. Postmortem examination of the brains of persons with schizophrenia subsequently demonstrated a reduction of dendritic spines, and of synapses, in prefrontal and temporal cortices. Studies in nonhuman primates, taken together with human postmortem and neuroimaging studies, suggest that loss of dendritic arbors does not result from antipsychotic medications taken by many individuals with schizophrenia. The onset of cognitive impairment and negative symptoms during this period is consistent with the idea that synaptic pruning somehow goes haywire, damaging the ability of the cerebral cortex to process information. When the overpruning hypothesis was first enunciated in the

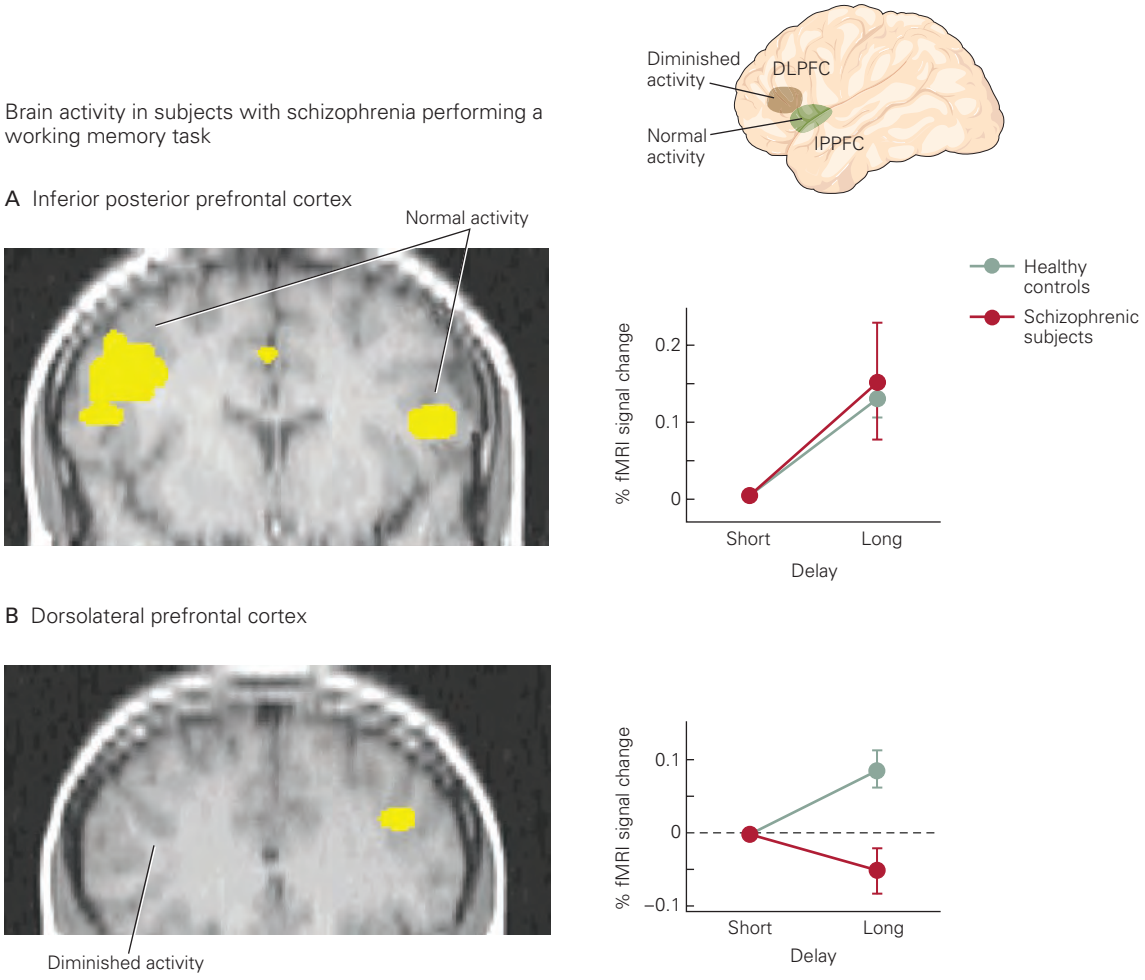

Figure 60–4 Deficits in the function of prefrontal cortex in schizophrenia. Functional magnetic resonance imaging (**fMRI**) was used to test the hypothesis that in patients with schizophrenia working memory engages circuits in the prefrontal cortex differently than in controls. Activity in the prefrontal cortex of two groups—patients with schizophrenia (first-episode patients who had never been given antipsychotic drugs) and healthy controls—was examined while subjects performed a working memory task. Subjects were presented with a sequence of letters and instructed to respond to a particular letter (the "probe" letter) only if it immediately followed another specified letter (the "contextual cue" letter). Demands on working memory were increased by increasing the delay between the cue and the probe letters. The greater demand on working memory requires greater activation of prefrontal cortical circuits. (Adapted, with permission, from Barch et al. 2001.)

A. In both patients with schizophrenia and controls, normal increases in activation within inferior posterior regions of prefrontal cortex (**IPPFC**; Brodmann's area 44/46) as a function of demand on working memory suggest that the function of these regions remains intact in schizophrenia. The plot shows the fMRI signal change that occurs in the right side of the prefrontal cortex in the long-delay and short-delay conditions in healthy controls and in patients with schizophrenia. Similar effects were observed for the left side.

B. There is less activity in Brodmann's area 46/49, a region of dorsolateral prefrontal cortex (**DLPFC**), in patients with schizophrenia relative to healthy controls. Unlike Brodmann's area 44/49 (shown in part **A**), Brodmann's area 46/49 is not activated normally in subjects with schizophrenia, consistent with the deficit in working memory seen in patients with schizophrenia. Selective impairment of one region of prefrontal cortex alongside other regions that appear to have normal function suggests that the impairment is due to a regionally specific process rather than a diffuse and nonspecific pathological process.

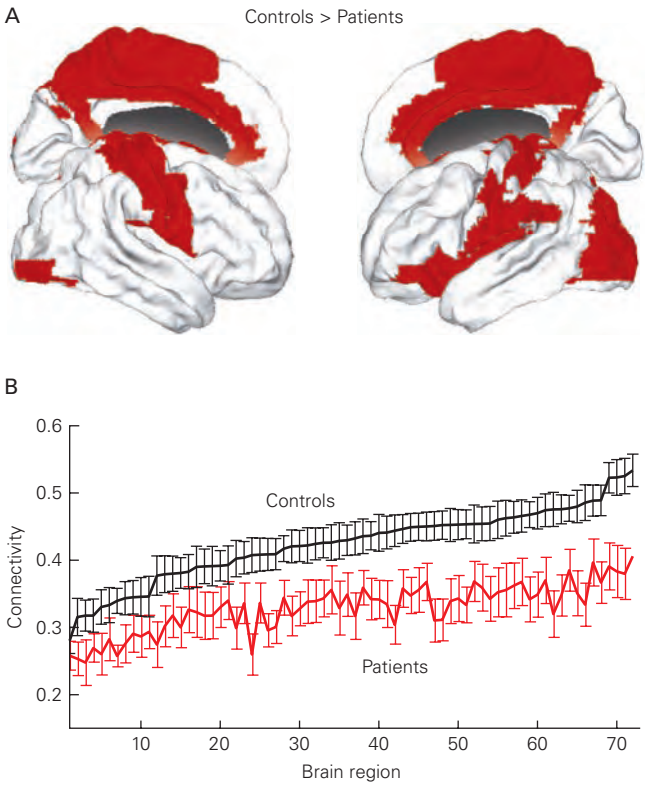

Figure 60–5 Decreased functional connectivity in schizophrenia. Correlations in neural activity between 72 defined brain regions were measured in patients with schizophrenia and in control subjects by resting state functional magnetic resonance imaging. (Reproduced, with permission, from Lynall et al. 2010.)

A. Brain regions that showed statistically significant reductions in functional connectivity in patients compared to controls are highlighted in **red**.

B. Mean (+/– standard error of the mean) functional connectivity between each brain region and the rest of the brain for patients and healthy controls.

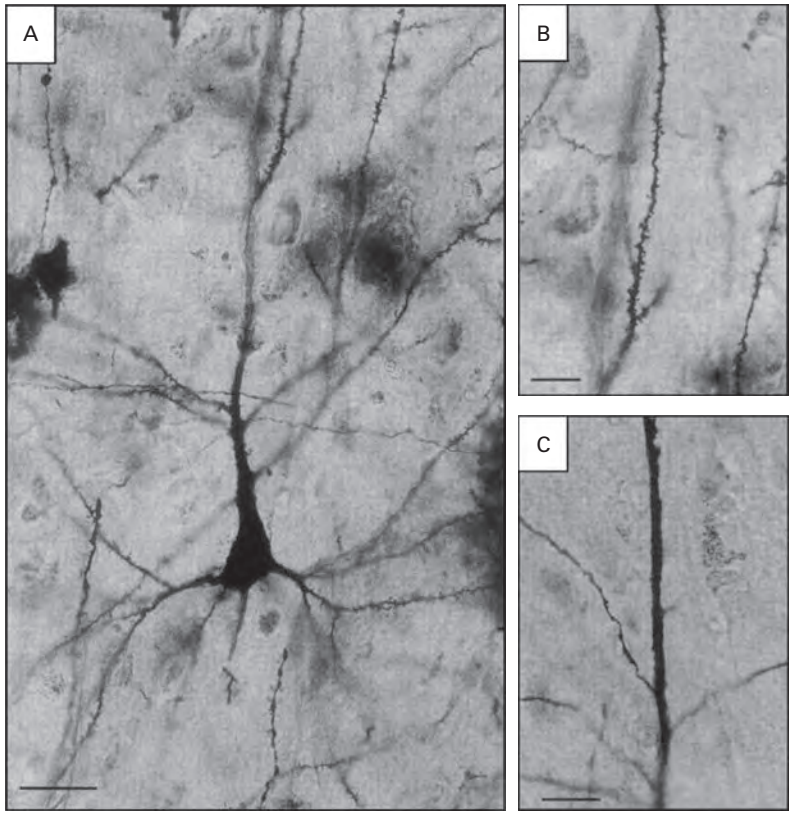

Figure 60–6 Photomicrographs of pyramidal neurons from the cerebral cortex from human brains stained by the Golgi method.

A. A layer III pyramidal neuron from a control brain, showing its morphology and its dendrites which are studded with spines.

B. A higher power view showing spines on a dendrite of a pyramidal neuron from a control brain.

C. A segment of a dendrite devoid of spines from the cerebral cortex of a person who had schizophrenia. (Scale: **A:** 30 µm; **B:** 20 µm; **C:** 15 µm.) Spine numbers are a rough proxy for the number of synaptic contacts onto the dendrite from other neurons; thus the paucity of spines in schizophrenia is consistent with fewer synaptic contacts than are found in the cerebral cortex of healthy brains.

(Reproduced, with permission, Garey et al. 1998. With permission from BMJ Publishing Group Ltd.)

1980s, it lacked a plausible molecular or cellular mechanism that might explain how synaptic pruning might go awry in schizophrenia. Recent genetic analysis may have provided a solution.

Unbiased, large-scale genetic studies have found that the strongest association with risk for schizophrenia lies within the major histocompatibility (MHC) locus on chromosome 6. The MHC locus encodes many proteins involved in immune function. Fine mapping of the locus pinpointed the largest genetic association signal to the genes encoding complement factor C4, a component of the classic complement cascade that, outside the brain, is involved in tagging microbes and damaged cells for engulfment and destruction by phagocytic cells. Subsequent analysis showed that the risk for schizophrenia is elevated as a function of increased expression in the brain of C4A (one of two isoforms). This finding adds support to the overpruning hypothesis because one function of the complement system in brain is to tag weak or inefficient synapses for removal by microglia (Figure 60–7).

Elevated expression of the complement factor C4A involved in synaptic pruning is certainly not the only mechanism leading to schizophrenia. As with any polygenic disorder, no one gene is necessary or sufficient for the disease phenotype. Thus, not everyone with schizophrenia has a high-risk C4A genotype, and not everyone with a high-risk C4A genotype develops schizophrenia. Many other genes are implicated in the risk for schizophrenia. Several such risk factors other than C4 are involved in regulation of the complement cascade, but the vast majority are not. Many of the genes associated with schizophrenia that have been identified to date are involved in various aspects of the structure and function of synapses; several encode ion channels. Thus, it seems likely that the genetic risk for schizophrenia involves, at least in part, synaptic function, synaptic plasticity, and synaptic pruning, and overpruning of synapses during adolescence is one plausible mechanism that should be explored further in studies of youth at high risk for schizophrenia. Nevertheless, other pathways, as yet less well characterized, may also turn out to be important. We have a long way to go in understanding the pathogenesis of schizophrenia.

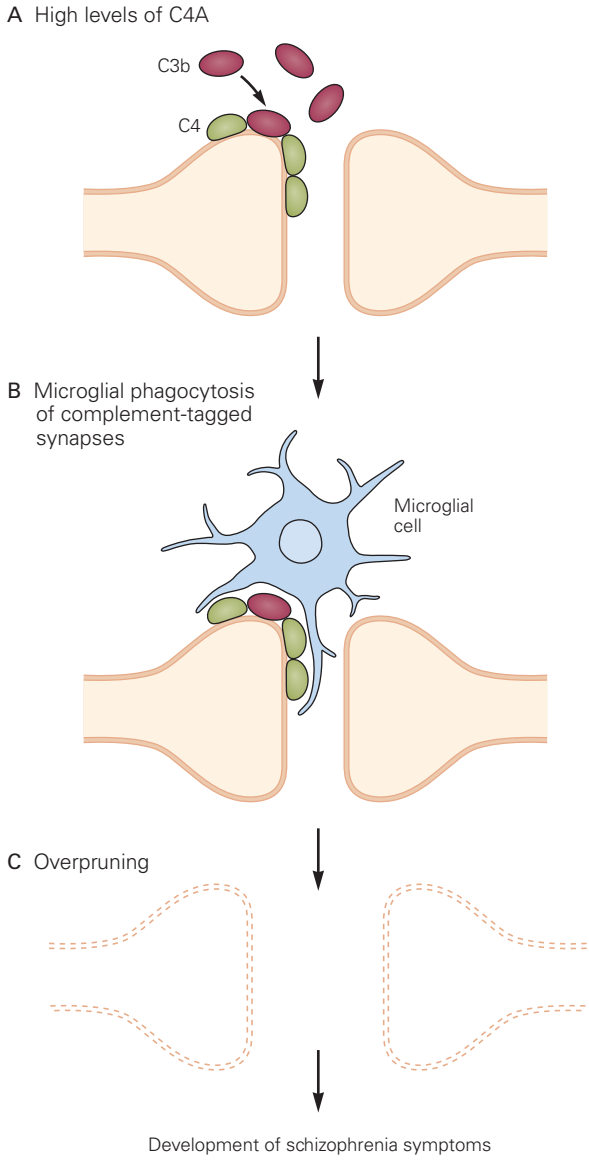

Figure 60–7 Complement factors and microglia have a role in synapse elimination. Maturation and plasticity of the nervous system involve both synaptogenesis and elimination of weak synapses. Complement factor 3b (**C3b**) is thought to serve as a "punishment signal" that identifies weak synapses for phagocytosis by microglia. Complement factor 4 (**C4**), a component of the complement cascade, is synthesized by neurons and astrocytes and recruits C3b to weak synapses. In humans, a complex genomic locus on chromosome 6 contains varying numbers of copies of the genes that encode the complement factor C4 proteins, C4A and C4B. Variants within this locus that give rise to high levels of C4A expression in brain increase schizophrenia risk. (Reproduced, with permission, from Christina Usher and Beth Stevens.)

Antipsychotic Drugs Act on Dopaminergic Systems in the Brain

All current antipsychotic drugs produce their therapeutic effects by blocking D_2 dopamine receptors in the forebrain. These drugs have many other effects at

various neurotransmitter receptors and intracellular signaling pathways, but these other actions primarily influence their side effects, not their main therapeutic mechanisms (Figure 60–8).

The first effective antipsychotic drug, chlorpromazine, was developed for its antihistaminic and sedating effects and was first investigated as a surgical preanesthetic by Henry Laborit in 1952. Based on its sedating effects, it was tested in psychotic patients soon thereafter. These tests showed, surprisingly, reduced hallucinations and delusions; indeed, the sedative effect of chlorpromazine is now considered a side effect. The success of chlorpromazine led to attempts to discover other antipsychotic drugs. Although many chemically diverse antipsychotic drugs are now in use, all share the same initial action of chlorpromazine in the brain, the ability to block the D_2 dopamine receptor. As a class, these drugs ameliorate psychotic symptoms not only in schizophrenia, but also in bipolar disorder, severe depression, and various neurodegenerative disorders. None of the antipsychotic drugs provide effective treatment for the cognitive impairments or deficit symptoms of schizophrenia.

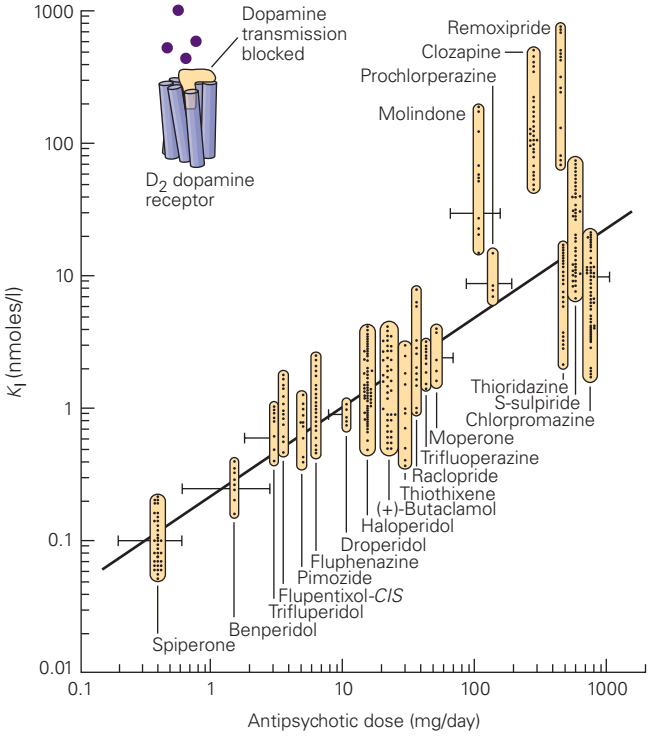

Figure 60–8 The potency of first-generation antipsychotic drugs in treating psychotic symptoms correlates strongly with their affinity for D_2 dopamine receptors. On the horizontal axis is the average daily dose required to achieve similar levels of clinical efficacy. On the vertical axis is K_i, the concentration of drug required to bind 50% of D_2 receptors in vitro. The higher the drug concentration required, the lower is the affinity of the drug for the receptor. One caveat is that the measurements on the two axes were not entirely independent of each other, as the ability of a drug to block D_2 receptors in vitro was often used to help determine doses used in clinical trials. Clozapine, which does not fall on the line, has significantly greater efficacy than the others. The mechanism of its greater efficacy is not understood. (Adapted, with permission, from Seeman et al. 1976.)

Among their side effects, chlorpromazine and related drugs caused Parkinson-like motor symptoms. Because Parkinson disease is caused by the loss of dopaminergic neurons in the midbrain, the occurrence of Parkinson-like side effects suggested to Arvid Carlsson that these drugs acted by decreasing dopaminergic transmission. Following up on this idea, Carlsson established that the antipsychotic drugs block dopamine receptors. Two families of dopamine receptors are known. The D_1 family, which in humans includes D_1 and D_5, are coupled to stimulatory G proteins that activate adenylyl cyclase. The D_2 family, which includes D_2, D_3, and D_4, are coupled to the inhibitory G protein (G_i) that inhibits the cyclase and activates a hyperpolarizing K^+ channel. A second signaling pathway for D_2 receptors is mediated by β-arrestin. The D_1 receptor is expressed in the striatum and is the major class of dopamine receptor in the cerebral cortex and hippocampus. The D_2 receptor is expressed most densely in the striatum, cerebral cortex, amygdala, and hippocampus. Correlations between receptor binding studies and clinical efficacy on psychotic symptoms indicated that the D_2 family is the molecular target for the therapeutic actions of antipsychotic drugs.

Clozapine, an antipsychotic drug discovered in 1959, had a low liability for causing Parkinson-like motor side effects. However, because it had some severe side effects, including a small chance of causing a potentially lethal loss of blood granulocytes, its use was discontinued until a clinical trial in the late 1980s clearly showed that it had greater efficacy than other antipsychotic drugs. Clozapine caused improvement in some individuals who had not responded to other antipsychotic drugs. It was reintroduced in conjunction with weekly monitoring of white cell counts; attempts to equal the efficacy of clozapine also motivated the development of second-generation antipsychotic drugs that mimicked some of its receptor binding properties, notably the ability to block serotonin 5-HT_{2A} receptors, an action that appears to diminish motor side effects. Large-scale clinical trials of the second-generation antipsychotic drugs have shown that their efficacy is no greater than the first-generation drugs, with none

having efficacy equal to clozapine. The liability of second-generation drugs for causing Parkinson-like motor side effects is lower than that of the first generation, but they typically cause more severe weight gain and other metabolic problems.

Because drugs that reduce psychotic symptoms do so by blocking D_2 receptors, investigators have asked: What is the role of dopamine in the symptoms of schizophrenia? Although some drugs that block D_2 receptors reduce psychotic symptoms, other drugs that increase dopamine at synapses, such as amphetamine and cocaine, can produce psychotic symptoms when taken chronically at high doses. Thus, Carlsson suggested that dopaminergic systems are hyperactive in schizophrenia. Evidence for this hypothesis has been difficult to obtain. The most direct evidence for this idea comes from studies begun in the mid-1990s that found that amphetamine-induced increases in dopamine release were greater in patients with schizophrenia than in healthy subjects. These studies suggest that abnormalities in amphetamine-sensitive processes—such as dopamine storage, vesicular transport, dopamine release, or dopamine reuptake by presynaptic neurons—may lead to hyperactivity in the subcortical dopaminergic systems and could contribute to the psychotic symptoms of schizophrenia, the symptoms that respond to antipsychotic drugs.

Although dopamine activity may increase in subcortical regions of the brain in schizophrenia, it may decrease in cortical regions; such a decrease might contribute to the cognitive impairments seen in schizophrenia. In particular, there may be fewer D_1 receptors in the prefrontal cortex in schizophrenia, which would be consistent with the observation that D_1 receptors in the prefrontal cortex normally play a role in working memory and in executive functions.

Highlights

1. Schizophrenia is a chronic, profoundly disabling disorder characterized by dramatic psychotic symptoms as well as deficits in emotion, motivation, and cognition.
2. Risk for schizophrenia is an inherited, polygenic trait.
3. Antipsychotic drugs are effective in reducing hallucinations, delusions, and thought disorder but do not benefit the cognitive and deficit symptoms of schizophrenia.
4. Cognitive impairments reduce the ability of people with schizophrenia to regulate their behavior in accordance with their goals. As a result, people with schizophrenia are frequently unable to succeed in school or to hold down jobs, even at times when antipsychotic drugs effectively control their hallucinations and delusions.
5. Postmortem and neuroimaging studies document loss of gray matter in the prefrontal and temporal cerebral cortex in a pattern that is consistent with cognitive impairments, such as deficits in working memory.
6. The gray matter loss results from decreased dendritic arborization and decreased dendritic spines, which implies that synaptic connections are also reduced. One hypothesis consistent with these anatomic findings and with the typical age of onset in adolescence is that schizophrenia is triggered by excessive and inappropriate synaptic pruning in the prefrontal and temporal cerebral cortices during adolescence and young adulthood.
7. Progress in the genetic analysis of schizophrenia combined with the use of new tools to study systems-level neuroscience promises to help attain the much needed advances in understanding disease mechanisms and in discovering new therapeutics.

Steven E. Hyman
Joshua Gordon

Selected Reading

Barch DM. 2005. The cognitive neuroscience of schizophrenia. Annu Rev Clin Psychol 1:321–353.

Nestler EJ, Hyman SE, Holtzman D, Malenka RJ. 2015. *Molecular Neuropharmacology: Foundation for Clinical Neuroscience*, 3rd ed. New York: McGraw-Hill.

Owen MJ, Sawa A, Mortensen PB. 2016. Schizophrenia. Lancet 388:86–97.

Stephan AH, Barres BA, Stevens B. 2012. The complement systems: an unexpected role in synaptic pruning during development and disease. Annu Rev Neurosci 35:369–389.

References

Addington J, Heinssen R. 2012. Prediction and prevention of psychosis in youth at clinical high risk. Annu Rev Clin Psychol 8:269–289.

Barch DM, Carter CS, Braver TS, et al. 2001. Selective deficits in prefrontal cortex function in medication-naïve patients with schizophrenia. Arch Gen Psychiatry 58:280–288.

Brans RG, van Haren NE, van Baal GC, et al. 2008. Heritability of changes in brain volume over time in twin

pairs discordant for schizophrenia. Arch Gen Psychiatry 65:1259–1268.

Cannon TD, Thompson PM, van Erp TG, Toga AW. 2002. Cortex mapping reveals regionally specific patterns of genetic and disease-specific gray-matter deficits in twins discordant for schizophrenia. Proc Natl Acad Sci U S A 99:3228–3233.

Feinberg I. 1983. Schizophrenia: caused by a fault in programmed synaptic elimination during adolescence? J Psychiatr Res 17:319–324.

Fisher M, Loewy R, Hardy K, Schlosser D, Vinogradov S. 2013. Cognitive interventions targeting brain plasticity in the prodromal and early phases of schizophrenia. Annu Rev Clin Psychol 9:435–463.

Fusar-Poli P, Borgwardt S, Bechdolf A, et al. 2013 The psychosis high-risk state: a comprehensive state-of-the-art review. JAMA Psychiatry 70:107–120.

Garey LJ, Ong WY, Patel TS, et al. 1998. Reduced dendritic spine density on cerebral cortical pyramidal neurons in schizophrenia. J Neurol Neurosurg Psychiatry 65: 446–453.

Glantz LA, Lewis DA. 2000. Decreased dendritic spine density on prefrontal cortical pyramidal neurons in schizophrenia. Arch Gen Psychiatry 57:65–73.

Gottesman II. 1991. *Schizophrenia Genesis: The Origins of Madness.* New York: Freeman.

Gur RE, Cowell PE, Latshaw A, et al. 2000. Reduced dorsal and orbital prefrontal gray matter volumes in schizophrenia. Arch Gen Psychiatry 57:761–768.

Kambeitz J, Abi-Dargham A, Kapur S, Howes OD. 2014. Alterations in cortical and extrastriatal subcortical dopamine function in schizophrenia: systematic review and meta-analysis of imaging studies. Br J Psychiatry 204: 420–429.

Kane J, Honigfeld G, Singer J, Meltzer H. 1988. Clozapine for the treatment-resistant schizophrenic. A double-blind comparison with chlorpromazine. Arch Gen Psychiatry 45:789–796.

Kety SS, Rosenthal D, Wender PH, Schulsinger F. 1968. The types and prevalence of mental illness in the biological and adoptive families of adopted schizophrenics. J Psych Res 6:345–362.

Lesh TA, Niendam TA, Minzenberg MJ, Carter CS. 2011. Cognitive control deficits in schizophrenia. Mechanisms and meaning. Neuropsychopharmcology 36:316–338.

Lieberman JA, Stroup TS, McEvoy JP, et al. 2005. Effectiveness of antipsychotic drugs in patients with chronic schizophrenia. N Engl J Med 353:1209–1223.

Lynall M-E, Bassett DS, Kerwin R, et al. 2010. Functional connectivity and brain networks in schizophrenia. J Neurosci 30:9477–9487.

McGrath J, Saha S, Welham J, El Saadi O, MacCauley C, Chant D. 2004. A systematic review of the incidence of schizophrenia: the distribution of rates and the influence of sex, urbanicity, migrant status, and methodology. BMC Med 2:13.

Mortensen PB, Pedersen CB, Westergaard T, et al. 1999. Effects of family history and place and season of birth on the risk of schizophrenia. N Engl J Med 340:603–608.

Rapoport JL, Giedd JN, Blumenthal J, et al. 1999. Progressive cortical change during adolescence in childhood-onset schizophrenia. A longitudinal magnetic resonance imaging study. Arch Gen Psychiatry 56:649–654.

Schizophrenia Working Group of the Psychiatric Genomics Consortium. 2014. Biological insights from 108 schizophrenia-associated genetic loci. Nature 511:421–427.

Seeman P, Lee T, Chau-Wong M, Wong K. 1976. Antipsychotic drug doses and neuroleptic/dopamine receptors Nature 261:717–9.

Sekar A, Bialas AR, de Rivera H, et al. 2016. Schizophrenia risk from complex variation of complement component 4. Nature 530:177–183.

Suddath RL, Christison GW, Torrey EF, Casanova MF, Weinberger DR. 1990. Anatomical abnormalities in the brains of monozygotic twins discordant for schizophrenia. N Engl J Med 322:789–794.

Thompson PM, Vidal C, Giedd JN, et al. 2001. Mapping adolescent brain change reveals dynamic wave of accelerated gray matter loss in very early-onset schizophrenia. Proc Natl Acad Sci USA 98:11650–11655.

Vidal CN, Rapoport JL, Hayashi KM, et al. 2006. Dynamically spreading frontal and cingulate deficits mapped in adolescents with schizophrenia. Arch Gen Psychiatry 63:25–34.

61

Disorders of Mood and Anxiety

Depression, bipolar disorder, and anxiety disorders have been well documented in medical writings since ancient times. In the fifth century BC, Hippocrates taught that moods depended on the balance of four humors—blood, phlegm, yellow bile, and black bile. An excess of black bile (*melancholia* is the ancient Greek term for black bile) was believed to cause a state dominated by fear and despondency. Robert Burton's *Anatomy of Melancholy* (1621) was not only an important medical text but also viewed literature and the arts through the lens of melancholia. Such texts describe symptoms that remain familiar today; they also recognized that symptoms of depression and of anxiety often occur together.

In this chapter, we discuss mood and anxiety disorders together, not only because they frequently cooccur but also because of overlapping genetic and environmental risk factors and some shared neural structures, including regions of the amygdala, hippocampus, prefrontal cortex, and insular cortex.

Mood Disorders Can Be Divided Into Two General Classes: Unipolar Depression and Bipolar Disorder

There are no objective medical tests for mood and anxiety disorders. Thus, diagnosis depends on observation of symptoms, behavior, cognition, functional

impairments, and natural history (including age of onset, course, and outcome). Patterns of familial transmission and response to treatment can also inform diagnostic classification. Based on such factors, it is possible to distinguish between two major groupings of mood disorders: unipolar depression and bipolar disorder. Unipolar depression, when severe and pervasive, is classified as major depression or major depressive disorder. Major depression is diagnosed when people suffer from depressive episodes alone. Bipolar disorder is diagnosed when episodes of mania also occur.

The lifetime risk of major depressive disorder in the United States is approximately 19%. Within any 1-year period, 8.3% of the population suffers major depression. The prevalence of depression differs in different countries and cultures; however, in the absence of objective medical tests, such epidemiologic data are subject to diagnostic and reporting biases, and thus, it is difficult to draw comparative conclusions. The World Health Organization reports that depression is a leading cause of disability worldwide, and other studies find it to be a leading cause of economic loss from noncommunicable disease. These dire social and economic consequences occur because depression is common, often begins early in life, and interferes with cognition, energy, and motivation, which are all necessary to learn in school and to work effectively.

Bipolar disorder is less common than unipolar depression, with a prevalence of approximately 1% worldwide. Its symptoms are relatively constant across countries and cultures. The incidence of bipolar disorder is equivalent in males and females.

Major Depressive Disorder Differs Significantly From Normal Sadness

Several factors distinguish major depression from transient periods of sadness that may occur in everyday life and from the grief that often follows a personal loss. These include the life context in which symptoms occur, their duration and pervasiveness, and their association with physiological, behavioral, and cognitive symptoms (Table 61–1). In healthy people, mood alternates between low and high, with timing and intensity phased appropriately with interpersonal interactions and life events. Mood states that are contextually inappropriate, extreme in amplitude, rigid, or prolonged are suggestive of either depression or mania, depending on their valence.

Depressive episodes, whether associated with unipolar or bipolar illness, are characterized by negative mood states such as sadness, anxiety, loss of interests, or irritability lasting for most of the day, day in and day out, and unrelieved by events that were previously enjoyable. This loss of interest is well expressed

Table 61–1 Symptoms of Mood Disorders

Five or more of the following symptoms have been present during the same 2-week period and represent a change from previous functioning. At least one of the symptoms is either (1) depressed mood or (2) loss of interest or pleasure.

1. Depressed mood most of the day, nearly every day, as indicated by either subjective report (eg, feels sad, empty, hopeless) or observations made by others (eg, appears tearful).
2. Markedly diminished interest or pleasure in all, or almost all, activities most of the day, nearly every day (as indicated by either subjective account or observation made by others).
3. Significant weight loss when not dieting, or weight gain (eg, a change of >5% of body weight in a month), or decrease or increase in appetite nearly every day.
4. Insomnia or hypersomnia nearly every day.
5. Psychomotor agitation or retardation nearly every day (observable by others, not merely subjective feelings of restlessness or being slowed down).
6. Fatigue or loss of energy nearly every day.
7. Feelings of worthlessness or excessive or inappropriate guilt (which may be delusional) nearly every day (not merely self-reproach or guilt about being sick).
8. Diminished ability to think or concentrate, or indecisiveness, nearly every day (either by subjective account or as observed by others).
9. Recurrent thoughts of death (not just fear of dying), recurrent suicidal ideation without a specific plan, or a suicide attempt or a specific plan for committing suicide.

Source: Adapted from the American Psychiatric Association. 2013. *Diagnostic and Statistical Manual of Mental Disorders*, 5th ed. Washington, DC: American Psychiatric Association.

by Hamlet's complaint, "How weary, stale, flat, and unprofitable seem to me all the uses of this world!" When depression is severe, individuals may suffer intense mental anguish and a pervasive inability to experience pleasure, a condition known as anhedonia.

Physiologic symptoms of depression include sleep disturbance, most often insomnia with early morning awakening, but occasionally excessive sleeping; loss of appetite and weight loss but occasionally excessive eating; decreased interest in sexual activity; and decreased energy. Some severely affected individuals exhibit slowed motor movements, described as psychomotor retardation, whereas others may be agitated, exhibiting such symptoms as pacing. Cognitive symptoms are evident in both the content of thoughts (hopelessness, thoughts of worthlessness and guilt, suicidal thoughts and urges) and in cognitive processes (difficulty concentrating, slow thinking, and poor memory).

In the most severe cases of depression, psychotic symptoms may occur, including delusions (unshakable false beliefs that cannot be explained by a person's culture) and hallucinations. When psychotic symptoms occur in depression, they typically reflect the person's thoughts of being undeserving, worthless, or bad. A severely depressed person might, for example, believe that he is emitting a potent odor because he is rotting from the inside.

The most severe outcome of depression is suicide, which represents a significant cause of death worldwide; the World Health Organization estimates that there are 800,000 deaths by suicide annually. More than 90% of suicides are associated with mental illness, with depression being the leading risk factor, especially when accompanied by substance use disorders.

Major Depressive Disorder Often Begins Early in Life

Major depressive disorder often begins early in life, but first episodes do occur across the life span. Those who have had a first episode in childhood or adolescence often have a family history of the disorder and have a high likelihood of recurrence. Once a second episode has occurred, a pattern of repeated relapse and remission often sets in. Some people do not recover completely from acute episodes and have chronic, albeit milder, depression, which can be punctuated by acute exacerbations. Chronic depression, even when symptoms are less severe than those of an acute episode, can prove extremely disabling because of long-term erosion of a person's ability to function in life roles. Major depressive disorder in childhood occurs equally in males and females. After puberty, however, it occurs more commonly in females; the ratio of females to males is approximately 2:1 across countries and cultures.

A Diagnosis of Bipolar Disorder Requires an Episode of Mania

Bipolar disorder is named for its chief symptom, swings of mood between mania and depression; indeed, the influential 19th-century psychiatrist Emil Kraepelin called this condition the manic-depressive insanity. By convention, a diagnosis of bipolar disorder requires at least one episode of mania. Mania is typically associated with recurrent episodes of depression, whereas mania without depression is distinctly uncommon.

Manic episodes are typically characterized by elevated mood, although some individuals are predominantly irritable. During manic episodes, individuals have markedly increased energy, a decreased need for sleep, and occasionally a decreased desire for food (Table 61–2). People with mania are typically impulsive and engage excessively in reward-directed

Table 61–2 Symptoms of a Manic Episode

A. A distinct period of abnormally and persistently elevated, expansive, or irritable mood, and abnormally and persistently increased goal-directed activity or energy, lasting at least 1 week (or any duration if hospitalization is necessary).

B. During the period of mood disturbance and increased energy or activity, three (or more) of the following symptoms (four if the mood is only irritable) have persisted and have been present to a significant degree:
   1. Inflated self-esteem or grandiosity.
   2. Decreased need for sleep (eg, feels rested after only 3 hours of sleep).
   3. More talkative than usual or pressure to keep talking.
   4. Flight of ideas or subjective experience that thoughts are racing.
   5. Distractibility (ie, attention too easily drawn to unimportant or irrelevant external stimuli).
   6. Increase in goal-directed activity (either socially, at work or school, or sexually) or psychomotor agitation (ie, purposeless non–goal-directed activity).
   7. Excessive involvement in pleasurable activities that have a high potential for painful consequences (eg, engaging in unrestrained buying sprees, sexual indiscretions, or foolish business investments).

Source: Adapted from the American Psychiatric Association. 2013. *Diagnostic and Statistical Manual of Mental Disorders*, 5th ed. Washington, DC: American Psychiatric Association.

behaviors, often with poor judgment characterized by extreme optimism. For example, a person may go on spending sprees well beyond his or her means or on uncharacteristic binges of drug and alcohol use or sexual behavior. Self-esteem is typically inflated, often to delusional levels. For example, an individual might falsely believe himself to have extensive influence on events or to be a significant religious figure. In antiquity, mania was described as "a state of raving madness with exalted mood." However, such elevated mood may be brittle, with sudden intrusions of anger, irritability, and aggression.

Mania, like depression, affects cognitive processes, often impairing attention and verbal memory. During a manic episode, a person's speech is often rapid, profuse, and difficult to interrupt. The person may jump quickly from idea to idea, making comprehension of speech difficult. Psychotic symptoms commonly occur during manic episodes and are generally consistent with the person's mood. For example, people with mania may have delusions of possessing special powers or of being objects of adulation.

The depressive episodes that occur in bipolar disorder are symptomatically indistinguishable from those in unipolar depression, but are often more difficult to treat. For example, they are often less responsive to antidepressant medications. Longitudinal studies have found that the most common affective state of bipolar patients between severe acute episodes of mania or depression is not healthy mood (euthymia), as was often taught in older textbooks, but a state of chronic depression.

Historically, the concept of bipolar disorder described patients who experienced full manic episodes, which often included psychotic symptoms and necessitated hospitalization (Table 61–2). In recent decades, diagnostic classifications have added type 2 bipolar disorder in which mild manias (also called hypomanias) alternate with depressive episodes. The manic episodes of type 2 bipolar disorder are, by definition, not accompanied by psychosis or severe enough to require hospitalization. Whether this represents a variant of classic (type 1) bipolar disorder or some other pathophysiology is not yet known, although genetic dissection of mood disorders may offer some clarification in the near future.

Bipolar disorder generally begins in young adulthood, but the onset may occur earlier or as late as the fifth decade of life. Many manic episodes often lack an obvious precipitant; however, sleep deprivation can initiate a manic episode in some individuals with bipolar disorder. For such individuals, travel across time zones or shift work represents a risk. The rate of cycling among mania, depression, and periods of normal mood varies widely among bipolar patients. Individuals with short, rapid cycles tend to be less responsive to mood-stabilizing drugs.

Anxiety Disorders Represent Significant Dysregulation of Fear Circuitry

Anxiety disorders are the most common psychiatric disorders worldwide. In the United States, 28.5% of the population suffers from one or more anxiety disorders over the course of their lifetimes. Some anxiety disorders are mild, such as the simple phobias that involve rarely encountered stimuli; others, such as panic disorder or posttraumatic stress disorder, are often highly debilitating based on the severity of symptoms, interference with functioning, and chronicity.

Anxiety and fear are related emotional states; both are critical to surviving dangers that might be encountered throughout life. The major distinction is that fear is a response to threats that are present and clearly signify danger, whereas anxiety is a state of readiness for threats that are less specific either in proximity or timing. The neural circuits of fear and anxiety strongly overlap, as do their physiological, behavioral, cognitive, and affective aspects.

Fear is normally a transient adaptive response to danger that, like pain, serves as a survival mechanism. Like pain, fear is alerting and aversive and motivates more or less immediate behavioral responses. Thus, fear interrupts ongoing behaviors, supplanting them with such responses as avoidance or defensive aggression. To prepare the body to cope physiologically, fear circuitry activates the sympathetic nervous system and causes release of stress hormones. This "fight or flight" response facilitates blood flow to skeletal muscle, increases metabolic activity, and elevates pain thresholds. Like reward and other survival-relevant emotional responses, fear strongly facilitates the encoding and consolidation of both implicit and explicit memories that prepare an organism to respond rapidly and effectively to future predictive cues. (Fear circuitry is described in Chapter 42.)

Many cognitive and physiological components of anxiety are similar to fear, but typically exhibit lower intensity and a more protracted time course. Anxiety is adaptive when proportionate to the probability and likely severity of a threat, leading to appropriate levels of arousal, vigilance, and physiological preparedness. Given the dangerous, indeed potentially lethal, consequences of ignoring even ambiguous threat cues, failure to mount appropriate anxiety responses can prove

highly maladaptive. However, excessive contextually inappropriate and prolonged vigilance, tension, and physiological activation can be the basis of distressing and disabling anxiety disorders or anxiety symptoms that may accompany depression. Risk factors for anxiety disorders include a person's genetic background, developmental experience, and lessons learned not only from direct experience but also taught by families, peers, schools, and other institutions.

Cues that elicit anxiety may be environmental or interoceptive (ie, arising from within the body, such as abdominal discomfort or heart palpitations). Social cues and social situations can be a major source of anxiety. In humans, anxiety states can also be initiated by trains of thought that elicit memories or imagination of danger. Anxiety can also arise from stimuli that are processed unconsciously because of their brevity or ambiguity, and the resulting emotion might then be experienced as arising spontaneously. In contrast to fear, which is initiated and terminated by the presence or termination of clear stimuli denoting threat, anxiety has a more variable time course. Anxiety states may be prolonged if the potential for danger or harm is long-lasting or if there is no clear safety signal.

Anxiety disorders and the anxiety that may accompany major depression are associated with diverse symptoms. Affected individuals may develop excessive preoccupation with possible threats and attentional biases toward cues interpreted as threatening. Such cognitive states are often associated with persistent worry, tension, and vigilance. Common physiological symptoms include hyperarousal, as evidenced by a low threshold for being startled, difficulty sleeping, and sympathetic nervous system activation, including a rapid, pounding heartbeat. Individuals with anxiety may become exquisitely aware of their heartbeat or breathing, which can become a source of preoccupation and worry in their own right. Sympathetic nervous system activation may reach extreme levels of intensity during a panic attack, one of the most severe manifestations of anxiety.

In anxiety disorders, cognitive, physiological, and behavioral responses that would be adaptive in the face of a serious threat may be maladaptively activated by innocuous stimuli, may be inappropriately intense for the situation, and may have a protracted time course in which safety signals fail to terminate the symptoms. Affected individuals may avoid places, people, or experiences that, although objectively safe, have become associated with perceptions of threats or the experience of anxiety. When severe, such avoidance can impair the ability of affected individuals to function in different capacities or roles.

Because there are no biomarkers or objective medical tests for particular constellations of anxiety symptoms, current psychiatric classifications such as the fifth edition of the *Diagnostic and Statistical Manual of Mental Disorders* (DSM-5) classify anxiety disorders based on clinical histories, such as the nature, intensity, and time course of symptoms, the role of external cues in triggering episodes, and associated symptoms. The DSM-5 divides pathological anxiety syndromes into several distinct disorders: panic disorder, posttraumatic stress disorder, generalized anxiety disorder, social anxiety disorder (previously called social phobia), and simple phobias. For heuristic purposes, these disorders are discussed below, but current evidence from long-term clinical observation and from family, twin, and epidemiological studies does not support dividing anxiety symptoms into discrete nonoverlapping categories. Rather, the evidence suggests that pathological anxiety symptoms and symptoms of depression might be better conceptualized as a continuum or spectrum in which individuals experience varying symptoms that cross current DSM boundaries.

Consistent with the concept of a symptom spectrum, anxiety disorders and depression do not often occur together across generations in families as distinct DSM-5 categories; instead, diverse patterns of anxiety and depressive symptoms are typically observed among affected family members. Twin studies that compare concordance for traits in monozygotic and dizygotic twin pairs find significant shared genetic risk across multiple anxiety disorders and major depression. In addition, epidemiological studies find that individuals diagnosed with one categorical DSM-5 anxiety disorder, during, for example, teen years, have a high probability of developing new anxiety or depressive symptoms over the next decade that could result in the person being diagnosed with multiple disorders based on DSM-5 classifications. The high frequency at which putatively distinct DSM-5 anxiety disorders and depression co-occur and the results of family and twin studies suggest significant sharing of etiologic factors and pathogenic mechanisms among anxiety disorders and major depression. Nevertheless, individual disorders that are listed in DSM-5 are briefly described below.

Panic attacks are a severe manifestation of anxiety. They are characterized by discrete periods (that can last for many minutes) of intense foreboding, a sense of doom, fear of losing control over oneself, or fear of death. They are associated with prominent bodily symptoms such as heart palpitations, inability to catch one's breath, sweating, paresthesias, and dizziness (Table 61–3).

Table 61–3 Symptoms of a Panic Attack

A discrete period of intense fear or discomfort in which four (or more) of the following symptoms develop abruptly and reach a peak within 10 minutes.

1. Palpitations, pounding heart, or accelerated heart rate
2. Sweating
3. Trembling or shaking
4. Sensations of shortness of breath or smothering
5. Feeling of choking
6. Chest pain or discomfort
7. Nausea or abdominal distress
8. Feeling dizzy, unsteady, lightheaded, or faint
9. Chills or heat sensations
10. Paresthesias (numbness or tingling sensations)
11. Derealization (feelings or unreality) or depersonalization (being detached from oneself)
12. Fear of losing control or "going crazy"
13. Fear of dying

Source: Adapted from the American Psychiatric Association. 2013. *Diagnostic and Statistical Manual of Mental Disorders*, 5th ed. Washington, DC: American Psychiatric Association.

Panic attacks often give rise to anxiety about future episodes such that the contexts in which attacks have occurred can become phobic stimuli that trigger subsequent attacks (fear conditioning). As a result, some severely affected individuals restrict their activities to avoid situations or places in which panic attacks have occurred or from which they fear they might not be able to escape should they experience an attack. The most severely affected may develop generalized phobic avoidance, leading them to become housebound, a state described as agoraphobia. Current diagnostic classification systems such as the DSM-5 define panic disorder based on the number and frequency of attacks and whether or not a phobic trigger can be identified. Such detailed criteria lack a strong empirical basis, but it is certainly the case that individuals who have recurrent panic attacks along with other anxiety symptoms are not only highly distressed but may also be significantly disabled.

Posttraumatic stress disorder (PTSD) follows an experience of severe danger or injury. Under different names and descriptions, including shell shock, a term coined during World War I, PTSD has long been recognized as a result of combat. More recently, civilian traumas such as assault, rape, or automobile crashes have been recognized as potential causes of PTSD. The current approach to PTSD was formalized by the American Psychiatric Association based on the experience of Vietnam War veterans.

PTSD is initiated by a traumatic experience. Its cardinal symptoms include intrusive reexperiencing of the traumatic episode, typically initiated by cues such as sounds, images, or other reminders of the trauma. For example, a person who has been assaulted might respond potently to an unexpected touch from behind. Such episodes are often characterized by activation of the sympathetic nervous system and, when severe, may be characterized by "fight or flight" responses. The reexperiencing of a traumatic event may also occur in the form of nightmares. Other symptoms of PTSD include emotional numbness that may interfere with relationships and social interactions, insomnia, chronic hyperarousal including excessive vigilance, sympathetic nervous system activation, and an exaggerated startle response to an innocuous stimulus such as a touch or sound.

Generalized anxiety disorder (GAD) is diagnosed when a person suffers chronic worry and vigilance not warranted by circumstances. The worry is accompanied by physiological symptoms such as heightened sympathetic nervous system activation and motor tension. GAD commonly co-occurs with major depressive disorder.

Social anxiety disorder is characterized by a persistent fear of social situations, especially situations in which one is exposed to the scrutiny of others. The affected person has an intense fear of acting in a way that will prove humiliating. Stage fright is a form of social anxiety that is limited to circumstances of performance, such as public speaking. Social anxiety disorder can lead to avoidance of verbal classroom participation or communicating with others at work and can therefore prove disabling as well as distressing.

Simple phobias consist of intense and inappropriately excessive fear of specific stimuli, such as elevators, flying, heights, or spiders.

Both Genetic and Environmental Risk Factors Contribute to Mood and Anxiety Disorders

Bipolar disorder, major depression, and anxiety disorders all run in families. Twin studies that compare the rate of concordance of monozygotic and dizygotic twin pairs demonstrate significant heritabilities among these disorders, where heritability represents the percentage of the variation in a phenotype explained by genetic variation. Among mood and anxiety disorders, bipolar disorder has the highest heritability (70%–80%); major depression and anxiety disorders exhibit lower but still significant heritabilities (approximately 35%), with greater roles for developmental

and environmental risk factors. Although there is an important role for genes in the pathogenesis of mood and anxiety disorders, all of them exhibit non-Mendelian patterns of transmission across generations, including frequent co-occurrence of major depression and anxiety disorders. Such patterns reflect the complexity of genetic and nongenetic risk factors.

Molecular genetic studies aimed at discovering the precise DNA sequence variants (alleles) that predispose to mood and anxiety disorders have been initiated. Such studies are challenging because the risk architecture of these, and indeed all, common psychiatric disorders is highly polygenic, meaning that population risk appears to involve many thousands of common and rare alleles linked to or contained within many hundreds of genes. Unlike some neurologic disorders such as Huntington disease, there is no "depression gene" or "anxiety gene." Disease-associated alleles confer small additive effects on the risk of an illness. The risk for any given individual results from genetic loading (comprised of diverse combinations of disease-associated alleles) acting in concert with developmental and environmental factors. This polygenic architecture explains non-Mendelian patterns of transmission and the diverse combinations of depressive and anxiety symptoms observed within families and across populations.

The lack of objective diagnostic tests for mood and anxiety disorders means that any study cohort is likely to have some proportion of diagnostic misclassification. As a result, the search for common disease-associated variants by genome-wide association studies (GWAS) and rare disease-associated variants by DNA sequencing requires significant statistical power conferred by very large cohorts and by meta-analyses conducted across multiple cohorts. Early results of GWAS have been reported for major depression and bipolar disorder; in both cases, several significant genome-wide loci have been found to date, but not yet enough to identify molecular pathways of pathogenesis with any certainty. Whole-exome sequencing (ie, DNA sequencing of all genomic regions that encode proteins) and whole-genome sequencing are being conducted for bipolar disorder.

The highly polygenic risk architecture of mood and anxiety disorders means that there is no diagnostic value in testing for one or a few risk gene variants that might be associated with these disorders. Rather, polygenic risk scores (PRS), based on the sum of all genetic risk variants for a trait, are emerging as useful tools to stratify individuals in epidemiological and clinical studies by severity of genetic risk. A discrepant PRS within a clinical cohort, eg, showing low depression risk in a study of people with major depression, would suggest misclassification. It is important to emphasize that the polygenic nature of risk for mood and anxiety disorders and the significant contribution of environmental risk factors mean that, like any genetic test, the PRS provides only a probability.

As more is learned, the PRS can be combined with other measures to yield a more predictive risk score, just as modern cardiac risk models increasingly include genetic measures, smoking history, lipid levels, and blood pressure. For mood and anxiety disorders, one type of measure that shows early promise is identification of intrinsic patterns of neural connectivity derived from resting-state functional magnetic resonance imaging (fMRI; imaging conducted when subjects are not engaged in task performance). Differing patterns of connectivity could potentially distinguish among different forms of disorder.

Epidemiological evidence has identified significant developmental risk factors for major depression and anxiety disorders. The best documented is a history of physical or sexual abuse early in life, serious child neglect, or other early, severe stressors. Investigations of such early stressors have focused on possible roles for altered reactivity of the hypothalamic-pituitary-adrenal (HPA) axis. Studies of early stress in animal models suggest that epigenetic regulation of gene expression may have a role in altering developmental trajectories. Such results cannot be readily followed up in humans because of lack of access to human brain tissue and thus remain hypothetical.

Other risk factors for depression and anxiety disorders include alcohol and other substance use disorders and the presence of other psychiatric disorders, such as attention deficit hyperactivity disorder, learning disorders, and obsessive-compulsive disorder. There is also evidence that alcoholism and other substance abuse disorders may be initiated by misguided attempts at self-medication of depression or anxiety, in turn worsening the underlying condition.

Environmental factors that may trigger new episodes of depression or anxiety include life transitions such as marriage, a new job, or retirement. Serious illness, whether acute or chronic, is also associated with the onset of major depression and anxiety. Some neurological disorders are associated with an elevated risk of depression, including Parkinson disease, Alzheimer disease, multiple sclerosis, and stroke. Some prescribed medications, such as interferons, also frequently trigger depression. When major depression accompanies a chronic illness such as type 2 diabetes or cardiovascular disease, the overall medical outcomes are worse, as a result of both the physiological

effects of depression, such as increased release of stress hormones (see below) and decreased motivation to engage in rehabilitative regimens.

Depression and Stress Share Overlapping Neural Mechanisms

Depression and responses to stress exhibit complex but significant interactions. As already noted, severe childhood adversity is a developmental risk factor for depression; moreover, depressive episodes may be initiated by a stressful experience. Conversely, the experience of depression is itself stressful because of the suffering it causes and its negative effects on functioning. Symptomatically, depression shares several physiological features with chronic stress, including changes in appetite, sleep, and energy. Both major depression and chronic stress are associated with persistent activation of the HPA axis (Figure 61–1).

Many but not all individuals with major depression and many in the depressed phase of bipolar disorder exhibit excess synthesis and secretion of the glucocorticoid stress hormone cortisol and the factors that regulate it, corticotropin-releasing hormone (CRH) and adrenocorticotropic hormone (ACTH). In a healthy state, a *transient* increase in cortisol secretion, as occurs in response to acute stress, shifts the body to a catabolic state (making glucose available to confront the stressor or threat), increases subjective energy levels, sharpens cognition, and may increase confidence. However, a *chronic* increase in glucocorticoids may contribute to depression-like symptoms. For example, many people with Cushing disease (in which pituitary tumors secrete excess ACTH, leading to excess cortisol) experience symptoms of depression.

Feedback mechanisms within the HPA axis normally permit cortisol (or exogenously administered glucocorticoids) to inhibit CRH and ACTH secretion and therefore to suppress additional cortisol synthesis and secretion. In approximately half of people with major depression, this feedback system is impaired; their HPA axis becomes resistant to suppression even by potent synthetic glucocorticoids such as dexamethasone. Although readily measurable disturbances of the HPA axis have not proven sensitive or specific enough to be used as a diagnostic test for depression, the observed abnormalities suggest strongly that a pathologically activated stress response is often an important component of depression.

The relationship of stress with depression has led to the development of several chronic stress paradigms in rodent models of depression. The reliance on

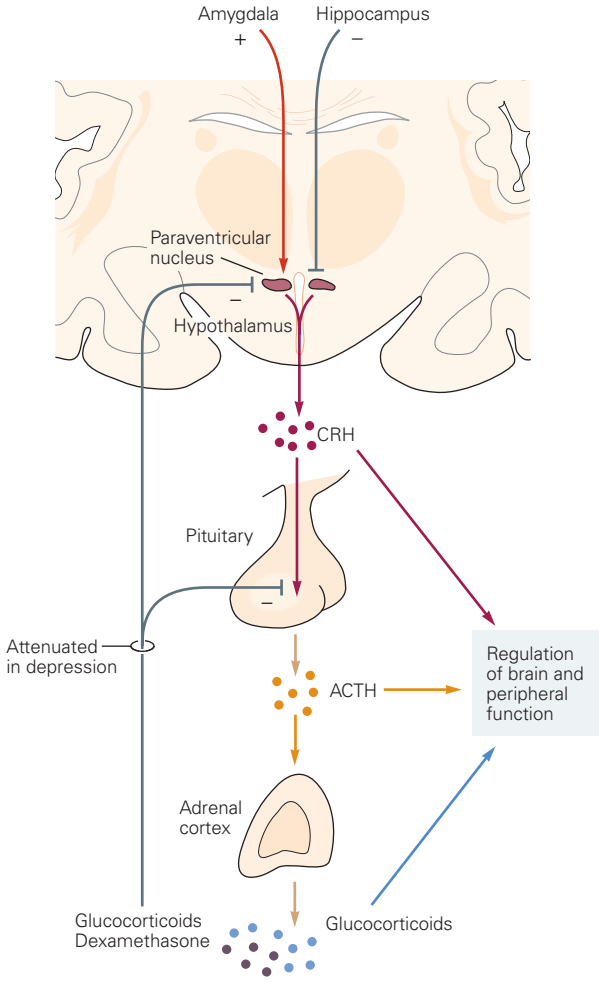

Figure 61–1 The hypothalamic-pituitary-adrenal axis. Neurons in the paraventricular nucleus of the hypothalamus synthesize and release corticotropin-releasing hormone (**CRH**), the key regulatory peptide in the hormonal cascade activated by stress. The CRH neurons have a circadian pattern of secretion, and the stimulatory effects of stress on CRH synthesis and secretion are superimposed on this basal circadian pattern. Excitatory fibers from the amygdala convey information about stressful stimuli that activates CRH neurons; inhibitory fibers descend from the hippocampus onto the paraventricular nucleus. CRH enters the hypophyseal portal system and stimulates the corticotropic cells in the anterior pituitary that synthesize and release adrenocorticotropic hormone (**ACTH**). The released ACTH enters the systemic circulation and stimulates the adrenal cortex to release glucocorticoids. In humans, the major glucocorticoid is cortisol; in rodents, it is corticosterone. Both cortisol and synthetic glucocorticoids such as dexamethasone act at the level of the pituitary and hypothalamus to inhibit further release of ACTH and CRH, respectively. The feedback inhibition by glucocorticoids is attenuated in major depression and the depressed phase of bipolar disorder. (Adapted, with permission, from Nestler et al. 2015.)

stress-induced syndromes in these animal models has been strengthened by the observation that many antidepressant drugs reverse stress-induced changes in physiology or behavior in these animals. However, the degree to which animals subjected to diverse chronic stressors actually model the disease mechanisms underlying depression in human beings remains unknown. Concern about overreliance on stress-based and other rodent models is indicated by the failure to identify new antidepressant mechanisms despite more than 50 years of trying. Drug screens using such models have only identified molecules with actions similar to prototype antidepressant drugs that were first identified by their unexpected psychotropic effects on humans.

Dysfunctions of Human Brain Structures and Circuits Involved in Mood and Anxiety Disorders Can Be Identified by Neuroimaging

Investigation of human brain regions and the neural circuitry involved in mood and anxiety disorders has relied on noninvasive structural and functional neuroimaging, neurophysiologic testing, and postmortem analyses. More recently, information is being gleaned from neuroimaging of patients being treated with deep brain stimulation.

Identification of Abnormally Functioning Neural Circuits Helps Explain Symptoms and May Suggest Treatments

Functional neuroimaging and electrophysiological studies are being pursued in order to elucidate abnormalities in circuit activity and in patterns of intrinsic connectivity in mood and anxiety disorders. Given the heterogeneity of major depression, bipolar disorder, and anxiety disorders defined by current diagnostic methods, it has been challenging to identify robust and replicable abnormalities. In addition, the use of diverse cognitive and emotional tasks to experimentally probe mood and anxiety disorders has limited researchers' ability to replicate and confirm findings. Overcoming the resulting uncertainties will require larger numbers of subjects, application of data standards that permit meta-analyses, and increasingly, methods such as use of the PRSs to stratify subjects.

Despite current limitations, fMRI and electrophysiological studies of mood and anxiety disorders have begun to provide initial empirical leads about circuit abnormalities in mood and anxiety disorders. Resting-state fMRI studies comparing subjects with major depression and healthy control subjects suggest differences in patterns of intrinsic connectivity, specifically within neural circuits that regulate "top down" control of cognition and emotion—the "cognitive control network"—and in circuits that process significant emotional and motivational stimuli—"the salience network" (Figure 61–2). Despite the need for replication, these findings are noteworthy because they are consistent with results from task-based imaging studies of humans (eg, studies of fear conditioning) and animal studies that investigate responses to aversive stimuli.

In healthy human subjects, regions of the amygdala are activated by threatening stimuli and during fear conditioning, such as pairing a previously neutral tone with a mild shock. Beginning with the work of Charles Darwin, human faces expressing fear have been recognized to elicit anxiety responses across diverse human cultures, presumably as a mechanism to communicate the presence of danger among members of a group.

The effects of fearful and other emotion-expressing faces on measurements of autonomic activity and brain activity measured by fMRI or by electroencephalography have been studied in subjects with anxiety disorders or with major depression. In one such paradigm, fearful faces are shown very briefly (33 ms) while the subject is in an MRI scanner. This presentation is followed by a neutral face (referred to as backward masking). Under such circumstances, subjects report that they have no awareness of having seen the fearful face. Yet they exhibit an altered galvanic skin response, a measure of sympathetic activation, as well as activation of the basal amygdala, the amygdala region that processes sensory inputs and that responds selectively to threat. Several functional neuroimaging studies of individuals with PTSD, other anxiety disorders, and major depression have demonstrated heightened activity in the amygdala, activation even to innocuous stimuli, and persistence of amygdala activity in contrast to normal patterns of adaptation (Figure 61–3).

Functional neuroimaging studies of anxiety disorders and major depression have also found decreased activity in prefrontal cortical regions that are interconnected with the basal amygdala. Studies of animals with prefrontal cortical lesions demonstrate that projections from the prefrontal cortex to the basal amygdala are necessary for cognitive control over aversive information. In individuals suffering from anxiety disorders or major depression, reduced activation of the prefrontal cortex by aversive stimuli is consistent with cognitive testing that demonstrates decreased cognitive control and might contribute to excessive and persistent anxiety and other negative emotions.

Electrophysiological and functional neuroimaging studies of both major depression and bipolar disorder

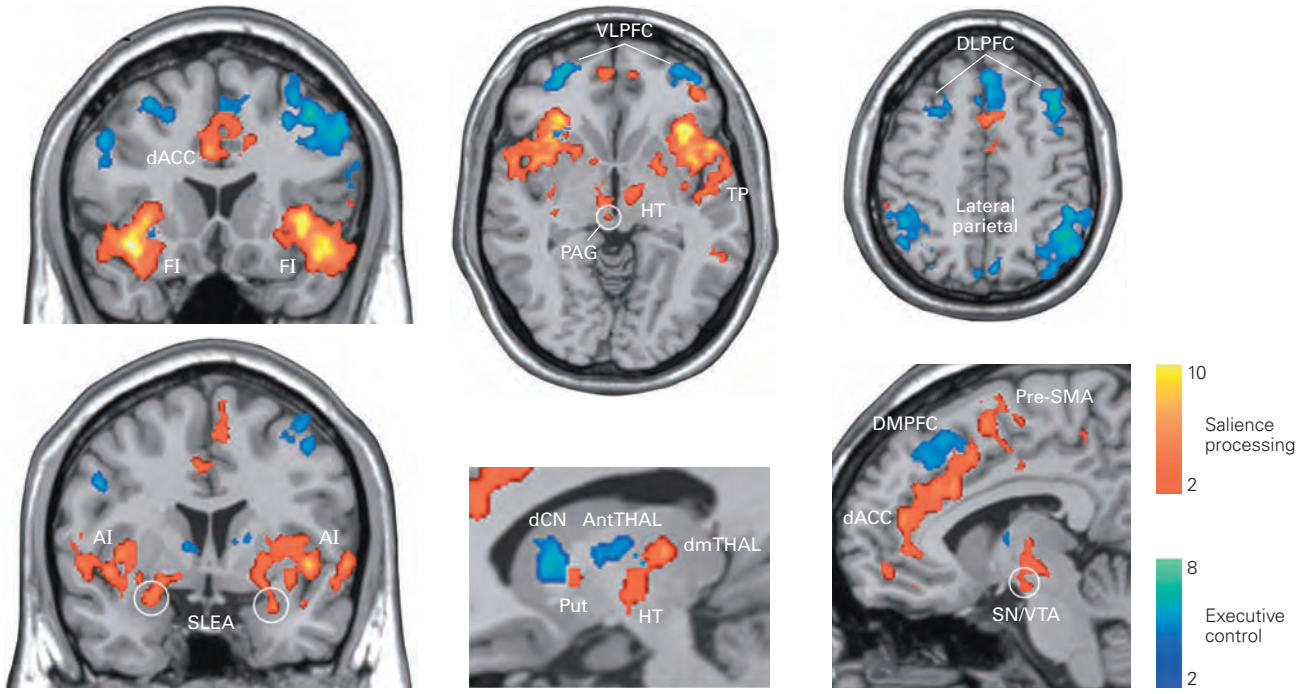

Figure 61–2 **Mood disorders involve independent neural networks associated with processing of emotional salience and cognitive control.** Statistical analysis (independent component analysis) applied to resting-state functional magnetic resonance imaging data identifies separable networks that compute emotional salience (**red-orange**) and regulate cognitive control/executive function (**blue**). The emotional salience network links dorsal anterior cingulate cortex (**dACC**) and frontoinsular cortex (**FI**) with subcortical structures involved in emotion. The cognitive control network links the dorsolateral prefrontal (**DLPFC**) and parietal cortices and several subcortical structures. The brain regions shown to be networked in this study have been implicated in major depression by multiple independent studies. (Abbreviations: **AI**, anterior insula; **antTHAL**, anterior thalamus; **dCN**, dorsal caudate nucleus; **DMPFC**, dorsomedial prefrontal cortex; **dmTHAL**, dorsomedial thalamus; **HT**, hypothalamus; **PAG**, periaqueductal gray matter; **Pre-SMA**, pre–supplementary motor area; **Put**, putamen; **SLEA**, sublenticular extended amygdala; **SN/VTA**, substantia nigra and ventral tegmental area of the midbrain; **TP**, temporal pole; **VLPFC**, ventrolateral prefrontal cortex.) (Reproduced, with permission, from Seeley et al. 2007. Copyright © 2007 Society for Neuroscience.)

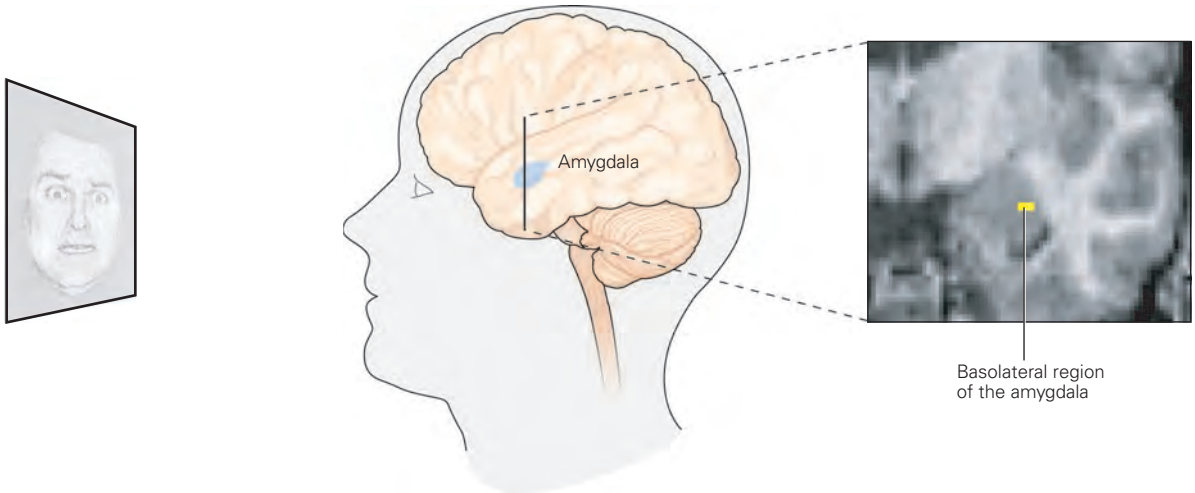

Figure 61–3 **Amygdala activation in response to a masked presentation of a fearful stimulus.** A human subject observes projected images while being scanned by magnetic resonance imaging. When a fearful face is presented for a very brief time followed by presentation of a neutral face, a protocol called backward masking, the subject is not consciously aware of the fearful face. Under these conditions, the basolateral region of the amygdala is more strongly activated in individuals with anxiety disorder than in normal individuals. (Reproduced, with permission, from Etkin et al. 2004.)

have shown abnormal functioning of the rostral and ventral subdivisions of the anterior cingulate cortex (ACC), a region of prefrontal cortex that participates in the emotional salience network. The rostral and ventral ACC have extensive connections with the hippocampus, amygdala, orbital prefrontal cortex, anterior insula, and nucleus accumbens and are involved in the integration of emotion, cognition, and autonomic nervous system function. The caudal subdivision of the ACC is involved in cognitive processes involved in control of behavior; it has connections with dorsal regions of the prefrontal cortex, secondary motor cortex, and posterior cingulate cortex.

Although abnormal function in both subdivisions of the ACC has been observed in depressive episodes, the most consistent abnormality observed in major depression and in the depressed phase of bipolar disorder is increased activity in the rostral and ventral subdivisions, especially in the subgenual region ventral to the genu (or "knee") of the corpus callosum. In a study using positron emission tomography, effective treatment of major depression with selective serotonin reuptake inhibitor antidepressants was correlated with decreased activity in the rostral ACC, whereas self-induced sadness in healthy subjects increased activity (Figure 61–4). Based on such studies, the rostral anterior (subgenual) cingulate cortex has been used as a target for electrode placement in deep brain stimulation for treatment-resistant major depression, which is operationally defined as depressive illness that has been unresponsive to antidepressant medication and psychotherapy.

Functional abnormalities of brain reward circuitry may also play a role in the symptoms of mood disorders. The reward circuitry comprises the dopaminergic projections from the ventral tegmental area of the midbrain to forebrain targets, including the nucleus accumbens, habenula, prefrontal cortex, hippocampus, and amygdala (Chapter 43). Under normal conditions, these pathways are involved in the valuation of rewards (eg, palatable food, sexual activity, and social interactions) and in motivating the necessary behavior to obtain them. Reward processing appears to be abnormal in depression, based on such symptoms as decreased interest in previously pleasurable activities, decreased motivation, and, when depression is severe, the inability to experience pleasure (anhedonia). Although less well studied, reward processing is also likely abnormal in mania, which is characterized by excessive engagement in goal-directed behaviors, even when they are maladaptive, such as uncontrolled spending, dangerous drug use, and promiscuous sexual activity.

In a recent analysis of resting-state fMRI, data showed that patients with major depression could be stratified based on connectivity patterns that correlated with their degree of anhedonia and anxiety. However, although modulation of the reward circuitry has been considered as a possible treatment for major depression, it has proven difficult in practice. For example, drugs known to activate this circuitry by

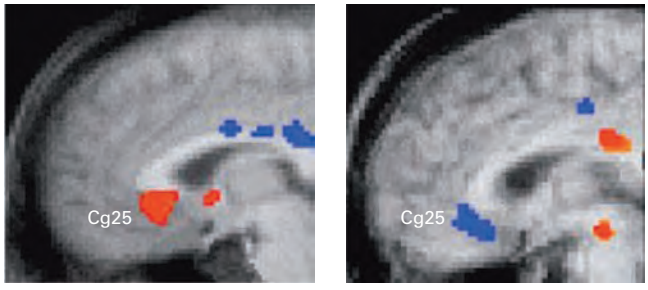

Induced sadness in healthy subjects Depression recovery with SSRI

Figure 61–4 Activity in the rostral anterior (subgenual) cingulate cortex is increased by sadness and decreased by successful treatment of major depression with an antidepressant. (Reproduced, with permission, from Mayberg et al. 1997.)

Left. Healthy volunteers provided a script of their saddest memory that was later used to generate transient sadness while undergoing positron emission tomography (PET). The rostral anterior cingulate cortex was activated (**red** pseudo-color in the sagittal section of the human brain) was activated when the sad story was read. **Cg25** is an alternative nomenclature for the cingulate gyrus, Brodmann area 25. The PET ligand was oxygen-15–labeled water, used to measure cerebral blood flow as a proxy for brain activity.

Right. Elevated metabolism in the rostral anterior cingulate cortex was confirmed in subjects with major depression. Following successful treatment with a selective serotonin reuptake inhibitor (**SSRI**) antidepressant, brain activity in Cg25 decreased (**blue** pseudo-color in the sagittal section of the human brain). The PET ligand was 2-deoxyglucose, used to measure cerebral metabolism as a proxy for brain activity.

increasing synaptic dopamine, such as amphetamine and cocaine, pose a high risk of overuse and addiction. More recently, tests of drugs that release reward circuits from inhibitory control, such as kappa opiate receptor antagonists, have been initiated in patients with major depression.

A Decrease in Hippocampal Volume Is Associated With Mood Disorders

The best-established structural abnormality in mood disorders is decreased hippocampal volume in individuals with major depression compared with healthy subjects. Recent studies of patients with major depression and bipolar disorder have found hippocampal volume loss in unmedicated subjects in regions of the cerebral cortex associated with the control of emotion. Such studies, which still need replication, show both overlapping and nonoverlapping patterns of volume loss in patients with major depression compared with bipolar disorder. Volume reductions observed in patients with major depression correlate with the duration of depressive episodes when controlling for duration of medication use. These findings suggest that in major depression the volume losses result from persistent illness and do not represent an antecedent risk factor. Some researchers have hypothesized that elevated cortisol levels in patients with major depression might be associated with reduced hippocampal volumes.

Reduced hippocampal volume has also been reported in cases of PTSD. In contrast with major depression, studies of monozygotic twins discordant for PTSD suggest that small hippocampi precede onset of the disorder and may thus represent a risk factor instead of a result of the disorder.

The acquired loss of hippocampal volume in major depression could result from loss of dendrites and dendritic spines, from decreased cell numbers (neurons or glia), or both. Given the relationship of stress and depression, excessive cortisol secretion could play a causal role in either type of loss. A decrease in hippocampal cell number could be explained by the fact that stress and elevated glucocorticoid levels suppress adult hippocampal neurogenesis, as shown in studies of several animal species.

In several mammals, including humans, new granule cells within the dentate gyrus of the hippocampus are produced during adult life. Studies of rodents have shown that these new neurons can be incorporated into functional neural circuits where they initially exhibit heightened structural and synaptic plasticity. A role for cell death as a balance to adult neurogenesis is less well studied.

In rodents, stressful or aversive treatments or administration of glucocorticoids inhibits the proliferation of granule cell precursors and thus suppresses normal rates of neurogenesis in the hippocampus. Antidepressants, including the selective serotonin reuptake inhibitors, exert an opposite effect, increasing the rate of neurogenesis. Thus, excess secretion of glucocorticoid stress hormones, as occurs in depression, could cause hippocampal volume loss by inhibiting neurogenesis over time. Because glucocorticoid receptors in the hippocampus are required for inhibitory feedback to hypothalamic neurons that synthesize and release CRH, impairments of hippocampal function could further impair feedback regulation of the HPA axis, creating a vicious cycle.

The hippocampus permits the brain to resolve differences among closely related stimuli (pattern separation) and provides contextual information that facilitates interpretation of the survival significance of a stimulus. Such information is needed by the organism to accurately identify threats that are signaled within a stream of complex sensory inputs. In animal studies, hippocampal lesions increase anxiety responses; it is thought that the resulting impairment of pattern separation and processing of contextual information permits threat-related memories to generalize inappropriately and thus to become associated with innocuous stimuli. Physiological and behavioral evidence suggests that newborn neurons within the dentate gyrus of the hippocampus play a particularly important role in pattern separation. Thus, inhibition of neurogenesis might contribute to anxiety symptoms that often accompany major depression, and abnormally low hippocampal volumes might increase the risk of PTSD.

Major Depression and Anxiety Disorders Can Be Treated Effectively

Major depressive disorder can be treated effectively with antidepressant drugs, cognitive psychotherapy, and electroconvulsive therapy. Major depressive disorder refractory to other interventions is being treated experimentally with deep brain stimulation targeted to the subgenual prefrontal cortex and other targets, including the nucleus accumbens.

Current Antidepressant Drugs Affect Monoaminergic Neural Systems

Named for their first clinical indication, the antidepressant drugs have broader utility than suggested by their name. Indeed, antidepressants are also the first-line

drugs for the treatment of anxiety disorders. Along with frequent co-occurrence and sharing of risk factors and some neural circuits, the overlap in effective treatment modalities is further evidence that mood and anxiety disorders are related.

All widely used antidepressant drugs increase activity in monoaminergic systems in the brain, most significantly serotonin and norepinephrine, although some antidepressants exert modest effects on dopamine as well. The relevant monoamine neurotransmitters—serotonin, norepinephrine, and dopamine—are synthesized by cells that reside within brain stem nuclei (Chapter 40). Serotonergic and noradrenergic neurons in the pons and medulla project widely to highly diverse terminal fields in brain regions that include the hypothalamus, hippocampus, amygdala, basal ganglia, and cerebral cortex (Figures 61–5 and 61–6). Dopaminergic neurons in the ventral tegmental area and substantia nigra pars compacta of the midbrain project to somewhat less widespread areas. Ventral tegmental neurons project to the hippocampus, amygdala, nucleus accumbens, and prefrontal cortex; substantia nigra neurons innervate the caudate and putamen. The widely divergent projections of these monoaminergic neurons permit them to influence functions such as arousal, attention, vigilance, motivation, and other cognitive and emotional states that require integration of multiple brain regions.

Serotonin, norepinephrine, and dopamine are synthesized from amino acid precursors and packaged into synaptic vesicles for release. Monoamines in the cytoplasm that are outside of vesicles are metabolized by the enzyme monoamine oxidase (MAO), which is associated with the outer leaflet of mitochondrial

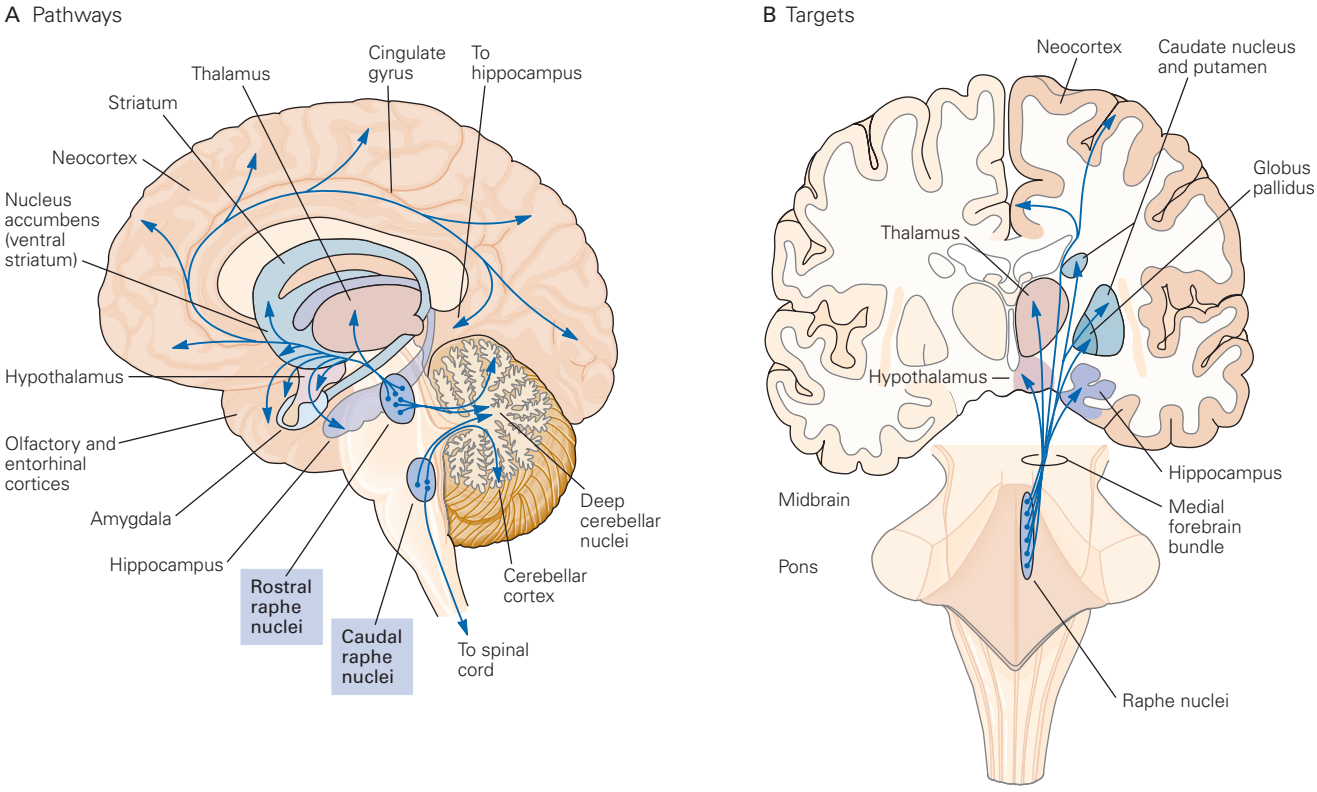

Figure 61–5 The major serotonergic systems in the brain arise in the raphe nuclei of the brain stem. Serotonin is synthesized in a group of brain stem nuclei called the raphe nuclei. These neurons project throughout the neuraxis, ranging from the forebrain to the spinal cord. The serotonergic projections are the most massive and diffuse of the monoaminergic systems, with single serotonergic neurons innervating hundreds of target neurons. (Adapted, with permission, from Heimer 1995.)

A. A sagittal view of the brain illustrates the raphe nuclei. In the brain, these nuclei form a fairly continuous collection of cell groups close to the midline of the brain stem and extending along its length. In the drawing here, they are shown in more distinct rostral and caudal groups. The rostral raphe nuclei project to a large number of forebrain structures.

B. This coronal view of the brain illustrates some of the major structures innervated by serotonergic raphe nuclei neurons.

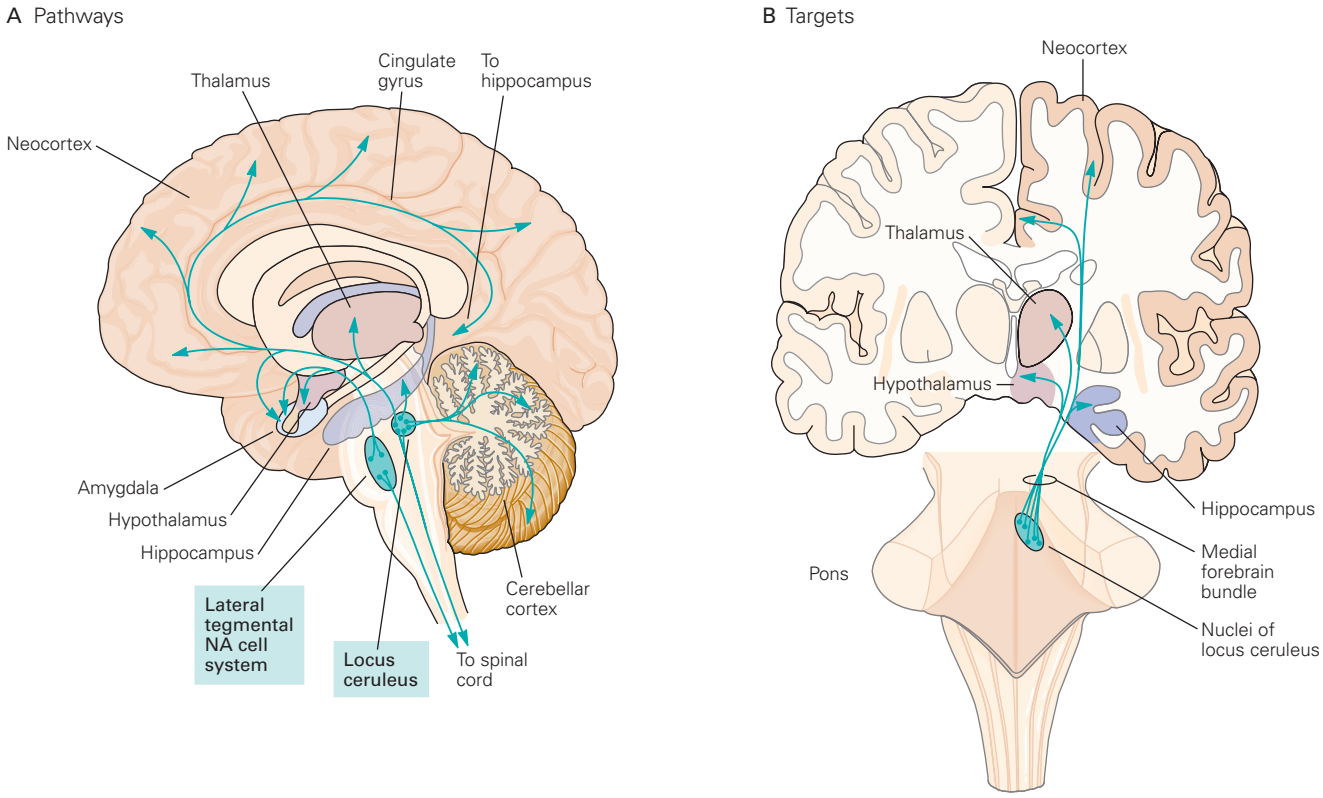

Figure 61–6 The major noradrenergic projection of the forebrain arises in the locus ceruleus. (Adapted, with permission, from Heimer 1995.)

A. Norepinephrine is synthesized in several brain stem nuclei, the largest of which is the nucleus locus ceruleus, a pigmented nucleus located just beneath the floor of the fourth ventricle in the rostrolateral pons. A lateral midsagittal view demonstrates the course of the major noradrenergic (NA) pathways from the locus ceruleus and lateral brain stem tegmentum. Axons from the locus ceruleus project rostrally into the forebrain and also into the cerebellum and spinal cord; axons from noradrenergic nuclei in the lateral brain stem tegmentum project to the spinal cord, hypothalamus, amygdala, and ventral forebrain.

B. A coronal section shows the major targets of neurons from the locus ceruleus.

membranes. After vesicular release, monoamine neurotransmitters bind synaptic receptors to exert their biological effect or are cleared from the synapse by specific transporter proteins located on the presynaptic cell membrane.

The most widely used antidepressant drugs fall into several major groupings, which affect monoaminergic neurons and their targets (Figure 61–7). The *MAO inhibitors* discovered in the 1950s, such as phenelzine and tranylcypromine, are effective against both depression and anxiety disorders but are rarely used today because of their side effects. MAO inhibitors block the capacity of MAO to break down norepinephrine, serotonin, or dopamine in presynaptic terminals, thus making extra neurotransmitter available for packaging into vesicles and for release.

Two forms of MAO, types A and B, are found in the brain. Type A is also found in the gut and liver, where it catabolizes bioactive amines that are present in foods. Inhibition of MAO-A permits bioactive amines such as tyramine to enter the bloodstream from foods that contain it in high concentrations, such as aged meats and cheeses. Transporters shuttle these amines into the terminals of sympathetic neurons, where they can displace endogenous vesicular norepinephrine and epinephrine into the cytoplasm, leading to nonvesicular release that causes significant elevations of blood pressure.

The *tricyclic antidepressants*, also first identified in the mid-1950s, include imipramine, amitriptyline, and desipramine; these block the norepinephrine transporter (NET), the serotonin reuptake transporter (SERT), or both. These drugs are effective in treating both depression and anxiety disorders. However, in addition to their therapeutic targets, the older tricyclic drugs also block many neurotransmitter receptors,

including the muscarinic acetylcholine, histamine H_1, and α_1 noradrenergic receptors, producing a panoply of side effects.

The *selective serotonin reuptake inhibitors* (SSRIs) such as fluoxetine, sertraline, and paroxetine, first approved in the 1980s, have no greater efficacy than the older tricyclic antidepressants and MAO inhibitors but are widely used because they have milder side effects and are far safer if taken in overdose. As their name implies, they selectively inhibit SERT. They are effective for major depressive disorder and many anxiety disorders. In high doses, selective serotonin reuptake inhibitors are also effective for symptoms of obsessive-compulsive disorder. Selective norepinephrine and serotonin-norepinephrine reuptake inhibitors have also been developed; these drugs have side effect profiles similar to those of selective serotonin reuptake inhibitors but are useful for some patients who do not benefit from inhibition of SERT alone.

Despite knowledge of the initial molecular targets that mediate the effects of antidepressant drugs, MAO or monoamine transporters, the ultimate molecular mechanisms by which they relieve depression remain unknown. One major challenge to understanding the therapeutic action of these drugs is the delay in their therapeutic effects. Although antidepressant drugs bind to and inhibit MAO, NET, or SERT with their first dose, several weeks of treatment are typically required to observe a lifting of depressive symptoms.

Several hypotheses have been put forward to explain this delay. One is that a slow buildup of newly synthesized proteins alters the responsiveness of neurons in a manner that treats the depression. Another is that increases in the levels of synaptic transmission of serotonin or norepinephrine rapidly increase plasticity in different emotion-processing circuits and that the latency to therapeutic benefit reflects the time it takes for new experiences to alter synaptic weights. A third hypothesis is that antidepressant efficacy is mediated in part by enhancement of hippocampal neurogenesis. Narrowing down the possible therapeutic mechanisms is challenging because of the lack of good animal models of depression. Without an animal model, it is not possible to know which of the many observable molecular, cellular, and synaptic changes cause depression or underlie the therapeutic actions of effective antidepressants.

Ketamine Shows Promise as a Rapidly Acting Drug to Treat Major Depressive Disorder

Ketamine, which blocks the *N*-methyl-D-aspartate (NMDA) glutamate receptor, is currently used in pediatric anesthesia for its ability to produce dissociative experiences as well as analgesia. It has been studied in randomized clinical trials with subjects suffering from major depression. In the trials, ketamine was administered by intravenous infusion; it produced an antidepressant effect within 2 hours, a significant advantage over existing antidepressant drugs that typically take weeks to show benefit. The therapeutic effects of ketamine last for approximately 7 days, after which second and third doses may continue to be effective. If such results become widely replicated, ketamine would represent the first antidepressant drug that does not exert its primary action on monoamine neurotransmission. Studies to identify mechanisms by which ketamine relieves depression, like those for older antidepressants, are challenging in part because of the lack of good animal models of depression.

At higher doses, ketamine is misused as a recreational drug to produce euphoria, dissociation, depersonalization, and hallucinations. Ketamine has also been used in laboratory settings to induce cognitive symptoms reminiscent of schizophrenia in human subjects. Although the advantages of a rapidly acting antidepressant would be significant, for example in treating acutely suicidal individuals, the unwanted psychotropic effects of ketamine make its use problematic. Attempts to develop alternative NMDA receptor blockers in which the antidepressant effects might be separated from psychotropic side effects are under way.

Psychotherapy Is Effective in the Treatment of Major Depressive Disorder and Anxiety Disorders

Short-term symptom-focused psychotherapies have been developed for depression and anxiety and tested in clinical trials. The best-studied psychotherapies are the cognitive behavioral therapies. Cognitive therapies that might be used to treat major depression focus on identifying and correcting excessively negative interpretations of events and of interactions with other people. For example, many depressed people exhibit a strong attentional bias toward negative information, automatically interpret neutral events as negative, and read evidence of disapproval into the behavior of others. Such automatic negative thinking, which can initiate or perpetuate depressed mood, can be much improved through cognitive psychotherapies.

Therapies with a more behavioral component have proven useful in the treatment of anxiety disorders such as phobias or PTSD. In exposure therapy, the affected individual is directed to vividly recollect phobic stimuli that trigger anxiety or avoidance. The therapist provides a safe context for such experiences

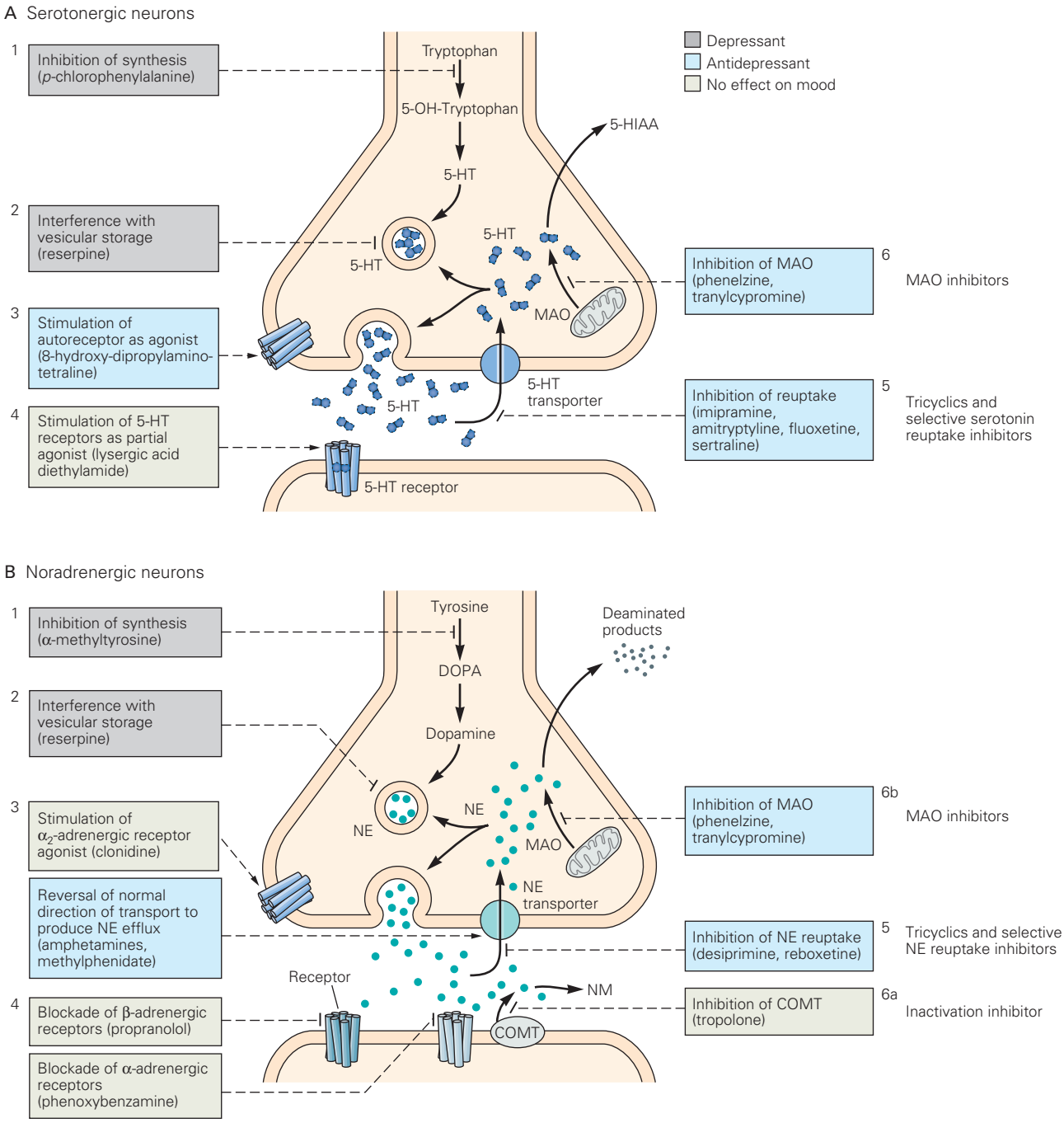
A Serotonergic neurons
Depressant
Antidepressant
No effect on mood
1
Inhibition of synthesis (p-chlorophenylalanine)
2
Interference with vesicular storage (reserpine)
3
Stimulation of autoreceptor as agonist (8-hydroxy-dipropylamino-tetraline)
4
Stimulation of 5-HT receptors as partial agonist (lysergic acid diethylamide)
Tryptophan
5-OH-Tryptophan
5-HT
5-HIAA
5-HT
5-HT
MAO
5-HT transporter
5-HT
5-HT receptor
Inhibition of MAO (phenelzine, tranylcypromine)
6
MAO inhibitors
Inhibition of reuptake (imipramine, amitryptyline, fluoxetine, sertraline)
5
Tricyclics and selective serotonin reuptake inhibitors
B Noradrenergic neurons
1
Inhibition of synthesis (α-methyltyrosine)
2
Interference with vesicular storage (reserpine)
3
Stimulation of α2-adrenergic receptor agonist (clonidine)
Reversal of normal direction of transport to produce NE efflux (amphetamines, methylphenidate)
4
Blockade of β-adrenergic receptors (propranolol)
Blockade of α-adrenergic receptors (phenoxybenzamine)
Tyrosine
Deaminated products
DOPA
Dopamine
NE
NE
MAO
NE transporter
Receptor
NM
COMT
Inhibition of MAO (phenelzine, tranylcypromine)
6b
MAO inhibitors
Inhibition of NE reuptake (desiprimine, reboxetine)
5
Tricyclics and selective NE reuptake inhibitors
Inhibition of COMT (tropolone)
6a
Inactivation inhibitor

Figure 61–7 (Opposite) Actions of antidepressant drugs at serotonergic and noradrenergic synapses. The figure shows the pre- and postsynaptic sides of serotonergic and noradrenergic synapses. Serotonin and norepinephrine are synthesized from amino acid precursors by enzymatic cascades. The neurotransmitters are packaged in synaptic vesicles; free neurotransmitter within the cytoplasm is metabolized by monoamine oxidase (**MAO**), an enzyme associated with the abundant mitochondria found in presynaptic terminals. Upon release, serotonin and norepinephrine interact with several types of pre- and postsynaptic receptors. Each neurotransmitter is cleared from the synapse by a specific transporter. The serotonin and norepinephrine transporters and MAO are targets of antidepressant drugs.

A. Important sites of drug action at serotonergic synapses. Not all actions described are shown in the figure.

1. *Enzymatic synthesis*. Inhibition of synthesis of the rate-limiting enzyme tryptophan hydroxylase by *p*-chlorophenylalanine initiates the cascade that converts tryptophan to 5-OH-tryptophan, the precursor of 5-hydroxytryptophan (**5-HT**, serotonin).

2. *Storage*. Reserpine and tetrabenazine interfere with the transport of serotonin and catecholamines into synaptic vesicles by blocking the vesicular monoamine transporter $VMAT_2$. As a result, cytoplasmic serotonin is degraded (see step 6 below), and thus, the neuron is depleted of neurotransmitter. Reserpine was used as an antihypertensive drug but commonly caused depression as a side effect.

3. *Presynaptic receptors*. Agonists at presynaptic receptors produce negative feedback on neurotransmitter synthesis or release. The agonist 8-hydroxy-diprolamino-tetraline (8-OH-DPAT) acts on $5\text{-}HT_{1A}$ receptors on the presynaptic neuron. The antimigraine triptan drugs (eg, sumatriptan) are agonists at $5\text{-}HT_{1D}$ receptors.

4. *Postsynaptic receptors*. The hallucinogen lysergic acid diethylamide (LSD) is a partial agonist at $5\text{-}HT_{2A}$ receptors on postsynaptic serotoninergic neurons. Second-generation antipsychotic drugs, such as risperidone and olanzapine, are antagonists at $5\text{-}HT_{2A}$ receptors in addition to their ability to block D_2 dopamine receptors. The antiemetic compound ondansetron is an antagonist at $5\text{-}HT_3$ receptors, the only ligand-gated channel among the monoamine receptors. Its key site of action is in the medulla.

5. *Uptake*. The selective serotonin reuptake inhibitors, such as fluoxetine and sertraline, are selective blockers of the serotonin transporter. The tricyclic drugs have mixed actions; some, such as clomipramine, are relatively selective for the serotonin transporter. Uptake blockers increase synaptic concentrations of serotonin. Amphetamines enter monoaminergic neurons via the uptake transporter and bind to the vesicular transporter found on the membranes of synaptic vesicles, causing reverse transport of the monoamine neurotransmitter into the cytoplasm. The neurotransmitter is then reverse-transported out of the neuron into the synapse via the uptake transporter.

6. *Degradation*. Phenelzine and tranylcypromine, both of which are effective for depression and panic disorder, block MAO-A and MAO-B. Moclobemide, effective against depression, is selective for MAO-A; selegiline, which has been used to treat Parkinson disease, is selective for MAO-B in low doses. (Abbreviation: **5-HIAA**, 5-hydroxyindoleacetic acid.)

B. Important sites of drug action at noradrenergic synapses.

1. *Enzymatic synthesis*. The competitive inhibitor α-methyltyrosine blocks the reaction catalyzed by tyrosine hydroxylase that converts tyrosine to DOPA. A dithiocarbamate derivative, FLA-63 (not shown), blocks the reaction that converts DOPA to dopamine.

2. *Storage*. Reserpine and tetrabenazine interfere with the transport of norepinephrine (**NE**), dopamine, and serotonin into synaptic vesicles by blocking the vesicular monoamine transporter $VMAT_2$. As a result, the cytoplasmic neurotransmitter is degraded (see below), and thus the neuron is depleted of neurotransmitter.

3. *Presynaptic receptors*. Agonists at presynaptic receptors produce negative feedback on neurotransmitter synthesis or release. Clonidine is an agonist at α_2-adrenergic receptors, inhibiting NE release. It has anxiolytic and sedative effects and is also used to treat attention deficit hyperactivity disorder. Yohimbine is an antagonist at α_2-adrenergic receptors; it induces anxiety.

4. *Postsynaptic receptors*. Propranolol is an antagonist at β-adrenergic receptors that blocks many effects of the sympathetic nervous system. It is used to treat some forms of cardiovascular disease but is commonly used to block anxiety during performance situations. Phenoxybenzamine is an agonist at α-adrenergic receptors.

5. *Uptake*. Certain tricyclic antidepressants, such as desipramine, and newer NE selective reuptake inhibitors, such as reboxetine, selectively block the NE transporter, thus increasing synaptic NE. Amphetamines enter monoaminergic neurons via the uptake transporter and interact with the vesicular transporter (the transporter on synaptic vesicles) to release neurotransmitter into the cytoplasm. The neurotransmitter is then pumped out of the neuron into the synapse via the uptake transporter acting in reverse.

6. *Degradation*. At the postsynaptic neuron, tropolone inhibits the enzyme catechol *O*-methyltransferase (**COMT**), which inactivates NE (**step 6a**). Normetanephrine (**NM**) is formed by the action of COMT on NE. At the presynaptic neuron, degradation by MAO is blocked by the MAO inhibitors phenelzine and tranylcypromine.

and also suggests new interpretations of such stimuli that help the patient cope with the experience. Where possible and when tolerable to patients, gradual transition to real-world exposures to phobic stimuli can be employed.

Exposure therapy produces extinction learning in analogy with studies of animal behavior. The memory of the phobic stimulus is not erased, but the fearful response is suppressed by new information that the stimulus and the context in which it is experienced are not dangerous. Animal physiology and lesioning studies and human imaging studies demonstrate that the prefrontal cortex is required for extinction learning and that the hippocampus is required for learning new contexts for familiar events or stimuli (eg, that a helicopter flying overhead does not portend an attack).

Electroconvulsive Therapy Is Highly Effective Against Depression

Although it still conjures up negative images in the popular imagination, electroconvulsive therapy (ECT) administered with modern anesthesia is medically safe and a tolerable patient experience, and it remains a highly effective intervention for the acute treatment of serious major depressive disorder. It is most often used when depressive symptoms are severe and medications and psychotherapies have proven ineffective. It is also effective in both the depressed and manic phases of bipolar disorder. It is not effective for anxiety disorders in the absence of a mood disorder and is not used to treat them clinically.

Generally, six to eight treatments are given, most commonly on an outpatient basis. Patients are anesthetized, and electrical stimulation is administered just above the threshold to produce electroencephalographic evidence of a generalized seizure. The major side effect is a variable degree of anterograde and retrograde amnesia. Amnesia can be minimized, but not eliminated, by placing the electrodes unilaterally and using the lowest level of electrical stimulation needed. Rodents given ECT exhibit massive release of neurotransmitters, which causes significant activation of gene expression, presumably leading to large-scale neural plasticity. However, the precise molecules, cells, and circuits involved in the therapeutic response remain unknown.

Newer Forms of Neuromodulation Are Being Developed to Treat Depression

Other forms of therapeutic electrical stimulation of the brain are being explored, motivated by the desire to improve upon the therapeutic effects of ECT while diminishing its side effects. These approaches are often described as "neuromodulation."

Transcranial magnetic stimulation (TMS) employs a device on the scalp to deliver brief pulses of rapidly alternating magnetic stimulation. This induces currents to flow within axons in regions of cerebral cortex beneath the device. Daily administration of TMS over the left prefrontal cortex is safe and was effective enough to have received regulatory approval by the US Food and Drug Administration. Nonetheless, in subsequent trials, its efficacy appears to be only modest. Additional clinical experiments are under way aimed at improving efficacy.

Alternative therapies under development include magnetic seizure therapy, an alternative to ECT in which a magnetic field is the used to produce a seizure. The hope for this experimental therapy is to reproduce the efficacy of ECT with less anterograde and retrograde amnesia.

Deep brain stimulation (DBS), mentioned above, is an invasive neuromodulatory treatment in wide use for treatment of the motor symptoms of Parkinson disease and of essential tremor. For treatment of Parkinson disease, an electrode is typically placed within the subthalamic nucleus, a component of basal ganglia circuitry involved in motor control that is well understood compared with circuits that regulate mood. A DBS electrode is connected by a wire that exits the skull and travels under the scalp and skin of the neck to a controller and battery pack that resides in the chest, much like a cardiac pacemaker battery. The rate at which the electrode stimulates its target can be controlled externally and is typically adjusted by the treatment team to optimize the therapeutic response. During the past decade, clinical trials of DBS have been extended from Parkinson disease and other movement disorders to psychiatric disorders. In addition to its use in treatment-refractory depression, DBS is being studied for the treatment of obsessive-compulsive disorder.

Several locations in the brain have been targets for DBS to treat depression. As described in Figure 61–4, the rostral anterior (subgenual) cingulate cortex is activated by sadness. Accordingly, it has been used as a DBS target for treatment-resistant depression (Figure 61–8). In some clinical series, 60% of treatment-resistant patients achieved stable improvement with stimulation of the subgenual cingulate cortex. However, similar levels of efficacy using this target could not be replicated in a large multisite clinical trial. Differences in patient selection, interindividual differences in brain anatomy, or small differences in electrode placement may account for the disparate results seen to date. To

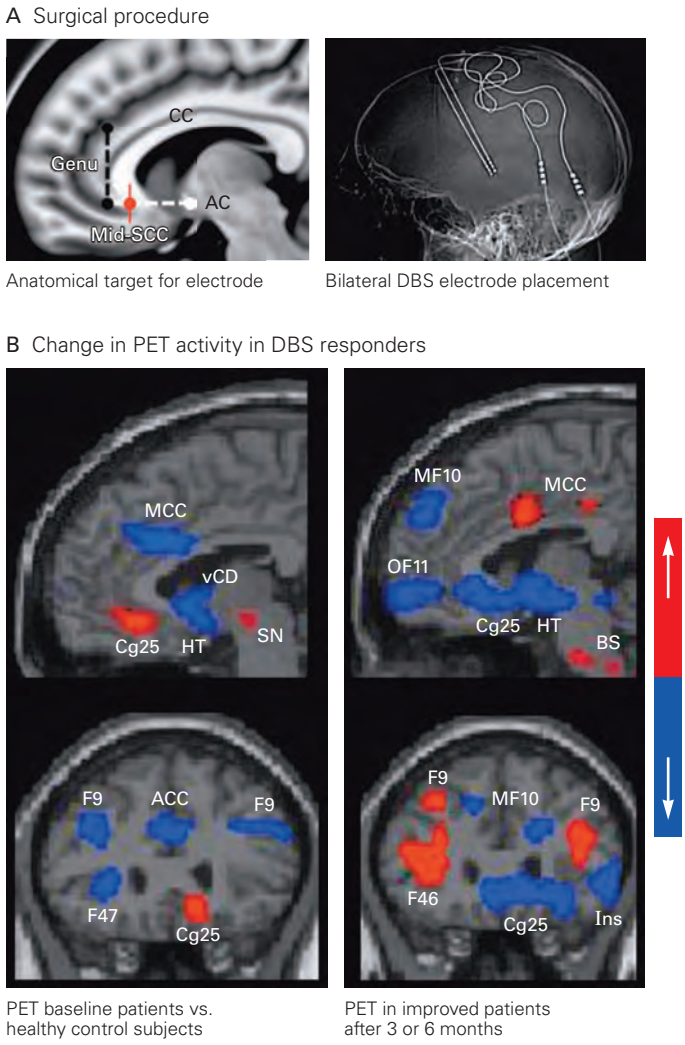

Figure 61–8 Electrode placement for deep brain stimulation (DBS) in the rostral anterior cingulate cortex and measurement of response by [18F] fluoro-2-deoxyglucose positron emission tomography (PET). (Reproduced, with permission, from Helen Mayberg.)

A. *Left:* The rostral anterior (subgenual) cingulate cortex, Brodmann area 25 (**Cg25**), is an anatomic target for DBS for patients with treatment-resistant depression. (Sagittal section; electrode site in **red**; corpus callosum is just superior and shown in **white**; **dotted line**, position of the electrode relative to the AC-genu line.) (Abbreviations: **AC**, anterior commissure; **Mid-SCC**, mid-subcallosal cingulate.) *Right:* A PET scan shows placement of the electrodes in the brain of a patient undergoing stimulation of the rostral anterior cingulate cortex. (Sagittal section.)

B. PET scans show the changes in activity in patients with treatment-resistant depression who have improved with stimulation of the rostral anterior cingulate cortex. The **top** panels are sagittal sections; the **bottom** panels are coronal sections. *Left:* Pretreatment metabolic activity in patients with treatment-resistant depression. **Red** pseudo-color denotes elevated metabolic activity compared with healthy control subjects (note elevated activity in Cg25 before DBS); **blue** denotes lower metabolic activity. *Right:* Averages of patients who have improved at 3 or 6 months after initiation of DBS. Activity in Cg25 is decreased (**blue**) in patients who have had a positive response to stimulation. (Abbreviations: **ACC**, anterior cingulate cortex; **BS**, brain stem; **F9**, dorsolateral prefrontal cortex; **F46**, prefrontal cortex; **F47**, ventrolateral prefrontal cortex; **HT**, hypothalamus; **Ins**, insula; **mF10**, medial frontal cortex; **MCC**, middle cingulate cortex; **OF11**, orbital frontal cortex; **SN**, substantia nigra; **vCD**, ventral caudate.)

put it simply, depression is highly heterogeneous, and it should not be surprising that a single DBS target is not useful for all treatment-resistant patients.

Lacking good animal models of mood disorders, human DBS treatment trials may provide a particularly important source of information about the brain circuitry responsible for the symptoms of mental disorders. Although careful attention must be paid to obtaining informed consent and to safety, especially when the judgment of patients is influenced by severe depression, DBS may provide an opportunity to learn about mood regulation. In particular, newly developed electrodes not only stimulate a DBS target but can also record extracellular neuronal activity. Such "read–write" electrodes, currently being used in research settings only, may not only improve clinical results but also advance our knowledge of circuit dysfunction and therapeutic modulation in psychiatric disorders.

Bipolar Disorder Can Be Treated With Lithium and Several Anticonvulsant Drugs

In 1949, John Cade discovered the calming effects of lithium in guinea pigs and, soon thereafter, in a small clinical trial in bipolar patients. Cade's observations initiated the modern era of psychopharmacology in which drugs, ultimately subjected to randomized, blinded clinical trials, were used to treat specific symptoms of mental disorders. Lithium eventually proved to be effective in treating acute episodes of mania and in stabilizing mood by reducing the frequency of cycling into mania and depression.

Several drugs initially developed to treat epilepsy, such as valproic acid and lamotrigine, have also been shown to be effective in treating acute mania and for mood stabilization and can serve as substitutes for lithium. In addition, antipsychotic drugs effectively

ameliorate symptoms of acute mania and, at low doses, can also help stabilize mood. None of these drugs exerts therapeutic effects rapidly; improvements in mental state and behavior may take several weeks.

The mechanisms by which lithium and anticonvulsant drugs exert beneficial effects on mania and on mood cycling are not known. Unlike the antidepressant and antipsychotic drugs, however, there remain open questions about the initial molecular target of lithium in the nervous system relevant to the initiation of its therapeutic effects. This lack of certainty reflects the many actions of lithium at therapeutic concentrations in the brain. The most likely molecular target is inhibition of glycogen synthase kinase type 3β (GSK3β), a component of the Wnt signaling pathway that has many functions in the nervous system. As in the case of other drugs to treat psychiatric disorders, investigation of the therapeutic mechanism of lithium and of the mood-stabilizing properties of anticonvulsants is impeded by the lack of an animal model of bipolar disorder.

Whatever the molecular mechanisms of lithium or the anticonvulsants, mood stabilizers appear to dampen the dynamics of mood regulatory systems. Mood is regulated by the external environment as well as several internal inputs, including the internal hormonal milieu, immune modulators, and circadian controls (eg, both the serotonergic and noradrenergic systems show diurnal variations closely coupled with the sleep–wake cycle). The integration of these systems is complex, involving dynamic interactions that are still poorly understood.

Second-Generation Antipsychotic Drugs Are Useful Treatments for Bipolar Disorder

All antipsychotic drugs act by blocking D_2 dopamine receptors, but these drugs have long been recognized to have therapeutic effects not only in the treatment of the psychotic symptoms of schizophrenia, severe mood disorders, and many other conditions, but also in the treatment of acute manic episodes. The side effects of first-generation antipsychotic drugs are severe, most prominently Parkinson-like motor side effects that result from D_2 dopamine receptor antagonism.

Most second-generation drugs have somewhat lower affinity for D_2 dopamine receptors than first-generation drugs and, in addition, have other receptor effects, such as blocking serotonin 5-HT_{2A} receptors, resulting in a lower liability for severe motor side effects. These drugs are by no means free of serious side effects; most cause weight gain and associated metabolic conditions. However, their relative tolerability and their effects on serotonin receptors have made them an important treatment for the depressed phase of bipolar disorder as well as the treatment of acute mania. They have gained an important role in therapeutics because bipolar depression is less likely to respond to antidepressant drugs than unipolar depression.

Highlights

1. Mood disorders are divided into unipolar and bipolar disorder based on whether depression occurs alone (unipolar) or whether a person also suffers from episodes of mania. Unipolar and bipolar disorders have different familial patterns of transmission.
2. Clinically significant unipolar depression, often denoted as major depressive disorder (major depression), differs from normal sadness by its persistence, pervasiveness, and association with physiological, cognitive, and behavioral symptoms.
3. Major depression is common (15%–20% lifetime prevalence) and disabling, making it a leading cause of disability worldwide. Bipolar disorder is less common (1% lifetime prevalence worldwide) but tends to produce severe symptoms that often require hospitalization.
4. Anxiety disorders are the most common psychiatric disorders. They range in severity from highly disabling cases of panic disorder and posttraumatic stress disorder (PTSD) to simple phobias. They often co-occur with major depression.
5. Mood and anxiety disorders have both genetic and nongenetic components of risk. Bipolar disorder is more heritable than major depression or anxiety disorders. Childhood adversity and later environmental stressors play a significant role in susceptibility to major depression and anxiety disorders. Genetic analyses of bipolar disorder, major depression, and PTSD are beginning to yield molecular clues to pathogenesis.
6. The neural circuitry of fear and anxiety disorders involves the amygdala and its interconnections with the prefrontal cortex. The neural circuitry of major depression and bipolar disorder is less well understood. However, neuroimaging in humans with major depression implicated circuits involved in the processing of emotional salience and in cognitive control.
7. Bipolar disorder can be treated with lithium, certain anticonvulsant drugs such as valproic acid, and second-generation antipsychotic drugs, although many patients have residual symptoms, most commonly depression.

8. Major depression and anxiety disorders can be treated with diverse antidepressant drugs and by cognitive and behavioral therapies. Electroconvulsive therapy is effective for major depression that is unresponsive to medications.
9. Experimental treatments such as deep brain stimulation are being investigated for treatment of major depression and other psychiatric disorders. The development of electrodes that can record as well as stimulate promise greater insight in human neural circuit function in disease and its treatment.

Steven E. Hyman
Carol Tamminga

Selected Reading

Nestler EJ, Hyman SE, Holtzman D, Malenka RJ. 2015. *Molecular Neuropharmacology: Foundation for Clinical Neuroscience*, 3rd ed. New York: McGraw-Hill.

Otte C, Gold SM, Penninx BW, et al. AF. 2016. Major depressive disorder. Nat Rev Dis Primers 2:16065.

Sullivan PF, Daly MJ, O'Donovan M. 2012. Genetic architecture of psychiatric disorders: the emerging picture and its implications. Nat Rev Genet 13:537–551.

Yehuda R, Hoge CW, McFarlane AC, et al. 2015. Post-traumatic stress disorder. Nat Rev Dis Primers 1:15057.

References

Adhikari A, Lerner TN, Finkelstein J, et al. 2015. Basomedial amygdala mediates top-down control of anxiety and fear. Nature 527:179–185.

American Psychiatric Association. 2013. *Diagnostic and Statistical Manual of Mental Disorders*, 5th ed. Washington, DC: American Psychiatric Association.

Anacker C, Hen R. 2017. Adult hippocampal neurogenesis and cognitive flexibility: linking memory and mood. Nat Rev Neurosci 18:335–346.

Bagot RC, Cates HM, Purushothama I, et al. 2016. Circuit-wide transcriptional profiling reveals brain region-specific gene networks regulating depression susceptibility. Neuron 90:969–983.

Besnard A, Sahay A. 2016. Adult hippocampal neurogenesis, fear generalization, and stress. Neuropsychopharm 41:24–44.

Cade JFJ. 1949. Lithium salts in the treatment of psychotic excitement. Med Australia 2:349–352.

Clementz BA, Sweeney JA, Hamm, JP, et al. 2015. Identification of distinct psychosis biotypes using brain-based biomarkers. Am J Psychiatry 173:373–384.

Cross-Disorder Group of the Psychiatric Genomics Consortium, Lee SH, Ripke S, et al. 2013. Genetic relationship between five psychiatric disorders estimated from genome-wide SNPs. Nat Genet 45:984–994.

Davidson RJ, Pizzagalli D, Nitschke JB, Putnam K. 2002. Depression: perspectives from affective neuroscience. Annu Rev Psychol 53:545–574.

Dayan P, Huys QJ. 2009. Serotonin in affective control. Annu Rev Neurosci 32:95–126.

Drysdale AT, Grosenick L, Downar J, et al. 2017. Resting-state connectivity biomarkers define neurophysiological subtypes of depression. Nat Med 23:28–38.

Etkin A, Klemenhagen KC, Dudman JT, et al. 2004. Individual differences in trait anxiety predict the response of the basolateral amygdala to unconsciously processed fearful faces. Neuron 44:1043–1055.

Fettes P, Schulze L, Downar J. 2017. Cortico-striato-thalamic loop circuits of the orbitofrontal cortex: promising therapeutic targets in psychiatric illness. Front Syst Neurocsci 11:25.

Fornaro M, Stubbs B, De BD, et al. 2016. Atypical antipsychotics in the treatment of acute bipolar depression with mixed features: a systematic review and exploratory meta-analysis of placebo-controlled clinical trials. Int J Mol Sci 17:241.

Heimer L. 1995. *The Human Brain and Spinal Cord*, 2nd ed. New York: Springer-Verlag.

Holtzheimer PE, Mayberg HS. 2011. Deep brain stimulation for psychiatric disorders. Annu Rev Neurosci 34:289–307.

Hui PS, Sim K, Baldessarini RJ. 2015. Pharmacological approaches for treatment-resistant bipolar disorder. Curr Neuropharmacol 13:592–604.

Hyde CL, Nagle MW, Tian C, et al. 2016. Identification of 15 genetic loci associated with risk of major depression in individuals of European descent. Nat Genet 48:1031–1036.

Ivleva EI, Morris DW, Moates AF, et al. 2010. Genetics and intermediate phenotypes of the schizophrenia: bipolar disorder boundary. Neurosci Biobehav Rev 34:897–921.

Johansen JP, Cain CK, Ostroff LE, LeDoux JE. 2011. Molecular mechanisms of fear learning and memory. Cell 47:509–524.

Kendler KS, Prescott CA, Myers J, Neale MC. 2003. The structure of genetic and environmental risk factors for common psychiatric and substance use disorders in men and women. Arch Gen Psychiatry 60:929–937.

Kessler RC, Bromet EJ. 2013. The epidemiology of depression across cultures. Annu Rev Public Health 34:119–138.

Kreuger RF, Markon KE. 2006. Reinterpreting comorbidity: a model-based approach to understanding and classifying psychopathology. Annu Rev Clin Psychol 2:111–133.

Mayberg HS, Brannan SK, Mahurin RK, et al. 1997. Cingulate function in depression: a potential predictor of treatment response. NeuroReport 8:1057–1061.

Mayberg HS, Liotti M, Brannan SK, et al. 1999. Reciprocal limbic-cortical function and negative mood: converging PET findings in depression and normal sadness. Am J Psychiatry 156:675–682.

Mayberg HS, Lozano AM, Voon V, et al. 2005. Deep brain stimulation for treatment-resistant depression. Neuron 45:651–660.

McClintock SM, Reti IM, Carpenter LL, et al. 2018. Consensus recommendations for the clinical application of repetitive transcranial magnetic stimulation (rTMS) in the treatment of depression. J Clin Psychiatry 79:1. doi:10.4088/JCP.16cs10905.

Miller BR, Hen R. 2015. The current state of the neurogenic theory of depression and anxiety. Curr Opin Neurobiol 30:51–58.

Moussavi S, Chatterji S, Verdes E, et al. 2007. Depression, chronic diseases, and decrements in health: results from the World Health Surveys. Lancet 370:851–858.

Muller VI, Cieslik EC, Serbanescu I, et al. 2017. Altered brain activity in unipolar depression revisited. Meta-analyses of neuroimaging studies. JAMA Psychiatry 74:47–55.

Neal, BM, Sklar P. 2015. Genetic analysis of schizophrenia and bipolar disorder reveals polygenicity but also suggests new directions for molecular interrogation. Curr Opin Neurobiol 30:131–138.

Nock MK, Borges G, Bromet EJ, et al. 2008. Cross-national prevalence and risk factors for suicidal ideation, plans and attempts. Br J Psychiatry 192:98–105.

Pizzagalli D, Pascual-Marqui RD, Nitschke JB, et al. 2001. Anterior cingulate activity as a predictor of degree of treatment response in major depression: evidence from brain electrical tomography analysis. Am J Psychiatry 158:405–415.

Ripke S, Wray NR, Lewis CM, et al. 2013. A mega-analysis of genome-wide association studies for major depressive disorder. Mol Psychiatry 18:497–511.

Seeley WW, Menon V, Schaztzberg AF, et al. 2007. Dissociable intrinsic connectivity networks for salience processing and executive control. J Neurosci 27:2349–2356.

Sheline YI, Sanghavi M, Mintun MA, Gado MH. 1999. Depression duration but not age predicts hippocampal volume loss in medically healthy women with recurrent major depression. J Neurosci 19:5034–5043.

Stoddard J, Gotts SJ, Brotman MA, et al. 2016. Aberrant intrinsic functional connectivity within and between corticostriatal and temporal-parietal networks in adults and youth with bipolar disorder. Psychol Med 46:1509–1522.

Trivedi MH, Rush AJ, Wisniewski SR, et al. 2006. Evaluation of outcomes with citalopram for depression using measurement-based care in STAR®D: implications for clinical practice. Am J Psychiatry 163:28–40.

Tye KM, Prakash R, Kim SY, et al. 2011. Amygdala circuitry mediating reversible and bidirectional control of anxiety. Nature 471:358–362.

Whiteford HA, Degenhardt L, Rehm J, et al. 2013. Global burden of disease attributable to mental and substance use disorders: findings from the global burden of disease study 2010. Lancet 382:1575–1586.

Zarate CA Jr, Singh JB, Carlson PJ, et al. 2006. A randomized trial of an N-methyl-D-aspartate antagonist in treatment-resistant major depression. Arch Gen Psychiatry 63:856–864.

62

Disorders Affecting Social Cognition: Autism Spectrum Disorder

Mental retardation, now referred to widely as *intellectual disability*, is currently defined as having an IQ below 70 accompanied by marked deficits in adaptive functioning. Both terms have been broadly used to label a variety of cognitive impairments linked to prenatal or early postnatal brain abnormalities. For decades, subsets of individuals with rare intellectual disability syndromes, such as Rett syndrome or fragile X syndrome, have been characterized by their genetic etiologies. We are now beginning to elucidate the complex genetics of more prevalent neurodevelopmental disorders without distinct physical features that distinguish them, including so-called *idiopathic* or *nonsyndromic* forms of autism spectrum disorder (ASD). The combination of insights resulting from the intensive study of rare genetic syndromes coupled with successes in unraveling the genetics underlying idiopathic ASD has transformed our understanding of normal and pathological development of the human brain.

Common to all of these disorders are mental impairments that persist throughout life, hampering development and learning. Generally speaking, even if all mental functions seem to be affected, conditions with distinct etiologies and natural histories can be differentiated because some cognitive domains tend to be

more impaired than others. And indeed, these differences are reified in diagnostic schemes that draw distinctions between developmental abnormalities that affect primarily general cognition, social cognition, or perception. These differential cognitive and behavioral vulnerabilities may provide useful clues about the origin and developmental time course of specific mental functions in normal development.

In this chapter, we focus principally on neurodevelopmental disorders that include abnormalities in social functioning, including ASD, fragile X syndrome, Williams syndrome, Rett syndrome, and Angelman and Prader-Willi syndromes. These conditions all impair highly sophisticated brain functions including social awareness and communication. ASD is a prime focus for several reasons: the high prevalence in the population; the overlap in genetic risks with other common neuropsychiatric conditions, including schizophrenia; and the absence of a defining neuropathology. They are also exemplars of the etiological and phenotypic heterogeneity common to many psychiatric syndromes. In this respect, ASD is a paradigmatic neuropsychiatric syndrome.

Autism Spectrum Disorder Phenotypes Share Characteristic Behavioral Features

Profound social disability has probably always been with us, but the characterization of autism as a medical syndrome was first described in the literature in 1943 by Leo Kanner and in 1944 by Hans Asperger. Today, clinicians and researchers think of autism as a spectrum of disorders with two defining but highly variable diagnostic features: impaired social communication and stereotyped behaviors with highly restricted interests.

Until recently, the term "Asperger syndrome" was used to describe individuals who met these two diagnostic criteria, but in whom language acquisition was not delayed and IQ was in the normal range. In the most recent edition of the standard psychiatric diagnostic manual, *Diagnostic and Statistical Manual of Mental Disorders, Fifth Edition* (DSM-5), Asperger syndrome along with a distinct disorder known as pervasive developmental disorder not otherwise specified—designed to capture individuals with deficits in social communication who did not meet full criteria in other areas—were eliminated in favor of including variations within a single spectrum construct.

Autism spectrum disorder is present in at least 1.5% of the population. Rigorous epidemiological studies estimate prevalence as high as 2.6% for the full spectrum of social disability, far higher than estimated only decades ago. The reasons for the increase in the prevalence over a relatively short time frame are of considerable interest and active debate, particularly among the lay public. Within the scientific community, a consensus has emerged that this increase reflects a combination of changing diagnostic criteria, increased awareness among families and health care professionals, "diagnostic substitution" (in which individuals who formerly would have been diagnosed with intellectual disability are now more likely to be identified as socially disabled), and some true increase in incidence. These issues will be discussed below with regard to genetic risks.

Autism spectrum disorders occur predominantly in males, although the typically cited 4:1 male-to-female ratio has recently been called into question based on concerns about male bias in the approaches used to ascertain the diagnosis, including the diagnostic instruments. Even accounting for these challenges, however, the cumulative evidence suggests a ratio bias of at least 2:1 to 3:1 male excess. Individuals across the IQ spectrum are affected, and based on current diagnostic practices, about half of all individuals with ASD also have intellectual disability. By definition, ASD must be detectable before 3 years of age, but recent studies have shown that it is possible to identify affected children in high-risk families well within the first year of life. ASD occurs in all countries and cultures and in every socioeconomic group.

Although ASD clearly affects the brain, no definitive biological markers have yet been identified; thus, diagnosis is based on behavioral criteria. This does not mean that there are not strong biological correlates, including specific gene mutations and neuroimaging findings, but none of these are sufficiently specific or predictive to be useful as an alternative to the gold standard of clinical assessment. Moreover, because behavior is variable during development and depends on a number of factors—age, environment, social context, and availability and duration of remedial help—no single behavior is likely ever to be conclusively diagnostic.

Like other neurodevelopmental syndromes, ASD typically endures throughout life. However, in recent longitudinal studies, approximately 10% of clearly affected children showed improvement, with little or no evidence of social disability later in life. Autism is not progressive. On the contrary, special educational programs and professional support often lead to improvements in behavior and adaptive functioning with age.

Autism Spectrum Disorder Phenotypes Also Share Distinctive Cognitive Abnormalities

Social Communication Is Impaired in Autism Spectrum Disorder: The Mind Blindness Hypothesis

One cognitive theory of social communication postulates that humans have a particularly well-developed ability to understand the mental states of others in an intuitive and fully automatic fashion. Watching a young person surreptitiously trying to open a car door without a key, you instantly understand that she believes she can break in while being unobserved, and you expect her to run away as soon as she realizes someone is watching. Thus, you explain and predict her behavior by inferring her mental states (desires, intentions, beliefs, knowledge) from her overt behavior. This so-called mentalizing ability, termed a *theory of mind*, is thought to depend on specific brain mechanisms and circuits underlying social cognition (Figure 62–1). Further, it is postulated that mentalizing is impaired in ASD, with profound effects on social development.

It is now generally agreed that insight into the mental state of others depends on the capacity to mentalize spontaneously. Spontaneous mentalizing allows us to appreciate that different people have different

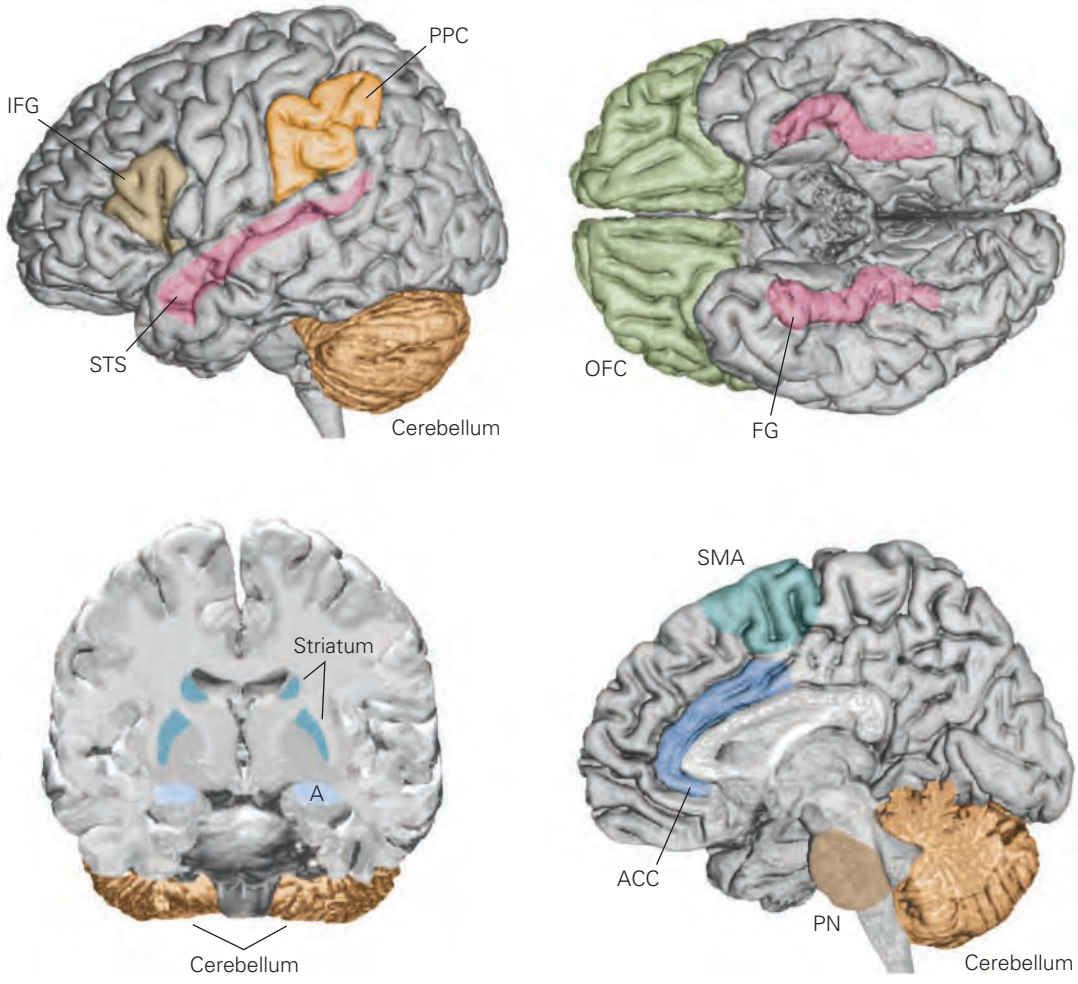

Figure 62–1 Brain areas implicated in the three core deficits characteristic of autism: impaired social interaction, impaired language and communication, and severely restricted interests with repetitive and stereotyped behaviors. Areas implicated in social deficits include the orbitofrontal cortex (**OFC**), the anterior cingulate cortex (**ACC**), and the amygdala (**A**). Cortex bordering the superior temporal sulcus (**STS**) has been implicated in mediating the perception that a living thing is moving and gaze perception. Face processing involves a region of the inferior temporal cortex within the fusiform gyrus (**FG**). Comprehension and expression of language involve a number of regions including the inferior frontal region, the striatum, and subcortical areas such as the pontine nuclei (**PN**). The striatum has also been implicated in the mediation of repetitive behaviors. (Abbreviations: **IFG**, inferior frontal gyrus; **PPC**, posterior parietal cortex; **SMA**, supplementary motor area.)

thoughts and that thoughts are internal and different from external reality.

The inability to mentalize, or "mind blindness," was first tested in children with autism using a simple puppet game, the Sally-Anne test. Young children with ASD, unlike those with Down syndrome or typically developing 4-year-olds, cannot predict where a puppet will first look for an object that was moved while the puppet was out of the room. They are not able to imagine that the puppet will "think" that the object will be where the puppet had left it (Figure 62–2). Many children with ASD eventually do learn to pass this task, but on average with a 5-year delay. Mentalizing acquired so slowly remains effortful and error-prone even in adulthood.

At the same time, young children with ASD show excellent appreciation of physical causes and events. For instance, a child who is incapable of falsely telling another that a box is locked is quite capable of locking the same box to prevent its contents from being stolen.

Variations of the Sally-Anne test and other mentalizing tasks have been used with children and adults with ASD since the mid-1980s (Figure 62–3).

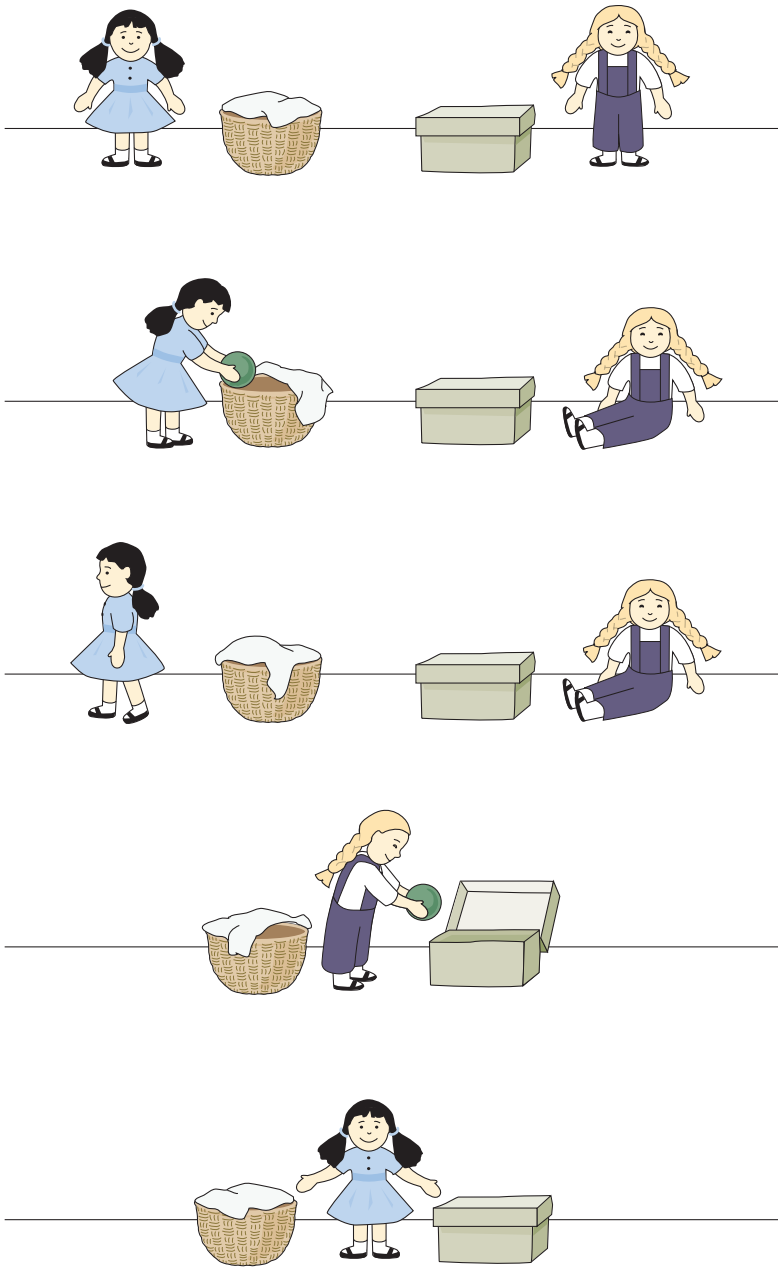

Figure 62–2 The Sally-Anne test. This first test of the "theory of mind" begins with a scripted performance using two dolls. Sally has a basket; Anne has a box. Sally puts a ball into her basket. She goes for a walk and leaves the room. While Sally is outside, naughty Anne takes the ball out of the basket and puts it into her box. Now Sally comes back from her walk and wants to play with her ball. Where will she look for the ball, the basket or the box? The answer, the basket, is obvious to most typically developing 4-year-olds but not to autistic children of the same or even higher mental age. (Adapted from original artwork by Axel Scheffler.)

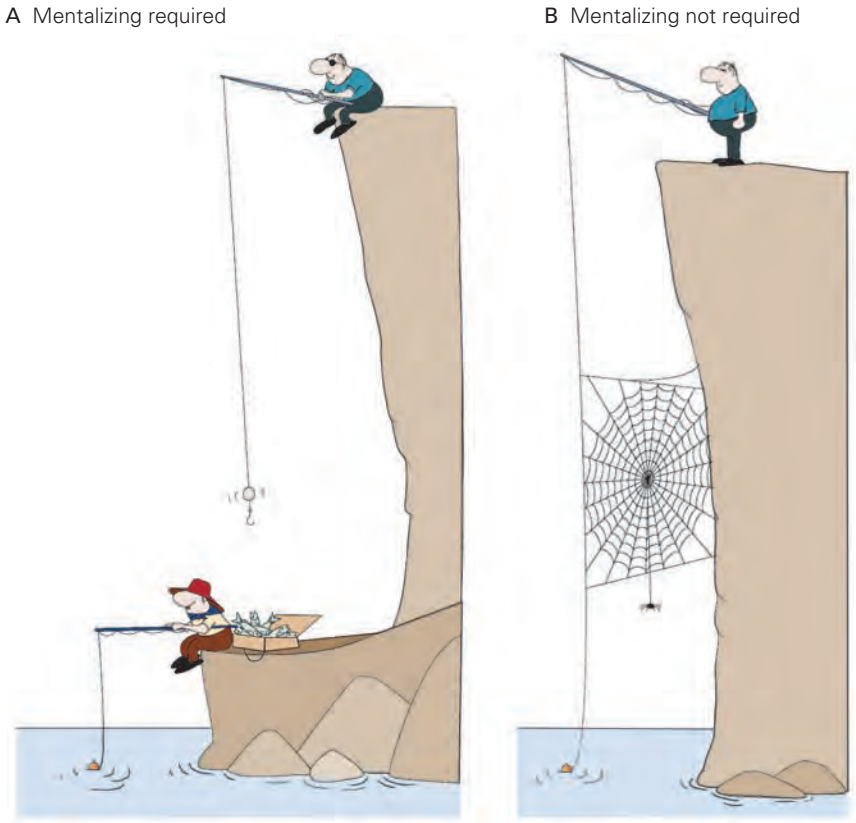

Figure 62–3 Examples of cartoons used in imaging studies of "mentalizing." Participants were asked to consider the meaning of each picture (silently) and then to explain them. In a functional magnetic resonance imaging study, normal adults passively viewed cartoons that require mentalizing versus those that do not. A characteristic network of brain regions is activated in each subject (see Figure 62–4). (Adapted from Gallagher et al. 2000.)

Functional neuroimaging has been used to examine activity in the brain of healthy subjects while they are engaged in tasks that necessitate thinking about mental states. A wide range of tasks using visual and verbal stimuli has been used in these studies. In an early positron emission tomography study, adults in a control cohort viewed silent animations of geometric shapes. In some of the animations, the triangles move in scripted scenarios designed to evoke mentalizing (eg, triangles tricking each other). In other animations, the triangles move randomly in a manner that does not evoke mentalizing. Comparison of the scans made while subjects viewed each type of animation reveals a specific network of four brain centers involved in mentalizing (Figure 62–4). Functional magnetic resonance imaging (MRI) studies using the same animations have shown that activity in this network is reduced in subjects with ASD.

This network has four components. The first, in the medial prefrontal cortex, is a region thought to be involved in monitoring one's own thoughts. A second component, in the temporoparietal region of the superior temporal lobe, is known to be activated by eye gaze and biological motion. Patients with lesions in this area in the left hemisphere are unable to pass the Sally-Anne test. The third region is the amygdala, which is involved in the evaluation of social and nonsocial information for indications of danger in the environment. The fourth region is an inferior temporal region involved in the perception of faces.

Recent studies have used stimuli intended to capture more nuanced and naturalistic social content, for example, using movies of actual social encounters as opposed to static pictures of facial expressions. These studies have identified, among other things, the role of the orbital frontal cortex in social cognition.

Other Social Mechanisms Contribute to Autism Spectrum Disorder

From birth, normal infants prefer to attend to people rather than other stimuli. An absence of this preference could lead to an inability to understand and interact with others. Indeed, the absence of preferential attention to social stimuli and mutual attention are widely acknowledged as early signs of ASD. These deficits may not involve problems with mentalizing, given that mutual attention normally appears toward the end of the first year when signs of mentalizing are still sparse.

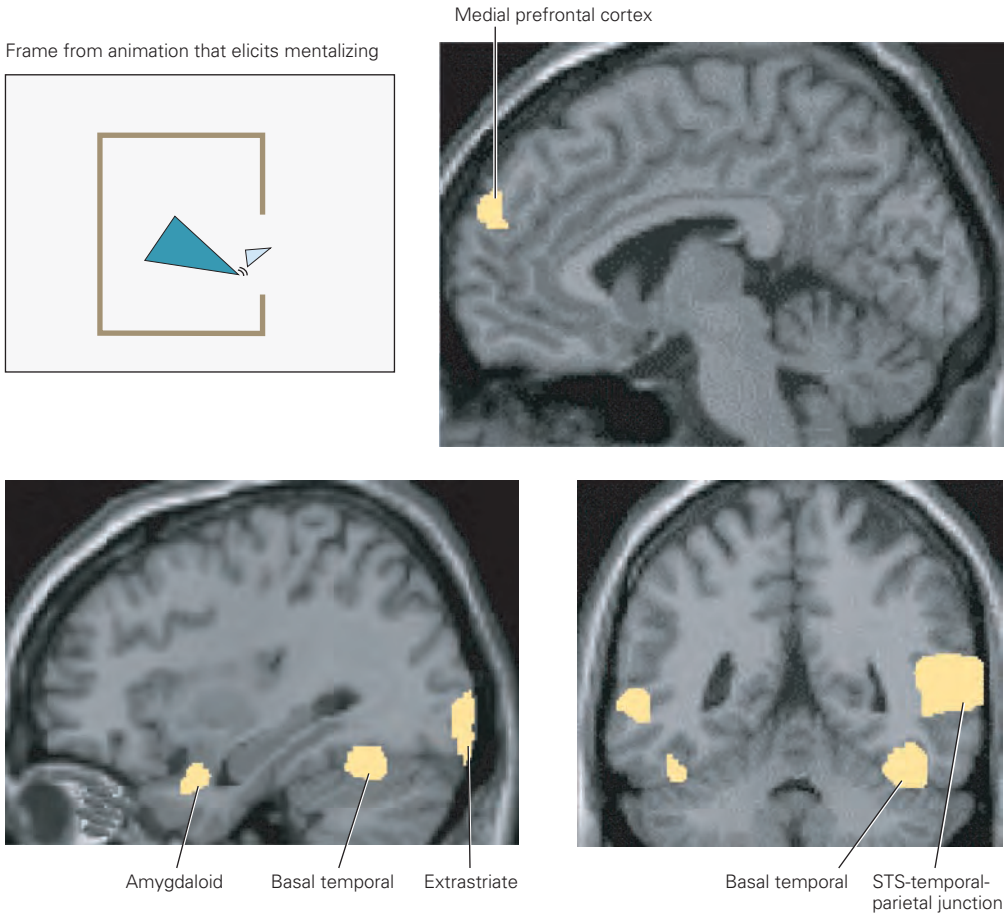

Figure 62–4 The mentalizing system of the brain. Healthy volunteers were presented with animated triangles that moved in such a way that viewers would attribute mental states to them. In the sample frame shown, the larger triangle was seen as encouraging the smaller triangle to leave the enclosure. They were also presented with animated triangles that moved in a more or less random fashion and thus would not elicit mentalizing. The highlighted areas show differences in the positron emission tomography scans of brain activation when these two viewing conditions were compared. (Abbreviation: STS, superior temporal sulcus.) (Reproduced, with permission, from Castelli et al. 2002. Copyright © 2002, Oxford University Press.)

Researchers have long considered the possibility that a specific neural mechanism underlies attention to social stimuli, such as faces, voices, and biological motion. In favor of this hypothesis, researchers found that the gaze of individuals with ASD is abnormal when watching social scenes. For example, multiple studies have found that individuals with ASD fixate on people's mouths instead of showing the normal preference for eyes (Figure 62–5).

People With Autism Show a Lack of Behavioral Flexibility

Repetitive and inflexible behavior in ASD may reflect abnormalities in frontal lobe executive functions, a wide array of higher cognitive processes that include the ability to disengage from a given task, inhibit inappropriate responses, stay on task (plan and manage sequences of deliberate actions), keep multiple task demands in working memory, monitor performance, and shift attention from one task to another.

Even ASD individuals with IQs in the normal range have problems in planning, organizing, and flexibly switching between behaviors. Irrespective of IQ, affected individuals have difficulties suggesting various different uses of a single object such as a handkerchief (used to block a sneeze, to wrap loose objects, etc.). Flexible thinking is also poor in patients with acquired damage to the frontal lobe.

Some Individuals With Autism Have Special Talents

A particularly fascinating feature of ASD in some individuals is "savant syndrome," defined by the presence

Figure 62–5 Individuals with autistic disorder often do not look into the eyes of others. Patterns of eye movements in individuals with autism were studied while the subjects watched clips from the film *Who's Afraid of Virginia Wolf?* When looking at human faces, the subjects tended to look at the mouth rather than the eyes, and in scenes of intense interaction between people, they tended to look at irrelevant places rather than at the faces of the actors. (Reproduced, with permission, from Klin et al. 2002. Copyright © 2002 American Psychiatric Association.)

of one or more exceptional skills that are in marked contrast to the individual's overall disability but also rare in the population at large. The most widely cited estimate is that 10% of individuals with ASD demonstrate such exceptional abilities compared to about 1 in 1,000 individuals with other forms of intellectual disability.

In the largest ASD cohort surveyed by self-reporting to date (about 5,000 families), 531 individuals were reported to have exceptional abilities in the following 10 areas (listed in descending frequency): music, memory, art, hyperlexia, mathematics, mechanical, coordination, directions, calendar calculating, and extrasensory perception. Subsequent small-scale studies have placed the prevalence of savant skills in ASD at between 13% and 28%.

A recently established savant syndrome registry now includes more than 400 people from 33 countries. Among a group of 319 individuals who met some criteria that earned them a savant diagnosis based on family or caregiver reports or self-reporting, 75% who showed savant skills in childhood were diagnosed with ASD. Approximately half reported a single exceptional skill and half reported multiple skills. Music was the most commonly reported exceptional skill, followed by art, memory, and mathematics. Calendar calculating, while present in many savants along with another skill, was the sole skill in only about 5% of the sample. Among this self- or family-selected group, the overall sex distribution mirrored that reported for ASD in general, with a male-to-female ratio of approximately 4:1.

One explanation for savant syndrome is that information processing is preferentially geared to tiny details at the cost of seeing the bigger picture. (For example, the drawing by the gifted artist with high-functioning autism in Figure 62–6 shows remarkably detailed cityscapes, as well as detailed numerical patterns and dates.) A similar hypothesis is that brain regions involved in perception are overfunctioning; another possibility is that there is a preference for manipulating the bits of information that fit within a strict framework such as calendar knowledge or a bus timetable. Neuropsychological data support both explanations, but decisive experiments to distinguish between them remain to be done.

Genetic Factors Increase Risk for Autism Spectrum Disorder

The earliest evidence that genes contribute to ASD arose from studies of twin pairs as well as familial aggregation. The former show from 60% to 90% concordance among monozygotic twin pairs; this wide range is due in part to previously used diagnostic criteria and classifications. For example, the highest estimates of monozygotic concordance are derived from observations of twins with any of three diagnoses that made up the social disability spectrum prior to the reformulations in the DSM-5. Only approximately 60% of monozygotic twins were found to be concordant for the "full diagnosis" of autism, which was defined at

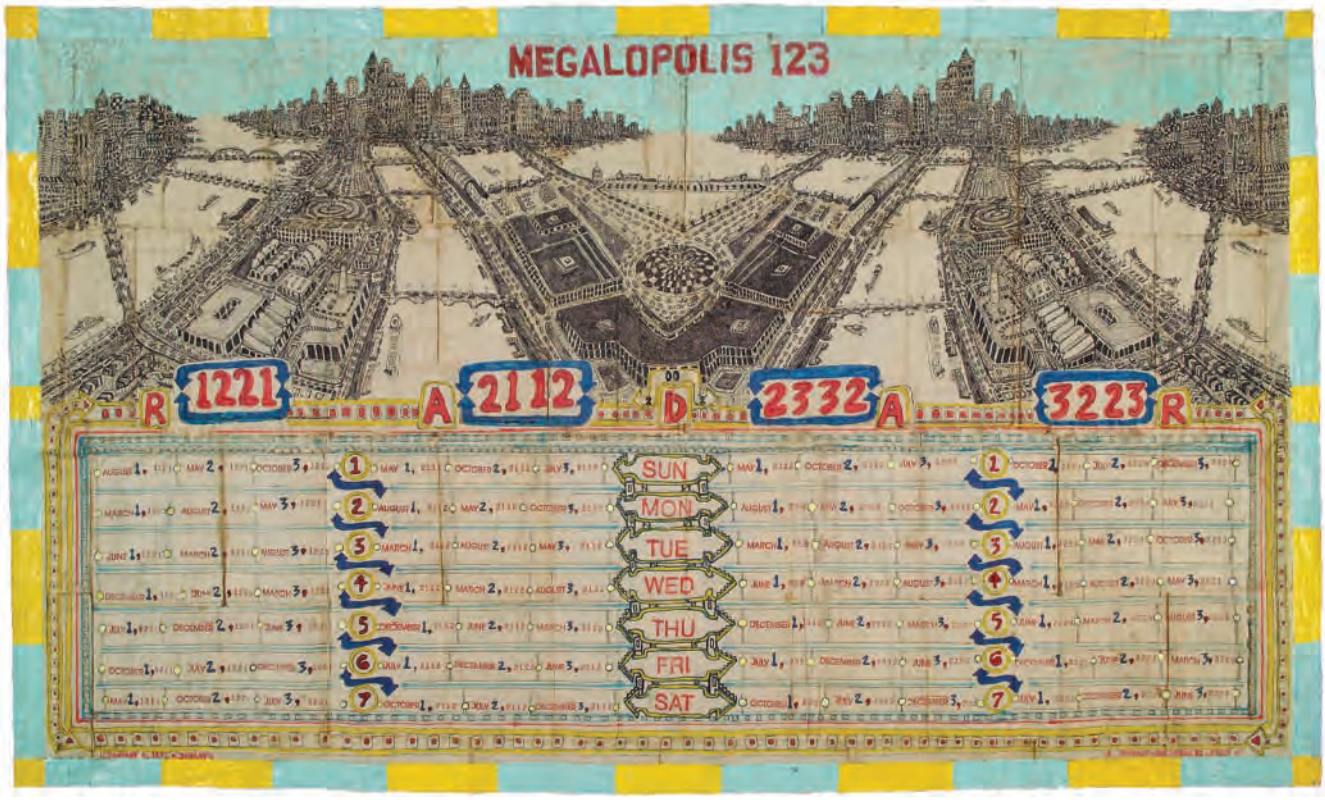

Figure 62–6 Strikingly beautiful art work by George Widener. George is a highly accomplished and much-admired outsider artist. In the attention to detail, this drawing resembles the drawings of other autistic savant artists. The intricate topographical detail of a symmetrically arranged city, with rivers, bridges, and tall buildings, is combined with minutely executed and seemingly abstruse calendar sequences. Mastery of the calendar and the ability to name the day of the week for any given date has often been described for autistic savants. The viewer of this drawing can partake in an otherwise very private world of space and time, numbers, and patterns. (Reproduced, with permission, from the Henry Boxer Gallery, London.)

the time as comprising fundamental impairments in each of three categories: social communication, language development, and restricted interests or repetitive behaviors. In contrast, dizygotic twins show 10% to 30% concordance—again with the lower number estimating concordance for the diagnosis of isolated autism, while the larger number encompasses any of three diagnoses on the autism spectrum.

This difference between the rates at which monozygotic and dizygotic twins share an ASD phenotype is attributed to differences in the amount of shared genetic material between the two types of twin pairs. Monozygotic siblings share all their DNA, whereas dizygotic twins share as much DNA as any sibling pair. In addition to these types of data, it has long been observed that ASD runs in families: Current estimates are that if parents have one child with ASD, the risk that a second child will be affected increases approximately 5- to 10-fold over the population base rate.

The most generous estimates of genetic contribution do not explain all risk for ASD in the population. Some contribution from the environment is a certainty. However, given the well-known public debate on the issue of whether immunization is a factor in ASD, it is important to note that there is no credible evidence that the increase in ASD prevalence is due to immunizations. The initial study that raised the issue of the contribution of the trivalent measles-mumps-rubella (MMR) vaccine has been retracted and thoroughly repudiated by the editors of the journal in which the article appeared, as well as by 10 of 12 of the original authors. A wide range of subsequent investigations, both of the MMR vaccine and of vaccines with the mercury-containing preservative thimerosal, has found no evidence for association with ASD risk.

The counter argument that certain rare individuals may be predisposed to a vulnerability to vaccines leading to ASD is nonfalsifiable. However, three lines of evidence suggest that such a contribution, if present, is

likely to be quite small. First, it is important to recall that the basis for the MMR hypothesis has been thoroughly debunked, and consequently, the prior probability that vaccines are major etiological factors is extremely low. Second, even in very large research cohorts, it has so far not been possible to detect a risk signal. Third, although there is a subset of children with ASD who show developmental regression in the second year of life, there is often evidence on careful examination of preexisting delay. In the final analysis, although the current level of understanding of pathophysiological mechanisms makes it impossible to definitively exclude any etiological contributor in a single individual, what is incontrovertible is that the risks to children of not receiving vaccinations are clear, measurable, and far greater overall than the role vaccines might play in ASD risk.

Although the evidence for a predominantly genetic contribution has been consistent, until recently, the search for risk genes contributing to nonsyndromic forms of ASD proved to be extremely challenging. Now, as will be discussed below, technological advances and changes in research culture have transformed the field. Moreover, critically important initial insights into both the genetics and neurobiology of ASD have emerged from the investigation of well-characterized genetic neurodevelopmental disorders, sometimes referred to as Mendelian syndromes (those with a single causative gene or genomic locus to the condition). These disorders typically manifest with intellectual disability, often with evidence of social impairment. Several of these syndromes, including fragile X, Rett, Williams, and Prader-Willi/Angelman syndromes, have been particularly important in beginning to elaborate the biology of ASD.

Rare Genetic Syndromes Have Provided Initial Insights Into the Biology of Autism Spectrum Disorders

Fragile X Syndrome

Fragile X syndrome is a common form of chromosome X–linked intellectual disability. Patients display a range of behavioral abnormalities including poor eye contact, social anxiety, and repetitive behaviors. In addition, approximately 30% of boys with fragile X meet the all diagnostic criteria for ASD. Moreover, in research with multiple cohorts, up to 1% of participants with apparently idiopathic ASD also carried fragile X mutations. The overall prevalence is approximately 1 in 4,000 boys and 1 in 8,000 girls.

The fragile X mutation is quite remarkable. The *FMR1* gene on the X chromosome includes the nucleotide triplet CGG. In normal individuals, this triplet is repeated in approximately 30 copies. In fragile X syndrome patients, the number of repeats is more than 200, with approximately 800 repeats being most common. This expansion of trinucleotide repeats has since been observed in other genes leading to neurological diseases, such as Huntington disease (Chapters 2 and 63). When the number of CGG repeats exceeds 200, the *FMR1* gene regulatory region becomes heavily methylated, and gene expression is shut off. Consequently, in these children, the fragile X mental retardation protein (FMRP) is lacking.

Lack of functional FMRP is considered responsible for fragile X syndrome. FMRP is a selective RNA-binding protein that blocks translation of messenger RNA until protein synthesis is required. It is found with ribosomes at the base of dendritic spines, where it regulates local dendritic protein synthesis that is needed for synaptogenesis and certain forms of long-lasting synaptic changes associated with learning and memory (Chapters 52 and 53). Interestingly, long-term depression of excitatory synaptic transmission, a form of long-lasting synaptic change that requires local protein synthesis, is enhanced in a mouse model of fragile X syndrome in which the gene encoding FMRP has been deleted. Loss of FMRP may enhance long-term depression by allowing excess translation of the messenger RNAs important for synaptic plasticity.

An exciting implication of these data is that antagonists of the type 5 metabotropic glutamate receptor (mGluR5), the activation of which is required for the enhanced protein synthesis underlying long-term depression, may lessen the excess protein translation. In fact, compounds with this activity have been found to rescue the mutant phenotype in mouse and fruit fly models. Thus far, clinical trials of mGluR5 antagonists for individuals with fragile X with ASD have not shown efficacy against the defined clinical end points. However, it is still too early to tell whether these initial forays into rational drug design for neurodevelopmental disorders may or may not be promising in the long run. A range of challenges have confronted these pioneering efforts, including measuring change in individuals with ASD, identifying ideal clinical end points, and determining the best age for evaluating interventions.

Rett Syndrome

Another single-gene disorder showing overlap with ASD is Rett syndrome, a devastating disorder that primarily affects girls. Affected females have normal

development from birth until 6 to 18 months of age, when they regress, losing speech and hand skills that they had acquired. Rett syndrome is progressive, and initial symptoms are followed by repetitive hand movements, loss of motor control, and intellectual disability. Often young girls will display symptoms indistinguishable from ASD early in the course of the syndrome, although social communication frequently improves later in childhood. Its prevalence is approximately 1 in 10,000 live female births.

Rett syndrome is an X-linked inherited disease caused by loss-of-function mutations in the *MECP2* gene, which encodes a transcriptional regulator that binds to methylated cytosine bases in DNA, regulating gene expression and chromatin remodeling. The gene product was initially thought to act predominantly as a transcriptional repressor, but studies of both the mouse model and human induced pluripotent stem cells have shown that overall gene expression is reduced when the gene is knocked out. Among the genes that have reduced expression in neurons is *BDNF*, encoding brain-derived neurotrophic factor. Studies in mouse models of Rett have found that overexpression of *BDNF* improves the knock-out phenotype. Other growth factors that increase gene expression but have more favorable neuropharmacological profiles, including insulin-like growth factor-1 (IGF-1), have also improved aspects of the mouse phenotype, leading to optimism about clinical trials of related compounds. Phase II human trials with both molecules are currently underway.

One might think that such a global abnormality in gene expression would lead to a very severe phenotype, but because females are mosaic, with approximately half of their brain cells expressing one normal copy of *MECP2* (due to random X-inactivation), they are viable but manifest the devastating Rett phenotype. Boys, who have a single X chromosome and thus a single copy of *MECP2*, typically die soon after birth or in infancy if they carry a loss-of-function mutation in *MECP2*.

The role of X-inactivation in the survival of female mutation carriers and the observation that favorable skewing (a shift toward preferential silencing of the mutant X) leads to a less severe clinical course have generated considerable interest in therapeutic strategies aimed at reactivating the normal but silenced X chromosomes in females with Rett syndrome. Although one can imagine considerable challenges resulting from the reactivation of many genes on a normally silenced chromosome, a recent study has reported a mouse mutation that leads to both alleles expressing MeCP2 without wholesale activation of genes on the X chromosome.

Interestingly, in 2005, duplications spanning *MECP2* were identified in males with severe intellectual disability. This condition, called *MECP2* duplication syndrome (MDS), includes autistic features, hypotonia, epilepsy, gait abnormalities, and recurrent infections. Like Rett syndrome, it has also been productively modeled in rodents. However, unlike Rett, the majority of identified cases are familial and not sporadic in nature. In these cases, female carriers are often healthy enough (due to favorable X-inactivation) to reproduce and transmit the duplication to boys with only a single X chromosome.

Williams Syndrome

Williams syndrome is caused by a segmental deletion of about 27 genes on the long arm of chromosome 7 and is characterized by mild to moderate intellectual disability, connective tissue abnormalities, cardiovascular defects, distinctive facies, and a behavioral phenotype characterized by increased sociability, preserved language abilities, affinity for music, and impaired visuospatial capabilities. The disorder occurs in 1 in 10,000 live births. The connective tissue and key cardiovascular symptoms have been attributed to the loss of the gene *ELN* (*elastin*), although no specific genes within the deleted interval have yet been definitively shown to result in the behavioral phenotype. Nonetheless, the social cognitive features of Williams syndrome are particularly intriguing: The degree of interest in social interaction is striking, leading to a nearly universal loss of reticence with strangers in children with the syndrome. In contrast to the almost complete absence of social anxiety, individuals with Williams syndrome have a high degree of general anxiety and isolated phobias. Finally, the affinity for and interest in music among a very large percentage of 7q11.23 deletion carriers, although less well characterized, are striking.

Conversely, duplication of the identical region of chromosome 7, including the same 26 to 28 genes, is a significant risk factor for ASD and other neurodevelopmental syndromes apart from Williams syndrome. The observation of contrasting social phenotypes depending on whether there is loss or gain of a small region of the genome is fascinating. Whether social functioning in William syndrome is truly the opposite of that seen in ASD, as is sometimes argued, seems less interesting than the conclusion that this region of the genome must contain one or more genes that modulate social affiliation. Consequently, the molecular characterization of these deletion and duplication syndromes and intensive investigation of their impact on the development of molecular, cellular, and circuit properties in the central nervous system are particularly important.

Angelman Syndrome and Prader-Willi Syndrome

Angelman and Prader-Willi syndromes are paradigmatic examples of genetic syndromes that result from mutations in genes subject to parental imprinting. To understand these conditions, one must not only know the associated DNA lesion but also its parental origin.

For example, both syndromes most often result from the loss of the identical region of chromosome 15 (15q11-q13) but have readily distinguishable phenotypes. Angelman syndrome is characterized by severe intellectual disability, epilepsy, absence of speech, hyperactivity, and inappropriate laughter. In contrast, Prader-Willi is characterized by infantile hypotonia, mild to moderate intellectual disability, obesity, highly perseverative behavior, social disability, and diminished or absent satiety.

How these contrasting phenotypes result from the loss of the identical set of genes confounded medical geneticists until about the year 2000. The mystery was solved by the discovery that the chromosomal interval is imprinted. Specifically, within this region, multiple genes are expressed only on the paternally inherited chromosome (*maternal* imprinting), whereas at least two genes, *UBE3A* and *ATP10C*, are expressed only on the maternally inherited chromosome (*paternal* imprinting) (Figure 62–7).

This discovery, along with a series of studies that allowed for fine mapping of the interval, provided a parsimonious explanation for the clinical observations. If the deletion of proximal chromosome 15 involved the maternal chromosome, the patient would suffer the loss of the protein product of *UBE3A*, a ubiquitin-protein ligase that stimulates the degradation and turnover of other proteins, leading to Angelman syndrome. Alternatively, if the paternal chromosome carried the deletion, *UBE3A* would be expressed normally, but a series of other genes, including several strongly implicated in Prader-Willi syndrome, would be lost.

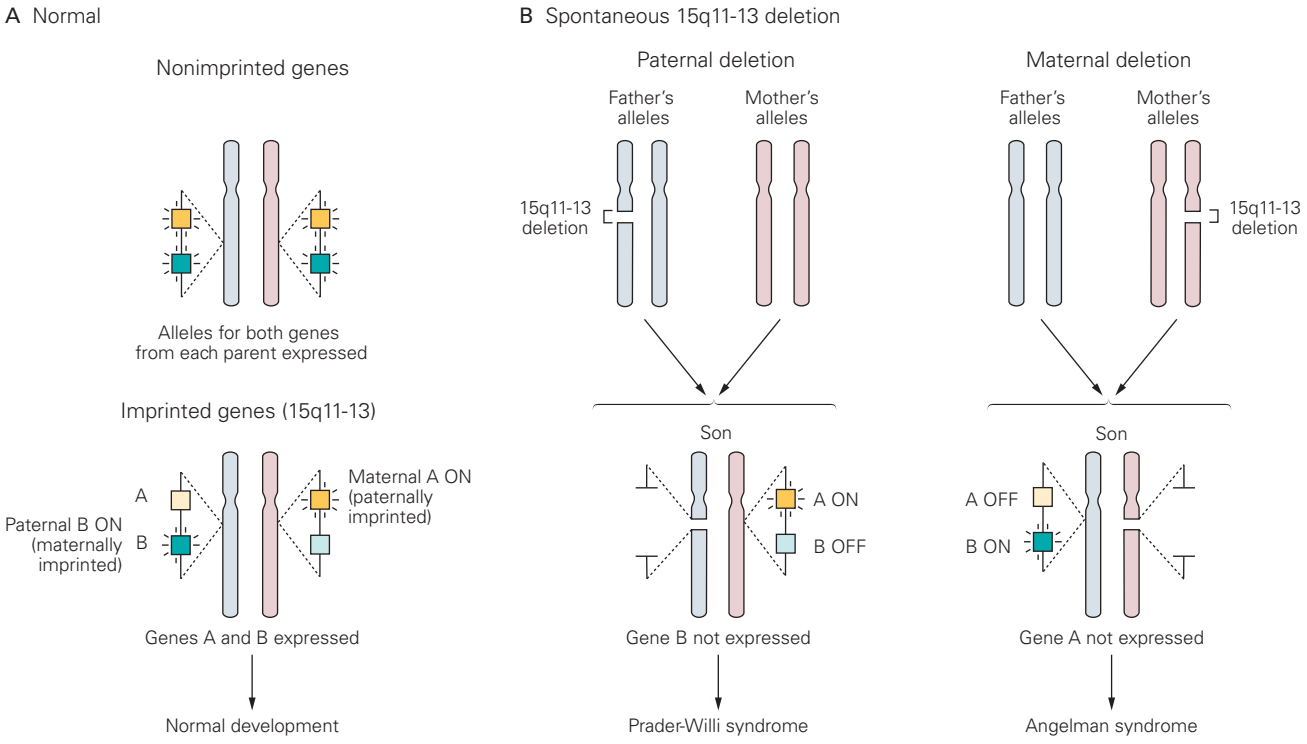

Figure 62–7 Imprinting in Prader-Willi and Angelman syndromes. Approximately 70% of Prader-Willi and Angelman syndrome patients inherit chromosome 15 from one parent with spontaneous (noninherited) deletions of the q11-13 interval. This interval contains imprinted genes with alleles that are either expressed or not depending on whether the chromosome was inherited from the father or mother. If the chromosome with the deletion is from the father, Prader-Willi syndrome occurs because maternally imprinted genes on the corresponding interval of the intact maternal chromosome (gene B, for example) are not expressed. If the chromosome with the deletion is from the mother, the gene for ubiquitin ligase (*UBE3A*) will not be expressed in offspring because of its normal inactivation on the paternal chromosome caused by imprinting; loss of expression of this gene leads to Angelman syndrome.

The solution to the phenotypic complexity seen in 15q11-13 deletion also led to a series of observations that revealed other previously unappreciated genetic mechanisms of behavioral pathology. For example, deletions on the maternal chromosome not directly involving the *UBE3A* gene were also observed in rare patients with Angelman syndrome, contributing to the identification of an Angelman syndrome *imprinting control* region mapping some distance from UBE3A but within the deletion interval. Similarly, the discovery of both Prader-Willi and Angelman syndromes in patients without deletions of any kind led to the recognition that in a small percentage of both conditions two copies of a chromosome from the same parent were present (with no representation from the other parent), a phenomenon called *uniparental disomy*.

Both syndromes have complex behavioral phenotypes. Social disability is characteristic of Prader-Willi; with Angelman syndrome, the overlap with ASD has been more difficult to establish because of the marked intellectual disability associated with the syndrome. Differentiating intellectual disability from ASD in individuals with very low IQ can be quite challenging. Nonetheless, there are multiple clear molecular and behavioral links with ASD. For example, duplications of the 15q11-13 region are a well-established risk factor for nonsyndromic ASD (see below), and functional de novo missense mutations in the gene *UBE3A* have been found in individuals with ASD without all of the features of Angelman syndrome.

Neurodevelopmental Syndromes Provide Insight Into the Mechanisms of Social Cognition

Although the fragile X, Rett, Williams, Angelman, and Prader-Willi syndromes collectively account for a small fraction of the burden of social disability in the population, studies of these disorders have contributed to major advances in the understanding of normal brain development, neurodevelopmental syndromes in general, and the mechanisms underlying social disability in particular. A number of biological processes identified in the study of these disorders—including the contribution of epigenetic mechanisms and chromatin dynamics, synaptic dysfunction, and the role of aberrant local protein synthesis—have all turned out to be important initial clues to the biological and developmental mechanisms underlying nonsyndromic forms of ASD. Moreover, characterization of the genetics underlying certain neurodevelopmental syndromes provided some of the earliest examples of a phenomenon that is now well accepted in ASD—either losses or gains of identical risk genes or regions may lead to neurodevelopmental disorders, sometimes with overlapping and sometimes contrasting phenotypes.

Importantly, in addition to the first clues regarding molecular mechanisms, recent studies of a number of Mendelian syndromes have challenged conventional wisdom by highlighting, in model systems, the potential reversibility of developmental phenotypes, even into adulthood. These observations, particularly with regard to Rett, Angelman, MDS, and fragile X syndromes, defied the long and generally held belief that the deficits associated with these types of severe syndromes are unchangeable. Moreover, the relevant studies have underscored the fact that a range of manipulations—from genetic, to pharmacological, to the more recent use of antisense oligonucleotides (in the case of *MEC2* duplication and Angelman syndromes)—have all been successful in reversing phenotype.

These findings provide not only an avenue forward for the development of rational therapies in humans but also a critical antidote to the penchant for nihilistic views of therapeutics development in neurodevelopmental disorders. In short, these findings have collectively, and now repeatedly, reinforced the notion that rationally designed therapies may reverse key symptoms long after initial pathology has begun to unfold in brain development. The question of how much of the core symptomatology seen in nonsyndromic ASD is a consequence of ongoing functional derangements, versus what would more traditionally be considered developmental pathology, remains to be clarified. One should note, however, that even with the limited treatments available, the observation that some children improve years after the onset of symptoms suggests that aspects of ASD pathology are not entirely static and may ultimately yield to the development of novel biologically driven treatment approaches.

The Complex Genetics of Common Forms of Autism Spectrum Disorder Are Being Clarified

The recent discovery of genes causing idiopathic ASD—once a scientific quagmire—has been among the most dramatic success stories in the field of human genetics. The combination of high-throughput genomic technologies—including the ability to assay common and rare variations in both the sequence and structure of DNA—the consolidation of large patient cohorts, and considerable investment in ASD research has transformed the field.

Initial breakthroughs can be traced to studies of the genes encoding the family of neuroligins—cell

adhesion molecules found at postsynaptic densities of glutaminergic synapses (Chapter 48). At the beginning of this century, the group led by Thomas Bourgeron, a geneticist at the Pasteur Institute, first identified putatively deleterious coding mutations in the genes coding for neuroligin 4X (loss-of-function) and neuroligin 3X (missense). About 6 months after the initial report on the loss-of-function mutation in *NLGN4X*, a nearly identical loss-of-function mutation in the same gene was found linked to both intellectual disability and ASD in a large pedigree. The relevance of the neuroligin 3X mutation to ASD has taken longer to clarify. Contemporary studies provide statistical evidence that *NLGN3X* is a probable, but not yet definitive, ASD risk gene. Additional studies of large cohorts will clarify this question.

In retrospect, these findings were prescient. The two papers on neuroligins pointed to the importance of loss-of-function heterozygous mutations leading not only to ASD but to a wide range of neurodevelopmental phenotypes and highlighted a role for synaptic proteins at the excitatory synapse. Moreover, in addition to being a harbinger of the contributions of both rare and de novo mutations (Chapter 2), the reported findings from Bourgeron's group also hinted, in retrospect, at a female protective effect as well as a paternal origin of de novo point mutations. In the initial report, the unaffected mother carried a de novo loss-of-function mutation on her paternally inherited X chromosome, which she passed to two affected sons.

Several years later, two key findings further ushered in the modern age of reliable and reproducible genetic studies in ASD. First, papers in 2006 and 2007 reported on the observation of rare de novo heterozygous copy number variations (Chapter 2) in children with ASD and intellectual disability. These studies focused specifically on idiopathic, nonsyndromic ASD and on families with only a single affected individual (simplex families). Both papers reported high rates of relatively large copy number variations among individuals with both intellectual and social disability. Second, it was not clear if individuals with ASD simply had more chromosomal abnormalities than those without. However, this question was soon answered by studies from multiple laboratories. De novo copy number variations did not appear to be distributed randomly throughout the genome but tended to cluster in distinct regions of the genome, suggesting that the increased rate in such cases was a consequence of an accumulation of specific risk events. Moreover, as higher-resolution genomic assays began to be applied, similar results emerged: Only certain subsets of mutations (eg, point mutations that disrupt gene function) proved to be elevated in individuals with autism, pointing to the aggregation of causal mutations in affected individuals, not hypermutability, as an explanation for the excess rate(s) of de novo events in affected individuals.

A considerable investment in studying copy number variations in simplex families has resulted in a steadily expanding list of copy number variations that clearly and dramatically increase the risk for ASD. At present, about a dozen genomic intervals reach genome-wide significance based on genome-wide screening of cases for de novo mutations (Figure 62–8). As a result, the American College of Medical Genetics now considers screening for copy number variations the standard of care for an individual presenting with ASD of unknown etiology.

Studies of de novo mutations have advanced throughout the second decade of this millennium, leading to the discovery that, similar to de novo copy number variations, de novo changes in the sequence of DNA—both single nucleotide variants and insertions or deletions (indels)—also contribute to ASD risk and can similarly be used to identify specific risk genes. Recent reports have now leveraged this approach to include more than 100 genes carrying large-effect single nucleotide variants and indel mutations that disrupt the function of the encoded protein (ie, likely gene-disruptive [LGD] mutations) (Chapter 2).

Several associated findings deserve mention here. First, although the contribution of de novo mutations to the risk for ASD in the total population is quite small (in the neighborhood of 3%), the proportion of individuals with large-effect de novo mutations who are seen in clinical settings and recruited for genetic studies is quite significant, as high as 40% of girls. The reason for this apparent contradiction is that most of the risk to the population writ large is carried in small-effect common variations that in most individuals are not sufficient to result in them crossing a diagnostic threshold for ASD. In short, most individuals carrying some degree of risk in the population never show overt social impairment and do not come to clinical attention. Conversely, individuals with large-effect de novo copy number variations, single nucleotide variants, and indels are much more likely to have significant clinical manifestations and seek medical attention.

Second, studies of de novo single nucleotide variants and indels in ASD using exome sequencing have found that the rate of de novo mutations increases with the father's age. Consistent with this observation is the finding that the vast majority of deleterious de novo sequence mutations in ASD cases are present on the paternally inherited chromosome. Although the

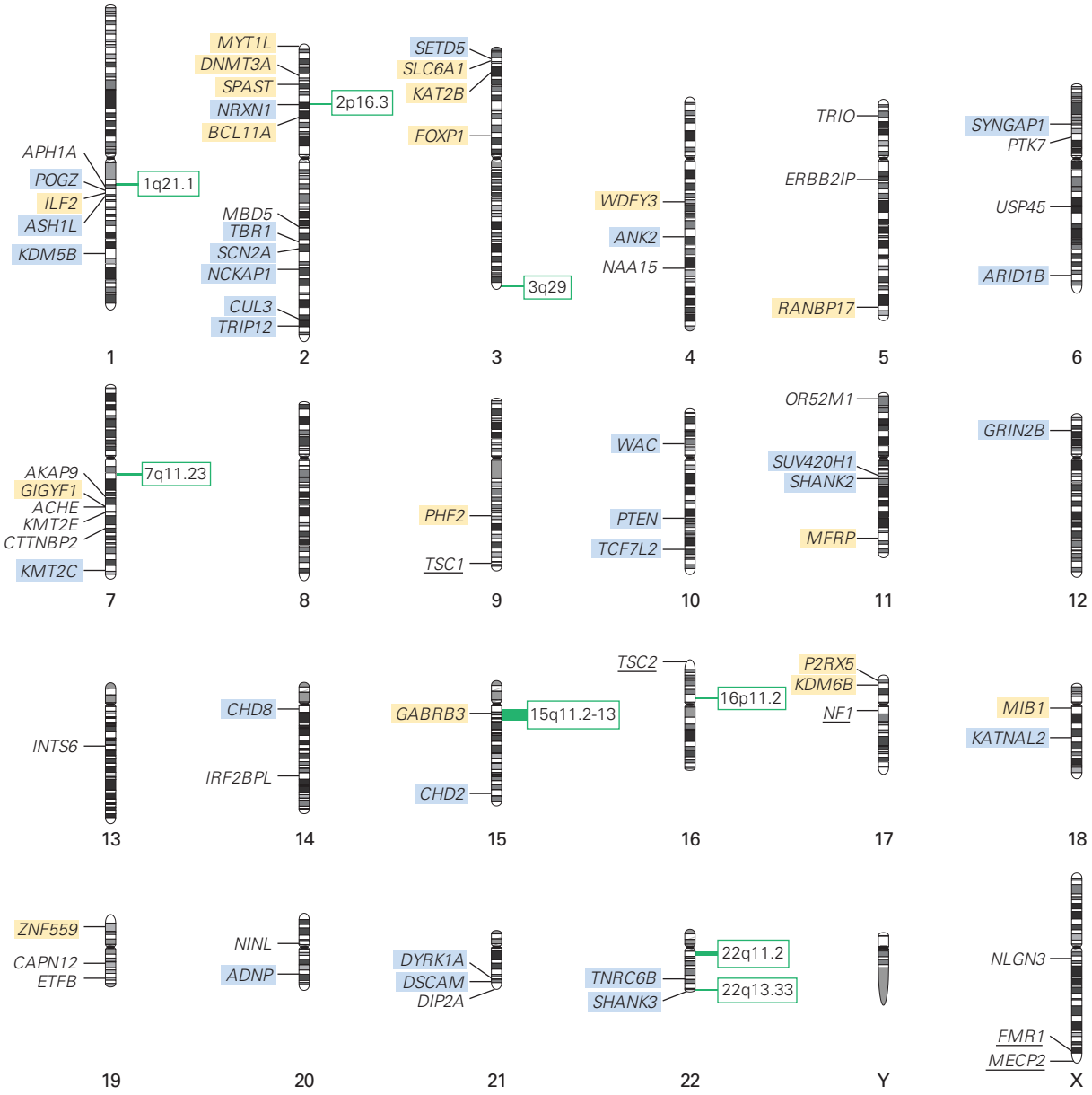

Figure 62–8 **Multiple genes and copy number variations that have been strongly associated with idiopathic risk for autism spectrum disorders (ASDs).** The figure identifies 71 genes and copy number variations (CNVs) associated with risk for ASDs based predominantly on the recurrence of de novo mutations. Abbreviations in **blue shading** denote genes with a false discovery rate (**FDR**) less than 0.01; abbreviations in **yellow shading** denote an FDR between 0.01 and 0.05; and abbreviations with **no shading** denote an FDR greater than 0.05 and less than 0.1. **Green bars** identify CNVs with an FDR less than 0.05. Data from Sanders et al. 2015. Statistical analysis was performed using the methods described in Sanders et al. 2015. Five additional genes with names underlined cause the syndromic forms of ASD discussed in the chapter text. Gene identification in ASD is continuing at a rapid pace. Up-to-date lists of associated genes and genomic regions can be found at https://gene.sfari.org.

absolute increase in risk with age is small, this observation nonetheless provides a conceptual framework for understanding secular increases in ASD prevalence. It also sets the stage for further studies of the impact of environmental factors in increasing de novo mutations and thereby potentially increasing the true incidence of clinical ASD cases.

The relationship of de novo large-effect mutations to intellectual disability has been the subject of considerable discussion, with some contending that de novo

large-effect mutations are typically seen in ASD with intellectual disability. Although it is the case that de novo mutations that are damaging (either copy number variations or single nucleotide variants) are more prevalent in ASD patients with lower IQ, it is also the case that mutations that confer ASD risk are found across the entire IQ spectrum, reinforcing the idea that domains of cognitive and social functioning are to some degree separable.

One notable difference between the genetics of ASD and other common disorders, including schizophrenia, has been the lack of progress using genome-wide association studies (Chapter 2). To date, only a handful of common genetic variants have been found that are significantly and reproducibly associated with ASD risk. Moreover, earlier conventional wisdom about the contribution of candidate genes such as *5-HTT*, *MTHFR*, or *OXT* polymorphisms is highly uncertain, based on the lack of findings from genome-wide association studies and the fact that these associations derived from an approach that has been shown empirically to be unreliable for gene discovery in complex common disorders. On the other hand, as noted, there is very strong evidence that common variation plays a substantial role in the population risk for ASD. Indeed, genome-wide association studies that have inferred the degree of contribution from this type of variation agree that the lion's share of vulnerability resides in common variation. One can reconcile these observations by noting that for those disorders, such as ASD, that markedly impair reproductive fitness, only common genetic variations carrying small effects remain in the human population over many generations. Those with larger effects would either be driven to low frequencies or removed entirely by natural selection. In addition, sample sizes for case-control genome-wide association studies of ASD to date have been more modest than those that have led to the marked success in identifying common polymorphisms associated with schizophrenia. In short, limited power is almost certainly a key limitation in identifying the common small-effect alleles contributing to ASD.

The relative success in identifying de novo mutations does not suggest that these are the only important mechanisms of ASD risk. Recent progress in this area is the result of a fortuitous combination of the large-effect size of the mutations, their location in the most easily interpreted portion of the genome (the coding region), and their low base rate in typically developing individuals. With regard to population risk, however, common noncoding, small-effect alleles are likely to collectively account for a greater overall proportion of the liability for ASD compared to rare high-effect variants. Moreover, there is evidence for recessive forms of ASD as well. These have initially been identified predominantly in consanguineous populations via the identification of homozygous loss-of-function mutations—that is, the identical damaging allele on both the paternally and the maternally inherited chromosomes—including in the genes *CNTNAP2*, *BCKDK*, and *NHE9*. Moreover, several recent studies have highlighted the contribution of compound heterozygote mutations to ASD risk—that is, different mutations mapping to the same gene on the maternally and paternally inherited chromosome—in populations with low rates of consanguinity.

A key point is that the pursuit and discovery of different types of mutations may help advance the science in different ways. For example, rare de novo high-effect mutations can be quickly studied in model systems. Also, common variants provide an opportunity to assess overall polygenic risk in research cohorts, an approach that may be highly useful for multimodal studies, such as those that integrate neuroimaging with genetic data, or other investigations linking human behaviors to genotypes. Finally, very rare homozygous/recessive variants mitigate some of the challenges of modeling haploinsufficiency.

Even though heritability—the proportion of the phenotypic variance due to genetic factors—is very high for ASD, environmental factors also play a role, although few specific environmental factors have been conclusively identified. Infections by viruses (eg, rubella, measles, influenza, herpes simplex, and cytomegalovirus) in utero may contribute to the etiology of ASD. There is substantial evidence that mediators of immune functions also play a role in brain development including synaptogenesis. Given the complexity of ASD and its various forms, it is likely that a variety of etiologies will ultimately be discovered—some purely genetic, others that depend on combinations of genetic risk factors and environmental factors, and some purely environmental causes.

Genetics and Neuropathology Are Illuminating the Neural Mechanisms of Autism Spectrum Disorder

Genetic Findings Can Be Interpreted Using Systems Biological Approaches

The recent advances in gene discovery are a particularly exciting development, offering many opportunities for biological analyses using an increasing armamentarium of in vitro and in vivo methods. In addition,

contemporary genomic approaches, examining large sections of the genome simultaneously, allow for unbiased approaches to be used in the study of groups of risk genes in an effort to identify points of convergence among disparate ASD genes.

To date, biological approaches that examine multiple systems have been divided roughly into two types of efforts: those that attempt to identify the types of biological processes reflected in the growing list of ASD genes and those that attempt to identify biological points of convergence at either the molecular or cellular level. The latter approach is based on the notion that multiple types of genetically driven perturbations in differing pathways may lead to a common phenotype due to their convergence on specific cell types, regions, or circuits at specific time points during the development of the human brain.

Biological processes or pathways in which ASD risk genes are present in a greater proportion than expected under the null hypothesis include chromatin modification, synaptic function, the WNT signaling pathway, and targets of FMRP. This list is clearly not exhaustive. For example, what we learned from genes involved in genetic syndromes as well as genes that cause nonsyndromic or idiopathic ASD implicates synaptic local protein synthesis as well as neurogenesis as points of potential biological convergence of disparate risk mutations.

Some variability in these findings is almost certainly attributable to different selection criteria for ASD risk genes as well as differences in the data used to annotate their function. This latter issue is important to keep in mind as numerous confounding factors are inherent in current efforts to annotate the biological processes assigned to a given gene or protein. These include the sources of data. For example, the assigned function of a gene can be markedly influenced by publication bias, whether in vitro or in vivo assays were employed, and what types of tissues and model systems were used to generate the data. Moreover, most functional annotations provide limited information on the time course of function for genes that may be developmentally regulated and biologically pleiotropic. Nonetheless, it is the increasing consistency in findings that is most striking. Despite the varying approaches, the biological processes noted above have been repeatedly identified among diverse rigorous studies.

As noted, an alternative approach to determining where multiple autism risk genes overlap involves examining not just their function but also their developmental expression pattern. Such studies are predicated on the notion that multiple risk genes may have different overt functions but share the ability to disrupt the same circuit, cellular, or developmental process. For example, a mutation in a gene encoding a protein known to mediate synaptic adhesion and a separate mutation in a gene encoding a chromatin modifier may both lead to identical abnormalities in the development of early cortical striatal connections. In such cases, the timing and location of the perturbation may be as relevant as a specific molecular pathway or the assigned molecular function of the individual gene(s). These studies have also tended to rely on assaying developmental expression trajectories genome-wide to minimize some of the confounding factors associated with other available annotation systems. For instance, it is now possible to assay essentially every gene in the genome simultaneously—eliminating the need to rely on prior research to assign a specific function to a gene. Moreover, such studies increasingly examine gene expression in human and/or nonhuman primate brain, mitigating some of the challenges of relying on in vitro data. Of course, such studies must still contend with the limits of resolution of expression analyses as well as a less than complete (and potentially biased) representation of different brain regions. Nonetheless, to date, the degree of agreement among varying studies is reassuring.

Despite differences in analytical and statistical approaches used in these types of studies, there has been general agreement to date that ASD risk genes point to vulnerability in human mid-fetal cortical development. There is also emerging evidence that these genes point to the involvement of both deep and upper layer projection neurons in cerebral cortex and of striatum and cerebellum (although the data on developmental expression in these regions remain limited in publicly accessible databases compared to cortical regions).

Autism Spectrum Disorder Genes Have Been Studied in a Variety of Model Systems

As a result of the tremendous progress of late, even a cursory description of the literature on the study of ASD in animal models is beyond the scope of this chapter. In part, this is a consequence of the sheer number of studies; in part, it is a product of the marked differences in the type of perturbation studied (eg, well-validated genetic models, "candidate gene" models, pharmacological models such as valproate exposure, or maternal immune activation). Moreover, differences in brain regions, cell types, developmental periods, and the biological processes assayed make summary generalizations problematic. In short, no consensus has yet been reached regarding the range of pathophysiological mechanisms relevant to ASD.

Nonetheless, given recent progress in human genetics, it is increasingly important to distinguish between models based on reproducible genetic findings, including those leading to syndromic ASD, and models based on unreliable candidate gene loci or solely on behaviors (ie, those that appear to reproduce human symptoms). Given the multiple options now available to study genetic variations that demonstrably increase the risk in humans for ASD in the phenotypes of interest, the study of models with more tenuous links to human pathophysiology is increasingly difficult to justify.

Many publications reporting rodent models of ASD, regardless of their origins, focus on phenotypes that resemble symptoms seen in the human syndrome, including changes in social interactions, vocalizations, and behaviors reminiscent of human anxiety or aggression. Even with a bias toward publishing positive findings, results vary dramatically. Of note, there has been a long-standing debate over the relevance of animal models for ASD, given the important differences in brain development, organization, and function between humans and the most commonly used experimental animals. Nevertheless, unbiased assessments of a wide range of animal behaviors—not necessarily prioritizing those that "look" like core ASD symptoms—may well provide a valuable window into pathophysiological mechanisms. For example, some of the most commonly observed phenotypes reported to date across various ASD genetic models (and by various laboratories) involve motor behavior. In this case, it seems far less important that the observed behaviors are reminiscent of core diagnostic features in humans than that the observations suggest an important point of biological convergence, providing clues to cell types, circuits, and processes involved in ASD.

Although rodent models continue to dominate the ASD literature, a wide range of other models have already provided important insights into biology. These include the fruit fly, worm, zebrafish, frogs, voles, nonhuman primates, induced pluripotent stem cells and brain organoids, and human postmortem samples. Given the complexity of the problems at hand, the differing strengths and limitations of various models, and the important differences in brain structure and development across species, continued progress will likely require integrating data across a wide range of existing models, from flies and worms to humans.

Postmortem and Brain Tissue Studies Provide Insight Into Autism Spectrum Disorder Pathology

The neuropathology of autism at a microscopic level is also not yet clear, but several studies provide evidence for the potential for multiple anatomical correlates. The multiple correlates may in part be due to the small number of brains available for pathological analysis. Moreover, only a small fraction of these have undergone quantitative analysis. Another problem is the frequent occurrence of epilepsy. Approximately 30% of individuals with autism also have seizure disorders, and seizures may damage the amygdala and many other brain regions implicated in ASD.

One of the earliest and most consistent anatomical findings in ASD has been the lower number of Purkinje cells in the cerebellum in some individuals. When neural stains are used to mark cell bodies, gaps in the orderly arrays of Purkinje cells are noticeable. Whether this reduction in cell number is because of ASD, epilepsy, or the co-occurrence of both disorders is not clear. It is also not clear whether the reduced number of Purkinje cells is characteristic of ASD in particular or neurodevelopmental disorders more generally. A wide variety of cerebellar changes were identified in cases of idiopathic intellectual disability, in Williams syndrome, and in other neurodevelopmental disorders. A few cases of alterations of brain stem nuclei that are connected to the cerebellum, such as the olivary complex, have also been reported. Finally, contemporary analyses have found considerable heterogeneity in cell number, with only a subset of samples showing a decrease in the number of Purkinje cells.

Microscopic abnormalities have also been observed in the autistic cerebral cortex, including defects in the migration of cells into the cortex, such as ectopias (nests of cells in white matter that failed to enter the cortex). It has also been proposed that the columnar organization of the autistic cortex is abnormal. These findings still await confirmation in larger studies using quantitative strategies. Finally, one study found fewer neurons in the mature amygdala of people with ASD without epilepsy.

In one of the few reported descriptions of live pathological tissue samples from patients with ASD (removed from three patients during surgery for intractable epilepsy), multiple cytoarchitectural abnormalities were identified in the temporal cortices. These individuals all carried rare recessive loss-of-function mutations in the gene *contactin associated protein-like 2*. Multiple histological abnormalities were observed in these patients, including areas of cortical thickening and blurring of the boundary between gray matter and white matter. Moreover, the authors described neurons in multiple cortical regions that were abnormally organized into tightly packed columns or clusters. In both the hippocampus and temporal cortex, the number of neurons was increased, and many of the

neurons had abnormal shapes instead of their pyramidal morphology. Given the presence of gross temporal lobe abnormalities visible on MRI in two of the three patients, the rare recessive genetic contribution, and the particularly severe seizure disorder, the generalizability of these findings to idiopathic ASD remains in question.

The notion overall that there are neuroanatomical changes in some ASD patients is supported by several other lines of evidence. A number of well-supported and well-characterized ASD risk genes (eg, *PTEN* mutations) are associated with increases in brain size ranging from modest (eg, *CHD8* loss-of-function mutations) to frank macrocephaly. In addition, ASD is often associated with microcephaly. Girls with Rett syndrome have acquired microcephaly, suggesting, not surprisingly, that multiple anatomical derangements may occur in social disability phenotypes.

Advances in Basic and Translational Science Provide a Path to Elucidate the Pathophysiology of Autism Spectrum Disorder

A full understanding of the neurobiological basis of the many neurodevelopmental disorders that lead to social and intellectual disability will require the convergence of neuroscience, other medical disciplines, computational biology, and genomics. A bottom-up approach—progressing from the identification of genes responsible for cognitive and behavioral disorders to an understanding of their effects on brain development—is already providing some key insights. At the same time, a top-down approach may also be highly productive by identifying and defining critical neural circuits involved in social function and dysfunction.

Fortunately, the tools available to pursue both approaches are increasingly accessible, from high-throughput whole-genome sequencing to rapidly advancing informatics pipelines, genome editing, optogenetics and other methods to study circuits in vivo, single cell technologies, improved neuroimaging methods and technologies, and the development of tractable human and nonhuman primate neural models, including brain organoids.

Although there has been great progress in elaborating the genetics and biology of ASD and other neurodevelopmental disorders, the findings from genomic studies have also pointed to some key challenges: At the most basic level, the translation of these discoveries to an understanding of pathophysiology is limited by the current state of knowledge regarding brain organization and development. It seems likely that without a detailed cellular understanding of the brains of humans, nonhuman primates, and other model systems, it will be challenging to interpret the wide variety of genetic perturbations and move from an understanding of the biology to any understanding of the pathogenesis. It is also reasonable to presume that to be most useful for the disorders of the type discussed in this chapter, this type of map will have to capture developmental dimensions. It is exciting and heartening, then, that the recent BRAIN Initiative, other large-scale governmental efforts, and the efforts of private foundations have all highlighted foundational knowledge as a key to success.

There is little doubt that the distance between our knowledge of clinical phenomenology, genetics, imaging, and neuropathology on the one hand and, on the other, the development of novel treatments that will profoundly improve the lives of severely affected individuals can seem daunting. At the same time, it is heartening to see the progress with Mendelian neurodevelopmental disorders, where some clinical trials of rational therapies have been completed and others are currently underway. Although some of the early results have been disappointing, the mere fact that the understanding of these syndromes has advanced to this point is cause for continued optimism. Along these lines, it is useful to consider the required extent of revision of this chapter from the prior volume to the current one. The ability to confidently assign large-effect genetic risk at nearly 100 genomic loci and genes, the emerging consensus regarding what types of molecular processes and pathways are involved, the first glimpses of the developmental characteristics, and the initiation of biologically driven therapeutic trials have all emerged over a relatively short period of time. It is exciting to speculate where the field could be by the publication of the next revision of this book.

Highlights

1. Neurodevelopmental syndromes can involve varying degrees of impairment in different cognitive domains. Syndromes that involve dysfunction in the social realm, with or without involvement of general cognition or perception, are the focus of this chapter.
2. Autism is the paradigmatic social disability syndrome, first described in the literature in 1943 by Leo Kanner. Today, autism is considered a spectrum of disorders with two defining diagnostic features: fundamentally impaired social communication and stereotyped behaviors and/

or highly restricted interests. The prevalence of autism spectrum disorder (ASD) is estimated to be at least 1.5% in developed countries and is much more frequent in males than females.

3. Both environmental factors and myriad genes contribute to ASD risk. This genetic complexity resulted for several decades in scant progress in efforts to map specific ASD risk genes and genomic regions (loci).
4. The earliest clues to both the genetics and neurobiology of ASD emerged from early investigations of neurodevelopmental syndromes that manifest both with intellectual disability and social impairment. These include, among others, fragile X syndrome, Rett syndrome, Williams syndrome, and Prader-Willi and Angelman syndromes.
5. High-throughput genomic technologies, the consolidation of large patient cohorts, and considerable investment in ASD research have transformed the field of gene discovery in idiopathic ASD. At present, dozens of specific genes and genomic regions have been reliably and reproducibly associated with risk for ASD.
6. Recent progress in the genetics of common forms of ASD has emerged from a focus on rare and sporadic (de novo) mutations in the coding portion of the genome. On average, these mutations carry much larger biological effects than have been identified in studies of other psychiatric disorders, such as schizophrenia, where many common genetic risk variants have been identified, each with a small effect.
7. Studies of both genetic syndromes and idiopathic ASD have begun to reveal processes, pathways, and developmental epochs involved in pathophysiology. These include epigenetic mechanisms and chromatin dynamics, synaptic dysfunction, and the role of aberrant local protein synthesis. Recent studies of genetically determined ASDs have also shown that human mid-fetal cortical development and glutamatergic neurons are particularly vulnerable.
8. The current availability of a significant number of confirmed ASD loci, both for syndromic as well as idiopathic forms of the disorder, provides a solid foundation for neurobiological studies. These advances provide a strong link to human pathophysiology, including potential traction on the question of cause versus effect, given that germline genetic changes are present prior to the earliest stages of brain development.
9. In addition to providing some of the first clues regarding molecular mechanisms of idiopathic ASD, studies of Mendelian syndromes have challenged conventional wisdom by highlighting the potential reversibility of developmental phenotypes. These observations, particularly with regard to Rett syndrome and fragile X syndrome, have generated renewed optimism about the opportunities for rational development of therapeutic treatments.
10. Multiple methods are now converging to elaborate the pathology underlying ASD, including gene discovery and systems biology, model systems approaches, neuroimaging studies, and neuropathological studies. The key challenge going forward will be to move from a general understanding of biology to an actionable understanding of pathophysiology.

Matthew W. State

Selected Reading

de la Torre-Ubieta L, Won H, Stein JL, Geschwind DH. 2016. Advancing the understanding of autism disease mechanisms through genetics. Nat Med 22:345–361.

Frith U. 2008. *Autism: A Very Short Introduction*. Oxford: Oxford Univ. Press.

Happé F, Frith U (eds). 2010. *Autism and Talent*. Oxford: Oxford Univ. Press. (First published as a special issue of *Philosophical Transactions of the Royal Society, Series B*, Vol. 364, 2009.)

Klin A, Jones W, Schultz R, Volkmar F, Cohen D. 2002. Defining and quantifying the social phenotype in autism. Am J Psychiatry 159:895–908.

Sesan N, State MW. 2018. Lost in translation: traversing the complex path from genomics to therapeutics in autism spectrum disorders. Neuron 100:406–423.

Zoghbi HY, Bear MF. 2012. Synaptic dysfunction in neurodevelopmental disorders associated with autism and intellectual disabilities. Cold Spring Harb Perspect Biol 4:a009886.

References

Amaral DG, Schumann CM, Nordahl CW. 2008. Neuroanatomy of autism. Trends Neurosci 31:137–145.

Anderson DK, Liang JW, Lord C. 2014. Predicting young adult outcome among more and less cognitively able individuals with autism spectrum disorders. J Child Psychol Psychiatry 55:485–494.

Baron-Cohen S, Cox A, Baird G, et al. 1996. Psychological markers in the detection of autism in infancy in a large population. Br J Psychiatry 168:158–163.

Baron-Cohen S, Leslie AM, Frith U. 1985. Does the autistic child have a "theory of mind"? Cognition 21:37–46.

Bear MF, Huber KM, Warren ST. 2004. The mGluR theory of fragile X syndrome. Trends Neurosci 27:370–377.

Cassidy SB, Morris CA. 2002. Behavioral phenotypes in genetic syndromes: genetic clues to human behavior. Adv Pediatr 49:59–86.

Castelli F, Happé F, Frith CD, Frith U. 2002. Autism, Asperger syndrome and brain mechanisms for the attribution of mental states to animated shapes. Brain 125:1839–1849.

De Rubeis S, He X, Goldberg AP, et al. 2014. Synaptic, transcriptional and chromatin genes disrupted in autism. Nature 515:209–215.

Deuse L, Rademacher LM, Winkler L, et al. 2016. Neural correlates of naturalistic social cognition: brain-behavior relationships in healthy adults. Soc Cogn Affect Neurosci 11:1741–1751.

Dolen G, Bear MF. 2009. Fragile x syndrome and autism: from disease model to therapeutic targets. J Neurodev Disord 1:133–140.

Ecker C, Bookheimer SY, Murphy DG. 2015. Neuroimaging in autism spectrum disorder: brain structure and function across the lifespan. Lancet Neurol 14:1121–1134.

Gallagher HL, Happé F, Brunswick N, et al. 2000. Reading the mind in cartoons and stories: an fMRI study of "theory of mind" in verbal and nonverbal tasks. Neuropsychologia 38:11–21.

Gaugler T, Klei L, Sanders SJ, et al. 2014. Most genetic risk for autism resides with common variation. Nat Genet 46:881–885.

Grove J, Ripke S, Als TD, et al. 2019. Identification of common genetic risk variants for autism spectrum disorder. Nat Gen 51:431–444.

Halladay AK, Bishop S, Constantino JN, et al. 2015. Sex and gender differences in autism spectrum disorder: summarizing evidence gaps and identifying emerging areas of priority. Mol Autism 6:36.

Happe F, Ehlers S, Fletcher P, et al. 1996. "Theory of mind" in the brain. Evidence from a PET scan study of Asperger syndrome. Neuroreport 8:197–201.

Hill E. 2004. Executive dysfunction in autism. Trends Cogn Sci 8:26–32.

Iossifov I, O'Roak BJ, Sanders SJ, et al. 2014. The contribution of de novo coding mutations to autism spectrum disorder. Nature 515:216–221.

Jacquemont ML, Sanlaville D, Redon R, et al. 2006. Array-based comparative genomic hybridisation identifies high frequency of cryptic chromosomal rearrangements in patients with syndromic autism spectrum disorders. J Med Genet 43:843–849.

Jamain S, Quach H, Betancur C, et al. 2003. Mutations of the X-linked genes encoding neuroligins NLGN3 and NLGN4 are associated with autism. Nat Genet 34:27–29.

Jin P, Alisch RS, Warren ST. 2004. RNA and microRNA in fragile X syndrome. Nat Cell Biol 6:1048–1053.

Kana RK, Keller TA, Cherkassky VL, Minshew NJ, Just MA. 2009. Atypical frontal-posterior synchronization of theory of mind regions in autism during mental state attribution. Soc Neurosci 4:135–152.

Kim YS, Leventhal BL. 2015. Genetic epidemiology and insights into interactive genetic and environmental effects in autism spectrum disorders. Biol Psychiatry 77: 66–74.

Klei L, Sanders SJ, Murtha MT, et al. 2012. Common genetic variants, acting additively, are a major source of risk for autism. Mol Autism 3:9.

Koldewyn K, Yendiki A, Weigelt S, et al. 2014. Differences in the right inferior longitudinal fasciculus but no general disruption of white matter tracts in children with autism spectrum disorder. Proc Natl Acad Sci U S A 111:1981–1986.

Kovács ÁM, Téglás E, Endress AD. 2010. The social sense: susceptibility to others' beliefs in human infants and adults. Science 330:1830–1834.

Kumar RA, Marshall CR, Badner JA, et al. 2009. Association and mutation analyses of 16p11.2 autism candidate genes. PLoS One 4:e4582.

Laumonnier F, Bonnet-Brilhault F, Gomot M, et al. 2004. X-linked mental retardation and autism are associated with a mutation in the NLGN4 gene, a member of the neuroligin family. Am J Hum Genet 74:552–557.

Lombardi LM, Baker SA, Zoghbi HY. 2015. MECP2 disorders: from the clinic to mice and back. J Clin Invest 125:2914–2923.

Marshall CR, Noor A, Vincent JB, et al. 2008. Structural variation of chromosomes in autism spectrum disorder. Am J Hum Genet 82:477–488.

Morrow EM, Yoo SY, Flavell SW, et al. 2008. Identifying autism loci and genes by tracing recent shared ancestry. Science 321:218–223.

Nakamoto M, Nalavadi V, Epstein MP, et al. 2007. Fragile X mental retardation protein deficiency leads to excessive mGluR5-dependent internalization of AMPA receptors. Proc Natl Acad Sci U S A 104:15537–15542.

Neale BM, Kou Y, Liu L, et al. 2012. Patterns and rates of exonic de novo mutations in autism spectrum disorders. Nature 485:242–245.

Novarino G, El-Fishawy P, Kayserili H, et al. 2012. Mutations in BCKD-kinase lead to a potentially treatable form of autism with epilepsy. Science 338:394–397.

Ozonoff S, Iosif AM, Baguio F, et al. 2010. A prospective study of the emergence of early behavioral signs of autism. J Am Acad Child Adolesc Psychiat 49:256–266.

Ozonoff S, Macari S, Young GS, Goldring S, Thompson M, Rogers SJ. 2008. Atypical object exploration at 12 months of age is associated with autism in a prospective sample. Autism 12:457–472.

Parikshak NN, Luo R, Zhang A, et al. 2013. Integrative functional genomic analyses implicate specific molecular pathways and circuits in autism. Cell 155:1008–1021.

Pinto D, Delaby E, Merico D, et al. 2014. Convergence of genes and cellular pathways dysregulated in autism spectrum disorders. Am J Hum Genet 94:677–694.

Raznahan A, Wallace GL, Antezana L, et al. 2013. Compared to what? Early brain overgrowth in autism and the perils of population norms. Biol Psychiatry 74:563–575.

Samson D, Apperly IA, Chiavarino C, Humphreys GW. 2004. Left temporoparietal junction is necessary for representing someone else's belief. Nat Neurosci 7:499–500.

Sanders SJ, Ercan-Sencicek AG, Hus V, et al. 2011. Multiple recurrent de novo CNVs, including duplications of the 7q11.23 Williams syndrome region, are strongly associated with autism. Neuron 70:863–885.

Sanders SJ, He X, Willsey AJ, et al. 2015. Insights into autism spectrum disorder genomic architecture and biology from 71 risk loci. Neuron 87:1215–1233.

Sanders SJ, Murtha MT, Gupta AR, et al. 2012. De novo mutations revealed by whole exome sequencing are strongly associated with autism. Nature 485:237–241.

Satterstrom FK, Kosmicki JA, Wang J, Breen MS, et al. 2020. Large-scale exome sequencing study implicates both developmental and functional changes in the neurobiology of autism. Cell 180:568–584.

Schultz RT, Grelotti DJ, Klin A, et al. 2003. The role of the fusiform face area in social cognition: implications for the pathobiology of autism. Philos Trans R Soc Lond B Biol Sci 358:415–427.

Sebat J, Lakshmi B, Malhotra D, et al. 2007. Strong association of de novo copy number variation with autism. Science 316:445–449.

Senju A, Southgate V, White S, Frith U. 2009. Mindblind eyes: an absence of spontaneous theory of mind in Asperger syndrome. Science 325:883–885.

State MW, Sestan N. 2012. Neuroscience. The emerging biology of autism spectrum disorders. Science 337:1301–1303.

Strauss KA, Puffenberger EG, Huentelman MJ, et al. 2006. Recessive symptomatic focal epilepsy and mutant contactin-associated protein-like 2. N Engl J Med 354:1370–1377.

Sztainberg Y, Chen HM, Swann JW, et al. 2015. Reversal of phenotypes in MECP2 duplication mice using genetic rescue or antisense oligonucleotides. Nature 528:123–126.

Sztainberg Y, Zoghbi HY. 2016. Lessons learned from studying syndromic autism spectrum disorders. Nat Neurosci 19:1408–1417.

Weiss LA, Shen Y, Korn JM, et al. 2008. Association between microdeletion and microduplication at 16p11.2 and autism. N Engl J Med 358:667–675.

Willsey AJ, Sanders SJ, Li M, et al. 2013. Coexpression networks implicate human midfetal deep cortical projection neurons in the pathogenesis of autism. Cell 155:997–1007.

Yang DY, Beam D, Pelphrey KA, Abdullahi S, Jou RJ. 2016. Cortical morphological markers in children with autism: a structural magnetic resonance imaging study of thickness, area, volume, and gyrification. Mol Autism 7:11.

63

Genetic Mechanisms in Neurodegenerative Diseases of the Nervous System

The major degenerative diseases of the nervous system—Alzheimer, Parkinson, and the triplet repeat diseases (Huntington disease and the spinocerebellar ataxias)—afflict more than six million people in the United States and more than 25 million throughout the world. Although this is a relatively small percentage of the population, these diseases bring a disproportionate amount of suffering and economic hardship, not only to their victims but also to the families and friends of the afflicted.

Most of these disorders strike in mid-life or later. Aging itself may contribute to susceptibility. The first symptoms to appear often involve loss of fine motor control. Huntington disease can first manifest itself in cognitive deficits, and this is certainly the case for Alzheimer disease. Nevertheless, the end result is the same: A period of slow deterioration, usually 10 to 20 years, robs afflicted patients of their abilities and eventually their lives.

The late-onset neurodegenerative diseases can be divided into two categories: inherited and sporadic (ie, of unknown etiology). Alzheimer and Parkinson diseases are predominantly sporadic; nevertheless, inherited forms, which afflict only a small number of patients, have provided some insight into the pathophysiology of these diseases. Huntington disease, the spinocerebellar ataxias, dentatorubropallidoluysian atrophy, and spinobulbar muscular atrophy are inherited, the result of polyglutamine or CAG triplet repeat diseases.

The triplet repeat diseases are notable for being caused by a "dynamic" mutation: The disease proteins contain a CAG repeat tract that codes for glutamine

and can undergo expansion during DNA replication. Unfortunately, the longer the CAG tract, the more likely it is to further expand, which accounts for the striking phenomenon of *anticipation*: Younger generations within a family have longer repeats and develop more severe symptoms at an earlier age than their parents. Identification of the molecular basis of these disorders has facilitated diagnosis and provides hope for eventual treatment.

Huntington Disease Involves Degeneration of the Striatum

Huntington disease usually strikes in early or middle adulthood and affects 5 to 10 people per 100,000. Symptoms include loss of motor control, cognitive impairment, and affective disturbance. Motor problems most commonly manifest first as chorea (involuntary, jerky movement that involves the small joints at first but then gradually affects the legs and trunk, making walking difficult). Fast, fluid movements are replaced by rigidity and bradykinesia (unusually slow movements).

Cognitive impairment—especially difficulty in planning and executing complex functions—may be detected by formal neuropsychological testing even prior to motor dysfunction. Affected individuals may also have disordered sleep and affective disturbances such as depression, irritability, and social withdrawal. About 10% of patients experience hypomania (increased energy), and a smaller percentage experience frank psychosis.

In adult patients, the disease progresses inexorably to death some 17 to 20 years after onset. Juvenile-onset patients suffer a more rapid course and typically develop bradykinesia, dystonia (spasms of the neck, shoulders, and trunk), rigidity (resistance to the passive motion of a limb), seizures, and severe dementia within only a few years.

The pathological hallmark of Huntington disease is degeneration of the striatum, which can show up in neuroimaging as much as a decade prior to the onset of symptoms. The caudate nucleus is more affected than the putamen. Loss of the medium spiny neurons, a class of inhibitory interneurons in the striatum, reduces inhibition of neurons in the external pallidum (Chapter 38). The resulting excessive activity of the pallidal neurons inhibits the subthalamic nucleus, which could account for the choreiform movements. As the disease progresses and striatal neurons projecting to the internal pallidum degenerate, rigidity replaces chorea. Disruption of the corticostriatal projections leads to thinning of the cortex. In addition to this central nervous system pathology, patients can suffer from immune system and metabolic disturbances, testicular atrophy, cardiac failure, osteoporosis, and skeletal muscle wasting. Cases of juvenile Huntington disease are more severe, and the pathology progresses more rapidly and broadly; for example, degeneration of cerebellar Purkinje cells can occur.

Huntington disease is an autosomal dominant disorder and one of the first human diseases whose gene was mapped using polymorphic DNA markers. It is caused by expansion of a translated CAG repeat that encodes a glutamine tract in the huntingtin protein. Normal or wild-type alleles have 6 to 34 repeats, whereas disease-causing alleles typically have 36 or more repeats that are quite unstable when transmitted from one generation to the next, especially through paternal germ cells. Disease severity, age of onset, and speed of progression correlate with repeat length; individuals with 36 to 39 repeats have later onset and milder disease, while those with more than 40 repeats will have earlier onset and a more severe course. Those carrying more than 75 repeats will develop the disease as juveniles.

The expanded glutamine tract causes a gain of function in huntingtin, a 348-kDa protein that is well conserved in nature from invertebrates to mammals. It is expressed throughout the brain as a soluble cytoplasmic protein, with a minor fraction present in cell nuclei. It is particularly abundant in somatodendritic regions and axons and has been found to associate with microtubules. Although its precise functions are not fully understood, huntingtin is essential for normal embryonic development. Based on a wide array of protein interactors that function in metabolism, protein turnover, cargo trafficking, and gene expression, it has been postulated that huntingtin functions as a molecular scaffold. Its large size, stability, and ability to switch between multiple conformations suggest it brings together multiple proteins into macromolecular complexes.

Huntingtin has multiple protein domains, the best studied of which is the N-terminal region, which contains the polyglutamine expansion and a nuclear localization signal. The N-terminal region consists of an amphipathic α-helix, which creates a structure critical for the protein's retention in the endoplasmic reticulum. The N-terminus undergoes extensive posttranslational modification by acetylation, ubiquitination, phosphorylation, and sumoylation, all of which affect huntingtin clearance and subcellular localization. Interestingly, the polyglutamine repeats in exon 1 are followed by a proline-rich domain, which, unlike the other exons, has been poorly conserved during evolution.

The remaining 66 exons outside the N-terminus, which account for about 98% of the protein, are far less well characterized. Several HEAT repeats are important for protein–protein interactions. These interactions allow the huntingtin protein to adopt a large number of three-dimensional conformations (up to 100 in vitro). Furthermore, the *HTT* gene produces two different mRNA transcripts, a short and long form. The long form contains an additional 3′ untranslated region and is enriched in the brain. Rare alternative splicing produces isoforms that skip exons 10, 12, 29, and 46 or include exon 41b or a fragment of intron 28, but their significance has not been determined. The diversity of these isoforms might be important during development and could expand the variety of protein interactions available to huntingtin.

Spinobulbar Muscular Atrophy Is Caused by Androgen Receptor Dysfunction

Spinobulbar muscular atrophy (SBMA, also known as Kennedy disease) is the only X-linked disorder among the neurodegenerative diseases discussed in this chapter. It is caused by expansion of a translated CAG repeat in the androgen receptor protein, a member of the steroid hormone receptor family. Only males manifest symptoms: The mutant androgen receptor is toxic only when localized to the nucleus, and this localization is dependent on the hormone androgen.

Proximal muscle weakness is usually the presenting symptom; eventually, the distal and facial muscles weaken as well. Muscle wasting is prominent, secondary to degeneration of motor neurons. Loss of androgen function typically leads to gynecomastia (growth of breast tissue in men), late hypogonadism, and sterility. Because individuals who lose androgen receptor function from other causes do not develop motor neuron degeneration, it seems that the glutamine expansion in SBMA causes both a partial loss of function that accounts for the secondary sexual characteristics and a partial gain of function that damages neurons and produces the neurological dysfunction.

Hereditary Spinocerebellar Ataxias Share Similar Symptoms but Have Distinct Etiologies

The spinocerebellar ataxias (SCAs) and dentatorubropallidoluysian atrophy (DRPLA) are characterized by dysfunction of the cerebellum, spinal tracts, and various brain stem nuclei. The basal ganglia, cerebral cortex, and peripheral nervous system can also be affected (Table 63–1).

Two clinical features common to all the SCAs, ataxia and dysarthria, are signs of cerebellar dysfunction. These typically appear in mid-adulthood and gradually worsen, eventually making walking impossible and speech incomprehensible. Brain stem dysfunction in advanced disease causes difficulties in keeping the airway clear; patients often die of aspiration pneumonia. Some SCAs are associated with additional symptoms such as chorea, retinopathy, or dementia, but these are too variable to support a differential diagnosis. Even individuals within the same family can present quite different clinical pictures. Thus, although the SCAs are single-gene Mendelian disorders, individual genetic makeup and environmental influences affect the clinical-pathological picture.

For example, Machado-Joseph disease and SCA type 3 (SCA3) had been regarded clinically as distinct diseases before it was discovered that they are caused by mutations in the same gene. The clinical confusion arose by historical accident. The most prominent features of the families of Azorean descent who were first studied were bulging eyes, faciolingual fasciculations, Parkinsonism, and dystonia; this syndrome was named Machado-Joseph disease. Subsequently, a group of European geneticists studied patients who had symptoms more reminiscent of SCA1—hypermetric saccades and brisk reflexes in addition to the characteristic ataxia and dysarthria. This constellation of symptoms was therefore called SCA3. It took several years before it became clear that the genetic locus of the two diseases was the same, but still both names (Machado-Joseph disease and SCA3) are used. We now know that the differences observed in the original two groups of patients are at least partially attributable to differences in length of the CAG repeats. Nonetheless, differences in the activity of other proteins caused by genetic variations are probably also at play.

The age of onset within each type of ataxia depends on the number of CAG repeats in the gene (Figure 63–1), although the toxicity of different repeat lengths depends on the protein context. For example, the CAG expansion in SCA6 is the shortest of all the SCAs: Normal alleles have fewer than 18 repeats, and pathological repeats have only 21 to 33 repeats. Yet, tracts of the very same length are completely nonpathogenic in other SCAs. In fact, the gene responsible for SCA7 normally tolerates a few dozen CAG repeats and, in the disease state, can undergo expansion to hundreds of CAGs, the largest expansions seen in any SCA.

Table 63–1 Pattern of Inheritance and Main Clinical Features of Neurodegenerative Diseases Caused by Unstable CAG Trinucleotide Repeats

Disease	Inheritance	Typical presenting features	Principal regions affected
SBMA	X-linked recessive	Muscle cramps, weakness, gynecomastia	Lower motor neurons and anterior horn cells
Huntington	AD	Cognitive impairment, chorea, depression, irritability	Striatum, cortex
Huntington-like 2	AD	Cognitive impairment, chorea, depression, irritability	Striatum, cortex
SCA1	AD	Hypermetric saccades, ataxia, dysarthria, balance, nystagmus	Purkinje cells, brain stem
SCA2	AD	Ataxia, hyporeflexia, slow saccades	Purkinje cells, granule cells, inferior olive
SCA3	AD	Ataxia, gaze-evoked nystagmus, bulging eyes, dystonia, spasticity	Pontine neurons, substantia nigra, anterior horn cells
SCA6	AD	Ataxia, late onset (>50 years of age)	Purkinje cells, granule cells
SCA7	AD	Ataxia, visual loss due to retinal degeneration, hearing loss	Purkinje cells, retina (cone-rod degeneration)
SCA8	AD	Scanning dysarthria, ataxia	Purkinje cells
SCA10	AD	Ataxia and seizures	Purkinje cells
SCA12	AD	Early arm tremor, hyperreflexia, ataxia	Purkinje cells, cortical and cerebellar atrophy
SCA17	AD	Dysphagia, intellectual deterioration, ataxia, absence seizures	Purkinje cells, granule layer, upper motor neurons
DRPLA	AD	Dementia, ataxia, choreoathetosis	Dentate nucleus, red nucleus, globus pallidus, subthalamic nucleus, cerebellar cortex, cortex

AD, autosomal dominant; DRPLA, dentatorubropallidoluysian atrophy; SBMA, spinobulbar muscular atrophy; SCA, spinocerebellar ataxia.

Besides tolerating different CAG repeat lengths, the gene products of mutated genes in polyglutamine diseases vary widely in function:

- The gene product in SCA1, ataxin-1 (ATXN1), is predominantly a nuclear protein that forms a complex with the transcriptional repressor Capicua (CIC). The expanded glutamine tract alters ATXN1's interaction with CIC in the cerebellum, which helps explain this region's vulnerability to SCA1 pathophysiology.
- SCA2 is caused by a CAG trinucleotide expansion in *ATXN2*. Genetic ablation of *Atxn2* increases global transcript abundance, indicating that it may work as an RNA-binding protein. More recent studies revealed that it interacts with TDP43, a protein involved in amyotrophic lateral sclerosis (ALS10), and mutations in *ATXN2* may contribute to amyotrophic lateral sclerosis.
- Impaired protein clearance is a theme among the SCAs, insofar as elevated levels of the disease-causing protein seem to drive pathogenesis. In the case of SCA3, the relationship is more direct in that ataxin-3 (ATXN3) is a deubiquitinating enzyme, and the expanded version cannot remove ubiquitin from proteins slated for clearance. More recently, ATXN3 has been linked to DNA damage repair.
- The affected gene product in SCA6, CACNA1A, is the α_{1A}-subunit of the voltage-gated Ca^{2+} channel; interestingly, loss-of-function mutations in the gene (not gain of function caused by CAG repeats) have been reported in patients with episodic ataxia and familial hemiplegic migraine.

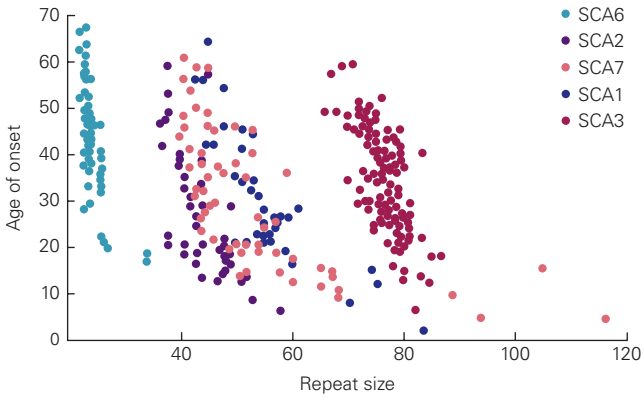

Figure 63–1 The length of the CAG repeat and age of onset in spinocerebellar ataxia (SCA) are inversely correlated. The longer the CAG tract, the earlier is the onset for a given disease. Specific repeat lengths, however, have different results depending on the host protein. For example, a 52-repeat of CAG causes juvenile onset of symptoms in spinocerebellar ataxia type 2 (**SCA2**), adult onset in spinocerebellar ataxia type 1 (**SCA1**), and no disease in spinocerebellar ataxia type 3 (**SCA3**).

- In SCA17, the affected gene product is the TATA box-binding protein, an essential transcription factor.
- Atrophin-1, the disease-causing protein in DRPLA, is thought to be a corepressor based on functional studies of its probable ortholog in *Drosophila*.

Despite these differences, some pathogenetic mechanisms may be common to the polyglutamine diseases, as discussed later in this chapter.

CAG repeats in coding regions are not the only dynamic mutations occurring in the SCAs (Table 63–2). SCA8 involves expansion of both a CAG tract and its complementary CTG repeat on the opposite strand in the 3′ untranslated region of a transcribed RNA with no open reading frame. The mutation responsible for SCA12 is a CAG repeat, but it occurs in a noncoding region 5′ upstream of a brain-specific regulatory subunit of the protein phosphatase 2A. SCA10 is caused by massive expansion of a pentanucleotide (ATTCT) repeat in the intron of a novel gene.

So far, a total of 33 SCAs have been identified. For the SCAs whose underlying pathogenesis is better understood, the most promising therapeutic approach seems to be to reduce the levels of the disease-driving protein. In the SCA7 mouse model, reducing the amount of both mutant and wild-type ATXN7 by RNA interference greatly improves the behavioral and pathological signs of disease. Likewise, in both *Drosophila* and mouse models of SCA1, genetic or pharmacological downregulation of several components of the RAS-MAPK-MSK1 pathway decreases ATXN1 levels and suppresses neurodegeneration.

Parkinson Disease Is a Common Degenerative Disorder of the Elderly

Parkinson disease, one of the more common neurodegenerative disorders, affects approximately 3% of the population older than age 65 years. Patients with Parkinson disease suffer from a resting tremor, bradykinesia, rigidity, and impairment in their ability to initiate and sustain movements. Affected individuals walk with a distinctive shuffling gait, and their balance is often precarious. Spontaneous facial movements are greatly diminished, creating a mask-like, expressionless appearance. The pathological hallmarks of Parkinson disease are the progressive loss of dopaminergic neurons, mainly in the substantia nigra pars compacta (Chapter 38), and the accumulation of proteinaceous aggregates termed Lewy bodies and Lewy neurites throughout the brain.

Although most cases of Parkinson disease are sporadic, studies of rare familial cases, which can be either autosomal dominant or recessive, have provided insight into the pathophysiology of this disorder and revealed novel risk factors for disease. To date, several genetic loci have been mapped (designated *PARK1–PARK22*), and the genes for all but four of these loci (*PARK3*, *PARK10*, *PARK12*, and *PARK16*) have been identified (Table 63–3). Of these mapped loci, the most studied and characterized are *PARK1/4*, *PARK2*, *PARK6*, and *PARK7*. Here, we focus on how the genetic basis of some forms of Parkinson disease provides insight into sporadic Parkinson disease.

Parkinson disease type 1/4 (4q2-22) is the locus for the dominantly inherited Parkinson disease caused by mutations in the gene *SNCA* encoding for α-synuclein. (As with Machado-Joseph disease and SCA3, Park1 and Park4 were initially thought to be two distinct variants.) Variants in the *SNCA* locus have been associated with increased risk of sporadic Parkinson disease, and several mutations in *SNCA* alter the conformation of the membrane-bound portion of the α-synuclein protein and cause it to aggregate. Duplications and triplications of *SNCA* have also been identified as causes of autosomal dominant Parkinson disease, indicating that elevated levels of even wild-type α-synuclein can cause disease. Patients with *SNCA* duplication have a disease course that resembles sporadic cases, but patients with triplication manifest an earlier-onset, more rapidly progressing disease with atypical features such as dementia and hallucinations.

Table 63–2 Hereditary Ataxias Caused by Expansion of Unstable CAG Trinucleotide Repeats

					Repeat lengths	
Disease	**Gene**	**Locus**	**Protein**	**Mutation**	**Normal**	**Disease**
SCA1	*SCA1*	6p23	Ataxin-1	CAG repeat in coding region	6–44[1]	39–121
SCA2	*SCA2*	12q24.1	Ataxin-2	CAG repeat in coding region	15–31	36–63
SCA3 (Machado-Joseph disease)	*SCA3, MJD1*	14q32.1	Ataxin-3	CAG repeat in coding region	12–40	55–84
SCA6	*SCA6*	19p13	α_{1A} subunit of voltage-dependent calcium channel	CAG repeat in coding region	4–18	21–33
SCA7	*SCA7*	3p12-13	Ataxin-7	CAG repeat in coding region	4–35	37–306
SCA8	*SCA8*	13q21	None	CTG repeat in the 3′ terminal exon (antisense)	16–37	110–250
SCA10	*SCA10*	22q13ter	Ataxin-10	Pentanucleotide (ATTCT) repeat in the intron	10–20	500–4,500
SCA12	*SCA12*	5q31-33	Protein phosphatase 2A	CAG repeat in 5′ UTR	7–28	66–78
SCA17	*TBP*	6qter	TATA-binding protein	CAG repeat in coding region	29–42	47–55
DRPLA	*DRPLA*	12q	Atrophin-1	CAG repeat in coding region	6–35	49–88
FXTAS	*FMR1*	Xq27.3	FMRP	CGG repeat in 5′ UTR	6–60	60–200

[1]Alleles with 21 or more repeats are interrupted by one to three CAT units; disease alleles contain pure CAG tracts.
DRPLA, dentatorubropallidoluysian atrophy; FXTA, fragile X–associated tremor ataxia; SCA, spinocerebellar ataxia.

Patients with *SNCA* mutations differ from those with sporadic Parkinson disease in that the age of onset is earlier (a mean of 45 years), and they exhibit fewer tremors and more rigidity, cognitive decline, myoclonus, central hypoventilation, orthostatic hypotension, and urinary incontinence.

Autosomal recessive juvenile parkinsonism is characterized by early-onset dystonia, brisk deep tendon reflexes, and cerebellar signs in addition to the classic signs of Parkinson disease, all as early as 3 years of age. Mutations in *PARK2*, *PARK6*, and *PARK7*—which encode parkin, PTEN-induced putative kinase 1 (PINK1), and protein deglycase DJ-1, respectively—have been confirmed as causes of this disease. Mutations in *PARK2* are much more frequent than mutations in *PARK6* and *PARK7*, and more than 60 different inactivating mutations have been identified; autosomal recessive juvenile Parkinsonism is thus caused by loss of function of the gene product rather than a gain of function. The pathology is also characterized by loss of dopaminergic neurons, but Lewy bodies are not as common as in sporadic or *PARK1/4* cases. Parkin is an E3 ubiquitin ligase of the RING finger family that transfers activated ubiquitin to lysine residues in proteins destined for degradation by proteasomes. Studies in the fruit fly *Drosophila melanogaster* revealed that parkin and PINK1 work together to promote healthy mitochondria. Interestingly, DJ-1, the third cause of autosomal recessive juvenile parkinsonism, is also involved in mitochondrial function, acting as an oxidative stress sensor.

Not all genetic causes of Parkinson disease exhibit complete penetrance. Such is the case with mutations in the gene encoding the leucine-rich repeat kinase 2 (*LRRK2*, *PARK8*). Interestingly, *LRRK2* mutations are a risk factor for sporadic Parkinson disease. Another genetic risk factor for Parkinson disease is the gene coding for glucocerebrosidase-1 (*GBA1*): Heterozygous carriers of *GBA1* mutations are at increased risk of developing Parkinson disease later in life, whereas homozygous carriers develop a recessive disorder known as Gaucher disease. There are undoubtedly additional genetic risk factors for Parkinson disease, and efforts to identify them are ongoing.

Table 63–3 Genetics and Main Clinical Features of Inherited Parkinson Disease

Disease	Locus map	Inheritance pattern	Gene	Main features
PARK1/4	4q21	AD	*SNCA*	Early onset, rigidity, and cognitive impairment
PARK2	6q26	AR	*PARKIN*	Juvenile onset and dystonia
PARK3	2p13	AD	Unknown	Adult onset, dementia
PARK5	4p13	AD	*UCHL1*	Adult onset
PARK6	1p36.12	AR	*PINK1*	Early onset, dystonia
PARK7	1p36.21	AR	*DJ1*	Early onset, behavioral disturbance, dystonia
PARK8	12q12	AD	*LRRK2*	Classic PD
PARK9	1p36.13	AR	*ATP13A2*	Juvenile or early onset, cognitive impairment
PARK10	1p32	AD	Unknown	Classic PD
PARK11	2q37.1	AD	*GIGYF2*	Adult onset, cognitive impairment
PARK12	Xq21-25	X-linked	Unknown	Unknown
PARK13	2p13.1	AD	*Omi/HtrA2*	Classic PD
PARK14	22q13.1	AR	*PLA2G6*	Early onset, cognitive impairment, dystonia.
PARK15	22q12.3	AR	*FBXO7*	Juvenile onset or early onset
PARK16	1q32	Unknown	Unknown	Unknown
PARK17	16q11.2	Unknown	*VPS35*	Adult onset, cognitive impairment, dystonia
PARK18	6p21.3	Unknown	*EIF4G1*	Classic PD
PARK19a/b	1p31.3	AR	*DNAJC6*	Juvenile or early onset, cognitive impairment
PARK20	21q22.11	AR	*SYNJ1*	Early onset, seizures
PARK21	3q22	AD	*DNAJC13*	Classic PD
PARK22	7p11.2	AD	*CHCHD2*	Classic PD

AD, autosomal dominant; AR, autosomal recessive; PARK, PD, Parkinson disease.

Selective Neuronal Loss Occurs After Damage to Ubiquitously Expressed Genes

One perplexing aspect of these neurodegenerative diseases is that the altered gene products are widely and abundantly expressed not only in the nervous system but also in other tissues, yet the phenotypes are predominantly neurological. Moreover, the phenotypes usually reflect dysfunction in only specific groups of neurons (Figure 63–2), a phenomenon referred to as neuronal selectivity.

Why are striatal neurons the most vulnerable in Huntington disease, whereas the Purkinje cells are targeted in the SCAs? Why are the dopaminergic neurons in the substantia nigra pars compacta primarily affected in Parkinson disease even though α-synuclein, parkin, DJ-1, PINK1, and LRRK2 are abundant in many other neuronal (and even nonneuronal) groups? Although definitive answers are not yet available, some hypotheses have been advanced. One possibility was suggested by the finding that the dopaminergic neurons that are vulnerable in Parkinson disease exhibit an unusual physiological characteristic: They depend on Ca^{2+} channels to fire in a rhythmic pattern. This dependence on Ca^{2+} influx in the neuron is thought to cause baseline mitochondrial stress, which could explain why these neurons are so vulnerable to direct insults to mitochondrial recycling, such as caused by parkin, DJ-1, and PINK1 dysfunction, as well as additional stress caused by LRRK2 dysfunction and α-synuclein accumulation.

In the polyglutamine diseases, the selectivity of the cellular pathology diminishes as the length of the glutamine tract increases: The more severe the mutation, the greater is the number of neuronal groups affected. This is especially evident in the early-onset forms

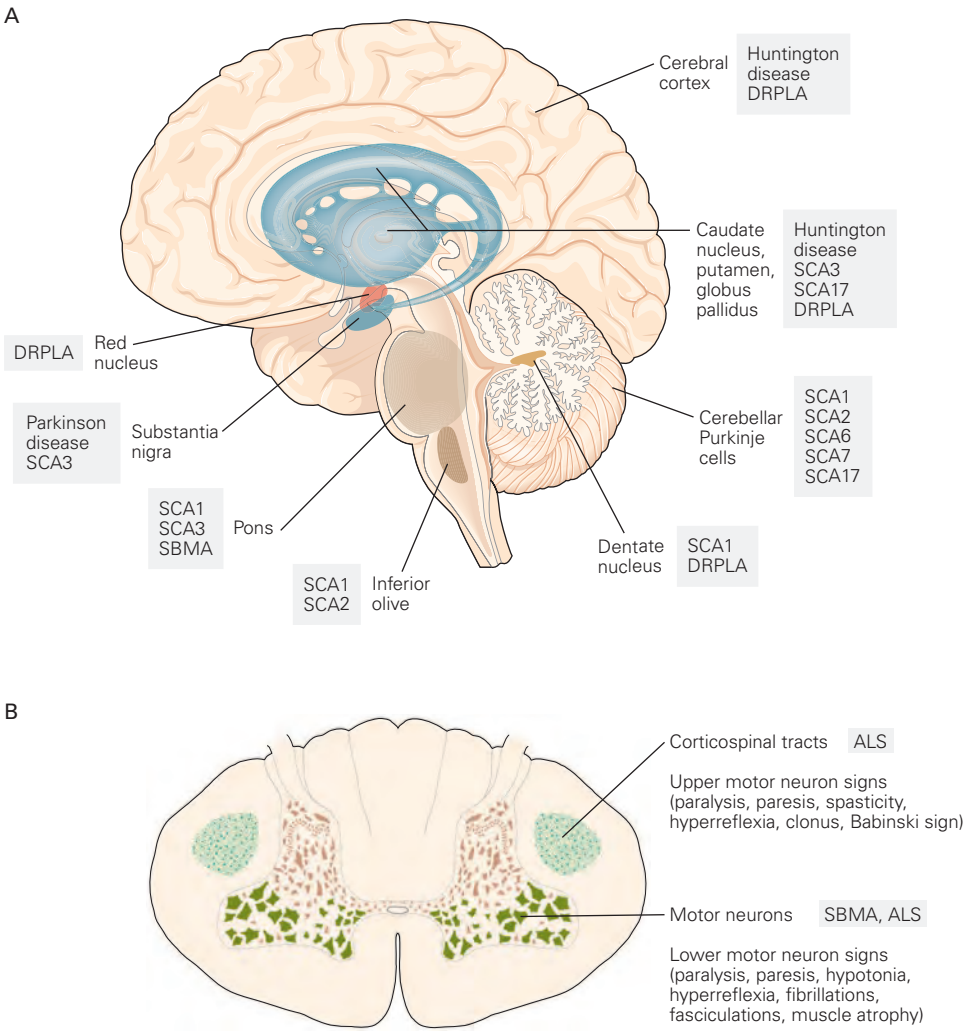

Figure 63–2 Neuronal selectivity illustrated by the primary sites of neuronal degeneration in the trinucleotide repeat diseases and Parkinson disease.

A. Brain regions most typically affected by adult-onset disease (see Table 63–1). (Abbreviations: **DRPLA**, dentatorubropallidoluysian atrophy; **SCA**, spinocerebellar ataxia.)

B. Comparison of neuropathology of amyotrophic lateral sclerosis (**ALS**) and spinobulbar muscular atrophy (**SBMA**).

characterized by extremely long repeats. Juvenile SCA1 can involve oculomotor abnormalities, for example, or cause dystonia, rigidity, and cognitive impairment, features that overlap with Huntington disease and DRPLA; death usually occurs within 4 to 8 years of symptom onset. Juvenile SCA7 patients can suffer seizures, delusions, and auditory hallucinations, and infantile disease also produces somatic features such as short stature and congestive heart failure. Infantile SCA7 causes progressive blindness by destroying both rods and cones; interestingly, infants with SCA2 can also suffer retinal degeneration. Such observations suggest that different cell types have different thresholds of vulnerability to toxic proteins with expanded glutamine tracts. Retinal cells, for example, seem more resistant to polyglutamine toxicity than cerebellar neurons, but more vulnerable than cardiac myocytes. Once the number of glutamines in the tract expands beyond a certain length—which varies from one protein to the next—no cell is safe.

Studies using mouse models suggest that protein misfolding is responsible for polyglutamine disorders. The longer the glutamine tract, the more severe the misfolding, and the more resistance there is to clearance; thus, the slow accumulation of higher-than-normal protein levels is a feature common to neurodegenerative diseases. As the tracts become very long, even cells with lower concentrations of disordered gene product

become vulnerable. Indeed, studies of animal models show that even a doubling in concentration can be the difference between phenotypic manifestation and apparent normality. It is therefore conceivable that the neurons affected in each disease have more dysfunctional protein than do the less vulnerable neurons. Although not detectable by current immunolabeling techniques, this incremental increase would nevertheless be sufficient to interfere with cellular function if the neuron was exposed to the toxic protein over decades.

Other major contributors to selective vulnerability might be variations in the levels of proteins that interact with or help dispose of the mutant proteins. Variations in the genes encoding such proteins could contribute to the clinical variability that is so prominent among ataxia families.

Why are neurons affected before other cells? As the organism ages, slight insults that have small detrimental effects could be exacerbated by the extra challenge the toxic protein presents to the protein-folding machinery. Because neurons are postmitotic, they might be especially sensitive to perturbations in the balance of intracellular factors. If the organism could survive the neurological assault long enough, other tissues might also eventually show signs of distress.

Animal Models Are Productive Tools for Studying Neurodegenerative Diseases

Animal models have proven extremely valuable for probing the pathogenesis of various neurodegenerative diseases and investigating therapies. The mouse has been the favored animal for modeling neurological disorders, but the *Drosophila* fly and the worm *Caenorhabditis elegans* have also proven useful in delineating genetic pathways.

Mouse Models Reproduce Many Features of Neurodegenerative Diseases

With the exception of the autosomal recessive juvenile forms of Parkinson disease, the neurodegenerative diseases discussed here primarily reflect gain-of-function mutations. Thus, most of the genetically engineered mice that model these diseases are created using one of two techniques. In the transgenic approach, an allele harboring the mutant gene is overexpressed, whereas in the knock-in approach, a human mutation, such as an expanded CAG tract, is inserted into an endogenous mouse locus to promote expression of the gene product at the correct time in development and in the right cells.

In some transgenic models, such as those generated for SCA types 1, 2, 3, and 7 and DRPLA, a full-length cDNA with either wild type or expanded alleles is overexpressed either in a particular class of neurons or in a larger population of cells (Figure 63–3). In other transgenic models of SCA3 and in models of SBMA, truncated versions of the coding regions are expressed. Both full-length and truncated huntingtin have been used in transgenic models.

Knock-in mice have been generated for Huntington disease, SBMA, and SCA types 1 and 7. These models confirm that sequences other than the expanded glutamine tract can produce toxic protein. Moreover, the same expansion in two different host proteins can affect cells differently. For example, in humans, 33 repeats cause SCA2, whereas 44 to 52 CAG repeats may or may not develop SCA3 (Figure 63–1 and Table 63–2). In mouse models, however, the relationship of the length of the tract to the rest of the protein is a good predictor of toxicity: Severe, widespread, nonselective neuronal dysfunction occurs in transgenic mice bearing a truncated protein with a relatively large glutamine tract. In contrast, mice that express full-length proteins containing the same CAG repeat length develop a milder neurological syndrome that progresses more slowly. Weakly expressing promoters also tend to produce more selective neuronal dysfunction. In some cases, expression of the full-length protein with even a moderately large expansion does not cause neurological dysfunction, but a truncated version bearing a similar repeat size does produce the disease phenotype. In sum, a glutamine tract of a certain length is more toxic when expressed in isolation or flanked by short peptide sequences, that is, when it occupies a larger proportion of the protein.

In SCA1 knock-in mice with 78 glutamine repeats, neurological dysfunction is barely detectable; only when the repeat length is expanded to approximately 154 glutamines does a neurological phenotype become apparent. Longer repeats are necessary to see a phenotype during the short life span of a mouse because polyglutamine toxicity takes time to exert its effects. In transgenic mice, however, massive overproduction of the mutant protein compensates for a moderate repeat length and brevity of exposure. Indeed, in mice, even overproduction of wild type ataxin-1 results in mild neurological dysfunction, and overexpression of wild type human α-synuclein is enough to cause parkinsonian symptoms.

Analysis of brain tissue from humans and various experimental mice reveals that misfolded proteins

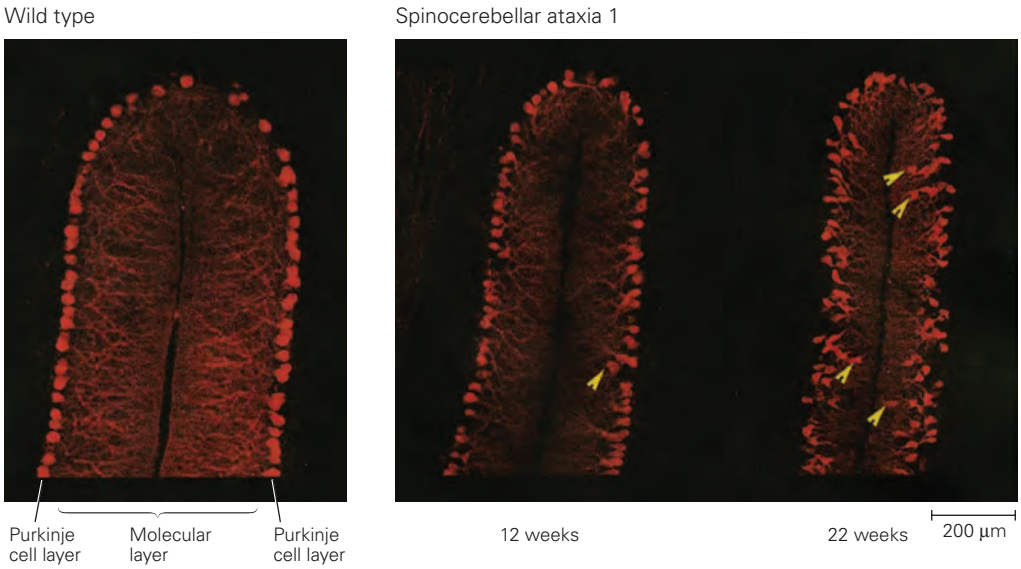

Figure 63–3 Progressive Purkinje cell pathology in spinocerebellar ataxia type 1 transgenic mice. Cerebellar sections from a wild type mouse and mice expressing a spinocerebellar ataxia type 1 (SCA1) transgene with 82 glutamines in Purkinje cells at 12 and 22 weeks of age. Calbindin immunofluorescence staining marks the Purkinje cells and their extensive dendritic arbors. In SCA1, there is progressive loss of dendrites, thinning of the molecular layer, and Purkinje cell displacement (**arrowheads**). (Images reproduced, with permission, from H.T. Orr.)

tend to accumulate in various neurons, often forming visible aggregates (Figure 63–4). Lewy bodies and abnormal accumulation of α-synuclein develop in mouse models of Parkinson disease, just as in humans. Although protein accumulation is common to all these neurodegenerative disorders, the location of the accumulated protein in the cell varies, and location within the cell is a factor in the protein's pathogenicity. For example, mutant ataxin-1 that accumulates in the cytoplasm instead of the nucleus (because its nuclear localization signal is disabled) exerts no detectable toxic effects.

The fact that mutant proteins accumulate both in mouse models that do not overproduce the proteins and in human patients who carry a single mutant allele suggests that neurons have difficulty clearing the proteins. This hypothesis is supported by the finding that ubiquitin and proteasome components, the machinery of protein degradation, are found with protein aggregates in both human and mouse tissues.

Invertebrate Models Manifest Progressive Neurodegeneration

Several invertebrate models have been used to study polyglutamine proteins, α-synuclein, parkin, and PINK1. The similarities in the pathogenic effects of these proteins across species are remarkable.

Flies with high levels of human α-synuclein develop progressive degeneration of dopaminergic neurons and have α-synuclein–immunoreactive cytoplasmic aggregates reminiscent of Lewy bodies. As in the mouse model, high levels of α-synuclein in flies carrying either the wild-type or mutant allele induce this phenotype. Additionally, flies with PINK1 or parkin mutations have dopaminergic neuron defects and motor abnormalities. Overexpression of wild type or mutant ataxin-1 in flies induces progressive neuronal degeneration that correlates with protein levels, but of course is more severe for flies with the mutant protein.

Polyglutamine toxicity has also been evaluated in the nematode *C. elegans* by expressing an amino terminal fragment of huntingtin containing glutamine tracts of different lengths. Neuronal dysfunction and cell death occur in worms expressing expanded tracts embedded within a truncated protein.

The Pathogenesis of Neurodegenerative Diseases Follows Several Pathways

Protein Misfolding and Degradation Contribute to Parkinson Disease

The gradual accumulation of neurodegenerative disease proteins along with chaperones and components

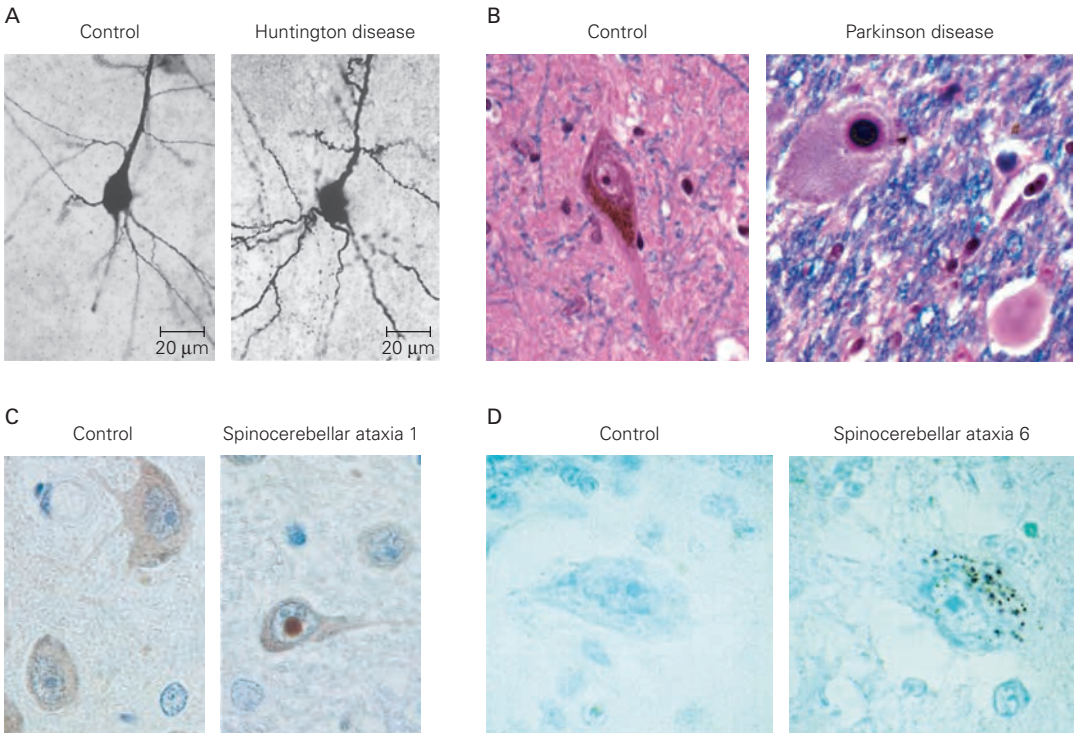

Figure 63–4 Neuropathological features of selected neurodegenerative disorders.

A. Comparison of a normal spiny neuron from the caudate nucleus and a spiny neuron affected by Huntington disease. Note the marked recurving of terminal dendritic branches in the diseased neuron. (Image of Huntington neuron reproduced, with permission, from Marian Di Figlia and J.-P. Vonsattel.)

B. A pigmented dopaminergic neuron in the substantia nigra with a classic cytoplasmic inclusion (Lewy body). The circular cytoplasmic inclusion is surrounded by a clear halo. Recent electron-microscopic and biochemical evidence indicates that the primary components of Lewy bodies are synuclein, ubiquitin, and abnormally phosphorylated neurofilaments that form a nonmembrane-bounded compacted skein in the cell body. Extracellular Lewy bodies occur following neuronal cell death and disintegration.

C. A neuron with a typical nuclear inclusion, almost as large as the nucleolus, and another Purkinje cell with a sizable vacuole and axonal swelling known as a torpedo.

D. Because spinocerebellar ataxia type 6 results from a repeat expansion in *CACNA1A*, which encodes a calcium channel, *CACNA1A* labeling occurs diffusely throughout the cytoplasm rather than in the nucleus.

of the ubiquitin-proteasome degradation pathway suggests that expansion of the glutamine tract alters the folding state of the native protein, which in turn recruits the activity of the protein-folding and degradation machinery. When that machinery cannot process the protein molecules, they accumulate, eventually forming aggregates. Evidence in support of this idea first came from observations in cell culture that overproduction of chaperones reduces protein aggregation and mitigates the toxicity of expanded glutamine tracts in proteins. In contrast, blocking the proteasome inhibits protein degradation and thus enhances aggregation and toxicity. Genetic studies in flies and mice provide even more compelling evidence. Overproduction of at least one chaperone, such as Hsp70, Hsp40, or tetratricopeptide protein 2, suppresses polyglutamine toxicity in *Drosophila* and reduces degeneration in mouse models of Parkinson disease and several types of ataxia. Conversely, loss of chaperone function worsens the neurodegenerative phenotypes (Figure 63–5).

The importance of the ubiquitin-proteasome pathway and protein degradation in the SCAs is further supported by genetic modification in animal models. In a *Drosophila* model of SCA1, haploinsufficiency for ubiquitin, ubiquitin carrier enzymes, or a ubiquitin carboxyl-terminal hydrolase worsens neurodegeneration. It appears that inclusions are part of the cell's attempt to sequester the mutant protein and thereby limit its toxic effects. Cells that are unable to form aggregates suffer the worst damage from polyglutamine toxicity. Indeed, the knock-in mouse models of SCA types 1 and 7 show conclusively that cells that

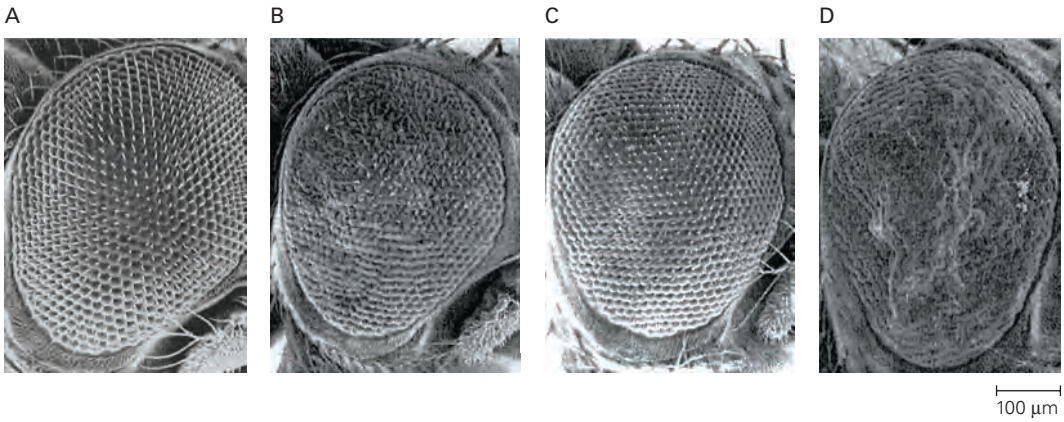

Figure 63–5 Polyglutamine-induced degeneration in the *Drosophila* eye and the effect of modifiers. (Images reproduced, with permission, from J. Botas.)

A. A scanning electron micrograph depicts the eye of a fly with normal ommatidia.

B. Ommatidia of a transgenic fly bearing a protein with expanded glutamine repeats.

C. Owing to the mitigating effect of over-producing a heat shock protein on the polyglutamine-induced phenotype, the ommatidia appear almost normal.

D. Absence of another heat shock protein aggravates the polyglutamine-induced phenotype.

form aggregates survive longer; cerebellar Purkinje cells, the prime targets in this disease, are the last to form nuclear aggregates.

In Huntington disease, the expanded huntingtin protein is readily cleaved by proteases, but the fragments are toxic to the cell, interfering with transcription and dysregulating the activity of dynamin-1. Expanded huntingtin activates the autophagy pathway via repression of mammalian target of rapamycin (mTOR) kinase, but the resulting autophagosomes are defective and cannot help the neurons degrade aggregated proteins. Finally, the expanded huntingtin protein forms aggregates. Some studies suggest these aggregates are harmful to the cell, while other studies have shown them to be protective because they reduce the circulating level of the soluble toxic protein. Their role in pathology might depend on the disease stage and which interacting proteins co-accumulate in the aggregates.

Studies of Parkinson disease further underscore the importance of the ubiquitin-proteasome pathway and reveal additional parallels with the polyglutamine diseases. First, studies focused on α-synuclein have shown that ubiquitinated forms of the protein accumulate in Lewy bodies and that ubiquitination regulates α-synuclein stability. Second, recent studies have identified NEDD4 as an E3 ubiquitin ligase that targets α-synuclein, and USP9X as a de-ubiquitinating enzyme that removes the modification. Other studies have identified parkin as an E3 ubiquitin ligase that targets many different mitochondrial proteins and is important for mitochondrial quality control.

How do misfolded α-synuclein or expanded glutamine tracts disrupt neuronal function? A protein that resists degradation might linger too long in the cell, performing its normal function longer than it should; the altered conformation might also cause it to favor certain protein interactions over others. This is what happens with glutamine-expanded ataxin-1: Part of the gain of toxic function involves prolonged binding with Capicua and subsequent alterations in its transcriptional activity.

Protein Misfolding Triggers Pathological Alterations in Gene Expression

One of the key consequences of misfolding as a result of expanded glutamine tracts is alteration in gene expression. This was first suspected when it was realized that most of the mutant proteins accumulate in the cell nucleus and that they interact with or affect the function of key transcriptional regulators. For example, huntingtin interacts with the transcription factors CREB-binding protein, NeuroD, specificity protein-1, nuclear factor-κB, and tumor suppressor protein 53 (p53), among others. Disruption of these interactions secondary to the polyglutamine expansion leads to myriad transcriptional changes seen in the disease state.

Alterations in gene expression are among the earliest events in pathogenesis, occurring within days of

expression of the mutant transgene in mouse models of SCA1 and Huntington disease. Many of the genes whose expression is altered are involved in Ca^{2+} homeostasis, apoptosis, cell-cycle control, DNA repair, synaptic transmission, and transduction of sensory events into neural signals. In fly models of SCA1, several modifiers of the neurodegenerative phenotype are transcriptional cofactors. Overproduction of polyglutamine proteins also can reduce levels of histone acetylation in cells, an effect that can be reversed by overproduction of CREB-binding protein. Finally, ataxin-1 is in a native complex with the transcriptional repressor Capicua; thus, some of the gain-of-function effects involve a gain of enhanced Capicua-mediated repression.

Mitochondrial Dysfunction Exacerbates Neurodegenerative Disease

Both morphological and functional studies provide evidence of mitochondrial dysfunction in polyglutamine disorders and Parkinson disease. Lymphoblast mitochondria from patients with Huntington disease as well as brain mitochondria from a transgenic mouse model for Huntington disease have a lower membrane potential and depolarize at lower Ca^{2+} loads than do control mitochondria.

Several proteins implicated in Parkinson disease affect mitochondrial function and integrity. For example, studies in *Drosophila* showed that the loss of PINK1 leads to mitochondrial dysfunction, dopaminergic neuron impairment, and motor abnormalities that can be rescued by parkin. These studies led to the finding that PINK1 and parkin regulate mitochondrial turnover in the cell in a process termed mitophagy. Thus, given the functions and interactions of these proteins, mitochondrial dysfunction is likely to be a key contributor to the Parkinson disease phenotype.

Apoptosis and Caspases Modify the Severity of Neurodegeneration

Although studies of most neurodegenerative diseases demonstrate that symptoms appear long before detectable cell death, loss of neurons is a hallmark of the end stage of all these disorders. Two major factors are implicated in the death of neurons: altered Ca^{2+} homeostasis and decreased induction of neuronal survival factors, such as brain-derived neurotrophic factor in Huntington disease. There is, however, specific evidence that the caspase activity critical for apoptosis is a contributing factor in neurodegenerative diseases. Some of the polyglutamine proteins, such as huntingtin, androgen receptor, ataxin-3, and atrophin-1, are substrates for caspases in vitro. This raises the possibility that caspase liberates the fragments of these proteins with expanded glutamine tracts. As noted above, such fragments are even more damaging than the full-length protein.

Intranuclear huntingtin increases production of caspase-1 in cells; this could lead to apoptosis and caspase-3 activation. Hip-1, a protein that interacts with huntingtin, forms a complex that activates caspase-8. This process might be enhanced by the glutamine expansion in huntingtin because Hip-1 binds less avidly to mutant huntingtin than to the wild type protein. In *Drosophila*, production of the antiapoptotic protein p35 results in partial rescue of the pigment loss induced by mutant ataxin-3.

In summary, expansions of polyglutamine tracts as well as several missense mutations in proteins implicated in neurodegenerative diseases alter the host protein, leading to its accumulation or abnormal interactions. The neuronal dysfunction results from the downstream effects of such abnormal interactions (Figure 63–6).

Understanding the Molecular Dynamics of Neurodegenerative Diseases Suggests Approaches to Therapeutic Intervention

The discovery of the genetic bases and pathogenic mechanisms of various neurodegenerative diseases offers us hope that therapies for these diseases will soon emerge. Dopamine replacement therapy has so far been the only pharmacological option for Parkinson disease, but it is not ideal. Patients tend to develop tolerance and require higher and higher doses of the drugs, which in turn cause a side effect known as levodopa-induced dyskinesias. The uncontrollable movements of dyskinesia soon become as disruptive as the motor symptoms originally being treated. Advancements in deep brain stimulation are promising, but the procedure is invasive and therefore reserved for medication-refractory Parkinson disease.

Patients with Huntington disease and SCA are worse off. No treatments that slow the progressive loss of motor coordination are currently available. However, several exciting therapeutic approaches that show great promise are under investigation. The most exciting therapeutic advances are those related to gene silencing of pathogenic products, including editing the genome, turning down transcription, or reducing expression of the protein. The most promising of these approaches in Huntington disease is the use of antisense oligonucleotides (ASOs). ASOs are small single-stranded molecules designed to bind to complementary sequences found within the mRNA product

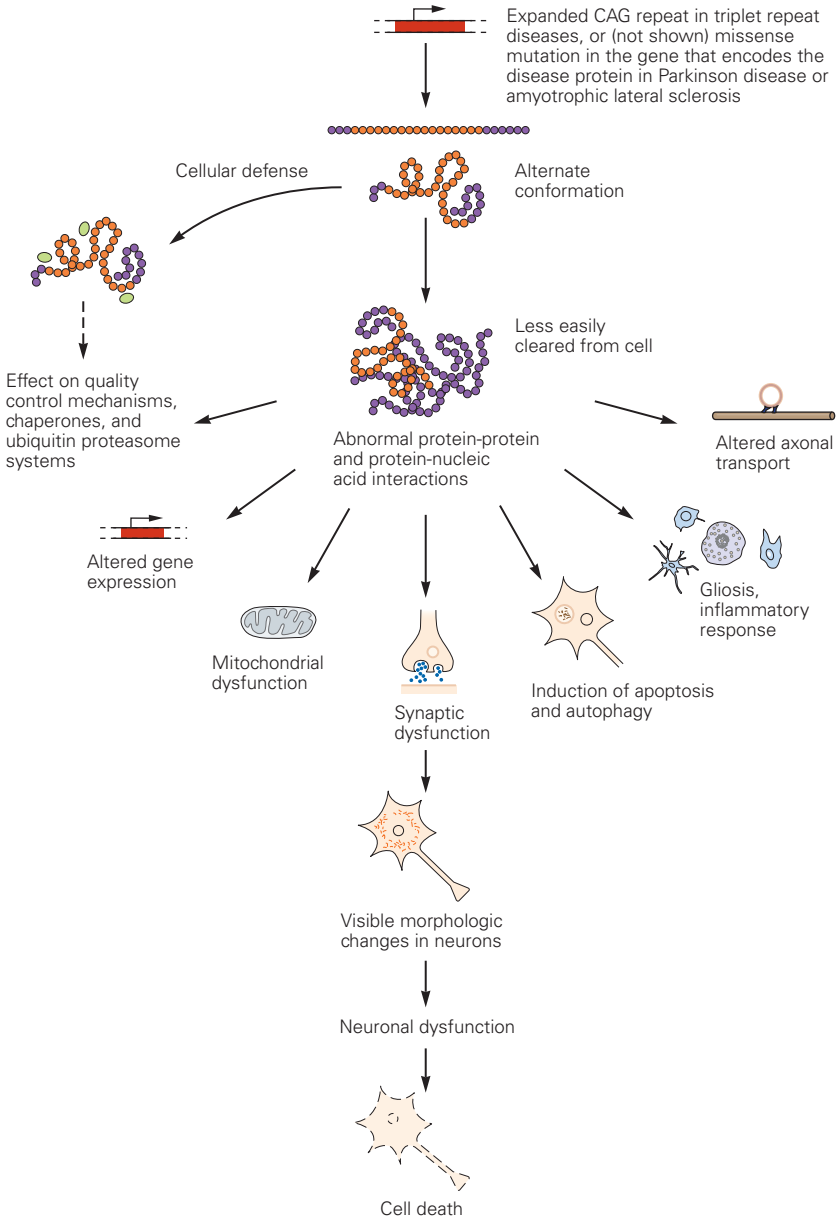

Figure 63–6 Current model for pathogenesis of the proteinopathies. The disease-causing protein adopts an alternative conformation that changes its interactions with other proteins, DNA, or RNA, altering gene expression and perhaps generating an inflammatory response. These early events in pathogenesis occur years before symptoms appear. Since this alternative conformation is more difficult for the cell to refold or degrade, steady-state levels of the mutant protein rise slowly over a period of decades. As levels of the mutant protein rise, the neuron attempts to sequester the mutant protein and forms aggregates. As disease progresses, these proteinaceous deposits themselves may affect protein interactions or compromise the protein quality-control system.

one wants to downregulate. When an ASO binds its mRNA target, it triggers degradation of the mRNA through RNAse H activity while at the same time sparing the ASO itself, thereby allowing it to bind to another mRNA molecule. In Huntington disease, several ASOs have been successfully used to reduce huntingtin protein levels. In fact, this approach is currently being utilized in clinical trials and holds promise for other diseases such as Parkinson disease.

Ideally, therapies should be targeted at some of the earliest pathogenic stages, when intervention could in theory halt the disease or even allow recovery of function. Indeed, studies of mouse models of Huntington disease and SCA1, in which expression of the mutant gene can be turned off, have shown that the neuronal dysfunction is reversible. When expression of the transgene is turned off, the neurons have a chance to clear the mutant polyglutamine protein and regain normal activity.

Because most neurodegenerative diseases progress over a period of decades, pharmacological interventions that even slightly modulate one or more of the pathways described above could delay disease progression or improve function, which would greatly enhance the quality of life for patients suffering from these devastating disorders.

Highlights

1. Late-onset neurodegenerative diseases collectively afflict more than 25 million people throughout the world, and it is anticipated that the prevalence of Alzheimer and Parkinson diseases will rise, given the increasing trend in life expectancy.
2. The identification of genes causing several forms of Parkinson disease and the various polyglutamine neurodegenerative diseases has allowed the accurate diagnosis and classification of these clinically heterogeneous disorders.
3. Although the gene product driving disease is widely expressed in the brain, there is selective neuronal vulnerability in all adult-onset neurodegenerative disorders. Perhaps a slight increase in abundance of the disease-driving protein and/or its interactors might explain such selective vulnerability.
4. Mitochondrial dysfunction is common in Parkinson disease; some of the genes mutated in Parkinson disease regulate mitochondrial turnover.
5. Studies in cell culture and model organisms have revealed a pathogenic mechanism common to adult-onset neurodegenerative diseases: protein misfolding. Mutations that cause the respective proteins to adopt an altered conformation gradually induce neuronal dysfunction either because of abnormal protein interactions or because of intracellular protein accumulation and altered activity.
6. The accumulation of polyglutamine-expanded proteins causes a variety of molecular changes in the cells, including alterations in gene expression, alterations in Ca^{2+} homeostasis, mitochondrial dysfunction, and activation of caspases.
7. The discovery that many adult neurodegenerative disorders are reversible in mouse models gives hope that some of the neuronal dysfunction can be rescued if a treatment is implemented early enough in the disease course before cell death occurs.
8. The identification of pathways that mediate some of the pathogenic effects is likely to lead to the discovery of drugs that can first be tested in animals and then applied in humans.
9. Lowering the levels of disease-driving proteins can ameliorate their toxic effects. This opens the way for therapeutic strategies that either employ antisense oligonucleotides that target the toxic RNA or that use small molecules to target regulators of the toxic protein.

Huda Y. Zoghbi

Selected Reading

Gatchel JR, Zoghbi HY. 2005. Diseases of unstable repeat expansion: mechanisms and common principles. Nat Rev Genet 6:743–755.

Gusella JF, MacDonald ME. 2000. Molecular genetics: unmasking polyglutamine triggers in neurodegenerative disease. Nat Rev Neurosci 1:109–115.

Haelterman NA, Yoon WH, Sandoval H, et al. 2014. A mitocentric view of Parkinson's disease. Annu Rev Neurosci 37:137–159.

Laforet GA, Sapp E, Chase K, et al. 2001. Changes in cortical and striatal neurons predict behavioral and electrophysiological abnormalities in a transgenic murine model of Huntington's disease. J Neurosci 21:9112–9123.

Moore DJ, West AB, Dawson VL, Dawson TM. 2005. Molecular pathophysiology of Parkinson's disease. Annu Rev Neurosci 28:57–87.

Pickrell AM, Youle RJ. 2015. The roles of PINK1, parkin, and mitochondrial fidelity in Parkinson disease. Neuron 85:257–273.

Sherman MY, Goldberg AL. 2001. Cellular defenses against unfolded proteins: a cell biologist thinks about neurodegenerative diseases. Neuron 1:15–32.

Steffan JS, Bodai L, Pallos J, et al. 2001. Histone deacetylase inhibitors arrest polyglutamine-dependent neurodegeneration in *Drosophila*. Nature 413:739–743.

Wong Y, Krainc D. 2017. α-Synuclein toxicity in neurodegeneration: mechanism and therapeutic strategies. Nat Med 23:1–13.

Zoghbi HY, Orr HT. 2009. Pathogenic mechanisms of a polyglutamine-mediated neurodegenerative disease, spinocerebellar ataxia type 1. J Biol Chem. 284:7425–7429.

References

Alexopoulou, Z, Lang J, Perrett RM, et al. 2016. Deubiquitinase Usp8 regulates α-synuclein clearance and modifies its toxicity in Lewy body disease. Proc Natl Acad of Sci U S A 113:4688–4697.

Alves-Cruzeiro JM, Mendonça L, Pereira de Almeida L, Nóbrega C. 2016. Motor dysfunctions and neuropathology in mouse models of spinocerebellar ataxia type 2: a comprehensive review. Front Neurosci 10:572.

Auluck PK, Chan HY, Trojanowski JQ, Lee VM, Bonini NM. 2002. Chaperone suppression of α-synuclein toxicity in a *Drosophila* model for Parkinson's disease. Science 295:865–888.

Bonifati V. 2012. Autosomal recessive parkinsonism. Parkinsonism Relat Disord 18:S4–S6.

Bonini NM, Gitler AD. 2011. Model organisms reveal insight into human neurodegenerative disease: ataxin-2 intermediate-length polyglutamine expansions are a risk factor for ALS. J Mol Neurosci 45:676–683.

Burré, J. 2015. The synaptic function of α-synuclein. J Parkinson Dis 5:699–713.

Chai Y, Koppenhafer SL, Bonini NM, Paulson HL. 1999. Analysis of the role of heat shock protein (Hsp) molecular chaperones in polyglutamine disease. J Neurosci 19:10338–10347.

Chesselet M.-F, Richter F, Zhu C, et al. 2012. A progressive mouse model of Parkinson's disease: the thy1-aSyn ('Line 61') Mice. Neurotherapeutics 9:297–314.

Cummings CJ, Mancini MA, Antalffy B, et al. 1998. Chaperone suppression of ataxin-1 aggregation and altered subcellular proteasome localization imply protein misfolding in SCA1. Nat Genet 19:148–154.

Cummings CJ, Sun Y, Opal P, et al. 2001. Over-expression of inducible HSP70 chaperone suppresses neuropathology and improves motor function in *SCA1* mice. Hum Mol Genet 10:1511–1518.

Davies SW, Turmaine M, Cozens BA, et al. 1997. Formation of neuronal intranuclear inclusions underlies the neurological dysfunction in mice transgenic for the HD mutation. Cell 90:537–548.

Feany MB, Bender WW. 2000. A *Drosophila* model of Parkinson's disease. Nature 404:394–398.

Fernandez-Funez P, Nino-Rosales ML, de Gouyon B, et al. 2000. Identification of genes that modify ataxin-1-induced neurodegeneration. Nature 408:101–106.

Fryer JD1, Yu P, Kang H, et al. 2011. Exercise and genetic rescue of SCA1 via the transcriptional repressor Capicua. Science. 334:690–3.

Fujioka S, Wszolek ZK. 2012. Update on genetics of parkinsonism. Neurodegener Dis 10:257–260.

Gennarino VA, Singh RK, White JJ, et al. 2015. Pumilio1 haploinsufficiency leads to SCA1-like neurodegeneration by increasing wild-type Ataxin1 levels. Cell 160:1087–1098.

Hagerman RJ, Hagerman PJ. 2002. The fragile X premutation: into the phenotypic fold. Curr Opin Genet Dev 12:278–283.

Holmes SE, O'Hearn EE, McInnis MG, et al. 1999. Expansion of a novel CAG trinucleotide repeat in the 5′ region of PPP2R2B is associated with SCA12. Nat Genet 23:391–392.

Huynh DP, Del Bigio MR, Ho DH, Pulst SM. 1999. Expression of ataxin-2 in brains from normal individuals and patients with Alzheimer's disease and spinocerebellar ataxia 2. Ann Neurol 45:232–241.

Huynh DP, Figueroa K, Hoang N, Pulst SM. 2000. Nuclear localization or inclusion body formation of ataxin-2 are not necessary for SCA2 pathogenesis in mouse or human. Nat Genet 26:44–50.

Kegel KB, Kim M, Sapp E, McIntyre C, Castano JG, Aronin N, DiFiglia M. 2000. Huntingtin expression stimulates endosomal-lysosomal activity, endosome tubulation, and autophagy. J Neurosci 20:7268-7278.

Koob MD, Moseley ML, Schut LJ, et al. 1999. An untranslated CTG expansion causes a novel form of spinocerebellar ataxia (SCA8). Nat Genet 21:379–384.

Kruger R, Kuhn W, Muller T, et al. 1998. Ala30Pro mutation in the gene encoding α-synuclein in Parkinson's disease. Nat Genet 18:106–108.

La Spada AR, Fu YH, Sopher BL, et al. 2001. Polyglutamine-expanded ataxin-7 antagonizes CRX function and induces cone-rod dystrophy in a mouse model of SCA7. Neuron 31:913–927.

Leroy E, Boyer R, Auburger G, Leube B, et al. 1998. The ubiquitin pathway in Parkinson's disease. Nature 395: 451–452.

Lucking CB, Durr A, Bonifati V, et al. 2000. Association between early-onset Parkinson's disease and mutations in the *parkin* gene. N Engl J Med 342:1560–1567.

Luthi-Carter R, Strand A, Peters NL, et al. 2000. Decreased expression of striatal signaling genes in a mouse model of Huntington's disease. Hum Mol Genet 9:1259–1271.

Masliah E, Rockenstein E, Veinbergs I, et al. 2000. Dopaminergic loss and inclusion body formation in α-synuclein mice: implications for neurodegenerative disorders. Science 287:1265–1269.

Matsuura T, Yamagata T, Burgess DL, et al. 2000. Large expansion of the ATTCT pentanucleotide repeat in spinocerebellar ataxia type 10. Nat Genet 26:191–194.

McCampbell A, Taye AA, Whitty L, Penney E, Steffan JS, Fischbeck KH. 2001. Histone deacetylase inhibitors reduce polyglutamine toxicity. Proc Natl Acad Sci U S A 98:15179–15184.

Miller J, Arrasate M, Shaby BA, Mitra S, Masliah E, Finkbeiner S. 2010. Quantitative relationships between huntingtin levels, polyglutamine length, inclusion body formation, and neuronal death provide novel insight into Huntington's disease molecular pathogenesis. J. Neurosci. 30:10541–10550.

Nakamura K, Jeong SY, Uchihara T, et al. 2001. SCA17, a novel autosomal dominant cerebellar ataxia caused by an expanded polyglutamine in TATA-binding protein. Hum Mol Genet 10:1441–1448.

Nalls MA, Pankratz N, Lill CM, et al. 2014. Large-scale meta-analysis of genome-wide association data identifies six new risk loci for Parkinson's disease. Nat Genet 46:989–993.

Nucifora FC, Sasaki M, Peters MF, et al. 2001. Interference by huntingtin and atrophin-1 with cbp-mediated transcription leading to cellular toxicity. Science 291:2423–2428.

Orr HT, Zoghbi HY. 2007. Trinucleotide repeat disorders. Annu Rev Neurosci 30:575–621.

Panov AV, Gutekunst CA, Leavitt BR, et al. 2002. Early mitochondrial calcium defects in Huntington's disease are a direct effect of polyglutamines. Nat Neurosci 5:731–736.

Park J, Al-Ramahi I, Tan Q, et al. 2013. RAS-MAPK-MSK1 pathway modulates ataxin 1 protein levels and toxicity in SCA1. Nature 498:325–331.

Piedras-Renteria ES, Watase K, Harata N, et al. 2001. Increased expression of alpha 1A Ca^{2+} channel currents arising from expanded trinucleotide repeats in spinocerebellar ataxia type 6. J Neurosci 21:9185–9193.

Polymeropoulos MH, Lavedan C, Leroy E, et al. 1997. Mutation in the α-*synuclein* gene identified in families with Parkinson's disease. Science 276:2045–2047.

Ramachandran PS, Boudreau RL, Schaefer KA, La Spada AR, Davidson BL. 2014. Nonallele specific silencing of ataxin-7 improves disease phenotypes in a mouse model of SCA7. Mol Ther 22:1635–1642.

Ravikumar B, Vacher C, Berger Z, et al. 2004. Inhibition of mTOR induces autophagy and reduces toxicity of polyglutamine expansions in fly and mouse models of Huntington disease. Nat Genet 36:585–595.

Rott R, Szargel R, Haskin J. 2011. α-Synuclein fate is determined by USP9X-regulated monoubiquitination. Proc Natl Acad Sci U S A 108:18666–18671.

Saudou F, Humbert S. 2016. The biology of huntingtin. Neuron 89:910–926.

Sidransky E, Lopez G. 2012. The link between the GBA gene and parkinsonism. Lancet Neurol 11:986–998.

Singleton AB, Farrer M, Johnson J, et al. 2003. α-*Synuclein* locus triplication causes Parkinson's disease. Science 302:841.

Smith WW, Pei Z, Jiang H, et al. 2005. Leucine-rich repeat kinase 2 (LRRK2) interacts with parkin, and mutant LRRK2 induces neuronal degeneration. Proc Natl Acad Sci U S A 102:18676–18681.

Surmeier JD, Guzman JN, Sanchez-Padilla J, Schumacker PT. 2011. The role of calcium and mitochondrial oxidant stress in the loss of substantia nigra pars compacta dopaminergic neurons in Parkinson's disease. Neuroscience 198:221–231.

Valente EM, Abou-Sleiman PM, Caputo V, et al. 2004. Hereditary early-onset Parkinson's disease caused by mutations in PINK1. Science 304:1158–1160.

Vonsattel JP, DiFiglia M. 1998. Huntington's disease. J Neuropathol Exp Neurol 57:369–384.

Warrick JM, Chan HY, Gray-Board GL, Chai Y, Paulson HL, Bonini NM. 1999. Suppression of polyglutamine-mediated neurodegeneration in *Drosophila* by the molecular chaperone HSP70. Nat Genet 23:425–428.

Wyant KJ, Riddler AJ, Dayalu P. 2017. Huntington's disease—update on treatments. Curr Neurol Neurosci Rep 17: 1–11.

Zhang S, Xu L, Lee J, Xu T. 2002. *Drosophila* atrophin homolog functions as a transcriptional corepressor in multiple developmental processes. Cell 108:45–56.

Zu T, Duvick LA, Kaytor MD, et al. 2004. Recovery from polyglutamine-induced neurodegeneration in conditional SCA1 transgenic mice. J Neurosci 24:8853–8861.

64

The Aging Brain

The average life span in the United States in 1900 was about 50 years. By 2015, it was approximately 77 years for men and 82 for women (Figure 64–1). The average is even higher in 30 other countries. These increases result largely from a reduction in infant mortality, the development of vaccines and antibiotics, better nutrition, improved public health measures, and advances in the treatment and prevention of heart disease and stroke. Because of increased life expectancy, along with the large cohort of "baby boomers" born soon after World War II, the elderly are the most rapidly growing segment of the US population.

Increased longevity is a double-edged sword since age-related cognitive alterations are increasingly prevalent. The magnitude of the change varies widely among individuals. For many, the alterations are mild and have relatively little impact on the quality of life—the momentary lapses we jokingly call "senior moments." Other cognitive impairments, although not debilitating, are troubling enough to hinder our ability to manage life independently. The dementias, however, erode memory and reasoning and alter personality. Of these, Alzheimer disease is the most prevalent.

As the population ages, neuroscientists, neurologists, and psychologists have begun to devote more energy to understanding age-related changes in the brain. The primary motivation has been to find treatments for Alzheimer disease and other dementias, but it is also important to understand the normal process of cognitive decline with age. After all, age is the greatest risk factor for a wide variety of neurodegenerative disorders. Understanding what happens to our brains as we age may not only improve the quality of life for the general population but may also provide clues that will eventually help us vanquish seemingly unrelated pathological changes.

With this in mind, we begin this chapter with a consideration of the normal aging of the brain. We then turn to the broad range of pathological changes in cognition, and finally focus on Alzheimer disease.

The Structure and Function of the Brain Change With Age

As we grow old, our bodies change—our hair thins, our skin wrinkles, and our joints creak. It is no surprise then that our brain also changes. Indeed, the widespread behavioral alterations that occur with age are

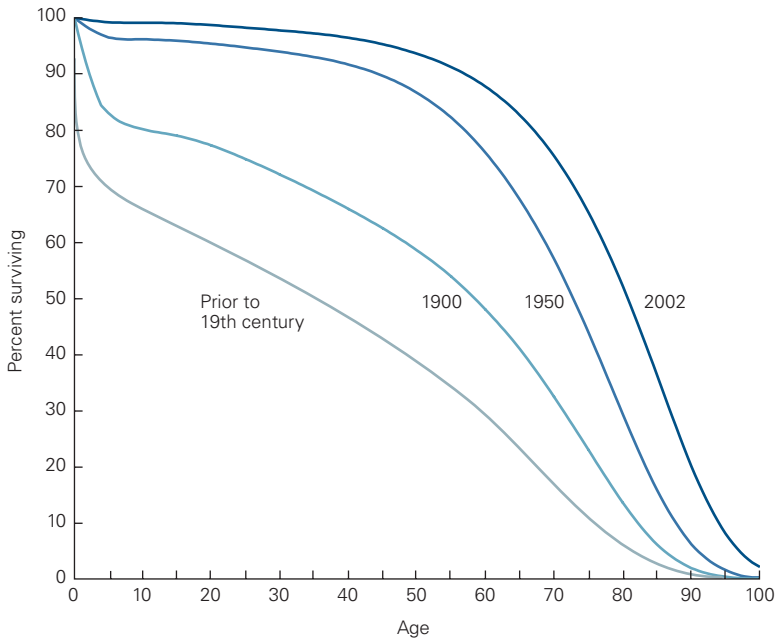

Figure 64–1 The human life span is increasing. The average life span in the United States has increased rapidly over the past 100 years. (Adapted from Strehler 1975; Arias 2004.)

signs of underlying alterations in the nervous system. For example, as motor skills decline, posture becomes less erect, gait is slower, stride length is shorter, and postural reflexes often become sluggish. Although muscles weaken and bones become more brittle, these motor abnormalities result in large part from subtle processes that involve the peripheral and central nervous systems. Sleep patterns also change with age; older people sleep less and wake more frequently. Mental functions ascribed to the forebrain, such as memory and problem-solving abilities, also decline.

Age-related declines in mental abilities are highly variable, in both rate and severity (Figure 64–2A). Although most people experience a gradual decline in mental agility, for some, the decline is rapid, whereas others retain their cognitive powers throughout life—Giuseppe Verdi, Eleanor Roosevelt, and Pablo Picasso are well-known examples of the latter category. Titian continued to paint masterpieces in his late 80s, and Sophocles is said to have written *Oedipus at Colonus* in his 92nd year. The fact that elderly people with completely preserved mental function are rare suggests that there may be special properties in the life experiences or genes of these people. Accordingly, there has been great interest in studying individuals who retain nearly intact cognition into their tenth or even eleventh decade. These centenarians may provide insight into environmental or genetic factors that protect against normal age-related cognitive decline or the more devastating pathological descent into dementia. One protective gene variant, discussed below, is the epsilon 2 allele of the apolipoprotein E gene.

An interesting finding that has emerged from studies of many individuals is that some cognitive capacities decline significantly with age while others are largely spared (Figure 64–2B). For example, working and long-term memories, visuospatial abilities (measured by arranging blocks into a design or drawing a three-dimensional figure), and verbal fluency (measured by rapid naming of objects or naming as many words as possible that start with a specific letter) usually decline with old age. On the other hand, measures of vocabulary, information, and comprehension often show minimal decline in normal individuals well into the 80s.

Age-related changes in memory, motor activity, mood, sleep pattern, appetite, and neuroendocrine function result from alterations in the structure and function of the brain. Even the healthiest 80-year-old brain does not look like it did at the age of 20. Elderly people exhibit mild shrinkage in the volume of the brain and a loss in brain weight, as well as enlargement of the cerebral ventricles (Figure 64–3A). The decreases in brain weight average 0.2% per year from college age onward, and about 0.5% per year in the 70s.

These changes could result from death of neurons. Indeed, some neurons are lost with age. For example, 25% or more of the motor neurons that innervate skeletal muscles die in generally healthy elderly individuals. As we will see, neurodegenerative diseases such as Alzheimer disease markedly accelerate the

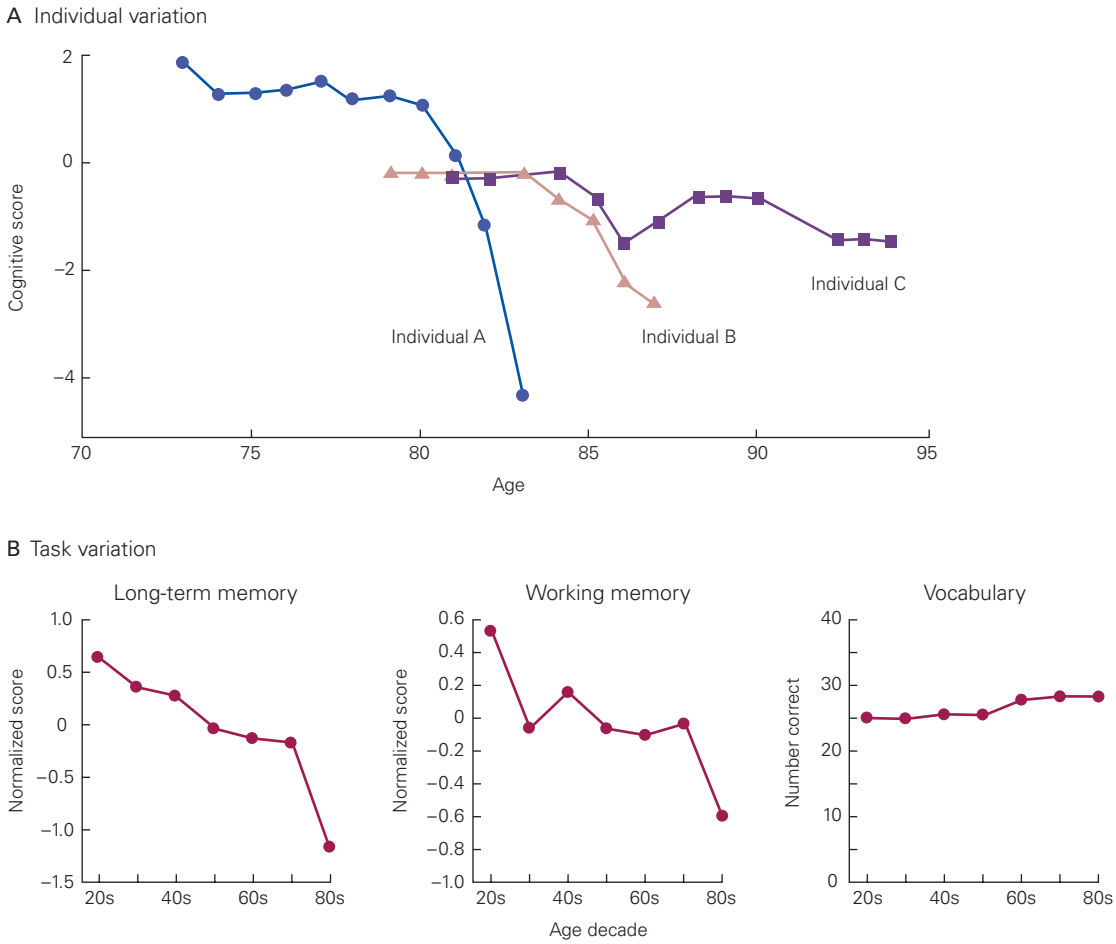

Figure 64–2 There is variation in age-related cognitive decline.

A. Scores of three people who were given a battery of cognitive tests annually for decades. Person A declined rapidly. Persons B and C showed similar cognitive performances into their 80s but then diverged. (Adapted from Rubin et al. 1998.)

B. Average scores on several cognitive tests administered to a large number of people. Long-term declarative memory and working memory decline throughout life and more so in advanced age. In contrast, knowledge of vocabulary is maintained. (Adapted from Park et al. 1996.)

death of neurons (Figure 64–3B). In most parts of the healthy brain, however, there is minimal to no neuronal loss simply because of age, so brain shrinkage must arise from other factors.

In fact, analysis of the brains of humans and experimental animals reveals structural alterations in both neurons and glia. Myelin is fragmented and lost, compromising the integrity of white matter. At the same time, the density of the dendritic arbors of cortical and other neurons decreases, resulting in shrinkage of neuropil. Levels of enzymes that synthesize some neurotransmitters, such as dopamine, norepinephrine, and acetylcholine, decrease with age, and this decline presumably results in functional defects in synapses that use these transmitters. Synapse structure is also altered, at least at the neuromuscular junction (Figure 64–4), raising the possibility that structural changes also lead to functional deficits at central synapses. Finally, the number of synapses in the neocortex and many other regions of the brain declines (Figure 64–5).

These cellular changes interfere with the integrity of the neural circuits that mediate our mental activities. Age-related loss of synapses along with impairment in function of remaining synapses are thought to be important contributors to cognitive decline. Changes in white matter are widespread but are especially notable in the prefrontal and temporal cortex. They may underlie alterations in executive functions

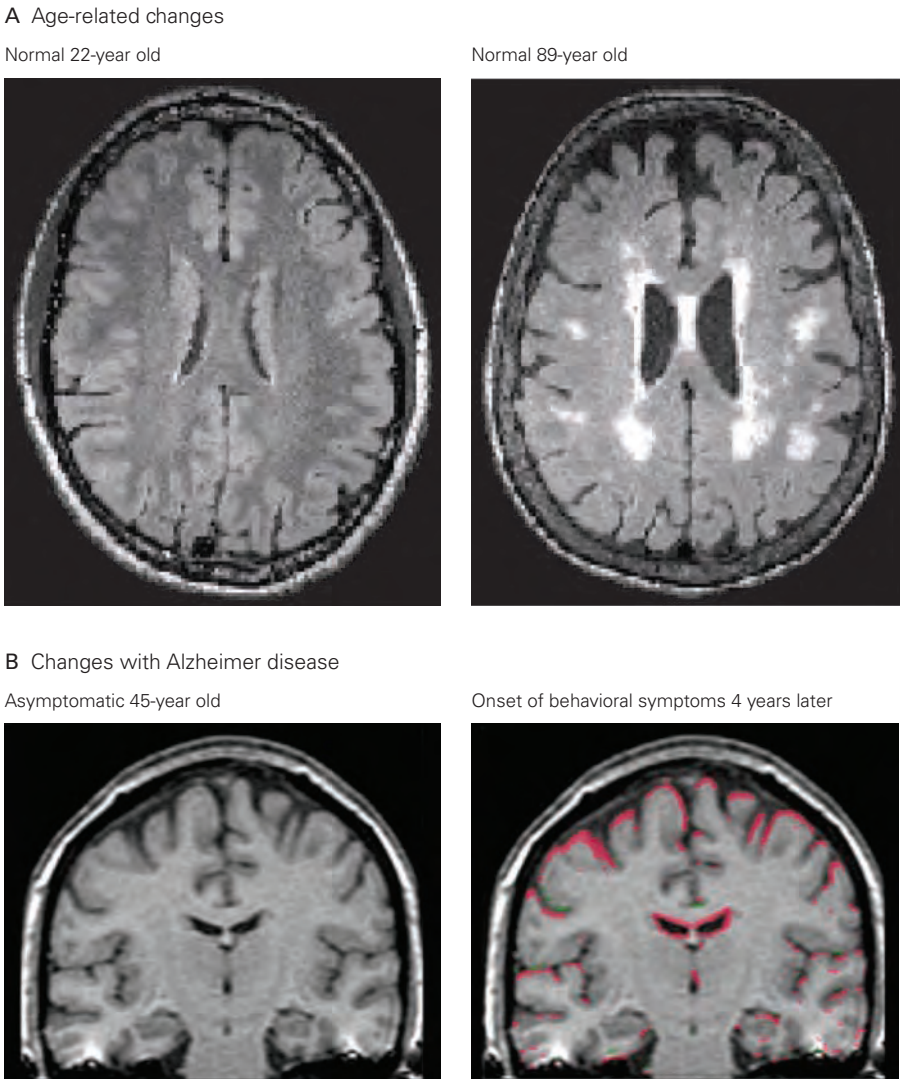

Figure 64–3 Changes in brain structure with age and at the onset of Alzheimer disease. (Also see Figure 64–8.)

A. Images of normal 22- and 89-year-old brains reveal changes in the structure of the living brain. (Reproduced, with permission, from R. Buckner.)

B. Images of the same individual over a 4-year period illustrate the progressive shrinking of cortical structures and the beginning of ventricular enlargement (**red**). These structural changes are evident prior to the onset of behavioral symptoms. (Reproduced, with permission, from N. Fox.)

and the ability to focus attention and encode and store memory, functions that are localized in frontal-striatal systems and the temporal lobes. The loss of white matter may also help explain the recent finding that the elderly brain is less able to support synchronization of activity in widely separated areas that normally work together to carry out complex mental activities. Disruption of these large-scale networks could be an important cause of cognitive decline.

It was long thought that aging resulted from progressive deterioration of cells and tissues due to accumulated genetic damage or toxic waste products. In support of this idea was the finding that mitotic cells removed from animals and placed in a tissue culture dish divide only for a limited number of times before they age and die. This view of "preordained" aging has changed radically over the past 10 to 20 years, primarily as a result of the discovery in model organisms of mutations that significantly extend life span (Figure 64–6).

Such dramatic discoveries established that the aging process is under active genetic control. One such regulatory pathway that has been characterized includes insulin and insulin-like growth factors, their receptors, and the signaling programs they activate. Disruption of these genes actually increases the resistance of cells to lethal oxidative damage. It is thought that the normal forms of these genes have been selected through evolution because they benefit the organism during the reproductive period. Their deleterious effects on longevity, once the animals are past reproductive age, may be an unfortunate side effect about which evolution cares little.

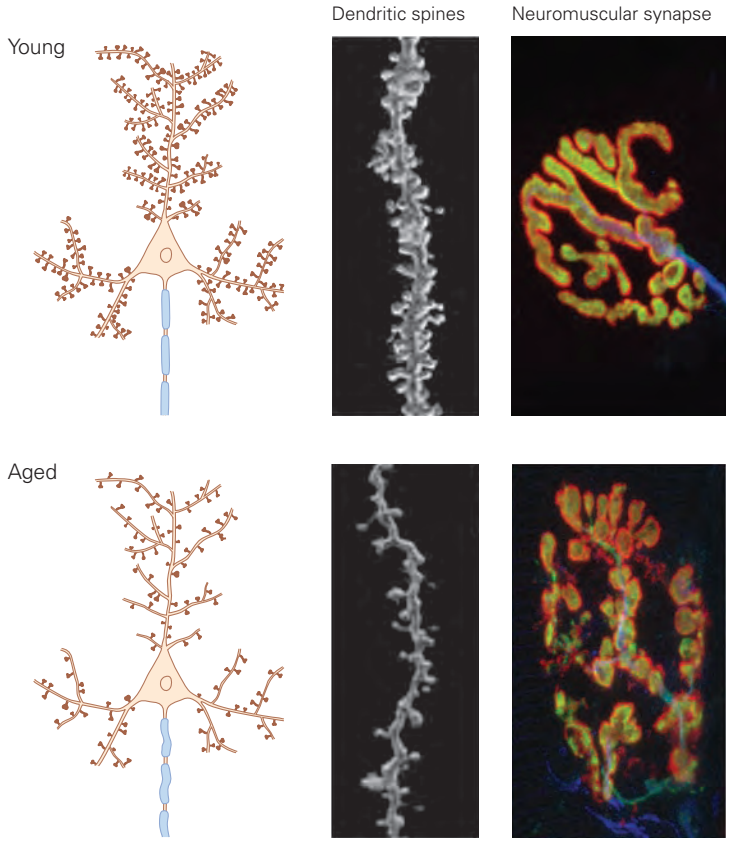

Figure 64–4 Age-related changes in dendritic and synaptic structure. Cortical pyramidal neurons in rodents lose dendritic spines with age. Neuromuscular synapses in rodents also exhibit age-related changes in structure. (Spine images reproduced, with permission, from J. Luebke; synapse images reproduced, with permission, from G. Valdez.)

These findings have two major implications for understanding how aging affects the nervous system. First, the biochemical mechanisms that lead to, or protect us from, the ravages of age are likely contributors to the changes in neurons that lead to age-related cognitive decline. Research to explore this link between cellular change and cognitive functioning is now underway in model organisms. Second, and perhaps more exciting, research on the pathways uncovered by genetic studies can identify pharmacological

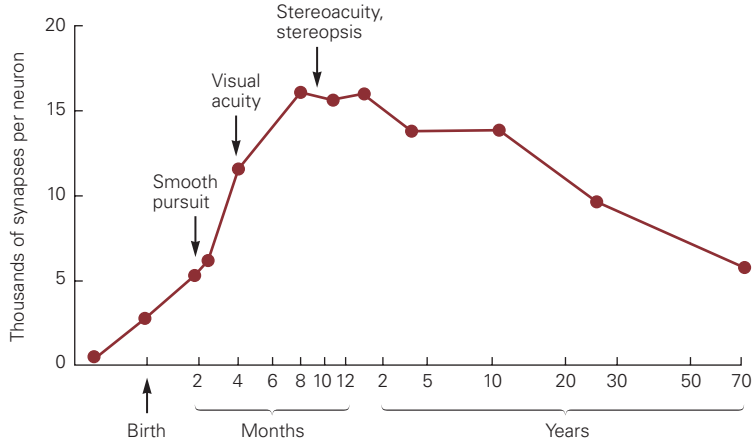

Figure 64–5 Age-related changes in synaptic density. Early cognitive development is accompanied by a marked increase in synapse density in different regions of the human cerebral cortex. Developmental landmarks through age 10 months are indicated. The density of cortical synapses declines with age. (Adapted from Huttenlocher 2002.)

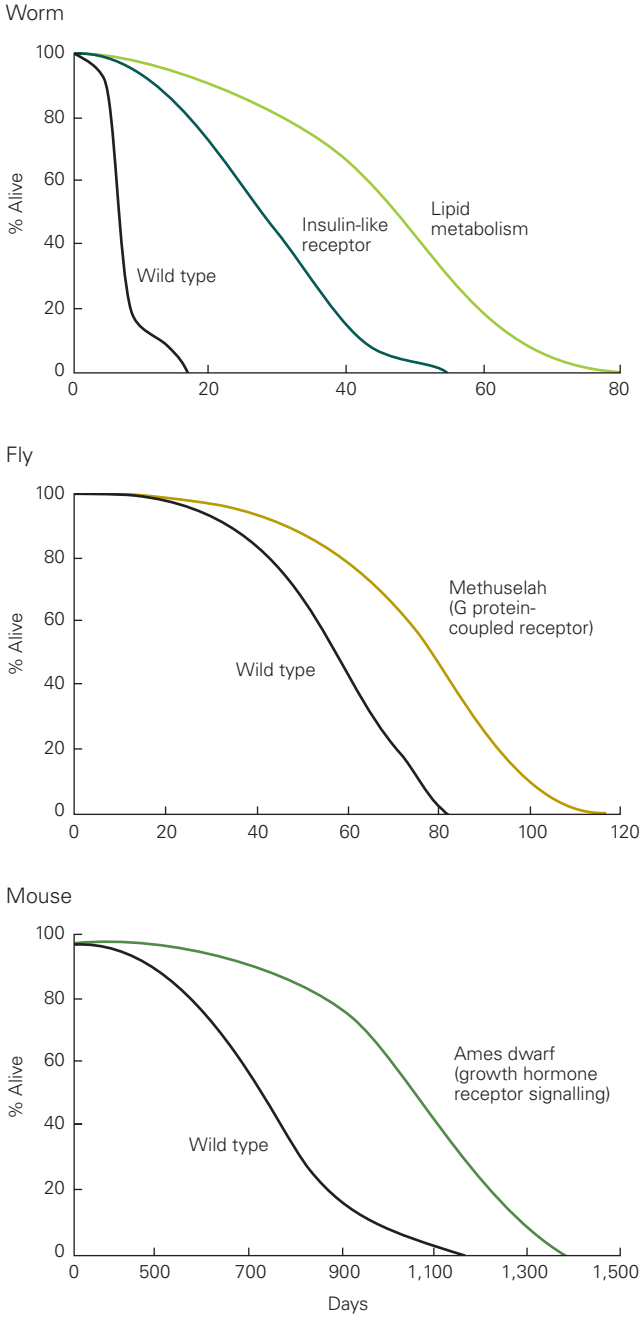

Figure 64–6 Life span can be increased through genetic mutation. Genetic mutations in specific receptors and signaling proteins markedly enhance life span in mutant strains of the worm, fly, and mouse, indicating that genetic regulatory mechanisms affect aging and life span. (Top adapted from Hekimi and Guarente 2003; middle reproduced, with permission, from Yi, Seroude, and Benzer 1998. Copyright © 1998 AAAS; bottom adapted from Brown-Borg et al. 1996.)

or environmental strategies for extending life span or health span (the period during which one remains generally healthy).

To date, the best-validated environmental strategy for extending life span (in organisms ranging from yeast to worms to primates) is caloric restriction. It appears that caloric restriction acts through genes in the insulin pathway mentioned above and may involve a set of enzymes called *sirtuins*. The sirtuins are activated by the compound *resveratrol*, originally isolated from red wine. Resveratrol, in turn, retards some aspects of aging, including cognitive decline, when administered to mice. While it is unlikely that resveratrol will serve as a fountain of youth in humans, it nevertheless exemplifies the new chemistries that are currently under consideration. These chemical strategies use model organisms to explore not only the positive factors that lead to aging but also the constraints that prevent model organisms, and presumably humans, from remaining generally healthy throughout their life span.

Cognitive Decline Is Significant and Debilitating in a Substantial Fraction of the Elderly

In most people, age-related cognitive changes do not seriously compromise the quality of life. In some elderly people, however, cognitive decline reaches a level that can be viewed as pathological. At the lower end of the abnormal range is a constellation of changes known as mild cognitive impairment (MCI). This syndrome is characterized by memory loss with or without other cognitive impairments that go beyond what is seen in normal aging. Individuals with MCI may be able to carry out most activities of daily living, although the impairments are noticeable to others and often influence the ability of the affected person to carry out certain activities that are important or pleasurable to them, such as managing finances or playing word games.

Importantly, MCI is a syndrome, not a diagnosis. Many underlying problems such as depression, overmedication, strokes, and neurodegenerative diseases can contribute to MCI. Approximately half of individuals with MCI have underlying Alzheimer disease, and more than 90% of this group will progress to full-blown dementia within 5 years from the time of diagnosis of MCI (Figure 64–7). As discussed below, there are now biomarkers that can suggest the presence of underlying Alzheimer disease pathology. As yet, however, there are no good biomarkers for predicting progression to dementia in people with MCI resulting from diseases other than Alzheimer.

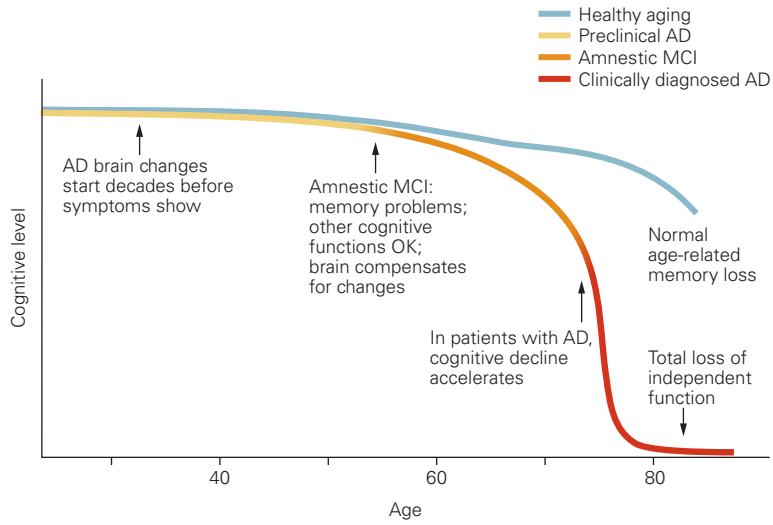

Figure 64–7 Cognitive performance can vary widely with age. The chart shows current thinking about the etiology of Alzheimer disease (**AD**). This gradual process, which results from a combination of biological, genetic, environmental, and lifestyle factors, eventually sets some people on a course to mild cognitive impairment (**MCI**) and then dementia. Other people, with a different genetic makeup or a different combination of factors over a lifetime, continue on a course of healthy cognitive aging. (From the National Institute on Aging: http://www.nia.nih.gov/alzheimers/publication/part-2-what-happens-brain-ad/changing-brain-ad.)

Like MCI, dementia is also a syndrome that involves progressive impairment of memory as well as other cognitive abilities such as language, problem solving, judgment, calculation, or attention. It is associated with a variety of diseases. The most common is Alzheimer disease, as discussed below. The second most common cause in the elderly is cerebrovascular disease, particularly strokes that lead to focal ischemia and consequent infarction in the brain.

Large lesions in the cortex are often associated with language disturbances (aphasia), hemiparesis, or neglect syndromes, depending on which portions of the brain are compromised. Small infarctions in white matter or deeper structures of the brain, termed *lacunes*, also occur as a consequence of hypertension and diabetes. In small numbers, these infarctions may be asymptomatic, or they may contribute to what appears to be normal age-associated cognitive decline or certain cases of MCI. As vascular lesions increase in number and size, however, their effects accumulate, and eventually, they can lead to dementia.

Numerous other conditions can lead to dementia, including Parkinson disease, Lewy body dementia, frontotemporal dementia, alcoholism, drug intoxications, infections such as HIV and syphilis, brain tumors, subdural hematomas, repeated brain trauma, vitamin deficiencies (notably lack of vitamin B_{12}), thyroid disease, and a variety of other metabolic disorders. Repeated brain trauma can result in what is termed chronic traumatic encephalopathy (CTE). Numerous cases of CTE in American professional athletes have recently been reported. In some patients, schizophrenia or depression may mimic a dementia syndrome. (Emil Kraepelin chose the term "dementia praecox" to describe the cognitive disease that we now call schizophrenia.) Because some dementias can be treated, it is important for the physician to probe differential diagnoses of dementia based on clinical history, physical examinations, and laboratory studies.

Alzheimer Disease Is the Most Common Cause of Dementia

In 1901, Alois Alzheimer examined a middle-aged woman who had developed a progressive loss of cognitive abilities. Her memory became increasingly impaired. She could no longer orient herself, even in her own home, and she hid objects in her apartment. At times, she believed that people intended to murder her.

She was institutionalized in a psychiatric hospital and died approximately 5 years after she was first seen by Dr. Alzheimer. After death, Alzheimer performed an autopsy that revealed specific alterations in the cerebral cortex, described below. The constellation of behavioral symptoms and physical alterations was subsequently given the name Alzheimer disease (AD).

This case caught Alzheimer's attention because it occurred in middle age; the initial clinical manifestations of AD (usually memory loss and decreased executive function) most commonly appear after age 65. The prevalence of AD at age 70 is about 2%, whereas after age 80, it is greater than 20%. Early-onset cases before age 65 are often familial (autosomal dominant AD), and gene mutations have been discovered in many of these patients, as we shall discuss below. In fact, new genetic tests on preserved brain samples from Alzheimer's first case recently showed that her disease resulted

from a mutation of a gene called presenilin-1, the most common cause of familial or dominantly inherited AD. Late-onset AD (onset at age 65 or greater) is more often sporadic, implying that there is no single causative gene as occurs in dominantly inherited AD. Nonetheless, it is clear that genetics contribute greatly to risk for even late-onset AD more likely through variants that affect susceptibility, along with environmental and other contributing factors that are just now being uncovered.

Both early-onset and late-onset varieties of AD usually present with a selective defect in episodic memory and executive function. At first, language, strength, reflexes, and sensory abilities and motor skills are nearly normal. Gradually, however, memory and attention are lost, along with cognitive abilities such as problem solving, language, calculation, and visuospatial perception. Unsurprisingly, these cognitive losses lead to behavioral alterations, and some patients develop psychotic symptoms such as hallucinations and delusions. All patients suffer progressive impairment of mental functions and activities of daily living; in the late stages, they become mute, incontinent, and bedridden.

Alzheimer disease affects approximately one-eighth of people older than 65 years. More than 5 million people in the United States now suffer from dementia due to AD. Because the elderly population is increasing rapidly, the population at risk for AD is growing rapidly. During the next 25 years, the number of people with AD in the United States is expected to triple, as will the cost of caring for patients no longer able to care for themselves. Thus, AD is one of society's major public health problems.

The Brain in Alzheimer Disease Is Altered by Atrophy, Amyloid Plaques, and Neurofibrillary Tangles

Three categories of brain abnormalities are found in AD. First, because of neuronal and synaptic loss, the brain is atrophied, with narrowed gyri, widened sulci, reduced brain weight, and enlarged ventricles (Figure 64–8). These changes are also seen in milder forms in cognitively intact elderly people who die from other causes. Thus, AD is a neurodegenerative disease.

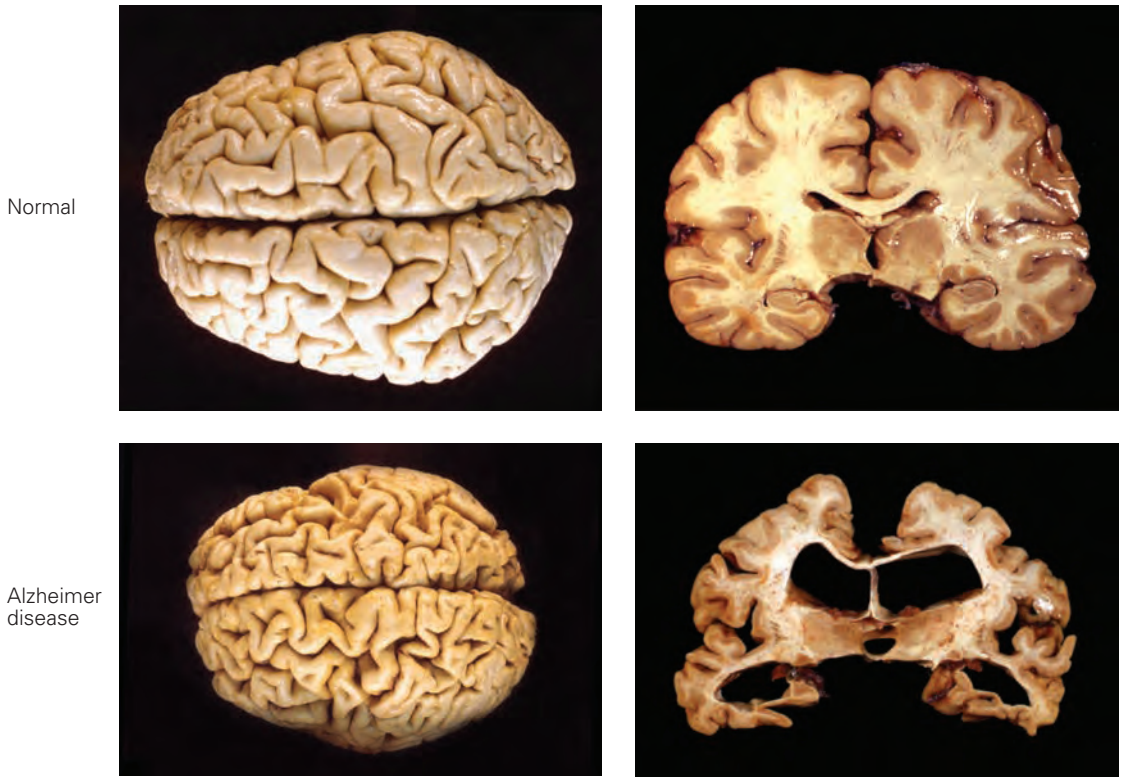

Figure 64–8 Overt pathological changes in the brain of individuals with Alzheimer disease. When compared to age-matched normal brains, the brain of an Alzheimer patient displays marked shrinkage and ventricular enlargement. (See also Figure 64–3.) (Whole brain photos reproduced, with permission, from University of Alabama at Birmingham Department of Pathology © PEIR Digital Library [http://peir.net]; brain slice photos reproduced, with permission, from A.C. McKee.)

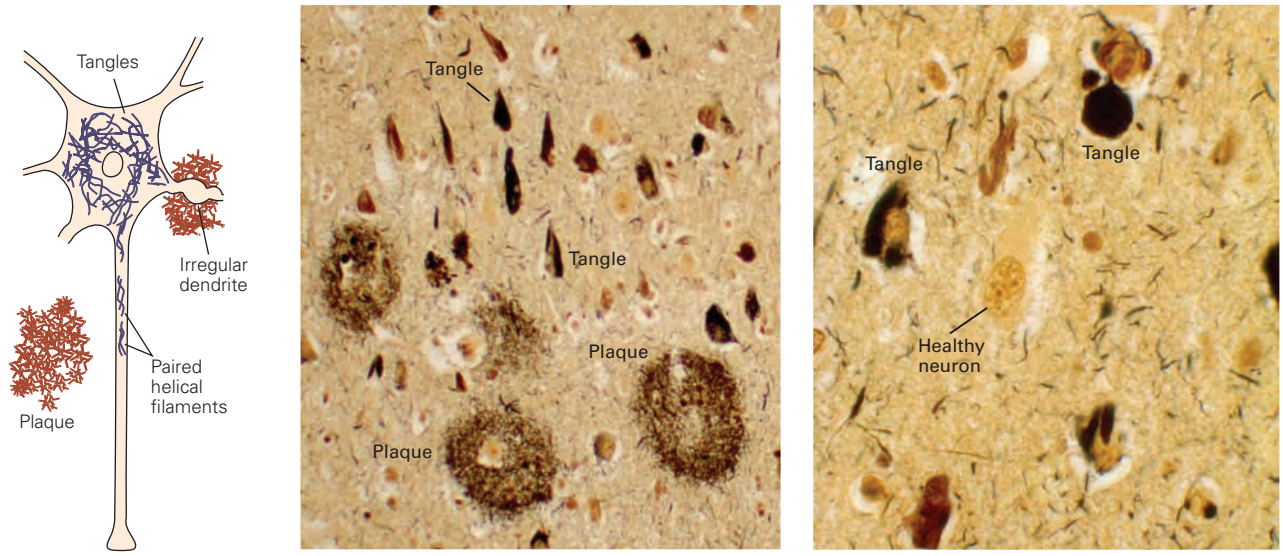

Figure 64–9 Plaques and tangles in the Alzheimer brain. A section of cerebral cortex from the brain of an individual with severe Alzheimer disease shows characteristic plaques and neurofibrillary tangles. (Images reproduced, with permission, from James Goldman.)

Left: The diagram shows a neuron containing neurofibrillary tangles in the cell body and axon. Amyloid plaques are shown in the neuropil; one of them surrounds a dendrite, which displays an altered, swollen shape. Tangles, composed of bundles of paired helical filaments, are comprised of abnormal polymers of hyperphosphorylated tau protein, and amyloid plaques are extracellular deposits of polymers of the amyloid-β (A4) peptide.

Middle: A section of neocortex from a patient with Alzheimer disease treated with a silver stain shows neuronal cell bodies containing neurofibrillary tangles and neuropil containing amyloid plaques.

Right: A higher magnification of the cortex shows neurofibrillary tangles in neuronal cell bodies and a healthy neuron without a tangle. Many thin silver-positive cell processes are seen in the neuropil.

Second, the brains of AD patients contain extracellular plaques composed predominantly of an aggregated form of a peptide called amyloid-β, or Aβ, which is cleaved from a normally produced protein. Aggregates of Aβ are called amyloid plaques. Much of the Aβ in plaques is fibrillar; aggregates of Aβ appear in a β-pleated sheet conformation along with other proteins that co-aggregate with Aβ (Figure 64–9). Amyloid can be detected when stained with dyes such as Congo red, and is refractive when viewed in polarized light or when stained with thioflavin S and viewed with fluorescence optics. The extracellular deposits of amyloid are surrounded by swollen axons and dendrites (neuritic dystrophy). These neuronal processes in turn are surrounded by the cell processes of activated astrocytes and microglia (inflammatory cells). Aβ can also form amyloid deposits in the walls of arterioles in the brain, producing what is known as cerebral amyloid angiopathy. This occurs to varying extents in up to 90% of patients who develop AD, but it can also occur independently of AD. Cerebral amyloid angiopathy can lead to ischemic stroke, and it is a common cause of hemorrhagic stroke in the elderly.

Third, many neurons that are affected by Alzheimer pathology but still alive have cytoskeletal abnormalities, the most dramatic of which is the accumulation of neurofibrillary tangles and neuropil threads (Figure 64–9). The tangles are filamentous inclusions in the cell bodies and dendrites that contain paired helical filaments and 15-nm straight filaments. These filaments are made up of an aggregated form of the normal microtubule-associated protein tau.

In AD, tangles do not occur uniformly throughout the brain, but rather affect specific regions. The entorhinal cortex, the hippocampus, parts of the neocortex, and the nucleus basalis are especially vulnerable (Figure 64–10). Alterations in the entorhinal cortex and hippocampus likely underlie the problems with episodic memory that are among the first symptoms of AD. Abnormalities in the basal forebrain cholinergic systems may contribute to cognitive difficulties and attention deficits. These cholinergic abnormalities contrast with those in frontostriatal circuits that correlate with age-related cognitive decline in normal subjects. The combination of anatomical differences, pathological changes, widespread neuronal death, and genetic

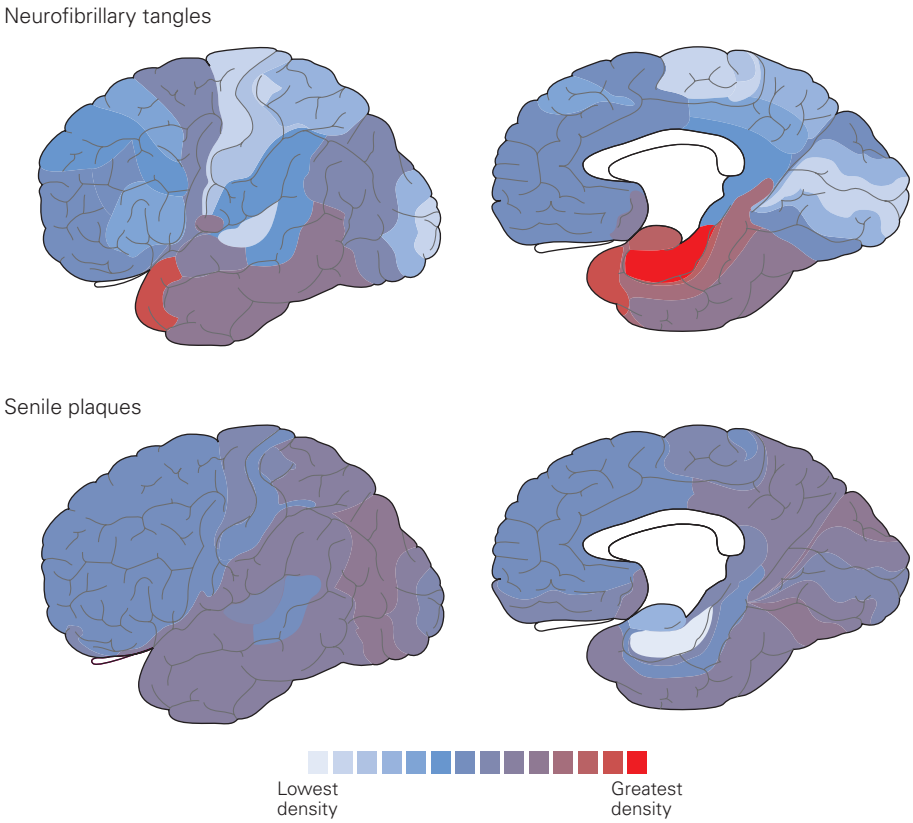

Figure 64–10 Neurofibrillary tangles and senile plaques are concentrated in different regions of the Alzheimer brain. (Adapted, with permission, from Arnold et al. 1991. Copyright © 1991, Oxford University Press.)

mutations (see below) argue against the idea, once prevalent, that AD is an aberrant form of normal aging processes.

Amyloid Plaques Contain Toxic Peptides That Contribute to Alzheimer Pathology

The main constituent of amyloid plaques, aggregates of Aβ peptides, were first isolated in the early 1980s by centrifugation, based on their low solubility. The predominant peptides were 40 and 42 amino acids in length (the 40 residues plus two additional amino acids at the carboxy terminal end). Biochemical studies showed that the Aβ42 peptide nucleates more rapidly than Aβ40 into amyloid fibrils.

Considerable experimental evidence indicates that Aβ42 drives the initial aggregation, although Aβ40 also accumulates to a significant extent, especially in cerebral amyloid angiopathy. For neurons in culture, the forms of the Aβ42 peptide that are larger than a monomer are generally more toxic than aggregated forms of Aβ40. These results implicate Aβ42 as a key driver of amyloid formation as well as Aβ toxicity.

Once it was discovered that Aβ peptides 38 to 43 amino acids in length are formed by cleavage of a precursor protein, researchers set out to isolate the precursor. The precursor was found in the mid-1980s, molecularly cloned, and named the *amyloid precursor protein* (APP). It is a large transmembrane glycoprotein that is present in all types of cells but is expressed at its highest levels in neurons. The normal functions of APP in the brain are not understood.

How is APP processed to form Aβ peptides? The answer has turned out to be complex. Three enzymes, α-, β-, and γ-secretase, cut APP into pieces. The β- and γ-secretases cleave APP to generate soluble extracellular fragments that are released into the interstitial fluid. These are the Aβ peptides, which include part of the transmembrane segment of APP (Figure 64–11). The cleavage by γ-secretase is unusual in that it occurs in a membrane-spanning portion of APP, a region long thought to be immune from hydrolysis because it is surrounded by lipids rather than water. Cleavage by α-secretase in the middle of the Aβ sequence prevents the formation of Aβ peptides.

The enzymes that account for α-, β-, and γ-secretases have been isolated and characterized. The enzyme α-secretase is a member of a large family of extracellular proteases called ADAM (a disintegrin and metalloproteinase) that are responsible

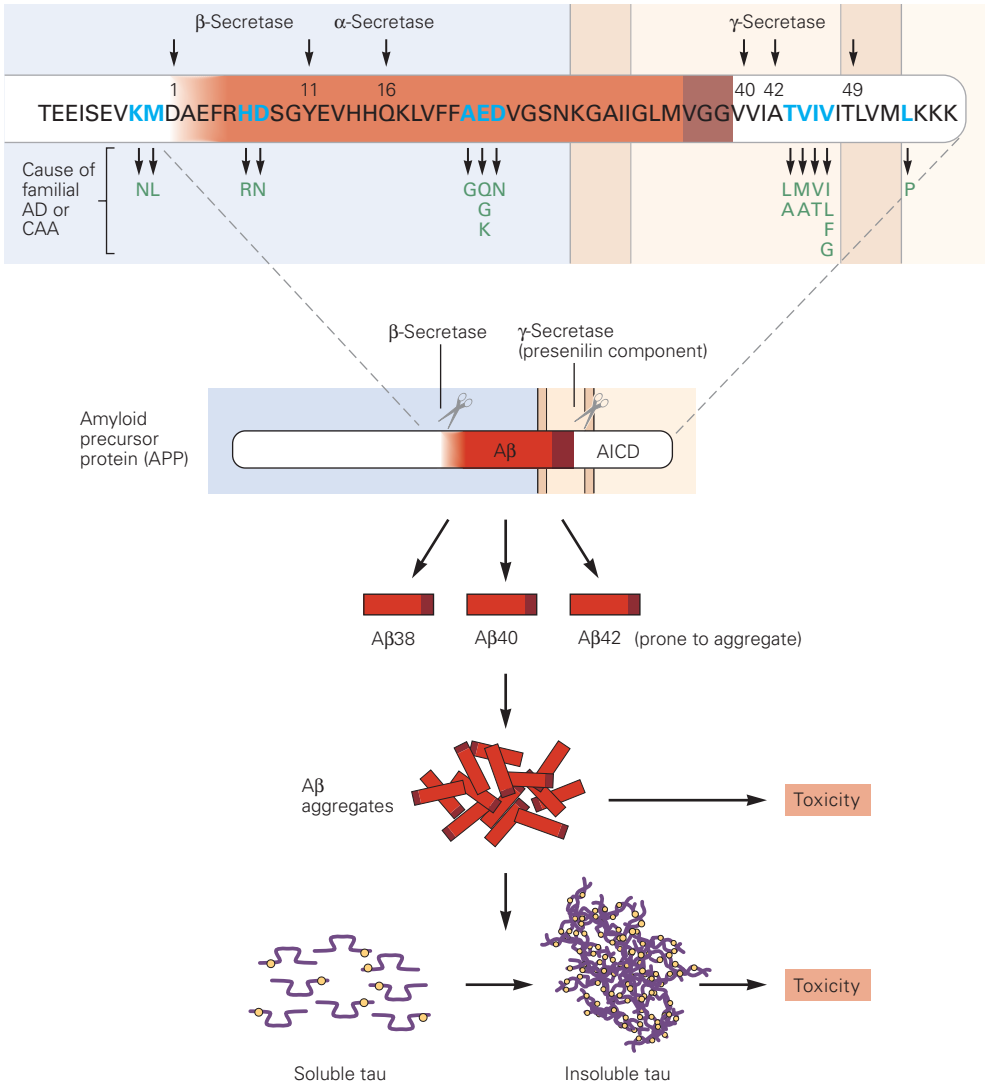

Figure 64–11 Processing of the amyloid precursor protein, generation of the Aβ peptide, and downstream effects on tau aggregation. The Aβ peptide is produced from the amyloid precursor protein (**APP**), a transmembrane protein, via cleavage by two enzymes, β-secretase and γ-secretase. (Cleavage by α-secretase prevents Aβ production.) Presenilin is the active enzymatic component of the γ-secretase complex and cleaves APP at several sites within the membrane to produce Aβ peptides of different lengths such as Aβ38, Aβ40, and Aβ42. Several mutations in APP that are just outside of the Aβ region or within the coding sequence of Aβ cause forms of autosomal dominant Alzheimer disease (**AD**). The amino acids (**blue**) in the APP/Aβ amino acid sequence represent the normal amino acids in APP; amino acids in **green** (below the normal sequence) are those that cause familial AD or cerebral amyloid angiopathy (**CAA**). Aβ is predominantly produced from APP within endosomes. A variety of molecules and synaptic activity regulate Aβ levels. There is evidence that Aβ aggregation is influenced by the Aβ-binding molecules ApoE and clusterin, which likely interact in the extracellular space of the brain. A variety of molecules and processes affect Aβ clearance from the interstitial fluid (ISF) that is present in the extracellular space of the brain, including neprilysin and insulin-degrading enzyme (IDE), as well as cerebral spinal fluid and interstitial fluid bulk flow. LRP1 and RAGE (receptor for advanced glycation end products) appear to influence Aβ transport across the blood–brain barrier. The concentration and type of Aβ influence aggregation (Aβ42 is more fibrillogenic). Once it aggregates into oligomers and fibrils, it can be directly toxic to cells, induce inflammation, and exacerbate the conversion of soluble tau to aggregated tau through mechanisms that remain unclear. In addition to Aβ, a variety of factors influence tau aggregation and toxicity, including tau levels, sequence, and phosphorylation state. (Abbreviation: **AICD**, APP intracellular domain.)

for degrading many components of the extracellular matrix. β-Secretase, called BACE1 (β-site APP cleaving enzyme 1), is a transmembrane protein in central neurons that is concentrated in synapses. Brain cells derived from mutant mice lacking BACE1 do not produce Aβ peptides, proving that BACE1 is indeed the neuronal β-secretase. γ-Secretase, the most complicated of the three, is actually a multiprotein complex that cleaves several different transmembrane proteins. As would be expected, given its peculiar ability to act within the membrane, γ-secretase itself includes several transmembrane proteins. Two of these are called presenilin-1 and presenilin-2, reflecting their association with AD. Other components of the complex include the transmembrane proteins nicastrin, Aph-1, and Pen-2.

Although the biochemical properties of Aβ and APP are interesting, the critical question is whether they have a part in the debilitating symptoms of AD. The disease might be caused by Aβ accumulation, but Aβ might itself be a result of another pathological process or even be an innocuous correlate. Genetic evidence in humans and experimental animals has been critical in demonstrating that APP and, specifically, Aβ play a central role in AD.

The first clue came from the observation that the APP gene lies on chromosome 21, which is present in three copies rather than the normal two in people with Down syndrome (also known as trisomy 21). All people with Down syndrome who live to middle age develop AD pathology and dementia, with onset around 50 years. This association is consistent with the idea that APP predisposes to AD by overproducing APP and Aβ by 50% throughout life. Nevertheless, copies of many genes are present in three copies in individuals with trisomy 21, and initially, it was not clear that triplication of APP in Down syndrome was responsible for AD in this population. Subsequently, rare families were found in which both AD and cerebral amyloid angiopathy developed in the absence of Down syndrome due to duplication of just the APP locus on human chromosome 21. This is strong evidence that overexpression of APP alone is enough to lead to AD and cerebral amyloid angiopathy.

More direct genetic evidence came from analysis of the rare patients with dominantly inherited AD, in whom the onset of symptoms is usually between 30 and 50 years of age. In the late 1980s, several research groups began using methods of molecular cloning to identify the genes mutated in dominantly inherited AD. Remarkably, the first three genes identified were those encoding the proteins APP, presenilin-1, and presenilin-2 (Figure 64–12). Many different mutations in these three genes have been found, and the majority influence cleavage of APP, increasing the production of Aβ peptides or specifically the proportion of the more aggregation-prone Aβ42 species. Interestingly, some APP mutations occur within the Aβ sequence itself and do not affect Aβ production but do affect Aβ aggregation and clearance from the brain.

Some APP mutations are amino acid substitutions flanking the Aβ region. Cells that express a double mutation at the β-secretase cleavage site (the so-called Swedish mutation), which is required for Aβ formation, secrete several-fold more Aβ peptide than cells expressing wild type APP. Interestingly, another mutation in APP adjacent to the β-secretase site was recently discovered. This mutation appears to protect against AD by decreasing Aβ production. Yet another APP mutation causes γ-secretase to generate a greater proportion of longer Aβ species, such as Aβ42, in relation to shorter species such as Aβ40. Likewise, in most presenilin mutants the mutant γ-secretase has higher than normal activity or generates peptides with an increased ratio of Aβ42 to Aβ40.

These human genetic studies offer compelling evidence that (1) cleavage of APP to generate Aβ and the propensity of Aβ to aggregate play key instigating roles in some cases of dominantly inherited early-onset AD and (2) less Aβ production decreases the risk for late-onset AD. Genetic studies in mice have also strengthened the case that APP cleavage and specifically Aβ aggregation contribute to AD. Transgenic expression or knock-in of mutant APP forms identical to those found in autosomal dominant AD leads to the appearance of amyloid plaques in the hippocampus and cortex, dystrophic neurites in proximity to Aβ deposits, decreased density of synaptic terminals around amyloid plaques, and impairments in synaptic transmission. Several mouse models develop functional abnormalities such as deficits in spatial and episodic-like memory. Alterations are more severe in transgenic mice that express altered forms of both APP and presenilin-1. It is important to note that although these mice do not develop tau aggregation or neurofibrillary tangles, lesions believed to be important in the cognitive decline seen in AD, they remain invaluable models for addressing the mechanistic role of Aβ and related pathology in the pathogenesis of AD, especially the role of Aβ, and for testing potential therapies.

Given the strong evidence that APP cleavage is involved in the pathogenesis of AD, the next question is: How does the accumulation of cleavage products contribute to symptoms and ultimately dementia? There are three sets of cleavage products: the secreted extracellular region (ectodomain), the Aβ peptide, and

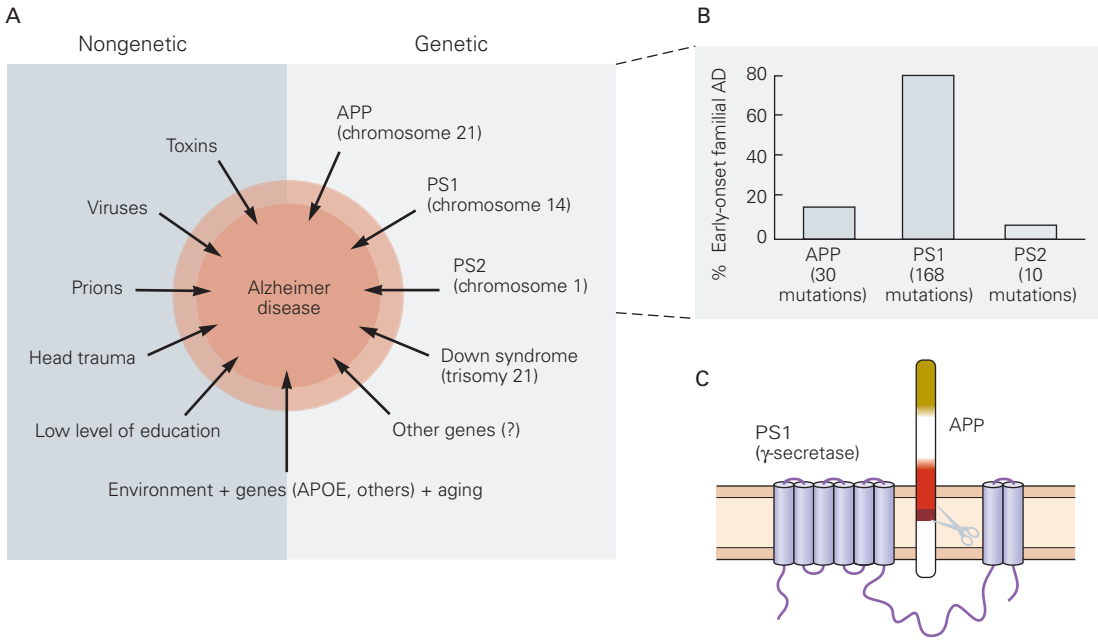

Figure 64–12 Environmental and genetic factors play a role in Alzheimer disease.

A. Environmental and genetic factors. (Abbreviations: **APOE**, apolipoprotein E; **APP**, amyloid precursor protein; **PS1**, presenilin-1; **PS2**, presenilin-2.)

B. Specific genes involved in early-onset Alzheimer disease (**AD**).

C. Presenilin-1 (a component of the gamma secretase enzyme complex) is associated with the APP protein within the plasma membrane.

cytoplasmic fragment. Although all three fragments can have deleterious effects on neurons in experimental animals, the Aβ peptides have received the most attention, and evidence for their involvement is strongest. There is evidence that different aggregated forms of Aβ such as oligomers, protofibrils, and fibrils can lead to synaptic and neuronal damage that might contribute to AD.

Neurofibrillary Tangles Contain Microtubule-Associated Proteins

Until around 2005, most research on the molecular and cellular basis of AD focused on Aβ peptides and amyloid plaques, but tau aggregation in neurofibrillary tangles appears to play a key role in the progression of AD (Figure 64–9). Molecular analysis revealed that these abnormal inclusions in cell bodies and proximal dendrites contain aggregates of hyperphosphorylated isoforms of tau, a microtubule-binding protein that is normally soluble (Figure 64–13). The tau protein plays a key role in intracellular transport, particularly in axons, by binding to and stabilizing microtubules. Impairments in axonal transport compromise synaptic stability and trophic support. While the mechanism by which aggregation and hyperphosphorylation of tau lead to toxicity is still not understood, tau accumulation is clearly associated with neuronal degeneration.

Although tangles are a defining feature of AD, it was initially unclear what role tangles and hyperphosphorylated forms of tau play in the pathogenesis of the disease. Whereas mutations of APP and presenilin genes can lead to AD, no mutations of the tau gene have been found in familial AD. Nevertheless, there is now a great deal of evidence indicating that tau aggregation is a key factor in the neurodegeneration that occurs in AD.

First, filamentous deposits of hyperphosphorylated tau are seen in a variety of neurodegenerative disorders, including AD, forms of frontotemporal dementia, progressive supranuclear palsy, corticobasal degeneration, and CTE. Second, mutations in the tau gene have been found to underlie another form of autosomal dominant neurodegenerative disease: frontotemporal dementia with Parkinson disease type 17 (FTPD17). These patients develop tau aggregation together with brain atrophy in specific brain regions in the absence of Aβ deposition. Third, progressive symptoms of AD correlate much better with the number and distribution of tangles than with the amyloid plaques

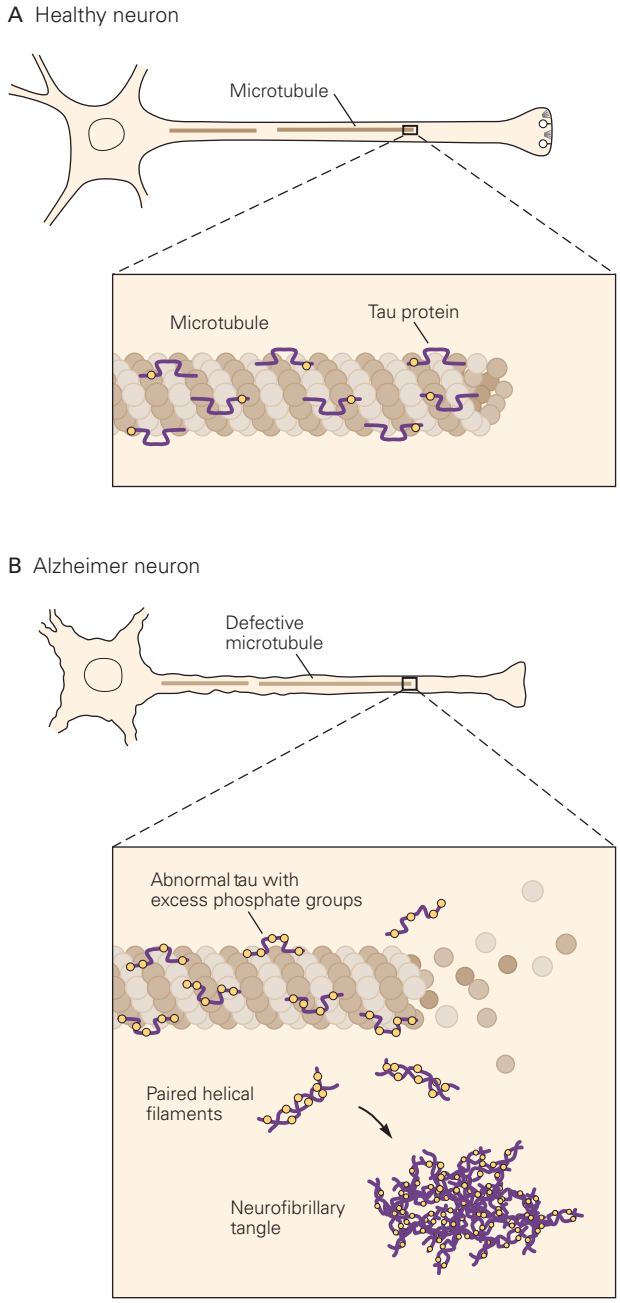

Figure 64–13 Formulation of neurofibrillary tangles.

A. In healthy neurons, tau protein associates with normal microtubules but not as paired helical filaments, and contributes to the structural integrity of the neuron.

B. In a diseased neuron, the tau protein becomes hyperphosphorylated and loses its association with normal microtubules, which begin to disassemble. It then forms paired helical filaments, which become sequestered in neurofibrillary tangles.

seen in autopsy. For example, tangles are usually first evident in neurons of the entorhinal cortex and hippocampus, the likely site of early memory disturbance, before plaques appear in this area (see Figure 64–16).

For many years, controversy raged between those who believe that Aβ is the main causal agent of AD and those who believe that tau-rich tangles play a major role. These partisans have been called "Baptists" and "Tauists," respectively. Baptists pointed to the fact that during the development of AD pathology, which begins about 15 years before symptom onset, accumulation of neocortical Aβ precedes the development of neocortical tau pathology. More recent evidence suggests, however, that Aβ accumulation appears to somehow drive tau aggregation and spreading in the brain. Thus, Aβ aggregation probably instigates the disease and tau aggregation and spreading likely contribute in a major way to neurodegeneration. For example, transgenic mice that express both mutant APP and mutant tau develop much worse tau pathology.

There appears to be interplay between plaques and tangles. Injection of Aβ42 into specific brain regions of transgenic mice that express a mutant tau protein increases the number of tangles in nearby neurons. Further, a manipulation that reduces the number and size of plaques leads to a decrease in levels of hyperphosphorylated tau. Importantly, recent experiments suggest that Aβ deposition in some way promotes spreading of tau aggregates from one brain region to another, possibly transsynaptically in a prion-like fashion. The details of this process remain to be worked out and are likely to be extremely important.

There is now abundant evidence from cell culture and studies in animal models that several proteins that aggregate in neurodegenerative diseases, including tau and synuclein, can spread from cell to cell in a prion-like manner. This is particularly important as a potential disease mechanism. For example, if the cell-to-cell spreading of misfolded proteins occurs in the extracellular space, this process might be interrupted with antibodies directed against the appropriate disease-associated protein. In fact, this now serves as the basis of several clinical trials in humans targeting tau and synuclein.

Risk Factors for Alzheimer Disease Have Been Identified

Very few individuals develop AD because they bear autosomal dominant mutant alleles of the APP or presenilin genes, and these are generally of the early-onset variety. Hardly any cases of late-onset AD are due to mutations in APP or presenilin genes. Can we, then, predict AD in such individuals?

The major risk factor is age. The disease is present in a vanishingly small fraction of people younger than age 60 (many of those being autosomal dominant cases), 1% to 3% of those between ages 60 and 70, 3% to 12% of those between ages 70 and 80, and 25% to 40% of those older than age 85. Knowing that elderly people are prime candidates for AD is of little therapeutic use, however, because modern medicine can do nothing to slow the passage of time. Therefore, there has been intense interest in other factors that affect the incidence of AD.

To date, the most significant genetic risk factors discovered for late-onset AD are the alleles of the gene *APOE*. The ApoE protein is an apolipoprotein. In the blood, it plays an important role in plasma cholesterol metabolism. It is also expressed at high levels in the brain, most prominently by astrocytes and to some extent by microglia. In the brain, where its normal function has not been clarified, it is secreted as a component of high density-like lipoproteins. In humans, there are three alleles of the *APOE* gene, *APOE2*, *APOE3*, and *APOE4*, which differ from each other by at most two amino acids. People with the *APOE4* allele are at risk for AD, whereas those with the *APOE2* allele are protected against AD relative to people who have the most common *APOE3/APOE3* genotype. The *APOE4* allele is present in about 25% of the general population but present in as many as 60% of those with AD. One copy of the *APOE4* allele increases the risk of AD by about 3.7-fold, and two copies by about 12-fold, relative to someone who is *ApoE3/E3* (Figure 64–14). One copy of the *APOE2* allele decreases the risk for AD by about 40% relative to being *APOE3/APOE3*.

The mechanism by which *APOE4* predisposes to AD and *APOE2* protects against AD is uncertain, but ApoE4 clearly promotes Aβ aggregation by diminishing Aβ clearance and promoting fibrillization (ApoE4 > ApoE3 > ApoE2). It may also act through additional mechanisms such as influencing tau, the innate immune system, cholesterol metabolism, or synaptic plasticity, although these pathways remain to be worked out.

A number of other genes and genetic loci influence risk for late-onset AD. Some are common variants that alter risk only slightly, whereas other rarer variants increase risk to a greater extent (Figure 64–14). For example, relatively rare mutations in the gene *TREM2* double or triple the risk for AD, similar to having one copy of the *APOE4* allele. This is interesting because *TREM2* as well as another gene associated with risk

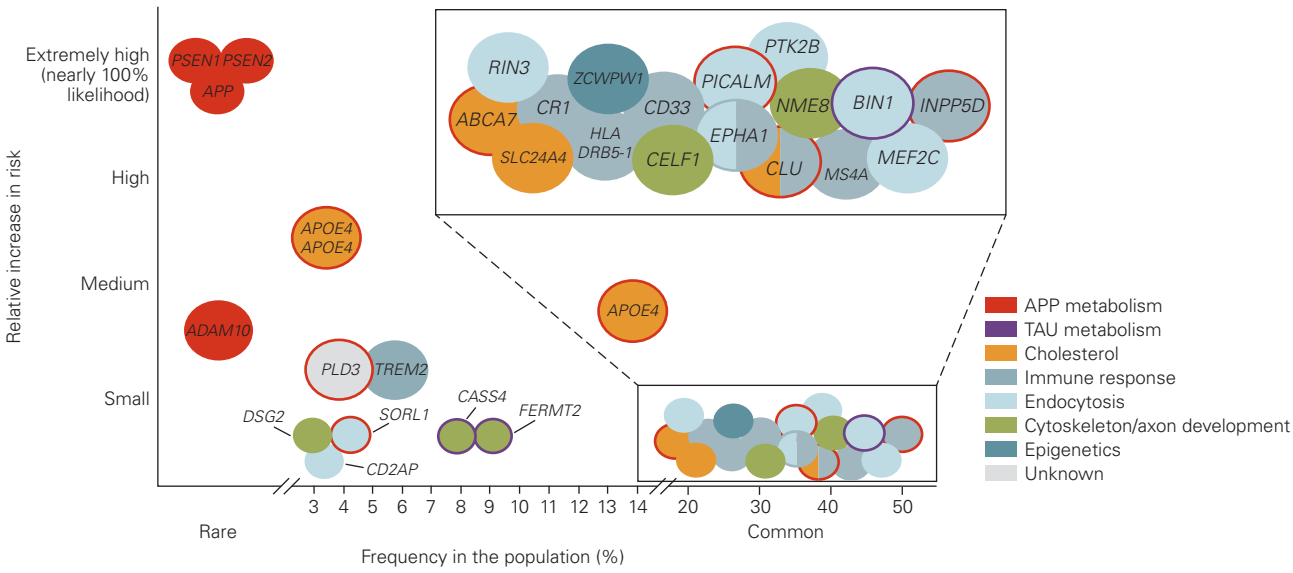

Figure 64–14 The risk for Alzheimer disease due to rare and common genetic variants. Data are from genome-wide association studies (GWAS). Mutations in the three genes that cause early-onset familial Alzheimer disease (*PSEN1*, *PSEN2*, and *APP*) are rare but result in Alzheimer disease in virtually 100% of people with these mutations if they live to middle age. There have been a number of common genetic changes found located in regions around or in genes that are relatively frequent in the population (eg, *ABCA7*, *CLU*, *BIN1*) that affect risk for Alzheimer disease but to a very small degree. The one common and strong genetic risk factor for Alzheimer disease that is present in about 20% to 25% of the population (allele frequency ~15%) is *APOE4*. One copy of *APOE4* increases risk approximately 3.7-fold and two copies increase risk approximately 12-fold relative to people who are homozygous for *APOE3*. (Adapted, with permission, from Karch and Goate 2015.)

for AD, *CD33*, are expressed only in microglia. Along with other emerging cellular and animal model data, this finding suggests that the innate immune system is involved in AD pathogenesis. A number of other rare variants that increase risk to varying degrees are under investigation. It seems likely that these developments will ultimately result in a more personalized clinical approach to determining risk for AD, especially as treatments for the disease emerge.

Alzheimer Disease Can Now Be Diagnosed Well but Available Treatments Are Unsatisfactory

Diagnosing AD at its earliest stages in the absence of biomarkers can be challenging, as its initial symptoms can be similar to those of normal age-related cognitive decline or of other related diseases. Nevertheless, diagnosis of mild to moderate dementia due to AD is usually fairly accurate. In fact, during the past few decades, the ability to accurately diagnose the disease has improved, largely because of three factors.

First, protocols for physical, neurological, and neuropsychological examination have become more sophisticated and standardized. Second, increased knowledge of the structural changes revealed by magnetic resonance imaging (MRI) have helped in diagnosing AD at early stages. For example, it is now possible to predict, with approximately 80% accuracy, which patients with MCI will develop AD based on the cortical thinning and ventricular enlargement visible by MRI. These imaging and diagnostic methods also assist in distinguishing dementia syndromes from each other and relating structural to functional defects. For example, patients with the disease known as *behavioral variant of frontotemporal dementia* experience personality changes early on, and MRI at that stage reveals atrophy of the frontal and/or temporal lobes. Likewise, initial difficulties in AD usually center on memory and attention, and MRI reveals initial alterations in the medial temporal cortex and hippocampus.

Third, and perhaps most promising, amyloid plaques and neurofibrillary tangles can be visualized by positron emission tomography (PET) using compounds that avidly bind fibrillar forms of Aβ or aggregated forms of tau. The first of these, Pittsburgh compound B (PIB), binds with high affinity to fibrillar Aβ; its radioactive form, labeled with short-lived isotopes of carbon or fluorine, is readily detected by PET (Figure 64–15). The US Food and Drug Administration (FDA) has approved three amyloid imaging agents: florbetapir (Amyvid), flutemetamol (Vizamyl), and florbetaben (Neuraceq).

The availability of safe molecular markers of AD allows early stages of the disease to be identified before clinical symptoms are present. Of equal importance, it allows for improved selection of patients for clinical trials and keener selection of subjects for detailed analyses of normal aging. It is important to note that these changes can also be detected in the cerebrospinal fluid, where the level of Aβ42 drops when amyloid deposition is present and total tau and phosphorylated forms of tau increase with neurodegeneration and tau aggregation.

Of course, improved diagnosis of AD is most useful if treatments are available that can halt or slow its progression at an early stage. While we still do not

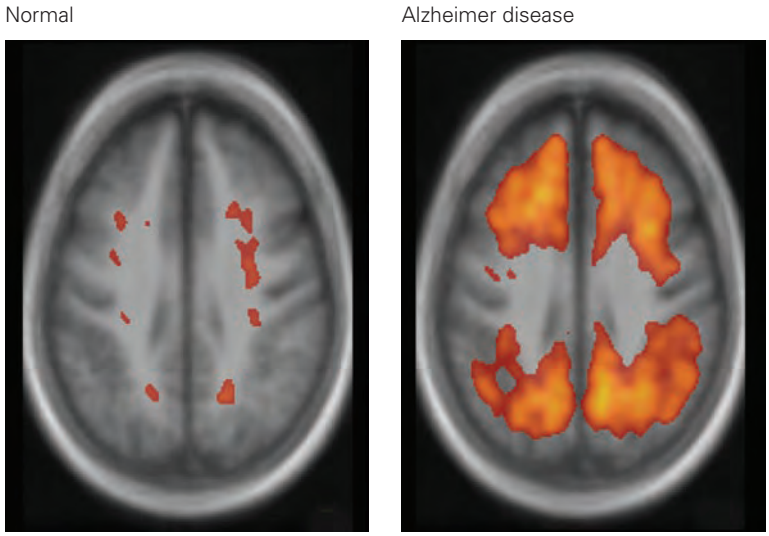

Figure 64–15 Positron emission tomography scans can visualize amyloid plaques in the living brain. The density of Aβ plaques is indicated by the red regions in these images made after administration of Pittsburgh compound B (PIB), a fluorescent analog of thioflavin T. (Images reproduced, with permission, from R. Buckner.)

have a treatment that delays the onset or slows the progression of AD, there is hope that we are not too far off from being able to mitigate symptoms. Although there is no definitive proof, there is good evidence that a variety of lifestyle factors decrease risk for AD. These include high levels of education, cognitive stimulation, staying socially engaged, regular exercise, not being overweight, and getting appropriate amounts of sleep. Present-day therapies focus on treating associated symptoms such as depression, agitation, sleep disorders, hallucinations, and delusions.

One of the principal therapeutic targets to date has been the cholinergic system in the basal forebrain, a region of the brain that is damaged in AD and that contributes to attention. Acetylcholinesterase inhibitors increase levels of acetylcholine by inhibiting its breakdown and represent one of the few drug classes approved by the FDA for treatment of AD. Another drug, the *N*-methyl-D-aspartate (NMDA) receptor antagonist memantine, also improves symptoms in individuals with mild to moderate dementia due to AD. It is believed that memantine's action modulates glutamate-mediated neurotransmission. Nevertheless, these drugs exert only a modest effect on cognitive functions and the activities of daily living.

Recent advances in our understanding of the cell-biological basis of AD have produced several promising new therapeutic targets, all of which are being explored intensively. One approach is to develop drugs that reduce or modulate the activity of the β- and γ-secretases that cleave APP to generate Aβ peptides and the associated soluble extracellular and intracellular fragments. In fact, decreasing either β- or γ-secretase levels in transgenic mice that overexpress mutant APP decreases Aβ deposition and, in some cases, functional abnormalities.

Accordingly, pharmaceutical companies have developed drugs that decrease or modulate levels of β- and γ-secretases in humans. An obstacle to this approach is that the secretases also act on substrates other than APP, so decreasing their levels can have deleterious side effects. This is especially true for γ-secretase, whose inhibition has led to toxicity in human trials for AD. There are now several β-secretase inhibitors in clinical trials for AD, and it is likely such drugs will also move into trials for what is called preclinical AD, when AD pathology is accumulating but there is no sign yet of cognitive decline (Figure 64–16). The goal of this therapy would be to delay or prevent the onset of cognitive decline and dementia.

Another approach is to decrease levels of Aβ through immunological means. Both immunization with Aβ, which leads to generation of antibodies to Aβ, and passive transfer of Aβ antibodies have been

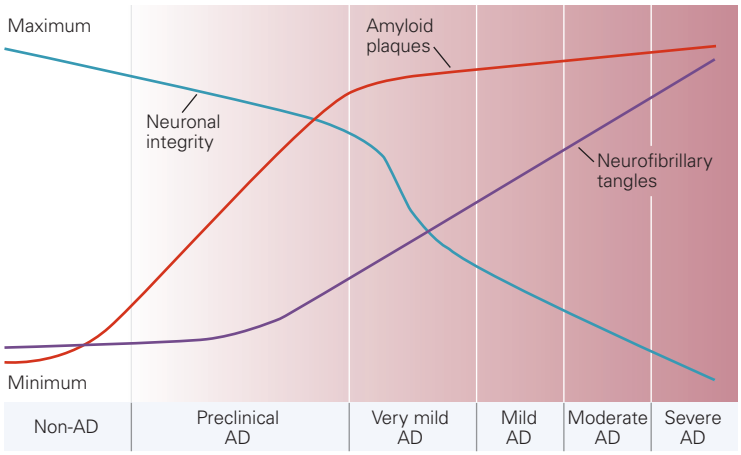

Figure 64–16 Relationship of biomarker changes to cognitive and clinical changes in Alzheimer disease (AD). In cognitively normal people who are going to develop AD dementia, one of the first physical signs is the initiation of Aβ aggregation in the brain in the form of amyloid plaques. While people are still cognitively normal, amyloid plaques continue to accumulate. At some point, about 5 years before any clear-cut cognitive decline, tau accumulation begins to increase in the neocortex, inflammation and oxidative stress increase, and brain network connections and metabolism begin to decline. Neuronal and synaptic loss and brain atrophy also begin. This period—when the patient remains cognitively normal but AD-type pathology is building up—is termed preclinical AD. Once there is enough neuronal and synaptic dysfunction as well as cell loss, very mild dementia and mild cognitive impairment become detectable. At that time, amyloid deposition has almost reached its peak. As dementia worsens to mild, moderate, and severe stages, neurofibrillary tangles form, and neuronal and synaptic dysfunction, inflammation, cell death, and brain atrophy worsen. (Adapted, with permission, from Perrin, Fagan, and Holtzman 2009.)

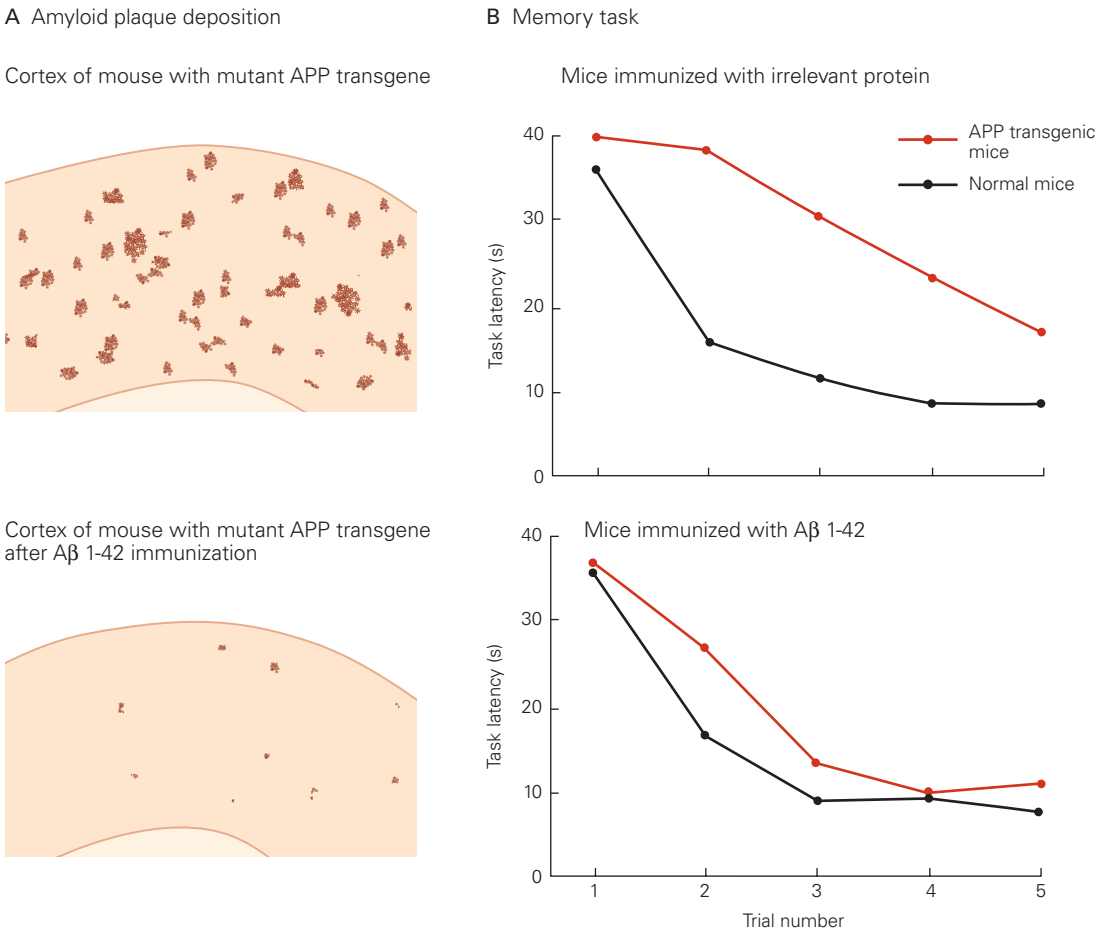

Figure 64–17 Immunization with antibodies to the Aβ peptide clears amyloid plaques and preserves cognitive performance in mice expressing the peptide. Mice that develop Aβ deposition in the form of amyloid plaques were immunized with the Aβ peptide. This led to production of antibodies against Aβ.

A. Comparison of amyloid plaque deposition in the cerebral cortex of mice overexpressing a mutant APP transgene (APP transgenic mice) that develop amyloid plaques. The mice that were immunized with the Aβ peptide have substantially reduced amyloid plaque deposition. (Adapted from Brody and Holtzman 2008.)

B. Cognitive performance (a memory test) in two groups of APP transgenic mice. One group was immunized with an irrelevant protein, the other with the Aβ peptide. The mice vaccinated with Aβ performed at levels close to normal animals, whereas mice immunized with the irrelevant protein showed severe impairment in memory. (Adapted, with permission, from Janus et al. 2000.)

tested in transgenic mouse models of AD. Both treatments have been shown to reduce levels of Aβ, Aβ toxicity, and plaques (Figure 64–17). The mechanisms of enhanced Aβ clearance are not completely clear. Serum antibodies likely serve as a "sink," resulting in Aβ peptides with low molecular weight being cleared more extensively from the brain into the circulation, thus changing the equilibrium of Aβ in different compartments and promoting removal of Aβ from the brain.

It is also clear that in the brain several anti-Aβ antibodies bind either soluble or fibrillar Aβ, or both. Those that bind to aggregated forms of Aβ can stimulate microglia-mediated phagocytosis to remove Aβ, although there is also plaque removal that is not dependent on microglial-mediated phagocytosis. Antibodies to soluble Aβ that enter the brain may decrease soluble Aβ toxicity. These findings suggest that immunotherapeutic strategies may be successful in AD patients, especially if they are given early enough in the disease course, prior to significant neuronal damage and loss. There are multiple human trials underway using active and passive immunotherapies against Aβ both in preclinical and mild AD.

In addition to targeting Aβ, clinical trials have also begun targeting tau. This is being done with active and passive immunization against tau as well as with small molecules that, in cell culture and animal models, can decrease tau aggregation. A number of studies in animal models have shown that certain anti-tau antibodies can decrease the amount of aggregated, hyperphosphorylated tau in the central nervous system and in some cases improve function. Although tau is predominantly a cytoplasmic protein, one of the reasons that anti-tau antibodies may be having an effect is that, as discussed above, tau aggregates may spread from cell to cell in the extracellular space in a prion-like fashion. It is in this space that an antibody may be able to interact with tau and block this process.

Highlights

1. It is only in the past 50 years that a large percentage of the population has lived into the eighth to tenth decades of life. With this increase, neuroscientists have been able to study changes in the brain that occur with normal aging as well as in individuals who develop age-related brain disorders.
2. Subtle changes in a variety of brain functions occur with age, including declines in speed of processing and memory storage and changes in sleep. The underlying basis for these changes is likely brain atrophy and loss of white matter integrity. In general, however, there is not a significant decrease in neuronal number that accounts for changes in brain function that occur with normal aging.
3. The changes in cognition that occur in normal aging are not disabling. When memory and often other areas of cognitive function decline more than is expected with age such that it is noticeable to others and mildly affects one's day-to-day life, this syndrome is called mild cognitive impairment (MCI).
4. MCI is not a disease, it is a syndrome. About 50% of individuals with MCI have Alzheimer disease (AD) as the underlying cause of the MCI. Other conditions that can cause MCI include depression, cerebrovascular disease, Lewy body disease, metabolic disorders, and drugs, prescribed for other diseases, that cause central nervous system side effects.
5. AD is the most common cause of dementia and manifests as loss of memory and other cognitive abilities sufficient to impair social and occupational functions. AD accounts for about 70% of cases of dementia in the United States, with the remainder caused primarily by cerebrovascular disease, Parkinson and Lewy body dementia, and frontotemporal dementia.
6. The pathology of AD is characterized by the accumulation of aggregated forms of two proteins in the brain, the Aβ peptide and tau. Aβ accumulates in a fibrillar form in extracellular structures called amyloid plaques in the brain parenchyma as well as in the walls of arterioles (where it is called cerebral amyloid angiopathy). Tau accumulates in neurofibrillary tangles in cell bodies and dendrites.
7. In addition to the accumulation of protein aggregates in the Alzheimer brain, marked brain atrophy as well as synaptic and neuronal loss occurs as the disease progresses. There is also a strong neuroinflammatory response, especially around amyloid plaques, which involves microglia and astrocytes.
8. The pathology of AD begins about 15 years prior to the onset of cognitive decline or the MCI phase of the disease. Aβ accumulation in the neocortex appears to initiate the disease with markedly abnormal levels, followed by the spread of tau aggregates from the medial temporal lobe to other regions of the neocortex. This phase of Alzheimer pathology prior to symptom onset is known as preclinical AD.
9. Significant data suggest that certain aggregated forms of the Aβ peptide lead to synaptic and neuronal damage in the Alzheimer brain, but a much better correlate of the cognitive decline is the presence and accumulation of aggregated forms of the tau protein.
10. There are two major forms of AD. The first is a dominantly inherited AD, which accounts for less than 1% of Alzheimer patients and is caused by mutations in one of three genes encoding the proteins APP, PS1, and PS2; this form leads to clinical disease onset between the ages of 30 and 50. Genetic, biochemical, and other studies have shown that the genes that cause autosomal dominant AD do so through early accumulation of the Aβ peptide in the brain. The second form, late-onset AD, with an age of onset of 65 years or later, accounts for more than 99% of cases. Although age is the greatest risk factor for late-onset AD, genetics also contribute. The *APOE* gene is by far the biggest genetic contributor to AD, with the *APOE4* variant increasing risk and the *APOE2* variant decreasing risk. There are a number of

other common genetic variants in other genes that influence risk. There are also rare variants in other genes such as *TREM2* that increase risk to a level similar to that associated with one copy of *APOE4*. Nonetheless, there is general agreement that major features of pathogenesis are similar in sporadic and familial AD.

11. Besides clinical symptoms and signs of AD, amyloid and tau imaging and cerebrospinal fluid markers can determine that Alzheimer pathology is present in a living person with or without cognitive decline.
12. There are currently only symptomatic therapies for AD that have modest benefit at best. A number of potential disease-modifying therapies that influence the production, clearance, and aggregation of either Aβ or tau are being tested in humans. Although none of these therapies is yet approved, there is hope that over the next several years one or more of these therapies will begin to show a clear benefit.

Joshua R. Sanes
David M. Holtzman

Selected Reading

Brody DL, Holtzman DM. 2008. Active and passive immunotherapy for neurodegenerative disorders. Annu Rev Neurosci 31:175–193.

Buckner RL. 2004. Memory and executive function in aging and AD: multiple factors that cause decline and reserve factors that compensate. Neuron 44:195–208.

Goedert M, Eisenberg DS, Crowther RA. 2017. Propagation of tau aggregates and neurodegeneration. Annu Rev Neurosci 40:189–210.

Haass C, Selkoe DJ. 2007. Soluble protein oligomers in neurodegeneration: lessons from the Alzheimer's amyloid beta-peptide. Nat Rev Mol Cell Biol 8:101–112.

Holtzman DM, Herz J, Bu G. 2012. Apolipoprotein E and apolipoprotein E receptors: normal biology and roles in Alzheimer disease. Cold Spring Harb Perspect Med 2:a006312.

Holtzman DM, Morris JC, Goate AM. 2011. Alzheimer's disease: the challenge of the second century. Sci Transl Med 3:77sr1.

Kenyon C. 2005. The plasticity of aging: insights from long-lived mutants. Cell 120:449–460.

Musiek ES, Holtzman DM. 2015. Three dimensions of the amyloid hypothesis: time, space and "wingmen." Nat Neurosci 18:800–806.

Sanders DW, Kaufman SK, Holmes BB, Diamond MI. 2016. Prions and protein assemblies that convey biological information in health and disease. Neuron 89:433–448.

References

Andrews-Hanna JR, Snyder AZ, Vincent JL, et al. 2007. Disruption of large-scale brain systems in advanced aging. Neuron 56:924–935.

Arias E. 2004. United States Life Tables, 2001. *National Vital Statistics Reports*, Vol. 52, No. 14. Hyattsville, MD: National Center for Health Statistics.

Arnold SE, Hyman BT, Flory J, Damasio AR, Van Hoesen GW. 1991. The topographical and neuroanatomical distribution of neurofibrillary tangles and neuritic plaques in the cerebral cortex of patients with Alzheimer's disease. Cereb Cortex 1:103–116.

Bard F, Cannon C, Barbour R, et al. 2000. Peripherally administered antibodies against amyloid beta-peptide enter the central nervous system and reduce pathology in a mouse model of Alzheimer disease. Nat Med 6:916–919.

Bateman RJ, Xiong C, Benzinger TL, et al. 2012. Clinical and biomarker changes in dominantly inherited Alzheimer's disease. N Engl J Med 367:795–804.

Bishop NA, Lu T, Yankner BA. 2010. Neural mechanisms of ageing and cognitive decline. Nature 464:529–535.

Brown-Borg H, Borg K, Meliska C, Bartke A. 1996. Dwarf mice and the ageing process. Nature 384:33.

Cai H, Wang Y, McCarthy D, et al. 2001. BACE1 is the major beta-secretase for generation of A–beta peptides by neurons. Nat Neurosci 4:233–234.

Choi SH, Kim YH, Hebisch M, et al. 2014. A three-dimensional human neural cell culture model of Alzheimer's disease. Nature 515:274–278.

Cleary JP, Walsh DM, Hofmeister JJ, et al. 2005. Natural oligomers of the amyloid-beta protein specifically disrupt cognitive function. Nat Neurosci 8:79–84.

Cohen E, Dillin A. 2008. The insulin paradox: aging, proteotoxicity and neurodegeneration. Nat Rev Neurosci 9:759–767.

Corder EH, Saunders AM, Strittmatter WJ, et al. 1993. Gene dose of apolipoprotein E type 4 allele and the risk of Alzheimer disease in late onset families. Science 261:921–923.

De Strooper B, Saftig P, Craessaerts K, et al. 1998. Deficiency of presenilin-1 inhibits the normal cleavage of amyloid precursor protein. Nature 391:387–390.

Dickstein DL, Kabaso D, Rocher AB, Luebke JI, Wearne SL, Hof PR. 2007. Changes in the structural complexity of the aged brain. Aging Cell 6:275–284.

Fitzpatrick AWP, Falcon B, He S, et al. 2017. Cryo-EM structures of tau filaments from Alzheimer's disease. Nature 547:185–190.

Glenner GG, Wong CW. 1984. Alzheimer's disease: initial report of the purification and characterization of a novel cerebrovascular amyloid protein. Biochem Biophys Res Commun 120:885–890.

Goate A, Chartier-Harlin MC, Mullan M, et al. 1991. Segregation of a missense mutation in the amyloid precursor protein gene with familial Alzheimer's disease. Nature 349:704–706.

Guerreiro R, Wojtas A, Bras J, et al. 2013. TREM2 variants in Alzheimer's disease. N Engl J Med 368:117–127.

Hansson O, Zetterberg H, Buchhave P, Londos E, Blennow K, Minthon L. 2006. Association between CSF biomarkers and incipient Alzheimer's disease in patients with mild cognitive impairment: a follow-up study. Lancet Neurol 5:228–234.

Hebert LE, Scherr PA, Bienias JL, Bennett DA, Evans DA. 2003. Alzheimer disease in the US population: prevalence estimates using the 2000 census. Arch Neurobiol 60: 1119–1122.

Hekimi S, Guarente L. 2003. Genetics and the specificity of the aging process. Science 299:1351–1354.

Hsiao K, Chapman P, Nilsen S, et al. 1996. Correlative memory deficits, Aβ elevation, and amyloid plaques in transgenic mice. Science 274:99–102.

Huttenlocher PR. 2002. *Neural Plasticity: The Effects of Environment on the Development of the Cerebral Cortex.* Cambridge, MA: Harvard Univ. Press.

Janus C, Pearson J, McLaurin J, et al. 2000. A beta peptide immunization reduces behavioural impairment and plaques in a model of Alzheimer's disease. Nature 408:979–982.

Johnson KA, Schultz A, Betensky RA, et al. 2016. Tau positron emission tomographic imaging in aging and early Alzheimer disease. Ann Neurol 79:110–119.

Jonsson T, Atwal JK, Steinberg S, et al. 2007. A mutation in APP protects against Alzheimer's disease and age-related cognitive decline. Nature 488:96–99.

Kang J, Lemaire HG, Unterbeck A, et al. 1987. The precursor of Alzheimer's disease amyloid A4 protein resembles a cell-surface receptor. Nature 325:733–736.

Kang JE, Lim MM, Bateman RJ, et al. 2009. Amyloid-beta dynamics are regulated by orexin and the sleep-wake cycle. Science 326:1005–1007.

Karch CM, Goate AM. 2015. Alzheimer's disease risk genes and mechanisms of disease pathogenesis. Biol Psychiatry 77:43–51.

Klunk WE, Engler H, Nordberg A, et al. 2004. Imaging brain amyloid in Alzheimer's disease with Pittsburgh Compound-B. Ann Neurol 55:306–319.

Lesne S, Koh MT, Kotilinek L, et al. 2006. A specific amyloid-beta protein assembly in the brain impairs memory. Nature 440:352–357.

Levy-Lahad E, Wasco W, Poorkaj P, et al. 1995. Candidate gene for the chromosome 1 familial Alzheimer's disease locus. Science 269:973–977.

Morgan D, Diamond DM, Gottschall PE, et al. 2000. A beta peptide vaccination prevents memory loss in an animal model of Alzheimer's disease. Nature 408:982–985.

Morris JC, McKeel DW Jr, Storandt M, et al. 1991. Very mild Alzheimer's disease: informant-based clinical, psychometric, and pathologic distinction from normal aging. Neurology 41:469–478.

Oddo S, Caccamo A, Shepherd JD, et al. 1996. Mediators of long-term memory performance across the life span. Psychol Aging 11:621–637.

Park DC, Smith AD, Lautenschlager G, et al. 1996. Mediators of long-term memory performance across the life span. Psychol Aging. 11:621–37.

Perrin RJ, Fagan AM, Holtzman DM. 2009. Multimodal techniques for diagnosis and prognosis of Alzheimer's disease. Nature 461:916–922.

Price JL, Davis PB, Morris JC, White DL. 1991. The distribution of tangles, plaques and related immunohistochemical markers in healthy aging and Alzheimer's disease. Neurobiol Aging 12:295–312.

Rubin EH, Storandt M, Miller JP, et al. 1998. A prospective study of cognitive function and onset of dementia in cognitively healthy elders. Arch Neurol 55:395–401.

Sanders DW, Kaufman SK, DeVos SL, et al. 2014. Distinct tau prion strains propagate in cells and mice and define different tauopathies. Neuron 82:1271–1278.

Schenk D, Barbour R, Dunn W, et al. 1999. Immunization with amyloid attenuates Alzheimer-disease-like pathology in the PDAPP mouse. Nature 400:173–177.

Sevigny J, Chiao P, Bussière T, et al. 2016 The antibody aducanumab reduces Aβ plaques in Alzheimer's disease. Nature 537:50–56.

Shi Y, Yamada K, Liddelow SA, et al. 2017. ApoE4 markedly exacerbates tau-mediated neurodegeneration in a mouse model of tauopathy. Nature 549:523–527.

Sperling RA, Aisen PS, Beckett LA, et al. 2011. Toward defining the preclinical stages of Alzheimer's disease: recommendations from the National Institute on Aging-Alzheimer's Association workgroups on diagnostic guidelines for Alzheimer's disease. Alzheimers Dement 7:280–292.

Strehler BL. 1975. Implications of aging research for society. Fed Proc 34:5–8.

Valdez G, Tapia JC, Kang H, et al. 2010. Attenuation of age-related changes in mouse neuromuscular synapses by caloric restriction and exercise. Proc Natl Acad Sci U S A 107:14863–14868.

Van Broeckhoven C, Haan J, Bakker E, et al. 1990. Amyloid beta protein precursor gene and hereditary cerebral hemorrhage with amyloidosis (Dutch). Science 248:1120–1122.

Yanamandra K, Kfoury N, Jiang H, et al. 2013. Anti-tau antibodies that block tau aggregate seeding in vitro markedly decrease pathology and improve cognition in vivo. Neuron 80:402–414.

Yi L, Seroude L, Benzer S. 1998. Extended life-span and stress resistance in the *Drosophila* mutant Methuselah. Science 282:943–946.

This page intentionally left blank

Index

The letters b, f, and t following a page number indicate box, figure, and table.

B

C

D

E

F

G

H

I

J

K

L

M

N

O

P

Q

R

S

T

U

V

W

X

Y

Z

Symbols

C Capacitance (measured in farads).

c_m Capacitance per unit length of membrane cylinder.

C_m Membrane capacitance: either total input capacitance of a cell (measured in units of F) or capacitance of a unit area of membrane ($F \cdot cm^{-2}$), depending on context.

E Equilibrium (or Nernst) potential of an ion species, e.g., E_{Na}, or reversal potential for current through an ion channel.

F Faraday's constant (9.65×10^4 coulombs per mole).

G Conductance (measured in siemens).

g Conductance of a population of ion channels to one or more ion species, e.g., g_{Na}.

g_l Resting (leakage) conductance; total conductance of a population of resting (leakage) ion channels.

I Current (measured in amperes). The flow of charge per unit time, $\Delta Q/\Delta t$. Ohm's law, $I = V \cdot G$, states that current flowing through a conductor (G) is directly proportional to the potential difference (V) imposed across it.

I_c Capacitive current; the current that changes the charge distribution on the lipid bilayer.

I_i Ionic current; the resistive current that flows through ion channels.

I_l Leakage current; the current flowing through a population of resting ion channels.

I_m Total current crossing the cell membrane.

i Current flowing through a single ion channel.

Q Excess positive or negative charge on each side of a capacitor (measured in coulombs).

R Gas constant ($1.99\ cal \cdot °K^{-1} \cdot mol^{-1}$).

R Resistance (measured in ohms). The reciprocal of conductance, $1/G$.

R_{in} Total input resistance of a cell.

R_m Specific resistance of a unit area of membrane (measured in $\Omega \cdot cm^2$).

r Resistance of a single ion channel.

r_a Axial resistance of the cytoplasmic core of an axon, per unit length (measured in Ω/cm).

r_m Membrane resistance, per unit length (measured in $\Omega \cdot cm$).

V_m Membrane potential, $V_m = Q/C_{in}$ (measured in volts).

V_r Resting membrane potential.

V_t Threshold of membrane potential above which the neuron generates an action potential.

V_{in} Potential on the inside of the cell membrane.

V_{out} Potential on the outside of the cell membrane.

Z Valence.

γ Conductance of a single ion channel, e.g., γ_{Na}

λ Cell membrane length constant (typical values 0.1–1.0 mm). $\lambda = \sqrt{r_m/r_a}$

τ Cell membrane time constant; the product of resistance and capacitance of the membrane (typical values 1–20 ms). $\tau = R_m \cdot C_m$

Units of Measurement

A Ampere, measure of electric current (SI base unit). One ampere of current represents the movement of 1 coulomb of charge per second.

Å Ångström, measure of length (10^{-10} m, non-SI unit).

C Coulomb, measure of quantity of electricity, electric charge (expressed in SI base units $s \cdot A$).

F Farad, measure of capacitance (expressed in SI base units $m^2 \cdot kg^{-1} \cdot s^4 \cdot A^2$).

Hz Hertz, measure of frequency (expressed in s^{-1}).

M Molar measure of concentration of a solution (moles of solute per liter of solution).

mol Mole, measure of amount of substance (Sl base unit).

mol wt Molecular weight.

S Siemens, measure of conductance (expressed in SI base units $m^{-2} \cdot kg^{-1}. s^3 \cdot A^2$).

V Volt, measure of electric potential, electromotive force (expressed in SI base units $m^2 \cdot kg \cdot s^{-3} \cdot A^{-1}$). One volt is the energy required to move 1 coulomb a distance of 1 meter against a force of 1 newton. Measurements in cells are in the range of millivolts (mV).

Ω Ohm, measure of electric resistance (expressed in SI base units $m^2 \cdot kg \cdot s^{-3} \cdot A^{-2}$).